TRANSACTIONS

OF THE

AMERICAN INSTITUTE

OF

ELECTRICAL ENGINEERS

VOLUME 68
1949
PART I

PUBLISHED BY THE
AMERICAN INSTITUTE OF ELECTRICAL ENGINEERS
33 WEST 39TH STREET
NEW YORK 18, N. Y., U. S. A.

Copyright 1949
by the
American Institute of Electrical Engineers

Printed in the United States of America by
The Mack Printing Company, Easton, Pa.

TRANSACTIONS

OF THE

AMERICAN INSTITUTE

OF

ELECTRICAL ENGINEERS

VOLUME 68
1949
PART II

PUBLISHED BY THE
AMERICAN INSTITUTE OF ELECTRICAL ENGINEERS
33 WEST 39TH STREET
NEW YORK 18, N. Y., U. S. A.

Copyright 1949
by the
American Institute of Electrical Engineers

Printed in the United States of America by
The Mack Printing Company, Easton, Pa.

AIEE Transactions Index for 1949

(Complete Index for Parts I and II of Volume 68)

1. Technical Subject Index

Accessory Design Utilizing New Laboratory Techniques, Cable. Bosworth, Farr.......1268–73; disc. 1273
Adjustable-Speed Drive, A Wide-Range. Conrad, Tribken..........789–90
Adjustable Speed Motors, Limitations in Design of D-C. Opel..........1095–8
Adjusting Radiosonde Recorder, Automatic Range-. Beggs..........602–07
Advances in Technique of Lightning Measurements. Brownlee..........515–19
AIEE-ASME Governor Performance Specification, Governors and the. Schwendner, Astley...1330–2
Ailments, Diagnosis of Rectifier. Dortort....1298–1304
Air-Break Switches for Protection of Transformer Stations, Automatic Grounding and. Ricker..........851–6; disc. 856
Air Circuit Breaker, A New 69-Kv Compressed-. Baker, Frisch..........363–8; disc. 369
Air-Core Reactors as Fault Limiting Means on High Interrupting Capacity Controllers, The Use of. Leitch..........469–74; disc. 474
Aircraft, An Electric Deicing System for. Gilloy..........1051–7
Aircraft Cable, Current Ratings of. Askew, McClinton..........988–92
Aircraft Carbon-Pile Voltage Regulators, Fundamentals, and Design Improvements. Austin, Richards..........983–7
Aircraft, Lightning Stroke Damage to. Hagenguth..........1036–44; disc. 1044
Aircraft Propellers, Development and Application of Electric Heating to Deicing of. Sheets, Sand..........1068–72
Aircraft Transformers, Lightweight. Stephens..1073–8
Airplane Main Bus, Protection of the. Exner..........979–82
Alarm and Control System for Remote Control of Coaxial Cable Stations, B-1. Hearn, Weber...622–6
A-C Generators, A Semiempirical Approach to Voltage Dip—with Suddenly Applied Loads on. Rosenberg..........160–6; disc. 166
A-C Network Analyzer, An Improved. Morgan, Rothe, Winsness..........891–5; disc. 895
A-C Resistance of Segmental Cables in Steel Pipe. Meyerhoff, Eager..........816–29; disc. 829
A-C Tripping and Reclosing of Line Sectionalizing Circuit Breakers. Winegartner, Bonheimer...1357–9
A-C Voltmeter, A New Expanded Scale. Millar..........641–3
Altitudes, A Small High-Voltage Bushing Design for High. Vogel, Hart..........761–4
Ampere Demand Meter, A New Thermal Volt-. Douglass, Morong..........79–83; disc. 83
Amplifier—Class A Operation, The Dynamoelectric. Saunders..........1368–73
Amplifier Stabilized for Gain and for Zero, Wide-Band D-C. Williams, Amey, McAdam..........811–15; disc. 815
Amplifiers, An Analysis of Rotating. Litman..1111–17
Amplifiers with Feedback, Analytical Determination of Characteristics of Magnetic. VerPlanck, Finzi, Beaumariage..........565–70
Amplifiers, Self-Saturation in Magnetic. Dornhoefer..........835–46; disc. 846
Analog Computer to Nonlinear Mechanics and Servomechanisms, Application of the California Institute of Technology Electric. McCann, Wilts, Locanthi..........652–60
Analog Computers, Comparison of Long-Time and Short-Time. Paschkis..........70–3
Analogs of Linear Vibration Problems, Summary of Transformations Useful in Constructing. Corbett..........661–4
Analogy, The Transient Behavior of the Two-Stage Rototrol Main Exciter Voltage Regulating System as Determined by Electrical. Carleton.....59–63
Analysis of Relay Servomechanisms, An. Kahn..........1079–87; disc. 1087
Analysis of Results to Research Problems in Magnetic Recording, Application of Experimental Test Procedures and Methods of. Thompson......407–17
Analysis of Rotating Amplifiers, An. Litman..1111–17
Analysis, The Torques of the Synchronous Tie—A Steady-State. Finzi, McConnell..........1147–52
Analytical Co-ordination Method, Field Tests of Oil Circuit Recloser Substantiate. Auer, Branflick, Woodward, McKinley..........801–08; disc. 808
Analytical Determination of Characteristics of Magnetic Amplifiers with Feedback. VerPlanck, Finzi, Beaumariage..........565–70
Analyzer, A New Fourier Coefficient Harmonic. Charp..........644–9; disc. 649
Analyzer, An Improved A-C Network. Morgan, Rothe, Winsness..........891–5; disc. 895
Analyzer to Determine Plant Loading Schedules, Coordination of Fuel Cost and Transmission Loss by Use of the Network. George, Page, Ward..........1152–60; disc. 1160
Application Engineering on Diesel-Electric Locomotives in Railroad Service. Bevan..........125–31
Application of Electric Heating to Deicing of Aircraft Propellers, Development and. Sheets, Sand..........1068–72
Application of Experimental Test Procedures and Methods of Analysis of Results to Research Problems in Magnetic Recording. Thompson..........407–17
Application of Multifrequency Pulsing in Switching. Dahlbom, Horton, Moody..........392–6
Application of the California Institute of Technology Electric Analog Computer to Nonlinear Mechanics and Servomechanisms. McCann, Wilts, Locanthi..........652–60
Applications, Microwave Channels for Power System. (Committee Report)..........40–2; disc. 42
Applications, Two Gas Turbines for Power Generation and Other. Howard..........461–5; disc. 465
Approach to the Design of High-Voltage Cable Joints, A Theoretical and Practical. Short..........1275–80; disc. 1280
Arc, Instrumentation for the Evaluation of the Stability of the Welding. Winsor, Schetky, Wyant..525–33
Arc Paths, Deionization Time of High-Voltage Fault. Harrington, Starr..........997–1003; disc. 1003
Armature Iron Losses in Series Motors. Chang, Karr..........262–4; disc. 264
Arrangements and Protective Practices for Shunt Capacitor Banks, Connection. Clark, Farnham..........1226–30; disc. 1231
ASME Governor Performance Specification, Governors and the AIEE-. Schwendner, Astley......1330–2
Aspects of Relay Circuits, Sequential. Ritchie..577–81
Attenuation and Delay Equalizers for Coaxial Lines. Lundry..........1174–9
Audio Noise Problems on an Electric Power System, Transformer. Murray..........740–7; disc. 747
Automatic Control Systems, The Design of D-C Motors for Use in. Lebenbaum..........1089–94
Automatic Grounding and Air-Break Switches for Protection of Transformer Stations. Ricker..........851–6; disc. 856
Automatic Load Control for Turbine Generators, A New. Ruud, Farnham.......1337–42; disc. 1342
Automatic Range-Adjusting Radiosonde Recorder. Beggs..........602–07
Auxiliary Circuits of Single-Phase Induction Motors, Design of. Thacker, Gopalakrishna.......1373–9

B

B-1 Alarm and Control System for Remote Control of Coaxial Cable Stations. Hearn, Weber.....622–6
Backlash, Instrument Inaccuracies in Feed-Back Control Systems with Particular Reference to. Marcy, Yachter, Zauderer..........778–88
Band Coupling of Power-Line Carrier Equipment, A Proposal for Broad-. Miller...1028–30; disc. 1030
Band D-C Amplifier Stabilized for Gain and for Zero, Wide-. Williams, Amy, McAdam..........811–15; disc. 815
Band of Governors on Steam Turbine Generators Under System Load Conditions, Determining Incremental Regulation and Dead. Tornquist, Wade..1343–7
Bandwidths, The Distinction Between Effective and Circuit. Kessler..........98–9
Bank, The Temperature Rise of Cables in a Duct. Neher..........540–6; disc. 546
Banks, Connection Arrangements and Protective Practices for Shunt Capacitor. Clark, Farnham..........1226–30; disc. 1231
(Basic Sciences) A Derivation of Heaviside's Operational Calculus Based on the Generalized Functions of Schwartz. Smith, Alger........939–44; disc. 944
(Basic Sciences) Dielectric Strength of Oil with Variations of Pressure and Temperature. Hoover, Hixson..........1047–50
(Basic Sciences) Formulas and Tables for the Calculation of the Magnetic Field Components of Circular Filaments and Solenoids. Grover..........665–75
(Basic Sciences) General Theory, and Experimental Confirmation, of the Moving Coil Fluxmeter. Higgins, Robertson..........897–907; disc. 907
(Basic Sciences) Nonharmonic Oscillations as Caused by Magnetic Saturation. Rudenberg..........676–85
(Basic Sciences) Self-Saturation in Magnetic Amplifiers. Dornhoefer..........835–46; disc. 846.
(Basic Sciences) The Vector Power Factor of Unbalanced Sinusoidal 3-Phase Circuits. Lamb, Brandt..........507–09
Behavior of the Two-Stage Rototrol Main Exciter Voltage Regulating System as Determined by Electrical Analogy, The Transient. Carleton..........59–63
Board of Directors, Report of the..........1383–1408
Boilers and of Hydro Units, Outage Rates of Steam Turbines and. (Committee Report)........450–7
Bolometer, Detection of Overheated Transmission Line Joints by Means of a. Leslie, Wait..64–8; disc. 68
Bonneville Power Administration Transmission System, Matching Electrical Characteristics of McNary Generators and Transformers with. Hoard, Weiner..........1022–5; disc. 1026
Braking Control of D-C Series Motors—Experimental Study of Speed-Torque Curves, Dynamic. Heumann..........560–4
Breaker, A New 69-Kv Compressed-Air Circuit. Baker, Frisch..........363–8; disc. 369
Breakers, A Manually-Operated Spring Mechanism for Medium Voltage Oilless Circuit. Wyman, Casey..........357–61; disc. 361
Breakers, A-C Tripping and Reclosing of Line Sectionalizing Circuit. Winegartner, Bonheimer....1357–9
Breakers, Insulator Flashover Deionization Times as a Factor in Applying High-Speed Reclosing Circuit. Boisseau, Wyman, Skeats......1058–66; disc. 1066
Broad-Band Coupling of Power-Line Carrier Equipment, A Proposal for. Miller.......1028–30; disc. 1030
Brushes, Progress Report on AIEE Test Code for Electric. (Committee Report)..........1126–8
Buried Cables and Pipes, The Temperature Rise of. Neher..........9–17; disc. 17
Bus, Protection of the Airplane Main. Exner...979–82
Bushing Design for High Altitudes, A Small High-Voltage. Vogel, Hart..........761–4
Busses, Trolley Coaches Replace. McMillon...403–06

C

Cable Accessory Design Utilizing New Laboratory Techniques. Bosworth, Farr......1268–73; disc. 1273
Cable Circuits in Philadelphia, 69-Kv Pipe-Type. Kidder, Van Antwerp..........550–6; disc. 556
Cable, Current Ratings of Aircraft. Askew, McClinton..........988–92
Cable for Carrier Current Installation on Power Lines, Line Tuning Equipment Used With Coaxial. Sutton..........44–8; disc. 48
Cable Impregnated with Extra-High-Viscosity Oil, High-Pressure Gas-Filled. Sticher, Doan, Atkinson, Meyerhoff..........336–45; disc. 345
Cable Joints, A Theoretical and Practical Approach to the Design of High-Voltage. Short..........1275–80; disc. 1280
Cable Overhead-Conductor 132-Kv Transmission Line at Carrier Current Frequencies, Loss Measurements Made on Underground-. Cornelius, Storer..........597–601
Cable Stations, B-1 Alarm and Control System for Remote Control of Coaxial. Hearn, Weber...622–6
Cables and Pipes, The Temperature Rise of Buried. Neher..........9–17; disc. 17
Cables, Heating of Radio-Frequency. Macalpine..........283–8
Cables in a Duct Bank, The Temperature Rise of. Neher..........540–6; disc. 546
Cables in Steel Pipe, A-C Resistance of Segmental. Meyerhoff, Eager..........816–29; disc. 829
Cables, The Power Rating of Radio-Frequency. Mildner..........289–98; disc. 298
Cables, Transient Temperature Phenomena of 3-Conductor. Wollaston..........1284–95; disc. 1295
Cage Induction Motors, General Theory of Multiple. Chang..........1139–43

Calculated Risk of Operating Capacitors Without Individual Fuses, The. Brooks....1219–25; disc. 1225
Calculation of the Magnetic Field Components of Circular Filaments and Solenoids, Formulas and Tables for the. Grover........................665–75
Calculus Based on the Generalized Functions of Schwartz, A Derivation of Heaviside's Operational. Smith, Alger...................939–44; disc. 944
California Institute of Technology Electric Analog Computer to Nonlinear Mechanics and Servomechanisms, Application of the. McCann, Wilts, Locanthi..652–60
Capacitor Banks, Connection Arrangements and Protective Practices for Shunt. Clark, Farnham..................................1226–30; disc. 1231
Capacitors, Report of a Survey on the Performance of Shunt. (Committee Report)..1200–06; disc. 1206
Capacitors, Report on the Operation and Maintenance of Shunt. (Committee Report)..........1208–18
Capacitors Without Individual Fuses, The Calculated Risk of Operating. Brooks....1219–25; disc. 1225
Capacity Controllers, The Use of Air-Core Reactors as Fault Limiting Means on High Interrupting. Leitch........................469–74; disc. 474
Carbon-Pile Voltage Regulators, Fundamentals, and Design Improvements, Aircraft. Austin, Richards..983–7
Carrier Current Frequencies, Loss Measurements Made on Underground-Cable Overhead-Conductor 132-Kv Transmission Line at. Cornelius, Storer..597–601
Carrier Current Installation on Power Lines, Line Tuning Equipment Used With Coaxial Cable for. Sutton..............................44–8; disc. 48
(Carrier Current) Microwave Channels for Power System Applications. (Committee Report)..40–2; disc. 42
Carrier Equipment, A Proposal for Broad-Band Coupling of Power-Line. Miller..1028–30; disc. 1030
Carrier for Relaying and Joint Usage, Power Line. Part I. Hampe, Storer..........864–7; disc. 867
Carrier System, Stability of Tandem Regulators in the L-1. Kinzer..........................1179–86
Centralized Traffic Control for Railroads. Hailes..1167–73
Changing Temperature, The Measurement of Dielectric Loss at High Frequencies and Under. Whitehead, Rueggeberg..............................520–4
Channels for Power System Applications, Microwave. (Committee Report)...............40–2; disc. 42
Characteristics of D-C Motors and Generators, Transient. McClinton, Brancato, Panoff......1100–06
Characteristics of Distribution Systems, Voltage-Recovery. Witzke.................172–80; disc. 180
Characteristics of Lightning Protective Devices, Performance. (Committee Report)..............1333–6
Characteristics of Magnetic Amplifiers with Feedback, Analytical Determination of. VerPlanck, Finzi, Beaumariage..............................565–70
Characteristics of McNary Generators and Transformers with Bonneville Power Administration Transmission System, Matching Electrical. Hoard, Weiner..................................1022–5; disc. 1026
Characteristics of Two-Phase Servomotors, Operating. Koopman......................319–27; disc. 327
Characteristics, Rectifier Transformer. (Committee Report)..............................1305–11
Charged Dust in Rooms, Electrically. Penney, Hewitt..278–82
Charging Currents on Transmission Lines as Affecting Ground-Fault Neutralizers, Report on Survey of Unbalanced. (Committee Report)..1328; disc. 1329
Chart Methods Applied to Frequency Response Curves, Control. Mundel........................424–7
Chesapeake and Ohio Railway Company Steam Turbine-Electric Locomotives, Electric Equipment for. Atwell, Baston..............................145–8
Circuit Bandwidths, The Distinction Between Effective and. Kessler..............................98–9
Circuit Breaker, A New 69-Kv Compressed-Air. Baker, Frisch..........................363–8; disc. 369
Circuit Breakers, A Manually-Operated Spring Mechanism for Medium Voltage Oilless. Wyman, Casey..........................357–61; disc. 361
Circuit Breakers, A-C Tripping and Reclosing of Line Sectionalizing. Winegartner, Bonheimer...1357–9
Circuit Breakers, Insulator Flashover Deionization Times as a Factor in Applying High-Speed Reclosing. Boisseau, Wyman, Skeats......1058–66; disc. 1066
Circuit Conditions, Heating of Transformers Under Short-. Montsinger, Halsey.....947–52; disc. 952
Circuit Currents and Recovery Voltages on Rural Distribution Systems, Short-. Eason, Johnson, Kalb, Peterson..........................930–7; disc. 937
Circuit of D-C Motors and Generators, Solid Short. Linville, Ward.................119–23; disc. 123
Circuit Recloser Substantiate Analytical Co-ordination Method, Field Tests of Oil. Auer, Branflick, Woodward, McKinley...............801–08; disc. 808
Circuits for Power-Flow Studies, Equivalent. Ward..373–80; disc. 380
Circuits for Protective Relays, Novel Test. Sonnemann..1249–54
Circuits in Philadelphia, 69-Kv Pipe-Type Cable. Kidder, Van Antwerp...........550–6; disc. 556
Circuits, Insulation Level of Relay and Control. (Committee Report)..........................1255–7
Circuits of Single-Phase Induction Motors, Design of Auxiliary. Thacker, Gopalakrishna.......1373–9
Circuits, Relay "Trees" and Symmetric. Washburn..582–6
Circuits, Sequential Aspects of Relay. Ritchie..577–81
Circuits, The Logic of Relay. Keister..........571–6
Circuits, The Vector Power Factor of Unbalanced Sinusoidal 3-Phase. Lamb, Brandt..........507–09
Circular Filaments and Solenoids, Formulas and Tables for the Calculation of the Magnetic Field Components of. Grover........................665–75
Clamps, Magnetic Heating of Transmission Line. Crabb, Sheadel..........................1032–5
Class A Operation, The Dynamoelectric Amplifier—. Saunders..............................1368–73
Class-H Insulation and Silicone Varnish, Motor Tests Evaluate Thermal Endurance of. Grant, Kauppi, Moses, Gibson..............................1133–8
Coaches Replace Busses, Trolley. McMillon...403–06
Coaxial Cable for Carrier Current Installation on Power Lines, Line Tuning Equipment Used With. Sutton..............................44–8; disc. 48
Coaxial Cable Stations, B-1 Alarm and Control System for Remote Control of. Hearn, Weber.....622–6
Coaxial Lines, Attenuation and Delay Equalizers for. Lundry..............................1174–9
Coaxial Lines, Equalization of. Gould.......1187–92
Coaxial Systems, Power Supplies for. Spencer...627–30
Coaxial Systems, Television Terminals for. Morrison..1193–9
Code for Electric Brushes, Progress Report on AIEE Test. (Committee Report)..............1126–8
Code Selector Supervisory System, Space. Forrest, Schirmer..................1312–15; disc. 1315
Codes and Translations. Myers...............592–7
Coefficient Harmonic Analyzer, A New Fourier. Charp..............................644–9; disc. 649
Coil Fluxmeter, General Theory and Experimental Confirmation of the Moving. Higgins, Robertson..................................897–907; disc. 907
(Committee Report) Insulation Level of Relay and Control Circuits..............................1255–7
(Committee Report) Microwave Channels for Power System Applications..............40–2; disc. 42
(Committee Report) Outage Rates of Steam Turbines and Boilers and of Hydro Units............450–7
(Committee Report) Performance Characteristics of Lightning Protective Devices.............1333–6
(Committee Report) Progress Report on AIEE Test Code for Electric Brushes..................1126–8
(Committee Report) Protection of Stations Without High-Voltage Switching........226–31; disc. 231
(Committee Report) Rectifier Transformer Characteristics..............................1305–11
(Committee Report) Report of a Survey on the Performance of Shunt Capacitors......1200–06; disc. 1206
(Committee Report) Report on Survey of Unbalanced Charging Currents on Transmission Lines as Affecting Ground-Fault Neutralizers....1328; disc. 1329
(Committee Report) Report on the Operation and Maintenance of Shunt Capacitors.............1208–18
(Committee Report) Stray Load Losses Measured in D-C Motors..................219–23; disc. 223
(Committee Report) Temperature Rise Values for D-C Machines. Part I.............206–12; disc. 212
(Committee Report) Temperature Rise Values for D-C Machines. Part II..........1118–23; disc. 1123
Committees and Officers—1949–1950..........1409–28
(Communication) A Method for Designing Pulse Transformers. Kirschbaum, Warren............971–8
(Communication) A Time Division Multiplexing System. Boothroyd, Creamer.................92–7
(Communication) Application of Experimental Test Procedures and Methods of Analysis of Results to Research Problems in Magnetic Recording. Thompson..............................407–17
(Communication) Application of Multifrequency Pulsing in Switching. Dahlbom, Horton, Moody...392–6
(Communication) Attenuation and Delay Equalizers for Coaxial Lines. Lundry................1174–9
(Communication) B-1 Alarm and Control System for Remote Control of Coaxial Cable Stations. Hearn, Weber..............................622–6
(Communication) Centralized Traffic Control for Railroads. Hailes..........................1167–73
(Communication) Codes and Translations. Myers..592–7
(Communication) Considerations on Facsimile Transmission Speed. Burkhard.......418–23; disc. 423
(Communication) Control Chart Methods Applied to Frequency Response Curves. Mundel......424–7
(Communication) Counting with Relays. Frost..587–91
(Communication) Equalization of Coaxia Lines. Gould..............................1187–92
Communication Equipment for Land-Mobile Services Operating on Frequencies Between 152–174 Megacycles, Design of Mobile Radio. Beers, Harris, Zappacosta..............................1232–9
(Communication) Power Supplies for Coaxial Systems. Spencer..............................627–30
(Communication) Power Supplies for Microwave Relay Systems. Ward..........................631–6
(Communication) Radio Influence from High-Voltage Corona. Slemon..............198–204; disc. 204
Communication Relay System, A Microwave. Boothroyd, Churchill..........................637–41
(Communication) Relay "Trees" and Symmetric Circuits. Washburn..........................582–6
(Communication) Rubber Insulators for Pole Lines. Wheeler, Markley..........................195–7
(Communication) Sequential Aspects of Relay Circuits. Ritchie..............................577–81
(Communication) Stability of Tandem Regulators in the L-1 Carrier System. Kinzer.........1179–86
(Communication) Television Terminals for Coaxial Systems. Morrison.......................1193–9
(Communication) The Distinction Between Effective and Circuit Bandwidths. Kessler...........98–9
(Communication) The Logic of Relay Circuits. Keister..571–6
(Communication) Vibrating Reed Selective Signaling System for Mobile Telephone Use. Pruden, Hoth..387–91
(Communication) Vibrating Reed Selectors for Mobile Radio Systems. Keller, Bostwick...........383–6
Commutation of D-C Machines and Its Effects on Radio Influence Voltage Generation. Motter..................................491–5; disc. 495
Commutation, Oscillographing. Baldwin..................................100–05; disc. 105
Commutation with an Indicating Instrument, Measuring. Lundy..............................1380–2
Commutator Surface Film Conditions on Commutation, Effects of. Lynn, Elsey........106–112; disc. 112
Comparative Performance Records—Steel and Wood Transmission Lines. Booker......686–9; disc. 689
Comparison of Long-Time and Short-Time Analog Computers. Paschkis..............................70–3
Comparison of Steady-State and Transient Performance of Servomechanisms. Chestnut, Mayer....765–77
Components and Systems, Graphical Determination of Transfer Function Loci for Servomechanism. Thomas, Easton................307–14; disc. 314
Components of Circular Filaments and Solenoids, Formulas and Tables for the Calculation of the Magnetic Field. Grover..............................665–75
Compressed-Air Circuit Breaker, A New 69-Kv. Baker, Frisch........................363–8; disc. 369
Computer to Nonlinear Mechanics and Servomechanisms, Application of the California Institute of Technology Electric Analog. McCann, Wilts, Locanthi..............................652–60
Computers, Comparison of Long-Time and Short-Time Analog. Paschkis..............................70–3
(Computing Devices) An Improved A-C Network Analyzer. Morgan, Rothe, Winsness..891–5; disc. 895
(Computing Devices) Summary of Transformations Useful in Constructing Analogs of Linear Vibration Problems. Corbett..............................661–4
Conditions, Determining Incremental Regulation and Dead Band of Governors on Steam Turbine Generators Under System Load. Tornquist, Wade..1343–7
Conditions During Operation of Hydroelectric Units, Some Oscillographic Methods of Investigating Mechanical and Hydraulic. Engvall.......993–6
Conditions, Fundamental Theory of Inherent-Overheating Protection Under Running Overload. Veinott, Schaefer..........................266–70; disc. 270
Conditions, Heating of Transformers Under Short-Circuit. Montsinger, Halsey.......947–52; disc. 952
Conditions on Commutation, Effects of Commutator Surface Film. Lynn, Elsey......106–12; disc. 112
Conductor Cables, Transient Temperature Phenomena of 3-. Wollaston............1284–95; disc. 1295
Conductor Economics, Distribution Transformer and Secondary. Brady..............483–6; disc. 486
Conductor, Hy-Therm Copper—Improved Overhead Line. Hickernell, Jones, Snyder.....22–7; disc. 27
Conductor 132-Kv Transmission Line at Carrier Current Frequencies, Loss Measurements Made on Underground-Cable Overhead-. Cornelius, Storer..597–601
Confirmation of the Moving Coil Fluxmeter, General Theory and Experimental. Higgins, Robertson..................................897–907; disc. 907
Connection Arrangements and Protective Practices for Shunt Capacitor Banks. Clark, Farnham..................................1226–30; disc. 1231
Considerations on Facsimile Transmission Speed. Burkhard..........................418–23; disc. 423
Contaminants on Electrical Insulation, Methods for Determining the Effects of. Mathes, Sieffert, Walker, Lindsey................113–18; disc. 118

Control Chart Methods Applied to Frequency Response Curves. Mundel.....424–7
Control Circuits, Insulation Level of Relay and. (Committee Report).....1255–7
Control for Railroads, Centralized Traffic. Hailes.....1167–73
Control for Turbine Generators, A New Automatic Load. Ruud, Farnham.....1337–42; disc. 1342
Control of D-C Series Motors—Experimental Study of Speed-Torque Curves, Dynamic Braking. Heumann.....560–4
Control System, A New 2-Signal Synchronous Supervisory. Derr.....857–63; disc. 863
Control System for Remote Control of Coaxial Cable Stations, B-1 Alarm and. Hearn, Weber.....622–6
Control Systems, The Design of D-C Motors for Use in Automatic. Lebenbaum.....1089–94
Control Systems with Particular Reference to Backlash, Instrument Inaccuracies in Feed-Back. Marcy, Yachter, Zauderer.....778–88
Controllable Reactors, Universal Curves for D-C. Johnson, Merrell, Alley.....31–7; disc. 37
Controlled Reactors with Resistive Load, Some Fundamentals of D-C. Storm.....188–94; disc. 194
Controlled Temperature and Insulation Protection in the Operation of Power Transformers. Satterlee, Reed.....753–8; disc. 759
Controllers, The Use of Air-Core Reactors as Fault Limiting Means on High Interrupting Capacity. Leitch.....469–74; disc. 474
Convenient Method for Determining Generator Reserve, A. Seelye.....1317–20
Converter for Telemetering and Totalizing, A Thermal. Downing.....879–84; disc. 884
Co-ordination Method, Field Tests of Oil Circuit Recloser Substantiate Analytical. Auer, Branflick, Woodward, McKinley.....801–08; disc. 808
Co-ordination of Fuel Cost and Transmission Loss by Use of the Network Analyzer to Determine Plant Loading Schedules. George, Page, Ward.....1152–60; disc. 1160
Co-ordination of Oil Insulated Transformers, Extremes in the Insulation. Vogel.....965–8; disc. 968
Copper—An Improved Overhead-Line Conductor, Hy-Therm. Hickernell, Jones, Snyder.....22–7; disc. 27
Corona, Radio Influence from High-Voltage. Slemon.....198–204; disc. 204
Cost and Transmission Loss by Use of the Network Analyzer to Determine Plant Loading Schedules, Coordination of Fuel. George, Page, Ward.....1152–60; disc. 1160
Counting with Relays. Frost.....587–91
Coupling of Power-Line Carrier Equipment, A Proposal for Broad-Band. Miller.....1028–30; disc. 1030
Cumulative and Differential Series Fields in the Parallel Operation of D-C Motors, Use of. Kimball.....1098–1100
Current Frequencies, Loss Measurements Made on Underground-Cable Overhead-Conductor 132-Kv Transmission Line at Carrier. Cornelius, Storer.....597–601
Current Installation on Power Lines, Line Tuning Equipment Used With Coaxial Cable for Carrier. Sutton.....44–8; disc. 48
Current Ratings of Aircraft Cable, Askew, McClinton.....988–92
Currents and Recovery Voltages on Rural Distribution Systems, Short-Circuit. Eason, Johnson, Kalb, Peterson.....930–7; disc. 937
Currents on Transmission Lines as Affecting Ground-Fault Neutralizers, Report on Survey of Unbalanced Charging. (Committee Report)..1328; disc. 1329
Currents, Rectifier Fault—II. Herskind, Schmidt, Rettig.....243–51; disc. 251
Curves, Control Chart Methods Applied to Frequency Response. Mundel.....424–7
Curves, Dynamic Braking Control of D-C Series Motors—Experimental Study of Speed-Torque. Heumann.....560–4
Curves for D-C Controllable Reactors, Universal. Johnson, Merrell, Alley.....31–7; disc. 37
Cycle Out-of-Step Relay Equipment, One Slip. Morris.....1246–8

D

Damage to Aircraft, Lightning Stroke. Hagenguth.....1036–44; disc. 1044
Damper Stabilized Instrument Servomechanisms. Hall.....299–306; disc. 306
Data, Prediction of Ultimate Temperature Rise from Early Heat Run. Ryan.....1164–6
Dead Band of Governors on Steam Turbine Generators Under System Load Conditions, Determining Incremental Regulation and. Tornquist, Wade.....1343–7
Deicing of Aircraft Propellers, Development and Application of Electric Heating to. Sheets, Sand.....1068–72
Deicing System for Aircraft, An Electric. Giloy.....1051–7
Deionization Time of High-Voltage Fault-Arc Paths. Harrington, Starr.....997–1003; disc. 1003
Deionization Times as a Factor in Applying High-Speed Reclosing Circuit Breakers, Insulator Flashover. Boisseau, Wyman, Skeats.....1058–66; disc. 1066
Delay Equalizers for Coaxial Lines, Attenuation and. Lundry.....1174–9
Demand Meter, A New Thermal Volt-Ampere. Douglass, Morong.....79–83; disc. 83
Demand Meters, Heat Flow Ratio as a Design Parameter in Thermal. Nelson.....885–90; disc. 890
Derivation of Heaviside's Operational Calculus Based on the Generalized Functions of Schwartz, A. Smith, Alger.....939–44; disc. 944
Design and Experience with 4-Kv Primary Network Systems in the Washington Area. Lank.....712–16; disc. 716
Design and Performance Based on Direct Lightning Strokes, Transmission Line. Harder, Clayton.....439–46; disc. 447
Design and Ventilation, Transformer Manholes and Vaults: Porter.....534–9
Design Features—Steam-Electric Generating Station P of the Pacific Gas and Electric Company, Electrical. Benson.....1013–20; disc. 1020
Design for High Altitudes, A Small High-Voltage Bushing. Vogel, Hart.....761–4
Design Fundamentals of Potheads 69,000 Volts and Below. Nicholas.....1263–7; disc. 1267
Design Improvements, Aircraft Carbon-Pile Voltage Regulators, Fundamentals, and. Austin, Richards.....983–7
Design of Auxiliary Circuits of Single-Phase Induction Motors. Thacker, Gopalakrishna.....1373–9
Design of D-C Adjustable Speed Motors, Limitations in. Opel.....1095–8
Design of D-C Motors for Use in Automatic Control Systems, The. Lebenbaum.....1089–94
Design of High-Voltage Cable Joints, A Theoretical and Practical Approach to the. Short.....1275–80; disc. 1280
Design of Mobile Radio Communication Equipment for Land-Mobile Services Operating on Frequencies Between 152–174 Megacycles. Beers, Harris, Zappacosta.....1232–9
Design of Traction Motors, Twenty-Five Years Progress in the. Baldwin.....132–7
Design Parameter in Thermal Demand Meters, Heat Flow Ratio as a. Nelson.....885–90; disc. 890
Design Utilizing New Laboratory Techniques, Cable Accessory. Bosworth, Farr.....1268–73; disc. 1273
Designing Pulse Transformers, A Method for. Kirschbaum, Warren.....971–8
Detection of Overheated Transmission Line Joints by Means of a Bolometer. Leslie, Wait. 64–8; disc. 68
Determination of Characteristics of Magnetic Amplifiers with Feedback, Analytical. VerPlanck, Finzi, Beaumariage.....565–70
Determination of Transfer Function Loci for Servomechanism Components and Systems, Graphical. Thomas, Easton.....307–14; disc. 314
Determining Generator Reserve, A Convenient Method for. Seelye.....1317–20
Determining Incremental Regulation and Dead Band of Governors on Steam Turbine Generators Under System Load Conditions. Tornquist, Wade.....1343–7
Determining the Effects of Contaminants on Electrical Insulation, Methods for. Mathes, Sieffert, Walker, Lindsey.....113–18; disc. 118
Development and Application of Electric Heating to Deicing of Aircraft Propellers. Sheets, Sand..1068–72
Developments, Electronic Relay. Loving.....233–40; disc. 240
(Devices) A New Fourier Coefficient Harmonic Analyzer. Charp.....644–9; disc. 649
(Devices) Comparison of Long-Time and Short-Time Analog Computers. Paschkis.....70–3
Devices, Performance Characteristics of Lightning Protective. (Committee Report).....1333–6
Diagnosis of Rectifier Ailments. Dortort....1298–1304
Die-Cast Rotors for Induction Motors. Packer.....253–60; disc. 260
Dielectric Loss at High Frequencies and Under Changing Temperature, The Measurement of. Whitehead, Rueggeberg.....520–4
Dielectric Strength of Oil with Variations of Pressure and Temperature. Hoover, Hixson.....1047–50
Diesel-Electric Locomotives in Railroad Service, Application Engineering on. Bevan.....125–31
Diesel-Electric Rig for Deep-Well Drilling, Performance of. Clark, Moore.....497–506
Diesel-Electric Switching Locomotives, Industrial Plants Prefer. Woods.....697–700
Differential Leakage of the Different Patterns of a Fractional Slot Winding. Liwschitz.....1129–31; disc. 1131
Differential Series Fields in the Parallel Operation of D-C Motors, Use of Cumulative and. Kimball.....1098–1100
Dip—with Suddenly Applied Loads on A-C Generators, A Semiempirical Approach to Voltage. Rosenberg.....160–6; disc. 166
D-C Adjustable Speed Motors, Limitations in Design of. Opel.....1095–8
D-C Amplifier Stabilized for Gain and for Zero, Wide-Band. Williams, Amey, McAdam.....811–15; disc. 815
D-C Controllable Reactors, Universal Curves for. Johnson, Merrell, Alley.....31–7; disc. 37
D-C Controlled Reactors with Resistive Load, Some Fundamentals of. Storm.....188–94; disc. 194
D-C Machine Performance, The Eccentric Pole Face—A Means to Better. Baker.....1107–10
D-C Machines and Its Effects on Radio Influence Voltage Generation, Commutation of. Motter.....491–5; disc. 495
D-C Machines, Temperature Rise Values for. Part I. (Committee Report).....206–12; disc. 212
D-C Machines, Temperature Rise Values for. Part II. (Committee Report).....1118–23; disc. 1123
D-C Motors and Generators, Solid Short Circuit of. Linville, Ward.....119–23; disc. 123
D-C Motors and Generators, Transient Characteristics of. McClinton, Brancato, Panoff.....1100–06
D-C Motors for Use in Automatic Control Systems, The Design of. Lebenbaum.....1089–94
D-C Motors, Stray Load Losses Measured in. (Committee Report).....219–23; disc. 223
D-C Motors, Use of Cumulative and Differential Series Fields in the Parallel Operation of. Kimball.....1098–1100
D-C Series Motors—Experimental Study of Speed-Torque Curves, Dynamic Braking Control of. Heumann.....560–4
Direct Lightning Strokes, Transmission Line Design and Performance Based on. Harder, Clayton.....439–46; disc. 447
Distance Relays During Faults and Power Swings, Graphical Method for Estimating the Performance of. Warrington.....608–20; disc. 620
Distinction Between Effective and Circuit Bandwidths, The. Kessler.....98–9
Distribution System, Lightning Investigation on a Rural. MacCarthy, Stann, Edge, McKinley.....428–37; disc. 437
Distribution System, Operation of a Ground-Fault Neutralizer on a Regulated. Tomlinson, Hunt.....1321–6; disc. 1326
Distribution System, Overcurrent Investigation on a Rural. Lincks, Edge, McKinley, Leh.....915–27; disc. 927
Distribution Systems, Short-Circuit Currents and Recovery Voltages on Rural. Eason, Johnson, Kalb, Peterson.....930–7; disc. 937
Distribution Systems, Voltage-Recovery Characteristics of. Witzke.....172–80; disc. 180
Distribution Transformer and Secondary Conductor Economics. Brady.....483–6; disc. 486
Division Multiplexing System, A Time. Boothroyd, Creamer.....92–7
(Domestic) The Heat Pump—Its Significance as a Potential Residential Electric Load. Bary.....1–8
Drilling, Performance of Diesel-Electric Rig for Deep-Well. Clark, Moore.....497–506
Drive, A Wide-Range Adjustable-Speed. Conrad, Tribken.....789–90
Drives for Looms, Selection of Electric. Demartini, Lukens.....349–56
Duct Bank, The Temperature Rise of Cables in a. Neher.....540–6; disc. 546
Duquesne Light Company System, Primary Networks on the. Holben, Lange.....704–09; disc. 709
Dust in Rooms, Electrically Charged. Penney, Hewitt.....278–82
Dynamic Braking Control of D-C Series Motors—Experimental Study of Speed-Torque Curves. Heumann.....560–4
Dynamoelectric Amplifier—Class A Operation, The. Saunders.....1368–73

E

Eccentric Pole-Face—A Means to Better D-C Machine Performance, The. Baker.....1107–10
Economic Loading of a Transformer System. Levine Smith.....733–8; disc. 738
Economics, Distribution Transformer and Secondary Conductor. Brady.....483–6; disc. 486
Effect of Leakage Reactance, Saturation. Chang, Lloyd.....1144–7
Effective and Circuit Bandwidths, The Distinction Between. Kessler.....98–9
Effects of Commutator Surface Film Conditions on Commutation. Lynn, Elsey.....106–12; disc. 112
Effects of Contaminants on Electrical Insulation, Methods for Determining the. Mathes, Sieffert, Walker, Lindsey.....113–18; disc. 118
Electric Analog Computer to Nonlinear Mechanics and Servomechanisms, Application of the California Institute of Technology. McCann, Wilts, Locanthi.....652–60

Electric Brushes, Progress Report on AIEE Test Code for. (Committee Report)........1126–8
Electric Deicing System for Aircraft, An. Giloy........1051–7
Electric Drives for Looms, Selection of. Demartini, Lukens........349–56
Electric Equipment for Chesapeake and Ohio Railway Company Steam Turbine-Electric Locomotives. Atwell, Baston........145–8
(Electric Heating) The Measurement of Dielectric Loss at High Frequencies and Under Changing Temperature. Whitehead, Rueggeberg........520–4
Electric Heating to Deicing of Aircraft Propellers, Development and Application of. Sheets, Sand........1068–72
Electric Load, The Heat Pump—Its Significance as a Potential Residential. Bary........1–8
Electric Locomotives in Railroad Service, Application Engineering on Diesel-. Bevan........125–31
Electric Motive Power, The Renaissance of. Candee........138–44
Electric Power System, Transformer Audio Noise Problems on an. Murray........740–7; disc. 747
Electric Rig for Deep-Well Drilling, Performance of Diesel-. Clark, Moore........497–506
Electrical Analogy, The Transient Behavior of the Two-Stage Rototrol Main Exciter Voltage Regulating System as Determined by. Carleton........59–63
Electrical Characteristics of McNary Generators and Transformers with Bonneville Power Administration Transmission System, Matching. Hoard, Weiner........1022–5; disc. 1026
Electrical Design Features—Steam-Electric Generating Station P of the Pacific Gas and Electric Company. Benson........1013–20; disc. 1020
Electrical Insulation, Methods for Determining the Effects of Contaminants on. Mathes, Sieffert, Walker, Lindsey........113–11; disc. 118
Electrically Charged Dust in Rooms. Penney, Hewitt........278–82
(Electronic Instruments) A Square-Law Power-Level Recorder. Clark, Turner, Williams........476–82
(Electronic Power Converters) Diagnosis of Rectifier Ailments. Dortort........1298–1304
(Electronic Power Converters) Rectifier Fault Currents—II. Herskind, Schmidt, Rettig..243–51; disc. 251
(Electronic Power Converters) Rectifier Transformer Characteristics. (Committee Report)....1305–11
Electronic Relay Developments Loving........233–40; disc. 240
(Electronics) Analytical Determination of Characteristics of Magnetic Amplifiers with Feedback. VerPlanck, Finzi, Beaumariage........565–70
(Electronics) Electrically Charged Dust in Rooms. Penney, Hewitt........278–82
(Electronics) Heating of Radio-Frequency Cables. Macalpine........283–8
(Electronics) The Power Rating of Radio-Frequency Cables. Mildner........289–98; disc. 298
Electro-Optical Shutter for Photographic Purposes, An. Zarem, Marshall, Poole........84–91
Endurance of Class H Insulation and Silicone Varnish, Motor Tests Evaluate Thermal. Grant, Kauppi, Moses, Gibson........1133–8
Energy, Measurements of Erythemal. Scott....725–29
Engineering on Diesel-Electric Locomotives in Railroad Service, Application. Bevan........125–31
Equalization of Coaxial Lines. Gould........1187–92
Equalizers for Coaxial Lines, Attenuation and Delay. Lundry........1174–9
Equipment, A Proposal for Broad-Band Coupling of Power-Line Carrier. Miller...1028–30; disc. 1030
Equipment for Chesapeake and Ohio Railway Company Steam Turbine-Electric Locomotives, Electric. Atwell, Baston........145–8
Equipment for Land-Mobile Services Operating on Frequencies Between 152–174 Megacycles, Design of Mobile Radio Communication. Beers, Harris, Zappacosta........1232–9
Equipment, One Slip Cycle Out-of-Step Relay. Morris........1246–8
Equipment, Reduction of Interference from Radio-Frequency Heating. Klingaman..718–24; disc. 724
Equipment Used With Coaxial Cable for Carrier Current Installation on Power Lines, Line Tuning. Sutton........44–8; disc. 48
Equivalent Circuits for Power-Flow Studies. Ward........373–80; disc. 380
Erythemal Energy, Measurements of. Scott....725–29
Evaluate Thermal Endurance of Class H Insulation and Silicone Varnish, Motor Tests. Grant, Kauppi, Moses, Gibson........1133–8
Evaluation of the Stability of the Welding Arc, Instrumentation for the. Winsor, Schetky, Wyant........525–38
Excitation Relay for Synchronous Generators, A New Loss-of-. Mason........1240–5
Exciter Voltage Regulating System as Determined by Electrical Analogy, The Transient Behavior of the Two-Stage Rototrol Main. Carleton........59–63
Expanded Scale A-C Voltmeter, A New, Millar..641–3
Experience With 4-Kv Primary Network Systems in the Washington Area, Design and. Lank........712–16; disc. 716
Experimental Confirmation of the Moving Coil Fluxmeter, General Theory and. Higgins, Robertson........897–907; disc. 907
Experimental Study of Speed-Torque Curves, Dynamic Braking Control of D-C Series Motors—. Heumann........560–4
Experimental Test Procedures and Methods of Analysis of Results to Research Problems in Magnetic Recording, Application of. Thompson........407–17
Extremes in the Insulation Co-ordination of Oil Insulated Transformers. Vogel........965–8; disc. 968

F

Face—A Means to Better D-C Machine Performance, The Eccentric Pole. Baker........1107–10
Facsimile Transmission Speed, Considerations on. Burkhard........418–23; disc. 423
Factor of Unbalanced Sinusoidal 3-Phase Circuits, The Vector Power. Lamb, Brandt........507–09
Fault-Arc Paths, Deionization Time of High-Voltage. Harrington, Starr........997–1003; disc. 1003
Fault Currents, Rectifier—II. Herskind, Schmidt, Rettig........243–51; disc. 251
Fault Limiting Means on High Interrupting Capacity Controllers, The Use of Air-Core Reactors as. Leitch........469–74; disc. 474
Fault Locator for High-Voltage Transmission Lines, A Transient. Spaulding, Diemond........1005–1010; disc. 1010
Fault Neutralizer on a Regulated Distribution System, Operation of a Ground-. Tomlinson, Hunt........1321–6; disc. 1326
Fault Neutralizers, Report on Survey of Unbalanced Charging Currents on Transmission Lines as Affecting Ground-. (Committee Report)........1328; disc. 1329
Faults and Power Swings, Graphical Method for Estimating the Performance of Distance Relays During. Warrington........608–20; disc. 620
Features—Steam-Electric Generating Station P of the Pacific Gas and Electric Company, Electrical Design. Benson........1013–20; disc. 1020
Feedback, Analytical Determination of Characteristics of Magnetic Amplifiers with. VerPlanck, Finzi, Beaumariage........565–70
Feed-Back Control Systems with Particular Reference to Backlash, Instrument Inaccuracies in. Marcy, Yachter, Zauderer........778–88
Field Components of Circular Filaments and Solenoids, Formulas and Tables for the Calculation of the Magnetic. Grover........665–75
Field Fluxes of the Shaded-Pole Motor, The. Kimberly........273–7
Field Tests of Oil Circuit Recloser Substantiate Analytical Co-ordination Method. Auer, Branflick, Woodward, McKinley........801–08; disc. 808
Fields in the Parallel Operation of D-C Motors, Use of Cumulative and Differential Series. Kimball........1098–1100
Filaments and Solenoids, Formulas and Tables for the Calculation of the Magnetic Field Components of Circular. Grover........665–75
Film Conditions on Commutation, Effects of Commutator Surface. Lynn, Elsey...106–12; disc. 112
Flashover Deionization Times as a Factor in Applying High-Speed Reclosing Circuit Breakers, Insulator. Boisseau, Wyman, Skeats........1058–66; disc. 1066
Flow Ratio as a Design Parameter in Thermal Demand Meters, Heat. Nelson........885–90; disc. 890
Fluxes of the Shaded-Pole Motor, The Field. Kimberly........273–7
Fluxmeter, General Theory and Experimental Confirmation of the Moving Coil. Higgins, Robertson........897–907; disc. 907
Formulas and Tables for the Calculation of the Magnetic Field Components of Circular Filaments and Solenoids. Grover........665–75
Fourier Coefficient Harmonic Analyzer, A New. Charp........644–9; disc. 649
Fractional Slot Winding, Differential Leakage of the Different Patterns of a. Liwschitz........1129–31; disc. 1131
Frames, Stationary Networks and Transmission Lines Along Uniformly Rotating Reference. Kron........690–6
Frequencies and Under Changing Temperature, The Measurement of Dielectric Loss at High. Whitehead, Rueggeberg........520–4
Frequencies, Loss Measurements Made on Underground-Cable Overhead-Conductor 132-Kv Transmission Line at Carrier Current. Cornelius, Storer........597–601
Frequency Cables, Heating of Radio-. Macalpine........283–8
Frequency Cables, The Power Rating of Radio-Mildner........289–98; disc. 298
Frequency Heating Equipment, Reduction of Interference from Radio-. Klingman..718–24; disc. 724
Frequency Response Curves, Control Chart Methods Applied to. Mundel........424–7
Fuel Cost and Transmission Loss by Use of the Network Analyzer to Determine Plant Loading Schedules, Co-ordination of. George, Page, Ward........1152–60; disc. 1160
Function Loci for Servomechanism Components and Systems, Graphical Determination of Transfer. Thomas, Easton........307–14; disc. 314
Functions of Schwartz, A Derivation of Heaviside's Operational Calculus Based on the Generalized. Smith, Alger........939–44; disc. 944
Fundamental Theory of Inherent-Overheating Protection Under Running Overload Conditions. Veinott, Schaefer........266–70; disc. 270
Fundamentals, and Design Improvements, Aircraft Carbon-Pile Voltage Regulators. Austin, Richards........983–7
Fundamentals of D-C Controlled Reactors with Resistive Load, Some. Storm.....188–94; disc. 194
Fundamentals of Potheads 69,000 Volts and Below Design. Nicholas........1263–7; disc. 1267
Fuses, The Calculated Risk of Operating Capacitors Without Individual. Brooks...1219–25; disc. 1225

G

Gain and for Zero, Wide-Band D-C Amplifier Stabilized for. Williams, Amey, McAdam..811–15; disc. 815
Gas-Filled Cable Impregnated with Extra-High-Viscosity Oil, High-Pressure. Sticher, Doan, Atkinson, Meyerhoff........336–45; disc. 345
Gas Turbine Power Plant, A 3,000-Horsepower. Haverstick........458–60
Gas Turbines for Power Generation and Other Applications, Two. Howard........461–5; disc. 465
Gas Turbines in Stationary Power Generation. Hague........467–8
General Theory and Experimental Confirmation of the Moving Coil Fluxmeter. Higgins, Robertson........897–907; disc. 907
General Theory of Multiple Cage Induction Motors. Chang........1139–43
Generating Station P of the Pacific Gas and Electric Company, Electrical Design Features—Steam-Electric. Benson........1013–20; disc. 1020
Generating Station, Relaying of Transmission Lines from the New. Green, Oewel, Ramsaur........873–7; disc. 877
Generation and Other Applications, Two Gas Turbines for Power. Howard........461–5; disc. 465
Generation, Commutation of D-C Machines and Its Effects on Radio Influence Voltage. Motter........491–5; disc. 495
Generation, Gas Turbines in Stationary Power. Hague........467–8
Generator Reserve, A Convenient Method for Determining. Seelye........1317–20
Generators, A New Automatic Load Control for Turbine. Ruud, Farnham........1337–42; disc. 1342
Generators, A New Loss-of-Excitation Relay for Synchronous. Mason........1240–5
Generators, A Semiempirical Approach to Voltage Dip—with Suddenly Applied Loads on A-C. Rosenberg........160–6; disc. 166
Generators and Transformers with Bonneville Power Administration Transmission System, Matching Electrical Characteristics of McNary. Hoard, Weiner........1022–5; disc. 1026
Generators, Solid Short Circuit of D-C Motors and. Linville, Ward........119–23; disc. 123
Generators, Transient Characteristics of D-C Motors and. McClinton, Brancato, Panoff......1100–06
Generators Under System Load Conditions, Determining Incremental Regulation and Dead Band of Governors on Steam Turbine. Tornquist, Wade........1343–7
Geometric Loci of the Synchronous Tie, The. Finzi, Wellard........168–71
Governors and the AIEE-ASME Governor Performance Specification. Schwendner, Astley........1330–2
Governors on Steam Turbine Generators Under System Load Conditions, Determining Incremental Regulation and Dead Band of. Tornquist, Wade........1343–7
Graphical Determination of Transfer Function Loci for Servomechanism Components and Systems. Thomas, Easton........307–14; disc. 314
Graphical Method for Estimating the Performance of Distance Relays During Faults and Power Swings. Warrington........608–20; disc. 620
Ground-Fault Neutralizer on a Regulated Distribution System, Operation of a. Tomlinson, Hunt........1321–6; disc. 1326
Ground-Fault Neutralizers, Report on Survey of Unbalanced Charging Currents on Transmission Lines as Affecting. (Committee Report)........1328; disc. 1329

Grounding and Air-Break Switches for Protection of Transformer Stations, Automatic. Ricker........851–6; disc. 856

H

Harmonic Analyzer, A New Fourier Coefficient. Charp........644–9; disc. 649
Heat Flow Ratio as a Design Parameter in Thermal Demand Meters. Nelson........885–90; disc. 890
Heat Pump—Its Significance as a Potential Residential Electric Load, The. Bary........1–8
Heat Run Data, Prediction of Ultimate Temperature Rise from Early. Ryan........1164–6
Heating Equipment, Reduction of Interference from Radio-Frequency. Klingaman..718–24; disc. 724
Heating of Radio-Frequency Cables. Macalpine..283–8
Heating of Transformers Under Short-Circuit Conditions. Montsinger, Halsey........947–52; disc. 952
Heating of Transmission Line Clamps, Magnetic. Crabb, Sheadel........1032–5
Heating to Deicing of Aircraft Propellers, Development and Application of Electric. Sheets, Sand..1068–72
Heaviside's Operational Calculus Based on the Generalized Functions of Schwartz, A Derivation of. Smith, Alger........939–44; disc. 944
High Frequencies and Under Changing Temperature, The Measurement of Dielectric Loss at. Whitehead, Rueggeberg........520–4
High-Pressure Gas-Filled Cable Impregnated with Extra-High-Viscosity Oil. Sticher, Doan, Atkinson, Meyerhoff........336–45; disc. 345
High-Speed Reclosing Circuit Breakers, Insulator Flashover Deionization Times as a Factor in Applying. Boisseau, Wyman, Skeats........1058–66; disc. 1066
High-Voltage Bushing Design for High Altitudes, A Small. Vogel, Hart........761–4
High-Voltage Cable Joints, A Theoretical and Practical Approach to the Design of. Short........1275–80; disc. 1280
High-Voltage Corona, Radio Influence from. Slemon........198–204; disc. 204
High-Voltage Fault-Arc Paths, Deionization Time of. Harrington, Starr........997–1003; disc. 1003
High-Voltage Switching, Protection of Stations Without. (Committee Report)........226–31; disc. 231
High-Voltage Transmission Lines, A Transient Fault Locator for. Spaulding, Diemond........1005–1010; disc. 1010
Horsepower Gas Turbine Power Plant, A 3,000-. Haverstick........458–60
Hydraulic Conditions During Operation of Hydroelectric Units, Some Oscillographic Methods of Investigating Mechanical and. Engvall....993–6
Hydro Units, Outage Rates of Steam Turbines and Boilers and of. (Committee Report)........450–7
Hydroelectric Units, Some Oscillographic Methods of Investigating Mechanical and Hydraulic Conditions During Operation of. Engvall........993–6
Hy-Therm Copper—An Improved Overhead-Line Conductor. Hickernell, Jones, Snyder........22–7; disc. 27

I

Impregnated with Extra-High-Viscosity Oil, High-Pressure Gas-Filled Cable. Sticher, Doan, Atkinson, Meyerhoff........336–45; disc. 345
Improved A-C Network Analyzer, An. Morgan, Rothe, Winsness........891–5; disc. 895
Improvements, Aircraft Carbon-Pile Voltage Regulators, Fundamentals, and Design. Austin, Richards........983–7
Improvements to Oklahoma City Primary Network. Brady........701–02; disc. 702
Incandescent Lamps, Saving Time in Testing Life of. Purcell........730–2
Incremental Regulation and Dead Band of Governors on Steam Turbine Generators Under System Load Conditions, Determining. Tornquist, Wade........1343–7
Indicating Instrument, Measuring Commutation with an. Lundy........1380–2
Indicator, Polar Vector. Walker, Waynick, Sulzer........154–9
Induction Motors, Die-Cast Rotors for. Packer........253–60; disc. 260
Induction Motors, Design of Auxiliary Circuits of Single-Phase. Thacker, Gopalakrishna....1373–9
Induction Motors, General Theory of Multiple Cage. Chang........1139–43
(Industrial Control) Prediction of Ultimate Temperature Rise from Early Heat Run Data. Ryan...1164–6
(Industrial Control) The Use of Air-Core Reactors as Fault Limiting Means on High Interrupting Capacity Controllers. Leitch.....469–74; disc. 474
(Industrial) Dynamic Braking Control of D-C Series Motors—Experimental Study of Speed-Torque Curves. Heumann........560–4
Industrial Plants Prefer Diesel-Electric Switching Locomotives. Woods........697–700
(Industry) Selection of Electric Drives for Looms. Demartini, Lukens........349–56
Influence from High-Voltage Corona, Radio. Slemon........198–204; disc. 204
Influence Voltage Generation, Commutation of D-C Machines and Its Effects on Radio. Motter........491–5; disc. 495
Inherent-Overheating Protection Under Running Overload Conditions, Fundamental Theory of. Veinott, Schaefer........266–70; disc. 270
Installation on Power Lines, Line Tuning Equipment Used With Coaxial Cable for Carrier Current. Sutton........44–8; disc. 48
Instrument Inaccuracies in Feed-Back Control Systems with Particular Reference to Backlash. Marcy, Yachter, Zauderer........778–88
Instrument, Measuring Commutation with an Indicating. Lundy........1380–2
Instrument Servomechanisms, Damper Stabilized. Hall........299–306; disc. 306
Instrumentation for the Evaluation of the Stability of the Welding Arc. Winsor, Schetky, Wyant........525–33
(Instruments) A New Expanded Scale A-C Voltmeter. Millar........641–3
(Instruments) A New Thermal Volt-Ampere Demand Meter. Douglass, Morong........79–83; disc. 83
(Instruments) A Transient Fault Locator for High-Voltage Transmission Lines. Spaulding, Demond........1005–10; disc. 1010
(Instruments) An Electro-Optical Shutter for Photographic Purposes. Zarem, Marshall, Poole..84–91
(Instruments) Automatic Range-Adjusting Radiosonde Recorder. Beggs........602–07
(Instruments) Polar Vector Indicator. Walker, Waynick, Sulzer........154–9
(Instruments) Surge Protection in a Modern Watt-Hour Meter. Busch, Williams........74–7; disc. 77
(Insulated Conductors) A-C Resistance of Segmental Cables in Steel Pipe. Meyerhoff, Eager........816–29; disc. 829
(Insulated Conductors) High-Pressure Gas-Filled Cable Impregnated with Extra-High-Viscosity Oil. Sticher, Doan, Atkinson, Meyerhoff........336–45; disc. 345
(Insulated Conductors) The Thermal Movement of Moisture in Soil. Mickley........330–3; disc. 333
(Insulated Conductors) Transformer Manholes and Vaults: Design and Ventilation. Porter....534–9
Insulation and Silicone Varnish, Motor Tests Evaluate Thermal Endurance of Class-H. Grant, Kauppi, Moses, Gibson........1133–8
Insulation Co-ordination of Oil Insulated Transformers, Extremes in the. Vogel........965–8; disc. 968
Insulation Level of Relay and Control Circuits. (Committee Report)........1255–7
Insulation, Methods for Determining the Effects of Contaminants on Electrical. Mathes, Sieffert, Walker, Lindsey........113–18; disc. 118
Insulation Protection in the Operation of Power Transformers, Controlled Temperature and. Satterlee, Reed........753–8; disc. 759
Insulator Flashover Deionization Times as a Factor in Applying High-Speed Reclosing Circuit Breakers. Boisseau, Wyman, Skeats........1058–66; disc. 1066
Insulators for Pole Lines, Rubber. Wheeler, Markley........195–7
Interference from Radio-Frequency Heating Equipment, Reduction of. Klingaman........718–24; disc. 724
Interrupting Capacity Controllers, The Use of Air-Core Reactors as Fault Limiting Means on High-. Leitch........469–74; disc. 474
Investigating Mechanical and Hydraulic Conditions During Operation of Hydroelectric Units, Some Oscillographic Methods of. Engvall........993–6
Investigation on a Rural Distribution System, Lightning. MacCarthy, Stann, Edge, McKinley........428–37; disc. 437
Investigation on a Rural Distribution System, Overcurrent. Lincks, Edge, McKinley, Leh........915–27; disc. 927
Iron Losses in Series Motors, Armature. Chang, Karr........262–4; disc. 264

J

Joint Usage, Power Line Carrier for Relaying and. Part I. Hampe, Storer........864–7; disc. 871
Joints, A Theoretical and Practical Approach to the Design of High-Voltage Cable. Short........1275–80; disc. 1280
Joints by Means of a Bolometer, Detection of Overheated Transmission Line. Leslie, Wait....64–8; disc. 68

L

Laboratory Techniques, Cable Accessory Design Utilizing New. Bosworth, Farr.....1268–73; disc. 1273
Lamps, Saving Time in Testing Life of Incandescent. Purcell........730–2
Land-Mobile Services Operating on Frequencies Between 152–174 Megacycles, Design of Mobile Radio Communication Equipment for. Beers, Harris, Zappacosta........1232–9
(Land Transportation) Application Engineering on Diesel-Electric Locomotives in Railroad Service. Bevan........125–31
(Land Transportation) Electric Equipment for Chesapeake and Ohio Railway Company Steam Turbine-Electric Locomotives. Atwell, Baston........145–8
(Land Transportation) Industrial Plants Prefer Diesel-Electric Switching Locomotives. Woods..697–700
(Land Transportation) Selenium Rectifiers in Motor Vehicle Power Systems. Ramsey..149–53; disc. 153
(Land Transportation) The Renaissance of Electric Motive Power. Candee........138–44
(Land Transportation) Trackless Trolley Operation in Rhode Island. Blomquist........397–402
(Land Transportation) Trolley Coaches Replace Busses. McMillon........403–06
(Land Transportation) Twenty-Five Years Progress in the Design of Traction Motors. Baldwin....132–7
Law Power-Level Recorder, A Square. Clark, Turner, Williams........476–82
Leakage of the Different Patterns of a Fractional Slot Winding, Differential. Liwschitz........1129–31; disc. 1131
Leakage Reactance, Saturation Effect of. Chang, Lloyd........1144–7
Level of Relay and Control Circuits, Insulation. (Committee Report)........1255–7
Level Recorder, A Square-Law Power-. Clark, Turner, Williams........476–82
Life of Incandescent Lamps, Saving Time in Testing. Purcell........730–2
(Light) Measurements of Erythemal Energy. Scott........725–9
(Light) Saving Time in Testing Life of Incandescent Lamps. Purcell........730–2
Lightning Investigation on a Rural Distribution System. MacCarthy, Stann, Edge, McKinley........428–37; disc. 437
Lightning Measurements, Advances in Technique of. Brownlee........515–19
Lightning Protective Devices, Performance Characteristics of. (Committee Report)........1333–6
Lightning Stroke Damage to Aircraft. Hagenguth........1036–44; disc. 1044
Lightning Strokes, Transmission Line Design and Performance Based on Direct. Harder, Clayton........439–46; disc. 447
Lightweight Aircraft Transformers. Stephens...1073–8
Limitations in Design of D-C Adjustable Speed Motors. Opel........1095–8
Limiting Means on High Interrupting Capacity Controllers, The Use of Air-Core Reactors as Fault. Leitch........469–74; disc. 474
Line at Carrier Current Frequencies, Loss Measurements Made on Underground-Cable Overhead-Conductor 132-Kv Transmission. Cornelius, Storer..597–601
Line Carrier Equipment, A Proposal for Broad-Band Coupling of Power-. Miller...1028–30; disc. 1030
Line Carrier for Relaying and Joint Usage, Power, Part I. Hampe, Storer........864–7; disc. 871
Line Clamps, Magnetic Heating of Transmission. Crabb, Sheadel........1032–5
Line Conductor, Hy-Therm Copper—An Improved Overhead-. Hickernell, Jones, Snyder........22–7; disc. 27
Line Design and Performance Based on Direct Lightning Strokes, Transmission. Harder, Clayton........439–46; disc. 447
Line Joints by Means of a Bolometer, Detection of Overheated Transmission. Leslie, Wait........64–8; disc. 68
Line Sectionalizing Circuit Breakers, A-C Tripping and Reclosing of. Winegartner, Bonheimer....1357–9
Line Tuning Equipment Used With Coaxial Cable for Carrier Current Installation on Power Lines. Sutton........44–8; disc. 48
Linear Vibration Problems, Summary of Transformations Useful in Constructing Analogs of. Corbett........661–4
Lines, A Transient Fault Locator for High-Voltage Transmission. Spaulding, Diemond........1005–10; disc. 1010
Lines Along Uniformly Rotating Reference Frames, Stationary Networks and Transmission. Kron........690–6
Lines as Affecting Ground-Fault Neutralizers, Report on Survey of Unbalanced Charging Currents on Transmission. (Committee Report)....1328; disc. 1329
Lines, Attenuation and Delay Equalizers for Coaxial. Lundry........1174–9
Lines, Comparative Performance Records—Steel and Wood Transmission. Booker.....686–9; disc. 689
Lines, Equalization of Coaxial. Gould........1187–92
Lines from the New Sunbury Generating Station, Relaying of Transmission. Green, Oewel, Ramsaur........873–7; disc. 877
Lines, Rubber Insulators for Pole. Wheeler, Markley........195–7

Load Conditions, Determining Incremental Regulation and Dead Band of Governors on Steam Turbine Generators Under System. Tornquist, Wade..........1343–7

Load Control for Turbine Generators, A New Automatic. Ruud, Farnham..........1337–42; disc. 1342

Load Losses Measured in D-C Motors, Stray. (Committee Report)..........219–23; disc. 223

Load Reduction, The Performance of a Topped Steam Power Plant on Sudden. Noest..........1348–56

Load, Some Fundamentals of D-C Controlled Reactors with Resistive. Storm..........188–94; disc. 194

Load, The Heat Pump—Its Significance as a Potential Residential Electric. Bary..........1–8

Loading of a Transformer System, Economic. Levine, Smith..........733–8; disc. 738

Loading Schedules, Co-ordination of Fuel Cost and Transmission Loss by Use of the Network Analyzer to Determine Plant. George, Page, Ward..........1152–60; disc. 1160

Loads on A-C Generators, A Semiempirical Approach to Voltage Dip—with Suddenly Applied. Rosenberg..........160–6; disc. 166

Locator for High-Voltage Transmission Lines, A Transient Fault. Spaulding, Diemond..........1005–1010; disc. 1010

Loci for Servomechanism Components and Systems, Graphical Determination of Transfer Function. Thomas, Easton..........307–14; disc. 314

Loci of the Synchronous Tie, The Geometric. Finzi, Wellard..........168–71

Locomotives, Electric Equipment for Chesapeake and Ohio Railway Company Steam Turbine-Electric. Atwell, Baston..........145–8

Locomotives in Railroad Service, Application Engineering on Diesel-Electric. Bevan..........125–31

Locomotives, Industrial Plants Prefer Diesel-Electric Switching. Woods..........697–700

Logic of Relay Circuits, The. Keister..........571–6

Long-Time and Short-Time Analog Computers, Comparison of. Paschkis..........70–3

Loss at High Frequencies and Under Changing Temperature, The Measurement of Dielectric. Whitehead, Rueggeberg..........520–4

Loss by Use of the Network Analyzer to Determine Plant Loading Schedules, Co-ordination of Fuel Cost and Transmission. George, Page, Ward..........1152–60; disc. 1160

Loss Measurements Made on Underground-Cable Overhead-Conductor 132-Kv Transmission Line at Carrier Current Frequencies. Cornelius, Storer..........597–601

Loss-of-Excitation Relay for Synchronous Generators, A New. Mason..........1240–5

Losses in Series Motors, Armature Iron. Chang, Karr..........262–4; disc. 264

Losses Measured in D-C Motors, Stray Load. (Committee Report)..........219–23; disc. 223

M

Machine Performance, The Eccentric Pole Face—A Means to Better D-C. Baker..........1107–10

Machine, The Negative-Sequence Reactances of an Ideal Synchronous. Duesterhoeft..........510–13; disc. 513

Machines and Its Effects on Radio Influence Voltage Generation, Commutation of D-C. Motter..........491–5; disc. 495

Machines, Temperature Rise Values for D-C. Part I. (Committee Report)..........206–12; disc. 212

Machines, Temperature Rise Values for D-C. Part II. (Committee Report)..........1118–23; disc. 1123

Machines, Transients in 2-Phase Synchronous. Wilson..........1360–7

Magnetic Amplifiers, Self-Saturation in. Dornhoefer..........835–46; disc. 846

Magnetic Amplifiers with Feedback, Analytical Determination of Characteristics of. VerPlanck, Finzi, Beaumariage..........565–70

Magnetic Field Components of Circular Filaments and Solenoids, Formulas and Tables for the Calculation of the. Grover..........665–75

Magnetic Heating of Transmission Line Clamps. Crabb, Sheadel..........1032–5

Magnetic Recording, Application of Experimental Test Procedures and Methods of Analysis of Results to Research Problems in. Thompson..........407–17

Magnetic Saturation, Nonharmonic Oscillations as Caused by. Rudenberg..........676–85

Main Bus, Protection of the Airplane. Exner..........979–82

Maintenance of Shunt Capacitors, Report on the Operation and. (Committee Report)..........1208–18

Manholes and Vaults: Design and Ventilation, Transformer. Porter..........534–9

Manually-Operated Spring Mechanism for Medium Voltage Oilless Circuit Breakers, A. Wyman, Casey..........357–61; disc. 361

Manufacture of Soldered Porcelain Potheads, A New Technique in the. Papp, Nicholas..........1258–60; disc. 1261

Matching Electrical Characteristics of McNary Generators and Transformers with Bonneville Power Administration Transmission System. Hoard, Weiner..........1022–5; disc. 1026

McNary Generators and Transformers with Bonneville Power Administration Transmission System, Matching Electrical Characteristics of. Hoard, Weiner..........1022–5; disc. 1026

Means on High Interrupting Capacity Controllers, The Use of Air-Core Reactors as Fault Limiting. Leitch..........469–74; disc. 474

Measurement of Dielectric Loss at High Frequencies and Under Changing Temperature, The. Whitehead, Rueggeberg..........520–4

Measurements, Advances in Technique of Lightning. Brownlee..........515–19

Measurements Made on Underground-Cable Overhead-Conductor 132-Kv Transmission Line at Carrier Current Frequencies, Loss. Cornelius, Storer..........597–601

Measurements of Erythemal Energy. Scott..........725–29

Measuring Commutation with an Indicating Instrument Lundy..........1380–2

Mechanical and Hydraulic Conditions During Operation of Hydroelectric Units, Some Oscillographic Methods of Investigating. Engvall..........993–6

Mechanics and Servomechanisms, Application of the California Institute of Technology Electric Analog Computer to Nonlinear. McCann, Wilts, Locanthi..........652–60

Mechanism for Medium Voltage Oilless Circuit Breakers, A Manually-Operated Spring. Wyman, Casey..........357–61; disc. 361

Megacycles, Design of Mobile Radio Communication Equipment for Land-Mobile Services Operating on Frequencies Between 152–174. Beers, Harris, Zappacosta..........1232–9

Meter, A New Thermal Volt-Ampere Demand. Douglass, Morong..........79–83; disc. 83

Meter, Surge Protection in a Modern Watt-Hour. Busch, Williams..........74–7; disc. 77

Meters, Heat Flow Ratio as a Design Parameter in Thermal Demand. Nelson..........885–90; disc. 890

Method, Field Tests of Oil Circuit Recloser Substantiate Analytical Co-ordination. Auer, Branflick, Woodward, McKinley..........801–08; disc. 808

Method for Designing Pulse Transformers, A. Kirschbaum, Warren..........971–8

Method for Determining Generator Reserve, A Convenient. Seelye..........1317–20

Method for Estimating the Performance of Distance Relays During Faults and Power Swings, Graphical. Warrington..........608–20; disc. 620

Methods Applied to Frequency Response Curves, Control Chart. Mundel..........424–7

Methods for Determining the Effects of Contaminants on Electrical Insulation. Mathes, Sieffert, Walker, Lindsey..........113–18; disc. 118

Methods of Analysis of Results to Research Problems in Magnetic Recording, Application of Experimental Test Procedures and. Thompson..........407–17

Methods of Investigating Mechanical and Hydraulic Conditions During Operation of Hydroelectric Units, Some Oscillographic. Engvall..........993–6

Metropolitan Area, A 66-Kv Subtransmission Plan for a. Smith, Michelson..........908–12; disc. 912

Microwave Channels for Power System Applications. (Committee Report)..........40–2; disc. 42

Microwave Communication Relay System, A. Boothroyd, Churchill..........637–41

Microwave Relay Systems, Power Supplies for. Ward..........631–6

Mobile Radio Communication Equipment for Land-Mobile Services Operating on Frequencies Between 152–174 Megacycles, Design of. Beers, Harris, Zappacosta..........1232–9

Mobile Radio Systems, Vibrating Reed Selectors for. Keller, Bostwick..........383–6

Mobile Telephone Use, Vibrating Reed Selective Signaling System for. Pruden, Hoth..........387–91

Modern Watt-Hour Meter, Surge Protection in a. Busch, Williams..........74–7; disc. 77

Moisture in Soil, The Thermal Movement of. Mickley..........330–3; disc. 333

Motive Power, The Renaissance of Electric. Candee..........138–44

Motor Tests Evaluate Thermal Endurance of Class-H Insulation and Silicone Varnish. Grant, Kauppi, Moses, Gibson..........1133–8

Motor, The Field Fluxes of the Shaded-Pole. Kimberly..........273–7

Motor Vehicle Power Systems, Selenium Rectifiers in. Ramsey..........149–53; disc. 153

Motors and Generators, Solid Short Circuit of D-C. Linville, Ward..........119–23; disc. 123

Motors and Generators, Transient Characteristics of D-C. McClinton, Brancato, Panoff..........1100–06

Motors, Armature Iron Losses in Series. Chang, Karr..........262–4; disc. 264

Motors, Design of Auxiliary Circuits of Single-Phase Induction. Thacker, Gopalakrishna..........1373–9

Motors, Die-Cast Rotors for Induction. Packer..........253–60; disc. 260

Motors—Experimental Study of Speed-Torque Curves, Dynamic Braking Control of D-C Series. Heumann..........560–4

Motors for Use in Automatic Control Systems, The Design of D-C. Lebenbaum..........1089–94

Motors, General Theory of Multiple Cage Induction. Chang..........1139–43

Motors, Limitations in Design of D-C Adjustable Speed. Opel..........1095–8

Motors, Stray Load Losses Measured in D-C. (Committee Report)..........219–23; disc. 223

Motors, Twenty-Five Years Progress in the Design of Traction. Baldwin..........132–7

Motors, Use of Cumulative and Differential Series Fields in the Parallel Operation of D-C. Kimball..........1098–1100

Movement of Moisture in Soil, The Thermal. Mickley..........330–3; disc. 333

Moving Coil Fluxmeter, General Theory and Experimental Confirmation of the. Higgins, Robertson..........897–907; disc. 907

Multifrequency Pulsing in Switching, Application of. Dahlbom, Horton, Moody..........392–6

Multiple Cage Induction Motors, General Theory of. Chang..........1139–43

Multiplexing System, A Time Division. Boothroyd, Creamer..........92–7

N

Negative-Sequence Reactances of an Ideal Synchronous Machine, The. Duesterhoeft..........510–13; disc. 513

Network Analyzer, An Improved A-C. Morgan, Rothe, Winsness..........891–5; disc. 895

Network Analyzer to Determine Plant Loading Schedules, Co-ordination of Fuel Cost and Transmission Loss by Use of the. George, Page, Ward..........1152–60; disc. 1160

Network, Improvements to Oklahoma City Primary. Brady..........701–02; disc. 702

Network Systems in the Washington Area, Design and Experience With 4-Kv Primary. Lank..........712–16; disc. 716

Networks and Transmission Lines Along Uniformly Rotating Reference Frames. Kron..........690–6

Networks on the Duquesne Light Company System, Primary. Holben, Lange..........704–09; disc. 709

Neutralizer on a Regulated Distribution System, Operation of a Ground-Fault. Tomlinson, Hunt..........1321–6; disc. 1326

Neutralizers, Report on Survey of Unbalanced Charging Currents on Transmission Lines as Affecting Ground-Fault. (Committee Report)..........1328; disc. 1329

New Automatic Load Control for Turbine Generators, A. Ruud, Farnham..........1337–42; disc. 1342

New Expanded Scale A-C Voltmeter, A. Millar..........641–3

New Loss-of-Excitation Relay for Synchronous Generators, A. Mason..........1240–5

New 69-Kv Compressed-Air Circuit Breaker, A. Baker, Frisch..........363–8; disc. 369

Noise Problems on an Electric Power System, Transformer Audio. Murray..........740–7; disc. 747

Nonharmonic Oscillations as Caused by Magnetic Saturation. Rudenberg..........676–85

Nonlinear Mechanics and Servomechanisms, Application of the California Institute of Technology Electric Analog Computer to. McCann, Wilts, Locanthi..........652–60

Novel Test Circuits for Protective Relays. Sonnemann..........1249–54

O

Officers and Committees—1949–1950..........1409–28

Oil Circuit Recloser Substantiate Analytical Co-ordination Method, Field Tests of. Auer, Branflick, Woodward, McKinley..........801–08; disc. 808

Oil, High-Pressure Gas-Filled Cable Impregnated with Extra-High-Viscosity. Sticher, Doan, Atkinson, Meyerhoff..........336–45; disc. 345

Oil Insulated Transformers, Extremes in the Insulation Co-ordination of. Vogel..........965–8; disc. 968

Oil with Variations of Pressure and Temperature, Dielectric Strength of. Hoover, Hixson..........1047–50

Oilless Circuit Breakers, A Manually-Operated Spring Mechanism for Medium Voltage. Wyman, Casey..........357–61; disc. 361

Oklahoma City Primary Network, Improvements to. Brady..........701–02; disc. 702

One Slip Cycle Out-of-Step Relay Equipment. Morris..........1246–8

Operated Spring Mechanism for Medium Voltage Oilless Circuit Breakers, A Manually-. Wyman, Casey..........357–61; disc. 361

Operating Capacitors Without Individual Fuses, The Calculated Risk of. Brooks...1219–25; disc. 1225
Operating Characteristics of Two-Phase Servomotors. Koopman....319–27; disc. 327
Operation and Maintenance of Shunt Capacitors, Report on the. (Committee Report)....1208–18
Operation in Rhode Island, Trackless Trolley. Blomquist....397–402
Operation of a Ground-Fault Neutralizer on a Regulated Distribution System. Tomlinson, Hunt....1321–6; disc. 1326
Operation of D-C Motors, Use of Cumulative and Differential Series Fields in the Parallel. Kimball....1098–1100
Operation, The Dynamoelectric Amplifier—Class A. Saunders....1368–73
Operational Calculus Based on the Generalized Functions of Schwartz, A Derivation of Heaviside's Smith, Alger....939–44; disc. 944
Optical Shutter for Photographic Purposes, An Electro-. Zarem, Marshall, Poole....84–91
Oscillations as Caused by Magnetic Saturation, Nonharmonic. Rudenberg....676–85
Oscillographic Methods of Investigating Mechanical and Hydraulic Conditions During Operation of Hydroelectric Units. Engvall....93–6
Oscillographing Commutation. Baldwin....100–05; disc. 105
Outage Rates of Steam Turbines and Boilers and of Hydro Units. (Committee Report)....450–7
Overcurrent Investigation on a Rural Distribution System. Lincks, Edge, McKinley, Leh....915–27; disc. 927
Overhead-Conductor 132-Kv Transmission Line at Carrier Current Frequencies, Loss Measurements Made on Underground-Cable. Cornelius, Storer....597–601
Overhead-Line Conductor, Hy-Therm Copper—An Improved. Hickernell, Jones, Snyder....22–7; disc. 27
Overheated Transmission Line Joints by Means of a Bolometer, Detection of. Leslie, Wait....64–8; disc. 68
Overheating Protection Under Running Overload Conditions, Fundamental Theory of Inherent-. Veinott, Schaefer....266–70; disc. 270
Overload Conditions, Fundamental Theory of Inherent-Overheating Protection Under Running. Veinott, Schaefer....266–70; disc. 270

P

Pacific Gas and Electric Company, Electrical Design Features—Steam-Electric Generating Station P of the. Benson....1013–20; disc. 1020
Parallel Operation of D-C Motors, Use of Cumulative and Differential Series Fields in the. Kimball....1098–1100
Parameter in Thermal Demand Meters, Heat Flow Ratio as a Design. Nelson....885–90; disc. 890
Paths, Deionization Time of High-Voltage Fault-Arc. Harrington, Starr....997–1003; disc. 1003
Patterns of a Fractional Slot Winding, Differential Leakage of the Different. Liwschitz....1129–31; disc. 1131
Performance Based on Direct Lightning Strokes, Transmission Line Design and. Harder, Clayton....439–46; disc. 447
Performance Characteristics of Lightning Protective Devices. (Committee Report)....1333–6
Performance of a Topped Steam Power Plant on Sudden Load Reduction, The. Noest....1348–56
Performance of Diesel-Electric Rig for Deep-Well Drilling. Clark, Moore....497–506
Performance of Distance Relays During Faults and Power Swings, Graphical Method for Estimating the. Warrington....608–20; disc. 620
Performance of Servomechanisms, Comparison of Steady-State and Transient. Chestnut, Mayer....765–77
Performance of Shunt Capacitors, Report of a Survey on the. (Committee Report)....1200–06; disc. 1206
Performance Records—Steel and Wood Transmission Lines, Comparative. Booker....686–9; disc. 689
Performance Specification, Governors and the AIEE-ASME Governor. Schwendner, Astley....1330–2
Performance, The Eccentric Pole Face—A Means to Better D-C Machine. Baker....1107–10
Phenomena of 3-Conductor Cables, Transient Temperature. Wollaston....1284–95; disc. 1295
Philadelphia, 69-Kv Pipe-Type Cable Circuits in. Kidder, Van Antwerp....550–6; disc. 556
Photographic Purposes, An Electro-Optical Shutter for. Zarem, Marshall, Poole....84–91
Pile Voltage Regulators, Fundamentals, and Design Improvements, Aircraft Carbon-. Austin, Richards....983–7
Pipe, A-C Resistance of Segmental Cables in Steel. Meyerhoff, Eager....816–29; disc. 829
Pipe-Type Cable Circuits in Philadelphia, 69-Kv. Kidder, Van Antwerp....550–6; disc. 556
Pipes, The Temperature Rise of Buried Cables and. Neher....9–17; disc. 17
Plan for a Metropolitan Area, A 66-Kv Subtransmission. Smith, Michelson....908–12; disc. 912
Plant, A 3,000-Horsepower Gas Turbine Power. Haverstick....458–60
Plant Loading Schedules, Co-ordination of Fuel Cost and Transmission Loss by Use of the Network Analyzer to Determine. George, Page, Ward....1152–60; disc. 1160
Plant on Sudden Load Reduction, The Performance of a Topped Steam Power. Noest....1348–56
Plants Prefer Diesel-Electric Switching Locomotives, Industrial. Woods....697–700
Polar Vector Indicator. Walker, Waynick, Sulzer....154–9
Pole Face—A Means to Better D-C Machine Performance, The Eccentric. Baker....1107–10
Pole Lines, Rubber Insulators for. Wheeler, Markley....195–7
Pole Motor. The Field Fluxes of the Shaded-. Kimberly....273–7
Porcelain Potheads, A New Technique in Manufacture of Soldered. Papp, Nicholas..1258–60; disc. 1261
Potential Residential Electric Load, The Heat Pump—Its Significance as a. Bary....1–8
Potheads, A New Technique in Manufacture of Soldered Porcelain. Papp, Nicholas.1258–60; disc. 1261
Potheads 69,000 Volts and Below, Design Fundamentals of. Nicholas....1263–7; disc. 1267
Power Factor of Unbalanced Sinusoidal 3-Phase Circuits, The Vector. Lamb, Brandt....507–09
Power-Flow Studies, Equivalent Circuits for. Ward....373–80; disc. 380
(Power Generation) A New Automatic Load Control for Turbine Generators. Ruud, Farnham....1337–42; disc. 1342
Power Generation and Other Applications, Two Gas Turbines for. Howard....461–5; disc. 465
(Power Generation) Determining Incremental Regulation and Dead Band of Governors on Steam Turbine Generators Under System Load Conditions. Tornquist, Wade....1343–7
(Power Generation) Electrical Design Features—Steam-Electric Generating Station P of the Pacific Gas and Electric Company. Benson...1013–20; disc. 1020
Power Generation, Gas Turbines in Stationary. Hague....467–8
(Power Generation) Governors and the AIEE-ASME Governor Performance Specification. Schwendner, Astley....1330–2
(Power Generation) Outage Rates of Steam Turbines and Boilers and of Hydro Units. (Committee Report)....450–7
(Power Generation) Some Oscillographic Methods of Investigating Mechanical and Hydraulic Conditions During Operation of Hydroelectric Units. Engvall....993–6
(Power Generation) The Transient Behavior of the Two-Stage Rototrol Main Exciter Voltage Regulating System as Determined by Electrical Analogy. Carleton....59–63
Power-Level Recorder, A Square-Law. Clark, Turner, Williams....476–82
Power-Line Carrier Equipment, A Proposal for Broad-Band Coupling of. Miller....1028–30; disc. 1030
Power Line Carrier for Relaying and Joint Usage. Part I. Hampe, Storer....864–7; disc. 871
Power Lines, Line Tuning Equipment Used With Coaxial Cable for Carrier Current Installation on. Sutton....44–8; disc. 48
Power Plant, A 3,000-Horsepower Gas Turbine. Haverstick....458–60
Power Plant on Sudden Load Reduction, The Performance of a Topped Steam. Noest....1348–56
Power Rating of Radio-Frequency Cables, The. Mildner....289–98; disc. 298
Power Supplies for Coaxial Systems. Spencer..627–30
Power Supplies for Microwave Relay Systems. Ward....631–6
Power Swings, Graphical Method for Estimating the Performance of Distance Relays During Faults and. Warrington....608–20; disc. 620
Power System Applications, Microwave Channels for. (Committee Report)....40–2; disc. 42
Power System, Transformer Audio Noise Problems on an Electric. Murray....740–7; disc. 747
Power Systems, Selenium Rectifiers in Motor Vehicle. Ramsey....149–53; disc. 153
Power, The Renaissance of Electric Motive. Candee....138–44
Power Transformers, Controlled Temperature and Insulation Protection in the Operation of. Satterlee, Reed....753–8; disc. 759
Power Transformers, Use of Thyrite. Meador....959–64; disc. 964
Practical Approach to the Design of High-Voltage Cable Joints, A Theoretical and. Short....1275–80; disc. 1280
Practices for Shunt Capacitor Banks, Connection Arrangements and Protective. Clark, Farnham....1226–30; disc. 1231
Prediction of Ultimate Temperature Rise from Early Heat Run Data. Ryan....1164–6
Pressure and Temperature, Dielectric Strength of Oil with Variations of. Hoover, Hixson....1047–50
Pressure Gas-Filled Cable Impregnated with Extra-High-Viscosity Oil, High-. Sticher, Doan, Atkinson, Meyerhoff....336–45; disc. 345
Primary Network, Improvements to Oklahoma City. Brady....701–02; disc. 702
Primary Network Systems in the Washington Area, Design and Experience With 4-Kv. Lank....712–16; disc. 716
Primary Networks on the Duquesne Light Company System. Holben, Lange....704–09; disc. 709
Problems in Magnetic Recording, Application of Experimental Test Procedures and Methods of Analysis of Results to Research. Thompson....407–17
Problems on an Electric Power System, Transformer Audio Noise. Murray....740–7; disc. 747
Problems, Summary of Transformations Useful in Constructing Analogs of Linear Vibration. Corbett....661–4
Procedures and Methods of Analysis of Results to Research Problems in Magnetic Recording, Application of Experimental Test. Thompson...407–17
Progress in the Design of Traction Motors, Twenty-Five Years. Baldwin....132–7
Progress Report on AIEE Test Code for Electric Brushes. (Committee Report)....1126–8
Propellers, Development and Application of Electric Heating to Deicing of Aircraft. Sheets, Sand....1068–72
Proposal for Broad-Band Coupling of Power-Line Carrier Equipment, A. Miller....1028–30; disc. 1030
Protection in a Modern Watt-Hour Meter, Surge. Busch, Williams....74–7; disc. 77
Protection in the Operation of Power Transformers, Controlled Temperature and Insulation. Satterlee, Reed....753–8; disc. 759
Protection of Stations Without High-Voltage Switching. (Committee Report)....226–31; disc. 231
Protection of the Airplane Main Bus. Exner...979–82
Protection of Transformer Stations, Automatic Grounding and Air-Break Switches for. Ricker....851–6; disc. 856
Protection, Shipshaw Relay. Madill, Duffy....50–5; disc. 55
Protection Under Running Overload Conditions, Fundamental Theory of Inherent-Overheating. Veinott, Schaefer....266–70; disc. 270
(Protective Devices) Lightning Investigation on a Rural Distribution System. MacCarthy, Stann, Edge, McKinley....428–37; disc. 437
(Protective Devices) Operation of a Ground-Fault Neutralizer on a Regulated Distribution System. Tomlinson, Hunt....1321–6; disc. 1326
Protective Devices, Performance Characteristics of Lightning. (Committee Report)....1333–6
(Protective Devices) Report on Survey of Unbalanced Charging Currents on Transmission Lines as Affecting Ground-Fault Neutralizers (Committee Report)....1328; disc. 1329
(Protective Devices) Voltage-Recovery Characteristics of Distribution Systems. Witzke..172–80; disc. 180
Protective Practices for Shunt Capacitor Banks, Connection Arrangements and. Clark, Farnham....1226–30; disc. 1231
Protective Relays, Novel Test Circuits for. Sonnemann....1249–54
Pulse Transformers, A Method for Designing. Kirschbaum, Warren....971–8
Pulsing in Switching, Application of Multifrequency. Dahlbom, Horton, Moody....392–6
Pump—Its Significance as a Potential Residential Electric Load, The Heat. Bary....1–8

R

Radio Communication Equipment for Land-Mobile Services Operating on Frequencies Between 152–174 Megacycles, Design of Mobile. Beers, Harris, Zappacosta....1232–9
Radio-Frequency Cables, Heating of. Macalpine....283–8
Radio-Frequency Cables, The Power Rating of. Mildner....289–98; disc. 298
Radio-Frequency Heating Equipment, Reduction of Interference from. Klingaman..718–24; disc. 724
Radio Influence from High-Voltage Corona. Slemon....198–204; disc. 204
Radio Influence Voltage Generation, Commutation of D-C Machines and Its Effects on. Motter....491–5; disc. 495
Radio Systems, Vibrating Reed Selectors for Mobile. Keller, Bostwick....383–6
Radiosonde Recorder, Automatic Range-Adjusting. Beggs....602–07
Railroad Service, Application Engineering on Diesel-Electric Locomotives in. Bevan....125–31
Railroads, Centralized Traffic Control for. Hailes....1167–73

Railway Company Steam Turbine-Electric Locomotives, Electric Equipment for Chesapeake and Ohio. Atwell, Baston....................145–8
Range Adjustable-Speed Drive, A Wide-. Conrad, Tribken....................789–90
Range-Adjusting Radiosonde Recorder, Automatic. Beggs....................602–07
Rates of Steam Turbines and Boilers and of Hydro Units, Outage. (Committee Report)............450–7
Rating of Radio-Frequency Cables, The Power. Mildner....................289–98; disc. 298
Ratings of Aircraft Cable, Current. Askew, McClinton....................988–92
Ratings, Standardization of Reactor. Kierstead, Thomason....................955–7; disc. 957
Ratio as a Design Parameter in Thermal Demand Meters, Heat Flow. Nelson.....885–90; disc. 890
Reactance, Saturation Effect of Leakage. Chang, Lloyd....................1144–7
Reactances of an Ideal Synchronous Machine, The Negative-Sequence. Duesterhoeft....................510–13; disc. 513
Reactor Ratings, Standardization of. Kierstead, Thomason....................955–7; disc. 957
Reactors as Fault Limiting Means on High Interrupting Capacity Controllers, The Use of Air-Core. Leitch....................469–74; disc. 474
Reactors, Universal Curves for D-C Controllable. Johnson, Merrell, Alley............31–7; disc. 37
Reactors with Resistive Load, Some Fundamentals of D-C Controlled. Storm.........188–94; disc. 194
Recloser Substantiate Analytical Co-ordination Method, Field Tests of Oil Circuit. Auer, Branflick, Woodward, McKinley............801–08; disc. 808
Reclosing Circuit Breakers, Insulator Flashover Deionization Times as a Factor in Applying High-Speed. Boisseau, Wyman, Skeats......1058–66; disc. 1066
Reclosing of Line Sectionalizing Circuit Breakers, A-C Tripping and. Winegartner, Bonheimer...1357–9
Recorder, A Square-Law Power-Level. Clark, Turner, Williams....................476–82
Recorder, Automatic Range-Adjusting Radiosonde. Beggs....................602–07
Recording, Application of Experimental Test Procedures and Methods of Analysis of Results to Research Problems in Magnetic. Thompson.........407–17
Records—Steel and Wood Transmission Lines, Comparative Performance. Booker....686–9; disc. 689
Recovery Characteristics of Distribution Systems, Voltage-. Witzke....................172–80; disc. 180
Recovery Voltages on Rural Distribution Systems, Short-Circuit Currents and. Eason, Johnson, Kalb, Peterson....................930–7; disc. 937
Rectifier Ailments, Diagnosis of. Dortort...1298–1304
Rectifier Fault Currents—II. Herskind, Schmidt, Rettig....................243–51; disc. 251
Rectifier Transformer Characteristics. (Committee Report)....................1305–11
Rectifiers in Motor Vehicle Power Systems, Selenium. Ramsey....................149–53; disc. 153
Reduction of Interference from Radio-Frequency Heating Equipment. Klingaman....718–24; disc. 724
Reduction, The Performance of a Topped Steam Power Plant on Sudden Load. Noest..........1348–56
Reed Selective Signaling System for Mobile Telephone Use, Vibrating. Pruden, Hoth............387–91
Reed Selectors for Mobile Radio Systems, Vibrating. Keller, Bostwick....................383–6
Reference Frames, Stationary Networks and Transmission Lines Along Uniformly Rotating. Kron....................690–6
Regulated Distribution System, Operation of a Ground-Fault Neutralizer on a. Tomlinson, Hunt....................1321–6; disc. 1326
Regulating System as Determined by Electrical Analogy, The Transient Behavior of the Two-Stage Rototrol Main Exciter Voltage. Carleton..........59–63
Regulation and Dead Band of Governors on Steam Turbine Generators Under System Load Conditions, Determining Incremental. Tornquist, Wade....................1343–7
Regulators, Fundamentals, and Design Improvements, Aircraft Carbon-Pile Voltage. Austin, Richards....................983–7
Regulators in the L-1 Carrier System, Stability of Tandem. Kinzer....................1179–86
Relay and Control Circuits, Insulation Level of. (Committee Report)....................1255–7
Relay Circuits, Sequential Aspects of. Ritchie..577–81
Relay Circuits, The Logic of. Keister..........571–6
Relay Developments, Electronic. Loving....................233–40; disc. 240
Relay Equipment, One Slip Cycle Out-of-Step. Morris....................1246–8
Relay for Synchronous Generators, A New Loss-of-Excitation. Mason....................1240–5
Relay Protection, Shipshaw. Madill, Duffy....................50–5; disc. 55
Relay Servomechanisms, An Analysis of. Kahn....................1079–87; disc. 1087
Relay System, A Microwave Communication. Boothroyd, Churchill....................637–41
Relay Systems, Power Supplies for Microwave. Ward....................631–6
Relay "Trees" and Symmetric Circuits. Washburn....................582–6
Relaying and Joint Usage, Power Line Carrier for, Part I. Hampe, Storer..........864–7; disc. 871
Relaying of Transmission Lines from the New Sunbury Generating Station. Green, Oewel, Ramsaur....................873–7; disc. 877
Relays, Counting with. Frost....................587–91
Relays During Faults and Power Swings, Graphical Method for Estimating the Performance of Distance. Warrington....................608–20; disc. 620
Relays, Novel Test Circuits for Protective. Sonnemann....................1249–54
Remote Control of Coaxial Cable Stations, B-1 Alarm and Control System for. Hearn, Weber....622–6
Renaissance of Electric Motive Power, The. Candee....................138–44
Report of a Survey on the Performance of Shunt Capacitors. (Committee Report)....1200–06; disc. 1206
Report of the Board of Directors..........1383–1408
Report on AIEE Test Code for Electric Brushes, Progress. (Committee Report)....................1126–8
Report on Survey of Unbalanced Charging Currents on Transmission Lines as Affecting Ground-Fault Neutralizers. (Committee Report)...1328; disc. 1329
Report on the Operation and Maintenance of Shunt Capacitors. (Committee Report)........1208–18
Research Problems in Magnetic Recording, Application of Experimental Test Procedures and Methods of Analysis of Results to. Thompson........407–17
Reserve, A Convenient Method for Determining Generator. Seelye....................1317–20
Residential Electric Load, The Heat Pump—Its Significance as a Potential. Bary....................1–8
Resistance of Segmental Cables in Steel Pipe, A-C. Meyerhoff, Eager..............816–29; disc. 829
Resistive Load, Some Fundamentals of D-C Controlled Reactors with. Storm..........188–94; disc. 194
Response Curves, Control Chart Methods Applied to Frequency. Mundel....................424–7
Results to Research Problems in Magnetic Recording, Application of Experimental Test Procedures and Methods of Analysis of. Thompson.......407–17
Rhode Island, Trackless Trolley Operation in. Blomquist....................397–402
Rig for Deep-Well Drilling, Performance of Diesel-Electric. Clark, Moore....................497–506
Rise from Early Heat Run Data, Prediction of Ultimate Temperature. Ryan....................1164–6
Rise of Buried Cables and Pipes, The Temperature. Neher....................9–17; disc. 17
Rise of Cables in a Duct Bank, The Temperature. Neher....................540–6; disc. 546
Rise Values for D-C Machines, Temperature. Part I. (Committee Report)............206–12; disc. 212
Rise Values for D-C Machines, Temperature. Part II. (Committee Report)..........1118–23; disc. 1123
Risk of Operating Capacitors Without Individual Fuses, The Calculated. Brooks......1219–25; disc. 1225
Rooms, Electrically Charged Dust in. Penney, Hewitt....................278–82
Rotating Amplifiers, An Analysis of. Litman...1111–17
(Rotating Machinery) A Semiempirical Approach to Voltage Dip—with Suddenly Applied Loads on A-C Generators. Rosenberg.....160–6; disc. 166
(Rotating Machinery) A Wide-Range Adjustable-Speed Drive. Conrad, Tribken....................789–90
(Rotating Machinery) Armature Iron Losses in Series Motors. Chang, Karr..........262–4; disc. 264
(Rotating Machinery) Design of Auxiliary Circuits of Single-Phase Induction Motors. Thacker, Gopalakrishna....................1373–9
(Rotating Machinery) Die-Cast Rotors for Induction Motors. Packer..............253–60; disc. 260
(Rotating Machinery) Differential Leakage Patterns of a Fractional Slot Winding. Liwschitz....................1129–31; disc. 1131
(Rotating Machinery) Effects of Commutator Surface Film Conditions on Commutation. Lynn, Elsey....................106–12; disc. 112
(Rotating Machinery) Fundamental Theory of Inherent-Overheating Protection Under Running Overload Conditions. Veinott, Schaefer....................266–70; disc. 270
(Rotating Machinery) General Theory of Multiple Cage Induction Motors. Chang..............1139–43
(Rotating Machinery) Limitations in Design of D-C Adjustable Speed Motors. Opel............1095–8
(Rotating Machinery) Measuring Commutation with an Indicating Instrument. Lundy...........1380–2
(Rotating Machinery) Methods for Determining the Effects of Contaminants on Electrical Insulation. Mathes, Sieffert, Walker, Lindsey....................113–18; disc. 118
(Rotating Machinery) Motor Tests Evaluate Thermal Endurance of Class-H Insulation and Silicone Varnish. Grant, Kauppi, Moses, Gibson......1133–8
(Rotating Machinery) Operating Characteristics of Two-Phase Servomotors. Koopman....................319–27; disc. 327
(Rotating Machinery) Oscillographing Commutation. Baldwin....................100–05; disc. 105
(Rotating Machinery) Saturation Effect of Leakage Reactance. Chang, Lloyd....................1144–7
(Rotating Machinery) Solid Short Circuit of D-C Motors and Generators. Linville, Ward..119–23; disc. 123
(Rotating Machinery) Stray Load Losses Measured in D-C Motors. (Committee Report)....................219–23; disc. 223
(Rotating Machinery) The Design of D-C Motors for Use in Automatic Control Systems. Lebenbaum....................1089–94
(Rotating Machinery) The Dynamoelectric Amplifier—Class A Operation. Saunders...........1368–73
(Rotating Machinery) The Eccentric Pole Face—A Means to Better D-C Machine Performance. Baker....................1107–10
(Rotating Machinery) The Field Fluxes of the Shaded-Pole Motor. Kimberly....................273–7
(Rotating Machinery) The Geometric Loci of the Synchronous Tie. Finzi, Wellard............168–71
(Rotating Machinery) The Negative-Sequence Reactances of an Ideal Synchronous Machine. Duesterhoeft....................510–13; disc. 513
(Rotating Machinery) The Torques of the Synchronous Tie—A Steady-State Analysis. Finzi, McConnell....................1147–52
(Rotating Machinery) Transient Characteristics of D-C Motors and Generators. McClinton, Brancato, Panoff....................1100–06
(Rotating Machinery) Transients in 2-Phase Synchronous Machines. Wilson....................1360–7
(Rotating Machinery) Use of Cumulative and Differential Series Fields in the Parallel Operation of D-C Motors. Kimball....................1098–1100
Rotating Reference Frames, Stationary Networks and Transmission Lines Along Uniformly. Kron....................690–6
Rotors for Induction Motors, Die-Cast. Packer....................253–60; disc. 260
Rototrol Main Exciter Voltage Regulating System as Determined by Electrical Analogy, The Transient Behavior of the Two-Stage. Carleton......59–63
Rubber Insulators for Pole Lines. Wheeler, Markley....................195–7
Run Data, Prediction of Ultimate Temperature Rise from Early Heat. Ryan....................1164–6
Running Overload Conditions, Fundamental Theory of Inherent-Overheating Protection Under. Veinott, Schaefer....................266–70; disc. 270
Rural Distribution System, Lightning Investigation on a. MacCarthy, Stann, Edge, McKinley....................428–37; disc. 437
Rural Distribution System, Overcurrent Investigation on a. Lincks, Edge, McKinley, Leh....................915–27; disc. 927
Rural Distribution Systems, Short-Circuit Currents and Recovery Voltages on. Eason, Johnson, Kalb, Peterson....................930–7; disc. 937

S

Saturation Effect of Leakage Reactance. Chang, Lloyd....................1144–7
Saturation in Magnetic Amplifiers, Self-. Dornhoefer....................835–46; disc. 846
Saturation, Nonharmonic Oscillations as Caused by Magnetic. Rudenberg....................676–85
Saving Time in Testing Life of Incandescent Lamps. Purcell....................730–2
Scale A-C Voltmeter, A New Expanded. Millar..641–3
Schedules, Co-ordination of Fuel Cost and Transmission Loss by Use of the Network Analyzer to Determine Plant Loading. George, Page, Ward....................1152–60; disc. 1160
Schwartz, A Derivation of Heaviside's Operational Calculus Based on the Generalized Functions of. Smith, Alger....................939–44; disc. 944
Secondary Conductor Economics, Distribution Transformer and. Brady.............483–6; disc. 486
Sectionalizing Circuit Breakers, A-C Tripping and Reclosing of Line. Winegartner, Bonheimer..1357–9
Segmental Cables in Steel Pipe, A-C Resistance of. Meyerhoff, Eager..............816–29; disc. 829
Selection of Electric Drives for Looms. Demartini, Lukens....................349–56
Selective Signaling System for Mobile Telephone Use, Vibrating Reed. Pruden, Hoth..........387–91
Selector Supervisory System, Space Code. Forrest, Schirmer....................1312–15; disc. 1315
Selectors for Mobile Radio Systems, Vibrating Reed. Keller, Bostwick....................383–6
Selenium Rectifiers in Motor Vehicle Power Systems. Ramsey....................149–53; disc. 153
Self-Saturation in Magnetic Amplifiers. Dornhoefer....................835–46; disc. 846
Semiempirical Approach to Voltage Dip—with Suddenly Applied Loads on A-C Generators, A. Rosenberg....................160–6; disc. 166
Sequence Reactances of an Ideal Synchronous Machine, The Negative-. Duesterhoeft....510–13; disc. 513

Sequential Arpects of Relay Circuits. Ritchie...577–81
Series Fields in the Parallel Operation of D-C Motors, Use of Cumulative and Differential. Kimball..........1098–1100
Series Motors, Armature Iron Losses in. Chang, Karr..........262–4; disc. 264
Series Motors—Experimental Study of Speed-Torque Curves, Dynamic Braking Control of D-C. Heumann..........560–4
Services Operating on Frequencies Between 152–174 Megacycles, Design of Mobile Radio Communication Equipment for Land-Mobile. Beers, Harris, Zappacosta..........1232–9
Servomechanism Components and Systems, Graphical Determination of Transfer Function Loci for. Thomas, Easton..........307–14; disc. 314
Servomechanisms, An Analysis of Relay. Kahn..........1079–87; disc. 1087
Servomechanisms, Application of the California Institute of Technology Electric Analog Computer to Nonlinear Mechanics and. McCann, Wilts, Locanthi..........652–60
Servomechanisms, Comparison of Steady-State and Transient Performance of. Chestnut, Mayer..........675–77
Servomechanisms, Damper Stabilized Instrument. Hall..........299–306; disc. 306
(Servomechanisms) Instrument Inaccuracies in Feed-Back Control Systems with Particular Reference to Backlash. Marcy, Yachter, Zauderer.....778–88
Servomotors, Operating Characteristics of Two-Phase. Koopman..........319–27; disc. 327
Shaded-Pole Motor, The Field Fluxes of the. Kimberly..........273–7
Shipshaw Relay Protection. Madill, Duffy..........50–5; disc. 55
Short-Circuit Conditions, Heating of Transformers Under. Montsinger, Halsey.....947–52; disc. 952
Short-Circuit Currents and Recovery Voltages on Rural Distribution Systems. Eason, Johnson, Kalb, Peterson..........930–7; disc. 937
Short Circuit of D-C Motors and Generators, Solid. Linville, Ward..........119–23; disc. 123
Short-Time Analog Computers, Comparison of Long-Time and. Paschkis..........70–3
Shunt Capacitor Banks, Connection Arrangements and Protective Practices for. Clark, Farnham..........1226–30; disc. 1231
Shunt Capacitors, Report of a Survey on the Performance of. (Committee Report)......1200–06; disc. 1206
Shunt Capacitors, Report on the Operation and Maintenance of. (Committee Report)........1208–18
Shutter for Photographic Purposes, An Electro-Optical. Zarem, Marshall, Poole..........84–91
Signal Synchronous Supervisory Control System, A New 2-. Derr..........857–63; disc. 863
Signaling System for Mobile Telephone Use, Vibrating Reed Selective. Pruden, Hoth..........387–91
Silicone Varnish, Motor Tests Evaluate Thermal Endurance of Class-H Insulation and. Grant, Kauppi, Moses, Gibson..........1133–8
Single-Phase Induction Motors, Design of Auxiliary Circuits of. Thacker, Gopalakrishna..........1373–9
Sinusoidal 3-Phase Circuits, The Vector Power Factor of Unbalanced. Lamb, Brandt..........507–09
66-Kv Subtransmission Plan for a Metropolitan Area, A. Smith, Michelson..........908–12; disc. 913
Slip Cycle Out-of-Step Relay Equipment, One. Morris..........1246–8
Slot Winding, Differential Leakage of the Different Patterns of a Fractional. Liwschitz..........1129–31; disc. 1131
Soil, The Thermal Movement of Moisture in. Mickley..........330–3; disc. 333
Soldered Porcelain Potheads, A New Technique in the Manufacture of. Papp, Nicholas..........1258–60; disc. 1261
Solenoids, Formulas and Tables for the Calculation of the Magnetic Field Components of Circular Filaments and. Grover..........665–75
Solid Short Circuit of D-C Motors and Generators. Linville, Ward..........119–23; disc. 123
Some Fundamentals of D-C Controlled Reactors with Resistive Load. Storm..........188–94; disc. 194
Space Code Selector Supervisory System. Forrest, Schirmer..........1312–15; disc. 1315
Specification, Governors and the AIEE-ASME Governor Performance. Schwendner, Astley...1330–2
Speed, Considerations on Facsimile Transmission. Burkhard..........418–23; disc. 423
Speed Drive, A Wide-Range Adjustable-. Conrad, Tribken..........789–90
Speed Motors, Limitations in Design of D-C Adjustable. Opel..........1095–8
Speed-Torque Curves, Dynamic Braking Control of D-C Series Motors—Experimental Study of. Heumann..........560–4
Spring Mechanism for Medium Voltage Oilless Circuit Breakers, A Manually-Operated. Wyman, Casey..........357–61; disc. 261
Square-Law Power-Level Recorder, A. Clark, Turner, Williams..........476–82
Stability of Tandem Regulators in the L-1 Carrier System. Kinzer..........1179–86
Stability of the Welding Arc, Instrumentation for the Evaluation of the. Winsor, Schetky, Wyant..........525–33
Stabilized Instrument Servomechanisms, Damper. Hall..........299–306; disc. 306
Standardization of Reactor Ratings. Kierstead, Thomason..........955–7; disc. 957
Station P of the Pacific Gas and Electric Company, Electrical Design Features—Steam-Electric Generating. Benson..........1013–20; disc. 1020
Station, Relaying of Transmission Lines from the New Sunbury Generating. Green, Oewel, Ramsaur..........873–7; disc. 877
Stationary Networks and Transmission Lines Along Uniformly Rotating Reference Frames. Kron..........690–6
Stationary Power Generation, Gas Turbines in. Hague..........467–8
Stations, Automatic Grounding and Air-Break Switches for Protection of Transformer. Ricker..........851–6; disc. 856
Stations, B-1 Alarm and Control System for Remote Control of Coaxial Cable. Hearn, Weber......622–6
Stations Without High-Voltage Switching, Protection of. (Committee Report)........226–31; disc. 231
Steady-State Analysis, The Torques of the Synchronous Tie—A. Finzi, McConnell..........1147–52
Steady-State and Transient Performance of Servomechanisms, Comparison of. Chestnut, Mayer..........765–77
Steam-Electric Generating Station P of the Pacific Gas and Electric Company, Electrical Design Features—. Benson..........1013–20; disc. 1020
Steam Power Plant on Sudden Load Reduction, The Performance of a Topped. Noest........1348–56
Steam Turbine-Electric Locomotives, Electric Equipment for Chesapeake and Ohio Railway Company. Atwell, Baston..........145–8
Steam Turbine Generators Under System Load Conditions, Determining Incremental Regulation and Dead Band of Governors on. Tornquist, Wade..........1343–7
Steam Turbines and Boilers and of Hydro Units, Outage Rates of. (Committee Report)..........450–7
Steel and Wood Transmission Lines, Comparative Performance Records—. Booker....686–9; disc. 689
Steel Pipe, A-C Resistance of Segmental Cables in. Meyerhoff, Eager..........816–29; disc. 829
Stray Load Losses Measured in D-C Motors. (Committee Report)..........219–23; disc. 223
Strength of Oil with Variations of Pressure and Temperature, Dielectric. Hoover, Hixson....1047–50
Stroke Damage to Aircraft, Lightning. Hagenguth..........1036–44; disc. 1044
Strokes, Transmission Line Design and Performance Based on Direct Lightning. Harder, Clayton..........439–46; disc. 447
Studies, Equivalent Circuits for Power-Flow. Ward..........373–80; disc. 380
(Substations) A New 2-Signal Synchronous Supervisory Control System. Derr.........857–63; disc. 863
(Substations) Automatic Grounding and Air-Break Switches for Protection of Transformer Stations. Ricker..........851–6; disc. 856
(Substations) Space Code Selector Supervisory System. Forrest, Schirmer..........1312–15; disc. 1315
Subtransmission Plan for a Metropolitan Area, A 66-Kv. Smith, Michelson..........908–12; disc. 912
Suddenly Applied Loads on A-C Generators, A Semiempirical Approach to Voltage Dip—with. Rosenberg..........160–6; disc. 166
Summary of Transformations Useful in Constructing Analogs of Linear Vibration Problems. Corbett..........661–4
Sunbury Generating Station, Relaying of Transmission Lines from the New. Green, Oewel, Ramsaur..........873–7; disc. 877
Supervisory Control System, A New 2-Signal Synchronous. Derr..........857–63; disc. 863
Supervisory System, Space Code Selector. Forrest, Schirmer..........1312–15; disc. 1315
Supplies for Coaxial Systems, Power. Spencer..627–30
Supplies for Microwave Relay Systems, Power. Ward..........631–6
Surface Film Conditions on Commutation, Effects of Commutator. Lynn, Elsey......106–12; disc. 112
Surge Protection in a Modern Watt-Hour Meter. Busch, Williams..........74–7; disc. 77
Survey of Unbalanced Charging Currents on Transmission Lines as Affecting Ground-Fault Neutralizers, Report on. (Committee Report)..........1328; disc. 1329
Survey on the Performance of Shunt Capacitors, Report of a. (Committee Report)....1200–06; disc. 1206
Swings, Graphical Method for Estimating the Performance of Distance Relays During Faults and Power. Warrington..........608–20; disc. 620
Switches for Protection of Transformer Stations, Automatic Grounding and Air-Break. Ricker..........851–6; disc. 856
(Switchgear) A Manually-Operated Spring Mechanism for Medium Voltage Oilless Circuit Breakers. Wyman, Casey..........357–61; disc. 361
(Switchgear) A New 69-Kv Compressed-Air Circuit Breaker. Baker, Frisch..........363–8; disc. 369
(Switchgear) A-C Tripping and Reclosing of Line Sectionalizing Circuit Breakers. Winegartner, Bonheimer..........1357–9
(Switchgear) Field Tests of Oil Circuit Recloser Substantiate Analytical Co-ordination Method. Auer, Branflick, Woodward, McKinley..........801–08; disc. 808
(Switchgear) Insulator Flashover Deionization Times as a Factor in Applying High-Speed Reclosing Circuit Breakers. Boisseau, Wyman, Skeats..........1058–66; disc. 1066
Switching, Application of Multifrequency Pulsing in. Dahlbom, Horton, Moody..........392–6
Switching Locomotives, Industrial Plants Prefer Diesel-Electric. Woods..........697–700
Switching, Protection Stations Without High-Voltage. (Committee Report)..........226–31; disc. 231
Symmetric Circuits, Relay "Trees" and. Washburn..........582–6
Synchronous Generators, A New Loss-of-Excitation Relay for. Mason..........1240–5
Synchronous Machine, The Negative-Sequence Reactances of an Ideal. Duesterhoeft..........510–13; disc. 513
Synchronous Machines, Transients in 2-Phase. Wilson..........1360–7
Synchronous Supervisory Control System, A New 2-Signal. Derr..........857–63; disc. 863
Synchronous Tie—A Steady-State Analysis, The Torques of the. Finzi, McConnell.......1147–52
Synchronous Tie, The Geometric Loci of the. Finzi, Wellard..........168–71
System, A Microwave Communication Relay. Boothroyd, Churchill..........637–41
System, A New 2-Signal Synchronous Supervisory Control. Derr..........857–63; disc. 863
System, A Time Division Multiplexing. Boothroyd, Creamer..........92–7
System Applications, Microwave Channels for Power. (Committee Report)..........40–2; disc. 42
System as Determined by Electrical Analogy, The Transient Behavior of the Two-Stage Rototrol Main Exciter Voltage Regulating. Carleton......59–63
System, Economic Loading of a Transformer. Levine, Smith..........733–8; disc. 738
System for Aircraft, An Electric Deicing. Giloy..........1051–7
System for Mobile Telephone Use, Vibrating Reed Selective Signaling. Pruden, Hoth.......387–91
System for Remote Control of Coaxial Cable Stations, B-1 Alarm and Control. Hearn, Weber....622–6
System, Lightning Investigation on a Rural Distribution. MacCarthy, Stann, Edge, McKinley..........428–37; disc. 437
System, Matching Electrical Characteristics of McNary Generators and Transformers with Bonneville Power Administration Transmission. Hoard, Weiner..........1022–5; disc. 1026
System, Operation of a Ground-Fault Neutralizer on a Regulated Distribution. Tomlinson, Hunt..........1321–6; disc. 1326
System, Overcurrent Investigation on a Rural Distribution. Lincks, Edge, McKinley, Leh..........915–27; disc. 927
System, Primary Networks on the Duquesne Light Company. Holben, Lange......704–09; disc. 709
System, Space Code Selector Supervisory. Forrest, Schirmer..........1312–15; disc. 1315
System, Stability of Tandem Regulators in the L-1 Carrier. Kinzer..........1179–86
System, Transformer Audio Noise Problems on an Electric Power. Murray..........740–7; disc. 747
Systems, Graphical Determination of Transfer Function Loci for Servomechanism Components and. Thomas, Easton..........307–14; disc. 314
Systems in the Washington Area, Design and Experience with 4-Kv Primary Network. Lank..........712–16; disc. 716
Systems, Power Supplies for Coaxial. Spencer..627–30
Systems, Power Supplies for Microwave Relay. Ward..........631–6
Systems, Selenium Rectifiers in Motor Vehicle Power. Ramsey..........149–53; disc. 153
Systems, Short-Circuit Currents and Recovery Voltages on Rural Distribution. Eason, Johnson, Kalb, Peterson..........930–7; disc. 937
Systems, Television Terminals for Coaxial. Morrison..........1193–9
Systems, The Design of D-C Motors for Use in Automatic Control. Lebenbaum..........1089–94
Systems, Vibrating Reed Selectors for Mobile Radio. Keller, Bostwick..........383–6
Systems, Voltage-Recovery Characteristics of Distribution. Witzke..........172–80; disc. 180
Systems with Particular Reference to Backlash, Instrument Inaccuracies in Feed-Back Control. Marcy, Yachter, Zauderer..........778–88

T

Tables for the Calculation of the Magnetic Field Components of Circular Filaments and Solenoids, Formulas and. Grover....665–75
Tandem Regulators in the L-1 Carrier System, Stability of. Kinzer....1179–86
Technique in the Manufacture of Soldered Porcelain Potheads, A New. Papp, Nicholas....1258–60; disc. 1261
Technique of Lightning Measurements, Advances in. Brownlee....515–19
Techniques, Cable Accessory Design Utilizing New Laboratory. Bosworth, Farr..1268–73; disc. 1273
Telemetering and Totalizing, A Thermal Converter for. Downing....879–84; disc. 884
Telephone Use, Vibrating Reed Selective Signaling System for Mobile. Pruden, Hoth....387–91
Television Terminals for Coaxial Systems. Morrison....1193–9
Temperature and Insulation Protection in the Operation of Power Transformers, Controlled. Satterlee, Reed....753–8; disc. 759
Temperature, Dielectric Strength of Oil with Variations of Pressure and. Hoover, Hixson....1047–50
Temperature Phenomena of 3-Conductor Cables, Transient. Wollaston....1284–95; disc. 1295
Temperature Rise from Early Heat Run Data, Production of Ultimate. Ryan....1164–6
Temperature Rise of Buried Cables and Pipes, The. Neher....9–17; disc. 17
Temperature Rise of Cables in a Duct Bank, The. Neher....540–6; disc. 546
Temperature Rise Values for D-C Machines. Part I. (Committee Report)....206–12; disc. 212
Temperature Rise Values for D-C Machines. Part II. (Committee Report)....1118–23; disc. 1123
Temperature, The Measurement of Dielectric Loss at High Frequencies and Under Changing. Whitehead, Rueggeberg....520–4
Terminals for Coaxial Systems, Television. Morrison....1193–9
Test Circuits for Protective Relays, Novel. Sonnemann....1249–54
Test Code for Electric Brushes, Progress Report in AIEE. (Committee Report)....1126–8
Test Procedures and Methods of Analysis of Results to Research Problems in Magnetic Recording, Application of Experimental. Thompson....407–17
Tests Evaluate Thermal Endurance of Class H Insulation and Silicone Varnish, Motor. Grant, Kauppi, Moses, Gibson....1133–8
Tests of Oil Circuit Recloser Substantiate Analytical Co-ordination Method, Field. Auer, Branflick, Woodward, McKinley....801–08; disc. 808
Theoretical and Practical Approach to the Design of High-Voltage Cable Joints, A. Short....1275–80; disc. 1280
Theory and Experimental Confirmation of the Moving Coil Fluxmeter, General. Higgins, Robertson....897–907; disc. 907
Theory of Inherent-Overheating Protection Under Running Overload Conditions, Fundamental. Veinott, Schaefer....266–70; disc. 270
Theory of Multiple Cage Induction Motors, General. Chang....1139–43
Thermal Converter for Telemetering and Totalizing, A. Downing....879–84; disc. 884
Thermal Demand Meters, Heat Flow Ratio as a Design Parameter in. Nelson....885–90; disc. 890
Thermal Endurance of Class H Insulation and Silicone Varnish, Motor Tests Evaluate. Grant, Kauppi, Moses, Gibson....1133–8
Thermal Movement of Moisture in Soil, The. Mickley....330–3; disc. 333
Thermal Volt-Ampere Demand Meter, A New. Douglass, Morong....79–83; disc. 83
Three-Phase Circuits, The Vector Power Factor of Unbalanced Sinusoidal. Lamb, Brandt....507–09
Thyrite in Power Transformers, Use of. Meador....959–64; disc. 964
Tie—A Steady-State Analysis, The Torques of the Synchronous. Finzi, McConnell....1147–52
Tie, The Geometric Loci of the Synchronous. Finzi, Wellard....168–71
Time Division Multiplexing System, A. Boothroyd, Creamer....92–7
Time in Testing Life of Incandescent Lamps, Saving. Purcell....730–2
Time of High-Voltage Fault-Arc Paths, Deionization. Harrington, Starr....997–1003; disc. 1003
Times as a Factor in Applying High-Speed Reclosing Circuit Breakers, Insulator Flashover Deionization. Boisseau, Wyman, Skeats....1058–66; disc. 1066
Topped Steam Power Plant on Sudden Load Reduction, The Performance of a. Noest....1348–56
Torque Curves, Dynamic Braking Control of D-C Series Motors—Experimental Study of Speed-. Heumann....560–4
Torques of the Synchronous Tie—A Steady-State Analysis, The. Finzi, McConnell....1147–52
Totalizing, A Thermal Converter for Telemetering and. Downing....879–84; disc. 884
Trackless Trolley Operation in Rhode Island. Blomquist....397–402
Traction Motors, Twenty-Five Years Progress in the Design of. Baldwin....132–7
Traffic Control for Railroads, Centralized. Hailes....1167–73
Transfer Function Loci for Servomechanism Components and Systems, Graphical Determination of. Thomas, Easton....307–14; disc. 314
Transformations Useful in Constructing Analogs of Linear Vibration Problems, Summary of. Corbett....661–4
Transformer and Secondary Conductor Economics, Distribution. Brady....483–6; difc. 486
Transformer Audio Noise Problems on an Electric Power System. Murray....740–7; disc. 747
Transformer Characteristics, Rectifier. (Committee Report)....1305–11
Transformer Manholes and Vaults: Design and Ventilation. Porter....534–9
(Transformer) Some Fundamentals of D-C Controlled Reactors with Resistive Load. Storm....188–94; disc. 194
Transformer Stations, Automatic Grounding and Air-Break Switches for Protection of. Ricker....851–6; disc. 856
Transformer System, Economic Loading of a. Levine, Smith....733–8; disc. 738
(Transformer) Universal Curves for D-C Controllable Reactors. Johnson, Merrell, Alley...31–7; disc. 37
Transformers, A Method for Designing Pulse. Kirschbaum, Warren....971–8
(Transformers) A Small High-Voltage Bushing Design for High Altitudes. Vogel, Hart....761–4
Transformers, Controlled Temperature and Insulation Protection in the Operation of Power. Satterlee, Reed....753–8; disc. 759
Transformers, Extremes in the Insulation Co-ordination of Oil Insulated. Vogel....965–8; disc. 968
Transformers, Lightweight Aircraft. Stephens..1073–8
(Transformers) Standardization of Reactor Ratings. Kierstead, Thomason....955–7; disc. 957
Transformers Under Short-Circuit Conditions, Heating of. Montsinger, Halsey....947–52; disc. 952
Transformers, Use of Thyrite in Power. Meador....959–64; disc. 964
Transformers with Bonneville Power Administration Transmission System, Matching Electrical Characteristics of McNary Generators and. Hoard, Weiner....1022–5; disc. 1026
Transient Behavior of the Two-Stage Rototrol Main Exciter Voltage Regulating System as Determined by Electrical Analogy, The. Carleton....59–63
Transient Characteristics of D-C Motors and Generators. McClinton, Brancato, Panoff....1100–06
Transient Fault Locator for High-Voltage Transmission Lines, A. Spaulding, Diemond....1005–10; disc. 1010
Transient Performance of Servomechanisms, Comparison of Steady-State and. Chestnut, Mayer....765–77
Transient Temperature Phenomena of 3-Conductor Cables. Wollaston....1284–95; disc. 1295
Transients in 2-Phase Synchronous Machines. Wilson....1360–7
Translations, Codes and. Myers....592–7
(Transmission) A 66-Kv Subtransmission Plan for a Metropolitan Area. Smith, Michelson....908–12; disc. 912
(Transmission) Connection Arrangements and Protective Practices for Shunt Capacitor Banks. Clark, Farnham....1226–30; disc. 1231
(Transmission) Deionization Time of High-Voltage Fault-Arc Paths. Harrington, Starr....997–1003; disc. 1003
(Transmission) Design and Experience With 4-Kv Primary Network Systems in the Washington Area. Lank....712–16; disc. 716
(Transmission) Hy-Therm Copper—An Improved Overhead-Line Conductor. Hickernell, Jones, Snyder....22–7; disc. 27
(Transmission) Improvements to Oklahoma City Primary Network. Brady....701–02; disc. 702
Transmission Line at Carrier Current Frequencies, Loss Measurements Made on Underground-Cable Overhead-Conductor 132-Kv. Cornelius, Storer....597–601
Transmission Line Clamps, Magnetic Heating of. Crabb, Sheadel....1032–5
Transmission Line Design and Performance Based on Direct Lightning Strokes. Harder, Clayton....439–46; disc. 447
Transmission Line Joints by Means of a Bolometer, Detection of Overheated. Leslie, Wait....64–8; disc. 68
Transmission Lines, A Transient Fault Locator for High-Voltage. Spaulding, Diemond....1005–10; disc. 1010
Transmission Lines Along Uniformly Rotating Reference Frames, Stationary Networks and. Kron...690–6
Transmission Lines as Affecting Ground-Fault Neutralizers, Report on Survey of Unbalanced Charging Currents on. (Committee Report)....1328; disc. 1329
Transmission Lines, Comparative Performance Records—Steel and Wood. Booker..686–9; disc. 689
Transmission Lines from the New Sunbury Generating Station, Relaying of. Green, Oewel, Ramsaur....873–7; disc. 877
Transmission Loss by Use of the Network Analyzer to Determine Plant Loading Schedules, Co-ordination of Fuel Cost and. George, Page, Ward....1152–60; disc. 1160
(Transmission) Primary Networks on the Duquesne Light Company System. Holben, Lange....704–09; disc. 709
(Transmission) Report of a Survey on the Performance of Shunt Capacitors. (Committee Report)....1200–06; disc. 1206
(Transmission) Report on the Operation and Maintenance of Shunt Capacitors. (Committee Report)....1208–18
Transmission Speed, Considerations on Facsimile. Burkhard....418–23; disc. 423
Transmission System, Matching Electrical Characteristics of McNary Generators and Transformers with Bonneville Power Administration. Hoard, Weiner....1022–5; disc. 1026
(Transmission) The Calculated Risk of Operating Capacitors Without Individual Fuses. Brooks....1219–25; disc. 1225
(Transportation, Air) Aircraft Carpon-Pile Voltage Regulators, Fundamentals, and Design Improvements. Austin, Richards....983–7
(Transportation, Air) An Electric Deicing System for Aircraft. Giloy....1051–7
(Transportation, Air) Current Ratings of Aircraft Cable. Askew, McClinton....988–92
(Transportation, Air) Development and Application of Electric Heating to Deicing of Aircraft Propellers. Sheets, Sand....1068–72
(Transportation, Air) Lightning Stroke Damage to Aircraft. Hagenguth....1036–44; disc. 1044
(Transportation, Air) Lightweight Aircraft Transformers. Stephens....1073–8
(Transportation, Air) Protection of the Airplane Main Bus. Exner....979–82
(Transportaton, Land) Application Engineering on Diesel-Electric Locomotives in Railroad Service. Bevan....125–31
(Transportation, Land) Centralized Traffic Control for Railroads. Hailes....1167–73
(Transportation, Land) Electric Equipment for Chesapeake and Ohio Railway Company Steam Turbine-Electric Locomotives. Atwell, Baston....145–8
(Transportation, Land) Industrial Plants Prefer Diesel-Electric Switching Locomotives. Woods..697–700
(Transportation, Land) Selenium Rectifiers in Motor Vehicle Power Systems. Ramsey..149–53; disc. 153
(Transportation, Land) The Renaissance of Electric Motive Power. Candee....138–44
(Transportation, Land) Trackless Trolley Operation in Rhode Island. Blomquist....397–402
(Transportation, Land) Trolley Coaches Replace Busses. McMillon....403–06
(Transportation, Land) Twenty-Five Years Progress in the Design of Traction Motors. Baldwin....132–7
"Trees" and Symmetric Circuits, Relay. Washburn....582–6
Tripping and Reclosing of Line Sectionalizing Circuit Breakers, A-C. Winegartner, Bonheimer...1357–9
Trolley Coaches Replace Busses. McMillon....403–06
Trolley Operation in Rhode Island, Trackless. Blomquist....397–402
Tuning Equipment Used With Coaxial Cable for Carrier Current Installation on Power Lines, Line. Sutton....44–8; disc. 48
Turbine-Electric Locomotives, Electric Equipment for Chesapeake and Ohio Railway Company Steam. Atwell, Baston....145–8
Turbine Generators, A New Automatic Load Control for. Ruud, Farnham....1337–42; disc. 1342
Turbine Generators Under System Load Conditions, Determining Incremental Regulation and Dead Band of Governors on Steam. Tornquist, Wade....1343–7
Turbine Power Plant, A 3,000-Horsepower Gas. Haverstick....458–60
Turbines and Boilers and of Hydro Units, Outage Rates of Steam. (Committee Report)....450–7
Turbines for Power Generation and Other Applications, Two Gas. Howard....461–5; disc. 465
Turbines in Stationary Power Generation, Gas. Hague....467–8
Twenty-Five Years Progress in the Design of Traction Motors. Baldwin....132–7
Two Gas Turbines for Power Generation and Other Applications. Howard....461–5; disc. 465
Two-Phase Servomotors, Operating Characteristics of. Koopman....319–27; disc. 327
Two-Stage Rototrol Main Exciter Voltage Regulating System as Determined by Electrical Analogy, The Transient Behavior of the. Carleton....59–63

U

Unbalanced Charging Currents on Transmission Lines as Affecting Ground-Fault Neutralizers, Report on Survey of. (Committee Report)........1328; disc. 1329
Unbalanced Sinusoidal 3-Phase Circuits, The Vector Power Factor of. Lamb, Brandt..........507–09
Underground-Cable Overhead-Conductor 132-Kv Transmission Line at Carrier Current Frequencies, Loss Measurements Made on. Cornelius, Storer........597–601
Units, Some Oscillographic Methods of Investigating Mechanical and Hydraulic Conditions During Operation of Hydroelectric. Engvall.......993–6
Universal Curves for D-C Controllable Reactors. Johnson, Merrell, Alley............31–7; disc. 37
Usage, Power Line Carrier for Relaying and Joint. Part I. Hampe, Storer..........864–7; disc. 871
Use of Air-Core Reactors as Fault Limiting Means on High Interrupting Capacity Controllers, The. Leitch........................469–74; disc. 474
Use of Thyrite in Power Transformers. Meador........959–64; disc. 964

V

Values for D-C Machines, Temperature Rise. Part I. (Committee Report)............206–12; disc. 212
Values for D-C Machines, Temperature Rise. Part II. (Committee Report)..........1118–23; disc. 1123
Variations of Pressure and Temperature, Dielectric Strength of Oil with. Hoover, Hixson....1047–50
Varnish, Motor Tests Evaluate Thermal Endurance of Class-H Insulation and Silicone. Grant, Kauppi, Moses, Gibson..........................1133–8
Vaults: Design and Ventilation, Transformer Manholes and. Porter............................534–9
Vector Indicator, Polar. Walker, Waynick, Sulzer........154–9
Vector Power Factor of Unbalanced Sinusoidal 3-Phase Circuits, The. Lamb, Brandt............507–09
Vehicle Power Systems, Selenium Rectifiers in Motor. Ramsey........................149–53; disc. 153
Ventilation, Transformer Manholes and Vaults: Design and. Porter............................534–9
Vibrating Reed Selective Signaling System for Mobile Telephone Use. Pruden, Hoth............387–91
Vibrating Reed Selectors for Mobile Radio Systems. Keller, Bostwick..........................383–6
Vibration Problems, Summary of Transformations Useful in Constructing Analogs of Linear. Corbett........661–4
Viscosity Oil, High-Pressure Gas-Filled Cable Impregnated with Extra-High-. Sticher, Doan, Atkinson, Meyerhoff...........336–45; disc. 345
Volt-Ampere Demand Meter, A New Thermal. Douglass, Morong...................79–83; disc. 83
Voltage Dip—with Suddenly Applied Loads on A-C Generators, A Semiempirical Approach to. Rosenberg.........................160–6; disc. 166
Voltage Fault-Arc Paths, Deionization Time of High-. Harrington, Starr............997–1003; disc. 1003
Voltage Generation, Commutation of D-C Machines and Its Effects on Radio Influence. Motter........491–5; disc. 495
Voltage Oilless Circuit Breakers, A Manually-Operated Spring Mechanism for Medium. Wyman, Casey........357–61; disc. 361
Voltage Recovery Characteristics of Distribution Systems. Witzke..................172–80; disc. 180
Voltage Regulating System as Determined by Electrical Analogy, The Transient Behavior of the Two-Stage Rototrol Main Exciter. Carleton.....59–63
Voltage Regulators, Fundamentals, and Design Improvements, Aircraft Carbon-Pile. Austin, Richards..................................983–7
Voltage Transmission Lines, A Transient Fault Locator for High-. Spaulding, Diemond........1005–10; disc. 1010
Voltages on Rural Distribution Systems, Short-Circuit Currents and Recovery. Eason, Johnson, Kalb, Peterson.......................930–7; disc. 937
Voltmeter, A New Expanded Scale A-C. Millar..641–3
Volts and Below, Design Fundamentals of Potheads 69,000. Nicholas.............1263–7; disc. 1267

W

Washington Area, Design and Experience With 4-Kv Primary Network Systems in the. Lank........712–16; disc. 716
Watt-Hour Meter, Surge Protection in a Modern. Busch, Williams..................74–7; disc. 77
Welding Arc, Instrumentation for the Evaluation of the Stability of the. Winsor, Schetky, Wyant..525–33
Well Drilling, Performance of Diesel-Electric Rig for Deep. Clark, Moore..................497–506
Wide-Band D-C Amplifier Stabilized for Gain and for Zero. Williams, Amey, McAdam.811–15; disc. 815
Wide-Range Adjustable-Speed Drive, A. Conrad, Tribken..............................789–90
Winding, Differential Leakage of the Different Patterns of a Fractional Slot. Liwschitz........1129–31; disc. 1131
Wood Transmission Lines, Comparative Performance Records—Steel and. Booker.....686–9; disc. 689

Z

Zero, Wide-Band D-C Amplifier Stabilized for Gain and for. Williams, Amey, McAdam........811–15; disc. 815

2. Author Index

Abetti, P. A. Disc..........................944
Adams, J. A. Disc..........................749
Alexander, E. H. Disc......................474
Alger, P. L. Disc...................214, 1131
Alger, P. L.; J. J. Smith. A Derivation of Heaviside's Operational Calculus Based on the Generalized Functions of Schwartz...........939–44; disc. 945
Alley, R. E., Jr.; W. C. Johnson, B. C. Merrell. Universal Curves for D-C Controllable Reactors........31–7; disc. 39
Amey, W. G.; A. J. Williams, Jr., Will McAdam. Wide-Band D-C Amplifier Stabilized for Gain and for Zero.......................811–15; disc. 815
Andrews, F. E. Disc........................447
Asbury, C. E. Disc................871, 877, 927
Askew, Wade H.; A. T. McClinton. Current Ratings of Aircraft Cable.........................988–92
Astley, Wayne C.; A. F. Schwendner. Governors and the AIEE–ASME Governor Performance Specifications...........................1330–2
Atkinson, R. W. Disc...............557, 1281
Atkinson, R. W.; Joseph Sticher, G. H. Doan, Louis Meyerhoff. High-Pressure Gas-Filled Cable Impregnated with Extra-High-Viscosity Oil........336–45; disc. 347
Atwell, C. A.; C. E. Baston. Electric Equipment for Chesapeake and Ohio Railway Company Steam Turbine-Electric Locomotives..............145–8
Auer, G. G.; R. A. Branflick, L. J. Woodward, W. C. McKinley. Field Tests of Oil Circuit Recloser Substantiate Analytical Co-ordination Method.........801–08; disc. 810
Austin, B. O.; H. H. C. Richards. Aircraft Carbon-Pile Voltage Regulators, Fundamentals and Design Improvements...........................983–7

B

Baker, B. P.; E. Frisch. A New 69-Kv Compressed-Air Circuit Breaker................363–8; disc. 371
Baker, M. A. The Eccentric Pole Face—A Means to Better D-C Machine Performance........1107–10
Baker, M. A. Disc...................215, 1123
Baldwin, M. J. Oscillographing Commutation........100–05; disc. 105
Baldwin, M. J. Twenty-Five Years Progress in the Design of Traction Motors................132–7
Barnett, H. G.; D. F. Shankle. Disc.............914
Bary, Constantine. The Heat Pump—Its Significance as a Potential Residential Electric Load.......1–8
Baston, C. E.; C. A. Atwell. Electric Equipment for Chesapeake and Ohio Railway Company Steam Turbine-Electric Locomotives..............145–8
Bauer, C. A.; H. Halperin. Disc...............1296
Beaumariage, D. C.; D. W. VerPlanck, L. A. Finzi. Analytical Determination of Characteristics of Magnetic Amplifiers with Feedback............565–70
Beaumariage, D. C.; L. A. Finzi, D. W. VerPlanck. Disc...................................846
Beck, E. Disc..............................185
Beers, R. A.; W. A. Harris, A. D. Zappacosta. Design of Mobile Radio Communication Equipment for Land-Mobile Services Operating on Frequencies Between 152–174 Megacycles.............1232–9
Beggs, George E., Jr. Automatic Range-Adjusting Radiosonde Recorder......................602–07
Behn, Eric R. Disc.........................306
Bellaschi, P. L. Disc...............447, 759, 969
Bennet, W. R. Disc.........................260
Bennon, S. Disc............................748
Benson, Francis S. Electrical Design Features—Steam-Electric Generating Station P of the Pacific Gas and Electric Company......................1013–20
Berkowitz, R. Disc.........................649
Bevan, G. T. Application Engineering on Diesel-Electric Locomotives in Railroad Service...125–31
Bewley, L. V. Disc.........................447
Bills, Glenn W. Disc.......................381
Blake, D. K. Disc..........................915
Blomquist, E. A. Disc......................747
Blomquist, H. R. Trackless Trolley Operation in Rhode Island..........................397–402
Boisseau, A. C.; B. W. Wyman, W. F. Skeats. Insulator Flashover Deionization Times as a Factor in Applying High-Speed Reclosing Circuit Breakers........1058–66; disc. 1066
Bonheimer, H. E.; C. E. Winegartner. A-C Tripping and Reclosing of Line Sectionalizing Circuit Breakers.................................1357–9
Bonneville Power Administration, Engineers of. Disc.........27
Bonneville Power Administration, Engineers of the. Disc...................................69
Booker, C. A. Comparative Performance Records—Steel and Wood Transmission Lines........686–9; disc. 689
Boothroyd, Wilson P.; H. J. Churchill. A Microwave Communication Relay System............637–41
Boothroyd, W. P.; E. M. Creamer, Jr. A Time Division Multiplexing System.................92–7
Borden, Perry A. Disc......................884
Bostwick, L. G.; A. C. Keller. Vibrating Reed Selectors for Mobile Radio Systems.............383–6
Bosworth, Phillips N.; H. K. Farr. Cable Accessory Design Utilizing New Laboratory Techniques........1268–73; disc. 1274
Brady, Bryce. Distribution Transformer and Secondary Conductor Economics...........483–6; disc. 489
Brady, Bryce. Improvements to Oklahoma City Primary Network................701–02; disc. 703
Brancato, E. L.; A. T. McClinton, R. Panoff. Transient Characteristics of D-C Motors and Generators........1100–06
Brandt, D. B.; J. F. Lamb. The Vector Power Factor of Unbalanced Sinusoidal 3-Phase Circuits..507–09
Branflick, R. A.; G. G. Auer, L. J. Woodward, W. C. McKinley. Field Tests of Oil Circuit Recloser Substantiate Analytical Co-ordination Method........801–08; disc. 810
Brooks, Hamilton. The Calculated Risk of Operating Capacitors Without Individual Fuses.....1219–25
Brown, J. Stanley. Disc....................361
Brown, W. T. Disc..........................488
Browne, T. E., Jr. Disc...................1003
Brownlee, Theodore. Advances in Technique of Lightning Measurements......................515–19
Brownlee, W. R. Disc.......................856
Brownlee, W. R.; J. A. Elzi. Disc..............738
Buckland, Mrs. B. O.; T. M. Linville. Disc.......218
Buller, F. H. Disc..................546, 830
Burkhard, Henry F. Considerations on Facsimile Transmission Speed............418–23; disc. 423
Busch, F. H.; G. D. Williams. Surge Protection in a Modern Watt-Hour Meter.........74–7; disc. 78
Butler, F. H. Disc..........................17

C

Cahen, Francois. Disc......................204
Caldwell, B. H. Disc................223, 1124
Caldwell, B. H.; G. H. Gunnoe. Disc............212
Campbell, H. E. Disc................486, 702
Candee, A. H. The Renaissance of Electric Motive Power..............................138–44
Carleton, James T. The Transient Behavior of the Two-Stage Rototrol Main Exciter Voltage Regulating System as Determined by Electrical Analogy........59–63
Carlisle, R. W. Disc.......................423
Casey, E. J.; B. W. Wyman. A Manually Operated Spring Mechanism for Medium Voltage Oilless Circuit Breakers..................357–61; disc. 362
Chang, Sheldon S. L. General Theory of Multiple Cage Induction Motors.................1139–43
Chang, S. S. L. Disc.......................327
Chang, Sheldon S. L.; J. H. Karr. Armature Iron Losses in Series Motors..........262–4; disc. 265
Chang, Sheldon S. L.; T. C. Lloyd. Saturation Effect of Leakage Reactance.....................1144–7
Charp, S. A New Fourier Coefficient Harmonic Analyser...........................644–9; disc. 649
Chestnut, Harold; R. W. Mayer. Comparison of Steady-State and Transient Performance of Servomechanisms...........................765–77
Churchill, Harold J.; W. P. Boothroyd. A Microwave Communication Relay System............637–41
Ciscel, Ben. Disc.........................1087
Clark, E. C.; B. L. Moore. Performance of Diesel-Electric Rig for Deep Well Drilling.......497–506
Clark, N. R.; S. B. Farnham. Connection Arrangements and Protective Practices for Shunt Capacitor Banks.......................1226–30; disc. 1231
Clark, W. R.; W. R. Turner, A. J. Williams, Jr. A Square-Law Power-Level Recorder........476–82
Clayton, J. M.; E. L. Harder. Transmission Line Design and Performance Based on Direct Lightning Strokes......................439–46: disc. 448

Cohen, S. B. Disc....846
Cole, Harold. Disc....487
Concordia, C. Disc....166
Conrad, A. G.; E. R. Tribken. A Wide-Range Adjustable-Speed Drive....789–90
Corbett, James P. Summary of Transformations Useful in Constructing Analogs of Linear Vibration Problems....661–4
Cornelius, H. A.; B. W. Storer. Loss Measurements Made on Underground-Cable Overhead-Conductor 132-Kv Transmission Line at Carrier Current Frequencies....597–601
Crabb, V. L.; J. M. Sheadel. Magnetic Heating of Transmission Line Clamps....1032–5
Crary, S. B. Disc....1161
Creamer, E. M., Jr.; W. P. Boothroyd. A Time Division Multiplexing System....92–7

D

Dahlbom, C. A.; A. W. Horton, Jr., D. L. Moody. Application of Multifrequency Pulsing in Switching....392–6
Davis, S. Disc....327
deBellis, A. M. Disc....370
Del Mar, W. A. Disc....17, 832
Demartini, R. J.; A. F. Lukens. Selection of Electric Drives for Looms....349–56
Dent, William U. Disc....1030
DePuy, S. M. Disc....270
Derr, W. A. A New 2-Signal Synchronous Supervisory Control System....857–63; disc. 863
Derr, W. A. Disc....1315
Diemond, C. C.; L. R. Spaulding. A Transient Fault Locator for High-Voltage Transmission Lines....1005–10; disc. 1011
Dillow, N. E. Disc....958
Doan, G. H.; Joseph Sticher, R. W. Atkinson, Louis Meyerhoff. High-Pressure Gas-Filled Cable Impregnated with Extra-High-Viscosity Oil....336–45; disc. 347
Dodds, G. B.; R. S. Smithley. Disc....716
Dornhoefer, W. J. Self-Saturation in Magnetic Amplifiers....835–46; disc. 846
Dortort, I. K. Diagnosis of Rectifier Ailments....1298–1304
Douglass, M. E.; W. H. Morong. A New Thermal Volt-Ampere Demand Meter....79–83; disc. 83
Downing, William C., Jr. A Thermal Converter for Telemetering and Totalizing....879–84; disc. 884
Downing, Wm. C., Jr. Disc....800
Duesterhoeft, William C. The Negative-Sequence Reactances of an Ideal Synchronous Machine....510–13; disc. 513
Duffy, F. H.; J. T. Madill. Shipshaw Relay Protection....50–5; disc. 57
Dunn, Charles. Disc....489
Dupuis, H. P. Disc....620
Dupuis, H. P.; D. C. Harker. Disc....57
Dwight, H. B. Disc....20

E

Eager, G. S., Jr.; L. Meyerhoff. A-C Resistance of Segmental Cables in Steel Pipe...816–29; disc. 833
Earle, R. H. Disc....187
Eason, W. H. Disc....964
Eason, W. H.; I. B. Johnson, J. W. Kalb, H. A. Peterson. Short-Circuit Currents and Recovery Voltages on Rural Distribution Systems....930–7; disc. 938
Easton, E. C.; C. H. Thomas. Graphical Determination of Transfer Function Loci for Servomechanism Components and Systems....307–14; disc. 318
Edge, D. R.; G. F. Lincks, W. C. McKinley, J. H. Leh. Overcurrent Investigation on a Rural Distribution System....915–27; disc. 928
Edge, D. R.; D. D. MacCarthy, D. A. Stann, W. C. McKinley. Lightning Investigation on a Rural Distribution System....428–37; disc. 437
Elsey, H. M.; C. Lynn. Effects of Commutator Surface Film Conditions on Commutation....106–12; disc. 112
Elton, M. B. Disc....489
Elzi, J. A. Disc....231, 957
Elzi, J. A.; W. R. Brownlee. Disc....738
Engvall, Lenard R. Some Oscillographic Methods of Investigating Mechanical and Hydraulic Conditions During Operation of Hydroelectric Units....993–6
Estcourt, V. F. Disc....1020
Exner, D. W. Protection of the Airplane Main Bus....979–82

F

Falck, Knute. Disc....361
Farnham, S. B.; N. R. Clark. Connection Arrangements and Protective Practices for Shunt Capacitor Banks....1226–30; disc. 1231
Farnham, S. B.; H. B. Ruud. A New Automatic Load Control for Turbine Generators....1337–42
Farr, Harold K.; P. N. Bosworth. Cable Accessory Design Utilizing New Laboratory Techniques....1268–73; disc. 1274
Finzi, L. A. Disc....39
Finzi, L. A.; H. M. McConnell. The Torques of the Synchronous Tie—A Steady-State Analysis....1147–52
Finzi, L. A.; D. W. VerPlanck, D. C. Beaumariage Analytical Determination of Characteristics of Magnetic Amplifiers with Feedback....565–70
Finzi, L. A.; D. W. VerPlanck, D. C. Beaumariage. Disc....846
Finzi, L. A.; L. C. Wellard. The Geometric Loci of the Synchronous Tie....168–71
Forrest, E. F.; P. W. Schirmer. Space Code Selector Supervisory System....1312–15; disc. 1315
Frick, C. W. Disc....495, 724
Frisch, E.; B. P. Baker. A New 69-Kv Compressed-Air Circuit Breaker....363–8; disc. 371
Frost, G. R. Counting with Relays....587–91
Fugill, A. P. Disc....747
Fujimura, Y. J. Disc....1010
Fuller, John L. Disc....214

G

Gault, J. S. Disc....1131
George, E. E.; H. W. Page, J. B. Ward. Co-ordination of Fuel Cost and Transmission Loss by Use of the Network Analyzer to Determine Plant Loading Schedules....1152–60; disc. 1162
Gibson, G. P.; G. Grant, T. A. Kauppi, G. L. Moses. Motor Tests Evaluate Thermal Endurance of Class-H Insulation and Silicone Varnish....1133–8
Gilchrist, A. D. Disc....153
Giloy, E. W. An Electric Deicing System for Aircraft....1051–7
Gmeiner, John B. Disc....241, 808
Goldberg, Edwin A. Disc....815
Goodrich, R. D., Jr. Disc....380
Gopalakrishna, H. V.; M. S. Thacker. Design of Auxiliary Circuits of Single-Phase Induction Motors....1373–9
Gordy, T. D. Disc....750
Gould, K. E. Equalization of Coaxial Lines...1187–92
Grant, George. Disc....216
Grant, George; T. A. Kauppi, G. L. Moses, G. P. Gibson. Motor Tests Evaluate Thermal Endurance of Class-H Insulation and Silicone Varnish....1133–8
Green, H. H.; J. A. G. Oewel, O. Rasmaur. Relaying of Transmission Lines from the New Sunbury Generating Station....873–7; disc. 877
Gross, Eric T. B. Disc....895, 914, 1329
Gross, I. W. Disc....1206
Gross, I. W.; Philip Sporn. Disc....969
Grosser, E. H. Disc....1281, 1295, 1336
Grosser, E. H.; H. L. Pedley. Disc....1273
Grover, Frederick W. Formulas and Tables for the Calculation of the Magnetic Field Components of Circular Filaments and Solenoids....665–75
Guess, L. T. Disc....487
Gunnoe, G. H.; B. H. Caldwell. Disc....212

H

Hadley, W. A. Disc....20, 334
Hagenguth, J. H. Lightning Stroke Damage to Aircraft....1036–44; disc. 1046
Hague, F. T. Gas Turbines in Stationary Power Generation....467–8
Hailes, W. D. Centralized Traffic Control for Railroads....1167–73
Halfmann, E. S. Disc....346
Hall, Albert C. Damper Stabilized Instrument Servomechanisms....299–306; disc. 306
Halperin, Herman. Disc....19, 333, 1336
Halperin, Herman; C. A. Bauer. Disc....1296
Halsey, G. H.; V. M. Montsinger. Heating of Transformers Under Short-Circuit Conditions....947–52; disc. 954
Hampe, G. W.; B. W. Storer. Power Line Carrier for Relaying and Joint Usage. Part I..864–7; disc. 872
Harder, E. L.; J. M. Clayton. Transmission Line Design and Performance Based on Direct Lightning Strokes....439–46; disc. 448
Harker, D. C.; H. P. Dupuis. Disc....57
Harrington, Everett J.; E. C. Starr. Deionization Time of High-Voltage Fault-Arc Paths....997–1003; disc. 1004
Harris, W. A.; R. A. Beers, A. D. Zappacosta. Design of Mobile Radio Communication Equipment for Land-Mobile Services Operating on Frequencies Between 152–174 Megacycles....1232–9
Harrison, L. P. Disc....1044
Hart, H. A.; F. J. Vogel. A Small High-Voltage Bushing Design for High Altitudes....761–4
Hart, Stephen V. Disc....241
Hatcher, C. T. Disc....558, 829
Hathaway, C. B. Disc....217, 224
Haverstick, J. S. A 3,000-Horsepower Gas Turbine Power Plant....458–60
Hayes, V. J. Disc....231
Hearn, R. B.; L. A. Weber. B-1 Alarm and Control System for Remote Control of Coaxial Cable Stations....622–6
Herskind, C. C.; A. Schmidt, Jr.; C. E. Rettig. Rectifier Fault Currents—II....243–51; disc. 252
Heumann, G. W. Dynamic Braking Control of D-C Series Motors—Experimental Study of Speed-Torque Curves....560–4
Hewitt, G. W.; G. W. Penney. Electrically Charged Dust in Rooms....278–82
Hickernell, L. F.; A. A. Jones, C. J. Snyder. Hy-Therm Copper—An Improved Overhead-Line Conductor....22–7; disc. 29
Higgins, Thomas J.; Glenn Robertson. General Theory and Experimental Confirmation of the Moving Coil Fluxmeter....897–907; disc. 907
Hill, V. E. Disc....913
Hinton, C. B. Disc....1326
Hixson, W. A.; W. G. Hoover. Dielectric Strength of Oil with Variations of Pressure and Temperature....1047–50
Hoard, B. V.; Lewis Weiner. Matching Electrical Characteristics of McNary Generators and Transformers with Bonneville Power Administration Transmission System....1022–5; disc. 1027
Holben, W. P.; J. E. Lange. Primary Networks on the Duquesne Light Company System....704–09; disc. 711
Holtz, F. C. Disc....77
Hoover, D. B. Disc....105
Hoover, W. G.; W. A. Hixson. Dielectric Strength of Oil with Variations of Pressure and Temperature....1047–50
Horton, A. W., Jr.; C. A. Dahlbom, D. L. Moody. Application of Multifrequency Pulsing in Switching....392–6
Hoth, Daniel F.; Harold M. Pruden. Vibrating Reed Selective Signaling System for Mobile Telephone Use....387–91
Howard, Alan Two Gas Turbines for Power Generation and Other Applications....461–5
Hull, Francis M.; W. A. Sinclair. Disc....558
Hunt, F. B.; H. R. Tomlinson. Operation of a Ground-Fault Neutralizer on a Regulated Distribution System....1321–6; disc. 1326
Hutchinson, Chase. Disc....489, 809

I

Imburgia, C. A.; H. P. St. Clair. Disc....1160

J

Jancke, G. Disc....1004
Johnson, I. B.; W. H. Eason, J. W. Kalb, H. A. Peterson. Short-Circuit Currents and Recovery Voltages on Rural Distribution Systems....930–7; disc. 938
Johnson, I. B.; J. W. Kalb. Disc....181
Johnson, Walter C. Disc....194, 649
Johnson, Walter C.; B. C. Merrell, R. E. Alley, Jr. Universal Curves for D-C Controllable Reactors....31–7; disc. 39
Jones, A. A.; L. F. Hickernell, C. J. Snyder. Hy-Therm-Copper—An Improved Overhead-Line Conductor....22–7; disc. 29

K

Kahn, David A. An Analysis of Relay Servomechanisms....1079–87; disc. 1088
Kalb, J. W.; W. H. Eason, I. B. Johnson, H. A. Peterson. Short-Circuit Currents and Recovery Voltages on Rural Distribution Systems....930–7; disc. 938
Kalb, J. W.; I. B. Johnson. Disc....181
Karr, J. H.; S. S. L. Chang. Armature Iron Losses in Series Motors....262–4; disc. 265
Kauppi, T. A.; G. Grant, G. L. Moses, G. P. Gibson. Motor Tests Evaluate Thermal Endurance of Class H Insulation and Silicone Varnish....1133–8
Keister, W. M. The Logic of Relay Circuits....571–6
Keller, A. C.; L. G. Bostwick. Vibrating Reed Selectors for Mobile Radio Systems....383–6
Kenefake, E. W. Disc....1031
Kessler, William J. The Distinction Between Effective and Circuit Bandwidths....98–9
Kidd, K. H.; J. R. Leslie. Disc....1011
Kidder, A. H. Disc....831
Kidder, A. H.; G. S. Van Antwerp. 69-Kv Pipe-Type Cable Circuits in Philadelphia....550–6; disc. 559
Kierstead, F. H. Disc....475
Kierstead, F. H.; J. L. Thomason. Standardization of Reactor Ratings....955–7; disc. 958
Kimball, A. W. Use of Cumulative and Differential Series Fields in the Parallel Operation of D-C Motors....1098–1100

Kimbark, Edward W. Disc.....382, 895
Kimberly, E. E. The Field Fluxes of the Shaded-Pole Motor.....273–7
Kinzer, J. P. Stability of Tandem Regulators in the L-1 Carrier System.....1179–86
Kirschbaum, H. S.; C. E. Warren. A Method for Designing Pulse Transformers.....971–8
Klingaman, G. W. Reduction of Interference from Radio-Frequency Heating Equipment.....718–24; disc. 724
Kochenburger, R. J. Disc.....1087
Komives, L. I. Disc.....1261, 1267, 1273, 1280
Koopman, R. J. W. Operating Characteristics of Two-Phase Servomotors.....319–27; disc. 328
Kron, Gabriel. Stationary Networks and Transmission Lines Along Uniformly Rotating Reference Frames.....690–6
Kusters, N. L. Disc.....68

L

Lamb, J. F.; D. B. Brandt. The Vector Power Factor of Unbalanced Sinusoidal 3-Phase Circuits..507–09
Lange, J. E.; W. P. Holben. Primary Networks on the Duquesne Light Company System.....704–09; disc. 711
Lank, W. J. Design and Experience with 4-Kv Primary Network Systems in the Washington Area.....712–16; disc. 716
Lawton, F. L. Disc.....56
Lebenbaum, Paul, Jr. The Design of D-C Motors for Use in Automatic Control Systems.....1089–94
Leeds, W. M. Disc.....1066
Leh, J. H.; G. F. Lincks, D. R. Edge, W. C. McKinley. Overcurrent Investigation on a Rural Distribution System.....915–27; disc. 928
Leitch, John D. The Use of Air-Core Reactors as Fault Limiting Means on High Interrupting Capacity Controllers.....469–74; disc. 475
Lensner, H. W. Disc.....48, 240, 871
Leonard, M. G. Disc.....488
Leslie, J. R.; K. H. Kidd. Disc.....1011
Leslie, J. R.; J. R. Wait. Detection of Overheated Transmission Line Joints by Means of a Bolometer.....64–8; disc. 69
Levine, D. L.; H. E. Smith. Economic Loading of a Transformer System.....733–8; disc. 739
Lewis, W. A. Disc.....513
Lincks, G. Fred. Disc.....937
Lincks, G. F.; D. R. Edge, W. C. McKinley, J. H. Leh. Overcurrent Investigation on a Rural Distribution System.....915–27; disc. 928
Lindsey, R. H.; K. N. Mathes, L. E. Sieffert, H. P. Walker. Methods for Determining the Effects of Contaminants on Electrical Insulation.....113–18; disc. 118
Linville, T. M.; H. C. Ward, Jr. Solid Short Circuit of D-C Motors and Generators.....119–23; disc. 123
Linville, T. M. Disc.....225
Linville, T. M.; Mrs. B. O. Buckland. Disc.....218
Litman, Bernard. An Analysis of Rotating Amplifiers.....1111–17
Liwschitz, M. M. Differential Leakage of the Different Patterns of a Fractional Slot Winding.....1129–31; disc. 1132
Lloyd, T. C.; Sheldon S. L. Chang. Saturation Effect of Leakage Reactance.....1144–7
Locanthi, B. N.; G. D. McCann, C. H. Wilts. Application of the California Institute of Technology Electric Analog Computer to Nonlinear Mechanics and Servomechanisms.....652–60
Looms, Selection of Electric Drives for. Demartini Lukens.....349–56
Loving, James J., Jr. Electronic Relay Developments.....233–40; disc. 242
Lukens, A. F.; R. J. Demartini. Selection of Electric Drives for Looms.....349–56
Lundry, W. R. Attenuation and Delay Equalizers for Coaxial Lines.....1174–9
Lundy, R. T. Measuring Commutation with an Indicating Instrument.....1380–2
Lunge, G. S. Disc.....884, 1315, 1342
Lush, Morley J. Disc.....907
Lynn, C.; H. M. Elsey. Effects of Commutator Surface Film Conditions on Commutation.106–12; disc. 112
Lynn, C. Disc.....224

M

Macalpine, William W. Heating of Radio-Frequency Cables.....283–8
MacCarthy, D. D.; D. A. Stann, D. R. Edge, W. C McKinley. Lightning Investigation on a Rural Distribution System.....428–37; disc. 437
Madill, J. T.; F. H. Duffy. Shipshaw Relay Protection.....50–5; disc. 57
Mahoney, J. H. Disc.....750
Mansfield, C. G. Disc.....333
Marcy, H. Tyler; M. Yachter, J. Zauderer. Instrumen Inaccuracies in Feed-Back Control Systems with Particular Reference to Backlash.....778–88
Markley, W. F.; H. H. Wheeler. Rubber Insulators for Pole Lines.....195–7
Marshall, F. R.; A. M. Zarem, F. L. Poole. An Electro-Optical Shutter for Photographic Purposes....84–91
Maslin, A. J. Disc.....251
Mason, C. R. A New Loss-of-Excitation Relay for Synchronous Generators.....1240–5
Mason, V. V. Disc.....952
Mathes, K. N.; L. E. Sieffert, H. P. Walker, R. H. Lindsey. Methods for Determining the Effects of Contaminants on Electrical Insulation.....113–18; disc. 118
Mayer, Robert W.; H. Chestnut. Comparison of Steady-State and Transient Performance of Servomechanisms.....765–77
McAdam, Will; A. J. Williams, Jr., W. G. Amey. Wide-Band D-C Amplifier Stabilized for Gain and for Zero.....811–15; disc. 815
McCann, G. D.; C. H. Wilts, B. N. Locanthi. Application of the California Institute of Technology Electric Analog Computer to Nonlinear Mechanics and Servomechanisms.....652–60
McClinton, A. T. Disc.....118, 1123
McClinton, A. T.; Wade H. Askew. Current Ratings of Aircraft Cable.....988–92
McClinton, A. T.; E. L. Brancato, R. Panoff. Transient Characteristics of D-C Motors and Generators.....1100–06
McConnell, H. M.; L. A. Finzi. The Torques of the Synchronous Tie—A Steady-State Analysis.....1147–52
McGrath, M. H. Disc.....18, 1295
McKean, A. L. Disc.....1267, 1281
McKenzie, D. A. Disc.....55
McKinley, W. C.; G. G. Auer, R. A. Branflick, L. J. Woodward. Field Tests of Oil Circuit Recloser Substantiate Analytical Co-ordination Method.....801–08; disc. 810
McKinley, W. C.; G. F. Lincks, D. R. Edge, J. H. Leh. Overcurrent Investigation on a Rural Distribution System.....915–27; disc. 928
McKinley, W. C.; D. D. McCarthy, D. A. Stann, D. R. Edge. Lightning Investigation on a Rural Distribution System.....428–37; disc. 437
McMillon, A. B. Trolley Coaches Replace Busses.....403–06
Meador, J. R. Use of Thyrite in Power Transformers.....959–64
Meador, J. R. Disc.....968
Merrell, B. C.; W. C. Johnson, R. E. Alley, Jr. Universal Curves for D-C Controllable Reactors.....31–7; disc. 39
Merrell, Edwin J. Disc.....345, 1273
Meyerhoff, L.; G. S. Eager, Jr. A-C Resistance of Segmental Cables in Steel Pipe...816–29; disc. 833
Meyerhoff, Louis; Joseph Sticher, G. H. Doan, R. W. Atkinson. High-Pressure Gas-Filled Cable Impregnated with Extra-High-Viscosity Oil.....336–45; disc. 347
Michelson, E. L. Disc.....232
Michelson, E. L.; K. M. Smith. A 66-Kv Subtransmission Plan for a Metropolitan Area.....908–12; disc. 914
Mickley, A. S. The Thermal Movement of Moisture in Soil.....330–3; disc. 334
Mildner, R. C. The Power Rating of Radio-Frequency Cables.....289–98; disc. 298
Millar, N. P. A New Expanded Scale A-C Voltmeter.....641–3
Miller, R. H. A Proposal for Broad-Band Coupling of Power-Line Carrier Equipment.....1028–30; disc. 1031
Montgomery, T. B. Disc.....166
Montsinger, V. M. Disc.....759
Montsinger, V. M.; G. H. Halsey. Heating of Transformers Under Short-Circuit Conditions.....947–52; disc. 954
Moody, D. L.; C. A. Dahlbom, A. W. Horton, Jr. Application of Multifrequency Pulsing in Switching.....392–6
Moore, B. L.; E. C. Clark. Performance of Diesel-Electric Rig for Deep Well Drilling.....497–506
Morgan, W. A. Disc.....1026
Morgan, W. A.; F. S. Rothe, J. J. Winsness. An Improved A-C Network Analyzer....891–5; disc. 896
Morong, W. H.; M. E. Douglass. A New Thermal Volt-Ampere Demand Meter.....79–83; disc. 83
Morris, W. C. One Slip Cycle Out-of-Step Relay Equipment.....1246–8
Morrison, L. W., Jr. Television Terminals for Coaxial Systems.....1193–9
Moses, Graham Lee; G. Grant, T. A. Kauppi, G. P. Gibson. Motor Tests Evaluate Thermal Endurance of Class-H Insulation and Silicone Varnish.....1133–8
Motter, D. P. Commutation of D-C Machines and Its Effects on Radio Influence Voltage Generation.....491–5; disc. 495
Mundel, A. B. Control Chart Methods Applied to Frequency Response Curves.....424–7
Murray, C. S. Transformer Audio Noise Problems on an Electric Power System.....740–7; disc. 751
Murray, C. S. Disc.....751
Myers, E. H. Disc.....495
Myers, Oscar. Codes and Translations.....592–7

N

Narbutovskih, Paul. Disc.....953
Nau, Robert H. Disc.....361, 369
Neher, J. H. The Temperature Rise of Buried Cables and Pipes.....9–17; disc. 20
Neher, J. H. The Temperature Rise of Cables in a Duct Bank.....540–6; disc. 548
Neher, J. H. Disc.....830
Nelson, J. S. Heat Flow Ratio as a Design Parameter in Thermal Demand Meters.....885–90; disc. 890
Nesbit, D. E. Disc.....710
Nicholas, J. H. Design Fundamentals of Potheads 69,000 Volts and Below.....1263–7; disc. 1267
Nicholas, J. H.; A. E. Papp. A New Technique in the Manufacture of Soldered Porcelain Potheads.....1258–60; disc. 1261
Noest, John G. The Performance of a Topped Steam Power Plant on Sudden Load Reduction..1348–56
Nye, H. V. Disc.....362, 370

O

Oewel, J. A. G.; H. H. Green, O. Ramsaur. Relaying of Transmission Lines from the New Sunbury Generating Station.....873–7; disc. 877
Olmsted, Leonard M. Disc.....28, 69, 183, 709, 809
Opel, L. G. Limitations in Design of D-C Adjustable Speed Motors.....1095–8
Opsahl, A. M. Disc.....181, 437

P

Packer, L. C. Die-Cast Rotors for Induction Motors.....253–60; disc. 261
Packer, L. C. Disc.....264, 271
Page, H. W.; E. E. George, J. B. Ward. Coordination of Fuel Cost and Transmission Loss by Use of the Network Analyzer to Determine Plant Loading Schedules.....1152–60; disc. 1162
Panoff, Robert; A. T. McClinton, E. L. Brancato. Transient Characteristics of D-C Motors and Generators.....1100–06
Papp, A. E.; J. H. Nicholas. A New Technique in the Manufacture of Soldered Porcelain Potheads.....1258–60; disc.1261
Parks, C. E. Disc.....381, 1207
Paschkis, Victor. Comparison of Long-Time and Short-Time Analog Computers.....70–3
Pease, W. M. Disc.....306
Pedley, H. L.; E. H. Grosser. Disc.....1273
Peltosalo, A. E. Disc.....1231
Penney, G. W.; G. W. Hewitt. Electrically Charged Dust in Rooms.....278–82
Peterson, H. A.; W. H. Eason, I. B. Johnson, J. W. Kalb. Short-Circuit Currents and Recovery Voltages on Rural Distribution Systems.....930–7; disc. 938
Poole, F. L.; A. M. Zarem, F. R. Marshall. An Electro-Optical Shutter for Photographic Purposes...84–91
Porter, L. F. Transformer Manholes and Vaults: Design and Ventilation.....534–9
Pruden, Harold M.; Daniel F. Hoth. Vibrating Reed Selective Signaling System for Mobile Telephone Use.....387–91
Puchstein, A. F. Disc.....264
Purcell, W. R. Saving Time in Testing Life of Incandescent Lamps.....730–2

R

Ramsaur, O.; H. H. Green, J. A. G. Oewel. Relaying of Transmission Lines from the New Sunbury Generating Station.....873–7; disc. 877
Ramsey, Glen. Selenium Rectifiers in Motor Vehicle Power Systems.....149–53; disc. 153
Rauth, A. W. Disc.....56
Raymond, A. E. Disc.....1045
Reed, R. D.; W. W. Satterlee. Controlled Temperature and Insulation Protection in the Operation of Power Transformers.....753–8; disc. 759
Rehberg, Charles F. Disc.....314
Rettig, C. E.; C. C. Herskind, A. Schmidt, Jr. Rectifier Fault Currents—II.....243–51; disc.252
Richards, H. H. G.; B. O. Austin. Aircraft Carbon-Pile Voltage Regulators, Fundamentals, and Design Improvements.....983–7
Ricker, E. A. Automatic Grounding and Air-Break Switches for Protection of Transformer Stations.....851–6; disc. 856
Ridgway, W. Disc.....1021
Ritchie, A. E. Sequential Aspects of Relay Circuits.....571–81

Robertson, Glenn; Thomas J. Higgins. General Theory and Experimental Confirmation of the Moving Coil Fluxmeter........897–907; disc. 907
Roehmann, L. F. Disc...........................298
Rorden, Harold L. Disc.........................204
Rosenberg, L. T. A Semiempirical Approach to Voltage Dip—With Suddenly Applied Loads on A-C Generators.....................160–6; disc. 167
Rothe, F. S.; W. A. Morgan, J. J. Winsness. An Improved A-C Network Analyzer....891–5; disc. 896
Rudenberg, Reinhold. Nonharmonic Oscillations as Caused by Magnetic Saturation...........676–85
Rueggeberg, W.; J. B. Whitehead. The Measurement of Dielectric Loss at High Frequencies and Under Changing Temperature...................520–4
Runciman, A. S. Disc...........................68
Ruud, H. B.; S. B. Farnham. A New Automatic Load Control for Turbine Generators..........1337–42
Ryan, J. E. Prediction of Ultimate Tempera[illegible] Rise from Early Heat Run Data..................1164–6
Rydbeck, V. A. Disc...........................716

S

St. Clair, Harry P. Disc..................1067, 1231
St. Clair, H. P.; C. A. Imburgia. Disc.........1160
Sand, Edward. Disc.............................224
Sand, Edward J.; Jack H. Sheets. Development and Application of Electric Heating to Deicing of Aircraft Propellers.........................1068–72
Satterlee, W. W.; R. D. Reed. Controlled Temperature and Insulation Protection in the Operation of Power Transformers.............753–8; disc. 759
Saunders, Robert M. The Dynamoelectric Amplifier—Class A Operation......................1368–73
Schaefer, L. C.; C. G. Veinott. Fundamental Theory of Inherent-Overheating Protection Under Running Overload Conditions...........266–70; disc. 272
Schart, W. J. Disc............................1087
Schetky, L. McDonald; L. P. Winsor, R. A. Wyant. Instrumentation for the Evaluation of the Stability of the Welding Arc......................525–33
Schifreen, C. S. Disc..........................1273
Schirmer, P. W.; E. F. Forrest. Space Code Selector Supervisory System...........1312–15; disc. 1315
Schirmer, P. W.; J. J. Winsness. Disc............863
Schmidt, A., Jr.; C. C. Herskind, C. E. Rettig. Rectifier Fault Currents—II..........243–51; disc. 252
Schwendner, A. F.; Wayne C. Astley. Governors and the AIEE-ASME Governor Performance Specification..............................1330–2
Scott, F. M. Disc..................112, 123, 216
Scott, Hoyt S. Measurements of Erythemal Energy..725–29
Scoville, M. E. Disc...........................1206
Seely, R. E. Disc..............................271
Seelye, Howard P. A Convenient Method for Determining Generator Reserve..............1317–20
Seelye, Howard P. Disc.........................487
Shankle, D. F.; H. G. Barnett. Disc.............914
Shanklin, G. B. Disc....................346, 558
Sheadel, J. M.; V. L. Crabb. Magnetic Heating of Transmission Line Clamps................032–5
Sheets, Jack H.; E. J. Sand. Development and Application of Electric Heating to Deicing of Aircraft Propellers..........................1068–72
Shores, R. B. Disc.............................369
Short, H. D. A Theoretical and Practical Approach to the Design of High-Voltage Cable Joints.................................1275–80; disc. 1282
Short, H. D. Disc..............................1296
Sieffert, L. E.; K. N. Mathes, H. P. Walker, R. H. Lindsey. Methods for Determining the Effects of Contaminants on Electrical Insulation.................................113–18; disc. 118
Silsbee, F. B. Disc............................1046
Sinclair, W. Allistair; F. M. Hull. Disc..........558
Skeats, W. F. Disc.............................370
Skeats, W. F.; A. C. Boisseau, B. W. Wyman. Insulator Flashover Deionization Times as a Factor in Applying High-Speed Reclosing Circuit Breakers.................................1058–66; disc. 1066
Slemon, Gordon R. Radio Influence from High-Voltage Corona.................198–204; disc. 205
Smith, Frank V. Disc.......................19, 547
Smith, H. B. Disc.............................1161
Smith, H. E.; D. L. Levine. Economic Loading of a Transformer System.............733–8; disc. 739
Smith, J. J.; P. L. Alger. A Derivation of Heaviside's Operational Calculus Based on the Generalized Functions of Schwartz..........939–44; disc. 945
Smith, K. M.; E. L. Michelson. A 66-Kv Subtransmission Plan for a Metropolitan Area.................................908–12; disc. 914
Smith, S. R., Jr. Disc..........................809
Smithley, R. S.; G. B. Dodds. Disc..............716
Snyder, C. J.; L. F. Hickernell, A. A. Jones. Hy-Therm Copper—An Improved Overhead-Line Conductor.................................22–7; disc. 29
Sonnemann, W. K. Novel Test Circuits for Protective Relays...........................1249–54
Spaulding, L. R. Disc..........................1031
Spaulding, L. R.; C. C. Diemond. A Transient Fault Locator for High-Voltage Transmission Lines.................................1005–10; disc. 1011
Specht, T. R.; E. C. Wentz. Disc.................38
Spencer, H. H. Power Supplies for Coaxial Systems..627–30
Sporn, Philip. Disc.....................466, 1067
Sporn, Philip; I. W. Gross. Disc................969
Squires, R. B. Disc.............................895
Staats, G. W. Disc.............................166
Stann, D. A.; D. D. MacCarthy, D. R. Edge, W. C. McKinley. Lightning Investigation on a Rural Distribution System............428–37; disc. 437
Starr, E. C.; E. J. Harrington. Deionization Time of High-Voltage Fault-Arc Paths.................................997–1003; disc. 1004
Steinberg, M. J. Disc..........................1160
Stephens, D. S. Lightweight Aircraft Transformers..1073–8
Stevens, R. F. Disc.............................42
Sticher, Joseph; G. H. Doan, R. W. Atkinson, Louis Meyerhoff. High-Pressure Gas-Filled Cable Impregnated with Extra-High-Viscosity Oil.................................336–45; disc. 347
Stoelting, H. O. Disc...........................186
Stokes, H. E. Disc.............................215
Storer, B. Wade; H. A. Cornelius. Loss Measurements Made on Underground-Cable Overhead-Conductor 132-Kv Transmisson Line at Carrier Current Frequencies..........................597–601
Storer, B. W.; G. W. Hampe. Power Line Carrier for Relaying and Joint Usage. Part I.864–7; disc. 872
Storm, H. F. Some Fundamentals of D-C Controlled Reactors with Resistive Load.............188–94
Storm, H. F. Disc.......................37, 847
Streiff, A. Disc................................489
Sulzer, P. G.; E. A. Walker, A. H. Waynick. Polar Vector Indicator.........................154–9
Sutton, Howard J. Line Tuning Equipment Used With Coaxial Cable for Carrier Current Installation on Power Lines,.....................44–8; disc. 49

T

Tallent, R. J. Disc.............................381
Taylor, P. L. Disc.............................369
Teague, Wm. L. Disc............................969
Terrant, F. R. Disc.............................214
Terwilliger, D. D. Disc.........................318
Thacker, M. S.; H. V. Gopalakrishna. Design of Auxiliary Circuits of Single-Phase Induction Motors...............................1373–9
Thomas, C. H.; E. C. Easton. Graphical Determination of Transfer Function Loci for Servomechanism Components and Systems........307–14; disc. 318
Thomas, E. R. Disc................1273, 1281, 1295
Thomason, J. L.; F. H. Kierstead. Standardization of Reactor Ratings................955–7; disc. 958
Thompson, C. S. Application of Experimental Test Procedures and Methods of Analysis of Results to Research Problems in Magnetic Recording..407–17
Tomlinson, H. R. Disc...........................181
Tomlinson, H. R.; F. B. Hunt. Operation of a Ground-Fault Neutralizer on a Regulated Distribution System........................1321–6; disc. 1326
Tornquist, E. L.; I. L. Wade. Determining Incremental Regulation and Dead Band of Governors on Steam Turbine Generators Under System Load Conditions............................1343–7
Travers, Paul. Disc.............................315
Tribken, E. R.; A. G. Conrad. A Wide-Range Adjustable-Speed Drive.........................789–90
Turner, W. R.; W. R. Clark, A. J. Williams, Jr. A Square-Law Power-Level Recorder.........476–82

U

Umphrey, D. M. Disc...........................1004

V

Van Antwerp, G. S.; A. H. Kidder. 69-Kv Pipe-Type Cable Circuits in Philadelphia....550–6; disc. 559
Veinott, C. G.; L. C. Schaefer. Fundamental Theory of Inherent-Overheating Protection Under Running Overload Conditions...........266–70; disc. 272
VerPlanck, D. W.; L. A. Finzi, D. C. Beaumariage. Analytical Determination of Characteristics of Magnetic Amplifiers with Feedback............565–70
VerPlanck, D. W.; L. A. Finzi, D. C. Beaumariage. Disc...................................846
Vikoren, O. B. Disc............................371
Vogel, F. J. Extremes in the Insulation Co-ordination of Oil Insulated Transformers.....965–8; disc. 970
Vogel, F. J. Disc...............................759
Vogel, F. J.; H. A. Hart. A Small High-Voltage Bushing Design for High Altitudes..............761–4
Von Voigtlander, F. Disc..................153, 751

W

Wade, I. L.; E. L. Tornquist. Determining Incremental Regulation and Dead Band of Governors on Steam Turbine Generators Under System Load Conditions............................1343–7
Wait, J. R.; J. R. Leslie. Detection of Overheated Transmission Line Joints by Means of a Bolometer.................................64–8; disc. 69
Waite, G. G. Disc..........................77, 83
Walker, E. A.; A. H. Waynick, P. G. Sulzer. Polar Vector Indicator.........................154–9
Walker, H. P.; K. N. Mathes, L. E. Sieffert, R. H. Lindsey. Methods for Determining Effects of Contaminants on Electrical Insulation.113–18; disc. 118
Wall, H. R. Disc...............................912
Ward, H. C., Jr.; T. M. Linville. Solid Short Circuit of D-C Motors and Generators...119–23; disc. 123
Ward, H. M. Power Supplies for Microwave Relay Systems.............................631–6
Ward, J. B. Equivalent Circuits for Power-Flow Studies.....................373–80; disc. 382
Ward, J. B.; E. E. George, H. W. Page. Coordination of Fuel Cost and Transmission Loss by Use of the Network Analyzer to Determine Plant Loading Schedules...................1152–60; disc. 1162
Warren, C. E.; H. S. Kirschbaum. A Method for Designing Pulse Transformers................971–8
Warrington, A. R. Van C. Graphical Method for Estimating the Performance of Distance Relays During Faults and Power Swings........608–20; disc. 621
Washburn, S. H. Relay "Trees" and Symmetric Circuits...............................382–6
Watchorn, C. W. Disc...........................1161
Waynick, A. H.; E. A. Walker, P. G. Sulzer. Polar Vector Indicator.........................154–9
Weber, Laurance A.; R. B. Hearn. B-1 Alarm and Control System for Remote Control of Coaxial Cable Stations...........................622–6
Weiner, Lewis; B. V. Hoard. Matching Electrical Characteristics of McNary Generators and Transformers with Bonneville Power Administration Transmission System..........1022–5; disc. 1027
Welchel, C. C. Disc............................1021
Wellard, L. C.; L. A. Finzi. The Geometric Loci of the Synchronous Tie.....................168–71
Wenner, Frank. Disc............................907
Wentz, E. C.; T. R. Specht. Disc.................38
Wheeler, H. H.; W. F. Markley. Rubber Insulators for Pole Lines..............................195–7
Whitehead, E. R. Disc..........................968
Whitehead, J. B.; W. Rueggeberg. The Measurement of Dielectric Loss at High Frequencies and Under Changing Temperature.............520–4
Wild, Earle. Disc..............................689
Williams, A. J., Jr.; W. G. Amey, Will McAdam. Wide-Band D-C Amplifier Stabilized for Gain and for Zero....................811–15; disc. 815
Williams, A. J., Jr.; W. R. Clark, W. R. Turner. A Square-Law Power-Level Recorder........476–82
Williams, G. D.; F. H. Busch. Surge Protection in a Modern Watt-Hour Meter.........74–7; disc. 78
Wilson, N. E. Transients in 2-Phase Synchronous Machines...........................1360–7
Wilson, W. A. Disc.............................465
Wilts, C. H.; G. D. McCann, B. N. Locanthi. Application of the California Institute of Technology Electric Analog Computer to Nonlinear Mechanics and Servomechanisms...................652–60
Winegartner, C. E. Disc.........................362
Winegartner, C. E.; H. E. Bonheimer. A-C Tripping and Reclosing of Line Sectionalizing Circuit Breakers..............................1357–9
Winsness, J. J.; W. A. Morgan, F. S. Rothe. An Improved A-C Network Analyzer....891–5; disc. 896
Winsness, J. J.; P. W. Schirmer. Disc............863
Winsor, Lauriston P.; L. M. Schetky, R. A. Wyant. Instrumentation for the Evaluation of the Stability of the Welding Arc......................525–33
Wiseman, Robert J. Disc..............546, 556, 832
Witzke, R. L. Voltage-Recovery Characteristics of Distribution Systems.............172–80; disc. 187
Witzke, R. L. Disc.............................938
Wollaston, F. O. Transient Temperature Phenomena of 3-Conductor Cables.........1284–95; disc. 1297
Woodrow, C. A. Disc............................913
Woods, Thomas J. Industrial Plants Prefer Diesel-Electric Switching Locomotives..........697–700
Woodward, L. J.; G. G. Auer, R. A. Branflick, W. C. McKinley. Field Tests of Oil Circuit Recloser Substantiate Analytical Co-ordination Method.................................801–08; disc. 810
World, Richard W. Disc.........................620
Wray, G., Jr. Disc..............................748
Wyant, Robert A.; L. P. Winsor, L. M. Schetky. Instrumentation for the Evaluation of the Stability of the Welding Arc......................525–33
Wyatt, K. S. Disc...............................29
Wyman, B. W.; A. C. Boisseau, W. F. Skeats. Insulator Flashover Deionization Times as a Factor in Applying High-Speed Reclosing Circuit Breakers.................................1058–66; disc. 1066

Wyman, B. W.; E. J. Casey. A Manually-Operated Spring Mechanism for Medium Voltage Oilless Circuit Breakers................357–61; disc. 362

Y

Yachter, M. Disc..............................315

Yachter, Morris; H. T. Marcy, J. Zauderer. Instrument Inaccuracies in Feed-Back Control Systems with Particular Reference to Backlash......778–88

Z

Zappacosta, A. D.; R. A. Beers, W. A. Harris Design of Mobile Radio Communication Equipment for Land-Mobile Services Operating on Frequencies Between 152–174 Megacycles.............1232–9

Zarem, A. M.; F. R. Marshall, F. L. Poole. An Electro-Optical Shutter for Photographic Purposes....84–91

Zauderer, Jerome; H. T. Marcy, M. Yachter. Instrument Inaccuracies in Feed-Back Control Systems with Particular Reference to Backlash......778–88

Preface

The 1949 TRANSACTIONS (volume 68) of the American Institute of Electrical Engineers will be published in two parts.

Part I contains technical program papers and related discussions presented at general meetings and District meetings during the first half of the calendar year as follows:

1. Winter General Meeting, New York, N. Y., January 31–February 4, 1949.
2. South West District Meeting, Dallas, Tex., April 19–21, 1949.
3. Summer General Meeting, Swampscott, Mass., June 20–24, 1949.

Forty-two Summer General Meeting papers are included in Part I. The remainder of the Summer General Meeting papers will be included in Part II together with the approved papers and related discussions presented at the Pacific General Meeting and the Fall General Meeting.

Full correlation of all material in this volume has been accomplished by means of the multientry index beginning on page 791. Reference to any of the several subject entries for a technical paper will lead directly to the paper and to any published discussion on that paper.

Statements and opinions given in papers and discussions published in TRANSACTIONS are the expressions of contributors for which the American Institute of Electrical Engineers assumes no responsibility.

Part II of Volume 68 is expected to be available for distribution early in 1950.

The Heat Pump—Its Significance as a Potential Residential Electric Load

CONSTANTINE BARY
MEMBER AIEE

THE NAME heat pump as used herein describes a device which transfers heat from one temperature level to another by means of an electrically-driven compressor. When such a device takes heat from a source of relatively low temperature and makes it available at a higher one, it is said to operate on a "heating cycle," and conversely, when it removes heat from a space of relatively high temperature and discharges it elsewhere (at a still higher temperature) it is said to operate on a "cooling cycle." In either case, fundamentally it does not create heat energy as such; it only conveys the available heat of a particular source from one temperature level to another, and thus combines within itself the ability to either heat or cool a given space.

The fundamental thermodynamic principles of this device have been known for almost a century. Its operation on the cooling cycle has had extensive practical application in refrigeration, and in air conditioning of homes and other buildings. But, because of many technical difficulties and relatively high first cost, its operation on the heating cycle has had only limited application. For the most part it has been confined to commercial establishments largely in the southern part of the United States, or where reliable supplies of underground water are available. More recently, however, and due to certain technical developments, extensive interest has been shown throughout the electric utility industry, and by the public at large, in its possibilities for a practical method of heating homes electrically with the accompanying advantages of cleanliness, absence of combustion, ease of operation and general comfort and convenience.

The use of electricity in one form or another for heating homes has been considered off and on over a span of many years throughout the electric utility industry. It is generally conceded, however, that, at the existing state of the art, electricity cannot compete in cost for house heating, on a direct energy conversion basis, with other fuels such as coal, oil, or gas customarily used. This is true even under existing inflated prices in territories where a good grade of furnace coal for household use sells for about $15 per ton, fuel oil for about $0.10 per gallon and manufactured gas for about $0.70 per thousand cubic feet. There are three fundamental reasons for this handicap:

1. The present-day over-all efficiency involved in producing and distributing electricity from the heat contained in the fuel at the generating station to the heat contained in the electric energy delivered to the premises of residential customers is comparatively low, being in the order of 15 to 25 per cent, even though this is offset to a considerable extent by the fact that the effective utilization of the heat in fuels such as coal, oil, or gas by conventional house heating equipment is in the order of 50 to 75 per cent, as compared to 100 per cent utilization of the heat energy in electricity for heating purposes.

2. The magnitude of the investment required for the production, bulk power, transmission, transformation and distribution facilities with the related costs in carrying charges and operating expenses.

3. The relatively low diversified and undiversified annual load factors produced by the heating load of an average home result in comparatively high unit cost per kilowatt-hour.

Table I illustrates this point, using a home requiring 100,000,000 Btu during an average heating season at fuel prices now generally prevailing in a large metropolitan area of the Middle Atlantic states. The price of electricity is assumed at $.025 per kilowatt-hour to approximate the cost of supplying this service under the low annual load factor of the house heating load. The comparison is confined to costs applicable to fuel only. These numbers do not purport to represent a complete comparison of the total costs of heating with various fuels, since investment costs, maintenance costs, and cost equivalents of many intangibles have been omitted purposely to simplify the illustrations of the major features of such a comparison.

It will be noted from Table I that, at the stated prices, the seasonal cost applicable to fuel (exclusive of fixed charges, maintenance, and intangible costs) of heating a house by electric resistance-type heaters is about four times that with manufactured gas, and about six times that with oil or coal.

Since, for a given method of electricity production and distribution its cost per kilowatt-hour depends primarily upon the annual diversified load factor of the load served, and since the annual diversified load factor of the house heating load is largely fixed by prevailing climatic conditions of the territory, it becomes evident that if it were possible to reduce the quantity of electricity required to do the job of house heating, say, by four times, then the total seasonal cost of electricity for heating would become as low as that of gas, the nearest high-grade house heating service.

This is where the heat pump fits into the picture. It can be used to multiply the effectiveness of electricity for heating purposes, and thus make practicable the economical supply of energy for residential

---

Paper 49-1, recommended by the AIEE domestic and commercial applications committee and approved by the AIEE technical program committee for presentation at the AIEE winter general meeting, New York, N. Y., January 31–February 4, 1949. Manuscript submitted April 12, 1948; made available for printing November 4, 1948.

CONSTANTINE BARY is rate research engineer, Philadelphia Electric Company, Philadelphia, Pa.

The author acknowledges the valuable suggestions received from N. E. Funk, I. L. Craig, E. H. Bromer, A. H. Kidder, and G. E. Klapper of the Philadelphia Electric Company on the original manuscript of this paper, and the assistance of A. Abramovitz of that company in preparing the material contained therein.

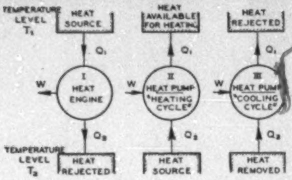

$$Q = KT$$

$$\text{I ENGINE EFFICIENCY} \text{———} = e = \frac{W}{Q_1} = \frac{Q_1 - Q_2}{Q_1} = \frac{T_1 - T_2}{T_1}$$

$$\text{II COEFFICIENT OF PERFORMANCE} = COP_h = \frac{Q_1}{W} = \frac{Q_1}{Q_1 - Q_2} = \frac{T_1}{T_1 - T_2}$$

$$\text{III COEFFICIENT OF PERFORMANCE} = COP_c = \frac{Q_2}{W} = \frac{Q_2}{Q_1 - Q_2} = \frac{T_2}{T_1 - T_2}$$

Figure 1. Principles of operation and performance of a heat engine and heat pump on a Carnot cycle

house heating by electric utilities, because, from thermodynamic considerations, a heat pump can be made to deliver from three to five kilowatt-hours in equivalent heat for every one kilowatt-hour required for its operation.

Scope

The object of this paper is to direct attention to the significant load characteristics that may be produced by the residential heat pump. This paper will touch briefly upon the general thermodynamic principles of heat pump operation; it will comment upon the nature of heat sources available for use with the heat pump and upon the applicability of several methods of heat distribution throughout the house; and it will demonstrate the major probable effects of the residential heat pump upon the load characteristics of the residential class of service. The actual values used herein represent experience with the load of one large electric utility system operating in metropolitan, suburban, and rural territories of the Middle Atlantic states.

A complete and precise picture of the significance of the residential heat pump cannot be made at this time, largely because this device is so new that its actual and possible engineering performance features are not firmly established, and because little if any experience is available as to its ultimate load characteristics. In this paper, however, recourse is made to the adaption of known characteristics of residential gas house heating loads, as determined by extensive tests made on a large system. It is assumed that these characteristics would be representative of the residential heat pump load as well.

No matter what ideas one may have at this time on the future heat pump situation, one is likely to be proved wrong by what actually may happen. But, notwithstanding the difficulty of foreseeing the future clearly and the futility of trying to determine precisely the world of tomorrow, it nevertheless seems highly desirable to obtain some idea now on the possible effects of the future residential heat pump load, so that the electrical industry can continue discharging its responsibility to broaden its usefulness just as in the past.

General Thermodynamic Principles of Heat Pump Operation

Figure 1 illustrates the well-known relationships of efficiency and coefficient of performance of an ideal Carnot heat engine, and that of a heat pump reflecting the ideal Carnot cycle of operation. In this figure, T_1 and T_2 are absolute temperatures, 460 + F (degrees Fahrenheit), with T_1 being higher than T_2; Q_1 and Q_2 the quantities of heat received from, or exhausted to some outside body, and W the work done by or on the system.

It will be noted from the formulas shown that since the difference between the temperatures T_1 and T_2 is always less than T_1, the coefficient of performance of a heat pump operating on a heating cycle will be always greater than unity. By algebraic transformation it may be shown too that for given temperature levels, the coefficient of performance for the heating cycle (COP_h) is equal to one plus the coefficient of performance for the cooling cycle (COP_c).

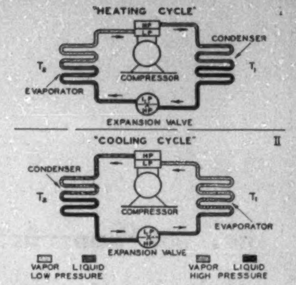

Figure 2. Schematic diagram of heat pump operation

Figures 2 and 3 illustrate schematically and by means of a pressure–enthalpy diagram respectively, the fundamental thermodynamic principles of operation of a heat pump on an ideal vapor cycle, with its irreversible processes, employing as a working medium a fluid which can be made to absorb and surrender heat by an alternate process of vaporization and condensation.

When operating on a heating cycle (Figure 2-I) the low-pressure vapor, in the ideal case, coming from the evaporator at a low temperature, enters a compressor, where the vapor is compressed, with a resulting increase in its temperature and pressure. It is then passed to the condenser where it is made to give up its latent heat, and in doing so is condensed to a liquid which, flowing through an expansion valve, is reduced in pressure and temperature and is then returned to the evaporator, where it is turned to vapor by absorbing heat from an outside source which is at a higher temperature than the low-pressure liquid coming from the expansion valve.

More specifically from the pressure-enthalpy diagram of the ideal cycle (Figure 3) the vapor from the evaporator at point h_1 is compressed isentropically to h_2 through the application of work done on it from outside (so that the enthalpy at $h_2 = h_1 + W$). The compressed vapor is then condensed at a constant pressure to a liquid at point h_3, and in doing so it liberates the amount of heat $Q_1 = h_2 - h_3$. The liquid then is expanded at constant enthalpy through an expansion valve proceeding to the evaporator, where, in ab-

Table I. Comparison of Cost Applicable to Fuel for Heating a Home Which Requires 100,000,000 Btu During a Heating Season From September to May

Kind of Unit	Electric Resistance Heating (Kilowatt-hours)	Manufactured Gas (Thousand Cubic Feet)	Fuel Oil (Gallons)	Coal (Net Tons)
Btu per unit employed	3,415	520,000	140,000	24×10^6
Efficiency, per cent	100	75	65	50
Useful heat delivered to house per unit-Btu	3,415	390,000	91,000	12×10^6
Units required to heat house	29,283	256	1,099	8.33
Cost applicable to fuel:				
Price per unit	$0.025	$0.70	$0.10	$15
Cost of fuel	$732	$179	$110	$125
Cost of electricity for auxiliaries			$8	
Total	$732	$179	$118	$125
Approximate relation to cost of electric resistance heating	1	1/4	1/6	1/6

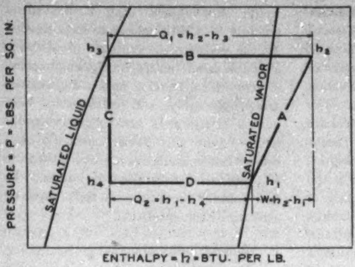

$$COP_h = \frac{Q_1}{W} = \frac{h_2-h_3}{h_2-h_1}$$

$$COP_c = \frac{Q_2}{W} = \frac{h_1-h_4}{h_2-h_1} = \frac{h_1-h_3}{h_2-h_1}$$

Figure 3. Pressure-enthalpy diagram of ideal vapor cycle for heat pump operation

A—isentropic compression
B—constant pressure condensation
C—constant enthalpy expansion
D—constant pressure evaporation

sorbing heat from the outside, it vaporizes and in doing so gains heat $Q_2 = h_1 - h_3$, completing the cycle by returning to the compressor.

When operating on a cooling cycle, the process is reversed, the evaporator becoming the condenser, and the condenser the evaporator. (Figure 2-II.)

The coefficients of performance of this ideal cycle are expressed by the following relationships:

When operating on a heating cycle

$$COP_h = \frac{Q_1}{W} = \frac{h_2-h_3}{h_2-h_1} \qquad (1)$$

and when operating on a cooling cycle

$$COP_c = \frac{Q_2}{W} = \frac{h_1-h_3}{h_2-h_1} \qquad (2)$$

Since $COP_h = 1 + COP_c$, the foregoing equations may be rewritten to:

$$COP_h = 1 + \frac{h_1-h_3}{h_2-h_1} \qquad (3)$$

The coefficient of performance of the actual cycle of a heat pump will be lower than that of the ideal by the high- and low-side frictional pressure drop losses occurring in the actual cycle, the electrical losses of the motor driving the compressor, and the mechanical losses of the compressor. However, some of this decrease in the actual coefficient of performance may be offset by employing liquid-subcooling and liquid-suction vapor heat exchange.

Expressing these effects in terms of factors for application in the coefficient of performance formula of the ideal cycle, the formula for the actual cycle with subcooling and liquid suction heat exchange becomes

$$COP_h = 1 + e f_l f_h z \frac{h_1-h_3}{h_2-h_1} \qquad (4)$$

Where

e = the isentropic efficiency of the compressor-motor combination
f_l = the low-side pressure drop correction factor
fh = the high-side pressure drop correction factor
z = liquid subcooling and vapor heat exchange correction factor

Under a proper design and within the practical range of heat pump operation, the factors f_l and f_h will be always lower than unity and the factor z will be generally higher than unity, with their product approximating unity. Therefore the isentropic efficiency of the compressor-motor combination is left as the major determining factor in establishing the coefficient of performance of an actual cycle as compared with an ideal one.[1]

In actual practice, in addition to the electric energy requirements of the compressor-motor, there may be energy required for auxiliaries such as fans and pumps which are functional parts of the heat pump. The energy used by them must be considered in establishing the over-all coefficient of performance of a heat pump assembly.

Figure 4 is presented from data recently developed by W. Parkerson[2] to illustrate the practical range of variation in the coefficient of performance of a heat pump (exclusive of auxiliaries) operating on a heating cycle for selected values of condenser and evaporator temperatures, and for performance cycles ranging from the ideal Carnot cycle through to the actual cycles utilizing Freon 12 (CCl_2F_2), and employing ideal, possibly attainable and present-day efficiencies of compressor-motor combinations. It will be noted that, the smaller the difference between the condenser and the evaporator temperatures, the higher is the coefficient of performance, indicating that for any given condenser temperature, one should strive for as high an evaporator temperature as possible in order to obtain the highest coefficient of performance of the heat pump; and similarly for any given evaporator temperature, one should strive for as low a condenser temperature as possible to obtain the highest coefficient of performance.

It is for this reason that temperature characteristics of heat sources become of major significance in the practical performance of heat pumps, and that temperature levels of heat distribution media become of great importance in the design of the heating system employing a heat pump.

Heat Sources and Heat Distribution

There are three principal heat sources available to a heat pump today: air, water, and earth. They may be used separately or in combination. Each has

Figure 4. Range in coefficient of performance of heat pump on a "heating cycle" for selected suction and condensing temperatures

1. Carnot cycle
2. Ideal cycle with Freon-12 (isentropic compression with 100 per cent compressor—motor efficiency, no super-heat, no sub-cooling)
3. Possibly attainable with Freon-12 (compressor efficiency 85 per cent, motor efficiency 85 per cent, 10 degrees super-heat, 10 degrees sub-cooling)
4. Present-day commercial-type compressor (5 horsepower)

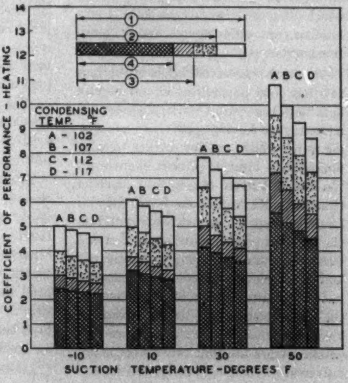

its own physical and economic advantages and disadvantages.

The air possesses the advantage of being universally available, free of charge. However, possible wide fluctuations of its temperature and especially the level of its dew point temperatures, are limiting factors in its universal use as a practical heat source for heat pumps. Its temperature is lowest at times when house heating requirements are at a maximum, which is obviously the reverse of what is required to limit the size of installed capacity of the heat pump and to obtain the highest coefficient of performance. It is for this reason that the practical application of air as the sole source of heat for house heating at present is limited to climates where the temperature does not drop much below 35 to 40 degrees Fahrenheit. However, in climates where the temperature drops below those values, for part of the total heating season, it still may be an economical source of heat for the heat pump in combination with another heat source, which would be called upon, at intervals, to supply either the deficiency in, or even the total heat of, the requirements during that time. In a climate such as is experienced in the Middle Atlantic states, about 50 per cent of the heating requirements as measured by degree days for an average heating season, occur at times when the daily mean outdoor temperature is 35 degrees Fahrenheit and higher.

Water from a flowing stream, from wells, or from city water mains is a good source of heat. It possesses the advantage of a relatively high temperature which is not subject to very wide fluctuations, but its disadvantages are that it is not universally available free of charge, and its use, in comparatively large quantities is undesirable, and usually entails costs which often are so high as to make it prohibitive from an economic and competitive point of view.

The earth several feet below the surface also has good possibilities as a source of heat for a heat pump.[3,4] It possesses the advantage of having relatively high temperatures which are not subject to wide fluctuations. But, at present, there is not too much known of its heat transfer characteristics at various levels for different soil types, moisture content and for the different conditions of extraction and dissipation under varying temperatures; and the ultimate effects of unbalanced heat withdrawal from, and absorption by, the earth upon its long-term temperature levels are a matter of conjecture now. Its disadvantages are that this source is not universally available in the quantities and qualities required, and heat from it cannot be obtained free of charge, since work would be needed to embed into the earth, at the desired depth necessary, lengths of piping for the purpose of heat extraction or dissipation, as the case may be. The possibilities for its use as a heat source are so attractive, however, that in recent years they have aroused considerable interest in the subject of application of the heat pump principles for the heating of homes even in the northern and middle temperature zones of the United States, which contain by far the major portion of the country's population. As a matter of fact, it is the opinion of the author and many others, that at the existing state of development of the art, unless the earth proves to be an economical heat source, the application of the heat pump principle for heating homes through the middle and northern belts of the United States can be relegated to the realm of theoretical discussion rather than be considered as a large volume commercial reality for the immediate future.

While the heat source is of major significance in the practical application of the heat pump, the medium employed for conveying the heat throughout the house is equally significant. As pointed out in Figure 7, the higher the temperature of the condenser the lower the coefficient of performance. The temperature level in the condenser coils is limited by the existing availability of refrigerants and by the practical considerations of higher pressures (required by the higher temperatures) on the design of compressors, piping, joints, and valves. Thus, from the standpoint of the heating cycle alone, practical condenser temperatures cannot be expected to be much above 120 degrees Fahrenheit. This level of temperature rules out steam for a heating medium, circumscribes greatly the conventional application of hot water, and frequently requires a redesign of heat distribution facilities when using air for the heating medium; and from the standpoint of the cooling cycle, the air as a cooling medium appears at this time to be the only practical means for accomplishing the desired job.

In addition to the foregoing considerations of heat sources and methods of heat distribution in the home, present indications are that the "first cost" and maintenance cost of a heat pump would be higher than those of conventional fuel-fired heaters and about the same as the sum of the costs for a conventional fuel-fired heater and a central system summer air conditioner.[5]

Looking realistically at the problem, it would thus appear that a substantial amount of additional research is needed on the economical methods of utilizing available heat sources, on the engineering of economical heating media and on the design, assembly, and operation of heat pumps, refrigerants, and accessory equipment, before this device could be considered as a commercial reality, within the reach of a large number of homes. To find popular acceptance it must have at least nine basic qualities:

1. High reliability of operation.
2. High efficiency of performance.
3. Low maintenance cost.
4. Reasonable "first cost."
5. Compactness.
6. Neat appearance.
7. Easy accessibility of all parts for repair, maintenance, and replacement.
8. Minimum noise level and vibration.
9. Adaptability to wide application in new, as well as in existing, home heating systems.

Effects on Residential Load Characteristics

Although the use of the heat pump for the heating of homes at present is far from a commercial and large volume reality, it possesses so much appeal to the popular mind on its cleanliness, convenience, and a year-round job of automatic air comfort in the home, that it cannot be ignored by either the utilities or manufacturers of equipment as to its future possibilities and probable effects on the load characteristics of the utility supplying the electric service for its operation. The potential magnitude of this load is great as evidenced by the fact that, if only 10 per cent of the residential customers of the system referred to in this paper were to be equipped with this device, under the performance levels now thought possible, there would be obtained an addition to that system's peak of about one-sixth of its entire 1947 peak load from all classes of service: residential, commercial, industrial, municipal, traction, and sales to other electric utilities. This increase in system peak is about equal to the peak load of the entire residential class of customers represented by a community of some 3,000,000 people. Obviously, a potential load of this magnitude deserves careful study as to its economic implications, especially since, in addition to its size, all indications are that its annual load factor and group coincidence factor[6] will be much different from those experienced by the present size and volume load of the residential class of customers.

There is no precise way to determine the average size of the house heating heat pump load which may be served in the future by any given utility system, because of the many variables involved in such a determination. At the beginning, and for many years to come, until substantial levels of saturation of this device are obtained, the average size of heat pumps may vary from year to year, depending upon the kind of homes in which they will be installed, the relative penetration of the various segments of the residential market, and the types of heat pumps used.

If past experience in the acquisition of the gas space heating load is any indication of the probable trends in the acquisition of the residential electric heat pump load, one may expect, at the start, the average size of heat pumps to be comparatively high, gradually decreasing with an increase in the saturation of this device. To give some indication of this probable average unit size of the heat pump load for saturations, equivalent to those now expected to be obtained for gas space heating in this territory, the assumption will be made that the heating requirements of an average home using a heat pump will approach the average size of the gas space heating installations, which experience indicates will approximate 250,000 cubic feet of 520 Btu manufactured gas per installation for a heating season having a normal temperature deficiency of 4,750 degree days. Based on these data, and an assumed gas heater efficiency of, say 75 per cent, the calculated heat input to the house for a 70 degree Fahrenheit differential will be close to 55,000 Btu per hour. But the heater capacity of such an average home, on the basis of actual experience with gas heating installations in this territory, should be close to 100,000 Btu per hour. The difference between the calculated heating requirements, and the actual heater capacity of an average installation is due to many factors which, among other things, include the provision for the desired quickness of heat recovery from a given low temperature level in the house, the effects of high-wind velocities on days of low outdoor temperature, which are not reflected by the above calculations, and the practical necessity for selecting heaters of a size next higher to the capacity indicated by calculations, because of the availability in practice of heating units only in standardized sizes.

It is possible that heat pump installations need not provide for such a wide margin between capacity and calculated maximum requirements, and that users of heat pumps must be taught to use this device differently from a conventional fuel-fired heating installation. Also, the economics of heat pump installations may preclude the use of such wide margins. But to assure adequate home heating service with heat pumps, practical necessity will require the provision of some definite margins. What the actual magnitude of this margin may be for an average installation is at this time only a matter of opinion; but for purposes of this paper it will be assumed that an average home with heat requirements, as calculated previously, of 55,000 Btu per hour will use a heat pump installation of 85,000 Btu per hour capacity at an outdoor temperature of zero degrees Fahrenheit. Its electrical input will be close to 7 kw with a coefficient of performance of $3^{1}/_{2}$ which, although not as high as desirable, appears to be at this time realistically attainable for the climatic conditions experienced in this territory. Assuming the annual coefficient of performance to be $3^{1}/_{2}$ also, such a heat pump on its "heating cycle" of operation would require about 8,200 kilowatt-hours for a normal heating season. For its "cooling cycle" of operation during a normal summer season it would require an additional amount of some 800 kilowatt-hours, based on results of tests made by the author in Philadelphia area on central system air conditioning installations in homes. The total electric energy consumption of such an average heat pump installation in this territory should thus be close to 9,000 kilowatt-hours for a normal year-round job of heating and cooling. The net additional amount of electric energy requirements, however, will be somewhat lower, because of displacement of existing electric equipment used in the home in connection with fuel-fired furnaces and summer ventilation. However, these effects will be neglected for purposes of this discussion.

For illustrative purposes, the 30-minute maximum demand of an average heat pump in this territory will be assumed at 7 kw. The corresponding diversified maximum 30-minute demand of this load on an average day of the coldest week in a year, approximating a daily mean temperature of 22 degrees Fahrenheit and an outdoor temperature at 7:00 a.m. of about 17 degrees Fahrenheit, will be around 4.9 kw per average installation, based on results of actual tests conducted by the author on residential gas space heating loads. Thus the annual diversified load factor of the heat pump load for its heating cycle of operation is assumed here to be substantially the same as that of the gas house heating load. In actual practice, however, it may be either higher or lower depending on the design of the unit, its relative efficiency of performance on cold days in comparison with the over-all record for the entire heating season, and whether a constant temperature is set on the house thermostat throughout the entire day, or if there is a higher setting during the daytime and at a lower one at night.

These factors, and others, will have a definite bearing upon the electric energy use during a heating season and upon the diversified maximum demands of the heat pump, which, in turn will influence the magnitude of its annual load factor.

Figure 5 shows illustrative winter period daily load curves of three types of average residential customers:

Curve A. A present-day type of ordinary-use customer having electric lighting, refrigeration, and small miscellaneous appliances.

Curve B. A present-day type of heavy-use customer having, in addition to the ordinary use, an electric range and a water heater.*

Curve C. An all-electric type customer, having, in addition to the heavy-use, a heat pump.

It will be noted from Figure 5 that on the average day of the coldest week of the winter period, the maximum diversified demand of the all-electric customer is estimated to be about 17 times that of the ordinary-use customer; and about three times that of the heavy-use type. Since the present saturation of electric ranges and water heaters in the Philadelphia area is relatively low, perhaps in the vicinity of 10 per cent for electric ranges and 5 per cent for electric water heaters, the size load of the all-electric customer of some 17 times that of the ordinary-use customer is more indicative of the magnitude of the problem faced by the utilities in meeting the requirements of this potential load by providing the necessary facilities in distribution lines, transformers, substations, transmission and generation than a comparison of it with the heavy-use customer. From Figure 5 it will be noted, too, that the peak load of the all-electric customer will occur in the morning, around 8 a.m., and that the load between 5 and 6 p.m. (the period of the present-day peak load of the residential class) will be about 65 per cent of the morning peak load, thus indicating that the heat pump load possesses diversity with respect to the present-day peak load of the residential class.

Figures 6 and 7 show respectively an

---

*All references to electric water heaters in this paper apply to single-element heaters which operate on a time-control basis, the elements being disconnected from electricity supply from 4 p.m. to 10:30 p.m.

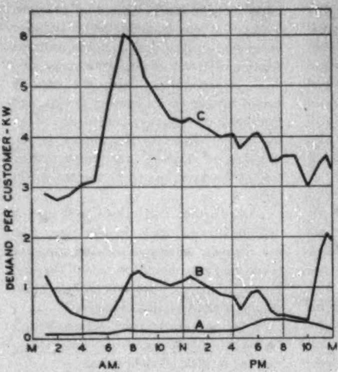

Figure 5 (left). Average weekday load curves for the coldest week of winter period for three groups of residential customers (Based on one-half hour integrated demands)

A—Ordinary-use (lighting, miscellaneous appliances and refrigeration)

B—Heavy-use (ordinary-use plus electric range and water heater)

C—All-electric (heavy-use plus heat pump)

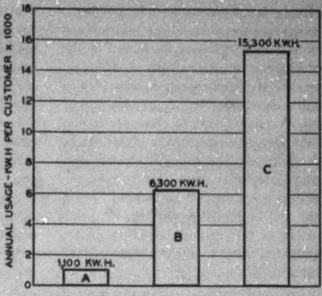

Figure 6 (right). Annual energy usage of three types of residential customers

illustrative comparison of the relative annual energy requirements of the three types of average residential customers, and the relative monthly distribution of this energy throughout the year. The annual energy requirements of the all-electric customer (bar C) are estimated to be about 15 times that of the ordinary-use customer (bar A), and about two and one-half times that of the heavy-use type (bar B). The monthly distribution of energy indicates that, while the winter months requirements for December, January and February of the all-electric customer (curve C) will be over 20 times the requirements of the ordinary-use customer (curve A), and from three to four times the requirements of the heavy-use type (curve B), the summer months' energy requirements of such a customer will be only ten times higher than those of the ordinary-use type, and only one-half higher than those of the heavy-use customer.

The principal data applying to the three types of average residential customers are summarized in Table II.

From the foregoing, it becomes evident that the annual load factor of an average all-electric customer with a heat pump will be lower than that of either the ordinary-use or the heavy-use residential customers, and that the coincidence factor of such a customer will be higher than that of both of these types. However, these comparisons alone are not fully indicative of the significance of the heat pump load because they fail to reflect the effects of the diversity which would exist between the peak load of an average all-electric customer having a heat pump and the peak load of the present-day residential class.

To illustrate this latter effect, Figure 8 is presented. It shows the progressive change in the annual load factors of the entire residential class load with an increase in the saturation of all-electric customers having heat pumps (curve X) and with an increase in the saturation of heat pumps for a given saturation of electric ranges and water heaters (curves Y and Z).

Among the many factors which enter into the appraisal of the economic significance of a given load supplied by an electric utility, the annual load factor is of major importance. It is a well-known fact that, with all other things equal, cost per kilowatt-hour of supplying electric service varies inversely with load factor in accordance with the laws of a hyperbola. The higher the load factor, the lower the unit cost per kilowatt-hour and conversely, the lower the load factor, the higher such unit cost becomes.

Curve X in Figure 8 shows the results for a residential class that starts out by having no electric ranges and water heaters, thus depicting the volume of the ordinary-use of the residential class load, which approaches the conditions now existing on the system referred to in this paper, and curves Y and Z show the results for a residential class that starts out by reflecting the present-day volume of the ordinary-use and stated electric range and water heater saturations. Curve Y illustrates the relationship for a 50 per cent electric range and 25 per cent electric water heater saturation, which may be considered to be within the practical range of accomplishment at some time in the future; and curve Z—for a 100 per cent saturation of these major appliances which can only be considered of theoretical significance depicting the possible (but not necessarily probable) upper limit in the saturation of these appliances. All three curves cover the range up to a 20 per cent heat pump saturation, which, from practical considerations, may not be reached for decades to come.

Curve X indicates that the addition of all-electric customers to an existing residential load of ordinary-use, at first improves the annual load factor of the residential class of this type. This improvement reaches a maximum at about an 8 per cent heat pump saturation and thereafter begins to recede reaching the same class load factor value at a heat pump saturation of 17 per cent as actually exists at 0 per cent. Beyond this point, however, a continued addition of this type of load results in a progressively diminish-

Table II. Electric Load Characteristics of Three Types of Average Residential Customers

	Type of Average Residential Customers Ordinary-Use A	 Heavy-Use B	 All-Electric C
Annual energy usage, kilowatt-hours	1,100	6,300	15,300
Annual diversified 30-minute integrated demand, kilowatts			
Winter average weekday maximum	0.35	2.0	6.0
Absolute maximum	0.41	2.1	7.0
Annual noncoincident 30-minute integrated maximum demand, kilowatts	1.0	5.0	12.0
Annual diversified load factor, per cent			
Based on winter average weekday maximum demand	35.9	36.0	29.1
Based on absolute maximum demand	30.6	34.2	25.0
Coincidence factor, per cent			
Based on winter average weekday maximum demand	35.0	40.0	50.0
Based on absolute maximum demand	41.0	42.0	58.3

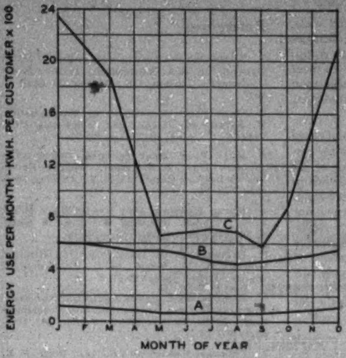

Figure 7. Monthly distribution of annual energy usage of three types of residential customers

A—Ordinary-use (lighting, miscellaneous appliances and refrigeration)

B—Heavy-use (ordinary-use plus electric range and water heater)

C—All-electric (heavy-use plus heat pump)

ing load factor of the class, approaching, at very high saturations, the value shown in Table II for the all-electric customer.

Curve Y indicates that the addition of heat pumps to a present-day residential load composed of ordinary-use and a 50 per cent electric range and a 25 per cent electric water heater saturation, improves the annual load factor of the residential class of this type within a rather small range of heat pump saturation. This improvement reaches a maximum at a heat pump saturation of about 2 per cent and thereafter begins to recede, reaching the same class load factor value at a heat pump saturation of around 4 per cent as actually exists at 0 per cent. Beyond this point a continued addition of heat pumps results in a progressively diminishing load factor of the class, but beyond an 8 per cent heat pump saturation, the annual load factor of this type of residential class is not much different from that of the residential class reflected by curve X for comparable heat pump saturations.

Curve Z indicates that the addition of heat pumps to a present-day residential load composed entirely of heavy-use customers (thus reflecting a 100 per cent electric range and water heater saturation) improves the annual load factor of the residential class of this type over a somewhat wider range of heat pump saturation. As indicated in the note on Figure 8, this improvement reaches a maximum at a heat pump saturation of about 25 per cent and, thereafter, begins to recede in a manner similar to that shown by curve X, and finally approaches at very high saturations the value shown in Table II for the all-electric customer.

The facts thus depicted in Figure 8 lead to the unavoidable conclusion that for electric utilities in the United States, geographically located in the latitude of the system referred to in this paper, the heat pump load does not offer possibilities of substantial improvement in the annual load factor of the residential class of service, within the probable saturation levels of this device which may be expected to be attained for some years to come. This fact, in turn, indicates that, with all other things equal, it would be impractical to justify a lower average rate per kilowatt-hour to the heat pump load than is obtained now from the addition of uncontrolled electric loads of other major usages in the home. As a matter of fact, under certain conditions, to cover all costs for the load factors of the residential class obtained with the heat pump, the average rate per kilowatt-hour applicable to this device may have to be even higher than is now available generally for uncontrolled usage of electric service in the home at the prices of the end blocks of residential rates. These prices now average over $0.017 per kilowatt-hour in the 16 largest cities of the United States, in the northern and middle temperature zones.

The inherent lack in ability of the heat pump by itself to improve the residential class annual load factor, at least insofar as these zones of the country are concerned, and its relatively large requirements for the supply of electric service, emphasizes the necessity for a proper engineering and design of the various component parts of the device to obtain maximum efficiency of performance, reliability of operation, and applicability in new and existing homes; and to minimize its first cost and all undesirable electrical features such as high-starting current, low-power factor, and high demand, which, otherwise, would have adverse economic effects upon the electric supply system and thus result in economic handicaps in the utilization of the electric service by this device.

It should be noted, however, that, for utilities located in territories similar to that referred to in this paper, the acquisition of the year-round heat pump load, with its inherently lower summer than winter electrical requirements, carries with it the ability to improve the economic significance of the residential summer air conditioning load which by itself in large quantities is not desirable, because of its low annual load factor. A proper implementation of the year-round heat pump load with additional summer air conditioning load for customers with

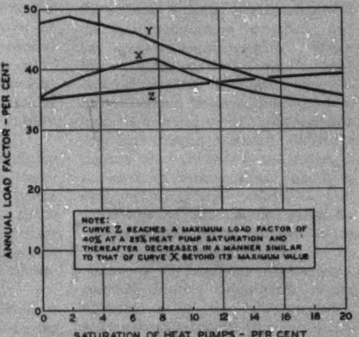

Figure 8. Relationships of trends in residential class annual load factors with increasing saturation of heat pumps

(Based on maximum diversified demands of average weekday for the coldest week of winter period)

X—Addition of all-electric customers with heat pumps to a residential class consisting of ordinary-use customers

Y—Addition of heat pumps to a residential class consisting of ordinary-use customers with a 50 per cent electric range and 25 per cent electric water heater saturation

Z—Addition of heat pumps to a residential class consisting of heavy-use customers (reflecting a 100 per cent electric range and electric water heater saturation) conventional heating systems, will tend to improve the over-all economic significance of the combined residential heating and cooling loads.

Conclusions

From the foregoing discussion it is possible to make the following observations:

1. The heat pump possesses the thermodynamic ability of removing the inherent economic handicaps present in electric resistance-type house heating. But to make it a commercial reality and within the reach of a large number of homes, it requires a substantial amount of additional research on the economical methods of utilizing available heat sources and on the engineering, design, and operation of compressor-motor assemblies, refrigerants, accessory equipment, and methods of heat distribution.

2. The electric load of an all-electric residential customer with a heat pump will be very large in comparison with the load of present-day average residential customers. The potential magnitude of this load and the difference in its load characteristics, from those of the present-day residential class, deserve careful study by electric utilities and manufacturers of power system equipment, to understand and be ready to meet the economic implications of this load upon the distribution, substation, transmission, and production systems.

3. By and large, within the practical range of probable heat pump saturations for residential house heating in the order of 20 per cent, the electric load of this device in the northern and middle temperature zones of this country will neither improve nor affect adversely (to any large extent) the annual load factor of the residential class of service. But for very large saturations of the device, substantial reductions in the annual load factor of this class of service can be expected, because of the inherently low annual load factor of the heat pump load.

4. To attain the optimum in the over-all competitive ability of the heat pump in regard to other methods of house heating, all efforts must be directed toward obtaining for this device the highest efficiency of performance, the highest reliability of operation, the lowest first cost, and the minimum of undesirable electrical features such as those of high-starting currents, low power factors, and high demands.

References

1. Losses in the Cycle of a Heat Pump Using a Ground Coil, **R. A. Budenholzer.** Midwest Power Conference, Chicago, Ill., March 31–April 2, 1947.

2. Heat Pump Coefficient of Performance. **W. Parkerson.** *Heating and Ventilating* (New York, N. Y.), May, 1947, pages 63–7.

3. Heat Pump Heat Sources, Earth as a Source of Heat, **E. N. Kemler.** *Bulletin*, Edison Electric Institute (New York, N. Y.), October, 1946, pages 339–46.

4. House Heating with Earth Heat Pump, **A. C. Crandall.** *Electrical World* (New York, N. Y.), November 9, 1946, pages 94–5.

5. Possibilities of Heat Pump for Heating Homes, **R. U. Berry.** AIEE Transactions, volume 63, 1944, pages 619–22.

6. Coincidence-Factor Relationships of Electric-Service-Load Characteristics, **Constantine Bary.** AIEE Transactions, volume 64, 1945, pages 623–28.

7. Progress Report on the Heat Pump, **E. R. Ambrose, E. N. Kemler, M. M. Smith, W. L. Holladay.** *Heating, Piping and Air Conditioning* (New York, N. Y.), December, 1946, pages 68–82.

8. The Heat Pump, **Report of the Indoor Climate Committee.** *Publication number 6*, Edison Electric Institute (New York, N. Y.), July 1947.

9. Heat Pumps, **Philip Sporn, E. R. Ambrose, Theodore Baumeister. John Wiley and Sons,** New York, N. Y., 1947.

No Discussion

The Temperature Rise of Buried Cables and Pipes

J. H. NEHER
MEMBER AIEE

IN THE calculation of the temperatures attained by underground cable systems, the first practical calculation of that portion of the temperature rise occurring in the earth was presented by Doctor A. E. Kennelly in 1893.[1] The formula which he developed expresses this temperature rise as a function of the heat loss of the cable system, its geometry, and the thermal resistivity of the earth.

As factual data bearing on this aspect of the problem have been accumulated over the intervening years, a disagreement has been observed between values of earth thermal resistivity measured in the laboratory and the values of thermal resistivity required by the Kennelly formula in order to account for the temperature rises actually observed under field conditions. Modifications of the formula have been proposed as a result, and alternate procedures have been adopted. At the present time, the situation in this respect is confused and badly in need of clarification.

Apparently the objections to the use of Kennelly's method are caused by misunderstanding the relationships involved. As a starting point in obtaining a generally acceptable method of calculating the temperature rise in the earth, therefore, it seems desirable to review the conditions under which the Kennelly formula applies. It then will be practical to consider the effects of deviations from these conditions. As this investigation progresses, it will explain why values observed heretofore in the field and in the laboratory are in apparent disagreement, and also will clear up certain misconceptions as to the direction of heat flow from the cable system.

The Problem and Its Solution

The basic problem with which we have to deal consists of the determination of the temperature which will be attained by a cable system dissipating heat to the surrounding earth, which may have varying initial temperatures at different points due to the influence of other heat fields which are present. The potential complications of such a situation are obvious. In order to effect a practical solution, it is necessary to idealize it by simplifying the conditions considerably. The solution so obtained then must be checked by tests to establish the validity of the assumed simplifications.

The geometry is idealized by assuming the radiator to be cylindrical in shape. This is obviously valid for a cable buried directly in the earth, or for a pipe. In the case of a rectangular duct system, however, it requires the conversion of the basic dimensions to the radii of equivalent cylindrical surfaces.

Since we must deal with superimposed heat fields, it is necessary to consider the thermal resistivity of the medium as being unaffected by the temperatures which may be attained at various points in the general field. We further will idealize the conditions by assuming the thermal resistivity to be a constant throughout the field. Under this condition the superposition theorem becomes applicable; that is, the temperature change existing at any point in the general heat field becomes equal to the sum of the temperature changes produced at that point by each of the respective heat fields operating as if by itself. Thus, the temperature rise of any point in the field of a thermal radiator buried in the earth (including points on the surface of the radiator), above the initial or ambient temperature of that point, may be determined by considering only the temperature rise which would accompany the heat flow from the radiator into a medium assumed to have been initially at uniform ambient temperature throughout.

It is most important to recognize the fact that the resultant heat flow considered in this portion of the solution cannot represent the actual heat flow in the general field, which is a combination of effects caused by this and other heat sources. This feature will be discussed later in considerable detail.

For the purposes of obtaining a solution, therefore, the problem may be reduced to the determination of the temperature rise of a cylindrical radiator in the earth, as if the earth were initially at the same temperature throughout and has constant thermal resistivity. If the thermal radiator were located at the center of the earth, the ultimate temperature rise would be great, since the heat from the radiator would flow through a very large thermal resistance. With the radiator relatively close to the surface of the earth, as in the practical case, however, a relatively large portion of the heat will flow to the surface of the earth in the vicinity of the radiator, provided that it can escape to the atmosphere. The remainder of the heat flows into the earth, gradually heating it up until, in the ultimate, all of the heat eventually reaches the atmosphere.

The coefficient of heat transfer at the surface of the earth also is a factor. The conventional treatment is to assume that heat can pass freely to the atmosphere; because of the motion of air over the surface of the earth, there is no appreciable

---

Paper 49-2, recommended by the AIEE insulated conductors committee and approved by the AIEE technical program committee for presentation at the AIEE winter general meeting, New York, N. Y., January 31–February 4, 1949. Manuscript submitted November 8, 1948; made available for printing November 12, 1948.

J. H. Neher is senior engineer with the Philadelphia Electric Company, Philadelphia, Pa.

The author wishes to acknowledge the very helpful contributions made by W. O. Smith, United States Geological Survey; F. H. Buller, General Electric Company; W. T. Brown, F. H. Housel and A. S. Mickley, all of the Philadelphia Electric Company; and to L. R. Ingersoll of the University of Wisconsin.

rise of temperature in this transfer. Conventionally, therefore, the surface of the earth is treated as if it were an isothermal plane. The refinement of accounting for the effect of the surface resistivity of the earth can be made later, without much difficulty.

We also must consider the time during which the heat flow from the cable system has been in effect, thus distinguishing between ultimate or steady-state, and transient conditions. In cable calculations it is customary to consider the steady-state rise, and we will solve the problem on this basis, indicating later the effect of time durations less than the theoretically infinite time implied.

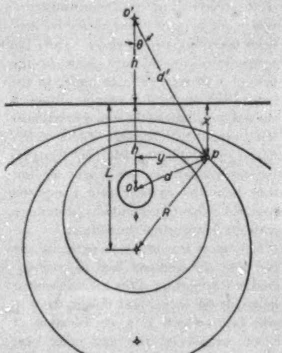

Figure 1. The development, in cross-section, of the isothermal surfaces surrounding a cylindrical thermal radiator in a uniform medium bounded by a parallel isothermal plane

The problem as now set up then is solved conveniently, as indicated in Figure 1, by the method of images given in detail in Appendix I. The resultant equation for temperature rise at any point P, in terms of the distances to the thermal center of the radiator d and to its image d', the heat flow Q_c, and the thermal resistivity ρ is

$$\Delta T_p = Q_c \frac{\rho}{2\pi} \log_e \frac{d'}{d} \text{ degrees centigrade} \quad (1)$$

It readily may be shown that the locus of all points having the same value of ΔT is a cylinder which is not concentric with the thermal center of the radiator, although, for relatively small diameters with respect to the buried depth, the eccentricity is negligible. Equation 1 may be rewritten in terms of the radius of any isothermal cylinder R, and the depth of its center L below the surface of the earth as

$$\Delta T_1 = Q_c \frac{\pi}{2\pi} \log_e \frac{L+\sqrt{L^2-R^2}}{R}$$

degrees centigrade (2)

This equation applies not only to the isothermals in the field of the radiator but to the surface of the radiator itself, if the radiator is, or may be considered to be, cylindrical in form. In this application, it has come to be known as the long form of the Kennelly formula.[1] For values of R small in comparison with D, both equations 1 and 2 reduce to the familiar form commonly known as the short form of the Kennelly formula

$$\Delta T_s = Q_c \frac{\rho}{2\pi} \log_e \frac{2L}{r} \text{ degrees centigrade} \quad (3)$$

If the thermal radiator is spherical in shape, the comparable form of equation 1 is

$$\Delta T_p = Q_c \frac{\rho}{4\pi} \left(\frac{1}{d} - \frac{1}{d'} \right) \text{ degrees centigrade} \quad (4)$$

and the resulting isothermals are distorted ellipsoids of revolution. (See Appendix I.)

Strictly speaking, the surface of the earth above a thermal radiator is not maintained as an isothermal plane, as is well evidenced by the fact that snow will melt directly above a buried steam main. This modification has been approached by Poritsky,[2] by assuming a constant and uniform surface resistivity β at the earth's surface. The resultant solution, as given in Appendix II, may be expressed as an additional term to be included in equation 1.

For practical purposes this additional term may be simplified to the form given below

$$\Delta T_p = \frac{Q_c}{2\pi} \left(\rho \log_e \frac{d'}{d} + 1.90 \frac{\beta \cos \theta}{d'} \right)$$

degrees centigrade (1a)

in which β is expressed in degree centigrade square centimeters per watt, d' in centimeters, and θ is the angle which d' makes with the vertical (See Figure 1).

In general, the effect of the additional term upon the temperature rise at the surface of the radiator is relatively small, and it usually may be neglected. Considering ρ to equal 60 degree centigrade centimeter per watt and β to equal 2,000 degree centigrade square centimeters per watt, which is felt to be conservatively high, and an 8-inch diameter radiator buried to a depth of 40 inches, its effect constitutes 9 per cent of the temperature rise at the surface of the radiator.

The effect at other points in the field may be more pronounced. At the surface of the earth directly above the radiator in the above case, the temperature rise is 16 per cent of the temperature rise at the radiator. At a distance 40 inches away on the surface of the earth, the temperature rise is 9.5 per cent of that at the surface of the radiator.

When equation 1a is used, the resulting isothermal surfaces, of course, will not be cylindrical.

Heat Flow from the Radiator

As indicated previously, the actual course of heat flow from the radiator is dependent upon all of the heat fields present. One of the objections most frequently raised to the use of the Kennelly formula arises from the mistaken notion that the formula infers that all of the heat from the radiator is always flowing to the surface of the earth.

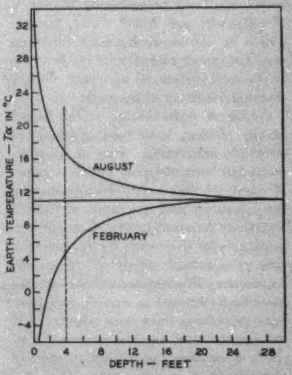

Figure 2. Typical vertical temperature gradients in the earth at extreme seasons of the year

To illustrate this point, let us consider the normal seasonal heat field present in the earth. This heat field results from a combination of the heat always flowing outward from the central core of the earth as it cools, and the heat received by solar radiation. In the summertime, heat is received from the sun, and as a result, the temperatures of the earth decrease with depth. In the wintertime the earth gives up heat to the atmosphere, and the temperature gradient is reversed. It will be found, by observation, that the average temperature over the year at any depth is quite constant, and that the difference between maximum and minimum temperatures decreases with the depth. Figure 2 shows the results of measurements made over a season in Philadelphia. Almost never is the earth at the same temperature at all depths, although this condition is approached roughly at midseasons.

Let us now assume that we have a cylindrical radiator buried in the earth to a depth equal to 10 times its radius, and that Q_c and ρ in equation 3 are such as to give a temperature-rise of 40 degrees centigrade at the radiator. By the relationships indicated in Appendix I, a family of eccentric circles, each representing a given value of temperature rise, may be determined and plotted on rectangular co-ordinates.

If at midseasons the earth were at a uniform temperature of 11 degree centigrade, each of these circles would represent an isothermal, the temperature of which is equal to the value of its temperature rise plus the 11 degrees centigrade. The resulting isothermals are indicated in Figure 3.

The lines of heat flow must pass from a higher isothermal to a lower isothermal in such a manner that they are always normal to the isothermals. Since, in this case, the isothermals are circles, the lines of heat flow are also circles, as shown in the dotted section of Figure 3, and all heat flow is ultimately toward the surface.

If we consider the earth's situation in February, the normal gradients are horizontal planes (lines in section), as indicated by Figure 2, and as shown at the extreme right-hand edge of Figure 4. By superimposing these horizontal ambient temperature lines upon our plot of temperature rises, we can determine, by addition, the resultant temperatures at the points of coincidence. The isothermals then can be drawn by the same procedure as is used in drawing topographical contour maps. Practically, it is more advantageous to solve directly for the rectangular co-ordinates of any point on a chosen isothermal. For a particular isothermal T_t and at a given depth (x co-ordinate) at which the ambient temperature is T_a, the value of temperature rise $\Delta T = T_t - T_a$. The horizontal position (y co-ordinate) of the point then is interpolated from the plot of temperature rises for the given depth.

Figure 4 shows the resulting isothermals determined by this procedure for February. The distortion of the isothermals from true circles is apparent, but it will be noted that the flow of heat is still upwards towards the surface.

Finally, if we go through the same process for the normal gradients existing in August, we obtain the interesting configuration shown in Figure 5. Here it will be noted that none of the heat liberated by the radiator goes directly toward the surface of the earth during this season, since the heat always flows in the direction from the higher toward lower isothermals.

It should be realized that Figures 3 to 5 are of academic interest only, and in no way contribute to the solution of the problem at hand. They have been included merely to indicate how the isothermals, which are actually present during stated conditions and which control the direction of heat flow from the radiator, may be synthesized by application of the principle of superposition.

Effect of the Time Factor on the Kennelly Formula

The Kennelly formula represents ultimate or steady-state conditions, which will be achieved strictly only after an infinite time, since the earth has thermal capacitance as well as thermal resistivity. In practical cable calculations, it is customary to reduce the cyclic heat flow from the duct system to an equivalent constant flow based on the average daily power loss. This equivalent constant heat flow is assumed to continue indefinitely, and we therefore are interested in the ultimate temperature rise as given by the Kennelly formula. In any attempt to back-calculate the thermal resistivity of the earth, however, by the application of the Kennelly formula to field tests which of necessity cannot be continued indefinitely, it is necessary to consider the attainment factor which represents the per cent of ultimate ΔT which will have been attained in the elapsed time t.

The attainment factors at the surfaces of cylindrical and spherical radiators are developed in Appendix III, and are plotted in Figure 7 against the dimensionless quantity $t\ \alpha/r^2$, in which α is the thermal diffusivity of the earth which is in turn equal to the reciprocal of the product of the thermal resistivity and the thermal capacitance.

Typical values for α, measured in Philadelphia, range from 23 to 42 square centimeters per hour. Thus, for an 8-inch diameter radiator buried 40 inches, it will be seen that, after 400 hours with $\alpha = 25$, the attainment factor is 0.85. In this connection it is well to note that a plot of ΔT versus t on rectangular co-ordinates is quite misleading, for if the curve is plotted to only 400 hours, it will appear that the ultimate substantially has been reached, whereas actually 15 per cent remains to be attained.

It should be noted that during the transient period, the loci of points having the same temperature rise are not circles, although the inner curves approximate this condition. By means of the formulas

Figure 3. Typical isothermals and lines of heat flow at midseasons

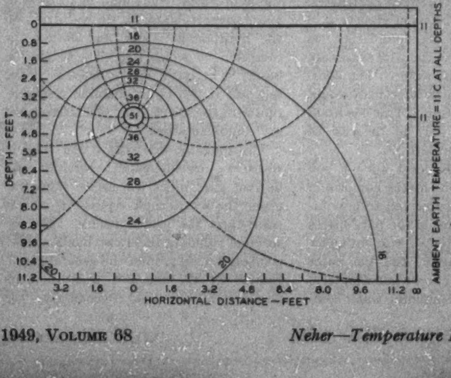

Figure 4. Typical isothermals and lines of heat flow at winter extreme

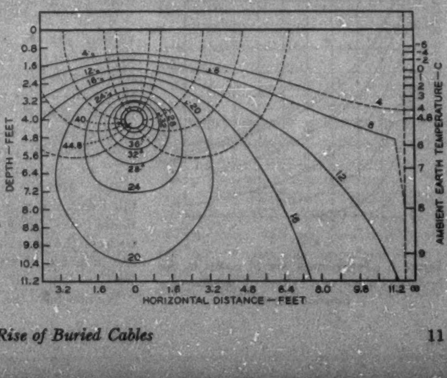

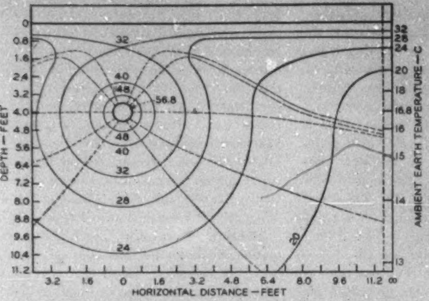

Figure 5. Typical isothermals and lines of heat flow at summer extreme

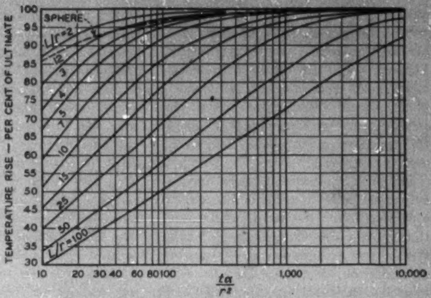

Figure 7. Attainment factors for cylindrical and spherical radiators

given in Appendix III, these loci may be plotted, and the isothermals, at any time after the inception of heat flow from the radiator and for any seasonal heat field condition, may be determined in the manner previously described if so desired.

Figure 6 shows the relative temperature rises of points in the horizontal plane through the center of a cylindrical radiator buried to a depth 10 times its radius, in terms of the ultimate temperature rise at the surface and for various values of $t\alpha/r^2$. From this it will be seen that, during the transient period at a given time, the relative temperature rise of a given point in terms of the corresponding rise at the surface of the radiator is less than that which will obtain after infinite time. In other words, the horizontal temperature gradient will be steeper than indicated by equation 1. This fact often has been observed during tests and has been interpreted incorrectly as a disagreement with the Kennelly formula. Actually, it is merely an indication that, at the time of the test observations, the heat field of the radiator was still in the transient period during which the Kennelly equation does not apply.

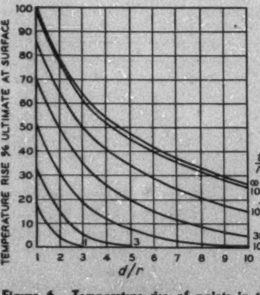

Figure 6. Temperature rise of points in the horizontal plane of a cylindrical radiator as a function of time

Thermal Resistivity of Soil and Moisture Migration

Thermal resistivity as a property of various soils in which the cable system may be located is a part of the science of soil mechanics, a subject with which cable engineers in general are not very familiar. While it is manifestly impossible to cover this extensive field in this paper, it does seem desirable to state briefly certain general principles and terminology which have important bearings on the problem at hand.

The thermal resistivity or conductivity of a given soil depends essentially on the type of soil, its structural arrangement, and its moisture content. Soil consists of discrete particles of irregular shapes and various sizes.[8] In the natural state, colloids are present which coat the sand and silt particles and collect them into aggregates. The pore spaces between the particles within the aggregates are quite different in size and must be distinguished from the pore spaces between aggregates.

Water is held in this soil structure in various degrees of freedom. Let us suppose first that all of the pore spaces are filled completely with water. The addition of any further water effectively would put the soil in suspension. This condition is of interest to us only in the case of cables located in river bottoms.

If we now suppose that such a soil sample, with the pore spaces completely filled with water, is subjected to gravitational forces, the water in the pore spaces between the aggregates will run out under the influence of gravity, and the water thus lost is termed "gravitational water."

We now have the remaining water completely filling the pore spaces within the aggregates, where it is held by capillary attraction. The amount of water present, expressed as a percentage of the dry weight of the soil sample is termed the "moisture equivalent" or "field capacity."

Proceeding further, let us assume that gravitational force is effectively increased (by a centrifuge) on our soil sample, so that the moisture is driven out of the capillary spaces within the aggregates, the water thus lost being termed "capillary water." This process will not continue until all of the water is withdrawn because some of the water is held very strongly as a thin film on the soil grains and on the colloid particles. The water thus held is the "hydroscopic water," and its amount on the basis of the dry weight is termed the "hydroscopic equivalent."

A point in the moisture scale slightly above the hydroscopic equivalent, termed the "wilt point," is of particular interest to agriculturists because plants are incapable of extracting moisture from the soil if the moisture present is less than this value.

If we now place our sample reduced to the hydroscopic equivalent in an oven at 105 degrees centigrade, we will drive off the hydroscopic water and obtain the condition on which the "dry weight" is based. There still will be moisture in the soil, but it will be in chemical combination with the soil elements; it is identified as "combined water."

The moisture content of the soils in which we are interested, therefore, will be that part which lies in the range between the hydroscopic equivalent or wilt point, and the field capacity. The respective values of these two limits are dependent not only upon the general classification of the soil but also upon its porosity in the field. Similarly, the

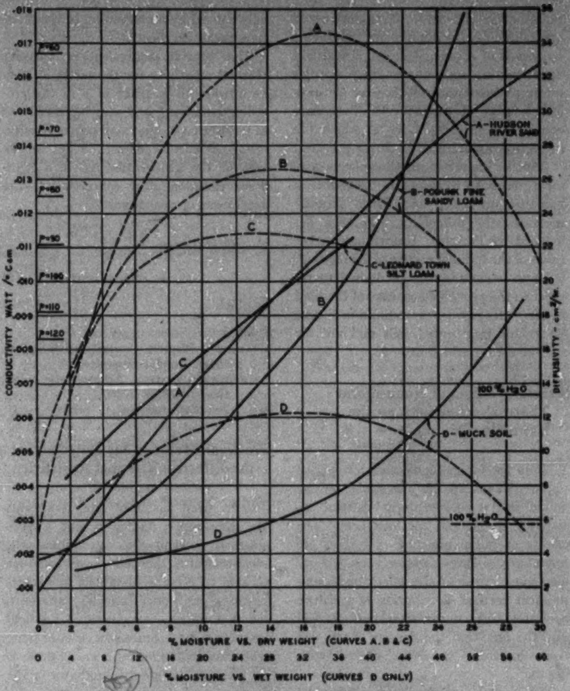

Figure 8. Values of thermal conductivity (solid lines), and diffusivity (dashed lines) of certain fragmented soils at various moisture contents, as given by Patten

thermal resistivity of the soil will depend upon these factors and the amount of capillary water present. It should be evident, therefore, that correct determination of the thermal resistivity indicative of field conditions must involve tests on an undisturbed sample extracted from the field.

This fundamental fact has been disregarded in most laboratory determinations on samples taken from actual cable locations intended to establish the proper value of thermal resistivity for use in the Kennelly formula.

W. O. Smith has investigated the relationship between the thermal resistivity of samples in the natural state and after fragmentation, and his published results on dry soils indicate that the thermal conductivity is higher in the natural state.[4,6] Similar investigations on moist soils have not been published yet, but the differences observed are in the same direction.

Of course, the soil in the vicinity of a new cable installation cannot be considered strictly as virgin soil, but after a period of time, if undisturbed, it will approach this condition, and the above generalization holds: that the thermal resistivities obtained in the laboratory, after the soil has been dug up and then packed into the measuring device, will be higher than those actually pertaining in the field.

There is another effect of major importance which must be considered. Smith[6,7] and others have observed that when moist soils are subjected to a thermal gradient, some of the moisture will move in the direction of heat flow. The amount of such moisture migration is a function of the thermal gradient, and of the moisture content of the sample. This effect is negligible both at the wilt point and at field capacity. For intermediate moisture contents, moisture migration will take place, reaching a maximum at an initial moisture content which has been referred to as the "thermal critical moisture-content."[7]

In our case, this phenomenon will result in a nonuniform thermal resistivity throughout the heat field of the radiator. The increase of the thermal resistivity, above the inherent value for the given conditions of soil and initial moisture content, is progressively less as the distance from the center of the radiator increases, and, practically, is of significance only within relatively short distances from the radiator. This corresponds with the observed higher values of thermal resistivity found near the surface of a sphere, both by the British[11] and those obtained by us in measuring the temperature rise of the earth at points close to the surface of spherical heat radiators.

To solve the problem rigorously from a mathematical standpoint, it is necessary to determine an expression for the variation of thermal resistivity as a function of temperature gradient and initial moisture content, and to introduce this relationship into the basic differential equation from which equations 1, 2, and 3 are derived. (See Appendix I.) This procedure is outlined in Appendix IV, where it will be seen that the resulting solution for the temperature rise at the surface of the radiator is similar to equation 2, with two additional terms which are functions of known parameters, and a moisture migration factor K_m. At the present time, K_m cannot be evaluated too accurately because of the lack of good experimental data. Using the best data available, however, for an 8-inch cylinder dissipating 38 watts per foot and buried to a depth of 40 inches in a soil of 60 degree centigrade centimeters per watt initially, the effect of maximum moisture migration is to increase the temperature rise at the surface of the cylinder by only 5 per cent, although the thermal resistivity at the surface has been increased by 21 per cent. For a radiator three times as large under the same conditions, the temperature rise at the surface is increased only 2.5 per cent with maximum moisture migration, and the thermal resistivity at the surface, by 6 per cent.

It will be apparent that the inherent moisture migration, occurring during laboratory thermal resistivity tests on samples of moist soils, will result in the indication of thermal resistivities higher than those truly representative of the initial moisture content. The magnitude of this discrepancy will vary with the type of equipment and test procedure used, but in most cases it is appreciable in contrast to the relatively small effect cited above for the case of typical cylindrical radiators in the field. Shanklin[8] noted great difficulty in obtaining measurements by means of a concentric cylindrical test apparatus on soils at certain particular moisture contents, which may be presumed to be the thermal critical moisture contents mentioned above at which the moisture migration effect is the greatest.

A rather interesting method of measurement, designed to eliminate the effects of moisture migration and which actually measures the diffusivity, has been developed by Patten.[9] Unfortunately, because of the indirect nature of the method, it leaves something to be desired in respect to the probable accuracy of the final results. His results, reproduced in Figure 8, are for fragmented soils and not for soils in the natural state.

Practical Effect of Nonuniform Thermal Resistivity on the Kennelly Formula

From the foregoing discussion it will be apparent that, in the practical case, we would not expect uniform thermal resistivity throughout the heat field. The effects of radial moisture migration are apparently of minor importance, but we also must consider the effect of a nonuniform vertical distribution of moisture as water sinks down after rainfall, and also the fact that the density of the soil itself increases in some degree with depth.

The solution of the basic differential equation with the thermal resistivity decreasing in some manner with depth presents a mathematical problem of considerable complexity. Nevertheless, attempts are being made currently to effect such a solution. At the present time, we probably are justified in the assumption that the Kennelly formula may be applied involving an over-all equivalent thermal resistivity which is momentarily constant but which, of course, will vary in some degrees seasonally.

It should be noted that, in all of the modifications to the Kennelly formula or alternate procedures of calculation proposed, the assumption of a constant thermal resistivity in the earth has been retained.

While it would be extremely difficult to solve each particular problem otherwise, it does seem desirable to complete the previously mentioned mathematical study, and to conduct a series of carefully controlled and co-ordinated tests to throw further light on this matter, particularly in respect to the limits at which the so-called "runaway" condition commences, and which is undoubtedly caused by an extension of the moisture migration effect.

This over-all equivalent or effective thermal resistivity for the earth, ρ', may be introduced in place of ρ in the preceding equations, and may be considered as including the effects of surface resistivity at the earth's surface. Thus, we obtain for the temperature rise of a cylindrical radiator, after converting to the usual units of measurement

$$T = 0.0120\, Q\rho' \log_{10} \frac{L+\sqrt{L^2-R^2}}{R} \quad \text{degrees centigrade} \qquad (5)$$

in which

Q = heat flow, in watts per foot
ρ' = earth's effective thermal resistivity, in thermal ohm centimeters
L = depth of the center of the radiator below the surface, in inches
R = radius of the radiator, in inches

Practical Methods for Determining the Effective Thermal Resistivity

From what has been said, it appears that laboratory testing is not a very practical method for determining the effective earth thermal resistivities applicable to cable installations in various locations and under seasonal variations, and that direct observations in the field are preferable. Since the use of long cylindrical radiators on a grand scale is not feasible, the spherical radiator or the short cylindrical radiator appears to offer the best compromise.

These test radiators, the equations for which are developed in Appendixes I and III, have the advantage of requiring a minimum amount of trench digging, and have a relatively high attainment factor for relatively short times, see Figure 8. The British have employed such test radiators,[11] and in this country the Philadelphia Electric Company, The Consolidated Edison Company, and The Detroit Edison Company[12] are employing them. Such installations should include the measurements of temperatures of the earth at various short radial distances from the radiator, in order that the moisture migration effect may be studied at the same time.

While the theory presented would predicate slightly different effective thermal resistivities for various values of heat flow, it would appear, in the light of experience, that sufficiently close approximations to the values applicable to long cylindrical radiators will be obtained if the test radiator is operated at the same temperature rise as that expected of the long cylindrical radiator.

Correction for the effect of the attainment factor on the field values obtained for both spheres and long cylinders readily is made by plotting the observed temperature rise at the surface of the radiator against time (with constant heat flow) on log–log paper. The comparable curve from Figure 8 is plotted on a similar sheet. The curve sheets are then superimposed, and the upper portions of the curves are brought into the best alignment, keeping the axes of the two sheets parallel. When so aligned, the 100 per cent attainment factor will fall on the ultimate temperature rise; also, the relationship between t and $t\alpha/r^2$ is established. From this, the effective diffusivity may be determined.

Conclusions

1. The Kennelly formula properly may be used to calculate the ultimate temperature rise of a horizontal cylindrical thermal radiator buried in the earth, with sufficient accuracy for cable-system temperature calculations.

2. The effective thermal resistivity of the earth, which is an inherent part of the formula, must be determined properly for the particular field conditions pertaining.

3. Most laboratory determinations of the thermal resistivity of soils commonly cited, do not represent conditions as faced in practical installations. Corresponding determinations made in the field, by back calculations by the Kennelly formula, will be too low unless correction is made for the time factor involved.

4. The spherical test radiator offers a very practical method for determining the effective thermal resistivity of the soil in which a cable system is to operate.

Symbols

α = thermal diffusivity, in square centimeters per hour
β = thermal surface resistivity, in degree centigrade square centimeters per watt
C_f = field capacity of the soil
d = distance from a point P in the heat field to the thermal center of the radiator, O, in centimeters
d' = distance from a point P in the heat field to the thermal center of the image, O', in centimeters
F = the correction factor for surface resistivity
G_c, G_s = geometric factors which are functions of t, α, and d
h = distance from the thermal center of the radiator or its image to the isothermal plane (surface of the earth)
K_m = moisture migration factor, in watts per degree centigrade squared
κ = thermal conductivity, in watts per degree centigrade centimeter
l = length of a short cylindrical radiator
l' = axial distance of a point P on the surface of a short cylindrical radiator from its center

L = distance from the physical center of the radiator to the surface of the earth
M = moisture content of the soil
ΔM = change in moisture content of the soil
Q_c = heat loss from a long cylindrical radiator, in watts per centimeter
Q_s = heat loss from a spherical radiator, in watts
Q_{sc} = heat loss from a short cylindrical radiator, in watts
r = radius of the radiator, in centimeters
R = radius of an isothermal surface for a cylindrical radiator, and also the radius of a cylindrical radiator where $D > h$
ρ = thermal resistivity, in degree centigrade centimeters per watt
ρ_i = initial thermal resistivity of the soil
ρ_p = thermal resistivity of the soil at a point P in the heat field
ρ' = effective over-all thermal resistivity
T = temperature, degrees centigrade
ΔT = temperature rise above ambient temperature
t = time, in hours
θ = the angle which d' makes with the vertical (See Figure 1)
x, y = rectangular co-ordinates of a point P in the heat field

Appendix I. Temperature Rise of Cylindrical and Spherical Thermal Radiators in a Medium of Constant Thermal Resistivity Bounded by an Isothermal Plane

Assume that a long, straight filament continuously radiating Q_c watts per unit length, is located in an infinite medium of constant thermal resistivity ρ. This location is shown in cross-section in Figure 1 at the point O. The differential equation governing this heat flow as a function of the temperature T at any radius r is

$$\frac{dT}{dr}+\frac{Q_c\rho}{2\pi r}=0 \qquad (6)$$

The temperature rise at any point such as P at a distance d from O is obtained by integrating equation 6 between the limits $r=\infty$ and $r=d$. Thus

$$\Delta T_p=\int_\infty^d -\frac{Q_c}{2\pi r}\rho\, dr \text{ degrees centigrade} \qquad (7)$$

Let us now assume that a similar parallel filament located at point O' continuously is absorbing $-Q_c$ watts per unit length. If the distance of P from O' is d', the temperature rise resulting at P may be found in a similar manner.

If these two heat flows operate simultaneously, by the superposition theorem, the resulting temperature rise is given by

$$\Delta T_p=\int_\infty^d -\frac{Q_c}{2\pi r}\rho dr+\int_\infty^{d'}\frac{Q_c}{2\pi r}\times \rho dr = Q_c\frac{\rho}{2\pi}\log_e\frac{d'}{d} \text{ degrees centigrade} \qquad (1)$$

If, in equation 1, the ratio d'/d be represented by k, and the position of the point P be represented in rectangular co-ordinates, as indicated in Figure 1, then

$$d'^2=(h+x)^2+y^2;\quad d^2=(h-x)^2+y^2 \qquad (8)$$

and, by introducing k, we obtain

$$\left\{x-h\left(\frac{k^2+1}{k^2-1}\right)\right\}^2+y^2=4h^2\left(\frac{k}{k^2-1}\right)^2 \qquad (9)$$

This will be recognized as the equation of a circle of radius

$$R=2h\left(\frac{k}{k^2-1}\right) \qquad (10)$$

whose center lies at a distance below the origin

$$L=h\left(\frac{k^2+1}{k^2-1}\right) \qquad (11)$$

$$L^2-R^2=h^2 \qquad (12)$$

Thus, for various constant values of ΔT_p in equation 1, the locus of point P is a family of eccentric cylinders (circles in section in Figure 1) about the point O if ΔT_p is plus, and about O' if ΔT_p is minus. These isothermal cylinders increase in diameter as the value of $\log d'/d$ (k in equation 10) decreases, and for $\log d'/d=0$, they merge into a plane bisecting and perpendicular to the line O-O'. For all positions of P on this plane, the value of ΔT_p is zero.

If by some means we are able to maintain this plane as an isothermal at zero temperature-rise, it is evident that equation 1 represents the temperature rise of any position of P below the plane, resulting from the heat liberated at point O and regardless of what happens above the plane.

By solving equations 10 and 11 for k in terms of L/R and substituting in equation 1, the following expression is obtained in terms of the radius R of any isothermal cylinder and the depth L of its axis below the isothermal plane

$$\Delta T=Q_c\frac{\rho}{2\pi}\log_e\frac{L+\sqrt{L^2-R^2}}{R} \text{ degrees centigrade} \qquad (2)$$

In the case of a spherical radiator, the radiator and sink are point sources radiating and absorbing Q_s and $-Q_s$ watts, respectively.

$$\frac{dT}{dr}+\frac{Q_s}{4\pi r^2}\rho=0 \qquad (13)$$

and

$$\Delta T_p=\int_{d'}^d -\frac{Q_s}{4\pi r^2}\rho dr=Q_s\frac{\rho}{4\pi}\left(\frac{1}{d}-\frac{1}{d'}\right) \text{ degrees centigrade} \qquad (4)$$

The isothermal surfaces resulting from equation 4 are distorted ellipsoids of revolution merging into a median plane, as in the case of equation 1. For relatively small values of d in comparison to d', the isothermal surface is, for practical purposes, spherical in form and concentric with point O. Thus, equation 4 may be used in determining the temperature rise of a small spherical radiator.

Short cylindrical radiators sometimes are employed as an alternate to spherical test radiators. By considering the heat flow per unit length to be distributed along the axis of the radiator, we can, by integrating a modification of equation 4, determine the temperature rise resulting at any point in the heat field, which may be effectively a point on the surface of the radiator.

Let L be the depth to the center of such a radiator of length l and radius r, and let l' represent the axial distance of a point P on the surface of the radiator from the center and x the axial distance from P of the unit heat source. Thus, from the first term of equation 4, which represents the source portion, we may write by application of the superposition principle

$$\Delta T_p=\int_0^{\frac{l}{2}+l'}\frac{Q_{sc}\rho}{4\pi l}\frac{dx}{\sqrt{x^2+r^2}}+\int_0^{\frac{l}{2}-l'}\frac{Q_{sc}\rho}{4\pi l}\frac{dx}{\sqrt{x^2+r^2}} \text{ degrees centigrade} \qquad (14)$$

The effect of the sink may be developed in similar manner, but, from a practical standpoint, the second term of equation 4 may be employed with negligible error.

It will be noted that ΔT_p will vary with l', the position of the point P along the radiator. Practically, because of the high conductivity of the surface of the radiator, the temperature rise of all points on the surface will tend to equalize. The effect may be cared for by reintegrating equation 14 with l' as the variable. Thus, the complete expression for the temperature rise at the surface of the radiator is given by the expression

$$\Delta T=\frac{2}{l}\int_0^{\frac{l}{2}}\Delta T_p dl'-\frac{Q_{sc}\rho}{4\pi}\frac{1}{2L} \text{ degrees centigrade}$$

$$=\frac{Q_{sc}\rho}{2\pi l}\left[\log_e l/r+\sqrt{(l/r)^2+1}+r/l-1-l/4L\right] \text{ degrees centigrade} \qquad (15)$$

In the usual application, $l=8r$ and $L=4l$, approximately. Under these conditions equation 15 reduces to

$$\Delta T=0.115\frac{Q_{sc}\rho}{l}=0.0144\frac{Q_{sc}\rho}{r} \text{ degrees centigrade} \qquad (16)$$

where l or r is measured in inches.

Appendix II. The Effect of Surface Resistivity at the Isothermal Plane

The heat field in the uniform medium must satisfy Laplace's equation, see Figure 1

$$\frac{\partial^2T}{\partial x^2}+\frac{\partial^2T}{\partial y^2}=0 \qquad (17)$$

The boundary condition at the surface of the cylindrical radiator at the point ($y=0$, $x=h$) is

$$\frac{\partial T}{\partial r}+\frac{Q_c\rho}{2\pi r}=0 \qquad (18)$$

At the isothermal plane of surface resis-

Table I. Values of G_c for a Long Cylindrical Radiator

$t\alpha/d^2$	G_c	$t\alpha/d^2$	G_c	$t\alpha/d^2$	G_c
0.05	0.001	2.30	0.873	100	2.708
0.07	0.003	4.00	1.129	156	2.931
0.10	0.012	6.93	1.390	278	3.218
0.14	0.033	11.10	1.620	625	3.624
0.20	0.073	17.35	1.839	2,500	4.317
0.30	0.146	25.0	2.019	3,090	4.422
0.40	0.216	30.9	2.123	3,910	4.540
0.50	0.280	39.1	2.240	5,100	4.673
0.70	0.390	51.0	2.373	6,950	4.827
1.00	0.522	69.5	2.527	10,000	5.010

tivity β ($x=0$), the boundary condition is

$$\frac{\partial T}{\partial y}-\frac{\rho}{\beta}T=0 \tag{19}$$

The solution of equation 17 with the boundary conditions imposed by equations 18 and 19, as developed by Poritsky,[3] takes the form

$$\Delta T_p=Q_c\frac{\rho}{2\pi}\,\mathcal{R}\left[\log_e\frac{d'}{d}-2\epsilon^{\frac{\rho}{\beta}d'}E_i\left(-\frac{\rho}{\beta}d'\right)\right]$$

degrees centigrade (20)

in which $\mathcal{R}$ denotes "the real part of" the following complex expression, d' and d being vectors, and E_i denotes the exponential integral of the expression contained in parentheses.

Equation 20 is readily soluble as it stands for locations of the point P on the line O-O' ($x=0$), since under this condition, the expression contained within the brackets is not complex. For other locations of P, equation 20 may be converted to an asymptotic series in the form

$$\Delta T_p=Q_c\frac{\rho}{2\pi}\left(\log_\epsilon\frac{d'}{d}+F\right)$$

degrees centigrade (21)

where

$$F=2\sum_{1}^{\infty}\frac{-(-1)^n(n-1)!\cos n\theta}{\left(\frac{\rho}{\beta}d'\right)^n}$$

$$=1.90\frac{\beta\cos\theta}{\rho d'} \tag{22}$$

approximately, and θ is the angle between O'-O and O'-P, see Figure 1.

Appendix III. The Temperature—Time Transients of Cylindrical and Spherical Radiators

The Fourier equation for the heat flow from a cylindrical radiator in an infinite medium is

$$\frac{\partial^2 T}{\partial r^2}+\frac{1}{r}\frac{\partial T}{\partial r}=\frac{1}{\alpha}\frac{\partial T}{\partial t} \tag{23}$$

in which α, the thermal diffusivity of the medium, is equal to the reciprocal of the product of the thermal resistivity by the thermal capacitance. It may be shown[10] that the solution of this equation for temperature rise at any point in the heat field, as a function of elapsed time t, may be represented with sufficient accuracy for our purposes by the expression

$$\Delta T_p=\frac{Q_c\rho}{2\pi}\int_{\frac{1}{2}\sqrt{\frac{d^2}{t\alpha}}}^{\infty}\frac{\epsilon^{-\beta^2}}{\beta}\,d\beta$$

degrees centigrade (24)

From the theory of images outlined in Appendix I, for the case of a horizontal cylindrical radiator buried beneath an isothermal plane

$$\Delta T_p=\frac{Q_c\rho}{2\pi}\left[G_c(d)-G_c(d')\right]$$

degrees centigrade (25)

where

$$G_c=\int_{\frac{1}{2}\sqrt{\frac{d^2}{t\alpha}}}^{\infty}\frac{\epsilon^{-\beta^2}}{\beta}\,d\beta \tag{26}$$

The value of equation 26 for various values of $t\alpha/d^2$ is given in Table I.

Figure 7 shows the value, attained by equation 25, for the temperature rise at the surface of the radiator as a percentage of the ultimate temperature rise in infinite time, equation 3, plotted against $t\alpha/r^2$ for several values of the ratio L/r.

Similarly, for a spherical radiator, the Fourier equation for heat flow is

$$\frac{\partial^2 T}{\partial r^2}+\frac{2}{r}\frac{\partial T}{\partial r}=\frac{1}{\alpha}\frac{\partial T}{\partial t} \tag{27}$$

The solution of this equation by operational calculus and the application of the theory of images, where the spherical radiator is buried beneath an isothermal plane, yields the following expression

$$\Delta T_p=\frac{Q_s\rho}{4\pi}\left[\frac{G_s(d)}{d}-\frac{G_s(d')}{d'}\right]$$

degrees centigrade (28)

in which the value of G_s for various values of $t\alpha/d^2$ is given in Table II.

The values, attained by equation 28, for the surface of a sphere having a L/r ratio of 12 as a percentage of the ultimate temperature-rise in infinite time, equation 4, also are shown in Figure 7.

Appendix IV. The Effect of Radial Moisture Migration in the Heat Fields of Buried Cylindrical and Spherical Thermal Radiators

A. S. Mickley[13] has developed the following theoretical expression which checks very nicely with the data determined by Smith[5] on moisture migration in moist soils

$$\Delta M=k_1\frac{dT}{dr}\left[\left(\frac{M_i}{C_f}\right)^2-\left(\frac{M_i}{C_f}\right)^3\right]\text{ per cent} \tag{29}$$

in which ΔM is the change in moisture content per unit volume expressed as a percentage of dry weight per unit volume; k_1 is a constant for the particular soil condition; dT/dr is the temperature gradient across unit radius in degrees centigrade per centimeter; M_i is the initial moisture content, and C_f is the field capacity, both expressed on the same basis.

Since a change in moisture content will result in a change in thermal conductivity, and since the change in moisture content will be relatively small in proportion to the total moisture content, it is justifiable to assume a linear relationship between these changes. Thus

$$\Delta\kappa=k_2\Delta M$$

watts per degree centigrade centimeter (30)

The thermal conductivity of any point in the field is given by the expression

$$\kappa_p=\kappa_i+\Delta\kappa=\frac{1}{\rho_i}+\Delta\kappa=\frac{1}{\rho_p}$$

watts per degree centigrade centimeter (31)

Combining equations 29, 30, and 31, and solving for ρ_p

$$\rho_p=\frac{\rho_i}{1+\rho_i\frac{dT}{dr}K_m}$$

degree centigrade centimeters per watt (32)

where

$$K_m=k_1k_2\left[\left(\frac{M_i}{C_f}\right)^2-\left(\frac{M_i}{C_f}\right)^3\right]$$

watts per degree centigrade squared (33)

The expression within the brackets in equation 33 represents the variation of moisture migration with initial moisture

Table II. Values of G_s for a Spherical Radiator

$\frac{t\alpha}{d^2}$	G_s	$\frac{t\alpha}{d^2}$	G_s	$\frac{t\alpha}{d^2}$	G_s
0.01	0.104	0.70	0.523	40.0	0.912
0.02	0.142	1.00	0.572	70.0	0.933
0.04	0.191	2.00	0.663	100	0.944
0.07	0.240	4.00	0.744	300	0.968
0.10	0.276	7.0	0.799	1,000	0.982
0.20	0.356	10.0	0.829	3,000	0.990
0.40	0.446	20.0	0.877	10,000	0.994

content, and reaches a maximum value of 0.32 at the "thermal critical moisture content." While firm values indicative of the constants k_1 and k_2 are not presently available, Smith's data[5,13] seem to indicate a maximum value of 9.6 per cent centimeter per degree centigrade for k_1. From Figure 9, a representative value of 0.0006 watt per degree centigrade centimeter per cent is indicated for k_2. Thus, the value of K_m for maximum moisture migration effect is in the order of 0.002 watt per degree centigrade squared.

As indicated in Appendix I, the basic differential equation for the heat flow from a cylindrical radiator is

$$\frac{dT}{dr}+\frac{Q_c\rho_2}{2\pi r}=0 \tag{34}$$

Substituting equation 32 in 34 and solving for dT

$$dT=\frac{-1\pm\sqrt{1-A/r}}{2\rho_1K_m}\,dr \quad \text{degrees centigrade} \tag{35}$$

where

$$A=\frac{2}{\pi}\rho_1{}^2Q_cK_m \text{ centimeters} \tag{36}$$

If $K_m=0$ be substituted in equations 35 and 36, the resulting expression is either indeterminate or infinite, according to whether the plus or minus sign is used before the second term of the numerator. Since, under this condition, dT has a finite value, as indicated by equation 34, the plus sign should be used.

Expanding equation 35 into a binomial series and integrating, we obtain the following expression for the temperature rise of a point P in the heat field

$$\Delta T_P=\frac{Q_c\rho_1}{2\pi}\left[\log_e\frac{d'}{d}+\frac{A}{4}\left(\frac{1}{d}-\frac{1}{d'}\right)+\frac{A^2}{16}\left(\frac{1}{d^2}-\frac{1}{d'^2}\right)\ldots\right] \text{ degrees centigrade} \tag{37}$$

By solving equations 32 and 34 simultaneously to eliminate dT/dr, an expression for ρ_p is obtained

$$\rho_p=2\rho_1\frac{d}{A}\left[1-\sqrt{1-\frac{A}{d}}\right] \text{ degree centigrade centimeter per watt} \tag{38}$$

Similarly, in the case of a spherical radiator, the following comparable equations are obtained

$$dT=\frac{-1+\sqrt{1-B/r^2}}{2\rho_1K_m}\,dr \quad \text{degree centigrade} \tag{39}$$

where

$$B=\frac{1}{\pi}\rho_1{}^2Q_sK_m \text{ square centimeters} \tag{40}$$

$$\Delta T_P=\frac{Q_s\rho_1}{4\pi}\left[\frac{1}{d}-\frac{1}{d'}+\frac{B}{12}\left(\frac{1}{d^3}-\frac{1}{d'^3}\right)+\frac{B^2}{40}\left(\frac{1}{d^5}-\frac{1}{d'^5}\right)\cdots\right] \text{ degree centigrade} \tag{41}$$

$$\rho_p=2\rho_1\frac{d^2}{B}\left[1-\sqrt{1-\frac{B}{d^2}}\right] \text{ degree centigrade centimeter per watt} \tag{42}$$

References

1. ON THE CARRYING CAPACITY OF ELECTRIC CABLES SUBMERGED, BURIED OR SUSPENDED IN AIR, A. E. Kennelly. *Minutes*, Ninth Annual Meeting, Association of Edison Illuminating Companies (New York, N. Y.), 1893.

2. ON REFLECTION OF SINGULARITIES OF HARMONIC FUNCTIONS CORRESPONDING TO THE BOUNDARY CONDITION DU/DR+AU=0, H. Poritsky. *Bulletin*, American Mathematical Society (New York, N. Y.), December 1937, page 873.

3. WATER RELATIONS OF SOILS, L. B. Olmstead, W. O. Smith. United States Department of Agriculture *Yearbook* Separate Number 1658, reprint from pages 897–910. United States Government Printing Office, 1939.

4. THE THERMAL CONDUCTIVITY OF DRY SOILS OF CERTAIN OF THE GREAT SOIL GROUPS, W. O. Smith. *Proceedings*, Soil Science Society of America (Morgantown, W. Va.), volume 3, 1938, page 13.

5. THERMAL CONDUCTIVITY IN MOIST SOILS, W. O. Smith. *Proceedings*, Soil Science Society of America (Morgantown, W. Va.), volume 4, 1939, page 32.

6. THE THERMAL CONDUCTIVITY OF DRY SOIL, W. O. Smith. *Soil Science* (Baltimore, Md.), volume 53, number 6, June 1942, page 435.

7. TEMPERATURE TRANSFER OF MOISTURE IN SOILS, W. O. Smith. *Transactions*, American Geophysical Union (Washington, D. C.), volume 24, 1943, page 511.

8. THE EFFECTS OF MOISTURE ON THE THERMAL CONDUCTIVITY OF SOILS, G. B. Shanklin. AIEE TRANSACTIONS, volume 41, 1922, pages 94–101.

9. HEAT TRANSFERENCE IN SOILS, H. E. Patten. *Bulletin number 59*, United States Department of Agriculture, Bureau of Soils, 1909.

10. HEAT CONDUCTION, WITH ENGINEERING AND GEOLOGICAL APPLICATIONS (book), Ingersoll, Zobel and Ingersoll. McGraw-Hill Book Company (New York, N. Y.), 1948.

11. CURRENT RATINGS OF CABLES FOR TRANSMISSION AND DISTRIBUTION, Whitehead, Hutchings. *Journal*, Institution of Electrical Engineers (London, England), volume 83, 1938, page 525.

12. THERMAL CHARACTERISTICS OF A 120-KV HIGH PRESSURE GAS-FILLED CABLE INSTALLATION, W. D. Sanderson, J. Sticher, M. H. McGrath. AIEE TRANSACTIONS, volume 67, 1948, Part I, pages 487–98.

13. THE THERMAL MOVEMENT OF MOISTURE IN SOIL, A. S. Mickley. AIEE TRANSACTIONS, volume 68, 1949, pages 330–35.

Discussion

W. A. Del Mar (Phelps Dodge Copper Products Corporation, Tarrytown, N. Y.): The author's paper is one of two papers by him which are the culmination of long discussions which have taken place, first in voluminous correspondence between the engineers of cable companies, then in the cable subcommittee of the old transmission and distribution committee of the Institute, and, finally, in the cable characteristics subcommittee of the present committee on insulated conductors. The other paper we hope to see later this year.

The discussion originated in the rivalry of oil-filled cables in ducts and the various types of pressure cables in pipes. The problem was to estimate the relative carrying capacities of cables of the two types. The difficulty arose from the fact that the usual method of estimating the carrying capacity of duct cables makes use of elements of thermal resistance which were derived from measurements made on cables in ducts without taking into account the thermal resistance of the surrounding soil, whereas the carrying capacity of pipe cables is estimated by means of a formula in which the thermal resistance of the soil is an important factor It, therefore, became necessary to ascertain, if possible, what soil resistivity was inherent in the commonly accepted duct constants. Estimates varied over a range of 3-to-1.

The cable characteristics subcommittee undertook to solve this problem. As chairman of the subcommittee, I tried to bring out the various points of disagreement, and, finding that these seemed to be lodged mostly in the minds of manufacturers' engineers, it seemed advisable to give the utility men the job of dislodging the various prejudices and differences of opinion. I counted myself very fortunate in enlisting the interest of Neher, and feel very grateful to him for his painstaking work, and to the Philadelphia Electric Company's engineers for enabling him to devote so much time to it. This has not been simply a matter of doing some mathematics and writing a paper but it has been a continuous tussle with some of the best minds in the industry. This paper has been rewritten several times to meet the keen criticism of committee members. Whether all differences of opinion have been resolved should appear from the discussion to follow.

Mickley's paper[1] is not only a valuable contribution to this subject, but also should be useful to designers of heat pump systems.

REFERENCE

1. See reference 13 of the paper.

F. H. Buller (General Electric Company, Schenectady, N. Y.): Neher has made a valuable contribution to the theory of heat flow from buried cables and pipes.

It might be pointed out that the Kennelly formula, in both the long and the short forms, is well known in British technical literature on buried cables; that Poritsky provided the solution for the effect of soil surface thermal resistivity; that Ingersoll developed the equation for attainment factor, and Mickley developed the one covering the effect of moisture migration. All this is perfectly true. Neher's contribution involved a synthesis of all these solutions, and an analysis which throws a flood of light on the general problem.

To appreciate what Neher has accomplished and what remains to be done, it is necessary to consider the state of the art at the time when he started his work. The Kennelly formula was well known and universally accepted in Britain, but most American engineers seemed to accept it with some mental reservations. Some, in fact, did not accept it at all. Certain engineers contended that the thermal resistance of the earth was equal to that of a cylinder of soil with a radius equal to the depth of burial of the cable; some went so far as to question the validity of the principle of superposition.

This should make it clear that the state of the art was one of considerable confusion until it was clarified by the sort of study and analysis which Neher has presented so ably. To anybody who thinks this was easy I suggest the careful consideration of the following questions which arose during the analysis.

The Kennelly formula leads to the conclusion that all the heat from the cable in the steady state eventually finds its way to the earth's surface, under the conditions on which the formula is based. This conclusion is absolutely correct but by no means obvious. The reason is that, after an infinite time, the average over-all earth surface temperature is actually the coolest within reach.

If we accept the foregoing statement, would the Kennelly formula apply in the practical case where the earth's surface temperature may actually be higher than the cable temperature? The Kennelly formula and the principle of superposition must be combined to answer this one; the engineer who does not accept the principle of superposition is going to have a hard time finding out what happens. However, he need only study Figures 3, 4, and 5 of the paper and the text to discover the right answer.

It might be mentioned that one of Neher's achievements is to make clear how closely the principle of superposition really does apply, and to what extent it is invalidated by moisture migration. His conclusion is that the effect of moisture migration is slight enough to permit the principle to be used.

Although all the heat eventually reaches the surface of the earth in the wintertime, the increase of moisture content and the decrease in soil thermal resistivity with depth undoubtedly will tend to cause more heat to start off in the downward direction than the Kennelly formula would call for. Just how much is very hard to determine exactly.

One formidable obstacle in the path of progress was the British 2/3 factor. The British found that measurements on soil samples made in the laboratory gave a soil thermal resistivity about 50 per cent in excess of that calculated by means of the Kennelly formula from field tests on buried cables. The following points, between them, probably explain the discrepancy:

1. The attainment factor caused by the very high thermal capacity of the earth, which even after 400 hours leaves 15 per cent of the ultimate temperature to be attained in a certain typical case
2. The variation of soil thermal resistivity with depth, due to the approach to the water table, and the presence of solid rock and earth packing
3. The effect of soil disturbance on laboratory samples, and above the cable in the field.

Neher shows that the second point involves a difficult mathematical problem if this effect is to be evaluated numerically. Moreover, it will be necessary to establish some law of variation of soil thermal resistivity with depth to be used in such a solution if it is to be anything but a mathematical exercise. As previously pointed out, it will result in more downward movement of heat than would be expected from the Kennelly formula.

It may be that, if enough data were available, it would be possible to correlate effective soil thermal resistivity with laboratory measurements taken on suitable samples of the soil at the depth at which the cable is buried, and with the law of soil resistivity variation with depth, when and if this law definitely is established.

The latter part of the third point is mentioned incidentally by Neher. It also would involve a very difficult mathematical analysis if a rigorous numerical evaluation were desired; however, a comparatively easy approximate analysis indicates that the action of the cable ditch as a dry drain may possibly account for a 10- to 15-per cent decrease in effective soil thermal resistivity. If this factor is as important as it looks, a good part of the 2/3 factor would be accounted for.

Incidentally, Neher well might sound a word of warning in this connection. If, as he suggests, the soil around the cable ultimately returns to something approximating the virgin state, its thermal resistivity may be expected to rise, perhaps enough to raise the effective over-all thermal resistivity of the earth as much as 10 to 15 per cent as far as the cable is concerned. A test on a recently buried cable thus might give a temporary soil thermal resistivity lower than that which ultimately will exist when the soil has stabilized over a period of years.

An organized group of utility engineers is in the process of obtaining a good deal of soil thermal resistivity data from buried radiators, and also some heat-run data on buried cables in pipes. The publication of such data would be very helpful, since it would contribute materially to the settlement of the vexed question of soil thermal resistivity in general.

M. H. McGrath (General Cable Corporation, New York, N. Y.): Neher has made a valuable contribution to the determination of the current ratings of underground power cables. His critical review of the Kennelly assumption establishes the latter premise as the logical basis for the further development of rational methods of current rating for all the usual types of installation such as duct lay, direct earth burial, and pipe type. By "rational" methods, we refer to ones in which the heat flow path from conductor to earth is broken up into a series of component parts, and the thermal resistance of the individual parts determined separately and then combined. In recent years, there has been a growing tendency in this country to employ a single over-all transfer coefficient or "correction factor" to cover a large number of the component parts of the thermal path. Even though the latter procedure provides what initially may seem to be a simple way out, experience has shown that it ultimately leads to misunderstanding and confusion. Lack of confidence in the applicability of the Kennelly assumption to the problem has been perhaps the most persistent reason advanced in support of the use of such over-all coefficients. Neher demonstrates clearly that there is little if any need for concern on this score.

Neher gives short and long forms of the Kennelly formula. These result in the following expressions for the external thermal resistance of a buried cylindrical structure

$$R_G=\frac{\rho}{2\pi}\log_e\left(\frac{2L}{R}\right)$$

degrees centigrade per watt per centimeter (43)

$$R_G=\frac{\rho}{2\pi}\log_e\left(\frac{L}{R}+\sqrt{\left(\frac{L}{R}\right)^2-1}\right)$$

degree centigrade per watt per centimeter (44)

Equation 43 assumes that the heat flow lines emerge from the geometric center of the structure. Strictly speaking, the heat flow lines terminate at a small distance vertically above the geometric center of the structure. Equation 44 takes this displacement into account. The magnitude of this displacement or eccentricity is given by

$$e=(L-h)=R\left[\left(\frac{L}{R}\right)-\sqrt{\left(\frac{L}{R}\right)^2-1}\right]$$

centimeter (45)

As Neher correctly points out, for most applications of practical interest, the short form can be employed. The magnitude of the error involved in using the short form, equation 43, in place of the long form, equation 44, is evident from Table I of the discussion which gives, for various L/R ratios, the results obtained by the short form in per cent of the values given by the long form.

In practice, L/R is seldom less than 10, and the error introduced by the use of the short form is entirely negligible.

So-called Kennelly formulas have appeared in many technical articles. In some cases, the forms appear at first sight to be at variance with those given by Neher. For example, Whitehead and Hutchings give the following equation[1]

$$R_G=\frac{\rho}{2\pi}\log_e\left[\frac{\sqrt{(L^2-R^2)}+(L-R)}{\sqrt{(L^2-R^2)}-(L-R)}\right]$$

degrees centigrade per watt per centimeter (46)

By rationalizing the term in brackets, it is found that equation 46 is identical to the long form as given by Neher. In other articles, the following formula appears

$$R_G=\frac{\rho}{2\pi}\cosh^{-1}\left(\frac{L}{R}\right)$$

degree centigrade per watt per centimeter (47)

This also is identical to the long form as given by Neher because

$$\cosh^{-1}\left(\frac{L}{R}\right)=\log_e\ \left(\frac{L}{R}\right)+\sqrt{\left(\frac{L}{R}\right)^2-1}\Bigg]$$

Table 1. Comparison of Long and Short Forms

L/R	$\frac{\text{Equation 43}}{\text{Equation 44}}$ per cent
1.5	114
2.0	105
3.0	102
5.0	101
10.0	100

Table II. Results Obtained with Line and Cylindrical Source Assumption

		Temperature Rise, per cent Ultimate	
L/R	$\frac{t\alpha}{R^2}$	Cylindrical Source (Figure 7 of paper)	Line Source (Reference 12 of paper)
2	10	87	88
2	100	99	99
10	10	51	52
10	100	86	87
10	1,000	98	98
100	10	30	30
100	100	51	51
100	1,000	73	73

Mansfield gives the following expression[2]

$$R_G=\frac{\rho}{2\pi}\log_e\frac{R}{e} \text{ degree centigrade per watt per centimeter} \quad (48)$$

Here again, we have an expression which is identical to the long form of Neher because, from equation 45, we can write

$$\frac{R}{e}=\left[\left(\frac{L}{R}\right)+\sqrt{\left(\frac{L}{R}\right)^2-1}\right]$$

Neher's analysis also provides all that is required to take account of mutual heating between adjacent cylindrical structures. Thus, for a group of equally-loaded structures, the thermal resistance R_M caused by mutual heating at a point P, may be written from Figure 1 of the paper as

$$R_M=\frac{\rho}{2\pi}\sum_1^n\log_e\frac{d_n'}{d_n}$$

degree centigrade per watt per centimeter (49)

where d_n and d_n' are defined as:

d_n = distance from the point where the heat flow lines of the nth adjacent structure terminate, to the point P on the structure under consideration

d_n' = distance from the point where the heat flow lines of the image of the nth adjacent structure terminates, to the point P on the structure under consideration

In rectangular co-ordinates, equation 49 from Figure 1 of the paper becomes

$$R_n=\frac{\rho}{2\pi}\sum_1^n\times \log_e\left[\frac{(x+(L_n-e_n))^2+(y-y_n)^2}{(x-(L_n-e_n))^2+(y-y_n)^2}\right]^{1/2}$$

degree centigrade per watt per centimeter (50)

Whitehead and Hutchings give the following expression for the mutual effect at the highest point of any one structure in the group[1]

$$R_M=\frac{\rho}{2\pi}\sum_1^n\log_e\left[\frac{(L_1+L_n-R)^2+y_n^2}{(L_1-L_n-R)^2+y_n^2}\right]^{1/2}$$

degree centigrade per watt per centimeter (51)

where

L_1 = axial depth of structure considered, centimeters

L_n = axial depth of each other structure of group, centimeters

R = radius of cylindrical structure, centimeters

Y_n = horizontal axial distance between structure considered and each other structure in group, centimeters

This equation follows directly from equation 50 if the heat flow lines are assumed to terminate at the geometric centers, in which case the eccentricity becomes zero.

A further expression which has been suggested takes the form

$$R_M=\frac{\rho}{2\pi}\sum_1^n\log_e\left[1+\left(\frac{2L_n}{y_n}\right)^2\right]^{1/2}$$

degree centigrade per watt per centimeter (52)

This form follows directly from equation 51 on making the assumption that all structures are buried at the same depth, and by using that isothermal of the nth structure, which passes through the axis of the structure under consideration in place, of the isothermal passing through the highest point.

Simmons suggests the following expression for the mutual thermal resistance[3]

$$R_M=\frac{\rho}{2\pi}\sum_1^n\log_e\left(\frac{2L_n}{y_n}\right)$$

degree centigrade per watt per centimeter (53)

This equation follows directly from equation 52 on making the assumption that the horizontal axial spacing between structures is small in comparison to twice the depth of burial. However, if the axial spacing should be greater than twice the depth of burial, use of this approximation results in a negative term, implying a cooling instead of a heating effect.

It is of interest to compare the attainment factors for cylindrical radiators as given by Neher in Figure 7 of the paper with those obtained using the somewhat simpler solution outlined elsewhere[4] for a continuous line source of constant strength. Table II of the discussion indicates that, for the range covered by Figure 7 of the paper, the line source assumption gives results closely equal to those obtained with the cylindrical source assumption.

REFERENCES

1. See reference 11 of the paper.

2. NEW 138-KV CABLE LINES IN LOS ANGELES, Carroll G. Mansfield. AIEE TRANSACTIONS, volume 63, 1944, pages 1240–49.

3. CALCULATION OF THE ELECTRICAL PROBLEMS OF UNDERGROUND CABLES. D. M. Simmons. *Electric Journal*, (East Pittsburgh, Pa.) volume 29, 1932, page 398.

Herman Halperin (Commonwealth Edison Company, Chicago, Ill.): The author is to be complimented for his patience in investigating this subject and for his ingenuity in developing new thoughts. The Association of Edison Illuminating Companies' cable engineering section, of which I am chairman, is very appreciative of Neher's efforts. The section also has been stimulating field tests on pipe-type cables to obtain a more complete picture for the industry of the variations that occur in thermal properties for different types of installations. The section has been promoting the idea of the reports on findings by utilities being made available to all concerned through the AIEE.

The author has indicated that, in 400 hours of continuous heating, the attainment of the ultimate temperature rise of the earth around the pipe is 85 per cent of the ultimate value. This is quite interesting to C. A. Bauer and me in connection with our activities in Chicago, because we have been assuming that the attainment at that time would be about 95 per cent.

We are obtaining further data in connection with this problem through tests being made on seven 20-foot lengths of pipe that are buried in different types of soil and at different depths. Heating elements are inserted in the pipes and the temperatures on the surface of the pipe will be varied. Furthermore, the tests will include determining effects of continuous heating as against heating part of the time each day.

In the second part of his conclusion, the author speaks of the "effective thermal resistivity of the earth." We have found over the years that, in some cases where conduits develop high temperatures, there seems to be an especially high temperature gradient develop in the earth adjacent to the conduit; this high gradient, usually associated with rather poor types of soil from the thermal standpoint, can be greatly reduced by replacing the soil immediately around the conduit with sand and small gravel. Likewise, with pipe installations in earth where the soil immediately adjacent to the pipe may develop a high thermal gradient incidental to heating to calculated temperature of, say, 70 degrees centigrade, it seems to us that the layer of earth around the pipe may have a much higher thermal resistance than the balance of the earth. Not only do we recognize this in the calculations, but, for one installation of buried cables that was under consideration, we would have made a change in the earth. In that case we would have substituted several inches of sand and small gravel for the earth at the location involved, that earth being in the nature of a heavy clay.

Frank V. Smith (Sargent and Lundy, Chicago, Ill.): Neher has contributed an important paper which should be of great service to the industry. It puts together in a very satisfying form the basic theory of the heating of buried cables and pipes. The methods of taking care of surface resistivity, moisture movement, and transient conditions represent important additions to the literature.

The industry will look forward to the results of the tests being carried out by several of the operating companies on the thermal resistivity of the soil in place by means of spherical or cylindrical radiators, particularly if a comparison can be made between the results obtained by this method and tests carried out in the laboratory with samples of soil.

One point of interest is the temperature rise produced by one cable or pipe on adjacent cables or pipes. The superposition method which Neher has used throughout is an important contribution to the understanding of the way in which heat flows in the earth and can be applied to this problem.

Figure 6 of the paper shows that, for a cable placed $10r$ below the surface, at the end of an infinite time the temperature rise at a horizontal distance $10r$ from the cable is 27 per cent of the temperature rise at the surface of the cable. At a distance of $5r$, it is 47 per cent. If this is translated into the effect on the current-carrying capacity of two similar cables which are to attain the same total surface temperature, it will be found that two cables located $10r$ apart must have their watts loss reduced to 79 per cent of the value for a single cable, and at a distance of $5r$, to a value of 68 per cent of a single cable. If this procedure is extended to the thought of a concrete duct run in which r is the equivalent radius of a group of ducts of perhaps 1 foot or more, it will be seen that the effect of a second duct run spaced 5 or 10 feet away is greater than has been generally considered.

H. B. Dwight (Massachusetts Institute of Technology, Cambridge, Mass.): The flow of electric current into the ground from a buried horizontal cylinder, such as a buried ground wire or counterpoise, and the flow of heat from a buried cable or duct bank might seem at first glance to be similar problems, to be calculated by the same formulas. However, they are not the same, as is shown admirably by J. H. Neher in this paper.

Since air is an insulator to electricity, there is no flow of electric current across the ground surface, which is a flow line in the current flow map. In winter, the heat from a duct bank flows rather directly to the ground surface and crosses it practically at right angles, as in Figure 4 of the paper. In summer, the interest is in the hottest condition, for determining the power rating of the duct bank, and the ground surface may be hotter than the temperature around the duct bank. The flow of heat from the duct bank at such a time is into the ground and not up to the ground surface. The mathematical solution for electric current flow into the ground nevertheless should not be used. There is still heat flow either into or out of the ground surface.

It is much better to use the method of Neher's paper, in which the heat flow is divided into two components, one being the heat from the duct bank, assuming it to be the only source of heat, and the other being the heat to or from the ground surface when the duct bank is considered absent. The solutions for heat flow and temperature rise for the two components can be superposed. That is, for any time of year, equation 1 or 1*a* gives the temperature rise of the surface of the buried cylinder, or other point, above what the temperature would be if there were no cylinder.

For testing purposes, a small sphere would seem to be better than a short cylinder, since there is a reliable formula for resistance to ground of the sphere by which a temperature measurement can give a direct determination of earth resistivity. Since the escape of heat from the buried object is entirely by conduction, there may be some question about calling it a radiator.

If measurements are to be made comparing the heat flow from small finite objects, such as spheres and short cylinders, to the surrounding material, which is a geometrical problem, it would seem better to take advantage of the established precise type of measurement of the flow of electricity from a metal object to a liquid in which it is immersed. The direct measurement of thermal resistivity of the earth would, of course, have to be made by the more uncertain measurement of heat flow in the earth, and the most favorable shape of metal object then could be used.

The use of equation 22 to account for the ground surface resistivity seems to be more of a complication than is needed. The loss of heat from the ground surface is approximately proportional to the temperature rise of the ground above the air. This is the assumption made for deriving equation 22 where the surface resistivity is taken to be a constant, β. The usual formulas for emission of heat from a warm surface have a result the same as if the surface were covered with a layer of undisturbed air about 1/4 to 1/2 centimeter thick. The outer surface of the layer is taken to be at the ambient air temperature, and the transfer of heat is taken to be by conduction only. Since a layer of undisturbed air has a resistivity of 3,800 degrees centigrade for one watt through one centimeter cube at 25 degrees centigrade, this would mean a surface resistivity of $\beta = 1/2 \times 3{,}800 = 1900$ degrees centigrade for one watt through one square centimeter, if the layer is taken to be 1/2 centimeter thick.

If ρ for the earth is 60, and β is 2,000, as given in the paragraph following equation 1*a* of the paper, then the layer of air is equivalent to a layer of earth of thickness

$$\frac{2000}{60} = 33 \text{ centimeters}$$

which is 13 inches, or 1.1 feet.

This would mean that the flow of heat and the temperatures may be computed as if 1.1 feet, or less, of earth were added at the top of Figures 3 and 4; that is, the cylinder would be at a depth of 5.1 feet instead of 4 feet. Since 1.1 feet is small compared with other dimensions in Figures 3 and 4, the flow lines through the added layer of earth would be almost straight and vertical, and there does not seem to be need to use a 2-layer calculation. The computation made by adding a layer of earth at the ground surface is especially desirable since the second term in equation 1*a* is the approximate sum of an infinite series, the convergence of which is unsatisfactory because of the presence of $(n-1)!$ in the numerators of the terms.

W. A. Hadley (Columbia University, New York, N. Y.): I think Neher is to be commended on his excellent paper. It explains many of the discrepancies previously noted between laboratory and field test data with regard to the Kennelly formula. To the best of my knowledge, it is also the first paper to evaluate the effect of moisture movement on heat transfer in soils.

I am in agreement with Neher's conclusion that thermally-actuated moisture migration is a minor consideration with respect to buried cables. In this instance the loss of moisture around the cable probably is small, and the attendant thermal effects likewise will be small.

However, in the reverse case, where a buried pipe acting as a thermal receiver is being considered, as in a heat-pump ground coil, the effects of thermally-actuated moisture migration may be significant. With a heat sink, the moisture migration is toward the pipe, which will saturate the soil around the pipe. In fact, if freezing conditions exist around the pipe, it is possible for the moisture to be trapped by freezing and to produce a moisture concentration greater than saturation. As varieties in moisture content may cause a tenfold increase in thermal conductivity, according to certain published data, this is very significant.

In fact, recent studies I have just completed on some heat-pump ground-coil data, in which I used essentially the method of Neher, much closer agreement was obtained between the calculated values and the field-test data when moisture migration was included than when constant properties were used. Unfortunately, there has been very little work done on moisture migration in soils.

J. H. Neher: I am greatly indebted to Del Mar for explaining why this somewhat mathematical exposition has suddenly appeared on the cable scene, and also to Buller for indicating some of the difficulties met with in its preparation. In approaching the practical problems of cable-in-duct installations, which, as Del Mar has indicated, occasioned this study and which will be the subject of a forthcoming paper, I felt that it was highly desirable to first review and obtain an agreement on the fundamental principles underlying the calculation of the temperature rise of buried thermal radiators.

Also, I wish to thank McGrath for his demonstration that the various versions of the Kennelly formula appearing in the literature are directly reducible to the form which I have chosen to use. It is assuring to note too, that the Ingersoll solution for the earth long-time transient which I have employed, is checked by the French formula[1] as cited by McGrath, as well as by the British formula.[2]

Halperin has discussed the attainment factor of 85 per cent given in the paper for a particular pipe-type cable installation after 400 hours. It may be of interest to demonstrate more fully how this may be obtained by graphical means. The upper curve of Figure 1 of the discussion shows the measured temperature rise—time transient plotted on a log-log scale. The points spotted are those measured at the times indicated. Actually the curve was first drawn on rectangular co-ordinates on the basis of many more test points than actually are shown.

The lower curve of Figure 1 of the discussion represents the theoretical temperature rise—time transient, taken from Figure 7 of the paper and plotted to the same log–log scale. By superimposing this curve upon the test curve as shown to obtain the best fit, we establish the ultimate temperature rise as 41 degrees centigrade, and, incidentally, the apparent value of the diffusivity of the earth. In this case the attainment factor after 400 hours is 80 per cent, whereas the 85 per cent figure cited in the paper was obtained from the best fit with the diffusivity (lateral position of the theoretical curve) pegged at 25 square centimeters per hour.

As Halperin points out, especially high thermal gradients may develop in the earth

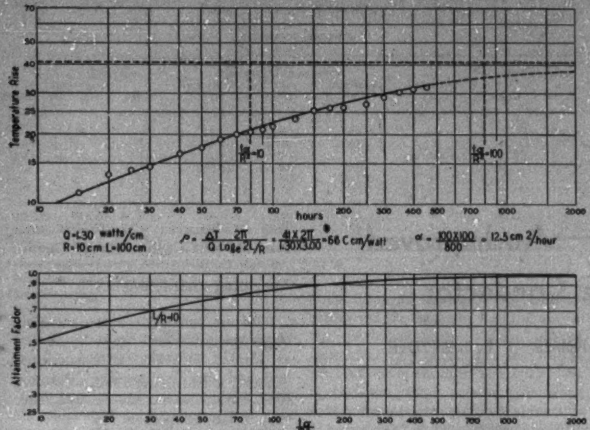

Figure 1. Measured and theoretical temperature—time transients

adjacent to the conduit; this is indicated by the theory presented. It is difficult, though, to understand how this condition may be improved by the substitution of sand or gravel in this region since, like earth, they have relatively high thermal resistivities when dry. What we really need is a material of low inherent thermal resistivity or one which more effectively will retain its moisture against the migration effect discussed. Bentonite clay has been suggested in connection with heat-pump ground coils, and its use may offer some advantages in cable applications.

The use of an "effective thermal resistivity" is admittedly an approximation intended to round out these effects and those resulting from nonuniformity with depth, as discussed by Buller. When and where these effects may be evaluated more fully for a particular critical installation, they should be taken into account. As Buller points out, the drainage-ditch effect of a new installation may outweigh the inherent increase in thermal resistivity of the disturbed soil, with the net result that, as the soil returns slowly to its virgin state, the effective thermal resistivity of the installation may rise.

As Smith has pointed out, the effect of adjacent cables or duct banks on the temperature rise of the particular system under investigation often may be greater than generally is supposed. This effect is calculated readily by use of equation 1 of the paper.

I am very glad that Dwight has mentioned the so-called Rudenberg formula for the electrical resistance of grounded conductors, because this formula has been cited incorrectly in text books and articles as applying to thermal flow as well. Dwight has explained nicely why the electrical formula is not applicable in this instance. As he points out, my use of the word "radiator" is not strictly accurate, but probably is no less so than the application of this term to the modern household article.

I feel that the method of caring for surface resistivity effects at the earth's surface suggested by Dwight is a definite simplification and improvement over the method presented, and suggest that it be used instead whenever such a correction is necessary.

Hadley mentions the effect of moisture migration in the case of a heat-pump ground soil. In this connection I should like to point out that the equation showing the effect of moisture migration on cable temperature rise given in the paper is not reversible. This is because in its derivation the effect of moisture moving outward in increasing the initial moisture content at a given radius is negligible because of the rapidly increasing volume per unit of radius, and may be neglected. With moisture moving inward, however, this effect is appreciable and must be considered. From what we have observed on our own heat-pump installations, and from Hadley's analysis of Coogan's tests, we believe that the practical result is to saturate completely the earth around the ground coil. From the point of view of cable engineers, it is indeed unfortunate that this moisture migration effect is not just the opposite.

References

1. L'Interpretation des Regimes Transitoires par L'Integrale de Fourier et Le Calcul Symbolique—Application au Calcul de L'Echauffement des Cables Enterries, P. Prache. *Bulletin de la Société Française des Electriciens* (Paris, France), volume 7, April 1947, (equation 55).

2. Current Rating of Cables for Transmission and Distribution, S. Whitehead, E. E. Hutchings. *Journal*, Institution of Electrical Engineers (London, England), volume 83, October, 1938, page 528 (equation 9.2).

Hy-Therm Copper—An Improved Overhead-Line Conductor

L. F. HICKERNELL
FELLOW AIEE

A. A. JONES
MEMBER AIEE

C. J. SNYDER
ASSOCIATE AIEE

THE SIZE of conductors for overhead lines generally is selected on the basis of obtaining the required voltage regulation and most economical power loss. Usually, these criteria result in a larger size than would be necessary from a thermal limitation. Indeed, many transmission text books and reference books do not even consider thermal limits of conductors.

On the assumption that copper anneals at 100 degrees centigrade, continuous current-carrying capacities of hard-drawn copper conductors using a maximum temperature below this value and under various operating conditions have been published as, for example, those shown in Table I.

Wartime conditions have focused attention on the determination of both the maximum continuous and short-time emergency overload capabilities of the conductors. Papers have been published which present methods of calculation considering these conditions.

Recent meetings[14–17] and papers [18–25] have pointed out the need for certain data, up to now unavailable, which are required to accurately determine current ratings for overhead-line copper conductors. Attention was directed specifically to:

1. The effect of noncuprous elements on the annealing characteristics of commercial copper conductors.[19–23] This may be considered in two parts: the effect of silver; and the effect of other constituents (including oxygen).

2. The effect of heat and time (annealing characteristic) on the strength of the conductor.[19–24]

3. The effect of initial hardness and tensile strength on the annealing characteristic.[19] This involves the influence of manufacturing technique; such as, size of hot-rolled rod, number of draws, reduction per draw, intermediate anneals, and so forth.

4. The effect of intermittent heating on the annealing characteristic.[19,23]

5. The effect of tension applied to the conductor on the annealing characteristic.[19–22]

6. The effect of vibration on the annealing characteristic.[19,23]

7. The correlation between change in elastic limit with ultimate strength.[21,24]

8. The effect of wire movement while hot on the annealing characteristic.[21]

In March 1943, following an informal conference,[26] an investigation was initiated to obtain the answers to some of these questions.

Hy-Therm Copper

A new brand of copper has been developed by the Anaconda organization which has improved annealing characteristics permitting higher current loading. It is produced by adding minute amounts of hardening agents to very pure electrolytic copper. This brand of copper due to its controlled composition, has consistently uniform properties. The types and amounts of added material are so chosen that their effect on purity and conductivity are negligible, as shown below:

	Hy-Therm Typical Values	ASTM *B5–43* Specified Minimum
Copper (including silver), per cent	99.953	99.900
Conductivity at 20 degrees centigrade, per cent of international annealed copper standard	100.9	100

For identification, this new copper has been trade-named "Hy-Therm" and branded "*AHT*" (*A*naconda *Hy-T*herm).

Annealing Characteristics

Data are presented on the annealing characteristics of hard-drawn copper wire as affected by chemical composition; heat and time—no tension; heat and time—with tension; intermittent heating; and manufacturing technique.

Effect of Chemical Composition

Data on the effect of various noncuprous elements (metallurgically referred to as "impurities") common to commercial brands of copper were published some years ago. More recently, the effect of iron, nickel, cobalt, silver, cadmium, tin, antimony, and tellurium on the conductivity and softening point of pure copper was covered excellently by Smart and Smith.[27,28] The effect on the annealing point of each element, both with and without oxygen, was shown. Since the effects of various elements on annealing are known to be not additive, and since some elements, especially oxygen, counteract the effect of others, the application of these data to commercial brands of copper containing various small amounts of each of 8 or 10 different elements becomes a difficult problem.

In 1940, for manufacturing purposes a study was conducted of the chemical, electrical, and annealing properties of 21 different brands and/or grades of commercial copper. Table II shows a summary of the chemical composition and conductivity found in common commercial wire-bar copper.

The complexity of correlating chemical composition, usually involving 11 variables, with annealing data made it impossible to draw very definite conclusions.

Paper 49-3, recommended by the AIEE transmission and distribution committee and approved by the AIEE technical program committee for presentation at the AIEE winter general meeting, New York, N. Y., January 31–February 4, 1949. Manuscript submitted October 18, 1948; made available for printing November 19, 1948.

L. F. Hickernell is chief engineer; A. A. Jones is manager, engineering department; and C. J. Snyder is supervisor, metallurgical laboratory; all with the Anaconda Wire and Cable Company, Hastings-on-Hudson, N. Y.

Table I. Thermal Limitations

Continuous Loading

Temperature Reference			Operating Temperature			Air Velocity, fps	Formula Reference	
Date	Reference Number*	Page	Ambient Air °C	Rise °C	Maximum °C		Number	Page
1922	1	43	25	40	65	still	2	208
1926	3	184	25	40	65	still	4	127
1927	5	80		5–40		outdoors	2	208
1930	6	153	40	30†	70†	2	6	154
1931	7	466	40	10–60	50–100	2	6	154
1933	8	419	25	50	75	2	6	154
1934	9	912	40‡	55	95	2.93	6	154
1941	10	1,197	25	50	75	2	6	154
1942	11	30	25	50	75	2	6	154
1942	12	1,203	40	40	80	2	6	154

*These numbers refer to references at end of paper.

†For outdoor substation busses.

‡Summer rating.

Table II. Chemical Composition and Electrical Conductivity

21 Different Brands and Grades of Copper

	Chemical Composition		
Element	Maximum, Per Cent	Minimum, Per Cent	Average, Per Cent
Silver	0.0253	0.00016	0.00309
Gold	0.00006	trace	0.000016
Oxygen	0.048	0.000	0.0317*
Sulphur	0.0041	0.000	0.0009
Arsenic	0.0012	0.0003	0.0007
Antimony	0.0015	0.0003	0.0007
Lead	0.0133	0.0003	0.0013
Selenium	0.0016	0.0004	0.0010
Tellurium	0.0012	0.0004	0.0010
Nickel	0.0027	0.0001	0.0010
Iron	0.0036	0.0015	0.0025
Tin	0.0014	nil	0.0005
Copper and silver	99.997	99.940	99.959
	Electrical Conductivity at 20 degrees Centigrade		
	Maximum, Per Cent IACS†	Minimum, Per Cent IACS	Average, Per Cent IACS
Annealed copper	101.96	100.30	101.09

*Average of tough-pitch samples only.

†International annealed copper standard.

Figure 1. Effect of heat and time—no tension

Brand *B*—hard-drawn wire

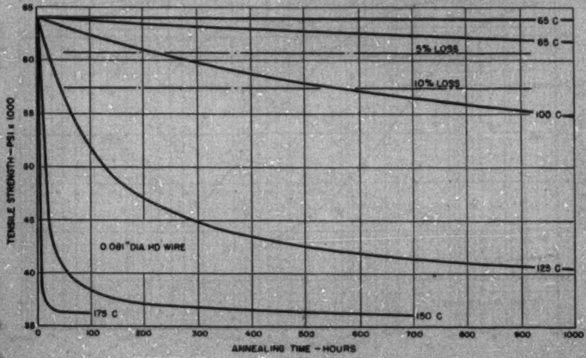

Some elements appeared to counteract others and the extremes were not always the controlling factor. "Lake" copper containing 7.67 ounces per ton (0.0253 per cent) silver annealed at a much lower temperature than another containing only 0.48 ounce per ton (0.0016 per cent). However, the sample lowest in silver (0.00016 per cent) was the easiest to anneal. Oxygen content had no noticeable effect on annealing. One oxygen-free copper was near the highest and another near the lowest of the group. The sample highest in antimony and arsenic was also the most difficult to anneal, but other samples of comparatively moderate antimony and/or arsenic content were also difficult to soften. Here again, however, the samples lowest in antimony and arsenic were the fastest to anneal. Nickel had no outstanding effect.

In correlating these annealing data with those from other tests, it was noted that fairly consistent results were obtained on copper from the same refinery brands. It, therefore, appears that the annealing characteristics of copper depend on a particular combination of elements which originates in one particular ore or mine, and which has been refined by a specific routine. The curve of the effect of silver, Figure 3, shown by Seelye and Malmstrom[20] would not apply to commercial copper unless, perhaps, all other elements were held constant. Likewise, their curve for the effect of oxygen, Figure 4,[20] would apply only if other elements such as iron were present, in which case the element would be oxidized and its effect reduced by the presence of oxygen.

Since the chemical composition or annealing characteristic of an overhead-line conductor are likely unknown to the operating engineer, current ratings should be based upon data obtained on commercial brands and/or grades of copper used in the industry.

Accordingly, based on previous investigations of manufacturing process anneals, three brands of copper were selected for this series of long-time, low-temperature tests which would produce annealing ranges as follows:

Brand *AHT*—Hy-Therm copper (having highest resistance to annealing).

Brand *B*—Representative commercial copper.

Brand *C*—Very pure copper (having lowest resistance to annealing).

EFFECT OF HEAT AND TIME—NO TENSION

The annealing characteristics of three brands of copper in the form of hard-drawn wire under no tension are shown in the following figures:

Figure 1—Brand *B* (rectangular co-ordinates).

Figure 2—Brand *C* (semilog co-ordinates).

Figure 3—Brand B (semilog co-ordinates).

Figure 4—Brand *AHT* (semilog co-ordinates).

In Figure 1, data are plotted on rectangular co-ordinates which give the true mental conception of the temperature-time (annealing) characteristic. Annealing starts as soon as heat is applied and progresses at a rate depending upon the temperature until the wire approaches a soft recrystallized state. However, in order to present data for long periods of time, it has been necessary to use a log scale for the annealing time (abscissa) in the remaining figures. It is hoped that this expedient will not lead to the erroneous impression that the wire resists softening for a certain period of time after which it suddenly and rapidly anneals.

Figures 2, 3 and 4 show that 5 per cent loss in strength occurs at various annealing temperatures at the times listed in Table III.

Figure 5 shows a comparison of the annealing characteristics of hard-drawn wire

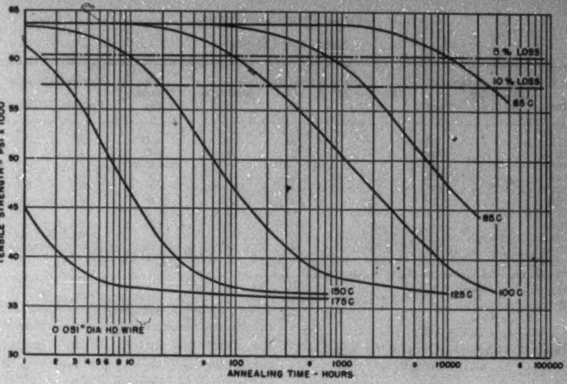

Figure 2 (top). Effect of heat and time—no tension

Brand C—hard-drawn wire

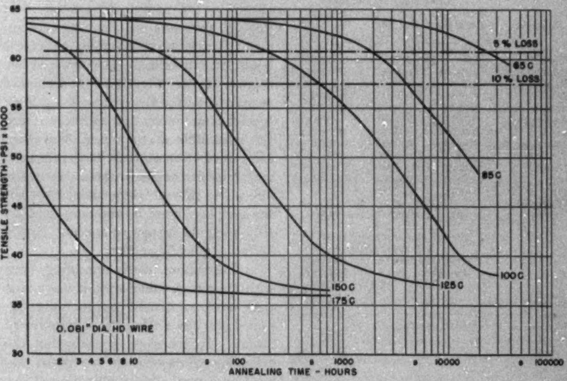

Figure 3 (center). Effect of heat and time—no tension

Brand B—hard-drawn wire

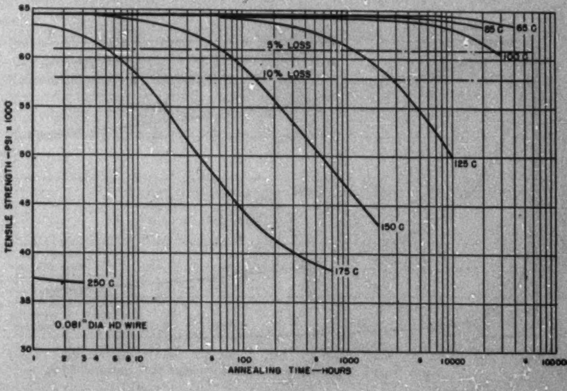

Figure 4 (bottom). Effect of heat and time—no tension

Brand *AHT*—hard-drawn wire

for the three brands at the lower operating temperatures (65, 85, 100, 125 degrees centigrade).

Comparing these data with those published previously, it would appear that previously available commercial copper wire anneals at a lower temperature than indicated by Seelye and Malmstrom,[20] Olmstead[24] and George;[25] also that extrapolating the data of Pilling and Halliwell[29] to temperatures below 100 degrees centigrade is not permissible.

Figure 6 shows a comparison between the authors' data and that of Seelye and Malmstrom (Figure 2)[20] for the time required at different temperatures for a 5 per cent loss in strength for hard-drawn wire. Fortunately, there appears to be some temperature at which no annealing will occur. If this be true, the data for 60 and 47.5 degrees centigrade shown by Olmstead (Figure 7)[24] appear questionable for representative commercial copper, and certainly so for Hy-Therm copper.

EFFECT OF HEAT AND TIME—WITH TENSION

Duplicate samples were heated at 150 degrees centigrade while held under tension equal to 25 per cent of the original breaking strength of the wires. This corresponds to normal working tension in overhead-line operation.

Figure 7 shows the effect of tension on the 150 degrees centigrade annealing

Table III. Temperature/Time Relation

For Five Per Cent Loss in Initial Strength

Annealing Temperature, Degrees Centigrade	Annealing Time for 5 Per Cent Loss in Strength Hard-Drawn Copper Wire Brand *AHT*, Hours	Brand *B*, Hours	Brand *C*, Hours
65	(a)	24,000	10,500
85	(a)	1,950	770
100	24,000	200	95
125	1,100	15	9.5
150	63	2.3	1.4

(a) Indeterminate to date; 1.4 per cent loss in strength occurs in 40,000 hours at 65 degrees centigrade and 21,000 hours at 85 degrees centigrade.

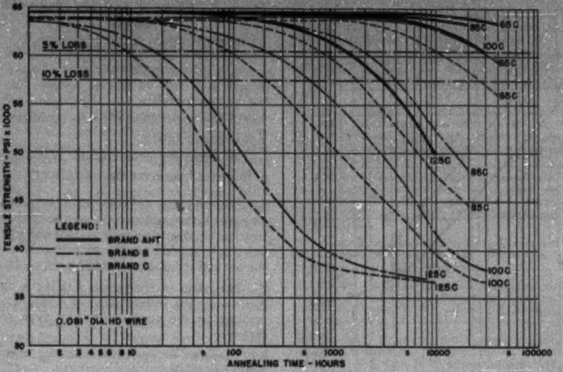

Figure 5. Effect of kind of copper—no tension

Hard-drawn wire

characteristic for hard-drawn wire of brand *B* copper. The rate of annealing is noticeably increased by the application of tension. Under the conditions stated, the reduction in annealing time is approximately 50 per cent. At lower annealing temperatures, it is expected that this effect would be considerably less.

It has been stated in the past[20,24,29] that the annealing rate, or recrystallization, of copper wire increases with increase of hardness caused by cold drawing. If cold drawing were considered as producing internal stresses in the wire in proportion to the total reduction of area after the last-process anneal, and if any external tensile stress on the wire were considered as adding algebraically to the internal stresses, the effect of both temper and tension is to anneal the copper wire at a rate proportional to the total stress in the wire.

Effect of Intermittent Heating

Duplicate samples were heated only eight hours out of each working day in the constant temperature oven used for all 125 degrees centigrade tests.

In Figure 8, the 125 degree centigrade continuous heating curve is reproduced (from Figure 3) and the values obtained on the intermittent heating cycle are plotted.

In four different sets of tests, the effect on annealing was directly cumulative in proportion to the number of hours heated.

Effect of Manufacturing Technique

It is probable that different manufacturing technique would have a small effect on the annealing characteristics of copper wire. Different routines would have an effect on the grain size and the final temper of a wire which, in turn, would be reflected in its annealing characteristic. In general, a fine-grained wire will work-harden faster and anneal at a lower temperature than a coarse-grained wire.[20]

However, the routines for drawing the common sizes and temper of commercial copper wire are so standardized that little variation from this source will be found. Commercial bare wire is produced to specifications which allow little leeway for variations in the manufacturing operations. Weatherproofed wire might show some variations due to the mechanical working and saturating processes.

Table IV. Increased Current Ratings Using Hy-Therm Copper

Conductor Size, (American Wire Gauge or Thousands Circular Mils)	Current Rating Commercial Brands, 75C (Amperes)	Current Rating Hy-Therm (Brand *A HT*), 100C (Amperes)
Solid		
6	120	145
4	165	195
Stranded		
2	230	270
1–0	305	365
2–0	355	425
3–0	415	490
4–0	480	570
350	665	790
500	835	995

Basis:

Method of calculation—Schurig and Frick (*General Electric Review*, March 1930, page 141).

Ambient temperature—25 degrees centigrade.

Air velocity—2 feet per second (1.36 miles per hour), crosswise.

Conductor resistance—96.16 per cent IACS conductivity (ASTM *B1–47*). D-c resistance increased 2 per cent for stranding and converted to operating temperature. A-c resistance determined by Bwan method (*General Electric Review*, April 1930, page 249).

Conductor surface—average tarnished.

Current Ratings

The data presented herein will enable the operating engineer to determine more accurately the thermal limit for existing and future lines based upon his local conditions (relation of peak load to ambient temperature, expected coincidental wind velocity, and so forth).

Continuous Loading

For design purposes, a thermal limit of 75 or 80 degrees centigrade has been used

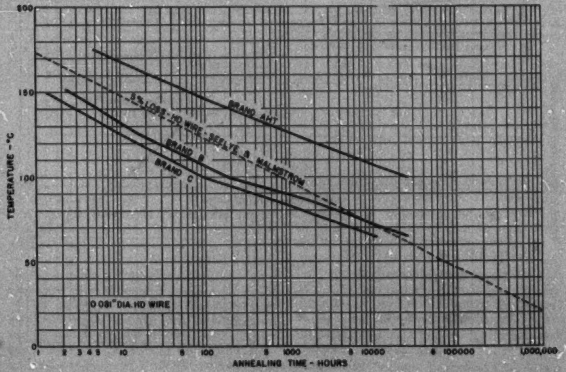

Figure 6. Comparison of annealing characteristics for 5 per cent loss in strength—no tension

Hard-drawn wire

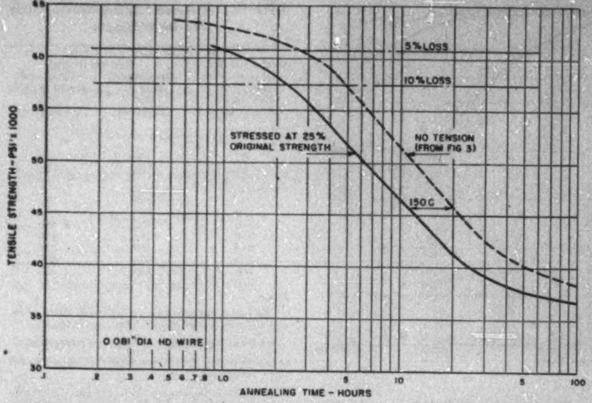

Figure 7. Effect of heat and time—with tension

Brand *B*—hard-drawn wire, 25 per cent original strength

for the commercial brands of copper available previously. These data indicate that hard-drawn copper wire made from these brands will undergo some loss in strength due to annealing even at these operating temperatures. Since no known adverse experience has resulted from ratings based upon these temperatures, it is concluded that under actual operation, these temperatures have not been obtained for a sufficient time to produce annealing due to atmospheric conditions (such as wind velocity) being more favorable than those upon which the ratings were based.

If it is accepted that maximum operating temperatures of 75–80 degrees centigrade have been satisfactory, on an equivalent annealing basis, Hy-Therm copper could be rated at 115 degrees centigrade. However, since it is probable that future lines will be designed to closer operating limits than formerly, it is suggested that a more conservative value of 100 degrees centigrade be selected.

Increasing the permissible maximum continuous operating temperature to 100 degrees centigrade will result in a substantial increase in current-carrying capacity, as shown in Table IV.

SHORT-TIME EMERGENCY LOADING

For commercial hard-drawn copper wire, manufactured to meet the requirements of American Society for Testing Materials specifications, the annealing characteristics are related primarily to the chemical composition of the brand of copper from which it is manufactured.

Brand *B* is representative of the commercial brands of copper more commonly used for overhead-line conductors.

Accordingly, for existing lines, in lieu of actual data on the brand used, it is suggested that short-time emergency current-rating calculations be based upon the annealing characteristics of brand *B* and consideration of local atmospheric conditions (ambient temperatures, wind velocities, and so forth) as proposed by others.[18,20,23,24]

For lines using Hy-Therm copper, these ratings will, of course, be much higher, since, for a given time, the annealing temperature is much higher.

Summary

A new brand of copper has been developed which, by virtue of increased resistance to annealing, permits higher current-carrying capacity and longer useful life under load with no significant loss in conductivity.

The annealing characteristic of copper is influenced by a number of factors:

1. The effect on annealing of noncuprous elements is the resultant of a complex interrelationship due to many variables and the net result appears to depend primarily on the ore and refining processes.
2. The effect of continuous heating is to start annealing immediately at a rate depending on the temperature and type of copper.
3. The effect of intermittent heating is directly cumulative.
4. The effect of externally-applied tension is to increase the rate of annealing.

These data enable continuous and short-time current-carrying capacities of overhead lines to be calculated more accurately.

Appendix—Test Procedure

Specimen Preparation

Three sets of wire samples were prepared from three 250-pound wire bars, one each of brands *AHT*, *B* and *C*. Each bar was hot-rolled to 5/16-inch diameter and the rods processed to 0.081-inch diameter hard-drawn wire.

Figure 8. Effect of intermittent heat and time—no tension

Brand *B*—hard-drawn wire

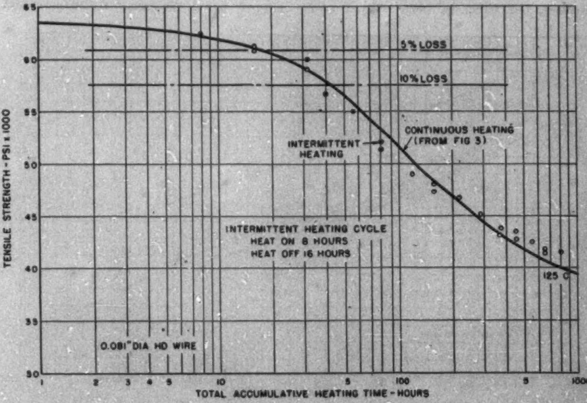

Annealing Without Tension

Tests were made at temperatures of 65, 85, 100, 125, 175 and 250 degrees centigrade by inserting a large number of duplicate 18-inch lengths of wire in a heating medium or oven and withdrawing two test pieces at scheduled intervals. Circulating-air ovens controlled within ±1 degree centigrade were used for the 65 to 125 degree centigrade tests. An oil bath controlled within ±2 degrees centigrade was used for the 150 and 175 degrees centigrade tests. A salt-bath tempering furnace controlled within ±5 degrees centigrade was used for the 250 degrees centigrade tests.

Annealing With Tension

In a circulating-air oven with a 32-inch effective heating length, duplicate samples were heated at 150 degrees centigrade controlled within ±1 degree centigrade while held under tension by calibrated springs. The springs were designed so that 1/16-inch extension exerted 1-pound pull at the working tension. Each spring was calibrated in a tensile-testing machine. The wires were threaded through closely-fitting holes in the ends of the oven and were fastened to a frame with the springs outside the oven. The oven was loaded with 12 samples and one sample withdrawn for test at scheduled intervals. A tension equal to 25 per cent of the original breaking strength of the wires was maintained throughout the tests.

Tensile-Testing Machine

Tensile-strength tests were made on a Southwark Tate-Emery testing machine having a 600-pound dial range reading in 0.5-pound divisions. The samples were pulled at a loading rate of 200-pounds-per-minute unless it was indicated that they were sufficiently annealed that an increase in testing speed had little effect on the results.

References

1. Electrical Characteristics of Transmission Circuits, **William Nesbit.** Westinghouse Electric and Manufacturing Company (Pittsburgh, Pa.) Reprint 82, February 1922.

2. Electrical Engineer's Pocket-Book, **Horatio A. Foster.** D. Van Nostrand Company, New York, N. Y., fifth edition, 1908.

3. Electrical Characteristics of Transmission Circuits, Westinghouse Engineers (compiled by William Nesbit) Westinghouse Technical Night School Press (Pittsburgh, Pa.) third edition, 1926.

4. Current Capacity of Wires and Cables, **G. E. Luke.** *Electric Journal* (East Pittsburgh, Pa.), volume 20, number 4, April 1923, page 127.

5. Overhead Systems Reference Book. National Electric Light Association (Edison Electric Institute, New York, N. Y.) Publication 267–5, 1927.

6. Heating and Current-Carrying Capacity of Bare Conductors for Outdoor Service, **O. R. Schurig and C. W. Frick.** *General Electric Review* (Schenectady, N. Y.), volume 33, number 3, March 1930, page 41.

7. Current-Carrying Capacity of Bare Cylindrical Conductors for Indoor and Outdoor Service, **C. W. Frick.** *General Electric Review* (Schenectady, N. Y.), volume 34, number 8, August 1931, page 464.

8. Symmetrical Components, **C. F. Wagner and R. D. Evans.** McGraw-Hill Book Company, Inc., New York, N. Y., first edition, 1933.

9. Conductor Load Limits Readily Determined, **E. P. Peck and H. B. Vincent, Jr.** *Electrical World* (New York, N. Y.), volume 103, June 23, 1934, page 912.

10. Standard Handbook for Electrical Engineers, **A. E. Knowlton.** McGraw-Hill Book Company, Inc., New York, N. Y., seventh edition, 1941.

11. Electrical Transmission and Distribution Reference Book. Westinghouse Electric and Manufacturing Company (Pittsburgh, Pa.), first edition, 1942.

12. Current Ratings for Electrical Conductors, **L. F. Hickernell.** Anaconda Wire and Cable Company (Hastings-on-Hudson, N. Y.), Publication C-51, October 1942. (For method of calculation, see Reference 13.)

13. Current Ratings of Overhead Conductors, **L. F. Hickernell.** Minutes of 29th Meeting, Transmission and Distribution Committee, Cincinnati, Ohio, October 19–20, 1942. Edison Electric Institute (New York, N. Y.), Appendix X, 1942, page 81.

14. Current-Capacity Ratings of Overhead Conductors (Roundtable Discussion). Minutes of 29th Meeting, Transmission and Distribution Committee, Cincinnati, Ohio, October 19–20, 1942. Edison Electric Institute (New York, N. Y.), 1942, page 19.

15. Conference on Emergency Loading of Transmission Systems. 1943 National Technical Meeting, AIEE. Electrical Engineering, volume 62, number 3, March 1943, page 121. (For summary, see Reference 16.)

16. Interim Report on Emergency Overloads on Overhead Conductors. AIEE Working Group on Towers, Poles and Conductors. Electrical Engineering (AIEE Transactions), volume 62, September section, 1943, pages 588–90.

17. Current-Carrying Capacity of Overhead Conductors. Minutes of 30th Meeting, Transmission and Distribution Committee, Pittsburgh, Pa., February 11–12, 1943. Edison Electric Institute (New York, N. Y.), 1943, page 14.

18. Ampere Load Limits for Copper in Overhead Lines. **A. H. Kidder and C. B. Woodward.** Electrical Engineering (AIEE Transactions), volume 62, March section, 1943, pages 148–52.

19. Current Rating of Overhead Conductors, **H. P. Seelye and A. L. Malmstrom.** Minutes of 30th Meeting, Transmission and Distribution Committee, Pittsburgh, Pa., February 11–12, 1943, Edison Electric Institute (New York, N. Y.), Appendix VII, 1943, page 64. (See Reference 20.)

20. Determining Current Ratings of Overhead Conductors, **H. P. Seelye and A. L. Malmstrom.** *Electric Light and Power* (Chicago, Ill.), part I, volume 21, December 1943, page 42; and part II, volume 22, January 1944, page 60.

21. Calculation of Current-Carrying Capacity of Overhead Conductors, **H. A. Enos.** Minutes of 30th Meeting, Transmission and Distribution Committee, Pittsburgh, Pa., February 11–12, 1943. Edison Electric Institute (New York, N. Y.), Appendix IX, 1943, page 67. (See Reference 22.)

22. Current-Carrying Capacity of Overhead Conductors, **H. A. Enos.** *Electrical World* (New York, N. Y.), volume 119, May 15, 1943, page 60.

23. Thermal Rating of Overhead Line Wire, **Myron Zucker.** Electrical Engineering (AIEE Transactions), volume 62, July section, 1943, pages 501–07.

24. Safe Ratings for Overhead Line Conductors, **L. M. Olmstead.** AIEE Transactions, volume 62, 1943, pages 845–53.

25. Electrical Heating Characteristics of Overhead Conductors, **E. E. George.** *Electric Light and Power* (Chicago, Ill). Part I, volume 22, December 1944, page 48; Part II, volume 23, January 1945, page 78; Part III, volume 23, April 1945, page 58; and Part IV, volume 23, December 1945, page 94.

26. Luncheon Conference during 30th Meeting of Transmission and Distribution Committee, Pittsburgh, Pa., February 12, 1943. Edison Electric Institute (New York, N. Y.).

27. Effect of Iron, Cobalt and Nickel on Some Properties of High-Purity Copper. **J. S. Smart, Jr. and A. A. Smith, Jr.** *Transactions*, American Institute of Mining and Metallurgical Engineers (New York, N. Y.), volume 147, 1942, page 48.

28. Effect of Certain Fifth-Period Elements on Some Properties of High-Purity Copper. **J. S. Smart, Jr. and A. A. Smith, Jr.** American Institute of Mining and Metallurgical Engineers (New York, N. Y.) *Transactions*, volume 152, 1943, page 103.

29. Softening of Hard-Rolled Electrolytic Copper, **N. B. Pilling and G. P. Halliwell.** *Proceedings*, American Society for Testing Materials (Philadelphia, Pa.), volume 25, part 2, 1925, page 97.

30. Copper and Copper Base Alloys, **R. A. Wilkins and E. S. Bunn.** McGraw-Hill Book Company, Inc., New York, N. Y., first edition, 1943, pages 5–9.

31. Effect of Temperatures Attained in Overhead Electric Transmission Cables, **A. v. Zeerleder and P. Bourgeois.** *Journal*, Institute of Metals (London, England), volume 42, 1929, page 321.

32. The Comparative Properties of Several Types of Commercial Coppers, as Cold Worked and as Recrystallized. **L. R. Jackson, A. M. Hall, and A. D. Schwope.** *Technical Publication number 2274* American Institute of Mining and Metallurgical Engineers (New York, N. Y.), September 1947.

Discussion

Engineers of Bonneville Power Administration (Portland, Oreg.): The authors describe a new brand of copper called "Hy-Therm" which appears to have improved annealing characteristics, permitting higher current loadings.

The Bonneville Power Administration generally uses a thermal limit of 75 degrees centigrade (50 degrees centigrade rise above an ambient of 25 degrees centigrade with 1.4 mile-per-hour wind) which is based upon 75 per cent of the maximum current carrying capacity of the conductor. The new *AHT* (Anaconda Hy-Therm) copper is claimed to operate comparably at 115 degrees centigrade; however, 100 degrees centigrade is suggested as a conservative value for design.

If 100 degrees centigrade is used for this *AHT* copper, the authors point out that for 500,000-circular mil conductors the current rating could be increased from 835 to 995 amperes for a 19.6 per cent increase over commercial brand copper.

It would, perhaps, be undesirable, if this conductor were used, to increase the present current in the conductors of the Bonneville Power Administration system by 19.6 per cent because of the increase in the power losses. However, the use of *AHT* copper appears to provide a safety factor which could result in a considerable reduction in annealing effects during overload conditions.

Both system stability and power loss would limit the advantageous use of this conductor in the Bonneville Power Administration system, except in short heavily-loaded transmission lines.

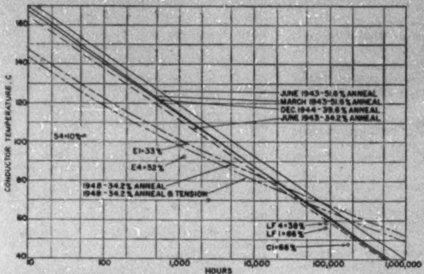

Figure 1 (left). Allowable time at various conductor temperatures for hard-drawn copper

Ultimate strength 64,000 pounds per square inch, design limit 50 per cent ultimate

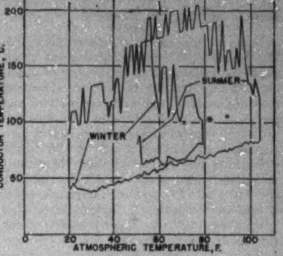

Figure 5 (right). Conductor temperature range of number 4/0 7-strand bare copper at 760 amperes

Leonard M. Olmsted (Duquesne Light Company, Pittsburgh, Pa.): This paper is a most welcome addition to the technical information required for intelligent and safe loading of hard-drawn copper conductors. Now, for the first time, operating engineers are able to discard approximations derived from various and scattered sources and to make use of an authoritative and comprehensive survey of the effect of operating temperatures upon the tensile strength of hard-drawn copper conductors.

A group of papers published early in 1943 reported the efforts of several engineers to make higher ratings available for war-time use on overhead circuits. In our own case, the beginning was late in 1938, nearly 12 years ago, when we were contemplating an increase in peak from 367 megawatts to a maximum of approximately 460 megawatts. With only slight changes, other than adding generating capacity, this bulk power system has since carried 719 megawatts.

Under such circumstances, it is quite natural that each important addition to the technical literature has been reviewed carefully to determine whether the original premises were sound, and to improve upon the accuracy of our ratings. The effect of several such reviews is shown in Figure 1 of the discussion. These time-temperature curves are plotted, not for an arbitrary five per cent loss of strength, but for what was considered to be the limit before replacement would be necessary. The curve entitled "March 1943—51.6 per cent anneal" reproduces the data used in our earlier technical paper. Additional data secured from discussion of this paper justified revision to the curve entitled "June 1943—51.6 per cent anneal." Tests of elastic limit after partial annealing during 1944 forced us to revise the time-temperature limit to the curve entitled "December 1944—39.6 per cent anneal," which was used for some time as the basis for our overhead line ratings.

Subsequent to the termination of hostilities, our thinking relative to ratings has become somewhat more conservative, particularly reflected in the additional restriction that the factor of safety should be maintained above 1.66 in order to comply with the general requirements of the National Electric Safety Code. The data presented in this paper have been plotted accordingly as shown by the dash line entitled "1948—34.2 per cent anneal." Inasmuch as the paper also shows an accelerated loss of strength under tension, a further reduction has been estimated in deriving the final curve entitled "1948—34.2 per cent anneal and tension." In my opinion, there is surprisingly close agreement between curves derived from these two radically different sources, the principle difference being in the slope of the curves. The time-temperature limits deduced from the original 1943 curve and from the final 1948 curve are shown by the circles "C 1" representing 1943 continuous, "LF 1" 1943 load factor, "LF 4" 1948 load factor, "E 1" 1943 emergency, and "E 4" 1948 emergency after "S 4" switching period. The change in these time-temperature limits is well within the 20 per cent margin recommended to cover suspected inaccuracies in the 1943 data, and the final ratings are almost identical.

Figure 2. Wind velocities recorded at various air temperatures

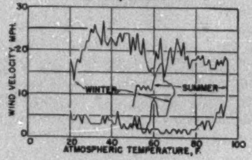

Figure 3. Wind velocities recorded at various effective air temperatures including sub heating

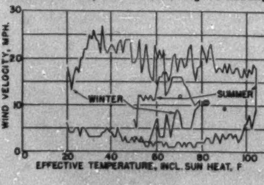

Figure 4. Conductor temperature range of number 4/0 7-strand bare copper at 510 amperes

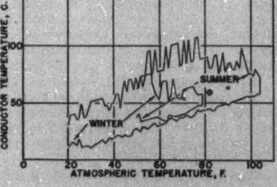

The authors' discussion of the effects of chemical composition, tension loading, intermittent heating, and manufacturing technique helps greatly to settle the questions which have persisted about these aspects of the thermal capability of copper conductors. Their treatment of current ratings, however, could prove somewhat misleading. After showing that a maximum temperature of 75 degrees centigrade on hard-drawn average copper causes a five per cent loss of strength in 7,000 hours, they then propose to rate the conductors for that temperature with 25 degrees centigrade ambient air moving at 1.36 miles per hour crosswise to the conductor, giving a rating of 480 amperes continuous for number 4/0 stranded copper. While the probable distribution of coincident velocities and air temperatures in this latitude is such that the temperature of the conductor would seldom exceed 75 degrees centigrade, and much of the time would be materially lower, short-time emergency ratings appreciably higher than 480 amperes are necessary to make firm this continuous rating.

Data from a recent analysis of 4/0 conductor loading at 510 amperes illustrate this point. Figure 2 of the discussion shows the range of coincident wind velocities and ambient temperatures from approximately 10,000 hourly observations. Figure 3 of the discussion shows the same data with the temperature adjusted during sunshine hours for sun heating, indicated as "effective temperature." Here the concentric circle denotes the annual equivalent effective temperature and wind velocity, and the single circles show the summer and winter allocations of it. Applying these cooling limitations to a 4/0 conductor carrying 510 amperes continuously gives the conductor temperature pattern shown in Figure 4 of the discussion. A practical emergency short-time rating to use with a 510-ampere normal rating would be 760 amperes; the conductor temperature pattern for this current is shown in Figure 5 of the discussion. The temperature reaches such a high level that there seems to be no practical way to maintain safe clearance over ground and structures underneath the spans, and there is considerable doubt that permanent splices and joints could be made.

This recent analysis was made primarily to check the validity of our earlier estimate that a 20-year life represented an economic balance of carrying costs, maintenance costs and line losses. It was found that a life span on the order of 75 years gives a lower annual cost per ampere without serious

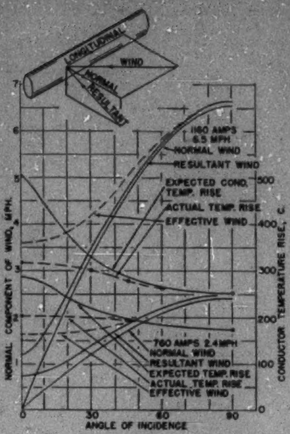

Figure 6. Effect of wind angle upon conductor cooling

sacrifice of ratings. These ratings, incidentally, are 420 amperes normal at system load factor, and 580 amperes for an emergency day following a 1-hour switching period at 630 amperes. The maximum conductor temperature is 125 degrees centigrade, which is about the highest value for which we believe it is feasible to provide and maintain satisfactory clearances to ground and structures beneath the line.

Calculations of the dissipation of heat from conductors must assume some definite angle of incidence of the moving air against the conductor. Common practice is to reduce the wind velocity by some arbitrary factor and assume the angle to be 90 degrees. Figure 6 of the discussion is presented to show the importance of this angle of incidence. Theoretically wind in a longitudinal direction has no normal component, consequently its cooling effect upon the conductor should be similar to still air, and the only normal component of wind would be in a vertical direction caused by heating of the air surrounding the conductor. For other angles between 0 and 90 degrees, the resultant of this vertical movement and the normal horizontal movement is plotted together with the expected conductor temperature rise, for two different conductor currents and wind velocities. Plotting on this same diagram the limited experimental data, shown by circles, implies that the actual temperature is not nearly as severe as calculations indicate. Inasmuch as the cooling effect of a minimum wind at zero angle establishes the maximum conductor temperature for which clearance must be provided, sometimes at considerable cost, this problem appears to justify further investigation.

After such a discussion, you may well wonder what value can be attached to the development of Hy-Therm copper for conductors. Economic considerations are such that utilization of the greater available normal capability does not appear attractive, but there is no question that a considerable factor of safety has been added. The restriction of emergency ratings for present copper solely to conditions arising from accidental loss of capacity certainly could be liberalized, particularly to facilitate maintenance work. It must be assumed, of course, that these improved thermal characteristics have been attained without sacrificing any qualities which are important in overhead conductors.

In closing this discussion, I wish once more to compliment the authors for their valuable contribution to the literature on copper conductors and to state the opinion that it, together with concurrent developments in related materials, will enable utility operating engineers to establish safer and more satisfactory ratings for their overhead plant.

K. S. Wyatt (Phelps Dodge Copper Products Corporation, Yonkers, N. Y.): This paper on the uses of coppers with higher annealing points for over-head conductors to permit higher normal and emergency current loading is very interesting. The authors are to be congratulated.

They have raised the annealing point without appreciable change in electrical conductivity by adding trace elements to a pure grade of electrolytic copper. In Table II they list 12 such elements. It should be pointed out that it is important to control the quantities of certain of these trace elements within narrow limits, otherwise the development loses its significance.

Of course, the pronounced effect of trace elements on the properties of copper is not entirely unknown, in fact considerable work has been done in this field, as is evidenced by the list of references in the authors' paper. The use of these trace elements commercially is, however, a relatively new and important departure.

It must not be thought that there is one, and only one, combination of these trace elements which yields a copper with a high anneal point. Our own metallurgical department has had considerable experience in this field. They report that they have developed a high anneal point copper having similar properties to the copper described by the authors, and are currently supplying the requirements of utility engineers for this type of conductor.

L. F. Hickernell, A. A. Jones, and C. J. Snyder: In general, the comments by the discussors appear to center more on the bases chosen for comparison, rather than on the experimental data presented in the paper. In this connection, it was not our intention to establish absolute methods (as for current-carrying-capacity calculations) or bases (such as ambient temperature, permissible loss in strength, wind velocity, and so forth) for making the comparisons, but instead to use those accepted most generally in the literature so that some approximate evaluation could be made of the new material.

It appears that Olmsted is in general agreement with our approach to the annealing problem and that he does not question the data presented. Some leeway must be allowed and judgment exercised in the choice of a suitable limiting parameter of loss in strength. Strictly for purposes of comparison, we chose the 5 per cent reduction because it is conservative and has been used previously (see reference 20 of the paper). Similar comparisons could be made on the basis of elastic limit after annealing (but there is a scarcity of authoritative data on this characteristic) or final factor of safety (ratio of partially annealed strength to design tension). The general results of such comparisons would be similar.

The discussion of current ratings also was included only for purposes of comparison. For this reason, only a relatively few ratings were given, sufficient only to establish that the allowable increase is in the order of 20 per cent. The choice of 75 degrees centigrade operating, 25 degrees centigrade ambient temperature and 2 feet-per-second crosswise wind was based on rather widespread usage of these conditions for tabular ratings (see reference 11 of the paper) with no indication that they have not proved satisfactory in service. Basic data on long-time annealing characteristics of commercial coppers were presented in such form that the user could apply them to determine current ratings under any particular set of local weather conditions in which he was interested. This applied equally to continuous ratings and emergency ratings.

We believe the possible increase in sag and decrease in line clearance due to higher operating temperatures has been overestimated. For example, with a number 4/0 American wire gauge 7-wire hard-drawn copper conductor on a 500-foot span, the increase in sag due to an increase in operating temperature from 75 to 100 degrees centigrade is only 1.3 feet. National Electrical Safety Code clearances are set at 60 degrees Fahrenheit and presumably they are sufficiently conservative to provide adequate clearance at any operating temperatures under all normal conditions of line installation. The slight increase in sag due to higher conductor temperatures shown before indicates this to be so. Similarly, if the span length is adjusted to maintain the same sag, only a slightly larger number of supports is required. For example, using the same conductor cited before, the sag in a 478-foot span at 100 degrees centigrade is the same as that in a 500-foot span at 75 degrees centigrade and the corresponding numbers of structures per mile are 11.1 and 10.6, an effective increase of one structure in two miles of line.

There are so many varieties of connectors used in line construction that no general statement regarding their thermal capacity is possible. However, tests on splicing and dead-end connectors of the type which we make, have shown that they run considerably cooler than the conductor to which they are attached (see reference 13 of the paper). Therefore permanent splices could be made for operation at the higher temperatures.

The discussion of angle of incidence of wind to the conductor appears to be correct theoretically but is difficult to apply practically because of the many variables involved.

Changes in line direction and in contour, sag in the conductor, and continual variation in wind direction all contribute to producing a higher component of wind normal to the conductor. As a matter of fact, Olmsted's data show this to be true, because "actual" temperature rises plotted in his Figure 6 show little variation with angle of incidence.

The improved thermal characteristics of Hy-Therm copper have been obtained without sacrificing any qualities which are important in overhead conductors. Hy-Therm is a commercial copper, developed to have the outstanding property of resistance to annealing. Its purity, electrical conductivity, strength, elongation, fatigue resistance, and crystal structure are all similar to regular copper wire. It meets all existing industry specification requirements for electrolytic copper wire and cable.

Referring to the discussion by the engineers of the Bonneville Power Administration: we appreciate that there are factors other than annealing (such as system stability and power loss) involved in selecting ratings of transmission conductors under normal operating conditions. In many cases, these other factors will govern in establishing normal operating ratings. However, the additional resistance to annealing inherent in Hy-Therm copper is of real value in permitting higher emergency loadings, as for example in the case of failure in one circuit of a double-circuit line and the remaining circuit has to carry practically double load for some time.

Answering Wyatt's discussion, the chemical analysis given in Table II of the paper is a composite list of the 12-trace elements which occurred in a total of 21 brands of copper.

Not all these elements occur in any one brand. Furthermore, only a few of them have any appreciable effect on the annealing characteristic. In Hy-Therm copper the complexity of control is avoided by using a very pure electrolytic copper to which small quantities of simple hardening agents are added.

It was not our intent in the paper to imply that only one combination of elements could accomplish the result desired. It is recognized that the annealing resistance of other brands of copper could be increased by suitable adjustment of their chemical composition. If this has been done commercially, published data similar to that given for Hy-Therm would be of interest to the industry.

Universal Curves for D-C Controllable Reactors

WALTER C. JOHNSON
MEMBER AIEE

B. C. MERRELL
STUDENT MEMBER AIEE

R. E. ALLEY, JR.
ASSOCIATE AIEE

Synopsis: This paper describes a graphical method for calculating the steady-state characteristics of d-c controllable reactors, using universal curves drawn on a per-unit basis. The phenomenon of d-c flux reduction, caused by the alternating current acting on the nonlinear flux path, is pointed out, and certain general conclusions are drawn. Comparison with experimental results indicates that the accuracy is reasonably good.

A D-C controllable reactor is an iron-cored inductor in which the a-c impedance can be varied over wide limits by magnetically saturating the iron with an auxiliary d-c winding. Because of its ruggedness, ease of control, and low losses, it has found ever wider application as a control device.

Many of the applications and general characteristics of the d-c controllable reactor have already been described in the literature,[1-10] but no reasonably complete quantitative theory of its operation has hitherto been published. The widespread use of these devices has made it seem desirable to investigate their properties analytically. The purpose of this paper is to present in an easily usable form the method and results of such an analysis. The present paper treats the steady-state characteristics only. The results are applicable to the calculation of the characteristic curves of a reactor from either its d-c or its a-c saturation curve. The computation can be made on either an rms or an average current basis. The universal curves presented herein can be used in a straightforward quantitative fashion, or they can be used in a qualitative or semiquantitative fashion, to enable one to determine, for example, the effect of using a magnetic material with different characteristics. The analysis also enables one to calculate the d-c flux linkage, a quantity which is difficult to measure in the d-c controlled reactor and which, as will be shown, is only partially determined by the control current. A knowledge of the d-c flux linkage is, of course, essential to the computation of transient characteristics.

The method of calculation has been checked experimentally for a number of 60-cycle reactors with silicon steel cores and for two 400-cycle reactors with high-permeability cores. The error in the computed rms alternating current has been generally less than ten per cent for silicon-steel reactors. The error in the average alternating current is generally smaller than that of the rms current. A somewhat greater error is obtained with high-permeability cores, ranging sometimes up to 15 per cent on the conservative side. These errors are within the expected limits for calculations on nonlinear circuits.

Description of Operation

A highly important phenomenon in the operation of the d-c controlled reactor is the reduction in d-c flux caused by the alternating current acting on the nonlinear flux path. Consequently, a brief description of the operation of the reactor will be given with the view of showing how this phenomenon takes place.

Figure 1 shows schematically three familiar forms of the d-c controlled reactor. In each case, the two a-c windings can be connected either in parallel, as shown, or in series. The same theory applies to all three forms of the reactor and, for definiteness and convenience, we shall refer to that of Figure 1(c). This latter type is the only one in which the a-c and d-c flux paths are congruent. Therefore, for the other types, additional current for the extra d-c flux path must be added to the direct current as read from the universal curves.

A-C COILS IN PARALLEL

Referring to the reactor of Figure 1(c), and considering for the moment the condition of zero direct current, it can be seen that each half of the device behaves separately as an iron-cored reactor, with the coil current corresponding to the magnetizing current of a transformer. Since the a-c fluxes in the two halves are in opposite directions with respect to the d-c coil, very little a-c voltage is induced in the d-c winding.

Assume, for convenience, that the a-c and d-c turns are equal and that hysteresis is negligible. If direct current is applied to the d-c winding, a certain d-c flux will be set up in the path shown in Figure 1(f). The magnetization curve for the left half of the reactor is shown in Figure 2(a). The net flux linkages in this element consist of the d-c linkages, ψ_0, plus an a-c component which depends upon the applied voltage. The time variation of the flux in the left element is shown in Figure 2(a), assuming a sinusoidal voltage. The current wave shape can now be traced point by point from the magnetization curve, with the result shown in the lower right-hand quadrant of Figure 2(a), in which the time axis for the current runs vertically downward. Since no direct current will be present in the a-c coil winding in steady state, the average value must represent the current in the d-c winding. The variation about this average is the current in the a-c coil, and is redrawn in Figure 2(b).

Paper 49-4, recommended by the AIEE transformer committee and approved by the AIEE technical program committee for presentation at the AIEE winter general meeting, New York, N. Y., January 31–February 4, 1949. Manuscript submitted October 21, 1948; made available for printing November 24, 1948.

WALTER C. JOHNSON is professor of electrical engineering at Princeton University, Princeton, N. J.; B. C. MERRELL is an engineer at Procter and Gamble, Cincinnati, Ohio; and R. E. ALLEY, JR., is assistant professor of physics at the University of Richmond, Richmond, Va.

The work presented in this paper has been supported in part under a contract with the General Electric Company.

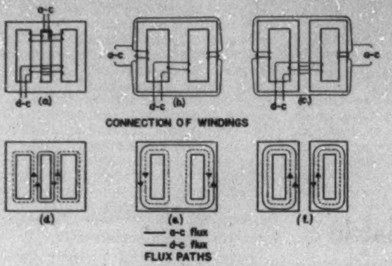

Figure 1 (left). Schematic diagrams of different types of d-c controllable reactors

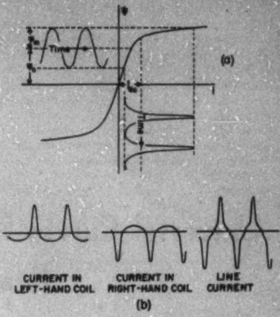

Figure 2 (right). Flux linkage and current relations

We now can observe the important point that, because of the nonlinearity of the magnetization curve, we must expect that the average flux and the average current will not intersect on the curve; in particular, ψ_0 will always be lower than the intersection of I_{dc} with the curve. Under the usual operating conditions, the effect is very much greater than can be shown in the illustration, a ratio of ten or more between I_{dc} and the intersection of ψ_0 being not at all unusual. The d-c flux and direct current will intersect on the magnetization curve only when the a-c voltage is extremely small. The reduction in ψ_0 with increasing a-c voltage can be regarded as caused by a demagnetizing action that the alternating current exerts on the d-c flux path because of the nonlinearity in the characteristics of the core material.

Considering next the right-hand half of the reactor, it can be seen from symmetry considerations that the alternating current will be similar to that in the left-hand half, but reversed and shifted in phase position by half a cycle. This is shown in Figure 2.

The alternating line current is the sum of the two coil currents, and, as shown in Figure 2, contains odd harmonics only. The even harmonics circulate between the two coils.

A-C Coils in Series

The foregoing discussion has assumed that the a-c coils are connected in parallel. With this arrangement, a sudden change in the control voltage will cause a transient current to circulate between the two a-c coils, temporarily bucking out the normal d-c flux and slowing down the response of the reactor. When a somewhat greater speed of response is desired, the two a-c coils may be connected in series, thus eliminating the path for the circulating transient. However, this does not permit the flow of even harmonics of current between the a-c coils, and, instead, even harmonics appear in the d-c winding. The ratio of d-c to a-c turns is often rather large, and if the source of direct current offers a high impedance to the flow of harmonic currents, the a-c voltage at the terminals of the d-c winding may become large. In the following discussion of the series connection, we shall assume that the d-c source has a low a-c impedance.

If the series-connected reactor of Figure 3 is controlled from a low-impedance d-c source, no appreciable a-c voltage can be developed across the d-c coil. Since the a-c and d-c coils on each core are closely coupled, this can be true only if the instantaneous voltages across the two a-c coils are at all times equal and in phase. Otherwise, transformer action would result in a net a-c voltage appearing across the d-c coil. If the applied voltage is sinusoidal, the voltage across each a-c coil will be a sine wave of half the line amplitude.

Assuming a unity turns ratio for simplicity, and designating the instantaneous magnetizing currents of the two halves by i_{m1} and i_{m2} respectively, we have, by reference to Figure 3

$$i_a+i_b=i_{m1} \tag{1}$$

and

$$i_a-i_b=i_{m2} \tag{2}$$

Adding and subtracting equations 1 and 2, we obtain for the instantaneous currents in the a-c and d-c windings respectively,

$$i_a=\frac{i_{m1}+i_{m2}}{2} \tag{3}$$

and

$$i_b=\frac{i_{m1}-i_{m2}}{2} \tag{4}$$

In contrast with this, we have for the parallel case $i_{\text{line}} = i_m + i_{m2}$ and $i_b =$ average value of i_{m1}.

If the line voltage considered in the discussion of the parallel case is doubled in magnitude and applied to the series-connected reactor, the voltage which the a-c coil of each half must absorb is the same as that causing the variation of flux linkages shown for the parallel case in Figure 2(a). The magnetizing currents will be the same as for the parallel case; therefore, referring to equation 3, the line current will be of the same form as previously but will have half the former magnitude. The current in the d-c winding will contain harmonics of even order (see Figure 4(b)), as can be shown from equation 4.

Method of Analysis and Assumptions

The mathematical analysis of circuits containing saturable iron depends primarily upon the use of an equation to represent the magnetization curve of the iron. Various methods have been suggested in the past, including the hyperbolic tangent, the power series, and a representation by the segments of straight lines. It has been recognized that the power series offers the possibility of considerable accuracy, but the objection has been that a series containing even a moderate number of terms is difficult to manipulate. The present analysis is based on the representation of the magnetization curve by an equation contain-

Figure 3. Series connection of a-c coils

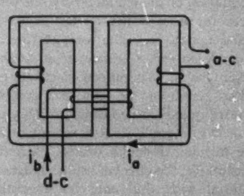

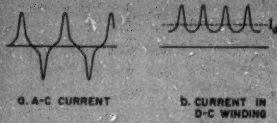

Figure 4. Currents with series connection; low a-c impedance in d-c supply

ing only one power term in combination with a linear term. The basic equation is

$$i = C_1\psi + C_n\psi^n \tag{5}$$

where

i = the instantaneous current,
ψ = the instantaneous flux linkage,
C_1, C_n, and n are constants which depend upon the shape of the magnetization curve.

The choice of this equation represents a compromise between the desire for accuracy and the need for simplicity in a difficult nonlinear problem. The equation lends itself to manipulation better than most, and experience with a number of different reactors has indicated that a wide variety of magnetization curves can be fitted with good accuracy. No provision has been made for the reverse curvature found at the lower end of the magnetization curve. For the present purpose, this was not of great importance, as it would affect the results mainly at the lowest a-c flux densities. A term representing hysteresis was originally added, but this was dropped because the additional complication did not seem to be justified.

In the analysis, the equations for the d-c magnetization curve and for the a-c saturation curve are related to each other. Calculations are then made for the unsymmetrically magnetized condition and the results are presented in the form of universal curves plotted in terms of dimensionless groups for n = 5, 9, and 15. Other values of n can be used by interpolation.

In addition to the assumptions mentioned in the foregoing paragraphs, the following assumptions were made so as to simplify the analysis without unduly affecting the accuracy.

1. The analysis is based upon a sinusoidal variation of flux with time. When the d-c excitation of the reactor is small, the impedance will be large, and most of the supply voltage will appear across the reactor. Under these conditions the flux will be nearly sinusoidal. Increased d-c excitation will reduce the impedance of the reactor; consequently, the current will increase and the reactor voltage will decrease. Under these conditions the terminal voltage and hence the flux may not be sinusoidal. However, it has been shown previously[11] that under low-voltage high-current conditions the characteristic curves of the reactor are little affected by the form of the voltage. Hence, in the working range of the reactor, reasonably accurate results can be obtained from computations made on the basis of a sinusoidal flux.

2. It is assumed that the flux follows the normal magnetization curve when the core is magnetized unsymmetrically. Experiments made on the usual types of transformer steel[13] have shown that this assumption should produce but little error except at low a-c flux densities. At low densities, the actual unsymmetrical hysteresis loop may be considerably inclined from the angle of the normal magnetization curve, and it is to be expected that the actual impedance will be lower than calculated. The error is in such a direction as to make the design more conservative.

3. The analysis assumes either that the a-c coils are connected in parallel or, if they are connected in series, that the source of direct current has a low a-c impedance.

4. Leakage flux is neglected.

The Universal Curves and Their Use

Preliminary Procedure

The universal curves are designed to be used in connection with the a-c saturation curve of the reactor as measured from the terminals of the a-c winding. As will be shown later, however, one can also work from the normal magnetization curve of the core material.

We shall assume that data are available on the relation between rms voltage and current as measured at the a-c terminals with zero direct current. The straight-line portion of the saturation curve (analogous to the air-gap line in machinery calculations) is first removed by subtracting the currents corresponding to this straight line. The saturation curve with the straight-line portion removed will be called the "reduced saturation curve." A base current, I_b, is then selected. The exact magnitude of this is not important, but it should be at least as large as the greatest expected alternating current in the reactor. The a-c voltage corresponding to I_b on the reduced saturation curve will be called the base voltage, E_b.

Since we are attempting to fit a power function, it might seem logical to plot the reduced saturation curve on log-log paper and measure the slope to the best straight line. However, this procedure is likely to overemphasize the lower portion of the curve and underemphasize the important top portion. Better results have been obtained by plotting the reduced saturation curve on the chart of Figure 5 and comparing with the power curves given. A per-unit basis is used in this chart, that is, one plots E/E_b and I/I_b. Interpolation can be used to find powers between the three shown. Reactors with silicon-steel cores have been found to fit a power curve remarkably well, as is illustrated in Figure 5 for a commercial reactor. The saturation curves of high-permeability cores do not fit as well, but the accuracy is still within reasonable limits.

The Universal Curves

Once the appropriate power has been determined for the reduced saturation curve, the universal curves of Figures 6 to 12 can be used directly to relate the a-c voltage and current, the required direct current, and the d-c flux of the reactor

Figure 5. Chart for fitting a power to a saturation curve

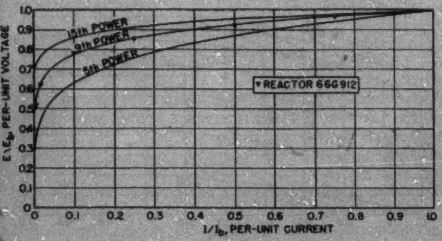

Figure 6. Universal curves for a fifth-power saturation curve, plotted in terms of effective current

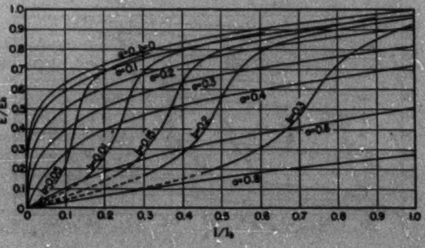

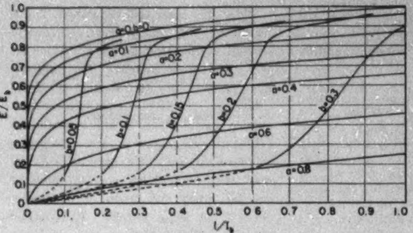

Figure 7. Universal curves for a ninth-power saturation curve, plotted in terms of effective current

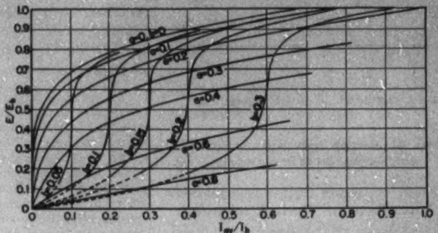

Figure 9. Universal curves for a fifth-power saturation curve, plotted in terms of average current

when operating with d-c saturation. A correction, generally small, must be added to take account of the straight-line portion previously removed from the saturation curve. This correction can be made graphically and is described later. Interpolation between the powers given can be made as necessary.

Figures 6 to 8 show, on a per-unit basis, the relations in terms of the rms current and voltage. Figures 9 to 11 show the corresponding relations for the average alternating current. In Figure 12 a comparison of the average currents obtained with curves of different powers is shown, together with the corresponding curves that would be obtained if the core material had ideal characteristics with a vertical side and a horizontal top. The small difference between the various average-current curves is striking.

The curves are plotted in terms of the following dimensionless groups:

E/E_b, where E is the rms voltage applied to the a-c terminals, and E_b is the rms base voltage selected previously.

I/I_b, where I is the rms alternating line current neglecting the straight-line correction, and I_b is the rms base current selected previously.

I_{av}/I_b, where I_{av} is the average alternating line current neglecting the straight-line correction.

$a=\psi_0/\psi_b$, where ψ_0 is the d-c flux linkage of one a-c coil, and ψ_b is the maximum a-c flux linkage which would be caused by the base voltage, E_b. ($\psi_b=\sqrt{2}E_b/\omega$).

$b=\dfrac{I_0}{I_b}\dfrac{N_{dc}}{N_{ac}}$, where I_0 is the current in the d-c winding, neglecting the straight-line correction. The quantity N_{dc} is the number of turns on the d-c winding; N_{ac} is the number of turns on one a-c coil in the parallel case, and is the total number of turns on both a-c coils in the series case.

STRAIGHT-LINE CORRECTIONS

The straight-line portion of the saturation curve adds a correction to the alternating current at any given a-c voltage as follows: to the rms current, I, as obtained from the universal curves, add the current given by the straight-line portion of the saturation curve at the given voltage to obtain the total rms line current; for the average current, I_{av}, as obtained from the universal curves, add 0.9 of the straight-line portion of the saturation curve to obtain the total average line current.

The straight-line portion of the saturation curve also adds a correction to the direct current. From the universal curve, read $a = \psi_o/\psi_b$ and compute a fictitious voltage $E_o = aE_b$. (Physically, this represents the a-c voltage which would produce a peak a-c flux equal to the d-c flux). Read the current corresponding to E_o from the straight-line portion of the saturation curve (see I_o' in Figure 13), and add to the direct current the following amount

$$\text{Additional direct current} = 0.707 I_o' \frac{N_{ac}}{N_{dc}} \quad (6)$$

ADDITIONAL D-C FLUX PATHS

When the reactor has a portion of the d-c flux path which is not traversed by the a-c flux, as in the reactors of Figure 1a and b, the additional direct current required for the added path can be found approximately as follows:

Compute the fictitious voltage $E_0 = aE_b$. At the value of voltage given by E_0, go horizontally across to the point P shown in Figure 13, which is located so that $m = 0.65\ n$. This point can be located with sufficient accuracy by eye. Read the current I_0'', and add to the direct current the following amount:

$$\text{Additional direct current} = 0.707 I_0'' \frac{N_{ac}}{N_{dc}} \; \frac{\text{Length of additional d-c flux path}}{\text{Length of a-c flux path for one a-c coil}} \quad (7)$$

EXAMPLE

The calculation of one point for the General Electric reactor Number *66G912* will be given to illustrate the method. The reactor is of the type shown in Figure

Figure 8. Universal curves for a fifteenth-power saturation curve, plotted in terms of effective current

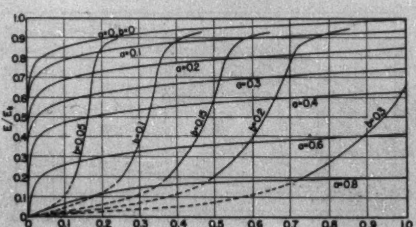

Figure 10. Universal curves for a ninth-power saturation curve, plotted in terms of average current

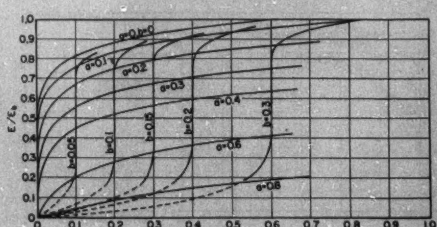

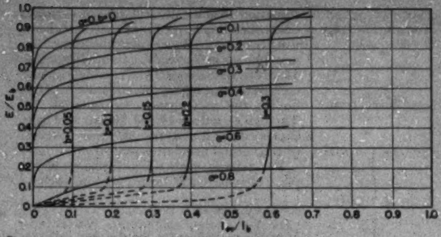

Figure 11. Universal curves for a fifteenth-power saturation curve, plotted in terms of average current

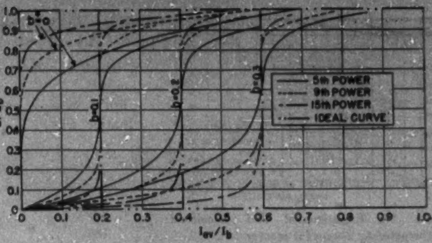

Figure 12. A comparison of the average-current curves

1(a), and, with the a-c windings connected in parallel, has the a-c saturation curve given by the top solid curve of Figure 14. Several points on this saturation curve have been plotted on the chart of Figure 5, using the base values $I_b=28$ amperes and $E_b=200$ volts. The curve is seen to fit a ninth-power equation quite well without removal of a straight-line portion. The reactor has $N_{ac}=230$ for one a-c coil and $N_{dc}=4{,}000$.

We shall calculate the direct current necessary to produce an alternating current of 20.9 rms amperes at 140 rms volts. Using the ninth-power chart, Figure 7, with $E/E_b=140/200=0.7$ per unit and $I/I_b=20.9/28=0.746$, we read from the chart $b=0.25$ and $a=0.32$. Then, from the definition of b, we have

$$I_o=b\,I_b\frac{N_{ac}}{N_{dc}}$$

$$=0.25\times 28\times\frac{230}{4000}=0.403 \text{ ampere}$$

Since no straight-line portion was removed from the saturation curve, the only other calculation necessary is the direct current required for the additional d-c flux path in the outer legs. The ratio of this length to the length of the a-c flux path for one a-c coil is measured to be 0.60. We compute the fictitious voltage $E_o=aE_b=0.32\times 200=64$ volts, and, following the method shown in Figure 13, we use Figure 14 and find I_o'' to be 0.3 ampere. Then, from equation 7, we have

$$\text{Additional direct current}=0.707\times 0.3\times\frac{230}{4000}\times 0.60=0.007 \text{ ampere}$$

The total required direct current for $E=140$ volts, $I=20.9$ amperes, is therefore

$$I_{dc}=0.403+0.007=0.410 \text{ ampere}$$

The measured value at this point was 0.416 ampere.

A complete set of calculated points for both rms and average currents is shown in Figure 14, together with the characteristic curves obtained experimentally.

Discussion of the Results

In the section entitled Description of Operation, the demagnetizing action of the alternating current upon the d-c flux was mentioned. This phenomenon is shown quantitatively in all of the universal curves, for, if one follows a curve of constant per-unit direct current, b, in the direction of increasing alternating current, the value of d-c flux linkage decreases markedly, as indicated by a reduction in the quantity $a=\psi_o/\psi_b$.

An interesting comparison is obtained between the values of direct current required for core materials with different saturation characteristics. Considering first Figures 6 to 8 for the rms current, it can be seen that the fifth-power curve for a per-unit direct current of 0.2 corresponds roughly with the fifteenth-power curve for $b=0.15$. The reduction in d-c excitation afforded by the much sharper-breaking curve is appreciable but perhaps not as great as one might expect. The reason is that the phenomenon of d-c demagnetization is stronger for the faster-breaking curves and tends to reduce their effectiveness. Figure 12 shows a similar comparison on an average alternating current basis, and here the difference between the various powers is strikingly small. In the lower-voltage region the sharper-breaking curves have an appreciable advantage, but at the higher voltages the reverse is actually true. Even the ideal magnetization characteristic with a vertical side and horizontal top does not affect the results greatly. For this latter case, the average-current characteristic curves have vertical sides at $I_{av}/I_b=2b$, that is, at $N_{ac}I_{av}=2N_{dc}I_o$, as has been shown previously by Uno Lamm.[1] The average-current curves are, of course, the important ones in circuits where the output is rectified, including those in which rectified feedback is employed.

The order of magnitude of the straight-line corrections is interesting. The correction is most important when the value of a is large, that is, at the lower voltages. In the region of low a-c voltage and current, the percentage increase in direct current due to the straight-line correction may be considerable in some cases. At the higher a-c voltages it is often negligible.

In the universal curves of Figure 6 to 11 it will be seen that the characteristics at low a-c voltages are shown dotted. In this region one should deal with the incremental permeability, and, since the present analysis assumes that the flux follows the normal magnetization curve, the figures do not give reliable information at low voltages. In general, the a-c impedance in the very-low-voltage region will be somewhat smaller than the figures indicate.

An aspect of the calculations which has not been emphasized is the fact that the charts make it possible to calculate the

Figure 13. Graphical method for computing the additional direct current required for an added d-c flux path

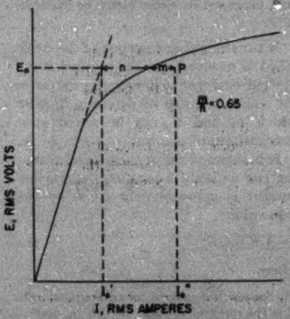

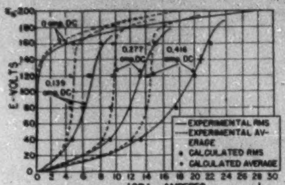

Figure 14. Experimental and calculated characteristic curves for reactor *66G912*

d-c flux in the reactor without difficulty. This quantity is of major importance in the transient operation of the reactor. It can not be measured easily under operating conditions because of the slowness of response of the reactor, and, as has been mentioned previously, it is not simply related to the direct control current. Work has been started on an investigation of the transient response of reactors, using the computed values of d-c flux as a basis for calculation. The preliminary results have been encouraging, and we hope to report on this work later.

Relation between Normal Magnetization Curve and A-C Saturation Curve

In some cases, it may be found desirable to make calculations from the normal magnetization curve of the core material rather than from the a-c saturation curve. The analysis shows that the following relations hold with good accuracy.

We first assume that the normal magnetization curve can be represented by the expression

$$i=C_1\psi+C_n\psi^n \qquad (8)$$

where

i is the instantaneous current in one a-c coil
ψ is the instantaneous flux linkage of that coil, expressed in weber-turns, or maxwell-turns$\times 10^{-8}$.

If the straight-line portion of the curve $(C_1\psi)$ is removed and the reduced curve plotted on a per-unit basis on Figure 5, the value of n can be determined, after which C_n and C_1 can be found in a straightforward manner.

It is shown in the analysis that, assuming two a-c coils in parallel, the rms line current is approximately given by the expression

$$I=A_1E+A_nE^n \qquad (9)$$

where

I is the rms line current for two parallel coils
E is the rms coil voltage $A_1=2C_1/\omega$, and

$$A_n=2\sqrt{\frac{\Gamma(n+1/2)}{\sqrt{\pi}\,\Gamma(n+1)}}\left(\frac{\sqrt{2}}{\omega}\right)C_n \qquad (10)$$

in which Γ indicates the gamma function.[13,14]

For n = 5, 9, and 15, we have from equation 10

$$\left.\begin{aligned}A_5&=\frac{5.61}{\omega^5}C_5\\A_9&=\frac{19.5}{\omega^9}C_9\\A_{15}&=\frac{138}{\omega^{15}}C_{15}\end{aligned}\right\} \qquad (11)$$

For two series-connected a-c coils, the foregoing values of A should be divided by 2, and E represents half the line voltage.

The foregoing relations make it possible to predict the wave shape of the magnetizing current from a knowledge of the shape of the a-c saturation curve. An in-phase current representing iron losses should be added to the current computed from equation 8 when necessary. The results of such a calculation are shown in Figure 15 for the reactor used in the previous example. The crosses mark calculated points and the solid curve shows a half cycle of the actual wave shape as obtained from an oscillogram. The agreement is seen to be quite good.

Appendix I. Analysis

Rms Current

Consider the equation which expresses the instantaneous current in one a-c coil in terms of the flux linkages

$$i=C_1\psi+C_n\psi^n \qquad (12)$$

If the alternating voltage is sinusoidal and there is no d-c saturation, the flux linkages can be expressed as

$$\psi=\psi_m\sin\omega t \qquad (13)$$

where

$$\psi_m=\frac{\sqrt{2}E}{\omega}\text{ weber turns} \qquad (14)$$

and E is the rms coil voltage.

Substituting equation 13 into 12, squaring, and integrating, we obtain for the mean squared coil current

$$I_c^2=\frac{C_1^2\psi_m^2}{2}+\frac{2C_1C_n\Gamma[(n+2)/2]}{\sqrt{\pi}\,\Gamma[(n+3)/2]}\psi_m^{n+1}+\frac{C_n^2\Gamma(n+1/2)}{\sqrt{\pi}\,\Gamma(n+1)}\psi_m^{2n} \qquad (15)$$

For values of n that are not too large, equation 15 is nearly a perfect square, and its approximate square root is

$$I_c\approx\frac{C_1}{\sqrt{2}}\psi_m+\sqrt{\frac{\Gamma(n+1/2)}{\sqrt{\pi}\,\Gamma(n+1)}}\,C_n\psi_m^n \qquad (16)$$

Equation 16 generally will give good results even when n is large, for the second term is usually the major one, and the error that arises in the cross-product term of equation 15 is then not serious. For two identical a-c coils connected in parallel, the line current is double the value given by equation 16. Through equations 14 and 16, we now have expressed the a-c saturation curve in terms of the normal magnetization curve.

When d-c saturation is present, we use in place of equation 13 the expression

$$\psi=\psi_0+\psi_m\sin\omega t \qquad (17)$$

in which ψ_0 represents the d-c flux linkage. Substituting equation 17 into equation 12, expanding the quantity ψ^n by the binomial theorem, and then expanding the powers of the sine function into harmonics, we obtain a Fourier series for the required magnetizing current. This series contains (1), a constant term which represents the required direct current, (2), even harmonics, which circulate between the two a-c windings in the parallel case and flow in the d-c winding in the series case, and (3), odd harmonics, which constitute the alternating line current. For example, the d-c term for $n=5$ is

$$I_{dc}=C_1\psi_0+C_5\psi_0(\psi_0^4+5\psi_0^2\psi_m^2+1.87\psi_m^4) \qquad (18)$$

and, for two a-c coils in parallel, the magnitude of the fundamental component of the line current is

$$I_1=2C_1\psi_m+10C_5\psi_m(\psi_0^4+1.5\psi_0^2\psi_m^2+0.125\psi_m^4) \qquad (19)$$

The influence of the a-c flux on the required direct current for a given value of ψ_0 is seen clearly in equation 18.

The expressions for the amplitudes of the various odd harmonics are squared and added, the results being nearly a perfect square. The approximate square root yields an expression for the rms value of the line current. For example, for $n=5$ and $\psi_0/\psi_m=0.5$, we obtain

$$I_{rms}\approx\sqrt{2}C_1\psi_m+4.20C_5\psi_m^5 \qquad (20)$$

Similarly, from equation 18, we have for $\psi_0/\psi_m=0.5$

$$I_{dc}=C_1\psi_0+1.59C_5\psi_m^5 \qquad (21)$$

Now, we subtract the straight-line portions of both expressions, then express ψ_m in terms of E by means of equation 14, and finally divide both sides by the base current $I_b=5.61C_5(E_b/\omega)^5$. Thus, we obtain the following expressions for the alternating and direct currents with the straight-line portions removed (the turns ratio will now be taken into account for the direct current)

$$I/I_b=4.24(E/E_b)^5 \qquad (22)$$

and

$$I_0N_{dc}/I_bN_{ac}=1.60(E/E_b)^5 \qquad (23)$$

By means of these relations, various points can be found along a curve corresponding to $n=5$ and $\psi_0/\psi_m=0.5$.

Similar computations will yield curves for other values of ψ_0/ψ_m and n. In plotting the charts, the parameter $a=\psi_0/\psi_b=(\psi_0/\psi_m)(E/E_b)$ was used instead of ψ_0/ψ_m, as the former is more convenient in practical calculations.

Average Current

For the condition of no d-c saturation, we substitute equation 13 into 12 and integrate to find the average current over one-half cycle. This yields the following result

$$I_{av} = \frac{2}{\pi} C_1\psi_m + \frac{\Gamma[(n+1)/2]}{\sqrt{\pi}\Gamma[n/2+1]} C_n\psi_m^n \text{ amps per coil} \quad (24)$$

For two identical a-c coils connected in parallel, the average line current is double the foregoing value.

When d-c saturation is present, we return to the previous analysis used for the rms case and integrate the current composed of all the odd harmonics. For example, for $n=5$ and $\psi_0/\psi_m=0.5$, we obtain for the average line current

$$I_{av} = \frac{4}{\pi} C_1\psi_m + 3.22 C_5\psi_m^5 \quad (25)$$

If we now subtract the straight-line portion of this expression, then express ψ_m as $\sqrt{2}E/\omega$, and finally divide both sides of the equation by the base current $I_b = 5.61 C_5(E_b/\omega)^5$, we obtain the relation

$$\text{Reduced } I_{av}/I_b = 3.25(E/E_b)^5 \quad (26)$$

By means of equations 23 and 26, points can be found along a curve corresponding to $n = 5$ and $\psi_0/\psi_m = 0.5$. Similar calculations will yield the curves for other values of ψ_0/ψ_m and n.

Appendix II. Direct Current Required for Additional D-C Flux Path

In this section, we shall derive an approximate graphical method for computing the additional direct current required for the portion of the d-c flux path that is not traversed by the a-c flux. If we assume that this additional path has the same magnetic characteristics as the main flux path, the equation $i = C_1\psi + C_n\psi^n$ will apply, provided that the coefficients are altered to take into account the turns ratio and the different length involved. Therefore, the additional exciting current is given by the expression

$$I_0' = \frac{N_{ac}}{N_{dc}} \frac{\text{length of additional d-c flux path}}{\text{length of flux path for one a-c coil}} \times (C_1\psi_0 + C_n\psi_0^n) \quad (27)$$

Now, we know that

$$\psi_0 = a\psi_b = \frac{\sqrt{2}aE_b}{\omega} \quad (28)$$

Hence, substituting equation 28 into 27 and using equation 10 to eliminate C_1 and C_n in favor of A_1 and A_n, we obtain

$$I_0' = \frac{N_{ac}}{N_{dc}} \times (\text{ratio of lengths}) \times \left[\frac{A_1}{\sqrt{2}}(aE_b) + \frac{A_n}{\sqrt[n]{\frac{\Gamma(n+1/2)}{\sqrt{\pi}\Gamma(n+1)}}}(aE_b)^n \right] \quad (29)$$

This can be rewritten as follows, using E_0 to denote the product aE_b

$$I_0' = \frac{N_{ac}}{N_{dc}} \times \text{ratio of lengths} \times \frac{1}{\sqrt{2}}(A_1E_0 + kA_nE_0^n) \quad (30)$$

where

$$k = \frac{1}{\sqrt{2}\sqrt[n]{\frac{\Gamma(n+1/2)}{\sqrt{\pi}\Gamma(n+1)}}} \quad (31)$$

The value of k does not vary rapidly with n and a mean value will be chosen for the range of interest. For $n=5$, 9, and 15, we compute from equation 31 that $k=1.44$, 1.64, and 1.86, respectively. If we choose a mean value of 1.65, the additional direct current can be read off the rms saturation curve at the voltage $E_0 = aE_b$ by increasing the contribution of the n-th power term by 65 per cent. This method is illustrated in Figure 13. The correction is, in general, only a small part of the total direct current, and the error made in supposing that k is always 1.65 is of little consequence.

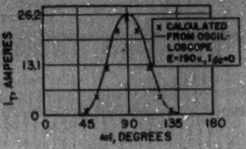

Figure 15. Current wave shape for reactor 66G912

References

1. The Transductor (D-C Pre-Saturated Reactor), with Special Reference to Transductor Control of Rectifiers (book), Uno Lamm. Esselte Aktiebolag (Stockholm, Sweden), 1943.

2. Theory of D-C Excited Iron-Core Reactors and Regulators, A. Boyajian. AIEE Transactions, volume 43, 1924, pages 919–36.

3. Application of Saturated Core Reactors and Regulators, D. K. Blake. AIEE Transactions, volume 43, 1924, pages 937–940.

4. Controlled Reactor, E. C. Wentz. *Electric Journal* (East Pittsburgh, Pa.), October 1931, page 561.

5. Mathematical Analysis of Non-Linear Circuits, A. Boyajian. *General Electric Review* (Schenectady, N. Y.), September and December 1931, pages 531 and 745.

6. Beitrag zur Qualitativen Theorie Gleichstromvormagnetisierter Eisenkern-Drosselspulen, G. Hauffe. *Archiv fur Electrotechnik* (Berlin, Germany), volume 33, 1939, pages 41–7.

7. Uber Gleichstromvormagnetisierte Wechselstromdrosselspulen und deren Ruckkopplung, Th. Buchhold. *Archiv fur Electrotechnik* (Berlin, Germany), volume 36, 1942, pages 221–38.

8. D-C Saturable Reactors, H. Holubow. *Electronic Industries* (New York, N. Y.), March 1945.

9. Saturable Reactors for Automatic Control, W. D. Cockrell. *Electronic Industries* (New York, N. Y.), December 1946.

10. Saturable Reactors for Load Control, P. A. Vance. *General Electric Review* (Schenectady, N. Y.), August and September 1947, pages 17 and 42.

11. An Experimental Verification of a Method of Calculating the Characteristics of Saturated Iron Cored Reactors, Reuben E. Alley, Jr. Master of Science thesis, department of electrical engineering, Princeton University (Princeton, N. J.), June 1940.

12. Unsymmetrical Magnetic Hysteresis, Robert G. Adamson. Master of Science thesis, department of electrical engineering, Princeton University (Princeton, N. J.), June 1938.

13. A Short Table of Integrals (book), B. O. Pierce. Ginn and Company (Boston, Mass.), 1929, third revised edition, page 140.

14. Tables of Functions (book), E. Jahnke, F. Emde. Dover Publications (New York, N. Y.), 1945, page 14.

Discussion

H. F. Storm (General Electric Company, Schenectady, N. Y.): This discussion intends to elaborate on one of the many interesting problems which are effectively described and clearly analyzed in this important paper, namely the phenomenon of d-c flux depression in the presence of an a-c flux. Without repeating the explanation, it is the object of this discussion to relate certain manifestations of this phenomenon which, without further knowledge, are quite puzzling.

Consider the two iron-core transformers which, as shown in Figure 1 of the discussion, are connected to form a saturable reactor. For a given control voltage E_d, a control current i_d will flow through the control windings W_2, the magnitude of this current being indicated by the d-c ammeter. The load consists of a resistance, for instance incandescent lamps. Suppose now that the load current is increased by connecting additional lamps into the circuit. As a result, the ammeter will indicate the intriguing fact that the control current i_d will also increase, though transiently, and then return slowly to its previous magnitude. For a decrease of load current, the control current

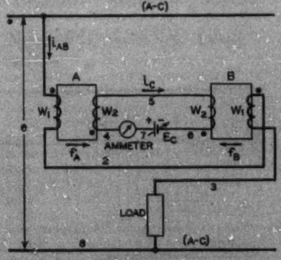

Figure 1 (right). Circuit diagram

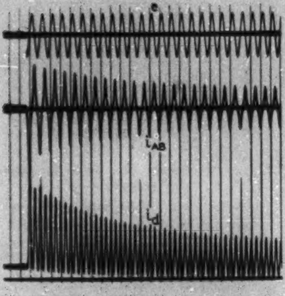

Figure 2. A-c voltage "e" suddenly applied near crest value

will transiently decrease and then build up to its previous value. Similar effects are obtained if the a-c voltage changes, no matter whether the load resistance is finite or zero.

One may be inclined to attribute these transient currents to the induction of electromotive forces from the W_1 windings into the W_2 windings. This, however, is not true. If the impedance in the control winding is low, and the load resistance is zero, the line a-c voltage divides equally between the two W_1 windings of transformers A and B. The voltages induced in the W_2 control windings are equal (providing the turn ratios are the same) but are opposing each other, as shown by the polarity marks. As a result, no net voltage is induced in the control circuit and therefore no current can be caused by these voltages.

The explanation of the phenomenon lies in the fact that by increasing the a-c flux, the d-c flux becomes smaller. The control current i_d causes a positive magnetomotive force f_A in core A, and a negative magnetomotive force f_B in core B, as shown by the polarity marks and arrows in Figure 1 of the discussion. Consequently the d-c flux is considered positive in core A and negative in core B. If an a-c flux is now superimposed, the absolute magnitude of the d-c flux decreases as shown in the author's paper. A decrease in the absolute magnitude of the d-c flux in core A means a change in a negative direction, and a change in core B in a positive direction. Therefore, the resulting electromotive forces will be positive at terminal 5 with respect to terminal 4 on transformer A, and positive at terminal 6 with respect to 5 on transformer B. These two electromotive forces are connected in series and are the cause for the transient current in the control circuit.

Figure 3. A-c voltage "e" interrupted

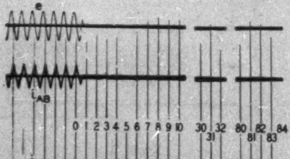

Figure 2 of the discussion shows an oscillogram of this phenomenon. First, without alternating current the control current i_d is seen as a constant quantity. Then when the alternating current has been connected to the circuit, at an instant corresponding to its crest value, the control current i_d is seen to surge up rapidly, thus causing a sharp increase of its average value; the ripple in the control current is caused by even harmonics, which are also present during steady-state operation. The average value of control current gradually subsides and reaches asymptotically the original value of i_d (this last phase is not shown in the oscillogram). It will also be observed that the load current i_{AB} is very large at the beginning of the transient and gradually declines to its steady-state value. This proves that the impedance of a saturable reactor changes transiently with a variation of load or a variation in supply voltage.

Figure 3 of the discussion shows a case where the a-c voltage was suddenly removed. The average value of the control current i_d drops very sharply upon the removal of the a-c voltage and then gradually increases to its original value.

E. C. Wentz and T. R. Specht (Westinghouse Electric Corporation, Sharon, Pa.): This paper should take its place as one of the important contributions to the basic theory of the d-c controllable reactor, and is the first, as far as I know, to relate basic simple data, such as the saturation curve, to the performance of the reactor.

The paper makes some assumptions which are admittedly not very close approximations to the facts. In discussing the paper, I believe we should examine some of the discrepancies with the idea of determining if further corrections can be made and if they are necessary for practical work.

The assumption that the saturation curve can be represented by the simple equation

$$= C_1\psi + C_n\psi^n$$

probably introduces relatively unimportant errors. In fact, many reasonably useful analyses has been done on the basis of the two-straight-line saturation curve, which is much less accurate.

The assumption that the flux is sinusoidal is approximate only for those applications where a sinusoidal voltage is maintained across the reactor. This is true for the current transductor, and for other current amplifiers where the impedance in series with the a-c winding is relatively small; consequently the application of this particular analysis is sharply limited. But the general method demonstrated in this paper can still be used for applications where the voltage is not sinusoidal, providing that it is some function which can be handled mathematically. Mathematical analysis will probably be more difficult for some of the other connections where the flux will not be sinusoidal, but the authors have shown a method of attack which is useful generally for other conditions besides that which they analyze.

The same comment applies to their assumption that the d-c circuit, or its equivalent, is able to carry or supply any amount of second harmonic current. This is frequently not true, but the analysis of the condition where it is true throws a great deal of light on the phenomena occurring when it is not true.

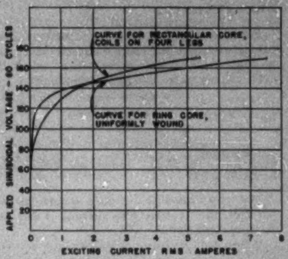

Figure 4. Saturation curves for two types of core—coil arrangement, using the same material

The most serious limitation of the method is its assumption that leakage flux can be neglected. Actually the authors do not quite mean what they say, because the saturation curve which they use has a great deal of leakage flux in it. That is, some of the flux which induces the voltages which are measured and plotted on the saturation curve is not confined entirely to the iron, but leaves the iron as soon as it can after going through the a-c coil and goes off into the air. When the iron is saturated, as it is in this type of reactor, the amount of flux which links the coil and then leaves the core is by no means negligible. This is shown in a semiquantitative way by Figure 4 of the discussion. The saturation curves in Figure 4 were made with two cores of the same cross-section and mean length of magnetic turn, but one was a ring core, with a winding uniformly distributed so that no flux would leave the core at any point, while the other was a rectangular core with coils on all four legs, a configuration which confines the flux to the core more effectively than if the coils were on only two legs of the core, but not as effectively as does the ring winding. The curve for the rectangular core shows that a very appreciable amount of this flux must be linking the turns in the coils without passing through much of the iron, because the curve rises considerably above the ring-core curve, and shows little sign of flattening off.

Another way of expressing the same thing is that it is necessary to consider the air-core inductance of the a-c coils. This is not an exact statement of the necessity, however, because the phenomenon of flux leaking from

Figure 5. Another type of reactor construction

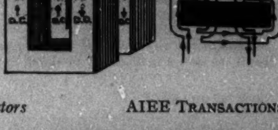

the saturated core into the air is not very closely equivalent to the flux which would link the coils if the core were entirely absent.

Now it is possible that someone in the near future will devise a simple method of taking leakage flux properly into account. The authors, as we have seen, have really taken it into account, in a way which seems to give satisfactory results, by using the measured saturation curve for the core. The limitation which must be kept in mind is that the saturation curve, however measured, is not a saturation curve for the magnetic material, but a curve for the complete structure, and that any change in configuration of the core or coils will probably bring about a significant change in the saturation curve, even though the material of the core is not changed.

Even the curve for a toroidal core is not entirely the same as the curve for the material, because even in a toroidal winding some flux flows around the outside, inside, and at both axial ends of the core which may link the winding without ever entering the core.

If the ampere-turn-per-inch values are relatively low, the leakage flux may still be negligible. In a reactor with the a-c coils in parallel, the magnitude of the a-c ampere-turns is approximately instantaneously equal to that of the d-c ampere-turns, and it is quite possible that the leakage flux produced by these ampere-turns may be small for a particular reactor, especially one of low power. For one of much higher power, however, the leakage flux cannot be even approximately neglected. It is not quite clear from the example given in the paper whether the leakage flux (roughly equivalent to air-core inductance of the a-c coils) is negligible.

In devices in which the linear relation between d-c and a-c ampere-turns is important, the leakage flux presents an even more difficult problem, because it effectively prevents linearity by introducing a very considerable effective constant inductance in series with the a-c circuit.

The leakage of d-c flux is probably nearly as important as leakage of the a-c flux, but can be reduced to reasonably small values by the use of the double-core reactor in which the d-c coil is closely coupled to the a-c coils, as in Figure 5 of the discussion. (United States Patent Number 2,374,059.) Other means of accomplishing the same result are known.

One other interesting conclusion follows from the fact that the effective saturation curve for a magnetic material does not necessarily represent the curve for the reactor. In order to take proper advantage of the high-permeability materials which are supposed to be the secret of success in magnetic amplifier construction, very careful consideration must be given to elimination of leakage flux paths. The authors show very clearly too that the fast-breaking saturation curve, even if it can be obtained, does not result in a reactor with significantly different characteristics from that with a slow-breaking curve. Evidently the specialized materials will not be either as useful or as essential as might be thought.

Tests were made on a 30-kva saturable core reactor. This reactor was of the two separate core type, with the a-c coil in parallel. Table I gives a comparison of the direct current needed for various alternating currents and voltages. The calculated direct current was determined from the test excitation curve.

Table I. Test and Calculated Performance of a Saturable Core Reactor

30 Kva, 480 Volts, 62.5 Amperes, Alternating Current

Volts, alternating current	Amperes, alternating current	Calculated I_{DC}	Test I_{DC}
543	60.3	1.00	1
387	50.2	1.00	1
171	40.4	1.12	1
102.6	30	1.05	1
74.3	65	2.10	2.3

The correlation between calculated and test values are within engineering accuracy. If curves for $b = 0.25$, 0.35, and 0.4 were given, the usefulness of the curves would be increased, although if I_b were chosen when making the tests so that I/I_b were always less than 0.7, the curves would be adequate.

The limitations of this paper are not really basic. The problem of calculation of reactor performance has not been solved by the authors for all possible connections of this type of reactor, and probably never will be. The authors have devised a general method, of which this paper demonstrates only one application. The general method, however, should be applicable to many other problems, and this paper should certainly be studied carefully by all those who intend to design or to apply saturable reactors, with the thought that this general method will probably be the fundamental basis for eventually complete design literature.

L. A. Finzi (Carnegie Institute of Technology, Pittsburgh, Pa.): W. C. Johnson and his associates attack the problem of the performance of magnetic amplifiers in terms of the true variables defining the operation, that is the average core flux and the crest value of the alternating superposed flux. The fitting of the normal *B-H* curve with an analytical function is a very skillful one. Another, somewhat similar analysis has been made by my associates and myself at Carnegie Institute of Technology. We have fitted the experimentally obtained normal *B-H* curve of the core materials with a power series, and also with combinations of hyperbolic sines, and from these we have obtained expressions for the current, which in each case checks with the experiment, with the same order of agreement as Johnson obtains. We have also obtained a satisfactory agreement in somewhat more involved cases, such as amplifiers with external feedback or with self-feedback. Here disturbing phenomena as "commutation" occur during the cycle. As D. W. VerPlanck reported at the National Electronics Conference at Chicago in 1948, the feed-back winding cuts itself loose during the cycle from the output circuit and behaves as a winding, short circuited through the rectifiers. This phenomenon complicates the analysis, since the instants in the cycle at which commutation begins and ceases, have to be determined by matching at boundaries, and so forth. In this case, too, our analysis checks surprisingly well with the experiments.

The agreement reported by the authors, and that which we have also found, leads to the conclusion that the basic simplifying assumptions (that is sinusoidal flux, use of normal *B-H* curves, and so forth) are sound, and that the general method of attack is correct, at least for silicon steel, and similar materials. In any case the analytical fit of the *B-H* curve has to be close over the whole range of operation, extending far above the knee. Less careful fitting, as has been suggested in some old German literature (for example, by means of a single hyperbolic sine), does not seem adequate. On the other hand, the function chosen should lead to expressions for the currents that are easy to compute numerically. The author's analysis leads to gamma-functions, while our analysis leads to modified Bessel functions, both of which are tabulated.

The studies to which I refer have appeared as Report Number 5 in a series of reports prepared at Carnegie Institute of Technology under United States Navy Contract.

I should like to add a further comment. The authors mention the fact that the average flux of the core, with superposed alternating magnetization, is lower than at first expected. In our experimentation, we have observed that small values of the alternating magnetization may cause a small increase of the average flux as reported by T. Spooner.[1] This is a phenomenon also which does not seem to be related to the circuitry of such nonlinear elements; and can probably be explained in terms of the structure of the magnetic material. For the cores used in our experiments (hypernik) this phenomenon was not important enough to modify the basic analysis, but it would be of interest to hear whether this has been found more important for different core materials.

REFERENCE

1. PROPERTIES AND TESTING OF MAGNETIC MATERIALS (book), T. Spooner. McGraw-Hill Book Company, New York, N. Y., 1927.

W. C. Johnson, B. C. Merrell, and R. E. Alley, Jr.: We wish to thank the discussers for their interest in the paper and for their many helpful comments. Storm's presentation of oscillographic evidence of the depression of d-c flux is convincing and very pertinent. In this laboratory we have made calculations recently of similar transients in saturable-reactor circuits and find good agreement between calculated and experimental results. We hope to report on this work in a later paper.

Wentz and Specht are quite correct in pointing out that our analysis takes account of flux which leaves the iron and passes through the air. It is necessary here to distinguish between two uses of the term "leakage flux". It may mean all the flux which passes from the iron into the air, or it may mean the portion of the above-mentioned flux which links one winding, but not both. Our analysis takes account of the flux which links both windings, regardless of its path. However, it does not take into account the flux which leaks between the coils and links only one winding. The latter was what we meant when we stated the assumption relating to our neglect of "leakage flux."

Experiments indicate that our analysis, based though it is on a sinusoidal variation of flux, is surprisingly good under load conditions with a rather high series impedance when the flux is certainly not sinusoidal at all. Therefore, this assumption seems not as restrictive as might be thought. This is certainly reassuring, for one needs to simplify these nonlinear problems just as much as possible in order to make the results at all usable.

We are aware of the excellent results obtained by VerPlanck and Finzi and their associates, and are glad for this opportunity to acknowledge their work.

The analysis which we present in this paper represents our third attempt to find a reasonably simple and usable presentation of the results of our original work. Alley's first analysis of the problem was presented in his master of science thesis in the spring of 1940. Our results at that time were as correct and accurate as those we have finally presented in this paper, but they required rather laborious calculations. We have spent considerable time and effort in simplification, and feel that it has been time well spent. The problem of presenting the results of a nonlinear analysis in useful form is a difficult one indeed.

Microwave Channels for Power System Applications

AN AIEE COMMITTEE REPORT

THE microwave system is a very high frequency beamed radio channel for transmitting information from point-to-point. It was highly developed during the war and promises to become a valuable tool to electrical power systems as a channel for the transmission of information which it is desired to send from point-to-point in the normal operation of the system. Relaying, telemetering, supervisory control, and communication are functions which could use such a channel. The information required by these functions now is being sent over pilot wires and power line carrier channels for the necessary communication media. The microwave channel, by virtue of its air-line transmission, and the large number of quantities which can be transmitted from point-to-point on a single beam, opens up application possibilities which cannot be handled with present methods. Spectrum crowding of power line communication channels has occurred. In most cases of spectrum crowding, considerable communication traffic of one kind or another exists and the installation of a microwave channel may easily be justified. While microwave channels will in some cases be used to replace pilot wire and power line carrier channels their major advantage will probably lie in supplementing existing methods and thus extending the possibilities of the use of communication channels for the transmission of intelligence necessary to obtain better power system operation.

Characteristics of Microwaves

Microwaves are radio waves in the region from a few hundred megacycles up. These correspond to wavelengths from about 100 centimeters down. For example, the 10-centimeter and 3-centimeter waves used in radar are considered to be microwaves. Radio waves of these short wave-lengths travel generally in a straight line like light and cannot be picked up if intervening objects such as hills, buildings, or the curvature of the earth interfere.

A line tangent to the surface of the earth rises to a height of $0.66S^2$ feet where S is the distance in miles from the point of tangency. For example, the line of sight would be 66 feet above the surface of an assumed perfectly spherical earth at a point ten miles from the point of tangency. As this height varies with the square of distance, it would be 264-feet above the surface when 20 miles away. Thus it would be theoretically possible to go about 35 miles line-of-sight between two 200-feet towers. It may be necessary for the line of the microwave beam to clear the nearest obstruction by some 50 feet. Tests show this is too conservative but this safety margin should be retained for the time being. Adding this 50-foot clearance, the tower height required on the average for different transmission distances is indicated in Table I. It would be possible to transmit approximately half this distance with only one tower of the indicated height and the other antenna 50 feet above the earth.

From Table I, it will be seen that a pair of towers a little over 100-feet high are good for 20 miles and towers about 200-feet high are good for 30 miles. These are average figures and in many cases favorable terrain will make much greater distance of transmission feasible and the converse is also true.

The number of microwave communicating channels which can be used is dependent on three factors:

1. Line-of-sight characteristic.
2. Angular directional characteristic.
3 Frequency selection.

Fifty miles away from a given installation, the line-of-sight of that installation would be 1,650 feet above the earth's surface and the same frequencies could generally be used over again. Thus the entire available spectrum may be thought of as being available in each 100-mile-square area. However, a great many channels could be used at the same frequency because of the directivity of the pattern. In other words, the antennaes are directional to a fairly high degree. Taking a conservative figure of 20 degrees, it is entirely possible that four signals could be sent in four directions from a given point without interfering, although reflections from buildings will need to be considered. There are several frequency bands which are available on an experimental license basis for power system applications using microwaves some of which are for commercial use (power, gas, water and steam utilities) some for government use, and some for joint use as shown in Table II.

For the purpose of an example for this report, consider the band from 952 to 960 megacycles. Channels could be spaced 100 kc apart, and there would be 80 such channels using the 8-megacycle band mentioned. It is easy to demonstrate with a hypothetical system the relatively enormous number of channels that a microwave system can provide. For example, a given 100-kc channel could be occupied by a microwave carrier together with modulation of the microwave carrier at audio (or modulated subcarrier) frequencies. Assume that six communication channels (voice channels) can be accommodated in each 100 kc of band

Paper 49-5, recommended by the AIEE carrier current committee and approved by the AIEE technical program committee for presentation at the AIEE winter general meeting, New York, N. Y., January 31-February 4, 1949. Manuscript submitted October 12, 1948; made available for printing November 29, 1948.

This report of the AIEE carrier current committee was prepared by S. C. Leyland, manager, relay engineering, Westinghouse Electric Corporation, Newark, N. J.

Table I. Average Distance of Microwave Transmission with Two Towers of the Indicated Height

Half This Distance for One Tower with the Other Tower 50 Feet High

Transmission Distance, Miles	Required Antenna Height*
5	54
10	67
15	87
20	116
25	153
30	199
35	252
40	314
45	385
50	462

(Based on spherical earth with line-of-sight always 50 feet minimum above the surface.)

*Note: If the effective earth radius is four thirds the actual radius, an approximation to account for the bending of the rays around the earth, then the antenna height required is three quarters of the values shown.

width. These channels can be used for voice only, or a combination of voice and about four audio tones, or for about ten audio tones without voice. Using these figures, a single microwave channel can accommodate 6-voice and 24-tone channels, or a total of 60-tone channels without voice. See the summary in Table III.

This illustrates that in the 952-to-960-megacycle region, 1,920 voice channels or 19,200 audio tone channels could be made easily available in each 100-mile-square area. This may be compared very roughly with a saturation limit of the order of 30-voice channels or 300-tone channels available over power line carrier. Roughly 60 times as many channels are available with the microwave and they can be repeated oftener. In addition, the higher frequency microwave bands will accommodate more audio channels than the 952–960 megacycle band.

Advantages of the Microwave System

Channel Reliability. A microwave channel is as reliable as the atmosphere through which transmission takes place. It is not dependent on the continuity of transmission line conductors or pilot wires for reliable operation. Microwave channels would not be subject to the same degree to conditions such as sleet, windstorm, airplane damage, and so forth, which might render wire channels inoperative.

Facilities per Channel. The intelligence required by a large number of different functions can be transmitted on a single microwave channel using modulated subcarriers as described. The maximum number of channels which can be provided is dependent on the type of multiplexing equipment used. Time division multiplexing, for example, will make many more channels possible than the use of subcarriers only. Therefore the number of channels or facilities per channel is very flexible and the type of multiplexing equipment used will largely be determined by economic factors.

Freedom from Interference. Interference in the microwave band is very small and may even be a negligible factor. This is true both from the standpoint of the microwave channel interfering with other facilities, and of other facilities or external interference, interfering with the microwave channel. An exception might be interference caused by an airplane flying directly in the path of the beam near one of the antennas. Rain and snow do not noticeably affect transmission in any of the lower frequency bands. However, frequencies in the order of 10,000 megacycles are subject to atmospheric absorption and refraction, and their variations cause attentuation and fading, but suitable safety factors may be possible with adequate design.

Maintenance. Since the microwave channel and terminal equipment are independent of the power system, maintenance can be performed without the necessity of having any part of the power system out of service. This simplifies and makes safer the maintenance problem particularly in those cases where in a carrier installation, maintenance on the coupling capacitor or line trap is necessary.

Disadvantages of the Microwave System

Line-of-Sight. The necessity of line-of-sight will have a number of disadvantages associated with it. In some cases it will necessitate repeater stations and the reliability of power supply at this repeater must be assured.

Power Supply. The higher voltage requirement necessitates the use of an a-c power supply with any equipment foreseen for some time. This is no particular disadvantage for some uses but for others, where reliability is of particular importance as in relaying, it will be necessary to use a continuous d-c to a-c power supply unit in order to use station battery power. In other communication and telemetering installations, it will be necessary to have transfer equipment to go over on the battery in event of loss of the a-c supply at the station.

Structure Rigidity. There may be a problem of directivity and loss of contact due to deflection of the antennae or structures upon which they are mounted. It is believed, however, that with a comparatively broad beam, this factor can be kept under control. Construction cost of suitable structure for mounting the antenna may be high.

Table II. Present Frequency Assignments for Point-to-Point Service

Band	Megacycles	Type of Service
952	960	Commercial
1,700	1,850	Government
1,850	1,990	Commercial
2,110	2,200	Commercial
2,200	2,300	Government
2,400	2,700	Commercial
4,400	5,000	Government
6,575	6,875	Commercial
7,125	8,500	Government
9,800	9,900	Commercial and Government
9,900	10,000	Commercial
12,200	12,700	Commercial
13,200	16,000	Government

Possible Applications

In view of the advantage and disadvantages of microwave channels as compared to power line carrier or wire channels, the following application possibilities are typical:

Telemetering. A microwave channel provides an ideal means of transmitting a large number of telemetered quantities from point-to-point. This would be particularly valuable for those locations where line-of-sight is possible from the load dispatcher's headquarters to one or more different points on the system, and carrier or wire facilities are not available for accommodating the large number of quantities desired.

Supervisory Control. Application requirements similar to those necessary for telemetering channels also would make microwave channels attractive for the transmission of a large number of super-

Table III. Possible Channels in Each 100 Mile Square

Item	Number
Direction	4
Microwave frequencies	80
Sub-carriers	6
Audio-tone	10
Total	19,200
or	
Voice and tone combination	5
Total	9,600
or	
Voice alone	1
Total	1,920

visory control functions from point-to-point.

Relaying. For locations where a large number of circuits exists between two points on a power system, and all the relaying requirements for the transmission of intelligence can be served by a single microwave channel. In this category would be stations interconnected by power cables, where the use of a carrier or pilot wires would not be possible or economical.

Communication. Important communication facilities necessary for dispatching purposes where other kinds of channel were not considered economically or technically possible.

Combined Services. It is expected that microwave channels will be most effective where large numbers of different types of intelligence must be transmitted between points on a power system or from the system to the load dispatcher's office. Combinations of telemetering, supervisory control, relaying, and communication will be the more common, but other services such as transfer tripping, teletype, telegraph, and load control, would be possible users of the microwave channel.

Part of a Communication Network. It is expected that the use of microwave channels in conjunction with existing or contemplated carrier or wire channels will greatly increase the utility of these channels by extending the scope of the entire communication system.

Conclusions

It is quite apparent from the economic and engineering possibilities of this system, from its successful use during wartime, and from the general interest in it throughout the country by responsible individuals that this field will definitely develop. It will occupy part of the place now occupied by carrier but will probably never displace carrier completely, and it will open new fields which are not now economic by carrier or wire channels. It will also provide power companies with an increased opportunity to control their own communicating facilities for important dispatching services and control functions.

Discussion

R. F. Stevens (Bonneville Power Administration, Portland, Oreg.): As the first power utility to adopt microwave radio as a major part of its communication network, the Bonneville Power Administration (BPA) has an especial interest in the appraisal of this new tool by the carrier current committee.

The conclusions agree well with those of our own studies on this subject, which we started immediately after the war, and which resulted in the purchase in 1948 of equipment for four microwave stations. These stations, plus three others, should be in operation by the end of 1949, and will form a multichannel link, 200 miles in length, connecting our Portland-Vancouver headquarters and dispatchers' offices with points in the Puget Sound area. This system operates in the 1,700–1,850 megacycle band using pulse time modulation. The network will be extended later to other important centers in our region.

The decision to use microwave was based in part on the crowding of the carrier spectrum, which had become quite serious. Careful cost comparison between carrier and microwave, based on typical conditions on our system, provided an equally compelling argument. The curves, shown in Figure 1 of the discussion, prepared from these studies show rapidly increasing savings from use of microwave as the number of channels along a given route is increased beyond four. On the other hand they indicate saving for carrier where but one or two channels are required. This has led us quite naturally to a decision to use microwave for our backbone communication routes, and carrier for radial branches. It also has provided confirmation for the opinion of the carrier current committee that microwave is not likely to completely supplant carrier at any time in the near future.

While our curves should be applied with caution to other situations, where basic conditions are different, the same general pattern can be expected; namely, a comparatively constant cost per channel for carrier and a high-minimum cost and low-incremental cost per channel for microwave.

It also should be remembered that the cost of power line carrier is pretty well stabilized, whereas the cost of microwave is likely to decline as development costs are written off and greater production is achieved.

Our comparison is based on microwave equipment which can be expanded to provide 23 or more channels relayed through many stations in tandem. We feel there is a definite field also for simpler and less expensive equipment for perhaps 2-, 3- or 4-voice channels. Such equipment would be used for links of short over-all lengths, or for short branches from the main microwave link, and need not meet the same distortion limitations necessary where many relay stations are in tandem. Such equipment also might open to microwave part of a field which we, in our thinking, have assigned to carrier.

ADDITIONAL ADVANTAGES OF MICROWAVE SYSTEM

The following advantages might be added to those listed in the paper:

Superior Voice Quality. A well-designed microwave system provides an extremely flat frequency response even though the signal must pass through many relay stations in tandem. This permits better voice quality; also successful multiplex transmission of a greater number of telemetering signals over a single voice channel. Attainment of comparable quality is impractical in many carrier installations.

Microwave Provides Full 2-Way Communications. Power-line carrier systems often must use the same frequency in both directions to conserve spectrum. This requires use of a push-to-talk switch or a voice relay. In contrast, standard microwave systems permit simultaneous 2-way transmission.

Availability of Wide Spectrum. In contrast to the crowded carrier spectrum, the available microwave spectrum is tremendously wide.

Use with Fixed-to-Mobile Radio. A microwave system can be connected readily to, and used in conjunction with, very high frequency radio stations transmitting to mobile units. Very high frequency transmitters can be installed at microwave relay tower sites, which are usually well suited to the purpose. Access roads and power supply lines can be used in common.

Use During Construction. Microwave stations can be installed in advance of transmission lines and used during the construction period at a power project.

Low Incremental Cost when more Channels are Needed.

ADDITIONAL DISADVANTAGES OF A MICROWAVE SYSTEM

More Eggs in One Basket. Trouble in the radio-frequency, or in parts of the multiplexing equipment may involve many channels and thus be more serious than failure of a single-carrier channel. This will become less serious as life expectancy of tubes and other parts is improved. Further, this dis-

Figure 1.

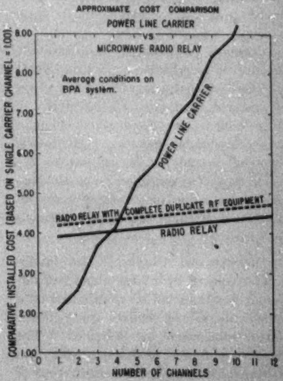

advantage can be overcome, at price, by duplicate equipment or duplicate routes, with automatic cut-over. In this case channel reliability will be better than for carrier.

The three other disadvantages listed in the paper can be overcome by proper design and by paying the necessary cost. The cost of overcoming these disadvantages is included in our comparison with the carrier.

Applications. Our plans for use of microwave confirm the prediction of the committee that it will find its greatest application where many different types of intelligence are to be transmitted over a given route. Of the applications suggested (telemetering, supervisory control, relay and communications, teletype, telegraphy, and load control) we will eventually use all (except perhaps teletype and telegraphy) and will add one or two additional uses. One of these may be facsimile. A more novel use planned is for instantaneous transmission line fault location using a system developed at BPA and described in a paper published in 1948.[1] The theory is very simple and is based on the fact that a transmission line fault sends travelling waves down the line in both directions at the speed of light. With the aid of a single timing pulse sent over the microwave system, the difference in time of arrival of these travelling waves at opposite ends of the line will be measured, from which the distance to the fault in miles will automatically be computed and printed on a chart.

Power Line Relaying. We believe that application of microwave to power line relaying offers more than the mere substitution of one type of channel for another. New approaches to the whole power line relaying problem become possible when it is not necessary to assume that the signalling channel may be out of service at the time of a transmission line fault. It should be possible to decrease by a significant amount the time required to clear both ends of a faulted line, and thus to permit also faster automatic reclosing. Preliminary studies indicate the resulting gain in stable transmission power limit may in itself alone justify a heavy microwave investment. This subject is being actively studied by BPA.

Layout of Beam Paths. Table I of the paper is of interest in indicating the distance between stations which might be expected under average conditions. It is often possible to take advantage of terrain. However, mountainous country is often less favorable than flat country, due to intervening hills or ridges that always seem to appear at the wrong places. For the 200-mile BPA link, the longest distance between stations is 54 miles. The average length of path is 32 miles with short branches respectively 12 and 15 miles in length. The average tower height is 96 feet. The two highest towers will be 145 feet high. Ground elevations at the towers vary from 180 feet to 1,980 feet. Most sites in our region above 2,000 feet in elevation, as well as really high points such as Mt. Hood, Mt. St. Helens, and so forth from which great distance can be seen, are impractical as radio sites due to lack of accessibility for roads and power. Most commercially developed equipment also lacks the power output at present to take advantage of extremely long paths.

Opinions seem to vary as to whether actual earth radius or the four-thirds value should be used in laying out beam paths. The paper makes no recommendation, other than that a 50-foot clearance between beam and intervening terrain, and suggests that this may be found conservative.

Based on experience reported from a prominent eastern installation, and on a desire to be conservative on our first installation, we have used true radius and a minimum clearance of 100 feet in our design work.

Since the most adverse conditions in the propagating medium may occur at very rare intervals, operating experience over a long cycle of years may be necessary before we can determine definitely whether we have been more cautious than necessary.

While tower height is not the major item in the over-all cost, it is still an important one. Lower towers result both in lower first cost and in more convenient and less costly maintenance. More complete studies and advance test data which will permit more exact determination of minimum tower heights therefore are needed.

REFERENCE

1. A TRANSMISSION LINE FAULT LOCATOR USING FAULT GENERATED SURGES, R. F. Stevens, T. W. Stringfield. AIEE TRANSACTIONS, volume 67, part II, 1948, pages 1168–79.

Line Tuning Equipment Used With Coaxial Cable for Carrier Current Installation on Power Lines

HOWARD J. SUTTON
ASSOCIATE AIEE

THE ADVANTAGE of using low-loss coaxial cable in conjunction with power line carrier equipment has been recognized for some years. The use of this cable has made it possible to locate the carrier transmitter-receiver near the equipment associated with it, rather than out near the capacitor which couples the carrier signal to the power line. Coaxial-cable connections have made carrier installations much more flexible than was possible before this type of cable was used.

Although the advantage of using coaxial cable has been known for some time, very little information has been published relative to its use for power company installations. A lack of knowledge on the part of the user makes it difficult to obtain the best operating adjustment of the equipment, or to select the most economical equipment. It is the purpose of this paper to discuss some of the theoretical and practical problems pertaining to the use of coaxial cable. The paper will be limited to the connection between the transmitter-receiver and the coupling capacitor, and to carrier current by-pass circuits.

To understand the behavior of coaxial cable, we must consider this type cable as a network rather than a simple conductor. As shown in Figure 1, this network is made up of series impedance branches and shunt admittance branches.

The resultant series impedance branch is equal to

$$Z=R+j\omega L \qquad (1)$$

The resultant shunt admittance branch is equal to

$$Y=G+j\omega C \qquad (2)$$

The values R and L represent total resistance in ohms and total inductance in henries of the cable used, while the values G and C represent the total shunt conductance in mhos and shunt capacitance in farads of the same cable.

The network or cable has a characteristic or surge impedance, Z_o, equal to

$$Z_o=\sqrt{\frac{R+j\omega L}{G+j\omega C}} \qquad (3)$$ [1,2]

On short lengths of low-loss cable, 1/12 wave lengths or less, the R and G values may be neglected without changing the results appreciably and equation 3 becomes

$$Z_o=\sqrt{\frac{j\omega L}{j\omega C}} \text{ or } \sqrt{\frac{L}{C}} \qquad (4)$$

The characteristic impedance is an important value when considering a network. A network terminated in an impedance equal to its characteristic impedance will also have an input impedance equal to the characteristic impedances and there will be no standing or reflected waves encountered in the network. In simpler terms a coaxial cable terminated in any value other than its characteristic impedance will introduce distortion or higher losses in the circuit. The amount of distortion or loss is dependent upon the length of cable compared with the wave length of the carrier frequency and the magnitude and type of load on the end of the cable. A coaxial cable with a characteristic impedance of 65 to 70 ohms is usually used for carrier applications.

Sometimes it is desirable to terminate a cable in an impedance different from the characteristic impedance, see Figure 2. When this is the case the impedance as seen at the sending end, Z_s, of a low-loss coaxial cable terminated in an impedance of any magnitude or type, Z_R, can be determined from the following equations

$$R_e=\frac{Z_o^2R}{(Z_o\cos\beta 1-X\sin\beta 1)^2+(R\sin\beta 1)^2} \qquad (5)^*$$

$$X_e=Z_o\frac{(Z_o^2-X^2-R^2)\dfrac{\sin 2\beta 1}{2}+Z_oX\cos 2\beta 1}{(Z_o\cos\beta 1-X\sin\beta 1)^2+(R\sin\beta 1)^2} \qquad (6)^*$$

Where

$$Z_s=R_e+jX_e \qquad (7)$$

$Z_o=Z_c=$ characteristic impedance of cable
$Z_R=R+jX=$ terminating impedance
$\beta_1=$ electrical length in degrees
$\beta_1=\frac{1}{\lambda}\times 360$ degrees (λ for coaxial cable is approximately 55 per cent of value in air)

From equations 5 and 6 it can be seen that when

$$Z_o=Z_R, \text{ and } Z_R=R_R+j0 \qquad (8)$$

$$Z_s=Z_R=Z_o \qquad (9)$$

Equation 9 is then in agreement with a statement made previously that when a network is terminated in its characteristic impedance, the input impedance will also be equal to the characteristic

---

Paper 49-6, recommended by the AIEE carrier current committee and approved by the AIEE technical program committee for presentation at the AIEE winter general meeting, New York, N. Y., January 31–February 4, 1949. Manuscript submitted October 13, 1948; made available for printing November 29, 1948.

HOWARD J. SUTTON is with the Gulf States Utilities Company, Beaumont, Tex.

The writer wishes to acknowledge and express his appreciation for the helpful comments and suggestions made by N. L. Jacklein, A. P. Cummins, E. W. Kenefake of the General Electric Company; J. M. Nelson and S. C. Leyland of the Westinghouse Electric Corporation; and to R. O. Hopkins and W. W. Eckles of the Gulf States Utilities Company.

*Equations 5 and 6 from E. W. Kenefake, General Electric Company, Schenectady, N. Y. These equations hold true for a dissipation less line or low loss cable, and can also be derived from the following equation appearing in another publication[1]:

$$Z_s=Z_o\frac{Z_R+jZ_o\tan\beta 1}{Z_o+jZ_R\tan\beta 1}$$

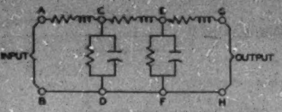

Figure 1. Equivalent coaxial cable network

impedance. Calculations were made at various frequencies for two sample lengths of coaxial cable (195 feet and 1000 feet) with terminating impedance of $Z_R = 500 - j10^6/2\pi f \times 0.003$ and the results were plotted as curves, see Figure 9. A study of equations 5 and 6 or the curves will indicate that the difference between the apparent input impedance Z_s and the terminating impedance Z_R becomes greater as the length of the cable increases. In the case of the 1,000 foot cable the capacitance load at the terminating end appears as an inductive load at the sending end at 150 kilocycles.

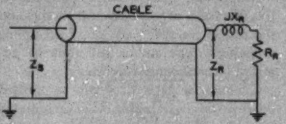

Figure 2. Schematic diagram for equations 5 and 6

The previous discussion has pointed out that coaxial cable should be considered as a network and has given formulas for calculations. Before studying several different coaxial transmission circuits, consideration should be given to the type of circuit a power line presents to radio frequency. For simplicity, only carrier coupling to a single conductor with ground return will be discussed. A single conductor will introduce resistance and inductance. In addition the shunt capacitance to ground will be an appreciable value. The power line can also be broken down into a network as shown in Figure 1.

The characteristic impedance of a line can best be determined by tests. From tests made on the Gulf States Utilities system the characteristic impedance has been found to be between 300 to 600 ohms. The coupling between the conductor connected to the carrier and the other conductors of the line plus the coupling between other lines makes it very difficult to calculate the impedance from equation 3.

Three different types of coaxial transmission circuits will be discussed. To assist in the description, the circuits will be called types *A*, *B*, and *C*.

Type A Circuit

The type *A* circuit as shown in Figure 3, may be used with coaxial cable without limitation at carrier frequencies. In this circuit the tuning inductance is adjusted so that its reactance is equal numerically to the capacitive reactance of the coupling capacitor. By the above tuning, the condition of connecting *G* directly to *J* is approximated. The surge or characteristic impedance of the power line is assumed to be 500 ohms.

A transformer *EFGH* is used for matching the line impedance to that of the cable. Winding *EF* is connected to the coaxial cable. The connection to *GH* winding is varied so that the 500-ohm load appears as a 70-ohm load across the *EF* winding. The coaxial cable is then matched to its characteristic impedance and maximum efficiency or low attenuation is obtained.

A carrier by-pass circuit similar to the foregoing circuit would be connected as shown in Figure 4. Carrier by-pass circuits are used when it is desired to provide a low-impedance circuit around one or two circuit breakers (one of which might be opened) or a power transformer bank. For this circuit a tuning inductance is provided on each end of the circuit to cancel out the reactance of the coupling capacitors. Both of the impedance transformers are connected so as to present 70-ohms load on each end of the coaxial cable.

In order to obtain a comparison between the type *A* line tuning circuit as shown in Figure 3, and the other two types to be discussed, tests were performed using three different lengths of coaxial cable, 61 feet, 195 feet and 1,000 feet. The results of these tests were plotted as curves, see Figures 10, 11, and 13. These curves show the total loss in the circuit in decibels at various frequencies from 30 to 150 kilocycles. For tests, a coupling capacitor of 0.003 microfarad was used in series with a 500-ohm resistance load. The 500-ohm load represents a high-voltage transmission line. These curves show the type *A* circuit to be the most efficient except at the highest frequency.

In addition to the type *A* circuit being the most efficient, it has the additional advantage of presenting very nearly a resistance-type load to the carrier transmitter throughout the frequency range.

The chief disadvantage of the type *A* circuit over the other types to be discussed is the cost of the equipment and the additional cost of installing the equipment. In the case of the carrier by-pass the additional cost is doubled because the coaxial cable is terminated at each end in a type *A* circuit, see Figure 4. Refer to Figure 16 for typical type *A* line tuning equipment.

Type B Circuit

This coaxial transmission circuit is the same as the type *A* circuit, see Figure 5, except the line tuning inductance (*GI*) of Figure 3 is omitted. The apparent impedance of the line shown in Figure 5 is then $(500 - j/\omega C)$ ohms. The value of 500 ohms is the assumed characteristic impedance of the power line. *C* is the capacity of the coupling capacitor in farads. To tune this circuit the connection to winding *GH* is varied so that the load on this winding appears as a 70-ohm load across the *EF* winding.*

In the case of a carrier by-pass, the circuit will be the same as type *A* circuit, see Figure 6, except both line tuning in-

---

*The impedance matching transformers used for the tests had two separate windings with a powdered iron core. Winding *EF* was designed for use with 70-ohm cable. The other winding or secondary has a range of 70 to 1,900 ohms. The transformers had very low losses between 50 and 150 kilocycles.

Figure 3. Type *A* line tuning circuit

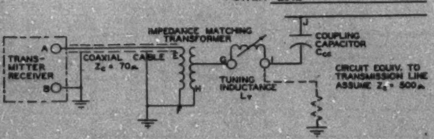
POWER LINE
J
IMPEDANCE MATCHING TRANSFORMER
COUPLING CAPACITOR C_{cc}
A
TRANS-MITTER RECEIVER
B
COAXIAL CABLE $Z_c = 70\Omega$
E
G
I
H
TUNING INDUCTANCE L_T
CIRCUIT EQUIV. TO TRANSMISSION LINE ASSUME $Z_s = 500\Omega$

Figure 4. Type *A* by-pass circuit

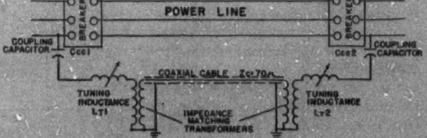

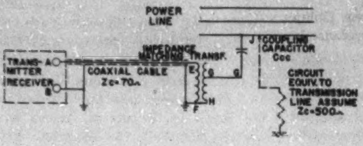

Figure 5 (left). Type *B* line tuning circuit

Figure 7 (right). Type C line tuning circuit

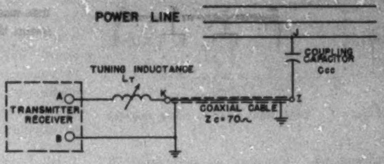

ductances will be omitted. The tuning of the by-pass circuit will be same as described in the previous paragraph.

Since the reactance of the coupling capacitor has not been cancelled by a tuning inductance, the cable will be terminated in a load with a high capacitance component which might be objectionable. Because of this fact, the use of the type *B* circuit is limited by the capacitance of the coupling capacitor and the length of the coaxial cable. From tests made it has been found that the type *B* circuit can be used in a frequency range of 75 to 150 kilocycles if the capacitance of the coupling capacitor is 0.00275 microfarad or greater, and the coaxial cable does not exceed 400 feet in length. Under these conditions, the capacitive component of load will be sufficiently low to be used with a typical carrier transmitter and the losses will be only slightly different than that of the type *A* circuit.

The tests indicated that the impedance matching transformer in transforming from a high impedance to a low impedance decreased the capacitive component, which meant that the cable was terminated in a load of a lower capacitive component than would be expected. The tests also indicated that the type *B* circuit could be successfully used between a frequency range of 100 to 150 kilocycles if the capacitance of the coupling capacitor was 0.0015 or greater and the cable 400 feet or less in length.

The type *B* circuit is much more economical to install than the type *A* circuit. The impedance matching transformer is mounted in the base of the coupling capacitor, see Figures 14 and 15. It is therefore necessary to provide only a conduit from the transmitter to the base of the coupling capacitor. The advantage of the type *B* carrier by-pass is even more pronounced because only mounting details for the two coupling capacitors and a path for the coaxial cable must be provided.

A reference to curves Figures 10, 11, and 13 will show that the losses of type *B* circuit, when used as recommended in the preceding paragraphs, are not enough greater to warrant the added expense of the type *A* circuit. Another advantage of the type *B* circuit is that one setting of the impedance transformer will pass a wide band of frequencies with very little difference in losses. A double frequency type *A* tuner might be required to pass the same band of frequencies.

Type C Circuit

This type circuit is connected as shown in Figure 7. The equivalent circuit is shown in Figure 7A. In this case the tuning inductance is located inside in the transmitter-receiver cabinet. This circuit will be tuned when sufficient inductive reactance is added to counteract the capacitive reactance as seen at the sending end of the coaxial cable. When tuned, the load on the transmitter will appear as a resistance load.

As an example, refer to curves shown on Figure 9 for the sending end impedance, Z_s, of the 195 feet cable for 50 kilocycles. From the curve $Z_s = 62 - j404$ ohms. If an inductive reactance of $+j404$ ohms is inserted in series, then the transmitter should be adjusted for a 62-ohm resistance load. If we should consider the transmitter end as the receiving end of the coaxial then $Z_R = 62 + j404$ ohms. The $+j404$ figure is the reactance of the line tuner and 62 ohms is the approximate impedance of the transmitter. Substituting the above values of Z_R in equations 5 and 6, we find that $Z_s = 500 + j1060$ ohms. Referring to Figure 7 the impedance of the cable circuit at *I* will be $500 + j1060$ ohms. Under the condition specified for curves Figure 9 the impedance of the line at point *I* will be $500 - j10^6/2\pi f \times 0.003$ or at 50 kilocycles it will be $500 - j1061$ ohms. The inductive reactance of the cable will then cancel the capacitive reactance of the coupling capacitor. The circuit will then be adjusted for maximum efficiency.

The use of type *C* circuit is limited because the coaxial cable is not terminated in an impedance approximately equal to its characteristic impedance. This fact is evident from the example given in the previous paragraph. Because this circuit is not matched with the cable, the problem of distortion from reflected waves becomes more troublesome as the length of cable increases, or as the frequency increases. If the use of this circuit is confined to short lengths of cable, approximately 200 feet or less, or to low frequencies, 100 kilocycles or less, the behavior of the coaxial cable will approximate that of a simple conductor. The amount that the foregoing range can be extended is dependent upon the impedance of the coupling capacitor and on the amount of distortion which can be tolerated.

The type *C* by-pass circuit is connected as shown in Figure 8. Inductance *AK* is adjusted so that its reactance will counteract the reactance of capacitor *AC* and likewise inductance *JI* is adjusted to counteract capacitance *JL*. If care is exercised in adjusting the circuit one of the foregoing inductances might be omitted.

Figure 6. Type *B* by-pass circuit

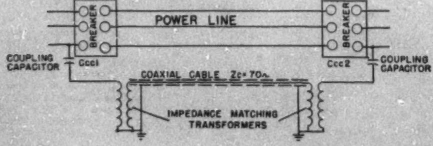

Figure 7A. Schematic diagram of type C line tuning circuit

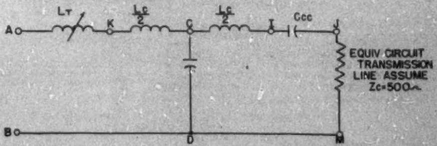

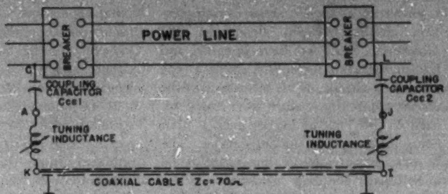

Figure 8 (right). Type C by-pass circuit

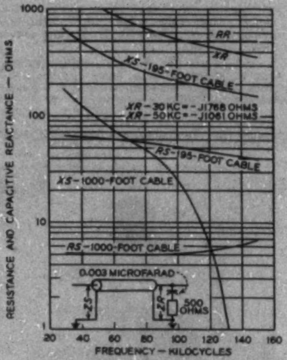

Figure 9. Calculated sending end impedance for receiving end impedance of $Z_R = 500 - j10^6/\omega \times 0.003$

Figure 10. Loss curves for line tuning equipment with 61 feet of coaxial cable

Load $= Z_R = 500 - j10^6/\omega \times 0.003$ except for curve 4

1. Type *A* line tuning
2. Type *B* line tuning
3. Type *C* line tuning
4. Same as curve 2 except $Z_R = 500 - j10^6/\omega \times 0.0015$

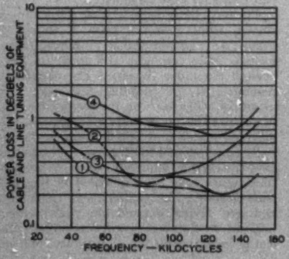

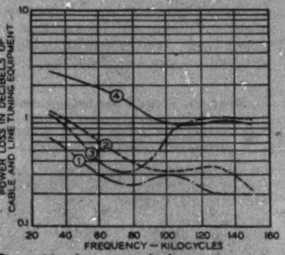

Figure 11. Loss curves for line tuning equipment with 195 feet of coaxial cable

Load $= Z_R = 500 - j10^6/\omega \times 0.003$ except for curve 4

1. Type *A* line tuning
2. Type *B* line tuning
3. Type *C* line tuning
4. Same as curve 2 except $Z_R = 500 - j10^6/\omega \times 0.0015$

Figure 12. Loss curves of by-pass equipment with 195 feet of coaxial cable

2. Type *B* by-pass circuit refer to Figure 6, *CC1* and *CC2* = 0.003 microfarad
3. Type *C* by-pass circuit refer to Figure 8 except only one tuning inductance used. *CC1* and *CC2* = 0.003 microfarad

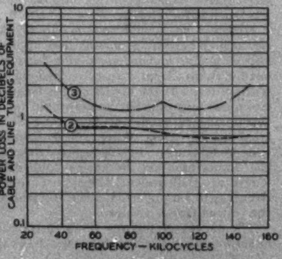

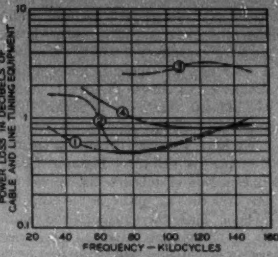

Figure 13. Loss curves for line tuning equipment with 1,000 feet of coaxial cable

Load $= Z_R = 500 - j10^6/\omega \times 0.003$ except for curve 4

1. Type *A* line tuning
2. Type *B* line tuning
3. Type *C* line tuning
4. Same as curve 2 except $Z_R = 500 - j10^6/\omega \times 0.0015$

The advantage of the type *C* circuit over the type *A* circuit is in the cost of equipment and installation. The type *C* circuit can be used in the lower frequency range where the type *B* circuit should not be used. This circuit also presents a resistance load to the transmitter whereas the type *B* presents a load with a capacitive component. As stated previously the use of the type *C* circuit should be limited to short lengths of cable 200 feet or less and to low frequencies 75 kilocycles or less. A reference to loss curves, Figures 10 and 11, will show that in the recommended range of use, the type *C* circuit compares favorably with the type *A*. With the 1,000 feet of cable, Figure 13, distortion was so pronounced that points for 30 and 50 kilocycles were not plotted. The losses for the remaining frequency range were much greater than for either the type *B* or type *A* circuits. A comparison of losses between the type *B* or type *C* by-pass circuits is shown in Figure 12.

Combination of Type B and Type C Circuits

By the addition of a line tuning coil inside the transmitter receiver cabinet the range of use of the type *B* circuit can be extended. The objection to the capacitive component to the transmitter can also be removed.

Summary

The tests providing the basis of this paper were performed in an effort to determine the best type of carrier by-pass to use on our line between Beaumont, Tex. and Baton Rouge, La. An effort was made to determine how much line tuning equipment was required for various installations. The tests were also made to eliminate considerable field work in making adjustments.

Upon the basis of our tests we have decided to use type *A* carrier by-pass circuits in phase "A" of our line for our communication circuit between Beaumont and Baton Rouge. This carrier will operate on two frequencies of 51 and 68 kilocycles over a 132-kv line through coupling capacitors of 0.0015 microfarad. A reference to comments under type *B* circuits or to curves Figures 11 and 13 will indicate that type *B* circuit should not be used for this application.

We have, however, decided to use type *C* by-pass as shown in Figure 8 for the transmission of telemetering carrier signals over the "C" phase of the same 132-kv line. These carrier channels are in the 30- to 34-kilocycle band. The required tuning inductances will be located in the same cabinet as the equipment for the type *A* circuit.

In an 85-kilocycle carrier communication circuit between Beaumont and Navasota, Tex., we have installed and had in operation for nearly a year a type *B* by-pass circuit. This by-pass is in the circuit at all times since wave traps are used to prevent the carrier energy from being dissipated in the substation. The by-pass is on a 69-kv line using 0.003 microfarad coupling capacitor. The connecting coaxial cable is approximately 200 feet long.

We have had several type *B* line tuning carrier relay circuits in operation for several years. Two terminals are on the 69-kv lines using 0.003 microfarad coupling capacitors. The cable lengths are under 100 feet and the frequency over 100 kilocycles. The balance of the type *B* circuits are on 34.5-kv lines. The longest length of cable is 330 feet.

It is hoped that this paper might stimulate other papers on the same subject and that information of value may be obtained from this paper and other papers to be written.

References

1. TRANSMISSION LINES ANTENNAS AND WAVE GUIDES, **King, Minno, Wing.** McGraw-Hill Publishing Company, New York, N. Y., first edition, 1945.

2. ELECTRICAL ENGINEER'S HANDBOOK, **H. Pender, K. McIlwain.** John Wiley and Sons, New York, N. Y., communication-electronics volume, third edition, 1936.

Figure 14. Type *B* line tuning circuit

Note transformer in base of capacitor

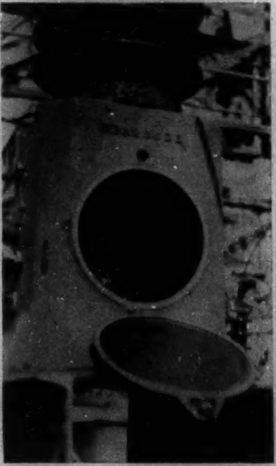

Figure 15. Type *B* line tuning circuit

Note conduit from inside carrier equipment terminates in base of capacitor

Figure 16. Typical type *A* line tuning circuit

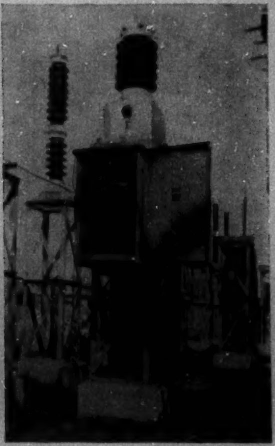

Discussion

H. W. Lensner (Westinghouse Electric Corporation, Newark, N. J.): Sutton has presented an interesting paper which includes some valuable data on limitations of frequency and cable lengths for various simplified line tuning systems. The simplification in equipment and adjustment as described is obtained at the expense of flexibility in choice of frequency, however, and as more carrier channels are added to a power system, the problem of frequency allocation becomes more complex.

Modern carrier transmitters using pentode or beam-power output tubes operate best when fed into a resistive load. The reactive termination presented to the transmitter with the type *B* tuning system can cause considerable harmonic output which may interfere with other services. This would not be of much consequence with unmodulated carrier which operates only occasionally, such as for relaying.

However with amplitude-modulated carrier at high percentage modulation, appreciable distortion and accompanying harmonic output results from a reactive load on the transmitter. At the higher carrier frequencies now in use, the harmonics would fall in the broadcast band, and with tone-modulated carrier telemetering, severe interference would result. In this respect, although the limitations on frequency and cable length are still present, the type *C* tuning circuit is to be preferred, since the load on the transmitter is resistive.

The curves of Figures 10 to 13 indicate losses which are considerably lower than that of other published data.[1,2] This raises a question as to the method of measurement of losses[2] and whether all the losses of the circuit elements were included.

The writer has made tests on a line tuning system similar to the type *B* circuit of Figure 5. The impedance matching transformer, however, was designed to have enough reactance to cancel the capacitive reactance of the coupling capacitor. By means of a few taps on the secondary side, it was possible to provide a reasonable impedance match and still present an essentially resistive load to the carrier transmitter over the carrier frequency band. Several of these units have been installed in the field with coaxial cable lengths up to 1,000 feet, and are giving dependable performance. Laboratory tests on the units including 1,200 feet of coaxial cable gave a total loss of from

0.9 to 1.6 decibels for a 0.004 microfarad coupling capacitor and 1.6 to 2.2 decibels for a 0.00129 microfarad capacitor. Even with the reasonably good impedance match, cancellation of reactive component and resulting reduction of standing waves provided by this special matching transformer, the measured loss figures are higher than the results shown in this paper.

The simplified tuning systems seem to be particularly well suited to use as by-passes around a transformer bank or open circuit breaker, especially if two or more frequencies are to be transmitted through them. The elimination of a multiplicity of tuning coils and trap circuits makes the systems described especially attractive.

References

1. Power Line Carrier Channels, M. J. Brown. Electrical Engineering (AIEE Transactions), volume 64, May 1945, pages 246–51.

2. Application of Carrier to Power Line, F. M. Rives. AIEE Transactions, volume 62, 1943, pages 835–44.

3. Method of Measurement at Carrier-Current Frequencies. AIEE Carrier Current Committee. AIEE Transactions, volume 67, part II, 1948, pages 1429–32.

H. J. Sutton: The writer wishes to express his appreciation for the comments made by Lensner. The primary purpose in presenting the three types of circuits was to bring out the characteristics of coaxial cable circuits in a discussion of practical applications. As a secondary consideration, the type *B* and type *C* circuits were recommended for limited applications.

Lensner, in his discussion has brought out some of the objections to the use of the simplified tuning circuit, particularly the type *B* circuit. The writer perhaps did not emphasize sufficiently that the impedance matching transformer used for the tests of this paper added inductive reactance which partially overcame the capacitance of the coupling capacitor. In the range recommended for the use of the type *B* circuit, the load on the transmitter was very close to unity power factor, and no trouble should be experienced from harmonics or distortion.

The tests were made in a laboratory using mica coupling capacitors rated at 2 500 volts direct current. No drainage coils or lightning arrester gaps were included in the tests. Otherwise the tests included all losses present on actual installation. The following instruments were used:

Thermo-coupled milliammeters, ±5 per cent accuracy.

(Note all milliammeters checked against standard and correction factor used.)

Vacuum tube voltmeter, ±2 per cent accuracy.

Cathode-ray oscilloscope, to check wave form and phase angle.

Electronic switch, to check phase angle. Possible ±10 per cent accuracy.

Considering the instruments used, a possible error of 5 to 10 per cent or 0.2 to 0.4 decibels may be present in the actual losses. A comparison of the differences in losses, type *A* and type *B* circuits, as shown on curves Figures 10, 11, and 13 agrees within 0.2 decibel of differences in coaxial cable losses as obtained from the manufacturer's published losses. The loss curves were used for comparison between the three circuits, and for this purpose the possible error in results would not make any appreciable differences in our conclusions.

Shipshaw Relay Protection

J. T. MADILL
MEMBER AIEE

F. H. DUFFY
ASSOCIATE AIEE

Synopsis: This paper will describe the relay protection of the Shipshaw Number 2 Generating Station of the Aluminum Company of Canada, Limited, and will draw attention to particular points of interest in design considerations and will outline some operating results and experience. In particular the excellent performance of one type of generator winding protection will be outlined. This protection has established a new record by detecting faults at a stage earlier than recorded hither-to-fore in the literature. In general this paper will illustrate modern protection for a large-unit type hydroelectric generating station.

AN ELEMENTARY 1-line diagram of the station will be seen in Figure 1. The basic design is the unit system; one 75,000-kva 13.2-kv generator, one 90,000-kva transformer bank, one 2,500-000-kva high-tension circuit breaker, and one 154,000-volt transmission line, with no low-tension or high-tension busses between units. In the case of the center six units, minor modifications are made for local and auxiliary power supply, but still no interconnection exists, because of interlocks. Almost the total output of the 1,200,000-horsepower Shipshaw Number 2 Station is transmitted at 154,000 volts, just two miles to the Arvida aluminum ingot production works.

Most of the relay protection is located on the back of the unit duplex switch boards, on the front of which the unit meters are mounted. Figure 2 shows the relays of one unit, and Figure 3 shows one unit diagrammatically. The most important sections of the protection are indicated on this latter diagram.

The ordinary generator percentage differential protection extends from the neutral leads to the phase leads of the generator. Both sets of current transformers have a ratio of 4,000/5 amperes and are the bus-bar type. Instantaneous balanced-beam percentage differential relays having two restraining coils, one in series with each set of current transformers, and one operating coil, connected between the junction of the two restraining coils and the neutral lead, are used. These relays are connected on their most sensitive tap, and will operate with a minimum of 80 milliamperes unbalance or 1.8 per cent of full load current. They have a 2.5 per cent characteristic, that is at any current, a difference of 2.5 per cent between the line and neutral currents will cause the relays to close contacts. This percentage protection was used because it was of the high-speed type, not the induction-time type, and was very sensitive.

It was believed that the transformer protection, while better than most, was not fast enough at low currents, or sensitive enough, for the generator, and the split-phase protection was untried.

The eight parallels of each generator phase are connected in two groups of four each, and leads are brought out from each group as shown in Figure 3 to permit the application of split-phase protection. These leads are brought in opposite directions through the two primary windings of the split-phase current transformers, which have a double primary and single secondary winding. The ratio is 500/500/5 amperes. The balanced-beam instantaneous overcurrent relays connected in the secondary circuits are set to have a minimum operating current of 0.5 ampere which is 1.3 per cent of full load current.

Figure 4 shows one split-phase current transformer. The double-primary, single-secondary construction permits very sensitive relay settings because there is no unbalance between current transformers. Currents are bucked against each other in one transformer and only the difference flux produces secondary current. Therefore saturation or burden present no problems and cannot cause false operation. Twenty-five amperes circulating between the winding halves or 50 amperes unbalance between the halves will cause these relays to close contacts. With a generator maximum current of 3,750 amperes, this gives a sensitivity of 1.3 per cent. Though the current transformer nominal ratio is 500/500/5 amperes, each half of the transformer is rated at 2,000 amperes continuously, and when connected in series on test, with a current of 3,000 amperes flowing, the maximum acceptable secondary current is 0.05 ampere. This current is of such small magnitude that normal generator unbalances due to design and construction details become the limiting factor in the relay settings.

The generator standby, or phase protection is connected to three Y-connected 4,000/5 ampere bus-bar type current transformers located on the generator neutral leads. The voltage-restrained inverse-time overcurrent relays, of the induction-disk type are calibrated to have a minimum operating current of 4.0 amperes and an operating time of 135 cycles at eight amperes with voltage restraint. This provides a setting of about 70,000 kva. With the voltage restraint this is increased to about 105,000 kva which provides ample margin for load currents. From Figure 5 it may be seen that it is necessary for this protection, to clear phase-to-phase faults on the low-tension side of the step-down transformer bank at Arvida, and this influences the settings. This standby protection must be able to operate on the sustained short-circuit current of one isolated generator which in the case of large hydroelectric generators, may not be much in excess of the load current. For the case under consideration, the minimum fault current which must be detected is 132 per cent of full load current. One of these relays is shown in Figure 6.

Paper 49-7, recommended by the AIEE relay committee and approved by the AIEE technical program committee for presentation at the AIEE winter general meeting, New York, N. Y., January 31–February 4, 1949. Manuscript submitted October 27, 1948; made available for printing December 13, 1948.

J. T. MADILL is electrical engineer and F. H. DUFFY is system protection engineer with the Aluminum Company of Canada, Ltd., Shipshaw, Quebec, Canada.

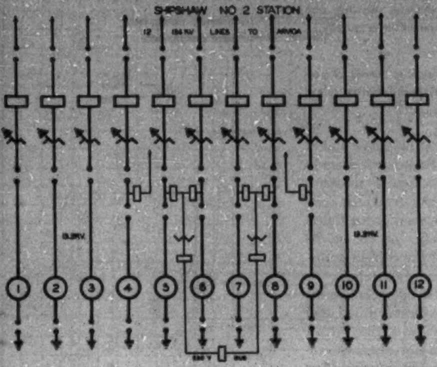
SHIPSHAW NO 2 STATION
12
154 KV
LINES
TO
ARVIDA
13.2KV
13.2KV
1
2
3
4
5
6
7
8
9
10
11
12
550 V
BUS

Figure 1. Elementary 1-line diagram of station

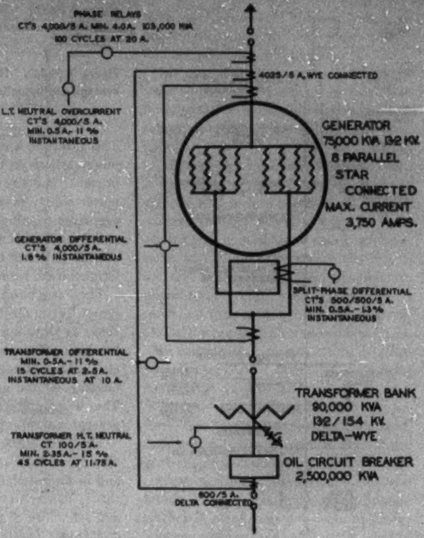
PHASE RELAYS
CT'S 4,000/5 A. MIN. 4.0A. 103,000 KVA
100 CYCLES AT 20 A.
4025/5 A. WYE CONNECTED
L.T. NEUTRAL OVERCURRENT
CT'S 4,000/5 A.
MIN. 0.5 A.- 11 %
INSTANTANEOUS
GENERATOR
75,000 KVA 13.2 KV.
8 PARALLEL
STAR
CONNECTED
MAX. CURRENT
3,750 AMPS.
GENERATOR DIFFERENTIAL
CT'S 4,000/5 A.
1.8 % INSTANTANEOUS
SPLIT-PHASE DIFFERENTIAL
CT'S 500/500/5 A.
MIN. 0.5A.- 13 %
INSTANTANEOUS
TRANSFORMER DIFFERENTIAL
MIN. 0.5A.- 11 %
15 CYCLES AT 2.5A.
INSTANTANEOUS AT 10 A.
TRANSFORMER BANK
90,000 KVA
13.2/154 KV.
DELTA-WYE
TRANSFORMER H.T. NEUTRAL
CT 100/5 A.
MIN. 2.35 A.- 15 %
45 CYCLES AT 11.75 A.
OIL CIRCUIT BREAKER
2,500,000 KVA
600/5 A.
DELTA CONNECTED

Figure 3 (right). 1-line diagram of one Shipshaw unit

The low-tension neutral or generator 13.2-kv ground relay is connected in the neutral of the Y-connected 4,000/5 ampere standby current transformers. It is an instantaneous balanced-beam type overcurrent relay. The operating current is 0.5 ampere or 11 per cent of full load. With the neutral point of the generator solidly grounded, this ground relay covers the transformer bank low-voltage winding, the 13.2-kv bus and all of the generator winding coils, with perhaps the exception of those particular coils connected right at the neutral point. It provides fairly sensitive, high speed, duplicate protection on the 13.2-kv equipment at just the cost of the relay and hence is easily justifiable.

The transformer bank or over-all differential protection extends from the generator neutral leads to the line side of the high-tension circuit breaker. The current transformers on the high-tension side are the bushing-type with a 600/5 ampere ratio and are delta connected. The second set is located, for convenience and extra protection, on the generator neutral leads. These current transformers have a normal ratio of 4,025/5 amperes and are tapped to exactly match the transformer bank turns ratio on each transformer tap. Also their saturation characteristics were designed to match those of the high-tension type. The characteristics of these current transformers are such that under the worst condition, a fault immediately outside of the high-tension circuit breaker, the transformers are operating well below the knee of their saturation curve and false tripping is definitely avoided.

Figure 2 (left). Relays of one Shipshaw unit on duplex panel

Top row—standby or phase protection

Second row—transformer differential relays

Third row—low tension neutral, generator split-phase and high tension neutral relays

Fourth row—trip relays and generator differential relay. The current transformer test blocks are at the bottom

The relays are the induction-disk low-energy very inverse-time overcurrent type with instantaneous overcurrent attachments, which have a better characteristic for transformer bank protection than the percentage type relays.

Figure 7 shows on the same co-ordinates, the time curves of a differentially-connected induction-type overcurrent relay with an instantaneous attachment, a high-speed transformer percentage differential relay set on its lowest tap, 25 per cent, and an induction-type transformer percentage differential relay. For severe faults the two former relays both operate in one cycle. The minimum operating current for the percentage relay is two amperes, while that for the induction-type overcurrent relay is 0.5 ampere. This latter relay is therefore four

Figure 4. One split-phase current transformer

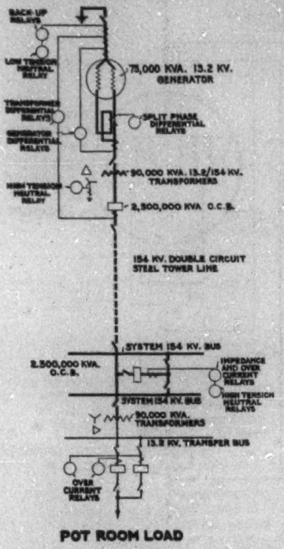
BACK-UP RELAYS
LOW TENSION NEUTRAL RELAY
75,000 KVA. 13.2 KV. GENERATOR
TRANSFORMER DIFFERENTIAL RELAYS
SPLIT PHASE DIFFERENTIAL RELAYS
GENERATOR DIFFERENTIAL RELAYS
90,000 KVA. 13.2/154 KV. TRANSFORMERS
HIGH TENSION NEUTRAL RELAY
2,300,000 KVA O.C.B.
154 KV. DOUBLE CIRCUIT STEEL TOWER LINE
SYSTEM 154 KV. BUS
2,300,000 KVA. O.C.B.
IMPEDANCE AND OVER CURRENT RELAYS
SYSTEM 154 KV. BUS
HIGH TENSION NEUTRAL RELAYS
90,000 KVA. TRANSFORMERS
13.2 KV. TRANSFER BUS
OVER CURRENT RELAYS
POT ROOM LOAD

Figure 5 (left). 1-line diagram showing one Shipshaw unit and connection to system

Figure 7 (right). Time-current curves of percentage and induction-type differential relays

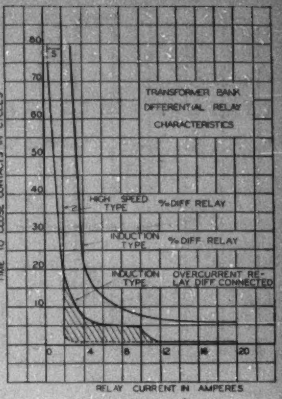

times as sensitive as the percentage relay and does not have the complications of voltage or harmonic restraint. Many installations do not operate the percentage relays on the lowest ratio, consequently the sensitivity may be even poorer. It should also be noted that as many windings and/or connections, from either the high tension or the low tension, as desired, can be accommodated with the overcurrent relay system, whereas the percentage relay is definitely limited in this regard.

This principle is used at Shipshaw and at other stations on the Saguenay system to prevent faults on local and auxiliary power supply systems at generator voltage, from tripping the transformer differential protection falsely. Of course, no scheme is better than the current transformers used, regardless of the relays.

There was no object in not including the generator in the transformer differential zone, as there are no low-tension circuit breakers. Four sets of current transformers are located together on one capacitor bushing on the generator neutral leads. Thus extra protection is available for the generator at no extra cost.

The price of the induction-type relay is about one-sixth of the percentage relay and in an installation involving 36 relays this is of some interest. The simplicity and reliability of this relay make it very desirable. The induction element is set to operate at 0.5 ampere which is 11 per cent of full load current and to have a time delay of 15 cycles at 2.5 amperes. The instantaneous attachment is set at 10 amperes or 200 per cent of full load. It might be noted that the 11 per cent setting was the most sensitive transformer bank differential relay setting reported in an AIEE survey made during 1946. This differential protection has never tripped falsely for faults just outside its zone, even though voltage recovery may impose some magnetizing transients on the relays.

An exactly similar installation is used at a station which has a low-voltage bus. Here transformer banks are energized at full voltage from either the high-tension or the low-tension side and no trouble with false tripping is experienced from either the time or instantaneous elements. No other type of protection is as suitable for covering a complete zone from circuit breaker to generator.

The high-tension neutral, or transformer bank ground relay is operated by a 100/5 ampere current transformer connected between the transformer bank Y-point and ground. The inverse-time overcurrent relay has a minimum operating current of 2.35 amperes, that is, 15 per cent of full load. The time delay is set at 45 cycles at 11.75 amperes. From Figure 5, it may be seen that this time delay is necessary to provide selective clearing of faults on other lines connected to the same section of the Arvida high-tension bus. The faulted line will be cleared from the system by ground relays at Arvida in 10 cycles on a 60-cycle base, and therefore the time delay in the Shipshaw ground relays is permissible. From Figure 5 it may be seen that the transmission line protection could only be solved, as far as the generating station is concerned, as it was, or by pilot wire or carrier current relaying, and either of the latter two would have to be considerably

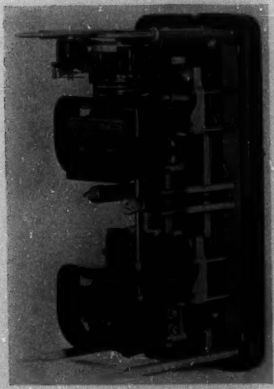

Figure 6 (left). Voltage restrained overcurrent relay used for standby phase overcurrent protection

Figure 8 (right). Location of gas detector relay on transformer bank

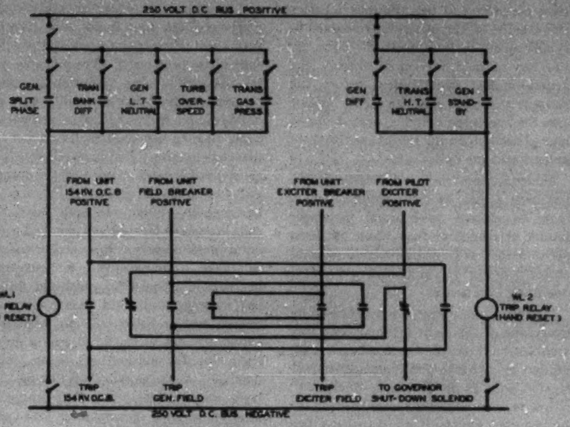
250 VOLT D.C. BUS POSITIVE
GEN. SPLIT PHASE
TRAN BANK DIFF
GEN L.T. NEUTRAL
TURB OVER-SPEED
TRANS GAS PRESS
GEN DIFF
TRANS H.T. NEUTRAL
GEN STAND-BY
FROM UNIT 154 KV O.C.B POSITIVE
FROM UNIT FIELD BREAKER POSITIVE
FROM UNIT EXCITER BREAKER POSITIVE
FROM PILOT EXCITER POSITIVE
WL 1 TRIP RELAY (HAND RESET)
WL 2 TRIP RELAY (HAND RESET)
TRIP 154 KV O.C.B.
TRIP GEN. FIELD
TRIP EXCITER FIELD
TO GOVERNOR SHUT-DOWN SOLENOID
250 VOLT D.C. BUS NEGATIVE

Figure 9. 1-line diagram of d-c tripping circuits

more complicated than in the case of an ordinary 2-terminal line. Because of the short lines, carrier current did not seem attractive and it developed that pilot-wire relaying, because of cost and reliability, was not selected either. This was because the high ground fault currents and rocky terrain required lead covered cable, and a 1,900-foot river crossing made this difficult. It was considered too risky to put the protection for all 12 lines in one cable, and without this the cost of the line protection became about 40 per cent of the cost of the transmission line itself. This is very difficult to justify, bearing in mind the bus arrangement already in existence to a large degree, at Arvida. There were no suitable commercial telephone channels available for lease. Therefore ground relaying and phase standby protection were used. This was relatively low in cost, simple and reliable, and has given satisfactory results.

Each transformer at Shipshaw is equipped with a gas detector relay of the Bucholz-type having a gas accumulation element, which operates an alarm, and a pressure element which operates one of the trip relays. The relay is located as shown in Figure 8, on the top of the transformer proper, and at one side for convenience of access during service.

The generator a-c overvoltage protection is provided by a solenoid self-resetting relay connected to a 13,200/110-volt potential transformer. The relay operates at 114 per cent voltage to energize a light and bell circuit, and through a contactor to add resistance to the field circuit of the main exciter.

The pilot exciter d-c overvoltage relay is energized directly by the output voltage of the pilot exciter. It operates at 120 per cent of normal pilot exciter voltage to insert a block of resistance in the field of the pilot exciter and thus limit the voltage to 120 per cent of normal under almost any overspeed condition.

The generator field ground detector is a solenoid-type relay connected between the center tap of a high resistance and one side of a 110-volt 60-cycle circuit. The resistance is connected across the generator field leads and the other side of the 110-volt circuit is connected to ground. The relay is set to operate with about 0.5 ampere ground current and covers the complete d-c circuit to which it is connected. This protection only operates an alarm.

The turbine overspeed consists of a centrifugal device on the permanent magnet generator which operates mercury switches to sound an alarm and energize the trip relay at 130 per cent speed.

Figure 9 shows the d-c control circuit for all of the relays which have tripping action. It may be seen that some sensitive and some high-speed protection for both the generator and transformer bank is connected to operate each trip relay. That is, the generator differential operates one trip relay, the split-phase protection the other. The transformer differential energizes one while the standby operates the other trip relay. Two trip relays were used so that the failure of one trip relay coil, mechanism, or contacts would not make all of the protection inoperative. Hand reset relays were used because of their simplicity in construction and in associated wiring, and because of their reliability.

All d-c circuit sources are separated back to the main d-c bus, but there was no alternative to paralleling the two trip relays, since both must energize the same coils.

All relays are calibrated annually using a test board which contains a cycle counter and meters of suitable range for current and/or voltage indications on each relay, as well as a switch arrangement to facilitate the use of the instruments. A very careful check of minimum operating currents and time setting is made, all dust or dirt particles removed, and any worn or defective parts replaced. This calibration, properly made, requires two men for $2^1/_2$ to 3 hours for each Shipshaw unit.

Annual relay calibration records for five years show that for the induction-type relays a change greater than 2 per cent may be expected in the minimum current setting in five relays per one hundred relay years, and a change in time setting of more than one cycle in 4.8 relays per one hundred relay years. In the high-speed type relays there is no apparent deviation in operating time, but the minimum current setting may be expected to change more than 2 per cent in 2.7 relays per one hundred relay years. The variation outside this 2 per cent figure is still only of the order of 6 per cent.

Turning now to operating experience, the gas detector accumulation elements have detected ten incipient low-tension winding joint failures, as reported previously[1] long before total failure. Complete confidence is placed in these elements and it was decided that their operation has been so excellent, and has indicated the trouble at such an early stage, that a check of all transformers is not justified. In other words, operating experience has led to the conclusion that

Figure 10. Hot joint in neutral ring bus detected by split-phase relay

Figure 11. Turn-to-turn coil fault involving only two turns detected by split phase relay

Figure 12. Turn-to-turn coil fault on generator detected by split phase relay

complete reliance in these elements is justified. There have been no faults for the pressure elements to detect, but to-date this element has never caused a false trip. With proper technical supervision and sampling devices there is no difficulty in interpreting indications from the gas detector accumulation elements.

Upon several occasions, rheostat trouble caused the loss of field on one 75,000-kva generator, when loaded to about 65,000 kw. This loss of field was always picked up by the relay protection, though no element was particularly designed for this. If the field decay took place rather slowly, the armature current in the generator, because of decreasing voltage, increased sufficiently slowly to permit the back-up or phase relays to close contacts and trip the unit. Under this condition, the generator remained in synchronism until tripped. If, however, the loss of field was more abrupt, the generator lost synchronism before the phase relays could close contacts. In this case the overspeed switch operated almost immediately upon the loss of synchronism and tripped the unit.

Including construction difficulties, there has been a total of eight troubles which may be classed as internal generator faults. At the same time, there has been accumulated at Shipshaw about 62 generator years or $4^{3}/_{4}$ million kva years of operating experience.

The split-phase protection operated on every one of the eight internal generator troubles. Three of the faults were to ground or phase-to-phase and other protection, such as the generator differential, or low-tension-neutral operated during the same cycle. One fault was a turn-to-turn one which broke down to ground but was detected so rapidly by the split-phase protection that no other relays operated. Four faults could be detected only by the split-phase relays.

One of these four was a hot joint in one neutral ring bus of one generator. The joint resistance finally unbalanced the winding currents and operated the split-phase protection. This fault is shown in Figure 10. Considering that this was in the neutral bus of a solidly grounded generator, it is difficult to see how any other protection could possibly have detected this fault until it had developed to the major proportions of a serious fire and/or a phase-to-phase bus short circuit.

Three of the four faults were turn-to-turn short circuits detected only by the split-phase protection. The machine was tripped without any system fault occurring and without any internal fire or arc or burning. In two different generators these turn-to-turn coil faults have been detected by the split-phase relays. The generator has been tripped off the system with no apparent fault jar, or arc, or burning, or ground. In both cases, the coils have been located and changed without a break occurring through the coil insulation. A simple and reliable method has been developed by which the faulty coil is determined, and thus no iron is burned and no other coils are damaged. Obviously this is the ideal condition as there is the minimum possible fault damage. As far as is known this has not been done before on a large-capacity solidly-grounded generator. This protection has been most satisfactory. Figure 11 shows the first signs of one fault as the coil insulation was being removed. About half the coil side insulation had been removed at this point. Figure 12 shows one fault in one coil, which involved only two of the three turns.

Checks on split-phase currents have indicated that the maximum unbalance in any generator is about 28 amperes or 0.75 per cent. The average unbalance of the 36 phases is only about 14 amperes or 0.37 per cent. Thus, it may be seen that the designers have done an excellent job of balancing the windings.

So far, no false trips can be definitely attributed to this protection, though one case is suspect. However, several definite experiences have shown stability or non-operation of this protection for through faults. In one, a fish wire established a double-line-to-ground fault on the 13.2-kv leads from one generator to its transformer. This was detected by the low-tension neutral and by the transformer

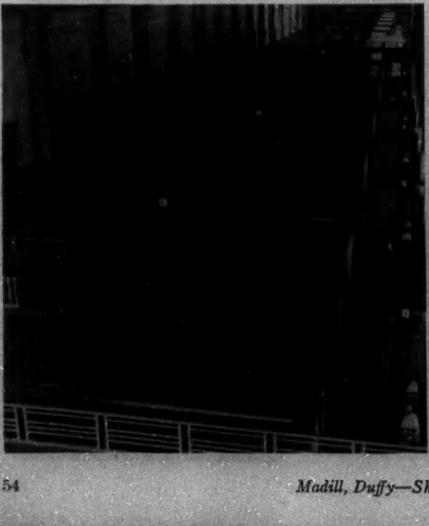

Figure 13 (left). Interior view of Shipshaw powerhouse

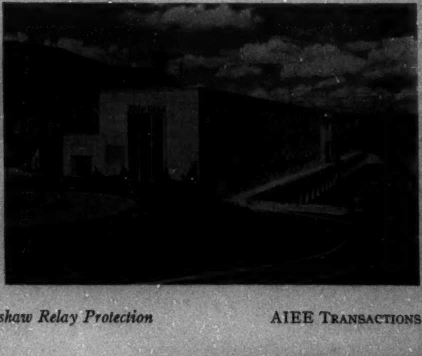

Figure 14 (below). Exterior view of Shipshaw powerhouse differential relays, but the generator split-phase relays did not operate. The fault current supplied by the generator was about 10,300 amperes. In another case, a dead line-to-ground fault occurred six feet outside of one high-tension oil circuit breaker. This was detected by the high-tension neutral relay and no other protection operated. In this case, the bank supplied about 1,150 amperes to the fault. In any future station of the unit type, it is thought that with split-phase generator protection, and with transformer differential protection which includes the generator, no percentage generator differential protection would be necessary. This would eliminate two sets of current transformers and one set of relays. However, Shipshaw Number 2 station was one of the first applications of this type of split-phase protection and it was felt that the percentage differential relay was desirable. In summing up, the following points stand out:

1. On the Saguenay system, with the very short lines and with the bus system as installed at Arvida, the rather simple combination of the back-up or phase relays and the transformer bank high-tension neutral relays have handled the line faults adequately.

2. The relays used have maintained their settings excellently and have been very reliable.

3. The transformer gas detector protection has given results far better than anticipated and has proved to be extremely valuable. This protection should always be used on any conservator-type transformer over 6,000 kva rating. The transformer differential has not been called upon to operate for winding faults, but has detected any faults in its zone and has not operated falsely for faults immediately outside of its zone.

4. The back-up or phase relays, combined with the overspeed trip have proved a reliable combination to detect loss of synchronism, and in turn loss of field. Some element of the generator relay protection should always be capable of detecting this latter condition.

5. The generator split-phase protection has been the outstanding feature of the generator protection. Its ability to detect turn-to-turn coil faults, and series faults as well as all of the usual short-circuits, has not been available previously. It is of the high-speed 1-cycle type and is very sensitive, 1.3 per cent. It has never missed an internal unbalance and has not operated falsely. This protection is most highly recommended.

Therefore, in conclusion, it would seem that by a judicious choice of relay methods, some of which were relatively new and untried, combined with a careful co-ordination of current transformers, and careful balancing of generator winding design, excellent protection has been secured with relatively simple elements, and is retained by careful, systematic maintenance.

The magnitude of the development on which this protection has been applied may be judged by Figure 13 which shows the generator room and Figure 14 which shows the Shipshaw Number 2 Station.

Reference

1. Typical Transformer Faults and Gas Detector Relay Protection, J. T. Madill. AIEE Transactions, volume 66, 1947, pages 1052–60.

Discussion

D. A. McKenzie (The Hydro Electric Power Commission, Toronto, Canada): We have been very much interested in the paper presented by Madill and Duffy on Shipshaw Relay Protection. The schemes selected are simple and reliable, and in view of the perfect performance record it would seem that nothing further could be asked in the way of protection. We should be glad, however, to have certain points clarified.

Differential Protection for Generators

While it would appear from the information submitted covering actual performance that the differential protection for the generators (percentage type) is faster than the over-all differential protection on the generator and transformer, as might be expected from the types of relays used; it would appear that this protection could safely have been omitted as has been suggested by the authors.

Split-phase Protection for Generators

Since generator protections based upon the similarity of the currents in circuits of multicircuit windings have been used for many years, we must assume that the statement that the "Shipshaw Number 2 station was one of the first applications of this type of split-phase protection" refers to the use of the special 2-primary current transformer. This type of current transformer, with normally zero secondary current, should of course, provide more sensitive and stable protection than could be expected from schemes in which standard current transformers are used and their secondary currents combined. However, some sensitivity is lost by the necessity of combining the circuits into two groups (to suit the 2-primary current transformer) since current could still circulate between the circuits without leaving the group.

It would be understood from the reference to 36 phases that the unbalances referred to have been obtained on the secondaries of the special 2-primary current transformers, but no mention is made regarding the load on the generator at the time these unbalances were measured. While balance between the two groups of circuits per phase is very good, this does not preclude the possibility of circulating currents between the circuits of the group. It might be mentioned that on several generating units which have recently only been placed in service, the circulating current between the two groups has been of such magnitude that the sensitivity of this type of protection has been very seriously affected.

It would have been expected that this protection would have functioned so rapidly in all cases that no other protective scheme could have indicated operation. Would it be probable, that in the cases where the generator differential or the low-tension neutral schemes functioned, the fault current reached high values very quickly?

Mention is made of an operation of this protection for a hot joint in the neutral ring bus of a generator. It would be of interest to know the exact location of this joint, that is, whether it was in the connection of one of the circuits to the group bus or in the connection of the group bus to the lead to the neutral.

Differential Protection for Generator-Transformer Group

This protective scheme should provide very satisfactory protection against faults within the zones covered by its current transformers, especially when combined with the split-phase protection which, of course, only covers the generator.

It is not quite apparent from an inspection of Figure 7 how the comparisons between the three types of relays which were considered for this protection, were obtained.

Loss of Field Protection in Generators

The interest in protections to function on loss of field has been developing during the past few years and the occurrences at this plant indicate that this matter requires serious attention. It would appear that an additional protection to provide high-speed operation is required. It should be feasible to provide more sensitive protection than the back-up relays and faster protection than the overspeed protection.

Generator Neutral Grounding

The fact that there are no interconnections at generator voltage is, of course, most favorable to the direct connection of the generator neutral to ground.

The employment of a current transformer in the neutral connection, of a suitable range, would have provided a more sensitive and stable ground protection than the residual current from the three 4,000/5 ampere current transformers installed for the standby relays.

It is interesting to note that no burning of iron has been experienced with the neutrals connected directly to ground.

It would have been of interest to have employed the recently developed method of grounding generator neutrals through a suitable capacity service-type transformer, on some of the generators in this plant to obtain comparative information on performance. In view of the apparent high incidence of faults in these generators, comparative information could be obtained in a relatively few years. This method provides sufficient current to enable reliable and fast operation of the protective schemes to be obtained and yet limits the fault current to values which will not result in burning of the iron. Moreover, by proper selection of the resistance burden on the transformer secondary, resonance is prevented and the scheme provides all the advantages of the dead grounded neutral with none of its disadvantages.

Overspeed Protection on Generator Unit

It is noted that the overspeed protection is mechanical, a centrifugal device within the permanent magnet generator, supplying power for the drive for the governor flyball head.

The setting of 130 per cent of normal speed for this protection seems somewhat low for use on hydraulic turbines but in view of the layout of this station and its type of load, it is probable that unnecessary operations of this protection would not be objectionable. Would the authors state how many operations of this protection have been experienced even if in conjunction with other protective schemes? Would they also advise if the shutdown solenoid of the governor operates through the governor valves, or if there is any provision for high-speed closure of the gates? In view of the independent drive on the governor head, it would be expected that the governor would be adequate to take care of overspeeds due to loss of load on the unit and that this device would not add to the plant security in such cases.

It is suggested that since the tachometers on these turbine governors are undoubtedly voltmeters calibrated in terms of speed, the simplest and most reliable overspeed protection would be obtained by use of a suitable overvoltage relay. This relay could be checked for operation at will and its setting changed as desired.

The maintenance and adjustment of the mechanical overspeed protection is an expensive and somewhat hazardous matter.

Overvoltage Protections on Generator Unit

The detector for grounds on the generator field is of a type which has given excellent service for many years.

The protections against overvoltage on the pilot exciter and on the main generator a-c winding are, of course, desirable in plants designed for normal service and it is of interest that even in this rather specialized plant it has been considered desirable. The functioning of the a-c overvoltage protection to add resistance in the field circuit of the main exciter appeals to us as fast and reliable but we should be glad to know if provision is made for this element to reset automatically.

Transformer Protection—Gas Detector Relays

The record of operations of the gas-detector relays installed on these large transformers is of very special significance, particularly when the method of installation of the relay is considered. The relay is shown mounted at the extreme edge of a large flat top surface which must have supports beneath it, and unless some means has been provided within the transformer to collect any gas generated and direct it to the location of the gas-detector relay, it would seem probable that only a very small percentage coverage in the matter of gas collection is obtained. Even the small opening in the cover adjacent to the relay probably would collect many times the amount of gas required to operate the relay before any gas would find its way to the relay. Also the openings in the cover leading to the conservator tank and to the explosion vent would provide means for the gas to escape without proceeding to the relay. Therefore, the detection of ten incipient cases of fault is an amazing performance, especially since none of the faults had progressed to the point where the operation of the transformer was affected. However, it would be quite reasonable to assume that many similar faults can be progressing and we would feel that a careful check on all transformers would be justified and at the earliest possible date. While it is necessary to locate these relays so that they may be inspected and reset, when desired, with the transformer remaining in operation, we believe that the importance of this type of protection will justify either the employment of several of these relays properly located on the top of the transformer, or the use of some means within the transformer to ensure that a fairly high percentage of any gas generated will be directed to the gas-detector relay. In the employment of this latter expedient, care must be taken that the entrance of the pressure wave to this relay is not impeded. If a single relay is employed, the European practice of mounting it on the connection to the conservator tank would appear to have considerable merit, even though some of the sensitivity of the pressure wave element would be lost.

It is noted that these relays have not yet been required to function on an actual case of trouble in a transformer. From a considerable amount of experience with these relays, it may be reliably expected that this protection normally will function in advance of the differential protection even of the sensitivity employed in this station on actual faults within the transformer. Even failures of high-voltage bushings have been cleared by these relays.

It has been a pleasure to study a paper such as this which shows evidence of such careful study of the various factors involved, and which frankly admits to an astonishing number of faults.

A. W. Rauth (Consumers Power Company, Jackson, Mich.): This paper discussing the relay protection of the Shipshaw Hydro Station is well written and interesting. In addition it shows how a relay problem is solved, and it should have far reaching value in demonstrating what can be done when full co-operation is obtained from everyone concerned. This has special reference to co-operation in solving protective problems pertaining to generation, distribution, and transmission.

The Shipshaw Station as demonstrated by the paper is one of the largest hydro stations of the world. It therefore required considerable study and ingenuity to make sure that the best type of equipment was used that such equipment was protected by the simplest, most effective protective scheme, and that the scheme was one which required the least amount of maintenance for the protection received. The operating results as given in the paper clearly show that all three of these things were accomplished. It also shows that the scheme of protection used could have been accomplished only by the complete co-operation of the protective engineer, the design engineer, the equipment engineer, and the operating engineer. This certainly should be an example of one method of solution to all major electrical protection problems. Perhaps those concerned with relay problems should be complimented in being able to obtain the results indicated in the paper.

In solving many protective problems pertaining to electrical transmission, distribution, and generation, it would appear that at times the design and equipment engineers complete their job and then ask the relay engineer or protective engineer to apply his ingenuity in protecting the equipment so that good service is maintained. The result in many cases is that the protective engineer must resort to highly specialized, complicated schemes which require considerable attention and frequent testing and calibration to provide adequate protection. The Shipshaw protective scheme clearly illustrates that important protective problems involving the protection of large generating stations can be solved by a simple, inexpensive protective scheme requiring practically no maintenance. The important thing is that the scheme used even though simple, provides better protection than some of the more complicated highly-specialized protective devices.

Without question, to my mind it seems that this is one of the outstanding power generating installations which clearly demonstrates what can be done with a simple protective scheme, if the protective engineer is given an opportunity to use his ingenuity before the generating and distribution designs are completed. It also illustrates that the thinking of the protective engineer is just as important as that of any group of engineers in designing generating or transmission systems.

F. L. Lawton (Aluminum Company of Canada, Montreal, Canada): Having been closely associated with the Saguenay system from the days when the Isle Maligne hydroelectric generating station was under construction, and with the design and construction of Shipshaw Number 2 power plant, it will not be inappropriate to comment briefly on the paper and certain of the points mentioned by previous discussers.

The authors have described the Shipshaw relay protection and the results achieved, results which surpass anything hitherto obtained with large hydroelectric generating stations, particularly as regards the split-phase feature. It should be emphasized that the excellent performance is due to full co-operation between the owner's engineers, fully conversant with system background, the consulting engineers responsible for design, and the manufacturers' engineers from the early stages of design. The relatively simple but well-balanced protection, properly designed and installed initially, has been well maintained, with the optimum performance noted.

The decision to solidly ground the generator neutrals stems from past experience on the Saguenay system. The generators at the 12-unit 450,000-kva Isle Maligne hydroelectric generating station were originally operated with isolated neutrals. Differential protection consisted of the type available in the early 1920's, differentially-connected current transformers and so-called instantaneous plunger-type solenoid relays.

Although single-phase-to-ground faults, with isolated generator neutrals, involved negligible burning of stator iron, some 50 per cent of all such faults developed into multiphase faults, frequently with excessive damage to stator iron.

As a result, groups of generators were operated in parallel at generator voltage and were arranged so that one generator in a group would be grounded through a neutral resistor of moderate value. Percentage differential relays were installed. This resulted in improved relay performance and a decrease in multiphase winding faults but too much burning of stator iron still occurred during such faults.

Thus our thinking was oriented over a period of years towards solid grounding of generator neutrals to eliminate multiphase faults, to sensitive and reliable differential relays which could detect low-fault currents, and to generator field circuit breakers to minimize duration of fault current after the quick-acting differential relays had operated—hence the generator protection adopted at Shipshaw with solidly-grounded generators. However, provision was made for the installation of generator neutral impedances should experience warrant their installation.

It may seem to some, for our stated experience with gas-detector relays at Shipshaw, that we have had an excessive number of faults with the 36 single-phase step-up transformers. Actually, all the troubles have been of a similar nature, that is, defective brazing of the heavy cable connections between the two low-tension windings. This defect appears to have resulted from poor workmanship by one individual which was not picked up by the factory inspection. In any case, there have been no actual faults (only incipient faults) all detected well in advance of actual failure, so that the transformer in question could be removed at our convenience without an interruption to service.

In fact, our experience with gas-detector relays at Shipshaw, and elsewhere on the Saguenay system, is such that we are convinced no large power transformer (5,000 kva and over, of the conservator type) should ever be installed without a gas-detector relay. Ours certainly have paid for themselves many times over.

Reference has been made to the short 154-kv transmission lines (two miles) connecting Shipshaw Number 2 generating station and the load center at Arvida. This voltage was decided on for two reasons: first, because the Saguenay system had been planned for 154 kv, and second, because far less strategic materials were required during the war emergency.

H. P. Dupuis, D. C. Harker (Commonwealth and Southern Corporation, Jackson, Mich.): The authors are to be congratulated on the excellent presentation of the application of the split-phase differential relay scheme for the protection of generator armature windings. It has long been recognized in the relay art that it is difficult to obtain protection of faults near the generator neutral by the usual current-differential scheme. Although the split-phase scheme of generator protection is not new, it is gratifying to learn that it has shown such an excellent performance record. The detection of a hot joint in a generator neutral ring even before it becomes a fault is indeed noteworthy. Similarly, turn-to-turn faults have been exceedingly difficult, if not impossible, to detect by conventional schemes before breakdown to ground occurs, with resultant possible serious and costly burning of the generator stator iron. The split-phase scheme of protection is, therefore, to be commended particularly for its ability to detect these faults so rapidly that in most cases the machine is tripped before any disturbance to the system occurs, and without any internal fire or burning; in fact, for two of the cases cited, even before any breakdown occurred in the coil insulation. Since there has been no false tripping due to the unusual sensitivity of the scheme, it appears that the split-phase arrangement of generator protection approaches the ideal for large vertical waterwheel generators. It would be interesting to know whether the split-phase scheme has been, or could be, applied to high-speed turbo-alternators where space and turn limitations enter into consideration.

Of particular interest is the ingenious method of using two current transformers having a common magnetic circuit to balance any saturation effect. Also of considerable interest is the excellent record of the gas-accumulator relay for the protection of transformer faults. This augments the present splendid record for this type of transformer protection, and perhaps may be instrumental in extending the application of this type of relay in the United States.

Eight generator faults out of 12 installed units in approximately five years appears to be an unusually high record of field trouble for this type of equipment. Presumably, this is due to war-time manufacturing conditions. However, it causes some concern to contemplate what loss of vital aluminum production during the war years might have resulted had not the split-phase scheme provided such adequate generator protection.

One cannot agree with the implication that $4^3/_4$ million kva-years is indicative of long experience, because so many kilovolt-amperes are involved. However, it is hoped that the continued use of the split-phase scheme of generator protection will prove to be as satisfactory as the experience so far has indicated.

The paper points out that a saving in cost of the relay installation is achieved by using induction-type instead of percentage relays, and in this particular installation there are probably factors which warrant the use of the less expensive type of relay. Where alternate relay schemes provide equal protection, the least expensive and simplest probably should be chosen. However, if one scheme provides better and more complete protection than is obtained in another, then other factors being equal, it would seem that the amount of money which could be spent justifiably on protection is a function of the value of the equipment to be protected; that is, buying relay protection is similar to buying insurance.

It is noted that the output of the Shipshaw Number 2 generating station is transmitted at 154 kv to its load at Arvida, only two miles distant. It would be helpful to know the factors leading to the choice of this particular voltage. Perhaps, too, a very brief description of the connections and relaying at the Arvida terminal would be of assistance to relay engineers in obtaining a better overall picture of the back-up relaying.

The magnitude of the power involved is impressive. In looking at the interior view of the power house, one realizes that he is looking at a concentration of generation sufficient to supply the entire requirements of many of the larger power systems in the United States.

F. H. Duffy: The authors are indebted to all of the discussers for the interest they have shown in this paper and their remarks concerning it, all of which have added to the general value of the paper.

A number of questions have been asked and additional information requested, particularly by McKenzie, and it is felt that the best way to answer these questions is in the order given.

As stated in the paper, the authors feel that in any future station of the unit type, with split-phase generator protection, and with transformer-differential protection which includes the generator, no generator differential protection would be necessary. However, without the experience which has been obtained at Shipshaw in the reliability of the split-phase relaying, it would have been rather difficult, at the time the Shipshaw station was designed to eliminate the generator differential protection.

The authors are aware that split-phase protection in other forms had been used previous to the construction of Shipshaw, but the double-primary single-secondary type of current transformer was relatively new and untried, and other forms of this type of protection had not been found to be as sensitive.

In regard to the unbalances on the 36 phases, these were measured with normal full load on the generators and therefore it is felt that the designers and erectors of these units have done an excellent job. However, as pointed out previously, unbalances due to design and construction will be the limiting factor in the setting of the split-phase relay.

For cases where the generator differential or low-tension neutral relay operated at the same time as the split-phase relay, it should be noted that all of these relays are of the instantaneous or balanced-beam type and operate in one cycle or less. Therefore even though the split-phase relay may have operated first there is a matter of some five cycles before the fault is cleared by the circuit breaker which provides ample time for other instantaneous relays to operate.

The hot joint detected in the neutral ring bus was in the group bus to the neutral lead.

The time-current curves shown in Figure 7 are standard curves which may be found in the data obtainable from any of the relay manufacturers, or which may be obtained on particular relays by measurement.

As mentioned in the paper, the authors feel that the combination of back-up and overspeed relays have done an excellent job in detecting loss of field on a generator, even though not particularly designed to do this. It was not intended to imply that this combination was either the only or the best method of detecting this trouble.

It is felt that the 13.2-kv ground protection at Shipshaw is as sensitive as necessary and that the installation of special current transformers in the neutral connection for this protection alone would hardly be justified.

Lawton, in his discussion has outlined the reasoning behind the solidly grounded neutrals at Shipshaw. It might be added that experience has not shown any justification for more complicated grounding schemes.

The overspeed relays have maintained their settings very well, and while occasional operations of this protection may be obtained after a unit has been tripped by other protection, this is not a serious difficulty, and the sensitive setting is available when necessary for troubles such as loss of field. Maintenance and adjustment of these relays have presented no insurmountable difficulties during the years Shipshaw has been in operation. The governor solenoid operates through the valves, and there is no provision for high-speed closure of the gates.

The a-c overvoltage protection used at Shipshaw resets automatically. Experience with the gas-detector relay at Shipshaw does not bear out the arguments put forth by McKenzie. In a number of cases where relay operations have been obtained, the manhole covers have been checked for entrapped gas and very little or none was found. While it is not denied that gas could be trapped in any pockets formed by the windings, or core, or bushings, it would seem to be rather excessive to cover the top of the transformer with these relays, not to mention the expense involved. It should be emphasized that at Shipshaw reliance on these relays in their present location is considered to be justified completely. Lawton's discussion of this point probably has clarified somewhat the impression of an excessive number of incipient transformer faults.

One or two other questions have been raised by the other discussers, and should be mentioned.

Dupuis and Harker's question, concerning the use of 154-kv transmission voltage for just over two miles, has, we think, been answered by Lawton.

The authors do not feel that they are in a position to say whether split-phase protection could be applied to turbo-alternators. This would be a matter for the designers and manufacturers to decide, but it appears to be a matter worthy of some investigation by those who are interested. The point should be emphasized that relay protection is insurance, and that the expenditure on it should be a function of the value of the protected equipment. All other things being equal however, the cost becomes the main consideration. The connections at the Arvida terminal are basically a series of duplications of the connections shown in Figure 5 with proper bus segregation facilities. The protection at Arvida is primarily neutral overcurrent relaying as mentioned in the paper, but space does not permit any complete description of it here.

The apparently high incidence of faults on both transformers and generators at Shipshaw has been mentioned. It has been stated previously that all of the transformer troubles were of one type and the reason given. Similarly, the majority of the internal generator troubles have been on one generator. This unit, owing to wartime conditions, was installed at Shipshaw using reinsulated coils, after about two years of heavily loaded operation in another station. This was necessary in order to obtain power to meet wartime aluminum production demands. This unit is at present being completely rewound using new coils.

Rauth's reference to the co-operation of all the engineering groups involved is worthy of further emphasis. Without this co-operation, the construction of Shipshaw in record time, with the necessary attention to details, would have been impossible.

The Transient Behavior of the Two-Stage Rototrol Main Exciter Voltage Regulating System as Determined by Electrical Analogy

JAMES T. CARLETON
ASSOCIATE AIEE

THE excitation requirements of large turbogenerators necessitate an exciter which can develop several hundred kilowatts. On the other hand, the power available to control the exciter is often in the magnitude of milliwatts. This is especially true if static networks, utilizing nonlinear circuit elements are used to provide the reference standard.[1]

The 2-stage Rototrol main exciter provides the necessary excitation with a minimum of control power being required.[2]

In voltage-regulator systems it is desirable to maintain the output voltage of the generator within specified fixed limits through large variations of load and wide temperature ranges. Present voltage regulator practice requires that the voltage be maintained within one-half of one per cent of the desired value from zero to full load, and in the case of turbogenerators over a temperature range of from 20 to 80 degrees centigrade.

The self-energizing effect of the Rototrol series field can ideally supply full Rototrol excitation. However, due to slight changes in the generator field resistance, the Rototrol may be imperfectly adjusted. In this case the necessary Rototrol excitation must be supplied by a static network. It is then, that the high amplification of the 2-stage Rototrol is advantageous in maintaining voltage within the desired limits.

The introduction of the 2-stage Rototrol main exciter is of great advantage inasmuch as it provides the necessary excitation with sufficiently high system amplification to permit the use of a static network containing no batteries or electronic parts and using only one rotating d-c machine.

Furthermore, the fact that the Rototrol is series excited is of great importance when considering the effect of a short circuit on the generator. The transient field current produced by the short circuit[3] flowing through the series field increases the excitation and raises the internal voltage, thus adding greatly to the power system stability.

Description of the Regulating System

Figure 1 illustrates the voltage-regulating system under study.[2] The main unit is a 70,000-kva 3,600-rpm turbogenerator. The excitation is supplied by a 200-kw 2-stage Rototrol. The static network consists of a saturating reactor, the impedance of which is automatically compared with a capacitive reactance of constant value. As the generator voltage increases, the reactance of the saturating reactor decreases until at the regulated voltage, the reactances of both elements are equal. In this manner a reference point is obtained. The output of the static network is rectified by dry-type rectifiers and introduced into the control field of the Rototrol. The 2-stage Rototrol[4] itself consists of a 2-pole pilot exciter superimposed upon a 4-pole compound excited d-c machine. The control field is wound upon poles one and three. The armature is wound without equalizers. The control field flux produces an armature voltage, e_f, between brushes one and three. Had equalizers been placed on the armature, this voltage would be short circuited. However, in the case of the 2-stage Rototrol, this voltage produces a current i_f in windings connected between brushes one and three. Current, i_f, flows through a forcing winding which produces a flux in the 4-pole machine. This flux produces the voltage e_1 between brushes one, three and two, four. Voltage e_1 is applied to the generator field through a series field having sufficient turns to self-excite completely the Rototrol 4-pole machine when loaded with the generator field resistance. Hence it can be seen that the Rototrol is capable of supplying generator excitation due entirely to the flux produced by the series field.

A damping transformer, which is a mutual reactor providing derivative feedback, is placed across the output voltage of the Rototrol to stabilize the system.[1] The object of this investigation is to determine the optimum parameters to be used in the design of this transformer.

Stability of Regulator Systems

The Rototrol voltage regulator is a closed cycle regulating system of the proportional type. An error in output voltage, such as may be produced by a change in load, produces a proportional compensating change in excitation. Hence the generator output voltage is maintained within close limits at all operating conditions within the rating of the generator.

If the regulating circuit were opened at point X (see Figure 1), and a voltage e_0 were applied, it would be found that $e_0 = e_0Ae^{ja}$ where both A and a are func-

---

Paper 49-8, recommended by the AIEE power generation and computing devices committees and approved by the AIEE technical program committee for presentation at the AIEE winter general meeting, New York, N. Y., January 31–February 4, 1949. Manuscript submitted November 16, 1948; made available for printing January 7, 1949.

JAMES T. CARLETON is with the Westinghouse Electric Corporation, East Pittsburgh, Pa.

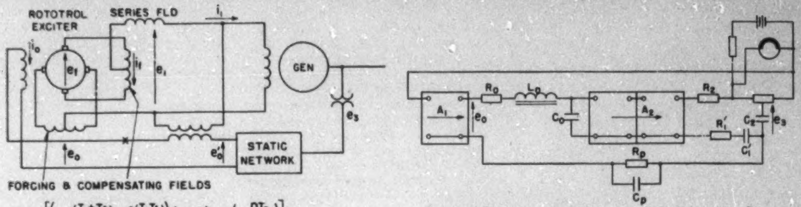
ROTOTROL EXCITER
SERIES FLD
i_1
i_0
e_f
i_f
e_1
GEN
e_3
e_0
e_0'
STATIC NETWORK
FORCING & COMPENSATING FIELDS
A_1
e_0
R_0
L_0
C_0
A_2
R_2
R_1'
C_2
C_1'
e_3
R_p
C_p

$$e_0 = B\left[\left(1+p\left(\frac{T_0+T_f}{1+a_f}\right)+p^2\left(\frac{T_0T_f}{1+a_f}\right)\right)(1+pT_2)-a_1\left(1+\frac{pT_0}{1+a_f}\right)\right]e_3 \qquad (1a)$$

$$e_0 = -A\left(1+p\,\frac{t_1(1+pT_2)}{(1+pT_{p1})}\right)e_3 \qquad (2a)$$

WHERE

T_0 = TIME CONSTANT OF CONTROL FIELD
T_f = " " " FORCING "
T_2 = " " " GENERATOR
t_1 = " " " DAMPING TRANSFORMER = $\frac{M}{R_p}B'$
T_{p1} = " " " " TRANS. PRIMARY
a_f = PER UNIT EFFECT OF ARMATURE REACTION
a_1 = " " SELF ENERGIZING EFFECT OF ROTOTROL

$A = -\frac{\Delta e_0'}{\Delta e_3}$
$B = \frac{\Delta e_0}{\Delta e_3}$
$B' = \frac{\Delta e_1}{\Delta e_0'}$
SERIES FIELD NOT CONNECTED SYSTEM OPEN AT POINT "X"

$$e_0 = \left(\frac{1}{A_2}\right)\left[(1+pR_0C_0+p^2L_0C_0)(1+pC_2R_2)-\left(\frac{A_2C_2}{C_1'}\right)(1+pR_1'C_1')\right]e_3 \qquad (1b)$$

$$e_0 = -A_1\left(1+\frac{pR_pC_0(1+pC_2R_2)}{A_2(1+pR_pC_p)}\right)e_3 \qquad (2b)$$

WHERE

$R_0C_0 \equiv \frac{T_0+T_f}{1+a_f}$ $\qquad \frac{R_pC_0}{A_2} \equiv t_1$
$L_0C_0 \equiv \frac{T_0T_f}{1+a_f}$ $\qquad A_1 \equiv A$
$C_2R_2 \equiv T_2$ $\qquad A_2 \equiv \frac{1}{B}$
$R_pC_p \equiv T_{p1}$ $\qquad \frac{A_2C_2}{C_1'} \equiv a_1$

Figure 1. Two-stage Rototrol regulating system

(Left) schematic diagram, (right) analog

tions of the frequency of the applied voltage.

The nature of this transfer function determines the stability (antihunt characteristic) and the transient behavior of the system.

Classical mathematical methods may be used to determine the transient response of simple regulating systems.[5]

$$f(p)e_3 = g(t)$$

The above equation must be solved and initial conditions determined for the given disturbance, $g(t)$. If the function, $f(p)$, where p is taken to represent the operator d/dt, is of an order greater than the second and it is necessary to vary the circuit parameters to obtain the desired re-

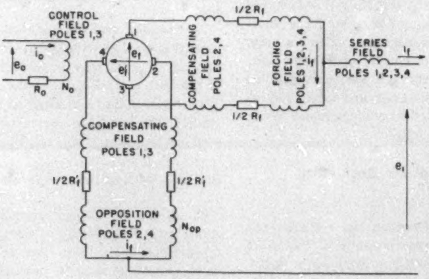
CONTROL FIELD POLES 1,3
e_0
i_0
R_0
N_0
e_f
e_f'
1
2
3
4
1/2 R_f
COMPENSATING FIELD POLES 2,4
FORCING FIELD POLES 1,2,3,4
i_f
SERIES FIELD POLES 1,2,3,4
i_1
COMPENSATING FIELD POLES 1,3
1/2 R_f'
OPPOSITION FIELD POLES 2,4
N_{op}
e_1

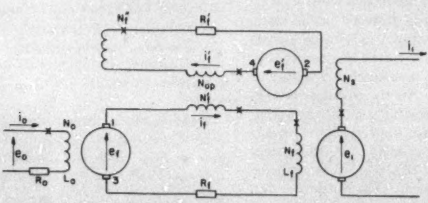
N_f''
R_f'
i_f'
N_{op}
e_f'
4
2
N_f'
i_f
i_0
N_0
e_0
R_0
L_0
e_f
1
3
R_f
N_f
L_f
N_s
e_1
i_1

i_fN_f' = UNCOMPENSATED ARMATURE REACTION IN POLES 2,4
i_fN_f'' = " " " " " 1,3
$K_f' = \frac{e_f'}{i_f}$ WHEN $i_f' = 0$
IF $N_0 \gg N_f''$ $\qquad i_f' = i_f\left(\frac{1}{\frac{N_{op}}{N_f'}+\frac{R_f'}{K_f'}}\right)$

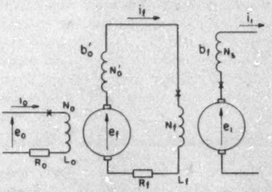
i_f
i_1
b_0'
N_0'
b_f
N_s
i_0
N_0
e_0
R_0
L_0
e_f
N_f
e_1
R_f
L_f

WHERE

$N_0' = N_f''\left(\frac{i_f'}{i_f}\right)$, $b_0' = \frac{N_0}{N_0'}$, AND $b_f = \frac{N_f}{N_s}$

$$e_0 = e_f\frac{R_0}{K_0}(1+pT_0)+\frac{i_fR_0}{b_0'} \qquad (1)$$

$$e_f = \frac{R_fe_1}{K_f}(1+pT_f)-\frac{i_1R_f}{b_f} \qquad (2)$$

$$e_1 = K_f\left(i_f+\frac{i_1}{b_f}\right) \qquad (3)$$

$$e_0 = \frac{R_0R_f\;1+a_f}{K_0K_f}\left[\left(1+p\left(\frac{T_0+T_f}{1+a_f}\right)+p^2\left(\frac{T_0T_f}{1+a_f}\right)\right)e_1-R_1a_1\left(1+p\left(\frac{T_0}{1+a_f}\right)\right)i_1\right] \qquad (4)$$

$T_0 = \frac{L_0}{R_0}$ = TIME CONSTANT OF CONTROL FIELD
$K = \frac{e_f}{i_0}$ = GENERATING CONSTANT OF CONTROL FIELD
$T_f = \frac{L_f}{R_f}$ = TIME CONSTANT OF FORCING FIELD
$K_f = \frac{e_1}{i_f}$ = GENERATING CONSTANT OF FORCING FIELD
$a_f = \frac{K_0}{b_0'R_f}$ = PER UNIT EFFECT OF ARMATURE REACTION
$a_1 = \frac{K_f}{b_fR_1}$ = PER UNIT SELF ENERGIZING EFFECT OF SERIES FIELD

Figure 2. Two-stage Rototrol

(Upper left) schematic diagram, (lower left) equivalent circuit, (right) simplified equivalent circuit sponse characteristic, the classical method becomes cumbersome and impractical.

Transfer function plotting may be used to estimate transient behavior of the regulating system.[6]

Probably the most practical method of determining the response of a regulator system is by the use of an electrical analog. When large quantities of data for a considerable range of variables are required, the use of the electrical analog computer is definitely indicated.

By writing the differential equations that express the action of the various elements of the regulating system, one can by inspection or by circuit synthesis, devise electric circuits having exactly the same differential-integral equations as the original regulating system. These circuits form the analogy of the electromechanical regulating system and can be set up readily on the electrical analog computer for study. A disturbance $g(t)$ is introduced, and the transient behavior is measured with an oscilloscope. Parameters may be varied to determine the effect on the system and optimum proportions of components may be determined.

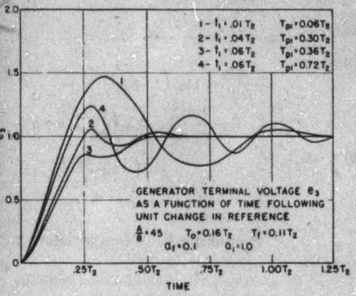

Figure 3 (left). Response of 2-stage Rototrol main exciter voltage regulating system

Figure 4 (right). Response showing effect of primary delay M/R=0.04 per unit

(Upper left) zero primary delay, (upper right) 18 per unit primary delay, (lower left) 0.30 per unit primary delay, (lower right) 0.36 per unit primary delay

Transient Behavior After Change in Reference as an Indication of Performance

In order to apply initial conditions to the system solution, a disturbance may be imposed upon the system. The type of disturbance most commonly encountered in voltage regulator systems of this type is a change in load. The disturbance may be considered to consist of two components: first, a change in internal voltage reference to compensate for the load flowing through the reactance of the machine, and second, an initial rate of change of generator voltage produced by increased inductance-reactance drop in the generator field.[1]

The ratio of the initial magnitudes of these components is determined by the nature of the load and the characteristics of the machine. However, since the total effect of the change in reference is predominant, for a general study of a large number of similar regulator systems that might be applied to water-wheel generators, turbogenerators, and synchronous condensers, a disturbance consisting of a change in reference only can be considered as representative.

Performance Criteria

In order to determine the optimum parameters for a regulating system, some measure of performance must be adopted. A criterion, to be applicable, must possess the following characteristics:

1. It must be a measure of the performance or transient behavior of the system and be of physical significance.
2. It must be calculable.
3. It must be measurable.

The criterion adopted for this study is as follows:[6]
Let e be the error voltage produced by unit change in reference voltage, then

$$T=\int_0^\infty e^2dt$$

if T is the criterion factor. By adjusting T to a minimum the error is compared to zero error by the method of least squares. T can be calculated by classical mathematical methods. If T is to be determined by electrical analog, an rms voltmeter may be used to read it directly. The actual regulator system T may be determined from oscillograms, by a recording voltmeter or by a watt-hour meter.

Should it be desirable to combine the effect of several components of disturbance each of which has been computed separately, the theorem of superposition may be utilized.

$$T^{1/2}=T_1^{1/2}+T_2^{1/2}\quad T^{1/2}\ldots\ldots\ldots\ldots$$

Analysis of System

Two-Stage Rototrol

Conventional Rototrol theory requires that the machine operate on the straight portion of the saturation curve. Therefore, the design of the 2-stage Rototrol is such that saturation is negligible throughout the operating range of the machine.

Figure 2 illustrates that, neglecting saturation and assuming balance between all four poles, the 2-stage Rototrol can be considered as three independent machines superimposed on one magnetic structure. Poles one and three, and poles two and four with associated brushes constitute two 2-pole machines. All the poles constitute a 4-pole machine.

An examination of machine constants reveals that current i_f' is approximately proportional to current i_f. A simplified equivalent circuit consisting of two compound wound d-c machines is obtained, the laws of which can be expressed by simple differential equations.

Damping Transformer with Primary Delay

Damping transformers in previous considerations[1,7] have been assumed to introduce a voltage into the control system proportional to the rate of change of the voltage that excites the transformer primary. This is true only if the time constant (L/R) of the primary is small. In that event, the primary current is proportional to the exciting voltage, producing in the secondary winding a voltage

MPe/R. Should the primary delay be appreciable, as is generally the case, the primary current is delayed and the induced secondary voltage $e' = tPe/1+TP$. Inclusion of the primary delay of each transformer increases the order of the system differential equation one degree, thus making a solution by classical mathematical methods more tedious.

OTHER COMPONENTS

Other components consist of the generator and the static network,[5] the analysis of which are amply described in the literature.

System Analog

The system analog is determined by inspection.[9] A form of inductive reasoning is employed. Blocks of previously used analogies are grouped together as suggested by the arrangement of the actual system. A trial analogy having been produced, its differential equation is written and compared with the differential equations of the actual system. If the equations of the analog circuits are identical, to those of the actual system, the analogy is acceptable.

In the analogy shown in Figure 1, R_2 C_2 represents the generator delay; R_0, L_0, C_0 represents the Rototrol delay; C_1, R_1 represents the self-energizing effect of the series field; and R_p, C_p represents the damping transformer with primary delay. Amplifiers supply system amplification A_1 A_2.

Conditions simulating change in reference and load are produced by the synchronous switch and battery combination shown.

Conclusion

In a previous study[1] it was observed that the generator voltage damping transformer, with negligible primary delay, is more effective than an exciter voltage damping transformer. However, a generator damping transformer is less desirable because rectifier and potential transformers are required. Therefore it was felt that an exciter voltage damping transformer having an appreciable primary delay might approach the performance of the generator damping transformer.

Figure 3 illustrates response to unit change in reference for several typical values of damping. Curve 2 having a mean square error of 0.085 T_2 second is the response obtained with optimum damping transformer parameters. It is interesting to note that the optimum value of primary delay is about 30 per cent of the generator, time constant.

The effect of delay in the damping transformer primary is illustrated in Figure 4. Mutual inductance is maintained constant at 4 per cent of the generator time constant, and L/R is varied.

The wide variations in performance indicate that primary delay is an important consideration in the design of a damping transformer.

Appendix I. Derivation of 2-Stage Rototrol Transfer Function

Consider the equivalent circuit of the 2 stage Rototrol illustrated in Figure 2. Let us demonstrate that i_f' is approximately proportional to i_f.

Writing the equation for voltage drops in the loop in which i_f flows we find:

$$e_f' = \left(R_f + pL_0 \frac{N_f''^2 + N_{0p}^2}{N_0^2}\right) i_f' - p\times\left(\frac{L_0 N_f''}{N_0}\right) i_0 - p\left(\frac{L_0 N_f' N_{0p}}{N_0^2}\right) i_f \qquad (1)$$

and

$$e_f' = K_f'\left(i_f - \frac{N_{0p}}{N_f'} i_f'\right) \qquad (2)$$

combining and assuming for the present that

$$i_o = \frac{i_f R_f}{K_o}(1+pT_f)$$

we find

$$\left(R_f + \frac{K_f' N_{0p}}{N_f'}\right)\left(1 + p\frac{\left(\frac{N_f'^2 + N_{0p}^2}{N_0^2}\right)}{R_f + K_f'\frac{N_{0p}}{N_f'}} L_0\right) i_f' = K_f'\left(1 + p\left(\frac{L_0 N_f' N_{0p}}{K_f' N_0^2} + \frac{L_0 N_f''(1+pT_f)}{K_f' K_0 N_0}\right)\right) i_f \qquad (3$$

Determining the numerical values of the time constants involved

$$\left(R_f + \frac{K_f' N_{0p}}{N_f'}\right)(1 + p1.24\times 10^{-3}) i_f = K_f'(1 + p(1.28 + 3.42(1+pT_j))10^{-3}) i_f \qquad (4)$$

It can be seen that first and second derivative terms are very small, (1 per cent of the control field delay) and may be neglected; therefore:

$$i_f' = \frac{K_f'}{R_f + \frac{K_f' N_{0p}}{N_f'}} = \frac{N_f'}{N_{0p}} i_f \text{(approximately)} \qquad (5)$$

Since i_f' is proportional to i_f the simplified equivalent circuit is valid where

$$N_0' = \frac{N_f' N_f''}{N_{0p}} \text{ and } b_0' = \frac{N_0'}{N_0}$$

Referring to the simplified equivalent circuit and writing the voltage drop in the control field we find

$$e_0 = i_0 R_0\left(1 + p\frac{L_0}{R_0}\right) - p\frac{L_0}{b_0'} i_f \qquad (6)$$

$$e_1 = K_0\left(i_0 - \frac{i_f}{b_f}\right) \qquad (7)$$

combining

$$e_0 = \frac{R_0}{K_0}(1+pT_0) e_f + \frac{i_f R_0}{b_0'} \qquad (8)$$

$$e_f = \frac{e_1 R_1}{K_f}(1+pT_f) - \frac{i_1 R_f}{b_f} \qquad (9)$$

$$e_1 = K_f\left(i_f + \frac{i_1}{b_f}\right) \qquad (10)$$

combining and letting

$$a_f = \frac{K_0}{b_0' R_f} \text{ and } a_1 = \frac{K_f}{b_f R_1'}$$

$$e_0 = \frac{R_0 R_f}{K_0 K_F}(1+a_f)\left(1 + p\frac{(T_0+T_f)}{1+a_f} + p^2\frac{T_0 T_f}{1+a_f}\right) e_1 - R_1 a_1\left(\frac{R_0 R_f}{K_0 K_f}\right)(1+a_f)\times\left(1 + p\frac{T_0}{1+a_f}\right) i_1 \qquad (11)$$

Appendix II. Nomenclature

n = Subscript denoting location of parameter
e_n = A voltage at location n
i_n = A current produced by e_n
R_n = A resistance through which current i_n flows
L_n = An inductance through which current i_n flows
$T_n = \frac{L_n}{R_n}$ = A time delay through which current i_n flows
$k_n = \frac{e(n+1)}{i_n}$ = A voltage generated due to a field through which current i_n flows
$a_n = \frac{k_n}{R_n}$
$b_n = \frac{N_R}{N_n'}$ = Ratio of turns of control field through which current i_n flows to turns of another field on the same machine
t_n = Time constant of damping transformer upon which e_n is imposed
T_{np} = Primary time constant of damping transformer upon which e_n is imposed

Table of Subscripts

n	Output Voltage of:	e_n
0	voltage regulator	e_0
1	pilot exciter	e_1
2	main exciter	e_2
3	generator measured at the secondary of regulator potential transformers	e_3
f	forcing voltage of 2-stage Rototrol	e_f
e	current in self-excited field of main exciter	i_e
s	current in shunt field of Rototrol	i_s
r	amplification of regulator	A

References

1. Solution of the General Voltage Regulator Problem by Electrical Analogy, E. L. Harder. *Thesis*, University of Pittsburgh (Pittsburgh, Pa.), 1946, page 7.

2. Main Exciter Rototrol Excitation for Turbine Generators, C. Lynn, C. E. Valentine. AIEE Transactions, volume 67, part I, 1948, pages 535–39.

3. Symmetrical Components (book), C. F. Wagner, R. D. Evans. McGraw-Hill Publishing Company, New York, N. Y., 1933, pages 74–83.

4 Two-Stage Rototrol for Low Energy Regulating Systems, A. W. Kimball. Electrical Engineering, volume 66, November 1947, page 1127.

5. Theory of Servo-mechanisms (book), H. M. James, N. B. Nichols, R. S. Phillips. McGraw-Hill Publishing Company, New York, N. Y., 1947.

6. Regeneration Theory, H. Nyquest. *Bell System Technical Journal* (New York N Y.) volume XI, 1933, page 126.

7. Recent Developments in Generator Voltage Regulation, C. R. Hanna, K. A. Oplinger, C. E. Valentine. AIEE Transactions, volume 59 1939, pages 838–45.

8. Static Voltage Regulator for Rototrol Exciter, C. E. Valentine, E. L. Harder. Electrical Engineering (AIEE Transactions), volume 64, August 1945, pages 601–06.

9. Electrical Analogy Methods Applied to Servo-mechanism Problems, G. D. McCann, S. W. Herward, H. S. Kirschbaum. Electrical Engineering (AIEE Transactions), volume 65, October 1946, pages 636–39.

No Discussion

Detection of Overheated Transmission Line Joints by Means of a Bolometer

J. R. LESLIE
ASSOCIATE AIEE

J. R. WAIT
NONMEMBER AIEE

THE LOCATION of high-resistance transmission line joints on circuits long in service has been an almost routine procedure of many utilities for some time past. Considerable effort has been expended by The Hydro-Electric Power Commission of Ontario in making such measurements. Many of the circuits, of aluminum cable steel reinforced (ACSR) construction, are now over 25 years old. Bearing in mind the limited knowledge of techniques for joining aluminum conductors which existed at that time it is not surprising that some conductor joints began failing after a useful life of 25 or 30 years. The seriousness of such failures regarding danger to life, and interruption to service, is apparent.

The greatest offender has been the screw-type compression joint used on the early 110-kv circuits. This joint had an aluminum compression sleeve in two parts which threaded together. The screw portion in many cases was found to be the source of the high resistance. In some cases this portion must have become almost an open circuit, whereupon the line current passed through the steel sleeve. The resulting temperature rise was sufficient to soften the steel until the joint pulled apart. In other instances the current distribution was found to be nonuniform, a few strands carrying most of the current.

About 1939, the failures had reached sufficient proportions to warrant a full-scale investigation. Joint testers were constructed using a Wheatstone bridge circuit, the joints being compared with an adjacent portion of the cable of equal length. This testing was carried out by means of lineman's trolleys, with the line out of service but otherwise normal. Many miles of line were examined in this manner, during the years 1939 to 1941.

During the war, the development of infrared bolometers for heat detecting purposes progressed to a remarkable extent. The Germans had equipment of this nature which was capable of accurately tracking the course of a ship through the English Channel. The detectors, which were mounted on the Cliffs near Calais, France, picked up radiation from the ship's funnel.

The sensitivity of these devices, and their robustness was such that their application to the detection of overheated joints was considered practical. The authors describe such a device which was developed in the research division of The Hydro-Electric Power Commission during 1947 and 1948, following upon the prior description of a somewhat similar device by D. C. Niven, National Research Council, Ottawa, in a private communication.

With the infrared detector, joint temperatures can be measured with the line in normal service by merely setting up the detector's tripod to one side of the line and sighting the bolometer on the joint. This procedure takes less than five minutes time.

During the past two months, more than 300 transmission line joints have been checked. Present performance is such that, depending on terrain, and so forth, 25 or 30 joints may be measured on good days on a double circuit line. The temperature can be measured to ±5 degrees centigrade providing the joint is more than 10 degrees centigrade above ambient. The approximate joint resistance can be calculated.

Application of the device to heavy-current switch contacts and miscellaneous clamps also has been made. Of the first 12 switch contacts measured, one was found which was dissipating almost 200 watts on the contacts.

The demands on the apparatus for all this work are such that a 2-man crew is presently working full time with the apparatus.

Description of Instrument

The infrared detector or bolometer, is shown on its tripod in Figure 1. It consists of two parts—a parabolic mirror which collects the heat radiation from the joint, and a heat sensitive element mounted at the focus of the mirror. The sensitive element is a resistor with a high negative temperature coefficient. The change in resistance is a measure of the heat radiation falling on the mirror.

The parabolic mirror is made of glass, eight inches in diameter with a six-inch focal length. It is precision ground and has an aluminized front surface. The long wave infrared radiations given off by the joint do not pass through glass so that the polished aluminum must be on the front of the mirror.

The sensitive element is a Western Electric thermistor bolometer type *V651*,[1] developed by the Bell Telephone Laboratories. The active area (termed a flake by the manufacturer) is 2 millimeters by 0.2 millimeter, being about 10 microns thick. Thermistors are thermal resistors with a temperature coefficient of about −4 per cent per degree centigrade. The element is enclosed with a compensating element in a small housing with a rock-salt window through which the radiations pass without absorption.

The circuit is so arranged that the voltage across the thermistor is proportional to the resistance, and the sensitivity is given as 250 microvolts per microwatt incident radiation.

A front end view of the bolometer,

Paper 49-9, recommended by the AIEE transmission and distribution committee and approved by the AIEE technical program committee for presentation at the AIEE winter general meeting, New York, N. Y., January 31–February 4, 1949. Manuscript submitted November 12, 1948; made available for printing December 28, 1948.

J. R. Leslie and J. R. Wait are both with the research division of The Hydro-Electric Power Commission of Ontario, Toronto, Ont., Canada.

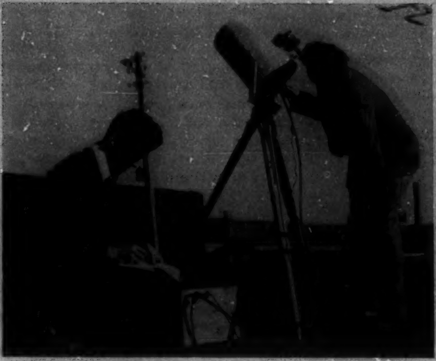

Figure 1. Bolometer in use

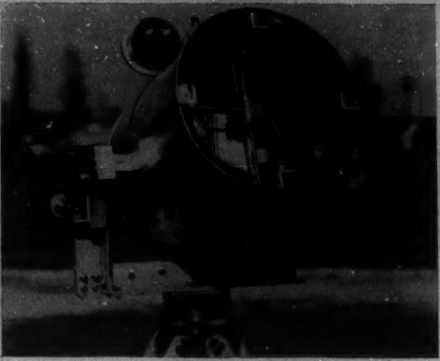

Figure 2. Bolometer, front end view

showing the general construction features, is shown in Figure 2.

In order to facilitate the amplification of the minute voltages set up by the bolometer, the incoming radiation is interrupted at a regular rate (15 cycles per second) by means of a rotating semicircular sector disk mounted in front of the element. The thermistor element is heated cyclicly at the disk frequency and cools by virtue of its small size each time the radiation is interrupted.

The disk is driven with an elastic band and pulley arrangement from a small motor mounted to one side of the mirror axis. The output of the bolometer is thus a 15-cycle square wave which can be amplified in a stable manner. The driving motor is a reed-synchronous type[2] having a speed variation of less than ±0.3 cycle per second. It is driven from a 6-volt motor cycle battery. The amplifier is tuned to the disk frequency so that it is insensitive to extraneous voltages. The box containing the amplifier and batteries is shown beside the tripod in Figure 1.

The use of a rotating sector disk has a further major advantage in that the chopping disk can be made of material (glass, mica, quartz) which is opaque to long wave radiations but passes the visible and near infrared waves. The latter are thus not modulated and produce only a d-c component (steady heating) which is not amplified by the tuned amplifier. The instrument thus becomes insensitive to visible light

It is shown below that although the total sky radiation may exceed that from a joint, it can be selectively filtered to a negligible value by the use of a glass or mica sector disk.

Thermal Properties of Joints

The total input power to a high-resistance joint consists of two parts, the I^2R power generated internally, and the incident radiation from the sun, called solar radiation.

The power losses are those due to radiation and convection.* Equating these two sets of power, we have

$$I^2R+P_s=P_r+P_c$$

Or

$$I^2R=P_r+P_c-P_s \qquad (1)$$

The bolometer enables only the first term (P_r) to be evaluated. The others must be calculated or determined experimentally. We shall deal with each separately.

Radiation Losses (P_r)

The radiated power from a cylindrical conductor of length, L, diameter D in centimeters has been given[3] as

$$P_r=18.55\times10^{-12}LDE(T_2^4-T_1^4)\text{ watts} \qquad (2)$$

where

E = the emissivity of the surface
T_2 = the conductor temperature, degrees absolute
T_1 = the ambient temperature, degrees absolute

The emissivity of a body is defined as the ratio of the power radiated per unit area of the material to that radiated by unit area of a perfectly black body at the same temperature.[4] The emissivity of bright aluminum is given as 0.1 or less. A light layer of soot increases E to as much as 0.8. Hence eight times as much power is radiated from a soot-covered joint at temperature T as from a new joint at temperature T. On the basis of an investigation by Hutchings and Tuck,[5] lines more than two years old should have E values of 0.5 or higher. Obviously this value will depend on the presence of factories, trains and so forth, close to the line. This uncertainty in the value to be ascribed to E may be one of the largest sources of error in calculating the resistance from the temperature.

Using the following typical values in equation 2, we have: $T_1=22$ degrees centigrade = 295 degrees Kelvin; $D=1.8$ inches = 4.6 cm.; $T_2=50$ degrees centigrade = 323 degrees Kelvin; $E=0.5$; and $L=24$ inches = 61 centimeters. Therefore $P_r=9.2$ watts.

Assuming spherical radiation, the intensity in watts per square foot at a distance of say 70 feet is easily calculated. The power finally incident on the thermistor works out to 38 microwatts. For a sensitivity of 250 microvolts per microwatt, we have E_r = 9.6 millivolts, which is easily measured.

Convection Losses (P_c)

In still air the joint is cooled not only by radiation but by natural convection. The air film adjacent to the joint surface becomes heated by conduction and hence rises. These gravity air currents dissipate a considerable portion of the power input to the joint.

Forced convection is caused by a wind which displaces this air film in a horizontal direction causing further cooling. For a joint at 60 degrees centigrade in a two miles-per-hour wind the total forced convection heat loss is about four times the radiated power loss.

---

* Conduction losses were found to be negligible.

Curves of natural convection and forced convection losses for various temperatures and wind velocities are calculated for the joint from both theoretical[4] and empirical[5] data.

From the foregoing data it is possible to calculate the total power dissipation (P_r+P_c). If the forced convection is great enough, then it can be reasonably assumed that the natural convection is completely replaced. However for low-wind velocities of the order of 0.5 mile per hour the calculated forced invections loss is of the same order of magnitude as the natural convection. Hence the assumption adopted is to evaluate the combined convection loss by taking the square root of the sum of the squares of both losses. In this way the natural convection is conceived of as a vertical current of air whereas the forced convection is a horizontal current of air.

For a given temperature, the total power being lost from the joint is the sum of the combined convection loss and the radiation loss. For example, when the joint temperature is 60 degrees centigrade the power radiated is $P_r = 14$ watts for an emissivity of 0.5 with an ambient of 22 degrees centigrade. If the wind is two miles per hour, the forced convection loss is 52 watts. The natural convection is calculated as 25 watts. The power loss or total wattage dissipation in the joint will be equal to

$$P_r+P_c=14+(52^2+25^2)^{1/2}=72 \text{ watts}$$

In this way a set of curves of total wattage (P_r+P_c) is plotted versus temperature rise for various wind velocities. See Figure 3.

Figure 3. Power dissipation and temperature rise for a joint

Joint diameter 1.8 inches, emissivity 0.5

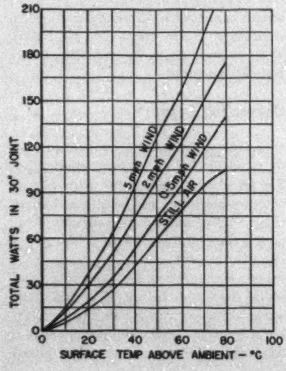

Using an actual high-resistance joint with currents up to 400 amperes, the calculated wattage dissipation curves were checked to about 10 per cent, which is within the experimental error in measuring wind velocity and other factors.

Solar Heating (P_s)

As mentioned, the power input to a joint is equal to the sum of the current heating plus the solar heating.

The intensity of solar radiation at the earth's surface neglecting atmospheric absorption is given[6] as 137 milliwatts per square centimeter at right angles to the sun's rays.

However, actual measurements on the earth's surface during a clear day indicate values of the order of 100 milliwatts.[7]

Hence the wattage incident on the joint will be the intensity of radiation multiplied by the projected area. The absorption coefficient (= emissivity) will be taken as equal to 0.5. If the joint diameter is 1.8 inches (4.6 centimeters) and the length is 30 inches (76 centimeters), then the total wattage absorbed by the joint is given by

$$P_s=0.10\times0.5\times4.6\times76=18 \text{ watts}$$

Sky Radiation

The thermistor element "sees" the back of the sector disk on one-half cycle of the disk's rotation and the joint plus a fringe of sky on the other half cycle. The bolometer measures the difference between the effective temperatures in each case.

To reduce as far as possible the effect of the extraneous sky radiation it is desirable to make the effective sky temperature equal to the effective disk temperature. Then with the sky reading equal to zero the bolometer reading will be proportional to the difference of the joint and disk temperatures.

With a clear blue sky, where there is little direct infrared radiation, the use of a polished copper disk was found to result in a low sky reading. The effective temperature of a polished copper disk is very low due to its low emissivity. This same disk, however, gave an excessive reading on clouds or haze.

With a cloudy sky, glass, mica, and lithium fluoride disks were used which all gave low readings on a uniform grey sky whether dark or light. The effective temperature of a cloud is lowered with these disks because part of the radiation produces a d-c output only, which does not contribute to the reading.

Although the complete explanation is more complicated than this, the experimental data show the same sensitivities for a copper disk and a blue sky as with a mica disk and a cloudy sky. The calibration curves for the infrared radiation are not affected by changing disks because both disks interrupt such rays.

Calibration

Having been provided with a curve, Figure 3, showing temperature rise above ambient for any wattage loss in the joint, it is only necessary to measure the temperature with the bolometer to enable I^2R, hence R, to be found. The bolometer calibration curve was obtained experimentally.

Because a high-resistance joint was not available early in the investigation, an artificial "hot" joint was constructed using a standard aluminum compression sleeve with short lengths of conductor (605,000 circular mils) in which the steel sleeve was replaced with a length of glass-insulated nichrome resistance wire. The ends of this wire were brought out of the sleeve through the holes normally used to insert No-oxid grease. The surface temperature of the sleeve and the bolometer reading were then obtained for different heater powers.

Figure 4 shows the response of the bolometer to this joint when soot covered, for various temperatures. Because the image

Figure 4. Bolometer response

Valid to ±5 degrees centigrade for distances from 50 to 65 feet. Conductor joint 30×1.8 inches. Surface color—dark grey

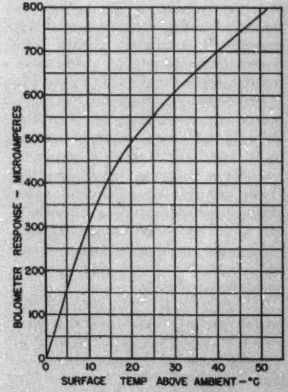

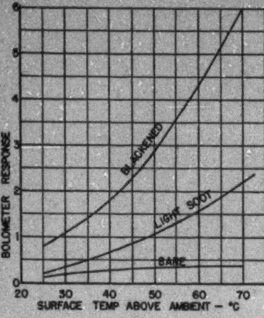

Figure 5. Effect of surface condition

of the joint at the focus is larger than the area of the thermistor flake for this particular joint, the reading is independent of distance over the limits 35 to 70 feet.

Figure 5 shows the effect on the response of varying the surface finish or emissivity. All the older joints in Southern Ontario would be of the blackened type, at least on their under surface. In northern regions this may not be the case. An individual calibration is planned for each typical case.

It was decided also that calibration curves would be desirable for each of the different types of joints, parallel clamps and so forth. These were simply obtained by heating the latter with a blow torch, then reading the bolometer over a half-hour period as it cooled, the temperature being measured with a thermocouple.

After the first high-resistance joint was found, and cut out of the line, it became possible to obtain a direct check on the radiation and convection loss calculations. The joint, of 2,000 microhms resistance, was set up in the laboratory and typical currents were passed through it. The effect of wind cooling on surface temperature was obtained directly using a large fan. The curves obtained theoretically in Figure 3 were checked and found to be substantially correct.

Field Tests

After many preliminary tests, routine measurements were started about August 1, 1948. Readings can be obtained only on days with little or no wind, as the theoretical considerations show that the cooling in a ten miles per hour or higher wind becomes many times the radiation loss. Thus very few joints would run hot on these days. In addition, the accuracy with which the total watts loss can be found is very low with high winds. Of course the bolometer measures at all times the actual temperature irrespective of wind.

Table I. Test Results on First Overheated Joints

Circuit	Current	Wind	Sun	Estimated Temperature Rise, Degrees Centigrade	Calculated Resistance, Microhms
1. *Y3T*	100	0	Bright	35	4000
2. *Y3T*	100	0	Obscured	30	3000
3. *B2 HS*	100	5	Bright	35	3000

First tests were performed on two double circuit lines ($5^1/_2$ and $6^3/_4$ miles long) both having screw-type compression joints, 110-kv construction, and 477,000 circular-mil aluminum cable, steel-reinforced. These lines were placed in service in 1924–25. Three joints (out of 30) showed signs of overheating. The data are given in Table I.

These joints were subsequently cut out and tested in the laboratory. Joint number 1 alone was very high in resistance, measuring 2,000 microhms compared to a normal value of 45 microhms. Joints 2 and 3 were 38 and 96 microhms respectively. The latter two were then placed under tension and again measured. Joint 3 was unstable and had then increased to 280 microhms, joint 2 did not change. A current of 200 amperes was then passed through these two joints while still under tension. Joint number 3 had increased to over 300 microhms after three days.

Measurements at a much earlier date (1940) on a similar high resistance joint showed it to have a resistance inversely proportional to the current. The voltage drop across this joint for heavy currents of different values was constant.

It was also noted that joint number 3 had been made using a sleeve larger in size than the others (probably a 795,000 circular-mil sleeve). Compressing it originally over the 605,000 circular-mil conductor had cracked the aluminium in two places.

A double circuit line, 26 years old running from Queenston, G.S., to Hamilton was then tested. This line of 605,000 circular-mil aluminum cable, steel reinforced, 40 miles long had 310 screw-type joints. They were tested by a 2-man crew in less than two weeks time. Eight overheated joints were found, the hottest running at about 50 degrees centigrade over ambient with a line current of the order of 280 amperes. Table II lists these joints together with their estimated temperature rise, the wind velocity, type of sky, and line current. The final column in Table II shows the results of resistance measurements on seven of the eight joints. The line was taken out of service and the resistance obtained from a millivoltmeter reading using 100 amperes direct current. The first four resistances were measured by lowering the conductor to the ground without disturbing the joint. They measure five to ten times normal. Two of the remainder, which do not measure high in resistance, were measured using a lineman's cable seat. The trolley in passing over the joints

Table II. Overheated Joints on a 40-Mile Double Circuit Line

Tower	Test	Wind, Miles Per Hour	Sun	Line Current	Estimated Temperature Rise, Degrees Centigrade	Measured Resistance, Microhms
231	1	0	Bright	280	50	300
	2	3	Bright	130	30	
205	1	4	Bright	150	30	250
	2	5	Bright	280	50	
186	1	8	Bright	200	40	450
	2	7	Bright	180	30	
181	1	5	Bright	200	30	450
	2	7	Bright	150	20	
217	1	3	Bright	130	30	
	2	2	Bright	270	45	
174	1	10	Bright	200	30	48*
	2	7	Bright	200	25	
109	1	5	Cloudy	200	30	31**
	2	4	Bright	180	30	
84	1	8	Bright	180	30	50*
	2	4	Bright	200	35	

Total number of joints tested—310.
Conductor—605,000 ACSR.
Ambient temperature, 22 degrees centigrade approximately.

*Measured using lineman's cable seat.
**Partially lowered, reached by ladder.

may have altered their resistance. The third was partially lowered, then reached by means of a ladder.

The authors concluded from all these tests that the resistance of a faulty joint is an extremely variable quantity. Removing or increasing the tension or handling of any nature could cause the resistance to vary in an unpredictable manner. This is natural considering that the resistance must lie in thin films of oxide or contamination, these films being easily broken by removing the strains in the material.

Using the value of emissivity and solar heating quoted before, these joints were all estimated to have over 1,000 microhms resistance so that the theoretical curves relating watts loss to temperature rise (Figure 3) may be in error. Further experience will enable more accurate curves to be drawn. The arbitrarily chosen value of 0.5 for the emissivity may be high. The effect of solar heating on temperature rise has not been checked experimentally.

Tests on Disconnect Switches

Twelve 13.2-kv disconnect switches were tested at Leaside transformer station. These switches connect four 25,000-kva synchronous condensers to the 220-kv system of The Hydro-Electric Power Commission of Ontario.

They were carrying 1,300 amperes at the time of test.

The bolometer was set up about 50 feet from the switching structure and sighted on the contacts. One switch was found to be running at a temperature estimated to be 65 degrees centigrade. The remainder were at less than 30 degrees centigrade. The overheated switch was taken out of service at the earliest opportunity (and found to be still warm one-half hour after the interruption). From the measured resistance it must have been dissipating about 200 watts across the contact fingers.

Conclusion

Temperature measurements on conductor joints and switch contacts are believed to be rapidly and simply made with the infrared detector described. The accuracy obtained is thought to be better than five degrees centigrade.

The prediction of the power dissipation or resistance of the joint or switch is a more difficult matter. In fact there is strong evidence to support the view that these high resistances are an extremely variable quantity, and that temperature rise may be the most reliable index of a joint's condition.

Further studies of the influence of wind cooling, solar heating and the condition of the surface on temperature rise are indicated.

Application of the bolometer to temperature measurements on rotating parts may be possible.

References

1. Thermistor Bolometers, W. H. Brattain, J. A. Becker. *Journal*, Optical Society of America (New York, N. Y.), 1946, page 354.

2. Anglo Corporation, Chicago, Ill.

3. Safe Ratings for Overhead Line Conductors, L. M. Olmsted. AIEE Transactions, volume 62, 1943, pages 845–853.

4. Heat and Thermodynamics, (book) J. K. Roberts. Blackie and Sons, London, England, 1933.

5. Current Carrying Capacity of Bare Stranded Conductors, E. E. Hutchings, W. D. Tuck. *ERA Technical Report F/T142*. The British Electrical and Allied Industries Research Association (London, England), 1941, 19 pages.

6. Mathematical and Physical Tables 1939, J. B. Clark, Oliver and Boyd, London, England.

7. The Albedo of the Ground and Atmosphere, S. Fritz. *Bulletin*, American Meteorological Society, June 29, 1948, pages 303–12.

Discussion

N. L. Kusters (National Research Council, Ottawa, Canada): A project similar to that described by the authors of this paper has been in progress at the Canadian National Research Council since 1946.

Early in our investigation we chose to use a-c amplification following the infra-red sensitive bridge, because of the difficulty of achieving high stability in a d-c amplifier for portable use. Having made this decision, an investigation was made of systems using: a circuit-breaker type of chopper to interrupt the output of a d-c volometer bridge; a radiation chopper in connection with a d-c bolometer bridge as used by the authors of this paper; and an a-c bolometer bridge.

It was found that the circuit-breaker type of chopper was satisfactory for use only with low-impedance bolometers, such as the German antimony bolometer, due to capacitive pickup difficulties.

The radiation chopper system, as used by the authors, was tested using the Western Electric *V651* bolometer and a low-impedance platinum bolometer from Baird Associates. Various forms of chopping disks, concentric tubes, and so forth, were used, but early in 1947 this system was abandoned for the following reasons:

1. Difficulty was experienced in maintaining the back of the chopper, which is the reference level for measurement, at a constant temperature.
2. Chopped systems do not provide indication of both hotter and colder bodies as readily as the a-c bridge.
3. As pointed out by P. Moon in 1935, there is no conversion loss using a bolometer in an a-c bridge. With a radiation chopper or circuit interrupter there is about a 40 per cent loss.
4. The use of a motor-driven disk, as used in the authors' instrument and which must be changed for different sky backgrounds, was not considered suitable in a rugged, portable instrument.

The Western Electric bolometer was chosen as best suited for use with an a-c bridge, and a bridge supply frequency of 1,000 cycles was selected as a compromise between the shunting of the bolometer element by stray capacities at higher frequencies, and the use of large electrical components in the amplifier at lower frequencies.

The use of 1,000 cycles instead of the 15-cycle chopper permitted the use of three small plug-in units containing all the electronic circuitry including nine subminiature tubes. The battery drain is very small, so all batteries are mounted within the case of the instrument.

The theoretical maximum sensitivity of the National Research Council instrument is 0.18 microwatt for full-scale deflection. The noise level of about one microvolt permits a minimum detectible signal of the order of 0.01 microwatt.

The authors are to be complimented on the success they have achieved in the quantitative estimation of the temperature and the resistance of the joint. We believe, however, that it is more practical to limit the use of the instrument to an indication of the temperature difference between the joint and the conductor. The resistance of a faulty joint varies widely, as pointed out by the authors; also, the emissivity of the surface examined varies from about 0.04 for polished aluminum or copper, to 0.92 for glazed porcelain. These factors, together with the necessity for reference to a multitude of curves for various wind velocities, limit its practicability as a field instrument. Consequently, our instrument is designed to give the temperature of the joint relative to that of the conductor itself, and emphasis has been placed on portability and simplicity of operation and maintenance.

A number of field tests have been carried out since early 1947, in co-operation with the Shawinigan Water and Power Company. In these tests, clamps, compression joints, twisted joints, and wave traps were checked, with considerable success.

Reference

1. Theory of A-C Bolometer, P. Moon. *Journal*, Franklin Institute (Philadelphia Pa.), January 1935.

A. S. Runciman (The Shawinigan Water and Power Company, Montreal, Canada): This paper gives an excellent idea of what may be accomplished by using the bolometer method for locating overheated joints or fittings on transmission lines, either high or low voltage. The authors have done work which should be of considerable assistance to others later. They point out the cooling effect of even a light breeze; a wind 10 miles per hour prohibits satisfactory use.

It has been observed on the Shawinigan system that the background should be uniform and preferably blue sky as the authors indicate.

One point on which we would like to question the authors is the feasiblity of using the apparatus in cold weather. Nothing is mentioned in the paper about the circuits used; therefore, it is not possible to estimate the effect of changing temperature on the balance and indicating equipment.

Field tests carried out on the Shawinigan Company's system in 1947, located a defective screw-type aluminum compression joint on the first trial. It was not possible with the early apparatus to obtain quantitative measurements. The authors have gone a long way in developing apparatus which can determine within reasonable limits actual temperatures.

This paper, no doubt, will bring to mind many other uses; one very simple and much needed application might be entirely outside of the power field, that of indicating heat leak spots on buildings.

The National Research Council has developed similar apparatus using no mechanical chopper but a 1,000-cycle amplifier. The sighting system of their apparatus is an optical arrangement by which the observer sees the object and the instrument reading, in the one eye piece.

A recent field trial of this apparatus, located an overheated wave trap in a 220-kv line. The wave trap was radiating approximately 100 watts. This loss was compared with a 100-watt yard lighting lamp at approximately the same distance and equivalent indication obtained.

The authors are to be highly commended for establishing the practicability of using bolometers on field work.

Leonard M. Olmsted (Duquesne Light Company, Pittsburgh, Pa.): The authors have presented an interesting report on a unique method for determining the adequacy of transmission line joints with the lines remaining in service. It seems to me, however, that a slight change in point of view would eliminate their difficulty with several variables entering into determination of the joint resistance.

Fundamentally a joint should be looked upon merely as a means of joining line conductors. As such, its requirements can be defined as matching the characteristics of the conductor with respect to mechanical strength, current capability, and permanency. From this point of view, it seems entirely justifiable to measure the adequacy of the joint in terms of its performance relative to that of the conductors. If practically simultaneous measurements were taken with the bolometer of the temperature of the joint and the temperature of the conductor at a suitable distance from the joint, then any difference could be determined directly. It is entirely reasonable to assume that such variables as sun radiation, air movement, surface conditions, and atmospheric temperature would remain substantially the same during this comparative test and that any difference in the effect of these factors upon the temperature of the joint or the conductor would be so slight as to be considered negligible.

Joint resistance is, of course, a convenient basis of comparison for laboratory tests and manufacturing control. It is my opinion that the proper limits for joint resistance should be established by test of joints which have been proved satisfactory under field operating conditions, using the bolometer or other devices to ascertain the field condition. It does not appear necessary to measure the joint resistance in the field, and I strongly urge that the complications besetting such determinations be avoided by using the bolometer solely for comparative measurements.

Engineers of the Bonneville Power Administration (Portland, Oreg.): Application of the bolometer method to measuring heat radiation from conductor joints appears to us unique and to offer considerable possibilities in the utility field.

In reading the paper we note that no mention is made of the method of determining wind velocities, which have a most noticeable effect on convection losses (P_c). In making conductor vibration studies on the Bonneville Power Administration system, it is found that wind velocities vary considerably from the ground to the conductor level. For this reason it would seem desirable that an anemometer be installed near the conductor level in order to obtain more accurate wind velocities. The paper states that heat measurements are made in a short interval of time indicating that wind velocity measurements probably are not made at the conductor level. If the anemometer method is used to determine wind velocities for convection losses, it would obviously require considerably more time in making tests of each joint than that shown by the authors.

Since all of the lines of the Bonneville Power Administration system are less than ten years old and, also, since the approved-type compression joints are used on all connections, we have not experienced to date any unusual failures due to overheating of joints. Even though properly made compression joints are used on all of the transmission lines being designed at the preset time, there still is the apparent need for an occasional check for heating of joints, switch contacts, and other contact-making surfaces.

In our experience of checking overheating of contacts in our substations, we use what is probably the simple, universal method. Our low-voltage substation disconnecting switches are checked for overheating by means of a wax candle on a switch stick. If the switch is hot enough to melt the wax, the switch is taken out of service for maintenance at the earliest opportunity. This simple test is made at regular intervals by the substation operators, and seems to be quite satisfactory. As for the 115-kv and 230-kv disconnecting switches, they are generally not loaded to the point where heating is a problem, and periodic maintenance seems to keep them in satisfactory condition.

J. R. Leslie and J. R. Wait: Replying first to Kusters, it is true that the bolometer we have described gives no indication as to whether the body sighted on is hotter or colder than ambient temperature. However, in practice this has caused little difficulty. In the few questionable cases to date, the addition of a small amount of radiation such as from a match, or the hand held in front of the mirror indicates the proper polarity.

The authors are in favor of the use of a sector disk because of its ability to filter out a great part of the radiation from clouds. This radiation is thought to be scattered solar radiation of shorter wavelength than that from a joint. It is very difficult to sight on the conductor alone, therefore background radiation should be low.

The suggestion by Olmsted and Kusters that joint and cable temperatures be compared directly has been made. This procedure is sufficient only to show that no temperature difference exists. If a temperature difference is indicated, and it usually is, its significance must be determined. What is required is the maximum temperature which the joint can attain in the absence of wind. The curves relating forced convection loss to temperature rise, Figure 3, must therefore be used. With these curves, the temperature rise under the worst conditions may be estimated. It is apparent that with sufficiently strong winds, all temperature rises would be reduced to negligible values. With the use of the curves then, what is obtained is a number, the resistance, corresponding to the temperature rise without wind cooling.

In the practical use of the bolometer to date, none of the conductors has experienced a measurable temperature rise other than that expected due to solar heating. This is because of the rather low currents in the older circuits examined. Thus, all conductors have been "cold" as far as the bolometer is concerned. It is interesting to note that two idle conductors of different size, exposed to the sun's radiation, will not experience the same temperature rise.

Runciman inquired as to cold weather operation. The bolometer has not been in use during the winter months but should operate without difficulty. Temperature rise above that of the sector disk is measured at all times.

Replying to comments by Bonneville engineers, the present practice in determining wind velocity is to climb the tower to a height of about 20 feet and with an anemometer obtain the average velocity during a 1-minute interval. Errors due to turbulence around the tower may be appreciable, and a better procedure would consist of raising the anemometer on a long pole to conductor height. This idea was abandoned for reasons of safety.

A further uncertainty is caused by wind direction, convection loss in this case being difficult to obtain. Procedure now used is to list all of the joints giving evidence of overheating and to re-examine these under conditions of low or zero wind and with high load currents, when possible. This has not proved difficult to do as the number of overheated joints is small.

The need for an occasional check on the heating of joints, disconnects, and bushings has been proved to us by the frequency of requests for such measurements.

The interest shown by the discussors is appreciated. It is hoped that additional field data will be available in a few months time.

Comparison of Long-Time and Short-Time Analog Computers

VICTOR PASCHKIS
NONMEMBER AIEE

THE USE OF electrical analog computers for the solution of transient heat flow problems had been realized first by C. L. Beuken.[1] In the United States the early published accounts describe an apparatus erected at Columbia University,[2,3] now known as the Heat and Mass Flow Analyzer, and henceforth referred to as HMFA. Various less extensive versions of the Columbia University apparatus have been constructed elsewhere,[4,5] and a still further development has modified the technique of execution.[6,7,8]

These later modifications offer certain advantages but necessarily entail certain disadvantages. In view of the increasing significance of the analog computers, it is important to weigh the advantages and drawbacks of the various modes of execution of the analogy idea; such a comparison is the purpose of this paper. Of course such computers can be applied to a large variety of problems. This paper deals exclusively with their application to heat flow problems.

Basically, the analog computers for transient heat flow problems are resistance-capacitance networks with suitable power supply systems and measuring devices. In Figure 1 an example is shown of the so-called "1-dimensional network" used for the calculation of 1-dimensional heat flow problems. Figure 2 is an example of a 2-dimensional network.

Figure 3 is a plan view of the heat and mass flow analyzer laboratory which covers a floor space of 530 square feet. The circuit elements of the apparatus comprise 120 resistor sections and some 720 individual capacitors. One pole of each of the latter is permanently grounded. The total capacitance is approximately 3,000 microfarads. The units are so arranged that almost any combinations can be assembled readily. To that end, resistor sections, each consisting of four decades, are mounted on 20 boards—six sections on one board. From four to eight capacitor units are placed in one tray and a total of 108 trays are placed in four frames. The trays are equipped with jacks which are connected to the various capacitors of each tray. In each capacitor frame there are also four busboards, each containing 12 busses. For each experiment the capacitors required for any one section are connected by flexible leads to the busboards.

The ends of the busses as well as the two ends of each resistor section are connected in turn to the "main panel" shown in Figure 5, on which the network connections are made. The latter consists of five boards: one for the outlets of the resistors, two for the outlets of the ends of the capacitor buses, and, finally, two "grounding devices" which make a rapid discharge of the capacitors possible after each experiment. On the main panel, the circuit representing the body is prepared.

Overhead wires lead to an instrument panel on which the necessary recording instruments, power supplies, and similar equipment are mounted. Figure 4 shows part of the resistor and capacitor frames.

The various modifications of the Columbia University apparatus referred to before differ with regard to the time constant of the individual element. In carrying out electrical experiments it is not necessary that they last as long as the corresponding heat occurrence. A time scale may be applied, expressed by the "Time Ratio" (*TR*). In calculating a circuit to represent a thermal phenomenon the time ratio applied is given by

$$TR = \frac{\tau_E}{\tau_H} = \alpha CR \qquad (1)$$

Here τ_E and τ_H denote the "electrical" and the "heat" time respectively. C is the capacity (microfarad per cubic foot), R is the resistivity (megohm times feet) used in calculating the network, and α is the thermal diffusivity of the body subjected to heat flow. The dimensions megohm per foot and microfarad per cubic foot appear unusual and require explanation. In calculating the circuit to represent a body, the latter is being considered as being composed of a number of discrete parts or sections. Each section is represented by one "lump" in the network.

The electrical values for these lumps are calculated on the basis of the geometric dimensions of the section represented; the capacitance is proportional to the volume and the resistance to the ratio thickness per cross sectional area. Thus, a high value of time ratio, *TR*, indicates that a certain thermal phenomenon is represented by a longer lasting electrical experiment than with a small value of *TR*. The *HMFA* at Columbia University is designed so that, for any given process, a time ratio of much greater order of magnitude can be used than is possible with the later modifications of the analogy method. This, of course, means that the *HMFA* comprises a much larger total capacitance and resistance than the modification; in fact, this difference in capacitance and resistance is the distinguishing factor.

Significance of Time Constant

In connection with analog computers, the time constant *RC* (capacitance times resistance) has to be considered from various aspects, namely: instrumentation,

---

Paper 49-13, recommended by the AIEE computing devices committee and approved by the AIEE technical program committee for presentation at the AIEE winter general meeting, New York, N. Y., January 30–February 4, 1949. Manuscript submitted November 16, 1948; made available for printing January 17, 1949.

VICTOR PASCHKIS is technical director of the heat and mass flow analyzer laboratory of the department of mechanical engineering, Columbia University, New York, N. Y.

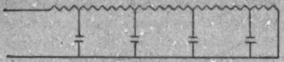

Figure 1. Equivalent network circuit for 1-dimensional problem

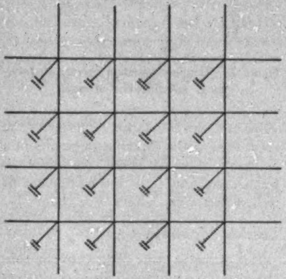

Figure 2. Equivalent network circuit for 2-dimensional flow

manipulation, leakage, and cost of equipment.

To put the problem into proper setting, it should be understood that runs on the *HMFA* last from several minutes to several hours, whereas on "short time apparatus" the phenomenon occurs in a fraction of a second. In way of example, take the case where an experiment on "short time apparatus" lasts 0.1 second; then the former needs 3,000 times the amount of *RC* used in the latter, and this is in no way extreme. An intermediate design uses time constants of such magnitude that the individual experiments last from fractions of a second up to several seconds.

INSTRUMENTATION

In order to register the readings—voltage and current—special instrumentation is required. The *HMFA* comprises modern fast-recording instruments, printing every two seconds. It is hoped that eventually even faster recording instruments will become available.

For many experiments with slow changes, the instruments can be either multiple-point recorders or slower recording instruments. In one run it usually is possible to record a number of variables—voltages at different points or voltage and current, and so on.

For the "short-time apparatus" the only possible recording device is the oscillograph. However, operation of an oscillograph requires more power than is available in short-time apparatus. A record can be obtained by filming the readings on an oscilloscope, showing the transient together with a time scale. Because of the high cost of the oscillograph, the short-time apparatus has been built to date with oscilloscopes for indicating measurements. For the "intermediate-time apparatus," pen-type recorders may be used, recording occurrences as short as 0.5 second. If, as is mostly the case, recordings at several points are required, a separate instrument for each point must be provided. Of course, sometimes several pens are combined in one instrument utilizing different parts of the total width of the paper. The width of any one record is limited compared with the records used for long-time experiments.

The accuracy of measurement on an oscilloscope is limited to probably 2 to 5 per cent of the full-scale value or less, and can be improved to 1 per cent only with extreme care; whereas the accuracy of the recording instruments used in long-time experiments is 1/5 to 1/3 per cent. It may appear, at first, as if an accuracy of 5 per cent might suffice, particularly in view of only an approximate knowledge of the thermal properties. Frequently, however, measurements at the lower end of the scale are required, where the percentage of error increases very markedly beyond that incurred with full scale.

This increase in error is proportional to the scale reading in recording instruments; it generally is more than proportional on oscilloscopes because of the lack of linearity in the tubes.

MANIPULATION

Under this heading several operations are covered. First, consider the boundary conditions. In some instances the impressed voltage may change with time, representing a time-dependent change of ambient temperature. Such a change can be represented on the *HMFA* in steps or continuously by manual control, because the experiment is slow enough to permit such operation. On intermediate-time apparatus and short-time apparatus, an input circuit is required to produce the desired voltage function. Hence, programs with frequently changing input conditions are solved more readily on the *HMFA* than on the two other types of equipment.

Figure 3. Plan view of heat and mass flow analyzer laboratory

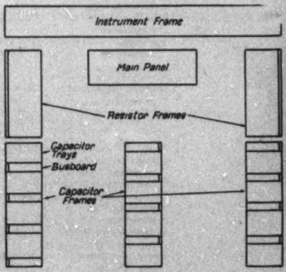

One of the very important objects of the electrical analogy work is the solution of problems with variable parameters, mainly with resistance and capacitance varying with voltage. This voltage dependence represents a temperature dependence of thermal conductivity and specific heat respectively. Of course the form and degree of dependence may be different for various materials.

In the case of short-time and intermediate-time apparatus, it is possible to obtain such variable parameters by designing electronic circuits to replace resistance and capacitance in the network, and to incorporate in the design the desired voltage dependence. However, different circuits have to be used for different degrees and modes of voltage dependence. For intermediate-time apparatus the use of cam-driven equipment is conceivable for changing parameters through relays.

On the *HMFA* changes of resistance and/or capacitance can be effected in steps. At those points in the network where "varying properties" prevail, the voltage is observed and, at certain predicted values, the resistances and capacitance of that section are changed manually by operating appropriate switches or relays. This method of operation is possible because the time

Figure 4. Resistor and capacitor frame, heat and mass flow analyzer laboratory

lapse between consecutive steps is sufficiently long to permit reading of instruments, and so forth.

Still another topic under the general heading of manipulation concerns problems where certain physical happenings are to be represented within the range of a heat flow problem. Consider, for example, a problem where two materials are alternately in and out of thermal contact. If this alternation is at regular intervals, depending on time only, no difficulty is encountered in using short- or medium-type apparatus. But if the intervals are irregular or depend on observation during the run of an experiment, only the long-time computer is feasible.

LEAKAGE

The accuracy of operation of analog computers hinges on keeping three sources of error small: errors because of leakage, lumping, and errors in instruments. The latter have been discussed in the section on instrumentation. The errors through lumping depend on the number of sections or lumps; if their number is kept constant, the error at any relative time (time from the start of experiment to a given instant, divided by total length of experiment) is independent of the length of the experiment.

The errors through leakage can be understood from Figure 6, which refers to a 1-dimensional network. Because the capacitors are not perfect, but have a leakage resistance, the equivalent circuit contains a shunt resistor for every capacitor. Moreover, in the physical arrangement of capacitances and resistances it is inevitable that leakage paths exist between the input point and various points in the circuit. Instead of the simple circuit, shown in Figure 1, the more complex circuit, Figure 6, must be used to represent the actual analog computer. The error incurred will vary depending on the relative size of the "useful" and the "leakage" resistances.

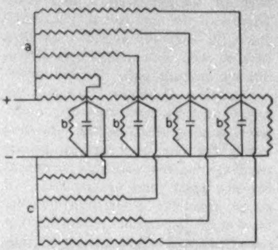

Figure 6. Equivalent network including leakage

a. Leakage from power supply to network
b. Leakage of capacitors
c. Leakage from network to ground

Figure 5. Main panel, heat and mass flow analyzer laboratory

Now, from the viewpoint of leakage, short-time and intermediate-time setups offer two advantages. First, the *RC* value is proportional to the length of the experiment. Hence, for short experiments it is possible to work with small capacitances. At least in the case of short-time computers and possibly even in the case of intermediate-time computers, the capacitances can be made so small that extremely high-quality capacitors, mica or polystyrene, become economically feasible. Secondly, the low value of useful resistance, required for the short time of the experiment, results in a favorable ratio of useful resistance to leakage resistance for the equipment as well as for the capacitors.

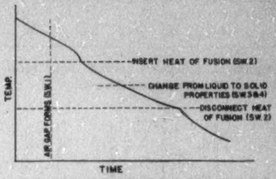

Figure 7. Time–temperature curve near interface; solidification of metal

COST OF EQUIPMENT

It is of course quite difficult to compare the cost of the various kinds of computers in a comprehensive way, because there is an infinite variety of possible designs for each of the three types.

The following general statements may be helpful. The cost of an analog computer comprises three groups of items: the input arrangement, the circuit elements (resistors and capacitors), and the measuring and recording devices. The input arrangement, if flexibility is desired, is more expensive for short- and intermediate-time computers than for long-time computers. The circuit elements, for work with constant parameters, are less expensive for short-time and medium-time computers than for long-time computers. If the parameters are not constant the conditions, generally, will be reversed and the long-time computer will be in the lead. The measuring equipment for equal performance (that is,

Table I. Analogy Equipment

Item		Short-Time	Medium-Time	Long-Time
Instrumentation	Type	Oscilloscope or oscillograph	Single-point high-speed recorders	Recording instruments
	Accuracy	Low	Fair	High
Manipulation	Constant boundary conditions	No difference between types		
	Varying boundary conditions	Special input circuit for every different boundary condition		Variation continuous or in steps with no special equipment required
	Voltage-dependent parameters	Resistors and capacitors replaced by electronic circuits which have to be different for each different function of property—voltage dependence		Manual by means of switches or relays—no special equipment required
Cost	Input device	High	High	Low
	Circuit elements, constant parameters	Low	Low	High
	Circuit elements, varying parameters	Very high	Very high	High
	Indicating measuring devices	Low		Low
	Recording measuring devices	Very high	High	Low

for recording) is more expensive for the short-time than for medium- or long-time apparatus. However, in general, no recording (oscillographs) is being done with short-time computers, since the oscilloscope is less expensive than the recording devices used in medium-time and in long-time apparatus. Between the latter two, the long-time computer probably is less expensive in instrumentation than the medium-time, because the former permits the use of multiple-point recorders.

Conclusions

As usual when different alternatives to an engineering problem are analyzed, there is no general answer possible which would hold for all cases. The proper selection depends on a number of variables.

One can conclude that short-time computers are well-suited for a more qualitative analysis of problems with constant parameters. Medium-time computers have their field of greatest significance in problems with simple operating conditions and constant parameters. The long-time computer is the most versatile apparatus and, so far, is indispensable for complex problems and for nonlinear parameters. Table I summarizes the characteristics of the three kinds of computers given in this paper.

In way of example of problems for which the *HMFA* seems better suited than any of the other equipment, the following three should be mentioned:

SOLIDIFICATION OF METALS

A hollow cylinder (mold) of great length is initially at uniform temperature. At time zero, the cavity is filled with a liquid metal of constant temperature. Because of the temperature difference the metal starts to cool. After a short time interval the metal shrinks away from the mold and any heat transferred from the cooling metal to the mold must pass through a thermal resistance represented by the airgap. As the temperature drops further, the metal reaches the upper end of the solidification range. At that point, heat (heat of fusion) starts to be liberated and continues to flow until the lower end of the solidification range is reached. Thermal properties of the metal are different for liquid and solid state and should be changed at the mean average temperature of the solidification range. All these changes take place in each section, but at different times in each section.

Figure 7 shows a schematic time–temperature diagram with all required changes indicated. The circuit used to represent the first section of the mold and the first section of the metal is shown in Figure 8. The switch S_1 is opened at a predetermined time; the switch S_2 is operated twice at a predetermined time—once inserting the "heat of fusion" into the circuit and once disconnecting it. Finally, switches S_3 and S_4 are to be operated between the two actions of switch S_2, at a predetermined temperature.

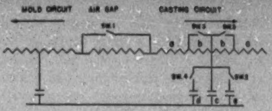

Figure 8. Circuit representing metal and mold near interface

a. One-half "solid resistance"
b. One-half difference liquid-solid resistor
c. Solid capacitance
d. Difference below liquid plus solid
e. Heat of fusion, capacitance

REGENERATOR OPERATION

A second problem refers to the operation of a regenerator, such as used for open-hearth furnaces, glass-melting tanks, and so forth. In many regenerators, the hot combustion gases are blown through refractory ducts for a predetermined period. Then the gas is shut off and cold air is blown through in opposite direction. The cold air picks up some of the heat stored in the refractory walls.

To represent this process, the "reversal period" (gas time and air time, respectively) is divided into several time steps. During each time step a certain amount of gas or air flows into the refractory flue, and the gas (or air) has a certain heat content per degree temperature difference. Now a network is built to represent the refractory flue. Then, at time zero, the first "gas capacitor", charged to the "gas voltage" (temperature), is connected to the first "flue section" across a boundary resistance. See Figure 9. After a time equivalent to one time step has lapsed, the gas capacitor has lost part of its charge to the flue section and, accordingly, its voltage has decreased. Now it is connected through a different boundary resistance to the second flue section, and a second gas capacitor, again charged to the gas voltage, is connected to the first flue section. After the second time step has elapsed, the first gas capacitor is connected to the third flue section, the second gas capacitor, to the second flue section, and a third gas capacitor, to the first flue section. This procedure is continued until the "gas period" is exhausted. Now uncharged "air capacitors" are connected to the individual flue sections in opposite directions, the air boundary resistances being different from the gas boundary resistances.

Figure 9. Circuit representing regenerator

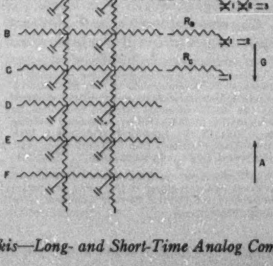

HOLLOW CYLINDRICAL THERMAL INSULATION

The third problem is a relatively simple one: that of intermittent operation of a hollow cylindrical thermal insulation, such as is used for steampipes. This problem can be set up easily on any one of the three types of analyzers. But the results, to be usable as general graphs, should be very accurate, and, therefore, again the long-time apparatus appears to be best.

References

1. IN ECONOMISH TECHNISH TIJDSCHRIFT, C. L. **Beuken.** Maastricht, Netherlands, 1937, number 1.

2. A METHOD FOR DETERMINING UNSTEADY-STATE HEAT TRANSFER BY MEANS OF AN ELECTRICAL ANALOGY, **V. Paschkis, H. D. Baker.** *Transactions*, American Society of Mechanical Engineers (New York, N. Y.), volume 64, 1942, page 105.

3. THE HEAT AND MASS FLOW ANALYZER LABORATORY—A TOOL FOR HEAT RESEARCH, **V. Paschkis.** *Metal Progress*, American Society for Metals (Cleveland, Ohio), volume 53, 1947, pages 813–818.

4. AN ELECTRICAL ANALOGY METHOD FOR FUNDAMENTAL INVESTIGATIONS IN AUTOMATIC CONTROL, **D. P. Eckman, W. H. Wannamaker.** *Transactions*, American Society of Mechanical Engineers (New York, N. Y.), volume 67, 1945, page 81.

5. ELECTRICAL DEVICE FOR ANALYZING OIL RESERVOIR BEHAVIOR, **W. A. Bruce.** *Transactions*, American Institute of Mining and Metallurgical Engineers, Petroleum Division (New York, N. Y.), volume 151, 1943, pages 112–124.

6. SIMULATING A JET ENGINE. *Electronics*, McGraw-Hill Publishing Company (New York, N. Y.), December 1947, page 188.

7. DESIGNING AUTOMATIC CONTROLLERS BY ELECTRICAL ANALOGS. *Electronics*, McGraw-Hill Publishing Company (New York, N. Y.), September 1947, page 136.

8. A LARGE-SCALE GENERAL-PURPOSE ELECTRIC ANALOG COMPUTER, **E. L. Harder, G. D. McCann.** AIEE TRANSACTIONS, volume 67, part I, 1948, pages 664–73.

No Discussion

Surge Protection in a Modern Watt-Hour Meter

F. H. BUSCH
MEMBER AIEE

G. D. WILLIAMS
NONMEMBER AIEE

RECENT trends in metering practice have imposed additional requirements upon the design of watt-hour meters, particularly from the viewpoint of surge protection. Most significant has been the change in the installation location, with the meter ahead of and remote from the fuse and switch box, and usually outdoors. This change, combined with the increasing number of meters installed on rural distribution systems, has indicated clearly that surge protection is of primary concern in evaluating the merits of any particular meter design.

Consideration of the over-all problem of surge protection for watt-hour meters is particularly appropriate at this time. Never before has the cost of labor in testing and maintaining the meters on a utility system been so great. In addition, maintenance of the growing number of meters installed on rural distribution systems, where lightning hazards are the most severe, is complicated by the greater distances involved.

Reduction of maintenance was the primary objective for the development of a new watt-hour meter, Figures 1 and 2. To accomplish this end, detailed consideration was given to the surge protection problem and to the provision of adequate protective features. By reducing the hazards of damage from surges, longer service periods without attention are possible. This objective has been further insured by other improvements. For example, the problem of bearing wear inherent in previous meter designs has been solved by suspending the rotor by means of two small magnets, one fixed to the meter frame and the other to the top of the shaft of the rotating disk. In this manner the previous use of a pivot or ball-on-sapphire bearing, operating at high-bearing pressures, has been eliminated.[1]

Types of Surge Protection Required

The modern meter, as exemplified by the design described in this paper, must be protected from surge current demagnetization of the permanent magnets and also from insulation damage caused by voltage flashovers. The types of protection and the meter components involved are as follows

A. Protection from demagnetization
   1. Braking magnets.
   2. Suspension magnets.

B. Protection from insulation damage
   1. Current coil.
   2. Potential coil.
   3. Terminals and mounting.

C. Protection from mechanical damage
   1. Disk and shaft.

That surge currents can be great enough to demagnetize the braking magnets is recognized. Damage of this type is of considerable concern to the operating company as it results in over-registration of the meter and, consequently, serious customer relation problems. During the last 15 years this hazard has been reduced effectively by using Alnico permanent magnets, or by encasing the magnets in a conducting covering.

The suspension of the meter disk and shaft by new magnetic components has been made possible by recent developments in magnetic materials. Protection of these magnets, as well as the braking magnets, must be provided.

Damage to insulation from lightning surges is the same for a watt-hour meter as for other electric equipment. The potential coil is made of many turns of small wire and is insulated from the frame or mounting of the meter. The most likely result of insulation puncture or flashover from the coil to the frame is the burnout of the small wire by either the surge current or the line-frequency ground current. This usually leaves the coil open circuited, and meter failure is evidenced by loss of registration. Meter current coils, on the other hand, are relatively heavy conductors and insulation puncture is not likely to result in open circuits. The hazard of short circuiting a portion of its turns is greater, however, and may result in under-registration of the meter. Terminal blocks or bases are subject to insulation flashover unless adequate insulation co-ordination is provided. The design considerations involved in providing this co-ordination are discussed in a later section of this paper.

The mechanical forces generated by severe surges can distort the watt-hour meter disk. A strong field in the current coils created by short circuit or surge current, acting on the aluminum disk, repels it violently, and may distort it sufficiently to prevent free rotation.

BRAKING MAGNETS

The braking magnets in the meter illustrated in Figure 3 utilize Alnico V, a highly coercive magnetic alloy having properties that make it especially suited to this application. Two C-shaped magnets are mounted diametrically opposite each other on a line passing through the axis of disk rotation. Actually they are cast as inserts in the die-cast aluminum alloy frame and are completely surrounded by the aluminum. Resistance to demagnetization by surge currents is attained by taking full advantage of the high-coercive force of Alnico V and by the eddy current shielding of the aluminum.

Alnico V has a coercive force of over 500

Paper 49-20, recommended by the AIEE instruments and measurements committee and approved by the AIEE technical program committee for presentation at the AIEE winter general meeting, New York, N. Y., January 31–February 4, 1949. Manuscript submitted July 19, 1948; made available for printing December 22, 1948.

F. H. BUSCH is section engineer and G. D. WILLIAMS is development engineer in the meter engineering division of the General Electric Company, West Lynn, Mass.

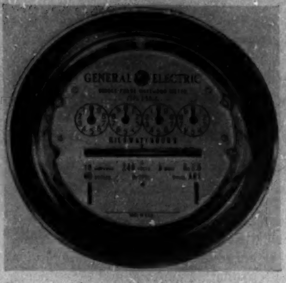

Figure 1. Detachable S-type single-phase watt-hour meter

oersteds as compared with just over 200 for cobalt steel, and less than 100 for chromium or tungsten steel. This high-coercive force has permitted an improved method of providing the stabilizing knockdown given the magnets before use on meters. Previously, the method was to knock down the magnets a fixed percentage of their saturated strength. The improved procedure is to use a demagnetizing field of a uniform strength to give the magnets the stabilization desired. The strength of this demagnetizing field exceeds the field which would be produced in the meter by the highest short-circuit current to which the meter is expected to be subjected. This method gives positive assurance of the stability of the magnets against short-circuit currents. The new method eliminates a hazard inherent in the former method of per cent knockdown, in which a magnet of high residual but low-coercive force appeared satisfactory, even though the magnet lacked the basic property, coercivity, which gives it resistance to demagnetizing fields. Figure 4 shows the means of attaining this stabilization in terms of the demagnetization curve for Alnico V. Note in particular how a magnet having satisfactory saturated strength but poor coercivity can be readily detected and rejected when all magnets are subjected to a fixed value of stabilizing field. On the basis of saturated strength both magnets would appear to be equally satisfactory. The field to which all magnets for this meter are subjected is strong enough to demagnetize completely previous types of chrome-steel magnets.

Figure 2. Front-connected A-type single-phase watt-hour meter

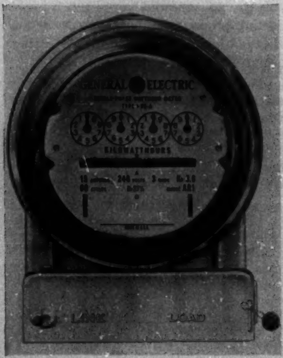

The second way in which resistance to demagnetization by lightning surge currents is attained is the eddy current shielding provided by the sheath of high conductivity aluminum enclosing the magnets. Eddy currents induced in the shield are effective in substantially reducing the magnetic field produced by steep-front surge currents as has been described previously.[3]

How effective this modern design is in protecting against decalibration by lightning-type surges is shown by Figure 5 which gives the results of laboratory tests with surge current values up to 40,000 crest amperes through the neutral conductor of a detachable S-type meter installation. These results show its definite superiority (meter A) as compared with chrome steel or Alnico II magnets used in previous designs (meters B and C), for the condition of the conductors passing behind the meter vertically (V) or horizontally (H). A test wave of relatively slow time-to-crest was used to insure as pessimistic test data as possible.

SUSPENSION MAGNETS

Surge protection of the suspension magnets, which support the disk with negligible bearing load, is assured by the same features as those used for the braking magnets. The magnetic alloy used for both inner and outer magnets is Cunico which has a coercivity of 700 oersteds. Full advantage of this property is taken by subjecting all magnets to a strong stabilizing field which is greater than the field established by the maximum short circuit or lightning surge current expected. The same principles as shown in Figure 4 apply.

In addition, eddy current shielding is obtained by enclosing the outer magnet in a jacket of conductive die-cast material, as well as by mounting it in an aluminum support. The location of the magnetic suspension at the top of the disk shaft, Figure 6, is particularly desirable because of its distance from the current coils which are the source of surge or short circuit fields. The concentric design of the magnets also contributes to the surge resistance, since the inner magnet is effectively shielded by the outer magnet.

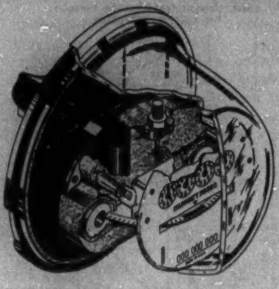

Figure 3. Cutaway diagram of new single-phase watt-hour meter showing location of braking magnets

A number of meters with magnetic suspensions have been submitted to both 60-cycle short-circuit tests and to lightning-type surges. Special care was taken to observe any change in the vertical position of the disk that would indicate weakened magnets. Tests were made with 60-cycle short-circuit currents up to 15,000 amperes through the current coils of a 15-ampere meter and with lightning surge currents up to 40,000 crest amperes through the vertical neutral of a detachable S-type meter installation. Even with the use of a microscope, any change of disk position was difficult to detect and in no case was greater than 0.002 inch.

These tests also showed that no damage occurred due to the mechanical forces

Figure 4. Stabilization of highly coercive magnetic alloy by application of uniform demagnetizing field

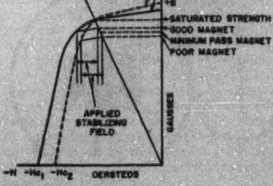

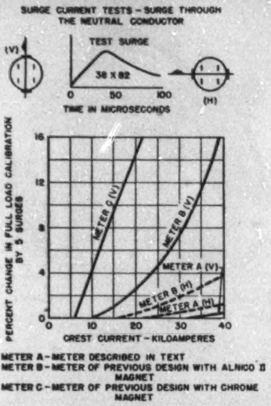

Figure 5. Curve showing results of lightning-type current surge tests on watt-hour meter calibration. Detachable-type meter

created in the disk by the surge current fields. Strength sufficient to prevent damage has been provided in this meter by a stiff aluminum disk, embossed to further increase its strength. This disk design has been used in previous meter designs and has proved satisfactory.

Insulation Coordination

The degree of improvement obtainable by practical improvements in sparkover levels of insulation cannot be expected to decrease substantially the hazard of surge damage to the meter insulations. Lightning discharges are considered to be the discharge of an electric charge between clouds and the earth. This discharge produces a current flow which will induce a voltage across any impedances encountered. The magnitude of the surge current and the steepness of its wave front are often such that the voltage induced across the meter windings would be many times the value to which it is limited by sparkover of the weakest point of insulation.

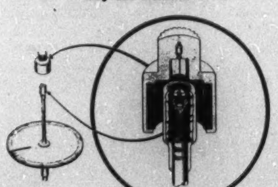

Figure 6. Magnetic suspension of rotating element of the new single-phase watt-hour meter with cutaway showing arrangement of magnetic elements

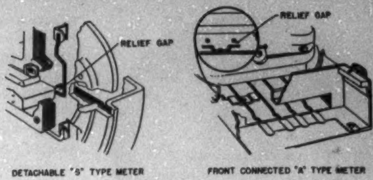

Figure 7. Cutaway diagrams showing location of relief gaps in new single-phase watt-hour meters

To reduce damage to the insulations to a minimum, the location of the sparkover point must be selected and predicted in the design, co-ordinating its impulse sparkover level with those of the other insulations. In the meter described, this has been accomplished by simple means. In the detachable S-type meter, brass pins riveted to the meter base provide controlled air gaps to the line leads. As shown in Figure 7 the pins are riveted through the base to stainless-steel spring clips which contact the lip of the socket when the meter is installed, thus completing the grounding circuit. Similarly, on the bottom-connected A-type meter, a formed clip provides the sparkover relief gap from the line leads to ground.

Figure 8 shows the improvement in appearance and mechanical nicety in the electromagnet design of this meter. Equally real, but not visibly evident, is the improvement in insulation strengths obtained. The current coils consist of round wire preformed to the required shapes. They are assembled onto the current laminations and held in position by means of a special mold. Butyl rubber is then molded and cured around the coils to provide for insulation both between coils and from the coils to the iron as well as to provide rigid mechanical positioning. This is in contrast to the usual practice of using taped or enameled wire coils which also must be separated from each other and from the lamination iron, usually by some form of paper or fiber.

Improved insulating techniques are also evident in the potential coil. Molding of the coil within an enclosure of polyethylene provides a straightforward solution to the difficulties of wrapping and insulating encountered with previous paper-insulated designs. The coil is layer wound with a thin insulating paper between each layer. The advantages of this construction in providing superior turn-to-turn and layer-to-layer insulation has been proved by many years of satisfactory experience. The enclosure of this coil within the molded polyethylene further improves the design by filling voids with insulating material and by reducing the possibility of corona as compared to previous constructions. The result is an increased impulse insulation level from windings to ground and also between the start and finish terminals of the coil.

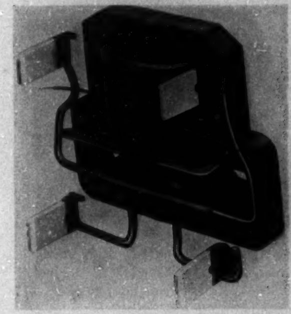

Figure 8. Electromagnet assembly of the new single-phase watt-hour meter

The requirement of long life was a major consideration in the choice of these materials for molding the current and potential coils. The improved sealing and omission of material provided by the molding processes materially reduces the effect of high humidity and insures higher insulation levels over a longer life.

The improved insulation strengths obtained permit satisfactory co-ordination of the insulation and the relief gaps. Fig-

Figure 9. Relative breakdown voltage of meter components showing co-ordination of insulation levels

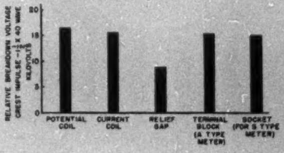

ure 9 shows the insulation co-ordination by comparing relative impulse voltage breakdown levels of the components of the meter with the relief gaps. The impulse level of the socket used for installing the detachable S-type meter is also shown since it is such an important part of the installation for this type meter. Variations between individual meters and for different test conditions are to be expected.

Summary

The growing number of watt-hour meters being installed outdoors with the new installation sequence have clearly established the necessity for protection against lightning surge damage. In a completely new meter this has been accomplished to a remarkable degree. Laboratory tests with lightning-type surges show the design to be definitely superior to previous designs.

Effective use of magnetic alloys has been made, combined with the additional protection offered by the conductive sheath enclosing the braking and suspension magnets. The insulation design of the potential and current coils has been improved through use of recently developed materials and methods of construction.

Insulation levels have been co-ordinated so that surge voltages will sparkover at relief gaps which have been incorporated to provide controlled points for sparkover with a minimum hazard of meter damage.

References

1. A New Watt-hour Meter, I. F. Kinnard. Electrical Engineering, volume 67, number 7, July 1948, pages 627–29.

2. Braking Magnets for Watt-hour Meters, I. F. Kinnard, J. H. Goss. AIEE Transactions, volume 60, 1941, pages 431–9.

Discussion

G. G. Waite (Sangamo Company, Ltd., Leaside, Ontario, Canada): Could the authors inform us of any statistics available as to the damage to meters from surges? Such statistics, with perhaps information as to the kind and extent of the damage, would be very relevant and would assist greatly in evaluating statements made in this paper.

F. C. Holtz (Sangamo Electric Company, Springfield, Ill.):

Braking Magnets

In order that the statements made in regard to the stabilization of magnets as used on watt-hour meters may not be misleading, it should be pointed out to the present authors that the practice of subjecting magnets to a "minimum" field for uniform stabilization is not new. For over twenty-five years, this has been the practice of the company with which I am associated. The magnets are subjected not only to a field in one direction, but to a revolving field which constitutes, in effect, a "washing" in the minimum field, so as to insure stability against stray-field demagnetization in substantially every direction. After such treatments, magnets with insufficient damping strength to meet the requirements of a particular meter are automatically rejected, as the authors indicate. Further demagnetization on the meter brings about correct calibration and adds further to surge resistance.

The use of modern magnet materials has in itself constituted the major gain in surge resistance. The effectiveness of any material is dependent upon its coercive force and the particular manner in which it is used. While the casting of magnets in aluminum or other metals is not new, the additional protection which it affords is achieved by other means, such as copper plating, or by designing the castings and brackets to which they are attached so that they provide short-circuited loops, preventing the rapid rise of magnetic flux within the areas they enclose.

As an indication of the extent to which surge-proofing has been attained, it may be said that, in the modern watt-hour meter using one of the better grades of Alnico magnet steel, not a single case of demagnetization from either short circuit or lightning surge has been brought to the writer's attention in the last nine years, since these meters were first introduced. In one instance where lightning had entered and where, perhaps because of a follow-up current, the lower bearing screw was burned off resulting in stopping the meter, the meter was found to be within calibration when the bearing was replaced. Such performance could not have resulted from some of the earlier-type meters; it was, in fact, their failure to withstand the effect of severe surges which brought about the general use of surge-resistant types. The ability to withstand these surges is a matter of engineering design and knowledge, and the modern meter can withstand repeated surges of a magnitude of the order indicated by the authors.

Insulation Co-ordination

The introduction of protective gaps in watt-hour meters has been suggested frequently as a means of preventing damage to its electric circuits. The effectiveness of such arrangements is dependent upon a number of conditions which should receive careful consideration. It must be said, however, in defense of such an arrangement that it does, as the authors point out, provide a weak link where, under favorable conditions, a surge may be by-passed to ground. When this occurs between electrodes, the path soon may be deionized and the insulation of the meter circuits restored. Had such surges taken place over insulating materials, a carbonized path might have been formed which would result in a power follow-up and resulting destruction of the meter. Where protective gaps are provided, as in the author's meter, the proper functioning may depend to a degree upon the available power level, in addition to the disruptive effect of the initial surge. Similar arrangements received the attention of the Sangamo Electric Company in 1937, at which time the subject was being discussed rather vigorously. Safety gaps of approximately 0.06- to 0.08-inch opening were placed between current-coil leads and ground. With the meter connected to a transformer of approximately 6-kilovolt-ampere capacity, it was possible to apply repeatedly a steep-front surge by means of a synchronized surge generator; the surge would discharge over the gaps and only show, at most, two to six cycles of power follow-up.

A possible improvement suggested itself in the form of a compression gap, comprised of rivetting a copper button into the inside surface of the meter base, adjacent to the heavy copper straps which connected to the main terminals. A porcelain bushing was placed over the button, just filling the space between the base and strap, thus providing what might be termed a compression gap with a specified opening. This type of gap gave more uniform results and led to power follow-up of not more than two cycles, even under the influence of heavy surges. This type of gap was pronounced superior to the open type and was considered satisfactory. A review of the tests then brought up the question of what might happen in the event the meter was connected by relatively low-resistance leads to a source of relatively high-power level.

The experiments therefore were repeated using two 50-kva transformers in parallel, having no limiting reactance or resistance in series except for the connecting cables. Several tests using the open gap indicated that serious damage resulted from power follow-up; except for the placement of an 80-ampere fuse in the ground circuit, the meter might have been destroyed. It also was observed that discharge frequently took place through air in other parts of the meter, where the separations were appreciably greater than in the protective gap.

Further tests made on the compression gap gave equally discouraging results because of power follow-up under the conditions mentioned in the preceding paragraph.

A review of the data at this time indicates that, whereas the crest values of the impulses used at that time were of somewhat the same order as those used by the authors, it is possible that protective gap openings somewhat larger than 0.06 to 0.08 inch might have lowered the power follow-up current.

A high insulation level in a watt-hour meter is most desirable, which raises the important question of preventing breakdown versus providing a weak link with the possibility of power follow-up damage. It would be interesting to have some further figures on the behavior of the authors' protective gaps when the meters are placed adjacent to large power transformers.

We might also ask for more information as to the magnitude of the gap spacings and how they are maintained in the ordinary process of manufacture.

F. H. Busch, G. D. Williams: The principal portion of the discussion presented by F. C. Holtz deals with the insulation co-ordination of this modern watt-hour meter. He agrees that a high insulation level in a watt-hour meter is most desirable. Next the question of preventing breakdown versus providing a flashover point is raised.

It must be made clear that the insulation voltage strength of this meter has been maintained at the same high level which has been found satisfactory through many years of experience. In the design of the new meter, it has been recognized that all breakdowns caused by surges cannot be prevented. This issue is not ignored, however, but rather the meter is designed to direct the puncture from any excessively high voltage to the point where it will do the least damage. This has been achieved by improving the insulation level of all the parts as compared to the present art, with the exception of the relief gap which is designed at the same level. In this way failure does not occur through or across organic insulation where a carbonized path might be formed, as pointed out by F. C. Holtz.

No attempt has been made to include a lightning arrester in the meter, but rather the emphasis has been to give the best coordination in insulation levels, taking maximum advantage of the properties of materials available commercially.

C. G. Waites' question concerning statistics available as to the damage to meters from surges, can be answered only to the extent that, to the author's knowledge, there are no comprehensive and sufficiently detailed data that permit ready evaluation. Various lightning investigations have shown the wide diversity of experience that occurs from place to place and from year to year. Since rural distribution systems notably offer greater exposure to lightning, the recent invesigation reported by MacCarthy, Stann, Edge, and McKinley should be pertinent.[1] It is interesting to note that the maximum values of discharge currents found in their study are approximately 30 kiloamperes, which is lower than the maximum currents used in the surge tests reported in this paper.

REFERENCE

1. LIGHTNING INVESTIGATION ON A RURAL DISTRIBUTION SYSTEM, D. D. MacCarthy, D. A. Stann, D. R. Edge, W. C. McKinley. AIEE TRANSACTIONS, volume 68, part I, 1949, pages 428–38.

A New Thermal Volt-Ampere Demand Meter

M. E. DOUGLASS
NONMEMBER AIEE

W. H. MORONG
NONMEMBER AIEE

THE PURPOSE of this paper is to describe the principles and to show the performance of a new meter for measuring single-phase volt-ampere demand, using thermal means. The discussion is limited to the technical principles and performance of such a meter, and does not consider the problems of rate structures and their relation to the units of demand measurement.

A study of the general problem of kilovolt-ampere measurement some years ago showed at least 40 patents issued on various methods of measuring and registering kilovolt-amperes. Many of the methods used required integrating devices and timing mechanisms to obtain a measurement of the demand. Since kilovolt-ampere-hours as such are used very little, thermal means of registering kilovolt-amperes, eliminating the integrating intermediary, are particularly adaptable. Table I, while not a complete summary of all the detailed methods proposed for measuring kilovolt-ampere does list the basic methods of combining the more common primary detectors with auxiliary devices to give an indication of volt-ampere demand.

Operating Principles

Of the four methods shown in Table I of using watt-hour meters and reactive volt-ampere-hour meters, all have been used to some extent.

In the first three methods, the requirement of two integrating units as primary detectors, and the complication of the ball mechanism or calculation of the vector sum of the meter indications, makes any one of them a relatively expensive means of obtaining billing information, justified only on large loads. The methods do provide true vector addition of active and reactive power to give volt-amperes.

The fourth method, that of adding the meter rotations through a series of differentials, requires many precisely made parts to minimize the friction load of the differentials and over-riding clutches, in addition to the problems of the first three. It indicates an approximation to kilovolt-ampere-hours or demand, good over a wide range of power factors.

The method of shifting the phase of the potential excitation of the watt-hour meter by the amount necessary to compensate for the average power factor angle of the load has been used. Devices of this kind measure a quantity that can be described by

$$EI \cos (A-B)$$

where E and I are voltage and current respectively, A is the power factor angle, and B is the angle of lag of the potential excitation. The registration is exact only when the power factor angle and the potential excitation lag angle are equal; the method, however, will permit deviations of about ± 11.4 angular degrees between A and B with errors of ± 1 per cent. To extend the range of power factors of this method, two or more watt-hour meters, with different values of B, may be combined through differential gearing. This is, of course, subject to the same comments on size and expense as the active-reactive vector addition methods mentioned in the preceding paragraphs.

In using an ampere-hour meter to give an indication of kilovolt-amperes, a shading coil, positioned by voltage, is inserted between the pole faces of the meter. The shading coil is suspended as a pendulous element in the air gap of the meter, with a torque to position the coil applied from an electromagnetic unit operated by voltage. The scheme provides a registration of kilovolt-amperes over a range of voltage, but it requires very careful leveling and mounting.

Thermal meters in both wattmeter and ampere meter form have been used for kilovolt-ampere measurement. Shifting the phase of the potential excitation (as described for watt-hour meters) is a method of obtaining an approximation to kilovolt-amperes over a range of power factors using a thermal wattmeter. The limitations of the method are the same as for the phase shifting method with a watt-hour meter. Multiplying the reading of an ampere meter by an assumed constant voltage is a method that has been used for measuring kilovolt-amperes with a thermal ampere meter. This method is obviously subject to errors due to line voltage differing from the assumed value.

Because all of these methods of registering kilovolt-ampere demands have either cost, maintenance, or accuracy problems involved in their application, they have not been used widely, and the extension of kilovolt-ampere metering rates by those who want them has been hampered. To meet the needs of those who wish to measure kilovolt-amperes demand, a parallel-circuit, voltage-compensating scheme for a thermal ampere meter to give an indication of kilovolt-amperes over a range in voltage has been developed.

Description of New Meter and Operation

An elementary diagram of the electrical circuit of the new meter is shown in Figure 1. The basic elements of the device are the bimetallic spirals, Figure 2; a resistance valve Figure 4; a load compensating resistor Figure 4; and the current and potential transformers.

Paper 49-22, recommended by the AIEE instruments and measurements committee and approved by the AIEE technical program committee for presentation at the AIEE winter general meeting, New York, N. Y., January 31–February 4, 1949. Manuscript submitted November 15, 1948; made available for printing January 7, 1949.

M. E. Douglass and W. H. Morong are both with the General Electric Company, West Lynn, Mass.

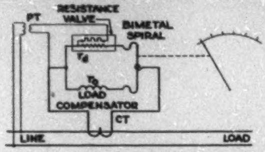

Figure 1. Thermal kilovolt-ampere-demand meter circuit diagram

The bimetallic spirals are thermally insulated so their temperature rise is directly proportional to the energy dissipated. They have the same torque change per unit temperature change, and are connected in opposition on a common shaft. The deflection of this shaft from the position of equal bimetallic temperatures is proportional to the temperature difference of the bimetallic spirals, and hence to the difference in energy input to the spirals.

The resistance valve is a temperature-sensitive resistor thermally coupled with a heating element, the assembly being encased in a glass envelope. The heating element is energized by the potential transformer; hence, its temperature, and the temperature of the associated resistor, is a function of voltage.

The load compensating resistor is a temperature-sensitive resistor, so adjusted that its resistance change as a function of current balances the resistance change as a function of current of the temperature-sensitive resistor in the resistance valve.

As current is drawn by the load, a current proportional to it flows in the secondary circuit of the current transformer. This secondary current divides between the two parallel circuits inversely proportional to their total resistances. Since the resistance of one side of the parallel circuit is a function of voltage, the ratio of the currents, and, hence, the difference in energy dissipated in the bimetallic spirals (that is, pointer deflection) is a function of voltage. As the line current changes, the difference in currents in the two branches of the circuit changes proportionally. Thus, the difference in energy dissipated in the two driving

Figure 2. Bimetallic spiral and insulating shield

Figure 3. Complete thermal unit

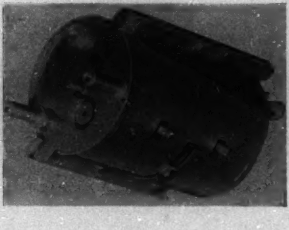

Figure 4. Resistance valve and load compensator

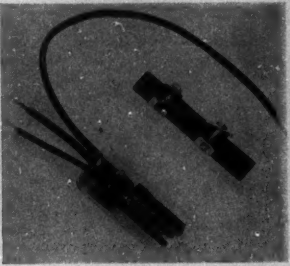

Table I. Volt-Ampere Demand Measurement Methods

Primary Detector	Auxiliary Means	Intermediate Means	End Device	Results
Watt-hour meter and reactive volt-ampere-hour meter	1. None	1. None	1. Demand register or recorder	1. Calculated volt-ampere demand
	2. None	2. Ball mechanism	2. Demand register or recorder	2. Direct indication or record of volt-ampere demand
	3. None	3. Contact device and ball mechanism	3. Demand register or recorder	3. Direct indication or record of volt-ampere demand
	4. None	4. Series of differentials with over-riding ratchets	4. Demand register or recorder	4. Approximate indication or record of volt-ampere demand
Watt-hour meter	1. Phase-shifting transformer for potential	1. None	1. Demand register or recorder	1. Approximate indication or record of volt-ampere demand
	2. Phase-shifting transformer for potential, with phase shift a function of power factor	2. None	2. Demand register or recorder	2. Direct indication or record of volt-ampere demand
	3. None	3. Mechanical means of making register ratio a function of power factor	3. Demand register	3. Direct indication of volt-ampere demand
Multiple watt-hour meters	4. Phase-shifting transformers	4. Mechanical detents	4. Demand register or contact device	4. Approximate indication or record of volt-ampere demand
Ampere-hour meter	1. None	1. Mechanical means of making register ratio a function of power factor	1. Demand register or recorder	1. Approximate indication or record of volt-ampere demand, good over a limited range of voltage
	2. Shading of ampere coils a function of voltage	2. None	2. Demand register or recorder	2. Approximate indication or record of volt-ampere demand, good over a limited range of voltage
D-C watt-hour meter or instrument	1. Rectifiers to change A-C to D-C	1. None	1. Demand register or recorder or indicating instrument	1. Indication or record of volt-ampere demand
Thermal wattmeter	1. Phase-shifting transformer	1. None	1. Scale and pointer or recorder	1. Approximate indication or record of volt-ampere, good over a limited range of power factor
Thermal ampere meter	1. None	1. None	1. Scale and pointer or recorder	1. Indication or record of ampere demand–multiplied by an assumed constant voltage approximates volt-ampere
Parallel circuit ampere meter	1. Resistance valve controlling current ratio as a function of voltage*	1. None	1. Scale and pointer or recorder	1. Indication or record of volt-ampere demand, good over a range of voltage

* General classification of method of meter described in the paper.

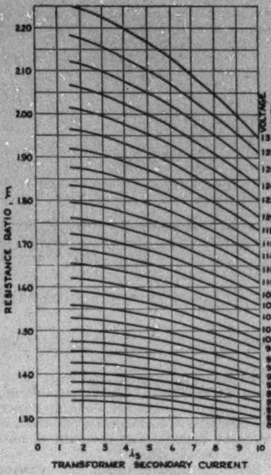

Figure 5. Curves of voltage, m, and i_s

spirals is a function of line voltage and line current.

For a correct volt-ampere indication, the deflection of the shaft, Θ, should be given by an expression which is of the form

$$\Theta = K_1(EI)^n \qquad (1)$$

where K_1 is a proportionality constant, E is the line voltage, I the line amperes, and n is an exponent of volt-amperes. This equation may be rewritten to be

$$\Theta = K_1E^nI^n \qquad (2)$$

which means that, for a correctly operating volt-ampere meter, the deflection must change according to the same function of volts and amperes over the range of voltage and current for which the device is to be used.

With the thermal unit and circuit described previously, the deflection of the shaft is given by the expression

$$\Theta = K_2 i_s^2 \left[\frac{kR_h \frac{m^2}{(m+1)^2}}{1 - ai_s^2 \frac{m^2}{(m+1)^2}} - \frac{R_c \frac{1}{(m+1)^2}}{1 - bi_s^2 \frac{1}{(m+1)^2}} \right] \qquad (3)$$

where K_2 is a proportionality constant, i_s is the transformer secondary current, k, R_h, a, R_c, and b are constants of the design, and m is the ratio of resistances of the parallel branches of the circuit. Equation 3 is derived in the Appendix.

Since in equation 3 the exponent of the secondary current, i_s, is two, the exponent n in equation 2 must also be two. Thus the expression in parenthesis in equation 3 must be proportional to the voltage squared, that is

$$\left[\frac{kR_h \frac{m^2}{(m+1)^2}}{1 - ai_s^2 \frac{m^2}{(m+1)^2}} - \frac{R_c \frac{1}{(m+1)^2}}{1 - bi_s^2 \frac{1}{(m+1)}} \right] = K_3E^2 \qquad (4)$$

where K_3 is a proportionality constant, and E is line voltage.

The term m is given by the expression

$$m = \frac{r_d + r_c}{r_o + r_h} = \frac{i_h}{i_c} \qquad (5)$$

where r_h and r_c are the resistances of the hot and cold spirals respectively, r_d and r_o are the resistances of the resistance valve and load compensator respectively and i_h and i_c are the current in the hot and cold spirals respectively.

Since r_d, equation 5, is the only component of m which is a function of voltage, the design problem is to make r_d change with voltage and current in such a way that m is the correct function of voltage and current to satisfy equation 4.

A solution of equation 4 is shown in Figure 5. In this illustration the transformer secondary current, i_s, is the abscissa and the resistance ratio, m, is the ordinate. On this co-ordinate system are plotted voltage index lines. From Figure 5, the required change in m to satisfy equation 4 can be found for any change in voltage or current. The required change in the resistance valve, r_d, can be calculated from equation 5.

Resistance Valve

Considering the resistance valve, as the voltage across the heater is increased, the temperature and resistance of r_d rise. This change of resistance with voltage may be expressed by the equation

$$\dot{r}_{de} = r_d \alpha \dot{\tau}_r \eta \dot{q}_h \qquad (6)$$

where $\dot{r}_{d_e}$ is the rate of change of r_d with voltage, α is the temperature coefficient of resistance of r_d, $\dot{\tau}_r$ is the rate of temperature change of r_d with heat input to it, η is efficiency, or the fraction of heat input to the heater that reaches r_d, and $\dot{q}_h$ is the rate of change of heat input to the heater with voltage.

The heater is not the only source of heat to r_d, however. The current passing through r_d also generates heat which causes changes in r_d as a function of current. This resistance change with current may be expressed by the equation

$$\dot{r}_{dl} = r_d \alpha \dot{\tau}_r \dot{q}_l \qquad (7)$$

where $\dot{r}_{dl}$ is the rate of change of r_d with current, α and $\dot{\tau}$ are the same as above and $\dot{q}_l$ is the rate of change of heat input to r_d with current.

Since the purpose of r_d is to change the ratio of currents, m, as a function of voltage independent of current, the value of $\dot{r}_{dl}$ must be minimized, and any residual value must be compensated by changes in the load compensator r_o. To make $\dot{r}_{de}$, the voltage sensitivity, large, it is necessary to have the items that make up the voltage sensitivity on the right hand side of equation 6 large. The first three items, however, r_d, α, and $\dot{\tau}_r$, are also components of $\dot{r}_{dl}$ which it is desirable to minimize. Thus, η, the efficiency of heat transfer and $\dot{q}_h$, the rate of heat input to the heater with voltage are the items that can be manipulated in design to best advantage.

Heat transfer by radiation increases with temperature much more rapidly at high temperatures than at low temperatures; for this reason, it was found desirable to transfer heat from heater to r_d by radiation. This was done by mechanically arranging the parts of the resistance valve so that r_d was in the form of a helically-wound ribbon with a straight rod of heater material on its axis. It is not

Figure 6. Temperature error curves

Type *IHE-1* single phase watt-hour and thermal volt-ampere demand meter, 50 amperes, 240 volt, 60 cycle, 3 wire
Temperature curve-demand meter element
Power factor = 1.0

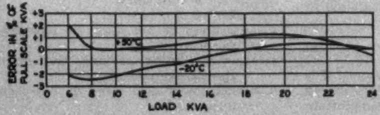

Figure 7. Voltage error curves

Type *IHE-1* single phase watt-hour and thermal volt-ampere demand meter, 50 amperes, 240 volt, 60 cycle, 3 wire
Voltage curve-demand meter element
Power factor = 1.0

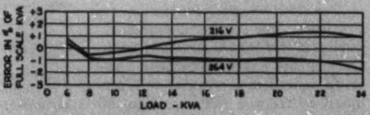

within the scope of this paper to treat the heat transfer method in detail. It can be shown, however, that with adequate shielding to conserve stray radiation, the factor η is not constant but is an exponential function of voltage that increases rapidly with voltage in the operating range. Thus an additional gain in r_{de} is realized by utilizing this heat transfer method that makes the efficiency of heat transfer a function of voltage. The shielding to conserve stray radiation consists of a double-walled cylinder of thin, bright nickel, closed at both ends except for openings for the leads, mounted concentrically about the heater and control resistance, r_d.

To make the value of $\dot{q}_h$, the rate of heat input to the heater with voltage, as large as possible, a heater material with a negative temperature coefficient of resistance is desirable since increasing voltage increases the heater temperature, and if, at the same time, this increase in temperature reduces the heater resistance, a further gain in heat input with voltage can be made. The material carbon fulfills these requirements; hence, it was the heater material selected.

With the factors η and $\dot{q}_h$ made as large as possible, it remains to compensate the heating effects of current in r_d. This was accomplished in two ways. It was found that the radiation loss from r_d could be minimized by providing an additional path for the conduction of heat, through the medium of an inert gas in the envelope. The presence of the gas also reduces the efficiency of heat transfer from the heater to r_d but the reduction in voltage sensitivity is not as great as the reduction in current sensitivity. Balancing one effect against the other to arrive at an optimum operating condition was done by controlling the pressure of the gas. It is known that the heat conductivity of a gas is proportional to the pressure, if the pressure is reduced to the point where the conduction path is shorter than the mean free path of the molecules. Thus, by controlling the gas pressure, an optimum ratio of voltage sensitivity to current sensitivity could be obtained. Helium, having the highest conductivity of the inert gases, provided the greatest degree of control.

The finally remaining current sensitivity of r_d was balanced by a temperature-sensitive resistor of nickel wire for r_o. The nickel wire was wound in the form of a helix. The cold or no current resistance of this helix is controlled by the diameter and length of the wire. The change in resistance with current is controlled by the wire diameter, helix diameter, and turn spacing, since these factors control the heat escape versus temperature characteristic of the helix.

Performance

With the use of temperature-sensitive elements in the meter, it might be imagined that ambient temperature would greatly affect the readings. This is not the case however, since in general the effects of ambient temperature are balanced in both the mechanical and electrical circuits of the meter. There is a net temperature effect on the meter that is compensated by a bimetallic spiral connected through a linkage to the thermal unit shaft. Performance curves on the meter, Figure 6 show that temperature variations from −20 degrees centigrade (−4 degrees Fahrenheit) to +50 degrees centigrade (122 degrees Fahrenheit) cause errors of less than ±3 per cent of full scale from one-quarter full-scale load to full-scale load.

The registration of the meters as a function of voltage and load is shown in Figure 7, and shows that for a range of ±10 per cent in voltage, the meters register within ±2 per cent of the correct value from one-quarter full-scale load to full-scale load.

The full-scale torque of the meters is 850 gram-millimeters with a power consumption of six watts in the potential circuit, and about 14 watts in the current circuit at full scale.

Power factor obviously does not influence the meter registration of kilovolt-amperes since the only interaction between voltage and current comes in the thermal coupling in the resistance valve. In Figure 8 is shown a finished, practical meter in combination with a watt-hour meter for registering kilowatt-hours and kilovolt-amperes demand.

Appendix. A New Thermal Volt-Ampere Meter

The purpose of this Appendix is to derive equation 3 quoted in the body of the paper.

As stated previously, the bimetallic shaft deflection is proportional to the difference in energy input to the bimetallic spirals. This is true only if the temperature rise per unit of energy input is the same for both spirals. Considering the general case, where this condition may not be met, the deflection of the thermal unit shaft will be given by equation 8

$$\Theta = K(kW_h - W_c) \tag{8}$$

where Θ is the deflection of the shaft, K is a proportionality constant between energy and deflection, k is the ratio of temperature rise per unit of energy input of the spirals, and W_h and W_c are the energy input to the hot and cold spirals respectively.

The energy input to the spirals is given by equations 9 and 10

$$W_h = i_h^2 r_h \tag{9}$$

$$W_c = i_c^2 r_c \tag{10}$$

where i_h and i_c are the hot and cold spiral currents respectively, and r_h and r_c are the hot and cold spiral resistances respectively.

Since resistance of the bimetallic spirals is not constant, but is a function of the temperature of the spiral, the resistance will be a function of current. This function is given in equations 11 and 12

$$r_h = \frac{R_h}{1 - a i_h^2} \tag{11}$$

$$r_c = \frac{R_c}{1 - b i_c^2} \tag{12}$$

where R_h and R_c are the no-current resistances of the hot and cold spirals respectively, and a and b are constants depending upon the temperature coefficient of resistance of the spiral material and upon the thermal insulation of the spiral.

From the parallel circuit the relations given in equations 13, 14, and 15 are obtained

$$i_c + i_h = i_s \tag{13}$$

$$i_c = i_s \frac{r_2}{r_1 + r_2} = i_s \frac{1}{m+1} \tag{14}$$

$$i_h = i_s \frac{r_1}{r_1 + r_2} = i_s \frac{m}{m+1} \tag{15}$$

where i_s is the secondary current of the transformer proportional to load current, r_1 is the total resistance of the resistance valve plus the cold spiral $(r_d + r_c)$, r_2 is the total resistance of the load compensator plus the hot spiral $(r_o + r_h)$, and m is the ratio of r_1 to r_2.

By substituting values from equations 9, 10, 11, 12, 13, 14, and 15 in equation 8, the expression for the deflection of the meter is obtained

$$\Theta = K i_s^2 \left[\frac{kR_h \dfrac{m^2}{(m+1)^2}}{1 - a i_s^2 \dfrac{m^2}{(m+1)^2}} - \frac{R_c \dfrac{1}{(m+1)^2}}{1 - b i_s^2 \dfrac{1}{(m+1)^2}} \right] \tag{3}$$

Symbols

Θ = deflection of bimetallic shaft, angular degrees
W_h = watts dissipated in hot spiral
W_c = watts dissipated in cold spiral
k = ratio of temperature rise per watt of hot spiral to temperature rise per watt of cold spiral
i_h = current in hot spiral
r_h = resistance of hot spiral
i_c = current in cold spiral
r_c = resistance of cold spiral
R_h = resistance of hot spiral at reference temperature
a = constant relating resistance to current through temperature rise
R_c = resistance of cold spiral at reference temperature

b = constant relating resistance to current through temperature rise
i_s = secondary current of current transformer
$r_1 = r_d + r_c$ = total resistance of cold spiral branch
$r_2 = r_o + r_h$ = total resistance of hot spiral branch
$m = r_1/r_2 = r_d + r_c/r_o + r_h$
K = proportionality constant between differential watts and deflection
K_1 = proportionality constant between volt-amperes squared and deflection for theoretically perfect meter
E = line voltage
I = line current
n = exponent of volt amperes

Figure 8 (left). Completed meter

$\dot{r}_{de}$ = rate of change of r_d with voltage
α = temperature coefficient of r_d
$\dot{r}_T$ = rate of change of temperature of r_d with energy input to r_d
η = efficiency of heat transfer from heater to r_d
$\dot{q}_h$ = rate of change of energy input to heater with voltage
$\dot{r}_{di}$ = rate of change of r_d with current
$\dot{q}_i$ = rate of change of energy input to r_d with current through r_d

References

1. The Basic Laws and Data of Heat Transmission, W. J. King. *Mechanical Engineering*, American Society of Mechanical Engineers (New York, N. Y.), March-August 1932, pages 275–80, 347–53, 492–97.

Discussion

G. G. Waite (Sangamo Company, Ltd., Leaside, Ontario, Canada): I would like to lend support to Perry Borden's suggestion that references to the prior art, be amplified in papers such as this one. Further, I can see no good reason for excluding references to patent numbers, as the authors have done.

The authors claim errors of less than 3 per cent of full scale for stated conditions of temperature and load, and 2 per cent for variations of 10 per cent in voltage. This is, perhaps, quite good considering the complexity of the compensation methods required. Why, however, do they choose to refer to only a ±1 per cent error for ±11.5 angular degrees deviation in the phase-shift method mentioned earlier in the paper, while talking about larger errors for their method?

M. E. Douglass, W. H. Morong: In regard to Waite's comments on accuracy of volt-ampere registration, we feel that a comparison of errors in two measuring methods should be referred to the same variable. With the new, thermal, volt-ampere demand meter the indication is independent of power factor, since the only interaction of voltage and current is obtained through the thermal coupling of the resistance valve; hence, the error caused by varying power-factor angle is zero. Furthermore, the quoted values of 2 and 3 per cent errors, given for the over-all performance, should not be compared with the fundamental error of the method only in the phase-shifting method. The selection of ±1 per cent was used purely as a convenient number to remember. The following table may help in clarifying the magnitude of the power-factor errors fundamental in the phase-shifting method. To these fundamental errors must be added any errors incidental to the measuring equipment.

It should be pointed out that the device must be calibrated to read one per cent fast at the assumed operating conditions to obtain the ±1 per cent error for ±11.5 angular degrees deviation from the assumed condition.

With regard to the complexity of the compensation: although the algebraic manipulations required to define the required compensation might be considered complex, the temperature coefficient of resistance of a metal, as an operating mechanism seems to us quite simple.

Deviation of Power Factor Angle from Value Assumed, Degrees		Effective Meter Power Factor, Per Cent	Error in Registration, Per Cent
20.0	Lead	94.0	—5.0
16.3		96.0	—3.0
11.5		98.0	—1.0
0		100.0	+1.0
11.5	Lag	98.0	—1.0
16.3		96.0	—3.0
20.0		94.0	—3.0

An Electro-Optical Shutter for Photographic Purposes

A. M. ZAREM
ASSOCIATE AIEE

F. R. MARSHALL
NONMEMBER AIEE

F. L. POOLE
MEMBER AIEE

Synopsis: This paper presents the theory and describes the development of a simple, reliable, and compact optical shutter which utilizes a Kerr cell as a light valve. With the aid of such a shutter, routine photographic studies of electric discharges have been made using an effective exposure time of 0.000,000,04 second. The novel feature of an electro-optical or Kerr cell shutter is that there are no mechanical moving parts, the speed of operation depending only upon the rapidity with which a required voltage can be applied to the Kerr cell electrodes. These electrodes are immersed in a fluid which exhibits uniaxial birefringence when under the influence of an electric field. Electrical birefringence is described and explained at some length and the optical transmission of a Kerr cell shutter as a function of applied voltage is derived and plotted for reference. With the advent of the "all-electric" shutter, some of the latest techniques of the electronic art become applicable to photographic work. The control can be made sufficiently positive and accurate to permit initiation of operation at any preselected instant with a precision of 5×10^{-9} second. This excellence of control has made possible the detailed photographic study of light from very rapidly changing self-luminous objects. The complete components of an electro-optical camera are described in some detail. Prints are included which show photographic records of the electrical vaporization of a fine wire taken with an effective exposure time of 0.000,000,04 second. Comments are made on the ultimate possibilities and further application of Kerr-cell shutters for ultra high-speed photographic work.

The phenomenon of electrical birefringence was discovered by J. Kerr in 1875.[1] One of the early applications of this effect was made in the construction of a light valve, now commonly called a Kerr-cell shutter, for the measurement of very small time intervals.[2] The ordinary Kerr cell is composed of two flat plates or electrodes immersed in a fluid which becomes birefringent upon the application of an electric field. When such a cell is oriented between two polarizers crossed for minimum transmission the arrangement constitutes an optical shutter. With no voltage applied to the cell, light cannot be transmitted because of the crossed polarizers. A voltage applied to the electrodes has the effect of altering the state of polarization of the light, and transmission through the second polarizer is accomplished.

The very small time lag between the application of voltage to the electrodes and the appearance of birefringence has led to the application of such shutters to: measurement of the time lag in fluorescence;[3] study of early stages in spark discharges;[4] spectral studies of electric discharges;[5] measurement of the velocity of light;[6] and modulation of light in telephotography.[7] In the first three activities listed, an electro-optical shutter was connected across a spark gap by means of an adjustable length of transmission line. As the gap voltage was increased the shutter opened. The occurrence of a discharge caused the cell voltage to collapse suddenly at a time which depended upon the length of the transmission line between the gap and the Kerr cell electrodes. By this means various stages during the spark discharge were examined. The last two programs listed utilized Kerr cells with varying voltages applied to their electrodes. There was, however, no intention of developing an optical shutter for use in a camera. In 1926 J. W. Beams introduced the first full cycle (closed-open-closed) shutter using an arrangement of two Kerr cells.[8] A preliminary review of published literature has indicated that no completely controlled full cycle operation of a Kerr-cell shutter for photographic purposes thus far has been reported. Such work, however, may have been done during the war. This very practical application has been slow in coming because successful optical shutters of large aperture require the accurate timing and control of high voltages. Interest in the photography of very high speed phenomena has increased steadily in recent years, and the development of the electric art has been so rapid, that simple techniques for generating and switching high voltage pulses, with great precision, are now standard practice.

The information presented in this paper is the result of work done in one part of a proposed program of basic research on electrical discharges. In order to make a complete optical study of a phenomenon with a duration of a few microseconds, it was necessary to use a camera with a very accurate controllable shutter that would enable the attainment of exposure times of less than a microsecond. The electro-optical shutter was chosen as the only solution to this problem. By controlling the type, duration, and instant of application of the voltage pulse applied to the cell electrodes, photographic records with an effective exposure time of 0.000,000,04 second have been obtained at preselected intervals during the life of the phenomena being studied.

The Electro-Optical Kerr Effect

If a beam of polarized light is passed through a medium which is optically anisotropic, the velocity with which the light travels in the material depends upon the direction of the electric vector in the incident light. This means the substance is birefringent, that is, the index of refraction depends upon the direction

---

Paper 49-24, recommended by the AIEE instruments and measurements committee and approved by the AIEE technical program committee for presentation at the AIEE winter general meeting, New York, N. Y., January 31–February 4, 1949. Manuscript submitted June 25, 1947; made available for printing January 7, 1949.

At the time this paper was written, A. M. Zarem was head, and F. R. Marshall and F. L. Poole were members of the electrical subsection, physics section, United States Naval Ordnance Test Station, Pasadena, Calif.

A. M. Zarem has since become chairman of physics research for the Stanford Research Institute, Stanford, Calif., and director of the Los Angeles division, Los Angeles, Calif.

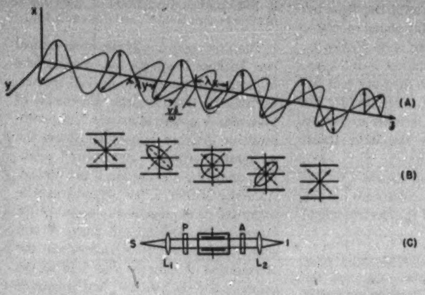

Figure 1. Principle of operation of a light valve

of propagation and the plane of polarization of the light traversing the medium. There are many known substances which are normally isotropic, but which exhibit the property of optical birefringence when subjected to an electrostatic field. This phenomenon is known as the electro-optical Kerr effect.[9]

In a simple case of a uniaxial birefringent material, there is one axis along which the index of refraction is not dependent upon the direction of the electric vector in the incident light. This axis is termed the optic axis of the material.[10] Substances which exhibit the electro-optical Kerr effect become uniaxially birefringent under the influence of an electric field, the optic axis being in the direction of the field.

According to the present state of the theory, the electro-optical Kerr effect is related intimately to molecular structure. It has been found that for a liquid or gas to exhibit a Kerr effect, it is essential that the individual molecules possess an aeolotropic optical polarizability with respect to a set of axes in the molecule. In addition, however, the molecules must have either a permanent dipole moment or be anisotropically polarizable by the application of an electric field, or both. It is not surprising, therefore, that the materials with the largest Kerr constants also have high dielectric constants.[11,12]

The statistically random orientation of molecules for liquids and gases in the normal state results in a condition of optical isotropy. In general, the application of an electric field produces a polarization assymmetry and also a tendency for the molecules to prefer a definite orientation mainly because of the permanent dipole moment. The orienting effect, although opposed by the thermal molecular motion, results in a more or less statistically-average regular arrangement of molecules under the influence of the applied electric field. Under these conditions the substance exhibits an overall molecular assymmetry and, generally, optical anisotropy. Orientation of the molecules is not a necessity, however, as the induced electrical polarization alone will cause optical anisotropy, but for substances with high Kerr constants, molecular orientation accounts for the largest part of the Kerr effect.[13] The rapidity with which the molecules of a substance assume a statistically-average preferred direction of orientation is related to the chemical structure, viscosity, and other factors, and can be determined approximately, using certain simplifying assumptions, by introducing the concept of relaxation time. The relaxation time for the Kerr effect is an average molecular time constant which may be considered as a measure of the effective time required for a substance to return to its optically isotropic state, after the electric field has been removed. For many substances this time is of the order of 10^{-9} second.[14]

Description of the Kerr Effect

For a clearer picture of the influence of an electric field upon a liquid which exhibits the Kerr effect, consider the arrangement of lenses L_1 and L_2, polarizers P and A, and the Kerr cell in Figure 1(c). S is a light source and I is its optical image. A beam of light, plane polarized at an angle φ with respect to the applied electric field, enters the cell. The electric vector in the incident light may be resolved into two components, one parallel and the other perpendicular to the applied field. These components traverse the cell fluid with different velocities, and as a result possess different wave lengths, as shown (much exaggerated) in Figure 1(a). As a consequence, if the applied electric field is kept fixed, the two components will differ more and more in space phase as they proceed through the liquid. This is the equivalent of stating that there will be a continuously increasing difference in time phase between the two components of light as they traverse the cell. Since the state of polarization of the light at any point is dependent upon the difference in time phase between the two components, the resultant light emerging from the cell will in general no longer be plane polarized. If the angle φ of the plane of polarization upon entering is 45 degrees, and the angular time phase difference between the components, δ, is an odd multiple of $\pi/2$, the light will become circularly polarized. If δ is an odd multiple of π, the emergent light will be plane polarized at 90 degrees to the plane of polarization of the entering light. For δ equal to an even multiple of π, the light leaves polarized as it entered. For all other values of δ the light will be elliptically polarized. The sketches of Figure 1(b) illustrate the states of polarization for $\delta = 0, \pi/4, \pi/2, 3\pi/4$, and π. The latter value represents the condition for full-open operation of the shutter.

One of the factors which determines the angular time phase δ is the Kerr constant of the fluid. The Kerr constant is defined by the equation

Table I

Substance	Kerr Constant	Resistivity	Dielectric Constant
Carbon disulphide CS_2	3.6×10^{-7}	10^{16}	2.5
Chloroform $CHCl_3$	-3.2×10^{-7}	10^{8}	5.0
Acetone C_3H_6O	16×10^{-7}	10^{7}	20.0
Nitrobenzene $C_6H_5NO_2$	400×10^{-7}	10^{10}	36.0

$$\frac{n_x - n_y}{\lambda} = KE^2 \tag{1}$$

where

n_x = refractive index in a direction parallel to the electric field
n_y = refractive index in a direction perpendicular to the electric field
λ = wave length in vacuo of the incident light in centimeters
E = applied electric field in electrostatic units

The time phase angle, see Appendix I, is given by

$$\delta = 2\pi l K E^2 \tag{2}$$

where

l = length of the light path under influence of the electric field in centimeters
E = applied electric field in electrostatic units
K = Kerr constant for the substance in centimeter-gram-seconds electrostatic units

Table I contains approximate Kerr constants, dielectric constants, and resistivities for various substances of interest in electro-optical work.

The Kerr constant for most substances depends not only upon temperature, but is a function of the wave length of the incident light as well. However, this is not too serious a difficulty even when careful quantitative work is to be done. It is a simple matter to keep the cell at constant temperature, and optical corrections for dispersion in the Kerr effect can be easily provided. These corrections were not required in the work described below.

Electro-Optical Characteristics of a Kerr Cell Shutter

The percentage optical transmission of a Kerr cell shutter[15] as a function of the applied electric field, may be obtained as in Appendix II, with the aid of equations 1 and 2 as

$$_{\varphi}T_{\alpha}=50[\cos^2(\varphi-\alpha)-\sin 2\varphi \sin 2\alpha \sin^2 \delta/2] \text{ per cent} \quad (3)$$

where

φ=angle between the plane of polarization of the entering light and the applied electric field

α=angle at which the analyzer is set relative to the applied electric field

$\delta=2\pi lKE^2$, angular time-phase difference between the emerging components of light parallel and perpendicular to the applied electric field

$_{\varphi}T_{\alpha}$=per cent optical transmission when the polarizer and analyzer angles are φ and α respectively

For optimum operation as a shutter, φ equals 45 degrees and α equals -45 degrees and the transmission therefore becomes

$$_{\pi/4}T_{-\pi/4}=50[\sin^2 \delta/2] \text{ per cent} \quad (4)$$

$$_{\pi/4}T_{-\pi/4}=50[\sin^2 (\pi lKE^2)] \text{ per cent}$$

If the electric field required for full-open operation is taken to be E_0, corresponding to an applied potential difference V_0, the transmission as a function of the potential difference, v, applied to the cell may be written:

$$_{\pi/4}T_{-\pi/4}=50\left[\sin^2 \frac{\pi}{2}\left(\frac{v}{V_0}\right)^2\right] \text{per cent} \quad (5)$$

Figure 2 shows the variation of transmission of an electro-optical shutter as a function of applied potential for several angular orientations of the plane of polarization of the entering light. The analyzer is fixed at α equal to -45 degrees. These curves were plotted using equation 3 which ignores the attenuation of light by the various components of the Kerr cell and does not take into account dispersion in the Kerr effect. The amount of light passed by the shutter increases with the applied potential until the light becomes polarized in the plane of transmission of the analyzer, *A* in Figure 1*c*. At this voltage, the shutter is full-open, but the transmission is fifty per cent because half of the light is rejected by the polarizer *P*. Further increase in voltage causes a decrease in the light transmitted.

From equation 3 and Figure 2 we observe two important conditions for the successful operation of the electro-optical shutter.

1. If there is to be zero transmission when no voltage is applied to the Kerr cell the polarizer and analyzer must be accurately crossed, that is $(\varphi-\alpha)=90°$.
2. The optimum condition of operation is obtained when $\varphi=45°$, see Appendix III.

The first condition is the more critical one, because it affects the completeness of closure of the electro-optical shutter. Fortunately the critical alignment of Polaroids is a simple matter if a photosensitive detector is used to obtain the minimum position. The second condition, namely $\varphi=45$ degrees is not critical. Accuracy within a few degrees can be tolerated. Equation 3 was obtained for operation of the Kerr cell under certain simplified conditions. Because of the attenuation of light by the fluid in the polarizer and the analyzer, and because of dispersion in the Kerr effect, neither full

Figure 2. Electro-optical characteristics of a Kerr-cell shutter

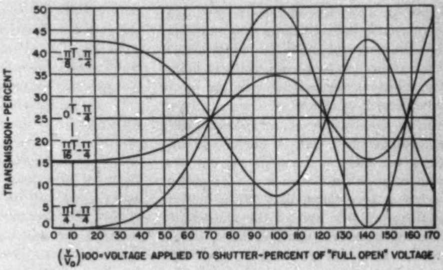

Figure 3. Components of a Kerr-cell camera

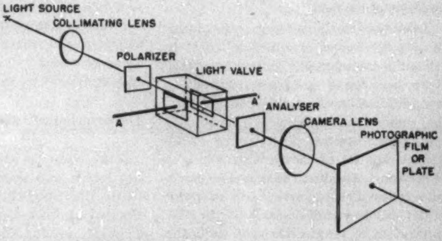

Figure 4. Characteristics of J-film Polaroid

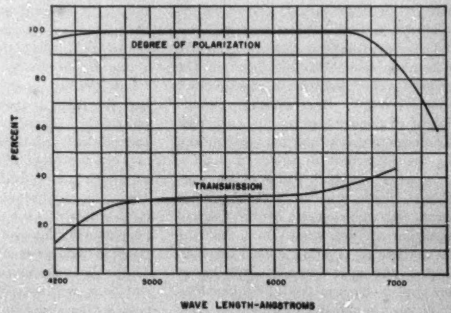

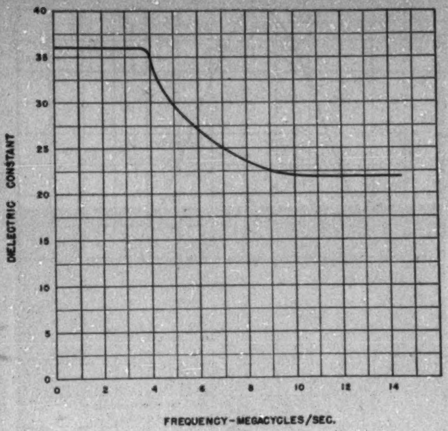

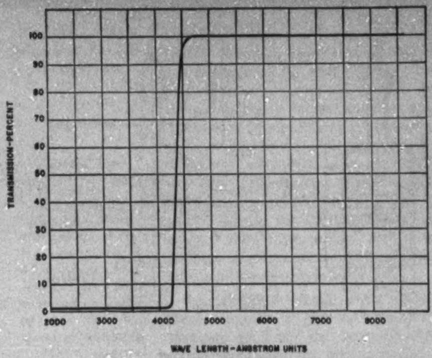

Figure 5 (left). Variation of dielectric constant with frequency for nitrobenzene

Figure 6 (above). Spectral transmission of nitrobenzene sample of 1 centimeter thickness

nor zero transmission actually is attained with increasing voltage applied to the cell.

Components of a Kerr Cell Camera

The components required to make a Kerr-cell camera are shown in Figure 3. Light from the source to be photographed is gathered and rendered parallel by the collimating lens. The polarizer and analyzer are accurately set at an angle of 45 degrees to the electric field and at 90 degrees to one another. For the camera lens and film combination we employed an *f*:4.5 Speed Graphic using 4 by 5 inch film or plate.

Several different polarizing agencies were tried. Nicol prisms, although having an excellent transmission characteristic, are bulky, expensive, and introduce a limited width of field. Polaroid glass is inexpensive, but zero transmission of a crossed pair was difficult to obtain—even with selected pairs. In addition, there were also mounting problems. Best over-all results were obtained with Polaroid J film sheets. This film comes in 12 by 12 inch sheets. It is inexpensive, and our experience has been that suitable uniform sections can be found in any sheet. These sections are easily cut out and properly oriented; they are fastened to the glass cell windows by means of scotch tape. Figure 4 shows the variation of degree of polarization and percentage transmission with wave length for Polaroid J film.[16]

The Kerr Cell Fluid

Among the fluids, nitrobenzene, $C_6H_5NO_2$, seems to have the highest Kerr constant. For this reason, it long has been used as the active substance in Kerr cell work. Commercially known as oil of mirbane, it is a straw-yellow oily liquid with a strong odor of shoe polish. It is very soluble in ether, alcohol, or benzene, but not in water. Nitrobenzene vapor is quite toxic, and the liquid can be absorbed by the body through the skin, causing blood poisoning. Care in handling is consequently essential.

The dielectric constant of nitrobenzene at 20 degrees centigrade is 36. The variation of the dielectric constant of nitrobenzene with frequency is given in Figure 5.[17] As shown, the dielectric constant decreases from 36 at three megacycles per second to 22 at 10 megacycles per second, and continues at the latter value up to 13 megacycles per second. Further data are not available. This would seem to indicate the existence of a first-order Kerr effect at frequencies at least as high as 10 megacycles per second. Experimental observations bear this out, as no time lag in the Kerr effect for pure nitrobenzene has been detected up to nearly 10^{-9} second.[18,19,20] Theory indicates that the relaxation time due to orientation should be of the order of 10^{-9} second.[21]

The absolute spectral transmission for a one centimeter path in very pure nitrobenzene resistivity of the order of 10^{10} ohm-centimeters, is given according to our measurements in Figure 6. The transmission cuts off almost completely at 4,200 Angstrom units.

There are other facts concerning nitrobenzene which are of interest. The refractive index is approximately 1.553. The dielectric strength of commercial oil of mirbane is about 45,000 volts per centimeter and its resistivity is of the order of 10^6 ohm-centimeters. When the liquid is purified, the dielectric strength may be increased to 150,000 volts per centimeter and its resistivity brought up to 10^{10} ohm-centimeters.[22] Under conditions of pulsed voltage, nitrobenzene undoubtedly will withstand much higher electrical stresses although no data have been found for such conditions. However, it has been reported that carbon

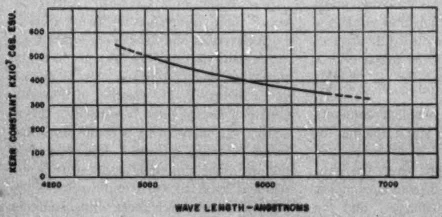

Figure 7. Dispersion in the Kerr constant for nitrobenzene

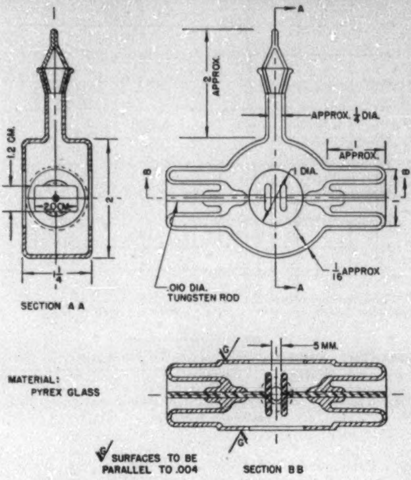

Figure 8 (above). Kerr-cell body

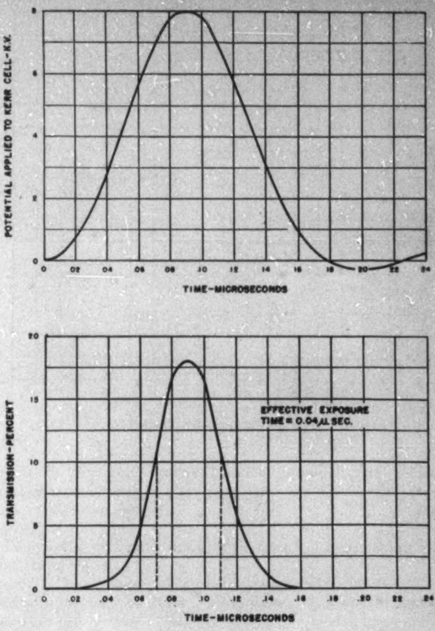

Figure 9 (right)

(a) Voltage applied to Kerr-cell terminals
(b) Kerr cell transmission for voltage pulse of (a) showing effective exposure time of 0.000,000,04 second

disulfide will withstand a gradient of 10^6 volts per centimeter for periods of the order of 10^{-7} second.

The Kerr constant for nitrobenzene as determined by electrostatic methods has been shown to be directly related to its purity as indicated by its resistivity. For this reason, elaborate precautions are usually made to obtain the highest possible purity and resistivity. Because nitrobenzene is a powerful solvent, great care is exercised in the cleansing and handling operations encountered in the construction of Kerr cells.[23] It should be noted here that the operation of a Kerr cell with voltage pulses of very brief duration (10^{-7} second) may not require nitrobenzene of the very highest degree of purity. This matter has not been fully investigated yet.

Figure 7 illustrates dispersion in the Kerr constant for nitrobenzene.[24]

The Kerr Cell Body

The heart of an electro-optical shutter is its Kerr cell unit. Figure 8 shows the structural details of a satisfactory model made of pyrex glass.[18,23] It is one of several designs used in our ultra high-speed photographic work. Circular openings are provided as shown, with suitably large areas about these openings ground flat to facilitate the attachment of the cell windows. These windows are directly in the optical path of the cell and consequently they must be strain free and optically flat enough to insure good photographic definition in the images formed by the associated lens system. Since polarized light is used with the cell, it is obvious that, if the windows are not strain free, they will produce alteration of the state of polarization. Poor operation of the light valve will result. The degree of optical flatness of the cell windows depends upon the use for which the camera is intended. Because the refractive index of nitrobenzene is much closer to that of glass than that of air, the tolerance on flatness for the inside surfaces of the windows can be as much as ten times greater than that for the outside surfaces.

The cell windows are usually completely masked excepting for a small opening for the passage of light. This serves two purposes: reflected light from the electrode faces is prevented from causing extraneous photographic images; and the useful light beam area is limited to a region of comparatively uniform electric field in the cell.

In the earlier models the glass windows were attached to the cell body with ceresin wax as a cement. Later, experimental cell models with fused windows were satisfactorily constructed, but those have not yet been used. The electrode plates were made of pure nickel, silver soldered to tungsten stems, which in turn were sealed into the pyrex body. The plates were rounded at the edges in order to minimize electrical stresses and the consequent possibility of breakdown.

Design Considerations

The design of a Kerr-cell shutter depends upon many factors which involve both electrical and optical considerations. After some thought has been given to the nature of the photographic problem in a given instance, the question of desirable shutter aperture must be settled. A good design will have to be a compromise between certain physical and electrical factors, since the possible aperture is dependent upon the width and spacing of the cell electrodes and these dimensions in

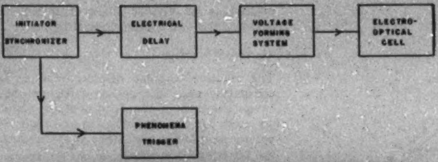

Figure 10. Block diagram of Kerr-cell camera system

Figure 11. Photograph obtained during vaporization of a fine tungsten wire. Taken at 0.60 microsecond after initiation of the electrical discharge

Effective exposure time: 0.000,000,04 second

turn are affected by the length of the electrodes and the availability of electrical means for obtaining and switching voltage to the electrodes. As an example consider equation 4. The condition for full open operation of a shutter is

$$\pi l K E_0^2 = \pi/2 \tag{6}$$

Taking $E_0 = V_0/d$ where d is the separation of the plates, this leads to

$$V_0 = 300d\sqrt{\frac{1}{2lK}} \text{ volts} \tag{7}$$

Since the Kerr constant K at best is of the order of 10^{-6}, shutters of wide aperture will require very high voltages. The alternative of increasing the length of the plates adversely affects the angular field and limits the rapidity with which the shutter can be operated by increasing the electrostatic capacitance of the cell. The Kerr cell shown in Figure 8 is full open with approximately 12,000 volts applied to the cell electrodes. Reference to Figure 2 will show that the most effective utilization of equipment will be obtained if the applied voltage is 80 to 90 per cent of the full-open voltage.

Voltage Forming System for a Kerr-cell Shutter

Up to this point we have discussed the Kerr-cell shutter alone and have given little attention to the electrical requirements which are necessary for its successful operation. To convert the device described to a useful instrument, it is necessary to be able to apply voltage pulses of suitable magnitude and duration to the Kerr cell at accurately predetermined instants. The general problem is too broad to be discussed here. It is sufficient to remark that a large variety of techniques are applicable, and that many elaborate control methods similar to those recently developed for radar may be adapted to this specific use. From the abundance of methods utilizing these techniques, one may choose those systems which best meet specific requirements of accuracy, stability, and simplicity. Since versatility in operation is a characteristic of most electronic control means, it will be found that a wide range of applications will be served by a single apparatus. For example, adjustments of the duration and magnitude of the voltage applied to the cell electrodes can be utilized to vary the effective exposure time over a wide range, and control of the instant of operation of the shutter allows selective photographic studies to be made.

The voltage forming system which was selected for use in obtaining photographic records of the various stages during the sudden electrical vaporization of fine wires provided an effective exposure time of 0.000,000,04 second when used with the Kerr cell shown in Figure 8. In operation, an accurately controlled initiating signal determines the instant at which the voltage pulse shown in Figure 9(a) is applied to the Kerr cell electrodes. This pulse reaches a magnitude of 8 kv and has a duration of 0.18 microsecond. All statements concerning timing have been checked experimentally with the aid of a high-speed oscillograph having a resolution time of 0.002 microsecond. The transmission of the shutter as a function of time, as shown in Figure 9(b), is obtained with the aid of Figure 2 or equation 5. Assuming 64 per cent as an average transmission for each polarizer, the over-all transmission of the shutter, including absorption by the polarizers, can be obtained by multiplying the ordinates of Figure 9(b) by 0.41. Seventy per cent of the area under the transmission versus time curve lies between 0.07 microsecond and 0.11 microsecond. The effective exposure time of the shutter is therefore given as 0.04 microsecond. This value has been checked approximately with the aid of a photosensitive detector.

For special problems, where photographic records of very brief exposure time are required, the accuracy with which the instant of maximum transmission for the shutter can be preselected may become an important matter. In general the midpoint of the exposure time will be determined by the electrical control of the voltage-forming system. Using standard pulsing techniques it was found that the initiation of operation of the shutter could be controlled to better than 0.005 microsecond.

Photographic Results

The Kerr-cell camera described in preceding paragraphs was used successfully to make complete optical studies during the sudden vaporization of various types of fine wires. These wires were supported in a horizontal position by clamping the ends between phosphor-bronze contactors. Vaporization was accomplished electrically by the controlled discharge of a capacitor. Other miscellaneous electrical discharges have also been studied and it is planned to present the results of these tests in a later paper.

The sequence of operations employed in our optical studies is shown in the block diagram of Figure 10. A passive network was used to obtain adjustable delay. By changing the amount of electrical delay, whole series of photographic records for various types of electric discharges were obtained at intervals as small as 0.025 microsecond after the discharge voltage was applied to the electrodes. One photograph was obtained during each discharge.

Figure 11 is a photograph taken at 0.60 microsecond after the application of voltage to a short length of tungsten wire. The effective exposure time was 0.04 microsecond.

Quite clearly the techniques which were employed are applicable, without much change, to other problems.

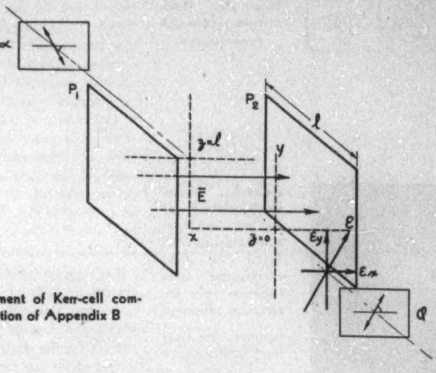

Figure 12. Arrangement of Kerr-cell components using notation of Appendix B

Conclusions

The electro-optical shutter appears to be an excellent instrument for obtaining controlled exposure times of less than 100 microseconds. For photographic studies which require exposure times of less than one microsecond the Kerr cell is almost the only practical solution. Since the inherent time lag in the electrical birefringence of nitrobenzene is of the order of 10^{-9} second, the attainable rapidity of shuttering is limited by the availability of suitable techniques for fast switching of voltage. The ease with which the operation of an "all-electrical" shutter can be synchronized with any phase of phenomena under study, gives these shutters an outstanding advantage over other types.

As an extremely fast photographic shutter, the Kerr cell will be an invaluable research tool in many fields. Among the high-speed self-luminous subjects which it is hoped to study with this device are: many types of electric discharges, the history of arc formation, cathode spot phenomena, the action of fuses, and so on. The instrument will also find applications in the study of certain basic problems in mercury-arc rectification, combustion problems, detonation phenomena, and ballistics. When non-self-luminous objects are to be photographed, the use of a Kerr-cell shutter in conjunction with a synchronous flash lamp makes possible far shorter exposure times than are attainable at present with flash photographic equipment. In addition to these applications, an entire field of "gated optics" optically analogous to radar is opened by use of the electro-optical shutter as a light modulator.

The use of a multiplicity of electro-optical shutters operated in rapid sequence offers a method of obtaining framing rates of many millions per second.

Appendix I

Using equation 1 of the text

$$\frac{n_x-n_y}{\lambda}=KE^2 \tag{8}$$

now

$$n_x=v/v_x$$

and

$$n_y=v/v_y \tag{9}$$

where

v = velocity of light in free space

v_x, v_y = velocity of the components parallel and perpendicular to the applied electric field in the Kerr cell.

Substituting equation 9 in equation 8 we obtain

$$\frac{v}{\lambda}\left(\frac{1}{v_x}-\frac{1}{v_y}\right)=KE^2 \tag{10}$$

Since

$$\nu=v/\lambda=\omega/2\pi$$

Equation 10 becomes

$$\omega\left(\frac{1}{v_x}-\frac{1}{v_y}\right)=2\pi KE^2 \tag{11}$$

Multiplying both sides of equation 11 by the length of the Kerr cell electrodes, l

$$\omega\left(\frac{l}{v_x}-\frac{l}{v_y}\right)=2\pi lKE^2 \tag{12}$$

now let

$t_x=l/v_x$ = time required for the x component of light to traverse the Kerr cell

$t_y=l/v_y$ = time required for the y component of light to traverse the Kerr cell

The difference in transit times may be expressed as an angular phase displacement between the two components of light

$$\omega t_x-\omega t_y=\delta_x-\delta_y=\delta \tag{13}$$

The relative angular displacement δ, is equivalent to a time phase difference between the two components of light which accounts for the alteration in the state of polarization of the total light as it traverses the birefringent medium.

From equation 12

$$\delta=2\pi lKE^2 \tag{14}$$

Appendix II

In Figure 12, P_1 and P_2 are the electrodes in a Kerr cell and $\boldsymbol{E}$ is the electric field applied. The polarizer is oriented at an angle φ with the applied field $\boldsymbol{E}$, and the analyzer is at an angle α as shown. Let $\boldsymbol{e}$ be the plane polarized light vector as it leaves the polarizer. Then using standard vector notation

$$\boldsymbol{e}=\boldsymbol{i}e_x+\boldsymbol{j}e_y \text{ for any } t, z \tag{15}$$

The components of the light vector can be written

$$\begin{aligned} e_x&=[e_0\epsilon^{-j\omega(z/v-t)}]\cos\varphi \text{ real part}\\ e_y&=[e_0\epsilon^{-j\omega(z/v-t)}]\sin\varphi \text{ real part}\end{aligned} \tag{16}$$

where e_0 is the magnitude of the electric vector in the incident light, and v is the velocity of propagation of light in the z direction.

Due to the applied electric field $\boldsymbol{E}$, the components e_x and e_y traverse the Kerr-cell field with velocities v_x and v_y respectively.

Hence

$$\boldsymbol{e}=\boldsymbol{i}e_0\epsilon^{-j\omega(z/v_x-t)}\cos\varphi+\boldsymbol{j}e_0\epsilon^{-j\omega(z/v_y-t)}\times \sin\varphi \text{ real part} \tag{17}$$

Using $v=\lambda\nu$, and taking $z=l$,

$$\begin{aligned} \frac{\omega z}{v_x}&=\frac{2\pi l}{v_x}=\delta_x\\ \frac{\omega z}{v_y}&=\frac{2\pi l}{v_y}=\delta_y\end{aligned} \tag{18}$$

Substituting equations 17 and 18, we get the vector expression for the electric field in the light at the analyzer ($z=l$) at any time t

$$\boldsymbol{e}=\boldsymbol{i}e_0\epsilon^{-j(\delta_x-\omega t)}\cos\varphi+\boldsymbol{j}e_0\epsilon^{-j(\delta_y-\omega t)}\times \sin\varphi \text{ real part} \tag{19}$$

The light which passes through the analyzer, is the component of $\boldsymbol{e}$ in the α direction

$$e_\alpha=\boldsymbol{e}\cdot\alpha_1 \tag{20}$$

where

$$\alpha_1=\boldsymbol{i}\cos\alpha+\boldsymbol{j}\sin\alpha \tag{21}$$

so

$$e_\alpha=e_0\cos\varphi\cos\alpha\epsilon^{-j(\delta_x-\omega t)}+ e_0\sin\varphi\sin\alpha\,\epsilon^{-j((\delta_y-\omega t)} \text{ real part} \tag{22}$$

At any instant, the magnitude of the light vector which passes through the analyzer will be given by the real part of the expression 22.

This equation may also be written in the form

$$e_\alpha = e_1 \epsilon^{-j(\theta - \omega t)} \qquad (23)$$

where e_1 is the maximum amplitude of the harmonically varying light vector $\mathbf{e}_\alpha$.

Since the intensity of the light emerging from the analyzer is proportional to the square of the maximum amplitude of the light vector, we have

$$e_1^2 = |\mathbf{e}_\alpha|^2 = \mathbf{e}_\alpha \mathbf{e}_\alpha^* \qquad (24)$$

where $\mathbf{e}_\alpha^*$ is the complex conjugate of $\mathbf{e}_\alpha$.

$$\mathbf{e}_\alpha^* = e_0 \cos\varphi \cos\alpha \epsilon^{+j(\delta_x - \omega t)} + e_0 \sin\varphi \sin\alpha \epsilon^{+j(\delta_y - \omega t)} \qquad (25)$$

and

$$|\mathbf{e}_\alpha|^2 = e_0^2[\cos^2\varphi \cos^2\alpha + \sin^2\varphi \sin^2\alpha + 2\sin\varphi \sin\alpha \cos\varphi \cos\alpha \cos(\delta_x - \delta_y)] \qquad (26)$$

Now

$$(\delta_x - \delta_y) = \delta$$

as in equation 14, Appendix I, and using the equation

$$\cos\delta = 1 - 2\sin^2 \delta/2$$

we obtain

$$|\mathbf{e}_\alpha|^2 = e_0^2[\cos^2(\varphi - \alpha) - \sin 2\varphi \sin 2\alpha \sin^2\delta/2] \qquad (27)$$

The transmission is defined as the ratio of intensities of emergent and incident light. Thus the percentage transmission is given by

$$T = 100 \frac{|\mathbf{e}_\alpha|^2}{e_0^2} \text{ per cent}$$

So

$${}_\varphi T_\alpha = 100[\cos^2(\varphi - \alpha) - \sin 2\varphi \sin 2\alpha \sin^2\delta/2] \text{ per cent} \qquad (28)$$

Since 50 per cent of the light incident on the first polarizer is rejected by it, we arrive at an expression for the over-all transmission of the Kerr cell unit by dividing equation 28 by two

$${}_\varphi T_\alpha = 50[\cos^2(\varphi - \alpha) - \sin 2\varphi \sin 2\alpha \times \sin^2\delta/2] \text{ per cent} \qquad (29)$$

For

$\varphi = 45$ degrees, $\alpha = -45$ degrees

$${}_{\pi/4}T_{-\pi/4} = 50[\sin^2 \delta/2] \text{ per cent} \qquad (30)$$

Using equation 14, Appendix I

$${}_{\pi/4}T_{-\pi/4} = 50[\sin^2(\pi lKE^2)] \text{ per cent} \qquad (31)$$

If the electric field for full-open operation is E_0 corresponding to an applied potential of V_0, the transmission at any applied potential, v, is

$${}_{\pi/4}T_{-\pi/4} = 50[\sin^2(\pi lKE^2)] \text{ per cent} \qquad (32)$$

$$= 50\left[\sin^2 \frac{\pi}{2}\left(\frac{v}{V_0}\right)^2\right] \text{ per cent}$$

Appendix III

The angular orientation of the "crossed" polarizers in order to allow maximum transmission for the Kerr cell may be obtained from equation 29 of Appendix II. Assuming perfectly "crossed" polarizers $(\varphi - \alpha) = 90$ degrees equation 29 becomes

$${}_\varphi T_\alpha = -50[\sin 2\varphi \sin 2\alpha \sin^2 \delta/2] \qquad (33)$$

$$= -50[\sin 2\varphi \sin 2(\varphi - 90°) \sin^2 \delta/2]$$

$${}_\varphi T_\alpha = 50[\sin^2 2\varphi \sin^2 \delta/2] \qquad (34)$$

$$\frac{\partial_\varphi T_\alpha}{\partial\varphi} = 200 \sin 2\varphi \cos 2\varphi \sin^2 \delta/2$$

To determine the maxima, equation 34 is set equal to zero yielding two solutions

$$\cos 2\varphi = 0$$

$$2\varphi = \pi/2,\ 3\pi/2, \text{ and so forth} \qquad (35)$$

$$\sin 2\varphi = 0$$

$$2\varphi = 0,\ \pi, \text{ and so forth} \qquad (36)$$

The values of φ given by equation 36 result in minimum or zero transmission. For maximum transmission the condition described in equation 35 will apply. Therefore

$\varphi = \pi/4,\ 3\pi/4$, and so forth

are positions of the polarizer for which transmission will be optimum.

The analyzer angle is found from the relation $(\varphi - \alpha) = \pi/2$

A specific example is

$\varphi = 45$ degrees, $\alpha = -45$ degrees

References

1. On a New Relation between Electricity and Light, **J. Kerr.** *Philosophical Magazine*, (London, England) 4th Series, volume 1, 1875, page 337.

2. Disparition instantanee du phenomene de Kerr, **H. Abraham and J. Lemoine.** *Comptes Rendus*, volume 129, 1899, page 206.

3. On Time Lags in Fluorescence and in the Kerr and Faraday Effects, **E. Gaviola.** *Physical Review*, American Physical Society, New York, N. Y., volume 33, 1929, page 1023.

4. On the Early Stages of Electric Sparks, **E. O. Lawrence and Frank G. Dunnington.** *Physical Review*, American Physical Society, New York, N. Y., volume 35, 1930, page 396.

5. The Time Intervals between the Appearance of Spectral Lines in the Spectra of Alkali and Alkaline Earth Metals, **G. L. Locher.** *Journal of the Optical Society of America*, American Institute of Physics, New York, N. Y., volume 17, 1928, page 91.

6. A Measurement of the Velocity of Light, **Wilmer C. Anderson.** *Review of Scientific Instruments*, American Institute of Physics, New York N. Y., volume 8, 1937, page 239.

7. Lehrbuch der Hoch frequenz technick (book), **F. Vilbig.** Edwards Brothers, Ann Arbor, Mich., volume II, 3rd edition, 1946, page 452.

8. A Method of Obtaining Light Flashes of Uniform Intensity and Short Duration, **J. W. Beams.** *Journal of the Optical Society of America*, American Institute of Physics, New York, N. Y., volume 13, 1926, page 597.

9. Electro-optic Observations on Various Liquids, **J. Kerr.** *Philosophical Magazine*, (London, England) 5th Series, volume 8, 1879, page 85.

10. Light Principles and Experiments (book), **G. S. Monk.** McGraw-Hill Co., New York, N. Y., chapter XIII, 1937.

11. Elektronentheorie des Naturlichen Optischen Drehungsvermogens isotroper und anisotroper Flussigkeiten, **M. Born.** *Annalen der Physik*, Leipzig, Germany, volume 55, 1918, page 177–240.

12. Dielektrizitatskonstante und elektrische Doppelbrechung, **R. Gans.** *Annalen der Physik*, Leipzig, Germany, volume 64, 1921, page 481.

13. Handbuch der Radiologie (book), **P. Debeye.** Academische Verlagsgesellschaft, Leipzig, volume 6, 1925.

14. Polar Molecules (book), **P. Debeye.** Dover Publishers, New York, N. Y., 1945, page 83.

15. The Kerr Electrostatic Effect, **E. F. Kingsbury.** *Review of Scientific Instruments*, American Institute of Physics, New York, N. Y., volume 1, 1930, page 22.

16. Polaroid Laboratory Products Bulletin Polaroid Corp., Cambridge, Mass.

17. Untersuchungen uber den Einfluss Verschiedener Substituenten und ihrer Stellung auf den Kerr-Effekt, Teil III, Untersuchungen uber die Frequenzabhagiogkeit der Dielektrizitatskonstante des Nitrobenzols und Beitrage zur Theorie des Kerr-Effekts, **O. Hilke.** *Zeits of Physik*, Berlin, volume 103, 1936, page 350.

18. The Electro-Optical Shutter: Its Theory and Technique, **F. G. Dunnington.** *Physical Review*, American Physical Society, New York, N. Y., volume 38, 1931, page 1506.

19. On Relaxation of Electric Fields in Kerr Cells and Apparent Lags of Kerr Effects, **J. W. Beams and E. O. Lawrence.** *Journal of the Franklin Institute*, (Philadelphia, Pa.) volume 206, page 169.

20. Operating Characteristics of the Electro-optical Shutter, **H. W. Washburn.** *Physical Review*, American Physical Society, New York, N. Y., volume 39, 1932, page 688.

21. Polar Molecules (book), **P. Debeye.** Dover Publishers, New York, N. Y., 1945, page 85.

22. Uber die Abhangigheit einiger Elektischer und Electro-optischer Konstanten von Nitrobenzol und Nitrotoluol von Reinheitsgrade, **F. Hehlgans.** *Physikalische, Zeit Schrift*, Berlin, Germany, volume 30, 1929, page 942.

23. The Technique of Kerr Cells, **Harry J. White.** *Review of Scientific Instruments*, American Institute of Physics, New York, N. Y., volume 6, 1935, page 22.

24. A Review of the Use of Kerr Cells for Measurement of Time Intervals and the Production of Flashes of Light, **J. W. Beams.** *Review of Scientific Instruments*, American Institute of Physics, New York, N. Y., volume I, 1930, page 780.

No Discussion

A Time Division Multiplexing System

W. P. BOOTHROYD
NONMEMBER AIEE

E. M. CREAMER, JR.
NONMEMBER AIEE

Synopsis: The paper describes a new multiplexing system employing time division. The system features pulse amplitude modulation with a filtering arrangement for minimizing the required transmission bandwidth. The distortion and crosstalk requirements for commercial applications are met over transmission paths including radio relay repeaters. A discussion of the channelizing, synchronizing, transmission equipment, and system performance data is included.

ELECTRICAL engineers working in the communications field are concerned with transmission systems for carrying messages over long distances with maximum fidelity. Usually such systems have terminal equipment for multiplexing many narrow band channels into a single wider band channel before transmission is started. Terminal equipments usually are divided into two groups according to their method of multiplexing. The frequency division group has been used widely,[1,2] and there have been many recent developments in the time division groups.[3,4] However, the time division systems previously described have required a transmission bandwidth many times greater than the bandwidth of the original total intelligence. Because of this, time division terminal equipments heretofore have been applicable only to radio relay systems employing pulse modulation. The terminal equipment described in this paper utilizes time division multiplexing but is characterized by requiring a transmission bandwidth approximating that of the original total intelligence. This low transmission bandwidth requirement makes the terminal equipment adaptable for use with either amplitude or frequency modulated transmission systems. The techniques to be described are applicable to amplitude modulated pulse multiplexing systems. The system described uses linear amplitude modulation but pulse-code modulation systems may be considered as a particular example to which these same techniques also may be applied.

As the art of radio relaying at microwave frequencies has advanced, the engineering problems inherent in the art have been defined more clearly. The direction of one solution to these problems is the use of a low bandwidth time division terminal equipment in association with a relay system using a frequency modulated carrier. If the required transmission bandwidth is sufficiently low the relay system may use either subcarrier modulation[5] or direct modulation with heterodyne remodulation.[6] With these transmission problems in mind the specific requirements for a multiplex terminal equipment which would function most effectively with a radio relay or coaxial cable transmission system were given attention. Out of this work has come the multiplexing system to be described.

General Description

The equipment is a time division system. The usual sending terminal has multiple band inputs, timing generator, sampling gates, and the combining stages from which the sending terminal output is derived. Amplitude modulated signals are handled throughout this equipment. Figure 1 is a block diagram of the sending terminal.

A carrier oscillator with a 60-kc sinusoidal output is used to trigger an 8-kc pulse generator. This is accomplished by frequency doubling and counting circuits together with gate circuits to insure uniform timing intervals. The pulse generator is arranged to have a generally triangular pulse output. The delay line distributor is a lumped constant transmission line or low pass filter made up of "M" derived sections such that its total time delay is 125 microseconds equally divided into 30 intervals of 4.16 microseconds. This line has a characteristic impedance of 2,500 ohms and a bandwidth of approximately 300 kc. The pulse generator output is applied to the line and the combination provides a traveling delay line signal which may be used to successively gate 30 band modulators at an 8-kc rate. The band modulators may have a voice band signal, or other signal with a frequency range of 60 to 3,300 cycles, applied to their inputs. The output of any individual modulator will be a pulse signal similar in shape to the delay line pulse signal but modulated in amplitude in accordance with the input signal amplitude at the time of application of the delay line signal. The time-spaced outputs of all of the modulators are combined into a pulse train, as shown at output terminal A. In order properly to index the receiver, one band modulator is modified to have two input terminals. One input is normally a 3,900-cycle indexing tone supplied from a suitable oscillator and the other input may be a voice band or order-band input having a frequency range of 60 to 2,500 cycles.

In conventional pulse amplitude modulation systems, output at A would be recognized as the normal sending-terminal output signal. It could be applied to any transmission medium having suitable passband characteristics. In the case of a microwave radio relay system, the signal could be used to frequency modulate the carrier or subcarrier of the radio relay. The output signal of the transmission medium should be a replica of the input signal ready for application to the receiving-terminal equipment.

The receiving-terminal equipment also follows the general pattern of similar time division systems. If the signal from output terminal A is applied to the receiving-terminal input it is necessary that we first

---

Paper 49-25, recommended by the AIEE communication committee and approved by the AIEE technical program committee for presentation at the AIEE winter general meeting, New York, N. Y., January 31–February 4, 1949. Manuscript submitted November 3, 1948; made available for printing December 29, 1948.

W. P. BOOTHROYD is a project engineer and E. M. CREAMER, JR. is senior engineer in the research division of the Philco Corporation, Philadelphia, Pa.

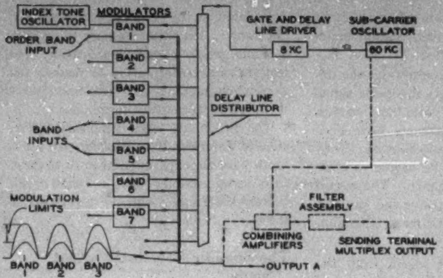
INDEX TONE OSCILLATOR
MODULATORS
ORDER BAND INPUT
BAND 1
BAND 2
BAND 3
BAND 4
BAND 5
BAND 6
BAND 7
BAND INPUTS
MODULATION LIMITS
BAND 1
BAND 2
BAND 3
GATE AND DELAY LINE DRIVER
SUB-CARRIER OSCILLATOR
8 KC
80 KC
DELAY LINE DISTRIBUTOR
FILTER ASSEMBLY
COMBINING AMPLIFIERS
SENDING TERMINAL MULTIPLEX OUTPUT
OUTPUT A

Figure 1 (left). Sending terminal

Figure 3 (right). Modulator schematic diagram

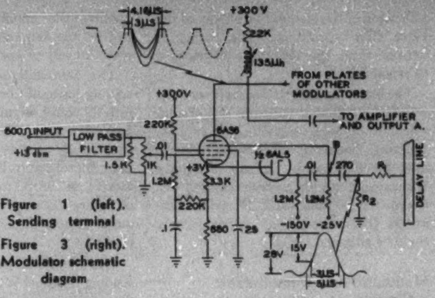
4.16µS
3µS
+300V
22K
135µh
FROM PLATES OF OTHER MODULATORS
+300V
TO AMPLIFIER AND OUTPUT A.
220K
6AS6
600Ω INPUT
+13 dbm
LOW PASS FILTER
.01
1.5K
1K
1.2M
+3V
3.3K
220K
½ 6AL5
.01
270
R1
B
R2
DELAY LINE
1.2M
1.2M
-150V
-25V
.1
680
25
28V
15V
3µS
5µS

produce and maintain proper registration or indexing of the voice bands, and second, demodulate the voice bands. Indexing and synchronizing are accomplished as two separate steps. The indexing problem is solved by the modulation of one of the bands by a tone slightly above the normal voice band passband such that the particular band is characterized by an unusual constant-tone modulation. The receiving terminal then is equipped with a single band having a means for recognizing this tone and indexing thereon. Until indexing is accomplished, the synchronizing circuits are disabled and the receiving-terminal timing generator repetition rate is made slightly different than the sending-terminal timing generator repetition rate so that slippage occurs between the received band pulses and the receiving-terminal gating pulses. When the proper channels are in register, the slip circuits are disabled and the receiver-terminal timing generator then is driven by the synchronizing circuits operating on the received signal. Synchronizing is accomplished by the transmission of band repetition rate frequency components in the sending-terminal signal. The signal energy of this frequency, called the carrier, is separated from the composite signal and, after amplification, may be used to control the timing generator in the receiving terminal. In order to index the receiving terminal, a slip-frequency oscillator is used as shown in Figure 2. The oscillator is crystal controlled to a frequency approximately 30 cycles higher or lower than the 240-kc carrier frequency of the sending terminal. During the indexing period, this slip frequency signal is applied to counter circuits and the timing generator to produce a delay line pulse as in the sending terminal, except that the repetition rate of this pulse is slightly slower or faster than the sending terminal pulse rate. Accordingly, there is a gradual drift of the receiver input signal with respect to the delay line keying signal. During each cycle of the slip frequency, a time of one-thirtieth of a second in this case, the bands drift into proper registration. During this brief interval of proper registration, the input signal is applied to the band separators as will be described. The presence of the indexing signal in its assigned band indicates proper register of the band pulses and the receiving-terminal separators, and this signal energy may be used therefore to operate a changeover circuit. This circuit, during the indexing interval, has connected the slip frequency oscillator to the timing generator. Once the bands have been indexed, the circuit discards the slip frequency oscillator and connects the derived sending-terminal carrier signal to the timing generator, thus locking the receiving-terminal gating rate to the sending-terminal sampling rate.

Proper indexing is insured by the deliberate modulation of one voice band with a tone which is higher in frequency (3,900 cycles) than the signals permitted in any other voice band, and by the provision in the corresponding voice band at the receiving terminal of a sharp bandpass filter responsive to this tone.

This indexing circuit has been given rigorous tests and has been found to index in less than one-thirtieth of a second following a signal interruption and to hold the receiving terminal in proper register with received signal-to-noise ratios as low as 0 decibel.

Voice-band demodulation is obtained by the progressive gating of pulse separators with subsequent filtering and am-

Figure 2. Receiving terminal

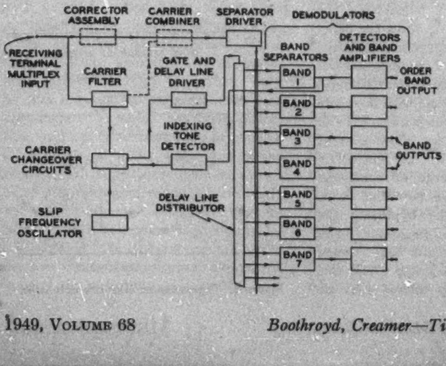
CORRECTOR ASSEMBLY
CARRIER COMBINER
SEPARATOR DRIVER
DEMODULATORS
RECEIVING TERMINAL MULTIPLEX INPUT
CARRIER FILTER
GATE AND DELAY LINE DRIVER
BAND SEPARATORS
DETECTORS AND BAND AMPLIFIERS
BAND 1
BAND 2
BAND 3
BAND 4
BAND 5
BAND 6
BAND 7
ORDER BAND OUTPUT
BAND OUTPUTS
INDEXING TONE DETECTOR
CARRIER CHANGEOVER CIRCUITS
DELAY LINE DISTRIBUTOR
SLIP FREQUENCY OSCILLATOR

Figure 4. Demodulator schematic diagram

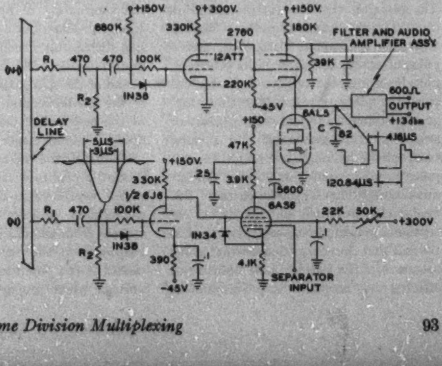
+150V
+300V
+150V
680K
330K
2700
180K
FILTER AND AUDIO AMPLIFIER ASSY
(+)
R1
470
470
100K
12AT7
39K
IN38
220K
600Ω
OUTPUT
+13dbm
R2
-45V
+150
6AL5
C
82
DELAY LINE
47K
4.16µS
5µS
3µS
+150V
.25
3.9K
120.84µS
330K
1/2 6J6
5600
6AS6
(-)
R1
470
100K
22K
50K
+300V
IN38
IN34
R2
390
.1
4.1K
SEPARATOR INPUT
-45V

plification of the modulation energy of the band pulse spectrum. The gating is derived from the delay-line distributor as explained.

The foregoing general description of the terminal equipment indicates one system whereby the basic functions of band multiplexing, indexing, and synchronizing may be performed. If an adequate transmission system were interposed between the sending and receiving terminals the desired band output signals could be obtained.

Modulator and Demodulator Circuits

Several specific circuits within the system described are worthy of more detailed description. The sending-terminal modulator and receiving-terminal demodulator are very important since, to a major extent, they determine the distortion and crosstalk levels within the system.

The modulator schematic for a single band is shown in Figure 3. The principal tube is a miniature pentode type *6AS6*. The triode section is operated class A with a prescribed amount of cathode degeneration. Voice band input at a rated level of +13 decibels (referred to one milliwatt in 600 ohms) is coupled to the control grid, g_1. The delay line pulse, obtained at the successive taps, is scaled by resistors R_1 and R_2 to the values shown and applied to the suppressor grid, g_3. This grid is normally so biased as to cut off the plate current except during the suppressor gating interval. In view of the relatively large cathode voltage swing (approximately four volts peak-to-peak) the suppressor is a-c coupled to the cathode so that the audio signal appears at *B*. R_1 and R_2 are relatively high value resistors to permit this. When the delay line pulse is applied, the high back resistance of the *6AL5* diode prevents loading of the circuit by the low cathode circuit impedance. The plate of the tube is connected in parallel with a group of plates of similar stages to a common plate load, and a pulse of approximately 2-volts peak amplitude, modulated ±0.7 volt, is derived from the plate circuit. The time-staggered outputs of this and other modulator stages are thus combined into a pulse train which is coupled through an amplifier or other combining stage to the terminal output *A*. A specific virtue of this modulator circuit, in addition to its exceptional amplitude linearity, is found in the fact that the energy distribution in the spectrum of the output pulse train is not affected by modulation. This makes possible the application of circuits to restrict the required transmission bandwidth as will be described.

The demodulator circuits in the receiving terminal convert this pulse signal into its many original voice band signals. Several circuit arrangements have been successfully used as demodulators. They vary considerably in the degree of complexity and in performance. The circuit of Figure 4 is representative and has adequate performance with reasonable simplicity.

The amplified pulse signal from the sending terminal is applied to the grid of the *6AS6* pentode, the cathode, grid, and screen of which are operated class A. The gating signal obtained from the timing generator through the delay line distributor cuts off the *6J6* triode unit and allows its plate and the *6AS6* suppressor, which have been residing at a negative voltage greater than suppressor cutoff, to rise. The suppressor rise is arrested by conduction of the crystal diode, thus holding the supressor at cathode potential. Since the latter moves with the control grid signal, the gating pulse is therefore superimposed on the modulation present on the band pulse and distortion due to curvature of the suppressor characteristic is eliminated. The plate current pulse is a true reproduction of the incoming signal during the interval allocated to that one band. If the plate circuit has sufficient bandwidth, then the charge drained from the storage capacitor *C*, via one half of the *6AL5* diode and the coupling capacitor will be proportional to the peak current in the tube. This charge is then trapped on the capacitor, since the diode cuts off as the plate swings positive with the signal, and all other leaks are purposely made high. The charge conditions on the coupling capacitor are restored by the other half of the *6AL5*.

The charge and hence the voltage across capacitor *C* remains substantially unchanged for a time interval of 120.8 microseconds. A new pulse from the timing generator coming down the delay line distributor encounters the discharge double triode *12AT7* 4.16 microseconds ahead of the *6J6* gating triode. The grid of the second section rises with the plate of the first as the latter is cut off; in so doing it passes cutoff and allows current to flow into the capacitor *C*. The *6AL5* diodes prevent a charge accumulation which would raise the potential on *C* appreciably positive by bypassing the current from the *12AT7* to ground. The output from the separator and storage circuit is the potential across *C* and this voltage when properly filtered may be considered as the demodulated output of the band. It is only necessary to provide suitable voice band amplification and impedance transformation to restore the original character of the voice band input to the multiplex output terminals.

The modulator and demodulator circuits as described have proved very satisfactory for the experimental work to date. Of course, simpler circuits with even better performance will be developed as the work progresses.

The Sending Terminal Output Signal

When one has terminal equipment of the type just described, or its equal, the problem of a transmission medium becomes most important. In our considerations we have been restricted primarily to the use of microwave radio relay systems and our study has concentrated on the known faults of such systems. Since

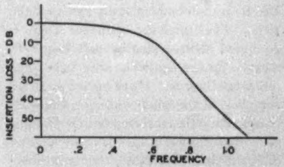

A. AMPLITUDE FREQUENCY RESPONSE

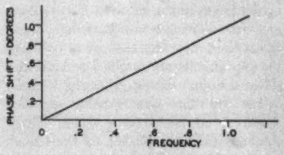

B. PHASE FREQUENCY RESPONSE

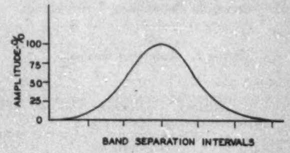

C. TRANSIENT RESPONSE

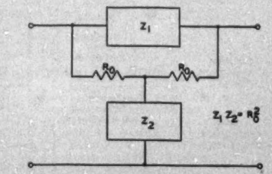

D BASIC FILTER CIRCUIT

Figure 5. Transmission filter characteristics

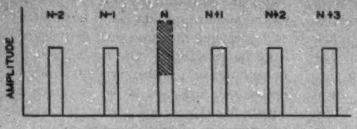

A. IDEALIZED BAND PULSES BEFORE FILTERING

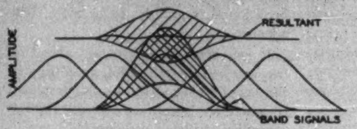

B. RESULTANT OF FILTERING BAND SIGNALS

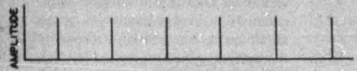

C. DETECTOR GATING INTERVALS

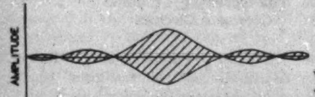

D. OUTPUT OF CORRECTOR

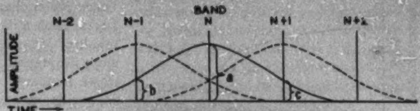

A. REPLICA OF BAND SIGNAL VOLTAGE IN CORRECTOR NETWORK AT TIME INTERVALS EQUAL TO BAND INTERVAL

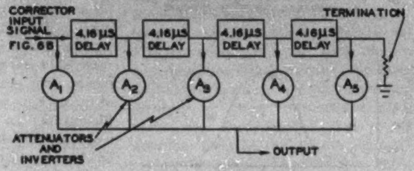

B. BLOCK DIAGRAM OF CORRECTOR

Figure 6 (left). Corrector operation

Figure 7 (above). Corrector characteristics

all types of radio relays cannot be considered in this brief paper; we shall consider the relay system which appears to be superior. Such a relay uses frequency modulation of the carrier and either a heterodyne type repeater, as has been previously described, or a locked oscillator type of repeater which will be described in a forthcoming paper. With a wide-band relay of this type it is possible easily to maintain good signal-to-noise ratios at reasonable modulation bandwidths but on account of the wide carrier frequency deviations used, the amplitude linearity of the system is not exceptional unless elaborate precautions are taken. These two primary factors, along with minor features, indicated that a time division multiplex system would match such a relay system best. With time division, only the signal of one channel is ordinarily present at any instant, hence the amplitude linearity and signal-to-noise ratio of the relay system need only be that required by the requirements of any single voice band. Harmonic distortion does not cause beat notes or noise in other bands. Further, distortions of the relay output signal due to multipath or other propagation or transmission defects will not be observed except as for their effect on each voice band individually.

Observing the advantages of time division multiplexing from the point of view of the radio relay requirements, we were disturbed by its one largest disadvantage; namely, that a modulated pulse train such as indicated at output terminal A of Figure 1 obviously required a bandwidth far in excess of the bandwidth of the intelligence being transmitted. In fact, for 30 voice bands representing approximately 100 kc of intelligence (neglecting guardbands) a low-pass bandwidth of approximately one megacycle would be required to satisfactorily resolve the sending-terminal output pulse train. Work on this phase of the project has progressed successfully and a technique has been developed whereby the required transmission bandwidth is comparable to the total input intelligence bandwidth by virtue of a coding arrangement using amplitude division. That is, the signal amplitude is shared among a few channels in a fixed proportion determined by the sending terminal equipment.

The apparatus for minimizing the required bandwidth is shown as the filter assembly on the output of Figure 1 and the corrector assembly at the input of Figure 2.

The filter assembly of Figure 1 performs the function of limiting the high frequency end of the spectrum of the signal from the sending terminal; thus the transmission equipment is called upon to handle a narrower band of frequencies than would be required otherwise. That this filtering function can be performed without distorting the modulation information in each voice band is evident from the Fourier analysis of the pulse train. Assuming a pulse train subject only to pure amplitude modulation (with no distortion of the pulse shape), this analysis shows the spectrum of the pulse train to be a fundamental frequency, corresponding to the basic sampling rate (8 kc) and its harmonics, each having an upper and a lower sideband produced by modulation. Thus modulation of one band will produce a spectrum of energy including the original modulation spectrum plus the band sampling rate and its harmonics, each of the latter having an upper and lower sideband. To discard some of the high frequency energy of this composite spectrum without distortion of the modulation information, it is required that the distribution of energy among the sampling frequency and its harmonics be a constant when the pulse train is modulated. This can be accomplished only with a modulator which is free of all modulations (width, shape, and so forth) other than amplitude. The modulator of Figure 3 is such a modulator, and no measurable increase in distortion occurs whether the sending terminal output is unfiltered or filtered.

If the foregoing requirements are met, the result of proper low pass filtering may be summed up as a failure to define the original pulse train. Therefore, a single band pulse is widened so as to overlap one or more adjacent band pulse intervals. The degree of this effect depends on how severely the bandwidth is curtailed and upon the transient response of the filter. This broadening of the pulse width by filtering, and its consequent overlap in time with the signal pulse of another band, results in a sharing of the total signal voltage from the sending terminal among a number of channels, and in the need for a compensating unit at the receiving terminal.

The extent of the basic pulse broadening is calculable from a statement of the

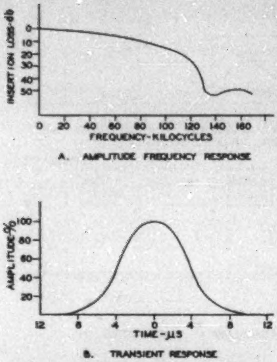

Figure 8. Typical filter characteristics

transient response of the filter. A filter with a symmetrical transient response approximating an error function shape $(f_t = e^{-a^2t^2})$ has been used for most applications. The typical responses of one such filter are shown in Figure 5*A* and 5*B* along with a calculated output pulse spread showing, in Figure 5*C*, corresponding interference in adjacent channels. In other applications a filter having a nonsymmetrical transient response possesses some advantage. Once a set of characteristics have been settled upon, the construction of the filter may be undertaken. It must be understood that since we are dealing with pulses, we are most interested in the transient response of the filter and not in its amplitude or phase response alone.

One actual filter unit used to accomplish this reduction in bandwidth is a low pass network of the constant resistance bridged-*T* variety,[7] successive sections of the composite network not necessarily being identical. A statement of the general characteristics which such a network ought to possess may clarify the design problem. Having specified a cutoff frequency at which the output shall be more than 40 decibels below the input, the variation of the transmission characteristics of the network for frequencies up to this limit are of concern. Certain responses are more desirable than others inasmuch as they make the compensation problem at the receiving terminal less complicated. A filter network whose characteristic transient is symmetrical and whose damping factor is just sufficient to prevent overshoots will provide, in general, a minimum of interference with adjacent bands.[8] The transmission characteristics of a network having such a characteristic are that the amplitude frequency response is a gradual slope throughout the pass band, while the phase frequency response is zero at zero frequency and increases linearly until after amplitude cutoff is reached. These responses are indicated in Figure 5*A* and 5*B* and serve to define network performance. The filter network chosen approaches these ideals quite closely with reasonably few parts and critical adjustments. The general form of one section of the network is shown schematically in Figure 5*D*. In cases where a nonsymmetrical transient response is desired, it has been found most expedient to obtain such responses by adding to the filter a required pattern of phase-equalizing circuits which are used to obtain the desired response without modifying the filter amplitude response.

In summary, the sending-terminal output is a pulse train which has been so filtered as to narrow the frequency spectrum of the signal energy while permitting a division of the instantaneous amplitude of the output signal among adjacent channels. Of course, from the filter characteristics, the amount of signal energy due to each channel is known, and, at the receiver, use is made of this information.

During field testing of this system of multiplexing using radio relays as the transmission medium, it was verified that, if desired, a relay system with a poor transient response might be used with this pulse system by accounting for the change in pulse shape introduced by the relay when making the initial receiving-terminal setup adjustments. This is of great importance in any practical radio relay network.

In preceding paragraphs it was noted that synchronization of the receiving terminal was obtained by the recovery of the carrier frequency. When a filter of the foregoing type is used it will be recognized that the normal carrier frequency, which is the 240-kc signal, is fully attenuated. The requirement for a carrier frequency signal at the receiving terminal is met therefore by the addition to the filtered output pulse train of a subcarrier which is at a frequency within the filter transmission band. There are two groups of choices for this subcarrier frequency: it may be a harmonic of the band sampling rate, or it may be midway between such harmonics. In the first, the receiving terminal input signal will show different voltage levels for successive signal bands but will not produce any undesired modulation signals. In the latter, each voice band will be modulated at a 4-kc rate due to the nonintegral relation of a subcarrier and sampling rate but such 4-kc signals may be rejected by the modulation recovery device. Either system is usable and a subcarrier at 60 kc is shown in Figure 1. The amplitude of the added subcarrier is controllable and a level of less than 10 per cent of the peak signal has been found in practice to be more than adequate.

It now remains to add the subcarrier frequency to the output of the filter and the signal output of the sending terminal is complete. Derived from the crystal controlled oscillator as shown in Figure 1, the subcarrier frequency is run through a band-pass filter of conventional design to eliminate undesired harmonics, phased to an advantageous position with respect to the composite output, and added thereto.

The Receiving Terminal Corrector Circuits

It is one of the design aims of the receiving-terminal common-band equipment to remove the mutual interference between channels, which interference was controllably introduced in the sending terminal, as completely as possible. At the same time, the equipment to accomplish this should remain simple, easy to adjust, and stable with time. The operation of the compensation system employed is based upon knowledge of the relative amplitude of the output of the sending terminal at time intervals corresponding to adjacent bands on either side of the interfering band, in terms of the output of the interfering band. In other words, for any band combination in which mutual interference results it always is known that the interference of one band on another is a fixed per cent of the peak of the interfering signal amplitude, the percentages of interference being specified by the filter transient response.

Figure 6 shows in some detail the results of filtering a typical multiband amplitude-modulation pulse train by a symmetrical transient filter. Figure 6*A* is an idealized section of the pulse train from the sending-terminal multiplex before filtering, with six of the band pulses present in the portion shown. If a band circuit is modulated, the modulation may vary the pulse amplitude between the limits shown crosshatched, and the crosstalk in adjacent bands will be known from the filter characteristics. As an example, the filter characteristics have been chosen to give adjacent-channel crosstalk only. Figure 6*B*, therefore, shows the component contributions of each band and the resultant output at the filter output terminals. In order to make clear the fact that the receiving-terminal channel detectors respond only to the peak of the modulation spread produced by the filtering action, it is emphasized that gated peak detectors are used, timed by the carrier transmitted with the multiplex signal. Interference of band N with bands $N-1$ and $N+1$ is readily visible. Figure 6*C* shows the effective gating function which the receiving terminal detectors exhibit. At the times labeled $N-1$ and $N+1$, corresponding to the opening of the band circuit separators, it is apparent that some signal from band N will be present also. It is the purpose of this discussion to show how this interference may be eliminated. The interference, however, will be corrected to zero only at the indicated gating instants. Basically, the corrector operates to cause the signal of any band to be zero at all times spaced by the band interval from the peak of the band modulation; that is, interference will be zero at the gating intervals of all other bands. Figure 6*D* illustrates a typical corrector output for the input signal of Figure 6*B*. It will be observed that the resultant signal amplitude is zero at the gating time of all bands other than the originally modulated band. Thus band interference has been eliminated. The block diagram for a corrector network which might be used to eliminate the interference shown by Figure 6*B* is shown in Figure 7*B*. It may consist of a series of delay networks driven from one end, with each delay unit having a time delay equal to the band interval. From the junctions of these networks, signals are fed through unilateral attenuators and polarity inverters, as required. They then are added to produce an output voltage which is used to energize the band separators. Proper adjustment of the attenuators permits the use of the signal of any band to cancel its own interference with all other bands. The operation may be visualized as follows: As the signal of any band passes through the delay network, the total output of the network is equal to the amplitude of the signal at that time, as shown in Figure 7*A*, multiplied by the corresponding attenuator gain. These outputs are shown in Table I for successive band gating intervals. By equating the outputs to zero at the adjacent band intervals the settings for the attentuators are calculable. Attenuator settings are also readily found experimentally when the equipment is initially adjusted. For correction of interference to absolute zero at all times, an infinite number of delay networks and attenuators would be required. However, the cancellation process can be made to converge rapidly for many useful transient responses such that, in practice, for as much as 30 per cent interference in adjacent channels, only six networks are required to reduce the crosstalk in all bands to negligible values. As an illustration, Table I indicates a residual output at channel $(N+3)$ and $(N-3)$ gating times. This ordinarily will be a negligible value, but it may be reduced as far as desired by the addition of more corrector networks.

The final practical limit to which this bandwidth reduction system can be extended has not yet been determined. A second paper to be published in the near future will treat the various criteria for satisfactory operation. To date, however, the 30-channel 240-kc pulse train system described has been operated successfully through a filter system having the amplitude characteristic of Figure 8*A* and a transient response of Figure 8*B* with a 10-section corrector reducing all crosstalk to 45 decibels below the output signal level. If the frequency scale of Figure 8*A* is multiplied by a factor of 1.15, a 6-section corrector will reduce the crosstalk level to 60 decibels below the output signal level.

Conclusions

It has been interesting to study the transmission characteristics of the sending-terminal filter assembly and the receiving-terminal corrector assembly when connected in series, and to consider their effect as a transmission medium on the signal to noise ratio of the signal. These calculations and equipment tests verify the conclusion that the bandwidth of a transmission system for use with the filter described by Figure 8*A* need not exceed 120 kc. Since the corrector adjustments have been found in practice to be stable and easy to adjust, the use of the techniques described makes possible the transmission of time-division multiplexed signals over a low bandwidth cable or over a radio relay system employing frequency modulation of the carrier. The high modulation index now possible with frequency modulation transmission systems results in favorable output signal-to-noise ratios.

From these characteristics it will be clear that no signal energy at frequencies above approximately 120 kc is required for the transmission of the complete signal. This compares favorably with the requirements for single-sideband amplitude modulation transmission, yet retains the features of pulse transmission. Of course, since the system is a pulse system, attention must be paid to the phase response throughout the entire pass band. It also will be understood that a low pass filter ordinarily is used ahead of the receiving-terminal input to eliminate any high-frequency noise which may have been added to the signal by the transmission system. This filter need be only slightly wider than the filter at the sending terminal, in order for its effect on the system transient response to be negligible. The amount of transmission loss inserted at frequencies above 120 kc makes no difference in the system operation. During field tests in June, 1948, the cooperation of the Western Union Telegraph Company in making available its radio relay circuits and its multiplexed telegraph voice band load signals, made possible a comprehensive testing program. From these tests the principles of operation were confirmed and new designs accommodating a greater number of voice bands are now in progress.

Table I. Output Voltage

Time	Output
N	$bA_2+aA_3+cA_4$ = desired signal
$N-1$	$bA_1+aA_2+cA_3=0$
$N+1$	$bA_3+aA_4+cA_5=0$
$N-2$	aA_1+cA_2 $=0$
$N+2$	bA_4+aA_5 $=0$
$N-3$	cA_1 = residual interference
$N+3$	bA_5 = residual interference
$N-4$	0
$N+4$	0

References

1. Frequency Division Techniques for a Coaxial Cable Network, R. E. Crane, J. T. Dixon, G. H. Huber. AIEE Transactions, volume 66, 1947, pages 1451–9.

2. A 150-Kilocycle Carrier System for Radio Relay Applications, J. E. Boughtwood. AIEE Transactions, volume 67, part I, 1948, pages 577–82.

3. Pulse Time Modulation, E. M. Deloraine, E. Labin. *Electrical Communication*, New York, N. Y., volume 22, 1944.

4. Pulse Code Modulation, H. S. Black, J. O. Edson. AIEE Transactions, volume 66, 1947, pages 895–9.

5. Preview of Western Union System of Radio Beam Telegraphy, J. Z. Millar. *Journal*, Franklin Institute, Philadelphia, Pa., volume 242, 1946, pages 23–46.

6. The Application of Heterodyne Modulation to Wide Band Frequency Modulated Television Relays, W. P. Boothroyd. AIEE Transactions, volume 66, 1947, pages 1126–30.

7. Radio Engineers Handbook (book), F. E. Terman. McGraw-Hill Book Company, Inc., New York, N. Y., 1943, Equalizers—pages 244–46.

8. Phase and Amplitude Distortion in Linear Networks, M. J. DiToro. *Proceedings*, Institute of Radio Engineers, New York, N. Y., volume 36, number 1, 1948, pages 28–31.

No Discussion

The Distinction Between Effective and Circuit Bandwidths

WILLIAM J. KESSLER
NONMEMBER AIEE

IN recent years, the term bandwidth has appeared so frequently that it appears desirable to discuss briefly the two major interpretations associated with this term. It is the primary purpose of this paper to cast into sharp relief the significant differences between the meaning of circuit bandwidth, which is employed to specify the frequency discriminating properties of networks; and the effective bandwidth, employed to specify the noise transmission properties of passive networks.

Despite the fact that electrical networks may display the same maximum sensitivity and the same selectivity, according to the standard definition, they will nevertheless display different sensitivities to noise. It is evident, therefore, that the results of noise measurements are meaningless unless accompanied by more adequate frequency response data of the measuring instruments reduced to a common basis. The concept of effective bandwidth, suitably defined, satisfies this requirement. The term "circuit bandwidth" is then reserved to specify the selectivity or frequency discriminating properties of any given network.

Figure 1. Squared response curve of physical network

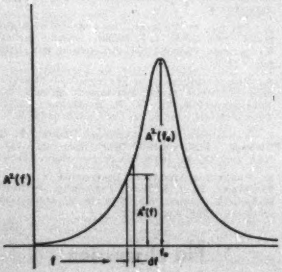

Definitions

Circuit bandwidth, usually represented by Δf, may be defined as the difference between the two frequencies at which the response is below the maximum a specified degree. When the specified attenuation is three decibels, these two frequencies are often referred to as the "half power" points. The definition for effective bandwidth B, however, is slightly more complex, since it is a measure of the network response to noise or other transient phenomena whose components are distributed throughout the frequency spectrum. For this reason, effective bandwidth is often referred to as the "noise" bandwidth. The effective bandwidth of any network of maximum response $A(f_o)$ is, therefore, defined as being numerically equal to the bandwidth of an equivalent network whose response is $A(f_o)$ throughout its entire transmission band, provided the noise powers developed across the output terminals of the two networks are equal for the same noise signal input.

Actually, the determination of the effective bandwidth of a network reduces to the problem of finding an equivalent rectangular response curve for the physical network. It is recognized readily that for the rectangular response curve there is little question as to the interpretation of bandwidth regardless of how arbitrary the definition might be in terms of relative response.

Theoretical Considerations

Response curves are, in general, graphical representations of voltage ratios as a function of frequency, which are in turn proportional to the square root of the power ratios. Since the average time rate of change of electric energy across the output terminals is proportional to the square of the voltage, Figure 1, it is possible to write the following differential equation

$$dP=\phi(f)A\ (f)df \tag{1}$$

where dP is the noise power contribution at each frequency and $\phi(f)$ is the energy-frequency distribution of the noise under consideration. Applying equation 1 to the physical and equivalent "rectangular" network exemplified in Figures 1 and 2, integrating over appropriate limits and under the conditions of the definition equating the two expressions, yields

$$\int_{f_o-B/2}^{f_o+B/2}\phi(f)A^2(f_o)df=\int_0^\infty \phi(f)A^2(f)df \tag{2}$$

Inspection of equation 2 discloses that further analytical progress is impossible unless the distribution of the noise is specified. Assuming the simplest possible

Figure 2. Squared response curve of equivalent network

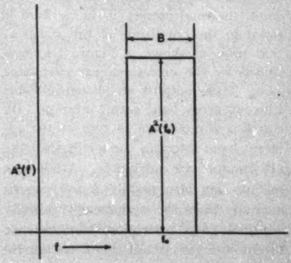

Paper 49-26, recommended by the AIEE communication committee and approved by the AIEE technical program committee for presentation at the AIEE winter general meeting, New York, N. Y., January 31–February 4, 1949. Manuscript submitted June 30, 1948; made available for printing January 4, 1949.

WILLIAM J. KESSLER is with the engineering and industrial experiment station, University of Florida, Gainesville, Fla.

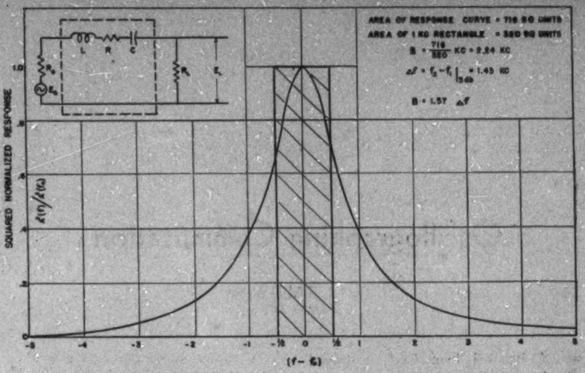

Figure 3. Squared response curve of physical network and 1-kc reference rectangle

distribution, one that is uniform and continuous such as "White" noise and approximated closely by random noise, equation 2 reduces to

$$KA^2(f_o)B = K\int_0^\infty A^2(f)df \tag{3}$$

where K is the constant form of $\phi(f)$ and evidently divides out. Thus the effective bandwidth B becomes

$$B = \frac{\int_0^\infty A^2(f)df}{A^2(f_o)} \tag{4}$$

Equation 4 shows that the effective bandwidth for any network is equal simply to the area under the squared response curve divided by the square of the maximum response.

Determination of Effective Bandwidth

The area under the squared response curve plotted on linear co-ordinate paper, and hence the effective bandwidth, may be determined by any convenient graphical or mechanical method. To obviate the necessity for converting the results of the mechanical integration into the dimensions indicated by equation 4, it is convenient to transform this expression for effective bandwidth into a simple ratio of areas multiplied by some arbitrary unit of bandwidth. Multiplying both the numerator and denominator of equation 4 by 1 kc, equation 5 becomes

$$B = \frac{\text{Total area under squared response curve}}{\text{Area of 1-kc rectangle}}\text{kc} \tag{5}$$

Thus the effective bandwidth may be restated as being numerically equal in kilocycles to the ratio of total area under the squared response curve to the area of a rectangle 1-kc wide whose ordinate is $A^2(f_o)$. Further simplification may be introduced by plotting the ordinates as squared response ratios $A^2(f)/A^2(f_o)$ rather than actual squared response, and the abscissa as the deviations from resonance $(f-f_o)$ in kilocycles rather than the actual frequency.

Conclusion

The concept of effective bandwidth, insofar as noise measurements are concerned, is most significant when dealing with networks characterized by gradually changing frequency response functions. For a single elementary inductive-capacitive resonant network, the effective bandwidth in cycles per second may be determined analytically and is found to be equal to $R(f_o)/4L$, where $R(f_o)$ is the total series resistance at resonance, and L the total inductance. The circuit bandwidth, however, is equal to $R(f_o)/2\pi L$, provided the network exhibits a value of Q of about ten or greater. It is evident, therefore, that for such elementary networks the ratio of the effective bandwidth to the circuit bandwidth is equal to $\pi/2$, or 1.57 as shown in Figure 3. This ratio approaches 1.07 as the number of such isolated elementary stages arranged in cascade increases,[1] and approaches unity as the over-all response curve approaches the rectangular form shown in Figure 2.

The noise power developed across the output terminals of a network is a linear function of the effective bandwidth only when dealing with noise phenomena uniformly distributed throughout the frequency spectrum such as random noise which is due usually to the spontaneous motion of free charge in electric conductors. Noise phenomena of other distributions expressed in terms of average, effective, or quasi-peak voltage may be treated approximately by revising the exponent associated with the expression for effective bandwidth.[2] The magnitude of the new exponent will depend on the nature of the noise that is, its frequency distribution, and the mode of measurement.

References

1. Survey of Existing Information and Data on Atmospheric Noise Level Over the Frequency Range 1–30 MC–S, **H. A. Thomas, R. E. Burgess.** National Physical Laboratory, (Washington, D.C.) February 21, 1944, pages 58–9.

2. An Experimental Investigation of the Characteristics of Certain Types of Noise, **Karl G. Jansky.** *Proceedings*, Institute of Radio Engineers (New York, N. Y.), volume 27, December 1939, pages 763–68.

No Discussion

Oscillographing Commutation

M. J. BALDWIN
MEMBER AIEE

TEXTBOOKS long have contained theoretical explanations of commutation, but the necessary tools have been lacking with which to obtain actual pictures indicating instantaneous values of current and voltage in coils undergoing this transition. The cathode-ray oscilloscope is the fundamental tool which now makes this possible. One method of obtaining such pictures is described in this paper, and is illustrated with typical oscillograms. The latter bear out, in general, the classical text-book material rather closely; in addition, the test curves are convincingly realistic, in that they are far from being smooth. This investigation was undertaken in an effort to obtain a better understanding of commutation, with the hope that this added knowledge might serve to point the way to improvements which would extend the range of application of d-c rotating apparatus.

Special Armature Used

The machine used for these experiments was a traction motor with series fields and a multiple-wound, three-coil-per-slot armature. The polycoil comprising these three coils was of the so-called "twisted-lead, orphan coil" type illustrated in Figure 1. Only one polycoil was used, on the assumption that all other polycoils, being normally of identical design, would have essentially equal characteristics. As indicated in Figure 2, the one polycoil used for the test essentially was normal in every respect, except that each individual coil had two small insulated wires, one electrically connected to the inside of the coil near each commutator riser (see points marked * in Figure 2), thence passing through the center of the conductor comprising the coil. These wires were brought out through a single small hole in the side of the loop, at the end of the coil opposite the commutator. The outside ends of each of these two small wires were connected to two slip rings. In order to investigate the three coils in the polycoil, therefore, a total of six slip rings was required, as is indicated in Figure 2. Figure 2 also indicates the designations used here for the six conductors, *A*, *B*, *C*, *a*, *b*, *c*, comprising the polycoil. In identifying a complete coil consisting of conductors *A* and *a*, the designation of the coil is the same as that of the top conductor, namely, *A* in this instance.

Figure 3 shows the connections schematically. It is easier to follow than Figure 2. For measuring current in any coil, the resistance drop in voltage caused by the flow of current is used. The coil becomes, in effect, a small d-c ammeter shunt.

Voltages which may be induced in the conductors are represented in Figure 3 by small arrows. If these voltages are added algebraically from slip ring 5 to slip ring 6, and if we assume the voltage induced in the coaxial wire in a conductor is equal to that induced in the conductor itself, then the only voltage which should appear across these two slip rings is that caused by the resistance voltage drop in the coil. Transient variations in this potential, therefore, may be considered as proportional to transient variations in the current flowing in the conductor. Similarly, variations in potential across slip rings 3 and 4 are proportional to variations in current in coil *B;* variations across slip rings 1 and 2 are proportional to corresponding variations in current in coil *C*.

It also is possible to read bar-to-bar voltage variations if we make one added assumption: namely, that the voltages induced in all conductors in a given slot are equal. In the commutating zone, where the flux density in the teeth is low, it would seem reasonable to make this assumption with negligible error. Referring to Figure 3, it will be found that coil *A* voltage can be read between rings 4 and 6; coil *B*, between rings 2 and 4; and coil *C*, between rings 1 and 3.

Typical Oscillograms

Figure 4 shows a series of 12 oscillograms, all for fixed values of load, speed, and rotation. The ones in the upper half show current in the three coils. The lower half shows voltages between the adjacent commutator bars to which the three coils are connected. In the top horizontal row and in the bottom horizontal row, each of the three current and voltage traces has been separated vertically to facilitate identification. The true vertical relationship is given in the two center horizontal rows of oscillograms.

The compensation adjustment producing the best observable commutation, by the black band method,[1] for this load and speed condition, is shown in the center column of oscillograms. For the oscillograms in the column at the left, the com-

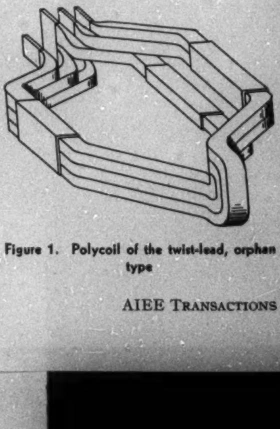

Figure 1. Polycoil of the twist-lead, orphan type

Paper 49-27, recommended by the AIEE rotating machinery committee and approved by the AIEE technical program committee for presentation at the AIEE winter general meeting, New York, N. Y., January 31–February 4, 1949. Manuscript submitted November 15, 1948; made available for printing December 20, 1948.

M. J. Baldwin is a design engineer of the motor engineering division, General Electric Company, Erie, Pa.

The author wishes to thank his associates for assistance given him in the preparation of this paper.

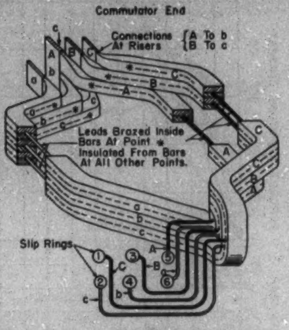
Commutator End
Connections At Risers
A To b
B To c
Leads Brazed Inside Bars At Point *
Insulated From Bars At All Other Points.
Slip Rings
A
B
C
a
b
c
1
2
3
4
5
6

Figure 2. Polycoil modified for test purposes

Indicating Connection of Coaxial Leads to Slip Rings at End Opposite Commutator. Core Portion Cut Away

mutating-pole strength was excessive, or, in other words, the motor was "overcompensated." For those in the column at the right, the opposite is true; the machine had insufficient commutating-pole flux, or, in other words, was "undercompensated." For both the undercompensated and the overcompensated conditions, the sparking was, on the average, grade *d*. For the intensity of this sparking, refer to Figure 6. For the best commutation, shown in the middle column, the sparking was *b*.

The time sequence is, in all cases, from left to right. Also, for this clockwise rotation, the three coils commutate in alphabetical sequence; *A* first, *B* second, and *C* last.

Elapsed time is indicated by the fourth trace. This indication is obtained by measuring voltage in units of segment pitch between adjacent bars, by means of a pair of small brushes mounted on the side of one of the motor brush holders.

Figure 5 contains a second set of oscillograms of the same machine operating at increased current and lower speed. Overcompensated and undercompensated sparking are about equal. Commutation is between *c* and *d*, as graded in accordance with Figure 6. For best compensation, the commutation is black.

In order to see better the proportions, and in order to have time reference points, the curves from Figure 2 have been replotted on rectangular co-ordinates. Figure 7 shows the commutation on coil *A*, the first coil commutated; Figure 8 shows coil *B*, and Figure 9 shows coil *C*. This particular set of oscillograms has been chosen because the changes in slope are so sharp.

Commutation Sequence

In order to understand the oscillograms, it is first necessary to determine the instant at which a given coil is either short- or open-circuited, and also the corresponding instant for any other coil, which may affect the rate of change of current or voltage in the coil under observation. Figures 7, 8, and 9 each have a time reference scale, the unit for which corresponds to the time for the armature to travel a distance equal to the width of one-half of one commutator bar. Figure 10 indicates which conductors are short-circuited for each time reference point at which the short circuits are made or broken for the three sets of curves shown in Figures 7, 8, and 9.

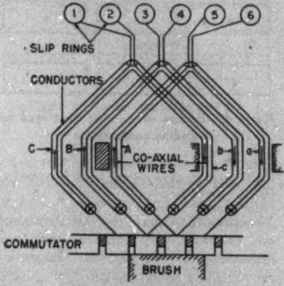

Figure 3 Schematic diagram of test polycoil connections

Bottom Conductors of all Coils are in Slot 1
Top Conductor of Coil *A* is in Slot 15
Top Conductor of Coils *B* and *C* are in Slot 16

Current Curves

Using the time sequence given in Figure 10, it is not difficult to discover the reason for most of the changes in slope of the current curves. Coil *A* is the first one commutated in this clockwise rotation, followed by the other two in alphabetical sequence. Coil *A* is short-circuited at time reference 0, and the short circuit is broken at time reference 5; coil *B* is short-circuited at 2 and the short circuit is removed at 7; coil *C* is short-circuited between 4 and 9.

Time reference point 9 marks the time of completion of commutation of the test polycoil. Point 6 would correspond to point 0 for the succeeding polycoil.

If the commutating pole is of correct strength, that is, the machine is correctly compensated, the current in the coil will reverse at a rate such that the current in the short circuit, at the time the short circuit is removed, is the same as the load current in the motor armature circuit. Coil *B* appears to meet this condition when correctly compensated, as shown at point 7 in Figure 8.

Neither coil *A* nor coil *C*, on the other hand, meets this requirement, either when "correct" or, especially, when "overcompensated." In both cases, the short-circuit current exceeds the load current for the point at which the short circuit is

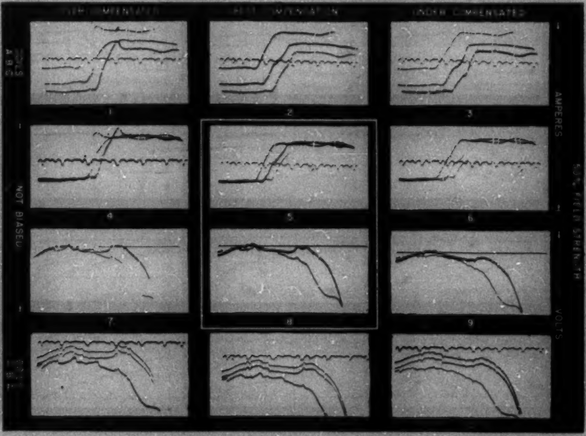

Figure 4. Oscillograms for 1,950 rpm, 450 amperes, clockwise rotation

broken. In spite of visual observation, the oscillograms appear to indicate overcompensation for the so-called "correct" condition. Point 9, "undercompensated," illustrates clearly the result of the commutating pole being too weak. The current in the short circuit here has not reached a value high enough at the time the short circuit is removed, and a spark is indicated in both current and voltage curves.

The rate at which current reversal in a coil takes place depends, in part, on the amount of commutating-pole excitation, but it also is altered by the presence of other short-circuited turns in the slot, which tend to reduce the speed of reversal. This is indicated by the change in slope of the correct curve at reference point 2 in Figure 7, when the rate of change of coil *A* is reduced by the short-circuiting of coil *B*. The reduction in the rate of change is even more pronounced for coil *B* at reference point 4 in Figure 8 when coil *C* becomes short-circuited by the brush.

The rate of change of current in a given coil, conversely, theoretically would be increased when the short circuit of the brush is broken in some other coil in that slot. At reference point 3 for coil *A*, the opening of a short circuit on coil *C* of the preceding polycoil increases the speed of reversal when undercompensated. Again, this is true of coil *C* for reference point 7 for the undercompensated condition. It is at this point that the short circuit on coil *B* is removed.

Voltage Curves

The voltage curves were taken principally in order to more accurately detect sparking, and as an auxiliary means of indicating time. The amplifier of the oscilloscope used did not have adequate capacitance-resistance product for the low frequency of the motor under test. Calculations would indicate about 32 per cent decay from the beginning of the voltage peak to the time when commutation begins. This accounts for the curves, shown in Figures 5 and 6, being below the zero axis instead of above. An approximate correction of 5 volts therefore, has been applied to the curves in replotting them for Figures 7, 8, and 9. The absolute values of the voltages shown are, therefore, very approximate. It is interesting to note how the changes in commutating conditions affect the shape of the voltage curves. Sparking is indicated rather clearly. Take time reference point 9, Figure 9, for example. Here we see overcompensation indicated by a peak upward; undercompensation, by a peak downward. It is doubtful if the voltage curves taken alone mean a great deal to an observer, but, in conjunction with the current curves, the two appear to tell whether there is sparking, and whether the sparking is caused by too slow or too rapid reversal of coil current.

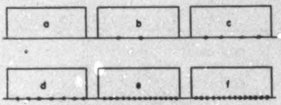

Figure 6. Portion of sparking chart used for grading commutation

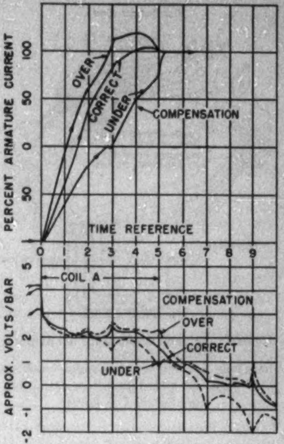

Figure 7. Commutation of coil *A*

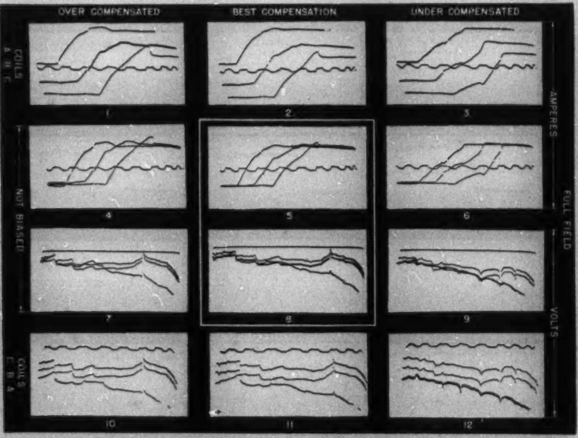

Figure 5. Oscillograms for 600 rpm, 830 amperes, clockwise rotation

Summary

To the designer of electric equipment, even these few curves indicate clearly the entire problem of commutation. The effect of variation in the adjustment of the commutating pole and of mutual inductance upon the rate of change of current is shown. The difficulty of getting the several coils in a slot to commutate equally is revealed. The need for brushes to absorb the residual voltages under the best of conditions is suggested. Commutation theory is proved to be correct, and a better understanding of commutation is promoted.

Beyond this point, what use can be made of the oscillograph in extending the range of commutation? At this time we cannot answer this question. It is like asking whether the microscope is of any use as an instrument after having employed it on but one specimen. If we consider as specimens each type of armature coil, pitching, and arrangement, and if we consider the oscilloscope as a microscope for the examination of each, this device could be the tool to assist the designer to select the ones that are better and, what is more to tell why they are better. In this manner, it ultimately may point the way to extension of the commutation range of d-c apparatus.

Appendix. Testing Technique

The oscillograms shown in this paper are typical. These, and others like them, were the result of a series of experiments performed with varying degrees of success. The remainder of this paper is devoted to a summary of what was learned regarding the technique of taking this type of oscillogram.

Magnetic Oscillographs

The magnetic oscillograph has two features which would seem to permit its use in connection with tests of this type. First, it usually can be used directly connected to the exploring coils without an amplifier. Second, it has several elements, permitting simultaneous photography of current or voltage in several coils.

On the other hand, the speed of response of all elements of the magnetic oscillograph must be exactly equal, and also must be adequate for the speed of machine to be tested. Although some oscillograms were attempted in connection with this particular test machine, the slow speed of response of available elements resulted in oscillograms of questionable value. At 1,950 rpm, the changes in the slope of the curves occur one-half of a commutator bar apart, corresponding to 82.5 microseconds. In order to give a good record, the oscillograph in this instance should be able to follow a square wave with a frequency of 6,050 cycles per second. The magnetic oscillograph was abandoned in this case because of the lack of matched elements good for this frequency.

Cathode-Ray Oscilloscope

The cathode-ray oscilloscope is suited better to this application than the magnetic oscillograph. This is principally because the electron beam has no inertia, and, for the frequency dealt with here, will follow the changes in rate accurately. The operator also is able to watch these changes take place. Some magnetic oscillographs, by means of revolving mirrors, possibly may permit some observation, but the cathode ray oscilloscope is excellent for large-scale images which readily may be photographed where oscillograms are desired.

The cathode-ray oscilloscope also must be of suitable size and design. If a 3-inch size otherwise is equipped suitably, it may prove adequate for preliminary observation, but, for photographs, a 5-inch size is much better. All oscillograms shown here were made with a 5-inch oscilloscope. The time constant of the resistance-capacitance network of the Y-axis amplifier should be as large as possible. These photographs were taken during the latter part of the war period, when any oscilloscope was difficult to obtain. The best one available had a time constant of about 0.050 second with which to measure commutation rate in zones occurring 0.025 second (at 600 rpm) apart. The decay in ampere signal can be accounted for easily as the current before and after the transient is of known value, but to estimate the voltage values in the commutating zone is not accurate, as has been noted already. Oscilloscopes now are available with Y-axis amplifiers good for much lower frequency than the one used here. The oscilloscope should be selected to suit the speed of the machine tested if voltage values are to be estimated accurately.

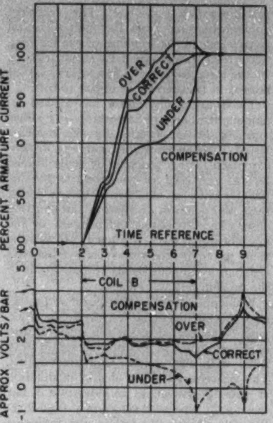

Figure 8. Commutation of coil *B*

The oscilloscope used should be provided with the single-sweep feature, which permits displacing the spot off the screen to the right, and initiating the sweep externally. The possible adjustment of sweep frequency should be adequate for the range of test-machine speed to be covered. While this is not important when the single sweep is being used, for visual observation it is desirable sometimes to use the recurrent sweep.

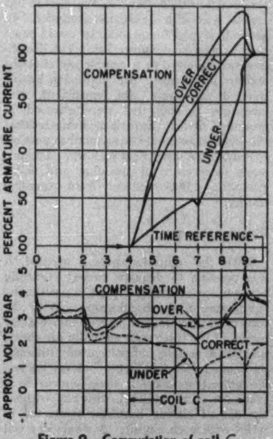

Figure 9. Commutation of coil C

Sweep Initiation

As has been noted, the oscilloscope was of the type permitting external initiation of the sweep. All the oscillograms shown were taken this way, using a small impulse generator for initiating at identically the same position on each revolution of the motor. A permanent magnet was mounted on the coupling of the machine being tested. As the machine revolved, this magnet passed across the face of a stationary electromagnet about the size of an ordinary spool of thread and induced an impulse in its winding. This impulse proved entirely adequate for initiating the sweep, with no amplification.

There were four of these electromagnets mounted on a yoke, each just ahead of a commutating zone. The yoke was arranged to be shifted, to obtain the desired points of initiation of the sweep. Between the external sweep terminals of the oscilloscope and the four coils, a selector switch was interposed in the circuit to permit the operator to examine quickly commutation at any of the four brush positions.

Experiments also were made using a photoelectric, light-sensitive cell to initiate the sweep. This cell would detect the reflection of light from a white dot on a revolving black drum, with sufficient output when amplified to initiate the sweep. Although not used for making these oscillograms, a photoelectric cell might prove to be a convenient means of initiating the sweep of the oscilloscope.

Time Indication

Time may be indicated on the oscilloscope in several ways. To be most useful, it needs to be indicated, not in terms of seconds, but in terms of commutator bars. The indication used here was obtained from two small brushes mounted on the edge of a brush holder, and separated just far enough apart to obtain an intermittent indication of bar-to-bar voltage when the two brushes spanned a mica. The brushes, when working properly, give a good time indication, as indicated in Figure 11. The upper curve indicates the signal obtained when connected to the vertical or Y oscillograph circuit. The lower is the same signal applied to the Z, or electron accelerator grid circuit, with the same sweep but no Y signal. Improved probes with coil-spring-backed, drafting pencil leads as brushes, have been developed subsequently, which should assist in obtaining better time indication curves in the future.

Slip Rings

The proper design of slip rings, brushes, and brush holders is important. Initial tests made, using a single brush per ring, were not satisfactory. Subsequent tests

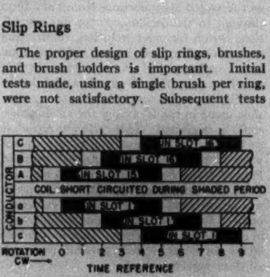

Figure 10. Commutation sequence

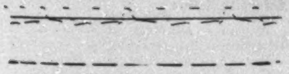

Figure 11. Typical time indications

with two brushes per ring turned out much better. Apparently, both brushes are not apt to lose contact with the ring surface at the same time, so two operate successfully where one does not. A reasonably well-ground surface on the rings, however, is essential. The slip rings necessarily do not require much space. In this test, six brush holders and rings were held within $2^{7}/_{16}$ axial inches. Figure 12 shows the final brush holder and the rings which are located below the armature back-end windings. The brushes used were of silver-graphite composition.

Multiple-Exposure Method

To compare the three coils from a commutation standpoint, photographs to the same scale and time reference were needed for all. Two methods were employed: the first simply being to adjust the oscilloscope and obtain one exposure for each coil and one for the time reference. The only difficulty found with this system was that there was enough creep in the length of the X axis, one way or the other, to throw off the timing before all the exposures were completed. It was not possible to switch from coil to coil without getting a powerful condenser discharge, sufficient to paralyze the oscilloscope temporarily. No common, full ground between two coils is possible, since such a connection would short-circuit the coil. The sweep being initiated once each revolution, the frequency of recurrence was sufficient to permit watching the effect of changing compensation without visual discomfort.

Single-Exposure Method

A second method of taking the oscillograms, therefore, was devised which permitted taking four exposures with one opening of the camera shutter. This was made possible by connecting the oscilloscope, in rapid succession, to each of these coils and to the timing-signal brushes. A revolving distributor was used, consisting of segmental copper rings with suitable brushes. This was arranged to connect one circuit at a time through to the oscilloscope for one revolution, switch for one revolution, connect for one revolution, and so on until all four curves had appeared on the screen. In this way it was possible to get the exposures in sufficiently rapid succession that any possible creep in the X axis of the oscilloscope could be neglected. This cycle was repeated as long as desired and was photographed when convenient. The pictures shown in Figures 4 and 5 were taken in this manner. From the visual standpoint, this method was not as good as the multiple exposure, because the same signal appeared but once in every eight revolutions. Despite the bad flicker, however, it was possible to watch all three coils commutate.

The paralyzing of the oscilloscope has been mentioned in connection with the multiple-exposure method. This discharge apparently came from the high dielectric capacitance of the windings of the machine under test. It was avoided in the distributor by the interposition of a temporary, partial ground in transferring from coil to coil.

The rotating distributor has several requirements that are important. It either must be driven directly by the machine tested, through a suitable gear box, or synchronized to that machine by some means. Selsyns were used for synchronizing the distributor with the machine on test in taking these photographs. Selsyns permit shutting down the distributor, independent of the machine under test. Arrangements must be made to remove the static charge from each distributor segment before connecting it to the oscilloscope.

When operating the distributor and working with the current curves, all circuits either must be connected to the slip rings in turn, or else grounded to prevent picking up stray fields with the unused, ungrounded line. This prevented the use of grid modulation of a straight sweep as an indication of bar spacing, at least with the circuits used here. For this reason, the timing was indicated by deflecting the spot along the Y axis, similar to upper timing wave shown in Figure 11, rather than by modulating the grid.

Shielding and Grounding

Nothing is more important in making preparations for a test of this type than to provide adequate shielding of circuits. The voltage drop in the armature conductor, when handling 830 amperes, is but 230 millivolts.

Every precaution is required to shield the circuits from the slip rings to the oscilloscope; otherwise the weak signal to be observed will be obliterated by stray field pick-up from other machines in the vicinity. Shielding is not as important when obtaining voltage curves. Twisted leads did not prove adequate unless wrapped with grounded copper wire. Final tests were conducted with nothing in the circuit but coaxial wire with all sheaths grounded. In general, it was found best to avoid more than one ground connection. The distributor was revolved in a completely enclosed and grounded case. All connection boards were of minimum size, consistent with creepages needed, and were encased in grounded covers. Experience indicates that the distributor should be as small as possible to reduce the stray field pick-up. The primary importance of shielding and single grounding was learned only from expensive testing.

Biasing Curves

With the multiple-exposure method, it was possible to displace curves vertically between exposures by using the positioning equipment of the oscilloscope. With the rotary distributor, the current and voltage curves of the three coils normally are superimposed, making identification difficult, particularly for the jagged voltage curves. To permit separation, these curves were taken for each condition, with and without the use of biasing batteries connected in series with each circuit. A single dry cell per circuit, shunted by an adjustable voltage divider, permitted reduction of the battery voltage to obtain the desired curve displacement.

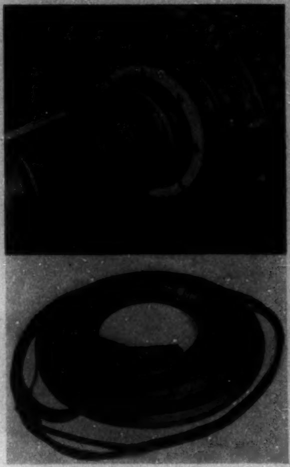

Figure 12. Brush holder and slip rings used in tests

For the voltage curves, a second set of batteries was needed which, in this case, was of the radio B-type. Only one set of batteries was connected at a time in order to keep stray pick-up at a minimum, particularly when working with the current curves. The rotary distributor served as a device for applying the d-c bias just ahead of the initiation of the sweep, thereby momentarily displacing the curve as desired.

Future Tests: Modified Multiple-Exposure Method

In the event that tests of a similar nature are to be made in the future, a modified form of the multiple-exposure method should be considered. A distributor of the type used for the single-exposure method would be provided, but would be operated only by hand, as a quick means of selecting the coil to be scanned. If, by the use of this device, the multiple exposure of the several coils can be accomplished within 30 seconds, no appreciable error in time relationship between the curves should result, as the creep of the X-axis sweep is perceptible only over several minutes.

The electronic switch also might be brought into use to permit observation of the current and voltage waves of a given coil simultaneously. To do so may require an oscilloscope larger than five inches. With the better visual condition resulting from the more frequent sweep, coupled with the ability to observe both rate of current change and voltage peaks at the same time, there would be little about the commutation that could not be seen at a glance. The necessity of changing grounds between coil observations will require the selector switch to be moved from coil to coil. This method then provides a means for visual observation of commutation, as well as for obtaining oscillograms.

Poor brush riding and improper brush fit may be detected. By switching the initiator selector from brush to brush, all brush positions may be examined. Such an arrangement might permit better commutation adjustment than can be obtained currently by the black band method.

Reference

1. The "Black Band" Method of Commutation Observation, T. W. Schroeder, J. C. Aydelott. AIEE Transactions, volume 60, 1941, pages 446–51.

Discussion

D. B. Hoover (Westinghouse Electric Corporation, East Pittsburgh, Pa.): The method described in the paper appears to be a good means of evaluating the merits of various types of d-c armature windings with respect to commutation. It stresses the importance of mutual inductance of the coil sides during commutation, and serves as a practical means of checking the effects of mutual inductance in any given winding.

The mutual inductance between coil sides of a given winding may be increased by increasing the number of bars spanned by the brushes, if it is assumed that the brushes maintain intimate contact with the commutator bars spanned. In this respect it would be interesting to study a plain, multiple-wound armature, say with two bars per slot and half slot chorded, using brush widths spanning two, three, and four bars. A study of this armature might prove the intimacy of contact that exists between the bars and the brushes.

It appears that the commutator roughness might affect the results of tests performed on some types of windings. Was this found to be the case on the machine tested?

M. J. Baldwin: As suggested by Hoover's discussion, a broad field of investigation is opened by the use of the oscillograph for studying commutation. So far, the only work done here has been with the winding described in the paper.

Oscillographs have been made with different brush widths. Perhaps the results of these tests may be published at some future date.

Although we do not have illustrations, the effect of poorly riding brushes has been observed. The current traces become erratic and nonrepetitive, whereas the opposite is true if the brushes are riding smoothly.

Effects of Commutator Surface Film Conditions on Commutation

C. LYNN
MEMBER AIEE

H. M. ELSEY
MEMBER AIEE

COMMUTATION, to the d-c designer, is considered fundamentally from the standpoint of the reactance voltage produced in the coils being short circuited by the brushes. This voltage can be considered as being produced by a changing and reversing current through the self and mutual inductance of the armature coils being commutated, or it may be thought of as being produced by the armature coils being commutated, cutting a resultant armature field, stationary in space, located in the interpolar space between each main pole and produced by load current in the armature coils themselves.[1] In any case, the designer is interested in proportioning his machine so that the magnetic structure and the winding combinations and commutator and brush rigging, give a structure which develops the desired voltage, carries the designed current and will commutate successfully. Successful commutation is defined in C-50 2.085[2] as follows: "Successful commutation is attained if neither the brushes nor the commutator is burned or injured in an acceptance test; or in normal service, to the extent that abnormal maintenance is required. The presence of some visible sparking is not necessarily evidence of unsuccessful commutation." In addition to the correct proportioning of the design of the d-c machine, which will reduce to a minimum the resulting reactance voltage of the coils being commutated, various other factors enter into the commutating problem. This paper primarily will discuss those effects on commutation produced by surface films of various types on the commutators, but in addition, it will necessarily also cover those other factors which are involved in the commutating problem.

Electrical and Mechanical Factors Affecting Commutation

Contact drop between the brushes and commutator surface and the resistance of the brush itself, as well as the resistance of the armature coils being commutated, limit the short circuit current which can flow in the brush and the coil being commutated. The lower the reactance voltage of commutation, the lower the short circuit current. Also, the higher the contact drop and the higher the resistance of the brush itself, the lower will be the short circuit current. However, since the load current, as well as the short circuit current, has to pass from the commutator to the brush and through the brush body, there is a limit to the permissible voltage drop at the contact and to the resistance of the brush body itself. Too high values for these will result in too great a loss at the brush contact surface. At some value of short circuit current, which is not a constant value, but which depends upon many factors, sparking at the brushes will occur. If the sparking is minute, it probably will not cause burning of the commutator bars or the brushes, and if it does not become cumulatively worse, no harm will result.

Assuming a correct design and correct electrical adjustment, commutation is adversely affected by lack of intimacy of contact between the brush and the commutator bars. It can be shown[3] that commutator bar to bar roughness as little as 0.0001 inch (this does not refer to eccentricity of the commutator as a whole) can cause sparking, while the same machine, with less than this bar to bar roughness, will have black commutation.

Commutator Films of Earlier Periods

Copper is used universally for the bars in commutators because; it is relatively cheap, mechanically it is fairly strong, it does not draw beads on arcing and because in uncontaminated atmospheres, it forms a film on its surface that assists commutation. Until recent years, the important part played by this film surface was not fully appreciated in the art. In the old days, the best operating d-c machines had chocolate colored commutators. This was before the days of high commutator surface speeds, when machines had low ratings, operated at slow speeds and had relatively easy load cycles. In those days, there were few brush grades, no treated brushes and much less was known about brushes and commutator surface films.

With the introduction of electrographitic brushes 30 or 40 years ago, and the building of larger, higher speed, d-c machines, with more difficult loading cycles and more contaminations of atmospheres in industrial plants, commutator surfaces of unfamiliar types and colors began to develop. With the introduction 20 to 25 years ago, of newer grades of electrographitic brushes produced under different manufacturing conditions, commutators with black surfaces began to develop in certain steel mill applications. Peculiar colored commutator surfaces occurred in chemical industrial plants and paper mills. Most of these machines with black commutators, operated successfully, but the customers objected to the color of the commutators. Cleaner or scouring brushes were brought out about this time. These brushes had the properties of mechanically abrading the commutator surfaces so as to reduce the amount of discolored film on the com-

---

Paper 49-29, recommended by the AIEE rotating machinery committee and approved by the AIEE technical program committee for presentation at the AIEE winter general meeting, New York, N. Y., January 31–February 4, 1949. Manuscript submitted November 22, 1948; made available for printing December 21, 1948.

C. Lynn is manager of the d-c engineering department, and H. M. Elsey is consulting chemist, research laboratories, Westinghouse Electric Corporation, East Pittsburgh, Pa.

mutator. These brushes were used, few in number, and were generally spiraled around the commutator, so as to continually lightly scrub the commutator film surface. The amount of scouring action was controlled by the number of brushes used on a given track. Even in case of bars, slightly burned from poor commutation, these brushes were used in maintaining a cleaner commutator surface. Usually, most machines, whose commutator surfaces have been reconditioned by grinding or handstoning, will commutate successfully, at least for a period of time.

When a new or freshly ground commutator is placed on load, and after a very few hours of operation starts to take on a reddish hue color, this is, in general, an indication that the film surface being formed on the commutator is of the right type to produce successful commutation.

Even before World War II started, the real importance of commutator films began to be appreciated. It was known that lightly loaded electro-graphitic brushes could develop a chatter on the commutator surface. This chatter was related to the type of film formed on the commutator surface by continued operation of these lightly loaded brushes. The brushes, themselves, developed an extremely high polish on their contact surfaces, and there was an appreciable movement of the brushes in the brush holder boxes. This could be determined by observing the polish on the sides of the brushes where they rode up against the brush box. The actual movement of the brush in the box was much greater than the actual out-of-roundness of the commutator, as could be proved easily by slightly sanding the commutator surface to remove the highly polished film. Usually machines which developed this chatter, would operate in a normal manner if the film was removed and if the load on the machine was such as to give a normal loading of the brushes, that is, current densities 40 to 60 amperes per square inch.

A phenomenon known as copper picking is sometimes experienced in the operation of commutating type d-c machines. When this occurs the surface of the brushes have small flakes of copper embedded in their surfaces. The size of these flakes may be extremely small, so that a magnifying glass is required to see them, although sometimes pieces of copper, up to a 1/16 inch square or even larger, may be found. This condition is always accompanied by threading or grooving of the commutator, because this results in certain portions of the commutator surface being rubbed by copper instead of by carbon. This condition usually occurs due to a build-up of surface on the commutator, and the finally breaking through of this surface at points on the brushes, with a resultant deposit of copper flakes on the brush at these points. When this happens, a lower resistance path to the flow of the current between the commutator and brushes occurs at these points, and the current distribution in the brushes is no longer even. Since it is impossible for all the current to be carried at these few points, other points will also be similarly affected and sometimes many of these threaded tracks occur on the commutator surface. This can lead to poor commutation. The only cure in this case is to remove the copper from the face of the brushes, either by picking it out with a knife or resanding the brush faces to accomplish the same purpose. The commutator surface should be reground so as to permit an even freshly ground copper surface, with the hope that a normal surface film will be formed evenly across the surface, and the picking up of copper eliminated. Certain other conditions, as will be mentioned later, also cause picking up of copper.

In the early 20's, it was discovered that in extremely cold weather, particularly in the northwest part of the country, brushes wore rapidly when the humidity was quite low. This applied to carbon, graphite, and copper graphite brushes. Sometimes a set of brushes would wear out overnight. Some substations in the north overcame this by humidifying the substation when the humidity became very low.[4] Machines have been built where humidification of the ventilating air to secure improved current collection, was an original part of the equipment. Experience in the past has indicated that more than normal brush wear will occur if the humidity content of the ventilating air of the conventional machine is less than $1^1/_2$ grains of water per cubic foot of air. This depends somewhat upon the current loading of the brushes. With the advent of d-c application to military aircraft, where generators had to operate at extremely high altitudes where the moisture and oxygen content in a given volume of air was low, extremely rapid brush wear was encountered.

Consideration of Commutator Surface Films

The first worker to seriously speculate as to the precise nature of the film which forms on the copper commutator in air was Baker.[5] He assumed that the film was composed essentially of copper oxide and that it ranged in thickness from 3×10^{-6} to 3×10^{-5} centimeters. Ten years later Van Brunt and Savage[6] stripped a film from a commutator bar and reported a total thickness of 5.4×10^{-6} centimeters of which only 2.1×10^{-6} centimeters was copper oxide. The balance of this film was found to consist essentially of an upper graphite layer which had a thickness of 3.3×10^{-6} centimeters. In interpreting this analysis and other data, these workers cited, assumed that there were at least three components in all normal films on commutators or copper slip rings which are operated in air, and of these constituents, they viewed the graphite as the most essential. This is the component which functioned as a lubricant. It is held to the tarnish film of copper oxide by bonds, which are greater than the bonds between adjacent layers within the graphite surface, and it performs its function as a lubricant through the presence of an absorbed layer of water vapor. For this reason brushes wear very rapidly in atmospheres of low absolute humidity and justifies the humidification of the ventilating air around current collecting parts of rotating machinery to a minimum of at least two grains of water per cubic foot of air. The lack of water vapor in the upper air was responsible for rapid wear of brushes on electric apparatus of high flying airplanes. Martinez[7] has observed a water content as low as 0.00075 grains per cubic foot at an elevation of 40,000 feet. If $1^1/_4$ grains of water vapor per cubic foot of air is absolutely necessary as a minimum for good brush life and performance at the earth's surface, it is no wonder that special treatments had to be discovered and applied to aircraft brushes which were forced to operate in exceedingly dry atmospheres encountered at high altitudes.

While admitting that graphite and copper oxide are both normally observed in commutator films, we suggest that a simpler mechanism of film maintenance and formation is more probable. In 1927 Vernon[8] reported that copper which was exposed to air, free of hydrogen sulphide, acquired an almost transparent tarnish film at room temperature, which was wholly composed of copper oxide and that this film was protective to the underlying copper in atmospheres which readily corroded unfilmed copper. However, if an unfilmed sample of copper was exposed to air containing as little as one part in 35 million parts of hydrogen sulphide, the tarnish film which formed was not protective to the underlying metal and contained sulphur out of all proportion to the concentration of hydrogen sulphide in the air. For example, while the oxygen content of the air is 210,000 parts per million and the hydrogen sulphide content was only 0.03 parts per million, the tarnish film formed in such an atmosphere consisted of 10 to 15 per cent of copper sulphide and 90 to 85 per cent of copper oxide. If an almost undetectable trace of gaseous impurity in the air can completely alter the character of the tarnish film on the copper by altering the character of the chemical reaction, there would seem to be no need to look for a complicated explanation for the effect of 3,600 parts of such a chemically active gas as water vapor on controlling the chemical nature of a tarnish film.

Hydrogen sulphide as an air impurity has been purposely chosen for discussion first, because this gas is present in many industrial atmospheres, and is the controlling cause of poor commutation and brush life in most steel mills, and even in some central station power plants. It is present in such high concentrations in certain areas in kraft paper mills and certain chemical industries, that it is almost impossible to operate commutating machines in those locations.

During the war, it was found that certain compounds, the metallic halides,[9] could be incorporated in brushes and that these treated brushes would give satisfactory life and performance on aircraft generators, when these were operated in air almost completely devoid of water vapor. Since this class of brush was apparently able to control the type of film on a commutator in the absence of water vapor, a gaseous constituent normally required for good commutation, it was thought that similar brushes might maintain satisfactory film conditions on industrial machines which were operating in atmospheres on the earth's surface containing such undesirable impurities as hydrogen sulphide. Many applications of brushes containing metallic halides, have been made and a substantial percentage of the large electric machines in steel mills now are fitted with so-called altitude treated brushes. Hydrogen sulphide has been the cause of poor commutation in so many industrial locations, that when a new complaint is received, it is well to look for evidences of this gas in the atmosphere. Its presence or absence is determined readily by the character of the film on the commutator outside of the brush tracks. The concentration which can cause trouble can be below that which is susceptible to the sense of smell. If there is no evidence of copper sulphide (and this is recognized readily by its characteristic color) on the edges of the commutator, or on the copper bus bar in the neighborhood of the machines, hydrogen sulphide is probably not present in damaging concentrations. Several instances of poor commutation and short brush life have been observed on machines in localities where hydrogen sulphide might be expected to be present on account of the nature of surrounding industrial plants.

In one instance, an exciter in a large power station at times sparked badly over extended periods, but close examination of the commutator and the surroundings indicated the complete absence of hydrogen sulphide. However, this station was not far distant from a battery of coke ovens, and it was found that whenever prevailing winds carried the gases from these ovens towards the station, poor commutation was observed and sparking decreased and at times even became black after periods of time, with the wind in the opposite direction. In this connection a most interesting discovery was made during one of the bad commutation periods. Through an accident, chlorine gas was released into the atmosphere of the station, from which the ventilating air of the exciter was secured, and the concentration was so high that it was necessary to open all the doors and windows to remove the irritating gas as quickly as possible. Immediately following this incident, it was noticed that the sparking had ceased and the commutation was black. There had been no change in load or any other operating conditions. The station operators had no clues as to the cause of the change in commutation, and it was only when an inspection of the commutator showed an indication of a change in color of the copper not covered by the brush tracks, that the incident of the release of chlorine gas was brought out. In our studies of this surface film commutation problem, we had found that traces of free halogen gases would form and maintain a copper oxide film on copper under high altitude conditions. Hence we at once assumed that it was the chlorine itself which was responsible for the improved commutation. Some weeks later, during another period of bad commutation, in the presence of a number of observers, we released a small quantity of chlorine gas into the entering cooling air for the exciter. Within a few seconds black commutation followed, and it was noted that no visible sparking was observed for a period of two weeks thereafter. From that time on, commutation was maintained at high quality by the occasional use of chlorine gas, until the installation of an air purifying equipment, which is described later, could be made.

Another power station located in the heart of the Allegheny Mountains, surrounded on all sides by hills, has located near it a burning culm heap. This station is in the heart of the Allegheny fog belt and is subject to bad down-draft conditions, which result in stack gases as well as fumes from the culm pile entering the station in relatively large volumes. Evidences of hydrogen sulphide were found on the bus bars in the station, and for that reason it might be assumed that this gas was responsible for the difficulties in commutation observed. It is, however, our feeling that in the case of this unit, the primary offender here is not hydrogen sulphide, but hydrocarbon vapors or other carbonaceous gases from the stack and the culm pile. An examination of the brushes on the machine showed nothing abnormal from a physical standpoint, but it was observed that the copper shunt wires were coated with black adherent deposits, which on analysis proved to be substantially carbon. Tinned copper surfaces were free of this tarnish. This observation suggests, therefore, that the possibility of a copper surface of a commutator, at times, may develop an objectionably high friction film which may be so thin as to be almost transparent, through the catalytic action of copper on carbonaceous vapors in the cooling air. It is well-known to chemists that copper greatly accelerates the formation of sludges in lubricating and transformer oils which are exposed to air. In a similar manner the hot copper on the surface of the commutator may convert the hydrocarbon vapors into resinous bodies which will adhere to the surface of the commutator as readily as they do to the copper wires of the shunts on the brushes. While pitch and other hydrocarbon fumes may not injure commutation through varnish formation, such a reactance mechanism would explain the damaging effects of the paraffin, oil, grease, and other carbon compounds when these are present at a brush copper interface through extended periods of time. It is well-known that a momentary application of paraffin may stop brushes chattering, but that a repeated use of this palliative will lead to undesirable commutation.

The use of chlorine in controlling the commutation in a central station when the air was contaminated with pitch fumes, was mentioned before. We have as yet suggested no mechanism for the improvement which was observed by the action of traces of this gas. It is one of those which is said to cause high friction and other undesirable commutating conditions when it is present in an industrial atmosphere. We have confirmed its effect on brush friction, but we cannot explain how an increase in brush friction will destroy a bad film condition and result in black commutation. It was our first thought that the poor commutation in question was caused by an inadequate copper oxide film on the commutator. We thought that the film was so thin that bare copper might be exposed, and it is known that the friction between bare copper and brushes is high and this could lead to chattering, with resultant sparking. We had assumed that the chlorine would attack the bare copper to form cuprous chloride and this in turn would be oxidized to copper oxide to form the desired normal film. Since, however, finding a resin or film on the copper shunt wires, we suspect that possibly chlorine functions by chemically attacking and destroying the undesirable varnish film formed from the pitch fumes. We are open to suggestions as to the true explanation of its beneficial effect, but we do think it most interesting that a trace of this corrosive, irritative, and otherwise highly objectionable gas, corrected bad commutation when all other attempted cures failed.

It is our belief that the phenomenon of copper picking, which is a very serious problem of commutation, is not caused by defective brushes of a given grade or by the application of an improper grade, but that this is associated with contaminated gaseous atmospheres. Experience has indicated, particularly heavy copper picking when machines operate in gaseous atmospheres containing hydrogen sulphide. Electrographitic brushes which are operated on a commutator which is filmed to a substantial percentage with copper sulphide, will almost always contain copper in the faces of the brushes. It is customary to assume that copper is transferred from the commutator to the brush face by some process similar to electrolysis, in which the copper dissolves at the anode, migrates through an electrolyte, and deposits on a cathode. Even if the existence of a mono-layer of tightly absorbed water vapor on a commutator film is assumed, we question if the mechanism by which the copper is transferred from the commutator to the brush bears any similarity to true electrolysis. We suspect that copper sulphide is not attached as firmly to the commutator copper as is the copper oxide, and that the sulphide film, in general, is thicker than the normal oxide film, and that fragments of copper sulphide break off and become embedded in the face of the brushes. Once embedded in the face of the carbon brush and removed from repeated exposure to the oxidizing action of the air, the sulphide particles are soon reduced by the carbon to metallic copper, and as such act as abrading or cutting tools on the commutator. Hence commutators are always found to be threaded or grooved, when copper is observed in the face of the brushes. An extreme grooving of commutators is customarily observed in areas contaminated heavily with hydrogen sulphide, particularly in kraft paper mills.

Current Collection in Hydrogen

The operation of brushes in a hydrogen atmosphere might be expected to avoid many of the troubles so frequently encountered in air operation. The reasons for operation of large a-c turbogenerators and synchronous condensers in hydrogen, have been covered in many papers in the past. D-c machines cannot make the same gains by similar operation and, therefore, there is not the demand for their operation in hydrogen. A turbogenerator requires the bringing out of the shaft through the case of the machine, for connection to the turbine shaft which drives it, and satisfactory operating hydrogen seals around the shaft have been developed. It is, therefore, quite simple to extend the shaft on the other end of the generator and operate the collector rings and the direct connected exciter for the unit in air. Operation of the collector rings and the exciter in hydrogen would result in many complications, particularly in regard to maintenance, especially since turbogenerator units are operated for periods of one in two years without a shut down. This necessitates changing both the collector ring brushes and the exciter brushes on the run, and suitable arrangements have been made for doing this.

In the case of synchronous condensers, some units have been built and are in successful operation, and other units are now building, using direct-connected exciters which together with collector rings, are operating in hydrogen. When this is done no shaft seals are required. Unfortunately, short brush life is not unknown on the collector rings of hydrogen cooled machines, with the collectors operating in hydrogen. Several years ago, after several brush grades had shown unsatisfactory wear on a hydrogen cooled synchronous condenser, a trial was made using halide-treated brushes. The original set of brushes is still in service on this machine. The quarterly inspection, to blow out carbon and metal dust and replace brushes, has been replaced by annual inspection, and the brushes promise an extremely long life as originally predicted by Baker[10] for brushes operating in hydrogen services. This original trial installation has been followed by others.

Commutation in hydrogen presents no particular problems. If the machine is designed so that it will operate satisfactorily in air with conventional brushes, it will also operate satisfactorily in hydrogen. If, however, sparking is present, the brush wear may be higher than in air and in that case the relative humidity should be kept below 10 per cent, otherwise extremely rapid brush wear will result. The voltage drop between the brushes and the commutator will be lowered somewhat when operated in hydrogen, as compared with operation in air, but this lowering is not so great as to adversely affect commutation.

Silicone Vapor Films

A very pronounced effect on commutation, of the action of a detrimental commutator surface condition, occurred during the war, when the first experimental submarine silicone insulated d-c motor was developed by Westinghouse. This double armature machine, which had about 40 per cent more rated output in the same weight and space, was totally enclosed and, of course, was worked very hard at the increased rating.

It was first tested as an open machine, taking air from the room at the middle, between the two armatures and discharging the heated air, back into the room, at the commutator ends. This unit was able to deliver 10 per cent additional output beyond its rating as a silicone insulated motor, under this condition of operation.

However, when it was enclosed and cooled by recirculated air, the commutation got bad after several days operation at this high loading. When this occurred, the voltage drop at the brush contact increased to two or more times normal values. By shunting current from the commutating field winding, it was possible to bring the brush potential curves, that is, the voltage drop at the brushes, back to a somewhat normal value and also materially reduce the sparking. The amount of current to be shunted was very great, corresponding to an excessively large commutating pole air gap. Continued operation in this manner, however, resulted in the commutation becoming bad again to the extent that the machine had to be shut down.

A film formed on the commutator surface, dark in appearance, which could be rubbed off easily. This was a carbon thrown down on the commutator and was responsible for the high voltage drop at the brushes and the resultant sparking.

Since the machine was operating at quite high temperatures, under this high loading, an attempt was made to cool the commutator by by-passing some of the air, directly from the outlet of the air-to-water heat exchanger. This resulted in some lowering of the commutator temperature but it did not improve the commutation. The commutator was cleaned and the test repeated with the same untoward results. However, when the same test was repeated, with the machine not enclosed and operated with a nonrecirculated ventilating system, it again successfully carried the 10 per cent overload continuously, without the formation of a detrimental film on the commutator or without the reappearance of the sparking. Once more, it was enclosed but this time it was operated at reduced load, with successful commutation. The load was increased until finally its rating (as a silicone insulated motor) was reached and it successfully passed the 17-day continuous load test at this load. The additional 10 per cent overload, as an enclosed machine, was just beyond its ability. This is the first instance on record of a large d-c motor encountering commutation trouble on account of the vapors of silicone varnish on its windings, forming a detrimental film on the commutator surface. In investigating this trouble, measurements were made to determine whether any vapors were given off by the silicone varnish, but none were found. Later investigations showed that the concentrations, which would give trouble in commutation, were far below that which could be determined by the apparatus used at that time, for detecting the vapor content.

At that time, it was not known that silicone vapor would cause rapid wear of the carbon brushes, even under a condition of successful commutation, as this large motor operated at relatively low speed and was not operated sufficiently long on test, for rapid brush wear to be encountered. This condition was first discovered at a Navy Laboratory, when a machine, that originally had class "B" insulation, was rewound with silicone-insulated coils. This was a relatively large high-speed d-c generator, totally enclosed, with a recirculatory ventilating system. The results were first indicated by the presence of low insulation resistance to ground of the windings. Upon opening up the machine, the presence of a large amount of carbon dust was found on the windings and a correspondingly short brush life. Further tests proved that rapid brush wear could be produced on a duplicate size generator, having class "B" insulation by simply placing into the ventilated air path, some coils covered with silicone varnish and heating the coils to any desired degree by passing current through the windings. Measurements have shown that a very minute amount of silicone vapor, 10 parts per million, show more than normal wear, while 200 parts per million produce ruinous wear, when recirculated air is used for cooling the machine. By opening the ventilating system to the atmosphere, the concentration will be reduced to a nondestructive value.

Duplicate results have been produced in the laboratory on small scale models, and attempts to thoroughly cure the silicone varnish by long time, high temperature bakes, have not produced a complete cure. Tests have indicated that it is possible to reduce the concentration, in a recirculatory system, to a sufficiently low value by suitable chemical filters. Operations, at lower than maximum permissible brush current densities, are a help in the right direction. The best method of eliminating the deleterious effects of silicone vapor on commutation, is to design and operate d-c machines, with silicone insulation, as open-type machines. A suggested design is to use separate ventilating systems for the current collecting parts of the machine and for the core and windings. This introduces some complications in design and operation.

Removal of Films by Scouring Action

Sometimes brushes, known as cleaner brushes, which are either inherently abrasive or have some cleaning action added to them, are used on machines for the purpose of removing or keeping the detrimental film from building up on the commutator. These brushes are usually few in number and are spiraled around the commutator in order to wipe the entire surface of the commutator, to an extent to keep the film from building up to a point where commutation or brush wear is adversely affected.

Cleaner brushes have no place on electric machines that are property designed and built, that are used within their designated ratings, that are fitted with the correct brush grade, that are satisfactorily installed and that are not operated under abnormal atmospheric conditions. If any one of these factors is ignored, cleaner brushes may be the economical way to mechanically remove the carbon smut laid down by a brush, because it is of poor quality or has been abused by an improperly designed or built machine, or because it has been installed incorrectly, or because of adverse loading or operating conditions. Cleaner brushes may also remove the undesirable films produced by hydrogen sulphide or other gases in the air, providing these filming gases are not too concentrated. In many contaminated industrial atmospheres, the use of cleaner brushes is not economical, because of their rapid abrasion of the copper of the commutators. In some cases, resin bonded grades have been substituted. This type of brush usually lays down a jet-black film which protects the copper from corrosive gases. The film seems to be composed of particles of brush dust bonded together and to the commutator, by a resin or varnish which may be formed from the brush bond (this may be Bakelite or other synthetic or natural resin) by a mechanism previously suggested in this paper. Unfortunately, the film is frequently high in resistance and must be removed from time to time if satisfactory service is to continue. The one big difficulty with cleaner brushes, is to secure a balance between the scouring action of the cleaner brushes and the formation of the undesirable film on the commutator. A solution is a cut and try proposition, and it is further complicated by a variation in the rate of build up of the film, which depends upon surrounding conditions, which may vary from time to time and upon the loading of the machines, which is usually not constant.

A Controlled Ventilating System

Figure 1, is a sketch of a turbogenerator exciter with an enclosed ventilating system installed in an atmosphere which has contaminating gases. A shaft mounted fan circulates the cooling air as indicated by the dotted lines of air flow. The air, discharged from the fan, first passes through a mechanical air filter to remove any carbon dust of worn brushes or other dirt that might get into the system. A water cooled heat exchanger removes the heat losses from the cooling air. The cooled air then flows back into

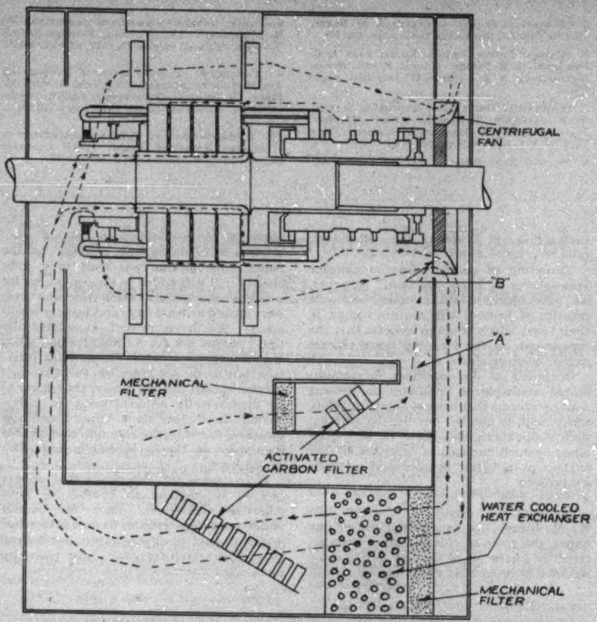

Figure 1—Turbogenerator exciter with recirculated ventilating system using mechanical filter, water cooled heat exchanger and activated carbon filter, with make-up air mechanically and chemically cleaned

the rear end of the exciter for again cooling the unit. Half of this air, leaving the cooler, passes through activated carbon cleaners which take the contaminants from that air. The activated carbon filter is more effective with cool air and is, therefore, located so that the air passes through it after passing through the cooler. The other half of the air passes through a restricted area, having the same pressure drop as that of the air passing through the activated carbon cleaners. Since the total air in the enclosure of the system is recirculated several times a minute, the entire volume of recirculated air is thus cleaned half as many times as the air is recirculated per minute. Such a scheme permits the air being effectively cleaned by the activated carbon at a velocity within the capacity of the cleaner and without requiring too large a cleaner installation.

Since it is not necessary, nor very practical, to make the enclosure vacuum tight, there will be some leakage of air out of the system at slight openings in the structure and duct system where the air pressure within is above the surrounding atmosphere and a corresponding volume of air leakage into the system at other points where the pressure is below atmosphere. These volumes are, of course, equal. By providing a definite opening into the system at point (A), which is adjacent to the inlet to the fan at point (B), where the pressure is the lowest value, all air leakage into the unit will occur through the opening at point (A), which is essentially at atmospheric pressure since the system is open to the atmosphere through a small filter there and all other points within the system will be above atmospheric pressure by an amount equal to the fan pressure, less the pressure drop in the system caused by the restriction of the air flow in the ducts and structure, at any point. Thus, any openings or cracks in the ventilating system will result in an air leakage outward and not inward. By installing a mechanical filter and an activated carbon filter in this intake opening to the ventilating system, any outside air going into the system, will be cleaned and freed of contaminated atmospheres. Such a system will operate continuously, essentially free of dirt and contaminating gasses that are harmful to successful commutation, from the standpoint of commutator surface film.

Conclusions

Commutator surface film conditions exert a large influence on the successful operation of a direct current machine from the standpoint of commutation. Duplicate machines of the same design, built on the same order in the factory, each successfully passing the manufacturer's tests, may have entirely different performance in the field. While loading conditions will have a pronounced effect frequently, the variable performance of identical machines is due to the surrounding atmospheres, under which the machines have to operate.

At the present time relatively little is known of the surface films themselves produced on commutators during operation under adverse conditions. The detrimental effects produced are recognized, but complete solutions in general for overcoming these troubles are not yet available. Machines operating under such conditions in many cases still have to be nursed along by giving attention to the commutator surface, either by the use of scouring brushes, grinding the commutator from time to time or installing protective ventilating atmospheres. The problem has also been attacked from the standpoint of producing brushes inherently designed or chemically treated during production to react with the film, supplying in some cases something missing from the atmosphere (as in the case of airplane generators) or producing a reaction which will permit the brushes to ride the film mechanically satisfactory and chemically successfully, so that acceptable commutation will result.

The authors want to point out that most commutating machines go into satisfactory service, with a minimum of commutator and brush maintenance. This paper has dealt, primarily, with those problems which are out of the ordinary; most of which come in the operating field alone and not in the design of the machine or the structure of a standard brush. Out of these troubles will come modifications in the design of the machines and development in the chemistry and processing of brushes, which will provide satisfactory operation under the present adverse conditions.

References

1. THEORY OF COMMUTATION AND ITS APPLICATION TO COMMUTATING POLE MACHINES (Electrical Engineering Papers), B. G. Lamme. Westinghouse Electric Corporation, East Pittsburgh, Pa., 1919.

2. Rotating Electrical Machinery, C-50-1943. American Standards Association (New York, N. Y.), page 13.

3. Influence of Temperature on Large Commutator Operation, **F. T. Hague, G. W. Penney.** AIEE Transactions, volume 48, April 1929, pages 666–77.

4. Humidity Control Prevents A-C Brush Disintegration, **E. F. Bracken.** *Electrical World* (New York, N. Y.), September 23, 1933, pages 410–11.

5. Electrical Sliding Contacts, **R. M. Baker.** *Electric Journal*, September 1934, pages 359–60.

6. Carbon Brush Contact Films, Part I, **C. Van Brunt, R. H. Savage.** *General Electric Review* (Schenectady, N. Y.), volume 47, July 1944, pages 16–19.

7. Electrical Units Seen Requiring Special High Altitude Treatment, **Karl Martinez.** *Journal*, Society of Automotive Engineers (New York, N. Y.), July 1948, pages 24–26.

8. Second Experimental Report to the Atmospheric Corrosion Research Committee, **W. H. J. Vernon.** Transactions, Faraday Society (London, England) volume 23, 1927, pages 113–204.

9. Treatment of High-Altitude Brushes by Application of Metallic Halides, **Howard M. Elsey.** Electrical Engineering (AIEE Transactions), volume 64, August 1945, pages 576–79.

10. Commutation and Current Collection in Hydrogen, **Robert M. Baker.** AIEE Transactions, volume 50, June 1931, pages 714–17.

Discussion

F. M. Scott (Allis-Chalmers Manufacturing Company, Milwaukee, Wis.): The fact that small amounts of chlorine immediately improved the commutation on a machine that was sparking apparently from the effect of hydrocarbon vapors was indeed surprising.

Although the authors are familiar with the effect of chlorine on commutator films it may be worth noting, particularly on this subject, the effect of chlorine on commutators. We have found that chlorine even in very small amounts will increase the brush friction greatly. It can be observed readily that the film on a commutator will be streaked almost immediately when a large amount of chlorine is drawn across a commutator. Selective commutation often results, and a brush and its connections are overloaded when the brush breaks through the film. If the surface is not corrected such action will sometimes burn off the pig tails.

Threading of commutators in chlorine atmospheres is very common. However, we have observed that usually only one polarity of brushes will contain copper in their faces, which tends to indicate that the copper got on the faces by some process similar to electrolysis.

Operating of d-c machines in contaminated atmospheres continues to present many problems that are not solved satisfactorily, and as pointed out by the authors, such applications may have to be nursed along by such methods as described by the authors until better brushes and methods are evolved.

H. M. Elsey: As we pointed out in our paper, the trace of chlorine must have altered the character of the film on the commutator in order that commutation should improve. As we pointed out in the verbal discussion following the delivery of the paper, the chlorine was used very judiciously. It was added to the cooling air for a few seconds only at each trial and these were spaced at least days and usually weeks apart. We have proved experimentally that chlorine does cause high friction when it is present at a brush commutator interface, but we do not know whether this high friction caused the bad film on the copper to be mechanically abraded away in a few seconds or whether the chlorine chemically attacked the objectionable film and altered its nature so that a desirable oxide film would form.

It has been our experience that copper picking is common to brushes of both polarities. Moreover, since we cannot understand how electrolysis can take place in the absence of an electrolyte, we believe that copper transfer must take place by some other mechanism than electrolysis.

Methods for Determining the Effect of Contaminants on Electrical Insulation

K. N. MATHES
MEMBER AIEE

L. E. SIEFFERT
NONMEMBER AIEE

H. P. WALKER
NONMEMBER AIEE

R. H. LINDSEY
NONMEMBER AIEE

SERVICE experience with electric apparatus has indicated that in many cases the presence of "contaminants" has contributed to the failure of electrical insulation. In the category of contaminants are included moisture, salt, oil, carbonaceous materials, and dust. Such contaminants may adversely affect both the physical and electrical properties of electrical insulation.

The General Electric Company under contract to the Bureau of Ships, United States Navy Department, has undertaken a program to develop laboratory test methods suitable for determining the effects of contaminants on electrical insulation. It is apparent that such tests to be significant must be applied to insulating materials in the form in which they appear in actual apparatus. Consequently it is best to develop test samples which consist of insulating materials in combination and which are characteristic of the combinations found in actual apparatus. This approach to the insulation problem has been described by one of the authors.[1]

It may be desirable to include this approach to the problem of writing new material specifications. There are two types of specifications for electrical insulating materials in common usage today:

1. *Material Quality Control Specification.*

Specifies tests on standard specimens and properties of the insulating material as manufactured, to determine that it is of the same quality as material previously found satisfactory by tests on the electric equipment in which it is used.

2. *Equipment Specifications.*

Specifies tests on and properties of the insulating materials indirectly by stipulating tests on and properties of the complete electric equipment in which the insulating materials are used.

It would be of obvious advantage to both insulating material and electric equipment manufacturers if means existed to predict, in advance of tests on the electric equipment itself, that the insulating material would be satisfactory in that equipment.

Material quality control specifications alone do not serve this purpose adequately. The principal reason for the inadequacy is the fact that insulating material quality control tests are conducted, and properties determined on the material as manufactured, whereas in the actual equipment such materials are used in combinations where design and construction factors play important roles not completely represented in the material quality control tests and properties.

There exists, therefore, a need for an additional type of specification.

3. *Simulated Component Specification.*

To determine the suitability of insulating materials in advance of tests on the complete equipment. This type of specification would give the tests to be conducted and properties to be determined on combinations of electrical insulating materials in a form simulating the design and construction in which the combination would occur in the electric equipment.

The purpose of this paper is to discuss the progress toward the development of test methods and synthetic contaminants suitable for evaluating the effect of contaminants on electrical insulation. The tabulated data in this paper is shown only to illustrate the type of information which can be obtained by the test methods developed, and to indicate the number of variables which may be involved. It is hoped that the success reported will serve as an incentive to the initiation of additional related programs by interested laboratories, so that eventually it will be possible to standardize on methods of tests which can be used to evaluate the suitability of insulating materials.

The Choice of Contaminants

In Navy applications a wide variety of contaminants may be deposited upon the electric apparatus. The following were considered to be most likely to occur in service.

1. Moisture—high humidity, leaking steam, mist, fog, and water.
2. Salt—salt mist, salt spray, or even salt water immersion.
3. Oil and gasoline—fuel, lubricants, and so forth.
4. Carbonaceous particles—soot and smoke from the stacks, and so forth.
5. Dust and dirt—suspended airborne soil, organic debris, and so forth.

To check these suppositions, a careful examination of the dirt scraped from representative surfaces on board ship was carefully examined and shown to contain at least the following: carbonaceous particles; lint; silica; clay; electrolytes (probably salt); and hydrocarbons (probably oil).

An enlargement of this contaminant is shown in Figure 1. Extraction and conductivity tests indicate that a relatively large proportion of oil, lint, and electrolyte is present.

It is obviously impossible to simulate in a test program the wide range of composition and character possible in each type of contaminant as it occurs naturally. In fact it is actually desirable to arrive at

---

Paper 49-35, recommended by the AIEE rotating machinery committee and approved by the AIEE technical program committee for presentation at the AIEE winter general meeting, New York, N. Y., January 31–February 4, 1949. Manuscript submitted November 12, 1948; made available for printing December 23, 1948.

K. N. MATHES and R. H. LINDSEY are development engineers in the general engineering and consulting laboratory of the General Electric Company in Schenectady, N. Y., L. E. SIEFFERT is materials engineer and H. P. WALKER is electrical engineer with the Bureau of Ships, United States Navy Department, Washington, D. C.

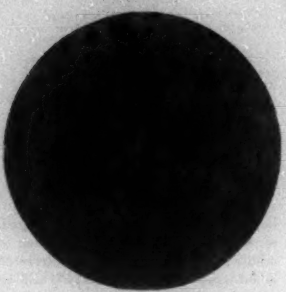

Figure 1. Dirt collected from insulation surfaces on shipboard

a definite and controllable formulation so as to permit reproducibility of test results. Moreover, the infinite variety of ways in which the contaminants may actually be deposited cannot be reproduced in tests, and an arbitrary method of applying the contaminants must be developed. However, the arbitrary materials and methods developed must be as representative as possible of actual service conditions with a tendency to emphasize the combinations and methods which produce the greatest deterioration. The development of the contaminants and methods of application actually has been carried out essentially by a process of "backing and filling"—the results of the tests on the physical and electrical properties of contaminated insulation with arbitrary contaminants has led to the formulation of different contaminants which in turn were evaluated electrically and mechanically. It is difficult and unnecessary to describe this study in chronological order but the approach and results will be described in the following sections.

Spreading of Liquid Contaminants—Contact Angles

At the beginning of the program it was apparent that the spreading of the liquid contaminants and the degree to which they "wet" various insulating surfaces should be important. To study this effect the contact angle was studied. Several such drops and their contact angles are shown diagrammatically in Figure 2. Contact angles for a number of liquids on different types of insulating surfaces are listed in Table I. A study of the relative angles for various liquids on different surfaces leads to a number of observations:

1. The contact angle of fuel oil is relatively small compared to water and salt water.
2. Number 1 fuel oil (kerosene) usually has a smaller contact angle than the more viscous oils, but this is not always the case. Apparently viscosity is not necessarily a controlling factor in determining the contact angle. Further reference to Table I will be made later in discussing the effect of liquid contaminants on physical properties.

Table II. Contact Angles

Distilled Water on Powdered Contaminants

	Adherent Liquids		
Contaminants	Turbine Oil (New)	Turbine Oil (Oxidized)	Nona-ethylene Glycol
Carbon black	131	125	0
Clay	0	0	0
1 part carbon black 5 parts clay	66	66	0
1 part carbon black 1 part clay 5 per cent salt	119	114	0

The relatively low contact angle for oils indicate that they would be the most likely to spread across a clean insulating surface and provide a base to which solid contaminants might adhere.

Table I. Contact Angles

Liquids on Various Insulation Surfaces

	Average Contact Angle						
Insulation Surface	Distilled Water	Tap Water	Sea Water	Con. Salt Solution	Turbine Oil	Gear Oil	Number 1 Fuel Oil
Short oil pigmented alkyd varnish air dried	75	70	69	71	5	11	5
Short oil pigmented alkyd varnish baked 6 hours at 160 degrees centigrade	79	76	78	79	5	10	5
Oil modified asphalt varnish air dried	90	84	88	92	12	20	5
Oil modified asphalt varnish baked 6 hours at 160 degrees centigrade	101	99	103	96	38	44	20
Medium length oil modified phenolic varnish, baked tackfree	83	80	84	90	14	17	14
Medium length oil modified phenolic varnish, baked 6 hours at 160 degrees centigrade	84	78	82	90	5	12	5
Medium length oil modified alkyd varnish, baked tackfree	82	70	76	76	8	32	5
Medium length oil modified alkyd varnish, baked 6 hours at 160 degrees centigrade	82	71	78	83	8	24	5
Paper base phenolic laminate-face surface	48	54	50	72	0	14	5
Paper base phenolic laminate-cross section	48	41	42	45	0	15	5
Glass base melamine laminate-face surface	68	66	72	77	32	28	5
Glass base melamine laminate-cross section	34	42	40	53	0	13	5
Cellulose acetate	59	58	58	62	18	31	5

Various methods of applying oil to the surface have been investigated; dipping in the oil or in the oil dissolved in solvent, vaporization, and condensation, spraying and atomizing, and simple smearing with a paper towel "wet" with the oil. Surprisingly the most uniform results were obtained with the simple smearing and this method has been adopted for most of the work.

Various methods of applying powdered solid contaminants to the oil coated surface have also been tried. In the method finally adopted, the powdered contaminant is dusted on the sample with a simple garden-type duster until the excess no longer sticks to the surface.

In service, moisture probably condenses on such dirty oily surfaces. The degree to which the condensed water spreads should affect the electrical characteristics.

Contact angles for water on various contaminants are listed in Table II. The contact angles of water on carbon black applied over an oily surface proved to be so high that an attempt was made to

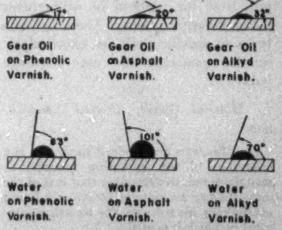
17°
20°
32°
Gear Oil on Phenolic Varnish.
Gear Oil on Asphalt Varnish.
Gear Oil on Alkyd Varnish.
83°
101°
70°
Water on Phenolic Varnish.
Water on Asphalt Varnish.
Water on Alkyd Varnish.

Figure 2. Diagrammatic representation of contact angles

Liquid contaminants on varnished surfaces

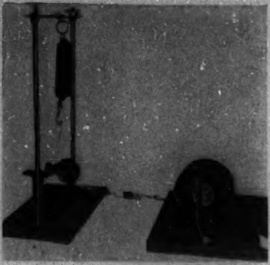

Figure 3. Wire helix bond test

Used to determine bonding strength of insulating varnishes

find a liquid which would provide adherence for the carbon particles and at the same time permit water to spread over the surface. Oxidized oil proved to be a small step in the right direction. Since it is difficult to reproduce the oxidized oil, a liquid with a definable composition was sought. Glycerine and several other liquids were tried without success. Finally nonaethylene glycol was found to combine the ability to stick carbon particles to surfaces and simultaneously to permit water to spread over the surface.

These observations of the spreading of liquid contaminants were used as a guide in developing the contaminants used for producing the physical and electrical deterioration described in the following sections.

Effect of Liquid Contaminants on Physical Properties

Only the liquid contaminants have been used in studying physical properties since it was believed that the solid contaminants could have relatively little, if any, effect. After trials with various methods of applying the liquid contaminants, total immersion in the liquid (hot or at room temperature) was adopted for most of the work as the easiest, most uniform, and in most cases, the most severe method. However, for the more volatile oils and fuels, results indicated that the vapors from the hot liquid in some cases might produce greater deterioration than immersion. Consequently, a number of samples also were tested in this way.

Four physical properties listed below were expected to be most affected by liquid contaminants.

1. Dimensional stability.
2. Strength (tensile, compressive, shear, and so forth.)
3. Plastic deformation and creep.
4. Abrasion resistance.

Dimensional change of solid insulating materials (such as plastics) exposed to moisture and water immersion have been studied in a number of investigations. The tensile and other strength characteristics of plastics after moisture exposure also have been studied. In view of this prior work, it seemed unnecessary to repeat such measurements. However, no measurements on insulating varnishes had been reported.

To study the strength characteristics of insulating varnishes, a varnished, magnet wire helix shown in Figure 3 was used. (The sample meets the objective of insulating materials in combination.) The tensile forces required to separate the turns of the helix before and after exposure to the contaminant are listed in Table III. It is of interest that exposure to the contaminant usually increased the bond strength. The helix bond test apparently evaluates a combination of the following physical properties:

1. Tensile strength of the varnish.
2. Shear strength of the varnish.
3. Adhesive strength of the varnish to the wire.
4. Ability of the varnish to elongate slightly.

It is probable that the liquid contaminants plasticize the varnish slightly so as to increase the helix bond strength.

To investigate the plasticizing action of the liquid contaminants, the cable coil sample[3] was used. This sample is made in the form of a concentric 7-strand cable of 0.032-inch insulated magnet wire with very low twist (1/3 turn per inch). Long lengths of the cable are dipped in varnish and baked or air dried. The cable is then

Figure 4. Cable coil deformation and creep test

Table III. Effect of Contaminants

Bond Strength—Varnished Formex* Helix

Varnish	Cure Time, Hours	No Contaminant	25C Immersion Distilled Water	25C Sea Water	25C Salt Water	25C Gear Oil	25C Turbine Oil	25C Number 1 Fuel Oil	95C Immersion Distilled Water	95C Sea Water	95C Salt Water	95C Gear Oil	95C Turbine Oil	95C Number 1 Fuel Oil
			Bonding Strength—Grams											
A	1	1,120	1,070	1,070	1,000	1,200	1,130	1,090	870	770	790	855	810	870
	24	910	890	930	920	970	970	1,030	1,070	960	980	800	920	790
B	1	635	700	650	690	690	670	295	595	570	550	610	635	350
	24	350	410	910	510	340	370	330	960	800	680	410	330	350
C	1	135	140	135	150	160	160	80	110	115	115	295	135	95
	24	90	80	80	80	130	90	130	70	90	70	130	180	130
D	1	170	315	310	300	270	210	230	170	195	190	150	150	160
	24	150	125	125	130	125	120	120	155	150	140	145	130	150
E	1	890	890	810	785	790	890	830	595	610	575	900	850	510
	24	1,670	1,550	1,490	1,370	1,660	1,730	1,800	1,190	1,220	1,190	1,550	1,630	1,490

A = unmodified phenolic varnish
B = medium length oil modified phenolic varnish
C = oil modified asphalt varnish
D = short oil pigmented alkyd varnish
E = medium length oil modified alkyd varnish
*Formex is a polyvinyl formal insulated magnet wire.

Table IV. Effect of Contaminants

Per Cent Elongation in Deformation and Creep of Cable Coils

Varnish Cure at 150 Degrees Centigrade	Hours	Uncontaminated		Immersed at 95 Degrees Centigrade					
				Turbine Oil		Number 6 Fuel Oil		Sea Water	
		DE*	CR**	DE	CR	DE	CR	DE	CR
Cotton Insulated Wire									
Unmodified Phenolic	1	0.01	0.001	0.01	0.001	0.01	0.001	0.01	0.001
Medium length Oil modified Phenolic	1	0.18	0.012	0.19	0.008	0.405	0.024	0.21	0.012
Oil modified	1	0.20	0.026	F†	F	F	F	0.26	0.043
Asphalt	24	0.09	0.001	0.14	0.007	0.48	0.043	0.02	0.005
Short oil	1	0.17	0.028	0.04	0.006	0.46	0.070	0.505	0.076
Pigmented Alkyd	24	0.01	0.001	0.01	0.001	0.02	0.001	0.02	0.001
Medium length Oil modified Alkyd	24	0.01	0.001	0.15	0.021	0.53	0.033	0.58	0.045
Formex Insulated Wire									
Unmodified Phenolic	1	0.01	0.001	0.01	0.001	0.01	0.001	0.01	0.001
Medium length Oil modified Phenolic	1	0.12	0.007	0.19	0.009	0.65	0.043	0.33	0.024
Oil modified	1	0.16	0.02	F	F	F	F	0.35	0.049
Asphalt	24	0.18	0.006	0.39	0.018	F	F	0.18	0.009
Short oil	1	0.08	0.014	0.13	0.028	0.90	0.088	1.1	F
Pigmented Alkyd	24	0.01	0.001	0.02	0.001	0.03	0.001	0.01	0.001
Medium length Oil modified Alkyd	24	0.02	0.001	0.03	0.003	0.48	0.025	0.54	0.042

*DE—deformation **CR—creepage † F—denotes complete mechanical failure

cut to a 4-inch length, supported at each end, and a load applied as shown diagrammatically in Figure 4. The deflection, five seconds after applying the load, is called the deformation, and the incremental deflection after an arbitrary two minutes, is called the creep. At the end of two minutes, an increased load is applied and the deformation and creep again determined. Table IV lists values of deformation and creep for samples before and after exposure to liquid contaminants. These results show a wide divergence in results for different varnishes and contaminants, and there were some differences between different magnet wire insulations. The cable coil sample and the deformation and creep test seems very suitable for determining the plasticizing action of liquid contaminants on varnish treated structures. Solid dielectrics such as plastics cut into rectangular bars also can be evaluated with the deformation and creep test as shown by the results in Table V.

A number of abrasion tests were tried without notable success in an attempt to evaluate the effect of contaminants on a variety of insulating materials. The most useful of the abrasion tests for this purpose has been described previously.[3] The carboloy washer abrasion test is shown in Figure 5. Two and a quarter turns of the cotton, asbestos, or glass fiber tape are wrapped about the 3/8-inch rectangular brass bar, fastened with small copper wires and varnish dipped and baked. The bar is rotated under the carboloy washer until the varnish tape abrades sufficiently to permit electrical contact between the washer and bar which stops the driving motor. Table VI compares abrasion resistance before and after immersion in contaminants. The most significant comparisons are obtained with varnished glass fiber tape, apparently because the glass fiber in itself has relatively low abrasion resistance.

Effect of Contaminants on Electrical Properties

In order to survey the effect of contaminants on electrical properties, simple rectangular plastic samples with bolts and washers for electrodes were used, Figure 6. After the first measurements of surface breakdown voltages were made, it became apparent that with either short time or step by step tests, the current flowing at the low voltage tended to dry the surface and prevent breakdown. To overcome this problem, a new technique for making surface breakdown tests was developed as follows:

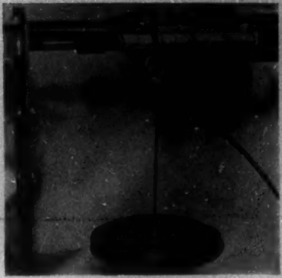

Figure 5. Carboloy washer abrasion test

1. Ten samples are used.
2. One sample is subjected to a short time breakdown test.
3. A voltage (125, 250, 500, 750, 1,000 1,300, 1,600, or 2,000) one step below the short time breakdown value is applied abruptly to three samples for five minutes and the number of failures recorded.
4. If two or three failures are obtained in Step 2, then three samples are subjected to a voltage one step below that of Step 2.

   If none or only one failure is obtained in Step 2 then three samples are subjected to a voltage one step above that of Step 2.
5. Dependent on the results obtained in Step 3, the three remaining samples are subjected to a higher or lower voltage step with the object of obtaining a voltage range—at the lowest voltage none or a maximum of one sample failed, at the highest voltage three or a minimum of two samples failed.

Table VII gives ranges of surface voltage breakdown for different contaminants under different humidity conditions. These results indicate that the effect of contaminants on surface breakdown is quite complicated. The choice of contaminants to give comparative results on different materials is restricted as outlined below:

1. The liquid used to supply adhesion for the solid contaminants should wet the solid

Table V. Effect of Contaminants

Per Cent Elongation in Deformation and Creep of Plastics

Laminate	Uncontaminated		Distilled Water				Gasoline	
			At 25° C		At 95°C		At 25°C	
	DE*	CR**	DE	CR	DE	CR	DE	CR
Paper base Phenolic laminate	0.01	0.001	0.01	0.001			0.01	0.001
Hard fiber	0.01	0.001	F†	F			0.01	0.001
Cellulose acetate	0.07	0.001	0.18	0.006	0.24	0.008		

*DE—deformation **CR—creepage † F—denotes complete mechanical failure

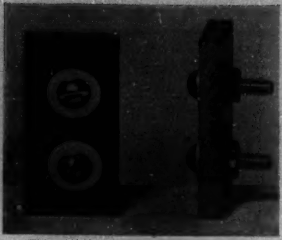

Figure 6. Rectangular plastic sample for surface breakdown test

Table VII. Surface Breakdown of Paper Base Laminate

Relative Humidity, Per Cent	Liquid Contaminant	Solid Contaminants Per Cent Clay	Solid Contaminants Per Cent Carbon	Solid Contaminants Per Cent Salt	Range Breakdown, Volts
100	*	80	20	0	1,600–2,000
100	**	80	20	0	>2,000
100	†	80	20	0	1,300–1,600
100	†	0	100	0	>2,000
100	†	90	10	0	1,500–2,000
100	†	80	20	0	1,300–1,600
100	†	70	30	0	500–750
100	†	80	20	0	1,300–1,600
100	†	80	19	1	1,000–1,300
100	†	79	19	2	250–500
100	†	78	18	4	250–500
100	†	80	20	0	1,300–1,600
96	†	80	20	0	>2,000
100	†	78	18	4	250–500
96	†	78	18	4	750–1,000
90	†	78	18	4	750–1,000
80	†	78	18	4	1,000–1,300
75	†	78	18	4	1,000–1,300
70	†	78	18	4	>2,000
100	*	78	18	4	250–500
96	*	78	18	4	>2,000

* new turbine oil ** oxidized turbine oil † nonaethylene glycol

contaminant and also be wet by water (nonaethylene glycol).

2. A carbonaceous conducting contaminant is required.

3. A powdered contaminant such as clay is required to increase the voltage breakdown to a value sufficient to permit comparison (carbon particles alone result in too low a surface breakdown voltage to permit comparison).

4. At relative humidities less than 100 per cent an ionizable contaminant (salt) is required to obtain surface failures at less than 2,000 volts. (Salt is best added by making a water paste with the carbon black and clay followed by drying and subsequent powdering in a ball mill.) The characteristics of the liquid contaminant also are important in this respect.

A contaminant system, such as described before, has been applied to samples designed to represent a varnished magnet wire winding. These samples are shown in Figure 7. A magnet wire is wound on a wooden core ($2^1/_4$ by 3/4 inches) in two cross-wise layers using 0.032-inch wire. The top layer is wound with a regular cross-over pattern so that there are two crossovers between each set of electrodes. The electrodes are narrow strips of silver paint spaced at 1/2-inch intervals. Lengths of braided 0.010-inch copper wire are wound around the samples over these electrodes and as support for the samples in the humidity box. Breakdown voltages between silver paint electrodes on the varnished magnet wire samples are compared for different varnishes and wires in Table VIII. A study of these results leads to at least two interesting observations.

1. Surface breakdown of contaminated surfaces is affected by the kind of varnish.

2. Surface breakdown is affected by the nature of the underlying magnet wire insulation as well.

Summary and Conclusions

A number of methods have been developed for evaluating the deteriorating effect of contaminants on both physical and electrical properties of insulating materials. Suitable contaminants have likewise been developed. The results bear out the need for samples which combine insulating materials in a manner similar to that in which they are actually used. For example, the surface breakdown of a contaminated varnished magnet wire sample depends on both the nature of the treating varnish and the type of magnet wire used. It is apparent that tests on the separate components could not provide the significant information obtained with the composite sample.

The large number of factors which enter into such evaluations is most striking. In consequence, the development of significant and useful material specifications covering the effect of contaminants on insulating materials appears to be difficult. It is likely that the methods described will be most useful at first in carrying out evaluations, which it is hoped may serve as a guide to the design engineer in his choice and use of insulating materials. Additional work is being done to learn more about the problem, eliminate unnecessary variables, and simplify tests. At the same time, results with methods described are being

Table VI. Carboloy Washer Abrasion Resistance

Insulation Surface	No Contaminant	Immersed in Number 1 Fuel Oil at 24 Degrees Centigrade 1 Hour	Immersed in Number 1 Fuel Oil at 24 Degrees Centigrade 24 Hours	Immersed in Number 1 Fuel Oil at 95 Degrees Centigrade 1 Hour	Immersed in Number 1 Fuel Oil at 95 Degrees Centigrade 24 Hours
Cotton Tape					
A	5	11	0	5	0
B	2,000+	2,000+	2,000+	2,000+	2,000+
C	2,000+	2,000+	2,000+	2,000+	2,000+
D	580	250	150	140	110
E	23	26	30	20	22
F	4	2	0	5	0
Glass Tape					
A	0	1	1	1	1
B	92	78	60	59	22
C	970	2,000+	2,000+	2,000+	2,000+
D	225	210	175	280	140
E	7	2	8	2	32
F	2	0	0	0	0
Asbestos Tape					
A	122	630	325	335	235
B	2,000+	850	1,525	1,000	975
C	2,000+	2,000+	2,000+	2,000+	2,000+
D	2,000+	2,000+	2,000+	2,000+	2,000+
E	750	156	225	365	485
F	435	225	95	152	85

A—untreated tape

B—medium length oil modified phenolic varnish, baked one hour at 150 degrees centigrade

C—unmodified phenolic varnish, baked one hour at 150 degrees centigrade

D—medium length oil modified alkyd varnish, baked one hour at 150 degrees centigrade

E—short oil pigmented alkyd varnish, air dried

F—oil modified asphalt varnish, air dried

Table VIII. Effect of Contaminants on Surface Breakdown Values in Volts, RMS, 60-Cycles Alternating Current

		Cure—1 Hour at 150° C				Cure—24 Hours at 150° C	
			Contaminant 5 Parts Clay 1 Part Carbon Black				
Varnish	Wire	No Contaminant	No Salt	1 Per Cent Salt	5 Per Cent Salt	No Contaminant	Contaminant 5 Parts Clay 1 Part Carbon Black 1 Per Cent Salt
Unmodified phenolic	HF	>2,000	500–750	250–500	250–500	>2,000	500–750
	DC	>2,000	>2,000	1,600–2,000	125–250	>2,000	1,000–1,300
Medium length Oil modified Phenolic	HF	>2,000	>2,000	750–1,000	125	>2,000	1,600–2,000
	DC	1,300–1,600	500–1,000	500–750	250–350	1,600–2,000	1,300–1,600
Oil modified asphalt	HF	2,000	>2,000	500–750	125	2,000	1,000–1,300
	DC	1,600–2,000	600–800	500–750	250–350	1,600–2,000	1,000–1,300
Short oil Pigmented Alkyd	HF	>2,000	1,000–1,300	1,000–1,300	750–1,000	>2,000	1,600–2,000
	DC	>2,000	1,000–1,300	750–1,000	750–1,000	>2,000	1,600–2,000
Medium length Oil modified Alkyd	HF	>2,000	>2,000	1,000–1,300	125	>2,000	1,600–2,000
	DC	1,600–2,000	1,600–2,000	500–750	125	>2,000	>2,000

HF—Heavy Formex DC—Double cotton

correlated with service experience. Eventually it may be possible to write material specifications which include the effect of contaminants on insulating materials in combination.

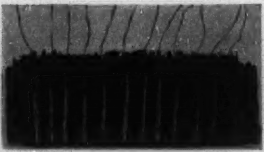

Figure 7. Varnished magnet-wire samples for surface breakdown test

References

1. Functional Evaluation of Insulating Materials, **K. N. Mathes.** AIEE Transactions, volume 67, part II, 1948, pages 1236–40.

2. Evaluating Insulating Varnishes, **K. N. Mathes.** *General Electric Review* (Schenectady, N. Y.), May 1948, volume 4, pages 20–28.

3. Fabric Abrasion Testing, **K. N. Mathes.** *General Electric Review* (Schenectady, N. Y.), November 1940, volume 43, page 467.

Discussion

A. T. McClinton (Naval Research Laboratory, Washington, D. C.): It is interesting to find that more people are now thinking in terms of evaluating the materials going into a piece of electric apparatus for its merits. This practice, which has long been recognized by a few, will lead to a more thorough understanding of the limitations in the design of equipment. It will not leave the engineer fumbling around in the dark wondering just how far he can go before he has approached or exceeded the design limitations.

Insulating materials are one of those components used in equipment about which so little is really known regarding its limitations and applications. Engineers have been working for years with specifications on spacing of live parts without any knowledge of the validity of those specifications nor how they were derived. The only check the engineer had on his design was the usual insulation tests plus service experience, neither of which informed him of the procedure he should follow in attempting to improve his design.

This paper, which presents one interesting approach to the problem, is of value in that it attempts to eliminate some of the unknown factors. There may be considerable disagreement with the techniques employed, and the numerical values obtained by the investigators, however, the purpose and ultimate goal is certainly of great importance. Its value will be greatest if it can cause others who are doing or have done similar work to publish their results.

The writers of this paper have commented on the desirability of approaching service conditions in the preparation of test procedures. This technique is unquestionably the best. However, there are actually two conditions that should be fulfilled in preparing test codes. One of these is as mentioned, namely, to simulate service conditions as nearly as possible. The second and of equal importance is to use a technique that can be duplicated readily by other laboratories. Unless this is done, obviously the procedure is of questionable value. There is considerable doubt as to how well the method of applying the contaminant, used by the authors, can be duplicated. The desirability of maintaining close control of the quantity of contaminant is demonstrated by the results in Table VII.

There are two questions concerning the procedure used, the answers to which may be of interest. These are:

1. What is the quantity of contaminant deposited per square inch of surface area?
2. Was the nonaethylene glycol used for any other purpose than as a wetting agent to provide uniform distribution of water over the surface of the test sample?

It is noted that complete surface breakdown resulting from one surge has been the technique employed in determining the electrical property of the insulation when contaminated. Certainly this is a simple test procedure and may give comparative data on different insulations with various contaminants. However, such a procedure does not consider all the factors, one of which is the effect on the breakdown voltage of repeated surges at lower voltages.

Concerning the results presented in Table VII, it would be of interest to know whether the authors have made sufficient tests to know how this data compares with that for other insulating materials. Also, information as to how quickly the breakdown was noted after application of the voltage in Step 3 might help the reader to understand some of the complexities of the effects of contaminants on surface breakdown. The statement has been made in the paper that "An ionizable contaminant (salt) is required if surface failures are to be obtained at less than 100 per cent relative humidity." This statement does not appear to be in agreement with the results presented.

K. N. Mathes, L. E. Sieffert, H. P. Walker, R. H. Lindsey: In reply to McClinton's specific questions, a uniform procedure has been developed for the application of the contaminants described which we believe will give reasonably reproducible results. The actual amounts of contaminant have not been measured directly, but insulation resistance measurements are being used to serve as an indication and control. The nonaethylene glycol used must "wet" the sample and the solid contaminant as well as providing a means for water to spread uniformly over the contaminated surface. In more recent work we have been able to obtain even more uniform results by using a combination of polyethylene glycol and glycerine.

We agree that the repeated application of voltage is an important service consideration and have made some preliminary investigations of this effect. Application of voltage tends to dry out the moisture at the surface of the sample. If sufficient time between applications of voltage is allowed so that the surface can soak up moisture, then a lower surface breakdown value will be obtained. For a thorough understanding of the problem the effect of repeated voltage applications should be investigated. It is believed, however, that the values after a single application of voltage give results which permit a comparison of materials.

Very recently quite a number of different insulating materials have been evaluated. Different surface breakdown values are obtained for different materials which indicates that the nature of the material is important. Most of the surface breakdowns occurred within 30 seconds after application of voltage, although a few were obtained throughout and even at the end of the 5-minute period of voltage application. Physical examination of the samples lends support to the theory that a progressive degradation occurs which is in conflict with the drying out that occurs at the same time. Breakdown occurs only when the rate of progressive deterioration outstrips the drying out which occurs simultaneously.

Failures at less than 100 per cent relative humidity can, of course, occur without ionizable contaminants if a sufficiently high voltage is applied. In the work described, however, voltages have been limited to 2,000 volts and within this range failure does not occur until an ionizable contaminant is present.

We wish to thank McClinton for the insights shown in the analysis of our work. Such suggestions are helpful in our program.

Solid Short Circuit of D-C Motors and Generators

T. M. LINVILLE
FELLOW AIEE

H. C. WARD, JR.
ASSOCIATE AIEE

Synopsis: In this paper the current of d-c machines on solid short circuit is expressed in terms of constant impedances similar to x_d' and x_d for synchronous machines. The outstanding advantage of this new result is that any number of d-c machines may be included in a network, with or without connection of batteries, rectifiers, or other machinery, and calculations may be made using a network analyzer, d-c calculating board or numerical calculation. The current in any machine, the total fault current, and so on, can be determined. Equations are given for d-c machines which are similar to the well-known equations for synchronous machines. Equations are given for the transient and steady-state resistances and for the decrement factors. The latter factors determine the rise and subsequent decline of current. Direct and simple expressions are given for the maximum rate of rise of current and for the maximum or peak value of current. Although design data is required for reliable calculations, useful preliminary estimates of current can be made using no data other than the resistance of the machine windings and a few dimensions which can be obtained from simple inspection of the machines. For this purpose, generalized values for design constants are given in the nomenclature.

IN A PAPER presented in 1946,[1] an analysis of short-circuit phenomena in d-c machines was described and formulas were derived for the current and torque. These formulas were expressed in terms of impedance which was variable with line current because of the influence of magnetic saturation in the armature teeth. Therefore, although the formulas were satisfactory for the case of one machine short circuited alone, when a number of machines were connected in a network the formulas were not suitable for simple calculations. Thus, there has been a need to derive the formulas in terms of constant impedances. Additional work has shown this can be done as described in this paper. Results are given in the following sections followed by an explanation of their derivation.

Short-Circuit Currents

Similarity between the new formulas and those for synchronous machines will be noted.[2,3] For a d-c machine the current on short circuit is

$$i_a=\frac{e_0}{r_d}-\frac{e_0}{r_d'}\epsilon^{-\sigma_a t}+e_0\frac{r_d-r_d'}{r_d r_d'}\epsilon^{-\sigma_f t}\text{ per unit} \tag{1}$$

where e_0 is the electromotive force existing in the machine just previous to short circuit (terminal voltage plus or minus winding and brush drop), r_d is the steady-state effective resistance of the machine, and r_d' is the transient-state effective resistance.

These quantities are all per unit. σ_a is the armature circuit decrement factor for the machine, and σ_f is the field circuit decrement factor.

The maximum short-circuit current is

$$I_a'=\frac{e_0}{r_d'} \tag{2}$$

The initial and also the maximum rate of rise of current is

$$\frac{di_a}{dt}=\frac{\sigma_a e_0}{r_d'} \tag{3}$$

since other terms in the derivative of equation 1 are negligible.

The field current is

$$i_f=\frac{e_0}{n_0}\left\{1+\frac{r_x'}{r_d' n_f}(\epsilon^{-\sigma_f t}-\epsilon^{-\sigma_a t})\right\}\text{per unit} \tag{4}$$

where r_x' is the per-unit transient-state compounding resistance, taking into account the effect of armature current on generated electromotive force; and n_f is the leakage flux coefficient for the field winding, ratio of total field flux linkages minus field linkages from flux-generating armature electromotive force to field linkages from flux-generating armature electromotive force.

Transient Resistances

The transient effective resistance is

$$r_d'=r_w+r_b'+r_x'+r_e \tag{5}$$

where r_w is the resistance of the windings, r_b' is the transient resistance of the brush contact, r_x' is the transient compounding resistance, and r_e is the resistance external to the machine if any; all quantities are per unit.

The resistance of the brush contact is derived in the previous paper as follows[1]

$$r_b'=E_R b\left(\frac{\epsilon^x+1}{\epsilon^x-1}\right)+V_c \tag{6}$$

where E_R is the average per-unit reactance voltage per armature coil at rated full-load current and at speed at which machine is short-circuited, b is the width of brush contact face in commutator segments, V_c is the normal per-unit full-load brush and brush contact voltage drop, and

$$x=\frac{E_R b}{V_c}$$

The effective compounding resistance, r_x', was treated in the previous paper as a variable.[1] It is the factor which measures the change in electromotive force between the initial electromotive force just before short circuit and the electromotive force existing when maximum armature current is reached. The new result for r_x'

Paper 49-39, recommended by the AIEE rotating machinery committee and approved by the AIEE technical program committee for presentation at the AIEE winter general meeting, New York, N. Y., January 31–February 4, 1949. Manuscript submitted November 16, 1948; made available for printing December 28, 1948.

T. M. Linville is staff assistant to the manager of engineering in the apparatus department, and H. C. Ward, Jr., is a member, advanced engineering program, General Electric Company, Schenectady, N. Y.

The authors wish to thank A. G. Darling and R. G. Rhudy for their assistance in making this paper possible and for the calculations given in Table I.

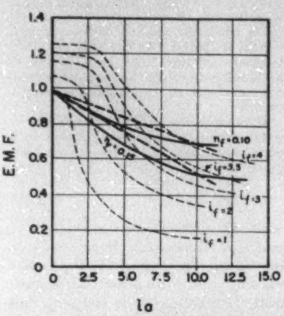

Figure 1. Relation between electromotive force, armature current, and field current

as a constant is, for machines without pole-face windings

$$r_x' = \frac{10 n_f e_o + n_f(K_1 + 10K_2)(10K_3 n_o - e_o)}{100(n_f + K_2) + 10K_1} \quad (7)$$

where

$$K_1 = \frac{p_p \phi_t}{p_a M_{a1}}$$

$$K_2 = \frac{C_s C_d K_\lambda g K_t}{0.85(g + d_s)} = \frac{1.25 g K_t}{g + d_s}$$

$$K_3 = \frac{(b \pm 2b_s) P M_{a1}}{B}$$

The symbols in these formulas for K_1, K_2, and K_3 are given in the nomenclature. ϕ_t on which K_1 is dependent is the flux in per unit determined by multiplying the average cross section of the armature teeth in square inches by the number of teeth in a pole arc by the intrinsic saturation density of 123,000 maxwells per square inch and dividing by unit flux in maxwells.

When a machine has pole-face windings and there is no serious distortion of flux in the main pole shoes and consequently no extreme saturation of the armature teeth, equation 7 becomes

$$r_x' = \frac{K_3 n_f n_o}{1 + n_f} \quad (8)$$

Steady-State Resistances

The steady-state effective resistance for separately excited machines is

$$r_d = r_w + r_b + r_x + r_e \quad (9)$$

where, for machines without pole-face windings

$$r_x = \frac{10e_o + n_o(10K_3 - I_{fo})(K_1 + 10K_2)}{100} \quad (10)$$

For a separately excited machine with pole-face windings

$$r_x = \frac{e_o + n_o(10K_3 - I_{fo})}{10} \quad (11)$$

The brush and brush contact resistance for either type of machine is

$$r_b = E_R(1 - E_c) b \left(\frac{\varepsilon^x + 1}{\varepsilon^x - 1} \right) + V_c \quad (12)$$

where

$$x = \frac{E_R(1 - E_c) b}{V_c}$$

and E_c is the estimated ratio, under sustained short-circuit conditions, of actual interpole field strength to field strength if no saturation occurred.

Decrements

The decrement factor σ_a for the armature circuit is

$$\sigma_a = \frac{r_d' 2\pi f}{C_x} \quad (13)$$

where f is the frequency of the machine in cycles per second at rated base speed, equal to number poles times revolutions per minute divided by 120, and C_x is the inductance coefficient. For machines without pole-face windings, C_x is about 0.6. For machines with pole-face windings, C_x is about 0.15. All factors in equation 13 are per-unit quantities except for frequency. The inductance L_a should be calculated from the dimensions of the windings and magnetic circuits whenever possible. Values given for C_x are preliminary and are subject to change when more test data is obtained. At best, C_x is an average coefficient and will vary quite widely between particular machines and between particular conditions of saturation.

Saturation will change the effective inductance, L_a, greatly. For example, when a machine without pole-face windings is excited at full rated excitation, it usually is operating above the knee of the saturation curve, and C_x, therefore, may be as low as 0.15. This is because in these machines a large part of the inductance is caused by flux in the main pole air gap caused by armature excitation. When a machine of this type at full excitation is excited above the knee of the saturation curve largely because of saturation in the armature teeth, the effective inductance from flux in the main pole air gaps will be reduced about in proportion to the ratio of the slope of the saturation curve at full excitation to the slope of the air-gap line, that is, the slope without saturation.

The decrement factor for the field circuit is

$$\sigma_f = \frac{r_f}{L_f} \quad (14)$$

where r_f is the resistance, which is simply the ratio of exciter volts to excitation amperes, and L_f is the inductance of the circuit, which is the flux linkages per ampere of the field coils times the number of coils in series times 10^{-8}. Saturation will change the effective value of L_f. Correction for it must be made. The simplest method is to reduce the flux linkages per ampere resulting from air-gap flux in proportion to the ratio of the slope of the saturation curve at the actual field excitation to the slope without saturation (slope of air-gap line).

Current Rise

It should be understood that the paper is concerned with the effect of saturation from two different causes. In the foregoing sections saturation existing before short circuit as a result of field excitation has been discussed. Now, in plotting the rise of current against time, account must be taken of the increase in σ_a caused by saturation resulting from the heavy load current.

To do this, the line given by equation 3 should be drawn remembering that, for machines without pole-face windings and with excitation before short circuit definitely above the knee of the saturation curve, C_x must be reduced to about 0.15. Assume that the current rises at this constant rate for a time interval of 0.67 σ_a seconds and thereafter goes parallel at all levels of current to equation 1 plotted with σ_a replaced by $3\sigma_a$.

This curve and the curve of equation 1 without modification can be expected to bracket the true current. The total change in σ_a during the rise in current is not likely to increase σ_a beyond $3\sigma_a$.

Per-Unit Quantities

All quantities for current, voltage, resistance, flux, magnetomotive force, and speed in the formulas are per unit, that is, each of these quantities has been divided by the corresponding base quantity. Base quantities are as follows:

V_1 = rated voltage, in volts
I_{a1} = rated full-load amperes
I_{f1} = rated full-load field amperes
$R_1 = V_1/I_{a1}$
N_1 = rated base speed
M_{f1} = field ampere turns per pole at rated voltage, rated base speed, no load
ϕ_1 = flux per pole in maxwells at V_1 and N_1

Assumptions

In our calculations, the following assumptions were made:

1. Saturation other than in armature teeth and pole-face teeth is neglected.
2. Leakage flux linkages of the field winding are proportional to field amperes.
3. Center of current in brush faces is at trailing edge of the brushes at instant of maximum current.
4. Change in commutating pole flux between instant of short circuit and instant of maximum current is negligible because of damping effects of solid steel frame, helped in many cases by solid steel poles.
5. Speed of the machine is maintained.

Discussion of Results

The calculation of sustained short-circuit current is included solely for completeness. It is not likely that machines of 250 volts and higher will reach sustained short-circuit current without flashing over or without such arcing at the brushes as to destroy the accuracy of the assumptions on which the paper is based.

It is to be expected that, in many cases, the current will be drawn out beyond the trailing edge of the brushes even at the moment of maximum current, causing measured current in cases where tests are made to be less than calculated current. To make calculations, it is necessary to fix the axis of armature reaction at some definite location, such as at the trailing edge of the brush, where the resulting error, if any, will yield a high current rather than a current lower than actual.

The use of the decrement factors requires use of good judgment in lieu of extensive calculations for inductance if the rise of current is to be plotted accurately. Otherwise, the inductance coefficient C_2 should be 0.15 for all machines with or without pole-face windings, and the current rise should be plotted as described in the section entitled "Current Rise" with the decrement factor σ_a increasing from σ_a to $3\sigma_a$.

Method and Basic Equations

For clarity and correction of the earlier paper,[1] the set of simultaneous equations whose solution gives the results presented in this paper are restated as follows.

The fundamental equation relating exciting flux, armature amperes, and field amperes is, for machines without pole-face windings

$$\phi_d' = \frac{M_f' p_p \phi_i}{M_a' p_a} + M_f' \rho \frac{\phi_1 K_1}{M_{f1}} \qquad (15)$$

where $\rho K = {}_1K_2$, as given in equation 7.

Equation 15 has two terms representing iron flux and space flux respectively. It was found necessary to divide the flux into these two components in order to take saturation of the armature teeth into account.[1] However, when there is no serious distortion of flux in the main pole shoes resulting from cross magnetization by armature magnetomotive force and consequently no extreme saturation of the armature teeth, equation 15 is not applicable. These conditions hold true in the case of machines with pole-face windings. Therefore, in this case the flux can be expressed as a function of the field-winding magnetomotive force alone as

$$\phi_d' = \frac{M_f' \phi_1 K_1}{M_{f1}}$$

This neglects all saturation, as is evident from line (*a*), Figure 2. So as not to neglect altogether the normal saturation, the saturation curve is taken as line (*b*), Figure 2, so that

$$\phi_d' = \frac{M_f' \phi_1}{M_{f1}} \qquad (16)$$

The fundamental equation relating field-circuit flux linkages immediately after short circuit to those immediately before short circuit, in accordance with the constant-linkage theorem,[4] is

$$\phi_d' + n_f \frac{\phi_1}{I_{f1}} I_f' = \phi_o(1 + n_f) \qquad (17)$$

The equation summing the voltages in the armature circuit is

$$I_a' = \frac{\phi_d' n_o}{r_w + r_b' + r_e} \qquad (18)$$

Equations 15, 17, and 18, or 16, 17, and 18, for machines without or with pole-face windings respectively, are the basic equations.

The effect of shift of the axis of armature magnetomotive force, caused by brush shift and by brush arcing, is included by replacing M_f' of the basic equations with M_d'. Assuming that brush arcing causes the axis of armature reaction to lie in line with the trailing edge of the brushes

$$M_d' = M_f' - \frac{(b \pm 2b_s) P M_a'}{B}$$

where M_d' is the net magnetomotive force in the main pole axis, M_f' is the field winding magnetomotive force, and M_a' is the armature reaction magnetomotive force. The brush shift from the polar axis, b_s, measured in commutator bars, is plus if with rotation, minus if against rotation. P is the number of poles. B is the total number of bars in the commutator. b is the brush width in bars.

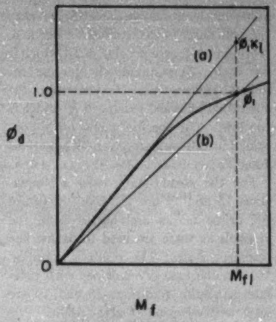

Figure 2. Saturation curve

Then, to express the basic equations in terms of the maximum armature current, I_a', and the maximum field current, I_f', the following relations are substituted

$$M_a' = \frac{M_{a1}}{I_{a1}} I_a'$$

$$M_f' = \frac{M_{f1}}{I_{f1}} I_f'$$

Each group of basic equations now can be solved for the maximum currents I_a' and I_f', obtaining results similar to those given in the earlier paper.[1] These results are complicated because the relation between armature electromotive force and armature current is not linear, as illustrated by the solid lines of Figure 1. An approximation can be made which is linear, as illustrated by the heavy dashed lines in Figure 1, by writing the change in electromotive force as equal to $I_a' r_x'$.

Then the flux, ϕ_d', responsible for electromotive force can be written

$$\phi_d' = \frac{e_o}{n_o} - \frac{I_a' r_x'}{n_o} \qquad (19)$$

where e_o is the electromotive force before short circuit, and n_o is the corresponding speed of the machine. By the simultaneous solution of equations 15, 17, and 19, or equations 16, 17, and 19 as the case may be, r_x', which is the slope of the heavy dashed lines in Figure 1, is found as a function of I_a'. However, if a specific value of 10 is assigned to I_a', the slope becomes specific as shown in Figure 1, and heavy dashed lines which are good approximations of the solid curved lines are obtained. It is apparent from Figure 1 that, for current values less than 10 per unit, this approximation will yield a value of electromotive force higher than the true value of electromotive force and, therefore, will give a value of I_a' which is too high. Correspondingly, for current values higher than 10 per unit, the equations will yield a value of I_a' which is too low. The specific values for r_x' obtained in this way are given by equations 7 and 8.

For the steady-state value r_x, equations 15 and 19 are the root equations. All prime marks are deleted from the symbols as these are used to denote the transient state. The result is equation 10. In the case of machines with pole-face windings, equations 16 and 19 are used, with equation 11 as the result.

Substitution of equation 19 in equation 18, and equation 5 into the result shows that $I_a' = e_o/r_d'$. Similarly, $I_a = e_o/r_d$. The complete current–time formula, equation 1, now can be developed. The armature current has the following components

Rise

$$I_a'(1-\varepsilon^{-\sigma_a t})$$

Decay

$$-(I_a'-I_a)(1-\varepsilon^{-\sigma_f t})$$

The time constants are so dissimilar that the components may be added together directly with negligible error, giving

$$i_a=I_a-I_a'\varepsilon^{-\sigma_a t}+(I_a'-I_a)\varepsilon^{-\sigma_f t} \tag{20}$$

Equation 1 follows when $I_a' = e_o/r_d'$ and $I_a = e_o/r_d$ are substituted in equation 20. Similarly, for the field current, the current starts with the initial current I_{fo} and has the following additional components:

Rise

$$(I_f'-I_{fo})(1-\varepsilon^{-\sigma_a t})$$

Decay

$$-(I_f'-I_{fo})(1-\varepsilon^{-\sigma_f t})$$

Adding these three components together

$$i_f=I_{fo}+(I_f'-I_{fo})(\varepsilon^{-\sigma_f t}-\varepsilon^{-\sigma_a t}) \tag{21}$$

Solving equations 17 and 19 for I_f' and substituting e_o/n_o for ϕ_o gives

$$I_f'=\frac{e_o}{n_o}+\frac{I_a'r_x'}{n_o n_f} \tag{22}$$

By putting $I_{fo} = (e_o/n_o)\ (I_{f1}/\phi_1)$ and $I_a' = e_o/r_d'$, equation 4 is obtained from equations 21 and 22 for the field current in per unit.

Conclusions

Calculations for several different types of d-c machines are given in Table I, showing that the current on dead short circuit with negligible external resistance is widely different between machines of different types and ratings. Therefore, short-circuit current cannot be determined without formulas such as given in this paper accounting for such important factors as r_x' and r_b' expressed in terms of measurable machine quantities. The authors feel sure that persons familiar with d-c machines will recognize the results given in Table I as typical of test results.

Comparison of calculations with test oscillograms in a few specific instances have shown good checks.[1] However, the rate of rise of current subsequent to the initial or maximum rate of rise is an estimate only. Also, the value for sustained current is mainly of academic interest especially in cases of high-voltage machines where flashover is more or less certain to occur. To account for the effect of changing magnetic saturation on the rise of current beyond an approximate method such as given here requires lengthy, step-by-step calculations.

Nomenclature

b = brush overlap, in segments
b_s = brush shift from polar axis, segments
B = total number of segments in commutator
C_s = air-gap slot fringing coefficient[1]
C_δ = air-gap duct fringing coefficient[1]
C_x = inductance coefficient, average value 0.15
d_s = depth of armature slot, inches
d_a = diameter of armature, inches
E_c = estimated ratio, under sustained short-circuit conditions, of actual interpole field strength to field strength if no saturation occurred. Generalized value = 0.3
e_o = armature electromotive force before short circuit, in per unit
E_R = average per-unit reactance voltage per coil at rated full-load current and at speed at which machine is short-circuited. At base speed, average value is $12n_oI_{a1}10^{-8}/d_a$ or, preferably, $5\times10^{9}lBI_cN_1n_o/V_1$
f = machine frequency at base speed, cycles per second
g = average length of main-pole air gap, inches
i_a = instantaneous short-circuit current, per unit
i_f = instantaneous short-circuit field current, per unit
I_a = steady-state short-circuit current, per unit
I_a' = maximum short-circuit current, per unit
I_{a1} = base amperes = rated full-load armature current, amperes
I_c = rated full-load armature amperes divided by number of circuits in armature winding. Number of circuits

Table I. Calculated Maximum Short-Circuit Current for Typical D-C Machines

Poles	Rating		Rpm	Volts	Pole-face Winding	Rating	Temperature Rise, Degrees	Ventilation	Maximum Amperes Per Unit
20	5,000	Hp	125	600	Yes	Continuous	40	Open	15.8
10	1,750		150	600			40		12.7
4	500		400	600			40		17.8
6	350		200	600			40		10.3
16	4,000		80	750			40	Forced	13.9
8	1,500		150	600			40		9.9
4	75	Kw	1,800	250	No		40	Open	9.4
4	125		1,800	125			40		6.3
4	150		1,800	250			40		12.1
4	50	Hp	1,150	230			40		6.9
4	150		850	230			40		10.3
6	600		850	230			40		13.1
4	25/30		400/1,600	230			40/50		7.0
6	200/		400/1,200	230			40/50		11.0
4	35		250/1,000	230			60	Forced	5.1
4	200		400/1,200	600			60		14.4
8	250	Kw	514	240			40	Open	11.4
6	30		1,200	120			40		7.4
4	70		1,500	70		1 Hour	50		4.0
4	5	Hp	1,025	230		1 Hour	75		5.0
4	100		485	230		1 Hour	75		8.4
4	15	Kw	1,750	125		Continuous	40		6.2
4	20		1,450	250			40		9.1
4	5		3,600	250			40		11.6
4	5	Hp	850	115			40		4.8
4	30		1,750	230			40		10.1
4	$7^1/_2$		1,750	230			40		7.6
4	3/5		300/1,200	230			40/50		6.6
4	$5/7^1/_2$		690/2,300	115			40/50		5.7
4	$5/7^1/_2$		575/2,300	230			40/50		8.0
6	500	Kw	900	250			40		14.2
8	600		900	250			40		11.0
8	1,250		720	250			40		11.5
12	1,500		514	250	Yes		40		14.8
6	1,250		750	600			40		17.3
8	1,500		514	600			40		17.2
12	2,500		514	600			40		15.6
16	4,000		300	600			40		15.0
16	4,000	Hp	80	750			40	Forced	13.9
8	2,000		400	600			40		17.0
8	1,500		70	600			40		9.9

usually is two in small machines and in medium and big machines is usually equal to number of poles

I_{f1} = base field amperes = field amperes at rated voltage, base rated speed, no load

K_1 = coefficient for flux ϕ_t. Generalized value = 0.92

K_2 = coefficient for permeance ratio Generalized value = 0.17

K_λ = pole tip flux fringing factor[1]

K_t = air-gap plus tooth ampere turns divided by air-gap ampere turns at rated voltage, base rated speed, no load

l = length of armature core, in inches

L_f = inductance of field circuit divided by unit ohms, R_1

M_{a1} = armature reaction magnetomotive force at full rated load, per unit. Representative value = 1.0

M_f' = maximum field ampere turns per pole, per unit

M_{f1} = base ampere turns = field ampere turns per pole at rated voltage, rated base speed, no load

n_f = ratio total field flux linkages minus linkages from flux responsible for armature electromotive force to linkages from flux responsible for armature electromotive force. Representative value = 0.15

n_o = speed at which machine is short-circuited, per unit

N_1 = base or unit speed = rated base speed, revolutions per minute

p_a = pole arc, inches

p_p = pole pitch, inches

P = number of poles

r_b = steady-state resistance of brush and brush contact, per unit

r_b' = transient resistance of brush and brush contact, per unit

r_d = steady-state effective total resistance of machine under short circuit, per unit

r_d' = transient effective total resistance of machine under short circuit, per unit

r_e = external resistance, per unit

r_f = resistance of field circuit, per unit

r_z = effective steady-state compounding resistance, per unit

r_z' = effective transient compounding resistance, per unit

r_w = effective total resistance of windings in armature circuit, per unit

R_1 = base ohms = V_1/I_{a1}

V_1 = base volts = rated voltage, volts

V_c = normal brush contact drop at full load, in per unit. Equals $3/V_1$ for graphitized brushes or $1/V_1$ for metal graphite brushes

ϕ_1 = base flux = flux per pole in maxwells at rated voltage, rated base speed, no load

ϕ_t = iron flux per pole, in per unit. Equals average section of armature tooth in square inches times number of teeth in pole arc × 123,000 lines per square inch divided by ϕ_1

ϕ_d' = flux responsible for armature electromotive force, per unit

ϕ_o = flux per pole before short circuit, per unit

σ_a = armature circuit decrement factor

σ_f = field circuit decrement factor, generalized value = 1.0

References

1. CURRENT AND TORQUE OF D-C MACHINES ON SHORT CIRCUIT, T. M. Linville. AIEE TRANSACTIONS, volume 65, 1946, pages 956–65.

2. SYNCHRONOUS MACHINES—IV, R. E. Doherty, C. A. Nickle. AIEE TRANSACTIONS, volume 47, April 1928, pages 457–92.

3. THREE-PHASE SHORT CIRCUIT OF SYNCHRONOUS MACHINES—V, R. E. Doherty, C. A. Nickle. AIEE TRANSACTIONS, volume 49, April 1930, pages 700–14.

4. A SIMPLIFIED METHOD OF ANALYZING SHORT-CIRCUIT PROBLEMS, R. E. Doherty. AIEE TRANSACTIONS, volume 42, 1923, pages 841–49.

Discussion

F. M. Scott (Allis-Chalmers Manufacturing Company, Milwaukee, Wis.): The procedure outlined in this paper for calculating the short-circuit currents of d-c machines is a practical method, particularly when it is necessary to consider several machines in a given system. The potential short-circuit current possibilities should be considered on any system containing a number of d-c machines. Installations such as hot strip mills can have values of short-circuit currents as high as 500,000 amperes. The actual occurrence of such faults on such systems has emphasized the need for such a procedure. A knowledge of values of current that are possible will allow proper preventive steps to be taken. Such known steps now are separating the two busses to minimize the possibility of faults, sectionalizing the bus sections with high-speed circuit breakers. Further development of better circuit breakers will be required.

The results in Table I of this paper are quite typical, but, as Linville pointed out, the actual short-circuit current calculation involves the consideration of many factors. We also have found the degree of saturation affects the results appreciably. Inductance varies with the degree of saturation, and is a factor that affects particularly the time required to obtain a given value of current.

There are so many variables such as speed drop, saturation, fault resistance, and so forth, that it almost is mandatory to use such a system as that outlined by the authors. The results obtained are quite safe as they are the maximum possible, and any actual values always would be less than those calculated. Such a paper as this requires a vast amount of computation and numerous tests. I believe that additional tests and investigations would be useful so that these previously indeterminate factors can be calculated with even closer accuracy.

T. M. Linville, H. C. Ward, Jr.: Questions have been asked about the accuracy which can be expected of the results and about the dimensional correctness of several of the equations. It also has been asked whether or not the equations are applicable at any initial value of speed, voltage, and load current, and whether they are equally accurate for very small as well as very large machines. The final question asked is: can the results be developed into a generalized method for the determination of short-circuit currents in d-c systems similar to the procedure already developed for a-c systems?

Accuracy is important of course, and the authors have found that the results usually will come very close to test values. This statement applies to the maximum value of current only. On solid short circuit, the current usually is drawn out from the trailing edge of the brushes rapidly in the form of heavy arcing, followed in many cases by flashing. This causes the current to be less than calculated, so that usually it is found that the calculated current is a little higher than actual. Calculation of the rate of rise of current depends upon the calculation of the inductance of the circuit as well as the effective circuit resistance. The inductance is affected, by magnetic saturation which varies with the value of currents in the armature and field circuits. However, calculation of the initial rate of rise (the maximum rate) will be found to be accurate, because the initial inductance can be calculated accurately, taking into account the saturation caused only by field current. It is important to remember that a machine at full excitation has a faster rate of rise than a machine at partial excitation. The time constant must be corrected for field-current saturation as described in the paper.

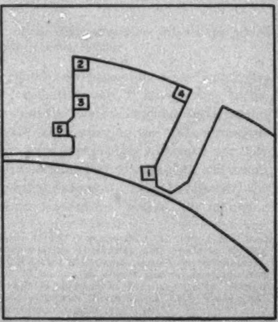

Figure 1

Care must be taken in making the calculations when a machine has a series field which is loosely coupled with the shunt field, and when a machine has a pole-face winding which gives incomplete compensation under the pole face. When the series field is loosely coupled, the formula for K_3 in equation 7 of the paper should become

$$K_3 = \frac{(b \pm 2b_s)PM_{a1}}{B} \pm k_s M_s$$

where k_s is a coefficient depending on the position of the series field, and M_s is the number of series-field ampere turns at rated full-load current in per unit. The sign of k_s is plus for differential series field and minus for cumulative series field when the machine is under short circuit. The following values of k_s are estimated for the positions shown in Figure 1 of the discussion:

Position	k_s
1	0.9
2	0.05
3	0.2
4	0.15
5	0.35

When the pole-face winding gives incomplete compensation, equation 7 should be used rather than equation 8, and K_1 should become

$$K_1=\frac{p_p\phi_t}{p_a M_{a1} k_c}$$

where

$$k_c=\frac{p_a M_{a1}-M_{b1}p_p}{p_a M_{a1}}$$

The importance of these corrections for series field and partial pole-face compensation has been shown by the results of tests made by the Naval Research Laboratory for the Bureau of Ships. Oscillograms from test are to appear in an AIEE paper, now in preparation. Their calculations checked test results closely when correction was made for a loosely-coupled series field, but did not do so using the bare formulas of the paper.

The authors undoubtedly owe an apology for not maintaining dimensional correctness of equations in which quantities are per unit. For example, equations 6 is actually

$$r_b'=E_R b\left\{\frac{\varepsilon^x+1}{\varepsilon^x-1}\right\}\frac{R_1}{V_1}+V_c\,\frac{R_1}{V_1}$$

Written this way the equation is dimensionally correct either with actual or per unit quantities. E_R is in volts per coil (volts per segment), b is in segments, R_1 is in ohms, V_1 is in volts, and V_c is in volts. r_b' is then in ohms. When all quantities are per unit, V_1 and R_1 are unit quantities. When one is substituted for each of them, the equation given in the paper is obtained. In all of the results, unit quantities have been dropped out and only per unit quantities retained.

The equations as given are applicable at any initial values of speed and voltage. n_o and e_o are fractional quantities according to the ratio of initial speed and voltage to rated speed and voltage, respectively. When there is an initial load current, I_a' and I_a are unaffected, but to make equation 20 correct, the initial load current I_o must be subtracted from I_a and I_a' in each place in the equation, and I_o must be added to the right-hand member of the equation as a new term.

The formulas are applicable to machines of all sizes.

The development of a new method often may be the start of a chain of progress and, therefore, the authors hope that calculations of a large number of machines, including all sizes and types, will be made, and that from resulting data, presented in suitable graphs and tables, it will be possible to find at a glance the maximum short-circuit current, maximum rate of current rise, and transient resistance for practically any machine whose nameplate data are known. It seems promising, therefore, that the design of machines, of bus structures, of circuit breakers, and the protection of equipment in d-c networks can be done more accurately and by substantially the same methods as have been developed for synchronous machines.

Application Engineering on Diesel-Electric Locomotives in Railroad Service

G. T. BEVAN
MEMBER AIEE

FORTY-FIVE per cent of the total operating expense of a railroad is affected by the character of motive power used. Consequently, very careful consideration should be given to the proper selection of locomotive power. From a strictly engineering viewpoint, a locomotive should be purchased as "a tool to fit the job," while from an economic standpoint, it is quite obvious that a complete cost study should be made before finally selecting the type of power.

This approach of "fitting the tool to the job" in the selection of Diesel-electric railroad power—as compared to the prior practice wherein steam locomotives were purchased and tested afterward with a dynamometer car to determine their hauling capacity—is now generally offered by the locomotive builders. This practice not only fits the correct Diesel-electric locomotive to the job, but also determines the economics involved, from an initial investment standpoint as well as from an annual operating expense comparison.

With the advent of the Diesel-electric locomotive, a new approach to train operation had to be established. The Diesel-electric locomotive can be overloaded to the point of damaging the electrical equipment if tonnage and grade conditions reduce the speed below a given continuous speed. This is not true of steam operation; a steam locomotive can be overloaded to the point of stalling without damage. It became necessary, therefore, for the Diesel-electric-locomotive manufacturer to establish a continuous as well as a short-time tonnage rating for any particular locomotive application.

Speed–distance curves enable the engineering and economic aspects of a given application to be readily understood. This graphical analysis is used as a basis for determining the fundamental application. It is the calculation of the operation of a train of predetermined size and weight at a certain speed over a given profile, in such a way that the complete running time as well as the continuous speed is obtained. A typical speed–distance curve is shown in Figure 1. From this basic information it is quite feasible to determine the economic aspect of a dieselization proposal, inasmuch as the total fuel consumption is readily obtained. The preliminary data needed to plot a speed–distance curve are:

1. Railroad profile, including rail weight, curve data, and elevation for plotting a condensed profile.
2. Employee's timetables, giving the number of stops and speed restrictions on the section under consideration.
3. Train performance data, giving information as to train size and weight in tons to be hauled.
4. Data as to equipment characteristics, such as air-conditioning, car weight, and so forth.
5. Train dispatcher's records for the period under consideration.

Before recommending a particular size of locomotive unit, it is necessary to determine the axle loading in order to permit a safe rail loading on the track structure. Excessive axle loading will cause not only rail and road-bed damage, but will result also in unsafe operation. In selecting the proper size of locomotive, the following data, giving the axle loadings permissible for different weights of rail, are helpful:

Rail Weight Pounds/Yard	Maximum Axle Load Per Pound of Rail Weight
0–60	500 pounds
61–90	600 pounds
91–152	700 pounds

For example: a 100-ton 4-axle locomotive will operate safely on 85-pound rail where the permissible loading is 85 ×600 = 51,000 pounds.

Tonnage Ratings

The next preliminary investigation is to determine the size of locomotive necessary to handle a given tonnage over the designated profile at a selected speed. Knowing the grade, curve, and train resistance and the tonnage to be hauled, the locomotive tractive effort and horsepower can readily be obtained. Let us assume a ruling grade of 1 per cent, a maximum curve of 4 degrees, a train resistance of 4.8 pounds per ton, and a freight tonnage of 70 cars at 40 tons per car. The total train resistance is the algebraic sum of the grade, curve, and train friction resistances. In this case the train resistance is 20 + 3.2 + 4.8 = 28 pounds per ton.

The continuous tractive effort of a typical single-unit 1,500-horsepower (115-ton) road locomotive, geared for a top speed of 65 miles per hour, is 42,500 pounds. Thus, knowing the locomotive weight, the required tractive effort can be derived from the following:

$$\text{Tractive effort} = \text{Train Resistance} \times (\text{Train weight} + \text{Locomotive weight})$$

or

$$\text{Train weight} = \frac{\text{Tractive effort}}{\text{Train resistance} - \text{Locomotive weight}}$$

$$= \frac{42{,}500}{28} - 115$$

$$= 1{,}400 \text{ tons (trailing)}$$

$$= 35 \text{ cars at } 40 \text{ tons/car}$$

Since one unit can handle 1,400 tons, a 3,000-horsepower 2-unit locomotive will handle the specified 2,800-ton train. The speed over the ruling grade will be 110

Paper 49-42, recommended by the AIEE land transportation committee and approved by the AIEE technical program committee for presentation at the AIEE winter general meeting, New York, N. Y., January 31–February 4, 1949. Manuscript submitted November 12, 1948; made available for printing January 1, 1949.

G. T. BEVAN is in the Alco-GE Division of the General Electric Company, Schenectady, N. Y.

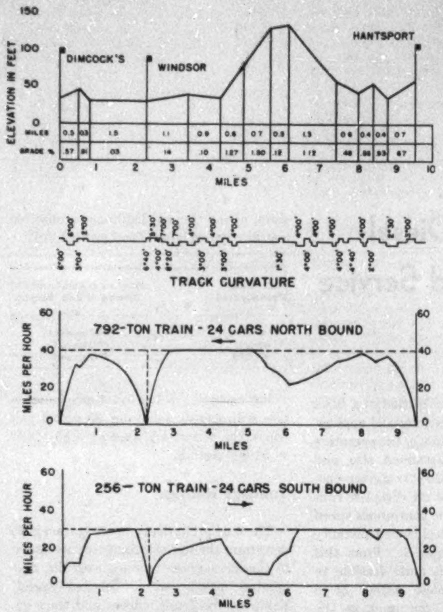

Figure 1. Condensed profiles and speed-distance curves, freight service

Alco-GE 2,000 horsepower (2-unit) locomotive. Speed restriction shown by broken lines

miles per hour, as shown on the characteristic curve for this locomotive.

Should it be desired, however, to handle a 1,400-ton train over the ruling grade at a speed between 25 and 30 miles per hour, a 3-unit 4,500-horsepower locomotive would be required. The tractive effort would be:

$$\text{Tractive effort} = 29.5\ (1{,}400 + 345) = 51{,}500 \text{ pounds}$$

This gives a speed over the grade of 27.5 miles per hour as noted from Figure 2. In this case, the running adhesion is comparatively low allowing minimum wheel slipping. The adhesion factor for a locomotive operating under these conditions is:

$$\text{Adhesion factor} = \frac{\text{Required tractive effort}}{\text{Weight on drivers, pounds}} = \frac{51{,}500}{345 \times 2{,}000} = 7.5 \text{ per cent}$$

The maximum running adhesion value with a dry, clean rail in good condition should not be over 20 per cent. Rail that is wet or in poor condition will necessitate the use of a lower adhesion value.

On relatively short grades over a rolling profile, the kinetic energy accumulated running down grade can be used to assist the train over the next ascending grade. After the momentum has been completely used up, it may be necessary to demand a locomotive output considerably higher than the continuous rating of the traction motors for a short time until the summit of the grade is reached. In this case, a short-time or overload rating may be used, provided, of course, that the adhesion factor of 20 per cent is not exceeded.

As an example, consider a rolling profile in which a ruling grade of one per cent for two miles is such that momentum operation could be employed. Assuming the curve resistance at one pound per ton and the train friction resistance at four pounds per ton of train weight, the continuous tonnage rating with a 4,500-horsepower (345-ton) locomotive would be:

$$\text{Trailing tons} = \frac{\text{Continuous tractive effort}}{\text{Train resistance}} - \text{Locomotive weight}$$

(Train resistance = Grade resistance + Curve resistance + Train friction resistance)

$$= \frac{127{,}500}{20+1+4} - 345 = 4{,}755 \text{ tons.}$$

Assuming 50-ton cars, this equals a 95-car train. Since the grade is only two miles in length, the short-time overload rating up to the slipping point (20 per cent) could be used. In this case, the momentum of the train would be considered run out in a train length or approximately 4,280 feet (95 cars × 45 feet length per car). Therefore, a distance of 6,280 feet or 1.19 miles is left to climb, in which the short-time rating could be used to advantage. At 20 per cent adhesion the tractive effort available is 0.20 × 345 × 2,000 or 138,000 pounds. The trailing tons that could be handled over this grade on a short-time basis is:

$$\frac{138{,}000}{20+1+4} - 345 = 5{,}175 \text{ tons or } 104 \text{ 50-ton cars}$$

The time on the grade at the short-time rating would be:

$$\text{Time (minutes)} = \frac{\text{Distance (miles)}}{\text{Speed (miles per hour)}} \times 60$$

$$= \frac{1.19}{9.5} \times 60$$

$$= 7.5 \text{ minutes}$$

Referring to Figure 2, it is seen that the speed over the grade at the short-time tractive effort rating is 9.5 miles per hour.

The capacity of a Diesel-electric locomotive is expressed in two ways, the continuous rating, and the short-time rating. The short-time rating is actually a $1^1/_2$-hour rating based on the temperature rise of the motor windings. Where the grades require over 90 minutes to ascend with a given train, the continuous rating must be used, otherwise the temperature rise will be excessive with consequent damage to the motor windings and insulation.

Speed and Acceleration

The correct size of Diesel-electric locomotive should be selected, furthermore from a preliminary investigation of the speed desired over the ruling grade with a given weight of train. Then a locomotive tractive effort–speed curve is made up which is used in calculating the speed of the desired train. In the usual manner, the grade, curve and train resistances are algebraically added to the tractive-effort values found from this curve, to obtain the net amount of tractive effort for acceleration of the train.

Since the grade, curve, and train resistance are expressed in pounds per ton, the locomotive tractive effort–speed curve is plotted on the same basis. The grade resistance is taken at 20 pounds per ton for each per cent of grade. The curve resistance is calculated at 0.8 pound per ton per degree of curvature. The train resistance is determined from the formulas developed by W. J. Davis.[1] These formulas are used to express the total resistance tending to reduce the locomotive

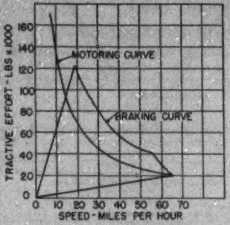

Figure 2. 4,500-horsepower Diesel-electric locomotive tractive effort and braking curves

speed, which consists of journal, flange, and air friction. The force required to accelerate one ton at one mile per hour per second is, for straight line acceleration, 91.1 pounds. This is derived from the well-known formula:

$$F=MA \qquad F=\frac{W}{32.2}\times 2{,}000\times A\times\frac{5{,}280}{3{,}600}$$

$$=\frac{W}{g}A \qquad =91.1WA$$

where

F = accelerating force in pounds
W = weight in tons
A = acceleration in miles per hour per second
M = mass
g = gravity constant

When the rotational inertia is taken into account, at approximately 10 per cent of the linear inertia, the total net force required to accelerate a ton of train weight at a rate of one mile per hour per second will be 100 pounds. Therefore if the net tractive effort available for accelerating a 1,000-ton train is 25,000 pounds, the acceleration will be

$$\frac{25{,}000}{1{,}000\times 100}=0.25 \text{ mile per hour per second.}$$

The ability of a loaded train to make a rapid acceleration depends upon a number of conditions, the most important of which is the coefficient of adhesion between the locomotive wheels and the rails. Numerous tests have proved that, on a clean dry rail, an adhesion factor of 30 per cent is the maximum that can be attained without excessive slipping of the driving wheels. Rails that are wet or that have poor running surfaces, such as driver burns and so on, will materially reduce these values.

In the normal application of Diesel-electric locomotives, rates of acceleration of 0.3 mile per hour per second for freight service and 0.75 mile per hour per second for passenger service have been proved practical by experience. Variations from these rates depend upon the characteristic and type of train being accelerated.

Horsepower and Fuel Consumption

By taking increments of the speed in accelerating a specified train, the time in seconds can readily be obtained. From this, the increment distance can be calculated. Thus, increment horsepower is obtained from the formula

$$HP=\frac{TE\times MPH}{375}$$

where

HP = horsepower
TE = tractive effort in pounds
MPH = speed in miles per hour

When the increment values of horsepower and time are known, the horsepower hours can be quite easily calculated. The total fuel consumption for a given operation can be obtained if the Diesel-engine fuel rate is known. Thus the speed–distance–time calculations and plotting of the data will give a complete history of the train movement.

Railroad operation requires four distinct locomotive services:

1. Yard-switching service includes switching work in passenger and freight terminals, classification yards, and local way-freight service.
2. Transfer service includes the movement of trains from one point to another, generally within a terminal territory.
3. Branch-line service includes freight and passenger operation on secondary lines of light traffic density.
4. Main-line service includes freight and passenger service in through main-line terminal-to-terminal operation.

Switching Service

The most striking replacement of steam locomotives has been in yard-switching service, principally because the Diesel-electric locomotive offers the following advantages:

1. Full utilization of Diesel-engine horsepower output.
2. Saving of time through higher acceleration rates.
3. Fuel savings up to as much as 50 per cent over steam.
4. Greater locomotive utilization.

A comparison of the tractive effort–speed curves for typical Diesel-electric and steam locomotives is shown in Figure 3. It is quite obvious that the full horsepower output of the Diesel-electric in the low-speed range gives this type of power supreme advantage in yard operation.

In the application of Diesel-electric locomotives to yard service, a knowledge of the particular operating conditions is necessary. The frequency of

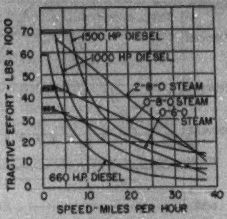

Figure 3. Comparison of tractive effort and speed characteristics of steam and Diesel-electric switching locomotives

yard movements, as well as the maximum number and tonnage of cars handled, must be determined first. As a general rule, a 660-horsepower Diesel-electric will replace a 6-wheel steam switcher; a 1,000-horsepower Diesel-electric will replace an 8-wheel steam switcher, and a 1,500-horsepower Diesel-electric will replace a Consolidation or a Mikado steam locomotive when used in yard service. The average yard operation is carried on at a speed of 6 to 8 miles per hour; consequently, speed–distance curves are of little value, since the distance a given train moves is comparatively small.

Transfer Service

In transfer, branch-line, and road service, however, the speed–distance curve is quite helpful in analyzing the scheduling of trains, and also in determing fuel consumption. Here again, a knowledge of the particular operations involved is necessary in order to establish the correct size of train. For instance, the line and profile may show that a 6,000-horsepower locomotive could handle a 125-car freight train.

Proper knowledge of the traffic conditions, the frequency of trains, or the length of passing sidings on single-track lines is also necessary to determine whether such a large-size locomotive can be used. There have been cases on several single-track railroads in which full utilization of the complete flexibility of the Diesel-electric locomotive could not be realized simply because the passing-track capacity limited the size of the train to be handled.

Furthermore, the Diesel-electric locomotive offers complete flexibility of motive power for around-the-clock operation. For example, in branch-line service a Diesel-electric road switcher of either the 1,000-horsepower or 1,500-horsepower size can perform passenger service in one direction on a run, and mixed-train or

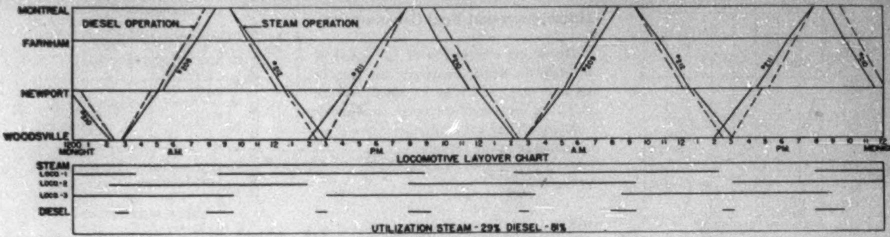

Figure 4. Graphic train sheet, steam versus Diesel-electric operation

way-freight service in the opposite direction, with equal efficiency. In this case, the scheduling of trains is such that one locomotive may make a complete round trip, whereas with steam-operation characteristics, passenger-train service may require a type of locomotive unsuited for the handling of a freight train on the return trip.

The flexibility of the Diesel-electric has been demonstrated further by the fact that this type of road-switcher locomotive has been used in triple-service around-the-clock operation on a railroad handling commuter traffic. During the rush hours, they handle commuter passenger trains. Then, during the daylight hours of industrial activity, these same locomotives are used in straight switching service. Finally, during the night hours, they haul freight trains on transfer runs, either singly or in multiple-unit operation.

Road Service

The Diesel-electric locomotive is ideally suited to this universal type of operation inasmuch as the Diesel engine develops constant horsepower over the entire locomotive speed range. The electric transmission in turn translates this horsepower into either high tractive effort at low speed or low tractive effort at high speed. This characteristic, by and large, makes a more dependable locomotive, both from the standpoint of schedules and of handling full tonnage under all kinds of climatic conditions. It is common practice with Diesel-electric locomotive operation to disregard the freight-train tonnage reduction formerly made in severe cold weather. The short-time overload capacity of the Diesel-electric enables it to start the same train in zero weather as in summer. In many instances with steam operation, the same train would require helper locomotives in cold weather.

In one instance, the supremacy of Diesel-electric was demonstrated by the complete elimination of steam-locomotive helper service over a ruling grade of 2.17 per cent for 1.5 miles. By taking advantage of the short-time overload capacity, the Diesel-electric was able to handle the full tonnage over this short, heavy grade without the use of helper locomotives.

The graphic train sheet, such as shown in Figure 4, has been used to considerable advantage in determining the number of locomotive units required to perform a given service. The Diesel-electric does not have to return to the engine house after every trip for cleaning of fires and replenishing of the water and fuel supply. Consequently, it can double back on a return trip within a few minutes after its arrival at a terminal. By analyzing the train movements graphically, therefore, maximum utilization of the Diesel-electric can be secured. In the case illustrated, one Diesel-electric can replace three steam locomotives.

One salient feature of the Diesel-electric locomotive that is of great value in mountainous territory is the dynamic brake, which uses the traction motors, acting as generators, to retard the train when descending heavy grades. On long, heavy, down-grade movements with steam operation, the air-brake retainer valves on the individual cars must be set before going down grade. This necessitates a stop at the top of the grade. If the grade is long and severe, two or three intermediate stops will be required to cool the brake shoes and wheels. One western railroad has indicated that, prior to the use of Diesel-electric locomotives, 2,500 wheels per month were removed on account of brake burns. Likewise, a considerable saving is realized by the elimination of the wear and replacement of brake shoes. The dynamic brake is much more reliable and results in safer operation, since the wheels and brake shoes do not become overheated.

As a general rule, Diesel-electric locomotives with dynamic braking can satisfactorily handle the same tonnage train either up or down grade. As a typical example, reference to the dynamic-braking curve in Figure 2 indicates that a 1,650 trailing-ton train can be handled down a 3 per cent grade with 6-degree curves, assuming 4.2 pounds per ton train friction. The total train resistance is the algebraic sum of the grade, curve, and train friction, or:

$-60+4.8+4.2=-51$ pounds per ton

(Train weight + Locomotive weight) × Total resistance = Braking effort

$1{,}650+345\times 51=101{,}745$ pounds

The braking curve, at 101,745 pounds braking effort, shows a speed of 5.5 miles per hour.

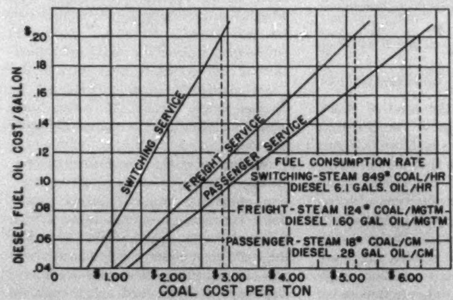

Figure 5. Comparison of fuel cost for steam and Diesel-electric operation

Table I. Steam versus Diesel Operation

Switching and Transfer Service. Grand Summary, 1947 Estimate

Steam

Operating Expenses I.C.C.*	Account Number	Per Hour	Per Annum
308	Locomotive repairs	$ 2.938	$ 50,325.48
378	Conductors and brakemen	4.659	79,780.08
380	Enginemen	2.875	49,232.88
382	Fuel	2.505	42,900.00
385	Water	0.021	360.00
386	Lubricants†		
387	Other supplies	0.735	12,510.48
388	Enginehouse expense†		
		$13.733	$235,108.92

Operating Data

Locomotive hours per year—17,124
Crew hours per year—17,124

Diesel

Operating Expenses I.C.C.	Account Number	Per Hour	Per Annum
308	Locomotive repairs	$ 0.840	$ 12,579.84
378	Conductors and brakemen	4.659	69,773.18
380	Enginemen	2.875	43,056.00
382	Fuel	0.640	9,584.64
385	Water		
386	Lubricants	0.064	958.46
387	Other supplies	0.735	11,007.36
388	Enginehouse expense	0.120	1,797.12
		$ 9.933	$148,756.60

Operating Data

Locomotive hours per year—14,976
Crew hours per year—14,976
Annual savings with Diesel operation—$86,352.32
Reduction of steam-operating expenses—36.8 per cent

Capital Investment

—1,000 Horsepower Diesel Switching Locomotives—$270,510**
Return on Capital Investment—32.0 per cent

*Interstate Commerce Commission.

†Expenses included in locomotive repair account 308.

**Includes freight charges to point of delivery at present rates.

Table II. Steam versus Diesel Locomotive Operating Costs

Branch Line Freight Traffic

Annual gross-ton miles	773,000,000
Annual train miles	356,000

I.C.C.* Account	Steam Costs Per Train Mile	Per 1000 GTM**	Per Annum
308 Locomotive repairs	$0.3878	$0.1786	$138,056.80
393 Fuel ($6.25 per ton)	0.8949	0.4121	318,582.42
397 Water	0.0406	0.0187	14,455.10
398 Lubricants	0.0229	0.0105	8,152.40
399 Other supplies	0.0120	0.0058	4,272.00
400 Enginehouse expense	0.1303	0.0600	46,386.80
392 and 401 enginemen and trainmen	0.8717	0.4014	310,323.25
	$2.3602	$1.0871	$840,228.77

I.C.C. Account	Diesel Costs Per Train Mile	Per 1000 GTM	Per Annum
311 Locomotive repairs	$0.1200	$0.0553	$ 42,720.00
393 Fuel (10.35 cents per gallon)	0.3952	0.1820	140,686.00
397 Water			
398 Lubricants	0.0395	0.0182	14,068.00
399 Other supplies	0.0120	0.0058	4,272.00
400 Enginehouse expense	0.0400	0.0184	14,240.00
392 and 401 enginemen and trainmen	0.8717	0.4014	310,323.85
	$1.4784	$0.6811	$526,309.85

Annual steam costs	$840,228.77
Annual Diesel costs	526,309.85
Savings	$313,918.92

First cost: 7—1,500 horsepower Diesel-electric road switchers........$920,500.00
Gross return on investment........34.1 per cent

*Intertstate Commerce Commission.

**Gross-ton miles.

In handling the same train up the grade, the tractive effort required will be:

$$(1{,}650+345)\times 69=137{,}500 \text{ pounds}$$

When exerting a tractive effort of 137,500 pounds, the locomotive speed will be 9.5 miles per hour as shown in Figure 2.

Analysis of Operating Expense

With a working knowledge of the train schedules and projected use of Diesel-electrics in the place of steam locomotives, the economics of the application can be determined, provided that additional data are available relative to the cost of operation. This information requires a complete breakdown of those operating expenses that are affected by motive-power operation. Railroad accounting classifies these expenses in eight different items as shown in the following tables. The largest saving of the Diesel-electric compared to the steam is in fuel expense. The reason for this is that the Diesel-electric has a thermal efficiency at the wheels of 25 per cent, whereas the corresponding figure for a modern steam locomotive is only 5 per cent.

Figure 5 shows the comparison between the costs of Diesel fuel oil and coal. The recent increases in fuel-oil cost have been paralleled by a corresponding increase in coal cost, so that the advantage of using fuel oil remains the same under the present price level. The savings in fuel cost with Diesel-electric operation may run as high as 60 per cent, depending, of course, on the relative prices of coal and oil.

Should the price of Diesel fuel oil advance to 20 cents per gallon, the cost of coal per ton for use in steam freight service would have to be $5.20 in order to match the fuel-oil cost. Any price higher than $5.20 would favor the Diesel-fuel cost and result in a saving over steam operation.

The second item reflecting a saving is the locomotive repair account. Steam locomotive repair cost is, on the average, approximately 10 per cent to 40 per cent higher than that of the Diesel-electric, depending upon the age of the steam motive power. The necessity of removing flues every four years, as well as costly firebox repairs, accounts for the increased maintenance on steam locomotives.

Engine house expense is the next item of comparison in which the Diesel-electric shows direct savings over steam operation. This expense covers the routine work at a terminal required to prepare a locomotive for its next run, including the cost of wiping and cleaning the locomotives,

Table III. Comparison of Steam and Diesel-Electric Operation of a Typical Major Class I Railroad

Freight—Passenger—Switching Service Annual Basis—Prorated from July 13–19, 1946 Traffic

Operating Expense

Steam				Diesel			
Freight Service							
I.C.C.* Account	Per Train Mile	Per 1000 GTM**	Per Annum	I.C.C. Account	Per Train Mile	Per 1000 GTM	Per Annum
308 Locomotive repairs	$0.4145	$0.2293	$1,585,021	311 Locomotive repairs	$0.2040	$0.0968	$ 669,837
392 Enginemen	0.2680	0.1483	1.025,095	392 Enginemen	0.3010	0.1424	985,066
394 Fuel	0.6882	0.3808	2,631,798	394 Fuel	0.3328	0.1576	1,089,213
397 Water	0.0311	0.0172	118,850	397 Water			
398 Lubricants	0.0160	0.0089	61,200	398 Lubricants	0.0401	0.0190	131,249
399 Other supplies	0.0081	0.0045	30,900	399 Other supplies	0.0081	0.0038	26,508
400 Enginehouse expense	0.1539	0.0852	588,500	400 Enginehouse expense	0.0409	0.0194	133,967
401 Trainmen	0.3409	0.1887	1,304,105	401 Trainmen	0.3409	0.1615	1,115,645
	$1.9207	$1.0629	$7,345,469		$1.2678	$0.6005	$4,151,48
Annual Gross-Ton Miles	6,911,249 (000)			Annual Gross Ton Miles			6,911,249 (000)
Annual Train Miles	3,824,355			Annual Train Miles			3,272,646
Annual Locomotive Miles	4,307,123			Annual Locomotive (Unit) Miles			5,581,978
Passenger Service							
I.C.C. Account	Per Train Mile	Per Car Mile	Per Annum	I.C.C. Account	Per Train Mile	Per Car Mile	Per Annum
308 Locomotive repairs	$0.3199	$0.0425	$ 503,842	311 Locomotive repairs	$0.1740	$0.0240	$ 241,447
392 Enginemen	0.2050	0.0273	322,864	392 Enginemen	0.2080	0.0244	288,562
394 Fuel	0.4605	0.0611	725,245	394 Fuel	0.2022	0.0236	280,490
397 Water	0.0185	0.0025	29,200	397 Water			
398 Lubricants	0.0088	0.0012	13,848	398 Lubricants	0.0252	0.0029	34,947
399 Other supplies	0.0053	0.0007	8,262	399 Other supplies	0.0053	0.0006	7,353
400 Enginehouse expense	0.0861	0.0114	135,540	400 Enginehouse expense	0.0298	0.0035	41,391
401 Trainmen	0.2150	0.0286	338,613	401 Trainmen	0.2150	0.0252	298,274
	$1.3191	$0.1753	$2,077,414		$0.8595	$0.1022	$1,192,464
Annual Car Miles	11,865,063			Annual Car Miles			11,865,063
Annual Train Miles	1,574,944			Annual Train Miles			1,387,318
Annual Locomotive Miles	1,599,500			Annual Locomotive (Unit) Miles			1,724,619
Switching Service							
I.C.C. Account	Per Hour		Per Annum	I.C.C. Account	Per Hour		Per Annum
308 Locomotive repairs	$ 1.2500		$ 86,895	311 Locomotive repairs	$0.8450		$ 58,740
380 Enginemen	3.1000		215,499	380 Enginemen	3.1000		215,500
382 Fuel	2.9132		202,233	382 Fuel	0.7960		55,335
385 Water	0.1329		9,242	385 Water			
386 Lubricants	0.0140		974	386 Lubricants	0.0796		5,533
387 Other supplies	0.0241		1,675	387 Other supplies	0.0210		1,460
388 Enginehouse expense	1.9693		136,900	388 Enginehouse expense	0.1440		10,010
378 Trainmen	4.8600		337,848	378 Trainmen	4.8600		337,848
	$14.2635		$991,266		$9.8456		$684,426
Annual Switching Hours	69,516			Annual Switching Hours			69,516
Annual Locomotive Miles	417,096			Annual Locomotive Miles			417,096

*I.C.C.—Interstate Commerce Commission.

**GTM—Gross-ton miles.

Annual Savings

Annual Savings	
Freight service	$3,193,984
Passenger service	884,950
Switching service	306,840
Total	$4,385,774

cleaning fires, dumping ashes, fire watching, and removing ashes.

The remaining items chargeable to locomotive operation include enginemen's and trainmen's wages, water, lubrication, and other supplies. With the exception of water account, which is considered negligible, these costs are approximately the same for Diesel operation, since the amount used for Diesel engine cooling and train heating is insignificant compared with that consumed in steam-locomotive operation.

A typical comparison of these eight items for steam and Diesel-electric operation for switching service is shown in Table I.

Since the daily mileage operated over by switching locomotives is rather low, and since considerable idling time has to be accounted for, it is necessary to use the hours operated per day as a means of comparison. Hence these switching-unit costs are based on locomotive hours.

In road work, on the other hand, the locomotive miles per day, month, or year give an indication of how much service a locomotive accumulates. Unit costs, therefore, are compared on the basis of train miles or locomotive miles. In the case of operating costs, a more correct comparison is obtained on the basis of the amount of work performed, which is represented in passenger service by car miles, and in freight service by thousands of gross-ton miles.

A comparison of the operating costs on a branch line of an eastern railroad where the steam locomotives are approximately 30 years old is shown in Table II.

A typical comparison of operating costs for a completely Dieselized, major Class-I railroad is shown in Table III. Here again, the operating savings in the fuel, locomotive repair, and engine house accounts are clearly evident. This program involves the replacement of 188 steam locomotives with 126 Diesel-electric locomotives. This replacement seems justified from an economic standpoint by the fact that a return of 24.2 per cent on the gross investment is possible. The reduction in operating expense accomplished by dieselization amounts to 42.5 per cent.

Conclusions

A locomotive, regardless of type, is more than a thermal and mechanical unit designed to develop ton-miles per hour. The first cost and efficiency of performance are the basic factors determining its selection. Efficiency of performance means not only availability, reliability, flexibility, and tractive-effort characteristics; but also includes costs of maintenance and operation.

From an initial investment standpoint, the first cost of steam motive power has advanced considerably in recent years, mainly due to the purchase of custom-built designs, and also to the smaller number of equipment manufactured. By comparison, the Diesel-electric has had a downward price trend largely due to standardization and quantity manufacturing practices. Consequently, on a dollar-per-horsepower basis, the operating savings with Diesel-electric motive power appear very attractive. The Diesel-electric locomotive, by its ability to operate on a round-the-clock performance, to operate in locations where water is hard to treat, and to eliminate costly engine house and other terminal inspections necessary with steam locomotives, has revolutionized the railroad industry. This newer type of motive power also has reduced, in many cases, the need for helper-locomotive service over mountainous routes. For these reasons the application of Diesel-electric locomotives to the railroad field has proved to be economically justified.

Reference

1. **W. J. Davis.** *General Electric Review* (Schenectady, N. Y.), October 1926.

No Discussion

Twenty-Five Years Progress in the Design of Traction Motors

M. J. BALDWIN
MEMBER AIEE

ALTHOUGH the traction motor at some 60 years of age is one of the oldest in the electrical industry, nevertheless it is a thriving oldster with an annual output of approximately 2,500,000 horsepower which has in the past quarter of a century staged a decided come-back due to the rapid development of the Diesel-electric locomotive.

This period has also been marked by the development of the PCC (President's Conference Car) standardized trolley car; the increasingly popular trolley coach; and by the application of 3,000-volt trolley power to commuter service multiple-unit cars and to new types of locomotives both here and abroad.

It is the purpose of this paper to review the progress that has been made in traction-motor design, and to note the particular design changes that have contributed to the improvements made.

Design Objectives

Traction motors are designed primarily for minimum weight. This is particularly true for trolley cars and coaches where weight is at a premium, and also, to a somewhat lesser degree, for rapid transit. For Diesel-electric locomotives where so much vertical space is required by the engine, a small wheel size is also important. On trolley locomotives, additional weight in the motors usually would be permissible, where ballast is used, to obtain required weight on the locomotive drivers. Large heavy motors have found, however, to add more to the cost of a locomotive than is saved in ballast.

Efficiency plays but a minor role in traction-motor design. Any increase in efficiency, if obtained at a cost of increased weight, tends in general to be offset by the added cost of hauling this extra weight around. Nevertheless there has been a decided gain in efficiency as speed and horsepower have increased.

Comparing Motors—Speed-Ratio Power

Two factors are of primary importance in measuring the application capacity of a traction motor: (1) continuous rated horsepower and (2) the ratio of maximum permissible to rated speed. The first factor, rated horsepower, requires no comment since this is accepted generally as the primary if not the only measuring unit. The traction motor, however, must be rated at a relatively low speed; and it must also be capable of operating at maximum permissible speeds ranging from two to five times its rated speed. If variation in rotation losses with speed could be ignored, and if the ratio of mechanical to electrical material could be assumed to be a constant, a motor with a speed ratio of five, would have five times the tractive effort and five times the size and weight of an equal horsepower purely hypothetical motor rating only at the maximum permissible speed. The product of these two factors: the ratio of maximum to rated speed, and the rated horsepower is here called "speed-ratio power" and is used to compare, in Figures 1 to 7 inclusive, the advances made over the years in the various lines of motors. Gains range from 70 to 300 per cent depending upon the application.

Speed-ratio power is an accurate measure if used to compare motors that are not too widely apart in peripheral speed at the rating. In each case, the comparisons here made are for a given class of service, and the error due to differences in peripheral speed is estimated to be not over five per cent.

Sources of Advancement

Advances in the design of a motor as old and established as the traction motor are arrived at generally in such small steps that it is not until the history over a relatively long period of time is reviewed, as has been done in the comparisons mentioned before, that the over-all progress can be appreciated. The advances have been brought about by an accumulation of quite a number of seemingly small changes.

Antifriction Armature Bearings

The first significant change that took place during the past 25 years was that from the waste-packed sleeve to the antifriction type of armature bearing. Compared to the sleeve type, any benefit that may have resulted from the reduction in friction due to the antifriction feature was incidental although there is no doubt some slight reduction in torque loss on an initial cold start. The antifriction bearing, however, does have three advantages over the sleeve: it operates at high speed with simple and reliable lubrication; it requires less axial space allowing room for increased active material; and the negligible wear with which it operates makes possible better maintenance of gear centers.

The principal problem in connection with the use of antifriction armature bearings has been to keep the lubricant in, and dirt and water out. The solution has been fairly well worked out for grease. Oil is an ideal lubricant for antifriction bearings and very little is required in the bearing at any time. Leakage and vaporization make it difficult to confine and means must be provided to continually

---

Paper 49-43, recommended by the AIEE land transportation committee and approved by the AIEE technical program committee for presentation at the AIEE winter general meeting, New York, N. Y., January 31–February 4, 1949. Manuscript submitted November 8, 1949; made available for printing December 27, 1948.

M. J. Baldwin is in the motor engineering division of the General Electric Company, Erie, Pa.

The author wishes to thank his associates for assistance given him in the preparation of this paper.

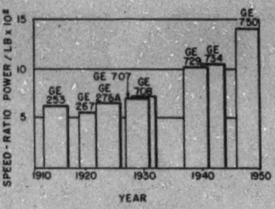

Figure 1. Progress of specific motor output, 3,000-volt locomotive motors

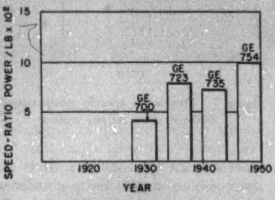

Figure 2. Progress in specific motor output, 3,000-volt multiple-unit car motors

replace that which is lost. Where oil is the gear lubricant, it is possible to obtain an adequate supply for the pinion-end bearing from the gear case. In this instance, however, general practice is followed in that the commutator-end bearing is grease-lubricated.

Gearing

On large-size traction motors at the beginning of this 25-year period, twin gearing usually was used. Two gears, pinions, and gear cases were required, one pinion being mounted on each end of the armature shaft, and one gear being mounted on the locomotive axle or wheel hub at each end of the motor. Equalization of gear loading was obtained by the use of springs between the rim and the center of each gear, tangential motion being permitted between the two parts in these spring or cushion type gears. About 20 years ago, twin gearing of this type was replaced by single gearing using solid gear, pinion, and gear cover. This change gained added space axially for active material in the motor core and effected an appreciable cost reduction.

Elimination of the second set of gears was in part made possible as a result of the better gear center distance maintenance resulting from the use of antifriction armature bearings, as has been noted; but there also were improvements made in the fundamental design of the gears and pinions. The gearing of the older twin-geared motor was cut and heat treated, but left relatively soft to permit wear in service to equalize cutting variations in the teeth and the tooth spacing. With the development of equipment for grinding tooth profiles after heat treatment, a harder, stronger gear material was used. The pressure angle of the teeth was increased to obtain more strength in bending. The two small fillets and short tangential section connecting adjacent teeth were changed to a single long radius fillet to minimize stress concentration in the pinion hub and gear rim. The grinding of the profiles improved the division of load on the teeth and minimized the torsional stresses in the armature shaft caused, particularly at high speed, by variation in spacing of the teeth.

Another popular way of obtaining high gear reduction is by making the pinion integral with a short shaft supported by bearings adjacent to the pinion on both sides. This so-called "straddle-mounted" pinion can be made unusually small. Its use has been found practical where the gear unit is separate from the motor, as is the case for truck or body-mounted motors used on PCC cars, trolley coaches, and at least one of the most recent medium-sized traction motors.

Double-Reduction Motors

In the past ten years, the double-reduction traction motor has come into widespread use for internally-powered locomotives operated principally in switching service. Motors of the general type shown at the right in Figure 5 have two reductions; the high speed being of the spur type, and the low speed being a hypoid. All bearings in the case, the pinion-end armature bearing, and also the axle linings are lubricated from the same oil bath. Only the commutator-end bearing of the motor is separately lubricated with grease.

Commutators

Increases in armature speed have been made possible largely as a result of corresponding improvements in commutators. On all high-speed motors, particularly those used in road service, the commutators are spun. This is the word generally used to designate the curing process. It consists of an indeterminate number of cycles of heating while revolving at high speed, cooling and tightening, which are repeated until a commutator surface is obtained that is smooth and relatively unaffected by variations in either speed or temperature. This process is expensive, but at present appears necessary to obtain commutators which are good for the maximum operating speed of approximately 10,000 feet per minute currently used for most railway motors. Increasing use of commutator spinning has been made from about 1925, the details of the process being continually the subject of developmental work, seeking means of obtaining better commutators.

Instead of the usual V-bound commutator, a few of the most recent motors have been equipped with arch-bound commutators. In this type the retaining V-shaped sections of the cap and shell

Figure 3. Progress in specific motor output, internal-power road locomotives

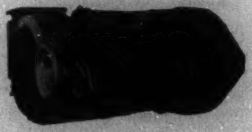

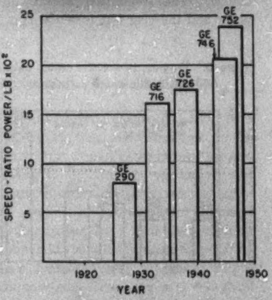

Figure 4. Progress in specific motor output, internal-power heavy switching locomotives

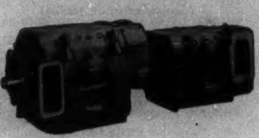

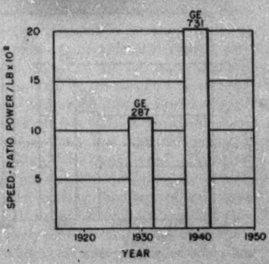

serve only as retractors to draw the bars in toward the center of the commutator and thereby build up tangential or arch pressure between the segments. In the so-called V-bound type, the bars are clamped axially between the V-shaped sections without developing high pressure between the bars. Of the two types, the arch-bound commutator generally has a somewhat better surface and requires less spinning.

Brushes

Along with improvements made in commutators there have been complementary improvements made in brushes. Brushes having a porous surface have been developed that are sufficiently nonresilient to follow the minute variation in the surface of commutators. Extensive use has been made during the past eight years of the split-type brush consisting of two parts, each half the thickness of the usual solid brush. Both the change in material and this splitting have resulted in the brushes maintaining more intimate contact with the commutators, particularly at high speed, and have effected a marked improvement in commutation.

Binding and Wedging

The windings of most armatures today are held in the core slots by means of wedges, where formerly magnetic steel binding wire was used. When nonmagnetic steel wire was developed, it was used where needed as a means of reducing cross slot flux, thereby improving commutation; and also as a means of reducing band losses, thereby improving rating. With further increases in core speed and corresponding increases in the required amount of binding wire, it became necessary about 1930 to begin to use slot wedges in the core portion. This change eliminated banding loss in this region entirely and increased heat dissipation from the core teeth. Core speeds today are approaching 13,000 feet per minute at the maximum permissible vehicle speed in service.

Figure 5. Progress in specific motor output, internal-power light switching locomotives (double-reduction gearing)

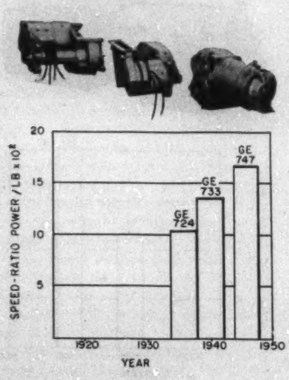

Reroll Banding

In order to bind the end windings down solidly, a relatively new practice termed "reroll banding" has been established on some of the higher speed motors. This operation consists of applying a layer of binding wire, anchoring it at both ends but running one strand over a pulley which is arranged to apply tension in this loop and to take up any slack. The wire is reeled over this pulley as the hot armature is rotated as shown in Figure 8 and the high-tension loop travels backward and forward across the winding surface distributing the pressure to all portions of the winding. In the core portion, a steel bar is temporarily laid along the coil in the top of each slot during the binding process. These bars are free to move radially and are of sufficient thickness so that the binding pressure is applied to them, and through them to the core portion of the winding. By means of the rest of the turns of wire, the pressure is retained until no additional slack can be taken by the traveling loop.

Truck-Mounted or Body-Mounted Motors

On most of the small railway motors, such as the ones used on PCC cars and trolley coaches, the axle-mounted motor has been abandoned in favor of a motor mounted on the truck frame or body of the vehicle. The connection between the motor and the gear box is of the double universal-joint type quite similar to the ones used on trucks and automobiles. Relatively high gear reductions are made possible in these automotive-type gear boxes. The corresponding increase in speed-ratio power per pound is indicated by comparing the older trolley-car motors with the PCC car motors in Figure 7.

Figure 6. Progress in specific motor output, 600-volt multiple-unit car motors

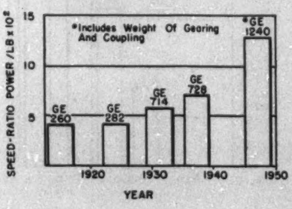

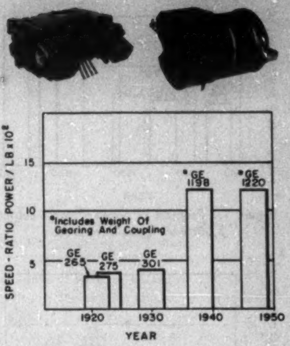

Figure 7. Progress in specific motor output, 600-volt street railway motors

Ventilation

Ventilation has been increased on most traction motors, particularly the larger sizes which today are blown somewhat harder than was considered economical a few years ago. Early traction motors were made to rely more upon thermal capacity than those designed today. Some 30 years ago motors were series ventilated, a practice which limited the amount of air to that which could be forced through the armature. Today practically all traction motors are multiple-ventilated, the air going through the machine in two parallel paths, one through the armature and the other through the air gap and between the stator coils. In the case of motors insulated for 600 volts or less, the air velocity has been increased in the last 10 years from about 3,000 feet per minute to its present approximate value of 5,000 feet per minute. On the higher voltage, thicker insulated motors it has not been found worthwhile to blow very hard due to the unaffected thermal resistance of this dielectric.

Insulation

The size of a given motor is affected to a marked degree by the thickness of the insulation. Thick insulation not only reduces the amount of available space for

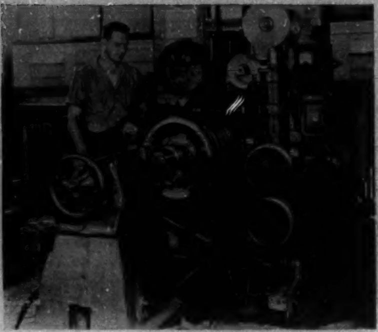

Figure 8 (left). Apparatus for re-roll binding of armatures

Figure 9 (right). Commutating field coil for motor used on internal-power locomotives

copper or steel, but also increases the resistance of the thermal path by which heat must escape from the copper. The problem is to obtain an insulation that is consistently good, that may be applied with normal shop handling without becoming damaged, and one that in service will stand class "B" temperatures or higher.

Class "A" materials are not being used on modern traction motors. Mica has been and still is the basic class "B" insulating material. Mica insulating tapes and sheets have been improved by the use of thinner retaining paper. This newly-developed material is but one-half mil in thickness—approximately half the former thickness—but has adequate strength. As this paper is permitted only as a means of applying the mica, the less used the more heat proof and more strictly class "B" is the insulation. Increasing use is being made of glass-baked mica tape which completely eliminates class "A" material from the insulation.

Glass outer protective insulation has largely supplanted asbestos. The glass has more per-unit tensile strength making possible a tighter taping or wrapping of coils, and also a saving in insulation space.

A change was introduced about eight years ago in the method of insulating commutating coils where fields may be connected in the circuit at approximately ground potential, and where the motor is for use on locomotives operating on internal power. The so-called "mummified" type of insulation in which the coil is completely taped together, has been abondoned as being unnecessarily large and heavy for this particular kind of service. Instead, the first two or three turns, depending upon creepage needed, are taped separately with ground insulation providing full thickness on the end turns and tapering the insulation to provide fewer tapings on the inner turns. Center turns are left bare. The commutating pole is wrapped with insulation, the coil assembled on the pole, the entire unit impregnated in synthetic varnish, clamped on blocks to simulate assembly in machine and cured in an oven into a practically incompressible, hard unit.

Coils of the type just described are used on small locomotives, where only one connection of motors is required. On larger locomotive motors where 2-motor combinations make necessary operation of field coils at more than ground potential, a similar coil is now being used mounted on a metal spool instead of directly on the pole. Here again this is done only for use on locomotives operating from internal power. Permafil, a new synthetic thermo-setting varnish, is used for mica insulation bonding and final impregnation. Center turns on these coils are individually glass taped. These coils are air-cured, clamped in a mold and heat-treated into an essentially incompressible, hard unit which, however, differs from the smaller coils in that the commutating pole is removable. The design is indicated in Figure 9. The coils are held in place on the pole by means of multiple-leaf, nonmagnetic spring pole tips.

Reduction in Use of Castings

The past quarter century has seen much of the work that was once done in the foundry transferred to the fabricating and welding shop. Only in the largest size magnet frames are castings more generally used than fabrication. Wherever possible frames have been changed from octagonal to round and formed by rolling at a reduction in cost. Where space limitations require a rectangular or octagonal shape of frame, the cost is marginal and the change to fabrication may or may not prove economical.

Fabrication of stators using punched sections welded together have been made on an experimental basis. Figure 10 shows how this type of frame appears after welding and before machining, and also the appearance of motor completed. These experimental machines have operated successfully in severest subway service for 15 years. This construction offers some advantages, particularly where electrical transients are severe.

While fabrication is used or not used largely on a cost basis, both the rolled plate and punched fabrication offer a more uniform flux-carrying medium than castings in which unseen blow holes and porosity are likely to occur.

Commutator shells and caps are now made generally from forgings instead of castings wherever the quantity involved is great enough that this construction proves most economical. Frameheads are being "hogged" more and more from ordinary welding plate instead of being made from castings.

Electrical Design

Although not so apparent, a number of changes in electrical design have been made during the past few years. Many of the more recent motors have made use of the twisted-lead type of armature winding, Figure 11, instead of the solid, deep bar; the stranded wire type, Figure 12; or the transposed bar types, Figures 13 and 14. The twist-lead type of armature coil offers high slot-space efficiency combined with low eddy-current loss, both effecting increases in armature capacity. The cost of the twist-lead type is also lower than that of the transposed-bar types. It is on the motors with three or more coils per slot that the twist-lead type of coil offers a gain in combined space efficiency and low loss as compared to coils of the other types. The more coils per slot, the more the gain on both counts, making this type of coil most useful in higher voltage motors, particularly for 3,000-volt trolley operation.

While resulting in a reduction in heating

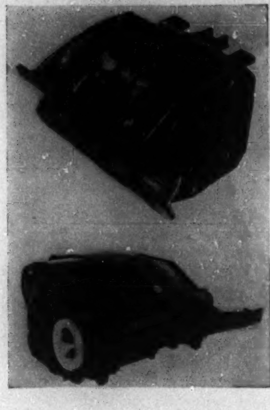

Figure 10. Motor with frame fabricated from punched shapes by welding

and increase in rating, the use of a shallow conductor increases the problem of obtaining a suitable adjustment of compensation to meet the requirements of all coils in a given slot. The eddy currents of the deep conductor tend to equalize the rate of change of current in the several coils during commutation, and also tend to cause some of the energy of commutation to appear in heat rather than sparking. The proper balancing of commutation difficulties against heat reduction is always a problem for any shallow conductor winding when it is used where commutation is inherently difficult.

Windings of the bar type have been used for many years in coils in which the back pitch is not a multiple of the coils per slot. Coils of this type are usually brazed at the end opposite the commutator, necessitating a removable flange and special molded flange insulation; all tending to make this type of coil expensive. There is, however, a definite gain in reduced commutator maintenance when this type of back pitching is used as compared to similar motors where the coil back pitch is a multiple of the coils per slot. In order to take advantage of the twist-lead coil and still use the special back pitching of the bar-type coil, many motors now use a modified form of this twist-lead type of coil which is ordinarily known as the "orphan coil." The design of this type of coil is indicated in Figure 15. Such windings have slot space efficiency comparable to the bar types and are somewhat less expensive in over-all armature cost.

About 1930, it was found advantageous

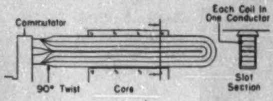

Figure 11. Twisted lead armature coil

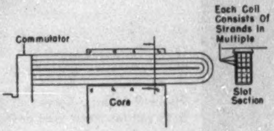

Figure 12. Conventional stranded conductor armature coil

to increase the amount of iron and decrease the amount of copper compared to the ratios used previously. The optimum proportion insofar as the armature is concerned has been found to be about two parts of iron to one part of copper in the effective circumference of the armature. This proportion works out well on motors having more than four poles. On 4-pole motors, it has generally been found advantageous to use a little higher percentage of copper to avoid excessive flux density in the armature core beneath the teeth.

In order to reduce peak voltage between adjacent commutator bars caused by flux distortion, it has been found desirable to increase the air gap from a minimum value at the main pole center to a maximum at the tips. Gaps flared in this way, in addition to reducing flux distortion, also tend to limit losses in the tips due to pulsation in flux caused by the passing of the armature teeth.

Standardization

In the last 20 years, much progress has been made in all lines of traction motors toward the adoption of standard machines. The adoption of a standard trolley-car motor as a result of co-operative developmental effort on the part of the car operators put this type of vehicle in competition with the gasoline coach. Similar co-operation between the operators and the manufacturers has resulted in the idea of a standard motor being carried over into the trolley bus application.

In the field of trolley locomotives, the manufacturers are attempting as much standardization of motors as the several gauges of track and variations in trolley voltage will permit. Designs in this field, however, are still largely determined by the customer through limiting specifications, although every effort is being made

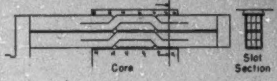

Figure 13. Double cross-over bar armature winding

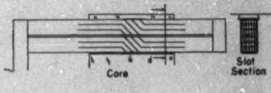

Figure 14. Folded bar armature winding

by the manufacturers in this country to adopt standards. Where complete motors are not standard, certain parts are being used as far as possible on different applications.

The internal-power locomotive offers the best possible opportunity for standardization on a widely-applicable motor for several different weights of locomotive. The motor shown at the right in Figure 5 is used on 25-, 45-, 50-, 65-, and 80-ton locomotives. Different numbers of motors per locomotive and different gear reductions are used depending on the maximum speed desired, which ranges from 25 to 50 miles per hour. This motor is made to be applicable on any track gauge down to 36-inch minimum.

For road locomotives of 50,000 pounds per axle or over, each manufacturer appears to have adopted a standard motor. Generators are designed to fit the motor since there is less than half the cost in the generator that there is in the motors of a 4-motor locomotive. Not only is there a greater percentage of the equipment cost in motors than in generators, but there is also a larger number of smaller units. Both of these considerations favor motor rather than generator standardization.

It is of interest to note that the motor for internally-powered locomotives is being reduced in size to a point where wheel diameter, instead of being deter-

Figure 15. Orphan-type armature coil

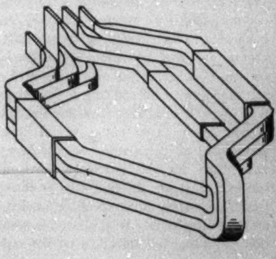

mined by motor size, is now in some cases on the heavier road locomotives being determined by the weight on the driver—that is by the per-square-inch pressure on the rail.

This situation is new and is welcomed as a possible aid to motor standardization. If the wheel rather than the motor does become limiting, a greater freedom is allowed in the choice of gearing for a small motor or, conversely, the way is opened for a more universal motor not requiring specialized gearing.

Standardization tends to reduce first cost and makes faster servicing possible, particularly where the volume is sufficient to make unit exchange possible.

Maintenance and Unit Exchange

The railway motor of today, like the automobile, is more complex, much more of a precision tool, and inherently more difficult to maintain than was the slower speed motor of 20 or 30 years ago. As in the automobile service shop, the problem of keeping the traction motor service shop fully informed regarding improved factory methods is one that is being solved by specialized training of service personnel supplemented by factory instruction sheets. The improved processes for binding, balancing, and spinning armatures and improved equipment for handling and testing is being used in the service shop as well as the factory in order to insure uniformly good operation from new and rebuilt equipment.

Little of the increased maintenance problem is apparent to the operating railroad which uses standardized motors where unit exchange is available. Under the unit-exchange system, the operator turns in a motor needing service and receives, with essentially no delay, a rebuilt motor in exchange. This method of handling service is one of the most important results of standardization which is not possible with custom-built apparatus. The system of unit exchange spreads the cost of specialized servicing equipment over many users of a given motor.

Conclusion

The principal way in which power per pound has been increased during the past 25 years has been by means of increases in speed. Considering the limitations imposed by available known materials—fundamentally copper, steel, and mica—this increasing of speed has proved to be the only way to accomplish progress in traction-motor design. Much work is being done currently in developing new synthetic insulating materials which may one day clear the way to increased specific output. Higher than class "B" temperatures are also being advocated for railway work. Further speed increases are to be expected despite increasing mechanical problems involved. The curves of output per pound are continually increasing. The interesting problem presented to the engineer is to see that they continue to do so.

Reference

1. The Design of New York Subway Motors for Dynamic Braking, B. A. Widell. AIEE Transactions, volume 66, 1947, pages 808–10.

No Discussion

The Renaissance of Electric Motive Power

A. H. CANDEE
NONMEMBER AIEE

THE DESIGN characteristics of the electric propulsion equipment of electric locomotives were thought to be well established by the development and use throughout the last half century of the trolley-electric or third-rail-electric locomotives which receive power from an external source. The widespread application of self-propelled electric locomotives and railcars over the past 23 years, however, and particularly the increased use of Diesel-electric locomotives (which have, within the past 12 years, threatened the existence of self-propelled steam locomotives) has developed new concepts of the design, arrangement, capacity, limitations, and advantages of electric propulsion apparatus for railroad motive power.

Any locomotive, whose propulsion is effected by means of electric motors mounted on it, is an electric locomotive, whether the propulsion power is generated elsewhere and transmitted to the vehicle, or whether it is generated on the locomotive itself. This term, then, is generic and embraces the trolley- or third-rail-electric, the gasoline-electric, the Diesel-electric, the steam-turbine-electric, the gas-turbine electric, and the storage-battery-electric locomotive. During the early stages of development, several builders of Diesel-electric locomotives purposely deleted the term "electric," claiming that the electric equipment was merely a transmission system and of secondary importance to the diesel engine, being a convenient but not entirely necessary accessory. Subsequent experience, however, has shown that many of the desirable operating characteristics of this type of motive power are directly attributable to the electric propulsion system, and that these same features are inherent in the steam-turbine-electric locomotive, the gas-turbine-electric locomotive, or any other self-propelled vehicle having electric drive. As a matter of fact, Diesel-engine-driven motive power would be highly impractical for general railroad use if it were not for the electric transmission and propulsion equipment, since there is no other torque-converting means with the wide range of application of the electric drive.

Tractive Force Improved by Electric Drive

Many railroad men have been astonished by the ability of a relatively low-powered Diesel-electric locomotive to outperform a high-powered (peak) reciprocating steam locomotive. This may be attributed, in part, to the tractive force characteristics of the electric system of power transmission and propulsion used with Diesel-electric motive power, which are available for any type of self-propelled motive power if electric drive is used.

In any properly designed electric drive, three characteristics are outstanding:

1. High tractive force for starting a train.
2. High available power at low train speeds.
3. The development of smooth, nonpulsating tractive force.

These factors, as compared to mechanical drives, permit easier and more positive starting of heavy trains, saving in time because of better acceleration, improved speeds on heavy grades, and fewer delays caused by wheels slipping.

The complication involved in driving the wheels of a self-propelled locomotive by mechanical means from a prime mover normally limits the number of wheels (or axles) that may be driven. Very few modern steam locomotives have more than four pairs of wheels (four axles) driven by a single prime mover, because such axles must be contained by a rigid frame and more axles make the rigid wheelbase too long for sharp track curvatures. In order to get high starting tractive force, then, the weight on this small number of driving axles must be high (if normal values of adhesion are considered), which is often impractical. This limitation is not present with electric drives, because traction motors may be applied to as many driving axles as may be found expedient. From this, it is clear that an electrically propelled locomotive may have vastly improved starting characteristics over any type of mechanical drive, and still stay within reasonable weights per axle and adhesive factors.

The power developed by a prime mover is a function of its speed. In any mechanical drive system, the speed of the prime mover and of the vehicle are related directly, so that full power is developed only at that vehicle speed corresponding to the full prime-mover speed. With a fixed relation between them, it is obvious that over the lower ranges of vehicle speed, only partial power can be obtained. In this respect, a self-propelled vehicle with an electric drive has a definite advantage. Since there is no mechanical connection between the prime mover and the drive wheels, the prime mover may be operated at its full speed and power at any locomotive speed. During acceleration of a train, or when negotiating severe grades, this feature is of considerable value in improving scheduled train speeds. Figure 1 illustrates the comparative speed—tractive-force—horsepower characteristics of a conventional steam locomotive and those of a self-propelled electric locomotive.

One characteristic of an electric traction motor is that its torque (tractive force) is

---

Paper 49-44, recommended by the AIEE land transportation committee and approved by the AIEE technical program committee for presentation at the AIEE winter general meeting, New York, N. Y., January 31–February 4, 1949. Manuscript submitted November 16, 1948; made available for printing January 5, 1949.

A. H. CANDEE is with the Westinghouse Electric Corporation, East Pittsburgh, Pa.

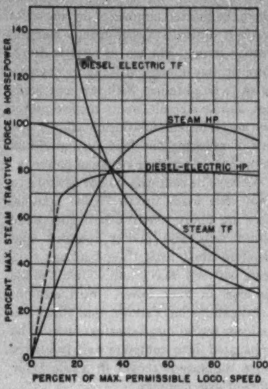

Figure 1. Comparison of locomotive characteristics

Reciprocating steam—4,250 horsepower at driver rims 4,000 horsepower Diesel-electric—3,350 horsepower at driver rims

of a continuous nature, without periodic variations or pulsation. In contrast, the tractive force of a reciprocating steam locomotive, especially at low speeds, is extremely variable (Figure 2). With such a locomotive designed for an average tractive force corresponding to a 25-per cent adhesive factor, the peak tractive force, which occurs once each wheel revolution, corresponds to an adhesive factor in excess of 30 per cent when starting a train. Since it is this peak force which determines the slipping point of the wheels, it follows that if a reciprocating steam locomotive does not slip at an average of 25-per cent adhesion (peak above 30 per cent), a locomotive with an electric drive will not slip at a tractive force corresponding to 30-per cent adhesion, and because of the continuous character of the force, this value may be maintained. By virtue of this, heavier trains may be started and handled much more easily than with a mechanical drive.

The preceding discussion has been based upon direct or geared drive by the traction motors. It should be recognized that when a traction motor or a prime mover drives wheels through a set of side rods, there may be an oscillation in the distribution of tractive force between the various pairs of wheels because of the reversal of side rod forces and clearances at the pins. These unequal tractive force values for the various wheels, then, may reduce the high effective adhesive values which are a normal characteristic of a direct or geared type of electric drive. It is considered inexpedient to apply electric drive through side rods if it can be avoided. It is preferable that direct gear drive be used wherever possible.

Most railroad motive-power men base their estimate of the worth of a locomotive on its tractive force characteristics rather than on its power. This is because, with a reasonable power output obtainable, high tractive forces for train starting and acceleration are of more importance than high power which can be developed only when operating at high train speed. This is one reason why the Diesel-electric locomotive, with its electric drive, has found favor among the operators of this type of power.

Independence of Prime Mover

Any prime mover, applied to a locomotive and transmitting its power to the driving wheels through a mechanical drive system, is subject to severe stresses and mechanical shocks, and definitely is limited in its application. The engines of a reciprocating steam locomotive have to be especially rugged because of this, but the simplicity of the connecting-rod and side-rod drive makes it desirable to accept this handicap. However, the connecting-rod and side-rod drive is limited in its application, since all drive wheels must be in a rigid frame for side-rod connection. As stated previously, this limits the number of axles which may be driven by a single pair of cylinders.

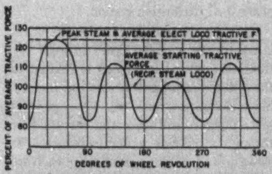

Figure 2. Tractive-force variation per wheel revolution, reciprocating steam locomotive

Electric locomotive can maintain 24 per cent higher tractive force than steam without exceeding steam locomotive adhesive limits

The application of an internal combustion engine with mechanical drive for locomotive propulsion is complicated somewhat because the engine must be kept running at all times even though the locomotive is stopped. This necessitates a clutch for disengaging the engine crankshaft from the drive mechanism. Also, since this type of engine is a relatively constant-torque machine, provision must be made for multiplication of the engine torque in inverse proportion to the locomotive speed. When such complication is added to that of driving a multiple number of wheels (or axles), the mechanical difficulties and the high maintenance expense make this type of drive impractical except for small locomotives and light duty. Furthermore, harmful road shocks are transmitted mechanically from the wheels to the engine. During accelerations with the engine at low speed, it is necessary to employ full engine torque, which is contrary to accepted practice for long service life of any internal combustion engine.

The use of an electric system of power transmission has contributed greatly to the success of the internal combustion engine (particularly the Diesel engine) as a prime mover for locomotives and railcars. Since the engine drives a generator for the conversion of its power into electric energy and is, therefore, independent of any mechanical relation to the driving wheels, this engine with its generator may be mounted in the most suitable location for accessibility and for weight distribution. Placing the power plant in a position where it readily may be inspected and repaired is conducive to its ready maintenance as an effective source of power, with a minimum risk of failure in service.

It is the present practice to design the automatic loading characteristics of an electric transmission system so that full torque will not be demanded of the prime mover until it approaches its full-load speed. This materially reduces engine stresses as compared with mechanical drives, and promotes long life as well as a reduction in repair expense. This electrical feature is considered to be one of the contributing factors to the success of the Diesel-powered electric locomotive.

The Hydraulic Drive

The transmission of power from the prime mover of a self-propelled vehicle to its driving wheels has been confined almost entirely to the mechanical or the electric system. Furthermore, the type of mechanical system which predominates is the side-rod drive of the conventional reciprocating steam locomotive, and the electric system has experienced its greatest application in connection with the Diesel engine. This raises the question as to why the hydraulic or fluid-drive transmissions have not been used more widely.

One of the most desirable characteristics of a power transmission system is the ability to drive any number of axles without mechanical complication, with whatever wheel arrangement may be found most desirable for the support of the locomotive structure and for good tracking characteristics. This requirement favors the use of individual drive of each axle. While the hydraulic drive—a fluid pump and one or more fluid motors—fulfills this basic requirement, the conduction of a large volume of fluid under extremely high pressure from the power pump to a multiple number of hydraulic motors mounted on and driving these individual axles, becomes a major problem—in fact, has been found entirely impractical. On the other hand, the fluid torque converter is not adaptable for individual axle drive, and has most of the disadvantages and complications of any mechanical system of power transmission.

Future of Electric Transmission Systems

Railroad motive power is undergoing a metamorphosis. For nearly 100 years the accepted type of power unit was the reciprocating steam locomotive. Then, the gasoline-engined railcar entered the field, inevitably followed by the Diesel-electric railcar and locomotive, which are rapidly replacing reciprocating steam power. Other locomotives have been built, or are under consideration, including steam-turbine units operating at conventional locomotive boiler pressures and with mechanical or electric drive, a steam-turbine-electric locomotive obtaining its steam from a new high pressure boiler, and the gas-turbine-electric locomotive. Because the advantages of electric drive are now recognized, it is predicted that few locomotives of the future, other than the reciprocating steam type, will be built with any drive other than electric.

Basic Type of Electric Transmission Equipment

The primary requirement of an electric power transmission system, as used for railroad locomotives and railcars, is the ability to convert the power available for propulsion into any desired speed-tractive-force combination necessary for the locomotion of the vehicle. Since horsepower is the product of the pounds of tractive force and speed (miles per hour) divided by 375, it follows that in any type of locomotive with a fixed maximum, prime-mover horsepower capacity, the speed of a locomotive changes in inverse relation to the tractive force requirement. Thus, the negotiation of a severe grade is always at relatively low speed, and high speeds are attained only when the resistance to train movement is reduced. Since the varying character of a railroad profile requires continual changes in the speed-tractive-force values, it is obvious that any electric drive system should permit an infinite variation in such relationship throughout the locomotive operating range, from the maximum tractive force required for train starting and acceleration to the maximum permissible locomotive speed.

D-c electric machinery is naturally adaptable to the variable requirements of self-propelled locomotives. By the use of a d-c generator (having means for varying its field strength) and series-type traction motors, variable values of speed and tractive force may be obtained in a very simple manner. As against this, nearly all of the simple and efficient a-c motors obtain their major speed variations through a change in pole combinations or in frequency of electric alternations. Since the generated frequency is a function of the prime mover speed, and since it is necessary to operate the prime mover at constant speed for obtaining its full power, any a-c system of locomotive power transmission becomes very complicated if variable frequency (and thus locomotive speed) is obtained. In the case of the electric locomotive receiving its power through a trolley wire from a single-phase a-c power supply, the disadvantage of a commutator-type a-c traction motor (which is a variable speed a-c motor) is accepted for the advantages of the a-c distribution system.

In a d-c system, tractive force is related to the current flow through the traction motors, and speed is related to the voltage impressed across the motors. Since electric power is a product of volts and amperes, and since the current flow through a traction motor increases as it slows down (such as caused by an increase in track grade) and vice-versa, it is only necessary to adjust the voltage of the generator in inverse relationship to the current flow in order to maintain constant power demand from the prime mover. The simplicity of this equipment and its regulation has resulted in a vast expansion in the use of d-c apparatus and has insured continued use of this system for railroad self-propelled electric vehicles.

Number of Traction Motors Per Locomotive

As has been mentioned, high axle loading has been the customary practice in reciprocating steam-locomotive design, where the limited number of driving axles makes it difficult to obtain high starting tractive force. The use of electric drive, however, has allowed still higher tractive forces to be obtained with low axle loadings, and as a result, many motive-power men are giving careful consideration to the idea of reducing the load on individual pairs of wheels with any type of power.

While some railroads do not hesitate to apply axle loads up to 70,000 pounds, there are many, many others that have lighter rails and poorer roadbed and therefore must limit their loadings to a figure between 50,000 and 55,000 pounds per axle, or even lower. Furthermore, investigations have shown that there is a tendency for rail-head shatter cracks to be propagated into complete rail fractures above the speeds shown in Table I for different axle loadings.

Table I. Rail Head Shatter Cracks Propagated into Complete Rail Fissures

Worn Wheel* Diameter, Inches	Axle Load, Pounds	Approximate Speed Limit, Miles Per Hour
36	50,000	90
36	55,000	72
36	60,000	56
36	65,000	42
38	50,000	105
38	55,000	85
38	60,000	67
38	65,000	52
40	50,000	120
40	55,000	98
40	60,000	78
40	65,000	62

*These wheel diameters are within the sizes used for self-propelled electric locomotives.

This further illustrates the desirability of low axle loadings in the interest of reduced rail failures. It is, of course, not always possible to keep to these low limits, but the figures serve as a goal toward which to strive.

It is apparent that low weight per driving axle may necessitate a large number of driven axles if high, starting tractice-force values are to be utilized at reasonable coefficients of adhesion between the wheels and the rail. It has been found that the practical starting tractive force values for the various types of railroad service are: switching service–50 to 65 pounds; passenger service–20 to 25 pounds; and freight service–35 to 45 pounds starting force per prime-mover horsepower. The preferred number of driven axles, then, may be calculated from these factors:

$$\text{Number of axles} = \frac{\text{Starting pounds per horsepower} \times \text{Prime mover horsepower}}{\text{Allowable pounds per axle} \times \text{Selected adhesive factor at start}}$$

Thus, for freight service, eight motored axles are desirable for a 3,000-horsepower Diesel-electric locomotive with a 55,000-pound axle loading and an allowable adhesive factor of 25 per cent, as follows:

$$\text{Number of axles} = \frac{35 \times 3{,}000}{55{,}000 \times 0.25} = 7.65 \text{ or } 8$$

Because of the electrical groupings of traction motors fed from a single generator, it is expedient at present to select the number of motors as a multiple of four or six. Diesel-electric locomotives are now available with 4, 6, 8, 12, 16, or 18 traction motors. In small sizes, one or two traction motors are sometimes sufficient.

Electrical Ratings

The use of an electric transmission system introduces a time factor into the application and use of self-propelled motive power which is not readily understood by the operating forces of a railroad who have been used to steam power with mechanical drive. This time factor is occasioned by the electric heating of the generators and traction motors.

Electric rotating-apparatus rating is based upon the current which can be carried continuously at a specified voltage without exceeding the safe temperatures established for its type of construction. This continuous current value is normally converted into a continuous tractive-force rating, and operation at a tractive force in excess of the rating will, if continued, cause the electric equipment temperature to exceed the established safe limit. However, if this overload tractive force is applied with the electric motors and generators at reduced temperatures, time elapses before the equipment reaches its maximum allowable temperature. It is these permissible overload ratings based upon time limits which confuse the average operating man.

The time factor is not a fundamental limitation of electric motive power, but is the result of commercial expediency. It is obvious that if large enough electric motors and generators were applied to give a continuous tractive-force rating exceeding the maximum that could ever be exerted (say, equivalent to 40-per cent adhesion between the wheels and rails), then no operating condition could ever arise which would overheat the equipment. This would require extremely large, heavy, and expensive electric machinery. In this age of modern self-propelled electric locomotives, competition makes it necessary to use motors and generators smaller than the ideal size in the interest of reduced equipment cost, and by so doing forces limitations in tonnage hauling capacity.

In reducing the capacity of electric machines from a size which will not overheat to that which is commercially practical, considerable judgment must be exercised and the results of actual operation analyzed. Unlike trolley-electric motive power, where schedules, grades and tonnages are rather well defined, the self-propelled locomotive must be built to fit an extremely wide range of operating conditions. Experience has shown that the practical minimums for the continuous tractive-force ratings of the electric equipment should approximate the values shown in Table II.

Table II. Preferred Minimum Continuous Tractive-Force Rating

Type of Service	Per Cent of Weight on Drivers
Switching service	13 to 15
High-speed passenger service	11 to 12
Medium-speed passenger service	15 to 16
Low-speed passenger service	17 to 18
High-speed freight service	14 to 15
Medium-speed freight service	17 to 18
Drag freight or transfers	20 to 22

For greatest utility, an electric locomotive must be given as high a tonnage-hauling rating as possible within the safe temperature limits of the electric motors and generators. The maximum tonnage rating of a mechanically driven locomotive for any section of a railroad is that load which can be hauled over the worst grade of that section without stalling. If this tonnage is exceeded and the train stalls, no harm is done to the motive power. This method of rating is not practicable when electric drive is used, for tractive-force values considerably in excess of the continuous rating may be developed without stalling, and correspondingly high ultimate temperature of the electric machinery may be reached. Thus, to determine the maximum tonnage rating of an electric locomotive, calculations or a test must be made to find the peak electric-equipment temperatures when negotiating the worst grades. Such calculations may involve short-time ratings.

Short-time ratings of electric locomotives must be applied with great care in establishing the tonnage-hauling capacity of a locomotive. Even though ample margins are allowed to insure safe temperatures of equipment under ordinary operating conditions, there are many unforeseen circumstances which may require more tractive force than estimated and thus increase the heating beyond safe limits, such as dragging train brakes, inaccurate estimate of train weight, excess proportion of high-resistance cars in the train, or deliberate overloading by uninstructed personnel. Where short-time ratings must be employed to keep within temperature limits, there is always considerable risk of exceeding these if anything goes wrong. For this reason, it is much safer to establish tonnage-hauling ratings for the longer grade zones upon the basis of the continuous tractive-force rating rather than on short-time values. Actual experience has shown that this results in increased operating reliability and reduced electrical repair expense.

Electrical Loading of Prime Movers

In the foregoing, a number of factors involved in the design of the self-propelled electric locomotive have been discussed, including the main electric components, the number of traction motors, the method of driving axles, and the traction motor capacity. Another very essential element to the success of this type of power is the system of control, by means of which full advantage may be taken of all of the power available whenever it becomes desirable to do so, but at the same time limits this load to the capabilities of the prime mover.

One of the important characteristics of a trolley-electric (or third-rail-electric) locomotive is the possible utilization of a relatively unlimited amount of power for propulsion purpose. In any self-propelled unit, the prime mover has a maximum output, usually varying somewhat with the mechanical condition of the plant and with atmospheric changes. Since this power is limited and is usually far below that which could be effectively utilized for propulsion, it is essential that the full available capacity of the prime mover be obtained when needed, whatever its output may be. Moreover, the determination of how much power the prime mover can develop safely should be automatic and not require judgment by the operator.

Various types of power plants—the gasoline engine, the Diesel engine, the steam boiler and steam turbine, and the gas turbine—have different limitations of their maximum capacity. The effect of an overload on a gasoline engine is to reduce its speed but not necessarily to stall it, whereas such an overload on a Diesel engine will usually stall it (assuming constant safe maximum fuel input).

The steam turbine, however, is not harmed when reasonable overloads are applied, and with a limited amount of excess energy stored in the steam boiler, such plants are capable of delivering more than their rated output for a short length of time without harmful effect. Gas turbine plants, being limited by gas temperature and blade materials, will probably not be given any overload factor until experience with such machines shows that overload ratings are permissible. Atmospheric conditions, however, effect big changes in its power output.

Automatic load regulation has attained its highest development in connection with Diesel-electric motive power. An essential of any such control system is simplicity, since adjustments often are made of equipment repaired by railroad personnel who are not trained electrical engineers. It generally has been found expedient to use the engine governor position as an indication of engine-loading conditions, since a tendency to admit more than full fuel means an overload, and action to reduce the fuel below the maximum allowable indicates an underload. Using the governor, then, to initiate action of the load control system, eliminates an extra device for this purpose and promotes simplicity. Full output of the engine is also assured, since the governor action always compares the full capability of the engine against the applied electric load. Such a load control system acts to vary the field strength of the main generator until the volt-ampere output of the generator corresponds to the power input.

In general, internal combustion engines should not be loaded to full torque at reduced engine speeds. Almost all modern control systems for Diesel-electric motive power take cognizance of this, applying electric load at very low torque at engine idling speed, and gradually building up to full torque only when the engine reaches the range of its full operating speed. This is illustrated by the diagram shown in Figure 3.

Traction Motor Connections

No comment need be made on the use of the series-type traction motors for railroad propulsion, because it is well known that their self-adjusting characteristics make them ideal for meeting the extremely variable tractive-force requirements of such service. However, the method of connecting them electrically to the source of power has a direct bearing on the operation of the locomotive.

In the case of a d-c trolley-electric locomotive, which uses motors similar in type to those of a self-propelled electric locomotive, the voltage of the system is relatively constant. To apply low voltage to the motors for starting and then to increase this for accelerating, means that resistance must be inserted in the motor circuits and then cut out in a series of steps until full operating voltage is impressed across the motors. Since the power loss in such resistors is a function of the square of the current value, it is usually expedient to connect the motors first in series relation to reduce the total current fed to the motors and the resultant high resistor loss, and then, when full voltage is impressed across them grouped in this manner, reinsert resistance and change the grouping to a parallel relationship. In this manner, accelerating losses in the resistors are reduced.

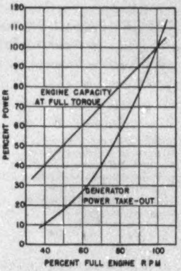

Figure 3. Diesel engine loading at reduced engine speeds

With the variable-voltage generator of a self-propelled locomotive, no accelerating resistor losses are involved. Under these circumstances, it is not necessary to connect motors first in series and then in parallel relationship. Nevertheless, several locomotive builders do resort to this practice, since it enables them to effect a slight reduction in generator size. However, by retaining a permanent relationship throughout the locomotive speed range, several important operating advantages are gained, which weigh heavily toward the adoption of this scheme of connections. Among these are:

1. Simplification of the control. The operator's attention is not distracted by the necessity for a change of connections at specified speeds or current values.

2. Power application is continuous and smooth. A change in traction motor connections is inevitably associated with a momentary unbalance of tractive force between groups of motors, causing rough handling of a train.

3. The possibility of overloading a generator is reduced. With series to parallel control, it is possible to draw excessive current from a generator with motors connected in parallel when they should have been series connected.

4. The smooth control of permanent motor connections reduces the tendency of wheels to slip.

In order to procure the maximum-tractive-force characteristics of a locomotive, it is customary to gear the traction motors with the maximum reduction which still will insure safe motor operation at the maximum permissible locomotive speed. With such gearing, the locomotive speed is usually low at the time that the maximum design voltage is impressed across each motor. In order to increase the locomotive speed, it is customary to weaken the traction-motor field strength by tapping or shunting the field windings in one or more steps. With a trolley-electric or third-rail-electric locomotive, the amount that the fields may be weakened is governed by the imminent possibility of sudden and violent rises in the voltage of the power supply system, which tends to cause motors to flash. Since such surges are not characteristic of an individual power plant, relatively weaker fields may be employed for self-propelled motive power, thus increasing the range of locomotive speed over which full power may be utilized.

Dynamic Braking

Dynamic braking is a system of electric braking in which the traction motors of an electric motive-power unit, when used as generators, convert the kinetic energy of the unit and its train into electric energy, thereby exerting a retarding force. This system has been used rather extensively with self-propelled electric locomotives as a by-product of electric propulsion, and has been found to be very useful for assisting the train brakes in descending long and steep grades at selected speeds. Its application for normal train decelerations when making a stop, however, has not been too popular because of the increased complication of electric circuits.

Dynamic braking is effected by separating the motor armature circuits from the field circuits, and by controlling the field excitation to adjust the voltage generated by the traction motor armatures to that which is required. In self-propelled electric motive power, the armatures are usually connected to a resistor for conversion of the electric energy into heat energy which is dissipated in the surrounding air. The generator of the power plant, being variable in voltage, is

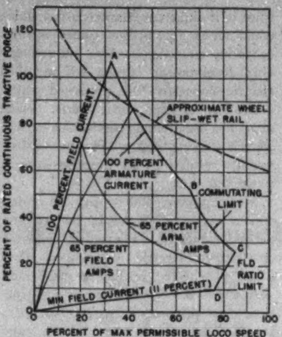

Figure 4. Dynamic braking envelope, resistance braking, fixed resistance value

an excellent source of power for excitation of the field circuits.

Many operating men are unfamiliar with the possible effective range of dynamic braking and expect full braking to be obtained regardless of the locomotive speed. As a matter of fact, such braking is subject to several limitations which allow full braking effect to be exerted over a relatively narrow operating speed range.

One of the prime limitations, of course, arises from the necessity of maintaining the current values through the motor armatures and through their fields, within limits which will not overheat the equipment. Another requirement is that the voltage generated by the armatures be held within accepted limits to reduce the possibility of insulation failures. A third consideration is the commutating characteristics of motors at high speeds when large currents are passed through the armatures; while a fourth limitation is the permissible ratio between the armature and the field currents, as established by the machine stability against flashing. All of these delineate the dynamic braking characteristics in terms of speed and tractive force.

Figure 4 shows a typical dynamic braking envelope of a Diesel-electric locomotive, wherein a single fixed value of dynamic braking resistance is provided. The curve from *A* to *B* is for continuous-rated armature amperes, the shape being determined by the maximum safe generated voltage. From *B* to *C*, the armature amperes must be reduced progressively as the speed rises because of the commutation characteristics at high amperes and high speeds. From *C* to *D*, a greater ratio of armature amperes to field amperes causes instability and possible flashing, while the line from *D* to *O* is the minimum desirable field current for stable control. The curve from *O* to *A* shows the rise in armature amperes with speed for a fixed (maximum) field current.

The dynamic braking characteristics of a locomotive at speeds above that of point *A* are somewhat inflexible, and are fixed by the characteristics of the electric traction motors. However, by reducing the value of the braking resistor, the curve *O–A* may be tipped upward and the braking effect increased at lower locomotive speeds. To reduce this in steps, of course, requires additional control equipment and is seldom found to be expedient for self-propelled motive power.

The efficacy of dynamic braking, as compared to the maximum braking which might be applied, is indicated by an approximate adhesion (wheel slip) curve drawn to the same co-ordinates. With the fixed value of braking resistance selected for illustration (which is in actual operation at present), full braking effect can be obtained only over 11 per cent of the locomotive speed range, or from 29 per cent to 40 per cent of the maximum permissible speed. Above 40 per cent and below 29 per cent speed, the braking force falls away rapidly from the curve which shows the maximum permissible braking as determined by wheel slippage. However, this envelope gives very satisfactory performance under heavy grade conditions when assisted by the train brakes. Care must be taken, however, to see that the locomotive brakes are not applied when braking dynamically, as the adhesive limit may be exceeded.

Resistance braking has had much wider application on Diesel-electric locomotives than on any other type of railroad motive power and has made the railroads conscious of this additional advantage of the electric locomotive. When dynamic braking is incorporated in trolley-electric locomotives, a regenerative type is normally applied so that the regenerated power may be returned to the power system, thereby increasing the operating economy. In most cases, this complicates the locomotive control circuits much more than the resistance type of braking used for self-propelled electric locomotives.

Ventilation

The rotating machinery of electric locomotives must be small, of light weight, and of relatively high capacity. This is especially true of the self-propelled electric locomotive, where the power plant and accessories occupy most of the space available above the locomotive deck and the predominance of the swivel-truck type of running gear limits the space for traction motors. In addition, the cost of self-propelled locomotives is high in relation to the reciprocating steam locomotive, which dictates that all production costs must be kept to the minimum. In the interest of low size, weight, and cost, such large capacity machinery must be force ventilated with cool air.

Very little heat is generated in the equipment compartment of an electric locomotive fed from an external power supply, and what little there is can be directed away from the electric motor ventilating systems. The reverse is true of the self-propelled electric locomotive having a power plant, because there is considerable waste heat, and special care must be exercised by both the locomotive builder and the railroad to insure a full supply of cool air at all times.

Accepted practice for self-propelled locomotive generators has been to mount a ventilating fan directly on the armature shaft. Since full load usually coincides with maximum prime-mover speed, full ventilation is available when needed. Blowers for traction motors are separate machines, driven electrically at times but more often directly from the prime mover. When driven electrically, full ventilation may be maintained at all times, but with a direct drive (or its electric equivalent where an engine-driven alternator and induction-motor fan drives are used) the ventilation fluctuates with the prime-mover speed.

As noted, with direct ventilating fan drives, full air volume usually coincides with full equipment heating. There are many times, however, when this is not the case. For instance, when pushing freight cars over a hump in order to classify them, full rated tractive force and equipment ventilation may be required, but, since the train speed is very low (three to four miles per hour), the horsepower requirements are low. In self-propelled electric locomotives, low horsepower is usually developed at low prime-mover speed, under which condition equipment ventilation is also low. Another case is in dynamic braking. At times, when full braking force is being developed and armature heat is generated at the full rate, the generator speed and consequently the traction motor ventilation is usually low, since only the power for energizing field circuits is taken from this source. These two cases illustrate the need for thorough consideration of the equipment ventilation problem in the design and application of self-propelled electric locomotives.

The operating personnel of the railroads is often neglectful of the equipment ventilating equipment. Fan drive belts may be loose and slipping, air passages may be partially obstructed so that hot air is taken from the engine room instead of from outside, or air connectors to the motors may leak. Any such conditions which tend to increase the temperature of ventilating air or reduce its volume are an invitation to failure in service and to increased equipment repair expense.

Improvements of Details

The tremendous growth in the use of electric motive power within the past 12 years has spurred the development of many details of electric equipment. Roller-type armature bearings are used almost invariably in modern motors and generators, while the felt-wick lubricator has replaced wool-waste packing for many types of bearings. Motors and generators for self-propelled electric motive power, not being subject to high voltage surges or lightning, need not be insulated as heavily as those for trolley-electric locomotives, thus leaving more space for copper. The use of fabricated steel frames, wedged armatures, non-magnetic bands, and improved copper sections have assisted greatly in increasing equipment capacity without increase in weight and size. Technological improvements of this kind, with a vast background of intense and varied Diesel-electric services, are exerting their influence on the designs of equipment for trolley-electric and third-rail-electric motive power.

Renaissance

Electric motive power has changed considerably in character since the advent of the self-propelled types of locomotives. Seldom are the merits of a high center of gravity now discussed in relation to a locomotive design, nor the necessity of a minimum of unsprung motor weight. Flexible drives between a motor and an axle no longer are considered essential for high-speed service. Swivel-truck designs are commonplace, where articulated-truck construction was once considered imperative for heavy-duty locomotives. Where high horsepower per driving axle was once deemed an accomplishment, the desirability of such construction is now very questionable except for locomotives which may be assigned to specific duties.

Almost all modern electric motive power now is being built with low weight and low horsepower per axle, the total locomotive horsepower required being obtained through the use of an increased number of axles. Since it is usually difficult to extend this to an unlimited number of axles under a single motive-power unit, the result is generally secured by coupling several smaller units together to form a locomotive. Such construction also improves the utilization of individual motive-power units, since one may be easily replaced for inspections or repairs without withdrawal from service of the whole locomotive.

The d-c axle-hung motor with a single, reduction spur-gear drive has proved to be entirely satisfactory for any type of self-propelled locomotive and for all classes of service. This is a definite simplification over many of the older trolley-electric locomotives.

The modern, high ventilation rates, resulting in high capacity with a minimum size and weight, are responsible in part for this result

The release of the electric locomotive from the confines of electrified tracks, by the addition of one or more prime movers to each locomotive, has disclosed some of its inherent characteristics which could not be fully utilized under previous operating conditions. Also, the remarkable development of the self-propelled electric locomotive has promoted standardization of equipment parts, which never has been found practical for trolley-electric locomotives. This has subsequently resulted in an immense savings to the railroads.

Motive-power philosophy has undergone a reversal because of the self-propelled locomotive. Where trolley-electric or third-rail-electric locomotives were fitted to specific operating conditions, with few locomotives of similar construction, mass production has necessitated a standardization of the former, and services are now fitted to the capabilities of these standard sizes of self-propelled units.

This procedure has been found entirely practical. The influence of the railroad operating personnel and the mechanical engineer has also been felt strongly. Instead of complicated electric control equipment, they have advocated, and in fact forced, the adoption of simple circuits and apparatus without loss of reliability. In this respect, modern self-propelled motive power has advanced a long way.

With the construction of new types of prime movers in progress, still further attributes of electric motive power are expected to emerge, especially as technological advances occur. One such improvement in prospect, as an example, is the use of high temperature (class *H*) insulation, which should reduce the service limitations now imposed by the time-temperature factors of commercial electric equipment application.

The electric locomotive, long thought to have reached its zenith, is again leading the way toward improved railroad transportation.

No Discussion

Electric Equipment for Chesapeake and Ohio Railway Company Steam Turbine-Electric Locomotives

C. A. ATWELL
MEMBER AIEE

C. E. BASTON
NONMEMBER AIEE

Synopsis: The successful operation of the three 6,000-hp turbine-electric locomotives that were placed in service by the Chesapeake and Ohio Railway Company in 1948 has demonstrated the reliability and adaptability of this type of coal-burning locomotive.

Several articles giving a general description of these locomotives have been published. It is the purpose of this paper to deal more particularly with the electric equipment used, its special requirements, and resulting performance.

Requirements Imposed by Prime Mover

The electric transmission equipment required for a steam turbine-powered locomotive is similar in many respects to that used on Diesel-electric locomotives. The principal differences are in the main generator and the control equipment. These differences result from the dissimilar speed-torque characteristics of the Diesel engine and the steam turbine. The steam turbine has a shaft speed many times that of the Diesel, will not stall if moderately overloaded, and its horsepower is practically constant over its operating range of speed. A comparison of these fundamental characteristics is shown in Figure 1 on the basis of percentages of full horsepower, torque, and speed. The important differences shown here are that the turbine torque rises rapidly as speed decreases and that its horsepower is much more constant from full speed to "idling" speed. These characteristics determine the way in which the generator must be controlled to properly utilize the power available. In the case of the Diesel-electric, considerable development of generator control devices has been necessary to prevent overloading or speed pull down of the engine. Such overloading is bad not only for engine life but any speed pull down means an almost proportional reduction in horsepower. The generator receiving power from a steam turbine does not need to be controlled to the same degree against speed pull down, since there is very little loss of power as speed is reduced over the operating range, and because operation at reduced speed at full throttle is not harmful to the turbine.

The type of service for which the Chesapeake and Ohio locomotives were built indicated a required net input of 6,000 horsepower to generators for traction. This net input produces approximately 5,000 horsepower at the rail. A turbine speed of 6,000 rpm was chosen to give an economical and reliable turbine design.

Main Generator Construction and Arrangement

The generator armature arrangement selected was determined by a combination of commutation, mechanical, ventilation, and motor grouping requirements. Two double-armature generators direct connected to two gear wheels driven by a turbine shaft pinion, proved to be an advantageous arrangement for meeting these requirements. The two generators are placed side by side in the locomotive and have a symmetrical mechanical relation to the turbine shaft. A 6-to-1 gear reduction gives the moderate speed of 1,000 rpm for the armatures. With 1,500-horsepower input to each armature at 1,000 rpm, good commutation and freedom from flashing are obtained without such special requirements as split-throw armature winding or pole-face compensating winding. Each of the four armatures supplies power to two traction motors in parallel. Four simplified independent power circuits are thus provided, any one of which may be removed temporarily from service without affecting the operation of the others

The two multiple-wound armatures of the double-armature generator are duplicates and are pressed onto a common shaft with the commutators at the ends. A heavy duty self-aligning roller bearing supports the outboard end of this shaft and a flange at the drive end is bolted solidly to the turbine gear flange.

Each armature has its own field structure including eight main and eight commutating poles and coils. The armature punching, coil, and commutator construction is the same as that used extensively on Diesel-electric locomotive generators. The field construction is different from the usual Diesel-electric generator in that a large part of the main field is self-excited and that an auxiliary separately-excited field is provided for external control. Also, no engine starting series field winding is required. The eight brushholders are mounted on an adjustable ring and are of the double-brush type with brushes inclined to the commutator surface. Each brushholder is supported by two sturdy insulated pins and can be adjusted easily in a radial direction.

The double armature arrangement is also advantageous for generator ventilation. The air for forced ventilation of the two generators is supplied from a turbine-driven blower to a duct which leads to the bottom center of each generator frame.

Paper 49-45, recommended by the AIEE land transportation committee and approved by the AIEE technical program committee for presentation at the AIEE winter general meeting, New York, N. Y., January 31–February 4, 1949. Manuscript submitted November 10, 1948; made available for printing December 27, 1948.

C. A. Atwell is design engineer and C. E. Baston is control and equipment engineer in the transportation engineering department of the Westinghouse Electric Corporation, East Pittsburgh, Pa.

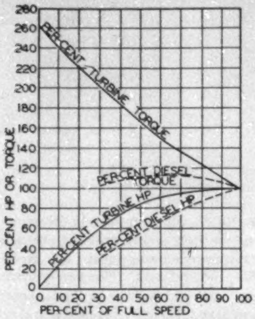

Figure 1. Comparison of speed, horsepower, and torque at full throttle—steam turbine and Diesel engine

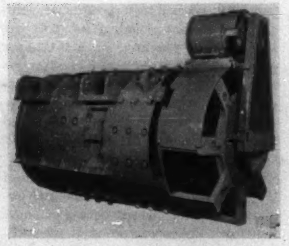

Figure 2. One of the double armature generators with auxiliary generator

From here, the air divides and flows in opposite directions between field coils and through longitudinal ducts in the armatures, past the brushholders and commutators and out through the openings in the end housings. In addition to this, smaller ducts are led from the supply duct underneath the generator frame and directed so they provide a blast of unheated air directly on the lower side of each commutator.

The generator frames are made of exceptionally rigid construction so that they act as stiffening members in the power plant assembly. This frame stiffness, together with a solid vertical mounting plate between the generators, allows a relatively light substructure for the power plant as a whole, yet provides an assembly that is sufficiently rigid to keep all rotating parts in accurate alignment. The entire power plant unit is supported at three points; two trunnions at the turbine end, and a rubber supporting pad under the generator mounting plate. This arrangement insures that stresses set up in the locomotive frame are not transmitted to the power plant assembly to disturb its alignments. A complete double-armature generator, Figure 2, weighs 25,800 pounds or 8.6 pounds per horsepower input.

Generator Performance

Each of the four armatures is rated continuously at 560 volts, 1,860 amperes, 1,000 rpm.

Figure 3 shows the voltage and speed regulation, efficiency, and horsepower input to one generator armature when operating at full throttle. This performance is obtained with the self-excited and separately-excited fields set with minimum external resistance. As mentioned before, the pull down of speed at heavy ampere loads is of little consequence, since the horsepower decreases but little with speed and operation at reduced speed is not harmful to the turbine. For example, at 75 per cent of full speed, the horsepower is still 96 per cent of that at full speed. Very little operating is done at full throttle at ampere loads greater than the continuous ampere rating of 1,860.

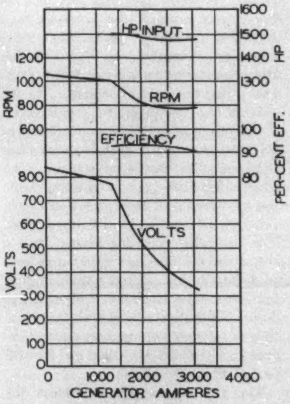

Figure 3. Performance of one generator armature at full turbine throttle

When the locomotive is ready to start, the turbine is idling at 63 per cent speed (3,780 rpm) and the generators are running at 630 rpm. The strength of the separately-excited fields is gradually increased in 11 steps (controller notches) by reducing the external resistance in that field circuit. The turbine speed is also increased slightly from the 6th to the 11th notches. Generator speed is 750 rpm on the 11th notch. As the separate field strength is increased, the self field strength also increases gradually. The separate field notches are small enough to increase gradually the load current supplied to the traction motors. This insures a smooth locomotive start under any condition of load or grade. When full excitation has been applied to the separate field, further movement of the master controller increases the turbine speed further. The self-excited field obtains its supply from the generator terminals through an adjustable resistance. This resistance is controlled automatically in two steps. The first step limits uncontrolled build-up and the second permits full voltage at the higher speeds.

Auxiliary Generator-Exciter

Each main generator is provided with a V-belt driven 9-kw 75-volt 120-ampere self-ventilated auxiliary generator, regulated to give constant voltage from 2,250 to 1,350 rpm. A maximum of 3 kw is required for the separately excited fields of the main generators. These auxiliary generators also supply low-voltage power for meter and indicator lights, control and other auxiliaries such as the mechanical lubricator pump and the air brake system. Either of the two auxiliary generators can supply all of the locomotive low-voltage requirements. Two were installed, however, so that normally they are operating well below their rating. This also made the construction of the right and left hand main generators duplicate at this end. A single regulator controls both auxiliary generators in parallel. Either may be cut out without affecting the operation of the locomotive. Each auxiliary generator weighs 570 pounds.

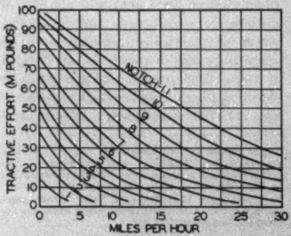

Figure 4. Locomotive performance at reduced turbine speed, showing starting notches

Traction Motors

The eight main driving motors are the Westinghouse type 370-F d-c motors which are widely used on large Diesel-electric locomotives. This motor rates 560 volts, 930 amperes, 750 rpm continuously with full field. This motor is 6-pole, series-wound, force ventilated, axle hung, and is geared to its driving axle with single reduction spur gearing of proved design. The entire motor is constructed for high-speed heavy-duty railway service, and its many successful applications have proved its reliability on both freight and passenger locomotives.

Electrical Control—General Features

The electrical control of a steam turbine electric locomotive bears some resemblance to that of a Diesel-electric locomotive. The differences arise from the different characteristics of the prime mover which has been described in detail before. The idling speed, being approximately 60 per cent of full speed, makes it necessary to apply field excitation to the main generators gradually. Thus the master controller, Figure 7, has two functions. One portion controls the contactors varying the resistance in the separately-excited fields of the main generators and the second portion controls the speed setting of the turbine governor. The field contactors are controlled by a series of contact units operated by cams on the master controller shaft. A cam on this same shaft varies the setting of an air pressure regulator which is connected by means of a control pipe to a spring loaded operating cylinder which is connected by a link to the governor actuating arm. Since no control battery is used on this locomotive, a second cam actuates an air valve which permits bringing the turbine up to the idling speed without control power being available.

Figure 5. Traction motor

An "idle" position is provided between the "off" and "on" positions of the master controller. Steam is admitted to the turbine on this notch and the motor switches are closed but no excitation is applied to the generators. A stop is provided on the master controller so that the handle is stopped in the "idle" position on a normal shut off. To move the handle to the "off" position and stop the turbine, a button in the end of the handle must be pressed.

The idling speed of the turbine is such as to cause the generators to build up as shunt excited machines with the normal field resistance in the circuit. To prevent this, a step of resistance is inserted which is above the critical value. This resistance is cut out of the circuit by means of contactors controlled by a voltage relay whose operating coil is connected across the generator armatures. These relays are set to operate at a voltage somewhat less than the maximum at which time the fields are approaching saturation so that the increased field current does not give a large tractive effort increment.

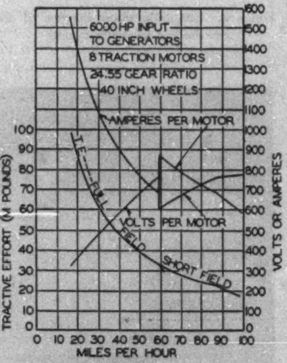

Figure 6. Locomotive performance at full turbine throttle

When the master controller is moved from the idle position to the first notch the field must build up, so the value of the field on the first notch was set to give a moderate tractive effort of 27 pounds per ton of locomotive weight. In practice, the time required for the field to build up softens the control so only a gentle response is obtained on the first notch, making for easy and safe coupling to a train. As the controller is advanced toward the 11th notch, the increments of separately excited field current become gradually smaller as the effect of the shunt field becomes greater. The net result is essentially uniform notching up to the 11th notch. Beyond this point, the quadrant is not provided with notches. The reason for this is that this portion of the master controller merely changes the speed setting of the governor which can be done smoothly without notches. The turbine speed indicator serves as a guide to the engineman in manipulating the master controller.

Figure 7. Master controller used on steam turbine-electric locomotive

Simplified Main Circuits

There is no interconnection between the four armature circuits. Each armature supplies two traction motors connected in parallel, thus the problems encountered in paralleling the generators were avoided, and in addition the cutting out of motors or generator armature is simplified. A small double-pole double-throw knife switch opens the motor switches and the generator fields in each circuit, thus preventing operation of damaged equipment. In the cutout position of this switch a replica resistor duplicating the field is connected across the excitation circuit. This maintains unchanged the other three fields that are connected in parallel with each other and in series with the single field resistor.

An adjustable resistor is connected in series with each separately excited field so as to permit compensating for slight differences in generator and motor characteristics. In practice, it has been found that only slight adjustment of these resistors has been necessary to balance the power equally on the four generators over practically the whole operating range and once set adjustment is permanent.

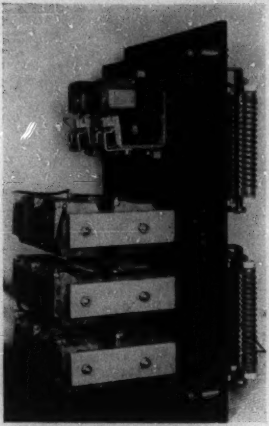

Figure 8. Control panel for self-excited fields of main generators

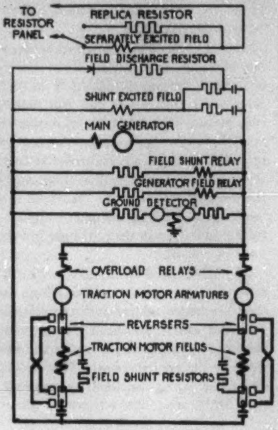

Figure 9. Schematic wiring diagram of one of the four generator circuits

One step of field shunting is provided by a noninductive resistance connected across the traction motor fields by an electro-pneumatic switch. This switch is controlled by a voltage relay connected across the generator armature.

Protection Provided Against Grounds, Overloads, and Wheel Slippage

The self excited fields of each main generator are controlled through a panel, Figure 8, on which are mounted the resistors on the back and the contactors and a Rectox unit on the front. This Rectox unit permits field discharge current to flow through the resistor but prevents any current flow through the field discharge resistor under normal conditions. A relatively low value of discharge resistance may thus be used to provide ample protection from inductive "kick" when the field current is suddenly decreased or the circuit opened.

Overload protection of the electric equipment is accomplished by relays that are arranged to de-energize the emergency trip valve thus shutting down the turbine without interrupting the load.

The parallel connection of the traction motors minimizes the effect of wheel slippage, but a slip relay is provided connected between the two traction motors which are connected to the same generator armature. The relay coil connection is made at the junction of the field and armature leads in each motor circuit. As long as the counter electromotive force, and consequently the speed of the two motors is equal, no current passes through the relay. If a wheel slips, the counter electromotive force of its motor increases and a current passes through the relay coil causing it to close its contacts and causes a warning buzzer to sound. It does not shut off or reduce power.

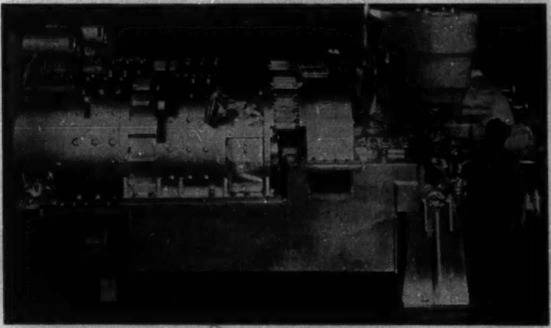

Figure 10. Side view showing mounting trunnions and foot of power plant assembly

The main and control circuits are not solidly grounded, but a simple ground detector is installed which provides a phantom ground midway between the positive and negative busses. This reduces the voltage strain and provides an indication but does not cause a locomotive failure when an accidental ground occurs. This permits the fault to be located and repaired before a second ground could occur and disable the locomotive.

From the diagram, Figure 9, which shows the main circuit of a single armature, the simplicity of which is readily apparent, it can be seen that the circuits involve a minimum of apparatus, the connections of which can be understood readily by the maintenance forces.

Conclusion

The electric equipment for these locomotives employs generators, motors, and control that were designed and built on well-known and proved electrical and mechanical principles. That these principles have been combined in a way especially suited to a steam turbine-powered locomotive of high horsepower is shown by the highly successful performance of this equipment in service.

References

1. Why a Turbine-Electric Steam Locomotive? **Charles Kerr, Jr.** *Westinghouse Engineer* (East Pittsburgh, Pa.), volume 7, September 1947, pages 130–32.

2. Power Plants for the C & O Locomotives. **T. J. Putz, C. E. Baston.** *Westinghouse Engineer* (East Pittsburgh, Pa.), volume 7, September 1947, pages 132–35.

No Discussion

Selenium Rectifiers in Motor Vehicle Power Systems

GLEN RAMSEY
MEMBER AIEE

FOR A GREAT many years, the electric power for automobiles, trucks, and busses, has come from d-c generators, and from storage batteries charged by these generators. Until recently, the capacity and performance of power systems of this kind has been satisfactory.

The progress in automotive research and development can be measured largely by the increases in electric load which these developments have brought about. Double horns; sealed-beam headlights; additional tail, parking, direction, and interior lights; radios; heaters; fuel pumps; and windshield defrosters are only a few examples.

Up to certain limits, increased load can be met by increasing the size of the battery, the generator, or both. Increasing generator capacity, of course, involves a problem of regulating the charge to the battery. Regulation of the generator field began in an experimental way as early as 1913. However, the present type of vibrating voltage regulator, which was one of the most important developments in automotive electric systems, did not come into general use until 1935.

It is interesting to note that the 1913 Cadillac had a voltage regulator which consisted of a mercury switch operated by a voltage coil solenoid. This regulator was not too satisfactory over the rough roads of that time. In 1914, it was replaced by a governor mechanism, which controlled the generator field current according to the engine speed. During World War I, vibrating-type regulators were built for special purposes, including some Liberty aircraft engines. About 1922, vibrating-type regulators for busses became available. Work was begun to adapt this type of regulator for automobile service in 1926. The "third brush" control, introduced by the Leece-Neville Company in 1914, was in general use at that time, and was used on some makes of cars until 1938.

As the electric loads increased, the electric system became more complicated, temperamental, and critical; most of this focused directly upon voltage regulation. High voltage was detrimental to lamp, radio tube, and electric-contact life; low voltage resulted in poor operation of all electric equipment. Unfortunately, most of the increased load was of the type which might be operated whether the engine was idling or running at normal speed. Above certain load limits, it becomes difficult to provide adequate voltage regulation over a wide range of motor speeds and load variations. These problems became especially acute in busses, trucks, police cars with 2-way radio systems, and taxicabs.

To meet these problems, a new approach has been taken—a new electric system consisting of a 3-phase alternator, a voltage regulator, and a rectifier. It might be stated more correctly that the system is new, but the approach has been gradual.

In about 1935, Chrysler Corporation proposed and patented such a system, consisting of a single-phase belt-driven inductor alternator, a voltage regulator, and a rectifier. Tests were made with a number of different types of rectifiers, Figure 1: copper oxide, copper sulphide, mercury vapor, tungar, and others. Several types of inductor alternators were designed, built, and tested, see Figure 2.

In 1936, a flywheel-type of inductor alternator was considered and designed, along with some seven other designs, including a 2-phase system. The increased efficiency offered by the 2-phase system compared to single phase, led to work on a 3-phase inductor alternator. Figure 3

Figure 1. Some of the copper oxide, copper sulphide, mercury vapor, and tungar rectifiers used in early tests with autmotive alternator-rectifier systems

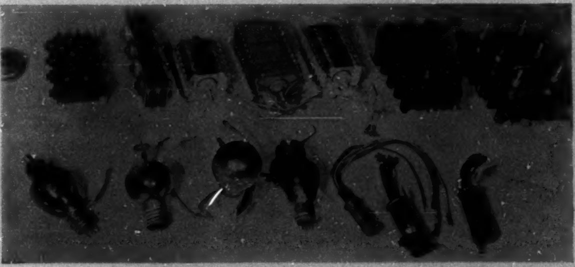

Paper 49-46, recommended by the AIEE land transportation committee and approved by the AIEE technical program committee for presentation at the AIEE winter general meeting, New York, January 31–February 4, 1949. Manuscript submitted October 13, 1948; made available for printing January 10, 1949.

GLEN RAMSEY is chief engineer of the rectifier division of Fansteel Metallurgical Corporation, North Chicago, Ill.

The author expresses his sincere appreciation for the assistance rendered by Gilbert C. Goode, F. J. Finkenauer, Jr., and O. E. Bowlus of Chrysler Corporation in collecting information on early history of the system; to B. M. Leece, S. Floyd Stewart, and A. D. Gilchrist of the Leece-Neville Company for information on present systems being manufactured, and also for assistance on the history of regulators; and to W. J. Rady and J. T. Fitzsimmons of Delco-Remy division, General Motors Corporation, for historical information on regulators.

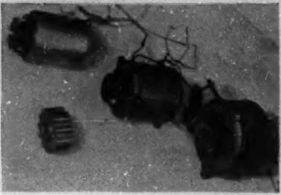

Figure 2. Typical single-phase belt-driven inductor alternators built and tested about 1935

illustrates one of the early flywheel-type single-phase units. Tests on a 3-phase system were made by the Chrysler Corporation, using copper oxide, copper sulphide, and selenium rectifiers.* At this same time, the company with which the author is associated was requested to supply a tantalum electrolytic rectifier, and it was then (1937) that the author first became aware of the scope of this development.

The flywheel-type inductor alternator proved to be noisy, and work on them was abandoned in favor of belt-driven inductor alternators in 1938. This change reduced the noise level, and resulted in a smaller, more compact inductor alternator, one of which is illustrated in Figure 4. The advantages of the 3-phase inductor alternator-rectifier system over the d-c generator were compactness and immunity to troubles arising from wide speed ranges of operation. The cost, unfortunately, was higher than that of equivalent d-c generator systems, which precluded its use in mass-produced vehicles.

The war stopped Chrysler Corporation's development work on the inductor alternator-rectifier systems. During the war, Chrysler Corporation developed a slip-ring alternator-rectifier system for military aircraft, and a number of these were used experimentally in fighters and bombers. Figure 7 illustrates an aircraft selenium rectifier rated at 200 amperes, 30 volts.

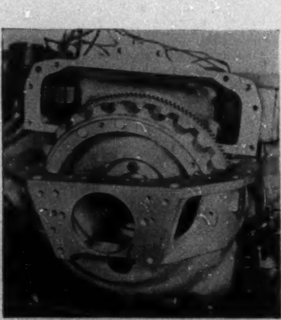

Figure 3. One of the first single-phase flywheel-type inductor alternators for automotive service

At the close of the war, Chrysler Corporation resumed development work on the alternator-rectifier system for automobiles. The important feature of low-speed cut-in was obtained by a simplified and improved field construction. Wartime experience meanwhile, had improved the construction, reduced the over-all dimensions, and lowered the cost of selenium rectifiers. Despite these improvements in the alternator and rectifier, the cost of the complete system did not justify its use in standard automobile production, largely because standard postwar designs do not require loads in excess of present d-c generator capacity.

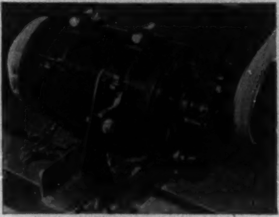

Figure 4. The belt-driven 3-phase inductor alternator proved to be smaller and more compact than the flywheel type

Cost limitations, however, did not keep the alternator-rectifier system out of markets where its use was economical. The Leece-Neville Company, Cleveland, Ohio, having worked with Chrysler Corporation during the war on regulators for the aircraft alternator-rectifier systems, realized the advantages of such a system when applied to vehicular service, and followed postwar developments. Production was begun by the Leece-Neville Company early in 1946, and many thousand units have been installed in busses, trucks, motor cars, and boats.

Early tests indicated, and subsequent tests have established, that for lowest cut-in and highest efficiency, the selenium rectifier is best. Because of lower costs, however, copper-sulphide rectifiers are being used at present in 6-volt systems, even though their characteristics are admitted to be not quite as good as those of selenium rectifiers. While the tantalum rectifier worked satisfactorily in tests, the lower efficiency, the problem of adding water, and the hazards of hydrogen precluded its use.

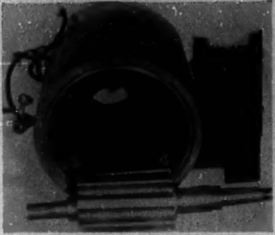

Figure 5. Partly disassembled view of 3-phase inductor alternator shown in Figure 4

At present, all systems of 12 volts or higher manufactured by the Leece-Neville Company employ selenium rectifiers. Selenium rectifiers are used in 6-volt systems only where lower cut-in is desirable or greater efficiency necessary.

The 3-phase alternator which Leece-Neville Company began to manufacture in 1946 was generally similar to the postwar designs developed by Chrysler Corporation. The generator, Figure 9, is a 3-phase, Y-connected, variable frequency 12-pole alternator. Slip rings feed the rotating field. The rotor, Figure 10, consists of two similar 6-legged forgings, making parallel magnetic paths excited by a single coil. Simple assembly and strong construction make the rotors suitable for high-speed operation. The one-turn machine-formed coils of the stator can be delta-connected, but the Y-connected circuit is used for better performance at lower speed, Figure 11.

The frequency in cycles per second of the alternating current generated in this unit is 0.1 times the rotor speed in revolutions per minute. Thus the minimum frequency at which full-load output is

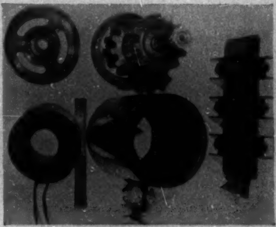

Figure 6. Disassembled view of experimental double-rotor 3-phase inductor alternator

---

* The selenium rectifiers used at this time were imported from Europe. Selenium rectifiers were not manufactured in the United States until 1938.

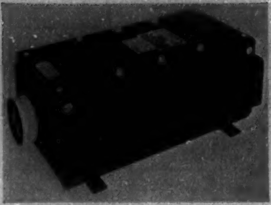

Figure 7. Selenium rectifier, rated 200 amperes at 30 volts, used in conjunction with alternator for aircraft service during the war

obtained in a 12-volt 100-ampere system is approximately 160 cycles. The maximum frequency at full engine speed is not likely to exceed 1,200 cycles. These frequencies are well within the range for best performance of selenium rectifiers.

In comparison with heavy-duty d-c generators, the alternator is very small. Over-all dimensions of the unit illustrated in Figure 9 are $6^{5}/_{8}$ inches diameter by $9\,^{5}/_{32}$ inches long. The weight is approximately 30 pounds.

Excitation of the field coil is accomplished by means of a load relay operated by the ignition switch, thereby exciting the field and connecting the battery to the rectifier. The current drawn by the field is approximately 2.0 amperes. Connections to the field coil are accomplished by brushes to two slip rings. Since the field polarity makes no difference in the operation of the alternator, nor does the direction of rotation, it is possible to rotate the alternator in either direction.

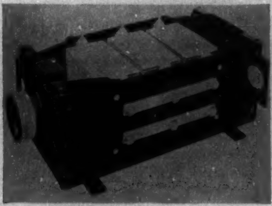

Figure 8. Selenium rectifier shown in Figure 7, with cover removed, showing stack and terminal construction and provision for ventilation through air intake at left

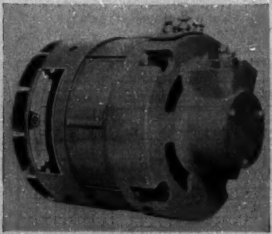

Figure 9. Modern 3-phase Y-connected variable frequency 12-pole alternator

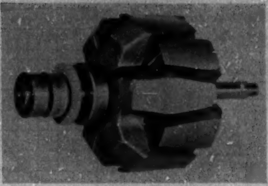

Figure 10. Rotor of alternator, shown in Figure 9, consists of 2 6-legged forgings, making parallel magnetic paths excited by a single coil

The system's control unit, Figure 12, consists of a voltage regulator, current limiter, and load relay. Response to the d-c output from the 3-phase full-wave bridge-type selenium rectifier, Figure 13, effects control by varying the field excitation in the alternator. The load relay is energized through the ignition switch, and is open when the ignition is turned off. In operation, the control-unit voltage-regulator-element primary coil establishes flux to offset mechanical spring tension, and a secondary coil keeps the armature vibrating at a high frequency. A low "point" resistance shunts the first set of operating contacts over a fair portion of the speed and load range of the alternator.

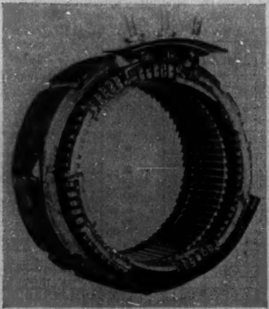

Figure 11. Three-phase Y-connected stator assembly of alternator shown in Figure 9

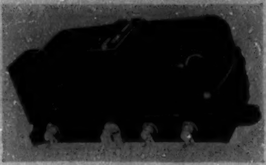

Figure 12. Voltage regulator (14 volts, 100 or 150 amperes) for alternator-rectifier system

When a resistance greater than this value is required to control the system, the regulator armature stops vibrating on the first contact and transfers to the second grounded contact, thereby collapsing the alternator field to the value needed to maintain the correct rectifier

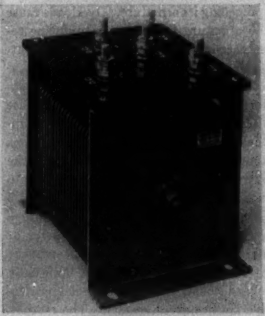

Figure 13. Three-phase full-wave bridge-connected Fansteel selenium rectifier, rated 100 amperes at normal 12 volts, converts the entire output of the alternator into direct current which supplies the load and charges the battery

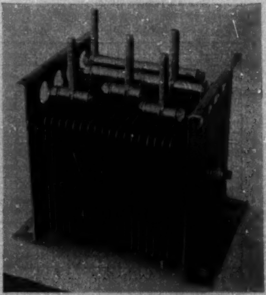

Figure 14. Selenium rectifier, shown in Figure 13, with terminal panel removed to show terminal construction

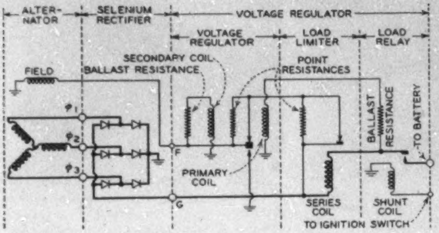

Figure 15. Schematic circuit of alternator-rectifier system, showing 3-phase alternator, selenium rectifier, and voltage regulator

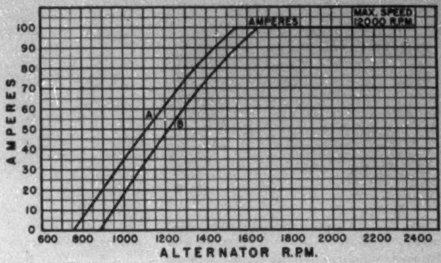

Figure 17. Typical current output of 12-volt 100-ampere alternator-rectifier system at various alternator speeds

Curve *A* shows performance at 12 volts, curve *B* at 14 volts

output voltage. The current limiter coil, in series with the load circuit, establishes flux which offsets spring tension controlling its armature. Overloads cause the armature to vibrate, introducing resistance into the field circuit to limit output current to a safe maximum value.

The selenium rectifier, Figure 13, converts the entire output of the 3-phase alternator into direct current which supplies all the load, with possible exceptions noted subsequently, and charges the battery. The rectifier uses cells 5 by 6 inches in dimension, arranged in 6-1-3 connection in a 3-phase full-wave bridge circuit. It is rated at 100 amperes at normal 12 volts. To withstand the rigors of automotive service, unusually rugged construction and special protective finishes are necessary. The rectifier must not only withstand vibration and mechanical shock, but must be protected against water, salt solution (from icy streets), abrasive dust, and sand. Several types of construction were tried before the design shown in Figure 13 was evolved.

Since the rectifier generates heat and requires ventilation, it is not always practicable to enclose the unit, although this has been done for some types of service. Normally, the rectifier is installed under the hood with the cells in a vertical position, and with the edges of the cells facing the source of ventilation, which may be the radiator fan, an auxiliary electric fan, or other means. Forced cooling permits overloading the rectifier, and permits safe operation in the high ambient temperatures encountered in motor compartments. Under these conditions, rectifier efficiencies range from 75 to 80 per cent. Naturally, the minimum amount of air required to cool the rectifier at full output depends upon the temperature of the cooling air. Figure 16 shows the minimum amount of air, in lineal feet per minute, required for adequate cooling at various air temperatures.

One of the most important advantages of the alternator-rectifier system is its low-speed cut-in. Figure 17 is a typical curve showing output in relation to speed for a 12-volt system. The high over-all efficiency of the alternator-rectifier system makes its use desirable. This efficiency is approximately 65 per cent at rated speed, as shown in Figure 18. (The rectifier efficiency as noted previously is 75 to 80 per cent.) While, under certain favorable conditions, the d-c generator has higher efficiency, the over-all conditions favor the alternator-rectifier system.

For low-speed performance, certainly it has a distinct advantage. At normal engine idling speed, 25 to 50 per cent of the system capacity is obtained, full output is obtained at vehicle speeds of 8 to 12 miles per hour in high gear.

The low-speed performance of the alternator-rectifier system is especially important in vehicles where the electric load is heavy while the unit is idling or running slowly. The city bus is an out-

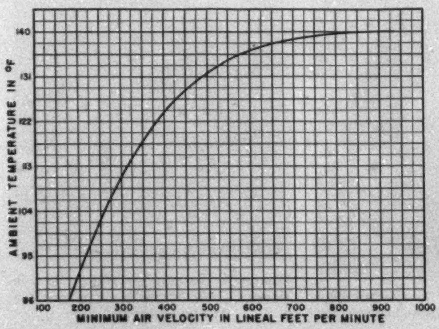

Figure 16. Minimum air velocity (lineal feet per minute) required for adequate cooling of automotive-type selenium rectifier at various air temperatures

Figure 18. Efficiency of alternator-rectifier system rated 100 amperes, 14 volts at alternator speeds of 1,660 to 12,000 rpm

Curve *A* shows generator efficiency, curve *B* shows selenium rectifier efficiency, and curve C shows over-all efficiency

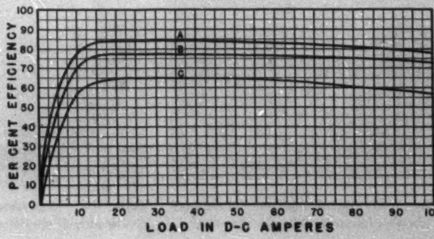

Figure 19. Typical installation of 3-phase alternator and selenium rectifier in a city bus

standing example, with its heavy electric load of lights, fans, and signals. In rush-hour traffic, these busses move slowly, and are stopped for a great portion of the time. Figure 19 illustrates a typical alternator-rectifier installation in a city bus, with sufficient capacity (100 amperes at 12 volts) to carry practically all the lighting load at idling speed. Fire vehicles, taxicabs, police cars, ambulances, utility company trucks, private cars equipped with radio-telephone, cross-country busses and trucks, marine engine plants, and heavy duty tractors also are using alternator-rectifier systems.

Another advantage of this system is that single-phase or 3-phase variable-frequency alternating current is available for windshield heating, fluorescent lighting, and other electric equipment. By means of suitable transformers, almost any desired voltage can be obtained. This offers the automotive engineer the possibility of incorporating both alternating and direct current in the design of new equipment.

While the alternator-rectifier system is confined to applications in a somewhat limited field at the present as compared to mass automobile production, it is believed that in time greater power will be demanded of batteries and generators in regular automobile service. This condition, along with the distinct advantages of this type of system, will lead eventually to much greater use in automobiles.

References

1. An A-C Vehicle Generating System, A. D. Gilchrist. Electrical Engineering, volume 66, August 1947, pages 779–80.

2. A Novel Rectified Alternating Current 6 and 12 Volt Power System. *Electrical Manufacturing* (New York, N. Y.), volume 39, number 5, May 1947, pages 104–5.

Discussion

F. Von Voigtlander (The Commonwealth and Southern Corporation, Jackson, Mich.): The author presents a very interesting application of variable-frequency variable-voltage 3-phase a-c generators without the need for mechanical speed-changing or governing devices to make their output useful. The use of a d-c field instead of a permanent magnet field seems surprising, inasmuch as the polarity of the d-c output is dictated by the rectifier connections, and is independent of direction of rotation of the alternator or its field polarity. The reason behind this choice of excitation would be of interest.

While a vibrating-contact regulator is undoubtedly economical and adaptable to regulating the output of this generator to match the requirements of the vehicle battery, the possibilities of output control by d-c-biased transformer action on the a-c generator output would seem to offer greater reliability and freedom from radio interference. The author's comments on methods of regulation would also be appreciated.

A. D. Gilchrist (The Leece-Neville Company, Cleveland, Ohio): We find Ramsey's paper very interesting. It will give other engineers, who are following this subject, a comprehensive review of the work that has been done on automotive rectified a-c battery-charging systems. We believe the following designed details will be of interest as a supplement to this paper. The alternator stator has 72 slots which makes it a two-slot per pole, per phase design. It is wave wound and series Y-connected to generate power at the lowest possible speed. Stator coils are made from rectangular Formex insulated wire, and are machine formed for high-production and low-cost purposes.

The rotor consists of two identical 6-legged Armco forgings, machined to assemble into the 12-pole field design. This design is very simple and mechanically rugged for wide speed range operation. The length to diameter ratio is very important. If the designer does not consider this initially, he may be surprised to find practically no room for the doughnut-shape coil after proportioning his magnetic circuit.

Another important characteristic of this style rotor is the 7-to-1 power ratio between the salient pole-type field and this rotor for the same system performance. Automotive voltage regulators can control only low amounts of field power for good contact life; thus, this field construction contributes a great deal to the outstanding performance of the system.

Commercial vehicle operation today commonly experiences 50 per cent idle engine speed operation. There are conditions where 70 to 75 per cent of the time the engines are idling; thus, ampere-hour or watt-hour calculations of the load versus the generating system capacity are necessary to obtain a reliable vehicle electric system. Therefore, the low-speed performance contributes an important portion of the power during the great amount of idle operation.

Glen Ramsey: Early models of the alternator had experimental permanent magnet fields. They were more difficult to regulate, as brute-force regulation had to be employed in the d-c circuit. This system was discarded in favor of the separately excited field because of cost and reliability. Voltage regulators of the vibrating type have been used with satisfaction for a great many years to control the field current of d-c generators.

Since it is possible to control a considerably greater amount of power in the alternator with the same amount of field current of a given d-c generator, this system of control was adopted. Therefore, the standard-type regulators were adapted to the alternator, with a gain in output in excess of two times.

Some of the other disadvantages of permanent magnet fields are:

In order to get the best low speed performance, higher flux densities are required than are obtainable in a given size with permanent magnet fields.

A permanent-magnet-field alternator has less maximum output for a given structure, over a wide speed range. Naturally, in this type of application, a wide speed range is essential to give desired performance.

Undoubtedly future developments in the art of magnetic amplifiers may produce a regulator of the saturable-reactor type which will be satisfactory. Naturally, such a system would be desirable. However, the size and cost, at the present state of the art, is prohibitive in the automotive industry. Such units are being suggested and developed at the present time, and it is hoped that in time these regulators can be made economical and reliable. In the meantime, the present vibrating-type regulator is being used.

Polar Vector Indicator

E. A. WALKER
FELLOW AIEE

A. H. WAYNICK
ASSOCIATE AIEE

P. G. SULZER
NONMEMBER AIEE

THE PROBLEM of determining the magnitude and phase angles of two or more voltages or currents frequently arises in circuit and instrumentation research. An excellent example of such a problem is the design of a feed-back amplifier or servomechanism. In more complex systems, the determination of the effect of changing certain circuit parameters is often as complex and time consuming as the initial analysis required in determining the characteristics and constants of the desired system.

A more elementary, but equally important, problem nearly always is encountered in the teaching of a-c circuit theory. It is customary to define sinusoidal current or voltage variations by means of equations and circle diagrams. This is easily understood by the average student. The transfer of these basic concepts to the use of vectors for the solution of more complex circuit problems, however, often is difficult for the student who has not developed the power of visualizing the meaning of the vector concept.

In view of the above, an electronic device[1] has been developed which has been found to be of great value in the solution of the preceding and similar problems. This device is called a polar vector indicator since it permits the delineation on a cathode-ray-tube screen of the magnitudes and phase angles of as many as three voltages or currents of the same frequency. In the instrument to be described, the frequency may be varied over the range of 15 to 300 cycles per second. Thus, the characteristics of an electric circuit or network may be determined quickly and visually in vector form, as a circuit or network parameter is changed, or as a function of frequency, or both. For the beginning student, this has been found to give meaning to the vector concept. In circuit analysis or research, the device permits simple and rapid determination of the effects of parameter modifications on the characteristics of the system under investigation.

The presentation appears on a cathode-ray-tube screen as a horizontal straight line for the reference voltage and as two dots for the two comparison voltages. By locating the center of the reference line at the center of a polar-co-ordinate system drawn on the cathode-ray-tube face, the magnitudes of the three voltages may be read directly by the length of the line and the radial displacement of the dots. The phase angles between the comparison and reference voltages also may be read directly from the angular displacement of the dots from the reference line.

Basic Circuit

The operation of the polar vector indicator is based on the use of an electronic switching system which permits polar deflections of the cathode-ray-tube spot, of such magnitudes as to indicate the amplitude and phase angle of the voltages or currents of interest. Referring to Figure 1, one of the voltages, generally the input to the device being investigated, is impressed through suitable circuits on the horizontal deflection plates of the cathode-ray tube. This appears as a horizontal line whose center is placed at the origin of a polar-co-ordinate screen. The length of the line is proportional to the amplitude of the impressed voltage. Its phase is chosen as the phase origin. Hence, the phases of the other voltages are established by the zero and 180-degree phase points, marked *B switch closed* and *C switch closed* in Figure 1.

Attention now will be confined to the second voltage input denoted as *B*. For the example of Figure 1, this has been chosen of equal amplitude to the reference voltage *A*, but leading it by 60 degrees. It will be noted that the magnitude of the *B* voltage, at the instant of zero phase of the reference voltage, is applied through the switching system to the vertical plates of the cathode-ray tube. A similar voltage is impressed on the horizontal deflecting plates at the same instant, but with its phase advanced 90 degrees by means of suitable networks in the instrument. The vector sum of the two voltages, illustrated at the right of the figure, is seen to be proportional to the magnitude of the *B* voltage, and its phase angle, for this example, leads the reference voltage by 60 degrees.

Similar statements apply for the third voltage, *C*, except that the phase origin, as far as switching is concerned, is chosen at the 180-degree phase point of the reference voltage. This is necessary in order to separate the *B* and *C* spot deflections from the *A* deflection. As described in the following, it is necessary to provide a 180-degree phase shift in the *C* circuits of the instrument so that phase coherence may be maintained.

Theory of Operation

The theory of the device is extremely simple, and will be given as a further aid in the explanation of the operation of the instrument.

Consider a sinusoidal reference voltage

$$e_A = E_B \sin \omega t$$

where, as usual, e_A indicates the instantaneous value of the reference voltage of angular frequency ω, and E_A is its maximum value, obtained when

$$\omega t = \frac{(2n-1)\pi}{2}$$

where n is a positive integer. Then for

Paper 49-47, recommended by the AIEE joint subcommittee on electronic instruments, and approved by the AIEE technical program committee for presentation at the AIEE winter general meeting, New York, N. Y., January 31–February 4, 1949. Manuscript submitted November 17, 1948; made available for printing December 27, 1948.

E. A. WALKER, A. H. WAYNICK, and P. G. SULZER are at the School of Engineering, Pennsylvania State College, State College, Pa.

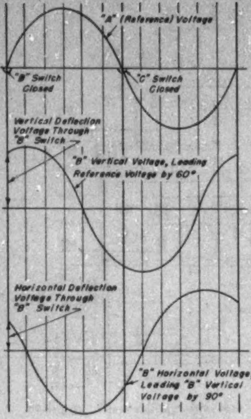
"A" (Reference) Voltage
"B" Switch Closed
"C" Switch Closed
Vertical Deflection Voltage Through "B" Switch
"B" Vertical Voltage, Leading Reference Voltage by 60°
Horizontal Deflection Voltage Through "B" Switch
"B" Horizontal Voltage, Leading "B" Vertical Voltage by 90°

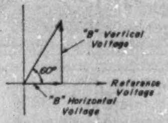
"B" Vertical Voltage
60°
Reference Voltage
"B" Horizontal Voltage

Polar Diagram Showing Addition of Horizontal and Vertical Components to Produce "B" Vector

Figure 1. Polar vector diagram and time sequence of switching

the instantaneous B voltage we may write

$$e_B = E_B \sin(\omega t + \phi_B)$$

where ϕ_B is the phase angle between e_A and e_B.

As indicated on Figure 1, two B deflection voltages are impressed on the cathode-ray tube as e_A goes through zero degrees. The vertical deflection voltage is given by

$$e_{BY} = E_B \sin(\omega t + \phi_B)$$

while the horizontal deflection voltage is given by

$$e_{BX} = E_B \sin\left(\omega t + \phi_B + \frac{\pi}{2}\right)$$
$$= E_B \cos(\omega t + \phi_B)$$

In these relations, ωt is restricted to the values

$$\omega t = 2n\pi$$

with n equal to zero or a positive integer, by the switching action occurring at these times with regard to the reference phase. The phase advance of $\pi/2$ in the X deflection voltage is obtained by a suitable network in the instrument.

The net deflection voltage determining the position of the cathode-ray-tube spot is then

$$e_B' = E_B (\cos \phi_B + j \sin \phi_B)$$

where j is a space operator accounting for the 90-degree position of the deflection plates and ωt has disappeared because of the preceding restriction. Hence, in polar co-ordinates, the net deflection voltage and consequently the deflection obtained is given by

$$e_B' = E_B e^{j \tan^{-1} \frac{\sin \phi_B}{\cos \phi_B}} = E_B e^{j\phi_B}$$

This indicates that the resulting spot deflection is proportional to the magnitude of the B voltage and leads the reference voltage deflection by ϕ_B as desired.

It is evident from Figure 1 that the third voltage, C, may be treated in the same manner, except that the C switches are actuated when $\omega t = (2n - 1)\pi$. An additional 180-degree phase shift in the C channel then provides phase coherence. It will be noted that the deflections proportional to the signals A, B, and C occur at different times. Visual integration is obtained by means of the cathode-ray-tube phosphor, so that the three deflections appear to be simultaneous to the observer.

Block Diagram

The block diagram of the instrument appears in Figure 2. The reference input, A, is applied through a continuously variable attenuator, to a 135-degree phase shift network whose function is described later. The output of the network is applied to a square-wave generator and, through a suitable isolation network which is not shown, to the horizontal-deflection amplifier of the cathode-ray tube.

The output of the square-wave generator is applied to two single-sided multivibrators or triggers through differentiating networks and half-wave rectifiers or clippers. By this means, the B trigger is actuated at the instant the A voltage goes through zero degrees, while the C trigger is actuated at the instant the A voltage goes through 180 degrees. The output of the B trigger actuates the horizontal and vertical B switches, while the output of the C trigger actuates the horizontal and vertical C switches. The outputs of both the B and C triggers are also used to actuate the intensifier amplifier, which is used to brighten the cathode-ray-tube spot during the triggering intervals.

Now consider the B signal circuit. The B signal input is applied through a step attenuator to 135-degree and 225-degree phase-shift networks. It will be noted that the phase difference between the outputs of these two networks is 90 degrees. It will be noted further that, due to the 135-degree network in the reference A circuit, the output of the 135-degree network is ϕ_B ahead of the corresponding point in the A circuit. The output of the 225-degree network is applied through the horizontal B switch to the horizontal-deflection amplifier. The output of the 135-degree network is similarly applied through the vertical B switch to the vertical-deflection amplifier.

Since the B switches are closed only when the reference signal goes through zero degrees, it is evident that the B deflection voltages will be applied only at this time. The trigger pulse, actuating the switches, is approximately 50 microseconds long. Thus, the B deflection voltages are applied for 300 × 360 × 50 × 10^{-6}, or 5.4 degree of a 300-cycle signal. This becomes 0.27 degree at 15 cycles, the lower frequency limit of the present equipment.

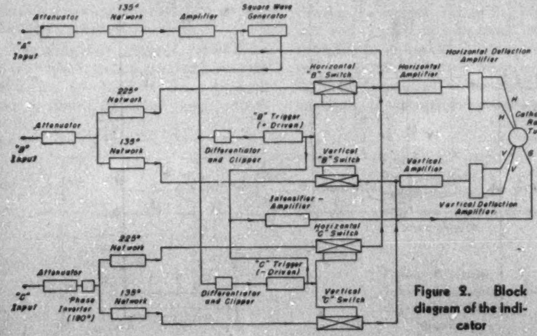
Attenuator
135° Network
Amplifier
Square Wave Generator
"A" Input
Horizontal Deflection Amplifier
Horizontal "B" Switch
Horizontal Amplifier
225° Network
"B" Trigger (+ Driven)
H
H
Cathode Ray Tube
Attenuator
"B" Input
135° Network
Differentiator and Clipper
Vertical "B" Switch
Vertical Amplifier
V
V
G
Intensifier - Amplifier
Vertical Deflection Amplifier
Horizontal "C" Switch
225° Network
"C" Trigger (– Driven)
Attenuator
"C" Input
Phase Inverter (180°)
135° Network
Differentiator and Clipper
Vertical "C" Switch

Figure 2. Block diagram of the indicator

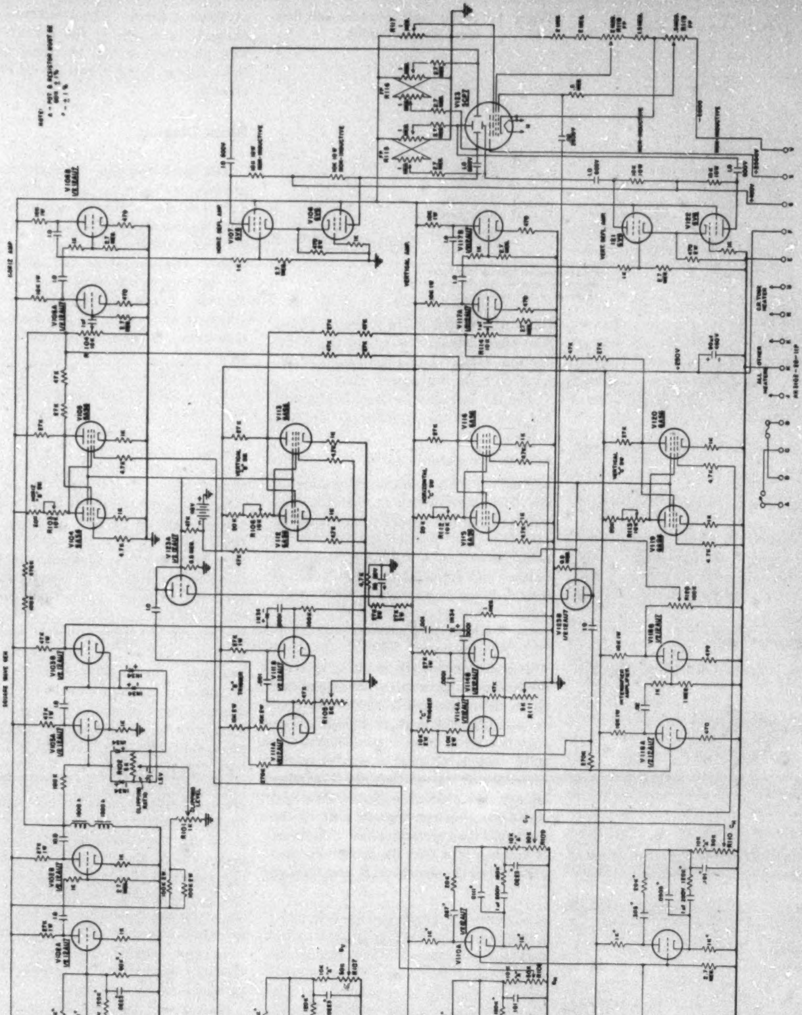

Figure 3. Complete schematic diagram

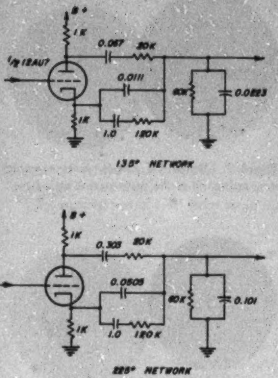

Figure 4. Phase shifting networks

The *C*-signal circuit is essentially the same as the *B* circuit except for the addition of the 180-degree phase inverter before the two phase-shift networks. Since the *C* switches close when the reference voltage goes through 180 degrees, this provides a common phase origin for the three inputs.

Schematic Diagram

The schematic diagram of the instrument appears in Figure 3. Certain portions of the complete schematic diagram have been drawn separately to aid in the description of the operation of the device, and appear in Figures 4, 5, 6, and 7.

Referring to Figure 3, the *A* input is applied through a phase inverter to a 3-section phase-shift network. The *B* input is applied to two phase inverters and associated phase-shift networks. The *C* input is connected through a 180-degree phase inverter to two phase inverters and associated phase-shift networks.

The phase shift networks, Figure 4, are of particular interest since they permit the successful operation of the equipment over a 20-to-1 frequency range without adjustment. It was mentioned in the theory section that a phase difference of 90 degrees is required between the horizontal and vertical deflection voltages in both the *B* and *C* channels. Dome[2] has described a method of satisfying these requirements by utilizing the difference in phase between two networks, so that the difference phase-frequency characteristic is approximately constant at 90 degrees over the preceding frequency range. The networks illustrated in Figure 4 provide a difference in phase shift of 90 degrees ± 3 degrees over the frequency range of 15 to 300 cycles per second.

The accurate determination of the zero-degree and 180-degree phase points of the reference signal is made possible, in a simple manner, with the aid of the rather unconventional square-wave generator or regenerative squarer, which is shown in detail in Figure 5. This circuit, designed by one of the authors, will be described in detail elsewhere.

The regenerative squarer provides a square-wave output for any input voltage between 5 and 50 volts. The switching time is less than five microseconds and switching consequently occurs within one-half degree of the zero-degree and 180-degree reference voltage points, for the highest frequency within the range of the instrument. The squarer consists of a 2-stage triode amplifier with regeneration occurring because of a common cathode resistor. Crystal diodes limit the positive and negative voltage swings at both grids, thereby producing a square-wave output.

It was found necessary to provide adjustments for both the clipping level, total limiter bias, and clipping ratio, ratio of positive to negative limiter bias, to reduce the switching error to the preceding figure. It is further necessary to utilize a low-resistance driving source for best operation. This is the purpose of the two series chokes used as the load for the amplifier driving the squarer, Figure 3. The circuit will oscillate at zero input, so it is necessary to utilize circuit parameters resulting in an oscillation frequency less than the lowest signal frequency to avoid ambiguity in the square wave produced.

The reference signal voltage utilized for driving the square wave generator is also applied, through a suitable isolation network, to the horizontal-deflection amplifiers. The resulting horizontal cathode-ray-tube deflection is proportional to twice the amplitude of the reference signal, and, as mentioned before, is chosen to have zero reference phase angle.

The output of the square-wave generator is applied to the inputs of the two trigger circuits through crystal diodes and differentiating networks. The crystal diodes and trigger inputs are connected so that the trigger circuit driving the *B*-channel electronic switches, is actuated by the positive pulse on the trigger input which occurs when the reference signal goes through zero degrees. Similarly, the trigger circuit driving the *C*-channel electronic switches, is actuated by the negative pulse on the trigger input which occurs when the reference signal goes through 180 degrees.

The trigger circuits[3] are quite conventional, as will be noted by referring to Figure 6, the *B*-channel trigger. The trigger output pulse length is adjusted to about 50 microseconds. Ideally, the trigger pulse length should be inversely proportional to the signal frequency, so that the electronic switch closure time would be constant in angular measure. The added circuit complications were not deemed worth-while in the present instrument. The results obtained with the instrument tend to bear out this assumption.

The outputs of the two triggers are combined through suitable isolation networks, and drive the input to the intensifier amplifier. The pulse output of either trigger is thus used to brighten the cathode-ray-tube trace.

Two other outputs from the *B*- and *C*-channel triggers are utilized to actuate the respective electronic switches in these two channels through delayed d-c restorers. Confining initial attention to the *B* channel, it will be noted that the output of the *B*, 225-degree, phase-shift network is applied to the control grid of the vertical *B* switch. The output of the *B*, 135-

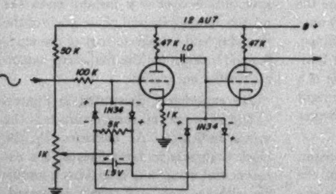

Figure 5 (left). Regenerative squarer showing input and output wave shapes

Figure 6 (right). Trigger circuit with differentiator for B channel

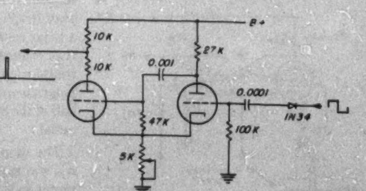

degree, phase-shift network is applied to the control grid of the horizontal *B* switch. Thus, upon actuation of the *B* trigger at the zero-degree point of the reference signal, the two *B*-channel switches are closed, permitting application of the vertical and horizontal *B*-channel outputs to the respective cathode-ray-tube deflection amplifiers during the trigger output pulse interval.

The type of transientless electronic switch[4] utilized contributed greatly to the success of the equipment. Referring to Figure 7, switching is accomplished by applying positive pulses to the suppressor grids of two tubes, one an amplifier and the other a sleeper. The plate current of both tubes is normally cut off by means of a large negative suppressor grid bias. As the bias is removed, by means of a switching pulse, and the plate current of both tubes increases, the negative transconductance from the suppressor to the screen grid of the sleeper tube matches the positive transconductance from suppressor grid to the plate of the amplifier tube. Consequently, the switching transients are balanced out, and the switching amplifier is turned on without distorting the amplified output obtained from the input signal.

Again referring to Figure 3, it will be noted that the *C* channel is identical to the *B* channel except for the addition of the input 180-degree phase-shift stage. The remaining portions of the circuit, such as the deflection amplifiers, cathode-ray-tube circuits, and so forth, are entirely conventional and require no further discussion. It will be noted that the power supply, also conventional, is not shown in the figure.

The complete instrument, without power supply, appears in Figure 8. As mentioned previously, the present model of the equipment is capable of operating over the power frequency range, from 15 to 300 cycles per second, without readjustment. The permissible input voltage range on any of the three channels is from 0.5 to 500 volts rms. The accuracy of the phase measurement is ±3 degrees, while the amplitude accuracy is ±10 per cent.

Figure 7. Electronic switch

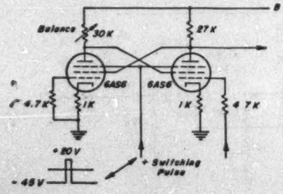

Results

Several simple experiments were devised to illustrate the operation of the instrument. Figures 9, 10, 11, and 12 incorporate the schematic diagram of the experimental setups on the right, with time-exposure photographs of the cathode-ray-tube face of the vector indicator appearing at the left. Each photograph indicates the locus of certain voltages for given circuit parameters as one of the parameters or the applied signal frequency is changed. All photographs were obtained during 10-second exposures. It has been found that similar visual results may be obtained by utilizing a long persistence screen in the vector-indicator cathode-ray tube.

Referring to Figure 9, a fixed-frequency, constant-amplitude voltage, E_1, was impressed across a series resistance-capacitance circuit and was also applied to the reference, *A*, channel of the vector indicator. The resulting vector-indicator deflection appears as the horizontal straight line on the photograph. The length of the line is proportional to twice the amplitude of E_1. It was found necessary to remove the polar co-ordinate grid, shown in Figure 8, in order to obtain a photographic reproduction suitable for printing. Consequently, it is necessary to visualize the photograph of Figure 9 as projected onto a polar co-ordinate screen. By so doing, it is evident that the center of the horizontal reference line lies at the center of a polar co-ordinate system, with the right half of the line lying along the zero-degree radial.

The drop across the variable resistor, E_R, was applied to the *B* channel of the vector indicator, and the resistance was varied from zero to, essentially, infinity. The resulting voltage locus in amplitude and phase, with reference to E_1, appears as the familiar semicircle whose diameter is equal to the amplitude of E_1.

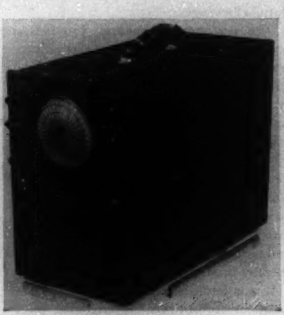

Figure 8. Vector indicator

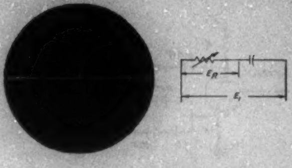

Figure 9. Series R-C circuit, voltage across resistance as the resistance is varied

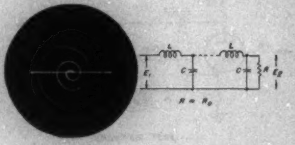

Figure 10. Locus of receiving-end voltage of artificial transmission line, terminated in its characteristic impedance, as the frequency of the input voltage is increased

A somewhat more interesting experiment is illustrated in Figure 10. As indicated by the schematic diagram at the right of the figure, the reference input voltage, E_1, was applied to the sending-end terminals of an artificial line, while the receiving-end terminals of the terminated line were connected to the *B* channel of the vector indicator. A 10-section artificial line terminated in its characteristic impedance was used. The output voltage E_2 was then determined in magnitude and phase, with reference to E_1, as the frequency of the applied voltage was varied, by means of a motor-driven oscillator, over the frequency range of the vector indicator.

As in the previous figure, the horizontal straight line is a measure of the sending-end voltage which was chosen to have zero reference phase. The spiral is the locus of the receiving-end voltage. The spot obtained at any instant gives the relative magnitude and phase angle of the receiving-end voltage to that of the sending-end voltage for the frequency associated with that instant.

The experiment illustrated in Figures 11 and 12 utilizes all three channels of the vector indicator. As indicated by the block diagrams in both figures, the experimental setup was a feed-back amplifier with the feed-back terminals opened.

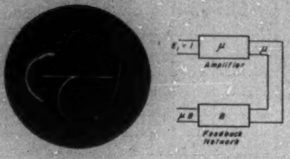

Figure 11. Feed-back amplifier characteristics showing μ and $\mu\beta$. Instability indicated by encirclement of 1, 0° point by $\mu\beta$

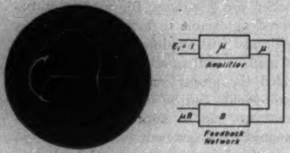

Figure 12. Feed-back amplifier characteristics showing stability resulting from incorporation of suitable notching filter in the β network

The input voltage, E_1, was set equal to unity and the complex amplification, μ, and the complex feed-back voltage, $\mu\beta$, were determined as the frequency of E_1 was varied over the range of the vector indicator.

Referring to Figure 11, the horizontal straight line is the unity-valued input voltage E_1, so that the right-hand end of this line denotes the point 1, zero degrees in the complex plane. The short arc at the left is the locus of μ. A single tube, with a voltage amplification of somewhat greater than unity at the center frequency, was utilized for the amplifier. This is illustrated by the fact that the μ locus passes through 180 degrees beyond the left-hand terminus of the reference line. The large arc is the locus of $\mu\beta$.

A short transmission line was utilized for the feed-back network. This resulted in a large change in $\mu\beta$, when compared with μ, as will be noted in the photograph. It should further be noted that $\mu\beta$ encircles the right-hand end—the 1, zero degrees point on the complex plane—of the reference line. Hence, according to Nyquist's criterion,[5] the feed-back amplifier should oscillate when the feed-back loop is closed. This was found the case.

Figure 12 illustrates the characteristics of the same feed-back amplifier used in obtaining Figure 11, with the feed-back loop open, but with the addition of a suitable notching filter to decrease $\mu\beta$ in the frequency range wherein $\mu\beta$ formerly encircled the point 1, zero degrees. Under this condition, the feed-back amplifier should be stable when the feed-back loop is closed. This was found to hold true.

Conclusion

The polar vector indicator has been found by experience to be an extremely useful tool in teaching and in research. Its great advantage over former methods of determining relative voltages, or currents, and phase angles is the ease and rapidity with which such measurements can be made. For example, the determination of the characteristics illustrated in Figures 11 and 12 by conventional methods would probably require two or three hours. These are obtained with the polar vector indicator in ten seconds. The instrument is particularly valuable when it is desired to investigate effects of parameter changes in a given system.

While the present instrument was designed for the power frequency range of 15 to 300 cycles per second, it would be a relatively simple matter to design a similar device for the lower frequency range commonly required in servomechanisms. It is thought that the instrument could be built to cover the audio frequency range, to 10 kc, by suitable broad-banding and relatively straightforward circuit design.

References

1. United States Patent, applied for April 10, 1948, A. H. Waynick.

2. Wide Band Phase Shift Networks, R. B. Dome. *Electronics* (New York, N. Y.), volume 19, December 1946, pages 112–115.

3. The Cathode Coupled Amplifier, K. A. Pullen, Jr. *Proceedings*, Institute of Radio Engineers (New York, N. Y.), volume 34, June 1946, pages 402–406.

4. Surgeless Volume Expander, A. N. Butz, Jr. *Electronics* (New York, N. Y.), volume 19, September 1946, pages 140–142.

5. Regeneration Theory, H. Nyquist. *Bell System Technical Journal* (New York, N. Y.), volume 11, January 1932, pages 126–47.

No Discussion

A Semiempirical Approach to Voltage Dip—with Suddenly Applied Loads on A-C Generators

L. T. ROSENBERG
MEMBER AIEE

THE variation in terminal voltage when load is suddenly applied to an a-c generator is of importance in the selection of machines required to start relatively large motors, to be sure the disturbance will not affect other motors or equipment on the system. It is also of interest when one or more generators are suddenly taken off the system imposing additional loads on the remaining units.

Point by point methods for calculating the voltage time curve, although accurate, have been found tedious and rather exacting. An analytical solution[2] has also been published based on the use of a voltage regulator and an exponential exciter build up curve corresponding to self excitation with little or no saturation in the operating range.

In these methods, the first few cycles are disregarded on the basis that no appreciable restoration of voltage begins within this interval anyway. While this may be substantially true today, developments in electronic and rotating-type regulators may ultimately lend more significance to this period.

The method presented here for determining the decay of voltage is sufficiently simple that the subtransient voltage drop can be included if desired. The exciter voltage build up is expressed by a form of exponential, well adapted to either separate excitation or self excitation with saturation. The equation for the build up of field current under ideal conditions is solved and the results expressed in a convenient single family of curves from which the entire current build up curve may be read directly. It is shown that with proper selection of time constant, this same family of curves may be used with good agreement for the build up of the sustained component of the terminal voltage. Oscillograms, covering tests on a 40,000-kva machine, are presented to show the accuracy to be expected.

Decay of Terminal Voltage

When induction motors or synchronous motors are started, the suddenly applied load may be considered as a short circuit through external impedance. The three components of short circuit current, sustained, transient, and subtransient, will result in three corresponding components of terminal voltage; e_2, e_2', and e_2'' respectively. The terminal voltage with fixed excitation is expressed in terms of these component voltages and the corresponding time constants, suitably corrected for external load, as follows

$$e_t=(e_2''-e_2')\epsilon^{-\frac{t}{T_{d1}''}}+(e_2'-e_2)\epsilon^{-\frac{t}{T_{d1}'}}+e_2 \qquad (1)$$

where

e_t = resulting terminal voltage at time t seconds
T_{d1}'' = corrected subtransient short circuit time constant
T_{d1}' = corrected transient short circuit time constant
e_2'' = generator terminal voltage immediately after the load change assuming generator internal reactance is x_d''
e_2' = the same based on x_d'
e_2 = the same based upon x_d/per unit excitation prior to loading

The calculation of the three voltage components may be done by any convenient method. While the present study and supporting test data are concerned only with static loads applied to an unloaded a-c generator, the method is believed applicable to loaded machines as well, and with modifications, to removal of load as well as addition of load, provided the proper values of the voltage components can be found and the time constants can be approximated for the range of loads involved.

If the initial and acquired loads are both static and linear with voltage, it is shown in Appendix I that the three voltage components can be expressed as

$$e_2,\ e_2',\ \text{or}\ e_2''=\sqrt{\frac{1+2b\sin\theta_1+b^2}{1+2a\sin\theta_2+a^2}} \qquad (2)$$

where

$b=\frac{I_1x_d}{K_1}$, I_1x_d', or I_1x_d'' respectively
I_1 = initial load current (per unit voltage of unity assumed)
K_1 = initial per unit excitation on generator
$\theta_1=\cos^{-1}$ (initial power factor)
$a=\frac{I_2x_d}{K_1}$, I_2x_d', or I_2x_d'' respectively
I_2 = final total load current after full voltage restored
$\theta_2=\text{Cos}^{-1}$ (final power factor)

For no initial load, the numerator under the radical becomes unity, and for the special case of reactive load

$$e_2,\ e_2'\ \text{or}\ e_2''=\frac{1}{1+a} \qquad (3)$$

In Appendix I, the voltages also are derived for initial and acquired loads whose currents and power factors are independent of voltage. This relation is

$$e_2,\ e_2',\ e_2''=\sqrt{\cos^2\theta_1+(b+\sin\theta_1)^2+a^2\cos^2\theta_2}-a\sin\theta_2 \qquad (4)$$

For more complicated loads, determination of the voltage components may be difficult or impossible except by interpolation between values for known

---

Paper 49-50, recommended by the AIEE rotating machinery committee and approved by the AIEE technical program committee for presentation at the AIEE winter general meeting, New York, N. Y., January 31–February 4, 1949. Manuscript submitted August 2, 1948; made available for printing August 23, 1948.

L. T. Rosenberg is a-c design engineer with the Allis-Chalmers Manufacturing Company, Milwaukee, Wis.

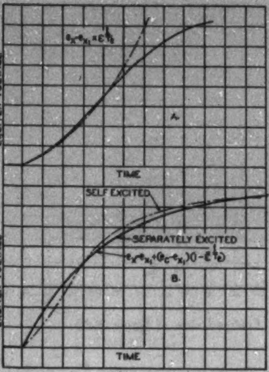

Figure 1. Equations for exciter build-up

(A) Self excited below saturation
(B) With saturation, or separately excited

conditions. Correction of the time constants also becomes increasingly difficult.

Exciter Voltage Build Up

The analytical treatment given previously[8] considered the exciter voltage to rise along a curve

$$e_x = e_{x1}\epsilon^{\frac{t}{T_e'}} \tag{5}$$

As shown in Figure 1(A), this approximates closely the rise for a self-excited exciter before appreciable saturation is reached. The relation used in what follows has the form

$$e_x = e_{x1} + (e_c - e_{x1})\left(1 - \epsilon^{-\frac{t}{T_e}}\right) \tag{6}$$

where

e_c = exciter ceiling voltage with generator field connected across its armature
e_{x1} = initial exciter voltage
T_e = exciter build-up time constant

which is shown in Figure 1(B) to agree closely with the general shape of a separately-excited exciter build-up curve and reasonably well with that of a self-excited exciter, operating well up on its saturation curve. The value of T_e in equation 6 can be found by any one of the three processes described in Appendix II.

Application of Exciter Voltage to Inductive Circuit

When the exciter voltage of the form (6) is impressed on an inductive circuit of constant inductance, L and resistance r, it is shown in Appendix III that the current will follow a curve

$$i_f = i_{f1} + \frac{(e_c - e_{x1})}{r\left(r - \frac{L}{T_e}\right)} \times \left[\left(r - \frac{L}{T_e}\right) - r\epsilon^{-\frac{t}{T_e}} + \frac{L}{T_e}\epsilon^{-\frac{r}{L}t}\right] \tag{7}$$

where

i_f = field current at time t
i_{f1} = initial field current
r = resistance in ohms of the inductive circuit
L = inductance in henrys of inductive circuit
T_e = exciter voltage build up time constant

Fortunately, this expression lends itself readily to quick application in the form of the curves of Figure 2. The initial field current, i_{f1}, is disregarded and the remainder of the right hand member of equation 7 is plotted as a fraction of its final value at $t = \infty$, for various values of time expressed in number of times the circuit time constant, L/r. For each ratio of $L/r/T_e$, only one curve applies. Interpolation between the various curves shown is readily accomplished, to obtain the field current build up for any desired L/r and T_e.

Effect of Eddy Current Paths

It has been shown by Weber,[1] that for magnetic circuits partially solid and partially laminated, the field current and flux do not build up at the same rate due to the eddy current paths in the solid material. In the tests presented herein and on other large machines of both cylindrical and salient pole types the time constant for the actual field current are found to be considerably less than those corresponding to the calculated short circuit time constants corrected for external load.

For the 40,000-kva machine, the actual time constant governing the field current is 2.8 seconds. With this value instead of the calculated T_{d1}' of 5.3 seconds, and with due allowance for the induced initial field current transient assumed to decay in accordance with this same time constant, 2.8 seconds, the generator field current build up obtained from Figure 2 agrees with tests, Figure 5.

The build up of flux on the other hand is found from Figure 2 to agree closely with tests when the calculated transient short circuit time constant, T_{d1}', is used.

Procedure in Determining Voltage-Time Curve

The application of Figure 2 to determine the voltage-time curve may be outlined as follows:

1. Determine the three voltage components of the decay curve and the time constants T_{d1}'' and T_{d1}' and plot.
2. Determine the exciter time constant T_e.
3. Choosing several time values in terms of T_{d1}', select the proper curve on Figure 2

List of Symbols

a = product I_2X, final current times internal generator reactance
b = product I_1X, initial current times internal generator reactance
e_c = exciter ceiling voltage
e_n = exciter nominal voltage
e_x = exciter voltage as a function of time
e_{x1} = initial value of exciter voltage
e_2'' = per unit generator terminal voltage immediately after load change assuming generator internal reactance is x_d'', (subtransient component)
e_2' = same assuming internal reactance is xd', (transient component)
e_2 = same assuming internal reactance is $\frac{x_d}{k_1}$, (sustained component)
$(e_2) = e_2''$, e_2', or e_2
e_t = generator per unit terminal voltage as a function of time
e_g = internal voltage behind subtransient, transient, or synchronous reactance drops
I_1 = per unit initial load current
I_2 = per unit final total load current
i_f = field current
i_{f1} = initial field current, $= \frac{e_{x1}}{r}$
K_1 = initial per unit excitation (based on air gap excitation = 1)
L = inductance of field in henrys, or of inductive circuit
q = ratio of $\frac{e_c - e_n}{e_n}$
r = resistance in ohms of inductive circuit, or field winding
t = time in seconds
T_{d1}'' = time constant governing decay of $(e_2'' - e_2')$, suitably corrected for load
T_{d1}' = time constant governing decay of $(e_2' - e_2)$, suitably corrected for load
T_e = time constant governing the voltage build-up of a separately excited exciter
T_e' = time constant governing the voltage build-up of a self excited exciter (unsaturated)
V = intercept of the straight line defining exciter response with the line $t = 0.5$
X = internal reactance of generator, may be x_d'', x_d', or x_d/K_1
x_d'' = direct axis per unit subtransient reactance
x_d' = direct axis per unit transient reactance
x_d = direct axis per unit synchronous reactance
x_2 = per unit negative sequence reactance
Z_2 = equivalent impedance of the final total load on the generator
ϵ = base of natural logarithms, 2.71828
$\theta_1 = \cos^{-1}$ (initial power factor)
$\theta_2 = \cos^{-1}$ (final load power factor)
∞ = infinity

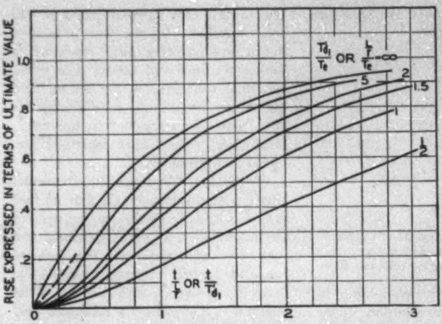

Figure 2(A). Family of build-up curves for field current or terminal voltage

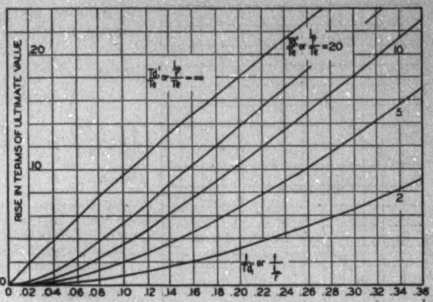

Figure 2(B). Enlarged view of Figure 2(A)

corresponding to the ratio T_{d1}'/T_e and determine the fraction of ultimate rise at each point.

4. These values are then multiplied by the ratio of $(e_c-e_{x1})/e_{x1}$ and by the sustained voltage component, e_2, and the products are added at each instant to the voltage decay curve of step 1, but offset to the right an amount equal to the time required for regulator contacts to close.

Step 4 assumes a linear relation between excitation and sustained component of terminal voltage, except for the substitution of T_{d1}', for the time constant of the actual field current. This means that whatever saturation was present at the initial excitation and sustained voltage, e_2, is assumed to increase proportionately with voltage. The agreement between test and calculated curves, indicates this assumption does not greatly affect the results.

Discussion of Tests

Figure 3, plotted from Film 8 indicates the voltage time curve of the 40,000-kva generator when a 1-ohm per leg reactive load is suddenly thrown on with fixed excitation. The terminal voltage was selected so that one ohm will take full load current at this voltage.

The field current is shown to decay with a time constant of 2.8 seconds, whereas the terminal voltage decay agrees closely with the calculated subtransient time constant of 0.06 second and the calculated transient time constant of 5.3 seconds.

Film 10, Figure 4, shows a sudden change in the voltage regulator control to require a 10 per cent voltage increase. From this film a plot on semilog paper gave a test value of exciter voltage build-up time constant T_e of 0.667 second, which checks the calculated value of 0.615 second obtained from design data fairly well. Figure 6, plotted from Film 15, indicates an even better check of T_e with calculation, in fact almost exact. Film 11, Figure 5, and Film 15, Figure 6, are both for 1-ohm per leg, suddenly applied under the action of a type *J* regulator, whereas Film 13, Figure 7, covers a 2-ohm reactive load, corresponding to 1/2 load current at the initial voltage. Finally, Figure 8, shows a single phase line-to-line load suddenly applied with one ohm in each of the two active phases.

For the single phase test, the voltages, e_2'', e_2', e_2, may be computed by symmetrical components, considering a short circuit through external impedance and solving for the voltage at generator terminals. The line-to-line voltages across the loaded phases by this method, agreed very well with those obtained from equation 3 when the generator reactance is made

$$\frac{x_d''+x^2}{\sqrt{3}},\ \frac{x_d'+x_2}{\sqrt{3}},\ \text{or}\ \frac{\frac{x_d}{k_1}+x_2}{\sqrt{3}}\ \text{respectively.}$$

However, as shown in reference 3, the oscillograms of short-circuit current do not truly indicate the same currents that are calculated by symmetrical components for single-phase faults. The presence of considerable distortion from 5 to 60 cycles flattened the peaks and made the line-to-line voltage wave appear low

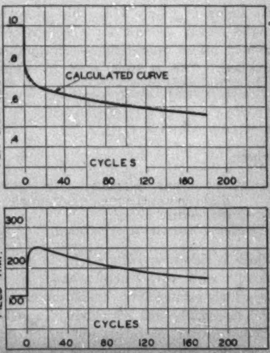

Figure 3 (right). Plot of generator terminal voltage and field current from Film 8, below. Full load thrown on, fixed excitation

[redacted]

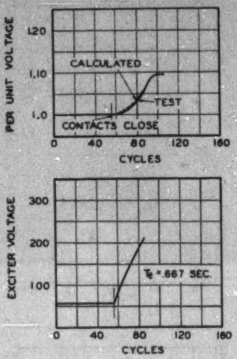

Figure 4 (left). Generator and exciter voltages from Film 10, above. Regulator control suddenly adjusted to raise voltage 10 per cent

in this interval. The line-to-neutral voltage time curve, on the other hand, had very sharp peaks and therefore appears higher than the calculated curve.

Conclusions

A relatively short procedure has been outlined for the calculation of voltage time curves of a-c generators under the control of voltage regulators acting upon separately excited exciters, during sudden load application. The simplifying assumptions permitting the use of the single family of curves to determine restoration of flux are shown by close agreement with tests to be justifiable within the scope of the present study.

Examination of Figure 2, reveals that for separately-excited exciters or self-excited exciters with appreciable saturation, the corrected short-circuit transient time constant is of prime importance in determining the rate of restoration of generator terminal voltage. Another major factor in the recovery time is seen to be the exciter ceiling voltage. The transient reactance is important in determining the maximum voltage dip. The ratio of T_{d1}'/T_e is significant in recovery time below values of 8 or 10, but little can be gained from here up to infinity.

Although the tests were made with the conventional type J contact-making rheostatic voltage regulator, the method of calculation is believed well adapted for the comparison of performance of different types of regulators. A companion paper is in the process of preparation covering tests with the regulex rotating amplifier type of regulator.

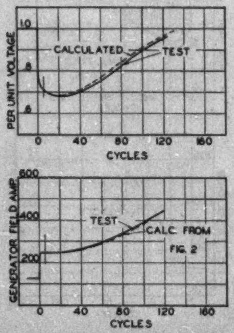

Figure 5 (left). Generator voltage and field current from Film 11, below. Full load thrown on, regulator in operation, first test

Appendix I. Expressions for e_2, e_2', e_2''

Case 1. Initial and acquired load currents and power factors not appreciably changed by the changing voltage. Referring to the vector diagram of Figure 9, e_g is assumed to remain constant as the load is suddenly changed from I_1 to I_2.

$$e_g^2 = I^2 + (I_1X)^2 + 2I_1X \sin\theta_1 = (e_2)^2 + (I_2X)^2 + 2(e_2)I_2X \sin\theta_2.$$

$$(e_2)^2 + (2I_2X \sin\theta_2)(e_2) + [(I_2X)^2 - (I_1X)^2 - 2I_1X \sin\theta_1 - 1^2] = 0.$$

Solving gives

$$(e_2) = \sqrt{(I_2X \sin\theta_2)^2 + 1 + 2I_1X \sin\theta_1 + (I_1X)^2 - (I_2X)^2} - I_2X \sin\theta_2.$$

Now let

$I_2X = a$; $I_1X = b$;

and simplifying

$$(e_2) = \sqrt{\cos^2\theta_1 + (b + \sin\theta_1)^2 - a^2\cos^2\theta_2} - a\sin\theta_2 \tag{4}$$

where (e_2) may be either e_2'' or e_2' from the above considerations for any machine if $X = x_d''$ or x_d'. The analysis is less rigorous for the sustained component e_2 except for cylindrical rotor machines. However, the use of e_2 from these equations with x_d/k_1

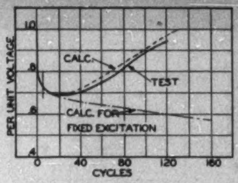

Figure 6 (right). Generator and exciter voltages from Film 15, above. Full load thrown on, second test

substituted for X, has proved sufficiently accurate on both salient and nonsalient pole machines.

Case 2. Both initial and acquired loads linear with voltage. Let I_2 = the final total current that would flow if $e_2 = 1.0$.

Let the final load impedance $= Z_2$, then $I_2 = 1/Z_2$, whereas the actual current after the load change, $I_s = (e_2)/Z_2$. In equation 4 we can therefore substitute $(e_2)I_2$ for the previous I_2 and hence $(e_2)a$ for the previous a, because $a = I_2x$. We may now write

$$(e_2) = \sqrt{\begin{matrix}\cos^2\theta_1 + (b + \sin\theta_1)^2 + \\ (e_2)^2a^2\cos^2\theta_2\end{matrix}} - (e_2)a\sin\theta_2$$

$$(e_2) = \sqrt{\frac{1+2b\sin\theta_1+b^2}{1+2a\sin\theta_2+a^2}} \qquad (2)$$

Appendix II. Method of Calculation of T_e

A. From exciter nominal response. Referring to Figure 10, the response with separate excitation for the main exciter is:

Response $= 2V/e_n$ where V is given by

$$4\int_0^{1/2} e\,dt - 2e_n$$

Response $= \dfrac{8}{e_n}\left[\displaystyle\int_0^{1/2} e\,dt - \frac{e_n}{2}\right]$; substituting $e = e_n + (e_c - e_n)\left(1 - \epsilon^{-\frac{t}{T_e}}\right)$, solving, and letting $\dfrac{e_c - e_n}{e_n} = q$

$$\text{Response} = q\left[8T_e\left(\epsilon^{-\frac{0.5}{T_e}} - 1\right) + 4\right] \qquad (8)$$

This relation is expressed as a curve, Figure 11, from which T_e may be read as a function of the nominal exciter response divided by q.

B. From the exciter voltage build up curve, when entire curve including ceiling voltage is known for the loaded condition. Subtract several ordinates of the exciter build up curve from ceiling voltage and plot differences against time on semilog paper. T_e is the time in seconds for the resulting straight line curve to drop to $1/\epsilon$ times its initial value.

C. From the exciter build up curve when only a portion of the curve is known. Select two time values t_1 and $2t_1$ (see Figure 12) covering the available range of the exciter build up curve or the portion of interest.

Measure the ordinates y_1 and y_2. Then

$$Te = -\frac{t_1}{\log_e\left[\dfrac{y_2}{2y_1} - \sqrt{\dfrac{(y_2)^2}{(2y_1)^2} - \dfrac{y_2}{y_1} + 1}\right]} \qquad (9)$$

Appendix III. Solution of Equation for Field Current Rise

Consider the circuit of Figure 13 with constant inductance and resistance, and an exciter voltage

$$e_x = e_{x1} + (ec - e_{x1})\left(1 - \epsilon^{-\frac{t}{T_e}}\right)$$

The equation for the circuit is

$$e_{x1} + (e_c - e_{x1})\left(1 - \epsilon^{-\frac{t}{T_e}}\right) - i_f r - L\frac{di_f}{dt} = 0 \qquad (10)$$

and its solution is

$$i_f = \frac{e_{x1}}{r} + \frac{e_c - e_{x1}}{r\left(r - \dfrac{L}{T_e}\right)}\left[r - \frac{L}{T_e} - r\epsilon^{-\frac{t}{T_e}} + \frac{L}{T_e}\epsilon^{-\frac{r}{L}t}\right] \qquad (7)$$

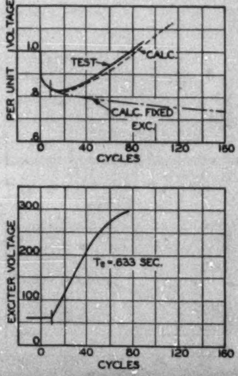

Figure 7 (right). Exciter and generator voltage from Film 13, below. Half load thrown on

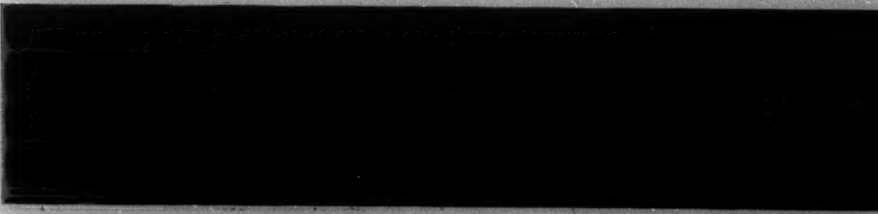

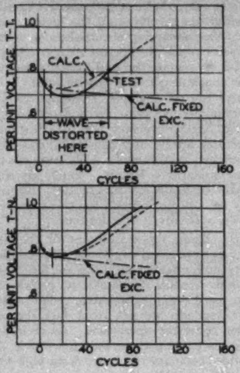

Figure 8 (left). Line-to-line and line-to-neutral voltages from Films 14 (top) and K, (above). Full load single-phase line-to-line thrown on

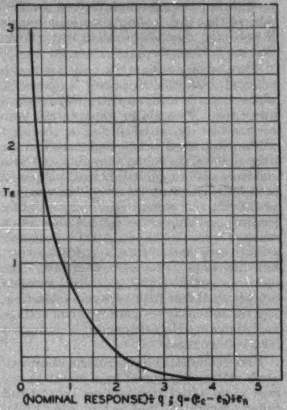

Figure 11 (right). T_e from nominal response, Equation 8

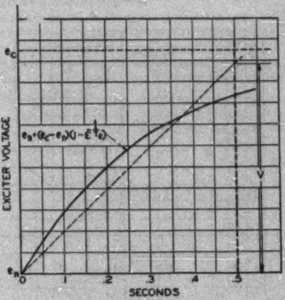

Figure 10 (below). Exciter voltage-time curve relating nominal response to time constant, T_e

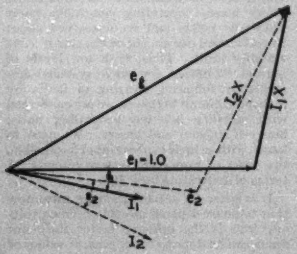

Figure 9 (left). Vector diagram showing initial voltage e_1 and final voltage e_2 during load change

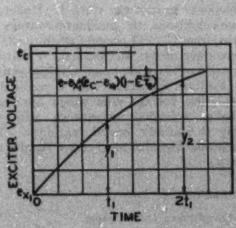

Figure 12 (right). Ordinates for equation 9

Appendix IV. Characteristics of Generator, Exciter, and Regulator

Generator

Rating 40,000 kva, 13,800 volts, 1,670 amperes, single circuit. Tested at 5,800 volts, two circuit, in order to circulate full load current, 3,340 amperes, with 1-ohm impedance per leg.

Reactances under this condition are as follows:

Synchronous reactance, $x_d = 1.92$
Transient reactance, $x_d' = 0.427$
Subtransient reactance, $x_d'' = 0.247$
Field resistance at 40 degrees centigrade $= 0.39$ ohm

Time constants:

Open Circuit $T_{d0} = 10.8$ seconds
Transient $T_{d1}' =$ Full load 5.3 seconds
Half load 6.68 seconds
Subtransient $T_{d1}'' =$ Full load 0.06 second
Half load 0.08 second

Per unit saturation 0.12 at no load, 5,800 volts.

Exciter

Rating 400 kw, 250 volts, shunt wound. Separately excited from 250-volt source. Ceiling voltage with 0.39-ohm load = 334 volts. Nominal voltage for test conditions = 170 volts. $T_e = 0.615$ second (calculated). Nominal response 1.24 (test).

Voltage Regulator

Allis-Chalmers type *J* contact-making rheostatic regulator.

Rating: Control element, 115 volts. Excitation voltage, 250 volts, 100 step bridge-type rheostat with high-speed contactors for sudden load changes.

References

1. Field Transients in Magnetic Systems, Ernst Weber. AIEE Transactions, volume 50, December 1931, pages 1234–46.

2. Regulation of A-C Generators with Suddenly Applied Loads, E. L. Harder, R. C. Cheek. Electrical Engineering (AIEE Transactions), volume 63, June 1944, pages 310–18.

3. Analysis of Short Circuit Oscillograms, W. W. Kuyper. Electrical Engineering (AIEE Transactions), volume 60, April 1941, pages 151–53.

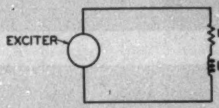

Figure 13. Inductive circuit

Discussion

G. W. Staats (Allis-Chalmers Manufacturing Company, Milwaukee, Wis.): Rosenberg's paper is doubtless a valuable addition to the existing literature on the phenomenon of voltage dips on generators due to suddenly applied loads, since it treats the problem in a forthright way and the method developed is readily applicable to actual situations. In addition, the equations derived are flexible, so that if it is desired to omit certain factors, for example, subtransient effects, this can be done easily.

The author mentions that the method is believed applicable to loaded machines as well as to static loads applied to an unloaded generator. It should be noted in this connection that the initial loading on a generator has, in general, only a slight effect on the magnitude of the voltage dip produced by a suddenly applied additional load. Figure 1 of the discussion serves to give an example of the effect of various conditions of initial loading, and shows the voltage dips which resulted when 1,500 and 2,000 horsepower motors were started from a 15,625 kva turbine generator of an eastern utility. The solid curves show the generator terminal voltage variation with constant excitation, and the dotted curves show terminal voltage variation when the field current is controlled by a voltage regulator.

Under voltage regulator control, the maximum voltage dip varied from about 11 per cent at no initial load to 9 per cent at full initial generator load when the 1,500-horsepower motor was started. Under the same conditions, the maximum voltage dip varied from 15 to 11 per cent when the 2,000-horsepower motor was started. This small variation over a wide range of initial generator loadings indicates that a method of calculating voltage dips which applies to initially unloaded generators will also apply to initially loaded machines. This conclusion was also reached by Harder and Cheek.[1]

Reference

1. See reference 2 of the paper.

C. Concordia (General Electric Company, Schenectady, N. Y.): The author of this paper refers to a previous analytical treatment in using his equation 5 for exciter voltage, but he prefers to use equation 6 of the paper. We should like to point out that equation 6 has also been used in a previous analysis. In particular, it was used in a paper by W. C. Johnson, Jr., published in 1930.[1] In fact, both equation 6 and equation 5 were used in Johnson's paper. Another analysis, using a linear variation of exciter voltage, was presented by H. C. Anderson, Jr. in 1945.[2]

References

1. Starting Induction-Type Motors from Systems of Limited Capacity, W. C. Johnson, Jr. *General Electric Review* (Schenectady, N. Y.) December 1930, page 712.

2. Voltage Variation of Suddenly Loaded Generators, H. C. Anderson, Jr. *General Electric Review* (Schenectady, N. Y.) August 1945, pages 25–33.

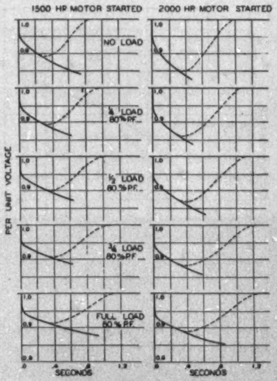

Figure 1. Effect of initial load on voltage dip of a 12.5-megawatt unit

T. B. Montgomery (Allis-Chalmers Manufacturing Company, Milwaukee, Wis.): In commenting on this paper I would like to direct my remarks from two points of view:

(A) The engineer applying regulators, of the modern high-speed type, to important generators on a system does not always have the time to do lengthy calculations to show what over-all results the use of such equipment is getting, and, as an application engineer he may not be accustomed to handling calculations involving all the factors, without time-consuming accumulation of data. He seldom has the correct exciter and generator characteristics and load short-circuit time constant conveniently at hand.

The control engineer, therefore, is especially happy to have a method of this type which merely involves the substitution of generator and exciter constants since these values can be obtained readily from the machine designer. Results, which are sufficiently accurate for all practical purposes, may be obtained quickly by those unaccustomed to involved calculations.

(B) From the standpoint of the user, since our standard practice for system stability under fault conditions on feeder and tie-lines remains dependent on clearing by high-speed circuit breakers, what salient advantage do we get from fast response under regulator operation? As recited in previous papers, those systems which, due to added capacity reactance from high-voltage cables as well as from static capacitors on distribution lines, find their excitation values under normal operating conditions lower than ever before and are concerned about the excitation margin above the steady state stability limit. Thus, with low levels of normal excitation (on such systems) immediately following clearing of faults by highspeed circuit breakers, we are concerned with stability between generating units, between stations and busses. We need to know, with as little expense labor as possible, the effect of excitation system response in terms of generating unit flux.

It is generally accepted among users now that response depends on exciter ceiling voltage (this is the primary factor since not much can be done to lower present values of inductance of generator field); on generator short circuit time constant T_{d1}'; exciter time constant T_e; and on regulator time response (this value is negligible on rotating amplifier type regulators).

The method presented is of particular value as a time saver in evaluating the effects of these four factors.

It appears that the success of application of the method depends very greatly on accurate determination of a short circuit time constant T_{d1}' corrected for load and of the exciter time constant T_e.

Since Figures 5 and 6 check fairly close, we would conclude that with high ratio of generator short circuit time constant to exciter time constant (T_{d1}'/T_e) the early part of the transient has an important bearing on the shape of the voltage time curve.

Since it has been customary to figure response under short circuit conditions only, the application of the method is useful especially in predicting the voltage fluctuation as influenced by changes in the control due to sudden load fluctuation. Although not definitely stated in the paper, for other conditions than the sudden short circuiting of the exciter rheostat, the value of T_e will not be related to the nominal exciter response curve as shown in Figure 11 because the build-up of the exciter will be dependent on the control signal that is, it will be proportional to the instantaneous change in output terminal voltage.

Equation 7 might be more conveniently expressed as follows if

$$\frac{L}{r} \text{ is replaced by } T'd,\ i_f = i_{f1} + \frac{(e_c - e_{x1})}{r\left(1 - \dfrac{T'd_1}{T_e}\right)} \times$$

$$\left[\left(1 - \frac{T'd_1}{T_e} - \epsilon^{-\frac{t}{T_e}} + \frac{T'd_1}{T_e}\,\epsilon^{-\frac{(t)}{T'd_1}}\right]$$

in this form it is more easily checked against the curves of Figure 2 of the paper which are given for various values of the ratio $T'd_1/T_e$.

L. T. Rosenberg: The curves presented by Staats cover a wide range in initial load, and yet show very little difference in minimum voltage. The effect of initial load at 80 per cent power factor lagging is shown to actually reduce the voltage disturbance. This is not true however of all types of initial load.

In practice, it is often more important to know the extent of the disturbance when the second motor is being started rather than the first, since with no initial load, there is nothing on the line to disturb. The expressions for the (e_t) values in equations 2 and 4 permit applying the method to two types of initial load.

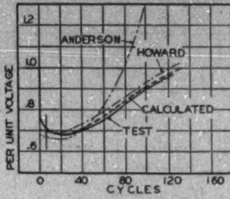

Figure 2. Voltage dip with full load suddenly added

For other types, similar relations may possibly be derived, or interpolation may be employed. As indicated in the paper, the expressions are suitable for removal of load also. If the entire load is removed, it will be noted the two relations, 2 and 4 become identical, as they obviously should.

I wish to thank Concordia for pointing out that equation 6 as well as equation 5 was also assumed for exciter build-up in a previous analysis by W. C. Johnson, Jr., and that a linear relation was used in a later paper by H. C. Anderson, Jr.

The treatment presented by Johnson covering equation 6 was credited to Alan Howard. Both the generator and the exciter voltages are assumed to follow a curve of the form 6 under suddenly increased field voltage. The operational expressions are then found for each circuit, and combined on the basis that the two circuits are linked only by a common electromotive force. The final solution for generator voltage, obtained by means of Heaviside's Expansion Theorem is very similar in form to equation 7 for generator field current.

The voltage components were expressed by Howard in terms of the ratios of external impedance to the total impedance behind synchronous and transient reactances. This limits their application to conditions of no initial load.

In Figure 2 of the discussion, the full-load test of Figure 5 is redrawn together with calculated curves based on both Johnson's and Anderson's papers. As may be expected the linear exciter voltage assumption of Anderson yields results in between those based on equation 5 and equation 6, and hence will only apply over a limited range. Like the other previous papers subtransient effects were not included.

With reference to part *B* of Montgomery's discussion, the value of quick-response excitation on generators and on intermediate synchronous condensers to augment inherent system stability has been recognized for many years, particularly in Europe where generator short circuit ratios of 0.4 to 0.5 are common. It is also well known that application of regulators to some machines on a system will yield more favorable results than to others, and that excessive amplification factors are not always justifiable. To properly evaluate the results of proposed regulating equipment, several alternate schemes must often be studied and compared.

Montgomery refers to Figures 5 and 6, both covering full load, 3-phase tests. Due to a faulty connection, the first test showed several momentary breaks in the exciter field current build-up after about 60 cycles, but the resulting generator voltage rise curves are almost identical. If the major part of the exciter voltage rise occurs in the early part of the disturbance, as it does with a high ratio of T_{d1}'/T_e, the remainder of the generator voltage build-up curve is governed mainly by T_{d1}'. This can be seen readily by reference to Figure 2 of the paper.

The use of Figure 11 to find T_e is confined only to cases where the regulator short circuits series resistance in the exciter field circuit, since nominal response is defined for this condition. Moreover, the curves of Figure 2 of the paper are valid only for exciter voltage build-up which can be approximated by equation 6. For other types of regulators, the actual exciter voltage build-up must therefore be determined, and then either method *B* or *C* of Appendix II may be used to find T_e.

Equation 7 was expressed in terms of *L* and *r* because its derivation is based on constant inductance and resistance of the field circuit.

In applying the curves of Figure 2 for voltage rise, the equation is more useful if expressed in terms of the two time constants T_{d1}' and T_e, as suggested by Montgomery.

The Geometric Loci of the Synchronous Tie

L. A. FINZI
ASSOCIATE AIEE

L. C. WELLARD
ASSOCIATE AIEE

Synopsis: A drive system consisting of two identical polyphase induction machines with their rotors interconnected and with additional secondary impedance networks is analyzed. General families of loci are obtained for the vectors representing the stator currents, and procedures are indicated for the determination of the torques.

TWO INDUCTION machines whose armature windings are supplied with polyphase alternating currents and whose rotors are interconnected, act as a positioning device; a rotation impressed on one of the shafts causes a corresponding motion of the second shaft, as if there were a mechanical coupling of some sort. If both shafts are stationary in arbitrary positions, the voltages induced in corresponding phase windings of the two rotors by the revolving air-gap fields differ in time phase by an angle which depends on the geometrical angle between the two shaft positions, and currents flow in the interconnected rotor circuits so as to generate torques which tend to line up the shafts in an equilibrium position of bucking induced rotor voltages. If both shafts are free to rotate, and if one of them is somehow displaced from such an equilibrium position, the other will follow. If the first is given a continuous rotation, the second also will rotate continuously at the same angular velocity, but with an angular displacement depending on its torque load.

As a remote positioning or indicating device this 2-machine drive falls in the category of the selsyns, while in industrial polyphase applications in which interchanges of considerable power are required, the names "synchronous tie," "synchro-tie," "synchro-lock," "electric shaft," and "power selsyns" are used.

The subject of the synchronous tie has been dealt with in the technical literature both in this country and abroad (See References 1–4). A most general treatment in terms of Kron's tensor analysis has also been developed.[5] The purpose of this paper is to present a steady-state analysis that applies to general drives as represented in Figure 1. The presence of external impedances in the rotor network introduces modifications in the torque–angle characteristics of the tie which may be of practical interest.

The Method of Analysis

In the following, two machines of identical design and size are considered, together with an additional rotor circuit network of balanced impedances which is reducible to a symmetrical *T*. The impressed stator voltages are of equal amplitude and frequency. These restrictions actually are not essential for a synchronous operation of the tie, since the only condition required for the existence of synchronizing torques is the equality of the frequencies of the induced rotor voltages. The restrictions are made chiefly in order to simplify the procedures and the form of the results.

The method of analysis is to establish an equivalent circuit, with the general procedures and assumptions which are customarily used in the circuit analysis of the induction machine. The currents in the various branches are obtained then by applying Kirchhoff's laws, and are functions of the two independent variables, per unit slip s, and relative phase angle δ, in electrical radians, of the two induced rotor voltages. Families of loci of the current vectors are derived, and, from these, torques and electrical and mechanical powers are evaluated for any steady-state operating condition.

It may be noted that names such as "transmitter" and "receiver," commonly used for selsyns, lead to confusion in this general case since they imply a definite flow of power from one shaft to the other while actual operating conditions are possible in which both shafts deliver (or absorb) mechanical power. It appears preferable, therefore, to distinguish between the two machines by means of the time phase of the induced rotor voltages. Thus, the machine of the synchronous tie whose induced rotor voltages lead in time the corresponding voltages of the other machine by a positive phase angle δ (ranging between zero and π) is called the "leader"; the other is called the "lagger." When the shafts rotate in directions opposite to those of their respective air-gap fields (that is, for slips greater than one), or when they rotate in the same directions as the fields but at a higher angular velocity (that is, for negative slips), the machine designated as leader, according to the definition above, is the one whose shaft leads that of the other in the direction of mechanical rotation. On the other hand, when the shafts rotate with the fields, but at a lower speed (that is for slips ranging between zero and one) the leader is the machine whose shaft is lagging in the direction of mechanical motion.

Figure 2(*a*) represents a single-phase equivalent circuit of the synchronous tie, with all secondary quantities reduced to primary terms. The subscripts *a* and *b* distinguish the two machines; 1, 2, and 0 refer to the stator, rotor, and exciting branches respectively, α and γ are used

---

Paper 49-51, recommended by the AIEE rotating machinery committee and approved by the AIEE technical program committee for presentation at the AIEE winter general meeting, New York, N. Y., January 31–February 4, 1949. Manuscript submitted November 15, 1948; made available for printing January 4, 1949.

L. A. Finzi is associate professor of electrical engineering, Carnegie Institute of Technology, Pittsburgh, Pa. L. C. Wellard, at present with the International Resistance Company, Philadelphia, Pa., was formerly a graduate student with Carnegie Institute of Technology and some of this paper was presented in partial fulfillment of the requirements for the degree of Master of Science.

The authors acknowledge the helpful criticisms of their associate, H. M. McConnell.

for the circuit parameters representing the external network, V is the line-to-neutral voltage. The phase angle existing between induced rotor voltages is introduced in the equivalent circuit by means of an ideal phase-shifter, *Ph*, with ratio of transformation 1:1.[6] According to the convention established, the machine *b* in Figure 2(*a*) is the leader.

Figure 2(*b*) shows a modified equivalent circuit in which the ideal phase-shifter has been transferred to the stator terminals of machine *b*. It is easy to verify that the use of either equivalent circuit leads to the same expressions for all branch currents designated with the same symbols in both figures.

In any case I_{a1} and I_{b1} are the line currents at the terminals of the two stators, while the current of slip frequency which actually flows into the shunt branch of the external impedance network has the value

$$I_\gamma = I_{a2} + I_{b2}\,\epsilon^{j\delta} \qquad (1)$$

(reduced to primary terms).

The Vectorial Loci of the Stator Currents for δ Constant and Variable s, (s-loci)

These loci are obtained in parametric form in equations 20 and 21 in the Appendix. For the simple synchronous tie without external networks (or also for the more general case in which an external network is added whose α branches consist of a resistor and an inductance in series and whose γ branch has only inductance), these equations simplify to

$$I_{a1} = V\frac{A+A's}{D+D's} \qquad (2)$$

and

$$I_{b1} = V\frac{B+B's}{D+D's} \qquad (3)$$

Thus the s-loci are circles whose centers and radii are obtained easily.

Figure 1. Synchronous tie with external impedances

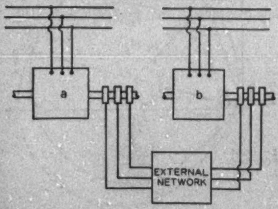

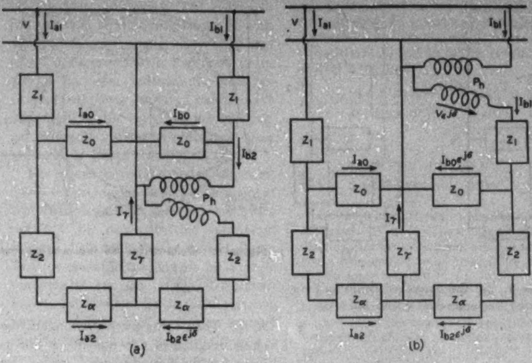

Figure 2. Equivalent circuits of the synchronous tie

$Z_0 = R_0 + jX_0$ $\qquad$ $Z_1 = R_1 + jX_1$

$$Z_2 = \frac{R_2}{s} \times jX_2$$

Z_α and Z_γ are functions of s

If, however, the γ-branch has resistance (that is $Z_\gamma = R_\gamma/s$ or $Z_\gamma = R_\gamma/s + jX_L$) equations 20 and 21 become

$$I_{a1} = V\frac{A+A's+A''s^2}{D+D's+D''s^2} \qquad (4)$$

and

$$I_{b1} = V\frac{B+B's+B''s^2}{D+D's+D''s^2} \qquad (5)$$

Thus the s-loci are bicircular quartics. These curves of the fourth order have a number of remarkable properties which may facilitate to some extent their construction by analytical or projective geometry procedures.[7]

If, as a further example, the external network consists of shunt capacitors (that is $Z_\alpha = 0$, $Z_\gamma = -jX_c/s^2$), the numerators and denominator of equations 20 and 21 and become polynomials of the fourth degree in s; this is the s-loci which are curves of the eighth order.

The Loci of the Stator Currents for s Constant and Variable δ (Delta-circles)

More convenient expressions for the stator currents are offered by

$$I_{a1} = V(H + K\epsilon^{j\delta}) \qquad (6)$$

and

$$I_{b1} = V(H + K\epsilon^{-j\delta}) \qquad (7)$$

For constant slip and variable δ, the loci of the current vectors are circles whose center and radius are obtainable from equations 15 through 19. A quicker determination of these delta-circles for any value of s is possible, however, if two s-loci are already known.

It is convenient to choose as basic s-loci for the construction of the delta-circles, the s-loci of I_{a1} for $\delta = \pi$ and $\delta = 0$. For these values of the phase angle, $I_{a1} = I_{b1}$, and, in view of the existing symmetry, the equivalent circuit simplifies to the circuits of Figures 3(*a*) and 3(*b*) respectively.

For $\delta = \pi$, no current flows in the γ-branch. If, in particular, $Z_\alpha = 0$, this locus coincides with the conventional circle diagram of one machine, and can be determined, from design or test data with any one of the various familiar procedures.

For $\delta = 0$, and no external networks (that is, $Z_\alpha = 0$, $Z_\gamma = \infty$), the s-locus shrinks to the tip of the vector representing the no-load current of a single machine. Hence the various delta-circles constitute a pencil of curves through this singular point. In the case of a simply-resistive shunt, the s-locus for $\delta = 0$ is again the circle diagram of a single machine, although with a different slip scale; while in the case of a simply-capacitive shunt, this locus becomes a bicircular quartic, whose determination, however, is still reasonably easy by means of the circuit of Figure 3(*b*).

In any event, for any conceivable type of external network, the s-loci for $\delta = 0$ and $\delta = \pi$ are easily obtained experimentally, within the range of speeds of practical

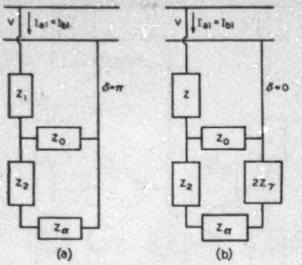
V
$I_{a1}=I_{b1}$
Z_1
$\delta=\pi$
Z_0
Z_2
Z_α
(a)
V
$I_{a1}=I_{b1}$
Z
$\delta=0$
Z_0
Z_2
$2Z_\gamma$
Z_α
(b)

Figure 3. (a) The equivalent circuit for $\delta=\pi$
(b) The equivalent circuit for $\delta=0$

interest, by simple tests performed on a single machine whose slip rings are connected to conveniently chosen external impedances.

The further use of these two particular s-loci for the general determination of the currents I_{a1} and I_{b1}, for any speed and angular displacement of the shafts, by means of constructed delta-circles is illustrated in Figures 4, 5, and 6.

Figure 4 refers to a simple synchronous tie without external network ($Z_\alpha=0$, $Z_\gamma=\infty$). As mentioned before, the s-locus for $\delta=\pi$ coincides with the circle diagram of one of the machines, while the s-locus for $\delta=0$ shrinks to the tip of the vector representing the no-load current. The constructions indicated with full lines lead to the determination of both stator currents for slip = 0.5, and for a relative rotor displacement of 60 electrical degrees. Also indicated, with dash-dot lines, are the vectors of the two stator currents for $s=1.4$ and for the same rotor angle, $\delta=60$ degrees. In either case, machine b is the leader in terms of induced rotor voltages, and absorbs electric power from the line, while machine a returns power to the line. For $s=1.4$ (this is rotation against the air-gap field), rotor b is also leading in terms of mechanical rotation; for $s=0.5$ (rotation with the field), rotor b, however, is lagging mechanically. Figure 4 applies to a set of two 10-horsepower 1,120-rpm 60-cycle 3-phase induction motors with the following per-unit impedances

$R_0=0.26$, $X_0=2.14$
$R_1=0.033$, $X_1=0.124$
$R_2=0.05$, $X_2=0.124$

(Unity current is defined as rated mechanical output per phase divided by rated stator voltage per phase.)

Figure 5 refers to the same tie with an additional shunt resistance ($Z_\alpha=0$, $Z_\gamma=R/s$). The s-locus for $\delta=\pi$ is again the circle diagram of one machine. The s-locus for $\delta=0$ is the same circle; its different slip scale is also indicated in Figure 5, in which it is assumed that $R_\gamma=0.10$. Constructions for $s=0.5$ and $\delta=60$ degrees are given. It may be noticed that for these values of the two independent variables, both machines absorb power from the line. As a matter of general interest, portions of the fourth order loci of I_{a1} and I_{b1} for $\delta=60$ degrees and variable slips, as obtainable from repeated constructions of delta-circles, also have been plotted in Figure 5.

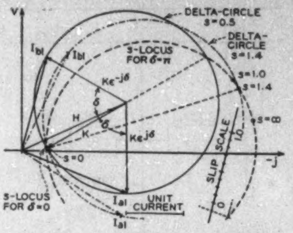
V
DELTA-CIRCLE s=0.5
DELTA-CIRCLE s=1.4
I_{b1}
I_{b1}
s-LOCUS FOR $\delta=\pi$
$K\epsilon^{-j\delta}$
δ
H
K
δ
$K\epsilon^{j\delta}$
s=1.0
s=1.4
s=∞
SLIP SCALE
1.0
0
s=0
-j
s-LOCUS FOR $\delta=0$
I_{a1}
UNIT CURRENT
I_{a1}

Figure 4. Delta-circles of the synchronous tie, $Z_\alpha=0$, $Z_\gamma=\infty$

Finally, Figure 6 refers to the tie with an additional shunt capacitance ($Z_\alpha=0$, $Z_\gamma=-jX_c/s^2$). Once more the s-locus for $\delta=\pi$ coincides with the circle diagram of one machine. A portion of the bicircular quartic, which is the s-locus for $\delta=0$, has been calculated numerically for a few values of s, assuming $X_c=3.62$ per unit. Constructions for I_{a1} and I_{b1} are indicated for $s=1.5$ and $\delta=60$ degrees.

The Torque Axes

Powers and torques for either machine of the tie can be obtained from the knowledge of I_{a1} and I_{b1} by means of customary procedures. A quick way for evaluating torque-angle characteristics at constant speed, however, is offered by the particular nature of the delta-loci. For this purpose the approximation is accepted that the power transmitted to the rotor of either machine by its revolving field, that is, the torque in synchronous watts, is expressed by:

air gap power = electric input − stator I^2R losses − no-load core losses

The torque is positive if acting upon the rotor in the direction of the revolving air-gap field. Whenever the locus of the stator current is a circle, it is possible to determine a straight line such that the distance between the tip of the vector representing the stator current and this line is proportional to the difference (power input—stator I^2R losses). The proof of this statement, as given in text books with particular reference to the circle diagram of the conventional induction motor,[8] is in fact valid quite generally, and applies to the delta-circles of the synchronous tie as well. The coefficients of the equation of this straight line depend on the coordinates of the center of the locus and on its radius. For the delta-circle of the stator currents $I_1=H+K\epsilon^{\pm j\delta}$, in a cartesian system of co-ordinates in which $H=y_h-jx_h$, the slope of the line is

$$\frac{dy}{dx}=\frac{x_h}{(V/2R_1-y_h)} \tag{8}$$

its intersection with the y-axis is

$$y_0'=-1/2\,\frac{x_h^2+y_h^2-K^2}{V_1/2R_1-y_h} \tag{9}$$

and

$$\text{(power input}-I^2R\text{ losses)}=m(V-2y_hR_1)\times d'$$

where m is the number of stator phases and d', read in the scale of the currents, is the distance between the tip of the

Figure 5. Delta-circles and s-loci, $Z_\alpha=0$, $Z_\gamma=\dfrac{R_\gamma}{s}$

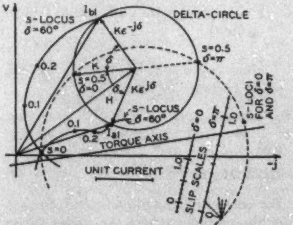
V
I_{b1}
s-LOCUS $\delta=60°$
DELTA-CIRCLE
$K\epsilon^{-j\delta}$
s=0.5 $\delta=\pi$
0.2
K
δ
s=0.5 $\delta=0$
δ
$K\epsilon^{j\delta}$
0.1
H
s-LOCUS $\delta=60°$
0.1
0.2
I_{a1}
TORQUE AXIS
s=0
$\delta=0$
$\delta=\pi$
1.0
s-LOCI FOR $\delta=0$ AND $\delta=\pi$
1.0
-j
UNIT CURRENT
SLIP SCALES
0
0

Figure 6. Delta-circles, $Z_\alpha=0$, $Z_\gamma=-j\dfrac{X_c}{s^2}$

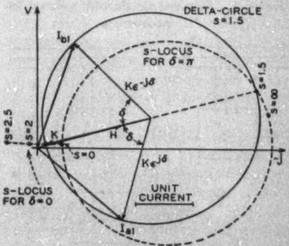
V
DELTA-CIRCLE s=1.5
I_{b1}
s-LOCUS FOR $\delta=\pi$
$K\epsilon^{-j\delta}$
s=1.5
s=∞
s=2.5
s=2
K
δ
H
δ
s=0
$K\epsilon^{j\delta}$
-j
s-LOCUS FOR $\delta=0$
UNIT CURRENT
I_{a1}

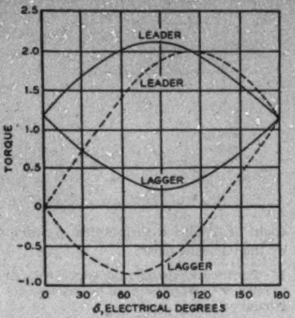

Figure 7. Examples of constant speed torque–angle characteristics

- - - - $Z_\gamma = \infty$

——— $Z_\gamma = \frac{R_\gamma}{s}$

current vector and this straight line, measured in the direction of the y-axis.

The air-gap power is obtained by further subtraction of the no-load core losses; thus the torque axis for the delta-circle in question results from a convenient parallel translation of the previous straight line in the y-direction, its intercept with the y-axis being

$$y_0 = y_0' + \frac{\text{no-load core loss}}{m} \times \frac{1}{V-2y_hR_1} \quad (10)$$

Hence air-gap power $= m(V-2\,y_h\,R_1)\,d$ where d is the distance between vector tip and torque axis, measured in y-direction.

Figure 5 indicates the construction of the torque axis for the delta-circle at $s=0.5$ for the case of the synchronous tie with external shunt resistance. It appears, from the position of this circle with respect to the co-ordinate axes, that the term $2\,y_h\,R_1$ may not be neglected in calculating the torque scale factor, as it may be practiced sometimes in simplified manipulations on the circle diagram of conventional induction motors.

Figure 7 shows plots of torque–angle characteristics for $s=0.5$; the dotted lines refer to the simple synchronous tie without external impedances, as obtained also by previous authors.[3,4] The curves in full line refer to the synchronous tie with external shunt resistance $R_\gamma=0.10$ analyzed in Figure 5. In Figure 7, unity torque has been chosen as the ratio between rated power output of one machine and rated motor speed; leader and lagger are defined in terms of induced rotor voltages, as stated initially.

The procedures established so far permit quick determination of the performance of the synchronous tie with external rotor networks for any operating speed and relative shaft angle, on the basis of design data or of simple tests made on a single machine of the set. In a subsequent paper, in preparation, these general methods will be used to discuss in more specific terms design considerations for a number of typical applications.

Appendix

For the equivalent circuit of Figure 3 the following loop equations are written

$$V = Z_1I_{a1} + Z_0(I_{a1} - I_{a2}) \quad (11)$$

$$V = Z_1 + I_{a1}(Z_2 + Z_\alpha)I_{a2} + Z_\gamma(I_{a2} + I_{b2}\epsilon^{j\delta}) \quad (12)$$

$$V\epsilon^{j\delta} = Z_1I_{b1}\epsilon^{j\delta} + Z_0(I_{b1}\epsilon^{j\delta} - I_{b2}\epsilon^{j\delta}) \quad (13)$$

$$V\epsilon^{j\delta} = Z_1I_{b1}\epsilon^{j\delta} + (Z_2 + Z_\alpha)I_{b2}\epsilon^{j\delta} + Z_\gamma(I_{b2}\epsilon^{j\delta} + I_{a2}) \quad (14)$$

Solving for I_{a1} and I_{b1}

$$I_{a1} = V\frac{N_a}{\Delta} \quad (15)$$

and

$$I_{b1} = V\frac{N_b}{\Delta} \quad (16)$$

with

$$N_a = [(Z_1+Z_0)(Z_2+Z_\alpha+Z_\gamma)+Z_1Z_1](Z_0+Z_2+Z_\alpha+Z_\gamma) - Z_\gamma^2(Z_1+Z_0) - Z_0^2Z_\gamma\epsilon^{j\delta} \quad (17)$$

$$N_b = [(Z_1+Z_0)(Z_2+Z_\alpha+Z_\gamma)+Z_1Z_0](Z_0+Z_2+Z_\alpha+Z_\gamma) - Z_\gamma^2(Z_1+Z_0) - Z_0^2Z_\gamma\epsilon^{j\delta} \quad (18)$$

and

$$\Delta = [(Z_1+Z_0)(Z_2+Z_\alpha+Z_\gamma)+Z_1Z_0]^2 - Z_\gamma^2(Z_1+Z_0)^2 \quad (19)$$

where Z_2, Z_α, and Z_γ are functions of the slip s. (It will be remembered, in fact, that, if the secondary network has resistors R and inductors and capacitors respectively of reactance X_L and X_c at line frequency, these elements shall be introduced in the equivalent circuit as R/s, X_L, and X_c/s^2.)

Equations 15 and 16 can be rewritten in general in the form

$$I_{a1} = V\,\frac{A+A's+A''s^2+\ldots+A^ns^n}{D+D's+D''s^2+\ldots+D^ns^n} \quad (20)$$

and

$$I_{b1} = V\,\frac{B+B's+B''s^2+\ldots+B^ns^n}{D+D's+D''s^2+\ldots+D^ns^n} \quad (21)$$

where the D are constant, while the A and B are functions of δ. Thus numerators and denominator are polynomials in s of nth degree, n depending upon the nature of the chosen rotor network.

For constant δ, 20 and 21 are parametric equations of the loci of the current vectors I_{a1} and I_{b1} in the complex plane, these loci being curves of order $2n$ (called s-loci in this paper).

Equations 15 and 16 can also be rewritten in the form

$$I_{a1} = V(H + K\epsilon^{j\delta}) \quad (6)$$

$$I_{b1} = V(H + K\epsilon^{-j\delta}) \quad (7)$$

where H and K are functions of s, seen by inspection of equations 17, 18, and 19.

Thus, for constant s and variable δ, the loci of the current vectors I_{a1} and I_{b1} become circles (called delta-circles in this paper).

References

1. SYNCHRONIZED OPERATION OF D-C MOTORS BY MEANS OF POLYPHASE INDUCTION MACHINES, M. Liwschitz. *Wissenschaftliche Veroeffentlichungen aus dem Siemens-Konzern* (Berlin, Germany), volume 5, 1926, page 26 (in German).

2. SYNCHROTIES TO HANDLE TORQUES OF MOTOR MAGNITUDES, C. W. Drake. *Electrical World* (New York, N. Y.), volume 104, August 1934, page 240.

3. INDUCTION MOTORS AS SELSYN DRIVES, L. M. Novacki. AIEE TRANSACTIONS, volume 53, 1934, page 1721–26.

4. SELSYNS INSTRUMENTS FOR POSITION SYSTEMS, T. M. Linville and J. S. Woodward. ELECTRICAL ENGINEERING (AIEE TRANSACTIONS), June 1934, pages 953–60.

5. DAMPING AND SYNCHRONIZING TORQUES OF POWER SELSYNS. C. Concordia, G. Kron. AIEE TRANSACTIONS, volume 64, 1945, pages 366–71.

6. THEORY OF THE INDUCTION MOTOR WITH DOUBLE STATOR, L. A. Finzi. *Archiv fuer Elektrotechnik* (Berlin, Germany), volume 27, 1933, page 813 (in German).

7. THE GEOMETRIC LOCI OF A-C CIRCUITS, (book) O. Bloch. Rasher and Company, Zurich, Switzerland (in German), 1917.

8. ELECTRIC MACHINERY, Volume II, A. C. MACHINES (book), M. Liwschitz-Garik. D. Van Nostrand, Incorporated, New York, N. Y., 1946, page 517.

No Discussion

Voltage-Recovery Characteristics of Distribution Systems

R. L. WITZKE
MEMBER AIEE

THE performance of distribution-system protective devices, such as expulsion-type lightning arresters, fuses, reclosers, and so forth, is influenced by the voltage-recovery characteristics of the system on which they are applied. Successful operation of a protective device requires proper co-ordination between the apparatus dielectric-recovery characteristics and the system voltage-recovery characteristics. The adequacy of the device is checked by employing laboratory test circuits having recovery voltages at least as severe as those experienced in practice on actual systems. The study reported in this paper was made to obtain the necessary fundamental data for predicting the most probable voltage-recovery characteristics of distribution circuits in the 2,400-to-13,800-volt classes. Previous papers[1,2,3] gave similar data for systems operating at the higher voltages, however, the results of these studies are not applicable generally to the lower-voltage systems because of the differences in source reactances, line lengths and conductor spacings. Furthermore, the development of procedures for estimating the characteristics of distribution systems, having a multiplicity of trunk lines, radial laterals, and so forth, was required.

A general study was made on the analog computer for a 4-wire multigrounded system, over a wide range of source reactances, line lengths and conductor sizes. Consideration was given to single- and double-line-to-ground faults and to fault location.

The final data give times to 90 per cent voltage and to the maximum recovery voltage as a function of source reactance and line length. Data on the maximum recovery voltage on these systems, for both single- and double-line-to-ground faults, also are included. Although the general study was made on the basis of a source and a single overhead circuit, methods are included for estimating the voltage-recovery characteristics of the more complicated, practical systems.

Additional studies were made for 3-phase, 3-wire and for single-phase systems to compare the characteristics of these systems with the corresponding characteristics of 4-wire systems. The effects of methods of system grounding, short sections of cable and fault resistance also were investigated.

List of Symbols

E_m = maximum recovery voltage in per cent of normal line-to-ground crest voltage
T_m = time to maximum recovery voltage in microseconds
$T_{0.9}$ = time to 90 per cent voltage, where 100 per cent is normal line-to-ground crest voltage
X = positive-sequence source reactance in ohms at 60-cycles
M = connected line in miles per phase

Summary and Conclusions

Previous studies,[1,2,3] and a review of protective device dielectric-recovery characteristics, showed that the significant points on a system recovery-voltage curve could be defined with practical accuracy by the following data:

1. The time required for the system voltage to recover to 90 per cent of normal line-to-ground voltage.
2. The magnitude of the maximum voltage, expressed in per cent of the normal line-to-ground crest voltage.
3. The time required for the system voltage to reach the maximum value obtained.

Theoretical considerations and analog computer studies showed that the X/M ratio of a distribution system, where X is the 60-cycle source reactance in ohms and M is the miles of connected line per phase, may be used as the fundamental variable in recovery-voltage studies, whenever the system natural frequencies are high by comparison to the fundamental system frequency, and losses are not a significant factor in determining the voltage-recovery characteristics. The natural frequencies of all solidly-grounded systems studied were high by comparison to 60 cycles, and losses had only secondary effects, even with number 6 conductors. This conclusion allowed expressing all significant data for solidly-grounded systems as a function of the X/M ratio, and greatly increased the possible scope of the studies, see Figures 7 and 8.

A general study was made for a 4-wire system, consisting of a solidly-grounded source and a single overhead circuit of average conductor configuration, for X/M ratios between 0.0625 and 8.0. Fault location was found to have an important influence on the data, so four fault locations were considered in each study, and the data giving the most severe recovery characteristics were used. Fault location was then eliminated in the final summaries on the basis that protective devices must be applicable to any location on a circuit. The times to 90 per cent voltage and to maximum voltage, divided by the line length in miles, were plotted as a function of the X/M ratio. Even though both single- and double-line-to-ground faults, and 4/0 and number 6 conductors were considered, the resulting times for a given X/M ratio did not vary more than 30 per cent from the minimum times obtained. In most cases the mini-

---

Paper 49-53, recommended by the AIEE protective devices committee and approved by the AIEE technical program committee for presentation at the AIEE winter general meeting, New York, N. Y., January 31–February 4, 1949. Manuscript submitted November 16, 1948; made available for printing December 27, 1948.

R. L. Witzke is with the Westinghouse Electric Company, East Pittsburgh, Pa.

The author wishes to acknowledge the assistance of A. M. Opsahl, who made many helpful suggestions in connection with the preparation of this paper, and T. J. Bliss who made the analog computer studies and analyzed the data.

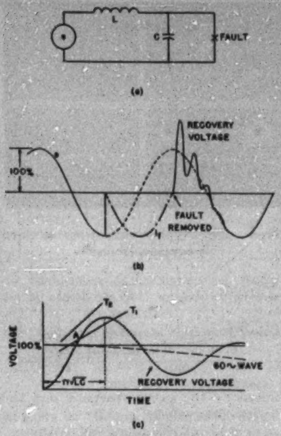

Figure 1. Recovery voltage-simple circuit

(A) Circuit
(B) Voltage and current relations
(C) Comparison of system recovery-voltage with expulsion-type lightning arrester dielectric characteristics, T_1 and T_2

mum times were at least 80 per cent of the maximum times recorded.

The maximum voltages obtained with 4/0 conductors (approximately 175 per cent for a single line-to-ground fault and 205 per cent for a double-line-to-ground) did not vary appreciably with the X/M ratio. With number 6 conductors, these voltages varied between 125 per cent at low X/M ratios, and the 4/0 conductor values at high X/M ratios. The main influence of conductor size was to change the phase angle of the fault path.

These results indicate one practical approach to the distribution-system recovery-voltage problem, and that is to eliminate conductor size as a variable, and use the same times to 90 per cent and maximum voltage for single- and double-line-to-ground faults.

A study of solidly-grounded systems with parallel circuits on the same bus led to conclusions, as follows:

1. The times to maximum recovery voltage decreased as the number of parallel circuits was increased, assuming the same total miles of connected line. These times could be estimated, for the limiting case of an infinite number of parallel circuits, by the simple relation

$$T_m = 15.9\sqrt{XM} \text{ microseconds}$$

2. The times to 90 per cent voltage could be estimated by one of the relations

$$T_{0.9} = 13.8\ NX \text{ microseconds}$$

or

$$T_{0.9} = 7.7\sqrt{XM} \text{ microseconds}$$

depending upon which gives the minimum time.

In the foregoing relations X is the 60-cycle source reactance in ohms, N the number of parallel feeders connected to the supply bus, and M the connected line, in miles per phase, including trunk feeders and laterals.

Special studies showed that the 4-wire system data could be applied to 3-wire and single-phase, solidly grounded systems. Reactance or resistance grounding decreases the severity of the recovery-voltage transients following single-line-to-ground faults, but increases the maximum voltages following double-line-to-ground faults.

Theory

The simple circuit in Figure 1(A) will be used to define system recovery voltage and to illustrate its influence on the performance of protective devices. In this circuit the power source is represented by a voltage and an inductance, and the line by a capacitance. Applying a short circuit across the capacitor is equivalent to applying a fault on a single-phase system. The fault current will lag the internal voltage of the source by 90 degrees as shown in Figure 1(A) because resistance has been neglected. When the fault is removed, at the instant the fault current passes through zero, the voltage across the capacitor returns to normal after a series of oscillations. The volt-time curve, measured across the capacitor following the removal of the fault, is referred to as the recovery-voltage of the circuit because it defines the manner in which the circuit voltage "recovers" after the fault is removed. This voltage will reach a maximum value equal to twice normal crest circuit voltage if losses are neglected. Losses will limit the maximum voltage to less than 200 per cent, and will damp out the oscillation after a number of cycles. The time to maximum recovery-voltage is equal to $\pi\sqrt{LC}$ for the simple circuit used in the illustration. As L depends on the source reactance and C is proportional to line length, the times associated with the voltage recovery characteristics of a system are a function of source reactance and line length.

The recovery-voltage curve of Figure 1(B) is replotted in Figure 1(C) with an expanded time scale. Also included are dielectric-recovery curves for two expulsion-type lightning arresters. The latter curves define the voltage that a lightning arrester can withstand at various time intervals after the lightning arrester ceases to conduct fault current. It will be remembered that a lightning arrester is a good conductor during the discharge and power-follow periods, and then must become a good insulator after the fault current is interrupted by the lightning arrester. This change from a conductor to an insulator does not take place instantly, but occurs gradually as indicated by the dielectric-recovery curves. For satisfactory performance, the lightning arrester characteristic curve must lie above the system recovery-voltage curve. Lightning arrester T_1 would restrike at point A, Figure 1(C), whereas lightning arrester T_2 would withstand the recovery voltage without restriking. Similar coordination between device and system characteristics is required for satisfactory performance of other protective devices such as fuses, reclosers, and so forth.

The voltage-recovery curve for a typical distribution system, shown in Figure 2(A), differs from the curve for the simple circuit of Figure 1(A) only in that it contains more than one natural frequency, and consequently is not a simple sine-wave function. Experience has

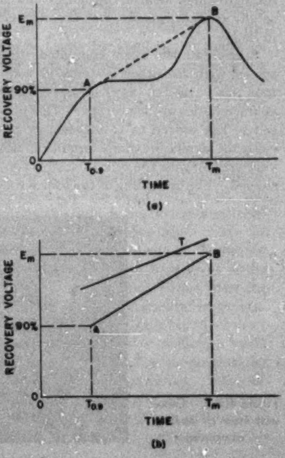

Figure 2. Recovery-voltage practical system

(A) Complete recovery-voltage curve
(B) Significant recovery-voltage data compared with expulsion-type lightning arrester characteristics represented by line T

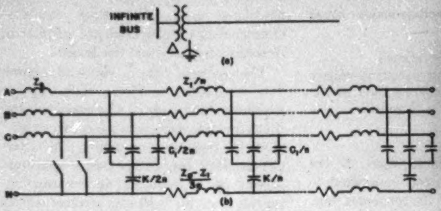

Figure 3. System used in general study

(A) One-line diagram
(B) Equivalent circuit
A, B, C, N-3-phase 60-cycle source
Z_s-source impedance
Z, Z_0-positive- and zero-sequence line impedances
C_1, C_0-positive- and zero-sequence line capacitances
n = number of π sections
$K = 3C_1C_0/(C_1-C_0)$

shown that only two significant points on the recovery-voltage curve are required to obtain co-ordination with protective-device characteristics. These are the time to 90 per cent voltage, and the time and magnitude associated with the maximum value of the recovery-voltage. These significant points, connected by a straight line, are compared with an expulsion-type lightning arrester characteristic curve in Figure 2(B).

Distribution Systems. The wide variety of systems in current use, and the range in circuit constants encountered, made it impractical to make general studies for all types of systems. For this reason, the more popular system, consisting of 4-wire multigrounded neutral primaries and a solidly grounded source, was investigated in detail.

Special studies then compared this system with the other systems in common use, insofar as recovery-voltage characteristics are concerned. This procedure has proved to be satisfactory because the significant characteristics do not vary greatly with the type of system considered. The grounding of the source was found to be an important factor, and was the basis of additional special studies.

The Analog Computer. Most of the studies reported were made on the analog computer;[4] a few special cases were calculated. The computer is essentially the same as the network calculator used in the 1938 recovery-voltage study; differing primarily in the number and characteristics of the circuit elements and voltage sources. The system studied is represented in miniature by means of inductors, capacitors, and resistors. Low-impedance 3-phase 60-cycle sources are available for representation of the fundamental-frequency system voltages. Faults are applied and removed with special synchronous switches to simulate the operation of protective devices. The transient being studied is repeated ten times per second and appears on a cathode-ray oscilloscope as a steady-state wave. Studies similar to the ones reported in this paper would be classified as impractical without an analog computer, or its equivalent.

The system selected for study and its equivalent circuit are illustrated in Figure 3. The system consists of a delta-star transformer bank, solidly grounded on the star side, and connected to an infinite bus on the delta side. The neutral wire of the single, 4-wire primary is assumed to be multigrounded. The impedance of the transformer supply is represented by three reactors in the 3-phase equivalent circuit. The line is represented by π sections, the actual number being determined by the source reactance and the length of the primary circuit. As many as eight π sections, requiring 68 circuit elements, were used in the general studies. The synchronous switches, representing ground faults, can be switched to any point in the equivalent line section by dial switches. In recovery-voltage studies a cathode-ray oscilloscope is connected to measure the voltage directly across the synchronous switches.

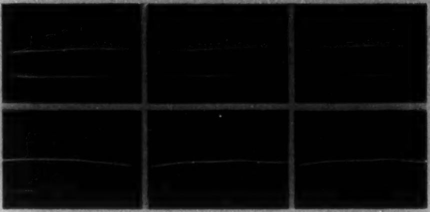

Figure 4(B). Typical oscillograms obtained in computer laboratory

Upper line—single-line-to-ground fault on sending end bus for 4, 16 and 64-ohm source reactances
Lower line—faults at sending end, center and open end of single-phase system

Figure 4(A). General view of analog computer

General Study

The important variables considered in the general 4-wire system study are as follows: source reactance; line length; conductor size; fault location; and type of fault, both single-line-to-ground and double-line-to-ground.

The positive-to-zero sequence reactance ratio of the source was made equal to one, corresponding to the assumption that all of the source reactance was in a solidly-grounded, delta-star transformer bank. The resistance of the source was represented by the inherent losses of the reactors used to represent the source reactance. The reactance-to-resistance ratio of these reactors was always higher than the probable ratio for distribution or power transformers, over the entire range of frequencies encountered in the study. Sixty-cycle source reactance of 2, 4, 8, 16, and 32 ohms, and line lengths of 2, 4, 8, 16, and 32 miles were considered. Data for systems outside of these ranges can be estimated from the data obtained.

Geometric-mean distances of 2.66 feet between phase conductors, and 4.1 feet between the phase and the neutral conductors were assumed. These spacings give reactances that are an average of the values obtained over the range of spac-

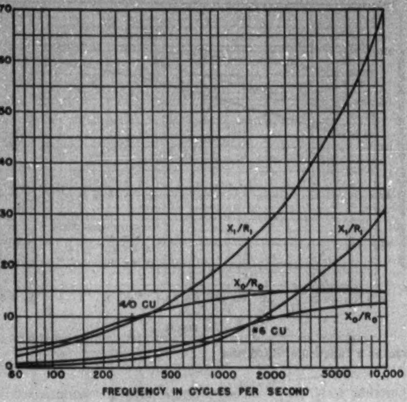

Figure 5. Variation of overhead-line reactance/resistance ratios with frequency

X_1/R_1—Positive-sequence ratio
X_0/R_0—Zero-sequence ratio

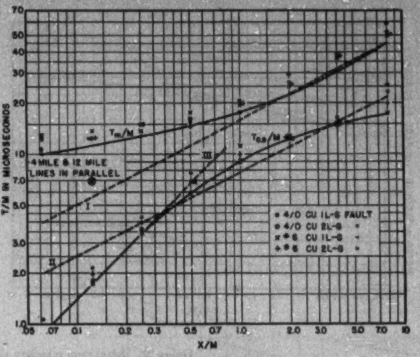

Figure 7. Times to 90 per cent and maximum recovery voltage referred to a 1-mile line basis

$T_{0.9}/M$, T_m/M—times to 90 per cent and maximum voltage divided by line length in miles
X—60-cycle source reactance in ohms
I. T_m/M neglecting line inductance
II. $T_{0.9}/M$ neglecting line inductance
III. $T_{0.9}/M$ neglecting line reflections

ings normally used between 2,400 and 13,800 volts. The small variations introduced by changes in spacing were not considered significant in the general problem. A conductor height of 30 feet and a ground resistivity of 100-meter ohms were used in all studies. The phase and neutral-conductor sizes were assumed to be the same, and were varied between 4/0 and number 6 copper. The line constants for these two extreme conductor sizes are included in Table I.

Fault location was found to have a significant effect so was retained as a variable. Previous studies[1,2] considered only one fault location, which was permissible because the circuits were grounded at both ends of the line section. In the present study, with only one ground point, the fault location could not be neglected. Faults were applied on the sending end bus and at the 1/4, 1/2 and 1.0 points, the latter being the open end of the line. Data were obtained for both single- and double-line-to-ground faults.

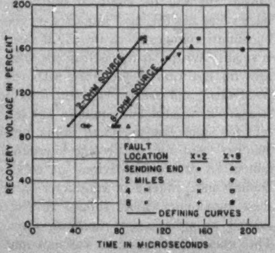

Figure 6. Method of recording and interpreting data illustrated for a single-line-to-ground fault on 8-mile, 4-wire system

Method of Study. The large number of conditions selected for study (five source reactances, five line lengths, four fault locations and two types of faults—a total of 200 cases) made it desirable to simplify and generalize the procedure as much as possible without introducing important errors. It was realized that two systems having the same X/M ratio (ratio of source reactance in ohms to line lengths in miles) would have the same recovery voltage curves, excepting for a difference in time scale. For example, the recovery voltage curve for a 4-ohm 4-mile system has the same shape as the curve for an 8-ohm 8-mile system. The times associated with the 8-mile case would be twice those for the 4-mile system. With this in mind, the X/M ratio was adopted as the fundamental variable in the general study. It was found that if data were obtained for X/M ratios between 0.0625 and 8.0, data for systems falling outside of these limits could be obtained with satisfactory accuracy by extrapolation. This procedure reduced the original 200 cases to the 64 actually studied on the computer. Eight systems, having different source reactances and line lengths, were selected to give the desired X/M ratios.

It should be noted that the foregoing procedure is permissible only when the natural frequencies of the systems considered are high by comparison to the fundamental system frequency, and when high-frequency losses are not too significant in the solution. The lowest natural frequencies of the selected systems ranged between approximately 600 and 18,000 cycles. The reactance-to-resistance ratios for overhead lines increase with frequency, and are reasonably large in the important frequency range, even with number 6 copper. As this ratio is a measure of decrement (a ratio of ten introduces a decrement factor of 0.85 per half cycle of a free oscillation), it was concluded that high-frequency losses were not particularly important in the study.

Some weight was given to high-frequency losses by leaving the faults on until most, if not all, of the initiating transients were damped out. This procedure is justified because of the high frequencies involved during single- or double-line-to-ground faults. For example, a 16-mile 8-ohm system has natural frequencies of at least 2,000 cycles during single-line-to-ground faults. Assuming the fault is applied at near crest line-to-neutral voltage, more than 33 half-cycles of the transient oscillation will elapse, before the fault is removed at the first current zero, which occurs after one half-cycle of the fundamental frequency. Giving some weight to the high-frequency losses of the source, this oscillation would be reduced to negligible proportions by the time the fault is removed. This conclusion was reached by assuming a source damping factor of 0.85 per half-cycle of the high-frequency oscillation. This

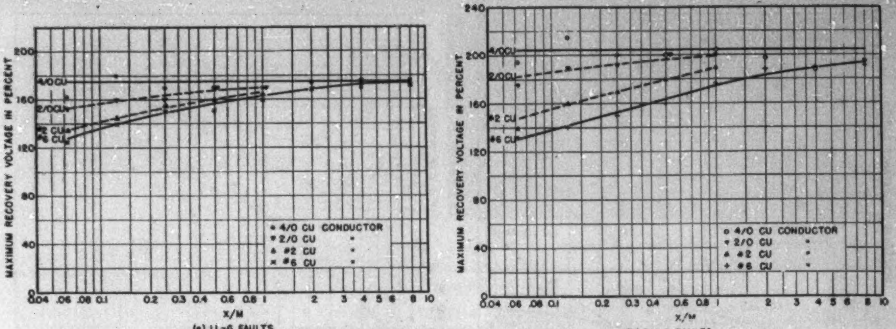

(a) 1L-G FAULTS

(b) 2 L-G FAULTS

Figure 8. Maximum recovery voltages as a function of *X/M* ratio

value has been proposed[5] as being typical for terminal equipment and appears to be within reason for the transformer sources considered in this study.

The initiating transient may have some small effect on the voltage-recovery characteristics of the 32-mile lines studied, especially with the larger source reactances. This, however, is not of practical importance because distribution systems having this much line would have a multiplicity of trunk feeders and laterals, which tend to decrease the magnitude of the recovery-voltage transients.

Previous studies[1,2] considered the effect of varying the point on the 60-cycle voltage wave where the fault is applied. This complication was not required in the present study because the instant of fault application is important only in those cases where the initiating transient has appreciable influence on the recovery-voltage transient.

It was found that the 60-cycle reactance-to-resistance ratios were important, and these were represented correctly, even where time-base multipliers were introduced to keep the system natural frequencies within the preferred frequency range of the Computer.

Results of General Study. The general studies were made by applying single- and double-line-to-ground faults at four locations, and recording the times to 90 per cent voltage, and the times and magnitudes associated with the maximum recovery-voltage transient. These data are illustrated in Figure 6 for the case of a single-line-to-ground fault on an 8-mile system. Time is expressed in microseconds and voltage in per cent of normal line-to-ground crest voltage. It is evident that fault location has considerable influence on the pertinent data. With a 2-ohm source, the time to 90 per cent voltage is a minimum for a sending-end fault, whereas a receiving-end fault dictates this time with an 8-ohm source. It will also be observed that the maximum voltages are obtained for faults away from the sending-end bus. However, many cases were noted where the maximum voltage did occur for sending end faults, especially where small line conductors were represented. This illustrates the complexity of the problem, and the need for considerable data before formulating conclusions.

As it would be impractical to summarize, in the form of useful curves, all of the data obtained, simple uniform method of interpretation was adopted. As a protective device must function at any location on a circuit, it is necessary to know only the most severe circuit conditions, regardless of fault location. With this in mind, a straight line was drawn to connect the points giving the minimum times to 90 per cent and maximum recovery voltage. This line then defines the voltage-recovery characteristics of the particular system. In certain cases, such as the 8-ohm system in Figure 6, the defining straight line was extended through one maximum voltage point to a horizontal line that intercepts the highest voltage recorded. This results in a simple method of plotting data without being ultra conservative. In the case illustrated, the maximum recovery voltage would be recorded as 170 per cent at 140 microseconds.

The times to 90 per cent and to maximum recovery voltage were obtained by plots similar to Figure 6. These times were then reduced to a 1-mile basis by dividing by the line length in miles; then plotted as a function of the *X/M* ratio (ratio of source ohms to line length in miles.) These data are summarized in Figure 7 for single- and double-line-to-ground faults, and 4/0 and number 6 copper conductors. It will be observed that the times, for a given *X/M* ratio, do not vary greatly with the type of fault or the conductor size, even though consideration has been given to various fault locations. For this reason, it was decided that practical answers could be obtained by drawing a single curve under each set of data. The differences between the actual times and those defined by the lower-limit curves were not considered important in view of the complexity of the over-all problem, and the complicated circuits encountered in practice.

The actual times for any given line length can be obtained by multiplying the values in Figure 7 by the line length in miles. Data obtained in this manner are plotted in Figure 9 for a range of source reactances and line lengths.

The maximum voltages measured are plotted in Figure 8 as a function of the *X/M* ratio. Values are included for four conductor sizes, which allows an evaluation of this variable on the voltages obtained. It will be observed that conductor size has the most influence on the maximum voltages when the *X/M* ratio is small. With 4/0 conductors the voltages do not vary appreciably with the *X/M* ratio, and can be represented by a straight horizontal line equal to 175 per cent for single-line-to-ground faults, and 205 per cent for double-line-to-ground faults. If protective devices are to be applied independent of conductor size, these maximum values should be considered as a basis for standardization. The maximum recovery voltages are plotted in Figure 10 as a function of source reactance in ohms and line length in miles. The voltages are expressed in per cent of

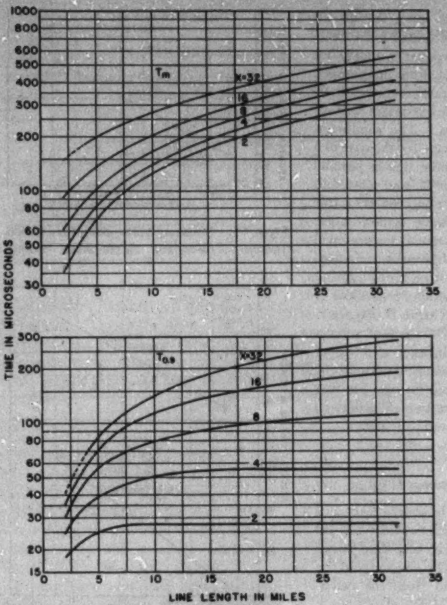

Figure 9. Times to 90 per cent and maximum recovery voltage for a system consisting of a solidly-grounded source and a single overhead circuit

normal line-to-ground crest voltage, and apply to systems in the 2,400-to-13,800-volt range.

Special Studies

A number of special studies were made to show the influence of a number of factors not included in the general study. The data in Figure 11 were obtained for a 3-wire system having the same equivalent phase conductor spacing as used in the 4-wire system study. The results are compared with the general curve data, Figures 9 and 10, to show the relative severity of the recovery-voltage transients on the 3-wire and 4-wire systems. These results indicate that satisfactory performance of protective devices would be obtained on solidly-grounded 3-wire systems, if designed to meet the conditions imposed by a 4-wire system.

Single-Phase System. Figure 12 summarizes the data obtained for a single-phase, multigrounded neutral system having a conductor spacing equal to the equivalent phase conductor to neutral conductor spacing of the 4-wire system. The comparison between these results and the single-line-to-ground fault data for the 4-wire system indicates that the general study results can be applied to single-phase systems with safety.

Unigrounded, 4-wire System. Although the unigrounded, 4-wire system was not studied on the computer, the recovery-voltage characteristics of this system should be no more severe than those for a 3-wire system. The data for this type of system can therefore be estimated with practical accuracy from Figures 9 and 10.

Effect of Load. Load will usually have a damping action on recovery-voltage transients, and so should introduce some margin in the results reported in this paper. The load on distribution systems may be quite small during light-load periods so should not be depended upon to limit transient voltages. One study made with an 80 per cent power-factor load equal to 20 per cent of the supply transformer rating did not show any important differences, with and without load.

Cable Terminations. Many overhead lines leave the substation through short sections of cable. Studies were made with 200-, 400- and 800-foot cables having a capacitance of 0.1 microfarad per 1,000 feet. These results, for a 16-mile line, are plotted in Figure 13, and indicate only minor differences as compared to the general study data.

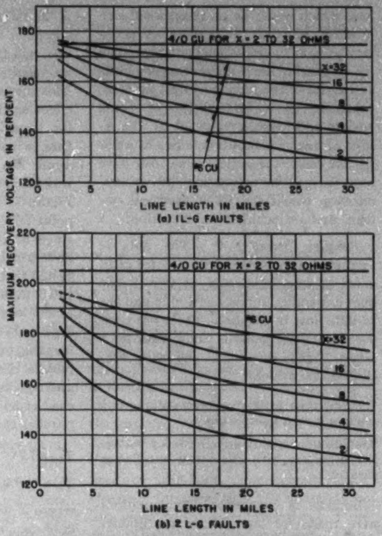

Figure 10. Maximum recovery voltages for a system consisting of a solidly-grounded source and a single overhead circuit

General Circuit Arrangements

The general curves, Figures 7 to 10, were obtained for a source and a single

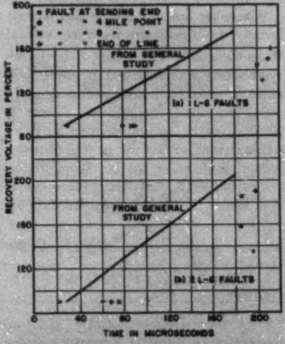

Figure 11. Recovery-voltage data for a 2-ohm 16-mile 4/0-copper solidly-grounded 3-wire system

line, which would be an exceptional condition in practice. It is therefore necessary to have available a definite procedure for estimating the voltage-recovery characteristics of the more practical systems, consisting of a multiplicity of trunk feeders and laterals. Guided by the results of analog computer studies of a few special cases, theoretical equations have been derived for estimating the voltage-recovery characteristics of practical systems, and are included in this section.

Parallel Circuit Data. The data in Figure 14 were obtained for a total of 16 miles of line, connected as two 8-mile lines in parallel, and as one 4-mile and one 12-mile lines in parallel. These are compared with the general study data for a single 16-mile line. The following conclusions are evident:

1. The time to 90 per cent voltage is a minimum with a single line.
2. The time to maximum recovery voltage is a minimum with more than one line in parallel.

Because of conclusion 2, calculations were made for the case of an infinite number of lines in parallel, which was done by neglecting all line inductance and representing the lines by lumped capacitances. This data, for a single-line-to-ground fault on a 2-ohm 16-mile system is given in Table II. The maximum voltages vary between 168 and 183 per cent, and compare favorably with the 175 per cent obtained in the general study for single-line-to-ground faults. The times to maximum voltage range between 90 and 103 microseconds, the shorter time being obtained with the smaller conductor on a 3-wire system. The time to 90 per cent voltage is also a minimum for this same system.

Whenever line inductance can be neglected, the significant recovery voltage times vary as $\sqrt{XM}$, where X is the 60-cycle source reactance and M is the total miles of connected line, assumed to be equal on the three phases. Curve I, Figure 7, is the calculated curve for times to maximum voltage for a single-line-to-ground fault on a number 6-conductor, 3-wire system. This straight-line curve, approaches the analog computer data for X/M ratios above 1.0, even though the computer data were obtained for a single line, and the calculated curve applies for an infinite number of lines in parallel. This shows that line inductance has little effect on the times to maximum voltage for large X/M ratios. The significant time to maximum voltage for the case of a 4-mile line and a 12-mile line in parallel was taken from Figure 14, and plotted in Figure 7. It will be observed that this point falls closer to curve I than to the single-line curve. As most systems will have a multiplicity of circuits, it is suggested that curve I be used for estimating times to maximum voltage, regardless of circuit arrangement. Curve II, Figure 7, represents the times to 90 per cent voltage for the case of an infinite number of parallel circuits. The times to 90 per cent and maximum voltage, for the limiting case of an infinite number of feeders in parallel, can be estimated as follows:

$$T_{0.9}=7.7\sqrt{XM} \text{ microseconds} \qquad (1)$$

$$T_m=15.9\sqrt{XM} \text{ microseconds} \qquad (2)$$

where X is the 60-cycle source reactance in ohms, and M is the connected overhead line in miles per phase, including trunk feeders and laterals. The constants in the equations were derived from the calculated times in Table II for a number 6 conductor, 3-wire system.

The computer data in Figure 7 fall close to curve II for X/M ratios larger than approximately 1/3. Below this ratio, the times for a single line are not a function of line length, but only of source reactance. The minimum times were obtained for single-line-to-ground faults on the sending-end bus, and the recovery voltage reached the 90 per cent values before reflections returned from the open end of the line. These times therefore vary directly with the 60-cycle source reactance, and follow curve III.

With several long feeders in parallel, and a low source reactance, the times to 90 per cent voltage will be independent of line length, and will vary directly with source reactance and with the number of feeders connected to the source bus. These cases could be represented in Figure 7 by additional curves in parallel with curve III, and with the times for a

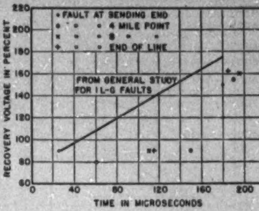

Figure 12. Recovery-voltage data for a 2-ohm 16-mile 4/0-copper single-phase system

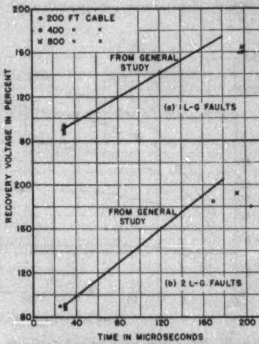

Figure 13. Effect of terminating cable on the recovery-voltage characteristics of a 2-ohm, 4/0-copper, 16-mile 4-wire system

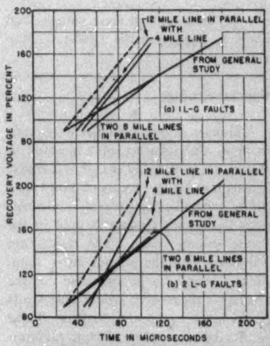

Figure 14. Effect of parallel lines on the recovery-voltage characteristics of a 2-ohm 16-mile 4/0-copper 4-wire solidly-grounded system

Dashed line—maximum voltage and time to 90 per cent voltage taken from general study. Time to maximum voltage was calculated for a single-line-to-ground fault, neglecting line inductance

Table I. Constants of Typical Lines

System	Copper Size	Z_1	Z_0	C_1	C_0
4-wire	4/0	$0.278+j0.615$	$0.564+j1.89$	0.0187	0.0078
	#6	$2.18+j0.756$	$2.93+j2.77$	0.0149	0.0069
3-wire	4/0	$0.278+j0.615$	$0.564+j3.15$	0.0187	0.0063
	#6	$2.18+j0.756$	$2.47+j3.29$	0.0149	0.0059
Single-phase	4/0	$Z=0.373+j1.04$			

All impedances in ohms per mile at 60-cycles. All capacitances in microfarads per mile.

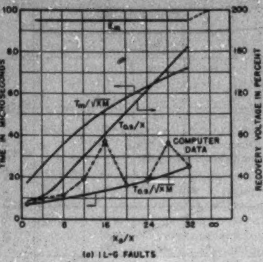

(a) 1 L-G FAULTS

Figure 15 (A. left, B. right). Reactance-grounded system recovery-voltage data

X_0=Zero-sequence source reactance
X=Positive-sequence source reactance

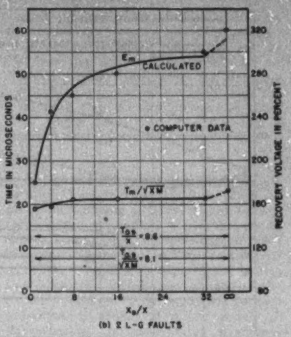

(b) 2 L-G FAULTS

given X/M ratio increased directly with the number of parallel feeders. The times to 90 per cent voltage for these long-line cases, where line reflections can be neglected, can be estimated from the following relation

$$T_{0.9}=13.8\ NX \tag{3}$$

where X is the 60-cycle source reactance in ohms and N is the number of long feeders in parallel. The constant in the equation is the calculated time to 90 per cent voltage for a system consisting of a 1-ohm source and a single number 6 copper overhead circuit.

In any particular case being studied, the time to 90 per cent voltage should be calculated by equations 2 and 3, and the minimum time thus obtained should be used. This procedure will result in conservative results for systems normally encountered in practice.

Impedance-Grounded Systems

Additional studies were made to show the effect of grounding methods on the voltage-recovery characteristics of distribution systems. As broad general studies of impedance-grounded systems were outside the scope of this paper, the data included should be used to indicate trends only. All investigations, excepting one, were based on a simple system representation in which line inductance could be neglected. This corresponds to actual systems having large X/M ratios, or a number of parallel circuits on a common supply bus.

Reactance-grounding. With a reactance-grounded source and the larger conductor sizes, resistance does not have any important influence on the significant voltage-recovery characteristics of a system. Assuming a given X_0/X ratio for the source, the times to 90 per cent voltage, with large X/M ratios, and to maximum voltage will vary directly with $\sqrt{XM}$. The time to 90 per cent voltage will vary directly with X if the X/M ratio is small. This allows plotting the data for reactance grounded systems on a general basis.

The data in Figure 15(A) apply for a single-line-to-ground fault on a 3-wire 4/0-conductor reactance-grounded system. The dashed curve, plotted from computer data, shows oscillations in the time to 90 per cent voltage as a function of the X_0/X ratio. These variations are present because the ratio of the positive- and zero-sequence natural frequencies vary with X_0/X. Similar variations would be produced by varying the X/M ratio of the system. For this reason it was concluded to draw a smooth curve below the computer data, and to use this curve in determining the time to 90 per cent voltage for large X/M ratios, where line inductance can be neglected. The $T_{0.9}/M$ curve was calculated by neglecting line reflections, and applies for low X/M ratios. In any given case, the time to 90 per cent voltage should be calculated by both methods, and the minimum time used.

The times to maximum voltage and the maximum voltages were calculated for X_0/X ratios that gave zero-sequence natural frequencies that were integral multiples of the positive sequence natural frequencies, in order to obtain the highest voltages. Smooth curves were then drawn through the calculated values. These calculations neglected line inductance, which case gives the minimum times to maximum voltage.

Figure 15(B) gives similar data for a double-line-to-ground fault on a reactance-grounded system. The times to 90 per cent voltage, neglecting line inductance or line reflections, were substantially constant over the reactance-ratio range considered, and so average values were used. The time to maximum voltage increases very slowly with increases in the X_0/X ratio. The maximum-voltage curve was estimated by multiplying the measured voltage of 180 per cent, for X_0/X = 1.0, by the calculated, sustained line-to-ground voltage during a single-line-to-ground fault. The computer data obtained by neglecting line inductance, falls close to the calculated curve, indicating that the increase in voltage is due to the higher dynamic voltage across the first phase to clear.

Ungrounded Systems. The data in Figure 15, for X_0/X ratios of infinity, apply for ungrounded systems. The recovery-voltage curve, following a single-line-to-ground fault on an ungrounded system, is a fully-offset cosine function, with 3,900 microseconds to 90 per cent voltage and 8,330 microseconds to 200 per cent voltage. The computer study gave a maximum recovery voltage of 320 per cent, following a double-line-to-ground fault, neglecting line inductance. The times associated with the recovery-volt-

Table II. Calculated Recovery-Voltage Data for a Solidly-Grounded System Consisting of a 2-Ohm Source and 16 Miles of Line

Conductor Size	System	$T_{0.9}$	T_m	E_m
#6	3-wire	43.5	90	175
4/0	3-wire	47.3	95	168
#6	4-wire	45.3	94	183
4/0	4-wire	49.6	103	180

The above data were calculated for a single-line-to-ground fault, neglecting loss and line inductance.

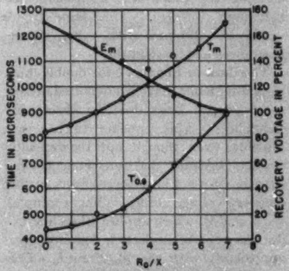

Figure 16. Recovery-voltage data for a single-line-to-ground fault on a resistance-grounded system

R_0—source zero-sequence resistance

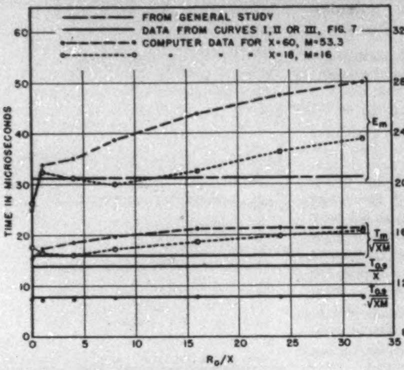

Figure 17. Recovery-voltage data for double-line-to-ground faults on resistance-grounded systems

R_0—source zero-sequence resistance

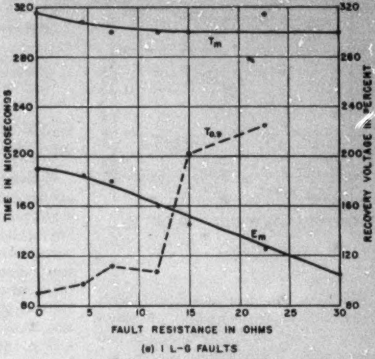

(a) 1 L-G FAULTS

Figure 18 (A. above, B. below). Effect of fault resistance on the recovery-voltage characteristics of a 3-wire system

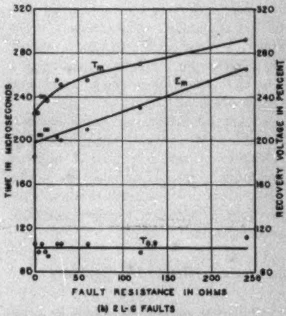

(b) 2 L-G FAULTS

age transients can be calculated using the data in Figure 15.

Resistance Grounding. The recovery-voltage data for resistance grounded systems cannot be generalized to the same extent as for reactance-grounded systems. For this reason, the information included here is of rather limited application, especially for single-line-to-ground faults.

The data in Figure 16 were obtained in an analog computer study of a 53.3-mile 4/0-conductor 3-wire system, having a source positive-sequence reactance of 60 ohms and a zero- to positive-sequence reactance ratio of unity. Line inductance was neglected. It is evident that resistance grounding decreases the severity of the recovery-voltage transients, following a single-line-to-ground fault, by increasing the times and decreasing the maximum voltages. This same trend would be obtained with other source reactances and line lengths.

The data in Figure 17 for double-line-to-ground faults, have been plotted on the same general basis used for reactance-grounding. This appears to be permissible, even though not theoretically correct, because the zero-sequence resistance does not have large effects on the recovery-voltage times. For example, $T_{0.9}/\sqrt{XM}$, which applies when line inductance can be neglected, does not vary appreciably with the R_0/X ratio. The plotted points, obtained for a 60-ohm, 53.3-mile system, fall very closely to the straight line curve, which applied for a solidly-grounded system (from curve II, Figure 7). The $T_{0.9}/X$ value in Figure 17 was taken from curve III, Figure 7. Both of these relations should be employed in estimating the time to 90 per cent voltage, in any particular application and the minimum value used. The times to maximum voltage were obtained for two systems having widely different XM products. Even though one XM product is over 11 times the second product, the $T_m/\sqrt{XM}$ values differ by less than 20 per cent. Indications are that this value will never be less than the corresponding value for a solidly-grounded system (curve I, Figure 7), which is plotted as a solid line in Figure 17.

The R_0/X ratio and the XM product have considerable influence on the maximum voltages, following double-line-to-ground faults. The highest voltages were obtained with the XM product of 3,200, which is larger than expected in practice. Practical XM products and R_0/X ratios would probably limit the voltages to values not much above the 205 per cent obtained for solidly-grounded systems.

Fault Resistance. Recovery voltage data, including the effects of fault resistance, were obtained for a 16-mile 3-wire 4/0-conductor system having a 16-ohm, solidly-grounded source. Line inductance was neglected. The single-line-to-ground fault data in Figure 18(A) shows that fault resistance decreases the maximum voltage produced, and increases the times to 90 per cent voltage. The times to maximum voltage are decreased slightly by fault resistance.

The double-line-to-ground fault data in Figure 18(B) do not indicate any important changes in the times to 90 per cent voltage, with fault resistance. The times and magnitudes associated with the maximum voltages increase with fault resistance, which means that fault resistance should be given consideration on 3-wire systems. On 4-wire systems, fault resistance is, in effect, in parallel with the neutral wire and would have less effect on recovery voltage than in 3-wire systems.

References

1. Recovery Voltage Characteristics of Typical Transmission Systems and Relation to Protector-Tube Applications, **R. D. Evans, A. C. Monteith.** Electrical Engineering, volume 57, August 1938, pages 432–43.

2. Power-System Voltage-Recovery Characteristics, **Harold A. Peterson.** AIEE Transactions, volume 58, 1939, pages 405–11.

3. Protector Tubes for Power Systems, **H. A. Peterson, W. J. Rudge, Jr., A. C. Monteith, L. R. Ludwig.** AIEE Transactions, volume 59, May 1940, pages 282–88.

4. A Large-Scale General-Purpose Electric Analog Computer, **E. L. Harder, G. D. McCann.** AIEE Transactions, volume 67, part I, 1948, pages 664–73.

5. Practical Calculation of Circuit Transient Recovery Voltages, **J. A. Adams, W. F. Skeats, R. C. Van Sickle, T. G. A. Sillers.** AIEE Transactions, volume 61, 1942, pages 771–79.

Discussion

H. R. Tomlinson (New England Power Service Company, Boston, Mass.): To correlate with the range used by the author, an investigation was carried out by the writer on the X to M ratio of several typical substations on the system with which he is associated. (See Table I of the discussion.) All feeders from the substations which were considered are overhead. Five stations have 2,300-volt ungrounded feeders and two stations have 4,000-volt ungrounded feeders. Total miles of equivalent 3-phase overhead circuits connected to the busses ranged from 21 to 64 miles. The minimum value of ohms of supply system reactance to the distribution substation bus, based on the nominal voltage of that bus, is 25.8×10^{-3} ohms and the maximum value 295×10^{-3} ohms, a range of approximately 1-to-11.

The X to M ratio for the 2,300-volt systems varies over a range of 1-to-15 with a minimum value of 4×10^{-4} ohms per mile and a maximum value of 61×10^{-4} ohms per mile. Intermediate values are 15×10^{-4}, 25×10^{-4}, and 48×10^{-4} ohms per mile. The two values for the 4,000-volt systems are 74×10^{-4} and 63×10^{-4} ohms per mile.

Table I

Name of Substation	Voltage	X	M	X/M
Gardner	2,300	0.0787	52.23	0.00151
Franklin	2,300	0.1225	47.47	0.00258
Uxbridge	2,300	0.0258	64.40	0.000400
Palmer	2,300	0.1285	21.0	0.00610
Rumford	2,300	0.210	43.2	0.00487
Arctic	4,000	0.295	39.6	0.00745
Knightsville	4,000	0.230	36.26	0.00635

X = ohms of supply system reactance to the distribution substation bus, based on the nominal voltage of that bus.

M = miles of equivalent overhead circuit connected to that bus.

I. B. Johnson, J. W. Kalb (General Electric Company, Pittsfield, Mass.): In comparing the results obtained by Witzke on the voltage-recovery characteristics of distribution systems with a similar study that we have made, we find a number of observations and conclusions that are in agreement. Whereas Witzke's study was primarily analytical involving the representation of systems in miniature, our study in addition to the miniature system included results obtained from a rural distribution system as basis for comparison, and as a basis for demonstration of the validity and ability of the miniature system to reproduce and extend the scope of the study. Comparing the miniature system results, these points of agreement were noted:

1. That in general the maximum recovery voltage to be expected for single-line-to-ground fault is approximately 175 per cent of line to neutral crest voltage.
2. That maximum recovery voltages are not obtained necessarily for faults at the sending-end bus. Witzke in his paper gives an example of this for an 8-mile line. One of our observations was made for a total of 220 miles of branched lines on the faulted phase.
3. That for small line conductors there was a tendency for the maximum recovery voltage to occur for sending-end faults.
4. That conductor size is effective in determining the phase angle of the fault path.
5. That in a broad general sense for short lengths of line of the order of six to eight miles in length involving single-line-to-ground faults, the time to maximum crest recovery voltage T_M and the time to nine-tenths normal crest voltage $T_{0.9}$ can be expected to be of the order of 150 and 70 microseconds, respectively when connected to an 8-ohm source.
6. That since distribution systems in general are a complex network and that since even for straightaway unbranched lines the determination of the maximum severity of the recovery voltage is a complex problem, the formulation of comprehensive conclusions requires further data and study.

A question for further discussion is this: Is or is not the degree of damping important when no lines or short lines connected to the substation bus are involved wherein relatively very high-frequency recovery voltages are experienced? Witzke makes two statements with regard to damping in his study; namely:

1. Theoretical considerations and analog computer studies showed that the X/M ratio of a distribution system, where X is the 60-cycle source reactance in ohms and M is the miles of connected line per phase, may be used as the fundamental variable in recovery-voltage studies, whenever the system natural frequencies are high by comparison to the fundamental system frequency, and losses are not a significant factor in determining the voltage-recovery characteristics.
2. The resistance of the source was represented by the inherent losses of the reactors used to represent the source reactance. The reactance-to-resistance ratio of these reactors was always higher than the probable ratio for distribution or power transformers, over the entire range of frequencies encountered in the study.

In comparing the magnitudes of the recovery voltages, the attenuation used in our miniature system study is greater than the results obtained by Witzke. Yet the attenuation evident in the field investigation is greater than that in our miniature system, particularly for cases of little or no line remaining connected to the substation bus. At the substation transformer bus with no lines emanating therefrom where the X/M ratio, or its equivalent, becomes very large and where the most severe recovery voltages might be expected to occur, the maximum recovery voltage from the field system study did not exceed normal crest voltage thus indicating a large amount of damping.

It is doubtful that this damping can be ascribed completely to after-conduction of the arc gases in the current interrupting device, since in many other instances of fault current interruption at the terminals of large kilovolt-ampere transformers, maximum recovery voltages of the order of only 125 per cent of crest line to neutral voltage have been recorded. To those who design and apply distribution system protective devices, this information in the region where the most severe recovery voltages are to be expected is extremely important. However, the question for this case, or any other similar case, of the relative amounts of damping contributed by the transformer, protective device or other factors remains unanswered.

It appears, therefore, that future studies and investigations might profitably be directed toward evaluating the damping factors that may be present in limiting the severity of the recovery voltages in those cases which apparently should result in severe recovery voltages.

A. M. Opsahl (Westinghouse Electric Corporation, East Pittsburgh, Pa.): Tests on expulsion lightning arresters require laboratory circuits to simulate the service conditions. These circuits must be concentrated in a relatively small space. It is impractical to attach several miles of overhead line to the laboratory transformer to modify the recovery voltage. It is impossible to have individual transformers which match all sizes that will be encountered in service. Reactors in the primary or secondary of the available test transformers can limit the current within the rating of the lightning arrester. Capacitors connected in shunt with the expulsion lightning arrester under test can simulate the effect of line capacitance in slowing down the recovery voltage following an operation which is initiated by a surge and followed by a half cycle of short circuit current.

Figure 1 of the discussion shows the voltage and current relations during the operation of an expulsion lightning arrester under a controlled laboratory test. Normal or generated voltage appears across the lightning arrester. At crest voltage, a surge is discharged through the lightning arrester and the voltage across the lightning arrester drops to a very low value establishing the follow current as limited by the impedance of the circuit at power frequency. Follow current through the lightning arrester causes some volatilization of fiber from the walls of the discharge path. The arc voltage

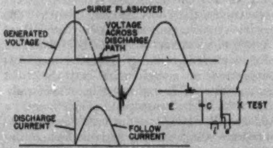

Figure 1. Voltage and current relations during the operation of an expulsion lightning arrester

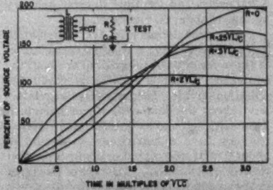

Figure 2. Natural frequency recovery voltage circuit characteristics

Units are: microhenries, microfarads, microseconds, and ohms

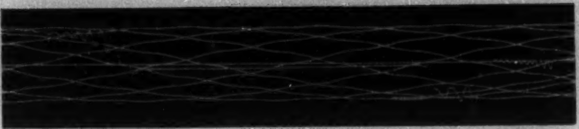

Figure 3. Section of cathode-ray oscillogram showing natural frequency oscillation on energizing the circuit, and recovery voltage oscillation following current interruption

builds up and may reduce the follow current. At follow current zero, the voltage across the lightning arrester begins to recover to generated voltage. However, the system is composed of an inductance in the form of the short-circuit reactance, and a capacitance in the transformer bushing and winding as well as any added capacitance. Charging the capacitance from line-to-ground through the circuit inductance causes the recovery voltage to oscillate around the instantaneous generated voltage at the natural frequency of the inductance-capacitance network. The network is in effect shocked into oscillation. The first half cycle of that oscillation determines the time to first crest of the recovery voltage. The lightning arrester discharge path must develop dielectric strength more rapidly than the voltage recovers or a second half cycle of follow current will be established.

The first half cycle of the recovery voltage is shown in more detail in Figure 2 of the discussion. The simple circuit of a single transformer energized from an infinite bus will serve to illustrate most cases as a single frequency oscillation from such test circuits is most frequently measured. The capacitance CT of the winding determines the shortest time to recovery voltage crest that can be expected from the transformer. The time to crest recovery voltage with no damping or loss in the circuit is $3.14\sqrt{L/C}$ as shown by the curve marked $R=O$. The recovery voltage reaches twice normal or generated voltage crest at the instant of follow current zero. If the inductance L is expressed in microhenries and the total capacitance C is expressed in microfarads, the time is in microseconds. For example, a 9,000-volt testing transformer delivering 560 amperes short circuit current has an inductance of 42,500 microhenries, and a capacitance of 0.0067 microfarad in the transformer winding and 0.002 microfarad in the cathode-ray oscillograph potentiometer. The natural frequency of the circuit is 8,200 cycles and the time to crest recovery voltage is about 60 microseconds.

Power transformers in the distribution voltage classes have a winding capacitance[1] in the order of 0.006 microfarad or about the equivalent of half a mile of overhead distribution circuit. Feeder voltage regulators have about the same capacitance from line-terminal-to-ground as transformers. Feeder reactors have a capacitance-to-ground of about 0.0001 microfarad or about 2 per cent that for transformers. The type of reactance in the source to a distribution circuit plays a part in determining the time of recovery voltage if the line is short enough that the addition of another half mile of line makes an appreciable difference.

In the laboratory test circuit, adding a capacitance C is the equivalent of adding a section of a distribution circuit. It increases the time-to-crest of the recovery voltage. By the addition of a resistance in series with the added capacitance, a degree of damping can be introduced. The inherent damping or loss in circuits without added capacitance is such that the recovery voltage is about 180 per cent of source voltage which in Figure 2 of the discussion is the equivalent of a resistance between $0.25\sqrt{L/C}$ and zero. Any resistance R added to the circuit reduces not only the crest of recovery voltage, but changes the wave shape so that the time to 90 per cent of source voltage $T_{0.9}$ will be shorter than in proportion to the time-to-crest recovery voltage T_m. This approaches more nearly the shape of the recovery voltage waves as determined by the analog computer studies, given in the author's paper and in field measurements.

A more exact representation of the rise of recovery voltage to the 90 per cent of normal could be obtained by splitting the reactance L into two parts and dividing the capacitance in two parts to provide a high and low frequency component of recovery voltage.[2] This is too complicated for use in these circuits where the required time to crest recovery voltage for all service conditions cannot be determined too accurately, but some time value must be set as the most severe condition to be regarded as standard for test purposes.

Previous studies indicate that recovery voltages can reach a maximum of 180 per cent of normal line-to-ground voltage following a single-line-to-ground, and 200 per cent of normal following double-line-to-ground faults on a grounded neutral system. These voltages on a 7,200/12,400-volt grounded neutral system would correspond to 144 and 160 per cent recovery voltage in a laboratory circuit using a 9,000-volt rms test voltage to match the standard lightning arrester rating. The circuit resistance R required to limit the recovery voltage to 160 per cent of normal is approximately $0.375\sqrt{L/C}$ assuming the inherent loss in the circuit and the transformer capacitance C_T can be ignored. A measurement of the recovery voltage must be made to check this approximate calculation.

Figure 4. Cathode-ray oscillogram of voltage during two follow current interruption tests

Such a selected percentage recovery voltage with a selected length of short distribution line, say 10 miles, in the case of the 7,200/12,400-volt class, could correspond to the most severe recovery voltage to be regarded as standard in service and to be required in a standard test. The capacitance of 10 miles of line is 0.13 microfarad. The actual time to crest recovery voltage is dependent on the reactance of the source as well as the capacitance of the line.

In service, any additional line length reduces the recovery rate or increase time to crest. Any arc voltage in the lightning arrester discharge path and resistance in the short circuit impedance will displace the current zero from the crest of generated voltage and reduce the maximum recovery voltage below the standard circuit condition. In fact, almost any other circuit changes are in the direction to reduce the severity of the recovery voltage.

The test circuit must be adjusted independently of the effect of a lightning arrester on the circuit. One method of making this check is to energize the primary of the transformer at crest of applied voltage. The circuit is shocked into natural frequency oscillation which is not affected by the lightning arrester. An oscillograph capable of responding accurately to the natural frequency of the circuit will record the recovery voltage magnitude and shape.

Figure 5. Cathode-ray oscillogram of voltage during two follow current interruption tests

Recovery voltage modified by capacitance and resistance

The oscillogram in Figure 3 of the discussion is interesting in that it illustrates the natural frequency of the test circuit without the effect of the lightning arrester, and with the effect of the lightning arrester. There were several revolutions of the film drum after the lightning arrester operation so there are a number of confusing lines which must be ignored. The length of the film covers about one-half of a 60-cycle wave. At the left, the circuit breaker between the generator and the transformer primary was closed at about crest voltage. The transformer was shocked into natural frequency oscillation, the voltage reaching about 180 per cent of the normal voltage at the instant. At the end of this oscillation, the surge generator discharged through the expulsion lightning arrester and the voltage dropped toward zero. After the surge current, the voltage attempted to recover without establishing follow current. The recovery voltage overtook the dielectric recovery strength of the lightning arrester under this condition, and follow current was established. Arc voltage built up with time during follow current and current zero occurred before power voltage crest. The lightning arrester withstood the recovery voltage. The surge timed to strike very early or late in the half cycle of power volt-

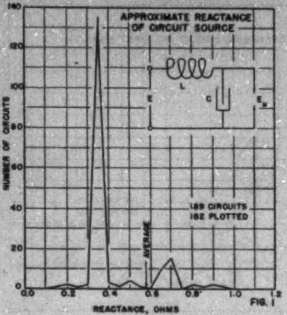

Figure 6. Approximate reactance of circuit source

age may not establish follow current due to this tendency of the expulsion to withstand recovery voltage following a surge discharge.

The cathode-ray oscillogram in Figure 4 of the discussion records the voltages during two operations of an expulsion lightning arrester on a 9,000-volt test transformer. There was no capacitance added to modify the recovery voltage. The follow current zero was ahead of generated voltage crest due to the relatively high arc voltage of the lightning arrester. The frequency of the recovery voltage is 8,200 cycles, and the time to maximum recovery voltage 60 microseconds.

The cathode-ray oscillogram in Figure 5 of the discussion records the voltage during two tests of an expulsion lightning arrester. The test transformer is the same as in Figure 4 of the discussion, but a reactor has been added to reduce the short circuit current from 560 to 150 amperes. A load capacitance of 0.08 microfarad increased the time-to-crest recovery voltage from 60 to 250 microseconds and a resistance of 1,000 ohms in the capacitor circuit limited the recovery voltage to 140 per cent of normal.

These oscillograms illustrate the tests that can be made in the laboratory with and without modification of recovery voltage. The determination of the complete dielectric recovery voltage curve for all expulsion lightning arresters at all currents is not feasible. A laboratory test circuit set up to duplicate the most severe conditions which can be justified on the basis of system studies can be established as a withstand test which is made quite readily. The recovery voltage in other studies has been expressed in terms of volts per microsecond. This terminology applied to an expulsion lightning arrester testing standard is awkward.

A standard circuit to control recovery voltage for expulsion lightning arrester testing could be specified as requiring:

1. A power source having a voltage equal to the maximum voltage rating of the lightning arrester.

2. A source reactance limiting the short circuit current within the lightning arrester rating.

3. A capacitance across the lightning arrester equivalent to the shortest length of distribution circuit that system studies indicates to be in common use.

4. A resistance in series with the capacitance to limit the crest recovery voltage to a value 160 per cent of the 60-cycle test voltage crest.

REFERENCES

1. PRACTICAL CALCULATIONS OF CIRCUIT TRANSIENT RECOVERY VOLTAGES, J. A. Adams, W. F. Skeats, R. C. Van Sickle, T. G. A. Sillers. ELECTRICAL ENGINEERING (AIEE TRANSACTIONS), volume 61, November 1942, pages 771–79.

2. TRANSIENT RECOVERY VOLTAGES AND CIRCUIT BREAKER PERFORMANCE, R. C. Van Sickle. ELECTRICAL ENGINEERING (AIEE TRANSACTIONS), volume 61, November 1942, pages 804–13.

Leonard M. Olmsted (Duquesne Light Company, Pittsburgh, Pa.): The two principal characteristics of recovery voltage are the maximum voltage and the time to maximum voltage. Witzke has reported the results of analyses and tests with the analog computer for several types of distribution circuits over a wide range of source reactances, line lengths, conductor sizes, and fault locations, which indicate that the maximum voltages usually are on the order of 175 per cent of normal crest voltage for single-line-to-ground faults and 205 per cent for double-line-to-ground faults. The purpose of this discussion is to present an analysis of voltage recovery time on a typical 4,160-volt distribution system consisting of 225 ungrounded circuits with lengths up to 44 miles and a great variety of combinations of source reactance, multiconductor cable, number and location of branches, and transformer locations. This total number of circuits includes 23 which are all cable and therefore omitted, and 19 other circuits which are fed from six common busses without individual reactors and hence were grouped into an equivalent six; the number of circuits considered for this investigation is thus established as 189.

It has been shown that the recovery characteristics of a circuit may be represented by the single line analogy shown in Figure 6 of the discussion, where *L* represents the inductance of the source, *C*, the equivalent shunt capacitance of the circuit, *E*, the impressed voltage, and E_R, the recovery voltage. It is more convenient to measure *L* in terms of the common 60-cycle reactance. The sources of the 189 circuits included in this survey have the reactances plotted in Figure 6 of the discussion; the most frequent value being 0.345 ohm which is a very common current-limiting reactor. Largely because of the higher impedance of a considerable number of unit stations, however, the system average is 0.58 ohm. The lowest reactance, 0.132 ohm, applies to one power circuit directly connected to the bus of a large substation.

The fundamental effect of the overhead line is to establish the value of capacitance. This is measured in terms of the circuit miles of 3-phase equivalent to the summation of the 1-, 2-, and 3-phase open-wire portions of the circuit. The values determined from this survey range from 0.3 to 44.4 miles, averaging 8.8 miles, with the distribution plotted in Figure 7 of the discussion. The open-wire distance to the most remote transformer on each of these circuits shows a range from 0.0 to 11.7 miles with an average of 2.8 miles as plotted in Figure 8 of the discussion. The distance to the first transformer varies from 0.0 to 3.2 miles with an average of 0.29 mile as plotted in Figure 9 of the discussion. The number of major branches from these circuits varies from 0.0 to 15, the latter figure derived from a group of five circuits which are fed without reactors from a common bus. The average number of branches is shown by Figure 10 of the discussion to be 3.5. The open-wire distance from the source to the first branch is plotted in Figure 11 of the discussion, which shows an average of 0.37 mile with a large number less than 0.025; the extreme distance is 3.4 miles. These considerations

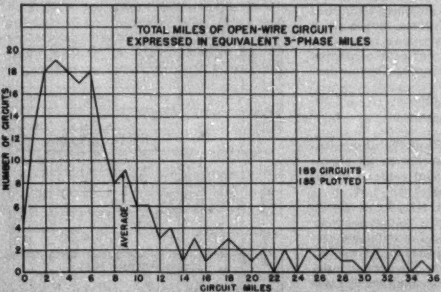

Figure 7. Total miles of open-wire circuit expressed in equivalent 3-phase miles

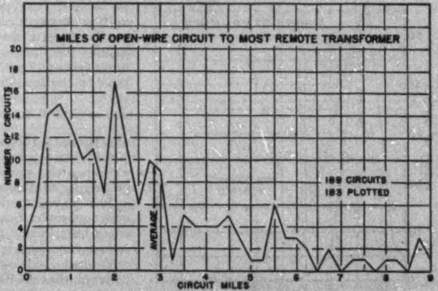

Figure 8. Miles of open-wire circuit to most remote transformer

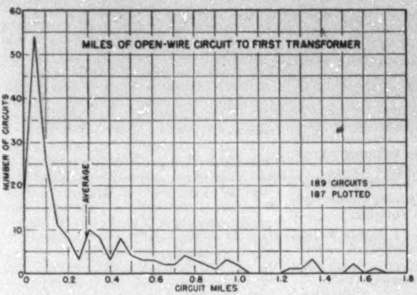

Figure 9(left). Miles of open-wire circuit to first transformer

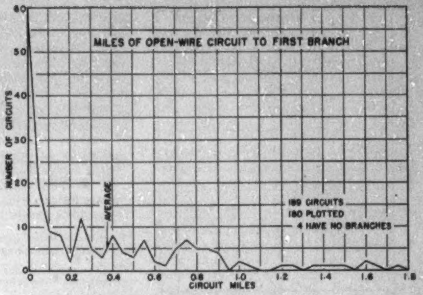

Figure 11 (right, above). Miles of open-wire circuit to first branch

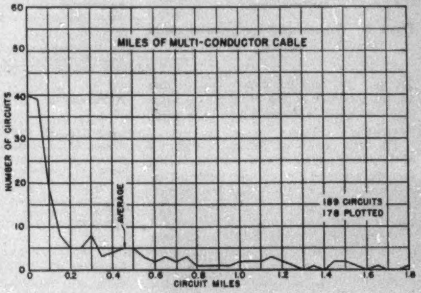

Figure 12 (right). Miles of multiconductor cable

indicate that the mileage of open-wire circuit is concentrated usually at a relatively short distance from the substation, which seems to justify the assumption that recovery voltage calculations can be based upon lumping the open-wire circuit capacity at the substation terminal.

Because of its relatively high capacity, compared with open-wire circuits, the amount of multiconductor cable is a very important factor The miles of cable on these circuits range from 0.0 to 4.8 miles with an average of 0.46 mile as plotted in Figure 12 of the discussion, showing a large number of circuits with less than 0.15 mile. Inasmuch as 0.15 mile of 3-conductor 350,000 circular mil cable is approximately equivalent to the capacity of nine miles of open-wire, it is clear that cable cannot be neglected in calculations of recovery voltage. Most of this cable is connected directly to the substation terminals; hence it is correctly represented by assuming all capacity to be lumped at that point. The combined capacitance of cable and open-wire, expressed in terms of the equivalent open-wire mileage, ranges from 0.30 to 304.6 miles with an average of 36.7 miles, as plotted in Figure 13 of the discussion.

Having determined the average of these seven characteristics of this group of circuits, it is interesting to observe the map of the circuit which most nearly approximates them. This circuit is shown as Figure 14 of the discussion and appears to be very typical.

The time to maximum recovery voltage has been calculated for each of these 189 circuits individually, using the method proposed by Witzke

$T_M = 15.9\sqrt{XM}$ microseconds

The M is shunt capacitance of wire and cable, expressed in equivalent 3-phase miles of open-wire. These values are plotted in Figure 15 of the discussion, showing a range from 14 to 120 microseconds (omitting three offscale values up to 205 microseconds), with a predominant value at approximately 40 and an average of 55 microseconds. T_M probably is the most significant time in voltage recovery calculations, but a point on the slope of the curve may have some value; the time to 90 per cent of normal line-to-ground crest voltage has been calculated by the equation

$T_{0.9} = 7.7\sqrt{XM}$ microseconds

and plotted on Figure 15 of the discussion, which shows a range of 6.8 to 99 microseconds with a predominant value of 20 and an average of 25 microseconds.

This survey should be considered only as a first approximation to the voltage recovery characteristics of a typical distribution system, as experience may indicate the need for refinements. It serves to demonstrate, however, that a 4,160-volt unigrounded system has surprisingly severe recovery voltage characteristics, in many cases worse than any shown by Witzke for star systems. The average circuit reaches 175 per cent of line-to-ground crest voltage in 55 microseconds, and one requires only 14 microseconds. Evidently present types of protective equipment have adequate provision for such recovery voltages, as their operating record appears generally satisfactory. The effect upon the design of future types of equipment is difficult to predict, however,

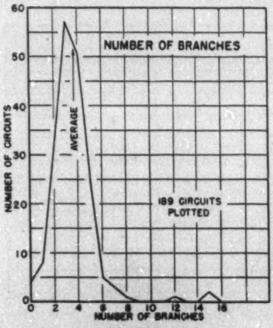

Figure 10. Number of branches

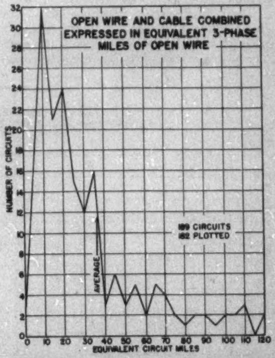

Figure 13. Open wire and cable combined expressed in equivalent 3-phase miles of open wire

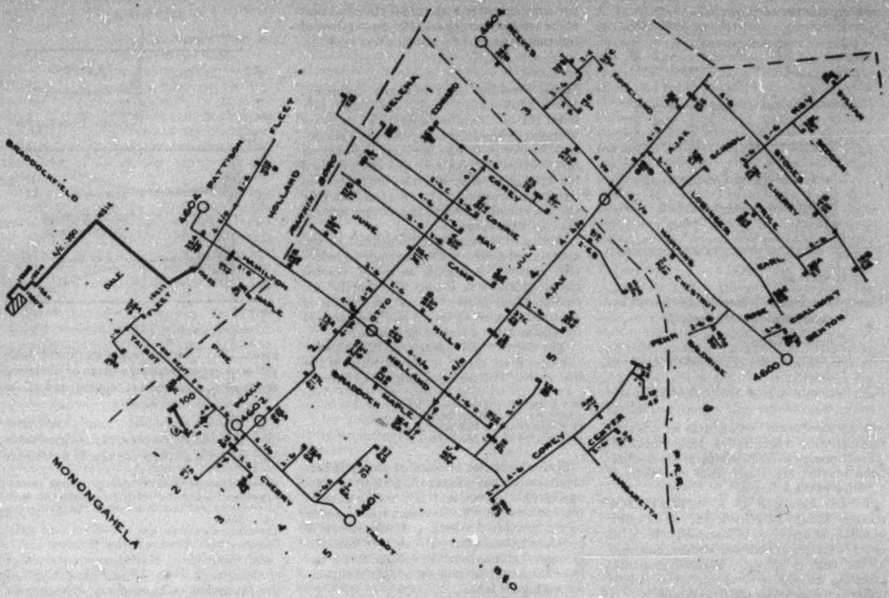
BRADDOCKFIELD
4404
PATTERSON
FLEET
HOLLAND
HELENA
HAMILTON
MAPLE
DALE
TALBOT
PEACH
4402
OTTO
HILLS
CAMP
JUNE
COREY
CARRIE
MAY
JULY
AJAX
REEVES
COPELAND
4400
BRADDOCK
CHERRY
4401
CENTER
MARIETTA
P.R.R.
CHESTNUT
PENN
ROSE
CHALMERS
BENTON
EARL
STOKES
MONONGAHELA
TALBOT
B&O

Figure 14. Typical 4,160-volt circuit

and appears to be a subject for careful investigation. It may prove necessary to establish zones for the application of certain devices within their voltage recovery capabilities, similar to present practice with the interrupting capacity of expulsion cutouts. It is highly desirable to avoid this complication if it is economically possible to design equipment for unrestricted application.

E. Beck (Westinghouse Electric Corporation, East Pittsburgh, Pa.): The papers presented on this subject are of great value. One of the services which they, probably supplemented by other work to follow, will render is the possibility of standardizing on duty cycle tests for distribution lightning arresters of the expulsion type. Such tests are, of course, made already by the various manufacturers of these devices but no standards for recovery voltage conditions exist. It appears that for the most part the service experience with expulsion lightning arresters has been highly satisfactory. The company with which this discussor is associated has manufactured such devices for about 17 years.

It is too soon to come to definite conclusions about the exact content of a standard. The complexity of the recovery voltage problem and the wide variations encountered in the studies indicate that the selection of a standard for laboratory test circuits will require considerable thought and perhaps compromise. Under certain system conditions and for certain locations of expulsion lightning arresters the recovery conditions may be exceedingly severe while for others they are more or less mild. The question will arise whether the test conditions selected shall be such that any expulsion lightning arresters will perform in the laboratory under the most severe conditions that may occur anywhere on any distribution system or whether a compromise should be adopted based on probabilities. This decision will affect design, construction, and costs.

The fact that the expulsion lightning arrester is affected by the recovery voltage characteristics of a system and the valve lightning arrester is not, may affect the decision. For example, it might be said that for some systems of large capacity, if all possible conditions are to be met, valve arresters should be used in the substations although expulsion lightning arresters are used everywhere else. For those who still entertain reservations about the ability of modern valve-type distribution lightning arresters to handle severe lightning discharges, it should be said that in a substation the duty on a valve-type lightning arrester is less severe than out on the line because of the presence, close by, of the

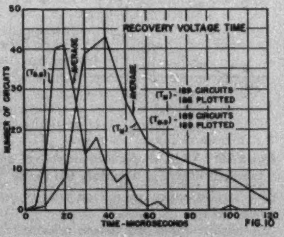

Figure 15. Recovery voltage time

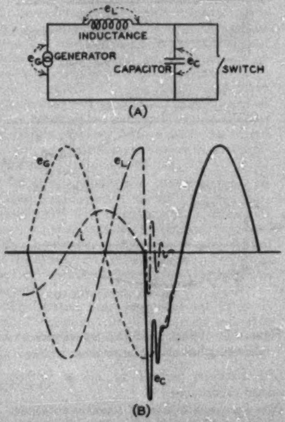
e_L
INDUCTANCE
e_G
GENERATOR
CAPACITOR
e_C
SWITCH
(A)
e_G
e_L
e_C
(B)

Figure 16. A simple recovery voltage circuit

(A) Circuit

(B) Current and voltage relationships

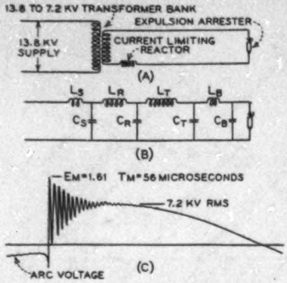

Figure 17. Typical laboratory test circuit and associated recovery voltage

(A) Circuit elements
(B) Inductances and stray capacitance of circuit (A)
(C) Recovery voltage of circuit (A)

source transformer which acts as a shunt for lightning currents of long duration. There appears to be no significant indication from service experience that one type is superior to the other.

In the approach to a standard these matters should be considered. It is quite possible to arrive at a standard which, in order to satisfy a condition whose occurrence in the field is unlikely, imposes economic penalties on the general use of a device under the conditions that predominate. It is also possible to temper the standard with a consideration of the probabilities and take whatever slight risk may lurk in those cases where the conditions defined in the standard are exceeded. It is further possible to approach the matter with the fact in mind that there already are available two types of lightning arresters for distribution systems.

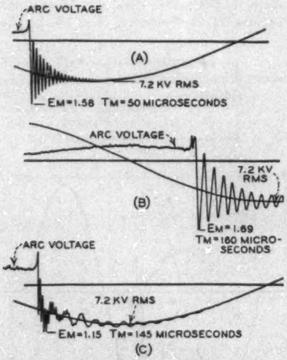

Figure 18. Effect of adding capacitance to a laboratory test circuit on recovery voltage

(A) Recovery voltage of circuit without added capacitance
(B) Recovery voltage of circuit with capacitance added in parallel to test specimen
(C) Recovery voltage of circuit with capacitance added in parallel to current-limiting reactor

H. O. Stoelting (Line Material Company, South Milwaukee, Wis.): This paper presents the first data on severity of recovery voltages on distribution systems. This discussion compares the recovery voltage on distribution systems with the circuits used for testing of fuse cutouts and expulsion lightning arresters. The effect of changing the test circuit constants on recovery voltage also are illustrated.

Recovery voltage can be defined as the charging of a capacitance through an inductive circuit. A simple recovery voltage circuit is shown in Figure 16(A) of the discussion. All inductance of the circuit is assumed lumped as shown and resistance is for the moment assumed negligible.

The current and voltage relationships for the circuit are shown in Figure 16(B) of the discussion. The curves shown are as follows:

e_G = generator voltage
i = current through the switch
e_L = voltage across the inductance
e_C = voltage across the capacitor

Since the circuit is assumed purely inductive, the current will lag the generated voltage by 90 degrees and the voltage across the inductance will be equal and opposite to the generated voltage. If the switch is opened at the normal current zero, both the generated voltage and the voltage across the inductance will be at crest, while the capacitor voltage is zero.

At the instant that the switch is opened the capacitor starts charging. The charging of the capacitor through the inductance causes the voltage of the capacitor to overshoot the normal voltage with a resulting oscillation due to an interchange in energy between the capacitor and the inductance.

If the circuit had no resistance the oscillations would continue indefinitely. Even slight amounts of resistance will cause the oscillations to damp out as shown.

Adding an additional series inductance and shunt capacitor to the right of the capacitor shown in Figure 16(A) of the discussion, will introduce a second frequency into the recovery voltage and make the analysis of the voltage relationships of the circuit much more difficult.

As Witzke pointed out, under certain conditions the reactance of the supply and the capacitance of the line of a distribution system can be considered as the inductance and capacitor respectively of Figure 1 of the discussion. Under most conditions, however, the reactance and capacitance to ground of the distribution lines must be considered as distributed. The usual method of representing this condition is by a large number of branches of inductance and capacitance in the circuit as was done in the transient analyzer studies.

A typical laboratory circuit for tests on 7.2-kv equipment is shown in Figure 17(A) of the discussion. This diagram shows only the elements of the circuit. The reactances and stray capacitances of the elements as shown in Figure 17(B) of the discussion are:

L_s = inductance of the supply line
C_s = capacitance of the supply line
L_r = inductance of the air core current limiting reactor
C_r = stray capacitance to ground of the reactor
L_t = leakage inductance of the transformer bank
C_t = stray capacitance to ground of the transformer bank
L_b = inductance of the bus
C_b = stray capacitance to ground of the bus

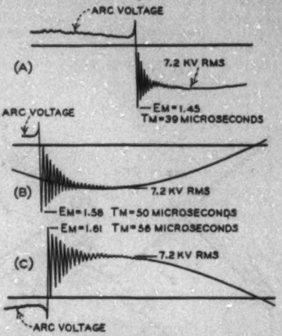

Figure 19. Effect of supply transformer kilovolt-amperes on recovery voltage of laboratory circuit of constant voltage, current, and power factor

(A) 200-kva single-phase supply transformer
(B) 300-kva single-phase supply transformer
(C) 400-kva single-phase supply transformer

An oscillogram of the recovery voltage of this circuit is shown in Figure 17(C) of the discussion. The recovery voltage crest of 1.61 times the normal voltage crest is somewhat lower than the maximum reported by Witzke.

The time to recovery voltage crest of 56 microseconds is of the same order as the minimum times to recovery voltage crest reported by Witzke. The studies in the paper presented indicate that a recovery voltage crest of 1.61 times the normal voltage crest associated with a time to crest of 56 microseconds is exceptional, so that the rate of rise of recovery voltage for the labora-

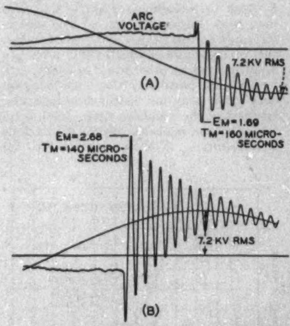

Figure 20. Effect of specimen arc voltage on recovery voltage of laboratory test circuit

(A) Low specimen arc voltage prior to recovery voltage
(B) High specimen arc voltage prior to recovery voltage

tory circuit is more severe than for the usual field condition.

The recovery voltage of Figure 17(C) of the discussion is predominantly single frequency, although a second frequency can be detected by drawing an envelope for the recovery voltage oscillations. In this instance, all of the inductance and capacitance branches of Figure 17(B) of the discussion with the exceptance of the inductance and capacitance of the supply transformer are negligible.

Studies were made to determine whether it would be possible to vary recovery voltages in the laboratory over the ranges found for distribution systems. The oscillograms of Figure 18 of the discussion were all taken on the same circuit but with a capacitor added to the circuit for Figures 18(B) and 18(C).

Figure 18(A) of the discussion shows the recovery voltage of the circuit normally used without a capacitor. Figure 18(B) was obtained by adding a capacitor in parallel to the test specimen. The added capacitance increased the recovery voltage crest 11 per cent and increased the time to crest by a factor of 3.2.

Figure 18(C) was obtained by adding a capacitance in parallel with the current limiting reactor. This change produced a double frequency recovery voltage of much lower crest value than for the other two conditions.

The time to 90 per cent of normal crest in this case is not a simple proportion of the time to crest as for the other two oscillograms of Figure 18 of the discussion.

A study of the effect of the supply transformer kilovolt-amperes on recovery voltage was undertaken to find out why some fuses would operate satisfactorily on one circuit, but would not clear on another circuit having the same voltage, current, and power factor, but with a different supply transformer kilovolt-amperes.

The oscillograms of Figure 19 were made on circuits having the same voltage, current and power factor, but with transformer banks of 200, 300, and 400 kilovolt-ampere single phase for Figures 19(A), 19(B), and 19(C) respectively.

Figure 19 shows that the effect of increasing the kilovolt-ampere of the supply transformer bank is to increase both the crest recovery voltage and the time to crest.

The analyzer studies reported by Witzke were made with a follow current interrupted at normal current zero. Under these conditions, the maximum recovery voltage can only theoretically reach a value of twice that of normal line voltage. The effect of arc voltage in a fault interrupting device is to force the current to zero before it normally would reach zero, and therefore increase greatly the severity of the recovery voltage.

The oscillograms of Figure 20 indicate the extent to which the arc voltage of a fault interrupting device can influence the recovery voltage of a circuit. Figures 20(A) and 20(B) were made on the same circuit, but with two different types of expulsion lightning arresters. The lightning arrester used in obtaining the oscillogram of Figure 20(A) had a very low rise in arc voltage just prior to current interruption compared to the lightning arrester used in the oscillogram of Figure 20(B). A slight difference in the design of the expulsion lightning arrester changed the recovery voltage crest from 1.69 to 2.68 times the normal voltage crest.

The influence of the arc voltage of a fuse or expulsion lightning arrester on the recovery voltage of a circuit must be recognized when recovery voltages are specified in industry standards. Since the recovery voltages of a circuit may be modified greatly by an arc interrupting device it will be essential to specify recovery voltage of the test circuit without the modifying influence of arc voltage.

R. H. Earle (Line Material Company, South Milwaukee, Wis.): This paper represents an excellent start on certain methods of test procedure which are of vital interest to manufacturers of circuit interrupting equipment for distribution systems.

In the development of fuses, circuit breakers, expulsion lightning arresters, and other apparatus whose function is to interrupt fault currents, it is highly desirable for the manufacturer to be able to reproduce actual service conditions in his laboratory.

Line voltage is known and can be reproduced accurately. The same is true of fault currents.

A third factor, namely, recovery voltage, is an entirely different question. Recovery voltage is the one that endeavors to restrike the arc after it has been extinguished by the device in question. The life of the device is measured frequently by the number of successful operations and this life is affected tremendously by the size and shape of these restriking voltages.

If during the development of a fuse for example, the designer chooses to test his device on recovery conditions that are too mild, the result may be a device which will prove inadequate in service. If on the other hand he chooses recovery conditions that are too severe, he may limit himself unduly from a design standpoint, and even abandon some designs which would be of considerable value if put into actual service.

These are not academic problems to the designer, but are of real practical importance in his daily work.

Industry standards have endeavored to take recovery voltages into account by requiring that rupturing tests be made at various low power factors. Low power factor is likely to be accompanied by severe recovery voltage conditions and low power factor is a step in the right direction in the testing of apparatus. Power factor is correlated with the recovery voltage only in a general way however and far more definite specifications are needed so that various laboratories can reproduce each others results.

Fortunately present day laboratory techniques and facilities permit the manufacturer to produce recovery voltages in his laboratory of almost any characteristics within reason, and he probably will have no trouble in establishing recovery conditions that are more severe than those occurring in all but the most exceptional service conditions.

The problem is to select suitable ones from the wide range of values available.

The work now in progress to determine the recovery voltages that actually exist under field conditions is of vital importance to the entire distribution industry.

R. L. Witzke: The number and character of the discussions presented indicates a real interest in the recovery voltage characteristics of distribution systems. The author expresses his appreciation for the comments given and for the valuable data included in the discussions. The acceptable agreement between field tests and miniature system studies, reported by Johnson and Kalb, is of particular interest because it substantiates our faith in the miniature system method of analyzing complicated system problems. When this method of analysis was introduced by Evans and Monteith[1] in 1937 there was considerable skepticism relative to its value. I feel we can now safely say it is an accepted tool in the field of power system engineering.

Johnson and Kalb point out that the attenuation used in their miniature system studies was greater than the attenuation shown by the analog computer results, and that the field studies showed still more damping. In the laboratory studies referred to by Johnson and Kalb, as well as in the analog computer studies, the losses in the transformer sources were represented by the inherent loss in the reactors used to represent the sources. The author kept the high-frequency reactance-to-resistance ratio of the sources to eight or ten, or higher, by a proper selection of miniature system constants, on the basis that the use of lower ratios might introduce losses not present on actual systems. A ratio of ten gives a damping factor of approximately 0.85 per half-cycle of a high-frequency oscillation, which value has been proposed[2] as being typical for terminal equipment. This decrement is in substantial agreement with the 180 per cent recovery voltage shown in Figure 3 of the discussion by A. M. Opsahl. The oscillograms in Stoelting's discussion show decrement factors per half-cycle of 0.88 in Figure 17 of the discussion and 0.92 in Figure 20 (B) of the discussion, which indicate even less decrement than we assumed.

As mentioned by Opsahl, the capacitance of terminal equipment, such as transformers and regulators, cannot be neglected if the total overhead line length is less than several miles. Also, as noted by Olmsted, many overhead circuits leave a substation through short sections of cable which may have appreciable capacitance. The influence of these terminal capacitances on the time to maximum recovery voltage can be estimated by converting the capacitances to an equivalent length of overhead line.

Opsahl's suggestion to base standards on a simple test circuit should be given consideration. The adequacy of a single-frequency test circuit must, of course, be established by further study of the relative shapes of the system recovery voltage and the protective device dielectric recovery characteristics.

The system data presented by Olmsted and Tomlinson will be extremely valuable in obtaining a broad picture of the recovery rates experienced on distribution systems.

REFERENCES

1. SYSTEM RECOVERY VOLTAGE DETERMINATION BY ANALYTICAL AND A-C CALCULATING BOARD METHODS, R. D. Evans, A. C. Monteith. ELECTRICAL ENGINEERING (AIEE TRANSACTIONS) volume 56, June 1937, pages 695–703.

2. See reference 5 of the paper.

Some Fundamentals of D-C Controlled Reactors with Resistive Load

H. F. STORM
ASSOCIATE AIEE

THE impedance of an iron-core reactor can be varied by introducing a magnetic bias, whose magnitude is controlled by a direct current in a separate winding. Such d-c controlled reactors commonly are called saturable reactors, or magnetic amplifiers.[1,2]

When a saturable reactor is connected to a load, as shown in Figure 1, an increase in the current in the d-c winding will increase the magnetic bias in the iron core. This will shift the alternating magnetic flux to a region of higher saturation, and hence decrease the impedance of the a-c winding. If the load consists of a resistance, a change in the direct current, and, therefore, in control power, is associated with a change in the load power. It will be found that a certain change in output power can be achieved with a much smaller change of input power; hence the term magnetic amplifier.

The ratio between output power and input power often is called the amplification factor. A typical value for the amplification factor is 100. To obtain amplification of higher order, several stages can be used, by feeding the d-c winding of the following stage with the rectified output current of the previous stage.[3] Another method for obtaining a higher amplification consists in rectifying the load current whose d-c component is used to aid the control-winding ampere turns;[4,5] amplification factors of 10,000 for a single stage can be obtained easily with ordinary transformer core materials.

The outward appearance of a saturable reactor is very similar to an iron-core transformer. Figure 2 shows a fairly large saturable reactor rated 25 kva, while Figure 3 shows one rated 1/2 volt-ampere.

Being an amplifying device, the saturable reactor, or magnetic amplifier, finds itself in competition with electronic amplifiers. There are fields of application where the choice is obvious, but in other cases a careful analysis will be required to decide which type of amplifier is preferable. At the present time, the application of the saturable reactor to frequencies of 100 kc and more is not considered practical because of excessive core losses. On the other hand, the amplification of small d-c voltages (millivolts) is a difficult matter for an electronic amplifier; however, a magnetic amplifier, being controlled by ampere turns, circumvents this difficulty.

Another distinct advantage of the magnetic amplifier over the electronic amplifier lies in the feasibility of applying a multitude of control signals simultaneously with freedom from voltage levels, by using several d-c windings acting on the same core. The comparative permanency of the components of magnetic amplifiers is an item which may sway the choice in favor of the magnetic amplifier.

Another advantage is seen sometimes in the high shock resistance of magnetic amplifiers; this feature, however, is not exclusive with magnetic amplifiers, as demonstrated by the electronic equipment used in the proximity fuse.

Applications

Saturable reactors often are used in theater lighting systems,[6] the incandescent lamps being connected in series with the a-c windings of the reactor. A similar arrangement is used for the heat control in electrical-resistance furnaces.[7] Firing circuits[8] for ignitrons and thyratrons use saturable reactors to effect phase shift. A great number of further applications are found in the literature.[9]

Basic Concepts

In its simplest form, a saturable reactor consists of an iron core with two windings: the a-c load winding, and the d-c control winding, Figure 4. The load winding is connected in series with the load, which may consist, for instance, of incandescent lamps, the control of their luminousity being the object. A d-c source of controllable magnitude energizes the d-c winding, thus effecting magnetic bias. Increasing the d-c current will increase the magnetic bias, shifting the core induction into regions of lower permeability, and thereby increasing the load current. The alternating current causes an alternating magnetomotive force f in the core. This induces an electromotive force in the d-c winding. If the inductor L were omitted, an appreciable amount of alternating current would flow in the d-c winding, causing unnecessary heat and power loss. However, the inductor L is undesirable. It involves extra cost and increases the time constant of the d-c control circuit, with attendant sluggishness of response on the part of the saturable reactors to a variation of the d-c control voltage, E_c.

Figure 1. Elementary diagram of d-c controlled reactor

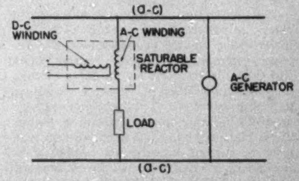

Paper 49-55, recommended by the AIEE transformer committee and approved by the AIEE technical program committee for presentation at the AIEE winter general meeting, New York, N. Y., January 31–February 4, 1949. Manuscript submitted August 2, 1948; made available for printing December 22, 1948.

H. F. STORM is in the control engineering divisions of the General Electric Company, Schenectady, N. Y.

Figure 2. Two d-c controlled reactors

Each: 25 kva, 60 cycles, approximately 675 pounds, 23 inches long

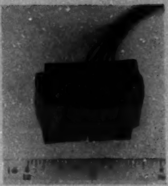

Figure 3. D-c controlled reactor with split core, 0.5 volt-ampere, 400 cycles

The induced electromotive force in the d-c winding consists of a large fundamental (line) frequency component and higher harmonics. By using two saturable reactors, they can be interconnected, Figures 5 and 6, so that the fundamental frequency components cancel out. Voltages of fundamental frequency still are being induced in the d-c windings between terminals Y_1 and Y_2. These voltages, being in phase with respect to the polarity marks, oppose each other, and a voltage of fundamental frequency does not appear across terminals 4–6. Thus, an inductor to suppress currents of fundamental frequency, as shown in Figure 4, becomes superfluous.

The control characteristics of the circuit in Figure 5 are shown in Figure 7. Supply voltage and frequency are held constant. Polarity of the direct current does not affect the load current I_{AB}.

The following paragraphs deal in greater detail with the harmonics appearing in core and windings, since these harmonics affect essentially the performance of the saturable reactor. Such interrelation is to be expected, because the operation of a saturable reactor is based on the nonlinearity of its inductance, and the higher harmonics are merely a manifestation of this nonlinearity.

For obvious reasons, the circuit in Figure 5 is called a parallel connection, whereas Figure 6 represents the series connection. It will become evident later that these two connections perform differently, the series connection being characterized by faster response.

As will be born out by oscillograms, the following simplifying assumptions can be made without impairing the validity of the conclusions:

1. The supply voltage is sinusoidal and the source impedance negligible.
2. Hysteresis effect and eddy current losses in the iron core are negligible.
3. Resistance and leakage reactances of the a-c windings are negligible.
4. The wave shapes are not affected greatly by the load resistance, hence the load is short circuited by closing switch *S*, Figures 5 and 6, further simplifying the theoretical analysis.

Next, polarities require definition:

Reactors *A* and *B* are identical; coil currents i_A, i_B, and i_{AB} are called positive when flowing in the direction of the associated arrows. Positive coil currents cause positive magnetomotive forces, f_A and f_B, whose positive direction also is indicated by the respective arrows. If a voltage pulse is applied which makes terminal *X1* positive with respect to terminal *X2*, a pulse will appear which is positive at terminal *Y1* with respect to *Y2* (as indicated by polarity signs); when current i_d flows in its positive direction, as indicated by the arrow, it causes a positive magnetomotive force, f_A, in coil *A*, but a negative magnetomotive force, f_B, in coil *B*.

Suppose an alternating voltage *e* is now applied to terminals *X1* and *X2*, Figure 5, and switch *S* closed. From Faraday's law the magnetic flux follows

$$e \quad \frac{d\varphi}{dt}N10^{-8} \tag{1}$$

$$\varphi=\frac{10^8}{N}\int edt \tag{2}$$

for

$$e=\sqrt{2}E\sin\omega t \tag{3}$$

and from equation 2

$$\varphi=-\frac{\sqrt{2}E10^8}{\omega N}\cos\omega t+\Phi_{dc} \tag{4}$$

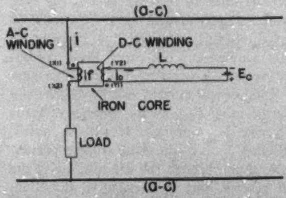

Figure 4. Schematic diagram of single, d-c controlled reactor

Substituting Φ_{ac}, for the factor of the cosine term

$$\varphi=-\Phi_{ac}\cos\omega t+\Phi_{dc} \tag{5}$$

where Φ_{dc} is an integration constant to be determined.

Equation 5 shows that the resultant flux φ in the core of the saturable reactor consists of a sinusoidally varying magnetic flux, φ_{ac}, which is lagging 90 electrical degrees behind the voltage, and which also may contain a superposed constant flux Φ_{dc}. These relations are shown graphically in the lower left-hand section of Figure 8. Subscripts *A* and *B* were added to refer to saturable reactor *A* or *B*, respectively. If Φ_{dc} is positive, the total flux φ_A will result; for a negative value of Φ_{dc} flux φ_B will result.

To produce the fluxes φ_A or φ_B, a magnetomotive force must be effective in the core. The relation between flux and magnetomotive force, in ampere turns, is shown in the graph in the upper left-hand section of Figure 8, and is referred to as magnetization line. For instance: for $\theta=150$ degrees, φ_A equals *MN;* the necessary magnetomotive force f_A is *PQ*. The magnetomotive force f_A is replotted, as a function of the electrical angle θ, in the upper right-hand part of the diagram. Because *PQ* was derived from the flux φ_A occurring at $\theta=150$ degrees, the same magnetomotive force *PQ* has to be erected over 150 degrees, as shown by *RS*. Other points of f_A are obtained in similar manner.

The magnetomotive force f_A may stem from ampere turns in the a-c winding, the d-c winding, or both. The currents in the windings of the saturable reactor can be determined from an analysis of the magnetomotive forces merely by dividing the magnetomotive force by the number of turns in the winding. To this end it will

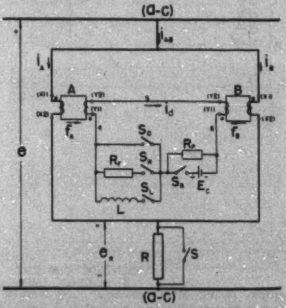

Figure 5. Parallel reactors with separate cores

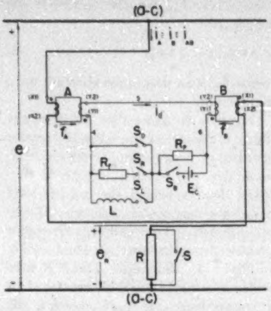

Figure 6. Series reactors with separate cores

be practical to break down the magnetomotive force of core *A* into three components: the constant term $F_{dc,A}$, the odd harmonics $f_{od,A}$, and the even harmonics $f_{ev,A}$. Applying a Fourier series[10]

$$f_A = F_{dc.A} + F_{1.A}\cos\theta + F_{2.A}\cos 2\theta + F_{3.A}\cos 3\theta + \ldots \quad (6)$$

If curve f_A were phase-shifted by 180 degrees and all signs were reversed, curve f_B would result

$$f_B = -F_{dc.A} - F_{1.A}\cos(\theta-180) - F_{2.A}\cos 2(\theta-180) - F_{3.A}\times \cos 3(\theta-180) + \ldots \quad (7)$$

Eliminating 180 degrees from equation 7

$$_B = -F_{dc.A} + F_{1.A}\cos\theta - F_{2.A}\cos 2\theta + F_{3.A}\cos 3\theta - \ldots \quad (8)$$

By addition and subtraction, one obtains

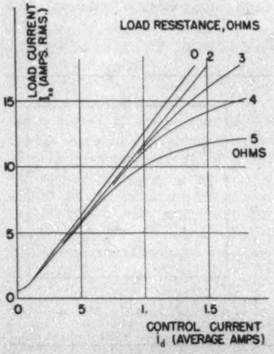

Figure 7. Control characteristics of circuit shown in Figure 5

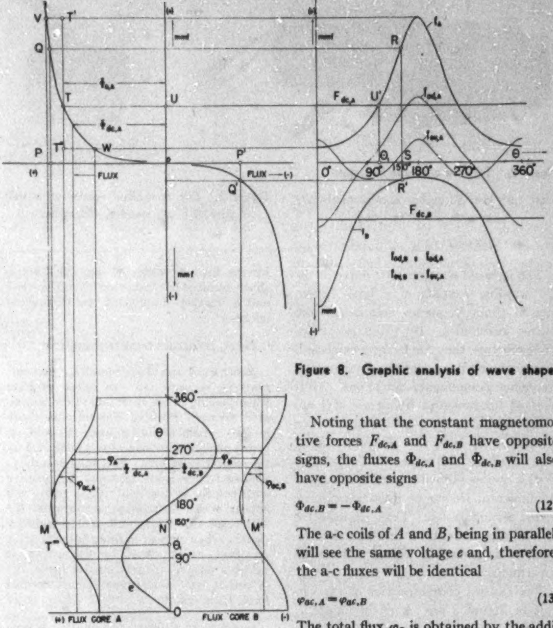

Figure 8. Graphic analysis of wave shapes

$$\frac{1}{2}(f_A+f_B) = F_{1.A}\cos\theta + F_{3.A}\cos 3\theta + \ldots = f_{od,A} \quad (9)$$

$$\frac{1}{2}(f_A-f_B) = F_{dc.A} + F_{2.A}\cos 2\theta + \ldots = F_{dc.A} + f_{ev.A} \quad (10)$$

Thus the odd harmonics, $f_{od,A}$, are the arithmetical mean between f_A and f_B. The constant term, $F_{dc,A}$, is obtained by averaging the area below curve f_A. The even harmonics, $f_{ev,A}$, follow from equation 10. The three components, $F_{dc,A}$, $f_{od,A}$, and $f_{ev,A}$, are shown in the right-hand section of Figure 8.

The current responsible for the constant magnetomotive force $F_{dc,A}$ must be produced in the d-c winding, because the a-c winding can not carry direct current during steady-state conditions. The magnitude of this current can be determined by dividing $F_{dc,A}$ by the number of turns in the d-c winding. It will be noted, Figure 5, that the same direct current also flows through the d-c winding of the *B* reactor, but in a negative direction, and

$$F_{dc,B} = -F_{dc,A} \quad (11)$$

Noting that the constant magnetomotive forces $F_{dc,A}$ and $F_{dc,B}$ have opposite signs, the fluxes $\Phi_{dc,A}$ and $\Phi_{dc,B}$ will also have opposite signs

$$\Phi_{dc,B} = -\Phi_{dc,A} \quad (12)$$

The a-c coils of *A* and *B*, being in parallel, will see the same voltage *e* and, therefore, the a-c fluxes will be identical

$$\varphi_{ac,A} = \varphi_{ac,B} \quad (13)$$

The total flux φ_B is obtained by the addition of $\Phi_{dc,B}$ and $\varphi_{ac,B}$, and is shown in the left-hand section of Figure 8. For $\theta = 150$ degrees, the total flux is now *M'N*. The required magnetomotive force *P'Q'* is obtained by the same process as *PQ*, and is plotted as a function of θ, resulting in *R'S*. Considering the symmetry of curves $\varphi_{ac,A}$ and $\varphi_{ac,B}$ with respect to the magnetization line, it will become apparent that *R'S* is one point of curve f_B, as obtained from equation 8. Hence f_B represents the magnetomotive force required by core *B*.

In terms of its own components

$$f_B = F_{dc.B} + F_{1.B}\cos\theta + F_{2.B}\cos 2\theta + F_{3.B}\cos 3\theta + \ldots \quad (14)$$

Comparing this expression with equation 8, it follows that

$$F_{dc.B} = -F_{dc.A} \quad (11)$$

$$F_{1.A} = F_{1.B} \quad F_{2.A} = -F_{2.B} \quad F_{3.A} = F_{3.B} \quad (15)$$

which means that

$$f_{od.B} = f_{od.A} \quad (16)$$

$$f_{ev.B} = -f_{ev.A} \quad (17)$$

Quiescent Flux

In the absence of an applied a-c line

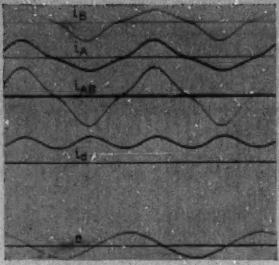

Figure 9. Oscillogram of circuit shown in Figure 5, S_D, S_B, and S closed

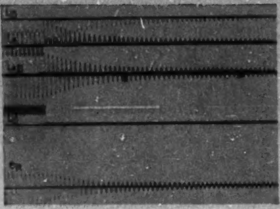

Figure 11. Oscillogram of circuit shown in Figure 5, S_B closed. S_D is closed at first. Opening S_D starts transient

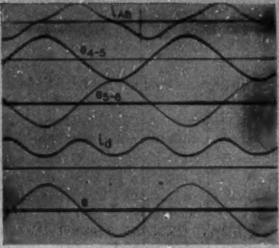

Figure 13. Oscillogram of circuit shown in Figure 6. S_D, S_B closed

voltage, the flux in core A will be $\Phi_{o,A}$ as indicated by the distance TU, obtained by intersecting $F_{dc,A}$ with the magnetization line. The flux $\Phi_{o,A}$ may be called quiescent flux, in analogy to the quiescent current in high-vacuum tubes when the grid voltage merely contains a d-c component. When steady-state a-c power is energizing the saturable reactor, the average flux $\Phi_{dc,A}$ is different from $\Phi_{o,A}$. This variation of flux has an important effect on the transient response of the saturable reactor as will be explained later. The cause of this variation can be seen as follows: the flux φ_A is obtained by operating f_A on the magnetization line. Magnetomotive force f_A consists of a constant term $F_{dc,A}$ and alternating part $f_A - F_{dc,A}$. The constant term $F_{dc,A}$ yields the quiescent flux $\Phi_{o,A}$. The effect of the alternating part is to alternately raise the flux to VT' and to lower it to WT''. The area of flux $\varphi_{dc,A}$ to the left of TT' is smaller than the area to the right of TT'', thus causing a negative flux average which lowers $\Phi_{o,A}$ to $\Phi_{dc,A}$. In high-vacuum tubes, an analogous deviation from the quiescent current takes place when an a-c grid signal is applied to the curved part of the tube characteristic; that effect is used for demodulation.

Parallel-Connected Reactors

The parallel a-c windings *X1–X2* of reactors A and B can carry currents of even and odd harmonics. The currents of even harmonics, equation 17, are in counterphase with respect to the polarity marks of the windings *X1–X2*, and, therefore, make no contribution to the total current, i_{AB}, Figure 5. The load current, i_{AB}, therefore contains odd harmonics only.

Suppose the control winding is energized through switches S_D and S_B. The resistance R_P is of very small value, in order to make the power supply a low-impedance source as seen from the terminals *Y1* of the d-c windings. Currents of odd harmonics cannot flow in the d-c windings, because the odd harmonics are in phase, equation 16, and the d-c windings are connected to each other with opposing polarity. For a similar reason, even harmonic currents, equation 17, are capable of flowing in the d-c winding. Thus the magnetomotive forces of even order can be produced by currents in the d-c windings, as well as by currents in the a-c windings. The partition of even-harmonic currents between a-c and d-c winding depends on the resistance and leakage reactance of the windings. Figure 9 illustrates this case. In this illustration the line voltage is e. The load current i_{AB} shows harmonics of odd order only. The d-c control current i_d exhibits considerable even harmonics, of which the second harmonic is most pronounced. Currents i_A and i_B show harmonics of odd and even order. Good coincidence is obtained between i_{AB}, i_d of the oscillogram, and the corresponding theoretical curves $f_{od,A}$ and $f_{ev,A}$ of Figure 8.

If a large inductance L is connected in the d-c circuit by closing switch S_L, and and switch S_D is opened, the flow of even-harmonic currents is impeded in the d-c circuit; therefore the a-c winding must carry the currents of even harmonics. Figure 10 shows this case. The wave shape of the total current i_{AB} is unaffected. The d-c control current i_d is nearly constant, and the voltage e_L appears across the inductor L. Currents i_A and i_B now carry practically all even harmonics in addition to the odd harmonics. Good coincidence is again obtained between the

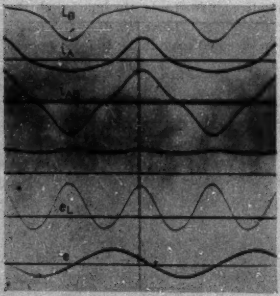

Figure 10. Oscillogram similar to Figure 9, except S_L closed and S_D open

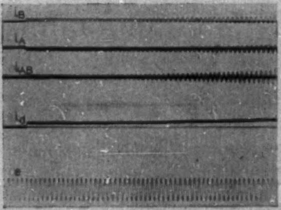

Figure 12. Oscillogram of circuit shown in Figure 5. S_B closed. Closing S_D starts transient

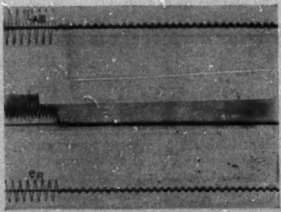

Figure 14. Oscillogram of circuit shown in Figure 6. S_B closed. S_D closed at first. Opening S_D starts transient

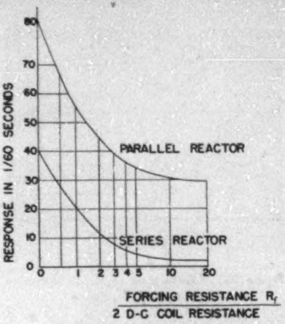

Figure 15. Transient response of parallel and series reactors

wave shapes of i_A and i_B of the oscillogram, and the theoretical curve, $f_A - F_{dc,A}$, in Figure 8.

The speed of response to a variation of control voltage, E_c, can be increased by placing a forcing resistor R_f in series with the d-c winding (S_R closed, S_D and S_L open). There is, however, a limitation to this speed-up. For a given line voltage, a change of impedance of the saturable reactor can be effected only by changing the average flux $\Phi_{dc,A}$ and $\Phi_{dc,B}$. This flux, however, can maintain constant flux linkages[11] through the a-c winding, even if the d-c circuit is interrupted; therefore, the fluxes $\Phi_{dc,A}$ and $\Phi_{dc,B}$ will not vanish instantly. If i_d is interrupted, transient currents will appear in the a-c coils. These currents will flow in a positive sense in reactor A, and in a negative sense in reactor B, thus forming a current circulating within the two reactors. Figure 11 shows the transient response of parallel-connected saturable reactors where the direct current i_d was suddenly interrupted by opening switch S_D. It can be seen that i_A immediately acquired a positive transient, whereas i_B exhibits a negative transient. As a result, the magnetic flux decays with the time constant of the a-c winding, and the change of impedance is manifested by the slowly decaying load current i_{AB}. With a load resistor R connected in series with the reactors (switch S open), the voltage across R is shown by e_R.

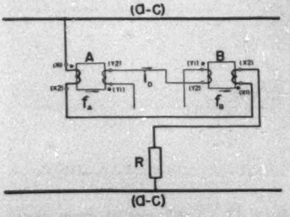

Figure 16. Arrangement similar to Figure 5 or Figure 6, except core *B* turned 180 degrees

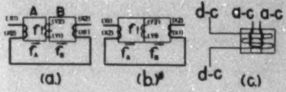

Figure 17. (a) Two cores using common control winding; (b) 3-leg core; (c) 4-leg core

Closing switch S_D will cause an abrupt start of i_d in the control winding, Figure 12, despite the large self-inductance of the control winding. The explanation[12] again lies in transient currents circulating between the a-c windings of the two reactors, maintaining constant flux linkage at the instant of switch closure. Figure 12 shows a negative transient of current i_A and a positive transient of current i_B. While the currents i_A, i_B, and i_d show abrupt changes, it is important to realize that the magnetic flux $\Phi_{dc,A}$ and $\Phi_{dc,B}$ will change only gradually, as evidenced by the slow increase in load current i_{AB}.

Series Reactor

Assume again that switch S, Figure 6, is closed. The a-c coils, being in series, make $i_A \equiv i_B \equiv i_{AB}$. No currents of even harmonics can flow in the a-c windings because such currents would have to be in phase opposition, equation 17, and the series connection between the a-c windings causes opposition of the two currents. Hence the a-c windings and the load current contain odd harmonics only. All even harmonics are flowing in the d-c winding, the d-c supply being connected by closing switches S_B and S_D. Figure 13 shows current i_{AB} as consisting of odd harmonics only. The control current i_d contains all even harmonics, of which the second harmonic is the most pronounced; e is the supply voltage for the saturable reactors. The series-connected saturable reactors can be used as a source of double-frequency power[13] by connecting a load in series with the d-c winding. In parallel-connected reactors, the even harmonics are forced into the a-c windings when their flow is impeded in the d-c winding, as previously explained. In the series-connected reactors, the a-c winding cannot carry even harmonics, and, therefore, such harmonics must appear in the d-c winding of the reactor.

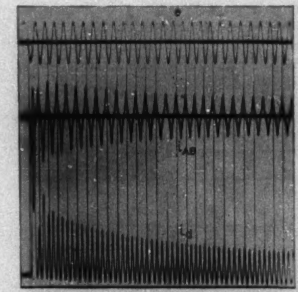

Figure 18. Oscillogram of circuit shown in Figure 6. Alternating current closed near phase angle where $i_{AB}=0$ during steady state

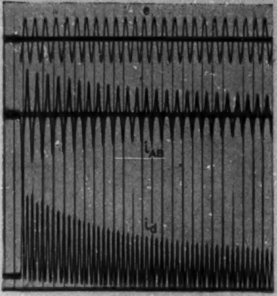

Figure 19. Oscillogram similar to Figure 18, except alternating current closed near phase angle where i_{AB} is maximum during steady state

If the flux $\Phi_{o,A}$ increases and flux $\Phi_{o,B}$ decreases (or vice versa) at the same rate, electromotive forces are induced in the a-c windings. These electromotive forces are of equal magnitude and of opposite

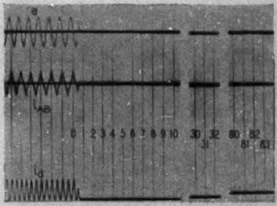

Figure 20. Oscillogram of circuit shown in Figure 6. Alternating current interrupted

polarity, and hence cannot cause a current to sustain constant flux linkages. The fluxes $\Phi_{o,A}, \Phi_{o,B}$ and hence the impedance of the saturable reactors, thus can be forced by the d-c ampere-turns. If, for instance, switch S_D is opened, the field collapses instantly, and the impedance of the reactor also changes instantly, as shown in Figure 14. When the control current i_d is interrupted, the load current i_{AB} declines immediately. In this case, switch S is open, and e_R is the voltage across the load resistance. It can be seen that the series-connected saturable reactor is capable of rapid response.

Comparison of Speed of Response

A comparison of response between the parallel and series reactor is shown in Figure 15. Circuits used are shown in Figures 5 and 6; switch S_B is permanently closed, switch S is kept open, and switching is done by S_B.

The response time is defined as the amount of time required for the peak value of the load current, i_{AB}, to pass through 0.63 (equals $1-1/\epsilon$) of the interval controlled by i_d. For a linear circuit this response time is usually called the "time constant."[14] The response times are shown as a function of "forcing," which is expressed as the ratio between the forcing resistance, R_f, and the resistance of both d-c windings. The curves show "turn-off" response from full-load current to minimum-load current. The "turn-on" response is similar.

Reactors with Common Control Winding

Suppose the electric connections of Figure 6 remain unchanged but reactor B is turned in space by 180 degrees, Figure 16. Considering the leg bearing the d-c winding, it can be seen that the magnetomotive forces $F_{dc,A}$ and $F_{dc,B}$ have the same direction in space. The even harmonics have the same direction in space as well, equation 17. Conversely, the magnetomotive forces of odd order have opposite directions in space, equation 16. If the two iron cores are now brought together, but an air gap left between the adjacent sides of the two reactors, and a common d-c winding placed around the adjacent legs, Figure 17a, the magnetic conditions in the cores will remain essentially the same. As far as the d-c coil is concerned, no odd-order voltage will be induced, because the odd-order fluxes in the two adjacent legs are of opposite phase. This is an advantage over the arrangements shown in Figures 5 and 6. While it is true that in Figures 5 and 6 the odd-order harmonics are cancelling at terminals *4* and *6*, these voltages nevertheless exist in each winding and may cause problems of over-voltage.

An important feature of this core arrangement is the existence of flux of fundamental frequency in the adjacent legs. If the control current is varied in opposite directions, residual magnetism causes the control characteristics, Figure 7, to shift. Also, if the control current i_d is turned off completely, residual magnetism would remain in the core surrounded by the d-c coil, and would prevent the magnetic amplifier from assuming its zero control-current position if it were not for the demagnetizing effect of the magnetomotive forces of fundamental frequency acting in the core. Such a core is shown in Figure 3.

Where residual magnetism is inconsequential, the two adjacent legs can be merged and a 3-leg reactor results, Figure 17b. The center leg carries a flux containing only the constant and even-order terms.

Another core construction is a 4-leg core, Figure 17c, where the two a-c windings are wound on the inner legs and the d-c winding is surrounding both a-c windings. While the basic function is the same as that of the 3-leg reactor, the 4-leg type has the advantage of smaller leakage reactance, and higher impedance with no d-c excitation. Such reactors are shown in Figure 2.

Transients

During the operation of saturable reactors, transient currents will be observed in the control windings: when the load current i_{AB} increases, the control current i_d will increase transiently, and vice versa.

Such a case is shown in Figure 18. This oscillogram was taken from the circuit of Figure 6, with S_D,S_B closed, and S open. At the start the a-c source was disconnected, $e=0$, $i_{AB}=0$, and only the control current i_d is flowing in the circuit. Near the crest value of e, the highly inductive a-c circuit was switched in. Two phenomena will be observed: the amplitude of i_{AB} is larger at the start and gradually decays to its steady-state value; secondly, the d-c component of the control current i_d rises very sharply, as evidenced by the average of i_d; this d-c transient gradually subsides, and during steady-state operation the average of the i_d-wave equals the value of i_d before the a-c source has been switched in. If the a-c source had been switched in at an instant essentially different from its crest value, additional d-c transients would be caused.[15] Such a case is shown in Figure 19.

The case where the load current i_{AB} is turned off is shown in Figure 20. The control current i_d contains, as usual, large even-order harmonic currents; the d-c component of i_d is obtained by averaging i_d. Then the load current i_{AB} was suddenly reduced to zero by opening the a-c circuit. It will be seen from Figure 20 that the d-c component of i_d suddenly drops to a very small value. Subsequently i_d increases gradually until it reaches, after approximately 80 cycles, the same value it had before the load current i_{AB} was cut out.

Both phenomena can be explained by the shift of the average magnetic flux, $\Phi_{dc,A}$ and $\Phi_{dc,B}$. Suppose that the a-c energization is interrupted at $\theta=90$ electrical degrees. The flux φ_A at this instant equals $\Phi_{dc,A}$. Due to the absence of alternating current, the magnetic flux will assume its quiescent value $\Phi_{o,A}$, which is larger than $\Phi_{dc,A}$. In reactor B the average flux, $\Phi_{dc,B}$ also is changing toward $\Phi_{o,B}$. This flux change is in the opposite direction to the flux change in reactor A. The voltages induced in the d-c windings, therefore, have opposite directions. However, the d-c windings are connected in opposition, hence the induced voltages are supporting each other. According to Lenz' law,[16] flux changes cause electromotive forces in the d-c windings, opposing the change. Hence the transient current caused by these electromotive forces will cause a temporary reduction of the direct current.

If the a-c power is increased, the direct-current will exhibit a transient increase. It is also important to note, however, that the change from $\Phi_{dc,A}$ to $\Phi_{o,A}$ cannot occur in zero time. The saturable reactor first will display a lower impedance which gradually will approach a higher steady-state value. As a result, the load current will display a larger magnitude at the beginning and will approach slowly its steady-state value.

Symbols

E = supply voltage, in rms volts
e = instantaneous value of supply voltage, in volts
$F_{1,A}$, $F_{1,B}$ = amplitude of fundamental component of f_A or f_B respectively
$F_{2,A}$, $F_{2,B}$ = amplitude of second harmonic of f_A or f_B respectively
$F_{3,A}$, $F_{3,B}$ = amplitude of third harmonic of f_A or f_B respectively
$F_{dc,A}$, $F_{dc,B}$ = constant part of magnetomotive force in core A or B respectively, in ampere-turns

f_A, f_B = instantaneous value of magnetomotive force in core A or B respectively, in ampere-turns
$f_{ev,A}$, $f_{ev,B}$ = instantaneous value of even-order harmonics of f_A or f_B respectively
$f_{od,A}$, $f_{od,B}$ = instantaneous value of odd-order harmonics of f_A or f_B respectively
I_{AB} = current in load, in rms amperes
i_{AB} = instantaneous value of alternating current in load, in amperes
i_A, i_B = instantaneous value of alternating current in reactor A or B respectively, in amperes
i_d = instantaneous value of control current, in amperes
N = number of turns of a-c winding, per reactor
t = time, seconds
ϵ = base natural logarithm, 2.718
θ = phase angle of time vector, in radians or degrees
$\Phi_{0,A}$, $\Phi_{0,B}$ = quiescent flux, in core A or B respectively, in maxwells
Φ_{dc} = constant part of φ, in maxwells
Φ_{ac} = peak value of a-c component of φ, in maxwells
φ = instantaneous value of core flux, in maxwells
φ_{ac} = instantaneous value of a-c component of φ, in maxwells
φ_A, φ_B = instantaneous value of core flux in core A or B respectively, in maxwells
$\varphi_{ac,A}\varphi_{ac,B} = \varphi_{ac}$ in core A or B respectively
ω = angular velocity of time vector, radians per second

References

1. Regulation of Electric Circuits, **C. F. Burgess, B. Frankenfield.** United States Patent 720,884, patented February 17, 1903.

2. Controlling Alternating Currents, **E. F. W. Alexanderson.** United States Patent 1,206,643, November 28, 1916.

3. Control System, **P. Thomas.** United States Patent 1,730,254, October 1, 1929.

4. Electrical Translating Apparatus, **P. H. Dowling.** United States Patent 1,739,579, December 17, 1929.

5. Electrical Control System, **M. A. Edwards.** United States Patent 2,169,093, August 8, 1939.

6. Application of Electron Tubes in Industry, **D. E. Chambers.** Electrical Engineering, volume 54, number 1, January 1935, page 87.

7. Installing, Maintaining, and Servicing Electronic Temperature Control Systems, **E. D. Schneider.** *Electrical Contracting* (Chicago, Ill.), volume 44, number 8, 1945, pages 149–157.

8. Industrial Electronic Circuits (book), **W. D. Cockrell.** McGraw-Hill Book Company, Inc. (New York, N. Y.), 1944, pages 140, 149.

9. Bibliography on Transductors, Magnetic Amplifiers, etc. (213 references). *Instruments* (Pittsburgh, Pa.), volume 21, April 1948, pages 332–362.

10. Ueber Gleichstromvormagnetisierte Wechselstromdrosselspulen und deren Rueckkopplung, **Th. Buchhold.** *Archiv fuer Elektrotechnik* (Berlin, Germany), volume 36, number 4, 1942, pages 221–238.

11. A Simplified Method of Analyzing Short-circuit Problems, **R. E. Doherty.** AIEE Transactions, volume 42, 1923, pages 841–849.

12. Theory and Calculation of Transient Electric Phenomena and Oscillations (book), **C. P. Steinmetz.** McGraw-Hill Book Company, Inc., New York, N. Y., third edition, 1920, page 141.

13. Principles of Radio Communication (book), **J. H. Morecraft.** John Wiley and Sons, Inc., New York, N. Y., third edition, 1933, page 742.

14. Electrical Engineers' Handbook (book), **H. Pender, W. A. Del Mar.** John Wiley and Sons, Inc., New York, N. Y., third edition, 1947, section 4–20.

15. Principles of Radio Communication (book), **J. H. Morecraft.** John Wiley and Sons, Inc., New York, N. Y., third edition, 1933, page 41.

16. Electric Circuits (book), Massachusetts Institute of Technology, members of the staff. First edition, 1940, John Wiley and Sons, Inc., New York, N. Y., page 4.

Discussion

Walter C. Johnson (Princeton University, Princeton, N. J.): H. F. Storm is to be commended for his clear and careful analysis of the operation of the saturable reactor. He has covered a wide range of phenomena in a manner which is very helpful.

The paper brings out clearly an important point which often is overlooked, namely, that the actual d-c flux in the reactor does not correspond with the intersection of the d-c magnetomotive force with the magnetization curve, but is considerably lower under operating conditions. This must be expected in a nonlinear circuit, and, as Storm points out, it is analogous to the deviation in direct current which occurs in a vacuum-tube circuit when the tubes are operated over a nonlinear portion of their characteristics. The effect is of major importance in the saturable reactor. To give a specific example:

For a particular reactor with a silicon-steel core, when operated in the middle of its normal range, the value of required control current is about 14 times what it would be if this demagnetizing action did not occur.

The effect increases with the nonlinearity of the magnetization curve, and explains why core materials with a sharp-breaking characteristic fail to produce results as spectacular as might be expected.

As the a-c voltage increases in amplitude, the alternating flux traverses a greater portion of the nonlinear magnetization curve, and the demagnetizing effect becomes increasingly severe. As a result, the d-c flux is reduced, and the alternating current changes by only a small amount. This, of course, is the basis for the application of the saturable reactor as a constant-current regulator.

For the reactor mentioned previously, when operating in the middle of its normal range, a doubled a-c voltage increases the rms alternating current by about 25 per cent, and increases the average alternating current by only about 9 per cent. The effect is more pronounced in reactors which have a very sharp-breaking magnetization curve. The demagnetizing effect is an overruling factor in the performance of the saturable reactor; its importance hardly can be overemphasized.

Rubber Insulators for Pole Lines

H. H. WHEELER
NONMEMBER AIEE

W. F. MARKLEY
NONMEMBER AIEE

LIKE SO MANY modern developments, the use of rubber insulators on pole lines is the unexpected outcome of research originally started in a somewhat different direction. Observations over many years had shown that substantial sums were spent annually in replacing glass insulators mischievously broken, and that such breakage was confined largely to specific and well-recognized locations which seemed especially to lure children or hunters to destructive activities; sometimes one or two poles in a particular area required insulator replacements almost weekly. Figure 1 shows an example of such mischievous breakage.

In the initial consideration of this problem, some thought was given to the idea of improving the glass itself, that is, making the insulator from tempered or shatterproof glass in order to improve its resistance to breakage, but it was found that such a design was impracticable. Thought was given also to the idea of surrounding the glass petticoat with an outer metallic skirt. Although this attachment gave a surprising degree of protection, it was not entirely satisfactory.

The next device that was tried was a moulded-rubber shroud over a small glass insulator of the pony type. This too developed a satisfactory degree of protection against blows, but was rather costly because of the volume of rubber required. It became obvious at this point that the real solution of the problem was to make the insulator itself of rubber. Although it was believed at the time that a suitable rubber compound could be developed possessing adequate physical characteristics and insulating properties, there was some question as to whether any such compound would have a useful life outdoors of more than three or four years.

Mechanically, the rubber composition had to be strong enough to carry the load of a telephone or telegraph wire, and yet be sufficiently resilient so as not to crack when struck. It was also important that the insulator maintain its resilience and not crack or check for a reasonable period when subjected to the heat and ultraviolet rays of the sun.

Considering electrical qualities, surface leakage obviously accounted for so large a fraction of the current losses that high volumetric resistivity of the material was not a necessary requirement. In a dry atmosphere, the surface leakage over any insulator is negligible, but in the presence of moisture two major conditions affect leakage. The first is the specific heat conductance of the material, or in popular expression, whether it feels cold or warm to the touch. On good heat conductors, water precipitates out of the atmosphere more freely and at smaller temperature differences than on poor heat conductors. The other condition has to do with the interfacial tension between water and the insulator surface, or more popularly, whether or not water "wets" the surface. A small quantity of water on a surface with which it has a high interfacial tension, tends to draw itself up into a series of discrete globules, not touching each other and with dry surfaces between. Such a condition is conducive to low electrical leakage over the surface. If, however, the interfacial tension is low, the water "wets" the surface, and it tends to spread out in a more or less continuous film over considerable areas. This gives rise to high electric leakage.

It was found that almost any rubber composition had an adequately low factor of heat conductance, but that extremely few compounds possessed the required inherent "nonwetting" surface characteristic desired for good insulating efficiency under conditions of rain or heavy fog.

Ultimately, a vulcanized rubber compound was developed having a reasonably satisfactory combination of essential qualities. This rubber compound was of the wax-bearing type, and the composition and extent of the wax ingredient and the technique of compounding were important characteristics in its manufacture. The wax component of the mixture blooms, or migrates to the surface, continuously for years, thereby maintaining in service high interfacial tension with water and insuring the desired "nonwetting" characteristic of the insulator. In addition, reasonable self-cleaning characteristics are afforded, as is almost complete freedom from surface checking under prolonged sun exposure. This wax component of the rubber compound represents one of the principal features of Western Union patents covering the product.

Two styles of single-petticoat rubber insulators, designated as types *R-1* and *R-2*, were designed for force-fit mounting on the spindle of a steel pin. A field trial of the *R-1* insulators showed the desirability of reinforcing the wire groove. Laboratory studies of the *R-2* insulator, which was designed to contain a minimum amount of rubber, indicated that the reduction in size was carried too far. The

Figure 1. Illustrating mischievous damage to glass insulators

---

Paper 49-59, recommended by the AIEE communication committee and approved by the AIEE technical program committee for presentation at the AIEE winter general meeting, New York, N. Y., January 31–February 4, 1949. Manuscript submitted October 22, 1948; made available for printing January 5, 1949.

H. H. WHEELER is lines engineer, and W. F. MARKLEY is assistant lines engineer with the Western Union Telegraph Company, New York, N. Y.

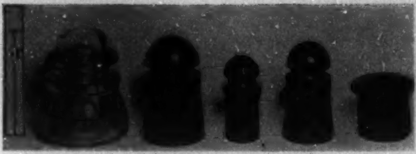

Figure 2. Glass and rubber insulators

Left to right:
Standard double-petticoat glass insulator
R-4 rubber insulator for use on wood pin
R-3 rubber insulator for mounting on spindle of steel pin
R-5 rubber insulator for use on telephone-type short-shank transposition pin
RC-1 rubber insulator for use with Case span-type transposition bracket

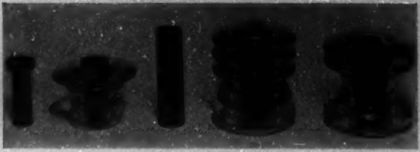

Figure 3. Rubber bushings

Left to right:
RB-1 flange-type rubber bushing
RB-1 rubber bushing in position in glass insulator, used on Case span-type transposition bracket
RB-2 straight-type rubber bushing
RB-2 bushing in position in dead-ending glass insulator
RB-2 bushing in position in power insulator

essential details of these two designs were combined in a third design, called type *R-3*, which is now standard for use with steel pins. A fourth design was tried, moulded so as to provide an inner petticoat, but moulding difficulties were encountered which made the cost of manufacture prohibitive.

The design of the type-*R-3* insulator is shown in Figure 2, along with other styles of rubber insulators that subsequently were developed for specific purposes. The type-*R-4* insulator shown was designed with an inner thread for use on wood pins, and currently is being employed in considerable quantities in the telephone industry. The type-*R-5* insulator, designed for use on telephone-type, short-shank transposition pin, was developed to meet requirements of two Canadian railroads. The type-*RC-1* insulator was designed for use on the Case span-type transposition bracket where the expense of replacing a broken glass insulator is sometimes prohibitive. The compound used in the type-*R-5* and type-*RC-1* insulators had to be modified somewhat to improve its toughness, to enable the insulators to withstand the continuous severe stresses encountered in service.

This latter compound was adapted subsequently for use as bushings in various types of glass insulators, as shown in Figure 3. It was found that this rubber composition not only provided adequate resilience for the assembly, but materially improved its over-all electrical efficiency The *RB-1* flange-type rubber bushing shown was designed for use with the glass insulator on the Case span-type transposition bracket. The *RB-2* straight-type rubber bushing was designed for the shackle-type glass insulator to replace the lead bushing which normally was used, but which was not entirely satisfactory. The *RB-2* bushing also is shown in position in a glass insulator for use in power work; this combination of rubber bushing and glass insulator is being used to replace porcelain insulators, and is an entirely new development in the power industry.

Rubber insulators moulded with these approved compositions definitely have solved the breakage problem, not only in service but also in shipping and handling. In actual tests, with insulators mounted on steel pins, loads that resulted in bending the pins left the rubber insulators unmarked. One such insulator, dropped from a 12-story window to the concrete pavement, was entirely unaffected. Bullets would pass through, but would not shatter the insulators. The smaller projected area made hits less likely, and the lack of any visible evidence on the insulator when struck discouraged its use as a target for marksmen.

The first extensive field installations of rubber insulators on steel pins were made in 1939 and 1940 in a wide variety of areas including Florida, representing severe sunlight exposure; the West Coast along San Francisco Bay, representing a difficult fog area; Nebraska, representing a heavy wind exposure; and the New York-Philadelphia area, representing a wide diversity of weather conditions, varying from dry to fog and heavy rains. Numerous small installations also were made in locations where the breakage of glass insulators was a major consideration.

After six years of service, a number of these insulators were removed from the various areas for rigorous laboratory inspection. It was observed generally that the insulators were practically as good as new, except those from the Florida area, which showed a slight superficial checking of the rubber. All of these insulators continued to maintain their original toughness and elasticity, as well as their self-cleaning and water-repellent characteristics.

In the heavy wind exposure in Nebraska, it was found that the rubber insulators are capable of satisfactorily supporting the relatively heavy loads resulting from large-gauge iron wires. Where the rubber insulators supported number 9 copper wire in this area, the resilience of the rubber materially reduced tie-wire breakage, and resulted in fewer fatigue breaks of the line wire.

In the New York-Philadelphia and the West Coast areas, the rubber insulators at critical points of support, such as at corners and terminals, showed no weakening under the severe mechanical strain encountered.

Because the line sections most vulnerable to insulator damage were selected initially for rubber insulator installations, the field reports indicated that the saving in broken glass insulators for the first year more than paid for the rubber insulators, and resulted in reduced material and labor costs. In addition, by eliminating the broken insulators which ordinarily caused increased leakage and wire trouble in wet weather, sustained line insulation was achieved, with consequent increased operating efficiency of the circuits.

The electrical performance of rubber insulators in the various classes of service has exceeded original expectations considerably. Relative insulation-resistance characteristics, determined from d-c leakage measurements on circuits insulated with rubber and with glass, respectively, are shown by the curves in Figure 4.

In Figure 4, the curves representing Elizabeth–Trenton circuits, comprising about 45 miles of open wire (approximately 3,100 insulators per circuit), indicate the average performance, during periods of heavy rain, of two rubber-insulated circuits and two glass-insulated circuits, all installed at the same time, as compared with old glass-insulated circuits that have been in service for 30 years or more.

These curves show that, after the first few months, the rubber-insulated circuits develop and maintain about a 100 per cent improvement over old glass-insulated circuits in insulating properties. On the other hand, while the new glass-insulated circuits appear to be nearly five times as good as the old glass-insulated circuits, and almost twice as good as the rubber-insulated circuits in the early stages of exposure, they deteriorate more rapidly in insulation resistance, so that after the first three or four years on the line, they approach the rubber-insulated circuits in insulating characteristics, and maintain this equivalent electrical performance on further exposure. Although these curves reveal that the circuits insulated with rubber and new glass maintain, on prolonged exposure, a two-to-one superiority over old glass-insulated circuits, field reports show no noticeable difference, under normal weather conditions, in the operating performance of any of these circuits, indicating that the old glass insulators still possess adequate insulation.

In Figure 4, the curve representing Pacific Coast circuits along San Francisco Bay, comprising about 22 miles of open wire (approximately 900 insulators per circuit), shows the average performance of two rubber-insulated circuits as compared with old glass-insulated circuits that have been in service for 30 years or more; no new glass-insulated circuits were erected in this section when the rubber insulators were installed. This curve indicates that, during periods of widespread fog, the rubber-insulated circuits during the first two years of service are 8 to 20 times as good as the old glass-insulated circuits from the standpoint of insulation resistance. The rubber-insulated circuits then reach a state of equilibrium, in which they appear to maintain a line insulation practically four times as good as old glass-insulated circuits. This relative performance is confirmed also by current field reports, which indicate that during periods of adverse weather, when all of the glass-insulated circuits are completely "fog-bound," the rubber-insulated circuits provide reasonably satisfactory operation.

These relatively extensive field tests with the steel-pin-type rubber insulators indicate generally that in normal telegraph service, the electrical efficiency of rubber-insulated circuits in heavy rain exposure can be expected to be about on a par with that of glass-insulated circuits of the same age, and superior to glass-insulated circuits in an area where heavy fog and high humidity are encountered. Similar results have been reported on the use of the wood-pin-type rubber insulators by the telephone industry.

Although no carrier circuits have been insulated as yet exclusively with rubber, short sections have been so equipped, with no apparent change in operating efficiency. Limited laboratory studies on the relative transmission efficiency of rubber- and glass-insulated circuits at various frequencies indicate that the a-c wet weather losses for both types of circuits are about the same for frequencies up to, and somewhat beyond, 30 kc. Because of limited experience with rubber insulators at frequencies appreciably higher than 30 kc, and because of the fact that at these frequencies electric losses mount rapidly, it is not possible to say at this time whether a circuit insulated entirely with rubber in this higher frequency range would provide acceptable operating efficiency, but it is believed that a small percentage of rubber insulators in such a circuit would not adversely affect its over-all transmission characteristics.

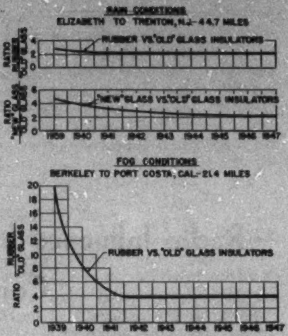

Figure 4. Relative insulation resistance of open-wire circuits

Rubber insulators never will equal in lasting qualities the more fortunate glass insulators, many of which, in their 50 or more years of existence, have outlasted not only the original crossarm on which they were mounted, but also its replacement. However, it is anticipated that the average life expectancy of rubber insulators will be 15 years or more, judging from their performance during the past nine years. Furthermore, their outstanding record of durability and over-all electrical and mechanical efficiency during these nine years warrants their continued use, even if it were not for the determining factor—that rubber insulators are, without question, the answer to the problem of mischievous breakage.

No Discussion

Radio Influence from High-Voltage Corona

GORDON R. SLEMON
ASSOCIATE AIEE

IN THE study of high-voltage power transmission, corona phenomena have received considerable attention. The power loss which accompanies corona has been investigated to the extent that general prediction may be made under most conditions. The increase in the voltage level of long-distance transmission lines, coupled with the extension of communication facilities, has created a demand for a more adequate knowledge of the radio-frequency propagations which may be expected from corona.

The experimental work of this project has been directed toward two main objectives. The first of these is a clarification and extension of the basic concepts of the space-charge phenomena which occur in corona. The general conditions under which radiating impulse currents will occur have been described, and an attempt has been made to show the effects of some of the variable factors. From the observations, certain additions and clarifications have been made in corona theory. With the aid of this firmer theoretical background, a beginning has been made in the field of radio-interference control under various voltage conditions.

Equipment

Because of the sensitive nature of the field measurements necessary in this corona study, the equipment was installed in a radio-frequency-shielded cage. This cage was ten feet square, eight feet high, and of standard construction with wire mesh on both inner and outer walls.

POWER SUPPLY

Supplies of 25, 60, and 500 cycles per second power, all at 110 volts, were brought into the cage through radio-frequency suppressors. Transformers were installed to supply continuously-variable voltages up to 50 kv at all three frequencies.

CONDUCTOR-PLANE CONFIGURATION

Separation of the effects of positive- and negative-potential corona discharges was accomplished by the use of a single conductor mounted parallel to a grounded plane. The electric field produced about this conductor is identical with that about one conductor of a 2-conductor, single-phase transmission line with double the conductor-to-plane spacing and operating at double the voltage.

The plane consisted of aluminum sheets connected mechanically and electrically to one wall of the cage. Bakelite post insulators were attached on a slide arrangement to the two adjacent walls. Most of the tests were made on a number 8 smooth solid conductor as this was the largest diameter which the 50-kv power supply would allow.

BRIDGE FOR CORONA CURRENT MEASUREMENTS

To separate the corona current from the capacitive charging current of the conductor, a simple capacitance-resistance bridge, Figure 1, was constructed using the conductor plane as one capacitance arm.[1] The bridge was balanced at a voltage below corona threshold. Above the threshold voltage, the detector voltage is a measure of the corona current.

MEASURING EQUIPMENT

High- and low-frequency radio noise meters were used for comparative measurements of the corona radio noise. Inside the cage, the induction field predominates. As there was some doubt of the accuracy of a rod-antenna instrument in this field,[2] no quantitative measurements of radio noise were made.

A communications receiver was fitted with a probe antenna for use in radio-noise location. For measurement of the intensity and phase of the audible corona discharge, a sound-level meter with microphone was employed. Also, it was thought advisable to analyse the visible spectrum radiations from corona. The output of a photoelectric cell was amplified with provision for differentiation, in order that constant and pulse radiations might be separated.

The outputs of all measuring devices could be applied to the plates of a double-beam oscilloscope for comparison.

A-C Corona Characteristics

The first set of tests were concerned with the corona characteristics of alternating voltage on a smooth, polished conductor. This surface does not represent a practical condition for service conductors but does eliminate a number of intangible factors. Later in the study, surface contaminations are reintroduced.

CORONA THRESHOLD VOLTAGE

To cause ionization of atoms by a single electron collision, a certain critical voltage gradient is required throughout the mean free path of the electron. This gradient is a function of the gas ionization potential and of the gas density. For air, the gradient required at the surface of a conductor of radius (r) is given in Peek's formula[3]

$$g_e = 29.8(K)\left(1+\frac{0.301}{\sqrt{K\cdot r}}\right) \text{ kv per centimeter}$$

where

$K = 3.92b/(273+t)$
b = pressure in millimeters of mercury
t = temperature in degrees centigrade

Paper 49-60, recommended by the AIEE communication committee and approved by the AIEE technical program committee for presentation at the AIEE winter general meeting, New York, N. Y., January 31–February 4, 1949. Manuscript submitted June 17, 1948; made available for printing December 28, 1948.

GORDON R. SLEMON is with The Hydro-Electric Power Commission of Ontario, and the University of Toronto, Toronto, Ontario, Canada.

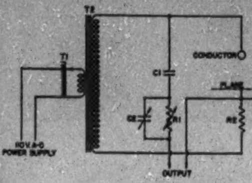

Figure 1. High-voltage circuit for corona current measurements

C1—20-micromicrofarad 50-kv parallel-plate air capacitor
C2—Variable capacitor to balance out residuals
R1—Variable resistance to balance capacitance-resistance bridge
R2—Fixed resistance in capacitance-resistance bridge
T1—Variac. Primary: 110 volts, 25 to 500 cycles per second. Secondary: 0 to 135 volts
T2—High-voltage transformer. Primary: 110 volts. Secondary: 50,000 volts

The voltage which will produce this surface ionizing gradient has been calculated as

$$e_c = g_c' r \frac{\left(\frac{s}{r}-1\right)}{\left(\frac{s}{r}+1\right)} \cosh^{-1}\frac{s}{r} \text{ kv peak}$$

where s is the spacing from the conductor center to the plane in centimeters.

The corona threshold voltage was observed experimentally by radio interference, audible noise, and visible light. All three propagations were initiated at the same voltages; this voltage corresponded closely in all cases to the critical corona voltage calculated above. The corona threshold was found to be independent of the frequency of the supply voltage over the range studied. The voltage of corona initiation with increasing voltage was found to coincide with that of corona extinction on decreasing voltage.

Figure 2. Radio noise versus supply voltage with various conductor-to-plate spacings

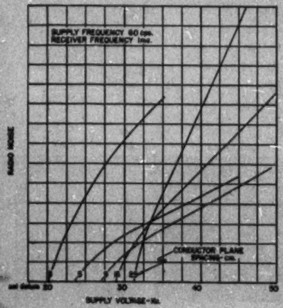

RADIO NOISE

Figure 2 shows a typical set of curves of radio noise with supply voltage as the independent variable. It is noted that the curves are very nearly linear, with the exception of the low intensity portion which has a greater slope. This would indicate that the magnitude of the radio noise from a smooth conductor is roughly proportional to the increase of the applied voltage over the threshold value.

In Figure 2 it is noted that the minimum slope occurs for the 5 to 9 centimeter region of spacing. In Figure 3 the same results are replotted on an abscissa of spacing. These curves indicate that, if radio noise is to be allowed, there appears to be an optimum spacing which will produce the lowest value of noise for a particular voltage. Since the amplitude of propagated radio noise is dependent on the complex factors of conduction and absorption of corona energy, there might be doubt as to the applicability of the conductor-plane results to a transmission line. There is some confirmation of possible analogy in this factor in the work of H. L. Rorden.[4] In his work on a 220-kv transmission line, he found that the radio noise at a short distance perpendicular to the line could be reduced by about half by a reduction in conductor flat spacing from 27 feet to 18 feet.

As to the relative intensities of radio noise over the radio-frequency spectrum, a reduction in noise intensity with increase in receiver frequency was noted in all cases.

PHASE ANALYSIS

The audio output of the radio noise meter and a voltage in phase with the supply voltage were applied to the vertical plates of a double-beam oscilloscope, Figure 4. It is observed that radio noise is produced, in this smooth-conductor case, only in the region of voltage about the negative peak of the wave. In the range of voltage up to double the threshold value, no radio noise occurred in the positive half-cycle.

The audio output of the meter appears as a series of random pulses of almost equal amplitude phased in a clearly defined group. As the voltage is increased above threshold, the phase width of the group increases; the amplitude of the group, however, remains almost constant. Accurate measurement of the phase limits of the group showed that the radio noise for the lower supply frequencies occurs only during that portion of the negative wave for which the voltage is in excess of the threshold value. Using a 500 cycle per second supply, the phase of corona initiation was advanced from 5 to 10 degrees beyond the 60 cycle per second case, indicating a possibility of residual ionization effect.

CORONA CURRENT

Observation of the corona current wave showed that the positive portion of the wave was smooth. On the negative portion, current pulses were superimposed Figure 5. The lower-frequency components of the corona current were removed by a short time-constant differentiating circuit, leaving only the high-frequency, noise-producing currents shown in Figure 6. These wave forms were compared with those of receiver audio output in Figure 4; the corresponding phases of initiation and extinction have been found to be identical.

AUDIBLE NOISE

When the time delay of sound travel from the conductor to the microphone was used as a correction, it was found that the initiation phase for audible sound corresponded closely with that of radio noise. No correlation could be expected on the phase of extinction because of the sound echoes throughout the cage.

VISIBLE CORONA

Wave forms of the amplified output of a photoelectric cell focused on the conductor were observed. It was found that the visible corona in the negative voltage cycle was of a pulsating nature, and that its phase limits corresponded closely with those of radio noise. The positive-voltage

Figure 3. Radio noise versus conductor-to-plane spacing for various applied voltages

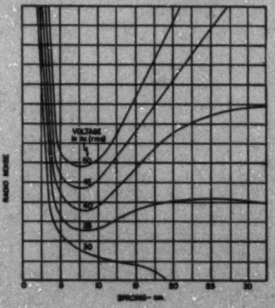

corona produced a relatively constant illumination during the ionized period.

Rectified Sine Wave-Form Characteristics

In some of the theories which have been advanced on the subject of conductor corona, the effects of residual ionization from the positive voltage cycle have been considered important in the transient phenomena noted during the negative half-cycle.[1] To analyse this interrelation, it was thought desirable to apply the positive and negative half sine waves of voltage to the conductor separately. To do this, a high-vacuum rectifier was placed in series with the high-voltage lead to the conductor.

With the positive sine wave, no radio propagation was observed up to the maximum voltage of 62.5-kv peak. The normal threshold voltage was 38.2-kv peak. The thresholds of audible and visible corona coincided with the alternating-voltage value. The nature of the audible noise was a low-amplitude, modulated hiss rather than the staccato pulse observed in alternating current. A bluish-white glow appeared about the conductor while in corona. The intensity was found to be roughly proportional to the excess of the applied voltage over threshold value.

Applying the negative sine wave of voltage, no noticeable difference was observed in the results of these tests and those made on alternating current. It would appear, then, that a theoretical analysis of corona in the negative cycle of an alternating-voltage wave will have to be based on charges produced during that negative cycle.

D-C Corona Characteristics

A study of the corona phenomena with direct current was indicated for several reasons. The effect of rate of change of voltage is eliminated from the list of variables, and direct current provides the simplest case for theoretical analysis of the phenomena which produce radio noise. Also, with the possible advent of d-c transmission, the results assume importance.

With positive direct current applied, no radio noise was radiated by the smooth, polished conductor up to double the normal ionization voltage. There was a barely-audible corona noise having the nature of a hiss, the frequency of which seemed to be dependent on voltage. A bluish-white glow appeared and was found to be unmodulated.

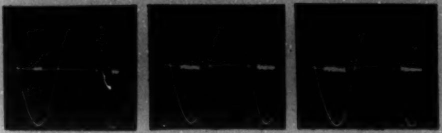

Figure 4. Radio noise from a smooth conductor at 30, 40, and 50 kv

60-cycle timing wave is in phase with supply voltage

As would be expected, radio noise was produced with negative voltage on a smooth conductor. However, the threshold of radio noise occurred at a voltage considerably higher than would be expected from the a-c tests. A typical pattern of negative d-c radio noise is shown in Figure 7. The wave form appears to be a mixture of pulses of random amplitudes and of repetition frequencies which increase with voltage increase. Actually, the interference to communications is not nearly so severe with the d-c radio noise because the continuous wave form has none of the lower harmonics of the power frequency present in a-c noise. The audio output of the receiver is a hiss which can be largely eliminated by limiting the high-frequency audio response of the receiver.

The audible noise from negative direct current shows characteristics which are almost identical with the receiver audio output. The visible corona appears as regularly spaced tufts along the conductor. These tufts are reddish in color and increase in number as the voltage is increased.

Effect of Contaminations

Up to this point in the study, all results have applied to smooth, polished conductors. To obtain a picture of what might be expected in service, contaminations were introduced.

Mutilations

As an introduction to the effect of surface roughness of conductors on corona, a single burr was produced on the conductor. This burr did not reduce the radio noise threshold. But, it is seen in Figure 8 that, while the negative-cycle radio noise remained unchanged, considerable radio noise was introduced into the positive-voltage cycle. Since this noise was caused by only one burr, positive-cycle radio noise promises to be severe on mutilated conductors.

Oil and Grease

On leaving the factory, new conductors often are coated with a film of die grease. This condition was produced on the test conductor, but no detectible change in radio-noise characteristics from those of a smooth conductor could be observed. Such was not the case, however, when irregular coatings of heavy grease were applied. With positive direct current and in the positive of the a-c cycle, corona brushes appeared, not from the projections, but from the thinly-greased areas. Radio noises occurred in the form of severe pulses, the pulse repetition frequency of which increased with increase in voltage.

Weathered Conductors

Prolonged corona on the conductor was observed to produce a surface condition similar to that of a slightly weathered conductor. Tests with this surface showed radio noise with negative direct current to be reduced by about 50 per cent in amplitude. When alternating current was applied, radio noise was produced more or less of equal magnitude in the positive and negative half-cycles, with a reduction of about 25 per cent in noise-meter reading. There is a possibility that tests on a conductor which had been fully weathered in service, would show a predominance of positive-cycle radio noise. The radio noise from newly-constructed transmission lines has been observed to reduce after the line has been in service for some time.[4] Generally, this characteristic has been explained by the fact that die grease and surface contaminations, incident to manufacture and stringing,

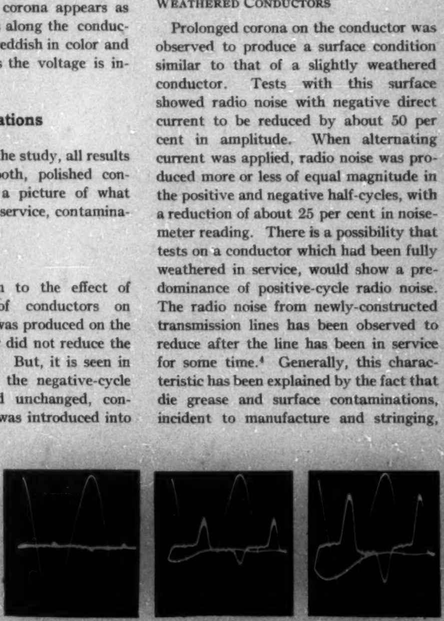

Figure 5. Corona current on a smooth conductor at 30, 40, and 50 kv

Same timing wave as in Figure 4

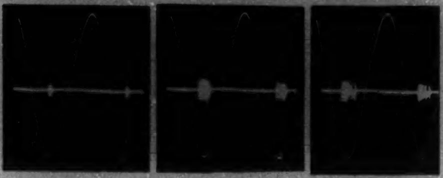

Figure 6. Radio-frequency components of the corona current shown in Figure 5

have been burned away by corona. The test observations indicate that this reduction may be effected partially by the added contaminations coincident with conductor weathering.

WATER

The severest case of corona occurs under weather conditions of rain, fog, sleet, and snow. Probably the most common and most important conductor surface contamination is, therefore, water. A fine mist of distilled water was produced about the conductor. With positive direct current, severe radio noise was initiated at about 60 per cent of the normal corona threshold voltage. When the mist cleared, leaving only the water droplets on the conductor, the radio-noise threshold voltage was increased slightly. It appeared, from the results of various tests, that water on the conductor is the important factor. Water in the surrounding dielectric caused changes, all of which were insufficient to warrant separate study. As with other contaminations the repetition frequency of the pulses increases with voltage increase, such that the most objectionable noise occurs in the low pulse repetition frequency range just above threshold voltage. With positive d-c transmission, the radio-noise threshold for a wet conductor probably would be considerably below the operating voltage, thus by-passing the most objectionable radio influence. The effect of water, however, may be the controlling factor in positive d-c work.

From previous work on contaminations, it was expected that water might have opposite effects with positive and negative direct current. It was found that, with negative direct current, water sprayed on the smooth conductor eliminated all radio noise. The radio noise did not recur until the water film was allowed to evaporate from the conductor surface. These results are substantiated by tests on transmission lines using alternating and direct voltages up to 300 kv. It was found that, for otherwise similar conditions, the ratio of positive d-c to negative d-c radio noise varied from three for fair weather conditions to about 100 for a heavy rain condition.[6]

Conductor Coatings

The effects of various conductor contaminations on radio frequency propagations have suggested the possibility of radio noise control by special conductor coatings. No attempt has been made here to develop practical coatings, but certain of the physical requirements will be indicated. The corona loss factor has not been considered in this study. It is probable that losses may be increased by the methods suggested here for radio-interference control.

POSITIVE DIRECT CURRENT

With a smooth conductor, the process of corona formation and maintenance takes place without radio-frequency radiation. When the conductor surface is contaminated or mutilated in any way, however, radio noise is produced. On all outside installations, the effect of atmospheric water is a controlling factor. Since water has a high dielectric constant and a high dielectric strength, it was doubtful if any insulating coating would be advantageous unless the insulation extended beyond the critical gradient region. A film of insulating varnish provided noise characteristics which substantiated this point.

Of the coatings tested, the only one which showed any advantage over the smooth condition was a conducting rubber. When water was sprayed on this coating, the radio-noise threshold was raised about 90 per cent above that of a smooth, wet conductor. The amplitude of the signal was comparatively low over the range above the threshold voltage. When dry, the radio noise increased until it was slightly below the value for the smooth, wet condition.

NEGATIVE DIRECT CURRENT

Radio noise with negative direct current has been shown to be most severe with a smooth, polished surface. Both insulating (water) and conducting (weathered) surfaces have tended to reduce the radiation. A carefully applied coat of varnish or enamel gave characteristics similar to those of water on the surface. Irregularities, however, produced severe radio noise.

A conducting coating of sodium chloride was applied as a saturated solution in water and allowed to crystallize. Over the greater part of the voltage range above threshold, the radio noise was reduced by over 90 per cent from its smooth value. This coating appeared to have the required structure and conductivity for radio-noise reduction. To determine the effect of water on this type of coating, a crystalline surface of dichloro-diphenyl-trichloroethane (DDT) was obtained. The reduction in radio noise was about 75 per cent from the smooth, dry condition. Water was sprayed on the conductor, and the radio noise was further reduced to about 70 per cent of the dry, coated value.

It was not certain whether the radio noise was reduced by the point structure of the coating or by its value of conductivity. Thus, a smooth coating of conducting rubber was tested with negative direct current. The radio noise was reduced by about the same percentage as for the DDT coating, but, since the audible noise was almost eliminated, the possibility arose that only a few points were producing severe radio noise. These points were isolated by detection of visible corona, but the surface could not be repaired easily. It is possible that a well-applied, pure coating of conducting rubber might have the same effect as a water film in noise reduction. Water sprayed on the imperfect rubber coating further reduced the noise to about 60 per cent of its dry, coated value.

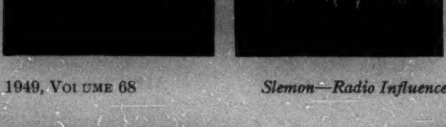

Figure 7. Radio noise from a smooth conductor with 50- and 60-kv negative direct voltage applied

Theory

The theory of ionization by collision is generally accepted as describing the process of breakdown of air under electrical stress. As the field potential gradient is increased, free electrons, present in atmosphere due to ultraviolet, cosmic, and radioactive radiations, attain a drift velocity proportional to the voltage gradient and inversely proportional to the gas density.

The general gradient and potential conditions to cause corona initiation have been discussed in the section on corona threshold voltage. There appears to be a slight difference in the voltage at which ionization is produced about positive and negative conductors. The production of space charges and the process of recombination differ widely for positive and negative conductor potentials. The cases, therefore, will be considered separately.

Positive-Potential Conductors

With positive potential on the conductor, free electrons in the surrounding region are attracted toward the conductor. As they reach the critical gradient, the ionization process establishes electron avalanches. A highly ionized region will exist about the conductor and may extend somewhat beyond the critical gradient region because of the average velocity of electrons moving inward in a field slightly lower than required for ionization. The electrons of ionization will be absorbed by the conductor. The positive ions will move outward in an ever-decreasing field such that few, if any, ionizing collisions may be accounted for by their motion. These ions provide the medium of current flow to the zero- or negative-potential plane.

The ionizing procedure is effected by a transfer of energy from the electric field to the acceleration of free electrons and, from these, to the high-energy electrons of ionization. No distinct electromagnetic radiation is produced in the process. Because of the outward motion of the ions and the process of ion neutralization by contact with negative ions, there is a continual ionization after the initial avalanche. The radiations produced throughout the ionized region by the deionization process appear to be confined to shorter wave length visual and ultraviolet bands. With a smooth conductor, no radio frequency propagation is noticeable.

This result would be expected from a study of the field configuration shown in Figure 9. The concentration of electrons passing into the conductor surface causes a reduction in surface potential. The positive-ion field increases the positive potential above the normal value at a distance from the conductor. This redistribution of the potential relieves the overstressed condition of the air; the potential gradient about the conductor is just sufficient to maintain ionization.

Negative-Potential Conductors

When negative potential is applied to the conductor, the free electrons in the immediate region are expelled and thus, are not available for continued ionization. The necessary electrons then must be emitted by the conductor. There are two probable means by which such emission could take place. The ions in the surrounding air will be accelerated toward the conductor. By bombarding the conductor surface with the energy received from the field, these positive ions may cause secondary emission. The process of secondary emission is somewhat inefficient; the number of electrons emitted is only a few per cent of the incident ions. However, only a few electrons are required to start the ionization process. The number of electrons available for ionization increases almost exponentially with distance from the conductor surface. Low-work-function surfaces would provide the best emitters in this case.

The other probable means of electron supply is field emission. Very high electrostatic fields are set up about surface irregularities, projecting crystals, and submicroscopic points. In these regions of high stress, the field energy may be sufficient to draw electrons out of the metal surface. Since the gradient at these points may be many times the average gradient, almost all the emission current is concentrated at these points. Field emission will be greatest for those surface impurities which have low work functions.

There is a certain similarity in the surface requirements for these two emission methods. Both are more efficient with low-work-function surfaces or surface impurities. Severe field accentuations about irregularities would have a greater effect on field emission than on ion bombardment.

In order to clarify the basis of certain observations, the following theory of negative corona is proposed. It is assumed that, under sufficiently high surface gradient, electrons will be emitted from the conductor surface by ion bombardment or field emission. When the potential is sufficient for ionization, electron avalanches occur outward from the conductor. These produce a positive-ion space charge, which increases exponentially with distance from the point until the potential gradient drops below ionization requirements, Figure 10(a). The positive-ion space charge causes an immediate increase in the gradient at the conductor surface with a proportional increase in emission current. The surface gradient continues to increase until the positive-ion space charge moves inward to contact the conductor. At this time, the surface potential is reduced greatly, and the gradient will drop considerably below ionization value. The ions are neutralized by contact with the conductor, giving a somewhat constant value of electron current from the conductor during this period. The space-charge distribution for this part of the cycle is shown in Figure 10(b). When the positive-ion charge is cleared, the gradient conditions are restored and electron avalanches again occur.

During this cycle, the electrons of ionization move outward into an ever-decreasing field. When their velocity is sufficiently small, negative ions are formed which drift toward the more positive potential.

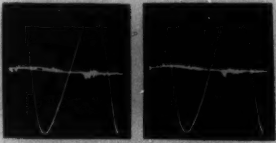

Figure 8. Radio noise with a single burr on an otherwise smooth conductor at 40 and 50 kv

Note the radio noise during the positive cycle of the voltage wave

Because of the large differences in electron and ion mobility, the period of ionization will be very short in comparison with the period of positive-ion neutralization. Thus, the corona current for each point will be a steep pulse followed by a slowly varying current of the same polarity for a period many times the pulse length.

A study of the potential distribution curve of Figure 10(b) shows that the gradient throughout the positive- and negative-ion regions is low. This increase in potential at some distance from the conductor distorts the potential-field lines in such a way as to reduce the gradient for a certain conductor length about the ionized region. Since the applied voltage determines the intensity of each electron avalanche and resultant ion cloud, only a certain discrete number of these corona tufts will exist simultaneously along the conductor length. These tufts will be spaced automatically such that they protect the intervening regions from excess gradients. The uniformity of the spacing

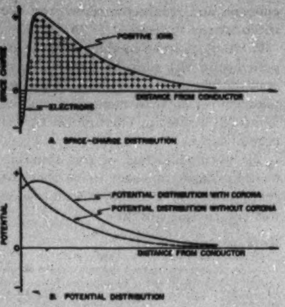

Figure 9. Field diagrams of corona from a positive-potential smooth conductor

will depend on the surface condition and the distribution of high-emissivity points on the surface. As the voltage increases, the corona tufts must be more closely spaced to cause a sufficient reduction in the field between these points.

Contaminations and Coatings—Positive Potential

We have observed that positive potential produces radio noise from a conductor only when the conductor surface is contaminated or roughened. Both insulating and conducting coatings produce similar impulse currents, but the mechanics of the discharges are somewhat different.

The effect of conducting coatings and contaminations may be explained partially by reference to Starr's work on high-voltage d-c point discharges.[6] Apparently, point discharge may be classified into three types. A sharp, slender point produces a small bead of ionization at its tip, with a tapering sheath of ionization extending back from the point. No normal radio noise accompanies this discharge. A polished conical point of about 60 degrees width produces a sharp ionized needle projecting some distance from the point and producing a harsh radio noise. The third type, a rough point or one of about 120 degrees width, has an ionized bead at the tip with a broad plume of discharge blossoms extending outward. The corona current is low; the radio noise is more regular and of higher repetition frequency.

Surface irregularities such as burrs, conducting coatings, and crystal points may be considered as separate discharge points. There will be certain mutual effects of adjacent discharges, but the theory of their radio-noise production will be similar to that of a combination of individual points. It was found that a needle point projecting from the conductor produced no radio interference. In this case, the positive space charge apparently builds up a stable equilibrium over a wide range of currents. This space charge, with its resultant effect on the potential gradient, blocks off the development of any positive streamers and hence no current impulses occur. This protective effect is similar to the case of a smooth conductor.

The mutilated or weathered surface presents many point structures which are of the second or third type. These points produce high regional gradients, and streamers composed of electron avalanches project from space toward the points The positive space charge thus created momentarily reduces the gradient and blocks further ionization until the ions have been cleared sufficiently from the point region. If the point is regular and symmetrical, a symmetrical field and charge structure will result. The discharge phenomena then should show a definite regularity. If the point is sharper as in the second type, the ion cloud produced does not provide as complete a shielding barrier. A more random discharge may be expected from these points.

The visual corona which will occur about this point-structure surface will depend upon the concentration of the points. If only a few are present, the normal bluish-white glow will exist about most of the surface. At the point, a needle or blossom corona tuft, reddish in color, will be observed. The normal glow in the surrounding region will be reduced or eliminated as a result of the tuft-gradient effect. As the points become more numerous, all corona will be concentrated at the points, and the gradients of all intermediate regions will be reduced by the projecting corona tufts. There will be a certain automatic spacing of tufts, just as in the case of negative potential.

If an insulator in the form of a water drop is placed on the conductor, a field distortion will occur. The water, being of high dielectric constant, will have a low voltage drop across it. Thus, the potential at the top of the drop is much greater than normally would exist at that distance from the conductor. As this provides the nearest and highest potential, electron avalanches will project toward this point. As the electron concentration builds up, the potential gradient through the drop increases until breakdown potential is reached. The result is a current surge into the conductor. It might be thought that breakdown would occur in the air about the drop rather than through it because of the higher dielectric strength of water. Observation, however, indicates the latter to be the general case.

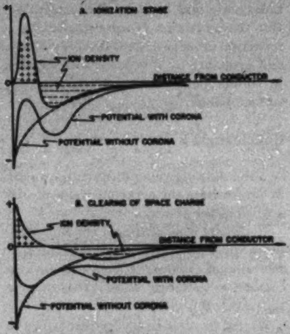

Figure 10. Space-charge distribution in negative-potential corona about a smooth conductor

Contaminations and Coatings—Negative Potential

The effect of any surface contamination will depend chiefly on two characteristics. Probably the most important factor is the increase in regional potential gradient caused by any point structure. The other factor is the electron emission characteristic of the coating. This will be controlled by the work function or ionization potential of the surface material.

There are then two possible approaches to the control of radio noise from a negative conductor. All emission may be eliminated up to a high potential by covering the surface with a smooth coating of high ionization potential. Water, which has an ionization potential of 12.56 volts, as compared with 7.68 for copper, and which also provides a smooth surface, was found to provide this effect up to a potential greater than twice the dry critical potential.

The other method of radio-noise control is exemplified by the crystalline coatings. In this case, the surface work function is intentionally lowered and the surface gradient increased. Under these conditions, the radio-noise-producing discharges are more numerous but less severe, and the advantages of lower-amplitude higher-repetition-rate pulses are obtained.

The first of these methods has certain advantages. From the radio-noise standpoint, complete elimination is naturally the more desirable. Also, the prevention of severe ionization about the conductor might result in a theoretical elimination of corona loss. With the other method, radio noise may be reduced considerably. But this reduction is accompanied by a reduction in radio-noise threshold voltage, and probably by a considerable increase in corona power loss over the smooth-surface value.

Conclusions

The following general conclusions may be drawn from the experimental work described in the preceding text:

1. There is an optimum conductor-to-plane spacing which will produce the lowest value of radio noise from corona on a conductor operating at a voltage above the corona threshold voltage.

2. An increase in the frequency of the supply voltage causes an increase in the magnitude of the radio noise, except at conductor spacings lower than the optimum value. The radio-noise threshold is independent of supply frequency.

3. Radio noise from corona on a smooth conductor is produced only during the negative peak of the applied voltage wave. The radio noise occurs within the time during which the negative voltage exceeds the corona threshold voltage for the lower power frequencies. An advance in the phase of radio-noise initiation was observed for supply frequencies of about 500 cycles per second. The effect of residual positive ionization from the positive half-cycle is shown to be a minor factor in the radio-noise phenomena of the negative-voltage cycle.

4. The phase of initiation of audible sound and visible light radiations coincides with that of radio noise.

5. Positive direct current on a smooth conductor produces no radio noise with voltages up to double the normal peak threshold voltage.

6. With negative direct current, the most severe radio noise occurs with a perfectly smooth conductor. Weathering and most contaminations reduce the radio noise considerably.

7. Water on the conductor causes severe radio noise with positive direct voltage but eliminates radio noise with negative direct voltage.

8. Radio noise from corona on conductors with negative potential may be controlled by two methods. A smooth coating of high work function will eliminate radio noise by preventing electron emission. A rough, pointed surface of low work function will facilitate electron emission and reduce the severity of the corona current pulses.

9. Radio noise on conductors which are periodically wet may be partially controlled in the positive d-c case by the application of a semiconducting coating which has a damping effect on the corona current surges.

10. A modification of this semiconducting coating appears to be the best compromise for control of radio noise with alternating current.

References

1. Some Characteristics of A-C Conductor Corona, **F. O. McMillan.** Electrical Engineering (AIEE Transactions), volume 54, 1935, pages 282–292.

2. Factors Affecting the Accuracy of Radio-Noise Meters, **H. E. Dinger, H. G. Paine.** *Proceedings*, Institute of Radio Engineers (New York, N. Y.), volume 35, 1947, page 75.

3. The Law of Corona and the Dielectric Strength of Air, **F. W. Peek, Jr.** AIEE Transactions, volume 30, part 3, 1911, pages 1889–1993.

4. Radio-Noise Influence of 230-Kv Lines, **H. L. Rorden.** AIEE Transactions, volume 66, 1947, pages 677–683.

5. Observations of Corona Losses and Radio Disturbances from High Tension D-C Lines with Heavy Conductors, **B. O. Henning.** Conference Internationale des Grands Réseaux Electriques à Haute Tension (Paris, France), June 27, 1946.

6. High Voltage D-C Point Discharge, **E. C. Starr.** AIEE Transactions, volume 60, 1941, pages 356–362.

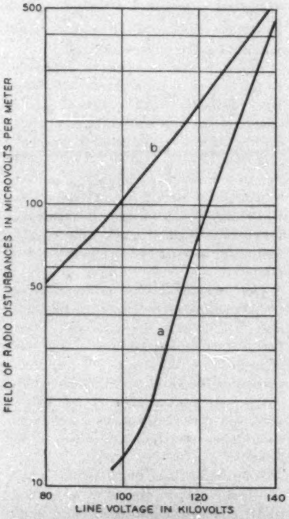

Figure 1. Radio disturbance field at 12 feet of an 0.325-square inch aluminum steel-reinforced cable (a) without, and (b) with a thread of one inch

Discussion

Francois Cahen (Electricite de France, Paris, France): Figure 2 of the paper represents the variation of radio noise versus supply voltage on a smooth and perfectly cleaned conductor. In the case of imperfectly cleaned cables such as cables in operation, the character of these curves differs in three ways from that of Figure 2 of the paper:

1. The level of disturbances is much higher.

2. Disturbances start at a voltage lower than the critical voltage.

3. Disturbances grow rapidly at first, then more and more slowly, to reach saturation point when the critical voltage is exceeded.

Therefore, the curves of Figure 2 of the paper must not be used as a basis for a study of the variations of transmission-line-radio disturbances versus voltage.

On the other hand, is not the shape of curves in Figure 3 of the paper caused by a deformation of the space charge due to the proximity of the plate which plays the part of a second electrode?

According to Slemon, the point of a needle sticking out of the cable would not cause any positive corona effect. We have obtained, at Chevilly, France, the contrary result.

The point of a needle placed on a cable was the center of positive brushes which were a source of power losses and radio disturbances. We even have plotted the curves pointing out the increase in disturbance field due to a needle point sticking out of the cable in Figure 1 of the discussion.

We always have observed positive brushes on all asperities visible to the naked eye, whereas negative brushes also occur on asperities invisible to the naked eye, but these can be removed by rubbing the conductor surface with chamois leather.

Maybe Slemon utilized too high a voltage for his experiments, as the explanation given by him of the nonappearance of brushes (on account of the space charge) applies only to voltages distinctly higher than the critical voltage, whereas brushes also appear when the voltage is lower than the critical voltage.

These observations set apart, the bulk of results described by Slemon tally perfectly with those we obtained at the Chevilly 500-kv experimental station, the latter forming the subject of a communication by Renaudin and Pelissier to the Societe Francaise des Electriciens which is to be published shortly.

Harold L. Rorden (Bonneville Power Administration, Portland, Oreg.): It is apparent that there still is considerable work to be done in our study of corona and radio noise before we can design transmission lines with good economy, and tolerable losses and radio-influence levels. Slemon's contribution to our knowledge of this subject is particularly enlightening with respect to several factors that require further study. He not only has given us a better understanding of the characteristics of corona generation, but he also has shown that it may be possible to reduce some of our radio-influence disturbances by relatively simple expedients. If, for example the optimum spacings mentioned by Slemon for the lowest value of radio influence emanating from a conductor could be determined for various operating voltages, we may have a simple and effective method of improving transmission design. The possible control of radio influence by means of conductor coatings appears to have some extensive possibilities. Should such an expedient become possible, it could be very helpful in mitigating troublesome conditions on existing transmission facilities, as well as to permit better economy in the design of future systems.

It also would be helpful if a method were devised for interpreting radio-influence measurements made by means of coupled circuits (the so-called National Electric Manufacturers' Association (NEMA) method) in terms of the magnitude of radio influence that produces disturbances in residences some distance away from transmission line conductors. The sources of corona are undoubtedly best studied by means of directly-coupled circuits, and Slemon's results amply demonstrate the adequacy of this method. At present it is difficult to specify the requirements for high-voltage transmission equipment, in microvolts measured by the NEMA method, in terms of the microvolts per meter that produce undesirable disturbances in household radios.

We hope that Slemon will continue his good work in the study of the causes and methods of mitigating radio disturbances.

Gordon R. Slemon: Cahen has indicated that radio influence may impose a more serious limitation on transmission-line designs than corona losses. From the viewpoint of economics, corona losses could be allowed to increase. The problem is therefore the prevention of increased radio influence with increase in corona loss. The first method by which this may be accomplished is by the use of phase-to-phase spacings which are smaller than would be indicated by normal practice. The corona loss and the radio-frequency energy are both increased by this reduced spacing. The radio-frequency propagations from the line, however, are reduced.

The second, and as yet undeveloped, method may be a conductor coating which will either prevent unstable ion concentrations or damp any impulses which occur. Rorden has indicated the potentialities of such a method of control. The development of such a coating presents severe mechanical as well as electrical problems. The needle points used in the study were attached to a small diameter conductor. The results obtained were found to correspond with those reported in reference 6 of the paper. It is possible that similar points attached to larger diameter cables may give rise to the radio influence noted at Chevilly, France. The author agrees with Cahen's observation that a more detailed study of corona in the critical-voltage region would be desirable.

Temperature Rise Values for D-C Machines

AN AIEE COMMITTEE REPORT

THIS REPORT gives the results of heat run tests made jointly by the Allis-Chalmers Manufacturing Company, Century Electric Company, General Electric Company, Reliance Electric and Engineering Company, and Westinghouse Electric Corporation on a motor exchange test program at the request of the AIEE rotating machinery committee. Motors tested ranged from 1/2 to 50 horsepower and were standard, open, general purpose, 40 degrees centigrade, 1,750 rpm. Temperature rise was determined for continuous and short time load runs by thermocouples built into the windings, by surface thermocouples, by surface thermometers, and by the resistance method. Each method of measurement is compared with the internal hot-spot measurement.

Based on the results, changes are recommended in the standard limits for temperature rise given in Table I of the American Standards Association (ASA) standard C-50 on Rotating Electrical Machinery.[1] These changes include values for class *B* insulation determined by applying the temperature ratios determined by the tests to the recognized thermometer temperatures for class *B* materials. The values for class *H* insulation establish conservative temperature limits for rise by thermometer, with the rise by resistance obtained by applying the temperature ratios as for class *B*.

It is recommended that Table I of the ASA standard be expanded to cover short-time rated motors, and values are given for this purpose.

In March 1945 the AIEE rotating machinery committee instituted a program for determining actual hot-spot temperatures in d-c machines and for comparing these hot spots with the temperature rise as measured by thermometer, resistance, and surface thermocouple. The test program looked toward placing the resistance method on a practical basis for short-time rated and continuous-rated machines, in order to permit its satisfactory use as an alternative method of test.

Efforts by manufacturers and purchasers to use the resistance method have resulted in difficulties and misunderstanding.

Table I of the ASA standard does not adequately cover the resistance method, particularly for machines having short-time ratings.

Method

Five standard, general purpose, open motors rated 1/2, 5, 10, 25, and 50 horsepower, 230 volts, 1,750 rpm, respectively, were tested. They were shunt wound or stabilized shunt with about 10 per cent regulation. Each motor was tested by its manufacturer and then shipped to one of the other participating companies and retested. Therefore, two tests on each motor are reported, with the exception of the 1/2-horsepower motor which was tested by its manufacturer only.

To determine the hot-spot temperature each motor was built with thermocouples embedded in the armature coils outside the conductor insulation but inside the coil insulation, placed one-third of the length of the slot from each end of the slot. An additional thermocouple was placed in the same manner in each end winding half way between the end of the slot and the end of the winding. Thermocouples were embedded in the coils on the main and commutating poles (at the center of gravity of the section of the coil) at the sides and ends of the coils on the respective center lines.

In most cases thermocouple leads were brought to plug receptacles on both the stationary and rotating parts. At the conclusion of each test run the motor was shut down quickly and thermocouple readings taken at time intervals beginning only a few seconds after removal of load. Curves of temperature were plotted against time and extended back to the instant of removing load. However, since the first reading was obtained so quickly there was virtually no extrapolation of the curves sufficient to cause error. It is particularly important to recognize that in such tests as these the thermocouple reading for the end winding at the commutator end may be rising during the first seconds after shut down, because of the heat flow from the hot commutator. Therefore, if readings are not taken quickly enough to determine this rise, erroneous extrapolation of the temperature-time curve will result.

Only temperature rise values at the instant of removal of load and for the highest of the several thermocouples at that instant are reported as hot-spot temperatures.

Thermometers were applied in all cases as specified by AIEE Test Code for D-C Machines[2] without preheating, except for test A of the 10-horsepower, and test B of the 5-horsepower motor, and the highest reading of the highest of the several thermometers is reported only.

Resistance readings were taken on all windings by Kelvin double bridge, and means were taken to get readings within a few seconds after removal of load and at

---

Paper 49-62, recommended by the AIEE rotating machinery committee and approved by the AIEE technical program committee for presentation at the AIEE winter general meeting, New York, N. Y., January 31–February 4, 1949. Manuscript submitted November 16, 1948; made available for printing December 29, 1948.

This report was prepared by the AIEE subcommittee on d-c machines of the rotating machinery committee.

Personnel of the AIEE subcommittee on d-c machines: T. M. Linville, *chairman*, Mrs. B. O. Buckland, W. E. Clancy, F. A. Compton, Jr., Lanier Greer, J. L. Hamilton, C. B. Hathaway, V. P. Hessler, W. R. Hough, P. Lebenbaum, C. Lynn, L. G. Opel, D. Ramadanoff, J. F. Sellers, V. B. Honsinger, L. N. Grier.

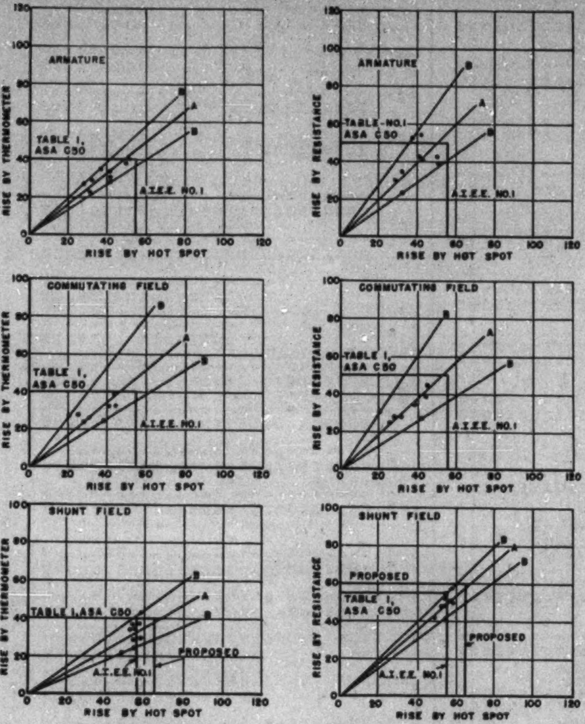

Figure 1. (top)
Figure 2. (center)
Figure 3. (bottom)

Figure 4. (top)
Figure 5. (center)
Figure 6. (bottom)

Figures 1 to 6. Thermometer, hot spot, and resistance data from Table II for 100 per cent continuous operation

Curves B show limits, curve A is average

short time intervals thereafter. The reason for this is the same as already described for the hot-spot readings; that is, to determine the temperature at the instant of load removal without possibility of extrapolating the curves erroneously. Only values for the instant of load removal are reported. The resistance of the armature winding was measured both cold and hot between the same two commutator bars marked for the purpose.

Surface thermocouples were applied adjacent to each thermometer and only the highest reading of the highest of the several thermocouples is reported in each case, the same as for thermometers.

All tests were made under carefully controlled conditions and many special provisions were made to eliminate sources of error.

The conditions for the nine tests made by each company on each motor are set forth in Table II which also gives the test results in degrees centigrade temperature rise. The ambient temperature measured in accordance with the AIEE D-C Test Code[2] was subtracted from each reading before it was tabulated.

Results

The results presented in Table II are used in Table III to show the ratio of the temperature rise measured by the different methods to the hot-spot temperature rise and also to the temperature rise as measured by thermometer. Table III is of special value as it relates the results to the two established, available, bases. These bases are, first, the recognized maximum hot-spot temperatures which insulation of the several classes will stand as given in AIEE standard number 1.[3] The second base is the recognized temperature rise allowed when the thermometer method

Table I. Limiting Observable Temperature Rises

The temperature rises in degrees centigrade in this table apply to the several classes of machines as given at the heads of the respective columns			General Purpose	Totally Enclosed		Short Time Rated						Special Purpose Continuous*		
			Continuous			30-Minute to 2-Hour Ratings, Inclusive			Ratings of 15 Minutes or Less					
			Class of Insulation											
			A	A	B	A	B	H	A	B	H	A	B	H
			Column											
Item	Machine Part	Method of Measurement	1	2	3	4	5	6	7	8	9	10	11	12
1	Armature windings	Thermometer	40	55	75	55	75	100	55	75	100	50	70	90
		Resistance	50	65	85	80	110	140	90	120	160	60	85	110
2	Shunt-field windings	Thermometer	40			55	75	100	55	75	100	50	70	90
		Resistance	60	70	90	70	90	120	70	100	130	70	90	120
3	Single-layer field windings with exposed copper	Thermometer	50	65	85	65	85	110	65	85	110	60	80	100
		Resistance	50	65	85	80	110	140	90	120	160	60	85	110
4	Cores and mechanical parts	Thermometer	40			55	75	100	55	75	100	50	70	90
5	Commutators and collector rings	Thermometer	55	65	85	65	85	110	65	85	110	65	85	110

* Generators having a 2-hour, 25 per cent overload rating will have temperature limits 10 degrees lower than as given in columns 10, 11, and 12 for the continuous load; and the same as given in columns 4, 5, and 6 at the end of the 2-hour overload.

Table II. Measured Temperature Rise Data

	Per Cent Load Current	Time	Per Cent Speed	Per Cent Volts	50-Hp Motor								25-Hp Motor							
					Hs		Res		Stc		Th		Hs		Res		Stc		Th	
					A*	B*	A	B	A	B	A	B	A	B	A	B	A	B	A	B
Armature	75	Cont.	100	100	36.5	40.0	28.0	34.5	28.5	31.0	30.5	31.0	32.5	35.0	32.5	46.8	24.5	28.0	25.0	29.0
	100	Cont.	100	100	50.0	51.0	43.0	39.5	41.0	39.5	38.5	40.0	41.0	37.0	42.5	52.5	28.5	26.0	28.0	35.0
	125	Cont.	100	100	64.5	65.0	56.5	59.5	49.0	52.5	48.0	51.0	56.0	67.5	57.0	86.6	39.5	43.5	40.0	46.5
	100	Cont.	50	50	55.5	61.0	48.5	50.5	45.5	46.0	44.0	45.5	43.5	58.0	41.5	61.0	29.5	36.0	30.5	40.5
	100	Cont.	100	50	34.5	40.0	32.5	34.0	31.0	26.5	31.5	29.0	36.0	34.0	35.5	43.0	24.0	28.5	24.5	28.5
	125	2 Hr.	100	100	65.0	62.0	52.0	57.5	49.5	57.5	51.0	55.5	55.5	59.0	57.0	74.0	38.5	45.3	38.0	48.5
	150	1 Hr.	100	100	80.5	79.0	73.0	69.0	61.5	55.5	62.5	59.5	75.0	72.0	76.0	88.0	47.0	48.5	48.0	54.5
	150	30 Min.	100	100	68.0	74.0	60.5	59.0	52.5	55.5	52.0	53.0	66.0	64.5	66.5	105.0	38.0	37.5	39.5	49.5
	200	15 Min.	100	100	84.5	90.0	87.0	80.0	57.5	56.9	61.5	56.0	91.0	81.5	94.0	114.0	45.0	66.5	47.5	55.5
Commutating field	75	Cont.	100	100	15.0	17.0	16.0	22.5	17.0	16.0	23.5	22.0	29.0	29.5	18.5	40.6	27.0	26.0	25.0	30.0
	100	Cont.	100	100	25.0	20.0	25.5	31.0	25.5	25.5	27.5	27.5	41.0	44.0	27.0	39.0	35.5	36.5	32.0	39.0
	125	Cont.	100	100	33.5	36.0	34.5	49.5	31.5	36.0	36.0	42.0	63.5	69.0	50.5	77.8	51.0	53.5	47.0	58.5
	100	Cont.	50	50	37.5	40.5	37.0	52.5	35.5	39.0	39.0	43.0	49.0	56.0	42.0	62.0	41.0	48.0	40.5	51.0
	100	Cont.	100	50	20.5	22.5	22.0	32.0	20.0	21.0	23.5	24.5	37.5	37.0	29.0	45.2	29.0	29.5	28.5	34.0
	125	2 Hr.	100	100	34.5	34.0	34.5	55.5	35.5	33.0	38.0	40.0	60.5	68.5	50.5	68.0	50.0	56.0	46.0	60.0
	150	1 Hr.	100	100	47.5	41.5	47.0	54.0	45.5	39.0	49.5	49.0	79.0	81.0	61.5	76.0	63.5	64.5	59.0	67.0
	150	30 Min.	100	100	40.5	28.0	38.5	48.0	37.0	26.0	42.0	40.0	58.5	65.0	47.0	73.0	50.0	53.5	43.5	56.0
	200	15 Min.	100	100	56.5	57.5	54.5	59.0	48.5	51.0	54.5	57.5	65.0	74.0	50.0	75.0	53.0	60.0	49.5	58.5
Shunt field	75	Cont.	100	100	45.5	47.5	41.2	40.5	24.0	26.5	26.5	32.5	52.5	49.0	42.3	53.1	36.0	30.5	33.0	40.5
	100	Cont.	100	100	52.5	54.0	48.5	53.0	32.5	31.5	33.5	36.0	54.0	58.0	42.0	49.4	38.5	34.0	34.0	43.5
	125	Cont.	100	100	56.0	52.0	54.5	59.5	40.0	38.5	40.0	46.5	60.5	58.5	51.0	63.6	45.0	42.0	41.0	49.5
	100	Cont.	50	50	60.0	62.5	56.5	50.5	42.5	46.0	41.0	48.5	57.0	58.3	46.5	53.6	41.0	39.0	37.5	48.5
	100	Cont.	100	50	18.5	10.5	15.0	12.0	20.0	23.0	24.5	20.0	18.5	17.5	14.5	16.9	17.0	20.0	18.5	23.0
	125	2 Hr.	100	100	58.0	63.0	53.5	50.5	40.5	46.0	41.0	45.0	57.5	60.5	48.5	56.5	43.5	44.5	41.0	50.5
	150	1 Hr.	100	100	60.0	60.0	41.5	48.0	49.0	49.0	49.5	48.5	53.5	52.5	44.0	47.5	45.0	45.0	43.0	46.0
	150	30 Min.	100	100	46.0	48.0	39.5	36.0	41.5	46.0	40.0	41.0	34.5	35.0	22.5	34.5	33.5	34.0	29.5	36.0
	200	15 Min.	100	100	37.5	39.0	32.0	26.5	51.0	64.0	48.5	48.0	19.0	20.0	18.0	18.0	23.0	44.0	26.5	26.5

	Per Cent Load Current	Time	Per Cent Speed	Per Cent Volts	10-Hp Motor								5-Hp Motor								½-Hp Motor			
					Hs		Res		Stc		Th		Hs		Res		Stc		Th		Hs	Res	Stc	Th
					A	B	A	B	A	B	A	B	A	B	A	B	A	B	A	B	A	A	A	A
Armature	75	Cont.	100	100	22.5	32.8	26.5	31.8			20.0	24.4	21.0	25.5	19.5	22.0			21.0	17.5	34.0	33.5		28.0
	100	Cont.	100	100	32.0	41.5	35.0	54.0			29.5	31.8	28.5	31.5	30.0	24.0			27.5	22.0	41.0	43.0		34.0
	125	Cont.	100	100	55.0	53.5	56.0	72.0			40.0	32.5	37.0	42.0	40.0	35.5			34.5	27.0	54.0	52.0		43.0
	100	Cont.	50	50	49.0	57.0	53.5	71.3			40.0	35.8	36.5	40.0	40.0	36.0			31.5	28.5	40.0	39.0		31.0
	100	Cont.	100	50	36.2	40.0	39.5	50.0			26.0	24.8	20.8	25.0	19.5	20.0			20.2	15.5	23.0	19.5		17.0
	125	2 Hr.	100	100	54.9	54.7	57.0	70.0			41.0	32.5	36.5	41.0	39.5	36.0			35.0	28.0	49.0	48.5		43.0
	150	1 Hr.	100	100	74.5	75.0	75.0	91.0			46.0	44.5	48.5	61.5	47.5	50.0			42.0	33.0	62.0	56.0		48.0
	150	30 Min.	100	100	66.0	52.0	65.0	71.0			38.0	29.5	45.0	46.0	42.5	45.5			36.5	32.0	53.0	52.0		40.0
	200	15 Min.	100	100	94.0	76.5	66.5	100.0			39.0	36.5	74.0	75.0	66.5	62.5			45.0	37.0	67.0	66.0		42.0
Commutating field	75	Cont.	100	100	25.0	28.0	24.5	40.7	18.9	23.7	14.0	22.5	21.5	20.0	19.0	20.0	18.0	16.0	20.0	16.5				
	100	Cont.	100	100	38.3	44.7	34.5	44.7	30.0	35.3	25.0	32.5	31.0	28.0	29.0	29.0	21.5	22.0	26.5	24.0				
	125	Cont.	100	100	60.0	64.3	56.5	60.0	44.0	46.5	37.0	44.5	46.5	41.5	42.5	39.0	27.5	29.5	35.5	32.5				
	100	Cont.	50	50	59.5	63.0	59.0	63.0	43.5	50.7	33.5	48.2	41.5	39.5	38.0	38.0	30.0	30.0	35.5	35.5				
	100	Cont.	100	50	36.5	41.0	36.0	28.0	27.5	29.3	21.5	28.0	24.0	24.0	22.5	20.0	15.0	15.5	18.5	18.0				
	125	2 Hr.	100	100	62.2	65.3	60.5	62.5	41.8	48.0	37.5	46.5	46.0	41.0	41.5	38.0	28.5	27.0	34.0	34.0				
	150	1 Hr.	100	100	83.0	85.0	75.5	82.3	56.7	60.5	40.0	57.0	59.0	52.0	54.0	51.0	35.5	34.0	45.5	41.0				
	150	30 Min.	100	100	64.0	62.8	63.5	52.0	45.2	42.5	30.0	42.0	49.0	48.0	46.5	48.0	29.0	32.0	37.5	35.5				
	200	15 Min.	100	100	73.0	73.5	70.5	67.5	51.0	58.3	32.0	42.2	61.0	54.0	55.0	52.0	31.0	32.5	39.0	39.0				
Shunt field	75	Cont.	100	100	45.0	54.2	49.0	51.0	29.9	36.0	25.0	35.0	55.0	53.5	50.5	48.0	24.5	24.0	27.0	21.0	47.0	41.5	30.0	19.0
	100	Cont.	100	100	54.0	57.7	54.0	50.5	35.0	40.0	28.5	37.2	58.0	54.5	53.0	49.0	27.5	27.5	29.5	24.0	48.0	42.0	31.0	21.0
	125	Cont.	100	100	59.2	62.0	58.5	55.8	41.8	48.5	35.5	40.5	61.0	57.0	54.0	49.5	31.5	32.5	34.5	26.0	53.0	47.0	36.0	24.0
	100	Cont.	50	50	69.5	81.5	69.5	67.0	47.4	53.0	42.0	52.3	68.5	67.0	59.0	62.0	35.0	36.5	38.0	34.0	54.0	44.0	38.0	25.0
	100	Cont.	100	50	18.9	23.0	11.0	22.9	17.8	19.4	14.5	17.7	16.5	13.5	17.5	13.5	13.0	10.5	14.8	10.0	12.0	9.0	8.0	5.0
	125	2 Hr.	100	100	61.2	60.0	60.5	59.1	39.0	43.0	35.5	41.6	62.0	57.0	57.5	55.0	32.5	30.5	34.0	26.5	51.0	46.5	33.0	23.0
	150	1 Hr.	100	100	62.5	63.5	59.0	59.6	46.0	45.0	39.0	43.0	62.0	57.0	56.5	55.0	34.5	31.5	38.0	28.0	52.0	48.0	36.0	25.0
	150	30 Min.	100	100	52.8	57.5	53.0	41.6	39.0	33.0	32.0	33.2	56.0	54.0	52.5	43.0	31.5	31.5	33.0	26.0	44.0	41.0	29.0	21.0
	200	15 Min.	100	100	41.8	35.5	44.0	30.0	35.3	26.0	30.0	22.3	38.0	41.0	43.5	39.0	30.0	26.0	28.0	20.0	38.0	32.0	27.0	22.0

HS = hot spot   Res = resistance   Stc = surface thermocouple   Th = thermometer   * A and B refer to tests

Table III. Ratio of Measured Temperature Rise Data

	Per Cent Load Current	Time	Per Cent Speed	Per Cent Volts	50-Hp Motor										25-Hp Motor									
					Res/Hs		Stc/Hs		Th/Hs		Res/Th		Stc/Th		Res/Hs		Stc/Hs		Th/Hs		Res/Th		Stc/Th	
					A	B	A	B	A	B	A	B	A	B	A	B	A	B	A	B	A	B	A	B
Armature	75	Cont.	100	100	0.77	0.86	0.78	0.78	0.84	0.78	0.92	1.11	0.93	1.00	1.00	1.34	0.75	0.80	0.77	0.83	1.30	1.61	0.98	0.97
	100	Cont.	100	100	0.86	0.78	0.82	0.77	0.77	0.78	1.12	0.99	1.06	0.99	1.04	1.42	0.70	0.70	0.68	0.95	1.52	1.50	1.02	0.74
	125	Cont.	100	100	0.88	0.92	0.76	0.81	0.74	0.78	1.18	1.17	1.02	1.03	1.02	1.28	0.71	0.64	0.71	0.69	1.42	1.86	0.99	0.94
	100	Cont.	50	50	0.88	0.83	0.82	0.75	0.79	0.75	1.10	1.11	1.03	1.01	0.95	1.05	0.68	0.62	0.70	0.70	1.36	1.51	0.97	0.89
	100	Cont.	100	50	0.94	0.85	0.90	0.66	0.91	0.73	1.03	1.17	0.98	0.91	0.99	1.26	0.67	0.84	0.68	0.84	1.45	1.51	0.98	1.00
	125	2 Hr.	100	100	0.80	0.93	0.76	0.93	0.78	0.90	1.02	1.04	0.97	1.04	1.03	1.25	0.69	0.77	0.68	0.82	1.50	1.53	1.01	0.93
	150	1 Hr.	100	100	0.91	0.87	0.76	0.70	0.78	0.75	1.17	1.16	0.98	0.93	1.01	1.22	0.63	0.67	0.64	0.76	1.58	1.61	0.98	0.89
	150	30 Min.	100	100	0.89	0.80	0.77	0.75	0.76	0.72	1.16	1.11	1.01	1.05	1.01	1.63	0.58	0.58	0.60	0.77	1.68	2.12	0.96	0.76
	200	15 Min.	100	100	1.03	0.89	0.68	0.63	0.73	0.62	1.41	1.43	0.93	1.02	1.03	1.40	0.49	0.82	0.52	0.68	1.98	2.05	0.95	1.20
Commutating field	75	Cont.	100	100	1.07	1.32	1.13	0.94	1.57	1.29	0.68	1.02	0.72	0.73	0.64	1.38	0.93	0.88	0.86	1.02	0.74	1.35	1.08	0.87
	100	Cont.	100	100	1.02	1.55	1.02	1.27	1.10	1.37	0.93	1.13	0.93	0.93	0.66	0.89	0.87	0.83	0.78	0.89	0.84	1.00	1.11	0.93
	125	Cont.	100	100	1.03	1.37	0.94	1.00	1.07	1.17	0.96	1.18	0.88	0.86	0.80	1.13	0.80	0.78	0.74	0.85	1.07	1.33	1.08	0.91
	100	Cont.	50	50	0.98	1.30	0.95	0.96	1.04	1.06	0.95	1.22	0.91	0.91	0.86	1.11	0.84	0.86	0.83	0.91	1.04	1.23	1.01	0.94
	100	Cont.	100	50	1.07	1.42	0.98	0.93	1.15	1.09	0.94	1.31	0.85	0.86	0.77	1.22	0.77	0.80	0.76	0.92	1.02	1.33	1.02	0.87
	125	2 Hr.	100	100	1.00	1.63	1.03	0.97	1.10	1.18	0.91	1.39	0.93	0.83	0.83	0.99	0.83	0.82	0.76	0.88	1.10	1.13	1.09	0.93
	150	1 Hr.	100	100	0.99	1.30	0.96	0.94	1.04	1.18	0.95	1.10	0.92	0.80	0.78	0.94	0.80	0.80	0.75	0.83	1.04	1.13	1.08	0.96
	150	30 Min.	100	100	0.95	1.71	0.91	0.93	1.04	1.43	0.92	1.20	0.88	0.65	0.80	1.12	0.85	0.82	0.74	0.86	1.08	1.30	1.15	0.96
	200	15 Min.	100	100	0.97	1.03	0.86	0.89	0.96	1.00	1.00	1.03	0.89	0.89	0.77	1.01	0.82	0.81	0.76	0.79	1.01	1.28	1.07	1.03
Shunt field	75	Cont.	100	100	0.91	0.85	0.53	0.56	0.58	0.68	1.55	1.25	0.91	0.82	0.81	1.08	0.69	0.62	0.63	0.83	1.28	1.31	1.09	0.75
	100	Cont.	100	100	0.92	0.98	0.62	0.58	0.64	0.67	1.45	1.47	0.97	0.87	0.78	0.85	0.71	0.59	0.63	0.75	1.24	1.14	1.13	0.78
	125	Cont.	100	100	0.97	1.14	0.71	0.74	0.71	0.89	1.36	1.28	1.00	0.83	0.84	1.09	0.74	0.72	0.68	0.85	1.24	1.28	1.10	0.85
	100	Cont.	50	50	0.94	0.81	0.71	0.74	0.68	0.78	1.38	1.04	1.04	0.95	0.82	0.92	0.72	0.67	0.66	0.83	1.24	1.11	1.09	0.80
	100	Cont.	100	50	0.81	0.73	1.08	1.39	1.32	1.21	0.61	0.60	0.82	1.15	0.78	0.96	0.92	1.14	1.00	1.31	0.78	0.73	0.92	0.87
	125	2 Hr.	100	100	0.92	0.80	0.70	0.73	0.71	0.71	1.30	1.12	0.99	1.02	0.84	0.93	0.76	0.74	0.71	0.83	1.18	1.12	1.06	0.88
	150	1 Hr.	100	100	0.69	0.80	0.82	0.82	0.83	0.81	0.84	0.99	0.99	1.01	0.82	0.90	0.84	0.86	0.80	0.88	1.02	1.03	1.05	0.98
	150	30 Min.	100	100	0.86	0.75	0.90	0.96	0.87	0.85	0.99	0.88	1.04	1.12	0.71	0.99	0.97	0.97	0.86	1.03	0.83	0.96	1.14	0.94
	200	15 Min.	100	100	0.85	0.68	1.36	1.64	1.29	1.23	0.66	0.55	1.05	1.33	0.95	0.90	1.21	2.20	1.39	1.33	0.68	0.68	0.87	1.06

	Per Cent Load Current	Time	Per Cent Speed	Per Cent Volts	10-Hp Motor										5-Hp Motor										1/5-Hp Motor				
					Res/Hs		Stc/Hs		Th/Hs		Res/Th		Stc/Th		Res/Hs		Stc/Hs		Th/Hs		Res/Th		Stc/Th		Res/-Hs	Stc/-Hs	Th/-Hs	Res/-Th	Stc/-Th
					A	B	A	B	A	B	A	B	A	B	A	B	A	B	A	B	A	B	A	B	A	A	A	A	A
Armature	75	Cont.	100	100	1.18	0.97			0.84	0.74	1.39	1.30			0.93	0.86			1.00	0.69	0.93	1.26			0.99		0.82	1.20	
	100	Cont.	100	100	1.09	1.30			0.92	0.77	1.19	1.70			1.05	0.76			0.96	0.70	1.09	1.09			1.05		0.83	1.26	
	125	Cont.	100	100	1.02	1.36			0.73	0.61	1.40	2.21			1.08	0.85			0.93	0.64	1.16	1.31			0.96		0.80	1.21	
	100	Cont.	50	50	1.09	1.25			0.82	0.63	1.34	1.99			1.13	0.90			0.89	0.71	1.27	1.26			0.98		0.78	1.26	
	100	Cont.	100	50	1.09	1.25			0.72	0.62	1.52	2.02			0.94	0.80			0.97	0.62	0.97	1.29			0.85		0.74	1.15	
	125	2 Hr.	100	100	1.04	1.28			0.75	0.59	1.39	2.15			1.08	0.88			0.96	0.68	1.13	1.29			0.99		0.88	1.13	
	150	1 Hr.	100	100	1.01	1.21			0.62	0.59	1.63	2.04			0.98	0.81			0.87	0.54	1.13	1.51			0.90		0.77	1.17	
	150	30 Min.	100	100	0.98	1.36			0.58	0.57	1.71	2.41			0.94	0.99			0.81	0.69	1.16	1.42			0.98		0.75	1.30	
	200	15 Min.	100	100	0.71	1.31			0.42	0.48	1.70	2.74			0.90	0.83			0.61	0.49	1.48	1.69			0.99		0.63	1.57	
Commutating field	75	Cont.	100	100	0.98	1.45	0.76	0.85	0.56	0.80	1.75	1.81	1.35	1.05	0.88	1.00	0.84	0.80	0.93	0.83	0.95	1.21	0.90	0.97					
	100	Cont.	100	100	0.90	1.00	0.78	0.79	0.65	0.73	1.38	1.37	1.20	1.09	0.94	1.03	0.69	0.79	0.85	0.86	1.09	1.21	0.81	0.92					
	125	Cont.	100	100	0.94	0.93	0.73	0.72	0.62	0.69	1.53	1.35	1.19	1.04	0.91	0.94	0.59	0.71	0.76	0.78	1.20	1.20	0.77	0.91					
	100	Cont.	50	50	0.99	1.00	0.73	0.80	0.56	0.76	1.76	1.31	1.30	1.05	0.92	0.96	0.72	0.76	0.86	0.90	1.07	1.07	0.85	0.85					
	100	Cont.	100	50	0.99	0.68	0.75	0.71	0.59	0.68	1.67	1.00	1.28	1.05	0.94	0.83	0.63	0.64	0.77	0.75	1.22	1.11	0.81	0.86					
	125	2 Hr.	100	100	0.97	0.96	0.67	0.74	0.60	0.71	1.61	1.34	1.11	1.03	0.90	0.93	0.62	0.66	0.74	0.83	1.22	1.12	0.84	0.79					
	150	1 Hr.	100	100	0.91	0.97	0.68	0.71	0.48	0.67	1.89	1.44	1.42	1.05	0.92	0.98	0.60	0.65	0.77	0.79	1.19	1.24	0.78	0.83					
	150	30 Min.	100	100	0.99	0.83	0.71	0.68	0.47	0.67	2.12	1.24	1.51	1.01	0.95	1.00	0.59	0.67	0.76	0.74	1.24	1.35	0.77	0.88					
	200	15 Min.	100	100	0.97	0.92	0.70	0.79	0.44	0.57	2.20	1.60	1.59	1.38	0.90	0.96	0.51	0.60	0.64	0.72	1.41	1.33	0.79	0.83					
Shunt field	75	Cont.	100	100	1.09	0.94	0.66	0.66	0.56	0.65	1.96	1.46	1.20	1.03	0.92	0.90	0.45	0.45	0.49	0.39	1.87	2.28	0.91	1.14	0.88	0.64	0.40	2.39	1.58
	100	Cont.	100	100	1.00	0.88	0.65	0.69	0.53	0.65	1.89	1.36	1.23	1.08	0.91	0.90	0.47	0.50	0.51	0.44	1.80	2.04	0.93	1.14	0.88	0.65	0.44	2.00	1.48
	125	Cont.	100	100	0.99	0.90	0.71	0.78	0.60	0.65	1.65	1.38	1.18	1.20	0.89	0.87	0.52	0.57	0.57	0.46	1.57	1.90	0.91	1.25	0.89	0.68	0.45	1.96	1.50
	100	Cont.	50	50	1.00	0.82	0.68	0.65	0.60	0.64	1.65	1.28	1.13	1.01	0.86	0.93	0.51	0.54	0.55	0.51	1.55	1.82	0.92	1.07	0.81	0.70	0.46	1.76	1.52
	100	Cont.	100	50	0.58	1.00	0.94	0.84	0.77	0.77	0.76	1.29	1.23	1.10	1.06	1.00	0.79	0.78	0.90	0.74	1.18	1.35	0.88	1.05	0.75	0.67	0.56	1.80	1.60
	125	2 Hr.	100	100	0.99	0.99	0.64	0.72	0.58	0.69	1.70	1.42	1.10	1.03	0.93	0.96	0.52	0.54	0.55	0.46	1.69	2.08	0.96	1.15	0.91	0.65	0.49	2.02	1.43
	150	1 Hr.	100	100	0.94	0.94	0.74	0.71	0.62	0.68	1.51	1.39	1.18	1.05	0.91	0.96	0.56	0.55	0.61	0.48	1.49	1.96	0.91	1.13	0.92	0.69	0.48	1.92	1.44
	150	30 Min.	100	100	1.00	0.72	0.74	0.57	0.61	0.58	1.66	1.25	1.22	0.99	0.94	0.80	0.56	0.58	0.59	0.48	1.59	1.65	0.95	1.21	0.93	0.66	0.51	1.95	1.38
	200	15 Min.	100	100	1.05	0.84	0.84	0.73	0.72	0.63	1.47	1.35	1.18	1.17	1.14	0.95	0.79	0.63	0.74	0.49	1.55	1.95	1.67	1.30	0.84	0.71	0.58	1.45	1.23

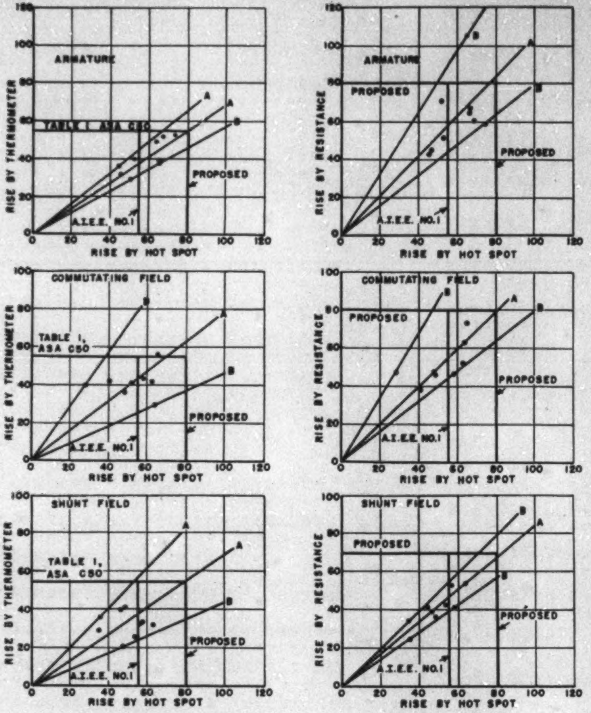

Figure 7. (top)

Figure 8. (center)

Figure 9. (bottom)

Figure 10. (top)

Figure 11. (center)

Figure 12. (bottom)

Figures 7 to 12. Thermometer, hot spot, and resistance data from Table II for 150 per cent, 30-minute operation

Curves B show limits, curve A is average

is used. These allowances measured by thermometer have given satisfactory life of electric apparatus for many years.

Therefore, there are two factors to keep in mind when setting up a table of limiting values covering all methods. First, it is not desirable to raise the recognized hot-spot limits. Second, it is not desirable to lower any of the thermometer limits which years of practice have proved satisfactory. The results show that the limits in both cases were originally established in a compatible manner so that a table of limiting values covering all methods can be set up based on the present results, without violating established general principles.

To correlate allowable maximum temperature rise by thermometer with the limiting hot-spot temperature rise, Figures 1, 2, and 3 are presented. These figures show for all tests made the rise measured by thermometer plotted against the hot-spot rise measured for each winding. Lines marked *B* show the limits of variation among the motors and the line marked *A* is the average result for all the motors.

From these figures a table of limiting values can be established. The vertical line representing the limiting hot-spot rise should be to the right of the test points but not higher than the established limit for the particular class of insulation. Since the test points are all for motors with class *A* insulation the vertical line in the figures is drawn correspondingly. The horizontal line representing the limiting thermometer rise is drawn to intersect the vertical line at line *A* or in order to be conservative, somewhat below it in some cases. It should also be higher than any of the test points.

To correlate allowable maximum temperature rise by resistance with the limiting hot-spot temperature rise, Figures 4, 5, and 6 are presented. The test points are plotted and the vertical and horizontal lines are drawn in the same manner as for Figures 1, 2, and 3.

Figures 7 to 12 inclusive give comparable data for 30-minute runs at 150 per cent load. These figures are used in the same way as before to determine limiting values for 30-minute rated machines.

Figures 13 to 18 inclusive give the data for 15 minute load runs at 200 per cent load. These figures are used to determine limiting values for 15 minute rated machines.

Discussion of Results

A number of questions arise about the data and results. For example, in the case of the 25- and 10-horsepower motors, Tables II and III show higher temperature rise measured by resistance than by the hot-spot thermocouples embedded in the armature winding. This result is caused by normal variations experienced in using the resistance method on armature windings where the mean temperature of the winding is nearly the same as the hot-spot temperature. This is the case for these two particular motors. Figures 4 to 6, 10 to 12, and 16 to 18 inclusive in each instance, show the variation in results which may be expected using the resistance method. Generally speaking, the lower the winding resistance and the lower the temperature rise, the greater is the variation.

Although the data show higher temperature rise by resistance than the hot-spot temperature rise in some instances for the 10-horsepower and 25-horsepower motors, the hot-spot temperature rise is normal in relation to the temperature rise measured by thermometer in the same instances. This fact indicates that the values for hot-spot temperature rise are reasonably accurate. When the data are used to determine allowable limits by the method shown in Figures 1 to 18 inclusive, the effect of inaccuracy of any particular test point is reduced.

Another point in question is the increase in the allowable hot-spot temperature from 55 to 65 degrees shown in Figures 3 and 6, and in Table I of this report. The figures show that there is no choice unless the time-honored allowance of 40 degrees centigrade rise by thermometer is to be lowered. It appears reasonable in the case of stationary field coils not to change the thermometer standard and to recognize the corresponding hot-spot temperature rise as 65 degrees centigrade.

A third question arises in regard to Figures 7 to 12 inclusive, where the hot-spot temperature rise is recognized as 80 degrees centigrade. This is done to hold onto the standard of 55 degrees centigrade as the temperature rise allowed by thermometer for short time rated apparatus consistent with AIEE standard number 1A[4] and Table I of ASA-C50.[1] The test data show that 80 degrees centigrade is the corresponding hot-spot temperature rise. This higher value is justified for the reasons given in AIEE standard number 1A, paragraph *1A-9*, explaining that the additional temperature rise is allowed to secure approximately the same life for short time rated machines as for continuous rated ones.

For the same reasons the hot-spot temperature rise for machines rated 15 minutes or less is recognized as 100 degrees centigrade, shown in Figures 13 to 18 inclusive, except for shunt field coils, Figures 15 and 18, where the hot-spot temperature rise is recognized as 80 degrees centigrade, corresponding to 55 degrees centigrade rise by thermometer and 70 degrees centigrade by resistance.

It should be recognized that on very brief load runs the surface of the shunt field winding is generally heated by radiation from the commutating field winding, causing the surface temperatures to be as hot as the mean temperature of the winding. It is not recommended that for class *A* insulated, short time rated

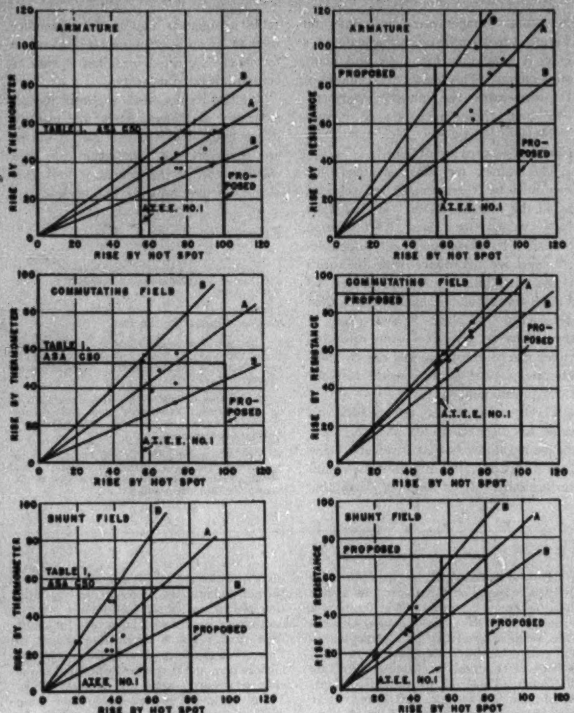

Figure 13. (top)

Figure 14. (center)

Figure 15. (bottom)

Figure 16. (top)

Figure 17. (center)

Figure 18. (bottom)

Figures 13 to 18. Thermometer, hot spot, and resistance data from Table II for 200 per cent, 15-minute operation

Curves B show limits, curve A is average

Table IV. Some Basic Test Conditions

Run Number	50-Horsepower Motor		25-Horsepower Motor		10-Horsepower Motor		5-Horsepower Motor	
	Test A	Test B	Test A	Test B	Test A	Test B	Test A	Test B
	Current for Runs in Order Appearing on Temperature Rise Chart							
1	137	136.5	68	69.4	28.65	28.5		
2	181.8	182	91	91.87	38.2	38		
3	227.4	230.4	114	114.8	47.75	47.5		
4	182.8	181	90.9	91.84	38.2	38	(Same for both)	
5	181.8	181	90.9	91.19	38.2	38		
6	227.4	227.5	114	114.8	47.75	47.5		
7	272.7	273	137	137.9	57.3	57		
8	272.7	273	137	137.9	57.3	57		
9	364	364	182	182.96	76.4	76.0		
	Cold Resistances							
Armature	0.007105	0.007107	0.05429	0.05433	0.2170	0.1752	0.4770	0.4497
(Degrees centigrade)	25	24	23.2	25	25.5	28	21.5	25
Shunt field	167	163.6	226	223.2	200	207.21	360.5	362
(Degrees centigrade)	26.5	24	25.4	25	27.5	28	27.5	25
Series field	0.003785	0.0045	0.005545	0.006162				
(Degrees centigrade)	25	24	231	25				
Commutating field	0.006615	0.006855	0.00994	0.01040	0.0509	0.05056	0.0885	0.0897
(Degrees centigrade)	25	24	23	25	25.5	28	23	25

machines a temperature rise by thermometer or resistance be allowed which is higher than that corresponding to 80 degrees centigrade rise at the hot spot.

Figures similar to 1 to 18 may be plotted for the 1-hour and 2-hour test runs. The results for these correspond closely to Figures 1 to 6 inclusive, for continuous load tests. That is, lines *A* and *B* of Figures 1 to 6 represent the 1-hour and 2-hour tests although the vertical and horizontal lines representing the maximum allowable temperatures should be changed to allow for the short time rating rather than continuous rating.

Basic test conditions are given in Table IV to help answer anticipated questions about variations between the test results.

Conclusion

The conclusions which have been drawn from the test results reported are given in Table I of this report. This table is formed by tabulating the values for the horizontal temperature rise lines on Figures 1 to 18 inclusive, as basic data for class *A* insulation for open and short time ratings. This results in no change in the temperature rise values by thermometer from those given in the present Table I of ASA-C50.[1] New values for rise by resistance are obtained.

The values for class *B* insulation measured by thermometer are retained as in the present Table I of ASA-C50. New values for class *H* insulation measured by thermometer are added determined in accordance with the principles of AIEE standard number 1.[3] Values measured by resistance are then determined for class *B* and class *H* insulations to give the same ratio between rise by resistance and rise by thermometer as was found from the tests for class *A* insulation.

Therefore, from the test results this table has been compiled and the committee recommends that it replace Table I of ASA-C50 (after due discussion and verification). It is believed that this table adequately covers the resistance method as an alternative test procedure for short-time rated machines as well as continuous rated machines.

The test results verify the interchangeable use of thermometers and surface thermocouples so that no special values are necessary for the latter. A free choice of either instrument is indicated except for motors below one horsepower.

References

1. Rotating Electrical Machinery. *ASA-C50*, American Standards Association (New York, N. Y.), 1943.

2. Test Code for D-C Machines. AIEE Standard Number 501, July 1941.

3. General Principles Upon Which Temperature Limits are Based in the Rating of Electric Machines and Apparatus. AIEE Standard Number 1, June 1947.

4. Report on General Principles for Rating of Electrical Apparatus for Short-Time Intermittent or Varying Duty. AIEE Standard Number 1A, September 1941.

5. The Application of Class B Insulation to Auxiliary-Type D-C Motors in Severe Duty Service, F. A. Compton, Jr. AIEE Transactions, volume 59, 1940, pages 828–34.

Discussion

B. H. Caldwell and **G. H. Gunnoe** (General Electric Company, Schenectady, N. Y.): Test results of temperature rise as measured by: embedded thermocouple; resistance; surface thermocouple; and surface thermometer are given for motors rated 1/2, 5, 10, 25, and 50 horsepower in the report. Based on the results of these tests, Table I is presented, which includes limits of temperature rise as measured by thermometer and by resistance. It is finally recommended by the committee that Table I of the report replace Table I of ASA-C50 (See Table I of this discussion).

Serious consideration of this proposal raises two questions. First, do test results indicate the resistance measurement to be a better method than the surface thermometer? In the discussion presented by M. A. Baker, a table is given (Table III of the discussion) which demonstrates that more consistent results were obtained in this series of tests by thermometer than by resistance. This result favors the use of the surface thermometer. However, the resistance method does, on the average, approach the hot-spot temperature more closely than does the surface thermometer. This is particularly true in the case of short time overloads. In this respect the resistance method is to be preferred.

The second question which arises is: are the results typical for all sizes of d-c machines? Since Table I of ASA-C50 applies for essentially the complete range in sizes and ratings of d-c machines, this question is of utmost importance. Data for medium size machines has been given to the committee and is summarized in M. A. Baker's discussion. Data for armored motors was given in a paper by F. A. Compton, Jr. in 1943.[1] Based on this paper and similar data on large d-c motors and generators, a Proposed New Table for "Limiting Observable Temperature Rise," was presented to the committee by T. M. Linville in 1945. A copy of this table is included with this discussion (Table II of the discussion). All of these data are in radical disagreement with the proposed revision of Table I, ASA-C50, now proposed by the committee (See Table I of the report).

Figure 1 of the discussion shows additional data which have been accumulated from tests taken on large d-c machines. Results are shown for machines with class *A*, *B*, and *H* insulation. All machines were larger than 1 horsepower per rpm. These data have been screened to eliminate questionable results, and it is felt that the points indicated represent best application of test procedure. All data represent continuous heat runs; none are for short time runs. The straight line shown in Figure 1 of the discussion, approximates the median line, and it is interesting to note the close agreement with the Proposed New Table. While it is clear both from these data, and from the data presented in the committee report, that there is no fixed ratio relating rise by resistance and rise by thermometer, it is evident that the average ratio for large machines differs greatly from that proposed in Table I of the report.

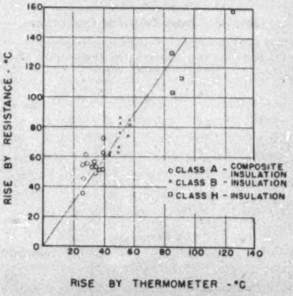

Figure 1. Comparison of armature temperature rise by resistance and by thermometer for large d-c machines

It is thus apparent that the proposed revision of Table I, ASA-C50, is not consistent with the present standards for large d-c machines. This proposal is equivalent to revising the present standards to limit rise by thermometer to 30 degrees centigrade for large, class *A* machines. The present practice has been in force for many years, and its successful operation needs no defense. Therefore, it would seem mandatory that the proposed revision be modified to permit limits of rise by resistance for large machines as indicated in the Proposed New Table (Table II of the discussion).

Even though the resistance method appears to be less accurate than the surface thermometer, the fact that it more nearly approaches the hot-spot temperature lends encouragement to its use. Of the various methods used, the embedded thermocouple has the dual advantage of accuracy and of allowing measurement of a temperature which closely approaches the hot spot value. Use of this technique, or a modification thereof, might prove feasible for large machines; just as in the case of large a-c machines the use of an embedded temperature detector is recognized and used.

Table I. Limiting Observable Temperature Rise

Reproduced from Page 10, ASA-C50-1943

Item	The temperature rises in degrees centigrade in this table apply to the several classes of machines as given at the heads of the respective columns Machine Part	Method of Temperature Determination to Be Employed	General Purpose Generators and Motors	Totally Enclosed, Totally Enclosed Fan-cooled, Explosion-proof, Waterproof, Dust-tight, and Submersible Motors		Generators Having a Nominal Rating at End of 2-Hour Overload		Generators Having a 2-Hour 25 Per Cent Overload Rating at Continuous Load		At End of 2-Hour Overload		Motors and Generators Other Than Col. 1–9 Inclusive	
			Class A Insulation Col. 1	Class A Insulation Col. 2	Class B Insulation Col. 3	Class A Insulation Col. 4	Class B Insulation Col. 5	Class A Insulation Col. 6	Class B Insulation Col. 7	Class A Insulation Col. 8	Class B Insulation Col. 9	Class A Insulation Col. 10	Class B Insulation Col. 11
1	Armature windings, and all windings other than 2 and 3	Thermometer See 2.054	40	55	75	55	75	40	60	55	75	50	70
2	Shunt field windings	Thermometer See 2.054	40*			55*	75*	40*	60*	55*	75*	50*	70*
		Resistance See 2.055	50*	60	80	65*	85*	50*	70*	65*	85*	60*	80*
3	Single-layer field windings with exposed uninsulated surfaces and bare copper windings	Thermometer See 2.054	50	65	85	65	85	50	70	65	85	60	80
4	Cores and mechanical parts in contact with or adjacent to insulation	Thermometer See 2.054	40			55	75	40	60	55	75	50	70
5	Commutators and collector rings**	Thermometer See 2.054	55†	65	85	65	85	55	70	65	85	65	85
6	Miscellaneous parts (such as brush holders, brushes, pole tips, and so forth) may attain such temperatures as will not injure the machine in any respect.												

* The method of temperature determination to be used shall be optional with the manufacturer unless otherwise agreed upon. Only one method of temperature determination shall be required in any particular case.

** The class of insulation refers to insulation affected by the heat from the commutator, which insulation is employed in the construction of the commutator or is adjacent thereto.

† The limiting observable temperature rise for commutators of generators for electrolytic service shall be 50 degrees centigrade.

Table II. Proposed New Table

Item	The temperature rises in degrees centigrade in this table apply to the several classes of machines as given at the heads of the respective columns Machine Part	Method of Temperature Determination	General Purpose Generators and Motors		Totally Enclosed, Totally Enclosed Fan-cooled, Explosion-proof, Waterproof, Dust-tight, and Submersible Motors Continuous Rated		Motor and Generators Rated One Hour		Motors and Generators Rated One-Half Hour		Generators Having a 2-Hour 25 Per Cent Overload Rating at Continuous Load		Generators Having a 2-Hour 25 Per Cent Overload Rating and Generators Having a Nominal Rating at End of 2-Hour Overload		Special Purpose Dripproof and All Motors and Generators Other Than Col. 1–12 Inclusive Continuous Rated	
			Class A Insulation Col. 1	Class B Insulation Col. 2	Class A Insulation Col. 3	Class B Insulation Col. 4	Class A Insulation Col. 5	Class B Insulation Col. 6	Class A Insulation Col. 7	Class B Insulation Col. 8	Class A Insulation Col. 9	Class B Insulation Col. 10	Class A Insulation Col. 11	Class B Insulation Col. 12	Class A Insulation Col. 13	Class B Insulation Col. 14
1	Armature windings, wire field windings, and all windings other than 2	Resistance See 2.055	60		70	100	80	110	90	125	60	90	75	105	70	100
		Thermometer See 2.054	40		55	75	55	75	55	75	40	60	55	75	50	70
2	Single-layer field windings with exposed uninsulated surfaces and bare copper windings	Resistance See 2.055	60		70	100	80	110	90	125	60	90	75	105	70	100
		Thermometer See 2.054	50		65	85	65	85	65	85	50	70	65	85	60	80
3	Cores and mechanical parts in contact with or adjacent to insulation	Thermometer See 2.054	40				55	75	55	75	40	60	55	75	50	70
4	Commutators and collector rings	Thermometer See 2.054	55	75	65	85	65	85	65	85	55	70	65	85	65	85
		Pyrometer	65	85	75	100	75	100	75	100	65	85	75	100	75	100
5	Miscellaneous parts (such as brush holders, brushes, pole tips, and so forth) may attain such temperatures as will not injure the machine in any respect.															

Any discussion of allowable temperature rise must recognize the type or class of insulation. The true limit is of course set by that value of temperature which permits satisfactory life. Thus, it is common practice to use a composite insulation for armature coils for large d-c machines; the insulation around the conductor and the main portion of the coil insulation being composed of mica. Even though rated as class *A*, for such an insulation the hot-spot temperature rise can safely approach the class *B* value, provided the temperature of the class *A* material which forms the external covering of the coil does not exceed its safe value. In this way composite insulation has been available for use in compensating for the little recognized yet wide discrepancy between temperature rise as measured by surface thermometer and the actual hot-spot value.

The present accelerated use of new synthetic materials offers the prospect of insulating materials with temperature endurance limits in between class *A* and *B* materials, as well as extending the limit recognized heretofore for class *B* materials. These developments promise new latitude for the design engineer, and it is to be hoped that revision of the standards can be accomplished so that efficient use of these new materials will be promoted rather than discouraged.

REFERENCE

1. TEMPERATURE LIMITS AND MEASUREMENTS FOR RATING OF D-C MACHINES, F. A. Compton, Jr. ELECTRICAL ENGINEERING (AIEE TRANSACTIONS), volume 62, December 1943, pages 780–85.

John L. Fuller (Reliance Electric and Engineering Company, Cleveland, Ohio): The report presents data on a well-conceived series of tests designed to establish suitable limits of temperature rise by resistance method. The results raise many questions, some of which were answered in the report.

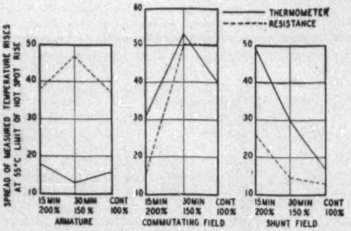

Figure 2. Spread of measured temperature rises versus hot spot

A most glaring result is the evidence of inability, even with the most carefully controlled laboratory techniques, to achieve anything approaching consistency in relationship of hot spot to temperature measurement by resistance or thermometer. This is particularly true for armature rise by resistance, which shows great variations.

As an aid to evaluating the spread of results, Figure 2 of the discussion shows the spread of measured temperature rise at the 55 degrees centigrade limit of hot-spot rise for each of the conditions represented in Figures 1 through 18 in the report. Data for Figure 2 of the discussion were secured from the points at which the upper and lower lines on Figures 1 through 18 cross the vertical 55 degree centigrade line.

From study of Figure 2 of the discussion, the following conclusions may be reached:

1. It is highly questionable, in view of the wide discrepancies in test results (about $2^1/_2$ times as much as by thermometer) whether or not a standard should be established for armature rise by resistance.

2. Shunt field rise can be measured more accurately by resistance method than by thermometer, and a standard should be established.

3. Commutating field rise can be measured about as well by resistance as by thermometer, and a standard for this is probably in order.

F. R. Terrant (Reliance Electric and Engineering Company, Cleveland, Ohio): Table I of the subcommittee's report proposes for motors rated 30 minutes to two hours a limiting observable temperature rise of 55 degrees centigrade by thermometer and 80 degrees centigrade by the resistance method for class *A* insulation. A study of tests on 26 30-minute and 60-minute duty motors, selected at random from our regular production test files, shows that the temperature rises by resistance range from 48 per cent above to 60 per cent below the rises by thermometer. Test department tests, although not as accurately made as the laboratory tests given in the report, do indicate that the majority of short-time rated motors meeting a 55 degree centigrade rise by thermometer would also meet the 80 degree centigrade rise by resistance which is 45 per cent above the 55 degrees centigrade by thermometer.

The temperature rise limits proposed for generators having a 2-hour 25 per cent overload rating as described in the footnote of Table I of the report would limit class *B* machines to 60 degrees centigrade by thermometer for the continuous rating. It would seem that the temperature rise is unduly limited in this instance and full advantage of class *B* materials would not be realized.

It is suggested that consideration be given to using column 11 directly for the continuous rating, and column 5 for the overload rating.

P. L. Alger (General Electric Company, Schenectady, N. Y.): This report gives important and interesting data relating the internal temperatures of small d-c machines to the measured values. Table I of the report summarizes the information in a very clear way, providing a basis for the intelligent development of better d-c machine standards.

There are three points I wish to emphasize in regard to Table I.

The purpose of the table is to limit the hot-spot temperatures to permitted values for each type of machine and service. The present method of setting temperature limits measured by thermometer is now shown to be a very crude way of accomplishing this, as the hot-spot temperature varies widely for a given thermometer rise, depending on the type of machine, and the duration of the test.

It is clear that the resistance rise method is preferable, as it gives a much closer approximation to the hot-spot temperature; but here also there are wide variations. The proposed new table (see Table I of the report) gives resistance rise values fairly equivalent to the thermometer values for the small or moderate sized open machines included in the test program given in the report, but the values do not apply to large or highly ventilated machines.

For, large machines with naturally high velocities of cooling air, and also highly ventilated small machines, will have considerable greater values of rise by resistance for the same thermometer rise than shown in Table I, due to the greater rate of heat flow through the insulation. I believe, for example, that many large continuous rated machines with less than 70 degrees centigrade rise by thermometer have actual values of armature rise by resistance of 100 degrees centigrade, or even more, as compared with the 85 degrees centigrade value given in column 11 of the table. Likewise, moderate sized machines, with short-time ratings of 15 minutes or less, which meet 75 degrees centigrade rise by thermometer, may have armature winding temperatures by resistance of the order of 150 degrees centigrade, as compared with the 120 degrees centigrade value given in column 8 of the table.

I believe that the resistance method should be recognized in the standards as an optional, but not a mandatory, way of measuring temperature, at least for moderate sized, and enclosed, d-c machines. The test data show wide variations in the temperature values found by different methods and different observers, the variations in the resistance values being generally somewhat greater than those between thermometer values. The resistance method is increasingly difficult to use, the lower the ohmic resistance to be measured, so that its regular use on large armatures may be a long time in coming. Nevertheless, I believe that the resistance method will be as reliable in most cases and more reliable in many than the thermometer method, besides giving temperatures much closer to the hottest-spot values. A statistical analysis of the ratios of resistance to thermometer and to hot-spot rises given in the report indicates that the errors in the resistance method are due largely to a displacement of all the values from the expected level, rather than errors in individual readings. This suggests that great improvements can be made with adequate experience and equipment.

In undertaking to define the desired hot-spot limits by resistance rise values, we should give the designers freedom to continue practices known to be satisfactory with existing thermometer limits. This in turn will permit higher hot-spot temperatures than the conventional limits of 105 and 130 degrees centigrade for class *A* and *B* materials; and it also will allow higher operating temperatures in some types of machines, for which the thermometer rise values have been unduly limiting in the past.

In undertaking this necessarily long range program of establishing new resistance rise temperature limits, three points need to be kept in mind:

1. In choosing the new resistance rise values, consideration should be given to the factors of overload capacity, temperature creep, stalled time limits, thermal expansion, and commutation and bearing limits, as well as the temperature life of the insulation itself, in the expected service. AIEE Standard Number 1[1] fully recognizes this need for choosing temperature limits on a broad economic basis, and encourages the adoption of different limiting values for different types of apparatus or service.

2. Existing AIEE standards for control equipment have for many years allowed 85 degrees centigrade rise by resistance with a 40 degree ambient, or 125 degrees centigrade hot-spot temperature, for class *A* coils in continuous operation. Also, the AIEE railway standards have for many years recognized 120 degrees centigrade rise by resistance for armatures, and 130 degrees centigrade rise by resistance for fields over a nominal 25 degrees centigrade ambient, or 145 to 155 degrees centigrade hot-spot temperature, for class *B* insulation. Thus, existing standards now recognize a spread of 20 to 30 degrees in hot-spot limits for the same insulation class, depending on the type of apparatus concerned.

3. I believe that the duty factor method of rating d-c machines for short-time or intermittent service should ultimately replace the present short-time rating methods in the standards. For, both the wide range of permissible values of hot-spot temperature for short-time rated machines, and the inaccuracies in measuring the rapidly changing temperature in such cases, make it impractical to set any new limiting values for them. On the other hand, the duty factor method of rating, in which the machine is run for definite time periods with intervals of rest between, allows the machine to reach a limiting temperature that is measured readily, and should be roughly the same for a wide variety of ratings. This method is now well recognized in the standards of the Iron and Steel Engineers, and, therefore, has the backing of long experience.

Summing up, I hope that the AIEE machinery committee and the standards committee will carry the development of new d-c machine standards forward with vigor, looking to improved techniques in the resistance method of measurement; to the recognition of the resistance method as the basic standard; the adoption of higher temperature limits by resistance, chosen on an economic basis; and the adoption of the duty factor method of rating in place of the short-time method.

Reference

1. See reference 3 of the report.

M. A. Baker (General Electric Company, Fort Wayne, Ind.): The motors tested in this AIEE test program are small machines and it is reasonable to expect different data on larger units which run at higher peripheral speeds and are often better ventilated. In fact, this is the actual case and a table of limiting temperature rise values covering d-c machines broadly must take into account experience with large machines and test results obtained on them.

The proposed new table (see Table I of the report) based on the data obtained from this test program proposes 50 degree centigrade rise by resistance and 40 degree centigrade rise by thermometer for armatures of class *A* continuous rated general purpose machines. For special purpose class *A* continuous rated machines, the proposed rise by resistance limit for armatures is 60 degrees centigrade. The ratio of rise by resistance to rise by thermometer is 1.25 for the armatures of general purpose class *A* machines, and 1.2 for class *A* special purpose machines. Five years ago, the General Electric Company submitted to this committee a summary of a number of heat runs taken on larger machines. These data indicated a rise by resistance to rise by thermometer ratio of 1.4 for continuous rated class *A* machines, and 1.6 for continuous rated class *B* machines. At that time, ratios of 1.4 and 1.43 were recommended for class *A* and *B* machines respectively. It appears that the new proposed table limits the rise by resistance on armatures to too low a value based on operating experience, and data obtained on larger units over a long period of time.

Table III of the discussion shows the per cent variation in the heat run results of the two independent tests made on the four motors. The per cent variation is calculated by taking the difference in temperature rise between heat runs *A* and *B*, and dividing the difference by the average temperature rise.

Table III. Per Cent Variation

Rating Horse-power	Armature, Res.	Armature, Th.	Commutating Field Res.	Commutating Field Th.	Shunt Field Res.	Shunt Field Th.
50	7.7	5.3	25.4	5.2	11.3	10.8
25	28.8	18.8	41.1	20.1	18.1	17.6
10	25.2	14.5	16.5	30.1	19.2	19.2
5	9.6	19.5	5.4	6.3	10.1	29.2
Average per cent variation	17.8	14.5	22.1	15.4	14.7	19.2

One of the conclusions that can be drawn from the data in Table III of the discussion, is that the temperature rise on low resistance circuits (armature and commutating fields) can be measured more consistently, by independent testers, by the thermometer method than it can by the resistance method. This is true in spite of the extraordinary care and laboratory equipment used in making these tests. If ordinary commercial test technique had been used, the resistance data would undoubtedly have shown still more variation.

Rise by resistance is a specialized tool by which we can get additional knowledge of our machines. However, standard commercial test practice should be limited to the thermometer method because of the special equipment and technique required and because of the relatively greater care that must be exercised to get equally reliable results. The test data show that the ratio of thermometer temperatures to internal hot-spot temperatures is as definite as is the ratio of resistance temperatures to hot-spot temperatures. Therefore, with proper allowances set up, the thermometer method is a reliable measure of internal hot-spot temperatures.

Since the resistance of the shunt field circuit is much higher than that of the armature and commutating field, the problem of contact resistance is not present. The resistance of shunt fields can be measured more accurately than that of the armature and commutating fields, so that rise by resistance is a reliable test for shunt fields. The foregoing data indicate that rise by resistance can be checked more consistently on shunt fields than can rise by thermometer. Based on many years of experience, the proposed increase in shunt field temperatures is entirely reasonable in the light of modern insulation. The increased rise by resistance limits proposed in the new table I for shunt fields is heartily indorsed.

Table IV. Ratio of Temperature Rise by Hot Spot to Temperature Rise by Resistance

Taken from Tests on Five Motors, Average Values

Armature	
Full load continuously	=0.985
25 per cent overload for 2 hours	=0.972
50 per cent overload for 1 hour	=1.031
100 per cent overload for 15 minutes	=1.005
Commutating Pole Coils	
Full load continuously	=1.038
25 per cent overload for 2 hours	=1.001
50 per cent overload for 1 hour	=1.039
100 per cent overload for 15 minutes	=1.065
Shunt Windings	
Full load continuously	=1.118
25 per cent overload for 2 hours	=1.093
50 per cent overload for 1 hour	=1.14
100 per cent overload for 15 minutes	=1.12

H. E. Stokes (Westinghouse Electric Corporation, East Pittsburgh, Pa.): The tests on which this report are based, were made on small industrial motors ranging from 1/2 to 50 horsepower at 1,750 rpm on standard open-type general-purpose motors. Table Number I of ASA C-50 1943 (See Table I of discussion), governs existing temperature rises for all classes of d-c rotating machines larger than 560 watts, and supersedes AIEE tables formerly applicable. Based on the tests made on these five relatively small motors, the report establishes ratios of rise by resistance/rise by hot spot; rise by resistance/rise by thermometer and so forth. Table III of the report tabulates all of these ratios which are obtained from the temperature rises given in Table II of the report. I have changed the form of these ratios to those shown in Table IV of the discussion, averaging the test results obtained on the five motors. The temperature rises obtained by thermometer and those obtained

Table V. Ratio of Hot-Spot Temperature Rise to Thermometer Temperature Rise

Tests Taken on Five Motors—50, 25, 10, 5 and 1/2 Horsepower Ratios Given are Average of the Five Motors

Armature	
Full load continuously	=1.23
25 per cent overload for 2 hours	=1.23
50 per cent overload for 1 hour	=1.42
100 per cent overload for 15 minutes	=1.7
Commutating Pole Coils	
Full load continuously	=1.16
25 per cent overload for 2 hours	=1.2
50 per cent overload for 1 hour	=1.07
100 per cent overload for 15 minutes	=1.396
Shunt Coils	
Full load continuously	=1.81
25 per cent overload for 2 hours	=1.72
50 per cent overload for 1 hour	=1.56
100 per cent overload for 15 minutes	=1.27

by surface thermocouple on the average may be taken as interchangeable and surface thermocouples are hereafter referred to as thermometer readings.

An inspection of Table IV of the discussion, which shows the ratio of hot-spot rise to/temperature rise by resistance for the armature, shows a ratio of 1.0 ± 3 per cent. For the commutating pole coils the ratio of hot-spot rise to/temperature rise by resistance is 1.0 plus a maximum of $6^{1}/_{4}$ per cent minus nothing. The shunt field coils show the only significant departure, where this ratio varies from 1.093 to 1.14.

Table V of the discussion shows corresponding values of 1.0 plus 23 per cent, plus 70 per cent for the armature, 1.0 plus 7 per cent, plus 40 per cent for the commutating pole coils and 1.0 plus 27 per cent, plus 81 per cent for the shunt fields.

In a similar manner Table VI of the discussion shows for these values armature, 1.0 plus 27 per cent, plus 76 per cent, commutating pole coils 1.0 plus 12 per cent, plus 36 per cent and shunt coils 1.0 plus 18 per cent, plus 64 per cent.

Tables IV, V, and VI of the discussion show the highest ratio of the fraction of hot-spot temperature rise to/thermometer-temperature rise, or the fraction, resistance-temperature rise to/thermometer-temperature rise to be 1.81. It should be remembered, however, that these ratios are obtained on small size industrial machines. If taken on large machines, the ratio fraction of hot spot rise to/rise by thermometer may be much greater, perhaps 50 per cent or more. The writer of these comments, therefore, feels that the values obtained on these small size machines cannot be used safely to amend temperature rise of Table I of ASA, C-50, 1943, which covers all sizes of machines above 560 watts.

Table VI. Ratio of Temperature Rise by Resistance to Temperature Rise by Thermometer

Tests Taken on Five Motors, Average Values

Armature	
Full load continuously	= 1.27
25 per cent overload for 2 hours	= 1.33
50 per cent overload for 1 hour	= 1.42
100 per cent overload for 15 minutes	= 1.76
Commutating Pole Coils	
Full load continuously	= 1.12
25 per cent overload for 2 hours	= 1.24
50 per cent overload for 1 hour	= 1.25
100 per cent overload for 15 minutes	= 1.36
Shunt Coils	
Full load continuously	= 1.64
25 per cent overload for 2 hours	= 1.56
50 per cent overload for 1 hour	= 1.4
100 per cent overload for 15 minutes	= 1.18

Past and present AIEE and ASA rules have probably shown a hot-spot temperature higher than the measured temperature rises by thermometer. This report shows that the difference between measured temperature rises and hot-spot temperature rises is appreciably higher than the values that have been used in the past. The writer would like to point out that over a period of decades, machines which have met the measured temperature rises have been operating with hot-spot temperatures actually higher than the values which have been set up in the past by standards for measured temperature rises with satisfactory operation from the standpoint of insulation, life, and general performance. Therefore, if the rules are changed to permit higher hot-spot temperatures, we would simply be recognizing conditions under which machines have been operating in the past, which conditions have actually been at higher temperatures than were considered in the past.

In this same connection most industrial-type machines have general ratios between armature diameters and core lengths. Large size power d-c machines, particularly motors, may have very large differences in the ratio of armature diameters to core length. Some machines have an armature diameter in the neighborhood of 4 feet and may have core lengths as short as 8 inches and as long as 48 inches. Obviously the hot-spot temperature distributions in the armature copper portion that is embedded in the slots, would be entirely different in a machine whose core length is six times as long as another machine. The end winding extensions in these machines of two extreme core lengths could be identical.

The new suggested Table I in the report should be restricted to small industrial-type machines only. Before the same kind of table is made available for large size industrial d-c machines, a considerable amount of tests and investigation will have to be carried out on the range of sizes of machines encountered for machines of this type, to determine what the actual hot-spot temperatures encountered are. Such tests are not as easy to make as in the case of the small industrial machines, since these large machines cannot be made for test and shipped to the various manufacturers for interchanging test procedures. They must be made on production machines going through for customers, and such procedure will take a long time, not only to obtain tests, but to correlate data and secure the same type of information.

F. M. Scott (Allis-Chalmers Manufacturing Company, Milwaukee, Wis.): The entire test program concerned the testing of motors up to and including 50 horsepower. The results obtained and the conclusions outlined in the report appear significant and logical. However, the application of these conclusions to large machines is not feasible.

Large machines, because of special requirements and varying speeds required, have drastically different ratios of diameter to length and large ranges of peripheral speeds. The few tests we have made on such machines, where temperature rise was determined by resistance rise, indicate that ratios of rise by resistance to rise by thermometer are considerably higher than those given in Table I of the report for all windings.

It has not been our practice to check temperature rise by resistance and consequently have very little test data we could furnish. We had in mind presenting the test results on the few machines we have checked, but such tests have varied so widely, with some ratios as low as 1.0 and some as high a 2.0, that we decided that it will be necessary to check a larger number of machines before submitting test data that we would consider reliable. Undoubtedly the tests made by General Electric and Westinghouse are significant as they have been made on a large number of machines.

Measuring temperature rise by resistance introduces new problems that must be overcome by the establishment of reliable commercial test procedure for such measurements. The percentage error due to contact resistance is definitely much greater on armature and interpole windings of large machines, and particularly so when compared with shunt field windings. As results vary so widely on small and large machines additional consideration will have to be given whether one table can be used later on all machines, or whether two or more tables will be necessary. It is possible that present division of motors below and above 200 horsepower could be used for such tables.

We recommend the acceptance of the proposed new table as part of ASA-C50 standards stipulating that this table is applicable for machines up to and including 50 horsepower, and the present table now listed in ASA-C50 apply to machines above 50 horsepower. We further recommend that the test program be continued on large machines so that results can be consolidated and averaged for a dependable comprehensive standard of temperature rise.

George Grant (Dow Corning Corporation, Midland, Mich.): This report is a significant study of the relation between hottest spot temperature rise and temperature rise as measured by thermometer, resistance, and surface thermocouples. There appears to be one error of fact, however, in the figures and in the discussion of them. Furthermore, no values are given for class *H* totally-enclosed motors rated for continuous operation and the values given in column 12 of Table I of the report are much more conservative than those given in columns 10 and 11. In view of the published and unpublished reports on the accelerated life testing of class *H* and other classes of insulation under carefully controlled conditions, exception is taken to this omission and to the ultra-conservative limits placed on this class of insulation.

In Figures 1 through 18 a vertical line is drawn at 55 degrees centigrade to represent the hot-spot temperature rise as given in AIEE Number 1,[1] wherein the hot-spot temperature rise for class *A* is set at 65 degrees centigrade.

Considering a vertical line representing AIEE Number 1, drawn at 65 degrees instead of 55 degrees centigrade in Figures 1, 2, 4, and 5 of the report it would appear that slightly higher values for temperature rise by resistance and by thermometer might be recommended for armatures and commutating fields. In Figures 3 and 6 a line drawn at 65 degrees centigrade coincides with the values proposed for shunt fields in this report and eliminates the need for paragraph 3 under Discussion of Results.

Relocation of the line representing AIEE Number 1 in the other figures reduces the proposed increase in hot-spot temperature from 25 to 15 degrees centigrade for all parts of motors with a short time rating of 30 minutes to two hours and for the shunt fields of motors having a rating of less than 15 minutes. Similarly proposed increases in hot-spot temperature for armatures and commutating fields rated for less than 15 minutes are reduced from 45 to 35 degrees

Table VII

		140°C. Hot-Spot Temperature Rise Class A Ratio	140°C. Hot-Spot Temperature Rise Class B Ratio	190°C. Hot-Spot Temperature Rise Class A Ratio	190°C. Hot-Spot Temperature Rise Class B Ratio
Armature windings	Thermometer	116	119	158	161
	Resistance	131	140	178	190
Shunt field windings	Resistance	140	152	190	205
Single layer field windings with exposed copper	Thermometer	131	140	178	190
	Resistance	131	140	178	190

centigrade. To maintain the increases in hot-spot temperatures proposed in this report, new hot-spot temperature rises of 90 and 110 degrees centigrade should be allowed, permitting somewhat higher thermometer and resistance values.

It is difficult to account for the omission of values for class *H* insulated, totally-enclosed motors rated for continuous operation. It is true that there has been some difficulty with commutation and brush wear in totally enclosed, class *H* insulated d-c motors, but a table of limiting temperature rises does not appear to be the proper place to resolve problems not related to the heat-stability of the insulating materials. The commutation problem may be solved before the proposed standards are adopted. In any case the solution will come more rapidly if limiting observable temperature rises for class *H* insulated motors of this rating are included in Table I of the report.

AIEE Standards Number 1 gives tentative approval to a hot-spot temperature rise of 140 degrees Fahrenheit for class *H*. This is a very conservative value as indicated by tests recently concluded and reported in a paper which will be submitted for presentation before the 1949 Midwest meeting of the AIEE. Test results reported in this report indicate that the life of class *H* and class *B* motors will be equal when the class *H* machine operates at a hot-spot temperature 100 degrees centigrade above that of the class *B*. This would indicate a hot-spot temperature rise of 190 degrees centigrade for class *H*.

Using these values, limiting observable temperature rises can be calculated for totally enclosed class *H* motors rated for continuous operation. This has been done by first determining the ratio of the values given in columns 2 and 3 to the hot-spot temperature rise values for class *A* (65 degrees centigrade) and class *B* (90 degrees centigrade) respectively. This ratio was then multiplied by the hot-spot temperature rise as set by AIEE Number 1 (140 degrees centigrade) as well as by that indicated by the tests recently concluded (190 degrees centigrade). These values are given in Table VII of the discussion.

It is suggested that consideration be given to the addition of a column to Table I giving values at least as great as those shown in Table VII of this discussion, for a hot-spot temperature rise of 140 degrees centigrade for class *H* totally-enclosed motors rated for continuous operation.

It is proposed in the report that the hot-spot temperature rises specified in the AIEE Standard Number 1[1] be increased by 15 and 35 degrees centigrade for short-time ratings, as shown in Figures 7 through 16 of the report. It would seem reasonable and consistent, therefore, to allow an equal increase for short time rated class *H* motors. The hot-spot values for class *H* would then be 155 and 175 degrees centigrade for these ratings. If a less conservative rating of 190 degrees centigrade hot-spot temperature rise were accepted for class H, continuous duty, the proposed temperature rises would become 205 and 225 degrees centigrade. Using these four values, the limiting observable temperature rises given in Table I, columns 6 and 9, have been recalculated. This has been done by first determining the ratios of the values given in columns 4 and 7 to the corresponding hot-spot values taken from Figures 7 through 16. These ratios were then multiplied by the hot-spot temperature rises proposed for short-time ratings. The results are given in Table VIII of the discussion.

It will be noted that the values, based on a continuous rating of 140 degrees centigrade hottest spot temperature rise, range from 4 degrees below to 16 degrees above the corresponding values given in columns 6 and 9 of Table I. The values given in column 6 of Table I average about 10 degrees centigrade below those shown in Table VIII of the discussion. The values given in column 9 of Table I are about the same as those shown in Table VIII.

The addition of 10 degrees centigrade to each of the hot-spot temperature rises used to calculate the values given in columns 6 and 9 of Table I would seem to be a minimum correction. Because the rating of 140 degrees centigrade hot-spot temperature rise for class *H*, AIEE Number 1, is ultra-conservative these hot-spot temperature rises might be increased by as much as an additional 50 degrees centigrade.

Table VIII

		Column 6 at 140°C. Continuous	Column 6 at 190°C. Continuous	Column 9 at 140°C. Continuous	Column 9 at 190°C. Continuous
Armature windings	Thermometer	107	141	96	124
	Resistance	155	205	158	202
Shunt field windings	Thermometer	107	141	107	141
	Resistance	136	179	136	179
Single layer field windings with exposed copper	Thermometer	126	167	114	146
	Resistance	155	205	158	202

The values given in Table I, column 12, for special purpose continuous duty motors are excessively conservative. They range from 30 to 40 degrees centigrade below the values based on AIEE Number 1 standards and suggested in this discussion for totally-enclosed, continuous duty class *H* motors. They are 70 to 80 degrees centigrade below the values based on a hot-spot temperature rise of 190 degrees centigrade for totally-enclosed continuous duty class *H* motors. It certainly seems conservative to suggest that the values given in column 12 of Table I be increased by at least 35 degrees centigrade.

Appropriate temperatures for cores and mechanical parts or for commutators and collector rings in class *H* motors are not suggested in this discussion because the data necessary for such calculations are not given in the report.

It has been suggested that limiting observable temperature rises for totally-enclosed class *H* motors rated for continuous duty be included in Table I. It has been suggested that the values given in columns 6 and 9 of Table I be increased by adding at least 10 degrees centigrade to the hot-spot temperature rises used in calculating these values. It has also been proposed that the values given in column 12 of Table I be increased by at least 35 degrees centigrade. These increases are consonant with the very conservative standards set for class *H* insulations in AIEE Number 1. All of these proposed increases are far below those which would be justified if the AIEE standard were revised to recognize hot-spot temperature rise of 190 degrees centigrade, for class *H*. These suggestions are intended to give design engineers an opportunity to exploit to the fullest extent the exceptional heat stability of class *H* insulations.

REFERENCE

1. See reference 3 of the report.

C. B. Hathaway (Westinghouse Electric Corporation, Buffalo, N. Y.): The report seemed to indicate that the present addition of 1 per cent of the output for the stray load losses is low. It is indicated that the actual stray load losses would be near 2 per cent. It must be recognized that these measurements were made on machines of 50 horsepower and smaller and the results, of course, are limited to this range. There is no evidence available as to what the losses may be in larger machines.

Furthermore, the values themselves are open to question. The method employed was by measuring the output with the dynamometer. A small quantity obtained by subtracting one large one from another large one is inherently subject to great error.

Therefore, it is my opinion that until a more accurate method can be developed to determine stray load losses that the present 1 per cent allowance should be allowed to stand.

T. M. Linville and Mrs. B. O. Buckland: Grant raises a question about the vertical line drawn at 55 degrees centigrade to represent the hot-spot temperature rise as given in AIEE Number 1.[1] It is true that AIEE Number 1 sets the hot-spot temperature rise for class *A* at 65 degrees centigrade. This corresponds to a hot-spot temperature of 105 degrees centigrade with an ambient temperature of 40 degrees centigrade. The corresponding rise by thermometer is 50 degrees centigrade. However, general purpose, class *A*, open motors are allowed only 40 degrees centigrade rise by thermometer based on a 40 degrees centigrade ambient. The corresponding hot-spot temperature rises are 95 degrees centigrade and 55 degrees centigrade respectively, in accordance with AIEE Number 1.

The method of the report is to establish the ratio of temperature rise by resistance to temperature rise by thermometer as given by the tests. Then this ratio is applied to the standard temperature rise by thermometer for class *A* and *B* insulations and for the several classes and ratings of machines in order to set up the new Table I for ASA-C50 so that it will properly cover the resistance method without any change in the present thermometer values.

This method should also be followed for class *H* insulation but in this case no thermometer values have been set as yet. Hence, the values given in the report for class *H* are highly preliminary and incomplete. All suggestions as to what these values should be is especially appreciated.

The report establishes and clearly shows in Figures 1 to 18 the values of hot-spot temperature rise which correspond to the standard thermometer values as shown by the tests. These are the hot-spot values which should be allowed if the thermometer values are left unchanged as is recommended. These hot-spot values are consistent with the principles set forth in AIEE Number 1A.[2]

Stokes has made an interesting presentation of the test data. He points out that the new Table I given in the report cannot be applied to large machines. He also points out that a long time will be required to get data on large machines and asks why, in view of the limitations of the paper, a definite recommendation is made to revise Table I of ASA-C50 (See Table I of the discussion) on an unrestricted basis.

In regard to the latter question, in the first place the test results show that expansion of Table I is definitely needed if the resistance method is to be a useful method of test. Furthermore, the conclusion seems reasonably justified that expansion of the table based on the tests covered by the report taken on small machines will not worsen the situation with respect to large machines.

As things stand now, it may be inferred from the standards (as is a fact in Navy specifications) that only 10 degrees centigrade additional rise is to be allowed for the resistance method over the thermometer method for all windings. For the purpose of keeping the standards up-to-date, an expansion of Table I is recommended now in view of the time necessary to obtain test data on large machines, remembering that the test program covered by the report was initiated in 1944.

Baker's comments represent a common desire to keep things simple. His tabulation of the data shows a larger variation in results with the resistance method than with the thermometer method. However, the purpose of all temperature tests is to measure the temperature of the hottest spot and because the resistance method comes closer to doing this than does the thermometer method for machines of normal proportions its accuracy is superior in spite of greater percentage variation in results. Moreover, the resistance method is the preferred standard method for railway motors and generators and its use by engineers to learn the maximum about machines of all types is commonly known. Therefore, there is need for standards covering its use so that where appropriate it can be used in commercial transactions without making special design of machines necessary.

Alger, who has been close to the test program given in the report and has contributed much to it, answers in his comments several of the questions raised by other discussors and outlines the program which the d-c subcommittee should carry forward vigorously in the interest of better standards and better machines as a result thereof.

Caldwell's and Gunnoe's discussion relates mainly to big machines and is important and encouraging for many reasons. It indicates that data very likely are already at hand among the manufacturers of big machines and possibly can be collected promptly by the d-c machine subcommittee (an exchange test program would obviously be impractical with big machines). It gives test results on a substantial number of big machines which support the "Proposed New Table" of 1945 which was derived from test results on 19 machines supported by theoretical data presented in 1945. Their discussion also presents data on class *A*, class *B*, and on 4 class *H* machines showing that there is a common average ratio between rise by resistance and rise by thermometer for all these classes as was assumed in the report. They present an alternative proposed new table (See Table II of the discussion) for consideration derived from tests on large machines by the same method as was used to derive Table I of the report from tests on small machines. In response to this discussion, it would appear that the d-c subcommittee should promptly seek similar information from other manufacturers and integrate it with the data of the report.

Fuller's discussion is similar to part of Baker's except that the average range of variation is not shown, undoubtedly on purpose, in order to focus attention entirely on the limits of variation in the test results. To get a true picture of the relative reliability of the test data, comparing the resistance method to the thermometer method, a thoroughgoing analysis should be made by the statistical methods used for modern quality control as suggested by Alger.

REFERENCES

1. See reference 3 of the report.
2. See reference 4 of the report.

Stray Load Losses Measured in D-C Motors

AN AIEE COMMITTEE REPORT

THIS REPORT gives the results of tests to measure stray load loss made jointly by the Allis-Chalmers Company, General Electric Company, Century Electric Company, Reliance Electric and Engineering Company, and Westinghouse Electric Corporation on a motor exchange program at the request of the AIEE committee on rotating machinery. Motors tested ranged from 1/2 to 50 horsepower and were standard, open, general purpose, 40 degree centigrade, 1,750 rpm.

Stray loss measurements are reported for 27 load conditions covering three values of load current, three values of excitation, and three values of speed. The variation of stray loss with these variables is given for each of the motors tested. By averaging the data, assuming that the variables are independent of one another and of saturation and all other factors, a general formula is derived expressing the stray loss as a function of these variables. The tests are not considered conclusive although the average results are held to be significant.

Stray load loss in d-c machines is the sum of:

1. Additional core loss due to flux from windings excited by load current.
2. Eddy current loss in the armature winding caused by the periodic reversal of current flow in the armature conductors.
3. Component of brush friction loss which varies with load current apart from brush friction measured at no load.
4. Brush contact loss caused by imperfect commutation and by current conduction apart from the conventional contact loss calculated for constant voltage drop.

All but negligible sources of loss can be grouped under these four items. None of these items are directly measurable.

For many years the standard practice has been to include these losses in all efficiency calculations by taking them to be equal to 1 per cent of the output. If this allowance has not been as large as the actual losses in particular cases, prime movers driving d-c generators have been required to furnish more than the rated power or, in the case of motors, the current input has been higher than expected. When the allowance has been more than the actual loss the conditions have been reversed. Moreover, engineers have recognized that stray losses can vary quite widely from motor to motor depending upon design proportions and, in any given motor they do not usually vary in direct proportion to the output. Therefore, in making calculations for fuel economy for engine driven generators, or for overall efficiency of motor-generator sets or in calculating temperature rise, and in other calculations, engineers have not been satisfied with the 1 per cent rule. There has been a steady desire for some simple but more realistic formula.

Accordingly, the subcommittee on d-c machines of the AIEE committee on rotating machinery asked the five manufacturers to measure the stray loss of motors on a co-operative test program. Motors tested were rated 1/2, 5, 10, 25, and 50 horsepower, open, general purpose, 40 degrees centigrade, 1,750 rpm. Each company contributed a motor and each motor was tested by its manufacturer and by one other company, except for the 1/2-horsepower motor which has been tested only by its manufacturer. An exchange program was worked out to accomplish this.

The committee undertook the work recognizing that the present allowance of 1 per cent applies to machines of all sizes and to all conditions of load, that is, any voltage, any speed, any load current on any size and type of machine. This allowance can be correct only as an average. The departure from this average allowance as either the size of motor or the load conditions change is not known generally. Therefore, the committee undertook the tests to determine how well the 1 per cent allowance fitted the particular group of motors to be tested.

It was found from the average of all test data that stray load loss was 3 per cent of output. This holds at the average output of all the test conditions but was found to vary so that, for example, at the average rated full load output of the motors it was 2 per cent.

The results make it possible to devise a simple expression for stray load loss as in equation 5. In the future it should be possible to use such a simple rule with several values for the coefficient and exponent, each value corresponding to a group of machines. The several groups of machines would be divided according to size and type (for example, pole face windings or not). Therefore, an important result of the present tests is to show what may be accomplished by future extension and improvement of the work. Until this can be done the committee recommends that the present flat allowance of 1 per cent be maintained.

At the risk of confusing the reader, the results are given in both watts and per cent of output. This amounts to two ways of expressing one set of results. The formula for stray load loss, equation 5, can be derived from either the data expressed in watts or the data expressed in per cent of output. The derivation given starts

---

Paper 49-63, recommended by the AIEE rotating machinery committee and approved by the AIEE technical program committee for presentation at the AIEE winter general meeting, New York, N. Y., January 31–February 4, 1949. Manuscript submitted November 16, 1948; made available for printing December 21, 1948.

This report was prepared by the AIEE subcommittee on d-c machines of the rotating machinery committee.

Personnel of the AIEE subcommittee on d-c machines: T. M. Linville, *chairman*, Mrs. B. O. Buckland, W. E. Clancy, F. A. Compton, Jr., Lanier Greer, J. L. Hamilton, C. B. Hathaway, V. P. Hessler, V. B. Honsinger, W. R. Hough, P. Lebenbaum, C. Lynn, L. G. Opel, D. Ramadanoff, J. F. Sellers.

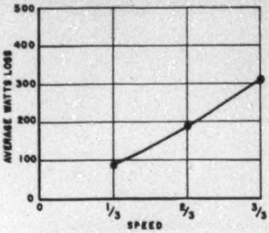

Figure 1. Watts versus speed

with the data in watts and ends by checking the formula against the data in per cent of output.

The reader is cautioned against attempting to attach importance to any single item of the data. Every engineer normally wants to feel that each element of a set of data is reliable and significant. But the committee feels that in this case the data must only be inspected in mass. When this is done the results have important value and real significance.

The discrepancy among the individual test results is a testimonial to the difficulty of measuring stray load loss. In future tests it will be helpful to extend the method to measure the loss of a machine twice, first driving it by the dynamometer and second driving the dynamometer by it. Moreover, it might be better to use two identical machines connected pump-back to read the total losses directly. Regardless of the method, large discrepancies are to be expected between the results of individual tests, because the brush loss due to friction and contact drop is subject to wide variations, and is commensurate in size with the stray load loss itself.

It has been suggested that the brush rigging be supported on bearings so that the friction can be measured continuously and that the brush contact voltage be read continuously through the use of an insulated brush. If this is done, a departure is made from the conventional definition of stray load loss which includes the vagaries of brush friction and contact loss as a part of stray loss. The committee believes that a great mass of test data is essential to find the general truth.

Method

In each test the power output of the motor was measured carefully with a dynamometer. The power input was measured by calibrated instruments. The difference between these two measurements gave the total losses of the motor. Total losses were measured in this way for 27 load conditions covering every possible combination of 1/3, 2/3, and 3/3 normal full-load speed, 1/3, 2/3, and 3/3 normal full-load flux, and 1/2, 2/2, and 3/2 normal full-load armature current.

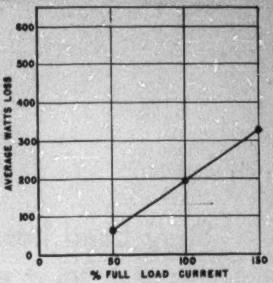

Figure 2. Watts versus current

The running light losses were measured directly by driving the motor from the dynamometer without armature current. Running light losses were generally checked by running the motor free of any connected load. Nine readings were taken by each method covering all combinations of speeds of 1/3, 2/3, and 3/3 of normal full-load speed and 1/3, 2/3, and 3/3 of normal full-load exciting flux. When the motor was driven electrically, the losses due to the input current were substracted from the input power. By these methods the running light losses comprising the loss due to bearing and

Table I. Measured Stray Load Loss (Watts)

		50 HP MOTOR									25 HP MOTOR								
Per Cent Current		50			100			150			50			100			150		
Test		A	B	Avg.	A	B	Avg.	A	B	Avg.	A	B	Avg.	A	B	Avg.	A	B	Avg.
1/3 Flux	1/3 Speed	0	11	6	67	100	84	224	330	277	58	179	119	139	328	234	344	257	301
	2/3 Speed	10	6	123	203	352	278	566	790	678	75	185	130	299	288	294	639	498	569
	Full Speed	104	97	101	415	600	508	1,137	982	1,060	112	355	234	450	673	561	784	988	886
2/3 Flux	1/3 Speed	67	29	48	180	193	187	459	425	442	76	83	80	165	288	227	367	438	403
	2/3 Speed	77	210	143	328	495	412	820	820	820	154	105	130	434	615	525	720	710	705
	Full Speed	192	141	167	670	755	713	1,301	810	1,056	158	356	257	506	1,156	831	787	1,186	987
Full Flux	1/3 Speed	28	−53	−10	165	280	223	422	212	317	31	149	90	107	359	233	240	294	267
	2/3 Speed	115	165	140	268	661	465	723	537	630	82	110	96	301	255	278	516	635	576
	Full Speed	65	142	104	431	1,145	788	980	1,669	1,324	169	39	104	487	669	578	795	1,609	1,202

10 HP MOTOR									5 HP MOTOR									1/3 HP MOTOR		
50			100			150			50			100			150			50	100	150
A	B	Avg.	A	B	Avg.	A	B	Avg.	A	B	Avg.	A	B	Avg.	A	B	Avg.	A	B	Avg.
2*	−25	−11	−2*	−2	−2	21*	309	165	−8*	0	−4	4*	21	13	40*	69	55	0.33	1.04	−0.43
11*	20	16	36*	0	18	161*	50	106	−5*	31	13	13*	49	31	57*	123	90		3.90	1.80
48*	360	204	111*	330	221	192*	310	251	1*	10	6	37*	93	65	99*	214	157	−0.60	−2.30	−0.60
−2*	−21	−12	−3*	−36	−20	12*	44	28	−15*	6	−5	−6*	38	16	14*	106	60	0.60	0.54	−0.80
19*	0	10	25*	90	58	76*	80	78	−7*	37	15	14*	116	65	43*	170	107	−2.60	1.82	0
54*	281	167	105*	241	173	174*	321	248	4*	63	34	49*	191	120	106*	270	188	−2.40	7.42	−6.00
−4*	27	12	−12*	−15	−14	10*	15	13	−9*	4	−3	−6*	37	16	6*	68	37	1.70	3.22	0
10*	148	79	20*	188	104	70*	428	249	−6*	55	25	8*	137	73	38*	227	133	−0.80	1.32	−2.10
23*	148	86	61*	258	160	129*	408	269	−1*	90	45	21*	146	84	61*	257	159	−2.70	2.72	0

Average of all data:

1/3 speed	86.1,	50 per cent current	60.7,	1/3 flux 174.3,	50 horsepower, 410.5
2/3 speed	183.9,	100 per cent current	191.6,	2/3 flux 210.6,	25 horsepower, 403.6
Full speed	313.3,	150 per cent current	330.7,	full flux 198.6,	10 horsepower, 98.0
					5 horsepower, 58.3
					1/3 horsepower, 0.18

*These data were taken at 1/3, 2/3 and full field current instead of 1/3, 2/3, and full flux

1/3 current = Approximately 39 per cent Flux

2/3 current = Approximately 75 per cent Flux

Full current = Full Flux

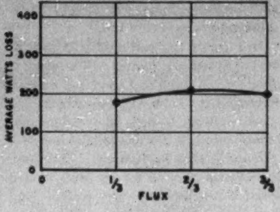

Figure 3. Watts versus flux

brush friction, the loss due to windage, and the open-circuit core loss were measured directly. The fact that the results gave smooth curves when plotted against flux and speed gave additional assurance of accuracy.

Copper loss for each load condition was determined by measuring the resistance of each winding, correcting it to the temperatures corresponding to each load condition, and multiplying by the square of the corresponding load current. Conventional brush contact loss was calculated for each load condition by multiplying the corresponding current by two volts for contact drop.

Stray load loss for each load condition was determined by subtracting from the total loss the sum of the running light losses, copper losses, and brush contact loss for the respective load conditions.

Results

Results expressed in watts are given in Table I. In Table II, the stray load loss is given expressed as per cent of motor output. Per cent of output is the recognized way of expressing the loss.

Because a general relation is being sought which will hold approximately for all conditions of operation and because error is expected in the stray loss measurement for each load condition, it is considered advantageous to average the results and to plot the average result as a function of each variable; that is, flux, load current, speed, and rated horsepower.

Figure 1 shows the average load loss in watts plotted against speed. The loss is proportional to speed raised to a power a fraction more than the first power.

Figure 2 shows that the average load loss plotted against load current varies about as the 3/2 power of current.

Figure 3 shows the average load loss plotted against flux, indicating some degree of independence of flux. It must not be imagined that the curve in this figure goes to zero loss at zero flux. If such were the case, the core loss determined by test under short circuit would be zero. If the load loss is truly independent of exciting field flux, then the losses under short circuit test which can be measured directly would give the true stray load loss when the corresponding brush friction, brush contact loss, and copper losses are subtracted from them. It has been recognized that short circuit core loss has some value as a measure of load loss. However, it cannot be calculated easily and no simple formula for it has been recognized any more than for load loss itself.

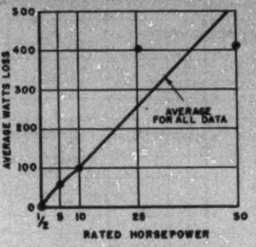

Figure 4. Watts versus rated horsepower

Figure 4 shows the average load loss for all of the tests on each motor plotted against the rated full-load horsepower.

Table II. Measured Stray Load Loss (Per Cent of Output)

	50 HP MOTOR									25 HP MOTOR								
Per Cent Current	50			100			150			50			100			150		
Test	A	B	Avg.	A	B	Avg.	A	B	Avg.	A	B	Avg.	A	B	Avg.	A	B	Avg.
1/2 Flux																		
1/3 Speed	0	0.54	0.27	1.57	2.44	2.01	3.58	5.74	4.66	6.19	21.9	14.05	6.94	18.90	12.92	11.43	8.62	10.03
2/3 Speed	0.24	6.17	3.21	2.42	4.37	3.40	4.66	6.69	5.68	4.04	10.65	7.35	7.72	7.42	7.57	10.82	7.39	9.11
Full Speed	1.74	1.63	1.69	3.35	5.00	4.18	6.03	5.44	5.74	4.18	11.56	7.87	8.02	12.25	10.14	9.16	14.50	11.83
2/3 Flux																		
1/3 Speed	1.58	0.70	1.14	2.11	2.32	2.22	3.54	3.50	3.52	3.80	4.17	3.99	3.97	6.42	5.20	5.92	7.15	6.54
2/3 Speed	0.92	2.58	1.75	1.93	2.96	2.45	3.24	3.28	3.26	3.87	2.64	3.26	5.30	7.72	6.51	5.74	5.74	5.74
Full Speed	1.55	1.15	1.35	2.65	3.00	2.83	3.42	2.13	2.78	2.71	6.30	4.51	4.19	9.96	7.08	4.24	6.47	5.36
Full Flux																		
1/3 Speed	0.44	−0.73	−0.15	1.27	2.19	1.73	2.20	1.11	1.66	1.02	5.03	3.03	1.68	5.86	3.77	2.48	3.08	2.78
2/3 Speed	0.92	1.34	1.13	1.04	2.64	1.84	1.84	1.40	1.62	1.37	1.86	1.62	2.45	2.04	2.25	2.75	3.36	3.06
Full Speed	0.35	0.75	0.55	1.25	3.05	2.15	1.71	2.96	2.34	1.95	0.44	1.20	2.66	3.65	3.16	2.83	5.85	4.34

	10 HP MOTOR									5 HP MOTOR									1/2 HP MOTOR		
Per Cent Current	50			100			150			50			100			150			50	100	150
Test	A	B	Avg.	A	B	Avg.	A	B	Avg.	A	B	Avg.	A	B	Avg.	A	B	Avg.	A	B	Avg.
1/2 Flux																					
1/3 Speed	0.48*	−5.8	−2.66	−0.22*	−0.20	−0.21	1.60*	30.40	16.00	−2.80*	0	−1.40	0.71*	4.90	2.81	4.90*	11.10	8.00	1.19	2.28	−0.60
2/3 Speed	1.41*	2.60	2.01	2.32*	0	1.16	7.44*	1.90	4.67	−1.00*	8.0	3.50	1.30*	5.80	3.55	3.80*	9.80	6.80		4.70	1.36
Full Speed	4.93*	46.70	25.82	5.35*	15.10	10.23	6.46*	8.70	7.58	0.20*	1.60	0.90	2.40*	7.30	4.85	4.45*	11.70	8.08	−1.29	−1.85	−0.31
2/3 Flux																					
1/3 Speed	−0.22*	−2.40	−1.31	−0.17*	−2.00	1.09	0.52*	1.70	1.11	2.70*	1.50	−0.60	−0.46*	4.50	2.02	0.90*	8.30	4.60	1.33	0.59	−0.55
2/3 Speed	1.09*	0	0.55	0.75*	2.60	1.68	1.62*	1.50	1.56	−0.80*	4.30	1.75	0.70*	6.70	3.70	1.20*	6.50	3.85	−3.24	0.98	0
Full Speed	2.18*	12.70	7.44	2.10*	4.80	3.45	2.45*	4.20	3.33	0.40*	5.00	2.70	1.60*	7.50	4.55	2.50*	6.80	4.65	−2.07	2.71	−1.41
Full Flux																					
1/3 Speed	−0.31*	2.12	0.91	−0.46*	−0.60	0.53	0.27*	0.37	0.32	−1.30*	0.63	−0.34	−0.50*	2.80	1.15	0.30*	3.40	1.85	3.82	2.38	0
2/3 Speed	0.40*	6.10	3.25	0.39*	3.60	2.00	0.99*	5.60	3.30	−0.30*	4.30	2.00	0.30*	5.20	2.5	0.90*	5.70	3.30	−0.91	0.50	−0.49
Full Speed	1.22*	4.10	2.66	0.83*	3.40	2.12	0.62*	3.50	2.06	0*	4.90	2.45	0.50*	3.60	2.05	1.10*	4.20	2.65	−2.34	0.69	0

Average of all data:
1/3 speed 2.84, 50 per cent current 2.64, 1/2 flux 5.65, 50 horsepower 2.41
2/3 speed 3.09, 100 per cent current 3.31, 2/3 flux 2.78, 25 horsepower 6.08
Full speed 4.29, 150 per cent current 4.26, full flux 1.82, 10 horsepower 3.61
5 horsepower 3.04
1/2 horsepower 0.29

* These data were taken at 1/3, 2/3, and full field current instead of 1/2, 2/3, and full flux
1/3 current = approximately 39 per cent Flux
2/3 current = approximately 75 per cent Flux
Full current = Full Flux

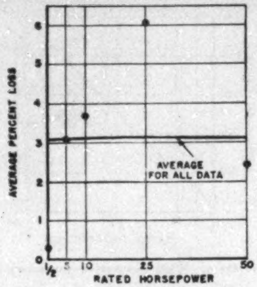

Figure 5. Loss versus rated horsepower

The solid line is drawn to have a slope determined by dividing the sum of the ordinates for all of the points by the sum of the abscissas.

Figure 9 is an enlargement of Figure 5. In this figure the heavy line represents the average result of 54 tests on each motor covering load outputs from 4 per cent of the rating to 150 per cent of the rating. The light lines in this enlargement show the wide variation of load loss as a percentage of output as measured in these tests. Tables I and II also show the wide differences in results.

Figures 6, 7, and 8 show the variation of load loss expressed as per cent of output with speed, load current, and exciting field flux respectively. These curves show average data obtained in the tests.

If, from inspection of Figures 1, 2, 3, and 4, it is assumed that the watts loss varies with the first power of the speed, with the 3/2 power of current, are independent of flux, and vary in proportion to the rated full-load horsepower, an expression for the dependence of the watts loss upon these variables may be established as follows

$$W=\frac{n}{n_r}\left(\frac{i}{i_r}\right)^{3/2} hp_r\, K \tag{1}$$

where

W = stray load loss at any operating condition in watts
n = speed of operation
i = load current
hp_r = rated full load horsepower
n_r = rated speed
i_r = rated full load current
K = constant factor

and if both sides of equation 1 are divided by the output load, *hp*, the resulting ratio of loss to output is

$$\frac{W}{hp}=\frac{n}{n_r}\left(\frac{i}{i_r}\right)^{3/2}\frac{hp_r}{hp}K \tag{2}$$

This ratio may also be expressed in terms of flux (the way it is shown in Figure 8) by substituting the following relation in equation 2

$$\frac{hp_r}{hp}=\frac{n_r}{n}\,\frac{i_r}{i}\,\frac{\phi_r}{\phi}\ \text{(neglecting part of the losses)} \tag{3}$$

giving

$$\frac{W}{hp}=\frac{\phi_r}{\phi}\left(\frac{i}{i_r}\right)^{1/2}K \tag{4}$$

where

ϕ = exciting field flux at output load
ϕ_r = exciting field flux at rated full load

The factor K can be evaluated from equation 2 using values which represent averages for all of the tests, that is, $W/hp = 0.03$ from Table II or Figure 5, $n/n_r = 2/3$, $i/i_r = 1$, $hp_r/hp = 9/4$, giving

$K = 0.02$

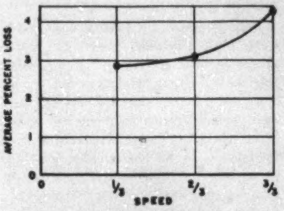

Figure 6. Per cent loss versus speed

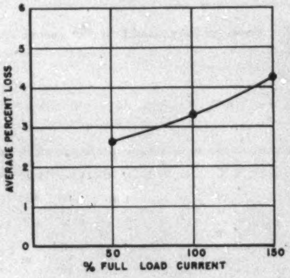

Figure 7. Per cent loss versus current

Therefore, the general expressions resulting from the average data are, from equation 2 and equation 4

$$\frac{W}{hp}=0.02\frac{n}{n_r}\left(\frac{i}{i_r}\right)^{3/2}\frac{hp_r}{hp}=0.02\frac{\phi_r}{\phi}\sqrt{\frac{i}{i_r}} \tag{5}$$

Equation 5 in either of its two forms may be used to check the curves of per cent loss versus speed, current, and flux as plotted in Figures 6, 7, and 8, respectively.

In Figure 6 the average loss of all tests at 1/3 speed are plotted. The same is done for 2/3 speed and also for 3/3 speed. Referring to Table II, the tests at 1/3 speed were made with all possible combinations of 1/3, 2/3, and full flux and 1/2, 2/2, and 3/2 full-load current. Therefore, the average flux, ϕ for the tests at 1/3 speed is 2/3 full flux, the average load current, i, is 2/2 full current, and hp/hp_r is 2/9 from equation 3. Substituting these values in either form of equation 5 yields $W/hp = 0.03$ or 3 per cent. For the tests at 2/3 speed the average values for flux, ϕ, and load current, i, are the same but now equation 3 yields $hp/hp_r = 4/9$. Using these values in equation 5 the answer again is $W/hp = 0.03$ or 3 per cent. Similar calculations for the average values at 3/3 speed give the same answer. Therefore, for comparison with the test results plotted in Figure 6, the calculated results using equation 5 are:

Speed	Per Cent Loss
1/3	3.0
2/3	3.0
3/3	3.0

In Figure 7, the average flux, ϕ, at each value of load current is 2/3 and the average speed, n, is also 2/3. By using equation 3 and the first form of equation 5 or by using the second form of equation 5 alone, the following calculated results are obtained for Figure 7:

Per Cent Current	Per Cent Loss
50	2.1
100	3.0
150	3.63

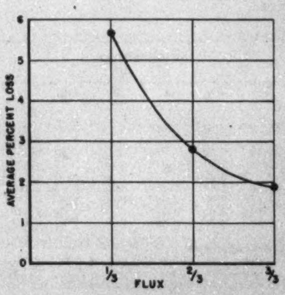

Figure 8. Per cent loss versus flux

In Figure 8, average values are, $n=2/3$, and $i=1.0$. Then from equations 3 and 5 the calculated results are:

Flux	Per Cent Loss
1/3	6.0
2/3	3.0
3/3	2.0

The general expressions of equation 5 may be used to check any of the test data in Tables I and II. By so doing any item of the test data may be compared with the result of the average "law," equation 5, derived from the mass of the data.

The mass of data summarized by the relations of equation 5 indicates that load loss is a fixed percentage of rated full-load output for the range of sizes tested but for fractional loads and speeds the loss varies in proportion to speed and in proportion to the 3/2 power of load current independent of exciting field flux. Although for the motors tested the mass of data indicates 2 per cent load loss at rated full load, it is certain that for very large motors the indicated percentage would be much less. Future work needs to be done to revise and establish general relationships similar to equation 5 so that the allowance for load loss for d-c machines can be specified in future standards on such a basis.

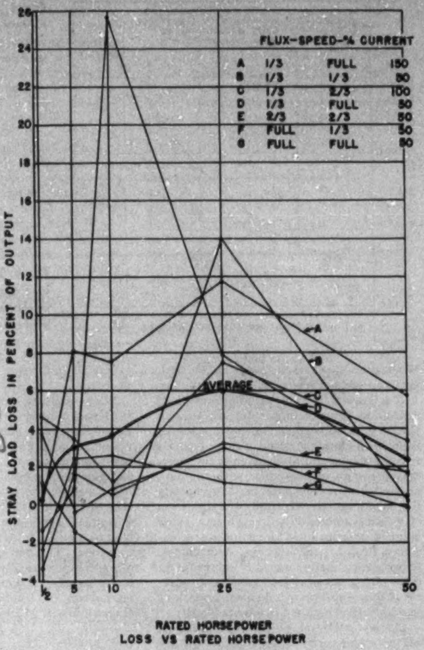

Figure 9. Enlargement of Figure 5, showing spread of data

All tests in which either a maximum or a minimum occurred are shown. The points are averages of two tests for the 5-, 10-, 25-, and 50-horsepower motors, and one test for the 1/2 - horsepower motor

Discussion

B. H. Caldwell (General Electric Company Schenectady, N. Y.): This report presents interesting data and emphasizes the lack of adequate information on this subject. It also directs attention to the difficulties involved in getting accurate and consistent data.

It is well known that brush friction and brush contact drop both vary widely even under closely controlled operating conditions, and these factors make it difficult to repeat results. The variations from the normal might be expected to be great for a machine with a small number of brushes. Conversely for a machine with a large number of brushes the variation from normal might be expected to be smaller. Data accumulated from factory tests would seem to confirm this, since it has been found possible to get good measurement on large machines of load loss with the application of proper test procedures.

Figure 1. Pump-back connections for measuring total loss for two d-c machines

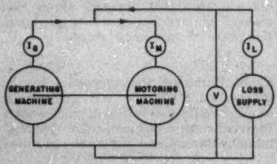

A direct measurement of total loss is to be preferred rather than measurement of input and output. The combined loss of two machines can be obtained readily from the relatively simple pump-back load test as shown in Figure 1 of the discussion. Here it is necessary only to meter the input current from the loss supply and the line voltage in order to compute the combined loss of the two machines. Other losses, having been predetermined by recognized methods, can be subtracted to give the combined stray load loss of the two machines. If the two machines are duplicate designs, then it is possible to assign the proper proportion of the combined load loss to each machine. It is only necessary to take account of the fact that the generating machine operates at the higher flux and the motoring machine operates at the higher armature current.

Data obtained in this manner are shown in Figure 2 of the discussion. The total loss was obtained by direct measurement. A number of tests were taken by different test crews over a period of several days. The points calculated from test data are indicated to show how well the data can be repeated. If other losses are calculated as specified in ASA, C-50[1] and subtracted from the total loss, resulting values of load loss as now defined are obtained. These values are plotted in Figure 3 of the discussion as curve 1.

A further refinement was added in the data plotted as curve 2 of Figure 3 of the discussion. The brush voltage drop was measured by using an insulated brush, and the brush drop loss was computed on this basis. Also the ohmic losses were corrected to apply at the measured temperature of the various elements. Two components which are normally included as part of load loss are thus eliminated. Variation of the brush friction loss from the value arbitrarily assigned is still included.

At rated load the load loss in this case is approximately 0.57 per cent. This compares with 2 per cent in the report and the present allowance in ASA, C-50 of 1 per cent. Similar data taken on large, compensated (pole-face winding) d-c machines shows the same general trends with load loss values which vary from a negative value of 0.09 to a positive value of 1.24 per cent at rated load. For variable speed mill motors in this class the load loss value is consistently higher at top speed than at base speed.

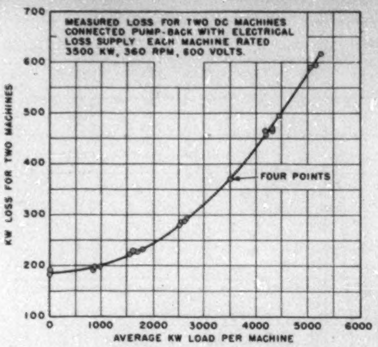

Figure 2. Loss for two machines versus average load per machine

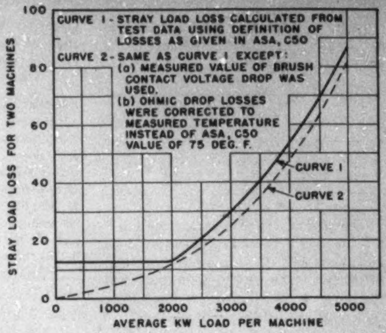

Figure 3. Stray load loss for two machines versus load per machine

With fixed speed there tends to be little variation of the load loss with change in flux.

It is known that the value of stray load loss is in general higher for an uncompensated machine than for a compensated machine. Thus, the value of 2 per cent for uncompensated machines given in the paper may prove to be consistent with the data presented here. It would seem appropriate to give serious consideration to modification of existing standards to recognize a lower value of stray load loss for compensated machines than for uncompensated machines. Other design factors are also important in determining the stray load loss, but the factor of compensation is a dominant one, and should be so recognized in our standards.

The committee should be encouraged to continue this project toward the end of accumulating sufficient data for intelligent revision of the existing 1 per cent rule. It is quite probable that the various manufacturers have considerable data available on this subject. The next step for the committee might well be to encourage the publication of these data.

In any further program for measuring stray load loss, a direct method of measuring the losses should be used. Various modifications of the pump-back method have been devised and described in the literature for doing this. The measurement so obtained is for two machines, so some uncertainty as to how the stray load loss should be divided is introduced. However, if the two machines are of duplicate design, the division of the losses can be assigned accurately.

Reference

1. Rotating Electrical Machinery. American Standards Association (New York, N. Y.), C-50-1943, 78 pages.

Edward Sand (Reliance Electric and Engineering Company, Cleveland, Ohio): Stray load loss tests taken at the Reliance laboratory in accordance with the method established by the subcommittee on d-c machines, showed the need of a better method of testing. Even after taking the tests several times in order to check the data, results showed that the stray load loss could vary over a wide range, depending on equipment accuracy and human error, because the value of loss which is small was obtained by taking the difference of two relatively large quantities.

When additional tests are to be made it is suggested that the Blondel opposition test method or some similar method be given consideration. This should reduce the testing errors as a percentage of stray load loss and give more consistent stray load results.

Essentially the Blondel method requires that the two identical machines to be tested be coupled together and to a small dynamometer to supply friction and windage and core loss. The two units are connected in opposition electrically with a boost-generator to supply the copper loss. More information on this method can be found in Direct Current Machinery.[1]

Reference

1. Direct Current Machinery, R. G. Kloeffler, J. L. Brenneman, R. M. Kirchner. The Macmillan Company, New York, N. Y., 1934.

C. Lynn (Westinghouse Electric Corporation, East Pittsburgh, Pa.): We have made very accurate tests of loss measurements on larger size compensated d-c machines having low-loss type of armature winding and have found that under full field conditions the load loss may be only one-half of 1 per cent as compared to load losses of up to 3 per cent or even more, on small noncompensated machines. It should, therefore, be strictly understood that the information in the report applies to small machines of the industrial type, since the data are based on tests of motors from 1/2 to 50 horsepower only.

The pump-back method of testing if carried out accurately, particularly on large size machines, is very accurate and much better than using a dynamometer. When a dynamometer is used full power measurements are made and any inaccuracies in readings affect the results directly. By the use of the pump-back method with each machine operated at exactly the same air gap flux and using a calibrated motor connected to the two machines for supplying the mechanical losses of the two machines under test, which in turn are mechanically connected together and loaded back one on the other, and by supplying the electrical losses from a separate electrical source, very accurate data can be obtained.

It is, of course, understood that the brush friction loss decreases with load current. When machines are operated for long periods of time at light loads, a heavy film builds up on the commutator which causes high brush friction and can lead to chatter of the brushes. The flow of current to the commutator from the brushes prohibits too high a build up of this film, and due to the electrolytic action of this flow of current, easier sliding of the brushes on the commutator results. Therefore, the measurement of the brush friction at no load and no voltage is not a true measurement of the brush friction that results under loaded conditions. To obtain this it is necessary for the brush rigging to be mounted in such a manner that direct torque measurements on it can be obtained. This should be done in such a manner that no appreciable movement of the brush rigging results, because if this occurs the fit of the brushes on the commutator is disturbed and the results will no longer be accurate. In addition commutation may be affected.

The stray load loss is a compensation for practically every separate loss considered in figuring the efficiencies of a machine, because all of these losses are different under load than when measured under no load conditions. For instance the armature copper loss considers only the armature current squared times the resistance of the armature winding. This resistance is taken on the basis of 75 degrees centigrade copper which, of course, will not be the actual temperature of the copper throughout its length. This loss will be very different even in machines of the same size and having the same d-c armature resistance, depending on the arrangement of the conductors in the slot. Certain design features can reduce eddy current losses appreciably. Also, commutation introduces additional loss in those coils being commutated. The core loss obviously under load is entirely different than that obtained at no load under a prorated flux condition simulating that of the machine when loaded.

C. B. Hathaway (Westinghouse Electric Corporation, Buffalo, N. Y.): The purpose of this investigation was to determine what the relation the actual temperature readings taken by thermometer and the rise by resistance bore to the hot spot in open, industrial-type d-c motors is. This purpose has been accomplished. The results, however, have been somewhat disconcerting.

Little change in the standards appear needed for the open, continuously rated motor. It seems desirable to modify but one item. There should be a differential of 20 degrees centigrade instead of 10 degrees for the shunt field when comparing rise by thermometer and rise by resistance.

The story is quite different for the short-time rated motors. There are great discrepancies between the thermometer readings on the one hand and the rise by resistance and the hottest spot on the other.

The allowable temperature of the hottest spot for class "A" material could be adjusted upward to 120 degrees centigrade for 1/2 hour ratings, and to 140 degrees centigrade for 15-minute or shorter ratings.

The tests also disclose that on short-time ratings the rise by resistance is much more closely related to the temperature of the hottest spot than it is to the rise by thermometer. This lends weight to the contention that for short-time ratings the rise by resistance and the rise of the hottest spot could be the same.

While the tests show clearly that the temperatures present in the machines are much higher than indicated by thermometer readings, there is no evidence or experience that indicates that the old method of applying motors with short-time ratings established by the thermometer method provides motors inadequate for the application intended.

T. M. Linville: Stray load loss is one of those perennial subjects which one may want to elude but cannot. It affects the heating of a machine and must be accounted for by a manufacturer in working out the utilization of material, the internal temperatures, and the ventilation of machines. It may affect the power input or output of a d-c machine by several per cent especially under light-load operation. Therefore, it will continue to be a problem and a worthwhile thesis topic for college students without abatement. We can hope that the combination of test data and theoretical analysis will lead to a wider understanding of it.

With respect to an industry standard to allow for stray load loss, it seems the best we can hope for is to leave its determination to the manufacturer just as we now do for open-circuit core loss or else accept a standard allowance which is an average for all machines and perhaps fits none precisely. Stray load loss is a catch-all for the changes caused by load current in each of the normal components of loss. It follows no simple formula for any one machine, but when the loss in all machines at once is studied it does appear to follow a pattern which can be defined. This definition in simple form is what we are seeking for use as a standard. It requires many tests and the determination of average results.

Fortunately the discussors have brought out in each instance important suggestions regarding the method of test. These will be helpful for a continuation of the program. In planning the program of the paper, all persons concerned anticipated a variation in results of the order of 100 per cent or more even assuming nearly perfect accuracy in measuring the stray loss. This was because in many of the tests the brush-friction and brush-contact electrical losses which are highly variable were to be of the same order of magnitude as the stray loss itself and, therefore, cause the stray loss to be highly variable.

In all machines stray load loss should be recognized as an unstable item changing with conditions of operation and the length of time between change of conditions, being less stable for some machines than for others.

It was expected that by measuring the separate no-load losses accurately both by dynamometer and running light input methods and plotting the results as a function of speed, or field current as the case might be, that the error in these losses would be reduced to a negligible factor even considering the amplification of error due to the small remainder when these losses were subtracted from the total losses. The real question concerns the measurement of the total losses. Here we felt confident that the input and output could be measured using carefully calibrated meters and dynamometers under laboratory conditions, so that when the output was subtracted from the input the accuracy of the remainder would be good. Those who have made stray load loss tests in similar motors will recognize that there can be large variations in results regardless of the method used. Nevertheless, the best method should be used and our first choice for future tests would undoubtedly be one of the methods giving a direct measure of total losses.

It should be recognized that 243 stray load loss tests were made and in the charts showing average loss against rated horsepower each point except one is the average for 54 tests; also in the charts for average loss plotted against speed, or flux, or load current, each point is the average of 81 tests. The tests are not each of equal weight but their weights are smoothly graduated and the tests where the probability for error is the greatest are those of least weight. Therefore, it would appear that the average results are truly characteristic of the motors. For example, the over-all average of the 243 tests gave the load loss as 3 per cent of the output and simultaneously the average output for the 243 tests was 4/9ths of rated full load power. This is considered a true characteristic of these motors.

We know that if additional tests had been made on larger motors the stray load loss as a percentage of output would be less as the discussors point out. The factor 0.02 in equation 5 of the report would be less, or more certainly the form of equation 5 would come out differently to show the loss as a function of physical size in addition to the other factors appearing in the equation. Furthermore, a discontinuity would be expected at the point in size where machines become compensated by pole face windings. Since an exchange motor test program is not practical with large motors and since perhaps the manufacturers already have test data at hand which could be made available to the committee, it behooves the committee to seek these data. Until it is accumulated and its meaning determined it is, of course, not proper to consider any proposal for change of the present standard allowance of 1 per cent of the output.

Protection of Stations Without High-Voltage Switching

AN AIEE COMMITTEE REPORT

In recent years there has been considerable interest in the tapping of high-voltage transmission lines to serve various types of loads and the installation of the transformers on these taps without high-voltage circuit breakers. The necessity to supply war loads with a minimum use of material provided a great incentive in this direction. Also, the present high costs of construction have increased the desirability of this type of installation.

It is well-known that the omission of the high-voltage circuit breakers complicates the problem of providing adequate relay protection for the line and the transformer tapped on the line. In some cases, the omission of high-voltage circuit breakers on tapped transformers makes it impracticable to obtain adequate line protection without the use of carrier-current or pilot-wire relays.[1] Protection for the tapped transformer requires tripping the high-voltage line circuit breakers which may be several miles distant from the transformer. Various methods are in use at the present time to accomplish this function.

In order to obtain information on the types of protective systems being used for the protection of stations without high-voltage circuit breakers, the AIEE relay committee has reviewed the practice being followed by the industry in this type of station. A questionnaire has been circulated covering the principal items under consideration, and answers have been received from a large number of representative companies from various parts of the United States and Canada. The answers received from these companies have been recorded in Table I. Various companies submitted detailed diagrams of their installations, and these have been grouped into the representative types shown in Figure 1. The stations without high-voltage circuit breakers can be classified into two categories; stations that are tapped to high-voltage transmission lines; and stations at which high-voltage lines are terminated without the use of a high-voltage circuit breaker.

The survey was limited to installations where the primary voltage was 66 kv or higher and involved those stations that have no form of local protection, such as a circuit breaker or a fuse.

Summary of Information Received

QUESTION NUMBER 1

How many stations without high-voltage switching are installed and how long have they been in service on your system?

Practically all companies answering the questionnaire indicated that they had some installations of stations without high-voltage switching. The 25 companies reporting had 169 installations, some of which had been in service up to 25 years. This would indicate general acceptance of this method of supplying substation loads and terminating high-voltage lines in order to obtain economical installations.

QUESTION NUMBER 2

What types of transformer protection are used for these installations?

The answers to this question agree substantially with the report presented in 1946[2] by the relay subcommittee on the

Summary of the Questionnaire Which Was Circulated

Question Number

1. How many installations of stations without high-voltage switching, and approximately how long have they been in service on your system?
2. What type of transformer protection is used for these installations?
3. What methods, if any, are used to trip the remote high-voltage line circuit breakers for trouble at the local station without high-voltage switching?
4. What size transformers are installed?
5. What is the largest size transformer that would be installed on your system without high-voltage switching?
6. What are the distances from the point where the station is located to the adjoining circuit breakers?
7. If an automatic grounding switch is used for protection, what is the time required for its operation?
8. If remote trip is used, describe the method. If pilot wire is employed, are the wires owned or leased?
9. If a reclosing system is employed on the high-voltage line, does the remote trip system lockout the reclosing procedure?
10. Experience Data: what has been your experience with this type of installation? Describe cases of failure if any have occurred.

Paper 49-65, recommended by the AIEE relay committee and approved by the AIEE technical program committee for presentation at the AIEE winter general meeting, New York, N. Y., January 31–February 4, 1949. Manuscript submitted November 8, 1948; made available for printing December 23, 1948.

This report was prepared by the project committee of the AIEE relay committee, power group.

The personnel of the project committee consists of: E. L. Michelson, *chairman;* L. F. Ferri, L. L. Fountain, V. J. Hayes, R. A. Larner and K. N. Reardon.

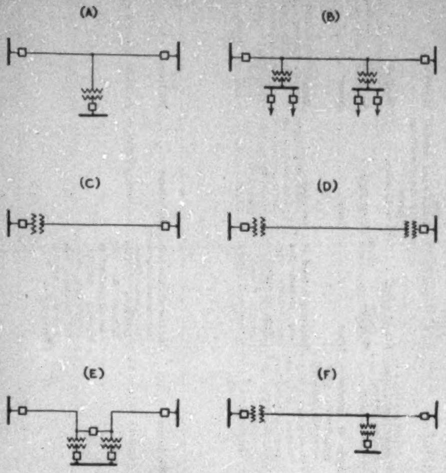

Figure 1. Typical stations without high-voltage switches

status of transformer protection. Various methods are used, depending upon the size of transformer and other considerations. In most cases, transformers of large size are equipped with differential relays. It should be noted that not all of the methods listed for each company are used on each installation.

QUESTION NUMBER 3

What methods, if any, are used to trip the remote high-voltage line circuit breakers for trouble at the local station?

The answers to this question indicate use of various methods to trip the remote line circuit breakers for trouble at the station without high-voltage switching. In 69 installations out of the total 169, there is no special method, and the only protection consists of the relays at the main terminals of the line, which are used primarily for line protection. On the remaining 100 installations, the methods used to produce remote tripping consist of special grounding disconnect switches or remote-trip relay schemes which function either through pilot-wire or carrier-current systems. These methods are described in more detail under a later question.

QUESTION NUMBER 4

What size are the transformers?

It was indicated there is practically no limit to the size of transformer installed without high-voltage switching, installations up to 100,000 kva being reported in this survey. Other cases up to 180,000 kva are known.

QUESTION NUMBER 5

What is the largest transformer that would be installed without high-voltage switching?

In most instances it was indicated that there was no definite limit.

QUESTION NUMBER 6

What are the distances from the point where the station is located to the adjoining circuit breakers?

The answers to this question indicated that distance was not an important factor, since such distances ranged from 100 feet to 100 miles.

QUESTION NUMBER 7

If an automatic grounding switch is used for protection, what is the time required for its operation?

The principle of the grounding switch is comparatively simple. It consists of a special disconnect switch arranged for high speed closing, with the closing circuit initiated by the protective relay used on the transformer without a high-voltage circuit breaker. When the grounding disconnect closes, it places a solid phase-to-ground fault on the transmission line, which permits the line relays at the main terminals of the line to de-energize the entire line. Closing times of six cycles to two seconds were reported, most of the installations being about 15 cycles.

QUESTION NUMBER 8

If a remote trip is used, describe the method. If pilot wire is employed, are the wires owned or leased?

The remote-trip schemes are based on the use of either pilot wires or carrier current. The use of pilot wires is comparatively simple, but the cost of pilot wires is the principal disadvantage of this scheme. Where pilot wires are used, the scheme generally consists of initiating a d-c signal by the differential or other relays that are used to protect the station without high-voltage switching. This d-c signal is received at the line terminals and provides for the tripping of the main circuit breakers. One advantage of this scheme is that high-speed tripping can be obtained safely by this method.

In some cases, separate wires are used for this function, but in many cases the d-c signal is superimposed on wires that are used for other purposes.

Where pilot-wires are used, there is no general agreement on the use of owned wires or leased wires, both being used.

On longer transmission lines the remote-trip function is accomplished by the use of carrier-current signals. Many special methods are being used at the present time to accomplish this function.

The principal problem in setting up a remote trip circuit by carrier current is to provide safe operation, considering the possibility of false signals being introduced into the line due to lightning, arcs at the terminals due to switching, and other causes.

One method for preventing false tripping which has been used successfully is to provide one signal which is on the line continuously and blocks the remote-trip function. In order to set up the remote trip circuit, it is necessary to shut off this blocking signal and introduce a tripping signal.

Another method is to use time as a factor by requiring that the remote trip signal be on for a period of time. The possibility of false operation is thereby reduced considerably.

In some cases it is necessary to consider the tapped transformer as a line terminal, with the result that a more elaborate relay scheme is required to obtain adequate system protection. This may mean carrier-current blocking equipment at the tapped installation (to prevent tripping the remote circuit breakers for low-voltage faults) or full carrier-current relay equipment if simultaneous fault clearing is necessary in order to permit automatic reclosing. Transformer faults then are cleared by adding to the carrier-current relaying scheme a remote trip function. In the case of short lines a

Table I. Summary of Protection of Stations Without High-Voltage Switching

Question	Company Number 1	Company Number 2	Company Number 3	Company Number 4	Company Number 5	Company Number 6	Company Number 7	Company Number 8	Company Number 9
1	20 stations—average nine years per station	6 stations—1 to 13 years	1 transformer bank, in service 11 years	1 station, in service seven years	4 stations—years not given	26 stations—up to 25 years	4—installed during war years	12 stations up to 18 years	None at present—had one in service 4 years
2	Banks under 5,000 kva: Overcurrent at remote ends—banks over 5,000 kva:—Differential, low-oil level low-oil pressure, and high temperature	Varies with stations—use combinations of: Differential - overcurrent-low oil-temperature	Differential and overcurrent	No protection (radial system)	Varies with stations—use differential ground, reactance, overcurrent, pilot wire, and carrier relays	High side fuses, thermal relays, overcurrent and differential relays	Carrier relays on terminals of line—distance relays on terminals of line and distance relays directional to bank on low side—differential relays which operate grounding switch	5 stations no protection; others have overcurrent relays	Differential relays
3	Single pole grounding switches closed by differential relays	4 stations—single pole grounding. One special case—phase to ground (Used because of ground fault neutralizer)	Current pilot wire relay scheme	Remote circuit breakers are not tripped for low-voltage faults	Pilot wire and carrier	Single pole grounding switches	None, except one station that has single pole grounding switch which is closed by differential relay	No remote tripping scheme	Automatic ground switch
4	1,000 to 20,000 kva banks	5,000 kva to 10,000 kva	40,000 kva	3,000 kva bank	30,000 kva to 75,000 kva	12,000 to 20,000 kva	9,000 kva to 12,000 kva	2,000 kva to 12,000 kva	15,000 kva
5	Size not considered a limiting factor	Do not know	Do not know	Do not know	No limit set (Based on using remote tripping)	No fast rule	No set standard	Transformer capacity not governing factor	15,000 kva
6	6 to 65 miles	6¼ to 26 miles	3.1 miles	6 to 12 miles	8 to 11 miles	60 miles (using fuse) 5 miles (others)	4 to 61 miles	5 to 15 miles	50 miles
7	30 cycles	9 to 12 cycles	None used	None used	None used	15 cycles or less	20 cycles	None used	15 cycles
8	Not used	Not used	Owned pilot wires	Pilot wires leased	Owned and leased pilot wires. Owned coaxial cable	None at present—proposed pilot wires will be owned	None	None	None
9	When 20 cycle reclosing employed. Carrier current relay signal is used to lock out reclosure. For normal automatic reclosure, the 1st reclosure delayed enough for transformer to be disconnected automatically by high voltage air break switch	Not used	Not used	Not used	Not used	Yes	Reclosing is used at one station—but no remote trip. None on others	Not used	None
10	No cases of failure	Experience satisfactory. No incorrect operation. One case where a grounding switch fell closed due to defective latch	Two cases of insulator failures which operated transformer differential relay and remote circuit breaker was properly tripped	No failures	No failures except two tripping operations due to double grounds on pilot wires in substation. Rectified by use of separate pilot wire battery	No failures	One transformer failure caused lockout on terminal circuit breakers. Two failures of tap change mechanism caused shorting switch to close, far terminal line circuit breaker tripped	No failures	No trouble

Table I. (Continued)

Question	Company Number 10	Company Number 11	Company Number 12	Company Number 13	Company Number 14	Company Number 15	Company Number 16	Company Number 17
1	3 stations—up to 22 years	10 stations, from 1 to 17 years	4 stations, from 1 to 17 years	2 stations from 2 to 7 years	15 stations from 1 to 19 years	5 stations—(years omitted)	16 stations from 15 to 20 years	2 stations, about 77 years
2	Use overcurrent, differential, directional overcurrent, and directional distance	Overcurrent, reverse overcurrent differential, thermal, reverse magnetizing, high-low oil; high-low gas, directional ground, and modified directional impedance relays in conjunction with carrier	Directional overcurrent, distance, directional overcurrent phase and ground, differential, ground, and pilot wire relaying	One station: percentage differential other: —differential ground and directional overcurrent. Oil temperature and gas pressure relays operate signal only	Overcurrent or directional phase and ground relays at source end of line; or differential relays	Differential relays	No local protection—protection obtained by overcurrent relays at remote line	Differential — directional distance—Overcurrent Phase and Ground—directional ground
3	One station none, one station pilot wire, other station carrier	Carrier with audio tones	For three stations tripping of remote high-voltage circuit breakers not initiated by local transformer relays. One station uses pilot wire for transfer tripping	Transfer trip via pilot wires at one station—carrier to be installed at other station	None. Depend upon line relaying at remote high voltage circuit breakers	Carrier—pilot wire—single phase grounding	Not used	Depend on directional distance protection at the far end
4	15,000 kva to 25,000 kva	7,500 kva to 67,000 kva	30,000 kva to 100,000 kva	24,000 kva to 50,000 kva	4,000 kva to 37,500 kva	7,500 kva to 40,000 kva	Largest—14,000 kva	25,000 kva
5	Probably 30,000 kva	80,000-kva auto transformer	Approximately 50,000 kva	Not known	Would not hesitate on size	No limit	No limit established	No limit established
6	3 to 28 miles	5 to 66 miles	5 to 15 miles	7.7 to 10.7 miles	5.4 to 41 miles	9.5–48.7 miles	Few miles to 20 miles	20 miles
7	None used	None used	None used	None used	None used	Not measured	Not used	Not used
8	Pilot wires leased—one station; —method is directional comparison by carrier directional distance relays plus carrier code transferred trip when low-tension circuit breaker opens on transformer differential	Remote trip uses carrier frequency plus audio tones of 150 and 208 cycles. The differential relays on the transformer energize an auxiliary lock-out relay, which in turn, trips the local circuit breaker and sends out the remote trip signal to the distant source terminal	Use pilot wire monitoring and transferred tripping relays on leased pilot wires	Owned pilot wire	None	Use 2-tone audio signal superimposed on carrier and time delay relay—also single-tone audio signal without time delay. Also leased pilot wire polarized d-c. Relay at remote end	None	None
9	Reclosing is manual, but hand reset lockout relay operated by remote trip warns operator not to reclose	Yes. The automatic reclosing on the local circuit breaker is locked out; and the receiving of a remote trip signal at a distant source locks out the automatic reclosing on the high-voltage line at that location also	Automatic reclosing not used—but the transferred tripping scheme locks out the closing circuits of the remote circuit breakers	Not used	Not used	Reclosing scheme is used only in case of automatic grounding switch and it is not lock-out	Not used	Not used
10	One failure on low side transformer leads operating differential relays and correctly operating remote trip. Two cases of incorrect operation of transformer differential relays resulting in operation of remote trip	No actual transformer failure calling for operation of remote trip. Two false trippings believed due to disturbances in the d-c supply to carrier audio tone transmitters and receivers causing trip signal to be sent out. Filters to be installed to prevent such disturbances	One case of trouble of high-voltage bushing flash-over on 30,000-kva transformer. Fault cleared by ground relay at remote end of line	No failures	Satisfactory — only two transformer failures	Several incorrect operations with tone - modulated carrier scheme	Satisfactory	Good—no failures of protective equipment

Table I. (Concluded)

Question	Company Number 18	Company Number 19	Company Number 20	Company Number 21	Company Number 22	Company Number 23	Company Number 24	Company Number 25
1	8 stations—up to 20 years	2 stations—each 8 years	2 stations—up to 6 years	3 stations—1 to 6 years	3 stations—2 under construction—1 to 5 years	13 stations from 1 to 20 years	8 stations from 2 to 20 years	1 station (years omitted)
2	Overcurrent relays; differential at one installation	Overcurrent at one station and overcurrent and differential at other	Overcurrent and differential	Differential	Overcurrent and differential	Differential, overcurrent, gas detector	Differential relays	Impedance and ground relays
3	Carrier plus backup relays. Also overcurrent relays	One station: single pole grounding switch actuated by differential relay	Carrier and pilot wire	Grounding disconnect	Grounding disconnect	Ground 1, 2, or 3 phases; relay on remote-end line protection	3 stations use transferred-tripping over relay pilot wires	Impedance and ground relays
4	30,000 kva to 60,000 kva	25,000 kva to 45,000 kva	45,000 kva to 100,000 kva	10,000 kva to 41,000 kva	15,000 kva to 52,000 kva	4500 kva to 50,000 kva	30,000 to 100,000 kva	30,000 kva
5	No limit	Unknown	100,000 kva	Not known	No limit	No set limit	100,000 kva	Would not install in future
6	20 to 90 miles	33 to 40 miles	3 to 52 miles	3.5 to 9 miles	1 to 27 miles	100 feet to 100 miles	5 to 15 miles	70 miles
7	None at present—to be installed on one bank—11 cycles	Instantaneous	Not used	Spring operated; 6 and 12 cycles, motor operated 2 seconds	18 cycles	Approximately 1 second	Not used	Not used
8	None at present—but under consideration	None	Radio frequency carrier current relaying with 3,000-cycle modulation trips the remote ends of the lines after 1/4-second delay. Also differential relays initiated the transfer trip by increasing the direct current transmitted over the owned differential pilot wire system	None	None	Not used at present. A carrier current remote trip scheme used for a while was not satisfactory	Superimposed direct-current over leased pilot wires used for a-c pilot wire relaying	Not used
9	None at present	Not used	Not used	Not used	Not used	No, permit one reclosure. Prefer delaying reclosure long enough for transformer to be disconnected automatically by motor-operated disconnects	Not used	Not used
10	Very good	Good—no failures	One case where relay in remote trip circuit failed to make contact. Routine tests also indicated: defective tubes in carrier radio equipment—3 cases faulty operation of relays—minor trouble in communication channel units. Some trouble in maintaining constant current in monitoring relay and pilot circuit, cause undetermined	Satisfactory	Satisfactory	Satisfactory. Motor-operated grounding switches more reliable than spring operated switches	No adverse experience	Satisfactory but residual currents at far end for ground faults near high-voltage side of transformer are too small for positive relaying

pilot wire scheme may be used to accomplish the same results.

Question Number 9

If a reclosing system is employed on the high-voltage line, does the remote trip system lock-out the reclosing procedure?

At the present time, reclosing systems are not generally used, as indicated by this survey. In those cases where reclosing is used, various schemes are employed. In some cases there is no lock-out system and the line is permitted to reclose on the fault. If the fault is in the transformer, or is some other type of permanent fault, the relay system will function to reopen the line. In other cases, a lock-out scheme is employed and the remote trip signal is used to prevent automatic reclosing.

In one case, the protective relays automatically open the transformer disconnects at the tapped station, and reclosing is permitted to take place within two seconds after the first opening.

Question Number 10

Experience data.

Practically all companies reported satisfactory experience with this type of installation. Some trouble has been reported with the remote-trip carrier schemes. The general opinion obtained from most companies would indicate that stations without high-voltage switching can be operated and protected successfully.

References

1. Relay Protection of Tapped Transmission Lines, M. A. Bostwick, E. L. Harder. Electrical Engineering (AIEE Transactions), volume 62, 1943, pages 645–50.

2. Relay Protection of Power Transformers, AIEE Relay Subcommittee. AIEE Transactions, volume 66, 1947, pages 911–17.

Discussion

V. J. Hayes (Connecticut Light and Power Company, Waterbury, Conn.): This report would indicate that, in general, satisfactory experience with this type of protection can be obtained. Out of the 25 companies reporting on a total of 169 installations, four found cases that could be considered as incorrect operation which might make desirable a change in the original design of the remote tripping scheme. One of these was on a pilot wire system where double grounds occurred. This type of trouble is not difficult to detect, and in the case reported a remedy was devised for it. A second company reported one case where a relay in the remote trip circuit failed to make contact. The other two companies reported difficulties which were associated with audio-tone-modulated carrier systems. One of these two attributed the false tripping to variations in the d-c supply to the audio-tone-trip signal transmitter and receiver units. It is possible that the operation of d-c equipment, such as motors, on the same source as the carrier sets caused a ripple in the d-c voltage containing frequencies that were within the operating range of the audio-tone-trip signal units. Filters to prevent such disturbances are mentioned as a remedy.

Another possible source of incorrect operation in tone-modulated carrier systems is due to beat frequencies caused by two or more simultaneous carrier frequency signals on such a system. Trouble is not likely to occur if two audio frequencies are used to supervise the remote tripping circuits, but field tests have shown that single audio-tone receivers will operate when the two or more simultaneous carrier frequencies produce a beat note within the operating range of that receiver. This can probably be avoided by separating the carrier frequencies employed on that system by an amount so that the combination of their nominal separation and drift in frequency of the individual carrier sets does not produce a beat note within the operating range of the audio-trip signal units.

J. A. Elzi (Commonwealth and Southern Corporation, Jackson, Mich.): We are all vitally interested in methods of accomplishing desired results as economically as possible without sacrificing reliability or introducing undue complications. This frequently calls for a great deal of ingenuity and study to make sure that the simplification used does this without introducing unforeseen hazards. A survey of actual field experience such as given in this report is therefore of very great interest and importance to the industry.

This report deals primarily with the protection of stations with particular emphasis on the protection of the power transformers at these stations. A recent AIEE paper on Relay Protection of Power Transformers[1] indicates that where switching equipment is provided for power transformers, differential protection is the generally accepted method of clearing transformer faults and that very few transformers are protected only by other back-up relays. In contrast to this, it is noted that out of a total of 169 installations without high-voltage switching, 69 provide no special method of protecting the transformer and the only protection consists of the relays at the main terminals. It would seem that we have unduly sacrificed transformer protection in stations without high-voltage switching. This may be due to undesirable features of available schemes of protection, a lack of reliabliity, or excessive costs.

Of the 100 installations that reported the use of some means of remote tripping, the special grounding switches seem to be used most frequently, and they also seem to indicate the greatest degree of reliability. There are, however, some very definite objections to placing a fault on a transmission line in order to clear a fault in a transformer. Also the time required to clear a transformer fault by this method is somewhat longer than by other methods so that this method cannot be said to give as good protection as would be provided by some of the other methods.

A few installations of remote tripping over pilot wire are mentioned and the answers to Question Number 10 indicate that some trouble has been experienced with this type of protection. This is not surprising in view of the very low current used for tripping in many of the pilot wire schemes. For example, one scheme requires only $1^1/_2$ to 2 milliamperes with a maximum of 5 milliamperes available for tripping, and another scheme requires 6 milliamperes for tripping with only 8 milliamperes available. Considering the number of cases of trouble reported compared with the number of installations reported as using the pilot wire remote tripping scheme, it would seem that there is a real need for improving this type of tripping scheme.

Under Question Number 8 the authors mention some of the possible causes of incorrect tripping when carrier current is used to provide the remote trip function. If we interpret this survey correctly, there are four of the reporting companies now using some form of carrier signals for remote tripping, and three of these reported trouble. Two companies have such equipment under consideration. One company reported that a carrier current remote trip scheme which was used for a while was not satisfactory and has been removed from service. The report therefore seems to definitely indicate that we do not have a reliable and satisfactory scheme of providing remote trip by carrier signals. The authors mention the introduction of time delay as a means of overcoming some of these difficulties. The length of time required is not given, but it can be seen that the introduction of appreciable time delay is very undesirable from the standpoint of providing adequate transformer protection.

It is felt that the statement made in this report under Question Number 10 is too optimistic and gives a false sense of security. Those companies using no remote tripping scheme are not providing transformer protection comparable to that provided where high-voltage switchgear is used. The line grounding switch seems to be the most dependable and reliable but introduces a certain amount of time delay and is somewhat undesirable inasmuch as it introduces a fault on the line. The pilot-wire and carrier-current remote trip schemes which would provide transformer protection comparable to that obtained with high-voltage switching are not shown to be very reliable by the report and should be made the subject of further study.

Reference

1. Relay Protection of Power Transformers, AIEE Committee Report. AIEE Transactions, volume 66, 1947, pages 911–16.

Chester E. Bauman (Harza Engineering Company, Chicago, Ill.): It probably is beyond the intended scope of this report to include the problem of stability in connection with low-voltage switching of transmission lines. We have found stability to be the important consideration. In one specific case where a large hydro was located 145 miles away, it was necessary to clear all "2-line to ground faults" on the lines in 0.1 second. This would not allow time for using any kind of short-circuiting switch on the transmission line. In fact, we found that the large change of transfer reactance occasioned by switching out the transformer at both ends along with the transmission line resulted in instability.

In one case where we employed low-voltage switching with transfer tripping operated by transformer differential relays, we experienced trouble due to automatic battery charger at one end causing false operation of transfer tripping. The exact cause of the trouble was not determined, but replacement of the automatic charger by a motor generator set eliminated the trouble. If similar trouble has been experienced by any other engineers, their comments will be appreciated.

E. L. Michelson: In Bauman's discussion he points out one of the limitations of the type of transmission line discussed in this report. The committee study did not encompass a study of the various applications of the tapped transmission line. While there are some limitations in its use, actual experience indicates that there are many instances where it is economical to install taps on high-voltage transmission lines.

All of the discussors point out the difficulties which have been experienced in setting up a reliable remote tripping scheme. We agree that this is one of the present limitations in the protection of tapped transmission lines. Undoubtedly, there will be further developments in this field, and improvements made in carrier-current and pilot-wire systems, to insure more reliable operation. The AIEE relay committee expects to continue its study of this subject and promote interest in the development of improved methods of remote tripping.

In the matter of tripping time for transformer faults, there appears to be some difference in opinion as to the need for very high-speed protection. While there obviously are advantages to 1-cycle protection under all conditions, on the other hand, no system difficulties may be experienced if protection for a low-voltage system, or a transformer, is delayed for a few cycles. The damage caused by a low-current fault may not be sufficient to justify very elaborate schemes to obtain 1-cycle operation.

Electronic Relay Developments

JAMES J. LOVING, JR.
MEMBER AIEE

THE NEW advances in electronics accelerated by the recent War offer many applications in addition to their use for military, aviation, or communication purposes. This paper describes briefly the results of some experimental and development work on the application of electronics to electric power system protective relaying. Heretofore, the use of electronic circuits in relaying schemes has been mainly as a supplement to the more conventional electromagnetic schemes, as for examples, the use of carrier current in a pilot directional scheme and auxiliary electronic relays for timing, and so forth. The purpose of the development work described here has been twofold—first, to apply the newer techniques to the fullest advantage and second, to employ electronic circuits so as to perform complete relaying functions in themselves.

The advantages offered by these electronic relay circuits as developed and compared with electromagnetic types or prior electronic types are as follows:

1. The number of moving parts and contacts has been reduced to an absolute minimum by having all functions of fault detection, determination of direction and distance, insertion of intentional time delays, and so forth, performed by the electronic elements, so that the only moving elements required are those in the actual tripping, indicator, and alarm circuits. A small mechanical relay is operated by the final output tube if circuit breaker tripping is required.

2. With a few minor exceptions, the circuits are constructed of standard electronic parts, the only special work required being the construction of a suitable chassis or housing unit and a few special windings on transformers.

3. A high degree of accuracy is obtainable in the determination of overcurrents, in the measurement of distances to faults, and in the insertion of intentional time delays. The characteristic curves are very flat throughout the operating range for such functions as fixed time delays, reach of distance elements with varying voltage and current, and operating time in the first zone of a distance relay application.

4. The sensitivity of the vacuum tube elements provides proper action with very low system voltages, and they respond during the first cycle of fault.

5. The only magnetic parts involved are the cores of radio-type transformers and consequently there are no adverse effects due to magnetic saturation as sometimes occur in electromagnetic relays when the fault current has a long d-c transient. The energy required for actuation of the electronic elements is very small, resulting in small burdens on potential and current transformers.

6. All vacuum tube circuits place very light loads on the tubes, with the development centered around the use of the *6SL7* and *6SN7* types, so that reliability and long tube life can be expected with the use of a minimum number of tube types.

7. In a carrier current relaying scheme, electronic elements can furnish directional control of the carrier channel, with actuation of the transmitter and utilization of the received signal being performed electronically. Since the transmitter can be turned on at very high speed, it is not necessary to start carrier by a distance element and stop it by a directional control, but rather the carrier transmitter is actuated by a distance-directional element responsive only to faults in the reverse direction. This allows very high speed tripping for internal faults.

The principal disadvantages of these electronic circuits stem from the fact that they depart considerably from standard relay practice in the past:

1. In the development, particular attention was paid to attaining reliability, but this remains an unknown factor until such time as extended tests in actual operation can be made.

2. Electronic applications are relatively new in the utility industry and in particular, relay operating engineers and maintenance men are not generally acquainted with electronic techniques.

3. The internal wiring is somewhat more complex than the electromagnetic equivalent, but this is probably compensated for by the simplification of the external wiring.

4. As at present developed, the circuits depend upon standard station battery of 125 volts for heating vacuum tube filaments and furnishing positive d-c potentials, and place a slight additional drain on these batteries.

5. Although built-in test switches can furnish a quick means of testing the functioning of all tube elements, periodic tests or replacements at fairly long intervals would still be required.

General Principles

In Figure 1 is a 1-line diagram of a section of a transmission line which illustrates the manner of applying electronic relays for protection of the line against faults. Electronic relays can be constructed for any type of relaying required and in most cases the relaying for phase faults would fall into one of three classifications: directional overcurrent, distance directional, and carrier current. The type of ground fault protection would be co-ordinated with the phase fault protection. Thus, a 3-phase electronic directional overcurrent inverse time-delay relay and an electronic ground directional relay could supply overcurrent protection for the line. Or a 3-phase electronic distance-directional relay with one, two, or three zones could supply faster tripping for the greater length of the protected line and back-up for the other zones. For best fault location and highest speed, electronic relays could be provided for furnishing directional control in a carrier current relaying scheme.

In Figure 2 is a block diagram illustrating the general method used with a

---

Paper 49-66, recommended by the AIEE relay committee and approved by the AIEE technical program committee for presentation at the AIEE winter general meeting, New York, N. Y., January 31–February 4, 1949. Manuscript submitted November 1, 1948; made available for printing December 23, 1948.

JAMES J. LOVING, JR. is an engineer in the research and engineering division of the Airborne Instruments Laboratory, Inc., Mineola, N. Y. The development work described in this paper was performed independently prior to his present affiliation.

Acknowledgment is made for the helpful assistance of the author's associate, Claude R. Durbin of Buffalo, N. Y.; also of Professor M. K. Akers of George Washington University, T. D. MacCoun of Link Radio Corp. and many operating and design engineers consulted.

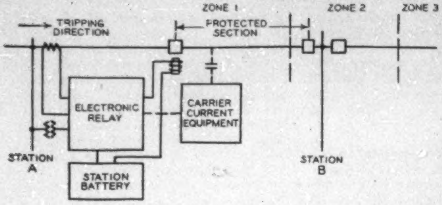
ZONE 1
ZONE 2
ZONE 3
TRIPPING DIRECTION
PROTECTED SECTION
ELECTRONIC RELAY
CARRIER CURRENT EQUIPMENT
STATION A
STATION BATTERY
STATION B

Figure 1. Application of electronic relaying to transmission line protection

3-phase electronic relay connected to a line through a set of potential transformers and a set of current transformers. Since the electronic elements are voltage actuated, the line currents are not utilized directly but are carried through the primaries of small coupling transformers included within the electronic relay, and the outputs of these transformers are used to reproduce the line currents. In order to make a comparison of phase and polarities of the line currents with other system conditions, such as the line voltages, the reproduced current waves are converted into series of sharp voltage pulses by electronic pulse forming circuits.

The pulses are first applied to fault-type detector circuits whose main function is to insure that the proper currents and voltages are compared in order to provide correct relaying. They are then applied to functional elements, such as directional and distance elements, with control voltages derived from the protected line. If these functional elements determine the fault to be within the protected section, the pulses are allowed to pass to an impulse circuit for actuating the tripping circuit. The dotted sections indicate that there are complete elements for each phase of the protected line and also there may be elements for ground protection. The actions of all the phases are combined in the impulse circuit. In Figure 2, the positive pulses sketched at the output of the pulse-forming circuits may be passed by the fault-type detector circuits as shown by (a) or they may be blocked or clipped as shown by (b). Similarly, the functional elements may pass the pulses as in (c) or block them as in (d). This description applies to any relaying scheme where instantaneous action is desired, but in overcurrent relaying with inverse time delay or in zone-type distance relaying, intentional time delays must be inserted to provide sequential operation. The method of applying inverse time delay is illustrated in Figure 3. In addition to actuating the pulse-forming circuits, the outputs of the current coupling transformers are rectified to provide a d-c voltage proportional to line current flowing. This d-c voltage provides a tripping impulse after a delay inversely proportional to line currents provided that the functional elements of the relay determine the fault to be in the tripping direction. The delay action is thus directional controlled.

Figure 2. Block diagram of general principles

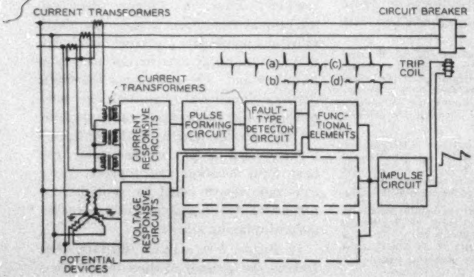
CURRENT TRANSFORMERS
CIRCUIT BREAKER
CURRENT TRANSFORMERS
(a)
(b)
(c)
(d)
TRIP COIL
CURRENT RESPONSIVE CIRCUITS
PULSE FORMING CIRCUIT
FAULT-TYPE DETECTOR CIRCUIT
FUNCTIONAL ELEMENTS
IMPULSE CIRCUIT
VOLTAGE RESPONSIVE CIRCUITS
POTENTIAL DEVICES

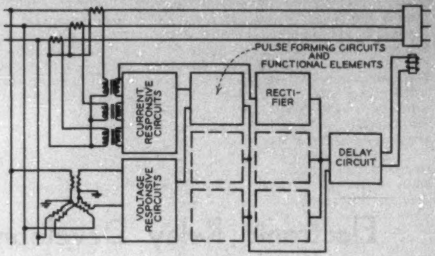
PULSE FORMING CIRCUITS AND FUNCTIONAL ELEMENTS
CURRENT RESPONSIVE CIRCUITS
RECTIFIER
DELAY CIRCUIT
VOLTAGE RESPONSIVE CIRCUITS

Figure 3. Block diagram of electronic relaying with inverse time delay

Where zone type protection is desired, the relay can be constructed as in Figure 4. Here there is a separate distance element for each zone of the protected line, and for the second and third zones fixed delay circuits are provided which are actuated only if the fault is within the particular zone. A fault in the first zone will operate the impulse circuit directly, but a fault in either of the other two zones will provide tripping only after the fault has persisted in that zone for a predetermined time period.

The method of combining electronic relaying with carrier current so as to provide an all-electronic directional controlled carrier relaying scheme is illustrated by the block diagram of Figure 5. Here a distance-directional element responsive to faults in the tripping direction actuates the impulse circuit. This causes circuit breaker tripping unless prevented by the blocking circuit controlled by the carrier current received from the remote end indicating that the fault is external to the protected section. A second distance-directional element responsive only to faults in the reverse direction actuates the carrier transmitter for preventing tripping at the remote end. Since the actuation of the transmitter is at very high speed, tripping for internal faults can also be at high speed since it is not necessary to turn on the transmitter in case of internal faults.

Figure 4. Block diagram of electronic relaying for zone-type distance protection

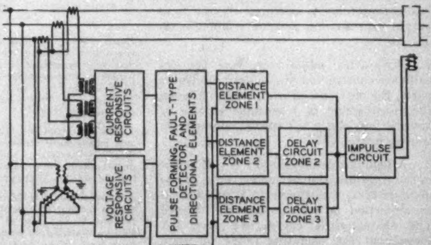
CURRENT RESPONSIVE CIRCUITS
VOLTAGE RESPONSIVE CIRCUITS
PULSE FORMING, FAULT-TYPE DETECTOR AND DIRECTIONAL ELEMENTS
DISTANCE ELEMENT ZONE 1
DISTANCE ELEMENT ZONE 2
DISTANCE ELEMENT ZONE 3
DELAY CIRCUIT ZONE 2
DELAY CIRCUIT ZONE 3
IMPULSE CIRCUIT

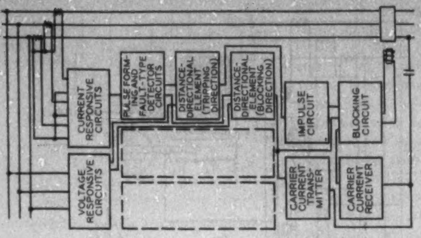
CURRENT RESPONSIVE CIRCUITS
PULSE FORMING AND FAULT-TYPE DETECTOR CIRCUITS
DISTANCE-DIRECTIONAL ELEMENT (TRIPPING DIRECTION)
DISTANCE-DIRECTIONAL ELEMENT (BLOCKING DIRECTION)
IMPULSE CIRCUIT
BLOCKING CIRCUIT
VOLTAGE RESPONSIVE CIRCUITS
CARRIER CURRENT TRANSMITTER
CARRIER CURRENT RECEIVER

Figure 5. Block diagram of all-electronic directional controlled carrier current relaying

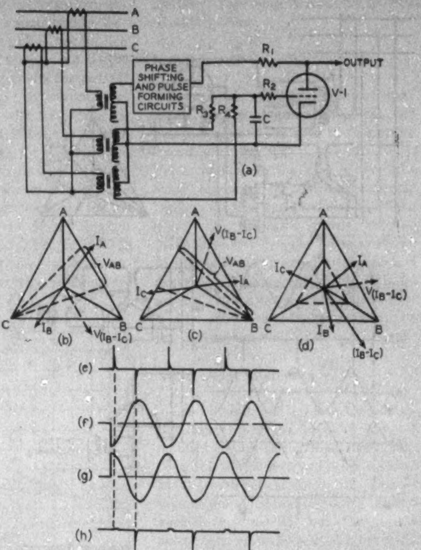
A
B
C
R1
OUTPUT
PHASE SHIFTING AND PULSE FORMING CIRCUITS
R2
V-1
R3
R4
C
(a)
A
IA
VAB
C
IB
(b)
V(IB-IC)
B
A
V(IB-IC)
VAB
IA
IC
C
(c)
B
A
IC
IA
V(IB-IC)
C
IB
(d)
B
(IB-IC)
(e)
(f)
(g)
(h)

Figure 7. Fault-type detector circuit

Pulse Forming Circuit

In order to provide a means of comparing the phase and polarity of the currents and voltage on a line so as to determine at high speed the direction and distance to a fault, the line current wave is converted into a series of sharp voltage pulses by the circuit shown in Figure 6(a). This circuit also serves as a means of detecting overcurrents and of providing phase shift in the current response of the relay when necessary. The secondary line current flows through a small coupling transformer and for a current wave form as shown in (b), the voltage output of this transformer leads the line current by 90 degrees as in (c). The phase-shifting circuit of R_1, C_1, R_2, and C_2 provides a voltage proportional to line current and approximately in phase with it as shown by (d). Electronic amplifier *V-1* is normally biased to cut-off and the time constant in the primary of the output transformer is made short so that the output of the amplifier will be a series of pulses as shown in (e). These are positive when the input voltage exceeds the cut-off level of the tube and negative when this voltage drops below cut-off. In place of the combination of current transformer and coupling transformer, it would be possible to use an air-core transformer in the line with output direct to the phase-shifting circuit.

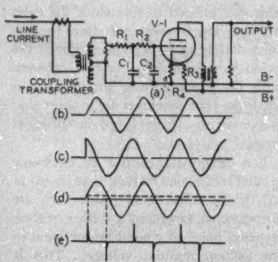
LINE CURRENT
V-1
R1
R2
OUTPUT
C1
C2
R3
B-
COUPLING TRANSFORMER
(a)
R4
B+
(b)
(c)
(d)
(e)

Figure 6. Pulse forming circuit

For use in an electronic overcurrent relay, the values of R_3 and R_4 providing positive cathode bias are selected so that utilization of the full output of the coupling transformer will provide pulses for a predetermined minimum line current, or in other words, the cathode bias determines the maximum sensitivity of the relay. The potentiometer at the output of the coupling transformer can be calibrated directly in terms of secondary line current.

For use in an electronic distance relay, the potentiometer is omitted and proper characteristics obtained by inserting a suitable phase-shift, as explained later in discussion of the distance element. The operating range in the phase overcurrent relays is 4-to-200 secondary amperes and in the distance and ground relays, 1-to-200 amperes. Greater sensitivity for the ground relays can be obtained by the use of taps in the coupling transformer.

The time constants R_1C_1 and R_2C_2 are both short when compared with the time constant of a normal d-c transient in the line current wave, and it can be shown mathematically that the response of the phase-shifting circuit will approach the steady-state after approximately one-quarter cycle, so that in the first peak the overswing of the transient is virtually eliminated. A transformer-coupled amplifier is used rather than a resistance-coupled amplifier so that fluctuations in battery voltage will not appear at the output.

Fault-Type Detector Circuit

In some applications it is necessary that the pulses caused by a particular line current be blocked from action in the relay unless the line current is due to a particular type of fault. One method of accomplishing this is demonstrated by the "fault-type" detector circuit of Figure 7(a).

The pulse-forming circuit is responsive to the line current in A phase so that pulses are produced for either an A-to-B fault or an A-to-C fault as shown in graph (e). These pulses are applied to the anode of *V-1* through resistor R_1 and the grid of *V-1* is controlled by a voltage proportional to (I_B-I_C) and shifted approximately 90 degrees ahead, this voltage $V_{(I_B-I_C)}$ being obtained from the coupling transformers associated with B-and-C phases through combining resistors R_3 and R_4.

For the case of an A-to-B fault as illustrated in the vector diagram (b), the voltage $V_{(I_B-I_C)}$ is negative at instants of the positive pulses as shown by graph (f)

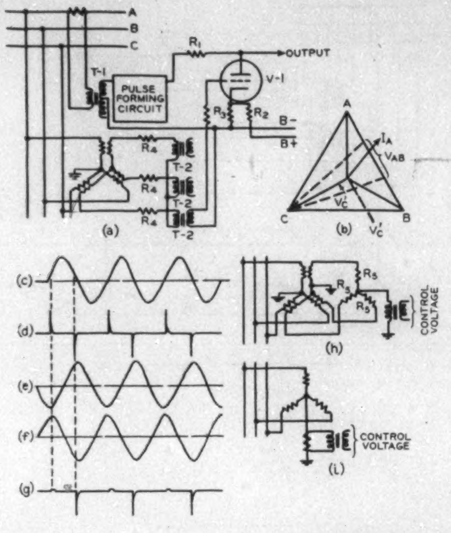

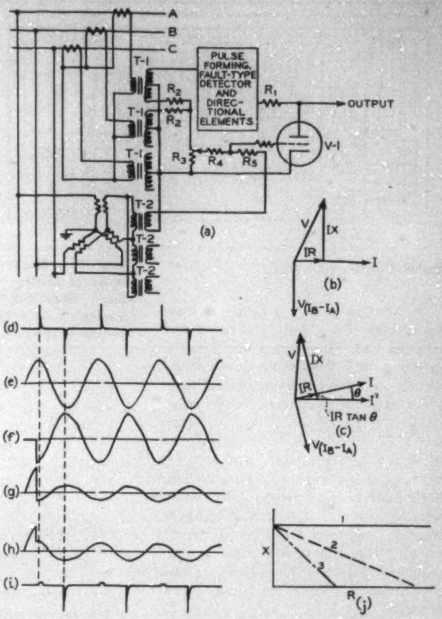

Figure 8 (left). Directional element

Figure 9 (right). Distance element

so that *V-1* is nonconducting at the instants of the positive pulses and they appear at the output. For the case of an A-to-C fault in the vector diagram (c), the control voltage as shown in (g) is positive at the instants of the positive pulses so that *V-1* is conducting and the pulses are dissipated through R_1 and the tube, and the output pulses are "clipped" as shown in the graph (h). This circuit performs correctly with or without load current in the line, as the fault current normally predominates over load current.

In order to allow the pulses to pass for the case of a 3-phase fault in the vector diagram (d), the capacitor *C* provides sufficient phase-shift in the control voltage

An alternate method of providing a response to an A-to-B fault but not to an A-to-C fault is to actuate the pulse-forming circuit by a voltage proportional to $(I_A - I_B)$ and to block the pulses by a voltage proportional to $(-I_C)$ and pass them by a voltage proportional to $(-I_A)$, this method requiring tube two elements instead of one.

For applications requiring ground preference relaying, a similar arrangement can be utilized with the control voltage actuated by ground current so as to block the pulses due to phase currents. Also the fault-type detector circuit can be applied to relaying involved in a single-pole reclosing scheme.

Directional Element

The circuit of Figure 8(a) demonstrates a directional element, with A-phase fault current as shown by graph (c) producing pulses as in (d). A voltage in phase with delta voltage V_{AB} is obtained by shifting the opposite star voltage V_C ahead 90 degrees, as shown by V_C' in vector diagram (b) for an A-to-B fault, and is accomplished by air-gap transformers *T-2* Y-connected through resistors R_4 to the secondary potentials. With a fault in the tripping direction, the control voltage (e) allows the positive pulses to pass, and with a fault in the reverse direction the control voltage (f) blocks or clips the pulses as shown in graph (g). Resistors R_2 and R_3 provide bias for *V-1* and this is adjusted so that with zero control voltage, the pulses are just blocked sufficiently to prevent relay action, thus obtaining high sensitivity.

If the pulses due to I_A are controlled by a fault-type detector circuit responsive only to an A-to-B fault, the action of this directional element will be correct no matter at what instant a fault occurs, as the current from phase A-to-B is caused by V_{AB} and will never turn positive when V_{AB} is negative. In the case of an A-to-C fault it is possible for I_A to be positive at the first instant of fault when V_{AB} is negative, so that without a fault-type detector circuit the arrangement cannot be used except where a slight time delay for tripping is allowed.

The opposite star voltage is used rather than using the delta voltage directly for two reasons. In case of dead short circuits, V_{AB} falls to zero whereas V_C retains full value. Also, it has been experienced that any coupling transformer of reasonable size utilized to reproduce the delta voltage directly will not drop to zero immediately at its secondary side if the primary voltage drops to zero, whereas with the phase-shifting arrangement as used, the time constants are so short that responses are accomplished in sufficient time.

For directional control in electronic ground relays, one method is as shown in (h), where three equal resistors R_5 are Y-connected, furnishing a voltage at their common point to ground proportional to the system residual voltage. This is coupled to the relay by a radio-type transformer, and the arrangement is possible because of the negligible energy

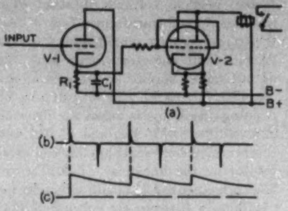

Figure 10. Impulse and tripping circuits

required. An alternate method is shown in (i) where the control voltage is obtained by causing the neutral current of a source of ground current to flow through a coupling transformer.

In the phase relays, by using the opposite star voltages, correct action is obtained for dead short circuits in either direction. For 3-phase faults, three-quarters volt rms (secondary) is required per phase to obtain tripping. In the ground relays, due to the gain in the coupling transformer, only one-third volt residual is required for tripping.

Distance Element

For determining distance to a fault, the phase-to-phase delta voltage is compared with the corresponding delta current. The method for doing this is illustrated in Figure 9(a). The pulses caused by A-phase line current are passed through fault-type detector and directional elements to determine if the fault is from A-to-B phases and in the tripping direction. A comparison is made between the A-B delta voltage on the line obtained from one of transformers *T-2* with a voltage proportional to (I_B-I_A) obtained from equal combining resistors R_2 and shifted ahead 90 degrees. This comparison is made by resistors R_4 and R_5 and the differential or balance voltage so obtained applied to the control grid of *V-1*. Graph (d) shows the pulses due to line current, (e) the delta voltage and (f) the voltage proportional to delta current. If in the balance voltage, the current predominates as in (g), the pulses will be passed to the output but if the voltage predominates as in (h), the pulses will be clipped as in (i). The distance setting is controlled by potentiometer R_3.

Figure 11. Time-delay elements

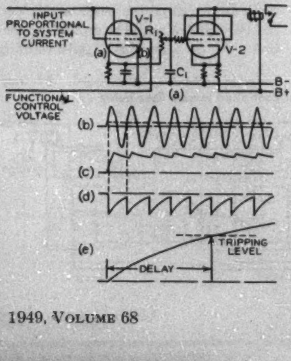

INPUT PROPORTIONAL TO SYSTEM CURRENT
V-1
R1
(a)
(b)
V-2
C1
B-
B+
(a)
FUNCTIONAL CONTROL VOLTAGE
(b)
(c)
(d)
(e)
TRIPPING LEVEL
DELAY

If the pulses are produced at the instants the line current passes through zero, the voltage $V_{(I_B-I_A)}$ proportional to (I_B-I_A) acts against the reactive component of the delta voltage as shown by vector diagram (b), so that the distance element acts as a reactance relay as indicated by curve 1 in Figure 9(j). If the pulses are produced after the current passes through zero as though the current were I' in Figure 9(c), the voltage $V_{(I_B-I_A)}$ must be slightly greater than the reactive component by an amount equal to $IR \tan \theta$. Or in other words, the reach of the distance element is reduced to $(X-R \tan \theta)$ resulting in the characteristic curve 2 of Figure 9(j). The distance measurement at the first instant of the transient is the reactance to the fault, as the delta voltage is compared with the rate of change of current. For 3-phase faults, the pulses are produced 30 degrees later resulting in the 3-phase fault characteristic of curve 3 in Figure 9(j).

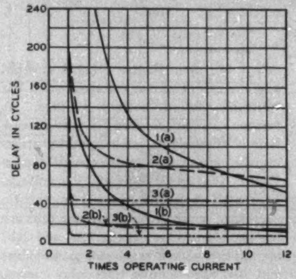

Figure 12. Characteristics of time-delay circuits

Since the fault currents are at low-power factor and load currents normally at high-power factor, the effect of load currents on the reach of the distance element is small.

The distance elements require that the protected line be of sufficient length to provide three secondary volts rms for minimum current faults at the far end of the line. The range is from 0.1 to 20.0 secondary ohms.

Impulse and Tripping Circuits

If any phase of a relay determines that circuit breaker tripping is required, the pulses are allowed to pass to an impulse circuit, as shown by *V-1* in Figure 10(a). Pulses applied to the grid of the tube cause capacitor C_1 to charge quickly through the tube and upon removal of the pulse, C_1 discharges slowly through cathode resistor R_1. The pulses as shown in (b) are thus converted into a series of decaying d-c voltages as in (c). This d-c voltage is then applied to tripping tube *V-2* for actuation of the plate circuit relay for tripping.

Time Delay Elements

For obtaining an inverse time delay, the circuit of Figure 11(a) is used. A rectified voltage proportional to a system current is obtained from *V-1*(a) as shown in (c) for the line current in (b). This d-c voltage is applied to capacitor C_1 through variable resistor R_1, but the voltage across C_1 is normally held at a low value by *V-1*(b). Upon the occurrence of predetermined fault conditions, the associated relay produces a negative voltage as shown by (d) which is applied to the grid of *V-1*(b), thus allowing capacitor C_1 to charge as in (e). The time delay circuit is thus functionally controlled, and after a time inversely proportional to

Figure 13. Laboratory version of electronic ground directional relay with inverse time characteristic

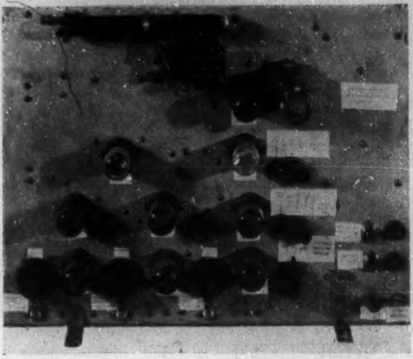

Figure 14. Laboratory version of 3-phase distance-directional relay

Figure 15. Model of electronic carrier current relaying for one terminal of transmission line

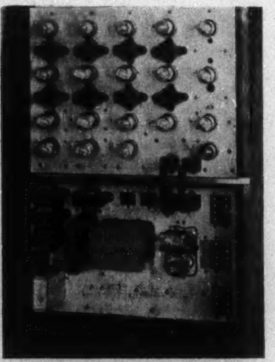

system current *V-2* becomes conducting. Upon removal of the fault, C_1 rapidly discharges through *V-1*(b) and allows quick reset of the tripping and timing circuits, this being accomplished in from three to six cycles even after very long delays.

In order to provide a fixed definite time delay, *V-1*(a) in Figure 11(a) is omitted and the source of d-c voltage used is the constant station battery voltage. A further variation resulting in very inverse time characteristics is obtained by utilizing the output of impulse circuit *V-1* in Figure 10(a) as the source of d-c voltage. Figure 12 shows the time characteristic curves, in which curves 1(a) and 1(b) are the typical inverse curves, 2(a) and 2(b) are typical very inverse curves and 3(a) and 3(b) fixed definite time delay curves. All of these are for short delays, with longer delays about four times as great obtainable for each type.

Complete Relay Models

A number of models have been constructed with Figure 13 showing a laboratory version of a ground directional relay and Figure 14 a 3-phase distance-directional relay. The application of electronic relaying to an all-electronic carrier relaying scheme has been accomplished in the model shown in Figure 15.

The schematic wiring diagram of a ground directional relay with directional controlled inverse time delay is in Figure 16. The relay is actuated by residual or ground current flowing through *T-1* and system residual voltages obtained from resistors R_{24} and transformer *T-5*. *V-1*(a) is a pulse forming circuit and *V-2*(a) a ground fault detector circuit with the output pulses applied to directional element *V-2*(b). If the ground fault is in the tripping direction the pulses are inverted and rectified by *V-3*(a) and *V-3*(b) and this negative d-c voltage applied to *V-4*(a) for starting the time delay. *V-4*(b) serves as an amplifier and *V-1*(b) as a rectifier for obtaining a positive d-c voltage proportional to ground current and for charging capacitor C_6 through variable resistor R_{18}. Tripping tube *V-5* conducts after a time delay inversely proportional to ground current, and upon clearing of the fault, *V-4*(a) becomes conducting again and C_6 discharges rapidly, thus allowing quick reset of the tripping circuit.

Figure 17 is schematic wiring diagram of a 3-phase distance-directional relay for protection of the first or instantaneous zone of a transmission line. The three secondary currents flow through transformers *T-1* and actuate elements for each phase of the relay. The center horizontal row of tubes is typical of the action in which *V-1*(b) serves as a pulse-forming circuit and *V-4*(a) as a fault-type detector circuit. The directional element is provided by *V-4*(b), the distance element by *V-5*(a), and for a fault within the protected section the pulses are allowed to actuate impulse circuit *V-5*(b) which in turn causes tripping tube *V-9* to operate the line circuit breaker. The tripping time for the majority of faults is one to two cycles, depending on the point in the voltage cycle at which the faults occur. The distance-directional characteristics of this particular relay are shown in Figure 18, the average tripping speed for faults at various locations in Figure 19 and a typical reactance characteristic in Figure 20.

In Figure 21 is a schematic wiring diagram of a 2-zone distance-directional controlled carrier relay including ground fault protection, in which the top row of tubes is typical of the phase action and the bottom row supplies ground protection. *V-1*(a) serves as a pulse-forming

Figure 16. Schematic wiring diagram of ground directional relay with directional controlled inverse time delay

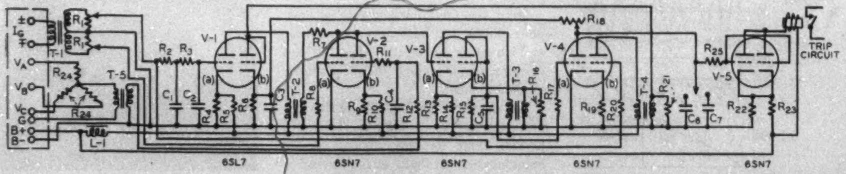

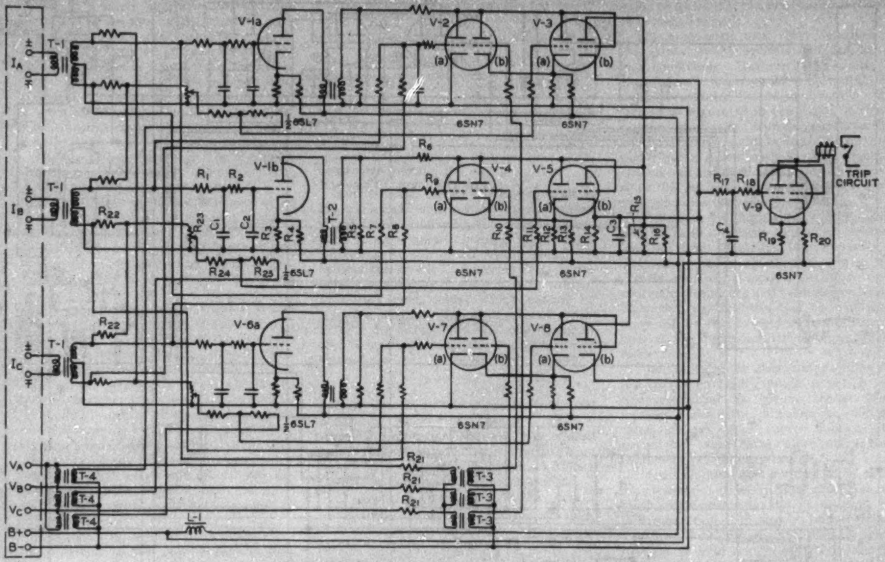

Figure 17. Schematic wiring diagram of 3-phase distance-directional relay

circuit, V-2(a) as a fault-type detector circuit and V-2(b) and V-3(a) the directional and distance elements respectively, for faults in the tripping direction. An impulse circuit V-3(b) causes circuit breaker tripping by V-16 if the fault is in the tripping direction and there is no received carrier from the remote end of the protected line. V-4(a) and V-4(b) furnish the directional and distance elements for faults in the reverse or blocking direction and actuate impulse circuit V-14(a) which in turn actuates the carrier transmitter by V-18. V-17 causes blocking of the tripping impulse if the fault is in the reverse direction or if there is a received carrier signal. In case of internal faults, tripping action is initiated in one-half to one cycle.

Figure 18. Tripping characteristics of distance-directional relay

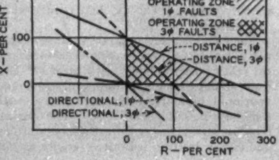

For simplicity, the foregoing wiring diagrams do not show details of the tripping, indicator, and alarm circuits used on the models, which are conventional. Test switches provide means for testing the function of all electronic elements in a very short period without the use of auxiliary equipment. These remove the electronic elements temporarily from their connections to the current coupling transformers and apply voltages to the elements simulating various types of faults.

Filaments are connected in series through a suitable dropping resistor, with each filament shunted so that in case of burn out of one tube the others will remain in use.

In addition to the detailed circuits shown, tests have been made on phase overcurrent directional-relay circuits with inverse or fixed time delays, zone-type distance-relay circuits and a simplified carrier relay using overcurrents for fault detection.

Figure 19. Operating time of distance-directional relay

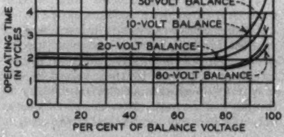

The models have all been tested on the miniature line shown in Figure 22 and have had intermittent laboratory duty for six months, including a 2-months continuous duty run, with no false operation or failures. Other extensive tests, such as effect of change in battery voltage on performance, effect of changes in tube characteristics, and so forth, indicate that no serious troubles should result from unusual operating conditions.

Conclusions

The development work described in this paper indicates that electronics can be utilized to obtain improvements in the

Figure 20. Reactance characteristic of distance-directional relay

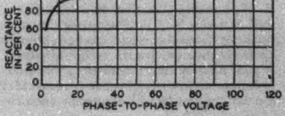

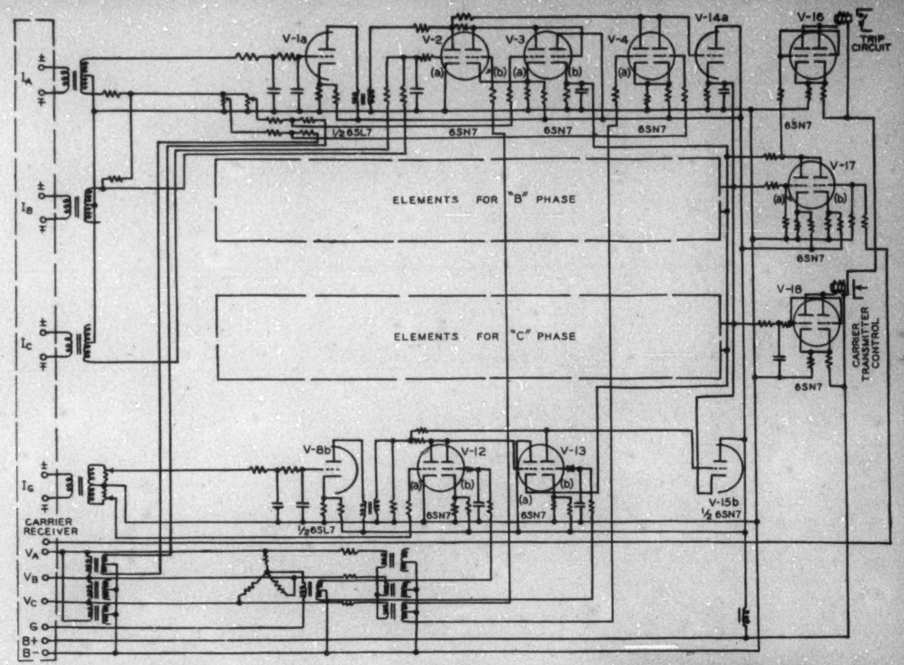

Figure 21. Schematic wiring diagram of electronic 2-zone distance-directional controlled carrier current relay including ground fault protection

accuracy, speed, and co-ordination of protective relays. By the use of standard electronic parts in their construction, the elimination of external auxiliary equipment and the provision for calibration by simple potentiometers, the electronic relays afford opportunities for savings in cost and simplification of maintenance. They require a minimum of tube types and are well suited to using ruggedized tubes; based on tube manufacturers' data and operating experience with other electronic equipment in utility applications, an average tube life of three to five years can reasonably be expected. Their versatility makes them adaptable to any relaying scheme by the combination of functions into integrated units or by simple circuit changes to obtain desired characteristics. In the development of the relay circuits, consideration was given to making them as nearly independent as possible of the uncontrollable factors that might be encountered in use, so that optimum performance would be obtained at all times.

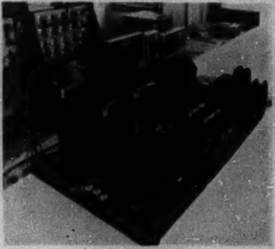

Figure 22. Miniature 3-phase transmission line (120/208 volts) with electronic relays being tested

---

Discussion

H. W. Lensner (Westinghouse Meter Division, Newark, N. J.): The use of electronic tubes for protective relays has been brought up from time to time in technical papers. It is of interest that practically every function now performed by a mechanical relay can be duplicated with electronic tube circuits. The general acceptance of electronic relays, however, depends on their advantages over equivalent mechanical relays.

The protective relays now in use represent years of development which have produced a device that approaches the ultimate in performance as proved by their record in use. It is not enough that an electronic relay do the job just as well. It must offer features not to be found in mechanical relays such as speed, burden, accuracy, and reduction in maintenance.

For example, it is claimed that electronic relays are faster in operation than mechanical relays. The curves of Figure 19 show time values that might well apply to a conventional high-speed distance relay, with tripping times of a cycle or so. The over-all tripping and reclosing time of a modern relay and circuit breaker is limited largely by the inertia of the circuit breaker mechanism and the de-ionization time of the arc path, and it seems that little increase could be made in the stability limit of a power system by paring a fraction of a cycle from the relay time. Electronic relays have no inertia, it is true, but the inertia of a mechanical relay is often of advantage in riding through a short transient on which it would be undesirable to trip.

The use of delay filters in the a-c input circuits may solve the problems of preventing false tripping on transients.

There is a limit to the possible speed of an electronic directional element as it may require nearly half a cycle to determine the direction of power flow. One apparent advantage of an electronic directional element is its ability to trip at high speed with very low a-c voltages.

The use of electronic protective relays always raises the questions of tube life and maintenance. The advent of the "ruggedized" tubes with a minimum life of 10,000 hours is one answer to this question. There still remains such problems as tube heater supply, battery drain, and failure alarm. A remote substation with perhaps dozens of mechanical relays requires a minimum of relay maintenance, and a station battery with a very low steady drain used primarily for tripping. With electronic relays, the demand on the battery is increased, and some alarm system would be desirable in event of tube failure.

It is too early to judge the value of electronic relays. A few years of field service, with ultimate improvements resulting from the experience gained, may put electronic relays in a prominent position for consideration in power system design.

Stephen V. Hart (Industrial Electronics, Inc., Detroit, Mich.): Loving's paper is impressive in that it demonstrates how those results in protective relaying which were heretofore achieved by electromagnetic means, can be achieved by electronic means. The circuit technique used, incorporates many features which were developed during the war for radar use. Attention is drawn to the pulse-forming circuits which make 1-cycle operation possible.

The usefulness of these circuits could be broadened if the following four steps were undertaken:

1. *Fail-safe Operation*

As they stand, many of the circuits would not indicate, by themselves, failure of tubes or associated components. It is believed that acceptance in practice will depend on the safety and reliability of these circuits. Redesign is advocated which will cause automatic alarm indication (or tripping of circuit breaker) should any vital component fail.

2. *Achievement of Novel Results*

The use of electronics opens the way to new applications in the power relaying field. It is not so much a matter of duplicating the performance of present electro-magnetic devices, but rather a step beyond, to achieve results not achieved heretofore. As an example, the over-current relay could be made sensitive to the slope of the initial transient, and could thus differentiate between a condition which may cause generators to fall out-of-step, and a fault which is within stability limits.

3. *Omit Conventional Transformers*

Often the current and potential transformers are the weakest link in the relaying system. By use of electronic amplification the use of the conventional types can be avoided. Air-core, toroidal transformers, and capacitive dividers are but two of many possibilities.

4. *Miniaturization*

The use of standard-size tubes has advantages, and the specialization on two tube types is desirable from the stockkeeping and replacement view point. However, the use of the mechanically more rugged miniature tubes and sub-miniature tubes should be considered, which, together with the latest miniaturization techniques would result in very compact and light-weight design. This would undoubtedly increase the appeal of the electronic relay to the power companies.

Summarizing, Loving's painstaking effort has introduced much of the latest thinking into the power relaying field and is an important step toward making these relays acceptable to the public utility field. To achieve this end it is suggested that the inherent possibilities of electronics be utilized to obtain new results which cannot be achieved electro-magnetically, and while making the circuits fail-safe, one may proceed to make the design more compact; this should provide a better relay at less cost.

John B. Gmeiner (The Commonwealth and Southern Corporation, Jackson, Mich.): A relay application engineer has several points to consider when he is applying a relay to perform certain functions. Among those to be considered are the following:

1. What burden will the device impose on the current and potential transformers?
2. If external continuous energy is required to operate the device, what are the requirements?
3. Will the relay give proper performance under heavy load conditions?
4. Will the relay perform accurately for repeated operation between maintenance and calibration periods?
5. If inverse time delay is involved, how will the relay characteristic curves coordinate with other relays and protective devices such as fuses?
6. If the relay is a distance-type relay, how well do the distance measuring characteristics perform the required job?
7. What special problems of maintenance are likely to be encountered?
8. What are the switchboard requirements?
9. What is the cost?

These are all questions that must be answered adequately before a relay is recommended for a particular application. How does the electronic relay as described by Loving fulfill the requirements listed above?

It is desirable that a relay does not impose more than a 1-ohm burden on a current transformer. The author indicates the burdens are low. While the input impedance of the various tube circuits described is probably in the thousands of ohms, with proper usage of matching input transformers, the reflected burdens on the current transformer and potential transformer circuits are probably low. It would be a helpful addition to the paper if specific values had been stated.

It is hoped the coupling transformers to the current circuit have been designed so they will not saturate when subjected to fault currents which may range from 50 to 100 amperes.

Most of the present-day relays do not require an external source of energy which is certainly desirable. What is the maximum value of watts that the electronic relay may be expected to use?

The overcurrent-type relay described in this paper should perform well for heavy load conditions. However, load ability of the distance relay would have to be examined carefully before application. Referring to Figure 18 in the paper, it would appear from the 3-phase characteristic curve, tripping might be initiated for high power factor heavy loading. It is assumed that second and third zone elements are used since this is the accepted practice for complete distance-type phase protection.

With the use of high quality circuit components and recently developed selected long-life radio tubes, the characteristics of electronic relays should not vary too greatly over any 6-months period between routine maintenance and calibration checks. However, it is doubtful that the electronic relay will be able to hold the calibration as well as the corresponding electromagnetic relay.

Upon plotting the characteristic time delay curves on log-log graph paper, it was discovered that the curves labeled "very inverse" had a rather flat slope beyond two times pickup. The curves labeled "inverse" were considerably more inverse than the ones labeled "very inverse." It would be desirable to have another time delay characteristic curve with a more inverse slope approaching that of a fuse curve.

Examination of Figure 18, tripping characteristics of distance-directional relay, brought to light several points of interest. The reach is quite different for phase-to-phase and 3-phase faults. This is a condition that is not desirable. Allowing for arc and transmission line impedance it may be seen that on a 3-phase fault, the relay will give coverage of only 60 to 70 per cent of the first zone setting. The straight line characteristic of the impedance relay will be susceptible to power swings which could cause unnecessary tripping. It would be more desirable to have an impedance circle or better yet an offset circle characteristic for the electronic relay.

The speed with which the electronic relay will operate has been stressed. Modern relays now operate in one or two cycles for first zone functioning. Due to transients and lack of necessity, it is doubtful whether faster operation than this is desirable or necessary.

With carrier current relaying becoming prevalent in most of the larger utility systems in this country, operating personnel are becoming acquainted with electronic equipments. Therefore, no great additional training of personnel should be necessary in the average application of this relay to provide proper maintenance. However, from past experience with electronic equipment, it is expected that more maintenance for electronic relays will be encountered than for a comparable electromagnetic relay.

From the illustrations in the paper, the space requirements of the relay appear to be somewhat less than for other types of relays. This might be true especially for the carrier relaying scheme.

It is to be hoped that these and other problems may be solved and the electronic relay can offer improvements over present relaying schemes. With further developments, the relay may be able to perform functions not now possible by present-day relays. Any new device meets a good deal of resistance in the field before widespread acceptance is made of that unit. Undoubtedly this will be the case with the new electronic relay. At the present time there are years of experience behind the development and application of electromagnetic relays. They are rugged and reliable in operation. Their limitations and capabilities are well known. The electronic relay does not have this background and will have to have several years of field use before its reliability is proved. However, the electronic relay should be a welcome addition in the field of relaying, especially if it shows advantages in performance, costs, and space requirements, and it is hoped that its use will fulfill the expectations of the author.

James J. Loving, Jr.: The discussers have raised a number of questions which were not adequately covered in the paper in order to hold it to reasonable length.

Lensner points out that the speed of operation of the electronic relay circuits as indicated by the curves of Figure 19 do not improve appreciably over the time characteristics for electromagnetic relays. In the final tripping circuit of the distance relay to which the curves apply, an intentional time delay of one cycle was inserted, so that the ultimate speed attainable by electronic relaying is greater than that shown by the curves.

The intentional delay was inserted because there is the possibility of false operation due to transient response of the coupling transformers for a small percentage of faults without the delay. In the case of application to carrier relaying, there is no possibility of failure to apply carrier in sufficient time, so that the very high tripping speed of one-half to one cycle is attainable. Also, the speed of response is relatively independent of system voltages, as is brought out by Figure 19.

The use of electronic relays would place an additional drain on station batteries, and if *6SL7* and *6SN7* tubes were used, this drain per relay would be in the order of 0.6 to 0.8 amperes, or about 75 to 100 watts. This additional battery load might be offset by the smaller requirements on potential and current transformers.

Gmeiner suggests that more specific values of burdens be stated. In the models constructed, the burdens on current transformers are about 0.2 volt-amperes per phase at normal current, and on potential transformers about 3 volt-amperes per phase for each function of the relay placing load on the potential circuit. The loading is due to the coupling transformers required, as the actual loading by the vacuum tube circuits is negligible. The small current coupling transformers used contain an air gap and show no indication of saturation at currents of 40 times normal.

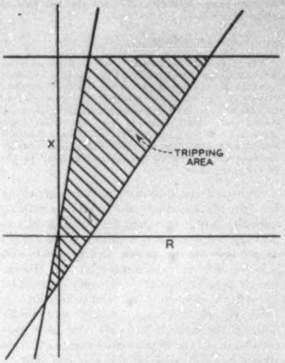

Figure 1. Tripping area enclosed by straight lines in electronic relaying circuit

Due to lack of data as to reliability, electronic relays would undoubtedly require more frequent maintenance checks until reliability is proved. However, the use of special built-in test switches could provide a means of checking very quickly whether all tubes were functioning properly. These switches place control voltages on the tube circuits similar to those encountered during a fault and thus no external test equipment is required except for re-calibration. The distance elements in the electronic circuits should hold their calibration even better than electromagnetic relays, as the comparisons of voltage and current magnitudes are made by simple resistor networks before application to the tube circuits.

The time delay characteristics and distance characteristics given in the paper are by no means the only ones obtainable by electronic circuits. It is possible to enclose any desired tripping area on the R–X diagram for a distance-directional relay by straight lines. In Figure 1 of the discussion, for example, the tripping area shown could be obtained by a relay constructed of a pulse forming circuit, a blocking circuit for each straight line of the area, and a tripping circuit. Also, it is possible to make the response to 3-phase faults identical with the response to single-phase faults by the addition of a separate set of tubes responsive only to 3-phase faults.

Hart mentions the desirability of designing the circuits so that a component failure would give an alarm indication. This could be done quite easily for the case of open-circuited tube filaments, but might be quite difficult and expensive for other component failures. The question of the reliability of the miniature-type tubes as against the normal size ruggedized tubes is one which could be settled only by trials with the different types. The electronic relaying circuits could undoubtedly be designed around the miniature tubes if this should prove more desirable.

It is probably possible to build an electronic relay which responds to the rate of rise or slope of the current during a fault or out-of-step condition. Some experimental work indicates that a circuit can be devised which duplicates the envelope of the current wave and then acts according to the relative steepness of the envelope.

There are possibilities in the simplification of current and potential reproducing devices over those now employed for electromagnetic relays. In the circuit of Figure 6 in the paper, an air core toroidal transformer placed around the line conductor could replace the current transformer and coupling transformer insofar as the need of a current transformer for an electronic relay is concerned.

Similar possibilities exist for simplification of potential circuits.

The discussers of the paper have made valuable comments and their interest is appreciated.

Rectifier Fault Currents—II

C. C. HERSKIND
FELLOW AIEE

A. SCHMIDT, JR.
MEMBER AIEE

C. E. RETTIG
NONMEMBER AIEE

A NUMBER of modes of circuit action may be obtained during faults on power rectifiers because of the variety of fault conditions and circuit parameters. Analyses of some of these have been treated in a previous paper.[1] This paper presents a further extension of this work with analyses of a number of idealized cases. An analysis is presented for the transient fault current during d-c short circuit and a procedure is outlined for analyzing the fault currents during arc-back with both a-c and d-c feed.

The objective of these studies is the development of a comprehensive procedure for the analysis of the circuit action and the determination of fault currents in rectifier circuits during d-c short circuits and arc-back. A complete treatment of the fault currents obtained in the widely used 6-phase double-Y circuit is particularly desired.

The results of fault current calculations and tests on a 200-kw 300-volt scaled ignitron rectifier equipment are compared. The wave forms and magnitudes of the fault currents obtained under various test conditions are shown by oscillographic records.

Data are presented showing the nature of the rectifier arc-drop at fault current levels. Some of the factors which influence the arc-drop are discussed. Methods for representing the effect of arc-drop in fault current calculations are proposed.

Types of Faults

Rectifier faults may be classified on the basis of the nature of the fault, the circuit pattern and action, and the analytical treatment which applies. In order to permit mathematical analysis, certain simplifying assumptions are necessary. These result in a number of idealized cases.

Rectifier faults are of two general types, namely, d-c short circuit and arc-back. Three idealized cases may be defined for each type as illustrated in Figures 1 and 2:

D-C Short Circuit

Case 1—primary impedance only
Case 2—secondary impedance only
Case 3—both primary and secondary impedances

Arc-Back

Case 1—a-c feed only
Case 2—d-c feed only
Case 3—both a-c and d-c feed

D-C Short Circuit

During d-c short circuit, the circuit action is determined by the relative magnitude and location of the various impedances in the rectifier unit and the short-circuit path. Three idealized cases are obtained with equivalent circuits and wave forms as shown in Figure 1. These three cases do not cover all the possible conditions which may be obtained as additional cases may be defined for d-c short circuits with impedance in the fault path and for other rectifier circuits.

CASE 1—D-C SHORT CIRCUIT WITH PRIMARY IMPEDANCE ONLY

In this case, it is assumed that the rectifier transformer d-c windings are perfectly interwound so that all the reactance may be considered to be located in the a-c windings and supply line as shown in Figure 1. The two tubes which are connected to the d-c windings of one phase of the rectifier transformer conduct current alternately so that the fault currents in the a-c winding are the same as in a 3-phase short circuit. Under sustained conditions each tube conducts current for 180 degrees.

STEADY-STATE CONDITIONS

Under sustained conditions, the anode current waves are sinusoidal in form, and each anode carries a half cycle of current whose crest value is

$$i_{as}=\sqrt{2}\,E_s/Z \tag{1}$$

The d-c short-circuit current is equal to the sum of the anode currents, and its average value is

$$I_{ds}=3\times\frac{2}{\pi}\times i_{as} \tag{2}$$

The sustained d-c short circuit current may also be expressed in the form

$$I_{ds}=\frac{2\sqrt{2}}{\pi}\times\frac{VA}{E_s\underline{Z}_c} \tag{3}$$

TRANSIENT CONDITIONS

Under transient conditions, immediately following the start of the short circuit, the fault-current waves in the transformer windings are displaced, and the current in the short circuit exceeds its sustained value. If it is assumed that the anodes are free to conduct at all times and that the fault is a bolted short circuit, the fault currents may be readily determined graphically by a procedure based on a single-phase analysis.

A graphic analysis of the current on d-c short circuit for a 6-phase double-Y rectifier is shown in Figure 3. In this analysis, the current in each pair of anodes is determined as for a single-phase circuit. The short circuit is assumed to occur at the beginning of the positive voltage wave on phase R_1, that is, at switching angle $\beta = 0$. The switching angles on the other two phases differ from this value by their phase displacements of 60 and 120 degrees.

The short-circuit current is obtained by adding the anode current waves which are indicated by the shaded areas. The construction shown is for a decrement

---

Paper 49-68, recommended by the AIEE electronic power converter committee and approved by the AIEE technical program committee for presentation at the AIEE winter general meeting, New York, N. Y., January 31–February 4, 1949. Manuscript submitted November 17, 1948; made available for printing December 22, 1948.

C. C. HERSKIND, A. SCHMIDT, JR., and C. E. RETTIG are all with the power electronics division of the General Electric Company, Schenectady, N. Y.

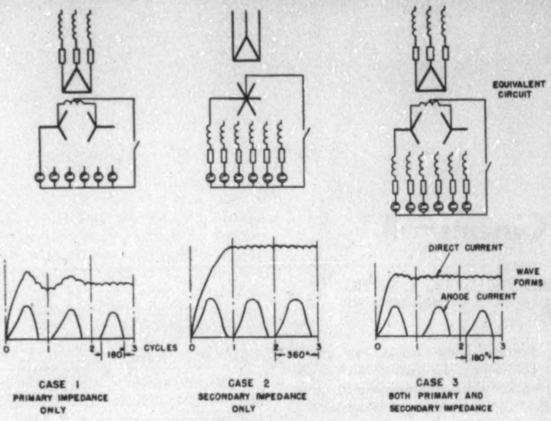
EQUIVALENT CIRCUIT
DIRECT CURRENT
WAVE FORMS
ANODE CURRENT
0
1
2
3
CYCLES
180°
360°
180°
CASE 1
PRIMARY IMPEDANCE ONLY
CASE 2
SECONDARY IMPEDANCE ONLY
CASE 3
BOTH PRIMARY AND SECONDARY IMPEDANCE

Figure 1. D-c short circuit—idealized conditions

factor $R/X = 0.3$. The maximum value of the fully displaced current wave, which would be attained with zero resistance, is also shown. Its value is twice the crest value of the sustained fault current.

The crest value of the instantaneous current depends upon the switching angle and the circuit reactance as expressed by the R/X ratio. Analyses show that the effect of switching angle is small and may be disregarded as it usually causes less than 5 per cent variation in crest current. However, the transient component due to reactance may cause the maximum instantaneous current to range in value from 1 to 2 times the sustained crest current. The maximum short circuit current may be expressed by the relation

$$i'_{ds}=K_p\frac{\pi}{3}I_{ds} \tag{4}$$

The value of the transient factor K_p for various R/X ratios is given in Figure 5.

Case 2—D-C Short Circuit with Secondary Impedance Only

The 6-phase star circuit shown in Figure 1 represents an idealized case having inductance and resistance that may be lumped in the anode leads. The absence of impedance on the primary side of the transformer permits a determination of the fault current on the basis of six single-phase circuits where the applied voltages have the phase relations determined by the transformer connection. In this case each tube acts independently; and under sustained conditions, the tube conduction period increases toward a value of 360 degrees as the circuit resistance is reduced to zero.

Steady-State Conditions

In contrast to Case 1, with its sinusoidal steady-state currents, the circuit arrangement in Case 2 causes the currents through the impedances to be discontinuous so that the transient is repeated each cycle. Therefore, the crest value of sustained anode current is the same as the maximum instantaneous value for Case 1 as given by

$$i'_{ds}=K_p\frac{\sqrt{2}E_s}{Z_c} \tag{5}$$

The crest value of the short-circuit current is larger than the maximum obtained in the transient state in Case 1 because of the longer conducting interval. The crest short circuit current is given by

$$i'_{ds}=K_s\times 2\frac{\sqrt{2}E_s}{Z_c} \tag{6}$$

Values of K_s may be obtained from Figure 4.

The average value of the short-circuit current may be determined for an idealized case with no resistance by the equation

$$I_{ds}=2\sqrt{2}\frac{VA}{E_sZ_c} \tag{7}$$

It should be noted that this value is π times the value obtained for Case 1 as given by equation 3.

When resistance is present the sustained short circuit current will have a lower value. This is shown in Figure 5.

Transient Conditions

Conduction During First Cycle. If the short circuit occurs at the instant the voltage on phase 1 is going through zero, conduction takes place initially in phases 5, 6, and 1. Sixty degrees later phase 2 starts conducting, and the remaining phases enter in sequence.

Neglecting resistance the currents in phase 1 and all succeeding phases are fully displaced. However, the short-circuit current does not reach its maximum value until phase 6 starts conducting a second time and steady-state conditions are reached.

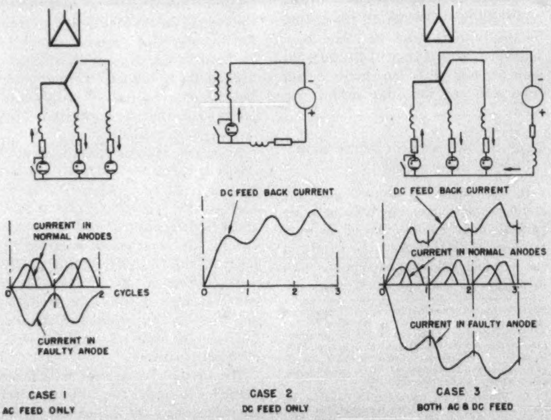
CURRENT IN NORMAL ANODES
CYCLES
0
1
2
3
CURRENT IN FAULTY ANODE
DC FEED BACK CURRENT
DC FEED BACK CURRENT
CURRENT IN NORMAL ANODES
CURRENT IN FAULTY ANODE
+
-
CASE 1
AC FEED ONLY
CASE 2
DC FEED ONLY
CASE 3
BOTH AC & DC FEED

Figure 2. Arc-back—idealized conditions

Figure 1 shows a sketch of the short-circuit current and the current in phase 1 that would exist in this case with a small R/X ratio.

Effect of Interphase Transformer. Neglecting the interphase transformer and treating the 6-phase star circuit yields results which apply with sufficient accuracy to the 6-phase double-Y circuit. Introducing the interphase transformer causes no change in the short-circuit current. Some redistribution of current among the anodes is caused, but the maximum change is less than 2.0 per cent of the crest value of anode current.

Case 3—D-C Short Circuit with Both Primary and Secondary Impedance

This is the general case which is usually encountered in practice. Its circuit action combines the effects obtained in the first two cases. With reactance and resistance in both primary and secondary windings of the rectifier transformer, the crest value of the anode current is still represented by the displacement factor K_p. X and R in this case are the sum of the components in the primary and secondary windings.

The short-circuit current has a peak value which falls between the two extremes represented by K_p and K_s in Figure 4. The exact value has not been determined, but it is dependent upon the ratios R_p/R_s, X_p/X_s and the total resistance to total reactance ratio R/X. The trend may be expressed as follows: For a given X_p/X_s ratio, the value falls upon the upper curve when the R/X ratio is equal to zero, but approaches rapidly the lower curve as the R/X ratio increases.

The ratios X_p/X_s and R_s/R_p determine the rapidity with which the value approaches the lower curve. The larger these ratios, the more rapidly the value approaches the lower curve.

For practical ratios of these quantities where no reactance is intentionally added in the anode leads, the lower curve applies for usual R/X ratios.

Arc-Back

During arc-back, the circuit action is determined primarily by the sources of voltage producing the fault current. Three idealized cases may be defined with equivalent circuits and wave forms as shown in Figure 2.

Case 1—Arc-Back with A-C Feed Only

In this case, the current flow in the faulty anode is established by the a-c supply and it is assumed that there is no other source of voltage. The equivalent circuit is shown in Figure 2. A 3-phase rectifier is assumed as it represents one commutating group of the rectifier. During arc-back, a reverse current flows in the faulty anode which is equal to the sum of the forward currents in the two normal anodes.

In the treatment presented in the original paper,[1] this case was referred to as arc-back in a wye and sustained values of current were given. Further studies indicate that the first cycle values are generally more important than sustained values in system studies.[5]

The first cycle crest values of the reverse current in the faulty anode and the forward current in the normal anodes may be determined by equations 8 and 9.

Crest reverse current in faulty anode is

$$i'_{ar} = K_r \frac{\sqrt{2}E_s}{Z_c} \qquad (8)$$

Crest forward current in normal anodes is

$$i'_{af} = K_f \frac{\sqrt{2}E_s}{Z_c} \qquad (9)$$

Values of the reverse current and forward current factors as a function of the R/X ratio are given in Figure 6. These factors give the crest value of current obtained during the first cycle when arc-back occurs at the end of conduction. It is assumed that the arc-drop is represented as an equivalent resistance in determining the R/X ratio.

Case 2—Arc-Back with D-C Feed Only

This is an idealized case where all the current in the faulty anode flows in the d-c system. The equivalent circuit is a single loop containing an alternating and a direct voltage in series. The current consists of an alternating component of constant magnitude and a direct component which increases exponentially with

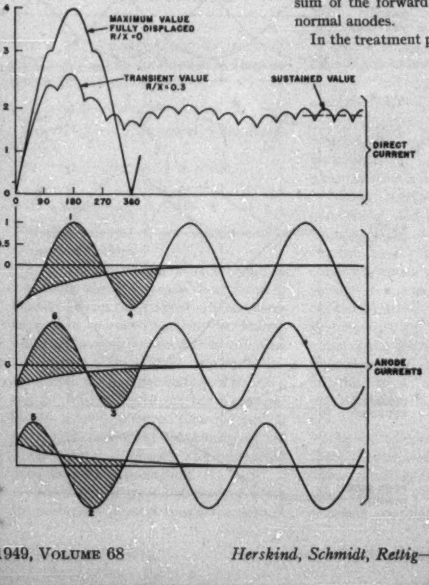

Figure 3 (left). Graphic analysis of transient current on d-c short circuit with primary impedance only

Figure 4 (below). Transient factors for determining crest values of anode current and d-c short-circuit current

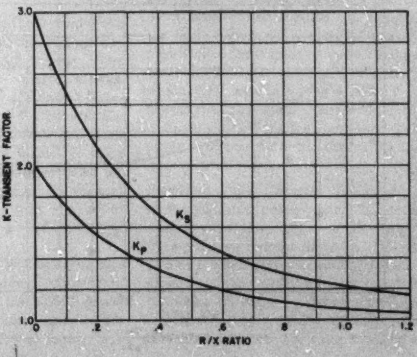

time until it is limited by resistance. Such a condition may be realized in practice if all the normal anodes of the rectifier are prevented from firing at the time of fault or may be approximated if a number of rectifiers are paralleled on the same d-c bus.

The reverse current in the faulty anode is given by the equation

$$i_{dr}=\frac{E_d'}{R_3}\left[1-\epsilon^{-\frac{R_d}{L_d}(t-t_1)}\right]+\frac{\sqrt{2}E_s}{Z_3}\times$$
$$\left[\sin(\omega t-\theta_3)-\epsilon^{-\frac{R_d}{L_d}(t-t_1)}\sin(\omega t_1-\theta_3)\right] \quad (10)$$

The idealized conditions are not closely approximated in practice and useful results of adequate accuracy may be obtained by an approximate expression based on the following assumptions: First, it is assumed that the arc-back occurs at the zero point of the a-c voltage wave when $t_1=0$. This is justified on the basis that the majority of arc-backs occur at the end of conduction which is usually within a few degrees of the zero point of the voltage wave. Second, it is assumed that the resistance of the fault path is low in comparison with the inductance so that $\theta=90$. The approximate value of the reverse current is given by the simplified equation

$$i_{dr}=\left[\frac{E_d'}{R_3}-\frac{\sqrt{2}E_s}{Z_3}\right]\left[1-\epsilon^{-\frac{R_3}{L_3}t}\right]+$$
$$\frac{\sqrt{2}E_s}{Z_3}[1-\cos\omega t] \quad (11)$$

CASE 3—ARC-BACK WITH BOTH A-C AND D-C FEED

This is the case usually encountered in practice and combines the action of the first two cases. In order to simplify the analysis, the action is considered on the basis of a single wye. During arc-back, the current in the faulty anode is a combination of a-c feed from the two normal anodes of the wye and d-c feed from a single d-c source representing all other anodes and parallel sources.

Currents feeding into an arc-back from a counter electromotive force load and from the normal anodes in a faulted wye are additive components of the current in the faulted phase. Each of these components is smaller than the value obtained in either Case 1 or Case 2, but their sum yields an arc-back current larger than either component considered separately. A method is described in the following analysis for obtaining the exact theoretical values of currents in the faulty anode, the normal anodes, and the d-c feed.

Circuit Analysis. The equivalent circuit for this case is shown in Figure 2. Paralleled converting equipment, counter electromotive force load, and the normal wye of the 6-phase double-Y rectifier are reduced to an equivalent voltage source E_d', resistance R_d, and inductance L_d. The action of individual phases is considered only in the faulted wye. The phases in this wye are designated in their normal conducting sequence. R_1 is the faulty phase and R_2 and R_3 are the normal phases in the faulted wye. L_c and R_c are the commutating inductance and resistance per phase. Arc-drop is treated as an equivalent resistance whose value is included in R_c.

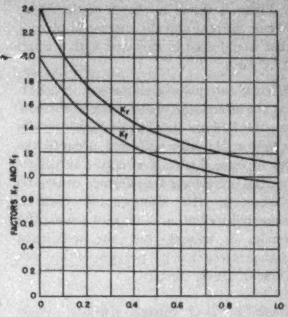

Figure 6. Factors for determining reverse and forward current during arc-back with a-c feed only

Circuit action during the first cycle following a commutation arc-back is shown in Figure 7. For purposes of defining circuit action, the cycle of operation is divided into four intervals. The divisions correspond to the instants at which a phase either starts or stops conducting. The current in phase 1 and the feed-back

Figure 5 (below). Average value of sustained d-c short-circuit current with secondary impedance only

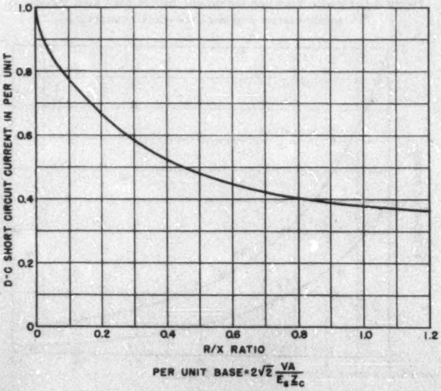

Figure 7 (right). Circuit action during arcback with a-c and d-c feed

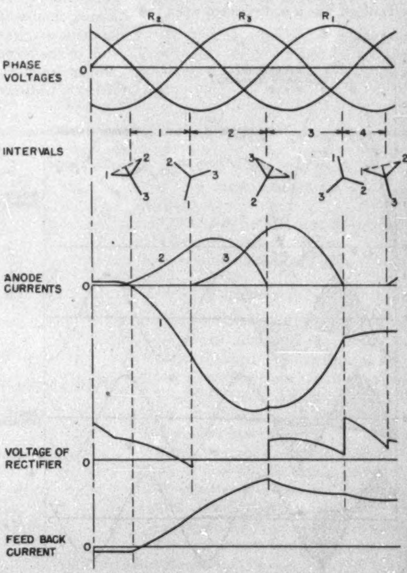

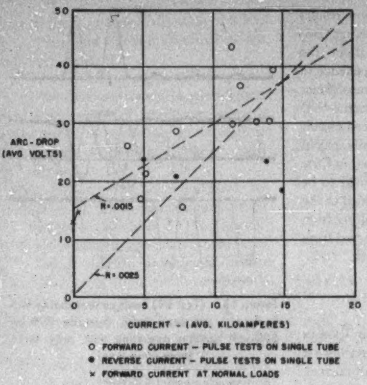

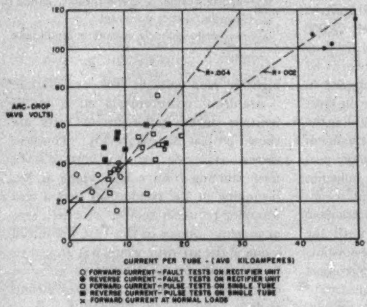

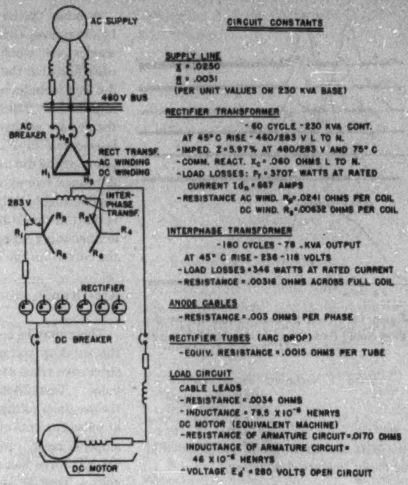
AC SUPPLY
460 V BUS
AC BREAKER
H1
H2
H3
RECT TRANSF.
AC WINDING
DC WINDING
INTER-PHASE TRANSF.
283 V
R1
R2
R3
R4
R5
R6
RECTIFIER
DC BREAKER
DC MOTOR
CIRCUIT CONSTANTS
SUPPLY LINE
X = .0250
R = .0031
(PER UNIT VALUES ON 230 KVA BASE)
RECTIFIER TRANSFORMER
- 60 CYCLE - 230 KVA CONT.
AT 45° C RISE - 460/283 V L TO N.
- IMPED. Z = 5.97% AT 460/283 V AND 75° C
- COMM. REACT. Xc = .060 OHMS L TO N.
- LOAD LOSSES: Pr = 3707 WATTS AT RATED CURRENT Idn = 667 AMPS
- RESISTANCE AC WIND. Rp = .0241 OHMS PER COIL
DC WIND. Rs = .00632 OHMS PER COIL
INTERPHASE TRANSFORMER
- 180 CYCLES - 78 .KVA OUTPUT
AT 45° C RISE - 236 - 118 VOLTS
- LOAD LOSSES = 346 WATTS AT RATED CURRENT
- RESISTANCE = .00316 OHMS ACROSS FULL COIL
ANODE CABLES
- RESISTANCE = .003 OHMS PER PHASE
RECTIFIER TUBES (ARC DROP)
- EQUIV. RESISTANCE = .0015 OHMS PER TUBE
LOAD CIRCUIT
CABLE LEADS
- RESISTANCE = .0034 OHMS
- INDUCTANCE = 79.5 X 10⁻⁶ HENRYS
DC MOTOR (EQUIVALENT MACHINE)
- RESISTANCE OF ARMATURE CIRCUIT = .0170 OHMS
INDUCTANCE OF ARMATURE CIRCUIT = 46 X 10⁻⁶ HENRYS
- VOLTAGE Ed' = 280 VOLTS OPEN CIRCUIT

Figure 8 (left, above). Arc-drop of sealed ignitron under fault current conditions

Figure 9 (left, below). Arc-drop of pumped ignitron under fault current conditions

Figure 10 (right). Power circuit during fault tests on 6-anode 200-kw 300-volt rectifier

current are continuous, and the intervals are determined by conduction in the two normal phases as follows:

Interval 1—conduction in phase 2.

Interval 2—conduction in both phases 2 and 3.

Interval 3—conduction in phase 3.

Interval 4—conduction in neither normal phase.

During interval 1, the circuit action proceeds as follows:

A current will start flowing from anode 2 to anode 1 with values as determined in Case 1. Upon this current will be superimposed a current from the d-c source, whose value is determined from equation 1. The a-c voltage which applies in this equation is the average voltage of phases 1 and 2. The current from the d-c source divides equally between phases 1 and 2, one-half its numerical value being added to the current in phase 1 and subtracted from the current in phase 2.

The end of interval 1 is reached when the voltage of phase 3 equals the voltage at the terminals of the rectifier as given by

$$e_d = E_d' - R_d i_{dr} - L_d \frac{di_{dr}}{dt} \tag{12}$$

where i_{dr} is the feed-back current during interval 1. A later time may apply if phase control is used.

During interval 2, all three anodes are conducting, and the net a-c voltage appearing in the d-c circuit is zero. The current from the d-c source divides equally between anodes 1, 2, and 3, one-third of its numerical value adding to the current in anode 1 and subtracting from the currents in anodes 2 and 3. The value of the d-c current is determined for the series circuit including E_d', L_d, R_d, and one-third of L_c and R_c with the initial value as determined at the end of interval 1.

The a-c components of current in the three transformer phases follow the values resulting from a complete 3-phase short circuit. The transient components maintain continuity between intervals 1 and 2 and decay with the exponential $(R_c/L_c)t$.

Interval 2 ends when the current in phase 2 reaches zero. Calculation of the currents in anodes 1 and 3 and in the d-c source at this time determines the initial conditions for interval 3.

The action in interval 3 is similar to that in interval 1 in that there are two conducting anodes. The average voltage of anodes 1 and 3 during this interval is opposed to the voltage of the d-c source and usually reverses the rate of rise of cathode current.

The transition from interval 3 to interval 4 is determined when the current in phase 3 goes to zero. The same current is then carried by the faulty anode and the d-c source during interval 4. Because the a-c voltage on phase 1 is opposed to the d-c voltage during most of this interval, the fault current is decreased. Interval 4 ends when the voltage of phase 2 exceeds the voltage at the rectifier terminals, at which time intervals 1 to 4 will be repeated with new initial conditions.

Appendix II gives the equations which apply to this circuit action during the four intervals.

Sustained Fault Current. The value of sustained fault current may be determined by carrying out the circuit analysis for a sufficient number of cycles. It may also be found by trial, assuming values of i_{dr} and t at the start of interval 1 and determining the resulting currents throughout the sequence. At $\omega t = 360$ degrees the current should have the value assumed at

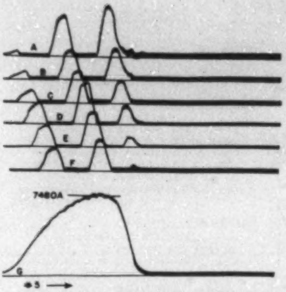

Figure 11. (Test 5) Fault current during d-c short circuit (inductance in the short), 6-anode 200-kw 300-volt rectifier

"A" to "F" inclusive—anode currents
"G" —cathode current

the start of interval 1, and anode 2 should be ready to start conducting.

Factors Modifying Circuit Action. The foregoing analysis describes a commutation arc-back in a free rectifier with three anodes. A number of factors may influence the circuit action, particularly the initial action.

Phase of Arc-Back—While arc-back commonly occurs at the end of commutation, it may occur at a later time during interval 1 or during intervals 2 or 3. The initial peak of reverse current is reduced in such cases. (Compare tests 43 and 45, Figures 17 and 18.)

Interphase Transformer—The interphase transformer acts as a large inductance to reverse current from the d-c load until saturation occurs. At the time of a commutation arc-back, the interphase transformer flux may have reached 0.1 to 0.5 times its saturation value, depending upon the design of the interphase transformer and the amount of phase control used.

Phase Control—Phase control may delay the entry of a normal anode and thereby reduce its contribution to the arc-back.

Approximate Solution. While the foregoing analysis for the case of arc-back with a-c and d-c feed constitutes an exact method of procedure, its use is likely to prove cumbersome and approximations of reasonable accuracy are well worth consideration.

The simplest approximation consists of determining upper limits for fault current values. Thus the current in the normal anodes cannot exceed the value for arc-back in a wye and the current in the d-c source generally cannot exceed the value for d-c feed only. The current in the faulty anode cannot exceed the sum of these values.

A more precise approximation results by assuming that on the average two anodes are conducting throughout the cycle and that the resulting impedance to d-c feed includes one-half the transformer impedance. A further assumption is that the net a-c voltage in the d-c feed circuit is one-half of E_s. This permits calculation of the d-c feed as described in Case 2. Since two anodes are assumed to be conducting, half this value is added to the current in the faulty anode resulting from arc-back in a wye and is subtracted from the current in the normal anodes.

Arc-Drop

There may be considerable variation in the arc-drop voltage across a rectifier on successive trials at the same fault current value. Tests 30 and 31 (Figure 16) show the arc-drop voltage in a pumped ignitron at pulse currents of approximately 25,000 amperes crest. In test 30, the arc-drop voltage wave has a rounded crest at 87 volts. Test 31 shows a sudden rise in voltage from 70 to 152 volts near the crest of the wave approximately doubling its value. In many cases, the crest value of the arc-drop voltage does not have particular significance insofar as its influence on the magnitude of fault current is concerned, since the break in the arc-drop voltage wave does not occur until the fault current has reached its crest value. Average values of the arc-drop voltage would appear to be more representative of the effect of arc-drop as they are a measure of both the volt-seconds appearing across the tube and the energy dissipated in the arc during the fault. Average values do not give undue weighting to high arc-drop voltages of short duration.

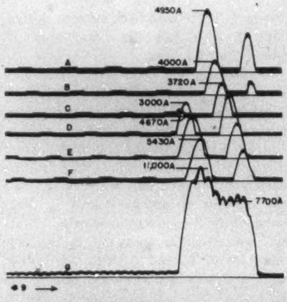

Figure 12. (Test 9) Fault current during d-c short circuit (bolted short), 6-anode 200-kw 300-volt rectifier

"A" to "F" inclusive—anode currents
"G"—cathode current

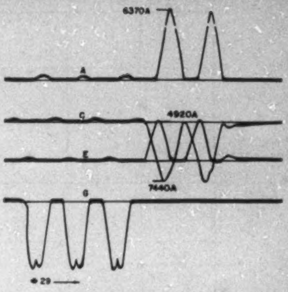

Figure 13. (Test 29) Fault current during arc-back with a-c feed only, 6-anode 200-kw 300-volt rectifier operating with only three tubes (one wye)

"A"—anode number 1 current
"B"—anode number 2 current (faulty anode)
"C"—anode number 3 current
"D"—anode-to-cathode voltage in faulty tube

Arc-drop measurements on a sealed ignitron during pulse-current tests are shown by test 23 (Figure 15). This test shows a triangular arc-drop voltage wave form starting from a high value at the beginning of the conduction period and dropping regularly to approximately zero at its end. Again in this case the initial value of the arc-drop would not appear to be as significant as its average value in determining the current obtained during faults.

The nature of the arc phenomena at fault current levels is not accurately known. In the case of the pumped ignitron, the sharp rise in voltage would appear to be the result of arc starvation. Observations show that this voltage occurs at a quite definite current level. When fault currents in excess of this critical value flow through the tube, the rise in voltage occurs before the current crest, causing a considerable increase in the averaged value of arc-drop voltage for a small increase in fault current. In the case of the sealed ignitron, observations show that when the tube is passing currents of fault magnitude, a considerable part of the cathode current is collected on the walls of the tube. The shorter arc-path which results may account for the reduction in arc-drop in the latter part of the conducting period.

Average arc-drop values for a sealed ignitron rectifier tube of the type used in units ranging in size from 200 to 500 kw for 250- and 600-volt applications are shown in Figure 8. Typical arc-drops for a pumped ignitron of the type used in units ranging in size from 1,000 to 2,500 kw for 250- and 600-volt applications are shown in Figure 9.

Two dashed lines representing equivalent resistance are shown in each figure. The lower value of resistance in each figure would be applicable to an equivalent circuit containing a battery and resistance.

The higher value of equivalent resistance is an approximation accounting for the total arc-drop. This approximation simplifies analytical treatment and is of commensurate accuracy with the determination of other circuit parameters.

Calculated and Test Results

Extensive fault-current tests were made on a 6-phase 200-kw 300-volt sealed ignitron rectifier. The complete circuit of the rectifier unit and the associated a-c supply and d-c load systems during these tests, together with the circuit constants, are shown in Figure 10. Oscillographic records of fault currents are shown by six tests included in the illustrations.

The fault current calculations are as follows:

D-C SHORT CIRCUIT

The total impedance of the circuit is determined as follows:

Rectifier Transformer

$\underline{Z}=0.0597$ (on 230-kva base)

$$\underline{R}=\frac{P_r}{VA}=\frac{3{,}707+346}{230\times 1{,}000}=0.0176$$

$$\underline{X}=\sqrt{\underline{Z}^2-\underline{R}^2}=0.0570=\underline{X}_p+{}^1/_2\underline{X}_s$$

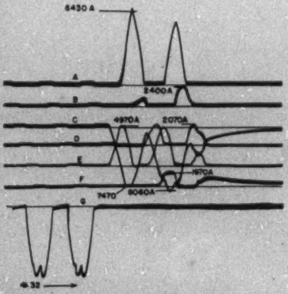

Figure 14. (Test 32) Fault current during arc back in double-Y circuit with no external d-c feed, 6-anode 200-kw 300-volt rectifier

"A", "B", "D", "E", and "F"—currents in normal anodes
"C"—current in faulty anode
"G"—anode-to-cathode voltage in faulty tube

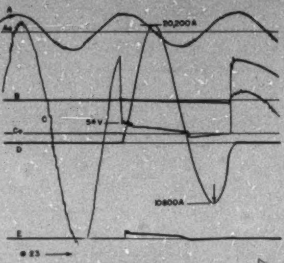

Figure 15. (Test 23) Arc-drop on sealed ignitron during current pulse

"A"—60-cycle timing wave
"B"—circuit-breaker voltage
"C"—anode-to-cathode voltage (arc-drop)
"D"—anode current
"E"—ignitor-to-cathode voltage

$$\text{Normal ohms on d-c winding}=\frac{3E_s^2}{VA}$$

$$=\frac{3\times 283^2}{230\times 1{,}000}=1.042$$

$$\underline{X}_c=X_c/1.042=0.060/1.042=0.0575=\underline{X}_p+\underline{X}_s$$

Anode Cables

$\underline{R}=0.003/1.042=0.00288$

Rectifier Tubes

$\underline{R}=0.0015/1.042=0.00144$

Using other values as given in Figure 10.

Total $\underline{X}_c=0.0250+0.0575=0.0825$
Total $\underline{R}_c=0.0031+0.0176+0.00288+0.00144=0.0250$
Total $\underline{Z}_c=0.0860$

Sustained Direct Current

$$I_{ds}=0.9\times\frac{VA}{E_s\underline{Z}_c}=0.9\times\frac{230{,}000}{283\times 0.0860}$$
$$=8{,}500 \text{ ampere (average value)} \quad (3)$$

Ratio $R/X=0.0250/0.0825=0.304$
$K_p=1.41$ (Figure 4)

Transient Direct Current

$$i_{ds}'=1.41\times\frac{\pi}{3}\times I_{ds}=12{,}500 \text{ amperes (crest value)} \quad (4)$$

ARC-BACK WITH A-C FEED ONLY

The ohmic value of commutating impedance is calculated from the total per unit value as determined for the case of d-c short circuit.

$$Z_c=\frac{3E_s^2}{VA}\,\underline{Z}_c=1.042\times 0.0860=0.0895 \text{ ohm}$$

Using the R/X ratio determined for d-c short circuit

$K_r=1.57$, $K_f=1.35$, (Figure 5)

Crest Reverse Current

$$i_{ar}'=K_r\frac{\sqrt{2}E_s}{Z_c}=1.57\times\frac{\sqrt{2}\times 283}{0.0895}=7{,}020 \text{ amperes} \quad (8)$$

Crest Forward Current

$$i_{af}'=K_f\frac{\sqrt{2}E_s}{Zc}=6{,}040 \text{ amperes} \quad (9)$$

ARC-BACK WITH D-C FEED ONLY

In calculating the fault current in this case, the total ohmic resistance of the d-c fault path is determined by adding the resistances of the various elements.

	Ohms
Supply line 0.0031×1.042=	0.00324
Rectifier transformer (3,707/230×1,000)1.042=	0.0168
Interphase transformer=	0.0016
Anode cable=	0.003
D-c cable=	0.0034
D-c motor=	0.0170
Total R_3=	0.0450

The tube arc-drop is not included as the

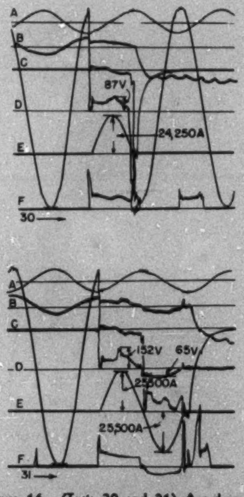

Figure 16. (Tests 30 and 31) Arc-drop on pumped ignitron during current pulse

"A"—60-cycle timing wave
"B"—grid-to-cathode voltage
"C"—grid current
"D"—anode-to-cathode voltage (arc-drop)
"E"—anode current
"F"—ignitor-to-cathode voltage

car-back was simulated by a switch.

The total inductance in the fault path is determined from the reactances of the various elements.

	Henrys
Supply line $0.025\times1.042/377=$	69.1×10^{-6}
Rectifier transformer $0.0575\times1.042/377=$	159.0
Interphase transformer =	15.8
D-c cables =	79.5
D-c motor =	46.0
Total $L_3=$	369.4×10^{-6}

The total reactance and impedance are

$X_3=\omega L_3=377\times369.4\times10^{-6}=0.139$ ohm

$Z_3=\sqrt{X_3^2+R_3^2}=0.146$ ohm

The ratio $R_3/X_3=0.324$.

The approximate value of the current in the faulty anode is given by the equation

$$i_{dr}=\left[\frac{E_d'}{R_3}-\frac{\sqrt{2}E_s}{Z_3}\right]\left[1-\epsilon^{\frac{-R_3}{X_3}\omega t}\right]+\frac{\sqrt{2}E_s}{Z_3}\left[1-\cos\omega t\right] \quad (11)$$

Substituting

$$\frac{E_d'}{R_3}=\frac{280}{0.045}=6{,}230 \text{ amperes}$$

$$\frac{\sqrt{2}E_s}{Z_3}=\frac{\sqrt{2}\times283}{0.146}=2{,}740 \text{ amperes}$$

at $\omega t=\pi$, $1-\epsilon^{-0.324\omega t}=0.632$, and $(1-\cos\omega t)=2$

$\omega t=3\pi$, $1-\epsilon^{-0.324\omega t}=0.950$, and $(1-\cos\omega t)=2$

$\omega t=5\pi$, $1-\epsilon^{-0.324\omega t}=0.995$, and $(1-\cos\omega t)=2$

The approximate currents in the faulty anode at the end of the first, third, and fifth half cycles are 7,680, 8,790, and 8,960 amperes, respectively.

ARC-BACK WITH BOTH A-C AND D-C FEED

If we assume that on the average, two phases are conducting and that the average a-c voltage in the circuit is one-half E_s, then

Total $L_1=255.4\times10^{-6}$ henries

$X_1=\omega L_1=0.096$ ohm

$R_1=0.0335$ ohm

$R_1/X_1=0.348$ ohm

$Z_1=0.101$ ohm

From equation 11

$$\frac{E_d}{R_1}=\frac{280}{0.0335}=8{,}400 \text{ amperes}$$

$$\frac{\sqrt{2}E_s}{Z_1}=\frac{\sqrt{2}\times283}{2\times0.101}=1{,}980 \text{ amperes}$$

The approximate currents in the d-c source at the end of the first, third, and fifth half cycles are respectively 7,280, 9,960, and 10,340 amperes.

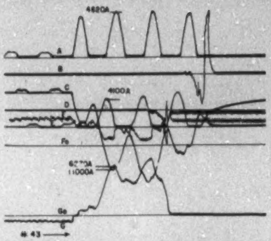

Figure 17. (Test 43) Fault current during arc-back with both a-c and d-c feed (arc-back approximately 120 degrees after end of conduction) 6-anode 200-kw 300-volt rectifier

"A"—anode number 1 current

"B"—a-c circuit breaker volts pole number 2

"C"—anode number 2 current (faulty anode)

"D"—d-c circuit breaker volts

"E"—anode number 3 current

"F"—d-c voltage

"G"—cathode current

The approximate current in the faulty anode is obtained by adding half these values to the value derived from Case 1. This results in an ultimate peak value of 7,020+10,380/2=12,210 amperes.

COMPARISON OF TEST AND CALCULATED VALUES

Test 9 (Figure 12) shows the fault currents during d-c short circuit with a bolted short. Calculated and test values are as follows:

	Calculated, Amperes	Test, Amperes
Average sustained current	8,500	7,700
Crest transient current	12,500	11,000

Test 5 (Figure 11) shows the fault current during d-c short circuit with inductance in the short. The average sustained current is 7,480 ampères and is only slightly below that obtained on test 9 (Figure 12).

Test 29 (Figure 13) shows the fault current during arc-back with a-c feed only with the rectifier operating on only three tubes. Calculated and test values are as follows:

	Calculated, Amperes	Test, Amperes
Crest reverse current	7,020	7,440
Crest forward current	6,040	6,370

A switch was used to short the faulty tube in making the arc-back test. Normal arc-drop was assumed in making the calculations, giving a calculated value which is too low.

Test 32 (Figure 14) shows the fault current during arc-back in a double wye circuit with no external d-c load. This record shows the effect of the current contribution of the anodes of the normal wye.

Test 45 (Figure 18) shows the fault current during arc-back with both a-c and d-c feed when the arc-back occurs at the end of conduction. Calculated and test values are as follows:

	Calculated, Amperes	Test, Amperes
Reverse current in faulty anode,		
At end of 1st half cycle	10,660	8,680
At end of 3rd half cycle	12,000	12,300
At end of 5th half cycle	12,200	12,900
Maximum d-c feed back	6,230	7,030

The effect of the time taken for saturation of the interphase transformer was not considered in the calculation. This results in too high a calculated value for the first half cycle.

Summary

A comprehensive procedure for the analysis of fault currents in power rectifiers has been developed and some of the more usual cases have been analyzed for the 6-phase double-Y circuit. However, further analyses are still required to cover all the conditions which may be encountered in practice and provide a ready means for determining fault currents.

Appendix I. Symbols

i=instantaneous current, also crest value of sinusoidal component of current

i'=crest value of instantaneous current including transient component

I=average value of current

First subscript:

a—anode (phase) current

d—d-c bus current

1, 2, 3—phase 1, 2, 3

Second subscript:

s—d-c short circuit

f—forward (normal) direction of flow

r—reverse direction of flow

1, 2, and so forth—start of intervals 1 and 2

e=instantaneous voltage

E_s=open-circuit, secondary voltage of rectifier transformer in rms volts

E_d'=counter electromotive-force component of d-c load voltage

L_c, R_c, $Z_c=\sqrt{R_c^2+X_c^2}$—line-to-neutral commutating inductance, resistance and impedance of rectifier

L_d, R_d=inductance and resistance of d-c circuit elements external to rectifier

L_p, R_p=inductance and resistance on primary side of rectifier

$R_s L_s$ = inductance and resistance on secondary side of rectifier transformer

Note

$L_p + L_s = L_c$

L_1, R_1, $Z_1 L_1 = L_d + {}^1/_2 L_c$, $R_1 = R_d + {}^1/_2 R_c$,
$Z_1 = \sqrt{R_1^2 + \omega^2 L_1^2}$

L_2, $R_2 L_2 = L_d + {}^1/_3 L_c$, $R_2 = R_d + {}^1/_3 R_c$

L_3, R_3, $Z_3 L_3 = L_d + L_c$, $R_3 = R_d + R_c$,
$Z_3 = \sqrt{R_3^2 + \omega^2 L_3^2}$

t_1, t_2, and so forth = time at beginning of intervals 1 and 2

Phase 2 voltage zero is the time reference for defining circuit action during arc-back with a-c and d-c feed.

β = switching angle (angle after voltage zero at which fault occurs).

$$\theta = \tan^{-1}\frac{\omega L}{R}$$

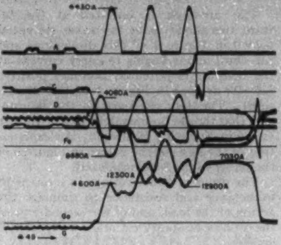

Figure 18. (Test 45) Fault current during arc-back with both a-c and d-c feed (arc-back at end of conduction) 6-anode 200-kw 300-volt rectifier

"A"—anode number 1 current
"B"—a-c circuit breaker voltage pole number 2
"C"—anode number 2 current (faulty anode)
"D"—d-c circuit breaker volts
"E"—anode number 3 current
"F"—d-c voltage
"G"—cathode current

Appendix II. Currents during Arc-back with A-C and D-C Feed

Interval 1 − t_1 to t_2

$$i_1 = I\left[\frac{\sqrt{3}}{2}\sin\left(\omega t - \frac{\pi}{6} - \theta\right) - \frac{\sqrt{3}}{2}\epsilon^{-\frac{R_c}{L_c}(t-t_1)} \times \sin\left(\omega t_1 - \frac{\pi}{6} - \theta\right)\right] + \frac{1}{2}i_d + \left(i_{11} - \frac{1}{2}i_{d1}\right) \times \epsilon^{-\frac{R_c}{L_c}(t-t_1)} \quad (13)$$

$$i_d = \frac{E_d'}{R_1}\left[1 - \epsilon^{-\frac{R_1}{L_1}(t-t_1)}\right] + \frac{\sqrt{2}E_s}{2Z_1}\left[\sin\left(\omega t + \frac{\pi}{3} - \theta_{d1}\right) - \epsilon^{-\frac{R_1}{L_1}(t-t_1)} \times \sin\left(\omega t_1 + \frac{\pi}{3} - \theta_{d1}\right)\right] + i_{d1}\epsilon^{-\frac{R_1}{L_1}(t-t_1)} \quad (14)$$

Interval 2 − t_2 to t_3

$$i_1 = I\left[\sin\left(\omega t - \frac{\pi}{3} - \theta\right) - \epsilon^{-\frac{R_c}{L_c}(t-t_2)} \times \sin\left(\omega t_2 - \frac{\pi}{3} - \theta\right)\right] + \frac{1}{3}i_d + \left(i_{12} - \frac{1}{3}i_{d2}\right)\epsilon^{-\frac{R_c}{L_c}(t-t_2)} \quad (15)$$

$$i_2 = I\left[\sin(\omega t - \theta) - \epsilon^{-\frac{R_c}{L_c}(t-t_2)}\sin(\omega t_2 - \theta)\right] - \frac{1}{3}i_d + \left(i_{22} + \frac{1}{3}i_{d2}\right)\epsilon^{-\frac{R_c}{L_c}(t-t_2)} \quad (16)$$

$$i_d = \frac{E_d'}{R_2}\left[1 - \epsilon^{-\frac{R_2}{L_2}(t-t_2)}\right] + i_{d2}\epsilon^{-\frac{R_2}{L_2}(t-t_2)} \quad (17)$$

Interval 3 − t_3 to t_4

$$i_1 = -\frac{\sqrt{3}}{2}I\left[\cos(\omega t - \theta) - \epsilon^{-\frac{R_c}{L_c}(t-t_3)} \times \cos(\omega t_3 - \theta)\right] + \frac{1}{2}i_d + \left(i_{13} - \frac{1}{2}i_{d3}\right)\epsilon^{-\frac{R_c}{L_c}(t-t_3)} \quad (18)$$

$$i_d = \frac{E_d'}{R_1}\left[1 - \epsilon^{-\frac{R_1}{L_1}(t-t_3)}\right] - \frac{\sqrt{2}E_s}{2Z_1} \times \left[\sin(\omega t - \theta_{d1}) - \epsilon^{-\frac{R_1}{L_1}(t-t_3)} \times \sin(\omega t_3 - \theta_{d1})\right] + i_{d3}\epsilon^{-\frac{R_1}{L_1}(t-t_3)} \quad (19)$$

Interval 4 − t_4 to t_1'

$$i_1 = i_d = \frac{E_d'}{R_3}\left[1 - \epsilon^{-\frac{R_3}{L_3}(t-t_4)}\right] + \frac{\sqrt{2}E_s}{Z_3}\left[\sin\left(\omega t + \frac{2\pi}{3} - \theta_{d3}\right) - \epsilon^{-\frac{R_3}{L_3}(t-t_4)} \sin\left(\omega t_4 + \frac{2\pi}{3} - \theta_{d3}\right)\right] + i_{d4}\epsilon^{-\frac{R_3}{L_3}(t-t_4)} \quad (20)$$

where

$$I = \frac{\sqrt{2}E_s}{Z_c}$$

$$\theta = \tan^{-1}\frac{\omega L_c}{R_c}$$

$$R_1 = R_d + \frac{1}{2}R_c \quad L_1 = L_d + \frac{1}{2}L_c$$

$$Z_1 = \sqrt{R_1^2 + \omega^2 L_1^2} \quad \theta_{d1} = \tan^{-1}\frac{\omega L_1}{R_1}$$

$$R_2 = R_d + \frac{1}{3}R_c \quad L_2 = L_d + \frac{1}{3}L_c$$

$$R_3 = R_d + R_c \quad L_3 + L_d = L_c$$

$$Z_3 + \sqrt{R_3^2 + \omega^2 L_3^2} \quad \theta_{d3} = \tan^{-1}\frac{\omega L_3}{R_3}$$

References

1. Rectifier Fault Currents, C. C. Herskind, H. L. Kellogg. Electrical Engineering (AIEE Transactions), volume 64, April 1945, pages 145–50.

2. Principles of Mercury Arc-Rectifiers and Their Circuits (book), D. C. Prince, F. B. Vodges. McGraw-Hill Book Company, New York, N. Y., 1927.

3. Mercury Arc Rectifier (book), Othmar K. Marti, Harold Winograd. McGraw-Hill Book Company, New York, N. Y., 1930.

4. Anode-Circuit-Breaker Design and Performance Criteria, E. W. Boehne, W. A. Atwood. Electrical Engineering (AIEE Transactions), volume 64, June 1945, pages 337–45.

5. Calculation of the Backfiring Phenomenon in Rectifiers, H. Forssell. Technical Achievements of ASEA Research, Vasteras (Sweden), 1946, pages 58–64.

Discussion

A. J. Maslin: (Westinghouse Electric Corporation, Sharon, Pa.): The treatment of short circuits and arc-backs presented in the paper by Herskind, Schmidt, and Rettig is an interesting addition to the published information on these subjects. In particular, the approximate solution for arc-back with a-c and d-c feed is most welcome, for it permits an estimate of the fault currents for this most important case, without laborious point-by-point computation of the current values in individual branches of the circuit. Everyone concerned with the design, application, or use of rectifier equipment will wholeheartedly endorse the authors' statement: "A complete treatment of the fault currents obtained in the widely used 6-phase double-Y circuit is particularly desired."

Generally, short circuits are relatively rare in comparison with arc-backs, and result in lower maximum fault currents in individual rectifying devices and transformer windings. As explained in the paper, all actual installation will have the a-c circuit impedance divided between the a-c winding and the d-c winding circuits. Because of the characteristics of rectifier transformers, the ratio X_p/X_s will usually be of the order of ten or more, hence the assumption that all impedance is located in the a-c winding circuit is usually completely justified. Short-circuit currents determined on this basis will be in error by being slightly too small.

Other factors, mentioned but briefly in the paper, are the inductance and resistance which are always present in the d-c circuit. Both of these operate to reduce the short-circuit current, usually to an extent more than sufficient to offset the error introduced by assuming all a-c circuit impedance located on the a-c winding side of the transformer. In the extreme case where the d-c circuit inductance is sufficient to completely smooth the direct current, the anode currents, instead of being sinusoidal with a crest value given by equation 1 of the paper, are approximately trapezoidal with a crest value only 87 per cent as great.

For most double-way circuits the location of the a-c circuit impedance is of no consequence. The short-circuit current is the same whether the impedance is all on the

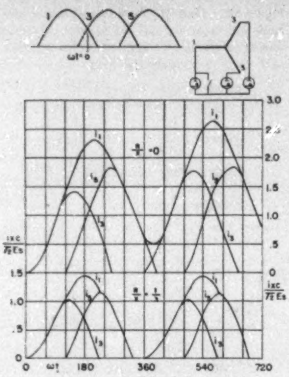

Figure 1. Arc-back, a-c feed only

a-c winding side, all on the d-c winding side, or divided between them.[1]

In spite of the great progress made in reducing the frequency of occurrence of arc-backs, they remain the most common rectifier fault. They are also the most severe, and are best isolated by high-speed anode-circuit switchgear. Because of this, experimental and analytical determinations of arc-back currents continue to receive a great deal of attention.

One of the simpler analytical treatments covers arc-back in a wye with a-c feed only, as presented in the paper. The values of K_r and K_f given in Figure 6 of the paper, however, appear to be rather high. Figure 1 of this discussion was calculated from equations which assume the arc to be equivalent to a resistance, and permit consideration of time of occurrence of the fault and amount of phase control. It applies to an arc-back occurring at no load, at the time $\omega t=0$, for a controlled rectifier operating with zero retard. The values of K_r and K_f from Figure 6 of the paper and Figure 1 of this discussion, as well as values of K_r taken from Figure 2 of a paper by H. Forssell,[2] are compared in Table I. It should be noted that Forssell's Figure 2 applies to arc-back in a wye with a-c feed only, at no load, and for an uncontrolled rectifier.

The arc-back is initiated at the instant two anodes have the same potential ($\omega t=0$ in Figure 1 of this discussion) and the third anode begins to carry current at the instant its potential becomes positive ($\omega t=90$ degrees in Figure 1 of this discussion). The data cited are for the assumption that the arc is equivalent to a resistance ($\alpha=0$ in Forssell's Figure 2). An explanation of the basis of the values in Figure 6 of the paper would be appreciated.

The use of a direct voltage in series with inductance and resistance to simulate the action of the load, and of the second wye of the 6-phase double-Y circuit, is a very useful artifice.

It was suggested but not developed in a previous paper.[3] A discussion,[4] however, presented a detailed comparison of test values of arc-back current in a double-Y circuit with calculated values for a single wye with both a-c and d-c feed. The equations used in this comparison permit taking account of the load being carried, the time of occurrence of arc-back, and the amount of phase control. These calculations, while they yield highly satisfactory results, are very laborious to make. The approximate solution demonstrated in the paper is therefore most welcome.

Whenever arc-back currents are calculated by these methods, the influence of switchgear must be given careful consideration. With high-speed switchgear, either cathode or anode, the crest calculated current will not be realized because the opening switch will introduce an important voltage drop into the d-c feed circuit, or the anode circuit itself, early enough to effect some degree of current limitation. A number of arc-back tests[5] on 600-volt 6-phase double-Y rectifiers, feeding regenerative loads through high-speed cathode circuit breakers, indicate that the first crest of arc-back current is about 90 per cent of that calculated on the basis of both a-c and d-c feed; while the second and subsequent crests are about 15 per cent greater than calculated on the basis of a-c feed only, this increase being due to the contribution of the other wye.

Table I

	K_r			K_f	
R/X	Figure 6 of Paper	Figure 1 of Discussion	Figure 2 of Forssell	Figure 6 of Paper	Figure 1 of Discussion
0	2.40	2.30	2.35	1.98	1.86
0.1	2.00		2.00	1.70	
0.2	1.75		1.73	1.50	
0.333	1.52	1.43	1.48	1.32	1.18
0.4	1.45		1.36	1.25	
0.5	1.35		1.23	1.16	
0.6	1.30	1.07	1.12	1.11	

References

1. The Three-Phase Full Wave Rectifier Circuit, **A. J. Maslin.** *Electronics* (New York, N. Y.), volume 9, December 1936, page 28.

2. Calculation of the Backfiring Phenomenon in Rectifiers, **Harry Forssell.** Technical Achievements of ASEA Research, March 1946, page 58.

3. Rectifier Fault Currents, **C. C. Herskind, H. L. Kellogg.** Electrical Engineering (AIEE Transactions), volume 64, April 1945, pages 145–50.

4. Discussion, **R. D. Evans, A. J. Maslin,** Loc. Cit., pages 441–42.

5. Arc-Backs in Rectifier Circuits—Artificial Arc-Back Tests, **R. D. Evans, A. J. Maslin.** Electrical Engineering (AIEE Transactions), volume 64, June 1945, pages 303–11.

C. C. Herskind, A. Schmidt, Jr., and C. C. Rettig: In his discussion, Maslin has compared values of K_r and K_f in Figure 6 of the paper with values calculated by himself and also by Forssell in another paper. The differences noted by Maslin may be explained as follows:

1. We have assumed a free rectifier, with conduction beginning as soon as the anode becomes positive. The per unit base for K_r and K_f is $\sqrt{2}E_s/Z$.

2. Maslin has assumed phase control which prevents conduction from starting for 30 degrees after the anode becomes positive with respect to the transformer neutral. While such phase control does not affect normal operation of the rectifier, it does serve to reduce the a-c feed during arc-back.

3. Forssell uses a base of $\sqrt{2}E_s/X$ instead of $\sqrt{2}Es/Z$. When this change in base is made, Forssell's curve agrees closely with ours. There is a slight difference at $R/X=0$, in the plotted curves. The calculated value of K_r at this point is 2.366.

The treatment of fault currents is by no means complete. Among the cases that merit consideration are:

1. Contribution of normal wye in arc back of double-Y rectifier.
2. Effect of impedance in d-c fault.
3. Circuits other than double-Y.

Die-Cast Rotors for Induction Motors

L. C. PACKER
MEMBER AIEE

Synopsis: There are many problems to solve in connection with the manufacture of die-cast rotors that require the co-ordinated efforts of the design and manufacturing engineers. Forcing molten aluminum under high pressures into the rotor slots causes excessive stray load losses unless the laminations are insulated properly and strain relieved, and the slots insulated from the cast aluminum conductors. Heating processes may be necessary after machining the surface. It is also necessary to select the best and most economical die casting methods, equipment, and furnaces. The moulds properly gated, holding pressure, pressure on the die-casting metal, and temperature are all important to the production of homogeneous die cast rotors free from impurities. With proper control, die-cast rotors can be manufactured to relatively close limits of rotor resistance and with the stray load losses reduced to a satisfactory value resulting in satisfactory performance, and generally at a lower cost than copper cage rotors. This paper explains the cause of the stray load losses, processing to reduce them, and suitable test methods. There are curves showing the effect of excessive stray load losses upon performance, results of various processes, and illustrations of die-casting methods and diagrams of equipment for testing die-cast rotors.

DIE-CAST rotors for ratings through 125 horsepower now are being produced in addition to those which have been manufactured for about 25 years in sizes ranging from about 1/200 to 50 horsepower in quantity production. They have many advantages to both the ultimate user and the manufacturer. The die cast rotor is a solid and fairly homogeneous mass that retains its balance, and in general gives the customer good all-around performance. The manufacturer can generally make die cast rotors at a lower cost than copper cage rotors, which is to the advantage of both the customer and manufacturer. Since World War II, aluminum, which is used in die-cast rotors, has been more plentiful and lower in cost than copper. The shortage of copper made it very difficult for manufacturers of copper cage rotors.

There are many pitfalls that must be guarded against in the successful manufacture of die-cast rotors. They are not just ordinary die castings and cannot be treated as such. Excessive stray load losses, porosity, and broken bars can be very detrimental to the performance, cause high factory rejects and trouble in operation. Some of these stray losses also can exist in copper cage rotors but to a much smaller degree. Therefore, before starting to lay out the design and manufacturing methods for die-cast rotors, it is advisable, first, to study the applications for which the motor is intended, and then the source of the losses in induction motors. Next to consider are the results of forcing pure aluminum or aluminum alloy into the rotor slots and making contact with the wall of the slots. If there is insulation on the laminations, there may still be exposed iron surfaces in the slots. If the source of the various losses, their effect upon the performance of the motor and the methods for reducing or eliminating them are known, then plans can be made to proceed with the details of design and processing methods.

A dependable method of testing die cast rotors is essential to control the quality.

There are die-casting problems, also, that must be worked out, and a study of equipment, gating, temperatures, and pressures must be made. Some of these problems can be worked out in pilot runs after the equipment is set up.

The main purpose is to point out the problems and give examples of experiences that lead up to production, and problems in manufacturing that affect the performance of the motor. Experience has proved that solving these problems makes it easier and less costly to get production up quickly and maintain the quality of the product.

This paper was prepared around data pertaining to fractional horsepower motors, but it may also apply to larger single-phase motors. The extent of the various losses and effects upon larger polyphase motors depends upon the design.

The source of most of the troubles, which will be discussed first, applies to both single-phase and polyphase motors.

Source of Losses in Induction Motors

In a copper cage rotor, the conductor may contact the walls of the rotor slots at various points if the conductor is buckled during the riveting process and due to skewing, but the points of contact are relatively few in the slot compared to the surface contact of the conductors in a die cast rotor.

In a die-cast rotor, hot aluminum is forced into the slots under pressure. It can short circuit all of the laminations, which in turn short circuit the conductors in part or throughout the slots, thereby causing a net-work of many circuits for circulating currents.

Losses in the ordinary squirrel-cage motor, not including the ordinary losses due to normal current in both windings, bearing friction, windage, and losses in the end bells, are those due to the fundamental frequency, tooth pulsation frequency, surface losses, losses due to spreading of the main flux back of the teeth, harmonics other than slot harmonics, and those caused by the eddy current in the rotor cage winding.

The stray load losses over and above

Paper 49-69, recommended by the AIEE rotating machinery committee and approved by the AIEE technical program committee for presentation at the AIEE winter general meeting, New York, N. Y., January 31–February 4, 1949. Manuscript submitted July 15, 1948; made available for printing December 28, 1948.

L. C. PACKER is manager of motor engineering, Westinghouse Electric Corporation, Springfield, Mass.

The author wishes to acknowledge the assistance of G. E. Monchamp, an associate, for his assistance in the development of the reverse rotation method of testing die-cast rotors and calculation of losses as used in this paper.

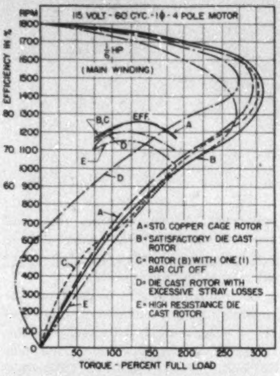

Figure 1. Speed-torque and efficiency on the main winding with typical cases of satisfactory and defective die-cast rotors and copper-cage rotors of single-phase motors

the normal inherent losses in a given design may be caused by bending of the laminations, punching strains, excessive pressure between laminations, poor interlamination insulation and burrs, plus the short circuiting effect in the slots of die-cast rotors.

Bending of the laminations and punching strains decreases the permeability of the steel and increases the magnetic densities, magnetizing current, and hysteresis iron loss. In single-phase motors the magnetizing current is relatively large. Any increase will increase the copper losses more than in polyphase motors. There also are harmonics due to hysteresis, the magnitude depending upon the saturation.

Burrs, insufficient interlamination resistance, and excessive pressure between laminations result in eddy current losses.

The tooth pulsation frequency losses have two causes:

1. High-frequency flux pulsations penetrating a short distance into the core.
2. High-frequency flux which extends throughout the whole magnetic circuit due to pulsation or reluctance as the teeth pass opposing teeth.

The high-frequency flux pulsations in the teeth also cause hysteresis and eddy current losses in the teeth.

The high-frequency circulating current in the cage winding of the rotor may damp out the high-frequency flux pulsations in the rotor teeth. However, it may cause the pulsations to be reflected to the stator teeth and produce large pulsation losses in the stator teeth. While the rotor tooth frequency may be partially damped, the high-frequency circulating currents in the cage winding may cause a high effective resistance due to the skin effect, thus increasing the losses.

Saturation of the teeth where tooth pulsations are present causes high-frequency leakage flux, both tangential and radial in the slots. This causes high eddy current losses in the conductors of the cage winding in the rotor. Therefore, there is a very rapid increase in the pulsation losses with increase in induction of the iron. There have, however, been instances indicating that, with higher fundamental flux density, the stray load loss is less for the same ampere turn value.

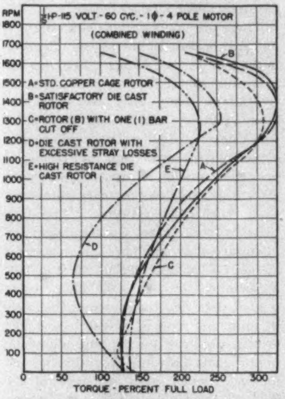

Figure 2. Speed-torque curves with the combined winding with typical cases of satisfactory and defective die-cast rotors and copper-cage rotors of single-phase motors

Same rotors as Figure 1

In fractional horsepower motors, punching strains penetrate farther into the teeth (compared with tooth width) than is the case in the larger industrial or power machines. Because of this, there is greater saturation in the small machines due to the decreased permeability and also high hysteresis losses.

Finishing the surface of the rotor core by machining, drives the tooth tips into the die-cast conductor. This increases the eddy current losses and short circuits the conductors within the slots. The bridges of a closed slot rotor also are driven into the die-cast conductor. In either case, the tooth tips or bridges are strained and thus saturated more than normal.

The Effect of Excessive Stray Load Losses and Rotor Resistance upon Performance

Stray load losses cause a reduction in efficiency, pull-up and breakdown torques. The effect is generally greater in single-phase motors than in polyphase motors. The starting torque is seldom reduced. If there is any change at all, it is a slight increase in starting torque. Apparently this is because the excessive iron loss has the effect of increasing the rotor resistance which increases the starting torque.

Probably the greatest effect of excessive stray losses is upon the pull-up torque. In some applications, this torque may be reduced so much that the motor cannot get the load up to speed. This is especially true with compressor applications.

The results of excessive rotor resistance are well known. The efficiency and breakdown torque are reduced and the starting torque and slip are increased.

Figures 1, 2 and 3 show typical cases of performance of die cast as well as copper cage rotors for a given design. Curve *A* is for standard copper cage rotors, curve *B* is for a satisfactory die-cast rotor, curve *C* is for rotor *B* with one broken bar, and curve *D* is a typical case of rotors with excessive stray load losses.

Figure 1 shows the test on the main winding only. Figure 2 shows the test on the combined main and starting winding single phase. Figure 3 shows test on

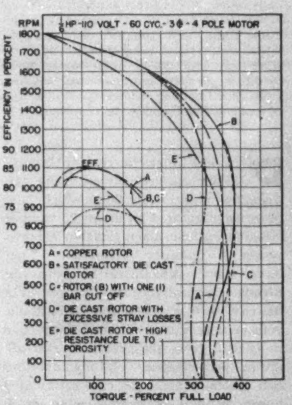

Figure 3. Speed-torque and efficiency curves of polyphase motor with typical cases of satisfactory and defective die-cast rotors and copper-cage rotors

Same rotors as Figures 1 and 2

three phase. Note the reduction in pull-up and breakdown torques and the efficiency caused by excessive stray load losses as shown by curve *D*. These curves were all produced by the motor driving a dynamometer. The stray load losses were so great in the motor (represented by curve *D* in Figure 1) that the torque was zero at approximately 630 rpm, and then the dynamometer drove the rotor.

The effect of excessive rotor resistance is shown by curves E in Figures 1, 2, and 3.

Figure 4 illustrates how the efficiency and torques vary with stray load losses. These curves represent the average values from tests on several hundred die-cast rotors, compared with average copper rotors of a certain design set up as 100 per cent. The curve of the torque at 600 rpm is shown because it is used as a test control point for this particular design of single-phase motor. When the breakdown torque on the main winding and the torque at 600 rpm on the combined winding are of acceptable values, the balance of the speed-torque curves are usually satisfactory. If the rotor resistance is excessive, the breakdown torque is usually too low.

Reduction of Stray Load Losses

The real problem with die-cast rotors resolves itself into eliminating, or at least reducing to a practical minimum, the eddy current and hysteresis losses in the laminations, eddy current losses in the rotor cage winding, and the short circuits between the conductor bars caused by contact between the conductor bars and the bare edges of the laminations. All of this is necessary to maintain the desired performance and eliminate rejects in the factory. A discussion of the means to accomplish the desired results follows.

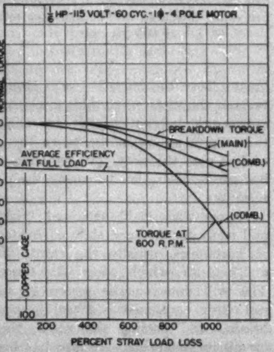

Figure 4. Torques and efficiency versus per cent of stray load losses with copper-cage rotors as 100 per cent

Design of Rotor

The design engineer may have either a program of superseding copper cage rotors with die-cast rotors or a new line of motors to design.

Die-cast rotors usually use pure aluminum or various aluminum alloys, depending upon the applications. Pure aluminum has a conductivity of approximately 60 per cent as compared to copper, but has only about 50 per cent conductivity when die cast. Therefore, in the laminations of a copper cage design, the pure aluminum conductor resistance is greater than for the copper bars. To have the same total resistance as for copper, the end rings must be of larger section than the copper rings. It may be an advantage in some cases to redesign the lamination to obtain a larger slot and also to decrease the tooth flux density.

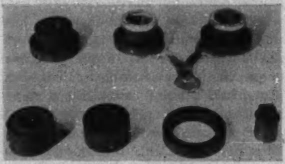

Figure 5. Sequence of operations in die-casting rotors

In a new design motor the slot combination of both stator and rotor may be changed to the advantage of the rotor, but again the designer should be very cautious about changing slot combinations, especially if he has a satisfactory fundamental line of combinations, since such a change may result in noise and cusps in the speed torque curve. However, conditions may be such that he can increase the diameter of the rotor and bore of the stator, and obtain the desired performance and cost without throwing the mechanical design of the motor out of line with standard sizes.

Larger slots, properly shaped, reduce the resistance and the high-frequency losses in the conductors. They also cause a reduction in the size of end rings, thus reducing the leakage losses. Lower teeth densities also will reduce the losses.

If the end rings are too large in section, they may cause casting difficulties and be more porous than small sections. Porosity means higher resistance. Large sections also increase the leakage between the rings and stator winding.

Figure 6. Front half of a die-casting mould

If the end rings are too thin, the cooling strains may cause a separation from the conductors. For motors that require cooling fans, there are further savings in cost by casting fan blades as a part of, and located at the end of, the rings.

For balancing the rotor, lugs can be cast onto the rings, and weights fastened to the lugs as required. A die-cast rotor should maintain its balance indefinitely whereas a copper-cage rotor may not. This is because the copper conductors do not fill the slot and may shift position a slight amount to change the balance. Recent improvements in copper-cage rotors have reduced this condition considerably, however, in die-cast rotors, the slots are filled solidly and therefore, no shifting can occur.

Processing of Rotor Laminations

The proper maintenance of the lamination dies will keep the punching strains and burrs to a minimum thus resulting in lower hysteresis and eddy current losses.

The eddy current losses can be reduced further by insulating the lamination surfaces to obtain sufficient interlamination resistance and to provide insulation between the slot walls and the die cast conductor bars. The insulation should be such that it will not be injured by the high temperature required for die casting, or forced out by the casting material. There are different methods of obtaining this insulation. The motor application may have some bearing upon the type of insulation used.

Strain relieving will reduce the hysteresis losses and increase the permeability of the steel.

Figure 7. Rear half of a die-casting mould

Die Casting Methods

There are two common methods of die casting rotors, namely, the closed-mould or high-pressure type and the end mould or "dunking" type. The centrifugal type is sometimes used, but is not as commonly used as the above types.

In the first type, the rotor core is placed into a 2-part mould and the mould closed. Hot metal is forced into the part of the mould which forms the rings and into the slots and then allowed to cool sufficiently to solidify the metal before removing the rotor. A close clearance between the mould and outside diameter of the rotor is desirable. A shoulder in the die at each end of the mould will eliminate any flash of metal around the outside of the rotor. A closed-slot rotor has advantages over a partially-open-slot rotor. There must be enough pressure against the laminations to prevent the hot metal from being forced between them and around the outside of the rotor. If this occurred, the eddy current loss would be increased. However, the pressure should not be so great that it will increase the eddy current losses.

In the closed-mould method rotors may be cast either singly or in multiples of six or more depending upon the size of the rotor and the size of the equipment. Rotors may be cast on special hubs or quills, or shafts if the production warrants it. However, means must be provided to prevent any of the laminations from moving and closing off the slots.

Figure 5 shows the different stages of a rotor from the laminations to the cast rotors. Figures 6 and 7 show the two halves of a typical mould with the rotor core assembled into one half of the mould ready to cast. Figure 8 shows a high-pressure die-casting machine.

In the end mould or dunking method, for small rotors the stack of laminations is assembled onto an arbor with a head on one end, or fastened to one end ring mould. There is a spiralled key on the arbor to skew the laminations, which cannot move when once assembled. End ring moulds are assembled to each end of the stack of laminations and the whole assembly tightened by a nut on the arbor. Unless properly controlled by using a torque indicator or torque wrench when tightening the nut, there may be excessive pressure exerted between laminations which will increase the eddy current losses. The normal frequency loss would not amount to very much but there can be considerable loss at tooth pulsation frequencies. The assembled unit is then placed into a well into which hot metal has been poured. The metal is forced under pressure through the ports in the lower ring mould, then into the slots and upper end ring mould. Ports in the upper mould permit the air and gases to pass through them.

The type of equipment, the pressures, temperatures, type of moulds, and gating of the moulds are very important to both methods of die casting in reducing the porosity and broken bars to a minimum.

The elimination of impurities in the die-cast metal results in more solid sections of the cast cage winding. This may be done by using nonmetallic linings for the melting pots and ladles.

Machining Rotor Surface

After the die-casting operation, the outside surface of the rotor is machined or ground to the proper finished diameter. For the motor's performance, grinding the outside diameter is generally more satisfactory for closed slots. Machining this surface results usually in higher stray load losses than by grinding. This is because the machining is more concentrated and drives the bridge or tooth tips into the conductor bars resulting in higher stray load losses. Grinding is generally unsatisfactory for partially-open-rotor slots as the grinding wheel may pick up too much die-cast metal and clog the wheel.

Heating the completed rotor at a reasonably high temperature, followed by proper cooling after machining or grinding the rotor surface, will break the conductor bars away from the slot wall and tooth tips or bridges. This process also breaks loose the burrs between laminations at the surface and adds some oxide between the laminations. It also relieves the strains set up in the tooth tips or bridges over the slots, thus reducing the hysteresis losses and increasing the permeability.

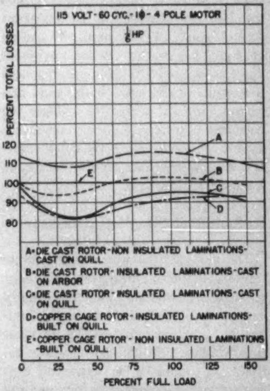

Figure 9. Per cent of total losses versus per cent load for various methods of processing die-cast rotors compared with copper-cage rotors as 100 per cent

Rotors with highly stressed bridges and teeth, for instance, show up hysteresis harmonics, usually the third, fifth and seventh, which affect the torque. This will show on the screen of special test equipment. After properly heating and cooling the rotor, these harmonics disappear. It also has been found that the conductivity of the material in the cage winding has been increased.

Figure 8. Die-casting machine using moulds in Figures 6 and 7 to die cast the rotors in Figure 5

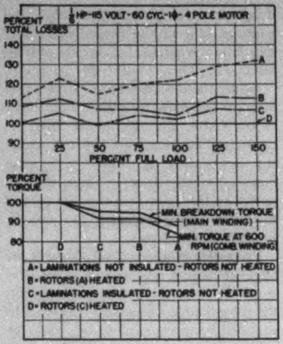

Figure 10. Upper curve is per cent of total losses versus per cent load for die-cast rotors with various processing

Lower curve shows the breakdown and torque at 600 rpm for the same rotors as above plotted against the process

Results Due to Processing

The results of various processes are shown in Figure 9 and compared with copper-cage rotors, *E*, which are considered as 100 per cent. Curve *A* shows die-cast rotors whose laminations and slots have not been insulated. Curve *B* is for die-cast rotors with laminations and slots insulated, assembled upon an arbor and locked in place with a nut ready for die casting. The higher losses are due to excessive pressure as compared to curve *C* whose laminations were insulated and assembled onto a quill. Curve *D* shows copper-cage rotors whose laminations were insulated. All laminations for the rotors shown by these curves in Figure 9 were made from the same lot of steel, and punched with the same dies.

There are four conditions shown in Figure 10: the laminations not insulated and not heated after machining; rotors heated to reduce the losses; laminations insulated but not heated; and the rotors heated. The upper set of curves show the per cent total losses plotted against per cent of full load for the different processes. Since process *D* was adopted for standard, it is set up as 100 per cent.

The lower curves in Figure 10 show the effect of the various processes upon the breakdown torque on the main or running winding and the torque at 600 rpm on the combined winding. The process *D* is considered as the standard and the minimum torques permissible are considered as 100 per cent. The lines between the points are connecting lines only to show the trend of results. All curves in Figure 10 are from results on die-cast rotors with a different type and gauge of steel than used in the previous tests.

The curves shown in Figure 11 are for the same die-cast rotors as Figure 10. The dotted lines are for the minimum, average, and maximum torque values at 600 rpm on the combined winding observed throughout the range of the lot tested, and are in per cent against the different processes. The minimum torque permissible is considered as 100 per cent torque for the process *D*. The solid lines show the corresponding stray-load losses obtained by testing the same rotors in a 3-phase stator. The type of service to which the motor will be subjected will determine whether or not it is necessary to insulate the rotor laminations and slots or heat the rotors after finishing the surface.

The results due to the number of times the rotors of a certain design are heated are shown in Figure 12. The rotors were all insulated prior to die casting. The condition where the rotors were not heated is considered as 100 per cent. When heated once the stray-load losses average about 72 per cent of the stray-load losses with no heating. The maximum improvement in the reduction with one heating shows a value of about 56 per cent of the value with no heating. There are sometimes instances where the burr condition of the laminations is very bad, in which case several heatings may be necessary. It has been found that there is very little improvement to be gained by heating the rotor more than three times unless there is a marginal case.

The per cent of total losses versus per cent full load for various processes is shown in Figure 13 for die-cast rotors operated as 3-phase motors. The rotors tested are the same rotors as shown as single-phase motors in Figure 9 and compared with the copper-cage rotors which are considered as 100 per cent.

Testing Die-Cast Rotors

Accuracy and consistency of test methods, equipment, and personnel are essential to reliable results during the development stage and for production testing. A satisfactory procedure for the development stage consists of using a standard single-phase stator and a 3-phase stator for checking performance and stray-load losses. These stators are kept as laboratory standards to check die-cast rotors of a given design.

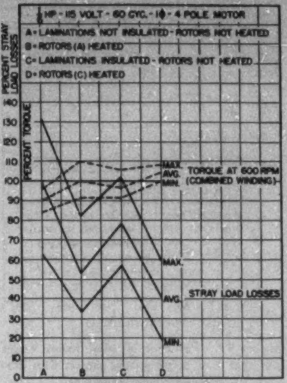

Figure 11. Per cent of stray-load losses and torque at 1/3 synchronous speed for the various processes of die-cast rotors

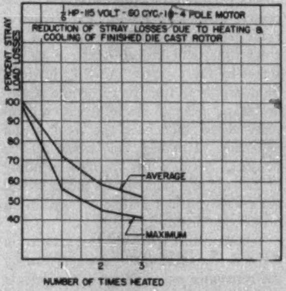

Figure 12. Reduction of stray-load losses due to heating the finished die-cast rotors

The stator and rotor are mounted in a frame in such a manner that the rotor is overhung from two ball bearings spaced apart sufficiently to maintain a uniform air gap. The frame is open on the one end as there is no end bracket. This makes it convenient to assemble rotors with uniform results. The bearing friction is maintained at about three watts for a 1/6 horsepower motor.

Rotors are checked for stray-load losses on 3-phase and correlated with the single-phase performance. Usually hundreds of rotors are tested so as to obtain minimum, average, and maximum values. There are then sufficient data for establishing limits and other data for production testing.

Many methods have been investigated but the foregoing method which is checking stray-load losses by the reverse-rotation method proved to be the most accurate and the fastest for both develop-

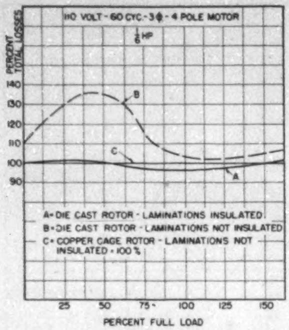

Figure 13. Per cent of total losses versus per cent load of polyphase motors with die-cast and copper-cage rotors

ment and production testing. By this method a production testing rate of 150 rotors per hour has been attained. Excessive stray-load losses, and excessive rotor resistance, insufficient skew of the rotor slots, and broken bars can be detected by this method. Actually it would be desirable to test the rotor in a standard stator prior to assembly into a complete motor and check the torques and efficiency. However, this would not be practical because the starting winding in the case of a single-phase motor would get excessively hot and soon burn up on production testing.

Testing rotors by the locked saturation method is satisfactory for measuring the resistance only. Most of the defects are due to stray-load losses. To check them the rotor must be revolved. However, a method for checking broken bars and high resistance is discussed at the end of this paper.

The production equipment consists of a polyphase, ball bearing motor driving the rotor to be tested through a shaft and coupling mounted on outboard ball bearings. The test stator has the same number of slots as the standard stator but oversize to reduce the heating. This equipment is shown diagrammatically in Figure 14. A rotor that represents the minimum acceptable performance is used for a standard. The watts input of the driving motor is correlated with the driving torque and stray load losses and the current in the test stator circuit determines whether the resistance of the rotor is excessive due to porosity or broken bars, in which case it will be lower than normal and it will be higher than established limits if the slots are not skewed the proper amount.

Figure 15 shows split-phase motor speed-torque curves, both positive and negative speeds, for a satisfactory and a defective rotor.

Figure 16 shows similar curves for a polyphase motor except that a rotor with a broken bar and another with excessive resistance are shown.

The method of calculating the stray-load losses of fractional horsepower motors was derived from data taken for the various known methods of calculating stray-load losses. It is also necessary to properly proportion the various losses, so that corrective measures can be applied to the processing of the rotors. The stray-load losses may be grouped according to the AIEE standard for polyphase motors.[19] Changed core loss and high frequency I^2R due to changed magnetic fields is the important item in moderate size motors.

Reverse Rotation Method of Determining Stray-Load Losses

The basis for these measurements was first taken from published works. However, refinements were made for this particular problem.

To outline briefly, the above consisted of applying a balanced polyphase voltage across the stator terminals and driving the rotor in the opposite direction to that of the revolving field. The stator input power, current, and stator resistance are measured during the test.

Denote the stator input by W_s.
Denote the stator copper loss by W_{cu}.
Denote the net stator input by W.
Let $W = W_s - W_{cu}$.

By means of a dynamometer, the rotor driving watts (P_r), and friction and windage (P_f) of the dynamometer and motor are measured. The net driving watts $= P$. Then, $P = P_r - P_f$.

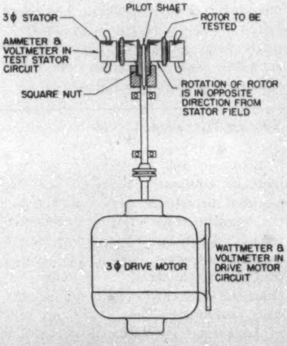
PILOT SHAFT
3ϕ STATOR
ROTOR TO BE TESTED
AMMETER & VOLTMETER IN TEST STATOR CIRCUIT
SQUARE NUT
ROTATION OF ROTOR IS IN OPPOSITE DIRECTION FROM STATOR FIELD
3ϕ DRIVE MOTOR
WATTMETER & VOLTMETER IN DRIVE MOTOR CIRCUIT

Figure 14. Schematic diagram of reverse rotation method of testing die-cast rotors for stray-load losses

Under these conditions the total power input is consumed in losses. In the case of the stator, the total power input W, consists of stator copper loss and power supplied to the rotor for part of the rotor double-frequency losses. The mechanical power to the rotor also supplies part of the rotor double-frequency loss and the tooth-frequency losses.

From the relation $R = R_2(1-s)/s$ we have at minus synchronous speed, $R = -1/2\ R_2$ which shows that one half (1/2) the rotor double-frequency losses must be supplied by mechanical power, while the other half must be supplied by the stator. Therefore, if we subtract the net stator power from the net driving watts, P, we have left the tooth frequency losses, or stray load loss $= P - W$.

At 1/2 synchronous speed in reverse direction from $R = R_2(1-s)/s$ we have $R = -1/3R_2$ which means that the mechanical power supplies 1/3 of the rotor loss due to the fundamental frequency and 2/3 the power supplied by the stator. Therefore, if we multiply the net stator input by per cent of synchronous speed, in this case 50 per cent, we have the net stator input $(2/3) \times 50$ per cent $= 1/3$ which is equal to the fundamental losses supplied by mechanical power.

By substituting the two values we again have stray-load loss, or for any speed, we have stray load loss $= P - W \times$ per cent synchronous speed.

Segregation of Eddy-Current and Hysteresis Losses

Stray load losses are caused by several factors. There are only two ways in which this power can be consumed, by eddy current, and by hysteresis losses. Since any increase in these losses at fundamental frequency is taken out in calculation of stray load loss, all we have left are these losses at tooth pulsation frequencies. Eliminating the design constant from the formulas for eddy current and hysteresis losses we have the equation for hysteresis loss

$$P_h = B^n f$$

and for eddy current loss

$$P_e = B^2 f^2$$

In these equations the machine constants are taken out since they are the same in the same machine.

Now let us take the measured stray loss at normal voltage and at minus

1,800 rpm, (assuming a 4-pole motor). We can then take this loss as made up of tooth pulsation eddy current and hysteresis loss, or

$$P_h+P_e=\text{stray load loss at minus } 1{,}800 \text{ rpm} \quad (1)$$

If we keep the flux density constant, and by regulating the voltage and dropping the speed to minus 900 rpm, the tooth pulsation frequency is half, therefore, we can set up equation 2

$$0.5\,P_h+0.25\,P_e=\text{stray loss at minus } 900 \text{ rpm} \quad (2)$$

in terms of equation 1.

Solving equations 1 and 2 simultaneously we get P_h and P_e at minus 1,800 rpm. From these values P_h and P_e can be calculated for any speed at this flux density.

For greater accuracy, the stray loss can be taken for any two speeds. For example, for minus 1,800 rpm and minus 900, the equation would be the same as equations 1 and 2.

The same thing could be done by holding the frequency constant and changing the flux density if the constant, n, in the hysteresis loss equation were known. However, Steinmetz's determination of the constant $n=1.6$ does not always apply to present-day materials. We have found that for present-day materials the constant n varies from 1.5 to 3.0 and it may not be constant for a given material. Thomas Spooner in his book[11] reported a similar range. The Massachusetts Institute of Technology staff[10] has done considerable work along this line and they report a value for this constant n varying from 1.5 to 2.5.

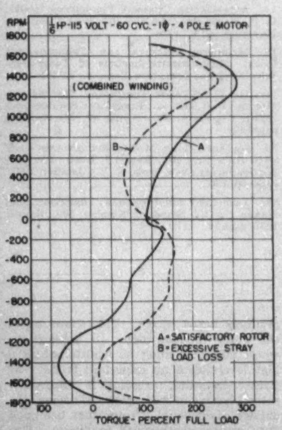

Figure 15. Positive and negative speed-torque curves of single-phase motors with die-cast rotors

Two examples of segregating the hysteresis and eddy-current losses are as follows for speeds of minus 900 and minus 1,800 rpm. The same stator was used with different die-cast rotors.

One motor had 155 watts stray-load loss at minus 1,800 rpm and 73 watts stray-load loss at minus 900 rpm. Let

$$P_h+P_e=155 \text{ watts at minus } 1{,}800 \text{ rpm} \quad (3)$$

$$0.5\,P_h+0.25\,P_e=73 \text{ watts at minus } 900 \text{ rpm} \quad (4)$$

which can be written

$$P_h+0.5\,P_e=146 \text{ watts} \quad (5)$$

Solving by subtracting equation (5) from equation (3)

$$0.5\,P_e=9 \quad (6)$$

$$P_e=18 \text{ watts or } 11.6 \text{ per cent of the total stray load loss} \quad (7)$$

Then

$$P_h=137 \text{ watts or } 88.4 \text{ per cent of the total stray load loss} \quad (8)$$

Another motor had 185 watts stray load loss at minus 1,800 rpm and 60 watts at minus 900 rpm.

Then

$$P_h+P_e=185 \text{ watts at minus } 1{,}800 \text{ rpm} \quad (9)$$

$$0.5\,P_h+0.25\,P_e=60 \text{ watts at minus } 900 \text{ rpm} \quad (10)$$

which can be written

$$P_h+0.5\,P_e=120 \text{ watts} \quad (11)$$

Solving by subtracting equation 1 from equation 9

$$0.5\,P_e=65 \quad (12)$$

$$P_e=130 \text{ watts or } 70.2 \text{ per cent of the total stray load loss} \quad (13)$$

Then

$$P_h=55 \text{ watts or } 29.8 \text{ per cent of the total stray load loss} \quad (14)$$

It is to be noted that the first motor had a high percentage of hysteresis losses whereas the second motor had a high percentage of eddy-current losses.

Stationary Method for Checking High Resistance and Broken Bars in Die-Cast Rotors

It is important for development work with die-cast rotors to be able to detect broken bars quickly and also to serve as a check for the people on production testing. It is also desirable to detect high resistance and the location of the high-resistance bars or high-resistance sections of the resistance rings of the rotor. The equipment shown in Figures 17 and 18 perform such duties as mentioned before.

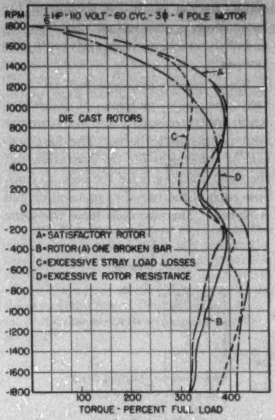

Figure 16. Positive and negative speed-torque curves of polyphase motors with die-cast rotors

One-third of a special stator core, having the same number of slots as the rotor to be tested, and skewed the same as the rotor is mounted on a supporting base. The teeth are removed except for two pairs, these forming two slots and convenient distance apart by several

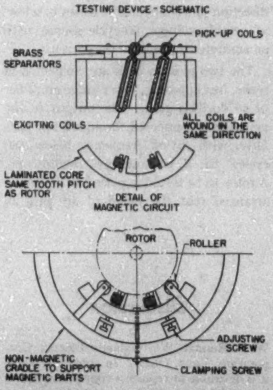
TESTING DEVICE-SCHEMATIC
PICK-UP COILS
BRASS SEPARATORS
EXCITING COILS
ALL COILS ARE WOUND IN THE SAME DIRECTION
LAMINATED CORE SAME TOOTH PITCH AS ROTOR
DETAIL OF MAGNETIC CIRCUIT
ROTOR
ROLLER
ADJUSTING SCREW
NON-MAGNETIC CRADLE TO SUPPORT MAGNETIC PARTS
CLAMPING SCREW

Figure 17. Schematic diagram of the excitation unit used in the method of testing die-cast rotors for excessive resistance, and uniformity of resistance in cage and broken bars

times the slot pitch. A section of the laminations is removed entirely near the end of the stack, dividing each tooth into two parts.

Brass spacers are arranged to separate the two sections of stackings which are bolted solidly into one structure with nonmagnetic bolts. The long section of stacking is for the excitation and the short stacking is for the pick up coils. Into each of the two slots an exciting coil is placed. The two coils have the same number of turns wound in the same direction and connected in series to a low, adjustable voltage, 60-cycle source, with an ammeter to measure the current.

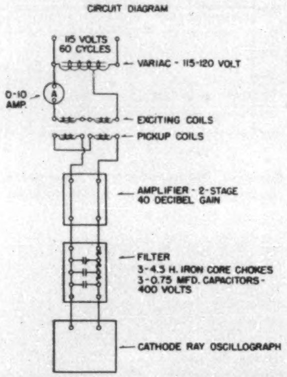

Figure 18. Circuit diagram of apparatus shown in Figure 17 plus the auxiliary equipment

The two pick-up coils are connected in series, but opposing, to a 2-stage amplifier of 40 decibels gain. The output of the amplifier is connected through a low pass filter, with cut-off frequency below 180 cycles to a cathode-ray oscilloscope. A rotor to be tested is placed on rollers so arranged that the standard air gap, as a motor, is maintained. A micrometer screw is used to adjust the position of the stator to make the air gap uniform for both sets of teeth. The exciting current is adjusted; the oscillograph sweep frequency is synchronized with the supply voltage so that one full wave of the differential pick-up voltage can be seen on the screen.

The rotor is turned slowly and variations of amplitude of this voltage observed on the oscilloscope. As the rotor is turned into a position of maximum coupling between two of its bars and exciting coils, the pattern on the oscilloscope is essentially a sine wave whose amplitude is adjusted to a convenient value by means of the gain control. An amplitude of about 1/4 of a full 5-inch screen is suitable. As the rotor is turned through the distance of one slot-pitch, the amplitude decreases a small amount and then returns to the same value as successive bar pairs pass through the maximum coupling position, provided the rotor bars are uniformly good and the equipment is in proper adjustment.

When a complete open bar passes the test position the amplitude increases momentarily by 250 to 400 per cent as the bar passes one coil and decreases or reverses as the bar passes the other coil, the total change in the second case being of about the same amount as in the first. Even though the rotor is turning quite rapidly this momentary increase of amplitude is observed readily. When a porous bar, whose resistance is considerably greater than normal, passes the test position the same effect is observed, the amount of deflection being less and dependent upon degree to which the porosity or flaw has increased the resistance of the bar relative to other bars on the same rotor.

If the rotors have been machined before testing, the presence of eccentric machining is evidenced by a gradual change of amplitude, maximum peak values appearing as that side of the rotor having more material removed passes the test coils.

References

1. High-Frequency Iron Loss, **Thomas Spooner.** AIEE Journal, volume 39, September 1920, pages 809–13.

2. Induction Motor Core Losses, **P. L. Alger, R. Eksergian.** AIEE Journal, volume 39, October 1920, pages 906–20.

3. Tooth Frequency Losses in Rotating Machines, **Thomas Spooner.** AIEE Journal, volume 40, September 1921, pages 751–56.

4. Surface Iron Losses with Reference to Laminated Materials, **Thomas Spooner, I. F. Kinnard.** AIEE Transactions, volume 43, February 1924, pages 262–81.

5. Tooth Pulsation in Rotating Machines, **Thomas Spooner.** AIEE Transactions, volume 43, February 1924, pages 252–61.

6. Effect of Punching Strains on the Magnetic Properties of Electrical Sheet Steel, **G. H. Cole.** *Electrical Journal*, (Pittsburgh, Pa.) volume 21, February 1924, pages 55–61.

7. Squirrel Cage Induction Motor Core Losses, **Thomas Spooner.** AIEE Transactions, volume 44, February 1925, pages 155–63.

8. No-Load Copper Eddy-Current Losses, **Thomas Spooner.** AIEE Transactions, volume 45, February 1926, pages 231–39.

9. Measurement of Stray Load Loss in Polyphase Induction Motors, **C. J. Koch.** AIEE Transactions, volume 51, September 1932, pages 756–63.

10. Stray Load Loss Test on Induction Machines, **Theodore H. Morgan, Paul M. Narbutovskih.** Electrical Engineering (AIEE Transactions), volume 53, February 1934, pages 286–90.

11. Properties and Testing of Magnetic Materials (book), **Thomas Spooner.** McGraw-Hill Book Company, New York, N. Y., 1927.

12. Reverse-Rotation Test for the Determination of Stray Load Loss in Induction Motors, **Theodore H. Morgan, William E. Brown, Arthur J. Schumer.** Electrical Engineering (AIEE Transactions), volume 58, July 1939, pages 319–24.

13. Stray Load Loss Tests on Induction Machines—II, **Theodore H. Morgan, Victor Siegfried.** Electrical Engineering (AIEE Transactions), volume 55, May 1936, pages 493–97.

14. Intersheet Eddy Current Loss in Laminated Cores, **L. V. Bewley, H. Poritsky.** Electrical Engineering (AIEE Transactions), volume 56, March 1937, pages 344–46.

15. Alternating Current Phenomena (book), **C. P. Steinmetz.** McGraw-Hill Book Company, New York, N. Y., 1908.

16. Magnetic Circuits and Transformers (book), **Massachusetts Institute of Technology.** John Wiley and Sons, New York, N. Y., 1945.

17. Die Cast Rotor Testing by Test Stator Method, **P. H. Trickey.** Electrical Engineering (AIEE Transactions), volume 65, March 1946, pages 139–41.

18. Squirrel Cage Motor Rotors Die Cast with High Economy, **Robert J. Reel.** *Electrical Manufacturing* (New York, N. Y.), January 1948, pages 96–100.

19. Test Code for Polyphase Induction Machines. AIEE Standard Number 500, August 1937, page 11.

Discussion

W. R. Bennet (Westinghouse Electric Corporation, Lima, Ohio): In some instances, it is desirable to replace a copper-cage rotor by an aluminum die-cast rotor. Larger end rings are, of course, required in the die-cast rotor and due to space limitations within the motor the end rings cannot always be made symmetrical. This means that one ring may have to be much thicker than the other to get the desired rotor resistance. I have had a case where one ring was made four times thicker than the other, but the performance of the die-cast rotor was in no way affected and equalled the performance of the copper-cage rotor. I know that Packer has had similar experiences in his design of die-cast rotors.

It has also been my experience that grinding the outside diameter of the die-cast rotor produces better rotors. This shows up in the motor performance. In applications where efficiency must be maintained at a high level this is an important factor. As Packer indicates, grinding is limited to rotors having closed slots. Turning the outside diameter of a rotor that has open slots, creates another bad condition. Aluminum particles are carried around the surface of the rotor by the turning tool; unless this aluminum is removed by heating, the result will be a motor with lower efficiency.

Various heat treatments are used on completed rotors to improve the motor performance. In some cases flame treatment for approximately one minute gives the desired result. This process consists of using oxygen and acetylene gas to give an intense heat; and revolving the rotor through this flame. This method is generally used on integral horsepower rotors. Heating rotors in an oven at the proper temperature gives good results for fractional horsepower rotors. I agree with Packer that the process of heating the rotor after machining is generally of such benefit that it should be seriously considered for die-cast rotors.

L. C. Packer: Bennet is correct relative to cases where one end ring may be much heavier on one end than the other. I have seen rings on one end from 25 to 50 per cent of the thickness at the other end and as thin as 1/8 inch for $3^{3}/_{4}$-inch diameter and as thin as 3/16-inch thick on about 5-inch diameter rotors. It is my understanding that no casting troubles are encountered with either of them, although fan blades are cast integral with each of them. The design will determine the practicability of thin section rings.

Grinding the outside diameter of rotors is generally limited to closed slot rotors as stated by Bennett and produces better rotors than those machined by ordinary methods. It might be added here that some recent experiments with shaving the outside diameter of closed-slot rotors has also produced some excellent results, but not enough of them were produced to permit drawing any definite conclusions.

The heating of the complete finished rotor has proved to be a necessity in order to produce uniformly good rotors. The method of heating employed depends a great deal upon the design, application, and factory conditions.

The greatest benefit from heating is derived by breaking the conductor away from the iron. The stray-load losses due to tooth pulsation frequencies and total 60 cycle iron losses are reduced in most cases. The rotor resistance is also reduced due partly to an increase in the conductivity of the aluminum after heating and also to breaking the conductors away from the iron. The short circuit and magnetizing reactances are in most cases increased slightly which reduces the magnetizing current. In some cases the magnetizing current has been increased due to too much oxidation, thus decreasing the sections of some of the magnetic paths.

A thin film of aluminum adhering to the surface of a finished rotor will reduce the breakdown, pull up, and in some cases the starting torque. The degree of the harmful effects depends upon the thickness and continuity of the film. This film must be removed if the motor is expected to perform properly.

Armature Iron Losses in Series Motors

SHELDON S. L. CHANG
STUDENT MEMBER AIEE

J. H. KARR
MEMBER AIEE

IN ORDER to calculate the performance of a-c series motors, it is necessary to predict the amount of iron loss as well as the way in which it is supplied. Tests results show that there exists a discontinuity in the armature iron losses supplied electrically and mechanically. The phenomena can be explained satisfactorily by the double revolving field theory.

Experimental

In order to illustrate experimentally the effect of speed (and rotor frequency) on iron loss distribution, a bi-polar series motor, rated at 1/3 horsepower, 5,000 rpm, was driven over a wide speed range for each of several selected values of excitation. The circuit arrangement for obtaining the data of Figures 1 and 2 is shown in Figure 3. Brushes of motor (B) were removed.

The wattmeter in the circuit of motor (B) reads field I^2R, field iron loss and that part of the armature iron loss supplied by the field. Figure 1 shows this input less field I^2R plotted against speed for several excitation values. Note the two regions on each curve showing essentially constant input, and the sharp reduction in the vicinity of 3,600 rpm.

Several general conclusions can be drawn from this. First, iron loss supplied by the field for given excitation is independent of speed (hence of armature frequency) for all speeds below and above synchronous speed. This means that no variable frequency armature iron loss is furnished by the field. Second, a constant component of field iron loss must be furnished by some other source than the field for speeds above synchronous.

Motor (A) in Figure 3 was calibrated so that the torque which the motor develops for any input and speed could be read from calibration curves. Thus, by reading the input to motor (A), the torque required to overcome friction and windage and armature iron loss of motor (B) can be obtained for various values of excitation and speed. These data are plotted in Figure 2. Note the abrupt rise in torque required in the region of synchronous speed.

Analysis

Consider the pulsating flux set up by the stator as being the result of two flux systems rotating at synchronous speed in opposite directions in accordance with the familiar double revolving field theory of the induction motor. Iron losses in the armature will then result from frequencies of $(f_r - f)$ and $(f_r + f)$, in which f_r is the frequency corresponding to armature speed and f is line frequency. Thus, at 2-pole synchronous speed $f_r - f = 0$.

The rotor of an ordinary polyphase induction motor revolves in the rotating, circular field at nearly synchronous speed. Rotor iron loss is neglected usually since the rotor frequency is very low.

If, however, the rotor revolves for any reason at a materially different speed in either direction relative to the revolving field, the rotor iron loss is no longer negligible. The rotor iron loss can be considered as a component of rotor current in stator terms, but not supplied necessarily by the stator. Let this component of current be $I_{r(h+e)}$. Then the actual rotor iron loss is

$$W_r = I_{r(h+e)} E_r \tag{1}$$

Where E_r is the voltage generated in the rotor in stator terms due to the air gap flux.

The stator air gap voltage E_s will be different than the rotor air gap voltage, E_r, because stator and rotor frequencies are, in general, not equal. Thus

$$E_s = E_r \frac{f}{f \pm f_r} \tag{2}$$

The rotor loss supplied by the stator will then be

$$W_F = I_{r(n+e)} E_s = I_{r(h+e)} E_r \frac{f}{f \pm f_r}$$
$$= (\text{actual rotor iron loss}) \frac{f}{f \pm f_r} \tag{3}$$

The remainder of the rotor iron loss must be supplied from the mechanical energy of the rotor, or act as a load on the rotor. Thus, the loss supplied by the rotor is

$$W_A = (\text{actual rotor iron loss}) \left(1 - \frac{f}{f \pm f_r}\right)$$
$$= (\text{actual rotor iron loss}) \left(\frac{\pm f_r}{f \pm f_r}\right) \tag{4}$$

in which the (−) sign is for the forward revolving field and the (+) sign is for the backward revolving field.

Let

W_{H+} = hysteresis loss in armature due to forward revolving field
W_{H-} = hysteresis loss in armature due to backward revolving field
W_{E+} = eddy current loss in armature due to forward revolving field
W_{E-} = eddy current loss in armature due to backward revolving field
W_{HO} = hysteresis loss in armature at zero speed
W_{EO} = eddy current loss in armature at zero speed

Then

$$W_{H+} = \frac{W_{HO}}{2} \left|\frac{f_r - f}{f}\right| \tag{5}$$

$$W_{H-} = \frac{W_{HO}}{2} \left|\frac{f_r + f}{f}\right| \tag{6}$$

$$W_{E+} = \frac{W_{EO}}{2} \left(\frac{f_r - f}{f}\right)^2 \tag{7}$$

$$W_{E-} = \frac{W_{EO}}{2} \left(\frac{f_r + f}{f}\right)^2 \tag{8}$$

Combining equations 3, 5, 6, 7, and 8, the expression for the armature iron loss

---

Paper 49-70, recommended by the AIEE rotating machinery committee and approved by the AIEE technical program committee for presentation at the AIEE winter general meeting, New York, N. Y., January 31–February 4, 1949. Manuscript submitted June 9, 1948; made available for printing December 20, 1948.

SHELDON S. L. CHANG and J. H. KARR are with Robbins and Myers, Inc., Springfield, Ohio.

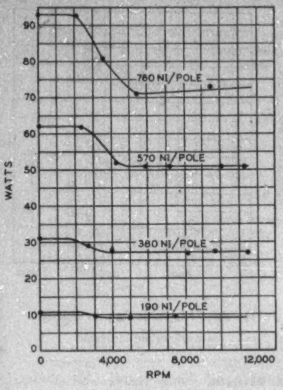

Figure 1. Effect of speed and excitation on field input

supplied by the field for $f_r > f$, that is, speed above synchronous, is

$$W_F = \left[\frac{W_{HO}}{2}\left(\frac{f_r - f}{f}\right) + \frac{W_{EO}}{2}\left(\frac{f_r - f}{f}\right)^2\right]\frac{f}{f - f_r} + \left[\frac{W_{HO}}{2}\left(\frac{f_r + f}{f}\right) + \frac{W_{EO}}{2}\left(\frac{f_r + f}{f}\right)^2\right]\frac{f}{f + f_r} = W_{EO} \tag{9}$$

Similarly, for $f_r < f$, the armature iron loss supplied by the field is

$$W_F = W_{HO} + W_{EO} \tag{10}$$

Combining equations 4, 5, 6, 7, and 8, the expression for armature iron loss supplied from mechanical energy of the armature, for $f_r > f$, is

$$W_A = \left[\frac{W_{HO}}{2}\left(\frac{f_r - f}{f}\right) + \frac{W_{EO}}{2}\left(\frac{f_r - f}{f}\right)^2\right]\frac{-f_r}{f - f_r} + \left[\frac{W_{HO}}{2}\left(\frac{f_r + f}{f}\right) + \frac{W_{EO}}{2}\left(\frac{f_r + f}{f}\right)^2\right]\frac{f_r}{f + f_r} = W_{HO}\frac{f_r}{f} + W_{EO}\left(\frac{f_r}{f}\right)^2 \tag{11}$$

Similarly, for $f_r < f$

$$W_A = W_{EO}\left(\frac{f_r}{f}\right)^2 \tag{12}$$

It will be seen that equations 9, 10, 11, and 12 are substantiated in a general way by the test results of Figures 1 and 2.

The power represented by equations 11 and 12 act as loads on the motor in the form of magnetic drag. This drag torque becomes

$$T_d = \frac{112.7\ W_{HO}}{syn} + \frac{112.7\ W_{EO}}{syn} \times \frac{\text{RPM}}{syn} \quad \text{ounce foot for } f_r > f \tag{13}$$

or

$$T_d = \frac{112.7\ W_{EO}}{syn} \times \frac{\text{RPM}}{syn} \quad \text{ounce foot for } f_r < f \tag{14}$$

Calculations

In order to compare test and calculated data, it is necessary to have iron loss curves showing hysteresis and eddy current losses separately. Such a set of curves at 60 cycles is shown in Figure 4 and was obtained from conventional curves which showed total iron loss versus flux density for several frequencies.

The magnetization curve for the motor under consideration is shown in Figure 5. It is proposed to compare experimental and calculated results for excitations of 190, 380, and 570 ampere turns per pole. Armature tooth area per pole is 1.395 square inches and core volume is 1.29 cubic inches. Sine wave distribution of air gap flux is assumed although it is recognized that the actual wave shape may deviate considerably from this. The standstill armature iron losses are calculated in the manner used usually for single-phase induction motor, that is, divide polyphase iron loss by two. The justification for this is that there is essentially no flux in the cross axis. The method is equivalent to assuming sinusoidal space distribution of flux.

Calculated rotor hysteresis loss is shown in Table I. In accordance with the

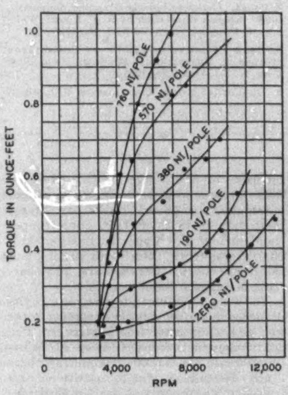

Figure 2. Friction and windage, and magnetic loading as functions of speed and excitation

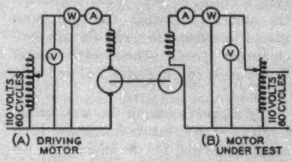

Figure 3. Diagram of motor connections

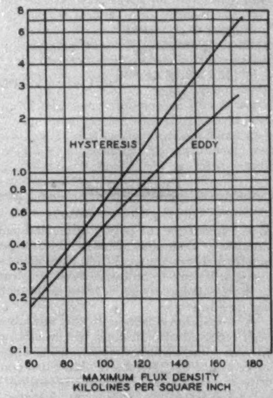

Figure 4. Hysteresis and eddy-current losses for 24-gauge electrical sheet steel

Table I

			Armature Core					Armature Teeth						
			Hysteresis		Eddy			Hysteresis		Eddy				
Ampere Turns (NI)	ϕ_{max}	B_c	Watts Per Cubic Inches	Watts	Watts Per Cubic Inches	Watts	B_t	Watts Per Cubic Inches	Watts	Watts Per Cubic Inches	Watts	W_{ho}	W_{eo}	Observed W_{ho} from Fig. 1
190	107,500	117,000	1.17	1.5	0.775	0.995	121,000	1.35	1.72	0.85	1.08	1.61	1.04	1.5
380	141,000	153,200	3.8	4.9	1.78	2.29	158,600	4.6	5.85	2.0	2.54	5.375	2.42	4.0
570	161,000	175,000	7.1	9.1	2.73	3.50	181,000	8.3	10.6	3.05	3.88	9.85	3.69	11.0

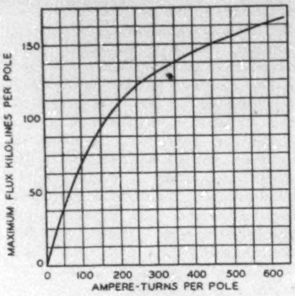

Figure 5. Magnetization curve

theory which has been presented, this is the amount by which the field input should be reduced in going through synchronous speed. These experimental values are shown in Figure 1 as well as in Table I.

The magnetic drag in the armature in terms of torque can be calculated from equations 13 and 14. As an example, for an excitation of 380 ampere turns per pole, this drag for speeds below 3,600 rpm is

$$T_d=\frac{112.7\ W_{EO}}{syn}\times\frac{\text{RPM}}{syn}$$

$$=\frac{112.7\times 2.42\times \text{RPM}}{(3{,}600)^2}=21\times 10^{-6}\times \text{RPM}$$

For the same excitation, and speeds above 3,600 rpm, the drag is

$$T_d=\frac{112.7W_{HO}}{syn}+\frac{112.7W_{EO}}{(syn)^2}\text{RPM}$$

$$=\frac{112.7\times 5.375}{3{,}600}+\frac{112.7\times 2.42\times \text{RPM}}{(3{,}600)^2}$$

$$=0.168+21\times 10^{-6}\times RPM$$

Likewise, the magnetic drag of 190 ampere turns and 570 ampere turns can be calculated:

190 Ampere Turns	
R.p.m. < 3,600	$T_d=9.05\times 10^{-6}\times$r.p.m.
R.p.m. > 3,600	$T_d=0.0504\ 9.05\times 10^{-6}\times$r.p.m.
570 Ampere Turns	
R.p.m. < 3,600	$T_d=32.1\times 10^{-6}\times$r.p.m.
R.p.m. > 3,600	$T_d=0.308\ 32.1\times 10^{-6}\times$r.p.m.

The foregoing results are plotted in Figure 6. Experimental data are shown by circled points. Experimental data shown in Figure 6 are deduced from the data of Figure 2, using the zero ampere-turn curve on the latter as representing friction and windage.

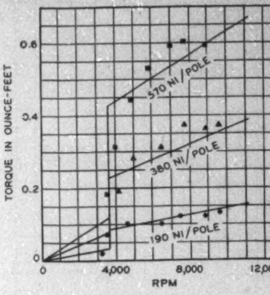

Figure 6. Magnetic drag on armature

Test values are indicated

References

1. Das Funken von Kommutator Motoren, **F. Punga.** Gebruder Janecke (Hanover, Germany), 1905. English translation by R. F. Looser, Whittaker & Company, New York, N. Y., 1906.

2. Iron Losses in Single-Phase Commutator Motors, **F. Niethammer.** *Electrical World* (New York, N. Y.), March 24, 1906.

3. Induction Motor Core Losses, **P. L. Alger, R. Eksergian.** AIEE Journal, October 1920, pages 906–20.

4. Effect of Superposed Alternating Field on Apparent Magnetic Permeability and Hysteresis Loss, **T. Spooner.** *Physical Review* (New York, N. Y.), volume 25, September 2, 1925, page 257.

5. Universal Electric Motors, **A. F. Puchstein.** *Bulletin 53*, Ohio State University Engineering Experimental Station, 1930.

6. Physical Conception of the Operation of the Single-Phase Induction Motor, **B. G. Lamme.** AIEE Transactions, volume 37, April 1918, pages 627–702.

7. The Apparent Impedance Method of Calculating Single-Phase Motor Performance, **W. J. Morrill.** Electrical Engineering (AIEE Transactions), volume 60, 1941, pages 1037–41.

8. The Revolving Field Theory of the Capacitor Motor, **W. J. Morrill.** AIEE Transactions, volume 48, April 1929, pages 614–32.

Discussion

A. F. Puchstein (The Jeffrey Manufacturing Company, Columbus, Ohio): This paper is useful to set the stage for experimental and calculation techniques which will lead to more satisfactory procedures in predicting such losses.

It would have helped if the tests had been repeated also at other frequencies, as 25 cycles, and on larger motors, using a sensitive torque dynamometer. The paper confirms the existence of the near-discontinuity in the vicinity of synchronism, Figures 1 and 6. No light is thrown on the effect of slot openings, length of air-gap, or shape of pole shoe. Commutation effects are not considered. These introduce circulating currents and commutated-coil magnetomotive forces which change the value and phase relation of the field flux relatively to the field magnetomotive forces and so have some effect on the iron loss. The data reported do not include the effect of armature reaction, which tends to increase the iron losses. It is not stated whether correction or compensation was made for meter losses.

In the analysis, some use is made of polyphase induction motor theory. As of today the losses of such a machine are considered to be stator copper (fundamental and upper harmonics, skin-effect), stator core, stator tooth, stator tooth surface, rotor copper (fundamental and upper harmonics, skin-effect, rotor tooth, rotor tooth surface, and rotor core losses. Occasionally, eddy currents in adjacent metal masses.

The torque produced in the rotor is the resultant due to all rotor bar currents, rotor iron eddy, and rotor iron hysteresis. The last of these acts forward for speeds below synchronism and backward above synchronism. Tooth losses due to rotation act as a brake at all speeds and are supplied mechanically. Reluctance torques due to magnetic dissymmetries tend to balance out over a revolution. Similar losses are present in the series motor.

From the view point of the physics involved, it would clarify the problem if experiments and calculations were set up to determine the dependence of the iron losses upon the time rate of change of flux-density, both when this density varies as a straight line function of time and when it varies in other ways. This should be done for alternating and rotating fields and combinations of them. In such experiments, transient or other effects would probably be absent. It should then be possible to work out a method of loss calculation which fits the actual conditions more closely than the commonly assumed sinusoids.

L. C. Packer (Westinghouse Electric Corporation, Springfield, Mass.): This is a very interesting paper. All of the iron losses in this paper are based on no-load flux. Under load conditions these losses will change due to distortion caused by the armature flux when current flows through the armature winding. The changes may be compensating as the iron losses will be lower with current in the armature due to the armature flux bucking down the field flux, but the rotational losses might be increased by increasing the flux density in the teeth.

The losses in both the field and armature will generally be greater than when calculated from Epstein tests because the eddy current and hysteresis losses are increased by the punching of the laminations and may be as much as 1.5 to 2.5 times higher unless the laminations are annealed after punching. It is assumed generally that the hysteresis component of the iron loss varies directly with the frequency. Due to flux distortion or skin effect at higher frequencies and also to possible differences in depth of penetration, this assumption is probably not strictly

Table

RPM	Field Amperes	Test Value, Losses	Calculated Values P_e	P_h	Total
Rotational Losses on Direct Current					
2,000	7	4.45	0.89	3.54	4.43
4,000	7	11.0	3.56	7.1	10.66
6,000	7	18.7	8.0	10.6	18.7
8,000	7	28.4	14.2	14.1	28.3
10,000	7	40.0	22.2	17.7	39.9
12,000	7	54.8	32.1	21.3	53.7
14,000	7	69.4	43.7	24.8	69.1
16,000	7	85.4	57.1	28.3	85.4 (Base)
Rotational Losses on 60-Cycle Alternating Current					
6,000	7	11.63	5.47	8.2	13.67
8,000	7	19.5	9.7	10.9	20.6
10,000	7	28.8	15.2	13.9	28.8
12,000	7	40.0	21.9	16.3	38.2
14,000	7	49.8	24.8	19.1	48.9
16,000	7	60.7	38.9	21.8	60.7 (Base)

true and the hysteresis loss per cycle may be considerably higher at relatively high frequencies. However, this direct proportion to frequency may be close enough for indicating relative values of hysteresis and eddy current losses.

I think for equations 5 to 8 inclusive, it might be mentioned that these equations can be used only when you have the same ampere turns per pole as used for determining the values of W_{ho} and W_{eo}.

It seems to me that in equation 12, it should also contain the term $W_{ho}(fr/f)$. It does not seem possible that there will be no hysteresis loss between the points $fr=f$ and $fr=0$. Assuming a-c operation, there is the fundamental hysteresis and eddy current loss present at zero speed. This loss will decrease, however, in the tenth to zero at synchronous speed. However, the surface losses (with slotted primary or pole face losses in a salient pole motor) will increase with the frequency due to rotational speed.

One method of breaking down the armature iron losses into its two components of hysteresis and eddy current losses is to use test data for two speeds at the same ampere turns per pole. It is better to select speeds at which the readings are relatively large to reduce errors. In this illustration a 13,000-r.p.m. motor is used.

Table I of the discussion is divided into two sections, one each for direct and alternating current. On direct current the fundamental frequency is zero. Then the rotational losses should be a function of the speed from zero r.p.m. The calculated values in the a-c table are based on the assumption that the rotational losses are independent of fundamental frequency but depend only on speed to a zero speed base. Let

P_e = eddy current loss
P_h = hysteresis loss

Select from the d-c table the values of total iron loss at 10,000 and 16,000 r.p.m.

At 16,000 rpm

$$P_h+P_e=85.4 \tag{15}$$

At 10,000 rpm = 5/8 of 16,000 rpm

$$5/8P_h+25/64P_e=40 \tag{16}$$

P_h varies directly with frequency
P_e varies as the square of frequency

$$P_h+5/8P_e=64 \tag{17}$$

Subtract equation 17 from 15

$$3/8P_e=21.4$$
$$P_e=57.1$$
$$P_h=28.3$$

Apply the same method to the a-c data. For any speed at same flux

$$P_h=P_h(\text{at } 16{,}000 \text{ rpm})\times\frac{\text{rpm}}{16{,}000}$$

$$P_e=P_e(\text{at } 16{,}000 \text{ rpm})\times\frac{(\text{rpm})^2}{(16{,}000)^2}$$

The values at 2,000 and 4,000 r.p.m. were so low that they were inconsistent and inaccurate.

Chang and Karr are to be commended for their paper. There is very little literature on the subject in connection with Universal motors and more papers should be encouraged. A paper has been under preparation for sometime by me on this subject which, it is hoped, will be presented at some future date.

Sheldon L. Chang and J. H. Karr: The writers appreciate greatly the comments of Packer and Puchstein. Some of their comments are answered in the following:

Packer states that equation 12 should contain the hysteresis term $W_{ho}(f_r/f)$, while one of the main purposes of this paper is to show that it does not. The armature iron loss has a hysteresis component at all speeds, below or above synchronism. Equations 9, 10, 11, and 12 state that this armature hysteresis loss is supplied exclusively by the magnetizing ampere turns at speeds below synchronism, and that it acts as a mechanical load at speeds above synchronism. These equations are the logical consequences of the double revolving field theory and they are substantiated by test results of Figures 1 and 6.

Apparently the hysteresis loss does not obey the principle of superposition. The theory deviates from the test results in that the theory predicts an abrupt change at synchronism as shown by the solid lines while the test shows a relatively gradual change.

This near discontinuity has been verified in every a-c series motor we have tested and the writers suspect that the motor Packer mentioned is not an exception. Packer omitted the values at 2,000 and 4,000 r.p.m. for 60 cycle because they were so low and inconsistent. If these values follow Packer's equation they would not be much lower than the corresponding values in the d-c motor. If the same dynamometer were used in these tests the same degree of accuracy should hold.

Packer shows a very practical method of separating hysteresis and eddy current losses by test. His method is preferable after the first test motor is built. The writers are more interested in predicting the motor performance before the lamination die is made. After that you will have to take it for what it is anyway. The hysteresis loss and eddy current loss curves are based on our experience with a particular grade of steel. They are generally higher than the values given by the steel manufacturer as Packer pointed out. The values of W_{ho} and W_{eo} are calculated for the entire range of magnetization. In calculating the load points, W_{ho} and W_{eo} are the values corresponding to the net ampere turns in the axis of the main field. Usually the reluctance in the cross axis is very high.

In series motors with laminated but not slotted field, the surface loss is negligible. In series motors with slotted field, the surface values loss can be calculated as in induction motors. An additional term of $W_{eo}(f_r/f)^2$ should then be added to equation 11 and 12.

The wave shape or the harmonics have an appreciable effect on the armature iron loss. However the harmonics are not as important in the a-c series motors as in induction motors, with equally bad wave shape, because the armature current of the series motor is unaffected by the harmonic flux.

In very bad cases the distorted wave shape due to armature ampere turns may increase the armature iron loss 20 per cent. Assuming that the armature iron loss itself reduces the output torque by 15 per cent, the effect of wave shape amounts to 3 per cent of the output at most.

Puchstein suggested a very interesting way of determining the effect of wave shape. We feel that the experiments he suggested are carried out and the results are put into a form easily applicable to a-c series motor design that would certainly be a very valuable contribution.

Fundamental Theory of Inherent-Overheating Protection Under Running Overload Conditions

C. G. VEINOTT
FELLOW AIEE

L. C. SCHAEFER
ASSOCIATE AIEE

SEVERAL papers have been written giving quantitative test results on the application of motor protective devices. The object of this paper is to discuss the fundamental theory of such devices, and to show how this theory may be applied to the selection of protective devices for fractional horsepower motors. This fundamental theory has been developed and used over the course of the last 15 years in the application of disk-type thermostats to obtain built-in thermal overload protection. How well built-in overload protection can work has been attested by results published in a number of papers and articles on the subject. An understanding of the theory presented in this paper will, the authors believe, help the thermostat application engineer in selecting the right thermostat for any particular motor, and will help the user of the protected motor to understand better how and why the devices can work so successfully when properly applied.

Probably the first use of built-in thermal overload protection to small motors occurred in 1928, when a few applications were made on portable drill motors. Undoubtedly the first large-scale commercial use was on a popular make of hermetic refrigerators in 1929. In this case the thermostats were mounted on the compressor unit and were responsive to both temperature and current. They were revolutionary in another sense—they were automatic-resetting. Now, 19 years later, use of an automatic-resetting thermostat, mounted on the compressor, is common practice in the hermetic refrigeration industry. In 1930, disk-type thermostats were applied by one of the authors to fractional horsepower induction motors and used in a limited number of motors commercially. In 1933, the advantages of such protection were pointed out in a technical article.[1] Use of such motors has been increasing ever since, and will probably continue to increase. By 1939 the Underwriters' Laboratories had recognized the advantages and safety features of motors with built-in thermal overload protection. They coined the very descriptive phrase "inherent-overheating protection" and adopted standards covering such devices.[2]

Partly because disk-type thermostats appear to be replacing other forms of built-in protective devices for fractional horsepower motors, and partly because the authors' experience has been almost entirely with this type of device, the theory and discussion in this paper are centered around disk-type thermostats, although the same fundamental principles should apply equally well to all types of thermal protective devices used. Probably the best way to introduce this discussion of inherent-overheating protection is to begin with the theory of current-operated thermal devices which appear to be more generally understood.

Tripping Characteristics of Current-Operated Devices

Usual current-operated devices offer only over-current protection. A familiar example is the common circuit breaker with a thermal tripping element. A magnetic circuit breaker is responsive only to current, but under conditions of severe over-current, the device trips within a fraction of a second. Such characteristics are undesirable in fractional horsepower motors because temporary overloads or line transients may cause nuisance trip-outs. Thermally operated circuit breakers would be better because they introduce a time lag sufficient to overcome this objection. This time lag, or characteristic inverse-time tripping curve, is shown in Figure 1. Here, the vertical asymptote is the value of current which, if maintained indefinitely, will ultimately cause the circuit breaker to trip, theoretically, in infinite time. This value of current is commonly referred to as the "ultimate tripping amperes." The horizontal asymptote is at zero time and infinite current. In practice, the maximum value of current may be limited either by the rupturing capacity of the contacts if all the heat is generated in the bimetal element, or by the current-carrying capacity of the heating element, if one is used. Current-operated devices usually carry an ampere rating of the order of 83 per cent of the ultimate tripping current. Thus, the actual current necessary to trip such a circuit breaker, in infinite time, is approximately 120 per cent of its rating. Often, the effect of ambient is neglected in rating such devices. In fact, attempts are often made to nullify the effect of any change in ambient by setting the operating temperature of the thermal element very high, or by using differentially opposed elements, making the device responsive to rate-of-rise rather than to actual temperature rise.

In selecting a current-operated device to protect a given motor, the first step is to determine the motor current corresponding to the maximum permissible temperature rise. Then a circuit breaker having an ultimate tripping current

---

Paper 49-71, recommended by the AIEE rotating machinery committee and approved by the AIEE technical program committee for presentation at the AIEE winter general meeting, New York, N. Y., January 31–February 4, 1949. Manuscript submitted July 27, 1948; made available for printing December 28, 1948.

C. G. Veinott is manager of the induction motor section and L. C. Schaefer is a design engineer, both of the industrial engineering department, small motor division, Westinghouse Electric Corporation, Lima, Ohio.

equal to this value is applied. Thus this device tends to limit the temperature rise of motor, rather than to limit total winding temperature.

Tripping Characteristics of Disk-Type Thermostats

A disk-type thermostat, mounted in a section of a motor end shield, is shown in Figure 2. This device has the same familiar inverse-time characteristic as the conventional over-current thermal relay just discussed, but the inherent-overheating device is intentionally designed to have its tripping characteristic affected in a predetermined manner by ambient temperature. But that is getting ahead of the story. In Figure 3, the tripping characteristic curves of a typical disk-type thermostat are plotted for different ambient temperatures. It is to be noted that the ultimate tripping current is definitely a function of the ambient temperature. Consequently, to see better the effect of ambient temperature on ultimate tripping current, the ultimate tripping amperes have been plotted as a direct function of ambient temperature in Figure 4.

At this point it seems most appropriate to introduce a new term—"ultimate tripping ambient." The ultimate tripping ambient, at a specified current, is that value of ambient temperature which makes the specified current equal to the ultimate tripping current. That is, if the ultimate tripping current is 7.3 amperes at 35 degrees centigrade, the ultimate tripping ambient, at 7.3 amperes, is 35 degrees centigrade. At first, introduction of this new term may seem to serve no useful purpose, but it will be shown later how this term helps one to grasp and retain certain fundamental principles applicable to inherent-overheating protection. In part, the concept of this term originated from one laboratory method of determination of the ultimate tripping characteristics of a thermostat, that is by holding the current constant and very slowly increasing the ambient temperature until the thermostat trips. A more conventional way is to hold the ambient constant, measuring the tripping time, at different currents, thereby obtaining a characteristic curve at a particular ambient such as Figure 3. Either method can be used to obtain a curve such as Figure 4.

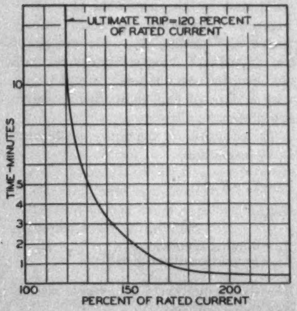

Figure 1. Time-current curve of thermally operated circuit breaker

Returning to Figure 4, it will be noted that the curve of ultimate tripping current versus ambient appears to be a parabola which, in fact, it is. Reason for the parabolic shape becomes more evident when the curve of rise of disk above ambient is plotted. The latter curve is obtained by subtracting the ultimate tripping ambient, for each current, from the disk-opening temperature. (The disk always opens at the same temperature, regardless of current or ambient temperature.) The temperature rise of the disk above its ambient is, of course, proportional to the watts generated in the thermostat, that is, to the I^2R losses. Hence, it is clear that the rise of the disk must be proportional to the square of the current, since the resistance of the nichrome heater is practically constant.

Now, the true interrelationship between ultimate tripping current, ultimate tripping ambient, and disk-opening temperature becomes apparent and we can create a word picture of this relationship as follows: Assume a given current of, say, 4.5 amperes to be passed through the thermostat continuously. The heater comes to a final ultimate temperature rise, heating the disk to a temperature somewhat below that of the heater. Say that the rise of the disk is 30 degrees centigrade above the thermostat ambient. Now, suppose the disk-opening temperature to be set at 120 degrees centigrade and further suppose that the ambient temperature of the thermostat be raised very slowly. This disk will always stay 30 degrees centigrade hotter than the ambient (assuming constant current, of course) so that when the ambient reaches 120–30 = 90 degrees centigrade, the disk will open. Hence, the ultimate tripping ambient for 4.5 amperes is 90 degrees centigrade for this thermostat. Or, in other words, the ultimate tripping current of this thermostat is 4.5 amperes at 90 degrees centigrade. Obviously, the ultimate tripping currents at other ambients can be determined similarly.

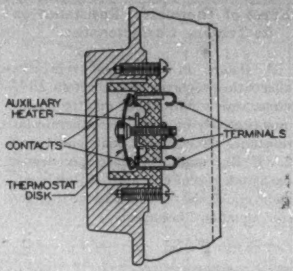

Figure 2. Cut-away view of disk-type thermostat mounted in motor end shield

Reduced to mathematical terms, the foregoing statements become

$$T_a = T_d - K_t I_u^2 \qquad (1)$$

where

T_d = disk-opening temperature
T_a = ultimate tripping ambient at current, I_u
I_u = ultimate tripping amperes at ambient, T_a
K_t = proportionality constant

Solving equation 1 for ultimate tripping current

$$I_u = \sqrt{(T_d - T_a)/K_t} \qquad (2)$$

Effect of Disk-Opening Temperature on Tripping Characteristics

Disk-opening temperature is, by itself a very important factor in inherent-overheating thermostats, because its value is a large factor in determining the effect of ambient upon tripping characteristics. In Figure 4, the disk-opening temperature was 120 degrees centigrade. Now suppose that the disk-opening temperature is raised, say 10 degrees centigrade. Then, at each value of ultimate tripping current, the ultimate tripping ambient is raised 10 degrees centigrade. This is a simple way to express the effect of disk-opening temperature on ultimate tripping characteristics.

The effect on the curve is to move the entire curve up 10 degrees centigrade, without changing its shape as has been done in Figure 5. This idea is expressed quantitatively in equation 1, and the effects of disk temperature on ultimate tripping current at a given ambient is expressed by equation 2.

To summarize: An increase or decrease of t degrees in the disk-opening temperature increases or decreases the ultimate tripping ambient at every current by t degrees.

Effect of Thermostat Resistance on Its Tripping Characteristics

A change in thermostat resistance affects the proportionality constant K_t in direct ratio. This effect may be shown quantitatively by introducing thermostat resistance directly into equations 1 and 2. If W_u equals the watts per degree centigrade rise of disk above its ambient, and r_t equals the resistance of the thermostat, equation 1 becomes:

$$T_a = T_d - (r_t/W_u)I_u^2 \tag{3}$$

and equation 2 becomes

$$I_u = \sqrt{(W_u/r_t)(T_d - T_a)} \tag{4}$$

From equation 4 it is apparent that the ultimate tripping amperes at a specific ambient will increase or decrease inversely as the square root of the change in thermostat resistance. This effect is shown graphically in Figure 6.

The constant, W_u, is a factor of thermostat design and is affected by the size and length of the heater element, by the relative location of the disk and heater element, by the apportionment of resistance between the heater and the disk, by the coefficient of radiation and absorption of the heater and disk materials respectively, and by the rate at which the heat is conducted from the disk by the electrical contacts and terminals. Outwardly, this appears to be quite an imposing list; however, many of the factors effecting W_u are constant within a particular line of thermostats and the determination of this constant is not unduly complicated. For a 1-inch diameter full round disk, W_u is approximately 0.05 to 0.06.

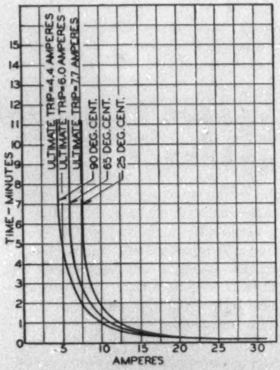

Figure 3. Time-current curves for typical disk-type thermostat at different ambients

Characteristics of Disk-Type Thermostats When Applied to a Motor

The next step is to extend and apply this basic theory to the application of inherent-overheating protection of fractional horsepower motors. Fundamentally, to realize true inherent-overheating protection, the temperature of the thermal disk should at all times follow that of the motor winding; thus the motor winding would always be protected to a definite temperature, regardless of conditions of line voltage, motor load, ambient, or ventilation. If it were possible to make the device infinitesimally small, so that it could be affixed directly to the stator copper beneath the wire insulation, ideal protection could be achieved. Since the thermostat is too large to be embedded in the windings it has to be located elsewhere. A common location is in the end shield as in Figure 7, where it is in as close a heat-receiving relationship to the stator windings as possible. If there were no auxiliary heater, the disk would tend to follow the temperature of the end shield fairly closely. However, the windings almost invariably get hotter than the end shield, by an amount that varies primarily with the current.

For purposes of analysis, it is most convenient to split the total temperature of a motor winding into three components, the sum of which gives the total temperature as follows:

1. Ambient temperature of motor.
2. Temperature rise of end shield above ambient.
3. Temperature rise of windings above end shield.

Now, factor (1) plus factor (2) equals the actual temperature of the end shield, which is the ambient temperature of the thermostat. The temperature of the end shield may be a function of many factors, including ambient temperature in which the motor operates, total losses of the motor (these are affected by voltage, frequency, load, bearing losses, and motor temperature), rpm of the motor, efficiency of the ventilating system, and so forth. Regardless of the number of factors affecting the temperature of the end shield, the thermostat assumes substantially that same temperature thus taking into account all conditions affecting the actual temperature of the end shield. If it were only the end shield temperatures that were significant, it would be sufficient to provide a thermostat responsive only to temperature and not affected by motor current; however, the winding temperature is the significant factor in motor protection, and since the windings get hotter than the end shield, the thermostat is provided with an auxiliary heater which heats the disk and makes the thermostat responsive both to temperature and to current. The problem of proper thermostat selection evolves itself into one of determining which combination of thermostat design features will allow the temperature rise of the disk above the end shield to follow the rise of the motor winding above the end shield.

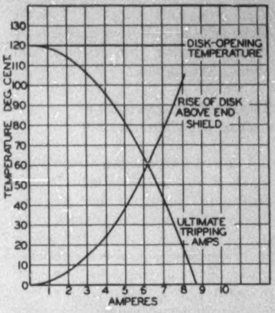

Figure 4. Typical curve of ultimate tripping characteristics for disk-type thermostat

Equation 1 shows that the rise of the disk above the end shield is proportional to the square of the current. With this relationship established, it is necessary to determine the relationship between the winding temperature and the end-shield temperature. In a normal motor, the temperature rise of the end extensions above the end shield is fairly nearly proportional to stator copper loss which in turn, is directly proportional to the square of the stator current. This fact is substantiated by the test data plotted in Figure 8. Here motor currents for various rises of the winding above the end shield are plotted on full logarithmic paper with the resultant curves being straight lines with a slope of two, indicating a square law proportionality.

The equation for the curve of Figure 8 is, by inspection,

$$T_w - T_a = K_m I^2 \tag{5}$$

Where

T_w = winding temperature
K_m = proportionality constant

Rewriting equation 1 to express rise of disk above ambient

$$T_d - T_a = K_t I_u^2 \tag{6}$$

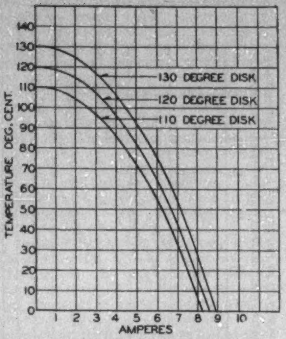

Figure 5. Effect of disk-opening temperature upon ultimate tripping characteristics

Now, since the motor and thermostat are connected in series, $I_u = I$, and the T_a in both equations are the same, it follows by comparing equations 5 and 6 that if

$$K_m = K_t \tag{7}$$

then $T_d = T_w$ for all values of I. That is, the disk temperature is the same as the winding temperature at all loads. All that remains, then, is to set the disk to open at the desired maximum winding temperature.

In other words, the steps in selecting the right thermostat for ideal protection are:

1. Determine K_m by a test on the motor.
2. Select a thermostat having a K_t equal to the tested value of K_m.

(Note: $K_t = (T_d - T_a)/I_u^2$).

3. Use a thermostat with a disk-opening temperature equal to the maximum desired temperature of the winding.

Application of Thermostats to a Line of Motors

If thermostats are applied to a line of motors, using equation 7 it would be necessary to take a test on each motor to determine the value of K_m. This procedure can be simplified by resolving K_m into two components. Let W_m equal total watts copper loss in the main winding per degree rise of winding temperature above end-shield temperature. Let r_1 = resistance of the main winding. Then, equation 5 can be rewritten

$$T_w - T_a = (r_1/W_m)I^2 \tag{8}$$

Now, in contrast with K_m, W_m will remain constant for a number of windings of varying resistance; it is dependent primarily upon the physical size of the motor, with which it can be correlated. Strictly speaking, the hot value of r_1 should be used, but the authors have found it more convenient to use the 25 degrees centigrade value of r_1 and making a slight compensating adjustment in W_m. For further simplification, the effect of ventilation efficiency and motor speed can be neglected by basing the value of W_m on an enclosed motor. Experience has shown that thermostats applied to open motors based upon constants for enclosed motors do not penalize seriously their overload capacity.

For ideal protection, that is, for the temperature of the disk to follow the temperature of the winding at all currents, it is necessary that

$$r_1/W_m = K_t = (T_d - T_a)/I_u^2 \tag{9}$$

When equation 9 is satisfied, the temperature of the disk follows the winding at all currents and ideal protection is obtained. Since the disk always opens at the same temperature, the winding is always protected to the same total temperature. This allows the motor to have appreciably more overload capacity when operating in a low ambient temperature without sacrificing protection in high ambients.

While equation 9 expresses the conditions for ideal protection, practical use of it in this particular form is not quite so easy because values of K_t are not ordinarily published; however, the disk-opening temperatures and ultimate tripping currents at different ambients are usually available. Equation 9 takes on a more usable form if we solve it for I_u, obtaining

$$I_u = \sqrt{(T_d - T_a)W_m/r_1} \tag{10}$$

Then, if we desire to protect the windings to a total temperature of 120 degrees centigrade, the disk-opening temperature, T_d, must also be made 120 degrees centigrade.

Tables for the ultimate tripping current at 90 degrees centigrade are available for 120 degrees centigrade thermostats. For this special case, equation 10 reduces to

$$I_{u90} = \sqrt{30W_m/r_1} \tag{11}$$

where I_{u90} = ultimate tripping amperes at 90 degrees centigrade.

If a thermostat can be found which has a disk-opening temperature of 120 degrees centigrade with an ultimate tripping current at 90 degrees centigrade as given by equation 11, ideal protection is obtained: that is, the thermostat will trip at a winding temperature of 120 degrees centigrade regardless of the load, ambient, or other condition. If the disk-opening temperature varies from 120 degrees centigrade, the ultimate winding temperature will vary by the same number of degrees. If the chosen thermostat has an ultimate tripping current higher than that given by the formula value, the winding temperature will be higher than 120 degrees centigrade. If the chosen thermostat has an ultimate tripping current lower than the formula value, the winding temperature will be limited to less than 120 degrees centigrade.

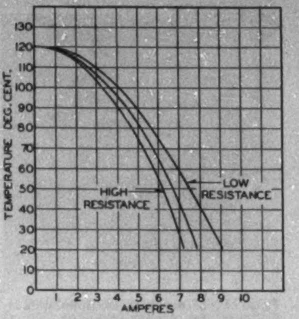

Figure 6. Effect of thermostat resistance upon ultimate tripping characteristics of disk-type thermostat

Some Practical Considerations

What effect do variations in thermostat characteristics have upon protection obtained? That is a question frequently asked. One of the biggest variations in production runs of thermostats is in the disk opening temperature which may vary as much as ± 5 degrees centigrade. Generally speaking, this will cause a variation in winding temperature of ± 5 degrees centigrade, that is, a variation of the same number of degrees as the disk opening temperature; the reasons for this statement are illustrated in Figure 5 and discussed earlier in this paper. Also, in applying thermostats by equation 10 allowance must be made for slight variations in W_m in different motors, and for variations in ultimate tripping current of the thermostats from the published values.

The authors recommend actual verification tests for active designs, but the formula value is usually close enough for low-activity designs. In verifying thermostat applications, the final tripping temperature of the winding should be approached slowly by gradual increases in

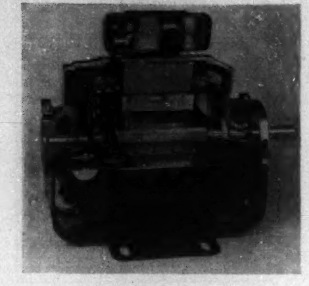

Figure 7. Section view of motor with inherent-overheating protection

Note location of thermostat in upper quadrant of front end shield

motor load allowing the temperature to stabilize between each load point. This type of load gives the highest winding temperature at thermostat trip and represents the worst possible loading condition. This fact is to be expected as the thermostat disk reaches its ultimate temperature more quickly than does the winding since the thermal capacity of the thermostat is smaller than that of the winding. Obviously if the winding and thermostat heater are so matched that ultimately the disk and winding reach the same temperature, the disk will always reach its ultimate temperature before the windings do. The significant conclusion is, that if the thermostat affords protection against a slowly increasing load, it tends to over-protect slightly in severe overloads; that is, in overloads so severe as to cause tripping of the thermostat in a relatively short time.

Summary and Conclusions

1. Inherent-overheating protection, utilizing disk-type thermostats, has proved itself over a period of 19 years. Millions of the devices are in service and their popularity is steadily increasing.

2. Current-operated devices, as distinguished from inherent-overheating devices, limit the current and temperature rise. On the other hand, a true inherent-overheating device limits the total temperature, not the rise, to a constant value.

3. A formula for the ultimate tripping current of a disk-type thermostat, in terms of its fundamental constants, has been derived, equation 4.

4. In deriving equations for the proper application of thermostats for inherent-overheating protection, the end-shield temperature, at the thermostat location, was used as a common reference point because:

a. It is the ambient of the thermostat.

b. It is closely related to the winding temperature.

c. It is less than the winding temperature by an amount proportional to the stator copper loss.

5. For ideal protection, the temperature of the disk should be made to follow the temperature of the winding at all currents. This is accomplished by the use of an auxiliary heater so chosen that the rise of the disk above the end shield is the same as the rise of the winding above the end shield. Since both of these temperature rises are proportional to the square of the current, the disk temperature can be made to follow the winding temperature at all load currents.

6. It follows logically from the foregoing that the disk-opening temperature should be made the same as the desired maximum winding temperature. On this basis, equation 10 has been derived for the ultimate tripping current of a thermostat to give this ideal protection.

7. A significant point brought out is that variations in the disk-opening temperature result in variations of the same number of degrees in the winding temperature.

8. All the considerations in this paper are based upon running overload conditions. Locked-rotor considerations often affect the selection of a thermostat, however, a full discussion of these is beyond the scope of this paper.

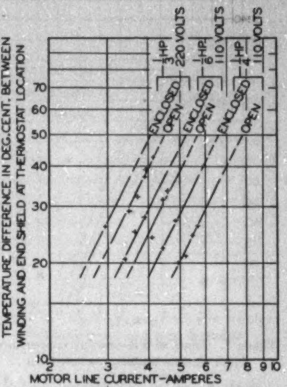

Figure 8. Relation of motor line current and temperature difference between winding and end shield at thermostat location for various motor ratings

References

1. Refrigerator Motors Need Thermal Protection, **E. B. Bremer, C. G. Veinott.** *Refrigeration News* (Detroit, Mich.), October 11, 1933.

2. Standard for Industrial Control, Underwriters' Laboratories (Chicago, Ill.), 1939.

3. Some Problems in the Standardization of Temperature Ratings of Fractional Horsepower Motors, **C. G. Veinott.** AIEE Transactions, volume 59, 1940, pages 1055–61.

4. The Inherent Overheating Protection of Single-Phase Motors, **C. P. Potter.** AIEE Transactions, volume 60, 1941, pages 993–96.

5. Principles of Aircraft Electric-Motor Protection, **V. G. Vaughan.** Electrical Engineering (AIEE Transactions), volume 62, December 1943, pages 760–65.

6. Inherent-Overheating Protection of D-C Aircraft Motors, **C. G. Veinott.** Electrical Engineering (AIEE Transactions), volume 63, December 1944, pages 920–25.

7. Overload Protection of Electric Motors, **E. F. Kurtz.** *Refrigerating Engineering* (New York, N. Y.), May, June, 1944.

8. Problems in Applying Protectors to Electric Aircraft Motors, **L. W. Buell.** AIEE Transactions, volume 63, 1944, pages 1250–58.

9. Fractional Horsepower Electric Motors (book), **C. G. Veinott.** McGraw-Hill Book Company, Inc., New York, N. Y., 2nd Edition, 1948.

10. A Method of Selecting Inherent-Overheat Protectors Based Upon Motor Design Information, **V. G. Vaughan.** AIEE Transactions, volume 67, Part II 1948, pages 1023–30.

Discussion

S. M. De Puy (General Electric Company, Schenectady, N. Y.): The authors have presented a simple and easily understood procedure for the selection of a running overload motor protector.

It should be pointed out that the procedure outlined for selecting a protector is based solely on limiting the temperature of the main winding during running overload. However, a number of factors equally as important as the running overload trip setting may influence the selection of the protector. This is particularly true in the case of a single-phase motor designed for automatic operation which may cycle with locked rotor. The omission of locked rotor protection from this discussion could lead one to believe that locked rotor overheating presents only a minor problem in the application of motors. Yet it is a fact that by far the greatest number of failures from burnout occur in the start winding.

The location, as well as the selection, of a protector has a pronounced effect on its ability to protect the start winding under locked rotor conditions. Veinott and Schaefer have indicated that the protector ambient should be "closely related to the winding temperature." If this relationship could be maintained equally well for running and locked rotor overload, a high degree of protection would result. Unfortunately, this is not always the case. Because of localized heating, high rate of rise, particularly in the start winding, and absence of air circulation, the temperature difference between winding hotspot and protector ambient may be much greater during locked rotor operation than during running overload. Also the protector heater input required becomes less as the protector ambient is made to approach winding temperature under running conditions. Consequently, less power is available to heat the protector element for rapid tripping under locked rotor conditions.

In order to provide satisfactory locked rotor protection, as well as protection for running overload, the protector ambient temperature should be lower than the winding temperature under ultimate tripping conditions by an amount sufficient to insure ample watts for tripping under locked rotor conditions. Fortunately, in many cases a protector, mounted in the motor end shield, will satisfy this requirement.

R. E. Seely (General Electric Company, Fort Wayne, Ind.): In general, I am favorably impressed with Veinott and Schaefer's theory of motor protection and feel that their work is an important step in providing an accurate method for applying motor protection thermostats. The great English physicist Lord Kelvin once said that you know little about a subject until you can measure it. The theory and equations as developed by Veinott and Schaefer enable an investigator to measure and express his results quantitatively. There are, however, a number of comments and suggestions which I would like to make concerning their paper.

The first suggestion which I would like to make is that the authors could perhaps have clarified their presentation if they had utilized a simple electrical equivalent circuit to represent the thermal conditions of a protected motor. In such equivalent circuits, heat flow in terms of watts is analogous to electric current; temperature is analogous to voltage; and thermal resistance is analogous to electrical resistance and can be expressed in terms of degrees centigrade per watt.

The simplest equivalent circuit would consist of three resistances arranged in the shape of a T. The resistance to the left of the vertical resistance would represent the thermal resistance between the stator windings and the end shield. The resistance to the right of the vertical resistance represents the thermal resistance between the disk of the thermostat and the end shield. The vertical resistance represents the thermal resistance between the end shield and the room ambient. The "thermal potential" or temperature of the winding, the disk, the end shield, and the room are T_w, T_d, T_a, and T_r. This means that there is a "thermal potential difference" or temperature difference of $T_w = T_a$ across the thermal resistance between the stator windings and the end shield which results from the flow of I^2R_1 watts through this resistance. It is apparent that the value of the thermal resistance and the end shield is equal to $1/W_m$. This means that the constant, W_m, as proposed by the authors, is in reality the thermal conductance between the stator windings and the end shield. You will note that W_m has the proper dimensions of watts per degree centigrade to indicate thermal conductance. In the same manner as we indicate the voltage drop across an electrical resistance as $E=IR$, we can say that $T_w-T_a=(I^2R_1)1/W_m$ which you will recognize as being the same as equation 8 in Veinott's and Schaefer's paper.

Similarly W_u is the thermal conductance from the disk to the end shield. Equating temperature difference to heat flow multiplied by the thermal resistance we obtain $T_d-T_a=(I^2r_t)1/W_u$ which you will recognize as being the same as equation 3 in the authors' paper.

Apparently, Veinott and Schaefer overlooked the highly desirable procedure of combining these two equations by eliminating T_a between them to obtain the following general equation

$$r_t=R_1(W_u/W_m)-W_u/I^2_c(T_w-T_d)$$

It will be noted that if $T_w=T_d$, the last term of this equation which involves I becomes zero and the equation is reduced to

$$r_t=(W_u/W_m)R_1 \text{ or letting } q=(W_u/W_m)$$

we get $r_t=qR_1$. (It might also be mentioned that this equation could have been derived very easily from Veinott's and Schaefer's equation 9). The fact that the last term of the general equation is reduced to zero when $T_w=T_d$ is in agreement with Veinott's and Schaefer's conclusion that if a thermostat is so selected to give $T_w=T_d$, then ideal protection, unaffected by current, is obtained. The reduced equation

$$r_t=qR_1$$

also indicates the direct relationship between the thermostat resistance and the stator winding resistance which results when ideal protection is obtained. This direct relationship between overload resistance and winding resistance has long been recognized. By using this equation it is possible to calculate the resistance of the thermostat which will give ideal protection once the thermal conductances W_u and W_m or their ratio q have been evaluated for a given line of thermostats and for a given line of motors.

In their paper Veinott and Schaefer have not outlined any test procedure whereby W_m and W_u can be evaluated. To evaluate W_m, I would propose that representative test motors be loaded until the winding temperature T_w is equal to the trip temperature of the thermostat T_d as obtained by heating the thermostat in an oil bath. For this test the thermostat would not carry current and T_a would be measured by means of a thermocouple on the disk of the thermostat. In this connection it has been our experience that T_a as measured in this manner is not the temperature of the end shield, but more nearly the temperature of the motor air. The thermal conductance W_m would be calculated from the formula $W_m=I^2R_1/(T_w-T_a)$ which is derived from Veinott's and Schaefer's equation 8.

Inasmuch as it has been our experience that W_u is somewhat affected by how the thermostat is mounted in a motor and upon the degree of motor ventilation as is W_m, I would propose that W_u be evaluated as follows. Hold the motor winding temperature constant and equal to T_d such that T_a can be assumed to remain constant and equal to its value as measured in determining W_m. Pass a very slowly increasing current I_u from a separate source through the thermostat until it trips. Calculate the thermal conductance W_u by using the formula

$$W_u=I_u^2r_t/(T_d-T_a)$$

which is derived from Veinott's and Schaefer's equation 3. Thermal conductance test made on a number of our fractional horsepower motors in this manner give values of W_m on the order of 1–5 watts per degree centigrade, of W_u on the order of 0.04–0.1 watts per degree centigrade, and of ratio q on the order of 0.012–0.04.

Our experience indicates this method is as accurate as any previous method for selecting motor protection thermostats and that, as pointed out by the authors, verification test of the actual application is still recommended.

It seems probable that Veinott's and Schaefer's method of selecting thermostats is capable of further refinement and of greater accuracy if further investigated in terms of a more exact electrical equivalent circuit for the thermal conditions of a motor.

L. C. Packer (Westinghouse Electric Corporation, Springfield, Mass.): The authors are to be complimented for their very fine paper which presents a problem of interest to all motor designers.

I would like to ask the authors if the constants as derived for their formulas would be adaptable to such special applications as hermetically sealed refrigerator motors. These are very special problems because of the differences in design which affect the gradient between the motor winding and the thermostat. It would be expected that such design variations as vertical versus horizontal motors, or internally spring-mounted as compared with non-internally spring-mounted compressors, or gas, oil, or air cooling would all affect the design of the thermostats and their constants.

In the usual hermetically-sealed compressor with Freon F-12 oil and with cellulose insulation in the motor excessive temperatures will greatly affect the life of the insulation and mechanical parts and will shorten their life to below normal, by first breaking down the insulation into moisture which in turn combines with the Freon to form hydrochloric acid. This acid even in small parts breaks down the oil. This in turn breaks down the insulation at a faster rate than the excessive temperature. Burned out motors, etched valves, and coated pistons and cylinders are the ultimate result of excessive temperatures at overloads, light loads, where gas cooling is used, and in some cases, cycling between drop out and pickup of the relay or under locked conditions.

Burned out starting windings is without doubt the cause of most of the failures of split-phase motors. The temperature of the starting winding will in most cases continue to rise above safe operating temperatures under locked and cycling load conditions with the starting winding in the circuit.

Again I want to compliment the authors

for their fine contribution and would suggest that they expand their methods to cover the special problems found in hermetic units, and also consider the problem of protecting the starting winding. It is very important that the manufacturers of thermostat protection also consider this problem.

C. G. Veinott: DePuy's kind remarks about our paper are appreciated. He is entirely correct in his comment that a number of other factors are equally as important as the running overload trip setting in the selection of a thermostat for inherent protection of a motor. We felt that the subject of locked-rotor protection was too important and too involved to be treated in this paper, if we were to cover running overload protection adequately. Hence the title of the paper indicated that the subject matter was confined to running overload protection. DePuy has not overstated the importance of locked-rotor protection as a factor in the selection of the thermostat. Many times an application, determined solely on the basis of running overload, has to be changed when locked-rotor conditions are covered. However, after a new selection is made, based on adequate locked-rotor protection, it is then necessary to check the correctness of this new application with respect to running overload protection.

During the first few cycles of thermostat operation with rotor locked, the thermostat functions virtually like a current-operated device, and it trips before any appreciable amount of the heat from the windings reaches the thermostat location; hence a definite heater effect is required. In general, we are in full accord with the ideas expressed by DePuy.

Seely's discussion is also very much appreciated. His analogy is very interesting and may help some to grasp the theory we presented in our paper. We suggest he complete his analogy by explaining how the two branches of the T are supplied. Since he took the resistance to the left as representing the thermal resistance between the windings and the end shield, he would have to feed a current into that branch proportional to the I^2r losses in the winding; likewise, into the resistance to the right he would have to feed a current proportional to the I^2r losses in the thermostat. A hydraulic analogy could be made the same way and would serve the purpose equally as well. We, too, think of W_u as the thermal conductance of the disk to end shield, and of W_m as the thermal conductance of the windings to the end shield.

Seely's approach of simplifying our equation 9, showing the thermostat resistance to be directly proportional to the resistance of the main winding was extremely interesting, for that is the first approach we developed to this problem years ago. In fact, we dropped this method with considerable reluctance because it appeared so beautifully simple. The catch is that the ratio q is not a constant, as pointed out by Seely himself; unfortunately, it is a function of the thermostat selected. Theoretically, it is impossible to use this approach because it is necessary to know what thermostat is to be used before a selection can be made, a rather anomalous condition. This tends to make this method somewhat of a cut-and-try method. We get around this difficulty by expressing the desired thermostat performance in terms of its ultimate tripping current, as in our equation 11, which is a very simple equation. The right-hand member of this equation contains no function of the thermostat design or characteristics as does Seely's "q".

Seely raises the question of testing for W_u and W_m. We find that these can be determined satisfactorily by measuring the actual opening temperature of the disk in an oil bath, and then taking an "ultimate tripping test" of the thermally-protected motor. This is done by applying an overload to the motor and allowing all the temperatures to level; the input current is increased by a small increment by increasing the load on the motor and the temperatures again allowed to level; this is continued until the thermostat finally trips. The measured values of current, winding temperature, and end-shield temperature at this point yield directly the values of K_t and K_m; these divided respectively into the thermostat resistance and winding resistance give the values of W_u and W_m. The value of W_u so obtained differs slightly from the value obtained by block test, a correction which has to be taken into account in applying the thermostat.

In reply to Packer's discussion, our method should apply to the application of thermostats to hermetically-sealed refrigerators in those cases where the design of the unit is such that W_m is essentially constant over the operating range. This would be approximately true if the stator laminations are pressed directly into the shell, if the shell receives substantially all of its heat from the motor and not from the compressor or refrigerant, and if the thermostat is mounted directly on the shell. Unfortunately all of these conditions are probably never obtained in a practical refrigeration unit. The applicability of the theory outlined in the paper is directly proportional to the closeness with which the foregoing conditions are realized. In a spring-mounted unit, where all of the motor heat has to be transmitted out through the refrigerant, the ideal conditions outlined are so far from being realized that the thermostat functions, to all intents and purposes, virtually like an external current-operated device and the theory outlined in the paper is probably of very little value.

The Field Fluxes of the Shaded-Pole Motor

E. E. KIMBERLY
MEMBER AIEE

THE pole-shading method of producing starting torque in single-phase a-c motors has been known so long that as early as 1895 at least one improvement patent was allowed.[1] While this type of motor is simplest of all to make, almost nothing has been published to clarify and catalog its field fluxes that make it so difficult to design.

In its simplest form the motor has two, or multiples thereof, salient poles every one of which has a portion of its airgap end surrounded by a short-circuited conductor of one or more turns similar to that shown in Figure 1. In the popular explanation of shading action, the total pole flux Φ is separated into two components of unshaded flux, Φ_u, and shaded flux Φ_s. Because of the inductance of the shading coil, Φ_s is caused to lag Φ_u in time phase α and thus produce a simulated rotating or gliding field of flux moving around the airgap from unshaded to shaded section of the pole. Inasmuch as Φ_u and Φ_s are unequal and their space and time angles (especially the time angle α) are less than 90 degrees, the rotating field is imperfect in that there is also a field moving in the backward direction. Assuming the space angle between Φ_u and Φ_s to be 90 degrees the magnitudes of the forward and backward rotating fundamental fields then may be calculated by 2-phase symmetrical component analysis. Because of over-simplification, this method proves to be only a scientific method of getting the wrong answer in calculating the performance of this type of motor.

At least as early as 1921 it was discovered that an improvement in performance could be achieved by encouraging a part of Φ_s to bypass the rotor through pole extensions (interleaving) from the shaded portion of one pole to the unshaded portion of the adjacent pole.[2] The fact was accepted and a questionable theory was offered. In 1923 the pole extensions idea was extended to include a complete path or bridge of iron from pole to pole around the rotor with only a butt-joint airgap at the mid-point.[3] In 1926, Chester I. Hall[4] used a modified form of the bridge and showed an understanding of its function. In some motors, the bridges are solid without gap of any kind as in Figure 2.

The Problem

The flux distribution in the airgap both as to space and time is affected by saturation and by simultaneous fluxes in opposite directions in the unshaded portion and in the shaded portion of a pole. The purpose of this experimental work is to determine the magnitude and speed of both fundamental and third harmonic fields in the airgap at standstill, at one-third full speed, and full speed. Other harmonic fields if present do not noticeably affect the performance of the special motor used and so have not been investigated. The results are intended to be qualitative rather than quantitative because of the innumerable variables that depend upon size and mechanical proportion.

The Experimental Motor

No available commercial motor is large enough to permit easy application of exploring coils large enough to operate electrical instruments without amplification and possible distortion. To overcome this inconvenience a large motor of dimensions shown in Figure 3, was built as a scale model (excepting the airgap length) of a core-type commercial fan motor or phonograph record-player motor. All tests were made with constant applied voltage rather than constant total armature leg flux because it was thought that the effect of changing the shading-coil resistance could be shown better in that way, inasmuch as the leakage flux in air is affected by change in the shading coil resistance. In order to emphasize the effect of the third-harmonic field which is sometimes annoying, the shading coil slot was made to open into the rotor bore at one-third of a pole pitch from the rotor horizontal center line or the theoretical pole tip.

The shading coils each were made of seven turns of the number 10 copper wire. The two coils were connected in series and to an external noninductive variable resistor. The data on shading-coil circuit resistance are given, however, on the basis of the equivalent single-turn coil. The apparent flux Φ_{sr} in the airgap facing the shaded portion of the pole was found from a 10-turn exploring coil surrounding that portion of the pole and cemented to it. The flux Φ_{ur}, in the airgap facing the unshaded portion of the pole was found similarly. The apparent flux in the shaded portion of the pole was found from an exploring coil around that portion and located adjacent to the shading coil at its end nearest the rotor. The rotor carried 47 round bars skewed one tooth pitch.

The airgap flux was measured from 18 exploring coils of one turn each, cemented to one pole face. Every coil subtended 10 degrees of arc and the 18 coils were distributed over one pole. In some cases where the flux distribution changed rapidly in space around the airgap, intermediate points were obtained. In drawing graphs of airgap flux density the distribution of flux was assumed to be the same under each pole.

The voltages from the exploring coils

Paper 49-72, recommended by the AIEE rotating machinery committee and approved by the AIEE technical program committee for presentation at the AIEE winter general meeting, New York, N. Y., January 31–February 4, 1949. Manuscript submitted October 27, 1948; made available for printing December 20, 1948.

E. E. KIMBERLY is in the Robinson Laboratory of the Ohio State University, Columbus, Ohio.

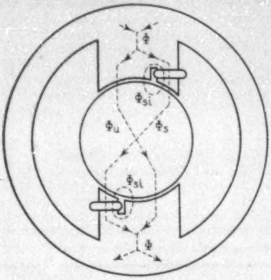

Figure 1 (left). Elemental 2-pole shaded-pole motor showing paths of flux components

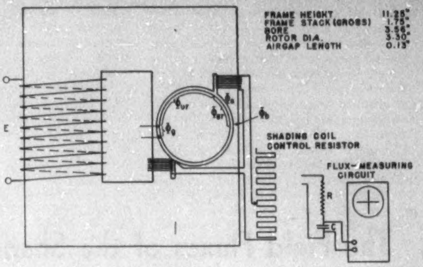

Figure 3 (right). Diagram of the experimental motor and flux measuring circuit

were fed into a reactance-capacitance integrating circuit which gave oscilloscope traces proportional to the net fluxes threading the coils.

The Fundamental Field with Rotor Blocked

To determine the flux distribution around the airgap at any chosen instant of time the magnitude of flux shown by the time trace on the oscilloscope screen at that instant as seen on the repetitive synchronized traces was recorded and plotted against space degrees around the airgap as the measuring circuit was switched to successive airgap exploring coils around the pole face. The same was repeated for instants of time successively later by 30 degrees until data for the six space plots of Figure 4 and Figure 10 were obtained. The fundamental and third-harmonic sinusoidal space component fields have been calculated by Fourier analysis and included in every case.

When the shading coil circuit was open the space waves plotted for 30-degree time intervals showed standing waves of both fundamental and third harmonic flux. Because that case is of slight importance, its graph has not been included, but was drawn to prove the soundness of technique in a simple case.

Figure 2. Core-type shaded-pole motor with bridges between poles showing paths of flux components

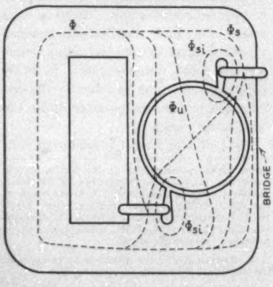

Figure 4 is a series of curves for the case when the shading coil circuit was closed with a little too much resistance (0.00063 ohm) to allow enough fundamental torque to pull the rotor through the cusp caused by the third harmonic field. The shifting of the fundamental field from a position of its maximum density at about the location of the shading coil slot (at 0 arbitrary angle) to advanced positions shown at 30-degree intervals of time is evident from the successive curves. The progress of the fundamental field around the airgap as a function of time is plotted against electrical degrees in the airgap in Figure 5, curve C.

The rotating field is born suddenly with its point of maximum density in the unshaded portion of the pole quite close to the shading coil slot, moves across the shaded portion at almost three times synchronous speed and slows to almost a stop about two-thirds of the way across the following unshaded portion of a succeeding pole. It is then again accelerated and continues its cyclic but erratic course. The field should then be said to sweep from the shaded area of one pole to the unshaded area of the succeeding pole rather than from unshaded to shaded area of the same pole as sometimes has been stated.

In Figure 5 also is plotted the progress of the fundamental component when the shading coil resistance is adjusted for maximum starting torque (b), and when the resistance is too low for maximum starting torque (a).

Action of the Shading Coil

The component of primary flux which passes through the shading coil acts as the mutual flux of a transformer of which the shading coil is the secondary. The magnetomotive force of the shading coil cur-

Figure 4 (below). Plot of instantaneous flux densities in airgap with rotor blocked and a little too much resistance in the shading coil to produce enough fundamental torque to overpower the third-harmonic torque at about one-third synchronous speed (fundamental)

$R_s = 0.00063$ ohm

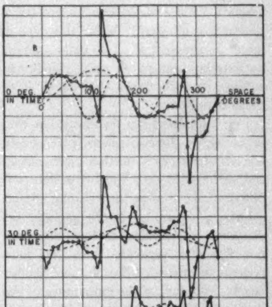

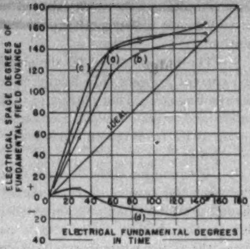

Figure 5. Plot showing space field advance around airgap as a function of time for three values of R_s

(a) Fundamental when $R_s = 0.000107$ ohm
(b) Fundamental when $R_s = 0.000315$ ohm
(c) Fundamental when $R_s = 0.00063$ ohm
(d) Third harmonic when $R_s = 0.000107$ ohm

rent acts on a complicated magnetic circuit in which the path taken by Φ_{st} of Figure 2 is most important. The flux Φ_{st} tends to saturate the shaded section of the pole at the airgap and so to crowd into the bridge that part of the mutual flux which would appear there with no shading coil current flowing. When R_s is decreased the net flux through the shading coil is decreased because of increasing I_s. A plot of this observed relationship is shown in Figures 6 and 7.

Figure 6. Phase relationship and relative magnitudes of fluxes in and around the shaded portion of the pole

t_1 bridge flux is zero. Φ_{sr} is sustained by I_s and is the same as Φ_s

t_2 flux Φ_s is apparently zero but is actually the instantaneous sum of the sustained Φ_{sr} and the reversed Φ_b

t_3 flux Φ_s is actually the same as Φ_b but shows less because there is a sustained Φ_{sr} in opposition

t_4 flux Φ_{sr} has subsided and Φ_b equals Φ_{sr}

However, the shaded portion of the rotor actually has a sustained flux magnitude equal and opposite to the reversed and rising Φ_s component of Φ_{sr}

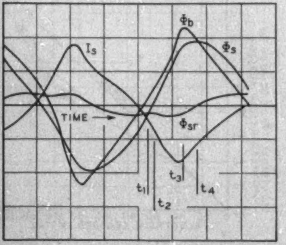

Figure 7 (right). Some effects caused by change in shading coil resistance

Φ_{sr} is flux entering the rotor opposite the shaded part of the pole. Φ_{ur} is flux entering the rotor opposite the unshaded part of the pole. I_s is the shading coil current. The fundamental components of Φ_{ur} and Φ_{sr} are calculated. Shading coil resistance R_s is varied in steps from 0.0007 to 0.0001 ohm

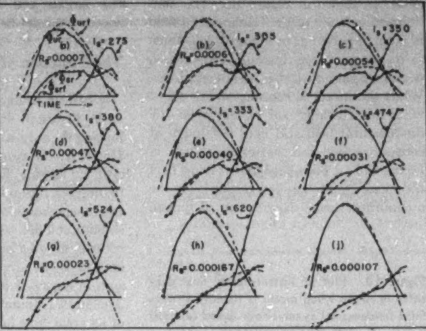

The complex interaction of fluxes Φ_s, Φ_b, and Φ_{sr} is partly shown in Figure 6, for a shading coil resistance which produces maximum starting torque. There is no obvious way to measure either the mutual flux, which is chiefly Φ_b, or Φ_s directly when both exist simultaneously.

In Figure 7, when the shading coil resistance is relatively high the net flux Φ_{sr} is composed largely of mutual flux (the earlier portion of rising Φ_{sr}) which lags behind Φ_{ur} by a small angle, and to a lesser extent by local flux Φ_{st} (the latter portion of rising Φ_{sr}) which is substantially in phase with I_s and lags Φ_{ur} by more than 90 degrees. As the shading coil resistance is decreased, I_s increases and flux Φ_{st} tends to dominate Φ_{sr} both as to magnitude and phase angle by which it lags Φ_{ur}. In Figure 7(J) when R_s is quite low the angle between the fundamental components of Φ_{ur} and Φ_{sr} is greater than 90 degrees. The starting torque produced by the fundamental components Φ_{urf} and Φ_{srf} is a function of $\Phi_{urf} \times \Phi_{srf} \times \sin \alpha$ where α is the time angle between Φ_{urf} and Φ_{srf} if the space angle is 90 degrees. In Figure 8 is shown a plot of starting torque so calculated plotted against R_s and compared with the starting torque as measured by prony brake. These curves show that in a motor as large as the one tested the shading coil resistance readily may be made too small to obtain the maximum starting torque. Under some conditions of shading when the shading coil resistance is too low, it is possible for the harmonic torque (third only investigated) to hinder the starting torque as shown by curve (d), Figure 5, in which the third harmonic flux appears to move backward most of the time.

Figure 8. Starting torque as a function of shading coil resistance

$\Phi_{urf} \times \Phi_{srf} \times \sin \alpha$ plotted from Figure 7 without units to show shape of curve only

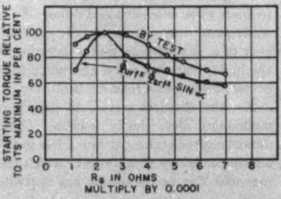

In Figure 9 is plotted the shading coil current and the net shaded section flux as a function of shading coil resistance. This flux curve should theoretically intersect the axes at point 0-0.

The Fundamental Field with Motor Running

When the rotor is permitted to run at about one-third synchronous speed with the shading coil circuit open it is found that the flux density around the airgap

Figure 9. Change in net flux through shaded portion of pole as the shading coil resistance is changed

Rotor blocked

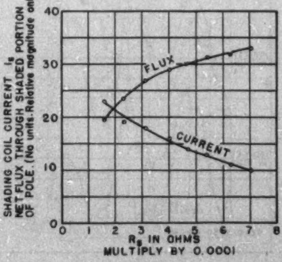

varies as shown in Figure 10. The nonuniform velocity of the fundamental field is again apparent as in Figure 4, inasmuch as its progress from instant to instant 30 degrees apart in time is not uniform. When the motor is running at full speed with the shading coil circuit open the fundamental field still does not move at constant speed but varies as shown in Figure 11. The double-revolving-field theory as usually applied accounts for the nonuniform space distribution of flux in the airgap and also for the variable speed of the net field.

Figure 10. Plot of instantaneous flux densities in airgap when motor is running at one-third fundamental synchronous speed (almost) with shading coil open

Six instants of time. Fundamental and third harmonic space components calculated

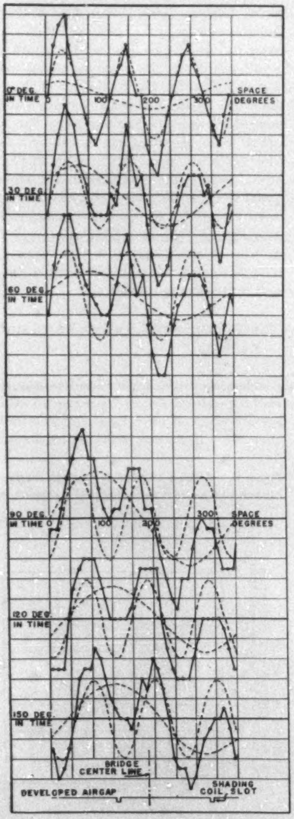

The Function of the Bridge

When no bridge between poles is used as in Figure 1, Φ_s passes into the rotor lagging Φ_u only a few degrees, α in time. However, the resulting shading coil current I_s, lagging Φ_s somewhat more than 90 degrees sets up its own local flux Φ_{st} which surrounds the slot in which the shading coil lies. The flux Φ_{sr} entering the rotor in an area opposite the shaded pole section is, at any instant, the algebraic sum of a part of Φ_s and the local flux Φ_{st}. The flux Φ_{st} is smaller than Φ_s but because of its great time lag, it causes Φ_{sr} to lag Φ_u more than if Φ_{sr} were composed of Φ_s only.

When the bridge is added it affords a superior path for Φ_s and increases its magnitude. Furthermore the bridge diverts most of Φ_s from its former path through the rotor under the shaded section of the pole. The magnitude of $\bar{I}_s$ and hence Φ_{st} is therefore increased and Φ_{st} becomes a dominating factor in controlling α which should be 90 degrees for maximum starting torque. It appears then that the shading coil side should lie close to the airgap in order to minimize the loss of Φ_{st} by leakage across the unfilled portion of its slot.

The Third-Harmonic Field

Inasmuch as the shading coil slot is located one-third of the way around the pole from the bridge center line, a marked third harmonic field is to be expected. In Figure 4, the third harmonic field is a standing wave and so contributes nothing to the starting torque. With the shading coil resistance adjusted for maximum torque, the third harmonic field moves forward at one-third synchronous speed and contributes to the starting torque. When the shading coil resistance is too low, the third harmonic field moves backward and detracts from the starting torque.

Conclusions

1. The classical rotating field theory without some extension and refinement is inadequate for calculating the performance of a shaded-pole motor because of the highly variable speed and magnitude of the fundamental rotating field.

2. The classical cross-field theory is inadequate also, chiefly because of the almost unpredictable pattern of flux in the airgap caused by conditions in which the magnetic flux in the airgap has opposite sense simultaneously at the shaded portion of a pole and also at the unshaded portion.

3. The flux produced by the shading coil current appears only locally around the shading coil. That portion of it that enters and leaves the rotor crosses the airgap twice near the embedded side of the shading coil.

4. The function of the bridge is that of diverting the mutual flux through the shaded portion of the pole (magnetizing flux in the shading coil) from a path across the airgap where its small lag angle is detrimental to starting torque. It also serves to increase the magnetizing component of shading coil flux and so to increase the shading coil current and the local flux which it produces with a great time lag behind Φ_{ur}. The magnetizing flux and mutual flux are identical.

5. The starting torque may be impaired by too little resistance in the shading coil. This condition is unlikely to occur in motors of 1/50 horsepower or less, however, because with the same pole section and shading coil proportions a small motor will have less magnetizing flux per ohm of shading coil resistance than will a larger motor. The magnetomotive force responsibilities of the shading coil are determined largely by the airgap length which does not decrease in proportion to the motor size. With less magnetizing flux in a smaller motor, the shading coil resistance should be less in proportion to that flux. It follows then that the shading coil size should not be proportionately reduced as the motor size is reduced.

6. The third harmonic field may cause a serious cusp in the speed-torque curve at about one-third synchronous speed and may even produce a negative torque at start.

Figure 11. Rate of field advance around airgap compared to the ideal when motor is running without load and with shading coil circuit open

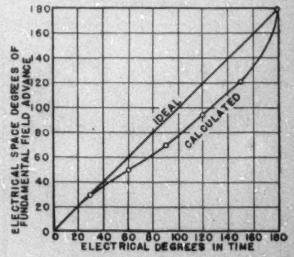

Appendix

The use of a resistance-capacitance circuit in connection with an oscilloscope to find the time function of a varying flux Φ by examining the induced voltage e_{rc} produced by it may need some justification.

In the circuit used, if the capacitor current i_c were controlled completely by the resistance R in series with it (effect of capacitor C ignored) then i_c would be a function of e_{rc} which is the exploring coil voltage

$$i_c = Ke_{rc}$$

$$\frac{d\Phi}{dt} = K'e_{rc}$$

$$\int \frac{d\Phi}{dt}\,dt = K'\int e_{rc}\,dt = \frac{K'}{K}\int i_c\,dt$$

$$\Phi = \frac{K'C}{K}\left[\frac{1}{C}\int i_c\,dt\right] = \frac{K'C}{K}e_c$$

Therefore

$$\Phi = K''e_c$$

If then R be made sufficiently large compared to $1/C$, the magnitude and phase angle errors, introduced by a circuit containing $R-jX_c$ instead of R alone, may be held to the same order as those of instrument reading. An analysis of airgap flux distribution with the shading coil open showed the fundamental and third space harmonics to be standing waves both passing through zero at the center line of the stator between poles and for that reason any accumulated errors are apparently negligible. To correct for this error in angle, if desired for accuracy, the flux fundamental or harmonic component under consideration should be set back (retarded in its space position) by the angle whose tangent is $1/\omega CR$.

References

1. United States Patent 534,151. H. R. Hassler. 1895.
2. United States Patent 1,495,827. H. E. Warren.
3. Landis and Gyr Haupt Patent 103,967 Zug Schweiz.
4. United States Patent 1,590,025. Chester I. Hall.

No Discussion

Electrically Charged Dust in Rooms

G. W. PENNEY
FELLOW AIEE

G. W. HEWITT
MEMBER AIEE

Synopsis: Inefficient electrostatic air cleaners may allow the escape of dust particles carrying electric charges of one sign. Such charged particles, suspended in the air of a room, create a space-charge potential. The resulting voltage gradient drives the charged particles toward the walls. Because of this space-charge effect, the full benefit of air cleaning may not be realized. In addition to the efficiency of the electrostatic air cleaner, other important factors are the concentration of particulate matter in the air, and room size and shape. Ordinarily, the space-charge problem can be solved by high-efficiency cleaning, under particularly severe conditions, such as especially dirty locations and large rooms (such as auditoriums), the use of a neutralizing device may be desirable.

WELL-DESIGNED installations of electrostatic precipitation equipment have given very satisfactory results in keeping buildings clean, but faulty design, installation, or maintenance can cause low efficiency and may result in serious trouble because of the electric charge on any dust escaping from the precipitator. The particles escaping from a precipitator normally carry a charge (usually positive). These charged dust particles suspended in the air in a room, give rise to an electric potential within the room which is a maximum at some central point and decreases toward the walls and other grounded objects. Thus a gradient of potential exists in such a direction as to drive the charged dust toward the walls. The full benefit of the air cleaner is not realized because charged dust near the walls, repelled by other charged dust suspended in the room air, travels more rapidly toward the walls than does uncharged dust. This paper discusses the nature of these effects and the various precautions that should be observed to minimize electrical deposition of dust on walls, so that the full benefit of removing a large percentage of the dust can be realized. This electric charge on dust suspended in the air is referred to in this paper as "space charge."

Demonstration of Space-charge Effects

In an electrostatic precipitator, the air first passes through an ionizer, then through a collector cell. The function of the ionizer is to give each suspended particle an electric charge of a given sign; the function of the collector cell is to remove these charged particles from the air stream by precipitating them upon its plates. If the cleaning efficiency is low because of faulty installation or maintenance, or because of overrating the precipitator, then an increased number of charged dust particles are carried by the air stream into the room.

Electric charges of one sign, carried by dust particles suspended in the air in a room, set up a space charge, resulting in an electrostatic field in the room. Persons in the room cannot sense the space-charge voltage because of the very low energy involved. To measure the resulting voltage, an extremely high-resistance instrument, like an electrostatic voltmeter, is required.

The voltage gradient produced by this charged dust is higher near any parts of the wall that project into the room. Conversely, it is lower on receding parts, such as inside corners or surfaces which are partially shielded by other surfaces. For example, the gradients at such projecting surfaces as those of light fixtures suspended from the ceiling are much higher than those at the wall surfaces. The rate at which dust moves toward surfaces varies directly with the gradient; hence surfaces projecting into the room are soiled rapidly.

These effects were demonstrated using an early precipitator installation from which unsatisfactory performance had been reported. It was found that the installation was such that all of the air passed through the ionizer, but that some ionized air could go through a passage by-passing the collector cells. Also, the precipitator being in a location which was difficult to service, collected dust was allowed to accumulate, almost blocking air flow through the collector cells and forcing about one-half of the air through the leakage path around the collector cells. The resulting efficiency was about 50 per cent, with the half of the dust remaining in the air fully charged. The results of this faulty installation and maintenance were studied in three ways:

1. An electrostatic voltmeter was set up to measure voltages within the room.
2. Specially-devised objects were hung in the room, some being at wall potential and some well-insulated from the walls to show the effect of gradient upon the deposition of dust.
3. The walls and furnishings were examined and pictures taken to show the nature of the dust deposits.

To measure the potential in the room, a disk electrode was mounted from the high-voltage terminal of an electrostatic voltmeter so that the electrode was $4^1/_2$ feet above the voltmeter. This is shown in Figure 1. Such an electrode normally would be very slow to come to the potential of its position in space, and because of some slight leakage, never would fully reach this potential. To increase the rate of response, and to decrease errors, a small amount of radioactive material was placed on the electrode. The material used emitted alpha particles which ionized the air for a distance of a few inches. The resulting air ions near the electrode had a relatively high mobility to move in an electric field, and since there were both positive and

---

Paper 49-74, recommended by the AIEE electronics committee and approved by the AIEE technical program committee for presentation at the AIEE winter general meeting, New York, N. Y., January 31–February 4, 1949. Manuscript submitted November 12, 1948; made available for printing December 24, 1948.

G. W. PENNEY is George Westinghouse Professor of Engineering, Carnegie Institute of Technology, Pittsburgh, Pa.; G. W. HEWITT is research engineer, electro-physics department, Westinghouse Research Laboratories, East Pittsburgh, Pa.

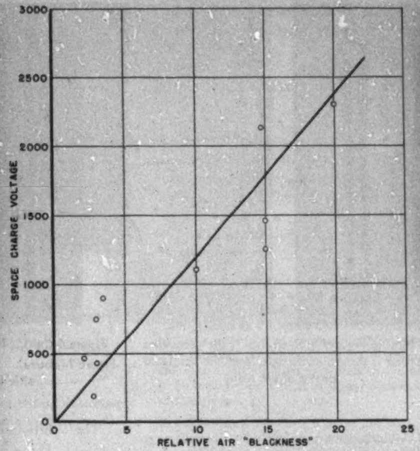

Figure 1 (left). Electrostatic voltmeter and radioactive disk electrode

Figure 2 (above). Space charge voltage versus air blackness in room *A*

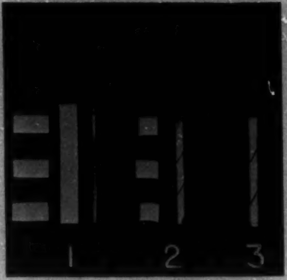

Figure 3. Assembly of paper-covered probes

1. Metal probe and paper strips
2. Spiral strip in place and bands partially curved ready to apply
3. Assembled probe

negative ions, the appropriate ion was always present to move to the electrode to bring it to the potential of the space.

Using this instrument, voltage measurements were made in a room supplied with the partially-cleaned air and designated as room *A*. At the same time the "dirtiness" or "blackness" of the air was measured by drawing a measured volume of air through filter paper and measuring the discoloration of the filter paper. The air blackness was evaluated by measuring the change in light transmission through the filter paper caused by the filtered dirt, using a standard illumination and a photocell. The reciprocal of the volume of air required to produce a given discoloration was used as a measure of the blackness.

These tests in room *A* indicated no voltage when the air was clean, while on some smoggy days, the potential in the room was over 2,000 volts. To show that this voltage was not a characteristic of the dirt in the air, duplicate measurements were made in a similar room not equipped with any air-cleaning device and designated as room *B*. In this second room the air was dirtier, but ordinarily there was no measurable potential in the room. The voltage and air blackness measurements for rooms *A* and *B* are given in Table I. Space charge voltage versus air blackness in room *A* is plotted in Figure 2. A rough correlation is evident. An exact correlation would not be expected, since the particle size and other factors vary from day to day.

To show the effect of the voltage gradient at a surface, small probes were made as illustrated in Figure 3. Each probe consisted of a 1/8-inch diameter copper cylinder on which a strip of white paper was spirally wrapped. Portions of this paper surface were covered by three cylindrical paper bands; and the rest was left exposed to the air. Figure 3 shows the construction in three steps. The small bands were used so that at the end of the test, the exposed surface could be compared with the clean unexposed surface.

In each of the two rooms, two probes were suspended, one by a grounded wire, and the other by a fine, waxed-silk thread. The two probes in each room were spaced far enough apart to prevent any appreciable influence upon each other. The grounded wire held its probe at wall potential although suspended in a high-potential region, so the gradient near the probe and rate of blackening was very high, much higher than at the walls of the room. On the other hand, the waxed-silk thread, because of its excellent insulating properties, allowed its probe to attain essentially the potential of the space; the gradient at its surface, therefore, was very low.

Typical probes after a test in room *A* are shown in Figures 4 and 5. In this room which had bad space-charge conditions, the probe at wall potential was badly discolored, while the insulated probe was only slightly discolored. The results of a similar test in room *B* are shown in Figures 6 and 7. In this room with negligible space charge, the grounded and insulated probes show almost the same discoloration.

The very slight discoloration of the insulated probe in room *A*, as compared with the grounded probe, might lead one to think that space-charge blackening of the walls could be eliminated by making the walls of highly-insulating material. This, however, is not true, since any air having a net electric charge must have a potential above its enclosing surfaces, so that insulating walls would primarily serve to raise the total potential, with practically no effect on the average discoloration of the walls. It would tend, however, to reduce the nonuniformity of this discoloration.

A typical example of the deposition of dust is shown in Figure 8. The wall consisted of asbestos-board panels with 5/16-inch-thick strips covering the joints between panels. In this picture the heavy deposit of dust on the projecting corners of the strip, and the absence of dust deposits in the protected corners, are very noticeable.

The tests on this faulty installation of electrostatic air cleaning demonstrated three things:

1. Voltages dependent on the amount of particulate matter in the air, can be measured in rooms supplied with air which has passed through an ionizer, but has bypassed the collector cell.

2. If a small surface can be sufficiently well insulated, it can project into the room without being blackened excessively; a

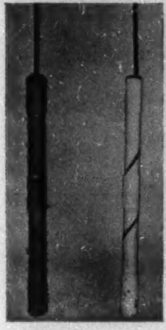

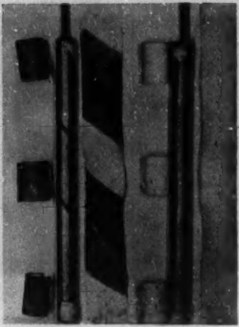

Figure 4 (above). Probes after test in room *A*

Figure 5 (right). Paper removed from probes after test in room *A*

Note: In Figures 4, 5, 6, and 7, the grounded probe is shown at the left, and the insulated probe at the right

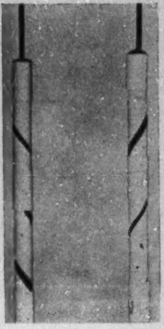

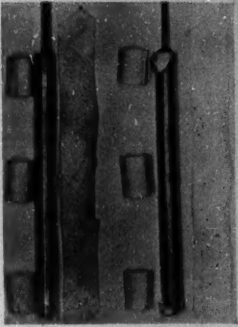

Figure 6 (left). Probes after test in room *B*

Figure 7 (above). Paper removed from probes after test in room *B*

similar grounded surface will be blackened very rapidly. This does not mean, however, that making the entire walls of highly-insulating material would eliminate blackening of such walls.

3. Blackening of walls due to space-charge voltages can be recognized by the pattern of the dust deposits, such deposits being heavy on surfaces projecting into the room and lighter on partially-shielded surfaces.

General Analysis

Poisson's equation expresses the relation between potential and position in the room

$$\frac{\partial^2 V}{\partial x^2}+\frac{\partial^2 V}{\partial y^2}+\frac{\partial^2 V}{\partial z^2}=\frac{-4\pi\rho}{k} \tag{1}$$

where

V = potential, statvolts
ρ = volume density of net charge, statcoulombs per cubic centimeter
k = dielectric constant
x, y, z = rectangular coordinates, centimeters

Assuming a uniform net-charge density in air (ρ constant throughout the space, and $k=1$), solutions may be obtained easily for bounding walls of certain simple shapes, such as two infinite parallel planes spaced a finite distance apart, or a spherical shell. The calculation of voltages in actual rooms becomes mathematically involved. It is not the purpose of this paper to treat these difficult cases, but rather to consider simple cases in order to find general trends.

SPACE CHARGE IN A LARGE, LOW ROOM

For the space between two infinite parallel planes, spaced a finite distance (H centimeters) apart in the x direction, the derivatives with respect to y and z are zero and equation 1 reduces to

$$\frac{d^2V}{dx^2}=-4\pi\rho \tag{2}$$

The solution of this is

$$V=-2\pi\rho x^2+C_1x+C_2 \tag{3}$$

where C_1 and C_2 are constants of integration.

Taking the origin at the center of the space, and letting both planes be at zero potential (ground), the constants can be evaluated from the conditions that $V=0$ at $x=H/2$ and at $x=-H/2$.

Then

$$V=(1/2)\pi\rho(H^2-4x^2) \tag{4}$$

and

$$\frac{dV}{dx}=-4\pi\rho x \tag{5}$$

The conditions in a large, unfurnished room with low ceiling are similar to the preceding, except in the regions near the vertical walls.

The maximum potential is in the center of the room, half-way from floor to ceiling, and is approximately

$$V_{\max}=1/2\pi\rho H^2 \tag{6}$$

The maximum voltage gradient is at the center of the floor and of the ceiling, and is approximately

$$\frac{dV}{dx_{\max}}=\pm 2\pi\rho H \tag{7}$$

SPACE CHARGE IN A SPHERICAL SPACE

Poisson's equation, in spherical co-ordinates, for space charge of uniform density in a spherical shell (R centimeters radius) is

$$\frac{2}{r}\frac{dV}{dr}+\frac{d^2V}{dr^2}=-4\pi\rho \tag{8}$$

The solution of this, by integration, is

$$V=-\frac{2}{3}\pi\rho r^2+\frac{C_1}{r}+C_2 \tag{9}$$

The constants may be evaluated by substituting the following boundary conditions:

The voltage gradient is zero at the center ($r=0$) of the spherically-symmetrical space charge, and $V=0$ when $r=R$, the spherical enclosing shell of radius R being at zero potential, that is, ground.

The potential equation is

$$V=2/3\pi\rho(R^2-r^2) \tag{10}$$

The maximum potential is at the center of the sphere ($r=0$)

$$V_{\max}=2/3\pi\rho R^2 \tag{11}$$

The gradient equation is

$$\frac{dV}{dr}=\frac{4}{3}\pi\rho r \tag{12}$$

The maximum voltage gradient is at the wall ($r=R$)

$$\frac{dV}{dr_{\max}}=\frac{4}{3}\pi\rho R \tag{13}$$

AVERAGE GRADIENT OVER BOUNDING SURFACES

The average value of the voltage gradient over the enclosing surface can be calculated very simply. Using the centimeter-gram-second electrostatic system, there are 4 π lines of flux associated with each statcoulomb of charge, and the voltage gradient in statvolts per centimeter is numerically equal to the number of these flux lines per square centimeter in a plane perpendicular to the gradient.

Considering geometrically similar shapes, let:

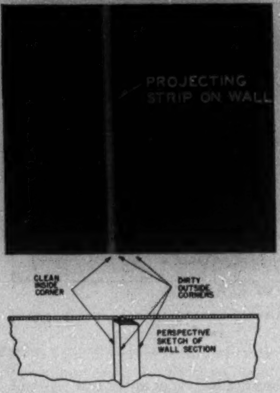

Figure 8. Typical space-charge blackening at a projecting strip on a wall (room *A*)

D = a characteristic linear dimension, centimeters
$v = C_v D^3$ = volume of room, cubic centimeters
$s = C_s D^2$ = area of bounding surfaces, square centimeters
C_v and C_s = factors depending upon room shape
ρ = average net charge density, statcoulombs per cubic centimeter
E_{ave} = average voltage gradient over bounding surfaces, statvolts per centimeter

Then

$$E_{ave} = \frac{4\pi\rho v}{s} = \frac{4\pi\rho C_v D^3}{C_s D^2} = 4\pi\frac{C_v}{C_s}\rho D \qquad (14)$$

For the case of the spherical space charge, the gradient over the whole spherical bounding surface is uniform and therefore equal to the average gradient given by equation 14. Let D = sphere diameter, centimeters. Then $C_v = \pi/6$, and $C_s = \pi$.

Substituting in equation 14

$$E_{ave} = 2/3\pi\rho D \qquad (15)$$

This agrees with equation 13, since $D = 2R$.

For a cube of height D centimeters, $C_v/C_s = 1/6$. Substituting this in equation 14

$$E_{ave} = 2/3\pi\rho D \qquad (16)$$

This shows that the average gradient at the walls would be the same for a cubical room as for a spherical room of equal height. However, the distribution of the gradient over the wall surface would be uniform for the sphere, but nonuniform for the cube. In the latter case, the gradient at the wall would be maximum at the center of the wall and minimum in the corners.

It is evident from equation 14 that for geometrically similar rooms, and a given charge density in the air, the average gradient over the enclosing surfaces is proportional to the size (linear dimension) of the room.

The distribution of this gradient over the bounding surfaces depends upon the configuration of the exposed surfaces. For geometrically similar rooms the distribution of gradient is independent of the size.

The following deductions are indicated by this analysis:

1. Assuming a given amount of dust per unit volume of air, and a given charge per particle, the voltage at the center of the room varies as the square of the dimensions of the room (rooms geometrically similar). The gradient at the wall, which determines the rate at which dust is driven to the wall, is directly proportional to linear dimensions of the room.

2. Assuming the charge to be proportional to the amount of dust per unit volume of air, the voltage gradient at the wall of a given room is proportional also to the concentration of dust in the air. The velocity with which the dust is driven towards the wall is proportional to the gradient, and the rate of precipitation on the wall is proportional to the product of the precipitation velocity times the dirt concentration in the air. In this way, the rate at which a surface becomes dirty is proportional to the square of the amount of dust per unit volume of air.

3. Consider an electrostatic precipitator supplying air to a given room: First, assume that the charge per unit of dirt leaving the precipitator remains constant, as the cleaning efficiency (e) of the precipitator is varied. Then, both the amount of dirt and the amount of charge per unit volume of air in the room varies as $(1-e)$. So the gradient at the walls and the velocity with which dust is being driven toward surfaces also vary as $(1-e)$, and the rate of precipitation upon the surface varies as $(1-e)^2$, that is, the product of precipitation velocity times dirt concentration. Actually, if the efficiency of the precipitator is decreased, either by increasing the air velocity or decreasing the plate length or voltage, the charge per unit of dirt probably will increase rather than remain constant; therefore, the actual rate of blackening of surfaces due to space-charge effects will probably vary more rapidly than $(1-e)^2$. This emphasizes the importance of utilizing the full ability of electrostatic precipitation to yield high efficiency of cleaning.

Engineering Solutions

Obviously, since the space-charge discoloration of surfaces varies more rapidly than the square of the amount of dirt escaping, it is very important to secure an efficient unit, properly installed and maintained. Experience has shown that if this is done, there will be ordinarily no difficulty with space charge in rooms of moderate size. The sealing of the unit so that air cannot by-pass the collector cell, and the distribution of the air so that at no point in the installation does the velocity exceed the rated value, are extremely important factors. Of course it is important to maintain proper voltage, and to clean the units thoroughly and regularly.

In large auditoriums and especially dirty locations, special consideration should be given to space charge because of

Table I. Space-Charge Voltage in Test Rooms

Date	Time	Space-Charge Potential, Volts (As Measured by Electrode on Electrostatic Voltmeter)		Relative Air "Blackness"	
		Room *A*	Room *B*	Room *A*	Room *B*
October 7	8:10 a.m.	210	*	*	*
9	8:20 a.m.	190	75**	2.7	3.6
	1:15 p.m.	*	*	*	2.5
10	8:06 a.m.	430	110**	3.0	4.0
11	8:10 a.m.	900	*	3.5	8.0
	2:30 p.m.	*	*	*	5.0
	4:30 p.m.	*	*	*	5.0
12	8:30 a.m.	1,100	*	10.0	20.
	1:30 p.m.	*	*	*	2.5
	4:45 p.m.	*	*	*	2.1
13	8:10 a.m.	750	*	3.0	4.5
	1:40 p.m.	*	*	*	1.7
	4:50 p.m.	*	*	*	3.0
14	8:10 a.m.	*	*	*	4.5
	10:30 a.m.	*	*	*	4.5
16	8:10 a.m.	1,250	*	15.0	31.0
	2:30 p.m.	*	*	*	3.0
17	8:10 a.m.	1,450	*	15.0	31.0
	2:30 p.m.	*	*	*	6.1
18	8:10 a.m.	2,130	*	14.7	31.0
	2:30 p.m.	*	*	*	1.6
19	8:10 a.m.	2,300	*	20.0	31.0
	12:00 noon	*	*	*	2.5
20	8:10 a.m.	460	*	2.1	4.0

*Too low to measure. Potential below 75 volts. Blackness below one unit.

**These potentials are believed to have been caused by high-voltage tests which were in progress in the room.

the variation of the effect with size of the room and with dust content of the air. Under particularly severe conditions, a neutralizing device may be desirable. Space-charge difficulties arise from the fact that all particles leaving the precipitator carry charges of one sign (generally positive).

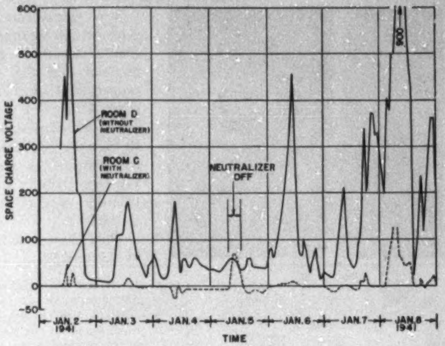

Figure 9. Comparison of space-charge voltages in rooms, with and without a neutralizer

This trouble might be eliminated by reversing the sign of one-half of the dust, or even by charging less than one-half of the dust strongly negative, so that the resultant positive and negative charges are balanced and well mixed.

The requirement of equal positive and negative charges could theoretically be met by operating one-half of the precipitator positive and one-half negative, but this increases the ozone generation (because negative ionizers generate several times as much ozone as positive ionizers) and introduces difficulties from the standpoint of mixing the air.

A method has been devised which uses a single, positive-polarity power pack which supplies both the electrostatic precipitator and a neutralizer which furnishes negative ions.[1] The neutralizer, with its ionizing wires at ground potential and its large electrodes at a high positive potential, takes only a fraction of the discharge air from the precipitator, but charges the particles strongly negative so that the total negative charge carried away approximately equals the total positive charge.

This system has been tested in the laboratory, using the defective precipitator described previously. In addition to the test room *A* this precipitator supplied air to two similar adjacent rooms, *C* and *D*. A neutralizer was installed in the air duct supplying room *C* only. An electrode, equipped with an alpha-particle emitter, was suspended centrally in each room, and connected to a recording electrostatic voltmeter. Records were taken over a period of several months, comparing the space-charge voltages in these two rooms. A plot of these voltages for several successive days is shown in Figure 9.

It was found that the voltage in the room equipped with the neutralizer (room *C*) seldom exceeded 10 per cent of that in the room without the neutralizer (room *D*). In order to demonstrate that this difference in voltage was definitely a result of neutralization, several tests were made with the neutralizer turned off. Under this condition the voltage in room *C* was substantially the same as that in room *D*.

Summary

Dust passing through an electrostatic precipitator carries a charge of one sign which produces a voltage in any room supplied with this air. This voltage tends to drive the charged dust onto walls and other exposed surfaces. The resulting discoloration varies as the first power of the room size (linear dimension), as the second power of the dust content of the air, and as a power of the inefficiency $(1-e)$, which is probably higher than the square, perhaps more nearly the cube.

Space-charge deposition of dust is particularly serious in large rooms, on columns, on hanging light fixtures, and on similar areas exposed to high voltage gradients.

Devices have been developed for neutralizing space charge, but the general experience, in ordinary locations and with moderate size rooms, has been that a unit of high efficiency, properly installed, will not give space-charge difficulties; however, proper installation and maintenance are of extreme importance. Special attention should be given to large rooms, such as auditoriums, and to especially dirty locations.

Reference

1. ELECTRICALLY NEUTRAL AIR CLEANING, G. W. Penney. United States Patent 2,318,093.

No Discussion

Heating of Radio-Frequency Cables

WILLIAM W. MACALPINE
MEMBER AIEE

THE THEORY of the heating of radio-frequency cables is developed, based upon the simplest physical and mathematical assumptions, and worked out with the physical picture in mind. The paper is essentially divided into two main parts: the electrical problem and the thermal problem. In the first part there is shown the generation of heat at any point of the conductors and in the dielectric, with its relationship to the standing waves on the cable. The second part treats the diffusion of the heat throughout the cable and its dissipation at the surface. Formulas are developed for computation of the steady-state distribution of temperature along each conductor and in the dielectric. The principal emphasis is upon the application to solid-dielectric coaxial cables. The paper concludes with an example, to illustrate more clearly the use of the theoretical results.

Symbols

Any system of units may be used with the symbols. In the example, unit length is taken to be one centimeter, and unit temperature difference, one degree centigrade. Subscripts 1 and 2 refer to the inner and outer conductors, respectively, while subscript p refers to the dielectric.

Mechanical Symbols

A_1 = cross-sectional area of inner conductor
A_2 = cross-sectional area of outer conductor
r = radius of a point in the dielectric core
r_1 = outside radius of inner conductor
r_2 = inside radius of outer conductor
r_3 = inside radius of jacket
r_s = radius of outside surface of the cable
x = distance along cable, measured toward the generator from a voltage standing-wave minimum

Electrical Symbols

C = capacitance, in farads, of unit length of cable
ϵ = dielectric constant of cable core
E = rms voltage at any location in cable
E_a = rms voltage of forward wave train
E_b = rms voltage of reflected wave train
E_{cr} = rms voltage at crest of standing wave
E_{tr} = rms voltage at trough of standing wave
E_{flat} = rms voltage when standing-wave ratio $=1.0$
e = instantaneous voltage
f = frequency in cycles per second
i = instantaneous value of current
I = rms current at any location in cable
I_p = rms current flowing radially in dielectric core
λ = electrical wave length of cable in centimeters $=3\times10^{10}/f\sqrt{\epsilon}$
P = net power delivered by cable to load
(pf) = power factor of the dielectric
$\psi=4\pi x/\lambda$
R_1 = resistance per unit length of inner conductor at frequency f
R_2 = resistance per unit length of outer conductor at frequency f
(swr) = standing-wave ratio $=E_{cr}/E_{tr}$
$\omega=2\pi f$
Z_0 = surge impedance of cable

Thermal Symbols

$\mathcal{E}$ = effective total emissivity (radiation and convection) of outer conductor acting through the jacket; in calories per second per unit area of outside surface of cable for unit temperature difference of outer conductor above ambient
$\mathcal{E}_s$ = total emissivity of outside surface of cable; in calories per second per unit area of surface for unit temperature difference of the surface above ambient
k_c = heat conductivity of conductor; in calories per second flow across unit cross-sectional area for unit temperature gradient normal to the cross-section
k_p = heat conductivity of dielectric-core material; in same units as k_c
k_s = heat conductivity of jacket material; in same units as k_c
q = rate of heat generation or flow; in calories per second
$q_1=q_1'+q_1''\cos\psi$ = rate of heat generation on inner conductor; in calories per second per unit length
$q_2=q_2'+q_2''\cos\psi$ = rate of heat generation on outer conductor; in calories per second per unit length
$q_p=q_p'-q_p''\cos\psi$ = rate of heat generation in a section of dielectric; in calories per second per unit length of section
u = temperature at any point referred to an arbitrary zero, which is usually the ambient unless otherwise indicated in the context (For subscripts see following paragraph)
u_0 = ambient temperature
U = maximum value of temperature rise when $u=U\cos\psi$ (For subscripts see following paragraph)

In order to specify the location of a temperature, or temperature rise u, and the heat source that causes the rise, the following system of subscripts and primes is used: The first subscript numeral or letter refers to the location of the temperature rise, while the second refers to the source of heat generation causing the rise. When a single prime is used, the rise is due to the part of the heat generation which is uniform over the length of cable in the vicinity of the point in question. A double prime refers to the rise due to the part of the heat generation which is a function of x or ψ. Thus,

u_{12} = rise of inner conductor due to heat generated on outer conductor
u_{21}' = rise of outer conductor due to q_1'
u_{p1}'' = rise of dielectric due to q_1''
U_{11} = maximum temperature of inner conductor due to q_1''

Electrical Problem

Although the losses in a cable cause both attenuation and the generation of heat, in most practical cases the attenuation per 1/2 wave length is so small that for present purposes it can be neglected in writing the voltage and current relations of the transmission line. The line then carries a forward wave travelling toward the load

$$e_a=\sqrt{2}E_a\sin(\omega t+2\pi x/\lambda) \tag{1a}$$

$$i_a=\sqrt{2}I_a\sin(\omega t+2\pi x/\lambda) \tag{1b}$$

and a reflected wave

Paper 49-77, recommended by the AIEE electronics committee and approved by the AIEE technical program committee for presentation at the AIEE winter general meeting, New York, N. Y., January 31–February 4, 1949. Manuscript submitted November 15, 1948; made available for printing December 29, 1948.

William W. Macalpine is with the Federal Telecommunication Laboratories, Inc., Nutley, N. J.

$$e_b = -\sqrt{2}E_b \sin(\omega t - 2\pi x/\lambda) \qquad (1c)$$

$$i_b = \sqrt{2}I_b \sin(\omega t - 2\pi x/\lambda) \qquad (1d)$$

where

$$\left.\begin{aligned} I_a &= E_a/Z_0 \\ I_b &= E_b/Z_0 \end{aligned}\right\} \qquad (1e)$$

and x is the distance along the transmission line measured from a voltage minimum to the point in question, x being positive toward the source. These voltages and currents and their resultants are shown in vector form in Figure 1.

The rms values of the forward and back voltages E_a and E_b are related to the crest and trough voltages of the standing waves along the line by

$$\left.\begin{aligned} E_{cr} &= E_a + E_b \\ E_{tr} &= E_a - E_b \\ E_a &= \frac{1}{2}(E_{cr} + E_{tr}) \\ E_b &= \frac{1}{2}(E_{cr} - E_{tr}) \end{aligned}\right\} \qquad (2)$$

In the generation of heat in the cable, the squares of the resultant rms voltage and current are important. By plane geometry, the diagrams show that

$$E^2 = E_a^2 + E_b^2 - 2E_aE_b \cos\psi \qquad (3a)$$

$$I^2 = I_a^2 + I_b^2 + 2I_aI_b \cos\psi \qquad (3b)$$

where $\psi = 4\pi x/\lambda$.

The power flowing toward the load is E_a^2/Z_0, and that flowing away from the load is E_b^2/Z_0. Then, the net power delivered to the load is

$$P = (E_a^2 - E_b^2)/Z_0 = E_{cr}E_{tr}/Z_0 \qquad (4a)$$

If the line were "flat," then $E_a = E_{flat}$ and $E_b = 0$, so

$$P = E_{flat}^2/Z_0 \qquad (4b)$$

For the same power in equations 4a and 4b there results

$$\left.\begin{aligned} E_{cr} &= E_{flat}\sqrt{(swr)} \\ E_{tr} &= E_{flat}/\sqrt{(swr)} \end{aligned}\right\} \qquad (4c)$$

where E_{cr}/E_{tr} = standing-wave ratio. Whence

$$\left.\begin{aligned} E_a &= (E_{flat}/2)\left[\sqrt{(swr)} + 1/\sqrt{(swr)}\right] \\ E_b &= (E_{flat}/2)\left[\sqrt{(swr)} - 1/\sqrt{(swr)}\right] \end{aligned}\right\} \qquad (4d)$$

and similarly for I_a and I_b.

The power loss in the cable orginates in the conductors and dielectric, these losses being proportional to I^2 and E^2, respectively. The average total power loss over 1/2 wave length is proportional to $E_a^2 + E_b^2$. Consequently, for the same power to be delivered to the load when the cable has standing waves as for a "flat" cable

$$\frac{\textit{Power loss}}{\textit{Loss for ``flat'' cable}} \approx \frac{1}{2}\left[(swr) + \frac{1}{(swr)}\right] \qquad (4e)$$

when the loss is small. The average temperature rise of each conductor, and that of the dielectric, is proportional to the power loss. Thus, the average rise of a cable with standing waves is to that of a "flat" cable as the preceding ratio of power losses. For example, compared to the attenuation and average temperature rise of a "flat" cable, these values must be multiplied by 1.25 for $(swr) = 2.0$, and by 2.125 for $(swr) = 4.0$.

Figure 2 shows the voltage and current waves E and I when $(swr) = 4.0$, and also the squares, E^2 and I^2. Note that whereas $E_{flat}^2 = 1.00$, the maximum E^2 is 4.0, and similarly for I^2. Thus, there are localized power losses of four times the uniformly distributed loss in a "flat" cable.

The rate of generation of heat on the surface of the inner conductor, in calories per second per unit length is

$$q_1 = 0.24I^2R_1 \qquad (5a)$$

and for the inside surface of the outer conductor

$$q_2 = 0.24I^2R_2 \qquad (5b)$$

For computing the heat generated in the dielectric, the cable is considered to be a capacitor with coaxial cylindrical plates of radius r_1 for the outside surface of the inner conductor, and r_2 for the inside surface of the outer conductor. In Figure 3, for a coaxial cylindrical shell or element in the dielectric, the capacitance per unit length is

$$0.0885\epsilon(2\pi r/dr)10^{-12}$$

farads. With a radio frequency current I_p flowing through the dielectric, between inner and outer conductors, the voltage across the cylindrical shell will be

$$dE = \frac{I_p}{\omega}\,\frac{10^{12}}{0.0885\epsilon}\,\frac{dr}{2\pi r}$$

Integrating between the limits r_1 and r

$$E = \frac{I_p}{\omega}\,\frac{\log_e(r_2/r_1)}{2\pi \times 0.0885\epsilon} \times 10^{12} = \frac{I_p}{\omega C}$$

where C is the capacitance in farads per unit length of the coaxial cable. The rate of heat generation in the cylindrical shell in calories per second per unit length is

$$dq_p = 0.24(pf)I_p dE = \frac{0.24(pf)\omega CE^2}{\log_e(r_2/r_1)} \cdot \frac{dr}{r} \qquad (6)$$

this being an incremental or infinitesimal quantity, because the volume of the shell is infinitesimal. If this quantity is integrated between r_1 and r_2, the total heat generated in a unit length of the dielectric is

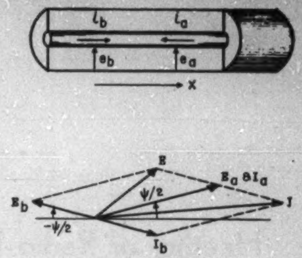

Figure 1. Voltages and currents on transmission line at time $t=0$

Each angle $\psi/2 = 2\pi x/\lambda$ where x is measured toward the generator from a voltage minimum

$$q_p = 0.24(pf)\omega CE^2 \qquad (7)$$

Thermal Problem

The general treatment of the thermal problem has been developed by J. B. J. Fourier (1768–1830),[1] and by numerous others, in works on partial differential equations as applied to such subjects as heat, sound, and electricity. The equations for heat flow are linear, since they involve only constants and the first power of the temperature u, and of its derivatives, and no products of such terms. Therefore, the principal of superposition may be applied. That is, if a source of heat is divided into two parts, or if there are several sources of heat, each source may be treated separately and the resulting temperature rises may then be added.

Heat flow is completely analogous to electric current; temperature difference, to potential difference; and thermal conductivity, to electric conductivity.

All heating of the cable causes temperature change with respect to the ambient temperature but independent of the ambient. This follows from the linear nature of the equations. Throughout the investigation which follows, it will be customary to set the ambient temperature $u_0 = 0$ in the equations and then to add that rise caused by the ambient (the latter is U_0 for some distance in the vicinity of the point in question when the ambient is constant) to the final rise.

In most practical cases, heat may be considered to flow only axially along the inner conductor. Although it flows both axially and radially in the outer conductor, usually the radial temperature gradient is negligibly small. This is because of the small radial dimensions of the conductor, compared to the thermal wave length of the cable (which is half the electrical wave length).

In the dielectric, on the other hand, the principal flow of heat is radial. The axial flow is usually much less than that in the copper, because the thermal conductivity of the dielectric is usually much lower than that of copper. The flow begins to deviate appreciably from the radial direction only when the thickness of the dielectric becomes an appreciable fraction of a thermal wave length. This is not usual in a coaxial cable, however. The axial flow in the dielectric is neglected in the present treatment. Correction terms have been developed in a previous paper,[2] where it is shown that the errors in temperature distribution, caused by neglecting the axial flow, are very small. Generally, the flow may be considered to have circular symmetry about the axis. This will not be quite true if the cable is attached to a surface, so that the dissipation at the outside jacket does not have circular uniformity, or if there is uneven heating of the surface by the sun or other source of radiation. Gas-filled lines may have the circular symmetry, as well as the axial flow, appreciably modified by convection.

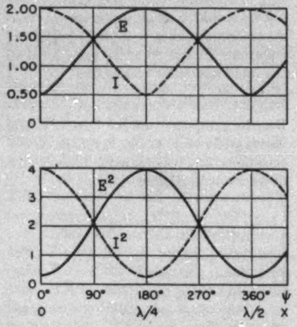

Figure 2. Standing waves, E and I, and their squares, E^2 and I^2, for a cable with standing-wave ratio = 4.0

Arbitrary units are used which would make $E_{flat}=1.00$ and $I_{flat}=1.00$ for the same power delivered to the load. Then $I_a=E_a=1.25$ and $I_b=E_b=0.75$. Average $I^2=I_a^2+I_b^2=2.125$

Some of the steps in the following development have been carried out in greater detail in the previous paper.[2]

Equations of Heat Flow

The conductor of Figure 4 may be solid, tubular, or stranded, but of equivalent thermal conductivity k_c and cross-sectional area A. At a plane normal to the axis, or x co-ordinate, heat flow per second in the direction of increasing x is

$$q=-k_cA\,du/dx \tag{8a}$$

where du/dx is the temperature gradient. At $x+\Delta x$, the temperature gradient is

$$\frac{du}{dx}+\frac{d^2u}{dx^2}\Delta x$$

The heat flow entering the element Δx through the conductor is the sum of that flowing into it across the surfaces x and $x+\Delta x$, or

$$\Delta q=k_cA\,(d^2u/dx^2)\,\Delta x \tag{8b}$$

This axial heat flow into the element, plus the heat generated therein, is equal to the radial flow out of its surface, under steady-state conditions.

In the dielectric of Figure 3, the heat flow at a point with coordinates r, θ, and x, may be resolved into three mutually-perpendicular directions. The net flow along the axial direction into an element $\Delta r\,\Delta\theta\,\Delta x$ is

$$k_pr\,\Delta\theta\,\Delta r\frac{\partial^2u_p}{\partial x^2}\,\Delta x \tag{9}$$

The net radial flow into the element, neglecting small second-order quantities is

$$k_pr\,\Delta\theta\,\Delta x\,\Delta r\left(\frac{\partial^2u_p}{\partial r^2}+\frac{1}{r}\,\frac{\partial u_p}{\partial r}\right) \tag{10}$$

In the third perpendicular direction the flow into the element is

$$k_p\,\Delta r\,\Delta x\frac{1}{r}\,\frac{\partial^2u_p}{\partial\theta^2}\,\Delta\theta \tag{11}$$

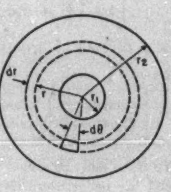

Figure 3. A section of the dielectric

Then total heat flow into the element is

$$\Delta q=k_pr\left(\frac{\partial^2u_p}{\partial r^2}+\frac{1}{r}\,\frac{\partial u_p}{\partial r}+\frac{\partial^2u_p}{\partial x^2}+\frac{1}{r^2}\,\frac{\partial^2u_p}{\partial\theta^2}\right)\times\Delta r\,\Delta x\,\Delta\theta \tag{12}$$

The quantity in parenthesis is the Laplacian, or the divergence of the gradient of u, expressed in cylindrical co-ordinates. In the case of circular symmetry, $\partial^2u_p/\partial\theta^2=0$, and $\Delta\theta=2\pi$. Also, in the event of negligible axial flow, $\partial^2u_p/\partial x^2=0$ for practical purposes, and

$$\Delta q=k_p2\pi r\left(\frac{\partial^2u_p}{\partial r^2}+\frac{1}{r}\,\frac{\partial u_p}{\partial r}\right)\Delta r\,\Delta x \tag{13}$$

This heat flow into the element, plus that generated therein by dielectric heating, is equal to zero in the steady state.

At the boundary between dielectric and inner conductor, the heat flow into the dielectric is, for circular symmetry

$$-k_p2\pi r_1\,\Delta x\frac{\partial u_p}{\partial r}\bigg]_{r_1} \tag{14}$$

and at the outer conductor

$$k_p2\pi r_2\,\Delta x\,\frac{\partial u_p}{\partial r}\bigg]_{r_2} \tag{15}$$

When no heat is generated in the dielectric, and under steady-state conditions with heat assumed to be flowing only radially through the dielectric from inner to outer conductor, the flow per unit axial length has the value, independent of r

$$q=-2\pi k_prdu_p/dr$$

Separating the variables u and r, and integrating between r_1 and any radius r, such as r_2

$$q=\frac{2\pi k_p}{\log_e\,(r/r_1)}\,(u_1-u_p)$$
$$=\frac{2\pi k_p}{\log_e\,(r_2/r_1)}\,(u_1-u_2) \tag{16}$$

It follows that the temperature in the dielectric is a function of r

$$u_p=u_1+(u_2-u_1)\,\frac{\log_e\,(r/r_1)}{\log_e\,(r_2/r_1)} \tag{17}$$

when no heat is generated therein and the flow is radial. This is the same law as that referring to the electric potential as a function of r.

This result can also be derived from equation 13.[2]

Phenomena taking place at the surface of the cable include the dissipation of the heat generated internally, and the heating of the cable by the external surroundings—radiation from the sun and so forth. If the dissipation of heat is the only matter of concern, then, per unit length

$$\Delta q=\mathcal{E}_s2\pi r_s\,\Delta x(u_2-u_0)$$

where $\mathcal{E}_s$ is the surface emissivity, a constant depending on the nature of the surface of the cable and on the medium in which it is immersed. The radius of the surface is r_s, while u_2 is the actual temperature of the outer conductor, and u_0

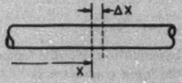

Figure 4. A portion of the conductor

the ambient temperature of the medium. If the cable has a jacket of conductivity k_s, inner radius r_3, outer radius r_s, and $\mathcal{E}_s$ is the surface emissivity of the jacket, then the dissipation per unit length is

$$\frac{2\pi k_s}{\log_e (r_s/r_3)}(u_2-u_3)=2\pi r_s\mathcal{E}_s(u_3-u_0)$$

where u_3 is the actual temperature of the outside of the jacket. This may be written

$$q=2\pi r_s\mathcal{E}(u_2-u_0) \tag{18a}$$

where 3 is now the effective total emissivity of the outer conductor to the surrounding medium, this being found by the relationship

$$\frac{1}{\mathcal{E}}=\frac{r_s}{k_s}\log_e\frac{r_s}{r_3}+\frac{1}{\mathcal{E}_s} \tag{18b}$$

which is analogous to two resistors in series.

Heat Generated on Inner Conductor

According to equations 3b and 5a, the heat generated on a section of the inner conductor of unit length is

$$\begin{aligned} q_1&=0.24R_1(I_a^2+I_b^2+2I_aI_b\cos\psi)\\ &=q_1'+q_1''\cos\psi \end{aligned} \tag{19}$$

which indicates a component uniformly distributed along the conductor, and a sinusoidally varying component. These two components may be treated separately, since the equations of heat flow are linear.

Taking the uniform part of the current-squared distribution, $I_a^2+I_b^2$, it is evident that, for a cable in a uniform medium of constant ambient temperature, or for a part of the cable at some distance from a variation in the medium, the temperature of each conductor will be independent of x, and there will be no heat flow parallel to the axis in either the dielectric or the conductors. The dielectric becomes a simple medium with heat conduction in accordance with equation 16. At the surface, by equation 18a

$$q=2\pi r_s\mathcal{E}(u_2-u_0) \tag{20}$$

per unit length.

The rate q in equation 20 is equal to q_1' in equation 19, being the rate of heat generation per unit length of the inner conductor

$$q_1'=0.24(I_a^2+I_b^2)R_1$$

Therefore, the temperature rise of the outer conductor, above ambient, is

$$u_{21}'=q_1'/2\pi r_s\mathcal{E} \tag{21a}$$

By equation 16, the temperature rise of the inner conductor is

$$u_{11}'=u_{21}'+\frac{q_1'}{2\pi k_p}\log_e\frac{r_2}{r_1} \tag{21b}$$

The variation of temperature with radius in the dielectric is given by equation 17.

The part of equation 19 which is a function of x is

$$q_1''\cos\psi=0.48R_1I_aI_b\cos\psi \tag{22}$$

which is the rate of generation of heat, per unit length. This is equivalent to a sinusoidal heating and cooling of the conductor with a wave length $\lambda/2$, since $\psi=4\pi x/\lambda$. Maximum heating occurs at the current-crest point of the standing waves on the cable, and maximum apparent cooling, relative to the heating caused by q_1', at the current trough.

In the complete cable, two simultaneous equations must be satisfied, one for each conductor. These follow from equations 8b, 16 and 18a, neglecting any axial flow in the dielectric

$$\left\{\begin{aligned} &k_cA_1\frac{d^2u_{11}''}{dx^2}+\frac{2\pi k_p}{\log_e (r_2/r_1)}(u_{21}''-u_{11}'')\\ &\qquad +q_1''\cos\psi=0 &\text{(23a)}\\ &k_cA_2\frac{d^2u_{21}''}{dx^2}+\frac{2\pi k_p}{\log_e (r_2/r_1)}(u_{11}''-u_{21}'')\\ &\qquad -2\pi r_s\mathcal{E}u_{21}''=0 &\text{(23b)} \end{aligned}\right.$$

For the solution, change the variable

$$\frac{d^2u}{dx^2}=\left(\frac{d\psi}{dx}\right)^2\frac{d^2u}{d\psi^2}=\left(\frac{4\pi}{\lambda}\right)^2\frac{d^2u}{d\psi^2} \tag{24}$$

Then

$$u_{21}''=U_{21}\cos\psi=\frac{q_1''\cos\psi}{2\pi r_s\mathcal{E}+\left(\frac{4\pi}{\lambda}\right)^2k_c(A_1+A_2)+\frac{k_cA_1}{2\pi k_p}\left(\frac{4\pi}{\lambda}\right)^2\times\left[k_cA_2\left(\frac{4\pi}{\lambda}\right)^2+2\pi r_s\mathcal{E}\right]\log_e\frac{r_2}{r_1}} \tag{25a}$$

$$u_{11}''=U_{11}\cos\psi \tag{25b}$$

$$U_{11}=U_{21}\left[1+\frac{k_cA_2\left(\frac{4\pi}{\lambda}\right)^2+2\pi r_s\mathcal{E}}{2\pi k_p}\log_e\frac{r_2}{r}\right] \tag{26}$$

To these must be added the ambient, u_0, and the temperature rises, u_{11}' and u_{21}', resulting from the constant component, q_1^1, of the generated heat. The temperature at any point in the dielectric is found by means of equation 17.

Consideration of equations 25a and 26 shows that when the wave length λ is very short, the temperature components U_{11} and U_{21} become negligibly small, as would be expected. When the wave length is very long, on the other hand, the equations reduce to forms similar to equations 21a and 21b. Then the maximum temperature rise, due to heat generated on the inner conductor, is the rise for a "flat" cable multiplied by the standing-wave ratio, and occurs at the voltage standing-wave minimum.

Similar results may be derived from the following equations for the temperature rise due to heat generated on the outer conductor and to heat generated in the dielectric. In the latter case, the maximum temperature rise occurs at the voltage standing-wave maximum.

Heat Generated on Outer Conductor

For heat generated on the outer conductor, the steady-state temperature rise above ambient resulting from the constant component $q_2'=0.24(I_a^2+I_b^2)R_2$ of equations 3b and 5b is the same for both the inner and outer conductors

$$u_{12}'=u_{22}'=q_2'/2\pi r_s\mathcal{E} \tag{27}$$

For the component of the heat that is a function of x or ψ, $q_2''=0.48\,I_aI_b\cos\psi$, the equations are, where axial flow in the dielectric is negligible

$$\left\{\begin{aligned} &k_cA_1\frac{d^2u_{12}''}{dx^2}+\frac{2\pi k_p}{\log_e (r_2/r_1)}(u_{22}''-u_{12}'')=0 &\text{(28a)}\\ &k_cA_2\frac{d^2u_{22}''}{dx^2}+\frac{2\pi k_p}{\log_e (r_2/r_1)}(u_{12}''-u_{22}'')\\ &\qquad -2\pi r_s\mathcal{E}u_{22}''+q_2''\cos\psi=0 &\text{(28b)} \end{aligned}\right.$$

Solving

$$u_{22}''=U_{22}\cos\psi \tag{29a}$$

$$u_{12}''=U_{12}\cos\psi \tag{29b}$$

$$U_{22}=\frac{q_2''}{2\pi r_s\mathcal{E}+k_cA_2\left(\frac{4\pi}{\lambda}\right)^2+1\Big/\left[\frac{\log_e (r_2/r_1)}{2\pi k_p}+\frac{1}{k_cA_1}\left(\frac{\lambda}{4\pi}\right)^2\right]} \tag{30}$$

$$\begin{aligned} U_{12}&=U_{22}\frac{2\pi k_p}{\log_e (r_2/r_1)}\,\frac{1}{k_cA_1\left(\frac{4\pi}{\lambda}\right)^2+\frac{2\pi k_p}{\log_e (r_2/r_1)}}\\ &=\frac{U_{22}}{1+\frac{k_cA_1}{2\pi k_p}\left(\frac{4\pi}{\lambda}\right)^2\log_e\frac{r_2}{r_1}} \end{aligned} \tag{31}$$

Heat Generated in Dielectric

When the heat conductivity of the dielectric is small compared to that of the conductor material, and for usual cross sections of cable, the axial heat flow in the dielectric can be neglected to a first approximation, as was done in the cases treated in preceding paragraphs. Then by equations 3a, 6, 7, and 13, the differential equation for the temperature distribution in the dielectric is

$$r^2\frac{d^2u_p}{dr^2}+r\frac{du_p}{dr}+\frac{q_p}{2\pi k_p\log_e (r_2/r_1)}=0 \tag{32a}$$

where

$$q_p=0.24(pf)\omega C(E_a^2+E_b^2 -2E_aE_b\cos\psi)=q_p'-q_p''\cos\psi \quad (32b)$$

A solution of equation 32a is

$$u_p=a+b\log_e\frac{r}{r_1}-\frac{q_p\left(\log_e\dfrac{r}{r_1}\right)^2}{4\pi k_p\log_e\dfrac{r_2}{r_1}} \quad (33a)$$

The boundary conditions are $u_p=u_1$ at $r=r_1$ and $u_p=u_2$ at $r=r_2$, whence

$$u_p=u_1+\left(\frac{u_2-u_1}{\log_e(r_2/r_1)}+\frac{q_p}{4\pi k_p}\right)\log_e\frac{r}{r_1} -\frac{q_p}{4\pi k_p\log_e(r_2/r_1)}\left(\log_e\frac{r}{r_1}\right)^2 \quad (33b)$$

It is to be noted that equation 33b is general; it includes the temperature distribution resulting from heat generated externally to the dielectric, as well as that generated internally. It reduces to equation 17 when $q_p=0$; and to equation 38 when $q_p''=0$, provided that only the heat generated in the dielectric is considered. This result may be derived also by simple integration.[2]

For the distribution of temperature along the conductors resulting from heat generated in the dielectric, it is noted that, in the steady state, the net heat flow into an element Δx of the conductor is zero. For the inner conductor, by equations 8b and 14; and for the outer conductor by equations 8b, 15 and 18a, letting $u_0=0$

$$k_cA_1\frac{\partial^2u_{1p}}{\partial x^2}+2\pi r_1k_p\frac{\partial u_p}{\partial r}\bigg]_{r_1}=0 \quad (34a)$$

$$k_cA_2\frac{\partial^2u_{2p}}{\partial x^2}-2\pi r_2k_p\frac{\partial u_p}{\partial r}\bigg]_{r_2}-2\pi r_s\mathcal{E}u_{2p}=0 \quad (34b)$$

Differentiating equation 33a or 33b

$$\frac{\partial u_p}{\partial r}=\frac{b}{r}-\frac{q_p}{2\pi rk_p\log_e(r_2/r_1)}\log_e\frac{r}{r_1} \quad (35)$$

which, substituted in equations 34a and 34b, gives

$$k_cA_1\frac{\partial^2u_{1p}}{\partial x^2}+2\pi k_p\frac{u_{2p}-u_{1p}}{\log_e(r_2/r_1)}+\frac{q_p}{2}=0 \quad (36a)$$

$$k_cA_2\frac{\partial^2u_{2p}}{\partial x^2}+2\pi k_p\frac{u_{1p}-u_{2p}}{\log_e(r_2/r_1)}+\frac{q_p}{2}- 2\pi r_s\mathcal{E}u_{2p}=0 \quad (36b)$$

Note that the heat entering the dielectric, the negative of the second plus third terms of equation 36a, plus the heat, q_p, generated therein, is equal to that leaving the dielectric, which is the second plus third terms of equation 36b.

Taking first the constant part q_p' of equation 32b, a reasonable supposition is that u_{1p} and u_{2p} are independent of x, as was the case for the constant part of the heat generated on the conductors. It follows that $\partial u_{1p}/\partial x=0$ and $\partial u_{2p}/\partial x=0$. From equation 34a, or from the fact that conditions are in equilibrium (no heat flow into or out of the inner conductor), it follows that

$$\frac{\partial u_p}{\partial r}\bigg]_{r_1}=0$$

Whence, from equation 36a

$$u_{1p}'=u_{2p}'+\frac{q_p'}{4\pi k_p}\log_e\frac{r_2}{r_1} \quad (37a)$$

and from equations 36a and 36b, or from elementary considerations

$$u_{2p}'=q_p'/2\pi r_s\mathcal{E} \quad (37b)$$

When equation 37a is substituted in equation 33b, it is found that the temperature distribution caused by q_p' acting alone is

$$u_{pp}'=u_{1p}'-\frac{q_p'}{4\pi k_p\log_e(r_2/r_1)}\left(\log_e\frac{r}{r_1}\right)^2 \quad (38)$$

The variable part of q_p, which is $-q_p''\cos\psi$ when substituted in equations 36a and 36b gives equations of a type similar to equations 23a and 23b. The solution is

$$u_{2p}''=U_{2p}\cos\psi \quad (39a)$$

$$u_{1p}''=U_{1p}\cos\psi \quad (39b)$$

The coefficients U_{1p} and U_{2p} are determined by subsituting equations 39a and 39b into equations 36a and 36b

$$-\left[k_cA_1\left(\frac{4\pi}{\lambda}\right)^2+\frac{2\pi k_p}{\log_e(r_2/r_1)}\right]U_{1p} +\frac{2\pi k_p}{\log_e(r_2/r_1)}U_{2p}=\frac{q_p''}{2} \quad (40a)$$

$$\frac{2\pi k_p}{\log_e(r_2/r_1)}U_{1p}-\left[k_cA_2\left(\frac{4\pi}{\lambda}\right)^2 +\frac{2\pi k_p}{\log_e(r_2/r_1)}+2\pi r_s\mathcal{E}\right]U_{2p}=\frac{q_p''}{2} \quad (40b)$$

The simplest means of solving equations 40a and 40b is to substitute the numerical values in the coefficients from the dimensions and constants of the cable. Then solve the resulting linear simultaneous equations for U_{1p} and U_{2p}.

The temperature distribution in the dielectric is given by equation 33b.

Example

As an example of the practical application of the equations developed in this paper, consider a type *RG-19/U* cable delivering 5 kw continuously to a load, the frequency being 100 megacycles per second. Two cases will be considered: *A*—where the cable is "flat," or standing-wave ratio = 1; *B*—where the standing-wave ratio is 2.0.

This cable is made up as follows:

Inner conductor: solid plain copper, 0.250-inch diameter
Cable core: solid polyethylene, 0.910-inch outside diameter
Outer conductor: single-layer braid, 48×9, 30-gauge (Brown and Sharpe) plain copper wires. Maximum (allowable but not necessarily actual) diameter is 0.990 inch
Jacket: synthetic resin, outside diameter 1.120 inches

The specified nominal characteristics are:

Surge impedance = 52 ohms
Capacitance = 29.5 micromicrofarads per foot
Attenuation = 0.68 decibel per 100 feet at 100 megacycles

Then, the various constants of the cable are:

$r_1=0.318$ centimeter
$r_2=1.16$ centimeters
$r_3=1.21$ centimeters (estimated average value)
$r_s=1.42$ centimeters
$A_1=0.317$ square centimeter
$A_2=0.220$ square centimeter
$k_c=1.0$ calorie per second per square centimeter for one degree centigrade per centimeter
$k_p=8\times10^{-4}$ calorie per second per square centimeter for one degree centigrade per centimeter
$k_s=4\times10^{-4}$ calorie per second per square centimeter for one degree centigrade per centimeter (estimated)
$\mathcal{E}_s=3\times10^{-4}$ calorie per second per square centimeter for one degree centigrade temperature difference (estimated: depends upon conditions of installation)

$\epsilon=2.3$ (dielectric constant of core)
$(pf)=4\times10^{-4}$
$C=0.97\times10^{-12}$ farad per centimeter
$Z_0=52$ ohms

From these constants other derived parameters are found:

$\mathcal{E}=2.6\times10^{-4}$ calorie per second per square centimeter for one degree centigrade temperature difference; by equation 18b
$R_1=1.48\times10^{-3}$ ohm per centimeter
$R_2=0.525\times10^{-3}$ ohm per centimeter

The values of R_1 and R_2 are taken to be slightly higher than the ideal theoretical values for 100 megacycles, but, together with the power-factor value listed, when used to calculate the attenuation of the cable, result in the specified value of 0.68 decibel per 100 feet.[1]

For the given frequency, power, and standing-wave ratio, the following quantities are found:

$\lambda=198$ centimeters

A. For the "flat" line, standing-wave ratio = 1:

$E_{flat}=510$ rms volts (4b)
$I_{flat}=9.80$ rms amperes (1e)

$q_1 = 34.1 \times 10^{-3}$ calorie per second per centimeter (5a)

$q_2 = 12.1 \times 10^{-3}$ calorie per second per centimeter (5b)

$q_p = 15.2 \times 10^{-3}$ calorie per second per centimeter (7)

B. For the line with standing-wave ratio = 2.0:

$E_a = 540$ rms volts (4d)

$E_b = 180$ rms volts (4d)

$I_a = 10.4$ rms amperes (1e)

$I_b = 3.46$ rms amperes (1e)

$q_1' = 42.5 \times 10^{-3}$ calorie per second per centimeter (19)

$q_1'' = 25.6 \times 10^{-3}$ calorie per second per centimeter (19)

$q_2' = 15.1 \times 10^{-3}$ calorie per second per centimeter

$q_2'' = 9.1 \times 10^{-3}$ calorie per second per centimeter

$q_p' = 19.0 \times 10^{-3}$ calorie per second per centimeter (32b)

$q_p'' = 11.4 \times 10^{-3}$ calorie per second per centimeter (32b)

Note that

$$q_1'/q_1 = q_2'/q_2 = q_p'/q_p = 1.25 \qquad (4e)$$

For the "flat" cable carrying 5 kw at 100 megacycles, the total heat generated is $q_1 + q_2 + q_p = 61.4 \times 10^{-3}$ calorie per second per centimeter, as tabulated in the preceding paragraph. The specified attenuation of the cable at 100 megacycles is 0.68 decibel per 100 feet, which is equal to 0.223×10^{-3} decibel per centimeter. This attenuation, acting on 5 kw, results in a loss of 0.258 watt per centimeter, or 61.7×10^{-3} calorie per second per centimeter, which checks closely the total heat generated.

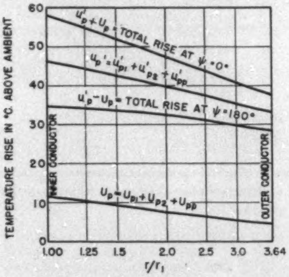

Figure 5. Temperature rise of the dielectric

Computed for a type *RG-19/U* cable carrying 5 kw continuously at 100 megacycles per second, with standing-wave ratio = 2.0. At inner conductor, $u_p' = u_1'$, while at outer conductor, $u_p' = u_2'$. Similarly for U_p and all other quantities with subscript *p*

For use in applying the formulas, certain quantities which occur several times are here evaluated

$\log_e (r_2/r_1) = 1.29$

$2\pi r_s \mathcal{E} = 2.32 \times 10^{-3}$

$2\pi k_p / \log_e (r_2/r_1) = 3.90 \times 10^{-3}$

$4\pi k_p = 10.1 \times 10^{-3}$

$4\pi k_p \log_e (r_2/r_1) = 13.0 \times 10^{-3}$

$(4\pi/\lambda)^2 = 4.05 \times 10^{-3}$

$k_c(A_1 + A_2)(4\pi/\lambda)^2 = 2.18 \times 10^{-3}$

$k_c A_2 (4\pi/\lambda)^2 = 0.89 \times 10^{-3}$

$k_c A_1 (4\pi/\lambda)^2 = 1.28 \times 10^{-3}$

$(k_c A_1 / 2\pi k_p)(4\pi/\lambda)^2 = 0.258$

The principal temperature rises are given in Table I and Figure 5. The data and curves are the result solely of computation from the specified dimensions and construction of the cable, and the published physical characteristics of its component parts. No experimental tests have been made in this connection to confirm the data. Some of the tabulated temperature rises for the 5 kw power value probably exceed the safe limit for this cable.

The column headed "If k_c were 0" gives hypothetical values which, when compared to the "Actual" column, show the effect of axial flow in the conductors in reducing temperature variation along the cable.

References

1. ANALYTICAL THEORY OF HEAT (book), J. B. J. Fourier, 1822. English translation by A. Freeman, Cambridge University Press (Cambridge, England), 1872. Reprinted by Stechert-Hafner, Inc. (New York, N. Y.), 1945.

2. HEATING OF RADIO-FREQUENCY CABLES, W. W. Macalpine. *Electrical Communication* (New York, N. Y.), volume 25, March, 1948, pages 84–99.

3. REFERENCE DATA FOR RADIO ENGINEERS (book), Federal Telephone and Radio Corporation, New York, N. Y., Second edition, 1946, page 206.

Table I. Type *RG-19/U* Cable Carrying 5 Kilowatts at 100 Megacycles

			Standing-Wave Ratio = 2			
			Part	Part Function of *x*		
Heat Source	Effect	Flat Line (*swr*) = 1	Independent of *x*	Actual	If k_c Were 0	From Equation
Inner conductor	q_1'	34.1×10^{-3}	42.5×10^{-3}			(19)
	u_{21}'	14.7°	18.3°			(21a)
	u_{11}'	23.4°	29.2°			(21b)
	u_{p1}'		*			(17)
	q_1''			25.6×10^{-3}		(19)
	U_{21}			4.6°	11.0°	(25a)
	U_{11}			13.0°	28.5°	(25b)
	U_{p1}			*		
Outer conductor	q_2'	12.1×10^{-3}	15.1×10^{-3}			
	u_{22}'	5.2°	6.5°			(27)
	u_{12}'	5.2°	6.5°			(27)
	u_{p2}'	5.2°	6.5°			(17)
	q_2''			9.1×10^{-3}		
	U_{22}			2.2°	3.9°	(30)
	U_{12}			1.6°	3.9°	(31)
	U_{p2}			*		(17)
Dielectric	q_p'	15.2×10^{-3}	19.0×10^{-3}			(32b)
	u_{2p}'	6.6°	8.2°			(37b)
	u_{1p}'	8.5°	10.6°			(37a)
	u_{pp}'		*			(38)
	q_p''			11.4×10^{-3}		(32b)
	U_{2p}			−2.4°*	−4.9°	(40a)
	U_{1p}			−2.9°	−6.4°	(40b)
	U_{pp}			*		(33b)
Inner and outer conductors and dielectric, combined	$q_1' + q_2' + q_p'$	61.4×10^{-3}	76.6×10^{-3}			By addition
	u_3'	22.8°	28.6°			≈ (18a)
	u_2'	26.4°	33.0°			(18a)
	u_1'	37.1°	46.3°			By addition
	u_p'		(Figure 5)			By addition
	$q_1'' + q_2'' + q_p''$			46.1×10^{-3}		By addition
	U_2			4.4°		By addition
	U_1			11.7°		By addition
	U_p			(Figure 5)		By addition

*Calculated for Figure 5, but individual components are not recorded here.

No Discussion

The Power Rating of Radio-Frequency Cables

R. C. MILDNER
ASSOCIATE AIEE

THIS paper deals with the limitations to the radio-frequency power which can be transmitted by cable. In the first place the normal electrical losses of the transmission line create heat within the cable. Secondly, excessive electrical stress may have two deleterious effects on the performance of the cable. The increased losses due to discharges may cause local overheating, or the discharges may cause a local deterioration of the insulation, leading to electrical breakdown.

The principles used in calculating the temperature rise are set down. The standard thermal rating of the cable is defined as the power that can be transmitted by the cable into a matched load with a given temperature rise for the steady-state condition. Suitable rating factors to deal with different maximum permissible temperatures and different ambient temperatures are proposed. The influence on the thermal and voltage rating of various operating conditions, such as modulation, standing waves, and load factor is briefly considered.

The principles outlined are applied to obtain the technical ratings of three, interesting ranges of cables and reference is made to the influence of various factors in the design.

The last decade has seen an amazing expansion in the use of high-frequency generators of high and medium powers. Among the applications of such transmitters may be included sound and vision broadcasting, communications systems, radar and navigational aids, medical appliances, and industrial heaters, using induction or dielectric heating effects. In most cases some form of transmission line is required to carry the radio-frequency power from the generator to the antenna, work coil, or operating electrode.

For all except the very highest frequencies, this transmission is by wire. For the highest powers, open-wire feeders have been used because their construction permits relatively wide spacing. This advantage is lost as frequencies of about 100 megacycles per second are approached, and the use of coaxial feeders has other attractive features. For mobile transmitters, flexible cables are almost indispensable and for fixed stations of medium power, cables or built-up coaxial feeders are commonly used.

On economic grounds the size of the cable would be determined by equating the rate of change of the annual charges associated with the cost of the cable to the rate of change of the annual cost of the energy lost in maintaining the required power at the antenna. Sometimes, however, the size of the cable to be used will be determined by technical considerations, namely, its ability to transmit the required power without damage to the cable structure. The power lost in the feeder will raise its temperature and may cause excessive deterioration by chemical or mechanical action due to thermal expansion or softening. The voltages associated with the input power will impose dielectric stresses on the cable insulation, and these may be sufficiently high to cause partial or complete electrical breakdown, with resultant over-heating or deterioration of the insulation. Either of these two processes may be effective according to operating conditions or cable design.

It is therefore important to establish for each cable type the maximum power it can carry safely without either of these effects intervening. These ratings will serve as a guide to the appropriate type to be used in any application.

Sometimes the equipment designer may require a practical test to establish that the feeder is able to carry the required power with a reasonable margin of safety. The results of such practical tests must be analysed to determine in what way the cable performance would be modified by the minor variations in quality which would be permitted by the acceptance specification. A study of the principles on which these ratings are based will indicate the manner in which such an analysis might be made.

Thermal Rating of Cables

In an earlier paper[1] the author considered the thermal rating of radio-frequency cables, more particularly from the standpoint of their use in equipment for the armed services. Specific ratings were proposed for a number of standard Uniradio and Duradio cables commonly used in England. The present section is therefore a development of the principles stated there, adapted to a wider field of application.

A theoretical basis of calculation, supplemented, where necessary by empirical constants, has been used throughout the paper, because it is necessary to state the precise location in the cable of the various sources of heat. The electrical losses, which are the source of heat, are calculated from the components of attenuation due to the inner conductor, the insulation, and the outer conductor. The thermal resistances of the component parts of a cable system are calculated from the dimensions and from the constants of the materials employed.

The methods used to calculate the temperature rise corresponding to a given heat loss are based partially on principles widely used in England to calculate the current rating of power-frequency cables,[2] since the methods used in the United States are not dissimilar and lead to com-

---

Paper 49-78, recommended by the AIEE electronics committee and approved by the AIEE technical program committee for presentation at the AIEE winter general meeting, New York, N. Y., January 31–February 4, 1949. Manuscript submitted November 22, 1948; made available for printing December 22, 1948.

R. C. Mildner is with the Telegraph Construction and Maintenance Company Ltd., Greenwich, London, England.

Table I. Field Factors for Stranded Conductors

Number of Strands n	m	Factors k_1	k_2
1	1	1.0	1.0
7	6	0.939	1.408
19	12	0.970	1.397
37	18	0.980	1.395
61	24	0.985	1.394
91	30	0.988	1.394

parable ratings, they may be found acceptable in the present instance. The permissible maximum temperature of operation determines the allowable heat dissipation in terms of the ambient temperature and this dissipation is converted readily into terms of input power.

Practical tests on a limited number of radio-frequency cables[3] have given overall temperature rises substantially in agreement with those predicted by the present treatment. It may therefore be accepted that the theoretical values constitute a reasonable basis for establishing power ratings.

In the equations for attenuation given later and in the theoretical treatment, the attenuation coefficient (α) is expressed in nepers per centimeter, whereas the tabulated values of cable characteristics are given in decibels per 100 feet; the attenuation in decibels per 100 feet is given by $2.65\times10^4\times\alpha$. The thermal coefficients are expressed in centimeter-gram-second and centigrade units. Practical units are used throughout the paper.

THE ATTENUATION COEFFICIENT OF CABLES

The theoretical attenuation of ideal coaxial and balanced lines formed by cylindrical conductors has been covered adequately in published literature. Practical cable constructions often deviate from this ideal form and the formulas given herein follow the classical lines, but include certain empirical factors to cover the effect of such divergences as stranding, braiding, and the use of bimetallic conductors. Considerable data on the attenuation of actual cables over a wide range of frequency have been amassed over the last few years, and the factors proposed here are based on part of that experience. In the normal run of production cables will exhibit a spread of results about the "standard" attenuation determined in this way. For the purpose of assessing the power rating of a given design of cable, a figure 10 per cent higher than the standard attenuation is proposed. This allowance is intended to cover minor variations of construction and of the quality of materials. Where a cable has to satisfy a specification calling for a maximum value of attenuation at the operating frequency, this maximum value should of course be used to estimate the power rating. For general purpose cables, the specified value is not likely to be greatly different from the value given here.

Table II. Calculated Values of Resistance Factor for Tinned Copper Surface

Thickness of Tin: 0.2 mil

Frequency, Megacycles per Second	K_ρ
1	1
5	1
20	1.03
100	1.16
200	1.26
600	1.96
1,500	2.65
3,000	2.92

Following classical theory, the attenuation of a transmission line at high frequencies is given by

$$\alpha=\frac{R}{2}\sqrt{\frac{C}{L}}+\frac{G}{2}\sqrt{\frac{L}{C}}\text{ nepers per centimeter} \quad (1)$$

where R, G, L, and C are the primary coefficients of the line. In this formula the first term is the conductor loss and the second the dielectric loss. For the case of the coaxial line, R is the sum of the resistances of the inner conductor, R_1, and of the outer conductor, R_2. Exact solutions for R_1 and R_2 have been obtained in terms of Bessel functions. Tabulated value of the appropriate function in terms of the parameter $\pi d\sqrt{2\mu f/\rho}$ have been published.[4] For values of this parameter which are greater than 70, the surface resistance of a conductor is given by

$2\pi\sqrt{\rho\mu f}$ ohms

to an accuracy better than 1 per cent. Since this condition obtains, for most practical cables, at frequencies not much greater than a megacycle, this latter value has been adopted in the following equation. In similar fashion, the inductance due to flux in the space between the "go" and "return" conductors is enhanced at low frequencies by the internal inductance of the conductors. This correction also may be neglected at very high frequencies as defined before. With small high-attenuation cables, the characteristic im-

List of Symbols

α_c = attenuation due to conductors, nepers per centimeter
α_{c1} = attenuation due to inner conductor, nepers per centimeter
α_{c2} = attenuation due to outer conductor, nepers per centimeter
α_d = attenuation due to dielectric, nepers per centimeter
α = total attenuation of cable, nepers per centimeter
d = outer diameter of inner conductor, centimeter
D = inner diameter of outer conductor, centimeter
D_s = diameter of outer surface of cable, centimeter
$f=\omega/2\pi$ = frequency, cycles per second
G_a = thermal resistivity of air, degrees centigrade, centimeters per watt
G_c = thermal resistivity of servings, degrees centigrade, centimeters per watt
G_d = thermal resistivity of dielectric, degrees centigrade, centimeters per watt.
G_g = thermal resistivity of ground, degrees centigrade, centimeters per watt
h = semispacing of conductors of balanced cable, centimeters
H_θ = dissipation, in watts per centimeter, corresponding to a temperature rise of θ degrees centigrade at the inner conductor
θ_i = temperature rise of inner conductor, degrees centigrade above ambient
θ_r = temperature rise of outer conductor, degrees centigrade above ambient
θ_s = temperature rise of surface of cable, degrees centigrade above ambient
k = thermal dissipation constant for surface in air
κ = permittivity of dielectric
K_b = ratio of resistance of outer conductor to that of equivalent cylindrical conductor (braiding factor)
K_ρ = proximity factor
K_ρ = ratio of resistance of outer conductor to that of a similar conductor constructed in the same material as inner conductor
K_s = ratio of resistance of stranded conductor to that of equivalent cylindrical conductor (stranding factor)
l = depth of cable axis below ground surface, centimeters
ρ = resistivity of conducting material, ohm-centimeters
ρ_1 = resistivity of inner conductor material, ohm-centimeters
μ = permeability of conducting material, henrys per centimeter
S_a = thermal resistance external to unit length of cable in air, degrees centigrade, centimeters per watt
S_c = thermal resistance of servings for unit length of cable, degrees centigrade, centimeters per watt
S_d = thermal resistance of insulant for unit length of cable, degrees centigrade, centimeters per watt
S_g = thermal resistance external to unit length of cable in ground, degrees centigrade, centimeters per watt
$\tan\delta$ = loss tangent of dielectric
P_0 = mean input power, watts
Z_0 = characteristic impedance of cable, ohms
E = voltage on cable, volts
I = current along cable, amperes

pedance may be complex, and higher than the value at very high frequencies, at frequencies of the order of one megacycle per second. In such cases the formulas given below will be subject to some error.

The constants given in the succeeding sections for the attenuation coefficients relate to atmospheric temperature (20 degrees centigrade). In calculating the thermal rating of cables, an enhanced value of this coefficient must be used to allow for the rise in temperature of the cable.

Since the conductor losses are proportional to the square root of the resistivity, the temperature coefficient of attenuation due to the conductors will be of the order 0.002 per degrees centigrade for most of the materials used in the construction of radio-frequency cables. Since the contribution of loss by the outer conductor is usually considerably smaller than that due to the inner conductor and since the ratings are based on relatively high values of ambient temperature, it has been considered sufficiently accurate to assume that the proportionate increase of loss is the same for the outer conductor as for the inner.

The temperature coefficient of attenuation due to the dielectric depends essentially upon the temperature coefficient of the power factor, which may be positive or negative, as explained in the section on Power Factor of Insulant. Since the attenuation due to the dielectric is based on a maximum value of power factor which is assumed to apply to all frequencies and temperatures, the corresponding temperature coefficient has been assumed to be zero for the purpose of these calculations.

ATTENUATION OF COAXIAL CABLES

At very high frequencies, as defined before, the attenuation is given approximately by the expression

$$\alpha = \frac{2.287\times10^{-7}\sqrt{\kappa\rho_1 f}}{\log_{10} D/k_1 d}\left\{\frac{K_s}{d}+\frac{K_b K_\rho}{D}\right\}+ 1.047\times10^{-10}\sqrt{K}f\tan\delta \quad \text{nepers per centimeter} \qquad (2)$$

The first term represents the attenuation due to the conductors, the two components of this term relating to the inner and outer conductor respectively: the second term gives the attenuation due to the dielectric. The factor k_1 allows for the effect of stranding on the capacitance and inductance of the cable. The factor K_s allows for the effect of the form of the inner conductor on its resistance, K_b allows for the effect of the form of the outer conductor on the resistance and K_ρ allows for the effect of the material of the outer conductor where it differs from that of the inner conductor. For the most general case, a factor K_p might have been included in the term giving the attenuation due to the inner conductor to account, for instance, for tinned conductors. This has been omitted in the interest of clarity.

Form of Inner Conductor. The factor, k_1, has been determined by A. L. Meyers[5] in a solution obtained by an extension of the theoretical results of T. Levi-Civita.[6] He gives values of k_1 for different values of m the number of closely-adhering strands in the outer layer of the stranded conductor having a total number of strands, n. These values are recorded in Table I.

The factor K_s is not amenable to calculation since it depends, to some extent, on the contact resistance of the inner conductor, and therefore varies with the material used and its cleanliness, and probably varies somewhat with frequency. Based on practical observations, a value of 1.30 is suggested as appropriate for the case of a reasonably clean 7-strand conductor in a solid-dielectric cable at all frequencies.

A similar factor may be taken for well-formed conductors having a greater number of strands, but the practical observations to support this are not extensive. In exceptional cases, the inner conductor may take the form of indented or corrugated longitudinal tapes or of helically-lapped tapes. The treatment proposed in such cases is outlined in the following section.

Form of the Outer Conductor. The factor, K_b, is intended to take care of deviations in the form of the outer conductor from the ideal cylindrical form. These deviations usually take one or other of the following forms:

1. Indented or corrugated longitudinal tapes.
2. Helically-lapped wires or tapes.
3. Braided wires, tapes, or bunched strands.

The factor corresponding to the first case can be estimated with sufficient accuracy by increasing the resistance of the equivalent ideal cylinder in proportion to the increase in length of the return path and the reduction in its effective periphery. The second case now is used rarely at high frequencies owing to the high attenuation and instability induced by poor contact resistance between neighboring elements except where a binding tape can be used to short circuit the neighboring ropes. Another exception is the overlapped tape applied with short lay, which tends to be unstable at low frequencies, but approaches the characteristics of a cylindrical conductor when frequencies are higher than about 10 megacycles per second. The case of braided conductors is of most practical importance.

The conditions of current flow in braids are far too complicated to be solved theoretically, although an elementary treatment has confirmed the effect of most variables of designs. Practical tests have shown that the use of short lays for the wire-braiding increases the radio-frequency resistance of the outer conductor, and that there is an optimum value for the filling factor of the braid, although this is not very critical provided that the braid is neither overfilled nor seriously under-filled. It also has been shown experimentally that the resistance factor increases as the core diameter increases. The following values of resistance factor based on practical observations are suggested as applying to present-day production.

Core Sizes Inches Diameter	K_b
0.25	2.0
0.50	2.5
0.75	3.0
1.00	4.0
1.50	5.0

These factors may be applied at all frequencies up to 3,000 megacycles per second. At higher frequencies up to about 10,000 megacycles per second contact resistance between wires appears to be responsible for the instability and the higher values of resistance which have been observed, and it may be found necessary to use silver-coated wires to achieve the resistance factors quoted before.

Material of Outer Conductor. In equation 2, the resistance factor relating to the material of the outer conductor is referred to that of the inner. For the case

Table III

Material	Symbol	Thermal Resistivity (Degrees Centigrade Cm/Watt)
Ground	G_g	120
Polyethylene	G_d	450
Servings (bituminized hessians or cottons)	G_s	500
Polyvinyl resin sheathings	G_s	1,200
Still air	G_a	4,100

of the homogeneous conductor at very high frequencies it is obvious that $K\rho$ is equal to the square root of the ratio of the resistivities of the outer and inner conductors.

For the case of bimetallic conductors, the resistance varies with frequency in a manner different from that of homogeneous conductors because an increasing proportion of the current flows in the outer layer as the frequency is raised. A theoretical solution for the resistance at very high frequencies by H. R. F. Carsten has been used.[1]

An important case of bimetallic conductors is involved in the use of tinned copper. A tin thickness of 0.2 mil has been assumed and the calculated values of $K\rho$ for various frequencies are given in Table II.

The application of this factor to tinned copper wire, as used in braids, is admittedly questionable, but it has been found to give a reasonable approximation to measured values.

The following values apply to materials which are of interest in radio-frequency cable construction:

Material	Resistivity in Ohm-centimeter	K_ρ
Copper	1.724×10^{-6}	1
Aluminum	2.825×10^{-6}	1.28
Lead	21.1×10^{-6}	3.5
Lead-tin alloy used in tinning	13.5×10^{-6}	(See Table II)

Permittivity of Insulant. The material of primary interest in flexible cables is polyethylene and this has a permittivity of 2.30 at all useful frequencies. However, in view of the fact that minute air films at the inner conductor have a marked effect on the effective permittivity of the cable insulation, a figure of 2.25 has been assumed for the practical case.

For the case of air-spaced and semi-air-spaced cable, the effective permittivity will vary with the construction and the following values are average practical values:

Semirigid air-spaced cables—1.1
Expanded polyethylene cables—1.2–1.3
Semi-air-spaced flexible cables—1.4–1.75

Power Factor of Insulant. The power factor of polyethylene is usually very low and rises slowly with increasing frequency. The presence of minute quantities of oxidation products may superimpose an absorption band spreading over a wide frequency range and having its peak at about 100–200 megacycles per second. As a consequence the temperature coefficient may be negative at low frequencies and positive at high frequencies.

For theoretical studies, a figure of 4×10^{-4} has been assumed for all frequencies and temperatures. This value is not usually exceeded in present-day production, except perhaps for a combination of extremely high frequency and temperature.

Attenuation of Balanced Cables

At very high frequencies the attenuation is given approximately by the expression

$$\alpha=\frac{2.287\times10^{-7}\sqrt{\kappa\rho_1 f}}{\log_{10}\left(2\nu\,\dfrac{1-\sigma^2}{1+\sigma^2}\right)}\left\{\frac{K_sK_p}{d}+\frac{4\sigma^2K_\rho}{D}\right\}+1.047\times10^{-10}\sqrt{K}f\tan\delta \text{ nepers per centimeter} \quad (3)$$

where

$\nu=2h/k_1d$
$\sigma=2h/D$

In equation 3 the two components of the first term refer to the losses in the conductors and screen respectively while the second term represents the dielectric loss. The significance of the empirical constants remains as in the previous section except where noted in the following.

Unscreened Balanced Cables. In this case $\sigma = 0$ so that the attenuation becomes

$$\alpha=\frac{2.287\times10^{-7}\sqrt{\kappa\rho_1 f}}{\log_{10}2\xi}\left(\frac{K_sK_p}{d}\right)+1.047\times10^{-10}\sqrt{K}f\tan\delta \text{ nepers per centimeter} \quad (4)$$

A doubt will often exist as to the appropriate value to assume for the effective permittivity. In the case of flexible solid-dielectric cables provided with belt insulation a value very little below that of the dielectric material itself is appropriate.

Carson[7] has given a formula for the proximity factor at very high frequencies

$$K_p=\frac{\nu}{\sqrt{\nu^2{}_{-1}}} \quad (5)$$

Rigid Screened Balanced Cables. In most practical designs, the proximity factor may be assumed to be unity in view of the proximity of the screen to the conductors.

Braided Flexible Balanced Cables. Where the screen consists of wire braid, it has been found that the attenuation depends greatly upon the contact resistance between the wires, in marked contrast to the coaxial case. In such cases the total attenuation at ultra high frequencies will often increase tenfold in a matter of days if the cable is left undisturbed. A partial recovery occurs if the cable is flexed vigorously, but the improvement is not maintained.

Table IV. Assumed Values of Convection Constant, K_c

Ratio of Air-space, Diameters, D_1/D_2	$K_c\times10^4$
0	16.0
0.2	10.5
0.4	5.8
0.6	3.1
0.8	1.4
1.0	0

In England it is customary to provide a metallized paper underneath the wire braid. This reduces the instability very markedly, but the attenuation is still appreciably higher than that given by equation 3.

It is recommended that measured values of attenuation should be used to calculate the power ratings of flexible balanced cables. The increment of attenuation over the theoretical value may safely be attributed to imperfections in the screen.

ESTIMATION OF THERMAL DISSIPATION

In the dissipation of heat from source to sink, conduction, radiation, and convection play their part. Since the two latter processes are not linear with temperature it is necessary to summate the temperature drops over different parts of the cable system to obtain the relationship between the heat dissipated and the total temperature rise. The problem is further complicated by the fact that, in the present case, there are various heat sources located at different parts of the cable system.

Thermal Resistance of Cable Insulation

Solid-dielectric Coaxial Cable. The thermal resistance per unit length of a long straight cylinder of material corresponding to the insulation of the cable is given by

$$S_d=\frac{G_d}{2\pi}\log_e(D/k_1d) \text{ degrees centigrade, centimeters per watt} \quad (6)$$

The appropriate value of G_d is given in Table III, in which the value proposed is higher than that of polyethylene itself and is based on actual cable measurements. The enhanced value is attributed to poor, and variable, thermal contact between the insulation and the adjoining conductors. The same remarks apply to

Table V. Assumed Values of Heat Emission Constant, k

Surface Condition	Constants of Heat Emission, $k\times10^4$ for Various Cable Diameters (cm) 1	2	3	5	7	10
Polyvinyl chloride sheathed or served	7.0	6.0	5.3	4.7	4.6	4.5
Plain lead sheath	6.1	5.1	4.6	4.2	4.1	4.0
Bright wire finish	5.2	4.2	3.9	3.8	3.7	3.5

the figures given for the polyvinyl resins.

Air-spaced Coaxial Cable. In this case heat transfer occurs by conduction, radiation, and convection. It is necessary to summate the heat flows corresponding to each process due to a given temperature difference, in a manner similar to that used to calculate the heat transfer from cables in ducts (see reference 2, page 530). This is repeated for several temperature differences over the interesting range, to yield the effective thermal resistance of the insulation over the same range.

The following equations apply

Conduction Loss

$$H_d=\frac{2\pi(\theta_1-\theta_2)}{G_a\log_e(D_2/D_1)}\text{ watts per centimeter}\tag{7}$$

Radiation Loss

$$H_r=\frac{4\pi D_1.\sigma(273+\theta_2)^3E_1E_2(\theta_1-\theta_2)}{E_1+E_2-E_1E_2}\text{ watts per centimeter (approximate)}\tag{8}$$

Convection Loss

$$H_c=K_cD_1^{3/4}(\theta_1-\theta_2)^{5/4}\text{ watts per centimeter}\tag{9}$$

where

σ = Stefan's constant $=5.71\times10^{-12}$

E = emissivity of the surface which is boundary to the air space

D = diameter of the boundary surface, centimeters

θ = temperature of the boundary surface, degrees centigrade

and the suffixes 1 and 2 refer respectively to the inner and outer surfaces which enclose the air space.

Table VI. Rating Factors for Various Operating Conditions

Ambient Temperature	Maximum Permissible Temperature 85°C.	75°C.	65°C.
40	1.58	1.20	0.82
55	1	0.63	0.29
70	0.45	0.13	
85	0		

The relationship between the constant K_c and the ratio of the dimensions of the air-space is given in Table IV, the values being taken from the British Electrical and Allied Industries Research Association report already quoted.[2]

In the absence of experimental data, the following values for thermal emissivity have been assumed:

Copper	0.10
Aluminum	0.25
Lead	0.25
Polyethylene (white)	0.40
Polyethylene (black)	1.00

Balanced Cables. An approximate solution for the thermal resistance between the two conductors and the screen of a balanced cable is as follows

$$S_d=\frac{G_d}{2}\log_e\left(\frac{\nu}{2\sigma^2}(1-\sigma^4)\right)\text{ degrees centigrade, centimeters per watt}\tag{10}$$

where

$\nu=2h/k_1d$

or

$\sigma=2h/D.$

This assumes that the screen is an isothermal. The same equation could be applied to unscreened balanced cable, with little loss of accuracy. In this case D represents the diameter over the solid-dielectric belt.

Thermal Resistance of the Cable Coverings

The thermal resistance of unit length of the coverings is given by the equation

$$S_c=\frac{G_c}{2\pi}\log_e D_2/D_1\text{ degrees centigrade, centimeters per watt}\tag{11}$$

where D_1 and D_2 are respectively the inner and outer diameters of the covering. In the case of armored cable, the armor wires or tape may be considered to have negligible temperature drop and the total thermal resistance will be the sum of the two terms corresponding to the bedding and outer servings.

Thermal Resistance External to the Cable

Cables Installed in Air. Comprehensive tests by the National Physical Laboratory have shown that the thermal emission from the surface of cables in air can conveniently be expressed by the empirical relationship.

$$H_\theta=\frac{Ak}{l}\theta_s^n\text{ watts per centimeter}\tag{12}$$

where A is the surface area (squared centimeters) and l is the length (centimeter). It has been found that a value of 5/4 for the index n satisfies practical conditions best.

The effective thermal resistance external to unit length of the cable is therefore given by

$$S_a=\frac{1}{\pi D_s\theta_s^{1/4}k}\text{ degrees centigrade, centimeters per watt}\tag{13}$$

The values of k for various conditions of surface are used in the present calculation shown in Table V and are based on information given in the British Electrical and Allied Industries Research Association report.

It is difficult to deal with the case of grouped cables theoretically, because, in contradistinction to the power cable case, it will be rare that similar cables carrying the same load will be involved. To show the order of effect involved the following observations may be made. It has been found that for two cables touching one another the appropriate value of k is that corresponding to a single core, reduced by 30 per cent and for three cables touching, the value of k is reduced by about 40 per cent.

Cable Installed in Ground. The thermal resistance of the ground is given approximately by

$$S_g=\frac{G_g}{2\pi}\log_e\frac{4l}{D_s}\text{ degrees centigrade, centimeters per watt}\tag{14}$$

where l is the depth of burial.

Thermal Dissipation of Cable Systems

In a radio-frequency cable, the inner conductor, the insulation, and the outer conductor are all sources of heat loss. In the case of a coaxial cable with a homogeneous insulation, it may be shown that the distributed loss in the insulation is accurately replaced by two lumped losses, each equal to one half of the total dielectric loss, located at either boundary. In the case of balanced cable it would appear to be reasonable to consider the total dielectric loss to be lumped at the conductors, although this obviously gives a slight over-estimate of the temperature drop.

Then, putting $\alpha_{c1}=k_1\alpha$, and $\alpha_d=k_d\alpha$, we may write, using the principle of superposition.

$$\theta_c=H_\theta[S_d(k_1+k_d/2)+S_c+S_a]\tag{15}$$

for a coaxial cable, and

$$\theta_c=H_\theta[S_d(k_1+k_d)+S_c+S_a]\tag{16}$$

for a balanced cable.

Since S_a varies with θ_s and, in the case

Table VII. Principal Dimensions of Solid Dielectric Cables

Characteristic Impedances: 50 and 75 ohms

Core Diameter, Inches	Diameter Over Braid, Inches	Diameter Over Sheath, Inches
0.125	0.160	0.200
0.250	0.285	0.345
0.500	0.540	0.630
0.750	0.790	0.900
1.00	1.040	1.180
1.500	1.540	1.740

of air-spaced cable, S_d varies with $(\theta_c - \theta_r)$, these equations are best solved graphically by plotting $(\theta_c - \theta_r)$, $(\theta_r - \theta_s)$, and θ_s against H_θ.

In the case of solid-dielectric cables buried in the ground this problem does not arise and the temperature rise of the inner conductor may be calculated directly, thus, for a coaxial cable

$$H_c = \theta_\theta / [S_d(k_1 + k_d/2) + S_c + S_g] \qquad (17)$$

ESTIMATION OF THERMAL RATING

Fundamentally the heat sources in a cable carrying a current I at voltage E are

$$I^2R + E^2\omega C \tan \delta \text{ watts per centimeter}$$

and this total heat loss must be equated to the heat dissipation calculated in the manner developed in the previous section. This method can conveniently be applied directly in cases where the loss due either to voltage or to current predominates. This condition often applies, for instance, in induction heating at low frequencies. For the general case it seems preferable to base the thermal rating on the mean power which can be transmitted continuously through a matched system, to cause a given maximum conductor temperature in a given ambient in a cable free from any longitudinal alleviation of temperature. This standard rating is a particular form of the general case considered before in which the ratio of the voltage and current is fixed and made equal to the characteristic impedance of the cable. From this basic rating, new ratings can be developed, by the application of "rating factors" to take care of variations in the operating conditions, and these are discussed later.

Determination of Basic Rating

For a matched system the power P transmitted along the cable is given by the expression

$$P = P_0 \epsilon^{-2\alpha x}$$

where x is the distance from the input end. The heat dissipation H at any point along the line can therefore be expressed in terms of the power being transmitted by substitution in the relationship

$$H = -\frac{d_P}{dx} = \frac{-d(P_0\epsilon^{-2\alpha x})}{dx} = 2\alpha P_0 \epsilon^{-2\alpha x} \qquad (18)$$

The dissipation H_θ corresponding to a specified maximum temperature rise θ is therefore given by the maximum value of the foregoing expression, or

$$P_\theta = \frac{H_\theta}{2\alpha} \qquad (19)$$

Maximum Temperature of Operation

In fixing the maximum permissible temperature of operation, several factors must be considered.

1. The temperature of the insulation must not approach the point at which softening occurs, so permitting displacement of the inner conductor or distortion of the cable.
2. Any chemical or physical action, which might deteriorate the insulation or impair the effectiveness of the waterproof coverings, must not be excessive.
3. Temperatures must be limited to avoid trouble due to differential expansion of the component materials used in the construction of the cable.

In the case of polyethylene-insulated cables, a maximum temperature of 85 degrees centigrade has been adopted in England for general use in the armed services. At this temperature the thermoplastic insulant is softened to the extent that it will not withstand severe mechanical stresses, but is satisfactory for normal usage. Some deterioration also will be experienced at these temperatures due to migration of the plasticizer in normal types of polyvinyl-resin sheathings. This causes a hardening of the sheathing material and an increase in the power factor of the insulant to an extent which may be serious at the higher frequencies. Sheathing materials with nonmigratory plasticizer should be used in such cases.

For commercial operation, a somewhat lower temperature of operation is desirable.

In air-spaced cables, the mechanical stresses on the insulant due to the inner conductor are inevitably higher than in solid-dielectric cables, and it is desirable that such cables should be rated still more conservatively.

In the present paper, basic ratings have been drawn up for three interesting ranges of cable and these have all been based for ease of comparison, on the same maximum temperature rise of 30 degrees centigrade. Other conditions of operation may, with little loss of accuracy, be met by multiplying the standard ratings by the rating factors, as will be indicated.

Ambient Temperature

The ambient temperature has a marked effect on the rating in view of the fact that the maximum permissible temperature may not be very much higher. The standard ratings for solid-dielectric cable have been based in the present instance on tropical use for which an ambient of 55 degrees centigrade has been assumed. Rating factors corresponding to use in temperate climates or in equipment are given in Table VI. The schedule proposed is based on the average of a wide range of cables. It should be noted that for use in equipment the ratings correspond to natural ventilation and if forced circulation is adopted some increase in rating might be permitted.

Effect of Modulation and Load Factor

It may be shown that for a system which is amplitude modulated by a factor, m, that the power transmitted and the heat lost in the cable is increased by a factor $1 + m^2/2$.

In practice the modulation varies usually between wide limits, but if the variation is reasonably rapid compared with the time-constant of the cable, the average value may be used. However, in general, equipment will be required to satisfy some arbitrary test involving operation for a given time at a given modulation and these conditions should set the requirements for the cable rating.

For pulse-modulated radio frequency, the mean power determines the rating and this may be taken as equal to peak power × pulse length × repetition frequency.

Calculations show that the thermal time-constant of solid-dielectric radio frequency cables in air varies between three minutes for a cable of 1/8 inch diameter over the insulation to about 90 minutes for a $1^1/_2$ inch cable. The time constant might be expected to vary at a rate proportional to the diameter raised to a power between 1.75 and 2. The time constant of buried cables is considerably higher, but since the cable ends will generally be above ground, advantage can rarely be taken of this condition. The figures just quoted show that the opportunities to increase the short-time rating of cables to take care of low load factors are extremely limited.

Effect of Standing Waves

The effect of standing waves on the temperature rise is very complex, and it is

Table VIII. Assumed Values of Attenuation for Solid Dielectric Cables, in Decibels per 100 Feet at 100 Megacycles per Second

Core Size, Inches	50-ohm Cables				75-ohm Cables			
	α_{c1}	α_d	α_{c3}	(Total) α	α_{c1}	α_d	α_c	(Total) α
0.125	2.95	0.166	1.38	4.45	3.01	0.166	0.922	4.10
0.250	1.47	0.166	0.692	2.33	1.51	0.166	0.461	2.14
0.500	0.737	0.166	0.461	1.36	0.752	0.166	0.288	1.21
0.750	0.491	0.166	0.346	1.00	0.502	0.166	0.231	0.90
1.000	0.368	0.166	0.346	0.88	0.376	0.166	0.231	0.77
1.500	0.245	0.166	0.307	0.72	0.251	0.166	0.192	0.61

difficult to express it in a concise form. The components of conductor and dielectric loss will vary along the line according to similar periodic functions which are 180 degrees out of phase and their combined effect will vary with the impressed frequency and the cable design. Two limiting cases will be recognized:

1. When the frequency is so high and the longitudinal transfer of heat is so effective that periodic maxima and minima of temperature tend to disappear. In this case it can be shown that the power transmitted along a cable of attenuation constant α, with a standing-wave ratio $s = E_{max}/E_{min}$ on the line, is given by

$$P=P_0 / \left[\epsilon^{2\alpha x}+\frac{(s-1)^2}{2s}\sinh 2\alpha x\right] \tag{20}$$

The maximum heat dissipation is therefore given by

$$H_\theta=\left(-\frac{dP}{dx}\right)_{x=0}=2\alpha P_0 \frac{s^2+1}{2s}\Bigg] \tag{21}$$

2. When the longitudinal transfer of heat along the cable can be neglected. Then remembering that the dielectric loss is proportional to the square of the voltage and the conductor loss is proportional to the square of the current, and putting $\alpha_d=k_d\alpha$, we may write for the maximum heat dissipation

$$H_\theta=2\alpha P_0\left[\frac{k}{s}+(1-k_d)s\right]$$

or

$$H_\theta=2\alpha P_0[ks+(1-k_d)/s]$$

whichever is the greater.

The most severe case occurs when either the conductor loss or the dielectric loss predominates. In this case, the dissipation will be increased, relative to a matched system, by a factor equal to the standing-wave ratio. The safe rating will be reduced correspondingly, or

$$P_0=\frac{H_\theta}{2\alpha s} \tag{22}$$

It is recommended that this criterion be used unless a more rigorous study can be made.

Voltage Ratings

The type of insulant used in radio-frequency cables usually precludes the appearance of any technical thermal instability process. The normal case of dielectric heating due to the applied voltage has been considered in the previous section, and it only remains to consider the effect of any nonlinear mechanism which may arise. Such limitations are most likely to arise for low-frequency applications or for the case of pulse-modulated systems.

Since the performance under transient voltage of solid-dielectric cables is quite different from that of air-spaced cable, the two cases are considered separately. It is useful however to make a preliminary survey of the nature of the voltage stresses which may be imposed on a transmission feeder.

The peak voltage due to a mean unmodulated power P_0 transmitted along a cable into a matched load, is given by the expression

$$E_p=\sqrt{2Z_0P_0} \text{ volts (peak)} \tag{23}$$

The ratio of the maximum voltage on the cable to the input voltage when the line is not correctly terminated at the load end depends upon the electrical length and attenuation of the line, and the nature of the mismatch. However this ratio cannot exceed the value of s, the standing wave ratio, and it is desirable to use this value for the general case, unless the special circumstances of an application justify a closer study.

If the input power is modulated by a factor m, the peak voltage will be increased by a factor $(1+m)$. For a pulse-modulated power application, the requirement for the cable usually will be expressed in terms of the peak power to be transmitted, and the peak voltage may be calculated directly.

Overvoltages, beyond the value calculated for the steady-state condition, as calculated before, will appear on the cable when the transmitter is switched, or when the constants of the terminating circuits are altered, whether by design or by accident. In certain cases, the antenna will be exposed to the possibility of a lightning stroke and although in such cases lightning protection would be provided, the voltages on the cable due to the resultant mismatch will be liable to exceed the maximum voltage which is normally present on the cable.

The maximum stress, g, in a coaxial cable with perfect cylindrical electrodes is given by

$$g=\frac{2E}{d\log_e D/d} \text{ volts per centimeter} \tag{24}$$

A. L. Meyers[8] gives a convenient expression for the effect of stranding, namely

$$g=\frac{2k_2E}{d\log_e D/k_1d} \text{ volts per centimeter} \tag{25}$$

where k_1 and k_2 are constants for any given strand formation. Some calculated values of these constants are given in Table I.

For a given voltage, the minimum value of g, with perfect cylindrical conductors, is attained when D/d has the value ϵ or 2.72. A somewhat lower value applies in the case of stranded conductors. The stress, g, may be converted readily in terms of the mean power by combining equations 23 and 24.

$$g=\frac{\sqrt{(120P_0\log_e D/d)}}{k^{1/4}}\times\frac{2}{d\log_e D/d}$$

$$=\frac{\sqrt{(480P_0)}}{k^{1/4}}\times\frac{1}{d\sqrt{(\log_e D/d)}} \text{ peak volts per centimeter} \tag{26}$$

This has a minimum value when $D/d=\sqrt{\epsilon}=1.65$, which corresponds to a characteristic impedance of 30 ohms for an air-spaced cable or 20 ohms for a polyethylene-insulated cable. This condition is rarely attained in practice because it is rather far removed from the condition for minimum attenuation.

Solid-dielectric Cables

For solid dielectric cables, we may usually dismiss the problem of transient voltages because the intrinsic surge strength of solid materials is usually extremely high compared with that of gases. Davis, Austen and Willis Jackson[9] have reported strengths for polythene of 1,650–2,000 kv per centimeter for single impulses and values of 1,000 kv per centimeter for more than 400 repeated pulses.

It has been established that minute

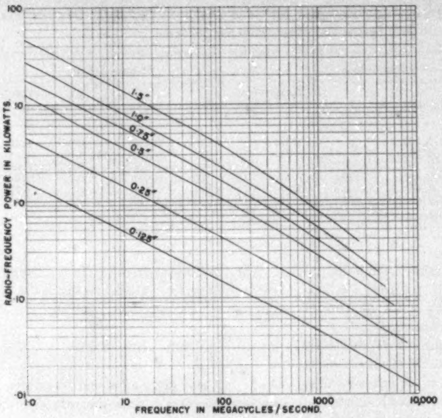

Figure 1. Power rating of some solid-dielectric flexible cables

Characteristic impedance, 50 ohms

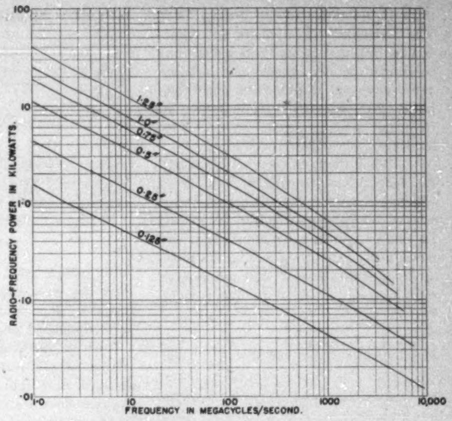

Figure 2. Power rating of some solid-dielectric flexible cables

Characteristic impedance, 75 ohms

cavities, in the form either of discrete bubbles or films in the neighborhood of the conductor, are often present in this type of cable. It has further been shown, by electrical tests at power frequencies and by visual tests at radio frequencies up to 2 megacycles per second that these cavities are the seat of electrical discharges when a certain critical voltage swing is exceeded. It is probable that this critical voltage does not greatly vary with frequency, certainly up to a few hundred megacycles per second. There is further limited evidence that the energy loss per cycle due to such discharges is of the same order, for a given impressed voltage, at power and radio frequencies. These discharges may cause direct electrical breakdown by disintegration of the molecules of the insulating material, or may cause overheating of the insulation by the superposition of the local energy loss on the general loss due to the cable attenuation. It has been proposed[3] that the radio frequency voltage rating should be equal to the power-frequency test voltage corresponding to a discharge of 2×10^{-12} coulombs for a 70-centimeter cable test piece.

It is inevitable, from the nature of the imperfections referred to, that the quality of cable judged in this way should vary within relatively wide limits. It has been found in England that the bulk of production of polyethylene radio-frequency cable is free from discharge at test voltages corresponding to 50 kv peak per centimeter, and that this discharge level is maintained during life when subjected to heating cycles. It is therefore proposed that the voltage rating of solid-dielectric cables should be based on a peak stress of 50 kv peak per centimeter, in the absence of specifications calling for a discharge initiation level which is appreciably higher than this value.

Since the criterion for the appearance of recurrent discharges is the total swing of voltage applied to the cable, the corresponding stress for cables subjected to unidirectional pulses is 100 kv per centimeter calculated from the total voltage swing of the pulse.

Air-spaced Cables

Considerable literature exists on the breakdown of air at high frequencies, although the consistency between the results obtained by different authorities is, at first sight, only fair. The probable reason for this will be revealed in the succeeding paragraphs.

Tested between sphere gaps in the region from 100 kc per second to 10 megacycles per second there is a drop in the breakdown strength of air, as compared with the 50 cycles-per-second value, of an amount not exceeding 20 per cent. Alford and Pickles[8] found no difference between breakdown values at 60 cycles-per-second and 13 megacycles per second whereas Cooper[9] has recently reported a reduction of 30 per cent, as compared with the direct voltage strength, at frequencies of 2,800 and 9,800 megacycles per second. The earlier results in the neighborhood of 1 megacycle per second have been attributed to the formation of a space charge due to the limited mobility of the positive ions. The precise band over which the process operates would appear to vary with the electrode configuration.

For needle gaps and for electrodes comprising point and plane, the reductions in strength, as compared with power-frequency values, are even more marked. Values of breakdown strength as low as 30 per cent of the 50-cycles per second value have been reported. This reduction of strength would again appear to be limited to the frequency band from 100 kc to 10 megacycles per second.

The effect of increased gas pressure has not been investigated widely, but tests in the neighborhood of atmospheric pressure have indicated that the normal air-density correction holds for radio frequencies of the order of a megacycle per second.

In dealing with the question of the electrical strength of air-spaced cables, it would appear that no form of electrical discharge can be tolerated. Two distinct conditions may be recognized.

In the first, the conductor surfaces are free from local irregularities and the variation of stress is restrained. The stresses in such cases are usually amenable to exact calculations. In the absence of comprehensive tests on air-spaced coaxial cables at radio frequencies, it seems safer to assume that the electrical strength at all radio frequencies of a cable satisfying these conditions may be about 20 per cent lower than the power-frequency strength.

In the second case there may be present

local stress concentrations, such as might be caused by burrs on the conductor, by small metallic slivers or by the presence of high-permittivity materials in the air space. It is, of course, quite impractical to attempt to calculate the maximum stress in these circumstances. It is therefore recommended that a further criterion be applied to determine the safe operating level of voltage. The critical power-frequency voltage, corresponding to the appearance of discharges, should be determined by one of the several methods which have been developed. The discharge detector used must be highly sensitive and the testing equipment itself should be free from discharge. This discharge initiation voltage should be taken as the ultimate strength of the cable at all radio frequencies. The same principles should be applied to the consideration of cables in which elevated gas pressures are used.

It is recommended that the electrical strength of the cable, calculated as before, should allow a factor of safety of not less than four on the maximum voltage normally arising on the cable, due allowance being made for the maximum permissible modulation coefficient and standing wave ratio. This factor of safety is intended to take care of switching transients.

Practical Application of Proposed Methods

The methods proposed in the preceding sections have been applied to establish the rating of three interesting classes of cable, namely:

1. 50-ohm flexible polyethylene-insulated cables.
2. 75-ohm flexible polyethylene-insulated cables.
3. 75-ohm air-spaced semirigid cables.

The individual cables in these classes are designated by their diameter over the insulation. The construction of the cables of the first two classes are in general accord with the United States Army-Navy specification for radio-frequency cables *JAN-C-17*. As proposed in the section The Attenuation Coefficient of Cables, an allowance of 10 per cent has been added to the attenuation coefficients quoted to allow for variations in materials and construction.

SOLID-DIELECTRIC FLEXIBLE CABLES

The 75-ohm cables are assumed to have a solid inner conductor while the 50-ohm cables have a 7-strand conductor. Both ranges have plain copper wire braids. The principal dimensions are given in Table VII.

Figure 3. Power rating of some air-spaced cables

Characteristic impedance, 75 ohms

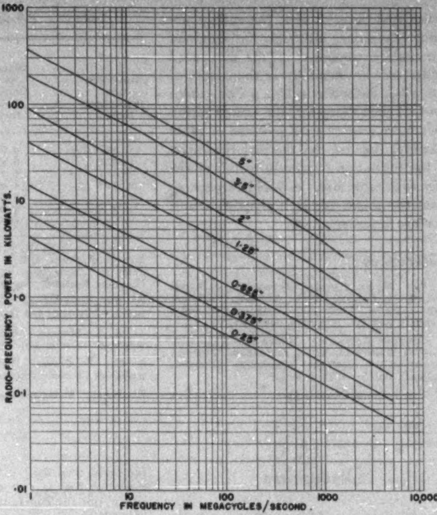

The components of attenuation assumed for these cables are given in Table VIII for a frequency of 100 megacycles per second. Corresponding values at other frequencies may be estimated readily on the assumption that the conductor losses vary as the square root of frequency, and that the dielectric losses are directly proportional to the frequency. The attenuation coefficients of the 75-ohm cables are about 10 to 15 per cent lower than those of the corresponding 50-ohm cable because the latter design assumes the use of a stranded conductor.

The power ratings for a matched load are plotted against frequency in Figures 1 and 2 for the 50- and 75-ohm cables respectively, for a maximum conductor temperature of 85 degrees centigrade, in an ambient of 55 degrees centigrade. A comparison of these figures shows that although the attenuation of the 50-ohm cables is higher, their power ratings are not less than those of the corresponding 75-ohm cables and are even 10 to 15 per cent higher for the larger cables. The difference is more marked at the higher frequencies where the dielectric loss is important. This result derives from the lower thermal resistance of the insulation of the 50-ohm cables, due to their lower diametral ratio, and from the fact that the thermal resistance external to the cable falls with increase in cable size whereas that of the insulation is of course unchanged.

75-OHM AIR-SPACED SEMI-RIGID CABLES

The cable type selected for the present theoretical study has a solid copper inner conductor and an extruded tubular return conductor of aluminum. This design lends itself to cable construction, is sufficiently flexible and robust for installation and has a transmission efficiency very close to the optimum obtainable. An effective permittivity of 1.10 and a power factor of 1×10^{-4} has been assumed. The principal dimensions and assumed attenuations of the range of cables studied are given in Table IX.

Figure 3 shows the mean power rating of these cables for a matched load over a range of frequencies. The assumed conditions were a maximum conductor temperature of 70 degrees centigrade, and an ambient of 40 degrees centigrade.

The calculations showed that the thermal resistance of the insulation was always many times that external to the cable, even with the larger cables where an enhanced degree of cooling of the inner conductor occurs due to convection. Consequently the outer conductor may be quite cool even when the inner conductor is very hot.

A rough comparison with the solid dielectric cables is possible because the maximum temperature rise above ambient is the same in each case. It will be noted that, size for size, the ratings are much the same, although the assumed attenuation constants of the air-spaced cables are very much lower than those of the solid dielectric cables. For cables above 1-inch diameter, the power rating rises more steeply with increase of cable diameter because the thermal resistance of the insulation continues to fall markedly with cable size. A 5-fold increase in diameter above one inch gives a 10-fold increase in power rating.

Table IX. Principal Dimensions and Assumed Attenuations of Air-Spaced Cable

Diameter over Insulation, Inches	Diameter over Aluminum Sheath, Inches	Diameter over Servings, Inches	Assumed Attenuation Decibels per 100 Feet at 100 Megacycles per Second			
			α_{c1}	α_d	α_{c2}	(Total) α
0.25	0.330	0.580	0.857	0.029	0.294	1.18
0.375	0.475	0.725	0.571	0.029	0.197	0.80
0.625	0.750	1.200	0.343	0.029	0.118	0.49
1.25	1.450	1.900	0.171	0.029	0.059	0.26
2	2.250	2.700	0.112	0.029	0.037	0.178
3.5	3.800	4.250	0.061	0.029	0.021	0.112
5	5.350	5.800	0.043	0.029	0.015	0.087

References

1. The Power Rating (Thermal) of Radio Frequency Cables, **R. C. Mildner.** *Journal,* Institution of Electrical Engineers (London, England), part III, July 1946, page 296.

2. Current Rating of Cables for Transmission, **S. Whitehead, E. E. Hutchings.** *Journal,* Institution of Electrical Engineers (London, England), October 1938, page 517.

3. The Voltage Characteristics of Polythene Cables, **R. Davis, A. E. W. Austen, Willis Jackson.** *Journal,* Institution of Electrical Engineers (London, England), part III, May 1947, page 154.

4. Radio-frequency Measurements, **L. Hartshorn.** Chapman and Hall, 1941.

5. **A. L. Meyers.** *Electrical Review* (London England), number 120, 1942, page 791.

6. **T. Levi-Civita.** Rendiconti Circolo Matematico of Palermo, volume 20, 1905, page 173.

7. Wave Propagation over Parallel Wires, the Proximity Effect, **J. R. Carson.** *Philosophical Magazine* (London, England), April 1921, page 627.

8. Radio Frequency High Voltage Phenonema, **Andrew Alford, Sidney Pickles.** Electrical Engineering (AIEE Transactions), volume 59, 1940, pages 129–37.

9. Experiments on the Electric Strength of Air at Centimeter Wavelengths, **R. Cooper.** *Journal,* Institution of Electrical Engineers (London, England), September 1947, part II, page 315.

Discussion

L. F. Roehmann (Anaconda Wire and Cable Company, Hastings-on-Hudson, N. Y.): Mildner's paper is excellent, and I say that not as a compliment but as a statement of fact. Particularly, his relation (18) between imput power and heat dissipated is lucid and revealing. True, he had it published previously in the Journal of the Institution of Electrical Engineers but it is now sandwiched between a host of less relevant equations, and its fundamental importance is thus played down.

There are a few comments from a power cable engineer's point of view, as follows:

1. While the discussor, and very probably his colleagues in the power field, have no difficulty in understanding the theory, problems arise when specific constructions are discussed which are familiar to the "coaxial boys" but not to them. How are balanced cables made up? And particularly, what is a "rigid screen" in a flexible cable? One sentence, or two, would put the reader at ease.

2. In speaking of the thermal resistance from the source to the "sink," power cable engineers distinguish basically between two thermal resistances; the (volume) thermal resistance of insulation, covering, and so forth, and the surface thermal resistance. The first is characterized by volume thermal resistivity and geometry, the second by surface thermal resistivity and geometry. For some unaccountable psychological reason there is a tendency to misname the second term "surface emissivity" though the word emissivity should be restricted to its distinct meaning in connection with radiation. Curiously enough, Mildner succumbed to the same mistake. E in equation 8 for the radiation loss is correctly defined as emissivity, but the constant k in Table V is misnamed emission constant though it is, dimensionally, a surface thermal conductivity.

3. Power rating, as the outcome of the investigation, is given in kilowatt as a function of frequency. Does that mean that a cable, rated 1 kw, may carry 1 ampere at 1 kv and equally well 1,000 amperes at 1 volt? Assuredly not! But who bridges the gap to the power engineer's concept who talks of rating only in terms of amperes, for a given voltage class? Or is it tacitly understood, amongst the coaxial boys, that the cables mentioned may not be operated at voltages in excess of certain unspecified limits? After all, at the frequencies under consideration, the current concept still holds true though standing waves introduce a complication which does not exist at power frequencies. This complication, however, is taken care of by the author, somewhat summarily, in such a way that the ratings will be conservative.

R. C. Mildner: The following brief description of balanced cables may serve to clear the difficulties to which Roehmann has drawn attention.

In a balanced cable, the two conductors comprising the transmission line are disposed symmetrically relative to earth or to a surrounding screen. In England it is usual to insulate each conductor separately, to cable the two conductors together with a length of lay from 2 to 5 inches, and to fill with insulating material to circular cross section. A belt of insulating material is sometimes applied additionally. I believe that it is more usual in the United States to arrange that the two conductors lie parallel without lay in a single extrusion of insulating material. Such cables may be left unscreened, or, in the case of flexible cables, provided with a wire braid (in England usually with a metalized paper as well). In the case of semirigid cables a lead sheath may be used as a screen.

I regret that, in dealing with the thermal resistance external to the cable, I have used a nomenclature which may be considered unorthodox in the United States. But I cannot accept that the terms which I have used and which are accepted in England are less logical than those quoted above. I feel that Roehmann attaches too narrow a meaning to the word "emission". Furthermore he overstates his case in claiming that the constant k in Table V has the dimensions of a surface thermal conductivity. This is clearly incorrect because k must be multiplied by a nonintegral power of temperature and by a distance to give the heat dissipation.

I know that the concept of power as opposed to current rating often creates difficulties for a power engineer. The section paper entitled Estimation of Thermal Rating attempted to make the position clear. For a cable having a characteristic impedance of 100 ohms, a power rating of 10 kw implies that the cable may carry 10 amperes at 1,000 volts. If, as is usual at low and medium frequencies, the conductor loss predominates, then the value of 10 amperes may be considered as the current rating of the cable. If the dielectric loss is appreciable, the current rating will be increased above the value of 10 amperes in proportion as the dielectric loss due to the applied voltage is reduced. I do not think it is practicable to give the general case with greater precision. The principles quoted in the paper will permit particular cases to be studied with sufficient accuracy.

Damper Stabilized Instrument Servomechanisms

ALBERT C. HALL
MEMBER AIEE

SERVOMECHANISMS are increasing in importance in this period of military and industrial mechanization, and are found performing tasks of variety limited only by the imagination of the engineer. A type of servomechanism that is very useful in both the military and industrial fields is termed the "instrument servomechanism." This term was employed originally to denote a servomechanism in which the output power required was primarily that necessary to operate itself. For example, a servomechanism operating a position indicator is called an instrument servomechansim because with reasonable design, the power required by the indicator is only a fraction of the power required by the servomotor. However, in more and more applications good reasons were found for coupling additional equipment to instrument servomotors, until in many cases the load power requirements became substantial. Consequently, today the term "instrument servomechanism" is used broadly to denote servomechanisms of any kind that develop an output power not more than about one-tenth horsepower.

Since a servomechanism is a closed-cycle system and contains power amplifying elements, the possibility always exists that the servo will be unstable if designed improperly. The servo engineer must concern himself with this possibility and design the system to avoid instability. Today, moreover, the science of designing closed-cycle systems has developed to the point where a "yes" or "no" answer to the stability question no longer is sufficient. In addition to being stable, the servomechanism must possess such a margin of stability that transients will be well damped and that the values of system parameters can have a reasonable tolerance. Today, therefore, the statement that a servomechanism is stabilized signifies that a satisfactory margin of stability exists in the system.

The technique chosen to stabilize a servomechanism is determined largely by the choice of servomotor, which, in turn, is likely to be specified by the application requirements. In many cases the servomotor is chosen with little regard for its dynamic properties but from considerations of efficiency, size, adaptability, type of power available and serviceability. Occasionally it is possible to employ in the application a servomotor and controller elements with such dynamic properties that the servomechanism will be stable without the use of compensating elements. More often the characteristics of the servomotor and other components of the servomechanism are such that it is necessary to provide compensating elements in the system to enable it to meet its dynamic requirements.

The stabilizing methods in common use are the following:

1. Cascade compensation.
2. Feed-back compensation.
3. Load compensation.

Figure 1 illustrates, in block diagram form, these three stabilizing methods. In cascade compensation a portion of the controller in cascade with the other system components, is designed to correct the characteristics of the servomotor and the remainder of the controller. Feedback compensation signifies that an appropriate signal from some point of the system is fed back around those system components, the dynamic characteristics of which require modification. In the third method of compensation, termed "load compensation," the characteristics of the system are corrected by altering the dynamics of the servo load. While cascade and feed-back compensation have been treated thoroughly in other literature[1,3,4] little has been written on the subject of load compensation. The subject of this paper, damper stabilization of servomechanisms, is an example of load compensation.

The simplest method of load compensation is that of applying to the servomotor output shaft a torque (viscous friction) proportional to the angular rate of rotation of the servomotor. This method of compensation is inefficient since it requires a power loss proportional to the rate of rotation of the servomotor. A more efficient type of load compensation element that has been employed with considerable success with instrument servomechanisms is the damper. One type of damper called the "viscous damper" in this paper, comprises a mass coupled to the servomotor shaft by means of viscous friction, as illustrated diagrammatically by Figure 2. The power loss in this unit is negligible since at constant servomotor velocity the external mass turns at the same velocity as the servomotor, and no power is absorbed by the viscous friction. A second type of damper, called the spring-coupled damper, also is illustrated by Figure 2. Here the rotating mass is coupled to the servomotor by means of a spring as well as by viscous friction. The advantages that result from the addition of the spring are made clear in later sections of the paper.

An instrument servomechanism with either type of damper can be designed

---

Paper 49-79, recommended by the AIEE servomechanisms committee and approved by the AIEE technical program committee for presentation at the AIEE winter general meeting, New York, N. Y., January 31–February 4, 1949. Manuscript submitted November 8, 1948; made available for printing December 22, 1948.

ALBERT C. HALL is associate professor at the Massachusetts Institute of Technology, Cambridge, Mass.

The author is indebted to Miss Constance Boyd for computation studies on the viscous-damper servomechanism, to Mrs. Elizabeth Kimball who made most of the computation studies on the spring-coupled damper, and to Donald McDonald who contributed greatly to the development of these servomechanisms, particularly to the design of the controller amplifier.

to have a well-damped natural frequency of 15 cycles per second or higher, and a correspondingly high ratio of torque output to error (sensitivity factor). While the configurations of both the viscous and spring-coupled dampers have been used as vibration absorbers in open-cycle systems, their design is entirely different if optimum operation in a closed-cycle system is to be secured. It is the purpose of this paper to develop the design criteria of these damper mechanisms and to discuss and compare their performance.

Method of Analysis

The steady-state sinusoidal analysis is employed to determine the optimum design parameters of instrument servomechanisms that employ damper stabilization. This method of analysis, in common use today among servomechanism engineers, considers the response of the system to a sinusoidal input whose frequency is varied from zero to a value well above the system natural frequency. The object of servo synthesis is to so adjust the system parameters that over as large a frequency band as possible the ratio of the amplitude of the output to the amplitude of the input is constant and the phase angle between the output and input is small. The ratio of amplitudes generally has a maximum at some frequency, and it is necessary to limit the ratio of this maximum to the zero-frequency-amplitude ratio to about four-thirds if the system is to have a satisfactory margin of stability.

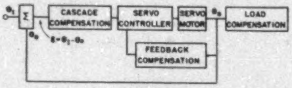

Figure 1. Servomechanism compensation methods

If the servo input and servo output are denoted θ_I and θ_o respectively it is common to express the sinusoidal characteristic of a servomechanism as $(\Theta_o/\Theta_I)(j\omega)$, written thus to emphasize the fact that the ratio is a function of the frequency ω. The ratio has vector properties and its amplitude may be written $|(\Theta_o/\Theta_I)(j\omega)|$.

A simplification of the analysis results if advantage is taken of the fact that the response of many servomechanisms is completely determined, except for a constant ratio, by the vector ratio of the servo output to the servo error. This vector ratio is called the transfer function and is written

$$\frac{\Theta_o}{E}(j\omega)=KG(j\omega) \tag{1}$$

in which K, the sensitivity factor, is invariant with frequency, while both the phase and magnitude of $G\,(j\omega)$ are functions of frequency. Since the error is given by

$$E(j\omega)=\Theta_I(j\omega)-\Theta_o(j\omega) \tag{2}$$

the system function $\Theta_o/\Theta_I(j\omega)$, is simply related to the transfer function by

$$\frac{\Theta_o}{\Theta_I}(j\omega)=\frac{KG(j\omega)}{1+KG(j\omega)} \tag{3}$$

The system response is thus completely determined by the transfer function, $KG\ (j\omega)$. Servomechanism synthesis, therefore, can be directed toward so prescribing the transfer function $KG\ (j\omega)$ that the system response has the proper characteristics.

The principles of servomechanism synthesis on the sinusoidal basis have been treated in other literature [1,3,4] and the analysis employed in this paper is no more than an application of these principles.

The method employed here is to plot the locus of the frequency dependent portion $G(j\omega)$ of the transfer function, and to determine from this plot the largest value of the sensitivity factor K, consistent with the maximum value of $|(\Theta_o/\Theta_I)(j\omega)|$, permitted by good servomechanism practice. With this restriction the system design is carried out to secure the desired system band width or the necessary system sensitivity.

The servomechanism design criteria may be summarized briefly as follows:

1. The amplitude response should be essentially flat to a frequency prescribed by the application requirements.
2. The maximum amplitude response should be not greater than about four-thirds its zero-frequency value.
3. The ratio of torque to error should be high with the actual value set by the system requirements.

The determination of the optimum system parameters for the damper-stabilized servomechanism is carried out with the foregoing criteria in view.

Design of Viscous-Damper-Stabilized Servomechanism

The synthesis of an instrument servomechanism stabilized by a viscous damper is considered first. Figure 3 represents the system diagrammatically. The torque developed by the servomotor is assumed to be proportional to the error except for the effects of a simple time lag and no viscous damping torques are considered to act upon the motor other than the one produced by the damper. While the latter assumption leads to slightly pessimistic results, the effect of viscous damping is a sufficiently small factor in the response of most high performance instrument servomechanisms to justify this simplification.

The differential equations of the system follow:

$$m=J_m\frac{d^2\theta_o}{dt^2}+f_A\frac{d\theta_o}{dt}-f_A\frac{d\theta_A}{dt} \tag{4}$$

$$f_A\frac{d\theta_o}{dt}-f_A\frac{d\theta_A}{dt}=J_A\frac{d^2\theta_A}{dt^2} \tag{5}$$

$$m+\tau_e\frac{dm}{dt}=k_e(N_I\theta_I-N_o\theta_o) \tag{6}$$

in which

θ_I, θ_o, and θ_A are the angular positions (as functions of time) measured with respect to a fixed reference of the servo input, the servo output, and the damper mass, J_A, respectively.

N_I and N_o are conversion constants relating the input and output of the servomechanism to voltages V_I and V_o, respectively, compared at the input to the servo controller.

f_A = torque acting upon the servomotor per unit relative velocity of the motor and the damper mass, J_A.

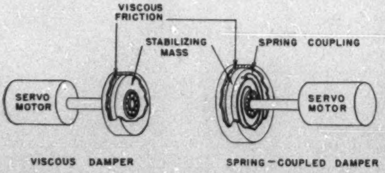

Figure 2 (left). Viscous and spring - coupled dampers

Figure 3. (right) Servomechanism stabilized by a viscous damper

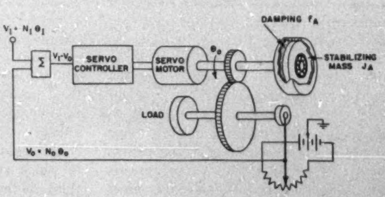

J_A = moment of inertia of the stabilizing mass of the damper.

J_m = moment of inertia referred to the servomotor of those moving parts of the system coupled rigidly to the servomotor shaft.

m = torque of the servomotor as a function of time.

k_c = proportionality constant between the torque m, and the system error.

τ_c = time lag between the generation of the servo error and the development of a torque by the servomotor.

The differential equations of a linear system have equivalent relations in terms of sinusoidal functions. The sinusoidal equations are found by replacing each variable by its vector counterpart and replacing dt by $j\omega$. Thus equations 4, 5, and 6 can be rewritten

$$M = J_m\Theta_o(j\omega)^2 + f_A(\Theta_o - \Theta_A)j\omega \tag{4a}$$

$$f_A(\Theta_o - \Theta_A)j\omega = J_A\Theta_A(j\omega)^2 \tag{5a}$$

$$M(1+j\omega\tau_c) = k_c(N_I\Theta_I - N_o\Theta_o) \tag{6a}$$

in which Θ_I, Θ_o, Θ_A, and M are vectors expressing the amplitude and phase of the sinusoidal functions corresponding to the time function θ_I, θ_o, θ_A and m.

The preceding equations may be solved algebraically to determine the system transfer function.

$$KG(j\omega) = \frac{N_o\Theta_o}{N_I\Theta_I - N_o\Theta_o} = \frac{k_cN_o}{J_m(1+r)(j\omega)^2} \times \frac{1+\dfrac{J_A}{f_A}j\omega}{1+\dfrac{1}{1+r}\dfrac{J_A}{f_A}j\omega}\,\frac{1}{1+j\omega\tau_c} \tag{7}$$

in which

$$r = \frac{J_A}{J_m} \tag{8}$$

The system function is related to the transfer function by

$$\frac{\Theta_o}{\Theta_I}(j\omega) = \frac{N_I}{N_o}\,\frac{KG(j\omega)}{1+KG(j\omega)} \tag{9}$$

The ratio N_I/N_o is a constant, independent of frequency.

It is convenient to transform equation 7 by changing the frequency variable. If a new frequency variable u is defined as

$$u = \tau_d\omega \tag{10}$$

where

$$\tau_d = \frac{1}{1+r}\,\frac{J_A}{f_A} \tag{11}$$

Equation 6 can be rewritten

$$KG(ju) = \frac{k_cN_o\tau_d^2}{J_m}\,\frac{1}{ju(1+ju)} \times \left[1+\frac{1}{j(1+r)u}\right]\frac{1}{1+j\dfrac{\tau_c}{\tau_d}u} \tag{12}$$

The form of equation 12 emphasizes the fact that the sensitivity factor is

$$K = \frac{k_cN_o\tau_d^2}{J_m} \tag{13}$$

and the frequency dependent portion of the transfer function $G(ju)$ is given by

$$G(ju) = \frac{1}{ju(1+ju)} \times \left[1+\frac{1}{j(1+r)u}\right]\frac{1}{1+j\dfrac{\tau_c}{\tau_d}u} \tag{14}$$

The usual method of studying such a function is to plot the locus of the frequency dependent function $G(ju)$ in the complex plane for each interesting combination of system parameters, and to so determine the sensitivity factor K, that the maximum value of $KG/1+KG$ does not exceed about four-thirds. In this particular case the number of loci can be substantially reduced if it is assumed that the time lag τ_c, can be made sufficiently small to be neglected. In most practical applications it is possible to so design the controller that the time lag τ_c is negligible. However, the possibility that the time lag may be appreciable should not be disregarded, and a permissible limit on its magnitude is determined in the latter part of this section of the paper.

When $\tau_c = 0$, Figure 4 is a plot of the loci of equation 14 for four values of r, the ratio of the moments of inertia J_A/J_m. The margin of stability of the system for a particular value of r is indicated by the proximity of the corresponding locus and the negative real axis. The sensitivity factor K should be adjusted so that the margin of stability is adequate as indicated by the maximum value of the amplitude response. The proper value of K can be determined by a simple graphical construction (reference 1, page 47) based upon the fact that if the amplitude response of the system is a constant, the locus of the transfer function is a circle. By this means it is easily shown that if r is two or four, respectively, it is not possible to so choose the sensitivity K, that the maximum value of $|(\Theta_o/\Theta_I)(j\omega)|$ is less than two or one and one-half, respectively.

On the other hand, if r is equal to or greater than six the sensitivity can be adjusted to limit the maximum amplitude ratio to four-thirds. The curves of Figure 5 were determined from the loci of Figure 4 and summarize the effect of sensitivity and ratio of moments of inertia upon the maximum amplitude ratio. Conservative servomechanism design in most cases would require that a value of r of about six be chosen. Thus the moment of inertia of the viscous damper should be about six times the moment of inertia of the motor and its load.

The ratio r of moments of inertia should always be as small as can be permitted by the stability requirements, in order to secure reasonable nonlinear operation of the servomechanism. If the servomechanism error should become very large (under synchronizing conditions, for example) the velocity of the servomotor will reach a high value in turning to its correct position. Since the maximum torque of the servomotor is limited by saturation in the controller and motor, an excessive transient time may be required to absorb the kinetic energy of the servomotor,

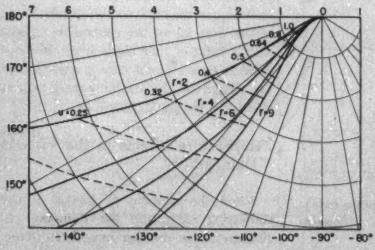

Figure 4 (left). Transfer function loci for the viscous-damper servomechanism

Figure 5 (right). Maximum amplitude ratio as a function of sensitivity factor for the viscous-damper servomechanism

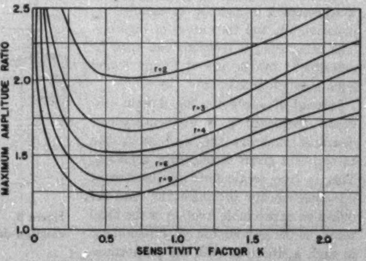

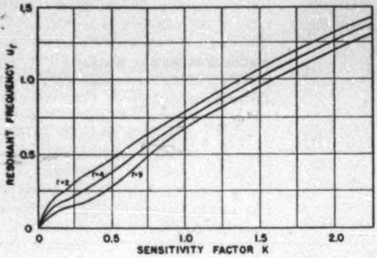

Figure 6 (left). Resonant frequency as a function of sensitivity factor for the viscous - damper servomechanism

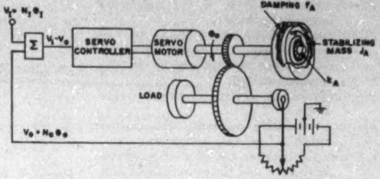

Figure 7 (right). Servomechanism stabilized by a spring-coupled damper

damper, and load. This transient time may be reduced by minimizing the total moment of inertia of the system. The system moment of inertia can be minimized by proper design of the servomotor and load, and by choosing the ratio r as small as is consistent with the desired margin of stability.

The resonant frequency of the instrument servomechanism also can be obtained from the loci of Figure 4 by the same graphical construction referred to before. The resonant frequency is the frequency at which the maximum amplitude occurs and is approximately equal to the system natural frequency, which is the frequency at which transients damp out. In Figure 6 is plotted the value of u_r at which resonance occurs as a function of the sensitivity factor. The resonant frequency ω_r, for a particular case, can be found from Figure 6 and the application of equation 10a.

$$\omega_r = u_r/\tau_d \tag{10a}$$

The curves of Figure 5 show that if the moment of inertia ratio r is six and the sensitivity factor K can be held at about six-tenths, the stability margin will be satisfactory. An additional system characteristic must be chosen in order that the system design may be completed. The characteristic commonly specified is either the system resonant frequency or the ratio of the motor torque to the error. If the resonant frequency is prescribed, the time constant τ_d can be determined by equation 10a and the curves of Figure 6. The other system relations can then be determined by the use of Figure 5 and equations 11 and 13.

Instead of specifying the system resonant frequency it is frequently more desirable to design the servomechanism to realize a given torque-error constant. This is true particularly of instrument servomechanisms in which the load requires an appreciable fraction of the total torque of the servomotor. It is important in such a situation that the proportionality constant relating the motor torque to system error be sufficiently large that the error caused by the load torque is limited to a tolerable value. If the magnitude of the load torque is known and the allowable error prescribed, the system torque-error constant can be calculated. The torque-error constant is the product k_cN_o appearing in equation 13, the expression for the system sensitivity factor K. Since the value of K may be selected from the curves of Figure 5, the ratio τ_d^2/J_m may be calculated, and the necessary value of the damping coefficient f_A, can be chosen once J_m, the combined moment of inertia of the motor and its load is known.

It is interesting to note that, according to the relations that have been presented here, both the resonant frequency and the torque-error constant can be increased indefinitely by making the damping constant, f_A, larger and larger. This anomaly is caused by the assumption that the time lag τ_c, is zero; that is, the torque developed by the servomotor has been assumed to be instantaneously proportional to the servo error. Actually the time lag τ_c is very small, and provided that it does not exceed a determinable value, it may be neglected and the preceding relations are valid.

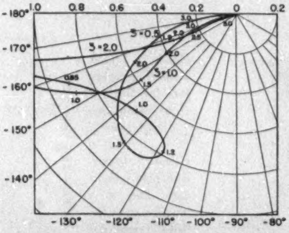

Figure 8. Transfer function loci for the spring-coupled-damper servomechanism. Moment-of-inertia ratio $r=1$

The lag τ_c appears in the lag factor $1/1 + j\,\tau_c/\tau_d u$ in equation 12. A safe criterion is to require the controller time lag τ_c, to be equal to or less than that value for which the lag factor introduces about five degrees phase shift in the transfer function at the system resonant frequency ω_r (reference 1, page 128). If the lag τ_c satisfies this requirement, the locus of the transfer function including the time lag term is essentially the same for important frequencies as the locus with the lag equal to zero. The criterion is expressed in equation form

$$\frac{\tau_c}{\tau_d}u_r \leq 0.1 \tag{15}$$

Since $u_r = \tau_d\omega_r$

$$\tau_c \leq \frac{0.1}{\omega_r} \tag{16}$$

If the time lag τ_c, is less than the above value it can be safely neglected provided the system without lag is adjusted to have a reasonable margin of stability. It is generally possible for the time lag τ_c to be as large as $0.2/\omega_r$ without seriously affecting the system response. If τ_c is larger than $0.2/\omega_r$, the effect of the lag should be determined by plotting the locus of the transfer function with the lag included.

The allowable time lag as determined from the preceding relations is small for a high-performance instrument servomechanism. For example, if a servo with a resonant frequency of five cycles per second is desired, the time lag of the controller should be less than about three milliseconds. If the time lag is more than twice this figure, appreciable deterioration in performance will occur, and the performance cannot be predicted without including in the analysis the specific value of the time lag of the controller. While such a value of time lag is small, it is not difficult to achieve if care is exercised in the design of the coupling and output circuits in the servo controller.

Temperature Effects in the Viscous Damper

When the moment of inertia of the stabilizing mass and the damping coefficient of the damper have been deter-

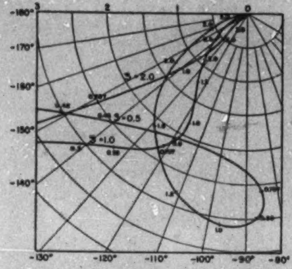

Figure 9. Transfer function loci for the spring-coupled-damper servomechanism. Moment-of-inertia ratio $r=4$

mined the mechanical design of the damper may be carried through. A damping medium must be chosen and while electromagnetic damping has the advantage of being independent of temperature the moment of inertia of the elements necessary to obtain a given value of the damping is excessive. Hydraulic fluids are available that provide high viscosity; unfortunately, the viscosity of the best of these fluids is by no means independent of temperature. There is no problem, of course, if the range of the operating temperature is small, since the viscosity of the oil and dimensions of the damper can be chosen to give almost any practical damping coefficient for a reasonable operating temperature. However, most military applications and some industrial applications require operation over a relatively large temperature range. For such applications the design of the damper is determined by the temperature requirements.

An example illustrates the importance of the temperature effect. The viscosity of a fluid (Dow Corning, type 200 Silicone fluid) with an unusually good temperature-viscosity characteristic varies by a factor of approximately three between a temperature of 35 and 130 degrees Fahrenheit. The damping coefficient f_A varies directly as the viscosity of the fluid, and the sensitivity factor K varies inversely as the square of the damping coefficient. (See equations 11 and 13.) If a servo using this fluid as a damping means must operate over this range of temperatures the damper design must provide for a nine-fold variation in K. Figure 5 indicates the effect of such a variation upon the maximum amplitude ratio. If the moment-of-inertia ratio is six or larger, this variation in K may be tolerable. For smaller values of moment-of-inertia ratio the maximum amplitude ratio at portions of the temperature range would normally be considered excessive. The larger the value of the moment-of-inertia ratio r, the wider can be the operating temperature range. Many military applications, however, require such a large range of operating temperature, as to exclude the possibility of employing a servomechanism stabilized with a viscous damper.

Design of a Spring-Coupled-Damper-Stabilized Servomechanism

The second type of load compensating element considered in detail is the spring-coupled damper. This device, shown schematically in Figure 2, operates in a substantially different manner than the viscous damper, and while somewhat more complex provides certain real advantages.

The block diagram of an instrument servo employing a spring-coupled damper for stabilization is shown in Figure 7. The differential equations of the system are as follows

$$m=J_m\frac{d^2\theta_o}{dt^2}+f_A\left(\frac{d\theta_o}{dt}-\frac{d\theta_A}{dt}\right)+k_A(\theta_o-\theta_A) \tag{17}$$

$$f_A\left(\frac{d\theta_o}{dt}-\frac{d\theta_A}{dt}\right)+k_A(\theta_o-\theta_A)=J_A\frac{d^2\theta_A}{dt^2} \tag{18}$$

$$m+\tau_c\frac{dm}{dt}=k_c(N_I\theta_I-N_o\theta_o) \tag{19}$$

in which k_A = spring constant of the spring coupling the damping mass to the servomotor and the other terms are defined following equation 6.

The sinusoidal relations equivalent to equations 17, 18 and 19 are

$$M=J_m(j\omega)^2\Theta_o+(\Theta_o-\Theta_A)(j\omega f_A+k_A) \tag{17a}$$

$$(\Theta_o-\Theta_A)(j\omega f_A+k_A)=J_A(j\omega)^2\Theta_A \tag{18a}$$

$$M(1+j\omega\tau_c)=k_c(N_I\Theta_I-N_o\Theta_o) \tag{19a}$$

The terms in these equations have been defined following equation 6a. The preceding equations may be solved algebraically and the system transfer function determined. If the frequency variable is transformed by

$$\frac{\omega}{\omega_0}=u \tag{20}$$

where

$$\omega_0^2=k_A/J_m \tag{21}$$

the transfer function can be written as follows

$$KG(ju)=\frac{k_cN_o}{k_A(1+r)}\,\frac{-ru^2+2j\zeta u+1}{-u^2\left(\dfrac{-u^2r}{1+r}+2j\zeta u+1\right)}\times\frac{1}{1+j\tau_c\omega_0u} \tag{22}$$

In equation 22

$$\zeta^2=\frac{f_A^2}{4k_AJ_m} \tag{23}$$

and the other terms have been defined in earlier parts of the paper.

The form of equation 22 emphasizes the fact that the sensitivity factor is

$$K=\frac{k_cN_o}{k_A(1+r)} \tag{24}$$

and the frequency dependent portion of the transfer function is given by

$$G(ju)=\frac{-ru^2+2j\zeta u+1}{-u^2\left(\dfrac{-u^2r}{1+r}+2j\zeta u+1\right)}\,\frac{1}{1+j\tau_c\omega_0u} \tag{25}$$

Reviewing for a moment the case of the viscous damper, the steps in the design study were first, the choice of the ratio r

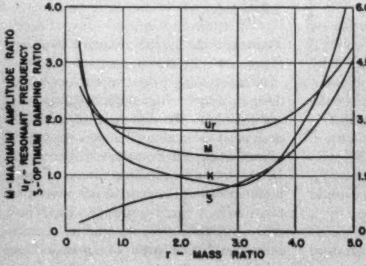

Figure 10 (left). Design curves for the spring-coupled-damper servomechanism

Figure 11 (right). Effect of variations in the damping ratio for the spring-coupled-damper servomechanism. Moment-of-inertia ratio $r=4$

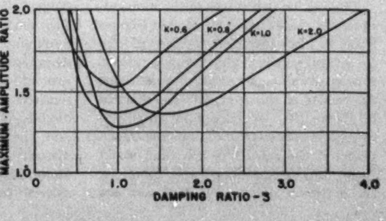

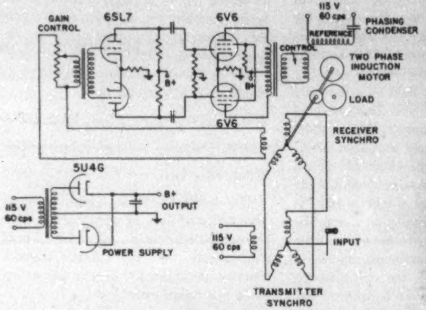

Figure 12. Diagram of instrument servomechanism stabilized with a spring-coupled damper

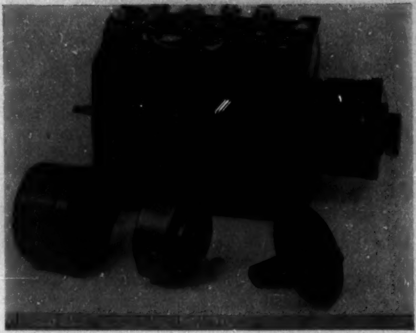

Figure 13. Induction-type servomotor and spring-coupled damper

(somewhat arbitrarily, initially) and plotting the corresponding transfer function locus; second, the determination from the locus of the maximum value of sensitivity K, consistent with the specified maximum amplitude ratio; and, third, repetition of the procedure for a range of values of r and comparison of the results.

The study of the spring-coupled damper is made similarly but is more lengthy because of the additional parameter, ζ, at the engineer's disposal.

Again it is expedient to neglect at first the controller time lag. After results have been obtained with zero controller lag, the upper limit of lag for which the results are valid can be determined. The steps in the design study are first, choose judiciously, if possible, the ratio r, and plot for a range of values of damping ratio ζ, the corresponding loci; second, determine from each locus the maximum value of the sensitivity, K, consistent with the permissible maximum amplitude ratio; third, choose as optimum that value of ζ that permits K to be maximum; and fourth, repeat the procedure for other values of r and compare the results. The optimum sensitivity K, the maximum amplitude ratio, and the resonant frequency are all determined by the graphical construction employed in the study of the viscous damper.

The loci for two values of the moment-of-inertia ratio r are illustrated in Figures 8 and 9. In each figure loci are plotted for several values of the damping ratio ζ. A range of values of r was investigated and the results of the study are summarized in Figure 10. A maximum amplitude ratio as low as four-thirds can not be obtained if the ratio r is less than about three. For r less than three, therefore, the optimum damping ratio ζ and the optimum sensitivity factor K, are chosen to minimize the maximum amplitude ratio. If the moment-of-inertia ratio r is larger than three, the damping ratio can be so selected that the maximum amplitude ratio can be less than four-thirds. Since in general there is no need for a larger stability margin the damping ratio when r is greater than three is chosen to permit the maximum sensitivity factor will not produce a peak amplitude response greater than four-thirds. For this reason the curve of M in Figure 10 is constant for r greater than three.

The resonant frequency that accompanies the choice of damping ratio ζ, and sensitivity factor K, is also plotted in Figure 10.

It is interesting to compare the results presented in Figure 10 for the spring-coupled damper and in Figure 5 for the viscous damper. For the viscous damper, the moment-of-inertia ratio must be at least six in order that the peak amplitude response be no larger than four-thirds. For the spring-coupled damper, however, the moment-of-inertia ratio need be only three to achieve the same result. Such a reduction in moment-of-inertia results in a real improvement in the synchronizing properties of the servomechanism.

The effect of temperature variation on the characteristics of the spring-coupled damper servomechanism is indicated by Figure 11, in which is plotted the maximum amplitude ratio as a function of the damping ratio ζ, for a moment-of-inertia ratio of four and several values of system sensitivity. The damping ratio ζ varies directly with the damping coefficient f_A, and therefore directly with the fluid viscosity. If the viscosity varies by a factor of three, as in the example considered earlier where the temperature ranged between 35 and 130 degrees Fahrenheit, the value of ζ will vary by three. The variation in the maximum amplitude ratio depends not only upon the variation in ζ but also upon its value at a particular temperature and the choice of sensitivity factor, K. Unlike the viscous damper, the sensitivity K, for the spring-coupled damper is independent of the damping coefficient. For a temperature range of 35–130 degrees Fahrenheit, an approximately optimum result is secured by choosing a sensitivity factor of 0.8 and a minimum ζ of 0.54. The maximum amplitude ratio is then the same at both ends of the temperature range and equal to 1.54. It is interesting to note that to limit the variation in the maximum amplitude ratio to this value for the viscous damper, a moment-of-inertia ratio of about 7.5 is required.

The criterion for the maximum permissible controller lag τ_c is the same as for the viscous damper. The term in which τ_c appears (see equation 22) should not introduce more than about five degrees phase shift at the system resonant frequency into the transfer function. This requirement is met provided

$$\tau_c \le \frac{0.1}{\omega_r}$$

where ω_r is the system resonant frequency expressed in radians per second.

It is revealing to contrast the optimum design of a spring-coupled damper for stabilizing a servomechanism with the design of a similar damper used as a vibration absorber on a rotating machine. In the latter case it is common to use a moment-of-inertia ratio of not more than one-fourth. Such a design, used in a servomechanism, would lead to a maximum amplitude ratio of at least three which today is considered entirely unsatisfactory. The difference in design arises from the difference in operation between open- and closed-cycled systems.

Example of an Instrument Servomechanism with Spring-Coupled Damper

During the last war there was a military requirement for an instrument servomechanism of good performance, minimum service requirements, and characteristics relatively independent of supply voltage, supply frequency, and temperature. Several types of instrument servomechanisms stabilized with spring-coupled dampers and employing induction motors as servomotors were developed in the servomechanisms laboratory of the Massachusetts Institute of Technology to meet these requirements. Their principal advantages are listed below.

Performance. These servomechanisms had an amplitude response essentially flat to 12 cycles per second. The performance was satisfactory for changes in the supply voltage and frequency of as much as 15 per cent. Some units were designed so that their performance essentially was unaltered for a change in operating temperature of 100 degrees Fahrenheit, and not seriously altered for a change in operating temperature of 150 degrees Fahrenheit.

Service Requirements. The induction motor is an ideal servomotor from the service standpoint. There are no brushes to wear out, and with conservative design the bearings and windings have an almost unlimited life. The spring-coupled damper employed was a sealed unit and required no attention. The amplifier controlling the servomotor contained no circuits requiring adjustment and included only one control, the gain control which was locked after initial adjustment. Since the amplifier was a proportional a-c amplifier, it required no special servicing techniques.

A diagram of one such unit is given in Figure 12. This servomechanism was used as a remote-position indicator and drove a relatively heavy mechanism.

The servomotor is a 4-pole, 60-cycle-per-second induction motor designed for a low moment of inertia of the rotor and a stalled torque of about four ounce inches. The data transmission system comprised two synchros, one geared to the servomotor, and the second remotely located. The electrical signal developed by the synchro coupled to the servo and supplied to the servo controller is proportional to the sine of the error of the relative position of the two synchros. The servo controller is a three-tube a-c amplifier with a power supply comprising a full-wave rectifier with capacitor filtering. The amplifier output is supplied to the control field of the induction motor, the second or reference field of which is connected to the a-c line through a phasing capacitor.

The induction motor has shafts extending from both ends of the rotor. One shaft couples the motor to the receiver synchro and load by means of a 100:1 gear reduction. The second shaft carries the spring-coupled damper. The servomotor and damper is shown in Figure 13. The damper housing is made of magnesium to minimize its moment of inertia, and completely encloses the damper in order to prevent leakage, eliminate dirt, and so forth. The damper moment of inertia is made of a lead alloy, and the housing is filled with a damping fluid with a viscosity of about 500 centistokes at room temperature.

The principal specification for this servomechanism was that it have a high torque-error constant, and this particular requirement determined the system design. It was desirable that the torque-error constant be about 0.2 ounce-inch per degree at the motor shaft, and this specification was met satisfactorily by the servo. This particular unit was required to operate over only a moderately wide temperature range and therefore a moment-of-inertia ratio r of three was chosen. The damper spring was selected to provide the specified torque-error constant, and since the moment of inertia of the motor rotor, damper housing, and load was about 0.1 ounce-inch squared, the natural frequency of the servomechanism was about 15 cycles per second. The time lag of the controller was kept at about one millisecond or less.

The servomechanism was tested by determining its transient response to certain test inputs. Three of the resulting records are given in Figure 14. The measurements were made by recording the receiver synchro voltage which is proportional to the servo error, except for inaccuracies in the data transmission system itself. In this type of test the data transmission errors should not be charged against the servomechanism. The test inputs were suddenly applied constant rotations of the transmitter synchro.

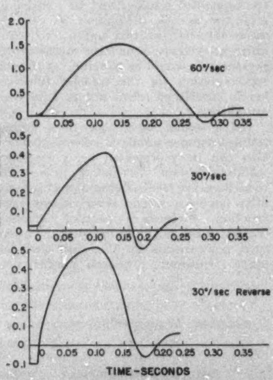

Figure 14. Transient responses of spring-coupled-damper servomechanism

Records are given of the servo response to velocity inputs of the transmitter synchro of 30 degrees per second, 60 degrees per second and a sudden reversal from 30 degrees per second in one direction to an equal velocity in the reverse direction. In all cases the transient has decayed in three-tenths second or less.

Conclusions

Load compensation of servomechanisms is a desirable method of stabilization under favorable circumstances. Compensation of certain types of instrument servomechanisms by either a viscous damper or a spring-coupled damper is effective. The spring-coupled damper is superior in that, for equal results it employs only about one-half the stabilizing moment of inertia required in the viscous damper.

The band width of instrument servomechanisms stabilized in this fashion can be made almost indefinitely wide provided the time lag in the controller and motor is made sufficiently small. With improperly chosen components, however, the nonlinear operation of such servomechanisms may not be satisfactory because of the larger moment-of-inertia coupled to the servomotor. An instrument servomechanism stabilized with a spring-coupled damper has been proved by service. This unit has a natural frequency of about 15 cycles per second and a torque-error constant of about 0.2 ounce-inch per degree measured at the servomotor shaft.

References

1. THE ANALYSIS AND SYNTHESIS OF LINEAR SERVOMECHANISMS, A. C. Hall. The Technology Press, Cambridge, Mass., 1943.

2. PARALLEL CIRCUITS IN SERVOMECHANISMS, H. T. Marcy. AIEE TRANSACTIONS, volume 65, 1946, pages 521–29.

3. APPLICATION OF CIRCUIT THEORY TO THE DESIGN OF SERVOMECHANISMS, A. C. Hall. *Journal*, The Franklin Institute (Philadelphia, Pa.), volume 242, October, 1946, pages 279–307.

4. PRINCIPLES OF SERVOMECHANISMS, G. S. Brown, D. P. Campbell. John Wiley and Sons, New York, N. Y., 1948.

Discussion

Eric R. Behn (Control Instrument Company, Brooklyn, N. Y.): Hall refers to a common figure of merit generally applied to servomechanisms, namely, the maximum amplitude response ratio should be not greater than four-thirds of its zero frequency value. In this connection, where the resonant frequency of an instrument servomechanism is high, say 15 cycles per second, it may present an interesting departure from this usually accepted design criteria. In the frequency analysis as applied in the laboratory, it is usual to adjust the amplitude of the sinusoidal input to be larger than any accumulated backlash. Such an analysis might show a maximum amplitude response greater than four-thirds of its zero frequency value, yet the servomechanism would not be necessarily unstable because the amplitude of a 15-cycle-per-second component in the input data is usually quite small and may readily be less than the lost motion in a gear train or linkage.

The limitation of the maximum amplitude response to four-thirds is still a good design figure of merit. It is merely suggested that where the natural frequency is greater than ten cycles per second, a careful analysis be made of the probable input data and component design before a design is rejected. The writer has designed and built a servomechanism with a natural frequency of 20 cycles per second, which is quite stable even though the maximum amplitude response is three times its zero frequency value.

W. M. Pease (Massachusetts Institute of Technology, Cambridge, Mass.): It is interesting to consider that damper-stabilization may be treated as a form of feedback compensation. The feed-back link consists of a device sensitive to rotation of the output shaft which produces torque acting in opposition to the electrically produced air-gap torque in the servomotor. Thus, the air-gap torque produced as a result of servomechanism error is degenerated through feedback as a function of the servomechanism output. When this feed-back concept is expressed in the form of a block diagram, similarities between damper-stabilized servomechanisms and feed-back stabilized servomechanisms can be recognized.

For the viscous-damper-stabilized servomechanism, Hall's basic equations lead to a feed-back representation which is identical with a case treated by Harris,[1] in which a servomechanism was stabilized by tachometric feedback through a simple high-pass filter. Since both Hall and Harris give numerical solutions for their systems, it is interesting to compare the results. This is done in Table I of the discussion.

The equation expressing the system transfer function as derived by Hall is identical with a generalized solution of Herr and Gerst[2] if secondary time lags are neglected. The results for this case are also given in Table I. The results have been reduced to the form of Hall's solutions to make comparison simple. Note that the parameter r, chosen nearly identically by the three authors, represents ratio of inertias in Hall's case, feed-back sensitivity in Harris' case and the ratio of time constants in the Herr-Gerst case. A similar divergence of physical meaning applies to other parameters. For the adjustments indicated, system sensitivity may have two values based on the same criterion of peak amplitude response. Hall indicates both values, but selects the larger of the two and, at the same time, permits a relatively small secondary delay. Harris, on the other hand, selects the smaller of the two and permits a relatively large secondary delay. Hall's choice of sensitivity seems to be based on providing the least sensitivity to variations in viscosity of the damper fluid, while Harris' selection of sensitivity seems to be based on permitting the largest possible secondary delay. Herr and Gerst chose the value of sensitivity for which $M_p = 1.25$ at only one frequency. This seems to correspond to Hall's selection.

Table I

	Parameter Ratio r	System Sensitivity, Nondimensionalized K_1	Permissible Maximum Secondary Time Lag, Nondimensionalized
Hall	9	0.37	0.02
		0.78	0.05
Harris	10	0.36	0.44
Herr-Gerst	9.6	0.76	0

Anyone attempting a comparison such as that in Table I will observe a weakness in the manner in which transfer functions for servomechanisms are represented. All three cases were nondimensionalized, but on different bases, and the similarity between the numerical results could be noted only after considerable calculation. Where the same transfer function applies to many different systems, a uniform mathematical presentation would be of value. A suitable representation for the transfer functions herein considered seems not to have been established.

Hall's second case, that of a spring-coupled-damper-stabilized servomechanism, also can be represented as a feed-back stabilized system. In this case, it is similar to tachometric feedback through a high-pass filter having a second order characteristic function. Because a parallel numerical treatment has not been found in the literature, comparisons for this case were not made. However, a general parallel does suggest itself. As the addition of the spring is beneficial to the damper-stabilized servomechanism, so is the use of a high-pass filter of second or higher order beneficial to the servomechanism stabilized by tachometric feedback.

REFERENCES

1. A Comparison of Two Basic Servomechanism Types, Herbert Harris. AIEE Transactions, volume 66, 1947, pages 83–93.

2. The Analysis and an Optimum Synthesis of Linear Servomechanisms, Donald Herr, Irving Gerst. AIEE Transactions, volume 66, 1947, pages 959–70.

Albert C. Hall: Behn, in commenting upon the design criterion that limits the maximum amplitude response of a servomechanism to approximately four-thirds has touched upon a very interesting point, namely, the determination of the margin of stability required in a closed-cycle system. The margin of stability is fixed generally by the following two considerations: First, the factor of safety required in order that maladjustments, component aging, and so forth will not produce actual instability; and second, the requirement that the servomechanism not magnify unduly the energy appearing in any particular frequency band of the signal. The determination of the maximum allowable amplitude ratio from either standpoint is a function among other things, of the type of servomechanism, the particular signals it must follow, and the service in which it may operate. Unusual conditions can affect appreciably the permissible maximum amplitude ratio. For example, if a servomechanism has a natural frequency of 20 cycles per second, but is subjected to input signal with negligible energy beyond two cycles per second, a much higher amplitude peak than four-thirds is permissible, provided component aging and maladjustments do not cause problems.

In general, however, servomechanisms are not designed with band widths ten times that required, and therefore appreciable signal energy does exist at all frequencies within the servo band pass. In addition, maladjustments are realistic service problems. For the majority of practical cases, therefore, a value of the maximum amplitude ratio of four-thirds to three-halves seems to give satisfactory results.

The comparison, provided by Pease, of the damper-stabilized servomechanism and the feed-back stabilized servomechanism is significant. It could have been extended as well to servomechanisms stabilized by cascade compensation. The agreement is illustrative of the fact that for the same system performance the transfer functions of either the cascade compensated, the feed-back compensated, or the load compensated servos will be the same. After proper transformation the design parameters of one system may be employed to determine parameters of either of the other two.

Graphical Determination of Transfer Function Loci for Servomechanism Components and Systems

C. H. THOMAS
ASSOCIATE AIEE

E. C. EASTON
MEMBER AIEE

IN the designing of a linearly operating control system it is desirable to determine for the uncompensated system the variation with frequency of amplitude and phase of the transfer function. As shown by a number of authors, this knowledge enables the designer to ascertain stability, and to synthesize compensating devices for improving the performance of the completed system. If the system can be described quantitatively, the transfer function locus may be calculated. In some systems it is possible to obtain the transfer function locus experimentally by introducing appropriate sinusoidal signals and measuring relative output and input amplitudes and phase. On the other hand, systems may be envisioned where both numerical mathematical representation and sinusoidal measurements are not feasible. It is the purpose of this paper to suggest a method for determining either the open- or closed-loop relative amplitude and phase diagrams from a single transient measurement. The input transient signal is not restricted in form particularly and may be of such nature that actual operating conditions of the system are duplicated approximately. Experimental results indicate the method to be practicable. The equations derived are applicable where the assumption of linearity and lumped parameters is reasonable.

Methods of Analysis

Laplacian Transform Equation

For generality a given open-cycle system, or isolated component of a more complex system, may be represented by a block as shown in Figure 1. The Laplacian transform equation relating input and output transforms is

$$F_o(s)=KG(s)F_i(s) \tag{1}$$

where $F_i(s)$ is the transform of the input signal $f_i(t)$, $F_o(s)$ is the transform of the output response $f_o(t)$, and $KG(s)$ is defined as the system transfer function.[1,2] The direct Laplace transforms of the input and output time functions are respectively

$$F_i(s)=\int_0^\infty f_i(t)e^{-st}dt \tag{2}$$

and

$$F_o(s)=\int_0^\infty f_o(t)e^{-st}dt \tag{3}$$

where $s=\sigma+j\omega$ and both σ and ω are real variables.[3] From equations 1, 2, and 3 there is obtained

$$KG(s)=\frac{\int_0^\infty f_o(t)e^{-st}dt}{\int_0^\infty f_i(t)e^{-st}dt} \tag{4}$$

Modifications of this expression, equation 4, for the transfer function are developed for special case applications in the following sections.

Bounded Transient Input Signal

Since it is desired to obtain the amplitude and phase of the transfer function $KG(j\omega)$ as a function of frequency, the complex variable s may be set equal to $j\omega$, and equation 4 becomes

$$KG(j\omega)=\frac{\int_0^\infty f_o(t)e^{-j\omega t}dt}{\int_0^\infty f_i(t)e^{-j\omega t}dt},$$

$$=\frac{\int_0^\infty f_o(t)\cos\omega t\,dt-j\int_0^\infty f_o(t)\sin\omega t\,dt}{\int_0^\infty f_i(t)\cos\omega t\,dt-j\int_0^\infty f_i(t)\sin\omega t\,dt} \tag{5}$$

Use of equation 5 requires the input signal and output response to be of such form that the integrals may be evaluated. This condition is realizable practically. The integrals may be evaluated by simple graphical procedures or by other convenient methods. It is necessary only to introduce into the system a bounded transient signal of more or less arbitrary form, taking simultaneous records of this signal and the system response. The duration time and maximum amplitude of the input signal should be so adjusted that the system is not overdriven or saturated. Furthermore if the duration time is made of the order of magnitude of the period of the highest frequency for which $KG(j\omega)$ is to be determined, graphical integration is much easier to perform. This is evident since over the finite interval of integration the number of positive and negative areas is reduced.

Step Function Input Signal

With a step function input the output response may be one of many possible forms depending on the nature of the particular system. For example the output voltage $e_o(t)$ as a result of a step input voltage $e_i(t)$ to a few simple electrical networks is sketched in Figures 2(a), (b), and (c). In Figure 2(d) is shown a sketch of the response of a second-order open-cycle servo system. In these examples, as well as many higher order systems, the steady-state component of the output response may be either zero, a constant, a linear function of time, or a constant

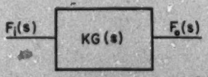

Figure 1. Block diagram of an open-cycle system

Paper 49-80, recommended by the AIEE servomechanisms committee and approved by the AIEE technical program committee for presentation at the AIEE winter general meeting, New York, N. Y., January 31–February 4, 1949. Manuscript submitted September 17, 1948; made available for printing December 21, 1948.

C. H. Thomas is instructor of electrical engineering at Harvard University, Cambridge, Mass. and E. C. Easton is the dean of the college of engineering at Rutgers University, New Brunswick, N. J.

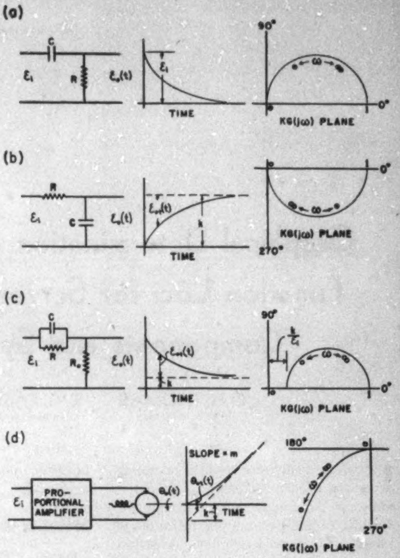

Figure 2. Transient responses to a step function and corresponding transfer function loci

(a). Simple differentiating type network

Time constant $T=RC$; output response:

$\epsilon_o(t)=\epsilon_i e^{-t/T}$; transfer function

$$KG(j\omega)=\frac{j\omega T}{j\omega T+1}$$
$$=\frac{1}{\epsilon_i}\left[\omega\int_0^\infty \epsilon_i e^{-t/T}\sin\omega t\,dt+ j\omega\int_0^\infty \epsilon_i e^{-t/T}\cos\omega t\,dt\right]$$

(b). Simple integrating type network

Time constant $T=RC$; steady-state component of response

$\epsilon_{oc}(t)=k=\epsilon_i$

Transient component of response

$\epsilon_{ot}(t)=-\epsilon_i e^{-t/T}$

Total output response

$\epsilon_o(t)=\epsilon_i(1-e^{-t/T})$

Transfer function

$$KG(j\omega)=\frac{1}{j\omega T+1}$$
$$=\frac{1}{\epsilon_i}\left[\epsilon_i+\omega\int^\infty(-\epsilon_i e^{-t/T})\sin\omega t\,dt+ j\omega\int_0^\infty(-\epsilon_i e^{-t/T})\cos\omega t\,dt\right]$$

(c). Differentiating type network

Time constant: $T=\dfrac{R_oRC}{R_o+R}$

Attenuation constant:

$\alpha=\dfrac{R_o+R}{R_o}$

Steady-state component of response

$\epsilon_{oc}(t)=k=\epsilon_i/\alpha$

Transient component of response

$\epsilon_{ot}(t=\dfrac{\alpha-1}{\alpha}\epsilon_i e^{-t/T}$

Total output response

$\epsilon_o(t=\dfrac{\epsilon_i}{\alpha}+\dfrac{\alpha-1}{\alpha}\epsilon_i e^{-T/t}$

Transfer function

$$KG(j\omega)=\frac{1}{\alpha}\frac{j\omega T\alpha+1}{j\omega T+1}$$
$$=\frac{1}{\epsilon_i}\left[\frac{\epsilon_i}{\alpha}+\omega\int^\infty\times\left(\frac{\alpha-1}{\alpha}\epsilon_i e^{-t/T}\right)\sin\omega t\,dt+ j\omega\int_0^\infty\left(\frac{\alpha-1}{\alpha}\epsilon_i e^{-t/T}\right)\cos\omega t\,dt\right]$$

(d). Second-order open-cycle servo system

Time constant, T; gain factor, K_a; steady-state component of response

$\theta_{oc}(t)=-k+mt$

Transient component of response

$\theta_{ot}(t)=ke^{-t/T}$

Total output response (angular position)

$\theta_o(t)=-k+mt+ke^{-t/T}$

Transfer function

$$KG(j\omega)=\frac{K_a}{j\omega(j\omega T+1)}$$
$$=\frac{1}{\epsilon_i}\left[(-k)+\omega\int^\infty ke^{-t/T}\times\sin\omega t\,dt-j\frac{m}{\omega}+j\omega\int_0^\infty ke^{-t/T}\cos\omega t\,dt\right]$$

where $\dfrac{k}{\epsilon_i}=K_aT$ and $\dfrac{m}{\epsilon_i}=K_a$

plus a linear function of time. Such a steady-state response may be expressed

$$_c(t)=k+mt \tag{6}$$

where k and m are constants, and t is the independent variable time. By superposition the total output response may be written as a sum of steady-state and transient components. Thus,

$$\begin{aligned}f_o(t)&=f_c(t)+f_t(t)\\&=k+mt+f_t(t)\end{aligned} \tag{7}$$

The direct Laplace transforms of step input ϵ_i and output $f_o(t)$ are respectively

$$F_i(s)=\int_0^\infty \epsilon_i e^{-st}dt=\frac{\epsilon_i}{s} \tag{8}$$

$$\begin{aligned}F_o(s)&=\int^\infty[k+mt+f_t(t)]e^{-st}dt\\&=\frac{k}{s}+\frac{m}{s^2}+\int_0^\infty f_t(t)e^{-st}dt\end{aligned} \tag{9}$$

Substituting equations 8 and 9 in 4 gives

$$KG(s)=\frac{1}{\epsilon_i}\left[k+\frac{m}{s}+s\int_0^\infty f_t(t)e^{-st}dt\right] \tag{10}$$

Setting $s=j\omega$ there is obtained

$$KG(j\omega)=\frac{1}{\epsilon_i}\left[k+\omega\int_0^\infty f_t(t)\sin\omega t\,dt- j\frac{m}{\omega}+j\omega\int_0^\infty f_t(t)\cos\omega t\,dt\right] \tag{11}$$

If the mathematical expression for the pure transient component $f_t(t)$ of the output response is uncertain, graphical integration as indicated by equation 11 yields the transfer function locus. Upon application of this expression to the responses illustrated in Figure 2, the transfer function loci shown are obtained.

Experimental Application

DESCRIPTION OF SYSTEM TESTED

For the purpose of testing the practicability of utilizing the relations derived in the preceding paragraphs a simple position control system was built. The schematic diagram of this system is shown in Figure 3. The principle components are as follows: selsyns for detection of position error, a demodulator for converting the 60-cycle error voltage to a d-c voltage, an electronic amplifier, an amplidyne, a d-c shunt motor, and a small d-c generator coupled directly to the motor shaft for the purpose of measuring motor speed. This setup was chosen for two predominant reasons, namely; (1) mathematical representation of the system is lengthy, since there are at least five time delays present, and (2) the transfer function locus is measurable directly and the calculated locus can be checked for accuracy.

DIRECT MEASUREMENT OF THE TRANSFER FUNCTION LOCUS

The schematic arrangement for the direct sinusoidal measurements is shown in Figure 4. The signal generator consists of two identical selsyns connected

Figure 3. Schematic diagram of system tested

R_1—Two potentiometers with shafts tied together, 40,000 ohms each
R_2 and R_3—200,000 ohms
R_4—5,000-ohm potentiometer
R_5 and R_6—12,000 ohms
R_7 and R_8—100,000 ohms
R_9—Two potentiometers 40,000 ohms each
C_1, C_2, C_3—0.50 microfarad
T_1 and T_2—Plate and filament transformer: 120/500/6.3 volts, high voltage winding center tapped

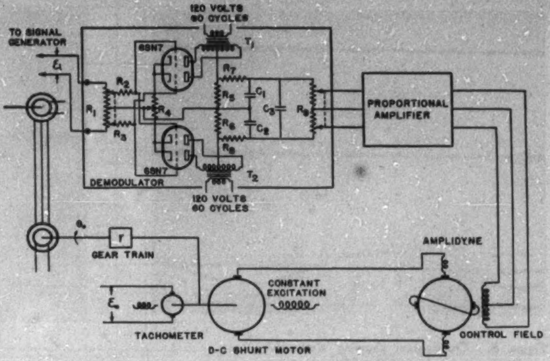
120 VOLTS 60 CYCLES
TO SIGNAL GENERATOR
ε_i
6SN7
T_1
R_2
R_1
R_4
R_3
R_7
R_5
C_1
C_3
R_9
R_6
C_2
R_8
6SN7
T_2
DEMODULATOR
120 VOLTS 60 CYCLES
PROPORTIONAL AMPLIFIER
θ_o
r
GEAR TRAIN
AMPLIDYNE
CONSTANT EXCITATION
ε_o
TACHOMETER
D-C SHUNT MOTOR
CONTROL FIELD

together by a differential and driven through suitable gear reduction by a constant speed d-c motor. In order to obtain the required low frequency signals the 60-cycle carrier voltage is modulated as desired by adjustment of the motor speed. The relative phase of the input and reference signals is controlled by changing the angle between the two selsyns through the medium of the differential. Relative phase may be read from a calibrated dial. The modulated reference signal and tachometer voltages feed through the continuous calibrator to the vertical and horizontal amplifier circuits of the cathode-ray oscilloscope. These two sinusoidally varying voltages form a pattern on the oscilloscope screen. The relative phase of the reference signal voltage envelope and the system output tachometer voltage may be adjusted to zero by changing the relative position of the reference selsyn. The phase shift through the system is thus obtained. The continuous calibrator[4] periodically disconnects the inputs to the oscilloscope for a brief interval of time and feeds variable calibrating voltages independently to the vertical and horizontal input circuits. A bright spot of light appears on the oscilloscope screen simultaneously with the pattern which is being studied. By means of two potentiometers on the panel of the calibrator the spot can be moved to any position on the screen. Two voltmeters on the panel read respectively the horizontal and vertical positions of the spot. By proper positioning of the spot the magnitudes of the two voltages being compared can be determined simultaneously.

Figure 5(a) shows the experimental setup, and Figure 5(b) shows the control panel of the continuous calibrator and the screen of the cathode-ray oscilloscope. The figure traced on the screen (long persistence type of screen) is that obtained when the phase difference of the reference signal and system output is zero. For this illustration, the input signal was being modulated at a frequency of one cycle per second. The calibrating spot has been moved to the upper right-hand portion of the screen so that it may be seen clearly. During actual measurements, readings were taken with the spot positioned to each of the four corners of the "bow tie" figure.

Figure 6 is an oscillogram showing waveforms of input signal and system output. Note that the output oscillation

Figure 4. Schematic setup for measuring the transfer function locus

A—Selsyn supplying input signal to the servo system
A—Selsyn supplying reference signal to the continuous calibrator
C—Differential gear
D—Small d-c motor
E—Dial calibrated in degrees

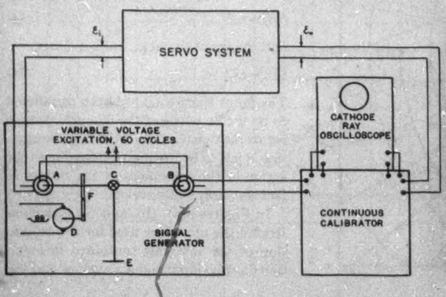
ε_i
SERVO SYSTEM
ε_o
VARIABLE VOLTAGE EXCITATION, 60 CYCLES
A
C
B
F
D
E
SIGNAL GENERATOR
CATHODE RAY OSCILLOSCOPE
CONTINUOUS CALIBRATOR

Figure 5. (a) (right, below) Experimental setup (b) (right) A typical pattern on the screen of the cathode-ray oscilloscope

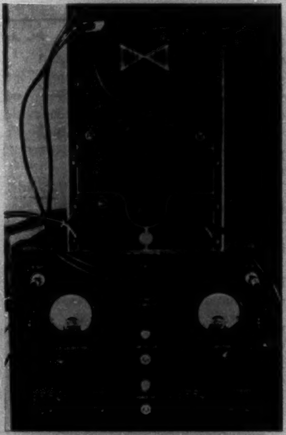

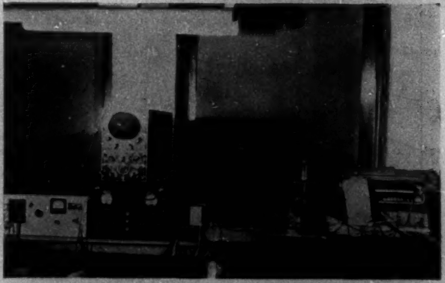

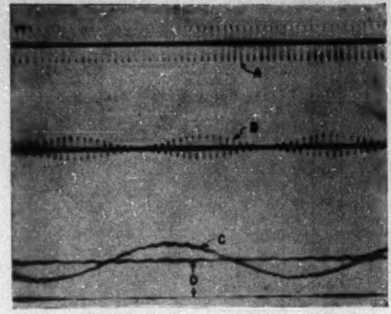

Figure 6. Oscillogram showing sinusoidal amplitude modulation of the 60-cycle input signal and the resulting oscillation of the servomotor. Motor running unidirectionally

A—Sixty cycles per second timing wave
B—Input signal
C—Servomotor oscillation
D—Average constant speed of the servo motor

is displaced by a constant value from zero. This was produced by a small unbalance of the demodulator and was purposefully done in order to compel the servo motor to run continuously in one direction. This reduced undesirable variations in friction and enabled the pattern on the oscilloscope screen to remain practically stationary.

The transfer function locus $E_o(j\omega)/E_i(j\omega)$ measured directly is shown in Figure 7. It should be pointed out that this plot relating the amplitude and phase of output and input voltages is not in the form most convenient for synthesis studies. Usually for a system such as this the output angular position and input angular error are related to form a transfer function. It may be shown very simply that this open-loop transfer function is

$$\frac{\theta_o(j\omega)}{\theta_i(j\omega)}=\frac{K_1}{rK_tj\omega}\,\frac{E_o(j\omega)}{E_i(j\omega)} \tag{12}$$

where $\theta_o(i\omega)/\theta_i(j\omega)$ is the ratio of output shaft angular position to input angular error, K_1 is the selsyn sensitivity expressible in volts per radian, K_t is the tachometer constant in volts per radian per second, r is the gear ratio between the servomotor and output shaft, and $E_o(j\omega)/E_i(j\omega)$ is the locus plotted in Figure 7.

Figure 7. Transfer function locus showing a comparison of measured and calculated points

x—Points determined by direct measurement
o—Calculated from the transient response to an arbitrary input signal
Δ—Calculated from the transient response to a step function input

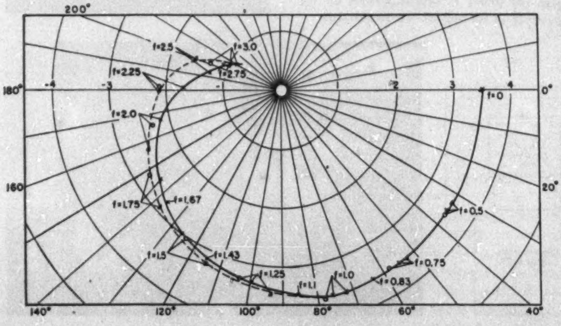

The transfer function locus, equation 12, is omitted since no object would be served unless the synthesis problem was carried to completion, and this is not the immediate aim of this paper. For methods of synthesis the reader is referred for example to references 1, 2, 5, 6, 7, and 8 listed at the end of this paper.

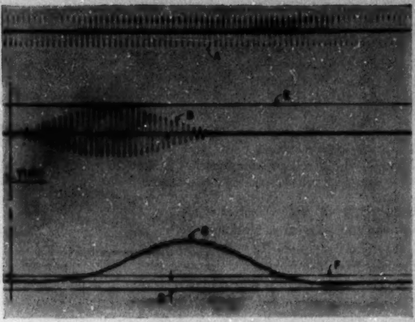

Figure 8. Oscillogram of arbitrary input signal and resultant servomotor speed response

A—Sixty cycles per second timing wave
B—Sixty cycle input signal with arbitrary envelope
C—Output speed response of servomotor
D—Initial and final value of servomotor speed
E and F—Calibration (2.05 volts)

CALCULATIONS BASED ON MEASUREMENT OF TRANSIENT RESPONSE TO A BOUNDED-INPUT SIGNAL

With gain adjustments in the system unchanged and with the setup as indicated in Figure 4, the oscillogram shown in Figure 8 was obtained. The input signal, the envelope of which is of haphazard form, was produced by varying the selsyn excitation. Note that the input starts at zero and returns to zero. It may be observed that the output response (tachometer voltage which is directly proportional to motor speed) begins at an initial small value and returns to this same value. Again the demodulator was purposely unbalanced so as to cause the motor to run continuously, thus avoiding frictional effects which arise when starting from standstill.

These waveforms are suitable for the application of equation 5, where as indicated in Figure 8, the output response is

$$f_o(t)=\epsilon_t(t) \tag{13}$$

and the input signal is

$$f_i(t)=\epsilon_i(t) \tag{14}$$

The input signal $\epsilon_i(t)$ has been considered to be the envelope of the 60-cycle voltage fed to the demodulator. Such an assumption is felt to be justifiable since due to the action of the demodulator, the system in fact sees only this envelope.

In Figures 9(a), (b), and (c) is demonstrated the procedure used for the evaluation of the integrals contained in equation 5. The input signal envelope and the

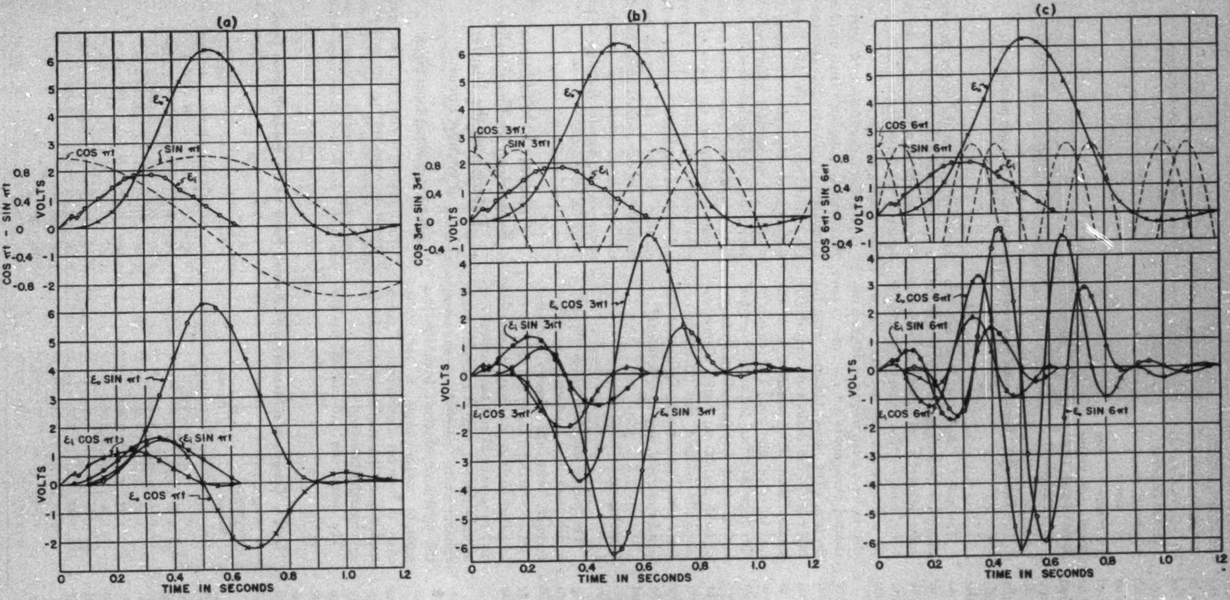

(a). One-half cycle per second

$\int_0^\infty e_i \cos \pi t \, dt = 0.364$ volt-second

$\int_0^\infty e_i \sin \pi t \, dt = 0.520$ volt-second

$\int_0^\infty e_o \cos \pi t \, dt = -0.084$ volt-second

$\int_0^\infty e_o \sin \pi t \, dt = 2.252$ volt-second

$$KG(j\omega)\Big|_{f=0.5} = \frac{-0.084 - j2.252}{0.364 - j0.520} = 3.55\underline{/-37.10^\circ}$$

(b). One and one-half cycles per second

$\int_0^\infty e_i \cos 3\pi t \, dt = -0.292$ volt-second

$\int_0^\infty e_i \sin 3\pi t \, dt = 0.0744$ volt-second

$\int_0^\infty e_o \cos 3\pi t \, dt = 0.304$ volt-second

$\int_0^\infty e_o \sin 3\pi t \, dt = -0.856$ volt-second

$$KG(j\omega)\Big|_{f=1.5} = \frac{0.304 + j0.856}{-0.292 - j0.0744} = 3.02\underline{/-123.80^\circ}$$

(c). Three cycles per second

$\int_0^\infty e_i \cos 6\pi t \, dt = -0.007$ volt-second

$\int_0^\infty e_i \sin 6\pi t \, dt = 0.012$ volt-second

$\int_0^\infty e_o \cos 6\pi t \, dt = 0.014$ volt-second

$\int_0^\infty e_o \sin 6\pi t \, dt = -0.012$ volt-second

$$KG(j\omega)\Big|_{f=3} = \frac{0.014 + j0.012}{-0.007 - j0.012} = 1.32\underline{/-199.0^\circ}$$

Figure 9. Graphical evaluation of the integrals of equation 5

output response, as obtained from the oscillogram in Figure 8, are replotted in each of the examples. The evaluation of each integral, the net area under the appropriate curve, was accomplished with the aid of a planimeter. The points on the transfer function locus determined thusly are plotted in Figure 7. It may be observed in Table I that the measured phase shift and the calculated phase shift for a particular frequency check to within four degrees or less except for the highest frequency (3 cycles per second) where the discrepancy is about 13 degrees. The measured and calculated amplitudes check to within 6 per cent or less over most of the locus, except for the highest frequencies. At three cycles per second the amplitude discrepancy is about 45 per cent.

The discrepancy mentioned above possibly may be explained as follows. Referring to Figure 9(c) it may be seen that the input signal duration time is nearly equal to two periods of the 3-cycle per second wave, and that all net areas measured with the planimeter were very small. Chances for making a large error thus were fairly great. A good criteria for this system and other similar systems appears to be "the duration time of the arbitrary input signal should be adjusted to be not greater than one to one and one-half times the period of the highest frequency for which the transfer function locus is to be evaluated." The optimum duration time of the transient input would also depend upon the number and magnitude of the time delays in the particular system.

CALCULATIONS BASED ON MEASUREMENT OF TRANSIENT RESPONSES TO A STEP FUNCTION INPUT SIGNAL

With a step function input signal the oscillogram shown in Figure 10 was obtained. Again the system responds only to the envelope of the input signal, and to a reasonable approximation this may be considered to be a step function. Equation 11, therefore, is applicable. The transient component of the output response is

$$f_t(t)=\epsilon_t(t) \tag{15}$$

and the constant k is the final change in the tachometer voltage. Note that the constant m is zero.

The method of evaluating the two integrals in equation 11 is demonstrated in Figures 11(a), (b), and (c). The graphical integration was carried out with the aid of a planimeter as in the preceding example. The points calculated for this case are plotted in Figure 7.

A—Step function input (2.70 volts peak)
B—Servomotor speed response
C—Initial speed of motor
D—Steady-state speed due to the input signal (9.40 volts equivalent)

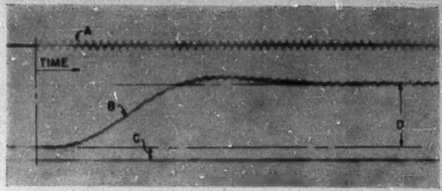

Figure 10. Oscillogram of servomotor speed response to a step function input

The points calculated from the two dissimilar measurements yield nearly the same locus for all practical purposes. Note, however, the frequency parameter for a given point does not check exactly, that is, for a given frequency the two calculated phase shifts differ by one to ten degrees. The phases obtained from the latter set of calculations are consistently smaller than those obtained from the first set of calculations. The reasons for this discrepancy are not entirely certain, but at least two contributing factors probably are, (1) the system is not linear as ideally assumed, and (2) changes in some of the parameters, mechanical friction for example, may have occurred.

Conclusion

The points calculated from the first measurement are in better agreement generally with the directly measured locus. For this reason and due to the fact that such an arbitrary input signal may be more easily realized practically, it appears the first type of transient measurement is to be preferred. In any event, the agreement obtained from the two separate measurements is sufficiently close to warrant further investigation toward using this technique as an aid in servomechanism design.

The amplitude attenuation of the measured locus at the higher frequency end relative to the calculated locus was due probably to a decrease in the gain factor of the demodulator in going from low to higher frequencies.

It is evident that if the time delays in the system are sufficiently large, graphical integration at the higher frequency end of the transfer function locus may be subject to intolerable errors. In some instances this undesirable feature may be avoided by breaking the system into two or more components, and by the methods described determine the locus of each component separately. The resulting loci may be combined by vector multiplication to obtain the over-all locus, providing the components are in cascade and there is no interaction effecting a change in the transfer function of the individual components.

Appendix I. Additional Expressions for Graphically Determining the Transfer Function Locus

Damped Exponential Input Signal

If it is possible to make the input signal a simple mathematical function, such as a damped exponential, the integrals in the denominator of equation 5 may be immediately determined and considerable

Table I. Comparison of Measured and Calculated Points on the Transfer Function Locus

Frequency, Cycles Per Second	$KG(j\omega)$ Measured Directly	Step Function Input	Arbitrary Input
0	$3.52\underline{/0^\circ}$	$3.49\underline{/0^\circ}$	$3.52\underline{/0^\circ}$
0.50	$3.50\underline{/-35.3^\circ}$	$3.54\underline{/-38.3^\circ}$	$3.55\underline{/-37.1^\circ}$
0.75	$3.53\underline{/-55.7^\circ}$	$3.57\underline{/-52.8^\circ}$	$3.52\underline{/-58.6^\circ}$
1.00	$3.53\underline{/-76.0^\circ}$	$3.58\underline{/-72.0^\circ}$	$3.61\underline{/-78.2^\circ}$
1.25	$3.30\underline{/-99.3^\circ}$	$3.43\underline{/-93.3^\circ}$	$3.26\underline{/-103.3^\circ}$
1.50	$2.98\underline{/-126.0^\circ}$	$3.23\underline{/-114.5^\circ}$	$3.02\underline{/-123.8^\circ}$
1.75	$2.60\underline{/-145.0^\circ}$	$2.91\underline{/-137.0^\circ}$	$2.76\underline{/-148.2^\circ}$
2.00	$2.16\underline{/-167.0^\circ}$	$2.52\underline{/-157.3^\circ}$	$2.32\underline{/-165.3^\circ}$
2.25	$1.69\underline{/-182.0^\circ}$	$2.14\underline{/-180.0^\circ}$	$2.18\underline{/-181.3^\circ}$
2.50	$1.27\underline{/-194.0^\circ}$	$1.58\underline{/-200.7^\circ}$	
3.00	$0.90\underline{/-212.0^\circ}$	$0.96\underline{/-215.7^\circ}$	$1.32\underline{/-199.0^\circ}$

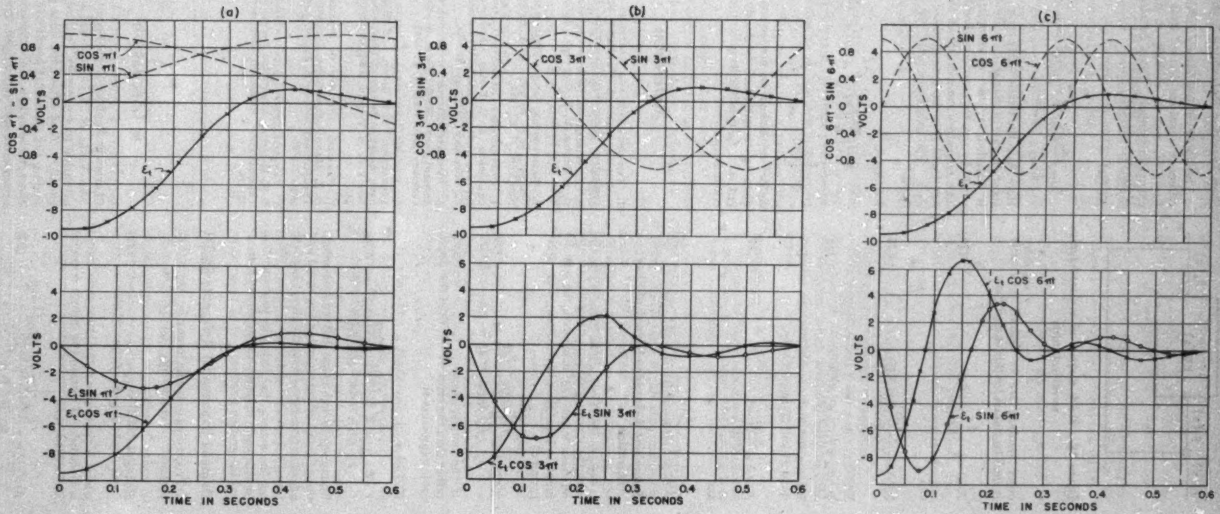

(a). One-half cycle per second

$\int_0^\infty \epsilon_t \sin \pi t\, dt = -0.448$ volt-second

$\int_0^\infty \epsilon_t \cos \pi t\, dt = -1.668$ volt-second

$$KG(j\omega)\Big|_{f=0.5} = \frac{1}{2.7}(9.40-0.448\pi-j1.668\pi) = 3.54\underline{/-33.3^\circ}$$

(b). One and one-half cycles per second

$\int_0^\infty \epsilon_t \sin 3\pi t\, dt = -1.380$ volt-second

$\int_0^\infty \epsilon_t \cos 3\pi t\, dt = -0.842$ volt-second

$$KG(j\omega)\Big|_{f=1.5} = \frac{1}{2.7}[9.40-(1.38)(3\pi) - j(0.842)(3\pi)] = 3.23\underline{/-114.5^\circ}$$

(c). Three cycles per second

$\int_0^\infty \epsilon_t \sin 6\pi t\, dt = -0.608$ volt-second

$\int_0^\infty \epsilon_t \cos 6\pi t\, dt = 0.080$ volt-second

$$KG(j\omega)\Big|_{f=3} = \frac{1}{2.7}[9.40-(0.608)(6\pi) + j(0.080)(6\pi)] = 0.960\underline{/-215.7^\circ}$$

Figure 11. Graphical evaluation of the integrals of equation 11

paper work saved thereby. Thus, if

$$f_i(t)=\epsilon_i e^{-bt} \tag{16}$$

then

$$KG(j\omega)=\frac{b+j\omega}{\epsilon_i}\left[\int_0^\infty f_o(t)\cos\omega t\,dt-i\int_0^\infty f_o(t)\sin\omega t\,dt\right] \tag{17}$$

The value of the damping factor b should be chosen with the view of making the graphical integration as simple as possible.

Step Sinusoidal Input Signal

For this case the input may be expressed

$$f_i(t)=\epsilon_i\cos(\lambda t+\alpha) \tag{18}$$

The total output response again may be written as a sum of steady-state and transient components. If the steady-state output is assumed to be of the same form as the input, then

$$f_c(t)=\epsilon_c\cos(\lambda t+\beta) \tag{19}$$

and

$${}_o(t)=\epsilon_c\cos(\lambda t+\beta)+f_t(t) \tag{20}$$

Taking the direct Laplace transforms of equations 18 and 20 and substituting in equation 4 there is obtained

$$KG(s)=\frac{\epsilon_c}{\epsilon_i}\frac{s\cos\beta-\lambda\sin\beta}{s\cos\alpha-\lambda\sin\alpha}+\frac{\lambda^2+s^2}{\epsilon_i(s\cos\alpha-\lambda\sin\alpha)}\int_0^\infty f_t(t)e^{-st}dt \tag{21}$$

Setting $s=j\omega$,

$$KG(j\omega)=\frac{\epsilon_c}{\epsilon_i}\frac{\lambda\sin\beta-j\omega\cos\beta}{\lambda\sin\alpha-j\omega\cos\alpha}+\frac{\lambda^2-\omega^2}{\epsilon_i(j\omega\cos\alpha-\lambda\sin\alpha)}\times\left[\int_0^\infty f_t(t)\cos\omega t\,dt-j\int_0^\infty f_t(t)\sin\omega t\,dt\right] \tag{22}$$

Again the transfer function locus may be found by graphical integration of the transient component of the measured response. Determination of the various quantities in equation 22 may become rather tedious, and in such a case this type of input signal may be undesirable. In the event the system is sufficiently simple, and a particular value of α may be found where no transient exists, the transfer function becomes

$$KG(j\omega)=\frac{\epsilon_c}{\epsilon_i}\frac{\lambda\sin\beta-j\omega\cos\beta}{\lambda\sin\alpha-j\omega\cos\alpha} \tag{23}$$

Appendix II. Determination of the Open-Loop Transfer Function From Transient Measurements on the Closed-Loop System

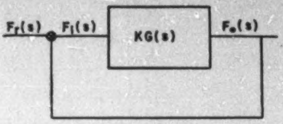

Figure 12. Block diagram of a closed-cycle servomechanism

One simple type of closed-cycle servomechanism may be represented as shown in Figure 12. The function $F_r(s)$ is the Laplace transform of the reference signal $f_r(t)$. The other symbols are as defined previously. It may be shown for this case[1,3] that

$$F_i(s)=\frac{1}{1+KG(s)}F_r(s) \tag{24}$$

and

$$F_o(s)=\frac{KG(s)}{1+KG(s)}F_r(s) \tag{25}$$

where

$$F_i(s)=F_r(s)-F_o(s) \tag{26}$$

Solving for the transfer function in equations 24 and 25 respectively,

$$KG(s)=\frac{F_r(s)}{F_i(s)}-1 \tag{27}$$

and

$$KG(s)=\frac{F_o(s)}{F_r(s)-F_o(s)} \tag{28}$$

Transient Reference Signal of Short Duration

For a transitory reference signal and with the input signal (error signal) $f_i(t)$ and reference signal $f_r(t)$ measured, the transfer function locus may be determined by application of

$$KG(j\omega)=\frac{\int_0^\infty f_r(t)e^{-j\omega t}dt}{\int_0^\infty f_i(t)e^{-j\omega t}dt}-1 \tag{29}$$

If the output response $f_o(t)$ is measured rather than the error signal, then the applicable expression is

$$KG(j\omega)=\frac{\int_0^\infty f_o(t)e^{-j\omega t}\,dt}{\int_0^\infty f_r(t)e^{-j\omega t}dt-\int_0^\infty f_o(t)e^{-j\omega t}dt} \tag{30}$$

Equations 29 and 30 are derived from equations 27 and 28 by replacing the signal and response transforms with the direct Laplace transform integral and setting $s=j\omega$. Writing the exponential terms in trigonometric form clearly indicates the necessary graphical integration process.

Damped Exponential Reference Signal

Proceeding as before it may be shown that for this type of reference signal $f_r(t)=\epsilon_r e^{-bt}$,

$$KG(j\omega)=\frac{\epsilon_r}{b+j\omega}\left[\frac{1}{\int_0^\infty f_i(t)e^{-j\omega t}dt}\right]-1 \tag{31}$$

which is applicable if the input error signal is recorded. If instead the output response is recorded, then

$$KG(j\omega)=\frac{(b+j\omega)(\int_0^\infty f_o(t)e^{-j\omega t}dt)}{\epsilon_r-(b+j\omega)(\int^\infty f_o(t)e^{-j\omega t}dt)} \tag{32}$$

Step Function Reference Signal

The applicable equations for this type of reference signal are derived from equations 8, 9, 27, and 28 making an appropriate change in symbols. Thus, for measurement of the error signal

$$KG(j\omega)=\frac{\epsilon_r}{k_i-j\frac{m_i}{\omega}+j\omega\int_0^\infty f_{it}(t)e^{-j\omega t}dt}-1 \tag{33}$$

Here, k_i is the steady-state error. The constant m_i, rate of change of steady-state error, is included for sake of completeness, but would be zero for most conceivable systems. The transitory component of the error is $f_{it}(t)$, and ϵ_r is the magnitude of the reference. For measurement of the output response

$$KG(j\omega)=\frac{k_o-j\frac{m_o}{\omega}+j\omega\int_0^\infty f_{ot}(t)e^{-j\omega t}dt}{\epsilon_r-\left[k_o-j\frac{m_o}{\omega}+j\omega\int_0^\infty f_{ot}(t)e^{-j\omega t}dt\right]} \tag{34}$$

As before, k_o and m_o are constants which describe the nature of the steady-state output, and $f_{ot}(t)$ is the transient component of the output.

References

1. THE ANALYSIS AND SYNTHESIS OF LINEAR SERVOMECHANISMS, A. C. Hall. Massachusetts Institute of Technology (Cambridge, Mass.) 1943.

2. PRINCIPLES OF SERVOMECHANISMS (book), G. S. Brown, D. P. Campbell. John Wiley and Sons, New York, N. Y., 1948.

3. TRANSIENTS IN LINEAR SYSTEMS (book), M. F. Gardner, J. L. Barnes. John Wiley and Sons, New York, N. Y., 1942.

4. CONTINUOUSLY CALIBRATED CATHODE-RAY OSCILLOSCOPE, E. C. Easton. *Review of Scientific Instruments*, (New York, N. Y.) volume 18, number 11, November 1947, pages 851–52.

5. NETWORK ANALYSIS AND FEEDBACK AMPLIFIER DESIGN (book), H. W. Bode. D. Van Nostrand Company, New York, N. Y., 1945.

6. DYNAMIC BEHAVIOR AND DESIGN OF SERVOMECHANISMS. G. S. Brown, A. C. Hall. *Transactions*, American Society of Mechanical Engineers, New York, N. Y., volume 63, July 1946, pages 503–24.

7. PARALLEL CIRCUITS IN SERVOMECHANISMS, H. T. Marcy. ELECTRICAL ENGINEERING (AIEE TRANSACTIONS), volume 65, August–September 1946, pages 521–29.

8. CONSIDERATIONS IN SERVOMECHANISM DESIGN, S. W. Herwald. ELECTRICAL ENGINEERING (AIEE TRANSACTIONS), volume 63, December 1944, pages 871–76.

Discussion

Charles F. Rehberg (New York University, New York, N. Y.): I should like to call attention to a paper by Bedford and Fredendall.[1] They attack the same problem of finding the sinusoidal amplitude and phase characteristics of a linear system from the experimentally determined transient response. Their method is essentially based on the Stieltjes integral representation

$$KG(s)=\int_0^\infty e^{-st}dA(t)$$

where $A(t)$ is the response of the system to unit step input. For purposes of numerical calculation, the integral may be replaced by an approximating sum, giving

$$KG(j\omega)\approx\sum e^{-j\omega t_k}[A(t_{k+1})-A(t_k)]$$

The latter may be evaluated by a geometric construction involving addition of vectors in the complex plane.

REFERENCE

1. ANALYSIS, SYNTHESIS, AND EVALUATION OF THE TRANSIENT RESPONSE OF TELEVISION APPARATUS, Bedford, Fredendall. *Proceedings*, Institute of Radio Engineers (New York, N. Y.) volume 30, October 1942, page 440.

Paul Travers (Servomechanisms Laboratory, Massachusetts Institute of Technology Cambridge, Mass.): In those cases where the control system or element whose transfer function is to be determined cannot be disconnected from an operating system, the following procedure is of interest. This method is based upon the a priori assumption that the component to be tested is linear and that its input can be characterized by a stationary random process.[1]

$I(t)$ is the input to the component under consideration. Its output $o(t)$ is given by

$$o(t)=\int_0^\infty h(x)I(t-x)dx \tag{1}$$

where $h(t)$ is the normal impulse response of the component. Under normal operating conditions the integrated magnitude of $I(t)$ does not converge and therefore $h(t)$ may not be obtained by transform methods.

However, since $I(t)$ is a stationary random process the input-output cross-correlation function may be defined as

$$\varphi_{IO}(\tau)\overset{\Delta}{=}\lim_{T\to\infty}\frac{1}{2T}\int_{-T}^{T}I(t)o(t+\tau)dt \tag{2}$$

Equation 2 is expanded by the substitution of equation 1

$$\varphi_{IO}(\tau)=\lim_{T\to\infty}\frac{1}{2T}\int_{-T}^{T}I(t)\int_0^\infty h(x)\times I(t+\tau-x)dx\,dt \tag{3}$$

The order of integration is then changed to give:

$$\varphi_{IO}(\tau)=\int_0^\infty h(x)\lim_{T\to\infty}\frac{1}{2T}\int_{T}^{T}I(t)I\times(t+\tau-x)\,dt\,dx \tag{4}$$

The definition of the autocorrelation of the input is[1]

$$\varphi_{II}(\tau)\overset{\Delta}{=}\lim_{T\to\infty}\frac{1}{2T}\int_{-T}^{T}I(t)I(t+\tau)dt \tag{5}$$

Equation 4 then becomes a convolution similar to equation 1

$$\varphi_{IO}(\tau)=\int_0^\infty h(x)\varphi_{II}(\tau-x)dx \tag{6}$$

Since the integrated magnitudes of $\varphi_{IO}(\tau)$ and $\varphi_{II}(\tau)$ converge, $H(\omega)$ may be obtained by the Fourier transformation of equation 6

$$H(\omega)=\frac{\int_{-\infty}^{\infty}\varphi_{IO}(\tau)e^{-j\omega\tau}d\tau}{\int_{-\infty}^{\infty}\varphi_{II}(\tau)e^{-j\omega\tau}d\tau}\overset{\Delta}{=}\frac{\Phi_{IO}(\omega)}{\Phi_{II}(\omega)} \tag{7}$$

In a manner similar to the foregoing exposition the cross-correlation may be obtained for a system which has two inputs,

$$I(t)=J(t)+K(t) \tag{8}$$

The cross-correlation for one input and the output is

$$\varphi_{JO}(\tau)=\int_0^\infty h(x)[\varphi_{JJ}(\tau-x)+\varphi_{JK}(\tau-x)]dx \tag{9}$$

If it is known that $J(t)$ and $K(t)$ are unrelated then $\varphi_{JK}(\tau)$ becomes zero and equation 9 reduces to

$$\varphi_{JO}(\tau)=\int_0^\infty h(x)\varphi_{JJ}(\tau-x)dx \tag{10}$$

$H(\omega)$ is then determined by equation 7.

It is concluded that the transfer function, $H(\omega)$, may be determined in the presence of disturbances which are stationary random processes and which are unrelated to the input.

REFERENCE

1. THEORY OF SERVOMECHANISMS, H. M. James, R. B. Nichols, R. S. Phillips. McGraw-Hill Book Company, New York, N. Y., 1947.

M. Yachter (M. W. Kellogg Company, Jersey City, N. J.): In this very interesting and important paper there is one weakness which, if not overcome, may reduce considerably the practical usefulness of the method studied by the authors. I refer to the numerical evaluation of the integral

$$I=j\omega\int_0^\infty f(t)e^{-j\omega t}dt=j\omega\int_0^\infty f(t)\times\cos\omega t\,dt+\omega\int_0^\infty f(t)\sin\omega t\,dt;\ j=\sqrt{-1}$$

where $f(t)$ is, as defined in the paper, the transient part of the output response to a step function (of constant amplitude or constant velocity) input so that

$$f(\infty)\to0$$

It is seen that if the transfer locus is to be calculated for, say, ten frequencies, 20 integrals must be evaluated. This is a very considerable amount of work.

Moreover, as ω increases the integrals oscillate more and more and their evaluation to any reasonable degree of accuracy becomes increasingly difficult. Indeed, the difficulty arises from the fact that in the limit $(\omega\to\infty)$ the integral I becomes indeterminate. For, one of the factors, $\omega\to\infty$ while the other factor

$$\int_0^\infty f(t)e^{-j\omega t}dt\to0$$

by the Riemann-Lebesgue lemma.[1] We see thus that the straight forward evaluation of the integrals for a reasonable range of frequencies is not practical. Now, this difficulty can be overcome by a very simple trick. The idea is merely to develop first the function $f(t)$ in some sort of a series

$$f(t)=\sum_0^\infty A_nU_n(t)$$

and such that the integrals

$$\int_0^\infty U_n(t)e^{-j\omega t}dt$$

can be integrated explicitly. Needless to add, the functions U_n should form an orthogonal set, so that the evaluation of the coefficients A_n is straightforward and convergence is, in general, assured (at least convergence "in the mean"). Now, there exist, of course, an infinite number of sets of orthogonal functions and the question is which of these should be used? On the basis of a one-degree of freedom system the following can be stated:

> If the (nondimensional) damping of the system is less than, say 0.7, then a Fourier series can be used to advantage. The number of terms required for good accuracy will be, at most, five (for $\zeta=0.7$).

If the damping of the system is greater than 0.7 then the orthogonal set of Laguerre polynomials[3], is generally more advantageous for convergence. Again, for $\zeta\geq0.7$, at most five terms may be necessary. Thus on the basis of a single degree of freedom system, $f(t)$ can be expressed in a series of at most five terms. The evaluation of the coefficients requires again the numerical evaluation of integrals essentially (for a Fourier series expansion exactly) of the same form as the integral I, but now only five (at most) integrals have to be evaluated instead of, say, 20 such evaluations. Once the coefficients have been found it is a very simple matter to calculate the transfer functions, and this in an exact manner. It may be added that the damping (and the natural frequency) can be estimated from the curves given in reference 3.

1. Suppose now that $\zeta\leq0.7$;

Let t_{ss} be the time at which $f(t)=\sim0$. That is $f(t)=0$ for $t\geq t_{ss}$.

Let now

$$\tau=\frac{\pi t}{t_{ss}};\ f(t)=F(\tau);\ \omega_{ss}=\frac{t_{ss}}{\pi}\omega \tag{1}$$

then

$$I=j\omega\int_0^{t_{ss}}f(t)e^{-j\omega\tau}dt$$
$$=j\omega_{ss}\int_0^{\pi}F(\tau)e^{-j\omega_{ss}t}d\tau;\qquad F(0)=f(0);\quad F(\pi)=0 \tag{2}$$

Write

$$F(\tau)=\sum_0^\infty A_n\cos n\tau$$

$$a_0=\frac{1}{\pi}\int_0^\pi F(\tau)d\tau;\ a_n=\frac{2}{\pi}\int_0^\pi F(\tau)\cos n\tau d\tau;\ (n=1,2,\ldots\infty) \tag{3}$$

Table I

ω	0	2.5	5	7.5	10	12.5	15	17.5	20
ω_{ss}	0	1/2	1	3/2	2	5/2	3	7/2	4
I	0 +0.j	0.833 +4.26j	3.867 +7.98j	9.075 +9.4j	13.9 +6.98j	15.6 +2.305j	13.1 −1.23j	11.17 −2.062j	9.64 −1.26j

Table II

ω	Author's Results	Fourier Series	Laguerre Series
π	$I=0.448\pi+1.668\pi j$	$0.44\pi+1.7\pi j$	$0.44\pi+1.667\pi j$
3π	$1.38\ (3\pi)$	$1.39\ (3\pi)$	$1.4\ (3\pi)$
	$+0.842\ (3\pi)j$	$+0.83\ (3\pi)j$	$+0.79\ (3\pi)j$
6π	$0.608\ (6\pi)$	$0.55\ (6\pi)$	$0.623\ (6\pi)$
	$-0.08\ (6\pi)j$	$-0.10\ (6\pi)j$	$-0.12\ (6\pi)j$

The values for $\omega=6\pi$ illustrate the difficulty of obtaining accurate results for higher frequencies.

Then we find

$$I=j\omega\int_0^\infty f(t)e^{-j\omega t}dt$$

$$=\sum_{n=0}^{\infty}\frac{a_n}{1-\left(\frac{n}{\omega_{ss}}\right)^2}[1-(-1)^n\cos\omega_{ss}\pi+ (-1)^n j\ \sin\ \omega_{ss}\pi] \qquad (4)$$

If $\omega_{ss}=m$, then the m^{th} term in the series becomes indeterminate, but this indeterminate form is easily evaluated to be

$$m^{th}\text{ term }=\frac{\pi}{2}\omega_{ss}a_m j \qquad (5)$$

If $\omega_{ss}=m$ or $\omega_{ss}=m+{}^1/_2$, where m is an integral number, the series (4) assumes a particularly simple form, thus

$$\omega_{ss}=m\begin{cases}I=2\sum\limits_{n=1,3\ldots}^{\infty}\dfrac{a_n}{1-\left(\dfrac{n}{m}\right)^2}+\dfrac{\pi}{2}ma_m j; & m\text{ even}\\ I=2\sum\limits_{n=0,2}^{\infty}\dfrac{a_n}{1-\left(\dfrac{n}{m}\right)^2}+\dfrac{\pi}{2}ma_m j; & m\text{ odd}\end{cases}$$

$$\omega_{ss}=m+{}^1/_2\begin{cases}I=\sum\limits_{n=0}^{\infty}a_n\dfrac{1+(-1)^n j}{1-\left(\dfrac{n}{(m+1/2)}\right)^2}; & m\text{ even}\\ I=\sum\limits_{n=0}^{\infty}a_n\dfrac{1-(-1)^n j}{1-\left(\dfrac{n}{m+1/2)}\right)^2}; & m\text{ odd}\end{cases} \qquad (6)$$

In general, evaluation of I for

$\omega_{ss}={}^1/_2,\ 1,\ {}^3/_2,\ \ldots\ 5$

is sufficient to determine the transfer function for the most practical range of frequencies. Thus it is seen that practically the main work consists in the evaluation of (at most) five integrals of the type

$\int_0^\pi F(\tau)\cos n\tau d\tau;\ (n=0,\ 1,\ \ldots\ 4)$, say

Limits

Suppose that

$\omega_{ss}=m\rightarrow\infty$

In general, it will be found (again say on the basis of a single degree of freedom) that

$$a_n\sim\frac{1}{n^2}$$

so that

$$\lim_{n\rightarrow m\rightarrow\infty}\frac{a_n}{1-\left(\frac{n}{m}\right)^2}\rightarrow 0$$

and in the limit

$\omega_{ss}=\infty$

we get

$$I=2(a_0+a_2+a_4+\ldots)=2(a_1+a_3+a_5+\ldots)=F(o)=f(o) \qquad (7)$$

That the above two expressions are equal to each other can be seen from the relations

$$a_0+a_1+a_2+\ldots=F(o);\qquad a_0-a_1+a_2-a_3+\ldots=0$$

Thus in the limit the imaginary part of I vanishes while the real part tends to the steady-state error. This will be the case if there is any inertia in the system.

2. Suppose now that $\zeta\geq 0.7$. It is now more advantageous to develop $f(t)$ into a series of Laguerre polynomials. The n^{th} normalized Laguerre polynomial is defined by

$$\varphi_n(\tau)=\frac{e^{-\tau/2}}{n!}Ln^{(\tau)};$$

$$\int_0^\infty\varphi_m(\tau)\varphi_n(\tau)d\tau=\begin{cases}0\text{ if }m\neq n\\ 1\text{ if }m=n\end{cases}$$

and

$$L_n(\tau)=e^{\tau}\frac{d^n}{d\tau^n}(\tau^n e^{-\tau})$$

$$=\sum_{k=0}^{n}(-1)^{n-k}\frac{[n(n-1)\ldots(n-k+1)]^2}{k!}\tau^{n-k}$$

so that,

$L_0=1;\ L_1=1-\tau;\ L_2=\tau^2-4\tau+2$ and so forth.

Let

$s=\xi+j\eta$

then, if $\xi<1/2$, we find

$$\int^\infty e^{s\tau}\varphi_n(\tau)d\tau=-\frac{1}{s-\frac{1}{2}}\left(\frac{s+\frac{1}{2}}{s-\frac{1}{2}}\right)^n \qquad (8)$$

The evaluation of equation 8 is somewhat lengthy, but is obtained by a continued integration by parts. Now let $F(\tau)$ be a function such that $F(\infty)=0$ and

$$\int_0^\infty[F^{(\tau)}]^2d\tau\neq\infty$$

which is surely true for transient response curves (that is the transient part $f(t)$); then it is possible to expand $F(\tau)$ in terms of the Laguerre polynomials

$$F(\tau)=\sum_0^\infty c_n\varphi_n(\tau);\ c_n=\int_0^\infty F(\tau)\varphi_n(\tau)d\tau \qquad (9)$$

with the assurance of convergence ("in the mean", see reference 2)

Hence we may write

$$\int_0^\infty F(\tau)e^{s\tau}d\tau=\sum_0^\infty c_n\int^\infty e^{s\tau}\varphi_n(\tau)d\tau$$

$$=-\sum_0^\infty\frac{c_n}{s-\frac{1}{2}}\left(\frac{s+\frac{1}{2}}{s-\frac{1}{2}}\right)^n$$

Let

$$A=\int_0^\infty f(t)e^{-st}dt;\ \tau=\alpha t;\ f(t)=F(\tau);\ \alpha>0; \qquad (10)$$

then,

$$A=\frac{1}{\alpha}\int^\infty F(\tau)e^{-\frac{s}{\alpha}\tau}d\tau$$

$$=\frac{1}{\alpha}\sum_0^\infty\frac{c_n}{\frac{1}{2}+\frac{s}{\alpha}}\left(\frac{\frac{s}{\alpha}-\frac{1}{2}}{\frac{s}{\alpha}+\frac{1}{2}}\right)^n \qquad (11)$$

Table III. The Normalized Laguerre Polynominals $\varphi_n(\tau)$

τ	φ_0	φ_1	φ_2	φ_3	φ_4
0	1	1	1	1	1
0.1	0.9512	0.8560	0.7650	0.6800	0.60
0.25	0.8825	0.6620	0.4680	0.2992	0.1528
0.5	0.7788	0.3894	0.0973	−0.1136	−0.2570
1	0.6065	0	−0.3032	−0.4033	−0.3785
1.5	0.4724	−0.2362	−0.4140	−0.3250	−0.1362
2	0.3679	−0.3679	−0.3679	−0.1226	+0.1228
2.5	0.2865	−0.4377	−0.2352	+0.0727	0.2583
3	0.2231	−0.4462	−0.1115	0.2232	0.3065
3.5	0.1738	−0.4350	+0.0218	0.3005	0.2464
4	0.1353	−0.4059	0.1353	0.3157	0.1353
4.5	0.1054	−0.3700	0.2242	0.2838	0.00906
5	0.08209	−0.3284	0.2873	0.2187	−0.1060
5.5	0.06393	−0.2875	0.3240	0.1369	−0.1940
6	0.04979	−0.2480	0.348	0.0497	−0.2485
6.5	0.03877	−0.2130	0.353	−0.0347	−0.2693
7	0.03020	−0.1812	0.347	−0.1107	−0.2603
7.5	0.02352	−0.1530	0.332	−0.1750	−0.2270
8	0.01832	−0.1282	0.311	−0.2260	−0.1770
8.5	0.01426	−0.1068	0.288	−0.2633	−0.1160
9	0.01111	−0.0889	0.261	−0.2887	−0.0511
9.5	0.008652	−0.0735	0.234	−0.3033	+0.0133
10	0.006738	−0.0605	0.209	−0.3073	0.0742
11	0.004087	−0.0409	0.161	−0.2953	0.175
12	0.002479	−0.0273	0.122	−0.2650	0.240

The problem now is what value to choose for α.

Of course, this choice can not influence the end results, but it can, and does, influence the convergence. Again, on the basis of a single degree of freedom system, it turns out that for optimum convergence one must choose $\alpha=2\omega_n$, where ω_n is the (approximate) natural frequency of the system (on a single degree of freedom basis). Let now

$$s=j\omega;\quad \omega_{ss}=\frac{\omega}{\omega_n};\quad \frac{s}{\alpha}=\frac{1}{2}j\omega_{ss} \tag{12}$$

then

$$A=\frac{1}{2\omega_n}\sum_0^\infty \frac{c_n}{\frac{1}{2}(1+j\omega_{ss})}\left(\frac{j\omega_{ss}-1}{j\omega_{ss}+1}\right)^n$$

and finally

$$I=s\int_0^\infty f(t)e^{-st}dt$$

$$=\frac{\omega_{ss}}{\sqrt{1+\omega_{ss}^2}}e^{j\psi}\sum_0^\infty(-1)^n c_n e^{jn\theta}$$

where

$$\psi=\tan^{-1}\left(\frac{1}{\omega_{ss}}\right);\quad \theta=\tan^{-1}\left(\frac{-2\omega_{ss}}{1-\omega_{ss}^2}\right);$$

$$0\leq\psi\leq\frac{\pi}{2};\quad -\pi\leq\theta\leq 0 \tag{13}$$

with

$$c_n=\int_0^\infty F(\tau)\varphi_n(\tau)d\tau;\quad \omega_{ss}=\frac{\omega}{\omega_n}$$

If $\zeta>1$, then one should choose $\omega_n=1/t_0$ where t_0 is the decay time.

It is seen that again I is expressed in the form of a Fourier series except that the coefficients c_n are those corresponding to the Laguerre polynomials, rather than the Fourier series.

For ease of computations it is better to write

$$\Phi_n(\omega_{ss})=\Phi_{n1}(\omega_{ss})+j\Phi_{n2}(\omega_{ss})=$$

$$\frac{\omega_{ss}}{\sqrt{1+\omega_{ss}^2}}e^{j(n\theta+\psi)} \tag{14}$$

so that,

$$I=\sum_{n=0}^\infty(-1)^n c_n\Phi_n(\omega_{ss}) \tag{15}$$

with tables for $\varphi_n(\tau)$ and $\Phi_n(\omega_{ss})$ it is just as easy to calculate I as in the case of the Fourier series. Such tables are added at the end of this discussion (Tables III and IV).

Finally, it may be added, that the same "technique" may perhaps be used to determine the transient response from a given frequency response or vice versa. However, because of lack of time the details have not as yet been worked out.

Numerical Examples

Consider the transient response curve e_t shown in Figure 11 of the paper under discussion. The damping factor and natural frequency are estimated to be

$$\zeta=0.56;\quad \omega_n=9.3\,\frac{\text{rad.}}{\text{sec.}};\quad t_{ss}=\frac{2\pi}{10}=0.628\text{ sec.}$$

According to what was said before, a Fourier series is more advantageous to use. However, the values of the integral I have been calculated by both methods.

Fourier Series

$$t_{ss}=\frac{\pi}{5};\quad \omega_{ss}=\frac{\omega}{5};$$

On the basis of 10 intervals, the following values for the Fourier coefficients have been found

$$a_0=2.66;\quad a_1=5.08;\quad a_2=2.22;\quad a_3=-0.262;\quad a_4=-0.201$$

The curve represented by the series of five terms follows the original quite closely except at the very end ($t=0.6$ sec.).

The values of I for a range of frequencies from $\omega=0$ to $\omega=20$ calculated from equation 6 is shown in Table I of the discussion.

Choose

$$\omega_n=10\,\frac{\text{rad.}}{\text{sec.}};\quad \omega_{ss}=\frac{\omega}{\omega_n}=\frac{\omega}{10}$$

for Laguerre expansion

The coefficients c_n have been calculated on the basis of 12 equal intervals, except that the first interval was subdivided into two half intervals, while the last two intervals have been taken as one. The values of the coefficients are:

$$c_0=15.24;\quad c_1=-5.707;\quad c_2=-3.55;\quad c_3=1.654;\quad c_4=1.264;$$

It is found that at $\tau=0$, these coefficients add up to 8.9 instead of to 9.42, which is the exact value. This shows that at least one more term is necessary in the series, and so for the value of $\zeta=0.56$, the Fourier series really gives better results as expected from theoretical considerations (on the basis of a single degree of freedom system).

Instead of calculating another term, the coefficients have been increased by weighted factors (inversely proportional to values of coefficients), so that the actual values used for calculating I are

$$c_0=15.26;\quad c_1=-5.66;\quad c_2=-3.47;\quad c_3=1.82;\quad c_4=1.48$$

The curve as represented by the Laguerre series with five terms follows the original curve less closely than the one given by the (finite) Fourier series, but is still a good approximation. With these coefficients the values of I have been calculated from equation 13 for $\omega=\pi$, 3π, 6π; for these frequencies the values of I have also been interpolated from Table I of the discussion. These values are compared with those obtained by the authors in Table II of the discussion.

Table IV. Values of $\Phi_n\omega_{ss}=\Phi_{n1}(\omega_{ss})+j\Phi_{n2}(\omega_{ss})$

ω_{ss} Degrees	ω_{ss} Radians	Φ_0	Φ_1	Φ_2	Φ_3	Φ_4
0	0	0	0	0	0	0
1	0.01745	0.0003042 +0.01745j	0.0009135 +0.01742j	0.001525 +0.01739j	0.002125 +0.01732j	0.002725 +0.01723j
3	0.05236	0.002745 +0.05230j	0.008175 +0.05170j	0.01353 +0.05060j	0.01872 +0.04885j	0.02370 +0.04660j
5	0.08727	0.007560 +0.08662j	0.02250 +0.08400j	0.03665 +0.07890j	0.04980 +0.07120j	0.06135 +0.06160j
7	0.12217	0.01473 +0.1204j	0.04335 +0.1133j	0.06940 +0.09970j	0.09135 +0.8010j	0.1080 +0.05560j
9	0.15708	0.02415 +0.1533j	0.06990 +0.1388j	0.1093 +0.1106j	0.1377 +0.07160j	0.1530 +0.02600j
11	0.19199	0.03595 +0.1848j	0.1015 +0.1583j	0.1530 +0.1097j	0.1827 +0.04500j	0.1863 −0.02907j
13	0.22689	0.04895 +0.2155j	0.1375 +0.1737j	0.1989 +0.09735j	0.2213 +0.001992j	0.2005 −0.09375
15	0.26180	0.06390 +0.2445j	0.1758 +0.1818j	0.2425 +0.0725j	0.2467 −0.05555j	0.1878 −0.1693j
20	0.34907	0.1085 +0.3110j	0.2785 +0.1761j	0.3275 −0.0357j	0.2342 −0.2315j	0.03910 −0.3270j
25	0.43633	0.1600 +0.3665j	0.3775 +0.1320j	0.3540 −0.1865j	0.1034 −0.3865j	−0.2125 −0.3390j
30	0.52360	0.2150 +0.4110j	0.4605 +0.0571j	0.3645 −0.3450j	−0.1078 −0.4510j	−0.4320 −0.09035j
40	0.69813	0.3285 +0.4700j	0.5540 −0.1462j	0.0539 −0.5705j	−0.5170 −0.2470j	−0.4100 +0.3230j
50	0.87266	0.4320 +0.4960j	0.5495 −0.3585j	−0.2833 −0.5935j	−0.6365 +0.2005j	+0.1142 +0.6475j
60	1.0472	0.5225 +0.5000j	0.4885 −0.5333j	−0.5445 −0.4760j	−0.4615 +0.5545j	0.5645 +0.4515j
70	1.2217	0.5980 +0.4910j	0.3625 −0.6845j	−0.7425 −0.2200j	−0.06890 +0.7710j	0.7700 +0.08490j
80	1.3963	0.6620 +0.4740j	0.2355 −0.7795j	−0.8130 −0.02287j	+0.2885 +0.7610j	0.6275 +0.5160j
90	1.5708	0.7135 +0.4535j	0.1663 −0.8140j	−0.8055 +0.2550j	0.5710 +0.6210j	0.3207 +0.7810j
110	1.9199	0.7850 +0.4080j	−0.1150 −0.8785j	−0.6540 +0.5970j	0.8640 +0.1930j	−0.3365 +0.8180j
130	2.2689	0.8395 +0.3695j	−0.2930 −0.8670j	−0.4440 +0.8015j	0.8915 −0.2145j	−0.7610 +0.5135j
150	2.6180	0.8740 +0.3335j	−0.4280 −0.8310j	−0.2345 +0.9050j	0.7780 −0.5190j	−0.9355 +0.1327j
170	2.9671	0.8990 +0.3035j	−0.5320 −0.7860j	−0.05220 +0.9470j	0.6150 −0.7230j	−0.9270 −0.2032j
190	3.3161	0.9170 +0.2763j	−0.6125 −0.7380j	+0.1020 +0.9535j	0.4420 −0.8505j	−0.8380 −0.4645j
210	3.6652	0.9210 +0.2515j	−0.6660 −0.6840j	0.2265 +0.9265j	0.2792 −0.9220j	−0.7105 −0.6535j
250	4.3635	0.9510 +0.2175j	−0.7600 −0.6110j	0.4185 +0.8810j	0.006050 −0.9755j	−0.4300 −0.8740j
290	5.0615	0.9620 +0.1910j	−0.8160 −0.5410j	0.5500 +0.8110j	−0.2003 −0.9600j	−0.1792 −0.9645j
330	5.7596	0.9710 +0.1686j	−0.8565 −0.4860j	0.6440 +0.7460j	−0.3535 −0.9190j	−0.2010 −0.9841j
360	6.2832	0.9750 +0.1549j	−0.8860 −0.4340j	0.7210 +0.6740j	−0.4935 −0.8660j	+0.2195 −0.9635j

REFERENCES

1. MODERN ANALYSIS, Whittaker, Watson. Cambridge, 1943, page 172.

2. METHODEN DER MATHEMATISCHEN PHYSIK, Courant-Hilbert. Volume 1, Berlin, Germany, 1931, page 79.

3. PRINCIPLES OF SERVO-MECHANISMS, C. S. Brown, D. P. Campbell. New York, N. Y., 1948, pages 54–5.

D. D. Terwilliger (The Glenn L. Martin Company, Baltimore, Md.): The authors mention that some systems may be envisioned where mathematical or sinusoidal measurements are not feasible. No specific cases are given. I should like to mention a very common one in the hydraulic servo using a variable stroke pump and motor.

In this system under sinusoidal test the oil lines become supercharged so that the effect of oil compressibility appears as two springs, one on each side of the output inertia.

This will produce a natural frequency $\sqrt{2}$ times greater than if the oil in only one line is considered effective.

In transient tests no supercharging effect is present so that a lower natural frequency should be measured. Some laboratory work has been performed to substantiate this effect.

The application of the author's technique will simplify calculations and permit more complete information to be obtained on this very important part of a hydraulic servomechanism.

C. H. Thomas and E. C. Easton: The authors wish to acknowledge with gratitude the discussions of their paper by Travers, Rehberg, Yachter, and Terwilliger. The method of evaluating the infinite integral suggested by Yachter, appears to be much simpler than the method used by the authors and should prove of considerable use to those who desire to utilize this method of determining transfer function loci. The discussions seem to bring out the fact that the authors' method of utilizing the Laplace transformation for determining transfer function loci from transient measurements is more general than other methods which have been described in the literature. This method is not restricted by input signal form and is applicable for practically any type of applied signal.

Operating Characteristics of 2-Phase Servomotors

R. J. W. KOOPMAN
MEMBER AIEE

IN THIS paper differences are pointed out between conventional 2- phase induction motors and 2-phase servomotors, both as to construction and operating conditions. An important feature of the construction differences is that they determine whether or not the servomotor will operate single phase.

Performance of a servomotor having typical equivalent-circuit parameters is analyzed by means of symmetrical-component theory. The usual assumption made in control-system analyses of linearity of torque with control voltage is shown to be fairly accurate, but the assumption of linearity of speed with control voltage is shown to be very limited. Internal damping varies widely with voltage and speed.

Numerous interrelations between motor design and control system design are pointed out and should be of interest to those engaging in either of these fields. A contribution to induction motor theory is made in showing how design factors may be combined to prevent the production of positive torque from single phase regardless of the speed that may be given to the rotor. A contribution to servomechanism design is made in showing how to obtain the relationships between control voltage and torque, and also the slopes of the speed-versus-torque curves. These are needed to calculate the period and the damping respectively of a closed cycle system.

In the last few years small 2-phase induction servomotors[1] have become quite popular for use in control systems where relatively small torques are required.

The usual construction employs a stator with windings located 90 electrical space degrees apart and a rotor of fundamentally the squirrel-cage type. The stator windings may or may not be balanced electrically. Fundamentally then, this type of motor is similar to the more familiar split-phase and capacitor motors, or in the case of electrically balanced windings it is similar to the 2-phase squirrel-cage induction motor.

However, there are some differences in design details which make important differences in performance. Also the conditions under which the servomotors operate are different.

The applied voltages are rarely balanced, for to achieve control of torque and direction of rotation, the control-winding voltage may be varied from rated value in one sense through zero to rated value in the opposite sense while the voltage on the other winding is held constant.

When it is necessary to have a fast acting yet stable closed-cycle control system, it is highly desirable that the torque-to-inertia ratio of the servomotor have a large value. For this reason the rotor often consists only of a thin hollow cup of light conducting material in order to reduce inertia. The magnetic path is completed by means of a stationary cylinder of iron placed inside the rotor. There are thus two clearance air gaps. Motors made in this manner are frequently called "drag cup" motors.

This type of construction means that the exciting current as compared with that of motors of conventional design, is relatively large. Closed-cycle control systems normally require a servomotor with characteristics typical of high-rotor resistance. High-rotor resistance may combine with high exciting current to produce conditions which prevent the motor from developing any running torque when operating single phase regardless of speed. This is a very desirable characteristic for many control applications although it is an intolerable condition in split-phase or capacitor motors.

Manufacturers of 2-phase servomotors usually give the speed-torque curves of their various models for balanced-voltage operation, that is, rated voltage on each winding. These curves are usually drawn from the no-load to zero speed. In predicting accurately the performance of a closed-cycle control system, it is really essential to have the speed-torque curves for various values of voltage on the control winding. However, for purposes of simplification the following assumptions are usually made:

1. Torque at a given speed is directly proportional to the voltage on the control winding.
2. Speed at a given torque is directly proportional to control-winding voltage.
3. The slopes of the speed-torque curves are constant.

These assumptions are quite different from the expected performance of the usual polyphase squirrel-cage induction motor.

The purposes of this paper are to:

1. Show how well the foregoing assumptions fit a typical case and to establish analytical bases for them where possible;
2. Show how the speed-torque curve usually given by the manufacturer for balanced-voltage operation can be utilized to calculate the speed-torque curves for variable control-winding voltages;
3. Show how high exciting current and high-rotor resistance combine to produce single-phase characteristics peculiar to servomotors.

A literal analysis of the circuital relationships involved will be presented. This will apply equally well to conven-

---

Paper 49-81, recommended by the AIEE rotating machinery committee and approved by the AIEE technical program committee for presentation at the AIEE winter general meeting, New York, N. Y., January 31–February 4, 1949. Manuscript submitted July 21, 1948; made available for printing December 21, 1948.

R. J. W. Koopman is an associate professor at Washington University, St. Louis, Mo.

The author is indebted to Walter R. Evans for data concerning the closeness of correspondence between speed-torque curves calculated from the balanced-voltage curve in the manner suggested by the writer and curves obtained by experimental observation.

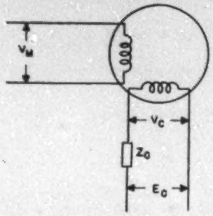

Figure 1. Servomotor circuits

tional 2-phase induction motors when operated under the conditions of unbalance common to servomotors. The results of applying the literal analysis to calculating the performance of a typical "drag cup" motor whose constants were determined by open-circuit and short-circuit tests in conjunction with consideration of actual performance will be presented in a group of curves. While no extensive laboratory checks were made on the performance curves, there is reasonably close general agreement between the theoretical results and those obtained in the laboratory and in practice. A more detailed appraisal of the expected correspondence between calculated and test results in general and a suggested method of measuring "constants" is given in Appendix III.

Analysis

SCOPE

This analysis is limited to control motors with electrically balanced windings 90 electrical space degrees displaced. It may be extended to motors in which the windings are electrically unbalanced by the argument followed in Appendix I. This paper deals mainly with the steady-state condition of operation. The transient condition also will be discussed, but it will be assumed that the electrical transients are fast and therefore negligible in comparison with the mechanical.

Two cases will be analyzed. In one case, the control voltage will be applied to the control winding through a resistance approximately equal to the average magnitude of the motor impedance. This corresponds in practice to supplying the winding from the plate circuit of a power amplifier tube matched to the motor winding through an impedance matching transformer. The second case will be that in which the control voltage is applied directly to the winding. This corresponds in practice to supplying the winding from a low-impedance generator, or the condition can be approached by the use of a feed-back amplifier.[2,3,4,5]

METHOD

The two voltages will be resolved into their symmetrical components in accordance with the methods developed by C. L. Fortescue.[6]

Although systems of polyphase vectors may be resolved into numerous equivalent systems,[7] the 2-phase system, a special case of 4-phase, may be and usually is resolved into two right-angled systems of opposite phase order.[8,9,10,11]

The main-winding voltage and the control-winding voltage, therefore, are resolved into two balanced 2-phase voltages of opposite phase sequence. The positive-sequence voltage produces positive-sequence current only and the negative-sequence voltage produces negative-sequence current only.[12,13] Total current and torque are found by the principle of superposition.[14,15]

For analytical purposes it is helpful to think of a polyphase induction motor operating on unbalanced voltages as equivalent to a system consisting of two identical motors mechanically coupled, one having impressed upon its windings the positive-sequence components of the unbalanced voltages and the other motor the negative-sequence components.[16,17]

This method of analysis has been tested in the laboratory and in practice and has been found to give good results when applied to standard polyphase induction motors under varying degrees of unbalance.[18,19,20] When applied to the servomotor with stationary "rotor" iron that is the drag cup motor, and the usual analytical assumptions[21] are met on the average, good agreement between experimental results and theory may be expected.

MATHEMATICAL DETAILS

Referring to Figure 1, which schematically represents the control motor in operation, the motor voltages V_M and V_C will be resolved into the two systems shown in Figure 2, as discussed previously. The voltage V_C must be expressed in terms of the drop through Z_C and the voltage E_C.

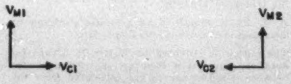

Figure 2. Symmetrical components of 2-phase voltages

From symmetrical component theory

$$V_M = V_{M1} + V_{M2} \tag{1}$$

$$V_C = V_{C1} + V_{C2} \tag{2}$$

From Figure 2

$$C_{C1} = -jV_{M1} \tag{3}$$

$$V_{C2} = jV_{M2} \tag{4}$$

Therefore

$$V_C = -jV_{M1} + jV_{M2} \tag{5}$$

$$jV_C = V_{M1} - V_{M2} \tag{6}$$

Adding equations 1 and 6

$$V_M + jV_C = 2V_{M1} \tag{7}$$

Likewise

$$V_M - jV_C = 2V_{M2} \tag{8}$$

From observation of Figure 1

$$V_C = E_C - I_C Z_C \tag{9}$$

It is assumed that

$$E_C = -jkV_M \tag{10}$$

where

$$k = \frac{|E_C|}{|V_M|} \tag{11}$$

and is regulated by the requirements of the control system.

Also from symmetrical component theory

$$I_C = I_{C1} + I_{C2} \tag{12}$$

$$I_{C1} = \frac{V_{C1}}{Z_1} = \frac{-jV_{M1}}{Z_1} \tag{13}$$

$$I_{C2} = \frac{V_{C2}}{Z_2} = \frac{jV_{M2}}{Z_2} \tag{14}$$

Where Z_1 and Z_2 are the impedances to positive- and negative-sequence currents in the motor respectively. Examples of the numerical calculation of these values from the induction motor equivalent circuit are in the literature.[10,18,19]

From equations 9, 10, 12, 13 and 14

$$V_C = -jkV_M - \left(-\frac{jV_{M1}}{Z_1} + \frac{jV_{M2}}{Z_2}\right)Z_C \tag{15}$$

From equations 7 and 15

$$2V_{M1} = V_M + j\left[-jkV_M + \left(\frac{jV_{M1}}{Z_1} - \frac{jV_{M2}}{Z_2}\right)Z_C\right] \tag{16}$$

and from equations 8 and 15

$$2V_{M2} = V_M - j\left[-jkV_M + \left(\frac{jV_{M1}}{Z_1} - \frac{jV_{M2}}{Z_2}\right)Z_C\right] \tag{17}$$

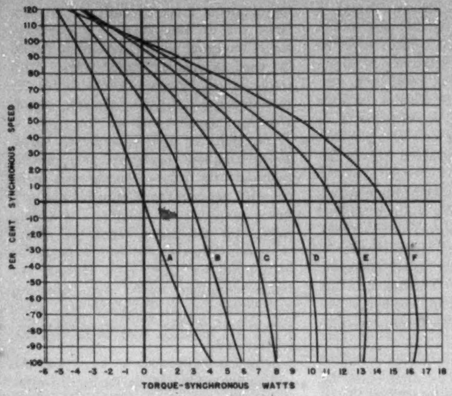

Figure 3. Per cent synchronous speed versus torque in synchronous watts for servomotor operating with $Z_c=0$

Curve "A" is for control voltage corresponding to $k=0$; "B", $k=0.2$; "C," $k=0.4$; "D," $k=0.6$; "E," $k=0.8$; "F," $k=1.0$

Equations 16 and 17 simplify as follows

$$V_{M1}=\frac{\frac{V_M}{2}\left[1+k+\frac{Z_C}{Z_1}\right]}{1+\frac{Z_C}{2Z_1}+\frac{Z_C}{2Z_2}} \tag{18}$$

$$V_{M2}=\frac{\frac{V_M}{2}\left[1-k+\frac{Z_C}{Z_1}\right]}{1+\frac{Z_C}{2Z_1}+\frac{Z_C}{2Z_2}} \tag{19}$$

These are the voltages applied to the two identical 2-phase motors fictitiously connected on the same shaft. The resultant torques can be calculated from the equivalent circuit noting that when the positive sequence motor is operating at a slip S_1, the negative sequence motor is operating at a slip $S_2=2-S_1$. Torque in synchronous watts is equal to the loss in the part of the equivalent circuit representing the rotor. Since the equivalent-circuit elements are considered constant, the torques on the two motors are proportional to the squares of their applied voltages. Negative-sequence torque subtracts from positive-sequence torque, because the negative-sequence voltage produces a magnetic field in the motor to which it is applied that is opposite in rotation to the shaft. Under these conditions the net torque is given by the following equation

$$T=T_{B1}\left(\frac{V_{M1}}{V_M}\right)^2-T_{B2}\left(\frac{V_{M2}}{V_M}\right)^2$$

synchronous watts (20)

Where T_{B1} is the torque produced by applying balanced 2-phase voltage of magnitude V_M to the motor windings at slip S_1 as read from a curve similar to curve "F" of Figure 3, and T_{B2} is taken from the same curve but at slip S_2. Examples of torque calculations are given in Appendix II.

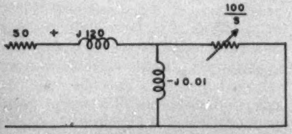

Figure 4. Servomotor equivalent circuit used in calculating performance curves

Balanced polyphase conditions

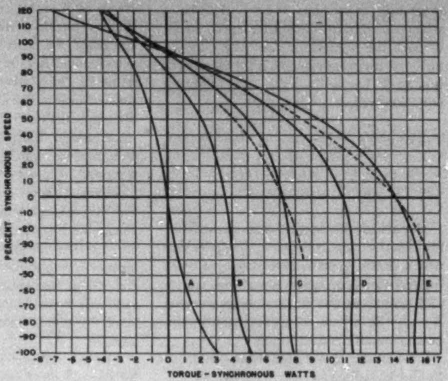

Figure 5. Per cent synchronous speed versus torque in synchronous watts for servomotor operating with $Z_c=200+j0$ ohms

Curve "A" is for control voltage corresponding to $k=0$; "B," $k=0.5$; "C," $k=1.0$; "D," $k=1.5$; "E," $k=2.0$

In the case where the control winding is supplied from a feed-back amplifier so that Z_C approaches zero, equations 18 and 19 are greatly simplified, for setting $Z_C=0$

$$V_{M1}=\frac{V_M}{2}(1+k) \tag{21}$$

and

$$V_{M2}=\frac{V_M}{2}(1-k) \tag{22}$$

For single-phase operation $Z_C=\infty$. The making of this substitution in both equations 18 and 19 results in the inde-

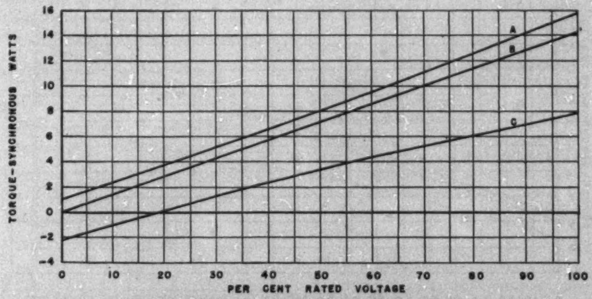

Figure 6. Torque in synchronous watts versus control-winding voltage expressed in per cent of rated voltage for servomotor operating with $Z_c=0$

Curve "A" is for 30 per cent synchronous speed in the reverse direction, or braking action; "B", zero speed; "C", 60 per cent synchronous speed in the normal direction terminate expression ∞/∞. However, when the derivative with respect to Z_C of both the numerator and the denominator of these expressions is taken according to l'Hospital's rule, the following equations result

$$V_{M1}=\frac{V_M Z_1}{Z_1+Z_2} \qquad (23)$$

$$V_{M2}=\frac{V_M Z_2}{Z_1+Z_2} \qquad (24)$$

Equations 18 and 19 are rather formidable for calculation. A simplification which holds approximately over a very limited range of speed about the standstill point can be made by considering $Z_1=Z_2=Z$, where Z is the motor impedance with blocked rotor.

On making this assumption equations 18 and 19 reduce to

$$V_{M1}=\frac{V_M}{2}\left[1+\frac{kZ}{Z_C+Z}\right] \qquad (25)$$

and

$$V_{M2}=\frac{V_M}{2}\left[1-\frac{kZ}{Z_C+Z}\right] \qquad (26)$$

Servomotor Performance—Application of Literal Analysis

STEADY-STATE PERFORMANCE

Control-Circuit Voltage Finite, but Different from Main-Winding Voltage. Figure 3 shows the speed-torque curves for control voltages corresponding to k values of 1.0, 0.8, 0.6, 0.4, 0.2 and 0 applied directly to the control winding of a motor having the equivalent circuit shown in Figure 4. This is the equivalent circuit of a control motor with stationary rotor iron as described previously. In separating the rotor and stator reactances, always a difficult problem with squirrel-cage rotors, the rotor reactance was considered to be zero inasmuch as it is relatively small because of the absence of conductors embedded in iron slots. Because of the large air gap, the exciting susceptance is so much larger than the conductance that this branch was considered purely inductive.

Figure 5 shows the speed-torque curves for the control winding voltage applied through a 200-ohm resistor, for k values of 2.0, 1.5, 1.0, 0.5 and 0. The curves are of steeper slope over the usual operating range near zero speed. The dash lines are obtained by use of the approximate equations 25 and 26 and are shown for comparison.

The calculations of torque are expedited by the use of the speed-torque curve for balanced operation, curve "F" of Figure 3. For any particular speed, the impedances Z_1 and Z_2 are calculated from the equivalent circuit Figure 4. These values are fed into equations 18 and 19, 23 and 24, or 25 and 26, whichever pair applies and the values of the positive- and negative-sequence voltages, V_{M1} and V_{M2}, are calculated.

Torque is then found by equation 20 and the speed-torque curve for balanced voltage.

When the control voltage is applied directly, the calculations are much simpler. The positive and negative components of voltage are given by equations 21 and 22. Torque is again found by equation 20. The speed-torque curve for balanced voltage on which the torques for the unbalanced conditions are based is calculated by the methods given in any standard text on a-c machinery or it may be obtained experimentally. However, since the exciting current is relatively large, the exact equivalent circuit should be used in making calculations. This curve is usually made available by the manufacturer of the control motor. However, usually only half the curve is given, that for positive-sequence speed. If the complete curve were given by the manufacturer from +100 per cent speed to −100 per cent speed, it would not take many minutes to calculate the data points for the whole family of curves shown in Figure 3. In fact, it would be economical of time even though the balanced-voltage curve were obtained experimentally to calculate the other curves rather than to obtain them experimentally.

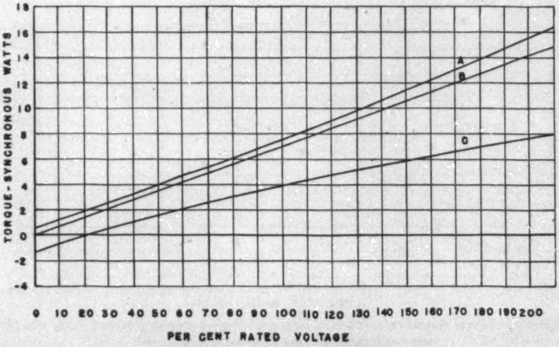

Figure 7. Torque versus control-winding voltage for servomotor operating with $Z_c=200+j0$ ohms, otherwise the same as Figure 6

It is not too serious to have only the positive-speed half of the balanced-torque curve given, as the remaining portion can be estimated with fair accuracy. Since V_2/V_M will be smaller than V_1/V_M for all cases except that of $V_C=0$, the effect of errors in the estimate will be reduced. At zero speed, of course, the calculation may be expected to be accurate, because this point is usually given on the torque curve for balanced voltage. This method has been used in the laboratory with good results.

Figures 6 and 7 show the validity of the assumption regarding linearity of torque with control voltage. The curves show that over a limited speed range this is nearly true. That it is exactly true at zero speed (assuming no variation in equivalent-circuit parameters with voltage) can be shown easily as follows

$$T=T_{B1}\left(\frac{V_{M1}}{V_M}\right)^2-T_{B2}\left(\frac{V_{M2}}{V_M}\right)^2 \qquad (20)$$

but at zero speed

$$T_{B1}=T_{B2}=T_B$$

therefore

$$T_0=\frac{T_B}{V_M^2}[V_{M1}^2-V_{M2}^2] \qquad (27)$$

Since

$$V_{M1}=\frac{V_M}{2}\left[1+\frac{kZ}{Z_C+Z}\right] \qquad (25)$$

and

$$V_{M2}=\frac{V_M}{2}\left[1-\frac{kZ}{Z_C+Z}\right] \qquad (26)$$

Equation 27 becomes

$$T_0=T_B\frac{kZ}{Z_C+Z} \qquad (28)$$

When

$$Z_c=0$$

$$T_0=kT_B \qquad (28a)$$

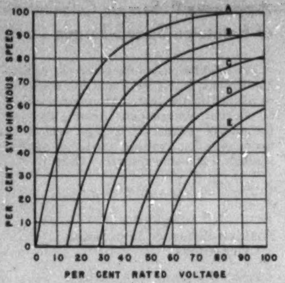

Figure 8. Speed in per cent of synchronous versus control-winding voltage in per cent rated for servomotor operating with $Z_c=0$

Curve "A" is for zero developed torque. Curve "B" is for developed torque of two synchronous watts; "C," $T=4$; "D," $T=6$; "E," $T=8$

Figures 8 and 9 show that the assumption of linearity of speed with control voltage is valid approximately only over limited ranges especially at higher torque loads.

Single-Phase Performance. The curve marked "A" in Figure 3 is a type of single-phase performance in which the voltage across the control winding is held at zero making $V_{M1}=V_{M2}=V_M/2$ at all values of speed. This is not truly single-phase performance as equations 23 and 24 show that the positive- and negative-sequence voltages vary with the impedances of these sequences and consequently the voltages vary with speed. The curve "A" of Figure 3 shows that the motor under discussion can not run with zero control-winding voltage, that is, with the winding short circuited.

This feature can be explained as follows. Since V_{M1} and V_{M2} always have the value $V_M/2$ the torque becomes

$$T=1/4(T_{B1}-T_{B2}) \tag{29}$$

For the motor under discussion, the balanced-voltage speed-torque curve crosses the zero-speed axis with negative slope and T_{B2} is always larger than T_{B1} for corresponding values of speed. Equation 29 then shows what the torque will be opposite to the rotation at all times. In the general-purpose 2-phase motor this curve would cross the zero axis with positive slope and such a machine would develop torque with one phase short circuited. Servomotors, however, must have a speed-torque characteristic crossing the zero axis with negative slope or they will be unstable (See the section on Application to Transient Analysis of Control Systems) in closed-cycle control systems unless there is sufficient load friction or derivative feedback is provided.

True single-phase operation (control winding open) can be explained in somewhat the same way except that the positive-and negative-sequence voltages do not remain constant. Figure 10 shows the relationships between V_1, V_2, T_{B1}, T_{B2}, (defined previously) T_1 and T_2 (positive- and negative-sequence torque for single-phase operation) and T the net torque. It can be seen that the net torque is always negative because of the shape of the balanced-torque curves and because there is not a large variation in the voltages V_1 and V_2. If V_1 had been larger and V_2 smaller at the higher speeds it is possible that this motor could have developed positive net torque single phase. It will be of interest to investigate the factors influencing the variation of the sequence voltages with speed.

Equations 23 and 24 are satisfied by the equivalent circuit of the single-phase induction motor shown in Figure 11.

Reference to this figure will show that the two impedances Z_1 and Z_2 will tend to remain equal if either the stator impedance is high or the impedance of the exciting circuit is low (conductance G and susceptance B large) in comparison with the rotor impedance. The stator and the blocked-rotor value of rotor impedance will normally be of the same order of magnitude. The exciting impedance is low in comparison with the usual induction motor because of the large air gap in the type motor being considered. Therefore Z_1 and Z_2 tend to remain nearly equal, and the voltages V_1 and V_2 tend to remain nearly equal. This coupled with a speed-torque curve which crosses the zero axis with negative slope prevents the motor from developing a running torque regardless of the speed at which the rotor may be caused to rotate. This facet of the discussion emphasizes the beauty of the two-revolving field theory of the single-phase induction motor.

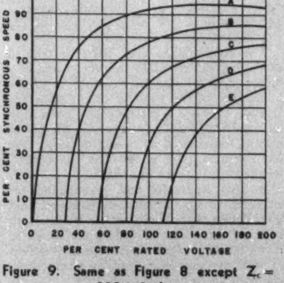

Figure 9. Same as Figure 8 except $Z_c=200+j0$ ohms

Application to Transient Analysis of Control Systems

The important electrical quantities in the transient performance of a servomotor in a control system are its internal damping and its torque-to-control voltage ratio.

It can be shown that the internal damping is equal to the negative reciprocal of the slope of the speed-torque curve.[22]

For a d-c motor with constant flux and neglecting stray load loss, core loss, friction, and windage

$$T=k_tI_a$$

$$I_a=\frac{V_t-k_vN}{R_a}$$

$$N=\frac{V_t}{k_v}-\frac{TR_a}{k_tk_v}$$

$$\frac{dN}{dT}=\frac{-R_a}{k_tk_v}$$

where

k_t = inch-ounces torque per ampere of armature current
I_a = armature current
N = speed in rpm
k_v = generated volts per rpm
V_t = terminal voltage
R_a = armature circuit resistance

The foregoing relations show that the speed-torque curves of a d-c motor are a family of straight lines each having a slope of $-R_a/k_tk_v$ and intercepts on the speed axis of V_t/k_v. Such characteristics permit the description of the transient performance of a motor in either open- or closed-cycle operation by linear differential equations. Although the torque-versus-control voltage curves are fairly straight lines in the case of the 2-phase motor, the damping factor is far from linear as shown by the curves of Figures 12, 13, 14, and 15. These curves show the variation in damping with voltage at several values of speed, also the variation in damping with variation in speed for several values of voltage. They were calculated by taking the instantaneous slopes expressed in terms of ounce-inches per revolutions per minute of the speed-torque curves under the stated conditions.

Curves are shown for both types of operation discussed previously, that is, $Z_C=0$ and $Z_C=200$ ohms resistance. Because of the nonlinearity of the damping and torque curves, control systems employing 2-phase servomotors cannot be described accurately by linear differential equations. It is beyond the scope of this

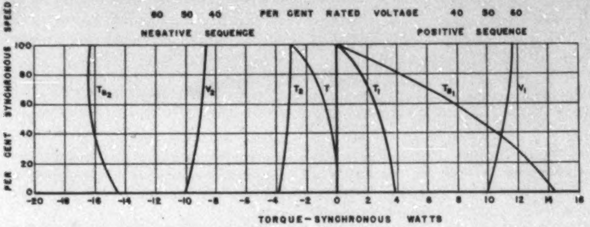

Figure 10. Curves used to explain single-phase performance of servomotors. Positive- and negative-sequence voltage in per cent rated versus speed in per cent synchronous. Torque in synchronous watts versus speed in per cent synchronous

Curve T_{B1} shows torque for operation on balanced 2-phase voltage applied to produce field rotation in direction of shaft rotation

Curve T_{B2} shows torque for operation on balanced 2-phase voltage applied to produce field rotation opposite to shaft rotation

V_1 and V_2 are curves of positive- and negative-sequence components of motor voltage respectively

T_1 and T_2 are curves of torque produced by the voltages V_1 and V_2 respectively

T is net torque T_1-T_2

paper to go any farther than to suggest that when the problem of analyzing the transient performance is met, the speed-torque curves be examined for the extreme of operation which will give minimum damping and again for that which will give maximum. Two solutions each using one extreme value of damping should bracket the actual performance provided the torque curves do not depart too greatly from linearity.

Conclusion

It is shown that the torque of the typical 2-phase servomotor discussed is approximately proportional to the control winding voltage over a normal speed range and that the torque at zero speed is directly proportional to control winding voltage for any servomotor of this type. The speed at constant torque is roughly proportional to voltage at only very limited ranges of low speed as contrasted with the d-c motor where speed at constant torque varies directly with voltage over a wide range in speed.

The damping factor is seen to be a function of speed and voltage and is far from being a constant value as in the d-c case.

Whether or not the motor will operate as a single-phase motor depends largely upon the exciting impedance as compared with rotor impedance and the slope of the balanced-voltage speed-torque curve near zero speed. The criteria are, that if the exciting impedance is low as compared with conventional values, and the balanced-voltage speed-torque curve crosses the zero speed axis with negative slope, the motor will not run single-phase.

Appendix I. Extension to Unbalanced Windings

It is assumed that the windings of the motor are such that sinusoidal magnetomotive-force space waves are produced by current in the windings. Let k_{bM} and k_{bC} be the breadth factors of the main and control windings respectively; k_{pM} and k_{pC} be the pitch factors of the main and control windings respectively; and N_M and N_C the number of turns in the main and control windings respectively.

Then $I_M k_{bC} k_{pM} N_M$ and $I_C k_{bC} k_{pC} N_C$ are the respective ampere turns in the main and control windings.

Assuming uniform permeance in the magnetic circuit, the flux waves produced by the two windings will be equal when

$$\frac{I_M}{I_C}=\frac{k_{bC}k_{pC}N_C}{k_{bM}k_{pM}N_M}=c \tag{30}$$

If $V_C^2=c^2V_M^2$, the same flux waves will be produced if an ideal transformer of turns ratio $c:1$ is placed across winding C and equal voltages applied to both windings. In this case $V_C=cV_M$; $I_C=I_M/c$ which satisfies equation 30. Normally, taking c as the ratio of the rated voltages of the windings should be sufficiently accurate.

The combination may then be treated as having the terminal characteristics of a motor having balanced windings.[23] If the impedance of the winding differs from the relation $Z_C=c^2Z_M$ the methods previously outlined may be used. That is, the motor may be considered as operating as in case one, with voltage applied to the control winding through an impedance.

In this Appendix and throughout the entire discussion it must be assumed that any circuit unbalance, either external or internal, must be confined to the stator as it can be shown that when unbalance occurs in both, the simple analysis by symmetrical components cannot be made.[24,25]

Appendix II. Sample Calculations of Points on Speed-Torque Curve

The calculations are based on the equivalent circuit of Figure 4 and the equations developed in the text. Assume a speed of 60 per cent synchronous. Assume also that the control voltage, E_C, is 50 per cent of the main winding voltage and is applied through a 200-ohm resistor. Then

$E_C=0.5V_M \qquad k=0.5$
$Z_C=200$

Positive-Sequence Impedance Calculations

Positive-sequence slip, $S_1=0.40$.

Positive-sequence equivalent rotor resistance, $R_R/S_1=100/0.4=250$ ohms. Assume that there is one ampere current in the equivalent rotor, then the voltage across the equivalent rotor and the exciting susceptance is $250+j0$. The exciting current is $250\times(-j0.01)=-j2.5$, and the total stator current is $1-j2.5$. The IZ drop through the stator is $(1-j2.5)\ (50+j120)=350-j5$ volts. The total voltage required to cause $1-j2.5$ amperes current in equivalent rotor is

$$350-j5+250=600-j5 \text{ volts}$$

$$Z_1=(600-j5)/(1-j2.5)=$$
$$600\underline{/-0.5}/2.69\underline{/-68.2^\circ}=223\underline{/67.7^\circ}$$

Negative-Sequence Impedance Calculations

Negative-sequence slip, $S_2=2-S_1=2-0.4=1.6$. Negative-sequence equivalent rotor resistance, $R_R/S_2=100/1.6=62.5$ ohms. Assume one ampere in the equivalent rotor, then the voltage across the exciting susceptance is $62.5+j0$; the exciting current is $62.5(-j0.01)=-j0.625$. The total stator current is $1-j0.625$. The drop through the stator is $(1-j0.625)\ (50+j120)=125+j88.75$.

$$Z_2=(187.5+j88.75)/(1-j0.625)=$$
$$207.5\underline{/25.3^\circ}/1.18\underline{/-32}=175.5\underline{/57.3^\circ}$$

Positive- and Negative-Sequence Voltage Calculations

$$V_{M1}=\frac{V_M(1+k+Z_C/Z_2}{2+Z_C/Z_1+Z_C/Z_2} \tag{18}$$

$V_M=75$ volts rated

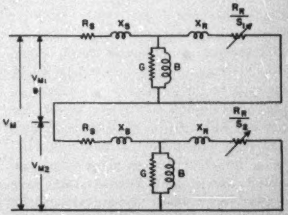

Figure 11. Equivalent circuit of single-phase induction motor

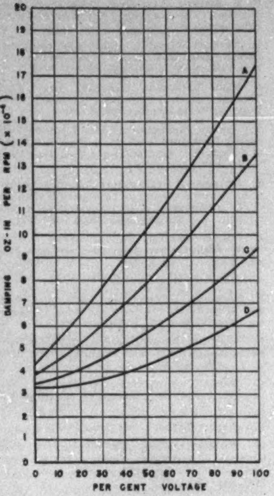

Figure 12. Internal damping factor in ounce-inches per revolutions per minute versus control-winding voltage in per cent rated for $Z_c=0$

Curve "A" is for a speed 60 per cent of synchronous; "B" for 40 per cent; "C" for 20 per cent; "D" for zero speed

$$V_{M1}=\frac{75(1+0.5+200/175.5\underline{/57.3^\circ}}{2+200/223\underline{/67.7^\circ}+200/175.5\underline{/57.3^\circ}}$$

$$=\frac{75(1.5+0.615-j0.96)}{2+0.34-j0.829+0.615-j0.96}$$

$$=\frac{75\times 2.32\underline{/-24.4^\circ}}{3.45\underline{/-31.2^\circ}}=50.4\underline{/6.8^\circ}\text{ volts}$$

$$V_{M2}=\frac{V_M(1-k+Z_C/Z_1)}{2+Z_C/Z_1+Z_C/Z_2} \qquad (19)$$

$$V_{M2}=\frac{75(1-0.5+200/223\underline{/67.7^\circ})}{2+200/223\underline{/67.7^\circ}+200/175.5\underline{/57.3^\circ}}$$

$$=\frac{75(0.5+0.34-j0.829)}{3.45\underline{/-31.2^\circ}}$$

$$=\frac{75\times 1.18\underline{/-46.0^\circ}}{3.45\underline{/-31.2^\circ}}=25.6\underline{/-15.4^\circ}\text{ volts}$$

Torque Calculations

The torque in the direction of motor rotation for balanced-voltage operation at 75 volts is found by standard methods to be 3.9 synchronous watts per phase at a slip of 0.4 or at 0.6 synchronous speed. The torque for reversed motor rotation at 0.6 synchronous speed (backwards) is also found by standard methods to be 8.2 synchronous watts per phase.

Calculating the net torque

$$T=\left(\frac{|V_{M1}|}{V_M|}\right)^2 T_{B1}-\left(\frac{|V_{M2}|}{V_M|}\right)^2 T_{B2}\text{ synchronous}$$

watts per phase, equation (20)

$$T=2\left[\left(\frac{50.4}{75}\right)^2 3.9-\left(\frac{25.6}{75}\right)^2 8.2\right]=$$

1.6 synchronous watts total

Calculations for Control Voltage Directly Applied

$Z_c=0$

Assume $k=0.6$, positive-sequence slip $=0.40$

$$V_{M1}=\frac{V_M}{2}(1+k) \qquad (21)$$

$$V_{M1}=\frac{75}{2}(1+0.6)=60\text{ volts}$$

$$V_{M2}=\frac{V_M}{2}(1-k) \qquad (22)$$

$$V_{M2}=\frac{75}{2}(1-0.6)=15\text{ volts}$$

Torque for balanced operation from above example $=3.9$ and 8.2 synchronous watts per phase for forward and backward rotation respectively.

$$T=2\left[\left(\frac{60}{75}\right)^2 3.9-\left(\frac{15}{75}\right)^2 8.2\right]$$

$=4.2$ synchronous watts total

Appendix III. Discussion of Correspondence between Experimental Data and Theoretical Performance

The equivalent circuit parameters of the motor used as an example in this paper were calculated from open-circuit and short-circuit tests and then modified so as to bring the calculated performance into reasonably good agreement with observed performance. Such procedure was necessary because of the normal difficulty involved in properly separating the rotor and stator reactances by means of blocked-rotor and no-load tests of squirrel-cage induction motors, a difficulty which is magnified in the present case because of the relatively large amount of exciting current.

However, the calculations are straightforward and if the parameters could be determined accurately for each value of positive- and negative-sequence slip, the results would be quite accurate. This is emphasized by the fact that when the experimental speed-versus-torque curve for balanced voltage was available, one of the writer's colleagues was able to predict the curves for various values of directly-applied control voltage with a high degree of accuracy.

When making performance calculations, it is desirable to assume that the leakage inductances and resistances remain constant in order to simplify the calculating procedure. This procedure was followed in constructing the several curves shown in the text material of this paper. There is perhaps more reason to assume that the stator leakage reactance and the exciting admittance remain constant in a "drag cup" motor than in a conventional motor because the large air gap is conducive to more constant saturation conditions.

The conditions in the rotor however are more adverse and it may be expected that the current distribution, and therefore the leakage inductance and the resistance, will change considerably with frequency or slip.

This should not cause great difficulty for the application engineer if the motor manufacturer would furnish the following experimental data:

1. Speed-versus-torque curve for balanced voltages for speed values ranging from 100 per cent positive rotation (slip = 0) to 100 per cent negative rotation (slip = 2).
2. Vector impedance values (as viewed from the terminals) for the same range in speed or slip.

The positive- and negative-sequence voltages could then be calculated by means of one of the following pairs of equations 18, 19; 21, 22; 23, 24; or 25, 26. Torque could be calculated by means of equation 27. Presumably quite accurate values of performance for a variety of operating conditions could be obtained. The accuracy of this method has been checked for the case where $Z_c=0$ as mentioned previously.

These methods, however, do not benefit the motor designer in the same degree. His problem concerns the finding of the various reactances and resistances which make up the terminal impedances. The determination of these values for varying frequency would make worthy subjects for future studies. Following is a description of a method which the writer hopes to use for

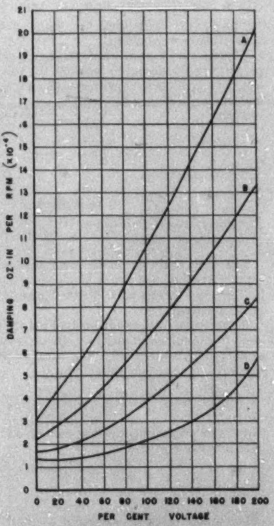

Figure 13. Same as Figure 12 except $Z_c=200+j0$

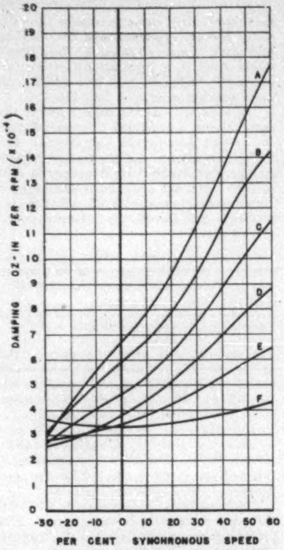

Figure 14. Internal damping factor versus speed for $Z_c=0$

Curve "A" is for control voltage corresponding to $k=1.0$; "B," $k=0.8$; "C," $k=0.6$; "D," $k=0.4$; "E," $k=0.2$; "F," $k=0$

experimentally separating the stator and rotor leakage reactances.

Assume that a search coil can be placed properly in the airgap to measure the voltage corresponding to that across the exciting admittance in Figure 4.

Then

$$V-I_sZ_s=E$$

where

V = terminal voltage
I_s = stator current
Z_s = stator leakage impedance
E = search coil voltage

This test could be made with blocked rotor. Another test could be made at no load or some chosen value of rotor speed in order to change I_s.

If the voltage, V, is adjusted so that the same E is obtained in each case (in order to avoid having to determine the turns ratio of stator coil to search coil), we have

$$V'-I_s'Z_s=E=V''-I_s''Z_s$$

where the primes signify first and second tests respectively, and

$$\frac{V'-V''}{I_s'-I_s''}=Z_s$$

The stator leakage impedance as calculated should remain fairly constant for reasons mentioned previously. The rotor impedances could then be calculated from measured terminal impedances for various slips.

Appendix IV. Nomenclature

V_M = terminal voltage of main winding
V_C = terminal voltage of control winding
V_{M1} = positive-sequence component of V_M
V_{M2} = negative-sequence component of V_M
V_{C1} = positive-sequence component of V_C
V_{C2} = negative-sequence component of V_C
V = terminal voltage for balanced polyphase
E_C = control voltage applied to motor winding in series with impedance external to winding
E = voltage induced in search coil by air-gap flux
k = ratio $|E_C|/|V_M|$
V_t = terminal voltage of a d-c motor
I_M = main winding current
I_C = control winding current
I_{C1} = positive-sequence component of I_C
I_{C2} = negative-sequence component of I_C
I_S = stator current balanced polyphase
I_a = armature current in a d-c motor
R_S = stator resistance
R_R = rotor resistance
X_S = stator leakage reactance
X_R = rotor leakage reactance
G = exciting circuit conductance
B = exciting circuit susceptance
S = slip for balanced polyphase
S_1 = positive-sequence slip, actually the same as S
S_2 = negative-sequence slip $=2-S$
Z_1 = total positive-sequence impedance as measured at the terminals (or calculated from equivalent circuit for balanced polyphase) with $S=S_1$
Z_2 = total negative-sequence impedance as measured from the terminals (or calculated from the equivalent circuit for balanced polyphase) with $S=S_2$
Z = total impedance with rotor blocked
Z_C = external impedance in control winding circuit
R_a = armature resistance of a d-c motor
k_t = developed torque per ampere
k_v = generated volts per rpm
N = rpm
T = net developed torque
T_0 = net developed torque at zero speed
T_{B1} = developed torque for balanced polyphase operation at slip of S_1
T_{B2} = developed torque for balanced polyphase operation at slip of $2-S_1$
T_1 = developed positive-sequence torque
T_2 = developed negative-sequence torque
T_B = developed torque at zero speed with balanced polyphase voltage applied
k_{bM} = breadth factor of main winding
k_{bC} = breadth factor of control winding
k_{pM} = pitch factor of main winding
k_{pC} = pitch factor of control winding
N_M = number of turns on main winding
N_C = number of turns on control winding
c = effective turns ratio between main winding and control winding

References

1. THEORY OF SERVOMECHANISMS (book), **H. M. James, N. B. Nichols, R. S. Phillips.** McGraw-Hill Book Company, New York, N. Y., 1947.

2. CONTROL OF THE EFFECTIVE INTERNAL IMPEDANCE OF AMPLIFIERS BY MEANS OF FEEDBACK, **H. F. Mayer.** *Proceedings*, Institute of Radio Engineers (New York, N. Y.), volume 27, March 1939, pages 213–7.

3. NETWORK ANALYSIS AND FEEDBACK AMPLIFIER DESIGN (book), **H. W. Bode.** D. Van Nostrand Co., New York, N. Y., 1945, pages 31–6.

4. RADIO ENGINEERS' HANDBOOK (book), **F. E. Terman.** McGraw-Hill Book Company, New York, N. Y., 1943, pages 402-3.

5. APPLIED ELECTRONICS (book), **Electrical Engineering Department Staff,** Massachusetts Institute of Technology. John Wiley and Sons, New York, N. Y., 1943, pages 525–36.

6. METHOD OF SYMMETRICAL COORDINATES APPLIED TO THE SOLUTION OF POLYPHASE NETWORKS, **C. L. Fortescue.** *AIEE Transactions*, volume XXXVII, part II, June 1918, pages 1027–1115.

7. CIRCUIT ANALYSIS OF A-C POWER SYSTEMS (book), **Edith Clarke.** John Wiley and Sons, Inc., New York, N. Y., page 55.

8. **Clarke,** op. cit. page 296.

9. SYMMETRICAL COMPONENTS (book), **C. F. Wagner, R. D. Evans.** McGraw-Hill Book Company, Inc., New York, N. Y., 1933, page 334.

10. ELECTRIC CIRCUITS, volume I (book), **O. G. C. Dahl.** McGraw-Hill Book Company, New York, N. Y., 1928, page 80.

11. THEORY OF ALTERNATING-CURRENT MACHINERY (book), **A. S. Langsdorf.** McGraw-Hill Book Company, New York, N. Y., 1937, page 127.

12. **Wagner, Evans,** op. cit. pages 341–2.

13. APPLICATIONS OF THE METHOD OF SYMMETRICAL COMPONENTS (book), **W. V. Lyon.** McGraw-Hill Book, Company, New York, N. Y., 1937, page 233.

14. **Dahl,** op. cit. pages 138–9.

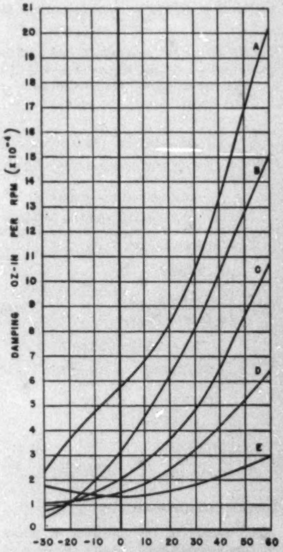

Figure 15. Internal damping factor versus speed for $Z_c=200+j0$

Curve "A" is for control voltage corresponding to $k=2.0$; "B," $k=1.5$; "C," $k=1.0$; "D," $k=0.5$; "E," $k=0$

15. **Lyon,** op. cit. page 230.

16. **Fortescue,** op. cit. page 1071.

17. **Langsdorf,** op. cit. page 682.

18. **Three-Phase Capacitor Motor, R. J. W. Koopman.** Master's Thesis, Yale University, New Haven, Conn., 1933.

19. **Polyphase Induction Motors on Unbalanced Voltages, H. R. Reed, R. J. W. Koopman.** *Electrical Engineering* (*AIEE Transactions*), volume 55, November 1936, pages 1206–13.

20. **Control of Slip-Ring Motors by Means of Unbalanced Primary Voltages, N. L. Schmitz.** *AIEE Transactions*, volume 66, 1947, pages 1103–13.

21. **Symmetrical Components as Applied to Single-Phase Induction Motors, F. W. Suhr,** *Electrical Engineering* (*AIEE Transactions*), volume 64, September 1945, pages 651–6.

22. **Servomechanism Fundamentals (book), H. Lauer, R. Lesnick, L. E. Matson.** McGraw-Hill Book Company, New York, N. Y., 1947, pages 97–100.

23. **Lyon,** op. cit. page 226.

24. **Lyon,** op. cit. page 276.

25. **An Extension of the Method of Symmetrical Components Using Ladder Networks, Waldo V. Lyon.** *AIEE Transactions*, volume 59, 1940, pages 1025–1030.

Discussion

S. Davis (Arma Corporation, Brooklyn, N. Y.): By making assumptions which apply specifically to the 2-phase, servo-type motor, Mr. Koopman has developed a simple set of formulas, which enables the application engineer to predict, from manufacturer's data, the performance characteristics of these motors under varied conditions of use.

The formulas, because of their simplicity, also are useful to the designer in checking performance with given circuit parameters. The clear statement of the criterion for avoiding single-phase operation of a servomotor is particularly helpful.

Mr. Koopman concerns himself primarily with the "drag-cup" motor. It should be pointed out that in the very small sizes, equally high torque to inertia ratios can be achieved by using more conventional rotors of relatively small diameter in comparison with the frame size. This design generally requires less power in the control field, because a smaller air gap is possible, although more care must be taken in design to avoid single-phase operation.

The assumption of negligible leakage reactance of the drag cup has been borne out by the experience of the writer.

Mr. Koopman indicates a procedure for measuring primary leakage by means of a search coil properly placed in the air gap. It is of considerable importance in this to distinguish between the fundamental and harmonic components of air-gap flux distribution. A full-pitch undistributed search coil, for example, would measure total air-gap flux, rather than the fundamental space component, including fluxes which properly are part of the differential leakage. In small motors having few slots per pole per phase, the differential leakage may be a large part of the total, and serious errors may result. The writer would be very interested in learning the results of such measurements.

S. S. L. Chang (Robbins and Myers, Inc., Springfield, Ohio): Mr. Koopman brings out some very interesting and significant relationships between the motor constants and the speed-torque characteristics. His paper is valuable to both servo and motor engineers. However, a more straightforward and exact analysis can be made by using the cross-field theory. For instance, one of the results of the cross-field analysis is that with zero-control-phase electromotive force, a motor would develop negative torque at all speeds if and only if $R_R > |Z_3|$, where Z_3 is the impedance shown in Figure 2A of the discussion.

The cross-field theory equivalent circuit[1] is shown in Figure 1 of the discussion, in which the same symbols are used except that S stands for the ratio of the actual speed to synchronous speed instead of the slip. The motor torque is given by equation 31.

Figure 1. The equivalent circuit for the 2-phase servomotor

On this diagram

$$R=\frac{SR_R}{1-S^2}$$

$$S=\frac{\text{actual speed}}{\text{synchronous speed}}$$

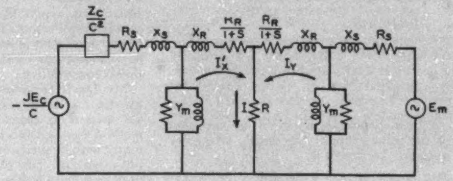

Y_m represents the magnetizing admittance. All the motor constants are in main winding terms

$$T=RI^2+\frac{2R_R}{1+S}I_x'I_y\cos(I_x',\ I_y)\quad\text{synchronous watts}\qquad(31)$$

The control-phase electromotive force is multiplied by $-j$. In case the actual control-phase electromotive force and the main-winding electromotive force are at an angle of 90 degrees, the two voltage sources shown on the equivalent circuit would be in phase.

Applying Thevenin's theorem to the circuit of Figure 1 of the discussion, it reduces to that of Figure 3 of the discussion. The impedances $\boldsymbol{Z}_3$ and $\boldsymbol{Z}_4$ are defined in Figure 2 of the discussion. The voltages $\boldsymbol{E}_3$ and $\boldsymbol{E}_4$ are given by the following equations

$$\boldsymbol{E}_3=-\frac{j\boldsymbol{E}_c}{c}\times\frac{1}{1+\boldsymbol{Y}_m\left(R_s+jX_s+\frac{\boldsymbol{Z}_c}{c^2}\right)}$$

$$\boldsymbol{E}_4=\frac{\boldsymbol{E}_m}{1+\boldsymbol{Y}_m(R_s+jX_s)}$$

The behavior of any servomotor, with or without external impedance, is fully represented by this 2-mesh circuit.

Take as a numerical example, the motor analyzed by Mr. Koopman with $\boldsymbol{Z}_c=200$. The impedances and voltages are calculated to be

$\boldsymbol{Z}_3=22.6+j80 \qquad \boldsymbol{E}_3=22.5k\underline{/48.6^\circ}$

$\boldsymbol{Z}_4=9.85+j57 \qquad \boldsymbol{E}_4=33.3\underline{/12.8^\circ}$

At slip 0.4 or $S=0.6$, the solution of the 2-mesh circuit is

$\boldsymbol{I}_x'=0.1382k\underline{/12.3^\circ}-0.1092\underline{/-42.4^\circ}$

$\boldsymbol{I}_y=0.228\underline{/-18.3^\circ}-0.0738k\underline{/-6.6^\circ}$

For $k=0.5$

$\boldsymbol{I}_x'=-0.0131+j0.0883$
$\boldsymbol{I}_y=0.180-j0.0674$
$\boldsymbol{I}=0.167+j0.021$
$T=93.7\times0.168^2-2\times62.5(0.0131\times 0.180+0.0883\times0.0674)=1.6$ synchronous watts

To obtain a general expression of motor torque with zero-control-phase electromotive force, $\boldsymbol{E}_3=0$. The currents $\boldsymbol{I}_x'$ and $\boldsymbol{I}_y$ can be expressed in terms of $\boldsymbol{I}$

$$\boldsymbol{I}_x'\left(\frac{R_R}{1+S}+\boldsymbol{Z}_3\right)=-\boldsymbol{I}\frac{SR_R}{1-S^2}$$

$$\boldsymbol{I}_x'+\boldsymbol{I}_y=\boldsymbol{I}$$

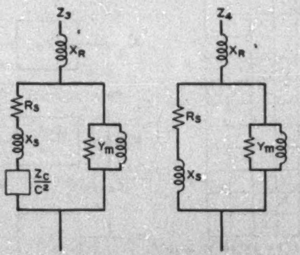

Figure 2. Definitions of Z_3 and Z_4

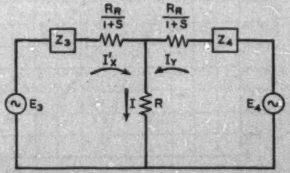

Figure 3. The simplified equivalent circuit

Substituting these expressions in equation 31 and simplifying the result, it yields

$$T=\frac{I^2R_RS}{1-S^2}\times\frac{|Z_3|^2-\dfrac{R_R^2}{1-S^2}}{\left|\mathbf{Z}_3+\dfrac{R_R}{1+S}\right|^2}\quad\text{synchronous watts}\qquad(32)$$

From equation 32, it is evident that

1. if $R_R>|Z_3|$,

torque is negative at all speeds

2. if $R_R<|Z_3|$,

torque is positive in the range

$$0<S<\sqrt{1-\frac{R_R^2}{|Z_3|^2}}$$

The cross-field theory gives an expression of the peak value of the double frequency pulsating torque, it is

$$T_p=RI|\mathbf{I}_x'-\mathbf{I}_y|\qquad(33)$$

For the numerical example cited, it is

$$T_p=93.7\times0.168\times|-0.193+j0.156|$$
$$=3.90\text{ synchronous watts}$$

The application of the cross-field equivalent circuit does not require any knowledge in electrical machinery. It also can be constructed in control winding terms and integrated into the amplifier circuit.

Reference

1. The Equivalent Circuit of the Capacitor Motor, S. S. L. Chang. *AIEE Transactions*, volume 66, 1947, pages 631–40.

R. J. W. Koopman: The writer is grateful to Mr. Davis for showing that his experience with 2-phase servomotors checks with the writer's deductions in the paper. Regarding the question of emphasis on the "drag cup" motor, the writer desires to state that drag cup motor constants were used in constructing the illustrative curves in the paper because they produced a more striking example of the phenomenon of negative torque on single phase than other typical constants which were available. When the usual assumptions[1] are met in like degree, the formulas developed apply equally as to "drag cup" motors as to those of more conventional construction.

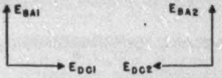

Figure 5. Components of voltage applied to servomotor through external impedances

Mr. Davis' last point concerns the experimental results of the search coil method for measuring primary impedance. This method was used on a small 2-phase drag cup motor with 2-layer winding consisting of one full-pitch coil per phase per pole. (The drag cup type was used because of a convenience which will be obvious.) The search coil was a full-pitch coil consisting of about ten turns of fine wire placed in the small openings between the teeth.

A terminal voltage V' applied to the stator with the rotor removed (simulating the no load condition for a conventional design) produced a voltage E on the search coil. With the rotor replaced and blocked, a different voltage V'' was required to produce the same E. From these readings, and current and phase-angle readings, the parameters for the equivalent circuit were calculated. From the equivalent circuit thus determined, speed-versus-torque curves were calculated in the usual manner, that is sinusoidal space distribution of flux was assumed. This curve then was corrected for the effect of the space harmonics. It was assumed that the flux wave produced by each phase acting alone was flat topped because of the single full-pitch coil winding. The amplitudes of the space harmonics fluxes are $1/n$ where n is the order harmonic and always odd. The correction was made by taking the harmonic torques as $1/n^2$ times the fundamental torque at the same slip and combining these with the fundamental, due regard being given to direction. The writer has not explored thoroughly the theoretical details involved, but the curve of Figure 4 of the discussion will show that good practical results were obtained in the instance cited.

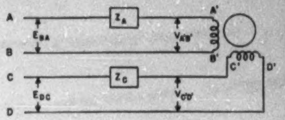

Figure 6. Servomotor circuit

The author also is grateful to Mr. Chang for bringing to his attention an equivalent circuit from which a quantitative criterion regarding single-phase operation is readily obtained. This circuit also facilitates the calculation or the actual measurement in a laboratory equivalent circuit of motor terminal impedances for various conditions of operation which is important in the application of motors in servomechanisms.

However, there also are some advantages over Mr. Chang's circuit possessed by the one given in a supplement to this closure and which is based on the revolving field theory and the induction motor equivalent circuit for balanced operation. If the latter were set up in the laboratory, torque could be obtained by the recording of two currents and two resistances whereas if Mr. Chang's circuit were used three currents, two resistances and one phase angle between currents would have to be recorded.

It has been known for years that the cross-field theory and the revolving-field theory of the single-phase induction motor lead to exactly equivalent results when equivalent design constants are used,[2] and more recently this argument has been extended to capacitor motor analysis.[3,4] Mr. Chang forged another link in the chain of this evidence when he calculated a performance point by means of formulas based on the cross-field theory and checked the calculations made by means of the formulas in the paper which are based on the revolving-field theory. Therefore, Mr. Chang's statement regarding a more "exact analysis" must be interpreted with care.

The question of which analysis is the more

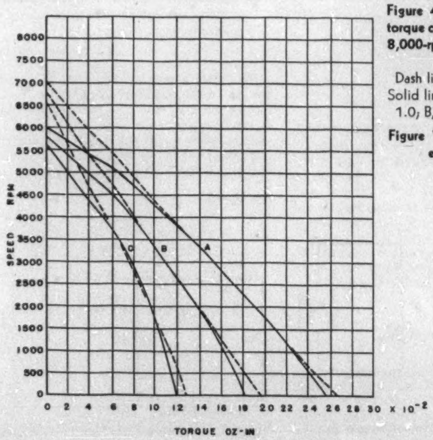

Figure 4 (left). Speed-versus-torque curves for small 2-phase 8,000-rpm synchronous speed servomotor

Dash lines, calculated curves
Solid lines, test curves. A, k=1.0; B, k=0.75; C, k=0.5

Figure 7 (right). Servomotor equivalent circuit

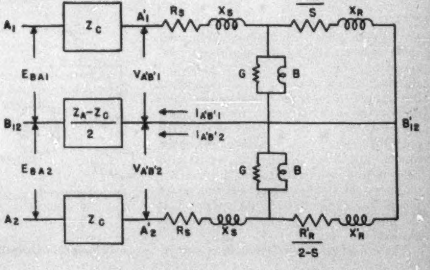

straightforward in general is a matter of opinion as has been pointed out in the literature.[4] It is the writer's opinion that an analysis, such as given in the paper, which is based on the equivalent circuit for the induction motor as it has been taught in electrical engineering schools for many years and symmetrical component theory, which also has been widely taught, is more straightforward than an analysis based on the cross-field theory.

SUPPLEMENT TO CLOSURE

In the paper under discussion it is obvious that the performance calculations for the more difficult cases are rather formidable even with the aid of a vector slide rule or calculating machine. Much time could be saved if an equivalent circuit were set up in the laboratory and direct measurements made. If the circuit were set up on a per unit[5] basis, a limited range of impedance units could be used to cover a range of ratings.

Such a circuit, quite similar to those developed by Kron[6,7] for the capacitor motor was derived by the writer from ordinary symmetrical component theory and the usual equivalent circuit for the induction motor on balanced voltages. An article on this was sent in to AIEE for review after the paper under discussion was preprinted. Slides showing the circuit were used by the author in his presentation of the paper under discussion. The essential details of this article are given here at the request of the reviewing committee.

All the formulas in the paper can be derived from this circuit.

The same assumptions regarding superposition, constancy of permeance, circuit balance, and sinusoidal time variation of current and voltage are made as in the paper. Fluxes also are assumed to have a sinusoidal space distribution as the inclusion of the space harmonics would lead to a cascade of equivalent circuits.[8]

DERIVATION OF AN EQUIVALENT CIRCUIT FOR 2-PHASE SERVOMOTORS

Method. The method of analysis consists in writing the symmetrical components of the applied voltages in terms of the voltage drops produced by positive- and negative-sequence currents flowing through the external impedances[9] and the positive- and negative-sequence terminal voltages on the motor.

These latter voltages are equal to the products of the respective sequence currents by the sequence impedances calculated from the "exact" induction-motor equivalent circuit using slip, s, for the positive sequence and 2-s for the negative sequence slip.[10]

Basic Equations. Unbalanced 2-phase voltages may be resolved into several equivalent systems.[10] However, the system chosen here is that shown in Figure 5 of the discussion.

When symmetrical components of voltage are applied directly to the terminals of the servomotor, they are related to the symmetrical components of current by the following equations.

$$V_{A'B'1}=I_{A'B'1}Z_{A'B'1} \tag{34}$$

$$V_{A'B'2}=I_{A'B'2}Z_{A'B'2} \tag{35}$$

where $V_{A'B'1}$ and $V_{A'B'2}$ are respectively the positive- and negative-sequence components of terminal voltages referred to the winding designated as $A'B'$ and with circuit direction of application designated by double-subscript notation,[12,13,14] $Z_{A'B'1}$ and $Z_{A'B'2}$ are the motor impedances to the positive- and negative-sequence components of current, $I_{A'B'1}$ and $I_{A'B'2}$.

Referring to Figure 5, the voltages applied to the complete system, servomotor and external impedances, may be resolved as follows[15]

$$E_{BA1}=\frac{E_{BA}+jE_{DC}}{2} \tag{36}$$

$$E_{BA2}=\frac{E_{BA}-jE_{DC}}{2} \tag{37}$$

The terminal voltages may be similarly resolved as follows

$$V_{A'B'1}=\frac{V_{A'B'}+jV_{C'D'}}{2} \tag{38}$$

$$V_{A'B'2}=\frac{V_{A'B'}-jV_{C'D'}}{2} \tag{39}$$

The currents may be resolved by means of equations paralleling 38 and 39. From Figure 6 of the discussion

$$E_{BA}=I_{A'B'}Z_A+V_{A'B'} \tag{40}$$

$$E_{DC}=I_{C'D'}Z_C+V_{C'D'} \tag{41}$$

From equations 36, 40 and 41,

$$E_{BA1}=\frac{I_{A'B'}Z_A+jI_{C'D'}Z_C+V_{A'B'}+jV_{C'D'}}{2} \tag{42}$$

Substituting an equivalent value for the right-hand voltage terms from equation 38

$$E_{BA1}=\frac{I_{A'B'}Z_A+jI_{C'D'}Z_C}{2}+V_{A'B'1} \tag{43}$$

Since the currents may be resolved into their symmetrical components,

$$E_{AB1}=(I_{A'B'1}+I_{A'B'2})\frac{Z_A}{2}+ j(I_{C'D'1}+I_{C'D'2})\frac{Z_C}{2}+V_{A'B'1} \tag{44}$$

From Figure 5

$$jI_{C'D'1}=I_{A'B'1}$$

$$jI_{C'D'2}=-I_{A'B'2}$$

hence

$$E_{BA1}=I_{A'B'1}\left(\frac{Z_A+Z_C}{2}\right)+ I_{A'B'2}\left(\frac{Z_A-Z_C}{2}\right)+V_{A'B'1} \tag{45}$$

Similarly

$$E_{BA2}=I_{A'B'1}\left(\frac{Z_A-Z_C}{2}\right)+ I_{A'B'2}\left(\frac{Z_A+Z_C}{2}\right)+V_{A'B'2} \tag{46}$$

It is evident that equations 45 and 46 are expressions of Kirchhoff's voltage law written around the two loops of the circuit shown in Figure 7 of the discussion. In applying the voltages E_{BA1} and E_{BA2} to the servomotor equivalent circuit they must act in the circuit direction indicated by the double subscripts.

The elements in Figure 7 of the discussion, R_S, X_S, R_R, X_R, G and B are respectively stator resistance and reactance, rotor resistance and reactance and the components of exciting admittance all for the servomotor considered as an ordinary polyphase induction motor. The symbols for rotor resistance and reactance in the lower part of the diagram are primed to indicate the possible desirability of making a correction in these values due to the higher frequency of the negative-sequence rotor currents.

The positive-sequence torque per phase in synchronous watts is the power in the resistive element, R_R/S, in the upper part of the circuit of Figure 7. The negative-sequence torque per phase is found from the power in the corresponding element $R_R/(2-S)$ in the lower half of the circuit. Net torque per phase is the difference between these two torques.

REFERENCES

1. See reference 21 of the paper.
2. ON THE EQUIVALENCE OF THE TWO THEORIES OF THE SINGLE-PHASE INDUCTION MOTOR, **V. Karapetoff.** *AIEE Journal*, volume XL, August 1921, pages 640–41.
3. THE CROSS-FIELD THEORY OF THE CAPACITOR MOTOR, **A. F. Puchstein, T C. Lloyd.** Discussion, **E. J. Schaefer.** *AIEE Transactions*, volume 60, 1941, pages 667–68.
4. Op cit, **Wayne J. Morrill.** *AIEE Transactions* volume 60, 1941, pages 669–70.
5. ALTERNATING-CURRENT MACHINERY (book), **J. M. Bryant, E. W. Johnson.** McGraw-Hill Book Company, New York, N. Y., 1935.
6. TENSOR ANALYSIS (book), **Gabriel Kron.** John Wiley and Sons, Inc., New York, N. Y., 1942.
7. STEADY-STATE EQUIVALENT CIRCUITS OF SYNCHRONOUS AND INDUCTION MACHINES, **Gabriel Kron.** *AIEE Transactions*, volume 67, Part I, 1948, pages 175–81.
8. LEAKAGE REACTANCE OF THE SQUIRREL-CAGE ROTOR WITH RESPECT TO THE STATOR HARMONICS AND THE EQUIVALENT CIRCUIT OF THE INDUCTION MOTOR, **M. M. Liwschitz.** *AIEE Transactions*, volume 66, 1947, pages 1407–08.
9. See reference 6 of the paper.
10. See reference 10 of the paper.
11. See references 12 and 13 of the paper.
12. A COURSE IN ELECTRICAL ENGINEERING (book), **Chester L. Dawes.** McGraw-Hill Book Co., Inc., New York, N. Y., 1947.
13. ALTERNATING-CURRENT CIRCUITS (book), **J. M. Bryant, J. A. Correll.** McGraw-Hill Book Co., Inc., New York, N. Y., 1931.
14. ELECTRIC CIRCUITS (book), M. I. T. Staff. John Wiley and Sons, Inc., New York, N. Y., 1940.
15. See reference 8 of the paper.

The Thermal Movement of Moisture in Soil

A. S. MICKLEY
ASSOCIATE AIEE

THIS paper develops a theory of moisture movement in soils under thermal gradients and demonstrates confirmation of test data published previously. A formula is derived to determine moisture movement quantitatively so that the precise effect on underground cable heating can be evaluated.

It has long been known that when a moist soil is subjected to a temperature gradient, the moisture will have a tendency to move in the direction of heat flow.

This migration will not continue until all of the moisture has been removed, but will cease after equilibrium conditions have been established. This phenomenon is of considerable interest in cable heating studies, because the thermal conductivity of the earth in the heat field involved will decrease as moisture is lost. If the loss is appreciable, it must be taken into consideration in temperature calculations.

The mechanism of moisture movement is thought to be due primarily to surface tension, although vapor movement also may be involved.

Surface Tension Movement

The moisture in the soil is considered to be held in droplets between soil particles, much as shown in Figure 1(a). The droplets are kept in place by surface tension forces, which must be in equilibrium in all directions. The irregular spaces between the soil particles give each moisture droplet an opportunity to take the shape necessary to satisfy the conditions of equilibrium.

To understand the mechanism, consider first a droplet of moisture between two horizontal flat plates as shown in Figure 1(b). The forces along the AB axis would be equalized as follows

$$F_A = F_B$$

or

$$4R_AS_A = 4R_BS_B \qquad (1)$$

where S is the surface tension in dynes per centimeter and R is the radius in centimeters. The factor 4 takes into account the integration of the A and B axis components of the surface tension radial forces, as well as the combined effects of the top and bottom meniscuses. Equation 1 is really an adaptation of the classical formula of force on a semicircular ring under normal pressure.

Force = diameter × unit pressure

Assume next that a temperature gradient is introduced so that the temperature at A is greater than at B. Surface tension varies with temperature T by the following relationship

$$S = S_0(1 - aT) \text{ dynes per centimeter} \qquad (2)$$

where S_0 and a are constants.

The surface tension at A will now be less than at B. To restore equilibrium the radii must change, R_A becoming greater and R_B less. This produces a distortion as indicated by the dotted line in Figure 1(b). The greater the gradient, the greater the distortion, hence we can write the relation

$$\text{Distortion} \propto \frac{dT}{dx} \qquad (3)$$

where dT/dx is the temperature gradient in degrees centigrade per centimeter.

Now in the course of distorting, the droplet may meet another droplet and merge to form a new, larger droplet. When a merger takes place, the surface tension forces are completely upset. The new droplet must seek to re-establish equilibrium by moving until it finds lodging in a crevice system whose shape produces the necessary equalization. It may even find another droplet in the course of this movement and have another merger. The resulting droplet must then start all over again to find equilibrium. It continues to move, therefore, until it can conform to the proper shape without touching off another merger in the process.

The movement of a droplet seeking equilibrium may be in any direction. In a temperature gradient field, however, the surface tension forces will be stronger in the cold direction. Among a large selection of droplets, therefore, the net effect will be a movement from hot to cold.

The distortion in a droplet, relation 3, is one factor. Its effect is modified, however, by the probability that a given amount of distortion will cause merger with an adjacent droplet. To develop this additional factor, assume a triangular arrangement of uniform soil particles as shown in Figure 1(c). Assume that the space between any two soil particles is a possible container of a droplet. A few spaces have been numbered for convenience. Take space number 1. This may be either occupied or unoccupied by a moisture droplet. The probability of its being occupied is

$$P_o = \frac{\text{total number of droplets}}{\text{total number of spaces}} = \frac{M_t}{F} \qquad (4)$$

where M_t is the initial moisture content and F is the field capacity, or the moisture content at saturation, both expressed in per cent of dry weight of soil.

Now consider the probability of the moisture in space 1 merging with the moisture in space 2. Any two adjacent

---

Paper 49-83, recommended by the AIEE insulated conductor committee and approved by the AIEE technical program committee for presentation at the AIEE winter general meeting, New York, N. Y., January 31–February 4, 1949. Manuscript submitted November 10, 1948; made available for printing December 17, 1948.

A. S. MICKLEY is with the Philadelphia Electric Company, Philadelphia, Pa.

The author wishes to acknowledge the helpful suggestions of A. H. Kidder, J. H. Neher and W. O. Smith.

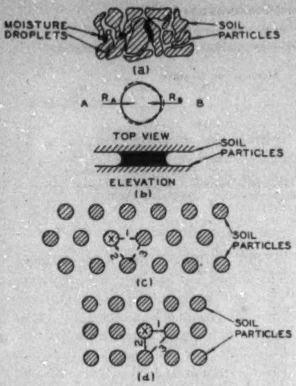

Figure 1. Soil particle moisture droplet relationships

spaces may be chosen. For a merger both must be occupied, the probability of which is $(M_i/F)^2$. If, however, spaces 1 to 3 are all occupied simultaneously as well as the spaces above and below particle X, this merger between 1 and 2 cannot take place, since they are already joined within an established water mass. The probability of this, $(M_i/F)^6$, must be subtracted from the total probability. The merger probability is therefore

$$P_m = \left(\frac{M_i}{F}\right)^2 - \left(\frac{M_i}{F}\right)^6 \qquad (5)$$

This relationship is seen to hold for both the triangular and rectangular structures of Figure 1(c) and 1(d).

The distortion and merger probability effects will be further modified by the particle size and by the distribution of particles of various sizes within a soil. These factors are taken care of by a constant of proportionality k, which is determined by test.

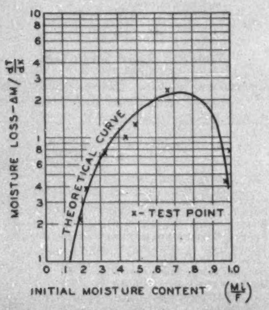

Figure 2. Thermal movement of soil moisture. Theoretical curve of surface tension movement plotted against data of Smith[1] for Barnes loam, horizon C

Relationships 3 and 5 are multiplied by the constant of proportionality to give the total movement equation

$$\Delta M = k\frac{dT}{dx}\left[\left(\frac{M_i}{F}\right)^2 - \left(\frac{M_i}{F}\right)^6\right] \qquad (6)$$

where

ΔM = moisture lost in per cent of dry weight (final moisture content $- M_i$)
M_i = initial moisture content in per cent of dry weight or the moisture content previous to application of a thermal gradient
F = field capacity of the soil in per cent of dry weight. (The moisture content of the soil at saturation is required here. There are a number of means of determination used by soil scientists based on various laboratory techniques. Either the field capacity or the moisture equivalent of a soil is satisfactory for use.)
dT/dx = temperature gradient degrees centigrade per centimeter
k = constant of proportionality, per cent centimeters per degree centigrade

Hot Radiator versus Cold

Equation 6 describes the tendency of soil moisture to move away from a hot radiator, such as a buried cable. It will not describe the effect of moisture collection around a radiator cooler than the surrounding soil, such as a heat pump circulating coil. In this case the coil surface forms a barrier which prevents any further moisture movement in the cold direction. The moisture accumulation cannot build up beyond the field capacity, however, since any moisture in excess of the field capacity will percolate down to the water table by gravitational flow.

Test Confirmation

W. O. Smith[1] has made very careful measurements of soil moisture movement under a thermal gradient, but has not attempted in published work to analyze his data on a mathematical or theoretical basis.

Smith's method was to place a soil sample between two parallel plates of different temperature. Measurements of soil moisture before and after 72 hours' exposure to the temperature gradient were made at three different points: the hot face, the cold face, and half way between. The movement of moisture away from the hot face and toward the cold face fits equation 6 quite well. The data plotted in Figure 2 are a typical example of one of the 18 samples Smith tested. In this particular soil, both the hot face measurements and the center measurements fit the curve. The cold face measurements do not fit, since the cold plate forms a barrier which causes the moisture to pile up artificially. In several soil samples, only the hot face measurements fit the theoretical curve, apparently because the cold barrier accumulation backs up into the center measurement point.

An analysis of the data presented by Smith[1] is given in Table I. From this it will be seen that the maximum value of k is 9.6 per cent centimeters per degree centigrade. Since the maximum value of equation 5 is 0.32, the maximum value of ΔM is 3.1 per cent per degree centigrade per centimeter.

Vapor Movement

No consideration of moisture movement would be complete without a discussion of the possibility of transfer by means of vaporization and condensation. To study this problem in soil, we must review some fundamental laws governing moist air:

1. A flat surface of water has a definite vapor pressure at a given temperature.
2. The vapor pressure above a curved liquid surface is less than or greater than the flat surface vapor pressure, depending upon whether the surface is concave or convex. The surface presented by water in a porous body is concave. For a concave surface the relationship is

$$V_P\ (\text{concave}) = V_p\ (\text{flat}) - \frac{v}{l-v}\,\frac{2S}{R} \qquad (7)$$

where

V_P = vapor pressure
v = vapor density
l = liquid density
S = surface tension
R = surface radius

3. The saturation point of a gas depends on Dalton's law of partial pressures, and the vapor content at saturation can be written

$$V = K\frac{P_s}{P - P_s} \qquad (8)$$

where

V = vapor content, pounds per pounds of dry air
K = constant
P_s = vapor pressure of liquid evaporating into gas
P = pressure of the gas and vapor mix

In a porous body, the surface tension forces are strongest in the smallest pores. The addition of a little moisture to a porous body will therefore tend to fill the smallest pores first. Looking at equation 7, we see then that the lower the moisture content, the lower R (radius of pore), and

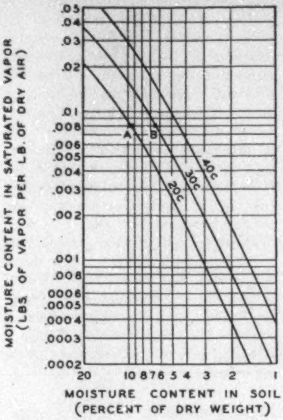

Figure 3. Moisture–vapor equilibrium chart for Sudan heavy clay[2]

Table I. Moisture Movement Constants From Smith

Values of *k* in Per Cent Centimeters Per Degree Centigrade

Soil Type	A	A_1	A_2	B	B_1	B_2	B_3	C
Barnes loam	4.2				3.3	4.2		7.0
Chester loam	6.8			6.2				9.6
Hermon sandy loam		†	†		.84	1.95	1.45	2.4
Kalkaska loamy sand		†	4.1		2.0	2.7		1.2

*Horizon is an agriculturist's expression for soil level. In general, horizon A includes the top soil, horizon B the subsoil, and horizon C the sub-stratum. Most cables are installed in horizons B and C.

†Inconclusive.

therefore the lower the vapor pressures within the porous body. By equation 8, the lower vapor pressures produce lower moisture contents in the saturated vapor. This is precisely what happens, and exact data are published[2] for certain African soils. Figure 3 is a calculated curve of moisture content of saturated vapor within moist soil in equilibrium with contained moisture, taking the published data.

For vapor equilibrium to prevail between two points in soil the following conditions must exist:

1. The partial pressure of vapor in air next to a moisture droplet must be equal to the vapor pressure of the surface of the droplet. In this case the air will be saturated with respect to the droplet.
2. The pressures of the air and vapor mixes at the two points must be equal.
3. The moisture contents of the saturated vapors must be equal.

If the two points are at different temperatures, they will satisfy these conditions if they are located on the same horizontal line in Figure 3. Thus we see that *Sudan A* at 20 degrees centigrade and 9.5 per cent moisture content can be in vapor equilibrium with *Sudan B* at 30 degrees centigrade if *B* has 6.5 per cent moisture content. There is, therefore, a tendency for moisture to move away from a hot body under a thermal gradient, but this can reach an equilibrium when the moisture content of the hot area has been sufficiently reduced.

Most investigators have felt that the vapor movement is negligible, or at least very slow. The effects may well be imperceptible in extremely fine grained soils, such as clay. In these cases the resistance to vapor flow is probably greater because of smaller passages.

Except for flow resistance, Figure 3 must always be satisfied for complete equilibrium to exist. Since the surface tension movement is likely to be quite rapid, this undoubtedly is greater initially. It can be seen that this movement is in the right direction for obtaining vapor equilibrium. The portion of vapor equilibrium achieved by surface tension movement may be large, and therefore the remaining vapor movement may be slight. An indication of this is that although Smith's tests were made on relatively coarse grained soils, his 72-hour data check the surface tension movement theory alone.

Application

Electric utilities, with large investments in underground cables, have for many years feared the effects of moisture migration on cable temperatures. In the absence of a means to evaluate this effect, they have limited the temperature of cables and ducts in direct contact with the earth, in the hope that a serious runaway of moisture would be prevented. This temperature limit is usually set at 50 or 55 degrees centigrade.

J. H. Neher[3] has applied equation 6 to the heat field of a buried cylinder for the purpose of providing a method to determine the effect of moisture movement on actual cable problems. The application of the method to two typical examples is given in Table II. These values are based on a movement constant of 9.6, the maximum value listed in Table I, and show that the effect is of little importance.

One should not expect that the moisture movement phenomenon discussed in this paper would be applicable at very high temperature gradients. Little is known about the critical temperature gradient, beyond which moisture will migrate until only dry earth remains. The author has had but one experience with this drying-out effect. This occurred as a result of an accidental overload applied to a heated sphere buried in clay loam. In this instance the drying-out effect started at 65 degrees centigrade and at a surface temperature gradient of 6.6 degrees centigrade per centimeter, but proceeded in an orderly fashion, with the effective earth resistivity stabilizing at a new level approximately 30 per cent greater than the original one. A summary

Table II. Examples of Moisture Movement Effects

	6-Cable Duct Bank	8-Inch Pipe
Maximum heat flow, watts per foot	30	38
Buried depth to center, inches	43	40
Initial earth resistivity, degrees centigrade centimeters per watt	75	60
Maximum temperature gradient, degrees centigrade per centimeter	.45	1.17
Temperature rise of structure, centigrade		
(a) Neglecting moisture movement	25.2	35.7
(b) With maximum moisture movement	26.0	37.5
(c) Per cent increase due to moisture movement	3.2	5.0

Table III. Buried Sphere Tests

Comparison of One Sphere Which "Ran Away," With One That Did Not

	"Run-away" Sphere	Stable Sphere
Sphere diameter, inches	6	8
Buried depth to center, inches	48	48
Watts	58	125
Ambient temperature, centigrade	19	23
Temperature at which drying-out started, centigrade	65	....
Ultimate temperature, centigrade	86	78
Earth resistivity, centigrade centimeters per watt		
At start	86.5	61
Ultimate	114	62
Temperature gradient at sphere surface, degrees centigrade per centimeter		
Before runaway	6.6	6.0

of this case is given in Table III, together with another case of operation without drying-out at 78 degrees centigrade.

Conclusions

1. The net direction of moisture movement in earth is from warm toward cool regions in the heat field surrounding a given underground heat radiator, or heat collector.

2. Moisture movement ceases when and if the resulting moisture distribution satisfies the conditions of surface tension and vapor pressure equilibrium at the temperatures and temperature gradients finally attained.

3. There is undoubtedly a critical temperature gradient for each soil, such that the soil will dry out altogether in any region exposed to an equal or greater temperature gradient. One unintentional test in clay loam indicated the critical gradient for that situation to be approximately six degrees centigrade per centimeter, or well beyond the probable limits of normal underground conduit design practice.

4. At normal maximum temperature gradients of less than two degrees centigrade per centimeter, the moisture movement effects appear to be almost negligible.

5. Vapor movement in the soils investigated accounts for very little of the net moisture movement in the vicinity of heated surfaces. Analysis of this factor, however, suggests that it might be found to account for appreciable moisture movement through very coarse-grained media such as gravel or crushed stone.

6. For underground heat collector coils, such as may be used with heat pumps, the cold surface of the coil or its frozen environment should be expected to form a liquid and vapor barrier in the vicinity of which moisture will accumulate in the liquid state until the earth becomes saturated. If there is additional moisture movement thereafter, the excess liquid will percolate downward gravitationally and away from the coil. It is therefore possible that the use of very coarse backfill around such coils might enhance considerably their heat collecting capacity.

References

1. Thermal Conductivities in Moist Soils, W. O. Smith. *Proceedings*, Soil Science Society of America (Morgantown, W. Va.), volume 4, 1939, pages 32–40.

2. The Relation Between the Vapor Pressure and Water Content of Soils, A. N. Puri, E. M. Crowther, B. A. Keen. *Journal of Agricultural Science* (Cambridge, England), volume 15, 1925, pages 68–88.

3. The Temperature Rise of Buried Cables and Pipes, J. H. Neher. AIEE Transactions, volume 68, Part I, 1949, pages 9-21.

4. General Physics for Students, Edwin Edser. MacMillan & Company Ltd., London, England.

Discussion

Herman Halperin (Commonwealth Edison Company, Chicago, Ill.): The author has focused attention on one important point in the heating of underground conduits and of pipes containing power cable. This paper, as well as the companion article by Neher,[1] is especially valuable at the present time, because the installation costs for underground conduit and pipes have risen by more than 100 per cent in the past ten years. It, therefore, becomes very necessary to know just how great the allowable heating may be in order to utilize conduit and pipes to the fullest possible.

Under the heading of "Application" the author mentioned a temperature limit of 50 or 55 degrees centigrade for cables and ducts in direct contact with the earth as being the limits in general use. In a paper I presented in 1942 "Load Ratings of Cable—II," I mentioned limits of 55 or 60 degrees for the duct temperature for normal operation and 5 degrees higher for emergency operation.[2] It seems to C. A. Bauer and myself that for the variety of soil conditions found in Chicago it is difficult to set an exact general limit.

For one set of conduits containing generator leads operating at a high load factor, we have set a limit of 70 degrees for the duct temperature and we have followed that location closely over the past several years; so far, with temperatures of about 65 degrees or so there has developed no run-away condition. The soil there is a sandy loam. For another location where there is heavy clay around the conduits, we have set a limit of 55 degrees centigrade for the duct temperature for normal operation. In the summer of 1948 there was a case of one conduit, having clay and loam fill around it, where a runaway condition tended to develop when the duct temperatures got to about 60 degrees centigrade. It was necessary to flood this conduit twice during the summer and also to install means for keeping the conduit wet into the fall.

It might be well if the author would discuss further the apparent inconsistency between the deductions that may be drawn between Table II and Table III. Table II shows only a three per cent increase in the temperature rise of an underground structure due to moisture movement, whereas Table III shows a change in the earth resistivity for the "run-away" sphere of 30 per cent. Furthermore, the heating load in Table III for the run-away sphere was about 1/6th less in watts per square inch of sphere surface than for the stable sphere.

Based on somewhat meager data, it seems to us that the limit of two degrees centigrade per centimeter given in conclusion 4 as the limit where moisture movement effects appear to be almost negligible may be a little too high.

References

1. See reference 3 of the paper.

2. Load Ratings of Cable, II, **Herman Halperin.** AIEE Transactions, volume 61, 1942, pages 930–42.

C. G. Mansfield (Water and Power Department, City of Los Angeles, Los Angeles, Calif.): The author has developed a fascinating hypothesis into an interesting and at least superficially plausible explanation of the migration of soil moisture along a temperature gradient. A more critical study of the assumptions and steps in this development raise substantial doubts as to whether the resulting formula is a true representation of the actual process, or whether the check with certain of the experimental data results from coincidence, aided by a rather liberal adjustment of the constant *k*, and elimination of the more unfavorable cases on the ground of artificial piling up of moisture at the cold end; an explanation which would appear to be acceptable only if the soil in that region becomes saturated. Following are some of the points which seem to the writer to be of doubtful validity, or to need further clarification or support.

One basic fault in the proposed theory is best visualized in the case of a homogenous soil with initially uniform moisture distribution, subjected to a uniform temperature gradient between parallel isothermal surfaces. Since the action at any point depends only on the thermal gradient and not at all on temperature, the moisture movement in all layers should be the same, and the end result would be a thin dry layer at the warm surface, a saturated layer at the cold surface having a thickness varying with the initial moisture content, but no change in the moisture content of the layers between them. This, I believe, is not in agreement with the observed facts.

The whole development is founded on the assumption that the moisture exists as discrete droplets presumably separated by dry surfaces, since if they were connected by surface films they would not wait for a droplet distortion to bring them into contact before merging. This condition would eliminate any possibility of capillary movement toward plant roots or toward an exposed surface at which evaporation is occurring. In fact, dryout by surface evaporation probably could not occur, since the temperature gradient established by sunshine or atmospheric temperature rise would drive the moisture deeper into the ground rather than bring it to the surface. Such an assumption, therefore, fairly demands further support, either by direct verification or by some rational explanation of the manner in which such a moisture distribution can be established. After the "gravitational water" has drained from an initially saturated soil, it is not at all clear why, in the process of further drying out by loss of moisture from the capillary spaces, the moisture remaining therein should break up into a large number of small droplets against their powerful tendency to reunite when brought into light contact by a minor distortion of shape. The two concepts seem directly contradictory, and we are required to believe that the initial dryout is accompanied by a decrease in average droplet size while a subsequent, or even simultaneous, local dryout due to a temperature gradient is accompanied by an increase in average size.

It seems reasonable to expect some distortion of a droplet due to nonuniform temperature, but the fact that this distortion, (expressed in some unit which the author does not define), increases with the temperature gradient does not necessarily mean that it is directly proportioned thereto as indicated in relations (3) and (6). In fact, both the geometric complexity of the droplet and the relation expressed in equation 2 raise considerable doubt as to the accuracy of that simple relationship. Incidentally, it seems very improbable that the picture of this distortion shown by the dash line in Figure 1 (b) can be correct since with a presumably uniform temperature gradient from left to right, the radius of curvature first decreases, then increases (at the tangent), and again decreases at the right end.

Numerous efforts to confirm the reality of a droplet distortion of significant magnitude have all given negative results. Droplets of various sizes were trapped between glass plates separated by one to three mils and observed through a 100x microscope while a temperature gradient was applied by placing a warm metal block on one end of the slide. In some cases the gradient was high enough to start rapid evaporation from the droplet edges within 30 seconds. In no case was there any observable distortion of the circular form when the gradient was applied. Possibly this means only that important distortion is confined to much smaller droplets, but this places serious limitations on the effective displacement of moisture which can result. When two particles of liquid merge under surface tension forces following contact, the resulting droplet occupies a position between the original ones, it is not projected forward as from a gun. It is therefore difficult to imagine any average displacement of the original moisture much in excess of the distortion of the droplets. It is not at all clear, in fact, just how the merger process can add anything to the effective displacement inherent in the distortion of the original droplet. And if significant distortion occurs only in the very small droplets, the effective moisture displacement must be correspondingly small and wholly inadequate to account for the movement observed in practice.

The character of the final result is largely determined by the probability equation 5, the development of which I find far from convincing. From equation 4 it would appear that for the theoretical development, the droplets and spaces are all conceived to be of the same size. If this be true, then droplets occupying two adjacent spaces would already be in contact and so would make any further "merger" impossible just as effectively as would occupancy of all four adjacent spaces. If "occupancy" is so defined as to avoid this difficulty, then the ratio of the distance between nominally "adjacent" droplets to the distortion becomes an important factor which does not seem to be reflected in the equations. The probability of secondary and later mergers also fails to appear in the equation, although it must certainly vary with the moisture content and so cannot be covered by constant k. It seems reasonable to expect that the product of a distortion factor and the probability of a resulting merger, as in equation 6, would represent the amount of moisture taking part in such mergers, but it can hardly be correct to speak of such moisture as "lost." It is still there, and not much more than a droplet's width away from its original location.

Finally there is the element of time. It would be expected that a low viscosity liquid such as water should adjust itself to a change in surface tension within, at most, a few minutes after the thermal gradient is established rather than after several days or weeks.

In view of the many questionable points involved in the development of this theory, it would seem prudent to use it with extreme caution until the facts are more fully established.

W. A. Hadley (Columbia University, New York, N. Y.): Mickley should be congratulated on his very excellent paper. There has not been very much work done on thermally actuated moisture migration and few investigations, if any, have attempted to express the phenomena mathematically.

The author limits his analysis to heat sources and states that his work is not applicable to heat pumps because the circulating coil would form a barrier, preventing moisture from migrating in the cold direction. He asserts that any moisture in excess of field capacity would percolate by gravity down to the water table.

From the results published by C. H. Coogan in his report, "The Residential Heat Pump in New England," it would appear that this may not be the case. Calculated values of the field capacity for the soil surrounding this ground coil indicate a field capacity of 31 per cent on the dry basis. However, samples of frozen soil chipped from the soil around the coil after the test period were found to range from 30 per cent to as high as 40 per cent wet. Perhaps the water is trapped by freezing, which in turn produces small cracks allowing more water to migrate in and thus yield concentrations in excess of the field capacity.

To investigate the application of Mickley's equation to heat pump ground coils, a calculation was made based on Coogan's experimental work. The soil surrounding the pipe was divided into annular zones, and it was assumed that all of the moisture lost by each of these zones appeared in the frozen soil around the pipe. Using the experimental temperature gradients, and the initial moisture concentration of 25 per cent, these losses were evaluated.

If a conservative value of 7.0 is used for k, the constant of proportionality, the final wetness around the coil is calculated to be 31.5 per cent, which falls within the measured moisture contents of 30 to 40 per cent. If we use the maximum value of k reported by Mickley, that is, $k=9.6$, the final moisture content is 33.9 per cent, which is still at the conservative end of the measured values. Perhaps additional experimental work will further substantiate this paper and may reveal higher values for the proportionality constant.

So far the results from this paper are encouraging, and at the present time it is by far the best interpretation of this phenomenon.

A. S. Mickley: Halperin's discussion confirms the thesis of the author that there is no definite value of soil contact temperature which is generally applicable, and that the use of too low a value can result in the loss of much inherent load capacity. Halperin's method of exceeding 50 degrees centigrade where necessary and maintaining a careful watch is a practical answer to this situation. It is hoped, however, that this paper may be helpful in line design, and may be useful in pointing the way to further study of the many variables in this problem.

The apparent inconsistency between Tables II and III is partially explainable in terms of temperature gradient. The maximum gradient in Table III is 6.6 degrees centigrade per centimeter, compared with 1.17 degrees centigrade per centimeter in Table II.

In addition, the tables treat two types of heat fields, the cylindrical and the spherical, which respond differently to the same conditions.

The comparison of watts per square inch of sphere surface, which Halperin cites, should be used with care, since it is not a fundamental measure which accounts for all variables, such as sphere diameter and depth of burial. It is true, however, that calculation indicates that both spheres should have run away, although only one did.

The fact that one was stable indicates either the constant k was too high for the particular soil, or that the moisture content was not at the movement curve peak of 75 per cent saturation, but was either very low or very high. Since this particular sphere was buried near a river, the moisture content was probably very high.

Mansfield's comments are much appreciated, since they afford the opportunity of more complete discussion of certain of the assumptions. The questions will be taken up in the order in which they were raised, except for the first question on uniform moisture distribution which, in the interest of a logical development, will be taken up last.

The inference that the surfaces between droplets are wet is correct. All soil particles must be covered with a water film, known as hygroscopic moisture, before capillary moisture can form. The thickness of this film has been estimated at between 15 and 20 molecules. The presence of this thin connecting film, however, does not nullify the possibility of further contact between droplets.

The natural drying out of the soil is brought about by three forces: surface evaporation, plant absorption, and downward percolation. Evaporation moisture is said to reach the surface either by capillary rise through an unbroken column, or by vapor movement. It is now thought that the bulk of plant moisture is obtained through the extension of root hairs to tap the capillary water directly. If these prevailing agricultural theories are correct, it is not apparent that they are fundamentally inconsistent with the local drying process described in this paper.

Mansfield questions the validity of equation 3. If equations 1 and 2 are combined we may write the following relationship

$$R_A = R_B\left[1+\frac{dT}{dx}\left(\frac{ax}{1-aT_A}\right)\right]$$

where

x = droplet diameter

If distortion is defined as the difference in radii, then distortion equals

$$R_A - R_B = \frac{dT}{dx}\left(\frac{ax}{1-aT_A}\right)R_B$$

Since the values in the parentheses are constants for a given droplet, proportionality is indicated.

From the objection to the egg-shaped dashed line of Figure 1(b), it appears that it has not been made clear that equation 1 is an integration of all the normal force components along a given axis. Since the normal forces at the tangent have relatively weak components along the A-B axis, they are not major contributors to equilibrium. The adjustment of radii at the tangent is geometrically necessary in order that the figure may close.

Mansfield has difficulty in accepting distortion as the trigger, or initiating force of movement. Smith[1] has advanced the hypothesis of the trigger action of surface evaporation and condensation, which Mansfield observed under his microscope. While it seems virtually impossible to isolate the two triggers by observation in actual soil, it is entirely conceivable that both triggers are operative. A complete analysis of the evaporation and condensation trigger may also confirm the proportionality to temperature gradient indicated by the test data.

When Mansfield describes how a merged droplet occupies the space between the two original positions, he is presumably thinking of cases in which this space is large compared with the droplets. Where this is applicable, however, the shape of the intermediate location may not be compatible with equilibrium of surface tension forces As described in the paper, the droplet may then have to travel a considerable distance before finding a crevice system exactly suited to the re-establishment of equilibrium. This distance could conceivably be much greater than the droplet width implied by Mansfield.

Any sample of soil contains a very large number of particles and droplets. In any given type, therefore, all samples should act reasonably alike. The assumption of uniform sizes and shapes to explain the probability relationship would seem justified under these conditions.

Mansfield recognizes the importance of the ratio of the distance between nominally adjacent droplets and distortion. A greater amount of distortion would be effective at greater distances, and would therefore touch off a greater number of mergers. It was reasoned that distortion was proportional to temperature gradient, dT/dx, which was then included in equation 6 to represent this factor. It is not clear, therefore, why Mansfield states that this factor is omitted.

The possibility of secondary and tertiary mergers has already been stated in the paper. They have not been specifically included in the formula, but it seems reasonable that they would follow, at least roughly, the over-all probability versus moisture law that governed the original merger. If this is true, the equation accounts for them through an increased constant k.

The distance through which a merged droplet may move can be greater than the width of a droplet, as has been stated before. The distance need not be great in terms of total soil volume, however. The concept of moisture "lost," with which Mansfield has difficulty, is merely net loss within a given area. Some moisture has moved in over the border and more has moved out, but the individual droplets themselves need not have moved relatively long distances.

There is nothing in the paper to contradict Mansfield's comment that surface tension movement must occur quickly. In fact, the tests have so far confirmed this. Since the movement is rapid, the factor M_t should include the moisture received from the adjacent warmer area. Such a complete consideration of M_t would eliminate the uniform distribution of final moisture between parallel plates, to which Mansfield objects in his second paragraph. This factor was included in the analysis of the center points of Smith's data. It was not considered in Neher's analysis, however, since this factor is of less importance in the case of hot pipes and cables, where the volumes of earth increase along the outward lines of heat flow, and since the error in its omission is on the conservative side, indicating more movement than can actually occur. This factor is of particular importance, however, in the case of the heat pump.

Hadley makes the observation that freezing earth around a ground coil may cause the moisture content to exceed the field capacity of the soil. This is undoubtedly the case, since the frozen soil interferes with the natural process of percolation which would otherwise relieve the soil of this excess moisture.

He also makes a very interesting application of equation 6 to actual heat pump data. A great deal remains to be done on this phase of the problem before all that happens in the field is completely explainable. The rigor of Hadley's application could be improved by the inclusion of two effects which tend to cancel in the final answer; the larger volumes between the nonconcentric outer isothermals, and the change of M_t in the inner rings. It is still a good approach to the problem, however, within the limits intended.

Reference

1. Thermal Transfer of Moisture in Soils, W. O. Smith. *Transactions*, American Geophysical Union (Washington, D. C.), 1943, page 522.

High-Pressure Gas-Filled Cable Impregnated with Extra-High-Viscosity Oil

JOSEPH STICHER
MEMBER AIEE

G. H. DOAN
MEMBER AIEE

R. W. ATKINSON
FELLOW AIEE

LOUIS MEYERHOFF
MEMBER AIEE

DURING 1941, a 7-mile circuit of 120-kv high-pressure gas-filled pipe-type cable known as the *SMD*-type cable was installed in the system of The Detroit Edison Company. This installation has been in satisfactory operation since it was energized on December 31, 1941, and has been described previously before the Institute.[1]

When this first *SMD*-type cable for commercial service was being contemplated, it was felt that an impregnating compound of much higher viscosity than that normally used in the mass-impregnation process should be employed. At that time, the status of the art was such that preimpregnation of the tapes seemed to be the only method of assuring satisfactory impregnation throughout the wall of insulation. Also, preimpregnation would provide sufficient channels in the insulation to assure ready access of gas to all locations in the insulation wall.

Another line of *SMD*-type cable is being installed now at Detroit, a 12-mile circuit connecting Warren and Northeast stations. When this new line was being contemplated, mass impregnation of the insulation was seriously considered. There were two main problems in conjunction with the question of mass impregnation versus preimpregnation. One was concerned with the question of whether satisfactory impregnation could be achieved by means of the mass-impregnation process, when a heavy wall of insulation was to be impregnated with a highly viscous oil of 3000 Saybolt Universal seconds (6 poises) at 100 degrees centigrade. The other one was whether, in a mass-impregnated cable, a supply of gas could be assured at all locations in the insulation to prevent ionization at operating voltage if, for instance, rapid cooling of the cable should occur, with consequent increase of the viscosity of the impregnant.

Characteristics of Saturant

High-pressure gas-filled cables require for their permanent integrity the retaining of a sufficient amount of their original impregnation to insure against ionization at operating voltage and to maintain satisfactory dielectric strength. Thus, the characteristics of the saturant with respect to their effect on the retention are a prime consideration in the design of high-pressure gas-filled cable.

It is believed that the saturant used in these cables (which will be designated, herein, as *HC-3,000*) is one of the most important elements, resulting not merely in the successful operation to date but in providing the basis for expectation of continued successful operation. For this reason, and because the characteristics of the saturant are so pertinent to the method of manufacture, these characteristics and their significance now will be described in greater detail than previously.

Essentially, viscosity is the important controllable property of the oil that is pertinent to drainage. The relationship between the viscosity of the oil and the changes in the cable caused by drainage has not been fully evaluated because the drainage of the saturant from a cable results from two radically different conditions. One of these has to do with the drainage of the saturant from between the layers and from the butt spaces. The other has to do with the drainage from the substance of the paper itself. Even with an oil such as is used in these cables, having a viscosity of the order of thirty times that of the usual solid-type cable oil, drainage of most of the oil from the spaces between tapes is relatively rapid where there is freedom for the oil to migrate. Drainage from the paper substance because of the very fine capillarity is another matter, and the time required is many times longer.

Comparative drainage of oil from saturated paper as a function of viscosity was studied on compactly-wound rolls of paper. The paper was 5 mils thick and 3/4 inch wide, and had a specific gravity of about 0.9. The rolls were about 2 inches in diameter and weighed about 20 grams. Four such rolls were dried thoroughly under heat and vacuum, and were saturated respectively in four oils having approximately the following Saybolt Universal viscosities at 100 degrees centigrade: 38, 65, 150, and 3,000. The dry weight of the paper was determined prior to saturation.

The impregnated rolls were placed in a horizontal position on blotting paper in an air oven maintained at 80 degrees centigrade. By periodic weighing of the rolls, the amount of oil drained from the rolls was determined, with the results shown in Table I.

It will be noted that the time required to drain 30 per cent of the oil is 100 times as great for the 3,000-second oil as for the 38-second oil, and is seven times as great for the 3,000-second oil as for the 150-second oil. It should be borne in mind that in the samples, drainage has been accelerated greatly over that which would occur in a cable, by the presence of the blotting paper and by the fact that the

---

Paper 49-84, recommended by the AIEE insulated conductor committee and approved by the AIEE technical program committee for presentation at the AIEE winter general meeting, New York, N. Y., January 31–February 4, 1949. Manuscript submitted November 16, 1948; made available for printing December 27, 1948.

JOSEPH STICHER and G. H. DOAN are with The Detroit Edison Company, Detroit, Mich., and R. W. ATKINSON and LOUIS MEYERHOFF are with the General Cable Corporation, Bayonne, N. J.

Table I. Drainage Characteristics of Saturated Paper Rolls as a Function of Viscosity of Saturant at 80 Degrees Centigrade

Viscosity of Saturant at 100 Degrees Centigrade		Hours Required to Drain Designated Percentage of Original Oil from Sample		
Saybolt Universal Seconds	Poises	Per Cent drainage 10	20	30
38	0.03	3	13	35
70	0.11	10	50	150
150	0.28	20	125	525
3,000	6.0	375	1,725	3,500

Note: Original oil is defined as obtained by extrapolation to zero time from measurements obtained at from 2 to 3½ hours.

vertical position of the oil spaces in the samples as placed in the oven is particularly conducive to drainage.

Consideration was given to various other oils of high viscosity. Reasons for discarding these in favor of the *HC* oil may be listed briefly. Although petrolatum would not migrate at temperatures below its melting point, usually about 50 degrees centigrade, it rapidly becomes fluid as the temperature is increased above that. Thus it is not good from the standpoint of migration, if used at the high temperatures often attained in American practice.

Although petroleum oil with rosin added will give high viscosity, such a mixture generally tends to separate and, moreover, does not produce the very low power factors obtained with the *HC* oil.

A high viscosity could be obtained with a composite consisting of a petroleum oil blended with a suitable plastic. In particular, such a composite can be made with the use of a very high molecular weight isobutylene polymer which, by itself, has the consistency of a sticky plastic solid. However, less assurance concerning ability to obtain initial uniformity and nonseparation thereafter was felt for such a composite than for the *HC* oil.

The constituents of the *HC* oil actually used have a fairly narrow range of molecular weights, and the oil is much more nearly homogeneous with respect to molecular type than are natural petroleum-oil saturants.

Continued experience with the *HC* oil has fully justified its original selection. This oil is produced by polymerization of refined low-molecular-weight olefinic gases. Following are listed some of its properties:

1. The viscosity at 100 degrees centigrade is about 3,000 Saybolt Universal seconds (6 poises), or about 30 times that of the higher viscosity petroleum oils most widely used for cable saturants. The viscosity at 40 degrees centigrade is about 250 poises. This characteristic is shown in Figure 1, together with that of a petroleum oil used widely for saturating solid-type cable.[9]

2. Although the viscosity is very high at high temperature, it is not so great as to prevent cable installation at the lowest temperature considered normal in American practice. Bending of the cable, or installation, presents no problem at −10 degrees centigrade.

3. The electrical properties are such that the oil contributes a negligible amount to the cable dielectric loss.

4. The resistance of this oil to the effects of electronic bombardment, such as occurs during ionization in a cable, is considerably more favorable than for petroleum oils.

One of the oustanding characteristics of the oil used for these cables and of the cables themselves is the low initial value of the dielectric loss and the stability with which this is maintained. Laboratory tests on sealed cable samples, maintained at 100 degrees centigrade and extending over more than 7 years, have shown the initial power factor of less than 1/2 per cent to have been maintained without increase. Similar data are reported later herein, showing no change in power factor of installed cables subjected both to high temperature and high voltage.

The inherently low dielectric loss of the *HC* oil does not result purely from the high viscosity but also from the low ion content. When an oil having high ion content, and having a low loss purely because of high viscosity, is blended with a fluid oil, the resultant mixture will have a high power factor. However, the *HC* oil used for these cables has an inherently very low ionic content, as evidenced by the fact that, even when it is mixed with a very fluid oil, the resultant power factor still remains very low.

The combination of low ion content and high viscosity plays a large part in the high stability of the cable made with this oil. For example, this oil, as opposed to one having a high ion content, is not subject to differential sorption by the paper, with the result that it has a power factor higher than would be explainable on the basis of simple saturation. The high viscosity of the oil will minimize power factor increases occasioned by contamination or even by changes within the oil itself.

Dielectric strength of the oil need be mentioned only in passing. This is considerably higher than for more fluid oils. It is not considered, however, that this high strength is particularly significant, nor that it makes any material direct contribution to the performance of the cable.

The *HC* oil is inherently of exceedingly low sulphur content, much lower than for natural petroleum oils, because of its production from low-molecular-weight gases which can be, and are, thoroughly freed from sulphur compounds. The process of producing it does raise a question of the possibility of a small content of organically-bound chlorine. An experimental lot of cable was produced with oil containing 0.03 to 0.04 per cent of chlorine and has been tested extensively. Rather extensive aging tests of paper impregnated with oil having a chlorine content of the order of 0.04 per cent have been made in comparison with control tests on similar paper with various oils of low chlorine content; these comparisons have shown no difference in the aging characteristics. All of the oil which has been used for the commercial production of the 1948 cable has a chlorine content of less than 0.01 per cent.

Typical data showing lack of influence of chlorine content of the saturant on the aging characteristics of saturated paper are given in Table II.

Preimpregnation and Mass Impregnation

At the time of the manufacture of the 1941 cable, it was not considered practical to impregnate this cable by means of the conventional methods involving mass impregnation, and the cable was made with preimpregnated tape, as stated in the beginning of this paper.

Preimpregnation

One satisfactory method of preimpregnation which has been used abroad is a continuous process in which rolls of paper are passed through oil of sufficiently high

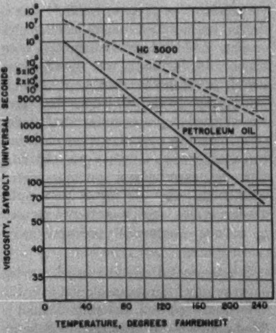

Figure 1. Comparison of the viscosity-temperature characteristics of *HC-3000* oil and a petroleum oil used widely in solid-type cables

temperature and for sufficiently long time. It then may be slit and wound into pads. In an alternate method, used in this country in the manufacture of the 1941 and 1948 preimpregnated cables, the pads of paper are heated and dried under vacuum and then impregnated in a manner similar to the impregnation of solid-type cables. With this latter method of impregnation, the oil readily reaches both faces of every portion of the tape by penetration through the space between tapes, as contrasted to the long and devious path the oil must follow in mass impregnation.

Application of preimpregnated tape presents two main problems. One of these is a simple mechanical one caused by the tendency of the sticky compound to get everywhere it is not wanted—on the taping machine and on the operator's hands and clothing. The only requirement resulting from the stickiness of the compound is that the taping machine must be so designed or so operated that the stickiness of the saturant shall not prevent the tapes from being applied in proper position and with suitable tension. In the manufacture of the 1941 cable, the difficulty was solved by a reduction in taping speed and by the use of additional manufacturing refinements.

The other problem is concerned with the humidity of the surrounding air and the tendency of the treated paper to reabsorb moisture. It has been found that control of the atmospheric moisture to values comparable with that of indoor air in the driest of winter weather (maximum of around 20 per cent) will bring down the rate of reabsorption to a point where no significant change in the properties of the paper takes place during the taping operation. The effective result of this is shown by so-called radial power-factor graphs, of which a great many have been made. In Figure 2 are shown three radial power-factor graphs, *A* and *B* being respectively of commercial preimpregnated cable manufactured under strict humidity control, and of mass impregnated cable. Graph *C* was obtained with an experimental preimpregnated cable made before the installation of the air-drying unit which was afterwards used in making commercial preimpregnated cable.

If a segmental strand is used, having paper or other fibrous insulation over the individual segments, the entire strand is dried and oiled, so that there will be no moisture to migrate from the insulation on the segments to the high-voltage insulation during the course of operation. This treatment also adds to the resistance between individual strands and results in an improvement of a-c resistance of the complete conductor, as compared with its resistance before treatment. Because of the effect upon the a-c resistance, the strand may be given such treatment for this purpose even though it may have no insulating materials which require drying. The shielding tapes over the strand, the preimpregnated insulating tapes, and the shielding and protective coverings are applied in a single machine operation. The coverings over the insulation include two metalized-paper shielding tapes, intercalated; one copper tape intercalated with polyethylene tape; an additional copper tape intercalated with polyethylene tape, and two copper D-shaped skid wires, applied open spiral. The coverings serve several purposes. They constitute an electrostatic shield. They furnish moisture protection to the insulation during handling and until installation of the cable. (They are supplemented in this function during shipment by a special weather-tight reel.) Finally, they act as a bedding for the skid wires.

Mass Impregnation

Various special manufacturing requirements for the use of preimpregnated tape indicated the desirability of reconsidering the possible use of the more conventional mass impregnation. A careful investigation disclosed that, with practical modifications of conventional methods, this would be entirely feasible.

Essentially this meant drying and impregnating at a temperature within the maximum range used for solid-type cable, but keeping the entire length at approximately this temperature. This contrasted with the considerable range of temperature which is permissible with solid-type cable. For solid-type cables, electrical drying had been used extensively for many years, but the choice between electrical heating and steam heating was essentially a matter of economics. In order to obtain the required uniformity of temperature for the mass impregnation with the high viscosity oil, electrical heating for drying became a requirement for long commercial lengths. With that, and with the use of pressure on the oil during the impregnation, complete impregnation could be assured with no longer exposure of the paper to high temperature than with previous good practice. Actual assurance of the impregnation of individual reels was facilitated by measurements of capacitance.

Contrary to the practice with solid-type cable, the oil was pumped from the tanks on the completion of impregnation while the cables were at high temperature. The resultant relative incompleteness of impregnation, about 7 per cent, caused by the contraction of the oil in cooling, leaves space in the insulation through which the gas may reach the entire mass of insulation. It also furnishes some reservoir of gas within the insulation body.

When it once was determined that satisfactory impregnation could be accomplished, the procedure for taping was carried through in a manner entirely normal for solid-type or low-oil-pressure cable. The metalized-paper shielding tapes were applied along with the paper insulation, but the copper tapes intercalated with the polyethylene tapes, and the D-shaped skid wires were applied subsequent to impregnation.

The mass-impregnated cable contains, at the time of manufacture, a greater amount of free oil in the butt spaces than does the preimpregnated. This results in a somewhat higher dielectric strength and a higher voltage at which ionization begins. Since, however, this difference cannot be considered permanent, it is accepted that this difference in dielectric strength may not be significant of long-time difference in performance.

The surge strength of the mass-impregnated cable has been found to exceed slightly the values previously reported for the preimpregnated type,[1] which are among the highest values published for any type of insulation.

On the mass-impregnated cable, dielectric loss values have been slightly

Table II. Effect of Chlorine Content of Oil on Tearing Strength of Impregnated Paper as a Function of Aging at 150 Degrees Centigrade

Aging, Hours	Tearing Strength, Grams					
	Paper Saturated in *HC-3000* Oil of:					
	Low Chlorine Content			High Chlorine Content		
	Minimum	Average	Maximum	Minimum	Average	Maximum
0	88	92	100	88	98	116
48	52	64	68	56	60	64
113	32	34	36	52	34	36

Four samples were measured in each set of determinations.

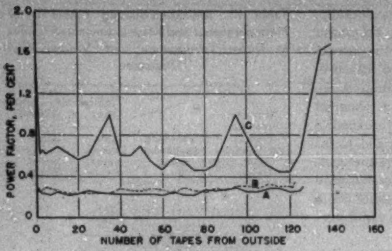

Figure 2. Radial power factor characteristics

A. Commercial preimpregnated cable
B. Commercial mass-impregnated cable
C. Experimental preimpregnated cable

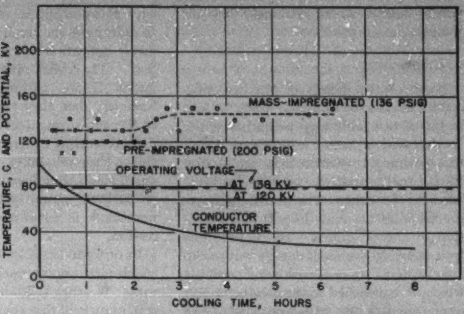

Figure 3. Comparison of ionization-starting potentials existing in mass-impregnated and preimpregnated cables during the cooling period of Test I

more uniform than on the commercial preimpregnated cable made in 1941. However, there is no significant difference observable in this respect between the mass-impregnated cable and the preimpregnated cable made in 1948.

Effect of Sudden Temperature Changes on the Electrical Performance of the Cable

It has been pointed out that satisfactory impregnation can be achieved by means of the mass-impregnation process even when a 600-mil wall of paper insulation is to be impregnated with an oil of a viscosity of 3,000 Saybolt Universal seconds at 100 degrees centigrade. Another question in connection with the use of such high-viscosity oil in the mass impregnation of high-pressure gas-filled cable, is one pertaining to the electrical performance of such cable in service operation.

Specifically, this question is concerned with the action of the very viscous oil when a heavy load on the cable is reduced suddenly to an extremely small load, especially during the winter season. This sudden and major reduction of load will result in a rapid cooling of the cable, with consequent rapid increase in the viscosity of the impregnating oil and decrease of the volume occupied by it. This contraction of the oil will result in enlarged void spaces; this condition, coupled with the possibility that the increased viscosity of the oil might result in the blocking of gas passages, might be thought to lead to the formation of low-pressure regions within the insulation of the cable. This mechanism might lower the gas pressure in the voids so much that the ionization-starting potential would be reduced to a dangerous value, and ionization might occur in the cable at operating voltage. It was pointed out, however, that two effects combine to prevent dangerous lowering of gas pressure. First, in the mass-impregnated cable, the gas spaces occupy a very significant volume, so that only a minor decrease in gas pressure may result from shrinkage of the oil. Second, the low-gas-pressure regions receive gas that has been sorbed by the oil at the higher pressure and is released by the oil upon pressure reduction in the adjacent gas spaces.

In order to obtain direct information concerning the effect of sudden temperature decreases on the ionization-starting potential, a series of tests was conducted.

Tests to Determine the Effect of Sudden Temperature Drops on the Ionization Starting Potential

After completion of a series of exploratory tests, a program was worked out for experimental study that included tests on samples of mass-impregnated cable and, for purposes of comparison, on samples of preimpregnated cable. It was expected that, in the case of preimpregnated cable, the relative freedom from oil of the butt spaces would largely eliminate the possibility that sudden decreases in temperature of such cables would produce low-pressure regions. Information concerning ionization-starting potential, obtained with preimpregnated cable under various conditions, would serve, therefore, as an excellent basis for comparison in determining the effect of mass impregnation on the ionization-starting potential under essentially identical conditions. For this purpose, tests were conducted on 600,000-circular-mil preimpregnated and mass-impregnated cable having an insulation thickness of 600 mils.

The test procedure was developed with the intention of reproducing important temperature variations to which a commercial cable installation or definite parts of it might be subjected during both normal and extreme conditions of service operations. In an attempt to cover the temperature variations that seemed most important from an operating point of view, the test procedure was arranged to include three successive tests.

In each of these three tests, the ionization-starting potentials were determined at significant periods by means of power factor–voltage measurements. The same test samples were subsequently employed in the study of the effect of sudden gas-pressure releases on both the a-c breakdown strength and the ionization-starting potential of this cable. This phase of the general study is reported in the next section of this paper.

One test was designed to simulate conditions that might exist for the buried-pipe installation during the summer season, when the ground temperature at the pipe level is at the maximum for the year, the cable is heavily loaded, the temperature conditions are at equilibrium, and the load is suddenly reduced to zero with the cable remaining energized.

A second test was to simulate conditions that might exist for the buried-pipe installation in the winter season, when the ground temperature at the pipe level is at the minimum, and other conditions are essentially the same as in the first test.

The third test to determine the effect of sudden temperature drops on the ionization-starting potential was concerned with conditions that might exist in connection with the cable in the vertical riser pipes at the terminals in the winter season when extremely low air temperatures prevail.

Test Procedure

Some of the details of the test procedure may be of interest. Each 33-foot length of test cable was covered, over the *D*-wire, with a heavy lead sheath which was reinforced with cotton and metal tapes to withstand the internal gas pressures to be used. The sheath was removed from the ends to permit application of the terminals. To prevent gas from entering the insulation by way of the ends, special copper lugs were provided which were attached to the conductor and were sealed to the adjoining part of the insulation by a long, tapered, taped joint. Added insulation was applied over the factory insulation, and 5-foot phenolic stop tubes with metal ends, similar to the stop tubes used in the service terminals, were employed to complete the pressure-tight gas container. One metal end of each phenolic stop tube was sealed to the conductor, and the other metal end to the sheath with its reinforcement, at both ends of the cable. The cable then was placed horizontally on tall wooden horses, with the cable ends sloping downward. Over the stop tubes were placed laboratory-type condenser terminals. To restrict still further any entrance of gas from the ends and to aid in the insulation of the terminals, high-viscosity oil was used to fill any remaining spaces within the stop tubes. Gas pressure then was built up as desired, and was maintained for several hours before a new stage of the test was begun.

Current for heating the conductor was provided by a transformer, the secondary of which was insulated from the primary and core to withstand the applied test voltages of up to 200 kv. Provision was made for determining the mean temperature of the conductor by measuring its resistance. This was done with a Kelvin bridge which could be switched on quickly after removal of the high voltage and high current. Sheath temperatures were determined by thermocouples soldered to it.

After determining the current–temperature characteristics of the cable, sufficient current was passed through the conductor to stabilize the temperature at the desired value. While current was flowing, measurements were made of power factor at different voltages up to 200 kv. With these completed, and with the dielectric-loss bridge in balance, the current was interrupted and the bridge promptly rebalanced. Comparison of the measurements made before and immediately after current interruption serves, incidentally, to determine the small error in the power factor indication as a result of the current flow. The chief value of the measurements before current interruption is, however, that they serve as a rehearsal of the measuring technique, to expedite the subsequent measurements and to increase their reliability. During the cooling of the cable following the interruption of current, power-factor measurements were made in series of tests in rapid succession.

In order to simulate the rate of cooling which might occur during extremely cold winter weather following removal of the maximum load that could be carried under such a condition, special provisions were made to cool the sheath. Four lead pipes about 1 inch in diameter were flattened and laid as elements against the reinforced sheath, equally spaced around the circumference. Provision was made to circulate cold brine through these, two pipes in parallel carrying the brine in one direction, with return through the other two. The brine was chilled by dry ice. The temperature was controlled by the rate at which dry ice was added.

Test Results and Conclusions

Prior to the heating and sudden cooling of the test samples, some information was obtained regarding the ionization-starting potentials at room temperature when various gas pressures are employed for various lengths of time. Representative results obtained with preimpregnated cable, as well as with mass-impregnated cable, are given in Table III.

It should be pointed out that these results refer to cables that had not been subjected to gas-pressure cycles before the values of ionization-starting potentials were obtained. When ionization-starting-potential determinations are made at room temperature and various pressures, on cables that have previously been subjected to gas-pressure cycles, then the values obtained will depend on the history of the cable, as is shown in the section dealing with the effect of sudden, repeated gas-pressure releases.

From the mass of information obtained during the three tests outlined previously, only those results will be considered that have a direct bearing on the ionization-starting potentials that prevail during the cooling periods of the three different heat cycles under consideration.

Test I. Pertinent results that were obtained during the test designed to simulate conditions that might exist in buried parts of the cable installation during the period of the year when ground temperatures are highest, are shown in Figure 3 for both the preimpregnated and the mass-impregnated cable samples. For the experimental determination of the ionization-starting potentials that prevail during such conditions, the cable samples involved in this test were heated by means of conductor circulating current until a conductor temperature of 100 degrees centigrade was reached. This temperature then was maintained until equilibrium of the system had been assured. With the cable assembly suspended in free air at the room temperature of approximately 25 degrees centigrade, all the load was dropped suddenly, and the cable was allowed to cool to room temperature. It should be noted that the preimpregnated cable was subjected to a nitrogen gas pressure of 200 pounds per square inch gauge, whereas the mass-impregnated cable sample was subjected to a nitrogen gas pressure of only 136 pounds per square inch gauge during the determination of the ionization-starting potentials. The mass-impregnated cable was therefore subjected to more unfavorable test conditions. The reason for the use of this lower gas pressure was that, at a pressure of 200 pounds per square inch gauge, the ionization-starting potentials were found to be above 200 kv during an exploratory test which was conducted previously on another specimen.

Table III. Ionization-Starting Potentials of Preimpregnated and Mass-Impregnated Cables at Room Temperature and Various Gas Pressures

Nitrogen Pressure, Pounds per Square Inch, Gauge	Pressure Application Time, Hours	Ionization-Starting Potential, Kilovolts	
		Pre-impregnated Cable	Mass-Impregnated Cable
0		21*	29*
50	1/2	48**	67**
50	1		75**
50	2		78**
150	1/2	130**	167†
150	8	130**	158**
150	11		170**
200	7		Above 200**

* Average of three determinations

** One determination

† Average of two determinations

In this graphical presentation, the ionization-starting potential is given as a function of time elapsed since the sudden termination of the heating of the cable. In order to enable correlation of the respective values with the temperatures prevailing at the conductor, the conductor temperature also is given as a function of cooling time. Only one temperature curve is given for both cables inasmuch as

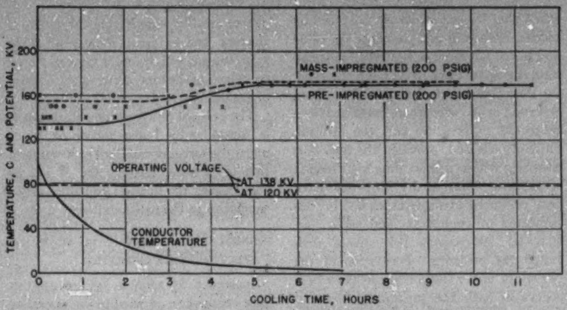

Figure 4. Comparison of ionization-starting potentials existing in mass-impregnated and preimpregnated cables during the cooling period of Test II

there was little difference in the temperature–time relations of the two cable types.

It can be seen that in some instances the measured values of the ionization-starting potentials show a considerable spread with respect to the curves plotted. It is nevertheless apparent that the curve drawn for the mass-impregnated sample indicates the true tendency of change in ionization-starting potential with respect to cooling time. Values of ionization-starting potential for the preimpregnated cable sample were determined only during the first 2¼ hours of the cooling period, but tests reported later herein leave no doubt that the character of the complete curve would be similar to that of the one given for the mass-impregnated sample.

It is concluded from the results obtained that no dangerous drop in ionization-starting potential is experienced when, with an ambient temperature of 25 degrees centigrade, the temperature of the insulation falls to ambient from that which exists when the conductor is at approximately 100 degrees centigrade. In order to indicate graphically how much the ionization-starting potentials are above the potentials that exist across the insulation during service conditions, these potentials are indicated in the graph for 3-phase operating voltages ranging from 120 kv to 138 kv. It should be noted that, for the properties of the thermal system involved, the "sudden" drop from a conductor temperature of 100 degrees centigrade to the ambient of approximately 25 degrees centigrade involved an interval of several hours.

Test II. The results of this test, which was to simulate conditions that might exist for the buried-pipe installation when the ground temperature at the pipe level is at the minimum, are shown in Figure 4. This test, in which the load was reduced suddenly to zero when the cable temperatures were stabilized with the cable suspended in free air at 25 degrees centigrade and a conductor temperature of 100 degrees centigrade, and in which a refrigerant at zero degrees centigrade was applied simultaneously with the removal of the load, was employed several times with each of the cable samples. During the repetitions of this test, gas pressures of nominally 150 pounds per square inch gauge were applied in some cases, and of 200 pounds per square inch gauge in others. In order to keep the presentation of the results as simple as possible, only the results obtained in one cooling period with a pressure of 200 pounds per square inch gauge are shown for each of the two types of cable.

From the results obtained in this test, the conclusion again is that no reduction in ionization-starting potential results from a sudden drop of cable temperatures, even though more severe test conditions are employed than in the case of Test I.

Test III. Ionization-starting potentials that were determined on the specimens of preimpregnated and mass-impregnated cables used in Tests I and II are shown in Figure 5 for the conditions that might exist in vertical risers when extremely low air temperatures prevail. In this test, the load current, which had produced stabilized conditions with the conductor temperature at approximately 50 degrees centigrade while a coolant at −20 degrees centigrade was being circulated around the outside of the cable, was reduced suddenly to zero. It is in this test that the first definite indication appears of a decrease in the ionization-starting potential as a consequence of rapid cooling of the cable. It also should be noted that only the mass-impregnated cable shows this drop.

From a study of these results, it is concluded that, although a definite drop of ionization-starting potential is found in the case of mass-impregnated cable, the minimum ionization-starting potential is still safely above potentials that occur during normal service operation (approximately 65 per cent above that for 138-kv operation). Also, attention should be called to the fact that even this small reduction of ionization-starting potential existed only for a brief period, beginning shortly after the removal of the load current and lasting until little more than one hour had elapsed after removal.

Conclusions

In connection with the observed spread of ionization-starting-potential values, a few words regarding the manner in which these values were determined may be in order. During the series of power factor–voltage determinations, the voltage usually was changed in 10-kv steps. Each power factor–voltage characteristic was plotted, and, from these smooth curves, the potential point was determined at which the curve deviated from a straight line.

In many cases, the change in power factor was so gradual that the ionization-starting potential could be determined only with an uncertainty amounting to ±5 kv, and in some cases an even greater uncertainty existed, particularly since the power-factor values were determined usually to within only 0.01 per cent.

The shape of the curves showing the change in ionization-starting potential with progressive cooling of the cable is of particular interest. It should be pointed out first that the gas pressure in the space surrounding the cable proper always was maintained essentially constant during the cooling period, that is, gas was allowed to flow into this space from a nitrogen tank in accordance with the requirements resulting from progressive cooling. Next, it should be recalled that, with respect to ionization-starting potentials, it is not only the absolute gas pressure that is of importance, even though in practical applications the gas pressure is taken as the criterion of prevention of ionization. When the chances for ionization to occur are judged only on the basis of changes in pressure in a given system, this can be done accurately only if constant temperature conditions prevail. When different temperature conditions are involved, however, as in this series of tests, then it is no longer the absolute pressure that is of importance, but it is the density of the gas which must serve as a basis for comparison.

From these considerations it is apparent that, if the absolute gas pressure is maintained at a constant value during the cooling period, not only in the gas space surrounding the cable but also within the voids of the cable insulation, an increase in the ionization-starting potentials must result with progressive cooling. Inasmuch as the gas pressure around the cable was maintained at a constant value during the cooling period, and inasmuch as in general the observed ionization potentials in these three tests did increase with progressive cooling, there can be little doubt that the gas supply had essentially free access to practically all the voids in the insulation.

If the inflow of gas with progressive cooling always had been sufficient to maintain constant pressure in all of the voids, and if there had been no dimensional changes in the voids occurring simultaneously with the progressive cooling, the increase in ionization-starting potentials would have progressed in strict conformity with the decrease in temperature. The observed characteristics of an *S*-shaped curve indicate, therefore, that dimensional changes of the void structure, or some other undetermined mechanism, did operate in such manner as to prevent complete conformity of increase in ionization-starting potentials, with concurrent decrease in temperature during the early part of the cooling periods. Whatever the responsible mechanism, it remains quite evident that even during the early part of the cooling periods, reductions in ionization-starting potentials were of minor importance.

Effect of Sudden, Repeated Gas-Pressure Releases

During the dissection of cable from an experimental installation of 120-kv high-pressure gas-filled cable of the preimpregnated type, a peculiar condition was noted which had the appearance of "dry" spots in the individual tapes of the oil-impregnated paper insulation. These dry spots were generally of small diameter and appeared in clusters, in the aggregate giving the paper surface a "peppered" appearance. When viewed by reflected light, the spots appeared lighter than the unaffected portions of the paper; when viewed with transmitted light, the spots appeared darker. Microscopic examination gave evidence of the presence of clusters of gas bubbles within the paper tapes at the dry spots.

Subsequent investigation has established that the dry spots are produced by sudden release of gas pressure. In cable which had not been subjected to gas pressure, dry spots have never been observed. On the other hand, dry spots have been observed in all cases where cable had been subjected to pressure and the pressure suddenly released, provided the cable was dissected within a short time after release of pressure. Similar dry spots also have been produced in single tapes and in rolls subjected to application and sudden release of 200-pounds per square inch gauge gas pressure. Formation of the dry spots, under the conditions described, occurs in both the preimpregnated and mass-impregnated types of cable. It also has been produced in the laboratory in tapes saturated with low-viscosity oil, so that the condition is not peculiar to the high-viscosity oil used in the cables here discussed.

Dissection of cable samples also has established that the dry spots may persist for many weeks after release of pressure, but that they become less prominent as time goes on. The dry spots disappear much more rapidly if the pressure is reapplied.

The formation of these dry spots can be explained in the following manner. When, after installation of the cable in the pipe, the gas pressure in the pipe is increased, the weight or amount of the gas sorbed in the oil will increase in proportion to the pressure, and, when the pressure in the pipe is decreased, the sorbed gas will be decreased in proportion to the pressure. The release of sorbed gas when the pressure is reduced, especially if the pressure reduction occurs at a high rate, is of particular significance with respect to the impregnating compound contained within each tape. The gas that was sorbed cannot readily escape from the inside of the tape, and, in forcing its way out of the tape, the gas will dislocate some of the oil contained in the tape, forming the clusters of gas bubbles or dry spots.

The gradual disappearance of the spots is caused by the redistribution of the oil under the forces of capillarity. Reapplication of pressure hastens the action by compressing the bubbles and thus aiding capillarity in the redistribution.

SIGNIFICANCE OF DRY SPOTS WITH RESPECT TO CABLE OPERATION

Inasmuch as sudden gas-pressure releases cannot be avoided in the operation of high-pressure gas-filled cables, it became important to investigate the significance of such dry spots with respect to cable operation. To determine the effects, the dielectric strength of tapes containing dry spots, and the a-c breakdown strength, the impulse strength, and the ionization-starting potentials of cables that had been subjected to a number of gas-pressure releases were determined.

DIELECTRIC STRENGTH OF TAPES CONTAINING DRY SPOTS

Dielectric-strength tests were performed on tapes removed from a length of unused cable which had been subjected to the following pressure program:

1. 200-pounds per square inch gauge nitrogen pressure for eight hours.
2. Sudden release of pressure to atmospheric.
3. Atmospheric pressure for 16 hours.
4. 200-pounds per square inch gauge nitrogen pressure for eight hours.
5. Sudden release of pressure to atmospheric.

The dielectric strength of tapes with

Table IV. Schedule of Gas-Pressure Changes Employed with Mass-Impregnated Cable Sample, and Key for Presentation of Results in Figure 6

Schedule			
Pressure, Pounds Per Square Inch, Gauge	Duration		Key to Results of Ionization-Starting Potential Measurements Presented in Figure 6
	Hours	Minutes	
0	15	23	Curve 1 ●——●
150	1	1	2 ●– – – – –●
200	3	1	2 ●— — — —●
0	4	15	3 ×——×
200	12		None
0	7	15	4 ○——○
150		55	5 ×– – – – –×
200	17	5	5 ×— — — —×
0	6		None
200	17	52	6 (one point ○)
0	5	58	7 △——△
150	1		8 ○– – – – –○
200	5		8 ○— — — —○
0	6		None
200	5	56	9 (two points △△)
0	5	29	10 ◇——◇

dry spots, removed 65 hours after the final release of pressure, was found to be 680 volts per mil; 2 weeks–840 volts per mil; 1 month–1,030 volts per mil. These values compare with 1,780 volts per mil on tape taken from a cable specimen which had not been subjected to gas pressure.

From these results it can be seen that there was a considerable decrease in dielectric strength as a result of the presence of dry spots, and that the dielectric strength improved with time elapsed since the last gas-pressure release. These dielectric-strength determinations were made with the tapes under atmospheric pressure, whereas under service conditions the tapes are under a pressure of approximately 200 pounds per square inch gauge. The dielectric strength of the portions of the tape that are well impregnated will be little affected by such an increase in pressure, but the dielectric strength of the clusters of gas bubbles or dry spots will be improved materially if the pressure in the dry spots is increased to 200 pounds per square inch gauge.

It is well to note here that the dielectric strength of the component tapes has only a limited bearing on the dielectric strength of the cable as a whole. The limiting dielectric stress in a cable is determined primarily by the dimensions and distribution of the butt spaces and by the electrical properties of the medium within these spaces, in the present case nitrogen at 200 pounds per square inch gauge. Even the spotty paper, having only about one-half the original dielectric strength of the saturated paper, is stronger electrically than the gas in the butt spaces.

In order to determine the practical significance of dry spots in high-pressure gas-filled cables, a-c breakdown and impulse tests were conducted on cable samples under a gas pressure of approximately 200 pounds per square inch gauge.

Effect of Gas-Pressure Releases on A-C Breakdown Strength

For the a-c breakdown test, two samples of 600,000-circular-mile cable provided with a 600-mil wall of insulation were used. One sample was of the preimpregnated type; the other, of the mass-impregnated type. Approximately ten pressure–release cycles, from 200 pounds per square inch gauge to atmospheric pressure, were applied to each sample immediately before the breakdown tests were started. In the breakdown tests, a voltage of 200 kv was applied for nine minutes; then the voltage was raised in 2-kv steps every nine minutes until 240 kv was reached; then at 8-minute intervals until 264 kv was reached, and then at 7-minute intervals until failure occurred. A nitrogen pressure of 200 pounds per square inch gauge was maintained in the samples during the breakdown tests. Under this treatment, breakdown occurred at 270 kv for the preimpregnated cable, and at 274 kv for the mass-impregnated cable. These breakdown values are in the same range as those of similar cables which had not been subjected to gas-pressure releases. These values cannot be compared properly with those of oil-filled or newly-made solid-type cables. The purposely-drained gas-pressure cables are not as well adapted as are these other types to withstand this particular kind of test. This does not, however, nullify the usefulness of the test for the comparison made.

Effect of Gas-Pressure Releases on Impulse Strength

For the first impulse-strength test, three specimens were used that were cut from a 95-foot length of cable removed from the experimental line. The cable had been in operation for $4^1/_2$ years, and during this time there had been approximately 20 gas-pressure releases. It was found that the impulse strength of these three specimens was somewhat higher than that of two other samples tested at the time of the installation of the experimental cable (640, 730, and 728 kv as against 700 and 500 kv). However, the impulse strength in either case was rather low, and the impulse failures occurred in regions of wide butt spaces. In this connection it should be mentioned that this experimental cable was the first one of this type manufactured and installed in this country. Further, this cable did not include several improvements in construction and uniformity of fabrication embodied in the original commercial line. The impulse-test results, therefore, were not necessarily conclusive with respect to the effect of dry spots on the impulse strength, inasmuch as other effects may have masked the effect of dry spots.

In order to obtain more reliable information concerning the effect of dry spots on the impulse strength of the cable, a specimen of mass-impregnated cable with 600,000-circular-mil conductor and an insulation thickness of 500 mils subsequently was subjected to impulse tests immediately after the cable had been subjected to ten gas-pressure release cycles. During these cycles a nitrogen pressure of 200 pounds per square inch gauge was maintained for approximately eight hours; then the pressure was released suddenly to atmospheric pressure, where it remained for 16 hours. Pressure at 200 pounds per square inch gauge then was applied, and two impulses were made at 680, 780, 860, and 955 kv. Full generator voltage of approximately 1,060

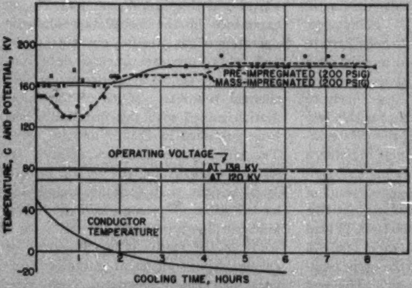

Figure 5. Comparison of ionization-starting potentials existing in mass-impregnated and preimpregnated cables during the cooling period of Test III

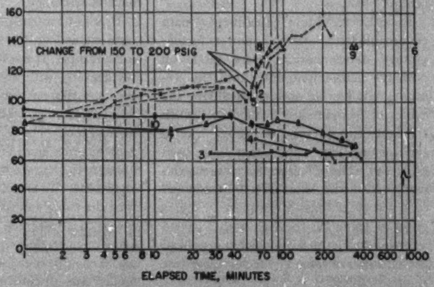

Figure 6, Ionization-starting potentials existing at various time intervals after gas-pressure changes were made on mass-impregnated cable

Table V. Power-Factor Values Obtained on Mass-Impregnated and Preimpregnated Cables in the Experimental Field Installation During Severe Loading Tests

Date	Mean Conductor Temperature, Degrees Centigrade	Power Factor Values, Per Cent		
		Mass-Impregnated Insulation		Preimpregnated Insulation
		500 Mil	600 Mil	600 Mil
8-5-47	18	0.30	0.345	0.40
8-14-47	60	0.27	0.265	0.335
8-20-47	70	0.26	0.25	0.32
8-26-47	75	0.25	0.23	0.295
10-21-47	80	0.27	0.26	0.31
1-14-48	35	0.35	0.36	0.45
1-26-48*	80	0.30	0.29	0.33
3-17-48**	85	0.27	0.25	0.315
6-14-48†	53	0.29	0.28	0.35

Power factor values refer to approximate operating voltage.

* After 88 cycles to approximately 100 degrees centigrade conductor temperature.

** After 139 cycles to approximately 100 degrees centigrade conductor temperature.

† After 226 cycles to approximately 100 degrees centigrade conductor temperature.

kv then was applied, and the sample failed during the eighth impulse at full generator voltage. Two similar samples of cable, but of the preimpregnated type and not subjected to gas-pressure releases, had been tested previously and had failed at 890 and 960 kv, respectively. It is evident from this that the surge strength of cable that has been subjected to gas-pressure releases is quite satisfactory.

EFFECT OF GAS-PRESSURE RELEASES ON IONIZATION-STARTING POTENTIAL

Another criterion that is of considerable importance in the operation of high-pressure gas-filled cable is the ionization-starting potential as affected by sudden gas-pressure changes. The reason for its importance is twofold: first, it may be used to determine how soon such a cable may be safely energized after pressure is restored subsequent to a pressure release to atmospheric pressure, and second, it may be a guide in determining how long the cable may remain safely energized when the gas pressure in the pipe is essentially lost.

In order to obtain experimental data concerning this criterion, power factor–voltage determinations were made on both the mass-impregnated and the preimpregnated cable specimens during the cycles of gas-pressure changes to which the cable samples were subjected prior to the a-c breakdown tests that have been discussed. The schedule of pressure cycles employed in the series of tests conducted on a sample of mass-impregnated cable is given in Table IV, together with a legend referring to Figure 6, in which a graphical presentation of some of the pertinent test results is given.

Only the results obtained with mass-impregnated cable are given, inasmuch as those obtained with preimpregnated cable are of essentially the same character. All the results given refer to conditions existing at room temperature. These series of gas-pressure changes were applied to the cable specimens that had been subjected to the three tests discussed under the previous section entitled "Effect of Sudden Temperature Changes on the Electrical Performance of the Cable."

From the results plotted in Figure 6, it can be seen that there is a tendency toward an increase in ionization-starting potentials with an increase in the number of gas-pressure applications and releases. Curves 2 and 7 from this figure are replotted in Figure 7, together with essentially corresponding results that were obtained in similar tests made on the preimpregnated-cable specimen. In this figure, potentials across the insulation wall that exist when the cable is in 3-phase operation at 120 kv and at 138 kv are indicated again in order to show the relation of the ionization-starting potentials to the potentials actually existing in normal operation.

It is not inappropriate to refer here to tests carried on for several months on a cable sample, at a voltage above operating voltage and with one end open freely to the atmosphere. The cable for this test was part of that made for the 1941 commercial line. The voltage was raised at a constant rate from 90 kv to 113 kv (compared with the rated voltage to ground of about 80 kv). During 2,800 hours of this time the cable was subjected to daily load cycles to 70 degrees centigrade, one end being open so that during the cyclic loading it could breathe in air. The test finally was discontinued without failure after a total time of 4,400 hours (about six months).

It is shown by ionization measurements made following sudden release of pressure, that the ionization voltage remains above operating voltage for several hours. Similarly, after reapplication of pressure, the ionization voltage rises so quickly above operating voltage that such cables may be energized safely immediately after service pressure is restored subsequent to a pressure release to atmospheric pressure. The long-time test at atmospheric pressure is of related significance in that it shows that even a short period of ionization, should it occur following sudden loss of pressure, does not produce rapid deterioration.

CONCLUSIONS CONCERNING THE EFFECT OF SUDDEN GAS-PRESSURE RELEASES

The results of this study of the cause and significance of dry spots observed in the insulation of high-pressure gas-filled cable lead to the conclusion that dry spots can be expected to appear in high-pressure gas-filled cable when the gas pressure is suddenly released, but that such dry spots apparently have no harmful effect under service conditions. Although these experimental results show no harmful effects even for repeated sudden pressure releases, such severity of conditions is not necessary and is not suggested for commercial installations. In order to insure against significant effects, it is desirable to arrange that sudden releases of pressure be made only at infrequent intervals.

Performance of Both Types of Cable in an Experimental Field Installation

An experimental field installation of pipe-type cable was completed in 1941 in the grounds of Warren Station of The Detroit Edison Company system. The purpose of this installation was to gain experience in the installation and the operation of gas-pressure pipe-type cable, and to procure experimental data concerning its electrical performance and thermal behavior. Much of the information gained with this installation has been published in 1942,[1,3] and in 1948.[4] The latter paper contains detailed information concerning the general layout. It is evident that such an installation lends itself readily to a study of various kinds of pipe-type cable, as well as to a study of the merits of modifications of existing types—for instance, the performance of mass-impregnated *SMD*-type cable as compared with that of preimpregnated *SMD*-type cable, as it was originally designed.

When the desirability of the use of mass-impregnated high-pressure gas-filled cable for the system of The Detroit Edison Company was being considered, two lengths of mass-impregnated cable and one length of preimpregnated cable were installed in one pipe section of approximately 660 feet in length. All three single-conductor cables that were used to make up the 3-phase cable in this pipe section had 600,000-circular-mil conductors, the two mass-impregnated cables having Compack-round conductors with 600-mil and 500-mil insulation, respectively, and the preimpregnated cable having a concentric-round conductor with 600-mil insulation.

This installation has been under test since the early part of August 1947, and has been subjected during that time to severe loading conditions. At first, continuous load was applied for about 180 hours with conductor temperatures at approximately 70 degrees centigrade, followed by 140 hours at 80 degrees centigrade, 145 hours at 90 degrees centigrade, and 1,475 hours at 100 degrees centigrade.

After continuous load had thus been applied for approximately 1,940 hours, the cable was subjected to daily load cycles of 12-hour heating and 12-hour cooling periods. During these load cycles, currents of sufficient magnitude were circulated to bring about a conductor temperature of approximately 100 degrees centigrade. To date these cables have been subjected to 310 such heat cycles. A potential of 120 kv, 3-phase, was applied to the cable during all loading schedules.

Power factor measurements were made initially and at various times during the load tests. The values shown in Table V are representative of the results obtained at operating voltage and indicate that little change has occurred in the insulation during the test.

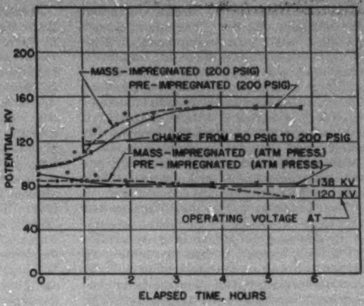

Figure 7. Comparison of ionization-starting potentials existing in mass-impregnated and preimpregnated cables at various time intervals after gas-pressure changes were made

Summary

1. The 7-mile circuit of 120-kv high-pressure gas-filled cable installed in 1941 has fulfilled, during seven years of operation, the favorable expectations indicated in an AIEE paper presented in 1942.[1]

2. Several engineering features of high-pressure gas-filled cable, concerning which there has been no previous publication, have been investigated and are described. The results obtained are favorable.

3. It is believed that the characteristics of the high-viscosity saturant used are very significant with respect to the performance which this cable has given and which may be expected from it. Reasons for this are given, and added details of the oil characteristics are shown.

4. Further tests on an experimental field installation are reported. These show favorable results concerning cable operation at high temperature for both the preimpregnated and mass-impregnated types.

5. A new installation of twice the power-carrying capacity and twice the length of the 1941 installation is nearing completion. Half of the cable is made with preimpregnated tapes, and, except for conductor size and for shipment without lead sheath, is substantially the same as that of the 1941 installation. The construction of the other half of the cable involves mass impregnation of the paper with the high-viscosity oil, in a manner generally similar to the impregnation of solid-type cable.

6. The ability of the mass-impregnated cable to meet special loading and other operating conditions has been ascertained by the rigorous tests reported in this paper.

References

1. 120-Kv High-Pressure Gas-Filled Cable, **I. T. Faucett, L. I. Komives, H. W. Collins, R. W. Atkinson.** Electrical Engineering (AIEE Transactions), volume 61, September 1942, pages 658–65.

2. Mineral Impregnating Oils for Paper Power Cables, **A. D. Pettee.** *Minutes*, Forty-Second Meeting, Transmission and Distribution Committee, Edison Electric Institute (New York, N. Y.), February 1947, pages A-133 to A-140.

3. 120-Kv Compression-Type Cable, **I. T. Faucett, L. I. Komives, H. W. Collins, R. W. Atkinson.** Electrical Engineering (AIEE Transactions), volume 61, September 1942, pages 652–57.

4. Thermal Characteristics of a 120-Kv High-Pressure, Gas-Filled Cable Installation. **W. D. Sanderson, Joseph Sticher, M. H. McGrath.** AIEE Transactions, volume 67, part I 1948, pages 487-98.

Discussion

Edwin J. Merrell (Phelps Dodge Copper Products Corporation, Yonkers, N. Y.): The following cable ionization data obtained in our laboratory are pertinent to this discussion. The measurements were made on two 50-foot samples of 138-kv cable mass impregnated with 3,000 Saybolt second at 100 degrees centigrade oil. One length was a round cable with taped sheath such as that described in the paper; the other was an oval compression-type cable with a continuous polyethylene sheath. The cables were installed in horizontal brass pipes under 200 pounds per square inch nitrogen, and terminated in condenser terminals, the ends being double guarded. Ionization factor was defined as the difference in room temperature power factors at atmospheric pressure, when measured at 20 volts per mil (11.2 kv to ground) and 143 volts per mil (80 kv to ground, rated voltage). Initial ionization factors were 0.01 per cent for both designs. After approximately 25 daily load cycles under 200 pounds per square inch pressure with the conductors heated by loading current for eight hours each day, from room temperature (about 25 degrees centigrade to between 100 and 105 degrees centigrade, the ionization factors were measured again. After one day at atmospheric pressure the ionization factors for the round and oval construetions respectively were 0.65 and 0.11; after five days, 2.22 and 0.21 per cent. Thus, in the taped sheath cable, oil pumped out on load cycle, leaving voids within the dielectric, thereby showing the ineffectiveness of the high-viscosity oil in preventing radial migration. On the other hand, the continuous sheath prevented loss of impregnant; moreover, the reversible elasticity characteristic of the polyethylene-sheathed compression cable, even with the conductor at 100 to 105 degrees centigrade, minimized gaseous void formation.

G. B. Shanklin (General Electric Company, Schenectady, N. Y.): The high-pressure gas-filled cable with preimpregnated insulation, as described in the paper, duplicates that used previously in Detroit, and is similar in principle to the Beaver-type cable. The characteristics are well understood and reliability in service at 200 pounds nitrogen gas pressure has been proved both in this country and abroad. Accordingly, no comments are required other than to point out the increased cost and manufacturing difficulties represented by this construction.

The gas-filled cable mass-impregnated with extra-high viscosity compound is something new and, as yet, untried in service. To a lesser extent, it also has inherently higher cost and represents a more difficult manufacturing problem than the more conventional designs used generally. The basic question is whether it offers sufficient advantages to overcome these handicaps. Only time and operating experience will fully answer this question. The makers and users deserve a great deal of credit for this contribution to the cable art.

We have been carrying out a systematic laboratory study of the polybutylenes for some years past, comparing them with the natural petroleum oils over the full range of available viscosities. At the higher viscosities, above the range of the natural oils, Vistanex has been added to obtain the desired viscosity in this comparison. Our conclusions have not always been in accord with those presented by the authors. For instance, it is stated that the polybutylene oils resist electronic bombardment from ionization considerably better than natural oils. On the contrary, we have found very definitely that at any given viscosity the natural oils with or without Vistanex are much more resistant to ionization bombardment. In fact, in this respect and in other ways polybutylenes closely resemble saturated highly-refined white oils.

Until some way is found of stabilizing the polybutylenes against ionization effects we would not care to use them in solid-type cable and low-pressure gas-filled cable where incipient ionization is always likely to occur, and where resistance to and a self-healing effect that extinguishes this incipient ionization are very important factors.

In high-pressure gas-filled cable there is a much wider margin between ionization starting voltage and normal operating voltage. This gives some assurance that incipient ionization will never start in service provided a sufficient pressure is maintained uniformly. If incipient ionization does occur it will lead to serious cumulative damage and with this type of oil it is very important to bear this in mind.

The effects outlined are aggravated by the extremely high viscosity of the oil and the relatively high operating pressure of the gas in the voids. According to our test study, extra-high viscosity oils of any type have no self-healing effect against incipient ionization because they cannot move freely in the paper insulation and accordingly are not drawn into the voids by electrostatic attraction. Also, the high energy in the electronic discharge at high pressure tends to aggravate accumulative action. The net result is that for successful operation there must always be a wide margin between ionization starting voltage and normal working voltage.

It might be pointed out that the drainage tests on rolls of impregnated paper as shown in Table I of the paper have no bearing on ionization characteristics in service as affected by compound drainage. The results in Table I as would be expected show a drainage in direct proportion to the viscosity of the impregnant and as the viscosity increases it requires a correspondingly longer time for the same degree of drainage. In a true gas-filled cable, surplus compound is drained off at the beginning and that which remains is held in place by capillary attraction. When voltage is applied, electrostatic attraction also tends to redistribute the compound in a favorable way provided the viscosity is sufficiently low to allow this. We have made many long-time load cycle aging tests with medium and low viscosity impregnants and under severe conditions of drainage. Many of these results have been presented in AIEE papers and will show that ionization characteristics are not affected by drainage as would be indicated by Table I.

The paper describes some interesting tests on gas pressure release and its effects on void formation and ionization characteristics. The conclusions are that gas pressure release within the minimum time limits that could occur in service has no important effect. We have made numerous tests of the same kind with a wide range of impregnant viscosities and would like to confirm this conclusion that such gas pressure release does not permanently affect the cable.

The test procedure on 33-foot lengths of cable as described in the paper is not entirely clear. No drawings are presented giving details of the end seals and the test terminals. From the description, however, it would appear that these lengths were tested strictly as compression cable, and had not been previously charged with gas to full working pressure. In other words, they were not tested as true gas-filled cable, since no gas in solution or otherwise was in the insulation. The pressure was applied externally on the impervious polyethylene sheath and presumably surplus compound had not been drained as it would be in a true gas-filled cable. The net result was a typical hydraulic compressive action, and about all these tests proved was that a round cable responds effectively to such hydraulic compressive action and is equal in this respect to the oval-shaped cable. If my interpretation is incorrect, it would be appreciated if the authors would explain this test in more detail. In service the cable will act as a true gas-filled cable, provided the gas pressure medium can penetrate and fully saturate the cable cross section to full working pressure and over a full length between joints that might be as much as 2,500 feet, or even more. Since the penetration and absorption of gas is not only a function of length but of compound viscosity also, it would appear that it will require an extremely long time for fully saturated and stabilized conditions to be reached.

One thing that puzzles me is how a preimpregnated insulation can perform as a true hydraulic compressive design. Because of the relatively large void spaces in a cable of this kind, it would appear that it could not possibly perform in this way and ionization would not be suppressed until and after the cable cross section is fully gas-saturated to working gas pressure. Perhaps the authors' comments will throw some light on this. Incidentally, the ionization characteristics as a function of pressure in Table III of the paper do not behave as expected in a true gas-filled cable. The plotted curves do not have a typical drop in ionization voltage as pressure increases. Instead, the curves tend to bend upward and the ionization voltage increases faster than the pressure. Even Paschen's law, which we all know is only approximate, is contrary to the unusual shape of these curves. This again indicates a compressive hydraulic action.

The aging tests on this cable at 100 degrees centigrade confirm the fact that, other things being equal, power factor stability under high-temperature aging improves with increase in viscosity of the impregnant. The reason for this is that conducting ions from the impurities released by heat disintegration are immobilized in the viscous material and their presence cannot be indicated by dielectric loss measurements, as it can with a lower viscosity impregnant. It does not mean that impurities cannot be present to an equal degree in both cases and it raises a question of whether dielectric loss measurements are a true criterion of aging under such conditions. It is a well-known fact that cellulose fiber does disintegrate at temperatures above 80 degrees centigrade, regardless of the impregnant.

It would appear that a good deal more work will be necessary before we will know all that is needed to be known about the characteristics of cable with super-high viscosity impregnants. Certainly, however, the results presented in this paper are promising and justify carrying this work to a full conclusion.

E. S. Halfmann (Philadelphia Electric Company, Philadelphia, Pa.): In describing the characteristics of the saturant, the authors make the following statement:

> "Although the viscosity is very high at high temperature, it is not so great as to prevent cable installation at the lowest temperature considered normal in American practice. Bending of the cable, or installation, presents no problem at —10 degrees centigrade."

This statement gives the reader the impression that cable impregnated with 3,000 Saybolt Universal second *HC* oil is capable of withstanding the bending during installation and the requirements of the Association of Edison Illuminating Companies' (AEIC) bend test as well as cable impregnated with a lighter oil. On the contrary, we have found that cable impregnated with 3,000 Saybolt Universal second *HC* oil would not pass a 16-diameter bend test performed at room temperature according to the AEIC specification for oil-filled cable,[1] while cable built by another manufacturer with the same conductor size and same insulation thickness but impregnated with a lighter oil passed a similar bend test performed on a 12-diameter mandrel.

For the purpose of this test the temporary lead sheath was removed from all cable samples. Of the four samples taken from different manufacturing lengths of cable which were mass-impregnated with 3,000 second *HC* oil, one sample was bent around a mandrel 12 times the diameter of the cable measured over the skid wire and three samples were bent around a mandrel 16 times the diameter of the cable measured over the skid wire. The tests were performed by the manufacturer in the presence of the writer, and followed the routine prescribed in the AEIC specification for oil-filled cable. Upon dissection, it was found that the number of torn tapes in each sample exceeded the number permitted by the AEIC specification by one or two tapes.

The manufacturer claims that bend tests on other samples have been performed successfully even at temperatures as low as −10 degrees centigrade. This inconsistency of results is extremely difficult to explain unless the high viscosity impregnant tends to cement adjacent tapes to each other in time. It is possible that the successful tests may have been made on newly impregnated cable and that the tests referred to in the preceding paragraph were made on cable which had been impregnated several weeks or months prior to the tests.

Reference

1. Specification for Oil-Filled Cable. Association of Edison Illuminating Companies (New York, N. Y.), fourth edition, June 1945.

Joseph Sticher, G. H. Doan, R. W. Atkinson, Louis Meyerhoff: The successful operation of the high-pressure gas-filled cable system installed in 1941 and of somewhat similar systems abroad, together with the extensive 1948 installations now in operation, has resulted in acceptance of the general system. Thus, the discussions of this paper have been concerned only with economics or engineering details.

Question has been made as to the performance under ionization of this *HC* oil. This is answered by the extensive comparison that has been made of the relative performance in cable under "load cycle aging tests" of the conventional petroleum oil saturant having a viscosity at 100 degrees centigrade of 100 Saybolt Universal seconds and of an *HC* oil of comparable viscosity. Data of some of these tests have been reported in a previous publication.[1] In these tests, the voltage was raised in geometric progression, over a period of weeks, at the rate of $1^3/_4$ per cent per day. The cable saturated with the *HC* oil withstood failure up to a voltage about 15 per cent higher than that at which the petroleum saturated cables failed—and for a correspondingly longer time.

Other data reported in 1940[2] include tests made by Mr. Halperin with similar excellent results on a slightly different load cycle aging test. The low over-all power factor and uniform radial power factor of this cable after the cyclic aging test are outstanding in comparison with the values that were shown by Mr. Halperin in 1939, as then typical for commercial cable. Some of the tests reported in 1940 were cited at that time to illustrate the value of shielding over the conductor, but they serve equally well to show the excellent performance of the saturant.

The results of these tests have now been confirmed by the exceedingly satisfactory service record of many hundreds of miles of cable made during the last nine years with this type of saturant.

We had once accepted the view now stated by Mr. Shanklin that any ionization at the stresses at which high-pressure gas-filled cable operates, would be destructive. Thus we were astonished at the extraordinary ability of this cable to withstand the ionization that occurs when it is tested at atmospheric pressure and at voltages well above the working voltage. Much higher stresses, indeed, than those used by Mr. Shanklin in his tests at a pressure of 12 pounds above atmospheric. Whatever may be the explanation of the "self-healing," the result is shown very convincingly by the long-time test at atmospheric pressure reported in this paper. This cable had 4,400 hours at average stresses varying from 150 to 190 volts per mil, all at atmospheric pressure. During this treatment the 20 volts per mil power factor, both at room temperature and at 70 degrees centigrade, rose gradually from the initial value of about 1/2 per cent to about 3/4 per cent. The ionization continued to decrease during the time that the cable was subjected to heat cycles. At atmospheric pressure and at 150 volts per mil, the power factor at room temperature dropped from 2.8 per cent to 0.9. At 70 degrees centigrade the drop was from 2.3 per cent to 0.9. Examination showed that these test conditions produced extensive wax formation in the butt spaces.

The ends of the cable were freely open to the atmosphere during these tests and free to breathe in and out during the temperature cycles. In view of Mr. Shanklin's comparison of his saturant with that used by the authors, it is very pertinent to contrast the stability of this cable with data reported by Mr. Shanklin. In 1942[3] Mr. Shanklin made pointed reference to the extreme sensitivity of his cables to exposure to oxygen of the air. He did this by reference to his Figure 11 which shows the effects of oxygen absorption during exposure to air for eight hours of the test length before it was sheathed, but otherwise complete. The 80 degrees centigrade, 20 volts per mil power factor of this cable was around 2 per cent for most of the 400-day test. Somewhat similar 20 volts per mil power factor increase is shown by Mr. Shanklin on various other curves. Thus he referred to his Figure 6 as showing typical test results and, on this, the power factor at 80 degrees centigrade and 20 volts per mil reached 2 per cent in two weeks and was at about this value or above for the remainder of the test. While these specific references apply to cable made with the medium viscosity saturant which he prefers, other references in this and his other papers indicate that his results with high-viscosity saturant were certainly no more satisfactory.

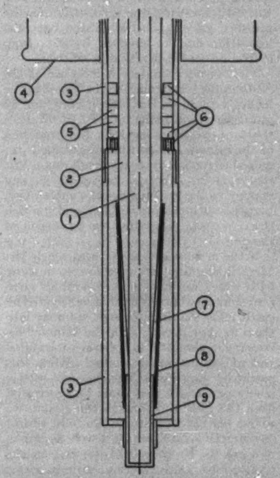

Figure 1. Sealing end for conductor, protruding through high-voltage end of terminal. Terminal, end of which only is shown, extends downward from cable test length

1. Cable conductor
2. Cable insulation
3. Brass tube
4. Condenser terminal
5. Rubber gaskets
6. Metal rings
7. Seal, composed of layers of Teflon and varnished cambric tape applied 1/2 lap
8. Butted turns of tightly wrapped copper wire
9. Conductor sealing tube (brass)

Mr. Shanklin's poor results with his polybutene oils may be explained by his description of his oils. Thus, he referred to the poor resistance of his polybutene oils to ionization bombardment and then said "In fact, in this and other ways polybutylenes closely resemble saturated highly-refined white oils." The polybutylene oils we use are not highly saturated, but on the contrary, consist almost wholly of unsaturated molecules. They combine the desirable very low initial power factor possessed by the "white" petroleum oils with the other essential property of cable oils, namely high degree of unsaturation, and this to a far greater degree than any practical natural oil. Mr. Shanklin is evidently talking about another material entirely! The vast difference in results is therefore not surprising.

We are glad to have Mr. Shanklin's confirmation of our tests and conclusions concerning the effect of gas pressure releases.

On the tests in which large loads were applied to the cable and then suddenly released, Mr. Shanklin concludes that the cable was not acting as a gas-saturated cable at all, but that the gas acted externally upon what he calls "the impervious polyethylene sheath" and that the "net result was a typical hydraulic compressive action" and that the tests prove simply "that a round cable responds effectively to such hydraulic compressive action and is equal in this respect to the oval-shaped cable."

There was no "impervious polyethylene sheath." The covering on the mass-impregnated cable consists of two pairs of intercalated copper and polyethylene tapes. This has been described previously[4] along with flow tests showing that these tapes furnish virtually no obstruction to flow into the cable, even of oil. Much less do they obstruct gas flow under pressure although they are adequate to minimize vapor diffusion into the cable. No polyethylene was present, in cable samples with preimpregnated tape, the copper tape being intercalated with a cotton tape. This length was, indeed, part of the original 1941 cable, taken from a stock reel.

The sealing of the ends of the cable was described in the paper and is shown in Figure

1 of this discussion. The mechanical arrangement shown, together with the use of the heavy saturant to fill the space within the inverted stop tubes, insures very thoroughly that the inner layers of the cable insulation cannot be gas filled by way of the ends, but must receive their gas supply through the coverings and insulation only. This diagram is given in response to Mr. Shanklin's request although the remaining emphasis in his discussion is not to question the adequacy of this seal, but to consider that the cable is so well sealed that gas did not get in at all.

Referring to the preimpregnated cable, Mr. Shanklin, in his subsequent discussion, makes a reply to his first conclusion that the cable behaves as if sealed off from the gas. He says "it would appear that it could not possibly perform in this way and ionization would not be suppressed until and after the cable cross-section is fully gas-saturated to working gas pressure." We presume his emphasis is upon the spaces not occupied by oil and that ionization will not be suppressed until these are occupied by compressed gas. With this we are in complete agreement and would point out, moreover, that it applies equally to the mass-impregnated cable. It must be remembered that after saturation of this cable, the oil is removed from the impregnating tank while still at 125 degrees centigrade and that no further oil enters the cable. The shrinkage of the oil to room temperature is about 7 per cent. A realistic conception of the physical characteristics of the paper tapes gives no basis for expecting them to yield by compression enough to fill this 7 per cent void space to a degree that would be required to affect the ionization voltage.

Mr. Shanklin says that "the ionization characteristics as a function of pressure in Table III of the paper do not behave as expected in a true gas-filled cable." The data shown in Table III cannot be used to determine the shape of the pressure-ionization curve because the lower pressures were not maintained to the point of stabilization. In most earlier ionization tests, gas was permitted to enter through the strand. The measurements at atmospheric pressure and at 50 pounds per square inch gauge were significant simply in showing that, even with the strand sealed, a major portion of the effect on ionization which could be expected from the application of 50 pounds per square inch gauge took place during the first half hour. Where the relationship between ionization voltage and pressure is to be determined carefully at pressures near atmospheric, full-pressure equalization may be very time-consuming because, at low pressures, a lack of equalization to the extent of even 5 or 10 pounds per square inch is so large a proportion of the total pressure. Lack of equalization at high pressures tends naturally to fall within the same absolute range (the same differences in pounds per square inch) as at low pressure. Whereas a lack of equalization of 5 or 10 pounds per square inch is very significant at low pressures, it is of no significance at all at, for instance, 200 pounds per square inch gauge.

Altogether, it is rather a fantastic thought, as Mr. Shanklin recognized, that in such cables ionization could be controlled purely by hydraulic compression, particularly that this could occur even at 50 pounds per square inch gauge. The thought could hardly have arisen without his erroneous impression that the cables were covered with an impervious sheath.

It is of interest that Mr. Merrell has succeeded in saturating laboratory lengths of cable, having a thick wall of paper, with high-viscosity oil, to the extent of obtaining at room temperature and atmospheric pressure an "ionization factor" as low as 0.01 per cent. However, as he shows, the mere heating of the cable not having an extruded sheath drives some of the oil out of the insulation and the ionization factor is no longer of the low initial value. In producing our cable we very definitely avoid the apparently complete saturation obtained by Mr. Merrell. We remove the oil from the impregnating tank while it is still at 125 degrees centigrade. Thus, we naturally obtain ionization at relatively low stress at atmospheric pressure as a result of the large shrinkage of the saturant as the cable cools. But this same shrinkage leaves space for the pressure gas to penetrate throughout the insulation and to produce freedom from ionization under practical conditions.

Mr. Merrell considers that his test on the round cable has significance in "showing the ineffectiveness of the high-viscosity oil in preventing radial migration." In this test, the pressure occurring from the expansion of the oil will rise to whatever value is required to force it from the insulation. But the resultant effect is not related in any manner to the performance of a cable which is purposely incompletely filled and in which there is space permitting the expansion of the oil.

If the unsaturated cable cores which Mr. Merrell saturated are comparable to those with which we have worked, and his saturant similar to ours, it must have required no small effort to force enough saturant into them as they cooled, with the saturant increasing in viscosity, to keep the cables filled and of low ionization factor. While this would be possible at high pressure with a laboratory length that could be penetrated from the ends and through the strand, we would not expect it to be practical with a commercial length, even if it were desirable.

What the purpose is of the test on the compression cable is not entirely clear. Mr. Merrell's tests show that the oval shape allows only partial accommodation for the expansion of the saturant, that is, the cable did not return entirely to its original condition after the heat cycles. But, more important than that, no less difficulty would be encountered with the oval cable than with the round in attempting to cause the cable to be completely oil-filled with the high-viscosity saturant at room temperature, for the reasons already stated. Although the fact is often overlooked, a compression cable cannot function as such and cannot have a good electrical performance unless the cable is full of oil under high hydrostatic pressure at all temperatures, even at the lowest operating temperatures.

In view of Mr. Halfmann's comment we repeat, with emphasis, and without qualification, the statement to which he takes exception "In spite of the high viscosity at high temperature, the viscosity is not so great as to prevent cable installation at the lowest temperature considered normal in American practice. Bending of the cable, or installation, presents no problem at −10 degrees centigrade." Mr. Halfmann's remarks would have been in better perspective if he had mentioned the following additional data concerning the tests he describes. In the cables which he examined, most of the tears were confined to the two metallized shielding tapes over the insulation. Only one insulating tape was torn. In view of the fact that metallized-paper tapes are included in the definition of the insulation thickness, the tears in these plus the tears in one insulating tape were held to constitute an excess over the two torn tapes permitted by the specification.

It may be remarked, further, that of course the purchaser accepted the cable and that it is in service. It is pertinent, also, that over 500,000 feet of cable of this general type was made and placed in service during the same year and that the only occasion for discussing this specification clause was this one with Mr. Halfmann.

Tests were made on a large number of specimens of cable of similar sort but made for three different utilities, and it is completely certain that the statement that was quoted and is requoted is entirely correct, and that this applies whether the cable is new or has been stored for a few months, or a few years.

While, except for some miles installed in San Francisco in the recent winter, all of the cable of this sort made in 1948 was installed in mild weather, a considerable amount of commercial cable in 1941 as well as various experimental lengths have been installed, without hesitation on the part of the manufacturer or the utility, in weather even colder than the minus 10 degrees centigrade of the standard specification.

References

1. Load Cycle Aging Tests Facilitate Cable Improvement. *Electric Light and Power* (Chicago, Ill), April 1940, pages 40–3 and 60–1.

2. Conductor Shielding Improves Paper Cable, **I. T. Faucett, R. W. Atkinson.** *Electric Light and Power* (Chicago, Ill), July 1940, pages 34–7 and 60.

3. Low-, Medium-, and High-Pressure Gas-Filled Cable, **G. B. Shanklin.** *Electrical Engineering* (*AIEE Transactions*), volume 61, October 1942, pages 719–26.

4. 115-Kv High-Pressure Oil-Filled Pipe Cable Installation at New Orleans, La., **W. R. Bullard, A. D. Pettee, G. L. Rhodes.** *AIEE Transactions*, volume 67, 1948, pages 475–86.

Selection of Electric Drives for Looms

R. J. DEMARTINI
ASSOCIATE AIEE

A. F. LUKENS
MEMBER AIEE

Synopsis: This paper outlines a method for calculating requirements of the drive for a weaving loom from knowledge of system constants and without the necessity for extensive testing. When electrical testing is performed, the pulsating character of the load must be taken into account in selection of instruments and in interpretation of data. The value of inertia in the successful drive also is discussed.

BECAUSE the load imposed on motors applied to conventional weaving looms is so complex, including many components of differing characteristics, proper application of such motors has required special skills and laborious techniques. Recently, a program of analytical testing directed at developing a simple straightforward method for selection of loom drives was completed. A new line of loom motors was developed and the methods discussed here played a prominent part in the formulation of final specifications. This paper has been prepared for the purpose of presenting a summary of the fundamentals and a discussion of basic mathematical relations evolved.

The Problem

What is desired is a method whereby, given basic physical constants of a loom, it will be possible to determine the characteristics of the proper drive for it. If the mechanical motions in loom operation can be reduced to a few basic mathematical relations built around values of the loom constants, the job to be performed by the drive may be clearly defined. With these mathematical tools at hand, the task of selecting the proper motor should be exceedingly simplified. This is precisely the approach described in this paper.

Ultimately, the drive chosen must conform to the following functional specifications:

1. The drive must have sufficient torque ability to operate the loom even under the extreme conditions exemplified by the high load break-in period and by those installations where supply voltage may be low.

2. Operation of the drive must be such as to impart the proper "feel" to the loom; a characteristic so important to the trained loom-fixer, and to be evaluated by him. The amount of speed variation pick-to-pick and the character and magnitude of loom vibration are factors which determine the feel. This factor has not yet been reduced to quantitative values.

3. The drive must operate on the loom load without overheating.

The Loom

Weaving, the process of interlacing two systems of filaments arranged in right-angle relation, is done on a machine known as a loom. In its earliest form, Figure 1, it consisted of any convenient horizontal beam from which the warp or lengthwise yarns were hung, a bobbin carrying the weft (or filling) or crosswise yarn, and a flat wand whose functions were to separate the warp ends in order that the bobbin might pass between them and to beat the weft into place after each insertion. Stones often were hung as weights at their lower extremities to maintain tension in the warp yarns during the weaving operation. To obtain a plain 1-up—1-down weave, alternate yarns were moved forward by rotation of the wand. The bobbin was handed across from right-to-left in the "shed" thus formed, and the filling yarn thus laid in position was beaten into the fabric. The wand then was withdrawn and reinserted between the ends, this time with the warp yarns which previously lay on the rear side brought forward, and those in front dropped to the rear. Again the bobbin was passed through the shed from left-to-right, and the wand was used to beat it up into the woven section. This process was repeated over and over to produce a web or fabric.

In Figures 2 and 3 the elements of a modern power loom are shown. In Figure 3(A) a modern loom is illustrated. The same basic functions as practiced in primitive weaving are incorporated in this automatic machine. Warp yarns, which here may number 10,000 to 15,000 or more, are many hundreds or thousands of yards long and are wound parallel on a large spool called a "beam." (This term has been carried over from the early loom construction.) This is placed at the rear of the machine, its center shaft set in bearings to permit rotation as the warp ends are paid off. All of those ends are led up over the guide roll (whip roll), divided into two equal-numbered systems, and laid over and under the lease rods. The principal function of the lease rods is to separate the closely-spaced ends, so that the weaver can trace more easily individual ends when tying broken ones. From here, each yarn is fed through its own "heddle," a steel wire with an eye through which the yarn passes in the harness frame. The raising and lowering of the harnesses, and thus the warp yarns, position those yarns above and below each weft thread in the order required to secure the pattern desired in the finished

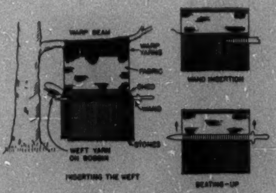

Figure 1. Early loom

Paper 49-86, recommended by the AIEE general industry applications committee and approved by the AIEE technical program committee for presentation at the AIEE winter general meeting, New York, N. Y., January 31–February 4, 1949. Manuscript submitted July 16, 1948; made available for printing December 21, 1948.

R. J. DEMARTINI is with the paper and textile division of the General Electric Company, Schenectady, N. Y. and A. F. LUKENS is with the induction motor division of the General Electric Company, Lynn, Mass.

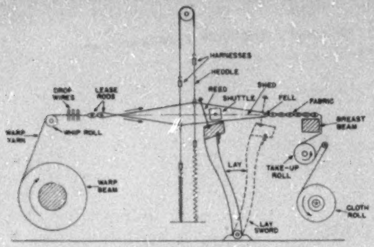

Figure 2. Diagrammatic cross-section view of loom

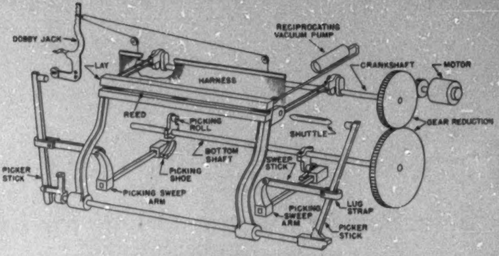

Figure 3. Diagrammatic 3-dimensional view of loom

fabric. In Figure 2 just two harnesses are shown; the requirement for producing a plain 1-up and 1-down weave. With each pick, or flight of the shuttle, one harness is raised and the other lowered. From each harness, the 2-yarn systems converge to enter the fabric, forming a shed. Between the harnesses and the fell (weaving point) of the cloth, the ends run through the slots (dents) formed between closely-spaced vertical flat wires of the reed, Figure 3. A bell-crank driven lever, called the "lay," carries the reed forward to push the weft yarn into the cloth and then back out of the shuttle's path. The woven fabric passes over the "breast beam," around a positively-driven take-up roll, and onto a winder, the cloth roll.

The shuttle, carrying the weft yarn, is propelled across the loom in flight under the impact of a blow from a rapidly moving lever, called the "picker stick." This stick, usually made of hickory wood, is accelerated rapidly by a cam control and suddenly imparts its energy to the metal-nosed shuttle as it strikes it. The shuttle darts across the loom, decelerating to a stop at the far side under the action of a spring-loaded friction drag in the "box."

In the weaving operation, each of the loom elements performs its function in proper sequence, as determined by cams and gearing. The order in which the operations occur are as follows:

1. Harnesses are positioned to raise some warp ends and lower others.
2. The lay, carrying the reed, moves to the back position toward the harnesses. As it approaches the end of its rearward travel, it is decelerated and its direction is then reversed.
3. Struck sharply by the picker stick, the shuttle flies across the loom, trailing the weft yarn behind it, and comes to rest in the box at the far side.
4. Meanwhile, the lay is accelerated forward, and the reed pushes the weft yarn into the fabric.
5. As it nears its frontmost position, the lay must be decelerated and its direction reversed once again.
6. A ratchet on the end of the take-up roll is notched forward by a pawl driven from the lay motion.

The cycle then repeats as the harnesses change position and the next pick is made.

In order to obtain uniformity in the finished product, the warp yarns must be held under tension at all times. A friction brake or other hold-back mechanism is applied to the warp beam to accomplish this.

Often, in order to secure particular patterns in the fabric, such special motions as the leno or jacquard attachments are added to the loom. Also, on some looms, there is furnished a reciprocating pump, Figure 3, whose function is to supply a vacuum to an automatic bobbin-changing mechanism. For purposes of this paper, the effect on load of such auxiliary equipment is not considered since they are not universally encountered.

Protection

If a warp or filling yarn should break, the loom must be stopped to prevent weaving any appreciable length of faulty fabric. Special electric and mechanical detection devices are provided on the loom to signal the occurrence of such a break and cause the clutch to become disengaged.

Occasionally, for any one of several reasons, shuttle speed on a pick may be slower than normal, or the shuttle may even fail to complete its flight. If the shuttle has not boxed by the time the lay swings forward to drive the weft yarn

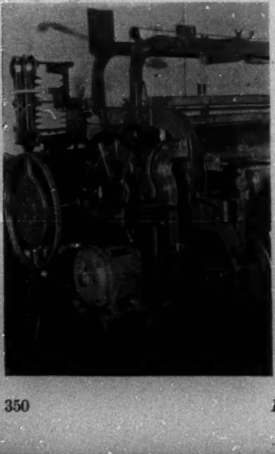

Figure 3A (left). Modern weaving loom

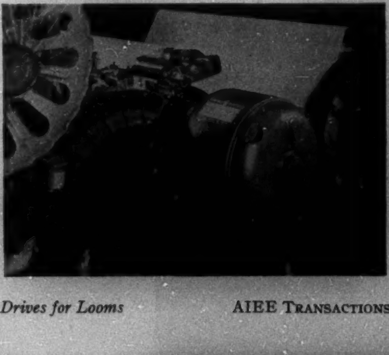

Figure 4 (right). Modern loom motor mounted on loom

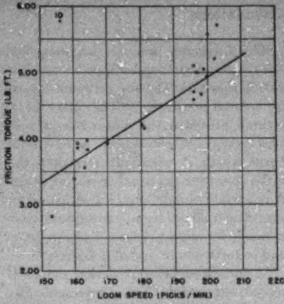

Figure 5. Plot of loom friction torque versus speed (based on 21 tests)

home, there is danger that it will be swept forward by the reed and pushed into the fell of the cloth. Many warp yarns would be broken and irreparable damage would be done to the fabric when the "smash" occurred, necessitating a relatively long shut-down for redrawing the broken warp yarns. To protect against such an occurrence, means are provided for checking on shuttle position to insure that its flight is true and on schedule early in the lay's forward swing. If the shuttle is not on its true course at this time, the "bang-off" protective mechanism operates to simultaneously declutch the motor and position a restraining rod, thus halting the forward travel of the lay. For such a brute-force method of stopping the loom to succeed without causing failure of mechanical elements, the clutch must be disengaged sharply. This occurs at that point in the cycle at which the energy stored in the loom parts is at a maximum.

The Loom Drive

The standard fly-shuttle loom drive consists of a full-voltage starting switch and a single induction motor, Figure 4, whose rating ranges from 1/2 to 2 horsepower and is of either 4- or 6-pole design. To protect against the possibility that the motors may become plugged with lint from the weave shed atmosphere, they are of totally enclosed construction. The sleeve-type, wool-yarn-packed bearing, which has proved successful over the years in loom motor applications, is standard today. The breakdown torque of the loom motor is approximately twice that of the general-purpose motor. The axial length of the motor is kept at a minimum so that it does not influence maximum over-all floor area.

The motor is coupled to the machine through a spur-gear reduction and a clutch. Starting and stopping the loom is accomplished by operation of the clutch mechanism, the motor being permitted to run continuously.

Loom Load

The load imposed on the motor by the various parts of the loom can be studied best by considering the energy required to drive each element individually. Since some of the parts have widely varying velocities, it is better to consider them on a torque basis and to refer the torques to the motor shaft. The more important components of the total load are:

1. Torque to overcome friction.
2. Torque to drive the lay.
3. Torque to drive the shuttle.
4. Torque to actuate the harnesses.
5. Torque to drive the air pump (if included).
6. Torque to actuate a leno motion or jacquard head (if any).
7. Torque to actuate many small devices, such as cloth beam, dobby (harness motion control), and so forth.

For analysis, one pick is considered as one cycle with zero degrees of the crank shaft taken at front dead center of the lay and with 180 degrees at back dead center.

The friction of the loom consists of the actual friction of all bearings, cams, and sliding contacts, and also the constant portion of the unrecoverable part of the energy that goes into driving each part. Friction is assumed constant for purposes of analysis, but in practice it varies widely in a relatively short time with changes in lubrication of the various bearings. Figure 5 is a plot of friction torque versus speed derived from 21 tests on a loom of one size and make. Although this machine was well run in and had expert attention while being tested, friction load varied at each speed considerably. Test 10 shows abnormally high friction preceding a bearing seizure, and, at the time of the test, no distress was noted. The high friction did not show up until the test results were analyzed.

Figure 6 shows, in graphic form, the torque required to drive each of the various loom parts. The torque is plotted against lay position and this also roughly represents time.

Friction is considered ideally constant and is represented by a horizontal line "A".

The lay is a heavy mass oscillating about its center, and requires considerable torque to accelerate and decelerate it. There are two accelerations and decelerations per pick, and so the frequency of the torque is twice that of the pickage, curve "B" Figure 6. During the deceleration, the energy can be recovered and returned to the system either as electric energy or as kinetic energy stored in the effective moment of inertia of the loom. The torque is thus a curve with equal areas above and below the zero line and is a sinusoid as a first approximation. The short connecting rods and the angularity of these rods introduce some harmonics which are not important as far as the motor is concerned, although they may be of considerable interest to the loom designer.

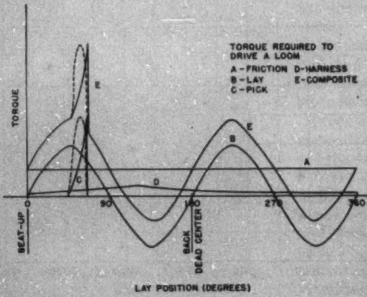

Figure 6 left). An analysis of the nature of components comprising the loom load

Figure 7 (right). An analysis of the manner in which energy is drawn from motor and rotating parts to drive a loom over its cycle

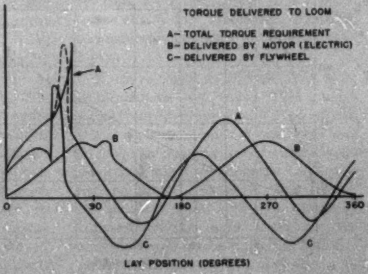

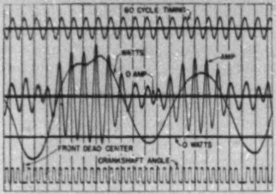

Figure 8. Oscillogram taken in loom test

The shuttle is struck by the picker stick, which in turn is struck by a cam with a very steep rise. This gives the picker stick its high acceleration and demands a sharp peak of torque from the drive system. The shape of the cam, adjustment of linkages, firmness of springs in the shuttle box, and probably several lesser factors affect the configuration and amplitude of the torque curve. The curve of Figure 6 labelled "C" is believed to be a fair representation of the actual values, but it can be approximated for purposes of calculation by a single loop of an eighth harmonic sine wave, as shown in dotted lines.

The torque required to actuate the harnesses, curve "D" Figure 6, is in most cases not great; its average value is included in the friction component. Unless the loom is fitted with a large number of harness frames and is weaving a complicated pattern that requires the lifting of nearly all of them at once, the variations in torque can be neglected. The load represented by the cloth-beam drive, dobby motions, and other lesser elements similarly may be regarded as constant and as a part of the friction factor.

The torque necessary to drive the loom is the summation of these components and is represented by the curve "E" of Figure 6.

This torque is supplied from two sources; the motor, and the inertia or flywheel effect of the revolving and oscillating parts of the system. The latter consists of the moment of inertia of the motor, of the revolving parts of the loom, and of the lay. The load at every instant is divided between the motor electrical torque, and energy from the rotating parts in varying proportions, depending on the motor speed–torque characteristics and the amount of system inertia.

For example, if the loom were driven by an infinitely-large synchronous motor, all the torque would be supplied electrically from the power line. The opposite extreme may be represented by a loom equipped with a large flywheel just after the motor has been disconnected from the line. In this case the flywheel would supply all of the torque. The actual case, of course, is a compromise between these two conditions, and the load is divided between the two sources in varying degree, as is illustrated in Figure 7.

Figure 8 is a tracing of an oscillogram of the current and watt input to a motor driving a loom. The similarity between the shape of the measured motor-input curve and that of the calculated total-load curve of Figure 7 is apparent.

Calculations

The foregoing analysis suggests that the motor output can be approximated by calculation provided the components can be treated additively. They may be so treated provided the motor operates on that portion of the motor speed–torque curve which is essentially straight; this is the case over the usual operating range. A relatively simple loom is considered for purpose of illustration; additional components for pump, heavy harness, leno, and so forth can be added if desired.

As indicated before, friction torque is considered constant and is represented by curve "A" of Figure 6.

The torque to drive the lay is treated as a sine wave with a frequency of twice the number of picks and is represented by

$$B \sin \frac{(4\pi P)}{60} t$$

where

B = peak accelerating torque
P = picks per minute

The variations in the harness torque are neglected, but the average of the torque wave is included in the friction torque A.

The torque to produce the pick is assumed to be a single positive loop of an eighth harmonic starting at the peak of the torque wave of the lay. The energy under this wave is made equal to the

Figure 9. Typical loom motor characteristic curves (steady state)

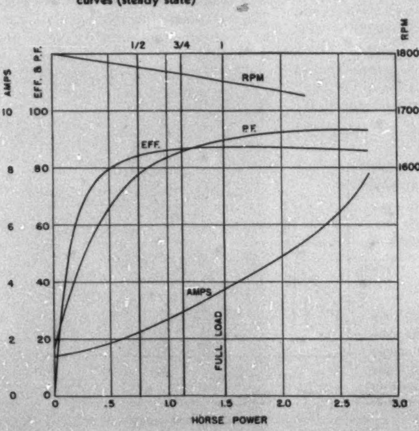

Figure 10. Typical loom motor curves of torque and losses versus watts input, based on data in Figure 9

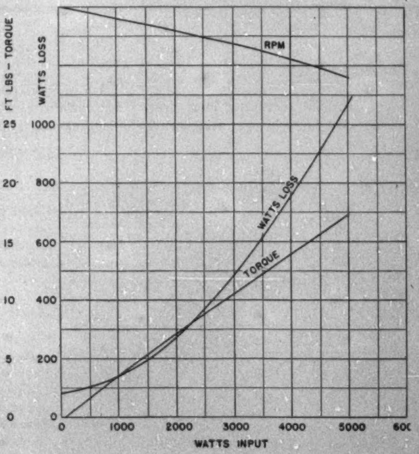

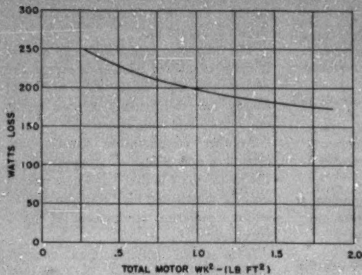

Figure 11 (left). Curve illustrating effect of inertia on loom motor losses

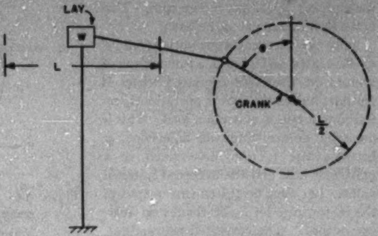

Figure 13 (right). Diagram of mechanics of lay drive

kinetic energy of the shuttle as it leaves the box, and the maximum value is represented by B'.

Motor torque can be approximated over the useful operating range by CS where S is the slip of the motor at any instant and C is the ratio of rated torque to rated slip.

The torque delivered by the flywheel is $I\ dS/dt$, where I is a function of Wk^2 and dS/dt is the acceleration of the flywheel.

These components of torques are equated and the differential equation reduced to the following.

$$T_{max}=A+\frac{B}{\sqrt{1+\left(\dfrac{PWK^2N_0^2S_{FL}}{7.75\ 10^6R}\right)^2}}+$$

$$\frac{B'}{\sqrt{1+\left(\dfrac{4PWK^2N_0^2S_{FL}}{7.75\ 10^6R}\right)^2}}=A+D+F$$

$$T_{rms}=(A^2+0.5B^2+0.048F^2+0.04AD+0.03DF)^{1/2}$$

$$N_{min}=N_0\left(1-\frac{T_{max}}{C}\right)$$

where

T_{max} = maximum torque imposed on the motor which is used in conjunction with the breakdown torque to determine the ability of the motor to carry the load under adverse conditions

T_{rms} = root-mean-square of the motor output, and is used to determine motor heating

N_{min} = minimum speed of the motor at the instant of heaviest load, and is used in estimating loom operation

A = friction torque

B = peak torque to accelerate lay

B' = peak torque to accelerate shuttle

P = number of picks per minute

Wk^2 = total system Wk^2 referred to motor

N_0 = motor synchronous speed

R = motor horsepower rating

S_{FL} = motor rated slip at full load

C = ratio of motor rated torque to rated speed

D = peak motor torque to drive lay

F = peak motor torque to drive shuttle

(See Appendix I for complete derivation)

Figure 12. Loom motor incorporating flywheel

All of the parameters, with the exception of friction torques, can be obtained by weighing and measuring, or are well known to loom designers. The friction must be estimated or determined by test. These equations lend themselves to fairly rapid columnar calculation, and, although only approximate, they are sufficiently accurate for motor application, as proved by comparison with oscillographic tests. By their use it is not difficult to compare the operation of motors with various combinations of characteristics, and to select the one with well-balanced performance.

Testing

Looms are tested to check motor operation and weaving ability, as outlined previously. In addition, tests can be used by the mill operator to determine that the loom fixer's adjustments hold friction and peak torques within limits anticipated by the loom designer.

From the oscillogram, Figure 8, it is apparent that watts input to the motor and the current input vary widely during different parts of the cycle. Ordinary meters connected to the circuit show wide needle swings and, unless properly read, give meaningless results. However, reliable results can be obtained if proper precautions and techniques are employed. Practical quantitative values descriptive of loom and motor operation are reduced from motor watt-input measurement and with due recognition of the two principles:

1. At any instant the input to the motor is the sum of motor output and motor losses.
2. Over a period of time, the average input to the motor is the sum of the average output plus the losses of the motor at the rms load.

Input can be measured in various ways, but the one that probably gives the greatest accuracy and the most complete information is an oscillographic recording of watts input to the motor. The oscillograph should be one that shows watts as an integrated curve and not as an envelope of an a-c wave. The average of the watt curve, Figure 8, is the average watt input to the motor and can be obtained by measuring ordinates or by means of a planimeter.

The rms of the watt trace can be calculated by measuring the ordinates, squaring them, averaging the squared values, and extracting the square root—a tedious process. The rms value also can be determined by the use of an Amsler mechanical integrator, a device that reads squared areas in the same manner that an ordinary planimeter reads areas; the rms value can be calculated as easily as the average.

The next step is to determine the watts loss of the motor. This can be done by referring to a test of the motor taken under steady load conditions, Figure 9, and determining the loss at the same watts input.

A curve such as Figure 10 is more convenient to work from. This is computed from efficiency data of Figure 9 and is a plot of watts input versus watts loss. In a similar manner, torque versus watts input and speed versus watts input also may be plotted, Figure 10. The average output of the motor is then the difference between average input watts and the watts loss, and can be converted to horsepower by dividing by 746, or to torque by multiplying by 7.04/average rpm. This is the friction torque of the loom.

Since the friction torque varies greatly, as illustrated in Figure 5, a comparison of motors on the basis of tested losses is fruitless unless the motor operation is referred to a common friction load. This is done by determining the difference, a, between the friction determined in a particular test and the accepted nominal value. Let rms_o be tested rms output of the motor, and let F_o be the tested average output. The corrected rms output, rms_c, is

$$rms_c = \sqrt{(rms_o)^2 + 2aF_o + a^2}$$

From the corrected rms output, the corrected losses are determined from the curve Figure 10, plotted from steady load conditions.

Peak values of torque and maximum and minimum values of speed can be determined, at least approximately, by entering Figure 10 with the proper ordinate of the watt trace.

Loom motors can be tested without the use of an oscillograph, with only a slight loss of accuracy and detail. The average watt input can be read on a polyphase wattmeter by reading the maximum and minimum positions of the needle as it swings through a rather wide range and then averaging the two readings. A better way is to use a watt-hour meter and count the revolutions of the disk for a minute or so, and get the average watts over this period of time.

The rms current can be measured with an ordinary electrodynamic or soft iron ammeter by noting the maximum and minimum positions of the needle and taking the reading halfway between the extremes. This is the rms value, since the scale of such an instrument is divided to read rms units. Calculations based on such test results are the same as outlined before, except that the rms load is determined from a current curve rather than from a watt curve. A hot-wire ammeter also can be used to advantage, since the needle swings are not as great as with the conventional type of indicating instrument. However, hot-wire instruments have practically no overload capacity, and are thus very prone to go out of calibration.

A fair approximation of peak torque can be obtained by measuring the peak value of watts input with a pointer-stop polyphase wattmeter. With this type of instrument, the needle is held up by an adjustable stop so that it moves from the stop only during the maximum part of the cycle. By using such a meter, the effect of the inertia of the meter itself is eliminated and a true peak value is observed. If a pointer-stop meter is not available, an ordinary instrument can be used by removing the cover glass and holding the needle in an elevated position with some small tool such as the blade of a penknife. This value of peak watts is used in the same manner as is that read from an oscillogram.

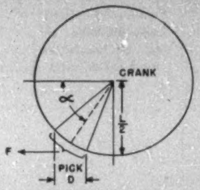

Figure 14. Diagram illustrating portion of crank cycle devoted to picking

A sample calculation of each type of measurement is given in Appendix II.

Effect of Wk^2

As explained before and as illustrated in Figure 7, the torque required to drive the loom is supplied in part from the power line and in part from the rotating parts of the system. The division of load varies depending on the amount of flywheel effect in the mechanical system and the slope of the motor speed–torque curve. Since the speed of the flywheel must drop to give up energy, it may be deduced that a motor with a sloping speed–torque curve is indicated. However, since the efficiency of a motor decreases with decreased speed and motor input, the sum of output and losses tends to increase. Thus, the gain expected from decreasing the load on the motor by letting the inertia do more work is offset to some degree by additional motor losses.

For this reason, a low-slip highly-efficient motor with high breakdown torque can be just as efficient, and give just as stable operation as one with greater Wk^2 but with lower efficiency, greater slip, and less breakdown torque. The operation of the loom is apparently exactly the same in both cases.

The addition of Wk^2 always reduces the amount of load on a motor of a given electrical design and reduces the motor losses as well as its speed variations when driving a pulsating load. The curve shown in Figure 11 illustrates how the losses of a given design of motor were reduced by the addition of Wk^2. It is apparent that the amount of reduction is appreciable, but the gains diminish after a reasonable amount of flywheel has been added. A motor with a built-in flywheel is shown in Figure 12.

The reduction in losses is so great that it often is entirely feasible to reduce the motor size one whole step and still satisfy the requirements of good motor application and loom operation.

Another consideration favoring inclusion of appreciable rotating inertia on the motor shaft is that 1,200-rpm motors may be substituted for 1,800-rpm motors without suffering an increase in speed variation.

This is not possible with conventional motors because the effective motor-rotor Wk^2, which varies with the square of the motor speed, is appreciably less when lower speed motors are used.

Motor Selection

In order to be sure that the motor will drive the loom without distress, two criteria are used:

1. The peak torque under maximum load on the motor should not exceed two-thirds of the breakdown torque of the motor.
2. The motor losses should not exceed the steady-state load losses which give a reasonable temperature rise.

By limiting peak torque to about two-thirds of breakdown torque, sufficient margin is provided to insure satisfactory operation under adverse conditions of 10 per cent under voltage and temporary load increase of about 20 per cent, as might be experienced during the loom break-in period. This safety factor assures that the speed will not drop so much that the picking becomes erratic.

Loom motors are rated 40 degrees centigrade rise on the windings at rated horsepower, this temperature being measured by thermometer during operation at rated load and under steady-state conditions. Traditionally, however, motors have been applied on the pulsating loom load to operate at about 55 degrees centigrade rise on the windings. (Overload protectors always have been selected in the range of 140–160 per cent of rated full-load current.) Although the method of rating and applying motors to looms differs from that for standard motors, the application specification that winding rise should not exceed 55 degrees centigrade is the same as for a conventional totally-enclosed motor. This is the maximum temperature rise considered for long trouble-free insulation life. As in any motor of this size, the outside temperature is considerably less than that of the winding and is generally in the 40 degrees centigrade rise range. Furthermore, this has become the practical limit in the minds of many, on the basis that a higher temperature affects the humidification around the loom. Therefore, a practical rule of application that insures meeting both requirements is to select a motor so that the temperature rise exceeds neither 40 degrees centigrade on the frame nor 55 degrees centigrade on the windings. Both temperatures are to be taken with mercury thermometers, or by an equivalent method.

The temperature rise of a motor on the loom cycle can be determined by comparing the rms losses, determined as outlined before, with the losses for a given temperature rise under steady-state conditions. This eliminates the necessity of conducting a heat run on the loom cycle.

Conclusions

1. The loom load is of a pulsating character, and the motor applied must have characteristics different from those of general-purpose machines Energy required at every instant must be supplied in part by electrical air-gap torque and in part from energy stored in the Wk^2.

2. Loom motors which give equivalent performance may be made with a wide range of designs, provided the characteristics are properly balanced.

3. The addition of a sizable flywheel reduces motor load, makes it possible to reduce the rating of the motor in some cases, and makes the operation of 1,200-rpm and 1,800-rpm motors equivalent.

4. Knowing only the basic constants of a loom and motor, performance of the combination may be calculated.

5. Motor tests on looms give results capable of reliable interpretation. Suitable instruments are:

a. An electrodynamic or soft-iron-type ammeter to read rms amperes.

b. A watt-hour meter or a polyphase wattmeter for reading average watts.

c. An a-c voltmeter to indicate line voltage. An oscillograph may be substituted for these three instruments for more precise results.

6. Friction load varies from loom to loom and from time to time on a given loom. This demands that a representative value of friction be established, and that all tests be corrected to a common base. In comparative testing, individual readings must be corrected to a nominal value before drawing conclusions.

Appendix I

This method of calculation is based on the assumption that the load consists of a constant part (broadly, friction), a sinusoid for accelerating the lay, and a single positive loop of an eighth harmonic for the pick. The torque is supplied electrically from the motor, and also from the flywheel. It further is assumed that the motor speed-torque curve is a straight line over the operating range.

The following must be known to make the calculation:

For the Loom

A = friction torque
H = weight of the shuttle
L = distance the lay moves
P = number of picks per minute
V = shuttle velocity as it leaves the box
W = weight of lay
$Wk_L^2 = Wk^2$ of the revolving parts of the loom (referred to the motor)

For the Motor

N_0 = synchronous speed of the motor
R = horsepower rating of the motor
S_{FL} = full load slip of the motor
$Wk_M^2 = Wk^2$ of the motor revolving parts
C = motor torque constant (see equation 13)

Additional Symbols

B = maximum torque to drive lay (4)
B' = maximum torque to pick shuttle (10)
E = energy of shuttle (5)
N = instantaneous motor speed (14)
N_{min} = minimum motor speed (27)
S = instantaneous motor slip
S_{FL} = full-load-motor slip (13)
S_0 = motor slip for friction (17)
S_1 = motor slip for lay (18)
S_2 = motor slip for pick (19)
T_{FL} = motor full-load torque (13)
T_L = torque to drive lay (4)
T_{max} = maximum torque motor delivers (24)
T_{rms} = rms torque motor delivers (26)
T_s = torque to drive shuttle (11)
Wk^2 = total Wk^2 referred to motors $= Wk_L^2 + Wk_M^2$ (14)
l = instantaneous movement of lay (1)
t = time
α = angle at which pick occurs (6)
θ = crank angle (1)
ω = angular velocity, radians per second, $= 2\pi P/60$ (1)
D = peak motor torque to drive lay (24a)
F = peak motor torque to drive shuttle (24a)

Torque to Drive the Lay

The lay is assumed to move in a straight line and to have an infinitely long connecting rod. See Figure 13.

The displacement of the lay from the center at any instant is

$$l = \frac{L}{2} \sin \theta = \frac{L}{2} \sin (1-S)P \frac{2\pi t}{60}$$

$$= \frac{L}{2} \sin (1-S)\omega t \qquad (1)$$

Acceleration of lay is

$$a = \frac{d^2l}{dt^2} = -\frac{L}{2}(1-S)^2\omega^2 \sin (1-S)\omega t \qquad (2)$$

Torque to drive the lay = −mass × acceleration × radius × cos θ

$$T_L = \frac{WL^2\omega^2(1-S)^2}{4_g} \sin (1-S)\omega t \cdot \times \cos (1-S)\omega t \qquad (3)$$

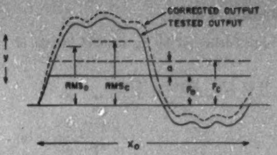

Figure 15. Correction for nominal friction

Since $(1-S)$ and $(1-S)^2 \cong 1$

$$T_L = \frac{WL^2P^2}{23500 \cdot N_0} \sin 2\omega t = B \sin 2\omega t \qquad (4)$$

Torque to Drive the Shuttle

The torque to drive the shuttle is assumed to be a single positive loop of an eighth harmonic.

Let

$$E = \text{energy of shuttle leaving the box} = \frac{HV^2}{2_g} \qquad (5)$$

E = average force × distance

and

$$\text{distance} = \left(\frac{1}{16}\right)(2\pi)\left(\frac{L}{2}\right) \sin \alpha = \frac{\pi}{16} L \sin \alpha \qquad (6)$$

(See Figure 14)

Therefore

$$\text{average force} = \frac{E}{\frac{\pi}{16} \sin \alpha} \qquad (7)$$

Torque = force × radius

$$= \frac{E}{\frac{\pi}{16} L \sin \alpha} \times \frac{L}{2} \sin \alpha = \frac{8E}{\pi} \qquad (8)$$

$$\text{Maximum torque} = \frac{\pi}{2} \frac{8}{\pi} E = 4E$$

(referred to crankshaft) (9)

Where

$$\frac{\pi}{2} = \frac{\text{peak}}{\text{average}} \text{ of sine wave}$$

$$\text{Maximum } T_s = \frac{4EP}{N_0} = B'$$

(referred to motor shaft) (10)

and

$$T_s = B' \sin 8\omega t \Big]_{\frac{3}{16}\frac{\pi}{\omega}}^{\frac{5}{16}\frac{\pi}{\omega}} \qquad (11)$$

that is, one positive loop of a sine wave extending from $t = 3/16$ to $t = 5/16$, since it is assumed that the pick occurs when the torque required to drive the lay is at a maximum.

Motor Electrical Torque

Electrical torque of motor = CS (12)

where

$$C = \frac{T_{FL}}{S_{FL}} = \frac{5250R}{S_{FL} N_0} \qquad (13)$$

Moment of Inertia

Torque delivered by moment of inertia of system

$$=\frac{Wk^2}{306}\frac{dN}{dt}=\frac{Wk^2N_o}{306}\frac{d(1-S)}{dt}=$$

$$-\frac{Wk^2N_o}{306}\frac{dS}{dt} \qquad (14)$$

$$=-I\frac{dS}{dt}$$

where

$$I=\frac{Wk^2N_o}{306} \qquad (15)$$

Maximum Torques

Equating the expression for total load torque with that for total driving torque

$$A+B\sin 2\omega t+B'\sin 8\omega t=CS-I\frac{dS}{dt} \qquad (16)$$

Since the equation is linear, it can be broken down to

$$A=CS_o \qquad (17)$$

$$B\sin 2\omega t=CS_1-I\frac{dS_1}{dt} \qquad (18)$$

$$B'\sin 8\omega t=CS_2-I\frac{dS_2}{dt} \qquad (19)$$

$$S=S_o+S_1+S_2 \qquad (20)$$

The similarity of equations 18 and 19 to the usual equation of harmonic current is apparent. The symbols of equations 21 and 22 are the usual electrical ones.

$$E\sin\omega t=iR-L\frac{di}{dt} \qquad (21)$$

The solution given in any text on alternating currents is

$$i=\frac{E}{\sqrt{R^2+(L\omega)^2}}\sin\left(\omega t-\tan^{-1}\frac{L\omega}{R}\right) \qquad (22)$$

By comparison, the following can be written from equations 17 through 22

$$T=A+\frac{BC}{\sqrt{C^2+(2I\omega)^2}}\times$$

$$\sin\left(2\omega t-\frac{1}{2}\tan^{-1}\frac{2I\omega}{C}\right)+$$

$$\frac{B'C}{\sqrt{C^2+(8I\omega)^2}}\sin\left(8\omega t-\frac{1}{8}\tan\frac{8I\omega}{L}\right) \qquad (23)$$

$$T_{max}=A+\frac{B}{\sqrt{1+\left(\frac{PWK^2N_o{}^2S_{FL}}{7.75\cdot 10^6R}\right)^2}}+$$

$$\frac{B'}{\sqrt{1+\left(\frac{4PWK^2N_o{}^2S_{FL}}{7.75\cdot 10^6R}\right)^2}} \qquad (24)$$

$$=A+D+F \qquad (24a)$$

Rms Torque

The equation of rms torque is

$$T_{rms}=\left(\frac{\omega}{2\pi}\left[\int_0^{\frac{3}{16}\frac{\pi}{\omega}}(A+D\sin 2\omega t)^2dt+\right.\right.$$

$$\int_{\frac{5}{16}\frac{\pi}{\omega}}^{\frac{2\pi}{\omega}}(A+D\sin 2\omega t)^2dt+$$

$$\left.\left.\int_{\frac{3}{16}\frac{\pi}{\omega}}^{\frac{5}{16}\frac{\pi}{\omega}}(A+D\sin 2\omega t+F\sin 8\omega t)dt\right]\right)^{1/2}$$

$$(25)$$

which reduces to

$$T_{rms}=(A^2+0.5D^2+0.048F^2+$$

$$0.04AD\quad 0.03DF)^{1/2} \qquad (26)$$

Minimum Speed

$$\text{Minimum speed}=N_{min}=N_o\left(1-\frac{T_{max}}{C}\right) \qquad (27)$$

Correction of Motor Rms Output to Nominal Friction

Refer to Figure 15.
Let

F_o = friction as tested
F_c = nominal friction
rms_o = Root mean square of output as tested
rms_c = Root mean square of output as corrected

$$a=F_c-F_o \qquad (28)$$

By definition

$$rms_o{}^2=\int_0^{x_o}\frac{y^2}{x_o}dx \qquad (29)$$

and

$$F_o=\int_0^{x_o}\frac{y}{x_o}dx \qquad (30)$$

Then

$$rms_c{}^2=\int\frac{(y+a)^2dx}{x_o}=\int\frac{y^2}{x_o}dx+$$

$$2a\int\frac{y}{x_o}dx+a^2\int\frac{dx}{x_o} \qquad (31)$$

$$=rms_o{}^2+2aF_o+a^2 \qquad (32)$$

$$rms_c=\sqrt{rms_o{}^2+2aF_o+a^2} \qquad (33)$$

Appendix II. Sample Calculation of Test Results

Test Data

1. Motor rating = $1^1/_2$ horsepower
2. Picks per minute = 202
3. Average watts (oscillogram) = 1,600
4. Average watts (indicating meter) = 1,620
5. Rms watts (oscillogram) = 2,160
6. Rms amperes (indicating meter) = 6 5

Calculation of Oscillogram Test

7. Watts loss (Figure 10) = 305
8. Average output = 1,600 − 305 = 1,295
9. Average torque = $\frac{1,295}{746}\times\frac{5,250}{1,750}=5.25$
10. Rms torque (Figure 10) = 7.5
11. Assumed average torque at 202 picks (Figure 10) = 5.00
12. Average torque correction, $a=5.00-5.25=-0.25$
13. Corrected rms torque = $rms_c=\sqrt{7.5^2-2(0.25)(5.25)+(0.25)^2}=7.4$
14. Corrected losses (Figure 10) = 295

Calculation of Indicating Instrument Test

15. Horsepower at 6.5 amperes (Figure 9) = 2.5
16. Efficiency at 2.5 horsepower (Figure 9) = 0.86
17. Rms loss = $2.5\times 746\ \frac{(1-.86)}{.86}=305$ watts
18. Average ouput = 1,620 − 305 = 1,315 watts

Then proceed through steps 9 to 14 inclusive.

No Discussion

A Manually-Operated Spring Mechanism for Medium Voltage Oilless Circuit Breakers

B. W. WYMAN
MEMBER AIEE

E. J. CASEY
MEMBER AIEE

Synopsis: Magnetic oilless circuit breakers rated 2,300 to 15,000 volts require high contact closing speeds in order to prevent excessive arcing during closing. As these contact speeds cannot be obtained manually, it has never been possible to operate magnetic circuit breakers of this class by manual mechanisms of the type frequently used to operate oil circuit breakers. In every case where medium voltage magnetic circuit breakers were applied, it was necessary, therefore, to install a reliable source of closing power. This requirement constituted a serious application handicap in some locations where a reliable source of closing power (normally storage batteries) is difficult and expensive to install. This paper describes a new type of mechanism for operating magnetic oilless circuit breakers rated 2,300 to 15,000 volts, which has been developed especially for such applications. Energy is manually supplied to this mechanism where it is stored in heavy compression springs until it is released to close the circuit breaker. Unlike previous mechanisms, when this mechanism is released, the springs transfer their energy to a rotating mass which in turn drives the circuit breaker contacts. As this rotating mass accelerates until the circuit breaker contacts meet, its entire energy is available for closing and latching the circuit breaker against the magnetic retarding forces of high current short circuits if the circuit breaker should be closed accidentally on a faulted circuit.

FROM the beginning of the electrical industry, many indoor oil circuit breakers, rated 15 kv and below, have been closed manually by hand-operated lever-type mechanisms. This type of operation was generally successful as long as short circuit currents were small. When short circuit currents increased to a certain value, however, the closing force and speed which an operator could supply manually were inadequate to close and latch the circuit breaker without stalling at the moment the contacts touched due to the high magnetic retarding forces of the short circuit current through the contacts. As these magnetic retarding forces varied as the square of the short circuit current, higher values of current actually reversed the motion of the contacts during the closing stroke. This sometimes resulted in excessive pressures being generated within the circuit breaker tank. For safety to personnel, therefore, the application of oil circuit breakers with manual mechanisms was limited to those locations where the maximum available short circuit current did not exceed 12,500 amperes. In locations where the available short circuit current exceeded this value, solenoid or other types of power operated mechanisms were used.

When magnetic air circuit breakers were developed for these voltages, it was found that higher closing speeds were necessary than had been common with oil circuit breakers to minimize arc prestriking between the contacts during closing. This was due to the lower dielectric strength of the air between the contacts as compared to oil in the oil circuit breakers. This meant that these oilless circuit breakers could not be operated by lever-type manual operating mechanisms even on load currents, and electrical operation was essential. Electrical operation was obtained on most magnetic oilless circuit breakers by means of solenoid mechanisms. In January 1946, a special solenoid mechanism using a flux shifting double air gap principle with high final output force was described before the Institute, which was capable of closing and latching magne-blast circuit breaker contacts on short circuit currents up to the full momentary current rating of the circuit breaker without disturbance or stalling of contacts.

Any solenoid mechanism, however, requires a reliable source of control power. As the most reliable source of power was normally considered to be storage batteries, they were used wherever possible. For isolated applications where storage battery installations were impractical, rectified alternating current from a control power transformer was used. Where these happened to be incoming line circuit breakers, however, the control power transformer had to be connected ahead of the circuit breaker in order for it to be energized when the circuit breaker was open.

This practice had the disadvantage that the circuit breaker afforded no protection in case of a short circuit in the control power transformer. For such isolated locations therefore, manual closing was desirable if some type of manual mechanism were available which had output force and speed characteristics similar to the output force and speed characteristics of the special high force solenoid mechanisms. A manual mechanism fulfilling these requirements obviously could not be of the simple hand-lever type, but would have to be of a stored energy type in which the charging energy could preferably be supplied by hand.

As magnetic air circuit breakers became more and more generally used in utility applications, various utility groups, such as the Edison Electric Institute and the Association of Edison Illuminating Companies, outlined the necessity for some type of manually operated stored energy mechanism which could be used to close magnetic-type oilless circuit breakers for locations where a satisfactory electrical

---

Paper 49-93, recommended by the AIEE switchgear committee and approved by the AIEE technical program committee for presentation at the AIEE winter general meeting, New York, N. Y., January 31–February 4, 1949. Manuscript submitted August 12, 1948; made available for printing December 20, 1948.

B. W. WYMAN and E. J. CASEY are with the circuit breaker division of the General Electric Company, Philadelphia, Pa.

control power source could not be obtained.

Requirements for Mechanism

In initiating the development of a manually operated stored energy mechanism to close magne-blast circuit breakers, the following requirements were established:

1. The mechanism should close the circuit breaker contacts with a closing speed at least equal to, or greater than 10 feet per second.

2. The mechanism should possess sufficient energy to not only close and latch the circuit breaker contacts on normal load currents, but also should close and latch the circuit breaker contacts without disturbance if the circuit breaker were closed accidentally on a short circuit up to the momentary current rating of the circuit breaker.

3. The mechanism should be capable of closing the circuit breaker with a minimum of time and effort on the part of the station attendant.

4. The mechanism should be sufficiently compact to be mounted on the front of the magne-blast circuit breaker without interfering with its installation in the metal-clad switchgear unit.

5. For safety to station attendant, the mechanism should be capable of closing and latching the circuit breaker with the door of the metal clad switchgear unit closed.

Figure 1. Experimental sample of mechanism using gun powder driven piston driving interposed mass

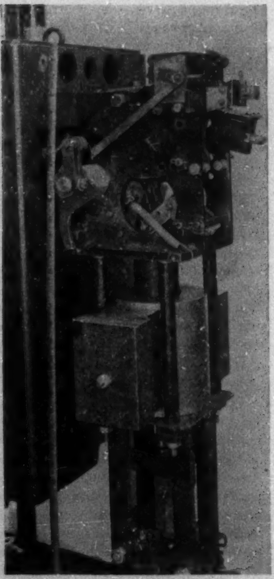

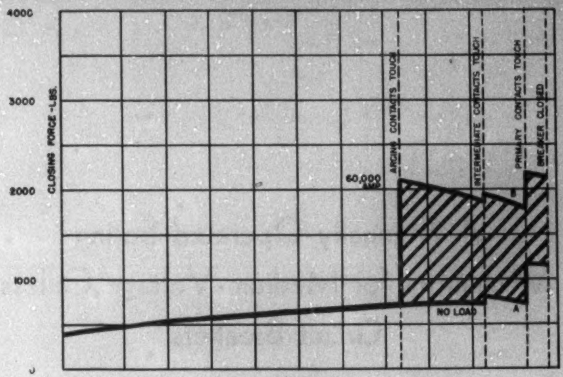

Figure 2. Closing force required at magne-blast circuit breaker linkage

A. Closing no-load. B. Closing against 60,000 amperes short circuit

Analysis of Possible Types of Mechanism

As it was realized that some source of stored energy would be necessary to meet the foregoing requirements, several sources of stored energy were considered. Among these were: a piston driven by high-pressure bottled gas; a piston driven by gun powder; a manually-charged spring which, when charged and released directly, drives the circuit breaker contacts; a manually-charged spring which, when charged and released, drives a mass which stores energy, and in turn drives the circuit breaker contacts. Table I lists some of the advantages and disadvantages of the various types of stored energy mechanisms which were considered.

A careful evaluation of the advantages and disadvantages of each type was made from the standpoint of: reliability; operation; maintenance and service; and manufacturing. To obtain a comparison from an operational standpoint

Table I. Comparison of Stored Energy Mechanisms

Type	Advantages	Disadvantages
1. Piston driven by gun powder	Light weight, compactness, pressure of 3,500 to 5,000 psi obtained. Burning gun powder permits small piston.	Extremely rapid burning of powder necessitates very large mass to store energy. Cylinder corrosion from high-temperature gases, requiring cleaning after operation. Gun powder must be kept in form of cartridges at all times.
2. Piston driven by high-pressure bottled gas	Compactness, ample energy and availability.	High-pressure gas must be kept available at all times. Available energy varies with temperature.
3. Direct spring drive	Simplicity, constant availability, and dependability.	Produces extremely high contact speeds. Produces greatest force at beginning of stroke, has little force at contact closing when required.
4. Spring-driven rotating mass	Simplicity, constant availability, and dependability. Capability of delivering full force at point of contact closing enabling circuit breaker to close and latch high momentary currents. Smoothness of closing operation. Instantaneous reclosing operation possible by energy stored.	Somewhat larger size and weight.

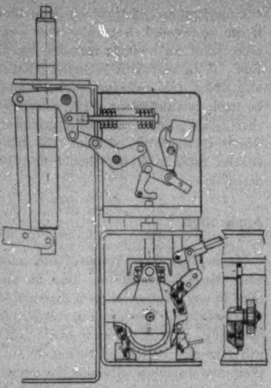

Figure 3. Cross section of manually-charged spring mechanism showing rotating mass driving crank shaft and connecting rod to supply closing energy to trip-free magne-blast circuit breaker linkage shown at top

between the various sources of stored energy, experimental samples of each type were built and tested. The most compact mechanism tested was the gun powder driven piston mechanism. Due to the fact that pressures up to 5,000 pounds per square inch are available from the gun powder, a very small piston could be used. Because of the extremely rapid burning rate of the gun powder, however, it was found on this mechanism that a mass had to be added which could be accelerated by the gun powder, and this mass then used to carry the circuit breaker closed, as shown in Figure 1. The disadvantages of this type of mechanism, which are listed in Table I, however, outweighed the advantages when compared with some of the experimental mechanisms using other sources of stored energy. A study of the advantages and disadvantages of each type built indicated that the spring-driven mass mechanism was the most desirable type for further development.

Development of Mechanism

In addition to satisfying the requirements already established, the output force supplied by the spring-driven mass mechanism must match the force requirements of the circuit breaker over the entire closing stroke, both when the circuit breaker was being closed on no-load, and when it was being closed on a faulted line with the maximum short circuit current flowing. Figure 2(A) shows the required force curve when closing the circuit breaker against no-load. It will be noted that the required closing force increases abruptly near the end of the closing stroke due to the heavy contact pressure. The abrupt increase in closing force required is the primary reason that the operating characteristics of the spring-driven mass mechanism are so superior to the direct-spring drive. With the direct-spring drive, most of the energy stored in the springs was already dissipated by the time the contacts touched. With a mass interposed, most of the spring energy in the first part of the stroke when the springs are fully compressed, goes into accelerating the mass, and all this energy is later available at the end of the stroke to overcome the contact pressure. The area under the force curve "A" in Figure 2 is the total energy required from the mechanism. Curve "B" in Figure 2 shows how this force curve is modified when the circuit breaker is closed on a short circuit current equal to the momentary current rating of the circuit breaker. It will be noted that the high magnetic retarding forces of the short circuit current through the circuit breaker contacts increase considerably the required force near the end of the closing stroke. The increase in area under this curve over that in curve "A" shown by the crosshatched area, represents an additional 1,010-inch pounds which must be available in the mechanism in order to prevent the circuit breaker contacts from stalling if they should be closed accidentally on a short circuit equal to 60,000 amperes. As the retarding force varies with the square of the short circuit current, this crosshatched area would increase to 1,800-inch pounds at 80,000 amperes. If the mechanism does not have available this amount of excess energy, the circuit breaker contacts would stall when trying to close against a short circuit, resulting in excessive arcing before the circuit breaker trip coil could operate to reopen the circuit breaker, possibly with disastrous consequences.

Under conditions of light load, or no-load, the excess energy which is provided for short-circuit conditions must be absorbed in some manner in the mechanism itself. As most of the circuit breaker operations will be under light load, or no-load, it is highly desirable that this excess energy be absorbed without shock to the mechanism or circuit breaker. The simplest manner of accomplishing this is to store the energy in rotation of the mass so that it acts as a flywheel to operate a crank shaft, and raise the mechanically trip-free circuit breaker linkage up on its prop, as shown in Figure 3. After the circuit breaker linkage has been raised up on its prop, the mass continues to rotate a partial revolution, thereby putting some compression back into the springs. The next manual charging of the springs, therefore, requires less energy input. If, however, the circuit breaker had closed on a heavy short circuit on the previous operation, there would be very little excess rotational energy left in the flywheel, and the next manual charging would have to supply almost the total spring energy. As this manual charging is obtained from a simple hand jacking on the rotating mass, it means that a few extra strokes will be required on the next operation. As the crank shaft motion

Figure 4A. Travel curve of circuit breaker contacts and crank shaft connecting rod when closing the magne-blast circuit breaker on no-load

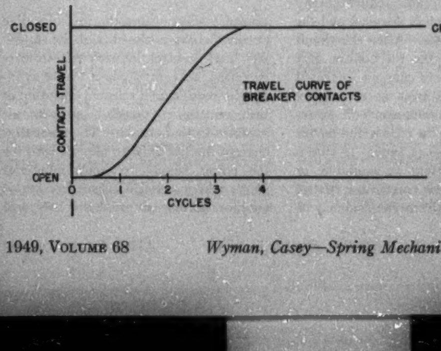

Figure 4B. Travel curve of circuit breaker contacts and crank shaft connecting rod when closing the magne-blast circuit breaker against a short circuit current of 60,000 amperes simulated by precompressed springs

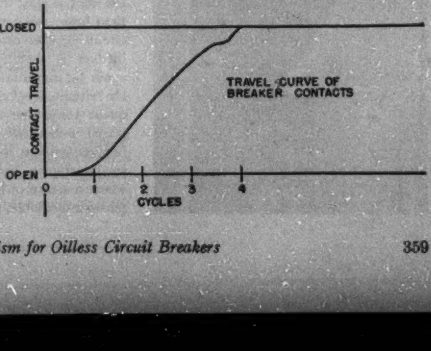

Figure 5. Magne-blast circuit breaker equipped with manually-charged spring operating mechanism ready for installation in metal clad switchgear. Charging handle shown in position

raising the crank linkage on its prop is a smooth (1-cosine) curve, this arrangement produces an extremely smooth operation of the circuit breaker contacts, both when closing against no-load and full short-circuit current. It eliminates the necessity of any buffers or dashpots required with most mechanisms, because the velocity of the contacts reduces smoothly to zero as the crank shaft reaches its uppermost position.

Figure 4(A) shows the travel of the circuit breaker contacts when closing against no-load. To determine the proper ratio of mass and compression springs to be used for the best over-all operation, tests were first made in which the short circuit magnetic retarding forces on the contacts were simulated by heavy additional springs fastened to the contacts. Figure 4(B) shows the travel of the circuit breaker contacts when closing against this extra retarding load with the ratios of spring and mass which were finally established for best operation. It will be noted that no stalling occurs in the contact travel when closing in against the maximum retarding force, and that actually only a very slight deviation can be seen between the travel at no-load and full retarding load.

Figure 6. Manual charging operation of spring mechanism on magne-blast circuit breaker installed in vertical lift metal clad switchgear and raised to operating position

After the best ratio of spring and mass had been determined, complete series of short circuit closing tests were made on the magne-blast circuit breaker with the circuit breaker closing and latching against fault circuits varying from no-load up through the momentary short circuit rating. A partial summary of these tests is shown in Table II. In these tests, the circuit breaker closed successfully and latched currents up to 92,000 amperes without excessive arcing at the contacts. As the mechanism uses the same mechanically trip-free linkage as is used on solenoid-type magne-blast circuit breakers, the tripping characteristics are unchanged, and the normal tripping time from trip impulses to interruption time varies between four and five cycles. Any standard means for tripping the magne-blast circuit breaker may be used when operated by this manually-charged spring mechanism; such as d-c potential trip, a-c potential trip, or instantaneous overcurrent trips energized by current transformers. Figure 5 shows a magne-blast circuit breaker equipped with a manually-charged spring mechanism.

Operation

Normal operation of the manually-charged spring mechanism is to first manually charge the springs by the jacking motion, as shown in Figure 6, which rotates the mass carrying the crankshaft just over center against a latch. To close the magne-blast circuit breaker at any time later, this latch is released and the circuit breaker closes. After the circuit breaker is closed, the mechanism may again be immediately charged so that if the circuit breaker trips at any subsequent time, the mechanism can be released immediately to reclose the circuit breaker without loss of time. In case a small tripping battery is available, or where a source of low current a-c control power is available, the mechanism may be equipped with an electrical release, so that it can be released electrically from a remote point for a single reclosing operation. If an automatic reclosing relay is also added, this reclosing operation may be made instantaneous. The extremely short closing time of the mechanism (three cycles after releasing the trip) enables rapid reclosing should that be desirable.

Application

Magne-blast circuit breakers with manually-charged mechanisms may be applied in any location where a dependable source of closing power is not available for operating solenoid mechanisms. This will generally be limited to remote stations, and usually to incoming line circuit breakers only. After the incoming line circuit breaker is closed, and the station bus and control power transformers energized, a-c control power will be available for rectifier and solenoid operation of the remaining magne-blast circuit breakers in that station. The manually-charged mechanism also may be used for the power supply to small industrial plants where a single circuit breaker is used for short circuit protection only, and

Figure 7. Magne-blast circuit breaker equipped with manually-charged spring operating mechanism removed from vertical lift metal clad switchgear

Table II. Short Circuit Test Data

3-Phase 60-Cycle Closing and Latching Tests

Test	Current Maximum Loop Peak	Current Maximum Loop Rms	Closing Speed, Feet Per Second	Degrees Excess Mass Rotation to Recharge Spring
1	1,130	680	16	67
2	1,250	750	16	66
3	65,000	39,000	16	62
4	69,000	42,000	16	67
5	87,000	51,000	16	62
6	87,000	51,000	16	62
7	105,000	61,000	16	54
8	100,000	63,000	16	54
9	152,000	92,000	16	41

where a control battery installation is not justified.

Summary

By means of the new manually-charged spring mechanism, magnetic oilless circuit breakers rated 2,300 to 15,000 volts for the first time may be applied where no dependable source of electrical control power is available. The output force of this mechanism is such that it will close and latch magne-blast circuit breakers against their full momentary current rating without excessive contact arcing, or without danger to operating personnel. Despite the high output force available, this mechanism is so designed that it absorbs without shock all excess force not required by the circuit breaker when it is closed on no-load, and therefore provides extremely smooth operation.

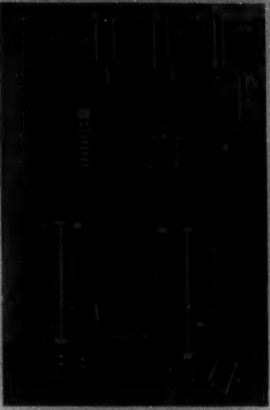

Figure 8. Close-up view of manually-charged spring operating mechanism with cover removed to show rotating mass and springs

References

1. Magne-Blast Circuit Breaker for 5,000-Volt Service, R. W. Boehne, L. J. Linde. AIEE Transactions, volume 59, 1940, pages 202–08.

2. A Magnetic Type Air Circuit Breaker for 15,000-Volt Services, L. J. Linde, B. W. Wyman. AIEE Transactions, volume 63, 1944, pages 140–44.

3. New Solenoid Mechanism for Magne-Blast Breaker, B. W. Wyman, J. H. Keagy. AIEE Transactions, volume 64, 1945, pages 268–74.

4. The Development Design, and Performance of Magnetic Type Power Circuit Breakers, L. J. Linde, B. W. Wyman. AIEE Transactions, volume 65, 1946, pages 386–93.

Discussion

Robert H. Nau (University of Illinois, Urbana, Ill.): I appreciate and am very much interested in the story of the development of the mechanically-stored-energy closing mechanism for the magne-blast circuit breaker of the General Electric Company. The given information is apparently accurate, and is quite convincing in that any remote installation may be assured the acme of protection by the "extremely smooth operation" of the main magne-blast circuit breaker on the incoming circuit.

Inasmuch as I and many other design and development engineers are fairly well informed, theoretically, concerning the perversity of kinetic energy of a moving mass I ask the authors to give to us, a complete technical discussion of the total mechanism used to impart the kinetic energy to a moving mass. That part of the mechanism used to harness this kinetic energy and hence deliver the positive closing-force to the hinged or pivoted contacts should be discussed. In order to clearly illustrate the action, I further ask the authors to support their discussion by sufficiently detailed elevation drawings, with legends.

By the general text of the paper, I gather that the mechanism is adequate to positively close the magne-blast circuit breaker only once against the optimum short circuit for each charge of hand-pumped mechanically-stored energy. Is this correct? I ask because the text in the section on "Operation" might give reason for implication that two closings per hand-pumped charge may be expected. I suspect that the authors meant to include that the circuit breaker would respond to a reclosure provided the station operator went to the particular circuit breaker and hand charged the mechanism after the circuit breaker had been closed, but before the circuit breaker was called upon to perform the reclosure cycle.

I ask another question. Can you now build or do you have the data for building one of the mechanically-stored-energy closing mechanisms for the magne-blast circuit breaker which will provide two closings of the circuit breaker on one hand-pumped charge for each of the conditions:

1. Both closures being against the optimum short circuit?
2. The first closure against rated full-load, and the second against optimum short circuit?

One more question. How will the 1-closure and the 2-closure mechanisms compare in space requirements, in weight, and in cost to the customer?

Knute Falck (Philadelphia Electric Company, Philadelphia, Pa.): The spring-operated mechanism described in this paper meets a real need. This may be further emphasized by pointing out that one of the major applications would be on customers' installations with single service. In most such cases the use of a battery is undesirable both from the cost and maintenance angle. Rectifier closing requires a tap on the line side of the circuit breaker which also is objectionable and introduces a metering problem. In general, the same difficulties are present in the power companies' own isolated installations.

The authors' method of analysis of the problem is thorough and systematic and their selection of this particular type of spring mechanism appears wise. The consideration given to the ability of the circuit breaker to close against a short circuit is well justified because the inherent characteristics of air circuit breakers of this voltage class are such that manual closing is unsafe, and if the circuit breaker mechanism is not capable of closing the circuit breaker against a short circuit, then it is no longer a truly protective device but a hazard.

Judging from the paper, it is believed that the spring mechanism subjects the structure to less shock and vibration than a solenoid mechanism, but it may be possible that the forces have been redistributed sufficiently to unbalance the previous over-all design and cause relay contact troubles. Has this been thoroughly tested?

One of the requirements listed is that the mechanism should be capable of closing and latching the circuit breaker with the door of the metalclad switchgear unit closed. The text refers to the jacking operation illustrated by Figure 7. This figure shows the door open. Is it correct to assume that the requirement has been met and that the door may be closed and the circuit breaker closed from the outside?

Has consideration been given to developing this type of mechanism for higher-voltage circuit breakers possibly including a motor operated charger?

The general impression of this mechanism is that it represents an effective application of fundamentally sound principles.

J. Stanley Brown (Duquesne Light Company, Pittsburgh, Pa.): The device discussed appears to be a practical solution to a problem that is sometimes met in practice.

We have recently had occasion to view with interest, a "bottle" operated mechanism for operation of 34.5-kv interrupter-type disconnecting switches. It performed very well. There is the possibility for application of a manually-stored energy closing and tripping device in this field because there is no place for operator hesitancy in operating disconnecting switches equipped with plunger or other type of interrupter units.

This new closing device, when proved in use, should be made available on competitive equipment.

It seems objectionable to be required to open the cubicle door to be able to manually charge the spring. This objection should be relatively easy for the designers to overcome.

Apparently the amount of stored energy left over after a normal closure is adequate for another normal closure, but not enough for a closure into a maximum fault. Therefore, if it is desirable to leave the circuit breaker set up for reclosure, the spring should be fully charged by the operator after the initial closing of the circuit breaker. This all then would seem to require some foolproof manner of assuring that the operator fully charges the spring. This subject is not clarified by the authors in their paper.

The powder- and bottle-operated mechanisms have appeal in those cases where it is desirable to leave the circuit set up for one or more reclosures. In the case of the powder-operated mechanisms, fouling should not be a problem when the proper ammunition is used.

Apparently, the greatest advantage of the accelerated mass design is associated with the self-snubbing shape of the closing curve permitted by the crank shaft action, while still permitting near maximum force to be available at the same time.

The authors should be complimented on their disclosure.

H. V. Nye (Allis Chalmers Manufacturing Company, West Allis, Wis.): This paper covers an interesting development of a manually-operated spring-closing mechanism for magnetic circuit breakers of the oilless type, for use in locations where no other means of operating power is available. Specifically designed for these locations as described in the paper, the mechanism seems to meet all of the requirements for such a device.

The discussion of alternative types of mechanism is interesting and indicates that considerable investigation of a gun powder operated mechanism was undertaken. The paper does not disclose, however, that an equally exhaustive investigation of a bottled-gas operator was conducted.

It seems to the writer that the mechanism described in this paper, although adapted to the application outlined, does not meet the need for an emergency closing device which can be applied to operate a solenoid-operated circuit breaker in case of control power failure or solenoid failure. The need for such an emergency closing device seems amply evident from the number of engineers who are asking for it. The spring-closed mechanism of this paper makes an excellent alternative closing mechanism but is distinctively an alternate to solenoid closing.

The disadvantages listed for the bottled-gas-driven piston are perhaps distinct disadvantages for any mechanism which is to be used for normal operation, but I cannot see that they are of importance if this method of operation is applied to an emergency closing device where a continuous and considerable supply of the operating gas is by no means essential.

To the advantages of this type of device can be added the statement that it is capable of being made as an auxiliary device for use in case of the failure of the source of power usually depended on, due to the compactness of the device and the facility with which it can be combined with a solenoid operated mechanism.

Consequently, it is my belief that circuit breaker engineers still have the problem of producing an auxiliary closing device that can be applied to the usual solenoid mechanism for emergency operation. Bottled-gas operation seems to be a distinct possibility for such an auxiliary operator, but does not preclude the use of other means. It does seem, however, that such a device must be very compact and comparatively inexpensive, and I believe the use of bottled gas has decided advantages from the standpoint of economy and availability.

Looking over the diagram showing the closing force required for closing in against a fault current compared with no-load operation, Fig. 3 of the paper will serve to impress on the reader the magnitude of closing force which must be available for such operation. It illustrates the problem a circuit breaker designer has in having this force available and yet controlling the operation under normal conditions so that the impact will not injure the operating mechanism or breaker. It might have been interesting to bring out the extent to which these required force variations can be equalized for the operator by the proper arrangement of levers and rotating centers in the mechanism itself. The methods employed in absorbing excess energy at the end of the closing stroke are also very important and might have been discussed.

C. E. Winegartner (Cleveland Electric Illuminating Company, Cleveland, Ohio): This manually-charged spring mechanism almost fills a long-felt need for a reliable source of closing power at a remote station with only a few circuit breakers, without the necessity of installing and maintaining a control battery. Almost, because it leaves the art of a-c tripping, without much needed improvement. If tripping batteries must be provided, then some of the advantages of manual closing is lost.

Either the contacts of circuit opening protective relays should be improved so that they can rupture without excessive maintenance the maximum short-circuit currents to which they may be subjected, or some form of network transformer should be developed into which the current transformers would feed, and the output used for tripping through protective relay contacts. With such improved a-c tripping, this manual operator promises better and more economical power supply to isolated load centers served by a few circuit breakers, with the improved service of a 1-shot reclosure, and without a battery problem.

B. W. Wyman and E. J. Casey: The authors are extremely gratified with the widespread interest which has been exhibited in the spring mechanism recently developed to manually operate the magne-blast circuit breaker. The discussions indicate that some points were not made entirely clear in the paper. Nye and Brown have both brought up the subject of the feasibility of operating with bottled gas rather than springs. The authors agree with Nye that there may be a place for bottled-gas operators for emergency operation of solenoid or compressed-air mechanisms. It is extremely doubtful, however, whether many station attendants would care to use bottled gas as a regular thing for all operations of a circuit breaker which had no source of electrical control power. To provide such operation with bottled gas, would require an appreciable reserve storage capacity of bottled gas maintained at all times to insure continuity of service during storm periods when a large number of trip-outs may follow each other in a short period of time. For manual operation under these conditions, the spring operator which can be charged by hand offers a distinct advantage.

Brown also questions whether some means of foolproofing has been added into the operation of the mechanism to prevent closing if the springs have not been completely charged. This is taken care of inherently in the design by the rotating mass starting position which must be at the upper end of the crank shaft motion to be released to close the circuit breaker. In this position the springs are always in the fully charged position, and therefore capable of closing and latching the circuit breaker against the maximum short-circuit current rating of the circuit breaker. This feature makes the mechanism more foolproof than any other possible method because the mechanism can not be released until the springs have been fully charged.

The charging operation illustrated in Figure 7 shows a man, manually charging the springs prior to closing the circuit breaker with the door of the metal-clad compartment closed. He would then close the door before releasing the springs to close the circuit breaker so that he would be afforded the full protection of the metal-clad structure during any operation of the circuit breaker.

Falck has questioned whether the jacking motion may be performed also while the door is closed. To do this would require a slot in the door for the manual handle to enter which could be included in any installation where this was considered desirable. The reduced amount of shock which this circuit breaker affords during a closing operation has been thoroughly tested to insure that it will not cause faulty operation of relays mounted on the equipment door. The primary reason for the reduction in shock is that excess energy is absorbed smoothly in the springs without being transmitted either to the circuit breaker frame or equipment structure. A-c tripping is possible without auxiliary tripping batteries through the use of over-current a-c trip coils mounted on the front of the mechanism if d-c tripping batteries are not available. Such trip coils provide accurate, positive operation on short-circuit currents where the magnitude of the current is high. They may however be less positive in their pick-up on overload currents near the pick-up point.

Nau questions whether two closing operations may be accomplished with this mechanism from one manual jacking of the springs. The inherent design of the mechanism is such that one closing operation is provided by each release of spring energy during a revolution of the rotating mass. Only one closing operation may therefore be obtained from each manual charging operation. As pointed out in the paper, this charging operation of the springs is independent of the position of the circuit breaker and the springs may be recharged after the circuit breaker is closed and latched. This energy is stored ready to reclose the circuit breaker immediately following a trip-out at any later time. This reclosing operation could be initiated automatically by reclosing relays, providing a small battery were available to release the spring latch.

A New 69-Kv Compressed-Air Circuit Breaker

B. P. BAKER
FELLOW AIEE

E. FRISCH
MEMBER AIEE

Synopsis: A metal-enclosed 3-phase 69-kv 3,500,000-kva 2,000-ampere compressed-air circuit breaker of the orifice type has been developed for outdoor service. The metal enclosure has six condenser bushings extending through the roof for connecting the circuit breaker terminals to the metal-clad bus structure. Each pole of the circuit breaker consists of an air reservoir, blast valve, isolating switch, and an interrupter. The interrupter assembly includes a moving-contact assembly, two orifice-type stationary contacts, and two exhaust gas receiving chambers, all clamped together by four spring-loaded wood Micarta rods. The isolating switches of the three poles are gang-operated by a single pneumatic mechanism mounted on the air reservoir of the center pole.

This circuit breaker has successfully passed all its commercial tests and has interrupted 37,500 amperes with 44 kv across a single pole.

IN LARGE metropolitan districts, such as Chicago, Philadelphia, and New York, the increasing power requirements of the congested residential and business districts necessitate the use of higher voltages for economical transmission and power distribution.

As the voltage increases, the necessary precautions to protect the power company personnel and the public from the attendant hazards become increasingly difficult and exacting. Not only must direct contact with the electric equipment be prevented and the danger of fire be reduced to a minimum, but it also is necessary that the operation of the equipment does not produce noise, radio interference, visible flashes, or other effects which in any way are annoying or disturbing to the public. In addition, outages must be limited to minimum, fault disturbances must be localized as much as possible, and the equipment must require only infrequent servicing and inspection. A practical solution for satisfying these requirements is offered by outdoor metal-enclosed switchgear which has gained wide acceptance.[1] Although the first cost is somewhat higher than for conventional equipment, it can be justified on the basis of lower installation cost, higher safety, fewer service interruptions, and reduced maintenance.

For a pioneering installation of this type on a 69-kv system capable of delivering 3,500,000 kva under fault conditions, the choice of a circuit breaker required considerable study. In general, there has been a tendency in this country to use compressed-air circuit breakers for indoor powerhouse service up to 34.5 kv, while oil circuit breakers are used for outdoor service up to the highest voltages. Since the circuit breakers for this installation will be installed outdoors, the normal selection, according to this practice, would have been the outdoor oil circuit breaker. Other considerations and requirements made it desirable, however, to extend the range of the indoor compressed-air circuit breaker and mount it in a weatherproof enclosure for this service.

Very satisfactory experience has been obtained with 34.5-kv indoor compressed-air circuit breakers when mounted in weatherproof metal housings for outdoor service. Also, several special 12-kv high-speed compressed-air circuit breakers have given an excellent account of themselves on the Pennsylvania Railroad system.[2] These circuit breakers, of indoor design, are placed in metal enclosures and installed outdoors.

Historical Review of Compressed-Air Circuit-Breaker Practice

The compressed-air circuit breaker first made its appearance about 20 years ago in Europe, where high cost of materials and low labor cost favor this type of circuit breaker. As a result, the efforts in Europe have been concentrated mainly on the development of compressed-air circuit breakers.

In this country, where conditions and requirements are different, oil circuit breakers are used for practically all high-voltage outdoor service and are available for up to 10,000,000-kva interrupting capacity.[3] Practically all development of compressed-air circuit breakers has been directed toward heavy-duty indoor powerhouse applications because of the insistent demand for reduction in fire hazard for this service. Circuit breakers of this type are available for 15-kv and 34.5-kv service with interrupting capacities of 2,500,000 kva. This line of circuit breakers,[4,5] with a 10-year service record, has proved very satisfactory and has received general acceptance as standard equipment.

For compressed-air circuit breakers, the orifice or nozzle type has become the general design practice in Europe where the kilovolt-ampere requirements are comparatively low. In this country, however, the cross-blast type of interrupter is used exclusively for 15- and 34.5-kv ratings, because it was found to be better suited for the much higher interrupting and current-carrying requirements.[6] Circuit breakers with cross-blast interrupters require only a single set of contacts, are simple in construction, and are easily accessible for inspection. They are available in up to 4,000- and 5,000-ampere current ratings, and are capable of interrupting in excess of 100,-

---

Paper 49-94, recommended by the AIEE switchgear committee and approved by the AIEE technical program committee for presentation at the AIEE winter general meeting, New York, N. Y., January 31–February 4, 1949. Manuscript submitted November 16, 1948; made available for printing December 20, 1948.

B. P. Baker and E. Frisch are with the Westinghouse Electric Corporation, East Pittsburgh, Pa.

The development of the circuit breaker described in this paper was undertaken as a natural part of the development of metal-clad equipment to meet the requirements of A. M. de Bellis, Consolidated Edison Company of New York.

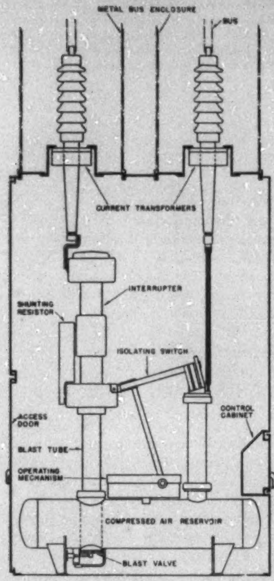

Figure 1 (left). Sectional view showing a 69-kv, 2,000-ampere, 3,500,000-kva compressed-air circuit breaker mounted in an outdoor dust-proof enclosure

000 amperes at 15 kv without the use of a shunting resistor. Some experience, however, has been gained in this country with the orifice type of circuit breakers for high-voltage outdoor service.[7,8] The results generally have been satisfactory, but because of the excellent performance of highly-developed dead-tank oil circuit breakers, their use has been confined to a few trial applications.

Summarizing, compressed-air circuit breakers of the orifice type are used in Europe for indoor low-voltage service as well as for outdoor high-voltage service. In this country, we have cross-blast compressed-air circuit breakers indoors and oil circuit breakers outdoors, with the possibility of the orifice-type compressed-air circuit breaker entering the outdoor field. If higher voltages move indoors, it is probable that the requirements for current-carrying and interrupting capacities would favor the orifice type of interrupter for these voltages.

The Circuit Breaker and Its Enclosure

Figure 1 shows a schematic drawing of a pole unit of a recently-developed 69-kv 3,500,000-kva 2,000-ampere orifice-type compressed-air circuit breaker, mounted in a steel enclosure for outdoor service. The enclosure, containing separate compartments for each of the three poles, includes six condenser bushings with current transformers. Although the upper ends of the bushings are porcelain clad, they will not be exposed directly to the weather, but will extend into the bus enclosure, which is shown attached to the roof of the circuit breaker enclosure. Each compartment is provided with a door and ventilating louvers. The doors are sealed with rubber to exclude rain and dust. The louvers are provided with dust filters.

The center compartment of the circuit breaker enclosure has a built-in control cabinet in which is located the control panel, auxiliary switches, pressure switches, gauges, control valves, and various interlocking elements. The interlocking system prevents access to the circuit breaker compartments without first tripping the circuit breaker and opening the disconnect switches.

Figure 2 shows a single pole unit as shown schematically in the enclosure of Figure 1. Each pole consists of an air reservoir on which is mounted the other elements of the circuit breaker. The breaker, therefore, is not dependent upon the metal enclosure for support. The only points of attachment are at the base and at the power connections to the condenser bushings.

The blast valve is mounted in a tube extending through the reservoir. It is of the differential-area air-actuated type, easily removable from the under side of the reservoir without disturbing the superstructure.

Above the blast valve is a heavy Micarta blast tube. This tube also serves as the support for the interrupter and forms the insulation to ground.

The contacts of the interrupter are normally biased to the closed position by springs except during the interrupting period, and, therefore, a series isolating switch must be provided. The lower end of the interrupter forms the hinge support for the isolating switch. The stationary contact of the isolating switch is supported by a second Micarta tube mounted at the opposite end of the air reservoir. The isolating switches of the three poles are gang-operated by a single pneumatic mechanism which is mounted on the air reservoir of the middle pole. The three poles, therefore, are tied together mechanically by the isolating switch shaft, pneumatically by a common control for opening the blast valves, and electrically through a single control system.

Method of Circuit-Breaker Operation

A schematic diagram of a complete 3-pole circuit breaker with its pneumatic system is shown in Figure 3. When the blast valve opens, compressed air at 200 to 250 pounds per square inch is admitted through the blast tube and the lower exhaust chamber to the space surrounding the moving-contact assembly. This assembly consists of two pairs of moving and stationary contacts connected in series. The moving contacts normally are biased toward the closed position by means of heavy contact-closing springs. As a result of the pressure exerted upon the lower moving contact by the compressed air, the contact opens, thereby interrupting the circuit except for the residual current which flows through a shunting resistor connected across the lower pair of contacts. This resistor consists of a number of cast grids with mica spacers, clamped together and mounted in an insulating tube. The upper contacts open in slightly less than one cycle after the opening of the lower contacts, as a result of the throttling action of the narrow space between the upper contact holder and the upper insulating tube. Because of this delay, the fault current is transferred to the shunting

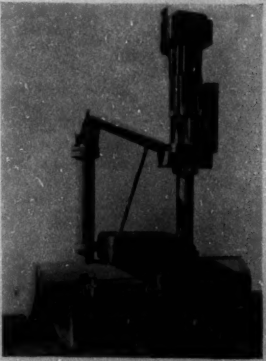

Figure 2 (right). Single pole unit of a 69-kv, 2,000-ampere, 3,500,000-kva compressed-air circuit breaker set up for interrupting tests in East Pittsburgh high power laboratory

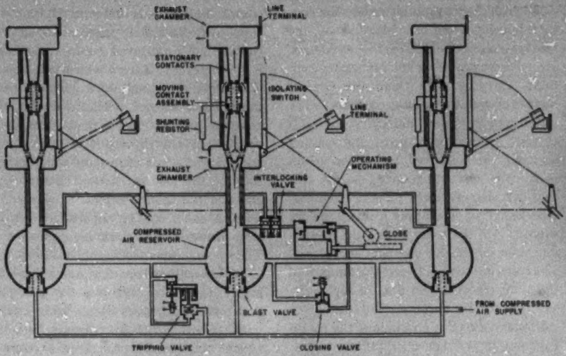

Figure 3. Schematic diagram showing the pneumatic system for a complete 3-pole compressed-air circuit breaker

Figure 4. Pneumatic mechanism for gang operation of the three isolating switches

Cover removed

resistor and greatly reduced before the upper contacts open.

When the moving contacts open, the orifice openings in the stationary contacts are uncovered. The high-pressure air forces the established arc toward the center of the opening and completely envelopes it with a high-velocity turbulent flow which sweeps the ionized gases through the hollow stationary contacts to the lower and upper exhaust chambers. Here, the gas is cooled before it is exhausted slowly to the surrounding atmosphere through mufflers. These restrictions to the free flow of the exhaust gases reduce noise and external demonstration to a minimum.

The three isolating switches are gang-operated by a single pneumatic mechanism through a rotating shaft and three wood Micarta rods. The shaft is connected to the piston of the mechanism through a rack and gear transmission, permitting 180 degree rotation. This places the mechanism in complete toggle in both the open and the closed position of the isolating switches. The movement of the piston is controlled by a sliding, cylindrical control valve on top of the mechanism cylinder. High-pressure air is admitted to either end of the valve as required, and causes movement of the valve to the corresponding operating position. In this position, the valve uncovers a port which admits high-pressure air to one side of the piston, resulting in either closing or opening the isolating switches.

At the same time, a second port is uncovered, through which the air on the other side of the piston is discharged to the atmosphere. This is required in order to obtain rapid opening of the isolating switches when they are being closed on a fault resulting in immediate tripping. The diameter of the "opening" end of the valve piston is slightly larger than the diameter of the "closing" end. Therefore, if control air for opening and closing of the isolating switch is applied to the mechanism at the same time, preference will be given to the opening operation. The circuit breaker, therefore, is pneumatically trip free.

High-pressure air for opening the isolating switches is taken from the blast tube on the middle pole. The air passes through an interlocking valve, connected pneumatically to the blast tubes of the two other poles. By this means, the high-pressure air is prevented from reaching the operating mechanism and opening the isolating switches until all blast valves are open and pressure is available in the interrupters for arc extinction. In addition, the blast valves are prevented by the electrical control from reclosing until the isolating switches are opened sufficiently to remove the voltage across the interrupters.

The operation of the three blast valves is controlled by a single electropneumatic tripping valve, mounted on the middle reservoir. When the tripping coil is de-energized, the tripping valve admits high-pressure air from the reservoirs to the underside of the blast valves, forcing them tightly against their seats. When the tripping magnet is energized, the tripping valve shuts off the high-pressure air supply and discharges the air under the blast valves, which then open by the air pressure on a portion of the upper side of the blast valves. The circuit breaker is closed by energizing the electropneumatic closing valve, which admits high-pressure air to the operating mechanism and closes the isolating switches.

The design of the operating mechanism is illustrated in Figure 4, which shows the mechanism with the cover removed. The two shock absorbers, shown in this illustration, serve to slow the speed of the isolating switches in the latter part of their travel in both closing and opening directions to lessen the shock of operation.

The Interrupter

The interrupter consists of two copper-alloy stationary contact members which are bolted to the upper and lower exhaust chambers, and a self-contained moving-contact assembly which is mounted in a centrally-located contact housing. The exhaust chambers with the stationary contacts, the contact housing with the moving-contact assembly and two insulating tubes used as spacing members, are clamped together by four spring-loaded, wood Micarta tie rods. The shop assembly of the interrupter, therefore, is extremely simple, a fact which

Figure 5. Exploded view of complete interrupter

Except for the removable contact assembly, all interrupter parts are clamped together by the four wood Micarta tie rods will be evident from examination of Figure 5, which shows an exploded view of all interrupter parts.

The moving-contact assembly, shown on top of the contact housing in the exploded view, is a self-contained unit consisting of a contact-support casting in which are mounted the two sets of moving main and arcing contacts with their heavy stainless-steel closing springs. The main contacts consist of a cluster of contact segments, each with two contact springs, mounted in a contact holder around the silver-tungsten-tipped arcing contact. With the contact assembly in place in the contact housing, the closing springs, acting on the contact holders, force the ends of the contact segments and the arcing contacts against the flat ends of the hollow stationary contacts, and cover the orifices in these contacts. The current is carried from the upper to the lower contacts on a stationary copper-alloy contact sleeve on which the contact segments slide.

When high-pressure air enters the contact housing from the blast valve, the moving-contact holders, acting as pistons, are forced away from the stationary contacts, carrying with them the contact segments and the arcing contacts. The latter remain closed and carry the fault current momentarily until the contact segments have moved a fraction of an inch, thus preventing arcing on the current-carrying surfaces of the contacts. The flange of the upper contact holder extends into the lower end of the insulating tube when the contacts are closed. The narrow space between the flange and the tube throttles the flow of high-pressure air to the space around the upper stationary contact, and delays the establishment in this space of sufficient pressure to open the contacts. The throttling effect is adjusted so as to delay the opening of the upper contacts till slightly less than a cycle after the opening of the lower contacts. The throttle opening is enlarged as soon as there is movement of the contact holder, thus removing all restrictions to free air flow, required for interruption. This delayed contact opening is an important feature which has made it possible to design the contacts for maximum efficiency. The lower set of contacts, which opens first, must be capable of interrupting very high currents, but the rate of rise and the magnitude of the restored voltage is low because of the shunting resistor. For this duty, a small contact separation and a large orifice opening are most effective. The upper contacts will not be subjected to a high-current arc, but must handle highly inductive and capacitive loads such as transformer-magnetizing currents and cable-charging currents, both of which may involve considerable overvoltage. For this interrupting duty, a smaller orifice opening and considerably more contact separation give the best results.

The contacts can be inspected by removing an inspection cover from the contact housing and by forcing the contacts to the full-open position by means of a special contact withdrawing tool. This brings both the moving and stationary contacts into full view. For closer examination, or for replacement of contact parts, the complete moving-contact assembly can be removed from the interrupter, as shown in the exploded view.

Table I. 69-Kv 3,500,000-Kva 2,000-Ampere Compressed-Air Circuit Breaker

Single-Phase Interrupting Tests

Test Number	Voltage Across Single Pole, Kv	Rms Amperes Interrupted	Circuit Breaker Time		Reservoir Pressure, Pounds Per Square Inch
			To Main Current Interrupted, Cycles	To Residual Current Interrupted, Cycles	
2-87639	50	180	1.8	2.9	230
640	50	190	1.9	3.0	230
641	50	340	1.9	2.9	230
642	50	330	1.9	2.9	230
643	50	630	1.9	2.9	230
644	50	630	2.0	2.8	230
645	50	1,370	1.9	2.9	230
646	50	1,400	1.8	2.8	230
647	50	2,620	2.0	3.3	230
648	50	2,600	1.9	3.3	230
649	50	4,300	1.9	2.8	230
650	50	4,400	1.9	3.2	230
651	50	380	1.8	2.9	230
652	50	7,000	1.8	2.7	230
653	50	7,100	1.9	3.2	230
654	50	10,400	1.9	2.7	230
655	50	10,100	1.9	2.8	230
656	44	11,700	2.0	2.7	230
657	44	16,600	2.4	2.6	230
658	44	17,100	1.8	2.6	230
659	44	22,000	1.9	2.7	230
660*	44	22,400	2.3	3.1	230
661	44	30,300	2.2	3.0	230
662*	44	37,500	2.2	2.8	230
2-89597	60	220	1.5	2.6	200
598	60	220	1.8	2.9	200
599	60	470	1.6	2.8	200
600	60	450	1.6	3.2	200
601	60	750	1.7	2.8	200
602	60	820	1.7	3.1	200
603	60	1,600	1.9	4.0	200
604	60	1,530	1.8	3.5	200
605	60	3,000	1.9	2.9	200
606	60	2,800	2.0	3.0	200
607	60	4,560	2.0	3.5	200
608	60	4,560	2.0	3.0	200
609	60	7,200	2.0	3.0	200
610	60	7,200	2.0	3.0	200
611	60	420	1.8	3.0	200
612	60	10,500	2.0	2.8	200
613	60	10,500	1.7	2.7	200
614	66	420	2.3	3.0	200
615*	60	12,800	2.2	2.7	200
616	33	5,100	1.9	2.7	200
617*	60	22,500	2.3	2.6	200

* Magnetic oscillograms of these tests are shown in Figures 6 and 7.

Test Results

Table I shows the results of several series of consecutive tests. Nineteen of these tests were made at 60 kv with currents ranging from 220 amperes to 22,500 amperes. Seventeen were at 50 kv with currents ranging from 180 amperes to 10,400 amperes. Seven were made at 44 kv with currents ranging from 11,700 amperes to 37,500 amperes. All tests were on a single-phase basis with full voltage across the interrupter. The interrupter consisted of two sets of contacts in series, one shunted and the other unshunted. The interrupting effort, therefore, is made in two steps. The first step covers the period from application of trip-coil voltage until the arc is interrupted on the lower or shunted set of contacts. Column 4 of Table I gives the time required for this step, which is a minimum of 1.5 cycles and a maximum of 2.4 cycles. The second step covers the interruption of resistor current on the upper unshunted contacts. Column 5 of Table I gives the total circuit breaker time from the application of trip-coil voltage to the extinction of the resistor current, the minimum time being 2.6 cycles and the maximum

4 cycles. The tests at 44 and 50 kv were made with a reservoir pressure of 230 pounds per square inch; the tests at 60 kv, with 200 pounds per square inch pressure. The tests were made at pressures somewhat below the normal operating pressure of 250 pounds per square inch to check the interrupting ability under conditions corresponding to a second operation with the reservoir sealed off from the air supply system.

Figure 6 shows magnetic oscillograms of two high-current interruptions at 44 kv. One represents the capacity of the laboratory on a symmetrical current basis of 22,400 rms amperes. The other represents the full capacity on an unsymmetrical current basis giving 37,500 rms amperes. Figure 7 shows magnetic oscillograms of two high-current interruptions at 60 kv. Both were at the full capacity of the laboratory, one being symmetrical and the other unsymmetrical.

Table II. 69-Kv 3,500,000-Kva 2,000-Ampere Compressed-Air Circuit Breakers

Single-Phase Tests, Interrupting Charging Current to a Capacitor Bank with Approximately 300-Ohm Series Resistor

Test Number	Voltage Across Single Pole, Kv	Charging Current, Rms Amperes	Circuit Breaker Total Time, Cycles	Reservoir Air Pressure, Pounds Per Square Inch	Maximum Overvoltage, Kv	Number of Restrikes
2-89570	60	45	2.7	200	163	0
571	60	45	2.8	200	154	0
572	60	45	2.9	200	147	0
573	60	45	2.7	200	158	0
574	60	45	2.7	200	158	0
575	60	45	2.6	200	161	0
576*	60	45	3.0	200	157	1
577	60	45	2.8	200	161	0
578	60	45	2.8	200	133	0
579	60	90	2.7	200	149	0
580	60	90	2.5	200	161	0
581	60	90	2.5	200	154	0
582	60	90	3.0	200	129	0
583*	60	90	2.8	200	161	0
584	60	90	2.8	200	168	0
585	60	90	2.8	200	147	0
586	60	180	2.9	200	168	0
587	60	180	2.6	200	154	0
588	60	180	2.9	200	164	0
589	60	180	2.9	200	112	0

* Magnetic oscillograms of these tests are shown in Figure 8.

Table II shows a series of 20 consecutive interrupting tests, all of which were made with 60 kv across a single interrupter. These tests were made to simulate conditions when opening a circuit consisting of an unloaded cable. Except for the normal impedance of the power circuit, the current for this group of tests was limited to 45, 90, and 180 amperes respectively by the use of a capacitor load in series with approximately 300 ohms of resistance. All tests were made with a reservoir pressure of 200 pounds per square inch. Column 4 of Table II shows the total circuit breaker time for interruption, from the application of trip coil voltage to the extinction of the residual current through the circuit breaker resistor. The times are very consistent, being maximum 3 cycles and minimum 2.5 cycles. The oscillogram of *test 2-89576*, which is given in Figure 8, records the only reignition observed during this entire set of tests. This reignition occurred before the upper contacts were fully separated, and, as is apparent, the voltage reached before breakdown was less than the voltage on the following half-cycle, which seems to have been influenced very little by the reignition. Column 6 of Table II is a tabulation of the maximum instantaneous values of voltage reached during the interruptions. The second oscillogram in Figure 8 is typical, and shows an instantaneous value of 161 kv. The maximum voltage observed during the series of tests was 168 kv.

It should be noted that the tests shown in Tables I and II were made on the interrupter as finally developed, but mounted on an experimental reservoir without a series isolating switch.

Table III shows a series of consecutive tests made on the complete circuit breaker unit shown in Figure 2. Eleven of these tests were made at 44 kv, 220 pounds per square inch reservoir pressure, single phase, on a close-opening basis. The

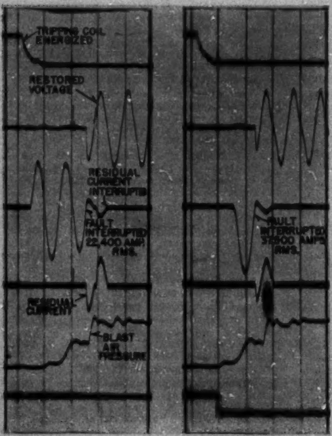

Figure 6 (left). Magnetic oscillogram showing single-phase current interruption of 22,400 and 37,500 rms amperes at 44 kv in 3.1 and 2.8 cycles respectively

Refer to Table I

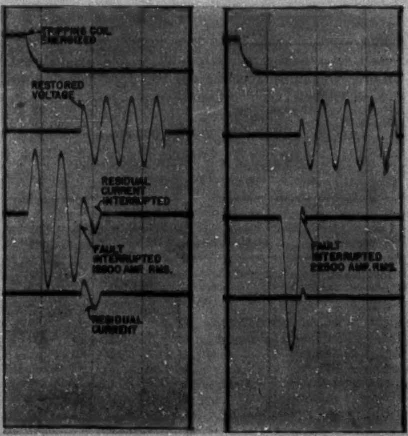

Figure 7 (right). Magnetic oscillogram showing single-phase current interruption of 12,800 and 22,500 rms amperes at 60 kv in 2.7 and 2.6 cycles respectively

Refer to Table I

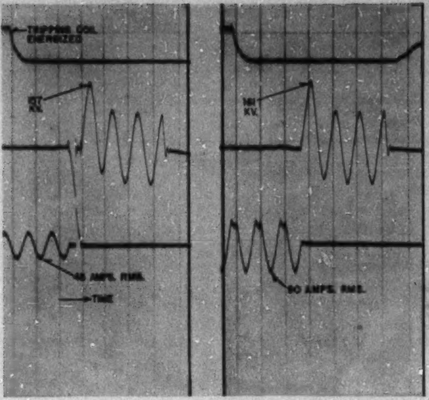

Figure 8. Magnetic oscillogram showing single-phase charging-current interruption of 45 and 90 rms amperes at 60 kv in 3.0 and 2.8 cycles respectively

Refer to Table II

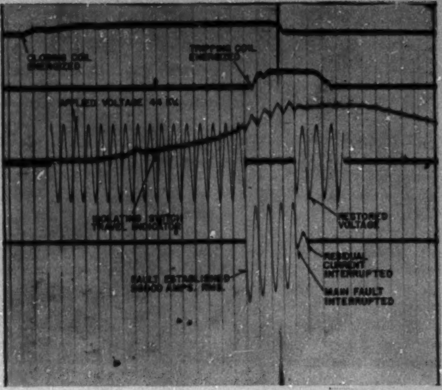

Figure 9. Magnetic oscillogram showing single-phase operation closing 26,000 rms amperes and opening 21,400 rms amperes

Fault duration 5 cycles including relay time. Refer to Table III

faults were closed on the isolating switch and opened in the interrupter.

The currents closed varied from 750 to 26,000 rms amperes. The currents opened varied from 710 to 21,400 rms amperes.

The circuit breaker was tripped by a current transformer and relay. When a high-speed relay was used, the total fault time, including relay and circuit breaker time, did not exceed 5 cycles.

Figure 9 shows the magnetic oscillogram of *test 2-91678*, when a current of 21,400 rms amperes was interrupted. At the conclusion of these tests, the interrupting contacts and isolating switch contacts were in excellent condition. Without cleaning or touching up, they successfully passed their momentary and 4-second tests at 57,500 and 36,500 rms amperes respectively. In order to demonstrate their ability to perform heavier-duty service, they were, without cleaning or touching-up subjected to momentary and 4-second tests of 100,000 and 59,400 rms amperes respectively, and were found to be in good operating condition at the conclusion of these tests. This circuit breaker also has passed the commercial impulse test of 350 kv, and a temperature test at 2000 amperes, 60 cycles, with a rise of 25.5 degrees centigrade.

Conclusions

Test results, simplicity, accessibility, safety, and ease of contact removal seem to indicate that this circuit breaker may find a field of usefulness for indoor service. When placed in a metal enclosure and equipped with condenser bushings, as shown in Figure 1, it appears to be competitive with oil circuit breakers, especially when used in combination with metal-clad bus structures. The circuit breakers, when equipped with porcelain weather casings, may be acceptable for general outdoor service, especially where current transformers and potential devices are not required.

Table III. 69-Kv 3,500,000-Kva 2,000 Ampere Compressed-Air Circuit Breakers

Single-Phase Close–Opening Tests, Reservoir Air Pressure, 200 Pounds per Square Inch, Circuit Breaker Tripped from Current Transformer Through Relay

Test Number	Voltage Across Single Pole, Kv	Rms Amperes, Closed	Rms Amperes, Interrupted	Duration of Fault Cycles	
2-91667	33	520	450	12	
68	44	750	710	12	
69	44	1,240	1,180	11.5	
70	44	2,000	Ampere setting	No oscillogram record	
71	44	2,100	2,200	5.0	
72	44	2,330	1,940	5.0	High-speed relay used in tripping circuit
73	44	4,000	3,900	5.0	
74	44	8,700	6,700	5.0	
75	44	9,600	9,200	5.0	
76	44	13,400	11,700	4.5	
77	44	18,800	15,400	5.0	
78*	44	26,000	21,400	5.0	

* Magnetic oscillogram of this test is shown in Figure 9.

References

1. METAL-CLAD UNIT-TYPE SWITCHGEAR FOR 33-KV SERVICE, C. H. Kreger. ELECTRICAL ENGINEERING (AIEE TRANSACTIONS), volume 65, June 1946, pages 360–68.

2. COMPRESSED-AIR CIRCUIT BREAKER IN A-C RAILWAY SERVICE, H. M. Wilcox, D. C. Harker. ELECTRICAL ENGINEERING (AIEE TRANSACTIONS), volume 64, March 1945, pages 141–44.

3. FIELD TESTS FOR DEVELOPMENT OF 10,000,000-KVA 230-KV OIL CIRCUIT BREAKERS FOR GRAND COULEE POWER PLANT, C. L. Killgore, W. H. Clagett. AIEE TRANSACTIONS, volume 67, part I, 1948, pages 271–87.

4. A 2,500,000-KVA COMPRESSED-AIR POWERHOUSE BREAKER, L. R. Ludwig, H. M. Wilcox, B. P. Baker. ELECTRICAL ENGINEERING (AIEE TRANSACTIONS), volume 61, May 1942, pages 235–40.

5. FIELD TESTS ON HIGH-CAPACITY AIR-BLAST STATION-TYPE CIRCUIT BREAKERS, H. E. Strang, W. F. Skeats. ELECTRICAL ENGINEERING (AIEE TRANSACTIONS), volume 61, February 1942, pages 100–04.

6. LARGE INDOOR POWER AIR BLAST CIRCUIT BREAKERS, G. E. Jansson. AIEE TRANSACTIONS, volume 67, part II, 1948, pages 1675–79.

7. A VERTICAL-FLOW COMPRESSED-AIR CIRCUIT BREAKER AND ITS APPLICATION ON A 132-KV POWER SYSTEM, H. A. P. Langstaff, B. P. Baker. ELECTRICAL ENGINEERING (AIEE TRANSACTIONS), volume 62, 1943, pages 188–92.

8. FIELD TESTS AND PERFORMANCE OF A HIGH-SPEED 138-KV AIR-BLAST CIRCUIT BREAKER, Philip Sporn, H. E. Strang. ELECTRICAL ENGINEERING (AIEE TRANSACTIONS), volume 61, January 1942, pages 1–6.

Discussion

P. L. Taylor (Allis-Chalmers Manufacturing Company, Boston, Mass.): We feel that the authors have done an excellent and thorough job of selecting, combining, and adapting the best principles developed in European air-blast circuit breaker practice, to achieve a 69-kv high interrupting capacity orifice-type indoor air blast circuit breaker design, arranged in an outdoor cubicle for application in congested residential areas.

The comprehensive series of tests reported on this circuit breaker further confirm evidence previously accumulated both in Europe and in the United States that the axial-blast contact arrangement of the orifice type circuit breaker is capable of excellent performance when interrupting currents of considerable magnitude. Western Europe is developing circuit breakers capable of interrupting 100,000 amperes and 3,000,000 kva.

The author's reference[8] on a 34.5-kv indoor station type air-blast circuit breaker, has been offered by them in substantiation of their statement that the cross-blast type of interrupter is used exclusively in the United States for 15- and 34-kv service because it is better suited for the higher interrupting and current carrying requirements.

To prevent misunderstanding, we should point out that the Jansson circuit breaker does not employ the cross-blast type of interrupter. It is provided with the contact arrangement usually associated with cross-blast circuit breakers, but the interrupting structure is of the orifice type. Thus it combines the advantages of both in what Mr. Jansson has called a cross-axial blast circuit breaker.

No doubt the authors have data to indicate the adequacy of 69-kv Micarta tubular insulation under the moisture condensation conditions encountered in outdoor metal-clad arrangements or they may have made special provisions to adequately control or eliminate the effects of such condensation. In either case the information would be of considerable interest to all.

Viewed fairly, this circuit breaker appears to fulfill many, if not most, of the special requirements for a high-voltage high interrupting capacity oilless circuit breaker for application in congested residential areas.

R. B. Shores (General Electric Company, Philadelphia, Pa.): The arrangement of an interrupter element and an isolator switch mounted on the unit's air storage tank has been used in several European air blast circuit breaker designs and results in a compact unit not requiring a separate framework to maintain alignment of the circuit breaker parts. Also, the rack and pinion type of operating mechanism with an overcenter arrangement to avoid springs and latches is simple, and has been in satisfactory use for some time on one American design of large indoor circuit breaker. However, this particular indoor 69-kv arrangement does not seem to lend itself to the use of a separating metallic barrier between the primary circuit elements of the circuit breaker and the mechanism. The cross-section of the circuit breaker in its enclosure indicates that inspection or maintenance of the mechanism must be performed by entering the primary compartment. It would be interesting to find out the user's reaction to the necessity of entering the primary compartment for any inspection of the circuit breaker mechanism, as to date most American circuit breakers have permitted the inspection or maintenance of the principle operating mechanism of either indoor or outdoor circuit breakers without necessarily getting dangerously close to primary circuit elements.

Reference in the paper has been made to electrical, mechanical, and pneumatic interlocks, and it would be inferred that these types back-up each other to give overlapping protection. However, it would appear from the schematic diagram that these interlocks are not successive stages against misoperation of some function of the circuit breaker, but are used independently depending on the convenience of each for the function to be interlocked. Is this correct, or is the failure for example of the pneumatic interlocking of the interrupting contacts, or of the blast valve, backed up by mechanical interlocking?

In considering the detail arrangements of the circuit breaker parts, it would appear that the location of the blast valve not only entails difficulties in inspection or maintenance, but might even act as a sump for the tank. Indoor compressed air circuit breaker tanks are normally provided with a blow-off valve as it is recognized that water may get into these tanks, especially during the initial placing in service of the circuit breakers. Is the blast valve inspection cover at the lowest point of the tank, and, if it is, has some means been provided to blow out the resulting sump?

Robert H. Nau (University of Illinois, Urbana, Ill.): According to a long established custom of the AIEE, the authors of a technical paper are more or less obligated to answer to the best of their ability all of the questions posed by an interested reviewer, providing he, the reviewer, has not by his investigative ability uncovered something which is considered confidential. Hence, I will assure you before I begin firing my questions that I have not been more intimate with this circuit breaker than having observed it casually and having studied the authors' present paper. Some of my questions may appear to have been answered by the text of the paper. In such cases I point out that the explanations have not been complete enough, and I would like for the authors to cover these particulars in greater detail. Please note that I have studied your paper forwards and backwards. Further, I have had considerable experience with contemporary circuit breakers, and hence know where to look for trouble points.

The abundance of test data on the new 69-kv compressed air circuit breaker substantiate its rating to interrupt short-circuit currents. However, you will note the restrikes or reignitions on each of the first oscillograms of each of Figures 6 and 8. Also, you will note that the second oscillogram of each of Figures 6 and 7 might be considered fortuitously lucky shots, catching the brunt on the little half-cycle of a highly asymmetrical current wave. There has been considerable contention concerning the validity of using oscillographic data for properly rating a circuit breaker when the arc is being quenched during the little half-cycle of a highly asymmetrical current wave. I refer you to my detailed closing discussion of a paper published in 1940.[1] I do not criticize the circuit breaker, but merely emphasize that these several phenomena indicate that the circuit breaker was operating at its optimum or maximum rating during these tests.

The remaining part of my discussion will deal more generally with the mechanical aspects of the 69-kv compressed-air circuit breaker. It is gratifying to see the rack mechanism put to work again, here as the link between the pneumatic operator and the disconnect or isolating switch. However, I ask the authors for the diameter of the associated gear and, also, the depth, breadth, and thickness of the teeth of the gear. Further, have you had or do you anticipate any alarming experience as concerns the teeth of this gear in shear?

The massive interrupter and its associated high-speed disconnect or isolating switch form an impressive podium when balanced or supported by the single Micarta tube, especially when there is no accompanying bracing. There is the thrust of the blast of air and the whipping action of the isolating switch for each operation. One would suspect that considerable stress would be encountered for each operation!

For circuit breakers of 2,000 to 5,000 amperes continuous current ratings the isolating switch becomes, by necessity, quite a mass in cantilever. Even with bumpers or shock absorbers incorporated in the pneumatic operator, I would suspect some difficulties especially if the isolating switch is given snappy action.

The main and arcing contact assembly intrigue me very much. Since the exploded view, Figure 5, is almost obscure, I would like to have a close-up or a detailed sketch that we may comprehend the construction. How much does each pair of main and arcing contacts weigh? How do you combat contact chatter and mushrooming during repetitive operation?

We are led to believe that the contacts may be inspected by removing the cover-plate window as shown in Figure 2, providing the mechanic has a specially-built contact retracting and revolving tool. However, it seems that a fairly large boom would be required to aid the mechanics in removing the massive interrupter podium from the supporting compressed air reservoir when more detailed inspection or repairs are necessary.

Please give us the following named dimensions:

1. The diameter and length of the compressed air tank.
2. The length and diametrical dimensions of the main supporting Micarta tube.
3. The height of the interrupter podium, from the top of the compressed air reservoir to the top of the upper muffler.

In the section Method of Circuit Breaker Operation, I presume the authors mean by "the throttling action of the narrow space between the upper contact holder and the upper insulating tube" that a slightly longer time is required for the pressure to build up in the more distant end of the tube before the second contact will open. The timed sequence of the opening of the two contacts is of some consequence! Besides taking design precautions in dimensioning the space between the upper contact and the insulating tube, how much have you considered varying the strength of the upper spring in relation to that of the lower spring? What are the magnitudes of these spring loads when the contacts are in closed position? How do you co-ordinate the dimensioning of the throttling space and spring loads when going from the 2,000 to the 5,000 ampere circuit breaker?

The questions which I have posed are more than academic, in fact, the operator will find them quite real. Hence, I ask, how well does the circuit breaker hang together, and how do the main contacts perform after a life test of 20,000 closing operations at no-load, or even after 5,000 operations?

As to the general trend in the design of compressed-air circuit breakers, I should like to emphasize that the European axial-blast or orifice-type circuit breaker has set the style pattern. It has been found expedient to resort to the famed cross-blast circuit breaker only when going to the lower voltages of the high-voltage classes where short-circuit currents of excessive values are encountered. I prognosticate that the axial-blast or orifice type of compressed air circuit breaker will be made to surpass even the cross-blast circuit breaker when our Westinghouse development engineers have completely co-ordinated the action of the paralleling resistor with the series and shunt orifices. The operation is most promising, and I feel that only a short time will pass before the voltage and kilovolt-ampere ratings will be extended to the highest transmission values. I suspect the orifice type of compressed-air circuit breakers will crowd all of the oil types.

REFERENCE

1. MAGNETIC "DE-ION" AIR BREAKER FOR 2,500–5,000 VOLTS, L. R. Ludwig, R. H. Nau. *Electrical Engineering* (*AIEE Transactions*), volume 59, September 1940, pages 519–22.

W. F. Skeats (General Electric Company, Philadelphia, Pa.): The authors are to be congratulated upon developing a 69-kv circuit breaker for operation in a metal enclosure. Certain questions present themselves, however, and I should like to address them to the authors.

1. It would be interesting to know whether the unit has been subjected to close or close-open duty within a metal enclosure such as is to be used in the installation. While such ionization as is produced by arcing at the isolating switch on closing is dissipated readily in the open air, experience has shown, on occasion, that it may be considerably more dangerous within a relatively tight enclosure.

2. The creepage distance across the Herkolite tube surrounding the upper break appears to be of the order of 12 inches both inside and outside. This insulation carries the full burden of maintaining an open circuit until the series isolating switch has achieved a substantial contact separation. According to Figure 9, this interval is about 20 cycles. Has this break been subjected to insulation tests, or is a somewhat reduced insulation for this period considered acceptable?

3. It appears from the oscillogram of Figure 9 that an interval of the order of 12 to 15 cycles elapses from the time the blast valve is opened for the interruption to the time when the isolating switch has built up a contact separation equal to that at which the arc strikes on closing a 44-kv circuit. Is air being lost through the blast valve during all of this period, or is there some provision for reducing its flow?

4. The contacts appear to perform in a rather unusual manner. It would be interesting to have more details of the arrangement for accomplishing the various functions in the proper sequence.

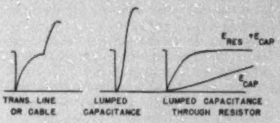

Figure 1. Voltages following restrike

5. The authors appear to have convinced themselves that a resistor is a reliable adjunct to a circuit breaker, and having done so, have built a resistor to pass quite substantial currents. Just what value of resistance is to be used is not quite clear, as Figure 6 shows a resistance current of about 3,800 amperes at 44 kv, corresponding to a value between 11 and 12 ohms, while Figure 7 shows a current of about 3,500 amperes at 60 kv, corresponding to a value of 17 ohms. Residual currents commonly used in recent practice have for the most part been about 10 per cent of the continuous current of the circuit breaker or less, but the values stated above are as high as the short-circuit current through 20 miles of transmission line at the rated voltage of the circuit breaker. The question may very well be raised whether currents of this magnitude are properly referred to as "residual." For the purpose of determining interrupting time, they should certainly be included.

6. The authors have used a peculiar circuit in their tests for interruption of cable charging current, in that a resistance of 300 ohms was inserted in series with the capacitance. This resistance corresponds reasonably well with the surge impedance of transmission lines, but since the authors particularly mention cable, which has a very much lower surge impedance, that fact presumably had nothing to do with the choice of value. Even with a resistance value corresponding to the surge impedance, however, the oscillations and overshoot associated normally with a restrike on either a lumped capacitance circuit, a transmission line, or a cable are substantially eliminated as indicated in Figure 1 of the discussion. The progressive build-up of voltage is, therefore, eliminated and the overvoltages greatly reduced. Performance on such a circuit can hardly be taken as a reliable indication of performance on field circuits.

A. M. de Bellis (Consolidated Edison Company of New York, Inc., New York, N. Y.): The 69-kv system which is planned for the East River Station 60-cycle development, of the Consolidated Edison Company is the first use of this voltage in New York City. Present-day conditions and particularly the increased cost of building structures and of switching equipment for the large kilovolt-ampere ratings have made it necessary to decentralize the switching galleries of the generating stations, by transmitting bulk power at high voltage to various distributing substations located at the load areas.

In distributing the large blocks of power which we have to handle in New York, it has become necessary to step up the generator voltage to 69 kv and then transform it back again to 13 kv at the area substations, even though the distance between the generating station and the substation may be short. With this arrangement some 69-kv switching equipment is required at the generating station.

In regard to the high-voltage circuit breakers it was our desire to avoid the use of oil and to adapt this equipment to newly designed 69-kv outdoor metalclad bus and disconnect switchgear equipment. We feel that the designers of the new air-blast circuit breaker, described in the paper, have accomplished the desired results in this respect. The design of this circuit breaker is unique since the usual outdoor circuit breaker of this voltage does not have a housing around it. This arrangement fits in very well with the metalclad isolated-phase type of bus construction and also permits the use of bushing current transformers over each circuit breaker terminal.

The circuit breaker designers are to be complimented for their courage in undertaking the construction of an air-blast circuit breaker for operation at 69 kv, and at the highest interrupting kilovolt-ampere rating now recognized in the new ASA Standards for this voltage class. The test results described in the paper show that the interrupter is efficient and is apparently capable of even greater interrupting capacity than its rated 3,500,000 kva. It would be interesting to see tests carried to higher levels of kilovolt-amperes to learn the actual interrupting limits of the circuit breaker.

Since this circuit breaker is to be used on a 69-kv cable system, we were particularly interested in its ability to interrupt cable charging currents. The test results showing only one "restrike" in 20 tests are reassuring so far as the possibility of imposing overvoltage on the cables, due to switching, is concerned.

H. V. Nye (Allis-Chalmers Manufacturing Company, Milwaukee, Wis.): The circuit breaker described in this paper differs from orifice-type circuit breakers presented previously to the Institute, largely in the use of a separate orifice and contact for introducing the series resistor. The use of a separate contact for this specific purpose may have some advantages, but I wish to point out that it has one distinct disadvantage. It adds approximately one second to the possible minimum arcing time obtainable. A study of Table I will illustrate this fact. The main current interrupting time varies from 1.5 cycles to 2.4 cycles depending on the load interrupted, but with a fixed time delay for the second orifice we find the total interrupting time runs from 2.6 to 4 cycles.

Previous air-blast circuit breakers have employed a probe in the arc path which serves to parallel the resistor with a portion of the arc and accomplish the purpose of the first orifice described by causing the portion of the arc paralleled to be extinguished leaving only the residual current through the resistor flowing. The residual current is then extinguished by the continued action of the air blast.

The advantage of this construction is that no mechanical timing is introduced for the transfer and it is accomplished as fast as the circuit conditions permit, usually in 1/2 to 1$^1/_2$ cycles. The extinction of the residual current then takes place very rapidly, in most cases only a fraction of a cycle. Consequently interruption in a total time of 1$^1/_2$ to 2 cycles are obtainable.

This may be of little importance so long as the operating time shown is acceptable, but indicates the ultimate possibility of shortening the operating time.

Other than above, the circuit breaker described by the paper seems to be well designed and the authors are to be complimented on presenting sufficient test data to give confidence in the circuit breaker rating.

The proposed outdoor construction with entrance bushings supported by an enclosure is interesting and helps solve the problem of bushing transformers.

In conclusion, the type of circuit breaker best adapted to American conditions, air blast, impulse, or ruptor types, will probably be determined largely through evaluation of the following factors, rather than by arcing times. These factors are: manufacturing cost; maintenance expense; and relative weight and space occupied.

This is due to the fact that adequately short arcing times are now possible with all three types of circuit breaker.

O. B. Vikoren (Philadelphia Electric Company, Philadelphia, Pa.): The authors are to be congratulated on their efforts to solve the problems confronting power companies which have to use increasingly higher voltages in congested metropolitan areas. We have in mind particularly the reduction of fire hazards, the totally-enclosed design of all high-voltage parts described, and the reduction in noise levels of this equipment. The paper indicates that no efforts have been spared to comply with the needs of the user in these respects. However, simplicity in design of switching equipment is generally a requirement, and although the authors appear to have tried to achieve this in the design of the 69-kv compressed air circuit breaker, the result leaves much to be desired. From the user's point of view it is believed that the compressed-air circuit breakers above 34.5 kv will have much wider acceptance in the industry if the mechanical parts of these circuit breakers, with respect to simplicity, would compare more favorably with those of oil circuit breakers. The authors could have explained in more detail their reasons why in the 69-kv, 3,500 megavolt-amperes compressed air circuit breaker a simple interrupter, without an external isolating switch, would not have been a suitable design. Visual inspection of the isolating switch does offer added insurance of safety, but this point can hardly carry much weight once the entire equipment is metal enclosed.

The 69-kv compressed-air circuit breaker with its many moving parts with precision tolerances can be expected to have higher maintenance costs than a switching device of equivalent rating, in which less precision work is required. It is recognized that the compressed-air circuit breaker is in the early stages of development and that many difficulties remain to be overcome. However, it is hoped that rapid progress will be made toward a design which will compete with established equipment in first cost, simplicity, and maintenance cost.

The authors might have emphasized earlier in the paper the fact that the compressed-air circuit breaker is suitable for outdoor installations in porcelain clad design. There may be many installations in which compressed-air circuit breakers are used in conjunction with transformers and similar equipment where the current transformer problem can be divorced from the circuit breaker entirely. In these cases there is often no need for the metal enclosure.

In general, the explanation of the operation of the circuit breaker is very thorough although it is unfortunate that the schematic diagram, Figure 3, is not clearer, since it does not convey the toggle action of the mechanism of the isolating switch, although it is indistinctly shown in Figure 4, a feature which is of extreme importance under through-fault conditions. In this connection it is believed that a few words about how the blast air passes the section of the air passage, which is shown as an exhaust port in Figure 3, would have been helpful.

From the test results it appears that the circuit breaker complies with the ASA requirements for speed with little or no margin. If this circuit breaker design is to be carried over into the 138-kv class and above, where three cycles interrupting time is required, it would be interesting to learn how the increased speed is expected to be obtained.

B. P. Baker and E. Frisch: It appears Mr. Taylor feels that the authors should not have used Mr. Jansson's paper as a reference for a cross-blast circuit breaker. If the reference has been misleading we wish to apologize. Mr. Jansson's paper shows very clearly that the heavy current carrying requirements are met by a contact structure quite similar to that used in the cross-blast circuit breaker. Also, the air blast is perpendicular to the motion of the contact as in the case of the cross-blast circuit breaker and since there has been no details shown on what Mr. Jansson calls the cross-axial blast we felt that any compromise design between the cross blast and axial blast would be more similar to the cross blast and could be classified as such. This appeared logical in view of the authors unsuccessful efforts to meet the heavy current requirements with a compromise design.

The use of Micarta insulation seemed justifiable on the basis of its satisfactory performance at 34.5 and 138 kv, where very liberal distances are provided, and when metal fittings at high potential are properly rounded and shielded. The condensation of moisture is precluded on the inner surfaces, by the use of predried air and on the outside surfaces by the application of heat and controlled ventilation.

We wish to point out to Mr. Shore that in addition to the conventional electrical interlocking between the closing and the trip circuit, the opening of the isolators pneumatically takes precedence over their closing. Also, unless blast air is available in all three interrupters, the isolators get no opening air. There is no mechanical interlock between the interrupters and the isolating switches.

The blast valves as located are quite accessible for inspection and maintenance. Removal of several bolts permits the entire valve and its associated parts to be removed as a subassembly. The reservoirs are provided with blow-off or drain valves located at the bottom, showing very indistinctly and almost covered by the air supply line, in Figure 2 of the paper. While the blast valve is removable from the bottom of the reservoir, it is actually located near the center of the reservoir, where it is impossible for water to get into it.

Mr. Skeats has questioned the ability of the circuit breaker to perform close or close-open duty when mounted in its metal enclosure. Apparently he feels that the ionization liberated may produce a breakdown to the surrounding, uninsulated grounded metal surfaces. At the time this paper was written the circuit breaker had not been tested in its metal enclosure. Since then tests have been made with the circuit breaker in its enclosure, and perhaps Mr. Skeats' question can best be answered by briefly describing the tests.

This series of 12 tests was made on a single-pole bus with 44 kv applied across the circuit breaker. The first ten consisted of five standard duty cycle tests, that is, a close-open–15 second–close-open with the circuit breaker reservoir charged to 250 pounds per square inch before the first close-open test and then sealed off from the air supply. The test results were as follows:

Numbers 1 and 2, 1,050 and 790 amperes crest cleared, 580 and 530 amperes rms opened.

Numbers 3 and 4, 5,000 and 5,300 amperes crest closed, 2,200 and 2,340 amperes rms opened.

Numbers 5 and 6, 9,600 and 18,700 amperes crest closed, and 4,050 and 7,400 amperes rms opened.

Numbers 7 and 8, 23,900 and 28,800 amperes crest closed, 13,700 and 13,700 amperes rms opened.

Numbers 9 and 10, 48,000 and 40,500 amperes crest closed, 18,900 and 18,700 amperes rms opened.

The maximum circuit breaker time including interrupting the residual current through the resistor was 5.6 cycles. The maximum duration of fault current was 7.9 cycles.

Two opening operations were made with the current completely asymmetrical and with anticipatory tripping of the circuit breaker to obtain two interruptions of 39,000 amperes rms. One test was made with the circuit breaker reservoir charged, to 250 pounds per square inch, the other at 210 pounds per square inch. At the conclusion of these tests the circuit breaker including the isolating switch seemed to be in excellent condition. No evidence of smoke or discoloration could be found on the walls of the metal enclosure adjacent to the isolating switch.

Mr. Skeats raises an excellent question regarding the flow of air from the time the blast valve is opened until the isolating switch is opened sufficiently far to withstand voltage. The air from the interrupters after having passed through the orifice is discharged into exhaust chambers as shown in Figure 3. The volume of these exhaust chambers is such that they receive gas from the orifices at acoustic velocities for several cycles, to provide ample time for arc extinction; after this time the back pressure in the exhaust chambers decreases the rate of flow until further use of gas is decreased to zero, except for extraneous leaks and that provide for slow escape through the muffled exhausts, from the exhaust chamber. The air consumption is, therefore, somewhat independent of the speed of the isolator switch operation.

Mr. Skeats' fourth question regarding the unusual manner of contact performance is a little difficult to understand. If he refers to the sequencing of interrupter contacts, I am afraid I cannot do much better than to refer to the third paragraph of the section under "The Interrupter." I may add that the "flange of the upper contact holder" is shown schematically in Figure 3 as the moving contact member which is biased upward by a spring in the section that is labeled "moving contact assembly." This member is shown in Figure 5. In referring to the lower end of the insulating tube, it may have been more nearly correct to say that insulating plate adjacent to the lower end of the insulating tube.

In Mr. Skeats' fifth question he feels that the authors have convinced themselves that "a resistor is a reliable adjunct to a circuit breaker." Personally I hope it is reliable. However, I have a very strong conviction that circuit breaker development engineers resort to the use of resistances as props when they are unable to find another practical solution With considerable chagrin I must confess that in this case, I could not find another way of making an orifice type of circuit breaker interrupt large values of current, at reasonable air pressure, and at high rates of rise of restored voltage. Under the conditions of many service applications and field tests, the use of resistance may not have been necessary. However, we felt that for this application we could not afford to take a chance.

Mr. Skeats questions the sufficiency of the tests shown in Table II, to prove the adequacy of the circuit breaker to interrupt cable charging current. The 300-ohm resistance used in series with the capacitor bank was placed there to protect the capacitors which were being worked considerably over their rating. If no restrikes were encountered it was believed that the voltage condition on the circuit breaker would not be affected appreciably providing some overvoltage was used to compensate for the small correction in power factor. For this reason 60 kv was used instead of 44 kv, the voltage at which the circuit breaker should normally be operated. Nevertheless we concede that Mr. Skeats has raised an excellent question and since the writing of this paper we have made a series of 30 tests at 44 kv in which no resistance was used in series with the capacitor bank. No restrikes at all were observed.

Mr. de Bellis has not asked any questions, nevertheless the authors wish to hereby acknowledge his very fine discussion and thank him for clarifying several points that have been in the minds of many of us.

Mr. Nye has ably pointed out the relative merits of the two methods for introducing series resistors. In self defense we can only add, that tests seemed to indicate that for 69 kv, the method we used was the only one which produced consistent successful results at high values of current. We agree that for high-speed interruption, 3 cycles or less as is required at very high voltage, this residual current persisting for another cycle will prolong the de-ionization across a flashed insulator which will in turn delay high-speed reclosures. Therefore, this method requires modification for high-voltage high-speed fast-reclosing circuit breakers; but again, in these cases, the magnitude of the current may not require the use of resistors.

Several discussors have evidenced interest regarding costs, maintenance expense, weights, and space occupied. Mr. Nye has pointed out that the general acceptance of the various types of circuit breakers will ultimately be dependent upon these factors. About all we can add, is that the manufacturing cost cannot be determined accurately until production volumes are known, and some standard is set up for applying accessories such as, current transformer, potential devices, mountings, and other applicational data. The same is true for weights and installation space requirements.

While the circuit breaker was designed for ease of inspection and maintenance, only time and experience will be able to determine maintenance expense.

Mr. Vikoren suggests that the authors could have explained in greater detail why an isolating switch external to the interrupter was used instead of building the isolating switch into the interrupter. Presumably Mr. Vikoren has in mind a 34.5-kv outdoor Westinghouse compressed air circuit breaker, which has been in service on their system in Philadelphia for several years. In that circuit breaker, the isolating gap is formed by simply elongating the interrupting gap. There, one line terminal is located vertically above the other and the entire circuit breaker forms a single vertical column. This type of structure seems desirable for outdoor porcelain-clad construction up to 115 or 138 kv. For a circuit breaker built into a metal enclosure which is equipped with two condenser roof bushings per phase, it seemed logical to use a horizontal isolating switch external to the interrupter as shown in Figure 1 of the paper. In this case the contacts of the isolator switch are in full view through glass windows in doors of the metal enclosure and very little additional space is required.

Mr. Vikoren inquires regarding the air flow shown in Figure 3. The arrows indicate that the flow is up through the blast tube, through bypasses in the lower exhaust chamber, through the space between the lower stationary contact members and the outside insulating wall, through the orifice and back through the lower stationary contact, through cored openings into the exhaust chamber. These cored openings may be seen in the far casting of Figure 5. In this figure they appear as supports for the stationary contact member or orifice.

This general type of construction can be carried to higher voltages such as 230 kv and obtain 3-cycle interruption from rise of trip coil current. It is accomplished by using a faster exhaust for the gas under the blast valve and by locating the blast valve near the interrupter with a minimum of space in the interrupter to be filled. To be sure, no time can be sacrificed for opening residual current through a resistor. However, at high voltages, and lower current, resistors should not be required.

Mr. Nau has raised a host of questions, a number of which have already been answered in my reply to other discussers. I regret that space allotted to our paper made it impossible to cover the circuit breaker in sufficient detail to meet with Mr. Nau's approval; although I doubt if the Institute is generally interested in many of these unimportant details, consequently I am hereby tendering Mr. Nau a cordial invitation to visit our factory if he wishes to obtain complete information on this circuit breaker.

Mr. Nau points out that the restrikes showing in Figures 6 and 8 indicate that the circuit breaker is operating near its maximum rating. We do not feel that this is the case, since these early unsuccessful attempts to interrupt the residual current are generally associated with the occurrence of a current zero at very short contact separation.

Mr. Nau feels that the tests shown in "the second oscillogram of each of Figures 6 and 7 might be considered fortuitously lucky shots, catching the brunt on the little half-cycle of a highly asymmetrical current wave." I believe that, had Mr. Nau looked more carefully at Table I he would not have drawn the above conclusion. *Test 2-87662* and *2-89617* referred to in Figures 6 and 7, show an extinction time for the main power are of 2.2 and 2.3 cycles respectively. *Test 2-89597* at very low current where the duty on the transfer contact is very light shows an interruption time of 1.5 cycles, and it is hard to conceive of this arc going out before the contacts part. Therefore, one must assume that the contacts part in at least 1.5 cycles.

Subtracting 1.5 from 2.2 and 2.3 leaves 0.7 and 0.8 cycles respectively as the arcing time for the tests shown in Figures 6 and 7. It is therefore, apparent that the contacts parted near the beginning of the large current loop and arced throughout its entirety which is certainly not fortuitous. Had the contacts parted just before the zero on which interruption occurred, I would agree heartily with Mr. Nau. The "brunt" was not caught on the little half cycle. On both tests the main power arc was interrupted before the little half-cycle.

The rack and gear have shown no evidence of distress in a life test consisting of several thousand operations, to be sure firm conclusions cannot be drawn without many breaker-years of experience.

Mr. Nau has asked several detailed questions regarding a 5,000-ampere contact. Such a contact has not been designed and consequently we are just as much in the dark as is Mr. Nau. I wish to assure Mr. Nau that we appreciate his interest in this paper even though space does not permit us to answer all of his questions in detail.

Equivalent Circuits for Power-Flow Studies

J. B. WARD
ASSOCIATE AIEE

PRESENT-DAY extensive interconnection between power systems complicates the analysis of steady-state network performance in the study of planning and operating problems. This complication of analysis is increasing continually with system expansion and additional interconnections. Network analyzer studies of power-flow conditions on large systems frequently require preliminary simplification and reduction of the network, because of limitations imposed by the number of analyzer circuits and generator units available.

In studies for determining the distribution of power flow over the lines of a system under various emergency operating conditions, or with proposed future developments, interconnections may have an important effect, particularly if two or more ties exist forming parallel paths through the adjoining system. The total interchange of power between separate companies usually is established by interchange contracts, but in order to determine the proper division of this power flow over several tie lines under various operating conditions, it may be necessary to set up the adjoining system or an equivalent circuit representation of it.

The problem of network reduction in power-flow studies is not related solely to inter-company ties. Some individual systems have grown to such an extent that the complete network of major lines, stations, and substations exceeds the capacity of the largest existing network analyzers. Even on smaller systems, simplification of the network by means of equivalent circuits can be employed advantageously, to speed up the progress of studies when interest is focused on a certain section.

This paper outlines briefly the existing commonly-used methods of network simplification, and presents additional methods for devising simple equivalent circuits which reproduce with reasonable accuracy the terminal performance of the actual system under conditions prevailing in the usual type of power-flow study. By these new methods an extensive power network, containing numerous loads and generators, is reduced to an equivalent circuit, as viewed from several selected terminals, requiring few network analyzer circuits and sources for its representation. Changes in generation or loads within the reduced system can be reproduced readily in the equivalent circuit. Although the methods are described, for the most part, in terms of the necessary tests and measurements on an a-c network analyzer set-up of the system to be reduced, derivation of the equivalent circuit analytically or by use of a d-c board is feasible. Based on constant-current representation of system loads and generation, the new methods will accomplish in many instances a greater simplification than previously-used equivalent circuits. Limitations of this treatment of loads and generation restrict application to load-flow studies, but in studies of this type acceptable accuracy can be attained.

Present Practice

Present practice in reducing the size of a network for analyzer power-flow studies is confined largely to two methods.

Method A. The network to be studied in detail is terminated at interconnecting points, and the adjacent system is represented by a load or generator attached at each of these terminals. Connections through the reduced system are omitted entirely, and an estimated tie line flow, based on system readings or previous studies, is reproduced in the stub loads and generators at the interconnection terminals. In system planning studies involving proposed future transmission development or location of new generating stations, the system changes are frequently so radical that it is not possible to predict, with sufficient accuracy, the loadings on the stub loads and generators used to represent multiple ties to an adjoining system.

Method B. The system to be simplified is replaced by an equivalent circuit in which the identity of the tie-line terminals and generator busses is retained, and the line network is represented by transfer impedances between these various busses. Equivalent load impedances appear as transfer impedances from each retained bus to neutral. The process of evolving this type of equivalent circuit from a network analyzer set-up of the system is outlined here for the dual purpose of providing a comparison with the new methods and of explaining certain steps in obtaining the new type of equivalent circuit.

A 1-line diagram of the system to be replaced by an equivalent circuit is represented in Figure 1. This diagram shows the loads, generators, and interconnection points, but the internal line connections are omitted. It is assumed that the system indicated in Figure 1 must be simplified before a detailed study of the adjoining network can be carried out. If tie-line terminals, generator busses, and neutral bus are to be retained, the branches of the resulting equivalent circuit, shown in Figure 2, can be obtained as follows.

Disconnect the generators and represent loads as constant impedances corresponding to the load real and reactive power at normal bus voltage. Connect an analyzer source from one of the terminals

---

Paper 49-96, recommended by the AIEE system engineering committee and approved by the AIEE technical program committee for presentation at the AIEE winter general meeting, New York, N. Y., January 31–February 4, 1949. Manuscript submitted October 4, 1948; made available for printing December 23, 1948.

J. B. Ward is with the School of Electrical Engineering at Purdue University, West Lafayette, Ind.

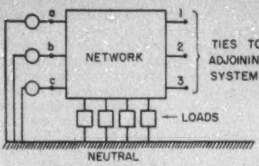

Figure 1. Typical system to be replaced by an equivalent circuit

to be retained, terminal 1 for example, to a new junction established at x, as shown in Figure 3. Connect zero-impedance metering circuits from junction x to all other terminals which are retained, including the neutral bus. Adjust the source at terminal 1 to an arbitrary value of voltage and read the current in each metering circuit. The impedance of the branch between terminals 1 and 2, in the equivalent circuit of Figure 2, is obtained by dividing the source voltage by the current in the metering circuit connected to terminal 2. It should be emphasized that all metering circuits are closed and carrying current simultaneously during this test. Similarly, the impedance of the equivalent branch between terminal 1 and neutral is the voltage at terminal 1 divided by the current in the metering circuit connected to neutral.

This process is repeated with the source connected successively to each retained terminal. At each step, all other terminals are connected to x through metering circuits. Thus, two measurements are obtained for each transfer impedance. The branches from the various generator and interconnection busses to neutral can be considered as equivalent loads. However, in the equivalent circuit derived in this way, the distinction between actual loads and line losses is lost.

The equivalent circuit, Figure 2, is connected at the proper points to the detailed set-up of the adjacent network. The desired internal generating schedule in the reduced system is established by adjusting sources connected to the generator busses of the equivalent circuit. If a different condition of loads is required in the reduced network, it is necessary to measure a new set of transfer impedances from the various terminals to the neutral bus. The transfer impedances, representing line connections between generator and interconnection busses, are modified only slightly by the presence of load impedances.

Certain branches of the resulting equivalent circuit are sometimes of such high impedance that they can be omitted entirely, but in general the number of branches is equal to $n(n-1)/2$, where n is the total number of terminals retained. The procedure just described is equivalent to applying star–mesh transformations to remove successively all busses except generator busses, tie-line busses, and neutral bus. The approximation of loads as constant impedances is required.

New Equivalent-Circuit Representation

The basis for the new equivalent circuit representation presented herein is the treatment of generation and loads, in the network being reduced, as constant-current quantities. By means of this approach, the internal generator busses as well as load busses in the reduced system can be eliminated, and the identity of only the tie-line terminals retained. The effects of suppressed generation and load are reproduced by an equivalent generator or load at each tie-line terminal, and the actual network of line connections is replaced by an equivalent mesh network interconnecting these terminals. The equivalent circuit of this type for the system of Figure 1 is shown in Figure 4. In principle the methods are rigorous for a hypothetical network in which all loads and sources are fixed impressed currents. The analysis of such a system is outlined in Appendix I, and, in the following paragraphs, the methods are adapted to the practical determination of simplified equivalent circuits for sections of power-system networks. Some of the important assumptions and approximations involved in this adaptation are listed briefly:

1. It is assumed that system loads can be considered as constant-current quantities. Usually loads are treated as constant impedances in analytical solutions of power-flow problems, and as constant-power loads in network analyzer studies. Differences in the three viewpoints become of major importance only under extreme voltage variations, as may occur during short circuits, for example.

2. Generators are usually held to a fixed power and voltage schedule, except for certain regulating machines. Reactive power generation may vary appreciably, but, as a rule, large blocks of reactive power cannot be transmitted economically over long distances. Furthermore, a large proportion of system studies are made at peak-load conditions, with generators operating at or near their maximum excitation. Hence, limited variation of power, reactive power, and voltage corresponds essentially to constant-current loading, in magnitude at least, on generators.

3. Angular displacements between bus voltages in a system usually are not large. Initial angles between various load and generator busses can be taken into account accurately, and then the assumption can be made that effects of subsequent variations in these angles can be neglected.

4. Synchronous condensers, static capacitors, and line charging capacitance can be treated as separate sources of reactive power or combined with nearby loads and generation.

5. Although the derivation of the equivalent circuit is based on the constant-current approach, it is assumed that the equivalent sources and loads, once determined, can be held at a fixed power schedule, for convenience in manipulation during studies.

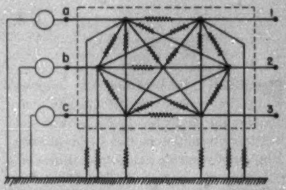

Figure 2. Equivalent circuit obtained by method B for the typical system of Figure 1

6. Initially, transformer turn ratios are assumed to be the same as ratios of the nominal voltages of the sections connected to the respective windings. Methods of handling transformer tap settings which result in other than nominal ratios are discussed in a later section.

7. It is assumed that, when a section of a power system is to be replaced by an equivalent circuit, detailed information on the performance of this section, with various line outages, for example, is not of immediate interest. Rather, the effect of this section during detailed study of the adjoining network is desired.

Determination of the Equivalent Line Network

After the section of the system to be reduced and the interconnecting terminals are decided upon, this section is set up in detail on a network analyzer, with all loads, generators, and capacitors open. The transfer impedances between the terminals to be retained are measured in the manner described under method B in "Present Practice," with the exception that, in the present method, only the points of interconnection are retained.

Equivalent Generators and Loads: Method I

Regardless of the number of internal busses suppressed in the reduced network, an equivalent generator and load can be established at each terminal of the equivalent circuit, corresponding to a given schedule of generation and loads at the actual stations. This can be accomplished through the medium of a set of distribution factors, determined as described in the following paragraphs. This description is given in terms of generation. The loads can be considered as negative generation and can be treated in exactly the same way.

1. In a detailed set-up of the network being reduced, with load and generator circuits disconnected, connect each interconnection bus to the analyzer neutral bus through a metering circuit. In the system of Figure 1, for example, connect points 1, 2, and 3 to the neutral bus.

2. Connect an analyzer source between one generator bus, such as terminal a in Figure 1, and the analyzer neutral bus. Adjust this source so that its output current is equal to one ampere or unit current. Measure the currents in the several metering circuits connecting the terminals to neutral.

These metering-circuit current readings are the distribution factors associated with the bus which is energized. If one of the interconnection terminals happens to be also one of the generator or load busses, it is not necessary to carry out the test for this bus. Unit-current input to this bus all would return to neutral through the metering circuit connected to the same bus. In this case, the one distribution factor is unity; the others are zero. With this exception, distribution factors are measured with unit current impressed successively at each bus.

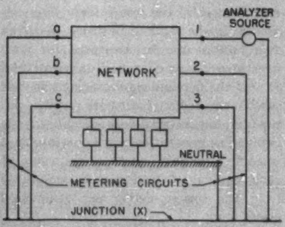

Figure 3. Network analyzer circuit connections for measuring transfer impedances

Usually, the metering circuit currents will be nearly in phase with each other and with the source current, if the ratio r/x of the major lines is reasonably uniform. If appreciable angular displacement appears, these currents or distribution factors can be measured as complex quantities, with the source current as reference, by means of the analyzer vector-metering equipment.

3. In order to establish a convenient notation for the distribution factors, let the internal busses be indicated by letters, and let the points of interconnection which are retained in measuring the equivalent line network be indicated by numbers. Use the first letters of the alphabet to indentify generator busses, and assign the remaining letters to load busses. If a load or generator appears at one of the retained busses, assign both a suitable letter and a number to this bus. When station a is energized by impressing unit current, denote the currents in metering circuits connected to terminals 1, 2, 3, . . . , by the symbols D_{a1}, D_{a2}, D_{a3}, . . . , respectively. Similarly, when unit current is impressed at station b, label the corresponding distribution factors as: D_{b1}, D_{b2}, D_{b3}, ...

4. The distribution factors are used to obtain an equivalent generation at each terminal of the equivalent line network, from known or specified power and reactive generation and bus voltages at generators in the reduced system. According to the usual practice in analyzer studies, voltages are expressed in per cent or per unit of a nominal base voltage, and power quantities are recorded either in terms of actual system value or in per unit.

Express the power and reactive loading of each station as a complex number in per unit of the chosen power base. Assuming that normal angular displacements between bus voltages are known, either from previous studies or from a special analyzer test made for this purpose, express each bus voltage in per unit as a vector quantity, with one of the retained terminals as reference. For each bus, the per unit current loading, corresponding to the scheduled power and reactive loading, is obtained by dividing the per unit vector power by the conjugate of the corresponding per unit bus voltage. If the bus angles are not known, the use, either of estimated angles or of only voltage magnitude may give sufficiently accurate results.

Represent the resulting per unit current loadings of stations a, b, c, . . . , by I_a, I_b, I_c, . . . , respectively. Denote by I_1, I_2, I_3, . . . , the equivalent generator per-unit-current loadings at terminals 1, 2, 3, . . . , respectively. The determination of these equivalent source loadings is indicated in equations 1

$$I_1 = D_{a1}I_a + D_{b1}I_b + D_{c1}I_c + \dots$$
$$I_2 = D_{a2}I_a + D_{b2}I_b + D_{c2}I_c + \dots \qquad (1)$$

and so on. The equivalent per unit source currents can be converted back into power and reactive loadings, using known or estimated tie-line terminal voltages.

5. The system generation and load can be reflected separately to the tie-line terminals in this manner, to appear as an equivalent generator and an equivalent load at each terminal, or the two can be combined into a net load or net generation at each terminal. If the currents I_a, I_b, I_c, . . . , on the right hand side of equations 1 include all busses, with the proper algebraic signs to distinguish between generation and load, these equations give the equivalent net current sources. The distribution factors, once determined, permit representation of any desired schedule of generation and load.

6. In reducing a large system containing many loads, this method may become quite lengthy and cumbersome. An approximate apportionment of the total system load at the terminals of the equivalent circuit can be carried out more rapidly as follows.

In the detailed set-up of the network being reduced, disconnect all generators, but represent all loads in the usual fashion as constant impedances to neutral, adjusted to consume the correct scheduled real and reactive power at normal bus voltage. Connect all the terminals retained in the equivalent line network through metering circuits to one terminal of a single analyzer source, which in turn is connected to neutral at the other terminal. Adjust this source to deliver unit current to the system. Read the currents in the metering circuits and label these currents d_1, d_2, . . . , as read in metering circuits to terminals 1, 2, . . . , respectively. These are treated as total-load distribution factors.

The equivalent load at terminal 1 is

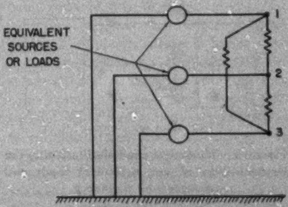

Figure 4. New simplified equivalent circuit for the system of Figure 1

taken as the product of d_1 and the total system load current. The equivalent load at terminal 2 is the product of d_2 and the total system load. The equivalent load at each of the other terminals is calculated in a similar fashion.

In the event that large loads, that is, low-impedance load circuits, appear at some of the terminals being retained, the accuracy of the equivalent loads determined in this way can be improved by modifying the procedure slightly. Disconnect large loads at any of the terminals before measuring the distribution factors. Apply the resulting factors to the total load, reduced by the total amount of load disconnected in the tests. Then, at each of the terminals where load was removed, increase the resulting partial equivalent load by the amount which was disconnected from that terminal during the measurements.

7. Another method for reducing all loads simultaneously to equivalent loads at the terminals suggests itself if the system loads are viewed as constant-impedance quantities.

Set up in detail the network to be reduced, leaving open all generator circuits, but representing loads by the proper impedance in the usual manner. Measure the transfer impedance, between the several retained interconnection points and neutral bus, as described under method *B*, and use these as the equivalent loads. If desired, the load real and reactive power can be computed, using known or estimated terminal voltages, and then these loadings can be combined at each terminal with the equivalent generator loadings.

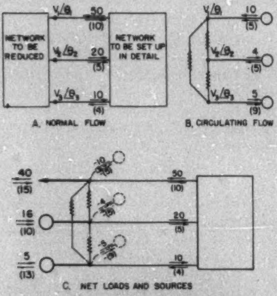

A. NORMAL FLOW

B. CIRCULATING FLOW

C. NET LOADS AND SOURCES

Figure 5. Numerical example illustrating the determination of net equivalent loads and generators by method II

Direction and magnitude of real and reactive power flows are shown. Reactive power is enclosed in parentheses

Equivalent Generators and Loads: Method II

The method outlined here resolves directly the equivalent net generation or net load, as the case may be, at each terminal, and can be employed if the system to be reduced is set up in detail, together with the adjoining network with which it is interconnected. It may not be necessary to represent the entire adjoining network if a portion adjacent to the interconnecting ties is sufficient to establish normal power flow and voltage at the points of interconnection. Some particular power-flow condition, here termed normal flow, serves as the basis for determining the equivalent net loads and generators.

1. First, establish the normal-flow condition on the analyzer set-up and measure carefully the voltage and angle at each interconnection bus. Measure also the normal power and reactive flow over the interconnecting ties.

2. Set up the equivalent line network, with only tie-line terminals retained, and connect an analyzer source to each terminal. Adjust these sources to reproduce the normal-flow values of voltage and angle at each terminal, and record the magnitude and direction of the resulting power and reactive loading of each source. Since loads are not represented in this test, the loadings of the sources consist of real and reactive power circulated between sources by the normal-flow terminal voltage and angle differences.

3. The measured circulating flow at each terminal can be combined with the normal-flow interchange at the same terminal, to determine the equivalent net load or generator which should be placed at each terminal of the equivalent circuit. This process of combination is described best by example.

Figure 5(A) shows the normal-flow interchange and terminal voltages in a system with three ties between the two sections. Figure 5(B) gives the flow circulated between the terminals by the same normal-flow terminal voltage conditions. Figure 5(C) illustrates how the equivalent load or generator at each terminal is deduced from the information given in Figures 5(A) and 5(B). The equivalent net load or generator at a given terminal contains the real and reactive power components required to attain a balance with the normal-flow interchange and with the normal circulating flow at that terminal. For convenience in calculating the net load or generator at each terminal, the normal circulating flow is indicated by dotted sources in Figure 5(C). In reality, these flows occur in the equivalent mesh network, but it is not necessary to determine their distribution in the various branches.

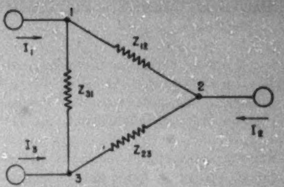

Figure 6. Typical equivalent circuit which is to be reduced further to one requiring a single source

4. When these tests are made, it is desirable to establish two or three additional conditions in the detailed portion of the set-up which represent extreme departures from normal flow, involving line outages or other emergency operating situations. The equivalent loads and generators, derived in the same way from these extreme conditions, will serve as an indication of the range of applicability of the normal-flow values, and also will serve as a guide for adjusting the equivalent reactive generation.

5. If it is desired to separate the equivalent net generation or net load at each terminal into the component parts contributed by the load and by the generation in the reduced network, distribution factors can be measured for each generator bus as described under method I. For the particular generating schedule within the reduced network, which was used in the normal-flow condition, the equivalent generation can be determined at each terminal, and then the value of each equivalent load can be separated from the corresponding net generation or net load.

Reducing the Number of Equivalent Generators

In cases where normal power interchange is from the reduced section to the rest of the system, the equivalent circuit probably will require a net generation at several of the terminals. If a sufficient number of power source units is not available on the analyzer to set up the equivalent circuit together with the adjacent detailed system, the method given here can be used to combine the generators appearing at several terminals of the equivalent circuit into a single source. The reduction to a single source introduces additional line circuits in the final equivalent network, but the shortage of analyzer sources often is more severe than that of line units.

The procedure is described in terms of an example involving a 3-terminal equivalent circuit, shown in Figure 6, with net generation appearing at each terminal. It can be extended, by analogy, to any number of terminals. In the following, all quantities are retained in literal form. A numerical example is given in Appendix II.

1. Figure 6 represents the equivalent circuit only, with connections to the adjoining detailed system not shown. The equivalent generator loadings in per unit current, complex or vector values, are indicated as I_1, I_2, I_3 at terminals 1, 2, and 3 respectively. Several intermediate steps are necessary in deriving the single-source circuit. Consider a star network, Figure 7(A), connecting three current sources equal to those shown in Figure 6. Arbitrarily assign a value of $(1.0+j0)$ to the impedance of the branch connected to terminal 1. If the other branches, Z_2' and Z_3', are chosen to satisfy the relation $I_1 \cdot 1.0 = I_2 \cdot Z_2' = I_3 \cdot Z_3'$, see equation 4, Appendix I, then the three source currents can be added together and impressed at the common junction of the star network without disturbing the terminal conditions.

2. Convert this star network to an equivalent mesh network, equation 2 of Appendix I, as indicated in Figure 7(B). Comparing the impedance values of this mesh network with those of Figure 6, multiply the impedances of Figure 7(B) by a complex constant, $\underline{/k\phi}$, which is chosen so that one branch of the resulting network is equal to the corresponding branch of Figure 6; at the same time, the other branches (those of Figure 7(B) multiplied by $k\underline{/\phi}$) are greater in magnitude than the corresponding branches of Figure 6. In this example, assume that the relation $Z_{12}' \cdot k\underline{/\phi} = Z_{12}$ satisfies this condition.

3. Next, calculate values of impedances Z_{23}'' and Z_{31}'' which, after being paralleled with $Z_{23}' \cdot k\underline{/\phi}$ and $Z_{31}' \cdot k\underline{/\phi}$ respectively, will be equal to the corresponding branches Z_{23} and Z_{31} of the original network, Figure 6. The network of Figure 8 then will have the same transfer impedances between terminals as that of Figure 6.

4. The mesh network composed of branches Z_{12}, $Z_{23}' \cdot k\underline{/\phi}$, and $Z_{31}' \cdot k\underline{/\phi}$ in Figure 8, is equivalent to the original star network of Figure 7(A), with each branch multiplied by $k\underline{/\phi}$. This star originally was established in such a way that the terminal current sources could be combined at the star point without changing terminal performance, and the constant factor $k\underline{/\phi}$ does not disturb this condition. The final equivalent circuit with a single source is shown in Figure 9.

If the source currents, representing either equivalent generation or net generation, have relatively large phase displacements with respect to each other, the procedure just outlined may produce negative resistance terms in the branches of the final equivalent circuit. It may be possible to avoid negative resistance by changing the angle ϕ. If this is done, one additional branch Z_{12}'' will appear between terminals 1 and 2.

Another way to avoid negative resistance is to divide each original source current into two parts, one a quadrature component which can be represented by a capacitor at each terminal, and chosen so that the remaining parts of all source currents are in phase. This can be stated more clearly in terms of power quantities. Assume that the terminal voltages in the present example are nearly in phase. Then, if the three generator loadings are at widely different power factors, negative resistance may appear. To avoid this, all of the real power generation is transferred from each terminal, at some convenient uniform power factor for all sources involved, to the star point; the balance of the reactive power is generated locally at each terminal by means of capacitors. If an equivalent source consumes reactive power, a shunt reactor can be used at that terminal instead of a capacitor.

This method of reducing the equivalent power sources to a single source is based on the assumption that the equivalent generator loadings are given in terms of fixed and known currents. In terms of power quantities, the single source located at the star point must generate the additional I^2R and I^2X losses incurred in the flow of current from the single source to the terminals of the equivalent circuit. This effect appears as a higher star-point voltage and as a shift in its angular position ahead of the terminal voltages. The star-point voltage and additional generation to supply losses can be estimated, in order to facilitate establishing the initial terminal conditions of the study. Then, in the course of the study, the single source is adjusted to produce the same total power and reactive input to the terminals as calculated for the original equivalent network from which the single-source circuit was derived.

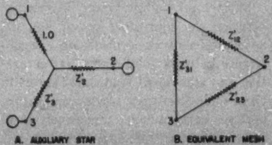

A. AUXILIARY STAR B. EQUIVALENT MESH

Figure 7. Auxiliary star network and its equivalent mesh, used in the derivation of the single-source circuit

If a change of internal generating schedule in the reduced system is to be simulated, a new single-source network must be computed, unless it can be assumed that all generation which has been shifted to the star point changes loading in the same proportion.

Transformer Taps

In network analyzer studies, convenient base voltages are chosen for the various transmission and subtransmission levels, and the analyzer voltage measurements usually are taken in terms of percentages of these nominal values. Very frequently, transformers represented in a study have actual turn ratios deviating from the ratios of the arbitrary nominal values assigned to the voltage levels interconnected by the transformers. Although nominal voltage transformations do not appear in the analyzer set-up, any such deviations from nominal ratio are represented at points of transformation by adjustable autotransformers provided for the purpose. The occurrence of off-nominal turn ratios within a system should be considered in devising an equivalent circuit for the system, because these ratios may have an important effect on terminal voltages and the distribution of reactive power. Since the possible situations in regard to off-nominal transformer tap settings are so numerous, a general treatment is not attempted. Several suggestions are offered to assist in reproducing, at least approximately, the effects of transformer turn ratios.

A residual, off-nominal turn ratio, encountered in tracing from one tie line terminal to another through the system being reduced, can be represented in the equivalent circuit by connecting an analyzer autotransformer in series with one of the terminals. If n terminals are retained, and a different residual turn ratio appears between each pair of terminals, these may be represented by $(n-1)$ autotransformers at any $(n-1)$ terminals. This assumes that the product of turn ratios around any closed loops in the reduced system is unity. If this is not the case, it is possible to encounter different residual ratios in tracing through different paths between two given terminals. Normally these differences will be small, or the paths involved will be of high impedance and an average ratio can be used.

A simple test on a network analyzer can be used to determine the net turn ratio between retained terminals in a complex network. A voltage of 100 per cent is impressed at one terminal on an analyzer set-up of the complete line network, with capacitors, loads, and generators open, and with all autotransformers adjusted to represent normal transformer tap settings. The voltages measured at the other terminals can be used to compute the net turn ratios between terminals.

Transfer-impedance measurements should be made with taps set at normal value if residual turn ratios between retained terminals are small or zero. If a relatively large turn ratio exists between one terminal and the rest, it may be possible to reduce this during impedance measurements by altering the tap settings of transformers at or near the terminal in question. Then, if the turn ratio is introduced in series with that terminal of the equivalent circuit, the transfer-impedance representation will be approximately correct.

The sum of the distribution factors described under method I may not be equal to unity in the presence of off-nominal turn ratios. The distribution factors as read with normal tap settings should be applied to the source and load currents. In applying method II to determine the equivalent loads and generators, residual turn ratios between terminals should be represented during the determination of normal-voltage circulating flow through the equivalent line network.

Using the Equivalent Circuit

After the desired equivalent circuit has been derived, it is set up, connected at the proper points to the detailed representation of the adjoining system, and the desired tests are carried out on this detailed portion. Some additional suggestions are given here on using the equivalent circuit during these tests.

If the information on equivalent loads and generation has been derived in terms of per unit current, the corresponding loadings in terms of real and reactive power can be calculated, using known or estimated voltages at the tie line terminals.

If it is necessary to estimate these voltages initially, the actual conditions are established by trial on the first analyzer study. During subsequent tests, the equivalent loads are held at constant values of real and reactive power.

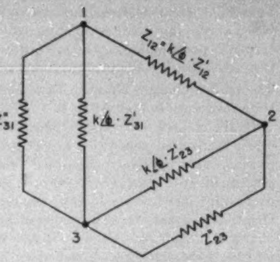
1
2
3
$Z_{12} = k\angle\theta \cdot Z'_{12}$
Z''_{31}
$k\angle\theta \cdot Z'_{31}$
$k\angle\theta \cdot Z'_{23}$
Z''_{23}

Figure 8. Mesh network equivalent to Figure 6

Assuming that generators in the reduced system are operated at a scheduled power output and fixed terminal voltage, the real power loading of the equivalent generators is held constant. The reactive loading of the actual generators, particularly those near the tie-line terminals, might vary during studies of different conditions in the adjoining system. This introduces a serious deviation from the basic assumption of constant-current sources, and gives rise to the problem of adjusting the reactive generation in the equivalent circuit. For the purpose of simplifying this problem, it is desirable to choose, as points retained in the equivalent network, busses where, in normal system operation, the voltage is held at a definite, known value. Then, only the power component of equivalent loads and generation need be determined. Equivalent reactive generation is adjusted to hold voltage. It may be helpful to calculate the equivalent generation at each terminal corresponding to the scheduled real power loading of all suppressed generators and the maximum reactive power capability of all generators and other sources of reactive power. This information can be used as a guide to avoid obtaining an unreasonable amount of reactive support from the equivalent circuit when some particularly severe emergency condition is being studied on the adjoining detailed network.

Since total tie-line power interchange between the equivalent circuit and the adjoining network depends on the difference between total equivalent generation and equivalent load, small errors in these quantities may assume major proportions in reproducing a relatively small power transfer. If inter-company ties are involved, the total transfer usually is specified. In other cases, it is well to check the initial measured transfer to or from the equivalent circuit, against the difference between generation and load plus estimated losses in the reduced system. The equivalent loads may be shaded, if necessary, to establish the correct total power interchange.

Conclusions

In steady-state power-flow studies, the treatment of system loads and generation as constant-current quantities gives a sufficiently realistic representation to warrant taking advantage of any simplification in analysis which may result. This assumption fails, however, to give a satisfactory reproduction of actual characteristics under certain conditions, notably short circuits and power swings.

A general statement on accuracy is not attempted, because the importance of various assumptions and the degree of approximation involved depend on the nature of the system being reduced. Trial on several types of power networks, and in actual system studies, has yielded good results. The equivalent circuits derived by these methods are capable, in the cases tried, of reproducing with acceptable accuracy the terminal performance of the reduced network with various emergency operating conditions represented in the adjoining system.

When an equivalent circuit is used to reproduce power flows over inter-company ties, accuracy requirements are not extremely rigid. One company, in the process of making a planning study of proposed future developments, usually has incomplete information on future plans of its neighbors, yet an approximate equivalent representation of neighboring systems may be necessary in the study. Joint studies of interconnection problems offer opportunities to obtain equivalent circuits of the systems involved as viewed from the inter-company boundaries. The methods described herein are well suited to this type of equivalent-circuit application.

Additional approximations can be employed to simplify determination of the equivalent circuit if the study at hand allows liberal accuracy limits. For example, the distribution factors in method I might be applied directly to kva loadings, neglecting voltage magnitudes and angles. A d-c board could be used to determine the distribution factors, if transformer taps are neglected and uniform impedance angles assumed.

In general, the new equivalent circuit representation occupies an intermediate position relative to methods *A* and *B* mentioned earlier in the paper. It is a more complete representation than method A, but it may lack some of the flexibility and accuracy of method B, through suppression of internal generating stations. It is intended to supplement existing methods; in practice, all three methods might be used simultaneously to advantage in some studies.

Appendix I. Analytical Methods and Basis for the Simplified Equivalent Circuit

The principles employed in methods I and II of the paper apply rigorously to an idealized network in which loads and generators maintain constant-current loadings, that is, currents fixed in magnitude and relative phase position regardless of bus voltage variations. Although these conditions are not realized in practice in a power-system network, such an idealized network is considered here for the purpose of illustrating the basis for practical applications. An analytical method is described for eliminating all busses, except the tie-line terminals in the section of the idealized network which is being reduced, and its equivalence to methods I and II is shown. This method can be adapted to the analytical determination of a power-system equivalent circuit if neither an a-c nor a d-c board is available for this purpose.

Referring to Figure 1 as an example, assume that the generators and loads satisfy the specified constant-current characteristics. Assume that connections exist to an adjoining network at the three points as indicated, and that it is desired to replace the system of Figure 1 with an equivalent circuit. Assume further that the neutral bus is common to both the section to be reduced and the adjoining section, and that the adjoining network contains at least one point of fixed or controlled voltage to neutral.

Under these conditions, the distinction between load and generation in Figure 1 is merely a matter of relative phase position of the current. Both the generators and loads can be treated alike as known, fixed, impressed currents. By Kirchhoff's law, the vector sum of the tie-line currents must be equal to the vector sum of the loads and sources (impressed currents). The equivalent circuit must reproduce the division of this total tie-line interchange among the several ties in the same manner as the actual network of Figure 1, when changes are being studied in the adjoining network. Within the section to be reduced, any bus or junction can be eliminated by a star–mesh transformation of the line impedances terminating at the junction. If an impressed current exists at the junction being eliminated, it can be removed, prior to the star–mesh transformation, by replacing it with separate currents at the neighboring junctions in such proportions that performance of the network beyond these adjacent terminals is not disturbed. New branches, appearing between neighboring junctions as a result of the star–mesh transformation, can be combined in parallel with circuits already existing between these junctions, and then the process repeated to eliminate another junction. In this way, all busses except the tie-line terminals can be eliminated, and, in the process, all source and load currents will have been shifted to these terminals to appear as equivalent impressed currents. As long as equivalence is maintained at each step, the final circuit, such as that shown in Figure 4 for the system of Figure 1, will reproduce the performance of the reduced network as viewed from the adjoining network. Hence, it is only necessary to show that this process is valid in eliminating the common junction of a general n-point star connection of impedances with a fixed current impressed at this common junction.

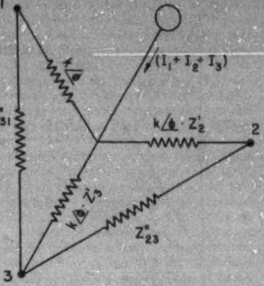

Figure 9. Final single-source circuit

The general star–mesh transformation is well-known, and is included here merely for convenience and consistent notation. Let Z_1, Z_2, $\ldots$, Z_n represent the impedances connected from the common junction to terminals 1, 2, $\ldots$, n, respectively, of an n-point star network. In general terms, let j and k denote any two of the n terminals. Then Z_{jk} represents the impedance between terminals j and k in the equivalent mesh network and its value is given by

$$Z_{jk}=Z_jZ_k\left(\frac{1}{Z_1}+\frac{1}{Z_2}+\frac{1}{Z_3}+\ldots+\frac{1}{Z_n}\right) \qquad (2)$$

An impressed current (representing either a source or a load) existing at the common junction of an n-point star can be divided into n parts and relocated at the n remote terminals of the star. If the total impressed current remains the same and the voltage differences between the terminals of the star are not disturbed, the performance of the network beyond the terminals of the star will be the same. In general terms, let I_k represent the portion of the original impressed current, I, which is shifted to terminal k. The following relations must be satisfied to preserve equivalence of the modified network

$$I=I_1+I_2+I_3+\ldots+I_n \qquad (3)$$

$$I_1Z_1=I_2Z_2=I_3Z_3=\ldots=I_nZ_n \qquad (4)$$

By combining the relations given in equations 3 and 4, the values of the new impressed currents at the terminals can be determined. In general terms, this leads to the following expression for the portion of the original impressed current to be transferred to terminal k

$$I_k=I/Z_k\left(\frac{1}{Z_1}+\frac{1}{Z_2}+\ldots+\frac{1}{Z_n}\right) \qquad (5)$$

This method of eliminating junctions containing impressed current accomplishes the same result as a reduction formula in matrix or tensor form discussed by Kron.[1] In the case where n is equal to two, equation 5 reduces to the familiar relation for replacing a tap load on a line section by equivalent loads at the two ends of the line.

In carrying out successive applications of this reduction, it is desirable to identify the original impressed currents by letters or symbols, and to retain them as literal rather than numerical expressions, keeping a record of the numerical coefficients of these currents as junctions are eliminated. When the process is completed, that is, when all except the tie-line terminals have been eliminated, all of the original sources and loads will have been shifted to the retained terminals with, in general, a portion of each appearing at each terminal. Upon collecting coefficients of like terms in the expression for the total equivalent impressed current accumulated at each tie-line terminal, the distribution factors of equations 1 will be obtained. Any desired schedule of source and load currents in the original network can be converted into equivalent currents impressed at the tie-line terminals by equations 1.

Either method I or method II of the paper can be applied to the idealized constant-current network to obtain the same result as that yielded by the analytical method just described. In the case of method II, the normal-flow interchange and the normal circulating flow would be expressed in terms of current rather than power quantities.

The equivalence of these different methods can be demonstrated by the principle of superposition. Any voltage differences existing between the tie-line terminals can be considered as arising from currents circulating through the line network of the reduced system, with the source of these circulating currents residing in the adjoining system. If the tie-line terminal voltages are equal, there can be no circulating currents; in the equivalent circuit, the impressed current at each terminal then will be equal to the tie-line flow at that terminal. In other words, the equivalent impressed currents are equal to the corresponding tie-line currents in the actual network, when the circulating currents are suppressed. In method I, the circulating currents are suppressed by connecting all tie-line terminals together. The resulting natural distribution of each internal impressed current in the tie lines is measured separately, and then equations 1 accomplish the proper superposition of the effects of all internal impressed currents.

In method II, any arbitrary "normal" operating condition of the complete network is used as a basis. The circulating-current components of the resulting tie-line flows are determined by impressing the "normal" voltage differences at the terminals of the equivalent line network, and then the equivalent impressed currents are obtained by separating the circulating components from the "normal" tie-line loadings.

Appendix II. Sample Calculation of Single-Source Equivalent Circuit

It is assumed that the equivalent circuit of Figure 6 has been derived to replace a power-system network, and that an additional reduction in the number of sources is necessary before this circuit can be used in the detailed study of an extensive system, to which it is interconnected at terminals 1, 2, and 3. The numerical values associated with the equivalent circuit are:

Impedances in per cent on 100,000 kva base

$Z_{12}=11+j40=41.4\underline{/74.6}$ degrees
$Z_{23}=6+j24=24.8\underline{/76}$ degrees
$Z_{31}=34.8+j118=123\underline{/73.6}$ degrees

Source currents in per unit (referred to voltage at terminal 1)

$I_1=0.57-j0.19=0.60\underline{/-18.5}$ degrees
$I_2=1.61-j0.70=1.76\underline{/-23.5}$ degrees
$I_3=0.10-j0.12=0.156\underline{/-50.2}$ degrees

It is assumed further that the impedance angles are sufficiently uniform to use scalar impedance with a constant impedance angle of 74 degrees, and that normally the interconnection terminal voltages are displaced only a few degrees. These latter assumptions are not required by the method, but they simplify calculations in cases where they can be made.

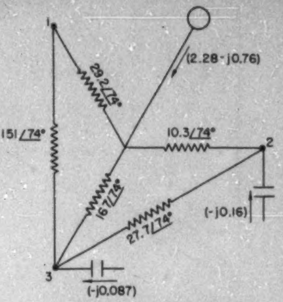

Figure 10. Single-source equivalent circuit derived in the numerical example

Values of current are in per unit; impedances are in per cent on a 100 megavolt-ampere base

In order to avoid negative resistance and to permit scalar computations, the original source currents are modified by separating each of the currents I_2 and I_3 into two parts: a quadrature component to be generated by a capacitor, and the remaining portion to be combined at a new junction established later. The portion of each which is to be moved to the new junction is chosen so that the phase angles of all three currents are the same. These modified source currents, used in subsequent calculations, are

$I_1=0.57-j0.19=0.6\underline{/-18.5}$ degrees
$I_2=1.61-j0.54=1.7\underline{/-18.5}$ degrees
$I_3=0.10-j0.033=0.105\underline{/-18.5}$ degrees

In the auxiliary star network of Figure 7(A) the values of Z_2' and Z_3' are $0.353\underline{/0}$ degrees and $5.71\underline{/0}$ degrees respectively, from the relation $0.6\cdot1.0\underline{/0}$ degrees $=1.7\cdot Z_2'=0.105\cdot Z_3'$; the branches of the equivalent delta, Figure 7(B) are: $Z_{12}'=1.42$, $Z_{23}'=8.06$, and $Z_{31}'=22.86$. By inspection, the ratio Z_{12}/Z_{12}' is larger in magnitude than the corresponding ratios of the other branches, hence the value of k/ϕ is taken as $(41.4\underline{/74}$ degrees$)/(1.42\underline{/0}$ degrees$)=29.2\underline{/74}$ degrees.

When the impedances in Figure 7(B) are multiplied by k/ϕ, the branch between terminals 1 and 2 in the resulting network is the same as the corresponding branch in the original equivalent circuit of Figure 6. Additional branches of the proper impedance can be connected between other pairs of terminals, see Figure 8, to make the resulting network entirely equivalent to that of Figure 6. This requires, in the present example: $(Z_{23}''\cdot k\underline{/\phi}\cdot Z_{23}')/(Z_{23}''+k\underline{/\phi}\cdot Z_{23}')=Z_{23}$; or $Z_{23}''=27.7\underline{/74}$ degrees, and, similarly, $Z_{31}''=151\underline{/74}$ degrees.

Since the network of Figure 7(B), with all branches multiplied by $k\underline{/\phi}$, is contained in Figure 8, this portion may be replaced by the star from which it was derived, Figure 7(A), with all impedances multiplied by k/ϕ. The sum of the modified source currents can be impressed at the common junction of this star, and the residual quadrature components of source currents can be impressed at the terminals to obtain the final equivalent circuit, requiring a single power source, as shown in Figure 10.

Reference

1. TENSOR ANALYSIS OF NETWORKS (book), **Gabriel Kron.** John Wiley and Sons, Inc., New York, N. Y., 1939, page 378.

Discussion

R. D. Goodrich, Jr. (United States Bureau of Reclamation, Denver, Colo.): Ward's introduction of the constant-current-type equivalent circuit is a distinct contribution to the technique of a-c network-analyzer operation. It provides a quick and simple method for representing the essential feature of a secondary network, namely, its ability to transfer power from one point of interconnection with the main network to another.

If power flow at the points of interconnection with the main network is the only purpose for which the equivalent circuit is required, it would appear that the equivalent generators in Figure 5(C) could be adjusted by trial rather easily, and thus the labor of computing the fictitious power outputs of these units could be avoided. If the equivalent generator at one point of interconnection is omitted, there should be only one combination of adjustments of the remaining generators which will yield the desired values of interchange power. The significance of individual generator powers in the equivalent circuit will, however, be lost.

Where a more complete equivalent circuit is required, as in stability studies, for example, it has been found convenient to use the star-type equivalent circuit, shown in Figure 1 of the discussion, corresponding to the mesh equivalent of Figure 2 of Ward's paper.

It can be proved mathematically that the two equivalent circuits are interchangeable. However, the star equivalent has the advantages that:

a. It requires less impedance units to set up.

b. It permits the elimination of an impedance leg, if no connection is to be made to it.

c. It allows, in some cases, the alteration of an impedance to simulate a change in line reactance, generator reactance, or total system load.

The star equivalent has the disadvantage that the evaluation of Z_a, Z_b, and so on requires the solution of a set of simultaneous equations, one equation for each unknown impedance. However, the symmetry of the coefficients of the unknowns simplifies the labor involved.

To determine the Z's, a reasonable power flow first is established in the secondary network on the network analyzer. Then the secondary network is disconnected from the main network and from the generator units, and a meterable jumper is connected to each point to be retained, including the ground bus. In some cases, it is permissible to bus together all of the points of generation in the secondary network, so as to retain a single equivalent generator. The final step of analyzer operation is to measure the impedance between each pair of jumpers, with the other jumpers separated electrically.

The series of readings obtained gives values of Z_a+Z_b, $Z_a+Z_c \ldots Z_2+Z_3$. Evidently, for the 7-point network shown in Figure 1 of the discussion, 21 such equations can be written, but, since there are only 7 unknowns, 14 of the equations are redundant. Although it has certain limitations, the method of least squares often is considered to yield the most reasonable values for the unknowns under these conditions. The least squares procedure is as follows: first, multiply each of the original observation equations by its coefficient of the first unknown, Z_a, and add the products. Since the coefficient of Z_a is one in six of the equations, and zero in the rest, six equations will be added together to yield a normal equation of the form

$$6Z_a+Z_b+Z_c+Z_G+Z_1+Z_2+Z_3=M_1$$

Next, multiply each observation equation by its coefficient of Z_b, and add the products. The second normal equation will, therefore, be

$$Z_a+6Z_b+Z_c+Z_G+Z_1+Z_2+Z_3=M_2$$

This process is repeated until seven normal equations have been formed; their solution will yield the impedances desired. The resulting equivalent circuit will be

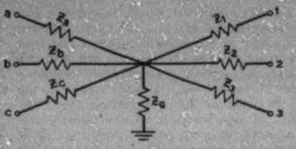

Figure 1. Star type of equivalent circuit

found to simulate very closely the effects of the original system, both for steady state and for transient conditions.

C. E. Parks (Public Service Company of Indiana, Inc., Indianapolis, Ind.): The author is to be congratulated for his novel approach to the subject of the setting up of equivalent circuits for power-flow studies on an a-c network analyzer.

Most electric utility companies are now employing the a-c network analyzer in the solution of present, and future, system operation and development problems. A large majority of the systems now being analyzed on the calculating board are interconnected with at least one other company. Where these interconnections become numerous, the problem of representing the adjacent system's transmission line set-up, taking into account that system's possible development in the future becomes a very important factor in the study under consideration. If the adjacent system is set up in detail, it usually requires that a joint study be conducted. While such joint studies are very desirable, they consume the time and effort of the operating engineers of both companies involved. Such an arrangement will result usually in abbreviating the system set-up for both systems involved, because of the limitations for board facilities, and further generally will limit the number of studies that can be conducted in a prescribed period.

The author of this paper, since he is engaged actively in power-flow studies of the numerous systems which employ the Purdue network analyzer, has appreciated this problem, and in his excellent paper, has presented a very sound solution of the problem.

The methods that he suggests have been employed in power-flow studies made by the Public Service Company of Indiana, Inc. It has been found, by actual practice, that the results obtained by using the equivalent circuits established by these methods has proved sufficiently accurate in the solution of the study being conducted. Other methods of representing the adjoining systems network have been tried out by our company, but it has been found that the method presented by the author in this paper produces by far the most accurate results.

Again, may I congratulate the author in his fundamental thinking in the development of the ideas presented in this paper, and express the hope that other operating companies will make use of this time- and labor-saving tool in their future studies.

Glenn W. Bills (Bonneville Power Administration, Portland, Oreg.): There is a definite need, by those engineers who use a-c network analyzers, for the type of equivalents introduced by this paper. It is a welcome contribution and should prove useful to most utilities that have calculating boards. Although the Bonneville Power Administration's a-c analyzer has 18 board generators, the Northwest Power Pool contains more interconnected systems than can be set up in detail; thus, we require equivalents.

In many problems on our board, these equivalents contain too many impedance units, since there are generators in the networks we desire to reduce. Ward's method supplies an ingenious method for reducing the number of impedances needed and allows for changes in loads and generation. In the majority of our studies, generators and loads are maintained at constant power output, and usually the reactive power changes very little so that it isn't necessary to be able to alter these. However, to be able to reduce the number of generator sources is of much value, and the author should be complimented on his neat scheme for reducing the number of equivalent generators.

We have attacked the problem of equivalents and solved it in another way. It is based on the fact that generators can be replaced by negative impedances in analytical solutions, assuming constant impedances. To do this on an a-c analyzer, we have developed an electronic negative impedance capable of use with the analyzer. This means that a system to be reduced can have its generators replaced by the negative impedances, and transfer impedances may be measured between the network terminals, as in method B described in the paper. Should any of these impedances contain negative resistances, one of our negative impedances can be used to represent it. In this fashion, it is possible to eliminate the use of distribution currents, which, as Ward has pointed out, can be quite "lengthy and cumbersome." Incidentally, these negative resistors can be used as board generators in conjunction with the ordinary board generators, as well as provide a representation of negative resistor elements. However, even with negative resistors, it is helpful to have a method for obtaining single-source equivalent circuits in parts of systems remote from the central portion being investigated. In this connection, negative impedances would simplify the procedure given by Ward to secure a single-source equivalent. In those cases where negative resistances appear, they easily can be represented by the electronic units, thus obviating the need for mathematical stratagems, such as "changing the angle ϕ," to eliminate negative resistances.

The author's pertinent comments on the effect of transformer taps in obtaining equivalents should be helpful to those who have had to contend with interconnected systems. Few, if any, articles have mentioned this subject, and the author deserves praise for bringing it to the attention of system engineers.

Now that at least two methods exist for obtaining satisfactory steady-state power-flow equivalents, it is desirable to obtain one which would be satisfactory for power-swing studies. In those cases where the generators are in an area electrically remote from the network upon which are inflicted shocks, such as line faults and line clearances, the generators usually oscillate together as a unit.

For such cases, equivalents are measured by means of method B, the generators in the network being represented by their transient impedances. The end result is an equivalent which contains a single equivalent generator. However, the equivalent rarely satisfies the initial steady-state conditions at the retained terminals and is not rigorous. It should be possible, by means of an extension of Thévenin's theorem to n terminals, or by some other device, to determine an equivalent which would be much more satisfactory than those used at present in swing studies. If any system engineers or network specialists know of such a method, it would be appreciated greatly if they would publish a paper on the subject.

R. J. Tallent (Ebasco Services, Inc., New York, N. Y.): Ward has developed equivalent-circuit methods which are quite an improvement over the old conventional methods. Power systems have grown so large, and interconnections have become so common, that it has become quite difficult to condense, by the conventional equivalent methods, some systems sufficiently to get them on the board. It has been a problem to set up the critical sections in enough detail so that line loadings and voltages may be observed, and yet leave enough board generators and impedance elements to accurately reproduce the adjoining system. By using Mr. Ward's method, it is possible to reduce considerably the number of elements in the adjoining-system equivalent.

The method in the paper described under method I, paragraphs 1 through 5, would give a flexible set of results suitable for readily representing a variety of load and generation conditions, but, as noted, the work involved in reducing a large system with many loads would become lengthy and time consuming.

The methods described under method II, paragraphs 1 through 5, are an improvement on the above insofar as reducing labor and time, but have the disadvantage of requiring both systems to be set up simultaneously. This requirement nullifies one big advantage of the method, since shortage of analyzer elements is frequently the motivating reason for using equivalents. Also, as recognized, results are not as flexible, since they pertain only to a given generation and load condition.

The method described in paragraph 6 under method I sounds promising and practical. However, as described, the results would not include the effect of varying generation in the neighboring system. This would limit its usefulness to a degree. If this method could be extended simply to include generation effects, it would find frequent application, since it would be very easy to carry out, requiring only one system set up at a time. Results would be accurate enough for a large variety of studies, presuming, of course, the studies deal with like load conditions and the same system.

Perhaps, by applying the superposition principle, it may be possible to extend this method to include generation effects without either increasing the work and time appreciably or causing need for major set-up reconnection, such as disconnecting loads.

This might be done in the manner described below.

1. Proceed as described in paragraph 6 and obtain load distribution factors for the interconnection points.

2. Next alternately and singularly connect, by a metering lead in parallel with the leads to the interconnection points, the various generating buses to the board generator. Adjust loads and record flows in each metering lead for each generating bus.

3. By application of the superposition principle, the distribution factor for each generating plant to the interconnection points may be obtained by subtracting results of step 1 from step 2, and dividing by the flow in the lead to generating bus.

4. The net load at each interconnection point may be computed by following equation:

$$Load_1 = D_1(Load) - D_{1a}(MW_a) - D_{1b}(MW_b) \ldots .$$

where

D_1 = distribution factor for loads as obtained in step 1 for interconnection point 1

Load = total system substation load

D_{1a}, D_{1b} = distribution factor for power plants *a* and *b* to the interconnection point 1

$Load_1$ = net load or generation at interconnection point 1

5. Adding these equivalent loads or generations to the interconnection points, and connecting these points by the transfer impedance between them, will give a close equivalent.

Edward W. Kimbark (Northwestern University, Evanston, Ill.): The representation of a multiterminal active network by a mesh of impedances, with a constant-current source at each terminal, as described by Ward, is really an extension of Norton's theorem to a network of more than two terminals.

Thévenin's theorem, in which a 2-terminal active network is replaced by an equivalent circuit consisting of a constant-voltage source and an impedance in series, is known and used now by many power engineers.

Norton's theorem, the dual of Thévenin's theorem, is not so well known. According to Norton's theorem, a 2-terminal active network can be replaced by the parallel combination of an impedance and a constant-current source. The impedance is the same as that of Thévenin's theorem. The current is equal to the short-circuit current of the original network.

Another fact not generally known is that Thévenin's and Norton's theorems can be extended to networks having more than two terminals. Instead of one impedance branch, there is now a branch between each pair of terminals. These impedances can be found by reduction of the original network after short-circuiting each constant-voltage source and open-circuiting each constant-current source in that network. Thévenin's equivalent circuit has a constant-voltage source in series with each terminal, except the reference terminal, equal to the open-circuit voltage between the corresponding terminal and the reference terminal. Norton's equivalent circuit has a constant-current source shunted between the reference terminal and each other terminal. The current of each source is equal to the short-circuit current of the corresponding terminal.

J. B. Ward: Tallent points out a disadvantage of method II in the necessity of setting up simultaneously the network to be reduced together with the section to be studied in detail. On the surface, if such a set-up were possible, it might seem that the equivalent circuit was not required. The author had in mind a particular situation in proposing method II, namely, the occasional necessity of interconnected operating companies making joint studies wherein skeleton representations of the major transmission networks are used to permit setting up simultaneously the several systems and studying interconnection problems of mutual interest. While such a set-up is available on the analyzer, it is a simple matter to obtain equivalent circuits by method II. Then these equivalent circuits will be useful in subsequent detailed studies made by the separate companies on their individual systems.

In connection with Tallent's comments on the approximate apportionment of load in paragraph 6 under method I, it was intended that the equivalent generation be obtained by separately measured distribution factors, with loads disconnected, as described in preceding paragraphs 1 to 5. Tallent's discussion outlines an interesting application of superposition, leading to essentially the same result with loads left connected.

The star-type equivalent circuit suggested by Goodrich is not interchangeable with the mesh circuit, Figure 2 of the paper, in the sense of exact general equivalence. For a general *n*-terminal circuit, a minimum of $n(n-1)/2$ links is required in an equivalent circuit.[1] The links of the circuit in Figure 2 of the paper, expressed as admittances, are the *D* coefficients of Starr's paper. The *C* coefficients of Starr's paper, which are commonly known as "self" and "mutual" constants,[2] may be arranged in an exact equivalent circuit, in the form of a star network with mutual coupling between branches. For the sample system of Figure 1 of the paper, this would appear as a star connection of six legs, with the common junction at the seventh terminal and with mutual coupling between each pair of the six legs, thus providing the required minimum of 21 impedances. Goodrich presents an interesting method for seeking the "best fit" of impedances in an approximate star network without mutual coupling. It is noted that the general "normal" equations for a given number of points of entry need be solved only once, since the coefficients are fixed by the number of terminals. Then this solution may be applied to any problem involving the same number of terminals. A simple relationship between self and mutual constants and the "through" impedances used by Goodrich is developed in Starr's paper.

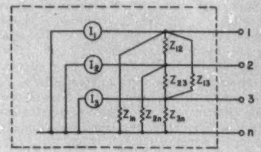

A. NORTON'S EQUIVALENT

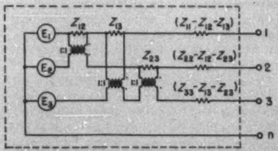

B. THÉVENIN'S EQUIVALENT

Figure 2. Generalized equivalent circuits

The reduction of a network containing sources as described by Bills treats both generation and loads as constant impedances, while, in the present paper, these quantities are considered primarily as impressed currents. The successful use of the two different approximations of power-system load and generator characteristics seems to indicate that, for the normal power-flow type of study, there is considerable freedom in designing equivalent circuits, based on combinations of the two viewpoints. If it is not necessary to deal with changes in loads, their representation as constant impedances lends itself more readily to wholesale reduction to equivalent loads at the tie-line terminals.

Kimbark's discussion brings out the close relationship between Norton's theorem and Thévenin's theorem. Although most power-system networks do not conform exactly with the idealized network characteristics on which these theorems are based, it is felt that there could be more widespread and effective application of these principles in power network analysis. Figure 2 of the discussion is submitted to supplement Kimbark's pertinent comments on extension of these theorems to more than two terminals. Two equivalent circuits are shown for a 4-terminal active network. Terminal *n* is taken as the reference terminal, corresponding to neutral in power networks. Note that the star-with-mutual circuit mentioned previously is shown in the generalized Thévenin equivalent circuit. This form yields a close analogy with the familiar 2-terminal case.

In the generalized Norton's equivalent, the links are transfer impedances, and the current sources are equal to the short-circuit currents obtained by connecting terminals 1, 2, and 3 simultaneously to *n*. The methods of the paper lead to a circuit of this type, and the impedances to neutral will appear if loads are retained as constant impedances. The voltage sources in the generalized Thévenin equivalent are the open-circuit voltages of the original network, measured with reference to terminal *n*. It should be emphasized that the self and mutual impedances appearing in Figure 2(B) of the discussion are not the same as the transfer impedances in Figure 2(A) of the discussion.

REFERENCES

1. EQUIVALENT CIRCUITS—I, F. M. Starr. AIEE TRANSACTIONS, volume 51, 1932, pages 287–298.

2. ELECTRICAL TRANSMISSION AND DISTRIBUTION REFERENCE BOOK. Westinghouse Electric Corporation (East Pittsburgh, Pa.), 1943, pages 87–96.

Vibrating Reed Selectors for Mobile Radio Systems

A. C. KELLER
ASSOCIATE AIEE

L. G. BOSTWICK
NONMEMBER AIEE

A NEW TYPE of signaling system has been developed for mobile radiotelephone service in the Bell Telephone System. This new system is described in a paper by H. M. Pruden and D. F. Hoth.[1] The basic selection of this system is performed by the use of vibrating reed selectors which are described in this paper.

Description of Selectors

A schematic diagram of the vibrating reed selector is shown in Figure 1. The vibrating reeds are attached to a block to form a small tuning fork, the tines of which are made of a suitably stable magnetic material, and are about an inch or less in length. A pole piece attached to a small magnet is positioned centrally between the ends of the tuning fork tines. Vibration of the tines takes place when the surrounding coil, shown in Figure 1, is energized with the proper voltage and frequency. The alternating magnetic field produced by the current through the actuating coil, increases and decreases the magnetic flux in the gap between the pole piece and the tines. This flux change in turn produces similar changes in the motion of the reeds. A light contact may be closed during a fraction of each cycle of vibration.

Two types of selectors are used in the mobile radio signaling system: the first, Figure 2, is a magnetically-operated tuning fork with an associated contact; the second, Figure 3, is similar except that the contact is omitted. The contactless type is used in a circuit to give filter characteristics as described later in this paper.

Vibrating reed selectors may be used singly or in groups, and in the latter case may be operated by a common actuating coil. The two types used in the new mobile radio signaling system are shown in Figures 4 and 5. Figure 4 shows the type used in the mobile station in which four selectors, each equipped with a contact, are operated by a common coil surrounding the four selectors. Figure 5 shows the type used in the fixed-station equipment, in which each selector is associated with an actuating coil. Each of the group of selectors shown in Figure 4 is provided with a plug-type base, so that they can be changed as needed. The four selectors, each of a different frequency, determine the mobile-station number or code. By changing the frequency of one or more of the selectors, the number of that particular mobile station is changed.

Use of Selectors in Signaling System

In designing a multifrequency signaling system using these selectors, a choice must be made as to the number of available frequencies, the number of selectors at each mobile station, and as to whether simultaneous or sequential operation be used.

It was decided to use simultaneous operation, that is, all frequencies to be transmitted at the same time. This was done to improve the margin of satisfactory operation in the presence of various types of noise, fading, and so forth, as compared with pulse or sequence operation of equal operating speed.

The number of frequencies required, and the number of frequencies needed at each mobile station, is determined by the number of different combinations it is possible to make. If n frequencies are available, it is possible to make ${}_nC_r$ different combinations of r frequencies where

$$ {}_nC_r = \frac{n(n-1)(n-2)\ldots(n-r+1)}{r!} $$

For common-carrier mobile-telephone service, it appeared necessary to be able to select any one of 10,000 stations. Such a large number of selections can be achieved by using different values of n and r as indicated below:

r	n	${}_nC_r$
3	41	10,660
4	24	10,626
5	19	11,628
8	16	12,870

As can be seen, 24 frequencies taken four at a time will provide more than 10,000 choices. However, to realize the full number of selections with this combination, requires a random code and more apparatus for translation, than with other values of n and r. For example, simpler translation of a 4-digit directory number designating a mobile station results from using two groups, each of 15 frequencies, with a combination of two frequencies, in one group associated with the thousands and hundreds digits, and a combination of two frequencies in the other group associated with the tens and units digits. There are, of course, many other possible combinations, but for reasons discussed in the contemporary paper already referred to, two groups of 16 frequencies, ranging from 350 to 850 cycles, are used in the mobile-radio system.

Performance Characteristics of Mobile Station Selectors

The suitability of these vibrating reed selectors for mobile-radio selective signaling depends primarily upon their sensitivity at their nominal frequencies, upon their selectivity or discrimination against other frequencies, upon their operate times, and upon their stability with temperature and time. The first three of

---

Paper 49-99, recommended by the AIEE communication committee and approved by the AIEE technical program committee for presentation at the AIEE winter general meeting, New York, N. Y., January 31–February 4, 1949. Manuscript submitted November 8, 1948; made available for printing December 22, 1948.

A. C. Keller and L. G. Bostwick are with the Bell Telephone Laboratories, Inc., New York, N. Y.

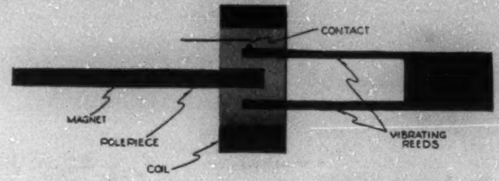

Figure 1 (left). Schematic diagram of vibrating reed selector

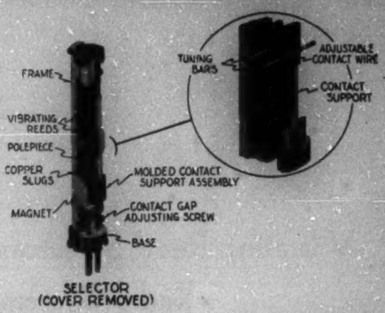

Figure 2 (right). Vibrating reed selector with contact

these factors in turn depend to a large degree upon the sharpness of tuning, or the Q of the mechanical vibrating system. In general, if the Q of a given fork is made larger, the current through the drive coil at the resonance frequency, necessary to vibrate the fork at the contact amplitude, becomes smaller in relation to the corresponding current at other frequencies. In other words, the higher the Q, the greater the sensitivity and selectivity. On the other hand, the operate time, or the time required for the tine amplitude to reach the contact amplitude, is also proportional to Q. If Q becomes too large, this build-up time becomes prohibitive. Furthermore, if Q is too large, the frequency bandwidth over which the sensitivity is within a 3-decibel range becomes so small that frequency drift in the electric supply source, and in the reeds themselves because of temperature changes and other causes, becomes troublesome in over-all system operation.

With these considerations in mind, and after some development experience in controlling frequency variations with temperature, a Q range was chosen to give a constant bandwidth (equal to resonance frequency/Q) of 1.2 cycles throughout the frequency range for selectors. This required that the Q vary directly with frequency, from about 300 at the lowest frequency to about 670 at the highest. With this choice of bandwidth, the operate time is always under 0.5 second for the lowest input level from the radio receiver, under the worst marginal conditions. The operate time is the time t required, after closing the circuit, for the fork tines to reach a contact amplitude a_t, and is related to the Q, the resonance frequency f, and the final steady state amplitude A as follows

$$a_t = A\left(1-\epsilon^{-\frac{\pi f t}{Q}}\right)$$

To obtain this adjustment of Q, electromagnetic damping was adopted, after considering other means, because of its relative independence of temperature. This damping is applied by means of copper collars slid over the pole piece to give short-circuited turns in the magnetic field, as shown in Figure 2.

The effect of the damping upon the sensitivity and the selectivity characteristics of the selector is shown by Figure 6. Plotted here on a relative decibel scale is the source power necessary to operate a selector with and without damping, and having Q values of 280 and 735, respectively.

The sensitivity of the selectors at their resonance frequencies depends upon several factors in addition to Q; these include the electromechanical coupling or force factor, the effective vibratory mass, the contact spacing, and the frequency. As used for mobile radio with four selectors in a common drive coil, about 0.7 milliwatt available source power is required at each frequency to operate the contacts.

The tuning of a selector is accomplished by bending the tuning bars as shown in Figure 2. By bending these toward the base of the selector, the frequency is increased; by bending away from the base, the frequency is lowered. This effect is the result of changing the effective mass of the reeds. With these tuning bars, it is possible to adjust the frequency of the selectors within 0.05 cycle of the desired frequency.

Avoiding excessive variations in the

Figure 3. Vibrating reed selector without contact

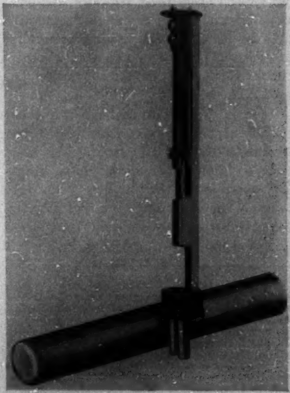

Figure 4. Mobile station selector set—four selectors in a common coil

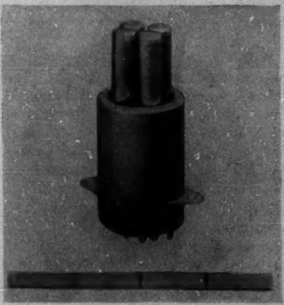

Figure 5. Filter selector in coil

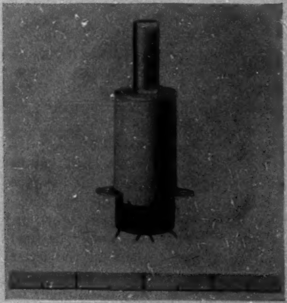

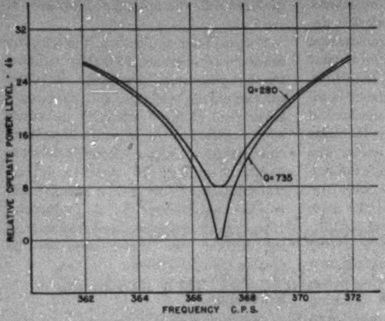

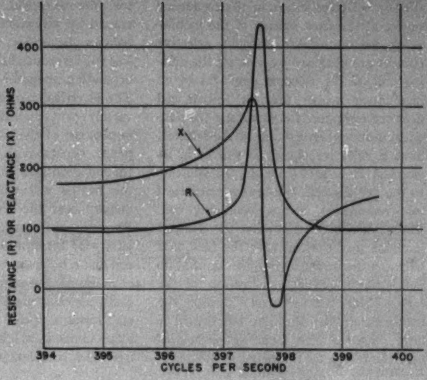

Figure 6 (left). Operate level–frequency characteristic of a selector with and without damping collars

Figure 9 (right). Electrical impedance characteristic of a filter selector

resonance frequency of the selectors with temperature has been one of the most difficult problems in the development. As used for mobile radio, selectors may be called upon to operate over a temperature range of −40 to +185 degrees Fahrenheit. Throughout this wide temperature range, the resonance frequency of the selector must not drift more than ±0.5 cycle from its nominal adjusted frequency at some median temperature, to meet over-all system requirements. Frequency changes with temperature occur primarily because of: changes in the elastic modulus of the time material; changes in dimensions, as effected by expansion; and changes in the flux density in the gap between the tines and the pole piece. This gap flux density affects the frequency because of the negative stiffness of the magnetic field, a well-known effect in electromagnetic driving systems. To keep changes in frequency within tolerable limits, materials have been used with low temperature coefficients of modulus and expansion, and with the most uniform magnetic characteristics. Furthermore, one effect has been used to compensate another, with the result that an integrated design has been achieved with temperature–frequency characteristics like those shown in Figure 7.

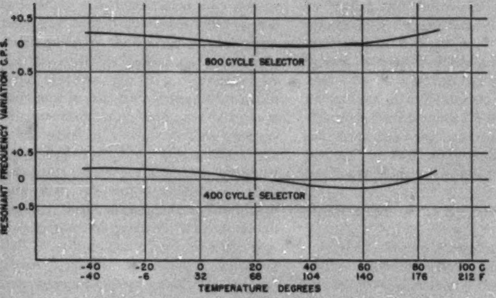

Figure 7 (above). Typical frequency—temperature characteristics of mobile station selectors

Performance Characteristics of Filter Selectors

As mentioned previously and as discussed in reference 1, vibrating reed selectors are used without contacts to provide

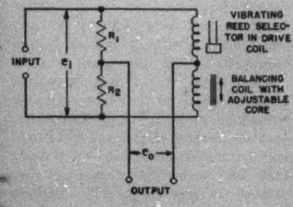
INPUT
e_1
R_1
R_2
VIBRATING REED SELECTOR IN DRIVE COIL
BALANCING COIL WITH ADJUSTABLE CORE
e_0
OUTPUT

Figure 8 (left). Vibrating reed-controlled selective circuit

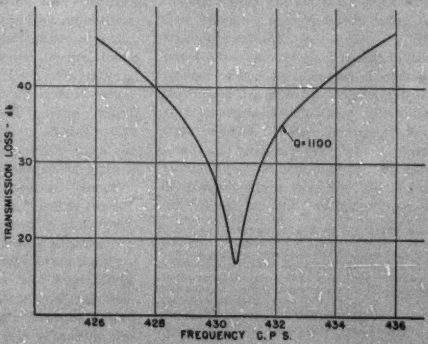

Figure 10 (right). Typical transmission loss characteristic of a reed filter sharply selective filters in the frequency source at the fixed station of the mobile-radio system. Such sharply selective circuits are obtained by making the driving coil of the selector one arm of an impedance bridge that is unbalanced near the resonance frequency by the electrical motional impedance of the selector. Such a selective circuit is shown in its simplest form in Figure 8. In addition to the driving coil, the bridge consists of two resistances and a balancing coil. The balancing coil simulates the damped impedance of the coil with the fork, and balances the bridge at frequencies that do not cause appreciable vibration of the fork. Under this balanced condition, the transmission loss through the bridge is large. On the other hand, at frequencies near the resonance frequency of the selector, the electrical motional impedance caused by vibration of the fork will unbalance the bridge, and the transmission loss will be reduced sharply, by an amount depending upon the degree of unbalance. The electrical motional impedance is inversely proportional to the mechanical impedance of the reed and has the same phase constant Q. Consequently, the transmission loss and phase shift through the bridge will vary rapidly with frequency near the resonance of the reed. For this mobile-radio application, a multiplicity of selectors, each with a driving coil and a balancing coil, are bridged on a common source of complex wave form. Each selector circuit, with its balancing coil, forms a bridge with two other common impedance elements, and selects from the complex wave form those frequencies near the resonance frequency of the fork.

For this filter application, the selectors are given a Q in excess of 1,000 by omitting the damping slugs previously described for the mobile selectors, and by using a cover shell of high resistivity to reduce eddy currents. A typical impedance characteristic of such a selector is shown in Figure 9. Figure 10 shows a typical transmission loss curve of a selective circuit like that in Figure 8. At frequencies 15 cycles or more away from resonance of the selector, the transmission loss is greater than 50 decibels.

Reference

1. Vibrating Reed Selective Signaling System for Mobile Telephone Use, H. M. Pruden and D. F. Hoth. AIEE Transactions, volume 68, part I, 1949, pages 387–91.

No Discussion

Vibrating Reed Selective Signaling System for Mobile Telephone Use

HAROLD M. PRUDEN
NONMEMBER AIEE

DANIEL F. HOTH
NONMEMBER AIEE

MOBILE telephone service is furnished by the Bell Telephone System through land radio stations connected to the wire telephone system. Since the number of radio channels available for this service is limited, it is necessary for a fairly large number of mobile stations to share the use of a single channel. In order that a mobile station may receive telephone calls, some means must be provided whereby the mobile-service operator may call the desired car. In many radio systems, this is accomplished by providing in each car a loud speaker which is in operation at all times, the desired car being called by voice. Such an arrangement has the disadvantage that the occupants of all the telephone-equipped cars hear all conversations on their channel. This is annoying and results in a reduction of privacy. Therefore, all Bell System common-carrier mobile-telephone systems use selective signaling arrangements, which enable the mobile-service operator to ring a bell in the desired car by dialing the car's telephone number.

The selective signaling system now in use involves the alternate transmission of a succession of 600- and 1,500-cycles per second pulses, under the control of the operator's dial. Each time the tone frequency is changed, a code wheel in the mobile station is stepped around one position. Five trains of pulses are transmitted, the total number of pulses being 23 or, in some cases, 25. If the proper number of pulses in each train is received, the code wheel steps to its 23rd position and the bell rings. If the wrong number of pulses in any train is received, the code wheel drops back to its starting position and therefore never reaches the 23rd position. This type of selective-signaling system, while reliable, has some disadvantages in that the mobile equipment is fairly expensive, physically large, requires a considerable amount of audio-frequency power from the radio receiver, and provides fewer number combinations than is desirable.

The vibrating reed selector, described by Keller and Bostwick,[1] provided an opportunity for the development of an entirely new type of selective-signaling system, a trial of which is now in progress. The new system has the principal advantages of a greater number of possible code combinations (10,000), and mobile signal-receiving equipment of lower cost and smaller physical size, requiring less audio-frequency power for operation.

Description of the System

Figure 1 shows a generalized block diagram of a mobile telephone system equipped for selective signaling. The land station is equipped with a signal-sending circuit, which, under control of the operator's dial, will deliver to the land radio transmitter a series or combination of audio-frequency tones peculiar to the mobile station being called. Each car is equipped with a signal-receiving circuit which is connected to the audio-frequency output of the radio receiver at all times except when a call is in progress. When the proper series or combination of tones is received, the signal-receiving circuit is actuated, ringing the call bell in the car. Except when maintenance or repair work is required, the land station is completely operated from the traffic switchboard by a telephone operator who may handle other types of telephone traffic as well. Therefore, the system is arranged so that its operation is, as nearly as possible, like that of other telephone facilities. Standard switchboard equipment and circuit arrangements are used.

The new signaling system, as well as the one now in use, fits into the type of radio system just described. However, the new system is basically different in the mode of operation. It was decided, early in the development program, to reject all systems requiring the transmission of a sequence of pulses to the mobile station, in favor of a type of signaling that could be applied continuously. A continuously applied signal is able to overcome difficulties caused by interference or fading, since it is necessary only to apply the signal for a sufficiently long interval to ring a bell. In contrast, signaling systems which depend on the transmission of a sequence of pulses are subject to failure or possible false operation whenever a pulse is mutilated or lost because of poor transmission conditions. The continuous-signal arrangement has the additional advantage that it makes possible an extremely simple signal-receiving circuit in the mobile station.

In the vibrating reed signaling system, the land station is equipped with a source of tones of 32 different audio frequencies. When the operator dials, a relay device, known as a sender, selects four of these tones, which are transmitted simultaneously over the land radio transmitter for a period of about four seconds.

Each mobile station is equipped with four vibrating reed selectors tuned to four different tone frequencies. A different combination is used at each mobile station. These selectors are miniature electrically-driven tuning forks equipped with contacts which close when the forks vibrate. When the proper four tones are received, the four selectors vibrate, their contacts close, and a circuit is operated which rings the bell in the car. Since no other mobile station is

---

Paper 49-100, recommended by the AIEE communication committee and approved by the AIEE technical program committee for presentation at the AIEE winter general meeting, New York, N. Y., January 31–February 4, 1949. Manuscript submitted November 15, 1948; made available for printing December 29, 1948.

HAROLD M. PRUDEN and DANIEL F. HOTH are with the Bell Telephone Laboratories, Inc., New York, N. Y.

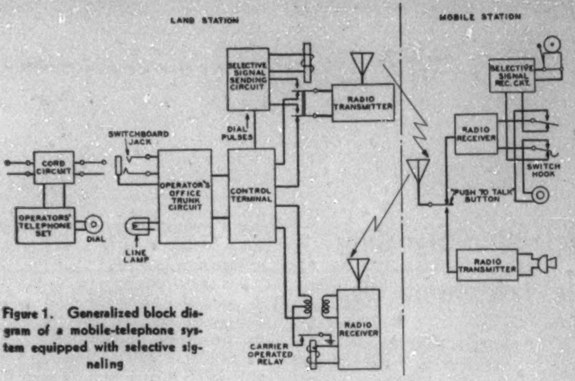

Figure 1. Generalized block diagram of a mobile-telephone system equipped with selective signaling

equipped to respond to the same combination of frequencies, no other bell rings.

The tone frequencies used are spaced 15 cycles per second apart. They are divided into two groups, the lower of which includes frequencies from 352.5 to 577.5 cycles per second, and the other includes frequencies from 607.5 to 832.5 cycles per second. This frequency range was chosen because it was suitable from the standpoint of design of the selectors. All tone frequencies are odd harmonics of 7.5 cycles per second. Therefore, even-order modulation products of the tones do not fall on other tone frequencies. As may be judged by the frequency spacing used, the selectors are tuned sharply, having an average bandwidth of 1.2 cycles per second. A power of only about 0.7 milliwatt is required to close their contacts.

The decision to use a total of 32 signaling frequencies, transmitted four at a time, was based on a number of considerations which may be of interest. First of all, the initial system requirements called for a total of 10,000 possible code combinations. This may seem an unnecessarily large number, since fewer than 100 mobile stations ordinarily operate on the same radio channel in any particular city. However, some of the mobile stations roam from one city to another. The numbers used by these stations, of course, cannot be duplicated in the cities in which they operate. The number capacity of the signaling system should therefore be as large as possible.

Telephone numbers ordinarily consist of a central-office code followed by a 4-digit number. It is desirable that the numbers for mobile-telephone service be assigned on a similar basis, and that the selective-signaling system have a capacity of 10,000 numbers, corresponding to the last four digits of the telephone numbers of the mobile stations.

The following table gives the minimum total number of signaling tones, n, which would be required for various numbers of tones, r, transmitted in each code (or numbers of vibrating-reed selectors per mobile unit):

r	n
1	10,000
2	142
3	41
4	24
5	19
6	17

It will be noticed that the value of n is very large when r is small, decreasing rapidly at first as r is increased, then more slowly.

It obviously would be impractical to use a system which required a very large number of different tone frequencies. On the other hand, increasing the value of r means a corresponding increase in the number of vibrating-reed selectors required per mobile station which increases the mobile station cost. It is apparent from the table that little advantage would be gained by increasing the value of r beyond four.

Another factor also entered into the choice of four is the number of selectors per mobile unit. The mobile signal-receiving circuit is subjected to speech and noise signals as well as the signaling tones. It must be designed so that it will not operate falsely on these signals. By requiring that a number of selectors all operate simultaneously to ring the call bell, the probability of false operation is kept small. Tests have shown that no trouble will be experienced with false operation from these causes when four selectors are used.

While a minimum of 24 tones will theoretically produce the desired 10,000 combinations, for practical reasons a larger number is used. It is a system requirement that the signal-sending circuit at the land station be controlled by a telephone dial at the traffic switchboard, and that only four pulls of the dial be required. In order to accomplish this, a register and a translator are used. The dial pulses are counted and registered on the register relays which, in turn, control the translator, which selects the tones corresponding to the desired code and connects them through to the land radio transmitter. Since no simple, orderly relationship exists between the original four-digit number and the combinations of 24 tones taken four at a time, the translator which would be required would be very complicated. On the other hand, if 40 tones were used, they could be divided into four groups of ten, and a tone from each group selected to represent the corresponding digit of the telephone number. The translation problem then would be extremely simple. However, the translation becomes nearly as simple if only 30 tones are used. These are divided into two groups of 15, one group representing the first and second digits of the telephone number, and the other group representing the third and last digits. From each group of 15 tones, it is possible to select 105 combinations of two, of which 100 combinations are used. With this arrangement, translation becomes simple enough so that it may be accomplished

Figure 2. Response curve of typical vibrating reed selector

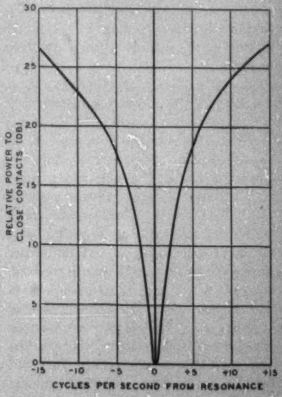

by using the contacts of the register relays; a separate translator is not required.

A further increase in the number of tones, to a total of 32, was adopted for another reason. The system must be designed so that false signaling does not occur in a mobile station when the land station transmits four tones of which three are the same as three tones of the code of the mobile station in question. The danger of false signaling is greatest when the fourth vibrating reed selector is subjected to two adjacent tones, one being one channel higher in frequency and the other one channel lower. This occurs only in mobile stations which are equipped with two selectors tuned to adjacent channels. Such codes may be eliminated by using two groups of 16 tones, or a total of 32.

Transmission Considerations

The system must be capable of operating over any useful radio circuit. Experience has shown that signaling is reliable, and normally will fail only on a much poorer radio circuit than is useful for speech transmission.

Tests also have shown that, in a properly designed and adjusted system, false signaling is virtually absent. However, there are a number of possible causes of false signaling. In the development of the system, it was necessary to give them careful consideration.

The possible causes of false signaling can be divided into two classes:

1. Those which occur when no signaling tones are being transmitted and thus simultaneously must operate all four vibrating reed selectors in the mobile station in order to produce a false signal.
2. Those which are the most serious when a code having three tones the same as the code of the mobile station in question, is being transmitted.

Causes of false signaling in the first class include noise, speech signals which are received during a call between the land station and another mobile unit, and the occasional transmission of various telephone-plant tones which possibly might contain frequency components corresponding to the resonant frequencies of the selectors in the mobile station in question. Tests have shown that no trouble may be expected from false signaling caused by any of these. Protection against such false signaling results from the fact that the selectors are tuned extremely sharply, so that the probability of sufficient energy falling within the bands of all four selectors to operate them is extremely small. As stated previously, the bandwidth of the vibrating-reed selectors is about 1.2 cycles per second. Figure 2 shows a response curve for a typical unit.

Causes of false signaling in the second class include cross-modulation products of the signaling tones, and adjacent-tone interference. Since the signaling tones are all odd harmonics of a basic frequency (7.5 cycles per second), even-order cross-modulation products always fall halfway between tone frequencies, and therefore would not be expected to cause trouble. On the other hand, odd-order products may fall directly on the signaling frequencies, and thus are potential causes of false signaling. However, tests have shown that there is ample margin against cross-modulation trouble in a well-designed system.

Tests made during the development of the system indicated that the most serious possible cause of false signaling was adjacent-tone interference. It was therefore necessary to give particular attention to this effect. The final system has been designed so as to be virtually free of such trouble.

Figure 2 shows that the steady-state discrimination of a typical selector against an adjacent tone 15 cycles per second away is greater than 25 decibels. Since the signaling-tone level applied to the selectors is normally about 8 decibels more than required just to close their contacts, the tone level would have to increase more than 17 decibels above normal for false operation to occur.

A peculiar type of interference, however occurs in moving vehicles when weak signals are received. Application of the system to date has been on frequency-modulation radio systems in the 150–160-megacycle band. Because of reflection of the radio waves, the signals almost always are transmitted from the transmitter to the receiver along two or more paths. Signals arriving by various paths may combine in or out of phase and thus, as the car moves along, the signal is alternately strong and weak as the path lengths vary. It can be shown that the minimum distance from one point of cancellation to the next is 1/2 wave length. As the car is moving along at about 35 miles per hour, fades can occur at rates as high as 15 per second. When the signal is strong, this fading does not affect the audio-frequency output of the receiver, since, in a properly designed frequency-modulation receiver with adequate limiting, variations in signal amplitude do not appear in the receiver output. However, when the signal is very weak, the limiter becomes ineffective and the audio-frequency signal level varies with signal strength. The rapid fading discussed, produces amplitude modulation of the signal. The result is that each tone has sidebands above and below its frequency. When the fading is at a 15-cycle-per-second rate, there are strong sidebands 15 cycles per second above and below the tone frequency or, in other words, at the resonant frequency of the next higher and lower vibrating-reed selectors. Under these conditions, discrimination of the selectors against adjacent tones is decreased markedly. Tests have shown a considerable decrease in margin against false signaling under these conditions. The interference is worst when the radio circuit is just too poor to be useful for voice transmission.

Adjacent-tone interference effects are most serious when the selectors in the car resonate at the frequency of three of the tones being transmitted, the fourth selector being between two tones 30 cycles per

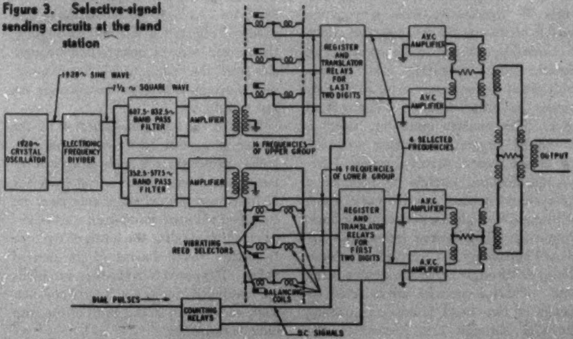
1920~ SINE WAVE
7½ ~ SQUARE WAVE
1920~ CRYSTAL OSCILLATOR
ELECTRONIC FREQUENCY DIVIDER
607.5-832.5~ BAND PASS FILTER
352.5-577.5~ BAND PASS FILTER
AMPLIFIER
AMPLIFIER
16 FREQUENCIES OF UPPER GROUP
16 FREQUENCIES OF LOWER GROUP
REGISTER AND TRANSLATOR RELAYS FOR LAST TWO DIGITS
REGISTER AND TRANSLATOR RELAYS FOR FIRST TWO DIGITS
A.V.C. AMPLIFIER
A.V.C. AMPLIFIER
A.V.C. AMPLIFIER
A.V.C. AMPLIFIER
4 SELECTED FREQUENCIES
OUTPUT
VIBRATING REED SELECTORS
BALANCING COILS
DIAL PULSES
COUNTING RELAYS
D.C. SIGNALS

Figure 3. Selective-signal sending circuits at the land station

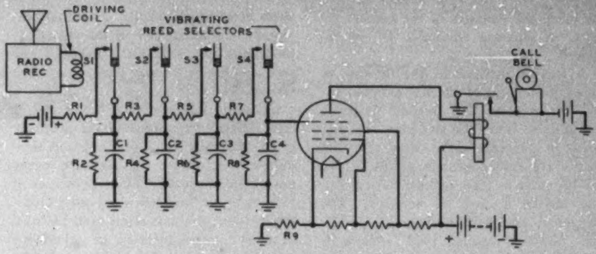

Figure 4. Simplified schematic diagram of selective signal receiving unit

second apart, 15 cycles per second from each. This can occur only in mobile stations having two adjacent selectors 15 cycles per second apart. Mobile stations having codes of this type occasionally may be signalled falsely, and therefore, as discussed previously, such codes have been eliminated by the use of 32 instead of 30 tone frequencies. Tests indicate that, with the 32-frequency arrangement, false signaling will be very rare.

Land Station Equipment

The selective-signaling circuits at the land station consist primarily of a source of tones of 32 different frequencies; a sender, which combines the functions of the register and translator previously discussed, and which counts the dial pulses and selects the proper four tones; amplifiers for amplifying the tones and precisely regulating their levels; and three transformers combining them on one pair of wires. A block diagram of these circuits is shown in Figure 3. When vibrating-reed signaling is provided on more than one radio channel at the same station, some of this equipment can be used in common for all or several of the channels.

The frequencies of the 32 tones must be held to about one part in 10,000, in order that most of the total frequency tolerance may be assigned to the selectors in the mobile station, where wide temperature variations may occur and stability is difficult to maintain. Suitable facilities are not available generally at the radio stations for readily measuring each tone frequency to the required accuracy. An arrangement therefore has been adopted for the 32-frequency source, which provides all frequencies from a common master oscillator, the frequency of which is checked by comparing the reading of an electric clock, operating from a submultiple of its frequency, with radio time signals or other suitable standards of time. The master oscillator, using a laminated crystal resonating at 1920 cycles per second, drives a series of frequency dividing circuits to produce a 7.5-cycle-per-second square wave which contains all the odd harmonics of the basic frequency. The desired frequencies are all odd harmonics of 7.5 cycles per second, the 47th through 111th harmonics being used. These harmonics are selected by means of two band filters, one passing the 47th through 77th harmonics, the other passing the 81st through 111th harmonics. Slope circuits are provided, so that all harmonics in each group appear at approximately the same level. These harmonics then are amplified and applied to 32 very-sharply-tuned filters, each of which selects one harmonic and rejects all others.

These filters use vibrating reed selectors as their frequency selective elements. The selectors differ from those used in the mobile stations only in their bandwidth, which is much narrower than that of the mobile selectors, and in that they do not have contacts. The selectors are used in bridge circuits which are well balanced to all frequencies in the signaling band, except the frequency at which the reeds vibrate. As a reed vibrates, the motional impedance of the selector unbalances the bridge circuit and causes the particular harmonic of the 7.5-cycle wave to which the selector is tuned to appear at its output terminals. The remaining harmonics are suppressed by at least 30 decibels.

The sender follows conventional telephone practice. The dial pulses from the operator's position are counted and registered on four groups of register relays, one group for each digit. The contacts on the register relays are connected to form two networks. The first contact network selects two frequencies from the 352.5- to 577.5-cycle-per-second group, as a result of registering the first two digits; the second network selects two frequencies from the 607.5- to 832.5-cycles-per-second group, as a result of registering the last two digits.

Each of the four tones selected by the sender is applied to an individual amplifier. Since there is some difference between the levels of the tones from the 32-frequency source, these amplifiers are equipped with automatic-gain-control circuits which regulate the levels of the tone to within ±1/2 decibel of the desired value. The outputs of the four amplifiers are combined through a hybrid-coil network and applied to the input of the land radio transmitter.

Mobile Station Equipment

A simplified schematic diagram of the mobile selector circuit is shown in Figure 4. The four vibrating reed selectors are driven by a common coil and are equipped with contacts which close when the reeds vibrate. The selectors fit into sockets inside the driving coil. The telephone number of the mobile station may be changed simply by plugging in a new set of selectors.

To insure maximum contact reliability, the contact current has been kept small. As a result, the selectors are not connected directly to the call bell but, instead, a d-c amplifier tube is used.

The contact closure of the selectors is not continuous but occurs over a short part of each cycle of vibration. The closure does not necessarily occur simultaneously in all four contacts. Therefore, the network consisting of *C1* through *C4* and *R1* through *R8* is used. Capacitor *C1* charges on closure of selector *S1*. Part of its charge is passed along to *C2* on closure of *S2*, and so on, the voltage finally being applied to the tube. Resistors *R2*, *R4*, *R6*, and *R8* discharge the capacitors in a short time after the selectors stop vibrating. Resistors *R1*, *R3*, *R5*, and *R7* protect the selector contacts by limiting the current through them.

The d-c amplifier tube is a pentode connected in an unusual manner. When the selector contacts open, the section of the tube consisting of the cathode and first and second grids acts as a triode with its control grid at nearly cathode potential. The second grid acts as an anode and its current is fairly large. Thus a voltage drop develops across resistor *R9*, raising the cathode above ground potential. The third grid is at ground potential, and is sufficiently negative with respect to the cathode that the plate current is nearly zero. When the selector contacts close, a positive voltage is applied to the third grid, and the plate draws current, operating the signaling relay. The bell in the mobile station continues to ring as long as the proper combination of tones is being received.

The d-c amplifier circuit was chosen because it is extremely stable. When the circuit is designed properly, using a suitable type of tube, the plate current is nearly zero when the third grid is at ground potential, regardless of wide variations in power-supply voltages.

The physical size of the mobile-station equipment required for reed signaling is considerably smaller than that of the corresponding equipment used in the present signaling system. The components shown in Figure 4 require a chassis area of about 10 square inches. In contrast, the corresponding elements of the present system require about 30 square inches. The volume of the present Western Electric type *38A* radio receiver, which is attributable to the built-in selective-signaling circuit, is about 200 cubic inches. The corresponding figure for vibrating-reed signaling is only about 40 cubic inches.

Advantages of the Reed Signaling System

The following are some of the advantages of the new system:

1. The mobile signal-receiving equipment is much smaller, adding only about 40 cubic inches to the volume of the mobile-station equipment instead of 200 cubic inches. This is a very important consideration since present types of mobile-radio equipment are much larger than desirable, and the selective-signaling equipment is an important element in the over-all size.

2. Less audio-frequency power is required from the mobile-radio receiver. In the new signaling system, about 18 milliwatts is applied to the selector driving coil, as against roughly 150 milliwatts applied to the old-type selective-signaling receiver. Since only about 10 milliwatts are required for talking purposes, the new signaling system permits the use of a radio receiver with smaller audio-frequency power capabilities. This reflects in design on the physical size of the receiver and on the current required from the car battery.

3. The new signaling system has a capacity of 10,000 codes, a much larger number than is available with the old system. As discussed previously, this is of importance because service is given to cars which roam from one radio system to another, and whose numbers may not be repeated, therefore, in any system in which they operate.

4. Only four instead of five pulls of the operator's dial are needed in the new system.

5. The selective-signaling portion of the mobile-station equipment for the new system is less expensive.

6. It is much easier to change codes in the new system, since it only is necessary to plug in a new set of vibrating reed selectors.

Reference

1. VIBRATING REED SELECTORS FOR MOBILE RADIO SYSTEMS, A. C. Keller, L. G. Bostwick. AIEE TRANSACTIONS, volume 68, part I, 1949, pages 383–86.

No Discussion

Application of Multifrequency Pulsing in Switching

C. A. DAHLBOM
NONMEMBER AIEE

A. W. HORTON, JR.
NONMEMBER AIEE

D. L. MOODY
MEMBER AIEE

MULTIFREQUENCY pulsing is a form of signaling with alternating current, which permits the rapid transfer over telephone trunks of the information required to select switch paths in local, toll, and tandem dial telephone systems. The multifrequency pulses consist of different combinations of two, and only two, of six frequencies. These six frequencies are spaced 200 cycles apart, from 700 to 1,700 cycles, inclusive. Each combination of two frequencies represents a pulse, and each pulse a digit. The pulses are sent over the regular talking channels and, since they are in the voice range, are transmitted as readily as speech. There are 15 pairs of frequencies possible from the group of six; ten of them are used for the digits 0 to 9, inclusive, and one each for signals indicating the beginning and end of pulsing. The remaining three possible pairs are available for future requirements.

The multifrequency system is arranged so that if more than two frequencies are received by the equipment, the operator who is setting up the connection receives a flashing cord lamp; then she must release the connection and start making the call over again in accordance with her instructions.

The first multifrequency pulsing system was installed at the toll board in Baltimore, Md., to permit the toll operators to complete calls to local crossbar offices without the aid of another operator, and without the use of senders in the toll office. Multifrequency pulsing next was used in connection with the new toll crossbar office installed in Philadelphia, Pa. In this installation calls were received over toll lines from distant points, as well as from switchboards within the city, by means of the multifrequency pulsing system. Today, installations of multifrequency pulsing arrangements are being made in many cities throughout the United States.

Applications of Multifrequency Pulsing

In applying multifrequency pulsing to the telephone plant, it must be kept in mind that the signals used in completing a normal connection in any of our dial telephone systems conveniently fall into two classes: supervision, and pulsing. Supervision includes the connect and disconnect signals going toward the called end, and the "on" and "off" switchhook signals going toward the calling end. The supervision signals can be used under certain conditions for other purposes; for example, to control the start of pulsing, and to recall an operator who may have been assisting in the establishment of the connection. The supervision channel must be ready at once to transmit signals, and, therefore, the supervision signaling equipment is provided individually to the trunk. On the other hand, pulsing signals are required only to set the switch paths and are sent toward the called end. Once the switch paths have been set, there is no longer any need for the pulsing channel, so the use of pulsing signals is limited to the time during which the connection is being established. Accordingly, the equipment used for pulsing can be detached from the connection as soon as it has been set up. In the case of multifrequency pulsing, therefore, the pulsing means are detached from the connection at both ends of the circuit as soon as the switching paths have been established.

OVER-ALL PLAN

The multifrequency pulsing system consists of:

1. The signaling current supply units and distribution arrangements with suitable protection and alarm features.
2. The signal transmitters, either manual multifrequency keysets or dial system multifrequency pulsing senders.
3. The signal receiver connected to the incoming sender or register.
4. The necessary additional maintenance facilities.

One arrangement of the system components for pulsing on a trunk between manual and dial system offices is shown in Figure 1. A local manual, dial system "A," or toll switchboard equipped with multifrequency key pulsing, is shown connected by a direct trunk arranged for multifrequency pulsing to a crossbar office equipped with incoming multifrequency pulsing senders. When an outward operator at a manual switchboard, as shown in Figure 2, handles a call which can be completed through the crossbar office, the first action is to connect a cord circuit to the trunk with the "talk" key operated and operate the *KP* (key pulsing) button of the keyset. The operation of the *KP* key operates a relay that transfers the cord from the telephone set to the keyset, lights a positional *KP* lamp, and prepares the keyset circuit to send the key pulse signal over the trunk as soon as the distant end signals that it is ready to receive pulses. Connection of the cord to the trunk gives a connect signal to the distant end which returns "off-hook" supervision to delay pulsing until a sender is found. When the sender at the distant end has been found, and the pulsing path has been completed, the supervision is changed to "on-hook" as a start-pulsing signal. This causes the *KP* pulse signal to go out automatically and lights the positional sender lamp.

Paper 49-101, recommended by the AIEE communication committee and approved by the AIEE technical program committee for presentation at the AIEE winter general meeting, New York, N. Y., January 31–February 4, 1949. Manuscript submitted November 16, 1948; made available for printing December 22, 1948.

C. A. DAHLBOM, A. W. HORTON, JR., and D. L. MOODY are with the Bell Telephone Laboratories, Inc., New York, N. Y.

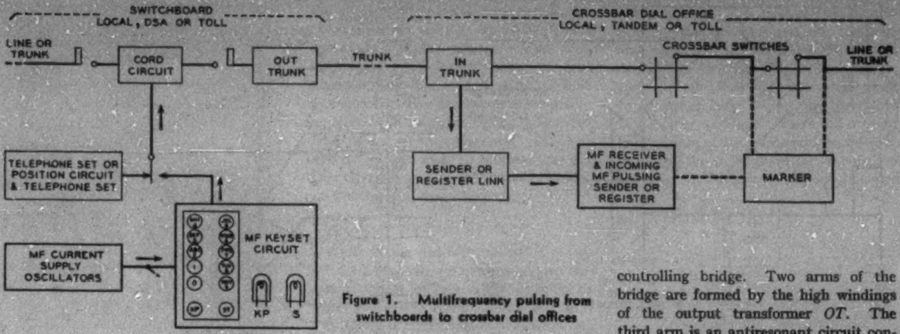

Figure 1. Multifrequency pulsing from switchboards to crossbar dial offices

Receipt of the *KP* signal at the distant end prepares the multifrequency receiver to accept the digits that are to follow. The operator may begin sending the digits of the called number as soon as the positional sender lamp is lighted. She will do this by pressing one button for each digit. Following the last digit, she presses the *ST* (start) button to indicate the end of pulsing. In addition to informing the distant sender that no more pulsing signals are coming, the operation of the *ST* key disconnects the keyset from the cord, reconnects the telephone set under control of the "talk" key, and also extinguishes the *KP* and sender lamps.

If the operator presses two buttons simultaneously, or if she presses the *KP* key after the positional sender lamp lights, a reorder signal is received from the distant end causing the cord supervisory lamp to flash, requiring the operator to release the connection and start the call over again.

Other Applications

In addition to the use of multifrequency pulsing from manual positions to local, toll and tandem crossbar offices, there is also a wide use of multifrequency pulsing between the incoming senders at the toll crossbar-switching offices and the local crossbar offices. In this case, the multifrequency pulses are sent out by a sender, instead of by a keyset. The rate of sending averages about seven digits per second, instead of the two digits per second normally keyed by the operators.

The toll crossbar and certain local crossbar offices are equipped to transmit, as well as receive, multifrequency pulses. A further application to toll switchboards has resulted in the use of multifrequency pulsing senders which will receive multifrequency pulses and transmit dial pulses. This arrangement is used to set up connections to the step-by-step type of office.

Multifrequency Current Supply

The current supply circuit consists of two groups of bridge-stabilized oscillators. Each oscillator group normally supplies one-half of the office load, but each oscillator group is capable of carrying the whole office load if failure occurs in either group. Each group consists of six oscillators operating at the frequencies 700, 900, 1,100, 1,300, 1,500, and 1,700 cycles respectively. The oscillator design is such as to provide constant frequency and amplitude output for normal variations in power supply and output load.

Description of Oscillator

One of the bridge-stabilized oscillators is shown schematically in Figure 3. It consists of a high-gain pentode vacuum tube *V*, operated as a class *A* amplifier, together with a frequency- and amplitude-controlling bridge. Two arms of the bridge are formed by the high windings of the output transformer *OT*. The third arm is an antiresonant circuit consisting of retardation coil *L* and capacitor *C* connected in parallel, while the fourth arm is a resistance *R* having a value slightly less than the impedance of the antiresonant circuit at the oscillator frequency. Part of the retardation coil is shunted by a thyrite varistor *VR*, whose impedance is responsive to amplitude variations. For low voltages, the varistor has a very high effective resistance, but its value decreases rapidly as the amplitude of the voltage is increased. Taps are provided to allow adjustment of the output voltage at the time of installation.

For the normal frequency F_0 and output voltage E_0, the impedance of the antiresonant network is resistive and slightly larger than the resistance arm of the bridge. Thus, a small voltage unbalance is applied to the grid of the *V* tube, and the oscillations are sustained. For frequencies above or below F_0, the antiresonant circuit reactance becomes capacitive or inductive, respectively; the magnitude of the reactance depending on how far the frequency shifts from the antiresonant frequency. These effects of frequency upon the phase angle of the impedance near antiresonance, and of amplitude upon the magnitude of the antiresonant impedance, are used to stabilize the frequency and amplitude of the oscillations.[1] The frequency control exerted by the tuned circuit depends upon the fact that the phase shift of the amplifier tube must be equal and opposite to that through the bridge circuit.

Figure 2. Outward operator at toll switchboard

Coding and Distribution of Frequencies

The output frequencies of the six oscillators are distributed to keysets, located in the various switchboard positions, and to outgoing senders in the switching equipment. A typical distribution plan is shown in Figure 4. The signaling frequencies have been desig-

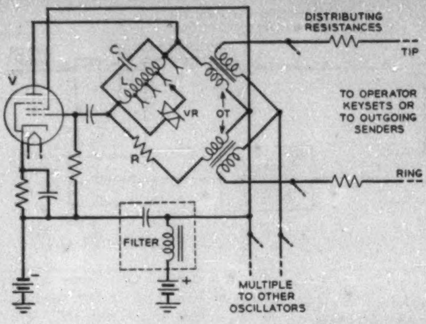
DISTRIBUTING RESISTANCES
TIP
TO OPERATOR KEYSETS OR TO OUTGOING SENDERS
RING
V
C
L
VR
OT
R
FILTER
MULTIPLE TO OTHER OSCILLATORS

Figure 3 (left). Bridge-stabilized oscillator, schematic diagram

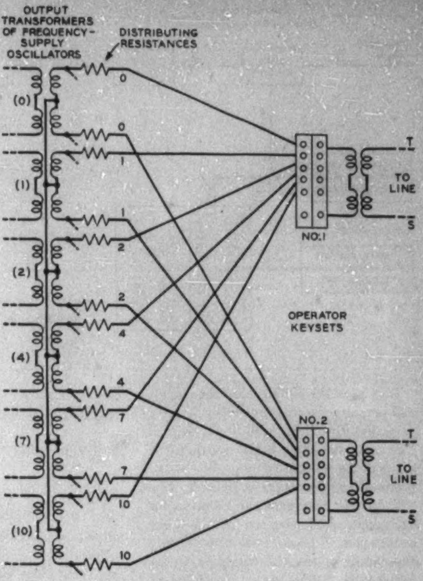

Figure 4 (right). Frequency-distribution plan

nated 0, 1, 2, 4, 7, and 10 for the 700, 900, 1,100, 1,300, 1,500, and 1,700 cycle frequencies, respectively. Frequencies 0 to 7 are used for the digit codes while frequency (10) in combination with the (2) or (7) frequency is used for special signals. The code which is referred to as an "additive code" is shown in Table I. Except for 0, *KP*, and *ST*, the frequency designations add to give a sum equal to the digit being transmitted. This feature of the code assists the maintenance forces when clearing troubles which may occur.

Alarm Features

Each group of oscillators is equipped with various types of alarm features. To guard against failure in the output, sensitive voltage relays are connected across the output circuits of the oscillators in pairs in differential relation. Therefore, if the output voltage of one individual oscillator departs more than 1.5 decibels from the output of its mate, the voltage relay operates and causes the load to be transferred automatically to the other oscillator group, and in addition sounds an alarm. Trouble grounds and power failures also are guarded against, and necessary alarms are given. In addition, an arrangement is provided whereby the transmission of number information, by sender equipment, is halted during the transfer interval and either transmission is resumed when the transfer is completed, or a reorder signal is given to the originating operator.

Figure 5 shows a typical installation of multifrequency supply oscillators, together with alarm relays.

Table I. Coding of Frequencies

Digit	Frequencies in cycles per second	Frequency designations
1	700+ 900	0+ 1= 1
2	700+1,100	0+ 2= 2
3	900+1,100	1+ 2= 3
4	700+1,300	0+ 4= 4
5	900+1,300	1+ 4= 5
6	1,100+1,300	2+ 4= 6
7	700+1,500	0+ 7= 7
8	900+1,500	1+ 7= 8
9	1,100+1,500	2+ 7= 9
0	1,300+1,500	4+ 7=11
KP	1,100+1,700	2+10=12
ST	1,500+1,700	7+10=17

Multifrequency Signal Receiver

The signal receiver is shown in Figure 6, and a simplified circuit schematic diagram is shown in Figure 7. Starting at the input from the line, there is: a shielded repeating coil, a gain adjusting pad, an impedance-controlling resistance, and a volume-limiting amplifier. The circuit branches at the output of the limiter, one branch going through the six channel filters, detectors, and relays, and the other going through a high-pass filter, detector, and a low-pass filter to the signal present *SP* relay. The operation of these relays controls the registration of the received signals in the sender which is associated with the receiver.

Operation of Receiver by Key Pulsing Signal

When the receiver is first connected to the line, possible false operation by speech prior to the start of pulsing is prevented by means of a slightly different relay arrangement from that shown in Figure 7. With this arrangement, it is necessary that the *KP* signal operate channels 2 and 10, and that all other channels remain unoperated, for a period of at least 55 milliseconds. At the end of this interval, the receiver is changed to the condition shown, and is prepared to accept the digits that are to follow.

Operation of Receiver by Digit Signals

When the receiver is in the pulsing condition, the two signal frequencies applied to the input are amplified or limited depending upon the received-signal power. The frequencies are selected then by the two appropriate channel filters and are detected. In the absence of incoming signals, plate current normally flows in the detectors. The presence of a signal biases the tube to reduce this current to a low value, which is more or less independent of the strength of the signal. The channel relays are energized by current from a battery through the *P* windings, and are prevented from operating by the plate current flowing in the *S* windings, which produces a flux which opposes and balances that caused by the current in the *P* winding. Consequently, when plate

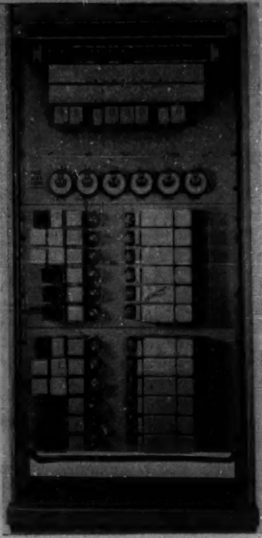

Figure 5. Oscillator and alarm unit

current is reduced sufficiently, the relay will operate. When the back contact of a relay is opened, ground is removed from a resistance and battery to reduce the screen voltage of the tube, which in turn further reduces the plate current, thereby producing a "snap" action to insure rapid and positive operation of the relay armature to the front contact. The reduction in plate current by this means is sufficient to prevent the release of the relay, even though the signal is subsequently removed. Thus, the relay is locked in the operate condition until the current in the *P* winding is interrupted by the sender after the registration has been completed.

Both signal frequencies enter the signal-present *SP* circuit and pass through a high-pass filter, the purpose of which is to reduce the effects of low-frequency noise, and operate the detector. The low-pass filter in the output of the detector serves to limit the fluctuations in the detector output, which occur at a frequency equal to the difference of the input frequencies, and to delay the operation of the signal-present relay. The front contact of this relay controls the operation of the sender to prevent duplicate registration of a digit in case a signal is unduly prolonged, and causes ground to be applied to the operate or *P* windings of the channel relays. This operation is delayed to reduce the effect of transients produced in the channel filters, which otherwise would operate falsely other channel relays. The back contact momentarily alters the grid biases of the limiter and signal-present detector to reduce effectively the relative sensitivity of the signal channels to avoid false operation by transients. The sensitivity is restored to normal as the capacitor associated with the back contact of the relay becomes charged.

CODE SELF-CHECKING FEATURE

Noise may cause false operation of one or more channels, or more than two frequencies may be received if an operator falsely operates two keys simultaneously.

Since each digit consists of exactly two frequencies, a check can be made that a bona-fide signal has been received. This is done as follows:

> Removal of ground by the back contact of a channel relay permits current to flow through a resistance to the relays *CK1*, *CK2*, *CK3*, and the current through the operate windings of these relays is proportional to the number of channel relays which are operated. The non operate bias of the *CK* relays are adjusted so that none will operate with a single channel relay operated, *CK1* and *CK2* will operate with two channel relays operated, and all three will operate when three or more channel relays are operated. These relays control the operation of the sender in such a way that the operation of a single channel relay is ignored, two channel relays operated permits registration of the appropriate digit, and with three operated the sender is informed that the signal is incorrect, where upon a reorder signal is transmitted to request retransmission of the number.

TRANSIENT PROTECTION BY TIMING

The receiver is required to operate on signals transmitted over lines which differ in attentuation and which have attenuation distortion or "twist." This requires that each channel shall be sufficiently sensitive to operate when the attenuation is a maximum, and not falsely operate on the filter transients when the attenuation is a minimum. To illustrate the significance of this problem and the methods used to satisfy the requirements, we will employ the formulas for the transient response of an ideal band-pass filter given by Guillemin,[3] and use only the envelopes of the filter response. When the applied frequency is at the midband frequency of the filter, the envelope of the response to a sine wave of unit amplitude is given by

Figure 6. Multifrequency signal receiver unit

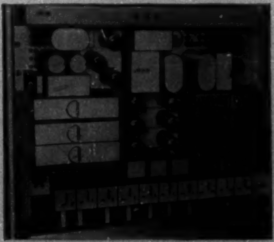

$$E(t)=\frac{1}{2}+\frac{1}{\pi}Si\left[\frac{w}{2}(t-t_d)\right]$$

where

$$Si(x)=\int_0^x \frac{\sin x}{x}dx$$

$$w=2\pi(f_2-f_1)$$

and f_2 and f_1 are the cut-off frequencies of the filter and t_d is the delay time of the filter. When the applied frequency is outside the pass band of the filter, the envelope of the response is given by

$$e(t)=\frac{1}{\pi}\frac{w}{\omega_m}\frac{\sqrt{\omega_m{}^2\cos^2\theta+\omega^2\sin^2\theta}}{\frac{\omega^2}{\omega_m{}^2}-1}\cdot\frac{\sin\frac{w}{2}(t-t_d)}{\frac{w}{2}(t-t_d)}$$

$\omega_m=\omega_1+\omega_2/2$ is 2π times the midband frequency, and θ is the phase angle of the applied wave. A plot of these equations is shown in Figure 8 for the case of a filter with a pass band 100 cycles wide and a midband frequency of 900 cycles. Since the results obtained with the filters actually used differ materially from those obtained with an ideal filter for times below 10 milliseconds, these portions of the curves are not shown. The top curve corresponds to an applied frequency of 900 cycles, and the bottom curve (drawn on an expanded amplitude scale) corresponds to an applied frequency of 700 cycles and a phase which yields the maximum amplitude. t_d was chosen arbitrarily as ten milliseconds. The first maximum of $e(t)$ is approximately 21 decibels below the final value of $E(t)$. Since we may have two frequencies present in channels adjacent to the one under consideration, the transient discrimination is 6 decibels less or only 15 decibels. Since the wanted signal does not reach its final value until about the time that the unwanted transient reaches its first minimum, it should be possible to increase the discrimination by about 9 decibels if operation of the channels is prevented until after the first minimum of the transient has occurred. This is ac-

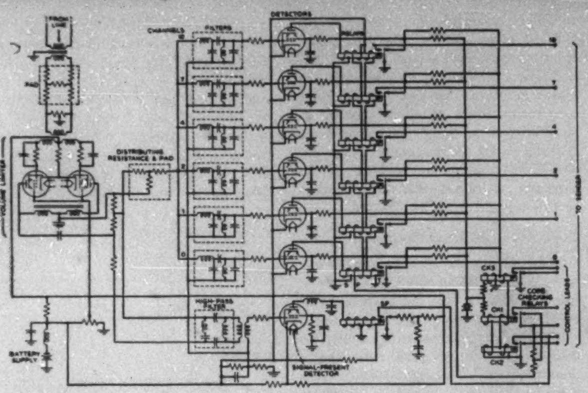

Figure 7. Multifrequency signal receiver, schematic diagram

complished by delaying the operation of the signal-present relay by means of a low-pass filter. To obtain this advantage, the time of occurrence of the minimum response must be the same in all channels. Reference to the foregoing formula shows that this requires the same bandwidth in cycles, and the same delay time for all the channel filters. With these conditions met, approximately equal discrimination, transient or steady state, is obtained with equal spacing of signal frequencies.

Transient Protection by Limiting

Additional protection against false operation by transients is secured by the use of a peak-limiting amplifier which acts as a linear amplifier for inputs up to a certain definite point called the point of limit; above this point the output is held constant. With a 2-frequency input to the limiter, it is necessary that the point of limit be at least six decibels above the single-frequency input which is just sufficient to operate a channel detector. If there is a difference in amplitude of the two input frequencies, the point of limit must be raised still further. For the case of n applied frequencies, let $V_1, V_2 \ldots V_n$ be the voltage amplitudes at the output of the limiter without limiting, and let V_L be the output voltage when limiting occurs. The point of limit is defined by

$$V_1+V_2+\ldots V_n=V_L$$

If L is the loss in decibels introduced by the limiter above the point of limit, we have

$$(V_1+V_2+\ldots V_n)10^{-\frac{L}{20}}=V_L$$

Without loss of generality, we can assume

$$V_1\leq V_2\leq\ldots\leq V_n$$

To insure operation on the minimum amplitude when limiting occurs, we must have

$$V_1 10^{-\frac{L}{20}}\geq V_0$$

where V_0 is the voltage required to just operate a channel detector. M is the margin in decibels between the just-operate voltage and the point of limit, measured with a single frequency, or

$$V_0 10^{\frac{M}{20}}=V_L$$

Figure 8. Envelopes of response of band-pass filters to applied sine wave

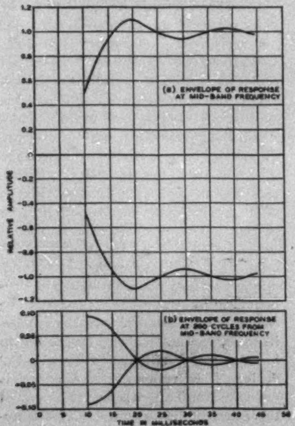

From the preceding equations we obtain as a condition for operation

$$\frac{V_1 10^{\frac{M}{20}}}{V_0+V_2+\ldots V_n}\geq 1$$

or

$$M20\log_1\geq_0\left(1+\frac{V_2}{V_1}+\ldots\frac{V_n}{V_1}\right)$$

Thus, the margin between "just limit" and "just operate" is determined by the number of frequencies, and is a function of the ratios of the larger voltages to the smallest one. For the case of $n=2$, M is shown in Figure 9 as a function of the difference in decibels of the tow voltages. With a nominal margin of 12 decibels, the maximum difference between two voltages is about 10 decibels.

When allowance is made for variations in components of the frequency sources and the receivers, the following operating characteristics are obtained:

Digit and ST signal duration, 27 milliseconds or greater.

KP signal duration, 55 milliseconds or greater.

Interval between signals, 20 milliseconds or greater.

Maximum receiver input power, 2 decibels above one milliwatt at each signal frequency.

Minimum receiver input power, 27 decibels below one milliwatt at each signal frequency, provided the difference in power between the two frequencies making up the signal does not exceed 6.5 decibels.

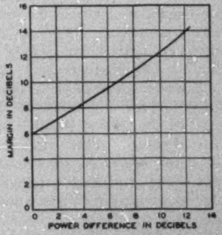

Figure 9. Required margin between "just limit" and "just operate" as a function of the power difference of two frequencies

References

1. The Bridge-stabilized Oscillator, L. A. Meacham. *Proceedings*, Institute of Radio Engineers (New York, N. Y.), volume 26, October 1938, pages 1278–94.

2. Communication Networks, Volume 2 (book), E. A. Guillemin. John Wiley and Sons, Inc., New York, N. Y., 1935, page 487.

Trackless Trolley Operation in Rhode Island

H. R. BLOMQUIST
MEMBER AIEE

Synopsis: This paper attempts to set forth the knowledge gained in operating a growing trackless trolley system over a period of 17 years. It in no way is intended to prove that the trolley coach is a cure-all for transit ills. Unbiased transit experts recognize the need for all types of vehicles in the industry: "A place for every vehicle–every vehicle in its place." We subscribe fully to this doctrine.

THE United Electric Railways Company serves a population of 594,000 persons living in 16 contiguous cities and towns covering an area of 334 square miles. It operates on 390 miles of road, and in 1947 operated 18,000,000 vehicle miles, carrying 142,000,000 passengers.

It was on this property that trackless trolley operations in New England was inaugurated at the very depths of a severe business depression. Earnings on the United Electric Railways Company property had dropped 28 per cent since the peak in 1926, and the transit industry generally was experiencing hard times. Ways and means of remaining solvent were needed sorely by the industry, as competition by private automobiles continued to cut deeply into the earning power of mass-transportation organizations.

In searching for a means to stem the tide of diminishing revenue, the company management decided to experiment with the trackless trolley. It was hoped that this modern-type of vehicle, through stimulated riding and reduced operating expenses, would stop the downward trend of earnings.

A few properties were already operating trackless trolleys, but little was known of their drawing power or operating problems. However, it appeared to incorporate in one vehicle the advantages of both the street car and the motor bus without their inherent disadvantages. It rolled on rubber, had maneuverability, smooth acceleration, good lighting, and operated quietly and without odor.

The Brook–Weeden Line, operating in Pawtucket, R. I., was selected as the "guinea pig." This was a cross-town street-car line about five miles long, operating between the east and west sides of the city by way of the downtown area, and would require only five vehicles. The route was primarily in a well built-up residential section and was earning about 41 cents per vehicle mile, as compared to the rail system average of 39 cents. The operation of this first trackless trolley line was watched with keen interest by the management, and the financial results of the first year surpassed their most optimistic hopes.

A study of the operating results indicated that substitution of trackless trolleys for street cars had resulted in an 11 per cent increase in revenue. The cost of maintaining the trackless trolley compared favorably with that of the motor bus, and no difficulties were encountered in keeping them in operation. The use of the trolley coach in a very short time had won enthusiastic supporters among the public and within the company.

From this inauspicious beginning has grown one of the largest trackless trolley systems in the world. Today it includes 80 miles of overhead and 330 vehicles which operate 8,500,000 miles per year, carrying 85,000,000 passengers. As a result of 17 years of experience in construction and operation, there have been developed many essential methods and techniques, some of which are today common to the industry, but some of which still are unique on this property. These cover such functions as vehicle storage, overhead construction, and vehicle maintenance.

Vehicle Storage

In spite of the rigors of New England winters, a decision to store trackless trolleys out-of-doors was reached in the early stages of development and has been adhered to through the years. It has proven to be a most suitable and economical procedure. There are two depots on the property today, out of which operate all of the trackless trolley lines. Typical of these vehicle storage areas is one at the Elmwood station. It occupies a corner lot 200 feet wide by 575 feet long, paved with a 2 inch sheet of asphalt on a 4-inch layer of crushed stone over a 6-inch banked-gravel base. The area is fenced on one side and an end, and is well illuminated with mercury-arc floodlights.

Vehicles are stored in 17 lanes parallel to the long dimension with 3-foot aisles between adjacent rows. Two 10-inch fire lanes are provided, at right angles to each other extending across the center of the lot, so that when the area is filled there are actually four blocks of vehicles

Figure 1. Trackless trolley storage area at Elmwood

Paper 49-104, recommended by the AIEE land transportation committee and approved by the AIEE technical program committee for presentation at the AIEE winter general meeting, New York, N. Y., January 31–February 4, 1949. Manuscript submitted November 16, 1948; made available for printing December 22, 1948.

H. R. Blomquist is with the United Electric Railways Company, Providence, R. I.

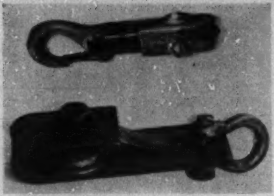

Figure 2. Rollers for tangent construction (above). Rollers for angle construction (below)

separated from each other by these fire lanes.

Readily accessible fire-fighting equipment, in standard hose houses as specified by the Fire Underwriters, is provided at several locations along these fire lanes. Overhead trolley wires are located so that each pair of wires serves two parking lanes, thus reducing to a minimum the overhead construction required, without hampering operations. The entire area contains 115,000 square feet and accommodates 185 vehicles with ample room for servicing.

The cost of this parking area over and above the land is approximately $80,000, broken down as follows:

Paving ($2.50 per yard), $32,000
Fire-fighting equipment, $5,000
Overhead construction including feeder, $40,000
Lighting, $3,000

Thus the cost of the area exclusive of land is equivalent to $432 per vehicle. Of the $40,000 for overhead construction, approximately one-half is for feeder. This is on account of the fact that the feeder requirements for an area of this sort are very heavy during the winter months, as the auxiliary electric heaters in the vehicles are used for warming up the coaches before they go into service. These auxiliary heaters are rated at 15 kw, so that with 185 vehicles stored the connected heater load is 2,775 kw.

Figure 3. Shop assembly of trackless-trolley intersection

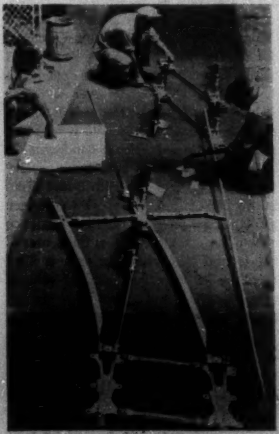

Overhead Construction

The trackless-trolley overhead system is one of the most critical parts of the entire plant. It is vitally important that these structures be erected economically and in such a manner that they will not be eyesores. Rubber-tired equipment has permitted mass-transportation vehicles to deviate from their former routes along main traffic arteries, and to wend their way into the very heart of residential areas. Here neatness of overhead lines is a must.

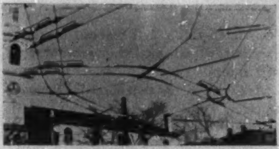

Figure 4. Trackless-trolley overhead—North Main and Waterman Streets, Providence, R. I.

1. The poles must be raked so that when load is applied they all shall be in the same line.
2. The span wires shall be sloped no more than is necessary and all in the same plane.
3. The contact wires on tangent construction shall be in a perfectly straight line.
4. Special work at intersections shall have no more supporting wires than is necessary.

These four items are the criterion of good overhead design and construction, and our methods were developed with these objectives in mind.

The construction of trackless trolley overhead can be broken down into five phases:

1. Installation of poles.
2. Installation of tangent spans.
3. Installation of curve segments.
4. Stringing trolley contact wire.
5. Installation of special work at intersections.

There have been developed special methods and tools for each of these phases which have reduced substantially the cost of installation, and at the same time result in an overhead structure which has been received very favorably by the community and is acceptable in residential area.

Poles were formerly ground-braced with heel and toe planking, the installation of which was time-consuming and difficult. When load was applied to the pole, the base invariably would shift in the ground because the pole was not bearing firmly against the planking. The degree of shift varied from pole to pole, resulting in an irregular lining up of poles. In order to eliminate this irregularity, it was decided to ground-brace poles with poured concrete and to do it in such a manner as to permit the pole to be readily removable in case of replacement. The pole is placed in the hole, the position and rake being adjusted and controlled by means of three wooden wedges placed around the pole. Two flat spades with long handles are then placed radially at the bottom of the hole, about 90 degrees apart at back of pole. Concrete is poured back of spades to a depth of one foot, and gravel is placed around the street side of the pole, watered and tamped. Spades are then removed, the hole filled with gravel to a point about 16 inches from ground grade, and wedges removed. The two spades are placed back in the hole on the street side, concrete poured at the front of the pole, and gravel placed at the rear. The spades are removed, and the remainder of the hole is filled with gravel, watered, and tamped. The pole is permitted to stand for about a week before any load is applied. The use of wedges for supporting pole during the setting operation has reduced the pole crew to seven men, and this crew with a foreman can set ten poles per day, including digging.

In order to speed up the installation of span wires in tangent areas without sacrificing the appearance of the finished job, the span wires are preloaded to get the correct length and height. We have standardized on a span-wire slope of one foot in eight feet, and the engineering department prepares a cross-section drawing showing the height of the point of attachment to the pole for each street width on the line. The first tangent span at any particular street width is installed by hanging two weights of 100 pounds each on the span wires, one at the point selected for the outbound pair of trolley wires and one at a point corresponding to the inbound trolley wires. The span wire is attached to the poles at the elevation specified by the drawing and then tensioned to 800 pounds.

The span wire is made fast to the pole, and the weight is removed. This span wire is now ready, properly tensioned and at proper height above the highway. It of course would be possible to repeat this performance at each span wire location, but this would be slow and cumbersome. To expedite the operation, a measuring device is used, consisting of a 50-pound weight fastened at the end of a telescopic rod, the length of which is adjustable. This measuring device is hung at the center of the span wire which has just been installed by the preloading method, and the length of the rod adjusted until the weight swings just clear of the roadway. We now have our measuring stick to use on all other spans installed along the line until a different road width is reached. This measuring device is hung at the center of each succeeding span, and the span wire tensioned until the weight swings clear. This method permits high-speed installation of all span wires in tangent areas. When a new street width is reached, the first span is again preloaded, the measuring device then is reset and used on the succeeding spans. The possible error created by the fact that some spans are from wood to wood, some from steel to steel, and others from steel to wood, is so slight that it has no apparent effect on alignment to completed line.

Because of the recent improvements in segment design, such as smooth underrun and long runners permitting high-speed operation, we use them almost exclusively for low-degree turns as well as at corners. Any curve calling for segment installation is covered by an engineering drawing, which shows not only the elevation of pole attachments and span wire tensions, but also shows the exact location of the segment with respect to two reference lines at right angles, selected so that they can be identified easily in the field. The line crew, using these reference lines, mark on the street the exact spot over which the segment is to be located, and the segment without runners is then installed by plumbing-down to this point.

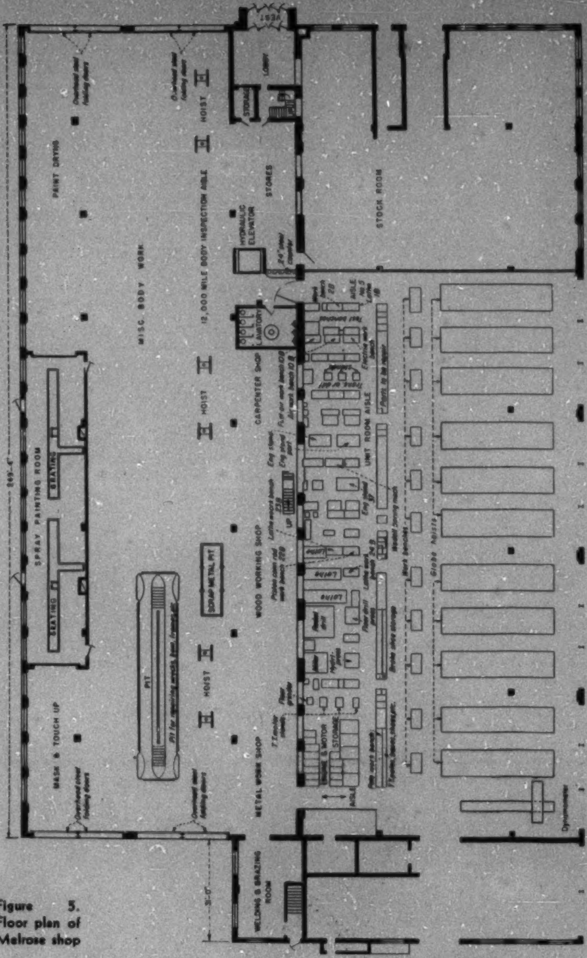

Figure 5. Floor plan of Melrose shop

The method of stringing trolley wire has been improved drastically by the use of a simple device designed in our own shops. This device, which we call an "anti-friction roller," consists of a small grooved wheel mounted in the hook of a J-shaped bronze casting about 1/2-inch wide and 3-inch long over-all. A spring clip closes in the top of the hook, and a snap hook fastened to the top of the *J* permits the device to be hooked onto a span wire. This roller is used on all spans in tangent areas where no side pull is developed when trolley wires are tensioned.

A similar roller, differing only in that it is larger and heavier, is used at segments and any other angle points. This angle roller is equipped with a length of wire cable and a 3-bolt clamp, so that it may be clamped to the segment-supporting wire or span to prevent any possibility of side slip.

After all span wires and segment plates have been installed on a new line the angle rollers are clamped in place at all angle points, and the job is ready for wire stringing.

A truck used in stringing wire is provided with a special wire reel stand equipped with a water-cooled brake drum. The wire is fed up over a tower truck following directly behind the wire truck; the tangent antifriction rollers are snapped onto the trolley wire and then onto the span as the trucks move along, and the contact wire is hooked into the rollers already in place at angle points. Ordinarily, the trolley wire for the entire line is strung before the tensioning is done. This is possible because the use of rollers reduces the friction to a minimum. By this method it is possible to string eight miles of wire per day with one crew. It is this speed which makes necessary the water-cooling of the brake drum on the reel stand. With the wire all in place, the tensioning is completed. Although long lengths are tensioned in one operation, it has been found that no more than three per cent of the tension is lost from one end of the line to the other.

The hangers and ears now are installed; the wire is removed from the rollers in tangent sections and is clamped in the trolley cars. This leaves only the angle rollers to be removed. The segment runners are installed, a chain jack is fastened to the pull-off wire, and loop is fastened between jack and trolley wire at the center of the segment. The jack is pulled up to remove the load from the angle roller. This is unhooked, and the jack is slacked off so that the trolley wire approaches the runner. The wire is guided by means of a Stillson wrench so that the groove is in proper location, and one of the segment clamps is tightened over the trolley wire when it is positioned properly. The loop is slipped over far enough to engage a second clamp, and this process continues until the loop is clear of the runner. The loop is then removed and placed on the opposite side of center clamp. The process is repeated until all clamps on this side are securely fastened to wire.

Engineering drawings of all junction points are provided, showing the exact location of all poles and special work, together with the elevations, tension, and length of all supporting wires. The intersection is assembled on the shop floor with all wires cut to length and tagged for identification. The material is then erected in the field by plumbing the location of each unit to a mark on the street. The preliminary shop work greatly expedites the field construction.

When the new line has been completed, a trial trackless-trolley run is made in order to check the need for any immediate adjustments. It is then turned over for regular operation and run for about a month before the final dressing up is made. At that time all trolley wire in tangent sections is lined up by means of a surveyor's transit; locations of all segments and special work is checked, and all supporting wires are clipped to proper length and the ends lashed.

A typical construction project was the erection of the trackless-trolley overhead for the Dyer–Plainfield Lines in 1946. It consisted of 177 solely-owned poles, 3.24 miles of 2-way overhead with 4 intersections, each having a leading switch, trailing switch, and crossover; 62 curve segments ranging from 2 degrees to 45 degrees, 2 terminal loops each made up of 8 curve segments and 2.82 miles of 500,000-circular-mil feeder cable. The number of poles set is low because the remaining poles were jointly-owned with the power company and/or the telephone company, and are not included in the analysis. The feeder installation is low, as a considerable part of the positive feeder used on the original rail lines was available and in place.

Figure 6. Portion of unit repair section at Melrose shop

The cost of the entire installation as described is shown in Table I, and is equivalent to $12,955.46 per mile.

Table I. Cost of Installation

	Labor	Material	Total
Poles......	$ 4,465.09..	$ 5,584.63..	$10,049.72
Feeder.....	5,063.96..	4,413.66..	9,477.62
Overhead...	7,460.71..	14,987.66..	22,448.37
Total......	$16,989.76..	$24,985.95..	$41,975.71

Vehicle Maintenance

One of the important decisions which had to be made when trackless trolleys became a part of our operations was that pertaining to vehicle maintenance. Should the vehicles be maintained by the rail mechanical department or the bus mechanical department? There were only a few companies operating trolley coaches at the time, and no pattern had been established which could be used in the solution of the problem. After considering local conditions and the vehicle itself, it was decided that they should be maintained by the bus mechanical department. The men in the department were schooled in the fundamental principles of electricity and electric motors in order that they might have some idea of the functions of the various parts of the propulsion and control equipment. This schooling, together with instructions from the manufacturers of the electric equipment, proved to be invaluable training for the bus mechanical staff.

The experience of the passing years has proved our original decision an excellent one. Some years before the inception of trolley coaches, the bus mechanical department had developed a system of protective maintenance for motor busses in which the frequency of inspections and maintenance of each part of the vehicle was based on mileage. The life of each part in miles had to be established by experience, but these had been pretty well-determined for motor busses. It was a simple matter, therefore, to set up a maintenance schedule for trackless trolleys for everything except the electric equipment. The chassis, steering mechanism, axle, and so forth were comparable to motor-bus equipment, and the maintenance of these parts was set up on the same mileage schedule. Temporary mileages were established for the propulsion and control equipment with the help of the manufacturers, and these have been adjusted as found necessary by operating experience.

The frequency of road failures served as an excellent criterion to determine the need for changes. Seventeen years of operations have served to stabilize maintenance mileages, and today our entire program is based on inspection and maintenance at 2,000 miles, 6,000 miles, and 24,000 miles. Obviously the higher mileages must be multiples of the lower mileages.

The 2,000 mile inspection includes the following operations:

Check motor brushes on traction motor, auxiliary motor, and auxiliary generator.
Drain air tanks, air system, and water separator.
Lubricate rear end.
Spray springs, rods, and so on, under vehicle at points of wear.
Check sanders.
Check wheel nuts.
Check for broken springs.
Test and adjust brakes.
Check all contact tips.
Check lights.

The 6,000 mile inspection consists of the following operations:

All work performed at 2,000 miles.
Clean brush holders and insulators.
Align front wheels.
Check for charged body.
Check switches and heaters.
Check points and adjust voltage regulator.
Check and clean auxiliary generator.
Check air cleaner.
Focus head lights.
Blow out motors and control cabinets with compressed air.

The 24,000 mile inspection includes the following:

All work performed at 2,000 miles and 6,000 miles.
Change retrievers and grease trolley base.
Check pole tension.
Change compressor oil and air cleaner.
Oil windshield wiper, door engine, and damper cylinder.
Change door air cleaners.
Change brake valve head.
Grease wheel bearings.
Adjust wheel stops.
Grease motor bearings.

At 240,000 miles, the propulsion motors are removed for complete overhaul, including dipping and baking of armature.

Busses are painted on a regular schedule which has been established through the years, and which has proved to be very satisfactory. This schedule consists of painting the outside, from the windowsill down, every six months; the entire outside every 12 months, and the inside every three years. This maintenance and paint schedule has resulted in excellent performance and appearance.

In 1947 there were 1,137 roadcalls because of electrical failures in 6,224,565 miles, which is equivalent to 5,476 miles per roadcall, and 3,713 roadcalls because of both electrical and mechanical failures, or 1,676 miles per roadcall. The direct charges for labor and material amounted to 2.81 cents per mile, broken down as follows:

Motors	0.13¢
Electric system	0.31
Line breaker	0.01
Air system	0.15
Control equipment	0.22
Overhead system	0.38
Rear end	0.21
Front axle	0.07
Steering post	
Brakes	0.28
Chassis	0.28
Body	0.56
Painting	0.16
Accidents	0.05
Total cost	2.81¢

Operating Results

The year 1948 saw the end of rail operation on the United Electric Railways Company property. From an all-rail system in 1921, it has been converted to a 100 per-cent rubber-tired system over a period of 27 years. Today the property consists of approximately one half motor busses and one half trackless trolleys. The majority of the urban lines are trackless trolley; the suburban lines, motor bus. This has proved to be, in our case, a very satisfactory balance. In only one instance have we found it necessary to second-guess a vehicle changeover, every other case having proved itself in actual operation over the years.

Trackless trolley operation has become a vital part of our system, as it earns 60 per cent of the revenue and accounts for 51 per cent of the vehicle mileage. As previously has been stated, the revenue of the original trackless trolley line increased about 11 per cent after the line was converted. This increase has been substantiated to a remarkable degree on each succeeding conversion. For example, one of the heaviest lines which was converted to trolley-coach operation in late 1940, showed a revenue increase of 12.17 per cent. Periodic checks on each of the lines indicates that the revenue increases have been sustained.

In 17 years there have been 30 lines converted from rail to trackless trolley operation. The routes of these lines range in length from 1.78 to 5.84 miles, and average 3.09 miles. In every case the speed has been increased, these increases ranging from 5.3 to 23.7 per cent. The present trackless trolley system speed, less layover, is 11.21 miles per hour; as rail operation these same lines averaged 9.56 miles per hour. Thus, the average increase in speed has been 17.3 per cent.

The earnings per route-mile range from $26,624 to $109,397, and average $53,541. The earnings per vehicle-mile range from 48.14 to 78.33 cents, with an average of 57.32 cents. It is obvious, from the range of these earnings, that the characteristics of the trackless trolley lines vary considerably. This, of course, is reflected in the amount of service required. Morning-peak headways range from $2^1/_2$ to 12 minutes. Off-peak head-

Table II. Trackless Trolley and Motor Bus Analysis

Trackless trolley			
Investment			
3.02 miles overhead at	$20,000	$ 60,400	
17 vehicles (including spares) at	17,000	289,000	
Total			$349,400
Operating Results			
Revenue			202,560
Expenses (less depreciation) at	42.90¢	$154,440	
Vehicle Depreciation (12 yr. life)		24,083	
Total			178,523
Net Earnings*			$ 24,037
Motor bus			
Investment			
17 vehicles (including spares) at	15,000		$255,000
Operating Results			
Revenue			193,352
Expenses (less depreciation) at	40.51¢	$145,836	
Vehicle Depreciation (8 yr. life)		34,000	
Total			$179,836
Net Earnings**			$13,516

*This is equivalent to 6.88 per cent return on the investment.

**This is equivalent to 5.30 per cent return on the investment.

ways range from 5 to 15 minutes, and evening-peak headways range from 2 to 10 minutes. The number of passengers carried in the maximum hour varies from a low of 285 to a high of 1,573, with an average per line of 699. This maximum hour occurs in the evening-peak outbound service. The average headway per line during this period is 4.49 minutes, which is equivalent to 13.35 trips per hour per line, thus, each trip averages 52.2 passengers.

The present trackless trolley fleet consists of 330 vehicles, and is made up of 74 40-passenger dual-motor coaches and 256 44-passenger single-motor coaches, with an average age of 5.83 years.

The 30 trackless trolley lines earn at the rate of $5,136,750 annually, operating 8,961,660 miles per year, which is equivalent to 57.32 cents per mile. The operating expenses on these lines range from 42.63 to 57.18 cents per mile, with a weighted average of 45.73 cents per mile. The net earnings are 11.59 cents per mile, or $1,038,656 per year. This is equivalent to an operating ratio of approximately 80 per cent. The breakdown of operating expenses is shown in Table III.

There are in the industry many yard sticks for determining the proper vehicle for a particular line. These yard sticks may include such items as passengers carried in the maximum hour, revenue per route mile, and revenue per vehicle mile. In the last analysis, however, the selection of the vehicle must be based on a thorough study of the particular line and area involved, together with a complete cost analysis covering each type of vehicle.

An example of this technique can be illustrated by the study made on the Hope Street Line prior to its conversion from rail to trackless trolley.

The Hope Street route is 3.02 miles long, extending from the center of Providence, R. I., through a high-grade residential area to the Providence–Pawtucket city line. It required 15 street cars in the evening-peak, operating on a $2\frac{1}{2}$-minute headway. The annual vehicle miles was 332,000 and the annual gross revenue was $184,145 in 1947.

It was determined by preparing a schedule, that 360,000 vehicle miles would be required with either motor bus or trolley coach and that 15 vehicles of either type would be required for service in the evening peak.

The trackless trolley and motor bus analysis worked out as shown in Table II.

It will be noted that a 10 per cent increase in revenue has been assumed for trackless trolley operation and a 5 per cent increase for motor bus operation. This is consistent with the results obtained on other lines.

It has been our policy throughout the entire conversion program to operate motor busses while the overhead was being constructed. The revenue has increased 5 per cent during this period.

A possible point of interest to power companies requested to serve trackless-trolley loads, is the fact that the maximum 15-minute demand-per-vehicle-in-service is 49.1 kw, metered at the generating station high-voltage bus. This peak occurs at about 5:30 p.m. although the maximum passenger load occurs at 5:00 p.m. The power consumption during the winter months equals 5.07 kilowatt-hours per vehicle mile, also measured at the a-c high-voltage bus.

Conclusion

The operating results on the United Electric Railways Company, and other properties throughout the United States, assures the future of the trackless trolley. Our operation has grown from 5 to 330 vehicles in 17 years. This is typical of the growth in the country as a whole. In 1931, there were 163 trolley coaches operated by six companies; today, there are over 6,000 vehicles in service on 42 properties.

The growth of their use on the United Electric Railways Company property is a tribute to the late Colonel Alonzo R. Williams, first vice president and general manager of the company from 1928 until his death in 1948. His steadfast courage and faith in trackless trolleys, in face of considerable early skepticism within the industry, were of immeasurable value in the establishment and growth of our trolley-coach operation, now among the largest in the country.

Table III. Trackless Trolley Operating Expenses in Cents Per Mile for the Year 1947

Operating Expenses	Cents Per Mile
Operating costs	
Garage and trackless trolley operation	
Removal of snow and ice	0.61
Superintendence	2.86
Station expense	0.01
Operators' wages	16.75
Garage employees	0.78
Garage expense	0.17
Electricity	6.58
Lubricating oils and greases	0.04
Miscellaneous transportation expense	0.79
Total garage and trackless trolley operation	28.59
General costs	
Advertising	0.04
Salaries and expenses of general officers	0.39
Salaries and expenses of general office clerks	1.06
General office supplies and expenses	0.22
Law expenses	0.05
Pensions	0.92
Miscellaneous general expenses	0.93
Injuries and damages	1.18
Insurance	0.12
Stationery and printing	0.22
Stores expenses	0.42
Total general costs	5.55
Total operating costs	34.14
Maintenance	
Telephone and telegraph lines	0.06
Poles and fixtures	0.21
Distribution system	0.69
Miscellaneous electric lines expenses	0.02
Garage buildings	0.06
Superintendence	0.36
Garage equipment	0.05
Shop expenses	0.37
Repairs, motive equipment	1.00
Repairs, chassis	1.12
Repairs, bodies	0.93
Tire repairs and renewals	1.17
Miscellaneous bus maintenance	0.16
Total maintenance	6.20
Depreciation	
Garage buildings	0.16
Trackless trolleys	2.67
Total depreciation	2.83
Taxes	2.56
Total operating expenses	45.73

No Discussion

Trolley Coaches Replace Busses

A. B. McMILLON
ASSOCIATE AIEE

ECONOMICS have precipitated the substitution of trolley coaches, which are electrically-propelled rubber-tired vehicles taking power from two overhead wires for self-propelled busses on lines of a number of urban-transit properties throughout the country. This affords an opportunity to accurately compare the two vehicles. The results of a number of these bus to trolley-coach changes are recorded here. They constitute significant reading for operators of transit systems and anyone interested in the problems of public transportation.

Need for Comparison

Rapidly rising costs and not-so-rapidly rising fares dictate the use of the most efficient means available for giving transit service. Thus it is particularly important at this time to define the proper range of service density for each type of vehicle at the disposal of our transit systems. Actual case histories are here used to establish the place for trolley coaches. Please note that no claim is made that the trolley coach is the answer to all transit problems. Busses, trolley coaches, modern street cars and rapid-transit equipment all have their place. For example; when modernizing a line with peak headways in the neighborhood of ten minutes or more, busses should be considered, because they have proved to be the most economical vehicle in this service range. When peak headways with large vehicles are less than two minutes the possibilities of the modern PCC (President's Conference Car) car should be investigated, for its economies begin to show up in such heavy service. The trolley coach belongs in the gap between the bus and the PCC car, where peak traffic ranges from 400 passengers per hour upward, or, in other terms, where peak headways are from two to ten minutes. A large majority of the trunk lines in our cities lie in this range.

The comparisons shown in this paper are taken from lines in the 2-to-10 minute headway range where trolley coaches have replaced busses.

Actual Cases

Trolley coaches have replaced busses on lines in Youngstown, Akron, Cleveland, Dallas, Little Rock, Des Moines, and Memphis. There are additional examples, but the substitutions in these cities are typical.

Youngstown, Ohio

Youngstown, Ohio, was first introduced to trolley coaches in 1936 when four motor-bus and two street-car routes were rearranged into four trolley-coach lines. With the new service, peak vehicles required was reduced from 33 to 29, schedule speeds increased 4 per cent and 8.6 per cent peak and base, and vehicle miles for the first three months of operation dropped 11.5 per cent below the same period the previous year. For this same period, passengers carried increased approximately 4 per cent. Youngstown's experience with this change resulted in subsequent conversion of a major part of the system to trolley coaches. In 1947, two-thirds of the total passengers were carried by trolley coaches.

Most of the conversion program in Youngstown was accomplished by forming new trolley-coach lines from combinations of street-car lines and motor-bus lines, but there were lines where the route traveled remained unchanged with the conversion. I have chosen such a motor-bus line for studying the results of trolley-coach substitution for motor busses in Youngstown.

The Mosier-Albert motor-bus line covering 12.20 round trip miles became a trolley-coach line during 1945–1946. Forty-passenger busses served the route before conversion and 44-passenger trolley coaches were substituted. Table I compares operation before and after conversion.

In order to analyze these statistics let us consider Table I item by item. Taking the first entry under Mosier-Albert Line, we see that total annual passengers carried decreased from 5,956,970 to 5,880,476, or 1.28 per cent. For the same period the passengers carried by the entire Youngstown Municipal Railway system fell off from 61,734,576 to 55,043,829, or 10.84 per cent; therefore, the net result is a 9.56 per cent increase in traffic for the Mosier-Albert Line as compared with the whole system. The table shows that annual vehicle miles went from 536,050 miles to 476,946 miles. This is an 11.02 per cent drop in miles over the road for a 1.28 per cent drop in people hauled. The result is a more favorable passengers-per-mile ratio which, according to the table, increased from 11.11 to 12.33. This simply means that each vehicle travels less miles to haul a given number of people, which is better efficiency.

Annual vehicle hours dropped from 51,629 to 49,906 hours. This represents a 3.36 per cent drop in platform expense.

It is interesting to observe that annual revenue for the Mosier-Albert Line went from $281,287.00 in 1944 when busses were running, to $303,528.00 in 1947 after conversion to trolley coaches. A point to note is that there was a 7.9 per cent rise in revenue on this line in the face of a decrease in riders and no raise in fare. This was explained by officials of the company who said that even though system traffic was down and total riders on this line had decreased, the increased revenue on Mosier-Albert was due to the people who did ride putting cash fare in the box

---

Paper 49-105, recommended by the AIEE Land Transportation Committee and approved by the AIEE Technical Program Committee for presentation at the AIEE winter general meeting, New York, N. Y., January 31–February 4, 1949. Manuscript submitted November 16, 1948; made available for printing December 27, 1948.

A. B. McMillon is Transportation Engineer with the General Electric Company, Erie, Pa.

Table I. Youngstown Operating Statistics for 1944 and 1947

System	1944	1947	Increase or Decrease, Per Cent
Total passengers carried	61,734,576	55,043,829	−10.8
Total passenger revenue	$3,019,470	$2,937,960	− 2.7
Mosier-Albert Line, 9½-minute peak headway	1944 (Bus)	1947 (Trolley Coach)	
Total annual passengers	5,956,970	5,880,476	− 1.3
Total annual vehicle hours	51,639	49,906	− 3.4
Total annual vehicle miles	536,050	476,946	−11.0
Total annual revenue	$281,287.70	$303,528.71	+ 7.9
Total annual operating expenses	$221,281.44	$229,363.33	+ 3.6
Total annual net revenue	$60,006.26	$74,165.38	+23.6
Revenue per mile	52.3¢	63.35¢	+21.1
Passengers per mile	11.11	12.33	+11.0
Revenue per passenger	4.71¢	5.14¢	+ 9.1

instead of buying tokens or weekly passes. The officials stated that these people paid cash because they were largely desire riders (people who did not have to ride public-transit vehicles, but who were attracted by the service). Here we have a definite picture of increased revenue resulting from the attractiveness of the service. It is also noteworthy that Mosier-Albert showed a 7.9 per cent rise in revenue while, for the same period, the system substained a fall in revenue from $3,019,470 to $2,937,960 or 2.7 per cent.

The rest of the comparisons speak for themselves. Net revenue jumped from $60,006 to $74,165 or 23.6 per cent. The revenue per mile went from 52.3 cents to 63.35 cents, a 21.1 per cent increase. Revenue per passenger increased because of more cash fares, as was explained before. Only one other item needs comment, and that is operating expenses. According to the statistics, trolley-coach operating expenses in 1947 show an increase over bus-operating expenses in 1944. This, at first glance, appears unfavorable to the electrically-propelled trolley coach, but the explanation is simple. There were three wage increases between 1944 and 1947 resulting in a labor cost increase of 22.65 per cent. Wages of drivers, mechanics and indirect labor constitute two-thirds of total operating expense. By adding this increase in labor expense only, to motor-bus expenses for 1944, the trolley coach shows a 10 per cent net advantage in operating expense.

Summarizing this example; when electrically-propelled trolley coaches replaced busses, revenue increased, vehicle miles and hours decreased, net revenue increased, passengers per mile increased, and (relative to the system) total passengers carried increased. Also, according to officials of the Youngstown Municipal Railway Company, the Mosier-Albert Line was given a considerably improved service when trolley coaches were installed.

This is not all of the Youngstown story, but the Mosier-Albert conversion is an example of what is being accomplished on this system through extensive use of electric transit. Youngstown hauls approximately 70 per cent of their traffic with trolley coaches.

Dallas, Texas

The first two trolley-coach installations made in Dallas replaced motor busses. The Vickery Line with 11.28 round-trip miles, converted in November 1945, was the first. The Capitol Line with 11.44 round-trip miles followed close behind with trolley coaches beginning operation in February 1946.

Evidence of the success of the Vickery Line conversion came early. Within the first three months of operation with trolley coaches on this line, patronage had increased 10 per cent. The new electric service on the Capitol Line was accepted in like manner by the public.

Table II. Statistics Before and After Trolley-Coach Installation, Dallas, Texas

Total Motor-Coach System Compared with Vickery and Capitol Lines, 4-to-5 Minute Peak Headway

	March to September 1945, Bus	March to September 1946, Trolley Coach	Per Cent Increase
Bus system revenue*	$1,404,776	$1,456,179	3.66
Capitol and Vickery revenue**	$ 220,252	$ 248,759	12.94
Bus system miles*	5,523,946	5,668,262	2.61
Capitol and Vickery miles	712,670	736,481	3.34
Bus system revenue per mile*	25.4¢	25.6¢	.80
Capitol and Vickery revenue per mile	31.0¢	33.8¢	9.00

* Total motor-coach system exclusive of Capitol and Vickery.

** Capitol and Vickery combined because the two routes serve contiguous territories.

The operating results following application of modern electrics on the Capitol and Vickery Lines has resulted in trolley coaches being included in subsequent modernization plans. The Mt. Auburn and Parkview Lines have since been converted to trolley coaches. Others being contemplated are the Harwood, Meadow, and Crosstown Bus Lines.

Table II gives the figures for these first two Dallas lines before and after conversion. These are self-explanatory.

Cleveland, Ohio

The Cleveland Transit System is providing transportation to over a million citizens of Cleveland and the adjacent communities with 284 trolley coaches, 75 PCC cars, 859 street cars, and 709 busses. Upon completion of their presently planned modernization program, however, the total number of rubber-tired electrics in Cleveland will be increased to 629 and trolley coaches will form the backbone of the system.

The first trolley coaches installed were on the Hough Avenue line in 1936. Difficulties during the war years prevented further modernization until 1945. Since then, however, six lines have been converted to trolley coaches. Among them was the Wade Park Line which was a motor-bus line with 11.16 round-trip miles. It was difficult to compare the bus service on Wade Park before the conversion to the new trolley-coach service for various reasons but according to a study made by the Cleveland Transit System preparatory to the Wade Park trolley-coach installation, busses and trolley coaches compared as shown in Table III.

Motor-bus lines included in future plans for trolley-coach conversion are Fulton, Clifton, and Woodland.

Akron, Ohio

The Akron Transportation Company serving nearly 350,000 people in Akron, Barberton, and Cuyahoga Falls, operates approximately 70 trolley coaches on its main trunk lines.

Trolley coaches were first operated in Akron in 1942 when the West Market Street Line, running 5-minute peak headways, was changed from motor-bus operation. The success of these first electrics is indicated by the statement of an official of the transportation company that out of the 32 trolley coaches on the property during the war, 32 were operated every day under the severest service conditions. The only exceptions to this were traffic accident repairs.

Another bus-to-trolley-coach conversion was the Cuyahoga Falls Avenue Line on December 17, 1945. Peak headways were 10 minutes. This line was made a through town route in 1948 and is now called the Bailey-Kenmore-Barberton Line. There is express operation to Cuyahoga Falls on this line during rush hours.

Actual comparative figures as to passengers carried, revenue, and so forth were not available because of a rearranging of the routes accompanying the substitutions, but a schedule speed comparison was obtained on the Cuyahoga Falls Line. The figures show trolley-coach rush-hour schedule speed to be 12 per cent faster than bus. In 1945, before trolley coaches were put in, round-trip time from Main and Exchange to the Bailey Loop was 75-minute rush and 70-minute base for the busses then operating as compared with 67-minute rush and 63-minute base for trolley coach. As a matter of record, the system average trolley-coach schedule speed in Akron for July, 1948, was 11.12 miles per hour including layover.

According to an Akron Transportation Company official, electric transit is the backbone of their system.

MEMPHIS, TENNESSEE

The Memphis Street Railway operates 204 rubber-tired electrics over 147 round-trip miles of route and there are more to come. The most recent change from bus to trolley coach was the Crosstown extension, a 7-mile round-trip run with peak headways from 4 to 5 minutes.

The next bus to trolley-coach conversion will be the Jackson Feeder Bus Line covering 4.0 round-trip miles. Following this will be the conversion of the Faxon Line covering 9.0 round-trip miles, running 3- to 4-minute peak headways. This expanded service will require a total of 18 additional coaches. The overhead line is now under construction.

Table III. Vehicle Comparison, Cleveland, Ohio

Wade Park Line Study, 2-to-3 Minute Peak Headways

	40 Passenger Gasoline Bus	40 Passenger Trolley Coach
Vehicles required	32	26
Annual rides	7,997,793	7,997,793
Annual miles	820,352	774,642
Annual hours	91,568	80,038
Annual expenses	$287,136.61	$244,176.32

Table IV. Statistics Before and After Trolley-Coach Installation, Des Moines, Iowa

Installed on Second Avenue Line, May 16, 1948, 6-Minute Peak Headways

Type Data	1947 June–July, Bus	1948 June–July, Trolley Coach	Increase or Decrease, Per Cent
System revenue	$543,399	$577,590	+ 6.3
Second Avenue Line revenue	14,623	18,083	+23.6
System miles	$1,438,195	$1,287,170	−10.5
Second Avenue line miles	48,519	45,552	− 6.5
System revenue per mile	37.8¢	44.9¢	+18.8
Second Avenue revenue per mile	30.1¢	39.6¢	+31.6

DES MOINES, IOWA

In Des Moines, trolley coaches are called "curbliners." The complete system includes ten curbliner routes, six street-car routes and eight motor-bus routes. The latest curbliner route was installed May 16, 1948. This was the Second Avenue Line which was served previously by motor busses. Comparing revenue for June and July 1947, before conversion, with the same period in 1948 shows a 23.6 per cent increase. System revenue showed a 6.3 per cent increase for the same period. Total miles operated on the Second Avenue Line in June and July 1948 as compared with the same period in 1947 showed a 6.5 per cent decrease.

The total result, considering the 23.6 per cent increase in revenue and the 6.5 per cent decrease in miles traveled indicates that in Des Moines more passengers are carried more efficiently with modern electric curbliners.

Additional proof of the quality of service rendered by trolley coaches in Des Moines lies in the statement by the Des Moines Railway Company that they operated every one of their 132 trolley coaches every day of every week for four years during the war, with the exception of vehicles with body damage caused by collisions.

LITTLE ROCK, ARKANSAS

The Capital Transportation Company has launched a modernization program which began December 26, 1947. At present, new electric passenger equipment on the property consists of 35 trolley coaches operated on what was formerly four lines. Of these four lines, two were converted from bus operation. They are the South Main, and West Ninth Street Lines. South Main is now combined with Pulaski Heights to make one route. West Ninth is combined with the Fair Park Line. These lines run 5-minute peak headways.

According to the company, future plans for trolley-coach installations include at least two other motor-bus lines.

Analysis of Cases

The facts and figures recorded in all of the foregoing examples compare the bus and trolley coach on two points as related to service on trunk lines in the 2-to-10 minute peak-headway range. These points are:

1. Ability to attract riders.
2. Operating economy.

The figures show the trolley coach to be superior on both points.

These points, which can be substantiated by an analysis of the actual cases, could stand further study. For example, why does the trolley coach serve a given line more economically than a bus?

Figure 1. Modern trolley coach

Economies offered by the trolley coach lie in:

1. Savings resulting from the smaller requirements as to quantity of vehicles and number of vehicle hours and miles.
2. Electric equipment maintenance being less expensive than engine and transmission maintenance.
3. Trolley-coach body and chassis maintenance being less expensive than bus maintenance because of smoother operating equipment on trolley coaches.
4. Electrical energy being more economical than petroleum fuels.
5. Brake maintenance advantage of the trolley coach due to electrical braking.
6. Tire and tube mileage advantage of the trolley coach due to less heat generated at the brake drums.

These factors generally add up to an expense comparison such as is shown by Table V.

The figures in Table V are further enhanced by the fact that trolley coaches will operate less miles and hours than busses in performing a particular service.

There are various reasons why trolley coaches are able to attract more revenue than busses. Important among them are the following:

1. Wide spacious aisles allowing more freedom of movement.
2. No engine roars, and a minimum of brake squeals.
3. Fast and comfortable.
4. Clean, well lighted, well ventilated, and devoid of the odor of engine exhaust gases.

Summary

This paper cites certain cases where trolley coaches replaced busses as indicative of a trend. Then the results of the replacements are recorded to explain the trend and the significance of sound vehicle selection.

For the most part, the routes chosen for this paper traversed the same streets before and after conversion. This type of route is necessary for accurate comparison of all the factors involved. Where the line in question changed, no attempt was made to compare figures which would be affected by the change. For example, if half of a line served a different area after conversion, no attempt was made to compare total revenue, passengers carried, or vehicle miles before and after conversion.

Table V. Typical Operating Costs

	Year	Trolley Coach	Bus
Boston, per vehicle mile	1946	36.7¢	43.5¢
San Francisco, per vehicle hour	1947	$3.39	$4.16

If detailed figures were not available, the conversion was merely cited, possibly with statements from the company, without making inferences or drawing any unfounded conclusions.

Conclusion

These actual case histories are good examples of how trolley coaches can improve gasoline-bus operation on a heavy-service line. The better operation which resulted in every case is indicative of the advantages of the trolley coach over self-propelled vehicles on trunk lines. More capacity, higher schedule-speed ability, less expensive maintenance and more attractive service enable this modern rubber-tired electric vehicle to give better service to the rider and greater economy to the operator. Thus the trolley coach confirms the fact that modern electric-transit equipment has a large field of application in our cities.

Confirmation also lies in the fact that almost every transit system cited here has plans for future bus to trolley-coach conversions. There are also companies whose experiences were not included here who have such conversions in their modernization plans. For example, the New Orleans Public Service, Inc., in New Orleans, La., plans to convert the City Park Line from the present bus operation to trolley coaches. Their modernization program at present calls for 169 trolley coaches.

To satisfy the mounting urgency for more efficient operation, we can expect the modern trolley coach to be applied at an increasing rate on heavy-service lines requiring peak headways of from two to ten minutes.

No Discussion

Application of Experimental Test Procedures and Methods of Analysis of Results to Research Problems in Magnetic Recording

C. S. THOMPSON
NONMEMBER AIEE

Synopsis: This paper discusses an investigation designed to determine, as functions of bias- and signal-current values and of recording media and recording and playback heads, the response characteristics of a magnetic recording system. The theoretical background presented permits the prediction of frequency response curves in terms of relative values. These curves are obtained from data determined by measurements, calculations, and experiments on the component parts of a magnetic recording system. Subsequent to the theoretical material there is a description of a systematic method for planning experimental procedure, plotting the results, and presenting the test data for a magnetic recording system. Other data displayed here proves the superiority of thin laminations (0.002 inch thick) over thick laminations (0.005 inch thick) as core material for the heads of a magnetic recording system.

MAGNETIC recording is a system for impressing time variations in magnetic field strength upon a ferromagnetic material, usually in the form of a fine wire or a thin film superimposed on a paper or plastic tape. The recording is accomplished as the tape or wire moves at a constant speed through the recording apparatus. Magnetic recordings also have been made on rotating disks or cylinders, but these are not a concern of this paper.

The variations in magnetic field strength to be recorded exist at the pole tips, in the boundary of an air gap in the core of an electromagnet. The magnetic field at the pole tips is produced by a current in the coils of the electromagnet. The electromagnet is referred to as the recording head. Variations of current strength in the recording head cause proportional variations in magnetic field strength to be recorded on the wire or tape. The most common use of magnetic recording is to record speech or music. Acoustic impulses may be translated into recording-head current variations by any conventional method.

Advantage is taken of the remanence of the magnetic recording medium to retain the effect of the magnetic field intensity existing in the air gap of the recording head at the instant in which any particular portion of the recording medium travels across the air gap.

Remanence is defined, according to the American Society for Testing Materials, as "the magnetic induction which remains in the magnetic circuit after the removal of the applied magnetic force. If there is an air gap in the magnetic circuit, the remanence will be less than the residual induction."

Residual induction is defined as "The magnetic induction corresponding to zero magnetizing force in a magnetic material which is in the symmetrically cyclically-magnetized condition." The difference between remanence and residual induction is caused by the demagnetization effect discussed later. Where remanence and residual induction are used in this paper, they are used in the sense of the preceding definitions.

Figure 1 (A) shows the signal to be recorded, as a sine wave of current in the coils of the recording head; Figure 1 (B) shows an enlarged view of the recording wire or tape. The small arrows represent symbolically the alignment of the so-called "molecular magnets." Immediately below the wire or tape, the recording head is shown with flux lines threading its core. The bottom leg of the core is surrounded by an energizing coil. The pole tips are marked with an assumed polarity indicated by the symbols *N* and *S*.

The recording medium enters the recording head, previous to time t_1, in the unmagnetized condition indicated by the heterogeneous state of the molecular magnets. At time t_1, the current starts to build up from zero. As the current increases in strength, more and more molecular magnets are aligned until, at time t_2, when the current has reached maximum value, the maximum number of magnets have been aligned and the maximum magnetic intensity along the wire is produced. Decreasing current produces less and less magnetic field strength at the pole tips, resulting in a decrease in magnetic intensity along the wire until, at time t_3, the intensity is reduced to zero. Increasing the current in the opposite sense repeats the process of aligning the molecular magnets in proportion to the current strength, but in the opposite direction.

As the recording medium moves along, the molecular magnets are removed from the magnetizing field. Thus the medium retains the magnetic intensity indicated by the remanence value. Notice that free magnetic poles are formed at the approximate times t_1 and t_3 and are indicated on the wire by the polar symbols *N* and *S*. The distance between these

---

Paper 49-107, recommended by the AIEE communication committee and approved by the AIEE technical program committee for presentation at the AIEE winter general meeting, New York, N. Y., January 31-February 4, 1949. Manuscript submitted December 3, 1947; made available for printing January 5, 1949.

At the time this paper was written C. S. THOMPSON was with the Franklin Institute Laboratories for Research and Development, Philadelphia, Pa. He is now a consulting engineer.

Information contained herewith was gathered in studies performed under research and development contracts with the Special Devices Center, Office of Naval Research, United States Navy.

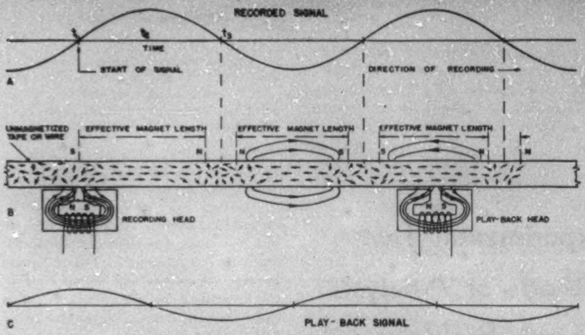
RECORDED SIGNAL
t_1
t_2
t_3
TIME
START OF SIGNAL
DIRECTION OF RECORDING
A
UNMAGNETIZED TAPE OR WIRE
EFFECTIVE MAGNET LENGTH
EFFECTIVE MAGNET LENGTH
EFFECTIVE MAGNET LENGTH
S
N
N
S
S
N
N
B
RECORDING HEAD
PLAY-BACK HEAD
C
PLAY-BACK SIGNAL

Figure 1. Diagram illustrating theory of magnetic recording

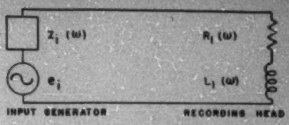
$Z_i\ (\omega)$
e_i
$R_1\ (\omega)$
$L_1\ (\omega)$
INPUT GENERATOR
RECORDING HEAD

Figure 3. Equivalent recording circuit

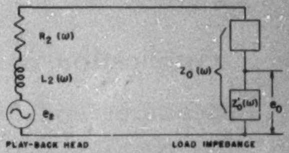
$R_2\ (\omega)$
$L_2\ (\omega)$
e_2
$Z_0\ (\omega)$
$Z_0'(\omega)$
e_0
PLAY-BACK HEAD
LOAD IMPEDANCE

Figure 4. Equivalent play-back circuit

poles indicates the approximate effective length of what will be referred to as the "fixed magnets" existing in the recording medium as a result of the recording process.

If a sample of the recording medium in ring or closed magnetic circuit form be measured by a B–H loop tracer, the residual induction will be that value of B, referred to as B_r, which corresponds to zero value of H. The fixed magnets in the recording medium, not being in a closed magnetic circuit when removed from the recording head, will exhibit a lower value of B, referred to as B_d, the remanence value. The maximum value of H at the tip of the hysteresis loop is the same in both the open and closed magnetic circuits. The reduction in B from B_r to B_d results from the demagnetization effect of the air-gap path of the return flux from the N pole to the S pole outside the recording medium.

The demagnetization effect, a function of the ratio of the thickness of the fixed magnets to their effective length, becomes greater as the ratio becomes greater. For a bar magnet with a length 100 times greater than its thickness, the demagnetization effect is negligible, and B_d may be taken equal to B_r.

Obviously, if a constant wire speed is assumed, the effective magnet length becomes shorter as the frequency of the recorded signal becomes higher. For very high frequencies the effective magnet length may approach, or become less than, the wire diameter. In such cases the demagnetizing effect is very powerful, resulting in a large attenuation of the value of magnetic intensity in the recording medium at high frequencies. This demagnetizing effect is one of the important sources of distortion in a magnetic recording system.

Another source of distortion is the nonlinear relation between B and H. This nonlinearity is severe, as can be seen by observing the familiar hysteresis loop.

Early investigators of magnetic recording were unable to overcome the serious distortion of the hysteresis loop (Figure 5) until it was discovered that, if the audio, or lower frequency, signal was mixed with a much higher frequency current and both recorded at their proper amplitudes, so far as the recorded signal was concerned, a linear relation between B and H was approached. The high-frequency current is referred to as the "bias current." Assuming an upper response curve cutoff frequency of 10 kc beyond which high-frequency components are sharply attenuated, and if the bias frequency is 30 kc or higher, no bias frequency component will be observed in the response of the recording system. The use of a biasing current does not make the relation between B and H completely linear, so that slight distortions due to nonlinearity still remain. D-c biasing has been used with only mediocre results.

Several detailed explanations of the action of high-frequency biasing currents have been published. Some of the explanations are at variance with each other as to the manner in which the biasing current acts to make the relation between B and H more nearly linear. While it is felt that the action of the bias current should be the subject of a more rigorous mathematical analysis, an article by Lynn C. Holmes and Donald L. Clark offers a well-thought-out theory.[1]

Figure 1(B) shows that, as the recording medium moves, it crosses the pole tips of the play-back head. Part of the flux surrounding the fixed magnet passing across the play-back head, threads through the core of the play-back head. The amplitude of the flux density thus set up in the play-back head, is proportional to the magnetic intensity existing in that part of the recording medium passing across the air gap. The directional sense of the flux is determined by a polarity of the fixed magnet. The building-up and dying-down of the flux in the core causes an electromotive force to appear at the terminals of the coil wound around the lower leg of the core of the play-back head. Again, this electromotive force is proportional to the magnetic intensity existing in the recording medium at the moment the medium passes across the air gap of the play-back head. The play-back signal produced by this passage is shown in Figure 1(C). The 90-degree shift in phase between the sine wave of magnetic intensity and the sine wave of electromotive force produced

Figure 2. Functional block diagram of magnetic recording system

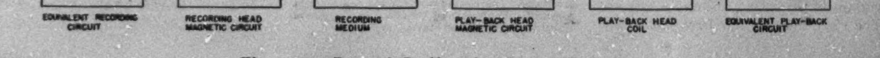
e_1
$\frac{1}{Z_1(\omega)+jL_1(\omega)+R(\omega)}$
i_1
$N_1 h_1(\omega)$
ϕ_1
$m(V_1\omega)$
ϕ_2
$h_2(\omega)$
ϕ_2
$N_2\omega$
e_2
$\frac{Z_0'(\omega)}{Z_0(\omega)+j\omega L_2(\omega)+R_2(\omega)}$
e_0
EQUIVALENT RECORDING CIRCUIT
RECORDING HEAD MAGNETIC CIRCUIT
RECORDING MEDIUM
PLAY-BACK HEAD MAGNETIC CIRCUIT
PLAY-BACK HEAD COIL
EQUIVALENT PLAY-BACK CIRCUIT

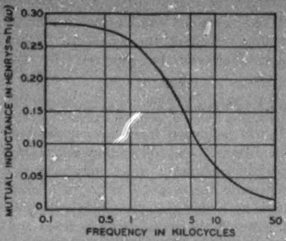

Figure 5. Mutual inductance of recording and play-back heads versus frequency

at the terminals of the play-back coil, is of mere academic interest.

The amplitude of the play-back electromotive force is at a rather low level, and must be amplified considerably before being used in a measuring instrument or loud-speaker.

In addition to the distortions produced by the demagnetization effect and the nonlinear relation between B and H, other magnetic, electrical and mechanical characteristics add to the distortion which may be produced in the magnetic recorder. The Bartol Research Foundation of The Franklin Institute, under contract to Special Devices Center, United States Navy, developed a theoretical background for the analysis of the factors influencing the response of a magnetic recorder. A summary of the analysis is presented here as the basis for the work covered by this paper.

Using data determined by measurements, calculations, and experiments, a concrete example of a frequency response curve, predicted from the known characteristics of each of the component parts of a magnetic recording system, has been worked out. It is not possible to obtain absolute values for the response curve, because some of the magnetic and electric loss factors can not be isolated experimentally, and because an exact mathematical solution to some of the problems is far too complex. Consequently, the theoretical work can provide a solution only in terms of relative values. This is a minor difficulty, however, since the value of the theoretical treatment lies in its ability to provide the tools for estimating the relative effects of suggested improvements, and to reveal the need for, and the nature of, improvements.

Figure 6. B versus H for recording-wire sample

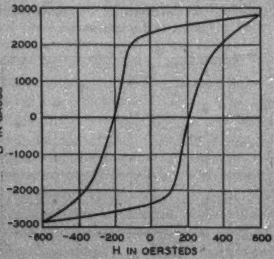

Mathematical Background

Assuming it is possible to evaluate the terms involved, the frequency response characteristics for the recording head, the play-back head, and the recording media (wire or tape) of a given magnetic recording system may be calculated from the following transfer equation established by Shutt

$$\frac{e_0}{e_i}=\frac{N_1N_2Z_0'(\omega)\omega h_1(\omega)m(\omega,v)h_2(\omega)}{[Z_i(\omega)+j\omega L_1(\omega)+R_1(\omega)][Z_0(\omega)+j\omega L_2(\omega)+R_2(\omega)]} \quad (1)$$

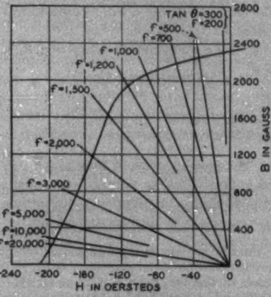

Figure 7. Second quadrant B–H curve

This formula is developed logically from the behavior of the elements of the magnetic recording system. It was presented by Ralph Shutt in an unpublished report to the Special Devices Section, United States Navy. ("Some Theoretical Considerations Concerning Magnetic Sound Recording," Bartol Research Foundation of the Franklin Institute, Swarthmore, Pa., October 22, 1946.)

The elements of the preceding equation are displayed functionally in Figure 2. Each box, corresponding to a functional element, contains the symbols describing its behavior as a function of signal frequency and the speed of the recording medium moving past the recording head and play-back head. The electric circuit elements involved are shown in Figure 3 for the input circuit, and in Figure 4 for the play-back circuit.

The symbols used in the diagrams and in the preceding equation are given in the list of symbols at the end of this paper.

THE FUNCTION, $h_1(\omega)$

The magnetic field in the pole tips of the recording head, available for magnetizing the wire or tape, is a function of the magnetic skin effect in the magnetic circuit of the recording head. The magnetic skin effect is represented by the function $h_1(\omega)$ for a given lamination thickness. Decreasing the lamination thickness reduces the magnitude of the magnetic skin effect. It can be shown that

$$h_1(\omega)\sim M_1(\omega) \quad (2)$$

where M_1 (ω) is the mutual inductance between the main coil of the recording head and an exploring coil wound on a pole tip. $M_1(\omega)$, obtained by means of an impedance bridge, is plotted against frequency in Figure 5. Since h_1 (ω) is proportional to M_1 (ω), and since absolute values are not concerned immediately, assume that

$$h_1(\omega)=M_1(\omega) \quad (3)$$

and substitute accordingly where h_1 (ω) appears.

THE FUNCTION, m (ω,v)

The symbol m (ω,v) represents the demagnetization effect existing in the wire or tape as it comes under the influence of the applied magnetic field in the gap of the recording head.

B–H curves are derived from samples having a large ratio of length to diameter; usually well above 50 to 1. This ratio, or a larger one, is used for the express purpose of obtaining a B–H curve under conditions free from any appreciable influence of the demagnetization effect. It is possible to predict the extent to which the remanence value would be lowered by the demagnetization in case a sample, measured under conditions of a large ratio of length to diameter, is to be used in a situation in which the ratio of length to diameter is small (less than 100 to 1). This prediction may be made, using methods devised to determine the magnitude of the demagnetization effect, by applying a correction factor to the standard B–H curve. The correction factor is calculated (in our case with the aid of predetermined graphs calculated by Shutt) from a knowledge of the ratio between the effective length and the thickness of the individual magnets appearing

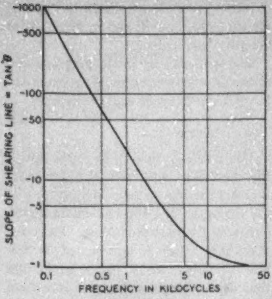

Figure 8. Slope of shearing line = tan θ versus frequency

Wire diameter = 0.004 inch
Wire speed = 5 feet per second

in the wire or tape during the recording process.

Figure 6 is submitted as the *B–H* curve of a representative sample of recording wire.

For our purpose, we are interested only in the second quadrant of the *B–H* curve. An enlarged view of the second quadrant is given in Figure 7.

Typical values of the magnitude of the demagnetization-effect correction factor are given by the curve in Figure 8, which shows the relation between the frequency and the slope of a shearing line. The slope of the shearing line is applied as a correction factor to the second quadrant of the *B–H* curve in Figure 7. Figure 8 is based on calculations by Shutt for the special case of 0.004 inch diameter wire moving at 5 feet per second.

The negative tangent of the angle θ, (slope of the shearing line) = the demagnetization factor if the B and H coordinates are drawn to the same scale. Since these co-ordinates are not drawn to the same scale in Figure 7, the actual slope of the shearing line is determined by applying the proper scale factor.

The slope of the shearing line is plotted against frequency for 0.004 inch diameter wire. One shearing line for each frequency is drawn on the curve in Figure 7. These lines are drawn radially from the origin, with the proper slope dictated by the frequency given in Figure 8. The intersections of the shearing lines and the *B–H* curve indicate B_d, the corrected values of B_r which correspond to the frequency under consideration, and which represent the relative value of the result of the demagnetization effect.

Figure 9 shows the plot of B_d, remanent magnetism, against frequency. For the purpose of this paper the function $m(\omega,v)$ is taken to be equal to the corrected B_r as a function of frequency, and, consequently the corrected B_r is the term used in the equation.

THE FUNCTION, h_2 (ω)

h_2 (ω) is a factor which decreases with frequency and may be shown to be composed of two parts

$$h_2(\omega) = h_2'(\omega) \times h_2''(\omega) \tag{4}$$

h_2' (ω) is quite similar to h_1 (ω) in that it is directly proportional to the mutual inductance between the main coil of the play-back head and an exploring coil wound on the pole tips. Since the functions h_1 (ω) and h_2' (ω) are similar, and the recording and pick-up heads may be almost identical (in some cases the same head is used both for recording and play-back), the curve of Figure 5 will be used to represent h_2' (ω) as well as h_1 (ω).

h_2'' (ω) is equivalent to a function, $h_3 \times \frac{(2\pi)}{\lambda}$ developed by Shutt where

λ = wave length of recorded signal
= 2 (effective magnet length)

The following concept may prove useful in describing the physical phenomena responsible for the frequency discrimination expressed by the function h_2'' (ω)

Fluctuating magnetic potentials are set up at the pole tips of the play-back head, as a result of the varying amounts of magnetization which were fixed in the wire or tape as it passed through the recording head. The effective permanent magnets found in the wire have a length inversely proportional to the signal frequency impressed at the recording head. When the effective length of these magnets approaches the dimension of the gap width in the play-back head, the geometrical distribution of the flux within the air gap, and consequently at the pole tips, becomes a function of the magnet length. For linear reproduction the flux in the pole tips should be proportional only to the intensity of magnetization. The departure from linearity resulting from changing geometrical flux distribution, caused by varying magnet length, is expressed by the function $h_2''(\omega)$, shown graphically by the curve of Figure 10. Negative values of $h_2''(\omega)$ indicate a reversal of phase of the play-back signal.

THE QUANTITY, ω

Assuming a constant rms value of alternating sine-wave flux, the output voltage of a transformer or other inductor is proportional to $d\phi/dt$ and, consequently, to the frequency, f. Therefore the output voltage of the play-back head is proportional to the signal frequency, as well as to the other factors mentioned in this summary.

The combined effect upon the output voltage of all of the significant factors mentioned can be expressed by the product

$$\omega \times h_1(\omega) \times m(\omega,v) \times h_2'(\omega) \times h_2'(\omega) \sim e_0 \tag{5}$$

It will be shown later that, under test conditions, the above product is the only part of equation 1 which influences significantly the response curve of a magnetic recording system. Calculating this product for the frequencies concerned, and plotting the results against frequency, one obtains the theoretical fidelity response curve of a magnetic recorder under conditions in which the current input to the recording head is constant. The resulting plot for this product, as developed from the functions outlined in this summary, is shown in Figure 11. Negative values of output indicate a reversal of phase of the output signal.

The response curve obtained under the foregoing outline is valid under the following conditions and assumptions:

1. The magnetizing current

$$i_1 = \frac{e_t}{Z_t(\omega) + j\omega L_1(\omega) + R_1(\omega)} \tag{6}$$

has been kept constant. This is one of the conditions of the experiment.

2. If the impedance Z_0 (ω) of the amplifier following the play-back head is large compared to the impedance $[j\omega L_2(\omega) + R_2(\omega)]$ of the play-back coil and if

$$Z_0'(\omega) = Z_0(\omega) \tag{7}$$

then

$$\frac{Z_0'(\omega)}{Z_0(\omega) + j\omega L_2(\omega) + R_2(\omega)} \approx 1 \tag{8}$$

Rewriting equation 1

$$e_0 = \frac{e i N_1 N_2 Z_0'(\omega) \omega h_1(\omega) m(\omega,v) h_2(\omega)}{[Z_t(\omega) + j\omega L_1(\omega) + R_1(\omega)][Z_0(\omega) + j\omega L_2(\omega) + R_2(\omega)]} \tag{9}$$

and observing that

$$i_1 = \frac{e_t}{Z_t(\omega) + j\omega L_1(\omega) + R_1(\omega)} = \text{Constant} \tag{10}$$

Figure 9. *Br* corrected for demagnetization effect versus frequency

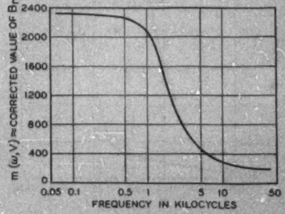

$$N_1N_2 = \text{Constant} \tag{11}$$

$$\frac{Z_0'(\omega)}{Z_0(\omega)+j\omega L_2(\omega)+R_2(\omega)} \approx 1 = \text{Constant} \tag{12}$$

Equations 10, 11, and 12 contribute nothing toward a study of the variations of e_0 with respect to frequency. This leaves for consideration only

$$e_0 \sim \omega h_1(\omega) \times m(\omega,v) \times h_2(\omega) \tag{13}$$

which is again proportional to

$$f \times h_1(\omega) \times m(\omega,v) \times h_2'(\omega) \times h_2''(\omega) \times h_2''(\omega) \tag{14}$$

which will be considered equal to e_0. e_0 is the output voltage, plotted against frequency in Figure 11. Equation 1 can be used to show what will happen when the input, e_1, varies; particularly what can be done when e_1 is controlled (pre-equalization). Equalization may also be accomplished by establishing and controlling the inequality, $Z_0'(\omega) \neq Z_0(\omega)$, as a function of frequency (post equalization). See equation 7.

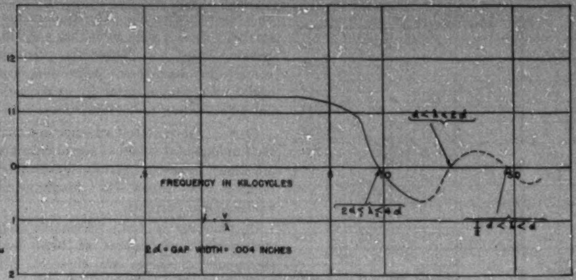

Figure 10. $h''(\omega)$ versus frequency. $v = 5$ feet per second

Development of Test and Analysis Methods

For the most part, the tests performed to date had for their purpose a determination of the influence exerted by component-part characteristics upon the over-all response. By altering a characteristic of the component part under tests, and by investigating again the over-all response, the influence of component-part characteristics upon over-all fidelity could be determined. One of the important objectives of the tests conducted at The Franklin Institute was the correlation of over-all fidelity with the influence of the various functions included in equation 5.

The nature of the project was such that the main interest lay in the effect of lamination thickness and of the *B–H* characteristics of the recording media, on the fidelity of reproduction.

The majority of the tests made on the magnetic recording system were in the form of sine-wave recordings, at various amplitudes and frequencies of the signal and bias currents. Experimental performance was judged from the results shown by fidelity curves drawn from the frequency versus response data obtained at the play-back head. Because of the nature of the project, it was considered desirable to measure the harmonics as well as the fundamental appearing at the output terminal of the play-back head.

Frequency versus response data was obtained with a General Radio Wave Analyzer. While response tests using an intermodulation measuring instrument may be conducted with profit, intermodulation testing does not estimate the harmonic content with ease, and, since an interest in harmonic content existed for special reasons, the majority of tests conducted up to the present time have been made with the conventional wave analyzer. It is planned that intermodulation tests will be conducted in the future as an aid to estimating the performance of magnetic systems used in recording speech and music.

Considering the complexity of the simultaneous action of bias and signal currents upon the nonlinear transfer characteristics of the loop, it is obvious that, in order to arrive at correct values of bias and signal currents, considerable experimenting must be done. It may be said that "optimum" values are desired. Optimum values may be defined as those values of bias current and of signal current which give maximum output, if these values are consistent with the requirement that the nominal operating range of signal current variation will be in the most linear portion of the signal (input versus output) saturation curve, that is, somewhere below the knee of the curve. This definition implies that operating in a part of the output curve which approaches linearity minimizes harmonic distortion.

An attempt to obtain optimum conditions discloses that the optimum bias current depends on the signal current chosen, and that the optimum signal current depends on the bias current chosen. The optimum bias current and the permissible range of signal current variation are quite interdependent.

Prevalent methods for adjusting the values of bias and signal currents consist of observing the effects on the output of varying the values of either the bias or the signal current, by means of an oscillograph which shows the received wave form, by using an intermodulation instrument or output meter, or by any other output-measuring device. Bias current adjustment is alternated with signal cur-

Figure 11. Fidelity characteristic for magnetic recorder

Voltage at play-back coil versus frequency at constant recording circuit

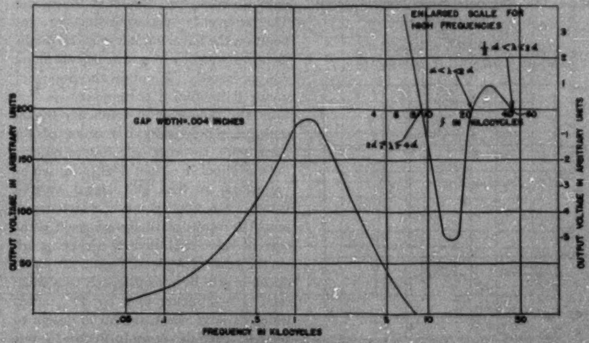

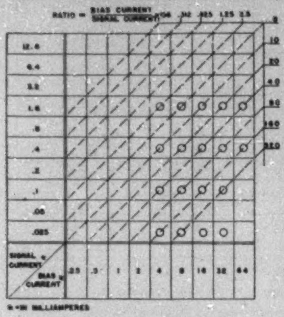

Figure 12. Test schedule sheet

rent adjustment until the operator judges that suitable operating values have been achieved. Most of the methods described in the literature seem to be based on similar cut-and-try procedure.

Considering the importance of determining correctly the proper operating values of bias and signal currents for a given magnetic recorder design, it seemed expedient to establish a suitable method for such a determination. The most reasonable procedure for this test was to obtain fidelity characteristics throughout a suitable range of both bias and signal currents, plot the results, and then determine from the plotted results which bias current could be considered "optimum" from the point of view of signal-current range and fidelity requirements. The information presented by the resulting graphs was complete, concise, and final.

A systematic plan for choosing a range of bias and signal currents was achieved. This plan involved choosing particular values of test currents at equal intervals on a logarithmic scale. The fundamental intervals chosen were such that each increasing value was double the previous value. In case these steps were too coarse, the fundamental intervals were halved according to the logarithmic scale.

Figure 12 shows a test schedule in which the fundamental values of signal currents are shown in the left hand column. The bottom row shows the fundamental values of bias currents.

In planning a test, reasonable and systematic combinations of bias- and signal-current values are chosen. For each of the chosen combinations, the frequency response curves are obtained. The selected combinations of bias and signal currents are indicated by placing a small circle at the intersection of the rows and columns of the test schedule sheet corresponding to the desired values of signals and bias currents. If the intervals between the fundamental current values shown on Figure 12 are too large, auxiliary sheets with half intervals may be prepared.

In order to analyze logically the characteristics of such component parts of a magnetic recording system as recording head, play-back head, and recording media, it has been found highly desirable and informative to obtain frequency response curves at each of a reasonable number of well-chosen combinations of bias and signal currents.

Some of the ways in which the frequency response data may be analyzed and presented will be described. Figure 13 shows a frequency response curve as obtained with the wave analyzer. These curves show the output of the fundamental frequency, together with the accompanying harmonic content, as functions of signal frequency. Each curve of harmonic content is labeled with a number representing the multiple of the fundamental frequency for that harmonic. The frequency corresponding to any point on the harmonic curve is the fundamental frequency at which the harmonic was measured. To obtain the frequency of the harmonic, it is necessary to multiply the fundamental frequency by the multiple representing the order of the harmonic. In order to estimate quickly the variations in output fidelity caused by variations in bias and signal current values, each fidelity curve, which represents the results of a test performed at the current value indicated by a check mark on the test schedule of Figure 12, is reduced in size by a pantograph to a small card, 1 $^{11}/_{16}$ inches long by $1^1/_4$ inches wide. A large sheet, similar in design to the test schedule shown in Figure 12, but with each square $1^{11}/_{16}$ inches long by $1^1/_4$ inches wide, is prepared. The rows and columns of this larger sheet, called the Test-result Schedule Sheet, designate bias and signal current values. The small cards, each containing a reduced fidelity curve, are affixed to the large sheet, in the appropriate space corresponding to the intersection of the row and column showing the value of the bias and signal current at which the fidelity curve was obtained.

Each card is ruled to a log–log scale. The left-hand edge of each card corresponds to the ordinate at 100 cycles per second, the second vertical line, to 1 kc; the third line, to 10 kc; and the right hand edge, to 100 kc. The bottom edge corresponds to an output level of 0.01 millivolt; the second horizontal line, to 0.1 millivolt; the third line, to 1 millivolt; the fourth line, to 10 millivolts; and the top edge, to 100 millivolts. It was preferred to plot the output in absolute values on a logarithmic scale, rather than in decibels on a linear scale.

The small cards show the fundamental as a heavy solid line, the second harmonic as a fine solid line, and the third harmonic as a dotted line.

Figure 14 shows a test-result schedule sheet which displays the variation of fidelity characteristics throughout a range of bias and signal current values. This test provided data on the fidelity characteristics of a magnetic recording system employing the commercially produced recording wire, designated as wire *A*. A similar test employing a commercial recording wire, designated as wire *B*, was performed with the results shown in Figure 15. Aside from a slight difference in the choice of the range of test values for bias and signal current and the difference in recording media, the test conditions and circuit elements of the entire recording system for the two investigations were identical.

The test results given by Figure 13 were not obtained from the investigations conducted on either wire *A* or wire *B*, and, consequently, are not to be found in the curves of either Figures 14 or 15.

The preceding *qualitative* method of presenting large amounts of data in a small space permits all variations in performance to be observed at a glance.

To provide a presentation of *quantitative* data in a concentrated form, additional graphs were prepared from data furnished by the original frequency response curves, the reduction of which is shown qualitatively by the Test-result Schedule Sheet. In order to make the best of the information obtained in the

Figure 13. Response curves, output versus frequency

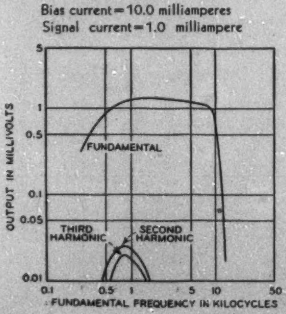

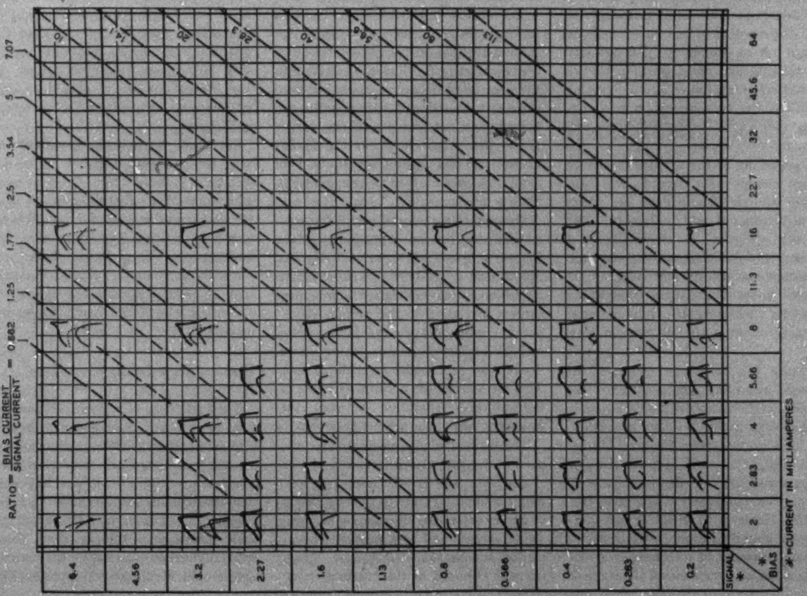

Figure 14. Response characteristics—wire A

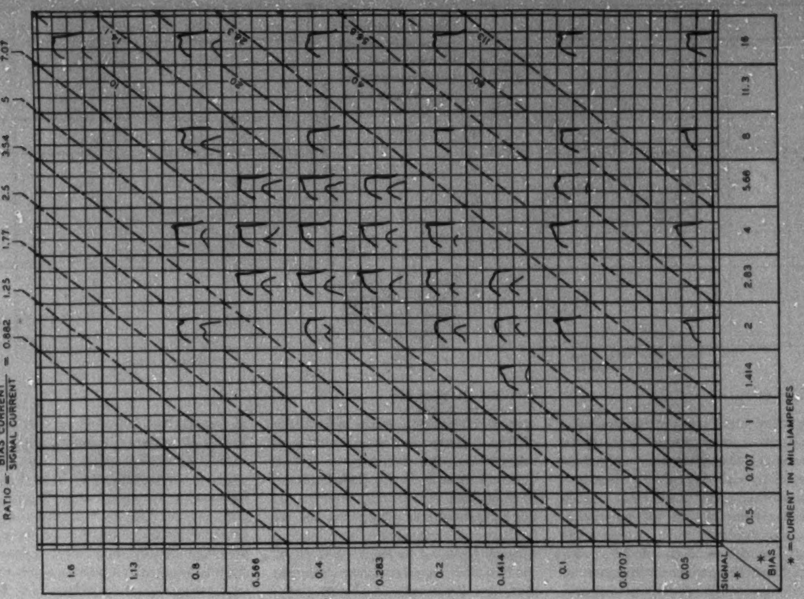

Figure 15. Response characteristics—wire B

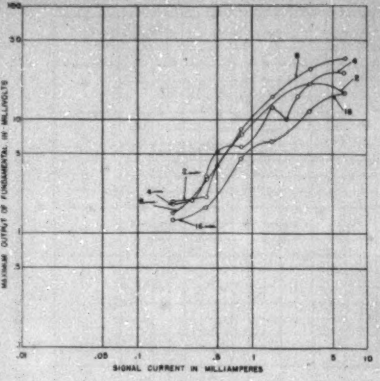

Figure 16 (left). Wire *A*—Maximum output of fundamental versus signal current at constant bias currents

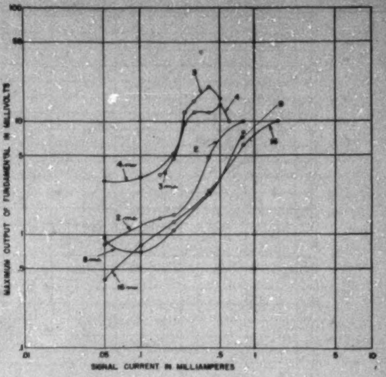

Figure 17 (right). Wire *B*—Maximum output of fundamental versus signal current at constant bias currents

basic curves, a number, representing magnitude or value, was assigned to an outstanding characteristic of the data presented by each curve sheet. Since each curve sheet represents data taken at a particular value of bias and signal currents, the "assigned value" corresponds to only one value of signal and bias current. Thus, the assigned value may be plotted against the variation of signal currents with the bias current held constant, or vice versa. Each assigned value should be regarded as a summation of all the data presented by one curve of output voltage versus frequency. Though this report treats bias and signal currents as adjustable factors, under actual operating conditions the bias current is held constant, while signal-current amplitude and frequency vary widely.

In preparing Figure 16, the maximum voltage output with wire *A*, was considered the significant data on which assigned values should be based. Consequently, Figure 16 shows assigned values at specific signal and bias currents. The extent to which the maximum output voltage varies with signal current is plotted for various values of bias currents. Figure 17 shows a similar plot for wire *B*.

Because the harmonics generated in magnetic recording are unwanted frequencies, and because the fundamental is the frequency in which we are interested, it is desirable to express the level of harmonic content in some definite relation to the amplitude of the fundamental. This may be done easily at any given frequency. However, it would be very convenient if a method could be contrived to express, by means of one number or assigned value, an over-all level of harmonic content with respect to the output level of the highest-amplitude harmonic in relation to the fundamental. This number or assigned value should attempt to express the difference in level between the highest-amplitude harmonic and the fundamental frequency throughout a wide range of the frequency covered by one frequency response curve. Assuming that what is needed is a number to express the average distance between the fundamental output level and the harmonic output level, the method chosen measures the area between the fundamental and the highest harmonic level. The area measurement is limited in all cases to the area lying between the vertical lines given by the 300 and 10,000 cycles per second points, and between the curves giving the output levels of the fundamental and the highest amplitude harmonic. This area was measured with a planimeter.

Since the area was measured on logarithmic paper in terms of linear dimensions (length squared), the area probably has no physical significance. However, from an arbitrary point of view, the area does express a relation to the average difference in level between the fundamental and its highest-amplitude harmonics in decibels, or in a similar logarithmic unit. This method affords a useful estimate of the average separation between the fundamental and the nearest harmonic.

The method of area measurement was used to compare the performance of wire *A* and with wire *B* with respect to harmonic content. Figure 18 shows a family of curves expressing the relation between signal current and area between fundamental and harmonic for wire *A*. Each curve is obtained at the constant value of bias current indicated on the curve. Figure 19 presents a similar graph for wire *B*.

The laboratory results, shown by the frequency response curve of Figures 14 and 15 and the quantitative-analysis curve of Figures 16 to 19 inclusive, were presented more for the purpose of demonstrating a logical system of analysis than for showing the results of any particular test. However, inspection of the curves of Figures 16 and 17 shows that, for a given signal current, the maximum output obtained from wire *B* is greater than that obtained from wire *A*. From the point of view of securing maximum output, the bias current for wire *A* should be eight milliamperes, and for wire *B*, three or four milliamperes.

Harmonic distortion is very nearly the same for both wires *A* and *B*. Minimum distortion is obtained for wire *A* by using a bias current of eight milliamperes, while the minimum distortion for wire *B* is obtained by using a bias current of four milliamperes. Thus, for maximum output with minimum distortion, a bias current of eight milliamperes should be chosen for wire *A* and four milliamperes for wire *B*.

Test for Thin-Lamination Head

The first phase of a significant investigation concerning the question of proper core lamination thickness for magnetic recording and play-back heads has been completed. Studies by Shutt indicated that considerable improvement in high-frequency response could be gained by using laminations thinner than those ordinarily employed in past commercial design and development work. The

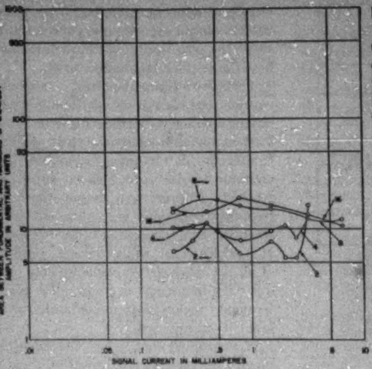

Figure 18 (left). Wire *A*—Area between fundamental and harmonic of greatest amplitude versus signal current at constant bias currents

Figure 19 (right). Wire *B*—Area between fundamental and harmonic of greatest amplitude versus signal current at constant bias currents

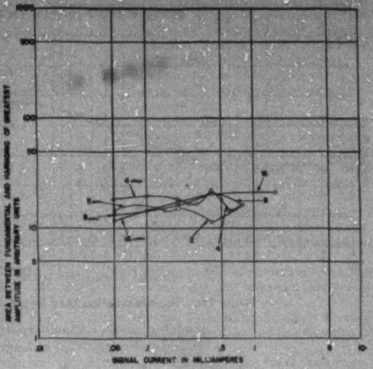

usual practice is to employ laminations of a thickness ranging from 0.005 inch to 0.015 inch. It was believed that laminations thinner than 0.005 inch would show a decided improvement in the high-frequency region. Accordingly, a play-back head having laminations of 0.002 inch in its core structure was built and tested.

Figure 20 shows a block diagram of the apparatus and instruments used in obtaining the frequency response characteristics for both the wire-comparison test and the thin-lamination test.

In order to obtain a direct comparison between the performances of thick and thin laminations, an experimental procedure was adopted which permitted frequency response curves to be obtained, under identical recording conditions, from a thick-lamination head, 0.005 inch thick, and a thin-lamination head, 0.002 inch thick, each in the play-back position. Both of these heads were of similar geometric design. The response curves in this test were obtained with an automatic sound-level recorder, rather than with the wave analyzer.

The advantage sought in using thin laminations is a greater fidelity than has been possible previously, in the high-frequency region. Thick laminations in the recording head result in high-frequency attenuation of the signals impressed upon the recording medium. Thick laminations in the play-back head result in a further attenuation, in the high-frequency region, of the reproduced signals. Thus, the use of a thin-lamination head in the play-back position avoids this second high-frequency attenuation. A system which employs a thick-lamination head in the recording position, and a thin-lamination head in the play-back position, should produce a fidelity superior to that of an arrangement in which a thick-lamination head is used in both the recording and the play-back positions. The fidelity superiority should correspond to an amount roughly proportional to the superiority of thin laminations over thick laminations. Such a comparison between the two systems was made.

Any difference between thin and thick laminations should show up to greater advantage in a test in which frequency response comparisons are made between thick laminations in both recording and play-back heads, and thin laminations in recording and play-back heads. High intensity of magnetization in the recording medium is necessary to raise the signal as far as possible above the noise level of the recording medium, and to eliminate the necessity for extreme amplification of signals appearing at the terminals of the play-back heads. This requirement demands a high-saturation-value material in the core of the recording head. Moreover, high-permeability material is required in the core of the play-back head, in order that the maximum flux be set up in the coil of the play-back head. However, at the time the test was made, thin laminations were available in only one material, high-permeability Mu-metal. This material has a low saturation value, rather than the high saturation essential for recording purposes in instances in which high flux density in the pole tip of the recording heads is needed to impress a high intensity of magnetization upon the recording medium. These restrictions prevented the use of thin laminations in the recording head, and thus confined their use to the play-back heads.

Throughout all tests reported in this paper the following test conditions prevailed:

Wire velocity = 5 feet per second
Bias frequency = 21 kc
Erase frequency = 20 kc
Recording and play-back air gap = 0.002 inch

Results

Figure 21 shows the fidelity response curve, taken with an automatic-level recorder, with a thick-lamination head in

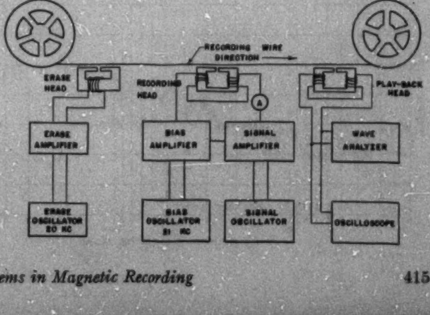

Figure 20. Block diagram of circuit used for obtaining fidelity characteristics

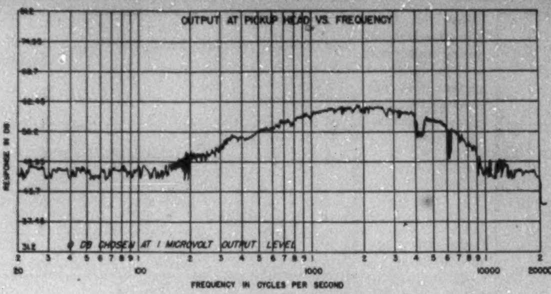

Figure 21. Thick-lamination head in play-back position

Bias current = 10 milliamperes
Signal current = 1.0 milliamperes

both the recording and play-back positions. The irregularities in the response were caused by local fluctuations in the magnetic properties of the recording wire, a characteristic possessed to a greater or lesser degree by all wires tested.

Figure 22 shows the frequency response of the thin-lamination head in the play-back position. The recording, made with the thick-lamination head, is the same one used to obtain the response curve of Figure 20, played through a thick-lamination head.

Observe that the response for the thin-lamination head holds at a high level up to 10 kc while the response for the thick-lamination head drops rapidly above 5 kc.

The response curve in Figure 22, taken with an automatic-level recorder, while not made from an identical recording, was made under the same operating conditions—with the same thick-lamination head in the recording position, the thin-lamination head in the play-back position and the same type of wire—as the response curve of Figure 13, taken with a wave analyzer. The same flatness of response in the region from 500 to 10,000 cycles per second is observed in both records.

None of the response curves shown in this paper were obtained with the aid of any inserted equalization whatever. The flat response of Figures 13 and 22 is caused by a fortuitous combination of the properties of the circuit components which are outlined in the mathematical background, and which may be analyzed in the manner outlined in preceding pages.

Except that the wire velocity, and bias and signal frequency ranges were the same, and that the thin-lamination head was used in the play-back position in both cases, the response curves of the Test-result Schedule Sheets of Figures 14 and 15 were made under test conditions, with circuit components differing from those used to obtain the response curves which show the superiority of thin-lamination heads over thick-lamination heads.

Figure 22. Thin-lamination head in play-back position

Bias current = 1.0 milliampere
Signal current = 1.0 milliampere

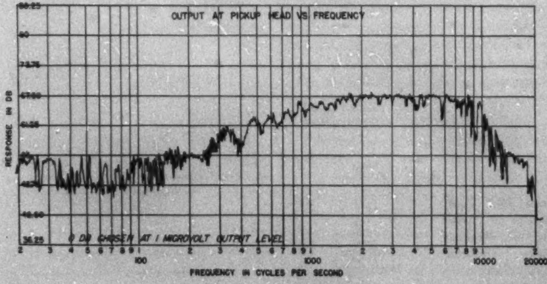

The wire-comparison-test response curves, combining circuit components having characteristics differing from those used in the thin-lamination test, do not exhibit the flat frequency response, but continue to rise until a sharp cut-off is reached. In every test, the superior high frequency response was obtained only when the thin-lamination head was used. It is evident that, while the contributions of all the other circuit elements may permit high-frequency response, the high-frequency region is attenuated unless thin laminations are used.

It was noted that, when the high-frequency response was improved by the use of the thin-lamination head, the high-frequency noise level was raised. Inspection of Figures 21 and 22, both made from the same recording, shows much more irregularity in the response of the thin-lamination head than in the thick-lamination head. It is concluded that the skin effect in the thick laminations attenuate the high-frequency noise components to the same extent that the high-frequency signal was attenuated.

Consideration of the theory of the demagnetization effect leads to the conclusion that a high-coercive-force recording medium tends to mitigate the demagnetization effect, and thus tends to raise the high-frequency response. A high residual induction tends to raise the over-all response level. Table I, obtained from the data of the comparison test of wires *A* and *B*, supports the theory.

Wire *A*, with the higher ratio of H_c to B_r, has its peak frequency occurring at the higher frequency, and possesses the lowest over-all amplitude. Wire *B*, with the lower ratio of H_c to B_r, has its peak frequency occurring at the lower frequency, and has the higher over-all amplitude.

Conclusions

For the purpose for which the analysis method was devised, it functions to give a more accurate and comprehensive understanding of the magnetic recording process than previous methods. It is recommended as a research method where a large mass of data must be collected and analyzed.

For an important experimental analysis of a magnetic recording system, a systematic investigation of fidelity characteristics throughout a reasonable wide range of operating conditions is necessary, if

Table I. Comparison of Wires A and B

	H_c Oersteds	B_r Gauss	Peak Fre-quency	Peak amplitude at 0.4 milliamperes signal current input
Wire *A*	400	1,350	10 kc.	3 millivolts
Wire *B*	245	8,100	6 kc.	20 millivolts

any degree of accuracy is to be expected from the experimental results. The trial and error method, adopted by some experimenters, is likely to leave unexplored some of the peculiar and, frequently, significant operating characteristics of a magnetic recording system. Usually, trial and error methods do not involve the keeping of a record of the trials, the errors, and the operating characteristics thus brought to light; the philosophy of systematic investigation is conducive to the keeping of written records.

The superiority of thin laminations over thick laminations is proved definitely. The Franklin Institute, under contract to the Special Devices Center, United States Navy, is constructing a series of recording and play-back heads to determine the extent to which it is necessary to go in the direction of using thinner laminations. It is expected that, with thin laminations in both recording and play-back heads, the superiority of thin laminations will be shown in greater contrast than is presented by the results shown here, in which only the play-back head employed thin laminations.

A method has been developed by which comparative response characteristics can be predicted from the known design, magnetic, and electrical properties of the recording heads, the play-back heads, and the recording media (wire or tape).

Symbols

B = magnetic induction

B_r = residual induction

B_d = remanent induction

e_0 = output voltage across a certain portion of the load impedance connected across the play-back head

e_1 = electromotive force of output coils of the audio transformer feeding the recording head

f = frequency in cycles per second

H = magnetizing force

H_c = coercive force

$M_1(\omega)$ = mutual inductance between the main coil of the recording head and an exploring coil wound on a pole tip

N_1 = number of turns in the recording coil

N_2 = number of turns in the play-back coil

N, S = conventional symbols to indicate magnetic polarity

t_1, t_2, t_3 = instantaneous times in process of recording sine wave on recording medium

The function, $h_1(\omega)$ = an expression representing the flux in the recording head as a function of ω under conditions of constant current and for a given lamination thickness. The variation of flux with frequency is referred to as the magnetic skin effect

The function, $h_2(\omega) = h_2'(\omega) \times h_2''(\omega)$. This quantity gives the flux threading the coils of the play-back head as a function of magnetic skin effect and the air-gap dimensions of the play-back head

The function, $h_2'(\omega)$ = the expression for the skin effect in the play-back head

The function, $h_2''(\omega)$ = an expression for the influence of the relation between effective magnet length and air-gap dimensions in the play-back head

The function, $L_1(\omega)$ = inductance of the recording head as a function of frequency

The function, $L_2(\omega)$ = inductance of the play-back head as a function of frequency

The function, $m(\omega,v)$ = a quantity expressing the remanent flux in the recording medium as a function of ω and velocity, the combination of which determines the effective magnet length; referred to as the demagnetization effect

The function, $R_1(\omega)$ = the effective resistance of the recording head as a function of frequency

The function, $R_2(\omega)$ = the effective resistance of the play-back head as a function of frequency

The function, $Z_0(\omega)$ = the total load impedance across the play-back head

The function, $Z_0'(\omega)$ = that part of $Z_0(\omega)$ across which the output voltage e_0 is taken for amplification

The function, $Z_1(\omega)$ = impedance in recording circuit external to recording head as a function of frequency

$\theta = \tan^{-1} B/H$

λ = wave length of recorded signal

ϕ = flux

ϕ_1 = flux in recording-head air gap effective in magnetizing recording medium

ϕ_m = flux surrounding the fixed magnets in the recording medium

ϕ_2 = flux produced in core of play-back head by passage of recording medium across head

$\omega = 2\pi f$

Reference

1. SUPERSONIC BIAS FOR MAGNETIC RECORDING, Lynn C. Holmes and Donald L. Clark. *Electronics* (New York, N. Y.), July, 1945, pages 126–136.

No Discussion

Considerations on Facsimile Transmission Speed

HENRY F. BURKHARD
NONMEMBER AIEE

PROBABLY one of the most pressing problems facing facsimile engineers is the requirement for greater speed of transmission. Several approaches to the problem have been made; namely, special scanning methods, improvement of means of modulation and demodulation, more efficient use of the frequency channel available, and the use of wider channels.

The speed of transmission of a facsimile copy depends upon the usable bandwidth of the available channel, the size of copy, and the definition required to adequately define the intelligence on the copy. Since scanning of large uniform areas results in the generation of low phototube signal frequencies which cannot be transmitted directly over most communication channels, the phototube signal must be used to modulate an audio-frequency carrier. Selection of the carrier is based upon the usable channel and the maximum phototube, or keying frequency which must be placed upon the carrier. The main item, therefore, which determines the speed of transmission, is the maximum keying frequency. This is a somewhat fictitious figure based upon the scanning of alternate black and white lines equal in width to the definition of the system as shown in Figure 1. Here the aperture is assumed to be a square also equal to the definition. The phototube signal is triangular and may be expanded into the Fourier series

$$F(t)=E+\frac{8}{\pi 2}E\left(\cos\frac{2\pi t}{T}+\frac{1}{9}\cos\frac{3(2\pi t)}{T}+\right.$$
$$\left.\frac{1}{25}\cos\frac{5(2\pi t)}{T}+\dots\right)$$

It is not anticipated that frequencies above the fundamental need be transmitted. The fundamental, therefore, is selected as being the maximum keying frequency. For present military equipment, this frequency is 900 cycles per second.

On normal copy, the sequence of lines shown seldom occurs. Usually spacing of lines is irregular, and large patches of white, gray, or black may be found. From a purely theoretical viewpoint, some advantage might be gained if the modulating frequency were a constant and were equal to the maximum modulating frequency. The significance of this may be determined from the two lower sketches of Figure 1 where various widths of light and dark areas are assumed. If the time required to scan from *a* to *b* is 1/1,800th second, the time required to scan from *b* to *d* should also be 1/1,800th second. This implies a much higher rate of scanning speed for the wider areas and lines. Preferably the scanning should take place in almost 1/1,800th second from *b* to *c* and then very rapidly from *c* to *d* in the order of 1/50,000th second. Although the side-band frequency would be a constant, the transmission of synchronizing signals such as a keyed tone would be necessary. The rapid acceleration of the scanning system would not be too fantastic if electronic scanning beams were employed.

Since most facsimile systems, however, are mechanical, this theoretic type of scanning cannot be realized. Probably the closest approach is the teleautograph system. In that system, a scribe is manipulated by the operator at the transmitting end so that the message to be transmitted is traced. Information on the orientation of the scribe is transmitted either by transmitting the *x* and *y* coordinates or by starting at a given point and transmitting relative motion. A pencil at the receiving end automatically follows the transmitting scribe. It is also necessary to transmit pencil-up and pencil-down information. This is a scanning type of system with almost all of the scanning taking place along the intelligence being transmitted. This results in relatively low modulating frequencies. It has the decided disadvantage that a transmitting operator must write out or trace the message, and therefore, the speed of transmission is limited. Practically all facsimile scanning, however, is not of this type but is sequential such as the scanning of a copy on a rotating drum by means of an optical system which slowly progresses parallel to the axis of the drum. One suggestion which has been made for increased speed on such a system is the use of specially-shaped letters and figures designed for the generation of a minimum[1] modulating frequency. This method is satisfactory for special cases, but the limitation caused by the requirement for a special typewriter and the impossibility of transmitting maps and sketches has discouraged general use.

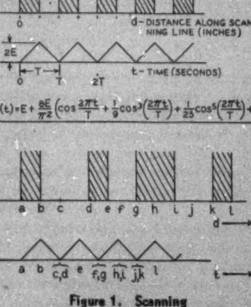
SCANNING APERTURE
0
d-DISTANCE ALONG SCANNING LINE (INCHES)
2E
T
0
T
2T
t-TIME (SECONDS)
F(t)=E+8E/π2(cos 2πt/T + 1/9cos3(2πt/T) + 1/25cos5(2πt/T)+)
a b c d e f g h i j k l
d
a b c,d e f,g h,i j,k l
t

Figure 1. Scanning

Paper 49-108, recommended by the AIEE communication committee and approved by the AIEE technical program committee for presentation at the AIEE winter general meeting, New York, N. Y., January 31–February 4, 1949. Manuscript submitted November 27, 1948; made available for printing December 21, 1948.

HENRY F. BURKHARD is a facsimile design engineer with the Signal Corps Engineering Laboratories, Fort Monmouth, and is assigned to the Coles Signal Laboratory, Red Bank, N. J.

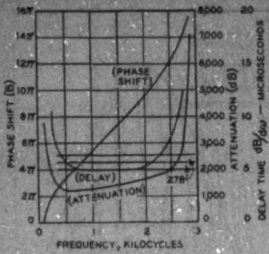

Figure 2. ***CF-1-B*, channel 1, and 20 miles "spiral four" cable**

A second approach on increasing the speed is through the more efficient use of the available frequency channel. Consider a channel having characteristics as shown in Figure 2. The pass band for ordinary use would be considered to be from 200 to 2,600 cycles per second. For facsimile, however, the usable portion of the band is limited by the delay distortion and is generally less than the pass band indicated by the attenuation curve. If the time of transmission through the system were the same for all frequencies, there would be no phase or delay distortion. The relation between phase shift, time delay, and frequency would be

$$B=\omega T$$

where

B = phase shift in radians
$\omega=2\pi f$
T = time delay in seconds

In actual transmission systems, however, the foregoing ideal condition is rarely found. For practically distortionless transmission of signals, it is necessary that the transfer impedance of the system have a constant amplitude and a phase angle linearly proportional to frequency with a phase angle value of $n\pi$ at zero frequency, where n = 0, 1, 2, 3, 4.... The phase shift relation then is

$$B=\omega t+n\pi$$

The value t represents the time it requires for the signal, or envelope, to travel through the transmission medium whereas the time required for various steady-state single frequencies to be transmitted is given by the total phase shift in radians at that frequency, divided by 2π times the frequency.

$$T=\frac{B}{2\pi f}$$

When the constant n has a value which is not an integer, a distortion sometimes called intercept distortion occurs. This distortion has little or no effect on the envelope wave shape. For a nonlinear relation between the phase shift and frequency, the envelope delay time at each frequency is given by $dB/d\omega$ and can, therefore, be found from the slope of the phase angle versus frequency curve. The acceptable limit for delay distortion is usually stated as an allowable number of microseconds plus or minus from the mean delay time of the envelope. This limit must be met over the frequency range required for the transmission. The figure generally used in the art has been ± 250 microseconds per 1,000 cycles of modulating frequency. Based upon a modulating frequency of 900 cycles, the limit for present military facsimile equipment would be found from 250 × 1,000/900 to be ± 278 microseconds. These limits have been superimposed in Figure 2 on the characteristics for the *CF-1-B* carrier channel and show a usable range for facsimile of about 900 to 2,300 cycles. Under Signal Corps contract for investigation of high-speed facsimile transmission, Radio Corporation of America engineers, Maurice Artzt and Charles Young, included study of the delay distortion requirements. The figure of ±250 microseconds per 1,000 cycles of modulating frequency was confirmed by tests employing vestigial sideband transmission. Of interest was the fact that when the curve of delay distortion versus frequency was irregular, a greater tolerance on delay distortion could be permitted if the carrier frequency were specially placed in the band. For a modulating frequency of 1,000 cycles, a carrier frequency (fc), and vestigial side band width (fv), the delay distortion over the band from (fc − fv) to (fc + fv) must not exceed ±250 microseconds. Outside this band of frequencies and out to the limit (fc−1,000), if the lower side band is being transmitted, or to (fc+1,000) if the upper side band is transmitted, the delay distortion must not exceed ±500 microseconds. The phase distortion limits for other maximum modulating frequencies are found from

Permissible delay distortion

$$=\frac{\text{(delay distortion at 1,000 cycles)}}{\text{modulating frequency in kilocycles}}$$

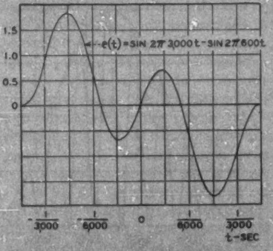

Figure 3. Single sideband signal

3,000 cycle carrier, 2,400 cycle modulation, carrier suppressed 6 decibels

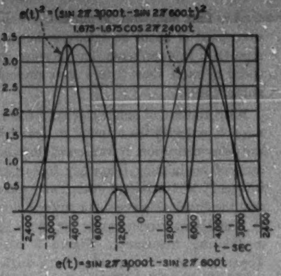

Figure 4. Full-wave square-law detected single sideband signal

Facsimile designs are always based upon available transmission channels and the delay distortion to be expected. Commercial lines used for speech have either no phase correction, or if they are corrected for delay distortion, the amount of correction is insufficient to be of appreciable value for facsimile. The exception to this is the case of a line leased specifically for picture transmission. Such a line is a standard voice channel specially corrected to decrease the delay distortion. In addition to the monetary consideration of such a line, there is the length of time often necessary to accomplish the delay correction. For military equipment intended for wire line transmission, therefore, the speed of transmission has been kept low to permit operation over normal uncompensated voice circuits. For a definition of 96 lines per inch, this has resulted in a scanning speed of about 12 square inches per minute. Due to integrated planning on the part of high military technical officers and engineers, the future military transmission channels are being designed with a view towards voice, teletype, and facsimile transmissions. Attempts are to be made to base initial designs of the channels on suitable phase as well as attenuation characteristics. This program prompted the study and establishment of phase distortion limits. It is expected that the available military channel will be from 300 to 3,500 cycles per second, and the aim will be to restrict the variation in envelope delay time of all frequencies in the range of 600 to 3,200 cycles per second to no more than ±100 microseconds from the mean delay time. This limit will permit a transmission speed of about 26 square inches per minute. It represents an increase in speed of more than 2 to 1 over present military sets.

With the use of single sideband transmission and with the attempt to diminish the delay distortion, it was found that the ratio of modulating frequency to carrier frequency was increased to such an extent that the envelope wave shape suffered due to insufficient carrier cycles per cycle of modulating frequency. Figure 3 and Appendix I show a sine wave with single sideband modulation where the modulation frequency is 4/5ths of the carrier frequency, and the carrier is attenuated 6 decibels. Figure 4 shows the result of full-wave square-law detection of the above wave; the envelope wave shape is very poorly defined. Artzt and Young of RCA Laboratories have evolved a method of demodulation based upon separating the wave into two parts and shifting components of one part of the wave forward and of the other part back 45 degrees. This is accomplished by heterodyning one portion of the wave with a sine wave and the other with a cosine wave. Each part is then detected by full-wave square-law detection and the two outputs superimposed, Appendix II. The sum of the two quarter phased signals is seen in Appendix III to add up to the modulating signal of $2-2\cos 2\pi 2{,}400t$.

Another modulating and demodulating system was devised by engineers of Radio Inventions, Inc. The scanner operates at a speed resulting in 2,400-cycle modulating frequencies. A carrier frequency of 10 kc is used giving a very satisfactory ratio of modulating to carrier frequencies. A filter in the output of the ring modulator which is employed eliminates most of the low sideband frequencies. The resulting signal is heterodyned with a 13-kc tone, thereby generating 23-kc and 3-kc carriers. By means of a special low-pass filter, only the lower carrier and its single sideband frequencies are selected for transmission over a line. At the receiver, the 600 to 3,000-cycle signal is heterodyned with a 13-kc signal as shown in Figure 5 in order to place the modulation back on a 10-kc carrier. Figure 6 shows the envelope of the 2,400-cycle modulation to be adequately defined by the full-wave rectified pulses of the carrier.

When some modulating methods such as the bridge modulator used by Times Facsimile Corporation are employed, the output signal from the modulator contains the modulator frequency, the carrier frequency, and sum and difference frequencies. The components proportional to the modulating frequency represent distortion of the modulated signal and will cause echoes due to delay distortion in the transmission medium. It is usually necessary, therefore, to eliminate the modulating frequencies from the transmitted signal by a filter. When the ratio of modulating to carrier frequency is less than one-half, the use of low-value coupling capacitors in the amplifier provides sufficient filtering action. When the ratio is increased, however, the use of filtering methods becomes more and more difficult. The Times Facsimile Corporation has recently perfected and adopted a revised modulating method. Referring to Figure 7, it is seen that the normal cell circuit at "*a*" generates a distorted wave. When light is applied to the phototube, the resistance of the cell drops, the capacitance increases, and a voltage is generated proportional to the so-called picture or keying frequency. It is this latter voltage which causes the distortion. The newer system contains a special phototube RCA type *5652* developed specifically for the purpose. It contains two emitting surfaces and is used in a circuit with practically no d-c anode bias. When light is applied to the phototube, the emissions from each cathode, which are caused directly by the light energy, produce an a-c voltage on the grid of the following tube instead of a pulsating d-c signal. A more symmetrical signal is produced as shown. In order to permit ready change from positive to negative types of modulating, the system has been worked into the normal Times Facsimile Corporation bridge-modulator circuit shown at "*c*."

A closer examination of the characteristics of the modulating-frequency signal is of interest. As mentioned previously, the allowable delay distortion is equal to ±250 microseconds per 1,000 cycles of

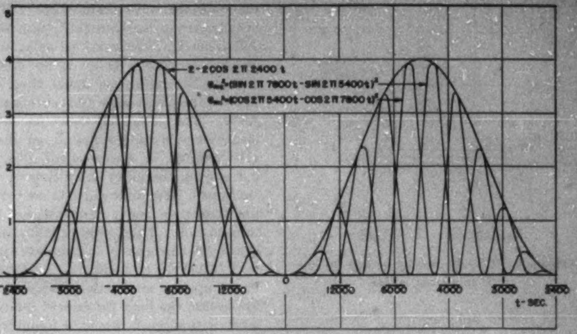

Figure 5. Heterodyne method of detection

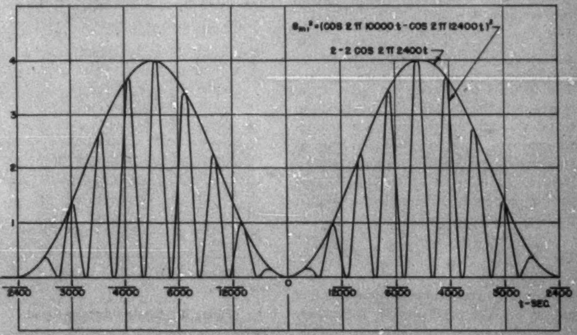

Figure 6. Heterodyne detection method

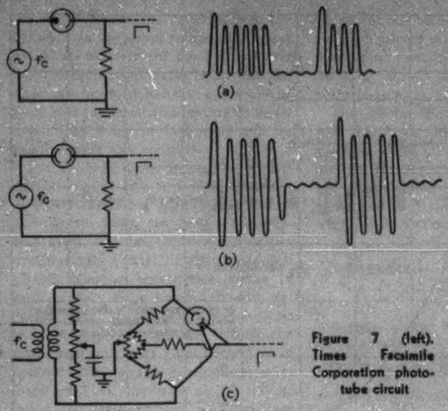

Figure 7 (left). Times Facsimile Corporation phototube circuit

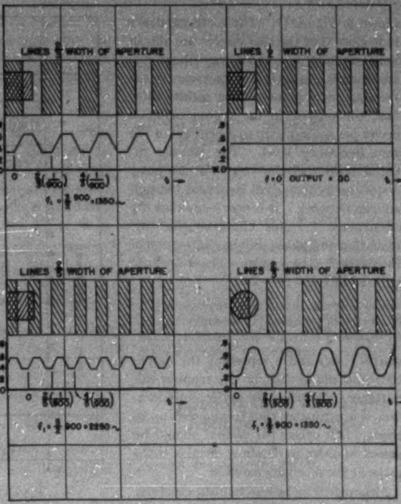

Figure 8 (right). Scanning of various line sequences

modulating frequency. This modulating frequency is computed on the basis of scanning alternate black and white lines where the width of the lines is equal to the definition of the equipment. Usually the aperture size is also equal to the definition. Under such conditions, the modulating wave shape as shown previously in Figure 1 is triangular with the Fourier series expansion shown. The fundamental of the series is considered usually to be the maximum frequency which must be transmitted. Naturally an improved wave shape would result if the harmonics were also transmitted, but this is not permissible due to the necessity to conserve bandwidth. In actual practice, the scanning of alternate black and white lines equal to the definition does not generate the maximum frequency. If the lines and spaces being scanned are not as wide as the aperture, higher frequencies are generated. Figure 8 shows various widths of recurring lines and spaces. When the line width and space width are each two-thirds of the aperture size, the wave shape is trapezoidal. A Fourier analysis results in a fundamental frequency of $1^1/_2$ times as much as for the case where the lines, spaces, and aperture were the same width. An interesting case occurs when the scanning lines and spaces are equal to one-half of the aperture. The output theoretically is pure direct current. This might be utilized as a means for measurement of the aperture size of a transmitter. Aperture distortion and halo, however, will add a slight ripple to the direct current. When the lines and spaces are two-fifths the width of the aperture, the fundamental frequency is five-halves the frequency of the case where lines, spaces, and aperture are equal. With the circular aperture, the wave shape is different, but the fundamental frequency is the same as for the square aperture. Naturally the special d-c case found for the square aperture is not encountered with the circular aperture. Normally facsimile systems are not designed to transmit lines finer than the aperture width, and reproduction of the finer lines considered before is not expected.

The second condition which involves additional frequencies from those which result from the scanning of alternate black and white lines is the scanning of isolated pulses. Two analytical methods will show the frequency distribution of the distribution of the components to be encountered. In both cases the line or spot to be scanned will be assumed to be equal to the width of the square aperture. Scanning will result in a linear rise and fall of signal, resulting in a triangular signal wave shape. The first method is to assume that the pulses occur repetitiously but are spaced a considerable distance apart. A standard Fourier series representation of the pulse may be found, Figure 9. For the military facsimile set *AN/TXC-1* with a single line on the copy, the repetitious rate is once a second, and width of pulse is 1/900 of a second. Using the formula and Figure 3 to be found on page 22 of the Radio Engineers' Handbook,[2] $2\pi k$ represents 1/900 of a second and $k=1/900$. A plot of the coefficients is also shown in Figure 9. The fundamental frequency is one cycle per second. It is to be noted that in the vicinity of 1,800 and 3,600 cycles per second, the output is zero.

A second more versatile analysis is to use the Fourier integral, as shown in Figure 10. Here the dot being scanned is assumed to be completely isolated from other dots and lines on the copy. Therefore, all transients resulting from scanning the dot will die away before the scanning of other dots. The equations of the two straight lines are found first. These give a description of the original pulse as a function of time. The frequency spectrum of the pulse is found from the equation

$$F(\omega)=\frac{1}{2\pi}\int_{-\infty}^{\infty} f(t)e^{-j\omega t}dt$$

As noted in Figure 10, the time function is substituted in the integral and by integrating term by term the result

$$F(\omega)=\frac{1{,}800E}{\pi}\left[\frac{1-\cos\frac{\omega}{1{,}800}}{\omega^2}\right]$$

is found. This represents a continuous frequency spectrum. In order to find the value at zero frequency, it was necessary to expand the cosine function before substituting $\omega=0$. A plot of this superimposed upon the Fourier series result is

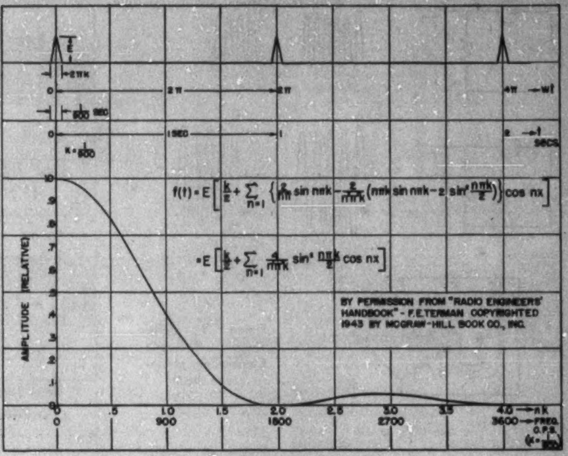

BY PERMISSION FROM "RADIO ENGINEERS' HANDBOOK" - F.E.TERMAN COPYRIGHTED 1943 BY MCGRAW-HILL BOOK CO., INC.

Figure 9. Scanning of widely separated thin lines

shown in Figure 11. The correspondence is so close that the two curves are almost indistinguishable. The very slight discrepancy is probably due to errors in extrapolation of points. The results show that the output in the region of 2,500 cycles per second is up to 5 per cent of the zero frequency level. The Fourier integral result permits study of the pulse distortion as the signal is passed through a given network. It is necessary that the admittance transfer characteristic (attenuation and phase shift) as a function of the frequency be known. These are substituted in

$$f(t) = \int_{\infty}^{\infty} F(\omega)\, Y(\omega) e^{i\omega t + a} d\omega$$

where $Y(\omega)$ and a represent the amplitude and phase shift of the transfer admittance. For the case under consideration, it is estimated that frequencies up to about 1,000 cycles per second should be passed in order to obtain a suitable wave shape at the receiving machine.

Although it appears that the analysis based upon scanning of alternate black and white lines equal to the aperture size is not adequate, it must be remembered that almost all applications of the results are based upon empirical data. For example, the figure of ±250 microseconds of delay distortion per 1,000 cycles of modulating frequency which is tolerable, was based upon actual test where the 1,000 cycles of modulating frequency really is a statement of linear scanning speed. Similarly the maximum modulating frequency allowable for a given carrier frequency was an empirical value found from actual test. The modulating frequency for any given definition, therefore, represents a maximum linear scanning speed which is tolerable. This factor coupled with the difficulty involved in solving the Fourier integrals for a given network have led most facsimile engineers to use the alternate line method of analysis.

The foregoing attempts to utilize more efficiently the available frequency spectrum of a voice circuit may at best produce about a $2^1/_2$-to-1 increase over the scanning speed of present military equipment. As facsimile transmissions assume more importance, this increase in speed may not be sufficient, and it is expected that the use of wider band channels will become imperative. Study of the problem was, therefore, undertaken by the Radio Corporation of America under a Signal Corps contract. This study was broken down to cover transmissions over channels 16-, 48-, 96-, and 192-kc wide. The limiting factor on the transmission speed was determined to be the delay distortion expected over practical carrier communication circuits. The requirement for the 16-kc channel is ±30 microseconds, for the 48-kc channel 11 microseconds, the 96-kc channel 5.5 microseconds, and the 192-kc channel ±2.75 microseconds. It is seen that as the spectrum is widened not only does the delay requirement become more stringent, but these tighter limits must be held over a wider frequency band. In addition to the excessive delay requirements for the two widest channels, it is not practical with ordinary techniques to record in daylight at the speeds of 333 and 667 square inches per minute which the channels permit. To ease both of these requirements, recording on wet electrolytic paper will be employed using several wires wrapped helically and spaced equidistant around the drum. (This method was first suggested to the Signal Corps Engineering Laboratories by engineers from Radio Inventions, Inc., and subsequently during discussions with engineers from RCA Laboratories.) The damp paper passes between the drum and a straight edged

---

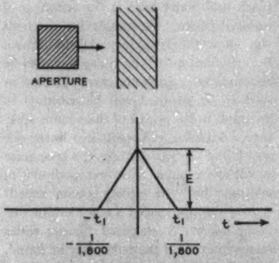

Figure 10. Frequency spectrum generated by scanning isolated spot

from

$-\infty t_0 - t_1\ F(t) = 0$
$-t_1$ to 0 $F(t) = 1{,}800Et + E$
0 to t_1 $F(t) = -1{,}800Et + E$
t_1 to ∞ $F(t) = 0$

The frequency spectrum is found by means of the Fourier Integral

$$F(\omega) = \frac{1}{2\pi}\int_{-\infty}^{\infty} F(t) e^{-i\omega t} dt$$

$$F(\omega) = \frac{1}{2\pi}\int_{-} (1{,}800Et + E) e^{-i\omega t} dt + \frac{1}{2\pi}\int_{0}^{t_1} (-1{,}800Et + E) e^{-i\omega t} dt$$

$$F(\omega) = \frac{E}{2\pi}\left[\int_{-t_1}^{0} 1{,}800te^{-i\omega t} dt + \int_{-t_1}^{0} e^{-i\omega t} dt - \int_{c}^{t_1} 1{,}800te^{-i\omega t} dt + \int^{t_1} e^{-i\omega t} dt\right]$$

$$F(\omega) = \frac{1{,}800E}{\pi}\left[\frac{1 - \cos\frac{\omega}{1{,}800}}{\omega^2}\right]$$

bar which presses the paper against the helices. As the drum rotates, the point of contact between the bar and any one helix wire progresses to the right. For the 48-kc channels, one helix wire will be used, and the drum will revolve at 2,500 rpm. One 8 by 10 inch copy will be printed every half a minute.

For the 96-kc transmission, the channel will be divided into two 48-kc channels. By means of dual scanning systems spaced 180 degrees apart, two lines of the original copy will be scanned simultaneously, and the signals from each photocell placed upon an appropriate carrier in each of two 48-kc bands. At the receiving end, two of the helices will be employed, spaced half way around the drum from each other. The bar will make contact with both helices simultaneously. Each band will supply the signals for one helix, and therefore, two scanning lines will be printed concurrently. The chief advantages are that the delay distortion over each 48-kc channel need only be held to ±11 microseconds instead of the requirement that the delay distortion over the wide 96-kc channel be ±5.5 microseconds. In addition, each helix wire need only print at the same rate of speed as in the case where the whole channel was 48-kc wide. Therefore, the actual linear speed of recording for each scanning line has not been increased. The recording power has been doubled because two lines are printed simultaneously, but the drum speed remains the same, 2,500 rpm. An 8 by 10 inch copy will be produced every 15 seconds.

The 192-kc channel likewise will be split into four 48-kc channels. Four scanning heads 90 degrees apart will be used for the transmitter, and four helices will be used at the recorder. Drum speed remains at 2,500 rpm, but an 8 by 10 inch copy will be produced every 7.5 seconds.

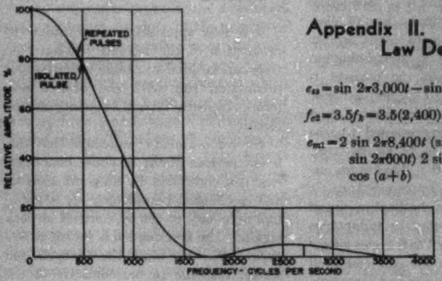

Figure 11. Frequency spectrum for short triangular pulses

Appendix I. Single Sideband Scan

Assume cosine modulation with zero initial phase shift

$$e=E(1-\cos 2\pi f_k t)\sin 2\pi ft$$

$$e=E\sin 2\pi ft-E\cos 2\pi f_k t\cdot\sin 2\pi ft$$

$$2\sin a\cdot\cos b=\sin(a+b)+\sin(a-b)$$

$$\cos 2\pi f_k t\cdot\sin 2\pi ft={}^1/_2\sin(2\pi ft+2\pi f_k t)+{}^1/_2\sin(2\pi ft-2\pi f_k t)$$

$$e=E\sin 2\pi ft-E/2\sin 2\pi(f+f_k)t-E/2\pi\sin 2\pi(f-f_k)t$$

For single sideband transmission, the carrier is usually attenuated 6 decibels. Assume that the upper sideband is eliminated.

$$e_{ss}=E/2\sin 2\pi ft-E/2\sin 2\pi(f-f_k)t$$

If, $f=3{,}000$, $f_k=2{,}400$, and $E=2$

$$e_{ss}=\sin 2\pi 3{,}000t-\sin 2\pi 600t$$

Appendix II. Quarter Phased Law Detection

$$e_{ss}=\sin 2\pi 3{,}000t-\sin 2\pi 600t$$

$$f_{c2}=3.5f_k=3.5(2{,}400)=8{,}400\text{ cycles}$$

$$e_{m1}=2\sin 2\pi 8{,}400t\,(\sin 2\pi 3{,}000t-\sin 2\pi 600t)\quad 2\sin a\cdot\sin b=\cos(a-b)-\cos(a+b)$$

$$e_{m1}=\cos 2\pi 5{,}400t-\cos 2\pi 11{,}400t-\cos 2\pi 7{,}800t+\cos 2\pi 9{,}000t$$

$$e_{m2}=2\cos 2\pi 8{,}400t\,(\sin 2\pi 3{,}000t-\sin 2\pi 600t)\quad 2\cos a\cdot\sin b=\sin(a+b)-\sin(a-b)$$

$$e_{m2}=\sin 2\pi 11{,}400t-\sin 2\pi 5{,}400t-\sin 2\pi 9{,}000t+\sin 2\pi 7{,}800t$$

If upper terms are removed by filtering

$$e_{m1}=\cos 2\pi 5{,}400t-\cos 2\pi 7{,}800t$$

$$e_{m2}=\sin 2\pi 7{,}800t-\sin 2\pi 5{,}400t$$

The demodulated wave $=e_{m1}^2+e_{m2}^2$

$$=(\cos 2\pi 5{,}400t-\cos 2\pi 7{,}800t)^2-(\sin 2\pi 7{,}800t-\sin 2\pi 5{,}400t)^2$$

This derivation is based upon the quarter phased method of detection proposed by Maurice Artzt and Charles Young of the RCA Princeton Laboratory.

Appendix III. Heterodyne Method of Detection

$$e_{ss}=\sin 2\pi 3{,}000t-\sin 2\pi 600t$$

$$e_m=2\sin 2\pi 13{,}000t\,(\sin 2\pi 3{,}000t-\sin 2\pi 600t)\quad 2\sin a\cdot\sin b=\cos(a-b)-\cos(a+b)$$

$$e_m=\cos 2\pi 10{,}000t-\cos 2\pi 16{,}000t-\cos 2\pi 12{,}400t+\cos 2\pi 13{,}600t$$

If the upper terms are removed by filtering

$$e_m=\cos 2\pi 10{,}000t-\cos 2\pi 12{,}400t$$

This is full law square law detected

$$e_m^2=(\cos 2\pi 10{,}000t-\cos 2\pi 12{,}400t)^2$$

This derivation is based upon the heterodyne method of detection proposed by engineers of Radio Inventions Incorporated.

References

1. R. W. Carlisle. United States Patents 2,255,408 and 2,210,706.

2. RADIO ENGINEERS' HANDBOOK, F. E. Terman. McGraw-Hill Book Company, New York, N. Y., 1943.

3. COMMUNICATION NETWORKS (book), E. A. Guillemin. John Wiley and Sons, Inc., New York, N. Y.

Discussion

R. W. Carlisle (Sonotone Corp., Elmsford, N. Y.): Burkhard's paper is a thorough résumé of the painstaking efforts of many investigators and it aggressively assembles their findings into one efficient facsimile system.

In connection with the scanning of facsimile print by sequential means, Burkhard has mentioned the writer's suggestion of using specially-shaped letters and figures designed for the generation of a minimum modulating frequency.*

This method consists of a series of steps:

> A typewriter roll is fitted with sprocket teeth at each end in the same manner as in various bookkeeping machines.
>
> A bold Gothic alphabet is used with a few of the letters re-shaped to emphasize certain portions for easy scanning.

The material to be transmitted is typed on this machine, using paper having sprocket holes along the edges.

This paper is then attached to a facsimile scanner equipped with pins to hold it in such an alignment that the scanning spot will exactly traverse the top and bottom edges and other predetermined bands in each line of type. The increase in scanning efficiency is well over 2 to 1, and may be estimated by study of relative shapes of type.

The use of this system does not put any restrictions on the use of the scanner for other material such as maps and sketches. Conversely, however, a facsimile system which has been designed for optimum transmission conditions will obviously be most efficacious for transmitting typed matter by this system.

---

* United States Patent 2,210,706.

Control Chart Methods Applied to Frequency Response Curves

A. B. MUNDEL
MEMBER AIEE

IT IS the purpose of this paper to present an application in which statistical control chart technique has assisted in the manufacture of an electro-acoustic transducer. The operation of a transducer will be described as well as the engineering considerations required before control chart techniques can be applied.

The use of control charts has been widely shown for maintenance of mechanical dimensions. The same techniques can be applied to obtain uniform frequency response curves from transducers. Not only does production benefit by reduced scrap and rework, but in addition a more uniform product is obtained.

Furthermore, two types of specifications will be discussed. First, the point by point system in which the response is specified at each frequency. Secondly, the sensitivity and frequency response shape system in which the sensitivity at a single frequency is specified, and the shape of the response curve is given using the response at the specified frequency as a reference level. Data obtained on an insert receiver will be presented to show the conditions under which each form of specification is preferable.

The Insert Receiver

The midget receiver shown in cross-section in Figure 1(a) will be discussed. It is desirable to maintain a high degree of uniformity both in sensitivity and in frequency response. The frequency characteristic of this receiver is shown in the conventional manner in Figure 2, which shows the response of three typical units.

Fundamentally, a receiver consists of a magnetic assembly which drives a diaphragm. The alternating current in the coil on the pole piece causes a variation in the magnetic flux which alternately assists and opposes the action of the "flux linkages" through the permanent magnet, the air gap, and the diaphragm and armature assembly, resulting in the vibration of the diaphragm. Vibration of the diaphragm gives rise to sound or acoustic energy.

At low frequencies the amplitude of vibration is governed by the total stiffness of the vibrating system. This stiffness is not only that of the diaphragm but also of the chambers V_1 and V_2. Acoustical engineers frequently make use of electrical circuit notation to assist in the analysis of vibrating system behavior. An electrical analog of the receiver is shown in Figure 1(b). The compliance or inverse stiffness of the chambers V_1 and V_2 (Figure 1(a)) is represented by the capacitances C_1 and C_2 in Figure 1(b). The compliance of the diaphragm assembly is represented by capacitance C_3. The equivalent mass of the diaphragm and armature are represented by inductance M_1. At approximately 1,200 cycles a resonance occurs between the stiffnesses and the mass of the diaphragm and armature. The sharpness of this resonance is controlled by an acoustic damping element placed in the receiver cap. At frequencies above this resonance another resonance occurs, due to the Helmholtz resonator effect occurring in the chamber immediately over the diaphragm. The acoustic compliance of chamber V_2 is represented by the capacitor C_2 which resonates with the mass of a slug of air moving in and out of the constricted area in the nub of the receiver and the tube connecting it to the 2-cubic centimeter chamber. This mass is shown as M_2 in the equivalent circuit. When measuring the acoustic sensitivity the receiver is driven at a constant power level by a signal generator and matching network. Acoustic output is measured by a calibrated microphone in a 2 cubic centimeter chamber connected to the receiver.[1] The compliance of this measuring chamber is represented by the capacitance C_4 in the electrical analog. The compliance of C_4 is sufficiently large to have little effect on the frequency characteristic. The measurements used in this discussion have all been obtained on a system such as shown in Figure 1(a). The units of measurement are decibels (db) above an arbitrary reference level.

It should be clear that this paper does not describe a new development in receiver design, but mainly the application of a production tool that simplifies the task of obtaining the desired qualities in the completed product.

Production Control of the Insert Receiver

It is now appropriate to consider the production of the receiver. What controls can be used to obtain a continuous production run with the desired uniformity, sensitivity, and frequency characteristic?

We have already indicated that different regions of the response characteristic are controlled by different acoustic and mechanical parameters. It is therefore necessary to set up controls at each region. The first control is set up at 400 cycles. We have found the 400 cycles per second response to be indicative of the general sensitivity of the receiver. This frequency is chosen for convenience; it would have been as effective to use 200 or 300 cycles per second as a control point. The sensitivity at 400 cycles is a function of the magnetic circuit performance, the air gap and the net stiffness of the system.

To find what level of sensitivity is

Paper 49-109, recommended by the AIEE communications committee and approved by the AIEE technical program committee for presentation at the AIEE winter general meeting, New York, N. Y., January 31–February 4, 1949. Manuscript submitted November 10, 1948; made available for printing January 7, 1949.

A. B. Mundel is with the Sonotone Corporation, Elmsford, N. Y.

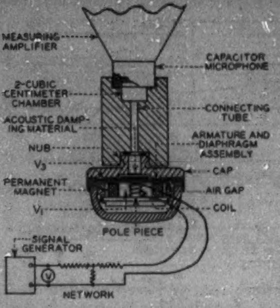

Figure 1(a). Cross section of miniature receivers

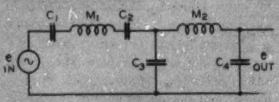

Figure 1(b). Electrical analog of vibrating system of receiver

maintained and to assist in the choice of corrective action if necessary, five sample receivers are taken at regular 2-hour intervals and measured for acoustic sensitivity. The average response and the range of the five samples at 400 cycles per second is plotted in Figure 3. The range is the difference between the maximum and minimum response of the sample of five. (Standard notation uses the symbols $\bar{X}$ and R for the average and range.) Figure 3 shows a control chart in which 19 samples of five have been taken and the average $\bar{X}$ and range R plotted. The grand average $\bar{\bar{X}}$ and the average range $\bar{R}$ also have been indicated. This chart is similar to the forms recommended in the ASTM Manual on the Presentation of Data, which contains a more complete discussion on applications of statistical techniques to engineering problems.[3]

Control limits for the averages and ranges are indicated by the dotted lines and are computable from the grand average and average range plus the factors A_2, D_3 and D_4 given in Table I of the previous reference. The points on the graph of Figure 3 should all lie within the indicated control limits if the process represented approximates a symmetrical bell-shaped frequency distribution as shown at the left of Figure 3. If all points do not lie within control limits there is evidence of variations due to assignable causes rather than to pure chance. A point outside of the control limits indicates that at least one controlling factor has changed. At this frequency (400 cycles per second) we must check the magnetic circuit, net stiffness, and air gap. We have found that these parameters are likely to drift in production unless watched in this manner, and that points outside of control limits are indicative of one or more of these items passing out of limits.

A histogram of the individual readings is shown at the left of Figure 3. The individuals, of course, have a wider variation than the averages shown on the control chart at the right of the figure. In the type of frequency distribution which we encounter so frequently (that is, a symmetrical bell-shaped normal distribution) we can expect about 99.7 per cent of the observations to occur within an interval extending 3σ units on each side of the average. A satisfactory estimate of σ can be obtained from the relation $\sigma = \bar{R}/d_2$. (Values of d_2 can be found in Table I, of the ASTM Manual).[3] Figure 3 shows a very satisfactory situation engineering-wise in that the entire production is well within the specification limits.

The next section at which a control chart (Figure 4(a)) is applied is at the first resonance. Since the first resonance occurs in the mesh containing the effective mass of the diaphragm and the effective stiffness of the vibrating system, variations in the frequency of this resonance are likely to occur simultaneously with variations in the low-frequency sensitivity. Increased stiffness is likely to result in lower sensitivity and higher resonance, as may be readily seen with reference to the equivalent circuit. The amplitude of this first peak is recorded on another control chart, Figure 4(b). The amplitude is a function of the damping rather than of the parameters mentioned previously. Excess peak amplitude can be corrected by increasing the acoustic damping which is placed at the entrance to the nub, as shown in the crossectional view.

To extend the frequency range of transducers, it is common practice to use auxiliary acoustic parameters effective at the high-frequency end of the spectrum. An example of this is the second peak which is due to the acoustic resonance occurring in the second mesh. This is controlled by the stiffness of the volume V_3 and the mass of the slug of air in the orifice previously referred to in the electrical analogue as C_3 and M_2 respectively. Variations in frequency of this resonance are usually due to variations in the clearance between the diaphragm and the cap. The control chart offers an effective means of watching this effect. Charts are kept as in Figure 4(c). The second resonance frequency is affected to a certain degree by its proximity to the first resonance. If the first and second resonances are too far apart, there will be a deep trough between. If this is worth watching, a control chart also may be set up as in Figure 4(e) and (f), using a pair of charts for valley frequency and amplitude. This is an effective method of checking the resonance peak separation. The amplitude of the peak of the second resonance control chart, Figure 4(d) is significant. High values usually correspond to low-resonant frequency. Conversely, low values of amplitude at this peak may be due to high frequencies of resonance but are more likely to occur when the cap and body are not effectively sealed together, or when there is an external leak from the volume V_3.

In selecting the data to be plotted on a control chart, it is essential to decide on regions that are important insofar as the applications are concerned and on regions which indicate what corrective action is appropriate. In our factory we have used these methods to warn us when variations in receiver manufacture occur.

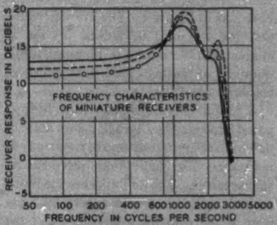

Figure 2. Typical frequency response of miniature receiver

Composite Curve of Receiver Response

By referring to the frequency characteristics of the midget receiver, Figure 2, it is apparent that plotting many curves on one sheet will cause endless confusion. On the other hand it is necessary to compare many curves during the production run, to determine the limits within which the response is likely to occur, or summarize the level at which production is running.

The control charts shown in Figure 4 do just this but they are not in a form usually understood in communication laboratories.

One method of summarizing many receivers on a single sheet is to draw an up-

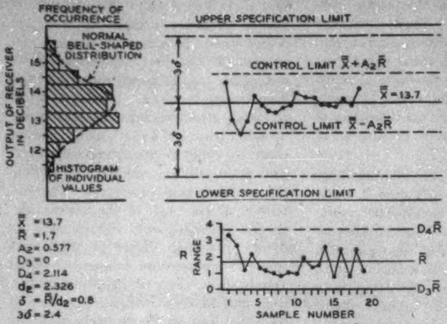

Figure 3 (above). Histogram and control chart of receiver response at 400 cycles per second

Figure 4 (right). Control charts for receiver at higher frequencies

$\bar{X}$ = average $\bar{\bar{X}}$ = grand average
R = range $\bar{R}$ = average range

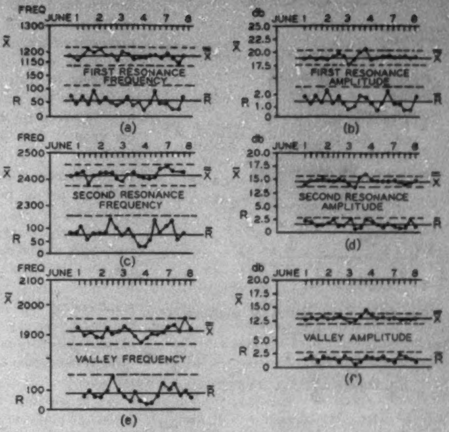

per and lower curve representing the maximum and minimum response. Another is to draw an average curve and specify tolerance limits from it at each frequency. It is more effective to use the data presented in the form of control charts as in Figure 4. The average values and the standard deviations (σ) for all characteristics charted in Figures 3 and 4 obtained by methods previously indicated are shown in Table I.

A graph (Figure 5) can then be prepared showing the average values and the 3σ limits of amplitude and of frequency at resonance for individual receiver response curve. The 3σ limits are the limits within which we would expect 99.7 per cent of the response curves to lie at the four indicated frequencies. The advantages of this presentation are that the variations likely to occur in resonant peaks and cutoff frequencies are better defined than by the upper and lower limit curve.

Table I. Receiver Characteristics Obtained from Control Charts of Figure 3

Characteristics	Grand Average $\bar{X}$	Average Range $\bar{R}$	Standard Deviation from $\sigma=\frac{\bar{R}}{d_2}$
Amplitude at 400 cycles per second (decibels)	13.7	1.7	0.73
First resonant frequency, cycles per second	1188.	56.	24.
Amplitude at first resonance, decibels	18.9	1.4	0.60
Frequency of valley between first and second resonance, cycles per second	2013.	94.	40.
Amplitude at valley, decibels	12.7	1.3	0.56
Frequency of second resonance, cycles per second	2420.	78.	33.
Amplitude at second resonance, decibels	14.6	1.4	0.60

Specification

The methods of statistical quality control are helpful in controlling the manufacture of a transducer and in representing its performance. A similar situation exists in writing the specification. Two forms of specification are used in discussing the characteristics of transducers. The first type of specification is form "A" in Table II wherein the average output and tolerance are specified for each frequency.

Another method of specifying the response characteristics of a receiver is form "B" in Table II. In this system the absolute value of the frequency response is listed at a single frequency and the frequency response curve is specified as the deviation from the 400 cycles per second response, in this instance. The proponents of form "A" claim that they are specifying the absolute levels more closely. The proponents of form "B" claim that they are specifying a more uniform frequency response. Form "B" may properly be used only within regions where the response is controlled by a single set of causes. Such a condition exists within the low-frequency region of the receiver described in this paper, but does not extend from the low-frequency region to the high-frequency region. The three top histograms of Figure 6 show the distribution of the outputs of a group of receivers at 200, 400 and 2,500 cycles per second above a single reference level. This is a form in which data might be submitted to indicate compliance with form "A" of the specification. If these same receivers had been manufactured for a customer using the specification in form "B", the lower histogram of Figure 6 would be submitted in support of the receivers meeting the specification. The 400 cycles per second condition is identical. The 200 cycles per second response shows that at this frequency the response is much like that at 400. The distribution is very narrow. The average value agrees with the specification but the distribution is narrower than the tolerance. The low-frequency response of the receivers is stiffness controlled. Both the 200 and 400 cycles per second response are controlled by the same system of causes. Here it seems legitimate to use form "B" of the specification.

At 2,500 cycles per second these same

Table II. Specification of Frequency Response

Form A		Form B	
Receiver Output under Standard Conditions, Decibels	Frequency, Cycles Per Second	Receiver Output under Standard Conditions, Decibels	Receiver Frequency Response Based on 400 Cycles Per Second Response as 0, Decibels
12 ±2.5	200		−0.5 ±2
12.5 ±2.5	400	12.5 ±2.5	0
13.5 ±2.5	600		+1.0 ±2
16.0 ±2	800		+3.5 ±2
18.0 ±2.5	1,000		+5.5 ±2
19.0 ±2.5	1,200		+6.5 ±2

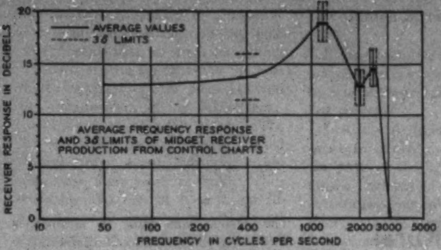

Figure 5. Curve showing 3σ (three sigma) limits of response of miniature receivers in production (data from Table I)

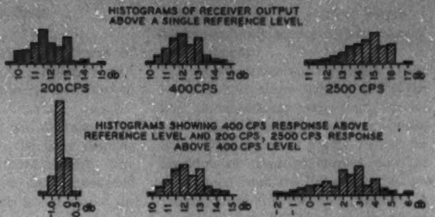

Figure 6. Histograms of receiver response at 200, 400, and 2,500 cycles per second

receivers now exhibit a wider range of variation than in the upper histogram. The 2,500 cycles per second response is not closely related to the 400-cycle response. It is actually a function of the Helmholtz resonator parameters, which are individually controlled. Hence this is a narrower distribution when viewed from a fixed reference level, as is done in the upper histogram. Specification form "A" appears preferable here.

At times the application of a transducer or the point of view of the specification writer has dictated the form in which the specification is written. In cases where the absolute value of the sound pressure output of the receiver must be controlled, the specification is written in form "A." In instances where the smoothness of the response is of primary concern, form "B" is used. When the manufacturer of the device writes the specification he should make it conform to the performance of the unit. Under such conditions it is possible that a portion of the specification such as the low-frequency response of the receiver will be written in form "B," and the remainder of the specification which covers the high-frequency response in form "A."

In all instances it is necessary to understand thoroughly the type of performance which is to be expected from the device and the reasons for the type of performance before plotting any control charts, or before choosing the form of the specification.

Conclusion

Although this paper has been confined to the discussion of control chart technique for simplifying the manufacture of a receiver to a desired sensitivity, uniformity, and quality, the principles involved are not restricted. We have kept similar plots and applied control chart technique to the control of manufacture of microphones, phonograph pickups, and to curves of the frequency response of amplifiers. There appears to be no reason why any series of characteristics mechanical, electrical, or physical could not be similarly treated, and the desired control obtained. Similarly it would appear possible to analyze and present composite pictures of response graphs whenever homogeneous data and operation under controlled conditions exists.

References

1. Tentative Code for Measurement of Performance of Hearing Aids. *Journal*, Acoustical Society of America (New York, N. Y.), volume 17, October 1945, pages 144–50.

2. A.S.T.M. Manual on the Presentation of Data. The American Society of Testing Materials (Philadelphia, Pa.), March 1941.

No Discussion

Lightning Investigation on a Rural Distribution System

D. D. MacCARTHY
MEMBER AIEE

D. A. STANN
NONMEMBER AIEE

D. R. EDGE
ASSOCIATE AIEE

W. C. McKINLEY
NONMEMBER AIEE

As rural electrification expanded, it became apparent that the requirements for supplying good service to consumers served by the long lines with low-load density, were different than for consumers in more thickly settled regions, for which equipment and operating practices had been developed. In rural territory the distribution system forms the main conducting network linking different areas, but in urban territory there are many other parallel conducting paths such as gas and water pipes, cables, and rails, which constitute extensive grounded networks. On these rural systems there are fewer consumers per mile, grounds are higher in resistance, lines are longer and higher in impedance. The lightning exposure is more severe, and the distances to be traveled in maintenance work are much greater. For these reasons, the construction and equipment typical of rural distribution systems became somewhat different from those typical of urban systems.

Several studies [1,2,3,4] have been made to investigate the effects of lightning on distribution systems, but none on a typical 7,200-volt multigrounded rural system. Hence, in 1944 the General Electric Company and the Central Electric Cooperative, Inc., at Parkers Landing, Pa., started a joint investigation aimed at the improvement of rural service.

The field work was in the charge of an engineer from the lightning arrester and distribution cutout division of the General Electric Company during the summers of 1944 to 1947 inclusive. The Central Electric Cooperative, Inc., made the investigation possible through the support of its board of directors and personnel.

Objectives

The principal objectives of the field investigation were:

1. To determine the nature and frequency of occurrence of lightning surges.
2. To measure the number, magnitude, and duration of 60-cycle transient currents.
3. To determine the short circuit and recovery voltage characteristics of the system.
4. To study each outage and to minimize consumer outages by improving the overcurrent protective system.
5. To learn the problems of operating a rural system from the viewpoint of the operating personnel so that practical improvements can be made.

The System Studied

The Central Electric Cooperative, Inc., serves an area of about 40 by 60 miles bordering on the Allegheny River in northwestern Pennsylvania, Figure 1. Isokeraunic maps predict 36 to 48 thunderstorm-days per year in this region. The system was built in accordance with Rural Electrification Administration (REA) Specifications. The first part of the system was energized in 1938, and the last large section was energized in 1941. It has continued to grow as more consumers were connected to existing lines and by adding numerous small extensions to the lines.

In 1947 there were 5,800 consumers supplied from 3,410 distribution transformers on 1,100 miles of line. The four principal feeders numbered 1, 50, 100, and 200 start as 3-phase lines from the substation and branch into single-phase lines. The substation contains two 900-kva banks of transformers rated 25-7.2/12.47 (Y-grounded) kv. Practically all apparatus on the system was made by one manufacturer.

All data are based on the equipment in service for the period of recording the data which was not constant during the four years of the study, due to system growth and changes made in the investigation as it progressed. Hence, data are reported in terms of installation-years; that is, lightning-arrester-years or oscillograph-years, and so forth.

Figure 1 also shows the location of the equipment used in the investigation. In 1944, 1,307 Hi-stroke expulsion lightning arresters, which had just been developed, were installed on feeder number 1 to study their performance. Each of them was equipped with surge crest ammeter links, hereafter referred to as links, to measure discharge current. Almost all the lightning surge measurements were made on this feeder.

Locations with Complete Magnetic Link Coverage

Magnetic links[5] were used extensively because they provide inexpensive, if approximate, measurement of surge current magnitude and polarity. Links were installed on each conductor connected to the group of distribution transformers where the cathode-ray oscillographs were and at other locations in their vicinity for the purpose of seeing how surge currents

---

Paper 49-110, recommended by the AIEE protective devices committee and approved by the AIEE technical program committee for presentation at the AIEE winter general meeting, New York, N. Y., January 31–February 4, 1949. Manuscript submitted November 15, 1948; made available for printing December 24, 1948.

D. D. MacCarthy and D. A. Stann are with the General Electric Company, Pittsfield, Mass.; D. R. Edge is with the Graybar Electric Company, Chicago, Ill.; and W. C. McKinley is with the Central Electric Cooperative, Inc., Parkers Landing, Pa.

The authors wish to acknowledge the valuable contributions made to this field investigation by the personnel of the Central Electric Cooperative, Inc. and by the following members of the General Electric Company: J. W. Kalb and W. H. Eason of the lightning arrester engineering division, and J. H. Leh of the Pittsburgh office engineering division.

were distributed, similar to Figure 2. Links were also installed on the pole ground wires; that is, wires connecting the system neutral conductor to the pole ground at many of the poles between these transformers giving rather complete coverage of 8.5 miles of line. The links at these locations were tested promptly after every lightning storm during the four years of study, thus minimizing the loss of records due to superposition of surges. All current determinations at these locations were made by calibrating the links individually to obtain greater accuracy than is possible if the magnetic characteristics are assumed to meet an average curve. A sensitive laboratory-type galvanometer was used to measure the residual magnetism.

With this technique and with the link spacings used, measurements were possible over a range of approximately 100 to 30,000 crest amperes.

By studying the polarity and magnitudes of the records, it was usually possible to determine how the surge arrived at a transformer location. By correlating the link records from adjacent locations, it was often possible to determine how the surge reached the part of the system covered by these link installations.

The Church Stroke Case

A very complete set of records was obtained from a stroke to a church served by one of the transformers with complete link coverage.

In this case, there was abundant evidence in addition to the links defining the path of the lightning current. The stroke terminated on an ungrounded ornamental zinc sphere at the top of the church steeple as shown by holes freshly burned in it. It jumped from the rod supporting the ornament to the steeple and shattered a 4 inch by 6 inch by 18 foot wooden rafter. It left the steeple, passed through the main roof of the church scattering more slate shingles, and terminated on the Romex wiring above the ceiling. On the ground floor, a 15-ampere plug fuse was shattered and an open knife switch was arced over. The filaments in some of the church lights were vaporized. In the basement, a 60-ampere cartridge fuse was blown. The current passing into the 150-ohm service ground is unknown. The currents measured in the secondary wires at the transformer traveled through the 3-wire Alnico magnet watthour meter which was tested and was not damaged or decalibrated. These currents reached the transformer over the 180-foot length of 3-wire secondary service without causing further damage.

The transformer was connected to the end of a short, single-phase branch of the line. A cathode-ray oscillograph was installed there in addition to the magnetic links. The arrows in Figure 2 show the direction of negative current flow, as determined from the links, and the adjacent figures give the crest currents. A total current of 31,700 crest amperes arrived at the transformer over the secondary service phase and neutral wires. This current, divided between several wires, 5,600 amperes went to ground via the ground and guy wires at the pole; 6,700 amperes went out on the system phase wire and were measured by magnetic links on the lightning arrester ground wire and by others on the system phase wire; 19,500 crest amperes went out on the system neutral wire. The sum of the current leaving the transformer is 31,800 crest amperes which is in unusually good agreement with 31,700 amperes, the total current measured in the secondary service wires. The cathode-ray oscillogram obtained is discussed under Cathode-Ray Oscillograms.

The transformer and pole wires were examined with great care, and the transformer was returned to the factory for test and detailed examination. No evidence of damage or flashover was found; hence, the currents of 8,200 and 11,000 amperes in the secondary phase wires passed through the transformer secondary windings to the grounded neutral.

The inductance of these windings is low for currents flowing in the same direction in the phase wires because the ampere-turns in the two halves of the secondary are opposed. The magnetic link records definitely show that a negative surge arrived at the transformer over the secondary service wires and then left

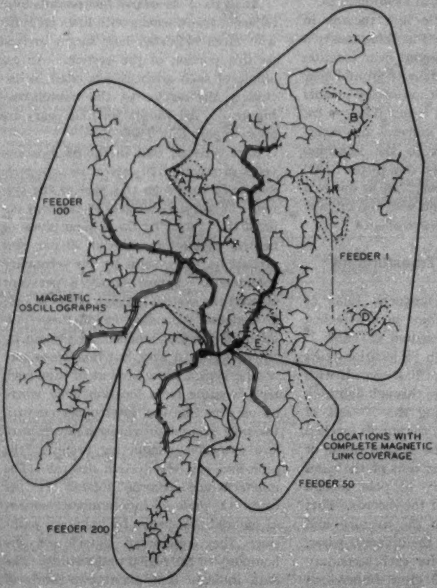

Figure 1. System map for Central Electric Cooperative, Inc.

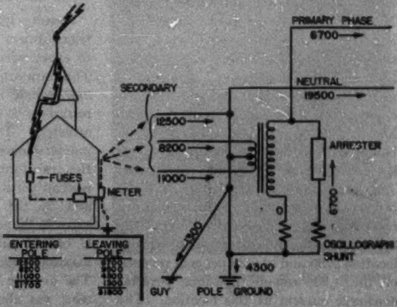

Figure 2. Path of stroke to church and resulting surge currents at transformer pole

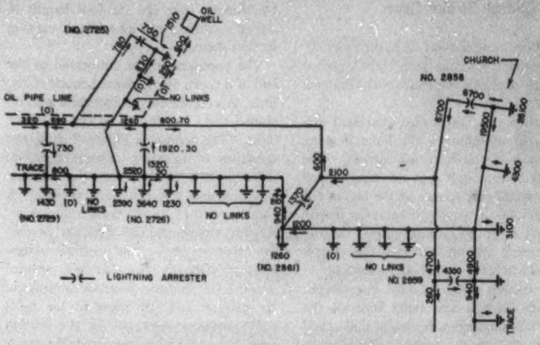

Figure 3. Distribution of the lightning surge currents for the church stroke case

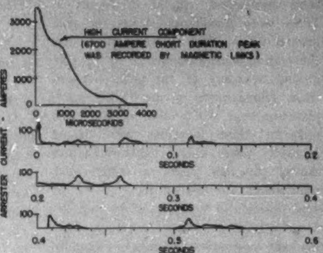

Figure 4. Replot of oscillogram showing long duration lightning arrester discharge resulting from stroke to church steeple

the transformer by every other connected wire.

Other records obtained in the vicinity of the church during the same storm illustrate the correlation often found between magnetic link records at adjacent transformers having links on each conductor connected to the transformer. Figure 3 is a diagram of the system phase and neutral wires in the vicinity of the church, which is at the right. The arrows near the lines give the direction of negative current flow and the adjacent figures, the magnitude. In cases where surge reversal was indicated, this value is given as a percentage following the crest magnitude. The currents in the indicated grounds are the algebraic sum of the currents in the guys, pole ground, and secondary phase, and neutral wires. In Figure 3, the 19,500 amperes leaving the church by the system neutral accounts for the negative currents measured to ground at transformer locations 2859 and 2861. The neutral current cannot be accounted for quantitatively because links were not installed on the ground wires at all of the intervening poles. However, the 6,700-ampere current leaving the church by the system phase wire shows up as 4,700 amperes at location 2859 and 2,100 amperes at location 2861, giving a sum of 6,800 amperes. The incoming and outgoing currents at both location 2859 and 2861 are in good balance. A current of 600 amperes left location 2861 by the system phase wire. This is considered to be the origin of the 560-ampere current of the same polarity recorded as a 70 per cent reversal of the 800 amperes in the system phase wire at location 2726 and as a 30 per cent reversal of the 1,920-ampere lightning arrester discharge current at this location. The surges from the church, indicated as reversals at location 2726, necessarily arrived after the larger surge currents had been recorded. Thus, one negative stroke entering the system via the secondary service wires at the church caused four lightning arresters to discharge over a total length of 1.25 miles of system. These lightning arrester discharges were 6,700 amperes positive at the church, and negative discharges of 4,300 amperes at location 2859, 1,370 amperes at location 2861, and 580 amperes at location 2726.

The other magnetic link records in Figure 3 are interpreted as being due to a negative stroke to ground near location 2726 and a positive stroke to ground near location 2729. The origin of the records at location 2725 is not clear. The system phase current of 780 amperes also measured as 750 amperes in the lightning arrester may have been due to the 1,260 amperes leaving location 2726, or due to a surge in the pole ground wire and oil pipe line at location 2725.

Surge Currents at Transformers

Results from the magnetic links at transformers where they were attached to every wire are presented in Table I. The data are based on 88 location-years and include 120 sets of link records with records of 86 discharges through lightning arresters. Disregarding the 20 sets of indeterminate records, the surges reached the transformer by the system phase or neutral wires in 64 per cent of the cases and by the secondary or pole ground wires in 36 per cent of the records. Part C of the table gives the average and maximum currents in the different wires. The average current for each secondary wire was about 1,000 crest amperes as was the average in the system phase wire. The average currents measured were 1,270 amperes in the system neutral wire, 1,670 amperes through the lightning arrester, and 2,240 amperes through the pole ground wire. The large number of records in all wires is a result of the lightning arrester providing a path between the system phase wire and the group of wires consisting of the system neutral, pole ground, and secondary wires.

How Surges Reach the System

Analysis of the sets of link records from adjacent transformers with links on every wire often indicated how surges arrived on this portion of the system. An example of such analysis was cited in discussing the stroke to the church, see Figure 3. All results for four years are given in part D of Table I.

It is believed that in the 88 location-years of record, 120 sets of records were due to 72 surges on this part of the system. Of these 72 surges, 29 per cent entered the system by the system phase or neutral conductors. About 29 per cent arrived on the system by the secondary conductors. Approximately 8 per cent entered the system through both the pole ground and secondary conductors. Another 12 per cent reached the system by the pole ground wire, but this figure may not be typical since six out of nine such records came from location 2725 where an oil pipe line was interconnected with the pole ground providing a junction of two extensive conducting systems, the pipe line and the system neutral. The indeterminate records totaled 21 per cent. Of these 15 indeterminate surges, 11 entered the system by unknown paths since they originated outside of the boundary of the region under study. The data indicate that about two-thirds of the surges may enter a rural system by the secondary or ground wires. This is due to the close proximity between the secondary circuits and exposed objects such as wired buildings or trees near the buildings, and the connection between the secondaries, out-buildings, and water systems. This result had not been anticipated.

Long Duration Lightning Surges

Cathode-ray oscillographs were used to measure long duration surges at a small group of distribution transformers on feeder number 1. Table II gives the characteristics necessary to understand the data. Each oscillograph had two cathode-ray tubes connected to shunts containing Thyrite to extend the measurable range. At the onset of a storm, the operator energized each oscillograph. The cathode beam initiated automatically in 20 to 50 microseconds when the transient current measured by either tube exceeded a value that depended somewhat on the wave shape. Six of these cathode-ray oscillographs were in operation during 1944. They were connected to measure both arrester and transformer primary currents. The impulse currents in the transformer primaries were measured to determine if they were capable of blowing transformer fuses. In 1945 a seventh oscillograph was installed, and four of them were changed to use both tubes to measure lightning arrester current over an extended range instead of measuring surge currents in the transformer primary winding. The oscillographs were operated in 1944 and 1945 but were then discontinued to enable the field engineer to concentrate on other aspects of the investigation. Magnetic links were installed on all wires connected to the distribution transformers at the oscillograph installations, see Figure 2. These links measured short duration surges that the oscillographs could not register.

During nine oscillograph-years of record, no lightning currents of significance were measured through the transformer primary. The lightning arrester was connected on the line side of the fuse. No transformer fuses were blown due to lightning at these locations.

Figure 5. Oscillogram of long duration discharge obtained at church

Table III summarizes the results from the 17 cathode-ray oscillograms of lightning arrester current. During the 13 oscillograph-years of record, the lightning arresters discharged 22 times as shown by oscillograms, magnetic link records, and scars on the electrodes of the expulsion lightning arrester series gaps. The electrodes were changed after each scar to relate the nature of the burns and the discharge currents. Five of the 22 discharges were too short in duration for the oscillographs to record. The crest current and total duration from beginning to the end of the discharge are given in Table III together with the crest current measured by the magnetic links.

Figure 4 is a replot of the oscillogram resulting from the stroke to the church. The record occupies 27 inches of film and the deflections are small making it impractical to reproduce the entire oscillogram; Figure 5 shows the first part of it. The peak current of 6,700 amperes recorded by the links was too short in duration for the oscillograph to record. The oscillogram shows an initial current peak of 3,500 amperes that reached a virtual zero in about 3,000 microseconds. There

Figure 6. Oscillogram of long duration discharge

Table I. Data from Magnetic Links at the Locations with Links on Every Conductor

A. Surges Causing Lightning Arrester Discharges

	1944 16 Locations	1945 17 Locations	1946 28 Locations	1947 27 Locations	1944, 1945, 1946, 1947 88 Locations
Number of surge records at transformers*	20	27	38	35	120
Number of lightning arrester discharges	15	21	27	23	86

B. Conductors Over Which Surges Arrived at Each Transformer

	1944	1945	1946	1947	1944, 1945, 1946, 1947	Percentage of Surges
Primary conductors	11	15	19	19	64	53.3
Secondary conductors	5	6	5	5	21	17.5
Pole ground	2	4	1	2	9**	7.5
Pole ground and/or secondary conductors	0	0	3	3	6	5.0
Undetermined	2	2	10	6	20	16.7
Total Surges	20	27	38	35	120	100.0

C. Surge Activity in the Different Conductors of Special Locations

	Maximum Number of Readings Possible From 120 Surges	Records Obtained			
		Number	Per Cent of Possible	Surge Current (Amperes)	
				Avg.	Max.
Primary neutral conductor	240	200	83.3	1,270	19,500
Primary phase conductor	219	194	93.0	1,070	21,700
Lightning arrester lead	120	86	71.7	1,670	17,500
Secondary conductor	120	94	78.3	3,060†	53,200
Pole ground	120	76	63.4	2,240	24,000

D. Conductors Over Which Surges Entered the System

	Surges					Percentages of Surges
	1944	1945	1946	1947	1944, 1945 1946, 1947	
Primary conductors	7	2	5	7	21	29.2
Secondary conductors	5	6	5	5	21	29.2
Pole ground	2	4	1	2	9	12.5
Pole ground and/or secondary conductors	0	0	3	3	6	8.3
Undetermined	2	0	9	4	15	20.8
Total surges	16	12	23	21	72	100.0

* 71.7 per cent of all surges reaching the transformer operated the Hi-stroke lightning arrester.

** Six of the nine pole ground surges occurred at one location where the pole ground was connected to an oil pipe line which branched to nearby oil wells.

† This value is the average sum of currents in all secondary conductors per surge.

Figure 7. Oscillogram of long duration discharge

Table II. Cathode-Ray Oscillograph Sensitivity and Initiating Current

	Tube 1 Lightning Arrester Current, Amperes	Tube 2 Transformer Primary Current, Amperes	Tube 1 Lightning Arrester Current, Amperes	Tube 2 Lightning Arrester Current, Amperes
Initiating current, amperes	90–200	4–6.5	90–200	90–200
Amperes for 1 millimeter deflection	100	3.5	100	15
Full scale deflection, 6.5 millimeter, amperes	5,000	200	5,000	500
Number of oscillographs in 1944	6		0	
Number of oscillographs in 1945	3		4	
Time sensitivity, 0.9 milliseconds per millimeter.				

were six subsequent long duration discharges in the stroke, none of them exceeding 90-amperes crest. The last of these discharges ceased after 0.55 second, which is the total duration given in the table. The individual discharges lasted from 0.017 to 0.071 second. The current was less than 10 crest amperes and may have been zero for a total of 0.3 second during the 0.55 second total duration of the discharge. This surge did not cause the primary fuse to blow, did not damage the Hi-stroke lightning arrester, nor was follow current established. However, follow current may have been established in one of the other lightning arresters which discharged simultaneously. Calculations show that this discharge was sufficient to blow primary fuses rated 30 amperes or less that might have been in its path. No current was recorded by the element connected to measure transformer primary current. This stroke produced the most severe record obtained. This oscillogram was preceded by another on a different time axis on the same film showing a positive current of 140 amperes, 500 microsecond duration through the lightning arrester, see Figure 5. This 140-ampere discharge was due to a negative lightning stroke which occurred at least 12 seconds before the steeple was hit and splintered a tree across the road from the church.

The second highest oscillographic record showed a crest current of 2,000 amperes and 5-milliseconds duration. It is reproduced in Figure 6. There was no follow current or transformer magnetizing transient. The set of link records indicates a negative surge arriving on the system phase wire recorded as 6,500 amperes in the lightning arrester and going out on the system neutral, pole ground, and secondary wires. The sum of the outgoing currents recorded is 5,700 amperes crest.

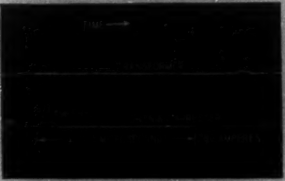

Figure 8. Cathode-ray oscillogram showing lightning arrester follow current

The 17-ampere 0.061-second oscillogram is reproduced in Figure 7 to illustrate a low current of long duration. Both traces show lightning arrester discharge current, the upper being from the oscillograph tube giving one millimeter deflection for 15 amperes, the lower from the other tube giving one millimeter for 100 amperes. This record was obtained at location 2725 during the same storm that produced the record at the church.

Many of the 17 oscillograms listed in Table III are not severe enough to be of importance. The first nine are traces merely showing long duration discharges through the lightning arresters. All of these traces are much less severe than a half cycle of follow current at these locations which would be recorded as 200 to 300 amperes crest and 8.3 milliseconds. The average current was usually much less than the crest. The current was apparently zero for more than 0.30 second during the 3,500-ampere record and for 0.16 second during the 40-ampere, 0.66-second record. The 2,000 and 3,500-ampere oscillograms listed last in Table III, Figures 4 and 6, are far more severe than the others. These oscillograms show that lightning arresters on rural distribution systems discharge long duration surges that occasionally, as in the case of the stroke to the church, may be of great severity. The probability of long duration discharges through lightning arresters is much greater on rural than on urban distribution systems because of the greater exposure, lower density of connected transformers, and absence of extensive systems of grounded conductors.

Only one cathode-ray oscillogram of follow current through arresters was obtained, see Figure 8. Since it showed no long duration lightning discharges, it was excluded from Table III. A second half cycle of follow current occurred five half cycles after the first; it was accompanied by a transformer magnetizing current transient shown in the upper trace. The link records of 300 amperes 100 per cent reversal in the lightning arrester and primary phase wires are believed to be the result of the follow current. The set of link records indicate that a negative surge totaling 1,150 amperes arrived via the secondary phase wires and went out on the system neutral and phase wires. It is surprising that 60-cycle follow current was started only once as shown by the oscillograms obtained from 13 lightning-arrester-years of experience since follow current was started readily at all of the oscillograph locations when each oscillograph was tested with a portable impulse generator to insure that it was in working order. The lack of follow currents is at least partly the result of several lightning arresters discharging simultaneously due to one surge on the system which could start follow current through only one of the lightning arresters. In other cases, the line may have been de-energized as by the operation of a recloser, or the lightning surges may have occurred near the zero point of power voltage wave.

Table III. Summary of the 17 Long Duration Lightning Strokes Obtained in 1944 and 1945

	Cathode-Ray Oscillograms		
	Crest Current, Amperes	Total Duration, Milliseconds	Crest Current Measured by Magnetic Links (Amperes)
Less than	−10	2.0	−150
	−10	1.5	−420
	+10	3.5	+160
	−10	1.0	−1,100
	−10	3.0	*
	+10	2.0	*
	−10	1.5	*
	+10	1.0	+200
	−10	2.0	−320
	−17	61.0	−750
	−40	660.0	−1,000
	+70	0.5	*
	+140	0.5	**
	−650	1.5	−700
	−680	0.5	−650
	−2,000	5.0	−6,500
	+3,500	550.0	+6,700

* Oscillograms obtained before magnetic links were installed at these special locations.

** Record obscured by subsequent +6,700-ampere record obtained during same storm.

Discharges Through Representative Groups of Lightning Arresters

Data from the links at transformers with links on every wire indicated that one surge frequently caused several lightning arresters to discharge and gave information on the number of times individual lightning arresters discharged. More information was desired, so in 1946 five widely separated groups of about 40 lightning arresters each were selected for a more detailed study, see areas A to E inclusive in Figure 1. Links at these transformer locations were installed on only the lightning arrester lead. The links in these five groups were checked 18 times between April 8 and November 25, 1946 to minimize the records lost by superposition. The average interval between inspections was 11 days and the maximum was 20 days. Currents below 5,000 amperes crest were determined from curves based on average link characteristics; larger currents were determined by calibration of the individual links.

Number of Lightning Arresters Discharging Due to One Surge

Link data from each of the five lightning arrester groups were spotted on system maps, see Figure 9. Many sets of records occurred in which every adjacent lightning arrester had discharged currents of the same polarity. These sets of discharge currents were interpreted as resulting from one surge on the system. The currents usually decreased at each successive lightning arrester away from the one with the highest current assumed to be nearest the stroke terminus. In a few cases, the polarity or magnitude of the currents indicated that one set of records was due to two separate surges.

This is illustrated by the records in the two lefthand sets of records in Figure 9. Each dot in this figure represents a lightning arrester; the polarity, crest current, and per cent reversal of the lightning arrester current are adjacent to the dots. The upper set of records was interpreted as five lightning arresters discharged by a negative surge resulting from a stroke nearest the lightning arrester which discharged 17,500 amperes, 2 per cent reversal. The trace at the extreme upper left was excluded because it was of positive polarity. On the basis of current magnitude, the middle set of records was interpreted as four lightning arresters discharging negative current resulting from another stroke. The set of records at the lower right is separated from the middle set on the basis of current magnitude and because one lightning arrester between the two sets did not discharge. This set of eight negative records, including traces, indicates eight lightning arresters discharged by one surge and is the maximum number found in these groups.

All data analyzed in this way are summarized in Table IV. The data are based on 293 lightning-arrester-years of experience. The 318 lightning-arrester discharges recorded are interpreted as resulting from 185 surges on the system or an average of 1.72 lightning arrester discharges for each surge. The number of lightning arresters discharging due to one surge ranged from one lightning arrester for 63 per cent of the surges; two lightning arresters for 19 per cent of the surges; on up to eight lightning arresters for one out of 185 surges. This surge caused discharges through lightning arresters on 1.8 miles of line.

In one case not included in these five groups, discharges were recorded through all 13 lightning arresters on three miles of line within a 1-mile radius of the lightning stroke terminus. The expulsion lightning arrester nearest the stroke burst due to the heavy surge current which exceeded 30,000 amperes, the upper measurable limit of the links. The currents were all of the same polarity and diminished in each successive lightning arrester away from the stroke terminus. These records show that surges may travel over long lengths of rural line and frequently cause more than one arrester to discharge.

Number of Times Individual Lightning Arresters Discharged

Table V summarizes the number of discharges per year for each arrester in the five groups, A to E, and for the lightning arresters at transformers with links on every conductor. Not all discharges were recorded since several discharges from multiple lightning strokes or from superposition of separate discharges in the interval between inspection contribute only one record. Based on 293 lightning-arrester-years, the lightning-arresters average 1.09 discharge per year as recorded by links; 32 per cent of the lightning arresters did not discharge;

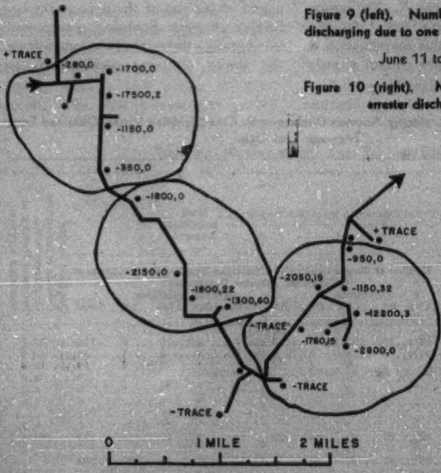

Figure 9 (left). Number of lightning arresters discharging due to one surge (Part of Group C)

June 11 to 28, 1946

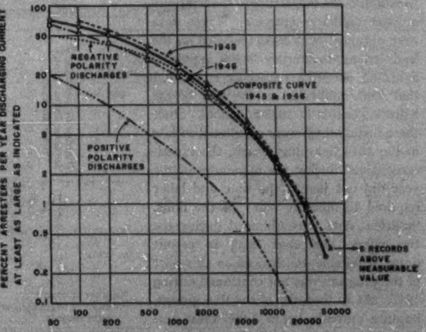

Figure 10 (right). Magnitude of lightning arrester discharge currents

40 per cent discharged once; and two lightning-arresters discharged at least four times during one year.

The variability in number of lightning arrester discharges is interesting. The 44 lightning arresters in group C averaged 1.5 discharge records per year, while the 43 lightning arresters in group A about 15 miles away averaged 0.67 during the same year.

Knowing the number of lightning arresters involved and the total discharges recorded, the law of independent trials can be used to calculate the number of lightning arresters expected to operate exactly once, twice, and so forth. This was done for the records from the 205 lightning arresters in groups A to E with the following results:

Records Per Lightning Arrester Per Year—Number, N	0	1	2	3	4	5
Calculated—Lightning arresters with exactly "N" records, per cent	32.2	36.6	20.4	7.5	2.1	0.6
Actual—Lightning arresters with exactly "N" records, per cent	29.3	39.5	21.0	9.3	1.0	0.0

The actual results show a trend toward fewer lightning arresters with no records and fewer with a large number of records than are calculated. This trend is consistent with the tendency for one surge to produce a record in more than one adjacent lightning arrester; that is, the average of 1.7 lightning arrester discharges per surge cited previously.

Impulse Currents Discharged by Expulsion Lightning Arresters

Link data obtained from the five groups and other locations on feeder number 1 selected for frequent inspection were used to estimate the frequency of lightning arrester discharges on this rural system. A larger amount of data were necessary to establish the magnitude of the lightning arrester discharge currents. These data were obtained from links installed on the leads of approximately 1,300 expulsion lightning arresters on feeder number 1 that were calibrated at the end of the lightning season in 1945 and 1946. Since these installations were completed so late in the 1944 lightning season, the experience gained during the remainder of the year did not justify the time and labor required to measure many of the links. Sufficient data were obtained during the two years, 1945 and 1946, to permit drawing reliable conclusions so this part of the program was not continued during 1947. As in the case of the five groups, impulse currents below 5,000 crest amperes were determined from average characteristic curves; larger currents were determined by calibration of the individual links with a sensitive laboratory galvanometer.

The magnitude of the impulse current obtained in this way is illustrated in Figure 10. The data for 1945 and 1946 are in good agreement. The composite curve represents the 1,685 impulse current records obtained during both years. It indicates 67.3 per cent of all the expulsion lightning arresters discharged at least once per year. This corroborates similar data obtained from the selected groups, see Table V. Only 0.36 per cent or six of the 1,685 records exceeded 30,000 crest amperes. Other curves based on 1,685 records separate the lightning arrester discharges according to polarity. Approximately three-quarters of the lightning arrester discharges were negative in polarity; this preponderance became more pronounced with increasing discharge currents. No positive arrester discharges greater than 15,000 crest amperes were measured. There were 26 negative discharges of 15,000 crest amperes or more.

A comparison of the results obtained by McEachron and McMorris[3] on rural systems with those from this investigation are summarized in Table VI. The results are in close agreement except for the lower currents. In this investigation a higher proportion of low current records was obtained because of the higher sensitivity of the instruments used.

Lightning Arrester Follow Currents

Automatic magnetic oscillographs recorded abnormal 60-cycle power currents such as lightning arrester follow currents, fault currents, and load inrush currents.

A magnetic oscillograph was installed on feeder number 1 approximately two miles from the substation during 1945, 1946, and 1947. The symmetrical short circuit current decreases with the distance from the substation. It was 700 rms amperes at the oscillograph and about 31 amperes at the extremity of the line. Any currents within this range in the phase conductors or in the neutral initiated the oscillograph within one half cycle. This oscillograph recorded follow currents through all expulsion arresters on feeder number 1 except 26 between the oscillograph and the substation.

Another magnetic oscillograph was located near the beginning of feeder 200 during 1946 and 1947. This oscillograph added data to the overcurrent investigation but not to the lightning study since the majority of the lightning arresters on this feeder were of the valve type and limited the follow current to values incapable of initiating the oscillographs.

The vibrators of each oscillograph measured the currents in phases A, B, C; the neutral current; and the voltages of phases A and C to ground. A short circuit through a 2-ampere fuse was placed at the end of the lines at the beginning of each lightning season and occasionally thereafter to demonstrate the ability of these oscillographs to

Table IV. Number of Lightning Arresters Discharged by One Lightning Stroke-Obtained From Magnetic Link Data

Number of Lightning Arrester Discharging Simultaneously	Number of Surges Causing the Indicated Number of Simultaneous Lightning Arrester Discharges: Group A*	B*	C*	D*	E*	Special Locations 1944	1945	1946	1947	Total	Per Cent Surges Causing Simultaneous Discharges of the Indicated Number of Lightning Arresters
1	18	19	23	13	15	7	4	11	6	116	62.7
2	3	8	4	5	4	4	1	5	1	35	19.0
3		2	2	4	8		1		2	19	10.3
4			3	1	1				1	6	3.2
5	1		2	1					1	5	2.7
6							2	1		3	1.6
7											
8			1							1	0.5
Number of surges	22	29	35	24	28	11	8	17	11	185	100.0
Number of Lightning arrester records	29	41	67	44	51	15	21	27	23	318	

* Special group records obtained during 1946.

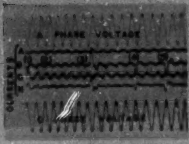

Figure 11. Magnetic oscillogram of follow currents resulting from multiple lightning stroke

initiate automatically due to the lowest fault current on the feeder.

Interpretation of Oscillograms

An interesting oscillogram resulting from a multiple stroke is reproduced in Figure 11 to illustrate the method of interpretation. Point 1 on this oscillogram indicates a lightning disturbance causing follow current through lightning arresters on B and C phases. The half cycle of follow current in each of these two phases was not recorded because of the time required to initiate the oscillograph. However the magnetizing transients are evidence that these lightning arresters discharged follow current. Point 2 shows lightning arrester follow current of a small magnitude in A phase lasting less than one half cycle. Half cycles of follow current in B phase are recorded at points 3, 4, and 5. The follow currents ranged from 50 crest amperes through the A phase lightning arrester at point 2 to 304 crest amperes through the B phase lightning arrester at point 3 presumably due to difference in timing angle. The duration of this multiple lightning stroke, which was taken as the time from first to the last half cycle of follow current inclusive, was 32 half cycles or 0.267 second. The time interval between the successive lightning arrester discharges was measured in half cycles between corresponding points at the beginning of each of the respective follow currents. For example, the time intervals between lightning arrester follow currents numbered 1 through 5 were 6, 11, 9, and 6 half cycles respectively.

Blowing of line fuses during a lightning storm with no corresponding record of fault current sufficient to blow the fuse was attributed to lightning.

Multiple Lightning Stroke Data

Oscillograms with intermittent half cycles of lightning arrester follow current, except where all follow currents occur simultaneously, are interpreted as due to multiple lightning strokes. By this definition, 22.5 per cent of the 1,481 follow current records obtained over a period of three years resulted from multiple lightning strokes, see Table VII.

Multiple stroke data were obtained by many investigators employing different measuring techniques. McEachron[6] obtained 184 crater lamp oscillograms showing follow current discharges through expulsion tubes on 138-kv lines; of these, 28 per cent were multiple. During another investigation conducted in the Pittsfield Lightning Observatory,[7] Hagenguth found that 37 per cent of the 619 lightning records obtained by means of a Boys camera were multiple in nature. Similarly the 65 Boys camera lightning records obtained during Schonland's Investigation[8] show that this percentage was 51. Stekolnikov and Valeev[9] used a Klydonograph with a fast moving film to show that 72 per cent of 25 records were due to multiple strokes.

All these different methods of recording multiple lightning strokes have limitations. Boys cameras may fail to record photographically weak lightning strokes. Electromagnetic oscillographs do not record strokes which fail to cause lightning arrester follow current, nor do they distinguish between successive surges occurring within the same half cycle. Klydonograph accuracy is limited by the film speed and the ability to interpret nearly superimposed Lichtenberg figures. All these instrument limitations tend to render too low a number of multiple stroke discharges.

Table VI. Comparison of Lightning Arrester Discharge Data

	McEachron and McMorris (Rural only)	Central Electric Cooperative, Inc. (Rural)
Number of lightning-arrester-years	1,709	2,503
Number of lightning arrester discharge records	909	1,685
Per cent lightning arresters discharging at least once per year	43.6	67.3
Per cent lightning arresters discharging per year currents greater than:		
1,000 amperes	28.9	25.0
5,000 amperes	7.3	6.0
15,000 amperes	1.75	1.4
Per cent of records that were of negative polarity	65.7	72 0

The maximum number of times follow current was started during this investigation due to one multiple stroke was 15. Analysis of 1,481 follow current oscillograms shows 22.5 per cent with follow current starting two or more times, 8.1 per cent three or more, 3.5 per cent four or more, and 1.9 per cent five or more.

All 333 multiple follow current oscillograms accumulated over a 3-year period were analyzed for total durations and the time intervals between separate lightning

Table V. Number of Discharges Per Lightning Arrester Obtained From Magnetic Link Data

(1946) Group	Total Lightning Arrester	Number of Lightning Arresters Contributing This Number of Records					Number of Records	Records Per Lightning Arrester	Lightning Arresters Contributing at Least One Record	
		0	1	2	3	4 at Least			Number	Per Cent
A	43	22	15	4	2	0	29	0.67	21	48.9
B	40	15	13	9	2	1	41	1.02	25	62.5
C	44	6	20	8	9	1	67	1.52	38	86.4
D	41	9	20	12	0	0	44	1.07	32	78.0
E	37	8	13	10	6	0	51	1.38	29	78.4
All groups	205	60	81	43	19	2	232	1.13	145	70.7
Per cent		29.3	39.5	21.0	9.3	0.98				
Magnetic Link Data Obtained From Special Transformer Locations During 1944–45–46–47										
1944	16	7	5	3	0	1	15	0.94	9	56.3
1945	17	8	4	2	0	3*	21	1.23	9	53.0
1946	28	7	15	6	0	0	27	0.96	21	75.0
1947	27	12	11	2	0	2	23	1.15	15	55.6
Grand total	293	94	116	56	19	8	318	1.09	199	67.9
Per cent		32.1	39.6	19.1	6.5	2.7				

* 2 out of 3 contributed 5 records.

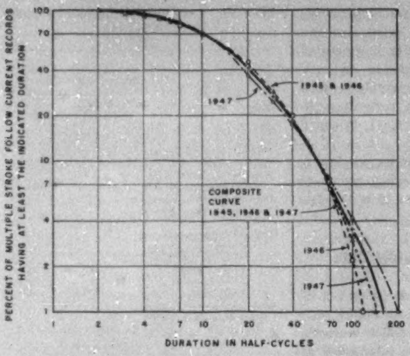

Figure 12 (above). Duration of multiple lightning strokes

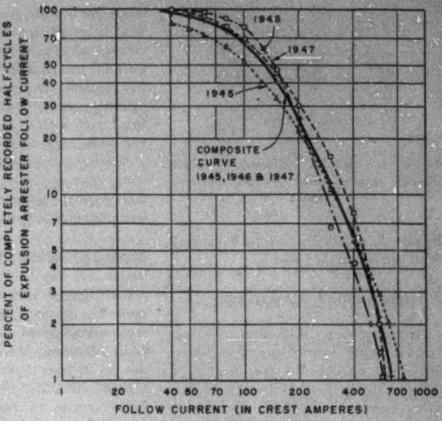

Figure 13 (right). Magnitude of lightning arrester follow currents

arrester follow currents. The total duration of these multiple follow currents is plotted in Figure 12 to show general trends. The yearly tendencies in multiple stroke duration were very consistent up to one second. Beyond this duration the number of oscillograms becomes progressively less; consequently, the curves show a greater divergence. The most probable, the average, and the maximum multiple stroke durations were 0.117, 0.19, and 1.83 seconds respectively. Similarly the most probable and the average time intervals indicated between individual discharges of multiple strokes were 0.084 and 0.17 second.

Expulsion Lightning Arrester Follow Currents

The 1,481 oscillograms with records of follow current covering 4,054 expulsion lightning-arrester-years of experience yielded a total of 2,479 half cycles of lightning arrester follow current. To compensate for the loss of oscillograms based on records of the short periods when oscillographs were inoperative, the total number of half cycles of follow current was estimated as 2,620. Using 2,620 half cycles of follow current, the average is 0.65 half cycle of follow current per lightning arrester per year, see Table VII. It must be remembered that the magnetic oscillographs recorded the number and magnitude of follow currents discharged through expulsion lightning arresters rather than the number of discharges or lightning strokes. These were precisely the data required to determine lightning arrester erosion life. Analysis of oscillograms shows that expulsion lightning arrester follow currents were interrupted at the first current zero in all but one per cent of the cases. Every such case resulted from a multiple stroke since there were several successive lightning arrester operations on the same oscillogram. These records are attributed to long duration discharges continuing for more than one half cycle or to several discharges which re-established follow current in successive half cycles.

To estimate the erosion life of lightning arresters, it is not only necessary to determine the number of half cycles of follow current discharged by lightning arresters but to measure the magnitude of the follow current. Because of the time required for initiation of the oscillograph, the crests of some half cycles of follow current were not recorded. The 693 crest values which were recorded are the basis of Figure 13. The average follow current magnitude was 182 crest amperes. Only 3.5 per cent of the follow currents were greater than 500 crest amperes. A probability curve drawn from these same data shows that the most probable follow current magnitude was 105 crest amperes. These figures apply only to this system.

A study was made to determine whether locations with high available short circuit current had a greater tendency to establish follow current. No correlation was found.

Single and multiple lightning arrester operations contributed a total of 1,481 follow current oscillograms with an average of 1.39 half cycles of follow current per lightning stroke. Considering only the multiple follow current records, this average was three.

Insofar as the authors are aware, this is the first investigation of the actual follow current duty of expulsion lightning arresters on a distribution system. Only 33 of the 1,481 follow current oscillograms show that follow current initiated five or more times. Furthermore, the average lightning arrester discharged only 0.65 half cycle of follow current which averaged 182 crest amperes. All data indicate that erosion is no problem for these expulsion lightning arresters when applied within their ratings. The erosion effect of impulse currents is negligible in comparison with erosion due to follow currents.

Line Flashovers

An average of three expulsion lightning arresters per mile of feeder number 1 was effective in reducing the number of line flashovers. Over a period of three years, 1,481 follow current oscillograms were obtained. To compensate for the time the oscillograph was inoperative, this number was increased to 1,577. Each of these would probably have caused a line flashover had the line not been protected by the expulsion lightning arresters. In addition to this, there were 1,046 temporary faults, or 0.7 per mile, on the line that cleared themselves or were interrupted by one oil circuit breaker opening. Therefore, assuming feeder number 1 was completely unprotected by lightning arresters and the 1,046 temporary faults were line flashovers, there would have been a potential total of 2,623 line flash

Table VII. Expulsion Lightning Arrester Follow Current Data—Feeder Number 1

Year	Lightning Arresters in Service	Number of $^{1}/_{2}$ Cycles of Follow Current, Recorded	Estimated	Half Cycles Follow Current Per Lightning Arrester Per Year
1945	1,307	673	800	0.61
1946	1,352	426	440	0.33
1947	1,395	1,380	1,380	0.99
Total	4,054	2,479	2,620	0.65 Avg.

Lightning Strokes—Feeder Number 1

Year	Records Showing Follow Current		Records Showing More Than One Lightning Arrester Operation Actual	Percentage of Multiple Strokes (At Least), Actual	Average $^{1}/_{2}$ Cycles Follow Current Per Stroke, Actual
	Recorded	Estimated			
1945	449	534	121	26.9	1.50
1946	280	291	79	28.3	1.52
1947	752	752	133	17.7	1.83
Total	1,481	1,577	333	22.5 Avg.	1.67 Avg.

overs on this line in three years, or 1.8 per mile of line each year.

Results and Conclusions

1. About one-third of the lightning surges arrived at distribution transformers by the secondary or pole ground wires.

2. About two-thirds of the surges reached the system phase and neutral wires from the secondary wires or pole ground wires.

3. The average surge current was about 1,000 amperes in each of the secondary phase and neutral wires, 1,070 amperes in the system phase wire, 1,270 amperes in the system neutral, 1,670 amperes through the arrester, and 2,240 amperes in the pole ground. The larger surges usually involved currents in all wires.

4. Seventeen long duration discharges through lightning arresters were recorded by cathode-ray oscillographs. These measurements indicate an average of 1.3 discharges per lightning arrester per year, although these data are too limited to establish a rate of expectancy. An oscillogram having a duration of 0.55 second was obtained of a severe discharge from a stroke which occurred near the oscillograph location.

5. Simultaneous discharge of lightning arresters at adjacent locations often occurred as a result of a single lightning surge. One severe surge discharged all 13 lightning arresters on three miles of line within a one-mile radius.

6. Expulsion lightning arresters on this system carry follow current less often than they discharge surge current since sparkover near power voltage zero may not start follow current and since only one arrester carries follow current when there is simultaneous discharge of lightning arresters on the same phase.

7. The number of times per year a lightning arrester discharges varies greatly with the locality and lightning severity. The links showed that 40 per cent of the lightning arresters discharged once; 19 per cent twice; 6.5 per cent three times; and 2.7 per cent four or more times per year. The lightning arresters averaged 1.1 discharge per year.

8. On a yearly basis, 0.36 per cent of lightning arresters discharged currents exceeding 30,000 amperes, 50 per cent at least 200 amperes, and 67 per cent at least 100 amperes

9. At least 22.5 per cent of the lightning strokes were multiple. These multiple strokes had an average duration of 0.19 second and caused an average of three separated half cycles of follow current through the expulsion lightning arresters.

10. The erosion duty was not severe for the expulsion lightning arresters used on this rural system since they discharged an average of only 0.65 half cycle of follow current per year with an average of 182 crest amperes.

11. The use of an average of three expulsion lightning arresters per mile reduced the number of line flashovers from an estimated 1.8 to 0.7 per mile of line per year.

References

1. Lightning Measured on 4-Kv Overhead Circuits, **Herman Halperin, K. B. McEachron.** Electrical Engineering (AIEE Transactions), volume 53, January 1934, pages 33–7.

2. Discharge Currents in Distribution Arresters, Part II, **K. B. McEachron, W. A. McMorris.** Electrical Engineering (AIEE Transactions), volume 57, June 1928, pages 307–14.

3. Measured Lightning Currents Through Distribution Arresters on 4,800-volt Rural Circuits, **H. R. Wilbur, W. A. McMorris.** *General Electric Review* (Schenectady, N. Y.), volume 44, March 1941, pages 159–65.

4. Lightning and Lightning Protection on Distribution Systems, **R. C. Bergvall, Edward Beck.** Electrical Engineering (AIEE Transactions), volume 59, August 1940, pages 442–49.

5. Direct Measurement of Surge Currents, **C. M. Foust, J. T. Henderson.** Electrical Engineering (AIEE Transactions), volume 54, April 1935, pages 373–78.

6. Multiple Lightning Strokes, Part II, **K. B. McEachron.** Electrical Engineering (AIEE Transactions), volume 57, September 1938, pages 510–12.

7. Photographic Study of Lightning, **J. H. Hagenguth.** AIEE Transactions, volume 66, 1947, pages 577–85.

8. Progressive Lightning II, **B. F. Schonland, D. J. Malan, H. Collens.** *Proceedings*, Royal Society (London, England), volume 152, 1935, page 595.

9. L'Etude de la Foudre dans un Laboratoire de Camtagne, **I. Stekolnikov, C. Valeev.** International Conference of High Voltage Electric Systems (Paris, France), report number 330, 1937.

Discussion

A. M. Opsahl (Westinghouse Electric Corporation, East Pittsburgh, Pa.): The authors state that in the church stroke case, there were currents of 8,200 and 11,000 amperes measured in the two outside wires of the secondary circuit or an unbalance of 2,800 amperes between the two windings. At the rate of change of current which can be expected in such lightning surges, how can it be explained that there was not sufficient voltage developed across the low- to high-voltage reactance of the transformer due to this 2,800 amperes unbalanced or uncompensated surge current to flash over the secondary bushing?

One conclusion of this investigation was that about one-third of the surges arrived at the transformers over the secondary wires. This is a high percentage. Was any record kept of secondary circuit disturbances such as bushing flashovers or trouble in the services? A few thousand amperes surge current over the secondary bushing will leave a mark which can be seen even though it cannot be classified as damage. Disturbances in dwellings due to lightning on the secondary circuits can occur and some might have been reported. There was considerable concern over a possible increase in secondary troubles when the interconnection of primary arrester ground lead and secondary neutral was up for code approval. No appreciable increase in secondary troubles was found.

The authors found that expulsion lightning arresters spaced three per mile reduced line flashovers from 1.8 to 0.7 per mile per year. What was the flashover of the insulation protected and what was the approximate span length in the area?

D. D. MacCarthy, D. A. Stann: Opsahl has raised an interesting question as to why the unbalanced currents measured in the secondary phase wires connected to the transformer at the church did not cause the secondary bushings to flash over. The same line of reasoning prompted us to make a very critical examination of this transformer immediately after the disturbance was reported.

When no evidence of flashover was detected in the field, the transformer was returned to the factory for disassembly and careful examination of the windings. There was no evidence of any flashover or other damage. There are two alternative explanations.

First, the current unbalance of 2,800 amperes was determined as the difference between the 11,000 and 8,200 ampere currents in the secondary phase conductors. Since the magnetic link readings were accurate to within ±10 per cent and the 2,800 amperes difference was small as compared to either phase conductor current, it is possible that the unbalanced current may have been appreciably less than 2,800 amperes; in which case, there would be insufficient current to cause bushing flashover.

Second, a simple calculation shows that the 2,800 ampere unbalance in discharge current could have occurred without resulting in a bushing flashover if it had a slow wave front. A reasonable value for the self-inductance of one 120-volt secondary winding is 500 microhenries, assuming the core does not carry flux due to the impulse current. This is consistent with the absence of current in the transformer primary in the cathode ray oscillogram of Figure 5. The flashover voltage of the secondary bushings is approximately 40-kv crest. Since this bushing did not flash over, the 2,800 ampere current flowing in the inductance of 500 microhenries could not have reached crest in less than 35 microseconds. Because the cathode-ray oscillograph did not record the front of the current, the time to crest current was less than the maximum initiating time of the oscillograph, which is 50 microseconds. With a time to crest current of 50 microseconds, the voltage on the secondary bushing would have been 28 kv, which is below the flashover value. Apparently, the unbalanced current at the transformer reached crest between the approximate values of 35 and 50 microseconds. Therefore bushing flashover would not be expected under these conditions.

Opsahl also has asked if records were kept of circuit disturbances. Evidence of damage was sought for correlation with the magnetic link records from transformers with links on each conductor. In some cases blown house fuses, damaged light bulbs, or struck trees in the vicinity of the house were found. On this system, the lightning arrester ground was always interconnected with the ground at the pole, the transformer tank, and the primary and secondary ground conductors. This interconnection may decrease the severity of the disturbances in the secondary circuit caused by surges originating on the secondary and would be expected to increase the number of small disturbances resulting from surges originating on the primary.

Information was requested on the line insulation to interpret the reduction in the number of line flashovers attributed to the expulsion lightning arresters. The line was built in accordance to REA specifications. On most of the system there was a ground at each pole with a ground wire brought up the pole and connected to the system neutral wire and extended within two inches of the pole top.

The primary phase conductors were carried on pin insulators that have a critical impulse sparkover voltage of 100 kv positive and 130 kv negative for 1.5 by 40 microsecond waves. The insulator pins were not connected to the ground wire. The pole-top gap between the primary phase conductor and the pole ground wire was about eight inches. It has a critical flashover value of approximately 160 kv positive and 185 kv negative for 1.5 by 40 microsecond waves. The pole span lengths were of the order of 350 to 400 feet.

Transmission Line Design and Performance Based on Direct Lightning Strokes

E. L. HARDER
FELLOW AIEE

J. M. CLAYTON
ASSOCIATE AIEE

IT IS well known that the insulation requirements of transmission lines are determined by lightning and switching transients rather than by the normal frequency voltage. For lines up to the highest voltages now in use, lightning is usually a principal factor. Consequently, a method for predetermining the design requirements to provide a desired immunity against lightning tripouts is essential.

A great deal of thought and effort has been devoted to developing such a method. Much painstaking work has been done in the collection of information regarding lightning currents to provide a fundamental basis for the estimates.

In this paper there is presented a method which has been in increasing use for a number of years for specific design calculations, and which is based on the stroke current probability data. This method now is extended into a complete set of estimating curves covering the full range of insulation levels, span lengths, and tower footings encountered on transmission lines. This is essentially a refinement and extension of the general curves given by Monteith.[1] However, it takes into account the improved knowledge of the lightning phenomenon obtained through field research and confirmed by actual line performance during the intervening years.

The previous curves were based on the stroke voltage which was considered to be constant irrespective of what line structure was hit. This required the assumption and use of a stroke surge impedance. In the present curves the stroke current is taken to be independent of the line structure hit so that the stroke surge impedance concept is not required and the method is tied more directly to measured currents. The latter representation is believed to be more nearly correct for reasons that will be outlined. In general the changes from the previous curves are not large, particularly for the lower tower footings of 20 ohms or less. There are some significant changes for higher tower footings encountered in certain territories and for the shorter spans used for lower-voltage wood-pole lines, such as 33 kv. These differences will be enumerated. The new general curves also include shorter span lengths than were included previously.

The new method of approach involving the treatment of the lightning stroke current as a constant fixed current rather than as a constant voltage back of a stroke surge impedance was introduced by G. D. McCann and C. F. Wagner,[2,3] several years ago and the quite extensive field data accummulated to that time indicated that this was a better representation and gave results which more strictly agreed with experience. The new method brought to bear on the problem the valuable field data which had been collected on stroke current and the accompanying theoretical approach enabled these data to be interpreted for comparative purposes on all forms of line design.

Mechanism of Stroke to Line. In all methods of estimating lightning performance the mechanism considered is as follows. The direct stroke theory being well established, it is known that in a region of average storm intensity of 30 storm days per year, the line will be hit by approximately 100 direct strokes per 100 miles per year on the average. Thus a shield wire must be used to receive these direct strokes and thereby shield the remaining conductors. This may be a ground wire which provides a suitable shielding angle or a top phase conductor equipped with protector tubes. The lightning current then is expected to take the path along the shield wire, down the tower or towers, and through the tower footing resistance to ground.

The entire tower top and connected ground wire rise to a high voltage principally because of the *IR* drop in the tower footing.

Neglecting coupling between the ground and phase wires, all this voltage would be impressed on the line insulation. Coupling elevates the phase wire voltages, so that the actual voltage impressed on the insulation is the tower-top voltage to ground times (one minus coupling).

It is evident that the tower lightning current required to cause flashover can be determined for any given insulation level, tower footing resistance, and coupling factor. The relation is:

$$\text{Tower current to cause flashover} = \frac{\text{insulation flashover voltage}}{\text{tower footing resistance} \times (\text{one minus coupling})}$$

The probability of line flashover is the same as the probability of tower currents equal to or greater than this value.

The problem is not as simple as outlined up to this point for a number of reasons. The insulation flashover voltage must be given for the wave shape of voltage to which it is exposed, which depends in turn on the wave shape of the stroke current and such factors as span length, tower footing, and so forth. Tower inductance is important as well as tower footing resistance when the latter is low (under 20 ohms). The coupling varies with corona which is a function of the voltage, spacings, and so forth. Finally, while the most extensive lightning data

---

Paper 49-111, recommended by the AIEE transmission and distribution committee and approved by the AIEE technical program committee for presentation at the AIEE winter general meeting, New York, N. Y., January 31–February 4, 1949. Manuscript submitted November 17, 1948; made available for printing December 27, 1948.

E. L. Harder is consulting transmission engineer and J. M. Clayton is central station engineer, Westinghouse Electric Corporation, East Pittsburgh, Pa.

available are tower crest current data, the tower currents resulting from given stroke currents vary with span length and to some extent with tower-footing resistance. Hence direct experimental tower current probability data can be used only for lines having the same order of span length and footing resistance as those on which the data were taken. For other lines some means of correction is necessary.

There also is the possibility of midspan flashover. The considerations are similar to those for tower flashover. The stroke current must be carried away by the ground wire and flashover will occur if the resulting voltage exceeds the air insulation strength from ground wire to phase conductors.

On many lines, midspan clearances required for mechanical reasons are such as to result in a negligible number of midspan flashovers, and for this reason, certain estimating methods consider tower flashovers only. However, for a general method intended to cover all cases, midspan flashovers must be included for in some cases they may be appreciable. It is the different treatment of these practical matters that has given rise to several distinct estimating methods.[4,5]

The authors recognize that the use of tower current data is the most direct and accurate approach to performance calculations of lines having about the same span length and midspan clearance as those on which the data were measured. However, to provide a general analysis applicable to the complete range of designs used in transmission practice, a more fundamental approach is necessary. This method is based on the stroke current, tower currents then being calculated for each different design. The stroke current is treated as independent of the terminating impedance which it strikes.

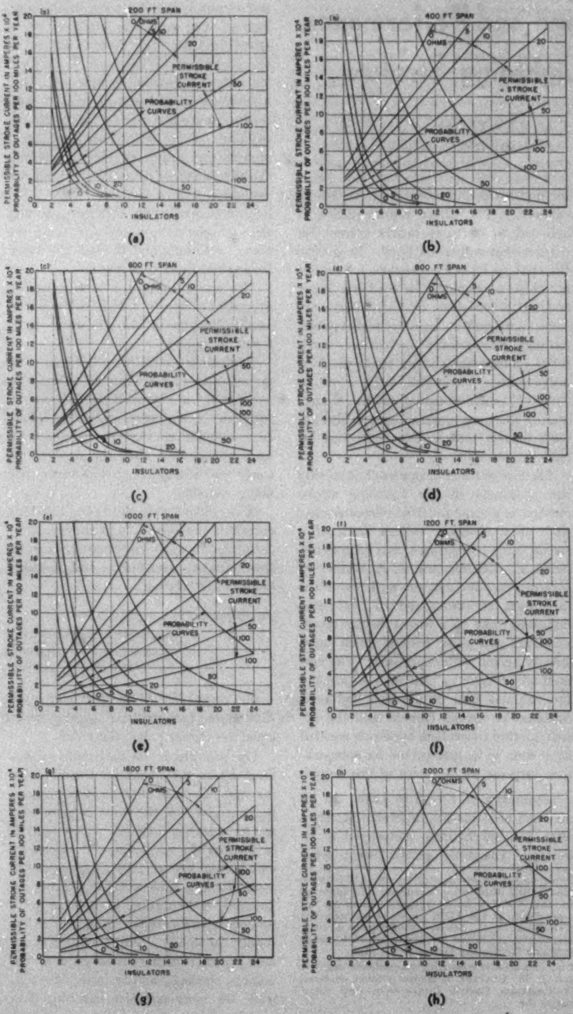

(a) (b) (c) (d) (e) (f) (g) (h)

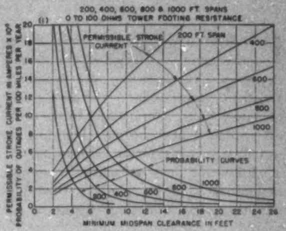

(i)

General Curves

It is evident from the foregoing discussion that the voltage to which the line

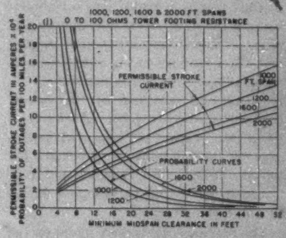

(j)

Figure 1. Curves for estimating line insulation and performance, based on 10-inch, $5^3/_4$-inch spaced suspension insulators, or equivalent, and an isoceraunic level of 30 storm days per year

The numerals on curves (a) to (h) indicate tower footing resistance, (i) and (j) length of span insulation is subjected depends on the following factors:

1. Stroke current magnitude and wave shape.
2. Tower footing resistance, and tower inductance.
3. Span length.
4. Line configuration including conductor spacings, height above ground, and so forth.

Using a typical line configuration and tower inductance and a 2-microsecond current wave, a general study has been made to determine the resulting voltages across the insulation at the tower and at midspan. The basis for the assumed parameters will be discussed later. This system was set up on the Anacom[8] (electric analog computer). The span length was varied from 200 to 2,000 feet and tower footing resistance from 5 to 100 ohms. This was done both for strokes entering at midspan and at tower. From the resulting potentials and wave shapes and the use of coupling factors taking into account corona, the stroke current required to cause flashover in each case was determined. These stroke currents are plotted in the general curves, Figure 1.

The probability of outage for a given case is simply the probability of stroke current in excess of that required to cause flashover. Figure 2 shows the stroke current probability curve used. The outage probabilities also are plotted in the general curves, Figure 1.

It will be noted that there are eight sets of probability curves, (a) to (h), giving outages for strokes to the tower for span lengths from 200 to 2,000 feet. Each set covers one span length giving the probability of outage as a function of number of insulators and the tower footing resistance for that particular span length. Where the insulation consists of wood or air in combination with porcelain the equivalent number of insulators should be determined as will be outlined subsequently. Each set of curves also gives the permissible stroke current as a function of the number of insulators and tower footing resistance. If more accurate stroke current probability data are available for the region being considered, these curves may be used.

Outage probabilities for midspan strokes are given in curves (i) and (j) of Figure 1 as a function of midspan clearance and span length only. This probability is substantially independent of tower footing resistance. For short spans the midspan flashovers would be slightly less than shown for any tower footings less than 100 ohms. However, for short spans the midspan flashovers shown are so low for practical spacings that this small reduction is unimportant.

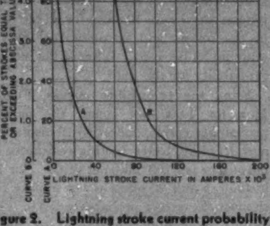

Figure 2. Lightning stroke current probability curve

Strokes per 100 miles of line per year for isoceraunic level of 30

Strokes to the line are assumed to be uniformly distributed along the line. It is further assumed that strokes within a quarter span length of the tower act as though at the tower, while strokes within a quarter span of the midspan act essentially like midspan strokes. Thus half the strokes are treated as strokes to tower and half are treated as strokes to midspan.

The probability curves, however, give the performance on the basis that all strokes are to tower, or all to midspan respectively. Thus it is necessary to average the two outage probabilities obtained from the tower and midspan curves respectively rather than add them. For a co-ordinated line, having equal probability of flashovers at the tower or at midspan either curve would give the complete outages for the entire line per hundred miles per year.

The probability curves are based on an isoceraunic level of 30 which denotes an average of thirty storm days per year. For other levels it is assumed that the outages will vary in direct proportion. An annual isoceraunic level map for United States is given in Figure 3.

The curves for estimating outages due to strokes to tower are based on a coupling factor corresponding to a 30-foot separation. For lower or higher separations the number of insulators should be corrected to allow for the corresponding change in coupling factor, the corrections being given in Figure 4. This correction is relatively unimportant for lines in the neighborhood of 132 kv, but becomes more important for the lower voltage lines such as 33 kv. The basis of this curve is given later.

On some lines the midspan clearance may be so high that even midspan strokes will cause flashover at the tower rather than at midspan. This can be determined by finding the permissible stroke current to tower and to midpsan. If the latter is more than twice the former, strokes to midspan can cause flashover at towers. In this case the outage probability for the line is the average of that corresponding to the permissible stroke current to tower and that corresponding to twice this stroke current. The resulting probability curve is given in Figure 5, the basis for which is stated in a subsequent section.

The general probability curves of tower outages have been plotted in terms of the number of $5^3/_4$-inch spaced insulators. Where other insulating media appear, they must be converted to equivalent insulators. The curves of Figure 6 provide a ready conversion from air or wood to equivalent number of insulators for estimating when more accurate data are not available. They are based on 100 kv per foot for wood and on the two microsecond time lag flashover values on $1^1/_2$—40 microsecond waves for air and for porcelain insulators. This wave shape is most representative of the tower-top potentials encountered. Conversions are discussed in greater detail later.

The probability curves are based on all

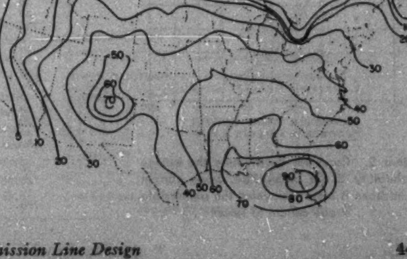

Figure 3. Annual isoceraunic map showing number of thunderstorm days per year

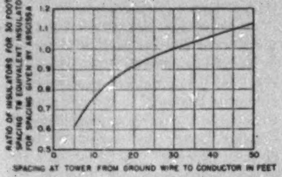

Figure 4. Correction factors for spacing at tower from ground wire to conductor

flashovers causing outages. All flashovers do not result in outages depending on the line insulation characteristics, and other factors. This reduction of outages is discussed in a later section.

Application of Curves. The use of the curves of Figure 1 in estimating the lightning performance of transmission lines will be illustrated by a few examples. The curves may be used for estimating the lightning performance of existing lines with various considered modifications. Or they may be used for estimating the insulation and midspan clearance required to obtain a desired lightning performance in the design of new lines. Because of the probabilities and assumptions involved the results should not be taken as rigorous. The chief value of the general curves lies in the facility provided for considering alternative designs on a comparative basis. A check of the estimating curves against a large amount of actual line experience does indicate quite good agreement.

Example I. A 220-kv steel-tower line, shielded by an overhead ground wire, located in a territory where the isoceraunic level is 50, has ten $5^3/_4$-inch spaced suspension insulators per string. The average span is 1,000 feet and the midspan clearance 24 feet. The tower footing resistances are 10 ohms for 20 per cent of the towers and 20 ohms for the remaining 80 per cent. What is the outage probability for this line?

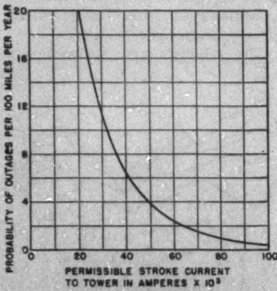

Figure 5. Curve for determining the outage probability if the permissible stroke current to midspan is more than twice the permissible stroke current to tower

From the probability curves, Figure 1(e), for 1,000-foot spans the outage probability corresponding to 10 insulators and 10 ohms tower footing resistance is 0.8 outage per 100 miles per year. For 10 insulators and 20-ohms tower footing resistance the outage probability is 3.0. The outage probability for strokes to tower along the entire line is (0.20 by 0.8) + (0.80 by 3.0) = 2.56 outages per 100 miles per year. The permissible stroke currents, Figure 1(e), to tower are 98,000 and 68,000 amperes for 10-ohms and 20-ohms tower footing resistances respectively.

From Figure 1(i) the outage probability is 1.0 outage per 100 miles per year for 1,000-foot spans with a midspan clearance of 24 feet. The permissible stroke current is 94,000 amperes.

The outage probability for strokes to tower and midspan is 1.78 outages per 100 miles per year for an isoceraunic level of 30; this is the average, (2.56 + 1.0)/2, of tower and midspan outage probabilities.

The outage probability for an isoceraunic level of 50 is 50/30 by 1.78 = 2.96 outages per 100 miles per year. This is the performance that should be expected of this transmission line.

Example II. A 33-kv wood-pole line, shielded by ground wire, located in a territory where the isoceraunic level is 30 has two $5^3/_4$-inch spaced suspension insulators per string. The minimum flashover path for any phase conductor is the porcelain plus 4 feet of wood. The average span is 200 feet and the midspan clearance 8 feet. The tower footing resistance is 50 ohms for all poles. The distance between ground wire and bottom phase conductor at the tower is 10 feet. What is the outage probability for this line?

From Figure 6, 4 feet of wood is equivalent to 2.6 insulators. The equivalent insulation of different insulating media may be added for estimating purposes. Thus the equivalent insulation is 4.6 insulators. Since the spacing from ground wire to conductor is considerably less than 30 feet, a correction is needed to compensate for the increased coupling. From

Table I. Computer Study Data

Span, Feet	Tower Footing Resistance, Ohms	Tower-Top Voltage per Unit of Stroke Current	Mid-Span Voltage per Unit of Stroke Current	Time Lag to Insulate (Microseconds): Insulator Flashover Characteristic Curves	Time Lag to Insulate (Microseconds): Rod Gap Flashover Characteristic Curves
200	5	11.6	27.5	2.0	2.0
	10	12.5	27.5	2.0	2.0
	20	16.3	28.5	2.0	2.0
	50	28.8	30.5	2.0	2.0
	100	45.0	40.5	2.0	2.0
400	5	13.2	45.0	2.0	2.0
	10	15.0	45.0	2.0	2.0
	20	21.0	46.5	2.0	2.0
	50	36.0	48.8	2.0	2.0
	100	57.5	56.3	2.0	2.0
600	5	14.0	65.0	2.0	2.0
	10	15.4	65.0	2.0	2.0
	20	21.5	67.5	2.0	2.0
	50	38.8	68.0	2.0	2.0
	100	64.0	72.0	2.0	2.0
800	5	14.0	86.0	2.0	2.0
	10	16.0	86.0	2.0	2.0
	20	22.0	87.5	2.0	2.0
	50	42.0	90.0	2.0	2.0
	100	72.0	92.5	2.0	2.0
1,000	5	14.0	110.0	2.0	2.0
	10	17.0	110.0	2.0	2.0
	20	24.5	110.0	2.0	2.0
	50	45.0	110.0	2.0	2.0
	100	75.0	113.0	2.0	2.0
1,200	5	14.0	125.0	2.0	2.0
	10	17.0	125.0	2.0	2.0
	20	24.5	125.0	2.0	2.0
	50	45.0	125.0	2.0	2.0
	100	75.0	130.0	2.4	2.0
1,600	5	14.0	158.0	2.0	2.0
	10	17.0	158.0	2.0	2.0
	20	24.5	158.0	2.0	2.0
	50	45.0	158.0	3.2	2.0
	100	75.0	158.0	3.2	2.0
2,000	5	14.0	167.0	2.0	2.0
	10	17.0	167.0	2.0	2.0
	20	24.5	167.0	2.0	2.0
	50	45.0	167.0	4.0	2.0
	100	75.0	167.0	4.0	2.0

Figure 4 the correction factor for a 10-foot spacing is 0.75. The effective insulation becomes 4.6/0.75 = 6.15 insulators.

From Figure 1(a) the outage probability for strokes to tower for 6.15 insulators and 50-ohms tower footing resistance is 12.6 outages per 100 miles per year; the permissible stroke current is 36,000 amperes.

From Figure 1(i) the outage probability for strokes to midspan for a 200-foot span with an 8-foot midspan clearance is 0.3 outage per 100 miles per year; the permissible stroke current is 120,000 amperes.

Since the permissible stroke current to midspan is more than twice the permissible stroke current to tower, strokes to midspan may cause flashovers and consequently outages at the tower. For this case, the outage probability is determined from Figure 5. The outage probability for a permissible stroke current to tower of 36,000 amperes is 8.0 outages per 100 miles per year. This is the outage probability assuming all lightning flashovers result in sustained power follow and trip-out. Since part of the insulating medium is wood, approximately 50 per cent of the flashovers will result in outages. Thus the outage probability is 0.50 by 8.0 = 4.0 outages per 100 miles per year for this line.

Example III. A transmission line is being constructed in a territory where the isoceraunic level is 30. The line will be shielded by ground wire and it is desirable to insulate the line so that outages due to lightning will be limited to 2.0 per 100 miles per year. A knowledge of existing lines in the territory indicates that tower footing resistances of 20 ohms can be obtained economically. Due to the choice of towers and conductors the average span will be 800 feet. The conductors and ground wire will be sagged to provide a midspan clearance of 18 feet. How many insulators are required to limit the outage probability to the desired number?

From Figure 1(i) the outage probability for strokes to midspan is 1.0 outage per 100 miles per year. The outage probability for strokes to tower must be 3.0 so that the over-all outage probability will be 2.0 outages per 100 miles per year. From Figure 1(d), the probability curves for 800-foot spans, nine insulators are needed for an outage probability of 3.0 when the tower footing resistance is 20 ohms. Thus nine insulators should limit the outage probability to 2.0 per 100 miles per year.

Basis for General Curves

Computer Study. To determine the tower-top and midspan potentials for strokes entering at those points respectively, a typical transmission line was set up on the electric analog computer.[6] Stroke currents were applied at tower and midspan and the corresponding potentials measured.

The computer set-up is shown in Figure 7, in which part (a) shows the line being represented and the stroke locations assumed. In part (b) is shown the analog or equivalent circuit of the transmission line, at the bottom, and the analog of the stroke, or surge current generator at the top. It will be noted that only the ground wire, tower, and footing constants are represented, the phase conductors having little effect on the ground wire potentials to ground caused by the stroke. Later the coupling is considered in determining the resulting voltage from ground wire to phase conductor.

In the operation of the Anacom, the forcing function which is the stroke surge current in this case, is repeated periodically so that the solutions, that is, the tower-top and midspan potentials, can be displayed on a cathode-ray oscillograph for observation and measurement. They are photographed for permanent records. Typical records of the stroke current waves and of the tower-top and midspan potentials are shown in Figure 8. Impedance in the transmission line analog are low compared with those in the current wave analog so that the line parameters can be varied over the desired range without altering the stroke current. In general, sufficient pi sections are used for the ground wire representation so that further subdivision has negligible effect on the results. Also a sufficient number of spans is represented so that further spans have a negligible effect. Advantage is taken of symmetry so that the line on only one side of the stroke needs to be represented.

The results of this study are summarized in Table I which gives the tower-top and midspan potentials per unit of stroke current, and the equivalent time lag referred to a $1^{1}/_{2}$—40 chopped wave.

Analysis Based on Computer Study. The outage probability curves were obtained from the results of the computer study in the following manner. To determine the insulators required to prevent flashover for any particular value of stroke current to tower the following relationship was utilized.

Insulation strength = stroke current × tower-top potential per unit stroke current × (1-coupling)

For this insulation strength the number

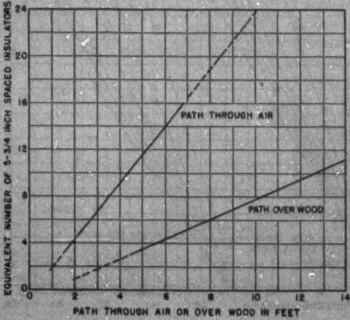

Figure 6 (left). Curves for converting wood and air insulating media to equivalent insulators

Figure 7 (right). (a) Lightning surging transmission line, and (b) current wave analog surging transmission line analog

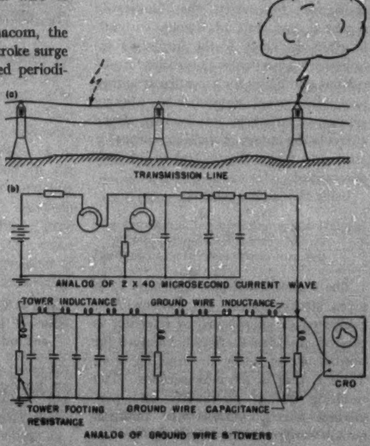

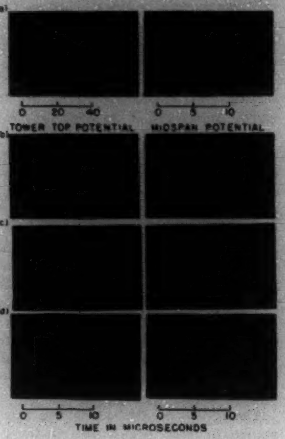

Figure 8(a). 2×40 microsecond current wave;

(b) typical tower-top and ground wire potentials, 1,000-foot span, 5 ohms tower footing resistance;

(c) 1,600-foot span, 10 ohms tower footing resistance; and

(d) 2,000-foot span, 100 ohms tower footing resistance

of insulators was then determined from the insulator curves of Figure 9, for positive waves using the time lag from Table I. The probability for this stroke current is given in Figure 2. Thus for a particular span length and tower footing resistance, for which the "tower-top potential per unit of stroke current" is given in Table I, the insulators required for a particular permissible stroke current and hence for a particular outage probability were determined. Making similar calculations for various stroke currents the outage probability curves for strokes to tower, Figure 1(a) to (h) were determined.

Using the similar relation,

Insulation strength required at midspan =
stroke current × midspan potential
per unit stroke current × (1-coupling)

The required midspan insulation for a given stroke current was obtained and converted to air spacing by referring to the rod gap characteristics, Figure 9 for positive waves, using the time lag from Table I, that is, 2.0 microseconds. The resulting outage probability and permissible stroke current for midspan strokes were plotted in Figure 1(i) and (j).

Stroke Current Magnitude and Wave Shape. The stroke current probability curve used is given in Figure 2. It is essentially that published by Waldorf[2] except that it has been modified slightly in the higher current region to allow for strokes up to 200,000 amperes which are known to occur from other field data. The reason for using these data rather than averaging other field data is that the figure of approximately 100 strokes per 100 miles per year for an isoceraunic level of 30, which is used to convert the percentage distribution curve to actual strokes per 100 miles exceeding certain values is based on these same data. However, for the more important high stroke current region, these data were in close agreement with the field measurements of stroke currents to wood pole lines.[7] A 2—40 microsecond current wave was used throughout this study as representative of the more severe lightning stroke currents of importance in estimating the lightning outages of transmission lines.

Ground Wires. The number of ground wires used to shield phase conductors is relatively unimportant as long as all conductors are properly shielded.

Figure 10 shows the relative positions of ground wire and phase conductors which permit 0.1 per cent exposure of the conductors. The general curves assume the shielding to be 100 per cent effective or that no strokes terminate on phase conductors. If the shielding[8] is inadequate strokes terminating on phase conductors must be added directly to the outages given by the general curves.

Consider a transmission line with two ground wires. Since strokes to midspan usually involve only one ground wire, the voltage across the insulation at midspan will be independent of the number of ground wires. For strokes to tower, the voltage across the insulation depends partly on the surge impedance of the ground wire and coupling between ground wire and conductor. Two wires in parallel have a lower surge impedance and higher coupling factor than a single wire; both of these factors tend to lower the voltage across the insulation. However, they are both minor factors as the voltage across the insulation depends principally on stroke current magnitude, tower inductance and tower footing resistance. Thus, the voltage across the insulation at tower will be slightly more for a line with a single ground wire than a line with two ground wires, other parameters being equal. For this reason, a transmission line with a single ground wire 1/2-inch diameter, 100 feet above the ground, having a surge impedance of 550 ohms is used for this study.

Towers. A separate study was made on the Anacom to determine the proper tower representation. The impulse value of tower footing resistance, on which the general curves are based, was represented by a linear resistor. For tower footings of 10 ohms or less the impulse value is only slightly less than the measured 60-cycle value and it is common practice to use the

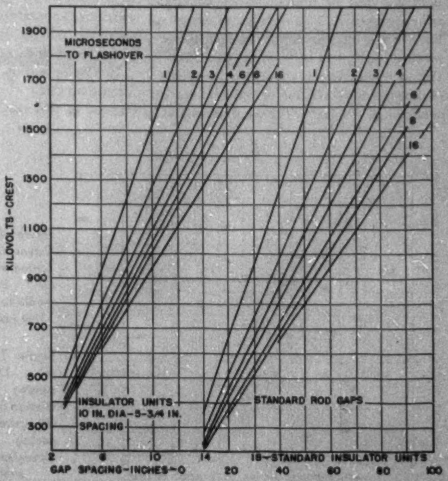

Figure 9. Characteristics of insulators and rod gaps

All values are based on positive waves and corrected to standard atmospheric conditions latter. For higher values the 60-cycle resistance should be converted[11,13] to the equivalent impulse value since the latter may be appreciably less than the former. The tower inductance of 20 microhenries, used throughout the study, was represented by inductance coils. This value represents a steel tower roughly 100 feet high assuming 0.2 microhenry per foot or a wood pole 50 feet high with a down lead taken as 0.4 microhenry per foot. Figure 11 shows the number of insulators required for different values of tower inductance. Tower capacitance to ground was neglected since it did not affect tower-top potential.

Coupling. The entire ground wire or tower-top voltage does not appear across the line insulation. A voltage is induced on the conductors of the same polarity as the ground wire voltage. The ratio of this induced voltage on the conductor to the ground wire voltage is the coupling factor. Thus, the voltage across the insulation is the ground wire voltage times (one minus coupling factor), neglecting normal frequency voltage.

Since coupling decreases as the distance from ground wire to conductor increases, the voltage across the insulator string of the conductor farthest from the ground wire will be greater than the voltages across the other insulator strings. This assumes that the ground wire and tower-top are at the same potential. A distance of 30 feet between ground wire and farthest conductor was assumed for calculating coupling factors.

The electromagnetic and electrostatic coupling factors are equal unless the effective radius of the ground wire is increased by corona, then the electrostatic coupling becomes greater and the electromagnetic coupling is believed to be unaffected. The coupling factor with corona considered is computed by the formula, coupling = $\sqrt{\text{electrostatic coupling} \times \text{electromagnetic coupling}}$; this is the geometric mean of the coupling factors.

The coupling is calculated by the equation

$$C = \frac{\log b/a}{\log \frac{2h}{r}}$$

where

C = coupling factor
b = distance from conductor to image* of ground wire
a = distance from conductor to ground wire
h = height of ground wire above ground
r = radius of ground wire

The electromagnetic coupling factor is calculated by using the actual radius of the ground wire, the electrostatic coupling factor is calculated by the same equation using the effective radius of the wire due to corona.

The effective radii of the ground wire due to corona are given by McCann.[9] The data in this paper are based on laboratory test with potentials up to 2,000,000 volts and then extrapolated so that the effective radii can be determined for potentials up to 6,000,000 volts. Using these effective radii the electrostatic coupling factors were calculated; the electromagnetic coupling factors were calculated using the actual radii. The geometric mean of these coupling factors was used in calculating the voltage across the insulation.

For strokes to midspan the ground wire voltage may exceed 6,000,000 volts. To determine the coupling for these higher voltages, the coupling factor versus voltage curves were extrapolated conservatively. The coupling increased with voltage to 7,000,000 or 8,000,000 volts and then remained constant for higher voltages. With this conservative extrapolation the coupling factors used for the higher ground wire voltages were not too large.

The Effect of Ground Wire to Conductor Spacing at Tower on Insulation Required. In calculating the coupling factors for the ground wire and phase conductor which is most likely to flashover, a 30-foot spacing was assumed. If the spacing is less than 30 feet the coupling factor will be larger, and consequently the voltage across the insulator string will be less. A means of correcting for the spacing is provided since a 30-foot spacing is not representative for all line configurations.

Coupling factors were calculated for spacings ranging from 5 to 50 feet for a particular ground wire potential. The voltage across the insulation and in turn the number of insulators required were determined. From this the ratio of insulators for a 30-foot spacing to the equivalent insulators for the particular spacing was determined. This was done for ground wire potentials ranging from 500,000 to 3,000,000 volts. The ratios were found to be almost independent of ground wire potential. Thus the average of the ratios for a particular spacing can be used irrespective of ground wire potential and not cause serious error.

These average values are plotted in Figure 4. By using the correction factor for the particular spacing, the general curves are applicable for all practical line configurations.

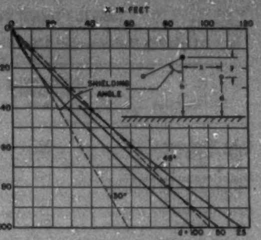

Figure 10. Configuration of shielding wire with respect to protected phase conductors for 0.1 per cent exposure

This correction factor also can be used for insulating the phase conductors so that all conductors have equal probability of flashover. The conductor nearest the ground wire will have the largest coupling factor and consequently the lowest voltage across the insulator string; thus fewer insulators can be used. If the insulation required for each phase conductor is determined in this manner, all phases have equal probability of flashover.

Tower Flashovers Due to Midspan Strokes. If the permissible stroke current to midspan is more than twice the permissible stroke current to tower, strokes to midspan may cause tower flashovers. Figure 5 provides a means of estimating the outage probability in such cases. This probability curve treats a current entering the tower through wire the same as a current of equal magnitude entering the tower through a stroke terminating on the tower.

This is not strictly true because the tower current will be reduced by reflected waves from both sides of the tower if the stroke is to tower. However, if the stroke is to midspan, the tower current will be reduced by reflected waves from one side of the tower only since the stroke channel is assumed to be of infinite impedance. However, this is a minor factor which can be neglected without causing serious error.

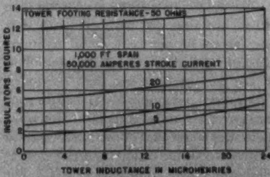

Figure 11. The effect of tower inductance on the number of insulators required

---

* The image of a wire is the same distance below the ground surface that the wire is above the ground surface.

Table II. Typical Values From the General Curves

Lightning Flashovers per 100 Miles per Year for an Isoceraunic Level of 30

Line Class	Tower Footing Resistance, Ohms	Span Length, Feet	Mid Span Clearance, Feet	Figure 1	Monteith[1]
33-Kv Wood pole	10	200	10	0.6	
BIL† = 700 kv	50	200	10	6.0	
Equivalent insulation = 7	10	400	12	1.1	1.5
5$^{3}/_{4}$-inch spaced insulators	50	400	12	9.5	4.0**
132-kv steel tower	10	600	16	0.6	1.0
BIL = 930-kv	50	600	16	5.0	2.5
Equivalent insulation = 10	10	1,000	24	0.9	1.2
5$^{3}/_{4}$-inch spaced insulators	50	1,000	24	7.6	3.5**
220-kv steel tower	10	1,000	24	0.5	0.7
BIL = 1,600 kv	50	1,000	24	2.0	1.5
Equivalent insulation = 18	10	2,000	30	1.2	1.4
5$^{3}/_{4}$-inch spaced insulators	50	2,000	30	3.7	3.4

† Basic insulation level.

** 6.8 for strokes to tower; 1.1 based on midspan, method not given for combining in case of noncoordination. Practice has been to average when estimates for tower and midspan not too far apart.

Wood and Air Insulating Media. For wood pole lines, the line insulation may be provided by a combination of porcelain, wood, and air. In this case it is necessary to find the equivalent number of insulators so that the general curves can be used. If the basic insulation level of the line is known, the equivalent number of insulators can be found from Figure 9. If not the probable flashover path must be determined. If the flashover path is through air or over wood, the equivalent number of insulators can be found from Figure 6. For estimating purposes it is sufficiently accurate to add the equivalent insulators of the different insulating media and use this value in the general curves.

Lightning Flashover and Power Follow. All lightning flashovers do not result in sustained power follow. The percentage of flashovers that result in power follow depends principally upon the type and length of the insulation path, the magnitude of the power follow current and the magnitude and duration of the lightning flashover current. Performance records[2] on various types of lines have yielded some data on the ratio of sustained power follow to flashover.

For the higher voltage, steel tower lines where the principal flashover path is in air, about 85 per cent of all lightning flashovers result in sustained power follow if the line length is less than 100 miles. The ratio is reduced to about 0.50 for such lines over 200 miles in length. For wood pole lines where part of the flashover path is over wood, the ratio of power follow to flashover ranges from 0.35 to 0.50. For 13- and 33-kv wood pole lines Ekvall[10] shows the sustained power follow to be a function of the length of flashover path divided by the normal frequency voltage.

If the characteristics of the line and line insulation result in a considerable reduction of the ratio of power follow to flashover, this should be considered in estimating the outage probability. To determine the outage probability taking this factor into account, multiply the ratio of power follow to flashover by the outage probability from the general curves. If the ratio is near unity, it can be neglected and the general curves will indicate a slightly pessimistic outage probability.

Experimental Verification. The general curves give results which are in accord with practically all of the published information on actual line performance. They are also in general agreement with the previous curves of Monteith except for the short spans and high-tower footings where some changes are required. In general it is known that 33-kv lines with basic insulation level of 700 kv and 10-ohms tower footing resistance result in two or three outages per 100 miles per year. The 132-kv lines of usual lightning-proof construction will have about one outage, and 220-kv lines with overhead ground wires and low-tower footings are practically lightningproof, having a small fraction of one outage per 100 miles per year.

Table II shows the predicted values from the new estimating curves for several typical cases, together with values from the earlier curves of Monteith. It will be noted that the new curves show slightly fewer flashovers for the more important case of 10-ohms tower footing. They indicate considerably more flashovers with high-tower footing since the stroke current treatment allows for no suppression of the stroke current by the high-footing resistance.

Conclusions

A method for estimating the lightning performance of transmission lines is presented. This method is based on the stroke current probability data and takes into account all the line parameters believed to affect the performance materially. The general curves with some auxiliary curves cover the complete range of transmission line designs.

The general curves may be used for estimating the performance of existing transmission lines or may be used for comparing the relative merits of changes proposed to improve the lightning performance of existing lines. The curves also may be used for estimating the insulation requirements of lines being designed for a predetermined lightning performance.

References

1. Line Design Based upon Direct Strokes, **A. C. Monteith.** Electrical Transmission and Distribution Reference Book (book), R. R. Donnelley and Sons Company, Chicago, Ill., 1942, pages 325–48.

2. Experience with Preventive Lightning Protection on Transmission Lines, **S. K. Waldorf** (Discussion, **C. F. Wagner, G. D. McCann**). AIEE Transactions, volume 60, 1941, page 702.

3. Lightning Surge Effects on Transmission Lines, **G. D. McCann.** *Electric Light and Power* (Chicago, Ill.), May 1945, pages 76–84.

4. Protection of Transmission Lines Against Lightning: Theory and Calculations, **L. V. Bewley.** *General Electric Review* (Schenectady, N. Y.), volume 40, April 1937, pages 180–88.

5. An Eight-Year Investigation of Lightning Currents and Preventive Lightning Protection on a Transmission System, **E. Hansson, S. K. Waldorf.** Electrical Engineering (AIEE Transactions), volume 63, 1944, May Section, pages 251–258.

6. A Large-Scale General-Purpose Electric Analog Computer, **E. L. Harder, G. D. McCann.** AIEE Transactions, volume 67, 1948, pages 664–73.

7. Lightning Investigations of 33-Kv Wood Pole Lines, **F. E. Andrews, G. D. McCann.** AIEE Transactions, volume 64, 1945. pages 768–77.

8. Shielding of Transmission Lines, **C. F. Wagner, G. D. McCann, G. L. MacLane, Jr.** AIEE Transactions, volume 60, 1941, pages 313–28.

9. The Effect of Corona on Coupling Factors Between Ground Wires and Phase Conductors, **G. D. McCann.** AIEE Transactions, volume 62, 1943, pages 818–26.

10. Minimum Insulation Level for Lightning Protection of Medium-Voltage Lines, **H. N. Ekvall.** . Electrical Engineering (AIEE Transactions), volume 60, 1941, March section, pages 128–32.

11. Impulse and 60-Cycle Characteristics of Driven Grounds, **P. L. Bellaschi.** AIEE Transactions, volume 60, 1941, pages 123–28.

12. Impulse and 60-Cycle Characteristics of Driven Ground—II, **P. L. Bellaschi, R. E. Armington, A. E. Snowden.** AIEE Transactions, volume 61, 1942, pages 349–63.

Discussion

P. L. Bellaschi (Consulting Engineer, Sharon, Pa.): Much in the way of labor and mathematics that normally would encumber a contribution of this character have happily been dispensed through the application of the electric analog computer. It would seem too that no excessive claims are made for the curves other than as a means of estimating purposes. In view of this and because of its simplicity and practical approach to the general problem, this paper by Harder and Clayton is well worthy of attention.

The following points have reference especially to the conditions surrounding the problem—for the end results are no better than the assumptions imposed. The basis of the analysis is summed up in the third paragraph under "General Curves." An examination of the curves in Figure 1 indicates that for 230-kv as well as 138-kv and 115-kv lines of usual design, the ratio of flashovers at midspan to tower-insulator flashovers is entirely on the high side. Referring to 230-kv design: 1,000-foot span, 32-to-36 foot clearances at midspan between line and ground conductors, 14 standard insulators and about 15-ohm tower footing resistance, according to the curves the relative flashovers at midspan and across the insulators at the tower are nearly the same. Field observations in general do not seem to bear this out. Because of the obvious practical difficulties, it could well be that midspan conductors have not been inspected in the past as diligently as at the tower position. To this we could add that long air spacings might be a factor in power quenching at midspan. Nevertheless, the high ratio of midspan to tower flashovers in the calculated curves very likely can be accounted in good measure from the assumptions imposed. One of these is that "a 2 by 40 microsecond current wave was used throughout the study as representative of the more severe lightning-stroke currents of importance in estimating the lightning outages of transmission lines." A second consideration affecting the results is the effect of the coupling factor between ground and line conductors at midspan and the fact that the data had to be extrapolated from 2,000,000 to 7,000,000 or 8,000,000 volts. Accordingly these assumptions bear further consideration. For instance, on the basis of average probability, a 2-microsecond front might in effect be too steep. Furthermore, there is some question as to whether the characteristics of the lightning stroke such as the surge impedance can be dispensed entirely.

It is clear that we do need more experimental data, especially in regard to coupling factors between conductors, up to possibly 8,000,000 or even 10,000,000 volts, and in regard to impulse sparkover for spacings 20, 30 and 40 feet. These as well as the related problems of grounds, power-quenching characteristics of wood and air, and so forth, can probably be settled economically and effectively in part through experimental work in the field conducted with portable lightning-stroke generators as it was indicated in the discussions at the Montreal summer meeting.[1]

It is well too to point out here that in estimating the lightning performance of a line due consideration has to be given to the distribution of lightning strokes along the entire length of the line, in the span and at the tower, to the effect of topography and terrain, and to similar factors. The significance to attach to Figure 3 is a matter that has to be weighed locally. To illustrate one instance, in a 230-kv line recently studied in some detail, practically all the strokes to the line were found to occur concentrated in two regions (creeks) which the line traverses, thus affecting only about 50 per cent of the total length of the line. Furthermore in this case the terrain plays a very important role.

In regard to the ratio of power follow to lightning flashovers, the paper gives a figure of 0.50 for lines over 200 miles in length. This figure, I would judge, is on the optimistic side insofar as it applies to high-voltage steel-tower construction. On the other hand, wood definitely offers possibilities of this order, and even greater advantage, as was discussed rather fully at a previous meeting.[1] Finally one can venture in saying—and this should not detract from the contribution under discussion—that in estimating line performance to lightning the method involving current in place of lightning voltage has been in use by the various investigators, Bell, Bewley, Waldorf, and others, in one form or another, for some time in the past.

Reference

1. Lightning and 60-Cycle Power Tests on Wood-Pole Line Insulation, P. L. Bellaschi. AIEE Transactions, volume 66, 1947, pages 838–50.

F. E. Andrews (Public Service Company of Northern Illinois, Chicago, Ill.): This paper is an especially timely step in progress of transmission line design because it brings practical field methods up-to-date to take into account the advances in knowledge and scope of application since Monteith's original work.[1] Extension to cover short-span wood pole lines is especially pertinent.

It may be of interest to report experience with shielding angle in relation to Figure 10.

In reference 7, the performance of 33-kv wood pole triangular construction with protector tubes on the pole top conductor (type III, Figure 9) is described. The x and y dimensions on Figure 10 for this construction are 4.6 feet and 6.2 feet respectively, which fall approximately on the $d=25$ foot curve, indicating good shielding. The operation of these lines has shown practically perfect shielding.

Figure 4, for coupling factor correction, makes use of the spacing at the tower between conductor and ground wire. It is assumed that the y dimension in Figure 10 also is intended to be taken at the tower. The question arises as to how differences in sag are taken into account. Were the curves based on average assumptions for midspan separation in relation to spacing at the tower, or is this difference unimportant?

Another question on which clarification seems desirable, is that of the wave shape used. It is stated that insulation flashover values and calculation of tower top potentials are based on $1^1/_2$ by 40 waves. In the section Stroke Current Magnitude and Wave Shape, reference is made to the use of a 2 by 40 current wave. An explanation to reconcile this apparent difference would be helpful.

Reference

1. See reference 1 of the paper.

L. V. Bewley (Lehigh University, Bethlehem, Pa.): The authors credit their associates, G. D. McCann and C. F. Wagner,[1] with having introduced the new method of using the lightning current, rather than the lightning voltage, as the parameter in calculating the lightning performance of transmission lines. In the opening paragraphs they speak of a still more fundamental approach leading to a general analysis in which the stroke current itself is used as a parameter. They also speak of their present paper as a refinement of Monteith's "complete set of estimating curves covering the full range of insulation levels, span lengths, and tower footing resistances encountered on transmission lines." May I point out that in reference 4 of the paper, which was published in 1937, and which itself was based on a previous paper, "Flashovers on Transmission Lines,[2]" I used the lightning current expectancy curve; gave the equations for placing all calculations on the basis of stroke currents, provided general formulas and estimating curves for strokes to towers and to midspan which included insulation, length of spans, coupling factors, tower footing resistance, and a factor to account for the effect of successive reflections; and in addition included the influence of the normal frequency voltage. The flashover equation given in reference 4 is

$$V=(1-C_s)\alpha R'I+e$$

in which

V = voltage across insulator
C_s = coupling factor (depends upon the number, configuration, and spacing of the conductors, and is modified by corona)
α = crest factor (depends upon the length of spans or the distance between expulsion gaps, tower footing resistance, lightning wavefront, and conductor surge impedance)
R' = effective resistance (depends upon the grounding resistance, and the surge impedance of the lightning stroke and of the stricken conductors)
I = lightning current which the stroke could deliver to a zero-resistance ground (which is equal to twice the traveling-wave current in the stroke)
e = effective instantaneous normal-frequency voltage (depends upon the normal-frequency polarities and the conductors involved)

Now the voltage at the stricken point is given by either $R'I$ or RI_B. But if we assume our lightning expectancy curve to be the total current delivered to all towers and ground wires we must use $R'I$. If, on the other hand, the expectancy curve refers to tower current only, then we have to use RI_B. But suppose this same stroke had hit a very high resistance ground. It would not deliver the same current. It is, therefore, highly preferable to base calculations on the current which the stroke could have delivered to a zero resistance ground, and to use a current expectancy curve with that understanding.

The authors include the inductance of the tower, but ignore the tower capacitance ". . . since it did not affect tower-top potential." Would the authors ignore the capacitance of the line conductors on the same basis? Actually the tower is a surge impedance of perhaps 100 ohms, and in the course of a few reflections (say, 0.5 microsecond) this surge impedance is wiped out, so that only the tower footing resistance remains. Since the crest of a 2/40 wave is substantially constant over a 0.5 microsecond interval, the tower surge impedance may be ignored. I believe the first to calculate the surge impedance of a tower was C. L. Fortescue.

The authors refer to G. D. McCann (reference 9 of the paper) for data pertaining to the effective radii of a ground wire with corona, and fail to state the origin of the geometric mean formula for the coupling factor with corona present. I believe the first to investigate the increase in diameter due to corona was E. M. Hunter.[3]

The minimum insulation of a line should be based on the maximum switching surge that can occur on the system, rather than on lightning surges (see Figure 4 and accompanying text in reference 4 of the paper). It is far cheaper to secure immunity from lightning by lowering the tower footing resistance than by increasing the insulation. A rule of thumb is "one ohm reduction in tower footing resistance is equivalent to one insulator disk."

REFERENCES

1. See references 2 and 3 of the paper.

2. FLASHOVERS ON TRANSMISSION LINES, L. V. Bewley. ELECTRICAL ENGINEERING, volume 55, April 1936, pages 342–54.

3. THE EFFECT OF CORONA ON GROUND WIRE PROTECTION, E. M. Hunter. *General Electric Review* (Schenectady, N. Y.), volume 33, February 1930.

E. L. Harder, J. M. Clayton: Andrews asks clarification of the use of the coupling-factor correction curve of Figure 4. This curve is used only for estimation of outages caused by strokes to the tower. Consequently it is the coupling factor at the tower which is being determined and the abscissa of Figure 4 refers to the ground wire to conductor spacing at the tower.

The estimating curves given for outages due to strokes at midspan involve midspan spacing from ground wire to phase wire as a parameter, see Figure 1, (i) and (j) and no single value was assumed for the midspan case. Hence no coupling factor correction curve is needed for the midspan estimates. The coupling factors used correspond to the actual midspan clearance with corona effect included.

Andrews' second question concerns wave shape. The 2—40 microsecond current wave was taken as most representative of the average severe lightning stroke current. With this wave introduced into the line the resulting voltage is not a 2—40 wave but is a complex shape dependent upon the impedances, reflections, and so forth. Typical resulting voltage waves are shown in Figure 8. The insulation is exposed to these voltages of complex shape and the problem is then to determine how much insulation is required to stand this voltage. The strength of insulating elements, wood, porcelain and air, is known and cataloged generally only for the $1^1/_2$—40s tandard wave. The strengths are known for full $1^1/_2$—40 waves and chopped $1^1/_2$—40 waves. The complex voltage wave must be converted to an equivalent standard wave so as to refer to the available data on insulation. There is no standardized way to make this conversion and the method adopted by the authors was based on a visual examination of the complex waves. As shown in Figure 8 they have the shape of chopped waves. We have therefore taken the equivalent chopped $1^1/_2$—40 wave as one which has the same crest value and has a chopping time corresponding to the time at which the abrupt drop takes place on the voltage oscillograms taken on the computer. These times vary somewhat from case to case and are given in Table I of the discussion. They are not less than two microseconds because no drop occurs as long as the surge current is rising, and are longer for high footing resistance with span above 1,000 feet. In these cases the reflections from adjacent towers are important and occur later than two microseconds.

At midspan the abrupt voltage drop corresponds to the cessation of surge current rise and is two microseconds for the 2-40 current wave used.

A careful analysis indicates that this relatively simple conversion of the experimentally determined voltage wave into an equivalent standard wave is as accurate as is needed or justified for this problem.

Bellaschi has raised a question regarding the relative number of midspan and tower flashovers predicted by the estimating curves. This is an important point and one which was given considerable study. His question applies to "230-kv as well as 138-kv and 115-kv lines of usual design". These we would like to discuss.

Consider first 230-kv lines. For a midspan clearance of 32 feet the curves give 0.2 flashovers per 100 miles per year based on half of the strokes occurring to midspan. They indicate that a stroke current of 116,000 amperes, occurring right at midspan is necessary to cause midspan flashover. This probability is extremely low which is in agreement with experience.

As to the experimental ratio of tower to midspan flashovers, two factors must be considered. First, more flashovers have occurred from lack of shielding than from insulation flashover by strokes contacting the ground wire on some 220-kv lines. For example, on the Pennsylvania Water and Power Company 220-kv lines "Three flashovers have occurred, two from lack of shielding, and one at a tower having a tower footing resistance of about 60 ohms."[1] The curves of Figure 1 predict only outages caused by strokes contacting the ground wires. All direct strokes to phase wires due to lack of shielding cause tower flashovers.

The second point is that some of the flashovers occur at towers where the footing is exceptionally high, and the case cited above is an example. In this case a stroke current of lower magnitude and far greater probability causes the outage and it is at the tower. The tower flashover probability can be considerably increased by a few towers of high footing, but the tower footing has very little influence on midspan flashover. Thus the only three cases of a flashover of these lines give no indication of the ratio of midspan flashovers to tower flashover for strokes contacting the ground wire on a line having a uniform 10-ohm tower footing. This probably explains the higher ratio of tower flashovers.

As pointed out in the paper total flashovers are the sum of those caused by lack of shielding and those caused by strokes contacting the ground wire. The latter are given by the general curves published in the paper and the former in reference 8 of the paper from which Figure 10 is derived.

Hansson and Waldorf[2] have analyzed a number of cases of midspan strokes of high current and have found that none caused midspan flashovers. These were cases in which large, substantially equal currents in two adjacent towers indicated the stroke to be to the ground wire of midspan. Lines from 66 kv to 220 kv were involved. These data are given in Table I of this discussion together with the midspan clearance required to prevent flashover according to the estimating curves given in Figure 1 (i) and (j) of this paper. Note that in 16 of the 17 cases the curves of the present paper also predict that the currents involved would not cause midspan flashover. Thus the curves are in good agreement with the Waldorf-Hansson data regarding the number of midspan flashovers.

Bellaschi questions the treatment of the characteristics of the lightning stroke and suggests the use of the stroke surge impedance. The constant current concept which assumes a high impedance stroke channel has been the basis for estimating line performance for a number of years and the authors believe this to be the best representation based on the present knowledge of the stroke channel. The stroke channel can be represented more accurately when more has been learned about it from field research.

Bellaschi points out that the distribution of lightning strokes along different lines varies depending on topography, terrain, and similar factors. This is quite true, but such considerations apply to a particular line and can not be considered in a general estimating method. The isoceraunic map of Figure 3 is the best available data for determining the average thunderstorm distribution neglecting minor factors that may influence a particular line.

Bellaschi questions the ratio of power follow to lightning flashovers of 0.50 for the steel tower lines over 200 miles in length.

Field data of this nature are quite incomplete and no attempt is made to cover this subject thoroughly in the paper. The subject is discussed in more detail in references 3 and 10 of the paper.

Bewley points out that in 1936 he published an estimating method based on the stroke current probability curve. The authors recognize that estimating methods based on lightning currents have been published previously. The general considerations of estimating method are discussed in the introduction of the paper.

Bewley's method is based on the stroke current which is taken to be dependent upon the terminating resistance. Also his method

Table I. Cases of High Midspan Stroke Currents Which Did Not Cause Midspan Flashover

Comparison of Actual Midspan Spacings with Those Required to Prevent Flashover According to the Estimating Curves of the Paper

Sum of Lightning Currents in Adjacent Towers[1]	Span Length in Feet[2]	Midspan Spacing Between Overhead Ground Wire and Nearest Line Conductor*	Minimum Midspan Spacing from Estimating Curves of This Paper
71,400	810	15.8	12.0
63,200	780	23.8	10.2
60,000	1,020	27.2	12.4
82,800	790	28.5	15.0
66,000	915	28.5	13.4
79,600	1,250	29.5	24.0
81,200	1,100	29.9	22.0
86,400	980	30.1	21.0
66,000	1,000	30.1	14.5
88,800	1,000	30.1	22.0
85,800	1,000	30.1	21.0
76,400	1,150	31.6	22.0
65,400	1,210	23.1	18.0
68,200	1,250	32.8	19.0
62,000	1,290	33.3	16.2
95,600	1,320	33.8	32.0
94,800	1,750	34.2	38.0*

* Only one case of flashover indicated by estimating curves.

requires the assumption and use of a stroke surge impedance.

The constant current method used in the paper assumes the stroke current to be independent of the terminating resistance. The authors do not believe this assumption results in appreciable error since the stroke current magnitudes recorded on lines of various tower footing resistances do not vary appreciably for the practical range of tower footings. Also the stroke current probability curve was obtained from strokes to transmission lines with tower footing resistances within the practical range. Thus no modification of the stroke current magnitude is needed for stokers terminating on lines with tower footings of the same order.

This method also assumes that traveling waves on the transmission line are not affected by the stroke channel. The velocity of the return stroke up the stroke channel is approximately one-tenth that of light. Thus the stroke channel behaves as a constant current source rather than a surge impedance.

Bewley states that "the tower surge impedance may be ignored." The study on the Anacom does not indicate this to be true.

For low (5 to 20 ohms) tower footing resistances, the tower top potential is increased appreciably by the tower inductance and can not be neglected. The tower capacitance was not ignored. It was considered and was varied from zero to the equivalent of several hundred feet of ground wire. Since it did not affect the tower top potential, it was eliminated from further studies.

The coupling factors measured by G. D. McCann are substantially the electrostatic coupling factors. The electromagnetic coupling factor is believed to be unaffected by corona and may be calculated by a conventional formula. With the electrostatic and electromagnetic coupling factors calculated independently, the coupling factors for practical considerations can be calculated from the equation given by Sunde[3] in his discussion of the McCann paper.

REFERENCES

1. TRANSMISSION OF ELECTRIC POWER AT EXTRA HIGH VOLTAGES, Philip Sporn, A. C. Monteith. AIEE TRANSACTIONS, volume 66, 1947, pages 1571–77.

2. See reference 5 of the paper.

3. THE EFFECT OF CORONA ON COUPLING FACTORS BETWEEN GROUND WIRES AND PHASE CONDUCTORS, G. D. McCann. Discussion, E. D. Sunde. AIEE TRANSACTIONS, volume 62, 1943, page 940.

Outage Rates of Steam Turbines and Boilers and of Hydro Units

AN AIEE COMMITTEE REPORT

THIS report makes available the forced outage data collected by committees of the Edison Electric Institute. It should promote an understanding of the definitions used in the collection of these data, which understanding is necessary if the data are to be properly used in calculations of system generating capacity requirements.

Part I, containing the steam turbine and boiler forced or emergency outage data collected by the Prime Movers Committee, Edison Electric Institute, was compiled by Philip Doane of the Consolidated Edison Company of New York, Inc.

Part II, containing comparable hydro unit data collected by the Hydraulic Power Committee, Edison Electric Institute, was compiled by E. S. Loane of the Pennsylvania Water and Power Company.

Part I. Forced Outage Rates of Steam Turbines and Emergency Outage Rates of Steam Boilers*

Classification of Outages in Edison Electric Institute Survey

The data collected apply to electric systems on which decreases in load at night and on Saturdays, Sundays, and holidays permit completion of all desired cleaning and minor maintenance work which can be postponed to such short intervals. All outages confined to light load hours of one day are excluded from the data. Outages on Saturdays, Sundays, and holidays have been given special treatment.

Outages widely controllable as to time of occurrence, which were or could have been postponed from one season to another, so that they could be fitted into the seasonal curve of load, were classified as scheduled turbine or overhaul boiler outages. These do not enter into the calculation of contingency reserve requirements; but many systems now find that capacity must be provided just to cover overhaul.

Boilers often require to be regularly cleaned and repaired once in every few months, so that provision for this must be made during the peak-load season regardless of time available in light-load seasons. Such outages, controllable as to time of occurrence within the cycle period of several months, which were or could have been postponed for several weeks were classified as boiler maintenance outages.

Maintenance outages can be scheduled to avoid encroaching on needed contingency reserves. On some systems they can be fitted into unused contingency reserve, while on other systems the amount of maintenance outage is so great that any emergency outage must be covered by additional reserve.

Work on turbines which could be confined to night-time light-load periods or to weekends is sometimes done for convenience during heavy load hours of weekdays. A transferable outage classification was provided for such cases.

All outages not covered by the foregoing classifications were considered to be forced turbine or emergency boiler outages. The separate tabulation of outage existing on weekdays made special classifications for "weekend work" unnecessary.

Turbine outages were also classified as chargeable to the turbogenerator unit, including its condenser and its own auxiliaries; or as chargeable to other cause, such as flood, bus failure, boiler or transmission line unavailability, or reconstruction to alter frequency or capacity as contrasted with rebuilding because of excessive failure rate.

Boiler outages were similarly classified as chargeable to the boiler, including its own piping and auxiliaries; or as chargeable to other cause, except that when a boiler was not operated because of turbine unavailability, the boiler was classified

Figure 1. Turbine weekday outage rates yearly 1939–1944 for units with pressure less than 1,000 pounds per square inch

Transferable outage, not separately shown, included in total

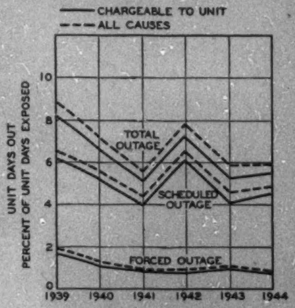

---

*Philip Doane.

Paper 49-112, recommended by the AIEE power generation and system engineering committees and approved by the AIEE technical program committee for presentation at the AIEE winter general meeting, New York, N. Y., January 31–February 4, 1949. Manuscript submitted November 16, 1948; made available for printing January 6, 1949.

This report was prepared by the AIEE joint subcommittee on application of probability methods to capacity problems.

Personnel of subcommittee: G. Calabrese, *chairman;* W. R. Blakeley, H. Duryea, R. G. Hooke, H. A. Lott, W. J. Lyman, K. W. Miller, H. W. Phillips, C. A. Roberts, H. B. Smith, H. P. St. Clair, G. M. Tatum, V. A. Thiemann, C. W. Watchorn.

as available but idle, rather than as out for other cause.

Reduction in boiler capacity by a major fraction because of mill or fan outage, and so forth was reported as partial outage. Reduced capacity operation of turbines was reported occasionally but was too infrequent to justify tabulation.

Questionnaires requested that when forced or emergency outages were extended to do general overhaul work, the time required for the forced or emergency repair be estimated and separated from the continuation as overhaul.

Provision was made for reporting days on which the turbine or boiler was operating, idle, or not installed.

The definitions for the various outage classifications were in general terms. (See Appendices I and II). In response to requests for some more definite if arbitrary demarkation, the following tabulation was included with the questionnaire instructions for reporting of 1941 and subsequent years:

	Criterion Postponability Approximately how long could outage have been postponed and rescheduled?	Criterion Predictability Is outage of kind for which advance provision is made as routine?	Classification
A–Turbogenerators			
	2 months or more		Scheduled
	Under 2 months		Forced
B–Boilers			
	2 months or more		Overhaul
	2 weeks to 2 months	Yes	Maintenance
	2 weeks to 2 months	No	Emergency
	Under 2 weeks		Emergency

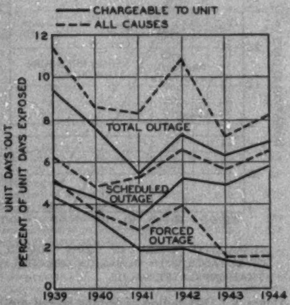

Figure 2. Turbine weekday outage rates yearly 1939–1944 for units with pressure 1,000 pounds per square inch or more

Transferable outage, not separately shown, included in total

Forced Turbine and Emergency Boiler Outage Rates

It has been assumed that turbine and boiler outage occurrences and outage times are proportional to the number of days on which the units operate. Thus, a day on which a unit started up and shut down twice, for a total of four hours of operation, is equated to 24 hours of operation without start-up or shutdown as a measure of the risk of outage. Use of the days on which a unit is in operation rather than of the hours in operation, or of the output per unit of capacity does give recognition to stresses in starting up and shutting down.

Summaries of the basic outage data are given in Tables I and II including data for all days as well as for weekdays. Figures 1 to 4, inclusive, show annual values of the several weekday outage rates. The small size of the annual sample for the high-pressure units is a factor in the variability of the corresponding outage rates.

For some calculations of capacity requirements the distribution of the outages according to length is a factor. Table III shows the summaries of the numerical details of these data and also the adjustment made to exclude an excessive number of "weekend" outages. The adjustment is made on the basis of the rate at which outages of three days or less occur, and are confined to weekdays. The summarized data for the entire period are shown graphically on Figures 5 and 7. Figures 6 and 8, respectively, show similar data, on an annual basis, for the low-pressure turbines and boilers.

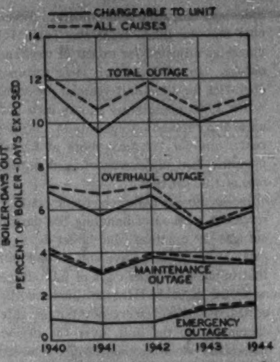

Figure 3. Boiler weekday outage rates yearly 1940–1944 for boilers with pressure less than 1,000 pounds per square inch, taking one day of partial outage as one-half day of full outage

The experienced unit-days of turbine forced outage chargeable to the unit in per cent of unit-days exposed (sum of

Table I. Summary-Performance of Turbine Generators for the Years 1939–1944 Inclusive. Unit-Days in Each Status

As Reported to Prime Movers Committee, Edison Electric Institute. Low-Pressure Turbines Operating at Pressure Less Than 1,000 Pounds per Square Inch with Capacity 20 Megawatts and Up,* and High-Pressure Turbines Operating at Pressure of 1,000 Pounds per Square Inch or More

	Total 1939–1944 Low-Pressure Units Only Weekdays† (1,521)	Total 1939–1944 Low-Pressure Units Only All Days (2,192)	Total 1939–1944 High-Pressure Units Only Weekdays† (1,521)	Total 1939–1944 High-Pressure Units Only All Days (2,192)
Number of unit-years reported on	2,148		253	
On forced outage chargeable to unit	4,531	7,581	1,099	1,818
On forced outage, other causes	762	1,637	485	868
On transferable outage	1,260	2,625	71	234
Sub-total on forced and transferable outage	6,553	11,843	1,655	2,920
On scheduled outage chargeable to unit	23,060	34,215	2,693	4,029
On scheduled outage, other causes	1,839	4,059	602	1,173
Sub-total on outage of all kinds	31,452	50,117	4,950	8,122
Available but not operated	42,341	92,768	494	1,793
Not installed	7,662	10,990	3,289	4,711
Total—not in operation	81,455	153,875	8,733	14,626
In operation	463,164	630,894	55,458	77,808
Total—unit-days	544,619	784,769	64,191	92,434

*Including units somewhat under 20 megawatts; 1 in 1939, 3 in 1940, 1 in 1941, 1 in 1942, 1 in 1943 and 1 in 1944.

†Weekdays exclude Saturdays, Sundays, and major holidays.

Note: Partial turbine generator outages neglected.
Table covers only status during heavy load hours of day.

unit-days operating and unit-days forced out) may be taken from the Table III values as adjusted for excess of weekend outage. In 1939 through 1944 turbines operating for 2,148 unit-years at pressures below 1,000 pounds per square inch had an average forced outage rate of 1.00 per cent; and for 253 unit-years at higher pressures had an average forced outage rate of 1.96 per cent.

In calculating boiler emergency outage rates one method of handling the partial outages is to treat the boiler-days of partial outage as equivalent to one-half that number of boiler-days of full outage as shown in Table III. On this basis the adjusted average emergency outage rate chargeable to the unit, over the period 1940–1944 inclusive, is 1.06 per cent for 1439 boiler-years operating at pressures under 1,000 pounds per square inch, and is 1.94 per cent for 351 boiler-years at the higher pressures.

Discussion

A classification of turbine outage different from the one employed for this report has long been in use by the Prime Movers Committee of the Edison Electric Institute and its predecessor. This older classification primarily distinguished outage during hours when the unit should have been in operation for best efficiency or for capacity needs, known as demand time, from outage during hours when the unit would not have run if it had been available, known as nondemand time. Since the speed with which repair work confined to nondemand time is done has no direct effect on the ability of the system to carry load or on its efficiency, some operators feel that nondemand outage should be excluded in calculating unit availability.

The contrast between demand outage and forced outage may be shown by the following cases. Assume two identical pairs of units, one pair of high efficiency, and the other pair of lesser efficiency. Load conditions are such that two units are needed, preferably the pair of high efficiency. Under the older classification of outages, if one of the higher efficiency units suffered an outage due to a broken shaft, such outage would be a demand outage. If one of the less efficient units suffered a similar outage, such outage would have been classified as a nondemand outage. However, under the classification used in this report, both units are on forced outage since there is no possibility of postponing the outage.

Now, suppose that, while there is nothing specifically indicating that the units could not go on running for another year without trouble, past experience suggests that, in the time since their last overhaul, blade erosion has progressed to a point making replacement desirable. Suppose further that the units are scheduled to be taken out of service at a time

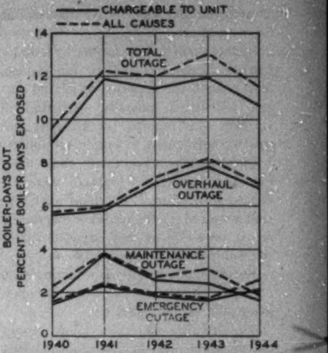

Figure 4. Boiler weekday outage rates yearly 1940–1944 for boilers with pressure 1,000 pounds per square inch or more, taking one day of partial outage as one-half day of full outage

Table II. Summary—Performance of Boilers for Years 1940–1944 Inclusive. Boiler-Days in Each Status

As Reported to Prime Movers Committee, Edison Electric Institute. For Boilers with Capacity of 200,000 Pounds of Steam per Hour or More.* Low-Pressure Boilers Operating at Pressure Less Than 1,000 Pounds per Square Inch and High-Pressure Boilers Operating at Pressure of 1,000 Pounds per Square Inch or More

		Total 1940–1944			
		Low-Pressure Units Only		High-Pressure Units Only	
		Week-days ϕ (1,269)	All Days (1,827)	Week-days ϕ (1,269)	All Days (1,827)
Number of boiler-years reported on		1,439		351	
On emergency outage, chargeable to boiler	Full	2,830	4,563	1,289	2,026
	Partial	1,157	1,728	348	481
On emergency outage, other cause	Full	136	243	119	216
	Partial	84	119	1	3
On maintenance outage, chargeable to boiler	Full	10,392	18,824	1,771	4,294
	Partial	1,253**‡	1,599**‡	151	255**
On maintenance outage, other cause	Full	489	980	240	486
	Partial	22	29**	18	32
Sub-total on emergency and maintenance outage		16,363	28,085	3,937	7,793
On overhaul outage, chargeable to boiler	Full	18,699	26,689	5,050	7,265
	Partial	127†	174**†	22	33
On overhaul outage, other cause	Full	1,175	1,746	166	274
	Partial	50	65	0	0
Sub-total on outage of all kinds		36,414	56,759	9,175	15,365
Available but not operated (excluding partial)		10,342	19,530	624	1,667
Not installed		6,141	8,806	4,197	5,990
Total not in full operation		52,897	85,095	13,996	23,022
In operation (excluding partial operation)		312,337	440,721	75,114	105,218
Total boiler-days		365,234	525,816	89,110	128,240

*Including low-pressure boilers with capacity somewhat under 200,000 pounds per hour: 9 in 1940; 11 in 1941; 11 in 1942; 10 in 1943 and 10 in 1944.

ϕ Weekdays exclude Saturdays, Sundays and major holidays.

**—Exclusive of boiler-days also reported as partial emergency outage chargeable to boiler.

†—Exclusive of boiler-days also reported as partial maintenance outage chargeable to boiler.

‡—Exclusive of boiler-days also reported as double partial maintenance outage chargeable to boiler.

Note: Table covers only status during heavy load hours of day.

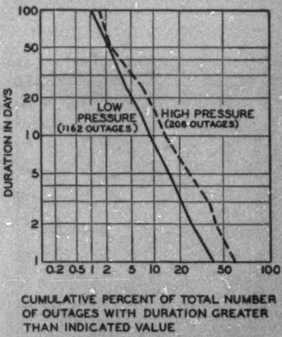

Figure 5. Distribution of turbine forced outage chargeable to unit according to duration, after adjustment to eliminate excess of weekend outage—turbines with pressure less than 1,000 pounds per square inch compared with turbines with pressure 1,000 pounds per square inch or more

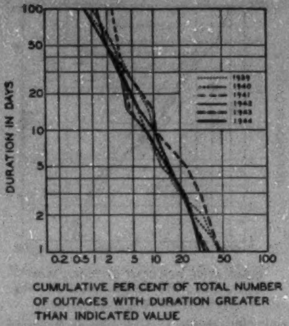

Figure 6. Distribution of turbine forced outages chargeable to unit according to duration, after adjustment to eliminate excess of weekend outage—turbines with pressure less than 1,000 pounds per square inch year by year

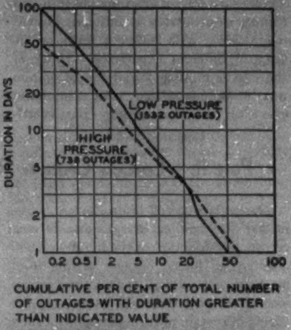

Figure 7. Distribution of boiler emergency outages chargeable to boiler (full plus partial) according to duration, after adjustment for excess of weekend outage—boilers with pressure less than 1,000 pounds per square inch, compared with boilers with pressure 1,000 pounds per square inch or more

when one unit of each pair can be out while still leaving a surplus of capacity over all requirements, and, that if available two of the four units, preferably the two most efficient would run. Then as before the more efficient unit will be out when in demand and the other will be out when not in demand. But in this case both outages are scheduled rather than forced, since they are taken when convenient.

Outage does not fall into the scheduled class merely because it is possible to postpone it for a few hours while replacement capacity is started, or because it happens to occur at a time when it falls within a surplus of available capacity over that wanted to cover load and all the reserve desired to meet contingencies. The essential feature is that the outage be of a kind that can be postponed for a length of time which would suffice, if the outage occurred at any time of the year, to allow the outage to be fitted into the overhaul schedule. The definition of nonforced outage used by the Hydraulic Power Committee of the Edison Electric Institute requires that the outage be postponable to a previously scheduled normal maintenance period for the unit, or for some other unit for which it might be substituted (or that the outage be confinable to night time or weekend periods). In this definition the required delay is variable with the circumstances of the case. Whether in the interest of uniformity a fixed period be preferable is a matter of opinion.

Valid criticism of the classification rests upon the use of an opinion as to what might happen for the basis of classification.

The criterion of time postponable is necessarily an estimate, even though it may rest on facts as to nature and amount of damage found in the actual repair.

Table III. Distribution of Certain Turbine Generator and Boiler Outages by Length, With and Without Adjustment for Excess of Short Outages on Weekends. For Outages Terminating in Period

Outages Chargeable to Unit Only

Outage Duration in Days	Turbine Forced Outages Full 1939–1944				Boiler Emergency Outages Full Plus One-Half of Partial 1940–1944				Boiler Maintenance Outages Full Plus One-Half of Partial 1940–1944			
	Pressure Less Than 1,000 Lb. per Sq. In.		Pressure 1,000 Lb. per Sq. In. or More		Pressure Less Than 1,000 Lb. per Sq. In.		Pressure 1,000 Lb. per Sq. In. or More		Pressure Less Than 1,000 Lb. per Sq. In.		Pressure 1,000 Lb. per Sq. In. or More	
	Actual	Adjusted	Actual	Adjusted	Actual	Adjusted	Actual	Adjusted	Actual	Adjusted	Actual	Adjusted
1	1,412	666	145	78	940½	664	278	252½	2,659½	1,047	497	96
2	363	178	113	30	408½	278	199½	166½	1,757	615	651½	72½
3	92	62	25	10	147	88½	101	71½	567½	394½	139	53
4	47	47	17	17	68	68	59	59	294½	294½	71½	71½
5	30	30	12	12	57½	57½	38½	38½	231	231	49	49
6–10	75	75	23	23	115	115	52½	52½	509	509	85½	85½
11–15	26	26	7	7	24½	24½	12½	12½	180	180	30	30
16–25	29	29	7	7	20	20	7½	7½	123	123	28½	28½
26–50	24	24	10	10	15½	15½	3½	3½	27	27	5	5
51–100	13	13	2	2	6	6	½	½	1½	1½		
101 up	12	12	3	3	½	½						
Total number of outages	2,123	1,162	364	208	1,803	1,337½	752½	664½	6,350	3,422½	1,557	491
Unit-days of outage**	7,803	6,597	1,810	1,550	5,417½	4,704½	2,243½	2,063½	19,674½	15,259	4,439½	2,622½
Outage-days prior to period, in above**	360	360	150	150	96½	96½	16	16	119	119	41½	41½
Outage-days in period, excluded above**	138	138	158	158	106	106	39	39	141	141	24½	24½
Outage-days in period**	7,581	6,375	1,818	1,558	5,427	4,714	2,266½	2,086½	19,696½	15,281	4,422½	2,605½
Average duration of one outage: days	3.7	5.7	5.0	7.5	3.0	3.5	3.0	3.1	3.1	4.4	2.9	5.3
Days of full operation in period	630,894	630,894	77,808	77,808	440,721	440,721	105,218	105,218	440,721	440,721	105,218	105,218
Days exposed in period‡	638,475	637,269	79,626	79,366	446,148	445,435	107,484½	107,304½	460,417½	456,002	109,640½	107,823½
Days exposed per outage‡	301	548	219	382	248	333	143	161	72	133	70	220
Number of unit-years	2,148*		253		1,439†		351		1,439†		351	

*Including turbines somewhat under 20 Mw. capacity; 1 in 1939, 3 in 1940, 1 in 1941, 1 in 1942, 1 in 1943, 1 in 1944.

†Including boilers somewhat under 200,000 lb. per hour capacity; 9 in 1940, 11 in 1941, 11 in 1942, 10 in 1943, 10 in 1944.

**Including one-half total days of partial outage.

‡Days of full operation plus outage-days, including one-half of total partial outage-days, for kind of outage considered.

There is no way of ensuring absolute uniformity of estimates by different individuals dealing with different units on the basis of different experience. However, the effects of such variations of opinion tend to be neutralized, with a minimum effect on the final results, particularly when a large amount of data is available. It is felt, therefore, that useful results are obtainable for which any deviations that may exist are hardly of sufficient magnitude to have any practical or significant effect on the results obtained by use of these data.

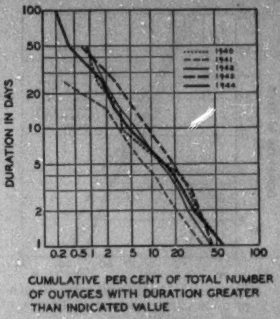

Figure 8. Distribution of boiler emergency outages chargeable to boiler (full plus partial) according to duration after adjustment for excess of weekend outage—boilers with pressure less than 1,000 pounds per square inch year by year

Part II. Forced Outage Rates of Hydroelectric Units*

The reliability of hydroelectric units, insofar as their capacity value is concerned, is a function of the frequency and duration of forced outages arising from mechanical, electrical, or structural failure associated with the units as well as the effects of certain natural phenomena such as low river flow, floods, and ice. This report is concerned only with those outages arising from the failure of the unit itself and which may be typical of all hydro units of the same general type. It is to be expected that the forced outage rate for hydroelectric units would be smaller than for steam-electric generators. In some cases the forced outage rate may be so low as to be negligible in comparison with probability of low-load carrying capability due to drought, floods, ice, or other natural causes, or it may be overshadowed by required outages for maintenance. These factors of river flow and temperature are peculiar to each system and have no significance as averages for a large number of hydro sites; but in most any case the data here reported will provide a reasonable basis for the consideration of hydro unit forced outages in an investigation of system generating capacity requirements.

The forced outage definition used here is essentially the same as that employed in the questionnaire on steam turbine outages. Much of the discussion in Part I of this report, relating to the distinction between different types of outage, is applicable to the data on hydro units. Although it is unnecessary here to supplement the comments and instructions which accompanied the hydro unit questionnaire and which are shown in Appendix III, one difference in the basis of outage rates should be noted.

It is to be expected, all other conditions being equal, that the occurrences of hydro unit forced outage will be approximately proportional to the time of unit operation. Because this quite reasonable assumption can be made with respect to forced outages of hydro units, their operating time and outage time have been reported in hours.

For steam units, however, a different assumption and basis of analysis was necessary. Because the strains of starting and stopping steam equipment are severe, it was felt that time alone was not a fair measure of the hazard of forced outage. It was initially assumed, and later supported by analysis of the steam unit data, that the number of days on which units operated was a more nearly correct measure of exposure than hours of operation.

Consistent with this measure of exposure, outage time was counted only in whole days, forced outage for any interval during the heavy load hours in a calendar day being considered as a day's outage. To provide hydro data on a basis comparable with that used for steam units, the over-all outage rate for hydro units has been determined on this whole day basis as well as on the actual hourly time of operation and outage.

Response to Questionnaire

The collection of forced outage data for hydroelectric units was undertaken in 1941, when a brief questionnaire was distributed to selected utilities in the United States and Canada. General distribution of the questionnaire was made only once; but the recipients were requested to report their forced outage experience for as many years as possible. A number of companies supplied the desired information for several years, some covering the entire experience of their hydro plants. A few utilities have continued to accumulate the outage data and have reported them to the Hydraulic Power Committee of the Edison Electric Institute, from time to time.

Although the study was undertaken at a time when questionnaires were in disfavor, and was not followed up in successive years, the response was sufficient to provide satisfactory indication of over-all outage rates. Data were not adequate, however, for analysis of outages by year of operation, or by size, type, or age of unit. Over 80 per cent of the reported data were for Francis units, the reports for Pelton and Kaplan wheels, being insufficient for separate analysis, were used in the computation of the over-all results.

Contributions of data, covering about 20 per cent of the installed hydro capacity in the United States and Canada, were received from 31 companies, 93 plants, and for 335 units with total capacity of 4,500,000 kw.

Forced Outage Data

The over-all results of the study, analyzed on both the hourly and daily basis are shown in Table IV.

On the whole-day basis the average duration is approximately 0.8 day longer than on the hourly basis, but the per cent outage time remains approximately the same.

The durations of individual forced outages also have been analyzed on the whole-day and actual-time bases. It has not been considered necessary to show hours of outage for durations above 72 hours since such a fine measure for the longer outages would have little significance.

Table IV

	Actual Time (Hourly Basis)	Whole-Day Basis
Unit years of record	1,448	1,448
Time of operation	9,292,300 hours	464,282 days
Forced outage time	42,559 hours	2,020 days
Exposed time	9,334,859 hours	466,302 days
Number of outages	297 hours	297 days
Forced outage in per cent of exposed time	0.46 hour	0.43 day
Average duration of outage	143 hours	6.8 days

---

*E. S. Loane.

Table V. Distribution of Outages by Duration

Hours	Outages	Days	Outages
1	57	1	161
2–4	41	2	34
5–7	25	3	14
8–12	28	4	17
13–24	27	5	8
25–36	14	6–10	24
37–48	5	11–15	11
49–60	11	16–25	9
61–72	9	26–50	10
		51–100	6
above 72	80	over 100	3
Total	297		297

The data shown in Table V include all weekend outages that were reported. Some companies reported such outages as forced, some did not. Analysis of the reported 1- and 2-day outages indicates that those occurring on weekends were somewhat less frequent (as they should be) than those occurring on Monday to Friday, inclusive. No adjustment, parallel to that made in steam unit data, was considered necessary for the hydro units.

An adjustment of the weekend outages, to eliminate them entirely or to approximate the number that should have been reported, would have insignificant effect on the outage rate. Because these are practically all 1-, or sometimes, 2-day outages, they do affect slightly the average duration, but would change the per cent forced outage time by less than 0.01 per cent.

Conclusion

The data presented are basic to determinations of system capacity requirements by probability computations. Applications have been discussed in other publications, particularly in a group of papers[1–4] presented at an AIEE meeting in November 1947. It is hoped that the material presented herein, as well as in these earlier papers, will be of service to those engineers engaged in studies of system capacity requirements, and should be a basis for more extensive use of such methods in the solution of system capacity problems.

Attention has been called to the fact that too few data are available for large, modern high-pressure steam turbines and boilers and for certain types of hydro units. General knowledge of the availability of data such as these and their usefulness in the industry should facilitate the future collection of such needed information. The outage rates reported in Table IV are not necessarily fixed quantities, and it would be desirable to collect further data at reasonable intervals.

Appendix I. Graphic Questionnaire. Summary System—Daily Record of Steam Turbine Operation and Outage[*]

Turbine Subcommittee, Prime Movers Committee, Edison Electric Institute

Reported Outage. In the analysis of reserve problems it is evident that only outages which reduce the margin between the daily peak load and the installed capacity need be considered. Any deficiencies in installed boiler capacity should be disregarded in figuring this margin between load and capacity. In general, any outage, regardless of length, that occurred or existed during the peak portion of the day is to be counted as one full day of outage, while an outage which was confined to off-peak hours of the day should be disregarded. An exception is an off-peak outage which has reduced the margin below that of the peak, so that it should be counted. Cases of successive nonoverlapping outages on the same day will have to be covered by remarks on the reverse side of the sheet. Outage days should be classified as described below.

Reduced Capacity Operation. Cases in which units either after or in anticipation of failure were repaired or altered for temporary operation at materially reduced capacity will have to be handled as remarks, giving capacity loss and dates. Remarks should be written on the reverse side of the form sheet.

Transferable Outage. Occasionally, on systems having a temporary superabundance of reserve capacity, units may have been out during the peak hours of weekdays for work which if the reserve had been normal could and would have been transferred and *confined* to off-peak hours of the day or to a nearby weekend or holiday period. These outages are classed as transferable. Evidently this classification is applicable only to 1-, 2- or at most 3-day outages that occurred on weekdays.

Scheduled Outage. A scheduled outage is one widely controllable as to time of occurrence so that it might have been or was postponed from one season to another, or even to another year. Such outages will usually have been planned months in advance. Annual overhaul is a typical scheduled outage. Scheduled outages are further classified as due to the unit (turbogenerator, condenser, and own auxiliaries); or as due to other cause such as: boiler, station or system rearrangement; or reconstruction of a unit to increase capacity, change frequency, and so forth as contrasted with reconstruction because of an excessive failure rate.

Forced Outage. All reported outages other than transferable or scheduled outages are classed as forced outages. Typically a forced outage is one due to causes requiring that the unit be taken out of service at once or within a few weeks, excepting transferable outages. Outages on weekends and holidays will be given separate treatment in the analysis of the returns; so that forced outages which were postponed to such days should be reported in the same way as any others. Forced outages are further classified as due to the unit (turbogenerator, condenser, and own auxiliaries) or as due to other causes such as boiler or transmission line unavailability, flood, bus failure, and so forth.

Combined Forced and Scheduled Outage. In certain cases of long forced outage the opportunity may have been utilized to schedule necessary overhaul work at the same time. The total duration of the outage may then have been determined by the overhaul. Since the primary interest of this questionnaire is forced outage, it is requested that in such cases the approximate outage time which would have been required without the overhaul be marked as forced outage and the remainder as scheduled outage.

Days Operated. If on any given day a unit was in service, that is, actually operated with switches closed to station bus for any length of time, however short, one full day of operation should be counted, unless a reported outage as defined above occurred on the same day.

Days Not Installed. Days prior to initial operation or following retirement of a unit should be marked days not installed. Days on which the generator was left uncoupled for operation as a synchronous condenser should also be marked days not installed.

Days Available But Not Operated. Obviously the days remaining after identifying outage days, days operated, and days not installed are days available, but not operated.

Treatment of Compound Units. In the case of 3-element cross-compound units; if the elements are regularly arranged so that the unit can be operated with any one element out, the elements should be reported as separate units.

Appendix II. Graphic Questionnaire. System Summary—Daily Record of Steam Boiler Operation and Outage[*]

Boiler Subcommittee, Prime Movers Committee of Edison Electric Institute

Boiler Unit. The boiler unit will be considered to include all components, fittings, piping, ducts and auxiliaries except those used or designed to be used in common with other boilers. Only boilers large enough to be important in fixing reserve requirements are included, the minimum size being set at 200,000 pounds per hour.

Reported Outages. In the analysis of reserve problems it is evident that only outages which reduce the margin between the daily peak load and the installed capacity need be considered. Thus in general any outage, regardless of length, which existed or occurred during the peak load portion of the

---

[1] For numbered references, see Bibliography at end of paper.

[*] Appendix I is a portion of the Explanatory Notes which accompanied the questionnaire sent to the reporting companies.

[*] Appendix II is a portion of the Explanatory Notes which accompanied the questionnaire sent to reporting companies.

day should be counted as one full day of outage, while an outage which was confined to off-peak hours of the day should be disregarded. Unavailability of turbines or load for the boiler does not constitute a boiler outage. Cases of successive nonoverlapping outages on the same day will have to be covered by remarks on the reverse side of the sheet. Outage days should be classified as described below.

Partial Outage. Where outage of some component, such as a mill or a fan, results in reducing capacity by a major fraction, as one half or one third, that outage should be reported as a fractional capacity outage in the manner indicated on the form. Cases in which boilers either after or in anticipation of failure were repaired or altered for temporary operation at materially reduced capacity also should be reported as partial outages.

Overhaul Outage. An overhaul outage is one widely controllable as to time of occurrence so that if desired it might have been or was avoided during the peak load season of the year. Such outages will generally have been scheduled months in advance. Overhaul outages are further classified as due to unit, for example, for renewal or repair of components or for correction of defects of the boiler itself or of its own auxiliaries; or as due to other cause, such as station rearrangement or alteration to increase capacity or to change the type of combustion equipment, and so forth.

Maintenance Outage. A maintenance outage is one which cannot be postponed from one season to another, but which can be assigned in advance so as to maintain an even or a minimum amount of simultaneous outage, or to utilize weekend time. Maintenance outages are further classified as due to unit or to other cause. A typical maintenance outage due to unit might be renewal of stoker parts or of furnace refractory in anticipation of failure; while one due to other cause might be replacement of a steam header valve beyond the boiler stop valve.

Emergency Outage. All reported outages other than overhaul or maintenance outages are classed as emergency outages, including in particular all cases which require a boiler to be taken out within a few hours and also those unforeseen outages of long duration which had not been regularly provided for in the normal maintenance schedule. Emergency outages are further classified as due to unit or to other cause. A typical emergency outage due to unit might be a tube rupture or the failure of the fan drive. An emergency outage due to other cause might result from failure of feedwater or coal supply.

Combined Emergency and Overhaul Outage. In certain cases of long emergency outage the opportunity may have been utilized to schedule necessary overhaul work at the same time. The total duration of the outage may then have been determined by the overhaul. Since the primary interest of this questionnaire is emergency outage, it is requested that in such cases the approximate outage time which would have been required without the overhaul be marked as emergency outage and the remainder as overhaul outage.

Days Operated. If on any given day a boiler was burning fuel for any length of time, however short and whether banked or steaming, one full day of operation should be counted unless a reported outage as defined above occurred on the same day.

Days Not Installed. Days prior to initial operation or following retirement of a boiler should be marked days not installed.

Days Available. Obviously the days remaining after identifying outage days, days operated, and days not installed, are days available but not operated. Days available will include days laid up.

Appendix III. Questionnaire on Hydroelectric Units—Forced Outages Chargeable to Units*

HYDRAULIC POWER COMMITTEE,
EDISON ELECTRIC INSTITUTE

An outage, to be classed as a forced outage, should be one resulting from the failure of the turbine, generator or any of their auxiliaries or pertinent structures extending from the water passages to the generator leads that requires that the unit be taken out of service. If the unit were taken out of service but could have been continued in operation had it been needed, without endangering life or property, until off-peak night hours, a weekend, or a longer previously scheduled normal maintenance period for that or some other unit for which it might have been substituted, and then have been repaired and returned to service during such period, the outage should not be classed as a forced outage.

It is recognized that, in some cases, the answers given will require considerable judgment as to what might have been done had some conditions been different from those actually experienced. If after due consideration doubt remains regarding the classification, the outage should be considered as forced.

If the outage were extended to permit work to be done on the unit other than the repair of the trouble that caused the forced outage or were extended simply because there was no immediate need for the unit to be returned to service, a reasonable estimate should be made of the minimum time that would have been required to return it to service had it actually been needed.

The primary purpose of this study is the consideration of the availability of hydroelectric units for capacity requirements. The critical hours for capacity for most systems, meaning the whole integrated interconnected system of which the hydro plant may be a part, is usually the heavy daily-load period extending from about 7 or 8 a.m. to about 10 or 11 p.m. on weekdays, which are commonly referred to as the peak hours.

An outage to be considered not forced must satisfy either one of the following conditions:

1. It is not necessary to immediately take the unit out of service and the eventual outage can be (or could have been) deferred to off-peak night hours, deferred to a weekend, or deferred for several months to a longer normally scheduled maintenance period for the unit taken out or some other unit for which it might be substituted in the normal maintenance schedule. The outage must be concluded and the unit restored to service before the next following heavy-load period or the end of the scheduled maintenance period, except that several such periods may be required and used provided the unit is available for service in the interim heavy-load periods.

2. It is necessary to immediately take the unit out of service but the outage occurs during off-peak night hours or a weekend. In such cases the outage must be concluded and the unit restored to service before the next following heavy-load period, even though further outage is required under the conditions specified in item (1) above.

Conversely, an outage to be considered forced must satisfy one of the following conditions:

3. It is not necessary to immediately take the unit out of service but the eventual outage cannot be taken care of during off-peak night hours, a weekend or normally scheduled maintenance period as described in item (1) above.

4. It is necessary to immediately take the unit out of service during the heavy load hours of a weekday.

5. It is necessary to immediately take the unit out of service during off-peak night hours or a weekend, but the outage cannot be concluded and the unit restored to service before the next following heavy load period.

Since the primary purpose of this study is the consideration of the availability of generating capacity, we must ask about each case whether the outage would have been taken immediately or would have been deferred had the unit at the time been needed for capacity purposes. The actual or possible need of a unit for energy generation, either firm or secondary, at the time of an outage has no influence on its classification as forced or not forced.

For example, a run of river plant with eight units may during a period of low flow be operating not more than four or five units during the heavy load hours of the day. An accident occurs which requires that one of the operating units be immediately shut down.

Such an outage is forced as defined under (4) above. Such an outage, however, would not be in demand were it possible to substitute one of the idle units for the one forced out.

Under the same situation as above, except that the unit could have been continued in service but was not simply because other units were available, the outage may or may not be forced. Its classification then depends on the necessary duration of the outage and would be covered by conditions (1) or (3).

In the same plant during high or sufficient flow all units may be in demand continuously. Nevertheless, outages may or may not be forced depending on the circumstances as they actually existed or would have existed had the units been needed for capacity rather than energy generation.

The same considerations apply to storage as well as run of river plants and to high and low flow equally well. The more familiar classification of in demand and not in demand are not related to the classifications forced and not forced. The tests outlined in (1) to (5) should cover all possible conditions which have bearing on the classification desired.

---

*Appendix III is a portion of the "Comments and Instructions" which accompanied the questionnaire sent to the reporting companies.

Bibliography

1. Generating Reserve Capacity Determined by the Probability Method, **G. Calabrese.** AIEE Transactions, volume 66, 1947, pages 1439–50.

2. Calculating Probability of Generating Capacity Outages, **W. J. Lyman.** AIEE Transactions, volume 66, 1947, pages 1471–77.

3. Outage Expectancy as a Basis for Generator Reserve, **Howard P. Seelye.** AIEE Transactions, volume 66, 1947, pages 1483–88.

4. Probability Methods Applied to Generating Capacity Problems of a Combined Hydro and Steam System, **E. S. Loane, C. W. Watchorn.** AIEE Transactions, volume 66, 1947, pages 1645–54.

5. Probability Theory Helps Determine System Reserve Generating Capacity, **G. Calabrese.** *Power* (New York, N. Y.), volume 92, July 1948, pages 423–6.

6. Flood Flows, **W. E. Fuller.** *Transactions*, American Society of Civil Engineers (New York, N. Y.), volume 77, 1914, pages 564–617.

7. Storage to be Provided in Impounding Reservoirs for Municipal Water Supply, **Allen Hazen.** *Transactions*, American Society of Civil Engineers (New York, N. Y.), volume 77, December 1914, pages 1539–1669.

8. Probable Variations in Yearly Run-Off as Determined from a Study of California Streams, **L. Standish Hall** (Discussion by **Allen Hazen**). *Transactions*, American Society of Civil Engineers (New York, N. Y.), volume 84, 1921, pages 191–257.

9. The Probable Number of Stops Made by an Elevator, **Bassett Jones.** *General Electric Review* (Schenectady, N. Y.), volume 26, August 1923, pages 583–87.

10. Theoretical Frequency Curves and Their Applications to Engineering Problems, **H. Alden Foster.** *Transactions*, American Society of Civil Engineers (New York, N. Y.), volume 87, 1924, pages 142–73.

11. Straight Line Plotting of Skew Frequency Data, **R. D. Goodrich.** *Transactions*, American Society of Civil Engineers (New York, N. Y.), volume 91, 1927, page 1.

12. Flood Flows (book), **Allen Hazen.** John Wiley and Sons, New York, N. Y., 1930.

13. A Method for the Economic Estimation of the Operating Standby Reserve in Electrical Systems, **R. A. Ferman.** *Electricity* (Russia), number 20, 1932.

14. Fundamental Considerations in Preparing Master System Plan, **W. J. Lyman.** *Electrical World* (New York, N. Y.), volume 101, number 24, June 17, 1933, pages 788–92.

15. Application of Duration Curves to Hydro Electric Studies, **G. H. Hickox, G. O. Wessenauer.** *Transactions*, American Society of Civil Engineers (New York, N. Y.), volume 98, 1933, page 1276.

16. Spare Capacity Fixed by Probabilities of Outage, **S. A. Smith, Jr.** *Electrical World* (New York, N. Y.), volume 103, February 10, 1934, pages 222–25.

17. Indices and Methods of Calculating Reliability in Power Economy, **B. M. Yakub.** *Electricity* (Russia), number 18, 1934.

18. Probability Theory and Spare Equipment, **S. A. Smith, Jr.** *Bulletin*, Edison Electric Institute (New York, N. Y.), volume 2, number 3, March 1934, pages 85–9.

19. Service Reliability Measured by Probabilities of Outage, **S. A. Smith, Jr.** *Electrical World* (New York, N. Y.), volume 103, March 10, 1934, pages 371–74.

20. The Use of the Theory of Probability to Determine Spare Capacity, **P. E. Benner.** *General Electric Review* (Schenectady, N. Y.), volume 37, number 7, July 1934, pages 345–8.

21. Duration Curves, **H. Alden Foster.** *Transactions*, American Society of Civil Engineers (New York, N. Y.), volume 99, 1934, page 1220.

22. Methods of Estimating Floods. From *Floods in the United States*, paper number 771, United States Geological Survey (Washington, D. C.), 1936, pages 28–67.

23. An Asymmetric Probability Function, **J. J. Slade, Jr.** *Transactions*, American Society of Civil Engineers (New York, N. Y.), volume 101, 1936, page 35.

24. Probable Outages of Shielded Transmission Lines, **S. K. Waldorf.** Electrical Engineering (AIEE Transactions), volume 56, 1937, pages 597–600.

25. Probability Distribution Curve for Flood Control Studies, **B. F. Kimball.** *Transactions*, American Geophysical Union (Washington, D. C.), 1938, pages 460–483.

26. Considerations Involved in Making System Investments for Improved Reliability, **S. M. Dean.** *Bulletin*, Edison Electric Institute (New York, N. Y.), volume 6, number 7, November 1938, pages 491–4.

27. Ratio Between Installed Capacity and Maximum Allowable Load of a Plant and of a Group of Interconnected Plants, **G. J. Th. Bakker, J. C. vanStaveren.** *Paper 331*, Conference Internationale Des Grands Reseaux Electriques A Haute Tension (Paris, France), 1939.

28. The Return Periods of Flood Flows, **E. J. Gumbel.** *Annals of Mathematical Statistics*, (Ann Arbor, Mich.), volume 12, number 2, June 1941, pages 163–90.

29. Probability Interpretation of the Observed Return Period of Floods, **E. J. Gumbel.** *Transactions*, American Geophysical Union (Washington, D. C.), August 1941, pages 585–1036.

30. Maximum Probable Floods on Pennsylvania Streams, **C. F. Ruff.** *Transactions*, American Society of Civil Engineers (New York, N. Y.), volume 106, 1941, page 1453.

31. Statistical Control-Curves for Flood Discharges, **E. J. Gumbel.** *Transactions*, American Geophysical Union (Washington, D. C.), 1942, pages 489–509.

32. Limited Type of Primary Probability Distribution Applied to Annual Maximum Flood Flows, **Bradford F. Kimball.** *Annals of Mathematical Statistics* (Ann Arbor, Mich.), volume 13, 1942, pages 318–25.

33. A Simple Method of Estimating Flood Frequency, **Ralph W. Powell.** *Civil Engineering* (New York, N. Y.), February 1943, page 105.

34. Methods of Estimating Flood Frequencies, **W. E. Howland.** *Civil Engineering* (New York, N. Y.), April 1943, page 185.

35. Statistical Analysis in Hydrology, **L. R. Beard.** *Transactions*, American Society of Civil Engineers (New York, N. Y.), volume 108, 1943, page 1110.

36. An Eight Year Investigation of Lightning Currents and Preventative Lightning Protection on a Transmission System, **E. E. Hansson, S. K. Waldorf.** AIEE Transactions, volume 63, 1944, pages 251–258.

37. On the Plotting of Flood Discharges, **E. J. Gumbel.** *Transactions*, American Geophysical Union (Washington, D. C.), 1944, page 699.

38. The Co-ordinated Operation of Hydro and Steam Capacity in Electric Power Systems, **G. W. Spaulding.** *Transactions*, American Society of Mechanical Engineers (New York, N. Y.), volume 66, August 1944, pages 545–9.

39. Floods Estimated by Probability Methods, **E. J. Gumbel.** *Engineering News Record* (New York, N. Y.), volume 134, June 14, 1945, pages 833–7. Also volume 135, August 9, 1945, page 188.

40. Simplified Plotting of Statistical Observations, **E. J. Gumbel.** *Transactions*, American Geophysical Union (Washington, D. C.), volume 26, part 1, August 1945, page 69.

41. Determination of Degree of Reliability of a Hypothetical Steam Electric Generating System, **E. S. Loane, C. W. Watchorn.** Pennsylvania Electric Association (Harrison Pa.), November 1945.

42. Synthetic Determination of Frequency and Duration of Multiple Forced Outages of Electric Generating Units, **E. S. Loane, C. W. Watchorn.** Pennsylvania Electric Association (Harrison, Pa.), November 1945.

43. Supplement to Synthetic Determination of Frequency and Duration of Multiple Forced Outages of Electric Generating Units, **E. S. Loane, C. W. Watchorn.** Minutes of thirty-eighth meeting of Electrical Equipment Committee, Edison Electric Institute (New York, N. Y.), February 1946.

44. Determination of Reserve Requirements of an Interconnected System, **H. W. Phillips.** *Bulletin*, Edison Electric Institute (New York, N. Y.), volume 14, number 4, April 1946, pages 117–120.

45. A New Approach to Probability Problems in Electrical Engineering, **H. A. Adler, K. W. Miller.** Electrical Engineering (AIEE Transactions), volume 65, 1946, pages 630–32, 1118.

46. Assignment of Frequencies to a Completely Ordered Set of Sample Data, **Bradford F. Kimball.** *Transactions*, American Geophysical Union (Washington, D. C.), volume 27, number 6, December 1946, page 843.

47. Service Continuity Standards Aid Economical Distribution Planning, **W. J. Lyman.** *Electric Light and Power* (Chicago, Ill.), volume 25, number 5, May 1947, pages 66–70, 112–13, also published in *Bulletin*, Edison Electric Institute (New York, N. Y.), September 1947, pages 325–39.

48. Determination of Required Reserve Generating Capacity, **W. J. Lyman.** *Electrical World* (New York, N. Y.), volume 127, number 19, May 10, 1947, pages 92–5.

49. Firm or Dependable Hydro Capacity, **E. S. Loane, C. W. Watchorn.** Pennsylvania Electric Association (Harrison, Pa.), October 1947.

50. Reserve Capacity Determined by the Probability Method, **G. Calabrese.** Minutes of forty-third meeting of Electrical Equipment Committee, Edison Electric Institute (New York, N. Y.), October 1947.

No Discussion

A 3,000-Horsepower Gas Turbine Power Plant

J. S. HAVERSTICK
ASSOCIATE AIEE

OVER THE past few years, several papers have been presented describing the gas turbine power plants with which the various manufacturers of turbines are working. The present paper describes a plant having somewhat different features than those described previously, and also presents performance characteristics of the plant which it is believed will be of value to those who must study and plan for the eventual use of gas turbine power.

Inasmuch as the compressor is a vital component of a gas turbine plant, much discussion has taken place concerning the relative merits of axial-flow and centrifugal machines; those who favor the axial-flow compressor usually claim a higher efficiency and less bulk, and those who favor the centrifugal compressor usually point to the broader range of operation and also indicate they believe that, with sufficient development, the efficiency of the centrifugal can be made to equal that of the axial. Herein, the compressor is a mixed-flow type which is adaptable to high-speed operation and, during its relatively short period of development, has proved that it is capable of high efficiency; its range of operation lies between those of the axial and centrifugal types.

A second distinguishing feature of the plant described herein is that the power output shaft is mechanically independent of the rotor of the compressor and compressor driving turbine. Such an arrangement is usually known as a split turbine design. It has the advantage of allowing the load to remain at constant speed while the compressor and its turbine are brought to their most desirable speed.

To allow even greater flexibility in the operation of the plant, a by-pass is placed around the power output turbine. It is only economical to use the by-pass during idling operation, but, on the other hand, its presence means that the plant may be used in applications where the simpler single-turbine plant is wholly unsuitable.

The cycle on which the design is based is the open cycle without intercooling of the compressor, regeneration, or reheating between turbines. It is accomplished by series flow through the compressor, combustors, high-pressure turbine, and power output turbine. All components are arranged along a common axis.

Design point conditions were chosen to be an ambient air temperature of 68 Fahrenheit degrees, a barometric pressure of 14.7 pounds per square inch, an over-all pressure ratio of 6 to 1, and a turbine inlet temperature of 1,300 Fahrenheit degrees with an output of 3,000 brake horsepower.

The general arrangement of the plant is shown in Figure 1 in which may be seen, starting at the left, the auxiliary housing, the compressor, the combustors, the high-pressure turbine, and the power turbine. All components other than the power turbine are in reality a power-gas generator, needed to produce the hot, compressed gases for the power turbine.

The compressor consists of three mixed-flow stages and is designed to deliver 44,500 cubic feet per minute at design air conditions when operating at 7,900 rpm. Each of the three impellers is made from forgings out of which the vanes and hub are machined to form an integral piece. Air enters the compressor radially and is turned immediately for axial entry into the first impeller. On being discharged from the rotor, the air enters a vaned diffuser which directs it radially outward. Following the diffusion it is brought back radially into the second stage, where the process is repeated. The casing and internal stator parts are all split on the horizontal center line for ease in handling during assembly and inspection. The rotor is supported at each end in sleeve-type journal bearings and is positioned axially by means of a Kingsbury-type thrust bearing. Labyrinth-type seals are used throughout, those between the suction of the first-stage impeller and the auxiliary housing being supplied with sealing air to insure that lubricating oil is not drawn into the main air stream.

The high-pressure turbine in this type plant is used primarily to drive the compressor, although, in addition, it drives the auxiliaries and may be adapted to supply a small amount of power for other services independent of the main power output. This machine is of the axial-flow type; it contains five stages, the rotating blades of each stage being attached to the rotor by fir-tree-type shanks fitted into corresponding slots

Figure 1. Gas turbine power plant

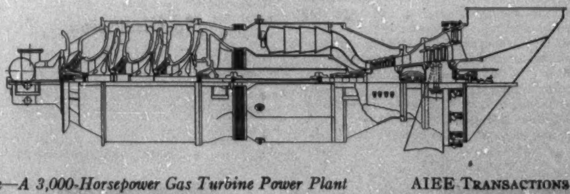

Paper 49-113, recommended by the AIEE power generation committee and approved by the AIEE technical program committee for presentation at the AIEE winter general meeting, New York, N. Y., January 31–February 4, 1949. Manuscript submitted November 16, 1948; made available for printing January 4, 1949.

J. S. Haverstick is the assistant chief engineer in the gas turbine department of the De Laval Steam Turbine Company, Trenton, N. J.

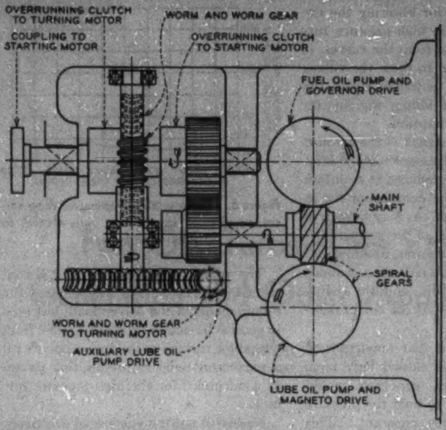
OVERRUNNING CLUTCH TO TURNING MOTOR
WORM AND WORM GEAR
COUPLING TO STARTING MOTOR
OVERRUNNING CLUTCH TO STARTING MOTOR
FUEL OIL PUMP AND GOVERNOR DRIVE
MAIN SHAFT
SPIRAL GEARS
WORM AND WORM GEAR TO TURNING MOTOR
AUXILIARY LUBE OIL-PUMP DRIVE
LUBE OIL PUMP AND MAGNETO DRIVE

Figure 2. Diagrammatic arrangement of auxiliaries

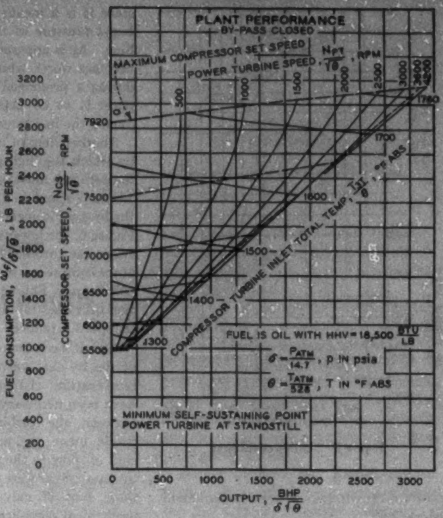

Figure 3 (right). Performance of power plant

machined axially in the rotor. The complete rotor is carried in two sleeve-type journal bearings located at each end; the axial position is determined by the compressor thrust bearing, the thrust being transmitted through to the compressor rotor. The casing is split on the horizontal center line as with the compressor.

The power turbine is of the same general design as the high-pressure turbine, but it contains only three stages and includes its own Kingsbury-type thrust bearing. It is designed to develop 3,000 brake horsepower at 4,200 rpm with the compressor set operating under its design conditions, and, of course, with the bypass valves fully closed.

In order to keep the machines symmetrical about the axis and thus maintain control of thermal expansions, the by-pass, from between the turbines to the exhaust, completely surrounds the power turbine and contains several valves equally spaced.

The combustors are set in a circle concentric with the axis of rotation; eight are used, and each consists of conical liners arranged to gradually mix the secondary air with the combustion products.

The arrangement of the auxiliary housing is shown in diagrammatic form in Figure 2. Included are a tachometer, a main lubricating-oil pump, an auxiliary lubricating-oil pump, a fuel-oil pump, an overspeed trip, a low lubricating-oil pressure trip, and the free-wheeling clutches for the starting motor and turning motor, as well as the speed governor. The turning motor serves as the motor for the auxiliary oil pump to insure that, as the plant is cooling off, the heat conducted to the bearings will be carried away by the flow of oil. Since the free-wheeling clutches are fully automatic and cannot transmit torque in the reverse direction, the turning motor and starting motor may be brought into operation at any time.

Dimensions of the plant as a whole are given by the maximum diameter of the casing (68 inches), and by the length from power output coupling to starting motor coupling (22 feet, 8 inches).

As shown in Figure 3, the performance of the plant may be shown on a single plot, provided, of course, that the by-pass valves are kept closed. Figure 3 was prepared for the plant performance with design ambient conditions of temperature and pressure, and can be used directly only when such conditions prevail.

Inasmuch as design ambient conditions are rarely encountered, it is usually necessary to correct existing conditions back to standard. The correction factors necessary for this purpose are given in the figure as factors of each variable.

It is interesting to note that, in a plant such as this one with a separate power turbine, constant speed for the output is attained by reducing not only the maximum temperature but also the speed of the compressor set. The consequent reduction of centrifugal stress in the highest temperature region should then contribute to longer life for these members of the turbine.

Corresponding to the constant speed line for 3,600 rpm in Figure 3, the fuel rate curve is plotted separately in Figure 4. It is based on fuel oil having a higher heating value of 18,500 Btu per pound.

Figures 3 and 4 are limited in that they do not carry on down to idling conditions; therefore, to illustrate performance in this range, Figure 5 is presented. It is to be noted that, as the compressor-set speed is reduced by reducing the quantity of fuel, the inlet temperature to the high-pressure turbine falls to a minimum value and then rises again with subsequent reduction of fuel. The temperature rise must, of course, be kept within safe limits; there is a point, therefore, below which it is necessary to shut off the fuel completely, and so shut down the plant or supply outside power from the starting

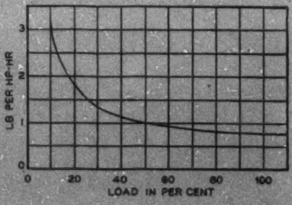

Figure 4. Fuel rate versus output at 3,600 rpm

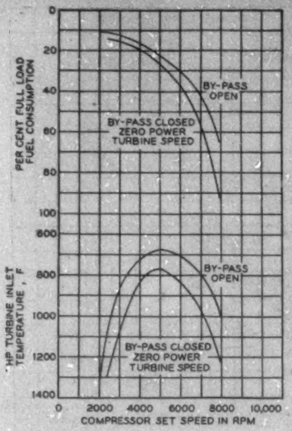

Figure 5. Idling conditions

motor if the compressor set is to remain in operation.

The amount by which the by-pass is opened affects the idling performance, since it is a means for lowering the exhaust pressure of the high-pressure turbine. As is apparent from the curves, it becomes worth while to open the valves during a prolonged period in which the plant is to be kept idling, thereby reducing the fuel consumption.

Another item of interest is the amount by which the high pressure turbine inlet temperature must be reduced to maintain constant speed in the compressor set as the by-pass is opened. As may be seen in Figure 6, the lowering of the pressure between the turbines requires, at full speed of the compressor set, a reduction of about 300 degrees Fahrenheit, and the reduction decreases rapidly as the compressor-set speed is reduced.

Had it been found that manipulation of the by-pass valves caused very large temperature changes, provision would have been necessary to hold the pressure between the turbines constant. This would mean the addition of valves to shut off flow to the power turbine as the by-pass valves were opened. The lack of these shut-off valves not only reduces mechanical complication, but, by allowing flow through the power turbine, maintains its temperature even at a standstill.

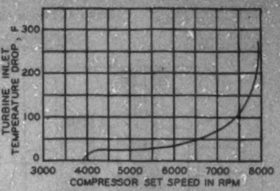

Figure 6. Turbine inlet temperature drop versus compressor speed from fully-closed to fully-open by-pass

The manner in which the plant is controlled is dependent, of course, upon the requirements of the driven load, but may in general be said to be speed control from the power turbine to the fuel supply, with a maximum temperature-limiting device as a safeguard for the high-pressure turbine.

Since it is not the purpose of this paper to discuss the possible applications for this type of power plant, details of the controls that might be used in different cases are omitted, but in conclusion, it may be pointed out that, since flexibility in operation is a main objective, many arrangements are possible.

No Discussion

Two Gas Turbines for Power Generation and Other Applications

ALAN HOWARD
MEMBER AIEE

Synopsis: This short paper, written as part of a symposium, outlines the status of a gas turbine development, briefly describes the two types of power plant resulting from this development to date, and outlines their applications.

THE GAS turbine, as in the case of most prime movers, has had a rather long history. It is, however, a new prime mover in being reduced to a form suitable for practical applications. A gas turbine may take a great many forms; throughout the world many designs are built and are in operation, and many more are underway. These range from the simplest type to very complex cycles which may involve both reciprocating and rotating equipment. These various types each have their attractive features and may fit particular applications to particular advantage.

Much has been written concerning the broad field available to the gas turbine as its development progresses. It does seem to be a type of power plant which will prove to be of wide usefulness. The gas turbine should prove its adaptability in two ways. First, even the simplest type of plant is, we believe, attractive for many applications without changing the basic unit. Second, as the over-all development progresses, further new types should become available with their own particular fields of superiority.

One important aspect of the gas turbine which is sometimes partly lost from sight among the glowing predictions for its future, is the fact that there is so far very little experience with it for general power purposes. Aside from process units designed for low temperatures, no really extensive operating experience has been reported anywhere.

During the war, two aircraft gas turbines of the axial flow type were developed by the General Electric Company at Schenectady, N. Y. These are shown in Figures 1 and 2. The *TG-100* has had many flights up to high altitude and has given a very good account of itself. The *TG-180*, and its successor the *TG-190*, are being used in a majority of the new jet

Figure 1. General Electric propjet aircraft gas turbine for propeller drive

Figure 2. General Electric axial-flow-type aircraft gas turbine for jet propulsion

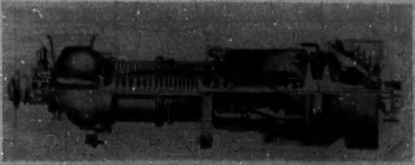

Figure 3. General Electric gas turbine for 4800-horsepower locomotive drive. Shaded longitudinal semisection

Figure 4. Gas turbine for 4,800-horsepower locomotive drive

External view, left to right: atomizing air compressor, accessories, compressor, combustion chambers, turbine, turbine exhaust

---

Paper 49-114, recommended by the AIEE power generation committee and approved by the AIEE technical program committee for presentation at the AIEE winter general meeting, New York, N. Y., January 31–February 4, 1949. Manuscript submitted November 17, 1948; made available for printing January 4, 1949.

Alan Howard is division engineer, gas turbine engineering division of the General Electric Company, Schenectady, N. Y.

Figure 5. Arrangement for test of 4,800-horsepower gas turbine for locomotive drive

fighters and bombers of the Air Force. Each of these is of the simplest type with one turbine, one compressor, and no intercooling or regeneration.

Based on this experience, but recognizing the difference in requirements for nonflying applications, a simple power plant with a design rating of 4,800 horsepower (at 1,500 feet altitude) has been designed, built, and tested in Schenectady. This power plant was designed particularly for locomotive applications, but with recognition that it should be attractive for many other types of installation also. Figures 3 and 4 show a cross-section and an external view respectively. The unit is approximately 19 feet long and weighs about five pounds per horsepower. Figure 5 shows the unit on test in Schenectady where it drove four d-c generators of the traction type through gearing. The tests and unit have been described in detail.[1,2] In summary, the power plant proved to more than meet its design rating and to be a little better in efficiency than the design predictions of 17 per cent based on net shaft power and the lower heating value of the fuel. Somewhat over 700 hours of operation have been accumulated. Some difficulties, of course, were encountered, but these were not of a basic nature.[2] Simple corrective measures were taken, and the over-all operation is considered very definitely encouraging. A majority of the running was on *Bunker C* (number 6) fuel oil, and a total of more than 230,000 gallons of this low-grade fuel has been burned.

The characteristics of this plant, based on the tests, are shown in Figures 6 and 7, while Figure 8 shows the effect of altitude. It will be seen that there is a definite effect of ambient temperature and of altitude. In these characteristics, the gas turbine is different from either steam plants or diesel engines; its features should be evaluated for each application. In cold weather, the power output obtainable increases substantially, whereas, in hot weather, the output falls off with exhaust temperature maintained constant. In dry locations, evaporative cooling of the inlet may be quite attractive since the wet-bulb temperature always may be attained. This will require on the general order of 1,500 to 2,000 pounds of water evaporated per hour. In at least one application, the incoming air will be cooled by a surface cooler.[3]

The exhaust temperature of the turbine varies with load and with ambient temperature, and the air flow also varies. This results in a variation of the heat available in the exhaust, as shown in Figure 7. This basic natural characteristic can be modified by the combustion of additional fuel in the exhaust gases prior to entering the waste heat boiler, or by throttling on the compressor inlet or

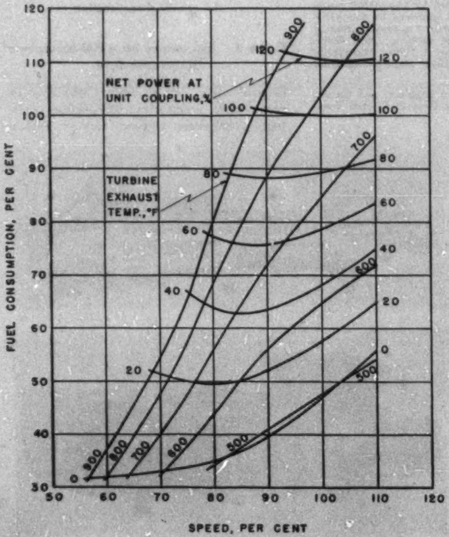

Figure 6. Tested thermal performance of a 4,800-horsepower gas-turbine power plant

100 per cent values correspond to 75,600,000 Btu/hour (based on the lower heating value), 6,700 rpm and 5,000 horsepower at sea level and 80 degrees Fahrenheit ambient

Figure 7. 3,500-kw gas turbine-generator estimated performance at sea level

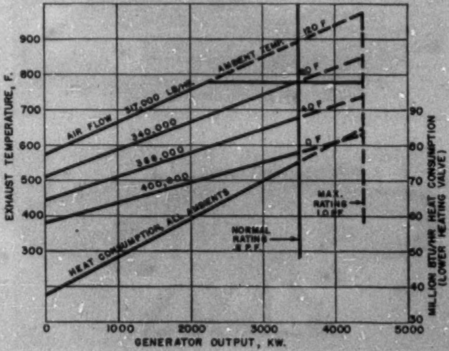

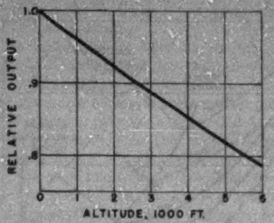

Figure 8. Effect of altitude on output and air flow

turbine discharge to raise the exhaust temperature at a given load. Of course, in doing this, the turbine exhaust temperature cannot be raised above the maximum permissible value. These possibilities of using waste heat are more fully covered elsewhere.[4]

Based on this successful operation, the power plant has been installed in a locomotive and is undergoing preliminary track tests as this is written. Furthermore, two of these power plants have been sold to public utilities for power generation purposes. In one of these applications, natural gas will be the fuel, and the exhaust will be used to heat the feed water of the existing steam power station in which the unit will be located. This application, which has been described in the technical press,[3] illustrates one of the adaptable features of this unit. An outline of the power plant, when used for power generation, is shown in Figure 9.

With this simple type of plant, the over-all efficiency is of a moderate value which indicates that the major application is expected to be where fuel is inexpensive, where the utilization of the waste heat is desirable, or where small size and light weight are important.

This type power plant requires cooling water only for lubricating oil, and even this can be dispensed with by the use of air-cooled radiators, if desired, so that the unit is particularly attractive where cooling water is difficult to obtain.

Since the power plant is relatively small, compact, and light in weight, simple, inexpensive foundations and housing are required, thus resulting in economical installations.

An attractive possibility for this simple unit is as a portable power plant, of which a preliminary outline is shown in Figure 10. While the details of this have not been developed fully, it appears likely that the generating plant could be put on one flat car with the fuel oil brought up in tank cars. Similar portable power plants well might form emergency units for pipe-line pumping spares, and probably could be transported in one or two trucks.

Other attractive applications for this plant should be in industrial power, gas or oil pipe-line pumping, and where the exhaust heat may be used directly, as in the drying of lumber.

For many applications, particularly the usual power generation case, a higher efficiency, both at full load and at part

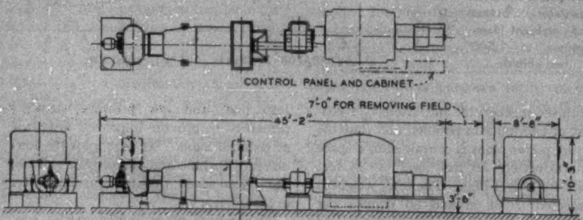

Figure 9. General Electric 3,500-kw gas turbine-generator set

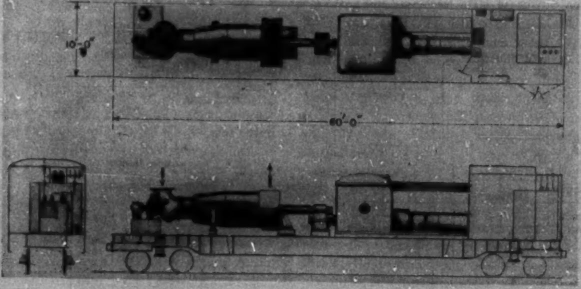

Figure 10. Preliminary shaded cross-section of General Electric 3,500-kw gas-turbine mobile power plant

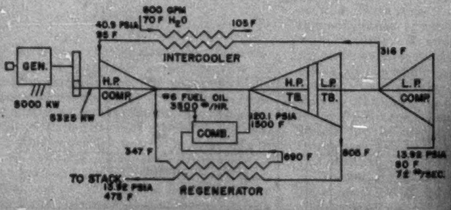

Figure 11. Cycle diagram with pertinent pressures, temperatures, flows, and output for design rating at 1,500 feet altitude

Figure 12. Artists' conception of 5,000-kw gas-turbine power plant as designed, with all components on one floor level

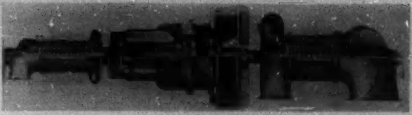

Figure 13. Cross-section of General Electric gas turbine for 5,000-kw turbine-generator set

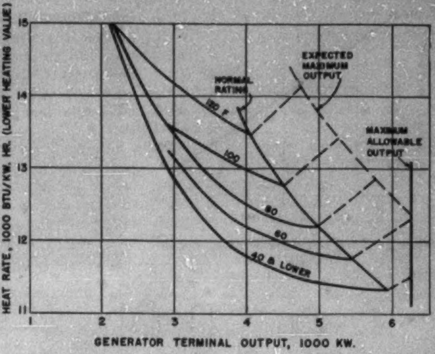

Figure 15. Estimated plant heat rate, based on lower heating value of gas or liquid fuel, versus generator output and ambient temperature at 1,500 feet altitude

load, than can be obtained with the simple cycle is desirable. Such increases in efficiency are obtained in the gas turbine primarily by using heat transfer elements in the form of intercoolers between stages of compression and regenerators making use of the turbine exhaust heat to preheat the air entering the combustion chambers. Figure 11 is a diagram of such a power-plant cycle, including temperatures and pressures at the various points in the cycle under the design conditions of 1,500 feet and 80 degrees Fahrenheit. Figure 12 is a perspective drawing of the physical appearance of such a plant, while Figures 13 and 14 show an approximate cross-section of the machinery and an installation outline. It will be noted that both the regenerator and intercooler consist of two units in parallel, and that the entire power plant is contained in a space approximately 50 feet long by 28 feet wide by 13 feet high. The total weight is expected to be around 60 pounds per kilowatt.

The turbine and compressor are divided into high and low pressure elements primarily to provide improved heat rate at reduced loads. At part load the low-pressure turbine and compressor will run at reduced speed, thus maintaining better cycle efficiency.

This power plant is now under construction, and the first of its type is ex-

Figure 14. Installation outline of main machinery and heat exchanger components

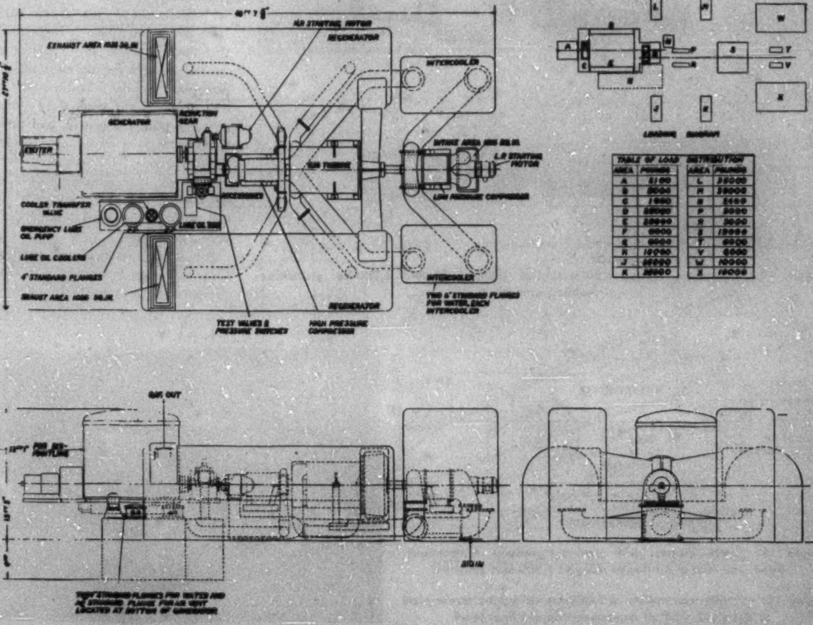
EXHAUST AREA 1025 SQ.IN.
H.P. STARTING MOTOR
REGENERATOR
INTERCOOLER
GENERATOR
REDUCTION GEAR
EXCITER
GAS TURBINE
INTAKE AREA SQ.IN.
L.P. STARTING MOTOR
LOW PRESSURE COMPRESSOR
ACCESSORIES
COOLER TRANSFER VALVE
EMERGENCY LUBE OIL PUMP
LUBE OIL TANK
LUBE OIL COOLERS
4" STANDARD FLANGES
EXHAUST AREA 1025 SQ.IN.
REGENERATOR
INTERCOOLER
TWO 6" STANDARD FLANGES FOR WATER, EACH INTERCOOLER
TEST VALVES & PRESSURE SWITCHES
HIGH PRESSURE COMPRESSOR
LOADING DIAGRAM
GAS OUT
DRAIN

TABLE OF LOAD		DISTRIBUTION	
AREA	POUNDS	AREA	POUNDS
A	2100	L	35000
B	8000	M	30000
C	1000	N	2400
D	25000	P	3000
E	20000	R	3000
F	6000	S	12000
G	6000	T	6600
H	10000	V	6000
J	25000	W	10000
K	25000	X	10000

pected to be in factory test operation within a few months.

It is designed for 5,000-kw generator-terminal output, and has an expected thermal efficiency of 28 per cent based on the generator terminal output and on the lower heating value of the fuel. This is a better efficiency than that attained by steam stations of comparable size.

The mechanical design has been described in detail in a recent paper,[5] which also gave the anticipated performance characteristics as shown in Figure 15. From this figure, it will be seen that the normal rating of the power plant is affected by ambient temperature as in the case of the simple type of power plant, but at a lesser rate. It is basically affected by altitude as shown in Figure 8, which applies approximately to any gas turbine. Relative to the normal rating, the maximum expected net output is about 15 per cent greater, which means that the full 5,000-kw net output should be maintained up to about 110 degrees Fahrenheit ambient. The part-load heat rate is higher than that at full load, but increases relatively slowly as load is reduced, so that at half power the heat rate should be only about 16 per cent higher than at full power.

This power plant requires relatively very little cooling water compared to a steam station of a similar rating. Normally, a total water flow, including intercoolers, oil coolers, and generator air coolers, of approximately 1,200 gallons per minute would be required. This is compared with around three to five times this value for a steam station. In addition to the good thermal efficiency and low cooling water requirements, this power plant is expected to have a relatively low installation cost. The version shown is essentially a one level plant with only the oil tank required to be below floor level.

In the perspective drawing, Figure 12, the exhaust openings from the regenerators are shown facing upward, and, in this case, the required exhaust ducting would be attached at these points and led in the most convenient manner to the outside. Alternatively, these regenerator outlets may be turned outward to each side or downward, if more convenient. Similarly, the inlet duct to the low-pressure compressor can be either along the floor or overhead. In common with the ducts for the 3,500-kw simple-cycle unit, these ducts normally would include simple sound absorbing means to suppress the high-frequency turbine and compressor noise. If desired, the regenerators can be left out and the turbine exhaust heat can be used for making steam or for other purposes, rather than preheating the combustion air. In this case the fuel rate would be increased by about one-third.

It is expected that these plants should be attractive for end-of-line installations, and for standby and peak-load operation where the quick starting feature would be of particular advantage. It is expected that completely automatic operation will be quite feasible.

As in the case of the 3,500-kw unit, this 5,000-kw plant is designed to be adaptable to the burning of a light or heavy fuel oil, including *Bunker C*, and to the combustion of gas. At the present time, three of these units have been ordered for installation in power stations; two of them will burn natural gas, while the other will burn *Bunker C* fuel.

In summary, a large-scale gas turbine developmental program is under way, including many component developments not outlined here. This development has resulted, so far, in the construction and test of the simple-cycle locomotive-type plant, the design and current construction of the high-efficiency 5,000-kw unit, the receipt of orders for both types for power generation, and the installation of the locomotive unit in a locomotive with preliminary track tests under way as this is written. This is all undertaken in the belief that the gas turbine will find wide use. However, it is not believed that it will displace in the near future other forms of prime mover, such as large steam turbines.

In this paper prepared for the symposium, a full description of these two power plants and their possibilities has not been attempted. It is hoped, however, that sufficient of the possibilities have been outlined to indicate the wide field to which we believe the present units are adaptable, and to indicate the general present state of development. It is anticipated that in the future other sizes and types of gas turbine will become available, and that experience with the present plants will prove them to have low maintenance and to be reliable and economical when properly applied. It is anticipated that, as developments progress, it will be possible to use coal as a fuel for gas turbines. This should considerably extend their field of usefulness.

References

1. DESIGN FEATURES OF A 4,800 HP LOCOMOTIVE GAS TURBINE POWER PLANT, **Alan Howard.** *Mechanical Engineering* (New York, N. Y.), volume 70, April, 1948, pages 301–06.

2. TEST OF A 4,800 HP GAS TURBINE POWER PLANT, **Alan Howard, B. O. Buckland.** American Society of Mechanical Engineers, New York, N. Y., 1948.

3. 3,500 KW GAS TURBINE RAISES STATION CAPABILITY BY 6,000 KW, **J. W. Blake, R. W. Tumy.** *Power* (New York, N. Y.), September, 1948, pages 518–25.

4. THE GAS TURBINE WITH A WASTE HEAT BOILER, **G. R. Fusner.** *Mechanical Engineering* (New York, N. Y.), June, 1948, pages 515–18.

5. A 5,000 KW GAS TURBINE FOR POWER GENERATION, **Alan Howard, Chapman J. Walker.** American Society of Mechanical Engineers, New York, N. Y., 1948.

Discussion

W. A. Wilson (Elliott Company, Jeanette, Pa.): The papers presented at the gas turbine symposium provide an exceptionally comprehensive view of current gas-turbine development in this country. In doing this they indicate a diversity of solutions of similar problems which may seem surprising or even alarming. This is a consequence of one source of the virility of the gas-turbine idea, that is, its extreme flexibility. The gas-turbine designer is "embarrassed with riches" when it comes to the number of degrees of freedom allowable in making his technical choices.

This is true not only with respect to mechanical design but, even more fundamentally, with respect to the choice of the thermodynamic processes to be employed. It is one of the most appealing virtues of the gas turbine that it is adaptable to the implementation of a whole range of cycles. Since none of these cycles has a clean-cut superiority on all counts, the choice between them is far from easy. Some insight into the reasons for the several selections indicated by the papers may be given by a brief exposition of the three "basic" gas-turbine cycles.

The simple gas turbine operates on the Brayton cycle—adiabatic compression, constant-pressure heat addition, adiabatic expansion. Theoretically, the efficiency of this cycle increases indefinitely with pressure ratio. At the same time, the ratio of useful output to turbine (and compressor) power decreases drastically. This latter circumstance makes the high-pressure-ratio simple-cycle extremely sensitive to component efficiencies. Simple-cycle gas turbines operating near 1300 degrees Fahrenheit usually are designed for operation at a pressure ratio of five or thereabouts. For this condition the output per pound of air handled is a maximum. A few more points of efficiency can be squeezed out by a considerable increase in pressure ratio, but at a less favorable air rate and by using more expensive compressors and turbines.

The introduction of a regenerator into the Brayton cycle creates the second basic gas-turbine process. This modification has more profound thermodynamic significance than usually is recognized. The ideal cycle—assuming complete recovery of available exhaust heat—has a maximum efficiency at unity pressure ratio equivalent to that of the Carnot cycle; instead of continually increasing as pressure ratio is raised, it declines. Actual gas turbines employing the Brayton cycle with practical degrees of regeneration have peak efficiencies at relatively low pressure ratios—approximately 5.0 for a 1300 degree Fahrenheit, 50 per cent regeneration plant. Since this corresponds reasonably closely to the optimum condition relative to air rate, the selection of a design pressure ratio is more straightforward than in the case of the non-regenerative plant.

The ultimate in ideal gas turbine processes is the Erricson full-regenerative cycle—isothermal compression, constant-pressure heating, isothermal expansion, constant-pressure cooling. The theoretical efficiency of this cycle is independent of pressure ratio, being everywhere equal to the Carnot efficiency. Compound cycles incorporating inter-cooling, reheat, and regeneration may be regarded as efforts to approximate this ideal. The independence of ideal cycle efficiency from pressure ratio is reflected in the flat performance curves of typical compound cycles. These more complicated plants pay off in other respects also: efficiencies are brought to high levels; output per pound of air may be double that for simple cycles; part load performance may be excellent, and at all loads is relatively insensitive to deterioration of component efficiencies. These advantages are gained, of course, only at the expense of additional rotating and stationary apparatus, but up to half the turbine power developed is useful power instead of a little over one third, and, for a given percentage of heat recovery, between one-third and one-half as much heat transfer surface is required per unit of plant output. It seems safe to predict that, if the gas turbine is to become more than a special purpose prime mover, it must embody a compound cycle. The selection of a particular version will involve compromise, based on judgment developed from experience in such endeavors as have been described at the symposium.

There is considerable question in the writer's mind as to whether simple open-cycle plants can be justified for power generation in capacities as high as the 7,500 kw indicated in Tucker's conference paper. Certainly increasing this capacity to 15,000 kw by essentially duplicating the compressor and turbine elements will be difficult to justify. The superposition of smaller high-pressure compressor and turbine elements, and incorporation of intercooling and reheating will develop nearly the same increase in capacity and at the same time nearly double the efficiency.

Philip Sporn (American Gas and Electric Service Corporation, New York, N. Y.): The authors are to be commended for presenting a series of papers which give us an authoritative picture of the present status of the gas-turbine power plant for application to public utility systems. It is this kind of approach which ultimately will serve to fill the vacuum in our knowledge of the performance of the gas turbine in industrial or power applications based upon application and operating experience.

The application of the gas turbine to the end-of-the-line situations may offer potentialities on a number of public utility systems. It doubtless can be used on such systems where oil and gas are economically available and are the prevalent fuels. However, for general application, a coal-burning unit will be required. This is a development still to be completed. While no basic difficulties stand in the way, the technical difficulties still are formidable.

Once the coal problem is solved, it should be possible to develop more clearly the particular place of the gas turbine in a general power supply picture—something very difficult to do now. There can be no question that every progressive power-system engineer and executive will be alert to new developments in that field, and that he will grasp every economically sound opportunity to exploit the gas turbine as a new tool in building the power system of tomorrow on the most economical power-supply base possible.

One line of development seems fairly obvious. Following the pattern of steam-turbine development, it is only natural to expect that the development of the gas turbines will be in the direction of higher and higher operating temperatures. This will bring about a material improvement in the thermal performance of the gas turbine and improve its competitive position. It will contribute to better designs of steam turbines as alloy steels for higher temperatures are developed, and this will serve to check the competitive gain of the gas turbine. However, it is important to point out that this development will not obviate the need of research in the direction of producing a coal-burning gas turbine which is so essential if such a machine is going to have widespread application.

The point about the moving target presented by the modern steam turbine should not be lost sight of. If the coal-fired gas turbine were available today for large-scale power generation, the steam-power mark it would have to strive to match or beat is that which is now possible with a 2,000 pounds per square inch, 1,050–1,000 degree reheat cycle, which is typical of some six large installations now in progress on the American Gas and Electric Company system, and which are designed to generate power at 9,300 Btu per kilowatt-hour net generation. It would be unsound, however, to assume that steam power will remain at this level during the period of development of the gas turbine. I feel that the goal for gas turbines in large-scale power generation will be even higher, as indicated by performance of a 2,000-pound 1,200-degree Fahrenheit steam reheat cycle which should be capable of generating at approximately 8,700 Btu per net kilowatt-hour. This projected steam cycle, utilizing 1,200 degrees as the operating temperature, is substantially higher than any steam equipment on which we presently have experience. The lessons learned on gas turbines should be helpful in this development.

Gas Turbines in Stationary Power Generation

F. T. HAGUE
ASSOCIATE AIEE

THE ULTIMATE possibilities of gas turbines for many types of application have been publicized widely. There is no lack of understanding of thermodynamic principles to hold up development progress. So many of the possibilities, on which improved performance at an economic cost is dependent, are in such a preliminary stage of research that it is manifestly impossible to put a time schedule on their reduction to practice, or to predict now the extent to which these possibilities ultimately will be incorporated in commercial gas turbines. This very uncertainty makes the future of the gas turbine intriguing to engineers.

The gas turbine is an economic and practical reality in its present stage of development for many types of application. Its acceptance as a high-speed-aircraft power plant is well established. It is pre-eminent in this field for one general reason—it does a better job than any competitive power plant. Doing a better job means that the integration and evaluation of its characteristics, that is, first cost, size, cost of power generation, life, maintenance, and reliability, puts it in a more favorable position than any other type of plant. Gas turbines will compete with and will supersede other types of power plants only when they "do a better job" in an evaluated sense.

In the stationary power generation field, the gas-turbine plant and the steam plant may be compared on an economic basis by arbitrarily assuming that the life, maintenance, and reliability characteristics can be made equal, leaving first cost and cost of power generation as the predominant criteria. Such an economic analysis has been described by A. Mendahl,[1] resulting in a simple diagram which permits the determination of the plant load factor at which two plants, of different first cost, have the same cost per unit of power generated for any specific fuel costs. Such an analysis of steam and gas-turbine plants of current design indicates that the present-day gas turbine has economic application possibilities in the stationary power generation field whenever the price of fuel is sufficiently low or the load factor is less than ten per cent, and then only when the gas turbine plant first cost is relatively low.

This is a reasonably encouraging outlook for a new type of stationary power-generation plant. It indicates the two lines along which the gas turbine probably will be introduced into the power-generation field. It also serves to give a quantitative answer to the usual question of how much improvement in the gas turbine plant's "first cost versus power generating cost" relationship must be achieved, by further research and development, before the gas-turbine plant can challenge the steam plant as an economic base-load operating unit for any specific set of fuel cost conditions. It appears that the gas-turbine plant will serve initially the stationary power-generation field not by challenging the steam plant, but by supplementing it. The gas-turbine plant, at its present stage of development, has the peculiar characteristics to give it an aptitude for economic peak-load service that the steam plant cannot match.

All gas turbines for stationary power generation, built or being built in both the United States and Europe, have been characterized by:

1. The availability of very cheap fuel, such as cheap oil from pipe lines, or gas costing one-third as much per heat unit as coal at the mine mouth in Pennsylvania.
2. Low load factor.
3. Experimental large plants, in England and France, subsidized by their governments.

In addition, there always will be special cases. A gas-turbine generating plant has been installed in an English factory as insurance against a national coal shortage, and a gas-turbine plant has been justified in the United States by using its exhaust heat, under exceptionally favorable circumstances, to increase the output of another generating unit.

There are very few locations in the world that present the same attractive combination of low fuel cost and large, industrial, electric power consumption as the cities located near the southern oil and gas fields of the United States. The availability of gas at one-third to one-fifth the cost of coal makes this a most attractive territory for the economic installation of gas-turbine plants. Low fuel costs permit the use of simple plants that are very desirable as initial installations of a new type of plant. Announcements have been made of three small gas-turbine generating units to be installed in this territory.

In Great Britain there is no cheap fuel. This condition favors the complicated type of gas-turbine plant where every effort is expended to attain low heat consumption per unit of power generated. This efficient and high-cost type of plant, using high-cost liquid fuel, is not economic at present cost levels, except for applications having very low load factors. The British Ministry of Supply has contracts for 15,000-kw units to be installed near New Castle and Manchester, and a 12,500-kw Escher-Wyss-type closed-cycle unit near Glasgow. These units will be installed in existing power stations which supply power to the national grid in Great Britain. As experimental installations, these units may be operated or tested as their availability permits.

Paper 49-115, recommended by the AIEE power generation committee and approved by the AIEE technical program committee for presentation at the AIEE winter general meeting, New York, N. Y., January 31–February 4, 1949. Manuscript submitted November 16, 1948; made available for printing January 4, 1949.

F. T. Hague is a consulting engineer with the steam and aviation gas turbine divisions of the Westinghouse Electric Corporation, Lester, Pa.

The English objective is both domestic and export, and reflects the opinion that long range benefits will accrue to Great Britain through the development and patent control of all types of gas turbines. These installations have the primary objective of giving their manufacturers an opportunity to "get their hand in" by actually designing, manufacturing, and operating these rather large size units, in order to get first-hand experience with the problems involved. At this stage of gas-turbine development they believe that actual experience, through construction and operation, is more important to further progress than long term component research in laboratories that are not available in England at this time.

The pattern of gas-turbine development for power generation in France is quite similar to that in England. Electricitie de France is the nationalized instrument which is financing three installations. None of these is economic as base-load installations; all of them have been promoted to get first-hand operating experience. These installations are all for suburban Paris stations as follows:

1. A 2,000-kw open-cycle unit of conventional type.
2. A 15,000-kw combined steam and gas-turbine unit employing some 30 free-piston gas generators.
3. A 12,500-kw closed-cycle unit being built by Escher Wyss of Zurich, Switzerland.

These English and French plants are a government investment in gas-turbine development, for the purpose of providing test plants from which constructional and operating data can be obtained and coordinated, and without which no real progress in this field ultimately can be made. Our industrial firms would have to invest several million dollars in a development and construction program, without reasonable assurance of an economic market for the end product, to gain comparable experience to that which will flow from these government-subsidized programs.

It is an almost unanimous opinion, both here and abroad, that there remains much work in research and development before the gas turbine can be considered as a practical and economic power plant for base-load power generation in competition with coal-fired steam plants. It will be found very attractive as a peak-load plant. It must burn coal if it is to compete with coal-burning base-load steam plants. Its cycle efficiency increases three times as fast as in a steam plant for higher top temperatures, so that its future promise for lower cost power generation is tied up largely with material development and constructional problems to utilize temperatures 300 to 500 degrees Fahrenheit above present-day levels. The limited availability, at times of national emergency, of the rare elements essential to higher-temperature materials is being given consideration in this materials research.

Continuing development of the gas turbine's major components—compressors, combustors, and turbines—is being accelerated, in the gas-turbine aviation engine program, by the availability of government-sponsored component research laboratories. At the same time several manufacturers are acquiring essential practical experience, by making applications of gas turbine plants in those fields where it is now economic, thereby laying the groundwork to use important research developments as they become available.

Reference

1. **A. Mendahl.** *Brown Boveri Review* (Baden, Switzerland), October, 1946.

No Discussion

The Use of Air-Core Reactors as Fault Limiting Means on High Interrupting Capacity Controllers

JOHN D. LEITCH
FELLOW AIEE

THE USE of air-core reactors as current limiting means is very old and well established. They are used in large power networks for the protection of generating equipment and the transmission system. Because of the large currents in such networks, the reactors have very small inductances to avoid excessive voltage drops and are made of large conductors to keep losses within reasonable values. The electromagnetic forces, experienced during a fault, demand very rigid construction, consequently they often are embedded in concrete. If, however, reactors are installed in feeder or branch circuits where the normal currents are of much lower values, their inductances can be increased proportionately, limiting fault currents to lower values.

For many years it has been the general practice to install motor controllers with moderate interrupting capacity (ten times their rating) in branch circuits without regard to the available fault kilovolt-amperes at the point of installation. It was considered adequate to provide protection for these and other branch circuits with a backup circuit breaker. In the event of a fault, the controller opens before the circuit breaker but often fails to clear the circuit, thus requiring operation of the circuit breaker, but not before considerable damage has been done. To overcome this, there recently has been an increase in the use of current-limiting fuses in conjunction with moderate interrupting capacity controllers. It is difficult to correlate such fuses and controllers so that the fuse clears the circuit on partial faults slightly above the interrupting capacity of the controller. This correlation is much easier when current-limiting fuses are used in conjunction with high-interrupting capacity controllers. In either case one or more fuses must be replaced after the interruption of a fault.

When air-core reactors are designed to limit fault currents below the interrupting ability of moderate interrupting capacity controllers, the required inductances are so high that the reactors become too large and costly and the voltage drops too great.

When the reactors are designed for use with high-interrupting capacity controllers (50,000 kva), the required inductances are very much less and this, combined with the smaller currents in the motor branch circuits, results in reactors of surprisingly small size and weight.

This paper deals with the design and application of air-core reactors for motor branch circuits in conjunction with high-interrupting capacity controllers. By selecting reactors capable of limiting a source of infinite power to 25,000 kva, much of the time-consuming calculation of system constants is eliminated. There are, however, two factors which limit the range of application of such air-core reactors. One is their increase in size and weight with increase in horsepower while the other is the reduction in voltage at the motor during starting. These limitations are discussed in detail.

In selecting circuit breakers for installation at various points in a power distribution system, it is customary to calculate, or in some way determine, the maximum available fault current at each point and to select circuit breakers having interrupting abilities in excess of these possible currents. Any subsequent increase in the available kilovolt-amperes necessitates a review of the system to determine the adequacy of the protection provided by existing circuit breakers.

Similar analysis is usually made prior to the selection of high-interrupting capacity controllers in motor branch circuits although calculations rarely go beyond the last bank of transformers. Having estimated that the maximum available fault might be 20,000 kva, it is customary to install starters having interrupting capacities of 25,000 or 50,000 kva depending upon the likelihood of increasing the available kilovolt-amperes at some future date. Frequently, however, the available kilovolt-amperes is increased beyond the interrupting capacity of the controller, necessitating a costly change.

By the introduction of adequate impedance in the branch circuit at the controller, the maximum fault can be limited to 25,000 kva. If, in addition, the controller itself has an interrupting capacity of 50,000 kva, adequate protection is provided in the circuit irrespective of any future increase in the available kilovolt-amperes of the system. If a particular feeder circuit supplies power to more than one motor, it might appear to be good practice to install one set of air-core reactors for the entire group of motors. Should additional motors be connected at some future time, new reactors would probably be required. By installing individual reactors for each motor, the reactors themselves are smaller and the installation is independent of future changes in feeder load.

In calculating the size and weight of many air-core reactors, it was surprising how small they actually are for application within an appreciable and important range of motor sizes. Before discussing the reactors themselves and their application limitations, it might prove worth-

---

Paper 49-117, recommended by the AIEE industrial control committee and approved by the AIEE technical program committee for presentation at the AIEE winter general meeting, New York, N. Y., January 31–February 4, 1949. Manuscript submitted November 15, 1948; made available for printing December 20, 1948.

John D. Leitch is chief engineer with the Electric Controller and Manufacturing Company, Cleveland, Ohio.

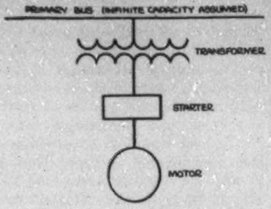

Figure 1. Motor feeder circuit

while to consider the characteristics of branch circuits.

Motor Circuits

When applying high-interrupting capacity controllers to motor circuits, it is customary to assume infinite available kilovolt-amperes at the primary of the feeder transformer, since the primary circuit impedance is usually low relative to that of the transformer itself and the motor lines. Figure 1 shows a typical motor circuit consisting of a transformer, a starter, and a motor. Other motors and starters may be on the same feeder, but need not be considered at present.

Assuming the transformer to have an impedance of 6 per cent, the maximum available kilovolt-amperes at its secondary terminals may be taken as its rated kilovolt-amperes divided by 0.06. The impedance of the transformer can be expressed as an equivalent secondary line reactance in equation 1.

$$\frac{E^2}{1{,}000X_L} = \text{maximum available kilovolt-amperes} \quad (1)$$

where E is the line to line open-circuit secondary voltage.

Table I lists the available kilovolt-amperes at the transformer secondary and the equivalent line reactance for a series of 6 per cent impedance transformers of different rated kilovolt-amperes having 2,300- and 4,600-volt secondaries.

The last four columns of Table I list the additional reactance per line necessary to reduce the available kilovolt-amperes to 25,000 and 50,000. For example, the equivalent line reactance of a 4,000-kva 6 per cent impedance transformer at 2,300 volts is 0.08 ohm, the reactance required to reduce infinite available kilovolt-amperes to 25,000 is 0.21 ohm, and the difference, 0.13 ohm, is the necessary additional reactance.

It is obvious that for transformers of lower rated kilovolt-amperes, there is no need for air-core reactors as a fault limiting means if controllers are used having interrupting abilities of 25,000 or 50,000 kva. The reactances of the lines themselves have been neglected, but if the lines are widely spaced and of considerable length they will reduce the available kilovolt-amperes at the motor. In applying air-core reactors as fault limiting means, it would be a waste of power and equipment to install them on a starter at the end of a long line.

Another impedance component between the transformer and the controller contacts is the overload relay. For a given design of magnetic overload relay, the coils are chosen according to the motor horsepower in such a way that the ampere-turns are essentially constant. This means that the number of turns varies inversely as the horsepower and the reactance varies inversely as the square of the horsepower. During a series of high-interrupting capacity tests, it was quite apparent that the overload relay coil impedance should not be neglected, especially at the lower horsepowers. Table II shows how the saturated impedance of an overload relay varies with the horsepower rating of its coil.

The saturated impedance of the 50-horsepower coil is about equal to that required per line to reduce infinite available kilovolt-amperes to 50,000 at 2,300 volts. It is therefore obvious that magnetic overload relays cannot be neglected on lower horsepower controllers and should be considered when applying fault limiting air-core reactors.

Table II. Saturated Impedance of Magnetic Overload Relay

Horsepower, 2,300 Volts	Turns	Saturated Impedance in Ohms (60 cycles)
25	120	0.361
50	65	0.104
100	34	0.028
300	12	0.0035
600	6	0.0009
1,200	3	0.0002

Table

Transformer Rating; Kva, 6 Per Cent Impedance	Available Kva at Transformer Secondary	Equivalent Line Reactance in Ohms		Additional Reactance Per Line Necessary to Reduce Available Kva			
				At 2,300 Volts		At 4,600 Volts	
		2,300 Volts	4,600 Volts	To 25,000	To 50,000	To 25,000	To 50,000
1,000	16,600	0.32	1.28	0	0	0	0
1,500	25,000	0.21	0.84	0	0	0	0
2,000	33,000	0.16	0.64	0.05	0	0.2	0
3,000	50,000	0.105	0.42	0.105	0	0.4	0
4,000	66,000	0.08	0.32	0.13	0.026	0.52	0.10
5,000	83,000	0.064	0.25	0.15	0.042	0.60	0.17
6,000	100,000	0.053	0.21	0.16	0.053	0.64	0.21
7,000	116,000	0.045	0.18	0.165	0.061	0.66	0.24
8,000	133,000	0.04	0.16	0.17	0.066	0.68	0.26
9,000	150,000	0.035	0.14	0.175	0.071	0.70	0.28
10,000	166,000	0.032	0.13	0.178	0.074	0.71	0.29
12,000	200,000	0.026	0.105	0.184	0.080	0.74	0.31

The possibility of designing magnetic overload relays which would at the same time serve as current-limiting reactors suggests itself. The conventional overload relay demands constant ampere-turns with variation in horsepower while the reactors demand constant inductance. In addition it is desirable that the power losses be constant over the horsepower range. Because of these limitations, the idea does not appear offhand to be economically practical.

Figure 2 shows graphically the reactance necessary to reduce any available kilovolt-amperes to 25,000 and 50,000 at 2,300 volts. These two curves differ in their ordinates by the constant amount 0.106 ohm, the reactance per line necessary to reduce 50,000 available kilovolt-amperes to 25,000. Referring to the ordinate for 200,000 available kilovolt-amperes, the amount of reactance required to reduce infinite available kilovolt-amperes to 200,000 is given by *BC* or *DE* on the two curves. This reactance (0.026 ohm) is only 14 per cent of that required (0.184 ohm) to reduce 200,000 available kilovolt-amperes to 25,000.

All the calculations so far have been based on steady-state fault currents. Actually the controller is called upon to interrupt currents of somewhat higher values because of the existence of transient d-c components. Under certain conditions if a short circuit is applied at the instant $E=0$, the current wave is displaced by an amount equal to the peak value of the steady-state wave. It can be shown easily that the total rms value of a completely displaced sine wave is equal to $\sqrt{3}$ times the rms value of the a-c wave alone. Actually the d-c component decays exponentially and disappears within a few cycles. If interruption occurs within the first half cycle (60 cycles per second), the total rms current interrupted might be as high as 1.5 times the rms value of the a-c component.

Should a completely displaced wave occur in one phase of a 3-phase system, the displacement in the other two phases will be half the a-c peak value and in the opposite direction since the sum of the d-c components is zero. This gives a total rms initial current of 1.23 times the rms value of the a-c wave and the average total rms initial currents for the three phases is 1.4 times the a-c rms current. A factor of 1.25 is often used in estimating the average of the total rms currents one half cycle after the fault, the difference between the 1.4 and 1.25 factors being an estimate of the decay of the d-c component during the first half cycle.

In applying current-limiting high-interrupting capacity fuses to motor feeder circuits, it is customary to multiply the available steady-state fault currents by 1.6 to obtain the total rms current that one of the three fuses may be called upon to interrupt during the first quarter cycle of a fault. In selecting circuit breakers for circuits having known available steady-state fault currents, the operating time of the circuit breaker is important, since the delay in opening is used along with the decrement characteristics of the circuit in determining the total rms current to be interrupted.

High-interrupting capacity controllers, which are not latched-in, start to part their contacts within a cycle of the instant of fault. Tests show the presence of total rms currents as high as 1.5 times the a-c component at the instant of interruption. Thus the interrupting capacity of the controller should be at least 50 per cent above the maximum available steady-state fault kilovolt-amperes. The present top rating of standard high-interrupting capacity controllers is 50,000 kva at 2,300 and 4,600 volts, based on the average of the phase currents including the d-c components. Therefore it was decided to use air-core reactors which would limit infinite available kilovolt-amperes to 25,000 steady state, thereby providing an additional factor of safety over that inherent in the controller.

Design and Application of Reactors

The reactance required to reduce any available kilovolt-amperes from one value to another is proportional to the square of the voltage, and the inductance corresponding to any reactance varies inversely as the frequency of the system. Table III lists the various inductances corresponding to the required reactances.

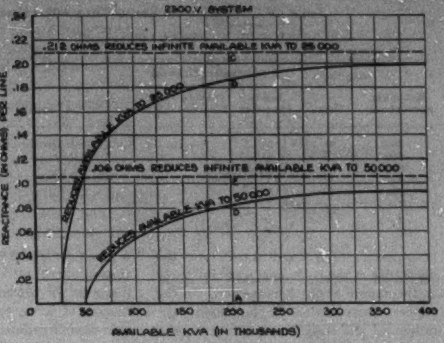

Figure 2. Reactance required to limit kilovolt-amperes to 25,000 and 50,000

Similar tables could be prepared for the inductances required to limit the available kilovolt-amperes to 50,000 and of course to extend the range in voltages and frequencies. This paper deals primarily with 2,300- and 4,600-volt systems, although comments will be made later regarding low-voltage systems. From an economic point of view, it is desirable to use a minimum number of reactors for a given range in motor sizes. By considering only infinite available kilovolt-amperes, the required number of reactors is reduced to a minimum and each installation is independent of the system constants and future changes in the available kilovolt-amperes.

Before a given reactor can be designed for a motor circuit of given horsepower, it is necessary to determine an acceptable power loss per coil at full load current. Heat tests were made in a controller enclosure, of approximately the anticipated size, to determine the temperature rise produced by various losses up to 200 watts per reactor. It was found that 100 watts per coil or 300 watts for a 3-phase controller gives a temperature rise less than 20 degrees centigrade and this was accepted as a reasonable power loss. In all of the design calculations which follow, this figure was used in determining the cross-section of the reactor winding.

The foregoing limitations can be used in conjunction with the well-known empirical formula[1]

$$L = \frac{aN^2}{238 \times 10^6} \text{ henries} \tag{2}$$

in designing air-core reactors. N is the number of turns and a is the radius of the mean turn in inches. This formula is very useful in making a rough estimate of the size of a given reactor and holds quite accurately where $a = 1.5b = 1.5c$, a, b, and c having the meanings shown in Figure 3.

A modification of the above formula is

$$L = aN^2 p \times 10^{-7} \text{ henries} \tag{3}$$

where the factor p is a function[2] of $b+c/2a$. This formula is useful where the above relationship between a, b, and c does not hold. There are other well-known empirical formulas,[3,4] of greater complexity which can be used where higher accuracy is required.

Using these formulas along with the power loss limitation, a series of air-core reactors was designed for 2,300-volt 60-cycle motors from 200 to 1,500 horsepower. The results of these calculations are listed in Table IV.

Table IV shows not only how rapidly the size of the reactor increases with horsepower, but how surprisingly small the reactors are for motors up to 600

Table III

Change in Available Kva From	To	Required Reactance 2,300 Volts	4,600 Volts	Required Inductance (in Millihenries) 2,300 Volts 60 Cycles	25 Cycles	4,600 Volts 60 Cycles	25 Cycles
Infinity	25,000	0.212	0.85	0.56	1.34	2.24	5.36
400,000	25 000	0.198	0.79	0.53	1.27	2.12	5.07
300,000	25,000	0.194	0.77	0.515	1.23	2.06	4.92
200,000	25,000	0.185	0.74	0.492	1.18	1.97	4.74
100,000	25,000	0.16	0.64	0.425	1.02	1.70	4.08
50,000	25,000	0.105	0.42	0.28	0.695	1.12	2.78

Tab.e IV. Variation in Reactor Size with Horsepower

(0.56 Millihenry)

Maximum Horsepower	Turns	Dimensions (Inches) Inside Diameter	Outside Diameter	Width	Size of Copper	Resistance in Ohms at 25° C	Weight in Pounds
200	66	$3\frac{3}{4}$	$7\frac{1}{2}$	2	Number 5 square	0.0243	12.25
400	54	$5\frac{3}{4}$	$12\frac{3}{8}$	3	$\frac{3}{32}\times1\frac{3}{4}$	0.0087	56.5
600	54	$5\frac{3}{4}$	14	4	$\frac{1}{8}\times1\frac{3}{4}$	0.0050	114
1,000	38	12	$24\frac{3}{4}$	$6\frac{1}{4}$	$\frac{5}{16}\times2\frac{7}{8}$	0.00164	625
1,500	40	14	32	$11\frac{1}{2}$	$\frac{7}{16}\times5\frac{1}{8}$	0.0007	2,240

horsepower. For fixed watts loss, the resistance of the coils must vary inversely as the square of the horsepower. As the copper cross-section is increased, the radius of the mean turn increases and consequently the weight of the reactor increases faster than the square of the horsepower. Figure 4 shows graphically how the reactor weight varies with horsepower. It will be noted that the average gradient of this curve is quite low up to 600 horsepower and that thereafter it increases rapidly. This suggests placing an upper limit of about 600 horsepower on the application of air-core reactors on 2,300-volt 60-cycle systems. If this were the only reason for such a limitation, it might be acceptable to permit greater power loss per reactor for 1,000- and 1,500-horsepower motors. If, for example, the 600-horsepower reactor in Table IV were used with the 1,000-horsepower motor, the power loss would be increased to about 320 watts at full load current. Similarly if a new reactor were designed for the 1,500-horsepower motor allowing 400 watts loss per coil, its weight would be reduced to about 300 pounds. There is however another and more important limitation to the application of air-core reactors. This limitation will be discussed later.

It is desirable to use the same enclosure for all sizes of reactors within the range of a given controller. This places a limitation of about $14\frac{1}{2}$ inches on the outside diameter for the enclosure in mind. For reasons of economy in mounting, the inside diameter should be limited to one or two sizes. These conditions are met by the first three reactors on Table IV.

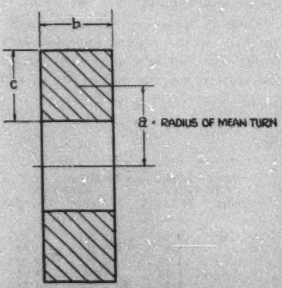

Figure 3. Cross section of reactor

If reactors are designed for various horsepowers at other voltages and frequencies, the same general results will be obtained. For 25-cycle systems, the inductances must be increased by the ratio 60/25 to obtain the same reactances, consequently the reactor size and weight will become quite large at about 300 horsepower.

For 4,600-volt 60-cycle systems, the reactors will have four times the inductances for 2,300-volt systems. For the same reactor dimensions, the reactance and resistance remain in the same ratio, consequently for the same power loss, the reactors again will become large at about 600 horsepower. Similarly 4,600-volt 25-cycle reactors will be limited to about 300 horsepower.

Table V lists eight reactors having weights less than 115 pounds and outside diameters less than $14\frac{1}{2}$ inches which may be applied to a wide range in motor sizes, a range which statistically represents more than 90 per cent of the total applications in this field.

Reactor 1, on Table V, weighs only $12\frac{1}{4}$ pounds. Obviously it would not be worthwhile considering additional reactors for motors lower than 200 horsepower. The power loss at full load current (50 amperes) is only 60 watts and of course will be less with smaller motors.

Had 50,000 been chosen instead of 25,000 as the limited kilovolt-amperes, the inductances required would have been halved and the maximum horsepower increased about 40 per cent. There is no reason why such a choice could not be made and the reactors used in conjunction with controllers or circuit breakers having interrupting capacities in excess of 50,000 kva. Such a procedure might be warranted for horsepowers above those listed in the last column of Table V.

Effect of Air-Core Reactors on Motor Voltages and Torque

It is important to know the effect of the air-core reactors on the motor torque during starting and running. Figure 5 shows the power circuit of a motor and controller with air-core reactors.

Assuming a star-connected motor and letting $\mathbf{Z}_m$ represent the equivalent impedance of each of the 3-phase windings at any motor speed, then

$$\mathbf{Z}_m=R_m+jX_m=\frac{E\underline{|0}}{\sqrt{3}I_m\underline{|-\theta}}$$
$$=\frac{E}{\sqrt{3}}\cdot\frac{\cos\theta+j\sin\theta}{I_m} \qquad (4)$$

where R_m and X_m are the equivalent resistance and reactance respectively of each of the windings and I_m is the current when the motor is connected directly to the line without reactors and θ is the angle of current lag behind the voltage.

When the air-core reactors are included, the total equivalent impedance per phase is given by

$$\mathbf{Z}_t=\mathbf{Z}_m+\mathbf{Z}_r=R_t+jX_t \qquad (5)$$

where $\mathbf{Z}_r$ is the reactor impedance. Neglecting the resistance of the reactors makes $R_t = R_m$ and

$$\mathbf{Z}_t=R_m+jX_t=\sqrt{R_m^2+(X_m+X_r)^2}\,\underline{|\theta_1} \qquad (6)$$

where

$$\theta_1=\tan^{-1}\left(\frac{X_m+X_r}{R_m}\right)$$

If I is the motor current with reactors

$$\mathbf{I}=\frac{E\underline{|0}}{\sqrt{3}}Z_t\underline{|\theta_1}=\frac{E\underline{|-\theta_1}}{\sqrt{3}Z_t} \qquad (7)$$

The drop in voltage across each reactor is given by

$$V_r=\mathbf{I}\mathbf{Z}_r=\frac{E}{\sqrt{3}}\cdot\frac{\underline{|-\theta_1}}{Zt}\cdot X_r\underline{|90\text{ degrees}}$$
$$=\frac{EX_r\underline{|90-\theta_1}}{\sqrt{3}Z_t} \qquad (8)$$

and the voltage across each phase winding of the motor is

$$V_m=\frac{E}{\sqrt{3}}-V_r \qquad (9)$$

The voltage at the motor with reactors expressed as a percentage of that without reactors is $\sqrt{3}\ V_m\times100/E$ while the per cent motor torque is $3V_m^2\times100/E^2$.

Applying these equations to the five reactors and the corresponding motors of Table IV and assuming the motors to have full-voltage locked-rotor currents of seven and ten times full load current, the effect

Table V. Application of Air-Core Reactors

Reactor	Inductance, Millihenries	Reactance, Ohms	Volts	Frequency	Maximum Horsepower
1	0.56	0.21	2,300	60	200
2	0.56	0.21	2,300	60	400
3	0.56	0.21	2,300	60	600
4	1.34	0.21	2,300	25	200
5	1.34	0.21	2,300	25	300
6	2.24	0.84	4,600	60	300
7	2.24	0.84	4,600	60	600
8	5.36	0.84	4,600	25	300

of the reactors on motor voltage and torque is shown in Table VI.

In making the calculations shown in Table VI the standstill power factor of the motors having an inrush of seven times full load current was assumed to be 0.35 and that for motors having an inrush of ten times full-load current 0.30. A full-load power factor of 0.85 was assumed for all motors. Table VI shows the small change in per cent power factor ($\cos \theta - \cos \theta_1$) $\times$ 100 caused by the air-core reactors at full load.

For a given series of reactors having a constant inductance, the voltage drop across the reactors is proportional to the horsepower of the motor. Obviously there will be a practical upper limit to the motor size with which the reactors can be used, and this will be decided by the reduction in motor torque that can be tolerated during starting. As in the case of the reactor size limitation, it appears that 600 horsepower on 60-cycle systems is a good practical limit of application, and that the starting torque requirements should be watched closely on large drives.

The effect of air-core reactors on motor torque during acceleration from rest is shown in Figure 6. The curves apply to a series of 2,300-volt 60-cycle motors having full voltage inrush currents of 6.65 times full-load current. These curves were determined from typical speed-torque and speed-current curves[5] for class *A* squirrel-cage induction motors, assuming a standstill power factor of 0.35 and a full-load power factor of 0.85.

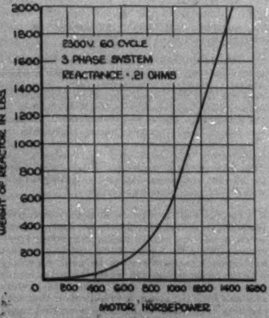

Figure 4. Weight of reactors versus motor horsepower

Air-core reactors used in this way, particularly on the larger sizes of motors, convert an "across-the-line" starter into an automatic reduced voltage starter without the use of an additional contactor and transfer relay.

Electromagnetic Forces

The method of mounting the air-core reactors in the controller enclosure is shown in Figure 7. The reasons for selecting such an arrangement of the coils are:

1. To reduce the mutual inductance between the coils and assure a reactance per line independent of phase sequence.
2. To provide individual and uniform mounting.
3. To provide simple and rigid assembly.

The eddy-currents induced in the wall of the steel cabinet are negligible at normal frequency. Any high-frequency oscillations during the interruption of the circuit will be damped more quickly by the eddy-current effect in the enclosure wall.[6]

With three coils mounted as shown in Figure 7, the electromagnetic forces between them produce torques about their perpendicular diameters, the greatest being that on the center coil marked (2). For coils of fixed dimensions and fixed spacing, the force between them is proportional to the square of the ampere-turns or proportional to LI^2 where L is the self-inductance of each coil. For the same fault kilovolt-amperes, the quantity LI^2 is constant for both 2,300- and 4,600-volt systems at the same frequency since the inductances are proportional to the square of the voltage and the fault current is inversely proportional to the voltage. The inductances also vary inversely with system frequency while the fault currents are independent of the frequency, hence the electromagnetic forces on reactors used on 25-cycle systems will be 2.4 times the corresponding forces on 60-cycle systems.

Three reactors were arranged for test as shown in Figure 7, reactors (1) and (3)

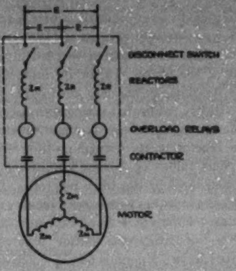

Figure 5. Motor and controller with reactors

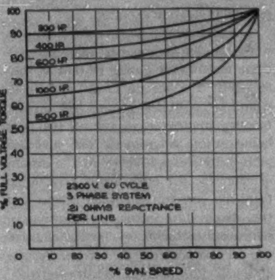

Figure 6. Effect of reactors on motor torque

Table VI. Effect of Air-Core Reactors on Motor Voltage and Torque, 2,300-Volt 60-Cycle Systems, 0.21 Ohm Reactance per Line

	Full Load Conditions				Starting Conditions					
					Inrush Currents		Motor Volts in Per Cent Line Volts		Motor Torque in Per Cent Full Voltage Torque	
Maximum Horsepower	Current	Motor Volts in Per Cent Line Volts	Motor Torque in Per Cent Full Voltage Torque	Reduction in Per Cent Power Factor	7×Full Load Current	10×Full Load Current	7×Full Load Current	10×Full Load Current	7×Full Load Current	10×Full Load Current
200	50	99.5	99.0	0.3	333	465	95.1	93.0	90.5	86.4
400	100	99.0	98.0	0.6	685	868	90.6	86.9	82.0	75.3
600	150	98.9	97.7	1.0	905	1,220	86.5	81.2	74.4	66.1
1,000	250	97.9	95.8	1.8	1,387	1,810	79.4	72.5	63.0	52.5
1,500	375	96.7	93.2	3.0	1,873	2,390	71.7	63.3	51.2	40.1

being rigidly fixed while the center reactor (2) was carefully pivoted about its vertical diameter. Current was led in and out of the center reactor by immersing the terminals in mercury-filled cups. An accurately calibrated spring was used in determining the torque required to return the reactor to its normal position when various values of 3-phase currents were passed through the three reactors. The measured torques were proportional to the square of the currents as expected, and by extrapolation the torque was estimated to be 75 pounds feet at 6,250 amperes, the current corresponding to 25,000 kva at 2,300 volts. If the current were reversed in reactor (3) the torque was negligibly small as expected.

The particular reactors used in the test were the 200-horsepower 2,300-volt 60-cycle reactors on Tables IV and V, consequently the torque for 25-cycle coils would be about 180 pounds feet. These torques are the mean values, the peak being twice as great or 150 and 360 pounds feet respectively. At the instant of fault the d-c components give initial total rms currents somewhat in excess of the steady-state currents. Allowing an additional factor of two for the effect of the d-c components, the torques become 300 and 720 pounds feet respectively. Unbalanced faults may increase these forces up to 50 per cent but even then the torques do not present any mounting difficulties.

Short-Time Current Ratings

Short-time current ratings of conductors are expressed in amperes for one-quarter second, one-half second or any other short time interval. The short-time current ratings of the reactors and any other components of the controller must be in excess of the maximum anticipated fault currents for the time the controller takes to interrupt the circuit. The smallest of the eight reactors, in Table IV, is wound with number 5 square wire and has a one-quarter second rating of 12,000 amperes. This is considerably in excess of that required since the interrupting time of the controller is of the order of 0.05 second.

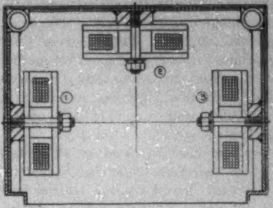

Figure 7. Arrangement of reactors in controller enclosure

Low-Voltage Applications (Up to 600 Volts)

A similar study was made of low-voltage systems with a view to determining the practical range of application of air-core reactors. The size and weight of the reactors themselves and their effect in reducing the voltage at the motor, particularly during starting, were the critical factors.

About 95 per cent of the activity in the low-voltage field is covered by motors up to 200 horsepower. In general, transformer banks are not larger than 3,000 kva, giving a maximum available kilovolt-ampere of about 50,000 at 6 per cent impedance. This results in fault currents of considerable magnitude on 'ow-voltage systems, for example 65,700 amperes at 440 volts. By a study similar to that made in the case of 2,300- and 4,600- volt systems, it can be shown that for maximum available fault currents in excess of 30,000 amperes, reactors may as well be designed for an assumed infinite available fault current. This is comparable to the conditions found with high-voltage reactors where available kilovolt-ampere is in excess of 200,000.

Following the same procedure as in the case of high-voltage systems, it was necessary to choose a limit for the fault current. If 10,000 steady-state amperes is chosen, and similar limitations in weight and starting torque are accepted, it appears that the range of application would be 100 horsepower at 220 volts and 200 horsepower at 440 and 550 volts. The 10,000-ampere limitation demands the use of controllers having rated interrupting capacities of 15,000 amperes or better including the d-c components.

References

1. ESSENTIALS OF TRANSFORMER PRACTICE (book), **E. G. Reed.** D. Van Nostrand Company, Inc., New York, N. Y., 1927, 2nd Edition, page 233.

2. MERCURY ARC POWER RECTIFIERS (book), **O. K. Marti, H. Winograd.** McGraw-Hill Book Company, New York, N. Y., 1930, page 424.

3. STANDARD HANDBOOK FOR ELECTRICAL ENGINEERS, 5th Edition. McGraw-Hill Book Company, New York, N. Y., 1922, section 2-70, page 72.

4. BUREAU OF STANDARDS BULLETIN. United States Department of Commerce, Washington, D. C., volume 8, number 1.

5. STANDARD HANDBOOK FOR ELECTRICAL ENGINEERS, 7th Edition. McGraw-Hill Book Company, New York, N. Y., 1941, section 7-239, pages 715-16.

6. TEST CODE FOR OIL CIRCUIT BREAKERS. American Standards Association (New York, N. Y.), C37.9, 1945, pages 41-2.

Discussion

E. H. Alexander (General Electric Company, Schenectady, N. Y.): In this paper the author has treated, in a thorough manner, the design and use of air core reactors for the special requirements of mounting within the enclosure of a high-voltage high-interrupting-capacity controller. The recognition of the need for controllers of adequate interrupting capacity is indeed timely for it has long been a neglected equipment in the circuit between the source of power and the power utilization apparatus as far as interrupting capacity is concerned.

Recently, air-core reactors also have gained somewhat in popularity as a means for limiting short circuit current on low voltage a-c systems, especially in the case of relatively low ampere feeder circuits originating from a bus of high short-circuit capacity where the economics of a full capacity or cascaded circuit breaker is unattractive. This is recognized in the Leitch paper. In this case, as in the case of the high-voltage motor controller, the current limiting reactor as a means of reducing fault current has to be appraised on the basis of cost, physical size, energy losses, and the penalty of voltage drop which it produces under various conditions of load.

There are several points in Leitch's paper which I feel should have further amplification and clarification, as follows:

1. From the standpoint of a co-ordinated equipment, it is assumed that the hook-operated disconnecting switches, shown schematically in Figure 5 of the paper, have ample momentary current ratings to withstand the magnetic effects of the short-circuit currents permitted by the reactor. This, of course, pre-supposes the short circuit to be at or beyond the load side of the reactor. These currents could be as high as 10,800 amperes. It is for this same reason that a 50,000-kva controller was selected, even though the steady-state fault currents were limited to 25,000 kva.

2. The short-circuit values calculated for Table I give values at the transformer secondary which originate from the transformer only. The table does not take into consideration an allowance for induction or synchronous motor contribution on the low-voltage side of the transformer. In practical short-circuit studies, better evaluations or assumptions can often be made, without seriously complicating the short-circuit calculations, and these more careful results could lead very easily to different conclusions, in certain circumstances, with regard to equipment selection.

3. The effect of the reactors on motor torque plotted in Figure 6 of the paper does not appear to be a severe penalty to pay for the average motor application. While the author has stated frankly that application precautions must be used, especially with the larger motors and where the motor torque requirements tend to be close to the normal values available from the motor, it would appear that such checking may have to be done somewhat more carefully than he implies to be sure of avoiding trouble. Such applications as ball mills, tube mills, positive displacement pumps and crushers would certainly be examples requiring more elaborate

investigation to determine if the reduced torque caused by the reactors could be tolerated. On the other hand, leading power factor synchronous motors, when running in synchronism, would actually have their terminal voltage slightly increased by the presence of the reactor.

4. The thermal and mechanical phases of the reactor design were not covered in great detail. As far as the losses in the reactor are concerned, we would presume from the paper that they were 100 watts or less per reactor. I would like to ask the author what he considers good engineering practice for the temperature rise limitations of the copper used on the reactor winding for the various conditions of normal running current; prolonged high starting currents; and short-circuit conditions. The extrapolation of the torque values produced by the electromagnet forces between the reactors was treated in the paper. Whereas sound conclusions may be arrived at by such a method, it would seem that more reliable data could be obtained by full capacity overcurrent tests on completely co-ordinated motor controllers, not only to check the mutual forces between the reactors, but also to check the mechanical or bursting strength of each individual reactor.

5. With available power switching equipment limited to 150,000 kva interrupting capacity at 2,400 volts and 250,000 kva interrupting capacity at 4,160 volts, the need for embracing systems in excess of these values is rather small. That there are such systems, in excess of the above values in existence, is fully recognized but they are fortunately few and far between, and are by no means a compliment to sound distribution engineering.

F. H. Kierstead (General Electric Company, Pittsfield, Mass.): Leitch is to be complimented on his development of reactors for this service that are so small, light, and inexpensive.

The description shows the reactor to be a simple back-turn section coil without ventilating ducts. The dimensions of the conductor given in Table IV appear to be in error inasmuch as 3/32 by $1^{1}/_{4}$ inches fit the dimensions of the coil, the resistance and the weight that are given.

In achieving simplicity of construction, a sacrifice has had to be made to eddy losses in the winding and to ventilating area. This results in high watts per square inch of dissipating surface and, one would expect, high coil temperature rises over surrounding air. The losses in the metal nut welded to the enclosure under the coils are probably fairly high, and if so would furnish additional heat to the coils by conduction.

The losses in the reactor coils and the losses which these coils generate in the enclosure walls contribute to a general rise in air temperature within the enclosure.

Leitch has pointed out that this rise is 20 degrees centigrade above outside ambient.

One would expect the accumulated effect of these factors to result in rather high coil temperature rises above outside ambient. Perhaps Leitch will want to say what the actual ultimate rise was when carrying the full 100-ampere load current of the motor, and also, what class of insulation was used.

With the back-turn section used and the dimensions of the coils as given, the distance between the ends of the winding cannot be much greater than 3/8 inch. This distance has to stand 75 per cent of the line to neutral voltage of the circuit, $(0.75\times2{,}300/\sqrt{3})$ when undergoing short circuit. Furthermore, if these coils are built to American Standards Association specifications for current limiting reactors used on 2,300-volt circuits, they will have to stand 25 kv applied between winding and ground as well as 25 kv applied between terminals.

It is quite possible that the insulations standards set up for current limiting reactors are too stringent for industrial applications. The possibility of setting up an industrial standard could be explored profitably. However, the establishing of two insulation standards would have several disadvantages, and should be adopted only after careful consideration of all factors. Leitch may want to state what insulation level his coils will meet.

John D. Leitch: The hook-operated disconnecting switches shown in Figure 5 are provided with blade locks.

Table I was intended primarily to show how little additional reactance is required to take care of infinite available kilovolt-ampere compared with that required for 200,000 kva. The decision to design for infinite available kilovolt-amperes eliminates the necessity of considering the existence of any synchronous machines on the secondary side of the transformer.

Alexander is quite correct in stating that care must be taken in applying fault limiting air-core reactors to motors of larger horsepower to assure adequate starting torque. This limitation is covered in detail on Table VI. Frequently reduced voltage starting is a requirement on higher horsepower drives.

The paper is somewhat longer than the usual six pages, consequently space was not available to go into the thermal and mechanical details of the reactors. Only sufficient information was given to show how surprisingly small the reactors can be.

The 200-horsepower coil on Table IV has a temperature rise of 90 degrees centigrade at its rating. The 400-horsepower coil was never built, but from tests on other coils of approximately the same size, its temperature rise should not exceed 100 degrees centigrade at its rating. The thermal capacity of the reactors is quite large and will withstand repeated starts equally as well as the motor. Class "B" insulation is used throughout the coils and according to NEMA Industrial Control Standards[1] a temperature rise of 105 degrees centigrade is permitted although such standards do not specifically include air-core reactors.

The I^2R losses at 25 degrees centigrade should be kept as low as practical in order to reduce the total watts including eddy-current losses in the winding. A slight increase in the weights and greater consideration to the proportions of the coil not only reduce the I^2R losses but also the eddy current loss per pound. This results in less total watts and greater surface area and consequently lower temperature rise. It is quite possible to obtain a series of coils having less than 80 degrees centigrade rise with very little additional copper.

It is acknowledged that the determination of the electromagnetic forces is only approximate. Prior to the presentation of the paper, arrangements had been initiated for tests such as those suggested by Alexander.

Kierstead points out that in achieving simplicity in construction and mounting, a sacrifice has been made to eddy-current losses within the winding and to the ventilating area of the coil. This is the penalty that must be paid for such compactness and ruggedness.

The total flux is proportional to the current or horsepower for a given series of coils having approximately the same number of turns. The effect of this flux on the mounting stud and welded nut is negligible for the lower horsepowers, but is significant at 400 horsepower and up. It becomes necessary to use nonmagnetic stainless steel in mounting the larger coils and to increase the distance between the coil face and the wall of the enclosure. This demands consideration of enclosure size for the larger horsepowers. With increase in size of the coils, there is also an increase in the total watts, requiring a larger and perhaps louvered enclosure. Such ventilation is hardly necessary with the smaller coil particularly when the enclosure is large because of the presence of disconnect switches and bus bars above the reactors.

Kierstead discloses an error on Table IV. This is a typographical error, the 400-horsepower coil winding should be 3/32 by $1^{1}/_{4}$ inches not 3/32 by $1^{3}/_{4}$ inches, as stated.

It is fully appreciated that the coils must have high insulation levels. The double glass wire wound coils have been abandoned in favor of strap wound coils. The insulation between turns is 0.010-inch glass cloth impregnated with thermal-setting varnish. On test this insulation breaks down at 3,500 rms a-c volts. The strap wound coils indicated in the paper are of the 2-layer back-turn construction with 1/4-inch insulation between layers. This insulation extends beyond the outside diameter of the winding giving a creepage distance of $1^{1}/_{4}$ inches between outside turns which is more than adequate for 25,000 volts.

It is somewhat premature to discuss standards for current limiting reactors used with motor starters. It is possible to meet the present ASA standard C57-16, 1948[2] as far as continuous temperature rise and insulation levels are concerned.

REFERENCES

1. INDUSTRIAL CONTROL STANDARDS. *Publication 45–97*, National Electrical Manufacturers Association (New York, N. Y.), September 1945.

2. AMERICAN STANDARD FOR CURRENT LIMITING REACTORS, C57-16. American Standards Association (New York, N. Y.), 1948.

A Square-Law Power-Level Recorder

W. R. CLARK
MEMBER AIEE

W. R. TURNER
ASSOCIATE AIEE

A. J. WILLIAMS, JR.
MEMBER AIEE

Synopsis: A square-law power-level recorder is described which is a new and improved version of a type of recorder which measures a-c voltage (or power level) on a linear decibel scale by means of a motor-balanced slide-wire attenuator.[1] The detector, which is responsive to the mean square of the instantaneous voltage of its input, and the problems encountered in the insertion of this detector into the instrument, are described in detail. Other improvements in the circuit with the resulting improved performance are presented.

THE DEMAND for more accurate measurements of power levels, as well as the increasing interest in the frequency characteristic of voice and carrier channels, filters, high fidelity amplifiers, and so forth, has created the need for an instrument to record quickly and accurately these measurements.

In this recorder, the voltage to be measured is applied to the input terminals of a ladder-type slide-wire attenuator which is adjusted by the balancing motor so that the output voltage of this attenuator is always returned to a standard value. This method, which is the same as the standard manual method of making attenuation measurements, eliminates the need of designing an a-c amplifier having reproducible characteristics over a large range of input voltage, and also eliminates the need for a dynamic element with a logarithmic response.

In the operation of the recorder it is essential that a d-c voltage be produced which is related to the magnitude of the a-c input signal. This detector may be designed to function from its peak input voltage, from its average input voltage after rectification, or, preferably, from the mean of the square of its instantaneous input voltage. This "square-law" type of detector is preferred, because it handles an input composed of two or more components of different frequency in such a way that their relative phase has no effect upon the mean detector output.

The development of this type of recorder, which employs a square-law detector and incorporates other circuit improvements to obtain better performance, was started during the war to meet a specific need of the Naval Ordnance Laboratory.

The resulting instrument, Figure 1, has a scale linear in decibels, and a range of 40 decibels above a zero reference level of 0.0002 milliwatt with a 125-ohm input impedance. (Recorder ranges of 20 decibels, 50 decibels and 60 decibels also have been built.) The frequency error is less than 0.1 decibel between 20 and 200,000 cycles, Figure 2. Abrupt changes of power level of 30 decibels can be recorded in 1.5 seconds. The limit of error is ±1/3 per cent of full scale over its frequency range, provided peaks in the wave form of the voltage being measured do not exceed four times the rms value of that voltage. The performance of the recorder is independent of line voltage variations or changes in frequency of the line voltage. It requires no batteries, being entirely a-c operated. The record is made with ink on a chart 10 inches wide, driven by a synchronous motor at standard speeds of 2 inches per minute or 4 inches per hour.

Figure 3 shows a sample chart made by a 40-decibel recorder. It was obtained by connecting the recorder to a decade attenuator which was supplied from a constant 1,000-cycle source. The attenuator was changed in 3-, 10- and 30-decibel steps, causing the recorder to plot the chart shown. It is apparent from this record that even though the recorder is fast, its error is less than 1/3 per cent of full scale, the dead range is negligible, and the recorder draws a smooth curve without overshooting the balance point.

General Description

In the operation of the recorder, the a-c voltage to be measured is connected to a ladder-type slide-wire attenuator, Figures 4 and 5. The attenuator output is amplified by an a-c amplifier; it then goes through an inverter stage before being "detected." A full-wave detector employing two pentodes is used. The circuit constants of the tubes are adjusted so that the detector has a square-law response. In order to obtain the same type of recorder performance for increasing signals as for decreasing signals, the output of the detector is filtered and limited. This d-c voltage is reduced by a standard d-c voltage and by the d-c voltage generated by a tachometer, the remainder being amplified by a d-c amplifier. The tachometer, mounted on the slide-wire motor shaft, generates a voltage proportional to the speed of the recorder and thus prevents overshooting. The output voltage of the d-c amplifier goes to the grids of the double-triode converter. This tube controls the firing of the two thyratrons that control the direction of rotation of the slide-wire motor. When the voltage across the grids of the double-triode has one polarity, one thyratron will fire, and the motor will move the slide-wire attenuator towards the balance position. A reversal of polarity causes the second thyratron to fire and the motor to move the attenuator in a reverse direction, but again towards the balance position. In all cases the motor moves

---

Paper 49-120, recommended by the AIEE joint subcommittee on electronic instruments and approved by the AIEE technical program committee for presentation at the AIEE winter general meeting, New York, N. Y., January 31–February 4, 1949. Manuscript submitted November 15, 1948; made available for printing December 27, 1948.

W. R. Clark is supervisory technologist, and A. J. Williams, Jr. is chief of the electrical division, of the research department of the Leeds and Northrup Company, Philadelphia, Pa. W. R. Turner formerly with the Naval Ordnance Laboratory, White Oak, Md., is now in Pasadena, Calif.

The authors are very grateful to R. E. Watson for his assistance in this development.

Also presented at the National Electronics Conference, Chicago, Ill., November 4–6, 1948.

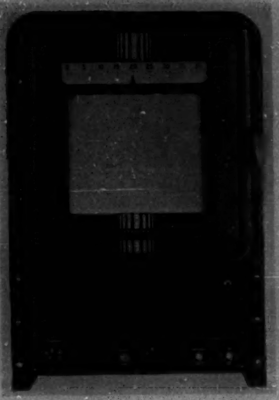

Figure 1. Square-law power-level recorder

the attenuator so that the input to the a-c amplifier is always brought to the same a-c voltage when the recorder is at the balance position.

The position of the slide-wire attenuator, which is indicated by the pointer of the recorder and recorded by the pen on the chart, is a measure of the power level of the input to the recorder above the zero reference level.

Component Parts

Slide-Wire Attenuator

The slide-wire attenuator, Figure 6, is a continuously-variable unbalanced-π-section attentuator, in which the series coils are the equal sections of a tapped slide-wire; the shunt coils are connected to these taps. Since the attenuator is contiuuously variable, the recorder will plot a smooth record. The decibel range of the recorder is determined by this attenuator.

The frequency characteristic of the recorder depends on the frequency characteristic of the attenuator, as well as that of the a-c amplifier, inverter, and detector. As can be seen from the inserts of Figure 6, the slide-wire is wound reversed-turn with constantan wire on a hard-rubber rod, and the shunt coils are woven resistors of manganin that have negligible reactance at the frequencies used.

Since the attenuator is at the input end of the recorder, Figures 4 and 5, the input impedance of the recorder is the characteristic impedance of the slide-wire attenuator.

In an attenuator of this type, the attenuation in decibels at successive shunt coils varies linearily with slide-wire position, but between shunt coils the variation is not linear. However, by using sufficient shunt coils, this error can be made negligible. If the decibel range of the recorder and the allowable error are known, the number of sections that should be used can be determined easily. (Equations and graphs used in determining this are given in the Appendix of W. R. Clark's paper.[1])

A-C Amplifier

The output of the attenuator is amplified by the a-c amplifier, Figures 4 and 5, which has a flat frequency response, caused by low-value plate resistors, large coupling condensers, and low-frequency compensation networks.

The gain of this amplifier determines the input level at which the recorder will operate. The lowest input of all standard recorders is 0.2 microwatt or 5 millivolts.

A gain control, marked "Input Level," Figure 5, is provided so that the input level can be adjusted over a range of almost ten decibels without otherwise affecting the operation of the recorder.

Inverter

A conventional single-tube-type inverter is used which employs equal resistors in the plate and cathode circuits

Detector

The desired property for the plate-rectification-type of vacuum-tube square-law detector is that the change in its plate current be proportional to the square of the instantaneous signal voltage. This change of plate current must develop a voltage across a load resistor at the input to a resistance-capacitance (*RC*) filter. Because of the averaging action of this filter, its output (measured from the quiescent state) will be proportional to the square of the instantaneous voltage applied to the detector input.

The search for the tube with the desired properties for a square-law detector started with the realization that a perfect linear variation of transconductance with control-grid voltage means a perfect quadratic variation of plate current with grid voltage see Figure 7. Certain pentodes, in particular the *12SH7*, approach this characteristic, under selected values of the operating parameters.

Since the quiescent grid voltage is at or very near to cutoff, negative swings of the grid are off the quadratic curve; hence, another tube must be used, with its grid driven from the other half of the phase inverter. The two tubes share a common plate load resistor which serves to combine their outputs. The two-tube detector practically eliminates the fundamental frequency from the detector output, and so eases the low-frequency requirements of the *RC* filter which follows the detector.

There is overlapping of the two tubes during those parts of the cycle for which the signal amplitude is less in value than the margin between bias and cut-off. Owing to the addition of the plate currents while the signal is in this region, it is not required that the cut-off of the tubes be as sharp as Figure 7 suggests.

It was found necessary to age new detector tubes 48 hours, with normal heater and plate currents, before their characteristics became stable. It was

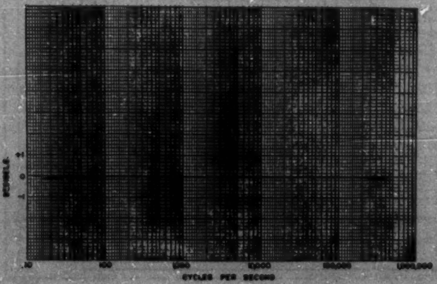

Figure 2 (left). Frequency characteristic of the recorder

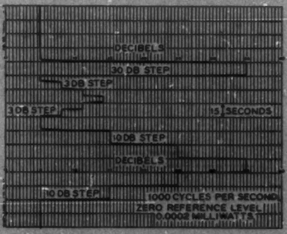

Figure 3 (right). Chart made by recorder

Figure 4. Block diagram of recorder

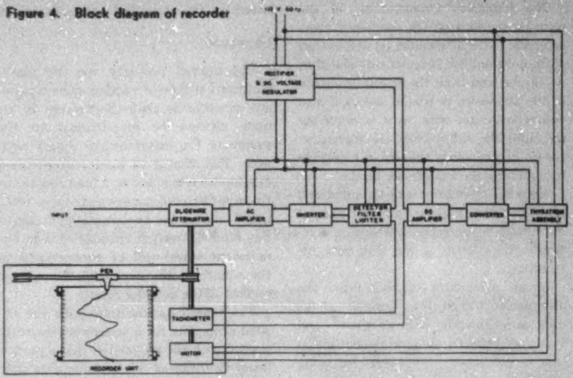
115 V 60 ~
RECTIFIER & DC VOLTAGE REGULATOR
INPUT
SLIDEWIRE ATTENUATOR
AC AMPLIFIER
INVERTER
DETECTOR FILTER LIMITER
DC AMPLIFIER
CONVERTER
THYRATRON ASSEMBLY
PEN
TACHOMETER
MOTOR
RECORDER UNIT

necessary to match tubes for the detector, and all tubes could not be used. Out of the 24 tubes tested, eight sets (16 tubes) were obtained.

In order that the d-c output would vary only with a-c input and would be independent of line voltage variations, it was necessary to use a well-regulated d-c supply voltage. Since this same regulated voltage supply is used to operate the d-c amplifier, and since direct coupling is used between the detector and the d-c amplifier, it was desirable to limit the plate voltage of the detector circuit to 45 volts, in order to have sufficient voltage available for the d-c amplifier to obtain the required power output.

It was not convenient to test the relation between instantaneous detector output and its instantaneous input, hence steady sine-wave signals were applied to the input, and the filtered d-c output was measured with the limiter and d-c amplifier disconnected. (A method of testing the square-law response of the complete recorder is described in the Appendix.) The results are plotted in Figure 8. It can be seen that the characteristic of each tube individually deviates from a square-law, but that the two tubes together do

Figure 5. Schematic wiring diagram of recorder

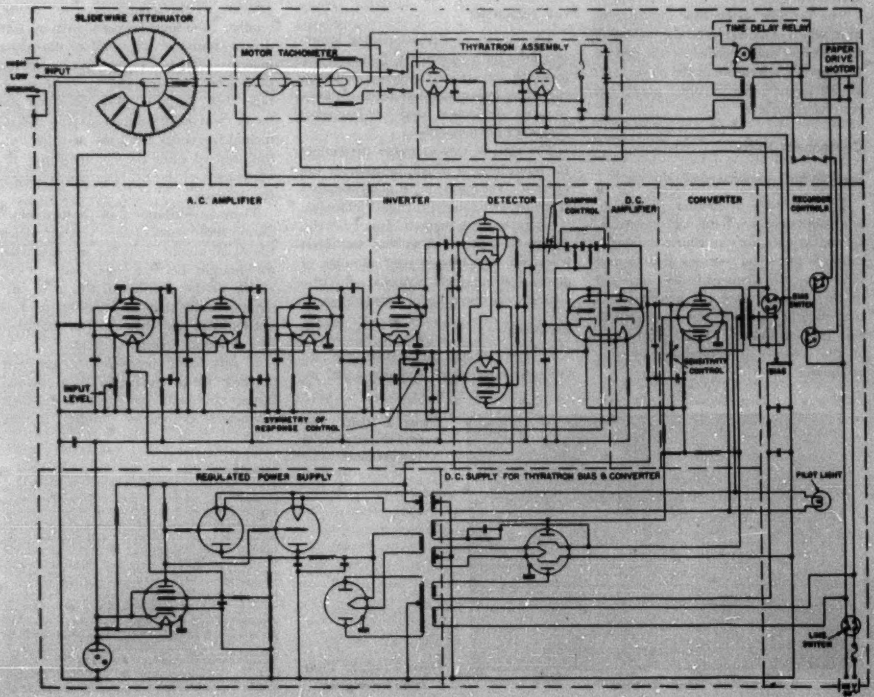
SLIDEWIRE ATTENUATOR
HIGH
LOW
GROUND
INPUT
MOTOR TACHOMETER
THYRATRON ASSEMBLY
TIME DELAY RELAY
PAPER DRIVE MOTOR
A. C. AMPLIFIER
INVERTER
DETECTOR
DAMPING CONTROL
D.C. AMPLIFIER
CONVERTER
RECORDER CONTROLS
BIAS SWITCH
INPUT LEVEL
SYMMETRY OF RESPONSE CONTROL
SENSITIVITY CONTROL
BIAS
REGULATED POWER SUPPLY
D.C. SUPPLY FOR THYRATRON BIAS & CONVERTER
PILOT LIGHT
LINE SWITCH

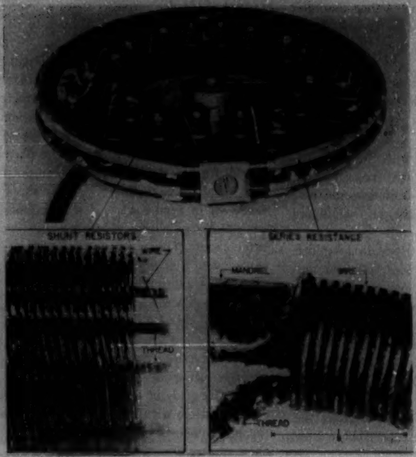

Figure 6 (above). Slide-wire attenuator

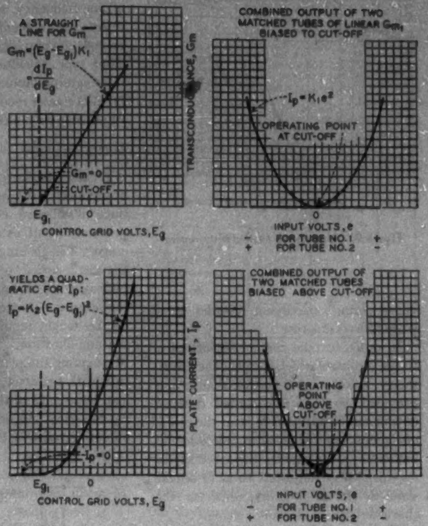

Figure 7 (right). Theoretical square-law detector characteristics

produce a square-law relation. The resistors in the screens of each tube extend the range of the square-law relation upward, as can be seen from the same figure.

The setting of the bias of the tubes controls the slope of the logarithmic curve relating the a-c input signal to the d-c output voltage. For the given operating conditions, a grid bias of -1.85 volts gave a very good square-law response. Larger values of negative grid voltage give a higher power law, while smaller values give a lower power law.

It is important that the square-law relation hold for a considerable range of voltages above and below the operating point, in order to adequately take care of peaked wave shapes. In the final design the square-law relation held over a decade of a-c input voltages, and the operating point was set at the mid-point ($\sqrt{10}$) of this range. Voltage peaks may therefore reach a value of $3\sqrt{2}$, or approximately four times their rms value, without causing overload and departure from square-law performance.

The characteristics of the tubes used, in addition to determining the law of the response, also affected slightly the operating level and, to a lesser degree, the frequency characteristic. However, the characteristics of the tubes, after aging, remained stable and did not vary appreciably with time.

The resistor and capacitor between the detector tube and the next tube, the limiter, are used as a filter to smooth out the output of the detector and thus obtain a steady a-c voltage. The time constant of this resistance-capacitance network must be low enough not to affect the speed of the recorder, yet not so low as to provide insufficient filtering at the low frequencies. Insufficient filtering causes the recorder to move back and forth continuously at the balance point, in an attempt to follow the instantaneous value of the voltage applied to the grid of the d-c amplifier.

In order to obtain proper operation of the recorder, and insure that upscale unbalances require the same time for rebalancing as downscale unbalances of the same magnitude and have the same type of response without overshooting, it was necessary to limit the effective output of the detector, to obtain the symmetrical curve of limited detector d-c output (linear scale) versus logarithm of a-c amplifier input voltage shown in Fig. 9. A triode, connected as a diode with proper d-c bias, was used to perform this limiting function. In order that it should not enter into the detector action, it is placed after the *RC* filter following the detector.

Since the slide-wire position is linear in decibels and logarithmic with voltage, this curve can also be considered as a limited detector-output versus slide-wire-position curve. When the recorder is balanced, the limited detector output is at the balanced position, Figure 9, which is the center of the *S*-shaped curve. Since the parts of this curve on either side of the balance position are symmetrical, a given displacement of the recorder from the balance position, in either direction, will produce the same change in the limited detector output, and will cause the recorder to rebalance with the same speed in either direction. This type of response

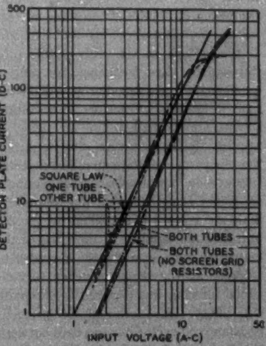

Figure 8. Square-law response of detector

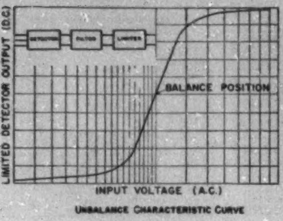

Figure 9. Unbalance characteristic curve

curve permits maximum recorder speed without overshooting.

In order to take care of variations in tubes, a control which is called the "Symmetry of Response" control, Figure 5, is provided, so that the limited detector output can be adjusted to be at the center of symmetry when the recorder is balanced. This enables the speed of the recorder to be adjusted so as to be the same in either direction whenever the characteristics of the tubes change.

The d-c voltage from the detector is opposed by a standard d-c voltage obtained from the regulated power supply, and by the tachometer voltage. The resulting voltage is applied to the d-c amplifier. This standard d-c voltage is equal to the output of the detector-limiter combination for a pre-selected input to the a-c amplifier, and is used to bring the input to the d-c amplifier to zero and thus permit the recorder to balance. The use of the tachometer voltage for damping is well known.[2]

The square-law detector presents a difficulty in the filtering problem. The action of the converter, as described later in the paper, depends upon having line-frequency (60 cycles) alternating voltage for the plate supply of its double triode. If the voltage on the grids of this tube differs from line frequency by only a small amount, the recorder will follow the beat frequency. Therefore, if a voltage having about one-half line frequency is applied to the recorder, the frequency doubling action of the square-law detector produces in its output a voltage having a frequency near that of the line frequency. This a-c voltage is amplified by the d-c amplifier and applied to the grids of the converter tube, causing the recorder to respond at the beat frequency. Additional filtering was required to eliminate this effect. A 3-terminal *RC* bridged-resistance 60-cycle filter was used between the limiter and the d-c amplifier. Tests of the recorder's action, with large changes of line frequency, showed that this filter rejects over a band of frequencies broad enough to completely solve this problem. This type of filter provides sufficient filtering with minimum time constant, and permits greater recorder speed than would be possible with filters of other types.

D-C Amplifier

A change in the a-c input voltage to the attenuator of 0.1 per cent does not produce a sufficient change in the limited detector output to operate the converter stage. A single-stage triode d-c amplifier, Figures 4 and 5, provides sufficient amplification to obtain enough sensitivity for even a 10-decibel range. Higher decibel ranges require a reduction in the d-c amplification. This is accomplished by shunting the plate of the d-c amplifier tube with a resistor, thereby lowering the load impedance of this stage and decreasing the gain. In order not to affect the operating point of the tube, this resistor is connected from the plate of the tube to a point on the voltage divider equal in d-c potential to that of the plate when the recorder is balanced. A capacitor across the load resistor in the plate circuit smooths out any pulses which may be present.

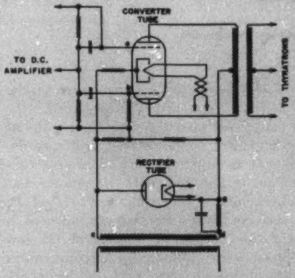

Figure 10. The converter (thyratron firing circuit)

Converter

The purpose of the converter, Figure 10, is to take the output of the d-c amplifier, Figures 4 and 5, and use it to operate the correct thyratron, so that the recorder slide-wire will be driven to the balance position. A further complication occurs since the thyratrons are at ground potential, while the d-c voltage obtained from the d-c amplifier is 105 volts above ground. Insulating transformers are used, and the converter changes the d-c output of the d-c amplifier to an a-c voltage, of the correct phase to operate the proper thyratron.

Each plate of the double triode, Figure 10, is connected to one end of a center-tapped primary winding of a transformer. The secondary winding of the transformer supplies voltages of the proper phase to the grids of two thyratrons. The plate supply for the double triode is obtained from a half-wave rectifier; its wave shape is shown in Figure 11. If this rectifier were perfect, there would be no negative component. This wave shape occurs because when *d* is minus with respect to *c* current flows through the rectifier, and the voltage drop across it is very low, but not quite zero, thereby making *e* minus with respect to *c*. When *d* is plus with respect to *c*, the rectifier does not pass current, and the voltage across it is high. When one of the grids of the double triode becomes positive with respect to the other, the plate current of that triode will become greater than the plate current of the other triode. At time *t*, Figure 11, the supply voltage goes sharply to zero and reverses polarity. This supplies negative plate voltage, but, what is more important, it also supplies negative grid-bias voltages to the triodes. This rapid shift of the grids to the negative region cuts off the plate currents of the triodes very sharply, and the rapid collapse of the flux in the output transformer produces a peaked wave in its secondary. Without this cutoff, the current would continue as a result of the inductance of the output transformer. The triode having the more positive grid passes more plate current than the other triode; thereby it determines the direction of this peak.

The secondary voltage from the transformer is used to turn on one or the other of the thyratrons. The polarity of the voltage across the grids *a* and *b* determines the phase of this peaked voltage, and so determines which thyratron is turned on, and also determines in which direction the motor is turned. The mag-

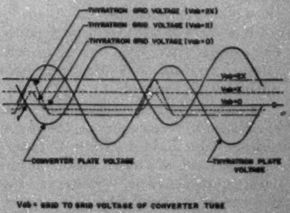
THYRATRON GRID VOLTAGE (Vab=2X)
THYRATRON GRID VOLTAGE (Vab=X)
THYRATRON GRID VOLTAGE (Vab=0)
Vab=2X
Vab=X
Vab=0
CONVERTER PLATE VOLTAGE
THYRATRON PLATE VOLTAGE
Vab = GRID TO GRID VOLTAGE OF CONVERTER TUBE

Figure 11. Wave shapes in converter circuits

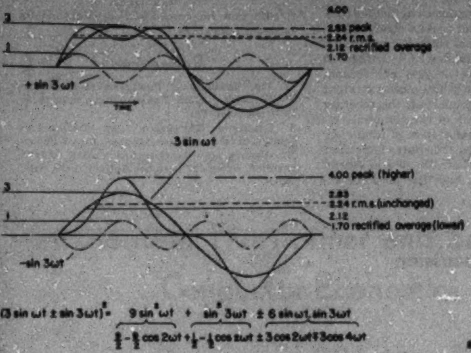

Figure 12. Effect of phase on peak, average, and rms values

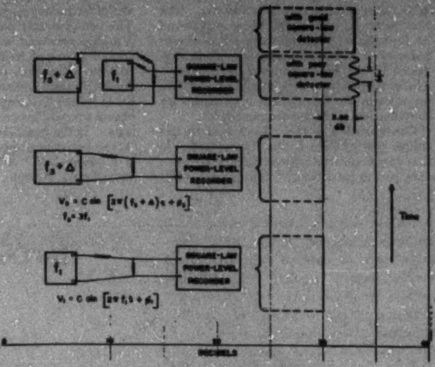
with good square-law detector
with poor square-law detector
$f_3+\Delta$
f_1
SQUARE-LAW POWER-LEVEL RECORDER
$V_3 = C \sin\left[2\pi(f_3+\Delta)t+\phi_3\right]$
$f_3 = 3f_1$
$V_1 = C \sin\left[2\pi f_1 t+\phi_1\right]$
Time
DECIBELS

Figure 13. Test for square-law response

nitude of this voltage across *a* and *b* determines the height and breadth of the pulse to the thyratrons. Since the higher peaks are broader at the base, they fire the thyratrons somewhat earlier in the cycle, thus giving a stronger pulse to the motor for large unbalances, which is desirable. When the recorder is balanced, the voltage across the grids *a* and *b* is zero, and there is no output voltage across the secondary of the output transformer.

The use of a peaked voltage to fire the thyratrons is a desirable feature of the circuit, since the phasing between this voltage, which is supplied to the grid of the thyratron, and the 60-cycle sine-wave plate voltage, does not have to be adjusted as accurately as is generally necessary when sine-wave voltages are used on the grid as well as on the plate of the thyratron.

The heater, plate, and bias voltages for the converter must be obtained from separate windings on the power-pack transformer, since they are also at 105 volts above ground. These voltages do not have to be regulated, since any change in their values, caused by normal line voltage variations, will not affect the operation of the converter. The plate and bias voltage, Figure 5, must be obtained from the same supply as the plate voltage of the thyratrons to ensure the correct phase relation between the two.

THYRATRON ASSEMBLY AND RECORDING UNIT

The output of the converter, as stated before, is applied to the grids of the thyratrons, Figures 4 and 5, which drive the three-lead, split-field, series reversing motor that is mechanically coupled to the slide-wire attenuator, the tachometer, and the pen. This part of the instrument is the same as the corresponding part in a standard type *A* Speedomax recorder.

POWER SUPPLY

The power supply for the recorder, exclusive of the plate and heater voltages for the converter and thyratrons, must be very well regulated, Figures 4 and 5. This is particularly true of the power supply for the detector, the d-c amplifier, and the standard-voltage supply, since any variation in their power supply enters directly into the operation of the recorder, and will affect its performance. Somewhat greater variations in the power supply of the a-c amplifier would be permissible, since these variations do not greatly affect its gain, which is all that need be held constant. Variations in the power supply of the converter will affect only the sensitivity of the recorder.

For stable recorder operation, especially on the low-decibel ranges, the d-c power supply must be held constant to 0.1 per cent. This requires an electronically-regulated power supply, Figure 5. Regulation obtained by this method was considerably better than that required. The heaters, as well as the plate, screen, and bias voltages, of all the tubes in the a-c amplifier, inverter, and rectifier, and the d-c amplifier, were supplied from this source.

Operation Controls

All controls are centralized on the front panel shown in Figure 1. There is a "Line" switch, Figure 5, to control the a-c power supply; two switches to control the paper drive; a "Bias" switch; a "Bias" control, used to adjust the bias of the thyratrons; and an "Input Level" control. This last control is provided so that the recorder can be adjusted to read decibels above or below a definite power level. To make this calibration, the external source should be adjusted to the desired power level and the "Input Level" dial adjusted so that the recorder balances at zero on its scale. These adjustments do not have to be made every time the recorder is used, but they should be checked occasionally.

Appendix. Over-all Test for Approach to Square Law

In the body of the paper, there is described the method used to determine the detector characteristic. By plotting the logarithm of detector output versus the logarithm of its input, the closeness of approach to the square law could be determined. These plots were essential in guiding the development work, but a simpler test was sought which would not require so much measuring and plotting, and which would not require breaking into the recorder circuit, but would test the recorder as a whole for that characteristic for which the square-law response was most desired.

Figure 12 shows how a sine wave, of amplitude three, and its third harmonic, of amplitude one, combine to form an irregular wave having a peak, rms and rectified average value. When the phase of the third harmonic is reversed, as shown at the bottom of the figure, the composite wave takes a very different shape. The peak value is obviously greater. The rectified average can be seen to be less (only one added area and two subtracted areas). The rms value is unchanged, being unaffected by the relative phase between the two components of different frequency, as is suggested by the brief equations in the figure. The cross-product term produces new frequencies in the output, but it produces no contribution to the d-c component.

Consideration of these facts lead to the simple test of Figure 13. The recorder is first connected through an isolating resistance pad to an oscillator delivering a voltage of frequency f_1, as shown at the bottom. The pen is steady and plots a straight line. f_1 is then removed, and there is connected a second source of frequency $3f_1+\Delta$ where Δ is only a fraction of a cycle per second. Again, the pen is steady and plots a straight line. When f_1 is reconnected, the recorder moves upscale because of the combined inputs. If the pen plots a wave of frequency Δ, the detector response deviates from that of a square law. When the pen is steady and plots a straight line, the detector response can be considered satisfactory for recorder operation.

References

1. THE "SPEEDOMAX" POWER-LEVEL RECORDER, W. R. Clark. AIEE TRANSACTIONS, volume 59, 1940, pages 957–64.

2. COMBINED THYRATRON AND TACHOMETER SPEED CONTROL OF SMALL MOTORS, A. J. Williams, Jr. ELECTRICAL ENGINEERING (AIEE TRANSACTIONS), volume 57 (October section), 1938, pages 565–8.

No Discussion

Distribution Transformer and Secondary Conductor Economics

BRYCE BRADY
MEMBER AIEE

Synopsis: The possibilities are investigated of lowering the cost of electric distribution in residential areas by using distribution transformers larger than required for thermal reasons to control voltage flicker; banking secondary mains to control voltage flicker; and using aluminum conductors instead of copper. The conclusion is reached that all three of these have a place in designing today's electric distribution systems.

MOST electric utilities operate more mileage of 120/240-volt single-phase secondary distribution mains than any other transmission or distribution voltage. It is important that such secondary lines and the size and spacing of the associated distribution transformers be designed for over-all economy.

The advent of more and more appliances which cause voltage flicker in residential areas makes control of flicker a prime design consideration. Most of the flicker voltage drop resulting from the starting of small motors occurs in the distribution transformers and the secondary conductors.

The most accurate approach is to design the transformer-secondary system for total allowable flicker and steady voltage drops, and to let over-all economics determine how much voltage drop should occur in the transformer and how much in the secondary main. The result of using this approach on a system with reasonably high service quality is that thermal capability ceases to be the governing factor in selecting transformer sizes in many residential areas.

Objectives

One of the objectives of this study is to determine the most economical loading of distribution transformers under various conditions. Another objective is to define the conditions under which secondary banking, as a means of controlling flicker, is economically justified. A third objective is to make an economic comparison of copper versus aluminum as secondary conductors under current price conditions.

Improving Existing Systems

The annual load growth on existing systems results usually in overloaded transformers, too much voltage drop, or excessive voltage flicker in the combined transformer-secondary system. In most cases such growth can be cared for by replacement and rearrangement of distribution transformers. On the system with which the author is associated, single-phase transformers up to and including 25 kva are installed at the top of the pole and can be moved from one pole to another without pole replacement and with little expense. Transformer locations are not considered permanent, but merely to be used until changing load conditions dictate that some other location would be more advantageous. The pertinent questions in periodic rearrangements to handle load growth are: What size transformers should be used, and how far apart should they be spaced?

Figure 1 shows the general form of the solution to this problem. This case is typical of nearly all of the practical situations encountered in distribution practice in that the most economical transformer size and spacing cannot be used because the quality of service would be unsatisfactory. The best that can be done is to choose the most economical transformer size and spacing which will meet the desired service standard.

In this example 10-kva transformers spaced 813 feet are more economical than either larger or smaller transformers where number 0 aluminum secondary conductors are used on the radial plan and the load density is 10 kva per 1000 feet.

The quality of service to be delivered by a distribution system has a great deal to do with its cost. In this and all other examples cited in this paper, steady voltage drop in the transformer plus the secondary main is limited to 6.6 volts. This is considered satisfactory on urban circuits equipped with voltage regulators. Flicker voltage drop in the transformer plus the secondary main resulting from the starting of 1/4-horsepower 115-volt motors is limited to four volts. This flicker is considered satisfactory provided it does not occur more often than six or seven times per hour. The same design limits the flicker resulting from the starting of 1/2-horsepower 115-volt motors to eight volts, which is considered satisfactory if it does not occur more often than once per hour. Larger motors are required to use the 230-volt connection. Transformer loading is limited to a maximum of 140 per cent of nameplate rating. No minimum transformer loading is recognized as a design limitation.

The total annual cost in Figure 1 includes taxes, interest, and depreciation on the investment in transformers, secondary conductors and variable appurtenances; cost of losses in transformers and secondary conductors; and maintenance of transformers and fuses. Iron losses are evaluated at $42 per kilowatt-year and copper losses at $14 per peak kilowatt-year. Other premises are listed in the Appendix and are used consistently throughout the paper.

The data from Figure 1 are plotted as

Paper 49-10, recommended by the AIEE transmission and distribution committee and approved by the AIEE technical program committee for presentation at the AIEE winter general meeting, New York, N. Y., January 31–February 4, 1949, and at the South West District meeting, Dallas, Tex., April 19–21, 1949. Manuscript submitted November 15, 1948; made available for printing January 5, 1949.

BRYCE BRADY is chief distribution engineer with the Oklahoma Gas and Electric Company, Oklahoma City, Okla.

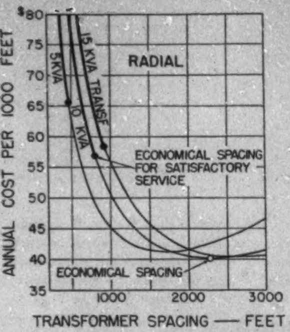

Figure 1. 10-kva transformers spaced 813 feet provide the most economical satisfactory service in a residential area where the load density is 10 kva per 1,000 feet and the 120/-240 volt secondary conductors are number 0 aluminum on the radial plan

functions of transformer loading in Figure 2. It is pertinent to note that 10-kva transformers loaded 82 per cent are more economical than smaller transformers loaded more heavily. This simply means that the capability to deliver the desired quality of service can be purchased more cheaply in a larger distribution transformer than in any other way.

In these examples the design limitation is the flicker resulting from the starting of small motors. If the secondary mains are banked so that starting current is supplied from two directions, and so that two or more transformers can contribute to the starting of the motor, then 15-kva transformers spaced 1,667 feet become most economical as shown in Figure 3. The result of banking is that the cost of distribution drops from $57 per 1,000 feet on the radial plan to $45 on the banked plan and the most economical transformer loading rises to 111 per cent as shown in Figure 4.

The most economical transformer size, spacing, and loading which will meet the required quality of service were ascertained in accordance with these methods for several types of conductor and a wide range of load densities. The results of this investigation are shown in Table I.

Where to Bank Secondary Mains

Distribution engineers do not all agree as to the merits of banking secondary mains. Most would undoubtedly agree that the principal advantage is reduction of voltage flicker. This is the only advantage evaluated in this paper. The conclusions which follow are, therefore, on the conservative side.

The total annual cost of each economical transformer-secondary combination listed in Table I is plotted in Figure 5, which shows that banking of secondary mains has too much merit to ignore at the lighter, and very commonly encountered, load densities. Nor can the advantages be dismissed as too much trouble, for the "trouble" has already been evaluated in the curves as the cost of two yearly inspections of secondary fuses plus 17 per cent replacement per year. Banking by means of circuit breakers instead of fuses would undoubtedly show similar results.

The curves show that secondary mains should be banked in all areas of less than 40 kva per 1,000 foot load density where number 6 copper is used; in all areas of less than 25 kva density where number 4 copper or number 2 aluminum conductor is used; and in all areas of less than 18 kva load density where number 2 copper or number 0 aluminum is used for secondary conductors. The curves are based on the premise that there are sufficient small 115-volt motors, existing or prospective, to justify holding the voltage flicker on all parts of the system to standards as discussed previously. Sufficient saturation of larger motors and electric ranges and the evaluation of the benefits of banking in equalizing steady voltage drop and transformer loads would extend the desirability of banking to higher load densities than shown.

Choice of Conductor for New Systems

Considerable labor is required to replace secondary conductors once they are installed and the service drops connected. It is usually most economical to make an initial installation of some size which will be suitable for continued use for many years as the load grows. Comparison of the annual cost curves in Figure 5 shows that number 4 copper is more economical than either larger or smaller copper conductor under the premises of this study. If a higher quality of service is to be rendered, then number 2 copper may be more economical. Similarly, it is apparent that number 0 aluminum is more economical than either smaller or larger aluminum conductor. This was found to be the most economical size whether the conductor is steel reinforced or not.

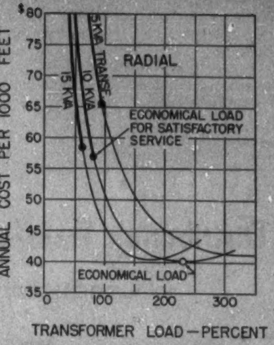

Figure 2. 10-kva transformers loaded 81 per cent are more economical than smaller transformers loaded more heavily under the conditions stated in Figure 1

Unfortunately it is impossible to attain 100 per cent banking of single-phase secondary mains because of irregular platting, necessity of balancing primary circuits, and similar reasons. Perhaps the best that can be done under average conditions is 50 per cent banked and 50 per cent radial. Making this assumption, the annual cost curves for number 4 copper, bare and weatherproof, and for number 0 aluminum, with and without steel reinforcing, are compared in Figure 6. Quite appreciable savings are available by using aluminum instead of copper.

Over a decade of experience with bare secondary conductors, in urban as well as rural areas, has led to the conclusion that weatherproof covering is an unnecessary luxury. All covering materials cost more per pound than copper. Bare conductors are inherently stronger by virtue of less weight, less resistance to wind, and less

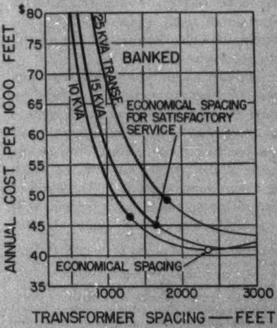

Figure 3. Banking of secondary mains reduces the total annual cost of the radial system in Figure 1 from $56.90 to $45.10

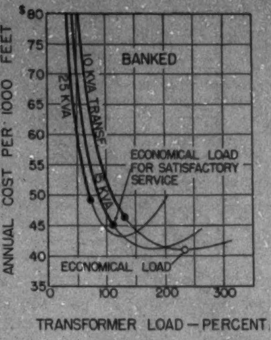

Figure 4. 15-kva transformers loaded 111 per cent are most economical if the secondary mains are banked

accumulation of glaze. Although arcing may be more frequent, it is less apt to cause burndown, because generally the arc does not remain concentrated at a single point. Altogether, it is the opinion of the company with which the author is associated, that part of the money which would be spent for weatherproof covering can be spent more wisely for increased clearance between the bare conductors; also that under current price conditions the savings that are possible by using aluminum instead of copper are worth going after.

Most Economical Transformer Loading

There can be no profit in loading distribution transformers to thermal capability, that is, to the peak load beyond which the life of the transformer is materially shortened, if it becomes necessary to make up for excessive flicker or steady voltage drop in more expensive ways. Likewise, it is a waste of time to calculate the most economical load on the transformer alone, without considering the secondary conductors, in situations where flicker or steady voltage drop in the transformer plus secondary circuit constitutes the design limitation.

The most economical transformer loadings which would render satisfactory service with a particular secondary conductor at a particular load density was ascertained in Figures 2 and 4 upon the premise that it is immaterial whether flicker and steady voltage drops occur in the transformer or in the secondary conductors. This premise is strictly correct in the case of flicker and is approximately

Table I. Most Economical Transformer Sizes, Spacings and Loadings Which Provide Satisfactory Service

Load Density Per 1,000 Feet	Transformer Size, Kva		Transformer Loading, Per Cent		Transformer Spacing, Feet	
	Radial	Banked	Radial	Banked	Radial	Banked
Number 6 Copper						
5	10	5	22	85	435	847
10	10	10	43	102	435	1020
20	10	15	87	107	435	800
30	10	15	130	121	435	606
50	15		140		420	
80	25		120		376	
Number 4 Copper						
5	10	5	30	121	600	1205
10	10	10	60	121	600	1220
20	10	15	120	121	600	909
30	15		136		680	
50	25		118		588	
80	25		136		424	
Number 2 Copper						
5	10	10	41	96	813	1923
10	10	15	81	111	813	1667
20	15		128		962	
30	25		114		955	
50	25		133		667	
80	37½		121		568	
Number 2 Aluminum						
5	10	5	30	121	600	1205
10	10	10	60	122	600	1220
20	10	15	120	121	600	909
30	15		136		680	
50	25		118		588	
80	25		136		424	
Number 0 Aluminum						
5	10	10	41	96	813	1923
10	10	15	81	111	813	1667
20	15		128		962	
30	25		114		952	
50	25		133		667	
80	37½		121		568	
Number 000 Aluminum						
5	10	10	53	123	1053	2460
10	10	15	105	126	1053	1887
20	15		140		1050	
30	25		126		1053	
50	25		140		700	
80	37½		136		637	

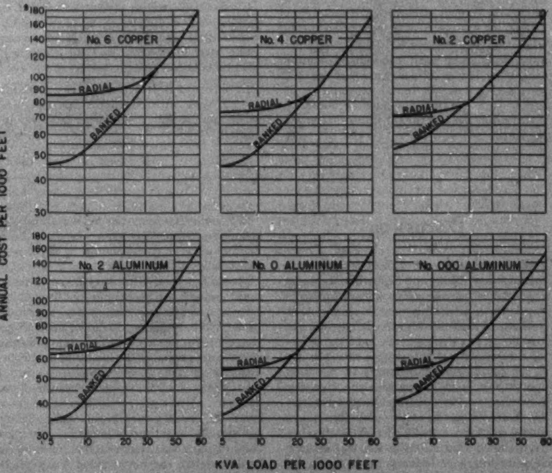

Figure 5. Economy of banking secondary mains is more pronounced at the lighter load densities

correct in the case of steady voltage drop, to the extent that voltage regulators on primary circuits are unable to compensate for noncoincident voltage drops of various magnitudes to different customers on transformer-secondary systems.

Each of the most economical transformer loadings for the various situations listed in Table I was determined upon this premise. The most economical transformer loading ranges from 22 per cent to 53 per cent depending upon the size of the conductor, on radial systems where the load density is 5 kva per 1,000 feet. At 10-kva density the most economical loading ranges from 43 per cent to 105 per cent. On banked systems and at higher load densities on radial systems, the most economical loading ranges from 85 per cent to 140 per cent. These percentages pertain to particular cost data and quality of service but are sufficiently general to justify careful appraisal of the over-all economy of loading distribution transformers to thermal capability in lightly loaded areas.

Conclusions

The premises and methods pursued in this study lead to the following conclusions:

1. The loading of distribution transformers to thermal capability of say 140 per cent is not economical if it is necessary to make up for the voltage drop in ways more expensive than installing larger transformers. On radial secondary systems it is not economical in general to load distribution transformers as high as 100 per cent of nameplate rating where the load density is 10 kva or less per 1,000 feet. The most economical loading may be as low as 22 per cent. On banked secondaries and on radial secondaries at higher load density, the most economical transformer loading ranges upward from 85 per cent.

2. The banking of secondary mains is definitely an economical method of limiting the flicker resulting from the starting of small motors in areas with load densities up to 18 to 40 kva per 1,000 feet, depending upon conductor size and material. Banking at higher load densities may be justified by other considerations.

3. Aluminum, with or without steel reinforcing, is attractive as a secondary conductor under current price conditions.

Appendix. Premises

1. Flicker voltage drop to be a maximum of four volts in transformer plus secondary produced by the starting of a 115-volt motor requiring 20 amperes at 60 per cent power factor.

2. Steady voltage drop to be a maximum of 6.6 volts in transformer plus secondary.

3. Transformers to be loaded a maximum of 140 per cent. No minimum.

4. Steady voltage drop in 120/240 volt 3-wire secondary based on unbalanced currents in the proportion of 83 per cent to 100 per cent.

5. 100 per cent load balance in transformer.

6. 90 per cent power factor.

7. Load distributed uniformly along secondary mains which are presumed to be straight without loops.

8. Transformers spaced uniformly along secondary main.

9. Diversity between loads on adjacent transformers is ignored.

10. Secondary conductor spacing to be 12 inches.

11. Annual cost on investment based on conductor prices of $0.31, $0.24, and $0.27 respectively for bare copper, aluminum cable steel reinforced, and all aluminum, plus installation costs.

12. Investment in secondary deadends (which vary with conductor material) and secondary banking fuses (where used) is included.

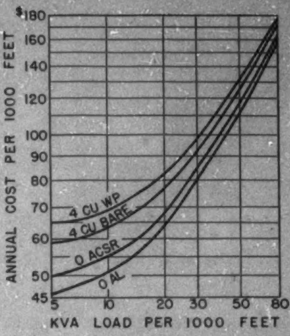

Figure 6. Worthwhile economy is available by using aluminum instead of copper for secondary conductors

13. Investment in poles and anchors is considered equal for all conductors studied, and is not included.

14. Transformer investment includes one fuse cutout, one lightning arrester, one ground and all installation costs.

15. Annual maintenance of transformers is included.

16. Annual maintenance cost of secondary banking fuses is included (two inspections plus 17 per cent replacement per year).

17. Copper loss in transformers and secondary conductors is based on 1,140 equivalent hours per year.

18. Iron loss is corrected to 122 volts.

19. Annual cost of 1-kw copper loss, $14 (includes energy cost plus demand cost in proportion to contribution to annual system peak load).

20. Annual cost of 1-kw iron loss, $42 (energy plus demand cost).

21. Transformers are mounted on the pole at primary voltage level and can be relocated at small expense (without pole replacement).

Discussion

H. E. Campbell (General Electric Company, Schenectady, N. Y.): The author shows us again the advantages of secondary banking. Figure 5 of his paper shows clearly that banking pays dividends especially when the load density is light and secondary conductors are small and the system must be designed for flicker conditions. It has been pointed out in his paper that the diversity between customers on different transformers has been omitted. However, this point should not be overlooked entirely. Studies have shown that distribution transformer capacity might be reduced by 10 to 15 per cent when transformers are banked as compared with radial systems at high load densities.

The point made by the author about the economies realized by using aluminum conductors on secondaries should be of interest to all utility men.

Brady has shown that for his system costs in some cases, it pays to operate distribution transformers underloaded. It is not clear to me from the paper just how the distribution transformers are changed around on the system to operate at the lowest annual cost. Table I of the paper shows the size of transformer and its loading for various load densities. Obviously, a system must grow from one density to a higher one. Many utilities have set up procedures whereby they change out a transformer when it is loaded up to a maximum value, and replace it with a larger one that will be loaded to only a fraction of its rating. I presume that this is the way Figure 5 was obtained.

I believe that the problem of economics of distribution transformers and secondary conductors is a little more complex than shown by this paper. The anticipated load growth and actual cost of changing transformers will influence the economics of changing transformers. Figure 1 of the discussion will show this point. Here a load growth of 10 per cent per year has been chosen, and the density has been plotted for an original value of 5 kva per 1000 feet for the next 15 years. Brady's paper indicates that when there is a number 0 aluminum secondary, a 10-kva transformer should be used for the first 13 years, and then a 15-kva transformer should be used. However, the difference in cost curve shown in Figure 1 of the discussion shows that over a 13-year period, it would cost only $18 extra to use 15-kva transformers instead of 10-kva trans-

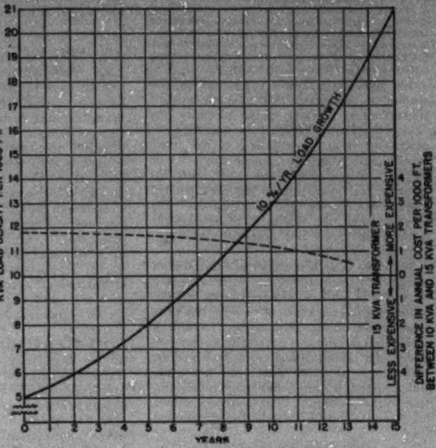

Figure 1. Dollars difference in annual cost between using a 10-kva versus a 15-kva transformer for a 10 per cent per year load growth

formers. Thus, if it cost more than $18 in labor to change a 10-kva transformer, then 15-kva transformers should have been installed originally. This cost of changing the size of transformers varies quite widely between utilities and between various sections of the country. Figures as low as $20 per installation for small transformers and as high as $80 per installation for large transformers have been quoted. This indicates that for this assumed load growth it would have been better to have installed the larger transformer initially.

The slower the load growth, the more one can afford to spend for changing transformers and vice versa. Load growth and cost of changing transformers, I believe, should be included in economic studies such as this.

L. T. Guess (Aluminum Company of America, Pittsburgh, Pa.): There are a number of technical papers on economic principles as applied to transmission lines. However, the technical literature as applied to distribution lines is rather limited. Perhaps this is because the factors peculiar to distribution systems do not lend themselves as well to analytical analysis. Even though it is not expedient usually to adopt the most economical size of conductor as calculated by Kelvin's classical theory, this "law" is generally recognized as a basis for economic studies. Application of this theory gives the most economical size for copper in circular mills to be equal to 590 $\sqrt{C/AP}$ and for aluminum to be 1,360 $\sqrt{C/AP}$ where C is equal to the cost per kilowatt-year of wasted energy, A is the per cent interest and depreciation, and P is the cost per pound of conductor installed. It is evident that if the most economic choice could be made on conductor and power-loss cost, it would be to use a larger size aluminum conductor than the equivalent copper conductor based on resistance. Naturally, the conditions peculiar to the distribution system under study will modify the choice. Brady's paper points out a logical approach to a distribution study and can be used as a guide by engineers who may wish to use slightly different assumptions.

Howard P. Seelye (The Detroit Edison Company, Detroit, Mich.): A comprehensive study of the various phases of the economics of secondary design, made in The Detroit Edison Company several years ago, indicated the same conclusion reached by Brady, that for light-load densities, excess transformer capacity is a cheaper means of limiting the voltage dips due to motor starting currents than the installation of unduly large conductors or the use of unduly close transformer spacing. In fact this same condition is true in the case of larger motors on heavier commercial secondaries. It should not be inferred, however, that this means that underloading of transformers in general is desirable or economical. In most cases, in urban distribution, the installation is providing for an increasing load and, although in the original condition with light loads the transformers may be appreciably underloaded, the same installation can take care of the increase up to the point where the load on the transformer reaches its thermal capability.

Since it is costly to replace conductors or to move transformers frequently, the most economical design will be that combination of wire size and transformer spacing which, within the voltage drop limits which have been assumed, will show the least cost over a considerable period of time with increasing load densities, the transformer size at any time being such as to provide adequately for the existing condition.

We also concur most fully with Brady's conclusion as to the advantages of banking transformers. The maximum voltage dips are cut in half by this practice. Although, as he indicates, banking may not be required to meet the 4-volt limit at the higher load densities, it is very desirable to reduce the dip below this amount if possible. Banking accomplishes this. There are also other advantages in banking in the better distribution of the loads among the transformers, leading to economy by higher average loading, and in the appreciable reduction in customer outage. The Detroit Edison Company has followed this practice for a great many years.

Harold Cole (The Detroit Edison Company, Detroit, Mich.): Brady's paper makes some very pertinent conclusions as to the best methods of reducing costs in a part of the distribution system which is an important element in the total cost of most distribution systems. Studies of this kind are very necessary if we are to keep our investment and operating costs at a minimum.

The advantage of banking transformers as an economical means of reducing voltage flicker has been given considerable emphasis in recent years with the more general use of motor-driven appliances. I also would like to point out that, in areas of light-load densities, banking has the further advantage of maintaining higher steady-state voltages in serving large concentrated loads, such as ranges, clothes dryers, and so forth.

It would appear from Brady's discussion of troubles connected with banking of transformers that he is considering only the "loose" banking method with fuses in the secondary mains midway between transformers. He finds it necessary to make two yearly fuse inspections and the replacement of 17 per cent of the fuses per year. This rate of fuse failure would indicate that blown fuses could remain unreplaced for several months, during which time the voltage flicker at the open ends of the secondaries might be double the permissible values, as I am assuming that not all of the fuse blowings were the result of a complete outage of the transformer. It would be interesting to know if the use of bare secondaries had any great effect on the number of fuse blowings. I would think it likely, however, that low-capacity fuses were used and that a large number of fuse blowings were due to load surges.

The method of banking transformers which we have been using for over 40 years may have its faults, but it results in much less frequent fuse blowing. In the past eight years the average rate of secondary fuse replacement in our Detroit district was 1.2 per cent per year. In our practice, there are no fuses in the secondary mains, but secondary fuses are installed in the connection from the transformer to the mains. These fuses are of such size that only secondary short circuits will cause them to blow. In spite of this fact, there were only 45 transformer failures due to overload or short circuit in our Detroit district. This is a failure rate of less than 0.2 per cent of the transformers involved.

In our case very few of the fuse blowings caused customer service outage, and the only interruptions from secondary causes were very occasional outages of a complete secondary bank, most of which occur in banks consisting of a few small transformers. As Brady points out, irregular platting of many residential areas sometimes makes it impossible to do any banking, and often makes it difficult to get the best conditions for solid banking, as proper arrangement of primary mains is essential to good performance. Where conditions are favorable for its use and it is properly maintained, a high degree of continuity is possible with solid banking with no increase in cost at least over a radial secondary system.

M. G. Leonard (Westinghouse Electric Company, Sharon, Pa.): This paper emphasizes the importance of quality of service as a factor of the design of a distribution system. We agree that this consideration is an important factor in laying out such a design.

Brady shows that, if a quality standard is set up on a basis which appears to be adequate, then the thermal capacity of the transformer tends to disappear as a design limitation. This is, no doubt, true for the assumptions made. We have some general questions however, in regard to these assumptions. In particular we would like to ask:

1. Are the calculations based on the performance of present-day distribution transformers? We have a line of transformers, for example, which are specifically designed for operation by copper temperature. In these transformers, the impedance drop has been kept to a low value. The regulation at full load and 90 per cent power factor is in the range of 2.1 to 2.7 per cent. At the low limit of 22 per cent load, which Brady mentions, this would result in only 1/2-volt drop in the transformer which seems to be a very small value.

2. A second question relates to whether there are not likely to be some conditions of abnormal loading which make copper temperature an important limitation. We believe such conditions should be considered even though they are not included in the system design. For example:

a. Excessive loads caused by peak demand or by faults on the secondary might be sufficiently probable to justify protective equipment on the transformer. The best way to obtain such protection is to use a circuit breaker, thermally co-ordinated with the transformer design.

b. Even though the system is initially laid out on a conservative basis as proposed by Brady, load growth may result in conditions which endanger the transformer, unless the thermal capacity limitation is recognized. Dangerous thermal conditions may not be known in time to permit adding or replacing a transformer before damage results.

We were particularly interested in the section of this paper dealing with banked transformers. Brady quite properly includes the cost of inspection and fuse replacement in his calculation of the most economical system for a specified quality of service. We would think that two inspections per year, plus 17 per cent fuse replacements, is a very generous estimate. He mentions the use of circuit breakers as a possible alternate, but does not carry this proposal any farther.

We have done a considerable amount of work on this subject, with a view to finding a practical and economical way of co-ordinating the circuit breaker with both the transformer characteristics and secondary service requirements. Several arrangements have been designed and tested. Based on this study, we have developed a system which affords a simple and economical solution to the problem. This system is shown diagrammatically in Figure 2 of the discussion.

Note that circuit breakers are built integrally with the transformers, and connected so that any section of circuit can be isolated by the tripping of adjacent circuit breakers. Thermal setting is adjusted to the capacity of the transformers. Thus we obtain protection for the secondary lines and for the transformer as well.

In case an outage does occur on this system, service can be restored merely by resetting the circuit breaker. Since the total kilovolt-amperes of the bank is relatively large (compared to a radial system) and all of the transformer capacity is available before the circuit breaker trips, many faults can be burned clear, and hence the number of outages is reduced to a minimum. This is, of course, also true of a fused system, except that if fuses are applied to protect the transformer on long-time loads, they do not make the full transformer capacity available for short-time loads.

Figure 2. Banked secondary system with circuit breaker integral with transformers

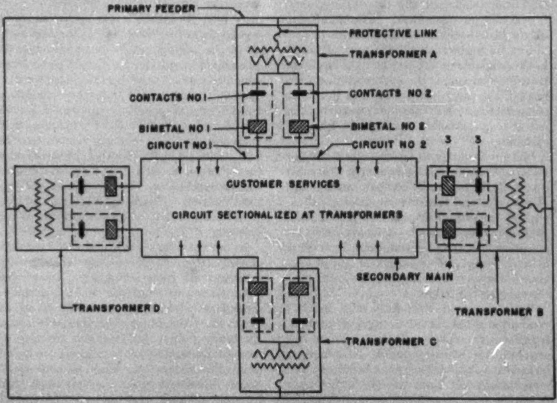

W. T. Brown (Philadelphia Electric Company, Philadelphia, Pa.): The secondary system is comprised of distribution transformers, secondary mains, secondary branches, and customer services. The design problem is, therefore, to obtain a combination of these elements to supply the secondary load at minimum over-all cost for fixed allowable voltage loss, (steady or flicker) in the secondary system.

Although the optimum loading of distribution transformers and secondary wire depends directly on the allowable voltage loss in the secondary system and the load density in the territory served, the optimum co-ordination of transformer size, secondary wire size, and transformer spacing can be shown to be essentially independent of these factors.

The best wire size for a given transformer size is essentially attained when the increased annual cost of a larger wire size per volt improvement thereby obtained, is just equal to the increased annual cost of a larger transformer size per volt improvement. Any other combination such as smaller transformer size and larger wire size required to remain within the permissible voltage loss limit, whether it be 5 per cent or 10 per cent will be more expensive. The annual saving due to a smaller transformer size would be more than offset by the annual cost of the larger wire. The cost of voltage improvement by increasing either the transformer size or the wire size is inversely proportional to the load supplied. Therefore, the economic co-ordination of wire size and transformer size is independent of load density except as it is somewhat influenced by annual copper loss evaluation.

The best transformer spacing for a given transformer size is also essentially attained when the increased annual cost of transformer capacity due to closer spacing per volt improvement thereby obtained, is just equal to the increased cost of a larger transformer size per volt improvement. Any other combination such as smaller transformer size and less transformer spacing required to remain within the permissible limits of voltage loss, would be more expensive. The annual saving due to the smaller size would be more than offset by the increased annual cost of the greater number of transformers to supply the area. The cost of voltage improvement by reducing the spacing of transformers is also inversely proportional to the load density and, therefore, proper spacing of transformers of a given size becomes independent of load density except as is slightly influenced by annual loss evaluation.

After the proper economic co-ordination of transformer size, transformer spacing and wire size has been determined according to the foregoing principles, then the particular ideal combination of secondary elements to serve a given load density within the permissible voltage loss can be determined. The particular combination to satisfy the given load conditions will therefore vary with the voltage loss permitted by the particular utility. On the other hand, the economic co-ordination of the elements to make up a particular ideal combination will vary essentially with the relative annual costs of the secondary elements and power factor of the load, but is essentially independent of the allowable voltage loss.

These fundamentals are not in variance with the author's paper. They indicate that although his analysis is based on an allowable 6.6-volt loss, the paper has general interest and broad implications.

Chase Hutchinson (Ebasco Services Inc., New York, N. Y.): Economic studies of transformer–secondary conductor which are a part of radial overhead systems are informative and often useful in guiding the operation of distribution systems. However, the choice of limiting conditions and premises may involve judgment and opinion, and it is in this respect that the writer disagrees with some of the conclusions of this otherwise excellent paper.

Banking of secondary systems to reduce flicker and losses, while not wholeheartedly accepted by the industry, is well known and has proved its value in many situations. Further application should be encouraged.

The use of aluminum conductor in lieu of copper, under present price conditions, will produce either a lower initial cost or a lower loss cost. Thus savings may either be taken immediately as a reduction in capital cost or over a period of time as a reduction in cost of losses. Under such conditions use of aluminum for secondary overhead conductor will no doubt expand considerably when the metal becomes more generally available.

Limiting noncyclic decrease in voltage with application of a 20-ampere 60-per cent power factor (lag) 115-volt load is taken as four volts. In the writer's opinion this value is too low and will result in unnecessary use of transformer capacity. This opinion seems to be borne out by the authors proposed use of maximum transformer loading of 80 per cent of rating in light density situations. Under a growing load condition, such a transformer might be loaded initially to values in the range of 40 to 60 per cent of rating. Thus acceptance of the values cited might mean doubling or tripling transformer capacity in the lighter density situations. Generally such situations can least afford the added expense.

The solution seems to lie in the acceptance of a more realisitic value for noncyclic decrease in voltage. Surveys in one area in which service is generally considered satisfactory indicated a value in the region of 10 to 12 volts to be reasonable. When such sudden decreases in voltage were in the range of 14 to 20 volts service was generally considered unsatisfactory.

With respect to Figure 2 of the paper the 10-kva transformer curve indicates the transformer secondary combination has an economical load for satisfactory service of 80 per cent of transformer rating and costs about $57 per year per thousand feet and has an economical load of 230 per cent of transformer rating. Does this mean that the 10-kva transformer installed with number 0 aluminum and a load density of 10 kva per thousand feet would not be loaded in excess of 8 kva? Or does it mean that where density is 10 kva per thousand feet nothing less than 10-kva transformers would be used initially, and as load grows these transformers would be loaded to as much as 140 per cent of rating before steps are taken to reduce the transformer load?

The assumption that secondaries are straight-line 2-way feed represents an extreme condition from the flicker and voltage drop standpoint. In many situations such a secondary layout is used commonly while in others a more complicated layout is attractive. Consider the case where secondary branches in three directions a few spans from transformer as indicated in Figure 3 of the discussion. Here flicker may be much less of a problem than indicated in the paper.

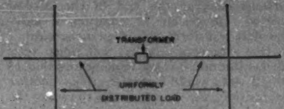

Figure 3. Branched secondary

Charles Dunn (Bonneville Power Administration, Portland, Oreg.): The paper by Brady has some good ideas, but the main criticism of this paper is that it is too specific in its assumptions and cannot be applied to most other systems because of this fact. For one thing, the load assumptions are altogether out of line with the loads which we have in the Pacific Northwest. Brady assumes the load density of 10 kva for 1,000 feet. This is very light loading for our distribution systems in this area. It is not uncommon to have loadings of five to ten times the values given by Brady, especially where house heating loads are involved.

Another assumption of Brady's is that transformer loading is limited to maximum of 140 per cent of name-plate rating. This is obviously a very conservative assumption, particularly in view of the loading which distributors have had to place on transformers during the winter peaks for short-time operation. Utilities in the Northwest believe this figure should be 150 to 175 per cent for short-time loadings.

Brady evaluates losses at certain specific figures which would only apply on his own system. Different figures would have to be used on the Northwest which could change the entire conclusions of his paper. We do not believe that bare aluminum without steel reinforcing should be used as a secondary conductor due to operating difficulties caused by burndowns.

M. B. Elton (Bonneville Power Administration, Portland, Oreg.): Brady states that "most of the flicker voltage drop resulting from the starting of small motors occurs in the distribution transformers and the secondary conductors."

Most of this flicker will be found to occur due to inadequate dwelling wiring over which the utility has little control, if any. Outside of the dwelling, the average allowable variation, in most cases, in the voltage from minimum to maximum will be as follows:

Service = 12.5 per cent or 1.2 volts
Secondary = 37.5 per cent or 3.6 volts
Transformer = 37.5 per cent or 3.6 volts
Primary = 12.5 per cent or 1.2 volts
Total = 100 per cent or 9.6 volts = (8 per cent for State of Washington for towns of 15,000 or more population)

In connection with the "choice of conductor for new systems" Brady speaks of the merit of using bare conductors because "weatherproof covering is an unnecessary luxury." It is true that, from a safety standpoint, the covering of most "weatherproof wires" is very inadequate and even constitutes a potential hazard, particularly if the wire drops to the ground and the unsuspecting public contacts the wire thinking it safe because it has a covering. However, most city ordinances still require weatherproof wires within city limits. Before bare wires could be used, therefore, the city ordnances would have to be changed. This would be a great step forward in permitting more modern engineering and operation practice within urban areas.

This paper contains a very logical approach to the growing problem of reducing voltage flicker due to small motors and to the most economical use of transformers on a network secondary system.

A. Streiff (Portland General Electric Company, Portland, Oreg.): The load density of this company varies from 50 to 100 kw per 1,000 feet in our residential district, and this occurs in the district with people of limited means as well as in our higher class districts. Due to our present rates, most of the people can afford range and water heater service and use electric heat to supplement other forms of house heating. There are also many houses which are electrically heated, and more would be totally electrically equipped if material and electrical power were available.

Due to the foregoing conditions we plan on loading our transformers about 150 per cent in the winter time as the load drops to approximately half this amount during the summer months. Practically all our transformer failures occur during the coldest days of the year.

Most of our secondary systems are radial although we bank two or more transformers together through secondary fuses. We have a number of banked secondary systems using the double circuit breaker current-protected transformers (Westinghouse type *CPB*) which have recently been installed, and which have given us satisfactory service to date.

Most of the secondary system consists of number 4 copper wire, but where the load density is large we use number 1 copper wire in the hot wires and number 4 copper wire in the neutral position. We have not been inclined to use aluminum wire in the more heavily loaded districts and have confined the use of aluminum wire to the rural districts.

However, within the past year we have used approximately 15,000 pounds of number 4 weather-proofed aluminum for service conductors.

Bryce Brady: Seelye has stated one of the conclusions so neatly that I would like to repeat it . . . "for light-load densities excess transformer capacity is a cheaper means of limiting the voltage dips due to motor starting currents than the installation of unduly large conductors or the use of unduly close transformer spacing."

During the war, heavy overloading of distribution transformers was practiced at all load densities. This undoubtedly helped the war effort by conserving copper and steel. Transformers are now more readily available and it appears timely that transformer sizes should be determined entirely in accordance with over-all economy.

Hutchinson asks, in regard to Figure 2 of the paper, if nothing smaller than 10-kva transformers would be used to serve a load density of 10 kva per 1,000 feet. The answer is yes, because the use of smaller transformers results in higher annual cost under the premises of this study.

Campbell asks if the initial installation of 15-kva transformers would not be more economical than 10-kva transformers, if the cost of future replacements were less than the accumulated difference in annual cost. The answer might be yes if the engineer could be certain larger transformers in the same locations would be the most economical arrangement at the end of the 13-year period. Respacing or addition of intermediate transformers is often economical.

One discussor thinks that four volts flicker limitation is not realistic and that 10 to 12 volts would be satisfactory; another states that it is very desirable to reduce the dips below four volts if possible. This divergence of opinion among utility engineers may indicate the need for further investigation of the border line between satisfactory and unsatisfactory service, taking into consideration both the magnitude and the frequency of occurrence of voltage dips in residential areas.

Brown's statement as to the independence of secondary wire size and load density is corroborated by Figure 5. If a median is drawn between the radial and banked curves, number 4 copper and number 0 aluminum conductors are more economical, with minor exceptions, than either larger or smaller conductors throughout the entire range of load densities studied.

As surmised by Cole, our company uses the largest size of secondary fuses at the midpoint between transformers, which will assure short circuit protection. We have not used solid banking because of fear of cascading, but from Cole's remarks such fears may not be justified.

The comments of Dunn, Elton, and Streiff, all located in the northwest, emphasize the divergence of load and operating conditions throughout the nation. The conclusions of the paper are valid where the 21 premises listed in Appendix are tenable. In other locations, the methods used in the study may be utilized with appropriate premises.

Commutation of D-C Machines and Its Effects on Radio Influence Voltage Generation

D. P. MOTTER
ASSOCIATE AIEE

FOR SEVERAL years the generation of radio influence voltage by rotating electric machinery has presented problems in radio frequency transmission and reception. This has been true particularly on aircraft. Radio communication, navigation, and other necessary radio and electronic equipment, along with many rotating electric machines are needed to perform various duties in attaining and sustaining flight and accomplishing the mission of the flight on present-day aircraft. Heretofore, the design of machinery has progressed with little or no thought toward reducing the radio influence voltage generated. Consequently, as aircraft functional performance necessitated more electric machinery, the problem of reducing radio influence voltage generated by the electric machinery resulted in the application of suppression harnesses in the form of radio frequency filters applied to almost every machine. With small d-c machines, satisfactory suppression harnesses often demand an overbearing weight and space requirement on the aircraft in proportion to that of the machines themselves.

In attempting to reduce the necessity of suppression harnesses, it is therefore of great value to study the basic causes of radio influence voltage generation in rotating electric machinery and attempt to reduce the radio influence voltage through design changes in the machines.

The Problem

It is of general knowledge to those who have worked with radio influence voltage generation in rotating electric machines, that radio influence voltage is generated as a result of passing a direct current from a stationary surface (such as a brush) to a revolving surface (such as a slip ring). The radio influence voltage generated under these conditions is considered random in character. The transient voltages generated do not reoccur in a definite pattern, or at a definite repetition rate and cannot be synchronized on the screen of an oscilloscope.

The magnitude of the conducted radio influence voltage measured across the brushes of a d-c commutating machine is often much greater than that measured across slip-ring brushes under identical test conditions. Oscillograms taken across the brushes of a d-c commutating machine indicate the predominance of transients reoccurring in a definite pattern and at a definite repetition rate.

The problem, therefore, is to determine the cause of these repetitive transients and to determine the significance of their possible reduction or elimination in reducing the radio influence voltage generated.

Selection of Machine for Tests

From a group of 30 d-c motors, generators, and dynamotors currently applied to United States military aircraft, a certain dynamotor was selected for the detailed tests. The reason for selecting this particular unit is that the radio influence voltage measured across the brushes of the high-voltage winding under normal operating conditions exceeded the radio influence voltage measured across the same brushes passing the same total current through a slip ring (of same diameter and peripheral speed) by a larger factor than any of the group of over 30 machines comparably tested. In making the selection of the test machine in this manner the effects of the repetitive type transients associated with commutation of current can be analyzed more clearly.

Curve "A" on Figure 1 shows the radio influence voltage measured across the two commutator brushes of the high-voltage winding of the test dynamotor. The machine was operated at rated speed, rated voltage, and load current.

Curve "C" on Figure 1 shows the radio influence voltage measured across the same two brushes riding on a slip ring. For these tests the same total brush current was supplied by batteries. All other test conditions were the same as those while making the tests on the commutator, including total brush current, peripheral speed, brush pressure, and brush-to-brush holder clearance. The data on curve "C" coincide with data taken across the brushes on the commutator with all commutator bars short-circuited, field poles removed, the same total brush current supplied by batteries, the same peripheral speed, and all other test conditions identical.

Test Conditions

The armature of the test dynamotor was driven at rated speed by a separate motor. The motor winding of the dynamotor was not used because the radio influence voltage generated in the motor winding would be coupled into the wind-

---

Paper 49-28, recommended by the AIEE rotating machinery committee and approved by the AIEE technical program committee for presentation at the AIEE winter general meeting, New York, N. Y., January 31–February 4, 1949. Manuscript submitted November 17, 1948; made available for printing December 27, 1948.

D. P. MOTTER is a design engineer with the General Electric Company, Fort Wayne, Ind.

This investigation was made by the author while engaged as a development engineer in the general engineering and consulting laboratory of the General Electric Company and under contract with Air Material Command of the United States Air Force, to which the author expresses his indebtedness for permission to submit this paper, and to C. M. Foust and C. W. Frick of the General Electric Company for their aid and general supervision in the investigation.

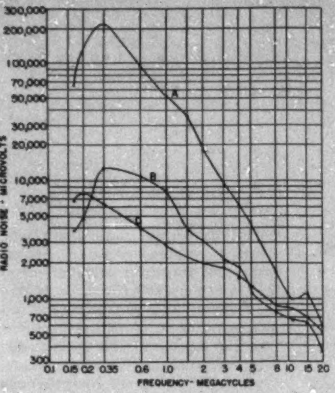

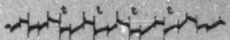

Figure 1 (left). Comparison of laminated brush (B) to normal brush (A) on commutator, and to normal brush on slip ring (C)

Figure 2 (above). Brush to brush oscillogram, 1/6 revolution, normal brushes

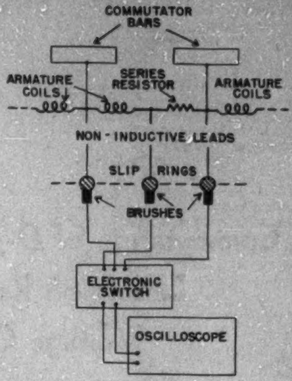

Figure 3 (right). Schematic diagram for measuring coil current and voltage simultaneously

ing under investigation. The shunt field was excited by batteries to provide rated output voltage, and the armature was loaded to rated load current by resistors. The brushes were removed from all commutators of the armature windings except the one under investigation which requires only two brushes. The brushes used for all tests were well seated and run in until all of the brush face area was polished and the commutator film build-up apparently at equilibrium. The same brush holders, nominal brush pressures, and brush-to-brush holder clearances were used in all tests. All radio influence voltage measurements (in microvolts) were made with a standard radio noise and field strength meter connected across the two commutator brushes, and were calibrated with a standard sinewave generator. All tests were made within a double screen shielded room.

Repetitive Transients Present

By connecting a cathode-ray oscilloscope across the two brushes on the commutator of the armature winding under investigation (with negative brush grounded), the presence of transients occurring at a definite repetitive rate is shown. Figure 2 is an oscillogram made under the test conditions stated before while employing the brush grade normally used on this winding of this machine. The radio influence voltage generated at frequencies between 0.16 to 20 megacycles is shown on curve "A" of Figure 1. No visible sparking could be seen during these tests, even in total darkness.

Many other standard grades of brushes were tested with approximately the same results in magnitude of repetitive transients as well as magnitude of radio influence voltage measured.

By properly synchronizing the sweep of the oscilloscope with armature rotation by means of a capacitive pick-up mounted on the revolving armature shaft, it was shown that the number of transients present is equal to the number of commutator bars multiplied by the number of armature circuits for each revolution. This indicates that a transient occurs each time an armature coil is commutated, but does not indicate at what time during the commutation period these transients are produced. It was therefore necessary to determine the differential armature coil currents and voltages during the commutation period of the armature coils.

Measurement Technique for Commutation Evaluation

To observe instantaneous values of armature coil voltage and current simultaneously, three slip rings were insulated from and mounted on the armature shaft between the commutator and bearing. These slip rings were connected to an armature coil by short noninductive leads and to a cathode-ray oscilloscope through slip-ring brushes and an electronic switch as shown in Figure 3. Thus, instantaneous armature coil voltage is measured across one armature coil and the instantaneous coil current is measured across the resistor in series with the armature coil.

The resistor in series with an armature coil on this diagram was a short piece of twisted resistance wire. It was mounted circumferentially along the armature shaft to eliminate the possibility of voltage being induced in it as a result of cutting the fringing flux of the poles. The impedance as well as the d-c resistance of this series resistor was very small in comparison to that of the armature coil so that dynamic balance of the armature circuits was not affected.

It has been determined that certain silver-graphite brushes generate less radio influence voltage on a slip ring than many other standard grades of brushes under the same conditions. These silver-graphite brushes were used on the slip rings and were specially selected and fitted in their brush holders to minimize the possibility of radio influence voltage generation from this source.

Sources of Transients

Figure 4 is a voltage and current oscillogram of one armature coil for approximately one armature revolution while employing the regular brushes on the commutator. The presence of transients on both the current (*I-I*) and voltage (*E-E*) traces is shown. The magnitude of the step (*X-Z*) in the voltage trace during the commutation period is equal to the *IR* change as a result of the change of direction of current of the armature coil under investigation.

Figure 5 is an oscillogram showing the

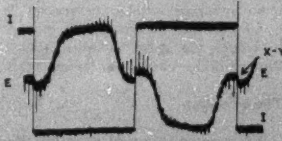

Figure 4. Voltage and current oscillogram, one armature coil, normal brushes

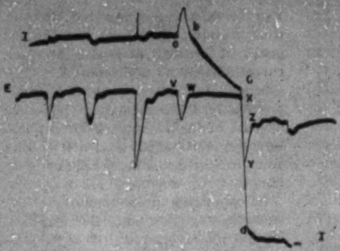

Figure 5 (left). Voltage and current oscillogram during commutation period, one armature coil, normal brushes

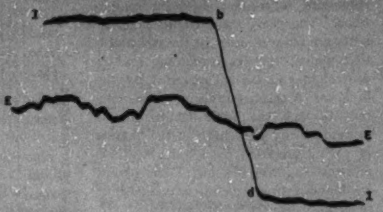

Figure 7 (right). Voltage and current oscillogram during commutation period, one armature coil, developmental laminated brushes

same voltage and current traces as Figure 4, but is expanded sufficiently along the *Y* axis and greatly along the *X* axis to show more detail of these traces during the commutation period of the armature coil under investigation. The sweep on this oscillogram is conventionally left to right. The points *b* and *d* represent the beginning and end of the commutation period respectively. The transients *X-Y-Z* appearing on the coil voltage trace coincides (in respect to time) with the relatively rapid rate of coil current change between points *c* and *d*. This was true for each armature coil investigated. It was therefore established that these transients were produced at the ends of the commutation periods of the armature coils.

It is interesting to note on Figure 5 that the transient (*V-W*) produced at the end of the commutation period in the coil immediately adjacent and in advance of the coil under observation produces a transient current rise in the coil under observation between the points *a* and *b*. The current in the coil under observation tends to oppose the change in current in the other coil since both coils are in the same armature slot and inductive coupling is relatively close.

There is a difference of induced voltage in the last coil in an armature slot with respect to the first coil in the next armature slot due to their circumferential position differences in the fringing flux field. There are three coils per armature slot on the test machine and the span of the brush is one commutator bar. Therefore another transient is produced at the end of the commutation period of every third coil. This transient is superimposed on the transient regularly appearing at the end of the commutation period and explains the greater magnitude of every third transient (*t*) shown on Figure 2.

Brush-to-commutator discontinuities of contact will produce objectionable transients either random or repetitive in character, depending upon the causes of the discontinuities. In the tests described in this paper, no such discontinuities were in evidence.

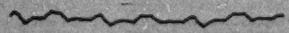

Figure 6. Brush-to-brush oscillogram, 1/6 revolution, developmental laminated brushes

Commutation with Standard Brushes and No Interpoles

Machine and brush designers are well acquainted with the problems involved in making it possible for the brush to largely control coil current reversal in d-c machines.

This is particularly a problem in the design of machinery for aircraft application wherein weight and space considerations are stringent. These considerations many times limit the possible employment of interpoles and prohibit their use on dynamotors. In addition, high contact drop brushes adversely affect machine efficiency.

On d-c machines, circulating current across the brush face is mainly affected by either or both the self-induced voltage of the armature coil opposing current change during commutation; and induced voltage in the armature coil during the commutation period resulting from the shift of the magnetic neutral with change in armature current. If either or both of these induced voltages are of sufficient magnitude, the brushes lose a large share of their control over coil current reversal. Circulating currents flow in the coil-bar brush-bar coil circuit, the rate of coil current change is not linear, and the greatest rate of coil current change occurs late in the commutation period as exemplified in Figure 5. The brush cross-face resistance is considerably lower than the contact resistance, and in many cases has relatively little significance in limiting the circulating currents. Of all the standard grades of brushes tested on this test machine, including brushes rated at "very high contact drop" as well as "very low contact drop," none showed marked improvement in commutation over the brushes normally used.

Commutation with New Laminated Brushes

New laminated brushes have been designed which improve commutation and reduce radio influence voltage generation over a rather wide range of armature currents.

With the new laminated brushes, the commutation of current in an armature coil depends largely upon the increase in resistance of each brush lamination as the commutator bar progresses from the leading edge to the trailing edge of the laminated brush. The thickness of each lamination in the brushes used on the test machine is equal to or less than the thickness of insulation between two adjacent commutator bars. Each brush lamination is insulated from all others (as well as from the brush holder) except at the pigtail end of the brush. A simple sketch of this brush structure is shown in Figure 8. As a result of this design the circulating current across the brush face must flow through the entire length of two brush laminations whose combined resistances are considerably larger than the resistance across the face of a nonlaminated brush or of a laminated brush not

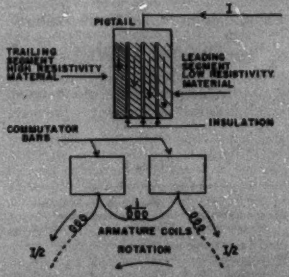
PIGTAIL
I
TRAILING SEGMENT HIGH RESISTIVITY MATERIAL
LEADING SEGMENT LOW RESISTIVITY MATERIAL
INSULATION
COMMUTATOR BARS
ARMATURE COILS
ROTATION
I/2
I/2

Figure 8. Developmental laminated brush showing division of current during commutation

employing insulation between laminations. Therefore, these circulating currents are reduced early in the commutation period, thereby promoting greater control of coil current reversal by the brushes. A relative division of line current through the brush laminations is represented by the length of the vectors in each lamination on Figure 8. This more or less forced division of line current is conducive to a more linear coil current reversal.

Figure 6 is an oscillogram taken across two developmental laminated brushes applied to the test machine. The absence of transients is noted. Test conditions were identical to those in making the oscillogram of Figure 2 with the normal brushes.

Figure 7 is an oscillogram showing the expanded voltage and current traces of an armature coil during commutation while employing the developmental laminated brushes. The rate of change in coil current is nearly linear during the commutation period (*b* to *d*), and absence of transients on both the current and voltage traces is noted. Test conditions were identical to those in making the oscillogram of Figure 5 with the normal brushes.

Radio Influence Voltage Reduction

Curve "B" on Figure 1 shows the magnitude (in microvolts) of the radio influence voltage generated while employing the developmental laminated brushes on the test machine over the frequency range 0.16 to 20 megacycles. The data for this curve were recorded during the time the oscillograms were taken, and coincides with data taken in other tests at frequent intervals during continuous operation of over 150 hours. The average radio influence voltage reduction provided by the laminated brushes as compared to the brushes normally used on this machine is shown in Table I.

Commutation Period Transposition

Figure 9 shows the change in magnitude of the radio influence voltage generated at 0.16 megacycle as the commutation period is shifted with respect to the magnetic neutral while employing standard grades of brushes (curve "B") and the laminated brushes (curve "A") on the test machine. For these tests a special vernier brush shifting mechanism was employed. The physical mid-point between the two field poles is marked zero degrees. Sufficient run-in time was permitted to assure the best possible brush seating for each test point. Load current was adjusted to rated load with brushes set in the best commutating position (27 degrees) as determined by oscillograms similar to Figure 5.

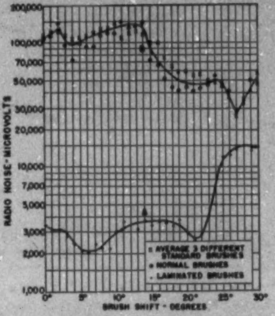

Figure 9. Comparison of laminated brushes (A) to normal and other standard brushes (B), brushes shifted with respect to magnetic neutral

Table I

Frequency Range, Megacycles	Average Radio Influence Voltage Ratio Normal		Laminated
0.16 through 1	12	to	1
1 through 5	6	to	1
5 through 20	2	to	1
0.16 through 20	10	to	1

The brush position for commutating full-load current at rated voltage at the minimum induced armature coil voltage position is at 22 degrees on Figure 9. This was determined by shifting the brushes into a position wherein the current trace started to cross the voltage trace at minimum coil voltage. Best commutation and minimum radio influence voltage generation occurred five degrees in advance of this position (27 degrees) while using standard grades of brushes as shown on curve "B."

From the radio influence voltage data and correlated oscillograms it was established that with standard brushes there is a finite position of the commutation period with respect to the magnetic neutral at which best commutation and minimum radio influence voltage is produced.

Curve "A" on Figure 9 shows that the radio influence voltage generated while using the laminated brushes is essentially constant over a 22 degree range of transposition of the commutation period behind the minimum induced armature coil voltage position. Oscillograms indicated better commutation with the laminated brushes over this wide range of commutation period transposition than the best commutation position with the standard grades of brushes. It is also shown on curve "A" that the radio influence voltage generated increases rapidly with transposition of the commutation period in advance of the minimum induced armature coil voltage position, and oscillograms indicated poor quality of commutation.

By comparing the performance of the laminated brushes and the standard brushes in this manner it may be concluded that better commutation will result and radio influence voltage will be reduced over a wider range of armature currents by utilizing the laminated brushes.

Design of Effective Laminated Brushes

The laminated brushes used on the test machine are made of four laminations of equal size, but each of different resistivities and total resistances from brush face to pigtail as shown in Table II.

Four other laminated brushes were designed identical to these brushes in every respect except resistivities of the laminations, and were tested on the test machine. In all designs wherein the leading lamination resistance was the same as shown in Table II, but the trailing lamination resistance was lower, and the second and third laminations of lower intermediate resistances, considerably less commutation improvement and radio influence voltage reduction was provided. From these tests it is concluded that for a given machine design there is a finite laminated brush design to provide an optimum performance by this method. The machine design factors most affecting the design of laminated brushes are those bearing upon the aggravation or amelioration of circulating current in the brush-commutator bar-armature coil-commutator bar-brush circuit. Other major considerations are the magnitude of armature current in various phases of operation (and including starting), current carrying capacity of brush laminations, whether or not interpoles are incorporated in the design, and

Table II

	Resistivity, Ohm-Inches	Total Lamination Resistance, Ohms
Leading lamination	0.000016	0.00192
Second lamination	0.0007	0.084
Third lamination	1.3	150.0
Trailing lamination	8.0	480.0

whether the machine is reversible or unidirectional.

Insulation between laminations must be provided to reduce circulating current across the brush face and be of such material as to prevent conducting brush material from depositing on it at the brush face and producing a low resistance path across the brush face.

Limiting the maximum thickness of each brush lamination to the thickness of insulation between commutator bars is essential in the design of effective laminated brushes for the test machine. This design requirement may not be necessary to provide optimum performance in applications on other machines.

Theoretically, an infinite number of brush laminations are necessary to eliminate transients appearing at the transition of one lamination to the next lamination. Actually, the machine constants and the economics of the design and manufacture of the brushes are the determining factors.

All short-circuit paths between brush laminations (except at the pigtail end of the brush) must be eliminated. This necessitates insulating the brush from the brush holder, or making the brush holder of insulating material.

By making each conducting brush lamination of the same material, and inserting the necessary resistances in each lamination at the pigtail end of the brush, the optimum performance characteristics of the brush may be realized over the entire life of the brush.

Conclusions

1. One of the main causes of radio influence voltage generation in d-c rotating machinery is transient voltages produced during commutation.

2. The magnitude of the transients and of the radio influence voltage generated is dependent upon linearity of armature coil current reversal.

3. Black band commutation is no assurance of the best quality of commutation to minimize radio influence voltage generation.

4. Where interpoles are not employed, there is a finite armature current at which commutation is of better quality and minimum radio influence voltage is generated while using standard brushes.

5. Developmental laminated brushes can improve linearity of armature coil current reversal and provide an appreciable reduction of radio influence voltage generation over a rather wide range of armature currents.

Discussion

C. W. Frick (General Electric Company, Schenectady, N. Y.): It has been known since the early development of radio communication that commutator motors and generators produce electric disturbances which may affect radio reception adversely under some conditions. While the presence of these disturbances has not been ignored, the common attitude has been that nothing could be done to prevent their occurrence. There were several reasons for this attitude. One reason was that the usual means for obtaining acceptable commutation failed to eliminate the disturbances. Another reason was that the earlier problems of radio interference were concerned largely with reception of standard broadcast signals. In that case it was usually an easy matter to eliminate or reduce the effects of the disturbance by adding a small capacitor to the commutator machine. This treatment does not attempt to deal with the cause of the disturbance and is known generally as suppression.

As pointed out in the paper, it was the use of radio communication in aircraft that brought attention to the need for a fundamental approach to the problem of reducing the radio influence of commutator machines. One of the accomplishments of the investigation reported is shown effectively by Figures 5 and 7 of the paper. Figure 5 shows armature coil current and voltage for a machine as originally tested. Current reversal instead of being smooth is characterized by a sudden jump at the end of the commutation period. Figure 7 shows the same current and voltage after means were applied to cause the current in the coil to reverse smoothly. In this case the treatment was the application of a specially-designed brush. A marked reduction of the transients in the voltage wave is apparent. The effectiveness with respect to radio influence is demonstrated by test with the radio noise meter which shows a 10-to-1 improvement over a widely used part of the radio spectrum. It is significant that the improvement is brought about by the treatment of conditions which cause the disturbances, not by suppression of disturbances after they have been produced.

This paper is a useful contribution to the attack of the problem of reducing the radio influence of machines of this type. Of course finding out how to do it is only part of the final answer. The design of commutator machines of many different sizes and performance characteristics has been developed over a period of many years. Changes which are introduced for a specific purpose need to be evaluated with respect to their effects on other performance characteristics. In order to apply successfully the ideas set forth in the paper such evaluations must still be made.

E. H. Myers (Westinghouse Electric Corporation, East Pittsburgh, Pa.): 1. This paper is one covering a subject on which very little is known, but one which is becoming increasingly important each year. This is particularly true on machines for naval and military use.

2. Most of our experience on the investigation of radio interference has been on much larger machines than those described by Mr. Motter. We were particularly interested in comparing the data presented in the paper with that which we took on much larger machines.

3. One rather interesting point is that the peak voltage given for the test machine with normal breakers was 220,000 microvolts, which was reduced to 13,000 microvolts by the use of a special laminated brush. From the paper it appears that the machine used was a small size noncommutating pole unit. We normally would expect such a machine to have rather easy commutating problems, due to the low reactance voltage and high armature resistance inherent with a very small machine. Mr. Motter confirms this somewhat by stating that no visible sparking could be seen during the tests. On a 300-kw 240/120-volt 1,200-rpm generator on which we carried out tests a few years ago, the peak radio noise without suppressors and with standard brushes, was about 26,000 microvolts.

4. A comparison of these data seems to indicate that the commutating poles on the larger machine on which we would expect to have more severe radio interference than on a smaller machine, have performed about the same function as the laminated brush on the smaller unit, that is, they force the current during reversal to approach a straight line variation.

5. We would like to know if Mr. Motter has had experience with laminated brushes on larger machines with commutating poles? If so, is the reduction as pronounced as on this small machine, and what reduced noise advantages were gained?

6. The reduced value of radio noise with laminated brushes of 13,000 microvolts as obtained on this small machine is, of course, way above the value normally accepted by purchasers of machines for military use, so that the use of a suppression circuit would be required in addition to the laminated brushes, in many cases. Could Mr. Motter give some information about the proportionate savings in size and weight of the filter by using laminated brushes? Were any data obtained on the basis of thicker laminations, that is, with laminations covering more bars?

D. P. Motter: Mr. Frick's discussion adds materially to the background of this paper, for which the author wishes to express appreciation. The author agrees that further evaluations need to be made in order to successfully apply the ideas set forth in the paper.

Mr. Myers' questions are answered below in the order in which they were presented in the discussion:

In items three and four of Mr. Myers' discussion it is assumed that the discussion refers to the repetitive type of transients as the cause of more severe radio influence voltage expected from the larger machines employing interpoles, and not the random type of transients which may be significantly greater in magnitude as associated with larger brush-face areas and at higher nominal current densities. It is true that higher reactance voltage generally associated with the machines of the size mentioned by the discusser do affect commutation. This effect exhibits itself at the trailing edges of the brushes, or near the end of the commutation period, in the form of arcing. In the author's opinion, at least some, if not all, of this electric energy could be absorbed in properly designed brush laminations at the trailing edge of the brushes. Such a design of laminations might require somewhat higher resistances near the main conducting portion of the brush and still higher resistances near the trailing portion of the brush to prevent resistance transitions of great magnitude, and therefore burning, between laminations.

In reference to item four of Mr. Myers' discussion, there is a question in the author's mind as to whether interpoles can be designed and constructed practically and economically to provide the necessary control of commutation apparently needed for radio influence voltage reduction.

Since the presentation of this paper at the AIEE Winter General Meeting, the author has had opportunity to evaluate the performance of a set of simple laminated brushes on a 100-kw, 240/120-volt 1,200-rpm d-c generator. These brushes were made up with three-quarters of the thickness (dimension in direction of rotation of commutator) of the brush of nearly the same material as the normal brushes used, and one-quarter of the thickness of somewhat higher resistance brush material at the trailing portion of the brush. Although the brushes did not operate satisfactorily at rated load current of the generator, the brushes operated satisfactorily and showed increased black band width and radio influence voltage reduction at load currents less than rated load current of the generator. With the generator loaded to one-quarter rated load current, and with no radio influence voltage suppression, the average of all readings from brush terminal studs to the grounded terminal frame while employing the simple laminated brushes, was 54 per cent lower than the average of the comparable readings while employing the brushes normally used on this machine. With a considerable degree of suppression, but with all other test conditions as shown, the average of all readings while employing the simple laminated brushes was 43 per cent lower than the average of all readings while employing the normal brushes. These tests covered a frequency range from 150 kc through 20 megacycles. Whether or not a brush of this type could be made that would carry the rated load current of the generator and obtain the same quality of improvement has not been evaluated.

In reference to item six of Mr. Myers' discussion, a careful evaluation of proportionate savings in size and weight of filters by using laminated brushes on a wide variety of machines is not available at this time. It is felt, however, that by reducing the radio influence voltage generation to the magnitude of that of the radio influence voltage generated by the random-type transients not associated with commutation of current, the filter requirement would not be as great. It has been shown that the repetitive type of transients generally are of much higher energy, and consequently are much more difficult to effectively filter than the random type of transients.

In the case of the test machine as reported in the paper, it would have been necessary to use a larger brush holder to evaluate the same number of laminations (with the same resistances in each lamination) but of greater thickness. However, the thought was that where a greater control of the commutation of current was needed (such as in the test machine) much could be gained by limiting the thickness of laminations to a dimension equal to or slightly less than the distance between commutator bars. From recent tests on larger machines employing interpoles it appears that the laminations can be thicker, that is, span more bars where less control of coil current by the brushes is required during commutation.

Performance of Diesel-Electric Rig for Deep-Well Drilling

E. C. CLARK
ASSOCIATE AIEE

B. L. MOORE
NONMEMBER AIEE

Synopsis: The successful operation of a big diesel-electric powered drilling rig has permitted the taking of accurate electrical data during normal deep-well drilling on each of the main motor drives and on the engine-generator sets. This paper presents: A description of the power plant and the main power equipment; an elementary power diagram showing the main d-c circuits; a discussion of the functions of the electrohydraulic governor which regulates engine speed from half speed to full speed; the operation of the rig as seen by the driller who is uninterested in the technical details of the governors and amplidynes; test data taken on the engine-generator sets showing how the governor regulates engine speed and limits engine loading; and test data taken on the drawworks motor, the mud pumps, and the rotary table motors and a discussion of the power requirements of each.

DIESEL-electric barge rig number 29 is one of the most powerful in operation today. The rig combines operating simplicity and flexibility with low fuel cost. Although designed primarily for economical drilling of deep wildcat wells, it is equally suitable for drilling production wells.

General Arrangement

POWER PLANT

The power for the rig is supplied by three 900-rpm 700-horsepower supercharged diesel engines each of which is equipped with an electrohydraulic governor.

Direct connected to each engine is a 500/375-kw 900-rpm 600/450-volt amplidyne controlled main generator. Top-mounted and belt-driven from each of the main generators is a 60-kw 125-volt 1,700/850-rpm auxiliary generator with a direct-connected exciter. Voltage regulators maintain a constant potential of 125 volts over the engine speed range.

DRAWWORKS

The 4-speed drawworks is driven by a 1,000-horsepower 75 degrees centigrade continuous 725-rpm 425-volt motor which has a peak rating of 1,667 horsepower. The drawworks provides step-down gear ratios from the motor shaft to the drum shaft of 9.06-1 (low-low), 5.73-1 (high-low), 3.65-1 (low-high), and 2.30-1 (high-high). The drum diameter is $30^{5}/_{8}$ inches.

Assuming that the effective drum diameter is $34^{1}/_{2}$ inches, the maximum hook speed that can be attained in high-high gear with eight lines to the traveling block is 540 feet per minute when the motor is operating at its rated (625 volt) maximum speed of 1,100 rpm. With ten lines to the traveling block, the maximum hook speed is 432 feet per minute.

MUD PUMPS

The two 480-horsepower 55-rpm $7^{3}/_{4}$ by 20 inch mud pumps are V-belt driven by two 500-horsepower 900-rpm 425-volt shunt-wound motors. Each pump will provide a maximum pressure of 1,200 pounds per square inch. The mud mixing pump which provides a maximum pressure of 1,160 pounds per square inch is V-belt driven by 60-horsepower 115-volt 690/1,380-rpm adjustable-speed shunt-wound motor.

ROTARY TABLE

The rotary table is driven by a 300-horsepower 875-rpm 425-volt shunt-wound motor through a 3.84-1 step-down gear. The 1,300-rpm maximum speed (625 volts) of the motor corresponds with a table speed of 340 rpm.

CORING REEL

The coring reel motor is a duplicate of the rotary table motor.

VENTILATION

The drawworks motor, the mud pump motors, the rotary table motor, the coring reel motor, the mud mixer motor, and the main control unit are ventilated by a

Figure 1. Diesel electric barge rig on location in Galveston Bay

---

Paper 49-121, recommended by the AIEE Chemical, Electrochemical, and Electrothermal Applications Committee and approved by the AIEE Technical Program Committee for presentation at the AIEE South West District Meeting, Dallas, Tex., April 19–21, 1949. Manuscript submitted March 8, 1948; made available for printing February 24, 1949.

E. C. CLARK is with the General Electric Company, Schenectady, N. Y., and B. L. MOORE is with the Humble Oil and Refining Company, Houston, Tex.

Figure 2. The 375-kw main generators and the top-mounted 60-kw auxiliary generators which supply power for rig number 29

central cooling system which is powered by a 30-horsepower 115-volt shunt-wound motor.

AUXILIARIES

The various rig auxiliaries are supplied with power by the three 125-volt d-c auxiliary generators. A list of the auxiliary drives is given in Table I.

Two emergency 9-kw 120-volt d-c engine-generator sets are available, one on the derrick barge and one on the power barge.

Rig Operation

POWER CONNECTIONS

The electric power connections for this rig are shown in Figure 5.

Each generator is provided with an isolating disconnecting switch and four motor selector switches which permit the generator to be connected to any main motor. Magnetic contactors (*H* and *D*) do all the power switching except for initial "set-up" switching. Relaying is provided so that the control switching automatically follows the power switching. When power switching has been properly done, the control circuits will be properly connected. A motor master switch conveniently located controls the operation of each motor regardless of generator selection.

Table I

Number	Motor Rating, Horse-power	Power Requirement, kilowatts	Equipment
1	60	51.0	Mud mixing pump
1	30	26.0	Blower
1	15	13.0	Air compressor
1	15	13.0	Fresh water pump
3	10	26.0*	Amplidyne exciter sets
10	$7\frac{1}{2}$	64.0**	Ballast pumps
1	5	4.3	Air compressor
3	3	7.6	Engine heat exchanger pumps
1	3	2.5	Fresh water pumps
1	3	2.5	Shale shaker
1	$1\frac{1}{2}$	1.3	Steam generator
6	2	10.2	Bug blowers
1	2	1.7	Fresh water pump
1	1	.9	Fuel transfer pump
1	1	.9	Dirty oil pump
4	1	3.4	Power barge exhaust fans
		10.0	Lights
		16.0	Motor fields
		254.13	Total kilowatts

* 16 kw is sufficient at one time, therefore, peak load is approximately 180 kw.

** Never operates simultaneously with other loads.

Deep-well drilling requires the simultaneous operation of two mud pumps, the rotary table, and the mud mixing pump. The rotary table and the two mud pumps may each be connected to any main generator through their *D* contactors while the mud mixer may be connected to any one of the three auxiliary generators.

The time spent in making a round trip is dependent upon the power supplied to the drawworks. As shown in Figure 5, the entire power output of the three engines may be supplied to the drawworks motor by closing the *H* contactors.

GOVERNOR OPERATION

The unique feature of the power system is the electrohydraulic engine governor. The governor is similar to those being used on diesel-electric locomotives, but it has never before been applied to a diesel-electric drilling rig.

The functions of the governors and associated amplidyne exciters are:

The Control of Engine Speeds

The engines operate over a speed range of 450–900 rpm. The governors permit the engines to operate at the lowest speeds compatible with the load requirements

The Limiting of Generator Loading

The governor limits generator loading to an amount that will not overload and stall the engine under any conditions

The Limiting of the Amount of Fuel Injected

The permissible maximum torque of a diesel engine varies with engine speed. The torque may be limited to the safe maximum value by limiting the amount of fuel injected. The governor limits the maximum amount of fuel that may be injected as a function of engine speed

The Control of Injection Timing

The proper injection timing of a diesel engine varies with speed. The governor regulates the timing as a function of engine speed (motor master switch position)

Figure 3. The driller operating the controls of the drawworks

The Limiting of Generator Currents

Over-current is destructive to d-c machinery because of heating and possible commutator damage. It might be destructive to driven equipment because of the excessively high torques it produces. The amplidyne exciters limit generator currents to safe preset values even though the motors may be stalled

The Control of Generator Voltage

Motor speed is determined primarily by generator voltage. The governor-amplidyne-exciter combination controls generator voltage and engine speed as functions of the position of the driller's master switch.

GOVERNOR CONTROLLED ENGINE GENERATOR CHARACTERISTICS

Test data were taken on one of the engine-generator sets to obtain a volt-ampere characteristic at various engine speeds. The results of this test for engine speeds of 516, 703, and 900 rpm are plotted in Figure 6. The 450-rpm curve is calculated from test data. As the engine speed is set entirely by the position of a master switch, these curves were taken by setting the master switch at several positions and varying the generator loads. In order to understand what the governor accomplishes as far as the speed and torque of the driven motor are concerned, it is necessary to be familiar with the characteristics of a d-c shunt-wound motor. Within reasonable limits,

Figure 4. Rear view of the drawworks showing 1,000-horsepower drawworks motor and ventilating duct on right

the torque of a d-c motor is directly proportional to the current. The speed of the motor is directly proportional to the voltage. Therefore, in a qualitative discussion of motor operation the terms speed and voltage and the terms torque and current may be used interchangeably.

Since all of the curves on Figure 6 are similar, the 900-rpm (engine speed) curve will be discussed only.

As the generator current is increased from zero (point *a*) to 940 (point *b*) amperes, the voltage drops slightly providing a desirable characteristic for stable motor operation. As the engine load increases from zero to full load (point *b*), the governor adjusts the position of the fuel rack so that the speed is maintained at 900 rpm regardless of the load and adjusts injection timing properly for 900-rpm engine operation.

With 940 amperes and 535 volts on the generator the fuel rack is in its limiting position (adjusted by governor as a function of speed) and the engine is fully loaded. A further increase in load will slow down and stall the engine.

When the attempt to further increase the generator load (beyond 940 amperes) is made, the engine slows down transiently as the amount of fuel injected cannot be further increased. The transient decrease in engine speed causes the governor to decrease the voltage and the load on the generator so that the engine accelerates again to 900 rpm with just the amount of load that it may carry at 900 rpm. Thus, as the current is varied from 940 (point *b*) to 1,640 (point *c*) amperes, the generator voltage is reduced by the proper amount to maintain constant load on the engine.

At 1,640 amperes (point *c*) the generator is near its maximum permissible current (rated 833 amperes). Further increase in the generator current causes the voltage to drop rapidly, decreasing the load on the engine. At 1,960 (point *d*) amperes output the generator voltage is zero and the power output from the engine is very small (losses only). Engine speed is maintained at 900 rpm.

The other characteristic curves shown on Figure 6 are similar to the 900-rpm curve.

The dotted, approximately vertical line shows the effect of the governor fuel limit cam. If these diesel engines were constant torque machines, this line would be vertical as constant current output would indicate approximately constant engine torque. However, these engines are equipped with turbochargers which are more effective when the engines operate at a high speed. Thus, as the engine speed increases, the maximum permissible engine torque also increases, giving an increase in engine power which is more than proportional to engine speed.

In order to illustrate the flexibility permitted with diesel-electric drive as provided on this rig, a simple arrangement of one generator supplying one motor is selected. The engine and the motor have identical horsepower and speed ratings of 700 horsepower and 900 rpm. The operation of each will be predicted from the test data on Figure 6.

For the first case, assume that the motor master-switch is in the full "on" position and that the motor torque is varied. The engine will run at 900 rpm. With zero torque on the motor and zero amperes output from the generator, the generator voltage will be 640 volts (point *a*), which will correspond to 150 per cent of motor speed (1,350 rpm). As the motor torque increases to 70 per cent rated torque (900 amperes), the motor speed will reduce to 126 per cent (point *b*) as determined by applied volts. As the torque on the motor is further increased, the speed will decrease but the horsepower output will remain constant at 100 per cent until 127 per cent (point *c*) torque is reached. At this point, current limit is reached and the motor speed will drop rapidly so that the motor will stall at 153 per cent torque (point *d*). When the motor stalls at 153 per cent torque, the generator voltage is practically zero and the generator load consists entirely of losses. Therefore, the engine is almost entirely unloaded. The engine speed remains at 900 rpm since engine speed is a function of master switch position only.

The 900-rpm (engine speed) curve of Figure 6 represents the speed-torque curve of the motor in this example with the abscissa representing motor torque (1,290 amperes = 100 per cent motor torque) and the ordinate representing motor speed (425 volts = 100 per cent motor speed).

The second example assumes a constant torque load on the motor and allows the motor speed to vary under control of the master switch in order to show the relation between motor speed and engine speed. A constant torque load of 50 per cent is assumed which corresponds with 650 generator amperes. In order to show clearly the relation between the engine speed and the motor speed, some of the data presented in Figure 6 are replotted in Figure 7 using different coordinates. Initially the motor speed is zero (point *a*, Figure 7).

As the master switch is moved forward, the speed of the motor increases without affecting the engine speed until the motor is operating at 66 per cent of rated motor speed (point *b*). As the motor speed is further increased, Figure 4 shows that the engine speed is also increased.

When the motor has reached a top speed of 133 per cent (point *c*), the engine speed has increased to 100 per cent. The torque load on the engine has been essentially constant as its speed increased from 50 to 100 per cent.

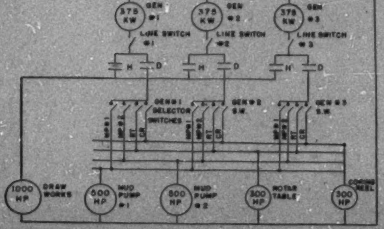

Figure 5 (above). Power connection diagram

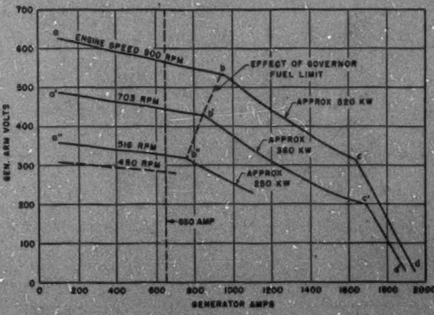

Figure 6 (right). Volt-ampere characteristic of governor controlled engine-generator set

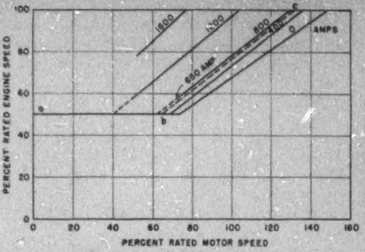

Figure 7. Approximate curve showing motor speed plotted against engine speed

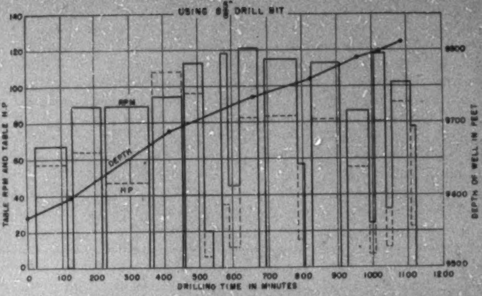

Figure 8. Rotary table horsepower, rotary table speed, and well depth plotted against drilling time

The first example allowed the motor torque to vary from zero to 150 per cent while the engine torque never exceeded 100 per cent. The governor makes it impossible to overload the engine regardless of the wishes of the operator.

The second example showed that as the motor speed was varied from zero to 133 per cent, the engine speed varied from a comfortable 50 per cent to a maximum of 100 per cent. It also showed that when the motor is driving a slow speed load, the engine will be operating at base speed. On a drilling rig, this is a very substantial part of the total operating time, and thus a great many unnecessary engine revolutions are saved.

Operation of the drawworks requires the use of all three generators in parallel for maximum power output. Provision is provided in the control system so this is easily done. Complete control of the drawworks motor, the three generators, and the three engines is from the drawworks master switch.

Operation of Rig by Driller

The only thing that concerns the driller is what happens when he operates the master switches, so it would be well to examine the operation of this rig from his point of view.

In order to start up this rig after a complete shutdown, the driller starts up the diesel engines and throws the switches to put auxiliary power on the lines. Going to the main control board, he may, for example, connect generator number 1 to mud pump number 1, generator number 2 to mud pump number 2, and generator number 3 to the rotary table (see Figure 5). He steps out to his position beside the drawworks and throws the drill-hoist selector switch to the drill position, closing all of the *D* contactors shown in Figure 5.

The rig now is ready to operate and the mud pumps and the rotary table are under control of their own driller's master switches. The mud mixer speed is controlled by its own field rheostat.

The driller need not concern himself with engine speed. He controls the speed of each main motor by its master switch and the engine speed is controlled automatically.

The driller has before him at all times electric meters indicating the speed of the rotary table, the torque of the rotary table, and the current of each mud pump motor.

After drilling for a period of time, the driller will find it necessary to make a round trip for any one of a number of reasons.

He operates the drill-hoist selector switch at the driller's position to close the hoist contactors which connects the three generators in parallel to the drawworks motor. The drawworks master switch has full control of the three generators. (It is not necessary that all of the generators be transferred to the drawworks motor if a different function is desired that requires the use of one. However, in general, all three generators are connected to the drawworks motor for a round trip.)

Starting the first hoist, he throws the drawworks master switch to the full "on" position.

The engines immediately accelerate to full speed and deliver maximum power to the drawworks. The driller does not have to worry about overloading any engine, or the motor, or about load division between engines as this is taken care of automatically by the governor and amplidyne system. When the hoist is completed, the driller stops the drawworks motor and the engines decelerate. The driller breaks the joint in the drill stem with the cathead and steps on the "spinout" switch, which operates the rotary table at a preset speed to unscrew the thribble. He then removes the disconnected thribble and drops the hook for the next hoist.

A drawworks motor ammeter located conveniently indicates to the driller the load on the drawworks motor and helps him to shift gears at the proper time for highest speed operation.

The next hoisting cycle will be exactly like the preceding one, except that the hook speed will be slightly higher. As the load on the hook is decreased, the speed will increase automatically if the driller takes advantage of the constant horsepower characteristic of the system.

If one of the diesels is not in operation at the time of a round trip, only two generators will be assigned to the drawworks. Two generators will provide more than sufficient torque on the drawworks motor for the heaviest hook load but maximum hook speed will be reduced.

Thus, after making the electric setup connections, normal operation of the rig requires the driller to control the following devices: the motor master speed controllers; the drill-hoist selector switch; the rotary table spinout switch; drawworks jaw clutches; and the drawworks brake.

Test Results

Tests were taken with recording voltmeters and ammeters on Cote Blanche number 1 at various depths from 9,000 to about 11,000 feet.

Rotary Table

Tests made on the rotary table showed a wide variation in table torque. The minimum torque noted occurred at 9,800 feet and at 80 rpm and was 1,550 pound feet. The maximum torque was 6,400 pound feet at 75 rpm. These values compare with a rated motor torque of

6,900 pound feet when referred to the rotary table.

The test records showed that a torque of 13,400 pound feet was maintained for approximately seven minutes at standstill or at creep speed. This is 195 per cent of rated motor torque and was the highest sustained torque noted during the tests. Unfortunately the testers were so busy elsewhere that they failed to note just what the driller was trying to accomplish. In general, the torque on the rotary table at approximately 10,000 feet was 5,000 pound feet or less.

The rotary table motor provides permissible speeds of the rotary table from 0 to 340 rpm. Maximum speed observed during the test was 135 rpm. Normal drilling speeds varied from 75 to 135 rpm.

The maximum power requirement noted (140 horsepower) occurred when drilling at 135 rpm with 5,400 pound-feet torque on the rotary table.

Figure 8 plots table horsepower, table revolutions per minute, and depth of well versus elapsed drilling time for a typical test. The variation in power requirements can be observed from a depth of 9,570 feet to a depth of 9,810 feet and for a period of elapsed drilling time of 18 hours. It can be seen that the ratio of horsepower to table revolutions per minute varies considerably, but is less than one in all cases, except from time = 360 minutes to time = 450 minutes. Thus, the usual "rule-of-thumb" that about one horsepower per table revolutions per minute is required seems to be borne out.

Figure 8 indicates that the minimum power requirements for rotation (with light weight on the bit) are quite low. This would indicate that a large percentage of the power input to the rotary table is actually required to overcome the friction due to mud drag and due to friction between the drill stem and the periphery of the hole. For deeper wells it appears that the rotary table power requirements would not greatly exceed present requirements for comparable speeds as the total drill stem torque is primarily bit torque.

Figure 9 is a typical section of a strip chart of rotary table current.

The maximum torque is approximately 12,500 pound feet at time = 10 minutes on the chart. On the average, the torque varies from 1,800 pound feet to 5,600 pound feet. The time variation of torque is not evident from this chart because of the slow speed of the chart.

Figure 10(A) is a 6-inch-per-minute strip chart taken when drilling at a depth of 10,900 feet, showing rotary table current (that is, torque). The maximum and minimum torques are approximately 4,250 and 1,800 pound feet.

Figure 10(B) shows the variation in speed (calculated from voltage) from 80 to 100 rpm accompanying the torque variation shown in Figure 10(A).

Examination of Figures 10(A) and 10(B) shows that the torque oscillation slowly builds to a maximum sustained value. The period of the oscillation is approximately 4.8 seconds.

A rough calculation of the natural frequency of a system consisting of a torsional spring (the drill stem) and an oscillating mass (the rotary table motor) gave a calculated natural period of 2.2 seconds. The analysis did not include the effect of the rotary table inertia or the effect of the engine-generator set inertia. Taking account of these factors would increase substantially the calculated natural period. Since the calculated period and the measured period are of the same order of magnitude, it is reasonable to assume that these oscillations are natural frequency oscillations of the drill stem.

Figure 11 shows another strip chart taken at 6 inches per hour when drilling at a depth of 11,000 feet. There is no appreciable natural frequency oscillation of the drill stem indicated in this chart.

The rotary table torque resulting from variations in the drill bit pressure are shown clearly. Between time = 5 minutes and time = 40 minutes particularly, the increase in rotary table torque which occurs when the driller jogs the drawworks to payout line is evident. The torque varies from approximately 2,200 pound feet to 7,800 pound feet. In general, torque variations resulting from this cause are of a smaller magnitude than in this example.

During the rotary table test, the maximum rotary table speed observed was 135 rpm (59 per cent of rated motor speed). Reference to Figure 7 will show that the engine supplying the rotary table motor operated at base speed at all times, since the sustained torque does not exceed 6,400 pound feet (515 amperes).

Mud Pump Tests

Spot checks were taken of the mud pump power requirements during normal operation with one mud pump in operation. The depth of the well increased

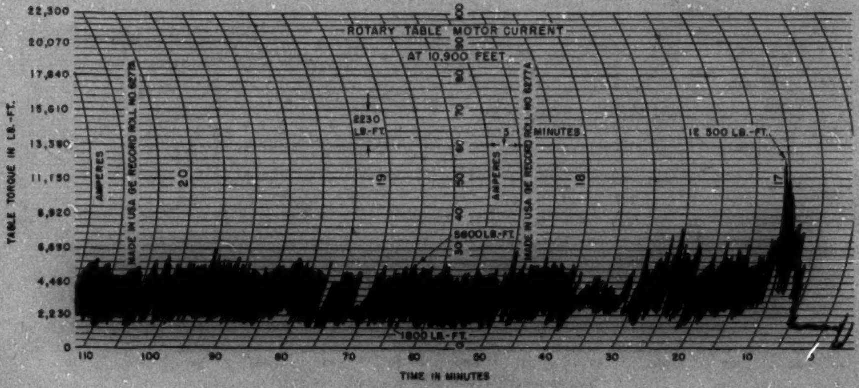

Figure 9. Section of rotary table motor current chart

Ordinate scale reads directly in pound feet of calculated table torque. Chart shows typical time variation of rotary table torque

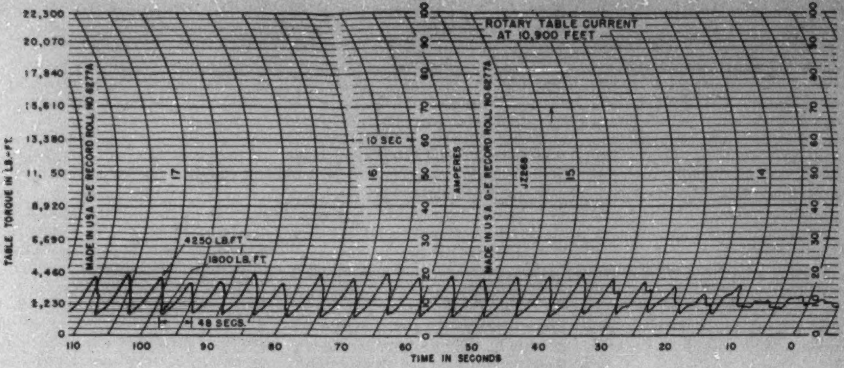

Figure 10(A). Section of rotary table motor current chart

Ordinate scale reads directly in pound feet of table torque. Chart shows periodic variation of motor torque resulting from drill stem oscillation

from 9,795 to 10,736 feet during the tests, while the pump pressure ranged from 1,000 to 1,150 pounds per square inch. The pump speed varied from 43 to 52 strokes per minute, (motor speed 87 to 105 per cent of rated) while the motor output varied from 272 to 448 horsepower. Reference again to Figure 7 will show that the engine supplying power to the mud pump operates at 65 per cent of rated revolutions per minute when supplying 272 horsepower (580 amperes, 87 per cent motor speed) and 82 per cent of rated revolutions per minute when supplying 448 horsepower (800 amperes, 105 per cent motor speed). Thus, the engines will operate from 65 to 82 per cent rated speed when driving the mud pumps.

Since these tests were taken, the mud pumps have been compounded (operated hydraulically in series), permitting maximum mud pressures of 2,400 pounds per square inch.

DRAWWORKS TESTS

A number of tests were taken on the drawworks motor to observe the driller's operation of the motor during the first half of a round trip (coming out of the hole).

Figure 12 shows the simultaneous speed and torque curves (calculated from voltage and current curves) of the drawworks motor plotted against time for hoisting one thribble with 118 thribbles of $5^1/_2$-inch drill pipe on the hook. The drawworks was in low-low gear (9.06/1) and there were eight lines to the traveling block. Two generators supplied power to the drawworks motor.

The driller's actions may be deduced from observation of the drawworks motor torque and speed curves. From 0 to 4 seconds, the driller was taking the slack out of the lines to make sure that he had a firm hold on the drill stem. At 5 seconds he turned the master switch to the full-speed position and the drawworks motor accelerated to maximum speed. At 20 seconds, the hook is traveling at its maximum speed which is determined by the maximum output power of the two engines. At 50 seconds, the end of the hoist is reached. At 54 seconds the driller started the drawworks motor, so that he could use the cathead to break the drill pipe joint. Between 57 and 64

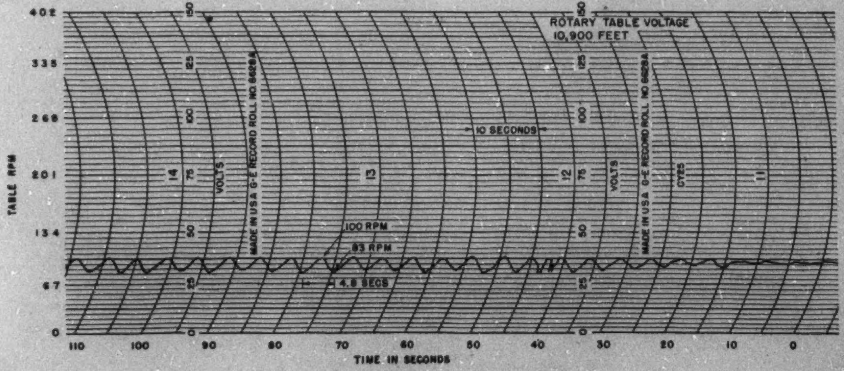

Figure 10(B). Section of rotary table motor voltage chart

Ordinate scale reads directly in calculated revolutions per minute of table motor. Chart shows periodic variation of motor speed seconds, the driller is unscrewing the thribble using the "spinout" arrangement on the rotary table. At 67 seconds the disconnected thribble is stacked at the side of the derrick. The hook is disconnected and dropped for the next hoist.

The engines accelerated to full speed at 5 seconds and remained at full speed until 45 seconds. At the beginning of the next cycle, the engines are again accelerated to top speed.

The next cycle would be almost identical with this one, except that the motor and hook maximum speeds would be slightly higher and the torque would be slightly lower. The time for the hoist would be reduced proportionately.

Figure 13 shows the operation of the drawworks motor during one complete hoisting operation. The tests were taken with a 10,691-foot hole, with eight lines to the block, with $5^1/_2$-inch drill pipe, and with two generators connected to the drawworks. For purposes of these curves one thribble is assumed to weigh 1,550 pounds net and the hook is assumed to weigh 20,000 pounds.

The curve shows the increase in motor speed as the load on the hook is reduced. Further calculations would show that the product of torque and revolutions per minute (power) as given in Figure 10 would not be constant as it should be if the possibilities of the system are utilized fully. The driller was not at all interested in making our test results beautifully consistent. As shown in Table II, the drawworks was operated with needlessly large gear ratios so that the motor speed was excessive. If the proper gear ratios had always been selected, the speed of hoisting could have been increased.

Table II

Gear Ratio	10 Lines: Minimum Weight in Pounds	10 Lines: Length of $5^1/_2$ Drill Stem in Feet	8 Lines: Minimum Weight in Pounds	8 Lines: Length of $5^1/_2$ Drill Stem in Feet
Three Generators				
Low-low	420,000	23,800	336,000	13,800
High-low	263,000	14,400	210,000	11,300
Low-high	163,000	8,500	130,000	6,500
High-high	0	0	0	0
Two Generators				
Low-low	280,000	15,400	224,000	12,100
High-low	175,000	9,200	140,000	7,100
Low-high	109,000	5,300	87,000	4,000
High-high	0	0	0	0
One Generator				
Low-low	140,000	7,100	112,000	5,500
High-low	88,000	4,000	70,500	3,000
Low-high	55,500	2,100	44,000	1,450
High-high	0	0	0	0

In Figure 14 the hook speed is plotted against the net weight of the drill stem using data from Figure 13. The figure shows that the operator shifted from low-low gear to high-low gear with 164,000 pounds net weight while Table II shows that the gears should have changed from low-low with 224,000 pounds net weight. The fact that the change in gear ratio gave no immediate increase in speed of the hook indicated that the driller could have shifted to high-low gear sooner with some benefit.

Figure 15 is based upon the same set of data as Figures 13 and 14 and shows the time of hoisting to remove a thribble plotted against the weight on the hook. The total cycle time, which includes the time between hoists, also is shown. The time between hoists varies quite widely and only those values which indicate that the crew is working constantly at a normal speed are used.

Figure 16 is based on test data and shows the amount of weight that can be lifted in any gear ratio and the proper gear ratio to use to take advantage of the constant horsepower characteristics of the system.

The horizontal broken lines enclosed by brackets show the upper and lower limits of drawworks motor current that should be used for best operation with three generators. The limits that should be used for one or two generators can be obtained by proper reduction of the limits shown for three generators. The top horizontal broken line shows the maximum current available from the three generators and indicates for any gear

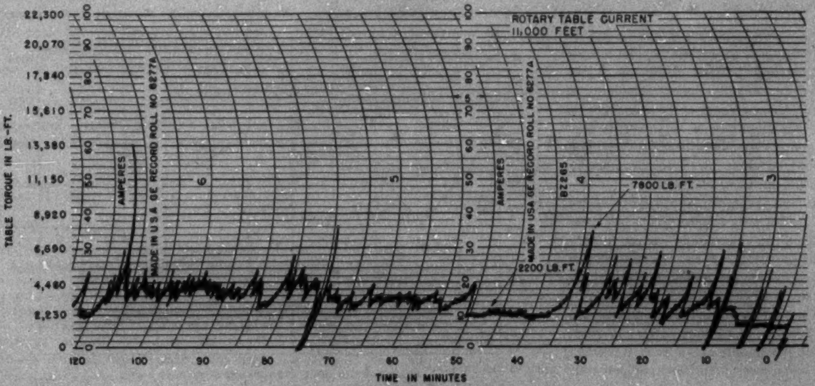

Figure 11. Section of rotary table motor current chart

Ordinate scale reads directly in terms of pound feet of calculated motor torque. Chart shows variation in table torque resulting from manual control of weight on drill bit ratio the amount of weight that may be lifted (no acceleration).

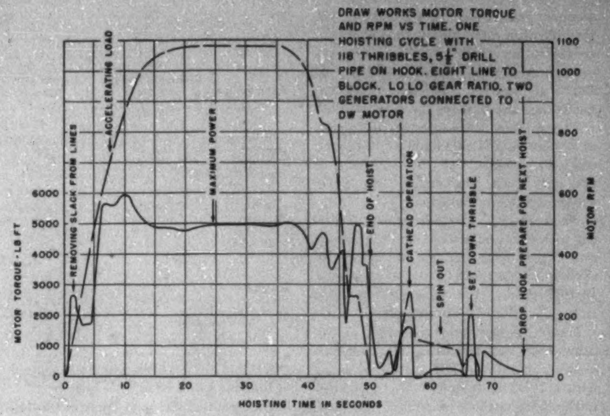

Figure 12. Typical drawworks motor torque and speed curves when "coming out of the hole"

Tests were taken while removing one "thribble" (90-foot section of drill stem)

The proper gear ratios to be used are shown in Table II.

If the values recommended here are checked against the weights at which the gears were shifted in Figure 13, the error becomes apparent.

The mechanical efficiency of the hoisting equipment from the motor shaft to the bottom of the hole was calculated to be approximately 70 per cent using the following definition of efficiency:

$$\text{Mechanical Efficiency} = \frac{W \times R}{N \times GR \times Tcalc}$$

where

W = total drill stem weight plus mud buoyancy factor + hook weight in pounds
R = drawworks drum radius in feet
N = number of lines to traveling block
GR = drawworks gear ratio
$Tcalc$ = calculated drawworks motor torque in pound feet necessary to lift weight W, without acceleration calculated from armature and field current

The losses included in the efficiency calculation are:

1. The drawworks chain drive and drum losses.
2. The line losses.
3. The crown block losses.
4. The traveling block losses.
5. The friction losses in the hole.

Discussion of Test Results

Rotary Table

As shown in Figure 8, the torque requirements of the rotary table for normal drilling will be one continuous horsepower per table revolution per minute or less. Although none of the tests taken on this rig show torque requirements substantially exceeding this value, provision should be made for higher torques for unusual operating conditions.

Since a properly designed electric drive will permit peak torques of 2 to $2^1/_2$ times normal, an electrically driven rotary table providing a normal rated torque of 1 horsepower per table revolution per minute is adequate.

The rig tested provided a normal rated table torque of 1.3 horsepower per revolution per minute and a peak torque of 3.4 horsepower per revolution per minute.

The oscillations shown in Figure 10(A) may occur with any type of rotary-table drive (electric, mechanical, or steam) although the natural period and magnitude may vary considerably. While this type of oscillation is known to exist in rotary tables driven by other types of drives, it can be measured and recorded most easily with the electric drive.

The variations in rotary table torque resulting from manual control of the weight on the drill bit are shown clearly in Figure 11. While it is recognized that the selection of the proper weight to be held on the bit is not an exact science, it is safe to say that either the weight corresponding to 7,800 pound feet torque was too high, or that the weight corresponding to 2,200 pound feet torque was too low for maximum drilling speed. This rig has a hydraulic drag device (not used during the tests) which simplifies greatly the problem of maintaining constant weight on the bit. The use of bit weight controlling equipment offers the following advantages:

1. The optimum weight on the bit may be held within close limits for a given strata resulting in the greatest drilling progress.

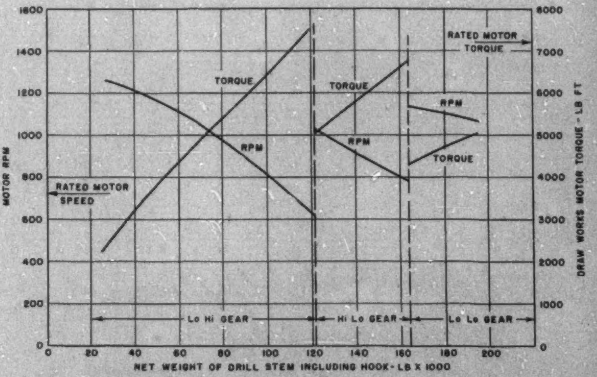

Figure 13. Motor torque and revolution per minute plotted against net weight of drill stem

Calculated from test data taken "coming out of the hole" from 10,691 feet with 8 lines to traveling block and using two engines

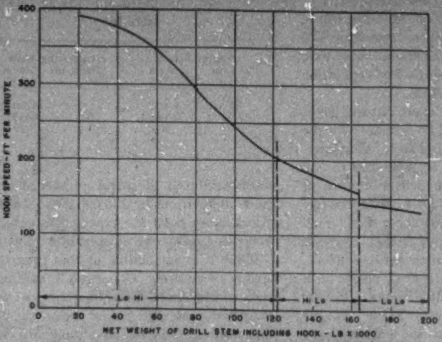

Figure 14. Calculated hook speed versus net weight of drill stem Data taken "coming out of the hole" from 10,691 feet with 8 lines to traveling block using two engines

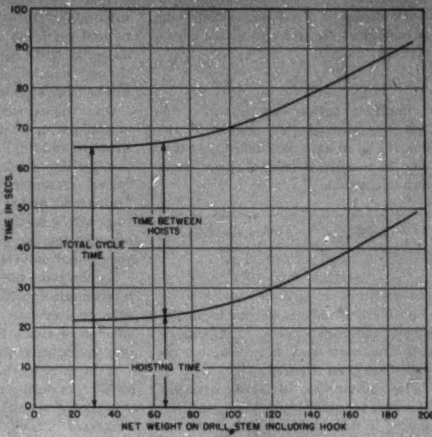

Figure 15 (right). Hoisting time to remove a "thribble" plotted against net weight of drill stem

2. The driller is relieved of the demanding and fatiguing duty of attempting to maintain proper bit loading manually.

Mud Pumps

Since the test data were taken the mud pumps have been operating compounded (hydraulically in series) by using a precharged air chamber as a surge tank between the two pumps. Operation has been satisfactory.

Drawworks

The test data indicated that 50 seconds was the average time between hoists (drawworks motor not rotating). An empirical equation expressing hoisting time as a function of net drill pipe weight and peak drawworks horsepower was set up. From these data an empirical equation relating the drawworks motor continuous horsepower rating, the drawworks motor peak horsepower and the maximum net weight to be hoisted was set up. The equation is

$$\frac{hp_c}{hp_p}=\sqrt[3]{\frac{hp_p+0.015W}{7.9hp_p+0.022W}}$$

where

hp_c = continuous horsepower rating of motor
hp_p = peak horsepower rating of motor
W = maximum net weight of drill stem to be hoisted in pounds

The preceding equation gives the continuous rating of the drawworks motor based upon heating considerations only. For reasonable values of hp_p and W, the ratio hp_p/hp_c will have a value of 1.6 to 1.8.

In order to calculate the amount of power required to hoist the drill stem, the following formula which assumes an efficiency of 65 per cent and a mud buoyancy factor of 0.85 may be used.

$$hp_p=\left(\frac{W_1}{25,000}+0.9\right)S$$

where

S = drill stem speed in feet per minute
hp_p = peak horsepower rating of motor
W_1 = total weight of drill stem in pounds (in air)

The 0.9 factor represents empty hook weight.

To the writers' knowledge, this rig operates with more power on the drawworks than any other rig now in existence. However the drawworks does not have more power than can be used effectively.

The power to be applied to the drawworks of a diesel electric rig is dependent primarily upon the selection of the other main drives. Engine-driven generators of proper size and number to provide power simultaneously to two mud pumps, one mud mixer, and the rotary table should be selected. The drawworks

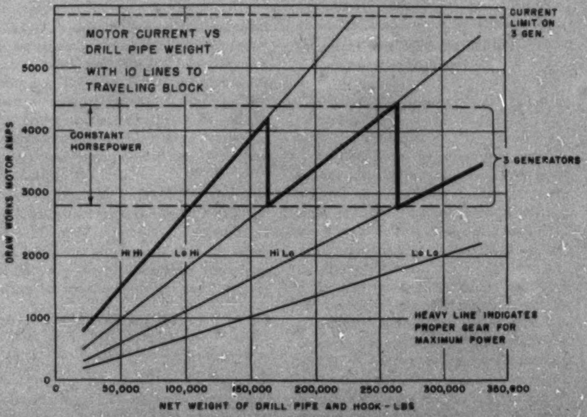

Figure 16. Curves calculated from test data indicating proper drawworks gear ratio to operate engine-generator sets on constant horsepower section of generator volt-ampere characteristic

motor should be of sufficient size to take advantage of the entire available engine capacity.

ENGINES

The diesel engines had been in operation approximately ten months at the time the latest data were taken. At that time the number of hours of operation on each engine was:

Engine	Hours, Operation
1	4,475
2	4,364
3	4,354

Insufficient time has elapsed to predict engine maintenance costs. The costs to date have been small as no major overhauls have been required.

Fuel consumption on this rig averages 25 barrels for a full day's operation. Assuming a delivered price of $0.07 per gallon, the fuel costs for a single day's operation is $74.

It is estimated that a heavy steam rig doing the same drilling duty would consume 1,000,000 to 2,500,000 cubic feet of natural gas in 24 hours. Based upon a charge of $0.13 per thousand cubic feet, the cost of fuel for a single day's operation will be from $130 to $325.

On a wildcat well where natural gas is unavailable, it would be necessary for the steam rig to burn liquid fuel. Consumption per day would be from 200 to 250 barrels. Assuming a delivered price of "Bunker C" fuel at $2 per barrel, the fuel costs will be $400 to $500 per day. Fuel consumption on heavy steam rigs has gone as high as 300 barrels per day ($600).

By analyzing the recording charts for a representative period of time, it is possible to calculate from Table III the amount of time that the engines have been operating at the various speeds.

If the three engines had been operating at 900 rpm during the total 13,193 hours of recorded operation, they would have completed 712,000,000 revolutions at top speed.

Actually, the electrohydraulic governor has required the engines to turn only 28,500,000 revolutions at top speed and has reduced the total number of required revolutions by 273,000,000. Low-maintenance costs are expected to result from this type of engine operation.

Table III

Engine Speed,		Operating Time	
Per Cent	Rpm	Per Cent	Hours
50	450	47	6200
50–85	450–765	49	6466
100	900	4	527

While it is impossible at this time to predict accurately the overall drilling costs of the large diesel electric rig as compared with the heavy steam rig, it appears that the cost advantage will be in favor of the diesel electric rig for production drilling when proper fuel charges are assigned.

Drilling a wildcat well where natural gas is unavailable will increase considerably the cost of operating the steam rig giving a substantially greater advantage in over-all drilling costs to the diesel electric rig.

No Discussion

The Vector Power Factor of Unbalanced Sinusoidal 3-Phase Circuits

J. F. LAMB
MEMBER AIEE

D. B. BRANDT
ASSOCIATE AIEE

WHEN the definitions of reactive power, vector power, and vector power factor,[1,2] of a polyphase circuit were established, the effects of unbalance were given considerable thought. Various suggestions[3,4,5] had been made to define "balance" or "unbalance" factors of different kinds in attempts to provide for the phenomena of power factor separately from those of unbalance. The development of the theory of symmetrical components led to the suggestion[4] of defining the power factor of an unbalanced polyphase load as being equal to the power factor of the positive sequence power input to the load.

During the time of this discussion, which was centered chiefly in the period from 1920 to 1935, many interesting facts regarding the effects of unbalance upon the power factor of a polyphase load were brought out. For example, it was well known that, with balanced line voltages. the vector power factor of a 3-wire 3-phase load became equal to the power factor of the positive sequence power input.

In some discussions, the authors confined their remarks to circuits having only current unbalance and assumed that line voltage unbalance could normally be neglected.

The reasons for many of the facts presented were often omitted, or, if included in the discussion, were usually of a specialized nature. The vast majority of the discussions were limited to the 3-wire 3-phase circuit.

The purpose of this paper is to develop expressions in which the part played by specific unbalance of current and voltage upon the magnitude of the vector power factor is clearly evident. The method of symmetrical components offers an approach by the use of voltage and current unbalance factors.

V. Genkin[6,7,8] has applied such unbalance factors to analyze the errors involved in the metering of reactive power and in investigating the "unbalance factor" of 3-phase, 3-wire loads. The unbalance factor considered by him was defined as the ratio of the pulsating component of 3-phase power to the vector volt amperes.

We are chiefly interested in the effect of unbalance upon the vector power factor, which quantity has been officially defined in the ASA Standards and is the basis for many power rates which include low power factor penalties. No official definition of power unbalance factor has as yet been incorporated into American standards.

Let us consider a 4-wire 3-phase star-connected load with the quantities of interest defined in Appendix I. All voltages and currents are assumed to be sinusoidal. We can at once write the vector expression for the volt-amperes[9,10] as

$$P+jQ=3E_1^*I_1+3E_2^*I_2+3E_0^*I_0=3\times(E_1I_1\cos\theta_1+E_2I_2\cos\theta_2+E_0I_0\cos\theta_0)+j3(E_1I_1\sin\theta_1+E_2I_2\sin\theta_2+E_0I_0\sin\theta_0) \qquad (1)$$

Expressing E_2, I_2, E_0, and I_0 in terms of the proper voltage and current unbalance factors multiplied by the corresponding positive sequence quantities, equation 1 then becomes

$$P+jQ=3E_1I_1(\cos\theta_1+K_{2v}K_{2i}\cos\theta_2+K_{0v}K_{0i}\cos\theta_0)+j3E_1I_1(\sin\theta_1+K_{2v}K_{2i}\sin\theta_2+K_{0v}K_{0i}\sin\theta_0)$$
$$=3E_1I_1(\cos\theta_1+K_2\cos\theta_2+K_0\cos\theta_0)+j3E_1I_1(\sin\theta_1+K_2\sin\theta_2+K_0\sin\theta_0) \qquad (2)$$

The vector power factor is then

$$\Lambda_v=\frac{P}{\sqrt{P^2+Q^2}} \qquad (3)$$
$$=\frac{\cos\theta_1+K_2\cos\theta_2+K_0\cos\theta_0}{[(\cos\theta_1+K_2\cos\theta_2+K_0\cos\theta_0)^2+(\sin\theta_1+K_2\sin\theta_2+K_0\sin\theta_0)^2]^{1/2}}$$

This expression can be reduced to

$$\Lambda_v=\frac{\cos\theta_1+K_2\cos\theta_2+K_0\cos\theta_0}{[1+K_2^2+K_0^2+2K_2\cos(\theta_1-\theta_2)+2K_0\cos(\theta_1-\theta_0)+2K_0K_2\cos(\theta_2-\theta_0)]^{1/2}} \qquad (4)$$

Equation 4 holds for a 3-phase, 4-wire circuit. For a 3-phase, 3-wire load, the zero sequence component of line current is zero, and hence K_0 is zero, and equation 4 reduces to

$$\Lambda_v=\frac{\cos\theta_1+K_2\cos\theta_2}{[1+K_2^2+2K_2\cos(\theta_1-\theta_2)]^{1/2}} \qquad (5)$$

An experimental check of equations 4 and 5 is given in Appendix II.

Practical Implications of the Derived Expressions

Referring to equation 4, the following points should be noted as applying to a 3-phase 4-wire load:

1. For both negative and zero-sequence unbalance, the effect of a given amount of unbalance in current is the same as that for an unbalance in voltage, since both K_2 and K_0 are the product of the corresponding voltage and current unbalance factors.

2. The vector power factor is dependent not only upon the magnitude of the unbalance factors but also upon the cosine of the angles θ_1, θ_2, θ_0, $\theta_1-\theta_2$, $\theta_1-\theta_0$, and $\theta_2-\theta_0$. However, the power factor is independent of the angles between the sequence voltages E_0, E_1, and E_2 once θ_0, θ_1, and θ_2 have been fixed. This means that the different sequence systems can be rotated independently of each other without affecting the vector power factor.

Paper 49-123, recommended by the AIEE Basic Sciences Committee and approved by the AIEE Technical Program Committee for presentation at the AIEE South West District meeting, Dallas, Tex., April 19–21, 1949. Manuscript submitted January 16, 1948; made available for printing February 24, 1949.

J. F. LAMB is with the University of Missouri, Columbia, Mo., and D. B. BRANDT is with the General Electric Company, Schenectady, N. Y.

Table I. Test Readings

Quantity	Test 1	2	3	4	5
Z_a ohms	10.3/83.5°	2.6/0°	10.3/83.5°	3.7/0°	10.3/83.6°
Z_b ohms	10.6/—88.8°	10.5/0°	10.6/—88.8°	10.4/0°	10.76/0°
Z_c ohms	10.9/—2.4°	15.6/0°	10.9/—1.1°	Infinity	10.9/—2°
E_a volts	48.6	22	73.5	24.8	83.5
E_b volts	57.5	57	50.4	53.5	46.8
E_c volts	101.3	84.8	89.3	113	29
E_{AB} volts	100	75.8	110.3	78.1	120.8
E_{BC} volts	98	88.3	72.9	108.4	44.6
E_{CA} volts	93.5	103.3	95.7	127.9	76
I_a amperes	4.68	8.6	6.94	6.66	7.88
I_b amperes	5.48	5.44	4.82	5.12	4.30
I_c amperes	9.16	5.42	8.22	0	2.80
I_n amperes			2.05	1.9	2.84
P_a watts	20	192	38	168	68
P_b watts	2	312	0	274	200
P_c watts	942	456	736	0	74
Q_a vars	—236	0	—520	0	—666
Q_b vars	326	0	252	0	6
Q_c vars	24	0	14	0	—2

3. If the line currents are balanced, both K_2 and K_0 will be zero and the vector power factor reduces to $\cos\theta_1$, regardless of the voltage unbalance. Likewise if the phase voltages are balanced, the power factor will reduce to $\cos\theta_1$, regardless of the current unbalance.

4. If the line voltages are balanced, K_2 becomes zero. However K_0 is not necessarily zero, since a shift in the voltage neutral can occur even with no negative sequence component in the line voltage. If K_0 is not zero, but K_2 is zero, then the power factor will reduce to an expression similar to equation 5 but involving K_0 and θ_0 instead of K_2 and θ_2.

5. In the event that Z_a, Z_b, Z_c are equal, passive impedances, $\theta_1=\theta_2=\theta_0=$ impedance angle of the load, and the vector power factor reduces to $\cos\theta_1$ regardless of the voltage unbalance. In this case also

$$K_{2i}=K_{2v},\quad K_{0i}=K_{0v},$$

because the load impedance is the same for all sequence components. These relations do not hold necessarily when the load includes mutual inductances between phases or rotating machinery for which the impedances, although balanced between phases, are not the same for all sequence components.

The 3-wire 3-phase load to which equation 5 applies, is a special case of the more general 4-wire connection. It is apparent that any shift of the voltage neutral due to zero sequence voltages will have no effect upon the vector power factor of a 3-wire circuit since the K_0 terms are missing from equation 5.

For a 3-wire load, the vector power factor becomes equal to the positive sequence power factor if either the line voltages or the line currents are balanced, or if the load consists of balanced, static impedances. If the load consists of rotating machinery having an impedance to negative sequence currents different from that to positive sequence currents, an unbalance in voltage implies an unbalance in current and the complete expression in equation 5 must apply.

For most practical circuits, the unbalance factors K_0 and K_2 are small, since they are the products of current and voltage unbalance factors, each less than unity. Multiplication by $\cos\theta_0$ or $\cos\theta_2$ and so forth, further reduces the magnitudes of some of the terms involved. Hence, even for badly unbalanced circuits, the vector power factor may often be approximately equal to $\cos\theta_1$. This is evident from the numerical examples worked out in Appendix II. Only in test 5, Table II, does the vector power factor differ markedly from $\cos\theta_1$.

In this connection, another point should be noted. For high power factor loads, $\cos\theta_1$ will be close to unity, and the unbalance terms will be small in comparison. For low-power factor loads, $\cos\theta_1$ will be small, as for example test 5, Table II, and the unbalance terms will have a relatively greater importance in the determination of vector power factor. The fact that $\cos\theta_0$, $\cos\theta_2$, and so forth can be negative for many loads complicates the detailed analysis for this point.

In conclusion, it is evident that the relations developed in equations 4 and 5 make possible a clear conception of the different effects of various kinds of unbalance upon the vector power factor of a 3-phase load for sinusoidal applied voltages and currents.

Appendix I. Nomenclature

The nomenclature is based upon a star-connected 3-phase load with sinusoidal currents and voltages. Phase A is used as the reference phase for symmetrical component quantities.

I_a, I_b, I_c, I_n = currents in the corresponding line wires and neutral wire respectively
E_a, E_b, E_c = phase voltages to neutral
E_{AB}, E_{BC}, E_{CA} = line voltages
$\mathbf{Z}_a$, $\mathbf{Z}_b$, $\mathbf{Z}_c$ = complex phase impedances
$\mathbf{I}_1$ = complex positive sequence component of line current
$\mathbf{I}_2$ = complex negative sequence component of line current
$\mathbf{I}_0=\mathbf{I}_n/3$ = complex zero sequence component of line current
$\mathbf{E}_1$ = complex positive sequence component of phase voltage
$\mathbf{E}_2$ = complex negative sequence component of phase voltage
$\mathbf{E}$ = complex zero sequence component of phase voltage
$\mathbf{E}_1^*$, $\mathbf{E}_2^*$, $\mathbf{E}_0^*$ = complex conjugate values of the corresponding sequence voltages
I_1, I_2, I_0, E_1, E_2, E_0 = magnitudes of the corresponding complex quantities
P_a, P_b, P_c = active power in watts in the corresponding phases

Table II. Computed Quantities

Actual Voltage Drop to Neutral Across Phase A is Used as the Reference Vector

Quantity	Test 1	2	3	4	5
E_0 volts	46.8/70.5	30.9/169.1	48.7/59.1	40.7/131	29.0/44
E_1 volts	55.8/—55	50.9/3.7	52.7/—46	59.1/—15.3	37.1/—37.9
E_2 volts	1.93/57.7	9.27/—80.5	12.6/—18	16.05/249.9	33.5/4.5
I_0 amperes	0	0	0.683/—108.7	0.595/—25.6	0.95/242.9
I_1 amperes	5.79/—49.1	6.2/0	6.13/—55.5	3.55/—22	4.73/—84.2
I_2 amperes	3.41/184	2.42/0	2.87/203.2	3.25/29.3	2.52/—72.4
K_{2i}	0.59	0.387	0.469	0.916	0.522
K_{2v}	0.0346	0.182	0.237	0.273	0.903
K_2	0.0204	0.0704	0.111	0.25	0.472
K_{0i}			0.1114	0.167	0.200
K_{0v}	0.84	0.608	0.924	0.79	0.782
K_0			0.1030	0.1155	0.1564
θ_0 degrees			—167.8	203.4	198.9
θ_1 degrees	5.9	—3.7	—9.5	—6.7	—46.3
θ_2 degrees	126.3	80.5	221.2	139.4	—76.9
$\cos\theta_1$	0.995	0.998	0.986	0.993	0.691
Power Factor*	0.994	1.00	0.957	0.998	0.462
Power Factor**	0.993	1.00	0.950	1.00	0.457

* = power factor computed from equation 4.

** = power factor computed from the sums of wattmeter and varmeter readings for all three phases.

Q_a, Q_b, Q_c = reactive power in vars in the corresponding phases

$P = P_a + P_b + P_c$ = watts total active power in the 3-phase load

$Q = Q_a + Q_b + Q_c$ = total reactive power in vars in the 3-phase load (algebraic summation)

θ_1 = time phase angle between E_1 and I_1

θ_2 = time phase angle between E_2 and I_2

θ_0 = time phase angle between E_0 and I_0

$K_{2I} = I_2/I_1$ and $K_{0I} = I_0/I_1$ = respective negative sequence and zero sequence current unbalance factors

$K_{2E} = E_2/E_1$ and $K_{0E} = E_0/E_1$ = respective negative sequence and zero sequence voltage unbalance factors

$K_2 = K_{2I} \times K_{2E}$ = negative sequence unbalance factor

$K_0 = K_{0I} \times K_{0E}$ = zero sequence unbalance factor

Λ_v = lambda, the vector power factor as defined in reference 1

Appendix II. Experimental Check

An experimental check of equations 4 and 5 was made by applying unbalanced voltages to several unbalanced 3-phase loads. The loads consisted of three impedances connected in star to form either a 3-wire or a 4-wire system. The test readings for five different examples are given in Table I. The results computed to within slide rule accuracy from the data of Table I are shown in Table II. No attempt was made to correct the test readings in Table I for ratio or phase angle errors involved in the use of current transformers. Potential circuit measurements were made directly without using potential transformers. The negative varmeter readings in Table I indicate inductive reactive power.

The agreement of the figures in the last two rows of Table II indicates that the experimental measurements checked the values computed using equations 4 and 5 very closely.

References

1. American Standard Definitions of Electrical Terms. ASA Standard C42-1941, pages 43-6.

2. Definitions of Power and Related Quantities, H. L. Curtis, F. B. Silsbee. *Electrical Engineering* (AIEE *Transactions*), volume 54, April 1935, pages 394–404.

3. Power Factor in Polyphase Systems, F. B. Silsbee. *AIEE Transactions*, volume 39, part 2, 1920, pages 1465–67.

4. Power Factor and Unbalance on a Polyphase System, C. J. Fechheimer. *AIEE Transactions*, volume 39, part 2, 1920, pages 1469–73.

5. Discussion on Report of Joint Committee. *AIEE Transactions*, volume 39, part 2, 1920, pages 1496–1520.

6. La Mesure Indirect de l'energie Reactive, V. Genkin. *Bulletin* la Societe Francaise des Electriciens (Paris, France), series 4, volume 6, 1926, pages 1148–57.

7. Mesure du Facteur de Puissance d'un Circuit Triphase non Equilibre, V. Genkin. *Bulletin*, la Societe Francaise des Electriciens (Paris, France), series 4, volume 6, 1926, pages 1158–66.

8. La Puissance Electrique dans un Circuit Triphase non Equilibre, V. Genkin. *Revue Generale de l'Electricite* (Paris, France), volume 19, January 30, 1926, pages 165–70.

9. Applications of the Method of Symmetrical Components (book), W. V. Lyon. McGraw-Hill Book Company, New York, N. Y., 1937, page 73.

10. Symmetrical Components (book), C. F. Wagner, R. D. Evans. McGraw-Hill Book Company, New York, N. Y., 1933, pages 312–13.

No Discussion

The Negative-Sequence Reactances of an Ideal Synchronous Machine

WILLIAM C. DUESTERHOEFT
ASSOCIATE AIEE

THE METHOD of symmetrical components is at present used widely in determining fundamental-frequency components of current and voltage in unbalanced 3-phase power systems. To apply this method, the sequence impedances of the various circuits which make up the system are required. As synchronous machines are present in all systems, determination of their reactances is of prime importance.

Before a specified reactance can be determined it must be definitely defined and, preferably, a method of testing for this reactance given. This is the general procedure followed by the Institute in standardizing electrical terms.[1] Because of saturation in synchronous machines, it may be necessary to specify the degree of saturation at which the test is to be made. This may be done by recognizing two values of reactance, one determined at rated current and the other at rated voltage. The two values should be identical if saturation is negligible.

As progress is made in the analysis of synchronous machine performance, it becomes necessary to specify the various reactances encountered with increasing accuracy. A paper discussing inherent errors in the prescribed AIEE method of determining direct-axis transient and subtransient reactances (x_d' and x_d''), by test, has been presented.[2]

The purpose of this paper is to show that there are many values of the negative-sequence reactance of a synchronous machine, as it is now defined. If only the machine is considered, without load and with negligible saturation, there are as many values of this reactance as there are types of unbalanced short-circuits; and none of these values is independent of the connected circuit. The number of negative-sequence reactances can be reduced readily to one by modification of the present definition. If so modified, the specified reactance may not be the proper one for use under all conditions where fundamental-frequency components of current and voltage are to be calculated by the method of symmetrical components, as conventionally applied. It would, however, have the advantage of being definite, and could be modified as required.

Definition of Negative-Sequence Reactance

In the American Standard Definition of Electrical Terms,[1] the following definition of negative-sequence reactance (x_2) is given under 10.35.170:

> "NEGATIVE-SEQUENCE REACTANCE (x_2)
>
> "The negative-sequence reactance is the ratio of the fundamental component of reactive armature voltage, due to the fundamental negative-sequence component of armature current, to this component of armature current at rated frequency.
>
> "The rated current value of negative-sequence reactance is the value obtained from a test with a current equal to rated armature current.
>
> "The rated voltage value of negative-sequence reactance is the value obtained from a line-to-line short-circuit test at two terminals of the machine at no-load and rated speed, and at rated armature voltage."

This definition of x_2 is somewhat ambiguous. It has been interpreted as implying that the only currents present are those of fundamental frequency. However, as this is not so stated, it is here understood to mean that there is no restriction on the harmonic currents and voltages which may be present.

If the first interpretation is accepted, there is only one definition of the negative-sequence reactance of an ideal synchronous machine. By this interpretation (see Appendix II, equation 22),

$$x_2=(^1/_2)(x_d''+x_q'') \tag{1}$$

where x_d'' and x_q'' are direct- and quadrature-axis subtransient reactances, respectively. Rated current value of x_2, as defined, is consistent with the first interpretation if "rated armature current" is understood to mean "fundamental-frequency negative-sequence current of rated magnitude." (Rated armature current usually signifies balanced currents of positive-sequence phase order.)

The rated voltage value of x_2, as defined, is only one of the many values of x_2 which are influenced by the presence of odd harmonic components of current. It is a special case, consistent with the second interpretation of the definition. This value of x_2, applicable for a line-to-line short circuit at the terminals of the machine at "no-load and rated speed, and at rated armature voltage," has already been given.[3,4] (See also Appendix III, equation 31). It is

$$x_2=\sqrt{x_d''x_q''} \tag{2}$$

where x_d'' and x_q'' are direct- and quadrature-axis subtransient reactances, respectively. A rated voltage value of x_2, consistent with the first interpretation of the definition, could be obtained from a test with impressed negative-sequence currents of fundamental frequency such as to produce a negative-sequence reactive armature voltage, equal in magnitude to rated armature voltage. In this test, as in the corresponding test for the rated current value of x_2, negative-sequence currents can be applied through high

---

Paper 49-127, recommended by the AIEE Rotating Machinery Committee and approved by the AIEE Technical Program Committee for presentation at the AIEE South West District meeting, April 19–21, 1949, Dallas, Tex. Manuscript submitted February 2, 1949; made available for printing March 10, 1949.

WILLIAM C. DUESTERHOEFT is with the Department of Electrical Engineering, the University of Texas, Austin, Tex.

The author gratefully acknowledges the helpful suggestions of Miss Edith Clarke in the preparation of this paper.

reactances to third-harmonic currents, so that third-harmonic voltages resulting from negative-sequence currents will exist at the machine terminals but will produce negligible currents.

Effect of Harmonics on Negative-Sequence Reactance

It has long been known that negative-sequence currents of fundamental frequency, flowing in synchronous machines in which the direct- and quadrature-axis reactances (x_d'' and x_q'') are unequal, produce positive-sequence third-harmonic voltages. When the system is unbalanced and the third-harmonic impedance is finite, positive-sequence third-harmonic voltage will cause both positive- and negative-sequence third-harmonic currents to flow and, in the case of ground faults in a grounded system, zero-sequence third-harmonic currents also. Negative-sequence third-harmonic currents produce positive-sequence fifth-harmonic voltages in the synchronous machine, and positive-sequence third-harmonic currents produce negative-sequence voltages of fundamental frequency. Negative-sequence currents of any odd harmonic order produce positive-sequence voltages of the next higher odd harmonic order; and positive-sequence voltages of any odd harmonic order above the fundamental produce negative-sequence voltages of the next lower odd harmonic order.[5] If the system is unbalanced and all impedances are finite, each harmonic voltage will produce positive- , negative- , and possibly zero-sequence currents, of the same harmonic order.

It can be concluded, therefore, that all odd-order harmonic currents will be present.

From the equations derived in the appendices and elsewhere,[3,4,5] it is evident that fundamental-frequency components of negative-sequence voltage or current, or both, are affected by the presence of odd harmonic currents in machines in which $x_d'' \neq x_q''$. Negative-sequence reactance, as now defined, will therefore be affected by their presence. It is only where negative-sequence reactance is defined in terms of applied currents of fundamental frequency (which implies that harmonic currents are prevented from flowing) that negative-sequence reactance has one definite value.

Negative-Sequence Reactance with Ground Faults

The negative-sequence reactance, as now defined, of an unloaded synchronous machine with a ground fault at its terminals will be influenced by the zero-sequence reactance x_0 viewed from the fault.

For a line-to-ground fault, from Appendix III, equation 37, x_2 by definition is

$$x_2=\sqrt{\left(x_d''+\frac{x_0}{2}\right)\left(x_q''+\frac{x_0}{2}\right)}-\frac{x_0}{2} \qquad (3)$$

For a double line-to-ground fault, from Appendix III, equation 50, x_2 is

$$x_2=\frac{2x_0\sqrt{x_d''x_q''}}{\sqrt{(x_d''+2x_0)(x_q''+2x_0)}-\sqrt{x_d''x_q''}} \qquad (4)$$

Negative-Sequence Reactance in Terms of Applied Negative Sequence Voltage

The following definition of negative-sequence reactance, analogous to that of the rated voltage value of a positive-sequence reactance, has been suggested:[4]

> Negative-sequence reactance is the ratio of applied negative-sequence voltage to the fundamental component of reactive negative-sequence current which it produces.

With balanced negative-sequence voltages applied to the machine terminals, from Appendix IV, equation 60, x_2 by this definition is

$$x_2=(2x_d''x_q'')/(x_d''+x_q'') \qquad (5)$$

As balanced voltages are applied, the positive-sequence third-harmonic voltages which are produced by the flow of negative-sequence currents are short circuited by the applied voltages and produce third-harmonic positive-sequence currents. However, since the system is balanced, no negative-sequence third-harmonic currents will flow. Third-harmonic positive-sequence currents, as previously explained, produce negative-sequence voltage of fundamental frequency which, in turn, produces negative-sequence currents. The resultant negative-sequence current is affected by the presence of the third-harmonic currents, while the applied negative-sequence voltage is unaffected.

The value of x_2 given by equation 5 is applicable only when the voltages at the machine terminals are balanced voltages of negative-sequence phase order.

Relative Values of x_2 Calculated from Equations 1–5

The greatest variation in the values of x_2 occurs in the case of a salient-pole machine without an amortisseur winding. For example, the values of x_2 calculated for a machine with $x_d''=0.30$, $x_q''=0.70$, $x_0=0.10$ are 0.500, 0.458, 0.451, 0.432, and 0.420 when computed from equations 1–5, respectively. A machine with amortisseur windings such that $x_d''=x_q''$ would have $x_2=x_d''=x_q''$.

Conclusions

1. Negative-sequence reactance x_2 determined in accordance with its present definition is a reactance which depends upon system conditions.

2. The rated current and rated voltage values of x_2, as now given, are special cases. These two values of x_2 are not the same in an unloaded machine of negligible saturation.

3. It is suggested that the definition be revised and x_2 be so defined that it has a definite value, affected only by saturation. This can be done by adding "with the effects of harmonics neglected" to the definition. The rated current value will then be consistent with the definition if "with a current equal to rated armature current" be replaced by "with fundamental negative-sequence current equal in magnitude to rated armature current." It is further suggested that the rated voltage value be changed to agree with the revised definition.

4. If the foregoing suggestions are adopted, x_2 will have a definite value: $x_2=(1/2)(x_d''+x_q'')$. Then, if harmonics are known to be appreciable, their effects can be considered separately and superposed.[5]

5. For unbalanced short circuits at the terminals of an unloaded machine, the values of x_2 given by equations 2, 3, and 4, which include the effects of harmonics, are applicable.

Appendix I

The method used to derive the equations of this paper utilizes Park's equations for the ideal synchronous machine,[6,7] expressed in terms of $\alpha\beta 0$ components.[8] These equations are used to determine expressions for the components of current which include the effects of all harmonics.

The fundamental-frequency components of these currents are found by the method of harmonic analysis.

On the assumption of constant unit rotor speed, Park's equations[7] for the ideal synchronous machine[6] during the first instant after fault, expressed in per unit of machine base quantities, become

$$\begin{aligned} e_d&=I_f-(px_d''+r)i_d+x_q''i_q\\ e_q&=-x_d''i_d-(px_q''+r)i_q\\ e_0&=-(px_0+r)i_0 \end{aligned} \qquad (6)$$

where I_f is the field current in per unit of that field current which produces unit armature voltage at no-load and rated frequency on the air-gap line. Subscripts d and q refer to direct and quadrature axes respectively; e indicates voltage and i current.

In terms of $\alpha\beta 0$ components of current and voltage, equations 6 become[8]

$$e_\alpha=-I_f\sin\theta-p(x+y\cos 2\theta)i_\alpha-\\ py\sin 2\theta i_\beta-ri_\alpha$$

$$e_\beta = I_f \cos\theta - py \sin 2\theta i_\alpha - p(x - y\cos 2\theta) i_\beta - r i_\beta \qquad (7)$$

$$e_0 = -(px_0 + r) i_0$$

where

$$\left.\begin{aligned} x &= \tfrac{1}{2}(x_d'' + x_q'') \\ y &= \tfrac{1}{2}(x_d'' - x_q'') \\ i_\alpha &= i_d \cos\theta - i_q \sin\theta \end{aligned}\right\} \qquad (8)$$

$$\left.\begin{aligned} i_\beta &= i_d \sin\theta + i_q \cos\theta \\ e_\alpha &= e_d \cos\theta - e_q \sin\theta \\ e_\beta &= e_d \sin\theta + e_q \cos\theta \end{aligned}\right\} \qquad (9)$$

The α, β, and 0 components of current i_α, i_β, and i_0, are defined in terms of the armature phase currents i_a, i_b, and i_c of phase order *abc* by the equations[4]

$$i_\alpha = \frac{2}{3}\left(i_a - \frac{i_b + i_c}{2}\right)$$

$$i_\beta = \frac{1}{\sqrt{3}}(i_b - i_c) \qquad (10)$$

$$i_0 = \frac{1}{3}(i_a + i_b + i_c)$$

The α component of current, i_α, is the component of armature current which produces a field in the axis of phase *a*; i_β is the component of armature current which produces a field in the common axis of phases *b* and *c* electrically perpendicular to the axis of phase *a*. Vectors representing sinusoidal i_α and i_β in the complex plane can be given in terms of the vectors representing positive- and negative-sequence currents. These vector equations[5] are

$$\left.\begin{aligned} \boldsymbol{I}_\alpha &= \boldsymbol{I}_{a1} + \boldsymbol{I}_{a2} \\ \boldsymbol{I}_\beta &= -j(\boldsymbol{I}_{a1} - \boldsymbol{I}_{a2}) \end{aligned}\right\} \qquad (11)$$

and

$$\left.\begin{aligned} \boldsymbol{I}_{a1} &= (\boldsymbol{I}_\alpha + j\boldsymbol{I}_\beta)/2 \\ \boldsymbol{I}_{a2} &= (\boldsymbol{I}_\alpha - j\boldsymbol{I}_\beta)/2 \end{aligned}\right\} \qquad (12)$$

The $\alpha\beta0$ components of voltage are related to the armature voltages and to symmetrical components of voltage by equations similar to 10–12 if *i* and *I* are replaced by *e* and ***E***, respectively, in these equations.

Armature resistances are usually small relative to reactances, and their omission does not affect appreciably the magnitudes or phases of the currents or voltages determined hereby solutions of equations 7. Decrement factors need not be considered as negative-sequence reactance is always a subtransient value. Equations 7 will be reduced on the assumption of negligible resistance to equations 13.

$$e_\alpha = -I_f \sin\theta - p(x + y\cos 2\theta) i_\alpha - py \sin 2\theta i_\beta$$

$$e_\beta = I_f \cos\theta - py \sin 2\theta i_\alpha - p(x - y\cos 2\theta) i_\beta \qquad (13)$$

$$e_0 = -px_0 i_0$$

Appendix II. Negative-Sequence Reactance to Applied Negative-Sequence Currents

If balanced fundamental negative-sequence currents are caused to flow in an unloaded machine, rotating at synchronous speed with the field winding short circuited but unexcited, $i_{a1} = 0$ and i_{a2} may be written

$$i_{a2} = I_2 \cos\theta \qquad (14)$$

Then, from equation 11

$$\left.\begin{aligned} i_\alpha &= I_2 \cos\theta \\ i_\beta &= -I_2 \sin\theta \end{aligned}\right\} \qquad (15)$$

When equations 15 are substituted in equations 13, the resultant α and β voltages at the machine terminals are

$$e_\alpha = -pI_2[x\cos\theta + y(\cos 2\theta \cos\theta - \sin 2\theta \sin\theta)] \qquad (16)$$

$$e_\beta = -pI_2[-x\sin\theta + y(\sin 2\theta \cos\theta + \cos 2\theta \sin\theta)] \qquad (17)$$

Since

$$\cos 2\theta \cos\theta - \sin 2\theta \sin\theta = \cos 3\theta$$

$$\sin 2\theta \cos\theta + \cos 2\theta \sin\theta = \sin 3\theta$$

Equations 16 and 17 can be simplified and differentiated to give

$$e_\alpha = 3yI_2 \sin 3\theta + xI_2 \sin\theta \qquad (18)$$

$$e_\beta = xI_2 \cos\theta - 3yI_2 \cos 3\theta \qquad (19)$$

If equations 18 and 19 are substituted in the voltage equations similar to equations 12, the resultant positive- and negative-sequence components of voltage, e_{a1} and e_{a2}, are found to be

$$e_{a1} = 3yI_2 \sin 3\theta \qquad (20)$$

$$e_{a2} = xI_2 \sin\theta \qquad (21)$$

The above development shows that fundamental negative-sequence current produces third-harmonic positive-sequence voltage and fundamental negative-sequence voltage. If the AIEE definition of negative-sequence reactance is taken to mean the ratio of the reactive fundamental negative-sequence voltage, produced by applied fundamental negative-sequence current, to that current, then

$$x_2 = \frac{1}{2}(x_d'' + x_q'') \qquad (22)$$

Appendix III. Negative-Sequence Reactances With an Unsymmetrical Short Circuit at the Terminals of the Ideal Synchronous Machine

An unloaded machine, operating at rated voltage and constant speed, will be assumed.

Line-to-Line Short Circuit

For a fault between phases *b* and *c*, conditions are $i_a = 0$, $i_b = -i_c$, and $e_b = e_c$. From equations 10

$$i_\alpha = i_0 = 0; \quad e_\beta = 0 \qquad (23)$$

If equation 23 is substituted in equation 13 and the resulting equation integrated, there results

$$i_\beta = \frac{I_f \sin\theta}{x - y\cos 2\theta} \qquad (24)$$

The integration constant is neglected since only the fundamental current is of interest, and the integration constant represents trapped flux which produces d-c and even harmonic currents. Equation 24 can be represented by a Fourier series of which the fundamental component $i_{\beta 1}$ is

$$i_{\beta 1} = \frac{2I_f \sin\theta}{(x + y) + \sqrt{x^2 - y^2}}$$

From equations 8

$$i_{\beta 1} = \frac{2I_f \sin\theta}{x_d'' + \sqrt{x_d'' x_q''}} \qquad (25)$$

The value of $i_{\beta 1}$ given by equation 25 is consistent with the value of i_b given by Doherty and Nickle.[8]

The symmetrical components of current, i_{a1} and i_{a2}, from equations 25 and 12 with $i_\alpha = 0$, are

$$i_{a1} = -i_{a2} = \frac{I_f \cos\theta}{x_d'' + \sqrt{x_d'' x_q''}} \qquad (26)$$

By the method of symmetrical components as conventionally applied, with resistance neglected

$$\boldsymbol{I}_{a1} = -\boldsymbol{I}_{a2} = \frac{\boldsymbol{E}_{a1}}{j(x_1 + x_2)} \qquad (27)$$

where $\boldsymbol{E}_{a1}$ is the vector representing the positive-sequence voltage at the machine terminals on open circuit. Its instantaneous value e_{a1}, from equations 12 and 13, is

$$e_{a1} = -I_f \sin\theta \qquad (28)$$

Therefore, instantaneous i_{a1} and i_{a2} are

$$i_{a1} = -i_{a2} = \frac{I_f \cos\theta}{x_1 + x_2} \qquad (29)$$

As the machine is operating at no-load and constant speed, with resistance neglected, fundamental positive-sequence currents appear in the direct-axis. Therefore

$$x_1 = x_d'' \qquad (30)$$

From equations 26, 29, and 30, it follows that

$$x_2 = x\sqrt{x_d'' x_q''} \qquad (31)$$

Line-to-Ground Short Circuit

The conditions are $i_b = i_c = 0$ and $e_a = 0$. From equations 10

$$i_\beta = 0; \quad i_\alpha = 2i_0; \quad e_\alpha = -e_0 \qquad (32)$$

If equations 32 are substituted in equations 13 and the resulting equations simplified and integrated to obtain a solution for i_α, with the integration constant neglected, there results

$$i_\alpha = \frac{I_f \cos\theta}{x + \dfrac{x_0}{2} + y\cos 2\theta} \qquad (33)$$

The above expression can be represented by a Fourier series of which the fundamental component i_{a1} is

$$i_{a1} = \frac{2I_f \cos\theta}{x_d'' + \dfrac{x_0}{2} + \sqrt{\left(x_d'' + \dfrac{x_0}{2}\right)\left(x_q'' + \dfrac{x_0}{2}\right)}} \qquad (34)$$

The fundamental-frequency symmetrical components of current, i_{a1}, i_{a2}, and i_0, from equations 12, 32, and 34, are

$$i_{a1}=i_{a2}=i_0=\frac{I_f\cos\theta}{x_d''+\frac{x_0}{2}+\sqrt{\left(x_d''+\frac{x_0}{2}\right)\left(x_q''+\frac{x_0}{2}\right)}} \quad (35)$$

In the symmetrical component method

$$I_{a1}=I_{a2}=I_0=\frac{E_{a1}}{j(x_1+x_0+x_2)}$$

and, since E_{a1} is the vector representing the voltage given by equation 28

$$i_{a1}=i_{a2}=i_0=\frac{I_f\cos\theta}{x_1+x_0+x_2} \quad (36)$$

If equation 30 and the discussion preceding it are considered, x_2 from equations 35 and 36 is

$$x_2=\sqrt{\left(x_d''+\frac{x_0}{2}\right)\left(x_q''+\frac{x_0}{2}\right)}-\frac{x_0}{2} \quad (37)$$

Double Line-to-Ground Short Circuit

With phases b and c grounded, $i_a=0$ and $e_b=e_c=0$. From equations 10

$$e_\beta=0;\ e_\alpha=2e_0;\ i_\alpha=-i_0 \quad (38)$$

If equations 38 is substituted in equations 13, these equations can be reduced to

$$p(x+2x_0+y\cos 2\theta)i_\alpha+py\sin 2\theta i_\beta=-I_f\sin\theta$$

$$py\sin 2\theta i_\alpha+p(x-y\cos 2\theta)i_\beta=I_f\cos\theta$$

The above equations can be integrated and, if the integration constant is neglected, become

$$(x+2x_0+y\cos 2\theta)i_\alpha+y\sin 2\theta i_\beta=I_f\cos\theta \quad (39)$$

$$y\sin 2\theta i_\alpha+(x-y\cos 2\theta)i_\beta=I_f\sin\theta \quad (40)$$

By simultaneous solution of equations 39 and 40

$$i_\alpha=\frac{(x-y)I_f\cos\theta}{x^2-y^2+2x_0x-2x_0y\cos 2\theta} \quad (41)$$

$$i_\beta=\frac{(x-y+2x_0)I_f\sin\theta}{x^2-y^2+2x_0x-2x_0y\cos 2\theta} \quad (42)$$

The above expressions for i_α and i_β can be represented by Fourier series of which the fundamental components $i_{\alpha1}$ and $i_{\beta1}$ are

$$i_{\alpha1}=\frac{2x_q''I_f\cos\theta}{x_q''(x_d''+2x_0)+\sqrt{x_d''x_q''(x_d''+2x_0)\times(xq''+2x_0)}} \quad (43)$$

$$i_{\beta1}=\frac{2(x_q''+2x_0)I_f\sin\theta}{x_d''(x_q''+2x_0)+\sqrt{x_d''x_q''(x_d''+2x_0)\times(x_q''+2x_0)}} \quad (44)$$

By the method of symmetrical components, the fundamental positive- and negative-sequence components of current I_{a1} and I_{a2} are

$$I_{a1}=\frac{E_{a1}}{j[x_1+x_0x_2/(x_0+x_2)]}=\frac{E_{a1}(x_0+x_2)}{j(x_1x_0+x_1x_2+x_0x_2)} \quad (45)$$

$$I_{a2}=\frac{-I_{a1}x_0}{(x_0+x_2)}=\frac{-E_{a1}x_0}{j(x_1x_0+x_1x_2+x_0x_2)} \quad (46)$$

The vectors representing $i_{\alpha1}$ and $i_{\beta1}$, determined by substitution of equations 45 and 46 in 11, are

$$I_{\alpha1}=(-jx_2E_{a1})/(x_1x_0+x_1x_2+x_0x_2) \quad (47)$$

$$I_{\beta1}=-E_{a1}(2x_0+x_2)/(x_1x_0+x_1x_2+x_0x_2) \quad (48)$$

Equations 43, 44, 47, and 48 give two expressions for the ratio of $I_{\alpha1}$ to $I_{\beta1}$. If these two ratios are equated

$$\frac{x_2+2x_0}{x_2}=\frac{[x_q''+2x_0][x_q''(x_d''+2x_0)+\sqrt{x_d''x_q''(x_d''+2x_0)(x_q''+2x_0)}]}{[x_q''][x_d''(x_q''+2x_0)+\sqrt{x_d''x_q''(x_d''+2x_0)(x_q''+2x_0)}]}$$

From the above expression, it is shown that

$$\frac{x_2+2x_0}{x_2}=\frac{\sqrt{(x_d''+2x_0)(x_q''+2x_0)}}{\sqrt{x_d''x_q''}} \quad (49)$$

and

$$x_2=\frac{2x_0\sqrt{x_d''x_q''}}{\sqrt{(x_d''+2x_0)(x_q''+2x_0)}-\sqrt{x_d''x_q''}} \quad (50)$$

Appendix IV. Negative-Sequence Reactance to Applied Negative-Sequence Voltage

If fundamental negative-sequence voltage is applied to a machine, rotating at synchronous speed with the field winding short circuited but unexcited, $e_{a1}=0$ and e_{a2} may be written

$$e_{a2}=E_2\cos\theta \quad (51)$$

From voltage equations similar to equation 11

$$e_\alpha=E_2\cos\theta \quad (52)$$

$$e_\beta=-E_2\sin\theta \quad (53)$$

If equations 52 and 53 are substituted in equations 13

$$p(x+y\cos 2\theta)i_\alpha+py\sin 2\theta i_\beta=-E_2\cos\theta \quad (54)$$

$$py\sin 2\theta i_\alpha+p(x-y\cos 2\theta)i_\beta=E_2\sin\theta \quad (55)$$

If equations 54 and 55 are integrated, the solution for i_α and i_β can be shown to be

$$i_\alpha=\frac{E_2(-x\sin\theta+y\sin 3\theta)}{x^2-y^2} \quad (56)$$

$$i_\beta=\frac{E_2(-x\cos\theta-y\cos 3\theta)}{x^2-y^2} \quad (57)$$

Substitution of equations 56 and 57 in equation 12 gives the positive- and negative-sequence components of current, i_{a1} and i_{a2}.

$$i_{a1}=\frac{yE_2\sin 3\theta}{x^2-y^2} \quad (58)$$

$$i_{a2}=\frac{-xE_2\sin\theta}{x^2-y^2} \quad (59)$$

The above development shows that if negative-sequence voltage is applied to the machine, third-harmonic positive-sequence and fundamental negative-sequence currents are produced. If negative-sequence reactance is taken as the ratio of applied fundamental negative-sequence voltage to the reactive fundamental negative-sequence current it produces

$$x_2=\frac{x^2-y^2}{x}=\frac{2x_d''x_q''}{x_d''+x_q''} \quad (60)$$

The above equation is given by Park and Robertson.[4] The development given here in terms of α and β components, however, is different.

References

1. American Standard Definitions of Electrical Terms. AIEE, 1942, page 70.

2. Inherent Errors in the Determination of Synchronous-Machine Reactances by Test, C. Concordia, F. J. Maginnis. *AIEE Transactions*, volume 64, 1945, pages 288–94.

3. Synchronous Machines IV—Single Phase Circuits, R. E. Doherty, C. A. Nickle. *AIEE Transactions*, volume 47, 1928, pages 457–87.

4. The Reactances of Synchronous Machines, R. H. Park, B. L. Robertson. *AIEE Transactions*, volume 47, 1928, pages 514–35.

5. Overvoltages Caused by Unbalanced Short Circuits (Effect of Amortisseur Windings), Edith Clarke, C. Concordia, C. N. Weygandt. *Electrical Engineering* (*AIEE Transactions*), volume 57, August 1938, pages 453–68.

6. Definition of an Ideal Synchronous Machine and Formula for the Armature Flux Linkages, R. H. Park. *General Electric Review* (Schenectady, N. Y.), volume 31, June 1928, pages 332–34.

7. Two Reaction Theory of Synchronous Machines—Generalized Method of Solution—Part I, R. H. Park. *AIEE Transactions*, volume 48, 1929, pages 716–27.

8. Circuit Analysis of A-C Power Systems, Edith Clarke. John Wiley and Sons, New York, N. Y., 1943.

Discussion

W. A. Lewis (Illinois Institute of Technology, Chicago, Ill.): The paper by Mr. Duesterhoeft is, I believe, the first to publish the value of the negative-sequence reactance of a synchronous machine which is applicable during a double-line-to-neutral short circuit. The previous discussion of a double line-to-neutral fault by Smith and Weygandt[1] develops expressions for the short-circuit currents but does not give a specific value of the negative-sequence reactance.

By extending that analysis, I have derived the value for it, which agrees with equation 4 of the present paper.

The value for a single line-to-neutral fault has been published previously.[2] With the addition of the value for the double line-to-neutral case, there are now five significant values of negative-sequence reactance, as follows

$$X_2=\frac{X_d''+X_q''}{2}$$

$$X_{2(LN)}=\sqrt{\left(X_d''+\frac{X_0}{2}\right)\left(X_q''+\frac{X_0}{2}\right)}-\frac{X_0}{2}$$

$$X_{2(LL)}=\sqrt{X_d''X_q''}$$

$$X_{2(2LN)}=\frac{2X_0\sqrt{X_d''X_q''}}{\sqrt{(X_d''+2X_0)(X_q''+2X_0)}-\sqrt{X_d''X_q''}}=\left[\frac{X_d''X_q''+\sqrt{X_d''X_q''(X_d''+2X_0)(X_q''+2X_0)}}{X_d''+X_q''+2X_0}\right]$$

$$X_{2V}=\frac{2X_d''X_q''}{X_d''+X_q''}$$

In the listing given here the five values have been arranged in descending order. The first value, denoted by X_2, for sinusoidal negative-sequence current applied, is the largest. The value for a single line-to-neutral fault, $X_{2(LN)}$, lies between the first value and the value for a line-to-line fault, $X_{2(LL)}$, and depends upon X_0. If X_0 is zero, the value for a line-to-neutral fault becomes the same as that for a line-to-line fault, and if X_0 is infinite, it can be shown, by expanding $X_{2(LN)}$ by the binomial expansion, that $X_{2(LN)}$ approaches X_2 as a limit. Similarly, $X_{2(2LN)}$, the value applicable for a double line-to-neutral fault, varies from $X_{2(LL)}$ to X_{2V}, the value applicable when sinusoidal negative-sequence voltage is applied. If X_0 is zero, $X_{2(2LN)}$ becomes the same as X_{2V}, and if X_0 is infinite, $X_{2(2LN)}$ approaches $X_{2(LL)}$ as it should. Thus, depending on the type of fault and the value of X_0, the negative-sequence reactance effective for a particular case may have any value between the maximum value, denoted by $X_2=(X_d''+X_q'')/2$ and the minimum value, $X_{2V}=2X_d''X_q''/(X_d''+X_q'')$. It is also of interest to point out that $X_2X_{2V}=X_{2(LL)}^2$.

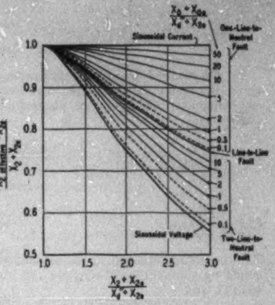

Figure 1. Correction factors for external reactance

The author suggests that the basic definition of X_2 should correspond to sinusoidal negative-sequence currents, namely $X_2=(X_d''+X_q'')/2$, and that the variation from this value for other cases should be allowed for separately, when correction is warranted. With this recommendation, I heartily agree. This value is the simplest and is the only one that is linear in X_d'' and X_q''. If external reactance is to be included, it may be added directly to this value of X_2, because X_d'' and X_q'' both will be increased by the amount of the external reactance. If any other of the five reactances is taken as basic, the inclusion of external reactance is much more complicated.

It is feasible to develop a general set of curves which give the correction factor by which the total value of nominal negative-sequence reactance, (X_2+X_{2e}), including any external reactance X_{2e}, is to be multiplied to determine the corrected or effective negative-sequence reactance for other cases. The correction factor may be expressed as a function of the parameters $(X_2+X_{2e})/(X_d''+X_{2e})=(X_d''+X_q''+2X_{2e})/2(X_d''+X_{2e})$, and $(X_0+X_{0e})/(X_d''+X_{2e})$, or some other combination of these same terms. Such a set of curves is shown in Figure 1 of the discussion.

It is evident that the correction factor differs little from unity unless X_2 differs considerably from X_d'', that is, unless X_d'' and X_q'' differ greatly. However, it is desirable to establish the basic relations in such a way that the corrections may be made easily whenever needed, and this is done most readily if the basic value of X_2 always is taken for sinusoidal negative-sequence currents. Since X_d'' and X_q'' are very nearly equal for turbine-driven generators and for salient-pole machines with an effective damper winding linking both axes, the correction will be small except for machines without damper windings or machines with a damper in only one axis.

REFERENCES

1. DOUBLE-LINE-TO-NEUTRAL SHORT CIRCUIT OF AN ALTERNATOR, **James B. Smith, Cornelius N. Weygandt.** *Electrical Engineering (AIEE Transactions)*, volume 56, September 1937, pages 1149–55.

2. NEGATIVE-SEQUENCE REACTANCE OF SYNCHRONOUS MACHINES, **W. A. Thomas.** *Electrical Engineering (AIEE Transactions)*, volume 55, December 1936, pages 1378–85. Discussion by **J. C. Balsbaugh,** *Electrical Engineering (AIEE Transactions)*, volume 56, July 1937, pages 903–04.

Advances in Technique of Lightning Measurements

THEODORE BROWNLEE
MEMBER AIEE

Synopsis: Improved measuring equipment and refinements of technique contributed materially to the number and accuracy of lightning records taken, in a 4-year study, on a rural distribution system. Special shunts were developed to match the expected lightning currents to the voltage sensitivity of automatic cathode-ray oscillographs. Modifications were made in the method of initiation of the oscillographs and in their operation so as to get the greatest possible accuracy and to extend their period of unattended reliable operation. Refinements were made to increase the accuracy and speed of magnetic link calibrations and to permit the calibrating equipment to be operated from a low-power 115-volt supply. The 60-cycle after effects of lightning disturbances on the system were recorded by an automatic magnetic oscillograph.

NATURAL lightning is so variable in its intensity and duration, and so erratic in its choice of a time and place to strike, that plans for measurements must be made with extreme care. In considerable measure, the success of a lightning investigation depends upon the use of special equipment custom-tailored to fit the particular job. It is the purpose of the present paper to describe the equipment used in a 4-year project of this kind and to explain the reasons for the designs used. The results of successful operation of the equipment are given in a companion paper.[1]

Along with the lightning investigation, studies were conducted of short circuits recovery voltages, and methods of protection against overcurrents. These are described in other companion papers.[2,3] The present paper also reviews the main features of the oscillograph used to study recovery voltage.

Automatic Cathode-Ray Oscillograph Equipment

A desire to obtain additional information on long duration lightning was responsible for the development of the *HC-10-G1* oscillograph. The standard model has been described before,[4,5] but considerable modification was made for the present investigation. It is a relatively inexpensive instrument and runs for several hours with no attention. A number of them can be spaced at distances limited only by the time required for the operator to visit each one and set it in operation when a storm is expected.

Each oscillograph consists of two 3-inch cathode-ray tubes mounted close together, so that a single lens can be used to record both traces on a rotating drum. This drum takes a film $3^{13}/_{16}$ by 31 inches and rotates once every 0.7 second. After an exposure, the drum automatically shifts axially so that four distinct records can be obtained. Figure 1 shows a complete instrument and Figure 2 shows the position of the cathode-ray tubes, lens, and film-driving mechanism. The oscillographs operate from a 115-volt 60-cycle source. A simplified wiring diagram is shown in Figure 3. In it are incorporated several changes which make the oscillograph more reliable and accurate. Part of these changes were suggested by a previous discussion of this oscillograph.[6]

Seven of these oscillographs were used in the lightning investigation. Some of them recorded lightning-arrester current only, with different sensitivities for the two traces, so that accurately measurable deflections could be obtained over a very wide range of currents. In the others, one tube recorded arrester current and the other the current in the ground side of the transformer protected by the arrester. To avoid loss of records, in case of power interruption, each oscillograph was provided with a storage battery, charger, and dynamotor to convert from 12 direct volts to 115 alternating volts at 60 cycles. All this equipment and the shunts were mounted in steel housings on the lower part of the transformer pole, as shown in Figure 4.

Initiation and Operation

When a lightning storm seemed likely, the dynamotor and film-drum driving motor were started up in each oscillograph. Power was applied to the cathode-ray tubes, but with sufficient grid bias to leave the electron beams turned off.

Figure 1. Automatic cathode-ray oscillograph

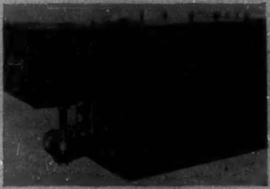

Figure 2. Oscillograph with top cover and film-drum housing removed

---

Paper 49-61, recommended by the AIEE Instruments and Measurements, and the Transmission and Distribution Committees and approved by the AIEE technical program committee for presentation at the AIEE Winter General Meeting, New York, N. Y., January 31–February 4, 1949. Represented at the Summer General Meeting, Swampscott, Mass., June 20–24, 1949. Manuscript submitted November 15, 1948; made available for printing December 17, 1948.

THEODORE BROWNLEE is with the High Voltage Engineering Laboratory, General Electric Company, Pittsfield, Mass.

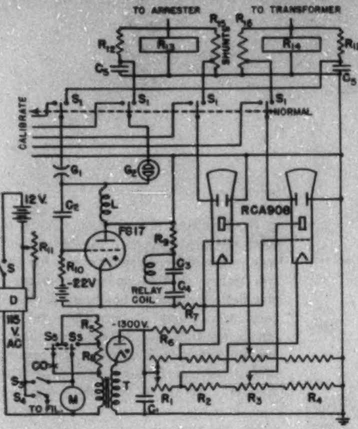

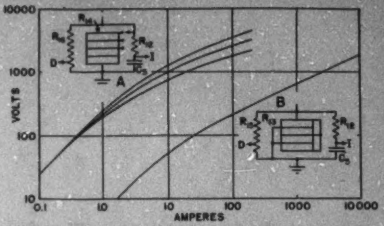

Figure 3 (left). Simplified wiring diagram of oscillograph

Figure 5 (above). Volt-ampere characteristics of shunts

A. Connections and curves for transformer current shunt using two, three, or four series Thyrite disks
B. Connections and curve for lightning-arrester current shunt using four parallel Thyrite disks
D. Connection to deflecting plate of oscillograph
I. Connection to initiating terminal of oscillograph

R_{12} 10,000 ohms $R_{15}=12.5$ ohms
$R_{16}=250$ ohms $C_5=0.001$ microfarad

At the top of Figure 3 shunts are shown as used in an installation to record both lightning arrester and transformer currents. While the two shunts are not identical, their principles are the same. Their physical features are described later. They are needed to provide the necessary voltage to turn on the electron beams and to deflect them so as to produce a record on the rotating film. For brevity the word "initiate" is used to denote the turning on of the electron beams as soon as a predetermined current flows through either shunt. The chief elements of the lightning-arrester shunt are the parallel resistors, R_{13} made of Thyrite, and R_{15} which is wire wound. The net resistance is made sufficiently high to initiate the oscillograph at the desired minimum current. Since this voltage exceeds the requirements for the deflection plates of the cathode-ray tube, the deflecting voltage is taken from a tap on R_{15}.

Both cathode-ray tubes use the same accelerating voltage supply and initiate simultaneously. The capacitor C_1 is negatively charged to 1,300 volts. Before initiation, C_2 and C_4 also are charged to the same voltage, and the *FG17* thyratron is held nonconducting by virtue of its 22-volt negative grid bias. When a voltage appears across R_{13} and R_{15}, the 0.001-microfarad capacitor C_5 charges up through the 10,000-ohm resistor R_{12}. This combination has a negligible effect on the shunt voltage drop and has a low enough time constant so that the voltage on C_5 is substantially the same as the total shunt voltage for waves that can be recorded by the oscillograph. G_2 is a glow tube which becomes conducting at a voltage corresponding to the minimum current it is desired to record. As soon as G_2 becomes conducting, C_3 oscillates with the inductance *L*, and the oscillating voltage is applied to the thyratron grid through C_2. Hence, irrespective of the original polarity of the lightning, the thyratron bias is overcome and the thyratron becomes conducting. When this happens, the lower side of C_4 goes to ground potential. This changes the bias on both cathode-ray tubes, and the beams turn on. At the same time, C_4 discharges through the relay coil. For simplicity the film-shift mechanism and controls are omitted. Actually, the relay coil shown picks up time delay relays, which cause the film shift to occur after the recording and then to reset for the next operation. When the voltage on C_4 is reduced, the thyratron becomes nonconducting and C_4 charges up again, thereby increasing the bias on the cathode-ray-tube grids and turning off the beams about 1.4 seconds after initiation. This means the record can last for two full revolutions of the drum, but the beam intensity gradually is reduced so that it is not difficult to interpret a record lasting from 0.7 to 1.4 seconds.

The rotating film-drum shaft is held in position by a nut on the threaded drive shaft. Ordinarily, the nut rotates on the shaft and the drum has no axial motion. After each record is taken, a solenoid moves an arm out which catches a pin in the nut and stops its rotation. Then the rotation of the shaft causes the nut and film drum to move downward. The time delay relays are adjustable to control the length of time the solenoid arm engages the pin. When set as in the lightning investigation, the axial motion starts five seconds after initiation and lasts for seven seconds. There is no period during which a record cannot be taken, for a second in-

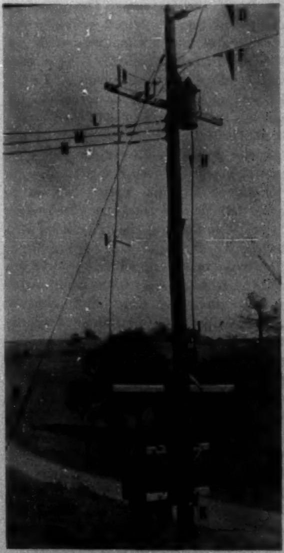

Figure 4. Typical pole installation with magnetic links and cathode-ray oscillograph

itiation can occur before the beam goes off, but, of course, the second record can be superimposed or but slightly shifted from the first, if initiations are not spaced by at least 12-second intervals. Originally, when the nut reached the end of its travel, a limit switch shut off the battery supply to the dynamotor to prevent mechanical damage. This might occasion the loss of an important record, so the solenoid arm was reshaped so as to leave the nut free to rotate after the third shift (and fourth record). Hence, there might be several superimposed records in the fourth position, but no records were lost because of run-down film drums.

The initiation from the transformer shunt uses the same inductance L as described previously, but an air gap G_1 is used instead of the glow tube G_2. This takes a higher voltage to spark, but was necessary because the current in the transformer increases gradually, and the glow voltage on the tube would prevent oscillation. The lightning-arrester current increases abruptly after the lightning-arrester sparks over, and, for steep wa[illegible] the glow tube has a sparkover vol[illegible] sufficiently above the steady glow voltage to insure oscillation.

Maintenance of Constant Sensitivity

Each oscillograph derives its power from a 12-volt battery through a dynamotor D, as shown schematically in Figure 3. R_{11} is a field rheostat to control the dynamotor speed. As the battery voltage runs down, the dynamotor voltage drops in proportion. This in turn changes the cathode-ray beam voltage and the sensitivity of the oscillograph. In addition, when C_4 is discharged through the thyratron, the voltage on C_1 is reduced for a few seconds until C_4 charges up again. By using a large value of five microfarads for C_4, the reduction is but eight per cent. The resultant small change in sensitivity is the same for every exposure and can be allowed for in the analysis of the oscillograms.

The change caused by reduced charge on the batteries was practically eliminated by using a ballast-tube resistor R_8 in series with the transformer T which charges up C_1. Without this ballast tube, the voltage on C_1 drops about 15 per cent as the battery becomes discharged; while with the tube, the change is about one per cent. The sturdy resistor R_5 has the same resistance value as R_8 at average operating conditions for R_8 and serves a dual purpose. Normally, when S_8 is closed to start the film motor M, S_6 is already in the left position, and R_5 acts as a current limiting resistor for R_8 while C_1 charges up. Then, when C_1 is charged up, S_6 is thrown to the right and R_5 is short-circuited. To avoid a loss of record, a Novalux cutout CO is used which becomes conducting if R_1 becomes open; then, when S_6 is thrown to the right, power is fed to the transformer through the cutout and R_6. During normal operation the battery chargers are left on continuously, and the oscillographs will run about 20 hours. If there is a power failure they will operate for four hours.

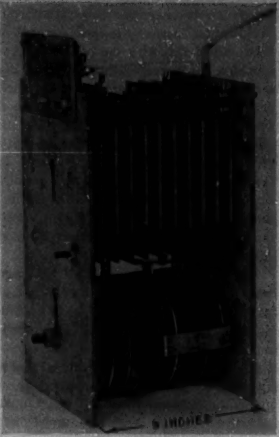

Figure 6. Combination shunt

Shunts

It was desired to measure the lightning currents flowing through transformers and lightning arresters on a 7,200-volt grounded system. It was relatively simple to insert shunts between these devices and the neutral conductor which is grounded at every pole. The desirable qualities for these shunts are enumerated here with explanations of how well these qualities were attained.

1. Ample discharge capacity. This was secured by using liberal-sized components with adequate clearances and insulation. The entire shunt structure was immersed in oil.

2. Stable characteristics. The resistor materials were carefully chosen. Laboratory measurements of the direct current and impulse characteristics were taken before and after the investigation with excellent agreement.

3. A nonlinear volt-ampere characteristic is desirable so that an extended range of currents can be measured with readable deflections. However, for best accuracy, the voltage range should not be compressed beyond that necessary to cover the required current range. Some special low-exponent Thyrite was used, shunted by comparatively high linear resistors. Figure 5 shows the characteristics of these shunts.

4. Accessible taps so that the current range to be studied can be varied if necessary. Since the voltage required for initiation is more than adequate for beam deflections, taps are provided on the linear resistance portion of the shunts. An entire shunt can be removed easily from its tank for tap changing.

5. Low inductance. The inductance was kept as low as possible. The inductance drop is negligible for currents that can be recorded by the oscillographs.

The lightning-arrester and transformer current shunts are mounted in a single frame with a common ground, as shown in Figure 6. The complete unit is set in a distribution transformer tank about 12 inches in diameter.

Calibration of Oscillograph

It is highly advantageous to be absolutely certain that the initiating and measuring circuits are in good condition. Hence, provision is made to check these circuits after the final installations. When switch S_1 of Figure 3 is thrown to calibrate position, the line-deflecting plates and initiating circuits of both tubes are connected to an octal socket at the rear of the oscillograph housing. A special calibrating box can be connected to any of the oscillographs.

Provision is made to supply to the deflecting plates 35 or 70 rms volts at 60 cycles, or 22.5, 45, 67.5, 90, or 112.5 direct volts. A dry cell, push button, and small step-up transformer are mounted in the same box and are used to check the initiation of either circuit. Suitable switches are provided on the box, so that all the checking can be done quickly, efficiently, and easily.

Testing with Impulse Generator

At the start of each season, an additional over-all check on the shunts and oscillographs was made, using a portable impulse generator which was discharged directly into the lightning arrester at each location. A 0.33 microfarad capacitor bank charged to 90 kv was used, with sufficient series impedance to give a crest current of about 3,000 amperes. The feeling of assurance that all equipment was ready to operate correctly was certainly well worth the expense of thorough checking.

Magnetic Link Calibrating Equipment

The use of magnetic links for measuring lightning currents is well known and has been described in previous articles.[5,6] In the lightning investigation, links were bracket mounted at spacings of 13/16 and $2^{3}/_{16}$ inches from the conductor with both links lining up with the flux lines which encircle the conductor when it carries current. With these spacings, and the technique described hereafter, crest currents in the range of 100 to 30,000 amperes could be measured with an accuracy of around 10 per cent. Figure 4 shows a typical multiple installation with 10 brackets, identified by letters, on a pole at the end of a feeder. Additional brackets were used in locations where there were more conductors arriving at, or leaving the pole. In addition to some 30 multiple installations like these, there were about 1,300 brackets, one per pole, to measure lightning arrester current.

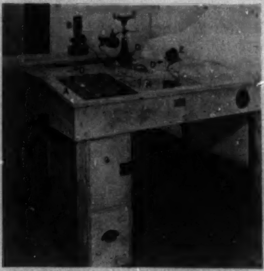

Figure 7. Calibrating table for magnetic links

A. Control panel
B. Galvanometer
C. Galvanometer coil
D. Openings for magnetizing coils (under top)
E. Demagnetizing coil
F. Capacitor cabinet
G. Adjustable d-c power supply
H. Safety glass above voltmeter

The usual surge-crest ammeter is a compact and easily carried instrument which can be used anywhere to measure the magnetism retained in the links. However, the individual links, while comparatively uniform at medium degrees of magnetization, vary considerably at low and at high degrees of magnetization. For the lightning investigation it was decided to use the ballistic galvanometer method of calibration developed by McEachron and McMorris.[7] In this discussion of magnetic links, the word "calibration" means the measurement of the retained flux with the ballistic galvanometer, using average link curves to determine the current and reversal which produced the retained flux. This method was used for the 1,300 installations to obtain statistical data on the probability of strokes of various magnitudes. It saved considerable time and was permissible for data of this sort, since the resultant curve is little affected by variations about the average in individual links.

For the 30 multiple installations it was desired to obtain much more precise measurements. Each pair of links was given an "individual calibration" meaning that, after galvanometer measurement, the links were demagnetized and a cut and try process of remagnetization applied to find out what kind of field must have produced the original retained flux.

Special Magnetic-Link Calibrating Table

In Figure 7 is shown a special table first used in the lightning investigation for magnetic-link studies. It is designed for convenience, speed, and accuracy in the calibration and demagnetization of links, and especially for the rapid individual calibration of pairs of links.

Calibration of Links

A link which is magnetized, as shown by a compass indicator, is first calibrated by rapidly withdrawing it from the magnetizing coil, which is in series with the ballistic galvanometer and a 4-position adjustable attenuator. The attenuator varies the sensitivity and gives approximately critical damping on all positions. This method is very sensitive; the coil has to be swivel mounted and set with the axis perpendicular to the earth's field to avoid errors. When the deflections for a pair of average links have been measured, curves can be used to determine the crest current and per cent reversal.[6]

Demagnetization of Links

The demagnetizing coil is similar to the measuring coil, but it is larger and is wound with coarser wire. It is connected to the 115-volt a-c supply through a push button and also is swivel mounted. A link is demagnetized by inserting it in the coil and then drawing it out slowly while the push button is held down. Unless the link is withdrawn axially with a motion perpendicular to the earth's field, it will not become completely demagnetized.

Individual Calibration of Links

The individual calibration of links is considerably slower than a curve calibration, but its accuracy is much better, and it was absolutely necessary to obtain the good correlations found in the lightning investigation. It is not practical to use currents and link spacings as encountered in the field, but substantially the same fields can be produced by coils with currents of 10 amperes or less. For some years such a coil has been used in connection with a d-c generator. However, about 5 kw are required to saturate a link, and, in the few seconds required to adjust and to read the current, the coil overheats. For the calibration table a new method was used which has the following improvements:

1. It operates from 115 alternating volts.
2. It takes very little power.
3. The coil overheating is eliminated.
4. Ample time is available for meter reading.
5. The inner and outer links can be calibrated simultaneously with any ratio of currents in the two coils.

Instead of using steady direct current for calibration, the coils are energized by capacitor discharges, with special care taken to prevent any reversal during the discharge. Figure 8 shows the circuit used in the special table. For any fixed values of *E*, *C*, *R*, and *L*, the crest current can be calculated—the current is always proportional to the voltage which can be read on the voltmeter. By changing the resistance in series with the outer link coil, the ratio of currents in the two coils can be maintained at any value corresponding to the spacings of the links from the lightning conductor. The coils are mounted on the underside of the rear table cover, with conical depressions in the cover to facilitate inserting and removing the link. They are located about three feet apart and at some distance from other equipment to avoid interaction with the calibrating fields. The coils are wound on a spool of 3.75-inch diameter and 1.125 inches wide. A total of 2,080 turns, in 52 layers, is used. The average coil diameter is 5.30 inches. The field strength on the axis can be calculated, and, over the active link length, the average field strength is within three per cent of the maximum field strength at the geometric center of the coil. The coils are large enough so that the presence of the link does not appreciably affect the total

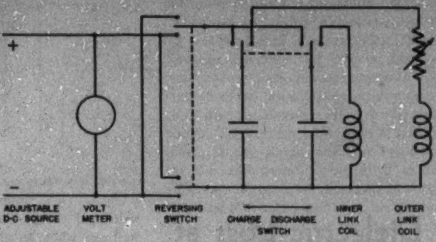

Figure 8. Simplified wiring diagram of impulse calibrating circuit for magnetic links

flux. As a safety precaution, the power pack and all live parts are interlocked so that the power supply must be interrupted and the capacitor banks discharged before any of the circuits are made accessible.

The Automatic Oscillograph (Duddell Type)

The automatic oscillograph was used in the studies reported in the three companion papers. It has been described fully before;[8,9,10] only the main features are reviewed here. It records six voltages or currents on a roll of photographic paper 4.5 inches wide and 200 feet long. The oscillograph is equipped with a mirror to provide the initial sweep motion and will record all but one-half cycle of a disturbance whose instantaneous current exceeds a predetermined value. The recording continues as long as the disturbance persists, at a rate of the order of one foot per second. The companion papers[1,3] give examples of the oscillograms.

In the present investigation, one or sometimes two of these oscillographs were used to record feeder phase and neutral currents near the substation or at the fault. Current transformers were inserted in all 3-phase wires, and another was inserted in the neutral. The secondaries of these transformers were all grounded on one side. An oscillograph vibrator was connected in series with each of the nongrounded terminals. The four vibrators were connected together on the ground side, but had the trip coil of the oscillograph inserted between the common point and ground.

The transformers were connected so that the current in the neutral added to the phase-wire current to facilitate the tripping. The sensitivity of the trip coil was such that a record would be taken if the current in a phase wire reached 40 amperes crest. The trip coil was shunted by a small Thyrite resistor to protect the coil and to keep down the burden on the current transformers.

Rotating-Drum 3-Element Cathode-Ray Oscillograph

The 3-element cathode-ray oscillograph used to study recovery voltages[2] was described previously by Rudge and Wade.[11] A rotating-drum-type film holder is used, with a top speed corresponding to 25 microseconds per millimeter. The oscillograms are obtained by photographing the phenomena on the fluorescent screen of the cathode-ray tube, using $f2.0$ lenses and 35-millimeter film. The magazine film drums hold 100 feet of film; means are provided for cutting off the exposed portions after each test. In the recovery-voltage tests, the oscillograph was coupled to the lines under study by compensated voltage dividers using resistance and capacitance elements. Typical oscillograms are shown in a companion paper.[2]

Conclusion

The findings of the three companion papers were made possible by the diligent efforts of a number of people, and also by the proper functioning of the equipment they used. The true value of this equipment is best demonstrated by the important disclosures in these papers.

References

1. Lightning Investigation on a Rural Distribution System, D. D. MacCarthy, D. A. Stann, D. R. Edge, W. C. McKinley. *AIEE Transactions*, part I, volume 68, 1949, pages 428–38.

2. Short-Circuit and Recovery Voltage Tests on Rural Distribution Systems, W. H. Eason, J. W. Kalb, H. A. Peterson, I. B. Johnson. *AIEE Transactions*, volume 68, 1949 (*Proceedings* T9177).

3. Overcurrent Investigation on Rural Distribution Systems, G. F. Lincks, D. R. Edge, W. C. McKinley, J. H. Leh. *AIEE Transactions*, volume 68, 1949 (*Proceedings* T9175).

4. The Cathode-Ray Oscillograph Applied to Long-Time Switching Transients, G. W. Dunlap, N. Rohats. *Electrical Engineering* (*AIEE Transactions*), volume 62, May 1943, pages 231–4.

5. Discussion, reference 4, J. H. Hagenguth. Page 445.

6. Direct Measurement of Surge Currents, C. M. Foust, J. T. Henderson. *Electrical Engineering* (*AIEE Transactions*), volume 54, April 1935, pages 373–8.

7. Discharge Currents in Distribution Arresters, K. B. McEachron, W. A. McMorris. *Electrical Engineering* (*AIEE Transactions*), volume 54, December 1935, pages 1395–9.

8. An Automatic Oscillograph (abstract), C. M. Hathaway, R. C. Buell. *AIEE Transactions*, volume 51, March 1932, pages 222–25.

9. The Automatic Oscillograph and Its Utility, A. D. MacAffer. *General Electric Review* (Schenectady, N. Y.), volume 38, number 3, March 1935, pages 146–151.

10. Special Uses for the Automatic Oscillograph, G. A. Powell, R. E. Walsh. *Electrical Engineering* (*AIEE Transactions*), volume 56, April 1937, pages 438–40, 476–7.

11. Expulsion Protective Gaps, W. J. Rudge, Jr., E. J. Wade. *Electrical Engineering* (*AIEE Transactions*), volume 56, May 1937, pages 551–57.

No Discussion

The Measurement of Dielectric Loss at High Frequencies and Under Changing Temperature

J. B. WHITEHEAD
FELLOW AIEE

W. RUEGGEBERG
ASSOCIATE AIEE

DIELECTRICS of all types are highly sensitive to change of temperature, dielectric losses especially rising rapidly with rise of temperature. Thus dielectrics to be used as insulators must be sharply limited as to dielectric loss and rise of temperature. On the other hand high dielectric losses are advantageous in composite materials requiring heating for curing or thermosetting. Industrial dielectric heating by high electric frequency, therefore, involves a new viewpoint as to desirable dielectric behavior, and demands a new survey and new methods of measurement of dielectric properties.

This paper describes a method of measuring the properties of a dielectric at any point in a high frequency heating cycle. Some of the results of measurements on several dielectric materials are given, with some general comments thereon. The paper however does not give complete numerical data on the materials studied, nor does it aim to analyze their behavior in terms of dielectric theory. The work was done in the School of Engineering of The Johns Hopkins University under the auspices of the Armstrong Cork Company.

Present Available Methods of Measurement

Of present available methods of measurement of dielectric properties under alternating stress all are limited apparently without exception to the steady-state condition with temperature constant. This applies also to a number of methods for frequencies in the megacycle range best suited for dielectric heating, such as American Society for Testing Materials shunted susceptance method,[1] bridge-type Q-meters, and others.

For two main reasons such methods are not suitable for following the dielectric through a high frequency heating cycle:

1. The low value of applied stress.
2. The difficulty of maintaining constant temperature during measurement.

An appreciable value of stress is necessary to liberate the internal dielectric losses. Moreover, once initiated, these losses increase with time over an appreciable period, thus precluding any effort to maintain constant temperature. A method is necessary in which temperature rise is caused by applied stress, and in which applied stress, current, and temperature, and also power input, may be measured at any stage in the heating cycle.

Method of Measurement

The method of measurement, described in a previous paper[2] is based on the conventional vector diagram of component voltages when an alternating electromotive force of any frequency is impressed on a cell containing a dielectric. The thermally-insulated cell is again shown in Figure 1, and the simple electric connections, with vector diagram of voltages, in Figure 2. In a heating run the current I in the sample is read directly by the thermoammeter F, the applied voltage E_0 by a vacuum-tube voltmeter, and the temperature at any point in the sample by thermocouples T, T, in Figure 1. Separate measurements are made of the impedance voltages E_z, E_{zr}, E_{zx}, of the ammeter and connections. Vector IR, however, cannot be measured directly.

Complete solution of the vector diagram, for dielectric constant, loss, and power factors, is obtained by finding the value of the vector IR, in which R is the effective resistance of dielectric loss. This vector cannot be measured directly, but its value is obtained by a separate calibration of the cell containing a second identical sample in which are imbedded thin high resistance grids (nichrome) heated with continuous current. Internal temperatures are read from thermocouples located as in the a-c heating run. After a

Figure 1. Test cell for 10 megacycles

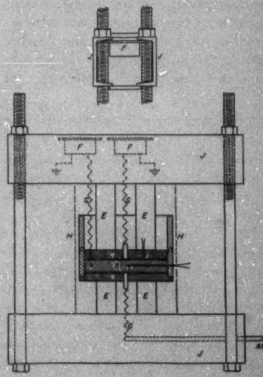

Paper 49-130, recommended by the AIEE Electric Heating and the Instruments and Measurements Committees and approved by the AIEE Technical Program Committee for presentation at the AIEE Summer General Meeting, Swampscott, Mass., June 20–24, 1949. Manuscript submitted March 4, 1949; made available for printing April 27, 1949.

J. B. WHITEHEAD, Professor of electrical engineering, and W. RUEGGEBERG are both with the School of Engineering, The Johns Hopkins University, Baltimore, Md.

Appreciation is extended to the Armstrong Cork Company and to Dr. G. W. Scott, Jr., for advice and support in furthering the progress of the work; also to Doctors C. F. Miller, F. Hamburger and W. B. Kouwenhoven of the University Staff for their co-operation, and to Messrs. F. H. Whelan, C. B. Boenning, and J. Mesmeringer, for participation in laboratory work.

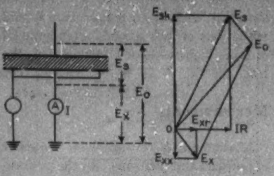

Figure 2. Vector diagram of test cell connections

$$E_{sk} = \sqrt{E_o^2 - (IR + E_{xr})^2} + E_{xx}$$

$$\text{Power Factor} = \frac{IR}{E_s}$$

$$E_s = \sqrt{E_{sk}^2 + IR^2}$$

$$K = \frac{I}{E_{sk}} \times \text{Constant}$$

$$IR = \frac{\text{Heating watts}}{I}$$

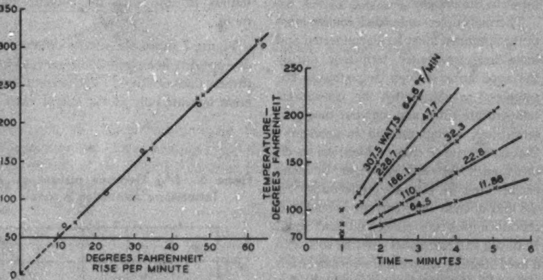

Figure 3. D-c calibration curves of sample in test cell

brief initial period the temperature of the sample increases linearly with time as shown in Figure 3 for several values of heating current.

Each of these curves in its linear portion represents a uniform rise of temperature, that is, a temperature-time gradient of so many degrees rise per minute, corresponding to a uniform supply of energy in watts due to the constant heating current. The family of heating curves may be combined in one curve showing heating watts as function of rate of rise of temperature, also shown in Figure 3. It will be noted that this curve is also a straight line up to 50 or 60 degrees Fahrenheit per minute; it passes through or near to a zero-point of no energy and no temperature rise.

Figure 4 shows the average location of the heating curves of two variations of the same material, each mixed with a binder, put under pressure in the cell of Figure 1, and heated by applying electric stress of 0.8 volt per mil at 10 megacycles. Temperature, current, and voltage can be read at one-half minute intervals. A tangent to the heating curve at any point gives the rate of temperature rise at that point. The corresponding rate of energy input, that is, watts, may be taken from the d-c calibration curve. If *R* is the effective resistance of dielectric heating, then the d-c watt input may be written as I^2R, in which *I* is the measured high-frequency current corresponding to the point in question on the heating curve. The vector *IR* of Figure 2 is now known and all quantities computed readily.

Improved Test Cell for 30 Megacycles

The duration of the heating cycle, that is the time required to reach a definite curing temperature, may be shortened by increasing the rate of energy input. This may be done by increasing the applied voltage, increasing the frequency, or by reducing the mass (for example, the thickness) of the sample. In the improved cell shown in Figure 5, all of these means have been employed. In the earlier work at 10 megacycles the duration of the heating cycle was from four to five minutes. In the present work cycles, from 20 to 40 seconds for temperatures up to 250 to 300 degrees Fahrenheit were common.

In the cell of Figure 5, the following modifications of the earlier cell may be noted:

1. *A* and *A* are duplicate samples, each five inches in diameter and 1/4 inch thick. *B* is the high-voltage electrode of nichrome foil, $3^1/_2$ inches in diameter. *G* and *G′* are the low-voltage guard ring electrodes, $2^1/_2$ inches and $3^1/_2$ inches in diameter, and also of nichrome foil. With these changes the cell has been carried to 1,200 volts, 30 megacycles, giving an applied stress of 4.8 volts per mil, which results in heating cycles from 16 to 40 seconds for the materials being studied.

2. The increase to 30 megacycles steps up markedly all electrostatic inductive disturbances. Complete and individual screening of all electrode connections and of back faces of electrodes becomes necessary. A metal housing completely enclosed the ammeters, *F*, *F*, and was tied to the immediately adjacent ground connection of the 2-kw Westinghouse oscillator by heavy copper strap. The high-voltage terminal of the generator and its short connection to the high-voltage terminal of the cell also were enclosed in double screening connected to ground.

3. In order to ensure uniformity of temperature in the test sample, it was found necessary to preheat the electrodes. This was done by inserting thin nichrome heating grids in the insulating backing of the low-voltage electrode and using a duplicate sample on the back face of the high-voltage electrode (see (4) below). A necessary condition in this electrode preheating was that no heat should pass from electrode into the sample. Test for this condition was made by thermocouples in the interface of sample and electrode and in the interface between back of electrode and adjacent insulation. As long as the former showed the higher temperature, the heat-flow was outward only. Subject to this restriction electrode preheating has the effect only of increasing the thermal resistance of the electrode insulating supports. Figure 6 shows that only after 20 seconds preheating of the electrode did any heat arrive at the outer surface of the sample. It was also found that throughout the a-c cycle, this surface was hotter than that between electrode and supporting insulation. The figure also shows a typical variation of temperature through the thickness of the sample.

4. The insulating supports of a high-voltage electrode are obviously subjected to electric stress and dielectric heating. The resulting losses are an additional

Figure 4. Heating curves of granulated cork

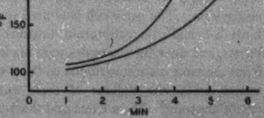

Figure 5. Test cell for 30 megacycles

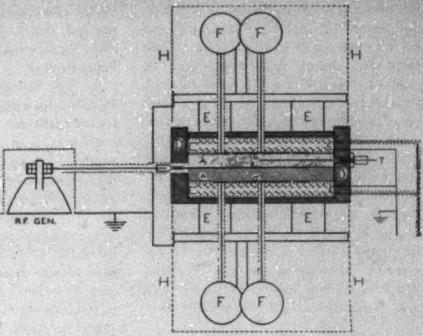

load on the generator, but cause no error in the measurement of loss in a sample. They do, however, at and above 30 seconds cause appreciable heating of the electrode insulating backing, and so may be utilized as electrode heating to help maintain uniform temperature in the sample (see (3) above).

The problem of the adjustment and measurement of this external electrode heating was met in the final form of cell by using two identical samples with a single or common high-voltage electrode between them, and with duplicate measuring electrodes and instruments as shown in Figure 5. In this way the high-voltage electrode is supported by the specimen itself, the temperature on both sides is the same, and thus results a maximum efficiency of electrode heating without either gain or loss of heat for either sample. As this balance obtains throughout the heating cycle, there is no necessity for preheating the high-voltage electrode.

5. In assembling the sample in the test cell, it was found necessary to use thin paper disks between sample and electrodes, and between sample and heater grids in the d-c calibration. Consequently part of the measured a-c input power goes into heating the electrodes and the paper disks. Separate measurements were made on the paper disks, and the heat to raise the mass of the electrodes could be computed readily; these two excess heating losses were deducted from the total a-c input values (at any desired temperature) as obtained from the d-c calibration. The same cell was used for both a-c and d-c calibration measurements, and since the electrodes were made from the same nichrome ribbon as the d-c heater grids, the volume of each was nearly the same. The a-c test and the d-c calibration samples were closely identical. The small excess losses referred to before were always a small fraction of the total input to the sample.

Thermocouples imbedded in the mass of the specimen must be disconnected and have low-capacitance terminals during the application of high frequency to the samples. Consequently for continuous temperature-time and current-time observations, a step method is necessary; that is, a series of runs on identical specimens, each one running longer, by some chosen interval, than its predecessor. At the end of each step, current is read and thermocouples are connected and read. Both cell and electrodes must be cooled to a fixed starting temperature between each step. Final temperatures for each step may be read with a needle thermocouple if the cycle is long and the material permits. However, for cycles as short as 30 or 40 seconds and a sample of small volume, temperature changes are rapid when voltage is removed and a faster temperature reading is necessary. A satisfactory solution was found in a pair of spring-operated contacts for the leads of imbedded thermocouples, and a Brown rapid temperature recorder. With this arrangement, temperatures could be read and recorded in one to two seconds after the removal of high-frequency voltage.

Experimental Accuracy

The accuracy of instruments and observations of the electrical quantities is better than two per cent, and this is well within the percentage variations of the materials both as furnished and after conditioning. It is believed that much the same may be said as to the temperature measured by the Brown recording instrument, with which temperature is read within one or two seconds after removal of the high-frequency voltage of the test.

Measurements

Measurements were made on a number of powders and preforms. In the preform the powder is compressed so that it retains a definite shape, in our case a disk, five inches in diameter and one-eighth inch thick.

Dry Materials. The normal heating or temperature-time curve of a dry thermosetting material is concave upwards. The corresponding current-time curve at first increases, then more slowly and finally passes through a maximum and decreases. The result of this relationship is a curve of loss factor and one of dielectric constant, both increasing at first, and each then passing through a maximum approximately in step with the current maximum.

Figure 7 shows the results on a certain dry powder, heated at 30 megacycles and three values of stress. The current maximum appears only at the lowest value of

Figure 6. (A) Electrode preheating. (B) Temperature distribution in sample

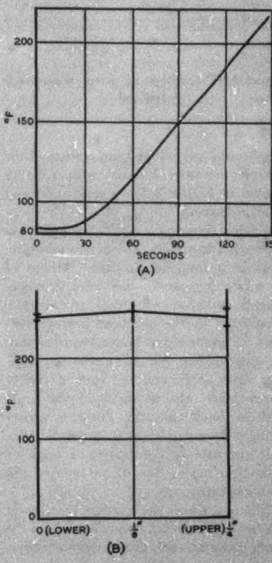

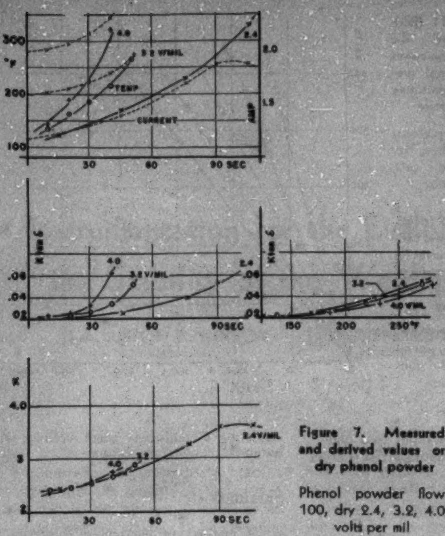

Figure 7. Measured and derived values or dry phenol powder

Phenol powder flow 100, dry 2.4, 3.2, 4.0 volts per mil

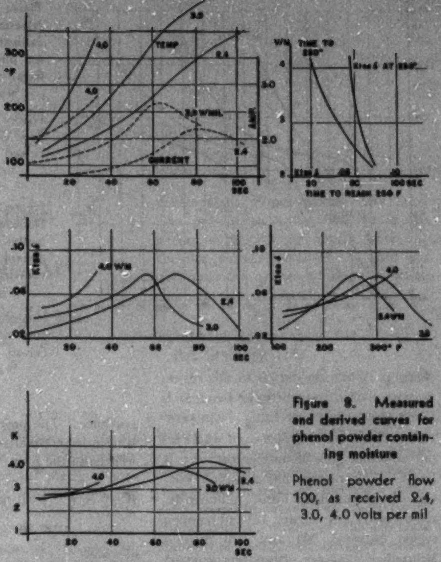

Figure 8. Measured and derived curves for phenol powder containing moisture

Phenol powder flow 100, as received 2.4, 3.0, 4.0 volts per mil

stress. A still lower value would be necessary and a longer heating cycle to bring out all of the behavior outlined in the foregoing paragraph.

Materials Containing Moisture. It is a long process to dry powders and preforms completely, and a relatively small amount of residual moisture causes an important variation of the behavior just described. In such cases the maxima of current, loss factor, and dielectric constant all appear, but earlier and in more pronounced character than in the dry specimens. Thus Figure 8 shows the results taken from a powder in the condition as received from the manufacturer and without preliminary drying. A somewhat extreme case is shown in Figure 9, for a preform not completely dry. In this case a loss factor of 0.2 is reached while the water is being driven off. In other cases, known to contain more moisture, much greater values of loss factor have been found.

The presence of water in a test sample is clearly shown by the d-c calibration curve. Figure 10 shows the measured and derived calibration curves of a dry powder, and Figure 11, the measured calibration curves of a preform with a moderate amount of absorbed moisture. In the latter, after initial temperature equalization, the curves are approximately linear between 110 and 200 degrees Fahrenheit. Between 200 and 220 degrees the curves flatten out sharply, and most of the heat input is expended in vaporizing the contained moisture. Above 220 degrees the rate of temperature rise again increases

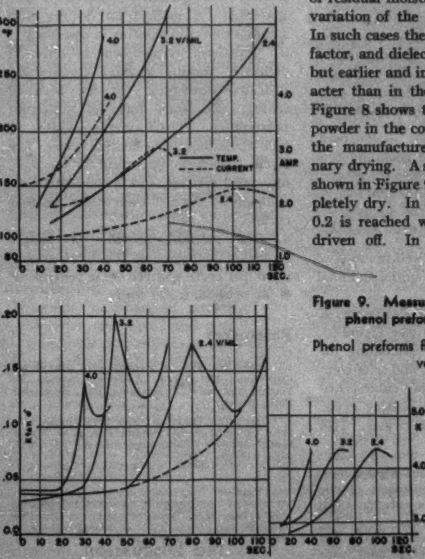

Figure 9. Measured and derived curves for phenol preform containing moisture

Phenol preforms flow 60, dry 2.4, 3.2, 4.0 volts per mil

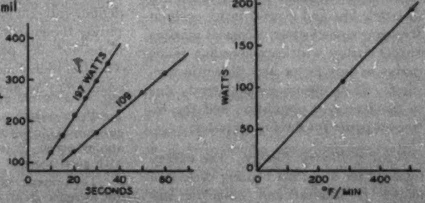

Figure 10. D-c calibration curves for dry phenol powder

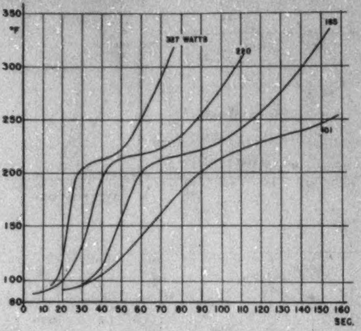

Figure 11 (left). Measured d-c calibration curves for phenol preform containing moisture

Phenol preforms flow 60, as received d-c calibration

Figure 12 (right). Derived d-c calibration curves for phenol preforms containing moisture

Phenol preforms flow 60, as received d-c calibration

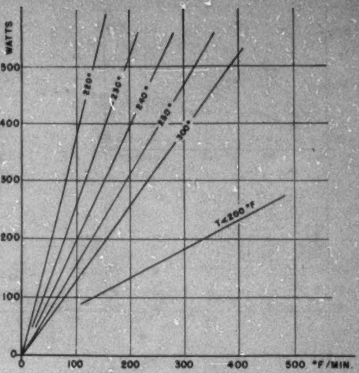

sharply. While the curves in this region do not at once resume linear form, it is found that at any one value of temperature the derived curve between watts input and time rate of temperature rise is linear. This means that a sample containing moisture has a family of linear derived curves (see Figure 12) and an open region between 200 and 220 degrees Fahrenheit. Under alternating current conditions in passing through this range, there is a large increase of loss factor. (See Figure 9.)

Dielectric Absorbtion as Heating Process. We have seen that in a dry powder under stress, 2.4 volts per mil, a maximum of current appears only after 100 seconds, whereas at 4.0 volts per mil, the temperature rises to 245 degrees Fahrenheit with 20 to 25 seconds at an approximately linear rate and without evidence of current maximum; loss factor, and dielectric constant remain constant.

These two types of behavior indicate that, since even the dry dielectric is complex, classical dielectric absorbtion may be present as a mechanism of heating. This phenomenon involves no molecular changes, is faster than molecular polarization, and simply heats the dielectric by an integrated i^2r process.

The presence of moisture increases the dielectric absorbtion and corresponding dielectric loss and gives a faster cycle at the same applied stress. Current maxima appear earlier with corresponding rising curves of loss factor and dielectric constant. These effects are apparently due to the increased absorbtion and the increased power for driving off water.

Input of Electric Energy. The energy required for a normal heating cycle is a matter of interest and economic importance. The power input to a dielectric subjected to alternating stress is often written in the form

$$W = 0.55\left(\frac{E_0}{d}\right)^2 fK \tan \delta 10^{-12}$$

watts per cubic centimeter (1)

in which

$\frac{E_0}{d}$ = applied stress, volts per centimeter
f = frequency, cycles per second
K = dielectric constant
δ = loss, or phase defect angle

It has long been known that for a complex dielectric K and δ may vary over wide ranges with change of temperature. Consequently equation 1, to be applicable for computing the energy input to a dielectric heating cycle must be written

$$\int_{t_0}^{t_T} W dt = 0.55\left(\frac{E_0}{d}\right)^2 \times f \times \left[\int_{t_0}^{t_T} K \tan \delta dt\right] 10^{-12}$$

watt-seconds per cubic centimeter (2)

in which $K \tan \delta$ is a derived function of time, and t_0 and t_T are the initial and final times of the heat cycle.

The computed curves of loss factor, $K \tan \delta$, as function of time (see Figure 9), afford a ready means of evaluating the definite integral indicated, and so of computing the energy input per cubic centimeter for any particular heating cycle. This has been done for many cases. Two results may be mentioned:

1. The energy input to reach a given temperature is generally independent of the applied stress, as is to be expected in a cell with good thermal insulation.
2. The presence of absorbed moisture does not increase greatly the energy input, thus indicating a relatively small volume of water.

Summary

1. A method of measuring the properties of a dielectric while its temperature is changing has been developed and applied to certain thermosetting materials under high-frequency heating.
2. The presence of absorbed moisture in small amounts has a pronounced influence on the dielectric properties of such materials. A method for dealing with samples containg moisture is described.
3. Two basic phenomena are active in dielectric heating at high frequencies: dielectric absorbtion (in the Maxwell sense); and some form of molecular polarization. The former is evident in high-stress short-time heating cycles. The latter is the more important for the thermosetting process, and is completely developed in longer lower-stress heating cycles.
4. The method provides a simple means of determining the total energy input per cycle and per cubic centimeter of the material under study.

References

1. TESTS FOR POWER FACTOR AND DIELECTRIC CONSTANT. *D150-47T*, American Society for Testing Materials (Philadelphia, Pa.), September 1947.

2. DIELECTRIC HEATING—THE MEASUREMENT OF LOSS UNDER RISING TEMPERATURE, J. B. Whitehead. *AIEE Transactions*, volume 66, 1947, pages 947-49.

No Discussion

Instrumentation for the Evaluation of the Stability of the Welding Arc

LAURISTON P. WINSOR
MEMBER AIEE

L. McDONALD SCHETKY
NONMEMBER AIEE

ROBERT A. WYANT
NONMEMBER AIEE

THE importance of the stability of the welding arc on both the ease of welding and the quality of the weld is fully recognized by everyone concerned with arc welding, whether he be a welding engineer or operator. The term arc stability is used widely by the industry, although too often it is loosely or poorly defined. Qualitatively, arc stability is understood to mean the ability of an arc to remain fixed in position, with uniform electrical characteristics, and uniform flow of heat to the weld. The arc should have no tendency to become extinguished and should have ample ability to recover from the frequent short circuits introduced by the deposition of weld metal. Quantitatively, it is difficult to express arc stability in terms that permit explicit definition or numerical measurement. Because of this, many decisions, such as the evaluation of the quality and performance of welding electrodes, machine characteristics, and recommended voltage and current ranges, are left largely to the personal opinions of expert welders. Their judgment is frequently supplemented by visual examination of the welds, metallurgical studies of the weld metal, and mechanical tests.

During the past two years, the Welding Laboratory at the Rensselaer Polytechnic Institute, under the sponsorship of the United States Navy Bureau of Ships, has been engaged in the development of instrumentation for the study of arc stability. A number of instruments have been developed, each of which measures some characteristic or parameter of the arc which is thought to influence arc stability, and which might serve as an indication of the degree of arc stability. These instruments have been designed to be simple in operation, easily read, readily reproducible, and portable enough to be taken from one laboratory to another and into the field to make measurements under actual welding conditions.

A rather extensive program of research utilizing the new instrumentation is now in progress in the laboratory. A general discussion of the scope of the over-all program, along with a review of the preliminary experimental data obtained, has been described in a recent publication.[1] The welding arc is being studied for a wide range of variables, such as electrode type, core and coating composition, arc current and voltage, and circuit characteristics. The new instrumentation is being supplemented by more conventional studies, such as depth of weld penetration, spatter loss, and visual observation of the arc and weld. When the results are assembled and correlated, it should be possible to make better evaluation of the worth of the newer instrumentation.

These results may reveal the measurements of one of these instruments to be more significant than the others, and lead to the adoption of that instrument as a major tool for further work. Or, they may show the need for modification of the present designs or even for further development along entirely new lines. The present paper is therefore in the nature of a progress report describing the instruments developed to date and outlining the research program being conducted to evaluate their merits.

Electrical Approach to the Study of Arc Stability

The over-all stability of the welding arc should be considered from three points of view: spatial; thermal; and electrical. These three stability characteristics are so interrelated that changes in spatial position or thermal equilibrium should be reflected in the electrical characteristics. Study of the electrical stability of the arc can therefore be used as one approach to the measurement of the total arc stability. This approach has been used as the basis of the instrumentation to be described. The electrical quantities that can be studied are the arc voltage, arc current, and power consumed. Typical arc voltage, current, and power characteristics of three representative types of electrodes on straight polarity direct current are shown by the oscillograms in Figure 1. All three were taken using the same welding head and arc welding generator. Figure 1(A) for a lightly coated (*class E-6045*) electrode and Figure 1 (B) for a heavily coated (*class E-6012*) electrode are representative of electrodes which deposit weld metal in the form of molten drops. Frequent short circuits are observed to occur when the metal globules being deposited momentarily short circuit the arc. These short circuits are accompanied by transient variations in the arc voltage, current, and power. The number, duration, and random distribution of these short circuits depend on many variables, such as electrode coating, arc length, arc current, and circuit characteristics. Between the short circuits, the arc voltage, current, and power values are subject to appreciable random fluctuation introduced by many factors such as motion of the arc, nonhomogeneity of the electrode core and coating, changing composition of the gases and vapors

---

Paper 49-131, recommended by the AIEE Instruments and Measurements Committee and approved by the AIEE Technical Program Committee for presentation at the AIEE Summer General Meeting, Swampscott, Mass., June 20–24, 1949. Manuscript submitted December 6, 1948; made available for printing May 10, 1949.

LAURISTON P. WINSOR is Assistant Professor, Department of Electrical Engineering; ROBERT A. WYANT is Associate Professor, Department of Metallurgical Engineering and L. McDONALD SCHETKY is a Research Fellow, all with Rensselaer Polytechnic Institute, Troy, N. Y.

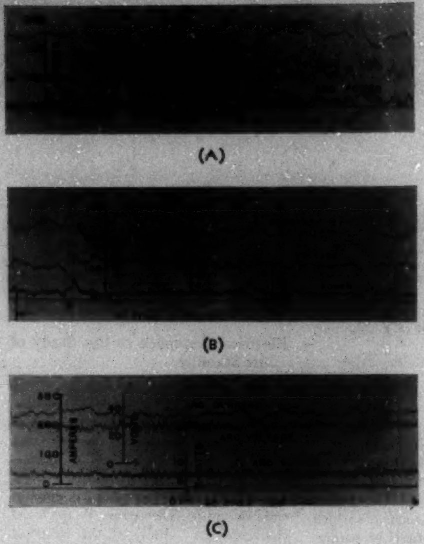

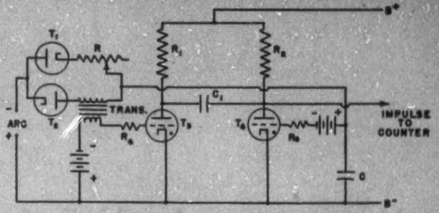

Figure 1 (left). Oscillograms of arc voltage, current, and power for typical welding arcs on straight polarity, direct current

(A) Lightly coated, class *E-6045* electrode
(B) Heavily coated, class *E-6012* electrode
(C) Heavily coated, class *E-6020* electrode

Figure 2 (above). Basic circuit of the short circuit detector

within and about the arc, formation and motion of molten drops on the end of the electrode, and turbulence in the crater. Figure 1 (C) for a *class E-6020* electrode is representative of those electrodes which deposit metal in the form of a spray of fine droplets. Here the short circuits introduced by droplet deposition of metal are entirely absent leaving the voltage and current characteristics with only the irregular fluctuations about the mean. Many oscillograms have been recorded of the characteristics of several electrode classes, over a wide range of arc current and voltage, and with both straight and reverse polarity. The electrical characteristics observed were all found to follow the same general pattern illustrated in Figure 1. The disturbances observed can be divided into two classifications for systematic study: fluctuations in the magnitude of arc voltage and current; and short circuits introduced by the deposition of metal.

Two approaches to the quantitative study of these disturbances were considered. One was a detailed study of the instantaneous variations in arc voltage, current, and power, placing emphasis on such characteristics as recovery from short circuits and the transient variations in the current and burning voltage. Since this approach would lead primarily to an oscillographic investigation, the study time would be limited to the relatively short duration of an oscillogram. The other approach was a statistical study of the variation of these parameters over a relatively long period of time, such as the deposition time of a 14-inch electrode. This seemed preferable for the present research program in which the arc is being studied under practical welding conditions. Owing to the time limitation imposed by the oscillograph, other forms of instrumentation were sought. Careful investigation of techniques to obtain the required information by direct measurements led to the development of a number of new instruments for arc studies. These are instruments to count the number of short circuits in the arc, to measure the proportion of the time the arc is short circuited, and to measure the rms deviation of the arc voltage and current.

The Short Circuit Counter

The rate of occurrence of short circuits in the arc stream is very irregular and usually of too high a frequency to permit counting directly with an electromechanical counter. The duration of the short circuits also is very irregular and often of too short duration to provide sufficient energy to operate a mechanical-type counter. Both of these obstacles are overcome easily by electronic counters because of their high speed and low energy requirements. Electronic counters have now reached a high degree of development due to the widespread requirement for counting pulses from radiation detectors and other pulse-making devices. Many satisfactory electronic counters are commercially available. Their application to the present problem, however, was handicapped because the pulse required to initiate the counter could not be obtained directly from the arc voltage.

The development of the short circuit counter hinged on the design of a satisfactory short circuit detector. Several requirements had to be satisfied. First, the detector should not be actuated by short circuits whose duration are less than a definite preassigned time. This limitation was imposed to eliminate counting extremely high-frequency voltage dips too short to be shown by the magnetic oscillograph. The detector should be actuated once, and only once, by each short circuit to be counted, regardless of its duration, and be reset immediately after removal of the short circuit. This condition eliminated a number of possible detector circuits which would be reset after a fixed time delay. Finally, the detector should not be sensitive to sharp changes in voltage, such as might be introduced by transient variations in burning voltage. This led to the requirement that the voltage actually drop to the short circuit value to be detected.

All of these requirements were met by the detector shown in elementary form in Figure 2. The basic circuit is a parallel inverter consisting of the thyratrons T_3 and T_4, current limiting resistances R_1 and R_2, and the commutating capacitor C. When the arc is burning, tube T_3 is conducting, while the negative arc voltage impressed across the capacitor

C holds the grid of T_4 more negative than the critical grid potential. When a short circuit occurs in the arc, the "arc" voltage drops to a low value, allowing the capacitor C to discharge through the resistance R and rectifier T_1. After the lapse of a short interval of time, determined by the time constant RC, the negative grid potential on tube T_4 is reduced sufficiently to cause the tube to conduct. Since the commutating capacitor C_1 was previously charged to the difference between line potential $B+$ and the relatively small burning potential of tube T_3, the sudden drop in the anode potential of tube T_4 caused by conduction suddenly reduces the anode potential of tube T_3 to a high negative value and extinguishes the tube. The capacitor C_1 then discharges and recharges with opposite polarity through resistance R_1 and thyratron T_4, thereby raising the anode potential of thyratron T_3 exponentially to full line value.

When the arc is re-established following the short circuit, capacitor C charges immediately through rectifier T_2 and the primary of the grid transformer. The transient surge of charging current through the transformer induces a momentary voltage peak across the secondary which fires tube T_3 and simultaneously extinguishes tube T_4. The subsequent reapplication of anode potential to tube T_4 resets the detector and leaves it in readiness to detect the next short circuit. The sharp exponential rise in potential on the anode of tube T_4 provides the triggering pulse that is fed into the counter stage to indicate the passage of the short circuit. An identical triggering pulse from the anode of tube T_3, indicating the time of initiation of the short circuit, was found to be equally satisfactory for registering the short circuit. Details of the short circuit counter are shown in Figure 3. The instrument is composed of four basic circuits or units: the short circuit detector; two counter stages; and a final counter circuit to register the results on an electromechanical counter. The detector stage is the same as described previously except for the addition of cathode biasing to the thyratrons. Separate biasing resistors are necessary because tube T_4 receives part of its biasing potential from the capacitor C. The detector is followed by the first of two identical counter stages. This is a conventional "scale of two" counting circuit, based on the circuit of Wynn-Williams[3] and is similar to those used in conjunction with Geiger counters. It is a parallel inverter circuit, which consists of the thyratrons T_6 and T_7 and the commutating capacitor C_3 and operates on the general principle described previously. Whenever a positive pulse is impressed on the parallel capacitor-resistor circuits C_4R_G and C_5R_G, a positive current pulse passes through both grid resistors and raises both grids to the firing potential. Whichever tube was not conducting previously is fired and the other tube is extinguished. As often as a positive pulse is received from the detector, the conduction is transferred from one tube to the other. The output of the detector circuit is coupled to the input of the inverter by the triode T_5. This is to prevent the possibility of negative pulses from the detector extinguishing the counting tubes to introduce an error in the count. Positive pulses to the grid of T_5 allow plate current to pass through the resistor R_5 to produce a positive voltage pulse which is fed to the counter inverter. Negative pulses have no effect on the plate current because of the high initial grid bias, and are not transmitted.

Every time the anode potential in tube T_7 goes positive, a positive pulse is transmitted to the second counter stage. Hence, for every second pulse from the detector circuit a positive pulse is transmitted to the second counter stage. The output of the second counter stage produces a pulse for every fourth signal from the detector, and so on. If n counting stages are incorporated, the final stage transmits a pulse for every $2n^{th}$ short circuit. As many counting stages should be used as is necessary to reduce the frequency of the pulses coming from the final stage to a number low enough to be handled by the mechanical counter. Two counter stages were found to be sufficient for the present application. The number of short circuits detected is obviously $2n$ times the reading of the mechanical counter.

The final counter circuit, which is based on the Pickering circuit[8] records the number of pulses from the last counter stage on a Cenco high-impedance counter. Thyratron T_{11} is normally prevented from conducting by the cathode bias maintained by the voltage divider R_{16}

Figure 3. Detailed circuit diagram of the complete short circuit counter

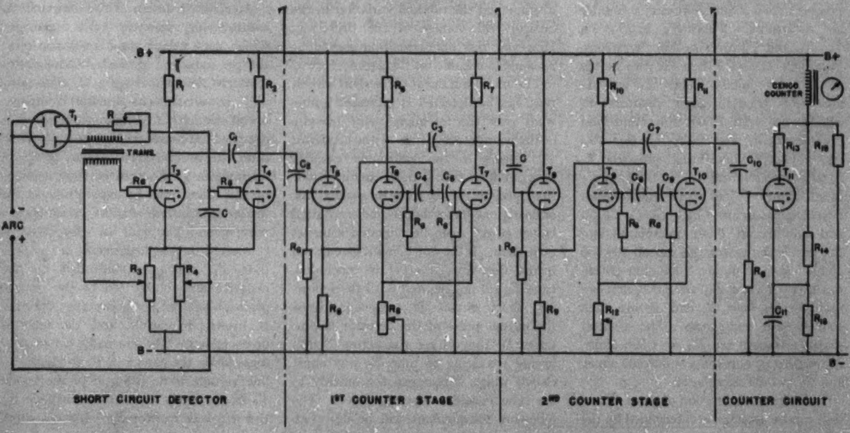

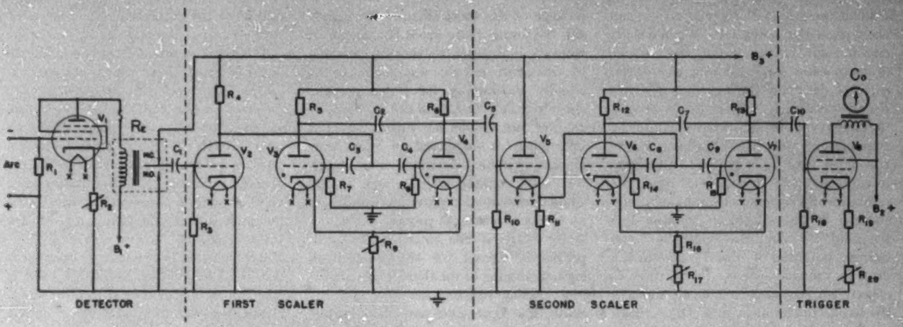

Figure 4. Circuit diagram of the modified short circuit counter

and R_{13}. The positive pulse transmitted from the last counter stage raises the grid of tube T_{11} sufficiently to cause it to conduct and pass current through the Cenco counter, R_{13} and C_{11}. The current surge quickly charges the capacitor to a high value of voltage which simultaneously decreases the tube current and increases the negative value of the voltage on the grid until the discharge through the tube is extinguished. Capacitance C_{11} then discharges through resistance R_{15} until the steady-state bias determined by the ratio between R_{14} and R_{15} is reached, and the counter is reset to record the next impulse. The resistance R_{16} conducts a small polarizing d-c current through the Cenco counter in order to speed its response when an impulse is received.

The circuit components used in the present model of the short circuit counter are as follows: Tubes T_3, T_4, T_6, T_7, T_9, T_{10}, and T_{11} are *type 884* thyratrons. Rectifiers T_1 and T_2 are the two halves of a *117Z6* tube. Tubes T_5 and T_8 are *6P5* triodes. Load resistors R_1 and R_2 are each 7,500 ohms, and load resistors R_6, R_7, R_{10}, and R_{11} are each 10,000 ohms. Commutating capacitor C_1 is 0.025 microfarad. C_3 is 0.05 microfarad, and C_7 is 0.10 microfarad. Coupling capacitors C_2, C_4, C_5, C_6, C_8, C_9, and C_{10}, are all 0.001 microfarad and the grid-leak resistors R_g are all 100,000 ohms. R_3 and R_4 are 3,000-ohm potentiometers, R_8 and R_{12} are 2,000-ohm potentiometers, and R_5 and R_9 are each 100,000-ohm resistances. The counter circuit elements are $R_{13} = 1{,}500$ ohms, $R_{14} = 800{,}000$ ohms, $R_{15} = 500{,}000$ ohms, and $C_{11} = 0.20$ microfarad.

The minimum duration of short circuit that can be detected is determined by the time required for the voltage across the capacitor C to drop from its normal value to a value low enough to allow tube T_4 to conduct. This time delay depends not only on the time constant RC but also on the voltage across C at the initiation of the short circuit. In order to maintain a fixed time delay, R is adjusted before each run to give the required time delay for the average arc voltage to be maintained during the weld. A delay of one millisecond has been adopted for the present. This is obtained by use of a fixed capacitor C of 0.01 microfarad and a resistor R, variable between 50,000 and 100,000 ohms, and calibrated in terms of the average arc voltage. It should be pointed out that the time delay thus determined is constant only to a first approximation because of the random fluctuation of the arc voltage from the average and the random variation in the critical grid voltage of the thyratron. However, this approximation should be reasonably reliable on the average.

The minimum duration of short circuit that can be detected is increased somewhat over the foregoing value because of the commutating time of the capacitor C_1. Owing to the additional cathode bias provided during the switching transient, probably about three time constants, or nearly one-half a millisecond is required before tube T_3 can be reignited after its extinction. If the short circuit is removed before this time interval is concluded, tube T_3 will not be fired until the following short circuit is removed. Since the output pulse of the detector is produced by the voltage rise across T_4 following the firing of tube T_3, any short circuit which is removed too quickly to fire tube T_3 will not be registered. The following short circuit will be detected, however, when tube T_3 is triggered by the removal of that short circuit. This effectively limits the minimum duration of short circuit that is counted to the sum of the time delay introduced by the RC circuit and the commutating time of the detector circuit. An exception would be two or more short circuits intermediate between the two limits in which case alternate short circuits would be detected. The commutating time of the detector also introduces a momentary "dead" period during the interval between the time tube T_3 is fired and the anode potential of tube T_4 is reapplied. Since this interval is shorter than the time delay introduced by the RC circuit to limit the minimum duration of short circuit detected, it does not affect the operation of the circuit. Slightly longer commutating times are allowed for counter stages since requirements for speed of response are reduced in each succeeding stage.

A modified design of the short circuit counter has recently been developed which uses a high-speed magnetic relay for the detector. Details of the circuit used are shown in Figure 4. The relay *RE* is a Stevens-Arnold Company, 6-volt *Model 172* Millisec relay which is designed to operate within one millisecond after it is energized. This speed of response is ideal since the time delay is of the same order of magnitude as the minimum duration of short circuit chosen previously. The coil of the relay is connected in the plate circuit of the pentode V_1, which is controlled by the negative arc voltage fed to the control grid. When the arc is burning, the tube is biased to cut-off and the relay is de-energized. The normally closed contacts allow the capacitor C_1 to charge to line voltage while the grid of the triode V_2 is effectively tied to the cathode by the grid leak resistor R_3. When a short circuit occurs, tube V_1 passes current through the relay which operates to ground the positive plate of the capacitor C_1. This capacitor discharges through R_1 to apply a negative pulse to the grid of V_2 and raise the potential of the plate of tube V_2 suddenly to line value. The sharp pulse from the plate of tube V_2 is fed into the first "scaler," or counter stage, to register the count. When the arc voltage is re-established, the relay is de-energized and the capacitor C_1 is recharged to reset the detector for the next short circuit. The output pulse of the detector is fed into "scaler" circuits which are identical to the two "counter" stages of the original instrument. The final stage which triggers the Cenco counter also was modified in the new design. Experience showed the thyratron circuit used previously to be somewhat critical to adjust and to require occasional readjustment. In the modified form, the Cenco counter is connected in the plate circuit of a *6L6* power amplifier tube V_3 which is normally biased sufficiently to prevent operation of the counter. When an output pulse is received from the final scaler through the coupling capacitor C_{10}, the potential of the control grid of the tube is momentarily raised to allow a surge of current to pass through the counter coil to register the count. The instrument is provided with a voltage regulated power supply to eliminate any instability that might be caused by plate supply disturbances. The complete assembly is housed in a metal chassis mounted on a steel rack which accommodates all the instruments used. The circuit elements used in the modified design are as follows: tube V_1 is a *6AG7* pentode, V_2 is a *6P5* triode, and V_3 is a *6L6* power amplifier; resistances R_1, R_3, R_4, and R_{14} are each 100,000 ohms, and R_2 and R_{20} are variable resistances of 3,000 ohms and 5,000 ohms maximum respectively; capacitance C_1 is 0.005 microfarad and C_{10} is 0.5 microfarad.

Both designs of the Short Circuit Counter have been used in the laboratory. The original design was used over a period of many months and furnished much useful data. The modified design proved to be less critical to adjust, however, and was adopted for general use. The latter instrument is unfortunately limited to studies of short circuits of a fixed minimum duration whose time is determined by the time delay of the relay used. If control over the duration of the short circuits counted should prove desirable, an electronic detector such as used in the original design of Figure 3 would be more flexible.

The Short Circuit Duration Indicator

A mere count of the number of short circuits in the arc includes no measure of their duration. An instrument to measure the average duration of the short circuits, or the proportion of the time the arc is short circuited, is therefore desirable. This need led to the invention of the Arcronograph by Ronay.[4,5] The original purpose for which the Arcronograph was developed was to measure the proportion of the total time that the arc burns. In the usual application, the instrument is used to study the rhythm of the occurrence of the short circuits. The practical design of the Arcronograph does not allow an absolute calibration in terms of the ratio of arcing time to the total time, however, so that the interpretation of the results depends to a large extent on the experience of the operator. To overcome this difficulty, the Short Circuit Duration Indicator shown in Figure 5 was developed for the present investigation. The per cent short circuit time was found to be a more convenient variable to use than the per cent arcing time because of the relatively small short circuit time exhibited by many modern electrodes.

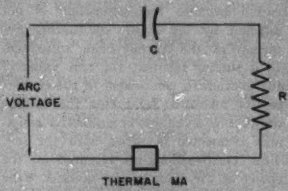

Figure 6. Elementary circuit to measure the standard deviation of a fluctuating direct voltage or current

The circuit is essentially a simple d-c amplifier consisting of the tube T_1 and load resistance R. The arc is connected between the grid and cathode so as to make the grid negative. When the arc is burning, the grid is biased to cut-off and the tube is nonconducting. The occurrence of a short circuit decreases the negative grid potential sufficiently to allow full plate current to flow. This is indicated by full scale deflection on the D'Arsonval milliammeter in the plate circuit. When the arc is short circuited, full scale current will pass through the milliammeter, while no current will pass when the arc is burning. If the frequency of the short circuits is high enough in relation to the inertia of the meter, the milliammeter will indicate the average value of the current. The ratio of the milliammeter reading to the full scale reading is obviously the ratio of the short circuit time to the entire time. If the milliammeter is calibrated in per cent, the instrument can be made direct reading.

Satisfactory operation of the circuit requires that the milliammeter current during a short circuit be absolutely independent of variations in the short circuit voltage caused by the short circuiting metal, and of any change in the plate supply voltage. Since modern tubes cannot be made to saturate, this requirement is insured by the addition of a clipping or by-pass circuit, consisting of the diode T_2 and the polarizing battery E_{bias} connected around the load resistance and milliammeter. As long as the current through the load is less than the predetermined value, the voltage drop across the load is less than the polarizing voltage on the diode, and the diode is nonconducting. When the load current reaches the specified value, the voltage drop exceeds the polarizing potential just enough to make the plate of the

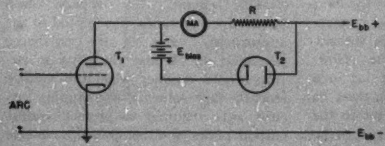

Figure 5 (left). Circuit diagram of short circuit duration indicator

Figure 7 (right). Circuit diagram of the first design of the rms voltage deviation meter

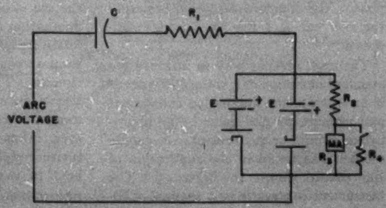

diode positive. Since the clipping circuit has negligible resistance, all current in excess of the specified value is shunted around the load, and the milliammeter current is limited to its full scale value. The values of E_{bias} and R are so chosen that the full scale current is one milliampere. The circuit elements used are as follows: tube T_1 is a *6C5* triode while T_2 is a *6H6* diode. The polarizing potential is provided by a 45-volt "B" battery, so that the resistance R is about 45,000 ohms. The final adjustment of R is made experimentally.

The present model is calibrated to give full scale deflection for 100 per cent short circuit time. The substitution of a multi-range milliammeter with more sensitive scales for the single-range milliammeter now in use would provide an instrument adjustable in range. This would make possible full scale deflection of the instrument with less than 100 per cent short circuit time. Such an increase in sensitivity would be useful for the study of electrodes which have only a relatively small short circuit time. If the full scale reading of the instrument is reduced below 100 per cent, however, care should be exercised to protect the milliammeter from unexpected long period short circuits, such as would occur if the electrode froze to the work. The indicating milliammeter used in the present instrument could easily be replaced by a recording milliammeter to provide a permanent record.

The Rms Voltage Deviation Meter

Turning from a study of the short circuits in the arc stream, valuable information on the stability of the arc can be obtained from a study of the variations in the burning voltage. One of the best mathematical methods of expressing statistical variation about the mean of a number of values of a quantity is the standard deviation. By definition, the standard deviation is the square root of the mean of the squares of the differences between the individual values and the mean value. In the case of a direct voltage or current with a fluctuating component, the standard deviation is simply the rms value of the fluctuating component.

The most obvious way to measure the standard deviation of a voltage or current is to separate the fluctuating component and measure its rms value by an appropriate circuit or instrument. A simple method was found in the application of the circuit shown in Figure 6. The instrument is essentially a thermal milliammeter connected in series with the resistance R and capacitance C across the arc voltage. The capacitor C charges to the average value of the arc voltage; therefore, the algebraic difference between the instantaneous and average values of the arc voltage is impressed across the resistance R. Since the current through the resistance is proportional to the impressed voltage, the current through the milliammeter is directly proportional to the fluctuating component of the voltage. An rms milliammeter can therefore be calibrated directly in terms of the rms value of the fluctuating component of the voltage. A thermal milliammeter is best suited for this application because the calibration is not affected by the highly fluctuating frequency of the current being measured. In a similar manner, the rms value of the fluctuating component of the current can be measured by taking the voltage drop across a suitable noninductive resistance connected in series with the arc. Two considerations are required for the choice of the value of resistance R: the sensitivity of the milliammeter and the range of voltage to be measured. The necessary resistance is obviously the ratio of the expected rms voltage to the full scale meter current. The value of capacitance is determined in turn from the resistance R and the circuit time constant, where the choice of time constant is governed by the length of the time base over which the voltage is to be averaged. Owing to the relative size of the meter resistance, the latter must be included in the total resistance R in the foregoing calculations.

The application of this circuit introduced one practical design problem. When the arc is suddenly short circuited, the voltage drops from the burning voltage of say 20 to 30 volts to less than 5 volts, a drop of 15 to 25 volts or more. Since the capacitor C remains charged to the average value, this difference in voltage is impressed across the resistance R and causes a proportional current through the milliammeter. Owing to the relatively smaller voltage fluctuation during the greater part of the time when the arc is burning, the rms value of the fluctuation over a long period of time is relatively small compared with the momentary peaks which accompany the short circuits. This would result in momentary peak currents through the thermocouple many times the rms value. However, in order to reduce time lag in a thermocouple, the heat storage must be kept to a minimum, and therefore the ratio of maximum allowable current to the rms current is limited accordingly. The choice of a thermocouple meter with sufficient sensitivity to give a reasonable deflection for the range of rms voltage encountered would therefore be severely overloaded by the short circuit peaks and would be burned out. A similar, although more serious, voltage peak will be impressed across the resistance if the arc is suddenly open circuited, and will likewise burn out the meter. The difficulty was overcome by limiting the thermocouple current to a safe value by the addition of a "clipping" circuit similar to that used in the Short Circuit Duration Indicator described previously.

Details of the first Rms Voltage Deviation Meter are shown in Figure 7. The milliammeter was an American Thermo-Electric Company *type 17A* vacuum thermocouple with a 200-microampere D'Arsonval instrument in the output circuit. A heater current of about 4.5 milliamperes was sufficient to cause full scale deflection. A total series resistance R of about 1,000 ohms provided the proper sensitivity for the range of voltage fluctuation usually encountered. The choice of time constant was somewhat flexible. The time constant should be large enough to average the voltage over a period long in relation to the period of fluctuation, yet short enough to allow the capacitor voltage to follow the long time drifts in the average arc voltage. A time constant of the order of 0.1 second was selected for trial and a number of test runs were made under identical test conditions with a number of values of time constant both above and below this value. No appreciable difference was observed in the value of the rms voltage measured over the range of time constant studied. A time constant of about 0.1 second was therefore adopted in the final design. This corresponded to a capacitance of the order of 100 microfarads. This had to be a paper capacitor, because the leakage current through an electrolytic capacitor would have been of the same order of magnitude as the current being measured.

A portion of the circuit resistance, consisting of R_2 of 120 ohms and the heater resistance R_4 of 60 ohms was utilized to determine the current limit set by the clipping circuit. The voltage drop across this resistance was limited to the approximate value of the polarizing potentials E, because the clipping circuits would conduct when the voltage reached this value. Two clipping circuits were required to protect against current peaks of either polarity. Single disk selenium rectifiers were used, with number 6 dry cells for the polarizing potentials to keep the resistance of the clipping circuit to a minimum. The voltage drop in the clipping circuit must be kept low compared with the polarizing potential to produce sharp clipping. The resistance R_1 constituted the remainder of the resistance R. Sensitivity control was obtained by shunting the resistance R_4 across the milliammeter.

The circuit described was used successfully in the laboratory for some time and found to be fundamentally satisfactory. A number of drawbacks were inherent in the design, however, and led to early work on a modified design. Most annoying of the disadvantages was the large value of capacitance required which resulted in an instrument both heavy and bulky. More serious technically, however, was the effective change in time constant introduced by shunting part of the circuit resistance during short circuits. This effect was held to minimum by keeping the ratio of R' to R_1 as small as possible, but could not be eliminated. In spite of these limitations, however, the basic simplicity of the circuit would probably have kept it in use indefinitely had it not been for faulty operation of the clipping circuit which occasionally allowed a thermocouple to be burned out. The use of a cathode-ray oscillograph revealed that although the clipping circuits worked satisfactorily on direct current and 60-cycle alternating current, sudden pulses were passed. A sufficient number of these would eventually burn out the thermocouple. The obvious solution to the problem would be the substitution of vacuum rectifiers, but the higher tube drop would require the use of a higher polarizing potential to produce sharp clipping action. This could be accomplished only by the use of a higher resistance R_2 and a correspondingly smaller resistance R_1. Because of the effect of clipping on the time constant described previously appreciable reduction in the value of R_1' would be undesirable.

The electronic modification of the circuit shown in Figure 8 proved the answer to all the problems encountered before. The basic element of the electronic circuit is still a resistance connected in series with a capacitance across the arc voltage. The voltage drop across a suitably tapped portion of the resistance is measured by a simple bridge-type vacuum tube voltmeter circuit consisting of the two triodes T_1 and T_2 and the two fixed resistances R_1. The input is to the grid of tube T_1 and the output is measured by a thermal milliammeter in series with the resistances R_4 and R_5 between the plates of the two tubes. Since the output current is proportional to the input voltage, the reading of the output meter is proportional to the rms value of the voltage deviation and is calibrated accordingly. A clipping circuit like that described previously is connected across the milliammeter and a suitable portion of resistance R_4. However, sufficient output voltage is available to allow a higher polarizing potential than before. This in turn permits the substitution of vacuum tubes for the selenium rectifiers without seriously decreasing the sharpness of clipping.

The substitution of the vacuum tube circuit for the milliammeter used previously to measure the voltage across R permits the value of R to increase to a value limited only by the maximum allowable grid resistance. A value of 200,000 ohms was satisfactory for the *type 45* tubes used in the design adopted. This permitted the use of relatively small capacitances to obtain the required time constant. Three values of capacitance C_1 of 0.25 microfarad, C_2 of 0.50 microfarad, and C_3 of 1.0 microfarad provide a time constant adjustment to values of 0.5 second, 1.0 second, and 2.0 seconds, respectively. Since the clipping circuit has been removed from R, it no longer has any effect on the circuit time constant. Tube T_2 receives its bias from the adjustable potentiometer R_3. This allows a balance adjustment to be made to compensate for inequalities between the two tubes. A d-c milliammeter (not shown in the diagram) can be connected in place of the thermal meter to provide a more sensitive balance indicator than the thermal meter. The thermocouple is an American Thermo-Electric Company, *type 17A*, vacuum thermocouple, the same as used in the previous instrument. A 200-microampere d-c indicating instrument was first used to measure the thermocouple output. This has since been replaced with a photoelectric potentiometer and recording milliammeter which furnishes a permanent record of the rms voltage deviation. The rectifiers T_3 and T_4 are the two halves of a *117-Z-6* duodiode and the polarizing potentials E are each 7.5-volt batteries. Other circuit constants are: $R_1 = 500$ to 1,000 ohms (variable), $R_3 = 50$ ohms, $R_4 = 2{,}000$ ohms, and $R_5 = 1{,}000$ ohms.

The calibration and clipping characteristics of the circuit with the constants just enumerated are shown in Figure 9

Figure 8. Circuit diagram of the electronic design of the rms voltage deviation meter

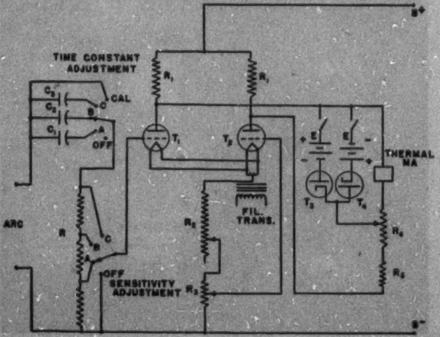

Figure 9. Calibration and clipping characteristics of the rms voltage deviation meter

(1) Adjusted for minimum clipping
(2) Adjusted for intermediate clipping
(3) Adjusted for maximum clipping

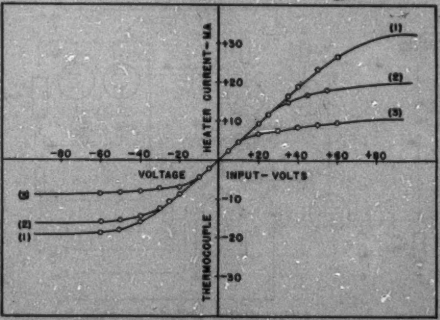

for three levels of clipping voltage and maximum circuit sensitivity (sensitivity control set on point C). In position 1, the adjustment is set for minimum clipping. The current calibration is essentially linear and independent of polarity over a wide range of voltage fluctuation. Some clipping is introduced in position 2 and still greater clipping in position 3. An intermediate setting between positions 2 and 3 is used generally since it clips at a sufficiently low level to protect the thermocouple, but at a high enough value to provide linear response over the normal range of voltage deviation. Some objection may be raised that the action of the clipping circuit eliminates the greater part of the voltage deviation introduced by the presence of short circuits from the measurement of the rms voltage deviation. This, however, appears to be an advantage as well as a disadvantage since it puts chief emphasis on the voltage deviation when the arc is burning. The inclusion of the short circuits in the measurement of rms voltage deviation would very largely obliterate the deviation introduced by factors other than short circuits. The effects of short circuits are properly studied by the other forms of instrumentation described previously. Precaution should be taken, however, to use the same clipping level for all comparable measurements since a change in the clipping level will modify the value of voltage deviation measured. This requirement not only fixes the position of potentiometer R_4, but effectively limits the setting of the sensitivity adjustment to one position; otherwise a change in the gain of the instrument with a fixed output clipping level would modify the clipping level relative to the input voltage. In practice, therefore, the sensitivity adjustment shown is set for maximum and the sensitivity is controlled by a shunt around the thermocouple.

The Rms Current Deviation Meter

The rms value of the current deviation is directly proportional to the rms voltage deviation across a noninductive resistance connected in series with the arc. When a pure resistance ballast is used to limit the arc current, the voltage drop across the resistance is of the same order of magnitude as the arc voltage. An rms deviation meter of identical design to that used for voltage measurements can therefore be used to measure that rms voltage deviation across this resistance. The rms value of the current deviation is computed by dividing the rms voltage deviation by the resistance. This method has proved quite satisfactory in the laboratory where considerable research has been done using a battery source of current with a pure resistance ballast. The substitution of a welding machine for the battery circuit would however prohibit the application of this method. A modified form of the rms deviation meter was therefore designed to measure the voltage deviation across a standard 0.01-ohm oscillograph shunt. This instrument has been designated as the Rms Current Deviation Meter.

Details of the Rms Current Deviation Meter are shown in Figure 10. The circuit used was suggested to the authors by Doctor Warren C. Stoker of the Department of Electrical Engineering of Rensselaer Polytechnic Institute. It is essentially that of the Rms Voltage Deviation Meter with an added amplifier stage to increase the sensitivity. The input voltage from the "shunt" is connected across the series circuit consisting of C_1 and R_1. The deviation voltage, which appears across R_1, is fed directly into the input terminals of the first stage of a balanced d-c amplifier. This amplifier stage is composed of the pentodes T_1 and T_2 and the load resistances R_2, R_3, and R_4. The output from this stage is taken between the plates of the two tubes and fed into the second or output stage cascaded above it. The second stage is almost identical to the circuit of the original Rms Voltage Deviation Meter except that the input is fed to both grids in push-pull. This stage consists of the tubes T_3 and T_4 and the load resistances R_6, R_7, and R_8. The resistance R_5 provides the cathode biasing. The output is taken from the plates of the tubes and measured by a properly protected thermocouple as in the previous instrument. The time constant of the Rms Current Deviation Meter has been retained at 0.1 second making C_1 equal to 0.2 microfarad and R_1 equal to 500,000 ohms. Tubes T_1 and T_2 are *6SJ7* pentodes while tubes T_3 and T_4 are *type 45* triodes. The resistances R_3 and R_4

Figure 10 (below). Circuit diagram of the rms current deviation meter

Figure 11 (right). Instrument assembly used for the study of the d-c welding arc

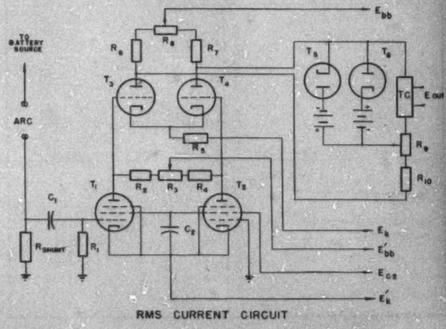

are each 25,000 ohms and R_6 and R_7 are each 2,500 ohms. The potentiometers R_3 of 100,000 ohms and R_5 of 1,000 ohms are included to provide balance adjustments to compensate for any inequalities in the tubes. An American Thermo-Electric Company, *type 19*, thermocouple with a maximum safe current carrying capacity of 10 milliamperes is used to increase the sensitivity of the instrument. The output can be fed either to an indicating microammeter or to a photoelectric potentiometer and recording milliammeter as in the Rms Voltage Deviation Meter. The latter method is being used currently. The design constants of the clipping circuit are the same as described for the previous circuit. The plate and screen grid potentials are obtained from a voltage divider connected across the output of a voltage regulated power supply.

Applications and Conclusions

The instruments described have evolved over a period of nearly two years of development, trial, and modification. Each is built on an independent steel chassis and provided with its own power supply so that it is readily portable. In the laboratory, the units are mounted one over the other on a steel rack as shown in Figure 11. Two Rms Voltage Deviation Meters are mounted at the top, followed by the Short Circuit Counter, the Rms Current Deviation Meter, and the Short Circuit Duration Indicator, in that order. The photoelectric potentiometers for the Rms Deviation Meters are located out of sight on the bottom shelf of the rack. The recording milliammeters, together with the recording meters for the average arc voltage and current, are shown at the right. The second Rms Voltage Deviation Meter was used originally to measure the rms current deviation before the present Rms Current Deviation Meter was built. It has been retained for the purpose of studying the effect on the rms voltage deviation of changes in such variables as the circuit time constant and the clipping level.

This instrumentation is now being used in the laboratory as an aid to the study of d-c welding arcs over a wide range of arc current and voltage, and for a variety of conditions of electrode coatings. Preliminary results from this investigation have been published previously.[1,6] They indicate that there are pronounced trends in the rms voltage and current deviations and the number of short circuits as the arc voltage and current are varied. These trends have been found to be different for different types of electrodes and even for different brands of electrodes of the same class. A marked contrast has been observed between the consistency of results with uniformly dried electrodes and electrodes taken directly from the package. These results indicate that the instrumentation is capable of distinguishing between different types of electrodes and different test conditions. Final evaluation of these instruments for arc studies must await the outcome of more extensive tests now being conducted in the laboratory. The results of this investigation may show one or more of these instruments to be superior to the others and lead to their adoption for future work. On the other hand, experience may suggest that some modifications in the present instrumentation would be desirable, or that further instrumentation should be sought.

References

1. An Investigation of Methods for Evaluating Welding-Arc Stability and Their Application, **Robert A. Wyant, Lauriston P. Winsor, L. McDonald Schetky.** *Welding Journal Research Supplement* (New York, N. Y.), volume 13, October 1948, pages 502-s to 514-s.

2. A Thyratron "Scale of Two" Automatic Counter, **C. E. Wynn-Williams.** *Proceedings,* Royal Society (London, England), volume 136, series A, 1932, pages 312–24.

3. A Circuit for the Rapid Extinction of the Arc in a Thyratron, **W. H. Pickering.** *Review of Scientific Instruments* (New York, N. Y.), volume 9, June 1938, pages 180–82.

4. Evolution of the Arcronograph, **B. Ronay,** *Journal American Society of Naval Engineers* (Washington, D. C.), volume 46, 1934, pages 285–98.

5. Arcronograph, **B. Ronay.** United States Patent 2,106, 190, Jan. 25, 1938.

6. Investigation and Development of Instrumentation for Evaluation of Welding Arc Stability, **L. P. Winsor, L. McD. Schetky, R. A. Wyant.** Report Number 1 on Research Contract NObs-2302 with United States Navy. Rensselaer Polytechnic Institute (Troy, N. Y.), December 31, 1947.

No Discussion

Transformer Manholes and Vaults: Design and Ventilation

L. F. PORTER
ASSOCIATE AIEE

DEMAND for electric power within urban areas, increasing at a rate greater than population growth, poses a problem of major magnitude to the public utilities whose obligation it is to supply that power with a maximum degree of safety, reliability, and economy to the public. This power demand falls within two classifications: domestic and small commercial or industrial users, whose individual demands do not exceed 100–200 kva each and may therefore be considered to constitute a generally distributed load without substantial concentrations; and the larger commercial and industrial users who individually require substantial blocks of power and sometimes present major problems of supply to the power company. The load growth in the latter classification stems from three sources:

1. New buildings whose design includes adequate space provision for the anticipated power requirements.
2. Older buildings whose demand is growing substantially beyond that originally contemplated because of the introduction of air conditioning, considerably increased lighting intensity, or change in the use of the building such as conversion from a warehouse to a loft building with increased lighting and miscellaneous power requirements.
3. Buildings that have been supplied by private plants which the owners have decided to discontinue in favor of purchased power.

Single buildings in the last classification have presented the problem of supplying new blocks of power in the order of 5,000 kva from the public utility's secondary network system and have required the construction of multibank transformer installations at two or more points.

This paper is concerned with the basic elements in the design and ventilation of transformer manholes and transformer vaults required to supply secondary network load. It is confined to network systems for simplicity, but structures for underground radial systems would be fundamentally the same with some modifications for different equipment.

General

Secondary network systems serving a distributed load without substantial concentrations of power generally are supplied from individual transformer installations strategically located for maximum economy in distribution. Such single-transformer installations are commonly located in the roadway where they may be subject to flooding; hence submersible equipment is used. Congestion of structures under city streets has led to the design of highly specialized top-connected transformer-network protector units which may be installed in minimum sized manholes. These manhole units are connected to the network secondary mains and usually have no customer service connection.

On the other hand, where substantial concentrations of load occur, say in the order of 200 kva or more, transformer installations adjacent to the customer's point of service connection are indicated. These transformers are generally located under the sidewalk or inside the building adjacent to the property line and either at the first basement level or at grade. Nonsubmersible vault-type equipment may be used as there usually is little danger of flooding through sidewalk gratings. These vault installations provide for a customer's service connection and have a secondary tie to the street network. Multiple installations of transformer manholes in the roadway are not practicable because of subsurface congestion by other structures and the difficulty of interconnecting secondary cables.

The number of banks required will be determined by the customer's maximum demand, the size of transformers used, the design of the secondary network system and the permissible loading of the transformers under emergency conditions.

Factors Affecting Design

The design for a specific installation is affected, and sometimes is governed, by conditions peculiar to the particular project such as are indicated below.

Space Available. This, particularly for multiple bank installations to be installed for existing buildings, often presents a problem of major difficulty. It frequently may tax the ingenuity of the designer to fit the necessary equipment into the space which can be obtained within reasonable distance of the customer's switchboard, and, at the same time, to obtain the area of grating or louvered panels essential for reliable cooling by natural ventilation. Since space is not generally available at grade for network transformer installations, only subgrade structures are contemplated here.

Type of Equipment Available. Dry-type transformers, for instance, with class *B* insulation may be considered ideal from the safety angle but require more space than liquid filled units, operate at a higher noise level which may be objectionable for certain installations, must be protected from rain unless submersible designs are used, and are not presently available at primary voltages above 15 kv.

City Codes and Regulations. These may impose restrictions as to location and

---

Paper 49-133, recommended by the AIEE Insulated Conductors Committee and approved by the AIEE Technical Program Committee for presentation at the AIEE Summer General Meeting, Swampscott, Mass., June 20–24, 1949. Manuscript submitted November 15, 1948; made available for printing April 26, 1949.

L. F. PORTER is an Assistant Engineer with the Consolidated Edison Company of New York, Incorporated, New York, N. Y.

dimensions of gratings which are required for ventilation and access, and thus directly affect the design and location of structures under the roadway or under the sidewalk.

Climate. Utilities, operating in areas with summer temperatures averaging above 30 degrees centigrade over a 24-hour period and having peak loads in summer, will require correspondingly larger ventilation gratings for transformer installations.

Nature of Load. A load cycle characterized by a peak demand of substantially over eight hours' duration—the maximum usually encountered on a network system—may require that the transformers be furnished with more ventilation than would be supplied otherwise.

Soil Conditions. Solid rock, or poor soil which would necessitate pile foundations, may make it advisable to seek space within the customer's building.

Design

A description of the basic features desired in the design of transformer manholes and vaults is offered as a means for measuring the adequacy of designs contemplated for specific instances. Adequately designed transformer manholes and vaults will provide:

1. Ventilation adequate for optimum utilization of the transformers and network protectors.

2. Direct and immediate access for maintenance crews 24 hours a day, preferably through street or sidewalk gratings.

3. Arrangement of transformers and associated equipment to provide approximately equal division of load among the transformers where two or more banks are paralleled on the same service bus.

4. Isolation of equipment to the extent of confining any fire or explosion, which may occur, to the vault in which the trouble originates so that the balance of the installation will operate unimpaired and the service will not be interrupted.

5. Isolation of service cables from transformer vaults and isolation of the cables associated with one transformer bank from other transformers.

6. Minimum size manhole or vault compatible with installation and with maintenance which includes: rolling out the network protector switch for maintenance and repair, repair of transformer terminals, sampling transformer fluid, removing debris which accumulates between the transformer and compartment walls, and replacing cables in case of failure. It is obvious that the design of equipment used is a major factor in determining space required; for instance, in the case of dry-type transformers, a minimum 12-inch separation between compartment walls and transformer is required to assure adequate air circulation, and, also, it is apparent from the construction of this type of equipment that space must be allowed to permit removing the transformer housing panels for cleaning purposes.

7. Adequate drainage, which is particularly important where nonsubmersible equipment is used, to avoid damage to equipment and possible loss of service.

Ventilation

Transformers may be loaded continuously to their full nominal rating only when the cooling air at no time exceeds 40 degrees centigrade and the average temperature of the cooling air during any 24-hour period does not exceed 30 degrees centigrade. Most of the heat released in the manhole or vault must be removed by ventilation, as only a minor part of the heat is dissipated through the walls. Heat loss through walls may be quite negligible where the transformers, in a multiple-bank installation, are on both sides of partition walls, and the vaults are located adjacent to a boiler room or steam mains.

Natural ventilation is essential for a maximum degree of dependability, for there are no thermostats, switches, wiring, motors or valves to get out of order and there is no failure of this type of equipment during peak load with consequent high transformer temperatures. Gratings in the sidewalk or roadway, or louvered openings in an outside building wall, afford the most reliable ventilation for subsurface vaults. It is essential that the transformers be close to these openings, both horizontally and vertically, for best results.

Ventilation ducts with horizontal offsets may be generally ineffective. Where vertical vent shafts are used for deeper vaults, separate inlet and outlet openings, properly located, may improve ventilation. Larger net vent opening may be required to offset the shaft resistance to air flow.

The effectiveness of the ventilation for a given vault does not lend itself readily to accurate determination because of the interrelation between vault dimensions, grating location, and the position of the transformer. Exposure to the sun also is believed to have an appreciable effect. Obviously, a full roof grating would permit a maximum transformer loading, but this is not generally obtainable in the sidewalk because of restrictions such as limited grating widths and prohibition of gratings in front of doors or under windows established by the city authorities, and customers' objections.

A minimum acceptable ventilation area must be established to avoid limiting unduly the loadability of the transformer installation.

The National Electrical Code minimum requirement of two square feet net vent area per 100 kva installed transformer capacity appears to provide adequate ventilation in most instances for cyclic loading where the 24-hour average ambient temperature does not exceed 30 degrees centigrade. On this basis, 500- and 1,000-kva installations (with total transformer and network protector losses of approximately 7 kw and 12.5 kw respectively at 100 per cent load) would be provided 10 square feet and 20 square feet net vent area respectively. Tests indicate that vaults or manholes, designed compactly and with transformers near or under the gratings and provided with 10 square feet or 20 square feet net vent openings, have heating constants, respectively, of approximately 4.0 and 2.5 degrees centigrade rise of vault air, above outside ambient temperature, per kilowatt loss. This "vault heating constant" is of direct value in computing the permissible loading of a transformer installation as recommended in ASA Standard C57.32.[1]

Vaults with heating constants of 4.0 and 2.5, equipped with 500- and 1,000-kva units respectively, will permit normal loading on standard network transformers in the order of 100 per cent of rating when operating on a typical industrial power cycle with a load factor of 60 per cent and an 8-hour peak load, and an average 24-hour ambient air temperature of 26 degrees centigrade. Since a network transformer cannot normally carry full load without being severely overloaded when adjacent banks are out of service, the critical condition for which the permissible loading of the transformer must be computed is the contingency of one or two adjacent banks out of service, depending upon the basis upon which the system is designed to operate. The frequency with which this emergency operation is expected to occur will guide the utility engineer in determining the maximum permissible copper hot-spot temperature, with its attendant sacrifice of life of the equipment, which should be tolerated.

Where the 24-hour average ambient temperature is above 30 degrees centigrade, auxiliary means of heat removal, such as a blower or water cooling, may be required. In every case, the use of the largest grating permissible is essential for maximum dependability of operation.

Ventilation should be provided for all subsurface vaults which do not contain transformers or network protectors and where moisture may accumulate, to check corrosion. Experience has shown that, where such subsidewalk vaults have the sidewalk access opening covered with checker plate instead of grating, steel and copper within the compartment have suffered severe corrosion.

Ventilation Ratio

Electrical failure within a liquid-filled transformer sometimes generates sufficient pressure to rupture the tank or blow off the cover with considerable force. If the transformer fluid is of the noninflammable type, this initial or "primary" explosion may be followed by nothing more than the generation of a highly noxious gas and black smoke in great volume. However, in the case of a primary explosion rupturing the tank of an oil-filled transformer, an oil fire may follow or, in some instances, a much more violent "secondary" explosion may occur. This secondary explosion results from the entire vault having been filled with an explosive gas generated by the action of an electric arc on the transformer oil.

It also may be noted at this point that a similar explosion sometimes follows a fault on cables in a poorly ventilated vault which has been filled with an explosive mixture generated by the distillation of insulation. Provision of limiter or fuse protection for cables will greatly reduce, but cannot entirely eliminate this hazard.

Although a secondary explosion following the failure of an oil-filled transformer is uncommon and although the similar "space" explosion following a cable failure is also unusual, either explosion may be highly destructive if the vault in which it occurs is not built sufficiently strong to protect from damage any equipment or personnel which may be near the wall of the vault when the explosion occurs. It is important, therefore, that walls be built sufficiently strong to contain such an explosion.

The amount of gas which can accumulate in a vault will be kept at a minimum by using the smallest size vault practicable, and by providing a maximum of ventilation to reduce the rate of gas accumulation. The smaller this ratio of vault volume to net vent area, the less will be the pressure developed within the vault should an explosion occur and hence the lighter will be the construction necessary to withstand the explosive force.

Data concerning the maximum pressures produced by the explosion of transformer-oil vapor or insulation-produced vapor mixtures are not available. However, data obtained from investigations of dust explosions in vented enclosures, when studied and correlated with data concerning the gaseous products of electric-arc-decomposed transformer oil, offer a rational basis for approximating the probable maximum forces that might result from an explosion within a transformer vault. Such a study has been made and is described in Appendix I. Briefly, these data indicate that the violence of an explosion of the gaseous products of electric-arc-decomposed transformer oil may be in the order of four times as great as that of alkali starch dust, which will produce one of the most violent dust explosions. Curve *A*, Figure 1, obtained from data published by Brown and Hansen of the Bureau of Chemistry and Soils,[10] shows how the pressure developed by alkali-dust explosion in a vented space will vary with the volume of the space per square foot of vent area. Curve *B*, Figure 1, showing the estimated maximum pressure which may be developed by a secondary explosion in a transformer vault, is obtained from Curve *A* by multiplying each ordinate by four. Curve *B* is therefore hypothetical, but there is strong evidence that it is of the right order of magnitude. It is offered tentatively as a basis of design in the absence of more accurate information.

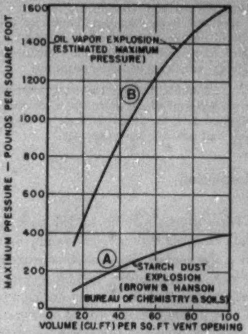

Figure 1. Approximate explosion pressures developed in vented enclosures

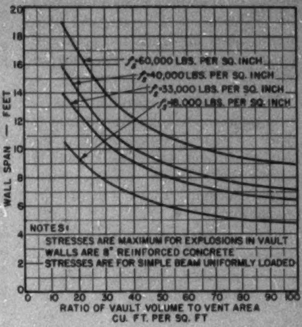

Figure 2. Stresses developed in vault walls by explosion of oil vapor

This curve is applicable where ventilation is so distributed that each unit of volume is afforded its share of vent opening. Thus, an explosion in a long narrow vault, with vent opening only at one end, might develop a substantially higher pressure than is indicated by the curve.

Figure 2 shows curves of constant stress in an 8-inch reinforced concrete wall, resulting from the explosion of an oil-vapor mixture within the vault, for various wall spans and volume–vent or ventilation ratios.

Construction

Transformer manholes and transformer vaults, to be built in unexcavated subsurface space, are best constructed of reinforced concrete for strength and water-tightness. Reinforced concrete is required for strength where explosion-proof vaults are to be built.

Vaults housing oil-filled transformers should be sufficiently strong to withstand an explosion, to the extent of protecting from damage or injury any property or persons that might be occupying space adjacent to the vault walls should an explosion occur within the vault. Explosion-proof construction also should be provided for all vaults containing cable, particularly where no short-circuit protection is provided and where ventilation is poor, for destructive explosions sometimes follow the distillation of cable insulation by short-circuit currents.

Askarel transformers should be housed in separate compartments and so ventilated that, should a failure rupture the transformer tank, the highly noxious fumes which may be generated in great volume, will not seep into the customers premises or deny access to adjacent vaults by operating personnel. Construction should be sufficiently sturdy to hold within the compartment any part of the transformer which may be thrown off by force when the tank is ruptured.

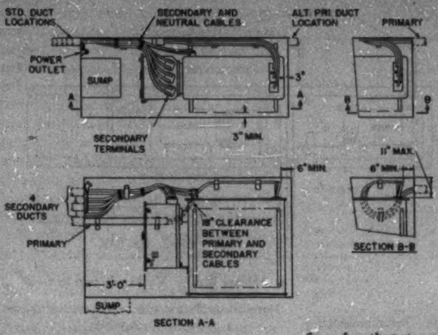
STD. DUCT LOCATIONS
SECONDARY AND NEUTRAL CABLES
ALT. PRI. DUCT LOCATION
PRIMARY
POWER OUTLET
SUMP
3"
A
A
B
B
SECONDARY TERMINALS
3" MIN.
11" MAX.
6" MIN.
6" MIN.
4 SECONDARY DUCTS
PRIMARY
18" CLEARANCE BETWEEN PRIMARY AND SECONDARY CABLES
3'-0"
SUMP
SECTION A-A
SECTION B-B

Figure 3. Installation of 500-kva submersible network unit in manhole

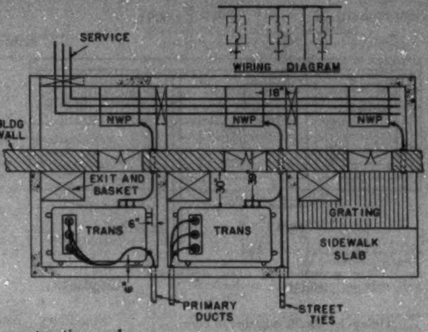
SERVICE
WIRING DIAGRAM
18"
BLDG WALL
NWP
NWP
NWP
EXIT AND BASKET
30"
TRANS
6"
TRANS
GRATING
SIDEWALK SLAB
PRIMARY DUCTS
STREET TIES

Figure 5. Vaults half-inside–half-outside building

Three 1,000-kva banks, typical layout

Experience also has shown that oil-filled potheads may explode violently upon failure.

Dry-type transformers with type *B* insulation, on the other hand, appear to offer a minimum of hazard to property in their immediate vicinity, but experience to date has been too limited to indicate whether, under fault conditions, explosive gases may be generated in sufficient volume to produce an explosive mixture within a vault. Vault-type units however, must be protected from the weather and the air must be reasonably free of dust if frequent cleaning is to be avoided.

Precast Concrete

Precast construction is particularly suitable and economical for transformer manholes wherever soil is sufficiently firm for that type of construction and wherever the space is not too congested by other subsurface structures. An equal or perhaps more important factor in favor of precast construction, in areas of heavy traffic, is the material reduction in the time the street is obstructed for construction. Transformer vaults also may be precast, but their use may be restricted by limitations in size and weight which can be transported, for vault-type equipment requires more space than the submersible top-connected equipment usually installed in manholes. Also, the inflexibility of precast designs sometimes will make field-poured construction necessary to use the limited space which may be available.

Roof and Gratings

The strength of the sidewalk or roadway roof slab and ventilation grating necessary for traffic is generally set by city code. Where vaults are located under the sidewalk adjacent to the curb, it is advisable to provide sufficient strength to sustain the wheel load of trucks that occasionally mount the curb. Where vaults are to be installed under driveways, roadway construction must be provided.

Sidewalk gratings which meet all these described loading conditions are commercially available which provide net ventilation openings of 63 to 70 per cent of the gross area, depending on weight of construction.

Providing a hinged exit and a permanently installed ladder will facilitate access for maintenance crews. In the case of street manholes, however, the hinged exit is hardly justified, as safety requires that a barricade be erected and a man be stationed at the open grating. Manhole gratings which have been made

Figure 4. Sub-sidewalk vaults at building line

Three 1,000-kva banks, typical layout

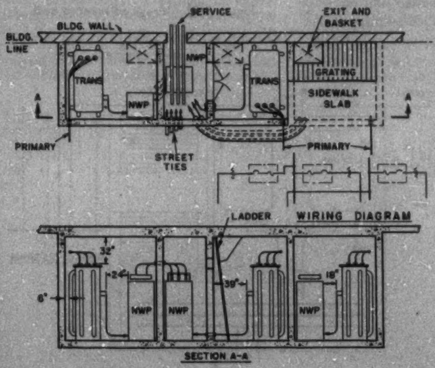
SERVICE
EXIT AND BASKET
BLDG. WALL
BLDG. LINE
TRANS
NWP
NWP
TRANS
GRATING
SIDEWALK SLAB
A
A
PRIMARY
STREET TIES
PRIMARY
LADDER
WIRING DIAGRAM
32"
24"
6"
39"
18"
NWP
NWP
NWP
SECTION A-A

Figure 6. Vaults inside building

Three 1,000-kva banks, typical layout

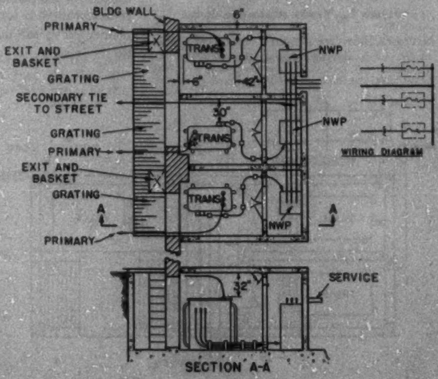
BLDG WALL
6"
PRIMARY
NWP
EXIT AND BASKET
TRANS
6"
42"
GRATING
SECONDARY TIE TO STREET
30"
NWP
GRATING
TRANS
PRIMARY
EXIT AND BASKET
TRANS
GRATING
NWP
WIRING DIAGRAM
A
A
PRIMARY
SERVICE
32"
SECTION A-A

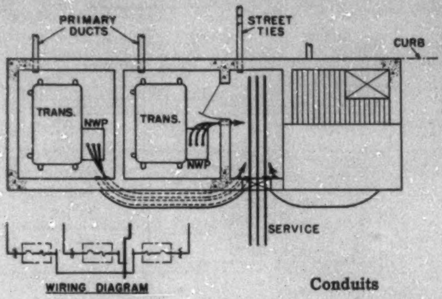

Figure 7. Vaults adjacent to curb

Network protector attached to side of transformer

in sections of two feet by five feet can be opened readily by two men.

Drainage

Where submersible equipment is used, drainage is desirable to reduce the cost of maintenance, if it can be obtained at moderate cost. Vault-type equipment, particularly the nonenclosed network protector, must be protected from flooding at all times. Frequently the impracticability of obtaining a gravity drain will force the use of a permanently-installed automatic sump pump. Where the probability of flooding the vault is very remote, a nonsubmersible motor, protected by a diving bell, may be used, but a sump pump which is apt to operate frequently should be provided with a submersible motor to avoid the overheating that may be caused by a diving bell.

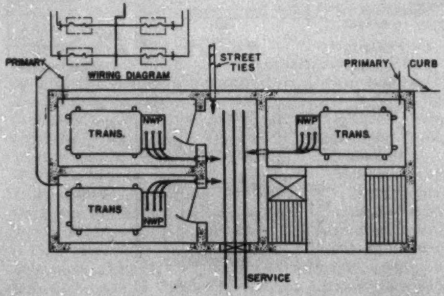

Figure 8. Vaults adjacent to curb

Network protector attached to end of transformer, scheme *A*

Conduits

Secondary conduits interconnecting transformer vaults are preferably of nonmagnetic material, such as Transite or concrete, to obtain a minimum impedance. This is particularly important where several transformers serving the same customer's switch are located at different distances, in order to obtain the best possible division of load. Conduits laid under floors in such a manner that water can be trapped, should be avoided where practicable. Where ducts are so installed, lead-covered cables should be used to protect the cable insulation from water absorption.

Design Illustrations

As an aid to clarifying and visualizing the design features described previously, several illustrative sketches have been prepared which include clearance dimensions that are the minimum considered acceptable with liquid-filled transformers to permit installation, maintenance, and repair of secondary cable terminals.

Figure 3 shows a transformer manhole installation. The transformer manhole offers the simplest design problem since it is installed as an isolated unit directly connected to the network mains and has no provision for a service connection.

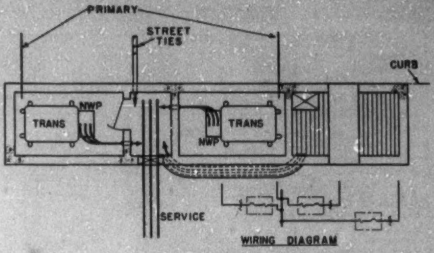

Figure 8(A). Vaults adjacent to curb

Network protector attached to end of transformer, scheme *B*

This illustration shows a combination-type unit, top-connected, installed in a transformer manhole which allows little space about the unit except at the network protector end, where a 3-foot space is provided for network protector maintenance. A full roof grating, made in 2-foot sections which can be handled by two men, provides a maximum of ventilation and accessibility. A drainage sump assists in maintaining a dry floor.

Figures 4, 5, and 6 show layouts for 3-bank vault installations with separately-mounted network protectors, located under the sidewalk at the building line, under the sidewalk with the network protectors inside the building at basement level, and entirely inside the building at basement level with sidewalk ventilation, respectively. A separately-mounted network protector affords a maximum of flexibility in the arrangement of equipment; this is sometimes of great importance where the available

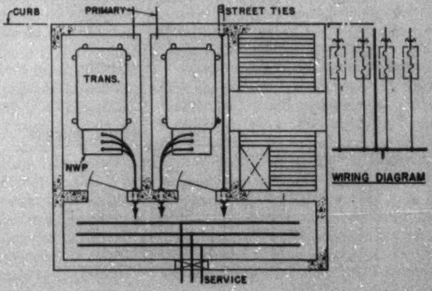

Figure 8(B). Vaults adjacent to curb

Network protector attached to end of transformer, scheme *C* space is very limited. Obviously, however, some space and labor of installation might be saved by mounting the network protector on the side of the transformer, as is shown in Figure 7. The network protector may be mounted on the end of the transformer and the compartments arranged as indicated in Figures 8, 8(A), and 8(B), but complications may arise in obtaining gratings where required, or the long vault construction may make it difficult to obtain the necessary space.

It will be noted in these figures that bus bars are indicated for service connections. This is a desirable feature to limit the number of cables which are connected to the bus. Also, a network protector is located under the service bus—a construction which is economical in the case of a separately-mounted network protector. This network protector is not considered a hazard to service continuity provided the bus is adequately supported with fire-resistant materials.

Appendix I

Published Data—Dust Explosions

The subject of dust explosions has received considerable study by the United States Department of Agriculture,[6,7,10] the United States Bureau of Mines,[8] and the Factory Mutual Laboratories.[9]

The United States Department of Agriculture published the results of tests on 133 materials for which they list a maximum pressure, average rate of pressure rise, and maximum rate of pressure rise for two concentrations of each dust used.[7]

It is stated in this article that the maximum pressure, maximum rate of pressure rise, and average rate of pressure rise are prime factors in determining the severity of an explosion. It is noted from the data that in comparing alkali starch, one of the most explosive dusts, with yellow corn meal, the ratio of the average of these factors is the same as that of their flame propagation rates. Results of tests on vented dust explosions, reported by Brown and Hansen of the Bureau of Chemistry and Soils,[10] show the relation between maximum pressure developed and vent area per unit volume of the test cubicle. Curve *A* of Figure 1 was obtained from these data. These investigators stressed that the shape of the compartment is important and that where the space is not a cube, the vent area should be distributed so that each unit of volume has its proportionate share of vent area.

Table I

Material	Per Cent By Volume Gas Hour Arc-Decomposed Oil[14]	Explosive Limits In Air[13] Per Cent	Maximum Rate of Flame Propagation, Centimeters Per Second	
Acetylene	23	2.5–82	304	Reference 13
Hydrogen	69	4.0–75	440	
Methane	5	4.7–15.5	110	
Ethylene	3	3.0–35	142	
Alkali starch dust			73	Reference 8

Explosion of Gaseous Products of Electric-Arc-Decomposed Oil

A correlation between alkali starch explosions and an explosion of the gaseous products of electric-arc-decomposed transformer oil would provide a means for approximating pressures which might develop in a transformer-vault explosion. One investigator states that, although explosive pressures of inflammable dusts may exceed those obtained from vapors of gasoline, acetylene, or hydrogen, the rate of flame propagation for a mixture of dust and air is slow compared with that for vapor explosions.[9]

Table I shows the approximate gas constituents of arc-decomposed oil, explosive limits in air, the maximum rate of flame propagation of each constituent, and the calculated rate of flame propagation in starch dust. The rate of flame propagation for the entire mixture of gaseous products is not known, but these data indicate it is probably at least 300 centimeters per second, or something over four times the rate for starch dust. Additional evidence of the rapid rate of pressure rise resulting from an oil and gas explosion is shown by W. Dann.[11] Although the scale of his curve is too small for accurate reading, it appears that the time required to reach maximum pressure is in the order of 0.02 to 0.03 second, as compared to 0.096 second for alkali starch.

It thus appears that the rate of flame propagation in an oil and gas mixture is approximately four times that of starch dust, and that the severity of the explosion will be about in that proportion. Using this ratio as a basis for correlation with alkali starch explosion, it is possible to arrive at a relation between maximum pressure and vent area for an oil and gas explosion.

References

1. Guides for Loading Oil-Immersed Distribution and Power Transformers. *ASA Standard C57.32*, American Standards Association (New York, N. Y.), 1932.

2. Considerations in Network Transformer Manhole and Vault Design, T. D. Reimers. *Minutes*, Transmission and Distribution Committee, Edison Electric Institute (New York, N. Y.), February 8, 1939.

3. The Thermal Time Constant of Dynamo-Electric Machines, A. E. Kennelly. *AIEE Journal*, volume 44, February 1925, pages 142–9.

4. Predetermination of Self-Cooled Oil-Immersed Transformer Temperatures Before Conditions Are Constant, W. H. Cooney. *AIEE Journal*, volume 44, December 1925, pages 1324–31.

5. National Fire Codes, Volume II—Dust Explosions (book). National Fire Protection Association (Boston, Mass.), 1946.

6. Dust Explosions and Fires in Grain Separators in the Pacific Northwest. *Bulletin 379*, United States Department of Agriculture (Washington, D. C.), August 1916.

7. Explosibility of Agricultural and Other Dusts as Indicated by Maximum Pressure and Rates of Pressure Rise, Paul Edwards. *Technical Bulletin 490*, United States Department of Agriculture (Washington, D. C.), October 1935.

8. The Explosive Limits of Petroleum Vapors, G. W. Jones, G. St. J. Perrott. *Quarterly Bulletin*, National Fire Protection Association (Boston, Mass.), volume 23, number 4, April 1930.

9. Venting Dusting and Solvent Vapor Explosions, A. L. Brown. *Quarterly Bulletin*, National Fire Protection Association (Boston, Mass.), volume 21, number 1, July 1927.

10. Venting Dust Explosions, H. R. Brown, R. L. Hanson. *Chemical and Metallurgical Engineering* (New York, N. Y.), volume 40, number 3, March 1933, page 116.

11. Transformer Explosions Artificially Produced, W. M. Dann. *Electric Journal* (Pittsburgh, Pa.), volume 31, November 1934, page 446.

12. International Critical Tables, Volume 2, National Research Council. McGraw Hill Publishing Company, New York, N. Y., 1927.

13. Researches on Circuit Breaking, Wedmore, Whitney, Bruce. *Journal*, Institution of Electrical Engineers (London, England), May 1929, pages 557–93.

No Discussion

The Temperature Rise of Cables in a Duct Bank

J. H. NEHER
MEMBER AIEE

IN THE calculation of the temperatures attained by underground cable systems installed in duct banks, it has been customary to base such calculations upon a set of experimentally determined thermal resistances commonly known as the "National Electric Light Association Duct Heating Constants" by which the temperature rise above ambient earth of cables located in the duct bank may be calculated under stated conditions of duct occupancy.

While this procedure has been satisfactory generally, there has been an increasing need for a fundamental method by which the temperature rise at the surface of the cables could be calculated in terms of the heat loss of the cable-in-duct system, its geometry, and the thermal resistivity of the earth. This would permit the clarification of certain ambiguities now attendant in the duct-constant method, and also would permit a direct comparison of the relative thermal efficiencies of the pipe-type and cable-in-duct transmission systems.

Methods of thus calculating the temperature rise of cables in duct are not new. A number of such methods have appeared in literature. These range from the fundamentally theoretical method discussed by Bailey,[1] to the quasi-empirical methods of Kirke[2] and Bauer.[3] Nevertheless, these methods have not found general favor among cable engineers, possibly because the basic theory is not understood thoroughly, or because of a natural hesitancy to use empirical methods based on someone else's power system.

This paper will discuss the fundamental theory applicable to a direct calculation of cable temperatures from the basic geometry and physical properties involved, and also such factual data as is available in support of the theory.

General Considerations

In a previous paper the author has discussed the solution for the temperature rise of a cylindrical radiator,[4] such as the pipe of a pipe-type cable system, buried in the earth, under conditions where the surface of the radiator is for all practical purposes an isothermal. Considering the simplest of cable-in-duct installations—a single cable in a single duct—the cable surface is an isothermal, but, strictly speaking, neither the duct wall nor the duct periphery are isothermals because the cable is not centered in the duct and because all points in the rectangular duct periphery are not equidistant from the cylindrical source of heat flow. In the case of a multicable-in-duct structure, the situation is further complicated by the usual dissymmetry of the cable positions and the interaction of the heat flow from the various cables.

A theoretical solution of this problem which is sufficiently simplified to be practical must involve the assumptions that the duct walls and duct periphery may be treated as cylindrical isothermal surfaces. Cable engineers are generally agreed on this point. The main points of diverging opinion concern the determination of the thermal resistance between cable and duct wall, and the formulation of the equivalent radius of an isothermal cylinder representative of a group of loaded ducts which properly accounts for the interacting heat flows from these ducts.

Of less importance is the matter of determining the equivalent radius of the duct structure, since this radius must appear in the calculations if differing thermal resistivities of the duct structure and earth are to be used.

If these values can be established, however, it follows from the Kennelly formula for the temperature rise of a buried cylindrical radiator,[4] that the temperature rise at the surface of a centrally-located cable in a duct can be given by the expression

$$\Delta T_s = Q_c H_{sd} + 0.012 Q_d' \times \left[\rho_d \log_{10} \frac{2L}{R_d} + (\rho_e - \rho_d) \log_{10} \frac{2L}{R_b}\right] \text{ degrees centigrade} \quad (1)$$

in which

Q_c = heat flow from given cable in watts per foot
Q_d' = effective total heat flow from all of the cables in the duct bank (including loss factor)
H_{sd} = thermal resistance between cable sheath and duct wall in degree centigrade feet per watt
ρ_d = thermal resistivity of the duct structure in degree centigrade centimeters per watt
ρ_e = thermal resistivity of the earth in degree centigrade centimeters per watt
R_d = equivalent radius of the group of loaded duct walls
R_b = equivalent radius of the duct bank
L = distance from center of duct bank to surface of earth

The use of the long form of the Kennelly formula in the development of equation 1 is not justified in view of the approximate nature of R_d and R_b.

Equation 1 assumes a uniform resistivity throughout the earth and neglects surface effects which may be included if desired.[4] If the duct structure is located beneath street paving of thermal resistivity ρ_p its effect may be cared for by the addition of another term within the

---

Paper 49-134, recommended by the AIEE Insulated Conductors Committee and approved by the AIEE Technical Program Committee for presentation at the AIEE Summer General Meeting, Swampscott, Mass., June 20–24, 1949. Manuscript submitted March 7, 1949; made available for printing April 26, 1949.

J. H. Neher is Senior Engineer with the Philadelphia Electric Company, Philadelphia, Pa.

The author wishes gratefully to acknowledge the help of G. B. Shanklin of the General Electric Company in establishing the average geometry involved in the tests from which the National Electric Light Association Duct Heating Constants were formulated; and the kindness of the Johns-Manville Company in furnishing their test data on fibre and Transite ducts.

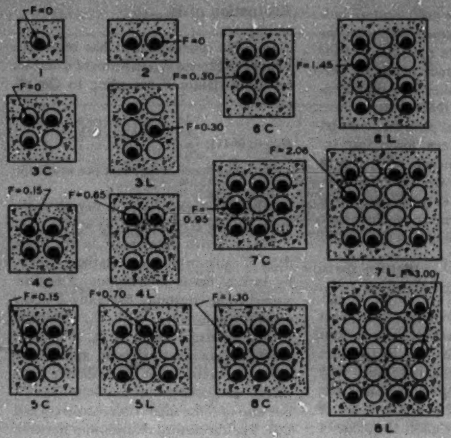

Figure 1. Typical duct bank configurations

brackets of equation 1, for which it is sufficiently accurate to use

$$(\rho_p-\rho_s)\log_{10}\frac{L}{L-p} \text{ degree centigrade centimeters per watt} \quad (2)$$

in which p is the thickness of the pavement.

As a practical matter, however, ρ_d, ρ_e, and ρ_p are of the same general magnitude, and since they will vary among themselves seasonally with the moisture content in a manner which cannot be predicted with any degree of accuracy, it often is sufficient to assume that they will have the same effective value ρ'. This matter is discussed in reference 4, together with methods of determining this effective value.

On this basis, equation 1 may be simplified to

$$\Delta T_s=Q_cH_{sd}+0.012\rho'Q_d'\log_{10}\frac{2L}{R_d} \text{ degrees centigrade} \quad (3)$$

Our problem, therefore, consists in the evaluation of H_{sd}, R_d, and R_b.

Evaluation of R_d

There appears to be a general feeling among cable engineers that, because of the complicated heat-flow pattern which exists in the immediate vicinity of the ducts of a multicable-in-duct installation, the value of R_d for use in equations 1 or 3 cannot be derived on a reasonably simple theoretical basis. As a result there is a tendency to accept the so-called "equal periphery" method as a simple and satisfactory means of evaluating R_d. In this method R_d is taken to be the radius of a circle whose perimeter is equal to the periphery of a boundary line drawn around, and tangent to, the inner walls of the loaded ducts.

It must be realized, however, that R_d and equation 1 or 3 are merely means to an end—the calculation of the temperature rise of a particular duct wall, assumed to be isothermal, which is operating in the vicinity of other loaded ducts. Looked at from this point of view, the value of ΔT_d may be determined graphically by plotting the lines of heat flow, as done by the British[5] and discussed by Bailey,[1] or, much more simply, by the application of the principle of superposition.[1,4] This procedure, outlined in Appendix I, results in an expression of the form

$$\Delta T_{d1}=0.012\rho \quad Q_1\log_{10}\frac{2L_1}{r_d}+ Q_2\log_{10}\frac{L_1+L_2}{d_{12}}+\ldots.+ Q_n\log_{10}\frac{L_1+L_n}{d_{1n}}\Bigg] \text{ degrees centigrade} \quad (4)$$

in which the numerical subscripts refer to arbitrary numbers assigned the individual loaded ducts in the bank, number 1 being the reference duct for which the temperature rise is desired. Thus, d_{12} is the center-to-center distance between the reference duct at depth L_1 and number 2 duct at depth L_2, and r_d is the duct wall radius. The temperature rise thus obtained is above earth ambient temperature at the depth L_1.

By the use of an ingenious electrical analogy consisting of a model test setup in which the thermal quantities are replaced by their corresponding electrical counterparts,[1] Bailey has demonstrated the correctness of equation 4 for the case of six isothermal duct walls buried in a uniform medium. Equation 4 does not take account of any empty ducts which may be present and which, having an effective thermal resistivity considerably higher than the duct structure itself, may be presumed to have some effect on the result. The magnitude of this effect may be obtained readily with the electrical counterpart equipment, but, unfortunately, this was not covered by Bailey. It is probable that the effect is minor and that its omission will not introduce any greater errors than some of the other assumptions which have been introduced.

In the majority of cable-in-duct calculations, the cables all dissipate the same amount of heat, or so nearly so that the values of Q in equation 4 may be taken as being equal to Q_d'/N, where N is the number of loaded ducts. Under these conditions equation 4 becomes

$$\Delta T_{d1}=0.012\rho\left[Q_d'\log_{10}\times\frac{L_1\sqrt[N]{2(1+L_2/L_1)(1+L_3/L_1)\ \ldots}}{\sqrt[N]{r_d\times d_{12}\times d_{13}\ldots}}\right] \text{ degrees centigrade} \quad (5)$$

Equation 5 results in a slightly different value for each loaded duct. If we consider a centrally-located loaded duct of depth L, equation 5 becomes substantially equal to

$$\Delta T_d=0.012\rho Q_d'\log_{10}\frac{2L}{\sqrt[N]{r_d\times d_{13}+d_{13}\ldots}} \text{ degrees centigrade} \quad (5a)$$

Hence, by comparison with the second term of equations 1 or 3

$$Rd=\sqrt[N]{r_d\times d_{12}\times d_{13}\ldots} \quad (6)$$

The procedure outlined is obviously suitable for determining the temperature rise of any point in the duct structure and thus the temperature rise of the air in any unoccupied or idle duct. The corresponding expression for R_i, the equivalent radius of an idle duct, is

$$R_i=\sqrt[N]{d_{12}\times d_{13}\times d_{14}\ldots} \quad (7)$$

Figure 1 shows a number of typical duct bank configurations with from one to eight loaded ducts. In Figure 1, C indicates close grouping and L indicates loose grouping. A determination of the degree of accuracy entailed in equation 5a as applied to these configurations, with consideration for possible effects of the empty ducts, could be readily made by means of the electrical counterpart equipment with insulating media inserted to represent the empty ducts. The procedure of Bailey[1] could be materially simplified by the use of a thin sheet or coated surface of uniform electrical-resistivity material instead of the water bath which he employed.

Any appreciable effect of the unoccupied ducts thus could be reduced to correction factors applicable to equations 6 and 7. Such a project would be of great value, and it is hoped that means may be found for undertaking it.

For comparative purposes, Table I has been prepared for the configurations of Figure 1, assuming the values for r_d, d and L therein stated. Values of the $\log_{10}$ ratio also are given. If a value of $\rho' = 83$ degree centigrade centimeters per watt be assumed, these values of the $\log_{10}$ ratio are equal to the thermal resistances involved, in degree centigrade feet per watt. It will be noted that the thermal resistance between a loaded duct wall and a centrally-located inside idle duct is inappreciable in respect to the total thermal resistance from loaded duct wall to ambient. This is merely a theoretical justification of a fact which may be deduced from a consideration of the heat flow paths involved, and, thus the temperature rise of an inside idle duct is justifiably employed as a bench mark by which the performance of a given duct bank readily may be determined.[6]

Two other significant points are indicated by Table I. The thermal resistance between the occupied ducts and an outside idle duct is too variable to permit the use of the temperature rise of an outside idle duct as a bench mark unless the particular geometry is taken into consideration. Also, over-all thermal resistances calculated by the equal periphery method average about 10 per cent lower than by the superposition principle, and slightly but not appreciably lower than the over-all thermal resistances of outside idle ducts. From this we must conclude that the equal periphery method is not a valid means of evaluating R_d.

Evaluation of R_b

As indicated previously, the exact evaluation of R_b is relatively unimportant since the thermal resistivity of the duct structure and the surrounding earth may be presumed to be so nearly the same that a considerable variation in the value of R_b will not appreciably affect the value of equation 1.

Equation 6 for the evaluation of R_d will be recognized as the equation for the "geometric mean radius" of a group of cylindrical conductors as commonly used in overhead transmission line calculations. For consistency, therefore, it would be logical to employ for R_b the corresponding expression for the geometric mean radius of a rectangle. This is equivalent to the geometric mean distance of a rectangle from its center, the expression for which, as given by Dwight,[7] is

$$R_b = 0.112 P_b \tag{8}$$

in which P_b is the periphery of the rectangular duct structure.

Table I. Geometric Constants for the Configuration of Figure 1

Assuming $r_d = 1.88$ inches, $d = 6.25$ inches, Depth of cover = 30 inches

Configuration	R_d	R_{ii}	R_{io}	R_d'	2L	$\log_{10}\frac{2L}{R_d}$	$\log_{10}\frac{R_{ii}}{R_d}$	$\log_{10}\frac{R_{io}}{R_d}$	$\log_{10}\frac{R_d'}{R_d}$
1	1.88			1.88	70.2	1.58			0
2	3.42			3.87	70.2	1.32			0.06
3*C*	4.18		7.00	5.01	76.6	1.26		0.23	0.08
3*L*	5.26		6.25	6.67	82.8	1.20		0.08	0.10
4*C*	5.05			5.85	76.6	1.18			0.07
4*L*	6.72		7.43	7.85	82.8	1.09		0.04	0.07
5*C*	5.25		9.00	7.27	82.8	1.20		0.13	0.14
5*L*	6.78	8.25	8.65	9.80	82.8	1.09	0.09	0.11	0.16
6*C*	5.75			7.95	82.8	1.16			0.14
6*L*	8.92	9.70	10.70	11.80	85.2	1.00	0.02	0.08	0.12
7*C*	7.20	7.25	11.10	9.27	82.8	1.06	0	0.19	0.11
7*L*	10.40	11.12	12.30	13.80	89.0	0.93	0.03	0.07	0.12
8*C*	7.82	7.45		9.85	82.8	1.03	−0.02		0.10
8*L*	12.70	13.00	14.00	15.80	95.2	0.87	−0.01	0.04	0.10

r_d = radius of duct wall

d = distance between duct centers

R_d = equivalent radius of centrally-located occupied duct, by equation 6

R_{ii} = equivalent radius of centrally-located inside empty duct, by equation 7

R_{io} = equivalent radius of centrally located outside empty duct, by equation 7

R_d' = equivalent radius of occupied ducts, by equal periphery method

L = depth of center of duct bank below earth's surface

Evaluation of H_{sd}

In cable calculations it has been customary to express H_{sd} in terms of a surface resistivity factor β according to the expression

$$H_{sd} = 0.00411 \frac{\beta}{D_s}$$

degree centigrade feet per watt (9)

in which β is expressed in degree centigrade square centimeters per watt.

This practice dates back to the early days of cable-in-duct calculations,[8] when, for lack of better information, β was assumed to be constant. Actually β is not constant and varies with D_s, although, within the usual range of D_s, β may be taken as constant without appreciable error. As indicated in Appendix II, H_{sd} is theoretically dependent not only upon D_s but also in some slight degree upon Q and D_d. The theoretical relationship between H_{sd} and D_s for average values of $Q = 10$ watts per foot and $D_d = 4$ inches is expressed in the form of a curve in Figure 2.

Because of the departure of the duct wall from an isothermal cylinder on which Appendix II is based, the theoretically-derived H_{sd} must be correlated with such test data as are available.

In a thesis written in 1925, Barenscher[9] gives the results of temperature measurements made at three points—top, bottom, and side—on a cable sheath and the corresponding three points on the inside of an enclosing fibre duct encased in a concrete envelope. These results, based on the average sheath and inner-duct-wall temperatures for $Q = 10$ watts, are given in Table II and are spotted on Figure 2. There obviously was something wrong with the $D_s = 2.13$ test, but otherwise the points fall on a curve parallel to the theoretical and about 0.55 degree centigrade feet per watt higher.

A more elaborate set of tests recently has been made by the Johns-Manville Company in which temperatures were measured at many more points around the cable sheath, and around the inner and outer surfaces of the enclosing fibre or Transite ducts. These tests involved a fibre duct in air, a fibre duct in a concrete envelope, a Transite (Korduct) duct in air, and a Transite duct in concrete envelope. The results, extrapolated back to a $Q = 10$ watts per foot, are likewise given in Table II and are spotted in Figure 2. It will be noted that the point for fibre duct in concrete falls on the curve through the Barenscher[9] points.

It is significant to observe from Table II that the thermal resistance between

Table II. Values of H_{sd} and H_{sd}' Obtained by Tests on Fibre and Transite Ducts

Q Watts Per Foot	D_s Inches	D_d Inches	H_{sd} Degrees Centigrade Foot Per Watt	*H_w Degrees Centigrade Foot Per Watt	H_{sd}' Degrees Centigrade Foot Per Watt	Condition	Source
10	0.69	3.50	4.70			Fibre duct in concrete	Reference 9
	1.13		3.35				
	2.13		2.70				
	3.13		1.50				
10	3.38	3.88	1.54	0.21	1.75	Fibre duct in air	Johns-Manville Company
			1.40	0.41	1.81	Fibre duct in concrete	
			1.25	0.15	1.40	Transite duct in air	
			1.07	0.13	1.20	Transite duct in concrete	

*The effective thermal resistivity of the duct wall may be determined from the expression

$$\rho_w = \frac{H_w}{0.012\log_{10}\dfrac{4.50}{3.88}} = 1{,}280H_w = \begin{array}{l}\text{400 degree centigrade centimeters per watt for fibre ducts}\\ \text{180 degree centigrade centimeters per watt for Transite ducts}\end{array}$$

cable sheath and the inside of the duct wall increases with an increase in thermal resistivity of the duct material. This is probably due to the departure of the duct wall from an isothermal surface. The data permit the projection of curves representing H_{sd} for fibre and Transite ducts. It may be presumed that the curve of equation 22 is a reasonably good representation in case of a terra-cotta duct which has a thermal resistivity of 100 degree centigrade centimeters per watt, as opposed to 180 degree centigrade centimeters per watt for Transite, and 400 degree centigrade centimeters per watt for fibre.

In the case of fibre and Transite ducts, it is most convenient to care for the additional thermal resistance of the duct wall itself by formulating H_{sd}' to include this resistance. Such curves are shown in solid section in Figure 2. In using these curves, r_d in equation 6 should be taken properly as the outside radius of the fibre or Transite duct, although practically this refinement is unnecessary. For most purposes, equation 9 may be used with β equal to 800 degree centigrade square centimeters per watt for terra-cotta ducts, 1,000 for Transite ducts, and 1,200 for fibre ducts.

It will be evident that a considerable amount of further work can be done profitably in this connection. The accuracy of the curves of Figure 2, however, probably is consistent with the accuracy with which the other components of the thermal circuit can be calculated.

Working Equations

As a practical matter, the separate calculation of R_d is somewhat laborious. The over-all procedure is simplified by setting up the working equations in terms of r_d the radius of a duct, d the distance between adjacent duct centers, and a factor F which is a function of the relative positions of the loaded ducts in the duct structure. The corresponding transformation of equation 5a is developed in Appendix III.

The complete over-all expression for the temperature rise of the surface of the given cable is therefore

$$\Delta T_s = 0.00411\,\frac{Q_c\beta}{D_s} + 0.012\,\frac{Q_d'}{N}\,\rho_d \times \left(N\log_{10}\frac{2L}{d} + \log_{10}\frac{d}{r_d} - F\right) + 0.012Q_d'\left[(\rho_e-\rho_d)\log_{10}\frac{2L}{R_d} + (\rho_p-\rho_e)\log_{10}\frac{L}{L-p}\right] \text{ degrees centigrade} \quad (10)$$

in which

β = 800 degree centigrade square centimeters per watt for terra-cotta ducts
1,000 degree centigrade square centimeters per watt for Transite ducts
1,200 degree centigrade square centimeters per watt for fibre ducts (11)

$$F = f_{12} + f_{13} + f_{14} \quad (12)$$

where the N-1 values of f for each loaded duct in respect to the reference loaded duct may be obtained from Figure 3. Values of F are shown in Figure 1 for the configurations there represented.

If a single equivalent value of thermal resistivity is used from the duct wall out, the last term (in brackets) of equation 10 becomes equal to zero.

The temperature rise of an idle duct is found by eliminating the first term in equation 10 and making $r_d = d$. The factor F will in this case be composed of N values of f.

A typical calculation for six equally located cables in a 2 by 3 duct bank is given in Appendix IV.

Comparison with Present Methods

The common method of calculating the temperature rise of cables in duct, and that adopted by the Insulated Power Cable Engineers Association,[10] is based on the use of equation 9 with β = 1,200 degree centigrade square centimeters per watt (for $D_s > 1.75$ inches) and the familiar National Electric Light Association duct constants.[8]

$$\Delta T_s = 0.00411Q_c\frac{\beta}{D_s} + Q_d'H \text{ degrees centigrade} \quad (13)$$

For a cable diameter of 2.5 inches the first term equation 13 represents a thermal resistance of 1.97 degree centigrade feet per watt, as contrasted with the corresponding value of 1.30 degree centigrade feet per watt obtained from equation 22. There has been considerable confusion as to the true significance of the first term of equation 13, but it is generally agreed that it represents a thermal resistance higher than that defined by H_{sd}. Hence

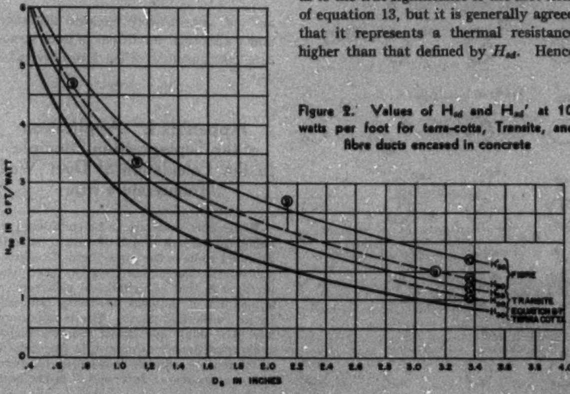

Figure 2. Values of H_{sd} and H_{sd}' at 10 watts per foot for terra-cotta, Transite, and fibre ducts encased in concrete

the duct constant H must represent a thermal resistance lower than that from the loaded duct wall to ambient. The value of the thermal resistance, $0.012\ \rho'\log_{10}(2L/R_s)$, represented by the second term of equation 3, on the other hand, involves the applicable value of the effective thermal resistivity of the earth ρ' and the geometry of the duct bank, which are inherently contained in the duct constant H.

While no true comparison can be made, therefore, it is well to note that, assuming a value of 75 degree centigrade centimeters per watt for ρ', $D_s=2.5$ inches, and the geometry given in Table I which is typical of average practice at the time the duct constants were formulated, the resultant values of the effective thermal resistance between sheath and ambient on a per-cable basis, H_{sa}, as calculated by equations 3 and 22 and as spotted on Figure 4 check reasonably well with the curve of equation 13 shown in the figure. For three or more loaded ducts the agreement is within 10 per cent, which is in the same order as the theoretical variations caused by a change in cable configurations for the same number of loaded ducts, and which is well within the variations which may be expected in ρ' for different locations.

For normal situations where ρ' has not actually been determined, therefore, a working figure of 75 degree centigrade centimeters per watt appears to be consistent.

Figure 3. Relative position factors f for ducts in a duct bank

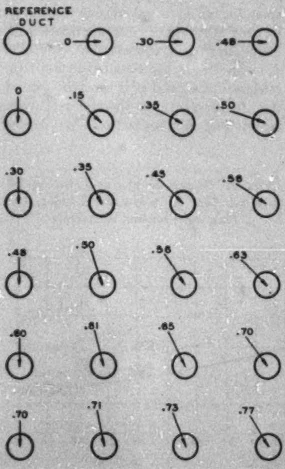

Conclusions

1. The basis for a theoretical method of calculating the temperature rise of cables in duct in terms of the geometry of the duct bank and the effective thermal resistivity of the earth has been indicated. The method is essentially simple and readily understandable. The slight additional labor involved over the conventional method is more than compensated by the increased accuracy of the method.

2. The accuracy of the method is dependent upon the refinement with which the basic quantities involved can be determined. Such refinements, involving further basic research and tests, have been indicated. At the present time sufficient data has been presented to permit calculations of equal accuracy with conventional methods under normal conditions, and of considerably greater accuracy under abnormal conditions of duct structure, configuration, or earth resistivity.

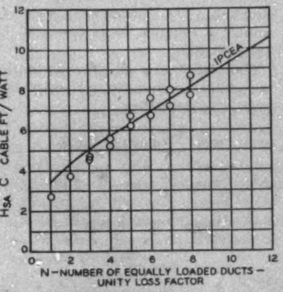

Figure 4. Comparison of H_{sa} as calculated for a 2.5-inch diameter cable and 75 degrees centigrade per watt thermal resistivity with the Insulated Power Cable Engineers Association values

Appendix I. Application of the Superposition Principle to the Calculation of Duct Wall Temperature Rise

If the duct walls are to be considered as being isothermal, and if the duct bank is assumed to have the same thermal resistivity as the surrounding earth, then the problem is that of cylindrical radiators in a medium of uniform resistivity bounded by an isothermal plane. The temperature rise of a single cylindrical radiator under these conditions is developed in Appendix I of reference 4, wherein it is shown that the temperature rise at any point P in the heat field of the radiator is given by the expression

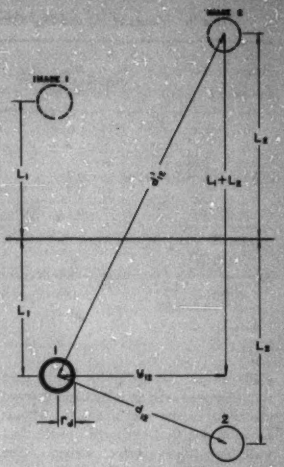

Figure 5. Development of the temperature rise of a duct wall by the principle of superposition

$$\Delta T_p = 0.012\rho Q \log_{10} d'/d \quad \text{degrees centigrade} \tag{14}$$

where d is the distance of the point from the thermal center of the radiator and d' is the distance of the point from the image of the thermal center of the radiator. If the radius r_d of the radiator is small in respect to twice its depth L below the isothermal plane, as is true in this case, the thermal center coincides practically with the physical center of the radiator.

The principle of superposition merely states that the temperature rise at any point such as P because of the simultaneous operation of a number of such radiators, is equal to the sum of the temperature rises produced at P by each radiator operating as if the other radiators were absent.

Consider the case of two such radiators located as shown in Figure 5, at depths L_1 and L_2 below the isothermal plane and liberating Q_1 and Q_2 watts per foot respectively. By the application of equation 14 and the superposition principle, the increase in temperature rise of radiator *1* due to the simultaneous operation of radiator *2* is given by the expression

$$\Delta T_{12} = 0.012\rho Q_2 \log_{10}\frac{d_{12}'}{d_{12}} \text{ degrees centigrade}$$
$$= 0.012\rho \times \left[Q_2 \log_{10}\frac{\sqrt{(L_1+L_2)^2+y_{12}^2}}{d_{12}}\right] \text{ degrees centigrade} \tag{15}$$

In the case of a duct structure, the maximum value of y is relatively small with respect to $2L$ so that d_{12}' may be taken equal to L_1+L_2. Thus the temperature rise of an isothermal duct wall due to the combined effect of all occupied ducts is

$$T_{d1}=0.012\rho\left[Q_1 \log_{10}\frac{2L_1}{r_d}+ Q_2 \log_{10}\frac{L_1+L_2}{d_{12}}\ldots+ Q_n \log_{10}\frac{L_1+L_n}{d_{1n}}\right] \text{ degrees centigrade} \quad (4)$$

Appendix II. Thermal Resistance between Cable Sheath and (Isothermal) Duct Wall

The mechanism of heat transfer between a cylindrical radiator and an enveloping isothermal enclosure through an intervening fluid medium is such that a portion of the total heat flow Q is carried by convection Q_{cv}, a portion by conduction Q_{cd}, and the remainder by radiation Q_r. In formulating the components of the thermal circuit, therefore, it is more convenient to work in terms of thermal conductances rather than thermal resistances, since the former quantities are directly additive. Thus, if ΔT is the temperature drop in degrees centigrade across the circuit

$$\frac{Q}{\Delta T}=\frac{Q_{cv}}{\Delta T}+\frac{Q_{cd}}{\Delta T}+\frac{Q_r}{\Delta T} \text{ watts per degree centigrade foot} \quad (16)$$

The phenomenon of convection involves the conception of the temperature drop being concentrated in two films, one at the surface of the cylindrical radiator, of diameter substantially equal to the diameter of the radiator D_s in inches; and one at the surface of the enclosing isothermal surface, which also will be considered as being cylindrical of diameter D_d. The following equation, based on McAdams' equation 42, page 254,[11] (first edition only) is applicable to either film when the fluid is air at atmospheric pressure and at 50 degrees centigrade.

$$Q_{cv}=0.092D_f^{3/4}\Delta T_f^{5/4} \text{ watts per foot} \quad (17)$$

The effect of normal temperature variations from 50 degrees centigrade is minor. The solution of equation 17 for the two films in series is given with sufficient accuracy by the expression

$$\frac{Q_{cv}}{\Delta T}=0.092\frac{D_s^{3/4}\Delta T^{1/4}}{1.39+D_s/D_d} \text{ watts per degree centigrade foot} \quad (18)$$

From a theoretical standpoint the expression for the conduction component should take into account any eccentricity between the cylindrical radiator and the enveloping isothermal enclosure. In the practical case of a cable in duct, the cable will not rest uniformly on the bottom of the duct, and also, in the case of a nonmetallic duct, the duct wall is not strictly maintained as an isothermal. Since these effects cannot be evaluated, the familiar expression for the resistance between two concentric cylinders in terms of the dimensions of the cylinders and the thermal resistivity of the medium, which has been taken as 3,900 degree centigrade centimeters per watt, will be used

$$\frac{Q_{cd}}{\Delta T}=\frac{0.0213}{\log_{10} D_d/D_s} \text{ watts per degree centigrade foot} \quad (19)$$

The radiation component is given with sufficient accuracy by the following expression based on McAdams' equation 17, page 63,[11] (second edition)

$$\frac{Q_r}{\Delta T}=0.102D_s\epsilon(1+0.0167T_m) \text{ watts per degree centigrade foot} \quad (20)$$

in which ϵ is the emissivity coefficient of the surface of the cable, and T_m is the average temperature of the air in the duct in degrees centigrade. Experience has indicated that the value of ϵ may be taken as 1.00. Thus, for an air temperature of 50 degrees centigrade, equation 20 becomes

$$\frac{Q_r}{\Delta T}=0.187D_s \text{ watts per degree centigrade foot} \quad (21)$$

Combining equations 16, 18, 19, and 21, we obtain for H_{sd}, the thermal resistance between cable and duct wall

$$H_{sd}=\frac{10.9}{\dfrac{D_s^{3/4}Q^{1/4}H_{sd}^{1/4}}{1.39+D_sD_d}+\dfrac{0.232}{\log_{10} D_d/D_s}+2.04D_s} \text{ degree centigrade feet per watt} \quad (22)$$

It will be seen that the primary variable in equation 22 is D_s. Since variations in Q, D_d, and T_m have minor effects on the final result, it is sufficient for practical purposes to assume average values for these quantities of 10 watts per foot, 4 inches, and 50 degrees centigrade, respectively. The resulting solution of equation 22 is plotted as the heavy curve in Figure 2.

Appendix III. The Relative Position Factors *F* and *f*

Equation 5a may be written as

$$\begin{aligned}\Delta T_d&=0.012\rho\frac{Q_d'}{N}(N\log_{10}2L- \log_{10} r_d-\log_{10} d_{12}-\log_{10} d_{13}\ldots)\\ &=0.012\rho\frac{Q_d'}{N}(N\log_{10} 2L- \log_{10} r_d+\log_{10} d-N\log_{10} d-\log_{10}\frac{d_{12}}{d}- \log_{10}\frac{d_{13}}{d}-\log_{10}\frac{d_{14}}{d}\ldots)\\ &=0.012\rho\frac{Q_d'}{N}\left(N\log_{10}\frac{2L}{d}+\log_{10}\frac{d}{r_d}-F\right)\end{aligned} \quad (23)$$

where

$$F=f_{12}+f_{13}+f_{14}\ldots \quad (12)$$

$$=\log_{10}\frac{d_{12}}{d}+\log_{10}\frac{d_{13}}{d}+\log_{10}\frac{d_{14}}{d}\ldots$$

The value of f for any relative position of a loaded duct with respect to the reference duct may be obtained from the diagram shown in Figure 3.

Appendix IV. The Solution of a Typical Problem

Given six 2.5-inch diameter equally-loaded cables with a loss factor of 0.85, located in a 2 wide by 3 deep duct bank consisting of 4.5-inch fibre ducts on 8.5-inch centers encased in concrete with over-all dimensions of 20 inches wide by 28.5 inches deep, and installed with a 30-inch cover of which 10 inches is concrete pavement, determine H_{sa} for a middle (hottest) duct.

> $r_d=2.25$ inches, $d=8.5$ inches, $D_s=2.5$ inches, $\beta=1{,}200$ degrees centigrade square centimeters per watt (equation 11); $F=0+0.15+0+0.15+0=0.30$ (equation 12 and Figure 3); $R_b=0.112\times2(20+28.5)=10.9$ inches (equation 8); $L=30+1/2\times28.5=44.3$ inches, $p=10$, $N=6$. Assume $\rho_d=100$, $\rho_c=65$, and $\rho_p=100$ degree centigrade centimeters per watt.
>
> By equation 10

$$\begin{aligned}H_{sa}=\frac{\Delta T_s}{Q_c}&=\left(\frac{0.00411\times1{,}200}{2.5}\right)+ (0.012\times0.83\times100)\times \left[\left(6\log_{10}\frac{88.6}{8.5}\right)+\left(\log_{10}\frac{8.5}{2.25}\right)-0.30\right]\\ &\quad+(0.012\times6\times0.85)\times \left[\left(-35\log_{10}\frac{87.6}{10.9}\right)+\left(35\log_{10}\frac{88.6}{78.6}\right)\right]\\ &=1.97+(0.012\times0.83\times100)(6.39)+ (0.012\times6\times0.85)(-30.0)\\ &=6.64 \text{ thermal ohm feet}\end{aligned}$$

If we assume an effective $\rho'=75$ degrees centigrade centimeters per watt

$$H_{sa}=\frac{\Delta T_s}{Q_c}=1.97+(0.012\times0.85\times75\times6.39) =6.86 \text{ thermal ohm feet}$$

present methods, equation 13

$$H_{sa}=\frac{\Delta T_s}{Q}=1.97+(0.85\times4.92) =6.15 \text{ thermal ohm feet}$$

Note that, for a corner duct, $F=0.80$ and H_{sa} becomes 6.14 thermal ohm feet.

References

1. Heat Flow from Underground Electric Power Cables, Neil P. Bailey. *AIEE Transactions*, volume 48, number 1, January 1929, pages 156–65.

2. The Calculation of Cable Temperatures in Subway Ducts, W. B. Kirke. *AIEE Journal*, volume 49, part II, 1930, page 855.

3. Operating Temperatures of Underground Cables, C. A. Bauer. Report of the Engineering Section, Great Lakes Section, National Electric Light Association (New York, N. Y.), 1930–31, pages 239–52.

4. The Temperature Rise of Buried Cables and Pipes, **J. H. Neher.** *AIEE Transactions*, volume 68, part 1, 1949, pages 9–21.

5. Current Rating of Cables for Transmission and Distribution, **S. Whitehead, E. E. Hutchings.** *Journal*, Institution of Electrical Engineers (London, England), volume 83, 1938, page 525.

6. Load Ratings of Cable, **Herman Halperin.** *Electrical Engineering* (*AIEE Transactions*), volume 58, October 1939, pages 535–55.

7. Geometric Mean Distances for Rectangular Conductors, **Herbert B. Dwight.** *Electrical Engineering* (*AIEE Transactions*), volume 65, August-September 1946, pages 536–8.

8. Calculations of the Electrical Problems of Underground Cables, **D. M. Simmons.** *Electric Journal* (East Pittsburgh, Pa.), volume 29, 1932, pages 237, 283, 336, 395, 423, 476, 527.

9. A Study of the Temperature Distribution in Electric Cables in Underground Ducts, **P. J. Barenscher.** *Thesis*, Department of Electrical Engineering, University of Wisconsin (Madison, Wis.), 1925.

10. Current Carrying Capacity of Impregnated Paper, Rubber and Varnished Cambric Insulated Cables. *Publication Number P-29-226*, Insulated Power Cable Engineers Association (New York, N. Y.), first edition, 1943.

11. Heat Transmission (book), **W. H. McAdams.** McGraw-Hill Book Company, New York, N. Y. second edition, 1942.

Discussion

Robert J. Wiseman (The Okonite Company, Passaic, N. J.): This paper by Mr. Neher helps to appreciate the various parts of the thermal circuit of a duct bank. A few years ago some of us, as members of a Subcommittee of the Power Transmission and Distribution Committee, engaged in a discussion as to what was meant by the duct heating constants which we use, and what earth thermal resistivity was associated with these constants. For a proper analysis, the structure of the duct bank and the position of the cables in the ducts have to be considered. The author has done a very nice piece of analysis of this problem and offers a method for future use. I think we should seriously consider his suggestions and decide if we are to adopt them or continue as we do now.

At the present time, the duct constants do not differentiate between the number of cables in a duct bank and the number of ducts, whereas the author shows us what the difference is, by what he calls close and loose configuration. As the allowable current is determined by the hottest cable, this current can be more accurately determined by using the author's method for calculating the duct bank thermal resistance. If the author's suggestions are adopted, the Insulated Power Cable Engineers Association's current loading tables will have to be revised. Before doing so, it seems advisable for both the Insulated Conductor Committee and the Insulated Power Cable Engineers Association to consider the matter.

The author makes several assumptions in order to arrive at reasonably simple methods of calculation. This is acceptable, provided assumptions do not go too far. Under Appendix IV he gives an example of how to use his method for computing the thermal resistance. I note that he uses a value of ρ for earth as 65 thermal ohm centimeters and then gives a new value for H_{sa} if $\rho = 75$ is taken assuming installation under paved areas. He shows in his paper that by using this value he obtains values of H_{sa} closely the same as for Insulated Power Cable Engineers Association's duct heating constants. Several years ago some of us who were studying this subject showed by very simple methods that the duct constants gave an apparent thermal resistivity of 65–75 thermal ohm centimeters and stated that if this were correct, we should use the same value for buried cables or pipes. We are not doing so, but using a value of $\rho_s = 80$. To be consistent, we should use $\rho_s = 80$ for duct systems also or revise both duct and buried pipe to $\rho = 65$, if in uncovered earth, or $\rho = 75$ if under paved areas. I hope that the Insulated Conductor Committee and Insulated Power Cable Engineers Association will take action to establish a uniform value for ρ when applied to duct or pipe cables.

This paper, along with the one previously presented, on buried cables and pipes,[1] have helped to show how the two systems compare thermally. It is up to us to take advantage of his investigation of the subject by accepting as our standard, his recommendations for methods of calculating the thermal resistance of ducts and buried cables with the correct thermal constants.

Reference

1. See reference 4 of the paper.

F. H. Buller (General Electric Company, Schenectady, N. Y.): Mr. Neher has again presented an interesting and valuable analysis of the problem of underground cable heating. This time he covers the case of cables in ducts. Some of the points which he brings up, however, would seem to merit a little further consideration.

First, there is the calculation of R_d and R_b. Mr. Neher evaluates these radii by the use of the principle of superposition, which leads to formulas involving the geometric mean distance between the cable under consideration and the other cables in the duct bank.

The principle of superposition is indeed a powerful tool whereby complicated problems can be greatly simplified; but it does have certain limitations. I propose to draw attention to a couple which are pertinent to the present study.

The first one is fundamental. The principal of superposition is rigorously valid only for situations where the effect is proportional to the cause. To illustrate this point, consider a current flowing through a resistance. If the resistance is constant, the voltage drop is given by Ohm's law $E = IR$. Here the effect (voltage drop) is proportional to the cause (current) and we would expect the superposition principle to apply, which it does. Double the current, and the voltage drop is doubled.

Now consider the loss in the same circuit. This is given by Joule's law — $W = I^2R$. Here the effect (watts loss) is not proportional to the cause (current) but to the square of the cause, and the principle of superposition cannot be expected to apply. Double the current, and the watts loss instead of being doubled, is quadrupled.

So long as Mr. Neher is dealing with thermal conduction, the superposition principle should apply. When he is considering the temperature rise in a duct due to losses in another loaded duct, convection and radiation come into the picture as well, in both ducts under consideration. In these phenomena the effect (temperature rise) is not proportional to the cause (heat flow). (See Mr. Neher's reference 11 and his Appendix II.) Hence the use of superposition in deriving equations 4 to 7 is at best an approximation.

The second limitation is practical. Before one can superpose several effects at any point, one must calculate these effects individually at that point. This is often a fairly straightforward process in a homogeneous medium; but the cross section of a duct bank is unfortunately far from homogeneous. The thermal resistance of the empty duct is much higher than that of the concrete; and the presence of metallic materials in the duct would on the other hand tend to reduce its thermal resistance. All this distorts the thermal field, thus placing Mr. Neher in the position of a man who tries to calculate the magnetic reluctance of a perforated steel plate in which some of the holes are partly filled with iron filings. This is a difficult problem; and the answer would not be the same as for a homogeneous unperforated steel plate, even if there is no saturation so that superposition could be applied directly. Thus, Mr. Neher's technique contains two approximations.

It also contains a third approximation which is introduced by the fact that the duct walls are not isothermals. This third approximation is at least as important as the other two.

Thus it would seem that Mr. Neher's technique of calculation R_d and R_b is actually no more rigorous than the equivalent periphery method even though it is based on the principle of superposition. However, it is reassuring to note that the two methods check within 10 per cent. If these radically different methods check so closely, the answers which they give should not be very far from the truth.

The man who wants to use Mr. Neher's results effectively would do well to subject the section Comparison with Present Methods in the paper to the most careful scrutiny. A careless reading of this section would give the impression that Mr. Neher believes that a soil thermal resistivity of 75 is the value on which the Insulated Power Cable Engineers Association's duct constants are based.

A more careful reading reveals that this is not the case; he has simply pointed out that if this value is used in his equations in combination with a cable diameter of 2.5 inches and a β value of 1,200, the values obtained by the Insulated Power Cable Engineers Association's method for H_{SA} will be checked within 10 per cent (see Figure 4 of the paper). This statement is correct; but it is not at all the same thing as saying that a value of 75 is representative for the soil thermal resistivity on which the

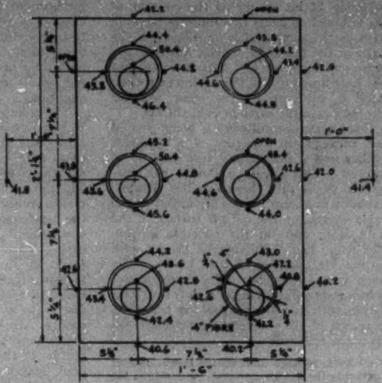

Figure 1. Temperature readings in concrete duct run in air

Cable outside diameter 2.52 inches. Chloroprene sheath. Loss=3.0 watts per foot per cable. Temperatures in degrees centigrade

Insulated Power Cable Engineers Association's duct constants are based.

The Insulated Power Cable Engineers Association also uses a value of $\beta = 1{,}200$; but all the test data on which their values of H are based were taken in outside idle ducts. Thus the value of $\beta = 1{,}200$ includes all the thermal resistance from the outside idle duct to the cable sheath; and a goodly portion of this thermal resistance occurs in the duct structure itself. This is borne out by various field tests made by different observers. The British get a value of about 675 for β, measured to the air of the loaded duct. Herman Halperin[1] gets something below 550 and other tests yield similar values. On the other hand for the portion of the thermal resistance in the duct structure itself W. B. Kirke[2] gets 0.75 degree centigrade per watt per foot; G. B. Shanklin in an unpublished memorandum on the Insulated Power Cable Engineers Association's duct constants obtains 1.32; and a recent heat run gave a value of 1.13 for one particular case. Since the soil heating term in Mr. Neher's formula is carried up to the loaded duct wall, these figures should be added to the Insulated Power Cable Engineers Association's duct constants when checking back on the soil thermal resistivity. If this is done the soil thermal resistivity in Mr. Neher's formulas which would check the revised Insulated Power Cable Engineers Association's duct constants when these are carried up to the loaded duct wall will be of the order of 100; and the difference between Mr. Neher's geometric mean distance method and the equivalent periphery method of calculating R_d and R_b could add another 10 per cent to this value.

To sum this point up, a soil thermal resistivity of 75 and a β value of 1,200 should be used in Mr. Neher's formulas to check sheath temperatures as obtained by the Insulated Power Cable Engineers Association's method, and to extend this method to other duct configurations; but these figures, while they fit the formulas, should be regarded as empirical coefficients rather than true thermal resistivity values. The true soil thermal resistivity which should be used in comparing performance of duct cables with buried cables and other buried systems is likely to be considerably higher than this.

If an exact comparison is required between the potential performance of duct cables and buried cable systems along some particular route, it is well to make a field survey covering the entire length of the projected cable line, at a dry season of the year; and even then a reasonable allowance should usually be made for a potentially drier season. If some point along the line is found to have a higher soil thermal resistivity than the rest of the line, either this point should be taken as the criterion, or oversized copper should be installed there, and the next hottest spot taken as the criterion of comparison.

REFERENCES

1. See reference 6 of the paper.
2. See reference 2 of the paper.

Frank V. Smith (Sargent and Lundy, Chicago, Ill.): A paper of the type that Mr. Neher has written has been needed for a long time. The inadequacy of the duct heating constants have been apparent to all those who have worked with them. The industry owes a debt of gratitude to Mr. Neher for the patience and perserverance he has shown in going through the great mass of historical material available in order to distill from it a method of analysis that it is hoped will be generally acceptable.

The degree of accuracy of any method of calculating the heat flow through duct structures and the earth cannot be too high, but what is important is that there be general agreement on the method of analysis and a proper sense of proportion so that the same approach can be used in making studies of alternate ways of handling a specific problem.

The duct heating constants were based on average conditions and were not designed to take account of changes in duct geometry, depth below the surface, earth resistivity, and so forth, factors which are different for every application. Large organizations have developed techniques suitable for their own local conditions, but it has not been possible to make these all consistent with one another.

Mr. Neher has discussed each of the debatable points in following the heat flow from the cable sheath to the earth and has produced a logical method of analysis with supporting data.

Mr. Neher's major contributions are:

1. Clarification of the thermal drop from the cable sheath to the duct wall. The experimental material in this field is still meager and additional test data are desirable.

2. A method of calculating the relative thermal resistances from various duct positions to earth. The method is based on a group of loaded ducts in a completely uniform medium and is to that degree an approximation, but still it does give reasonable results that allow differentiation between the temperature rises of different ducts in a bank. Additional test data here, too, would be welcome.

The effect of two of the factors ignored by the duct heating constants might be noted from an examination of Appendix IV of the paper. Here for a 6-duct run with 30-inch cover and earth with a thermal resistivity of 65, the total thermal resistance from the hottest cable sheath to the earth is calculated to be 6.64 thermal ohms per foot. If the cover were increased to 60 inches, the same method of analysis would show that the thermal resistance has increased to 7.45 thermal ohms, or a matter of 12 per cent. If the earth resistivity were doubled to 130 (a not unlikely figure), the thermal resistance will be found to increase to 10.05 thermal ohms per foot, or a matter of some 58 per cent. Such changes clearly make important differences in the temperature rise and cable rating.

We would like to comment on the application of the method to the case of a concrete duct run suspended in air. This is a situation that exists frequently in power station design where important generator leads may be carried through turbine rooms and boiler rooms. The paper is concerned with a duct bank in earth and the formulas are set up with this situation in mind. It will be noted that the second term in equation 1 could be written

$$0.012Q_d'\rho_d \log_{10}\frac{R_b}{R_d}+0.012Q_d'\rho_e \log_{10}\frac{2L}{R_b}$$

The first term could be interpreted as the thermal resistance from the loaded duct wall to the surface of the concrete and the second term as the thermal resistance from the surface of the concrete to the earth. If this were done in the case of Appendix IV of the paper, the distribution of thermal resistances would be as follows:

	Thermal Ohms
Sheath to duct wall	1.97
Duct wall to concrete surface	.95
Concrete surface to earth	3.72
Total	6.64

If the duct run were suspended in air, the last term would disappear and would be replaced by one giving the thermal drop from the concrete surface to the air, such as

$$Q_d'\frac{0.00411\pi\beta}{P_b}$$

where β is considered by the heating and ventilating engineers to be about 1,000 for still air and 300 for air moving at 22 feet per second.

Mr. Neher might not quite agree with this adoption of his theory as the concept of R_4 is based on ducts in a uniform medium such as the earth and is developed on the basis of the theory of images, but common sense and available test data indicate that the heat flow through the concrete duct run itself is substantially the same whether the duct is in the earth or is in the air.

Some experimental work is being carried out through the courtesy of a Midwest Utility and a preliminary test may be of interest. This covers a 6-duct run suspended in air with thermocouples installed as shown in Figure 1 of the discussion on the cable sheath, on the outside surface of the duct wall, and on the concrete surface. The cable had a chloroprene sheath with an outside diameter of 2.52 inches. The ducts were 4-inch fibre. The temperatures shown were obtained under steady load conditions with 3.0 watts per foot loss per cable. A review of the temperature readings will show the following:

> Using the average cable sheath temperature in relation to the average duct wall temperature, the value of β for the cable sheath becomes 1,020.
>
> Using the average duct wall temperature of the four corner ducts in relation to the average concrete surface temperature, the thermal resistance from duct wall to surface is 0.11 thermal ohms. (A calculation according to Mr. Neher's method using ρ for concrete of 100 would give 0.08 thermal ohms.)
>
> Using the average duct wall temperature of the two center ducts in relation to the average concrete surface temperature, the thermal resistance from a center duct wall to the surface is 0.16 thermal ohms. (Calculation according to Mr. Neher's method would give 0.19).
>
> Unfortunately ambient air temperatures were taken only at the sides of the duct run rather than also the top and bottom so that the average drop from concrete surface to air is not available, but the temperature drop from the sides of the concrete structure to the air in that vicinity shows an average temperature difference of 1.3 degrees centigrade which would correspond to β for the concrete surface of 480.

Paul Greebler (Johns-Manville Research Center, Manville, N. J.): Mr. Neher, in his paper, refers to tests conducted at the Johns-Manville Research Center on Transite and fiber duct. Although we plan in a forthcoming paper to give a complete discussion of the method and results of the tests, I would like at this time to give a brief description of the test assembly together with some practical calculations based upon our results and using Mr. Neher's working equations.

The cross-section detail for ducts encased in concrete in Figure 2 of the discussion shows the thermal heat flow components that were studied. The $3^1/_2$ inch lead sheath encloses a centered Calrod heater. Thermocouples for temperature measurements are located on the sheath surface, on the inside and outside duct wall surfaces, and around the outside of the concrete casing. Tests were conducted both for ducts in air and in concrete, the cross-section detail for the "in-air" tests being identical with that shown in Figure 2 of the discussion with the absence of the concrete casing. An 8-foot length of duct was used, measurements being made on a 2-foot test section in the center, the remainder of the duct length being employed as thermal guards to eliminate end effects. This test section might seem somewhat short. However, the many years experience in conducting thermal tests at Johns-Manville has shown that a small sample, properly guarded against end effects, gives results identical with those from a large sample.

The most critical measurements in the tests were those of the inside and outside duct wall surface temperatures. Figure 3 of the discussion shows the thermocouple assembly on the outside of a test section of fiber duct. There are 48 couples spaced around each surface in the form of a 3-turn helix with 16 couples per turn. The constantan wires are soldered to a thin copper strip cemented to the duct wall. They are run for about two inches along the duct surface, and then inserted into fine holes carrying them inside the duct. All constantan leads were carried through the inside of the duct to avoid abrasion when set in concrete.

Table I. Current Rating Calculations

3 Conductor, 500,000-Circular-Mil Compack Sector, 203 Mils Paper, 125 Mils Lead, 15-kv Grounded Neutral (6th Edition AEIC Specification)

Number of Loaded Ducts*	Amperes per Conductor		
	Transite	Fiber	Ratio: Transite/Fiber
One	456	423	1.078
Three	386	365	1.056
Six	325	312	1.042

* These calculations are based upon inside and outside duct wall surface diameters of 4.00 and 4.62 inches, a 30-inch cover, spacing of 6.6 inches between duct centers, and a 2-inch layer of concrete over the ducts. A 20-degree-centigrade earth ambient and a 75 per cent daily load factor are assumed.

Current rating calculations of cable in Transite and fiber duct, applying Mr. Neher's working equation with a 75 degrees centigrade centimeters per watt thermal resistivity outside the duct wall, are shown in Table I of the discussion. Thermal surface resistivity factors of 1,020 and 1,200 degrees centigrade square centimeters per watt are used respectively for Transite and fiber, these β values being based upon a heat flow of ten watts per foot and averaged for the tests in air and in concrete. The additional thermal resistance of the duct wall itself is considered by adding the term,

$$0.012\rho_w \log_{10} \frac{D_o}{D_i} \text{ where } D_o \text{ and } D_i \text{ are}$$

the outside and inside duct wall diameters, and ρ_w, the duct wall thermal resistivity, is 200 degrees centigrade centimeters per watt for Transite and 480 degrees centigrade centimeters per watt for fiber. These values are higher than those given by Mr. Neher in Table II of his paper since they are based upon two sets of tests, the calculations from the second test series having been completed too late for consideration by Mr. Neher in his paper. The ratio of current rating in Transite duct to that in fiber duct, shown in the third column of Table I of the discussion measures the practical effect of the duct wall thermal resistivity for one, three, and six loaded cables in a duct bank. The decrease in current rating ratio with increasing number of loaded ducts measures the rate at which the influence of the duct wall upon the thermal path decreases as the number of loaded cables in the duct bank increases.

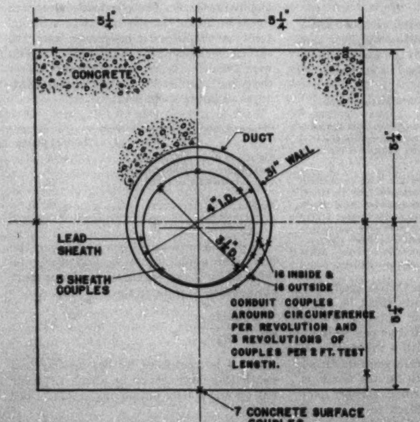
5¼"
5¼"
8¼"
8¼"
CONCRETE
DUCT
31" WALL
4" I.D.
3½" O.D.
LEAD SHEATH
5 SHEATH COUPLES
16 INSIDE & 16 OUTSIDE CONDUIT COUPLES AROUND CIRCUMFERENCE PER REVOLUTION AND 3 REVOLUTIONS OF COUPLES PER 2 FT. TEST LENGTH.
7 CONCRETE SURFACE COUPLES

Figure 2 (left). Cross-section detail for tests conducted with ducts encased in concrete

Figure 3 (below). Thermocouple assembly on the outside surface of a test section of fiber duct. An identical thermocouple assembly is employed on the inside surface

J. H. Neher: I am greatly indebted to the various discussers for reviewing the background of this problem, which explains in some measure why this particular paper has been written. The additional data presented by Mr. Smith and by Mr. Greebler on the thermal resistance between cable sheath and duct wall is most interesting and I am pleased to see how close an agreement is obtained between the measured and calculated difference between average duct wall temperature and average bank periphery temperature from Mr. Smith's data. This is a difficult part of the thermal circuit to calculate and fortunately it represents only a small part of the total.

It appears that the β values of 1,020 for Transite and 1,200 for fiber to the inside of the duct wall which Mr. Greebler derives from his tests, were obtained on the basis of a 3.5-inch cable in a 4-inch duct. I have indicated in the paper that the variation of H_{sd} with cable diameter is fundamental and that the derived quantity β is only approximately constant and increases with cable diameter. Hence if one insists in using β for convenience, β should be determined on the basis of an average size cable. The cable in this particular test was unusually large. A more representative cable size was used in determining the working values as given in the paper which, incidentally, include the additional drop through the duct wall.

The value of 1,020 which Mr. Smith derives from his data for a fiber duct is presumably to the outside of the duct wall and is based on an average size cable, but on a lower than average heat flow, the effect of which is to increase slightly the value obtained. Thus we must conclude that Mr. Smith's value for a fiber duct is some 20 per cent lower than that given in the paper. It is hoped that further test data of this type will soon become available so that the accuracy of this part of the calculation may be improved. Here again, however, H_{sd} represents a relatively small part of the total thermal circuit in the usual case.

Mr. Buller has nicely stated the limitations of the principle of superposition, and he has pointed out quite rightly that my solution of the problem involves three basic assumptions.

(1) The thermal resistivity at any point in the heat field is independent of the temperature existing at that point.

(2) The difference in effective thermal resistivity of the loaded or empty ducts from that of the duct structure may be neglected.

(3) The duct walls may be treated as isothermal cylinders.

The use of assumptions in the solution of a problem of this type is unavoidable, but the relative merit of the solution depends on whether these assumptions are the best that can be made and to what degree they are valid. These assumptions apply primarily within the duct structure. Beyond the duct structure the first assumption might be involved as a result of moisture migration, but as indicated in reference 1 of the paper, this effect is negligible because of the relatively large effective radius of the duct structure.

As indicated in the paper the errors introduced by all these assumptions may be evaluated by a number of carefully controlled tests and appropriate correction factors developed which would increase the accuracy of the procedure. Both theory and experience indicate, however, that a relatively small portion of the total thermal drop exists between the loaded duct walls and the duct bank periphery. The first two assumptions are, therefore, found to be essentially valid. It will be noted that Mr. Buller's preferred "equivalent periphery" method makes use of these same approximations.

The equivalent periphery method, however, is entirely arbitrary in its evaluation of the effective radius of the loaded duct walls, and one might equally well argue that the boundary should be drawn inside of empty outside ducts, or even that the solution should be based on the enclosed area rather than on the perimeter. On the other hand the method given in the paper is theoretically correct for the assumptions which have been made. A given problem may be solved just as quickly by the working equations given in the paper as by the equivalent periphery procedure.

The third assumption also is reasonable. The abrupt decrease in thermal resistivity occurring at the duct wall tends to equalize the temperature around the wall, as is indicated by the test data cited in the paper and presented by Mr. Smith. Furthermore as Mr. Buller has mentioned, there is a change in the mechanism of heat transfer at the duct wall which establishes it as a natural reference point in formulating equations for the overall thermal circuit.

In the Insulated Power Cable Engineers Association's procedure, the reference point was taken to be the air in outside idle ducts. This is not an altogether suitable bench mark, because the thermal resistance between it and the cable sheath is not only variable, but is a composite relationship which is difficult to deal with analytically. While experience has indicated that the Insulated Power Cable Engineers Association's procedure will yield rule of thumb answers which are quite satisfactory for most practical calculations, it is manifestly impossible to derive therefrom separate thermal resistances between sheath and duct wall and between duct wall and ambient earth from which the earth's effective resistivity might be determined. These quantities simply do not exist as distinct entities in the procedure.

The method given in the paper involves both the thermal resistivity of the earth and the geometry of the particular installation. By making the geometry conform to that involved in the formulation of the National Electric Light Association's duct constants, it becomes possible to determine empirically what approximate value of the thermal resistivity would cause this method to yield results comparable to the Insulated Power Cable Engineers Association's procedure. In this determination the value of β was taken as 800 corresponding to terra cotta ducts which presumably were used in the National Electric Light Association's duct constant determination and not 1,200 as Mr. Buller has indicated. The effective value of thermal resistivity thus determined is 75-thermal-ohm centimeters, and the agreement between the two methods is within ten per cent.

This does not mean that one should compare the performance of a pipe-type cable system calculated with a resistivity of 75 and a cable in duct system calculated by the Insulated Power Cable Engineers Association's procedure. One serious deficiency of this procedure is that it does not represent the geometry or the duct material currently used in high-voltage cable in duct installations. Valid comparison requires that both systems be appraised by the use of a method which consistently accounts for all of the significant factors involved.

Mr. Wiseman has indicated that he has been using a value of 80 rather than 75 for the effective earth resistivity in making these comparisons. We too have been using 80 because it more nearly represents the average dry season value obtained by sphere tests on our system. It is important to realize that the point-to-point variation over the system or in fact along a single line far exceeds the difference in these values, and thus the establishment of separate values for installations in covered or uncovered earth is not warranted.

Mr. Wiseman also has suggested the advisability of revising the Insulated Power Cable Engineers Association's current loading tables in the light of the method given in the paper. This would be a considerable procedure due to the number of variable factors involved, for each of which a representative value would have to be established and agreed upon. The resultant values would more nearly represent present duct construction practice, but would not necessarily represent a more accurate cable rating unless the particular geometry and resistivity prevailing happened to coincide with the values used in the preparation of the tables.

This and the preceding paper[1] have been prepared not with the idea of revising the present current loading tables, but to present consistent methods whereby the temperature rise of various specific cable installations might be more accurately calculated, and incidentally more accurately compared.

REFERENCE

1. See reference 4 of the paper.

69-Kv Pipe-Type Cable Circuits in Philadelphia

A. H. KIDDER
MEMBER AIEE

G. S. VAN ANTWERP
ASSOCIATE AIEE

THE Philadelphia Electric Company System has approximately 250 miles of 69-kv circuits, of which 74 miles are installed underground, along routes where right-of-way considerations have precluded using aerial construction. Prior to 1940, the system plans permitted 69-kv underground cable circuits to have ratings of 440 to 525 amperes under conditions satisfied by solid-type paper and lead cable. The 52 miles of underground circuit additions since 1940, including six miles recently contracted for, however, were required to have load ratings in the range from 660 to 880 amperes. Comparative cost studies showed the pipe-type of construction to have a somewhat lower cost than oil-filled cable.

Only one manufacturer would recommend a practical copper size for the desired 880-ampere rating in pipe for projects being planned from 1940 to 1945. The unanswered problems of pipe corrosion and practical cable fault locating techniques in pipe also handicapped the pipe-type systems. Consequently, conventional oil-filled cable was specified for the 13-mile Chester-Upper Darby 660-ampere line installed in 1942, and for the two $4^1/_2$-mile Southwark-Schuylkill 880-ampere lines then in planning stages.

Meanwhile the problems of load rating, pipe corrosion, and cable fault location were actively investigated. The 69-kv experimental Oilostatic cable installation at Plymouth Meeting Substation, in service since 1933, was disconnected in January 1945, and a 19-day 880-ampere low-voltage heat run was started March 1 on one 1,000,000 circular mil, 800-foot section. Thermocouples observed pipe temperature at approximately 100-foot intervals. Copper temperature was observed by d-c resistance measurements, and corrected for the natural temperature decrement during the few minutes interval between the instant of de-energizing the cable and that of each reading obtained. Ambient earth temperature was observed by several thermocouples, some in the earth and others on remote sections of the pipe excluded from the test. The total losses were read by the standard 3-wattmeter method. Figure 1 summarizes this test, from which the thermal resistivity of the earth at this open location was found to be 60 thermal ohm centimeters, or less than the 80 thermal ohm centimeters at which pipe-type circuits could be designed for loads above 800 amperes.

It soon became apparent that the section containing an oil pipe-type cable fault might be identified by the operation of suitable pressure diaphragms installed at the semistop joints and actuated by the transient oil pressure waves accompanying the fault. A more accurate location might then be obtained by use of the high-voltage bridge which has since been secured for this purpose.

Almost concurrently, the pipe corrosion investigations gave needed assurance that a high quality pipe coating should permit maintaining slightly cathodic potentials for preserving the integrity of the steel pipe as a pressure vessel during the expected life of the cable.

Orders for ten miles of 880-ampere oil pipe-type cable circuit were then placed and followed shortly by orders for a 3-mile circuit of similar design. The next project included a 6-mile 880-ampere circuit and two short 560-ampere circuits, all high-pressure gas in pipe through a tunnel constructed under the Schuylkill River. These three projects were completed respectively, ten miles of oil pipe in August 1947, three miles of oil pipe in

Figure 1. Measured heating characteristics of experimental cable installation at Plymouth Meeting Substation

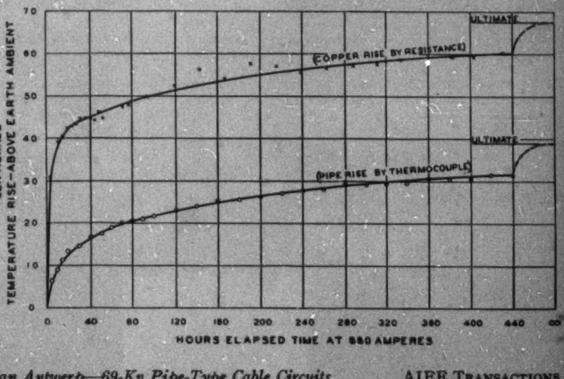

Paper 49-136, recommended by the AIEE Insulated Conductors Committee and approved by the AIEE Technical Program Committee for presentation at the AIEE Summer General Meeting, Swampscott, Mass., June 20–24, 1949. Manuscript submitted March 18, 1949; made available for printing April 26, 1949.

A. H. Kidder is Assistant Engineer in charge of Special Investigations and Testing Divisions, and G. S. Van Antwerp is General Superintendent, Transmission and Distribution Department, both with the Philadelphia Electric Company, Philadelphia, Pa.

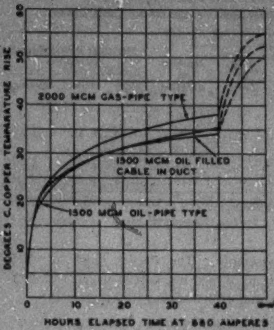

Figure 2. Comparative heating characteristics in 80 thermal ohm centimeter earth

July 1948, and seven miles of high-pressure gas pipe in September 1948.

It seems appropriate now to summarize briefly the significant features of the more interesting 880-ampere pipe-type circuit designs, one circuit using oil and one circuit using gas as the pressure medium for two quite different cable constructions.

Description of the Cables

The 1,500,000 circular mil oil-pipe cable construction consists of four compact segmental sectors, with two opposite segments insulated by two paper tapes and the assembly bound together with a 5-mil bronze binder tape intercalated with a paper tape; then metallized paper tapes and impregnated wood pulp paper insulation which, together, make a 315-mil wall; a 3-mil copper tape intercalated with cotton tape and one 102 by 204 mil copper D-shaped armor wire over-all, with a lay of 1.2 inches and making an outside diameter of 2.312 inches. The cable was mass-impregnated with a mineral base oil, having a viscosity of 2,600 Saybolt Universal seconds at 100 degrees Fahrenheit, and shipped in a 63-mil temporary lead sheath having a steel rip-wire to facilitate stripping.

The two respective constructions of 2,000,000-circular-mil gas-pipe cables were as follows:

1. 2,000,000-circular-mil compact segmental conductor with four segments, two opposite segments insulated by two paper tapes and the assembly bound together with a 5-mil bronze binder tape intercalated with an 8.5-mil manila paper tape; then 315 mils of paper insulation including metallized paper shielding tapes; a 4-mil copper tape intercalated with a 24-mil cotton tape and two 100 by 200 mil copper D-shaped armor wires over-all, equally spaced with a lay of 2.1 inches and making an outside diameter of 2.476 inches. The cable was mass-impregnated with a mineral base oil, having viscosity of 2,500 Saybolt Universal seconds at 100 degrees Fahrenheit, and shipped in a 90-mil temporary lead sheath having a steel rip-wire.

2. 2,000,000-circular-mil compact segmental conductor with four segments, three insulated with two paper tapes each and a 5-mil bronze binder tape over-all; then 315 mils of paper insulation including metallized paper shielding tapes; two 3-mil plain copper tapes without intercalated cotton and two 100 by 200 mil D-shaped copper armor wires over-all equally spaced with a lay of 2.1 inches and making an outside diameter of 2.412 inches. The cable was mass-impregnated with a synthetic oil having a viscosity of 140,000 Saybolt Universal seconds at 100 degrees Fahrenheit, and shipped in a 90-mil temporary lead sheath having a steel rip-wire.

Load Losses

In present designs of cables for pipe-type circuits, the proximity effect upon a-c conductor resistance substantially discounts the increase in load rating which accompanies a given increase in conductor size, particularly for sizes above 1,500,000 circular mils. Also, the parasitic energy losses in the binding tapes, skid wires, and in the pipe add materially to the heating effects.

Much remains to be learned concerning the sources and control of these various energy losses. For instance, low-voltage laboratory tests show the measured total energy losses at 880 amperes and 75 degrees centigrade conductor temperature to be in the order of 26 to 28 watts per foot for the two types of 2,000,000-circular-mil cables, as compared to 25 watts per foot observed on a similar test of the 1,500,000-circular-mil cable. Consideration of possible remedies for these unreasonably high losses suggests that the short-circuited sheath effects of metallic tapes and skid wires might be reduced appreciably by the use of high-resistance materials, also that there may be opportunity for drastic reductions in conductor losses as well.

The stranded segmental construction of these large conductors inherently transposes the strands in such a way that, if each strand were insulated, each should have essentially the same effective a-c impedance per transposition, and the current distribution should therefore be essentially uniform. This suggests that the controlled application of an insulating or high-resistance film on each of the copper strands of such conductors might almost eliminate proximity as a cause of extra a-c losses. If this reasoning can be confirmed by test, such an equalization of mutual reactance effects between strands would make 1,500,000-circular-mil conductors have approximately the same load rating as had been expected of the 2,000,000-circular-mil conductors in pipe.

It is important to realize that 25 watts per foot in a 6-inch pipe-type cable circuit are equal to the heat losses from a well designed 6-inch 150 pound-per-square-inch steam main. Cable engineers have learned to give steam mains the respect that is their due. Pipe-type circuit losses should have at least equal respect.

Load Ratings

The 1,500,000-circular-mil conductor size for oil pipe-type circuit was estimated to have essentially the same copper temperature at 880 amperes as that for 1,500,000-circular-mil oil-filled cable in duct. The larger 2,000,000-circular-mil conductor for high-pressure gas-pipe cable was specified to gain an expected lower copper temperature rise of 48 degrees centigrade ultimate, as compared to 50 degrees centigrade for oil-filled cable, and 52 degrees centigrade for the oil pipe-type cable. The comparative temperature rises are shown in Figure 2. Excessive losses in the gas-pipe cable designs have increased their ultimate temperature rises from the expected 48 to 55 degrees centigrade for the 26.5-watt construction and 58.5 degrees centigrade for the 28.4-watt construction. All of these calculations assume the earth to have a resistivity of 80 thermal ohm centimeters. A rather extensive program of tests begun in 1947 indicates that the average thermal resistivity of earth in Philadelphia is very nearly 75 thermal ohm centimeters; with a range from 34 minimum to 114 maximum in the characteristic clay subsoil, including seasonal variations.

Analysis of the thermal circuits involved was a large study in its own right The essentials of this work have been summarized in papers by J. H. Neher[1,2] and A. S. Mickley,[3] hence need not be reviewed here.

With but one exception, each of the pipe-type cable lines has a continuous service record of copper temperature, pipe temperature, ambient earth, and load. The copper temperature is obtained by adding the pipe temperature thermocouple output to that of a recently developed adjustable thermal circuit, calibrated to represent accurately the temperature rise from pipe to copper as determined by a test heat-run on the cable and pipe assembly.

Table I. Power Factor Tests on Oil Samples from Various 69-Kv Cable Lines

	Age in Years	Number of Samples	Per Cent Power Factor at 100° C		
			High	Low	Average
Low-pressure oil					
Chester-Upper Darby Line	6	60	7.83	0.48	2.91
200 pounds per square inch oil-pipe					
Plymouth Meeting Experimental Line	15*	3	2.21	1.66	1.99
South Delaware-Westmoreland Line	1½	12	1.00	0.265	0.58
Chester-Naamans Line	0	15	2.63	0.20	0.62

* In operation 12 years and de-energized three years, waiting changeover to high-temperature operation.

These particular pipe-type circuits were designed to operate under a load cycle which was recognized to place a severe limitation on load rating. From Figure 3 it will be seen that the 0.90 load factor is calculated to develop a 75 degree centigrade copper temperature, or 50 degree centigrade rise above no-load temperature, on 1,500,000 circular mil oil-pipe type cable at 860 to 900 amperes. The rectangular weekly load cycle is particularly severe, but characteristic of base load transmission operations for which these lines were designed. The standard daily load cycle and load factors in the range of 0.75 to 0.50 are representative of most other operations, for which the oil-pipe cable design of Figure 3 might have a 10 per cent to 35 per cent greater rating for the same copper temperature.

It was expected that the thermal resistivity of the earth would exceed 80 thermal ohm centimeters at some locations and in some seasons, as confirmed by subsequent tests. Therefore, the copper temperature in the design selected for the pipe-type cables was expected to exceed the normal operating limit of 75 degrees centigrade where such conditions prevail in small percentages of their length, but only if the operations at that particular season require the full-load rating under an adverse load cycle.

The maximum copper temperature recorded in nearly two years' operation of the oil-pipe cable line was 55.5 degrees centigrade in 44 thermal ohm centimeter earth at Southwark Station, or 31.5 degrees centigrade above earth ambient on August 28, 1948, when the load reached 980 amperes maximum at 0.655 load factor for the week. The maximum copper temperature recorded during 6 months' operation of the gas-pipe lines was 37 degrees centigrade at 892 amperes on December 12, 1948, or 25.5 degrees centigrade rise above earth ambient at 0.37 weekly load factor. From these observations it would appear that there is little risk of exceeding 75 degrees centigrade copper at the working load factors which have been well below the 0.90 specification for base load operations.

The sturdy qualities of high-pressure oil-pipe systems suggest it may be practical to accept the possibility of occasionally operating such cables at normal copper temperatures ranging up to 100 degrees centigrade. The occasions would be infrequent. The sheath crack problem is not present. Slight additional restraint against the somewhat greater expansion forces is provided readily. The only effect can be some life loss in scattered locations along the circuit. The experimental Oilostatic cable installation at Plymouth Meeting Substation is, therefore, about to be modified to operate in this higher temperature range.

Figure 3. Effect of load cycle on ampere rating for 1,500,000-circular-mil oil pipe-type installation in 80 thermal ohm centimeter earth

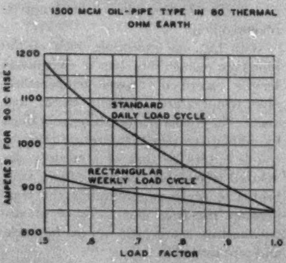

Connectors

The comparatively straight parallel lay of conductors in the pipe-type system which does not have the cable slack that is characteristic of duct and manhole installations, makes it imperative that the connector be designed to have substantial mechanical strength. The connectors for these pipe-type systems were designed to withstand about one-third the ultimate strength of the conductor. This is approximately twice the maximum stress which would accompany a possible 25 degree centigrade drop in conductor temperature after the connectors had been installed.

Figure 4 shows two designs of connectors, both of which have the required mechanical strength and ample electrical conductivity. Steel pin reinforcement was at first thought to be required. Simple radial compression has been found to be sufficient, but has the disadvantage that the press may require somewhat greater working space than can be provided conveniently in the joint casing assembly. The sleeves must be made from oxygen-free copper which will withstand deformation without cracking.

Insulation

The oil-pipe cable and about half of the gas-pipe cable had 315 mils of insulation mass-impregnated with mineral base oil having a viscosity of 2,500 to 3,000 Saybolt Universal seconds at 100 degrees fahrenheit. The remaining 2,000,000-circular-mil gas-pipe cable was mass-impregnated with a synthetic oil having a viscosity of 140,000 Saybolt Universal seconds at 100 degrees fahrenheit. The manufacturer of the synthetic oil made a substantial number of severe tests designed especially to determine whether the synthetic oil had the chemical, physical, and electrical stability required for this type of service. The results of these tests were very satisfactory and the synthetic oil was accepted.

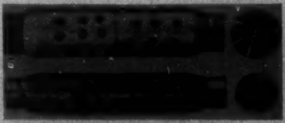

Figure 4. Types of connectors

(Above) 2,000,000-circular-mil connector, radial compression only

(Below) 1,500,000-circular-mil connector, circumferential compression with steel pin reinforcement

The gas-filled insulation was not expected to have the same rugged electrical qualities as high-pressure oil-filled cable insulation, although it had demonstrated sufficient strength at normal working pressures of 180 to 220 pounds per square inch. A disadvantage of the high-pressure gas-filled insulation is that the manufacturers are not willing to authorize operation at pressures below 100 pounds per square inch. This can become an im-

Table II. Typical High-Voltage-Time Test Data From Certified Test Reports on 69-Kv Cable

Test Voltage		Hours of Test Voltage Application					
		Low Pressure Oil Cables		200 Psi Gas Cables		200 Psi Oil Cables	
Kv	Avg. Volts per Mil	A	B	C	D	E	F
90	315	0	0	0	6	0	0
118	375	6	6	6	3	6	6
142	450	3	3	3	3	6	3
170	540	0.4	0.5	3	0.1	6	3
204	650	—	—	0.2	—	54	44.7 did not fail
204 to 354*	650 to 1,130*			—		9.1*	
Hours to breakdown		9.4	9.5	12.2	12.1	81.1	

* The voltage was raised continuously at the rate of 20 per cent in three hours.

portant consideration in case a serious leak should occur. The high-pressure gas-filled stop joints were designed for 115 kv at 200 pounds per square inch, in order to have the same 60-cycle strength as the 69-kv cable at 50 pounds per square inch. The high-pressure oil-pipe cable system requires only that the minimum pressure be kept above atmospheric pressure.

Experience to date suggests that the oil in the high-pressure oil pipe-type systems has considerably more stability than the highly refined oil in low-pressure oil-filled cable. Recent 100 degrees centigrade power factor tests of typical oil samples are summarized in Table I. Power factor is but one evidence of oil changes with time and exposure. There are cases where values above 10 per cent at 100 degrees centigrade have been considered tolerable, but operators naturally would prefer to have oils which age with minimum evidences of change from their initial condition.

Typical high-voltage 60-cycle breakdown test data are summarized in Table II from Certified Test Reports on cable supplied for these lines. The endurance of the 200 pound per square inch oil pipe-type cable construction seems almost phenomenal, in comparison to low-pressure oil and 200 pounds per square inch gas which failed at approximately one-half the 1,130 volts per mil breakdown for the oil pipe-type cable. Test F was not carried to failure, because the 204-kv maximum output of the test set was inadequate to cause breakdown within a reasonable time.

Figure 5. Effect of arc energy on maximum oil pressure for cable faults in oil-filled pipe

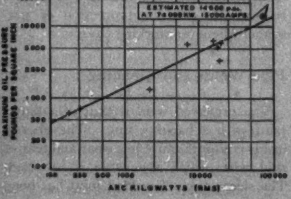

Cable designers no doubt would be interested in more detailed review of the technical differences between the respective cable constructions used. From the operating point of view, however, there appears to be no reason to expect the 69-kv high-pressure gas-filled insulation to be any less satisfactory than oil-filled cable insulation; provided the inherent design limitations are observed.

Pressure Media

A few significant characteristics of oil and gas respectively, as pressure media, are summarized in Table III, where P is absolute pressure in pounds per square inch.

Table III

	Oil	Gas
Viscosity at 100 degrees Fahrenheit		
In Saybolt Universal seconds	850	
In pounds per foot seconds, absolute	0.115	0.0000123
Density, in pounds per cubic foot, at 0 degrees centigrade	58.7	0.0055 P
Thermal expansion coefficient ($a = dV/Vd\theta$), per degree centigrade	0.00068	0.0039
Bulk modulus of elasticity ($B = VdP/dV$), in pounds per square inch	210,000	1.4 P
Maximum pressure change with temperature (aB), in pounds per square inch, per degree centigrade	143	0.0055 P

Gas pressure is seen to be relatively insensitive to temperature changes, whereas oil pressure is so sensitive as to require automatic compensation. To compensate for a 30 degree centigrade temperature drop in the $6^5/_8$-inch pipe, for instance, requires supplying 30 gallons of oil for each 1,500-foot pipe section between semistop joints. The Philadelphia oil-pipe system designs provide for pressure control at each end of the line so as to permit keeping the pipe full of oil at all times, even though sectionalized, as by freezing in order to permit cutting the pipe for cable repairs. The line is supplied normally from one plant.

The instantaneous maximum transient pressure which can be attained in the compression medium during conductor faults is determined by the rate at which the energy of the fault can be dissipated by the accompanying pressure wave within the pipe. These pressures are over four times as great in oil as in gas, being approximately

$$p = KI(t/A)^{1/3} \text{ pounds per square inch} \quad (1)$$

where

K = a coefficient which accounts primarily for the elastic and inertia properties of the fluid, being nine for oil and approximately two for 200 pounds-per-square-inch gas
I = the fault current in amperes
t = paper insulation wall thickness in inches
A = square inches gross area enclosed by the pipe

Figure 5 summarizes the pressures observed on several tests in oil-filled pipe. The two tests for staged faults having less than 300 arc kilowatts were made in 1934 by the Pennsylvania Railroad on a sample of 132-kv oil pipe-type cable. The fault currents were 410 and 465 amperes, respectively. The six remaining tests were made by The Okonite-Callender Cable Company, Inc. in 1945 on a sample 15-kv oil pipe-type cable installation at fault currents ranging from 4,650 to 11,380 amperes. Readings of arc amperes and arc voltage gave the direct indication of arc kilowatts used as the basis for correlating these tests, indicating arc resistances in the range of 2 ohms per inch of insulation thickness at very light faults down to 1 ohm per inch at 10,000 amperes.

The transient hoop stress is independent of pipe diameter, since the maximum hoop stress in the pipe is proportional to the product of the diameter by the instantaneous maximum transient oil pressure and the latter is inversely proportional to the diameter. The duration of the transient maximum stresses is so short as to preclude cold flow or necking down the pipe wall. Consequently, the transient ultimate strength of the pipe wall approaches a limit approximately equal to the product of its conventional ultimate strength by the ratio of the original to the necked down cross-sectional area of the test specimen at the break. The steel in question tested 60,000 pound per square inch ultimate strength and had a 50 per cent neck-down under the conventional test, which indicated a

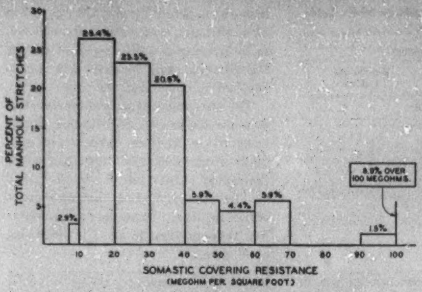

Figure 6. Somastic pipe covering insulation resistance for 90,000 feet of 6⅝-inch outside diameter pipe-type cable circuits in Philadelphia

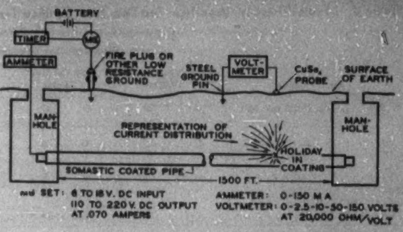

Figure 7. Method used for locating holidays in buried Somastic coated pipe

transient ultimate strength of 120,000 pounds per square inch maximum. Consequently, a 3/8-inch steel pipe wall was estimated to have just about the bursting strength required to contain a 15,000 ampere fault on 69-kv cable under the most adverse conditions.

Cable Failures

For an approximate appraisal of the probable failure record, it was assumed that oil pipe-type systems might have a record comparable to oil-filled cable which, in 2,307 cable-mile years of reported use from 1930 to 1942 inclusive, had experienced three cable failures and 13 joint failures. This amounted to 2.1 failures per 100 circuit-mile years for the three cable circuit designs considered. Examination of the physical relation between cable surfaces and the pipe wall suggested a probability that one-third of the failures would impinge upon and burn through the steel pipe wall having any practical thickness being considered.

It seemed extravagant to provide a 3/8-inch pipe wall and accept the additional energy losses in the hope that an occasional pipe burst might be thus avoided, with so low a failure rate and a probability that one-third of the failures would perforate the pipe at the point of failure in any event. The additional thickness could not be expected to have any practical effect upon life expectancy in exposures to corrosion or arc-burns. Hence, the 1/4-inch wall was preferred for oil as well as for gas.

Construction experience suggests that the simplest and least expensive fault repair procedure is to open the trench, freeze the oil, cut the pipe and make a buried-joint type of repair. The required parts and the construction specification are available for such use in case of need. Oil-contaminated earth can be replaced at little extra cost, if encountered. The alternative of replacing the three cables in a 1,500- or 2,000-foot cable section would almost certainly require more material, labor, and time. A comparable repair procedure also is provided for gas pipe-type cable failures.

Pipe Coating

All of the Philadelphia pipe-type circuits have a 7/16-inch wall of Somastic, Type II coating designed to maintain its integrity at temperatures up to 65 degrees centigrade, as needed for such construction. This coating is somewhat brittle at freezing temperatures, hence the location and repair of defects commonly known as holidays can be simplified considerably by avoiding winter construction schedules where practical.

The initial insulation resistance of this Somastic coating is above 10 megohms per square foot. Figure 6 summarizes the insulation resistance readings on 90,000 feet of pipe construction completed to date, as accepted after repairing known holidays.

Each length of the coated pipe is inspected above ground with a 40-kv spark test set constructed by this Company. The standard 20-kv test set did not have the strength found necessary to locate many pinholes, particularly in the pipe weld covering. The pipe is welded into sections up to 200 feet maximum length and laid or threaded into the trench, depending upon conditions imposed by obstructions, and the backfill is placed.

After each stretch of pipe is completed between manholes, a low-voltage insulation resistance test is made as a final check on the integrity of the pipe coating. This is done by applying an intermittent direct voltage of 100 or 200 from one end of the pipe to a nearby water pipe or driven ground.

The method of locating holidays is shown schematically in Figure 7. A holiday in the coating is located by moving a copper sulphate electrode along the ground surface at 3-foot intervals directly above the pipe and parallel to it. Experience has shown that larger intervals are impractical due to the fact that the sphere of influence about a small holiday is very limited. The electrode is connected through a high-resistance voltmeter, to a driven steel ground rod located 50 feet to 100 feet from the pipe. When the holiday is approached, the signal sent out by the automatic timer becomes discernible on the voltmeter, the extent of needle swing on the meter becoming greatest at a point directly over the holiday. The swings range from 0.05 volt to 0.5 volt depending on the size of the holiday, location of the copper sulphate cell and local earth resistivity. This method has located holidays which had passed inspection with a conventional 20-kv spark test set. The accuracy of location is usually within ±12 inches, even through concrete or granite block paving.

A recent check test on one 25,000-foot pipe circuit shows that the coating resistance still averages 1 megohm per square foot after two years of service. It has been found possible to keep the pipe at least 1/2-volt cathodic by proper bonding, with both ends solidly grounded. A driven ground connection is provided in each manhole and standard procedure requires its use for protection of personnel whenever working therein.

Pipe Welds and Cleaning

The preferred weld is that of a flared joint with a backing ring. The smooth inside contours cause less wear and tear of skid wires when the cable is installed. The sleeve-type of welded joint has been

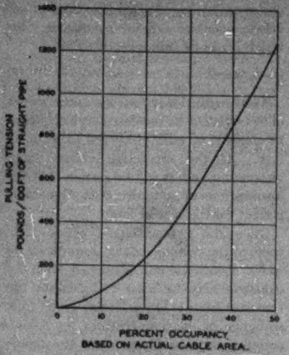

Figure 8. Cable pulling curve for straight sections of pipe-type cable installed in oil-lubricated pipe

used as an alternative, but is rougher and has an undesirable dirt accumulating pocket. Experiments with the use of a pneumatic internal expanding tool for aligning the pipe ends and temporarily backing the weld suggest that the method may considerably simplify fabrication and welding procedures. Each weld is proof-tested at 500 pounds per square inch, Somastic covered, and spark-tested.

Cleaning the inside of the pipe has been a problem now thought to have been solved by deferring the operation until just before the cable is installed. Each manhole-to-manhole section of pipe is then cleaned with a rotary wire brush tool, vacuum dried, and filled with dry nitrogen gas. The impracticability of preserving precleaned interior surfaces inviolate while storing, handling, and installing the pipe casts considerable doubt upon the integrity of such procedures. In fact, it is questionable whether practical precautions with the precleaning procedure will result in cleanliness comparable to the preferred alternative of cleaning in place.

Pulling Tensions

All manhole locations and related cable pulling lengths for the approximately 20 miles of pipe-type cable circuits installed to date, had to be established before any cable had been installed. It has since been found that somewhat longer cable pulling lengths are permissible. Using the percentage of total cable cross-section to internal area of the pipe as a measure of occupancy, the first two 1,500,000-circular-mil circuits occupied 41 per cent of their $6^{1}/_{8}$-inch inside-diameter pipes, the third 1,500,000 circular mil circuit occupied 45 per cent of its $5^{7}/_{8}$-inch inside-diameter pipe, and the 2,000,000-circular-mil circuit occupied 48 per cent of its $6^{1}/_{8}$-inch inside-diameter pipe. Forty per cent occupancy has been considered altogether reasonable, but the higher percentages required for the later installations were considerably beyond the limits of common practice. For instance, the circumscribing circle limit of three cables in a pipe is 65 per cent occupancy in the foregoing reference scale.

The $6^{1}/_{8}$-inch inside-diameter pipe was considered practically ideal for 1,500,000-circular-mil cable. For purposes of design, the maximum pulling tension is limited to the 10,000 pounds per square inch nominal elastic limit of soft drawn copper, with an assumption that one of the three conductors may be required to withstand as much as one-half of the total pulling tension.

Straight-away pulling tensions with properly lubricated pipe in sections without bends may be summarized for practical purposes as in Figure 8, in terms of percentage occupancy alone. The relationship has been found to be altogether dependable for 69-kv cable sizes ranging from 700,000 circular mils at 16 per cent occupancy to 2,000,000 circular mils at 48 per cent occupancy. The tensions shown in Figure 8 are about 15 per cent lower than were estimated from a review of published test data[4] on pulling tensions for smaller cables in duct.

The pulling tension added by a pipe-bend is determined predominantly by the cable tension at the entrance to the bend, the arc length of the bend and its radius. These relationships are summarized for convenient reference in Figure 9.

Figure 9. Tension added at pipe bends as determined by tension at bend entrance and the ratio θ of bend arc length to radius

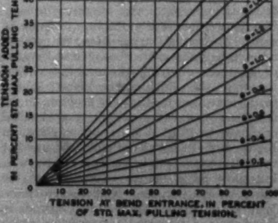

Total pulling tension then can be computed readily in steps and the cutting length determined when the total reaches the maximum permissible pulling tension which, of course, includes the braking and other friction losses at the cable feed-in point, as well as the weight of cable in such vertical pipe sections as may be encountered.

For practical purposes the layout can be simplified materially by allowing approximately 15 per cent of the maximum permissible pulling tension to account for the numerous small bends to be found in nominal straight-away construction, and accounting specifically only for the major bends accompanying major deviations from straight pulls. This was the method used in selecting manhole locations for the 35,000-foot pipe line now about to be installed.

Pressure Controls

The pressure controls for these pipe-type systems were engineered by the respective cable manufacturers. The gas-pressure controls are extremely simple, involving little more than high-pressure gas bottles, a pressure reducing valve and a low-pressure alarm. The comparative incompressibility of oil, its specific gravity and high viscosity, however, require a comparatively intricate system of pumps, reservoirs, and automatic controls.

In the oil-pipe circuits, there is a semistop joint at each cable joint, with by-pass piping and automatic valves designed to reduce materially the rate of oil supply to any section in which the oil pressure drops below 75 pounds per square inch for any reason, as in case of a pipe break.

The system has appeared to work very well when supplying oil demands from a pump at one end of a circuit so long as its length is in the order of 4.5 miles and 18 semistop joints. Some additional field tests will be required to determine whether it is practical to increase the length appreciably without any special provisions.

For illustration of the general relationships involved, consider the conditions for oil flow through the distributed resistance in the main pipe and the lumped resistances of the by-pass pipe assemblies at the semistop joints, as actuated by thermal expansion of the oil in the main pipe.

The critical velocity for turbulence in viscous oil appears to be well beyond the thermal displacement velocities expected.

For nonturbulent flow in an unobstructed pipe, the friction loss is given by Poiseuille's law

$$\frac{dp}{dx}=(k/D)^2\mu v \text{ pounds per square inch per foot} \quad (2)$$

where k^2 is a constant, μ is the absolute viscosity of the oil, v is the average velocity, and D is the pipe diameter. The obstructions offered by the cables in the main pipe, and by the fittings and valves in the by-passes, suggest that $(k/D)^2$ be treated as a constant to be evaluated by test on the particular pipe in question.

To evaluate the pressure losses accompanying the heating or cooling of the oil requires expressing the average velocity of displacement in terms of the distance from the closed end of the pipe. In the main pipe, with oil having a thermal expansion coefficient of (1/1,500) per degree centigrade and undergoing an r degrees centigrade per second change in temperature, the average thermal displacement velocity at distance x from the closed end is $v_m=(rx/1{,}500)$ feet per second.

By direct substitution in equation 2 and integrating for values of x between the limits of 0 and nL, where n is the number of sections and L is the length per section, the total pressure loss in the main pipe is found to be

$$p_m=(k/D)_m^2\mu r n^2L^2/3{,}000 \text{ pounds per square inch} \quad (3)$$

The velocity of oil flow is inversely proportional to the fluid cross-section and, if c indicates the ratio of main to by-pass fluid cross-sections, the velocity in the by-pass is $v_b=(crx/1{,}500)$ feet per second. Hence, the pressure loss in the by-pass pipe of length b becomes

$$p_b=c(k/D)_b^2\mu rbx/1{,}500 \text{ pounds per square inch} \quad (4)$$

in which the values of x are successively L, $2L$, and $(n-1)\,L$ for the respective by-pass locations at L-feet intervals in the line, so that the sum of these by-pass pressure losses is

$$p_b=c(k/D)_b^2\mu rbnL(n-1)/3{,}000 \text{ pounds per square inch} \quad (5)$$

and the total pressure loss from equations 3 and 5 is

$$p=p_m+p_b=\mu r(nL)^2G/3{,}000 \text{ pounds per square inch} \quad (6)$$

where

$$G=\left(\frac{k}{D}\right)_m^2+\frac{bc}{L}\left(\frac{k}{D}\right)_b^2\left(1-\frac{1}{n}\right)$$

p = pressure change caused by oil temperature changes, in pounds per square inch
μ = absolute viscosity of the oil, in pounds per foot seconds
r = time rate of oil temperature change, in degrees centigrade per second
n = number of main pipe sections
L = average main pipe section lengths, in feet
b = average by-pass pipe lengths, in feet
c = ratio of main to by-pass pipe fluid cross-section
$(k/D)^2$ = a constant for the particular pipe section

It will be seen that the pressure loss is jointly proportional to the viscosity, the rate of change in temperature and the square of the total length of the line, since G in equation 6 rapidly approaches a constant value as n increases. It will be observed that the greatest cooling rates occur at the higher operating temperatures which reduce materially the viscosity of the oil and the effective friction head. The total effective head against which the pressure control system must work is the algebraic sum of the friction and gravity heads.

For a given line, the value of G in equation 6 can be determined readily by a test at constant oil temperature and viscosity μ_0. By bleeding oil from the far end of the pipe while the oil supply pump is in active service, a predetermined pressure drop p_0 may be held constant and the resulting velocity v_0 of oil flow may be observed by measuring the rate of oil delivery under these conditions, for which it can be shown readily that

$$G=p_0/\mu_0 v_0 nL \quad (7)$$

As a precautionary measure, the values of G, or $(k/D)^2$ as the case may be, should be checked at each of several rates of oil flow. If the respective values agree reasonably well, it will be certain that the assumption of nonturbulent flow was correct for the case at hand.

Once the precautionary check tests confirm the validity of the assumption on which equation 6 was developed, then the equation may be used to calculate the transient friction loss p for any given time sequence of oil temperatures by taking account of their effects upon the factor μr.

Conclusion

High-pressure gas pipe-type construction avoids certain familiar inconveniences inherent in treating and handling cable oils. It remains to be demonstrated, however, that the gas-filled insulation will earn for itself a record of dependability approaching that already established by oil for use at 69 kv and upward. Meanwhile, Philadelphia Electric Company's seven miles of high-pressure gas pipe-type circuits should contribute a fair share to the necessary experience record.

References

1. THE TEMPERATURE RISE OF BURIED CABLES AND PIPES, J. H. Neher. *AIEE Transactions*, volume 68, part I, 1949, pages 9–21.

2. THE TEMPERATURE RISE OF CABLES IN A DUCT BANK, J. H. Neher. *AIEE Transactions*, volume 68, part I, 1949, pages 540–49.

3. THE THERMAL MOVEMENT OF MOISTURE IN SOIL, A. S. Mickley. *AIEE Transactions*, volume 68, part I, 1949, pages 330–35.

4. CABLE PULLING TENSIONS, Will G. Kelley. *Electrical World* (New York, N. Y.), volume 85, 1925, page 1015.

Discussion

Robert J. Wiseman (The Okonite Company, Passaic, N. J.): This paper reviews the many problems which faced us back in the early 1930's when we first introduced the high oil pressure pipe system, and the progress that has been made in design and installation procedure so that today we have a much better knowledge of its mechanical, physical, and electrical characteristics.

One of our big problems was the correct earth thermal resistivity to use when calculating the conductor size to carry the load. Should we follow the English practice of using 120 thermal ohm centimeters (net) or use a lower value as had been found by some of us when studying the problem? Fortunately, the Philadelphia Electric Company was willing to study the problem on the Oilostatic installation which was installed originally in 1932. The results as shown in Figure 1 of the paper not only told us what the effective earth thermal resistivity was, but gave us a chance to appreciate the shape of the transient temperature curve. We were able to use an empirical formula to calculate the transient temperature which checked the actual curve very nicely. Note that we obtained on this test as low as 60 thermal ohm centimeters, but to be conservative, we took a value of 80 for future calculations. This can easily cover any hot spots that may occur along a route. Any spots having higher values will probably be rare and of short length, and also actually exist for a very short time. It is not economically feasible to design a line for these isolated cases and the system can well handle them. The authors refer to this in the section on Load Ratings.

Although the authors state that the higher temperature rise for the 2,000,000-

circular-mil gas cable was due to the higher losses in the conductor over that for the 1,500,000-circular-mil oil cable, it also is a fact that the thermal resistance inside the pipe for the gas cable was about the same as for the oil cable, whereas it would have been lower if both systems had had the same thermal characteristics. We have made tests and found this to be so. As a result, we use a thermal resistivity for the insulation of 500 thermal ohms per centimeter for the Oilostatic (oil pressure) cable and 550 for a gas-pressure cable. For the pressure zone we have found we can get sufficiently accurate values of thermal resistance if we use $R_{th} = 1.60/D$ thermal ohms per foot for the Oilostatic cable and $R_{th} = 2.58/D$ thermal ohms per foot for a high gas-pressure cable where D is the diameter over the shielding tape on the single-conductor cable.

We are looking forward to the time when the authors will give us a progress report on the thermal operation of their lines.

We have no hesitancy in allowing the Oilostatic cable system to operate at 100 degrees centigrade conductor temperature under an emergency condition. We are wondering how closely we can approach this temperature for normal temperature. As far as insulation is concerned, thermal time tests indicate no physical or electrical deterioration when held at 100 degrees centigrade for at least three years, indicating at present, perhaps 85 or 90 degrees centigrade feasible. The limitation, as I view it, will be based on how much drying out of the soil around the pipe will occur. It may not be too great based on the ideas presented by A. S. Mickley.[1]

Reference is made to the modification in the experimental Oilostatic cable installation at Plymouth Meeting Substation to obtain a higher temperature range. The information given below may be of interest to those who are following the subject: An 800-foot section of the Oilostatic installation has three 400,000-circular-mil conductors in place of the 1,000,000-circular-mil conductor. With the contemplated load of 75 megavolt-amperes at 75 per cent load factor, we have estimated a pipe temperature of 59 degrees centigrade and a conductor temperature of 101 degrees centigrade, with an earth ambient temperature of 20 degrees centigrade. Will this pipe temperature cause drying out of the earth? Time will tell. It is expected that an emergency load of 103 megavolt-amperes may take place for several hours. If it follows the 75-megavolt-ampere load and the conductor has reached 101 degrees centigrade, then in two hours the conductor is estimated to reach 150 degrees centigrade and the pipe 72 degrees centigrade. We do not plan to let the conductor go over this temperature. We are looking forward to this study with great expectations.

Although it appears it is not necessary to use the steel pin reinforcing for connectors, we believe they are worthwhile as a further strengthening against excessive tensions if the cable goes to low temperatures.

We are interested in the authors stating that the gas-filled insulation was not expected to have the same rugged electrical qualities as high-pressure oil-filled insulation, shown in Table II of the paper. This brings up a point for discussion. If we are satisfied with the breakdown voltage obtainable with the gas-filled insulation, which is about the same as for low-pressure oil cables, then why not reduce the insulation thickness for high-pressure oil systems? We are ready to do so by 10 per cent and perhaps as much as 20 per cent. This also is in accord with the ideas advanced by Dr. L. Domenach.[2] We recognize that in some cases the impulse level of the insulation must be considered. However, Dr. Domenach has obtained some high impulse tests on his cable, partially due to using very thin tapes next to the conductor, but also I believe because of the high pressure that he uses.

There are several factors involved which influence the instantaneous pressure that is developed in case a short circuit takes place in a pipe system. For the gas type we have the formation of gas due to the burning of the insulation by the arc, and as the authors state, the pressure developed is not great because of the compressibility of the gas. In the case of the oil type, we have the formation of gas due to the arc burning oil and insulation, which creates a positive pressure and the stretching of the pipe, the absorption of gas by the oil and the propagation of the wave in both directions to the joints, all of which are negative, in that, they tend to hold down the pressure. The resultant pressure is not as large as one would expect. The authors show in Figure 5 of their paper the pressures that are liable to be expected. I would prefer to express it as a function of kilowatt seconds of energy as it is the latter which determines the amount of gas formed which causes the sudden pressure. Also in determining pipe thickness, we must keep in mind that it is the ability to withstand sudden pressures rather than a static pressure that is important.

In the beginning when setting up lengths of sections we believed it feasible to use 2,000-foot lengths. Conditions of installation showed 1,500 feet was a better average to take. We note that there is a trend toward longer lengths without getting excessive pulling tensions. I think this is good, but we must be careful in not going ahead too fast until data are collected showing what pulling tensions are found. It appears that 2,000-foot lengths are safe, and possibly 2,500 feet. I agree with the authors that percentage of occupancy is important, although I am more inclined to believe it is more important on the basis of allowable space for radial expansion of the cables, particularly when longer lengths of sections are used.

While pressure control of a gas system is relatively simple, it would appear that for an oil system such control is complicated. This is not true. It requires a storage tank for the oil supply, and since the oil changes in volume as its temperature changes, a pumping plant also is required to maintain the pressure. The superiority of the oil pressure system over the gas system justifies its extra pressure-control setup.

One of the problems that we have on an oil-pressure system is the building up of the pressure if the load is suddenly applied on a very long line when it is at a low temperature. Calculations have indicated, and actual tests have shown, that these pressures are not high enough to cause any damage to the system. Likewise when dropping load it is essential that the pump capacity be large enough to supply oil to the far end of the system and all restrictions to flow be kept to low values. Experience with the various installations that have been made has helped us to attain this end.

This paper should help weigh the evidence of the relative merits of the two systems as to their over-all design, installation, and operating characteristics.

References

1. The Thermal Movement of Moisture in Soil, A. S. Mickley. *AIEE Transactions*, volume 68, part I, 1949, pages 330–35.

2. Cables with Reduced Thickness of Insulant Under Pressure, Dr. L. Domenach. International Conference on Large High Voltage Electric Systems (Paris, France), June 1948.

R. W. Atkinson (General Cable Corporation, Bayonne, N. J.): The authors emphasize the undoubted desirability of reducing any unnecessary costs and complications during installation. It is helpful to consider several items involved in construction and to discuss the purpose of some of the refinements and the degree to which the means used are justified by the results.

1. The need for removal of the temporary sheath is disappearing with increasing acceptance of shipment of the cable without such a sheath.

2. One method of jointing produces a joint that is electrically as strong as the cable by virtually reproducing the mechanical and electrical equivalent of the factory applied insulation. Even where a joint can be made having a strength equal to the *specified* strength of the cable at lower cost or much more expeditiously, there seems to be grave doubt of the desirability of accepting anything that is not able to meet any tests which the cable actually can meet. In short, can a joint be acceptable if, on a type test, the joint fails and the cable does not fail? The answer to that question will have much to do with the direction of development of jointing.

3. Stop joints, complete or semistop, add much to the installation problem as compared to simple normal or nonstop joints. The suggestion toward reducing or eliminating these is noted. The experience at New Orleans with complete absence of stop joints helps to encourage that arrangement at least for high pressure oil-filled cables.

4. The difficulty involved in the production of high electrical strength of a joint is considerably increased if the connector greatly exceeds the conductor diameter. There has recently become available a connector which is satisfactory in conductivity and in mechanical strength and which is a little larger in diameter than the conductor. This connector materially reduces the cost and time required to produce a joint of high electrical strength as compared with earlier forms of solderless connectors which were significantly larger than the conductor.

5. In many of the existing high pressure oil systems, the pipe oil has been thoroughly degassed before it enters the system and means are taken to assure that it stays that way. This involves some degree of extra trouble and cost. In other systems, the oil is admitted under conditions which cause it to be gas-saturated at around atmospheric pressure. It should be recognized that this may result in a definite sacrifice in reference to the ability of the cable to be operated temporarily at pressures in the range of atmospheric. With the fully degassed oil operation at low pressure, when required, is

fully justified because this does not result in any tendency to form gas bubbles as would be the case where the oil does not remain fully degassed.

One wonders whether it is a significant handicap to the gas-pressure cable that it is undesirable for such a cable to be operated at pressures greatly under the normal values. Only a direct break in the pipe or end equipment need result in low pressures with gas whereas these and many other things, even a power failure to the supply pump may cause failure of oil pressure. In any event with gas pressure there is some evidence that temporary operation at low pressure may be found permissible. Indeed, some data have been found surprisingly favorable.

A word may be said here concerning pipe losses. These should be independent of the pipe thickness within the commercial range sizes. Due to skin effect in the pipe, only about the inner 1/16 inch plays a significant role in the losses due to the pipe. The remainder of the wall is pretty thoroughly screened from electrical current or magnetic field at the power frequency of 60 cycles.

It is of interest to note the close correlation between pulling tension and per cent occupancy of the duct, without any direct relation to the weight of the cable or size of the pipe. It will be of further interest to tie this in with previous data where the pulling tensions have been correlated with the weight, without reference to per cent of occupancy. It may be found that a still broader application of the data may be made by taking both into account than with either one alone.

W. Allistair Sinclair and **Francis M. Hull** (The Detroit Edison Company, Detroit, Mich.): The authors should be commended for their valuable contribution to the experience record of pipe-type cable. They state that because of the sturdy qualities of high-pressure oil-pipe systems it may be practical to accept the possibility of occasionally operating such cables at normal copper temperatures ranging up to 100 degrees centigrade. Sections of *SMD*-type high-pressure, gas-filled cable, having 600,000 circular-mil conductors insulated with both 600 mils of preimpregnated and mass-impregnated paper in a 7-inch outside diameter steel pipe have been operated at such temperatures on the Detroit Edison Company's 120-kv experimental line. The 700-foot cables have been operating with a potential of 69 kv between conductor and ground and the conductor temperatures have been maintained at approximately 100 degrees centigrade for 1,600 hours. These cables now are being subjected to further and more severe tests. They have been operated on a "12-hours on, 12-hours off" schedule for load current with loads up to 790 amperes per conductor for 310 days. High voltage to ground is maintained continuously. Power factor tests indicate no apprecciable deterioration of the insulation This schedule provides daily variations in conduetor temperatures of from 100 to 30 degres centigrade and constitutes a severed test of the ability of the cable to withstand rough usage.

It must be remembered, however, that theire is a limit to the number of watts which can be dissipated without encountering accumulative heating. Such a condition developed in January during the above cycling. The cables had been subjected to 70 days of cycling previous to the time that this condition developed. In seven days the shielding temperatures, at the end of each load period, increased 15 degrees. On each successive cycle the increase in temperature was rapidly becoming larger. During this interval the line was dissipating between 57 and 60 watts per foot.

At the start of the load period on the eighth day, the high voltage was removed but the temperature rise during the first six hours equalled that obtained during the previous 12-hour load period. The load was decreased from 770 to 500 amperes for the remaining six hours of the load period. The line was then left out of service for 36 hours during which time power-factor measurements were made. Since the results were of the magnitude expected, the line was placed back in operation. During the first load period, 500 amperes were applied at low voltage and the high voltage also was applied at the start of the load period of the second cycle. The load was increased on each successive cycle until on the sixth cycle the load was the same as that which existed at the time the runaway was detected. The cycling was then continued for 227 days without any long-time shutdowns. During this period there was no indication of a reoccurrence of the runaway condition.

Our new lines and terminal equipment, therefore, are being designed on the assumption that loads which will produce 100 degree centigrade copper temperature may be impressed ultimately.

Soldered-type, countersunk, copper connectors were used on our experimental and our first commercial lines. These connectors have a diameter the same as that of the cable conductor. Two cases of open circuits in joints have been encountered on the commercial line. Both of these open circuits occurred during periods that the line was out of service due to overhaul of the generator and, incidentally, during periods of the lowest ambient earth temperature.

Recently one of the joints on the experimental line was dismantled and it was found that the solder had been extruded at the end of the connectors. There also was some evidence that similar action had taken place at the center of the connector where the conductors butted. This particular joint had been subjected to 310 days of cycling load and it was possible that an open circuit would have occurred if the cycling had been continued.

Compression-type connectors were used on the line completed last year and is now our standard for pipe-type cable.

Somastic coating has been utilized on all the Detroit, commercial pipe-type circuits and the difficulties encountered were similar to those mentioned by the authors. It is interesting to note that their spark test voltage has been increased to 40 kv. However, it is not stated whether this is rms or peak voltage and where it is measured. In Detroit, each nominal 40-foot length of pipe is tested with a 20-kv rms voltage between points on the outside of the 1/2-inch covering and the pipe itself. This voltage is measured by means of sphere gaps. Each completed section of pipe between manholes is tested in a manner similar to that outlined in the paper.

Every reasonable effort is made to obtain a measured resistance (as accepted after repairing known holidays) from pipe to ground of not less than 10 megohms per square foot of the outside surface of the pipe. Table I of the discussion is a comparison of the insulation resistance readings on 65,000 feet of pipe construction completed during 1948 with the results shown in Figure 6 of the paper. This table shows the Detroit results to be higher than those obtained in Philadelphia. This might indicate the need for a specification covering the testing of the Somastic covering so that all construction would be tested on the same basis and directly comparable.

Table I

Somastic Covering-Resistance, Megohms Per Square Foot	Per cent of Total Manhole Stretches	
	Philadelphia	Detroit
0–10	2.9	3.4
10–20	26.4	26.7
20–30	23.5	10.0
30–40	20.6	3.3
40–50	5.9	10.0
50–60	4.4	13.3
60–70	5.9	3.3
70–80		
80–90		
90–100	1.5	6.7
Over 100	8.9	23.3

G. B. Shanklin (General Electric Company, Schenectady, N. Y.): The paper by A. H. Kidder and G. S. Van Antwerp represents a very useful contribution to the pipe cable art, where additional knowledge and experience of this kind is still badly needed.

The manufacturers and users of cable of this type are all working on the problem either individually or in co-operation. During the course of our work findings and conclusions on some aspects of the problem are not in full accord with those presented by the authors and it might be well to discuss these briefly.

The authors conclude that for the same loading and temperature rise pipe cable requires the same conductor size as single-conductor oil-filled cable in underground ducts. This same thought has been expressed by others on previous occasions, but according to all of the information we have been able to obtain the equivalent conductor size for pipe cable is from 25 to 50 per cent larger than that of single-conductor oil-filled in ducts. This is particularly true for the heavier loads and larger conductor sizes, such as the 1,500,000-circular-mil conductor mentioned in the paper. Like many of the present differences related to pipe cable, the a-c losses assumed in the calculations are undoubtedly involved. Recent studies of such losses show that the armour losses and the steel pipe losses are somewhat higher than previously assumed. On the other hand, losses in lead sheathed cable are already well established.

The authors also conclude that, other things being equal, a high pressure gas-filled pipe cable conductor should be at least 33 per cent larger than an equivalent oil-filled pipe cable conductor for the same loading. All of the test data we have been able to obtain would not indicate that this is so. As far as thermal characteristics are concerned, there is only a slight advantage in favor of oil-filled pipe cable and for all practical purposes the conductor sizes are the same for both. Here again the variable a-c losses found in pipe cable and the, as yet, lack of full control of these losses, may have influenced the authors' conclusion.

Table I of the paper gives measured power factor values on samples of oil withdrawn from low pressure oil-filled cable and high pressure oil-filled pipe cable after several years of service. Based on these measurements the authors conclude that the oil used in the pipe cable has greater temperature aging stability. We have made a number of aging tests on both types of oil and without exception the thinner oil used in oil-filled cable has shown greater aging stability. The primary reason for this is that this thinner oil was especially designed and developed as an insulating oil, while that now used in pipe cable was actually borrowed from the lubrication field. It undoubtedly has sufficient stability for all practical purposes, but this stability is definitely not equal to that of the other oil mentioned. It is true that, all other things being equal, aging stability of oils increases with viscosity, but it does not prove to be so in this case. The higher power factor of the thinner oil in Table I is actually due to the much more limited volume of oil in the self-contained type of cable and the large surface exposure to copper in the conductor core. Copper, of course, is a very active catalyzer of oil.

C. T. Hatcher (Consolidated Edison Company of New York, Inc., New York, N. Y.): The authors are to be complimented on presenting a comprehensive picture of the problems involved in selecting cables for a high-capacity tie system. Any utility engineer, who has been in the position to make a decision regarding the type and size of cable to be installed to meet a prescribed loading condition, knows some of the troubles which are experienced before the cable construction is decided upon.

The effect of binding tapes, skid wires, and pipe all add to the losses in the cables. This has been thoroughly shown in the paper presented by L. Meyerhoff and G. S. Eager.[1] Considerable work now is being carried on in regard to these losses and it is hoped that in the future the selection of cables will be somewhat easier since sound data will be available.

Limited test data to date on oil from our pipe systems indicates that the oil is stable. Sufficient data has not been collected to make a direct comparison between oil from low-pressure oil-filled cables and oil from the pipe systems.

Limited experience appears to confirm the authors' conclusion that the simplest and least expensive fault repair procedure is to open the trench, freeze the oil, cut the pipe, and change a relatively short length of cable.

I do not agree with the authors that cleaning the inside of the pipe at a coating plant and maintaining the pipe in a clean condition is an impractical procedure. Methods have been developed for providing a satisfactory internal coating at a central location and plugging the pipes during shipment so that the pipe is received in a clean and satisfactory condition. Receipt of pipe in this condition speeds up the installation and restoration of street conditions. Any cleaning of inside pipe scale in the field would apparently require time and it is questionable if the scale could be removed completely from a manhole-to-manhole section.

I also question the authors' statement that the length of a pipe system should be limited to $4^{1}/_{3}$ miles when supplied with one pumping plant. The length of a system to be supplied depends upon the restriction in the line, namely, by-pass connections at the semistop joints, and we have found that this situation can be controlled by installing larger by-pass pipe. At the present time we are installing a line approximately ten miles in length with approximately 20 semistop joint locations with a supply from only one end. Test data on existing lines indicates that this will be satisfactory.

REFERENCE

1. A-C RESISTANCE OF SEGMENTAL CABLES IN STEEL PIPE, L. Meyerhoff, G. S. Eager, Jr. *AIEE Transactions*, volume 68, part II, 1949 (*Proceedings* T9135).

A. H. Kidder: The authors appreciate deeply the interest shown by the several discussers and particularly their comments concerning points which merit additional consideration.

Mr. Atkinson has stated accurately on several points, a position which is almost in complete accord with our own. We were as surprised as he, to find that our maximum pulling tensions could be summarized entirely in terms of per cent occupancy. In fact, we obtained a better correlation on this basis than when we attempted to deal in terms of weight, friction coefficient, and assumed conductor configuration within the pipe. We think one of the difficulties with the latter method is that conductor configuration is unpredictable.

We shared Mr. Hatcher's preference for precleaning the pipe, until we were convinced that adequate cleaning could be accomplished at lower cost after the pipe had been installed. We have consistently avoided the use of any internal pipe coating, because we were uncertain of its compatibility with the oil, particularly when locally carbonized as during welding operations.

Our analysis of one test on Mr. Shanklin's 2,000,000-circular-mil pipe-type cable construction as supplied for one of our projects, suggests that its unusual high losses are attributable entirely to certain unexpected effects of hitherto commendable precaution against oxidation of the conductor strands during the course of cable manufacture and treatment.

Judged in terms of the tests reported in the AIEE paper by L. Meyerhoff and G. S. Eager, Jr.[1] however, it is now apparent that Mr. Shanklin's 2,000,000-circular-mil cable in pipe has approximately the same a-c conductivity as others have reason to expect from 1,600,000 circular mils. I therefore shall continue to disagree with Mr. Shanklin's often repeated claim that oversize conductors are required.

The 2,000,000-circular-mil conductor size for the gas pipe system was specified with Mr. Shanklin's consent in what we considered a reasonable attempt to avoid operating the gas-filled insulation at temperatures above 75 degrees centigrade in locations where the thermal resistivity of the earth might exceed 80 thermal ohm centimeters. In this case the 2,000,000-circular-mil conductor in high pressure gas has approximately the same temperature rise per watt of a-c losses as does the 1,500,000 cable in an oil-filled pipe. We shared his unwillingness to permit gas-filled insulation to operate at temperatures above 75 degrees centigrade and, consequently, specified the larger copper size in order to reduce the watts losses.

Mr. Shanklin's explanation of the lower measured power factor on samples of oil withdrawn from high-pressure oil-pipe cable is enlightening. We had thought the oil to have greater temperature aging stability. It is now apparent that the superior performance of the oil in pipe is in part, at least, attributable to the reduced exposure to copper as a catalyst—a factor which can be controlled even in oil-filled cable designs, as by coating the copper strands with a tin or lead alloy.

The experience of W. A. Sinclair and F. M. Hull with 100 degree centigrade operation on *SMD* type high-pressure gas-filled cable, is an antidote for our discomfiture in the knowledge that our gas-pipe cable has 15 to 23 per cent greater a-c resistance than had been expected. We are very much interested in their report of accumulative heating, with losses in the order of 57 to 60 watts per foot.

The spark test voltage in Philadelphia is measured only by means of point-to-point gaps in air. For testing the 7/16-inch Somastic coating on the pipe, the voltage is increased until the spark will jump a 3/4-inch gap setting. For testing the 1-inch thick molded Somastic covering over pipe welds, the voltage is adjusted to spark across a $1^{1}/_{2}$-inch gap setting. This is admittedly a much less accurate voltage measurement than that obtained by the use of sphere gaps as reported by Mr. Sinclair and Mr. Hull.

As Dr. Wiseman points out, a greater 60-cycle breakdown strength of insulation in high-pressure oil suggests considering a reduction in insulation thickness provided satisfactory impulse strength can be maintained.

Our analysis of the transient pressures summarized in Figure 5 of the paper should, perhaps, be amplified somewhat in the light of Dr. Wiseman's comment that kilowatt-seconds may be a factor. We found the pressures to be proportional to the square root of the arc-kilowatts, and apparently independent of arcing-time. This confirmed our mathematical analysis which had indicated that the maximum transient pressure should be a natural function of the maximum rate of fault energy input as measured in Btu per second or kilowatts. We, therefore, prefer to deal in terms of arc-kilowatts rather than in terms of kilowatt-seconds.

REFERENCE

1. A-C RESISTANCE OF SEGMENTAL CABLES IN STEEL PIPE, L. Meyerhoff, G. S. Eager, Jr. *AIEE Transactions*, volume 68, part II, 1949 (*Proceedings* T9135).

Dynamic Braking Control of D-C Series Motors—Experimental Study of Speed-Torque Curves

G. W. HEUMANN
MEMBER AIEE

Synopsis: This paper presents the results of tests to determine the speed-torque characteristics of a d-c series motor driving a crane hoist. Direct readings of speed and torque during dynamic braking lowering operation were taken for various values of resistance in the motor circuit branches. A comparison between test data and calculated performance, using a conventional method of calculation, indicates that calculation obtains performance curves which are sufficiently accurate to forecast the performance of a practical crane hoist controller.

WHEN a series motor is used to retard an overhauling load by dynamic braking, motor power circuits are represented by Figure 1. The series field and the armature are connected in parallel. In series with the series field, there is a block of resistance R_F which includes the internal resistance of the series field and the series brake.

In series with the armature, there is a block of resistance R_A which includes the internal resistance of the armature and commutating field, and the equivalent brush drop resistance. A series resistance R_S is connected in series with both the armature and the field. R_S includes the resistance of the power leads between the point of constant line voltage V and the motor.

For many years, control circuit designers have used a method of calculating speed-torque curves which was described by A. A. Merrill.[1] Expressing motor performance quantities in per unit, speed and torque can be calculated by the following equations.

$$S=\frac{E}{K} \tag{1}$$

$$T=KI_A \tag{2}$$

where

S = speed in per unit of rated speed
T = torque in per unit of rated torque
E = electromotive force in per unit of normal generated motor electromotive force at rated torque and rated speed
I_A = armature current in per unit of rated full-load current
K = a factor, expressed in per unit, which is a function of field current and armature current

Factor K (equivalent to the commonly used terms "torque per ampere" and "volts per revolution per minute") is determined from motor test data. For motoring operation, it is permissible to consider K as a function of field current only, as the effect of armature current is negligible. When the motor is operating as a generator, retarding an overhauling load, the effect of armature current on K must be considered.[2] Knowing K from motor test records, an analysis of the motor circuit can be made, using Ohm's law and calculating currents and voltages in the various branches of the motor circuit.[3] Knowing motor electromotive force, field current, and armature current for each assumed operating point, speed and torque can be calculated using equations 1 and 2.

Test Set-up

To check the accuracy of the aforesaid method of calculating dynamic braking motor performance, a series of tests was conducted on an experimental hoist. Figure 2 is a view of the motor driving the hoist, which is beyond the wall to the right. An electromagnetic torque meter, rated 1,000 pounds-feet, which is described elsewhere,[4] is mounted between the motor coupling and the hoist coupling. It reads the torque transmitted between motor and hoist shafts directly in pounds-feet. On the left side of the motor are the series brake and a d-c tachometer generator for reading motor speed on a voltmeter calibrated in revolutions per minute.

Test Motor

Tests were made with a series motor whose nameplate data included the following: C01830, 50 horsepower, 30 minutes, 550 rpm, 230 volts. All quanti-

Figure 1. Generalized dynamic braking power connections

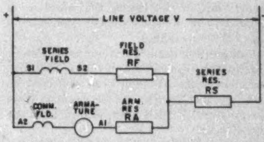

Figure 2. View of motor driving test hoist

Paper 49-138, recommended by the AIEE Industrial Control Committee and approved by the AIEE Technical Program Committee for presentation at the AIEE Summer General Meeting, Swampscott, Mass., June 20–24, 1949. Manuscript submitted February 8, 1949; made available for printing April 27, 1949.

G. W. Heumann is in the Control Engineering Divisions, Apparatus Department, General Electric Company, Schenectady, N. Y.

The author wishes to acknowledge the assistance given by K. A. Andrew and J. A. Hepperlen in obtaining the experimental data used in this paper.

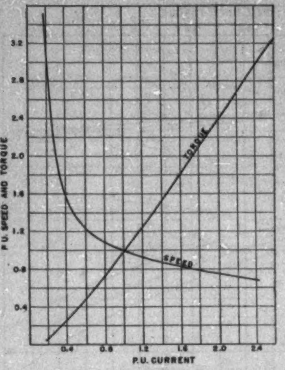

Figure 3. Per unit speed and torque versus current of test motor

ties relating to motor performance in this paper are given in per unit. The base quantities are as follows:

Base torque, 482 pound-feet
Base speed, 550 rpm
Base current, 185 amperes
Base voltage, 206 volts
Base resistance, 1.113 ohms

Internal resistances of the motor at rated temperature rise, expressed in per unit, are

Armature plus commutating field	0.079
Series field	0.037
Total	0.116

The fundamental characteristic of the motor is plotted in Figure 3. These data were taken from conventional test records of a motor of the same type as the test motor.

Curves for K as a function of field current and armature current are given in Figure 4. These data were obtained from special tests on a motor of the same type during which the motor was driving a load, or was driven as a generator, with various amounts of resistance in series with the field and the armature. Values of K were calculated from the measurements of torque, speed, and currents in the motor branch circuits. The dashed curve in the motoring quadrant has been calculated from Figure 3. This K curve obtains satisfactory calculated speed-torque curves for motoring operation.

Effect of Losses

Equation 2 for the calculation of torque is correct rigorously only when T is the internal developed torque of the motor, and K were determined on the same basis. The torque delivered at the shaft differs from the developed torque by the losses. Values of K, given in Figure 4, include losses, as they were determined experimentally from the shaft torque at each test point. When K is then used to calculate torque and speed for a different operating condition, losses are different. The question then arises what error is introduced in the calculations by the neglect of motor losses.

Core loss, friction, and windage are a function of speed, and core loss is also a function of field current. The sum of these losses, taken from test data of a motor of the same type as the test motor, expressed as per unit torque loss, is plotted in Figure 5 as a function of speed for various values of field current. The loss curves are straight lines. Friction and core loss change linearly with speed, except for very low speeds. Windage changes with the second power of speed, but as the test motor is totally enclosed, the windage loss is very small. At two per unit speed it is less than 0.001 per unit torque, thus its effect is negligible.

The dashed curve in Figure 5 represents losses with the motor operating as a straight series motor according to Figure 3. Thus, the dashed curve represents the losses included in the K factors of the dashed curve in Figure 4. During actual motor operation low speeds are associated with high-field currents and high speeds with low-field currents. Hence, Figure 5 indicates that neglecting core loss, friction, and windage introduces an error in the torque calculations of less than 0.01 per unit.

The foregoing discussion does not include the "load" or "stray" losses which are generally taken as a fraction of the core loss. Experience with similar motors, which has been set down in an AIEE Standard[6] indicates that the "load" losses vary between 22 per cent of the core loss at light load and 65 per cent at twice normal load. The error introduced in the torque calculations is less than 0.01 per unit, so that neglecting all losses introduces an error of less than 0.02 per unit in the calculated torque.

Effect of Resistor Heating

Cast grid resistors, which are applied on many crane installations, were used during the tests forming the subject of this paper. Cast grids have a comparatively high temperature coefficient. The increase in resistance is of the order of 7 per cent for each 100 degree centigrade rise. Since their permissible temperature rise is 350 degrees centigrade, it is necessary to consider the resultant increase in resistance when calculating speed-torque curves for installation.

To illustrate the effect of resistance changes due to heating, two sets of calculated dynamic braking curves are given in Figure 6, which are typical for low-speed and high-speed lowering points of a crane hoist controller. For each speed point, three curves are plotted. Curves (A) were calculated with the resistor at room temperature, and curves (B) and (C) were calculated with all resistance values increased 10 and 20 per cent respectively.

In the region of low speeds, which are

Figure 4. K-factor of test motor

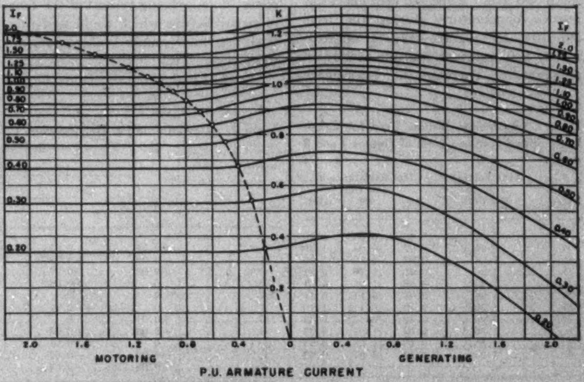

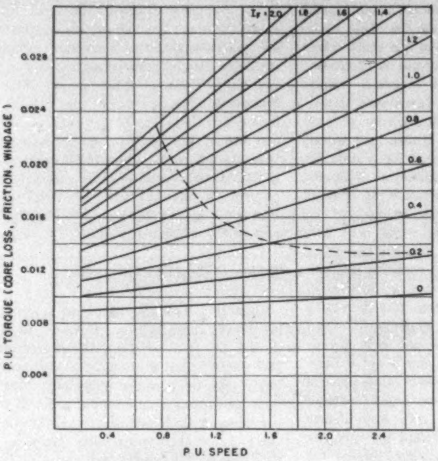

Figure 5. Core loss, friction, and windage of test motor

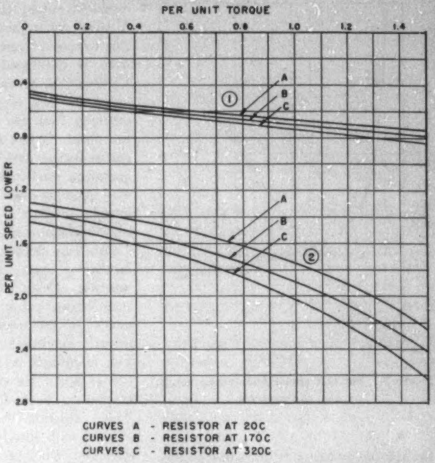

Figure 6. Typical calculated lowering speed-torque curves indicating effect of cast grid resistor heating

associated with high-field currents, the difference between cold and hot resistance has only a minor effect. However, in the region of high speeds, in which the field current is below normal current, a decrease in field current due to resistor heating results in a considerable decrease in factor K and a consequent rise in speed. For the tests on the experimental hoist, the cold resistance of each resistor section was measured by a bridge. The hoist was operated prior to each test until resistor temperature became stabilized and consistent speed and torque readings were obtained for each resistor setup and load. Repeated spot checks of resistor temperatures during the tests indicated an average rise of approximately 300 degrees centigrade over room temperature. Therefore the performance curves, with which test results are compared in the following paragraphs, were calculated with hot resistances, 20 per cent higher than measured cold values.

Test Data

The results of tests on a number of typical dynamic braking circuits are plotted in Figures 7 and 8. The resistances connected in the motor circuit branches, including internal motor resistance, are shown in Table I. These values were used to calculate the curves. The heavy dots are the test readings. The curves shown are not associated with any particular design of crane hoist controller. They were selected from a large number of test data as being typical of the range of circuit setups which could find practical use on dynamic braking lowering controllers.

Figures 7 and 8 contain the readings of 64 individual tests. In Table II the deviations between calculated and tested values are tabulated as per-unit differential in speed. Positive deviation means that measured speed is higher than calculated speed. The occurrence of the deviations is plotted in Figure 9, each dot representing the occurrence of a deviation in Table II.

The majority of the deviations occur within a band of ±0.03 per unit. It is generally accepted by control engineers that calculated speed-torque curves may reasonably be within 0.05 per unit deviation from actual speed. Therefore, the correspondence between calculated curves and test data is quite satisfactory for practical purposes.

The calculated speed-torque curves

Table I. Resistance Values Used for Calculating Speed-Torque Curves of Figures 7 and 8

Curve	Line Voltage Volts in Per Unit	Hot Resistance in Per Unit R_A	R_F	R_S
A	1.26	0.46	0.04	1.20
B	1.26	0.87	0.04	1.20
C	1.26	0.87	0.62	1.20
D	1.26	0.08	1.16	0.21
E	1.26	0.08	1.96	0.21
F	1.26	0.08	3.11	0.21
G	1.24	0.13	0.11	1.10
H	1.24	0.13	0.47	0.63
I	1.25	0.13	1.04	0.63
J	1.26	0.13	1.68	0.63
K	1.26	0.13	2.61	0.63

For Nomenclature Refer to Figure 1

Table II. Deviation in Per Unit Between Calculated and Measured Speeds for Tests Plotted in Figures 7 and 8

	At Load					
Curve	1	2	3	4	5	6
A	+0.01	+0.01	+0.01	−0.01	−0.01	−0.02
B	+0.03	+0.03	+0.01	+0.01	−0.01	−0.02
C	+0.03	−0.07	−0.03	−0.08	−0.03	−0.04
D	0	+0.03	+0.01	+0.02	+0.02	+0.03
E	0	0	+0.01	+0.03	−0.02	−0.02
F	0	−0.01	−0.01	−0.03		
G	+0.01	0	0	−0.01	+0.01	+0.03
H	−0.03	−0.03	−0.02	−0.03	−0.02	0
I	0	−0.01	0	−0.02	−0.02	+0.02
J	−0.02	−0.02	0	0	+0.01	+0.02
K	−0.05	−0.02	0	+0.02	+0.04	+0.09

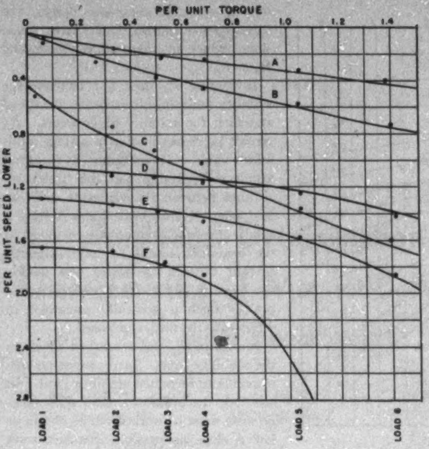

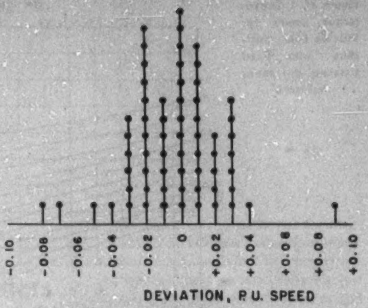

Figure 7(left). Comparison of calculated speed-torque curves and test readings

Tests A to F

Figure 9 (above). Occurrence of deviation between calculated and measured speeds

give a good indication of the load at which instability may occur. Consider curve (F) in Figure 7. With that circuit it was possible to lower load 4, which corresponds to approximately 0.70 per unit motor torque or rated load on an average crane hoist. When it was attempted to lower load 5, corresponding to approximately 1.15 per unit motor torque or 165 per cent load on the hook, it was impossible to obtain stable speed readings, as would be expected from the shape of curve (F).

Figure 8. Comparison of calculated speed-torque curves and test readings

Tests G to K

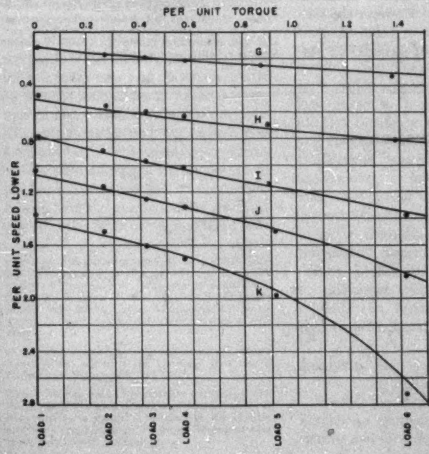

By comparison, refer to curve (K), Figure 8. This curve has considerably less slope in the range between 2.60 and 2.80 per unit speed, and it was possible to lower load 6, corresponding to approximately twice rated hook load, at stable speed. Part of the improved performance on curve (K) is due to reduction in no-load speed by using somewhat lower resistance in the field circuit, and part is due to increase in series resistance, the beneficial effect of which had been pointed out in a previous paper.[3]

Application to Hoist Controller Design

In the design of a d-c dynamic braking crane hoist controller, the first step is to select the speed-torque curves it is desired to realize on the various controller points. Good controller design should obtain as uniform a spacing as possible of no-load and full-load speeds between controller points. The speed-torque curve on the

Figure 10. Speed versus field resistance with fixed armature and series resistance

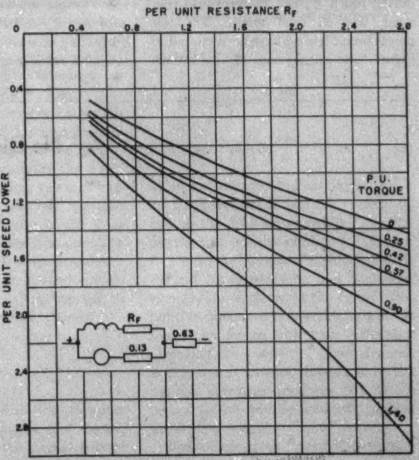

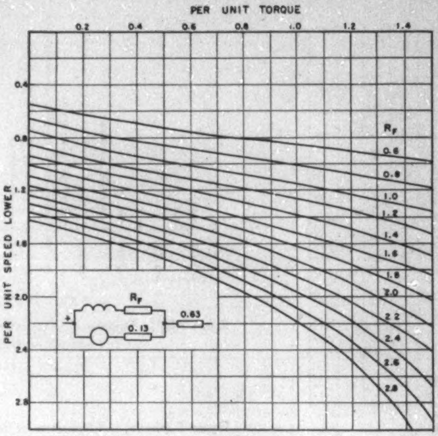

Figure 11. Speed-torque curves for variable field resistance with fixed armature and series resistance

final controller point should obtain as high no-load and full-load speeds as practicable, and still provide stable operation under overload.

In the range of high lowering speeds, control is essentially by inserting resistance in the motor field circuit. The amount of field weakening which can be safely employed limits the maximum speed for which the controller can be designed.

Figures 10 and 11 illustrate how the results of comparatively few tests can be utilized as an aid in controller design. As an example, consider tests H, I, J, and K, during which R_A and R_S were held constant, and R_F was varied. The test points from Figure 8 have been plotted in Figure 10 as speed versus R_F, for various values of torque. From this figure the speed-torque curves of Figure 11 have been drawn, giving speed versus torque for various values of R_F. This figure indicates the range of speed control which can be obtained by selecting various values of R_F. It also gives an approximate indication of the variation in speed due to resistor heating, as the effect of changes in R_F is large compared with changes in R_A and R_S.

An ideal crane hoist controller would have as little change as possible between no-load and full-load speed on each controller point. Theoretically, the flattest speed-torque curves would be obtained with zero R_A and R_S. However the stability limit of such curves would occur at too low a value of motor torque.[2] To obtain a workable controller design, the speed-torque curves must have some slope, which is increased by increasing R_A or R_S.

Increasing R_A does not increase the stability limit, it only increases the speed at which the stability limit occurs. R_A cannot be reduced below a certain minimum value. It contains the internal armature resistance and the trolley resistance between the armature and the controller. It may be desirable to leave a small amount of external resistance in the armature circuit to force sufficient current through the series field during acceleration, to insure that the series brake, which is generally connected in series with the field, is released.

Increasing R_S has a marked effect on the stability limit. Increased slope corresponds to increased stability limit. In selecting the proper value of R_S a compromise must be worked out to obtain as low a slope as possible, commensurate with sufficiently high stability limit. Any increase in no-load speed and any reduction in R_S reduce the torque at which unstable operation is to be expected.

References

1. The Speed Torque Curves of a Series Motor, **A. A. Merrill.** *General Electric Review* (Schenectady, N. Y.), October 1933, page 431–40.

2. Dynamic Braking Control of D-C Series Motors—Calculation of Stability Limit, **G. W. Heumann, W. P. Smith.** *Electrical Engineering* (AIEE *Transactions*), volume 65, July 1946, pages 454–57.

3. Magnetic Control of Industrial Motors (book), **G. W. Heumann.** John Wiley and Sons, New York, N. Y., 1947, pages 42–50.

4. Electromagnetic Torque Meter, **M. W. Hively, D. F. Livermore.** *Transactions*, American Society of Mechanical Engineers (New York, N. Y.), October 1946, pages 723–27.

5. American Standard for Rotating Electrical Machinery on Railway Locomotives and Rail Cars and Trolley, Gasoline-Electric and Oil-Electric Coaches. *AIEE Standard Number 11*, 1943, section 11-304e, page 15.

No Discussion

Analytical Determination of Characteristics of Magnetic Amplifiers with Feedback

D. W. VER PLANCK
MEMBER AIEE

L. A. FINZI
ASSOCIATE AIEE

D. C. BEAUMARIAGE
STUDENT MEMBER AIEE

Synopsis: An analytical method is developed for predetermining the steady-state characteristics of magnetic amplifiers with feedback. The magnetization curve is expressed in a convenient functional form and analytical relations among the direct control current, alternating output current and applied alternating voltage are derived for two different feed-back circuits. Magnetic amplifiers without feedback are included as limiting cases. Simultaneous conduction of the rectifiers which occurs in feed-back circuits during portions of the cycle is taken into account and explained. Experimental checks confirm the soundness of the analysis throughout.

A MAGNETIC amplifier consists of interlinked electric and saturable magnetic circuits arranged so that a small amount of direct current controls the reactance of an a-c circuit.[1,2,3] Thus the a-c power to a load may be regulated by a much smaller power in the d-c control circuit. Amplifiers of greatest sensitivity usually involve self excitation or feedback.[4,5,6,7] The steady-state theory of magnetic amplifiers without feedback has been established and means for predetermining the characteristics are available.[8,9] The addition of feedback, however, greatly complicates the analysis and published theories are either only qualitative[8] or if quantitative, require semigraphical procedures for their application.[10] The purpose here is to give a quantitative theory of the steady-state operation of magnetic amplifiers with feedback which permits analytical predetermination of their characteristics.

While the theory is general, it is presented by showing its application to a particular circuit. Some results of similar analyses for other cases are given.

Self Feed-Back Circuit

The circuit chosen for illustration is shown in Figure 1. It comprises two identical saturable cores, each having a d-c control winding N_1 and an a-c load winding N_2. The control windings are connected in series with a d-c source. The load windings are connected through identical rectifiers *a* and *b* to an a-c source and load as shown. An increase of control current, which saturates the cores, has the effect of increasing the load current. Because of the rectifiers, the load current links the cores alternately, so as to add to the bias already introduced by the control current, and thus feedback occurs. In distinction from other circuits no additional windings are needed to produce the regeneration; hence the term "self feedback."

Analysis

Briefly, the method is first to apply Kirchhoff's voltage law to the electric circuits and solve for the magnetic fluxes in the two cores; then to use the magnetization curve of the material expressed in analytical form to find the corresponding mmf's; next to use Ampere's law to relate the magnetomotive forces and currents; and finally to solve for the currents. This procedure is facilitated by the following simplifications:

1. Steady-state conditions exist.
2. The load is replaced by a short circuit so that a sinusoidal voltage is impressed directly on the amplifier terminals.
3. The voltage impressed on the control circuit is constant and its source has no impedance to harmonic currents.
4. Winding resistances are very small though not neglected entirely.
5. Leakage fluxes are neglected, and the flux density is uniform throughout each separate core.
6. Eddy currents and hysteresis are neglected and the magnetic flux density—magnetizing intensity relationship is given by the normal magnetization curve of the core material.
7. Rectifiers have infinite resistance in the reverse direction and a constant, but very small, resistance in the forward direction.

Application of Kirchhoff's voltage laws, to the circuit of Figure 1 with the load replaced by a short circuit gives

$$E_{dc}=2R_1i_1+N_1\left(\frac{d\phi_\alpha}{dt}+\frac{d\phi_\beta}{dt}\right) \tag{1}$$

$$E_m\cos\omega t=R_2i_2+N_2\frac{d\phi_\alpha}{dt}+V_a \tag{2}$$

$$E_m\cos\omega t=R_2i_3-N_2\frac{d\phi_\beta}{dt}+V_b \tag{3}$$

V_a is the voltage drop across rectifier *a* in the direction of positive current i_2; and V_b the drop across rectifier *b* in the direction of positive current i_3. R_1 and R_2 are the resistances of each of the coils N_1 and N_2 respectively, and the other symbols are as shown in the figure. The positive directions of currents and fluxes have been chosen arbitrarily. The sign preceding the number of turns of a coil is negative if current through it in the positive direction produces flux in its core opposite to the assumed positive direction of flux.

The voltage drops V_a and V_b determine

Paper 49-139, recommended by the AIEE Electronics Committee and approved by the AIEE Technical Program Committee for presentation at the AIEE Summer General Meeting, Swampscott, Mass., June 20–24, 1949. Manuscript submitted March 21, 1949; made available for printing May 3, 1949.

D. W. Ver Planck, L. A. Finzi and D. C. Beaumariage are all with the Carnegie Institute of Technology, Pittsburgh, Pa.

This work was done in part under a contract with the Office of Naval Research, and in part by D. C. Beaumariage in partial fulfillment of the requirements for the degree of Doctor of Science at Carnegie Institute of Technology.

the operation of the rectifiers as follows:

$$V_a>0, \quad i_2>0, \quad V_a=i_2R_r \tag{4}$$

$$V_a\leqq 0, \quad i_2=0 \tag{5}$$

$$V_b\geqq 0, \quad i_3=0 \tag{6}$$

$$V_b<0, \quad i_3<0, \quad V_b=i_3R_r \tag{7}$$

where R_r is the forward resistance of each rectifier, assumed constant.

Consideration of the circuit and the foregoing equations shows the possibility of three conditions in each a-c cycle as follows:

> Rectifier *a* conducts and *b* does not. This is described by equations 4 and 6 and is termed a ***positive*** conduction period.
>
> Rectifier *b* conducts and *a* does not, as described by equations 5 and 7. This is called a ***negative*** conduction period.
>
> Both rectifiers conduct in accordance with equations 4 and 7. This is commutation.

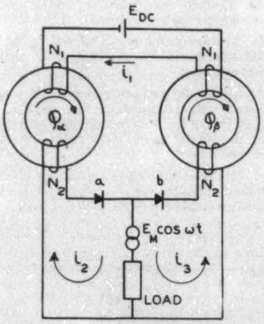

Figure 1. Magnetic amplifier with self feedback

The fluxes in the two cores are found for each of these periods by simultaneous solution of the appropriate ones of the voltage equations 1, 2, and 3 assuming that the resistance, drops, and consequently E_{dc}, are negligible. The flux densities in the cores, B_α and B_β respectively, are then found by dividing each flux by the core area A. For each period the result is the same, namely

$$B_\alpha=B_m \sin \omega t+B_0 \tag{8}$$

$$B_\beta=-B_m \sin \omega t+B_0 \tag{9}$$

where $B_m=E_m/N_2\omega A$. For each period a constant of integration arises, which can be shown to be the same for all periods and both cores, and equal to the average flux density. This quantity, identified by B_0, is as yet undetermined. For the commutation period only two of the three voltage equations available are needed to determine the flux densities; the third equation is utilized later.

The field intensities required in the cores are related to the flux densities through the magnetic characteristic of the material, assumed here to be the normal magnetization curve. This functional relationship has been represented analytically in several ways, for example by straight line segments,[11] the sum of a linear and a high odd powered term,[9] and the hyperbolic sine.[12] For the present purpose, a more satisfactory empirical expression is

$$H=U \sinh uB+vB \tag{10}$$

where U, u, and v are constants dependent on the shape of the magnetization curve. Using this form it was possible to fit the measured points to within the accuracy of the magnetic measurements for hypernik and silicon steel.

Substitution of equations 8 and 9 into equation 10 results in

$$H_\alpha=H_0+H_1 \sin \omega t+H_2 \cos 2\omega t+ H_3 \sin 3\omega t+H_4 \cos 4\omega t+\ldots \tag{11}$$

$$H_\beta=H_0-H_1 \sin \omega t+H_2 \cos 2\omega t- H_3 \sin 3\omega t+H_4 \cos 4\omega t-\ldots \tag{12}$$

where the coefficients of the series are in terms of modified Bessel functions of the first kind[13,14] as shown in Table I. If expressions other than equation 10 are used to represent the magnetization curve, equations 11 and 12 still apply but the formulas for the coefficients are not those in Table I. For instance if equation 10 is replaced by the sum of two hyperbolic sines, each harmonic coefficient has two terms each involving modified Bessel functions. A finite power series[15] instead of equation 10, gives coefficients which are polynomials in B_m and B_0. These other representations fit the magnetization curve of the material studied just as well as equation 10 and lead to equally good over-all checks, but they are less convenient mathematically.

Application of Ampere's law to each of the magnetic circuits relates the currents to the field intensities. Thus

$$N_1i_1+N_2i_2=LH_\alpha \tag{13}$$

$$N_1i_1-N_2i_3=LH_\beta \tag{14}$$

where L is the mean length of path for either core.

In the positive and negative conduction periods i_3 and i_2 are respectively equal to zero, and equations 13 and 14 suffice to determine expressions for the remaining two currents. With the aid of equations 11 and 12 the currents in these two periods are then expressed in terms of the harmonic components of field intensity as shown in Table II.

During commutation, however, all three currents exist simultaneously and a third equation is required for their determination. This is obtained by manipulation of the voltage equations 1, 2, 3, 4, and 7 so as to eliminate the time rates of change of flux but without ignoring the resistance drop terms as was done earlier. The resulting equation with equations 13 and 14 then leads to the expressions for the currents shown at the bottom of Table II. Here

$$k'=\left(\frac{R_2+R_r}{R_1}\right)\left(\frac{N_1}{N_2}\right)^2 \tag{15}$$

and

$$I_1=\frac{E_{dc}}{2R_1} \tag{16}$$

Although expressions for the currents in all periods of the cycle have been established, the times of transition between the periods have not been determined, nor is a relationship known connecting B_0, the time average of flux density, and I_1, the time average of control current. To break into the determination of these remaining unknowns the following significant facts are noted from a study of the expressions in Table II:

1. The output current (i_2+i_3) is given by the same expression throughout the cycle and passes through zero at $\omega t=0, \pi, 2\pi \ldots\ldots$ as indicated in Figure 2.
2. The expressions for the control current are such as to result in the symmetries about $\omega t=0, \pi, 2\pi \ldots\ldots$ and about $\omega t=\frac{\pi}{2}, \frac{3\pi}{2} \ldots\ldots$ indicated in Figure 2.

From this it follows that the times of transition between periods can be expressed in terms of a single angle σ as shown in Figure 2.

The angle of transition σ is determined by the voltage of equations 4 through 7. For instance at $\omega t=\sigma$, that is at the end of the commutation period (in which both i_2 and i_3 were flowing), just before positive conduction, i_3 and V_b are just reaching zero. Inserting these conditions in equations 1, 2, and 3 with $V_a=i_2R_r$ and eliminating the time rates of

Table I. Coefficients of Magnetomotive Force Harmonics

$H_0=U\mathrm{I}_0(uB_m) \sinh uB_0+vB_0$
$H_1=2U\mathrm{I}_1(uB_m) \cosh uB_0+vB_m$
$H_2=-2U\mathrm{I}_2(uB_m) \sinh uB_0$
$H_3=-2U\mathrm{I}_3(uB_m) \cosh uB_0$
$H_4=2U\mathrm{I}_4(uB_m) \sinh uB_0$
$H_5=2U\mathrm{I}_5(uB_m) \cosh uB_0$

$\mathrm{I}_n(x)$ is the modified Bessel function of the first kind.[13,14]

change of flux results in the relation between i_1 and i_2 which must hold at this instant. Then replacing i_1 and i_2 with their values for the commutation period as given in Table II results in the following equation connecting σ and N_1I_1

$$N_1I_1=L[(H_0+H_2\cos 2\sigma+\ldots)-(1+k')(H_1\sin\sigma+H_3\sin 3\sigma+\ldots)] \quad (17)$$

Consideration of the voltage conditions at the other transition times ($\omega t=\pi-\sigma$, $\omega t=\pi+\sigma$, and $\omega t=2\pi-\sigma$) in each case leads to this same relationship between σ and N_1I_1.

Another independent relation between N_1I_1 and σ is obtained by expressing the time average control current as

$$I_1=\frac{1}{2\pi}\int_0^{2\pi} i_1 d(\omega t) \quad (18)$$

using the expressions for i_1 given in Table II and integrating each between the proper limits. This results in

$$N_1I_1=LH_0-\frac{2L}{\pi(1+k')-2\sigma}\times\left[\left(\frac{H_2}{2}\sin 2\sigma+\frac{H_4}{4}\sin 4\sigma+\ldots\ldots\right)+(1+k')\times\left(H_1\cos\sigma+\frac{H_3}{3}\cos 3\sigma+\ldots\ldots\right)\right] \quad (19)$$

Elimination of N_1I_1 between equations 17 and 19 gives an expression from which σ may be determined if B_0 and B_m (which determine the H's) are known. To facilitate computation harmonic terms above the second order usually may be dropped without serious error. Doing this and making a number of transformations gives

$$\tan\sigma-\frac{1}{\frac{\pi}{2}(1+k')-\sigma}=\frac{1}{\tan\sigma+\frac{H_1}{H_2}(1+k')\sec\sigma} \quad (20)$$

The steps in determining the characteristics of a given magnetic amplifier with self feedback may now be summarized as follows:

1. Adjust the constants of equation 10 to fit the magnetization curve of the core material.
2. Calculate B_m for the applied alternating voltage desired.
3. Assume a value of B_0.
4. Use Table I to determine the harmonic coefficients H_n.
5. Use equation 20 to determine the angle of transition σ.
6. Calculate N_1I_1 from either equation 17 or 19 and use the other as a check on σ.
7. Calculate instantaneous currents using the expressions in Table II.

If the rectified average value of load current is desired, it may be calculated immediately following step 4 from

$$(i_2+i_3)_{\text{rectified average}}=\frac{4L}{\pi N_2}\left[H_1+\frac{H_3}{3}+\ldots\right] \quad (21)$$

If the rectifiers are omitted from the circuit under discussion, Figure 1, a familiar nonfeed-back magnetic amplifier with parallel load coils results. The foregoing analysis applies to this case also, if R_r is set equal to zero and the expressions in Table II for the commutation period are taken to apply throughout the cycle. The angle of transition σ has no meaning in this case. Integration of the expression for i_1 over the whole cycle leads to the result that $N_1I_1=LH_0$. The load current is given by equation 21 without modification.

Experimental Checks

Experiments were performed to check the validity of the assumptions made in the preceding analysis. For this, two shell-type hypernik cores with mean lengths of path of 7.12 inches and cross-sectional areas of 0.656 square inches were used.

A first set of experiments was directed to check the analytical predetermination of the average value of the alternating flux density B_0 as a function of B_m and of the control ampere-turns N_1I_1. For this, the amplifier with no feedback (Figure 1 with rectifiers omitted) was used. B_0 was measured by means of a fluxmeter inserted in an exploring circuit so as to eliminate odd harmonics of induced current through the fluxmeter coil. The results are shown in Figure 3. The calculated curves are found using the formulas $B_m=E_m/N_2A\omega$ and $N_1I_1=LH_0$ obtaining H_0 from Table 1 for assumed values of B_0. In these experiments $N_1=N_2=2{,}000$ turns, $R_1=115$ ohms, $R_r=100$ ohms, and the frequency of the a-c power source was 60 cycles per second. The curve for $B_m=0$ is the measured normal magnetization curve and for this case the approximation of equation 10 agrees within the accuracy of the magnetic measurements but is not plotted.

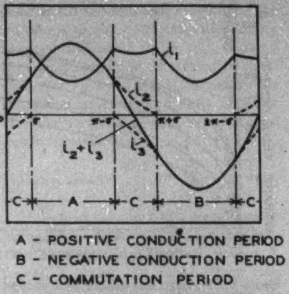

Figure 2. Representative current waveforms for magnetic amplifier with self feedback

A second set of experiments was made to check the analytical predetermination of the steady-state no-load characteristics of magnetic amplifiers with self feedback. Typical results are shown in Figure 4.

Figure 5 is typical of many comparisons of calculated instantaneous currents with oscillograms. It constitutes direct evidence of the phenomena of commutation or simultaneous conduction of the rectifiers.

Finally the effect of inserting a load was checked experimentally. It was found under conditions of equal control current (average value) and equal load current (rectified average value) that the

Table II. Instantaneous Currents in Self Feed-back Circuit

Period	Current
Positive	$i_1=\frac{L}{N_1}[(H_0+H_2\cos 2\omega t+\ldots)-(H_1\sin\omega t+H_3\sin 3\omega t+\ldots)]$ $i_L=i_2+i_3=\frac{2L}{N_2}\times[H_1\sin\omega t+H_3\sin 3\omega t+\ldots]$ $i_3=0$
Negative	$i_1=\frac{L}{N_1}[(H_0+H_2\cos 2\omega t+\ldots)+(H_1\sin\omega t+H_3\sin 3\omega t+\ldots)]$ $i_2=0$ $i_L=i_2+i_3=\frac{2L}{N_2}\times[H_1\sin\omega t+H_3\sin 3\omega t+\ldots]$
Commutation	$i_1=\frac{1}{N_1(1+k')}\times[k'L(H_0+H_2\cos 2\omega t+\ldots)+N_1I_1]$ $i_2=\frac{L}{N_2}[H_1\sin\omega t+H_3\sin 3\omega t+\ldots]+\frac{1}{N_2(1+k')}\times[L(H_0+H_2\cos 2\omega t+\ldots)-N_1I_1]$ $i_3=\frac{L}{N_2}(H_1\sin\omega t+H_3\sin 3\omega t+\ldots]-\frac{1}{N_2(1+k')}\times[L(H_0+H_2\cos 2\omega t+\ldots)-N_1I_1]$ $i_2+i_3=\frac{2L}{N_2}\times[H_1\sin\omega t+H_3\sin 3\omega t+\ldots]$

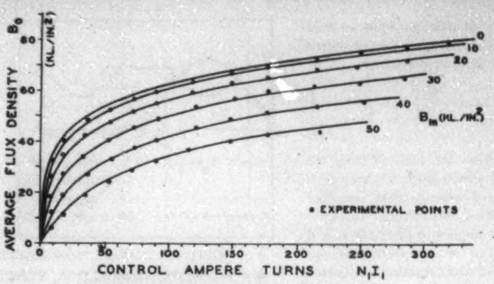

Figure 3. Average flux density as a function of average control ampere-turns and maximum alternating flux density

The upper curve is the measured normal magnetization curve of the material and the other curves are calculated

rms voltage drop across the amplifier terminals was substantially unaffected by the presence of resistance loads, even when the drop across the load was as high as 420 volts and that across the amplifier 140 volts. Moreover the current wave forms and the angle of commutation were not significantly altered by the load.

Physical Interpretation

It is to be emphasized at the outset that simultaneous conduction of the rectifiers is not caused by imperfections, for in the analysis the rectifiers have been assumed to have infinite backward resistance. To clarify this phenomenon of commutation, a consideration of the harmonic currents required for excitation is helpful.

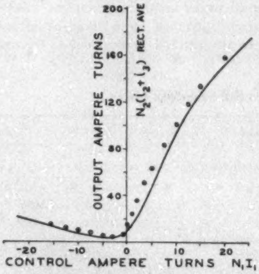

Figure 4. Characteristic of magnetic amplifier with self feedback

The curve is calculated, the points are measured experimentally. Core material as for Figure 3

$E_m=198$v, $\omega=2\pi 60$, $N_1=500$ turns, $N_2=4000$ turns, $R_1=31.5$ ohms, $R_2=240$ ohms, $R_r=50$ ohms

With the assumption of very small circuit resistances the fluxes must vary sinusoidally. That the flux in each core separately must vary sinusoidally in spite of the action of the rectifiers is a consequence of the coupling afforded by the control circuit. The displacement of the sinusoids of flux density, described by equations 8 and 9, results in part from the direct current in the control circuit, and requires magnetomotive forces having both odd and even harmonics as shown in equations 11 and 12.

Odd Harmonics of Magnetomotive Force

The odd harmonics of magnetomotive force, as shown by equations 11 and 12, have opposite signs in the two cores. When both rectifiers are conducting, the circuits and windings are so balanced that these odd harmonics can be produced only by identical components in the currents i_2 and i_3, see Table II, and these components can flow only through the a-c source. This occurs throughout the cycle in amplifiers without feedback. If, however, one rectifier is nonconducting, the current in the a-c winding of the core on that side is zero and the necessary odd harmonic components of magnetomotive force there have to be produced by current in the control circuit. But such a current in the control circuit produces odd harmonics of magnetomotive force of the wrong sign in the other core; hence the corresponding components of current in the load winding on that core must be double the former value. It will be seen that these conclusions agree with Table II.

Even Harmonics of Magnetomotive Force

The required even harmonics of magnetomotive force have the same signs in the two cores and therefore can be pro-

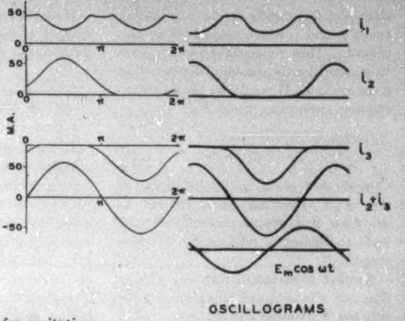

Figure 5. Calculated instantaneous currents (left) compared with oscillograms for the same conditions as Figure 4 and $N_1I_1=17$

The calculated curves are plotted to scales determined by the oscillograph sensitivity

duced by components of current i_1 or by components of currents i_2 and i_3 of equal magnitude but opposite signs. If the windings had zero resistance and there were no rectifiers the distribution of these components of current would be indeterminate.

Since the windings necessarily have resistance, voltages of corresponding harmonic frequencies have to be generated to balance the resistance drops which necessitate deviations from the initially assumed sinusoidal variation of the fluxes. These deviations are neglected in deriving equations 8, 9, 11, and 12, since the resistance drops are usually quite small in comparison with the impressed voltage, but it is recognized that small voltages of higher frequencies in fact must be induced in each winding to overcome the resistance drops. In the absence of rectifiers the currents which provide the needed even harmonics of magnetomotive force divide between the control winding and the external loop of the a-c windings in the inverse ratio of the resistances if the turns are equal, or in general in accordance with the factor k' defined by equation 15.

The rectifiers in no way alter the need for even harmonic components of magnetomotive force to sustain the displaced sinusoids of flux, but they do affect the way in which the currents to produce these magnetomotive forces are distributed between the control circuit and the external loop of the a-c windings. If either rectifier alone is conducting, the necessary component currents can flow only in the control circuit, the other possible path being interrupted. Consideration of the voltage relations shows, however, that as time goes on with one rectifier conducting there comes a moment when the voltage drop across the other rectifier passes through zero in the direction to cause conduction. Then for an interval both rectifiers conduct and the components of current which produce even harmonics of magnetomotive force divide between the two possible paths in accordance with the factor k' as they would with no rectifiers present. This condition persists until the current through the first rectifier drops to zero when conduction ceases and the second path for even harmonics is again interrupted.

External Feed-back Circuit

Another magnetic amplifier circuit providing feedback is shown in Figure 6. Here the feedback is obtained by rectifying the load current and passing it through a set of coils N_4 connected so that their magnetomotive forces reinforce those of the control coils N_1. The term external feedback is used to describe this circuit because coils external to the corresponding nonfeed-back circuit are required. The steps in analyzing the external feed-back circuit are similar to those for the self feed-back circuit and so only the important differences in the results will be indicated here.

Again it is found that there are three conditions in each a-c cycle.

1. A positive period when only the pair of rectifiers *aa* conducts and the feed-back windings N_4 are connected in series with the load windings N_2.
2. A negative period when only rectifiers *bb* conduct and the feed-back windings are again connected in series with the load windings but in opposite sense.
3. Commutation periods when all four rectifiers conduct simultaneously thus short circuiting the feed-back windings while the load windings alone support the impressed a-c voltage.

From voltage equations it is found that equations 8 and 9, and consequently equations 11 and 12, also apply to this case except that here $B_m=E_m/2N_2\omega A$.

Application of Ampere's law to the magnetic circuits leads to the expressions for the currents shown in Table III. Here I_1 is as given by equation 16, and

$$k''=\left(\frac{2R_4+R_r}{2R_1}\right)\left(\frac{N_1}{N_4}\right)^2 \tag{22}$$

where R_1 and R_4 are the resistances of single coils N_1 and N_4 respectively, and R_r is the forward resistance of a single rectifier. The factor k'' is analogous to k' defined by equation 15 and relates to the division of currents necessary to produce even harmonics of magnetomotive force between the two possible paths, in this case the control circuit and the short circuit through the feed-back coils when all rectifiers are conducting at once.

As in the self-feed-back case, the times of transition between the periods in each cycle may be expressed in terms of a single angle σ. Again two relations are found connecting σ and the average control excitation N_1I_1, one arising from consideration of rectifier voltage drops at the instants of transition, and the other from averaging the control current over the cycle. These relations are respectively

$$N_1I_1=L\left[(H_0+H_2\cos 2\sigma+\ldots)-\frac{N_4}{N_2}\times (1+k'')(H_1\sin\sigma+H_3\sin 3\sigma+\ldots.)\right] \tag{23}$$

$$N_1I_1=LH_0-\frac{2L}{\pi(1+k'')-2\sigma}\times \left[\left(\frac{H_2}{2}\sin 2\sigma+\frac{H_4}{4}\sin 4\sigma+\ldots.\right)+\frac{N_4}{N_1}\times (1+k'')\left(H_1\cos\sigma+\frac{H_3}{3}\cos 3\sigma+\ldots.\right)\right] \tag{24}$$

Eliminating N_1I_1 from these and dropping harmonics beyond the second results in

$$\tan\sigma-\frac{1}{\frac{\pi}{2}(1+k'')-\sigma} =\frac{1}{\tan\sigma+\frac{N_4}{N_2}\frac{H_1}{H_2}(1+k'')\sec\sigma} \tag{25}$$

Summarizing, the procedure for determining the characteristics of a magnetic amplifier with external feedback is the same as for self-feedback except that the transition angle σ is calculated using equation 25 instead of 20, N_1I_1 is found from equations 23 or 24 instead of equations 17 or 19, and Table III is used for the instantaneous currents instead of Table II. The rectified average value of load current is given by

$$(i_2)_{\text{rectified average}}=\frac{2L}{\pi N_2}\left[H_1+\frac{H_3}{3}+\ldots.\right] \tag{26}$$

If the feed-back turns N_4 are reduced to zero, Figure 6 becomes the familiar nonfeed-back circuit with load coils connected in series. In this limiting case, the instantaneous currents i_1 and i_2 are given by the expressions in Table III for the positive or negative period which become identical for $N_4=0$. The angle of transition σ in this case becomes zero and averaging the control current over the cycle gives $N_1I_1=LH_0$.

Comparison of Self and External Feedback

The expressions for instantaneous control and output currents in Table III for the external feed-back amplifier with series-connected a-c windings, Figure 6, become identical with the corresponding expressions in Table II for the self-feedback amplifier, Figure 1, if the comparison between the two is established as follows: equal core dimensions and materials; equal control windings and control currents; equal source voltages and a-c volts per turn; equal weights of copper for the a-c windings; and if it is further assumed for the external feed-back amplifier that the feedback and a-c windings have the same number of turns ($N_4=N_2$), mean lengths, and copper weights (which implies the availability of space for the feed-back winding). Under the terms of this comparison the total copper losses

Table III. Instantaneous Currents in External Feed-back Circuit

Period	Current
Positive.....	$i_1=\frac{L}{N_1}[(H_0+H_2\cos 2\omega t+\ldots)-\frac{N_4}{N_2}(H_1\sin\omega t+H_3\sin 3\omega t+\ldots)]$ $i_2=\frac{L}{N_2}[H_1\sin\omega t+H_3\sin 3\omega t+\ldots]$ $i_4=i_2$
Negative....	$i_1=\frac{L}{N_1}[(H_0+H_2\cos 2\omega t+\ldots)+\frac{N_4}{N_2}(H_1\sin\omega t+H\ \sin 3\omega t+\ldots)]$ $i_2=\frac{L}{N_2}[H_1\sin\omega t+H_3\sin 3\omega t+\ldots]$ $i_4=-i_2$
Commutation	$i_1=\frac{1}{N_1(1+k'')}\times[k''L(H_0+H_2\cos 2\omega t+\ldots)+N_1I_1]$ $i_2=\frac{L}{N_2}[H_1\sin\omega t+H_3\sin 3\omega t+\ldots]$ $i_4=\frac{1}{N_4(1+k'')}\times[L(H_0+H_2\cos 2\omega t+\ldots)-N_1I_1]$

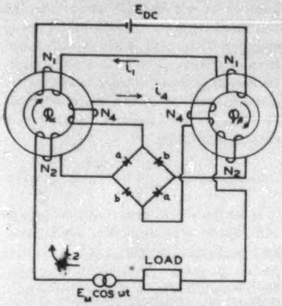

Figure 6. Magnetic amplifier with external feedback

are the same for both amplifiers. Thus the amplifier with self-feedback is superior to that with external feedback in that it gives identical performance with less material. It is to be noted, however, that the self feed-back circuit is less flexible in that there is no way to vary the amount of feedback as can be done by adjusting the number of turns N_4 in the external feed-back circuit.

Conclusions

An analytical predetermination of the no-load steady-state characteristic of magnetic amplifiers has been made possible in terms of design data and the properties of the core material. The operation of the magnetic amplifier depends basically on the fact that there is an average value of flux density and a superimposed alternating flux density; thus it appeared logical to develop expressions for the currents in the various circuits as functions of the two independent variables B_0 and B_m. Experimental checks agree closely with the results of calculation for a number of circuits with and without feedback using hypernik and silicon steel cores.

The analysis established here considers amplifiers with zero load impedance. This apparent limitation has the advantage of avoiding excessive analytical difficulty and eliminates the immediate need for considering the load impedance as a further variable. It is recognized that the presence of a load may alter the assumption of purely sinusoidal variation of core fluxes. An iterative process, initiated from the results of the present analysis appears possible, if needed, to study the true influence of a general load impedance. There is evidence however that such refinement may not be necessary. It is already customary to use experimentally-obtained no-load characteristics[3,4,16] of the type calculated here in the treatment of loaded amplifiers without feedback.[17,18] The work reported here indicates that the same procedures, based on conventional a-c circuit analysis, apparently also can be applied to feedback circuits.

References

1. Even Harmonics in A-C Circuits, **John B. Taylor.** *AIEE Transactions,* volume 28, part I, 1909, pages 725–36.

2. A Magnetic Amplifier for Radio Telephony, **E. F. W. Alexanderson, S. P. Nixdorf.** *Proceedings,* Institute of Radio Engineers (New York, N. Y.), volume 4, 1916, page 101.

3. Theory of D-C Excited Iron-Core Reactors and Regulators, **A. Boyajian.** *AIEE Transactions,* volume 43, 1924, pages 919–36.

4. Direct-Current Controlled Reactor, **E. C. Wentz.** *The Electric Journal* (Pittsburgh, Pa.), volume 28, 1931, page 561.

5. Über gleichstromvormagnetisierte Wechselstromdrosselspulen und deren Rückkopplung, **T. Buchhold.** *Archiv für Elektrotechnik* (Berlin, Germany), volume 36, 1942, page 221.

6. A Balanced Amplifier Using Biased Saturable Core Reactors, **H. S. Kirschbaum, E. L. Harder.** *AIEE Transactions,* volume 66, 1947, pages 273–8.

7. Some Fundamentals of a Theory of the Transductor or Magnetic Amplifier, **A. Uno Lamm.** *AIEE Transactions,* volume 66, 1947, pages 1078–85.

8. An Analysis of Interlinked Electric and Magnetic Networks with Application to Magnetic Amplifiers, **D. W. Ver Planck, M. Fishman.** *Proceedings,* Institute of Radio Engineers (New York, N. Y.), volume 37, 1949.

9. Universal Curves for D-C Controllable Reactors, **W. C. Johnson, B. C. Merrell, R. E. Alley, Jr.** *AIEE Transactions,* volume 68, 1949 (Proceedings T94).

10. An Analysis of Magnetic Amplifiers with Feedback, **D. W. Ver Planck, M. Fishman, D. C. Beaumariage.** *Proceedings,* Institute of Radio Engineers (New York, N. Y.), volume 37, 1949.

11. Mathematical Analysis of Non-Linear Circuits, **A. Boyajian.** *General Electric Review,* (Schenectady, N. Y.), volume 34, 1931, pages 531–37, pages 745–51.

12. Zur qualitativen Theorie gleichstromvormagnetisierter Eisendrosseln, **T. Wasserrab.** *Archiv für Elktrotechnik* (Berlin, Germany), 1937, page 814.

13. Bessel Functions (book), **A. Gray, G. B. Matthews, T. M. MacRobert.** MacMillan and Co. Limited, London.

14. A Five Figure Table of the Bessel Function $I_n(x)$, **H. B. Dwight.** *Electrical Engineering* (*AIEE Transactions*), volume 60, 1941, pages 135–36.

15. Beitrag zur qualitativen Theorie gleichstromvormagnetisierter Eisenkern-Drosselspulen, **G. Hauffe.** *Archiv für Electrotechnik* (Berlin, Germany), 1939, page 41.

16. Some Notes on the Design of Magnetic Amplifiers, **A. S. Fitzgerald.** *Journal,* Franklin Institute (Philadelphia, Pa.), volume 244, November 1947, pages 323–62.

17. Magnetic Amplifiers—Parts 1 and 2, **S. E. Tweedy.** *Electronic Engineering* (London, England), volume 20, February and March 1948, pages 38–43 and 84–88.

18. Magnetic Amplifiers—Circuits, Characteristics, Applications, *Bulletin Number VT-2000,* Vickers, Inc.. St. Louis, Mo.

No Discussion

The Logic of Relay Circuits

WM. KEISTER
NONMEMBER AIEE

MODERN telephone switching systems of the common control type such as the crossbar system, employ relay circuits which perform much the same actions as a human operator in setting up the connections for a telephone call. These relay circuits respond in an appropriate manner to signals of various types. They receive information in the form of a telephone directory number, evaluate it, locate suitable groups of trunks and paths through an interconnecting network of switches and from these groups choose a set of idle elements and connect them together for a telephone call. These telephone switching control circuits perform logical actions, and the design of such circuits is primarily an exercise in rigorous logic. The problem is usually one of producing specific effects in response to certain causes. Electric apparatus is merely a convenient means of detecting the causes and bringing about the desired effects.

A circuit designer in discussing the action of a relay circuit will often use such words as "tell," "remember," "know," and "choose;" words which are applied normally to rational mental actions and yet express with surprising accuracy the nature of actions performed in automatic switching systems. The actions, however, are not a result of independent thinking on the part of the units, but are more in the nature of automatic response to control signals. The designer has analyzed the situations which may occur, determined what shall be done for each one, and built into the control mechanisms a means for recognizing the situations and reacting accordingly. The machine then "knows" what to do for a definite set of circumstances and is able to analyze a combination of preconceived conditions and produce for each condition a result which agrees with the precise pattern of logic laid out by the designer.

The ways in which complex relay circuits such as those of telephone switching systems perform logical actions cannot be explained easily, without considerable discussion of technical details of the systems in which they are used. However a general discussion of a few fundamental ideas with simple examples will illustrate that the design of these circuits is basically a process of constructing a relay analogy of a chain of logical reasoning in which bits of information are received and correlated and suitable actions taken.

Contact Networks

A pair of mating contacts for making or breaking an electric circuit which will be called simply a contact, is basically a 2-valued device. At any given time it is either open or closed. In this respect a contact corresponds to an "open or shut" proposition in logic which can be demonstrated under given conditions to be either false or true. A 2-terminal network of contacts is similar to a single contact in that it is either open or closed for any given set of conditions. By 2-terminal network is meant a network consisting of individual contacts connected together in a configuration which provides but two entry points. Such networks connected in a circuit with a battery can control the actions of relays in a complex control circuit. A 2-terminal network corresponds to a proposition whose truth or falsity depends on the truth or falsity of a number of individual propositions, the individual propositions corresponding to the individual contacts in the network. The development of a contact network to perform a certain function is an exercise in logic of the kind which is used in building up a proof that a certain statement is true or false by demonstrating that a number of other statements are true or false. Furthermore, the arrangement of the individual contacts in the network is similar to the way the various statements are related to prove that the given statement is true or false.

Two-terminal contact networks correspond to propositions which may sometimes be true and at other times false and not to propositions which are basically true. (These would prove to be short circuits.) For example, the proposition that "the 5:30 train will arrive on time" may be either true or false and will depend on the truth of a number of other propositions such as (*a*) "it left the last station on time," and (*b*) "the track is blocked." The original proposition may be true if proposition (*a*) is true and (*b*) is false. The use of a false proposition to prove the truth of another corresponds to the use of break contacts on a relay which close a circuit path only when the relay is not operated. A relay may control two types of contacts, both makes which close when the relay operates and breaks which open when the relay operates. A complete relay may be compared to a proposition which is sometimes true (operated) and sometimes false (released) and the contacts on this relay correspond to the use of this proposition in proving other propositions. A relay circuit thus is a collection of open and closed propositions.

Requirements for relay circuits are usually stated on a cause and effect basis; that is, when "such and such" events happen in a certain way, certain effects will be produced. If a clear logical statement of the relations between certain causes and the desired effects can be made, it is usually a simple matter to construct a circuit of relays controlled by contact networks which is analogous to the logical statement and consequently produces the desired results. Flaws in the logical reasoning will produce corresponding flaws in the circuit leading to inopera-

---

Paper 49-145, recommended by the AIEE Communication Committee and approved by the AIEE Technical Program Committee for presentation at the AIEE Summer General Meeting, Swampscott, Mass., June 20-24, 1949. Manuscript submitted November 16, 1948; made available for printing May 4, 1949.

WM. KEISTER is with the Bell Telephone Laboratories, New York, N. Y.

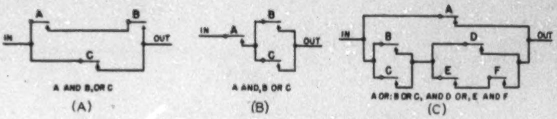

A AND B,OR C
(A)

A AND,B OR C
(B)

A OR: B OR C, AND D OR, E AND F
(C)

Figure 1 Circuit networks as statements of conditions for closing a path

tive conditions. Also restrictive conditions such as apparatus limitations may not always permit us to use the simplest straightforward solution.

The causes, constituting the input or control conditions for a relay circuit must result, directly or indirectly, in the closure (or opening) of an electrical contact suitable for operating a relay. Thus the control conditions may be: the manual operation of a push button; the closure of a contact by the mechanical motion of some instrument or machine; the insertion of a plug into a jack; or the closure of relay contacts in other associated circuits.

If the purpose of a relay circuit is merely to recognize the simultaneous occurrence of several control conditions and produce some output condition when this combination of conditions occurs, the correspondence between a statement of conditions and a relay contact network is very close. For example, if a lamp is to be lighted when two push button contacts, A and B, are both operated at the same time the statement of conditions for lighting the lamp is "A is operated *and* B is operated." The circuit path obviously is a series connection of make contacts. On the other hand, if the conditions are that the lamp shall light if "A is operated *or* B is operated," the circuit consists of a parallel connection of make contacts A and B. In the foregoing statements the words *and* and *or* have been italicized. These conjunctions in a careful statement of conditions for closing a circuit indicate whether a paralleled or series arrangement of the contacts is to be used, *and* indicating a series connection while *or* indicates a paralleled connection.

The same process may be applied to more elaborate statements. The path which is closed when "A *and* B are operated, *or* C is operated" is the series parallel arrangement of Figure 1(A) while the circuit which is closed when "A is operated *and* B *or* C is operated" is shown in Figure 1(B). A still more elaborate example is shown in Figure 1(C) where the path is closed when "A is closed *or:* B *or* C, *and;* D *or,* E *and* F are closed." The punctuation of the statement may become quite complicated but the above examples show that an accurate analysis of the requirements for closing a circuit will indicate directly a series parallel arrangement of the contact network. The point is not that a verbal statement of conditions for closing a circuit path is necessary or desirable but that the mental processes required in constructing and punctuating such a statement are the same as those required in designing the network. Note that the *or* indicating a parallel connection is not a mutually exclusive term. A parallel connection of two contacts A and B is a circuit which is closed when "A *or* B or *both* are closed."

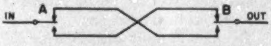

A AND NOT-B, OR NOT-A AND B

Figure 2. Use of break contacts

It is important that statements of circuit conditions mean precisely what is intended. For example, consider a statement describing the control of circuit paths X and Y by contacts on relays A and B, "When A operates, path X is closed but when both A and B operate only path Y is closed." This does not specifically state the conditions for closing path X. What is meant is that X closes when "A is operated *and* B is not operated." When it is necessary to state that a relay is not operated or some condition is not present in order to describe a control condition the use of a break contact is implied. Another example is a statement such as "the path is closed when either A or B is operated" where the *or* is mutually exclusive and the circuit is open when both A and B are operated. A more exact statement of these conditions is, "A operated *and* B not operated, *or* A not operated *and* B operated." The circuit is shown in Figure 2 where transfer contact arrangements are used.

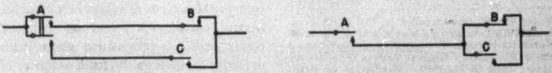

A AND NOT-B,OR A AND C
(A)

A AND,NOT-B OR C
(B)

Figure 3. Simplification by restatement

After a little study it becomes evident that the sketch of a network of contacts corresponds to a concise statement of conditions for opening or closing a circuit path The most concise statement of a set of conditions or, in other words, the contact network producing the desired results with the least number of contacts, is often reached only after several trials and restatements of the conditions. As a simple example, the circuit which is closed when "A is operated *and* B is not operated, *or,* A is operated and C is operated," as shown in Figure 3(A), may be restated as a circuit which is closed when "A is operated *and,* B is not operated, *or* C is operated." Since the element A is mentioned only once, a single A contact is sufficient as shown in Figure 3(B).

The practicing circuit designer seldom makes actual verbal or written statements of circuit conditions, but sketches the circuits themselves as the most direct way of expressing the requirements or conditions of a circuit. Often the original circuit contains many superfluous contacts, the important point at this stage being to insure that the various contact networks are closed for all required conditions and not closed for any conditions likely to produce undesirable reactions. Next comes the process of simplification, an elementary example of which was shown in Figures 3(A) and 3(B). All of this requires considerable attention to detail and logical analysis. The designer must keep in mind the positions of all relays of the circuit at any given time, and must visualize the reactions which take place when a contact network closes to operate a relay whose contacts in turn open or close to cause other relays to act, causing still further reactions. An experienced designer often conceives his original circuit network in their simplified forms. After a certain amount of practice, intuition for the construction and simplification of contact networks develops from the repeated application of logic to problems of cause and effect.

The algebra of logic, or Boolean algebra, has been applied to problems of contact network configurations.[1] This is a 2-valued algebra which deals with propositions in logic which are either true

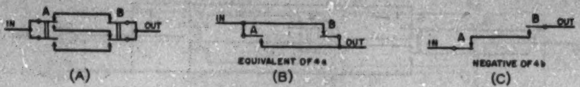

Figure 4. Negative reasoning

or false. Since a contact also is 2-valued, the theorems of this algebra concerning the combination of several propositions into a single proposition also apply to the combination of contacts into a single 2-terminal network. When a network which meets requirements has been devised from a study of the conditions of a problem, this algebra can often be used to great advantage in simplifying the network and eliminating superfluous elements.

A different type of reasoning often leads more directly to the desired form of a contact network. This is, thinking in terms of open circuits or considering the conditions which must open a circuit path, rather than those which close it, and designing a network to satisfy these open circuit conditions. This can be characterized as negative reasoning. For example, consider a network on the contacts of two relays, A and B, which must be closed when "A *and* B are released, *or*, A is operated *and* B is released, *or*, A *and* B are operated." The network corresponding to this statement is shown in Figure 4(A). However, an analysis of the conditions shows that the path is closed for three of the four possible combinations in which A and B may stand operated or released, and is open only when A is released and B is operated. This analysis gives us the equivalent circuit shown in Figure 4(B) which is open only on this condition and consists of a make contact on A in parallel with a break on B.

Now consider the condition "A released *and* B operated." The circuit closed for this condition, a break on A in series with a make on B is shown in Figure 4(C). This circuit, 4(C), is open when that of Figure 4(B) is closed and closed when 4(B) is open. The two circuits are said to be "negatives" of each other. Either one or the other is closed for any given set of conditions but they are never both closed at the same time. Comparing the circuits of Figure 4(B) and (C), we see that where one contains make contacts the other contains break contacts and a series connection in one becomes a parallel connection in the other. It turns out to be a general rule that the "negative" of any series parallel 2-terminal network of contacts can be constructed by substituting break contacts for make contacts and vice versa, and interchanging series and parallel connections. Two examples are shown in Figure 5. Obviously a circuit can be constructed directly from a statement of conditions for opening a path by changing meanings of *and* and *or* to parallel and series, respectively, and using break contacts on operated switches or relays and make contacts on unoperated switches or relays. The negative type of reasoning often leads more directly to simplified circuit arrangements. It may be used as a check on circuit arrangements obtained by direct reasoning and the ability to readily construct the negative of any given circuit is a convenient tool in developing relay control circuits.

Example 1

Now let us consider a simple problem in logic to illustrate how a contact network analogy may be constructed, choosing a problem which is obviously one of logic and not electrical circuits. In this it will be seen that in order to develop the circuit the logic must be completely reasoned through. When this logic has been incorporated in the circuit, the circuit then "knows" the correct answers and will deliver them without error. The problem is a simplified version of the well known "wolf, goat, and cabbage" puzzle:

A farmer has entrusted the care of a goat, a wolf, and a quantity of cabbages to a not-too-intelligent hired man. These items may be kept in either of two barns. If the goat is left alone with the cabbages it will eat the cabbages, while the goat himself is subject to being devoured by the wolf if the hired man is not present to intervene. The farmer desires a device to check on the hired man which is to consist of keys W, G, C, and M, representing the wolf, goat, cabbages, and hired man, respectively. By observing the contents of one of the barns and operating the corresponding keys, the farmer is to be warned by the lighting of a red lamp if the hired man is not properly fulfilling his duties.

For a logical analysis of the problem, first consider the situation in a particular barn under observation. If the hired man is not present and the goat is present with the wolf or the cabbages, trouble will occur in that barn. A more concise statement is "M absent *and* G present *and*, W *or* C present." Items absent from one barn must be present in the other so that a similar statement concerning items not observed describes conditions for trouble in the other barn. The statement is "M present *and* G absent *and*, W *or* C absent." Networks can be constructed from these statements, "present" indicating a make contact and "absent" a break. Since trouble will occur if one *or* the other of these statements is true the two net-

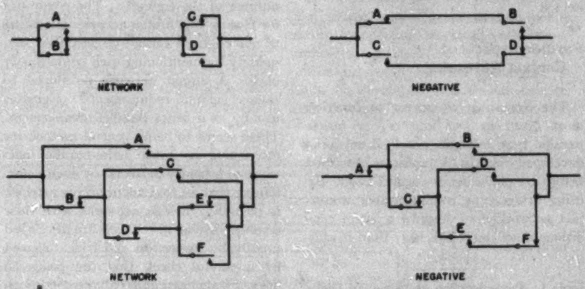

Figure 5. Examples of networks and their negatives

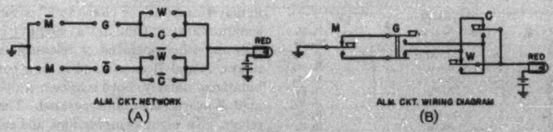

Figure 6. Alarm circuit

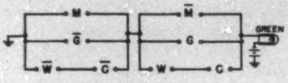

Figure 7. Check circuit

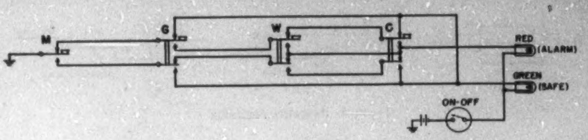

Figure 8. Complete circuit combining alarm and check actions

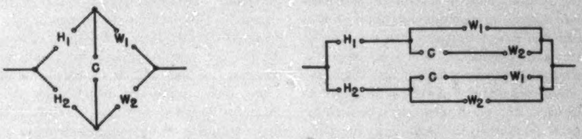

A SIMPLE BRIDGE CKT.
(A)

SERIES-PARALLEL EQUIVALENT
(B)

Figure 9. Bridge circuits

works must be placed in parallel. This is shown in Figure 6(A) where a bar over a designation indicates a break contact. The equivalent schematic is shown in Figure 6(B). With this device it is necessary only that a person be able to identify the items in one of the barns. No analysis or even knowledge of the habits of wolves or goats is required. The contact network having been developed to correspond to a logical framework will examine input conditions to produce answers according to this logic.

Now suppose that the farmer, after using the foregoing device for some time and losing a quantity of cabbages due to a burned-out warning lamp, requests that a green lamp also be provided to indicate as a check that conditions are satisfactory. Thus, the red lamp will light when the hired man is in trouble, and the green lamp when the situation is under control. For this circuit we may simply construct the negative of Figure 6(A) without further analysis of the problem. The resulting network is shown in Figure 7(A) which is the negative of Figure 6(A). An experienced designer will combine and rearrange the complete circuit for both lamps in the equivalent form shown in Figure 8. We leave to the reader the design of a suitable carrying case for the device.

Further Aspects of Contact Networks

The human mind seems to function most often in *and* and *or*, or series-parallel type reasoning, and all networks developed directly by processes described before are of the series-parallel type. By using bridge-type configurations, a contact network may describe a set of conditions much more concisely than it may be stated in words or even thought about. This can be shown by the example of the two jealous wives whose husbands may not take a canoe ride with the other wife except if accompanied by a chaperon. The conditions for a couple to take a canoe trip are concisely expressed by paths through the bridge network of Figure 9(A) where W_1 and W_2 represent the two wives, H_1 and H_2 their respective husbands and C designates the chaperon.

Table I. Representation of Numerical Digits

Digit	Code A	Code B
1	A_1	B_0-B_1
2	A_2	B_0-B_2
3	A_1-A_2	B_1-B_2
4	A_4	B_0-B_4
5	A_5	B_1-B_4
6	A_1-A_5	B_2-B_4
7	A_2-A_5	B_0-B_7
8	A_1-A_2-A_5	B_1-B_7
9	A_4-A_5	B_2-B_7
0	None	B_4-B_7

A bridge-type network is one which has one or more cross branches between parallel branches. Figure 9(A) is an example of the simplest bridge, and a series-parallel equivalent is shown in Figure 9(B) where it is necessary to duplicate a number of the contacts. The conditions for closing this bridge network consisting of five contacts cannot be described adequately by mentioning each contact only once. A circuit network developed to satisfy given requirements originates usually as a series parallel arrangement. There seems to be no general method for converting a given series-parallel network to a bridge network, or even determining that an equivalent bridge network is possible. Bridge networks with their resulting saving in contacts are developed usually by inspection and trial, followed by a careful check that the bridge is opened and closed under all the conditions of the original problem.

A given number of relays or switches, n, may stand open or closed in 2^n possible combinations. That is, a single relay may be either operated or released, two relays, A and B may stand in four combinations, namely, both released, A operated, B operated, or both operated. Three relays give eight combinations and each additional relay doubles the number of combinations. A circuit path can be developed for each of these combinations which is closed only when this combination occurs and open during all others. In fact, a network can be developed which is closed for any set of combinations and open for all others. In the problem of the farmer there are 16 ways in which the wolf, goat, cabbages, and man can be placed in and out of the barn and the circuit for the red lamp is closed for six of these combinations. A routine method for constructing

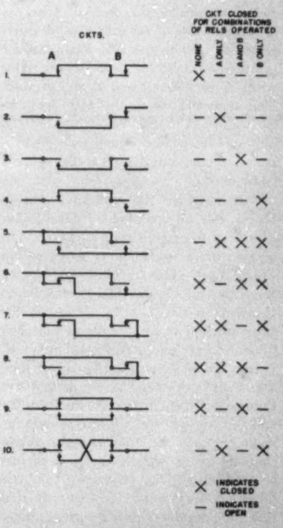

Figure 10. The ten different circuits on the contacts of two relays

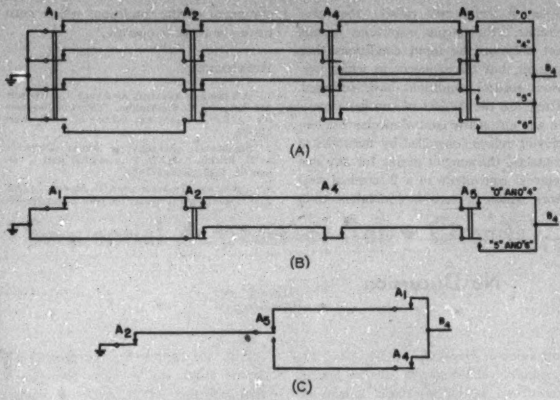

Figure 11. Development of network for one output lead

a network closed for any set of combinations of given relays is to first construct the path for each individual combination. Each of these consists of a series chain of one contact on each relay, the contact being a make or a break, depending on whether the relay is operated or released in that combination. The final network may be obtained by placing all of the individual chains in parallel and simplifying the resulting network.

A surprisingly large number of distinctly different paths may be constructed on the contacts of a few relays. Consider the case of two relays which may stand in for different combinations. The four combinations may be designated as either open or closed in 16 ways, and 16 corresponding circuits developed. Of these, one is an open circuit, one is a closed circuit, four require contacts on only one relay, and the remaining ten require contacts on both relays and are all different. These are shown in Figure 10. For three relays the number of distinctly different arrangements is 218, which indicate how rapidly the complexity of a relay circuit arrangement may increase as the number of relays increases.

EXAMPLE 2

An example from telephone switching practice will illustrate further the process of developing contact networks. In telephone switching systems numerical digits such as those of a directory number are recorded by operating a set of relays in distinctive combinations corresponding to the numerical digits. For various reasons a number of different "codes" are used and it is sometimes necessary to convert from one code to another.[3] Two such codes are shown in Table I.

The circuit example will be that of an arrangement to convert from code A to code B. The elements of code A consist of four relays designated A_1, A_2, A_4, and A_5 which are operated in combinations of one, two, or three at a time to represent the digits as shown. A contact network on these relays is required to ground five output leads, B_0, B_1, B_2, B_4, and B_7 two at a time as in code B. These codes are both additive codes in that the sum of the designation subscripts adds up to the digit value (with the exception of zero in the B code).

The procedure for developing the contact network is to first consider separately each output lead in the B code, examine the individual conditions which cause this lead to be grounded, and construct a contact network which is closed for only this set of conditions among all the conditions which may occur. When networks for all the output leads have been developed it may be possible to partially combine them to save contacts. To illustrate let us develop the network for output lead B_4. This must be grounded for four of the digits represented in the A code as shown in Table II.

Table II

Digit	A Code
4	A_4
5	A_5
6	A_1-A_5
0	None

In developing circuit paths, the effect of unoperated as well as operated relays must be considered. For example, the A code for digit four is not only A_4 operated but also A_1, A_2, and A_5 released. The corresponding circuit path consists of a series chain of breaks on A_1, A_2, and A_5 and a make on A_4. This path is shown together with those for the other three digits in Figure 11(A) where the branch paths are designated according to the digit they represent. This network meets the basic requirements for grounding lead B_4.

It obviously contains superfluous contacts and can be simplified by Boolean algebra or by inspection and logical analysis. An intermediate stage of the simplification is shown in Figure 11(B) and the final form in Figure 11(C). Note the curious fact that this particular network contains only one make contact. The circuit achieves the desired result mainly by opening the circuit path during undesired combinations.

The networks for the remaining B leads are developed in a similar manner and produce arrangements which are

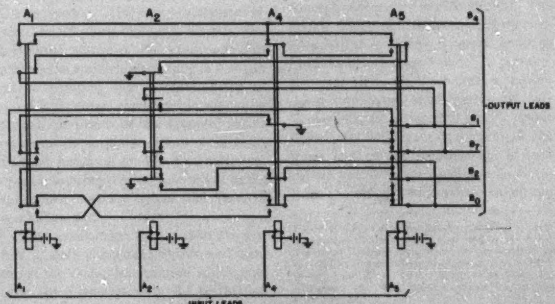

Figure 12. Complete code conversion circuit

somewhat more complex than that of the B_4 lead used for an example. The networks for all five of the B leads may be combined by inspection and analysis to produce the complete network shown in Figure 12.

Circuits such as this where there is a one-to-one correspondence between combinations of input control condition and output conditions are called "combinational circuits." In circuits of a higher order of complexity called "sequential circuits," the output conditions depend not only on the input conditions then present, but the sequence in which previous control conditions have occurred. These are the subject of another paper.[2] In any automatic control mechanism employing relays controlled by networks of contacts, the control means for any one relay is equivalent to a 2-terminal network which in turn is equivalent to a statement of the conditions which must cause the relay to operate.

References

1. A SYMBOLIC ANALYSIS OF RELAY AND SWITCHING CIRCUITS, C. E. Shannon. *Electrical Engineering* (*AIEE Transactions*), volume 57, 1938, pages 713–23.

2. SEQUENTIAL ASPECTS OF RELAY CIRCUITS, A. E. Ritchie. *AIEE Transactions*, part I, volume 68, 1949, pages 577–81.

3. CODES AND TRANSLATIONS, O. Myers. *AIEE Transactions*, part I, volume 68, 1949, pages 592–96.

No Discussion

Sequential Aspects of Relay Circuits

A. E. RITCHIE
NONMEMBER AIEE

IT IS well recognized that the electromagnetic relay is the basic circuit element employed in the control of present day automatic telephone switching systems. Although the relay is fundamentally a very simple device capable of assuming but two conditions, unoperated and operated with contacts correspondingly open or closed, it possesses certain properties which enable it to be woven into amazingly complex circuit arrangements. It is but a slight exaggeration to claim that relay circuits can be designed to perform any logical operation of which the mind of man can conceive, provided that there are a finite number of input and output conditions which can be translated into the relay "language."

The basis of relay circuit action is that a set of n of the 2-position devices can assume 2^n distinct combinational patterns. Thus a particular input condition can produce a particular relay pattern which by utilizing the contact configurations on the relays generates a corresponding output condition. A new input condition develops another output condition, and so on. This combinational aspect of relay circuits is the subject of other papers.[1,2]

Of equal importance with this concept is the realization that an input combination to a relay circuit can generate an internally-used condition which can be locked-in, so to speak, for future use. Such internal registrations can be employed to modify the reaction to subsequent input conditions or to originate a series of internally-controlled output conditions, which proceed, once started, independent of the input. These considerations all imply a sequential aspect to relay circuits which will be the subject of this paper.

An excellent example of the sequential capabilities of relay circuits is offered by the control circuits of a modern telephone switching system. Although in detail the control circuits are incredibly complex, the over-all input and output conditions are sufficiently well known to permit a ready understanding of the nature of sequential relay circuit action. A brief description of switching control will be followed by a discussion of some of the factors that enter into the design of sequential relay circuits.

The control action necessary to establishing a telephone connection can be broken down into two principal series of operations. One concludes when the subscriber hears dial tone; the second when a distant bell rings. The first is initiated when a subscriber lifts his receiver to place a call. This action produces a simple input condition to the switching system consisting of the closure of the conductor loop to the central office. Circuits within the central office recognize this loop closure and call into action associated circuits which interact with each other to find the one calling line out of perhaps 10,000, locate one out of perhaps 100 register circuits capable of receiving dialed instructions, and finally, test and set up a connecting path from line to register. This simple statement of what takes place indicates directly the sequential nature of the operation; implied is the sudden burgeoning of a single relay operation into a multiplicity of secondary control conditions in which the output conditions of one group of relays represent the input conditions of the next. In total, hundreds of individual relays cooperate to bring the dial tone signal to the subscriber, usually before the receiver reaches his ear.

The second input condition to the system is more complex in nature and comprises the dialed information which contains the directions as to the destination of the call. The very problem of accepting and registering this information requires for its solution an involved sequential-type relay circuit part of which is the subject of another paper.[3] However, assuming that the dialing of a 7-digit number represents a single input condition, consider the magnitude of the response required from the switching system. A particular 7-digit number is one condition out of a possible 10,000,000. Relay circuits must determine from this unique number the general location or central office of the called line and test and set up a connection to an idle path leading to that office. Complex signals representing the called line number are then transmitted over the established path and are registered at the distant office. This information must in turn be interpreted and used to control circuits which guide the connection toward the particular called subscriber. Finally, a bell starts to ring, and continues until the call is either answered or abandoned. At any point in this series of events, the relay circuits must be prepared to start out on alternate sequences of operations depending upon particular conditions encountered.

Basic Design Principles

This brief description is an oversimplification of the control features of telephone switching, but it will perhaps serve to illustrate the nature of the capabilities of relay circuits and to indicate the concept of sequence in such circuits. The actual design of circuits to perform such a variety of functions, however, is not as formidable as it may sound. In practice, the over-all control problem is broken down into many small parts and particular jobs are assigned to specific circuit units. By intelligent statement of the input and output requirements of each circuit unit a set of conditions is established, to satisfy which a relay circuit can

---

Paper 49-146, recommended by the AIEE Communication Committee and approved by the AIEE Technical Program Committee for presentation at the AIEE Summer General Meeting, Swampscott, Mass., June 20–24, 1949. Manuscript submitted November 16, 1948; made available for printing May 5, 1949.

A. E. Ritchie is with the Bell Telephone Laboratories, Inc., New York, N. Y.

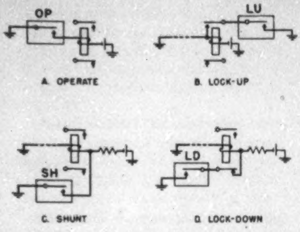

Figure 1. Basic control paths for a relay

be designed. The basic design technique for sequential-type circuits is outlined in this section and is followed in the next by an application to a practical design problem.

Underlying the technique of relay circuit design is an understanding of the basic relay control paths. There are four of these paths, illustrated on Figure 1, which may be defined as follows:

Operate. A battery-ground path in series with the relay winding and containing a network *OP* developed on the contacts of other relays. When the contact configuration closes the path, the relay operates; when it opens the path, the relay releases.

Lock-Up. A path to the relay winding through a make contact on the relay itself. The lock-up path is ineffective until the relay is energized through the operate path. Thereafter contact network *LU* on other relays can hold the relay operated until *LU* opens the lock-up path.

Shunt. A path in parallel with the relay to a series current limiting resistor. Its functioning is the inverse of the operate path. When the operate path has been closed, closure of contact network *SH* on other relays releases the relay; opening *SH* permits the relay to operate.

Lock-Down. A path shunting the relay winding through a break contact on the relay itself. When the relay is released, a closed-path through network *LD* on other relays prevents it from operating; opening *LD* permits it to operate. This path is ineffective when the relay is operated and is the inverse of the lock-up path.

Of these four paths, the operate and lock-up are by far the most frequently used. The two shunting paths, however, can be very useful in certain circuit situations which in general can be recognized easily. An example is when a relay is required to operate to record the termination of a pulse.

The nature of input conditions to a relay circuit is also obvious from Figure 1. In general they consist of the simple presence or absence of ground (or battery) on leads to the circuit. This statement ignores special relays which respond to polarity or to alternating current, and which are not considered in this paper. The complexity of a set of input conditions depends upon their combinational or sequential aspects rather than upon their basic nature. The output conditions which relays can establish are similar to the input conditions in that they consist of the closing or opening of paths. These paths can light lamps, ring bells, actuate other relays, and so forth, but again are fundamentally simple in nature.

It is convenient in designing relay circuits to associate a relay with each input path. These primary relays will then accurately follow the various input conditions and offer in effect sets of contacts for manipulation. If at a later stage in the design a primary relay is found to require only a single make or break contact, it can perhaps be dispensed with.

The input conditions to a relay circuit may consist of one or more unique signal combinations with each of which a particular and unvarying output condition is associated. Circuits of this type may be characterized as combinational. In this case contact networks on the primary relays alone can usually be designed to complete the circuit. The more usual situation, however, involves a sequence of input conditions in which the reaction at each change of input depends upon preceding events. A particular input combination may be repeated more than once with a different output condition associated with each appearance. An input condition may initiate a series of output conditions or a group of circuits may interact to provide each other with consecutive instructions which determine from moment to moment the subsequent action. Circuits of this type are known as sequential circuits. They invariably require the use of secondary relays whose function is to record preceding events, to differentiate between repetitions of the same input condition, and to control sequential output conditions. Control of the secondary relays is through contacts on both the primary and secondary relays.

Figure 2. An example of sequential design

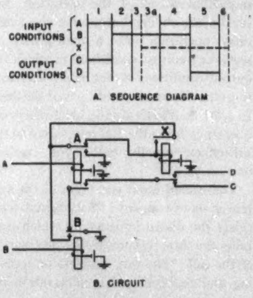

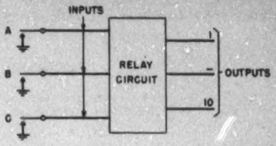

Figure 3. Block diagram of design problem

An illustration of a repetitive input condition is shown on Figure 2(A). The two horizontal lines *A* and *B* represent the sequential order of two input conditions which may be considered ground on leads *A* and *B*. The *A* condition first appears and then is joined by condition *B*. Condition *A* terminates and reappears during condition *B*, finally persisting for an interval beyond the removal of *B*. This representation constitutes a cycle and, if *A* and *B* are understood to be primary relays which follow the input signals, each successive relay combination is known as an interval. It can be seen that intervals 1 and 5 are identical as are 2 and 4. The circuit is required to develop distinctive output conditions for both intervals 1 and 5. Clearly an additional relay is necessary to differentiate between intervals 1 and 5. The secondary relay should, logically, be in an operated condition during one of the conflicting intervals and in an unoperated state during the other.

The general design procedure consists, first, of examining the sequence diagram to determine a plan of operation for the secondary relays or, basically, the intervals during which the secondary relays must be operated. Thereafter the control paths and the output paths can be designed. In this case, a single secondary relay (X) must operate after interval 1 and prior to interval 5. The primary combination to operate (X) must be chosen so that it does not appear before or during interval 1, and, in the general case, must not recur at any other time during which (X) must be released.

After the operate interval for (X) has been chosen, the release interval must be determined. Obviously, this must be later in the cycle than the intervals that (X) operated is required to distinguish and also it must not be duplicated within the operated period of (X). Once this interval has been established, the holding circuit for (X) can be developed in either

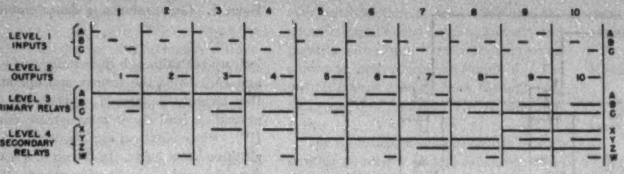

A. OVERALL SEQUENCE DIAGRAM

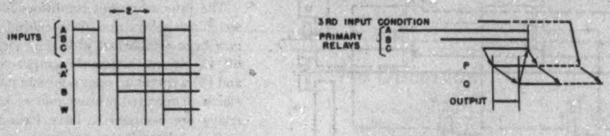

B. END-OF-PULSE DETECTION

C. OUTPUT TIMING AND RELEASE

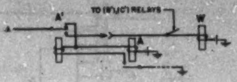

Figure 4 (left). Sequence diagram of design problem

Figure 5 (above). Circuit for detecting the end of a pulse

of two ways. One is to examine the release interval, determine a path through the primary relay contacts that is *open* only at that time, and connect the path to a lock-up contact on relay (X). The other method is to examine the intervals during which (X) remains operated, determine overlapping contact paths that remain *closed* until the release interval, and connect such paths in parallel to a lock-up contact on (X). Since the lock-up contact is closed only when (X) is operated, duplicate holding paths that are closed to this contact during intervals in which (X) is not operated can have no effect on circuit operation and need not be considered.

In the sequence diagram of Figure 2(A), interval 3 offers the unique primary combination of (B) alone operated for operating relay (X). Since (X) must remain operated through interval 5, a suitable holding combination persisting during intervals 3, 4, and 5 consists of (A) or (B) operated. The complete circuit for the three relays including the output paths is shown in Figure 2(B).

In the general case of more complex circuits, a great many secondary relays may be required. Control paths for these involve not only contacts on the primary relays, but on the secondary relays themselves. It is frequently necessary to operate a particular secondary relay two or more times during a cycle. This requires placing several operate paths in parallel. If lock-up paths are developed from overlapping holding combinations, several of these may be placed in parallel. On the other hand, if holding paths are derived from consideration of the release intervals and are chosen to open only at the correct instant, they may be placed in series. In any case, considerable care is necessary to determine the optimum position of a secondary relay in a cycle and to design good control paths.

A very important factor in design, mentioned earlier, is that a group of n relays is capable of assuming 2^n different combinational patterns. Since, in general, each interval of a complete cycle including both primary and secondary relays should represent a distinct combination, this is a clue to the maximum number of relays required. In Figure 2, the original statement of the problem called for five distinguishable intervals necessitating at least three relays. Introduction of the third relay into the cycle differentiated between intervals 4–5 and 1–2 and also created two new intervals, 3a and 6. These latter occur because of the finite operating time of a relay. It is generally true that, with the larger circuits, as the ratio of used combinations to total combinations increases, circuit complexity goes up rapidly. Therefore, it may be desirable to add more secondary relays to a circuit than logic strictly calls for.

The design of relay circuits in which sequential output conditions are generated internally by the circuit follows the same general technique as that described before. Building on a sequence diagram of input conditions, the output conditions are plotted and then the secondary relays are added to satisfy the requirements. Considerable care must be exercised in choosing the secondary relay pattern since the sequence may have a profound effect on the complexity of the over-all circuit. Frequently the design of internal control and output paths indicates desirable modifications of the cycle.

Design Problem

The discussion up to this point has been very general in nature, and perhaps requires an example of actual circuit design to illustrate the technique. The problem that follows is not taken directly from telephone switching systems, yet it is closely related to a type of circuit situation that recurs in switching design.

A 3-button key set, each button actuating a single make contact, is connected over three wires to the relay circuit to be designed. This is indicated on Figure 3. Input conditions consist of three successive key operations, with the restriction that the same key may not be operated twice in a row. This permits 12 permutations of key sequences of which ten are required to produce individual output conditions. The output conditions are to consist of a short ground closure, following the third key operation, to the one out of ten output leads corresponding to the input sequence. Following the output signal, the circuit must return to normal.

On levels 1 and 2 at the top of the sequence diagram of Figure 4(A) are plotted the ten individual input sequences or cycles, each associated with a particular numbered output. Since the only difference between the various input sequences lies in the order of key closures, basically the relay circuit must be a sequence-detecting device. Furthermore, it must recognize three key operations, not necessarily on three different keys, before producing an output.

Since the three input conditions of an individual sequence do not overlap, relays must record by locking-up that a particular input has occurred. In this particular case, it is advantageous to lock-up the primary relays for this purpose in order to simplify the control of secondary relays. On level 3 of Figure 4(A), the condition of primary relays as a result of this assumption is shown. It will be

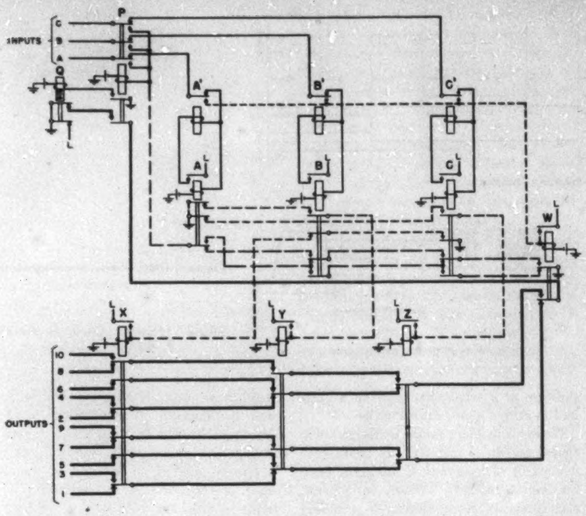

Figure 6. Circuit solution to design problem

noted that, at the end of each odd input cycle, all primary relays are operated; at the end of each even cycle, two of the three primary relays are operated. Clearly secondary relays are necessary to distinguish between the identical primary combinations.

If the primary cycles are examined in order, it is seen first that the final combination of cycle 3 must be differentiated from that of cycle 1. Since cycle 3 differs from cycle 1 only in that relay (C) operates before relay (B), a secondary relay (X) can be specified that will operate in cycle 3 through a make contact on (C) and a break contact on (B). This path, which detects sequence, is not closed in cycle 1. However, it is closed in cycles 4, 9, and 10 and relay (X) should be entered on the sequence diagram at all four places as shown on level 4 of Figure 4(A).

Similar analysis discloses that a secondary relay (Y) operating on the combination of (B) operated and (A) released will differentiate between cycles 1 and 5. Relay (Y) also operates during cycles 6, 7, 8, 9, 10. Interval 7 is now indistinguishable from interval 5. Therefore, relay (Z), which detects the sequence of (C) operating before (A) is added to cycles 7, 8, 9, 10. At this stage of the development a unique combination of relays (A), (B), (C), (X), (Y), (Z) exists at the end of each cycle and appropriate output paths could be constructed on the contacts of the relays.

However, further study of the sequential diagram will show that there is no present means of detecting the arrival of the third, duplicating, input on the even cycles. This is necessary primarily to indicate when the output path should be closed. A secondary relay (W), operating as shown on level 4 of Figure 4(A), could well perform this function. There is no convenient way, however, to provide the correct operating paths for (W) using only the relays already shown on the sequence diagram. Additional relays are required which can react to the termination of the first appearance of each input closure and prepare a path through which a second appearance can operate (W). The nature of the problem is such that it makes no difference which repeated input operates (W).

The sequence diagram for a typical individual cycle is shown on Figure 4(B). Input *A* causes primary relay (A) to operate and lock. Directly below (A) is shown an auxiliary relay (A′) which operates and locks when input *A* ends and which serves to provide a unique combination to operate (W) when input *A* reappears. Since the operating condition for auxiliary relay (A′) consists of the removal of a ground closure, a lock-down path is necessary for its control. A frequently used circuit arrangement that meets the sequential requirements perfectly is shown in Figure 5. Initial grounding of lead *A* operates relay (A), yet prevents (A′) from operating. When ground is removed from lead *A*, the series lock-up path through the windings of (A) and (A′) holds the former and operates the latter. A second appearance of ground on lead *A* can now operate relay (W). Since identical conditions apply to all three input leads, the circuit of Figure 5 can be used in conjunction with each of them.

The internal circuit conditions for the secondary relays and their control have now been established with the exception of: (1) means to time the output signal; and (2) a circuit to open a ground path to which all operated primary and secondary relays are assumed to have locked. A sequence diagram for two relays to perform these functions is shown in Figure 4(C).

Relay (P) operates when the third input condition in any cycle appears and must, first, close ground to the signal output paths on the secondary relays, and second, close a path to slow-acting relay (Q) which, when it operates after a time delay, will open the output path. If locking ground for the circuit as a whole is taken from a back contact on relay (Q), the circuit will release at the termination of the output condition.

A careful analysis of the conditions represented by Figure 4(C) will indicate the possibility of the third input condition persisting beyond the release of relay (Q). If this were to occur, a primary relay might reoperate to initiate falsely a new cycle. In order to prevent this, it can be decided now to take the input leads through break contacts on (P) and to provide locking contacts on (P) to permit the relay to hold to any activated input lead.

All information required for setting up the final contact paths of the completed circuit is now available. The circuit itself is sketched in Figure 6. The control paths for the primary relays (A), (B), (C) and their auxiliaries (A′), (B′), (C′), identical to that shown in Figure 5, are drawn in light lines. Control paths for secondary relays (W), (X), (Y), (Z), derived from sequence diagram levels 3 and 4 of Figure 4(A) and from Figure 4(B), are shown in short dashed lines on Figure 6. The operating path for relay (P) requires somewhat more consideration. Relay (P) must operate under a variety of conditions which include (A), (B), (C) all operated and [(A), (B)] or [(A), (C)] or [(B), (C)] operated in conjunction with (W). A path designed on this basis would be very cumbersome. However, all these conditions are embodied in the statement that (P) must operate when any three of relays (A), (B), (C), (W) are operated. This permits use of a symmetric three-out-of-four contact network,[2] shown in long dashed lines, to control (P). Also relay (P), as stated before, must lock to all input leads and must open the input leads to the primary relays.

The original conception of the output path network visualized contacts on relays (S), (Y), (Z), (A), (B), (C). However, introduction of relay (W) into the circuit simplifies the output network and permits use of the "tree" configuration[2] shown in heavy lines in Figure 6. The output circuit extends back through contacts on (P) and (Q) for timing purposes.

The final design detail consists of connecting all relay locking leads *L* back to a break contact ground on relay (Q). The circuit is now complete and may be checked against the initial statement of requirements.

References

1. The Logic of Relay Circuits, W. Keister. *AIEE Transactions*, part I, volume 68, 1949, pages 571–76.

2. Relay "Trees" and Symmetric Circuits, S. H. Washburn. *AIEE Transactions*, part I, volume 68, 1949, pages 582–86.

3. Counting with Relays, G. R. Frost. *AIEE Transactions*, part I, volume 68, 1949, pages 587–91.

No Discussion

Relay "Trees" and Symmetric Circuits

S. H. WASHBURN
NONMEMBER AIEE

BASICALLY, a telephone switching system performs a large majority of its functions as a result of the operation of groups of interconnected relays, or similar electromechanical devices. These relays control one another by means of contact networks, the configurations of which depend upon the requirements to be fulfilled by the relay circuits involved. Due to the complexity of modern switching methods there is an almost limitless variety of these circuits. However, there are certain types of circuit arrangements which are employed over and over again and have become, with usage, familiar to all engaged in the design of switching systems. This paper discusses two of these types: the relay "tree," and the symmetric circuit.

Relay "trees" and symmetric circuits are forms of combinational circuits. The combinational circuit, as opposed to the sequential type, recognizes and reacts to certain combinations of active input conditions, and establishes a particular output condition in response to each input combination. The operation of the sequential circuit, on the other hand, is further affected by the order in which input conditions are applied. For the purposes of this paper each input control lead to a circuit may carry an active input condition; the term "combination of conditions" refers to the state of a group of input leads, each lead in either an active or a passive state.

The number of relays in a combinational circuit and the number of combinations of active input conditions it can recognize are directly related. A single relay, a 2-valued device either operated or released, can respond to only a single active input condition; that is, it can be operated by that condition and released by the absence of the active condition. Two relays can respond to four combinations of conditions: one combination operating one relay; one operating the second relay; the third operating both; and the fourth operating neither. Such reasoning shows that the number of combinations of input conditions which an n-relay network can recognize is 2^n. For each combination of input conditions causing circuit action, the relay circuit can produce a unique output condition (a grounded lead, for example). Thus, the number of independent and mutually exclusive output conditions possible for an n-relay circuit is 2^n. This same relationship can be given by the expression

$$\sum_{r=0}^{n} C_r^n$$

the sum of combinations of n relays of which r are operated. This summation is the number of combinations in which n relays may be operated and is equal to the number of possible independent output conditions, 2^n.

Relay "Tree" Networks

The relay tree, so-called because of its configuration, is a special case of a multiterminal network of relay contacts comprising a single input terminal which may be connected to one of a number of output terminals. The path from each output terminal to the input end of the network passes through contacts on all of the relays upon which the network is constructed and all paths are disjunctive; that is, only one is closed at a single time and no two paths are connected together. The particular path closed through depends upon the combination of operated relays.

The Fully-Developed Tree

In the fully-developed tree there is an output terminal corresponding to each of the 2^n possible output conditions. As an illustration, consider the fully-developed 4-relay tree of Figure 1. This network has $2^4 = 16$ output terminals. If the acting times of the relays are assumed to be negligible, it then follows that one and only one path from the input to an output terminal is always closed, the particular path depending upon the input combination placed on the four input control leads. The use of break-before-make transfers in the tree insures that no output terminals are connected together at any time.

Due to the orderly pattern on which the fully-developed network is constructed, certain relations hold between the number of circuit relays, the number of contacts in the circuit, the maximum number of contacts, on a relay, and so on. Designating the circuit relays in order of increasing number of contacts, relay R_1 is equipped with one transfer-contact; relay R_2, two transfers; R_3, four transfers; relay R_n, the maximum number of trans-

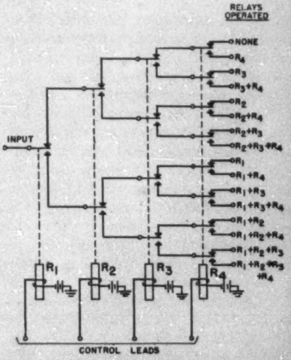

Figure 1. A fully-developed 4-relay tree circuit

Paper 49-147, recommended by the AIEE Communication Committee and approved by the AIEE Technical Program Committee for presentation at the AIEE Summer General Meeting, Swampscott, Mass., June 20–24, 1949. Manuscript submitted November 16, 1948; made available for printing May 4, 1949.

S. H. Washburn is with the Bell Telephone Laboratories, Inc., New York, N. Y.

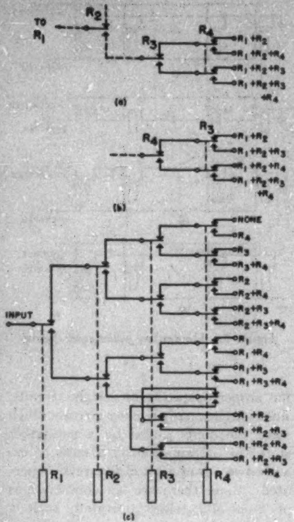

Figure 2 (right). Redistribution of the spring load on the relays of the tree

fers, 2^{n-1}. The total number of transfers in the circuit is the summation: $2^{n-1}+2^{n-2}+\ldots.2^1+2^0=2^n-1$.

An obvious disadvantage of the tree network in its general form is the unequal distribution of spring load on the circuit relays. A somewhat more uniform distribution may be obtained by manipulation of that portion of the network carried by all relays except the first, that equipped with the single transfer combination. Unfortunately, any contact rearrangement which adds to the spring load on the first relay greatly increases the total number of contacts in the circuit. This is not, of course, true of the trivial rearrangement in which all contacts on relay R_2 are transferred to relay R_1 and those on R_1 are placed on R_2.

The fully-developed n-relay tree may be considered as two $(n-1)$-relay trees, or as four $(n-2)$-relay trees, and so on, suitably connected. Inspection of the tree of Figure 1 indicates that it can be divided into two 3-relay trees, or four 2-relay trees. Contact rearrangement may best be carried out by successive manipulations of these minor trees, such manipulation having no effect upon the operation of the tree as a whole. There appear to be no specific rules for obtaining a rearrangement which provides a certain desired spring load distribution. The method of rearrangement described in the following must be applied on a successive-trial basis until a permissible distribution is attained.

The rearrangement of a minor tree consists merely of redesignation. For example, consider the lowermost of the four 2-relay minor trees on relays R_3 and R_4 of Figure 1, as redrawn in Figure 2(A). The designations of the two relays are interchanged, as far as this particular minor tree is concerned and, the output terminals are redesignated, as in Figure 2(B). Since the minor tree has a separate output terminal for each combination of the operated relays upon which it is built, such a redistribution of contacts results in a second minor tree which is the exact equivalent of the first. The rearranged minor tree of Figure 2(B), then, can be inserted in the complete tree in the place of the minor tree of Figure 2(A). This manipulation has, in effect, removed one transfer-contact from relay R_4 and has added it to the load on relay R_3, as shown in Figure 2(C).

Further load equalization is accomplished by rearranging the lower of the two 3-relay minor trees of Figure 2(C), interchanging the spring loads of relays R_2 and R_4 and thus moving two transfers from R_4 to R_2. The final exchange leaves the circuit with the following spring loads: R_1, one transfer; R_2, four transfers; R_3, five transfers; R_4, five transfers. In this manner the spring load may be shifted as desired, the total number of transfer-contacts always remaining 2^n-1.

THE PARTIALLY-DEVELOPED TREE

In many cases a tree network is not fully-developed; that is, not all possible combinations of operated relays have corresponding outputs. This type is more common in relay switching applications than the fully-developed form. As an illustration of the utility of a partially-developed tree, assume that a circuit is to be designed to fulfill the following requirements.

There are four leads a, b, c, and d which are grounded two at a time to indicate a digit from 1 through 5 in the following code: a and b = 1, a and c = 2, a and d = 3, b and d = 4, c and d = 5. The circuit to be designed is a translator which will ground one of five leads, each corresponding to an input digit. An additional requisite is that when any combination of grounded input leads other than those denoting the above codes occurs, no output lead is to be grounded. Output leads are to be disjunctive.

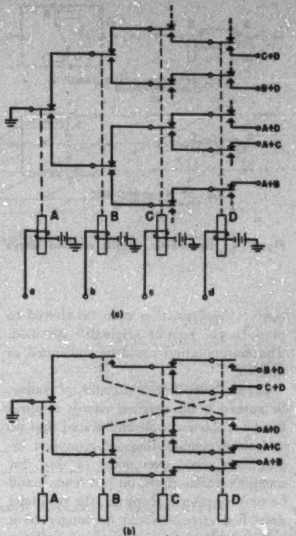

Figure 3. A partially-developed 4-relay tree used as a translation circuit

As a first step in synthesizing the desired circuit, relays (A), (B), (C), and (D) are provided, each relay to be operated when its corresponding input lead is grounded. The number of possible relay combinations for four relays, as has been indicated, is sixteen and, of these, five are to be used in the present circuit: an output lead, 1, is to be grounded when relays (A) and (B) are operated, output lead, 2, is to be grounded when relays (A) and (C) are operated, and so on. No lead is to be grounded for the remaining 11 combinations. The tree network of Figure 1 placed on the four relays will satisfy these requirements, and those elements of the tree which do not contribute to the grounding of the five required output leads can be eliminated. The resultant partially-developed tree is shown in Figure 3(A). Inspection shows that the circuit meets the original specifications.

The network of Figure 3(A) can be manipulated in a manner similar to that described previously. However, mere interchange of designations of the minor-tree relay contacts is not sufficient when the tree is not fully-developed. This is indicated in Figure 3(B) in which the upper minor-tree on relays (B), (C), and (D) of Figure 3(A) is rearranged. The

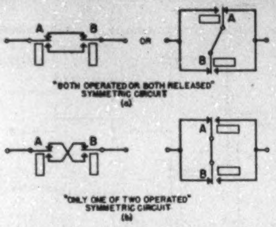

Figure 4. Symmetric circuits on two relays

contact configuration must be altered to produce the output originally specified. The manipulation could be continued as desired.

Greater simplification could, of course, be gained if the original circuit requirement for this example had stated that no undesired combinations of grounded input leads could ever occur or that, for certain combinations, output leads could be tied together. However, the resultant simplified circuit would no longer be a tree since, by definition, network paths in a tree must pass through contacts on all relays and must be disjunctive.

Symmetric Circuits[1]

A symmetric relay-contact network is one in which the conditions for closing a particular input-to-output path are given, not in terms of the designations of relays operated and unoperated, but in terms of the number of relays operated and unoperated. For example, a network which is closed when any three, and only three, out of five relays are operated is a symmetric circuit. A second example might be a network in which one path is closed when less than two circuit relays are operated and a second is closed for more than four relays operated. Chains and parallel groups of make-or-break contacts are elementary forms of symmetric networks since they can indicate conditions of all relays operated or released, or one-or-more relays operated or released.

There are two general symmetric networks which may be constructed on two relays, as shown in Figure 4, and each of these may be connected in two ways. These networks are closed for "both operated or both released" and "only one of two operated," respectively. This second network is of interest in that in the statement setting forth conditions for circuit closure, "relay (A) *or* relay (B) operated," the "or" indicates mutual exclusion: no path is closed when both (A) and (B) are operated. This "or," then differs from the "or" which appears in statements illustrating the operation of a network of parallel contacts.[3]

Numerous simple symmetric circuits based on chains of make-, break-, and transfer-contacts combined in various configurations can be developed. Some of these are shown in Figure 5 together with the associated conditions for circuit closure. For several of these networks two output terminals are shown, one for each closure condition of the network. The two terminals in these cases may be connected together if only a single path is desired for both conditions.

A network for any symmetric circuit may be constructed of series and parallel elements. Such a network, however, is generally complicated and uneconomical of contacts. A general type of lattice structure which gives the most satisfactory circuit is shown in Figure 6. This figure indicates the circuit in conventional form and also in a symbolic notation in which each contact is represented by a line segment. In this notation make-contacts are characterized by sloping lines and break-contacts, by horizontal lines. These elements are so arranged that contacts on a particular relay appear as line segments placed one above another, each vertical group of segments having the same designation as that of the corresponding relay. Inspection of the circuit in conventional notation indicates that the network paths are disjunctive and that the particular output terminal which is connected to the input terminal depends only upon the number of relays operated. The output terminals are designated to correspond to the number of operated relays or to the number of input control leads grounded.

The operation of the circuit can be seen more readily from the symbolic diagram. If ground is applied to the input terminal and no relays are operated, ground will be connected through a chain of break-contacts on the zero level of the diagram to the output terminal "O". If any one relay is operated, ground will pass along the zero level until it encounters the make-contact on the operated relay where it will be switched up to the next or first level. The ground then remains on the first level and appears on terminal 1. If more than one relay is operated, the ground is passed from one level to the next higher level at each operated relay. The highest level reached corresponds to the number of relays operated.

One important function which the symmetric circuit performs in telephone switching applications is that of checking for proper operation of certain circuits. For example, many register circuits which store the digits dialed by a subscriber store this information on a basis of exactly two out of a set of five relays operated. Since there are ten combinations of 2-out-of-5 relays operated, such a register can store any one of ten digits. However, under trouble conditions, more or less than two relays may become operated, mutilating the stored digit. So that this mutilation can not cause trouble in other circuits, it is desirable to include in the register arrangement a check circuit which will give an indication, or allow the stored digit to be passed on, only if the normal number of register relays are operated. A 2-out-of-5 symmetric circuit is an ideal arrangement for this application.

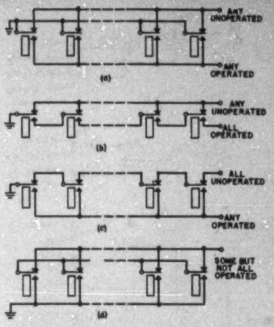

Figure 5. Elementary symmetric circuits

To satisfy a given condition with the general symmetric network, it is necessary only to connect to the input and to the desired output terminal. Superfluous contacts may be eliminated. The desired circuit for 2-out-of-5 relays operated is indicated in Figure 7, both as a lattice diagram and in more conventional form. Many of the junction points on the lattice diagram can represent transfers facing in either direction; an arrangement with fewer springs results if the circuit is drawn from both ends with transfers facing away from the end terminals. In the circuit of Figure 7 the (D) and (E) relays are inverted top-to-bottom to obtain a simpler schematic diagram.

SYMMETRIC CIRCUITS CLOSED FOR ONE CONDITION

As illustrated by the preceding example, if a symmetric circuit is closed for but one number of relays operated and the superfluous elements of the general symmetric

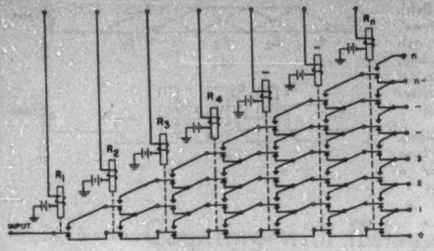

SCHEMATIC DIAGRAM
(a)

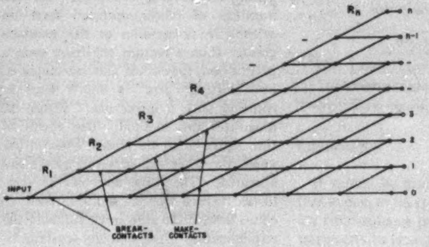

SYMBOLIC LATTICE DIAGRAM
(b)

Figure 6. General symmetric contact-network

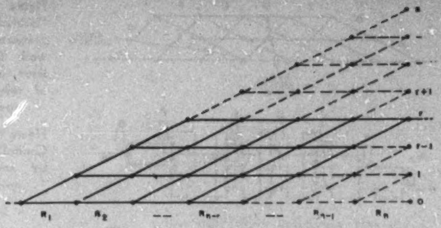

Figure 8. General single-condition symmetric network

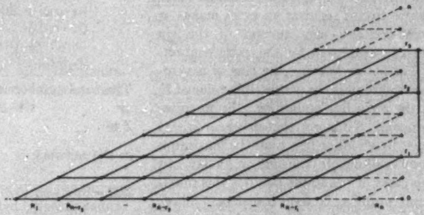

Figure 9. General multicondition symmetric network

are eliminated, the symmetric lattice becomes a parallelogram. A sloping side of this parallelogram consists of r elements, where r is the number of operated relays necessary for circuit closure, and the base is composed of $(n-r)$ elements, where n is the total number of relays in the circuit. The quantity $(n-r)$ has the significance of being the number of relays which must be *unoperated* to cause circuit closure. This generalized single-condition symmetric lattice is shown in Figure 8.

Considering the lattice, quantitatively, the total number of contacts, N, in the network is by inspection

$$N=(n-r)(1+r)+r(n-r+1)=2r(n-r)+n \tag{1}$$

The total number of make-contacts, M, represented by the sloping line segments, is

$$M=r(n-r+1)=r(n-r)+r \tag{2}$$

The total number of break-contacts, B, represented by horizontal line segments, is

$$B=(n-r)\ (1+r) \tag{3}$$

Considering now that make- and break-contacts may be combined to form transfer-contacts, either all makes or all breaks may be made parts of transfers depending upon which type of contact is lesser in number. The number of contacts which remain after the transfers are formed is given by

$$R=M-B=2r-n \tag{4}$$

The sign of R is positive if the remaining contacts are makes and negative if they are breaks.

The total number of transfers, T, is

$$T=(N-|R|)/2 \tag{5}$$

where $|R|$ is the absolute value of R.

Close inspection of the general symmetric lattice of Figure 8 indicates that the number of contacts on the most-heavily loaded relay depends not only upon the quantities n and r, but also upon whether $(n-r)$ is greater or less than, or equal to, r.

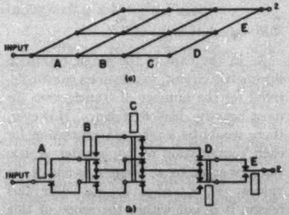

Figure 7. The 2-out-of-5 symmetric network

When $(n-r)>r$, or $n>2r$, the maximum number of contacts, N_1, on a relay is

$$N_1=2r+1 \tag{6a}$$

The number of transfers, T_1, obtained by combining these contacts, is

$$T_1=r \tag{6b}$$

and there is an extra contact, a break.

When

$(n-r)=r$, or $n=2r$,

$$N_1=2(n-r)=2r \tag{7a}$$

$$T_1=r \tag{7b}$$

and there are no extra contacts.

When

$(n-r)<r$, or $n<2r$,

$$N_1=2(n-r)+1 \tag{8a}$$

$$T_1=(n-r) \tag{8b}$$

and there is an extra make-contact.

These expressions make possible a determination of the symmetric networks of the greatest dimensions possible employing given relays. For example, assume that relays with a maximum of six transfers are available. If, however, the most-

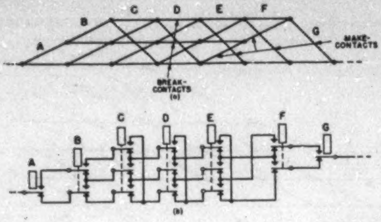

Figure 10 (left). "Shifted - down" symmetric network for zero, three, or six out of seven relays operated

Figure 11 (right). Control of a lamp by any of n switches

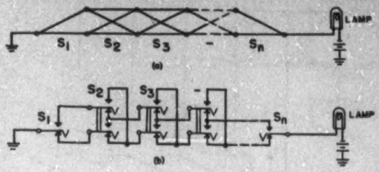

heavily loaded relay in a particular symmetric circuit requires an extra make- or break-contact, one transfer of the six must be employed for the extra contact.

The factor limiting the size of a symmetric circuit is the permissible value of T_1 in the preceding equations. From equations 6 and 8 it is seen that either r or $(n-r)$ must be equal or less than the maximum number of usable transfers on a relay. In the cases of equations 6 and 8 this maximum number is five transfers. Thus, either the number of operated relays r, or the number of unoperated relays $(n-r)$, necessary for circuit closure must be equal or less than five. Equations 7 indicate a special case where $r=(n-r)$, and r may be equal to six. With the relays available, then, symmetric circuits may be constructed for the following conditions:

n	r
12 or less	12 or less
13	8 or more, 5 or less
14	9 or more, 5 or less
n	(n—5) or more, 5 or less

SYMMETRIC CIRCUITS CLOSED FOR MORE THAN ONE CONDITION

Thus far, only symmetric circuits which are to be closed for a single value of r, have been discussed. Circuits closed for several values of r may be designed by connecting together outputs of the general symmetric lattice of Figure 6 corresponding to the desired values of r and eliminating unnecessary elements. In Figure 9 is shown a lattice which is closed for r_1, r_2, and r_3 relays operated.

Consideration of Figure 9 indicates that the expressions for the total number of contacts, the number of make-contacts, the number of break-contacts, and so on, may be written for a general symmetric network to be closed when any r_1, r_2, $r_3, \ldots,$ or r_m out of n relays are operated.

The total number of contacts is

$$\overset{m}{\Sigma} N=[2r_1(n-r_1)+n]+[2(r_2-r_1)(n-r_2)+(r_2-r_1)]+[2(r_3-r_2)(n-r_3)+(r_3-r_2)]+\ldots.+[2(r_m-r_{m-1})(n-r_m)+(r_m-r_{m-1})] \tag{9}$$

The total number of make-contacts

$$\overset{m}{\Sigma} M$$

in the network is

$$\overset{m}{\Sigma} M=[r_1(n-r_2)+r_1]+[(r_2-r_1)(n-r_2+1)]+[(r_3-r_2)(n-r_3+1)]+\ldots+[(r_m-r_{m-1})(n-r_m+1)] \tag{10}$$

The total number of break-contacts is

$$\overset{m}{\Sigma} B=[(n-r_1)(1+r_1)]+[(n-r_2)(r_2-r_1)]+[(n-r_3)(r_3-r_2)]+\ldots+[(n-r_m)(r_m-r_{m-1})] \tag{11}$$

As before, make- and break-contacts are combined into transfers, and the number of contacts which are left over is

$$\overset{m}{\Sigma} r=\overset{m}{\Sigma} M-\overset{m}{\Sigma} B=(2r_1-n)+(r_2-r_1)+(r_3-r_2)+\ldots+(r_m-r_{m-1})=r_1+r_m-n \tag{12}$$

If the sign of the summation is positive, the remaining contacts are makes, or are breaks if the sign is negative.

The total number of transfers is

$$\overset{m}{\Sigma} T=(\overset{m}{\Sigma} N-|\overset{m}{\Sigma} R|)/2 \tag{13}$$

where

$$|\overset{m}{\Sigma} R|=\text{absolute value of } \overset{m}{\Sigma} R$$

As in the case of the single-condition symmetric circuit, expressions can be derived for the number of transfers on the most-heavily loaded relay. However, there would be a separate expression for each combination of $2_p\mathrm{I}$, greater or less than, or equal to, n, where r_p is one of the values: r_1, r_2, r_3, …., r_m. For this reason it is not within the scope of this paper to derive these expressions for even a small number of closure conditions.

"SHIFTING DOWN" SYMMETRIC CIRCUITS

Where a contact network is to be closed for several conditions and the numbers of relays operated form an arithmetic progression or the numbers greater than a certain one form such a progression, the circuit may be simplified by "shifting down" a higher level to coincide with a lower one. Figure 10 illustrates this method. The circuit of this figure is to be closed when either none, three, or six of seven relays are operated. The third level of the symmetric lattice can be shifted down to coincide with the zero level, fulfilling the requirements. Note that any level can be "shifted down" to any other level to meet the particular circuit specifications.

Although the utility of the "shifted-down" symmetric circuit is not great, one familiar example makes use of this method. In this example, a lamp is controlled by a number, n, of 2-position switches, S. Any switch can light or extinguish the lamp regardless of the positions of the other switches. These requirements may be fulfilled by a circuit in which the path supplying current to the lamp is closed when 0, 2, 4, …. switches are in their operated positions and open when 1, 3, 5, …. switches are operated. This circuit can be the "shifted-down" symmetric lattice, as in Figure 11, in which the third level is made to coincide with the first. This is, of course, the arrangement used in practice when several wall switches are to control a single lamp.

References

1. A SYMBOLIC ANALYSIS OF RELAY AND SWITCHING CIRCUITS, C. E. Shannon. *Electrical Engineering (AIEE Transactions)*, volume 57, 1938, pages 713–23.

2. THE LOGIC OF RELAY CIRCUITS, W. Keister. *AIEE Transactions*, volume 68, part I, 1949, pages 571–76.

No Discussion

Counting with Relays

G. R. FROST
NONMEMBER AIEE

IN THESE days of automatic control of everything from scoring on pinball machines to supervision of big city subway systems,[1] relay circuits have become important to many engineers not heretofore concerned with such matters. The relay circuit has taken over, in recent years, many tasks formerly performed by the human hand or the mechanical cam and lever. This is evidenced in almost every engineering field. Widespread are the applications of relay circuits to counting, allotting, locating, preferential lockout,[2] and other performances. It is the purpose of this paper to correlate, from a telephone switching system viewpoint, some of the principles and practices involved in one of the most frequently used of the specific circuits, namely, counting. Counting circuits, besides performing their basic function of counting, form the basis for many other circuits of a sequential nature.

Counting Circuit Defined

A relay counting circuit is a circuit arrangement of relays which recognize the appearance and disappearance of electric pulses representing events to be counted, and establish unique conditions during and after each successive pulse, or after a particular number of pulses. The number of preceding pulses, therefore, can be determined by an examination of the combination in which the various relays are operated. A counting circuit usually must perform some external work, and the relays will carry contacts to perform external control functions. In this paper, however, only the means for controlling the action of the counting relays will be considered.

Limitations

It should be understood at the outset that events to be counted by relay counting circuits must be represented by electric pulses having certain characteristics of amplitude, duration, and interval; only events that may be so represented can be counted. The necessary characteristics are quite obvious. The pulse current amplitude must be of sufficient value to operate a relay within the counting circuit. The duration of the operating amplitude of the pulse and the interval between pulses must be sufficiently long to allow a relay to act fully. Thus, the allowable speed of repetition of events to be counted is directly dependent upon the operate and release times of the relays chosen. Presently available, common relays, being electromechanical devices exhibiting both electrical and mechanical inertia, limit the repetition frequency to under 50 pulses per second when directly fed. Transmission of the pulses over long circuits decrease this value because of the pulse mutilation that may take place.

Recognizing a Single Pulse

In order to detect the passage of a single pulse by means of a relay circuit, three distinct conditions must be recognized: pre-pulse, during-pulse, and post-pulse. Obviously these three conditions cannot be detected with a single 2-position relay. Two relays, at least, are necessary to produce a one-to-one correspondence between the three conditions and three unique combinations of the relay circuit. Figure 1 depicts the passage of a single pulse and a sequence of relay operations satisfying the circuit requirements. Here two relays, *A* and *B*, are normal during the pre-pulse condition; relay *A* alone is operated during the pulse, and relays *A* and *B* are operated after the pulse has passed.

A straightforward method of obtaining this action is shown in Figure 2. This circuit employs a pulse-repeating relay *X* to provide a back contact for the control of relay *B*. The pulse, entering on lead *P*, causes relay *X* to operate. Relay *X* operated, causes relay *A* to operate and to lock operated. The termination of the pulse allows relay *X* to release, which now supplies ground through its own back contact, through a contact on operated relay *A*, to relay *B*. Relay *B* operates and locks operated. This arrangement has two disadvantages: an additional relay is required and two relays must act in sequence during and after the pulse.

A second scheme using "shunt-down" operation is shown in Figure 3. The pulse on lead *P* causes relay *A* to operate and lock through its own front contact, but relay *B* is held shunted-down or inoperative by locking ground on one side of its winding and pulse ground on the other. With the disappearance of the pulse, relay *B* operates in series with operated relay *A*. This circuit sometimes is designated a prime pair, since the two relays usually are designated by the same letter, the shunted relay (see Figure 3) being designated the prime (′) relay.

Noninterfering Requirements

These two circuits of Figures 2 and 3 satisfy the original requirements for a

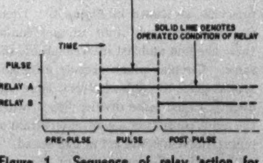
SOLID LINE DENOTES DURATION OF PULSE
SOLID LINE DENOTES OPERATED CONDITION OF RELAY
TIME
PULSE
RELAY A
RELAY B
PRE-PULSE
PULSE
POST PULSE

Figure 1. Sequence of relay action for recognizing a single pulse

---

Paper 49-148, recommended by the AIEE Communication Committee and approved by the AIEE Technical Program Committee for presentation at the AIEE Summer General Meeting, Swampscott, Mass., June 20–24, 1949. Manuscript submitted November 16, 1948; made available for printing May 4, 1949.

G. R. Frost is with the Bell Telephone Laboratories Inc., New York, N. Y.

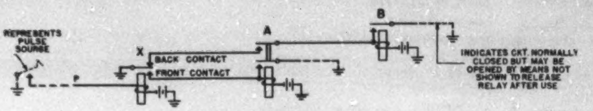
REPRESENTS PULSE SOURCE
X
BACK CONTACT
FRONT CONTACT
P
A
B
INDICATES CKT. NORMALLY CLOSED BUT MAY BE OPENED BY MEANS NOT SHOWN TO RELEASE RELAY AFTER USE

Figure 2. Simple pulse detector

single pulse counter having three distinct combinations, but they do not satisfy two noninterfering requirements that are frequently imposed. These are:

1. The circuit must not permit the back-up of a ground condition to the control (pulse) leads.
2. The circuit must ignore subsequent pulses or grounds on the control lead.

Circuits which satisfy these conditions will find much broader application, since the control lead may be reused for a subsequent control operation after a single pulse. The control lead may be freed from interference by passing it through a back contact of relay *B* in either Figure 2 or 3. Figure 4 shows isolation of control lead *P* of Figure 3.

Alternate Sequence

The above circuits are based on the operating sequence shown in Figure 1. This seems to prove the most satisfactory sequence for a non-interfering single pulse counter. An alternate sequence, shown in Figure 5(A) together with a nonshunting 2-relay scheme, Figure 5(B), based on this sequence, has been worked out. Several disadvantages are at once evident. Here again, the action of two relays in sequence is necessary, producing a slow circuit. The circuit is of the interfering type. Modification by isolation of the control lead *P*, as shown in Figure 5(C), produces pulse clipping to relay *A* which may interfere with locking relay *B* under severe contact stagger.

Pulse Dividers

A requirement might be placed on the 2-relay single-pulse counter that the relays recycle, returning to normal after the completion of a second pulse. One cycle for such a circuit then consists of five intervals, as shown in Figure 6. There are, however, only four unique conditions, the first and last intervals being the same. Circuits which recycle after the second pulse are pulse halvers, more frequently called pulse dividers since, when the input consists of a continuous train of pulses, the relays will act at half speed.

The pulse divider circuit of Figure 7 operates much like the prime pair of Figure 4 in that the first pulse ground on lead *P* causes relay *A* to operate while "shunting-down" relay *B*. The purpose of the continuity transfer contacts on relay *A* is to provide the lead *K* between relays *A* and *B* with an uninterrupted ground, either from lead *P* or from the locking ground, after the start of the cycle. Relay *A* is thereby locked operated and relay *B* held unoperated before lead *P* is opened at this contact. The termination of the first pulse removes the shunting ground from relay *B*, allowing it to operate to the locking ground on relay *A*. Operation of relay *B* extends lead *P* to the junction between resistor *RA* and relay *A* so that the second ground pulse releases relay *A* by shunting action. The continuity transfer on relay *A* again plays the role of securing the pulse ground on lead *K* to hold relay *A* unoperated and relay *B* operated during removal of the locking ground. Relay *B*, now held operated to the ground on lead *P*, releases with the termination of the second pulse, completing the cycle. Resistors *RA* and *RB* are necessary to protect the battery *BB* from direct ground over lead *P*.

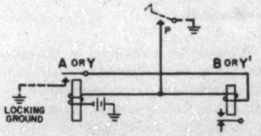

Figure 3. "Shunt-down" or prime-pair pulse detector

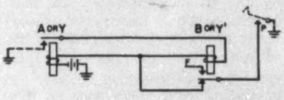

Figure 4. Isolation of control lead after pulse

The circuit of Figure 7 is widely used, where high speed is not essential to the particular application, in automatic telephone switching systems and is commonly called a *W-Z* combination, having been designated so in the first application. The combination has the disadvantage that it is inclined to be slow, particularly on the short-circuit release of the *W* relay.

Open *W-Z* Combination

Where faster operation than that provided by the shunt-type *W-Z* combination is required, the open *W-Z* combination of Figure 8 frequently is employed. It is somewhat faster than the shunt type, since *Z1* usually can be made to operate and release *W* in sequence faster than a single relay can be shunted down. A difficulty sometimes encountered is that the current surge, occurring when the shunt on the winding of *Z* is removed at the end of the first pulse, tends to kick *W* down, releasing the circuit.

Counting a Train of Pulses

The general problem of counting a train of any number of pulses immediately suggests the cascading of circuits such as Figures 4 or 7 to the desired number. It then is evident that the circuit will not only be capable of counting the desired number of pulses, but that it will count a train of any number of pulses less than this maximum. This is because the circuit holds its relays, through its own local circuit, in the combination set by the last received pulse. If, then, no further pulses appear on its input lead, the last set combination will remain indefinitely. As each combination corresponds to the total number of pulses received in the sequence, the number is identifiable.

Action on Maximum Pulses

A counting circuit, having received its maximum number of pulses, may: lock-up during this last pulse and ignore the

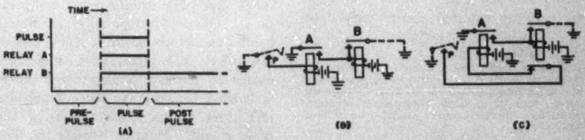

Figure 5. Alternate sequence and circuits for pulse detection

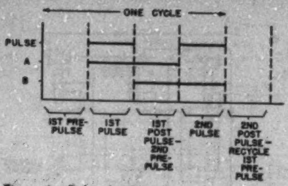

Figure 6. Pulse-divider relay action sequence

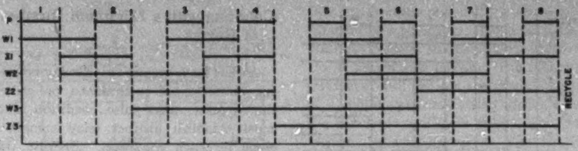

Figure 9. Relay sequence in counting with pulse dividers

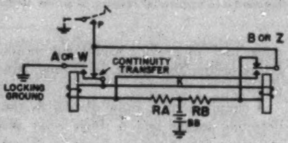

Figure 7. Pulse-divider circuit—W-Z shunt type

termination of this last pulse and any succeeding pulses; lock up at the termination of the last pulse and ignore succeeding pulses; or return all relays to normal on the termination of the last pulse, thus establishing a new cycle which will start the count over on succeeding pulses. The first two cases given are most common, although many circuits recycle part of their total relays.

Counting with Pulse Dividers

A *W-Z* combination counts and recycles on two pulses and, if a train of pulses is applied to the circuit, the *W* and the *Z* relays will act once for each two input pulses. If the *Z* relay then is made to control a second *W-Z* combination and this in turn similarly controls a third, a pulse-counting scheme results. Obviously, the scheme may be extended to count any number of pulses desired. The sequence of operation is shown in Figure 9; the circuit is shown in Figure 10.

One *W-Z* combination recognizes two pulses and recycles, two *W-Z* combinations "count" four pulses and recycle, while three count eight pulses. All relays of the three stages of Figure 10 return to normal at the termination of the eighth pulse. It thus may be seen that *D* pulse dividers of any type will count up to a maximum of 2^D pulses. A circuit using *D* pulse dividers will return to normal and start the count over after the 2^D pulse. If a record of the passage of 2^D pulses is to be retained, at least one more relay must be added to prevent recycling after the 2^D pulse.

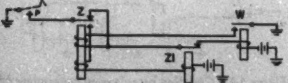

Figure 8. Pulse-divider circuit—open type

The circuit can be easily arranged to cut itself off from the pulse lead for ignoring further pulses after a given number of pulses have been received, if this number is less than the 2^D maximum. This may be accomplished by passing the control lead through contacts of relays which have completed their action following the end of the last desired pulse. For example, after the seventh pulse in Figure 9, the unique condition *W1*, *Z1*, *Z2*, *Z3* relays operated obtains. *Z1*, *Z2*, *Z3* is sufficient to define this interval, and the passage of the control lead through paralleled back contacts on these three relays will open the lead after the seventh pulse.

Two disadvantages are inherent in pulse-divider counting schemes. First, they are slow since, at a number of stages, several relays must act in sequence. For example, during the interval following pulse 2, relay *Z1* must release and *Z2* and *W3* operate in sequence. However, only the first pair of relays, *W1* and *Z1*, are controlled by the pulse and must complete their action during a pulse or interval between pulses. The sequential action of subsequent relays may lag over into the following interval of pulsing without adverse effect, since the control pulse to each succeeding *W-Z* combination doubles in time duration. Where information is used only after pulsing ceases, this is of no particular disadvantage, but where information must be obtained while pulsing is in progress, the arrangement may not be satisfactory.

Second, when the number of pulses to be counted is large, a large number of relays must be examined to determine the count at any stage. This means that, in order to close a circuit path during any one interval, a number of contacts are required. In large circuits this number may be excessive.

Prime Pair Counting

The noninterfering single-pulse prime-pair counter is especially adaptable to counting a series of pulses. Since relay *B* of Figure 4 acts after the pulse terminates, it may be utilized to switch the pulse lead without interfering with its own action or interrupting or clipping the length of a transferred control pulse. The transfer springs on relay *B* may be used to extend the control lead, through the front contact marked *F*, onward to a second similar circuit. Thus, a series of these circuits wired as shown in Figure 12 may be controlled in the sequence of Figure 11. This scheme may be extended to count any desired number of pulses *N*, and will automatically disregard any pulse after pulse *N*.

Various modifications of the basic circuit of Figure 12 may be made to satisfy special applications. For example, the *N'* relay may be required to close an external circuit at the termination of the *N* pulse under one condition or the *N-1* pulse under a second condition. If then

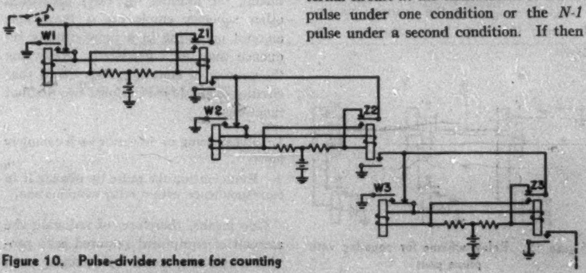

Figure 10. Pulse-divider scheme for counting

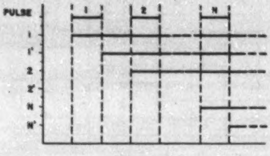

Figure 11. Relay action sequence for counting with prime pairs

the control lead is switched by external means to the armature spring of relay *2'*, as shown by dotted *X* wiring, the *N'* counter will be actuated when the *N-1* pulse terminates. This is a convenient arrangement when some function must be performed after a given number of pulses, and the number of pulses is variable but known in advance.

In Figure 12 each pair of relays is held operated by ground from a make on the nonprime relay. In order to release the relays, this ground must be removed by control means not shown. In Figure 13, the circuit is rearranged so that each pair of relays is released by the action of some higher numbered relay. In this case only one pair of relays remains operated after any given pulse. The last pair must be released by external means. It should be noted in this case that the pulse lead enters the controlling chain of contacts on the prime relays at the *N'* relay rather than at the *1'* relay of Figure 12. This modified circuit acts in the same sequence as that of Figure 12, but has the advantage of checking that all relays are normal before the first relay may act. Figure 12 may be modified to carry this reverse chain of contacts.

Many other variations of the prime-pair counting scheme are possible. For instance, the circuit may start with all relays operated by external means and locked under control of the prime relays, and permit the pulsing to release the relays successively, as shown in Figure 14. Such circuits may be more adaptable for connecting a group of external circuits, then opening the connections one by one, than for basic counting purposes.

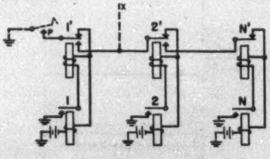

Figure 12. Relay scheme for counting with prime pairs

Counting with a Minimum Number of Relays

As has been mentioned, a relay counting circuit must recognize a pre-pulse, during-pulse, after-pulse condition, and must establish distinct relay combinations for each condition. Because the pre-pulse interval of every pulse except the first overlaps the after-pulse interval of the preceding pulse, the number of intervals required and, hence, the number of necessary relay combinations is $2P+1$, where P is the number of pulses. If, however, the circuit is allowed to lock during the last pulse, the last interval may be disregarded and the combination becomes $2P$.

As two relays may be operated in four combinations and three relays in eight combinations, the number of combinations in which N relays can be operated is 2^N. Now, if a circuit is to count a number of pulses, P, a number of relays N, such that 2^N is equal to or greater than $2P$ or $2P+1$, is the minimum required.

Circuits based on a minimum number of relays can be worked out,[3] but usually do not prove practical. Circuits which use a large portion of the possible relay combinations tend to produce large spring loads and complex contact circuits for their own control. Add to this the number of relays which must be examined to determine the count at any stage,[4] and the contact load becomes excessive. A judicial use of the number of combinations possible may, however, provide a very practical circuit for the establishing of a fixed-number pulse counter which loses or opens an external circuit after a particular number of pulses has been received.

Use of Common Relays

Having rejected pulse counting schemes using a relatively large number of the possible combinations of a small number of relays as too drastic a means of minimizing the number of relays necessary, other schemes employing a reasonable amount operating in a more orderly sequence may be considered. Analyzing the process of counting, it is found that circuits so employed perform two distinct functions:

1. Recognizing or detecting each complete pulse.
2. Enumerating the pulse by placing it in correspondence with a relay combination.

One means, therefore, of reducing the amount of equipment required is to provide a common means of detecting each pulse and to provide additional means for recording the count as pulsing progresses.

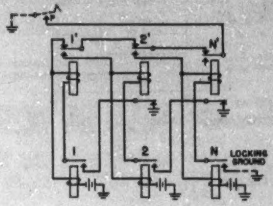

Figure 13. Sequential release of prime pairs

A circuit using a pulse divider as the detecting means and a single relay for recording each pulse is shown in Figure 15. Although the shunt-type pulse divider is shown, the faster open-type pulse divider may be used to advantage in some applications. In tracing the operation of this circuit, it will be found that *Z* operates at the end of the first pulse and grounds the odd lead operating relay *1*. At the termination of the second pulse, relay *Z* releases and grounds the even lead, causing the operation of relay *2*, and so on. Figure 16 illustrates the sequence for the circuit shown, and, also, for the case where relay *W* instead of relay *Z* carries the contact for transferring ground between the odd and even leads. Such circuits are usually called odd and even counters.

Partial Recycling Schemes

In the prime-pair counting schemes of Figures 12 and 13 and the odd and even counter of Figure 15, one prime pair and one relay, respectively, were assigned to each pulse of the count. The amount of apparatus necessary to count *N* pulses can be reduced by reusing these elements after their initial function has been performed. The principle of partial recycling of counting relays can be used to this end. As one example of this principle, consider the prime-pair circuit of Figure 13. In this circuit the operation of each prime

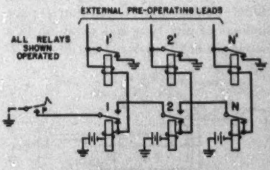

Figure 14. Counting by releasing preoperated prime pairs

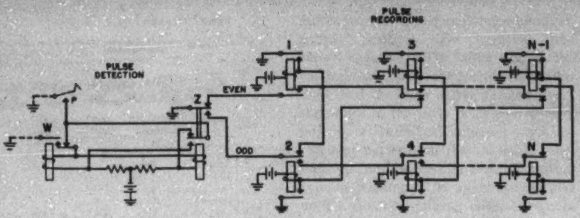

Figure 15. Separation of detecting and recording functions in pulse counting

relay, following the termination of a pulse, releases the preceding pair. After the last pulse, the *N* and *N′* relays are the only ones operated, and the action of the *N′* relay completely disconnects the pulse lead from the circuit. It is a simple matter to arrange this pulse lead, as shown in Figure 17, to make possible the reoperation of the first pair of counters. The sequence of operation is then as follows:

At the end of the first pulse *1* and *1′* are operated.

At the end of the second pulse *2* and *2′* are operated.

At the end of the third pulse *3* and *3′* are operated.

At the end of the fourth pulse *3* and *3′* and *1* and *1′* operated.

Thus, four pulses may be counted by means of three pair of counters or six relays. In extending this scheme, it will be found that ten pulses may be counted by means of 12 relays. Pulses beyond the maximum which may be counted by this scheme are disregarded, operating the unprimed counter of the next-to-last pair during the extra pulse and releasing it at the termination of the pulse.

Other circuits, such as the odd and even counters, also may be partially recycled to achieve economy in apparatus.

Conclusion

Three general types of counting circuits have been discussed and examples of each given. From these examples, which by no means exhaust the available counting-circuit arrangements, it may be concluded that relay counting circuits either are available or may be readily designed for any special application that, from a pulse repetition standpoint, falls within their scope.

In applying these circuits, one of two requirements usually must be satisfied. One requirement will call for the establishment of a condition, after a particular number of pulses has passed, for the control of an external circuit. The other requirement will call for the establishment of a unique condition either during or at the termination of each pulse. The first requirement may be best satisfied by the use of pulse-divider schemes or of circuits where the number of relays is held to a minimum but exceeds the $2={}^{N}2P$ value sufficiently to provide a practical spring load. In these cases the number of relays that must be examined to determine the count at any stage is of no concern. Only one combination is of interest.

The second requirement is satisfied more readily by the prime-pair type of circuit or by the use of common detecting and individual recording form of odd-even counting schemes. The necessity of $2P$ relays of the prime counters or the P plus the common pulse detector relays, may be minimized by the application of partial recycling operation.

References

1. Supervisory Control for New Chicago Subway, W. A. Derr, C. J. Buck, J. A. Stoos. *Electrical Engineering* (*AIEE Transactions*), volume 64, January 1945, pages 10–16.

2. Relay Preference Lockout Circuits in Telephone Switching, Amos E. Joel, Jr. *AIEE Transactions*, volume 67, part II, 1948, pages 1720–25.

3. Sequential Aspects of Relay Circuits, A. E. Ritchie. *AIEE Transactions*, part I, volume 68, 1949, pages 577–81.

4. The Logic of Relay Circuits, W. Keister. *AIEE Transactions*, part I, volume 68, 1949, pages 571–76.

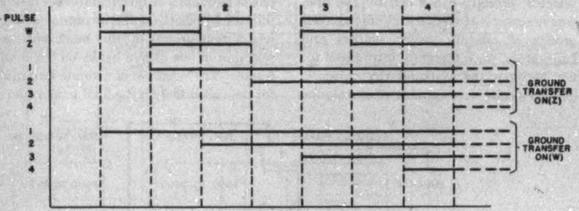

Figure 16. Relay action sequence for Figure 15

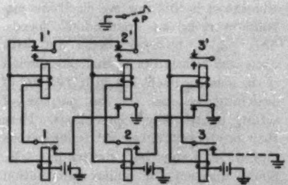

Figure 17. Partial recycle of prime-pair counting circuit

No Discussion

Codes and Translations

OSCAR MYERS
NONMEMBER AIEE

ONE of the problems which confronted S. F. B. Morse when he undertook to transmit intelligence by means of his "electric telegraph" was to devise a code suitable to the electrical circuit and mechanical apparatus which he had constructed. His solution was the familiar Morse code. The translators for encoding and decoding the electrical signals were the telegraph operators. Alexander Graham Bell's telephone avoided the need for translations through the use of conversion devices having simple mathematical relationships between the voice signals and their electrical equivalents; but the discrete, arbitrary relationships which characterize code methods have made their appearance in "pulse code modulation" recently devised for microwave transmission. The translators in this case are electronic circuits working at tremendous speeds. This paper, however, deals not with codes and translators for the transmission of the message itself, but with their use in switching systems for the purpose of setting up telephone connections. Here they have been developed in numerous and varied forms, both for sending telephone numbers, or similar information from one central office to another, and also within a central office for signaling from one component of a switching system to another. The forms of the codes and the electrical methods for transmitting them vary with the nature of the information, the form of the apparatus involved, and the character of the signaling channel. This paper describes some of the forms which have assumed importance in the design of switching systems.

Early Codes and Translations

When the first dial switching system was invented one of the basic requirements was a device for coding the called number and apparatus for translating this code into operations of the switching machine. The answers here were the dial and the step-by-step selector.

As the switching art progressed and the nomenclature and trunking problems of large multioffice cities were encountered, it became clear that, although it was desirable to retain the dial because of its simplicity, some recording and translating device other than the 10-level selector, directly controlled by the dial, was necessary at the central office. New groups of circuits, called senders and translators, were therefore introduced for use between the dial and the switches. These circuits were capable of storing the dial pulses and translating them into new electrical codes more suitable for controlling large nondecimal switches.

The first system which used senders and translators was the panel system. These circuits were able to translate the decimal dial pulse code into a nondecimal "revertive" code. (In revertive pulsing the translator presets the sender. The latter then starts the distant selector which, in advancing, sends back pulses which the sender counts. When the predetermined number of pulses has been counted, the sender stops the selector.) The sender also could change part or all of the number into a "call indicator" code for operating a bank of call indicator lamps to give a visual display of the called number at an operator's position in a manual office. Figure 1 is a schematic drawing of the terminating equipment in a panel office to show the background of the revertive pulse code. Selection of a subscriber line through the incoming and final frames requires the translation of the thousands and hundreds digit of the called number into a code which selects one of five banks of terminals (or one of five selector brushes) on the incoming frame, one of four groups on this bank and the selection of one of five banks on the final frame. The selection of a single terminal for the called line on the final bank is per-

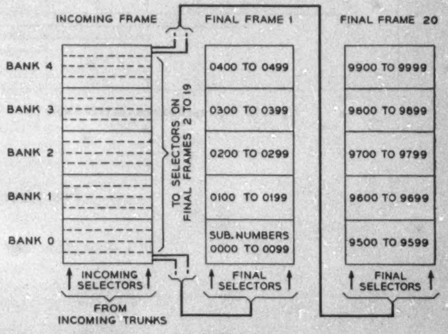

Figure 1. Panel system - terminating schematic

NOTES

1. ALL FRAMES HAVE 5 BANKS; EACH BANK HAS 100 TERMINALS
2. EACH BANK ON THE INCOMING FRAME IS DIVIDED INTO 4 GROUPS

Paper 49-149, recommended by the AIEE Communication Committee and approved by the AIEE Technical Program Committee for presentation at the AIEE Summer General Meeting, Swampscott, Mass., June 20–24, 1949. Manuscript submitted November 5, 1948; made available for printing May 12, 1949.

Oscar Myers is with the Bell Telephone Laboratories, Inc., New York, N. Y.

Table I. Call Indicator Codes

Segments	1	2	3	4
Thousands Digit	2	4	8	1
Hundreds, Tens and Units Digits	1	2	4	5

Thousands Digit	Party Letter	All Other Digits				
0		0		–		–
2		1	+	–		–
4	W	2		—		–
6	R	3	+	—		–
8	J	4		–	+	–
1	M	5		–		—
3		6	+	–		—
5		7		—		—
7		8	+	—		—
9		9		–	+	—

formed in two decimal steps called final tens selection and final units selection. It can be seen that the incoming bank selection is a choice of a block of 2,000 consecutive numbers, the incoming group selection is a choice of 500 consecutive numbers, and final bank selection is a choice of 100 consecutive numbers. Table I shows the combinations used in the call indicator code. Three kinds of pulses are used in sequential combination, namely positive, light negative, and heavy negative. The difference in the call indicator code between the thousands digit, and the other digits, resulted from the desire of the early designers to have both revertive and call indicator codes in a common pattern, so that a single relay register could be used for recording either type of pulsing. The panel system also used a d-c key pulsing code, shown in Table II. This was used for registering in a sender the called office designation and number which was keyed from an operator's position. The operator was furnished with a 10-button key set, each button representing one of the ten digits 0 to 9.

Later Examples of Codes and Translations in a Modern Telephone System

Further development of the telephone switching art has resulted in the introduction of what are called crossbar systems. The basic switching unit in these systems is a co-ordinate type of switch (crossbar switch) which is generally controlled by an external circuit. Since these systems require more common controls than the panel system, they employ even more coding and translation in the process of setting up a call. The following paragraphs describe briefly the various successive steps of coding and translating which are used in setting up a telephone

Table II. D-C Key Pulsing Code

Digit	Pulse on Tip Conductor	Pulse on Ring Conductor
0	L+	
1	H+	
2	L−	
3	H−	
4	L+	L−
5	L+	H+
6	H+	H+
7	L−	H+
8	H−	H+
9	L+	H−
Start	H+	L−

H+ = low-resistance ground
H− = low-resistance 48-volt battery
L+ = high-resistance ground
L− = high-resistance 48-volt battery

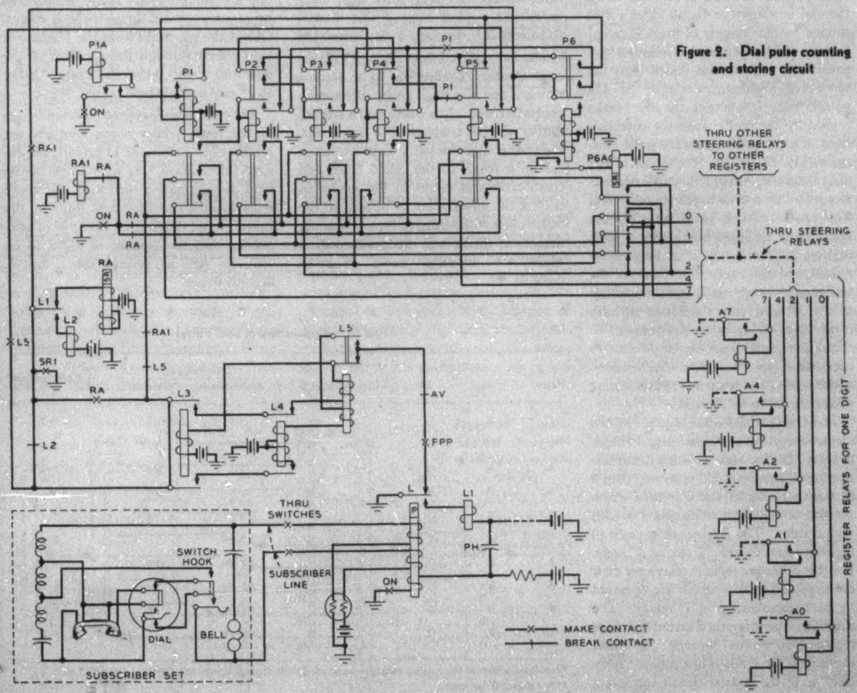
P1A
ON
P1
P2
P3
P4
P5
P6
P6A
RA1
RA
L1
L2
SR1
L5
L3
L4
AV
FPP
L
P
PH
THRU SWITCHES
SWITCH HOOK
SUBSCRIBER LINE
DIAL
BELL
SUBSCRIBER SET
THRU OTHER STEERING RELAYS TO OTHER REGISTERS
THRU STEERING RELAYS
0
1
2
4
7
A7
A4
A2
A1
A0
REGISTER RELAYS FOR ONE DIGIT
MAKE CONTACT
BREAK CONTACT

Figure 2. Dial pulse counting and storing circuit

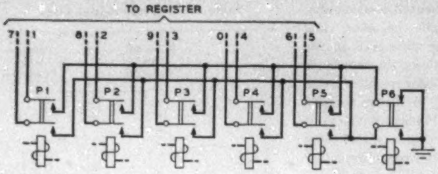

Figure 3. Relay tree for operating decimal register

connection in a crossbar system. The examples are presented in the order in which they might be encountered on a normal call.

REGISTERING THE NUMBER THE SUBSCRIBER DIALS

When a subscriber lifts his receiver one of a common group of senders or registers is temporarily attached to his line by switches to record the dialed number. Figure 2 illustrates a typical dial pulse counting and storing circuit of a crossbar sender or register which shows the process of number transformation prior to storage.

A dialed digit in a decimal system consists of a series of line breaks produced by the dial in which the digital value corresponds to the number of breaks (except for zero which is ten breaks) followed by a pause. To register this dialed digit the successive momentary releases of the pulsing relay *L* following the line breaks caused by the dial change the combinations of a group of temporary pulse storage relays, *P1* to *P6*. At the end of the digit there is an interdigital pause which is recognized by a slow to release relay *RA*. The release of this relay transfers the temporarily recorded number to a digit register which will hold it as long as required, and also causes the release of the temporary storage relays and the advance of the steering relays (register advance from which *RA* gets its designation) so that subsequent digits can be directed to succeeding registers. The combinations of the pulsing and temporary pulse storing relays are shown in Table III.

The transformation takes place in two steps. Step 1 is the operation and release of relays *L3*, *L4*, and *L5* which determine whether the pulse is odd or even. Step 2 is the operation of the *P* relays which provide a unique combination for each digital value. The *P* relays close paths to register relays in the "2 out of 5" code. For this code, five register relays per digit are provided, two of which are operated by each combination of *P* relays. The circuit for operating the 2-out-of-5 storage registers is woven through the lower contacts of the *P* relays in a typical "relay tree" to fit the register circuit employed. (A relay tree is an array of contacts on a group of associated relays which are interconnected in a pattern which resembles the branching of a tree.) This contact array is a small translator. If the register relays had been required in different combination, say a decimal code, a corresponding relay tree on the *P* relays would have translated the *P* relay combinations into this code as shown in Figure 3.

TRANSLATING THE OFFICE DESIGNATION

The office designation, when used, consists of the first one, two, or three dialed digits in a local (as distinguished from toll) system. For our example, let us assume a large city with three digit office codes. (A typical code of this kind is ACademy 2.) In such a city when the sender has received three digits it calls for a momentary connection to a marker which is one of a small group of common control circuits. In a fraction of a second, during which it is attached to the sender, the marker operates switches to set up the call to a trunk to the called office and combinations of relays in the sender to control the information to be sent to the called office with regard to type of pulsing, number of digits, and other information which the machine needs to complete its job.

Figure 4 shows, in simplified form, how the marker acts on the coded office designation to obtain the information which the marker and sender need for their subsequent action. Step 1 in the marker is the closure of a circuit to a single point ("code point") which corresponds to the office designation. With three digit designations this is the selection of one out of a thousand possible code points. Step 2 is the operation of a route relay to which the code point is cross-connected and the closure of variably cross-connectable contacts of the route relay to relays which record and check the data contained in the route relay cross-connections.

The operation in brief is as follows: A multiplicity of leads are closed to the marker from the sender by multicontact relays. Two of each of the three sets of five code input leads are grounded by operated register relays in the sender and operate corresponding relays in the marker. One of 20 50-contact relays is operated by the *A* relays and the "above or below five" circuit from the *B* relays. This relay is operated at the same time one of five 10-contact relays is operated by another circuit through the *B* relays. One of the ten paths from the *C* relays is thus closed through the contacts of the operated "tens" relays and "fifties" relay to ground a single code point.

The code point is cross-connected to one of the route relays whose contacts are further cross-connected to provide the desired information. As an example of the kind of information furnished, the route relay locates the busy test leads of the called group, determines the type of outpulsing and the number of digits to be sent, as well as several other miscellaneous items.

Table III. Registration of Dial Pulses

Pulse	L	L3	L4	L5	P-Relays Operated	P-Relays Released	$\frac{2}{5}$ Combination*
1	R	O			P1		0–1
	O	H		O			
2	R	R	O	H	P2	P1	0–2
	O		R	R			
3	R	O			P3	P2	1–2
	O	H		O			
4	R	R	O	H	P4	P3	0–4
	O		R	R			
5	R	O			P5	P4	1–4
	O	H		O			
6	R	R	O	H	P5–P6		2–4
	O		R	R			
7	R	O			P1–P6	P5	0–7
	O	H		O			
8	R	R	O	H	P2–P6	P1	1–7
	O		R	R			
9	R	O			P3–P6	P2	2–7
	O	H		O			
**10	R	R	O	H	P4–P6		4–7
	O		R	R			

*Indicates which of the correspondingly numbered digit storage relays are operated at end of digit.

**For digit "0" or zero.

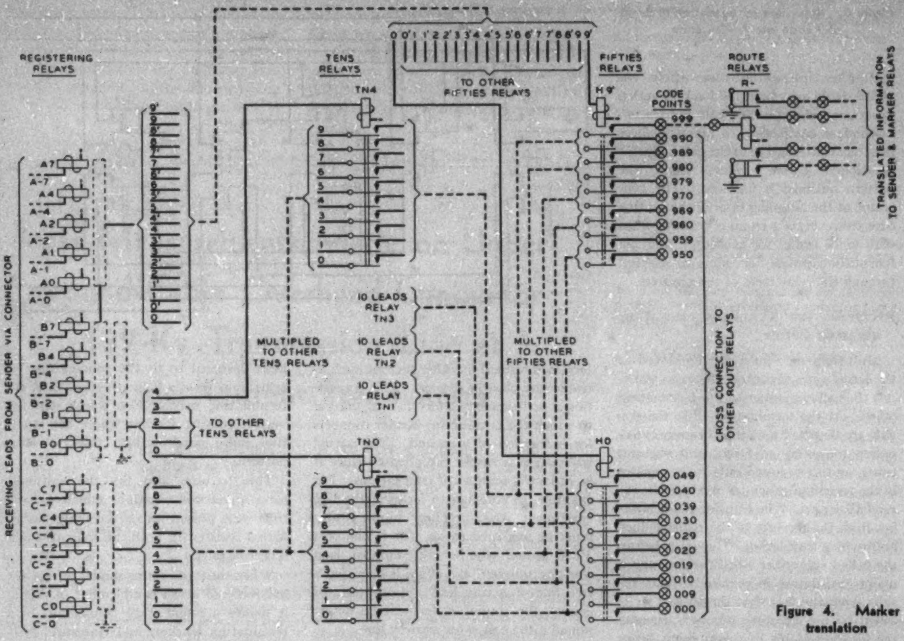
REGISTERING RELAYS
RECEIVING LEADS FROM SENDER VIA CONNECTOR
A7
A-7
A4
A-4
A2
A-2
A1
A-1
A0
A-0
B7
B-7
B4
B-4
B2
B-2
B1
B-1
B0
B-0
C7
C-7
C4
C-4
C2
C-2
C1
C-1
C0
C-0
TENS RELAYS
TN4
TN0
10 LEADS RELAY TN3
10 LEADS RELAY TN2
10 LEADS RELAY TN1
MULTIPLED TO OTHER TENS RELAYS
TO OTHER TENS RELAYS
0 0' 1 1' 2 2' 3 3' 4 4' 5 5' 6 6' 7 7' 8 8' 9 9'
TO OTHER FIFTIES RELAYS
FIFTIES RELAYS
H 9'
H0
MULTIPLED TO OTHER FIFTIES RELAYS
CODE POINTS
999
990
989
980
979
970
969
960
959
950
049
040
039
030
029
020
019
010
009
000
CROSS CONNECTION TO OTHER ROUTE RELAYS
ROUTE RELAYS
R-
TRANSLATED INFORMATION TO SENDER & MARKER RELAYS

Figure 4. Marker translation

SENDING TO THE TERMINATING OFFICE

A sender may be arranged to complete to several types of connecting offices. Assume that the sender under consideration is equipped to outpulse either multifrequency pulses or decimal pulses, or that it can signal the trunk to cut through with no pulsing. Assume further that the connecting office in this example is arranged to receive multifrequency pulses. (Multifrequency pulses are short spurts of pairs of frequencies in the voice range.) Since, as indicated previously, each digit register has two out of five relays operated, and since multifrequency pulsing is based on the same 2-out-of-5 code (as shown in Table IV), once the marker has indicated that multifrequency pulsing is required, it is merely necessary for the outpulsing control circuit of the sender to steer from digit to digit sending out the multifrequency pulses, each pulse consisting of two frequencies, corresponding to the operated digit register relays. The pair of frequencies for a digit are sent simultaneously and successive digits follow each other with a momentary open period between pulses.

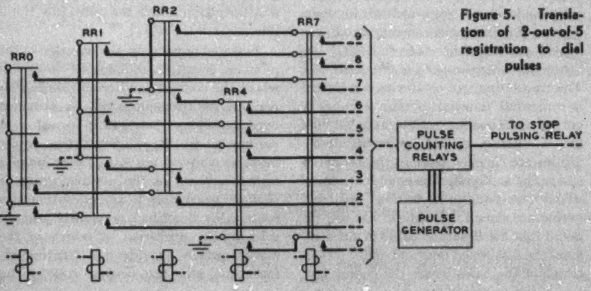
RR0
RR1
RR2
RR4
RR7
9
8
7
6
5
4
3
2
1
0
PULSE COUNTING RELAYS
PULSE GENERATOR
TO STOP PULSING RELAY

Figure 5. Translation of 2-out-of-5 registration to dial pulses

If the connecting office had been of the dial pulse receiving type, the outpulsing part of the sender circuit would have reversed the translation originally employed in registering the dialed digits. One method of doing this is shown in Figure 5. Here the relay-tree contacts are woven through the 2-out-of-5 register group to mark a stopping point in a chain of counters which can count ten pulses. Each pulse, of course, results in a line break to the equipment ahead, and a timed interdigital pause also is provided.

Other types of "in" and "out" pulsing also are available in the crossbar system. Revertive pulsing is provided to reach panel offices. D-c key pulsing is employed between operator positions and senders. However, broadly speaking, the basic design of the sender is the same for all types of pulsing. It consists of three parts:

1. A group of register relays which record the incoming pulses.

2. Tree circuits from the registers to prime the outpulsing relays.

3. A group of pulse generating elements (relays or oscillators or frequency generators) and control relays which cause the circuit to advance from digit to digit as required.

Figure 6. Relay tree for translation of 2-out-of-5 code into 4-relay code

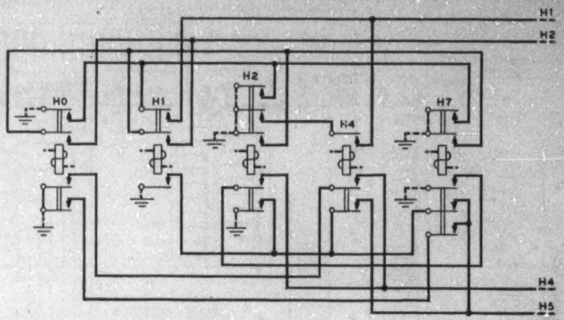

Another interesting case where the coded digits are converted back to verbal pronouncements, is the "call announcer" method of completion to manual offices used as an alternative to the call indicator mentioned before. Here again the pattern outlined is followed. The generator of the outgoing information in this case, however, is a group of rotating films with voice tracks for each digit and the four station letters. The films are selected through the relay trees of the registers

Receiving the Number at the Terminating Office

Multifrequency pulsing is employed in the latest type of central offices to transmit the called number to the terminating office. At the terminating office the signals are detected by a multifrequency receiver consisting of filters and vacuum tubes, and then stored on a relay register in the terminating sender of which the receiver is a part. The transfer of the number from the receiver to the register does not involve translation. However, before the called subscriber's bell can be rung a major translation is required. This results from the fact that the subscriber is called by his directory number, whereas the location of his line equipment bears no relationship to this number, being determined instead by other factors, such as traffic and class of service. This translation is performed by a terminating marker to which the terminating sender connects for a fraction of a second. The actual translation is rather complicated since it is, in fact, a number of translations. For example, in addition to locating the line equipment, the directory number also must be analyzed to see if it is one of a *PBX* group, whether the number is a working number, and if so, if it is also a free line or a coin line. In addition, of course, the ringing code must be determined if the call is for a party line.

Table IV. Multifrequency Code

Digit	Relay Combination	Frequency Combination, Cycles
0	4+7	1,300+1,500
1	0+1	700+900
2	0+2	700+1,100
3	1+2	900+1,100
4	0+4	700+1,300
5	1+4	900+1,300
6	2+4	1,100+1,300
7	0+7	700+1,500
8	1+7	900+1,500
9	2+7	1,100+1,500

Table V. Translation of 2-Out-Of-5 Code into 4-Relay Code

Digit	2-Out-Of-5 Relay Combination	Terminating Marker Relay Combination Thousands	Terminating Marker Relay Combination Hundreds, Tens, Unit
0	4+7	none	none
1	0+1	1	1
2	0+2	2	2
3	1+2	1+2	1+2
4	0+4	4	4
5	1+4	1+4	5
6	2+4	2+4	1+5
7	0+7	1+2+4	2+5
8	1+7	8	1+2+5
9	2+7	1+8	4+5

Briefly, the action is as follows: the multifrequency pulsing receiving circuit which is part of the terminating sender circuit receives the pulses transmitted over the trunk from the originating sender (or keyset, in some cases) in the 2-out-of-5 combinations listed previously, and stores this information on groups of relay registers through a relay steering circuit which advances after each digit. These registers are equipped with contacts to translate the 2-out-of-5 code into the code required by the terminating marker to which the number is transferred when complete. The translation consists of a change from 2-out-of-5 relays to "marks" or grounds on a set of four leads for each digit in combinations varying from "no leads" grounded for the digit "O" to "three leads" grounded for the digit "8". The translating tree on the digit registers is somewhat unusual in that it consists only of make contacts as illustrated in Figure 6. Errors caused by trouble conditions are checked both in the receivers and in the markers. The combinations to which the sender registrations are converted are shown in Table V. It will be noted that the thousands digit is different from the hundreds, tens and units. This is one of the cases where the coding has been designed to fit the connecting systems, and results from the fact that the terminating marker also works with revertive pulsing senders where the revertive pulse combinations fall into this pattern.

This pattern also fits the call-indicator pulse combinations which at one time were pulsed into a receiving circuit with a register for both call indicator and revertive pulses.

When the terminating sender or register has received a full complement of digits, it makes a momentary connection to a terminating marker, and transmits to it the called number in the code of Table V. The translation is somewhat different than in the originating marker, however. It is not economical to provide a route relay per line per marker. A compromise is employed instead. The four numerical digits consisting of thousands, hundreds, tens, and units are reduced to a "code point group" of terminals for a block of consecutive numbers. One of the functions of this set of terminals is to select one of a group of auxiliary circuits called "number groups." Each number group of several hundred directory numbers is subdivided into smaller directory number groups which the marker also selects. A final operation selects the called line, if it is idle.

As stated previously, the function of the number group is to provide a circuit where the contacts and cross-connections per line for translation can be provided once per office rather than to furnish a set per marker which, in a large office, might mean as many as ten sets. Selection of a set of contacts in the number group is similar in principle to the operation of a route relay described previously and results in the operation of relays in the marker which provide line locating information and the ringing code. The terminating marker sets up the connection in the called line and then puts itself back to circulation for handling other calls.

At the present time the Bell Telephone System is extending automatic switching to its toll plant. The problems met in this connection have in general, been solved by an extension of the coding and translating mechanisms already employed in the local crossbar systems. Future development of switching systems will undoubtedly be accompanied by improvements in translators which are becoming an increasingly important part of the control mechanisms.

No Discussion

Loss Measurements Made on Underground-Cable Overhead-Conductor 132-Kv Transmission Line at Carrier Current Frequencies

H. A. CORNELIUS
MEMBER AIEE

B. WADE STORER
ASSOCIATE AIEE

Synopsis: This paper discusses carrier current applications on a 132-kv line composed of underground cable and overhead conductors. The discussion includes some of the test procedures used at the carrier frequencies in measuring the losses in the various components of the circuit and some of the difficulties encountered. The measured results are compared on a decibel loss and on a watt loss basis. Some data on "ambient" noise levels and on signal to noise ratios also are included.

THE Commonwealth Edison Company of Chicago and the Public Service Company of Northern Illinois have an interconnecting 132-kv power line over which it is desirable to place a reliable carrier transmission channel for relaying and other purposes.

This particular line, which is roughly 37 miles in length, extends from Northwest Station in Chicago to Station 6 in Waukegan, Illinois. Although the line is not long, it presents many troublesome carrier problems. A single-line schematic diagram of the line is shown in Figure 1.

TROUBLESOME FACTORS IN THE APPLICATION

The carrier channel difficulties arise chiefly from the 5.8 miles of 600,000-circular-mil paper-insulated oil-filled lead-covered cable extending out from Northwest Station. This length of cable would not be particularly difficult were it not for the fact that it is equipped with sheath bonding transformers. These are used to reduce 60-cycle circulating currents in the sheaths, thus avoiding decrease in the cable load capacity. The sheath bonding transformers present a high loss return path to carrier frequency currents.

Adding to the carrier problems are the increased terminal equipment losses at Northwest Station. These losses are greater than for an overhead line terminal, due to the fact that the carrier energy is fed into the low impedance cable. The test results at Northwest Station show that about 71 per cent of the available carrier energy (at 75 kc), is lost in the terminal equipment before reaching the 132-kv cable.

Other factors that contribute to the carrier transmission losses are: the cable-overhead conductor mismatch at the Chicago city limits (see Figure 1); the line tap at Skokie Substation; the normal overhead conductor attenuation; and the carrier terminal equipment loss at Station 6 in Waukegan.

Losses and changes in attenuation also result from two other 132-kv lines that parallel the overhead section, and normal line noise is increased by an electric railway on the same right-of-way with the 132-kv line.

DIFFICULTIES ENCOUNTERED IN MAKING LOSS MEASUREMENTS

1. External conditions, such as pick-up from nearby broadcasting stations, and noise produced by the paralleling electric railroad mentioned before.
2. High residual currents, in the cable section and in the overhead section resulting from coupling to other 132-kv lines on the same right-of-way.
3. Difficulty in procuring adequate line outages for the tests at the time they were being conducted.
4. Lack of good communication facilities between the cable-overhead conductor junction and the line terminals.

LOSS MEASUREMENT PROCEDURE

The carrier loss measurements were divided into three general parts: the terminal equipment; the cable section; and the overhead section. The mismatch loss at the cable overhead junction was calculated from the impedance measurements made on the cable section and on the overhead section. The 200-foot line tap loss at the Skokie Substation was assumed to be three decibels. The test methods are shown in detail, and some calculations are included in an attempt to clarify decibel loss values for those reading this paper who may not be familiar with this method of loss evaluation.

Terminal Equipment Losses

NORTHWEST STATION

Wave Trap Loss. The impedance of the wave trap at the present operating frequency (75 kc) is 3,700 ohms. Since this high impedance in parallel with the low-impedance 132-kv cable produces very little loss, this small loss has been ignored at the Northwest terminal of the 132-kv line.

Coupling Capacitor and Drain Coil. The coupling capacitor plus drain coil loss, R_s (see Figure 2), was found by substituting a variable resistance and a variable air capacitor in a Q circuit. The upper end of the coupling capacitor was grounded, and the drain coil in the base

---

Paper 49-150, recommended by the AIEE Committee on Carrier Current and approved by the AIEE Technical Program Committee for presentation at the AIEE Summer General Meeting, Swampscott, Mass., June 20–24, 1949. Manuscript submitted March 21, 1949; made available for printing April 28, 1949.

H. A. CORNELIUS is Supervising Design Engineer with the Public Service Company of Northern Illinois, Chicago, Ill., and B. WADE STORER is an engineer in the Testing Department of the Commonwealth Edison Company, Chicago, Ill.

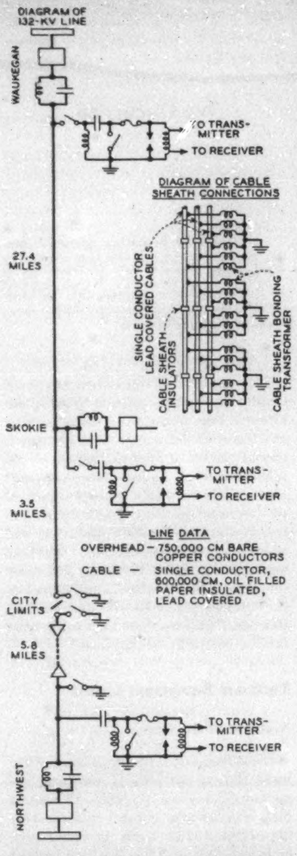
DIAGRAM OF 132-KV LINE
WAUKEGAN
TO TRANSMITTER
TO RECEIVER
DIAGRAM OF CABLE SHEATH CONNECTIONS
SINGLE CONDUCTOR LEAD COVERED CABLES
CABLE SHEATH INSULATORS
CABLE SHEATH BONDING TRANSFORMER
27.4 MILES
SKOKIE
TO TRANSMITTER
TO RECEIVER
3.5 MILES
LINE DATA
OVERHEAD – 750,000 CM BARE COPPER CONDUCTORS
CABLE – SINGLE CONDUCTOR, 600,000 CM, OIL FILLED PAPER INSULATED, LEAD COVERED
CITY LIMITS
5.8 MILES
TO TRANSMITTER
TO RECEIVER
NORTHWEST

Figure 1. One line diagram of underground cable overhead-conductor 132-kv line and diagram of cable sheath connections

of the capacitor was left in place during the tests.

The results obtained from the measurements are as follows:

Frequency in Kilocycles	50	75	100	150
R^s in ohms	36	30	26.5	22.5
Loss in decibels	3	2.8	3.0	3.2

The decibel loss remains approximately constant with increase in frequency. This is due to the fact that the cable input resistance declines at about the same rate that the coupling capacitor plus drain coil loss, R_s, declines.

Lead-in Wire. The lead-in wire from the coupling capacitor to the line tuning unit is 50 feet long. It is a weatherproof wire, supported by three post-type 33-kv insulators.

To obtain the loss in the lead-in wire only, a "no loss" air capacitor was substituted for the 132-kv 0.001 microfarad coupling capacitor, as shown in Figure 3. In addition, another circuit containing a variable air capacitor and a variable non-inductive resistor was used to determine the total power input to the lead-in circuit.

The method of procedure was to read I_s and I_c. A dummy load was then substituted by adjusting C_{as} and R_a to give the same current reading on I_s, as was obtained previously with C_a and R_c in the circuit. With these values and the cable input resistance (R_c) known, the loss in the lead-in wire was calculated from the ratio of the total power input to the power delivered to the cable. At 75 kc:

Power into lead-in wire:
$I_s^2R_a=0.38^2\times36.9=5.45$ watts
Power out of lead-in wire:
$I_c^2R_c=0.294^2\times33.2=2.87$ watts

$$\text{Lead-in loss}=10\log\frac{5.45}{2.87}=2.8\text{ decibels}$$

The result obtained, plus the cable input resistance measured were then used to calculate the equivalent resistance of the lead-in circuit, as follows:

$$\text{Loss}=10\log\frac{R_1+R_2}{R_2}$$

$$2.8=10\log\frac{R_1+33.2}{33.2}$$

$$10.28=\frac{R_1+33.2}{33.2}=1.905$$

$$R_1+33.2=1.905\times33.2=63.24$$
$$R_1=63.2-33.2=30.0\text{ ohms}$$

Figure 4 shows the equivalent loss circuit of lead-in, air capacitor, and cable.

The decibel loss (at 75 kc) to be expected in the lead-in circuit when the 0.001-microfarad coupling capacitor is used instead of the "no loss" air capacitor, is as follows:

$$\text{Loss}=10\log\frac{R_1+R_2}{R_2}=10\log\frac{30+63.2}{63.2}$$

$$=10\log\frac{93.2}{63.2}=10\log 1.48$$

$$=1.7\text{ decibels}$$

Figure 5 shows the equivalent loss circuit of lead-in, coupling capacitor and cable.

The results obtained in the lead-in wire circuit at four different frequencies are summarized as follows:

Kilocycles	50	75	100	150
Decibels measured in test circuit	2.8	2.8	2.6	2.7
Equivalent resistance in ohms	31.7	30.0	22.2	17.7
Decibel loss in normal circuit	1.6	1.7	1.5	1.5

LINE TUNING UNIT. The full resistance of the large 300-turn transmitter tuning coil in the equipment tested varies from 21 ohms at 50 kc to 60 ohms at 150 kc. The Q increases from 91 at 50 kc to 113 at 150 kc. At 75 kc, for the portion of the coil used, the resistance is 22.5 ohms and the Q is 57 (between taps 3 to 180).

WAUKEGAN STATION

Using the methods described previously the Waukegan terminal losses were found to be as follows:

Kilocycles	50	75	100	150
Decibel loss	3	3	2	2

132-Kv Cable Section Loss Measurements

The characteristic impedance, the resistance component of input impedance and cable attenuation were measured on the cable section. The methods used and results obtained are given below. The test circuit was arranged as shown in Figure 6.

Characteristic Impedance: The characteristic impedance, Z_o, of the cable was determined by reading the current and voltage input to the cable with the far end

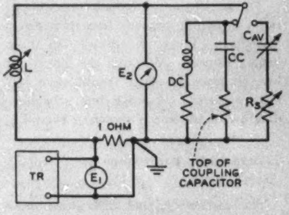
L
E2
DC
CC
CAV
RS
1 OHM
TR
E1
TOP OF COUPLING CAPACITOR

Figure 2. Coupling capacitor test circuit

TR = transmitter
L = tuning coil
E_1 = vacuum tube voltmeter
E_2 = vacuum tube voltmeter
CC = coupling capacitor
DC = drain coil
C_{as} = variable air capacitor
R_s = variable resistor

of the cable open circuited to give Z_{oc}, and with the far end of the cable short circuited to give Z_{sc}. Z_o was then calculated from the relation

$$Z_o=\sqrt{Z_{oc}Z_{sc}}$$

The loss in the cable was so great that no measurable difference was found between the open circuit and short circuit impedances.

The results are as follows:

Frequency in Kilocycles	50	75	100	150
Characteristic impedance	42.5	38.2	28.5	31.0

Input Resistance, Impedance, and Attenuation. The test procedure was as follows: The transmitter was tuned to maximum output into the cable, and the current I_1, and voltage E_1 were read. Because of the high loss mentioned previously in this cable, the transmitter loading was not affected by change in the terminating resistance R_2. To obtain the input resistance, therefore, it was only necessary to substitute the dummy load R_1, retune C_{av} and adjust R_1 to give the same I_1 reading. These steps gave the input impedance and input resistance

$$Z_{in}=\frac{E_1}{I_1}(R_{in}=R_1)$$

In order to obtain the minimum attenuation at each frequency in the cable, it was necessary to find the proper terminating resistance. This was done by varying R_2, reading E_2, for each value of R_2 over a reasonable range and then plotting the power absorbed from the cable for each setting of R_2. The maximum value of absorbed power (taken from the curve plotted) gave the proper terminating resistance, R_2, for the cable. The attenuation was then obtained from the ratio of the power input into the cable ($I_1^2R_1$) to the power received for this value of R_2, (E_2^2/R_2).

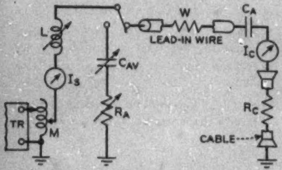

Figure 3. Lead-in wire test circuit

TR = transmitter
M = impedance matching transformer
I_s = radio frequency milliammeter
L = tuning coil
W = lead-in wire
C_A = air capacitor
I_c = radio frequency milliammeter
R_c = cable input resistance
C_{av} = variable air capacitor
R_a = variable noninductive resistor

$$\text{Attenuation}=10\log\frac{I_1^2R_1}{E_2^2/R_2}\text{ decibels}$$

The results are shown as follows:

Frequency, Kilocycles	Z Input, Ohms	R Input, Ohms	Attenuation, Decibels
50	42.5	35.0	25
75	38.2	33.2	29
100	28.5	27.0	36
150	31.0	20.5	53

Overhead Section Loss Measurements

The losses measured in the overhead section of the line, including the cable-overhead conductor mismatch loss calculations, are given below:

Overhead Conductor Losses: Using the above test methods, the losses in the overhead conductors between the Chicago city limits and Waukegan Station were measured.

Results obtained are shown as follows:

Frequency in Kilocycles	50	75	100	150
Decibel loss	4	5	6	9

It was found impossible to stop reflections on the overhead conductor section by terminating the line in a single resistance. At 75 kc, a minimum value of reflections was found by terminating the line in 435 ohms. Further tests on the overhead section are needed to complete this portion of the loss data.

Cable-Overhead Mismatch Loss. Looking from the 33-ohm cable section (at 75 kc) into the 435-ohm overhead conductor section, the mismatch loss at this frequency can now be calculated.

The cable may be considered as a generator having open circuit voltage E and internal resistance, $R=33$ ohms. The power transfer to the 435-ohm load would be

$$P_2=I^2435=\left(\frac{E}{33+435}\right)^2\times 435$$

$$P_2=\frac{E^2}{504}$$

Figure 7 shows the circuit used to calculate cable-overhead mismatch loss.

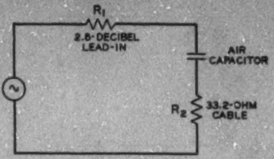

Figure 4. Equivalent loss circuit of lead-in, air capacitor and cable

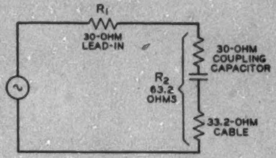

Figure 5. Equivalent loss circuit of lead-in, coupling capacitor, and cable

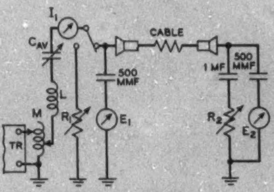

Figure 6. Cable section test circuit

TR = transmitter
C_{av} = variable air capacitor
L = tuning coil
R_1 = variable noninductive resistor
R_2 = variable noninductive resistor
E_1 = vacuum tube voltmeter
E_2 = vacuum tube voltmeter
I_1 = radio frequency milliammeter
M = matching transformer

If there were no mismatch the maximum available power to the overhead conductor would be

$$P_{max}=I_1^2 33=\left(\frac{E}{66}\right)^2 33=\frac{E^2}{132}$$

$$\text{Mismatch loss}=10\log\frac{P_2}{P_{max}}=10\log\times$$

$$\frac{\frac{E^2}{504}}{\frac{E^2}{132}}=10\log 0.262=5.8\text{ decibels}$$

In Figure 8 the theoretical circuit shows the overhead section matched to cable.

Skokie Tap Loss. It is assumed that with proper matching at the line tap that

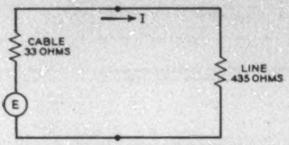
I
CABLE 33 OHMS
LINE 435 OHMS
E

Figure 7. Equivalent circuit used to calculate cable-overhead mismatch loss

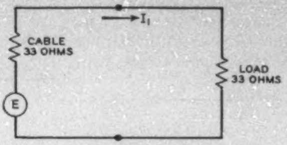
I1
CABLE 33 OHMS
LOAD 33 OHMS
E

Figure 8. Circuit showing overhead section matched to cable

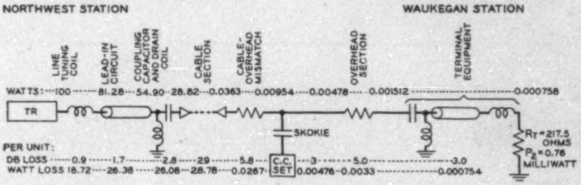
NORTHWEST STATION
WAUKEGAN STATION
LINE TUNING COIL
LEAD-IN CIRCUIT
COUPLING CAPACITOR AND DRAIN COIL
CABLE SECTION
CABLE-OVERHEAD MISMATCH
OVERHEAD SECTION
TERMINAL EQUIPMENT
WATTS: 100 81.28 54.90 28.82 0.0363 0.00954 0.00478 0.001512 0.000758
TR
SKOKIE
PER UNIT:
DB LOSS 0.9 1.7 2.8 29 5.8 3 5.0 3.0
WATT LOSS 18.72 26.38 26.08 28.78 0.0287 0.00476 0.0033 0.000754
C.C. SET
RT = 217.5 OHMS
P2 = 0.76 MILLIWATT

Figure 9. Summary of line losses at 75 kc

Total loss = 51.2 decibels

$$10 \log \frac{P_1}{P_2} = 51.2$$

$$\frac{P_1}{P_2} = 10^{5.12} = 10^{.12} \times 10^5 = 1.32 \times 10^5$$

For power input $P_1 = 100$ watts

$$P_2 = \frac{100 \times 10^{-5}}{1.32} = 0.000758 = 0.76 \text{ milliwatt}$$

Equivalent series circuit

$$\frac{R}{R_T} = 10^{5.12} = 1.32 \times 10^5$$

$$R = 217.5 \times 1.32 \times 10^5 = 28.69 \text{ megohms}$$

For 100-watt transmitter (*TR*)

$$I^2R = 100$$

$$I^2 = \frac{100 \times 10^{-6}}{28.69} = 3.485 \times 10^{-6}$$

$$I = 1.87 \text{ milliampere}$$

one half the carrier power would be absorbed at the Skokie Substation carrier set. This would be a 3-decibel loss in the Northwest to Waukegan carrier transmission.

Summary of Losses

A calculation and summation of the various losses along the line at 75 kc in transmitting carrier energy from Northwest Station to Waukegan Station is given in Figure 9. The losses are shown in decibels and in watts. The resistance values also are given in Figure 10 for a hypothetical series circuit that would deliver a current at the receiving end at Waukegan Station of the measured value.

In the circuits shown in these figures the overhead section of the line is terminated in 435 ohms resistance. Since the Waukegan Station terminal equipment loss, at the frequency for which the analysis is made, is three decibels, approximately one half of this resistance appears in the terminal equipment and the other half in the resistance load (R_T).

Signal-to-Noise Ratio Measurements

Signal plus noise and noise measurements were made at Northwest Station, Skokie Substation, and Waukegan Station, using a standard noise meter and a specially-designed converter unit to lower the frequency range of the noise meter to the 50-150 kc carrier band.

For these measurements the present carrier coupling capacitor was tuned at each location by means of a low-loss coil into a resistance load. A 500-ohm termination was used at Skokie Substation and Waukegan Station, and an 85-ohm termination was used at Northwest Station (coupling capacitor and lead-in 30 ohms each and line tuning coil 25 ohms). Since the noise power received was less than 10 per cent of the signal power, the signal plus noise readings were assumed to be signal power only.

The following signal-to-noise ratios were obtained on a clear, dry day at 75 kc:

Northwest = 314 to 1
Skokie = 105 to 1
Waukegan = 74 to 1

At the time the 74-to-1, (37 decibels) signal-to-noise ratio test was made at Waukegan, the noise power measured in the 500-ohm termination was 0.15 microwatt.

Assuming a 100-watt 90-decibel range, 75-kc transmitter-receiver carrier set were applied to the line, the following conclusions could be drawn for the 74-to-1 signal-to-noise ratio.

Minimum receiver power required, P_2

$$10 \log \frac{100}{P_2} = 90$$

$P_2 = 10^{-7}$ watts = 0.1 microwatt

Signal power, P_s, received at Waukegan through 51.2 decibels attenuation (see Figure 9)

$$10 \log \frac{100}{P_s} = 51.2$$

$P_s = 758$ microwatts

Noise power in 217.5-ohm termination, P_n

$$P_n = \frac{217.5}{500} \times 0.15 = 0.065 \text{ microwatt}$$

Signal-to-noise ratio would be

$$\frac{P_s}{P_n} = \frac{758}{0.065} = 11{,}660 \text{ or } 40.7 \text{ decibels}$$

These data show the noise power to be so low on a dry, clear day that it could hardly interfere with receiver operation.

To show the range available for the postulated conditions, it is assumed that

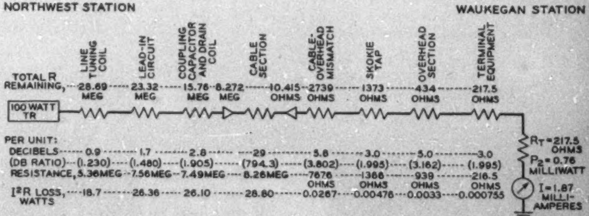
NORTHWEST STATION
WAUKEGAN STATION
LINE TUNING COIL
LEAD-IN CIRCUIT
COUPLING CAPACITOR AND DRAIN COIL
CABLE SECTION
CABLE-OVERHEAD MISMATCH
SKOKIE TAP
OVERHEAD SECTION
TERMINAL EQUIPMENT
TOTAL R REMAINING, 28.69 MEG 23.32 MEG 15.76 MEG 8.272 MEG 10.415 OHMS 2739 OHMS 1373 OHMS 434 OHMS 217.5 OHMS
100 WATT TR
PER UNIT:
DECIBELS 0.9 1.7 2.8 29 5.8 3.0 5.0 3.0
(DB RATIO) (1.230) (1.480) (1.905) (794.3) (3.802) (1.995) (3.162) (1.995)
RESISTANCE, 5.36MEG 7.56MEG 7.49MEG 8.26MEG 7676 OHMS 1366 OHMS 939 OHMS 216.5 OHMS
I²R LOSS, WATTS 18.7 26.36 26.10 28.80 0.0267 0.00476 0.0033 0.000755
RT = 217.5 OHMS
P2 = 0.76 MILLIWATT
I = 1.87 MILLI-AMPERES

Figure 10. Equivalent series resistance circuit to give the measured 75-kc loss values

the receiver would function satisfactorily on a 1.5-to-1 signal-to-noise ratio (0.1/-0.065 microwatt). With 90 decibels range carrier equipment, less the 51.2 decibels measured for the over-all line attenuation, 38.8 decibels is left to provide for changes in noise or signal power.

On the other hand, if it is assumed that the received signal power must be ten times the measured noise power (0.065 ×10 or 0.65), then the available receiver operating range would be:

$$\text{Decibel range} = 10 \log \frac{758}{0.65} = 10 \log 1{,}166$$

$$= 30.7 \text{ decibels}$$

In conclusion, sufficient data have not yet been obtained on signal-to-noise ratios under severe weather conditions. However, measurements made to date during light rains and snow conditions, indicate that the signal-to-noise ratios will permit securing a reliable carrier channel over this line.

No Discussion

Automatic Range-Adjusting Radiosonde Recorder

GEORGE E. BEGGS, JR.
ASSOCIATE AIEE

A RADIOSONDE is the air-borne unit of an air-to-ground telemetering system. This equipment transmits audio frequencies in time sequence which represent temperature and humidity, and a fixed reference signal. These signals constitute frequencies produced in the relaxation oscillator circuit of the transmitter, covering a range from 8 to approximately 200 cycles per second. A commutating switch, operated by an aneroid pressure cell, transfers the input terminals of the oscillator circuit from the temperature measuring element, to the humidity measuring element, to the reference signal circuit, in a definite sequence. Since the switch is actuated by an aneroid cell, each step of the switch represents a change of altitude. Thus temperature and humidity data are referred to altitude.

Air-borne radiosonde equipment, being of necessity lightweight, expendable, battery operated, and subject to wide variations of temperature, pressure, and humidity during balloon ascent, is subject to certain calibration drifts, exclusive of changes in primary measuring elements. The "reference frequency," transmitted periodically between indications of temperature and humidity, indicates the magnitude and direction of such drifts. Since this reference frequency drifts in the same proportion as the drifts occurring in the other indications, it has been used in the past as a secondary standard for manual range-readjustment of the recorder at the ground station. These frequent range changes, and the need for check calibration tests of ground equipment from time to time, demand skilled personnel in constant attendance.

Early recorders, used to record the audio frequency signals transmitted from an air-borne radiosonde, were primarily strip-chart single-range frequency recorders. Under a development contract between the Signal Corps Engineering Laboratories, Belmar, N.J., and the Leeds and Northrup Company, a recorder has been developed which performs automatically the functions of range-adjustment and calibration. Many of the features incorporated in this equipment represent joint efforts of the two organizations.

This radiosonde recorder includes a 10-inch strip chart covering the range 0 to 200 cycles per second; a frequency meter which converts incoming frequency, over the range from 8 to 200 cycles, to direct current proportional to frequency, in a linear fashion; a frequency standard with a limit-of-error of 0.01 per cent, or better, for automatic calibration and linearity checks, and a control panel having circuits for automatic range-adjustment of the recorder in accordance with the reference-frequency signals received. Drifts occurring in the airborne transmitter are cancelled out by this range-adjustment, resulting in corrected indications for temperature and humidity. An over-all limit-of-error of ±0.25 per cent, or better, is obtained, including the automatic, range-adjustment feature, the operation of frequency meter circuits, and automatic relay switching at the control panel.

Ease of service and maintenance, compactness, and convenience are secondary, but important, features. All units are designed for standard 19-inch relay rack mounting, each unit sliding into place in the rack and making connections automatically to the rack circuits as it is fastened in place, through the use of multiple-contact connectors. In some cases, as many as 60 connections are made when a unit is plugged in. A-c and d-c power and measuring circuits of various levels are carried in these connectors.

Complete System

The complete recorder, as shown in Figures 1, 3, and 4, comprises input switching and selector circuits followed by the frequency meter. The frequency meter is followed by a null-balance, potentiometer recorder with a full-scale range of approximately 20 millivolts. This full-scale range is variable by approximately ±15 per cent of nominal full-scale range, by either manual or automatic means.

The control panel includes relay and control circuits for automatic range-adjustment; for selecting appropriate input signals; for operation of the automatic stepping-switch of the frequency standard; for counting the number of automatic calibration sequences which have occurred; means for aural monitoring of incoming frequencies, and indicating instruments for observing line voltage and frequency.

The complete recorder is intended for use with standard air-borne radiosonde equipment, and new types under development. Battery voltage changes or temperature effects on the components of the radiosonde affect all signals of temperature, humidity, and reference in the same proportion. Accordingly, if the recorder is readjusted to read at the same chart position for each succeeding reference signal received, then temperature and humidity readings will be corrected for

---

Paper 49-152, recommended by the AIEE Instruments and Measurements Committee and approved by the AIEE Technical Program Committee for presentation at the AIEE Summer General Meeting, Swampscott, Mass., June 20–24, 1949. Manuscript submitted March 18, 1949; made available for printing April 28, 1949.

George E. Beggs, Jr., is with Leeds and Northrup Company, Philadelphia, Pa.

The writer is indebted to J. A. Siderman, Project Engineer, Meteorological Branch, Signal Corps Engineering Laboratories for technical advice; to E. W. Yetter (formerly of Leeds and Northrup Company) of Sun Physical Research Laboratory, for development of the frequency meter circuits; to W. R. Clark, David Clements, A. W. Kozak, and A. J. Williams, Jr., for advice and assistance in design and fabrication of this equipment.

drifts in their actual transmitted frequencies, assuming that the primary measuring elements themselves are correct.

The signal from the radiosonde transmitter is received by a radio receiver with its output circuit connected to the input circuit of the frequency meter. The corresponding d-c voltages produced by the frequency meter then cause the recorder to indicate these values on the chart. No signals above approximately 175 cycles are produced for any temperature or humidity condition. On the other hand, all reference signals utilized for range-adjustment of the recorder occur above 175 cycles. A recorder control cam (*B* cam) closes a relay circuit any time the recorder balances above nominal 175 cycles, thus recognizing the presence of a reference signal. This activates the automatic-range-adjustment circuits, causing the recorder to readjust its range. All reference signals are made to indicate 190 cycles on the chart by varying the slidewire voltage, until the d-c voltage corresponding to the incoming signal, and a tap point on the slidewire representing 190 cycles (95 per cent of full scale), are of equal value. This is the corrected, reference-point indication, resulting in corrected humidity and temperature indications. The 190-cycle value is used since this is the nominal value of the reference signal. The actual method of performing this function will be described briefly under the heading Control Panel.

Frequency Meter

The frequency meter is the heart of the system. Figure 2 is a block diagram of this unit. Incoming frequencies are amplified in a high-gain multistage, vacuum-tube amplifier and clipped so that square waves are produced from any incoming wave shape, independent of amplitude, within wide limits. By differentiation of these square waves in a resistance-capacitance circuit of very short time-constant, sharp positive and negative pulses are produced. An overbiased amplifier disposes of the negative pulses, allowing the positive pulses only to continue through the system.

These positive pulses, occurring at a rate determined by the incoming frequency, are then used to initiate the operation of a "one shot" multivibrator. This circuit produces a positive pulse of fairly constant width and height regardless of the shape of the incoming pulse, but the repetition rate of the pulses of this circuit is still dependent upon the original incoming frequency.

The pulse derived from the 1-shot multivibrator is then fed into a delay line, having a total delay of approximately 100 microseconds, from the input terminals of the line to the short circuit termination of the line and back to the input terminals of the line.

The delay line construction, shown in Figure 8, is comprised of an inductance-capacitance-type filter circuit in which mutual inductance is present between the adjacent coils to improve band-width of the circuit. This mutual inductance is determined by the amount of overlap between the coils, the overlap being determined by the slope of the mounting pieces.

The coils are connected in series, with shunt capacitors to ground, each coil and capacitor combination being mounted on a separate mounting form. The complete delay line comprises 30

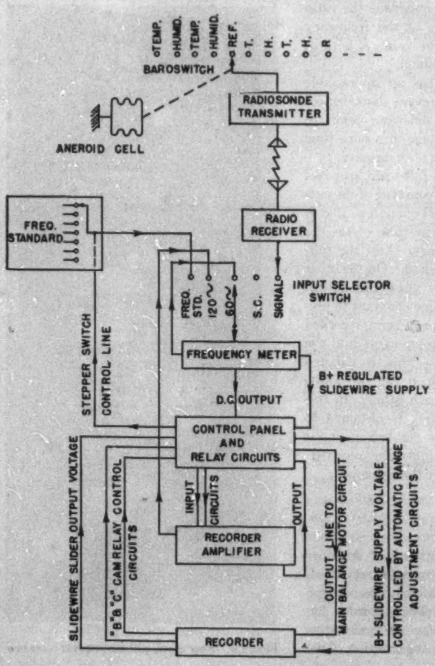
oTEMP.
oHUMID.
oTEMP.
oHUMID.
oREF.
oT.
oH.
oT.
oH.
oR
BAROSWITCH
RADIOSONDE TRANSMITTER
ANEROID CELL
FREQ. STANDARD
RADIO RECEIVER
FREQ. STD.
120~
60~
S.C.
SIGNAL
INPUT SELECTOR SWITCH
STEPPER SWITCH
CONTROL LINE
FREQUENCY METER
B+ REGULATED SLIDEWIRE SUPPLY
D.C. OUTPUT
CONTROL PANEL AND RELAY CIRCUITS
SLIDEWIRE SLIDER OUTPUT VOLTAGE
"B"&"C" CAM RELAY CONTROL CIRCUITS
INPUT
CIRCUITS
OUTPUT
RECORDER AMPLIFIER
OUTPUT LINE TO MAIN BALANCE MOTOR CIRCUIT
B+ SLIDEWIRE SUPPLY VOLTAGE CONTROLLED BY AUTOMATIC RANGE ADJUSTMENT CIRCUITS
RECORDER

Figure 1 (left). Block diagram, complete system

Figure 2 (below). Block diagram, frequency meter operation

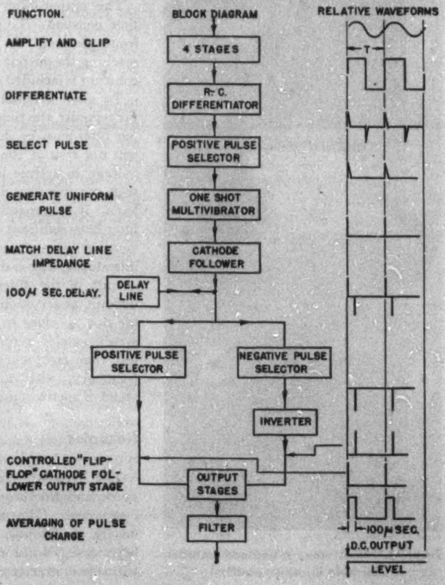
FUNCTION.
BLOCK DIAGRAM
RELATIVE WAVEFORMS
AMPLIFY AND CLIP
4 STAGES
T
DIFFERENTIATE
R-C. DIFFERENTIATOR
SELECT PULSE
POSITIVE PULSE SELECTOR
GENERATE UNIFORM PULSE
ONE SHOT MULTIVIBRATOR
MATCH DELAY LINE IMPEDANCE
CATHODE FOLLOWER
100μ SEC. DELAY.
DELAY LINE
POSITIVE PULSE SELECTOR
NEGATIVE PULSE SELECTOR
INVERTER
CONTROLLED "FLIP-FLOP" CATHODE FOLLOWER OUTPUT STAGE
OUTPUT STAGES
AVERAGING OF PULSE CHARGE
FILTER
100μ SEC.
D.C. OUTPUT
LEVEL

filter sections which are mounted in a sealed container.

The bandwidth of this delay line is made sufficient to prevent the pulse shape from being altered appreciably during its transmission down the line and back. This passive network determines the delay between the incoming positive pulse and the outcoming phase-inverted, or negative pulse, the time delay being fixed in value. The new, negative pulse produced in this fashion is inverted to become a second positive pulse. Then both positive pulses, now forming a pair of positive pulses separated by 100 microseconds, the pairs occurring at a repetition rate still determined by the incoming frequency, are amplified and applied to an output "flip-flop" circuit in such a manner that the first pulse turns the circuit on, and the second pulse turns it off, through control tubes.

Accordingly, in the cathode of the output stage a pulse is produced with its width determined by the time spacing between the two pulses in a pair, and its repetition rate determined by the incoming frequency.

The height of the output pulse is determined by the tube constants, the tube-heater temperature, and the plate-supply voltage. The plate-supply voltage is regulated by a vacuum-tube voltage-regulator circuit. In addition, the output-stage cathode temperature is maintained sufficiently constant by the inclusion of the heater of the output stage in the load circuit of the power supply. The use of a cathode-follower makes variation of tube constants relatively unimportant over a fairly wide range, as far as height of the output pulse is concerned.

Figure 3. Front view, radiosonde recorder, reroll table in writing position

These output pulses, essentially of the same height and of the same width, as determined by the passive delay line network, are averaged in a filter circuit which removes the a-c component, leaving a d-c voltage proportional to the incoming frequency. The output voltage of the filter circuit is measured by a potentiometer recorder. To minimize the error of the system, the potentiometer recorder circuit is modified so that the power supply for the slidewire, instead of being a battery, is obtained from the same plate, supply line as is used to operate the output cathode-follower stage. Therefore, any variations in the output voltage of the regulated power-supply are cancelled out, because the recorder measures the ratio of the output voltage of the frequency meter and the slidewire voltage, both of which vary in a like fashion.

The output filter has an appreciable time constant. To prevent disturbances from reaching the slidewire prior to reaching the output stage, the same time constant is included in both circuits.

To allow adequate full-scale speed of the recorder, the time constant of the output filter must be short enough so that it will not restrict the rise-time of the d-c voltage to a time longer than the full-scale recorder time desired. On the other hand, it is necessary that the output filter have sufficient time constant to prevent the lowest frequency being recorded introducing any a-c component into the output of the filter. This is not too difficult to accomplish, if the two limits are not too close to each other. In this system, stable recording is obtained to less than eight cycles per second input frequency, with a full-scale recorder-speed of approximately three seconds.

Recorder

The recorder comprises a modified Leeds and Northrup model *G* electronic instrument. The modifications are primarily mechanical. The recorder has been designed for relay rack mounting with file drawer type construction of the recorder proper, to improve accessibility for paper loading and pen service. The standard model *G* amplifier, including a vibrator-type converter, and amplifier stages, has been modified to allow mounting in a rack with plug-in features. The chart reroll device is of the type which can be swung back into a storage compartment giving a flush front recorder, or may be swung out and used as a writing table.

This reroll table includes a "window shade" type of roller mechanism with a solenoid-operated clutch, providing for examination of up to six feet of prior record by lifting the paper and pulling it out for examination. The paper will return to the storage compartment in the same manner as a window shade, following which normal reroll drive is activated by closure of a microswitch operated by paper tension. Hand advance of the paper can be accomplished by a knob on the reroll table, when desired.

Forty yards of paper are accommodated in the recorder and reroll table with a paper advance speed of one-half inch per

Figure 4. Rear view, with back cover removed

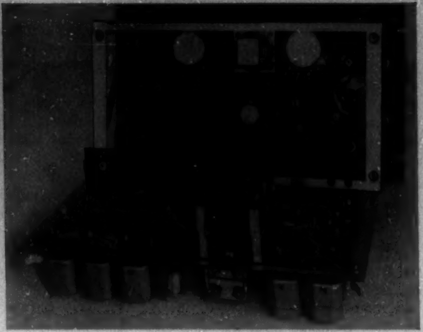

Figure 5 (left). Frequency meter removed from rack

Bails serve as bench chassis-jacks, carry handles, and guides to assure mating of multiple connectors

Figure 6 (right). Control panel removed from rack, rear view with back opened for service

minute, allowing about 48 hours of continuous recording.

Frequency Standard

In addition to the signals derived from the incoming radio signal from the radiosonde transmitter, signals also are available from an internal frequency standard which produces frequencies of 190, 160, 140, 120, 100, 80, 60, 40, 20, and 10 cycles with limit-of-error of 0.01 per cent, or better. This frequency standard, supplied by American Time Products, Inc., utilizes two hermetically-sealed low-temperature-coefficient tuning forks. Multivibrator circuits used with these forks produce the frequencies noted. These frequencies are selected by a stepper switch of the telephone type, operated either automatically or manually, for field check of the linearity of the recorder. Accordingly, the frequency standard acts as a primary standard for field use.

Other Input Sources

In addition to the radiosonde signal and the frequency standard signals, two other signal sources are provided for quick check of recorder operation. Both 60 cycles and 120 cycles are derived from the incoming line supply by tapping off a portion of filament supply in one of the units, and by full-wave rectification of this supply. These frequencies are available at the input selector switch on the main control panel, as are the frequencies from the radio receiver and from the frequency standard.

Control Panel

This unit furnishes automatic and manual control for the complete equipment. It comprises relay control circuits and switching circuits, plus monitoring facilities to allow checking of the whole system. An incoming signal is selected by the selector switch on the control panel and is applied directly to input terminals of the frequency meter. The output of the frequency meter returns to the control panel, goes through relay contacts used in the range-change circuit, and then connects to the recorder amplifier and slidewire circuits.

Automatic range-adjustment is performed at the control panel in the following manner. If an incoming signal, produced either by the radiosonde transmitter or by the frequency standard, has a value of approximately 175 cycles or greater, a cam switch on the recorder closes, activating a relay in the control panel. This relay initiates operation of one of two timers. This timer operates for a period of time, determined by its initial setting, to ascertain whether the input signal is sufficiently steady over this period of time to warrant an automatic range-adjustment. If the signal does not stay present for the selected time interval, the recorder moves downscale to a temperature or humidity reading, and the timer resets.

If the reference signal is present for the required length of time (up to 30 seconds) the output of the frequency meter is continued in its connection to one side of the recorder amplifier, but the slidewire contact is disconnected from the recorder amplifier, and a point representing exactly 95 per cent of the printed chart-width (that is, nominal 190 cycles) is connected to the other side of the recorder amplifier input circuit. Thus, the recorder amplifier compares these two input voltages. At the same time the output of the recorder amplifier is disconnected from the recorder balancing motor and is connected to an auxiliary balancing motor which drives a multiturn rheostat (Helipot or Micropot). This multiturn rheostat, the range-adjustment control, is in series with the slidewire voltage-supply. As its value is changed, it changes the total slidewire voltage and the voltage of the 95 per cent tap point proportionately. The motor driving the multiturn rheostat moves in the direction to reduce to zero the difference between the 95 per cent tap point (referred to usually as the reference point) and the output of the frequency meter, derived from the steady input reference signal. This action occurs in a period of approximately three seconds, determined by electronic delay circuits on the control panel.

At the end of this time, the recorder amplifier and recorder balancing motor are returned to their normal connections to the circuit, so that the input signal is recorded normally, now at exactly 95 per cent of chart-width. Since the slidewire is a linear device, the value of all other incoming d-c signals derived from the frequency meter will be changed in the same proportion. Actually this constitutes a range adjustment of the recorder to offset any changes or drifts which are not desired in the incoming signal.

Since the final record is produced on a strip of paper, it is desirable that the 95 per cent tap point of the slidewire and the 95 per cent point on the chart correspond at all times. Accordingly, the reference or 95 per cent point is adjustable over a range of approximately ±1 per cent to compensate for expansion or contraction of the paper which may occur with changes in humidity. The zero end of the paper is fixed by the sprocket pins. The setting of this reference point adjustment determines to what point the recorder will adjust incoming reference signals, during the automatic range-adjustment cycle.

To avoid repeated recycling of the automatic-range-adjust circuit, a second timer is provided. This timer, known as the "drop-out" timer, with a range of 60 seconds, operates as follows. If after return to normal recording following the automatic range-adjustment, the signal departs from the reference frequency (that is, frequency of 175 cycles or greater) other relay circuits operate to cause the recorder amplifier to switch from the frequency meter output to the 95 per cent reference point. The recorder then records 95 per cent of scale independent of the input signal. This condition continues until the drop-out timer has completed its operating cycle. If, at the completion of this cycle, the reference signal is still absent, that is, if a humidity or temperature signal is present, the recorder moves downscale and records this signal, which is below 175 cycles. As the recorder moves below 175 cycles, it releases all the relay circuits which have operated, so that they are ready for the next reference signal which may be received.

However, if the reference signal had returned during the time interval determined by the drop-out timer, so that it is present at the completion of the timer cycle, the timer resets, the recorder returns to recording the output of the frequency meter (190 cycles), and the drop-out timer "protection" is ready to repeat the operation noted before. This cycle can be repeated as many times as the reference signal drops out until such time as the reference signal drops out, and stays out, for a period of time longer than that determined by the drop-out timer.

Figure 7 is a sample chart record showing the record produced by the range-change operation. A signal which should read 80 cycles (40 per cent of full scale) on the chart, is shown initially with an error. The same proportional error exists in the corresponding 190-cycle position. The 30-second timer causes the recorder to observe this signal for 20 seconds prior to correcting the error.

After the automatic range-adjustment, return to normal recording of the 190-cycle signal occurs, for a period of 35 to 40 seconds. Then 80 cycles is reconnected to the input circuit. This produces a short downscale motion of the recorder, operating the drop-out timer control cam, and returning the recorder to the 95 per cent reference point for the 35-second setting of the 60-second timer, before allowing recognition and recording of the 80-cycle signal, which is still present at the end of the drop-out-timer period. The 80-cycle signal now records correctly.

The reason for the incoming time delay and the drop-out timer, is that under certain conditions the airborne commutating switch which selects humidity, temperature, and reference contacts may not make positive contact immediately. This may lead to very short reference signal indications which should be ignored by the recorder. The operator, by listening to the monitor speaker, can obtain information leading to proper setting of the timers to prevent this occurrence.

Since the reference signals are produced by a commutating switch operated by an aneroid cell, the number of times that a reference signal appears is an indication of the altitude attained by the balloon. An electrically-operated counter controlled by the relay circuits which operate the automatic range-adjustment circuit, counts the number of times frequencies above 175 cycles are received. The counter is prevented from making false counts by the same timers that prevent recycling of the automatic-range-adjustment feature.

Automatic Calibration

Automatic calibration utilizes signals derived from the frequency standard. If it is desired to have the frequency standard stepped from one frequency to the next, the automatic calibration switch on the control panel is depressed momentarily. The 60-second drop-out timer used previously for protection in the automatic-range-adjustment circuit is not needed for this feature, when the frequency standard is used as a signal source. Therefore, this timer is transferred to the automatic calibration circuit to determine the length of time that a given frequency is produced by the frequency standard. At the end of each time cycle of the 60-second timer, it causes the stepper switch on the frequency standard to move one step, so that a step record, first downscale and then upscale and then downscale again, is produced. Each time the stepper switch selects the 190-cycle point, an automatic range-adjustment occurs if the range-circuit switch is placed in the "automatic" position. However, if this is undesirable, the automatic range-adjustment feature may be disconnected by placing the switch in the "manual" position.

In addition, specific frequencies may be selected from the frequency standard by stepping the stepper switch with an auxiliary control switch on the control panel.

Other Features

Other check features also are provided on the control panel including means for short-circuiting the input circuit of the frequency meter to see if the output-stage voltage is actually zero when no input frequency is present. An output-short-circuit switch also is provided to short-circuit the output stage of the frequency meter. By comparing the input and the output short-circuit conditions, the condition of the output stage is determined. If there is no shift in zero position of the pen when input and output short-circuit conditions are compared, it may be assumed that the output tube is in good condition and that the output stage is operating properly. Variations of zero under these conditions usually indicate a faulty tube having heater-cathode leakage which may cause an error in the output d-c voltage.

Mechanical Features

All units slide into the rack and plug in. Units are removable and in most cases are self-powered so that they may be serviced on the bench without the necessity for interconnection to the rack. The bails on the chassis serve to guide the connectors into place when the units are slid into the rack, and as carrying handles and chassis jacks for service. Figure 5 shows the

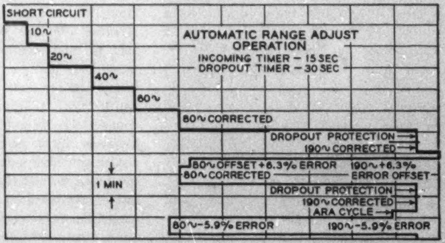

Figure 7. Sample chart record, showing two different automatic-range-adjustment cycles and portion of linearity check

Figure 8. Delay line construction

Partially assembled line (above), completely assembled and sealed line (below)

frequency-meter chassis removed from the rack for service.

Service is further facilitated by mounting the chassis in the vertical plane so that the usual bottom of the chassis opens at the front of the recorder rack and the tubes project horizontally from the back of the chassis. The front panels, which are held by separate screws, may be removed, but the chassis will stay in the rack, held by their own screws concealed under the panels. This allows accessibility to all circuits and tubes while the units are in the rack in operating condition.

A greater mechanical problem is involved in the design of the control panel assembly because it comprises not only 14 relays and circuits with associated tube controls, but also the indicating instruments, timers, input switch, control switches, counter, auxiliary balancing motor, and multiturn rheostat, audio circuits, and so forth. Therefore, the control panel is built in two parts. When it is pulled out of the rack and unplugs its connections, it may be set on the bench. Then the back panel of the control unit itself may be hinged down to allow accessibility to the inside of the control panel and to relay and tube-socket wiring and components, as shown in Figure 6. The relays are plug-in units utilizing 12-contact tube-bases and dust covers. They may be removed for replacement or service. The dust covers may be removed and the relays placed back in their sockets in case contact operation is to be observed.

Limit-of-Error

The limit-of-error of the system is determined by two factors. First, the linearity of the slidewire is extremely important. However, linear, accurate slidewires have been made for a number of years. Second, the a-c to d-c conversion linearity of the frequency meter must be well within the limits of the complete system, since all input signals are converted to direct current by this unit.

Extraneous pick-up in both the d-c and a-c circuits must be reduced to a value which will not affect the over-all limit-of-error. This is one of the major problems in a recorder of this type since there are so many different paths followed by the a-c and d-c circuits through the relays, and through the control-panel and rack cabling. Careful attention to magnetic loops in the circuits, and proper shielding, are essential. Appropriate relay contact materials must be used so that contact potentials and thermal potentials do not introduce errors in the d-c circuits. The complete recorder has a limit-of-error of ±0.25 per cent, or better, including operation of the automatic-range-adjustment circuit.

References

1. An Improved Radiosonde and Its Performance, **H. Diamond, W. S. Hinman, Jr., F. W. Dunmore, E. G. Lapham.** *Journal of Research*, National Bureau of Standards (Washington, D. C.), volume 25, 1940, pages 327–67.

2. Radiosonde Telemetering Systems, **V. D. Hauck, J. R. Cosby, A. B. Dember.** *Electronics* (New York, N. Y.), volume 19, number 5, May 1946, pages 120–23.

3. High-Speed Multiple-Point Potentiometer Recorder for Measuring Thermocouple Temperatures During Test-Plane Flights, **I. M. Stein, A. J. Williams, Jr., W. R. Clark.** *Transactions*, American Society of Mechanical Engineers (New York, N. Y.), volume 66 number 4, May 1944, pages 271–75.

4. Electronically-Balanced Recorder for Flight Testing and Spectroscopy, **A. J. Williams, Jr., W. R. Clark, R. E. Tarpley.** *AIEE Transactions*, volume 65, 1946, pages 205–08.

5. The Impulse Response of Electrical Networks, **M. Levy.** *Journal*, Institution of Electrical Engineers (London, England), volume 90, part 3, number 12, December 1943, pages 153–64.

No Discussion

Graphical Method for Estimating the Performance of Distance Relays During Faults and Power Swings

A. R. VAN C. WARRINGTON
MEMBER AIEE

THE impedance of a transmission line of a given conductor size and spacing is proportional to its length. This fact makes it possible to build distance relays which can determine the distance to a short circuit by comparing the current in the conductors with the potential between them, since the ratio V/I is the impedance which is proportional to the distance to the short circuit.

In order to measure correctly the distance to a fault between two phases of a 3-phase line, a relay must be provided which compares the voltage between those phases and the vector difference of the currents in them. Two more identical relays, similarly connected, are required to measure the distance to faults between the other phases of the line. Similarly for ground faults, three distance relays are required; each one compares the potential between a conductor and ground with the currents in the conductor and the ground.

With distance relays connected in this manner a fault involving the phase or phases associated with the relay will cause it to measure the true impedance of the line between the relay and the fault. However, since the other two relays are energized by the currents in these phases and the voltages across the other phases, this same fault will cause them to measure values other than the true impedance, the necessary determination of which involves rather complicated and tedious calculation. Similarly, power swings which result in large angles between voltages at the ends of the system may produce current-voltage relations which cause distance relays to measure impedances even more tedious to evaluate by mathematical computation. Finally the slow clearing of a fault may cause a power swing, so that there will be a combination of swing and fault conditions to analyze.

The purpose of this paper is to describe a method of determining quickly what impedances all phase and ground distance relays measure during all of these fault and swing conditions. The method is generally relatively simple, employing only a ruler and a protractor or a draftsman's 30- 60- 90-degree triangle, and requiring knowledge only of the positive and zero sequence impedances of the system.

The validity of the graphical method used is established in the section on Derivation of Construction for charts, where the calculations are summarized in the form of tables with all values given in terms of the phase sequence impedances of the system. The expressions in the tables and the vector algebra used in calculating them have been made as easy to read as possible by limiting the use of subscripts to one reference at a time and choosing them to be self-evident, so that constant reference to the nomenclature list is not necessary.

It was observed that there was a certain symmetry in the expressions for the impedances seen by the relays under different fault conditions and this indicated that relatively simple charts could be used to reduce the work of calculation and that relay performance would be predicted by drawing the relay characteristic on the same chart.

The protected section was assumed to be a single line. Parallel lines were not considered because they do not appreciably affect the results for faults near the ends of the protected section. These are the only faults that need be considered since this analysis is concerned only with the possibility of relays' tripping on faults beyond the end of the protected section.

Fault Charts

These charts show, as vectors on an impedance diagram, the relationship between the impedance seen by the relay in the faulted phase or phases and the impedances seen by the relays in the other phases. Line-to-line, line-to-ground, and double-ground faults are considered for phase relays and for ground relays. Three-phase faults were not considered because they are symmetrical so that all the relays are presented with the same impedance.

CONSTRUCTION OF TYPICAL CHART

When supplied with the proper currents and potentials, the relay associated with the faulted conductor or conductors measures the positive sequence impedance of the line between the relay and the fault, including any arc or contact resistance in the fault. The impedance and arc resistance measured by the relays in the phases not directly associated with the fault, differs from the true impedance by an amount which depends on the type of fault and which can be obtained graphically as shown in subsequent paragraphs.

Phase Relays with Line-to-Line Faults, Figures 1 (A), (B), and (C)

Figure 1(A) is an impedance diagram with resistance and reactance co-ordinates R and X. The line AB is a vector representing the true (positive sequence) impedance of the protected transmission line whereon F is the fault location. The lines AS and BL represent the total system impedance behind the relay and

---

Paper 49-154, recommended by the AIEE Relays Committee and approved by the AIEE Technical Program Committee for presentation at the AIEE Summer General Meeting, Swampscott, Mass., June 20–24, 1949. Manuscript submitted March 22, 1949; made available for printing April 28, 1949.

A. R. VAN C. WARRINGTON is with the General Electric Company, Philadelphia, Pa.

beyond the protected line respectively and can be calculated easily from a knowledge of the short-circuit currents at the line terminals *A* and *B*, deducting the current that flows through the line.

The impedance measured by the relay in the faulted phases *2-3* (neglecting arc resistance) is represented by the line *AF* which is the phase-to-neutral or positive-sequence impedance of the line between the relay and the fault, and is referred to as the true impedance. The phase *3-1* relay sees an impedance which is leading the true impedance, and the phase *1-2* relay a lagging impedance, which are obtained as follows: Join *SF* and draw lines from *S*, 60 degrees on each side of *SF*, to meet perpendiculars to *SF* drawn from *F* at *M* and *N*. *AM* is the impedance seen by the *3-1* relay and *AN* the impedance seen by the *1-2* relay.

In Figure 1(B), and all the ensuing diagrams, arc resistance is considered but, for the sake of simplicity in the explanation, all the impedances of the system are considered to be of the same phase angle, that is, the system is homogeneous and points *S*, *A*, *B*, and *L* are on the same straight line. As shown in the previous paragraph and in Figure 1(A), if the phase angle is not uniform throughout the system, it is necessary only to draw the extra line *SF*.

SM is drawn at 60 degrees leading *SF*, as in Figure 1(A), but the arc resistance R_F/C is added at 60 degrees leading the *R* axis so that the total impedance Z_{31}' seen by the phase *3-1* relay is the vector AF_{31}. Z_{12}' is found in a similar manner, but using a 60 degree lagging shift. By drawing the perpendiculars from *A* instead of *F* the points M_A and N_A can be found which give the impedances for a fault at the relay location *A*. The addition of the arc resistance locates the points A_{31} and A_{12} so that now four points have been located which define the fault areas; these areas are shaded in Figure 10 to show their relationship to typical relay tripping areas, which will be discussed later.

The arc resistance is expressed as R_F/C instead of R_F because only the fraction *C* of the fault current flows through the relay; the rest comes from the line section on the other side of the arc.

Ground Relays with Line-to-Line Fault, Figures 2 (A) and (B)

The procedure for Figures 2(A) and (B) is much the same as used in Figures 1(B) and (C). The diagrams are similar except for the facts that the angle which *SM* and *SN* subtend from *SF* is 30 degrees this time, and that the arc resistance is less by the ratio $\sqrt{3}$ and is drawn at 30 degrees from the *R* axis. These ratios and angles are summarized for the various faults in Table V. Z_1', the impedance presented to the phase *1* relay, is infinite and therefore not shown on Figures 2(A) and (B).

Phase Relays with a Line-to-Ground Fault, Figures 3 (A) and (B)

Figure 3(A) shows the impedance produced by a ground fault as viewed by the phase relays. The lines *SM* and *SN* are drawn at 30 degrees on each side of *SF* as in Figure 2(A) but they are now extended to *T* and *W* by the zero sequence component $Z_0/C\sqrt{3}$ because the ground circuit is involved. The arc resistance is then added as it appears to the relay. $\sqrt{3}R_F/C$, at 30 degrees from the *R* axis see Table V. Z_{23}' is not shown because it is infinite.

Ground Relays with a Line-to-Ground Fault, Figures 4 (A) and (B)

In this case the relay current is a mixture of phase and residual current and the value *C* is replaced by a hybrid value which we will call *C'* and which is $C-C_0 Z_0'/Zp'$. This means that *SM* and *SN* are no longer at 30 degrees or 60 degrees from *SP* but the angle depends on the relative values of *C* and C_0. The construction is therefore a little less convenient than before and is as follows: Draw a line *MN* through *F* at right angles to *SF* so that $FM=FN=\sqrt{3}Z_n/C'$. Draw $MT=\sqrt{3}Z_0/C'$ leading *SF* by 30 degrees and draw $NW=\sqrt{3}Z_0/C'$ lagging *SF* by 30 degrees. Finally draw the arc

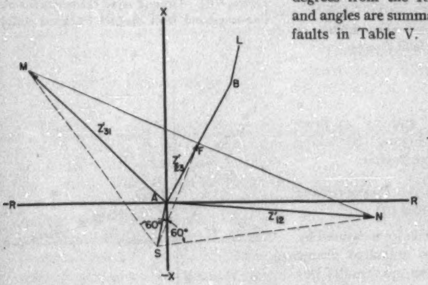

Figure 1(A) (left). Impedances seen by phase relays for phase 2-phase 3 fault at F (nonhomogeneous line)

$$FS=\frac{Z_n}{C}$$

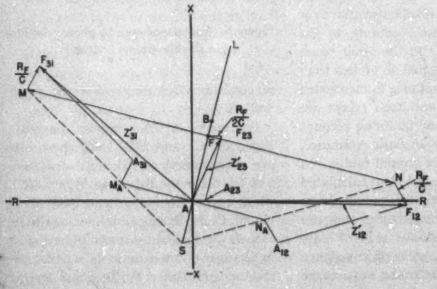

Figure 1(B) (lower left). Impedances seen by phase relays for phase 2-phase 3 fault at F (homogeneous line)

$$FS=\frac{Z_n}{C} \quad FM=\sqrt{3}\frac{Z_n}{C} \quad \text{Angle } FSM=60 \text{ degrees}$$

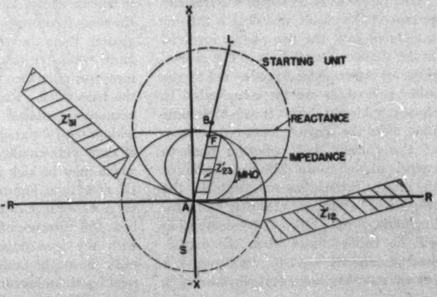

Figure 1(C) (below). Phase relay characteristics on line-to-line fault diagram

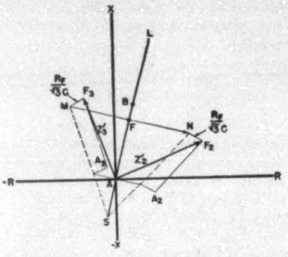
X
L
$\frac{R_F}{\sqrt{3}C}$
F3
M
B
Z_3'
F
N
$\frac{R_F}{\sqrt{3}C}$
F2
A3
Z_2'
-R
A
R
A2
S
-X

Figure 2(A). Impedances seen by ground relays with phase 2 to phase 3 fault at *F*

$FS=\frac{Z_n}{C}\quad Z_1'=\infty\quad \text{Angle } FSM=30 \text{ degrees}$

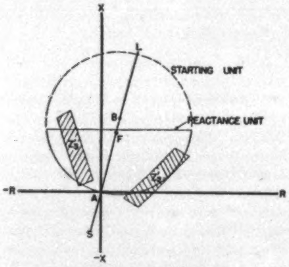
X
L
STARTING UNIT
B
REACTANCE UNIT
Z_3'
F
Z_2'
-R
A
R
S
-X

Figure 2(B). Ground relay characteristics on line-to-line fault diagram

$Z_1'=\infty$

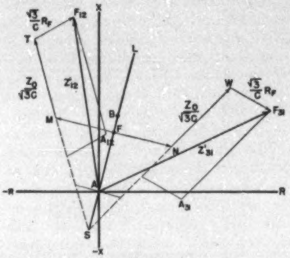
$\frac{\sqrt{3}}{C}R_F$
F12
X
T
L
$\frac{Z_0}{\sqrt{3}C}$
Z_{12}'
W
$\frac{\sqrt{3}}{C}R_F$
$\frac{Z_0}{\sqrt{3}C}$
F31
M
B
F
A12
N
Z_{31}'
-R
A
R
A3
S
-X

Figure 3(A). Impedances seen by phase relays for phase-1-to-ground fault at *F*

$FS=\frac{Z_n}{C}\quad Z_{23}'=\infty\quad MF=FN=\frac{Z_n}{\sqrt{3}C}$

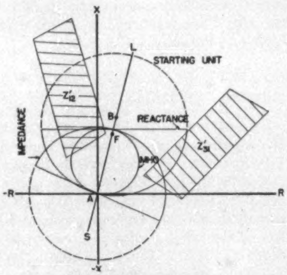
X
L
STARTING UNIT
Z_{12}'
B
REACTANCE
IMPEDANCE
F
Z_{31}'
MHO
-R
A
R
S
-X

Figure 3(B). Phase relay characteristics on line-to-ground fault diagram

$Z_{23}'=\infty$

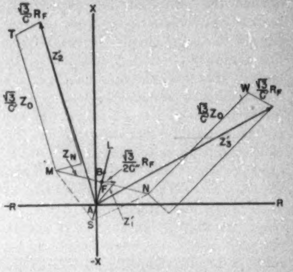
$\frac{\sqrt{3}}{C}R_F$
X
T
Z_2'
W
$\frac{\sqrt{3}}{C}R_F$
$\frac{\sqrt{3}}{C}Z_0$
$\frac{\sqrt{3}}{C}Z_0$
Z_3'
Z_N
L
$\frac{\sqrt{3}}{2C}R_F$
M
B
F
N
-R
A
R
S
Z_1'
-X

Figure 4(A). Impedances seen by ground relays with phase-1-to-ground fault (reduced scale)

$FS=\frac{Z_n}{C}\quad C'=C-C_0\frac{Z_0'}{Z_p'},\quad C''=2C+C_0\frac{Z_0'}{Z_p'}$

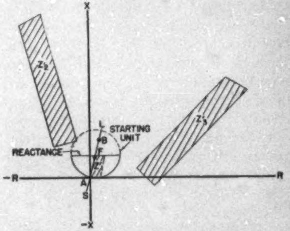
X
Z_2'
Z_3'
L
STARTING UNIT
B
REACTANCE
F
Z_1'
-R
A
R
S
-X

Figure 4(B). Ground relay characteristics on line-to-ground fault diagram (reduced scale)

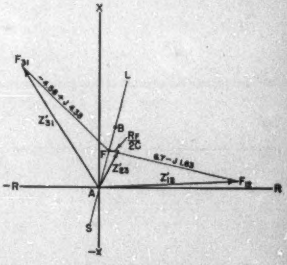
X
F31
-4.56+J4.38
Z_{31}'
L
B
$\frac{R_F}{2C}$
F
6.7-J1.63
Z_{23}'
Z_{12}'
F12
-R
A
R
S
-X

Figure 5. Impedance seen by phase relays for a double-ground fault at *F*

resistance component $\sqrt{3}R_F/C'$ at *T*, leading the *R* axis by 30 degrees and draw $\sqrt{3}R_F/C'$ at *W*, lagging the *R* axis by 30 degrees.

It will be noted that this chart was drawn to a smaller scale because the quantity $\sqrt{3}R_F/C'$ is too large for the same scale to be used.

Phase Relays with a Double-Ground Fault, Figure 5

One phase relay measures the true impedance to the fault, and that is the one associated with the two phases involved in the double-ground fault. The expressions for the impedances measured by the other two relays are too complicated to show graphically, but it is safe to assume that, since the zero sequence components of the current and potential tend to cancel out, due to the delta connections of the relay, the impedance measured by the relays will be similar to that for a line-to-line fault, Figure 1(B). This assumption will be verified later when the mathematical analysis is given. In Figure 5, a typical case has been worked out and it will be seen that Z_{31}' and Z_{12}' are practically the same as in Figure 1(B), taking into account the change in scale.

Ground Relays with a Double-Ground Fault, Figures 6(A) and (B)

Here again the impedance measured by the relays in the two unfaulted phases is too complex to show graphically, but it will be shown later that in one phase the relay measures a reactance equal to or greater than the true reactance to the fault, while the relay in the other phase measures reactance equal to or less than the true value. Reactance is mentioned because impedance and mho relays are seldom used for ground faults on account of their vulnerability to fault resistance, which may be high in ground faults. In the meantime, Figure 6(A) was calculated for a wide range of conditions and shows how the measured impedances compare with the true impedance *AF*. Figure 6(B) shows the fault areas of impedance seen by the relays under the same range of conditions for faults over the whole section.

Reference to the vector diagrams, Figures 6(C) and 6(D), will show why one relay measures too much reactance and the other too little. In Figure 6(C), which represents the general case where *C* and C_0 are comparable in magnitude, the relay potential V_2' is seen to be almost in phase with the current I_2' so that the reactance measured by the phase 2 relay

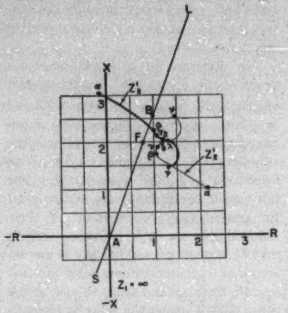

Figure 6(A). Impedances seen by ground relays with a double-ground fault at *F*

is small and the relay will overreach; the relay potential V_3' however is leading its current I_3' by a considerable angle so that its measured reactance is large and the relay will underreach. The true impedance would be roughly half the potential V_{23}' divided by one of the $I\phi'$ components. $I\phi'$ is the current that would flow between conductors if the ground were not involved.

Figure 6(D) represents the case where there is a grounded neutral transformer nearby, but little generation, so that C is small compared with C_0. In this case it can be seen that the phase *2* relay will measure the same as or greater reactance than the phase *3* relay.

DERIVATION OF PARAMETERS AND CONSTANTS

Z_0 can be obtained from the system impedance diagram. R_F can be estimated or can be calculated as explained in a previous paper.[1] C and C_0 can be either 0 or 1 on a radial system but, on the average system with many connections and parallel paths, they usually would be between 0.3 and 0.7. C also can have an angular component, for example, where there is double-end feed with a phase displacement between the generators at the two ends, the angular component of C would be leading on one side of the fault and lagging on the other, the sum of these two angles being equal to the angle between the sources of generation. For example, if there were 25 degrees between the generated electromotive force at *S* and the generated electromotive force at *L*, the angular component of C might be 12 degrees at *A* and 13 degrees at *B*, which can be neglected in most cases. The angular component of C_0 would be negligible, because the only source of zero sequence potential is the fault.

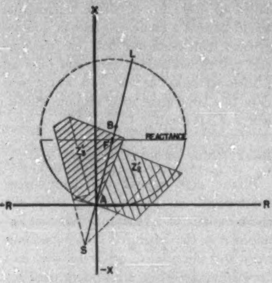

Figure 6(B). Ground relay characteristics on a double-ground fault diagram

$Z_1 = \infty$

In most cases the relays in the other phases will not operate for external faults by a considerable margin, so that the phase angle of C can be ignored. In a borderline case it would be advisable to recalculate, taking into account the angle of C. In the case of the ground relay with single-phase ground faults the value of $C - C_0\, Z_0'/Z_p'$ is usually small so that the impedance seen by the ground relays in the other phases is very large and need not be calculated since the relays will not operate.

SUPERPOSITION OF RELAY CHARACTERISTICS

The purpose of making these impedance charts is, of course, to find out how the relays respond when a fault occurs. This can be done quite accurately by drawing the relay characteristic on the diagram, using the same ohmic scale. Relays that have accurate and consistent characteristics will of course be easier to handle. In other words, if the relay has a perfectly circular characteristic which remains the same over a wide range of current or potential, the behavior of the relay can be ascertained at once by taking a pair of compasses and drawing the circle. If the relay characteristic is not circular, or if it varies, it will be necessary to draw a family of curves.

The relay characteristics shown superimposed on some of the diagrams are those of typical distance relays for long and short lines. The long line relay is a mho relay whose characteristic circle is the small one shown between the origin *A* (relay location) and the fault *F* as explained in previous papers.[1,2] The small characteristic of the mho relay is best for long lines because it is less liable to trip on power swings. It will be shown later that this smallness also is desirable on any line because, the smaller the characteristic, the more effectively the relay is confined to tripping only on faults within the zone, and phase with which it is associated.

The short-line characteristic is that of the reactance relay which was described in a previous paper.[3] The reactance relay is prevented from tripping on faults behind the bus by a directional starting unit which is also a mho unit, so that the tripping area is the area enclosed between the reactance characteristic and the larger mho circle. Earlier reactance relays

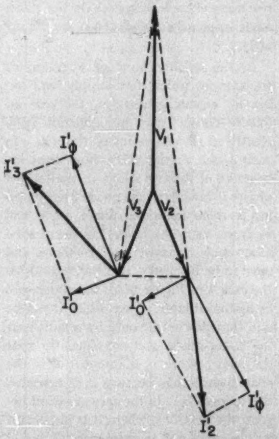

Figure 6(C). Vector diagram of double-ground fault average case

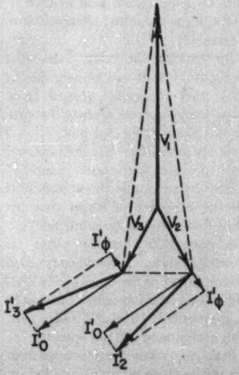

Figure 6(D). Vector diagram of double-ground fault at relay near grounding transformer (whose directional or starting units were polarized by potential from another phase pair) had an angle and diameter depending on the type of fault and the angle of the polarizing potential; for such relays the starting unit circle would have to be drawn in different positions depending on the phases with which the relays were associated.

FAULT AREAS

The arc resistance is a function of the fault current and the conductor spacing.[1] It is shown as a constant value in the diagrams for the sake of simplicity. In practice it will be less at the line terminal which has the heavier short-circuit current.

In Figure 1(B) the point M indicates the impedance measured by the relay in phase pair *3-1* for a phase *2*-phase *3* fault at F, while the point M_A indicates the impedance measured for a fault at A with solid faults in both cases. Similarly N and N_A are corresponding values measured by the phase *1-2* relay. The points F_{31}, A_{31}, F_{12}, and A_{12} are corresponding values for arcing faults.

BEHAVIOR OF PHASE RELAYS

Figure 1(C) shows the characteristics of typical distance relays superimposed on Figure 1(B). The directional starting unit which limits the characteristics of the reactance unit also is a mho unit and it is apparent that neither the reactance relay nor the mho relay can operate for faults in other phase pairs with this particular system arrangement. On the other hand, if the generator S were closer to the relay A, the points M_A and N_A would be closer to A and the phase *3-1* relay might operate. It is quite clear that neither of the relays in the unfaulted phase pairs would overreach.

By drawing the relay characteristics on Figure 3(A) it can be seen, in Figure 3(B), that a nearby ground fault in phase 1 may operate a phase distance relay in phase pairs *1-2* and *3-1*. This gives the advantage that the phase relays may provide high-speed tripping on nearby ground faults which would otherwise be tripped in a longer time by inverse time residual (ground) relays; the disadvantage is that the phase target showing at station A would contradict the ground target at the other end of the line and cause confusion unless this condition is appreciated. The *2-3* relay gets no fault current and will not operate.

Hitherto, when targets appeared on two of the phase relays at one end of the line and only one at the other, it was often assumed that one of the targets had failed to operate. A better explanation might be that a phase-to-phase or double-ground fault occurred and that the correct relays worked at each end plus an additional relay at the end which was close to a large generating station, that is, where AS is small.

BEHAVIOR OF GROUND RELAYS

Figure 2(B) shows the fault areas constructed in Figure 2(A) with the characteristic of a reactance relay superimposed on the diagram. The impedance relay and the mho relay circles were not drawn because they are seldom used for ground faults on account of the probability of appreciable resistance in ground faults. It can be seen that two ground reactance relays may operate on phase-to-phase faults, overreaching in the leading relay and underreaching in the lagging relay. Figures 6(B) and (C) show the same tendency in double-ground faults. It is for this reason that it has been customary to provide a blocking relay with ground distance relays which prevents them from tripping when the fault involves more than one phase. On the other hand, if the blocking relay were arranged to block only the ground relay that overreached, the other relay would operate correctly though it would not reach as far as its ohmic setting would indicate. This would increase the value of ground distance relays since they could back up the phase relays and, in some cases, could be used for all faults, their reach on phase faults being better on lines with a high ratio of X to R because the reactance error decreases as the line phase angle approaches 90 degrees, see Figure 6(A).

In the neighborhood of a grounding transformer which may supply load but has no nearby generation, the zero sequence current may preponderate sufficiently so that C_0 is many times C. In such a case Figure 6(D) shows that the behavior of the two relays in the faulted phases is reversed; the phase *2* relay now has a more favorable phase angle and measures more reactance, but the phase *3* relay may measure less reactance and have to be blocked. This corresponds to the case 4 in Figure 6(A) and which will be discussed later. Meanwhile, it can be said that this is true only for a fault near the transformer, and consequently near the relay, where it is immaterial if the relay overreaches because it is expected to trip anyway. In the case of a fault beyond the next bus, where it is important for the relay not to overreach, C_0 would be less and the phase *3* would be more likely to underreach. In intermediate cases both relays would measure the correct reactance so that it would not matter which was blocked.

The diagram for a single phase-to-ground fault, Figure 4(A), was drawn to a smaller scale because the term $\sqrt{3}Z_0/C'$ is a large quantity. Figure 4(B) shows the characteristic of a reactance relay superimposed on Figure 4(A). The impedance and mho characteristics are not shown because they are seldom used for ground faults on account of their vulnerability to fault resistance which may be high in ground faults. It can be seen that a ground distance relay will not operate for a ground fault on one of the other phases unless the relay is close to the bus of a large station so that Z_N and Z_0 would be small causing the fault area to be closer the relay at A. In other words, there is no chance of overreach on single-phase ground faults in other phases and practically no chance of having more than one target show.

OTHER RELAY CHARACTERISTICS

In the foregoing only distance relays with standard connections have been considered, but it is possible to superimpose the characteristics of any other type of relay. It must be remembered, however, that distance relays polarized by potential other than the one used for the restraint windings have a family of circles for different fault conditions and hence their characteristics are more difficult to show on an impedance diagram. Distance relays using current from only one phase require the calculation of a new table of impedances, since those given in this paper are based on the difference between two phase currents for the phase relays and the difference between the phase and ground currents for the ground relays which are necessary for accurate distance measurement.

The behavior of relays other than distance relays also can be analyzed. For instance, the pick-up of a residual power relay (V_0I_0) can be determined by reading off the values of V_0 and I_0 in Table I. Similarly the operation of a phase selector using $V_0 \times I_n$ or $V\delta \times I_0$ can be determined in its application to single-pole switching under different fault conditions. There also are polyphase directional relays, with and without voltage restraint, whose behavior can be predicted by this method.

Power Swing Charts

On a system where faults are cleared by high-speed (1 cycle) relays and fast circuit breakers (8 cycle or less) the effects of power swings can be considered alone because we can generally assume that the fault will be cleared before the system swings apart appreciably. On the other hand where low-speed (induction disk) relays are used, or a mixture of high-speed and slow relays are used, the swing may be appreciably under way before the fault is cleared and there may be a period where the swing and the fault are present simultaneously.

First the case of the power swing alone will be considered, and then the case of a power swing with a fault. The graphical method employed can be used, not only to check the relay operation in the different phases, but also to determine the maximum load that can be transmitted over a line without causing relay operation. It is also a guide to the selection of suitable types of phase relays.

In analyzing the effects of power swings on relays many of the variables which complicate system stability computations can be neglected, because they have

Table I. Currents and Potentials During Faults

QUANTITY	VALUES OF RELAY QUANTITIES FOR DIFFERENT TYPES OF FAULTS			
	THREE-PHASE	PHASE 2 - PHASE 3	PHASE 1-GROUND	PHASE 2 - PHASE 3-GROUND
KI'_P	C	C	C	$C(Z_N+R_F+Z_0+3R_G)$
KI'_N	0	$-C$	C	$-C(Z_0+\frac{R_F}{2}+3R_G)$
KI'_0	0	0	C_0	$-C_0(Z_N+\frac{R_F}{2})$
KI'_1	C	0	$2C+C_0$	$(C-C_0)(Z_N+\frac{R_F}{2})$
KI'_2	a^2C	$(a^2-a)C$	C_0-C	$C[a^2(Z_N+\frac{R_F}{2})+(a^2-a)(Z_0+\frac{R_F}{2}+3R_G)]-C_0(Z_N+\frac{R_F}{2})$
KI'_3	aC	$(a-a^2)C$	C_0-C	$C[a(Z_N+\frac{R_F}{2})+(a-a^2)(Z_0+\frac{R_F}{2}+3R_G)]-C_0(Z_N+\frac{R_F}{2})$
KV'_P	$CZ'+R_F$	$Z_N+CZ'_P+R_F$	$Z_N+Z_0+CZ'_P+3R_F$	$CZ'_P(Z_N+R_F+Z_0+3R_G)+(Z_N+\frac{R_F}{2})(Z_0+\frac{R_F}{2}+3R_G)+\frac{R_F}{2}(Z_N+Z_0+R_F+3R_G)$
KV'_N	0	$Z_N-CZ'_N$	CZ'_N-Z_N	$(Z_N-CZ'_N)(Z_0+\frac{R_F}{2}+3R_G)$
KV'_0	0	0	$C_0Z'_0-Z_0$	$(Z_N+\frac{R_F}{2})(Z_0-C_0Z'_0)$
KV'_1	CZ'_P+R_F	$2(Z_N+\frac{R_F}{2})$	$2CZ'_P+C_0Z'_0+3R_F$	$(Z_N+\frac{R_F}{2})[CZ'_P-C_0Z'_0+3(Z_0+\frac{R_F}{2}+2R_G)]$
KV'_2	$a(CZ'_P+R_F)$	$(a^2-a)CZ'_P+a^2R_F-Z_N$	$(a^2-a)Z_N-CZ'_P+(a^2-1)Z_0+C_0Z'_0+3a^2R_F$	$CZ'_P[a^2(Z_N+\frac{R_F}{2})+(a^2-a)(Z_0+\frac{R_F}{2}+3R_G)]-C_0Z'_0(Z_N+\frac{R_F}{2})+3R_G(a^2R_F-Z_N)+(a^2-a)\frac{R_F}{2}Z_0+(a^2-1)\frac{R_F}{2}Z_N+3a^2\frac{R_F^2}{4}$
KV'_3	$a^2(CZ'_P+R_F)$	$(a-a^2)CZ'_P+aR_F-Z_N$	$(a-a^2)Z_N-CZ'_P+(a-1)Z_0+C_0Z'_0+3aR_F$	$CZ'_P[a(Z_N+\frac{R_F}{2})+(a-a^2)(Z_0+\frac{R_F}{2}+3R_G)]-C_0Z'_0(Z_N+\frac{R_F}{2})+3R_G(aR_F-Z_N)+(a-a^2)\frac{R_F}{2}Z_0+(a-1)\frac{R_F}{2}Z_N+3a\frac{R_F^2}{4}$
KV'_{12}	$(1-a^2)(CZ'_P+R_F)$	$(a-a^2)CZ'_P+3Z_N+R_F(1-a^2)$	$3CZ'_P-(a^2-a)Z_N-(a^2-1)(Z_0+3R_F)$	$CZ'_P[(1-a^2)(Z_N+\frac{R_F}{2})+(a-a^2)(Z_0+\frac{R_F}{2}+3R_G)]+[3Z_N+(1-a^2)R_F](Z_0+\frac{R_F}{2}+3R_G)+(1-a^2)(Z_N+\frac{R_F}{2})\frac{R_F}{2}$
KV'_{23}	$(a^2-a)(CZ'_P+R_F)$	$2(a^2-a)(CZ'_P+\frac{R_F}{2})$	$(a^2-a)(Z_0+2Z_N+3R_F)$	$(a^2-a)[CZ'_P\{(Z_N+\frac{R_F}{2})+2(Z_0+\frac{R_F}{2}+3R_G)\}+\frac{R_F}{2}(Z_N+2Z_0+\frac{3}{2}R_F+6R_G)]$
KV'_{31}	$(a-1)(CZ'_P+R_F)$	$(a-a^2)CZ'_P-3Z_N+(a-1)R_F$	$-3CZ'_P+(a-a^2)Z_N+(a-1)(Z_0+3R_F)$	$CZ'_P[(a-1)(Z_N+\frac{R_F}{2})+(a-a^2)(Z_0+\frac{R_F}{2}+3R_G)]-[3Z_N+(1-a)R_F](Z_0+\frac{R_F}{2}+3R_G)-(1-a)\frac{R_F}{2}(Z_N+\frac{R_F}{2})\frac{R_F}{2}$
K	$\frac{1}{E}(Z_P+R_F)$	$\frac{1}{E}(Z_P+Z_N+R_F)$	$\frac{1}{E}(Z_P+Z_N+Z_0+3R_F)$	$\frac{1}{E}[Z_PZ_N+Z_NZ_0+Z_0Z_P+\frac{R_F}{2}(Z_P+Z_N+Z_0)+3R_G(Z_P+Z_N+R_F)+\frac{3}{4}R_F^2]$

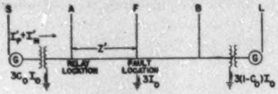

Figure 7. Simplified impedance diagram of a transmission system

negligible effect on the part of the power swing locus in the region of the relay characteristic.

The effect of these variables is to bend the extremities of the power swing locus up or down into a large circle, which goes through or near the electrical center of the system and some point on the X or $-X$ axis, but the portion of the locus which is within the relay tripping characteristic is not changed enough to affect the chance of tripping appreciably. On the other hand, the simplification of the diagram is very much worthwhile.

THE POWER SWING WITHOUT A FAULT

Figure 7 shows the electric circuit representing the system when all the generation beyond the two ends of the protected line are lumped to represent an equivalent machine at each end. Figure 8 shows the generated electromotive forces, E_S and E_L, at the two ends of the system and their difference voltage SL which exists across the system and causes the transfer current I_S to flow through it. This transfer current flows through the whole system so that, by dividing it into the voltages, an impedance diagram results, Figure 9.

The origin of the diagram is drawn at the relay location A so that the impedance will appear as measured from the location A. The relay at A, for instance, would measure an impedance value AB for a fault at B, but, in the case of power swing with angle θ_S between the generated voltages, it would measure the impedance AO. As the swing became more severe and the angle of separation increased to θ_S' the impedance measured by the relay would decrease to the value AQ' which might be within the tripping characteristic of the relay. Similarly, if the origin of the R and X axes had been drawn at B, a line drawn from B to any point would be a vector representing the impedance seen by a relay at B for a condition represented by that point.

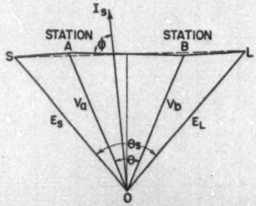

Figure 8. Simplified voltage diagram of a transmission system

Assuming equal generated electromotive forces, the power-swing locus will be the locus of the apexes of a series of isosceles triangles with a common base SL, so that the locus must be a straight line bisecting SL at right angles.

A practical example of the use of this method is to find approximately how far apart the system can swing without causing the relays to trip. Referring to Figure 10, AB is the impedance of the protected section, SA is the system impedance behind terminal A, and BL is the system impedance beyond terminal B. Draw a line perpendicular to SL through its midpoint. From the point O where this line cuts the relay characteristic, draw lines to L, S, A, and B. LOS is the smallest angle θ_S between the generated electromotive forces at L and S at which the relay at terminal A will trip. BOA is the smallest angle θ between the terminal voltages at A and B at which the relay at A will trip, and AO is the impedance it sees.

The power-swing locus shown in Figure 10 is for equal generated electromotive forces and no line capacitance. These assumptions simplify the construction and have negligible effect on the angles θ and θ_S at which the relay operates.

Where only high-speed relays are concerned, the fault will be cleared promptly before a power swing can progress very far but, while the circuit breaker is open, the system may continue to swing apart and may oscillate about a new position when the circuit breaker is reclosed. Consequently the behavior of the relays may be checked first with a fault chart such as described in the section on Fault Charts and then with the power swing diagram.

On the other hand, on systems where both fast and slow relays are used in different line sections, a fault may not be cleared promptly if it occurs in a section having a slow relay. While the slow relay is operating, the high-speed distance relays are subjected to a mixture of fault and swing conditions which are dealt with below.

POWER SWING ON A FAULTED LINE

In the following discussion only a phase-to-phase fault will be considered for the following reasons: in 3-phase faults the flow of power is completely interrupted by the fault and the three relays can see only the fault until it is cleared leaving only the power swing. Double-ground faults with a power swing involve a very complicated calculation and their effect on the ohmic reach of distance relays is sufficiently similar to the effect of a phase-to-phase fault to accept the results of the latter. A single-phase fault was not considered because it is not likely to produce a power swing sufficiently severe to cause relay operation unless the system is loaded close to its steady-state limit of stability.

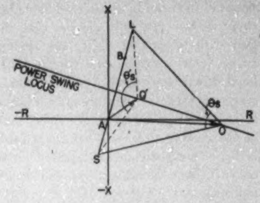

Figure 9. Simplified impedance diagram of a power swing

The effect of a phase *2* to phase *3* fault on Figure 10 is to change the length of the impedance vector SL representing the total system impedance and to shift it in the leading direction in phase *3-1*, and an equal amount in the lagging direction in phase *1-2*. SL is now multiplied by $2/\sqrt{3+(SL/SF)^2}$ and shifted through an angle ϕ_K-30 degrees where $\phi_K=\tan^{-1}SL/\sqrt{3}SF$. Figures 11 and 12 illustrate this change. It should be noted that, in Figure 11, the angle $S'O'L'$ is not the angle θ_S between the generated electromotive forces, but $\theta_s+\phi_K$, so that θ_S is $S'O'L'-\phi_K$. A similar consideration holds for Figure 12 except that $\theta_S=S'O'L'+\phi_K$.

The presence of the fault also tends to bend the power swing locus upwards so

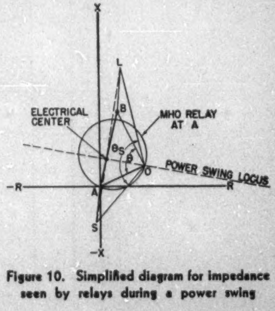

Figure 10. Simplified diagram for impedance seen by relays during a power swing

Table II. Currents and Potentials Supplied to Phase-Distance Relays

QUANTITY	VALUES OF RELAY QUANTITIES FOR DIFFERENT TYPES OF FAULTS			
	3ϕ	ϕ2-ϕ3	ϕ1-GROUND	ϕ2-ϕ3-GROUND
$K(I'_1+\frac{Z'_0-Z'_p}{Z'_p}I'_0)$	C	0	$2CZ'_p+C_0Z'_0$	$(C-C_0\frac{Z'_0}{Z'_p})(Z_N+\frac{R_F}{2})$
$K(I'_2+\frac{Z'_0-Z'_p}{Z'_p}I'_0)$	a^2C	$(a^2-a)C$	$-CZ'_p+C_0Z'_0$	$C[a^2(Z_N+\frac{R_F}{2})+(a^2-a)(Z_0+\frac{R_F}{2}+3R_G)]-C_0\frac{Z'_0}{Z'_p}(Z_N+\frac{R_F}{2})$
$K(I'_3+\frac{Z'_0-Z'_p}{Z'_p}I'_0)$	aC	$(a-a^2)C$	$-CZ'_p+C_0Z'_0$	$C[a(Z_N+\frac{R_F}{2})+(a-a^2)(Z_0+\frac{R_F}{2}+3R_G)]-C\frac{Z'_0}{Z'_p}(Z_N+\frac{R_F}{2})$
KV'_1	CZ'_p+R_F	$2Z_N+R_F$	$2CZ'_p+C_0Z'_0+3R_F$	$(Z_N+\frac{R_F}{2})[CZ'_p-C_0Z'_0+3(Z_0+\frac{R_F}{2}+2R_G)]$
KV'_2	$a(CZ'_p+R_F)$	$(a^2-a)CZ'_p-Z_N+a^2R_F$	$-CZ'_p+(a^2-a)Z_N+(a^2-1)Z_0+C_0Z'_0+3a^2R_F$	$CZ'_p[a^2(Z_N+\frac{R_F}{2})+(a^2-a)(Z_0+\frac{R_F}{2}+3R_G)]-C_0Z'_0(Z_N+\frac{R_F}{2})+3R_G(a^2R_F-Z_N)+(a^2-a)\frac{R_F}{2}Z_0+(a^2-1)\frac{R_F}{2}Z_N+\frac{3a^2}{4}R_F^2$
KV'_3	$a^2(CZ'_p+R_F)$	$(a-a^2)CZ'_p-Z_N+aR_F$	$-CZ'_p+(a-a^2)Z_N+(a-1)Z_0+C_0Z'_0+3aR_F$	$CZ'_p[a(Z_N+\frac{R_F}{2})+(a-a^2)(Z_0+\frac{R_F}{2}+3R_G)]-C_0Z'_0(Z_N+\frac{R_F}{2})+3R_G(aR_F-Z_N)+(a-a^2)\frac{R_F}{2}Z_0+(a-1)\frac{R_F}{2}Z_N+\frac{3a}{4}R_F^2$
K	$\frac{1}{E}(Z_p+R_F)$	$\frac{1}{E}(Z_p+Z_N+R_F)$	$\frac{1}{E}(Z_p+Z_N+Z_0+3R_F)$	$\frac{1}{E}[Z_pZ_N+Z_NZ_0+Z_0Z_p+\frac{R_F}{2}(Z_p+Z_N+Z_0)+3R_G(Z_p+Z_N+R_F)+\frac{3}{4}R_F^2]$
Z'_1	$Z'_p+\frac{R_F}{C}$	∞	$Z'_p+\frac{3R_F}{2C+C_0\frac{Z'_0}{Z'_p}}$	$Z'_p+\frac{3(Z_0+\frac{R_F}{2}+2R_G)}{C-C_0\frac{Z'_0}{Z'_p}}$
Z'_2	$Z'_p+\frac{R_F}{C}$	$Z'_p+\frac{Z_N-a^2R_F}{(a-a^2)C}$	$Z'_p+\frac{(a-a^2)Z_N+(1-a^2)Z_0-3a^2R_F}{C-C_0\frac{Z'_0}{Z'_p}}$	$Z'_p+\frac{3R_G(a^2R_F-Z_N)+(a^2-a)\frac{R_F}{2}Z_0+(a^2-1)\frac{R_F}{2}Z_N+\frac{3}{4}a^2R_F^2}{C[a^2(Z_N+\frac{R_F}{2})+(a^2-a)(Z_0+\frac{R_F}{2}+3R_G)]-C_0\frac{Z'_0}{Z'_p}(Z_N+\frac{R_F}{2})}$
Z'_3	$Z'_p+\frac{R_F}{C}$	$Z'_p+\frac{Z_N-aR_F}{(a^2-a)C}$	$Z'_p+\frac{(a^2-a)Z_N+(1-a)Z_0-3aR_F}{C-C_0\frac{Z'_0}{Z'_p}}$	$Z'_p+\frac{3R_G(aR_F-Z_N)+(a-a^2)\frac{R_F}{2}Z_0+(a-1)\frac{R_F}{2}Z_N+\frac{3}{4}aR_F^2}{C[a(Z_N+\frac{R_F}{2})+(a-a^2)(Z_0+\frac{R_F}{2}+3R_G)]-C_0\frac{Z'_0}{Z'_p}(Z_N+\frac{R_F}{2})}$

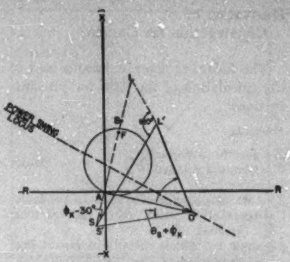

Figure 11. Simplified diagram for impedance seen by phase 1-2 relay during a phase 2-phase 3 fault with a power swing

that it will form a circle above the straight locus representing the power swing without the fault. The error in the impedance measured by the relay caused by assuming the power swing locus still to be a straight line is greater than the error caused by this assumption when no fault is present but, since the error will be substantially tangential to the relay characteristics where they meet the power swing locus earliest, it can again be accepted without much risk of a wrong prediction of relay performance. In borderline cases, or cases where E_S is greater than E_L, the relays can be checked more precisely by using the charts which are provided in Miss Edith Clarke's paper.[4]

The procedure for checking the relays, as before, is merely to draw the impedance characteristics of the relay upon the power swing diagram, using the same ohmic scale, as in Figures 10, 11, and 12. The impedance and reactance relay circles were not shown because such relays are not suitable for heavily loaded lines which are long enough to be liable to trip on power swings.

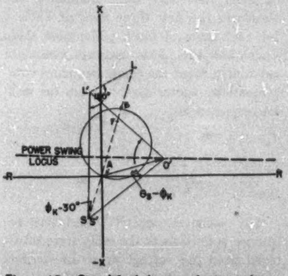

Figure 12. Simplified diagram for impedance seen by phase 3-1 relay during a phase 2-phase 3 fault with a power swing

Derivation of Construction for Charts

The following nomenclature is used in the calculation of the data for the illustrations:

Symbols

E = generated voltage
V = terminal voltage
I = current
Z = total impedance of system to the fault
C = distribution ratio, relay current/total current
ϕ = angle by which current in circuit lags potential
θ_S = angle between generated electromotive forces
θ = angle between two station voltages
a = operator equivalent to $1\underline{|120}$ degrees
j = operator equivalent to $1\overline{|90}$ degrees
R_F = fault resistance
R_G = resistance in ground return
S = leading or sending end of system
L = lagging or receiving end of system
A and B = stations where relays may be located
F = fault location

Other Subscripts

12, 23, 31 = refer to the three pairs of phases
p = positive sequence
n = negative sequence
0 = zero sequence

Primes

A single primed quantity pertains to the section protected by the relay.
Z' = impedance of protected section or as seen by a relay in the protected section
V' = voltage at relay terminal
I' = current measured by the relay

Figure 7 shows the equivalent impedance diagram of a transmission system. Figure 13 shows the positive, negative, and zero sequence impedance networks corresponding to Figure 7 for different types of faults. By a simple mathematical procedure, such as the use of Kirchoff's law, the currents in these networks can be calculated. The relay currents (which flow in the left-hand half of each network) thus calculated are shown in the first three lines of Table I for each type of fault. The next three lines show the phase currents which are calculated from the phase sequence components by vector algebra from the well-known relations

$$I_1 = I_p + I_n + I_0$$

$$I_2 = a^2 I_p + a I_n + I_0$$

$$I_3 = a I_p + a^2 I_m + I_0$$

The positive, negative, and zero sequence potentials at the relay were calculated from the voltage drops in the networks (which are shown in Figures 14, 15, 16, and 17) and the phase potentials were calculated from the phase sequence

Table III. Currents and Potentials Supplied to Ground-Distance Relays

QUANTITY	VALUES OF RELAY QUANTITIES FOR DIFFRENT TYPES OF FAULTS			
	3 ϕ	ϕ2-ϕ3	ϕ1-GROUND	ϕ2-ϕ3-GROUND
$K(I_1-I_2)$	$C(1-a^2)$	$C(a-a^2)$	$3C$	$C[(1-a^2)(Z_N+\frac{R_F}{2})+(a-a^2)(Z_0+\frac{R_F}{2}+3R_G)]$
$K(I_2-I_3)$	$C(a^2-a)$	$2C(a^2-a)$	0	$C[(a^2-a)\{Z_N+\frac{3R_F}{2}+2(Z_0+3R_G)\}]$
$K(I_3-I_1)$	$C(a-1)$	$C(a-a^2)$	$-3C$	$C[(a-1)(Z_N+\frac{R_F}{2})+(a-a^2)(Z_0+\frac{R_F}{2}+3R_G)]$
KV_{12}	$(1-a^2)(CZ'_p+R_F)$	$(a-a^2)CZ'_p+3Z_N+(1-a^2)R_F$	$3CZ'_p-(a^2-a)Z_N-(a^2-1)(Z_0+3R_F)$	$CZ'_p[(1-a^2)(Z_N+\frac{R_F}{2})+(a-a^2)(Z_0+\frac{R_F}{2}+3R_G)]-(1-a^2)(Z_N+\frac{R_F}{2})\frac{R_F}{2}+[3Z_N+(1-a^2)R_F](Z_0+\frac{R_F}{2}+3R_G)$
KV_{23}	$(a^2-a)(CZ'_p+R_F)$	$2(a^2-a)(CZ'_p+\frac{R_F}{2})$	$(a^2-a)(Z_0+2Z_N)+3(a^2-a)R_F$	$(a^2-a)(CZ'_p+\frac{R_F}{2}\{(Z_N+\frac{R_F}{2})+2(Z_0+\frac{R_F}{2}+3R_G)\}$
KV_{31}	$(a-1)(CZ'_p+R_F)$	$(a^2-a)CZ'_p-3Z_N+(a-1)R_F$	$-3CZ'_p+(a-a^2)Z_N+(a-1)(Z_0+3R_F)$	$CZ'_p[(a-1)(Z_N+\frac{R_F}{2})+(a-a^2)(Z_0+\frac{R_F}{2}+3R_G)]-(1-a)\quad(Z_N+\frac{R_F}{2})\frac{R_F}{2}-[3Z_N+(1-a)R_F](Z_0+\frac{R_F}{2}+3R_G)$
K	$\frac{1}{E}(Z_p+R_F)$	$\frac{1}{E}(Z_p+Z_N+R_F)$	$\frac{1}{E}(Z_p+Z_N+Z_0+3R_F)$	$\frac{1}{E}(Z_pZ_N+Z_NZ_0+Z_0Z_p+\frac{R_F}{2}(Z_p+Z_N+Z_0)+3R_G(Z_p+Z_N+R_F)+\frac{3}{4}R_F^2$
Z_{12}	$Z'_p+\frac{R_F}{C}$	$Z'_p+\frac{(a^2-a)}{C}Z_N-\frac{a}{C}R_F$	$Z'_p+\frac{(a-a^2)Z_N+(1-a^2)(Z_0+3R_F)}{3C}$	$Z'_p+\frac{[3Z_N+(1-a^2)R_F](Z_0+\frac{R_F}{2}+3R_G)+(1-a^2)(Z_N+\frac{R_F}{2})\frac{R_F}{2}}{C[(a-a^2)(Z_0+\frac{R_F}{2}+3R_G)+(1-a^2)(Z_N+\frac{R_F}{2})]}$
Z_{23}	$Z'_p+\frac{R_F}{C}$	$Z'_p+\frac{R_F}{2C}$	∞	$Z'_p+\frac{R_F}{2C}$
Z_{31}	$Z'_p+\frac{R_F}{C}$	$Z'_p+\frac{(a-a^2)}{C}Z_N-\frac{a^2}{C}R_F$	$Z'_p-\frac{(a-a^2)Z_N+(a-1)(Z_0+3R_F)}{3C}$	$Z'_p-\frac{[3Z_N+(1-a)R_F](Z_0+\frac{R_F}{2}+3R_G)+(1-a)(Z_N+\frac{R_F}{2})\frac{R_F}{2}}{C[(a^2-a)(Z_0+\frac{R_F}{2}+3R_G)+(1-a)(Z_N+\frac{R_F}{2})]}$

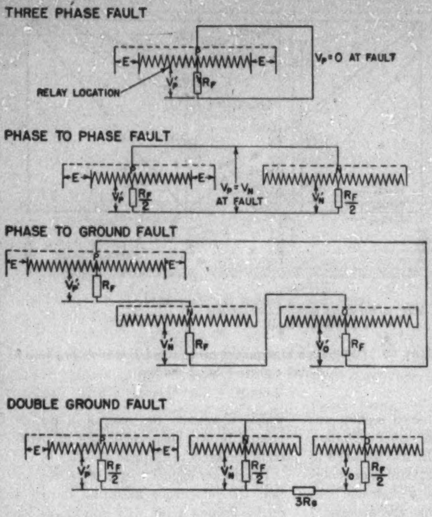

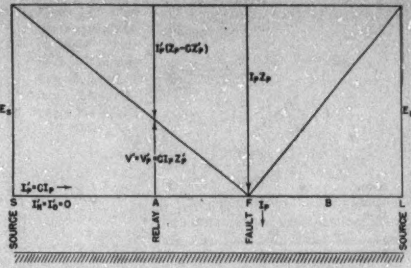

Figure 13 (left). Sequence networks on a transmission system

Figure 14 (above). Distribution of phase sequence currents and potentials (during a balanced 3-phase fault)

potentials by equations corresponding to the above. The phase potentials were then combined to give the line-to-line potentials in the last three lines of Table I. All these quantities have the same denominator for a given type of fault so, in order to simplify the tables, all quantities are multiplied by the denominator, *K*, for the particular fault.

In Table II these quantities were combined in the manner in which they are supplied to phase distance relays, and the impedances measured by the relays were calculated. Z_{12}', Z_{23}', and Z_{31}' are the impedances measured by the phase relays and Z_1', Z_2', and Z_3' are the impedances measured by the ground relays. Phase relays receive delta currents and potentials so that

$$Z_{12}' = \frac{V_{12}'}{I_1' - I_2'};\; Z_{23}' = \frac{V_{23}'}{I_2' - I_3'} \text{ and } Z_{31}' = \frac{V_{31}'}{I_3' - I_1'}$$

where the primed values refer to the protected section. Ground distance relays receive Y-potentials and a combination of phase and residual current (I_{res}), so that

$$Z_1' = \frac{V_1'}{I_1' + \dfrac{Z_0' - Z_n'}{3Z_p'} I_{res}'} = \frac{V_1'}{I_1' + \dfrac{Z_0' - Z_p'}{Z_p'} I_0'}$$

Similar expressions for Z_2' and Z_3' are shown in Table III.

The impedances measured by the relays are thus expressed in terms of the total system impedances Z_p, Z_n, and Z_0 and the arc resistance R_F. In the double-ground faults the term R_G is used to denote the resistance of the ground return path.

In Tables I, II, and III, the operator "a" was used for convenience in calculation. In constructing vector diagrams, however, it is easier to use a single operator having amplitude and angle such as $\sqrt{3}\,\overline{|90^\circ}$ rather than the corresponding function $(a^2 - a)$.

Inspection of Tables II and III will show that all the relays measure the true impedance Z_p' plus some additional terms. Table IV lists the additional impedance. The final step is to convert this information to something that can be drawn quickly.

Let us consider the first line of Table IV. The additional impedance for the *1-2* phase relay for a phase *2*-phase *3* fault is $(\sqrt{3}/C)\ Z_n\overline{|90^\circ} + (R_F/C)\overline{|60^\circ}$. Now Z_p can be substituted for Z_n without appreciable error and Z_p/C is the line impedance *SF* because $C = I_p'/I_p = Z_p/Z_F$ where Z_F is the positive sequence impedance on the relay side of the fault.

This means that $(\sqrt{3}/C)\ Z_n\overline{|90^\circ}$ can be simplified to $\sqrt{3}\ SF\overline{|90^\circ}$ which is the line *FN* on Figure 1(B). Or, as will be seen by the application of trigonometry, it is only necessary to draw a line at 60 degrees lagging *SF* to intersect a perpendicular from *F* and thus to find the point *N* which gives the impedance Z_{12}' seen by the *1-2* relay, excluding arc resistance. Arc resistance can then be added, if necessary, as described previously.

In two of the other cases in Table IV the first expression is $Z_n\overline{|90^\circ}/C\sqrt{3}$. Similarly, it can be shown that this vector can be conveniently constructed by drawing a line at 30 degrees to *SF* to intersect the perpendicular from *F* and thus to locate the points *M* and *N*.

In the expression for the impedance seen by ground relays during a single-phase-to-ground fault the denominator is not *C* but *C'* which is $C - C_0Z'/_0Z_p'$.

This means that the expression $(\sqrt{3}/C')\ Z_n\overline{|90^\circ}$ has to be drawn without recourse

Table IV. Impedance Measured by Relays in Addition to True Impedance

Relay	Three Phase	Phase *2*-Phase *3*	Phase *1*-Ground
Z_{12}'	$\frac{R_F}{C}$	$\frac{1}{C}\left(\sqrt{3}Z_n\overline{\vert 90^\circ}{}^* + R_F\overline{\vert 60^\circ}\right)$	$\frac{1}{C\sqrt{3}}\left(Z_n\underline{\vert 90^\circ} + Z_0\underline{\vert 30^\circ} + 3R_F\underline{\vert 30^\circ}\right)$
Z_{23}'	$\frac{R_F}{C}$	$\frac{R_F}{2C}$	∞
Z_{31}'	$\frac{R_F}{C}$	$\frac{1}{C}\left(\sqrt{3}Z_n\underline{\vert 90^\circ} + R_F\underline{\vert 60^\circ}\right)$	$\frac{1}{C\sqrt{3}}\left(Z_n\overline{\vert 90^\circ} + Z_0\overline{\vert 30^\circ} + 3R_F\overline{\vert 30^\circ}\right)$
Z_1'	$\frac{R_F}{C}$	∞	$\frac{3}{2C'}R_F$
Z_2'	$\frac{R_F}{C}$	$\frac{1}{\sqrt{3}C}\left(Z_n\overline{\vert 90^\circ} + R_F\overline{\vert 30^\circ}\right)$	$\frac{\sqrt{3}}{C'}\left(Z_n\underline{\vert 90^\circ} + Z_0\underline{\vert 30^\circ} + \sqrt{3}R_F\underline{\vert 60^\circ}\right)$
Z_3'	$\frac{R_F}{C}$	$\frac{1}{\sqrt{3}}\left(Z_n\underline{\vert 90^\circ} + R_F\underline{\vert 30^\circ}\right)$	$\frac{\sqrt{3}}{C'}\left(Z_n\overline{\vert 90^\circ} + Z'\overline{\vert 30^\circ} + \sqrt{3}R_F\overline{\vert 60^\circ}\right)$

* $\overline{|90^\circ}$ means lagged in phase by 90 degrees, and similarly $\underline{|90^\circ}$ means advanced in phase by 90°.

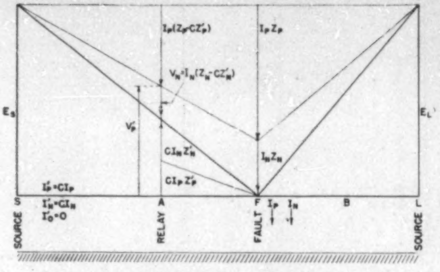

$V_{23}'=\sqrt{3}(V_P-V_N)$ AND IS ZERO AT THE FAULT

Figure 15. Distribution of phase sequence currents in potentials in phase 1 during a phase 2–phase 3 fault

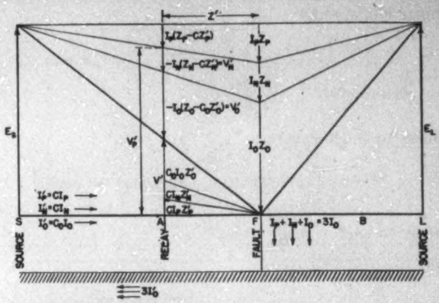

NOTE: V_N' AND V_0' ARE NEGATIVE (SEE ARROWS)
$V'=CI_PZ_P'+CI_NZ_N'+C_0I_0Z_0'$

Figure 16. Distribution of sequence currents and potentials in phase 1 during a phase-1 to ground fault

to the 60-degree projection line, which takes a little longer than the previous cases. Similar expressions for Z_0 and R_F also have to be worked out. Fortunately, this diagram is seldom constructed because the relays in the unfaulted phases measure such a high impedance that there is practically no chance of their operating.

PHASE RELAYS WITH DOUBLE-GROUND FAULTS

In the section on Fault Charts it was stated that the relays in one of the unfaulted phase pairs measured the correct reactance, or more, and that the other relay measured the correct reactance or less. This can be verified by working out a few cases, first of all limiting cases, such as for zero arc resistance, then a typical case with average values. For instance for a solid fault R_F and R_G will be zero and the expression for Z_{12}' in Table II will give

$$Z_{12}'=Z_p'+\frac{\sqrt{3}Z_nZ_0}{CZ_0\,\underline{|90°}+CZ_n\,\underline{|30°}}$$

Since Z_0 is usually several times Z_n, the term $Z_0\,\underline{|90°}$ will be the dominant figure in the denominator and the expression will approximate roughly to $Z_p'+\sqrt{3}Z_n\,\underline{|90°}$ which is similar to the expression for the phase 2-phase 3 fault. If R_G is infinite there will be no path through the ground and the expression will be exactly the same as for the phase 2-phase 3 fault.

A typical case was worked out using the following system parameters. The total system impedance, when simplified to a single impedance between two generating sources, was taken as 10 ohms secondary, at an angle of 70 degrees lag and the zero sequence impedance was taken as three times the positive. The impedance of the protected section was assumed to be $0.75+j2$ ohms secondary and the arc resistance R_F was assumed to be 1/2 ohm, which is 1/2 ohm in each network; C and C_0 were both made one half. Inserting these values in the expression for Z_{12}' under the column phase 2-phase 3-ground in Table II we get $Z_{12}'=Z_p'+6.7-j1.63$. Similarly for Z_{31}' we get $Z_p'-4.56+j4.38$. These values are plotted in Figure 5 and can be seen to lie close to the points corresponding to the phase 2-phase 3 fault, Figure 1(B).

GROUND RELAYS WITH A DOUBLE-GROUND FAULT

In the case of ground relays, the impedance measured is again too complex to show graphically, but an approximation can be made by considering the limiting cases. One extreme case is when the impedance of the ground circuit is infinite, so that the diagram is the same as for a phase-to-phase fault, Figure 2(B). When the arc resistance and ground resistance are zero, that is, R_F and R_G are made zero in the expressions for Z_2' and Z_3', it will be seen that the relays in phases 2 and 3 will both measure correctly for a 2-3, ground fault. Another limiting case is when Z_0 is assumed equal to Z_p and $R_G=0$, which represents the case of a perfect ground return; here again the measurement is correct in all three phases.

It appears logical therefore to assume that the impedance measured during a double-ground fault with conditions intermediate between these extreme cases would be on some locus between Figure 2(B) and the correct measurement. In order to verify this assumption, the expressions for the impedance measured by the relays were worked out for a number of typical cases, using the same system parameters as for the preceding discussion on the phase relays but varying C and C_0.

The values shown in Table V are to be multiplied by $1/D$ where D is the ohmic distance of the fault from the receiving end, L, expressed as a fraction of the total distance SL. Figure 6(A) shows the case where the fault is in the middle of the system ($D=0.5$). The points are lettered according to the cases in Table V. Figure 6(B) ignores case ψ, because it represents a special case, and shows the general areas of tripping for the phase-2 and phase-3 relays. Phase-1 relay gets negligible current and does not operate. The table shows that, for a fault between phases 2 and 3 and ground, the phase-2

Table V. Additional Impedance Measured by Ground-Distance Relays During Double-Ground Faults

Case	C	C_0	R_G	Z_2'	Z_3'	Comment
α	1	0	∞	$1.4-j\,1.01$	$-0.91+j\,1.01$	Phase-to-phase fault
β	1	0	$^1/_2$	$0.3-j\,0.27$	$0.24+j\,0.27$	Ungrounded generation behind relay
γ	1	1	$^1/_2$	$0.32-j\,0.11$	$0.31+j\,0.12$	Stub end feed
δ	$^1/_2$	1	$^1/_2$	$0.54-j\,0.04$	$0.54+j\,0.04$	Common case
λ	0.43	1	$^1/_2$	$0.58+j\,0$	$0.58-j\,0$	Both relays measure same reactance
ψ	0	1	$^1/_2$	$0.68+j\,0.53$	$0.58-j\,0.54$	Grounding transformer but no generation behind relay

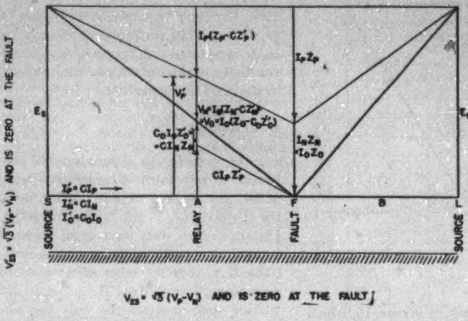

Figure 17. Distribution of phase sequence currents and potentials in phase 1 for a phase 2-phase 3 to ground fault

and phase-*3* relays would measure the correct impedance plus an additional impedance of the form $R-jX$. Ground-distance relays are usually of the reactance type so that they would ignore the additional resistance; the additional reactance is about the same for the two relays except that, if $C>0.43C_0$, it is positive for phase *3* and negative for phase *2*. If $C<0.43C_0$ the signs are reversed as in case ψ. It is seldom that $C<0.43C_0$ for a fault just beyond the end of the protected section where overreaching would be undesirable but, if such a case were encountered, it would be necessary to block phase *3* instead of phase *2* on a *2-3* ground fault.

This means that the reactance ground relay in phase *2* will overreach and the relay in phase *3* will underreach on double-ground faults in most cases, the additional impedance being zero if $C=0.43C_0$. It is the present practice with ground distance relays to block them on double-ground faults, but the foregoing reasoning shows that in most locations (where $C>0.43C_0$) the relay in the lagging one of the two faulted phases could be permitted to operate on all faults and hence greatly extend their usefulness.

POWER SWINGS

The construction of the power swing without a fault requires no further elucidation than has been given under Power Swing Charts. However, it must be repeated here that this construction is based on equal generated voltages at each end of the system and with no shunt loads or capacitances. These assumptions are permissible because the change in the power swing locus caused by allowing for shunt impedance and unequal voltages is substantially tangential to the relay characteristics where they intersect the power swing locus, so that it will have negligible effect on the behavior of the relays. More rigorous analyses have been given in previous papers.[4,5]

POWER SWING ON A FAULTED LINE

It can be shown that, during a power swing on a transmission line with two conductors short circuited together, as in Figure 18, the resultant current from faulted pair of conductors has only the fault current, and no swing component, and that the remaining pairs of conductors have a combination of the swing current and the fault current.

The following table is based on these premises and gives the swing and fault components of the current in the conductors at the end *S* and at the relay location *A*. Figure 18 shows the equivalent diagram of the system, and explains the terms Z_S, Z_r, and Z_F.

Current	Swing Component	Fault Component
I_1'........	$\frac{E_S-E_L}{Z_S}$........	0
I_2'........	$-\frac{E_S-E_L}{2Z_S}$........	$\frac{(a^2-a)E_S}{2Z_F}$
I_3'........	$-\frac{E_S-E_L}{2Z_S}$........	$-\frac{(a^2-a)E_S}{2Z_F}$

Distance relays are usually provided either with delta current or with double windings, so that the magnetic effect is the same as with delta current. The following are the currents supplied to the relays:

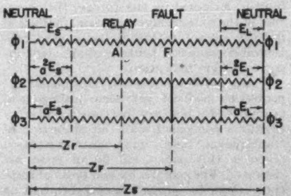

Figure 18. Simplified circuit of a transmission line with a line-to-line fault

$$I_1'-I_2'=\frac{3}{2}\cdot\frac{E_S-E_L}{Z_S}-\frac{(a^2-a)E_S}{2Z_F}$$

$$I_2'-I_3'=0+(a^2-a)\frac{E_S}{Z_F}$$

$$I_3'-I_1'=-\frac{3}{2}\cdot\frac{E_S-E_L}{Z_S}-\frac{(a^2-a)E_S}{2Z_F}$$

The potentials at the relay location can be derived in the usual manner subtracting the line drop from the generated electromotive forces

$$V_1'=E_S-I_1'Z_r=E_S-\frac{E_S-E_L}{Z_S}\cdot Z_r$$

$$\begin{aligned}V_2'&=a^2E_S-I'_2Z_r\\&=a^2E_S+\left(\frac{E_S-E_L}{Z_S}-\frac{(a^2-a)E_S}{Z_F}\right)\frac{Z_r}{2}\end{aligned}$$

$$\begin{aligned}V_3'&=aE_S-I_3'Z_r\\&=aE_S+\left(\frac{E_S-E_L}{Z_S}+\frac{(a^2-a)E_S}{Z_F}\right)\frac{Z_r}{2}\end{aligned}$$

The delta potentials can be derived from the Y-potentials as follows

$$V_{12}'=(1-a^2)E_S-3\left(\frac{E_S-E_L}{Z_S}-(a^2-a)\frac{E_S}{Z_F}\right)\frac{Z_r}{2}$$

$$V_{23}'=(a^2-a)E_S\frac{1-Z_r}{Z_F}$$

$$V_{31}'=(a-1)E_S+3\left(\frac{E_S-E_L}{Z_S}+(a^2-a)\frac{E_S}{Z_F}\right)\frac{Z_r}{2}$$

From the foregoing delta currents and potentials the impedance seen by the relays can be derived as follows. With a phase *2*- phase *3* fault the phase *12* relay measures $Z_{12}'=V_{12}'/(I_1'-I_2')$.

Hence

$$\begin{aligned}Z_{12}'&=\frac{(1-a^2)E_S-3\left(\frac{E_S-E_L}{Z_S}-(a^2-a)\frac{E_S}{Z_F}\right)\frac{Z_r}{2}}{\frac{3}{2}\cdot\frac{E_S-E_L}{Z_S}-\frac{a^2-a}{2}\cdot\frac{E_S}{Z_F}}\\&=\frac{2(1-a^2)E_S}{3\frac{E_S-E_L}{Z_S}-(a^2-a)\frac{E_S}{Z_F}}-Z_r\underline{/\phi}\\&=\frac{Z_S\left(1+\frac{j}{\sqrt{3}}\right)}{1+\frac{j}{\sqrt{3}}\cdot\frac{Z_S}{Z_F}-\frac{E_L}{E_S}}-Z_r\underline{/\phi_r}\end{aligned}$$

If

$$K=1+\frac{j}{\sqrt{3}}\cdot\frac{Z_S}{Z_F}$$

θ_S is the angle by which E_L lags E_S, ϕ_r is the phase angle of Z_r, ϕ_K is the phase angle of K, and R_V is the ratio E_L/E_S, then

$$Z_{12}'=\frac{2Z_S\underline{/\phi s+30^\circ}}{\sqrt{3}(K\underline{/\phi_K}-R_V\underline{/\theta_S})}-Z_r\underline{/\phi_r}$$

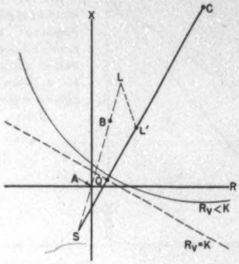

Figure 19. Locus of impedance seen by phase 1-2 relay during a line 2-line 3 fault with a power swing

The locus of Z_{12}' is a circle of radius

$$\frac{2R_VZ_S}{\sqrt{3}(K^2-R_V^2)}$$

and center

$$\frac{2KZ_S\underline{/\phi_S+30^\circ-\phi_K}}{\sqrt{3}(K^2-R_V^2)}-Z_r\underline{/\phi_r}$$

Similarly

$$Z_{31}'=\frac{2Z_S\underline{/\phi_S-30^\circ}}{\sqrt{3}(K\underline{/-\phi_K}-R_V\underline{/-\theta_S}}-Z_r\underline{/\phi_r}$$

where

$$K=1-\frac{j}{\sqrt{3}}\cdot\frac{Z_S}{Z_r}$$

whose magnitude is the same as before but with a negative phase angle. The locus of Z_{31}' is a circle of radius

$$\frac{2R_VZ_S}{\sqrt{3}(K^2-R_V^2)}$$

and center

$$\frac{2KZ_S\underline{/\phi_S-30^\circ-\phi_K}}{\sqrt{3}(K^2-R_V^2)}-Z_r\underline{/\phi_r}$$

which is a circle of the same radius as the Z_{12}' circle and displaced the same distance on the other side of the line impedance vector.

In the section on Power Swing Charts it was stated that, within the bounds of reasonable accuracy, the locus of the Z_{12}' and Z_{31}' impedances (Figures 11 and 12) could be drawn as a line bisecting at right angles the line SR' which was related to the total system impedance SR. This assumption is based on the following reasoning: referring to Figure 19, which corresponds to Figure 11

$$SQ=SC-CQ$$

$$=\frac{2Z_S(K-R_V)}{\sqrt{3}(K^2-R_V^2)}$$

$$\frac{2Z_S}{\sqrt{3}(K+R_V)}$$

If $K=R_V$, then $SQ=1/2SR'$, that is, Q bisects SR', hence $1/2\,SR'$, $=Z_S/\sqrt{3}\,K$. Now SC and the radius CQ tend to be infinite since they have $(K^2-R_V^2)$ in their denominators so that the locus will tend to be a straight line through Q which bisects SR'.

In practice $K>1$ and, on a line long enough to have power swing trouble, R_V would be equal to or slightly greater than unity, so that R_V would tend to be equal to K.

If $R_V<K$ the locus would be a circle with the center beyond C, but line capacitance would tend to curve it down towards the straight line. Hence in general the assumption of a straight locus is a reasonable one for a line long enough to warrant a check of this kind. As stated before, the error involved is negligible in predicting relay performance because the circle is so large that its periphery is substantially straight within the confines of the relay characteristic.

Conclusions

It is possible to determine the behavior of any form of protective relay under any system conditions by using the methods explained in the foregoing. Distance relays were used as an example because they combine the operating functions of most of the other relays and are more complicated than the others. By making such analyses not only can abnormal operations of distance relays be explained but applications of new relays can be made with greater confidence.

Superposition of the characteristics of the present standard types of distance relays upon these fault charts indicates that they are relatively free from incorrect operation if no power swing is present. It also has been shown that ground distance relays can be made more useful if properly connected.

References

1. APPLICATION OF THE OHM AND MHO PRINCIPLES TO DISTANCE RELAYS, **A. R. van C. Warrington.** *Electrical Engineering* (*AIEE Transactions*), volume 65, June 1946, pages 378–86.

2. THE MHO DISTANCE RELAY, **R. M. Hutchinson.** *Electrical Engineering* (*AIEE Transactions*), volume 65, June 1946, pages 353–60.

3. A NEW REACTANCE RELAY, **J. R. McGlynn, C. G. Dewey.** *Electrical Engineering*, volume 67, May 1948, page 445.

4. IMPEDANCES SEEN BY RELAYS IN THREE-PHASE SYSTEMS WITH AND WITHOUT FAULTS, **Edith Clarke.** *AIEE Transactions*, volume 64, 1945, pages 372–84.

5. PERFORMANCE REQUIREMENTS FOR RELAYS ON UNUSUALLY LONG TRANSMISSION LINES, **F. C. Poage, C. A. Streifus, D. M. MacGregor, E. E. George.** *Electrical Engineering* (*AIEE Transactions*), volume 62, June 1943, pages 275–83.

Discussion

H. P. Dupuis (The Commonwealth and Southern Corporation, Jackson, Mich.): The author is to be complimented on his very complete and concise presentation of this paper.

The graphical method for determining the settings of step-type relays has been in use for a number of years and has been of much assistance to relay engineers. The procedure given by Mr. Warrington in this paper should further assist in making more accurate settings and in checking probable causes of incorrect operation and therefore is a useful contribution to the art of relaying.

Phase relay characteristics for line-to-line faults shown in Figure 1(C) are of special interest in analyzing the operation of certain impedance relays having greater reach along the resistance axis. For nearby faults, two or even three targets may show where only one would be expected. Also of considerable interest is Figure 3(B) showing the characteristics of phase relays on line-to-ground faults. As noted by the author, the operation of the phase relays on ground faults is of definite advantage but it has caused considerable confusion because of apparent incorrect target indication.

The use of distance relays for ground fault protection has not yet come into general practice but it is a very live issue for all relay engineers concerned with the protection of transmission lines, and the information given in this paper will be of great assistance. The complexity and costs of step-type relays for ground fault protection as compared with a simple induction-type relay, will deter their general adoption, especially since fast clearing of ground faults is not generally considered as necessary as the fast clearing of phase faults. In addition to faster clearing of ground faults, the advantage of step-type ground relays is the same as for phase relays in that they are almost immune to system changes.

Richard W. World (United States Bureau of Reclamation, Denver Federal Center, Denver, Colo.): One fault condition not covered by the author, which I believe is of interest, is a line-to-line fault on the opposite side of a Y-delta or delta-Y-connected transformer bank. A practical case is that of a substation without high-voltage circuit breakers, since from a recent AIEE committee report[1] it appears that the practice is not uncommon of relying on remote line relays for transformer protection.

Figure 1 of the discussion is a curve which we have developed from mathematical analysis, showing the shorter distance relay reach for low-voltage line-to-line faults as compared with 3-phase faults. It appears that a graphical method for this fault condition would be the same as for a line-to-ground fault on the high-voltage side, except that the impedance would have no zero-sequence component. In Figure 3(A) of the paper if *AF* were the impedance seen for a low-voltage 3-phase fault, then *AM, AN,* and an infinite impedance would be seen by the 3-phase distance relays for a line-to-line fault at the same location. Is this correct? It would be interesting to know the reach of ground distance relays for this low-voltage fault, which has no effect on the usual residual current ground relay.

REFERENCE

1. PROTECTION WITHOUT HIGH-VOLTAGE SWITCHING, AIEE Committee Report. *Electrical Engineering*, June 1949, page 520, and *AIEE Transactions*, part I, volume 68, 1949, pages 226–32.

A. R. van C. Warrington: With the method described in the paper it is possible to determine accurately just what a phase or ground distance relay will do under any fault or power swing condition. With this knowledge relays can be selected with assurance that they will operate correctly, and an analysis can be made quickly to determine the cause of misoperation of relays in use.

Mr. Dupuis calls attention to two cases where relays have not necessarily tripped wrongly but provided misleading information through their targets. By comparing the targets shown at both ends of the protected section, the true story can be found. For instance, in the first case cited by Mr. Dupuis, in Figure 1(C), if the impedance *SA* were slightly smaller, the tripping areas would intersect the circle causing three impedance relay targets, which would indicate a 3-phase fault, whereas at the other end of the section only one impedance relay target would show, indicating a phase-to-phase fault.

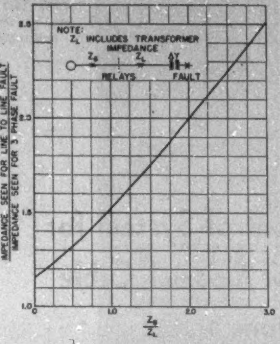

Figure 1. Reduction in relay reach for line-to-line faults on far side of delta-Y transformer bank

Reference to a diagram similar to Figure 1(C) would explain the true nature of the fault and would indicate the targets. In the past such an occurrence would have been construed as erratic operation of the targets.

The second case cited by Mr. Dupuis also shows how this method of analysis can be used to unravel target indications. Figure 3(B) shows that two phase relays may operate for a nearby ground fault while, at the other end of the line section, a ground relay and none of the phase relays will show targets. Again these indications may be misunderstood unless both ends are considered with reference to these diagrams.

I agree with Mr. Dupuis that ground distance relays are now a live issue as they are being used in increasing numbers.

Mr. World called attention to the fact that the paper does not cover the case of a fault on the opposite side of a Y-delta or delta-Y transformer. His analysis is correct for a 3-phase fault and his diagram is essentially correct for a system of homogeneous impedance.

There are obviously other conditions which could have been discussed but which could not be covered within the scope of a single Institute paper. However, these and other aspects of this subject should be covered, and it is to be hoped that other AIEE papers will be written on them using, if possible, a simple graphical method similar to that used in this paper.

B-1 Alarm and Control System for Remote Control of Coaxial Cable Stations

R. B. HEARN
MEMBER AIEE

LAURANCE A. WEBER
ASSOCIATE AIEE

THE *B-1* alarm and control system is an arrangement for providing remote control of stations on type *L* carrier telephone systems[1] over coaxial cables. There are two types of repeater stations: auxiliary stations which are spaced every 5-to-8 miles along the coaxial cable; and main stations which are spaced at intervals of 40-to-165 miles along the cable. Main stations perform many important functions such as supplying power to the auxiliary stations, receiving alarms from the auxiliary stations, providing line equalization, and cable switching. The alarm and control equipment is located in the main stations and permits remote control and supervision of many stations from one central control point. A typical coaxial maintenance and control section is shown in Figure 1(A).

Main stations are divided into groups, each group having one attended main station and one to ten unattended main stations. The attended main station exercises maintenance control over the unattended main stations in a group. Alarm registration devices, equipment for controlling the unattended stations, and equipment for indicating the conditions at any unattended station are installed in the attended station. Equipment for sending alarms, executing orders, and sending indicator signals are located in unattended stations.

Signals for the alarm and control circuits are transmitted between attended and unattended stations over channels obtained by compositing a 4-wire telephone order wire circuit which is provided for *L* system maintenance.

Figures 1(B) and 1(C) show the equipment of the *B-1* alarm and control system. Figure 1(B) shows the equipment used at the unattended station. The left-hand bay contains the relay equipment exclusive of that used to transmit signals. The right-hand bay contains the signaling equipment. Figure 1(C) shows the equipment at the attended station. In addition to the equipment shown in Figure 1(C), an additional bay similar to the signaling bay at the unattended station is provided.

Functions of System

The *B-1* alarm and control system has three distinct functions.

1. Alarm conditions at any unattended station are transmitted automatically to the controlling attended station indicating which station is in trouble and whether the alarm is of major or minor importance. The indication is on lamps and is accompanied by an audible alarm. This function is performed by the alarm circuit.

2. Orders or remote controls are transmitted to any unattended station by dial codes. Codes are available for 100 orders for each station. This function is performed by the director circuit.

3. One of the available orders causes equipment at an unattended station to send indicator signals back to the attended station. It is possible to indicate the condition of 168 circuits on a bank of neon indicator lamps in the main station. This function is performed by the indication circuit.

Composited Signaling Circuit

The signaling circuits are terminated at each end of the line section between two main stations by composited signaling terminals. A ground terminal is furnished at the end of each line section at or nearer to the attended station and a battery terminal is furnished at the other end. Three operating channels and a neutralizing channel are provided on a 4-conductor line. A typical layout is shown in Figure 2.

The first channel, shown in Figure 3, is a differential-duplex circuit used for transmitting alarms from all unattended stations to the main station. When an alarm condition occurs at any unattended station, the sending potential at that station is changed from battery to ground. This condition is repeated in each line section between the originating station and the attended station. When

---

Paper 49-155, recommended by the AIEE Communication Committee and approved by the AIEE Technical Program Committee for presentation at the AIEE Summer General Meeting, Swampscott, Mass., June 20–24, 1949. Manuscript submitted March 21, 1949; made available for printing April 28, 1949.

R. B. Hearn and Laurance A. Weber are both with the Bell Telephone Laboratories, Inc., New York, N. Y.

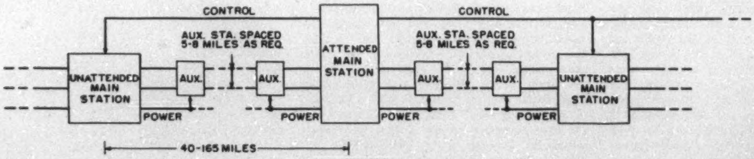

Figure 1(A). Typical cable maintenance section

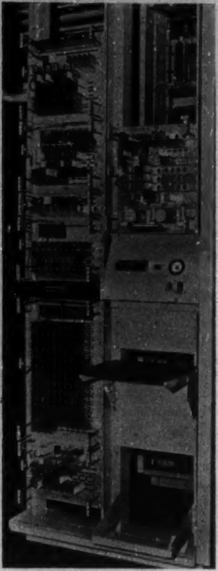

Figure 1(B) (left). Equipment at unattended station

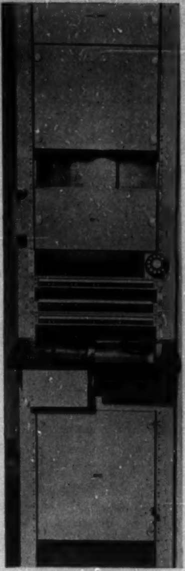

Figure 1(C) (right). Equipment at attended station

the attended station is ready to accept the alarm information, the sending potential at the attended station is changed from ground to battery which is likewise repeated into the next line section at each station between the attended and originating stations. On receipt of the battery signal, the originating station sends a code consisting of alternate battery and ground pulses. Both ends of the circuit are then restored.

The second channel is a differential-duplex circuit used for transmitting orders to the unattended stations and for sending synchronized stepping pulses for the indication circuit to the attended station.

The third channel is a 1-way polar circuit used to transmit indication signals to the attended station. The second and third channels are shown in Figure 4.

The fourth channel is used for neutralizing interference in the three operating channels. The neutralizing circuit duplicates the configuration and electrical constants of the operating channels, but is terminated in equal potentials obtained from potentiometers across the operating channel batteries. Differences in battery voltages at the two ends of a line section are partially compensated by this device. Because the operating channel balancing circuit is duplicated in the neutralizing channel large amounts of interference and ground potentials, either alternating or direct current can be tolerated by the system as the effect produced in the receiving relays due to extraneous currents in the operating channels is cancelled by a substantially equal current in the neutralizing channel.

Vibrating circuits are provided for receiving relays which are required to receive pulses except on the third channel where the retransmission of pulses is controlled by the second channel. The vibrating circuits increase the effective operating forces during the transition times when the circuits are most susceptible to interference, and they tend to correct signal distortion by lengthening short pulses and decreasing long pulses. Only one set of transfer contacts is avail-

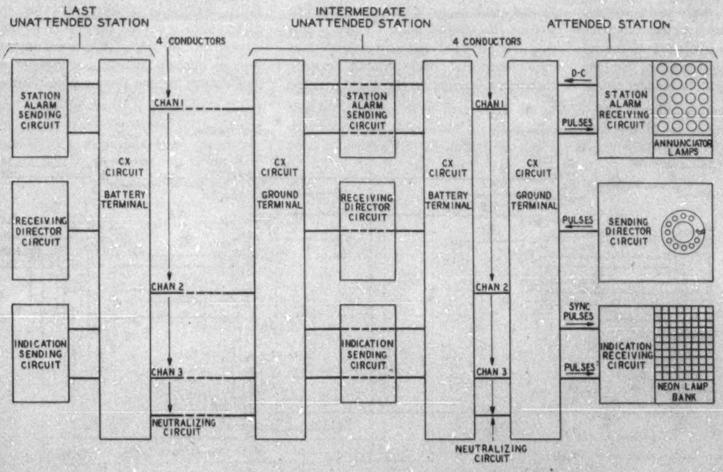
LAST UNATTENDED STATION
INTERMEDIATE UNATTENDED STATION
ATTENDED STATION
4 CONDUCTORS
4 CONDUCTORS
STATION ALARM SENDING CIRCUIT
RECEIVING DIRECTOR CIRCUIT
INDICATION SENDING CIRCUIT
CX CIRCUIT BATTERY TERMINAL
CHAN 1
CHAN 2
CHAN 3
NEUTRALIZING CIRCUIT
CX CIRCUIT GROUND TERMINAL
STATION ALARM SENDING CIRCUIT
RECEIVING DIRECTOR CIRCUIT
INDICATION SENDING CIRCUIT
CX CIRCUIT BATTERY TERMINAL
CHAN 1
CHAN 2
CHAN 3
NEUTRALIZING CIRCUIT
CX CIRCUIT GROUND TERMINAL
D-C
PULSES
STATION ALARM RECEIVING CIRCUIT
ANNUNCIATOR LAMPS
PULSES
SENDING DIRECTOR CIRCUIT
SYNC PULSES
PULSES
INDICATION RECEIVING CIRCUIT
NEON LAMP BANK

Figure 2. Block diagram of signaling system

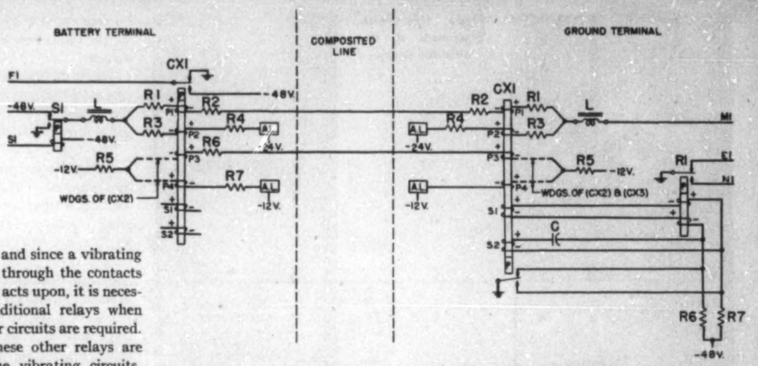

Figure 3. Alarm transmission channel

able on polar relays and since a vibrating circuit is controlled through the contacts of the relay which it acts upon, it is necessary to operate additional relays when contacts free of other circuits are required. The windings of these other relays are made a part of the vibrating circuits. The arrangement used permits a voltage swing on the vibrating circuit equal to twice the available battery voltage. This simplifies the design problem when the available battery voltage is low.

The windings of two additional relays are included in the vibrating circuit for the receiving relay of channel two at the ground terminal. The first relay follows the operation of the receiving relay at all times. The second relay follows the operation of the receiving relay except when prevented from doing so by the closure of a holding circuit through the contacts of the receiving relay of channel three. The holding circuit is connected through the normally-closed contact of the second relay, so that when the second relay operates from its idle position the holding circuit loses control. The indication signals are thus synchronized with the stepping pulses at each main station. Two or more indication signals occurring in sequence can be combined at the indication sending equipment into one long signal which will open the holding circuit at the first ground terminal for the required number of pulses.

The relay controlling the indication pulses will operate to the opposite contact during the idle period if the holding circuit is opened. It is necessary therefore to have a means of restoring the relay to its normal position if the holding circuit is opened momentarily by a trouble on channel three. A slow release relay provides a restoring circuit after a short interval if the holding circuit has been reestablished through the contacts of the third channel receiving relay.

Alarm Circuit

When an alarm condition occurs in any one of the remote main stations, the alarm sending circuit associated with that station seizes the alarm channel (channel 1) and sends a d-c signal along the line toward the control main station. This signal is received and retransmitted at each intermediate remote station between the station originating the alarm and the main station. The receipt of this signal by the intermediate stations serves to inform the alarm sending circuits at these stations that the alarm channel is in use so that any alarm originating at these intermediate stations will be stored until the alarm channel is free. Receipt of this signal by the control station causes operation of relays in the alarm receiving circuit which send an answering steady signal in the reverse direction, that is, toward the remote station. This station interprets this signal as an indication that the alarm channel is functioning correctly and is not transmitting an alarm from another station. It thereupon transmits a series of pulses at a rate of ten per second. The number of pulses sent out indicates the particular station sending the alarm and whether the alarm is of major or minor importance. Figure 5 shows the alarm circuits in outline form for the control station and for the nearest remote station on one side. Additional remote stations contain identical equipment as that shown for the first remote station.

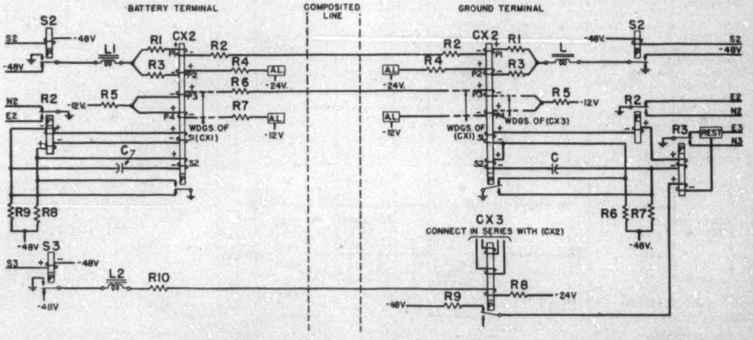

Figure 4. Director and indication transmission channels

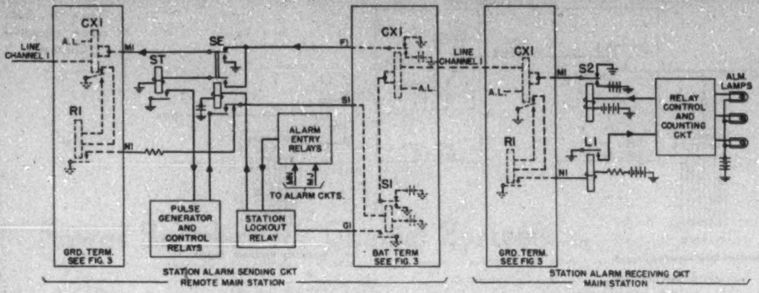
CX1
LINE CHANNEL 1
A.L.
M1
SE
ST
R1
N1
PULSE GENERATOR AND CONTROL RELAYS
STATION LOCKOUT RELAY
ALARM ENTRY RELAYS
TO ALARM CKTS.
GRD. TERM. SEE FIG. 3
F1
S1
G1
CX1
A.L.
S1
BAT TERM SEE FIG. 3
LINE CHANNEL 1
CX1
A.L.
M1
S2
R1
N1
L1
RELAY CONTROL AND COUNTING CKT
ALM. LAMPS
GRD. TERM. SEE FIG 3
STATION ALARM SENDING CKT
REMOTE MAIN STATION
STATION ALARM RECEIVING CKT
MAIN STATION

Figure 5. Alarm circuits — Channel 1

When an alarm condition originates at the remote station either a major *MJ* or a minor *MN* lead is grounded depending upon the class of the particular alarm. Each alarm source operates a particular alarm relay which in turn operates the seizure relay *SE* causing the alarm channel to be seized. The seizure changes the condition of the line, the line current dropping to zero or to a low value if small earth potentials are present. This change of line condition causes a signal to be sent to the *CX* signaling circuit at the main station where relays *CX1* and *R1* in that circuit and relay *L1* in the alarm receiving circuit operate. The alarm receiving circuit responds to this signal by operating relay *S2* which changes the line condition of the channel in the opposite direction sending an answering signal toward the remote station. When the signal is received at the remote station, it activates a pulse generator. The pulse generator supplies pulses at the rate of ten pulses per second to the *S1* relay and also to a local counting circuit. The pulses applied to the *S1* relay cause pulsed operation of the *L1* relay in the alarm receiving circuit. The local counting chain is arranged to stop the pulse generator when a particular number of pulses has been produced. Optional wiring to the counting circuit is different at each station so that the number of pulses which are sent out before the pulse generator is stopped is different for each station. The pulses received in the alarm receiving circuit drive another counting chain which registers the total number of pulses received, lighting an annunciator lamp and actuating an audible alarm in accordance with the meaning attached to the number of pulses.

When the pulsing is through, and the alarm information registered, the seizure signal is removed toward the control station. This results in the removal of the start signal from the line and the conditions revert to those encountered normally and the alarm channel is available for use by any other station having alarm conditions to be registered.

Director Circuit

When an attendant at the control station desires to perform some remote control action at any one of the remote main stations he dials a 3-digit code on the telephone dial associated with the sending director circuit. The first digit dialed corresponds to the station to which the order is directed and the second two digits represent the particular remote control action desired. Since 100 separate codes are available from 2-digit 10-pulse combinations a total of 100 orders is available for use at each of ten remote stations. Figure 6 shows the circuits for the director signals. In addition, Figure 6 shows parts of the indication circuits which also use channel 2, and which will be described in succeeding paragraphs.

When the attendant operates the dial key in the sending director circuit and dials the first digit he causes pulsed operation of relays *L1* and *S2* in the control station, and relays *CX2*, *R2*, and *L1* in all the remote main stations. All remote stations count the number of pulses contained in this first digit by means of local counting circuits driven from the *L1* relay in each receiving director circuit. In the particular remote main station to which the director signal was addressed, the local counting circuit is wired so as to respond only to the particular number which was dialed as the initial digit. When the receiving director circuit receives this first digit, it enables itself to accept the succeeding two digits which are dialed by the attendant.

The second digit dialed will again cause operation of relays associated with channel 2. Only the receiving director circuit

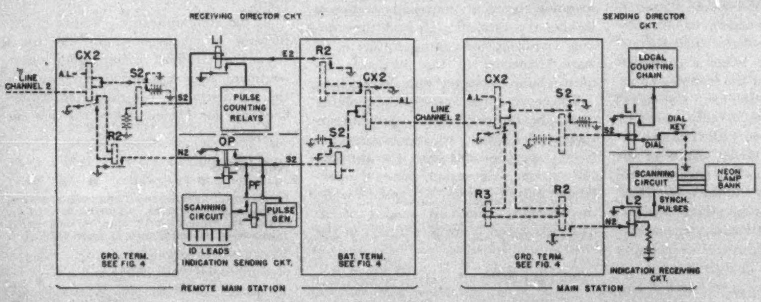
RECEIVING DIRECTOR CKT
LINE CHANNEL 2
CX2
A.L.
S2
S2
R2
L1
E2
PULSE COUNTING RELAYS
OP
N2
S2
PF
SCANNING CIRCUIT
PULSE GEN.
ID LEADS
INDICATION SENDING CKT.
GRD. TERM. SEE FIG. 4
R2
CX2
A.L.
S2
BAT. TERM. SEE FIG. 4
LINE CHANNEL 2
SENDING DIRECTOR CKT.
CX2
A.L.
S2
R3
R2
GRD. TERM. SEE FIG. 4
LOCAL COUNTING CHAIN
L1
S2
DIAL KEY
DIAL
SCANNING CIRCUIT
NEON LAMP BANK
L2
SYNCH. PULSES
N2
INDICATION RECEIVING CKT.
REMOTE MAIN STATION
MAIN STATION

Figure 6. Director and indication circuits—Channel 2

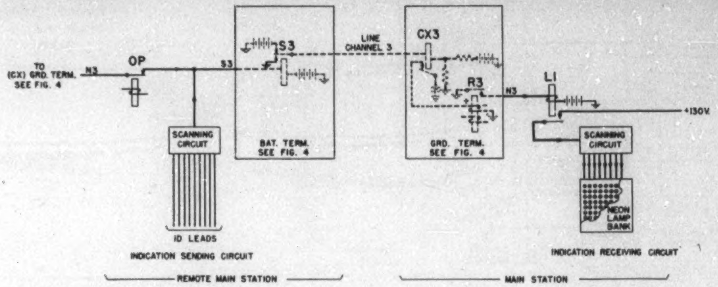

Figure 7. Indication circuits—Channel 3

associated with the station to which the first digit was directed, however, will count the second digit. All other remote stations will ignore this digit. This second digit will be counted by the counting chain in this station, and a particular final relay out of a total of ten will be energized after the digit has been received. In a similar fashion, the third digit is received by the selected remote station and causes a ground to be applied to a particular contact on the final relay which had been operated as a result of the registration of the preceding digit. This ground, which can occur on any one of the 100 leads can be used to operate relays in a local circuit for any particular control function. Typical controls for the *L* carrier system are: start gas engine; start indication circuits; and reset pilot level sensitrol relays.

Indication Circuits

One of the orders sent by the director circuit is used to start the indication circuit. This circuit transmits automatically the condition of as many as 168 circuits at the remote station. These indication signals appear at the main station as lighted neon lamps arranged in a convenient bank in a keyshelf. Information about the circuits at the remote station is obtained by scanning a group of 168 leads and ascertaining whether particular leads are grounded or not. When a grounded lead is encountered in the scanning process, a signal is sent to the main station to light the particular neon lamp which is permanently associated with that lead in the receiving lamp bank. Since 14 of these 168 leads are used in checking the identity of the station and the correctness of the received display, there remain available 154 indication signals which may be used to determine the status or condition of circuits at the remote point.

Figure 6 shows the circuits associated with channel 2 for the indication circuits. In addition, Figure 7 shows the circuit associated with channel 3 for the indication circuits. Channel 2 which was used for sending director signals in the direction from the main station toward the remote station also is used for sending synchronizing pulses in the opposite direction when indications are being transmitted. The director signal which sets the indication circuit in operation, energizes a pulse generator which begins to send out dial pulses at approximately ten pulses per second. These pulses are used to operate a local scanning circuit and are also transmitted over channel 2 to the main station where they operate an identical scanning circuit. The pulses transmitted to the main station are sent by operation of relays *PF* and *S2* in the remote station and relays *CX2*, *R2*, and *L2* in the control station. Thus two identical scanning circuits are driven simultaneously from one pulse generator. The scanning circuit at the remote main station looks at each one of the indicator *ID* leads in turn and the scanning circuit at the control station connects to each of the neon indicator lamps in turn. When the scanning circuit at the remote station is looking at a particular *ID* lead, the scanning circuit at the control station is always connected to the particular indicator lamp associated with that lead.

Whenever, in the course of the scanning cycle, the scanning circuit encounters a lead which is grounded, it sends a signal (see Figure 7) over channel 3 to the control station. This signal, causes the particular indicator lamp to operate when the scanning circuit is looking at it. Channels 2 and 3 are interlocked in the ground terminal composite signaling circuit at the main station, as has been described previously, in order to make certain that the synchronizing pulses and the marker pulses occur simultaneously so that the correct lamp will always be energized.

The indicator lamp bank is arranged under a frosted plastic cover of standard letter size paper so that a permanent record or log of the condition of all important circuits for a particular unattended station may be made by the attendant simply by checking the printed form which is placed over the plastic cover.

Summary

The *B-1* alarm and control system provides means of supervising and controlling as many as ten remote stations in a maximum of four directions from the control station. The maximum distance between the most distant stations in a maintenance group is 1,650 miles which certainly exceeds the range in which remote stations can be serviced efficiently from a single maintenance center. The system presages increasing use of automatically-obtained information about isolated stations and stepped-up use of remote control signals for the telephone plant.

As the communication circuits in use increase in complexity, and the trend toward centralized maintenance effort continues, reliable alarm systems such as the *B-1* alarm and control system will be necessary for efficient use of the new developments.

Reference

1. Coaxial Telephone-Television System Progress, L. G. Abraham. *Electrical Engineering*, volume 68, February 1949, page 147 and *AIEE Transactions*, volume 67, part II, pages 1520–27.

Power Supplies for Coaxial Systems

H. H. SPENCER
ASSOCIATE AIEE

THE TYPE *L* broad-band carrier telephone systems are in extensive use over nationwide coaxial-cable networks. Some use has been made of these facilities for transmission of television programs. The closely spaced repeaters needed for these systems to maintain proper transmission of the signal frequencies, approximately every five miles for 0.27-inch and every eight miles for 0.375-inch coaxials, has made it desirable to transmit 60-cycle power to auxiliary repeaters over the same conductors as used for the higher frequencies, rather than have a separate power supply at each repeater. This paper describes the power-supply system used, its regulation, and some of the features employed to guarantee continuous service. Communication and television features have been described previously,[1-3] and in this paper will be referred to only insofar as they are affected by the power supply.

Constant-Current Power System

The power transmission system involves a circuit in which the primaries of the power packs at each repeater are arranged in series with the inner conductors of the coaxials to form a series feed from a power sending station. With proper loading to compensate for shunt capacity, all power packs in a transmission circuit receive substantially the same line current. By regulating this current at the source, constant power supply is obtained at each repeater. Figure 1 illustrates a typical span of auxiliary repeaters between adjacent power sending stations. At the left, a terminal station supplies power to its own repeater and, over coaxials *1* and 2, to six auxiliary repeaters with the power circuit looped at the sixth repeater. The remaining five repeaters of the span are supplied from the main station shown at the right of Figure 1. Power is supplied from this station to repeaters in both directions. The power section west of the main station is not looped at the last repeater which it supplies, but is carried to the next repeater and looped there through a looping filter. This is done to maintain current in all cable sections, thus facilitating testing, both in locating faults and also in establishing that the sending-end voltage has been removed before workmen are allowed to open the cable.

The number of repeaters supplied in a span between power sending points depends on several factors, chiefly: availability of existing Bell System buildings and personnel along the coaxial cable routes, need for dropping circuits at intermediate points along the route, and availability of commercial power service. Spans will be as short as 40 miles to permit dropping circuits, but will average about 100 miles and may be as great as 165 miles. From a power standpoint, the maximum span is determined by the safe voltage which may be applied at the source to obtain the required line current. At present, the maximum rms 60-cycle voltage which has been applied to the power separation filters at the power sending station is 1,700 volts, 850 volts to ground. A line current or between 430 and 500 milliamperes is employed to supply the power-pack primaries.

Repeater Power Pack

Figure 2 shows more detail of the power circuits at main and auxiliary repeaters, including the power separation filters which separate the carrier frequencies from the low power frequencies so that the former may be amplified and returned to the coaxials for transmission to the next station. The power pack at each repeater includes a transformer having two primaries, one in series with each side of the power circuit. Its secondaries supply a-c filament power at approximately 6.7 volts, and, through a rectifier, d-c plate at approximately 140 volts. The rectifier is of the metallic type with filters to reduce ripple voltages. A large electrolytic capacitor across the rectifier output provides a hold-over plate supply to the amplifiers to maintain carrier transmission during short interruptions of power supply, such as a two cycle outage in switching from a regular to an emergency source. The plate windings of the power transformer are in series, so that the resultant plate voltage is not affected by any unbalance in the current flowing in the two sides of the power loop so long as the average current in the loop remains the same. However, the filament windings are individual to each coaxial amplifier, and, to prevent unequal heater voltages in the event of unequal line currents in the two coaxials, these windings are connected through load balancing coils so that they are at substantially the same voltage. These coils are designed as low-pass filters to prevent crosstalk between amplifiers. The power circuit is grounded at the midpoint of the supply transformer for safety reasons; unbalanced current in the two coaxials may be caused by unequal leakage to ground, shorts in the coaxials, or as has happened in a few instances, by induced currents resulting from heavy earth fault currents from a ground high-voltage commercial power feeder in the vicinity of the coaxial cables. Cover switches are provided at all points of access to the power circuit to short out the power supply in case the maintenance forces fail to turn down power before opening covers.

The power circuit is treated as a unity-power-factor load. Loading is added as required to practically equalize the line current throughout the circuit. The primary current at each auxiliary station

---

Paper 49-156, recommended by the AIEE Communication Committee and approved by the AIEE Technical Program Committee for presentation at the AIEE Summer General Meeting, Swampscott, Mass., June 20–24, 1949. Manuscript submitted March 21, 1949; made available for printing April 28, 1949.

H. H. SPENCER is with the Bell Telephone Laboratories, Inc., New York, N. Y.

Figure 1. Power transmission system

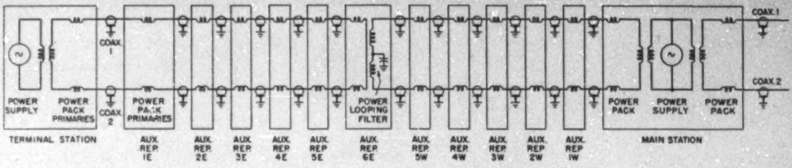
COAX.1
COAX.2
COAX. 1
COAX. 2
POWER SUPPLY
POWER PACK PRIMARIES
POWER PACK PRIMARIES
POWER LOOPING FILTER
POWER PACK
POWER SUPPLY
POWER PACK
TERMINAL STATION
AUX. REP. 1E
AUX. REP. 2E
AUX. REP. 3E
AUX. REP. 4E
AUX. REP. 5E
AUX. REP. 6E
AUX. REP. 5W
AUX. REP. 4W
AUX. REP. 3W
AUX. REP. 2W
AUX. REP. 1W
MAIN STATION

is the vector sum of the series line current, the shunt current which flows through the capacities of the power separation filters, and the distributed capacity of the cable itself. Taps on the transformer primaries at each repeater provide adjustment for variations in power-pack outputs. The adjustment of these taps and the line currents required for the power circuit are determined on a trial basis. Shunt loading, applied only at the source, and series loading shown in Figure 2, are employed as required depending on the length and number of repeaters in the power section.

Regulation of Coaxial Current

The voltage applied at the source to give the desired line current to a power section is obtained by adjusting the taps of the power-control transformer, shown in Figure 2, to get the proper transformer step-up ratio when approximately normal alternating supply voltage is applied to its primary. The coaxial current then is regulated at the desired value by automatic control of the motor-driven continuously-tapped variable transformer. This is accomplished by holding a constant drop across resistance *L* which is in series with the transformer secondaries. With the line current normal, voltage relay *VR* maintains a neutral position. If, however, the line current is away from normal by about ±1.5 per cent, this relay makes its high or low contact to operate raise or lower relays. These relays connect power to a reversing-type a-c motor which is geared to drive the variable-transformer brush at a speed of one revolution per minute. The motor, of course, is controlled to change the supply voltage in the direction to return the line current to its regulated value.

Regulation of the line current is required chiefly to correct for changes in the load resistance due to temperature, and for fluctuations in the alternating supply voltage. Automatic regulation provides protection against overload such as might occur if a coaxial should open or become short circuited. Where the overload is insufficient to blow the supply fusing, the controls reduce the line current to normal by dropping the voltage to the necessary value. Where the short circuit is near enough to the main station to blow a supply fuse, the control circuit functions to turn the variable transformer to minimum voltage, so that replacement of the blown fuse cannot cause a line-current surge. Again referring to Figure 2, the loss of line current releases relay *NV* to remove the "raise" signal from relay *VR*, and provides a permanent lower signal until the maintenance forces throw a key and manually restore the line current.

Uninterrupted 230-Volt A-C Supply

The 230-volt a-c supply for the coaxial power circuit is provided from continuously-operated alternators rather than direct from the commercial service, to reduce the effect on carrier transmission caused by power service fluctuations and outages. The alternators are self-excited and are driven normally by induction motors from the commercial service and, during emergencies, by d-c motors from the station's 130-volt battery. With stable power-supply frequency, induction motor speeds are practically constant, and as the sets are self-excited and the loads are practically constant, the alternator output voltage normally is held within close limits and is affected very little by commercial-power voltage variations. The alternators further serve to insulate the coaxial power supply from any power-line high-voltage surges, lightning hits, or power-service harmonic interference.

The d-c motor is connected to battery whenever the alternator is operating, but is kept from supplying any appreciable power, while the a-c motor is driving, by

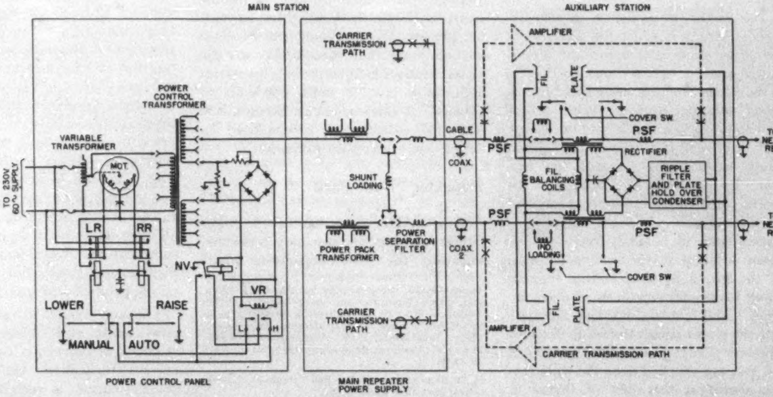
MAIN STATION
AUXILIARY STATION
POWER CONTROL TRANSFORMER
VARIABLE TRANSFORMER
MOT.
TO 230V 60~ SUPPLY
L
LR
RR
NV
VR
LOWER
RAISE
MANUAL
AUTO
L
H
CARRIER TRANSMISSION PATH
SHUNT LOADING
CABLE
COAX. 1
COAX. 2
POWER PACK TRANSFORMER
POWER SEPARATION FILTER
CARRIER TRANSMISSION PATH
AMPLIFIER
FIL.
PLATE
COVER SW.
PSF
PSF
PSF
PSF
RECTIFIER
FIL. BALANCING COILS
RIPPLE FILTER AND PLATE HOLD OVER CONDENSER
IND. LOADING
COVER SW
FIL.
PLATE
AMPLIFIER
CARRIER TRANSMISSION PATH
TO NEXT REP
TO NEXT REP
POWER CONTROL PANEL
MAIN REPEATER POWER SUPPLY

Figure 2. Repeater power pack

the insertion of a current-limiting resistance in its armature circuit. The field of the motor is connected to the battery side of this resistance. The setting of the field resistance is such that the counter electromotive force across the armature is practically equal to the battery voltage. Accordingly, when fast-acting relays short circuit the resistance in the armature circuit to cause the d-c motor to take over the drive, there is little or no inrush of armature current and, therefore, little change in alternator output. The d-c motor speed is unregulated and varies with the battery voltage, as the motor field rheostat remains at a fixed setting. As the battery is held within close limits to meet other station load requirements, the alternator output during emergency operation is well within a range for which the power-control circuits can maintain regulated coaxial-cable current.

Alternator Control

A simplified schematic of the 230-volt supply circuit is shown in Figure 3. As drawn, this circuit shows an alternator set ready to start, with its load being carried by an emergency alternator. The set is started with its d-c motor by operating the "start" key to bring in the current-limiting starter. When the alternator voltage builds up to its normal range, a voltage sensitive relay *LV*1 connected across the alternator output causes relay *MS* to operate and hold the d-c motor connected to battery. At the same time, relay *MS* causes relay *M* to disconnect ground from the winding of contactor *AR*, which releases and removes the short from resistance *AR*. This inserts resistance (*AR*) in the armature circuit of the d-c motor, limiting its driving power. Relay *M*, in operating, also connects the a-c motor to take over the drive of the set. The alternator now is ready to take over the load. This is accomplished by returning the start key to normal. This removes ground from the winding of relay *EC*, which releases and causes relays *A* and *E* to transfer the load from the emergency to the regular alternator. It may be noted that transfer of the drive from one motor to the other is controlled by relay *M*. With this relay operated, the set will be a-c driven; released, d-c driven. Operation of the "d-c mot test" key provides a manual means of motor transfer; release of relay *TR* or relay *MF* provides automatic transfer control.

Power Failure Transfer Control

The operation of relay *TR* is controlled by a voltage-sensitive relay *VR* connected to the commercial service through a rectifier and step-down transformer. This relay is adjusted, by means of rheostats *R*1 and *R*2 in series with its winding, to close its low contact *L* at supply voltages in the order of 85 per cent of the nominal service voltage value for the particular station. Above 85 per cent of normal line voltage, the slip in speed of an induction motor will be so small that the alternator output may be expected to remain within close limits during a-c drive. On closing its *L* contact in the event of low voltage, relay *VR* connects battery to operate relay *L* which locks operated to battery from contacts of timer *TD*. Operation of relay *L* removes ground from the *TR* relay winding to cause transfer to d-c motor drive. It will be noted that the *TR* relay winding receives its power from the commercial service through a transformer and rectifier. This provides a more rapid transfer of motor drive in the event of instantaneous outage of service voltage in that the *TR* relay releases from loss of power without waiting for the slower marginal-relay control cut-off.

Transfer back to a-c motor drive is delayed by timer *TD* after power is restored to normal, to prevent too many transfers with unstable power-supply voltage. In this respect, an additional feature is provided, requiring a return of the service voltage to above 90 per cent of the nominal value before transfer can be made to a-c drive. This feature consists of short-circuiting rheostat *R*2 with operated contacts of relay *L*, thereby increasing the current in the winding of relay *VR*. Under this condition, rheostat *R*1 adjustment is such as to cause relay *VR* to make its high contact *H* at the desired percentage of nominal voltage. When contact *H* has been operated long enough for timer *TD* to break the holding battery on relay *L*, relay *L* releases, causing relay *TR* to reoperate and transfer the drive back to alternating current. Release of relay *L* restores relay *VR* and the control circuit to normal.

A-C Motor Failure Transfer Control

Another motor-transfer control is provided in the event the alternator output should fall below its normal range for reasons other than low power service

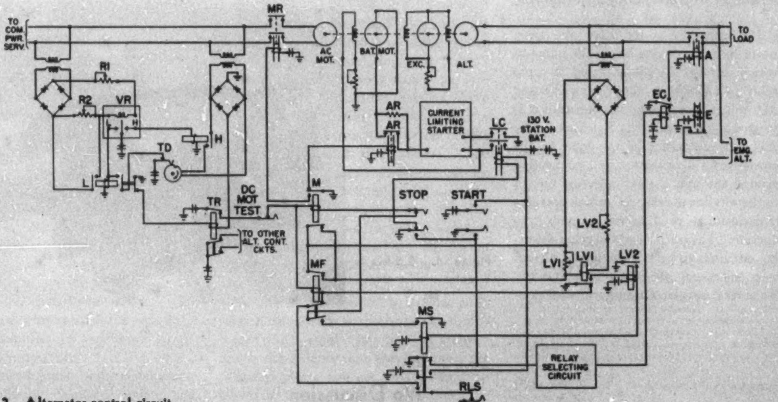

Figure 3. Alternator control circuit

voltage. For example, low line frequency without accompanying drop in line voltage would drop the alternator speed and output voltage, and no transfer in motor drive would result from the voltage control just described. Failure of the a-c motor could likewise drop the alternator voltage without the service voltage transfer control being affected. To care for these contingencies, rheostats *LV*1 and *LV*2, in series with relay *LV*1 across the alternator output, are adjusted so that relay *LV*1 will release at approximately 85 per cent of normal output voltage and cause relay *MF* to operate and open the grounded side of the winding of the *M* relay, thereby causing transfer to the d-c motor. Relay *MF* locks operated through closed contacts of operated relay *MS* to prevent transfer back to the a-c motor when the d-c drive brings the alternator voltage back to normal. When relay *MF* is operated, it also closes a short circuit around rheostat *LV*1, increasing the current in the winding of relay *LV*1 to make this relay reoperate and hold down to a lower value of voltage. This lower value of voltage is determined by the adjustment of rheostat *LV*2 and is used as an alternator cut-off control in case the d-c motor fails to maintain alternator output. If the d-c motor takes over the drive satisfactorily, relay *LV*1 is not released long enough to allow relay *LV*2 to release, as the latter is a slow-acting relay. Accordingly, the alternator will operate under d-c drive until an attendant releases the lock-up on the *MF* relay. The *MF* relay is kept from operating during power failure transfers by removal of battery from its winding during release of relay *TR*.

Transfer to Emergency Alternator

If, during d-c motor drive, the alternator output remains below the value at which rheostat *LV*2 is adjusted to cause relay *LV*1 to release, then relays *LV*2 and *MS* will release to stop the set until it is started again manually. Release of relay *MS* causes transfer of the load to the emergency alternator by connecting ground through a relay-selecting circuit to the winding of relay *EC*, which operates and causes relay *A* to release and *E* to operate. The purpose of the relay-selecting circuit is to permit the use of a common emergency alternator as a standby for several regular alternators, with control to prevent more than one load being transferred to the standby at one time. The emergency alternator is operated continuously at no load to reduce the outage time of the coaxial supply in the event of an emergency transfer. Manual transfer of the load to the emergency alternator may be accomplished by the "stop" and "start" keys whenever the regular alternators are to be shut down or operated for maintenance only.

Size of Alternators

Alternators usually are furnished on the basis of one alternator per pair of coaxials. In a station feeding power in one direction only, 1.5-kva alternators usually are used, but 2.5-kva and 5-kva sizes are available where it is desired to supply more than one pair of coaxials from the same machine. This usually is not done, however, in view of the large number of circuits affected if one machine should be down for maintenance and trouble should develop in another. In a main station feeding power to coaxials in two directions, 1.5- or 2.5-kva alternators are used, depending on the number of auxiliary repeaters supplied. A maximum of five alternators is required in such a station, for each 8-coaxial cable, one for each pair of coaxials, plus the common standby emergency alternator.

Unattended Operation

These power supplies are completely automatic for use in remote unattended stations, and because of this, they include alarms which are transmitted to an attended station to indicate abnormal conditions. Alarms are given if the coaxial current exceeds its normal limits, if drive is transferred to the d-c motor or if alternators fail along with other power plant alarms such as low battery voltage, battery fuse failure, engine failure, and so forth. Engine alternator standby for the commercial service generally is furnished, and, in unattended stations, the engine sets are started and controlled automatically. Station batteries also are charged automatically, using electron-tube-type rectifiers for battery voltage regulation. Station equipment such as order-wire circuits, alarms, and so forth, require 130-volt plate and 24-volt filament batteries. These are used, as has been previously stated, for 130-volt supply to the d-c motors and 24-volt supply for the various control circuits.

Terminal Equipment Power Supply

Power supplies for the terminal equipment used to bring telephone messages from the carrier down to voice frequency, usually are taken from the regular terminal station 130- and 24-volt plants. Particular care is taken in distributing these battery supplies, to prevent loss of service through accidental grounding, and to subdivide the fusing so as to reduce the number of circuits affected by the loss of any battery discharge fuse.

References

1. WIDE BAND TRANSMISSION OVER COAXIAL LINES, Lloyd Espenschied, M. E. Strieby. *Electrical Engineering (AIEE Transactions)*, volume 53, October 1934, pages 1371–80.

2. TELEVISION NETWORK FACILITIES, L. G. Abraham, H. I. Romnes. *AIEE Transactions*, volume 66, 1947, pages 459–64.

3. PROGRESS IN COAXIAL TELEPHONE AND TELEVISION SYSTEMS, L. G. Abraham. *AIEE Transactions*, volume 67, part II, 1948, pages 1520–27.

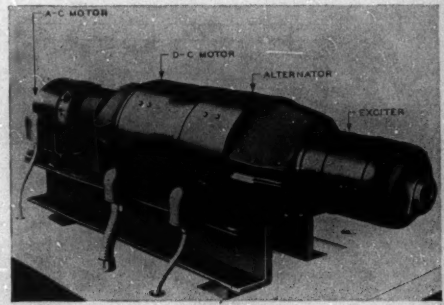

Figure 4. 2.5-kva 2-motor alternator set

No Discussion

Power Supplies for Microwave Relay Systems

H. M. WARD
NONMEMBER AIEE

Synopsis: The establishment of microwave relay systems, carrying large numbers of separate telegraph communication channels on a single radio circuit and having relay stations located every 30 or 40 miles, usually in remote country districts, has put a premium on dependability of power supplies. This paper describes the facilities that have been provided for regular and fall-back power supplies for the Western Union radio-beam triangle which interconnects New York, Washington, and Pittsburgh. Interruption of the regular commercial a-c supply at any point causes the radio beam to be switched, without any effect on its operation, to a-c power supplied from battery-fed vibrators. Simultaneously, an engine generator unit is started and takes over the load automatically as soon as it has reached a steady operating condition. The paper includes a brief discussion of operating experience.

MORE THAN a century ago, Samuel F. B. Morse transmitted the words "What hath God wrought!" from Washington to Baltimore, and thus became the first individual to make practical use of electric energy in the communications field as a substitute for physical exertion. For many years thereafter, simple primary-battery plants sufficed as the fundamental source of power, without which there would have been no telegraph industry. Subsequent improvements in the speed and efficiency of telegraph operations brought about greatly increased demands for power and have made the requirements as to stability and reliability much more exacting. It is the microwave radio-relay system, however, with its inherent capacity for large numbers of communication channels on a single circuit, that has emphasized the necessity for power supplies of maximum continuity and dependability.

In a microwave radio-beam system such as that built by Western Union, the volume of traffic on a radio beam, and hence the importance of the circuit, far exceed that of anything previously used in the telegraph industry. Furthermore, completely automatic operation of all relay stations, except during prolonged operation on emergency power, was essential as a fundamental requirement. The relay stations are substantial in number and are so widely scattered that the cost of providing attendants at each station on a 24-hour basis would have been prohibitive. Therefore, the importance of maintaining continuous operation, and the fact that each relay station would have to function entirely without human aid at all times, in all kinds of weather, made extreme reliability one of the prime objectives in the design of the power-plant equipment.

The Power Supply Problem

Radio beam "terminal" stations are located in cities where dependable power supplies already exist, but the "relay" stations, almost without exception, are located in remote country districts where the commercial power supplies are subject to frequent outages due to line breaks caused by ice and wind storms. The radio-beam equipment was designed for operation on 115-volt 60-cycle a-c commercial power. However, since a power interruption of even a fraction of a second would cause disturbance in the beam signals that would persist for an appreciable period of time—even after power is restored—it was essential to provide each relay station with auxiliary power equipment which would function so quickly and so dependably that any failure of the primary power sources would have no effect on the radio-beam operation.

From previous experience it was known that automatic transfer switch operation could be achieved with an interruption of only about 0.05 second. It also was known that the addition of capacitors in the plate supply units of the radio equipment would make continuous operation possible during interruptions of more than twice that interval. The problem, therefore, was to provide an auxiliary source of 115-volt 60-cycle alternating current which would function in less than 0.1 second after a fuse blew or a tree fell over the power supply line.

The Complete Power Plant

The major components of the power plants installed at all relay stations of the radio-beam system are shown in Figure 1. Commercial 115-volt 60-cycle a-c power service is used as the normal source of supply for operating radio equipment, battery-charging rectifiers, station and tower lights, oil-burner motors, and other miscellaneous loads. An engine generator is provided as the prime emergency power supply for protection against prolonged power failures. Vibrator units, operated from a storage battery, are provided as the initial "instantaneous" reserve source of alternating current to maintain radio operation during the early stage of a power interruption, until the engine generator has started and has reached a steady operating condition.

In the event of failure of the regular service, or of a drop in voltage from the normal 115–120-volt level to below 102 volts, the "secondary" relay-controlled transfer switch almost instantaneously connects the storage battery to the input side of the two vibrator units and transfers the radio load to them. Simultaneously, the "main" relay-controlled transfer switch is set to start the engine-driven generator, and to switch the load

---

Paper 49-157, recommended by the AIEE Communication Committee and approved by the AIEE Technical Program Committee for presentation at the AIEE Summer General Meeting, Swampscott, Mass., June 20–24, 1949. Manuscript submitted March 3, 1949; made available for printing April 28, 1949.

H. M. Ward is with the Western Union Telegraph Company, New York, N. Y.

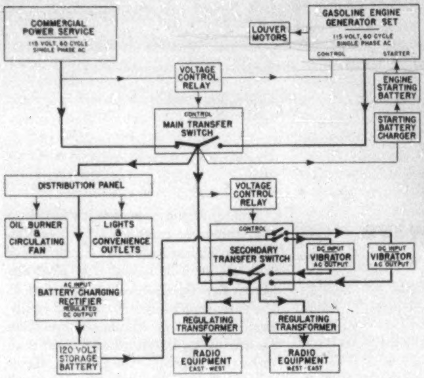
COMMERCIAL POWER SERVICE
115 VOLT, 60 CYCLE SINGLE PHASE AC
LOUVER MOTORS
GASOLINE ENGINE GENERATOR SET
115 VOLT, 60 CYCLE SINGLE PHASE AC
CONTROL
STARTER
VOLTAGE CONTROL RELAY
ENGINE STARTING BATTERY
CONTROL
MAIN TRANSFER SWITCH
STARTING BATTERY CHARGER
DISTRIBUTION PANEL
VOLTAGE CONTROL RELAY
OIL BURNER & CIRCULATING FAN
LIGHTS & CONVENIENCE OUTLETS
CONTROL
SECONDARY TRANSFER SWITCH
DC INPUT
VIBRATOR
AC OUTPUT
DC INPUT
VIBRATOR
AC OUTPUT
AC INPUT
BATTERY CHARGING RECTIFIER
REGULATED DC OUTPUT
REGULATING TRANSFORMER
REGULATING TRANSFORMER
120 VOLT STORAGE BATTERY
RADIO EQUIPMENT
EAST-WEST
RADIO EQUIPMENT
WEST-EAST

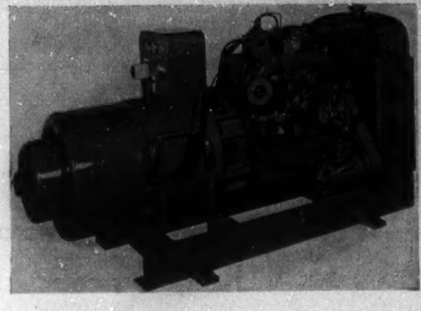

Figure 1 (left). Block diagram of relay-station power plant

Figure 3 (above). 10-kw engine alternator unit

to it just as soon as the latter comes up to full speed and voltage, which may be 30 seconds or more after the initial operation. Actual starting of the engine is delayed for approximately 15 seconds in order to avoid unnecessary starting during extremely short power failures. If for any reason the engine should fail to start, the radio load would remain on the vibrators.

Simultaneously with these operations, special signals are automatically transmitted to each terminal to indicate that a power interruption has occurred and whether the load is being carried on the vibrator unit or the emergency engine. These fault tone signals are sent by a code-keying unit, operating over the service channel of the radio-beam circuit.

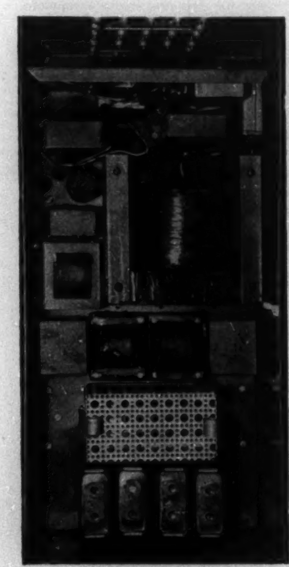

Figure 2. Vibrator unit

When regular power is restored, the load is transferred back automatically to that service; the engine unit is shut down, and the signals to the terminal stations are restored to normal. Here again, however, actual return to regular power is delayed for about five seconds after the commercial service reaches a minimum value of 108 volts, in order to make sure that the restoration is reasonably permanent. It often happens that, in the case of a power failure resulting from a short circuit or a grounded transmission line, the power-station attendant will make one or more attempts to reclose the circuit breaker feeding that line, only to have the breaker trip out again if the fault has not burned clear. The slight additional delay in transfer back to normal service almost entirely eliminates unnecessary switching operations and restarting of vibrators and engine unit under such conditions. Regulating transformers are interposed between the secondary transfer switch and the radio equipment in order to correct for variations in the commercial-service, engine-unit, and vibrator voltages.

Each station is provided with a small oil burner for heating purposes, not only to provide comfortable working conditions during emergencies, but to prevent condensation on radio and power equipment which could interfere with normal operation. The heating plant normally is operated so as to prevent the inside temperature dropping below 40 degrees Fahrenheit. This has the added advantage of facilitating the starting of the engine unit and preventing loss of battery capacity at excessively low temperatures.

Vibrators

The vibrators, which normally are intended to carry the radio load only until the engine unit has started and attained a steady operating condition, are big brothers to the units used for automobile radio operation, and are the largest size available which have been in use long enough to establish a satisfactory record of reliability. (See Figure 2.) Each vibrator has an output rating of 750 volt-amperes of 115-volt 60-cycle alternating current, and delivers its full-capacity a-c output almost instantaneously after closing of the d-c input circuit. Inasmuch as the radio load for a relay station, sending and receiving in two directions, is slightly in excess of 1 kva, it was necessary to divide the load between two 750-volt-ampere vibrator units. The units are supplied from the storage battery which is kept fully charged at all times.

Engine Generator Units

Inasmuch as remote-controlled automatic engine-generator units had been used by the thousands during the war in various branches of the armed services, there was considerable choice in the selection of such equipment. Various models produced by five of the larger manufacturers were inspected and compared, and a design worked out which incorporated the various features of the different makes that were considered essential for the radio-beam service. Four-cylinder gasoline engine drive (Figure 3), was selected in preference to a single or 2-cylinder diesel engine for two major reasons. First and foremost was the conviction that more reliable starting under cold weather conditions would be assured, particularly with unattended operation. Secondly, it appeared probable that the operation, adjustment, and emergency repair of gasoline engines would be more familiar to the average maintenance man because of similarity to the ordinary automobile engine. Use of the individual manufacturer's standard arrangement of starting and protective controls was adhered to so far as practicable, since these invariably had been used on a sufficient number of units to insure that basic faults had been eliminated.

The engines are radiator cooled. Two motor-operated louver openings are provided in the building wall for venting the heated radiator air and for admitting fresh cool air. The radiator-air exhaust opening is located directly in front of the engine; a canvas duct is provided between the front of the radiator and the opening to direct the air flow and to insure maximum discharge from the room, particularly during the summer months. Protective hoods are provided on the outside to prevent drifting snow, ice, or sleet from plugging the opening or interfering with the operation of the louvers, Figure 4. Only a very coarse 1/2-inch mesh screen was specified, to further reduce the possibility of restricting the air flow, either by the screen itself or as a result of snow or ice being deposited on the screen. Various protective devices, to shut down automatically the engine in the event of overheating, improper lubrication, or operation at excessive speed, are provided.

The alternator is equipped with a special voltage regulator, developed by the Electric Machinery Company. This voltage regulator has no moving part or contacts; this should reduce operating difficulties from such sources to a minimum. The engine governor is capable of maintaining a speed within limits of one per cent maximum variation at any given constant load, and four per cent maximum change between no load and full load.

An underground gasoline-storage tank of 120-gallon capacity is provided at each of the normal 1-beam stations. This will provide for about five or six days continuous operation, which is considered adequate to allow time for replenishment, even under severe weather conditions. The quantity in storage is limited purposely in order to minimize the possibility of gum formation which will occur when gasoline is stored for periods in excess of one year. Such gum formations easily could clog up the carburetor or fuel pump and cause failure of the plant to function, without prior warning.

Battery and Charging Rectifiers

In the majority of relay stations where only one radio beam is involved, a 57-cell 100-ampere-hour-capacity storage battery is used to supply the d-c input to the vibrator units. A somewhat larger battery is provided at stations such as Neshanic, where additional load is imposed by extra beam circuits. The battery is kept on trickle charge from a regulated-output selenium rectifier, developed primarily for this project. This rectifier maintains a constant voltage on the battery regardless of supply voltage variations within limits of 90 to 130 volts, so that the battery is kept fully charged at a rate just sufficient to offset internal losses. When the battery is used during a power failure, the charging rate is increased automatically until the battery is restored to a fully charged condition, at which time the trickle rate again prevails. The rectifier also is designed with inherent characteristics which prevent overloading and burning-out of the rectifier stacks or transformer.

A separate battery with rectifier charger is provided for starting the engine-generator unit.

Control Equipment

The major portion of the transfer switching and control equipment is incorporated on the main control panel, Figures 5 and 6, and is mounted immediately adjacent to the engine unit. This panel is enclosed in a metal cabinet with hinged double doors, front and back, to facilitate access. The two voltage-control relays, which constitute the "brain" of the plant, are mounted on rubber supports fastened to the side of the cabinet, to prevent vibration or jars from affecting their operation. Connections from the voltage-control relays to the panel are made through multiple-conductor plugs and receptacles to facilitate testing, removal, and replacement of the units. The upper control relay, shown on the left side of the cabinet in Figure 5, provides the signals required for starting and stopping the unit and for operation of the main transfer switch. The lower unit controls transfer of the radio load to and from vibrator operation.

The voltage-control relays were designed especially for this project, since nothing was commercially available which would provide the degree of sensitivity and other characteristics desired. The alternating voltage to be monitored is applied to a small bridge-type selenium rectifier, with a 75-microfarad capacitor

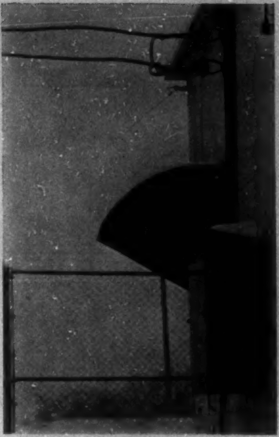

Figure 4. Air intake hood and power service entrance meter cabinet, gasoline tank

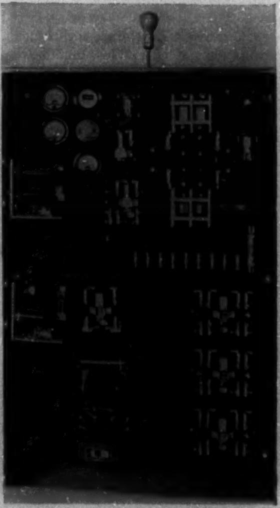

Figure 5. Main control panel, front

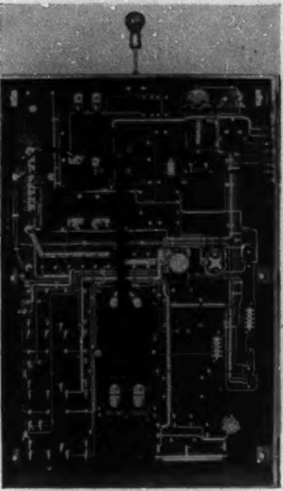

Figure 6. Main control panel, rear

across the d-c output of this rectifier as a filter. Variations in the alternating voltage are reflected directly in the direct output voltage of this small rectifier. A Western Union *41-C* relay, standard except for armature air-gap and contact-spring adjustments, is used to detect these variations. The two voltage-control relays are essentially identical except for the method used for obtaining the different time delay desired on the reclosing operation. In one, charging of a capacitor through a fixed resistor provides the desired 5-second delay; the other, shown in Figure 7, utilizes a small synchronous-motor-driven cam to provide a 1-minute delay, to give time for the engine unit to attain stable operation. Toggle switches are provided to by-pass the control relays, so that they may be tested and adjusted without unnecessary transfer of load to the engine unit or vibrators. A pilot light at the top of the control cabinet indicates when any of the special test switches are not in normal position for full-automatic control, to guard against the maintenance man inadvertently leaving the station without protection.

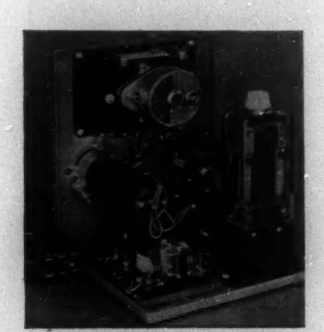

Figure 7. Voltage control relay for secondary transfer switch control

A special portable test set was designed for checking the adjustment of the voltage-control relays. Because of normal manufacturing variations in the small selenium-rectifier stacks, resistors, and other components, it is essential that each *41-C* relay be checked and adjusted in conjunction with the actual unit in which it is to be used. The relay test set provides a variable alternating voltage and an a-c meter, together with cord and plug connectors and indicator lights, so that the *41-C* relays may be checked conveniently in the required manner, without interference with operation of the radio circuit.

Meters on the main control panel show station load, voltage and frequency of outside power, engine, and vibrator units, and provide ready means for checking operation of the plant. An elapsed-time meter maintains a continuous record of hours of engine operation and shows whether any failures of regular power have occurred between inspections. A control switch is provided which permits testing of the engine unit either at no load or under load, simulating an actual power failure.

Also included on the main control panel are fuses for protection of load and control circuits, engine unit circuit breaker, auxiliary protective relays, and a selenium rectifier for charging the engine-starting battery. This battery is normally kept on a slow trickle charge in order to maintain it at full capacity. A higher charging rate is available from the rectifier for use if required.

The rectifier and its control components are housed in a rack cabinet, Figure 8, which also is used for mounting circuit breakers in the d-c input circuits to the vibrator units and the a-c input to the regulating transformers. The two vibrators and two regulating transformers required at the average 1-beam station are housed in this same cabinet, to simplify the installation of equipment. The main control cabinet, associated with the engine unit, and the rectifier cabinet were completely assembled, wired, and tested before shipment to the station. It then was necessary only to put these two units in place, to provide interconnections between them, and to the radio equipment, power service entrance switch, engine unit, and lighting cabinet, to complete the installation. Since many of the relay stations were in isolated locations, material savings in installation costs were thus effected.

Terminal Station Power

Because the terminal stations are manned 24 hours a day, the radio-system power facilities at these points are of a more usual type than described in the foregoing. Existing emergency supplies were utilized where available; vibrators were installed to serve as an instantaneous source of alternating current where an existing battery reserve was available. The same type of voltage-control relay as used in the relay stations was utilized at the terminal stations to control transfer of the radio load from regular to vibrator

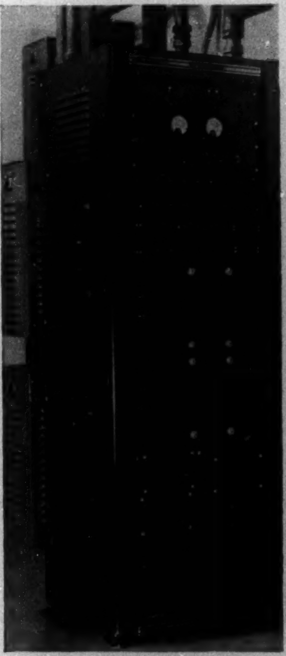

Figure 8. Relay-station rectifier and power equipment cabinet

Table I

Station	Number of Failures of Commercial Power Supply	Total Duration of Failures Hours	Minutes
Neshanic	12	31	43
Mount Laurel	4	15	3
Brandywine	0		
Elk Neck	2	6	1
Cub Hill	2	7	10
Severn	3	1	10
Washington Terminal	6	All momentary	
New York Terminal	0		
Total all stations	29	61	7

power. The regulating transformers and vibrators, voltage control relays, transfer switches and associated protective circuit breakers, and alarm equipment for a two-beam terminal are housed in a rack cabinet such as shown in Figures 9 and 10.

Operating Experiences

The preceding general description of the radio-beam power plants and some of the considerations which affected their design, necessarily lacks considerable detail regarding such items as the engine-starting control and protective devices, generator voltage regulators, radio shielding, power distribution to radio equipment on the tower, and actual circuit diagrams. Rather than attempt to describe these various details, it would seem more desirable to present a brief resume of the operating results experienced to date with the power equipment of the radio-beam system.

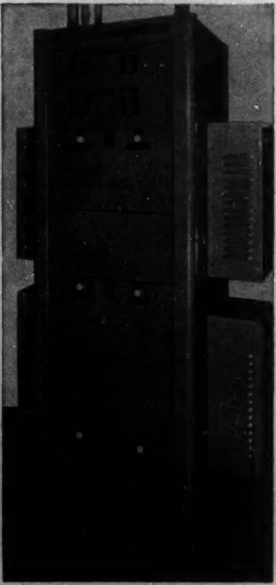

Figure 9. Terminal-station power equipment cabinet, front view

The New York–Philadelphia circuit was put into actual traffic operation late in 1947. The New York–Washington installation was completed and put into traffic operation on a trial basis during February, 1948. The New York–Pittsburgh and Washington–Pittsburgh circuits were completed and operated under test conditions a few months later. Operation was continued until late August, 1948, when regular operation was discontinued temporarily to permit changes in tower construction incidental to the installation of additional television channels between New York and Philadelphia, and to make adjustments in radio equipment, which operating experience had proved desirable. This, in effect, constituted the initial field trial of the power plants.

The emergency engine at Neshanic carried the station for a continuous period of over nine days, following the great ice storm of January 1–2, 1948. During this period, all power lines in the vicinity were down due to the storm, as were also all open-wire telegraph circuits between New York and Philadelphia. However, the radio system continued to function throughout the emergency and to provide reliable circuits for traffic service. Later, while the New York–Washington circuit was carrying traffic on a fairly regular basis, accurate records of operation were kept.

Table I shows the number and duration of power-supply failures occurring at each of the terminal and relay stations on that one circuit during the 3-month period between May 1 and August 1, 1948.

There was no interruption of the radio-beam circuit during that period, and no failure of the power equipment to function, indicating a high degree of reliability.

Subsequently, during a widespread snow, ice, and rain storm on December 15–16, 1948, at least 16 separate power failures occurred, affecting 10 of the 18 relay stations on the three beam circuits comprising the New York–Washington–Pittsburgh triangle. As many as six of these stations were operating on emergency power at a time, making it difficult for terminal station attendants to correctly interpret and accurately log the multitude of alarm signals being transmitted. Table II indicates the number and duration of failures, as accurately as could be determined from the log and subsequent detailed reports submitted by the maintainers. It will be noted that the outages of the commercial power sup-

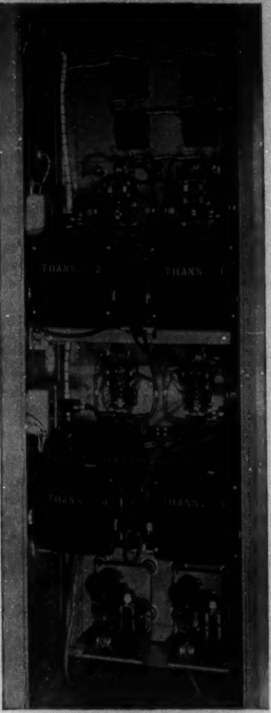

Figure 10. Terminal-station power equipment cabinet, interior view

Table II

Station	Number of Failures of Commercial Power Supply	Total Duration of Failures Hours	Minutes
Brandywine	3	3	23
Honeybrook	1	4	38
Red Lion	1	0	45
Blue Mountain	5	17	10
Allegheny	1	3	15
Bakersville	2	25	22
Jennerstown	1	0	38
Little Savage	1	81	8
Sidêling Hill	2	7	55
Gambril Park	1	7	20
Total all stations	18	151	34

ply add up to the rather astonishing total of approximately 150 hours.

Operation of the power-plant equipment was not perfect in all these instances, as there were two rather serious outages of the beam circuit caused by loss of power. One of these was caused by a regulating-transfer circuit breaker opening at the instant the load was transferred back to regular power, apparently because of faulty circuit-breaker operation, or because there was a current surge larger than had been designed for. In two other instances, these circuit breakers failed to function properly, but in these cases the maintainer was present and closed the circuit breaker immediately. Higher-capacity circuit breakers subsequently have been substituted at all stations.

In the other beam interruption, actual failure occurred because of a combination of circumstances. Here, the engine unit failed to start, and at the same time, the keying unit associated with the radio fault-tone alarm system failed to function, so that no one knew the power had failed until actual interruption of the beam occurred. Subsequent investigation showed that the station operated satisfactorily on battery power for at least nine hours after the regular power failed. Failure of the engine to start was apparently due to the exhaust pipe opening being completely clogged with ice, in spite of the precautions which had been taken to prevent such an occurrence. This constituted the only major interruption of the beam caused by lack of power during this entire interval.

In another case, the radio load remained on battery for two hours before being picked up by the engine unit, which then operated satisfactorily until the end of the power failure five hours later. There was no interruption to the radio beam.

What happened to the power unit only can be surmised from the fact that there were ice and carbon deposits around the exhaust pipe and muffler joints, quite similar to what were found in the previously described failure.

The operation of the power plants at the various radio-relay stations has been very gratifying. The reliability already demonstrated gives ample assurance that lack of power will not destroy the advantages of microwave radio beams for operation through fog, sleet, ice storms, and lightning, at times when these same elements may completely paralyze commercial power supplies.

No Discussion

A Microwave Communication Relay System

WILSON P. BOOTHROYD
NONMEMBER AIEE

HAROLD J. CHURCHILL
NONMEMBER AIEE

Synopsis: This paper describes the design of a microwave radio relay repeater suitable for use in communication systems requiring low distortion repeaters. The modulation bandwidth is approximately 500 kc for the illustrated design. The repeater employs negative feedback, and features extreme simplicity of electrical and mechanical design.

AT PRESENT, two general types of repeaters are in common use in the field. They are the subcarrier-type of remodulating repeater and the heterodyne-type repeater. Both types have features of excellence but are usually more complex than may be necessary for general communication service. The repeater to be described is advanced as an application and extension of techniques in related engineering fields to radio relay systems.[1,2]

This radio repeater is based on the use of a form of locked radio frequency oscillator. An incoming, frequency modulated, radio frequency carrier is used to cause a deviation of the oscillator output signal in accordance with the modulation of the incoming carrier. The oscillator signal is radiated as the repeater output signal. Figure 1 is a block diagram of a typical equipment. With the switch S open, the circuit is recognized as a conventional heterodyne receiver with the detected modulation of the incoming carrier appearing at the video amplifier output as a video signal. With the switch S closed this video signal is applied to the radio-frequency oscillator so as to cause its output signal to be frequency modulated in the same sense as the incoming carrier. Closing switch S thus closes the loop of a negative feed-back amplifier, and a study of the repeater performance can be made on the basis of feed-back amplifier analysis.

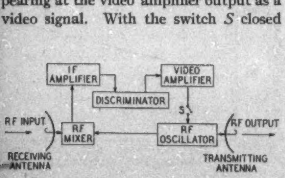

Figure 1. Block diagram of repeater

The performance of this type of repeater is measured by the accuracy with which the radiated radio-frequency oscillator signal corresponds to the incoming carrier signal in both magnitude and phase of modulation. The application of feedback in this repeater is operative in two major ways to minimize the distortions ordinarily encountered. First, the feedback decreases the distortion of nonlinear circuits, such as the control voltage versus output frequency characteristic of the radio-frequency oscillator. Second, the deviation of the intermediate frequency signal of the amplifier, which is the difference between the incoming carrier and the radio-frequency oscillator deviations, is small, so that phase and amplitude distortions in the intermediate-frequency amplifier are minimized. Other salient features of the repeater will be considered after an analysis of some general feed-back amplifier requirements.

General Feed-back Systems

A natural starting point in the analysis of the repeater is the standard inverse feed-back amplifier block diagram[3] shown in Figure 2.

$$E_o = \mu E_{IN} - \mu\beta E_o$$

where

μ = forward gain of the amplifier
β = fraction of E_o applied to amplifier input

$$E_o(1+\mu\beta) = \mu E_{IN}$$

$$\frac{E_o}{E_{IN}} = \frac{\mu}{1+\mu\beta}$$

The negative sign is used on the second term because this is an inverse feed-back system.

As applied to the repeater of Figure 1, the total voltage at the output of the amplifier is applied as a frequency control voltage to the local oscillator; therefore β equals 1, and the transmission equation becomes

$$\frac{E_o}{E_{IN}} = \frac{\mu}{1+\mu} \qquad (1)$$

In analyzing the repeater we prefer to consider the modulation on the incoming carrier as E_{IN} and the modulation of the radio-frequency oscillator output signal as E_o. It is further assumed that the modulation characteristics of the radio-frequency oscillator in each repeater shall be identical.

Equation 1 is the basic transmission equation of the system upon which the final calculations will be based. μ, the forward gain of the system, should be high in order that E_o/E_{IN} will approach unity. This ratio must be very close to one in order to make it possible to relay the modulation through multiple repeaters without serious loss of modulation. In any feed-back system, however, it is necessary that the feed-back factor $\mu\beta$ be less than one when the phase shift reaches 180 degrees. This is known as Nyquist's criterion.[4]

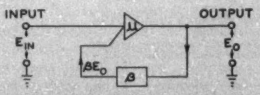

Figure 2. Basic feed-back diagram

Paper 49-158, recommended by the AIEE Communication Committee and approved by the AIEE Technical Program Committee for presentation at the AIEE Summer General Meeting, Swampscott, Mass., June 20–24, 1949. Manuscript submitted March 22, 1949; made available for printing April 29, 1949.

WILSON P. BOOTHROYD and HAROLD J. CHURCHILL are both with the Philco Corporation, Philadelphia, Pa.

Design of the Feed-back System

It is known from this criterion that an amplifying system will not oscillate if the magnitude of the amplifier forward gain at the 180 degree phase shift frequency is less than unity. The specifications for this repeater system require, in addition, that the ratio of E_o/E_{IN} with feedback shall be as nearly constant as possible throughout the desired modulation frequency range. In order to meet this last requirement it is usually desirable that the ratio $\mu/(1+\mu)$ should have an initial value at low frequencies, very near unity. In the following discussion, μ will be considered as a vector having both magnitude and phase components.

Figure 3 is a vector plot of the ratio $\mu/(1+\mu)$. In the first quadrant Figure 3(A) (phase shift of the μ circuit under 90 degrees) $\mu\underline{/\theta_1}/(1+\mu)\underline{/\theta_2}$ must always be less than unity since the real component of $\mu\underline{/\theta_1}$ is positive. Therefore the ratio of E_o/E_{IN} at low frequencies (where the phase shift is under 90 degrees) is less than unity, but will approach this value when the magnitude of μ is large. In the second quadrant (phase shift in the μ circuit between 90 and 180 degrees) $\mu\underline{/\theta_1}/(1+\mu)\underline{/\theta_2}$ will exceed unity if the real component of $\mu\underline{/\theta_1}$ is less than $-.5$. This is shown in Figure 3(B) and is undesirable, as this condition reveals regeneration within the amplifier. $\mu\underline{/\theta_1}/(1+\mu)\underline{/\theta_2}$ will be less than unity if the real component of μ/θ_1 is greater than -0.5. This is shown in Figure 3(C) and is the desired condition. Since both the magnitude and phase of the vector μ are functions of frequency, we are interested in a plot of the locus of the vector μ for all frequencies in the passband.

At this point it must be noted that a repeater as shown in Figure 1, involving both frequency modulation and amplitude modulation circuits as a part of the feedback loop, is unusual when analyzed to determine the parameters of the basic feed-back circuit. For example, the forward gain of the repeater is given by the equation

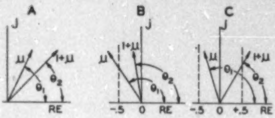

Figure 3. Plot of vectors μ and $1+\mu$

$$\frac{A_{osc}}{A_{disc}}\times G=\mu \tag{2}$$

where

A_{osc} = deviation characteristic in megacycles per volt of control voltage of the radio-frequency oscillator.

A_{disc} = discriminator characteristic in megacycles per volt of the video signal output of the discriminator, at the maximum carrier level provided by the intermediate-frequency amplifiers and limiters.

G = gain of the video amplifier circuits.

Since the A terms are constants not affected by the modulation frequency in the ideal case, the G term determines the relationship of the magnitude of μ to the modulation frequency. For reasons which will be developed later, the video amplifier must be a very narrow band amplifier with a bandwidth of approximately 1.3 kc. Thus the response of this amplifier may be taken as determining the magnitude of μ in accordance with equation 2. However, the phase angle of the μ circuit is determined by the complete amplifier. The phase characteristic calculations for a typical repeater composed of the circuits noted are shown in Table I. In these calculations, it has been assumed in each case that the carrier frequency is centered on the intermediate-frequency amplifier response, and that only envelope delay need be computed. This is not rigorous, but appears to be a necessary assumption in this first calculation. The video amplifier bandwidth is substantially less than the modulation frequencies tabled, therefore the phase shift of this amplifier is entered as a constant 90 degrees in the table. Figure 4 is a plot of the total phase shift taken from Table I. We can now progress to a determination of actual circuit values for a desired repeater performance characteristic.

Table I. μ Circuit Phase Response

Stage	Modulation Frequency 50Kc	100Kc	200Kc	500Kc	1Mc	1.75Mc
Intermediate frequency input stage (Double tuned, critically coupled, pole separation 16 megacycles)	0.32	0.64	1.28	3.20	6.5	11.7
6 Intermediate frequency stages (Double tuned, critically coupled pole separation 21 megacycles)	1.26	2.52	5.04	12.60	27.6	52.2
Discriminator (Pole separation 10 megacycles)	0.55	1.10	2.20	5.50	10.9	19.7
Discriminator (Reactance-capacitance output)	0.18	0.36	0.72	1.80	3.6	6.3
Narrow band amplifier (1.3 kc)*	88.50	89.30	89.50	89.70	89.90	90.00
Totals	90.8	93.9	98.7	112.8	138.5	179.9

*Note: In initial calculation when this bandwidth is not known, the amplifier phase shift can be entered as a constant 90.0 degrees.

Typical Design Calculation

It has been pointed out that the response of the video amplifier of the repeater is a very narrow band compared to the bandwidth of all other circuits. It is therefore the determining response of the gain versus frequency characteristic, and if the stage be a simple resistance-capacitance circuit (without peaking) then

$$\frac{\mu}{\mu_{max}}=\frac{1}{\sqrt{1+\left(\frac{f}{f_2}\right)^2}} \tag{3a}$$

where

f_2 = the cutoff frequency of the amplifier (3 decibels down)

μ_{max} = gain of amplifier at frequency 0 cycles per second

when

$$\frac{f}{f_2}>10$$

$$\frac{\mu}{\mu_{max}}\doteq\frac{f_2}{f} \tag{3b}$$

From Figure 4 we derive that the phase shift in radians for a frequency f (megacycles) is expressed by

$$f=1.10\theta-1.64 \tag{4}$$

in the region 0.5 to 1.0 megacycles.
From equations 3 and 4 we get

$$\mu\cos\theta=\mu_{max}\frac{f_2\cos\theta}{1.10\theta-1.64} \tag{5}$$

where

μ = the forward gain of the circuit at a frequency.

θ = the phase shift in radians at the same frequency.

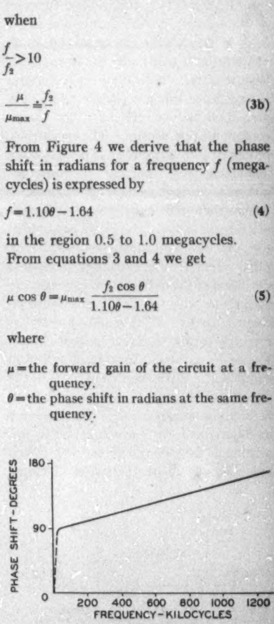

Figure 4. Plot of Table I

Table II. Repeater Tracking Coefficient

Frequency Kc/Second	$\mu/\underline{\theta_1}$	$(1+\mu)/\underline{\theta_2}$	Tracking Coefficient Per Cent	Degrees
0	$499/\underline{0^\circ}$	$500/\underline{0^\circ}$	99.80	0
1	$396/\underline{40.3^\circ}$	$396.76/\underline{40.21^\circ}$	99.80	0.09
10	$64.3/\underline{83.10^\circ}$	$64.43/\underline{82.22^\circ}$	99.80	0.88
50	$13.0/\underline{90.80^\circ}$	$13.024/\underline{86.40^\circ}$	99.81	4.40
100	$6.50/\underline{93.90^\circ}$	$6.509/\underline{85.08^\circ}$	99.86	8.82
200	$3.25/\underline{98.70^\circ}$	$3.253/\underline{81.00^\circ}$	99.92	17.70
500	$1.29/\underline{112.8^\circ}$	$1.2901/\underline{67.19^\circ}$	99.99	45.61
730	$0.891/\underline{124^\circ}$	$0.893/\underline{55.81^\circ}$	99.80	68.19
1,000	$0.65/\underline{138.2^\circ}$	$0.674/\underline{40.10^\circ}$	96.50	98.10
1,750	$0.37/\underline{180^\circ}$	$0.63/\underline{0^\circ}$	58.70	180

Now, in considering the locus of the vector μ, we wish to find the phase angle at which the real part of μ ($\mu\cos\theta$) is a minimum, in order to design our circuits so that the magnitude of the ratio $\mu\angle\theta_1/(1+\mu)\angle\theta_2$ shall never equal or exceed unity. This is assured by making $\mu\cos\theta$, at the frequency of its minimum value, greater than -0.5 as explained in Figure 3.

To find the phase angle at which $\mu\cos\theta$ is a minimum, differentiate $\mu\cos\theta$ as expressed in equation 5 with respect to θ, and solve for μ when $d(\mu\cos\theta)/d\theta=0$.

This gives $\theta=2.16$ radians $=124$ degrees but $f=1.10\theta-1.64$.

Therefore $f=0.73$ megacycles per second which is the frequency at which $\mu\angle\theta_1/(1+\mu)\angle\theta_2$ is a minimum. Since this ratio has been defined previously as E_o/E_{IN} and must be less than unity, we set the ratio equal to 0.998 which is the minimum ratio which we desire through the repeater passband.

Then at 730 kc

$$\frac{\mu\angle 124 \text{ degrees}}{(1+\mu)/\underline{\theta_2}}=0.998$$

which solves for $\mu=0.891$ at 730 kc.

For

$f>10f_2$

$$\mu_{max}=\mu\frac{f}{f_2}=\frac{(0.891)(730)}{f_2} \text{ from equation 3}$$

$$\mu_{max}f_2=650 \qquad (6)$$

μ_{max} has been defined as the absolute value of the forward gain at zero frequency, but at zero frequency the phase shift is also zero. Therefore setting E_o/E_{IN} at zero frequency equal to 0.998 (our minimum ratio)

$$\frac{E_o}{E_{IN}}=\frac{\mu/\underline{0}}{(1+\mu)/\underline{0}}=0.998$$

$$\mu/\underline{0}=499=\mu_{max}$$

Therefore, from equation 6, $f_2=1.3$ kilocycles per second.

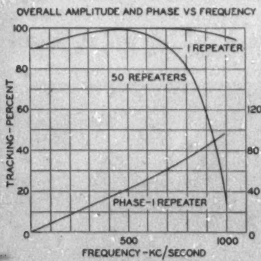

Figure 5. Tracking curves

Having found μ_{max} and f_2 these values can be substituted in equation 3 from which

$$\mu=\mu_{max}\frac{f_2}{f}=\frac{499f_2}{f}=\frac{650}{f}$$

where f is in kilocycles and is greater than $10f_2$.

Or, for all values of f in kilocycles

$$\mu=\frac{\mu_{max}}{\sqrt{1+\left(\frac{f}{f_2}\right)^2}}$$

$$=\frac{499}{\sqrt{1+\left(\frac{f}{1.3}\right)^2}}$$

from equation 3a.

We now have μ and θ, as a function of frequency for our specific design, hence we can now plot $\mu\angle\theta_1/(1+\mu)\angle\theta_2$ as a function of frequency to determine E_o/E_{IN} versus frequency. This is our original measure of performance of the repeater, and the results are shown in Table II and plotted in Figure 5. It is convenient to refer to these results as the "Tracking Coefficient" of the repeater versus frequency.

Figure 5 also includes the response curve of a 50-repeater chain. Variations of the foregoing analysis to obtain different performance curves are possible. For instance, a higher tracking coefficient over the same bandwidth can be obtained by increasing μ_{max} and decreasing f_2; alternately, a lower tracking coefficient can be maintained over the same bandwidth with a smaller μ_{max}.

However, the following summarizing statements will be true:

1. Due to the gain and phase shift characteristics of the system, the feed-back factor is a function of frequency, being highest at low frequencies.

2. The foregoing analysis is accurate only at frequencies where the feedback is adequate to reduce the carrier deviation in the intermediate-frequency amplifier so that the amplitude-modulation analysis of intermediate-frequency amplifier envelope delay does not introduce too large an error.

Considerations in the Design of Electrical Circuitry

The usual receiver design requires a prescribed bandwidth and associated linear phase response. The magnitude of the phase shift is usually not important. However, in this feed-back system, as in any other, the frequency should be as high as possible before the phase shift reaches 180 degrees. To obtain the necessary feed-back factor, a large gain also is necessary. The basic requirement, therefore, is that the ratio of gain to phase shift must be a maximum. A first detector-video amplifier-type of repeater is attractive in principle since a low-pass video-frequency amplifier has a single sided response, thus requiring only one-half the bandwidth of that of a band pass amplifier stage passing the same intelligence. This means that the gain per stage of a video amplifier would be double that of an intermediate-frequency amplifier for the same phase shift. However, the practical difficulties encountered in such a low level video amplifier makes it unfeasible, and various band-pass intermediate-frequency circuits must be considered.

The simplest type is the synchronous single-tuned type. For a given required gain the total time delay should be a minimum. This can be calculated by differentiating $n \tan\theta$ with respect to the variable Q and setting it equal to zero to obtain the minimum.

n = number of stages
θ = phase shift per stage
Q = Q for the resonant circuit

The optimum gain per stage is $\epsilon=2.73$. This result is independent of the intermediate frequency and the type of tubes used although a tube with a high figure of merit should be used to minimize the phase shift for the optimum gain per stage.

The synchronous, double-tuned intermediate-frequency amplifier was investigated next and found superior to the single tuned amplifier. For a given pole configuration, the unsymmetrically damped transformer gives the greatest gain per stage. As the coupling is increased beyond critical coupling, the gain at center frequency decreases slowly but the phase shift also decreases. The net result is that the ratio of gain to phase shift increases with coupling for a multistage amplifier. There is of course a limit to the degree of coupling that can be used. For the overcoupled case, tremendous peaks occur outside the desired passband thus increasing the noise bandwidth and reducing the selectivity of the amplifier. In our calculation, critically coupled circuits were used.

Rejection of amplitude modulation of the incoming carrier may be obtained by means of a conventional limiter following the intermediate-frequency amplifier, although such circuits have poor gain, phase shift characteristics, and a fast automatic gain control circuit appears to be more advantageous.

The conventional Foster-Seeley discriminator was chosen in our experiments for its sensitivity and bandwidth capabilities. The narrow-band video-amplifier stage can conveniently be made to have very high gain by supplying it with an adequate plate supply voltage, so that although it may have 90 degrees of phase shift throughout most of the useful band its gain to phase shift ratio is favorable. Further, it is often convenient to direct couple through all video circuits from the discriminator output to the radio-frequency oscillator control electrode. By this means automatic frequency control, whereby the oscillator is locked on the incoming carrier but differing therefrom by the intermediate-frequency center frequency, can be obtained with conventional circuitry, see Figure 6.

In most applications it will usually be found desirable to include some radio frequency preselection ahead of the first detector. This may take the form of a waveguide filter. Since it is outside of the feed-back loop, it does not affect the feed-back calculations and it must be treated as a parameter in the external transmission circuit.

Mechanical Considerations

In the application of any repeater, the mechanical properties may be as important as other characteristics. In one design, a parabolic antenna, employing a waveguide horn feed, was equipped on the rear with an insulated aluminum box measuring 14 by 12 by 8 inches. The entire assembly was designed for sealing and pressurization and, ready for mounting, would weigh under 50 pounds. Figure 7 is a typical waveguide assembly including the radio-frequency oscillator tube and mount, output transmission line, crystal mixer mount, and a triple tuned waveguide input preselector. The amplifier stages have been assembled on a 6 by 8 inch chassis which is mounted from the waveguide. This assembly did not include any provision for mounting a second or transmitting antenna, as this requirement would vary with installations.

It would not appear that this repeater would ordinarily be mounted on a tower since its size would permit satisfactory mounting from an "I" beam or pole. Similarly no power supplies are included in the basic design since the 35-watt total power requirement of the repeater may be obtained in many ways.

System Specifications

This paper cannot dwell at length on the specifications of a complete repeater system but a few highlights should be emphasized. First, the feed-back ratio of the repeater in our example is 54 decibels at zero frequency, and the ratio decreases from 51 decibels at 1.3 kc, at the rate of 6 decibels per octave, to a value of 3 decibels at 330 kc. Thus if the harmonic distortion of the repeater is at the level of −35 decibels below signal without feedback, the repeater with feedback could be expected to be improved by the above feed-back ratios. Also a considerable reduction in microphonic or other disturbances occurring within the feed-back loop can be expected.

A typical signal to noise calculation for a repeater operating with a transmitter power of 50 milliwatts might be as shown in Table III.

Table III

	Decibels
Transmitter power (50 milliwatts)	−10
Antennas gain (two 4-foot parabolic antennas at 6,500 megacycles)	+74
Transmission loss (25 miles)	−138
Converter and input circuit noise figure	−14
Receiver noise level (±7 megacycles bandwidth)	−133
Frequency modulation improvement (±3 megacycles deviation with 0.5 megacycles video bandwidth)	+20
Video signal/noise ratio	65

Conclusions

The radio repeater system described in this paper appears from calculations and tests to have many desirable characteristics when applied to the problem of relaying communication signals of medium bandwidth over long relay chains. The application of negative feedback ap-

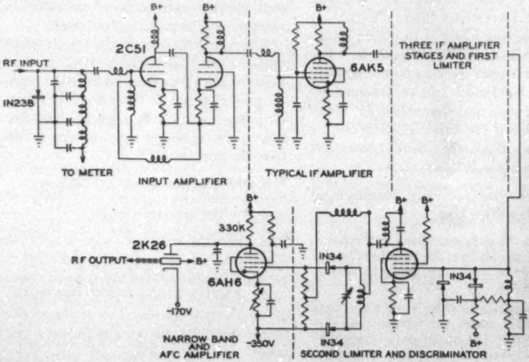

Figure 6 (left). Partial schematic diagram

Figure 7 (below). Repeater waveguide assembly

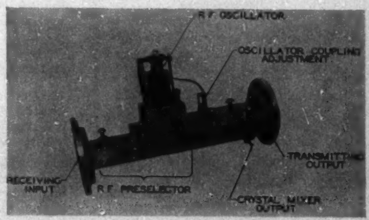

pears to have materially improved the performance of the remodulation type of repeater and thereby increased its application range and usefulness. Many avenues of improvement over the repeater described are still open for investigation, but the existing design represents the summation of our initial work.

References

1. Application of Negative Feedback to Frequency Modulation Systems, J. G. Chaffee. *Bell System Technical Journal* (New York, N. Y.), volume 18, July 1939.

2. Duplex System of Communication for Microwaves, R. V. Pound. *Proceedings*, Institute of Radio Engineers (New York, N.Y.), volume 36, July 1938.

3. Network Analysis and Feedback Amplifier Design (book), H. W. Bode. Van Nostrand Company, New York, N. Y., Chapter 19.

4. Regeneration Theory, H. Nyquist. *Bell System Technical Journal* (New York, N. Y.), volume 11, January 1932.

No Discussion

A New Expanded Scale A-C Voltmeter

N. P. MILLAR
ASSOCIATE AIEE

THE accurate measurement of power system voltage has become increasingly more important to the power station attendant than in former years. There are several reasons why this is true as the complexity of system operation has increased with the growth of household, commercial, and industrial power demands. A few of the more important reasons for voltage measurement are:

1. To facilitate interconnections between systems. All stations participating in interconnection activities must have their voltages set to within reasonable limits of each other.
2. To satisfy more critical home appliance voltage requirements, particularly for electric stoves and other heating devices.
3. To control central station bus voltages in order to keep operations within the capacity ratings of generating and distribution equipment.

Method Used for Scale Expansion

Heretofore, the measurement of voltage has been accomplished by conventional zero-left a-c moving-iron or electrodynamic voltmeters with square law scale distribution characteristics. Experience has shown that in many applications the measurement problem consists of detecting and measuring a variation of ±1 volt or less from a given reference voltage. This reference voltage is usually 120 volts or multiple thereof as determined by potential transformers. A 1-volt variation from 120 volts represents approximately $^3/_{64}$ inches of arc on a standard 250 degree scale concentric-type switchboard voltmeter, or approximately $^1/_{32}$ inches for conventional 6-inch rectangular voltmeters with 90 degrees scales. Frequently this is not enough of a deflection to read with the desired degree of certainty, since the smallest division on the 250 degree scale corresponds to two volts, and the 1-volt position has to be estimated while in the 90 degree scale instrument the smallest division is usually five volts.

Any instrument that is offered as a solution to this problem must have as a general objective a scale expansion characteristic within the range of the normal voltage variation that produces a scale length per volt of approximately four times that of the standard voltmeter. This gives a scale arc of approximately $^3/_{16}$ inches per volt for the 250 degree scale-type instrument only.

Two general engineering approaches that have been employed in the development of expanded scale voltmeters are:

1. A modification of the basic instrument mechanism.
2. The use of standard mechanisms with impedance networks, the outputs of which vary as some function of the voltage to be measured.

Modified Instrument Mechanisms

One of the simplest methods of modifying the basic instrument mechanism is to suppress the natural zero position of a standard a-c voltmeter. In an ordinary voltmeter, the normal unenergized position of the pointer is at the left end of the scale. Suppression of this zero is accomplished by shifting the position of the control spring on the pointer shaft in a direction to cause the zero to be located at a point beyond the left end of the scale. When this is done, the pointer is restrained by a stop at this end of the scale and will not deflect until an appreciable voltage is applied. A certain degree of scale expansion can be realized by this method, but there is a limit to the amount the zero position can be suppressed. As this amount is increased to give greater scale expansion, the instrument finally becomes unstable. Figure 1 shows by a plot of the dynamic and control spring torque curves the scale distribution that results before and after the zero has been suppressed. Near the point of instability, the torque gradient is nearly zero and the instrument behaves in a sluggish manner. Action of the pointer gives the impression of excessive jewel roll as indicated by gently tapping the instrument. When the instrument responds in this manner, the indicated measurement becomes unreliable. In general for 90 degree scale voltmeters of the moving-iron and electrodynamic types, the zero can be suppressed only 30 to 40 angular degrees.

An equally serious objection to the suppressed zero instrument is the loss of the natural zero setting. Since it is no longer possible to check visually the natural position of the pointer with the instrument unenergized, frequent checks of accuracy with a carefully controlled voltage reference are necessary to determine the constancy of the initial calibration.

Impedance Networks

There are numerous types of expanded scale voltmeters which function in response to the variation of an impedance in some kind of a network to produce an

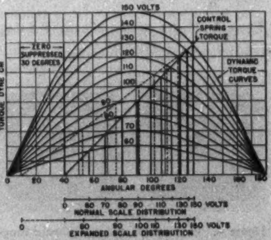

Figure 1. Scale distribution characteristics for a suppressed and unsuppressed zero instrument

---

Paper 49-161, recommended by the AIEE Instruments and Measurements Committee and approved by the AIEE Technical Program Committee for presentation at the AIEE Summer General Meeting, Swampscott, Mass., June 20–24, 1949. Manuscript submitted March 21, 1949; made available for printing April 29, 1949.

N. P. Millar is with the General Electric Company, West Lynn, Mass.

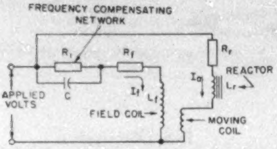

Figure 2. Schematic diagram of expanded scale voltmeter

R_f, L_f—Resistance and inductance of field coil
R_r, L_r—Resistance and inductance of reactor
R_1—C—Resistance-capacitance network for frequency compensation
I_f—Field current, amperes
I_a—Moving coil current

expanded scale distribution. These may have: (a) auxiliary means to produce a voltage that bucks down a portion of the measured voltage; (b) some sort of an electronic tube circuit that cuts out all but the desired voltage range and rectifies the output to be indicated on a conventional permanent-magnet moving-coil end device; or (c) nonlinear circuit parameters in suitable networks.

The most serious problem that confronts an engineer who chooses to develop an expanded scale voltmeter utilizing the afore-mentioned methods is one of component stability. Moreover, for the methods of types (a) and (b), power must be used which further complicates the design and application of the voltmeter.

Saturable Reactor Networks

The most practical solution to the problem of scale expansion is the use of an iron-core saturable reactor in combination with an instrument of the electrodynamic type. Of all the known types of nonlinear circuit components, the iron-core reactor gives the most stable and reproducible performance characteristics. If a voltage is applied across such a reactor, the exciting current will vary in a nonlinear fashion with the voltage. Any suitable a-c milliammeter connected in series with this reactor to measure the exciting current could have its scale calibrated in terms of volts. The scale distribution then would correspond to the nonlinear variation of the exciting current. The milliammeter, therefore, becomes an expanded scale voltmeter that has a good torque gradient and a natural zero position on the scale.

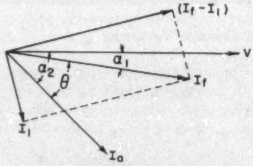

Figure 3. Vector diagram of expanded scale voltmeter

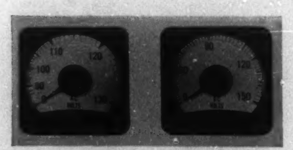

Figure 4. General Electric switchboard long-scale a-c voltmeters

Expanded scale (left) and standard scale (right)

Theoretically, an expanded scale voltmeter could be made using an a-c milliammeter as described, but the application would be impractical for two reasons: the volt-ampere burden would be excessive as compared to normal a-c voltmeter burdens; and the system would not lend itself to convenient and effective frequency compensation, which, it will be recognized, is necessary if a reactor is to be used. These objections can be overcome by placing the saturable reactor in series with the moving coil of a standard electrodynamic wattmeter mechanism and making connections to the voltage source as shown in the schematic diagram of Figure 2. It will be noticed that both the field and moving-coil circuits of the wattmeter are connected in parallel. Frequency compensation can be applied easily by placing a resistance-capacitance network in the field circuit and making the impedance predominantly capacitative. Corrective frequency action can be visualized to advantage by referring to a typical vector diagram of this application as shown in Figure 3.

As frequency increases, the magnitude of the moving-coil current I_a decreases and its phase angle α_2 increases. However, since the field circuit impedance is capacitative, the magnitude of the field current I_f and its phase angle α_1 varies in such a manner as to offset the effect of the armature current change. This results in the instrument torque remaining constant over a reasonable range of frequency variation. With the reactor placed in the moving-coil circuit where the current is small for wattmeter operation, the resulting total volt-ampere burden is comparable with that of the standard voltmeter.

This principle of scale expansion has been applied to an actual design which meets the general requirements of scale expansion without the instability characteristics of other methods.

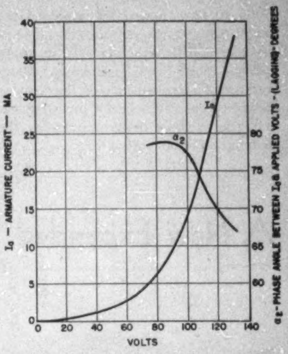

Figure 5. Variation of moving-coil current and phase angle with voltage—expanded scale voltmeter

Design and Performance of Saturable Reactor Voltmeter

The general appearance and design of an a-c expanded scale voltmeter that depends for its scale expansion on the nonlinear characteristics of a reactor follows the same pattern as that of the long-scale indicating instruments described elsewhere.[1,2] It maintains a 250 degree scale arc and utilizes approximately 220 degrees of that arc in expansion from 90 to 130 volts, where 0 to 130 volts is the volt-

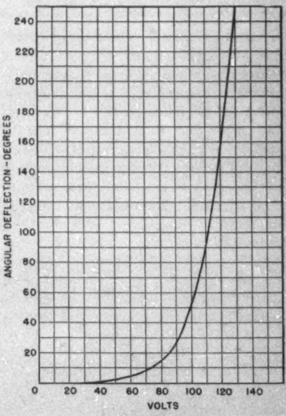

Figure 6. Voltage-deflection curve of expanded scale voltmeter

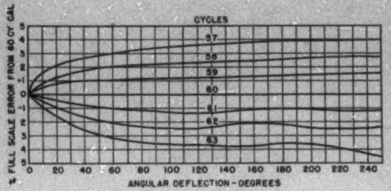

Figure 7. (left) Uncompensated frequency error of expanded scale voltmeter

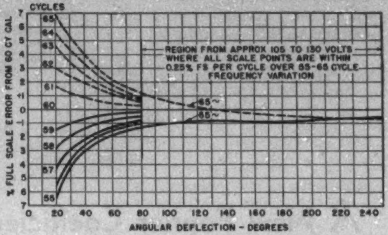

Figure 8. (right) Compensated frequency error of expanded scale voltmeter

meter rating. Figure 4 shows the actual scale distribution of this new device and, for comparison, the distribution of a normal 150-volt voltmeter also is shown.

The average torque on the moving-coil shaft can be written the same as that for any standard electrodynamic system, that is

$$T_{av} = kI_fI_a \cos \alpha$$

where

I_f = field current, amperes, rms
I_a = moving-coil current, amperes, rms
α = phase angle between I_f and I_a, degrees
k = constant of proportionality

In this application, however, current I_a is a nonlinear quantity that varies with voltage approximately as shown in Figure 5. Also shown is the moving-coil current phase angle α_1 as it decreases with increasing voltage. From the generalized circuit diagram, Figure 2, it will be noted that, as the applied voltage increases, the field current I_f also increases, thus aiding the expansion characteristic of the moving-coil current. Altogether, the combined effect produces a rather steep voltage-deflection curve or scale distribution as shown in Figure 6. One half-volt variations can be detected and read easily in the expanded region from 90 to 130 volts with an accuracy of $^1/_2$ per cent of full scale.

The theoretical method of frequency compensation was described in detail in the preceding section on the application of the saturating reactor to a generalized instrument. In practice it is possible to compensate the expanded scale voltmeter so that its frequency error is within ±1/4 per cent of full scale per cycle from 105 to 130 volts and over a ±5-cycle variation from a reference frequency of 60 cycles. Figures 7 and 8 show the frequency error of the expanded scale voltmeter before and after compensation respectively.

This device has a wave form error of less than one per cent of full scale when the voltage source contains both third and fifth harmonics of 5 per cent each. This distortion represents a maximum condition that may be encountered in a large number of power systems, and the average third and fifth harmonic voltages are in the order of 1 to 1.2 per cent of normal.

The average ambient temperature error is shown in Figure 9 in curve form. The temperature coefficient is plus 0.021 per cent per degree centigrade rise from plus 15 to plus 55 degrees centigrade.

The total volt-ampere burden of the voltmeter is nonlinear with the applied voltage as might be expected, and varies from 2.6 at 90 volts to 7.4 at 130 volts full scale, see Figure 10.

Table I lists the important physical constants of the expanded-scale a-c voltmeter in comparison of those of the standard 0-to-150-volt long-scale types.

Table I. Comparative Physical Constants

	Expanded Scale Voltmeter		Standard Voltmeter
Type	AB15	...	AB15
Rating, volts	130	...	150
Accuracy, per cent full scale	0.5	...	1.0
Scale length, inches	7.1	...	7.1
Expansion range, volts	90–130	...	none
Full scale torque, gram-millimeters	7.23	...	4.20
Full scale torque, weight	2.82	...	1.36
Damping factor	67/infinity	...	17.7/infinity
Response time, seconds	0.85	...	1.3

Conclusion

The successful application of a saturating core reactor to a standard electrodynamic wattmeter mechanism has resulted in an expanded scale a-c voltmeter with improved accuracy and reliability. The device is self-contained and requires no auxiliary means for operation. A natural zero has been maintained, and the moving-coil system operates with a high torque gradient for all scale points in the expanded region. A fast-responding moving system makes the device sensitive to small and rapid voltage fluctuations.

It is possible to apply this method of scale expansion to recording instruments and thereby obtain a permanent record of actual voltage fluctuations about a given reference. Since the device is extremely sensitive in the expanded region, the possibility also is suggested for using the principle to advantage in precise voltage control applications.

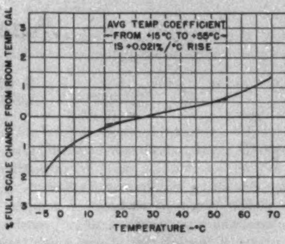

Figure 9. Average ambient temperature error of expanded scale voltmeter

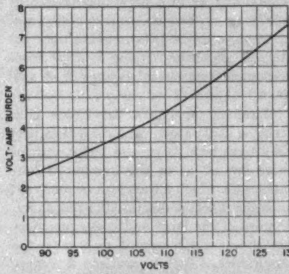

Figure 10. Volt-ampere burden of expanded scale voltmeter

References

1. Advancements in the Design of Long-Scale Indicating Instruments, R. M. Rowell, N. P. Millar. *AIEE Transactions*, volume 66, 1947, pages 155–60.

2. New Long Scale Instruments, R. M. Rowell, N. P. Millar. *General Electric Review* (Schenectady, N. Y.), volume 51, April 1948, pages 14–19.

No Discussion

A New Fourier Coefficient Harmonic Analyzer

S. CHARP
MEMBER AIEE

THE Fourier-coefficient harmonic analyzer is a machine designed primarily for evaluating the Fourier coefficients of periodic waves, or sections of complex waves which are assumed to be periodic outside of the interval within which the wave is to be analyzed. Its usefulness is not limited to any particular branch of engineering or to a particular branch of mathematics, and its general utility and application in the solution of a wide variety of problems ranging in scope from communications to medicine will be evident.

Harmonic analyzers have been constructed in the past, but for the most part they have been large and bulky and far more limited as to the number of harmonics for which a wave can be analyzed than the machine described in this paper. Typical of the large and bulky machines are those which accept as inputs the amplitudes of the sine and cosine components of a wave and produce, usually in the form of a curve, a composite trace of the harmonic components.[1,2] These machines can be used to a limited extent for harmonic analysis, but the range of harmonics which can be obtained is rather restricted. Only two harmonic analyzers have come to the attention of the author which in any way approximate this new machine as to physical size, but neither of them has the harmonic range, the ease of operation, nor the mechanical design features which are incorporated in the machine described.[3,4]

General Description of Machine

The Fourier-coefficient harmonic analyzer can be considered to be a small special-purpose differential analyzer, permanently set up to solve for the Fourier coefficients. It consists essentially of a number of ball-and-roller-type (Ford) integrators and interconnecting mechanisms and counters. Figure 1 is an overall view of the analyzer; Figure 2 shows the front view of the machine proper. The active components are mounted on an aluminum framework provided with free-rolling casters, allowing ready moving of the machine from place to place.

This analyzer carries out the integrations of the following equations which define the coefficients of the Fourier series

$$F(\theta)=A_0/2+\sum_{1}^{\infty}A_n\cos n\theta+\sum_{1}^{\infty}B_n\sin n\theta \quad (1A)$$

$$A_0=\frac{1}{\pi}\int_0^{2\pi}F(\theta)d\theta \quad (1B)$$

$$A_n=\frac{1}{\pi}\int_0^{2\pi}F(\theta)\cos n\theta d\theta \quad (2)$$

$$B_n=\frac{1}{\pi}\int_0^{2\pi}F(\theta)\sin n\theta d\theta \quad (3)$$

Use is made of some of the techniques peculiar to the operation of a mechanical integrator. In such a device, the integrand moves proportionally to the ordinate of the given curve, $F(\theta)$, to be analyzed, and the disk rotates in proportion to the independent variable θ. The incremental output, dA_0, of the integrator is proportional to the product of the two inputs, that is

$$dA_0\propto F(\theta)d\theta \quad (4)$$

Now, the right-hand side of this expression is included in the integrals defining A_n and B_n, hence, upon substitution, these latter coefficients assume the form, neglecting scale and proportionality factors

$$A_0=\frac{1}{\pi}\int_0^{2\pi}F(\theta)d\theta \quad (5)$$

$$A_n=\frac{1}{\pi}\int_{\theta=0}^{\theta=2\pi}\cos n\theta dA_0 \quad (6)$$

$$B_n=\frac{1}{\pi}\int_{=0}^{\theta=2\pi}\sin n\theta dA_0 \quad (7)$$

The implication of these equations is that if one integrator can be made to produce the term A_0 as an output-shaft rotation, then this quantity can be fed into other integrators as a differential input. The outputs of these latter integrators, when the integration is performed over the

Figure 1. Over-all view of the harmonic analyzer

Paper 49-163, recommended by the AIEE Computing Devices Committee and approved by the AIEE Technical Program Committee for presentation at the AIEE Summer General Meeting, Swampscott, Mass., June 20–24, 1949. Manuscript submitted August 11, 1948; made available for printing April 29, 1949.

S. Charp is Research Engineer at The Franklin Institute Laboratories for Research and Development, Philadelphia, Pa. The harmonic analyzer was developed while he was Research Associate in Electrical Engineering at the Moore School of Electrical Engineering, University of Pennsylvania, Philadelphia, Pa.

The author wishes to acknowledge the helpful suggestions of Dr. C. N. Weygandt and M. E. Nelson, and the valuable design efforts of M. Unis and J. P. Moore, all members of the Moore School staff.

Figure 2. Front view of the harmonic analyzer

proper interval, are the coefficients A_n and B_n. The use of integrators in this cascaded scheme differentiates this harmonic analyzer from the Henrici-Coradi analyzer, from the point of view of how the computations for the coefficients are mathematically carried out.

It is further to be noted that the coefficients A_0, A_n, and B_n are so defined only after the integration is carried out over one period of the independent variable, in this case the angular distance 2π radians.

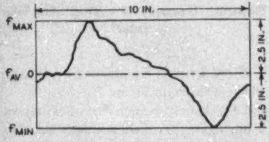

Figure 3. Plotted curve as used on harmonic analyzer

Stated in another way, the coefficients A_n and B_n can be written as

$$A_n=\frac{1}{\pi}\int_{\theta=0}^{\theta=2\pi}\cos n\theta d[\int F(\theta)d\theta] \tag{8}$$

$$B_n=\frac{1}{\pi}\int_{\theta=0}^{\theta=2\pi}\sin n\theta d[\int F(\theta)d\theta] \tag{9}$$

which is the form used in this harmonic analyzer.

Referring back to equation 1(A), it is seen that terms of like frequency appear as sines and cosines. These can be combined to obtain the magnitude and phase of each harmonic relative to the component of fundamental frequency. The final form of the Fourier series becomes

$$\begin{aligned}F(\theta)=A_0/2+C_1\cos(\theta-\phi_1)+\\ C_2\cos(2\theta-\phi_2)+\ldots.+\\ C_n\cos(n\theta-\phi_n)+\ldots\end{aligned} \tag{10}$$

$$F(\theta)=A_0/2+\sum_{n=1}^{\infty}C_n\cos(n\theta-\phi_n) \tag{11}$$

where

$$C_n=[A_n^2+B_n^2]^{1/2} \tag{12}$$

$$\phi_n=\tan^{-1}(B_n/A_n) \tag{13}$$

By applying equations 12 and 13, the magnitude and phase can be determined for each of the harmonics present in the given curve.

The preparation of a curve to be analyzed on this machine is straight-forward, the chief requirement being that the peak-to-peak excursion of the ordinate must be less than or equal to five inches, this size being most desirable from the point of view of maximum utilization of the integrator and hence for maximum accuracy. From the physical or experimental data from which the curve is to be plotted, one can determine the absolute maximum value of the function, f_{max}, and the absolute minimum, f_{min}. The average value, f_{avg}, is computed as the arithmetic mean value of the peak-to-peak values of the function

$$f_{avg}=\frac{f_{max}+f_{min}}{2} \tag{14}$$

The conversion factor for changing the physical measured data to inches displacement along the plotted curve is given by

$$K=\frac{5}{[f_{max}-f_{min}]} \tag{15}$$

and, in terms of inch displacement, the curve to be analyzed can be expressed as

$$f_{inches}=[f-f_{avg}]\times\frac{5}{[f_{max}-f_{min}]} \tag{16}$$

This last equation represents the displacement of the ordinate from the f_{avg} line as a fiducial zero.

If the curve to be analyzed has a peak-to-peak displacement of less than five inches, then substitute this value for the number *5* in equations 15 and 16.

The abscissa likewise has to be scaled, in this case to a 10-inch length. This distance represents period of the fundamental of the function to be analyzed, and corresponds to an angular measure of 2π radians.

Figure 3 shows the finished form of a plotted curve ready for analysis.

Block Diagram and Functional Layout

Of the four ball-and-roller integrators used in this machine, three are used to perform the integration process, and one is used as a variable speed drive, in discrete steps, obviating the use of change gears.

Figures 4 and 5 are over-all top views of the analyzer from the front and rear re-

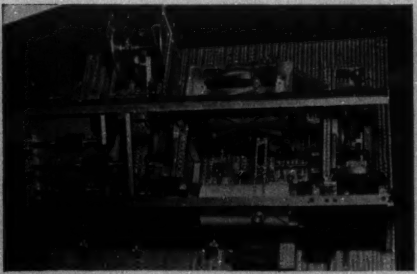

Figure 4. Top front view of the analyzer with plastic cover removed

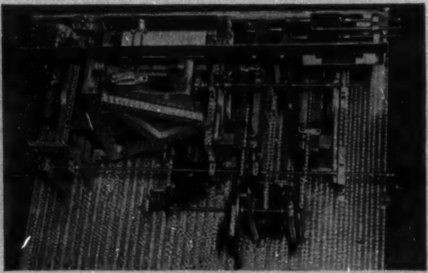

Figure 5. Top rear view of the analyzer with plastic cover removed

spectively, showing the integrator layout as well as the major components.

A functional block diagram of the analyzer is shown in Figure 6, the symbols used being those common in differential analyzer work. It is to be noted that no gear changes are required; the analyzer is totally self-contained. Scale factors chosen for the integrators are such as to use them to their fullest designed capacity.

At this point, a detailed account of the operation performed by each integrator is appropriate.

The 5-inch integrator is designed with an integrator constant equal to 8/3; that is, the integrator equation is $y=(8/3)\int R\,dx$, where y is the number of revolutions of the output shaft, R is the displacement of the balls off center in inches, and x is the number of revolutions of the integrator disk. In this analyzer, each integrator disk is driven through a gear ratio of 1-to-5; hence, the integrator constant is taken as 8/15, or $y=(8/15)\int R\,dx$.

INTEGRATOR I

Integrator I solves for the constant term A_0. It accepts as one input, to drive the ball carriage, information proportional to the instantaneous ordinate of the curve. The integrator disk, coupled to the drive motor, rotates an amount proportional to the variable of integration. Referring to Figure 6, it is seen that the output of the first integrator is given by

$$\frac{8}{15}\int_0^{2\pi} f_{inch}\, d\left[\frac{450\theta}{2\pi}\right]=\frac{8}{15}\times \frac{450}{2\pi}K\left[\int_0^{2\pi}F(\theta)d\theta-\int_0^{2\pi}f_{avg}\,d\theta\right] \quad (17)$$

$$\text{Output turns}=120KA_0-240Kf_{avg} \quad (18)$$

After passing through a fixed-gear-ratio chain drive, 48-to-10, the A_0 counter reads

$$576KA_0-1152Kf_{avg} \quad (19)$$

The constant term then becomes

$$A_0=\frac{\text{Counter Reading}}{576K}+2f_{avg} \quad (20)$$

INTEGRATOR II

The differential or integrator disk of Integrator II is driven directly by the output of Integrator I, while the integrand is moved by the Scotch yoke as a cosine function, with a maximum amplitude of $2^1/_2$ inches. The output roller then turns as

$$\frac{8}{15}\int_{\theta=0}^{\theta=2\pi} 2.5\cos n\theta d[120KA_0]=160KA_n \quad (21)$$

This rotation passes through a fixed-gear-ratio chain drive, 36-to-10, so that the A_n counter reads 576 K A_n. The amplitude of the *nth*-harmonic cosine wave is given by

$$A_n=\text{Counter Reading}/576K \quad (22)$$

INTEGRATOR III

In a similar manner it can be shown that Integrator III produces the amplitude of the *nth*-harmonic sine wave, given by

$$B_n=\text{Counter Reading}/576K \quad (23)$$

INTEGRATOR IV

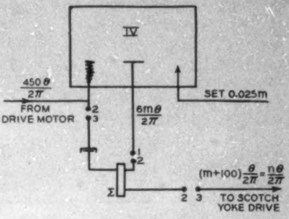

Figure 7. Method of production of the *nth* harmonic

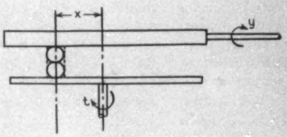

Figure 8. Geometry of ball-and-roller integrator

The fourth integrator is used as a variable-ratio device to produce a shaft rotation n times that of the fundamental. The entire range of harmonics from 1 to 100 is produced; the most accurate region of the integrator is utilized by means of a clutch by-pass circuit, a schematic of which is shown in Figure 7.

A calibrated precision lead screw having a pitch of 0.025 inch positions the carriage. The letter m, used in Figure 7, represents the complement of the harmonic number with respect to 100 with sign reversed; that is, the number of the harmonic, n, equals $100+m$, or $n=100+m$. Therefore, for the first harmonic, $n=1$ and $m=-99$. The output of the integrator is fed into one side of a mechanical adder device, the other side of which is fed through a clutch mechanism from the drive motor producing the independent variable. The output of the adder, after gear reduction, produces a shaft rotation just n times that of the fundamental. For harmonic settings less than 50, the clutch is engaged; the m settings are negative, in range from −99 to −50, producing harmonics from 1 to 50. Notice that the carriage setting is from −2.475

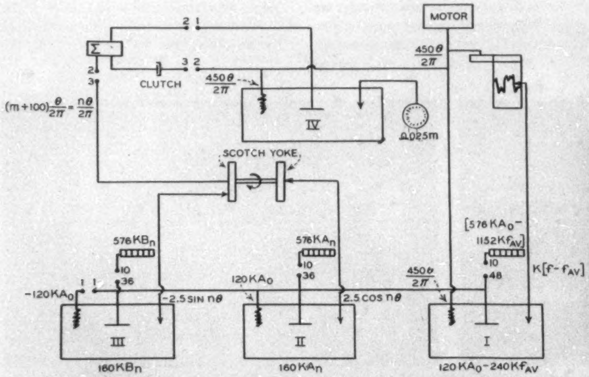

Figure 6. Block diagram of harmonic analyzer interconnections

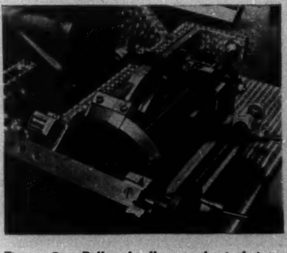

Figure 9. Ball-and-roller mechanical integrator partially opened

to −1.250 inches. For harmonics greater than 50, the clutch mechanism is disengaged; the m numbers are varied from 50 to 100, over the positive part of the integrator disk, that is, the carriage displacement is from 1.250 inches to 2.500 inches. The central part of the disk is not used. The by-pass adder circuit just described can be seen located between the Scotch yokes in Figures 4, 5, and 11.

Description of Major Components

DOUBLE-BALL INTEGRATOR

The most essential single mechanism of the harmonic analyzer is the mechanical ball-and-roller integrator,[5] a common component of many gun fire control computers. The mechanism has two input shafts and one output shaft, arranged so that the ratio of the incremental rotation of the output shaft to that of one of the input shafts is proportional to the rotation of the second input shaft

$$\frac{\Delta y}{\Delta t}=kx \tag{24}$$

$$y=k\int_{t_1}^{t} xdt \tag{25}$$

where

y = output shaft rotation
t = input shaft rotation
x = input shaft rotation

Figure 8 shows the geometry of a ball-and-roller integrator. Figure 9 is a photograph of integrator IV used in the machine, opened up to show construction details. The rotating integrator disk is used as one input, supplying the differential of equation 25. Two steel balls, one on top of the other, are held in position in a carriage which moves across the disk on a pair of guide rails. The position of this carriage with respect to the center of the disk, denoted by x in Figure 8, represents the integrand of equation 25. When the disk rotates about its center, and the carriage carrying the balls is displaced off the center of the disk, the motion of the bottom ball is transmitted to the roller shaft or output roller, yielding the value of the integral, equation 25, as a continuous function. This type of integrator is similar to the wheel-and-disk integrators used so extensively in the large multipurpose differential analyzers built in this country.[6]

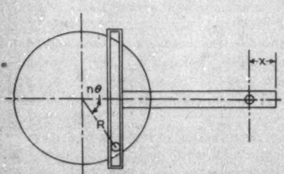

Figure 10. Geometry of Scotch-yoke mechanism

The mechanical integrator, performing a process of continuous addition, has no knowledge of the physical nature of the driving functions; that is, the x and t of equation 25 can be any functions whatsoever and the output will still be given, in functional form, by equation 25. In the particular case of the harmonic analyzer, the integrand is a sinusoid. Cosine $n\theta$ of equation 6 corresponds to the x of equation 25, and the differential dt in Equation 25 is represented by the function $d\,A_0$ of equation 6. Equation 25 then can be written in place of Equation 6, with the integration between the limits corresponding to $0 \leq \theta \leq 2\pi$.

SINE AND COSINE GENERATORS

The sine and cosine functions necessary for the integrations are generated by a finely-machined Scotch-yoke mechanism, similar to that shown in Figures 10 and 11. An aluminum disk has imbedded in it a hardened steel pin at a distance R from the center, equal to the amplitude of the sinusoid to be generated. This pin moves between two rails in a framework constrained to move along one axis only. Upon rotation of the disk the T-arm will move in translation, and the instantaneous displacement will be a true sinusoid, equal to $R \cos n\theta$, with zero theoretical error. It is most important that this mechanism be precisely built, since even a small amount of play or backlash between the steel pin and the guide rails may seriously impair the accuracy of the analyzer output.

Figure 11. Scotch-yoke mechanism showing adder by-pass circuit

Two Scotch-yoke mechanisms are utilized in the harmonic analyzer, one to produce the sine, the other the cosine, as shown in Figure 11. The two yokes are mounted on a common center, the pins being displaced exactly 90 degrees apart; hence, one unit generates the sine, the other the cosine, both at the same frequency. The integrals, given by equations 6 and 7, require the use of multiple-frequency sinusoids, that is, cos $n\theta$ and sin $n\theta$. The effect of a frequency higher than the fundamental is obtained by rotating the Scotch-yoke disk at a correspondingly higher speed than is used in scanning the curve under analysis. For example, if the base speed of rotation of the disk is that which obtains when the fundamental frequency is being generated, then the second harmonic is obtained by rotating the disk at twice base speed, the third harmonic by rotating at three times base speed, and so forth. The exact method of setting the frequency is outlined below.

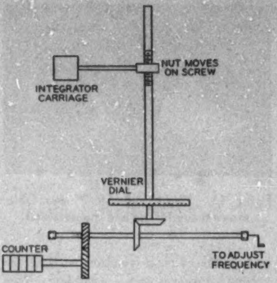

Figure 12. Details of the harmonic-setting mechanism

FREQUENCY-SETTING INTEGRATOR

A 5-inch ball-and-roller integrator is used as a variable gear ratio, whose function is to produce a shaft rotation proportional to the particular harmonic frequency to be investigated. As was noted above, any integrator has an incremental output given by

$$y=k\int_{t_1}^{t} xdt$$

where k is the integrator constant, x is the displacement from center of the integrator carriage carrying the balls, and t is the integrator-disk rotation. Obviously, if $x=c=$ constant, the output of such integrator, not including the initial offset, will be $k\,c\,t=k_1t$, or the output equals the input times the constant k_1. Use is made of this fact by driving the integrator disk with the independent variable θ, and ad-

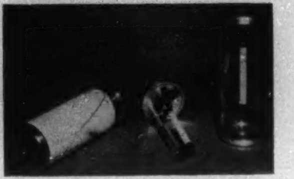

Figure 13. Plastic cylindrical curve table, shown ready for use and disassembled

justing the carriage position so that the output rotation is an *nth* harmonic. This *nth*-harmonic angle is used to drive the Scotch-yoke mechanism through either a direct or indirect path, producing sin $n\theta$ and cos $n\theta$.

Figures 9 and 12 show details of the harmonic-setting mechanism. The integrator carriage is carried along by a nut riding on a precision-ground lead screw having a pitch of 0.025 inch. Thus, each turn of the lead screw moves the carriage away from center by this amount. It will be shown later that each turn of the lead screw, or each advance of 0.025 inch, corresponds to another harmonic. When the frequency setting wheel is turned, during the machine adjustment period and prior to investigating for the presence of a harmonic in the given curve, the integrator carriage is displaced, and the counter, shown in Figures 9 and 12, indicates the distance of the carriage off center, to the nearest 0.001 inch. The vernier dial is graduated into 250 divisions; hence, each division represents a displacement of 0.0001 inch. It is thus theoretically possible to set the carriage to within ±0.00005 inch, but, because of certain inherent play and backlash in the ball carriage and the fact that the balls do not have a precise point contact, the actual precision of setting is not as accurate. A calibration chart is provided to relate the number of the harmonic to be investigated and the setting of the carriage.

INPUT TABLE

The curve whose harmonic content is to be investigated is plotted on a piece of paper to a standard size, 5 by 10 inches, the smaller dimension representing the maximum peak-to-peak excursion of the function, and the larger size representing the independent-variable scale. Linear graph paper having twenty lines to the inch, $7^1/_2$ by 10 inches ruled spacing with margin, has been found to be quite suitable.

The curve is wrapped around a plastic cylinder, shown in Figure 13, and inserted in the machine. This cylinder is shown in position in Figure 2. When the analyzer is in operation, the cylinder rotates an amount proportional to the independent variable, 0 to 2π radians, and the operator tracks the curve by sighting through an eyepiece and turning the tracking hand wheel located on the front panel. This latter motion is then transmitted to the integrator, which computes the constant term A_0 in the Fourier series.

Some thought was given to providing automatic curve following rather than hand tracking, and such feature may be incorporated into the machine at a later date. The use of an automatic curve follower would materially reduce the time to make an analysis, possibly by a factor of three.

The input cylinder assembly, shown in Figure 13, consists of the plastic cylinder proper, two aluminum end pieces, and a fluorescent light mounted within, with brush contacts brought out at one end. During operation, this internal light provides illumination behind the curve sheet.

The eyepiece is provided with a pair of adjusting screws which allows it to be displaced laterally over a distance of about 0.15 inch. This is most desirable, especially when adjusting for the zero line of the curve and the integrator.

OUTPUT COUNTERS

The results of the integrations of equations 5, 6, and 7 appear on counters located at the front upper-left-hand part of the analyzer. Except for a multiplying scale factor, these counters yield directly the magnitudes of the constant term and the sine and cosine amplitudes for each frequency investigated. Combination of the coefficients according to equations 11, 12, and 13 yield a resultant magnitude and phase relative to the fundamental. The counters are shown in Figures 2 and 4; they can be read to about 0.02 revolution.

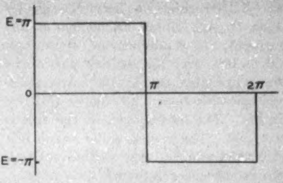

Figure 14. Square-wave used for checking purposes

Example of Square-Wave Analysis

The square wave, shown in Figure 14, was used to check the inherent accuracy of the harmonic analyzer. This is a particularly useful curve in this respect, because no tracking error is involved, except for an initial setting by eye of the tracking eyepiece.

Initial setting was by eye rather than by precise measurement in order to approximate the human setting error. The wave shown in Figure 14 can

Table I. Analysis of Square Wave

Amplitude = π $0\leq\theta\leq\pi$
Amplitude = $-\pi$ $\pi\leq\theta\leq2\pi$

Harmonic Number	Computed A_0	Computed A_n	Computed B_n*	True B_n	Per-cent Error in B_n
1	0.0056	−0.0247	3.9291	4.0000	−1.77
3	0.0004	−0.0102	1.3342	1.3333	+0.07
5	−0.0019	0.0019	0.8015	0.8000	+0.19
7	0.0077	0.0029	0.5727	0.5714	+0.23
9	0.0039	−0.0061	0.4455	0.4444	+0.25
11	0.0044	0.0050	0.3649	0.3636	+0.36
13	0.0104	0.0062	0.3079	0.3077	+0.07
15	0.0002	0.0046	0.2677	0.2666	+0.41
17	0.0111	0.0002	0.2388	0.2353	+1.49
19	0.0119	0.0011	0.2118	0.2105	+0.62
21	0.0003	0.0065	0.1910	0.1905	+0.26
23	0.0259	0.0025	0.1751	0.1739	+0.69
25	0.0133	0.0011	0.1607	0.1600	+0.44
27	0.0058	0.0027	0.1490	0.1481	+0.61
29	0.0131	0.0045	0.1380	0.1379	+0.07
31	0.0189	0.0057	0.1293	0.1290	+0.23*
33	0.0105	0.0069	0.1221	0.1212	+0.74
35	0.0004	0.0037	0.1142	0.1143	−0.08
37	0.0113	0.0048	0.1079	0.1081	−0.18
39	0.0033	0.0028	0.1024	0.1027	−0.29
41	0.0145	0.0028	0.0977	0.0977	0.00
43	0.0051	0.0028	0.0930	0.0930	0.00
45	0.0011	0.0059	0.0884	0.0888	−0.45
47	0.0074	0.0040	0.0847	0.0851	−0.47
49	0.0022	0.0044	0.0809	0.0816	−0.86

True A_0 and true A_n are both zero throughout (See text).

*Actual computed B_n was greater than this figure by 0.0055. This error is attributed to nonaccurate zero setting, hence this constant amount was subtracted from each entry.

be formally expanded in a Fourier series as follows

$$F(\theta)=\frac{4E}{\pi}\sum_{n=1,3,5\ldots}^{\infty}\frac{1}{n}\sin n\theta \qquad (26)$$

For the case of $E=\pi$, the series becomes

$$F(\theta)=4\sum_{n=1,3,5,\ldots}^{\infty}\frac{1}{n}\sin n\theta \qquad (27)$$

The constants necessary for the analysis are now determined as follows

$$f_{max}=\pi \qquad (28)$$

$$f_{min}=-\pi \qquad (29)$$

$$f_{avg}=(\pi-\pi)/2=0 \qquad (30)$$

$$K=5/2\pi=2.5/\pi \qquad (31)$$

$$f_{inches}=(2.5/\pi)F \qquad (32)$$

This latter equation allows the plotting of the curve from the original data. The integrated constants are as follows

$$\begin{aligned}A_0=A_n=B_n&=\text{Counter reading}/576K\\&=(\pi/1440)\times\text{Counter reading}\\&=0.0021816\times\text{Counter reading} \qquad (33)\end{aligned}$$

Table I shows the true and the computed values of the amplitudes of some of the harmonics in the square wave. The analyzer always computes all coefficients, A_0, A_n, and B_n. When only sine terms are theoretically present in a curve, and A_0 and A_n do not vanish, then their presence may give rise to an error in addition to any error in the computed amplitude of the sine curve.

From Table I, it is seen that the square wave analyzed produced coefficients for terms which are not theoretically present in this kind of wave. It is felt that these spurious coefficients are due almost entirely to tracking. In some cases, there is no appreciable error introduced by these terms. Consider, for example, the ninth harmonic, having $A_9=-0.0061$ and $B_9=0.4455$. The theoretical value of $B_9=0.4444$, and on the basis of the B_9 terms only, there is an error in the amplitude of this coefficient of 0.25 per cent. If the A_9 term is taken into account, the amplitude of the sinusoid remains the same to four significant figures, with the same accuracy as if this term were not present.

Only odd harmonics are present in the odd-function square wave, but the analyzer gave results of a rather constant but very small magnitude for the even harmonics; their contribution to the error was small.

The error inherent in the harmonic analyzer can be measured either with respect to the theoretically true value of the amplitude of the harmonic, or with respect to the contribution which this error makes to the over-all curve. It is an easy matter to measure the former, as is shown in Table I. As can be seen, even if the error in the amplitude of harmonic *49* is 0.86 per cent, the true amplitude of this harmonic still is only 2.04 per cent of the fundamental, and the net effect of the curve which would be synthetized from the Fourier series would be quite small.

Appendix I. Theoretical Error Due to Missetting of Frequency

The coefficients of the Fourier series are given exactly by the integrals

$$A_0=\frac{1}{\pi}\int_0^{2\pi}F(\theta)d\theta \qquad (1B)$$

$$A_n=\frac{1}{\pi}\int_0^{2\pi}F(\theta)\cos n\theta d\theta \qquad (2)$$

$$B_n=\frac{1}{\pi}\int_0^{2\pi}F(\theta)\sin n\theta d\theta \qquad (3)$$

only when the harmonic number n is, of course, an integer, and when the integration is carried out over exactly one period, $\theta=2\pi$. In this harmonic analyzer, the period of integration is determined by the curve sheet, that is, the distance along the independent variable axis, from beginning to end, is 2π, regardless of any setting of the harmonic. It is desirable, however, to investigate the error in the A_n or B_n counter reading representing the amplitude of a harmonic, when the frequency setting is a non-integer, that is, n is nonintegral. This necessarily must be the case, since n is an integrator setting. There will always be an error in setting, and a corresponding error in the output.

It is obvious that the constant term, A_0, will be independent of frequency errors, in fact the accuracy of this term is limited only by tracking errors, which now are neglected. The other integrals, however, contain n, and if this is nonintegral, then there will be error. The error is the difference between the true value and the computed value. If δ represents the nonintegral part of n, this error can be written as

$$\mathcal{E}_{A_n}=\frac{1}{\pi}\int_0^{2\pi}F(\theta)\cos n\theta d\theta-\frac{1}{\pi}\int_0^{2\pi}F(\theta)\cos(n+\delta)\theta d\theta \qquad (34)$$

$$\mathcal{E}_{A_n}=\frac{1}{\pi}\left|\int_0^{2\pi}F(\theta)[\cos n\theta-\cos(n+\delta)\theta]d\theta\right| \qquad (35)$$

Expanding the quantity in the bracket there results

$$\cos n\theta-\cos(n+\delta)\theta=2\sin\left(n+\frac{\delta}{2}\right)\theta\times\sin\frac{\delta}{2}\theta \qquad (36)$$

and since δ is very small, not greater than 0.01, the last factor can be approximated by a maximum value $\delta/2\times 2\delta=\delta\pi$. Equation 35 then becomes

$$\mathcal{E}_{A_n}\approx\frac{1}{\pi}\times 2\pi\delta\int_0^{2\pi}F(\theta)\sin\left(n+\frac{\delta}{2}\right)\theta d\theta \qquad (37)$$

$$\mathcal{E}_{A_n}\approx 2\delta\int_0^{2\pi}F(\theta)\sin n\theta\cos\frac{\delta}{2}\theta d\theta+2\delta\int_0^{2\pi}F(\theta)\cos n\theta\sin\frac{\delta}{2}\theta d\theta \qquad (38)$$

Making the same approximation as before

$$\mathcal{E}_{A_n}\approx 2\delta\pi B_n+2\pi\delta^2A_n\approx 2\pi\delta B_n \qquad (39)$$

The error in the B_n term can be written

$$\mathcal{E}_{B_n}=\frac{1}{\pi}\int_0^{2\pi}F(\theta)\sin n\theta d\theta-\frac{1}{\pi}\int_0^{2\pi}F(\theta)\sin(n+\delta)\theta d\theta \qquad (40)$$

$$\mathcal{E}_{B_n}=\frac{1}{\pi}\int_0^{2\pi}F(\theta)[\sin n\theta-\sin(n+\delta)\theta]d\theta \qquad (41)$$

Expanding the quantity in the bracket there results, for δ very small

$$\mathcal{E}_{B_n}\approx -2\delta\int_0^{2\pi}F(\theta)\cos\left(n+\frac{\delta}{2}\right)\theta d\theta \qquad (42)$$

$$\mathcal{E}_{B_n}\approx -2\delta\int_0^{2\pi}F(\theta)\cos n\theta\cos\frac{\delta}{2}\theta d\theta+2\delta\int_0^{2\pi}F(\theta)\sin n\theta\sin\frac{\delta}{2}\theta d\theta \qquad (43)$$

Again making the same approximations as previously

$$\mathcal{E}_{B_n}\approx -2\delta\pi A_n+2\pi\delta^2B_n\approx -2\pi\delta A_n \qquad (44)$$

References

1. A MECHANICAL SYNTHESIZER AND ANALYZER, F. W. Krauz. *Journal*, Franklin Institute (Philadelphia, Pa.), volume 204, number 2, August 1927, pages 245–62.

2. A SYNTHESIZER ANALYZER, S. L. Brown. *Journal*, Franklin Institute (Philadelphia, Pa.), volume 228, number 6, December 1939, pages 675–94.

3. THE HENRICI HARMONIC ANALYZER AND DEVICES FOR EXTENDING AND FACILITATING ITS USE, D. C. Miller. *Journal*, Franklin Institute (Philadelphia, Pa.), volume 182, number 3, September 1916, pages 285–322.

4. THE ANALYSIS OF PERIODIC WAVES, L. W. Chubb. *Electric Journal* (East Pittsburgh, Pa.), volume 10, 1914, page 91.

5. THE THEORY OF MATHEMATICAL MACHINES (book), Francis J. Murray. King's Crown Press, New York, N. Y., 1948.

6. A NEW TYPE OF DIFFERENTIAL ANALYZER, V. Bush, S. H. Caldwell. *Journal*, Franklin Institute (Philadelphia, Pa.), volume 240, number 4, October 1945, pages 255–326.

Discussion

R. Berkowitz (Moore School of Electrical Engineering, University of Pennsylvania, Philadelphia, Pa.): Since the completion of Mr. Charp's paper, some additional test work has been done on the Fourier coefficient harmonic analyzer at the Moore School of Electrical Engineering. Fourier coefficients were obtained both by the machine and by numerical computations for several types of functions, including triangular wave, approximation to random noise data made up of straight line segments, and composite sinusoidal wave containing 20 harmonics. In the discussion to follow the equations of operation are stated in simplified form and some conclusions resulting from the above mentioned tests as to sources of error and accuracy are presented.

Simplified Equations of Counter Outputs

Let A_{0c}, A_{nc}, B_{nc} T_c be the changes during a run of the readings of the A_0, A_n, B_n and "time" counters, respectively, and let $f_c + 97{,}500$ be the reading of the frequency counter. The curve to be analyzed is a function $y(x)$ plotted versus x starting at $x = 0$ on a piece of paper no larger than 5 inches (ordinates) by 10 inches (abscissas). Let u_y and u_x be respectively the numbers of y-units and x-units plotted per inch and let y_0 be that value of the ordinate corresponding to the machine zero (that value of ordinate occurring at the midpoint of the 5-inch maximum range).

The equations of operation are:

For the time counter (independent variable)

$$x = u_x T_c/45 \quad \text{or} \quad T_c = 45\, x/u_x \tag{1}$$

Frequency setting—causes Scotch yoke to generate $\sin 2\pi fx$ and $\cos 2\pi fx$, where

$$f = f_c/(250\, u_x) \quad \text{or} \quad f_c = 250\, u_x f \tag{2}$$

For A_0 counter reading

$$A_{0c} = \frac{115.2}{u_y u_x} \int_0^x [y(x) - y_0] dx \tag{3}$$

For A_n counter reading

$$A_{nc} = \frac{115.2}{u_y u_x} \int_0^x [y(x) - y_0] \cos 2f\pi x\, dx \tag{4}$$

For B_n counter reading

$$B_{nc} = \frac{115.2}{u_y u_c} \int_0^x [y(x) - y_0] \sin 2\pi fx\, dx \tag{5}$$

For harmonic analysis only one reading is taken for each frequency setting, at $x = x_m$, the highest value of the abscissa. Thus:

The final time counter reading

$$T_c = 45 x_m/u_x \tag{6}$$

The frequency setting for nth harmonic

$$f = n/x_m; \quad \therefore f_c = 250n\, u_x/x_m \tag{7}$$

The A_0 counter reads

$$A_{0c} = \frac{57.6\, x_m}{u_y u_x} \cdot \frac{2}{x_m} \int_0^{x_m} [y(x) - y_0] dx \tag{8}$$

The A_n counter reads

$$A_{nc} = \frac{57.6 x_m}{u_y u_x} \cdot \frac{2}{x_m} \int_0^{x_m} y(x) \cos 2\pi n \frac{x}{x_m} dx \tag{9}$$

The B_n counter reads

$$B_{nc} = \frac{57.6\, x_m}{u_y u_x} \cdot \frac{2}{x_m} \int_0^{x_m} y(x) \sin 2\pi n \frac{x}{x_m}\, cx \tag{10}$$

Thus the Fourier coefficients A_n and B_n are given by

$$A_n = \frac{u_y u_x}{57.6 x_m} A_{nc} = \frac{u_y}{1.28 T_c} A_{nc} \tag{11}$$

$$B_n = \frac{u_y u_x}{57.6 x_m} B_{nc} = \frac{u_y}{1.28\, T_c} B_{nc} \tag{12}$$

$$A_0 - 2y_0 = \frac{u_y u_x}{57.6 x_m} A_{0c} = \frac{u_y}{1.28\, T_c} A_{0c} \tag{13}$$

When the full 10-inch abscissa scale is used, $x_m/u_x = 10$, and thus

$$f_c = 25n \text{ (or one micrometer revolution per harmonic)} \tag{14}$$

$$T_c = 450 \tag{15}$$

$$A_n = \frac{u_y}{576} A_{nc} \tag{16}$$

$$B_n = \frac{u_y}{576} B_{nc} \tag{17}$$

$$A_0 = \frac{u_y}{576} A_{0c} + 2y_0 \tag{18}$$

Errors of the Machine Methods of Reduction

In actual runs to determine Fourier coefficients the following inaccuracies are immediately evident: (1) time counter does not read computed value at the end of the run; (2) Scotch Yoke has not returned to zero at the end of the run.

These effects are due to unavoidable slippage of integrators and looseness of gears. In many applications these effects are unimportant. However, if maximum accuracy is desired, the following procedure can be applied. At the end of a run, two values of the time counter reading are recorded: T_{c1}, the reading at which x_m has come under hairline, and T_{c2}, the reading at which the Scotch yoke has returned to zero. Suppose that $T_{c2} = T_{c1} + \Delta$. If for example Δ is greater than zero the implication is that the Scotch Yoke was moving too slow. Thus the run should be repeated with a higher value of f_c. In general, if Δ is greater in magnitude than some preassigned value depending on the degree of accuracy desired, the run should be repeated after the frequency counter setting has been changed by an amount δ, given approximately by

$$\delta \cong -\frac{11{,}250n}{T_{c1}^2} \Delta \tag{19}$$

In the normal case where $T_c \cong 450$, there results

$$\delta \cong -\frac{5}{90} n\ \Delta \text{ frequency counter divisions}$$

$$\delta \cong -\frac{5}{9} n\ \Delta \text{ frequency micrometer divisions,}$$

$$\text{since 25 counter divisions} = 250 \text{ micrometer divisions} \tag{20}$$

Note that in equations 19 and 20, n is the order of the particular harmonic being considered.

Accuracy of Fourier Harmonic Analysis

As a result of the tests made on the machine it is safe to say that with reasonably accurate tracking, harmonics of orders up to and including the 25th can be obtained with an expected error of less than approximately 20 counter divisions. It can be shown that maximum possible counter readings for any harmonic is about 735. Thus the expected error is less than 3 per cent of this maximum. It should be remembered that the actual number of counter divisions for a given harmonic will generally be considerably less than 735. As a result, the expected per cent error of a given harmonic will be correspondingly larger than the 3 per cent mentioned before.

Walter C. Johnson (School of Engineering, Princeton University, Princeton, N. J.): The harmonic analyzer described by Mr. Charp is ingenious and apparently very effective. The accuracy is quite good and is especially impressive at the higher harmonics. This speaks well for both the design and the construction of the device.

Regarding the analysis given in Appendix I for the maximum error to be expected from a slight mis-setting of the harmonic order, I agree with the author's general conclusion but not with his method of arriving at it. In finding the zeroes of the function $\cos(n + \delta)\theta - \cos n\theta$, he states in effect that if $\cos A = \cos B$, then $A = B + 2k\pi$, where k is an integer. From this he concludes that the zeroes of the function lie outside the interval $0 < \theta < 2\pi$, and so is able to use the mean-value theorem (equation 36)* to find the upper limit of the error. But the equation $\cos A = \cos B$ is satisfied also by $A = -B + 2k\pi$. Therefore, the function has additional zeroes given by

$$(n+\delta)\theta = -n\theta + 2k\pi$$

from which

$$\theta = \frac{k\pi}{n + \delta/2}$$

Thus, in the interval $0 < \theta < 2\pi$, the function has either $2n$ or $2n-1$ zeros, depending on whether the small number δ is positive or negative. The presence of the zeroes in the range of integration invalidates the result given in equation 41.

However, a direct calculation for a square wave shows a maximum error which is only double the limit indicated by equation 42, and it can be seen in an intuitive way that, so long as $\delta \ll 1$, the error can not be very large. The square wave defined by $f(\theta) = 1$ for $-\pi/2 < \theta < \pi/2$, $f(\theta) = -1$ for $\pi/2 < \theta < 3\pi/2$, has the Fourier coefficients $A_0 = 0$, $B_n = 0$, and

$$A_n = \frac{4}{n\pi} \sin \frac{n\pi}{2}$$

If the order of the harmonic is mis-set to $n + \delta$ instead of n, where $\delta \ll 1$, the coefficients become approximately

$$A_n' = \frac{4}{(n+\delta)\pi} \left(\sin \frac{n\pi}{2} - \delta\pi \cos \frac{n\pi}{2} - \pi\delta \right)$$

Approximating $1/(n + \delta)$ by $1/n - \delta/n^2$, the error is

---

* Editor's Note. Professor Johnson is referring to equation 36 in the preprint of the author's paper. This equation has since been corrected, as can be noted in the author's closure.

$$\epsilon = A_n - A_n' = \frac{2\delta}{n}\left(1 + \cos\frac{n\pi}{2} + \frac{2}{\pi n}\sin\frac{n\pi}{2}\right)$$

The function in parentheses has a maximum value of two when n is a multiple of four, whereas the maximum value of the function $f(\theta)$ is unity. Thus, for this function, the greatest error is double the limit given in equation 42.

S. Charp: Many thanks to Professor Johnson and Mr. Berkowitz for their comments. Notation of the additional zeros for the function $[\cos(n+\delta)\theta - \cos n\theta]$ mentioned by Professor Johnson were unfortunately omitted from the preprint of this paper. The existence of the additional roots was known and corrected for immediately after the preprint was issued. A slightly different analysis for the error due to mis-setting the frequency dial appears in this printed copy.

The use of the set of equations which were proposed by Mr. Berkowitz is optional on the part of the user of the harmonic analyzer. Equations are given in the body of the paper for the use of various scale factors which are easily related to those given by Mr. Berkowitz. The two sources of error noted by him may be the result of recent mechanical changes made in the original analyzer. For example, the machine as first constructed was equipped with a presetting time counter which automatically stopped the analyzer at the end of the prescribed period of the independent variable. Hence, the time counter always read the proper value at the end of a run.

The accuracy of a Scotch-yoke is, of course, dependent upon the tolerances set on the machining of its parts and the care taken in keeping it in adjustment. The fact that in recent operation the fiducial marker on the Scotch-yoke was not randomly offset from its zero position at the end of a series of runs would indicate that this source of error is not due to integrator slippage but rather to faulty maintenance, calibration, and operation of the analyzer. Improvements in these factors should increase the accuracy figure given by this discusser as well as increase the harmonic range of the machine bringing it closer to the fully designed value.

Application of the California Institute of Technology Electric Analog Computer to Nonlinear Mechanics and Servomechanisms

G. D. McCANN
MEMBER AIEE

C. H. WILTS
ASSOCIATE AIEE

B. N. LOCANTHI
NONMEMBER AIEE

Synopsis: This paper describes the non-linear elements and circuit techniques used with the California Institute of Technology electric analog computer. Their application to nonlinear mechanical vibratory systems and nonlinear servomotors is discussed in detail. These techniques have been found to be generally suitable for representing single valued nonlinear functions of a dependent variable. Nonlinear springs, spring loaded backlash, and nonlinear damping factors can be readily simulated as well as saturation effects and other single valued nonlinearities in servomotors. Methods of analysis are illustrated for several typical problems including a nonlinear rotating mechanical system and an autopilot employing a solenoid-operated rate and position limited hydraulic motor. Numerous servos of this type have now been studied and correlation of computer solutions with actual servo test data have shown in every case that the mathematical equations presented here accurately describe this type of motor.

THE California Institute of Technology electric analog computer has now been used for the solution and general analysis of a sufficient number of nonlinear servomechanisms and nonlinear mechanical vibratory systems to warrant a general discussion of the electrical techniques and analogies suitable for such problems. This paper deals particularly with its application to problems involving single valued nonlinear parameters that are a function of one dependent variable. The more common types of such nonlinearity in mechanical vibratory systems are nonlinear springs, backlash, and nonlinear damping such a coulomb friction. Many types of servomechanisms have nonlinearities of sufficient importance that their effects should be considered in analyzing system performance. Some of these nonlinearities are in the control system itself; others are in the system to be controlled. In position type controllers nonlinearities are commonly in the form of velocity or position saturation effects or limits, backlash, coulomb friction, or servos of the "on-off" type. Saturation effects such as occur in motors and generators of speed controllers and voltage regulators are sometimes important. The nonlinearities existing in the systems to be controlled may be of many types. In mechanical systems they may be in the form of nonlinear damping factors or spring constants, or they may be in the form of limits to certain motions being controlled. Certain thermal processes are inherently nonlinear. Some types of autopilot problems require consideration of the nonlinearities in the aerodynamic equations.

The California Technology electric analog computer has been described in detail in previous papers.[1-4] Suitable multipliers and nonlinear function devices now have been developed to enable its use for the rapid solution of a large number of problems of this type. These are described in detail in reference 4, and are only discussed briefly here with reference to their application to circuit analogies. The basic elements now being used in this computer are listed in Figure 1. The form of symbolization shown is that used in the California Technical Analysis Laboratory for preparing analogous circuits.

Description of Nonlinear Functions Devices

The devices for simulating nonlinear functions of a dependent variable are of two general types designated here as the "type I" and "type II" nonlinear functions devices. The first of these is essentially a nonlinear resistor in that it produces voltages that are arbitrary functions of currents or vice versa. The second type produces voltages that are arbitrary functions of another voltage.

TYPE I—NONLINEAR FUNCTIONS DEVICE

Diodes which conduct freely in only one direction can be used as the basic elements of a nonlinear device. In order to avoid power supply problems and to minimize the "forward resistance," crystal diodes have been used generally instead of vacuum diodes. The "back resistance" of the former elements is sufficiently high to meet most of the requirements in practical problems. Although these diodes can be associated with general impedance elements, this is usually undesirable because the forward and back impedances are resistive in nature and are most readily combined with other resistances. Nonlinear impedances can be achieved with diodes, however, through the use of amplifiers as will be described later.

The two basic elements of the diode nonlinear resistance are the voltage clipper and the current limiter shown in Figure 2. For the voltage limiter, batteries are connected with polarity opposing the normal direction of current flow, so that until the voltage exceeds the battery voltage, the effective resistance of the circuit is very high and is equal to one-half the back resistance of one diode. After the voltage exceeds this value, the

---

Paper 49-165, recommended by the AIEE Computing Devices Committee and the AIEE Joint Subcommittee on Servomechanisms and approved by the AIEE Technical Program Committee for presentation at the AIEE Summer General Meeting, Swampscott, Mass., June 20–24, 1949. Manuscript submitted November 22, 1948; made available for printing May 5, 1949.

G. D. McCANN, C. H. WILTS, and B. N. LOCANTHI are all with the California Institute of Technology, Pasadena, Calif.

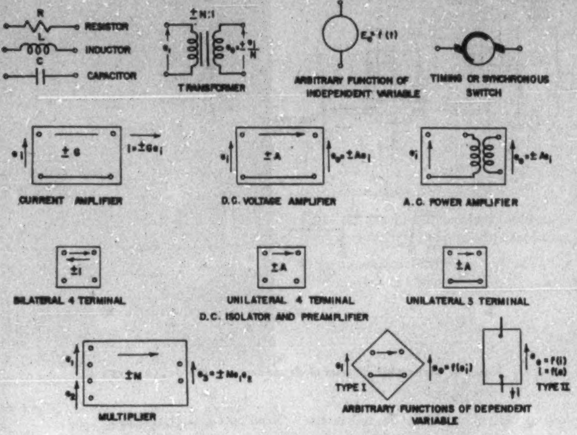
R
RESISTOR
L
INDUCTOR
C
CAPACITOR
±N:1
e_i
$e_o = \pm \frac{e_i}{N}$
TRANSFORMER
$E_o = f(t)$
ARBITRARY FUNCTION OF INDEPENDENT VARIABLE
TIMING OR SYNCHRONOUS SWITCH
e_i
±G
$I = \pm G e_i$
CURRENT AMPLIFIER
e_i
±A
$e_o = \pm A e_i$
D.C. VOLTAGE AMPLIFIER
e_i
$e_o = \pm A e_i$
A.C. POWER AMPLIFIER
±1
BILATERAL 4 TERMINAL
±A
UNILATERAL 4 TERMINAL
D.C. ISOLATOR AND PREAMPLIFIER
±A
UNILATERAL 3 TERMINAL
e_1
e_2
±M
$e_3 = \pm M e_1 e_2$
MULTIPLIER
e_i
$e_o = f(e_i)$
TYPE I
$e = f(i)$
$i = f(e)$
i
TYPE II
ARBITRARY FUNCTIONS OF DEPENDENT VARIABLE

Figure 1. Symbolization of basic computer elements

effective resistance is very low, the forward resistance of one diode plus that of the battery. For a typical *1N35* crystal, the ratio of the two slopes of the voltage-current characteristic is approximately 10,000. The current limiter utilizes two large resistors, R_1, to produce circulating currents in the two diode loops. Until the current inserted at the terminal equals this circulating current, the net resistance of the network is low and twice the forward resistance of one diode, while for larger currents it becomes large, essentially equal to the resistance R_1 in parallel with the back resistance of one diode. The ratio of the slopes of the resulting characteristic is not as great as that for the voltage limiter because of the addition of the resistor R_1. However, values of 200-to-1 for this ratio can be readily achieved.

In both limiters, the ratio of slopes can be reduced to any desired value by insertion of resistors in parallel and in series with the diode branches. Such a modification forms the basis of the general nonlinear device shown in Figure 3. The adjustable resistors are made relatively large compared to the forward impedance of the crystals so that the variations of the latter with current do not affect the overall impedance appreciably. If the switches are all thrown to the left in Figure 3, each parallel branch will not conduct current until the terminal voltage rises above the battery voltage of that branch. The resulting current voltage characteristic is composed of a series of straight lines, with the slope of successive segments decreasing as the voltage rises. Such a characteristic is shown in curve "A" of Figure 3.

If the switches are thrown to the right, a different characteristic results. Each branch produces a circulating current which passes through R_0. The battery voltage E_0 is provided to give zero terminal voltage when no external current enters the terminals. As voltage is applied, the current which flows is determined by the effective resistance of all branches in parallel. As soon as the terminal voltage rises above the lowest branch battery voltage, the current in that branch ceases to flow, and the effective impedance of the device is raised. As the voltage exceeds the highest battery voltage, the impedance becomes equal to R_0 alone, the maximum value. The resulting current-voltage characteristic is one of constantly increasing slope, as shown in curve "B". By combination of branches of each type, a characteristic may be achieved whose slope is alternately increasing and decreasing, provided the slope always remains positive. Curve "C," Figure 3, is typical.

A nonlinear resistor with 22 parallel branches, 11 each for positive and negative voltages is shown in Figure 5. The simpler voltage and current limiter is shown in the same figure.

Type II—Nonlinear Functions Device

Although the first nonlinear device described is essentially a resistance element, another nonlinear device has been constructed which produces a voltage that is an arbitrary (though necessarily single valued) function of any voltage however derived. This generator is based upon a principle developed elsewhere.[6,7] It utilizes a cathode-ray tube and photo cell for viewing the cathode-ray tube screen. The quiescent position of the electron beam is set to one side of the tube and the photo cell output is amplified and applied to the plates with a polarity which will drive the beam to the other side. If an opaque template is placed on the surface of the tube, as shown in Figure 4, the beam spot will be driven below the edge of

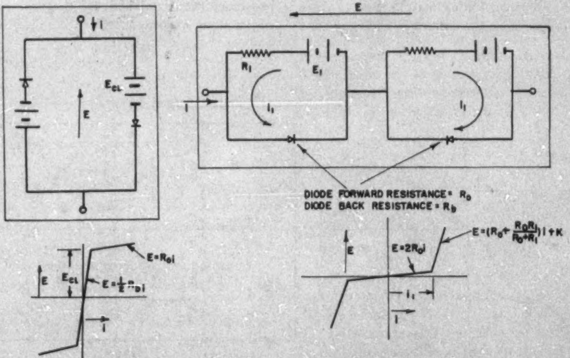
I
E_{CL}
E
$E = R_b i$
E
E_{CL}
$E = \frac{1}{2} R_D i$
i
E
R_1
E_1
I
I_1
I_1
DIODE FORWARD RESISTANCE = R_0
DIODE BACK RESISTANCE = R_b
E
$E = 2R_0 I$
$E = (R_0 + \frac{R_0 R_1}{R_0 + R_1}) I + K$
I_1
I

VOLTAGE LIMITER

CURRENT LIMITER

Figure 2. Schematic circuits of simple voltage and current limiters

the template until the light reaching the photo tube is just sufficient to produce a signal that will deflect the beam to the edge of the template. Since the beam will follow closely the template, and since the voltage required to deflect the beam is a linear function of the deflection, the output voltage of the device is proportional to the height of the template at the particular position of the beam. A generator of this type is shown in Figure 5. A typical characteristic is shown as viewed on an oscilloscope in Figure 4. A more detailed description of both of the nonlinear functions devices has been given elsewhere.[4]

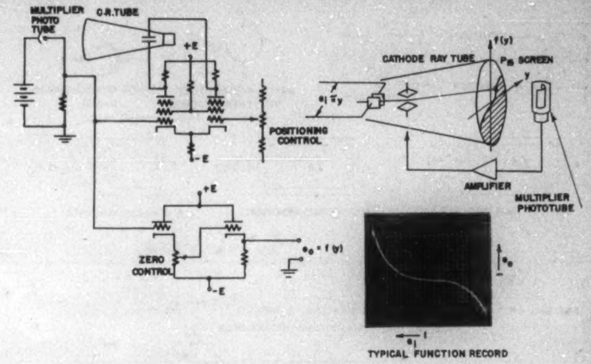

Figure 4. Schematic diagram of dependent variable device—type II

General Application of Nonlinear Devices

Voltage Clippers

In some physical systems a variable exhibits a linear characteristic until it reaches a limiting value which it cannot exceed. Such characteristics can be produced electrically with a voltage limiter if the voltage at some point in the electrical circuit can be made the analog of the variable in the physical system. The only important electrical requirement is that the voltage clipper be driven by a source with high impedance so that the forward resistance of the diode is very small compared with the source impedance. In typical cases the slope of the characteristic may be changed by a factor as large as 2,000.

As discussed later this principle can be used directly to simulate position and velocity stops in servomechanisms, coulomb friction, and backlash.

Current Limiters

A current limiter may be used in those cases where the current is analogous to a physical variable which is limited in its maximum value. Its application is discussed later with reference to rate limited hydraulic servos.

Nonlinear Gain Characteristics

The simulation of such nonlinear amplification characteristics as saturation effects in electronic amplifiers or rotating machines can be accomplished readily with either type of nonlinear functions device. The type II device need merely be inserted in cascade with linear amplifiers of the computer. The type I device also could be used in the same manner as illustrated later for simulating nonlinear springs.

However, it has usually been found more suitable to use it as a nonlinear feed-back resistor as shown in Figure 6. This type of circuit also is used where the resistance range provided by the type I device alone is too high.

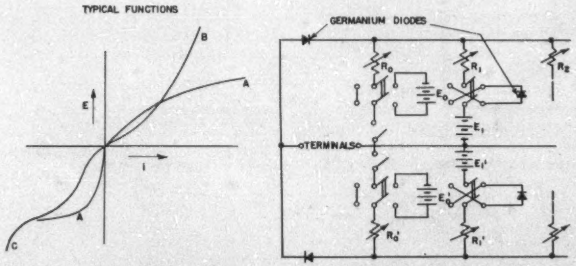

Figure 3. Schematic diagram of dependent variable device—type I

Nonlinear Impedances

The nonlinear terms arising in many physical or mathematical problems may be interpreted in the analog as nonlinear self or mutual impedances. It will be sufficient to describe methods of achieving nonlinear self impedances. The type I device must be used in conjunction with resistors to avoid unpredictable phase shift characteristics. In order to use this element, therefore, the voltage from a small impedance of the type specified must be applied to the nonlinear resistor by means of an amplifier, and the resulting nonlinear voltage reinserted in the circuit by means of another amplifier. Such a circuit and the resulting characteristic is shown in Figure 7. The use of the type II nonlinear device is shown in the same figure and requires no additional explanation.

As an example, suppose the charge flowing in a circuit is equal to a variable x, and a term $f(x)$ appears in the differential equation to be solved, then the impedance Z_0 would become a large capacitor and either nonlinear device would be adjusted to give an output voltage equal to $f(x)$. A correction would be applied if the voltage across the capacitor were appreciable in the circuit.

The accuracy obtained with the foregoing circuit techniques depends primarily upon how accurately it is attempted to simulate a given function. The type I device will simulate many functions with an error ranging from one to five per cent of the maximum value of the function. The type II device will simulate most functions to a somewhat greater accuracy, and is applicable to a wider variety of functions.

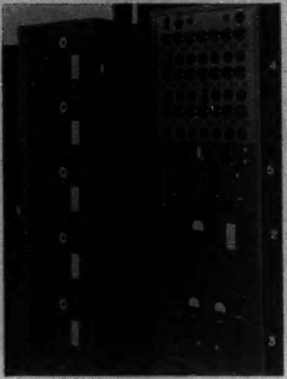

Figure 5. Nonlinear functions devices and other computer elements

1. Negative gain servo amplifiers
2. Positive gain d-c amplifiers
3. Voltage and current limiter
4. Arbitrary functions device—type I
5. Arbitrary functions device—type II

Nonlinearities in Mechanical Vibratory Systems

The preceding discussion makes it readily apparent that the nonlinear functions devices can be used to simulate most types of single valued nonlinearities occurring in mechanical systems. These are generally either nonlinear springs or damping factors. With the use of the force-voltage analogy, in which current is analogous to velocity and charge to position, it is evident that the nonlinear resistance devices can be used directly to simulate nonlinear mechanical damping. Their application to the analysis of problems involving coulomb friction has been discussed previously.[5]

NONLINEAR SPRINGS AND BACKLASH

The application of the nonlinear impedance circuits to mechanical systems with nonlinear springs and spring-loaded backlash is illustrated by the system of Figure 8. This is the rotating mechanical system of a radial aircraft engine that was studied quite extensively with the computer.

In this system all three shafts are geared and have appreciable spring-loaded backlash. In addition, shaft number 3 is nonlinear as is shown in Figure 9.

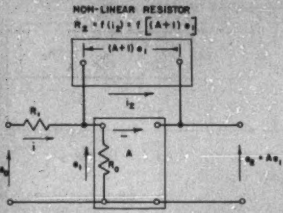

Figure 6. Circuit for nonlinear amplification factor or reduced impedance nonlinear resistor

e_0=input voltage from source of negligible impedance

$$e_1=\frac{R_2R_0e_0}{R_1R_2+R_2R_0+(A+1)R_1R_0}$$

if $R_1<<R_0$ and $A>>1$

$$e_1=\frac{R_2e_0}{R_2+(A+1)R_1}=\frac{e_0}{1+\frac{R_1}{R_2}(A+1)}$$

or if $\frac{R_1}{R_2}(A+1)>>1$

$$e_1=\frac{R_2e_0}{R_1(A+1)};\quad e_2=\frac{-AR_2e_0}{R_1(A+1)}$$

The following equations specify the system

$$\left.\begin{aligned}0&=Ip^2\theta_1+K_1(\theta_1-\theta_2)\\0&=I_2p^2\theta_2+K_1(\theta_2-\theta_1)+K_2(\theta_2-\theta_3)\\T&=I_3p^2\theta_3+K_2(\theta_3-\theta_2)+K_3(\theta_3-\theta_4)\\0&=I_4p^2\theta_4+K_3(\theta_4-\theta_3)\end{aligned}\right\}\quad(1)$$

where $p=\frac{d}{dt}$

If the spring characteristics were perfectly linear the analogous electric circuit would be that given in Figure 8(B) with simple capacitors representing the spring constants. The electric circuit equations would be the following

$$\left.\begin{aligned}0&=L_1p'^2q_1+\frac{1}{C_1}(q_1-q_2)\\0&=L_2p'^2q_2+\frac{1}{C_1}(q_2-q_1)+\frac{1}{C_2}(q_2-q_3)\\E_0&=L_3p'^2q_3+\frac{1}{C_2}(q_3-q_2)+\frac{1}{C_3}(q_3-q_4)\\0&=L_4p'^2q_4+\frac{1}{C_3}(q_4-q_3)\\p'&=\frac{d}{dt'}\end{aligned}\right\}\quad(2)$$

By establishing values for an impedance base factor (a) a time base change factor $\left(n=\frac{t}{t'}\text{ or }\frac{d}{dt'}=n\frac{d}{dt}\right)$ and a forcing functions ratio $r=\frac{T_0}{E_0}$ the following electrical parameters can be determined

$$L_1\ldots\ldots=I_1\frac{a}{n^2};\ \frac{1}{C_1}\ldots\ldots=aK_1;$$

$$\theta=arq;\ T=\frac{E}{r}\ \ldots\ldots\quad(3)$$

In the analysis of nonlinear problems of this sort, the proper representation of initial conditions is more difficult than for linear systems. This can be best illustrated by considering a specific type of disturbance, namely the torques produced by a cylinder misfire under a given load condition.

To simplify the initial conditions and the representation of the nonlinear springs for such a case a change can be made in the co-ordinate specifying the system such that the steady-state values of all functions are eliminated. Thus

$$T_0'=T_0-T_{0_{ss}};\ T_1'=T_1-T_{1_{ss}};$$
$$\theta_1'=\theta_1-\theta_{1_{ss}};\ \ldots\ldots\quad(4)$$

This changes the stress-strain curves representing the nonlinear springs in the manner illustrated by Figure 9(B). As shown in Figure 8(B) voltage clippers were used in the circuits of K_1 and K_2 to simulate the backlash. For shaft number 3 both the backlash and change of spring constant were simulated with the circuit of the type I functions device. However, in Figure 8(C) only those elements required are illustrated to clarify a detailed description of the analogy.

Referring to Figure 9(C) the charge flowing through the spring analogy circuit represents the strain and the voltage across it represents the stress. The analogous circuits of Figure 8 are actually positive self-impedance circuits that alter the effective capacities of the condensers C_1 and so forth, by a variable gain which is a function of (q_3-q_4) and is adjusted to properly fit the desired stress-strain curve. When the voltage E_1 exceeds the clipper voltage E_{c1} and the voltage E_2 is less than clipper voltage E_{c2}, Figure 8(C), the amplifier circuit has its maximum gain and the analogous spring factor for K_3 is a maximum given by the equation

$$aK_{3\max}=\frac{1}{C_{\min}}=\frac{1+kA_1A_2}{C_3}\quad(5)$$

where

$$k=\frac{R_1}{R_0+R_1}$$

Referring again to Figure 8(C), the backlash characteristic is simulated with the diode voltage clipper (E_{c1}). Whenever the voltage A_1E_0 plus E_1 is less than E_{c1} the clipper acts like an open circuit and amplifier A_2 puts out no voltage. Under these conditions the spring constant is

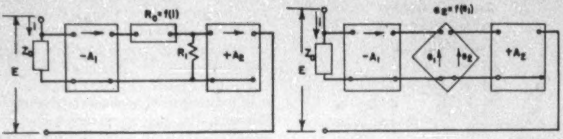

Figure 7. Circuits for obtaining nonlinear impedances with arbitrary functions devices

(Left) Using type I functions device

$$E=\left(Z_0+\frac{A_1A_2R_1}{R_1+R_0}Z_0\right);$$

$$Z=Z_0\left(1+\frac{A_1A_2R_1}{R_1+R_0}\right)$$

$$\text{if } R_0>>R_1 \text{ and } \frac{A_1A_2R_1}{R_0}>>1,\ Z\cong\frac{KZ_0}{R_0}$$

Interchanging R_1 and R_0 in circuit

$$Z=Z_0\left(1+\frac{A_1A_2R_0}{R_1+R_0}\right)$$

$$\text{if } R_1>>R_0;\ \frac{A_1A_2R_0}{R_1}>>1 \quad Z\cong KR_0Z_0$$

(Right) Using type II functions device

$$E=Z_0i+A_2f(A_1Z_0i)$$
$$E=Z(i)i$$

$$Z(i)=\left(1+\frac{A_2f(A_1Z_0i)}{i}\right)$$

---

very low and equal to the following

$$aK_{3\min}=\frac{1}{C_3} \tag{6}$$

It will have this characteristic over a range of q_0 given by the following equation

$$\frac{q_0}{C_3}A_1=2E_{c1};\ \Delta E=\frac{2E_{c1}}{A_1} \tag{7}$$

This slope can be made negligible by using a large value for A_1A_2 and C_3.

The stress-strain curve is shifted to the proper zero position by adjusting E_1 to satisfy the relation

$$A_2(E_1-E_{c1})=\frac{T_a}{r} \tag{8}$$

and then the actual circuit voltage is set to zero by adjusting E_3 until

$$E_3=-A_2(E_1-E_{c1}) \tag{9}$$

Additional changes in the spring constants are accomplished by additional voltage clippers such as E_{c2}. The spring constant above this level is given by the equation

$$aK=\frac{1+\frac{R_a}{k}A_1A_2}{C_3} \tag{10}$$

where

$$R_a=\frac{R_1R_2}{R_1+R_2}$$

Smooth variations in the spring factor can be accomplished by replacing the second voltage clipper with the arbitrary functions device type II.

The resistance R_n could be inserted to add enough negative resistance to the circuit to cancel the effect of the resistance at the output terminals of amplifier A_2 should it be appreciable. However, the positive gain amplifiers used in the computer have an impedance of only one ohm so that such compensation is rarely necessary. The voltages E_1 and E_2 are obtained by adjustment of the d-c amplifier zero-control. Figure 10 presents typical solutions for the transient torque pulse resulting from a single cylinder misfiring. As mentioned before, this was simulated as an applied voltage pulse having no steady-state value.

Another nonlinear spring problem studied with the computer is illustrated in Figure 11. This represents a one degree of freedom mechanical system (having a nonlinear spring) that is controlled with a servo using rate and position feedback. Figure 11 shows typical solutions for both the controlled and uncontrolled system under the influence of a suddenly applied constant disturbance torque. Linear feedback only is shown. However, this system was studied with nonlinear position feedback. It is readily apparent that if the servo time delays are not too great, the system can be linearized by the use of a nonlinear position feed-back characteristic that just counteracts the nonlinearity of the spring.

Nonlinear Servomotors

During the past year and a half the California Technology computer has been used extensively for the design analysis of guided missile control systems. This work has all been of a restricted nature and the studies cannot be described in detail. However, the analog techniques themselves are of sufficient interest to merit discussion. In most of these studies the aerodynamical equations have been linearized but some have included the effects of angle of attack and interaction between the three degrees of freedom of the missile. The latter type have included studies of "stabilized" platforms.

RATE AND POSITION LIMITED HYDRAULIC SERVO SYSTEMS

Several types of servomotors have been analyzed. One of the most important of the nonlinear motors studied extensively is the "rate limited" hydraulic motor. In

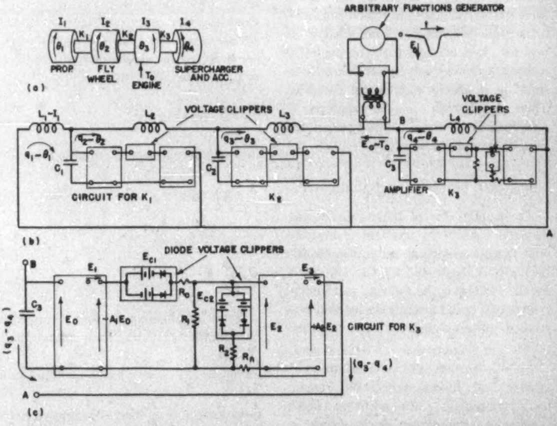

Figure 8. Analogy for radial aircraft engine with nonlinear spring constants and backlash

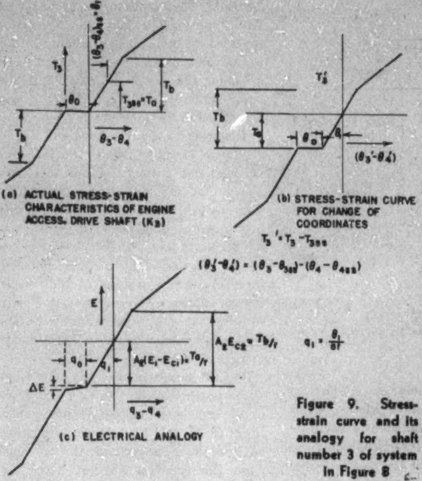
T3
(θ3-θ4)ss=θ1
θ0
T3ss=Ta
Tb
Tb
θ3-θ4
(a) ACTUAL STRESS-STRAIN CHARACTERISTICS OF ENGINE ACCESS. DRIVE SHAFT (K3)
T3'
Tb
Ta
θ0
θ
(θ3'-θ4')
(b) STRESS-STRAIN CURVE FOR CHANGE OF COORDINATES
T3' = T3 - T3ss
(θ3'-θ4') = (θ3-θ3ss)-(θ4-θ4ss)
E
AgEc2 = Tb/r
q1 = θ1/θr
q0
q1
Ag(E1-Ec1) = To/r
ΔE
q3-q4
(c) ELECTRICAL ANALOGY

Figure 9. Stress-strain curve and its analogy for shaft number 3 of system in Figure 8

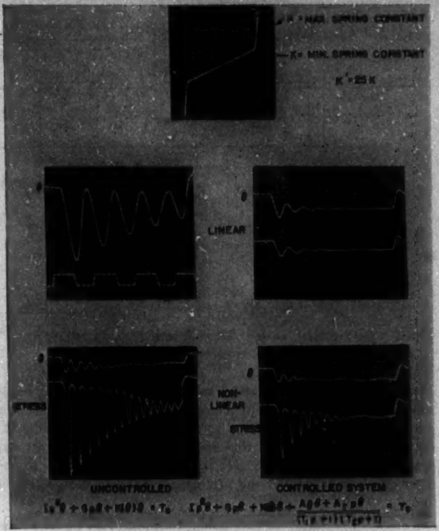

Figure 11. Computer solutions to servo controlled system with nonlinear spring

this a hydraulic valve is actuated, usually by an electromagnetic solenoid circuit. The valve controls the flow of the hydraulic line which will drive the missile control surfaces in either direction at a velocity proportional to the valve opening. However, the maximum control surface velocity is limited to a value corresponding to the full open position of

$$\omega_0=\frac{K}{I};\ \omega_0'=\frac{K+A_\theta}{I};\ \omega_0'=1.72\omega_0$$

T_0 = suddenly applied constant torque $=3.3T\alpha$

$$\frac{A_r}{A_\theta}\omega_0=0.49;\ T_1\omega_0=0.098;\ T_1\omega_0=0.196$$

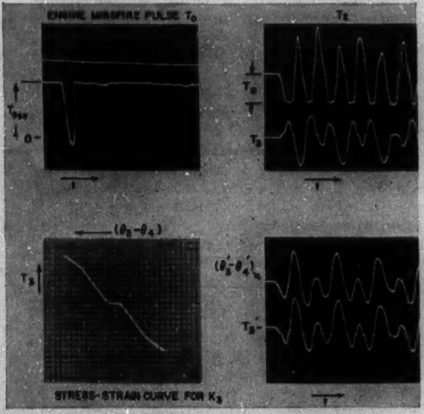

Figure 10. Typical solutions for system of Figure 8

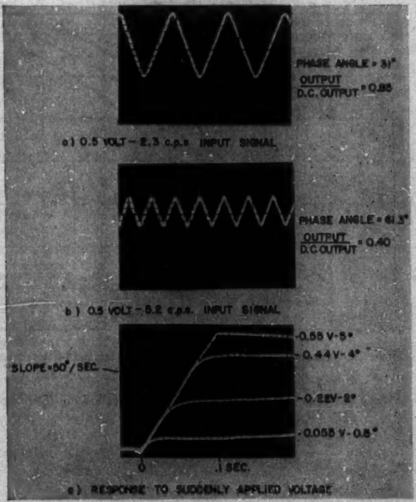

Figure 12 (right). Computer solutions for steady-state sinusoidal response and impulse response characteristics of rate and position limited hydraulic servomotor

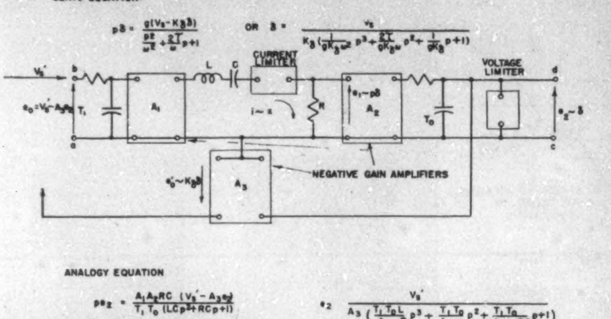
SERVO EQUATION:
$p\delta = \frac{g(V_s - K_\delta \delta)}{\frac{p^2}{\omega^2} + \frac{2T}{\omega}p + 1}$
OR $\delta = \frac{V_s}{K_\delta\left(\frac{1}{gK_\delta\omega^2}p^3 + \frac{2T}{gK_\delta\omega}p^2 + \frac{1}{gK_\delta}p + 1\right)}$
CURRENT LIMITER
VOLTAGE LIMITER
V_s'
b
L
C
d
$e_0 = V_s' - A_3 e_2$
T_1
A_1
$i \sim x$
R
$e_1 \sim p\delta$
A_2
T_0
$e_2 \sim \delta$
a
c
$e_0' \sim K_\delta \delta$
A_3
NEGATIVE GAIN AMPLIFIERS
ANALOGY EQUATION
$pe_2 = \frac{A_1 A_2 RC\ (V_s' - A_3 e_2)}{T_1 T_0 (LCp^2 + RCp + 1)}$
$e_2 \quad \frac{V_s'}{A_3\left(\frac{T_1 T_0 L}{A_{123} R}p^3 + \frac{T_1 T_0}{A_{123}}p^2 + \frac{T_1 T_0}{A_{123} RC}p + 1\right)}$

Figure 13. Electrical analog for rate and position limited hydraulic servomotors

the valve. Such a motor can generally be quite accurately specified by the mathematical equations of Figure 13. These equations are derived in the Appendix together with the electrical analogy. There both the electrical and mechanical elements of the solenoid are represented by one lumped transfer function. This usually provides a sufficiently accurate analogy. However, if desired the complete analogy for both the electrical and mechanical elements of the solenoid can be used. The nonlinearities in motors of this type can usually be accurately specified by assigning a definite maximum value to the rudder velocity and assuming the system to be linear below these limits. Rudder position stops can be treated in the same way.

Referring to the Appendix and Figure 13, these limits are accomplished with voltage and current limiters. It was found that the velocity limitations for some motors (although sharply defined) had a saturation characteristic which was not perfectly flat. This type of characteristic was studied by using an arbitrary functions device instead of the simple voltage clipper. The results of the study showed that sufficiently accurate results could always be obtained with the simple voltage clipper.

Typical impulse and steady-state sinusoidal response characteristics of a servomotor are shown in the computer solutions of Figure 12. Analog computer analyses have been made for systems using this type of motor in which the numerical parameters were obtained in several ways. In some cases the servo

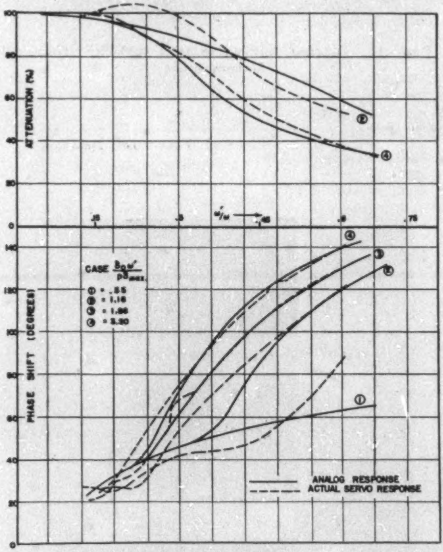

Figure 14. Frequency response curves comparing actual servomotor with electrical analogy

Motor parameters used with computer are the following (See Figure 12)

$\frac{2}{\omega} = 0.006;\ \frac{\omega}{gK_\delta} = 2.17$

δ_0 is steady-state rudder angle without position limitation

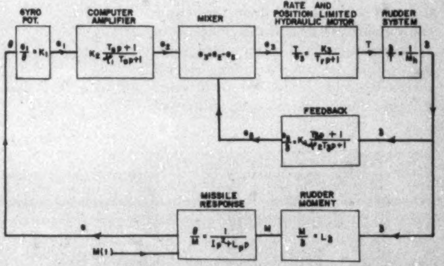
GYRO POT.
COMPUTER AMPLIFIER
MIXER
RATE AND POSITION LIMITED HYDRAULIC MOTOR
RUDDER SYSTEM
θ
$\frac{e_1}{\theta} = K_1$
e_1
$K_2 \frac{T_a p + 1}{\frac{1}{\gamma_1} T_a p + 1}$
e_2
$e_3 = e_2 - e_5$
e_3
$\frac{T}{e_3} = \frac{K_3}{T_f p + 1}$
T
$\frac{\delta}{T} = \frac{1}{M_h}$
δ
FEEDBACK
e_5
$\frac{e_5}{\delta} = K_4 \frac{T_2 p + 1}{\gamma_2 T_2 p + 1}$
δ
MISSILE RESPONSE
RUDDER MOMENT
θ
$\frac{\theta}{M} = \frac{1}{I p^2 + L_p p}$
M
$\frac{M}{\delta} = L_\delta$
δ
M(t)

Figure 15. Block diagram—rate and position limited hydraulic autopilot

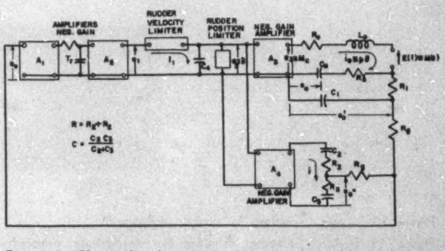
AMPLIFIERS NEG. GAIN
RUDDER VELOCITY LIMITER
RUDDER POSITION LIMITER
NEG. GAIN AMPLIFIER
e_0
A_1
T_7
A_2
e_1
I_1
C_4
$e_2\delta$
A_3
$e_3 = M_c$
R_0
L_0
$i_0 = \dot{\theta}$
$E(t) = m(t)$
C_0
R_5
e_0
C_1
R_1
e_0'
R_6
R = $R_2 + R_3$
C = $\frac{C_2 C_3}{C_2 + C_3}$
A_4
NEG. GAIN AMPLIFIER
C_2
R_2
R_4
i
R_3
C_3
e_0''

Figure 16. Electrical analog—rate and position limited hydraulic autopilot

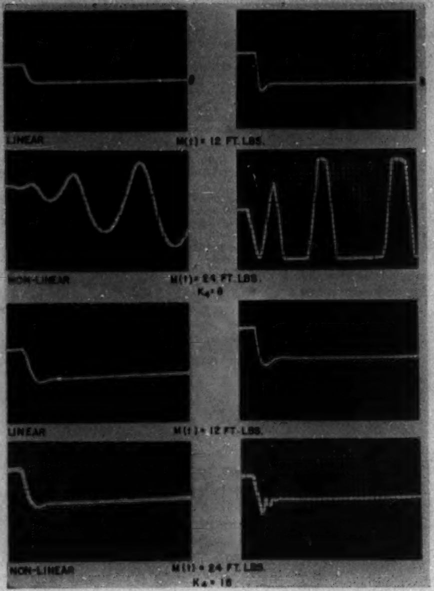

Figure 17. Response characteristics of autopilot system of Figure 15 instability induced by an applied torque exceeding the linear range of the control system, and corrected by an increase in K_4

$T_a = 0.06$ second; $T_\delta = 0$; $K_3 = 50$

parameters given in Figure 12 were obtained directly by test and used directly for specifying the proper analog parameters.

In other cases it was required to determine certain of the parameters by fitting frequency response curves as shown in Figure 14. Such curves can be run off very rapidly with a computer of this type so that it only requires a few hours to determine by trial and error the parameters that best simulate test data.

Figures 15 and 16 are typical examples of an autopilot employing a rate and position limited servomotor. This system was used for roll stabilization and the simplified form for the aerodynamic equations is shown. In the analogy, Figure 16, is shown a modified version of the motor analogy which can be used if the motor transfer function, Figure 13, can be expressed as a quadratic instead of a cubic equation. This analogy can be derived readily. In it the current i_1, Figure 16 is analogous to rudder velocity so that a current limiter is used for velocity limitation.

Computer solutions for the transient response characteristic of this type of servo system are given in Figure 17. These illustrate a condition found in several cases with the parameters of an actual proposed missile at certain points in its flight program. If optimum servo parameters were chosen from a perfectly linear analysis, well damped solutions such as given at the top of the figure result.

These solutions would correspond to those resulting from small disturbance torques in the actual systems. However, if the disturbance torque is sufficiently large the two nonlinearities can produce complete instability as illustrated by the second set of solutions. For this particular type of system the instability can be eliminated by increasing the rudder feed-back parameter K_4 as shown in the two bottom pairs of computer solutions, Figure 17.

With a computer of the type described here solutions can be obtained so rapidly that it is a relatively quick and simple matter to study the performance of a guided missile or autopilot over its complete range of flight conditions. Optimum servo parameters can thus be quickly determined.

In some cases a single set of servo parameters may be suitable. In others a schedule for varying the parameters may be desirable.

Appendix I. Derivation of the Equations and Analogy for Rate and Position Limited Hydraulic Servomotors

Let

V_s = control signal voltage
δ = rudder position angle
K_δ = feed-back constant from rudder position
e_0 = voltage applied to motor solenoid
$e_0 = V_s - K_\delta\delta$
M = mass of solenoid valve system
K = its spring constant
G = its damping factor
m = constant relating solenoid force to applied voltage e_c
k = constant relating rudder velocity to valve opening

$$\frac{d\delta}{dt} = p\delta = \frac{mk}{K}\cdot\frac{(V_s - K_\delta\delta)}{\frac{M}{K}p^2 + \frac{G}{K}p + 1} \tag{11}$$

δ and $p\delta$ are limited to either a specified maximum value or to a sharply defined saturation characteristic. Equation 11 can be rewritten as follows

$$p\delta = \frac{g(V_s - K\,\delta)}{\frac{p^2}{\omega^2} + \frac{2\tau}{\omega}p + 1} \tag{12}$$

where

$$g = \frac{mk}{K};\ \omega = \sqrt{\frac{K}{M}};\ = \frac{G}{2\sqrt{KM}}$$

Solving for δ gives the following equation

$$\delta = \frac{V_s}{K\left(\frac{1}{gK_\delta\omega^2}p^3 + \frac{2\tau}{gK\delta\omega}p^2 + \frac{1}{gK\delta}p + 1\right)} \tag{13}$$

Electrical Analogy. Referring to Figure 12, it can be seen that if V_s' is the analogous control signal voltage the input voltage e_0 is:

$$e_0 = V_s' - A_3e_2 \tag{14}$$

where e_2 is analogous to δ. The voltage e_1 is analogous to $p\delta$ and given by the equation

$$e_1 = \frac{-A_1RC(V_s' - A_3e_2)}{T_1(LCp^2 + RCp + 1)} \tag{15}$$

where T_0 is time constant of first integrating circuit.
As the relation between e_1 and e_2 we have the equation

$$e_2 = \frac{-A_2e_1}{T_0p} \tag{16}$$

where T_0 is the RC time constant of the second integrating circuit. Combining equations 14, 15, and 16

$$pe_2 = \frac{A_1A_2RC(V_s' - A_3e_2)}{T_1T_0(LCp^2 + RCp + 1)} \tag{17}$$

and solving for e_2

$$e_2 = \frac{V_s'}{A_3\left(\frac{T_1T_0L}{A_{123}R}p^3 + \frac{T_1T_0}{A_{123}}p^2 + \frac{T_1T_0}{A_{123}RC}p + 1\right)} \tag{18}$$

giving the transfer function analogous to that for the actual servo, equation 13. In this analogy the current in the *RLC* circuit is truly analogous to the solenoid position x which is proportional to $(p\delta)$. Thus by limiting this current with a current limiter the proper nonlinear conditions are imposed.

If a time base $\left(n=\frac{t}{t'}\right)$ is used where t' is computer time base and t actual time base the following relationships must be satisfied by the analogy

$$\left.\begin{aligned} &A_2=K_\delta & &\frac{T_1T_0}{A_{12}}=\frac{2}{2g\omega} \\ &\frac{T_1T_0L}{A_{12}R}=\frac{1}{n^2g\omega^2} & &\frac{T_1T_0}{A_{12}RC}=\frac{1}{ng} \end{aligned}\right\} \tag{19}$$

The following relationships establish the clipping current and voltages necessary to simulate the maximum permissible values for rudder velocity and position.

$$\text{Let } e_2=r\delta \text{ then } e_{2\max}=r\delta_{\max} \tag{20}$$

when e_2 and δ are expressed in volts and radians respectively

$$pe_{2\max}=nrp\delta_{\max}$$

or from equation 6

$$e_{1\max}i_{\max}R=\frac{T_0nr}{A_2}\,p\delta_{\max} \tag{21}$$

It should be noted that the rudder position and velocity limitations can be made different for the two directions. Equations 20 and 21 can be combined to give the following required relation between the two clipping voltages

$$\frac{e_1}{e_2}=\frac{T_0n}{A_2}\,\frac{(p\delta_{\max})}{(\delta_{\max})} \tag{22}$$

References

1. A New Device for the Solution of Transient Vibration Problems by Means of the Method of Electrical-Mechanical Analogy, H. E. Criner, G. D. McCann, D. E. Warren. *Journal of Applied Mechanics* (New York, N. Y.), volume 12, page 135.
2. The Mechanical Transients Analyzer, G. D. McCann. *Proceedings*, National Electronics Conference, volume 2, 1946, page 372.
3. A Large Scale General-Purpose Electric Analog Computer, E. L. Harder, G. D. McCann. *AIEE Transactions*, volume 67, part I, 1948, pages 664–73.
4. Electronic Techniques Applied to Analog Methods of Computation, G. D. McCann, C. H. Wilts, B. N. Locanthi. *Transactions*, Institute of Radio Engineers (New York, N. Y.).
5. The Effect of Coulomb Friction on the Performance of Servomechanisms, G. D. McCann, F. C. Lindvall, C. H. Wilts. *AIEE Transactions*, volume 67, part I, 1948, pages 540–6.
6. A High-Speed Electronic Function Generator, D. M. MacKay. *Nature*, (London, England) 159, 1947, page 406.
7. Electrical Analogue Computing, Part I, D. J. Mynall. *Electronic Engineering* (London, England), 1947, page 19.

No Discussion

Summary of Transformations Useful in Constructing Analogs of Linear Vibration Problems

JAMES P. CORBETT
NONMEMBER AIEE

THIS PAPER is concerned with the problem of representing linear vibrating systems in terms of electric circuits. The system under study is represented by a system of ordinary differential equations, linear, with constant coefficients. Such a system has an electric circuit representation if the vibrations are of stable type. However, the realization may require the use of ideal transformers and ideal unilateral impedances, and the number of such devices may be excessive. Again, the realization may require an excessive range of impedance values or may require linear behavior over too great a range of frequencies.

Difficulties arising from frequency requirements usually can be evaded by changes of time scale which compress the frequency range. Difficulties concerning the numerical ranges of impedance elements, capacitors for example, generally are eliminated by a combination of a change of time scale and a change of scale of current or charge.

In standard works it is shown that a system of linear differential equations with constant coefficients can be reduced to a triangular system by use of a system of multipliers with constant determinant. The use of a transformation of this type can result in considerable simplification. It is possible to alter the essential type of coupling appearing between loops of the circuits by this means. This transformation is particularly valuable, since it does not alter the dependent or independent variables and introduces only rational functions of the original parameters.

If the original system is expressed in terms of operators, it appears as an ordinary system of linear algebraic equations. In matrix form, this last transformation is simply a multiplication of this system on the left by a nonsingular matrix of constant determinant, that is, a set of row transformations of the original matrix. A corresponding column transformation of the system can be made—multiplication on the right by a nonsingular matrix of constant determinant. This transformation introduces new dependent variables, but there are cases in which this transformation can be kept sufficiently simple for practical use. By the use of the foregoing transformations, many systems which otherwise would be difficult or unwieldy are found to have simple passive representations.

A simple treatment of changes of independent variable for a general differential equation is given. Here the defining relationship among the derivatives may have simple discontinuities. The importance of this lies in emphasizing the way in which initial conditions are transformed. When the system to be analoged contains a nonlinear element or a simple discontinuity, the realization of initial or boundary conditions in the analog must be given careful attention. Even for linear systems, there is always the possibility of obtaining simplification in the analog through attention to the realization of a suitable set of initial conditions. In this last connection, the following important fact should be pointed out. In constructing an analog, it may be possible to avoid the necessity for exact simulation of an active element by proper attention to the initial conditions under which the analog is operated.

Change of Time Scale

It will suffice to illustrate this process for the equation

$$L\frac{d^2y}{dt^2}+R\frac{dy}{dt}+Ky=0 \qquad (1)$$

Let $y = f(t)$ be a solution of equation 1 and let $u = \eta t$ be the equation defining the change of time scale.

Then

$$y=\phi(u)=f(u/\eta) \qquad (2)$$

and differentiating this last equation with respect to t we obtain

$$\frac{dy}{dt}=\phi'(u)\frac{du}{dt}=\eta\phi'(u)$$

$$\frac{d^2y}{dt^2}=\eta^2\phi''(u) \qquad (3)$$

Substituting these values in equation 1

$$\eta^2L\phi''(u)+\eta R\phi'(u)+K\phi=0 \qquad (4)$$

Thus, $y = \phi(u)$ is a solution of the equation

$$\eta^2L\frac{d^2y}{du^2}+\eta R\frac{dy}{du}+Ky=0 \qquad (5)$$

Conditions under which this process is reversible are given in the Appendix. That is, given a solution $y = \phi(u)$ of a transformed differential equation, state conditions under which $y = f(t) = \phi[u(t)]$ is a solution of the original differential equation.

One use of this transformation is in obtaining a "dimensionless" form of a differential equation, as in the following example. Let the differential equation be

$$a_0y'''+a_1y''+a_2y'+a_3y=0 \qquad (6)$$

Set

$$a_3y=z$$

obtaining

Paper 49-166, recommended by the AIEE Computing Devices Committee and approved by the AIEE Technical Program Committee for presentation at the AIEE Summer General Meeting, Swampscott, Mass., June 20–24, 1949. Manuscript submitted November 26, 1948; made available for printing May 5, 1949.

James P. Corbett is with the Aerial Measurements Laboratory, Northwestern University, Evanston, Ill.

$$(a_0/a_3)z'''+(a_1/a_3)z''+(a_2/a_3)z'+z=0 \qquad (7)$$

Let

$$w(u)=z(\eta t)$$
$$\eta=(a_3/a_0)^{1/3}$$

then

$$w'''+(a_1/a_3)(a_3/a_0)^{2/3}w''+(a_2/a_3)(a_3/a_0)^{1/3}w'+w=0 \qquad (8)$$

which is a useful canonical form.[1]

Note that the initial conditions for operation of the analog are transformed according to equations 2 and 3.

Left Multiplication by a Nonsingular Matrix

In considering the system

$$U_i=\sum_{j=1}^{n}F_{ij}(D)y_j=0,\ (i=1,2,\ldots,n) \qquad (9)$$

a common procedure is to derive new equations by the operations of differentiation, multiplication by a constant, and addition or subtraction of the equations U_i. In other words the polynomials $F_{ij}(D)$ are considered as algebraic quantities, and the equations are manipulated according to the ordinary rules of algebra. If such operations are performed without restriction, extraneous solutions may be introduced, and the derived system will not form the basis for a usable analog. The foregoing process is equivalent to replacing the system of equation 9 by the system

$$V_k=\sum_{i=1}^{n}A_{ki}(D)U_i,\ (k=1,2,\ldots,n) \qquad (10)$$

where the elements, $A_{ki}(D)$, of the matrix are polynomials in D, and where the determinant of the matrix is not identically zero. The systems of equations 9 and 10 are equivalent if any solution of either is a solution of the other.

As an example, consider the system

$$U_1=(D+1)(D+2)y_1-(D+3)y_2=0$$
$$U_2=\qquad (D+2)y_1+\qquad y_2=0 \qquad (11)$$

Multiply the second equation of this system by $(D+1)$ and add to the first, obtaining

$$V_1=U_1+(D+1)U_2=-2y_2=0 \qquad (12)$$

and set

$$V_2=U_1=(D+1)(D+2)y_1-(D+3)y_2=0 \qquad (13)$$

The system consisting of the pair of equations 12 and 13 has among its solutions

$$y_2=0\quad y_1=e^{-t} \qquad (14)$$

which does not satisfy the original system. The solutions of the system of equation 11 are

$$y_2=0\quad y_1=ae^{-2t} \qquad (15)$$

This example shows the necessity for care in algebraic manipulation of a system of differential equations.

The systems of equations 9 and 10 are equivalent if, and only if, the determinant of the matrix $[A_{ki}(D)]$ is a constant (independent of D) different from zero. In the preceding example the value of this determinant is $-(D+1)$; hence equations 11 and equations 12 and 13 are not equivalent.

For our purpose, an important property of a transformation of the present type is that a system of differential equations of the form of equation 9 can be reduced to an equivalent triangular system

$$U_i=\sum_{j=1}^{n}F_{ij}(D)y_j=0 \qquad (16)$$

where $F_{ij}(D)=0$ if $i>j$, that is, in the matrix, all elements below the principal diagonal are zero. This reduction can be accomplished with any ordering of the variables, $y_1,\ldots.y_n$.[2]

It may be well to point out that solutions of the system of equations 9 by determinant theory will lead merely to the system

$$\Delta(D)y_i=0\ (i=1,2,\ldots n) \qquad (17)$$

where Δ (D) is the determinant of the system matrix, a result which may or may not be equivalent to the original system.

If the reduction to an equivalent triangular form is accomplished, the last equation of the system will be

$$F_{nn}(D)y_n=0 \qquad (18)$$

and hence the behavior of the element represented by y_n is described by the single differential equation given in equation 18.

A transformation of the foregoing type can be used to eliminate certain couplings from the system, as in the following example

$$U_1=(L_{11}D^2+R_{11}D)y_1-R_{12}Dy_2=0$$
$$U_2=\qquad -R_{21}D\ y_1+K_{22}\ y_2=0 \qquad (19)$$

If the voltage $R_{12}D\ y_2$ is to be supplied from the capacitor voltage $K_{22}\ y_2$, a differentiating amplifier would be required. This coupling can be eliminated in the following manner. Let the system of equations 19 be replaced by the system

$$V_1=aU_1+bDU_2=0$$

$$V_2=\qquad U_2=0 \qquad (20)$$

The equations making up the last system are

$$[(aL_{11}-bR_{21})D^2+aR_{11}D]y_1-(aR_{12}-bK_{22})Dy_2=0-R_{21}Dy_1+K_{22}y_2=0 \qquad (21)$$

Set

$$(aR_{12}-bK_{22})=0$$

then

$$a/b=K_{22}/R_{12}$$

If all the parameters of the system of equations 19 are positive, then a/b is positive.

The coefficient,

$$aL_{11}-bR_{21}$$

becomes

$$b(L_{11}K_{22}/R_{12}-R_{21})$$

If a and b are both positive, this last term will have the same sign as R_{11}, that is, a positive sign only if

$$L_{11}K_{22}-R_{12}R_{21}=0$$

The characteristic determinant of the original system is

$$(L_{11}K_{22}-R_{12}R_{21})D^2+R_{11}K_{22}D \qquad (22)$$

Hence, if the system is stable, the first coefficient must be positive and the trans-

Figure 1. Circuit representation of equations 23

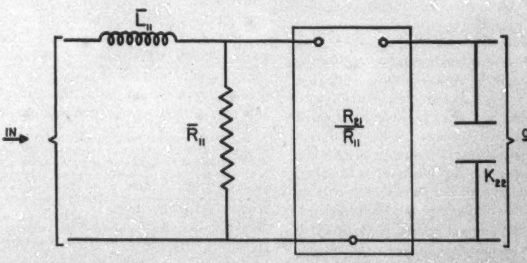

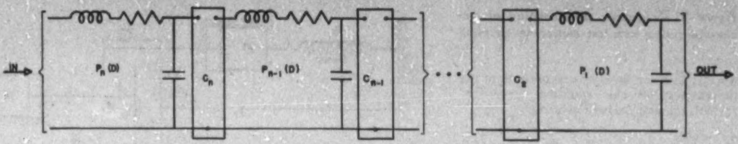

Figure 2. Circuit representation of differential equation, equations 24

formation can be made in the desired manner.

The new system, equation 20, therefore has the form

$$\begin{aligned}(\bar{L}_{11}D^2+\bar{R}_{11}D)y_1 \qquad &=0\\ -R_{21}D\ y_1+K_{22}y_2&=0 \qquad (23)\end{aligned}$$

where

$$\bar{L}_{11}=aL_{11}-bR_{21}>0$$
$$\bar{R}_{11}=aR_{11}$$

and is representable by the circuit shown in Figure 1.

A possible analog which will represent solutions of the differential equation

$$P_1(D)P_2(D)\dots P_n(D)y=1 \qquad (24)$$

will be shown to be the following system.

Let the system of equations be given

$$U_1=P_1(D)y_1-y_2=0$$
$$U_2=P_2(D)y_2-y_3=0$$
$$\cdot \quad \cdot \quad \cdot \quad \cdot$$
$$U_{n-1}=P_{n-1}(D)y_{n-1}-y_{n-1}=0$$
$$U_n=P_n(D)y_n=1 \qquad (25)$$

where

$$P_k(D)=a_kD^2+b_kD+c_k,\ (k=1,\ 2,\ \dots,\ n)$$

Replace this system by the equivalent system

$$V_1=U_1$$
$$V_2=P_2U_1+U_2$$
$$V_3=P_3P_2U_1+P_3U_2+U_3$$
$$\cdot \quad \cdot \quad \cdot \quad \cdot$$
$$V_k=P_kV_{k-1}+U_k \qquad (26)$$

and note that the determinant of this system is equal to one.

These equations when expanded in terms of the original system become

$$P_1(D)y_1-y_2=0$$
$$P_1(D)P_2(D)y_1-y_3=0$$
$$P_1(D)P_2(D)P_3(D)y_1-y_4=0$$
$$\cdot \quad \cdot \quad \cdot \quad \cdot$$
$$P_1(D)P_2(D)\dots P_n(D)y_1=1 \qquad (27)$$

The equivalent system, equations 25, then is an analog for the differential equation given in equations 24, as shown in Figure 2.

Transformation of Dependent Variables

We begin with the system

$$U_i=\sum_{j=1}^{n}F_{ij}(D)y_j=0,\ (i=1,\ 2,\ \dots,\ n) \qquad (28)$$

with the determinant of the matrix $(F_{ij}(D)) \neq 0$.

Let a transformation be defined by

$$y_j=\sum_{k=1}^{n}A_{jk}(D)z_k,\ (j=1,2,\dots,\ n) \qquad (29)$$

where the elements $A_{jk}(D)$ are polynomials in D.

The system of equations 28 then becomes

$$V_i=\sum_{j,k=1}^{n}F_{i}\ (D)A_{jk}(D)z_k=0,$$
$$(i=1,\ 2,\ \dots,\ n) \qquad (30)$$

If the determinant of the matrix $[A_{jk}(D)]$ is nonzero and independent of D, the variables z are uniquely expressible as

$$z_k=\sum_{j=1}^{n}B_{kj}(D)y_j,\ (k=1,\ 2,\ \dots,\ n) \qquad (31)$$

where $B_{kj}(D)$ are the elements of the matrix inverse to $[A_{ij}(D)]$ and, since the determinant of the latter matrix is constant, the elements $B_{kj}(D)$ are polynomials in D.

If z_k is a solution of equations 30, then the functions y_j defined by equation 29 are seen to be a solution of equations 28. If (y_j) are a solution of equations 28, then the functions (z_k) defined by equations 31, substituted into equations 30, yield

$$V_i=U_i=0$$

and hence these functions are solutions of equations 30.

This transformation may be exploited in a manner similar to that indicated in the example given under "Left Multiplication by a Nonsingular Matrix." This last example amounted to a row transformation of the matrix $[F_{ij}(D)]$. The present transformation represents a column transformation of this matrix.

The following example illustrates a transformation of this kind. We previously considered a system of equations

$$\begin{aligned}U_1&=(L_{11}D^2+R_{11}D)y_1-R_{12}Dy_2=0\\ U_2&=\qquad -R_{21}D\ y_1+K_{22}\ \ y_2=0 \qquad (32)\end{aligned}$$

Set

$$y_1=z_1$$
$$y_2=(R_{21}/K_{22})Dz_1+z_2 \qquad (33)$$

and the system of equations 32 becomes

$$\begin{aligned}V_1&=[(L_{11}-R_{12}R_{21}/K_{22})D^2+R_{11}D]z_1-\\ &\qquad R_{12}Dz_2=0\\ V_2&=\ \ K_{22}\ \ z_2=0 \qquad (34)\end{aligned}$$

and, as has been shown, if the original system was stable, the term $(L_{11}-R_{12}R_{21}/K_{22})$ is positive.

Let the system of equations 34 be replaced by

$$W_1=V_1+\frac{R_{12}}{K_{22}}DV_2=0$$
$$W_2=V_2 \qquad (35)$$

which, when expanded, becomes

$$W_1=\bar{L}D^2+\bar{R}Dz_1=0$$
$$W_2=K_{22}z_2=0 \qquad (36)$$

where

$$\bar{L}=(L_{11}-R_{12}R_{21}/K_{22})$$
$$\bar{R}=R_{11}$$

Appendix I. Change of Independent Variable in a System of Ordinary Differential Equations

Let a typical differential equation of the system have the form

$$F(x,\ y,\ dy/dt,\ \dots\ d^ny/dt^n)=0 \qquad (37)$$

where the arguments y, $dy/dt, \dots,\ d^ny/dt^n$ may be regarded as symbols for the set of arguments $y=(y_i)$ together with the successive derivatives of the elements y_i.

Suppose that a solution of equations 37, $y=f(x)$, is known. Let $x=x(u)$ be a transformation from the variable u to the variable x. In the range of definition of $x(u)$, it will be supposed that the first n derivatives of $x(u)$ exist, and that $dx/du \neq 0$ throughout the range.

Under these circumstances the inverse transformation $u=u(x)$ exists and has the same differentiability properties as $x(u)$. The successive derivatives of the function

Figure 3. Schematic representation of mechanical system with lost motion in coupling

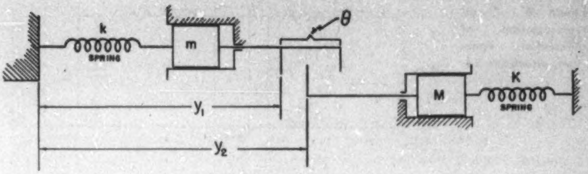

$y=f(x)$ then can be expressed in terms of the derivatives of the equation $y=\phi(u)=f[x(u)]$, the first derivative being

$$\frac{dy}{dx}=\frac{du}{dx}\frac{dy}{du} \tag{38}$$

By an induction it can be shown that

$$\frac{d^py}{dx^p}=A_{1p}\frac{dy}{du}+A_{2p}\frac{d^2y}{du^2}+\ldots+A_{pp}\frac{d^py}{du^p} \tag{39}$$

where the quantities A_{kp} are integral functions of the derivatives of $u(x)$ and where in particular $A_{pp}=du/dx$.

Equations 37 are thus to be transformed by replacing the derivatives d^py/dx^p by the linear expressions given by equations 39. Equations 37 then have the form

$$G\left(u, \frac{dy}{du}, \frac{d^2y}{du^2}, \cdots \frac{d^ny}{du^n}\right)=0 \tag{40}$$

In order to see that a solution of equations 37 can be recovered from a solution $y=\phi(u)$ of equations 40, we note that the system of linear equations, equations 39, has a unique inverse, since the determinant of the system is

$$\left[\frac{du}{dx}\right]^p \neq 0$$

Since the inverse is known to be unique, it is unnecessary to solve for the quantities d^py/du^p from equations 39. Instead, the chain rule for differentiation yields directly

$$\frac{d^py}{du^p}=B_{1p}\frac{dy}{dx}+B_{2p}\frac{d^2y}{dx^2}+\ldots B_{pp}\frac{d^py}{dx^p} \tag{41}$$

Substitution of these expressions into equations 40 must reduce it to the original differential equation, equations 37.

These considerations show that if $y=f(x)$ is any solution of the system of equations 37, then $y=\phi(u)=f[x(u)]$ is a solution of the transformed system of equations 40, and conversely, if $y=\phi(u)$ is any solution of the system of equations 37, then $y=f(x)$, $f(x)=\phi[x(u)]$ is a solution of the original system.

An application of this result is to the equations representing a simple mechanical system in which there is coulomb friction. The functional relationship, equation 37, in this case will be represented by

$$my''+ky+\epsilon f=0 \tag{42}$$

m, k, f, are fixed real constants

where

$\epsilon=1$ if $y'>0$
$\epsilon=-1$ if $y'<0$
$y'=0$ and $y\geq f/k$, then $\epsilon=-1$
$y'=0$ and $y\leq -f/k$, then $\epsilon=+1$

$y'=0$ and $|y|<f/k$, then $\epsilon=-\frac{k}{f}y$

To change time scales, it is only necessary to know that a solution exists. If $u=\eta t$, we obtain,

$$m\eta^2z''+\eta kz'+\epsilon f=0 \tag{43}$$

with the same conditions as above on ϵ relative to the functions, $z(u)$ and $z'(u)$.

Another example is for a system in which "backlash" or "lost motion" is present. See Figure 3. In a simple case the system is represented by the equations

$$my_1''+ry_1'+ky_1=0$$

$$My_2''+Ry_2'+Ky_2=0 \tag{44}$$

for

$y_1<y_2<y_1+\theta$

For the conditions, $y_1=y_2$, or $y_2=y_1+\theta$ it will be assumed that new boundary conditions may be computed according to the laws of conservation of momenta and energy.

Let $y_2(t_0)-y_1(t_0)=\theta$. The boundary conditions then may be expressed as

$$M[y_2'(t_0-0)]^2+m[y_1'(t_0-0)]^2$$
$$=M[y_2'(t_0)]^2+m[y_1'(t_0)]^2$$

$$My_2'(t_0-0)+my_1'(t_0-0)$$
$$=My_2'(t_0)+my_1'(t_0) \tag{45}$$

Setting $u=\eta t$, $z_1(u)=y_1(u/\eta)$, $z_2(u)=y_2(u/\eta)$, we obtain

$$\eta^2mz_1''+\eta=z_1'+kz_1=0$$

$$\eta^2Mz_2''+\eta Rz_2'+Kz_2=0 \tag{46}$$

and the boundary conditions become

$$M\eta^2[z_2'(u_0-0)]^2+m\eta^2[z_1'(u_0-0)]^2$$
$$=M\eta^2[z_2'(u_0)]^2+m\eta^2[z_1'(u_0)]^2$$

$$M\eta z_2'(u_0-0)+m\eta z_1'(u_0-0)$$
$$=M\eta z_2'(u_0)+m\eta z_1(u_0) \tag{47}$$

and the above equations are seen to be independent of the constant η.

References

1. SERVOMECHANISMS, CHART FOR VERIFYING THEIR STABILITY, Y. J. Liu. Massachusetts Institute of Technology (Cambridge, Mass.), 1941.

2. ORDINARY DIFFERENTIAL EQUATIONS (book), E. L. Ince. Dover Publishing Company, New York N. Y., 1934, page 149.

No Discussion

Formulas and Tables for the Calculation of the Magnetic Field Components of Circular Filaments and Solenoids

FREDERICK W. GROVER
MEMBER AIEE

THE calculation of the magnetic field strength at any point, due to a current in a circular filament or in a solenoid, is a problem having not only a theoretical interest but a practical importance in the shielding of apparatus and in the design of instruments for the control of electron flow.

Series formulas, both for circular filaments and for solenoids, involving zonal harmonics, were derived by Gray,[1] and extended by Dwight[2] to cover all possible cases. Dwight also has derived[3] formulas in hypergeometrical series which apply to short solenoids, and has shown how to take into account the correction due to the actual distribution of the current in a rectangular section.

Russell[4,5] expressed the magnetic field components of a circular filament in terms of elliptic integrals. A very full account of existing formulas and the cases to which they apply is given in chapter 32 of Dwight's book Electrical Coils and Conductors.[6]

The present paper has for its purpose the derivation of further formulas, both for circular filaments and solenoids. Particular attention is paid to the problem of routine calculations of magnetic field strength. Tables are provided for facilitating the computations.

Methods of Deriving Formulas for Field of a Circular Filament

If an expression for the magnetic potential ω is available, then the axial component H_z and the radial component H_r of the magnetic field strength are found by $H_z=-\partial\omega/\partial x$ and $H_r=-\partial\omega/\partial y$.

This is the method by which were obtained existing formulas[1,2] in zonal harmonics. Unfortunately, these expressions are not very rapidly convergent in certain cases.

The Biot-Savart formula for the magnetic field intensity due to an element of current, may be integrated around the circuit. The usefulness of this as a general method of attack is limited by the difficulty of performing the integration. This method was used by Russell[4,5] in deriving his elliptical integral expressions for the magnetic field components of a circular filament.

Dwight[3,6] has shown that the field components of a circular filament may be obtained by differentiation of any formula for the mutual inductance of two coaxial circles. If M_0 is the mutual inductance of two coaxial circles, one of which is the given filament and the other of radius y is passed through the point P (x,y), then

$$H_z=\frac{NI}{10}\frac{1}{2\pi y}\frac{\partial M_0}{\partial y} \tag{1}$$

$$H_r=-\frac{NI}{10}\frac{1}{2\pi y}\frac{\partial M_0}{\partial x} \tag{2}$$

The dimensions are in centimeters, the current in amperes, M_0 in abhenrys, and H_z and H_r are in gausses. The factor N is introduced to cover the case of a circular coil of N turns and negligible cross section, whose mean radius is a.

This is a very useful method, in that the differentiations always will be possible. Dwight's formulas 2 and 8, pages 274 and 278 of reference 6, for H_z and H_r were derived by differentiating a series expression for M_0 due to Havelock,[7] which is especially suitable for the purpose, since the dimensions of the problem appear in simple form in the general term of the series. However, many other formulas for M_0 are known[8,9] from which also formulas for the magnetic field components of a circular filament may be derived.

It is interesting to note, in passing, the relations between formulas 1 and 2 and the well-known formulas for the mechanical force exerted between the two coaxial filaments. The mechanical force, exerted in the axial direction, on each element ds of the circular filament of radius y through point P carrying a current of $i/10$ amperes, is $(iH_r/10).ds$. Substituting for H_r from formula 2, this is

$$-\frac{iI}{100}\frac{1}{2\pi y}\frac{\partial M_0}{\partial x}.ds$$

and integrating around the filament, the total axial force is

$$-\frac{iI}{100}\frac{\partial M_0}{\partial x}$$

the familiar formula.

Similar reasoning, using formula 1 for H_z, leads to the known expression for the mechanical force tending to increase the radial dimension of the circular filament.

Formulas 1 and 2 applied to the Maxwell elliptic integral formula[11] for the mutual inductance of coaxial circular filaments, leads to the Russell formulas[4,5] for the magnetic field components of a circular filament. Since these also are expressed in elliptic integrals, they are especially useful as a starting point for obtaining other formulas, since the elliptic integrals may be expanded in such various ways as in hypergeometric series, in q series, and in arithmetico-geometrical-mean expressions. Of these possible

---

Paper 49-167, recommended by the AIEE Basic Sciences Committee and approved by the AIEE Technical Program Committee for presentation at the AIEE Summer General Meeting, Swampscott, Mass., June 20–24, 1949. Manuscript submitted February 25, 1949; made available for printing May 5, 1949.

FREDERICK W. GROVER is Professor Emeritus of Electrical Engineering, Union College, Schenectady, N. Y.

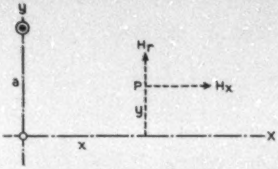

Figure 1. Field of circular filament, nomenclature

series only those in hypergeometric series will be considered here. The formulas obtained also may be derived by the use of formulas 1 and 2, but it is simpler to work from the Russell formulas.

Series Expansions for Circular Filaments

The Russell formulas are

$$H_x=\frac{2NI}{10r_1}\left[\frac{2a(a-y)}{r_2^2}\ E+(K-E)\right] \tag{3}$$

$$H_r=\frac{2NI}{10r_1}\left[\frac{2ax}{r_2^2}\ E-\frac{x}{y}(K-E)\right] \tag{4}$$

or, expressed in terms of space ratios

$$H_x=\frac{A}{\rho_1}\left[\frac{2(1-y/a)}{\rho_2^2}\ E+(K-E)\right] \tag{3a}$$

$$H_r=\frac{A}{\rho_1}\left[\frac{2x/a}{\rho_2^2}\ E-\frac{x}{y}\,(K-E)\right] \tag{4a}$$

where, as shown in Figure 1

a = radius of the filament
x, y = co-ordinates of the point P, referred to an origin at the center of the filament

$$r_1^2=(a+y)^2+x^2 \qquad \rho_1^2=(1+y/a)^2+\frac{x^2}{a^2}$$

$$r_2^2=(a-y)^2+x^2 \qquad \rho_2^2=(1-y/a)^2+\frac{x^2}{a^2}$$

$$A=2NI/10a$$

K and E are complete elliptic integrals with modulus given by $k^2=4ay/r_1^2$ and complementary modulus by $k'^2=r_2^2/r_1^2$. In Figure 1, the positive directions of H_x and H_r are as shown for the indicated direction of the current in the filament. From equations 3 and 4 it is evident that H_x reverses in direction for large values of y. H_r for a given value of y, changes sign in passing through the plane of the coil. These facts are in agreement with the familiar lines-of-force diagram of the filament.

Making use in equations 3(a) and 4(a) of the known expansions[12] of the elliptic integrals in powers, respectively, of k^2, k'^2, $\mu^2=k'^2/k^2=r_2^2/4ay$, and $\nu^2=k^2/k'^2=4ay/r_2^2$, and with the abbreviations $\lambda=\log_e 4/k'$ and $\lambda'=\log_e 4/\mu$, there result the following series expansions

$$H_x=\frac{\pi A}{\rho_1^3k'^2}\left[\left(1-\frac{k^2}{4}-\frac{3}{64}\,k^4-\frac{5}{256}\,k^6-\frac{175}{16{,}384}\,k^8-\frac{441}{65{,}536}k^{10}-\ldots\right)-\frac{3}{8}\,k^2\frac{y}{a}\left(1+\frac{k^2}{4}+\frac{15}{128}\,k^4+\frac{35}{512}k^6+\frac{735}{16{,}384}\,k^8+\ldots\right)\right] \tag{5}$$

$$H_r=\frac{3}{8}\ \frac{\pi A\dfrac{x}{a}\,\nu^2}{\rho_1^3}\left[1+\frac{k^2}{4}+\frac{15}{128}\,k^4+\frac{35}{512}\,k^6+\frac{735}{16{,}384}\,k^8+\ldots\right] \tag{6}$$

in powers of k^2, and

$$H_x=\frac{\pi A}{\rho_1^3k'}\left[\left(1+\frac{\nu^2}{4}-\frac{3}{64}\,\nu^4+\frac{5}{256}\,\nu^6-\frac{175}{16{,}384}\,\nu^8+\frac{441}{65{,}536}\,\nu^{10}-\ldots\right)-\frac{3}{8}\,\nu^2\frac{y}{a}\left(1-\frac{\nu^2}{4}+\frac{15}{128}\,\nu^4-\frac{35}{512}\nu^6+\frac{735}{16{,}384}\,\nu^8-\ldots\right)\right] \tag{7}$$

$$H_r=\frac{3}{8}\ \frac{\pi A\dfrac{x}{a}\,\nu^2}{\rho_1^3k'}\left[1-\frac{\nu^2}{4}+\frac{15}{128}\,\nu^4-\frac{35}{512}\,\nu^6+\frac{735}{16{,}384}\nu^8-\ldots\right] \tag{8}$$

in powers of ν^2. Also in terms of the complimentary modulus k'.

$$H_x=\frac{2A}{\rho_1^3k^2k'^2}\left[\left\{1+\frac{k'^2}{2}\left(\lambda-\frac{5}{2}\right)-\frac{5}{16}\,k'^4\times\left(\lambda-\frac{3}{20}\right)-\frac{9}{128}\,k'^6\left(\lambda-\frac{8}{9}\right)-\frac{65}{2{,}048}\,k'^8\left(\lambda-\frac{1{,}657}{1{,}560}\right)-\ldots\right\}-\frac{y}{a}\left\{1-\frac{3}{2}\,k'^2\left(\lambda-\frac{1}{2}\right)+\frac{3}{16}\,k'^4\times\left(\lambda+\frac{1}{4}\right)+\frac{3}{128}\,k'^6\left(\lambda-\frac{2}{3}\right)+\frac{15}{2{,}048}\,k'^8\left(\lambda-\frac{109}{120}\right)+\ldots\right\}\right] \tag{9}$$

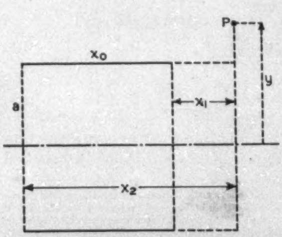

Figure 2. Field of thin solenoid or current sheet. Field at point P is difference of field due to two solenoids with point in end plane of each

$$H_r=\frac{2A\dfrac{x}{a}}{\rho_1^3k^2k'^2}\left[1-\frac{3}{2}\,k'^2\left(\lambda-\frac{1}{2}\right)+\frac{3}{16}\,k'^4\left(\lambda+\frac{1}{4}\right)+\frac{3}{128}\,k'^6\left(\lambda-\frac{2}{3}\right)+\frac{15}{2{,}048}\,k'^8\left(\lambda-\frac{109}{120}\right)+\ldots\right] \tag{10}$$

and in powers of μ^2

$$H_x=\frac{2A}{\rho_1^3\mu^2k}\left[\left\{1+\frac{1}{2}\,\mu^2\left(\lambda'+\frac{1}{2}\right)-\frac{1}{16}\,\mu^4\left(\lambda'-\frac{3}{4}\right)+\frac{3}{128}\,\mu^6\left(\lambda'-1\right)-\frac{25}{2{,}048}\,\mu^8\left(\lambda'-\frac{133}{120}\right)+\ldots\right\}-\frac{y}{a}\left\{1-\frac{3}{2}\,\mu^2\left(\lambda'-\frac{3}{2}\right)-\frac{9}{16}\,\mu^4\left(\lambda'-\frac{1}{12}\right)+\frac{15}{128}\,\mu^6\left(\lambda'-\frac{13}{15}\right)-\frac{105}{2{,}048}\,\mu^8\times\left(\lambda'-\frac{883}{840}\right)+\ldots\right\}\right] \tag{11}$$

$$H_r=\frac{2A\dfrac{x}{a}}{\rho_1^3\mu^2k}\left[1-\frac{3}{2}\,\mu^2\left(\lambda'-\frac{3}{2}\right)-\frac{9}{16}\,\mu^4\left(\lambda'-\frac{1}{12}\right)+\frac{15}{128}\,\mu^6\left(\lambda'-\frac{13}{15}\right)-\frac{105}{2{,}048}\,\mu^8\left(\lambda'-\frac{883}{840}\right)+\ldots\right] \tag{12}$$

These expressions have been checked by differentiation of the corresponding formulas[8,9,10] for M_0. In certain instances algebraic transformations have been applied to give more favorable numerical coefficients. In each case the factor A takes account of the current, number of turns, and the radius of the filament. The series involve space ratios only. Formulas 9 to 12 inclusive are useful for points near the filament and are very accurate for values of k'^2 and μ^2 less than about 0.2. Formulas 5 to 8, inclusive are very convergent for values of k^2 and ν^2 smaller than about 0.2 and find their usefulness for distant points. Formulas 11 and 12 are equivalent to Dwight's formulas 2 and 7, respectively, although expressed in more compact form. The other formulas are believed to be new.

In addition to the Russell formulas 3 and 4, other expressions in elliptic integrals may be derived by differentiation of other elliptic integral formulas[8,9,10] for M_0. Of these the most important is Maxwell's second formula.[11]

The resulting expressions are

$$H_x=\frac{A(\rho_1+\rho_2)}{\rho_1\rho_2k_1y/a}\left[\frac{k_1^2}{k_1'^2}\left\{1-2\frac{y}{a}\,k_1+k_1^2\right\}E_1+\left(\frac{y}{a}-k_1\right)k_1(K_1-E_1)\right] \tag{13}$$

$$H_r=A\,\frac{x}{y}\ \frac{\rho_1+\rho_2}{\rho_1\rho_2}\left[\frac{k_1^2}{k_1'^2}\,E_1-\frac{1}{2}(K_1-E_1)\right] \tag{14}$$

in which K_1 and E_1 are complete elliptic integrals to modulus

$$k_1=\frac{4y/a}{(\rho_1+\rho_2)^2}$$

and complimentary modulus

$$k_1'^2=\frac{4\rho_1\rho_2}{(\rho_1+\rho_2)^2}$$

These are not as simple as Russell's equations, but they may be expanded without difficulty. Of these expansions only those in powers of k_1^2 are given here

$$H_z=\frac{2\pi A}{\rho_1\rho_2(\rho_1+\rho_2)k_1'^2}\left[\left(1+\frac{k_1^2}{4}+\frac{k_1^4}{64}+\frac{k_1^6}{256}+\frac{25}{16{,}384}k_1^8+\frac{49}{65{,}536}k_1^{10}+\ldots\right)-\frac{3}{2}\frac{y}{a}k_1\left(1-\frac{k_1^2}{8}-\frac{k_1^4}{64}-\frac{5}{1{,}024}k_1^6-\frac{35}{16{,}384}k_1^8-\frac{147}{131{,}072}k_1^{11}-\ldots\right)\right] \tag{15}$$

$$H_r=\frac{3\pi A\frac{x}{a}k_1}{\rho_1\rho_2(\rho_1+\rho_2)k_1'^2}\left[1-\frac{k_1^2}{8}-\frac{k_1^4}{64}-\frac{5}{1{,}024}k_1^6-\frac{35}{16{,}384}k_1^8-\frac{147}{131{,}072}k_1^{10}-\ldots\right] \tag{16}$$

These give very accurate values up to about $k_1^2=1/4$, to which corresponds $k'^2=1/9$, so that they provide an overlap between formulas 5 to 8 and 9 to 12. Formulas 13 to 16 are believed to be new.

Routine Calculations of the Magnetic Field Components of a Circular Filament

The formulas listed by Dwight, together with those presented here, enable the magnetic field components of a circular filament to be calculated at all possible points. However, the number of formulas, their various ranges of convergence, and the number of geometrical parameters involved, tend to confuse the computer. A systematic procedure is desirable.

In the Russell equations 3 and 4 only two parameters appear, namely, ρ_1 and $k'^2=\rho_2^2/\rho_1^2$. The elliptic integrals depend upon the latter alone, and if tables of the elliptic integrals are at hand, the Russell equations provide a practical solution of the problem, without the necessity of investigating which of the series formulas is sufficiently convergent for the problem in question.

For numerical calculations using Russell's formulas tables of elliptic integrals based on k^2 or k'^2 as argument are especially convenient,[13] but for small values of k'^2 (points near the filament) these tables suffer from the usual difficulty due to the rapid increase of K with k. Interpolation is however rendered satisfactory if, instead of k'^2, log k'^2 is chosen as argument of the table. Table I has been calculated on this basis and suffices for the most precise work. The writer does not know of the existence of other tables based on this argument. This table is useful also for the case of a solenoid to be considered later. For many cases linear interpolation in the table will suffice, but for very precise work the second difference should be taken into account.

It is an advantage to use logarithms in the calculations. From the given coordinates, ρ_2^2 and ρ_1^2 and their ratio k'^2 are calculated, and from the logarithm of the latter the elliptic integrals are interpolated with a minimum of entries in the logarithm table. From the calculated values of H_z and H_r, the total magnetic intensity vector $\boldsymbol{H}$ and its direction θ with respect to the axis of the filament are found by the relations

$$\tan\theta=\frac{H_r}{H_z} \qquad \boldsymbol{H}=\frac{H_z}{\cos\theta} \tag{17}$$

Unfortunately, for the case of very distant points, the Russell formulas suffer from the disadvantage that the results are given by the small difference of nearly equal terms. For more precise work in such cases, series formulas 15 and 16 in terms of the modulus k_1 are recommended.

Example 1. For a circular filament with 10 centimeter radius, carrying a current 20 amperes, find the magnetic field components at the point $x=10$, $y=11$ centimeters.

Here $a=10$, $A=40/100=0.4$, $x/a=1$, $y/a=1.1$, $\rho_2^2=1.01$, $\rho_1^2=5.41$. Hence, log $\rho_2^2=0.0043214$, log $\rho_1^2=0.7331973$ and thus log $k'^2=9.2711241-10$. Interpolating in Table I for this value of log k'^2, there are found $E=1.16943$ and $(K-E)=1.11914$.

log $2(1-y/a)E=$ $n\bar{1}.3690042$
log ρ_2^2 $=$ 0.0043214
log difference $=$ $n\bar{1}.3646828$
$K-E$ $=$ 1.11914
minus difference $=$ -0.23157
Difference $=$ 0.88757
log Difference $=$ $\bar{1}.9482026$
1/2 log ρ_1 $=$ 0.3665986
$\bar{1}.5816040$
H_z $=$ $0.381595A$
$=$ 0.152638 gauss

The same example solved by the series formulas 9 and 11 give $H_z=0.381604A$ and $0.381591A$ respectively. For the radial component

$(2/\rho_2^2)E$ $=2.315703$
$(x/y)(K-E)=1.017400$
Difference $=1.298303$

and

H_r $=0.558184A$
$=0.223274$ gauss

By formula 10, $H_r=0.558180A$; by formula 12, $H_r=0.558183A$. Dwight's formula for this case gives $H_r=0.55846A$, but the value of $\mu^2=u^2/Dd$ is here too large for higher order terms to be neglected.

The calculation of the total magnetic field vector follows

log H_r $=\bar{1}.7467769$
log H_z $=\bar{1}.5816010$
log tan θ $=0.1651759$
log cos θ $=\bar{1}.7515563$
log $H_z/\cos\theta=\bar{1}.8300447$

or $\boldsymbol{H}=0.67615A=0.270460$ gauss, inclined to the filament axis by the angle $\theta=55$ degrees 38 minutes 31.7 seconds.

Example 2. In the case $x/a=10$ and $y/a=10$,

$\rho_2^2=181$ log $\rho_2^2=2.2576786$
$\rho_1^2=221$ log $\rho_1^2=2.3443923$
log $k'^2=\bar{1}.9132863$

and from Table I, $E=1.49710$ and $(K-E)=0.15306$.

$K-E$ $=$ 0.15306
$2(1-y/a)E/\rho_2^2=$ -0.14888
Difference $=$ 0.00418
H_z $=$ $0.0002812A$

The Russell formula is unfavorable, not only because of the smaller number of significant figures in the tabular value of $(K-E)$, but because of the near cancellation of terms.

By formula 15 log $k_1=\bar{2}.6978826$. In the series, terms in k_1^2 only have to be calculated.

First series $=1.000622$
Second series $=0.747892$
Difference $=0.252730$
$\therefore H_z=0.00028105_7A$ by equation 15
$=0.00028104_3A$ by equation 5
$=0.00028104_8A$ by equation 7

For the calculation of the radial component, the Russell formula gives

$[(2x/a)/\rho_2^2]E=0.165425$
$(x/y)(K-E)=0.15306$
Difference $=0.012365$

and

$H_r=0.0008318A$
$H_r=0.00083172\,A$ by equation 6
$H_r=0.00083171_9A$ by equation 8
$H_r=0.00083171_9A$ by equation 16

Table I. Complete Elliptic Integrals as Functions of Log$_{10}$ k'^2

Log$_{10}$ k'^2	K	Δ	K—E	Δ	E	Δ	Log$_{10}$ k'^2	K	Δ	K—E	Δ	E	Δ
$\bar{6}$.0	8.29405	−11513	7.29405	−11513	1.000004		$\bar{3}$.35	4.43915	5737	3.43473	5783	1.00441	15
.1	8.17892	11513	7.17892	11513	1.000004		.40	4.38178	5734	3.37690	5786	1.00488	47
.2	8.06379	11513	7.06379	11513	1.000006	1	.45	4.32444	− 5733	3.31904	− 5789	1.00539	57
.3	7.94866	11513	6.94866	11513	1.000007	2	$\bar{3}$.50	4.26711	− 5730	3.26115	5792	1.00596	62
.4	7.83353	11513	6.83353	11513	1.000009	2	.55	4.20981	5727	3.20323	5797	1.00658	69
$\bar{6}$.5	7.71840	−11512	6.71840	−11513	1.000011	3	.60	4.15254	5725	3.14526	5800	1.00727	76
.6	7.60328	11513	6.60327	11513	1.000014	3	.65	4.09529	5721	3.08726	5805	1.00803	84
.7	7.48815	11512	6.48814	11514	1.000017	4	.70	4.03808	− 5718	3.02921	− 5810	1.00887	92
.8	7.37303	11513	6.37300	11513	1.000021	6	$\bar{3}$.75	3.98090	5714	2.97111	5816	1.00979	102
$\bar{6}$.9	7.25790	11513	6.25787	11513	1.000027	6	.80	3.92376	5711	2.91295	5822	1.01081	112
$\bar{5}$.0	7.14277	−11513	6.14274	−11513	1.000033	8	.85	3.86665	5705	2.85473	5828	1.01193	122
.1	7.02764	11512	6.02761	11514	1.000041	10	.90	3.80960	5701	2.79645	5836	1.01315	136
.2	6.91252	11512	5.91247	11514	1.000051	10	$\bar{3}$.95	3.75259	− 5695	2.73809	− 5845	1.01451	148
.3	6.79740	11512	5.79733	11513	1.000061	16	$\bar{2}$.00	3.69564	− 1138	2.67964	− 1169	1.01599	32
.4	6.68228	11512	5.68220	11514	1.000077	20	.01	3.68426	1139	2.66795	1171	1.01631	32
$\bar{5}$.5	6.56716	−11512	5.56706	−11514	1.000097	21	.02	3.67287	1138	2.65624	1170	1.01663	33
.6	6.45204	11512	5.45192	11515	1.000118	32	.03	3.66149	1137	2.64454	1171	1.01696	33
.7	6.33692	11511	5.33677	11515	1.000146	34	.04	3.65012	1138	2.63283	1172	1.01729	34
.8	6.22181	−11511	5.22162	11515	1.000180	43	$\bar{2}$.05	3.63874	− 1137	2.62111	− 1172	1.01763	34
$\bar{5}$.9	6.10670	−11511	5.10647	−11515	1.000223	51	.06	3.62737	1137	2.60939	1172	1.01797	36
$\bar{4}$.0	5.99159	− 5755	4.99132	− 5759	1.000274	131	.07	3.61600	1137	2.59767	1172	1.01833	36
.05	5.93404	5755	4.93373	5758	1.000305	33	.08	3.60463	1137	2.58595	1173	1.01869	36
.10	5.87649	5755	4.87615	5759	1.000338	42	.09	3.59326	− 1136	2.57422	− 1174	1.01905	37
.15	5.81894	5755	4.81856	5758	1.000376	41	$\bar{2}$.10	3.58190	− 1136	2.56248	− 1174	1.01942	38
.20	5.76139	5754	4.76098	5759	1.000417	46	.11	3.57054	1136	2.55074	1174	1.01980	39
$\bar{4}$.25	5.70385	− 5754	4.70339	− 5759	1.000463	50	.12	3.55918	1135	2.53900	1175	1.02019	39
.30	5.64631	5754	4.64580	5760	1.000513	57	.13	3.54783	1135	2.52725	1175	1.02058	40
.35	5.58877	5753	4.58820	5760	1.000570	62	.14	3.53648	1135	2.51550	1176	1.02098	41
.40	5.53124	5754	4.53060	5760	1.000632	69	$\bar{2}$.15	3.52513	− 1134	2.50374	− 1176	1.02139	42
$\bar{4}$.45	5.47370	5753	4.47300	5761	1.000701	67	.16	3.51379	1134	2.49198	1177	1.02181	43
4.50	5.41617	− 5753	4.41539	− 5761	1.000777	85	.17	3.50245	1134	2.48021	1177	1.02224	43
.55	5.35864	5752	4.35778	5762	1.000862	94	.18	3.49111	1134	2.46844	1177	1.02267	44
.60	5.30112	5752	4.30016	5762	1.000956	103	.19	3.47977	1133	2.45667	1178	1.02311	45
.65	5.24360	5751	4.24254	5763	1.001059	115	$\bar{2}$.20	3.46844	− 1133	2.44489	− 1179	1.02356	46
.70	5.18609	− 5751	4.18491	− 5764	1.001174	127	.21	3.45711	1133	2.43310	1179	1.02402	46
4.75	5.12858	− 5750	4.12727	− 5765	1.00131	14	.22	3.44578	1132	2.42131	1180	1.02448	48
.80	5.07108	5750	4.06963	5765	1.00144	16	.23	3.43446	1132	2.40951	1180	1.02496	48
.85	5.01358	5749	4.01198	5766	1.00160	17	.24	3.42314	1132	2.39771	1182	1.02544	49
.90	4.95609	5748	3.95432	5767	1.00177	19	$\bar{2}$.25	3.41182	− 1131	2.38589	− 1181	1.02593	50
4.95	4.89861	− 5748	3.89665	− 5769	1.00196	21	.26	3.40051	1131	2.37408	1182	1.02643	52
$\bar{3}$.00	4.84113	5747	3.83896	5769	1.00217	23	.27	3.38920	1131	2.36226	1182	1.02695	52
.05	4.78366	5745	3.78127	5771	1.00240	26	.28	3.37789	1130	2.35044	1183	1.02747	53
.10	4.72621	5744	3.72356	5773	1.00266	28	.29	3.36659	1129	2.33861	1184	1.02800	54
.15	4.66877	5743	3.66583	−5774	1.00294	32	$\bar{2}$.30	3.35530	− 1129	2.32677	− 1185	1.02854	55
.20	4.61134	− 5741	3.60809	5777	1.00326	35	.31	3.34401	1129	2.31492	1185	1.02909	56
$\bar{3}$.25	4.55393	5740	3.55032	5778	1.00361	38	.32	3.33272	1129	2.30307	1186	1.02965	57
.30	4.49653	5738	3.49254	5781	1.00399	42	.33	3.32143	1128	2.29121	1186	1.03022	58
.35	4.43915		3.43473		1.00441		.34	3.31015		2.27935		1.03080	

Table I (Continued). Complete Elliptic Integrals as Functions of Log$_{10}$ k$'^2$

Log$_{10}$ k$'^2$	K	Δ	K—E	Δ	E	Δ
$\bar{2}$.34	3.31015		2.27935		1.03080	
		1128		1187		59
$\bar{2}$.35	3.29887		2.26748		1.03139	
		− 1127		− 1188		61
.36	3.28760		2.25560		1.03200	
		1127		1188		61
.37	3.27633		2.24372		1.03261	
		1127		1190		63
.38	3.26506		2.23182		1.03324	
		1126		1190		64
.39	3.25380		2.21992		1.03388	
		1126		1190		65
$\bar{2}$.40	3.24254		2.20802		1.03453	
		− 1125		− 1192		66
.41	3.23129		2.19610		1.03519	
		1125		1192		67
.42	3.22004		2.18418		1.03586	
		1125		1193		68
.43	3.20879		2.17225		1.03654	
		1124		1193		70
.44	3.19755		2.16032		1.03724	
		− 1123		− 1195		71
$\bar{2}$.45	3.18632		2.14837		1.03795	
		− 1123		− 1195		72
.46	3.17509		2.13642		1.03867	
		1122		1197		74
.47	3.16387		2.12445		1.03941	
		1122		1197		75
.48	3.15265		2.11248		1.04016	
		1122		1198		77
.49	3.14143		2.10050		1.04093	
		1121		1199		78
$\bar{2}$.50	3.13022		2.08851		1.04171	
		− 1120		− 1200		79
.51	3.11902		2.07651		1.04250	
		1120		1200		81
.52	3.10782		2.06451		1.04331	
		1120		1202		82
.53	3.09662		2.05249		1.04413	
		1119		1202		83
.54	3.08543		2.04047		1.04496	
		1118		1204		85
$\bar{2}$.55	3.07425		2.02843		1.04581	
		− 1118		− 1205		87
.56	3.06307		2.01638		1.04668	
		1117		1205		88
.57	3.05190		2.00433		1.04756	
		1117		1207		90
.58	3.04073		1.99226		1.04846	
		1116		1207		92
.59	3.02957		1.98019		1.04938	
		1116		1209		93
$\bar{2}$.60	3.01841		1.96810		1.05031	
		− 1115		− 1210		95
.61	3.00726		1.95600		1.05126	
		1115		1211		96
.62	2.99611		1.94389		1.05222	
		1113		1212		98
.63	2.98498		1.93177		1.05320	
		1114		1213		100
.64	2.97384		1.91964		1.05420	
		1112		1214		102
$\bar{2}$.65	2.96272		1.90750		1.05522	
		− 1112		− 1215		104
.66	2.95160		1.89535		1.05626	
		1111		1217		105
.67	2.94049		1.88318		1.05731	
		1110		1218		107
.68	2.92939		1.87100		1.05838	
		1110		1219		110
.69	2.91829		1.85881		1.05948	
		1109		1220		111
$\bar{2}$.70	2.90720		1.84661		1.06059	
		− 1109		− 1222		113
.71	2.89611		1.83439		1.06172	
		1108		1223		115
.72	2.88503		1.82216		1.06287	
		1107		1224		117
.73	2.87396		1.80992		1.06404	
		1106		1226		120
.74	2.86290		1.79766		1.06524	
		1106		1227		121
$\bar{2}$.75	2.85184		1.78539		1.06645	
		− 1105		− 1229		124
.76	2.84079		1.77310		1.06769	
		1104		1230		126
.77	2.82975		1.76080		1.06895	
		1103		1231		127
.78	2.81872		1.74849		1.07022	
		1103		1233		131
.79	2.80769		1.73616		1.07153	
		− 1102		− 1234		132
$\bar{2}$.80	2.79667		1.72382		1.07285	
		− 1101		− 1236		135
.81	2.78566		1.71146		1.07420	

Log$_{10}$ k$'^2$	K	Δ	K−E	Δ	E	Δ
$\bar{2}$.81	2.78566		1.71146		1.07420	
		1101		1238		137
.82	2.77465		1.69908		1.07557	
		1099		1239		140
.83	2.76366		1.68669		1.07697	
		1099		1241		142
.84	2.75267		1.67428		1.07839	
		1098		1242		144
$\bar{2}$.85	2.74169		1.66186		1.07983	
		− 1097		− 1244		147
.86	2.73072		1.64942		1.08130	
		1096		1246		150
.87	2.71976		1.63696		1.08280	
		1096		1247		152
.88	2.70880		1.62449		1.08432	
		1094		1250		155
.89	2.69786		1.61199		1.08587	
		1094		1251		157
$\bar{2}$.90	2.68692		1.59948		1.08744	
		− 1093		− 1253		161
.91	2.67599		1.58695		1.08905	
		1091		1254		163
.92	2.66508		1.57441		1.09068	
		1091		1257		166
.93	2.65417		1.56184		1.09234	
		1089		1259		168
.94	2.64328		1.54925		1.09402	
		1089		1260		172
$\bar{2}$.95	2.63239		1.53665		1.09574	
		− 1088		− 1263		175
.96	2.62151		1.52402		1.09749	
		1087		1264		177
.97	2.61064		1.51138		1.09926	
		1086		1267		181
.98	2.59978		1.49871		1.10107	
		1085		1269		184
$\bar{2}$.99	2.58893		1.48602		1.10291	
		1084		− 1270		187
$\bar{1}$.00	2.57809		1.47332		1.10478	
		− 1083		1273		190
.01	2.56726		1.46059		1.10668	
		1082		1276		193
.02	2.55644		1.44783		1.10861	
		1081		1277		197
.03	2.54563		1.43506		1.11058	
		1079		1280		200
.04	2.53484		1.42226		1.11258	
		1079		1282		203
$\bar{1}$.05	2.52405		1.40944		1.11461	
		− 1078		− 1284		207
.06	2.51327		1.39660		1.11668	
		1076		1287		210
.07	2.50251		1.38373		1 11878	
		1076		1289		214
.08	2.49175		1.37084		1.12092	
		1074		1292		217
.09	2.48101		1.35792		1.12309	
		1073		1294		221
$\bar{1}$.10	2.47028		1.34498		1.12530	
		− 1072		− 1297		225
.11	2.45956		1.33201		1.12755	
		1071		1299		229
.12	2.44885		1.31902		1.12984	
		1070		1302		232
.13	2.43815		1.30600		1.13216	
		1068		1305		236
.14	2.42747		1.29295		1.13452	
		− 1067		− 1308		241
$\bar{1}$.15	2.41680		1.27987		1.13693	
		− 1066		− 1311		244
.16	2.40614		1.26676		1.13937	
		1065		1313		249
.17	2.39549		1.25363		1.14186	
		1063		1316		253
.18	2.38486		1.24047		1.14439	
		1062		1319		257
.19	2.37424		1.22728		1.14696	
		1061		1322		261
$\bar{1}$.20	2.36363		1.21406		1.14957	
		− 1060		− 1325		265
.21	2.35303		1.20081		1.15222	
		1058		1328		270
.22	2.34245		1.18753		1.15492	
		1057		1331		275
.23	2.33188		1.17422		1.15767	
		1056		1335		279
.24	2.32132		1.16087		1.16046	
		1054		1337		283
$\bar{1}$.25	2.31078		1.14750		1.16329	
		− 1053		− 1341		288
.26	2.30025		1.13409		1.16617	
		1051		1344		293
.27	2.29974		1.12065		1.16910	
		1050		1348		297
.28	2.28924		1.10717		1.17207	

Table I (Concluded).

Log$_{10}$ k'^2	K	Δ	K—E	Δ	E	Δ	Log$_{10}$ k'^2	K	Δ	K—E	Δ	E	Δ
$\bar{1}$.28	2.28924		1.10717		1.17207		$\bar{1}$.64	1.91195		0.59400		1.31795	
		1049		1351		303			986		1520		534
.29	2.27875		1.09366		1.17510		$\bar{1}$.65	1.90209		0.57880		1.32329	
		1047		1355		307			− 985		− 1527		542
$\bar{1}$.30	2.25828		1.08011		1.17817		.66	1.89224		0.56353		1.32871	
		− 1046		− 1358		312			982		1532		550
.31	2.24782		1.06653		1.18129		.67	1.88242		0.54821		1.33421	
		1044		1362		318			980		1540		559
.32	2.23738		1.05291		1.18447		.68	1.87262		0.53281		1.33980	
		1042		1366		323			979		1546		568
.33	2.22696		1.03925		1.18770		.69	1.86283		0.51735		1.34548	
		1042		1369		328			976		1552		576
.34	2.21654		1.02556		1.19098		$\bar{1}$.70	1.85307		0.50183		1.35124	
		1039		1373		333			− 974		− 1559		585
$\bar{1}$.35	2.20615		1.01183		1.19431		.71	1.84333		0.48624		1.35709	
		− 1038		− 1377		339			972		1566		594
.36	2.19577		0.99806		1.19770		.72	1.83361		0.47058		1.36303	
		1037		1380		344			970		1573		603
.37	2.18540		0.98426		1.20114		.73	1.82391		0.45485		1.36906	
		1035		1385		350			968		1579		612
.38	2.17505		0.97041		1.20464		.74	1.81423		0.43906		1.37518	
		1034		1388		355			− 965		− 1587		621
.39	2.16471		0.95653		1.20819		$\bar{1}$.75	1.80458		0.42319		1.38139	
		1032		1394		361			− 963		− 1594		631
$\bar{1}$.40	2.15439		0.94259		1.21180		.76	1.79495		0.40725		1.38770	
		− 1030		− 1397		367			961		1602		640
.41	2.14409		0.92862		1.21547		.77	1.78534		0.39123		1.39410	
		1029		1402		373			959		1609		650
.42	2.13380		0.91460		1.21920		.78	7.77575		0.37514		1.40060	
		1027		1404		379			957		1616		659
.43	2.12353		0.90056		1.22299		.79	7.76618		0.35898		1.40719	
		1025		1410		385			954		1624		670
.44	2.11328		0.88646		1.22684		$\bar{1}$.80	1.75664		0.34274		1.41389	
		1023		1416		391			− 952		− 1632		680
$\bar{1}$.45	2.10305		0.87230		1.23075		.81	1.74712		0.32642		1.42069	
		− 1022		− 1420		397			950		1639		690
.46	2.09283		0.85810		1.23472		.82	1.73762		0.31003		1.42759	
		1020		1424		404			947		1648		700
.47	2.08263		0.84386		1.23876		.83	1.72815		0.29355		1.43459	
		1019		1428		410			945		1655		711
.48	2.07244		0.82958		1.24286		.84	1.71870		0.27700		1.44170	
		1017		1434		416			943		1664		721
.49	2.06227		0.81524		1.24702		$\bar{1}$.85	1.70927		0.26036		1.44891	
		− 1016		− 1438		423			− 940		− 1672		732
$\bar{1}$.50	2.05211		0.80086		1.25125		.86	1.69987		0.24364		1.45623	
		− 1014		− 1443		430			938		1681		743
.51	2.04197		0.78643		1.25555		.87	1.69049		0.22683		1.46366	
		1012		1448		436			936		1689		754
.52	2.03185		0.77195		1.25991		.88	1.68113		0.20994		1.47120	
		1009		1453		444			933		1699		765
.53	2.02176		0.75742		1.26435		.89	1.67180		0.19295		1.47885	
		1008		1459		450			931		1707		776
.54	2.01168		0.74283		1.26885		$\bar{1}$.90	1.66249		0.17588		1.48661	
		1005		1463		458			− 928		− 1716		788
$\bar{1}$.55	2.00163		0.72820		1.27343		.91	1.65321		0.15872		1.49449	
		− 1004		− 1469		465			926		1725		799
.56	1.99159		0.71351		1.27808		.92	1.64395		0.14147		1.50248	
		1002		1474		472			923		1735		812
.57	1.98157		0.69877		1.28280		.93	1.63472		0.12412		1.51060	
		1000		1479		479			931		1744		823
.58	1.97157		0.68398		1.28759		.94	1.62551		0.10568		1.51883	
		998		1485		487			918		1753		835
.59	1.96159		0.66913		1.29246		$\bar{1}$.95	1.61633		0.08915		1.52718	
		997		1491		494			−916		−1763		847
$\bar{1}$.60	1.95162		0.65422		1.29740		.96	1.60717		0.07152		1.53565	
		− 995		− 1496		502			913		1773		860
.61	1.94167		0.63926		1.30242		.97	1.59804		0.05379		1.54425	
		993		1503		510			911		1783		872
.62	1.93174		0.62423		1.30752		.98	1.58893		0.03596		1.55297	
		990		1508		518			908		1793		885
.63	1.92184		0.60915		1.31270		$\bar{1}$.99	1.57985		0.01803		1.56182	
		989		1515		525			− 905		− 1803		898
.64	1.91195		0.59400		1.31795		0.00	1.57080		0		1.57080	

The total field intensity is $H=0.00087784A$, and $\theta=71$ degrees 19 minutes 43.2 seconds.

Magnetic Field Strength Due to a Current in a Thin Solenoid

Formulas for the magnetic field strength due to a current in a thin solenoid may be obtained by the integration of the formulas for the field components of a circular filament. If, in Figure 2, it is assumed that the winding density of the solenoid of radius a is n turns per centimeter of axial length, we may multiply a suitable expression for H_x or H_r, due to a circular filament, by $n\,dx$ and integrate between $x=x_1$ and $x=x_2$, with $x_2=x_1+x_0$, to obtain the value of H_x or H_r due to the solenoid at the point. The integrated expression for the value $x_1=0$ is zero, so that the basic case is that of a solenoid of length x with the point P in its end plane. That is, the field strength at point P in Figure 2 is the difference of the values due to two solenoids, each of radius a, one of length x_1 and the other of length x_2, the point P being in the end plane of both. As Dwight pointed out, this method of treatment has the advantage that the two values, which are to be subtracted, do not have to be calculated by the same formula, but each may be obtained separately by the most favorable formula from the standpoint of convergence.

Of the available series formulas for the circular filament, not all are easily integrable, and some do not yield simple series expressions.

Dwight's formulas 3 and 9, given on pages 275 and 278 of reference 6, are in fact especially favorable. In general, the problem of the solenoid may be treated more easily by other methods. The radial and axial components will be separately treated here.

Radial Component H_r of a Thin Solenoid

Let

H_{r0} = the radial component due to a circular filament
H_{rs} = the radial component at P (Figure 2) due to a thin solenoid of length x_0 and radius a
n = winding density of the solenoid
M_0 = the mutual inductance of two circular coaxial filaments of radii a and y_0 with a distance x between their planes

Then

$$H_{rs}=n\int_{x_1}^{x_2} H_r dx$$

Substituting from formula 2

$$H_{rs}=-\frac{n}{2\pi y}\int_{x_1}^{x_2}\frac{\partial M_0}{\partial x}dx$$

$$=-\frac{n}{2\pi y}\left[M_{0x_2}-M_{0x_1}\right] \qquad (18)$$

in which M_{0x_2} and M_{0x_1} are, respectively, the mutual inductances of pairs of circular filaments of radii a and y with distances between their planes of x_2 and x_1.

From formula 18 it is evident that the radial component at point P due to the solenoid of Figure 2 may be calculated from the difference of the mutual inductances of two pairs of coaxial circles, and these may be calculated individually by any favorable formula of the large number known.

Since Dwight's[6] formula 7 for H_{r0} was obtained by the differentiation of Havelock's formula for the mutual inductance of two coaxial circular filaments with respect to x, while his equation 9 for H_{rs} is the result of integrating equation 7 with respect to x, between the limits zero and x, formula 9, therefore, should be equivalent to Havelock's formula, except for the factor $n/2\pi y$ the limits x and zero having been substituted and the results subtracted.

This conclusion can be verified readily. There is an advantage, however, in using equation 18 as it stands, without introducing the limit zero. This procedure avoids the difficulty that for $y=a$ and $x=0$, in formula 9, the term $\log_e(16Dd/c^2)$ becomes infinite.

Routine calculations of H_{rs} are very simple if the mutual inductances in equation 18 are computed with the aid of existing tables.[14] See example 5.

Formulas for the Axial Component H_z, of a Thin Solenoid

For the calculation of the axial component due to the solenoid, conditions are not so simple. It does not seem feasible to integrate Russell's equation 3 with respect to x. Of the series formulas 5 to 12, only formula 11 seems to yield a valuable formula. This is a result equivalent to Dwight's formula 3 page 275 of reference 6. The axial component, however, may be obtained by the differentiation of a suitable mutual inductance formula.

We may write, from formula 1

$$H_{z0}=\frac{-1}{2\pi y}\frac{\partial M_0}{\partial y}$$

and from Figure 2.

$$H_{z0}=n\int_{x_1}^{x_2} H_{z0}\,dx=\frac{n}{2\pi y}\int_{x_1}^{x_2}\frac{\partial M_0}{\partial y}dx$$

$$=\frac{n}{2\pi y}\frac{\partial}{\partial y}\left[\int_{x_1}^{x_2} M_0\,dx\right]$$

But

$$n\int_{x_1}^{x_2} M_0 dx$$

is the mutual inductance M_{s0} of the solenoid and a coaxial circle passed through point P; this also may be written

$$M_{s0}=n\left[\int_0^{x_2} M_0\,dx-\int_0^{x_1} M_0\,dx\right]$$

in which each of the integrals represents the mutual inductance of a solenoid and coaxial circle in its end plane. Thus, in general

$$H_{zs}=\frac{1}{2\pi y}\left[\left(\frac{\partial M_{s0}}{\partial y}\right)_{x=x_2}-\left(\frac{\partial M_{s0}}{\partial y}\right)_{x=x_2}\right] \qquad (19)$$

Any available formula for the mutual inductance of a solenoid and a circle in its end plane may be used for the differentiations indicated in equation 19. Since, in general, differentiation is always possible, this is an especially valuable method of attack.

Only two series formulas for the mutual inductance of solenoid and coaxial circle are known. One of these, which is rapidly convergent for short solenoids and a circle near the solenoid, is given by Dwight as formula 21 on page 245 of reference 6.

Differentiating this with respect to y and using formula 1 leads to the same equation 3, page 275 of reference 6, which Dwight[5] found by integrating his formula 2* with respect to x. This gives a check of the method.

A second mutual inductance formula, due to Rosa,[16,17] may be simplified by the substitution $x^2=r^2-A^2$ to give Dwight's equation 22, page 246 of reference 6.

This formula applies, either with the radius of the solenoid larger than that of the circle, or the reverse case, provided only that in either case A in the formula is understood to be the larger radius. Accordingly, in carrying out the differentiation of this expression with respect to y, the result is different, according as y is smaller or greater than a.

For the case $y<a$, points near the axis

$$H_{zs}=\frac{2\pi nIx}{10r}\left[1+\frac{3}{4}\alpha^2\rho^4-\frac{15}{16}\alpha^4\rho^6\xi_2+\right.$$
$$\frac{35}{32}\alpha^6\rho^8\xi_4-\frac{315}{256}\alpha^8\rho^{10}\xi_6+$$
$$\left.\frac{693}{512}\alpha^{10}\rho^{12}\xi_8-\frac{3{,}003}{2{,}048}\alpha^{12}\rho^{14}\xi_{10}+\ldots\right] \qquad (20)$$

where

$$\alpha=y/a$$

$$\rho^2=\frac{a^2}{x^2+a^2}=\frac{a^2}{r^2}$$

$$\xi_2=1-\frac{7}{4}\rho^2$$

$$\xi_4=1-\frac{9}{2}\rho^2+\frac{33}{8}\rho^4$$

$$\xi_6=1-\frac{33}{4}\rho^2+\frac{143}{8}\rho^4-\frac{715}{64}\rho^6$$

$$\xi_8=1-13\rho^2+\frac{195}{4}\rho^4-\frac{1{,}105}{16}\rho^6+\frac{4{,}199}{128}\rho^8$$

$$\xi_{10}=1-\frac{75}{4}\rho^2+\frac{425}{4}\rho^4-\frac{8{,}075}{32}\rho^6+$$
$$\frac{33{,}915}{128}\rho^8-\frac{52{,}003}{512}\rho^{10}$$

The ξ functions oscillate between plus one and a negative maximum not as great as one unit. Making use of the relation $x^2/r^2=1-a^2/r^2$, and the known expressions for $P_n'(\mu)$, it is easy to show that formula 20 is equivalent to Dwight's formula 42 on page 289 of reference 6, for the case that $t=0$. This latter expression is easy to use, if tables of $P_n'(\mu)$ are at hand. Otherwise formula 20 is compact and not difficult to calculate.

If $y>a$, points distant from the axis, differentiation of the Rosa-Dwight expression for M_{s0} results in the following simple formula, after having used the relation $y^2/r^2=1-x^2/r^2$

---

* This formula (2) should have $-c/d$ instead of $+c/d$ in the last line.

$$H_{zs}=-\frac{\pi nIa^2x}{10r^3}\left[1-\frac{3}{4}\frac{a^2}{r^2}\frac{P_3(x/r)}{x/r}+\frac{5}{8}\frac{a^4}{r_4}\frac{P_5(x/r)}{x/r}-\frac{35}{64}\frac{a^6}{r^6}\frac{P_7(x/r)}{x/r}+\ldots\right] \tag{21}$$

with $r^2=x^2+y^2$. The general term is

$$\frac{(-1)^{2n+1}3\cdot5\cdot7\ldots(2n+1)}{4\cdot6\cdot8\ldots(2n+2)}\frac{P_{2n+1}(x/r)}{x/r}\cdot\frac{a^{2n}}{r^{2n}}$$

in which P_{2n+1} is the zonal harmonic.

This formula is seen to be the same as Dwight's formula 39 page 288 of reference 6, for the case $t=0$. If tables of zonal harmonics are available, this is a very convenient formula for computation, in cases where the convergence is sufficiently rapid.

Unfortunately, these existing series formulas for H_{zs} do not overlap sufficiently well to allow very precise calculations in certain cases. An expression in elliptic integrals, which will apply in all cases, is much to be desired. The Jones-Campbell[18,19] elliptic integral formula for the mutual inductance of a solenoid and coaxial circular filament in its end plane furnishes this solution. The differentiation of this expression with respect to y is straightforward, but the algebraic manipulation is far from simple. In the course of this work, the writer discovered that Campbell[19] had made this differentiation, but for a different purpose, in his study of the most favorable dimensions for his standard of mutual inductance. No details of the work are supplied there.

The result given here although different in form, checks Campbell's differentiation completely. The result is

$$H_{zs}=\frac{nI}{10}\left[\frac{4ax}{r_1(a+y)}\cdot K\mp 2\psi\right] \tag{22}$$

$$=\frac{nI}{10}\left[\frac{4x/a}{\rho_1(1+y/a)}\cdot K\mp 2\psi\right] \tag{22a}$$

The upper sign is to be used when $y<a$, and the lower sign for $y>a$.* The function ψ is given by

$$\psi=KE'-(K-E)F'-\frac{\pi}{2} \tag{23}$$

in which K and E are complete elliptic integrals whose modulus k and complementary modulus k' are given by $k^2=4ay/r_1^2$ and $k'^2=\rho_2^2/\rho_1^2$, just as equations 3(a) and 4(a) for the circular filament. Note that here, however, x is the length of the solenoid. F' and E' are incomplete elliptic integrals with modulus equal to k' and amplitude $\beta=\sin^{-1} c'/k'$ with $c'^2=(y-a)^2/(y+a)^2$.

Routine Calculations for the Thin Solenoid

The complete elliptic integral K in equation 22 can be obtained from Table I for the given value of $\log_{10}k'^2$. Values of Ψ, which will be recognized as involving an elliptic integral of the third kind, give especial difficulty, since it depends not only on the modulus but on the parameter $c^2=1-c'^2$. Values of Ψ may be calculated from the defining equation 23, using Legendre's table of incomplete integrals[20] or the tables of Jahnke and Emde,[21] but in general the interpolations are tedious and time consuming. The tables presented here have the advantage that the interpolations necessary do not enter into the principal terms.

Writing $\Psi=(-\pi/2)+\beta+D$, the quantity $D=f_0k'^2\sin2\beta$ may be calculated from values of f_0 tabulated with $\log_{10}k'^2$ and β as arguments in Table II. The value of β in radians may be taken from the usual conversion table common in collections of formulas.

For values of k'^2 nearly unity it is better to write $\Psi=(-\pi/2)(1-p\sin\beta)$ and then to obtain values of $\log p$ from Table III for the given arguments $\log k'^2$ and β. In computing Table II a series expression for ψ in powers of k'^2, derived from known series[18] for F' and E' was used. For larger values of k'^2 the Legendre tables had to be used. For the calculation of $\log p$, a development for ψ in terms of

---

* For the special case $y=a$ in equation 22, $\psi=-\pi/2$, whatever the length x of the solenoid. Therefore, in the calculation of the axial component at the point P, the term ψ is the same both for the calculation for $x=x_1$ and $x=x_2$, and cancels in the difference. The axial component in this case is therefore given by the difference of the terms in K in equation 22 as calculated for the two values of x. In the basic formula for the point $y=a$ in the end plane, the point is in contact with the end of the winding, and the axial component is indeterminate. This difficulty does not arise for a winding of finite thickness.

Table II. Values of f_0 as Function of k'^2 and β

$\log_{10} k'^2$	$\beta=0°$	10°	20°	30°	40°	50°	60°	70°	80°	$\beta=90°$	$\log_{10} k'^2$
$\bar{4}$.0	1.37291	1.37291	1.37292	1.37292	1.37293	1.37293	1.37294	1.37294	1.37295	1.37295	$\bar{4}$.0
.2	1.31536	1.31536	1.31537	1.31538	1.31538	1.31539	1.31540	1.31540	1.31541	1.31541	.2
.4	1.25783	1.25783	1.25784	1.25785	1.25786	1.25787	1.25788	1.25789	1.25790	1.25790	.4
.6	1.20031	1.20031	1.20032	1.20034	1.20036	1.20038	1.20039	1.20040	1.20041	1.20041	.6
$\bar{4}$.8	1.14284	1.14285	1.14287	1.14289	1.14292	1.14294	1.14297	1.14299	1.14301	1.14302	$\bar{4}$.8
$\bar{3}$.0	1.08539	1.08540	1.08543	1.08546	1.08550	1.08554	1.08559	1.08562	1.08564	1.08565	$\bar{3}$.0
.1	1.05669	1.05670	1.05673	1.05677	1.05682	1.05687	1.05692	1.05697	1.05700	1.05701	.1
.2	1.02800	1.02802	1.02805	1.02810	1.02815	1.02823	1.02829	1.02834	1.02838	1.02839	.2
.3	0.99933	0.99935	0.99939	0.99945	0.99953	0.99961	0.99969	0.99975	0.99979	0.99980	.3
.4	0.97069	0.97071	0.97076	0.97083	0.97093	0.97103	0.97112	0.97119	0.97124	0.97126	.4
$\bar{3}$.5	0.94207	0.94209	0.94216	0.94225	0.94235	0.94248	0.94260	0.94269	0.94275	0.94277	$\bar{3}$.5
.6	0.91349	0.91352	0.91360	0.91371	0.91384	0.91399	0.91413	0.91424	0.91432	0.91434	.6
.7	0.88496	0.88499	0.88508	0.88522	0.88538	0.88556	0.88573	0.88587	0.88596	0.88599	.7
.8	0.85646	0.85650	0.85661	0.85677	0.85698	0.85720	0.85740	0.85757	0.85768	0.85772	.8
$\bar{3}$.9	0.82804	0.82809	0.82822	0.82842	0.82867	0.82893	0.82918	0.82937	0.82952	0.82957	$\bar{3}$.9
$\bar{2}$.0	0.79968	0.79973	0.79989	0.80014	0.80044	0.80076	0.80106	0.80131	0.80148	0.80153	$\bar{2}$.0
.1	0.77140	0.77146	0.77166	0.71196	0.77232	0.77271	0.77308	0.77338	0.77358	0.77365	.1
.2	0.74321	0.74330	0.74353	0.74390	0.74434	0.74481	0.74526	0.74562	0.74586	0.74594	.2
.3	0.71515	0.71525	0.71553	0.71597	0.71650	0.71707	0.71761	0.71806	0.71834	0.71844	.3
.4	0.68722	0.68734	0.68768	0.68820	0.68885	0.68954	0.69020	0.69073	0.69108	0.69120	.4
$\bar{2}$.5	0.65944	0.65958	0.65999	0.66063	0.66141	0.66224	0.66303	0.66368	0.66410	0.66425	$\bar{2}$.5
.6	0.63184	0.63201	0.63251	0.63327	0.63421	0.63522	0.63615	0.63695	0.63746	0.63763	.6
.7	0.60446	0.60466	0.60526	0.60617	0.60730	0.60852	0.60967	0.61061	0.61123	0.61145	.7
.8	0.57731	0.57756	0.57827	0.57937	0.58072	0.58219	0.58358	0.58474	0.58547	0.58574	.8
$\bar{2}$.9	0.55043	0.55073	0.55158	0.55290	0.55453	0.55629	0.55797	0.55935	0.56026	0.56058	$\bar{2}$.9
$\bar{1}$.0	0.52388	0.52422	0.52525	0.52682	0.52878	0.53090	0.53292	0.53460	0.53571	0.53610	1.0
.1	0.49769	0.49810	0.49931	0.50118	0.50354	0.50610	0.50855	0.51060	0.51196	0.51242	.1
.2	0.47187	0.47239	0.47380	0.47606	0.47886	0.48196	0.48493	0.48744	0.48908	0.48964	.2
.3	0.44619	0.44707	0.44878	0.45148	0.45485	0.45858	0.46222	0.46526	0.46735	0.46805	.3
.4	0.42161	0.42229	0.42432	0.42752	0.43159	0.43612	0.44057	0.44436	0.44686	0.44786	.4
$\bar{1}$.5	0.39726	0.39809	0.40049	0.40429	0.40921	0.41474	0.42029	0.42502	0.42824	0.42944	1.5
.6	0.37352	0.37448	0.37734	0.38188	0.38782	0.39463	0.40157	0.40767	0.41190	0.41341	.6
.7	0.35041	0.35154	0.35490	0.36035	0.36756	0.37607	0.38496	0.39300	0.39871	0.40079	.7
.8	0.32800	0.32932	0.33329	0.33932	0.34871	0.35949	0.37126	0.38246	0.39081	0.39391	.8
$\bar{1}$.9	0.30631	0.30786	0.31255	0.32041	0.33147	0.34406	0.36207	0.37922	0.39331	0.40570	1.9
0.0	0.28540	0.28721	0.29276	0.30230	0.31636	0.33574	0.36160	0.39567	0.44052	0.50000	0.0

arithmetico-geometric series was employed.

Example 3. To find the axial component H_{xs} due to a solenoid of radius $a=5$ centimeters, length $x=25$ centimeters, at a point in the end plane for which $y=20$.

Here

$r_2^2=(15)^2+(25)^2=850$
$r_1^2=(25)^2+(25)^2=1{,}250$
$c'^2=\left(\frac{15}{25}\right)^2$
$4ax=500$
$\log c'^2 \quad =\bar{1}.5563025$
$\log k'^2 \quad =\bar{1}.8325089$
$\log \sin \beta=\bar{1}.8618968$
$\beta=46$ degrees 41 minutes 10.1 seconds = 0.81483 radians
β = 46.6861 degrees
$\log \sin 2\beta=\bar{1}.99925$

From Table I, $K=1.72578$, and from Table II $f_0=0.35056$, while Table III gives $\log p=\bar{1}.96430$

$f_0k'^2 \sin 2\beta = 0.23797$
$\beta = \underline{0.81483}$
Sum $= 1.05280$
$-\pi/2 = \underline{-1.57080}$
$\psi = -0.51800$

$(\pi/2)p \sin \beta = 1.05274$
$-\pi/2 = \underline{-1.57080}$
$\psi = -0.51806$

A very accurate calculation of Ψ using arithmetico-geometric-mean series gave -0.518017. Using this value

$2\psi = -1.036034$
Term in $K = \underline{0.976249}$
Sum $= -0.059785$
$H_{xs} = -0.059785nI/10$

This result may be checked by formula 21, that is, Dwight's formula 39

$r^2=x^2+y^2=1.025$
$x/r=0.78087$

$$\frac{P_3(x/r)}{x/r}=0.0244$$

$$\frac{P_5(x/r)}{x/r}=-0.5325$$

$$\frac{P_7(x/r)}{x/r}=-0.2080$$

The terms in the series are $(1-0.000446-0.000198+0.000002)=0.999358$, and $H_{xs}=-0.0597950nI/10$. The negative sign signifies that the field is opposed in direction to that at points on the axis.

Example 4. For the case $a=5, x=50$, and $y=2$. $r_2^2=2509$, $\log c'^2=\bar{1}.2640464$, $4ax=1000$ $r_1^2=2549$, $\log k'^2=\bar{1}.9931309$, $K=1.57701$, $\beta=25$ degrees 35 minutes 34.5 seconds = 25.5929 degrees.

From Table III, $\log p=\bar{1}.99829$, $\psi=-0.89492$. A very accurate calculation of ψ gives -0.8949208.

First term $= 4.462226$
$2\psi = -1.789842$

Difference gives $H_{xs}=6.252068nI/10$. Using formula 20 $r^2=25+2{,}500=2525$, $\xi_2=0.98267$, and higher order terms are negligible. $H_{xs}=2\pi x/r(1.0000118)nI/10$ $6.252077nI/10$.

Example 5. A good illustration of the usefulness of the formulas and tables here developed is furnished by a study of Campbell's form of mutual inductance standard,[19] Figure 3. Two equal coils of radii 10 centimeters and axial lengths 5 centimeters are placed coaxial with a separation between their nearer ends of 10 centimeters. Each is wound with 10 turns per centimeter that is, a total of 50 turns. In the median plane is placed a coaxial circular coil with 1,000 turns, wound in a square cross section one centimeter on a side. The mean radius of this coil, $y=14.5$ centimeters was chosen so that the turns of this secondary lie in a region of nearly zero magnetic field intensity. Under this condition, the mutual inductance of the secondary on the two primary coils in series is nearly the same as though all the secondary turns were concentrated at the center of the cross section, point P.

By symmetry, with the two primaries aiding magnetically, their radial components cancel, and the resultant field at P is twice the axial component due to one. The axial component produced by each coil is equal to the difference of the values which would be produced by a solenoid 10 centimeters long and one 5 centimeters long with the point P in the end plane of each. These values are, respectively, $-6.6034I/10$ and $-6.6523I/10$, giving a resultant of $0.0489I/10$ and, for both coils, $H_{xs}=+0.0978I/10$. This case is unfavorable for the use of formulas 21 and Dwight's formula 3. For $x=10$, formula 21 gives $-6.5998I/10$ and for $x=5$, formula 3 gives $-6.472I/10$.

Repeating the calculation of H_{xs} for $y=14.6$, the resultant field is $-0.0210I/10$, which indicates that H_{xs} becomes zero at $y \cong 14.58$, which agrees with Campbell's estimate of 14.6.

It is to be noted that the calculation of H_{xs} using formula 22 depends on data useful also for calculating the mutual inductance by Campbell's formula.[19] Multiplying the mutual inductance of the turn at the center of the cross section by 1,000 gives a value of 9.17588 millihenrys, uncorrected for the effect of a finite cross section.

The mutual inductance per turn of the secondary is a maximum for a turn at the point of zero magnetic field intensity, but the maximum is very flat. The value for

Table III. Values of $\log_{10} p$ as Function of $\log_{10} k'^2$ and β

β	$\log_{10} k'^2 = \bar{1}.80$	Δ	$\log_{10} k'^2 = \bar{1}.85$	Δ	$\log_{10} k'^2 = \bar{1}.90$	Δ	$\log_{10} k'^2 = \bar{1}.95$	Δ	$\log_{10} k'^2 = 0.00$
0	$\bar{1}$.95427	1063	$\bar{1}$.96492	1115	$\bar{1}$.97607	1170	$\bar{1}$.98777	1223	0
	4		3		2				
5	.95431	1064	.96495	1114	.97609	1169	.98778	1222	0
	12		7		3				
10	.95443	1059	.96502	1110	.97612	1166	.98778	1222	0
	18		12		5		1		
15	$\bar{1}$.95461	1053	$\bar{1}$.96514	1103	$\bar{1}$.97617	1162	$\bar{1}$.98779	1221	0
	25		14		9		3		
20	.95486	1042	.96528	1098	$\bar{1}$.97626	1156	.98782	1218	0
	38		22		9		3		
25	.95524	1026	.96550	1085	.97635	1150	.98785	1215	0
	49		29		15		3		
30	$\bar{1}$.95573	1006	$\bar{1}$.96579	1071	$\bar{1}$.97650	1138	$\bar{1}$.98788	1212	0
	61		37		17		5		
35	.95634	982	.96616	1051	.97667	1126	.98793	1207	0
	81		50		25		6		
40	.95715	951	.96666	1026	.97692	1107	.98799	1201	0
	99		63		31		10		
45	$\bar{1}$.95814	915	$\bar{1}$.96729	994	$\bar{1}$.97723	1086	$\bar{1}$.98809	1191	0
	132		84		44		12		
50	.95946	867	.96813	954	.97767	1054	.98821	1179	0
	166		110		63		18		
55	.96112	811	.96923	907	.97830	1009	.98839	1161	0
	216		145		75		27		
60	$\bar{1}$.96328	740	$\bar{1}$.97068	837	$\bar{1}$.97905	961	$\bar{1}$.98866	1134	0
	281		195		112		36		
65	.96609	654	.97263	754	.98017	885	.98902	1098	0
	368		267		162		61		
70	.96977	553	.97530	649	.98179	784	.98963	1037	0
	485		363		230		96		
75	$\bar{1}$.97462	431	$\bar{1}$.97893	516	$\bar{1}$.98409	650	$\bar{1}$.99059	941	0
	633		496		356		163		
80	.98095	294	.98389	376	.98765	457	.99222	778	0
	831		683		494		285		
85	$\bar{1}$.98926	146	$\bar{1}$.99072	187	$\bar{1}$.99259	248	$\bar{1}$.99507	493	0
	1074		928		741		493		
90°	0	0	0	0	0	0	0	0	0

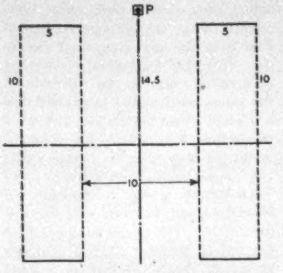

Figure 3. Arrangement of Campbell-type of mutual inductance standard

$y=14.6$ is only 30 parts in a million greater than that for $y=14.5$. The value, for given y, is a minimum in the median plane, as far as axial displacements are concerned, but this minimum also is very flat.

It is safe to assume that derivatives of M, with respect to either co-ordinate, of order higher than the second are negligible.

The value of the mutual inductance, taking into account the effect of a finite rectangular cross section of radial dimension c and axial dimension b, is, then

$$M_{corr.}=N_2\left[M_P+\frac{b^2}{24}\left.\frac{\partial^2 M}{\partial x^2}\right|_P+\frac{c^2}{24}\left.\frac{\partial^2 M}{\partial y^2}\right|_P\right] \tag{24}$$

or, making use of formulas 1 and 2

$$M_{corr.}=N_2\left[M_P-\frac{2\pi b^2 y}{24}\left.\frac{\partial H_{rs}}{\partial x}\right|_P+\frac{2\pi c^2}{24}\left(H_{zs}+y\frac{\partial H_{zs}}{\partial y}\right)_P\right] \tag{25}$$

The subscript P designates values at the central point P.

Campbell[19] solved for this correction by a quadrature formula derived from formula 24, which requires the calculation of M at points located at the centers of the sides of the rectangle, as well as at P. With $y=14.5$ for point P, $b=1$ and $c=1$, the correction is 12 parts in a million, the corrected value being larger than the uncorrected.

To apply formula 25, we already have from the calculations of H_{zs} at $y=14.5$ and 14.6, the derivative

$$\left.\frac{\partial H_{zs}}{\partial y}\right|_P=-1.188$$

We need the value

$$\left.\frac{\partial H_{rs}}{\partial x}\right|_P$$

To obtain this, we may calculate H_{rs} for $y=14.5$ and a displacement of $\Delta x=0.1$ centimeter. The required mutual inductances in formula 18 are for circles of radii 10 and 14.5, and with the distances between their planes to be shown. These mutual inductances will here be calculated from the formula $f\sqrt{ay}$ in abhenries, the values of f being interpolated from tables.[14,15]

Left hand coil

$x_2=9.9$
$r_2^2=(4.5)^2+(9.9)^2=118.26$
$r_1^2=(24.5)^2+(9.9)^2=698.26$
$k'^2=0.1693639$
$1000f=5.703$

$x_1=4.9$
$r_2^2=(4.5)^2+(4.9)^2=44.26$
$r_1^2=(24.5)^2+(4.9)^2=624.26$
$k'^2=0.0708999$
$1000f=10.111$

$$H_{rs}\ left=\frac{10\sqrt{145}(10.111-5.703)}{2\pi(14.5)}$$
$$=5.8260 \text{ radially outward}$$

Right hand coil

$x_2=10.1$	$x_1=5.1$
$r_2^2=122.26$	$r_2^2=46.26$
$r_1^2=702.26$	$r_1^2=626.26$
$k'^2=0.1740951$	$k'^2=0.073867$
$1{,}000f=5.574$	$1{,}000f=9.891$

$$H_{rs}\ right=\frac{10\sqrt{145}(9.891-5.574)}{2\pi(14.5)}$$
$$=5.7058 \text{ radially inward}$$

The resultant is, therefore, $5.8260-5.7058=0.1202$, radially away from the axis, and since H_{rs} at P is equal to zero, and $\Delta x=-0.1$,

$$\left.\frac{\partial H_{rs}}{\partial x}\right|_P=-1.202$$

This is checked by Dwight's formula 9. It is possible also to calculate this derivative by the formula

$$\left.\frac{\partial H_{rs}}{\partial x}\right|_P=2n\left(\underset{x=x_2}{H_{r0}}-\underset{x=x_1}{H_{r0}}\right) \tag{26}$$

obtained by the use of formula 1. This calculation thus is made to depend upon the radial components of circular filaments, using formula 4 and Table I. By this method only two values of H_{r0} have to be calculated, and the derivative so found applies strictly to point P if y is taken equal to 14.5 and the two values of x are taken as $x_2=10$ and $x_1=5$. Using this method there is found $(\partial H_{rs}/\partial x)_P=-1.2158$.

Calculating by formula 25 with

$$\left.\frac{\partial H_{rs}}{\partial y}\right|_P=-1.184$$

$$\left.\frac{\partial H_{rs}}{\partial x}\right|_P=-1.216$$

$H_{zs}=0.0978$

$M_p=9176$ abhenries

the correction factor is found to be 1.0000156, thus agreeing well with the value 1.000012 found by the quadrature formula.

Influence of Finite Cross Section on Calculation of H_z and H_r

The formulas of this paper refer, strictly, only to circular filaments and cylindrical current sheets. The correction of the values so calculated, to apply, respectively, to a circular coil of rectangular cross section and to a solenoid of finite thickness, have been thoroughly treated by Dwight in pages 292–6 and 276–280 of reference 6.* As would be expected, the corrections are greater, the larger the cross-sectional dimensions compared with the other co-ordinates involved, and the nearer, relatively, the point is situated to the winding. However, except in unfavorable cases and for calculations where a moderate accuracy suffices, the values calculated for a circular coil may be made assuming its turns to be concentrated at the middle of its cross section, and for solenoids with the assumption of its equivalence with a thin solenoid having a radius equal to the mean radius of the actual coil.

References

1. ABSOLUTE MEASUREMENTS IN ELECTRICITY AND MAGNETISM (book), **A. Gray.** Volume II, part 1, 1893, page 245.

2. MAGNETIC FIELD OF A CIRCULAR CYLINDRICAL COIL, **H. B. Dwight.** *Philosophical Magazine* (London, England), 11, 1931, pages 948–57.

3. FORMULAS FOR THE MAGNETIC FIELD STRENGTH NEAR A CYLINDRICAL COIL, **H. B. Dwight.** *Electrical Engineering (AIEE Transactions)*, volume 61, June 1942, pages 327–33.

4. ALTERNATING CURRENTS, **A. Russell.** Cambridge University Press (Cambridge, England), volume 1, 1914, equations 21 and 22, page 98.

5. THE MAGNETIC FIELD AND INDUCTION COEFFICIENTS OF CIRCULAR CYLINDRICAL AND HELICAL CURRENTS, **A. Russell.** *Philosophical Magazine* (London, England), 13, 1907, page 420.

6. ELECTRICAL COILS AND CONDUCTORS (book), **H. B. Dwight.** McGraw Hill Book Company, New York, N. Y., 1945.

7. ON CERTAIN BESSEL INTEGRALS AND THE COEFFICIENTS OF MUTUAL INDUCTION OF COAXIAL COILS, **T. H. Havelock.** *Philosophical Magazine* (London, England), 15, 1908, page 332.

8. FORMULAS AND TABLES FOR THE CALCULATION OF MUTUAL AND SELF INDUCTANCE, **E. B. Rosa, F. W. Grover.** *Scientific Paper* 169, National Bureau of Standards (Washington, D. C.), 1912, pages 6–18.

9. ADDITIONS TO THE FORMULAS FOR THE CALCULATION OF MUTUAL AND SELF INDUCTANCE, **F. W. Grover.** *Scientific Paper 320*, National Bureau of Standards (Washington, D. C.), 1918, pages 538–41.

---

* A more general procedure is to replace the coil by its equivalent circular filament as proposed by Lyle.[22,23] With n filaments, assuming N/n turns associated with each, the contribution of each to the magnetic field may be calculated by the Russell formulas. The number n will be larger, the larger the cross section. This procedure is to be recommended for solenoids when point P is very distant.

10. Methods for the Derivation and Expansion of Formulas for the Mutual Inductance of Coaxial Circles and for the Inductance of Solenoids, F. W. Grover. *Journal of Research*, National Bureau of Standards (Washington, D. C.), volume 1, October 1928, pages 487–512.

11. Electricity and Magnetism (book), John Clark Maxwell. Oxford University Press (Oxford, England), volume II, section 701, 1873. See also reference 17, page 6, formula 1.

12. Series for the Complete Elliptic Integrals K, E, K', E' and Certain Other Elliptic Integrals, T. J. Bromwich. *Journal of Pure and Applied Mathematics*, number 176, 1913, pages 363–80.

13. Tables of Theta-Functions, Elliptic Integrals K and E, and Associated Coefficients in the Numerical Calculation of Elliptic Functions, H. Nagaoka, S. Sakurai. *Scientific Papers*, Institute of Physical and Chemical Research (Tokyo, Japan), volume II, 1922, pages 1–67.

14. Tables for the Calculation of the Mutual Inductance of Circuits with Circular Symmetry About a Common Axis, F. W. Grover. *Scientific Paper 498*, National Bureau of Standards (Washington, D. C.), 1924, pages 1–18.

15. Inductance Calculations (book), F. W. Grover. Van Nostrand and Company, New York, N. Y., 1946, page 77.

16. Mutual Inductance of a Circle and Coaxial Single-Layer Coil, E. B. Rosa. *Scientific Paper* 56, National Bureau of Standards (Washington, D. C.), 1907, pages 209–236.

17. Formulas and Tables for the Calculation of Mutual and Self Inductance, E. B. Rosa, F. W. Grover. *Scientific Paper 169*, National Bureau of Standards (Washington, D. C.), 1912, page 101.

18. Mutual Inductance of Solenoid and Coaxial Circle, J. V. Jones. *Proceedings*, Royal Society of London (London, England), 1898, page 198. See also reference 17, page 99.

19. On a New Standard of Mutual Inductance, A. Campbell. *Proceedings*, Royal Society of London (London, England), 1907, pages 428–435. See also reference 17, page 100.

20. A. M. Legendres Tafeln der Elliptischen Normalintegrale, edited by Fritz Emde, Konrad Wittwer. (Stuttgart, Germany) 1931.

21. Tables of Functions, Jahnke, Emde. Dover Publications, 1943, pages 62–72.

22. Circular Filaments or Circular Magnetic Shells Equivalent to Circular Coils, T. R. Lyle. *Philosophical Magazine* (London, England), 3, 1902, pages 310–29.

23. Formulas and Tables for the Calculation of Mutual and Self Inductance, E. B. Rosa, F. W. Grover. *Scientific Paper 169*, National Bureau of Standards (Washington, D. C.), 1912, page 310.

No Discussion

Nonharmonic Oscillations as Caused by Magnetic Saturation

REINHOLD RÜDENBERG
MEMBER AIEE

MANY of the conventional methods of investigating free and forced oscillations in nonlinear circuits tend to approximate the problem in one way or another in order to attain a suitable analytical solution. A number of different approaches have been proposed as: limitation to the amplitudes of oscillation without concern about the wave shape; omission of higher order terms in a series expansion difficult to evaluate; approximation of the magnetic characteristic by a closed mathematical function; neglecting the transient part of the solution; decomposition of the characteristic into several linear portions; linearization by other analytical or geometrical approximations.

Valuable results have been derived from such analyses, for example the facts that no regular resonance effects can occur under sinusoidal excitation, that under equal over-all conditions there may develop more than one stable performance of the electric circuit, usually an ordinary state of low current and an extraordinary state of high current, and that particularly in the latter state intense higher harmonics and also subharmonics may occur.

Our present aim is to investigate in detail the effect on the wave shape* within every cycle, produced by the nonlinear characteristic of circuits containing capacitance and saturated inductance. In many examples of actual electric systems one or the other element has a curved characteristic and this always can be reduced to the analysis which we will develop. Usually, the characteristic is given graphically from experimental data, and this fact suggests deducing the solution also by some type of graphical evaluation. A rigorous method can be derived which for natural oscillations constitutes a closed formulation based on quadratures, whereas for forced oscillations a step-by-step method will be developed.

All of the methods discussed here† may be transferred easily to mechanical or other types of oscillations as it will be shown by one example.

Distortion of Natural Oscillations

We consider at first the electromagnetic oscillations of a saturated flux Φ, the exciting coil of which is connected to a capacitance C as indicated in Figure 1. The magnetic characteristic is shown in Figure 2, however, instead of flux Φ and exciting current i there are taken as variables the magnetic induction B and the linear current density A. These more specific magnitudes are correlated to Φ and i by the cross-section a of the magnetic circuit, its length l, and the number of turns N as

$$B=\frac{\Phi}{a};\qquad A=\frac{Ni}{l} \tag{1}$$

The differential equation for the natural oscillations is, in the absence of ohmic resistance

$$N\frac{d\Phi}{dt}+\frac{1}{C}\int i\,dt=0 \tag{2}$$

which changes by use of equation 1 into

$$aN\frac{dB}{dt}+\frac{l}{NC}\int A\,dt=0 \tag{3}$$

If we now introduce for abbreviation the parameter

$$\tau=\sqrt{C\frac{a}{l}N^2}=\sqrt{C\Lambda} \tag{4}$$

which we will term the intrinsic time of the device, equation 3 yields, after differentiation, the simple differential equation

$$\frac{d^2B}{dt^2}+\frac{A}{\tau^2}=0 \tag{5}$$

This characteristic equation which determines the performance of the electromagnetic circuit contains only two parameters, namely the intrinsic time τ which is a constant of the system, and the magnetic characteristic, as shown in

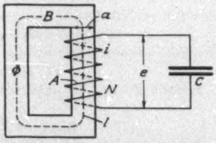

Figure 1 (above). Oscillatory electric circuit subjected to magnetic saturation

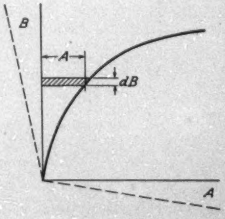

Figure 2 (right). Magnetic characteristic sheared by series and parallel air reluctance

---

* A bibliography at the end of this paper gives a survey of the theoretical and experimental literature.

† Taken from a book "Transient Performance of Electric Power Systems" soon to be published by McGraw-Hill Book Company.

Paper 49-170, recommended by the AIEE Basic Sciences Committee and approved by the AIEE Technical Program Committee for presentation at the AIEE Summer General Meeting, Swampscott, Mass., June 20–24, 1949. Manuscript submitted March 24, 1949; made available for printing May 16, 1949.

REINHOLD RÜDENBERG is Professor of Electrical Engineering at the Graduate School of Engineering, Harvard University, Cambridge, Mass.

The author wishes to express his appreciation for assistance given by Dr. K. Pohlhausen, Dr. E. Reimann, Mr. H. Brandt and Mr. B. Binson.

Special Letter Symbols

A = linear current density
b = harmonic induction amplitude
β = virtual permeability
ϵ = voltage ratio
ϑ = numerical time
Λ = self-inductance in air
ρ = resistance ratio
τ = intrinsic time

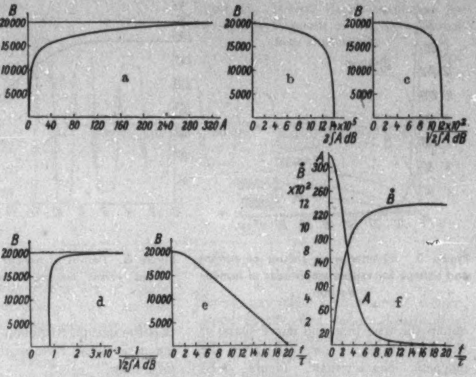

Figure 3. Successive integration of magnetic characteristic yielding the shape of natural oscillations

Figure 2, which is a graphically given function, analytically expressed either as $B(A)$ or as $A(B)$. According to equation 4 the intrinsic time is determined solely by the magnitudes of the capacitance C and a self-inductance Λ, the latter representing the inductance of the exciting coil if the iron of the magnetic circuit were replaced by air. Hence, τ appears as the natural period of an air flux, expressed in units of 2π seconds.

Any additional magnetic flux, either in leakage paths parallel to the steel yoke or in a constant inductance in series with the electric elements, can be considered by shearing the abscissa axis of Figure 2 into the dashed position. On the other hand, any air gap in the magnetic circuit or any constant inductance in parallel to the electric elements can be considered by shearing the ordinate axis of Figure 2 into the dashed position. Hence, the performance of a wide variety of saturated electromagnetic circuits can be described by the same differential equation 5.

This equation can be solved by separation of the variables. At first we multiply the equation by the derivative $\dot{B}=dB/dt$, yielding

$$\dot{B}\frac{dB}{dt}+\frac{d\dot{B}}{dt}\cdot\frac{A}{\tau^2}=0 \tag{6}$$

or, rewritten after cancellation of dt

$$\dot{B}d\dot{B}+\frac{1}{\tau^2}AdB=0 \tag{7}$$

This yields, when integrated

$$\frac{\dot{B}^2}{2}+\frac{1}{\tau^2}\int_{B_0}^{B}AdB=0 \tag{8}$$

The integration in the second term may be performed graphically by use of the characteristic in Figure 2, and the lower limit must be chosen according to the initial conditions. A continuous change of the upper limit gives directly the integral curve. Hereby the derivative

$$\frac{dB}{dt}=\dot{B}=\sqrt{-\frac{2}{\tau^2}\int AdB} \tag{9}$$

is graphically determined as function of B alone. A further integration after separation of the variables yields the elapsed time as

$$t=\tau\int\frac{dB}{\sqrt{-2\int AdB}} \tag{10}$$

This integral also can be evaluated rigorously. We may draw the reciprocal curve of equation 9 and integrate it with respect to B. Or, we may plot the curve from consecutive elements dB/dt determined from equation 9. We will denote the integral of equation 10, equal to the ratio t/τ as the numerical time of oscillation. It depends solely on the shape of the effective characteristic, whereas all constant parameters of the system are comprised in the intrinsic time τ. After having found the correlation of induction B and time t, we can easily return by use of equation 1 to current i and voltage e, yielding

$$i=\frac{l}{N}A;\quad e=N\frac{d\Phi}{dt}=aN\frac{dB}{dt} \tag{11}$$

wherein the last derivative is already expressed by equation 9.

Let us apply equation 10 analytically to the simple case of a linear characteristic, as present in Figure 2 in the neighborhood of the origin. Here B is proportional to A, namely

$$B=\mu A \tag{12}$$

wherein μ is the initial permeability of the electromagnetic system. This gives for equation 9

$$\sqrt{-2\int AdB}=\frac{j}{\sqrt{\mu}}B \tag{13}$$

and with use of equation 10

$$t=\tau\frac{\sqrt{\mu}}{j}\ln\left(\frac{B}{B_0}\right) \tag{14}$$

After inverting this expression and replacing the exponential function of complex argument by its trigonometric equivalent this yields

$$B=B_0\cos\left(\frac{t}{\tau\sqrt{\mu}}\right) \tag{15}$$

Thus, the intrinsic time τ together with the square root of the permeability determine the period of oscillation which is, with use of equation 4

$$T=2\pi\tau\sqrt{\mu}=2\pi\tau\sqrt{\mu\Lambda C}, \tag{16}$$

Herein $\mu\Lambda$ expresses the self-inductance of the iron circuit. The period of oscillation is independent of the amplitude B_0 of the oscillation as long as the linear part of the characteristic is not exceeded and μ is a true constant.

For an actual characteristic of the iron, as curved by saturation, Figure 3 presents the procedure to be taken in order to

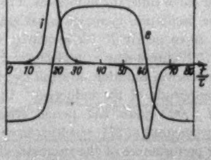

Figure 4. Wave shapes of current and voltage of saturated natural oscillations

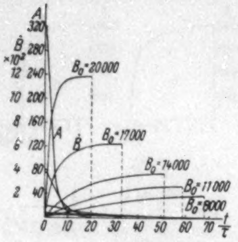

Figure 5. Quarter wave shapes of current and voltage for various amplitudes of iron induction

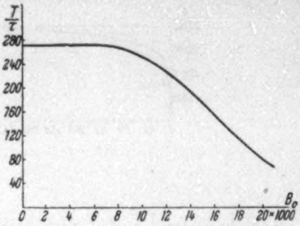

Figure 6. Period of natural electric oscillations versus maximum iron induction

obtain the true time and curve shape of the oscillations. Figure 3(A) gives the magnetic characteristic. Figure 3(B) shows the integral curve when starting at 20,000 gauss. The square root of this curve is taken in Figure 3(C). The reciprocal curve is shown in Figure 3(D) and this is integrated in Figure 3(E). The latter curve gives directly the correlation of time and magnetic induction and we see that the flux will decrease nearly linearly with time. Now we can correlate to each time, via the induction B, the current expressed by A from the original characteristic, and the voltage expressed by dB/dt from the abscissa of Figure 3(C), both as determined by equations 9 and 11. This is shown in Figure 3(F). Because of the complete symmetry, the curves are derived in Figure 3 for a quarter of a cycle only. From the last diagram the curves of current and voltage are plotted in Figure 4 for an entire cycle. The current has high peaks, the voltage very flat tops. The numerical period of oscillation evaluates to 80, whereas the same oscillatory circuit without iron would give only 2π, and both e and i would be sinusoidal.

Figure 5 shows the result of similar evaluations for smaller amplitudes B_0 than 20,000 gauss. Here also, only one-quarter of each cycle is shown for A and dB/dt representing current and voltage. We see that with decreasing amplitude the peaked and flat curves gradually lose their marked shape and approach for small oscillations a sine or cosine change. At the same time, the numerical duration of the oscillation increases considerably, from 20 to nearly 70 for a quarter of a cycle. Figure 6 shows the dependence of the numerical duration of a full cycle on the amplitude of the induction. Up to about 7,000 gauss the period remains nearly constant at 271, resulting from the linear performance of the magnetic characteristic. With further increasing amplitude the period decreases rapidly so that the natural frequency of the electromagnetic circuit rises greatly with higher saturation.

We see from this investigation that the natural oscillations of a magnetically saturated oscillatory circuit remain harmonic and have constant natural frequency only at small amplitudes. However, with increasing amplitude the curve shape of the oscillations becomes more and more distorted and simultaneously the natural frequency increases. These two properties, distorted curve shape and dependence of the natural frequency on the amplitude, are characteristic qualities of any nonharmonic oscillations.

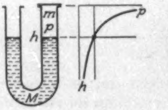

Figure 7. Oscillations of a gas volume in a liquid subjected to adiabatic compression

As a second example, let us investigate adiabatic oscillations of a gas bubble as they may occur in oil circuit breakers. We simplify the problem by considering the linear oscillation of a cylindrical gas volume v against a column of liquid mass M included in the same U-shaped guiding tube, as in Figure 7. Any motion of the level h produces a change in the pressure p on the surface area a between gas and liquid. The equilibrium of the forces on the liquid gives the differential equation

$$M\frac{d^2h}{dt^2}+ap(h)=0 \tag{17}$$

Introducing the specific volume v of the gas instead of the level h by

$$a\,dh=m\,dv \tag{18}$$

wherein m designates the mass of the gas, equation 17 yields

$$\frac{Mm}{a}\frac{d^2v}{dt^2}+ap(v)=0 \tag{19}$$

If we define the intrinsic time of this problem as

$$\tau=\frac{\sqrt{Mm}}{a} \tag{20}$$

we obtain the differential equation

$$\frac{d^2v}{dt^2}+\frac{p(v)}{\tau^2}=0 \tag{21}$$

This is of identical form to equation 5. Here, the intrinsic time depends on the product of the oscillating masses of liquid and gas related to their contacting area. Essentially, this is determined by the geometric mean length of the gas and liquid columns.

By analogy with equation 10 the solution of this problem is given by

$$t=\tau\int\frac{dv}{\sqrt{-2\int p\,dv}} \tag{22}$$

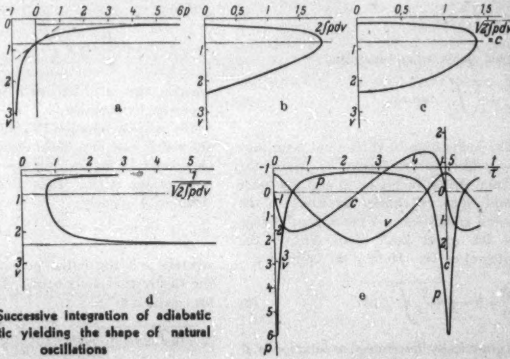

Figure 8. Successive integration of adiabatic characteristic yielding the shape of natural oscillations

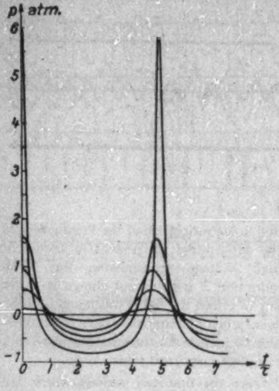

Figure 9. Wave shapes of gas pressure for various amplitudes of oscillation

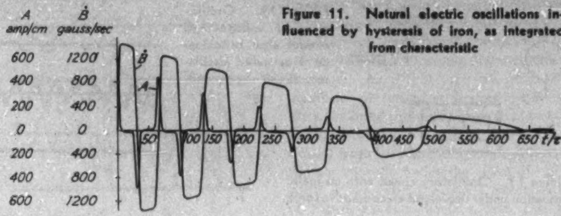

Figure 11. Natural electric oscillations influenced by hysteresis of iron, as integrated from characteristic

In Figure 8 the integration of the adiabatic pressure-volume curve of Figure 8(A) is carried out according to the same scheme as used in Figure 3. The integration results immediately in the curve of the gas volume v against time as shown in Figure 8(E), giving at the same time the level of the liquid column, see Figure 7. By transfer of the correlated values of pressure p from Figure 8(A) and velocity c from Figure 8(C), we obtain the various curves as plotted in Figure 8(E). We see that all the curves are unsymmetrical with respect to their mean axes and that the pressure curve forms a sharp positive peak and a flat negative saddle. This means that the oscillating liquid, by compression of the gas, will be very suddenly reflected as seen from the break in the v-curve, and this results from the gas pressure which increases very rapidly with decreasing volume causing also a nearly instantaneous change of the velocity.

The evaluation in Figure 8 is related to an initial pressure of 6 atmospheres. For some smaller amplitudes, the pressure oscillations are shown in Figure 9. We see that only small oscillations of the order of 1/10 atmosphere are of nearly sinusoidal shape, whereas large fluctuations of pressure produce very steep peaks.

The natural period of the oscillations is dependent only slightly on the amplitude, as seen from Figure 10. Although with larger fluctuations the duration of the excess pressure decreases, the period of suction increases and the sum changes slightly. Hence, such adiabatic pressure oscillations behave nearly isochronously.

If hysteresis is present in the magnetization curve, its ascending and descending branches must be distinguished in the evaluation of equation 10. This is done in Figure 11. Since now the initial energy is gradually dissipated by the hysteresis loss, a decay occurs and thus the oscillations pass through various wave shapes, as plotted in Figure 5. In Figure 12, an actual oscillogram of voltage and current of such an oscillation is shown which very nearly repeats the pattern of Figure 11, except that the damping is greater because of the additional losses in the ohmic resistance. In both these last figures the period of oscillation increases substantially during the decay up to a multiple of the initial value.

Transient Forced Oscillations

If the oscillatory circuit with magnetic saturation is fed by an external voltage $e(t)$ as in Figure 13, the complete circuit equation including the ohmic resistance, which we will no longer neglect, is

$$N\frac{d\Phi}{dt}+Ri+\frac{1}{C}\int i\,dt=e(t) \tag{23}$$

Herein, any effect of constant L is contained in the first term. Substituting again the specific values A and B for i and Φ as in equation 1, and the intrinsic time τ as in equation 4, we obtain

$$\tau\frac{dB}{dt}+\frac{RC}{\tau}A+\frac{1}{\tau}\int A\,dt=\frac{\tau}{aN}e(t) \tag{24}$$

If we now introduce abbreviations for the resistance factor and for the impressed electromotive force, namely

$$\rho=\frac{RC}{\tau}=\frac{R}{\sqrt{\Lambda/C}};\quad \epsilon(t)=\frac{\tau}{aN}e(t)=\sqrt{\frac{C}{al}}\quad e(t) \tag{25}$$

and designate the numerical time as ratio of elapsed time to intrinsic time by

$$\vartheta=\frac{t}{\tau} \tag{26}$$

equation 24 reduces to

$$\frac{dB}{d\vartheta}+\rho A+\int A\,d\vartheta=\epsilon(\vartheta) \tag{27}$$

This formulation comprises all the possible cases of saturated oscillations although it contains only four parameters. These are: the values of the constant τ and of the function $B(A)$ as formerly considered and defining the intrinsic time and the magnetic characteristic of the iron and air fluxes; and the new parameters of equation 25, namely the resistance ratio ρ designating the ohmic resistance as related to the oscillation resistance of the air-inductance, and $\epsilon(t)$ as the impressed voltage $e(t)$ related to a few

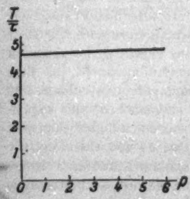

Figure 10 (left). Period of natural pressure oscillations versus maximum pressure

Figure 12 (right). Oscillogram of actual oscillation as influenced by resistance and hysteresis

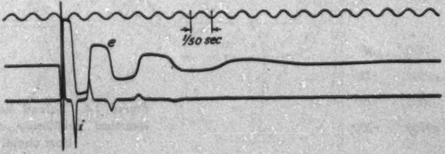

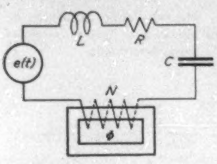

Figure 13. Oscillatory circuit with magnetic saturation under impressed electromotive force

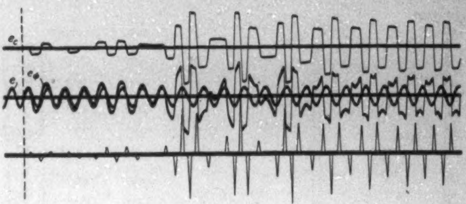

Figure 15. Oscillogram of voltages and current after switching-on a saturated oscillatory circuit at zero voltage

basic constants of the circuit. Thus, in equation 27 the first term is essentially determined by the shape of the magnetic characteristic, the second term by the value of the ohmic resistance, the third term by the performance of the capacitance, and the term on the right-hand side by the impressed voltage. Depending on the values of the parameters, the solution of equation 27 may have very different shapes. No assumption has been made about the curve $B(A)$ and thus, any actual form of the effective magnetic characteristic may be used for the evaluation.

If the elements of the circuit should not be connected in series, as in Figure 13, but in parallel, a formulation very similar to equation 27 can be derived. However, the second term will be $\rho' B$ rather than ρA and the resistance coefficient will be inverted to $\rho' = \tau/RC$.

For impressed direct voltage suddenly changing with time the transient performance can be found relatively simply because ϵ is constant before and after the jump. Hence, the perturbation term on the right-hand side of equation 27 has no further influence and the change in the deviations of B and A from the new steady state result from the left-hand side alone. This side, however, departs from equation 5 only by the resistance term ρA which can be handled during the integration as a correction. Therefore, oscillations will occur which are very similar in character to Figures 11 and 12, although they may be unsymmetrical in plus and minus values.

More interesting is the solution for alternating voltage. For the purpose of evaluation we rewrite equation 27 as

$$\frac{dB}{d\vartheta} = \epsilon(\vartheta) - \rho A - \int A\, d\vartheta \qquad (28)$$

Then we see that the change of the induction B with time is given in the first place by the impressed voltage, from which however, the resistance drop and the capacitive term must be deducted. The former is usually small, the latter, as an integral over time, also can be accurately obtained simultaneously with the development of the left-hand side. Figure 14 shows the curves for the inductive voltage $dB/d\vartheta$, the current A, and the capacitive voltage $\int A d\vartheta$, as derived in step-by-step construction from the impressed sinusoidal voltage $\epsilon(\vartheta)$ which suddenly is switched on. The graph is based on a circuit containing a moderately saturated transformer coil, a linear inductance in series, and some resistance of the conductors to the capacitance, as present in an actual high voltage transmission line. The induction B itself is not shown in order not to crowd the figure too much. However, when plotting the curve it is advisable to include all the variables used in a complete numerical table.

Over the first ten periods which are indicated in Figure 14 by dashed lines not a single cycle resembles any other. The phase angle of the voltage at the instant of switching is taken as zero and therefore an inrush current should be expected. However, by effect of the saturation such a peaked current develops gradually with large and irregular fluctuations of its amplitudes. By no means are these amplitudes alternating throughout. In many cycles two unidirectional amplitudes of current follow each other. No regular repetition of the phenomena is discernible during the time covered by Figure 14. The inductive voltage $dB/d\vartheta$ is fairly similar to the impressed voltage $\epsilon(\vartheta)$, although many irregular deviations are present. The capacitive voltage $\int A d\vartheta$ however, shows a very different performance consisting mostly of trapezoidal shapes with flat tops, the latter frequently extending over more than a full cycle. Thus, in contrast to any harmonic performance these curves indicate the occurrence of considerable nonharmonic currents and voltages, containing periods very different from that of the impressed voltage.

In Figures 15 and 16 some oscillograms are shown, taken when suddenly switching-on a highly saturated inductance-capacitance circuit, Figure 15 when switching near the zero angle of voltage, and Figure 16 near 45 degrees and 90 degrees. Here, after a short relatively tranquil transient performance, the state changes to a new violent performance for all the parameters measured, as flux, capacitor voltage, inductive voltage, and current. The resistance of this experimental circuit was much higher than that underlying Figure 14 and therefore, the transient time was much shorter. Nevertheless, the main features of the theoreti-

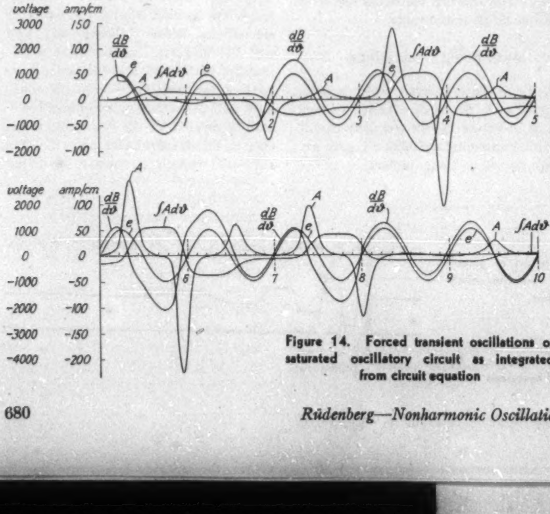

Figure 14. Forced transient oscillations of saturated oscillatory circuit as integrated from circuit equation

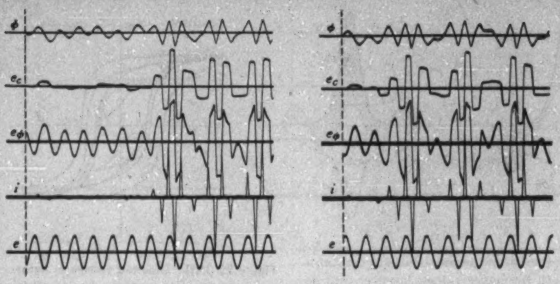

Figure 16. Oscillogram of voltages, current, and flux after switching-on a saturated oscillatory circuit

(left) near 45 degrees (right) near 90 degree phase angle of impressed sinusoidal voltage

cal curve shapes of Figure 14 also are visible in the beginning of Figures 15 and 16.

Steady State and Higher Harmonics

The oscillograms in Figures 15 and 16 indicate that even after the decay of the initial transient fluctuations there remain curve shapes of e and i which are markedly different from the sinusoidal shapes occurring in the steady state of nonsaturated circuits. Experiments show that the shapes are varying, depending on the degree of saturation and hysteresis, on the resistance of the circuit, and on the phase of switching. We know that for the amplitudes of the forced fundamental oscillations, the existence of two stable and one labile states is possible. Although rigorously no superposition can be expected, a consideration of the curve shape and the production of higher harmonics shall be developed here.

For this purpose, we linearize the problem by resolving the actual magnetic characteristic, as in Figure 17, into a proportional component βA and the remainder ΔB. Herein, β is a constant numerical factor designating a virtual permeability somewhere between 1 and μ, so that βA gives a linear rise of the induction and ΔB expresses essentially the nonlinear part of the variation of B. Thus, we set

$$B = \beta A + \Delta B(A) \qquad (29)$$

The latter magnitude is shaded in Figure 17 and changes from positive to negative values within the range of current considered. Substituting this expression into equation 27 and taking the nonlinear component to the right-hand side, we obtain

$$\beta \frac{dA}{d\vartheta} + \rho A + \int A\, d\vartheta = \epsilon(\vartheta) - \frac{d(\Delta B)}{d\vartheta} \qquad (30)$$

In this formulation, the left-hand side is linear and will follow the ordinary rules of proportionality and superposition. On the right-hand side an additional term is acting which can be conceived of as an impressed voltage. We see from Figure 17 that this voltage will change sign several times within every half cycle.

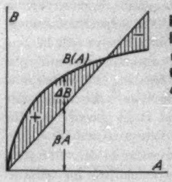

Figure 17. Resolution of curved magnetic characteristic into linear and nonlinear component

Equation 30 may be applied for deriving directly the curve shapes of the steady state oscillations. These were already found by use of the rigorous equation 27, however, they appear in purity only after the passing of the entire transient period which is very long at small resistance. In solving equation 30 we use the method of iteration. As a first step we omit the nonlinear perturbation function ΔB on the right-hand side and obtain in approximation by the conventional way a solution A' from the remaining linear differential equation 30 under the effect of $\epsilon(\vartheta)$. With A' we enter the true characteristic of Figure 17 and obtain a first $\Delta' B$ as function of time. Subtracting the derivative of this curve from the impressed voltage $\epsilon(\vartheta)$ on the right-hand side of equation 30 we solve again the linear equation for A. Either directly or by superposition we obtain an improved solution A''. With this, again, we enter the true characteristic, obtaining an improved $\Delta'' B(\vartheta)$. This procedure may be repeated until no further improvement in the stationary solution occurs. It is obvious that an originally harmonic curve shape of A' will be greatly distorted by this process of repeated introduction of the effect of curvature of the characteristic.

Since the position of the straight line βA in the characteristic diagram is arbitrary, both the left- and right-hand sides of equation 30 depend on the value of β. By suitable choice of β the evaluation may be greatly facilitated. Nevertheless the process is laborious and therefore, we will discuss the development of higher harmonics proper which produce the distortion of the curve shape. If the complete solution of A were present, as in Figure 14, we could directly resolve the total B, and thus $dB/d\vartheta$, into the two components of equations 29 and 30. The true ΔB of Figure 17 would appear as depending on time, as shown in Figure 18 together with the linearly behaving part βA. The two right-hand terms of equation 30 are acting independently and we see that a sinusoidal $\epsilon(\vartheta)$ will bring about a sinusoidal current of supply frequency while ΔB

Figure 18. Resolution of wave shape of induction into linear and nonlinear component

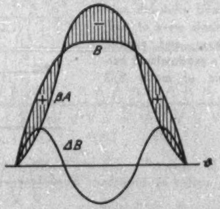

Figure 19. Wave shapes of distorted voltages and current of saturated natural oscillations in circuit without resistance

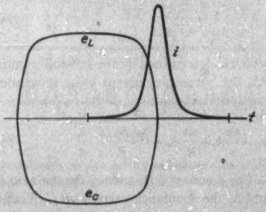

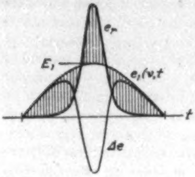

Figure 20 (above). Distorted voltage e_r necessary to compensate resistance drop of natural oscillations and its sinusoidal fundamental e_1 leaving a remainder Δe

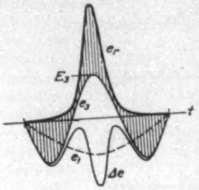

Figure 21 (right). Distorted voltage e_r necessary to compensate resistance drop of natural oscillations and its 3rd harmonic e_3 leaving a remainder Δe

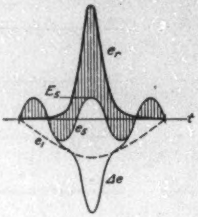

Figure 22 (left). Distorted voltage e_r necessary to compensate resistance drop of natural oscillations and its 5th harmonic e_5 leaving a remainder Δe

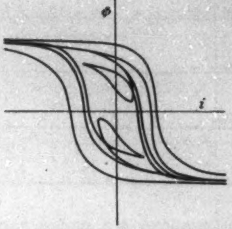

Figure 24 (above). Cathode-ray oscillogram of magnetic characteristic during forced oscillations indicating subharmonic of mode 1/5

will produce the sum of all the superposed higher harmonic currents. By this process we have quantitatively filtered out the cause of the nonsinusoidal behavior.

The nonharmonic voltage

$$\Delta e = \frac{d(\Delta B)}{d\vartheta} \tag{31}$$

contains an extensive series of individual harmonics comprising all the odd modes, and also the even modes if any unsymmetrical condition should be present. The current-amplitude a_ν of an individual higher frequency ν, produced under the effect of a certain sinusoidal amplitude b_ν of the perturbation function ΔB, can be determined from the linear left-hand side of equation 30, yielding

$$j\nu\tau\beta a_\nu + \rho a_\nu - \frac{j}{\nu\tau} a_\nu = -j\nu\tau b_\nu \tag{32}$$

Herein, τ appears as a factor to ν since the latter value refers to the absolute time t rather than to the numerical time ϑ, see equation 26. Thus, the amplitude of the harmonic current is

$$a_\nu = \frac{(\nu\tau)^2}{\sqrt{[\beta(\nu\tau)^2 - 1]^2 + (\rho\nu\tau)^2}} b_\nu \tag{33}$$

At the frequency

$$\nu = \frac{1}{\sqrt{\beta\tau^2}} = \frac{1}{\sqrt{\beta\Lambda C}} \tag{34}$$

which is determined by the self-inductance $\beta\Lambda$, the harmonic current has a resonance maximum of the magnitude

$$a_{\nu r} = \frac{\nu\tau}{\rho} b_\nu = \frac{\nu\Lambda}{R} b_\nu = \frac{\sqrt{\beta\Lambda/C}}{R} \cdot \frac{b_\nu}{\beta} \tag{35}$$

The resonance frequency depends on C and Λ, the resonance current on C, R, and Λ, these three parameters being constants. Both resonance values, however, will depend on β which is given by the position of the linear component of the characteristic in Figure 17. Since this position, and thus the value of β was arbitrarily chosen, such resonances are virtual and may appear for a number of higher harmonic frequencies ν, increasing the amplitudes of all of their currents.

These conclusions would be exact if the values of ΔB in Figure 17 would remain the same over a number of oscillations. However, as the rigorous Figure 14 indicates this is not necessarily so. Therefore, the variations in ΔB, and in βA, will often prevent the resonances from coming into prominence. Nevertheless our considerations show that by marked saturation of the magnetic characteristic in oscillatory circuits a substantial amount of higher harmonics always will be produced which may extend to high multiples of the supply frequency. This refers to the transient as well as to the steady state performance and is in accord with the oscillograms of Figures 15 and 16.

The same results can be derived from a corresponding formulation for parallel connection of a saturated inductance and a constant capacitance. However, the impressed nonharmonic forces now result from the deviation of the magnetizing current from a linear behavior. In either case, series or parallel connection, it is possible to extract one or more of the harmonics, as existing in the irregular curve shapes of current and voltage, by tuned external circuits containing constant inductance and capacitance and thus having a definite resonating frequency.

Subharmonic Resonance

The differential equation 27 and its rigorous solutions as described before implicitly contain the occurrence of all possible kinds of deviations from the simple harmonic behavior, caused by frequencies higher as well as lower than that of the impressed voltage. Since subharmonics occasionally are observed, in the laboratory and in the field, it is suitable to analyze the problem further in order to arrive at a plausible understanding of the physical causes of this complex phenomenon.

Let us consider the conditions for perfect resonance formation between an impressed voltage and the nonharmonic natural oscillations of the saturated circuit as derived before, for example in Figure 4. The inductive and capacitive

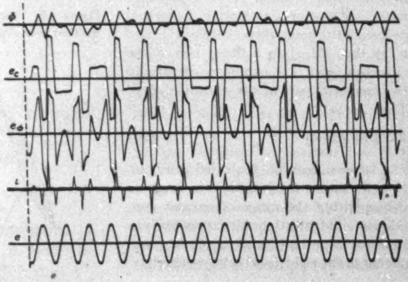

Figure 23. Transient and steady-state oscillations showing intense 3rd and weak 6th subharmonic wave of flux, voltages, and current, and a predominant harmonic of mode 5/3

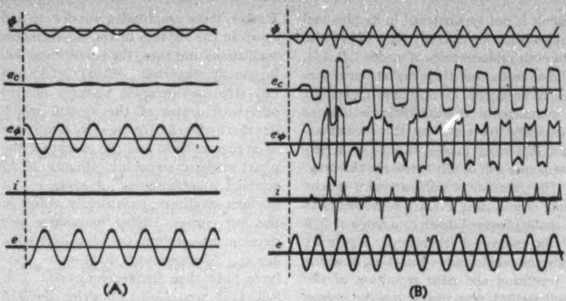

Figures 25(A) and (B). Low-current and high-current stable state of amplitudes of a saturated oscillatory circuit after switching-on at maximum and zero impressed voltage

voltages would be in equilibrium among each other with respect to magnitude, phase, and curve shape, and both these voltages would be oppositely equal, as shown in Figure 19. The current would have a peaked shape, as also transferred from Figure 4 to Figure 19, and this current and these voltages would satisfy equation 5, derived in absence of a dissipating resistance. In order to sustain these conditions the external voltage must have a value equal to *Ri*, since the impressed voltage has no other work to do than compensating the ohmic drop in the circuit. With currents and voltages as expressed by equation 5, the first and the third terms on the left-hand side of the complete equation 27 neutralize each other. Hence, in this case the external voltage must be chosen as

$$e(\vartheta)=\rho A,\ \text{or}\ e_r(t)=Ri \tag{36}$$

which is graphically represented in Figure 20.

Thus, in nonlinear oscillatory circuits true resonance can be sustained if the impressed voltage has a magnitude, frequency, and curve shape as given by the ohmic drop of the current constituting a nonharmonic natural oscillation. The smaller the resistance, the lower is the voltage necessary to sustain the resonance state. The voltage to be impressed can be conceived of as an infinite Fourier series

$$e_r(t)=e_1(\nu_1 t)+e_3(\nu_3 t)+e_5(\nu_5 t)+\ldots \tag{37}$$

wherein the functions $e(\nu t)$ are sine or cosine functions and ν_1 is the natural frequency of the circuit.

If the circuit is fed, not by this peaked voltage but by a sinusoidal voltage of the fundamental frequency ν_1 and the amplitude E_1 as indicated in Figure 20, then a voltage, as shaded in this figure, remains as a deficiency. This voltage Δe is separately plotted to the negative side in order not to crowd the figure. In the present case this voltage contains all the higher harmonics of equation 37, of which obviously the third is preponderant. The residual voltage Δe will produce currents and inductive and capacitive voltages changing the original curve shapes of Figure 19 until equilibrium is established. Because of the curved characteristic of the circuit, no linear superposition will occur. However, it is obvious that the actual currents and voltages will be so distorted that they contain a different amount of the third and higher harmonics than before.

Let us now feed the circuit by a voltage not of natural frequency ν_1 but of three times this frequency, as represented in Figure 21. The impressed voltage $e_3(\nu_3 t)$ is the second best approximation to the peaked voltage e_r originally required and there remains as a deficiency the voltage Δe, shown shaded and plotted in Figure 21. This residuum contains a substantial wave of natural frequency ν_1, as plotted dashed by e_1, which now acts as an uncompensated and thus, as a distorting voltage in the circuit. This will produce currents and voltages which are essentially of the natural frequency which the circuit had before, as in Figure 19. Thus, we see that impressing a voltage $e_3(\nu_3 t)$ on the saturated circuit will create, in addition to currents i_3, also substantial currents $i_1(\nu_1 t)$ and correlated voltages e_{C1} and e_{L1}. All of these have 1/3 of the supply frequency and therefore, constitute a subharmonic phenomenon with respect to the source. Further currents of frequencies 5/3, 7/3, and so forth, the supply frequency, and of different amplitudes, will be produced by the higher harmonics contained in Δe of Figure 21.

By the actual currents now flowing in the system, the curve shapes will deviate considerably from those of Figure 19. The current i and the voltages e_L and e_C will change in magnitude and thereby the natural frequency also will be changed Thus the two voltages will come out of shape and out of phase and hereby will be enabled to take up completely between them the feeding voltage e_3.

If we feed the circuit by a voltage $e_5(\nu_5 t)$ as indicated in Figure 22, there now remains in Δe as a main deficiency a voltage e_1 of 1/5 and a voltage e_3 of 3/5 the feeding frequency. The further development of currents and distortions corresponds to that described before, and we see that subharmonics of 1/5 and 3/5 the frequency of the feeding voltage may appear, and also higher order oscillations of the mode 7/5 and more. The same argument can be applied if the circuit is fed by a voltage of any harmonic frequency contained in the original ohmic voltage of the natural oscillation, as expressed by equations 36 and 37.

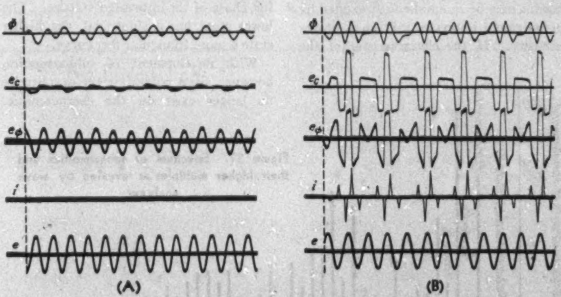

Figures 26(A) and (B). Two states of unstable amplitudes as caused by subharmonics under the same circuit conditions as before, except the switching-on exerted at two intermediate phase angles

Thus, we conclude that an oscillatory circuit of nonlinear characteristic is able to respond in its fundamental natural oscillation to impressed voltages of a frequency of any and all of its natural higher harmonics. This refers to any possible natural oscillation of the circuit. However, we have seen that the natural frequency depends greatly on the intensity of the oscillation, as shown by Figures 5 and 6. Hence, we realize that such subharmonic resonance can occur only if the current and voltages produced are of such intensity that the exact ratios 1:3, 1:5, 3:5, and so forth, between the fundamental natural frequency and the impressed frequency are established. This will require for every given characteristic a certain magnitude of the impressed voltage, or magnitudes between certain limits. Otherwise, the 1/3rd, 1/5th, and lower subharmonics cannot be excited by the mechanism described.

The ohmic resistance of the circuit plays a decisive part. At $R=0$, all the voltages of equation 37 can excite the circuit up to the necessary amplitude and thus, all the subharmonics of any mode might be created. At low resistance, relatively small voltages of the modes e_3, e_5, and so forth, will be sufficient to produce subharmonics. With greater resistance, much higher voltages are necessary to balance the ohmic drop as in equation 36 at a resonant amplitude, and only the highest mode, usually 1/3, may remain active. A further increase of the circuit resistance may be used to suppress entirely any accidental subharmonic resonance.

Depending on the resistance, a range of magnitudes in the impressed voltage is able to excite subharmonics and the various ranges of e_3, e_5, and so forth, even may overlap. Therefore, a number of subharmonic currents of different modes as 1/3, 1/5, and so forth, and their higher harmonics, may be simultaneously excited by an individual impressed voltage of proper intensity. If the characteristic of the circuit is not symmetrical in its plus and minus behavior, not only the odd but also the even subharmonics of modes 1/2, 1/4, and so forth, and their higher harmonics will be produced. It also can happen that a symmetrical characteristic is unsymmetrically traversed by the oscillations and that even modes of sub- or superharmonics will be self-excited in this way.

The creation of subharmonics in circuits of nonlinear characteristic has been actually observed down to a mode of 1/9 of the impressed frequency. Figure 23 shows an oscillogram versus time in which a repetition and near repetition of the fundamental phenomena can be recognized after every 6th and every 3rd cycle of the impressed voltage. Here the predominant oscillation of the flux is of the mode 5/3. The duration of the switching-on transients in this test which was taken with very high voltage, is conspicuously short. If the magnetic characteristic Φ versus i, or B versus A, is directly measured, for example on the screen of a cathode-ray oscillograph, an identical curve will be traced only after complete repetition. The intermediate traces can be made visible by a slight artificial displacement of the individual curves. Figure 24 shows such a cathode-ray oscillogram on which five traces can be distinguished, indicating that subharmonics of at least the 1/5th mode have been present.

The existence of two possible stable points of voltage and current on the magnetic characteristic is well established, one of low, another of higher current. This can be derived by sole consideration of the amplitudes of oscillations. The oscillograms of Figures 25(A) and (B) give an over-all picture of the transient and the steady state performances in these two states. The selection among the two states depends entirely on the switching phase of the impressed voltage. The lower state has a sinusoidal, the higher state a more triangular flux curve.

With development of subharmonics, however, fixed points for the amplitudes no longer exist on the characteristic. Rather, these amplitudes wander up and down in the rhythm of the subharmonic oscillations and thus, the equilibrium will be greatly distorted. Figure 26(A) and (B) give oscillographic pictures of two additional states of the system which develop under exactly the same conditions as in Figure 25(A) and (B) except for the phase angle of switching. Figure 26(A) contains a subharmonic of mode 1/3 of medium amplitude, as is clearly visible in the flux curve. Higher harmonics also develop, as seen from the capacitive voltage e_C. Measurements by a wave analyzer yield their frequencies as 5/3, 7/3, 9/3, 11/3, and 15/3. Of these, the 9/3 and 15/3 modes also could be conceived of as the 3rd and 5th harmonics of the supply frequency.

Very different is the appearance of Figure 26(B). Here, a weak subharmonic of mode 1/4 and a strong one of mode 1/2 are present, and in addition a very strong harmonic mode 3/2 followed by many odd and even multiples of the mode 1/4, as disclosed by the wave analyzer, the entire spectrum of which is shown in Figure 27. It is a remarkable way in which the curve shapes are hereby distorted, for example those of the current or the capacitive voltage. The predominant wave of the flux seems to be that of the mode 3/2, in accord with Figure 27, while in the capacitive voltage the mode 1/2 is intensely visible, distorting completely the symmetry in width and amplitude of every two subsequent oscillations.

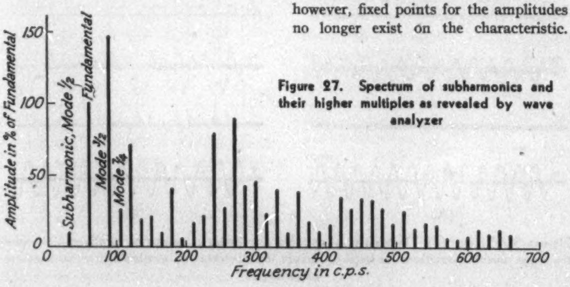

Figure 27. Spectrum of subharmonics and their higher multiples as revealed by wave analyzer

Summary

It is shown that the distorted curve shapes of natural oscillations can be rigorously derived from the saturation characteristic of the oscillatory circuit by means of simple integrations. The natural frequency is not constant as under linear conditions, but varies greatly with the amount of saturation.

For forced oscillations, a concise differential equation is given covering all possible cases by only four parameters. The solution can be evaluated for any initial conditions by a straight-forward step-by-step construction. It shows graphically strange curve shapes of flux, current, and voltages, of no regularity with respect to periodic repetition or symmetrical behavior during the transient state.

In the steady state, a rigorous linearization of the differential equation allows considering the effect of saturation quantitatively as a distortion of the impressed voltage. The final effect on magnitude and curve shape can be evaluated by repeated superposition of the residual distorting voltage. Intense higher harmonics are produced in this way.

Consideration of the resistance voltage as actually present in the state of free oscillations shows that natural oscillations can be sustained in true resonance by an impressed voltage of definite magnitude and curve shape, requiring in series circuits a highly peaked voltage curve. Hence, the saturated circuit can respond to any constituent harmonic of this shape, leading to the forced development of subharmonics to the frequency of the supply voltage within certain ranges of its magnitude. If the ohmic resistance is small a multitude of such subharmonics and all their higher harmonics may develop.

The theoretical results are illustrated by oscillograms taken on actual circuits of high saturation. These experiments confirm that, depending on the switching angle, many distinct oscillatory states of the circuit exist under the same over-all conditions, producing widely different currents and voltages. Within one subharmonic period of forced oscillation different parts of the characteristic may be subsequently traversed, creating odd and even sub- and super-harmonics even under externally symmetrical conditions.

Bibliography

1. On The Maintenance of Vibrations by Forces of Double Frequency, **Lord J. W. Rayleigh.** *Philosophical Magazine* (5) (London, England), volume 24, 1887, pages 145–59.

2. Uber Neue Resonanzerscheinungen in Wechsetstromkreisen, **O. Martienssen.** *Physikalische Zeitschrift* (Leipzig, Germany), volume 11, May 1910, pages 448–60.

3. Einige Unharmonische Schwingungsformen mit Grosser Amplitude, **R. Rüdenberg.** *Zeitschrift fuer Angewandte Mathematik under Mechanik* (Berlin, Germany), volume, 3, 1923, pages 454–67.

4. Experimentelle Untersuchungen uber Schwingungskreise mit Eisenkernspulen, **L. Casper, K. Hubmann, J. Zenneck.** Jahrbuch der Drahtlosen Telegraphie und Telephonie, volume 23, 1924, pages 63–77.

5. Uber Selbsterregungserscheinungen bei Systemen mit Gestorter Superposition, **K. Heegner.** *Zeitschrift fuer Physik* (Berlin, Germany), volume 29, 1924, pages 91–109.

6. Uber Systeme mit Gestorter Superposition, **K. Heegner.** *Zeitschrift fuer Physik* (Berlin, Germany), volume 33, 1925, pages 85–112.

7. Entretien d'une Oscillation libre non Sinusidale par Resonance de l'un de ses Harmoniques, **J. Fallou, A. Mauduit.** *Comptes Rendus* (Paris, France), February 1, 1926, pages 312–13.

8. Demultiplicateurs Statiques de Frequence, **J. Fallou.** *Revue Generale de l'Electricite* (Paris, France), volume 19, 1926, pages 987–91.

9. Aufnahme von Magnetisierungskurven mit der Braun'schen Rohre, **K. Kruger, H. Plendl.** Jahrbuch der Drahtlosen Telegraphie und Telephonie, volume 27, 1926, pages 155–61.

10. Frequency Multiplication by Shock Excitation, **E. Guillemin, P. Rumsey.** *Proceedings*, Institute of Radio Engineers (New York, N. Y.), volume 17, 1929, pages 629–51.

11. Mathematical Analysis of Nonlinear Circuits, **A. Boyajian.** *General Electric Review* (Schenectady, N. Y.), 1931, pages 531–7 and 745–51.

12. The Amplitudes of Nonharmonic Vibrations, **J. P. Den Hartog.** *Journal*, Franklin Institute (Philadelphia, Pa.), volume 216, 1933, pages 459–73.

13. Contribution a l'Etude Experimentelle de la Ferro-Resonance, **E. Rouelle.** *Revue Generale de l'Electricite* (Paris, France), 1934, pages 715–38; 763–80; 795–819; 841–58.

14. Quelques Nouvelles Experiences de Demultiplication de Frequence dans un Circuit Oscillant a Noyau de Fer, **E. Rouelle.** *Revue Generale de l'Electricite* (Paris, France) volume 40, December 1936, pages 811–19.

15. Uber das Wesen der Stabilen Gleichgewichtszustande bei Reihenschaltung von Eisendrossel und Kondensator, **A. Aretz.** *Elektrotechnische Zeitschrift* (Berlin, Germany) volume 58, 1937, pages 1160–62.

16. Analysis of Series Capacitor Application Problems, **J. W. Butler, C. Concordia.** *Electrical Engineering* (*AIEE Transactions*), volume 56, August 1937, pages 975–88.

17. Steady Oscillations of Systems with Nonlinear and Unsymmetrical Elasticity, **M. Rauscher.** *Journal of Applied Mechanics* (New York, N. Y.), volume 5, 1938, pages A169–77.

18. Subharmonics in Circuits Containing Iron-cored Reactors, **I. Travis, C. N. Weygandt.** *Electrical Engineering* (*AIEE Transactions*), volume 57, 1938, pages 423–31.

19. Resonance Theory of Series Nonlinear Control Circuits, **E. G. Keller.** *Journal*, Franklin Institute (Philadelphia, Pa.), volume 225, 1938, pages 561–77.

20. Subharmonics in Circuits Containing Iron-cored Inductors, **I. Travis.** *AIEE Transactions*, volume 58, 1939, pages 735–42.

21. The Generalized Solution for the Critical Conditions of the Ferro-Resonance Parallel Circuit, **W. T. Thomson.** *AIEE Transactions*, volume 58, 1939, pages 743–46.

22. The Engineer Grapples with Nonlinear Problems, **Th. von Karman.** *Bulletin*, American Mathematical Society (New York, N. Y.), volume 46, 1940, pages 615–83. (Contains bibliography of classical papers.)

23. An Experimental Investigation of Subharmonic Currents, **J. D. McCrumm.** *AIEE Transactions*, volume 60, 1941, pages 533–40.

24. Analytical Methods of Solving Discrete Nonlinear Problems in Electrical Engineering, **E. G. Keller.** *AIEE Transactions*, volume 60, 1941, pages 1194–1200.

25. The Effect of Initial Conditions on Subharmonic Currents in Nonlinear Circuits, **S. J. Angello.** *Electrical Engineering* (*AIEE Transactions*), volume 61, September 1942, pages 625–27.

26. Introduction to Nonlinear Mechanics, **N. Bogoliuboff, N. Kryloff.** Princeton University Press, Princeton, N. J., 1943. (Contains bibliography of Russian papers).

27. Abnormal Overvoltages Caused by Transformer Magnetizing Currents in Long Transmission Lines, **H. A. Peterson, T. W. Schroeder.** *Electrical Engineering* (*AIEE Transactions*), volume 62, January 1943, pages 32–40.

28. Sustained Subharmonics Response on Nonlinear Series Circuits, **C. F. Spitzer.** *Journal of Applied Physics* (New York, N. Y.), volume 16, 1945, page 105.

29. An Experimental Investigation of Forced Vibrations in a Mechanical System Having a Nonlinear Restoring Force, **C. A. Ludeke.** *Journal of Applied Physics* (New York, N. Y.), volume 17, 1946, page 603.

30. Negative Resistance Effects in Saturable Reactor Circuits, **J. M. Manley, E. Peterson.** *AIEE Transactions*, volume 65, 1946, pages 870–81.

31. Recherches sur la Demultiplication de Frequence Ferro-Magnetique, **M. R. Dehors.** *Revue Generale de l'Electricite* (Paris, France) 1947, pages 455–67.

32. Introduction to Nonlinear Mechanics, **N. Minorsky.** J. W. Edwards, Ann Arbor, Mich. 1947. (Contains bibliographies of mathematical papers.)

No Discussion

Comparative Performance Records—Steel and Wood Transmission Lines

C. A. BOOKER
NONMEMBER AIEE

THE PREPARATION of this paper has been suggested to stimulate thought and discussion on the question of wood versus metal transmission-line supports. It will present statistical performance records of several different types of steel- and wood-supported transmission lines.

The body of the paper should be prefaced with the statement that the comments and conclusions herein apply to New England territory which has an average of about 30 thunderstorm days per year, and may or may not be applicable in whole or in part in other regions. It also should be noted that the normal direction of storms is parallel with our main transmission lines, so that the exposure to each storm is prolonged sometimes for several hours.

Useful Life and Obsolescence

The data will show that most of our high-voltage lines, in keeping with the trend of thought at the time they were built, have employed steel supporting structures until quite recently. The principal reason for this was the relatively short life expectancy of wood structures. Various preservative treatments for field application have greatly increased this expectancy, and they, together with the development of full-length pressure-treated timber products, have done much to alleviate this major objection to the use of timber.

At the present time the useful life of treated timber corresponds roughly with the cycle of obsolescence. In the opinion of many engineers, a life of 30 or 40 years is one of the principal recommendations for wood construction, as it offers reasonably frequent opportunities to consider extensive modernization without the dead weight of a large unamortized capital investment.

Trend to Wood Structures

About 15 years ago, after an analysis of the operating histories of our various high-voltage lines, it was concluded that a properly designed wood line should give superior service from an interruption standpoint. It was felt that such a design would incorporate single-circuit construction, horizontal configuration, considerable wood insulation with no reduction in porcelain, an aerial direct stroke wire, reasonably short span lengths, low wire stresses, natural round rather than sawn or machine-shaved timbers, simple hardware, and a minimum number of wire guys.

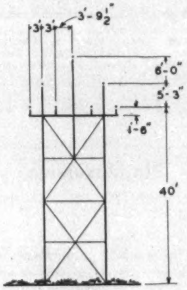

Figure 1*

Voltage	66,000
Constructed	1907–1910
Circuit-mile years experience	4,249
Impulse insulation, positive, kv	285
Lightning interruptions:	
Per 100 circuit-mile years	22.3
Per 100 structure-mile years	28.4
Per 100 right-of-way-mile years	31.7

A basic design embodying these requirements was worked out at the time; several variations have been built. The operating data presently available indicate that our objectives have been met with a degree of success.

Compilation of Operating Data

To put the story in pictorial form, the accompanying series of illustrations showing several types of lines extensively employed on our system, have been pre-

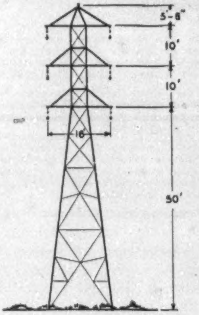

Figure 2*

Voltage	66,000
Constructed	1911–1915
Circuit-mile years experience	9,014
Impulse insulation, positive, kv	490
Lightning interruptions:	
Per 100 circuit-mile years	23.2
Per 100 structure-mile years	28.4
Per 100 right-of-way-mile years	29.8

---

*Estimated impulse value of porcelain and wood insulation $1^1/_2$ by 40 wave without including effect of aerial ground wires. The number of right-of-way miles is considered to be inversely proportional to the number of lines of structures thereon.

Paper 49-173, recommended by the AIEE Transmission and Distribution Committee and approved by the AIEE Technical Program Committee for presentation at the AIEE Summer General Meeting, Swampscott, Mass., June 20–24, 1949. Manuscript submitted March 21, 1949; made available for printing May 5, 1949.

C. A. Booker is a Transmission-line Engineer with the New England Power Service Company, Boston, Mass.

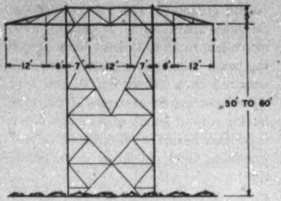

Figure 3*

Voltage	110,000	
Constructed	1924–1927	
Circuit-mile years experience	5,993	
Impulse insulation positive	615 kv	790 kv
Lightning interruptions:		
Per 100 circuit-mile years	20.6	12.8
Per 100 structure-mile years	23.4	16.3
Per 100 right-of-way-mile years	25.2	16.3

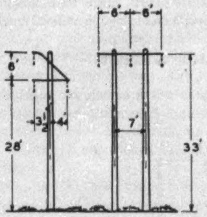

Figure 4*

Voltage	66,000
Constructed	1911–1935
Circuit-mile years experience	5,433
Impulse insulation, positive, kv	390
Lightning interruptions:	
Per 100 circuit-mile years	17.4
Per 100 structure-mile years	17.8
Per 100 right-of-way-mile years	24.0

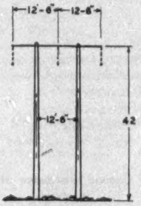

Figure 5*

Voltage	110,000
Constructed	1924–1928
Circuit-mile years experience	1,448
Impulse insulation, positive, kv	680
Lightning interruptions:	
Per 100 circuit-mile years	1.7
Per 100 structure-mile years	17.4
Per 100 right-of-way-mile years	17.4

pared, each with a brief summary of cumulative operating results covering the period from 1921 to 1947 inclusive. Brief historical comments will be required only to supplement and point up these data. Figures 1 to 9 inclusive, and Figure 10, show lightning outages for various types of line, the approximate construction dates of which are noted on the various figures.

Table I shows the cumulative record of structural failures under extraordinary external loading conditions.

The lightning outage experience record is presented on three different bases.

1. Interruptions per 100 circuit-mile years. This is based on the total number of circuit operations.

2. Interruptions per 100 structure-mile years. This eliminates the effect of simultaneous operations on 2-circuit tower lines and gives a figure comparable to the same structures carrying but one circuit. It also permits a determination of the per cent of double-circuit faults, which will be discussed later.

3. Interruptions per 100 right-of-way-mile years. These figures are included on the theory that a more or less definite number of lightning disturbances occur within limited areas such as a transmission line right of way, and that the strokes within such areas will be divided between the various available targets (or lines). That is, two parallel lines should together suffer a negligible increase in interruptions over a single circuit of the same design on the same right of way. This theory follows from the absence of simultaneous double-circuit operations on the large mileage of twin-circuit lines covered by this paper.

Lightning Disturbances—Early Double-Circuit Steel Lines

Figure 1 illustrates a double-circuit type of steel structure used rather extensively before suspension pin and cap insulators were satisfactorily developed. This line suffers 28.4 lightning disturbances per 100 structure-mile years. However, this number of disturbances results in a total of 44.6 switch operations, which indicates that 16.2 or 57 per cent must produce simultaneous faults in both circuits.

Figure 2 illustrates the type of structure which, with the advent of the disk insulator, supplanted that shown in Figure 1. Although from 5 to 7 disks in series were installed on such lines, no improvement in lightning outages occurred, possibly because the average height of wire and structure are greatly increased and consequently may be the target for a larger proportion of direct strokes. Sixty-three per cent of the lightning strokes result in double-circuit outages.

The severe sleet storms of November, 1921 and March, 1924 demonstrated that a vertical configuration of wires was a fertile cause of trouble under such conditions. It thereupon was determined to build all important future lines with a horizontal arrangement. Figure 3 is such a line, used on two important developments where the maximum service security was warranted. Here the wires are at an intermediate height between Figures 1 and 2. The difference in the record of the two lines reflects the use of different porcelain and arc-over devices. One of these lines suffers 76 per cent double faults and the other 57 per cent.

Lightning Disturbances—Wood Lines, No Aerial Ground

Figure 4 is a type of grounded-crossarm wood structure used extensively during and following World War I when steel was difficult to obtain. These lines usually are insulated with four disks. Each steel crossarm is grounded with a coil of wire at the pole butt. The apparent absence of adverse effect from the omission of an aerial ground wire, may be accounted for by better-than-average grounding conditions.

During the early 20's, less important lines were built using the grounded-crossarm H-frame structure illustrated in Figure 5. These lines have impulse insulation of the same order as Figure 3, but no aerial ground wire was installed so that the remarks in the caption of Figure 4 with respect thereto are also in order here.

Lightning Disturbances—Single-Circuit Steel Lines

In 1926 it became desirable to build a single-circuit line equivalent to Figure 3 but for about 50 per cent of the investment, as a second circuit would not be re-

Table I. Structure Failures During Severe Storms of Lines Located on Adequately Cleared Private Right of Way

Damaged and Leaning Structures Not Included

Date	Type of Storm	Failures	
		Towers	Poles
Dec. 22, 1916	Sleet	6	0
April 2, 1920	Sleet	1	0
Nov. 28, 1921	Sleet	150	3
Nov. 28, 1922	Sleet	0	8
March 11, 1924	Sleet	37	0
Sept. 21, 1938	Hurricane	49	0
Sept. 14, 1944	Hurricane	0	0
		243	11

---

*Estimated impulse value of porcelain and wood insulation 1½ by 40 wave without including effect of aerial ground wires. The number of right-of-way miles is considered to be inversely proportional to the number of lines of structures thereon.

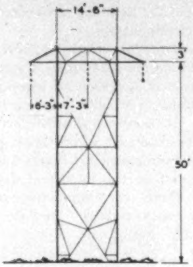

Figure 6*

Voltage	110,000
Constructed	1926–1939
Circuit-mile years experience	3,150
Impulse insulation, positive, kv	860
Lightning interruptions:	
Per 100 circuit-mile years	7.0
Per 100 structure-mile years	7.0
Per 100 right-of-way-mile years	14.8

quired for several years. Our studies resulted in a semiflexible steel structure of the type illustrated in Figure 6. The operating record of this type with eight and nine disks shows improvement over Figures 3 and 5, possibly because of the better shielding provided by the two aerial wires used in part to obtain longitudinal stability.

Later, the erection of a second circuit on the same right of way confirmed our hope that such independent circuits offered a practicable way to eliminate double-circuit interruptions. On our double-circuit towers as a whole, the foregoing figures show that about 60 per cent of the lightning strokes result in double-circuit outages. On parallel single-circuit lines, similar to Figure 6 or those to be hereinafter discussed, there have been no double-circuit interruptions during the time covered by this paper, a period encompassing 3,300 circuit-mile years of experience.

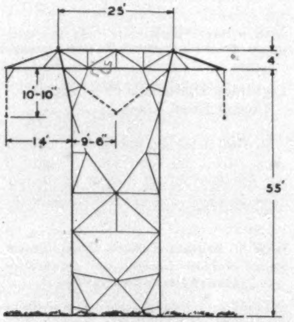

Figure 7*

Voltage	220,000
Constructed	1930
Circuit-mile years experience	4,290
Impulse insulation, positive, kv	1,345
Lightning interruptions:	
Per 100 circuit-mile years	2.75
Per 100 structure-mile years	2.75
Per 100 right-of-way-mile years	5.5

Figure 7 illustrates the principal features of our 220-kv transmission lines, which closely follow the design developed in Figure 6. Detailed information on this line has been published recently by Ohio Brass Company.[1]

Lightning Disturbances—Wood Lines with Aerial Ground

The opening remarks mention our present preference towards the use of timber structures. Figures 8 and 9 show these structures for 66 and 110 kv respectively. The 66-kv line introduces about 15 to 18 feet of wood insulation, which, for impulse frequencies, is equivalent to 15 to 24 disks, depending on wave shape as modified by reflections from adjacent grounds. The 110-kv structure provides about 25 to 27 feet of wood, equivalent to 25 to 35 disks on the preceding basis. No lightning interruption has occurred on a 110-kv line of this type. There now are six examples of this type, having a total length of 95 miles and an experience record of 267 circuit-mile years (including 1948, not shown in the tabulation).

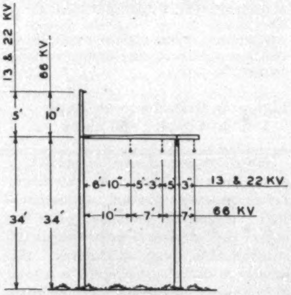

Figure 8*

Voltage	13,000 to 66,000
Constructed	1937
Circuit-mile years experience	347
Impulse insulation, positive, kv	1,500+
Lightning interruptions:	
Per 100 circuit-mile years	3.6†
Per 100 structure-mile years	3.6
Per 100 right-of-way-mile years	3.6

†This figure determined from that portion of this general type of construction on which completely segregated information is available.

Notes on Grounding Conditions

In the territory covered by this paper, the ground resistance at individual structures runs from 5 to over 1,500 ohms, with an average of about 390 ohms. Table II shows the range as determined from nearly 1,400 tests on about 150 miles of line.

Longitudinal counterpoise wires are being installed on some of the more important tower lines, and preliminary reports indicate very beneficial results.

Structural Failures

Table I is a cumulative tabulation of structural failures in our most severe

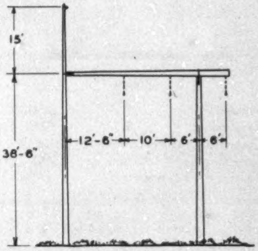

Figure 9*

Voltage	110,000
Constructed	1939
Circuit-mile years experience	192
Impulse insulation, positive, kv	2,200+
Lightning interruptions:	
Per 100 circuit-mile years	0
Per 100 structure-mile years	0
Per 100 right-of-way-mile years	0

Table II. Ground Resistance at Individual Structures

Per Cent	Footing Resistance Exceeding: Ohms
94	50
86	100
71	200
59	300
49	400
42	500
20	1000
8	1500

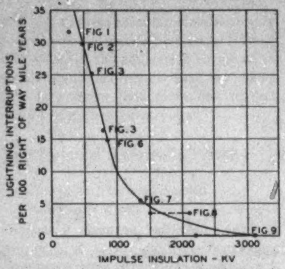

Figure 10. Curve showing relation of impulse insulation to lightning disturbances on lines with ground-wires

storms, when extensive damage occurred not only to utility plant, but to all types of structures. This table demonstrates the reliability of wood when properly used and maintained on transmission-line rights of way adequately cleared of trees. The ultimate replacement of wood structures or components may offer some problems if service interruptions are hard to schedule when the time arrives. These problems should not be difficult on our system as all important loads have alternate feeds.

Forest, brush, and grass fires frequently are mentioned as a possible objection to wood structures in timbered country. We have had many such fires cross our rights of way, and untreated poles are some times consumed where tall grass has grown around them. Creosoted poles in the same area and conditions have been charred, but none has ever been irreparably damaged.

Miscellaneous Remarks on Design

On future 110-kv extensions, we are contemplating the elimination of all guy wires by the use of brace poles or cross bracing. Also, it is worth noting in passing that in no case have any so-called Polarm structures been shattered by lightning after the aerial ground was in place. In some instances during construction, the top of the tall pole has been shattered when the pole ground only ran part way up the pole, before the longitudinal ground wire was run in and connected to the pole ground by the flying jumper which preserves the wood insulation.

Unfortunately, we have no comparative data to offer on the more conventional H-frame with two ground wires carried well above the crossarm. Such lines have not been used on our system because of our policy of avoiding any close approach to a vertical configuration, and our desire to obtain more of the benefits of wood insulation than practical H-frame dimensions allow. It would be necessary to use about a 50-foot crossarm to secure the same electrical characteristics in an H-frame that we have in a Polarm. When the extra protection of complete ground-wire shielding is desired, we use a separate ground-wire line with nothing else on it. This is considered only on single-circuit lines of the greatest importance.

Interruptions Related to Impulse Insulation

From the foregoing experience record, a curve has been prepared to reflect interruptions on a 100-mile right-of-way-year basis for lines having different impulse insulation levels and at least one aerial ground wire. This curve is shown in Figure 10 and convincingly shows the value of high impulse insulation and the relative ease of securing such insulation with wood structures.

Conclusion

A study of the various figures indicates that near immunity to lightning is obtained in this territory when a line incorporates in its design 2,500 to 3,000 kv of impulse insulation, corresponding clearances, and one or more ground wires. Lines operating at voltages up to at least 110 kv can be designed to meet these requirements without excess cost by taking advantage of the impulse insulating properties of wood.

Reference

1. Lightning Performance of Typical Transmission Lines. Ohio Brass Company, Mansfield, Ohio, 1948, pages 98–9.

Discussion

Earle Wild (Commonwealth Edison Company, Chicago, Ill.): Would Mr. Booker please give the correlation between the tower footing resistance and the excellent performance of the newer lines.

Is it not possible that these newer lines are the ones with the lower resistance so that they would logically have a better performance record than some of the earlier lines?

Also, how does the performance of your lines compare with the calculated theoretical performance as given by A. C. Monteith and others?

C. A. Booker: In reply to Mr. Wild's question, structure ground resistances on new lines average about the same as old. No special efforts to improve such conditions have been made except on some of the old tower lines where a longitudinal counterpoise wire is now being installed. Preliminary reports indicate considerable benefit from this installation.

Mr. H. R. Stewart, Electrical Engineer for our organization, stated that the line performance has been checked against the probability curves of A. C. Monteith[1] and also the later ones of E. L. Harder and J. M. Clayton.[2] The actual operating records are considerably less severe than the curve predictions. Possible explanations are that the tower footing resistance under lightning discharge conditions may be materially less than the values measured by the conventional reversed—d.c. "megger" method, or the number or severity of strokes per stormday in New England might be less than for the lightning data on which the published probability curves are based.

References

1. Transmission of Electric Power at Extra High Voltages, A. C. Monteith. *Electric Journal* (East Pittsburgh, Pa.), Feb., 1934.

2. Transmission Line Design and Performance Based on Direct Lighting Strokes, E. L. Harder, J. M. Clayton. *AIEE Transactions*, part I, volume 68, 1949, pages 439–49.

Stationary Networks and Transmission Lines Along Uniformly Rotating Reference Frames

GABRIEL KRON
MEMBER AIEE

Synopsis: This paper represents the first of a series of studies on the physical and mathematical analysis of the steady-state stability of conventional and long-distance transmission systems as influenced by the presence of voltage regulators and other control devices. As a first step attention is restricted to the transmission line as a component part of the over-all system and practical equivalent circuits are established for its representation, when the connected synchronous machines oscillate. For that purpose the basic equations of stationary networks are set up when viewed from uniformly rotating reference frames. An isolated inductor and capacitor, then a transformer, and finally a transmission line are used as examples. Their equations viewed from a simultaneously rotating and oscillating reference frame are given in reference 1.

THE CONCEPT OF "TRANSFORMATION OF REFERENCE FRAMES"

WHEN a stationary network is connected to a rotating machine, it usually is a simple matter to correlate their equations, since the latter are in most cases established along stationary axes for both machine and network. Difficulties arise, however, when the equations of the rotating machine happen to be established along rotating reference frames while the equations of the stationary network still retain their conventional form which is valid, of course, only for stationary reference frames. Such a case occurs, for instance, in transmission systems where synchronous generators are connected to a stationary transmission line.

In steady-state problems or in elementary small oscillation problems when the transmission line may be replaced by a tie-line (a single inductor) or when the synchronous machine may be considered balanced (no saliency, and so forth) the presence of a stationary network does not complicate the intended analysis. On the other hand, when in a hunting problem it is necessary to consider at the same time the shunt-capacitors of the transmission line and the saliency of the synchronous machine, lack of familiarity with the concept of "reference frames" and "transformation of reference frames" may lead to unnecessary complications.

THE METHOD OF REASONING OF CRARY AND CONCORDIA

In Park's method of analyzing synchronous machines the reference axes of both armature and field are rigidly connected to the field and rotate and oscillate (accelerate) with it. Hence no stationary network may be connected to the armature without further extension of the theory.

Crary[2] and Concordia[3,4] extended Park's equation to include any symmetrical stationary network connected to the armature. Their method of attack is as follows:

1. First they assume the synchronous machine axes not along the rotating (or accelerating) d, q, o axes, but along the stationary armature axes a, b, c, as Park originally did. In that case the synchronous machine equations are of the usual simplified form

$$e = Ri + p\psi = Ri + p(Li)$$

2. To this form they add the conventional equations of stationary networks connected to the a, b, c axes.

3. Afterward they transform both the machine and the network equations simultaneously from the a, b, c to the d, q, o axes in exactly the same manner as Park did for the machine alone.

The resulting equations are rather complicated. Also, it is difficult to add additional synchronous machines, say in the middle of the transmission line.

THE TENSORIAL METHOD OF ATTACK

Familiarity with the idea of transformation of reference frames would have suggested the following simpler method of attack for adding stationary networks to the armature of a synchronous machine:

1. First remove the stationary network from the synchronous machine.

2. Transform the machine and the network equations separately from the a, b, c to the d, q, o axes.

Since the transformed machine equations are already known, there was no need to establish them all over again. Hence it would have been sufficient to study the equations of only a stationary network along the accelerated axes d, q, o, or along any other arbitrary reference frame, along which a rotating machine itself was to be analyzed.

3. The resultant equations of the machine and of the network—both now being expressed along the same reference frame—are combined.

In fact, if the equivalent circuits of the machine and of the network are developed separately, it is sufficient to interconnect the networks themselves, without bothering to combine their equations first.

The foregoing reasoning is followed in this paper with the difference that the armature reference frame is assumed to rotate uniformly without any acceleration (small oscillation) in order to simplify the final equations. As a consequence it also will be necessary to study the small oscillations of synchronous machines along a uniformly rotating reference frame (Park

---

Paper 49-174, recommended by the AIEE Transmission and Distribution Committee and approved by the AIEE Technical Program Committee for presentation at the AIEE Summer General Meeting, Swampscott, Mass., June 20–24, 1949. Manuscript submitted January 26, 1949; made available for printing May 2, 1949.

GABRIEL KRON is a Consulting Engineer with the General Electric Company, Schenectady, N. Y.

and his followers assume a simultaneously rotating and oscillating reference frame). The study of the equivalent circuit of an oscillating synchronous machine along this new frame will form the subject matter of a consequent paper.

The Physical Reference Frame

Equation of Voltage Along Stationary Axes

It will be assumed that the three axes a, b, c of the armature at 120 degrees from each other are replaced by two axes α, β at 90 degrees apart, Figure 1. The zero-sequence o axis will exist, but will be left out of consideration.

Let two sets of stationary networks, each with any number of meshes, be given, that are to be connected to the armature axes α, β of a synchronous machine, (or to the slip rings on the rotor of an induction motor). The system must be a symmetrical R, L, C network (it may include rotating machines with symmetrical structure); that is if symmetrical components are introduced the positive-sequence network must be the same as the negative-sequence network, while the zero-sequence network may be anything. The impressed voltage need not be symmetrical. (If the network is not symmetrical, time harmonics have to be introduced.)

The equation of voltage of the network is

$$e=L\frac{d^2q}{dt^2}+R\frac{dq}{dt}+Sq$$

where the component impedance tensors L, R, and S are not functions of θ or of time.

Since it is not known how the charges are transformed when reference axes are changed, it is necessary to replaced the charges by another set of variables, $i=dq/dt$ as it is known how the i's are transformed with a change of axes. (In the language of dynamics a "nonholonomic" reference frame must be introduced.) In terms of current variables the equation of voltage of any stationary network along stationary reference frames is

$$\boxed{e=Ri+Lpi+S\frac{1}{p}i} \tag{1}$$

or

$$e=Zi \tag{2}$$

where

$$Z=R+Lp+S\frac{1}{p} \tag{3}$$

If sinusoidal currents flow in the network and if their frequency with respect to the stationary conductors is n, then p becomes $jn\omega$

$$\omega L=X_L \quad \Big| \quad S/\omega=X_c$$

and the impedance tensor becomes

$$Z=R+jX_Ln-jX_cn^{-1} \tag{4}$$

Here $\omega=2\pi k$ where k is some base frequency in terms of which X_L and X_c are calculated. The actual frequency n is expressed as a fraction of the base frequency k.

Introduction of Rotating Axes

Let now the stationary axes α, β of each set of two meshes be replaced, Figure 1, by the two rotating axes d, q (or the rotating axes α, β of the induction motor rotor by the stationary axes d, q). That is let the currents i be replaced by i' with the aid of the equation

$$i=Ci' \tag{5}$$

where C is a function of θ. If all axes rotate with the same instantaneous velocity $p\theta$, the transformation tensor C for a single-mesh 2-phase case is

$$C=\begin{array}{c|c|c|}
 & d & q \\
\hline
\alpha & \cos\theta & -\sin\theta \\
\hline
\beta & \sin\theta & \cos\theta \\
\hline
\end{array} \tag{6}$$

(For an induction motor θ has opposite sign.) Substituting, the equation of voltage (1) becomes

$$e=R(Ci')+Lp(Ci')+S\frac{1}{p}(Ci')$$

Multiplying by C_t

$$C_te=(C_tRC)i'+C_tLpCi'+C_tS\frac{1}{p}Ci'$$

If along the rotating reference frames the various impedance tensors are defined by their laws of transformation as

$$\begin{array}{l|l}
R'=C_tRC & S'=C_tSC \\
L'=C_tLC & e'=C_te
\end{array} \tag{7}$$

the new equation of voltage viewed from an arbitrarily rotating reference frame becomes

$$e'=R'i'+L'(C^{-1}pC)i'+S'\left(C^{-1}\frac{1}{p}C\right)i' \tag{8}$$

where p and $1/p$ refer to all expressions to the right of them.

The "Christoffel Symbols" V and Γ

Let for the time being the capacitor be absent and $S'=0$. Considering the inductor term only

$$\begin{aligned}pCi'&=(pC)i'+Cpi'\\&=\frac{\partial C}{\partial\theta}p\theta i'+Cpi'\end{aligned}$$

Substituting

$$e'=R'i'+L'pi'+L'C^{-1}\frac{\partial C}{\partial\theta}p\theta i' \tag{9}$$

The expression

$$\Gamma=C^{-1}\frac{\partial C}{\partial\theta}=\begin{array}{c|c|c|}
 & d & q \\
\hline
d & & -1 \\
\hline
q & 1 & \\
\hline
\end{array} \tag{10}$$

is analogous to the rotation tensor γ_t' used in rotating machine studies, it has the same components but a different definition, since

$$\gamma_t'=C_t\frac{\partial C_t^{-1}}{\partial\theta}=\gamma_{m}^{\cdot n}$$

Γ is the contravariant form of the "Christoffel symbol" V' (or rather of the "nonholonomic Christoffel symbol")

$$V'=L'\Gamma'=(C_tLC)C^{-1}\frac{\partial C}{\partial\theta}=C_tL\frac{\partial C}{\partial\theta} \tag{11}$$

Using index notation, V and Γ are special cases of several geometric objects, namely

$$V'=V_{mk}=\Gamma_{ks,m}=[ks,m]=-\Omega_{ks,m} \tag{12}$$

$$\Gamma'=L^{-1}V=V^{m}_{\cdot k}=\Gamma_{ks}^{m}=\begin{Bmatrix}m\\ks\end{Bmatrix}=-\Omega_{ks}^{m} \tag{13}$$

None of these concepts are tensors; all are geometric objects (see reference 5).

In direct notation two different symbols V and Γ must be used to represent the covariant and contravariant forms of the

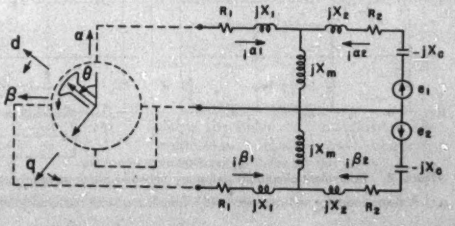

Figure 1. Stationary network, to be connected to a synchronous machine

same geometric object, though it is a very confusing practice. Hence occasionally the index notation also is used here to keep the physical concepts straight.

THE EQUATION OF VOLTAGE WITH NO CAPACITORS

In terms of Γ equation 9 becomes

$$\mathbf{e}'=\mathbf{R}'\mathbf{i}'+\mathbf{L}'\frac{d\mathbf{i}'}{dt}+\mathbf{L}'\boldsymbol{\Gamma}'\mathbf{i}'p\theta \tag{14}$$

and in terms of $\mathbf{V}$ it becomes

$$\mathbf{e}'=\mathbf{R}'\mathbf{i}'+\mathbf{L}'\frac{d\mathbf{i}'}{dt}+\mathbf{V}'\mathbf{i}'p\theta \tag{15}$$

$$e_m=R_{mn}i^n+L_{mn}\frac{di^n}{dt}+[ks,m]i^k\frac{dx^s}{dt}$$

It may be seen that when a stationary 2-phase inductor is viewed from a rotating frame, an apparent generated voltage appears as if the stationary inductor were a rotating machine. However, it is interesting and important to note that no torque is exerted on the stationary coil by the rotating axes since

$$\text{torque}=\mathbf{i}'^{*}\mathbf{G}'\mathbf{i}'$$

and the torsion tensor $\mathbf{G}'$ has no existence in the present dynamical problem (its place is being taken by $\mathbf{V}'$, a nontensor object).

THE "ABSOLUTE" TIME DERIVATIVE $\mathbf{p}$

For the purpose of the present paper still another form of the voltage equation will be employed. If $\mathbf{L}'$ in equation 14 is factored out, the equation assumes the form

$$\mathbf{e}'=\mathbf{R}'\mathbf{i}'+\mathbf{L}'(\mathbf{I}p+\boldsymbol{\Gamma}'p\theta)\mathbf{i}' \tag{16}$$

where $\mathbf{I}$ is the unit tensor. The expression in parenthesis is a tensor of valence two and will be denoted by $\mathbf{p}'$. It is a generalization of $p=d/dt$ and is called the "absolute" (or "covariant") time derivative δ/dt in tensor analysis

$$\mathbf{p}'=\frac{\delta}{dt}=\mathbf{I}p+\boldsymbol{\Gamma}p\theta=p_{\cdot n'}^{m'} \tag{17}$$

The voltage equation 16 in terms of $\mathbf{p}$ becomes

$$\mathbf{e}=\mathbf{R}'\mathbf{i}'+\mathbf{L}'\mathbf{p}'\mathbf{i}'=\mathbf{R}'\mathbf{i}'+\mathbf{L}'\frac{\delta\mathbf{i}'}{dt} \tag{18}$$

the same as that of a stationary impedance viewed from a stationary frame.

Comparing equation 18 with equation 8 it may be seen that the law of transformation of $\mathbf{p}'$ is

$$\mathbf{p}'=\mathbf{C}^{-1}\mathbf{p}\mathbf{C}\quad\Big|\quad p_{\cdot n'}^{m'}=p_{n\cdot}^{m}C_m^{m'}C_{n'}^{n} \tag{18A}$$

where along the stationary axes $\mathbf{p}=p\mathbf{I}=pI_{n\cdot}^{m}$. That is $\mathbf{p}$ is a once covariant and once contravariant tensor like $\gamma_t=\gamma_{\cdot n}^{m}$ and $\mathbf{C}=C_n^m$ are.

THE EQUATION OF VOLTAGE WITH CAPACITORS

Returning to the general equation of voltage, equation 8, with $\mathbf{S}$ different from zero, let it be written as

$$\mathbf{E}'=\mathbf{S}'\left(\mathbf{C}^{-1}\frac{1}{p}\mathbf{C}\right)\mathbf{i}'$$

where

$$\mathbf{E}'=\mathbf{e}'-\mathbf{R}'\mathbf{i}'-\mathbf{L}'\mathbf{p}'\mathbf{i}' \tag{19}$$

In order to get rid of the inverse p let first both sides be multiplied by $\mathbf{C}\mathbf{S}'^{-1}$

$$\mathbf{C}\mathbf{S}'^{-1}\mathbf{E}'=\frac{1}{p}\mathbf{C}\mathbf{i}'$$

and then by p

$$\mathbf{C}\mathbf{S}'^{-1}p\mathbf{E}'+(p\mathbf{C})\mathbf{S}'^{-1}\mathbf{E}'=\mathbf{C}\mathbf{i}'$$

($\mathbf{S}'^{-1}$ is not a function of θ or p.) Multiplying both sides by $\mathbf{C}^{-1}$

$$(\mathbf{I}p+\mathbf{C}^{-1}p\mathbf{C})\mathbf{S}'^{-1}\mathbf{E}'=\mathbf{i}'$$

The expression in parenthesis is $\mathbf{p}'$ and the equation may be written as

$$\mathbf{p}'\mathbf{S}'^{-1}\mathbf{E}'=\mathbf{i}'$$

Multiplying first by $\mathbf{p}^{-1}$, then by S'

$$\mathbf{E}'=\mathbf{S}'\mathbf{p}'^{-1}\mathbf{i}'$$

Substituting the value of $\mathbf{E}'$ the equation of voltage of a stationary network containing inductors $\mathbf{L}$ and capacitors $\mathbf{S}$, as viewed from arbitrarily accelerated reference frames, is

$$\boxed{\mathbf{e}'=\mathbf{R}'\mathbf{i}'+\mathbf{L}'\mathbf{p}'\mathbf{i}'+\mathbf{S}'\mathbf{p}'^{-1}\mathbf{i}} \tag{20}$$

This equation has the same form as equation 1

$$\mathbf{e}=\mathbf{R}\mathbf{i}+\mathbf{L}p\mathbf{i}+\mathbf{S}p^{-1}\mathbf{i}$$

representing their equation viewed from *stationary* reference frames, with the dif-

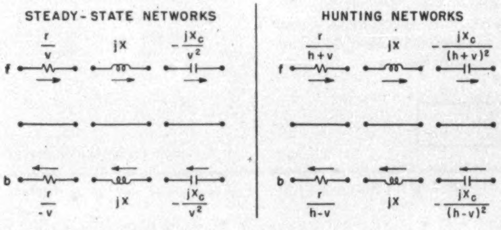

a) RESISTOR, INDUCTOR AND CAPACITOR

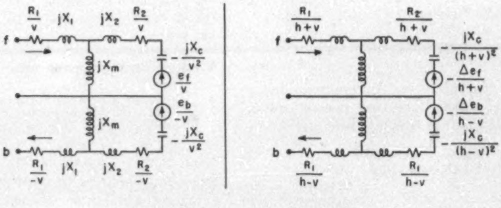

b) TRANSFORMER WITH CAPACITOR LOAD

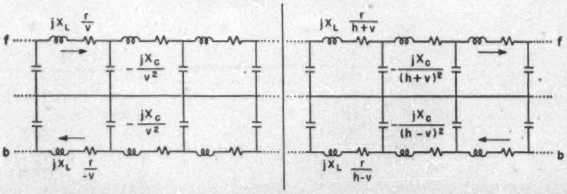

c) TRANSMISSION LINE

Figure 2. Equivalent circuits of stationary networks along uniformly rotating reference frame

(a) Resistor, inductor and capacitor (b) Transformer with capacitor load (c) Transmission line ference that all ordinary time derivatives $p = d/dt$ are replaced by "absolute" time derivatives $\mathbf{p} = \delta/dt$.

These last two equations are further illustrations of the "Generalization Postulates" (reference 5, page 115) whose purpose is to reduce the formulation of otherwise complex problems to the simplicity of common everyday usages. Equation 20 also may be written as.

$$\mathbf{e}'=\mathbf{Z}'\mathbf{i}' \tag{21}$$

where

$$\mathbf{Z}'=\mathbf{R}'+\mathbf{L}'\mathbf{p}'+\mathbf{S}'\mathbf{p}'^{-1} \tag{22}$$

Both equations are generalizations of equations 2 and 3 from stationary to uniformly rotating reference frames.

The definition of the "absolute" time derivatives $\mathbf{p}$ was already given in equation 17. It is still necessary to define its inverse, $\mathbf{p}^{-1}$.

CALCULATION OF $\mathbf{p}^{-1}$ WHEN $p\theta$ = CONSTANT

Later on it will be necessary to replace the general tensor equations by two sets of tensor equations, each relating to only one phase of a 2-phase system. For the present it will be sufficient to express only Γ and $\mathbf{p}$ along each of the phases in terms of compound tensors (namely in terms of tensors in which each component is a tensor) as

$$\Gamma=\begin{array}{c|cc} & d & q \\ \hline d & & -I \\ q & I & \end{array} \tag{23}$$

$$\mathbf{p}=\begin{array}{c|cc} & d & q \\ \hline d & pI & -p\theta I \\ q & p\theta I & pI \end{array}=\begin{array}{|cc|} \hline z_1 & z_2 \\ z_3 & z_4 \\ \hline \end{array} \tag{24}$$

where I is a unit tensor having as many diagonal components as the network has meshes (along one phase).

If, and only if, $p\theta$ is constant, then the inverse of $\mathbf{p}$ can be expressed as (reference 6, equation 10.43).

$$\mathbf{p}^{-1}=\begin{array}{c|cc} & d & q \\ \hline d & y' & -y'z_2y \\ q & -yz_3y' & y+yz_3y'z_2y \end{array}$$

$$y=z_4^{-1}=\frac{1}{p}I$$

$$y'=(z_1-z_2yz_3)^{-1}=\frac{p}{p^2+(p\theta)^2}I$$

Substituting, the 2-phase form of $\mathbf{p}'^{-1}$ is

$$\mathbf{p}'^{-1}=\frac{1}{p^2+p\theta^2}\begin{array}{c|cc} & d & q \\ \hline d & pI & p\theta I \\ q & -p\theta I & pI \end{array} \tag{25}$$

Comparing with equation 24 $\mathbf{p}'^{-1}$ can be expressed in the general (single-equation) form as

$$\boxed{\mathbf{p}'^{-1}=\frac{1}{p^2+(p\theta)^2}(Ip-\Gamma'p\theta)} \tag{26}$$

where $p\theta$ is a uniform rotation, a constant.

Comparing equation 20 with equation 8 it may be seen that the law of transformation of $\mathbf{p}^{-1}$ is the same as that of $\mathbf{p}$, namely

$$\mathbf{p}^{-1}=\mathbf{C}^{-1}\mathbf{p}^{-1}\mathbf{C} \quad | \quad p^{n}_{\cdot m'}=p^{m}_{\cdot n}C_{m'}^{m}C_{n}^{n'} \tag{27}$$

where along the stationary axes

$$\mathbf{p}^{-1}=p^{-1}\mathbf{I}=p^{-1}I_m^{\cdot n}.$$

Examples of the Physical Frame

SINGLE IMPEDANCES VIEWED FROM ROTATING AXES

For a single resistance, inductor or capacitor in each phase of the armature of an alternator, the individual impedance tensors along stationary axes are

$$\mathbf{R}=\begin{array}{c|cc} & \alpha & \beta \\ \hline \alpha & R & \\ \beta & & R \end{array}$$

$$\mathbf{L}p=\begin{array}{c|cc} & \alpha & \beta \\ \hline \alpha & Lp & \\ \beta & & Lp \end{array}$$

$$\frac{\mathbf{S}}{p}=\frac{1}{p}\begin{array}{c|cc} & \alpha & \beta \\ \hline \alpha & S & \\ \beta & & S \end{array} \tag{28}$$

The impressed voltage vector along stationary axes is

$$\mathbf{e}=\begin{array}{|c|c|} \hline e_\alpha & e_\beta \\ \hline \end{array}$$

Along uniformly rotating axes the impedance tensors of the individual coils become

$$\mathbf{R}'=\begin{array}{c|cc} & d & q \\ \hline d & R & \\ q & & R \end{array}$$

$$\mathbf{L}'\mathbf{p}=\begin{array}{c|cc} & d & q \\ \hline d & Lp & -Lp\theta \\ q & Lp\theta & Lp \end{array}$$

$$\mathbf{S}'\mathbf{p}^{-1}=\frac{1}{p^2+p\theta^2}\begin{array}{c|cc} & d & q \\ \hline d & Sp & Sp\theta \\ q & -Sp\theta & Sp \end{array} \tag{29}$$

The important fact should be noted that unilateral mutual impedances appear between the phases of an inductive or capacitive coil, as if they were two rotor phases of a rotating machine with magnetic or dielectric flux lines. The resistance tensor remains unchanged.

If the three coils of each phase are connected in series say when they represent a tieline with a series capacitor, the resultant impedance tensor becomes their sum

$$\mathbf{Z}'=\begin{array}{c|cc} & d & q \\ \hline d & R+\left(L+\frac{S}{p^2+p\theta^2}\right)p & -\left(L-\frac{S}{p^2+p\theta^2}\right)p\theta \\ q & \left(L-\frac{S}{p^2+p\theta^2}\right)p\theta & R+\left(L+\frac{S}{p^2+p\theta^2}\right)p \end{array} \tag{30}$$

The impressed voltage vector becomes

$$\mathbf{e}'=\begin{array}{c|c} d & q \\ \hline e_\alpha\cos\theta & e_\beta\sin\theta \end{array}$$

BALANCED 2-PHASE NETWORKS VIEWED FROM ROTATING AXES

The problem next is to replace the general tensor equations 20 to 22 by two sets of tensor equations, each relating to only one phase of a 2-phase system. The definitions of Γ, $\mathbf{p}$, and $\mathbf{p}^{-1}$ have already been replaced in equations 23 to 25.

Let the impedance tensor $\mathbf{Z}$ of a network with any number of meshes along phase α be the same as that along phase β. No mutual impedance is assumed between the two phases. Then along stationary axes the component impedance tensors are (expressed as compound tensors)

$$\mathbf{R}=\begin{array}{c|cc} & \alpha & \beta \\ \hline \alpha & R & \\ \beta & & R \end{array}$$

$$\mathbf{L}=\begin{array}{c|cc} & \alpha & \beta \\ \hline \alpha & L & \\ \beta & & L \end{array}$$

$$\mathbf{S}=\begin{array}{c|cc} & \alpha & \beta \\ \hline \alpha & S & \\ \beta & & S \end{array} \tag{31}$$

and the resultant impedance tensor, viewed from a stationary reference frame is

$$\mathbf{Z}=\begin{array}{c|cc} & \alpha & \beta \\ \hline \alpha & R+Lp+\frac{S}{p} & \\ \beta & & R+Lp+\frac{S}{p} \end{array} \tag{32}$$

where the index "α" includes all the meshes $\alpha_1, \alpha_2, \ldots \alpha_n$ along phase α, similarly the index β includes all the meshes β_1, β_2, $\ldots \beta_n$ along phase β.

The impressed voltage vector is

$$\boldsymbol{e}=\begin{array}{c|c} \alpha & \beta \\ \hline e_\alpha & e_\beta \end{array}$$

Let rotating axes $\boldsymbol{d}$ and $\boldsymbol{q}$ be introduced with the aid of

$$\boldsymbol{C}=\begin{array}{c|c|c} & d & q \\ \hline \alpha & \cos\theta I & -\sin\theta I \\ \beta & \sin\theta I & \cos\theta I \end{array} \qquad (33)$$

where I is the unit tensor. After transformation the matrices of $\boldsymbol{R}$, $\boldsymbol{L}$, and $\boldsymbol{S}$ happen to remain the same

$$\boldsymbol{R}'=\begin{array}{c|c|c} & d & q \\ \hline d & R & \\ q & & R \end{array}$$

$$\boldsymbol{L}'=\begin{array}{c|c|c} & d & q \\ \hline d & L & \\ q & & L \end{array}$$

$$\boldsymbol{S}'=\begin{array}{c|c|c} & d & q \\ \hline d & S & \\ q & & S \end{array} \qquad (34)$$

where now "$\boldsymbol{d}$" includes all the direct axes meshes $d_1, d_2, \ldots d_n$ and $\boldsymbol{q}$ includes all the quadrature axes meshes $q_1, q_2, \ldots q_n$. By equation 22 the resultant impedance tensor is

$$\boldsymbol{L}'\boldsymbol{p}=\begin{array}{c|c|c} & d & q \\ \hline d & Lp & -Lp\theta \\ q & Lp\theta & Lp \end{array} \qquad \boldsymbol{S}'\boldsymbol{p}'^{-1}=\frac{1}{p^2+p\theta^2}\begin{array}{c|c|c} & d & q \\ \hline d & Sp & Sp\theta \\ q & -Sp\theta & Sp \end{array}$$

$$\boldsymbol{Z}=\begin{array}{c|c|c} & d & q \\ \hline d & R+\left(L+\dfrac{S}{p^2+p\theta^2}\right)p & -\left(L-\dfrac{S}{p^2+p\theta^2}\right)p\theta \\ q & \left(L-\dfrac{S}{p^2+p\theta^2}\right)p\theta & R+\left(L+\dfrac{S}{p^2+p\theta^2}\right)p \end{array} \qquad (35)$$

Hence the effect of rotating axes is to introduce mutual impedances between each of the meshes of the two phases just as if each set of meshes were a rotating machine having both magnetic and dielectric flux lines.

It should be noted that the impedance tensor, equation 35, of any 2-phase network has the same form as that of two single meshes, equation 30, except that each scaler R, L, S is replaced by an appropriate tensor $\boldsymbol{R}$, $\boldsymbol{L}$, $\boldsymbol{S}$. This is another example of the Generalization Postulates facilitating the analysis of complex systems.

The impressed voltage vector is

$$\boldsymbol{e}'=\begin{array}{c|c} d & q \\ \hline \cos\theta e_\alpha & \sin\theta e_\beta \end{array}$$

EXAMPLE OF A 2-PHASE TRANSFORMER WITH CAPACITOR LOAD

To show an example where each of the phases has several meshes let the network on each phase consist of a 2-mesh transformer with a capacitive load as shown in Figure 1. Among the stationary axes of phase α the component impedance tensors are

$$\boldsymbol{L}=\begin{array}{c|c|c} & \alpha_1 & \alpha_2 \\ \hline \alpha_1 & L_1 & M \\ \alpha_2 & M & L_2 \end{array}$$

$$\boldsymbol{S}=\begin{array}{c|c|c} & \alpha_1 & \alpha_2 \\ \hline \alpha_1 & & \\ \alpha_2 & & 1/C \end{array}$$

and the resultant impedance tensor is

$$\boldsymbol{Z}=\begin{array}{c|c|c} & \alpha_1 & \alpha_2 \\ \hline \alpha_1 & r_1+L_1p & Mp \\ \alpha_2 & Mp & r_2+L_2p+\dfrac{1}{Cp} \end{array}$$

Then along the uniformly rotating axes the component tensors (still along one axes only) are

$$\boldsymbol{R}'=\begin{array}{c|c|c} & d_1 & d_2 \\ \hline d_1 & R_1 & \\ d_2 & & R_2 \end{array}$$

$$\boldsymbol{L}'=\begin{array}{c|c|c} & d_1 & d_2 \\ \hline d_1 & L_1 & M \\ d_2 & M & L_2 \end{array}$$

$$\boldsymbol{S}'=\begin{array}{c|c|c} & d_1 & d_2 \\ \hline d_1 & & \\ d_2 & & 1/C \end{array}$$

By equation 35 the transient impedance tensor of the resultant 2-mesh network along both axes is

$$\boldsymbol{Z}'=\begin{array}{c|c|c|c|c} & d_1 & d_2 & q_1 & q_2 \\ \hline d_1 & R_1+L_1p & Mp & -L_1p\theta & -Mp\theta \\ d_2 & Mp & R_2+\left[L_2+\dfrac{1}{C(p^2+p\theta^2)}\right]p & -Mp\theta & \left[-L_2+\dfrac{1}{C(p^2+p\theta^2)}\right]p\theta \\ \hline q_1 & L_1p\theta & Mp\theta & R_1+L_1p & Mp \\ q_2 & Mp\theta & \left[L_2-\dfrac{1}{C(p_2+p\theta^2)}\right]p\theta & Mp & R_2+\left[L_2+\dfrac{1}{C(p^2+p\theta^2)}\right]p \end{array}$$

STEADY-STATE EQUATIONS

If sinusoidal currents flow in the network and if their frequency with respect to the rotating reference frame is f then p becomes $jf\omega$, $p\theta$ becomes $v\omega$. Also if $\omega L = X_L$ and $S/\omega = X_c$ then along uniformly rotating axes the general equation 22

$$\boldsymbol{Z}=\boldsymbol{R}+\boldsymbol{L}\boldsymbol{p}+\boldsymbol{S}\boldsymbol{p}^{-1}$$

becomes

$$\boldsymbol{Z}_s=\boldsymbol{R}+jX_L(f\boldsymbol{I}-jv\Gamma)-jX_c\frac{f\boldsymbol{I}+jv\Gamma}{f^2-v^2} \qquad (36)$$

The 2-phase transient form, equation 35, becomes

$$\boldsymbol{Z}_s=\begin{array}{c|c|c} & d & q \\ \hline d & R+jfX_L-\dfrac{jfX_c}{f^2-v^2} & \left(jX_L+\dfrac{jX_c}{f^2-v^2}\right)jv \\ q & -\left(jX_L+\dfrac{jX_c}{f^2-v^2}\right)jv & R+jfX_L-\dfrac{jfX_c}{f^2-v^2} \end{array} \qquad (37)$$

If along the rotating axes the frequency is zero (as it is if the network is connected to a synchronous machine) $f=0$ and the above $\boldsymbol{Z}$ simplifies to

$$\boldsymbol{Z}_s=\begin{array}{c|c|c} & d & q \\ \hline d & R & -X_Lv-\dfrac{X_c}{v} \\ q & X_Lv-\dfrac{X_c}{v} & R \end{array} \qquad (38)$$

The Hypothetical Reference Frame

SYMMETRICAL COMPONENTS

In order to eliminate the unilateral mutual impedances between coils belonging to two different phases, symmetrical components (a set of hypothetical axes having no physical interpretation) are to be introduced along the physical $\boldsymbol{d}$, $\boldsymbol{q}$ axes. Let

$$\boldsymbol{C}_s=\frac{1}{\sqrt{2}}\begin{array}{c|c|c} & f & b \\ \hline d & I & I \\ q & -jI & jI \end{array} \qquad (39)$$

All tensors of valence two like $\boldsymbol{Z}$ are going to be transformed as

$$\boldsymbol{Z}'=\boldsymbol{C}^*{}_t\boldsymbol{Z}\boldsymbol{C}$$

Now the $\boldsymbol{R}$, $\boldsymbol{L}$, and $\boldsymbol{S}$ tensors of equation 34 remain unchanged. On the other hand the contravariant Christoffel symbol Γ, equation 23, assumes a diagonal form as

$$\Gamma=\begin{array}{c|c|c} & f & b \\ \hline f & jI & \\ b & & -jI \end{array} \qquad (40)$$

The absolute time-derivative $\boldsymbol{p}$, equation 24, and its inverse, equation 25, become also diagonal

$$\boldsymbol{p}=\begin{array}{c|c|c} & f & b \\ \hline f & (p+jp\theta)\boldsymbol{I} & \\ b & & (p-jp\theta)\boldsymbol{I} \end{array} \qquad (41)$$

$$\boldsymbol{p}^{-1}=\begin{array}{c|c|c} & f & b \\ \hline f & \boldsymbol{I}/(p+jp\theta) & \\ b & & \boldsymbol{I}/(p-jp\theta) \end{array} \qquad (42)$$

The transient impedance tensor, equation 35, becomes by equation 22

$$\boldsymbol{Z}=\begin{array}{c|c|c} & f & b \\ \hline f & R+L(p+jp\theta)+\dfrac{S}{(p+jp\theta)} & \\ b & & R+L(p-jp\theta)+\dfrac{S}{(p-jp\theta)} \end{array} \qquad (43)$$

showing the isolation of the two sequence equations. For a 2-phase transformer these equations become

$$\boldsymbol{Z}=\begin{array}{c|c|c|c|c} & f_1 & f_2 & b_1 & b_2 \\ \hline f_1 & R_1+L_1(p+jp\theta) & M(p+jp\theta) & & \\ f_2 & M(p+jp\theta) & R_2+L_2(p+p\theta)+\dfrac{1}{C(p+jp\theta)} & & \\ b_1 & & & R_1+L_1(p-jp\theta) & M(p-jp\theta) \\ b_2 & & & M(p-jp\theta) & R_2+L_2(p-jp\theta)+\dfrac{1}{C(p-jp\theta)} \end{array}$$

The couplings between the two phases have disappeared.

THE "ABSOLUTE" FREQUENCY TENSOR $\boldsymbol{n}$

If during steady-state the frequency of all currents with respect to the uniformly rotating reference frame is f then $p=jf\omega$ while $p\theta=v\omega$. Also $\omega L=X_L$ and $S/\omega=X_c$. Here f and v are fractions of the base frequency k in $\omega=2\pi k$ at which the reactances X_L and X_c happened to be calculated. The absolute time derivative $\boldsymbol{p}$ assumes the form

$$\boldsymbol{p}=\boldsymbol{I}p+\boldsymbol{\Gamma}p\theta=j\omega(f\boldsymbol{I}-jv\boldsymbol{\Gamma})=j\omega\boldsymbol{n} \qquad (44)$$

$$\boldsymbol{Z}=\begin{array}{c|c|c} & f & b \\ \hline f & R+jX_L(f+v)-\dfrac{jX_c}{f+v} & \\ b & & R+jX_L(f-v)-\dfrac{jX_c}{f-v} \end{array} \qquad (47)$$

where the "frequency tensor" $\boldsymbol{n}$ is defined along the hypothetical axes as

$$\boldsymbol{n}=\frac{\boldsymbol{p}}{j\omega}=f\boldsymbol{I}-jv\boldsymbol{\Gamma}=\begin{array}{c|c|c} & f & b \\ \hline f & (f+v)\boldsymbol{I} & \\ b & & (f-v)\boldsymbol{I} \end{array} \qquad (45)$$

Its physical interpretation is very important. It is built up of two components:

1. $-jv\boldsymbol{I}$ shows the speed (or frequency) of the reference frame with respect to the stationary conductors.

2. $f\boldsymbol{I}$ shows the frequency of the currents in the network with respect to the rotating reference frame assumed.

Hence their sum, the frequency tensor $\boldsymbol{n}$, shows the actual or "absolute" frequencies $\boldsymbol{n}$ of the currents in the conductors themselves. This property of $\boldsymbol{n}$ becomes very useful especially in the equivalent circuits of rotating machines where the conductors themselves are also rotating not only the reference frames. Knowledge of the frequencies of currents allows the determination of the torques of various frequencies. In terms of $\boldsymbol{n}$ the impedance tensors of equations 36 and 43 assume the form

$$\boldsymbol{Z}=\boldsymbol{R}+j\boldsymbol{X}_L\boldsymbol{n}-j\boldsymbol{X}_c\boldsymbol{n}^{-1} \qquad (46)$$

Comparing with equation 4 it may be seen that the equations of a stationary network remain unchanged if uniformly rotating axes are introduced and if in connection with them also hypothetical sequence axes are introduced. Only the frequencies entering into the equations have to be watched carefully, that is the scalar frequency n is replaced by the frequency tensor $\boldsymbol{n}$ (or the "absolute frequency" $\boldsymbol{n}$).

EQUIVALENT CIRCUITS ALONG THE ROTATING AXES

Since the equations $\boldsymbol{e}=\boldsymbol{Zi}$ of the armature axes of a synchronous machine equivalent circuit—to which the stationary network equivalent circuits are to be connected—have been divided by the frequency tensor $\boldsymbol{n}$, therefore all mesh equations of the stationary network also have to be divided by $\boldsymbol{n}$. Accordingly the impedance tensors of the equivalent circuits assume the form

$$\boldsymbol{Z}'=\boldsymbol{Rn}^{-1}+j\boldsymbol{X}_L-j\boldsymbol{X}_c\boldsymbol{n}^{-2} \qquad (48)$$

and the impressed voltages become

$$\boldsymbol{e}'=\boldsymbol{en}^{-1} \qquad (49)$$

The following two equivalent circuits will have to be then established:

1. For the steady-state networks $f=v$ hence $\boldsymbol{n}$ is v or $-v$

$$\boldsymbol{Z}_s=\begin{array}{c|c|c} & f & b \\ \hline f & \dfrac{R}{v}+jX_L-j\dfrac{X_c}{v^2} & \\ b & & -\dfrac{R}{v}+jX_L-j\dfrac{X_c}{v^2} \end{array} \qquad (50)$$

2. For the hunting network $j=h$ hence $\boldsymbol{n}$ is $h+v$ or $h-v$

$$\boldsymbol{Z}_h=\begin{array}{c|c|c} & f & b \\ \hline f & \dfrac{R}{h+v}+jX_L-\dfrac{jX_c}{(h+v)^2} & \\ b & & \dfrac{R}{h-v}+jX_L-\dfrac{jX_c}{(h-v)^2} \end{array} \qquad (51)$$

The negative sequence networks require negative resistances. The impressed voltages are

$$\boldsymbol{e}_s=\begin{array}{c|c} f & b \\ \hline \dfrac{\boldsymbol{e}_f}{v} & -\dfrac{\boldsymbol{e}_b}{v} \end{array}$$

$$-\Delta\boldsymbol{e}_h=\begin{array}{c|c} f & b \\ \hline -\dfrac{\Delta\boldsymbol{e}_f}{h+v} & -\dfrac{\Delta\boldsymbol{e}_b}{h-v} \end{array} \qquad (52)$$

The equivalent circuits (both steady-state and hunting) of three isolated coils and a transformer (to be connected to a synchronous machine) are shown in Figures 2(A) and 2(B). The equivalent circuit of a continuous transmission line is analogous to those of a transformer and is shown in Figure 2(C).

In view of the division by $\boldsymbol{n}$ it has to be remembered that the voltages (impressed or induced) on the equivalent circuits do not correspond to voltages in the physical networks, but rather to fluxes.

References

1. STEADY-STATE AND HUNTING EQUIVALENT CIRCUITS OF LONG-DISTANCE TRANSMISSION SYSTEMS, G. Kron. *General Electric Review*, (Schenectady, N. Y.) June 1943, page 337.

2. TWO-REACTION THEORY OF SYNCHRONOUS MACHINES, S. B. Crary. *Electrical Engineering* (*AIEE Transactions*), volume 56, January 1937, page 27–31, 36.

3. TWO-REACTION THEORY OF SYNCHRONOUS MACHINES WITH ANY BALANCED TERMINAL IMPEDANCE, C. Concordia. *Electrical Engineering* (*AIEE Transactions*), volume 56, September 1937, pages 1124–27.

4. NEGATIVE DAMPING OF ELECTRICAL MACHINERY, C. Concordia, G. K. Carter. *Electrical Engineering* (*AIEE Transactions*), volume 60, March 1941, pages 116–19.

5. A SHORT COURSE IN TENSOR ANALYSIS FOR ELECTRICAL ENGINEERS (book), G. Kron. John Wiley and Sons, Inc., New York, N. Y., 1942.

6. TENSOR ANALYSIS OF NETWORKS (book), G. Kron. John Wiley and Sons, Inc., New York, N. Y., 1939.

No Discussion

Industrial Plants Prefer Diesel-Electric Switching Locomotives

THOMAS J. WOODS
ASSOCIATE AIEE

DIESEL locomotives pulling long freight trains of several thousand tons on main-line railroads are a familiar sight, yet most people are not generally aware of the time and effort that must be expended in collecting and distributing this freight moving over the principal lines of the railways. The little known "workhorse" that performs the seemingly thankless task of collecting and distributing this freight to all industries is the switching locomotive, working at all hours of the day and night. Loaded cars are brought to a classifying point, where further switching and transfer work is required to "make up" a through freight train destined for movement over the main line.

Engines used in switching service may be classified broadly in two groups, depending upon ownership. A railroad switch engine is owned by the railroad and handles cars, not only on the railway property, but also in industrial plants where volume of traffic does not warrant the purchase of a locomotive. Industrial switch engines are used in many large plants for handling traffic within the plant or to a railroad exchange point. In many instances, the transportation system of an industrial plant may be larger and more complete than a fair-sized railroad, requiring, therefore, a large number of personnel for operation and maintenance of motive power.

To meet the specific requirements of this type of industrial service, there are many manufacturers who specialize in supplying industrial plants and railways with these smaller switching locomotives, weighing 80 tons or less, with horsepower ratings up to 600. Main-line locomotives are much larger and have been built in capacities of 500 tons and several thousand horsepower. These are specialized fields and usually are handled independently by different builders.

Development of the Diesel Engine for Railway Service

For many years the reciprocating steam locomotive handled practically all the transportation services in industrial plants. Little thought was given to the diesel engine which was proving itself to be an efficient and economical prime mover for stationary work, but these cumbersome slow-speed units were totally unsuited for railway vehicles. By 1925 it began to be recognized that the diesel engine offered considerable possibilities as a prime mover for locomotives; developments incorporating higher speeds, lower weights of parts, and more power concentrated in a small space were under way. In a comparatively few years—the early thirties to be exact—the diesel engine rapidly grew in popularity as a prime mover for railway work. Today, it enjoys a dominant position in the motive power field. The large percentage of locomotives now being ordered are of the diesel type. On December 1, 1948, there were 1,615 diesel locomotives on order for delivery to Class I railroads, as compared to 78 steam locomotives.

Electric Transmission

To the electric transmission can be traced the success of the diesel engine as a prime mover for locomotives. Locomotives must deliver high pulling capacity at low speeds and high horsepower at high speeds. As the engine is a relatively constant torque device, it cannot meet these conditions and, therefore, is not suited for a locomotive propulsion drive without the introduction of a torque-converting mechanism between the engine and driving wheels. The d-c generator and traction motors (the electric transmission) between engine and wheels are unsurpassed as a torque converter. The relatively unvarying torque of the diesel engine is converted to the correct type of power required at the driving wheels. This ranges between the high torque, sufficiently great to slip the wheels at starting, to the low torque values at high speed. In other words, the electric transmission permits utilization of full engine horsepower over the operating-speed range of the locomotive. Locomotive builders have available reliable and efficient electric transmissions, designed for

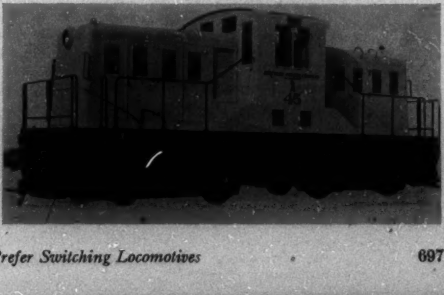

Figure 1. 65-ton 500-horsepower industrial switching locomotive with four traction motors

---

Paper 49-176, recommended by the AIEE Land Transportation Committee and approved by the AIEE Technical Program Committee for presentation at the AIEE Summer General Meeting, Swampscott, Mass., June 20–24, 1949. Manuscript submitted March 22, 1949; made available for printing May 3, 1949.

THOMAS J. WOODS is a Transportation Engineer in the Industry Engineering Department of Westinghouse Electric Corporation, East Pittsburgh, Pa.

the severe service encountered on locomotive applications and suitable for all sizes of locomotives. These electric machines present difficult design problems because of space limitations. To achieve required ratings in the limited space, not only are high-strength materials used, but it is also necessary to work the machines at temperatures well beyond those found practicable for stationary industrial applications.

Present Status of Diesel Motive Power

As the prime mover for a switching locomotive, the diesel engine is unsurpassed. It is efficient, uses a minimum of fuel, presents no water and ash problem, and has low standby losses. With electric transmission, it is possible to easily power any number of driving wheels to obtain high pulling capacity. So outstanding is the diesel-electric locomotive in these respects that it is rapidly replacing the steam locomotive for switching service. Practically no steam switching units are being built at present. As an indication of the rapid growth in popularity of diesel-electric motive power, Table I shows the cumulative total of small diesel locomotives sold through 1948.

Standard Locomotive Sizes

Industrial switching locomotives usually range in size from 20 up to about 80 tons on drivers. In a few large industrial plants, however, such as certain steel mills, 120-ton locomotives, commonly found in railway switching, are required to handle the heavier loads encountered. For the great majority of applications, it bears repeating that units of less than 80-tons weight are entirely adequate.

From the extensive application experience gained in this country and abroad, there has evolved a line of standard units suitable for industrial work. These are classified by weight on drivers. The most common types are the 25-, 35-, 44-, 50-, 65-, and 80-ton locomotives. There is a sufficient degree of flexibility in design of these locomotives to permit builders to supply locomotives with characteristics to meet special operating requirements of users. These special requirements are many. Both in this country and abroad, other than standard gauge is frequently encountered; also, unusual width and height limitations often are imposed.

Table I. Diesel Electric Locomotive Sales

Up to 80 Tons on Drivers

Year	Number of Units, Cumulative
1935	27
1940	213
1945	1,966
1948	2,500

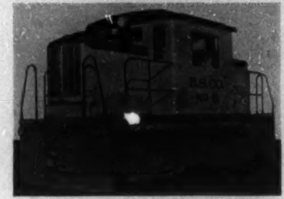

Figure 2. 50-ton 300-horsepower industrial switching locomotive with two traction motors

With the many types of engines and electric apparatus available, the locomotive builders have been able to supply industrial users with the required locomotive sizes and characteristics.

With industrial locomotives varying in weight from 20 to 80 tons, it is interesting to note that locomotives of about 50 tons weight have proved the most universally acceptable for plant switching. Following is a list of the percentage of locomotives sold with respect to weight on drivers. This includes all industrial-type locomotives under 80 tons weight sold through December 31, 1948.

Weight on Drivers, Tons	Per Cent of Total Sales
Below 20	3
21–30	10
31–40	3
41–50	49
51–60	3
61–70	24
71–80	8

Engine–Generator Sets

The builders of industrial locomotives do not manufacture diesel engines but purchase recognized makes for locomotive installation. These range in speed from 1,000 to 2,100 rpm and in horsepower from 100 to 600. In recent years, as engine design and reliability have improved, the trend has been toward higher speeds. A number of 2,100-rpm engines of 250 to 300 horsepower have been in service for several years with excellent operating results. In engines of 600-horsepower capacity, operating speeds of 1,000 to 1,200 rpm normally are not exceeded.

A single-bearing traction generator is recognized as the most acceptable for locomotive service. Coupling details vary. Many types of generators utilize a solid coupling between the armature and the crankshaft. On others, a steel-disc flexible coupling is used, with the generator frame bolted to the engine through a machined-fit bell housing. Either method of mounting results in a compact unit free from distortion caused by locomotive movement.

Traction Motors

Two types of traction motors are available for locomotive use—the heavy slow-speed type with the integral axle bearing using a single reduction gear, and the light-weight high-speed type utilizing multiple-reduction gearing. Careful analysis of service requirements will indicate which is better suited for a particular service. The slow-speed motor has a maximum speed of 2,000 rpm, as compared to 4,500 rpm for the high-speed motor. The following tabulation indicates the principal characteristics of each when geared for the same continuous tractive force.

	Motor Type	
	Slow Speed	High Speed
Weight, pounds	4,200	1,425
Rated tractive force, pounds	5,500	5,500
Gear ratio	4.4-to-1	22-to-1
Maximum locomotive speed, miles per hour	50	20

It is evident that the high-speed motor may be geared for the same continuous tractive force as the heavier slow-speed motor. This is done at a sacrifice in maximum locomotive speed. Under the stated conditions, a locomotive using the large low-speed motor is permitted a maximum speed of 50 miles per hour, while the smaller high-speed motor limits the maximum speed of the locomotive to 20 miles per hour. For industrial plants where the locomotive is restricted to slow-speed operation, the smaller motor is well suited. The thermal capacity of this motor is less than the heavy motor, resulting in a lower short-time rating. By proper consideration of axle loading and service requirements, it is possible to use the lightweight motor on locomotives requiring 25 to 35 miles per hour maximum speed.

Comparative Performance of Steam and Diesel-Electric Locomotives

One of the principal reasons the diesel-electric locomotive is supplanting the steam locomotive in industrial switching is its superior operating characteristics.

The operating cycle of a locomotive in switching service is short. It consists of accelerating from standstill up to approximately 10 miles per hour, then braking to a complete stop. The next operation may be in the reverse direction. As the time element is important, it is essential that the locomotive have the ability to respond quickly to throttle manipulation and to develop high tractive force at low speeds, in order to produce a high rate of acceleration. With an electric control system, the diesel responds to control manipulation faster than a steam engine of comparable size. The steam engine has a pulsating torque characteristic; the torque at the driving wheels of the diesel-electric is smooth. It has been found that the steam engine cannot be operated in excess of about 25 per cent adhesion; the diesel locomotive has a starting tractive force based on 30 per cent adhesion. Thus, with the same weight on drivers, the diesel has a starting tractive force 20 per cent greater than the steam engine, resulting in a higher rate of acceleration so necessary for switching service. The accelerating rate of the steam engine is further reduced by the nonadhesive weight carried on the tender and idle axles of the locomotive.

The diesel locomotive, with electric drive, is particularly well suited for short heavy-grade operation, often encountered in industrial plants. These grades may be in the form of ramps and may be quite steep. With the inherent ability of the electric equipment to withstand heavy overloads for short periods of time, the diesel locomotive may be worked up the short grade at tractive-force values approaching the slipping point of the wheels, and, for the reasons before mentioned, would excel a reciprocating steam locomotive of equivalent horsepower rating.

Most industrial plants do not require all locomotives to operate 24 hours a day. During the off period the diesel locomotive may be shut down and housed for the night. With the steam engine, there is the ever-present problem of maintaining fires. This may require additional personnel for the sole purpose of keeping the locomotives fired, thus adding to the cost of maintaining the transportation system.

Higher economy and greater availability are the principal factors sounding the "death knell" for the steam switching locomotive. Smoke-control ordinances of many communities merely increase the preference for diesel electrics. Although some progress is being made in reducing smoke from steam locomotives by using overfire air jets and controlled combustion, it is unlikely that the steam locomotive will ever be as clean as a diesel.

Table II. Comparison of Operating Costs of Steam and Diesel-Electric Locomotives Typical Steel Plant

	Dollars Per Hour	
	Present Steam	50-Ton Diesel
Fuel	$ 0.698	$ 0.330
Lubricants	0.045	0.033
Water	0.032	.....
Supplies	0.073	0.040
Repairs	1.272	0.350
Total	$ 2.120	$ 0.753
Hours per year	13,660	13,660
Annual operating expense	$28,959	$10,286
Annual operating savings by use of diesels		$18,673

Economies of Diesel Motive Power

In these days of increasing costs, efficiency is becoming increasingly important as premiums are set on economy of operation. From the standpoint of efficiency, the diesel switching locomotive is unexcelled. In most instances a considerable saving in operating expense results by the substitution of diesel power. A careful analysis of a switching service will indicate the advisability of replacing existing steam power with diesel-electric locomotives. The decision to substitute diesels for existing steam motive power usually depends on the number of hours the diesel may be used. The modern diesel locomotive has an availability of about 90 per cent, and it is desirable that it be utilized to the fullest extent in order to realize the greatest savings. For example, in a small plant requiring only eight hours of switching per day, it may be impossible to realize a sufficient saving in operating cost to justify the large expenditure for a diesel locomotive. In general, it may be said that a diesel will justify its purchase price if it can be used a minimum of 10 to 14 hours per day.

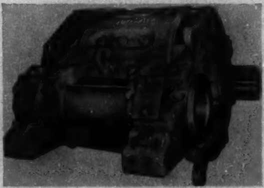

Figure 3. Axle-hung traction motor for 65- and 80-ton diesel-electric locomotive

The items of operating expense in which a diesel shows the greatest savings are fuel and repairs. With present prices of coal and diesel fuel, the diesel locomotive can do the same amount of switching work as a steam locomotive with 25 to 50 per cent of the fuel cost. There is a fixed relation between the coal burned in a steam engine and the fuel oil used in a diesel locomotive for a particular service. In switching service, this ratio is 100 to 140 pounds of coal to one gallon of diesel fuel. This variation is due to the difference in types of switching service, which is ascertainable by observation. The selling price of fuel oil and coal in a particular locality will cause further variation in relative fuel costs.

Data obtained from various operating companies indicate that diesel repairs average 30 to 50 per cent of comparable steam repair costs. A general figure for diesel repair expense cannot be established for a particular size diesel locomotive. This is particularly true in industrial plant switching. The repair expense has been found to vary greatly, depending on local conditions. With relatively few locomotives in service, for example, maintenance personnel must be retained even though they are not needed at all times. This results in a high repair expense chargeable to the locomotives. On the other hand, if there is a relatively large number of locomotives on the property, by proper scheduling, the unit repair expense will be low. It has been established, however, that on a particular property, there will be a definite relationship between maintenance costs for steam and diesel locomotives. If the steam repair costs are low because of efficient maintenance, then the diesel repair costs likewise will be low when diesel substitution is made. Taking these factors into consideration, it is possible to estimate with a considerable degree of accuracy the economic justification of diesel motive power.

To illustrate what may be accomplished by the substitution of diesel motive power, the results of a recent steel-mill-application study are shown in Table II. The mill has five steam locomotives in operation handling intraplant switching. Consideration is being given to the replacement of these units with diesel locomotives. An analysis of the system indicates that four 50-ton diesel-electric locomotives can replace existing steam power. The resulting savings will pay for the diesels in five to seven years. It may be seen that each diesel locomotive will average 3,415 hours of operation per year, and the annual savings in operating expense will approximate $18,673.

Conclusions

The position of the diesel-electric locomotive in the industrial-switching field is unchallenged, as evidenced by the large number in service and the rapid rate at which existing steam power is being replaced.

The versatility of this form of power is well suited for the many applications encountered ranging from heavy steel-mill work to light switching in small industrial plants.

The operating advantages and economies possible with diesel locomotives are obtainable by precision maintenance and repair. A diesel-electric locomotive is composed of many elements, requiring trained personnel for its proper upkeep and for realizing the high availability and low operating cost inherent in this type of motive power. A diesel locomotive functions best when properly maintained. By observing the necessary precautions with regard to operation, following recommended maintenance procedures, and keeping the locomotive equipment clean, the industrial user will achieve an economy of operation hitherto unattainable with reciprocating steam motive power.

No Discussion

Improvements to Oklahoma City Primary Network

BRYCE BRADY
MEMBER AIEE

Synopsis: The expansion of an existing 4.16-kv primary network in Oklahoma City has been found to be more economical than conversion to a radial plan of primary distribution. Some recent improvements are described; some operating problems are discussed.

THE SECOND oldest primary network in the United States has provided service to a typical residential section of Oklahoma City since 1931. When load growth recently made it apparent that major improvements would be required, a study was made to ascertain whether it would be more economical to retain and expand the network or to convert to a radial primary system such as is used in all other sections of Oklahoma City where the load density is of similar magnitude.

Premises

Load growth was projected three times its present magnitude, and both radial and network systems were designed to serve this future load. Every effort was made to keep the two plans as nearly comparable as possible. Service to all customers in both plans was made firm to the extent that loss of one 13.8-kv source line must not cause an outage, and that the overload on the remaining substation transformers and equipment shall not exceed 150 per cent. Both plans assume that sufficient capacitors will be added to the distribution lines from time to time to maintain approximately 0.90 power factor at peak load. Both plans include conversion from the present uniground neutral system to a common primary-secondary multiground neutral system.

Radial Plan

The radial plan proposes the installation of one centrally located substation to serve the entire area, which ultimately will consist of two 6,000-kva 3-phase transformers; six 4.16-kv outgoing feeders, each with reclosing circuit breaker and step-type voltage regulator; and three incoming 13.8-kv lines, with switches to isolate any faulted line. The 13.8-kv lines also would serve other load in adjoining areas. In order to limit the available fault current through the voltage regulators, the 4.16-kv bus would be split and would have an automatic tie breaker; that is, each 6,000-kva transformer normally would serve three outgoing 4.16-kv feeders. All load, however, would be switched automatically to the remaining transformer in case of transformer or 13.8-kv bus failure. This ultimate plan provides firm service to 9,000 kva of load. Of course, the necessary expenditure for the individual components would be deferred until required to serve the growing load.

Network Plan

Comparative cost estimates were prepared for various numbers, sizes, and arrangements of network stations. It was found that the most economical plan which would provide firm service to 9,000 kva of load, distributed according to the load forecast, would consist of four network substations, interconnected by five 4.16-kv mains and served by three 13.8-kv source lines. The two substations served by the same 13.8-kv source would not have a 4.16-kv tie main between them. The 13.8-kv lines also would serve other load. Each of the network stations was planned with tap changing under load-bus regulation—one master circuit breaker, and either two or three feeder circuit breakers as required. All automatic switching is to be done at 4.16 kv. Each component of expenditure would be deferred until required.

Economic Comparison

Cost estimates were made of both network and radial plans to provide firm service year by year during the next 17 years under assumed load growth conditions. These estimates show that the network plan will require less capital expenditure than the radial plan for improvements to the present system, both immediately and ultimately. The estimates compare as follows:

	Network	Radial
Immediate capital expenditure, per cent	100	114
Ultimate capital expenditure for 9,000-kva load, per cent	128	144

This comparison does not include cost of losses, nor does it recognize the different years during which improvements would be required. Evaluation of copper and iron losses shows an additional difference in favor of the network plan, by virtue of the decreased average distance from substations to load. The present worth at 6 per cent interest of the immediate and future capital expenditures plus the future copper and iron losses during the next 17 years compare as follows: If retention of the network plan, including losses, is taken as 100 per cent, then conversion to the radial plan under the same conditions is 134 per cent.

It must be remembered that these comparisons do not pertain to the establish-

---

Paper 49-178, recommended by the AIEE Transmission and Distribution Committee and approved by the AIEE Technical Program Committee for presentation at the AIEE Summer General Meeting, Swampscott, Mass., June 20–24, 1949. Manuscript submitted November 15, 1948; made available for printing May 3, 1949.

BRYCE BRADY is Chief Distribution Engineer of the Oklahoma Gas and Electric Company, Oklahoma City, Okla.

ment of a new primary network. They pertain to the alternatives of retaining and adding to an existing primary network, versus the conversion of this existing network to a radial system.

Operating Comparison

Service continuity has been equal to or slightly better during the last 17 years in the network area than in comparable radial areas. It is difficult to predict the future trend because of improvements that currently are being made in both the radial and network service areas. A carefully co-ordinated scheme of line-sectionalizing fuses and instantaneous and very-inverse-time-delay relays is being installed on all 4.16-kv radial circuits which, it is anticipated, will very materially improve service continuity to all customers. It does not appear that this plan of automatically ascertaining whether a fault is transient or permanent, and using fuses for automatic sectionalization in the latter event, can be applied to the network plan. Principally for this reason, it may work out that service continuity will be slightly better in the radial service areas in the future. Only time will answer this question.

Most of the operating difficulties on the primary network have arisen from the fact that two of the network stations are served directly from a generating station while the third network station is served from a 66-kv substation, with somewhat different phase angle at various hours of the day. This has resulted in some improper circuit breaker operations. These have not, in general, resulted in customer outage, but rather in pumping action and transfer of load between network stations. This problem has been serious but not insurmountable. Various solutions have been used, including reversal of the reactance setting of the line-drop compensators and desensitization of the network relays. The plan which is being used now and which appears to be the most satisfactory, is a network relay scheme whereby a network station is disconnected from source when the load current either reaches zero or reverses, and is restored to service when the source voltage is both higher in magnitude and leading in phase angle. At the present time, the reactance settings of the line-drop compensators are set on zero at two network stations and are reversed on the other two. Positive overcompensation of voltage drop, that is, delivery of higher voltage at peak load, then at light load, is accomplished solely with the resistance setting of the line-drop compensators.

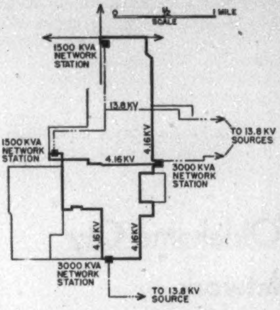

Figure 1. Oklahoma City primary network at present stage of development

The network and radial plans were kept comparable on the basis of voltage spread between first and last customer at the time the comparative cost estimates were prepared. There is no reason why this should not continue to work out in practice.

It is necessary to add supplementary sectionalizing devices on long radial extensions from the network ahead of the point where the available fault current would fail to actuate the circuit breakers, just as on a radial system. These devices may be either repeating fuses or pole-top reclosers.

Recent Improvements

As a result of this investigation, two 3,000-kva unit-type network stations of the factory-assembled-type have been purchased and are now in operation. Both of the stations were installed in well built-up residential areas and are located on lots immediately adjacent to residences. In one case we were able to secure a vacant lot; in the other case this could not be done, and we purchased a lot with a frame house, which dwelling was sold and removed. The feeders leave the new stations via 500,000 circular-mil paper-insulated lead-covered cables in underground ducts. All of the remainder of the 4-kv system is overhead and is illustrated in Figure 1. The mains are predominantly number 000 bare copper and 267,000 circular-mil bare aluminum without steel reinforcing. The laterals are predominantly number 6 hard-drawn copper and number 4 aluminum-cable-steel-reinforced conductor. The 13.8-kv connection to one of the new stations is overhead; to the other, underground. Each of the new stations will be landscaped with shrubbery and grass by spring 1949 to minimize any objection by those who live nearby.

Conclusions

The 4.16-kv primary network is a satisfactory and economical method of distributing electricity. Its relative economy depends upon the proximity of a suitable number of subtransmission voltage sources and the relative cost of extending these versus 4.16-kv feeders. In some cases it may be considerably more economical than a radial system made equally firm and reliable. All of the supply lines to a primary network should originate at one firm source, or from sources which do not have appreciable phase-angle differences. The relaying of primary networks is much more complicated than on radial systems. The copper loss on a primary network is considerably less than on a radial system, because energy is transmitted nearer to the load at high voltage, and because more advantage is taken of load diversity. Unit-type substations can be added near the load center of well built-up residential and commercial areas without excessive costs. There is probably no great difference in the quality of service rendered by a primary network as compared with radial feeders. It is anticipated that the radial circuits which are being equipped with sectionalizing fuses carefully co-ordinated with instantaneous and time-delay relays to secure automatic sectionalization of faults, will provide somewhat better service continuity than the primary network.

Discussion

H. E. Campbell (General Electric Company, Schenectady, N. Y.): It is gratifying to see the author's conclusion that the 4.16-kv primary network is a satisfactory and economical method of distributing electricity. This confirms our thoughts about the primary network system.

The author points out that he has experienced some difficulty in pumping action of the transformer circuit breakers and he found it necessary to desensitize the network relays. Is it possible that his difficulty could have been avoided if a less sensitive relaying scheme had been used in the beginning? And, would not a less sensitive relaying scheme make it unnecessary to conclude that all of the supply lines to a primary network should originate at one firm source or from sources which do not have appreciable phase angle differences?

If directional overcurrent relays, set to trip for currents of 100 per cent in the reverse direction, were used instead of the sensitive network relays, then some phase angle differences can be tolerated without any expected difficulty. As long as the magnitude of the power flowing out of the network is not great enough to overload any part of the network, there should be no objections to such a transfer of power.

The stipulation that all primary network substations be supplied from one firm source seems to be an economical hardship placed upon this type of system. Quite often sources of power for a primary network can be found at many locations throughout an area. If these cannot be tapped because of sensitive relaying, then subtransmission cost for the system might be excessive.

We have not considered it necessary to use sensitive relaying in order not to have an occasional power reversal through a network substation. We would appreciate the author's comments on this.

Bryce Brady: We agree with Mr. Campbell that there is no harm in having reverse current flow from the primary network, through a network station, into a source line under normal operating conditions.

Our concern is for the safety of the public under abnormal conditions such as with a broken conductor on a 13.8-kv source line. It is considered imperative that the network switch be opened to stop the back-feed into such a fault. All of our network transformers are connected delta on the 13.8-kv side and wye on the 4.16-kv side, and therefore deliver very slight current into this type fault.

While there are other methods of detecting line-to-ground faults, such as grounding potential banks, Thyrite ground indicators, and "over-and-under" voltage devices, we have found the modern network relay to be the most dependable. We set this relay to open the switch when load current either reaches zero or reverses, and to close the switch when the source voltage is both higher in magnitude and leading in phase angle.

This scheme, together with the reversal of the reactance settings of the line drop compensators, has apparently stopped all pumping action and transfer of load between stations, which action was quite bothersome some years ago.

Primary Networks on the Duquesne Light Company System

W. P. HOLBEN
FELLOW AIEE

J. E. LANGE
ASSOCIATE AIEE

THE 4-kv primary-network type of distribution system is used successfully in the Pittsburgh area. This is not a new development. In fact the design of the Verona–Oakmont 4-kv network, which was placed in service in 1931, was reported and described in considerable detail in a paper published in September, 1931.[1]

A report[2] of the first year of operating experience with this network system was presented in November 1932. A new feature was added to improve stability, to reduce circulating currents, and to reduce transformer circuit-breaker operations. The application of inverse reactive compensation to the induction voltage regulators provided a solution for these problems.

These two important contributions to technical literature provide a historical background for the primary network on the Duquesne Light Company system, and also have become a record of achievement in distribution engineering.

It is the purpose of this paper to present results of recent tests of the Verona–Oakmont network and to provide a 1931–1948 performance record. A new 4-kv primary-network installation for the Squirrel Hill area also will be discussed, with special reference to present-day practices and modern equipment that now is offered by manufacturers of distribution substation equipment.

Summary

1. Test results and operating experience confirm the effectiveness of inverse reactive compensation to provide satisfactory division of load between network units, to improve stability, and to reduce the circulating currents.

2. An 18-year performance record for 1931–1948 of the Verona–Oakmont 4-kv primary-network system provides convincing evidence of a high degree of service reliability.

3. The primary network is attractive from a system cost point of view, provided conditions in the area to be served include reasonably uniform load density, substantial overload relief requirements, and the need for a high degree of service reliability.

4. The interconnected mains between network substations, which provide 2-way service to all loads, permit circuit breaker or transformer maintenance without prearranged switching or outage to any customers. Only extended unit outages require the use of the mobile unit substation.

5. The Squirrel Hill network is equipped with modern network units of the factory-built package type. These units will be cable connected and completely metal clad, and have been selected with consideration for economical size. Other features include regulation by means of automatic tap changing under load with inverse reactive compensation and 4-kv air circuit breakers. All network units are installed outdoors with fenced enclosures.

Operating Elements of the Verona–Oakmont Network

Figures 1, 2, and 3 show the electrical and geographical arrangement of the network station units, the 4-kv circuits, the 22-kv subtransmission circuits, and a single-line diagram of the station equipment.

The network, which remains effectively the same as at installation, has three transformer units, each with a nameplate rating of 1,500 kva, which transform the voltage from 22 kv to 4 kv. The five network mains interconnecting these three units are 1/0 open-wire lines with cable connections to circuit breaker cubicles at the network substations. The 22-kv single radial connections to the network units are made with open-wire line extensions and underground cable to a 3-position switch on the network transformers. Each unit has a 4-kv bank circuit breaker and three single-phase induction bus regulators. The Hulton and Verona units each have three feeders or mains connected to the bus by oil circuit breakers, and the Oakmont unit has four feeders or mains and four oil circuit breakers.

The bank circuit breakers are equipped with network and reclosing relays; the transformers, with contact-making thermometers. The feeders are tripped by induction overcurrent relays and reclose automatically, once from each end, with the reclosing times staggered. The 4-kv bus is provided with differential protection using induction overcurrent relays.

For the purpose of obtaining experience with various types of installation, one unit was installed underground, one in a small building, and one outdoors. The transformer and regulator housing construction in all three is essentially the same. They were designed to be watertight units with wiped cable entrance connections. The circuit breakers in Hulton also were designed to be watertight, while those at Oakmont and Verona were designed as weatherproof cubicles. All the watertight equipment has removable flat plates held by nuts on stud bolts, gasketed with flat cork gaskets.

The regulators are induction type with a five per cent plus or minus regulating ability. They are equipped with the

---

Paper 49-179, recommended by the AIEE Transmission and Distribution Committee and approved by the AIEE Technical Program Committee for presentation at the AIEE Summer General Meeting, Swampscott, Mass., June 20–24, 1949. Manuscript submitted November 16, 1948; made available for printing May 3, 1949.

W. P. Holben and J. E. Lange are with the Duquesne Light Company, Pittsburgh, Pa.

The authors gratefully acknowledge the important contributions of G. N. Hoffman and L. M. Olmsted to this paper.

normal regulator control, except that the reactance section of the compensator has been reversed by changing connections internally.

Supervisory indications are transmitted to the System Operator's office to provide immediate information of abnormal operating conditions, such as open circuit breakers, high transformer temperature, control voltage failure, and deenergized station.

Some time after installation, the Hulton unit, which is underground in a vault, was equipped with additional control facilities located just under the street-level grating, so that manual operations could be performed even though the equipment was submerged. This unit also is equipped with a pump controllable from the grating opening and a hose connection at the same level, so that water can be discharged into the street.

Operating Experience

The annual peak loads from 1931 to the present time are shown in Figure 4, along with the adjustments of the contact-making voltmeter and voltage compensator. The network nameplate capacity of 4,500 kva was provided for an estimated 2,000 kva of load. Actually, because of conditions existing in the early thirties, the load did not reach this point until 1936. Now it is almost 4,000 kva, and because of the relatively large capacity originally installed, it has not been necessary to increase the number of units or the size of the transformers. Recent tests and studies resulted in an increase in the assigned capacity of the network, based on thermal capabilities, and further tests are expected to result in another increase in capacity ultimately. A study also is being made relative to the addition of a fourth unit.

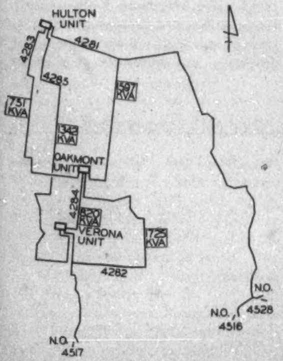

Figure 1. Verona–Oakmont network: map showing network units, 4-kv mains, and connected loads

The original inverse reactive compensator setting of 20 was determined by test and later raised to 24 because of a change in current-transformer ratio. Early experience indicated the impracticality of operation without this inverse reactive compensation. The regulators at the three units assumed widely divergent positions, and, as a result of the tendency of the bus voltages to be unequal, circulating currents of relatively high value occurred. At light load periods, this was sufficient to cause one of the unit-bank circuit breakers to trip repeatedly on current fed back into the transmission system from the other two units.

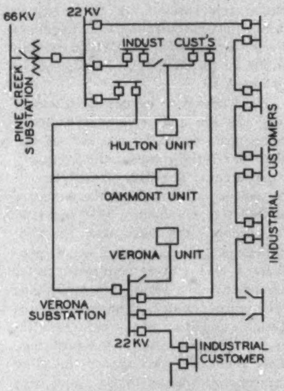

Figure 2. Verona–Oakmont network: schematic diagram of 22-kv connections

Theoretically, the highest inverse reactive compensation available that would not cause hunting would be desirable, since the current due to the tendency to different bus voltages would be held to a minimum; that is, a very small reactive current flowing would produce enough voltage at the contact-making voltmeter to cause it to change the regulator position to stop this flow, but not change it enough to reverse the flow. Another factor requires consideration, however. The reactive component of the load current will lower the entire network voltage, and, unless there is sufficient resistance compensation available to overcome this effect of the reactive load component and add whatever additional voltage is desired, a compromise setting must be used.

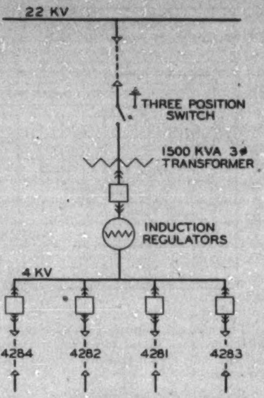

Figure 3. Verona–Oakmont network: schematic diagram of a network unit

With the relatively light loads of the first several years of operation, it was thought unnecessary to have any resistance compensation in the circuit. However, as loads increased, it became necessary to add resistance compensation to prevent lowering of the 4-kv bus voltage due to the effect of the reactive component of load, as previously explained. The present relation of reactive to resistance compensation of two-to-one will provide a constant bus voltage with a load power factor of 90 per cent.

All of the inverse-time feeder relays are set at the same pick-up and time values. Calculations of current division between the circuits during fault conditions indicated that sufficient time selection would be obtained to insure co-ordination. Operating results show satisfactory co-ordination, in that no feeders have tripped incorrectly during faults on other feeders. Clearing of faults on network feeders usually will be by sequential opening of the two ends of the feeder and will require, therefore, longer time than on radial feeders.

The operating experience with the unit in the underground vault has not been entirely satisfactory for the following reasons:

1. It is difficult to maintain watertight seals with flat gasketed plates that are removed frequently for testing, maintenance, and operation.

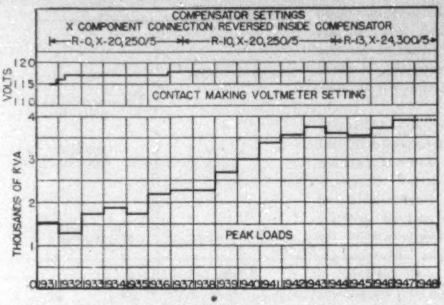

Figure 4. Peak loads, compensator settings, and contact-making voltmeter settings, 1931–1948

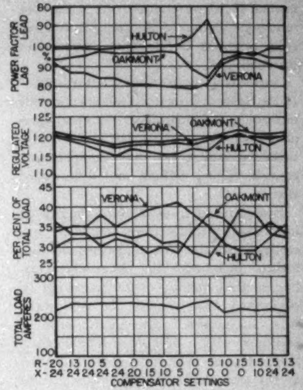

Figure 5. Effect of changes in compensator settings on load division, regulated voltage, and power factor of load current

2. Two men are required for work that one switchman does at all other nonattended stations. One man is required to guard the entrance.

3. Corrosion, dirt, and moisture are deteriorating the equipment in this unit more than at the two surface units.

4. It is necessary to tear up the street and interfere with traffic to effect removal and installation of major equipment.

It is recognized that improvements can be made that would minimize the above conditions. The experience has been, however, that this equipment cannot be maintained in the manner that surface-installed equipment is maintained.

Test Results

Figure 5 shows results of tests to determine the effect of compensation settings on operation of the network. These data indicate that the present settings of 13*R* and 24*X* produce satisfactory results and about the best combination of load division, voltage, and power factor for the conditions encountered. The power factor at time of test was higher than 90 per cent; the regulated bus voltage is correspondingly higher than the balance point.

The effect of increasing the inverse reactive compensation on the regulated voltage is clearly shown, as is the use of the resistance compensation in compensating for the undesirable lowering of bus voltage level.

The tendency to increase unbalance of load current and amount of reactive component carried by the various stations, as reactive compensation is cut out, is apparent. The data plotted for the 0–0 compensation setting is the average of several sets of readings that were obtained during this test setup. The regulators changed position and the distribution of load current and power factor among the units varied during the time this setting existed, demonstrating the unstable condition of the network without the inverse reactive compensation. This would be accentuated if the 22-kv transmission sources to the units were less solidly connected than they are in this installation.

The charts in Figure 6 indicate load current division with various operating conditions of the network. The tests in which the tie main between Verona and Hulton was open, were made to simulate conditions that would occur on a network where there would not be direct mains between each unit and each other unit. In one test the regulators at Verona were manually set in the neutral position with the main between Verona and Hulton open, to determine load division if the mobile substation unit, which is not regulated, were used in place of a regular network unit. The possibilities encountered under abnormal operating conditions are so numerous that general tests can provide only a general indication of what would take place. The number of units in the network, number of tie mains between units, impedance of these mains, compensation, and firmness of the high-tension sources all will contribute to the division of load under abnormal condi-

Table I. Verona–Oakmont Interruption Record

	1931	1932	1933	1934	1935	1936	1937	1938	1939	1940	1941	1942	1943	1944	1945	1946	1947	1948 9 months
Interruptions to Entire Network																		
Total Interruptions	0	2	0	1	2	2	0	0	0	1	0	0	0	0	0	1	0	0
Interruptions in excess of 2 minutes	0	1	0	0	1	1	0	0	0	0	0	0	0	0	0	0	0	0
Interruptions to Tie Mains																		
Circuit:																		
4,281 Hulton–Oakmont				3	0	1(1)	0	1	0	0	1	0	0	2	0	1(1)	0	0
4,283 Hulton–Oakmont				1(1)	0	5(2)	0	0	0	0	0	1(1)	0	0	0	0	0	0
4,282 Oakmont–Verona				0	0	1(1)	0	0	0	0	0	0	0	0	0	1	1(1)	1(1)
4,284 Oakmont–Verona				0	0	1(1)	0	0	0	0	0	0	0	0	0	0	0	0
4,285 Hulton–Verona				0	0	2(1)	1	0	0	1(1)	0	0	2	3(1)	0	0	0	0
Figures in parentheses indicate the number of these outages in excess of 2 minutes.																		
Interruptions to Units Due to Maintenance and Fault Conditions																		
Hulton Unit								3	8	7	11	10	9	17	7	10	12	8
Oakmont Unit								4	13	12	10	8	10	9	9	10	5	11
Verona Unit								3	10	4	2	6	4	6	4	3	3	5

1936 outages include flood outages.

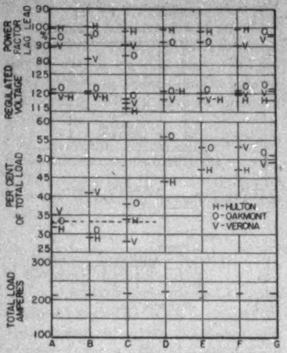

Figure 6. Effect of switching operations on load division, regulated voltage, and power factor of load current

A. Normal condition. All network mains closed
B. Main between Verona and Hulton open at Hulton
C. Main between Verona and Hulton open at Hulton, and regulators in neutral position at Verona
D. Main between Verona and Hulton open at Hulton and transformer circuit breaker open at Verona
E. All mains closed and transformer circuit breaker open at Verona
F. All mains closed and transformer circuit breaker open at Oakmont
G. All mains closed and transformer circuit breaker open at Hulton

tions. It appears that manual setting of regulators may be required to provide the distribution of load desired to prevent overloading some units, under conditions of a unit outage during peak load periods, where total load approaches total remaining load capability.

Network Performance: 1931-1948

Table I shows the outages to the network units and tie mains from all causes. The figures include both accidental or fault outages and planned or maintenance outages to the units. The outages to the tie mains are all caused by faults. The blank spaces indicate that no data were available for those periods.

During the 18 years of operation, there have been nine complete network outages. Three occurred during the following major system disturbances: generating-station bus failure, flood, and failure of a tie-line transformer on a circuit feeding this area radially during labor trouble in 1946. One network outage was caused by a fault on the 22-kv line which supplies Hulton. This line contacted a 4-kv circuit, with the result that Oakmont and Hulton bank circuit breakers opened due to current flow to the grounded neutral of the banks. The other five outages occurred when the four 22-kv transmission lines which energize the network were out of service simultaneously due to sequential faults and cross feed operations. During storms, lines became temporarily faulted, and because there was no automatic reclosing equipment at customer stations adjacent to Verona, a succession of these operations caused a complete outage. The installation of automatic reclosing at these adjacent stations, and various other improvements, reduced this type of operation to a point where it has occurred only once since 1936.

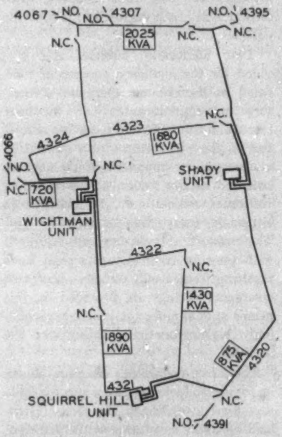

Figure 7. Squirrel Hill network: map showing network units, 4-kv mains, and connected loads

All of the faults on the distribution system have cleared without outage to other than the faulted circuit. There have been 30 faults causing circuit outages. Following 17 of these outages, the circuits were returned to service in two minutes or less.

There were two failures of station equipment at Verona, a potential transformer and a regulator, and a failure of the power transformer at Hulton, none of which caused any load to be dropped.

Analysis of the foregoing data indicates that there has been no load dropped as a result of inherent conditions of the network. The conditions causing total network outage would have resulted in distribution interruption if the circuits had been radial. As shown by the single-line diagram in Figure 2, the subtransmission circuits supplying the Verona-Oakmont network units all connect to the Verona bus. A network designed to have its transmission sources come from several transmission or switching stations, instead of all being connected to one bus, would be less subject to the condition of all circuits being deenergized at one time, although circulating currents may become a problem. Inverse reactive compensation normally corrects this tendency.

Flexibility in operation and ease of obtaining outages for maintenance and testing have been proved. Weekend outages and the planning of outages long in advance are unnecessary. While there are probably those who believe that well-planned switching procedures are acceptable at long intervals to clear station equipment without customer outages, as may be required with radial systems, most operating personnel will prefer equipment that can be removed from service almost at will, if it is otherwise economical.

The Squirrel Hill Network

This project provides overload relief for Schenley and East End substations and for 4-kv circuits originating at these substations. The area served is outlined in Figure 7, which also indicates the arrangement of 4-kv network mains, network-unit locations, and connected loads. The 22-kv transmission connections are

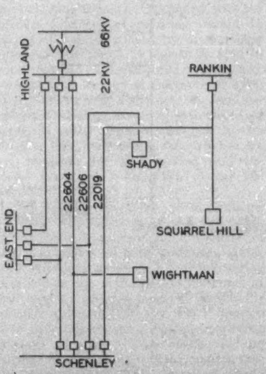

Figure 8. Squirrel Hill network: schematic diagram of 22-kv connections

shown in Figure 8; Figure 9 shows a typical network-unit diagram. The initial load being served is 7,500 kva in an area of three square miles, and the average load density is 2,500 kva per square mile. Service to this area was provided by one radial circuit from Schenley substation and two temporary 2,000-kva unit substations, which were installed to release a feeder from Schenley and another from East End substation.

The 4-kv network mains consist of overhead open-wire lines and underground cable lines. The overhead conductors are 1/0 and 4/0, and the cable sections are 350,000-circular-mil multiple-conductor cable.

For the 4-kv connections to network-unit circuit breakers, single conductor 500,000-circular-mil cable with oil-base rubber insulation, a neoprene jacket, and lead sheath will be used. This will avoid potheads in circuit-breaker cubicles where limited working space is available.

The unit-type network substation, illustrated on the location plan in Figure 10, includes a 3-position disconnecting switch for the 22-kv cable connections, a 3,750-kva transformer equipped with tap changing under load (*TCUL*), and inverse reactive compensation. The 4-kv transformer circuit breaker has network relaying for reverse current control and selective reclosing. The feeder circuit breakers connecting the network mains are relayed for overcurrent, timed reclosing, and bus differential protection, which also includes the transformer circuit breaker. The 4-kv automatic air circuit breakers are the truck-mounted withdrawal type, each enclosed in a separate cubicle.

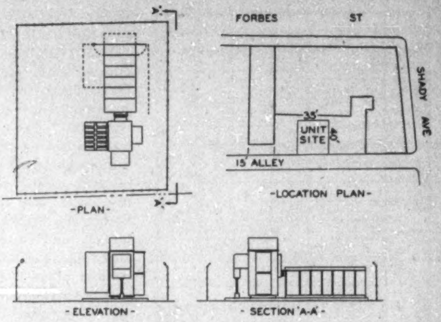

Figure 10. Squirrel Hill network: typical location plan of network-unit installation

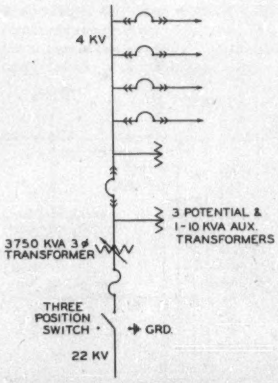

Figure 9. Squirrel Hill network: schematic diagram of a network unit

Two additional cubicles are provided for the auxiliary equipment indicated in the one-line diagram. Necessary metering includes one watthour meter and three thermal recording ammeters on the transformer; also three thermal recording ammeters which may be switched to any feeder, and a recording voltmeter which may be switched to either the transformer or the 4-kv bus. The network transformers are equipped with fans for cooling during peak loads resulting from a unit outage. Increased emergency ratings are provided by this means at minimum cost, with correspondingly higher functional ratings for the network.

The 22-kv connection diagram, shown in Figure 8, includes 22-kv subtransmission lines available in the area. Highland 66/22-kv substation is the principal source of supply for this area, with East End, Schenley and Rankin as switching stations which also serve as additional supply substations because of connections from other parts of the 66-kv system.

The Wightman, Shady, and Squirrel Hill network substations are supplied from 22-kv circuits *22,604*, *22,606*, and *22,019* respectively.

The 4-kv network diagram shows network tie mains, principal radial branches, and ties to adjacent radial circuits. These ties are part of the existing radial system and will be left in place to provide further overload relief, when required, and emergency service to portions of adjacent circuits in case of feeder faults or other emergency conditions. The connected light and power load in kilovolt-amperes is shown for each 4-kv network circuit.

New Features

The new features in the Squirrel Hill network as compared with the Verona–Oakmont network include the following items:

1. Larger and more economical size unit, that is, 3,750-kva instead of a 1,500-kva unit.
2. Regulation by means of tap changing under load in place of induction regulators. Inverse reactive compensation, however, is provided for both systems.
3. Air circuit breakers instead of oil circuit breakers for 4-kv switching.
4. Elimination of 4-kv potheads in circuit-breaker cubicles by using rubber insulated cable for connections to 4-kv circuits.
5. Factory-built unit-type equipment.
6. Alley locations for two out of three unit installations. The ground space at the third site is sufficient to accommodate the mobile-unit substation.

Advantages of Primary Networks

A comprehensive review of 4-kv radial and network systems shows the following advantages for the primary network:

1. Economical system investment is obtained by means of: single 22-kv connection per network substation; elimination of 22-kv automatic service restoration which is usually required with radial systems; the use of relatively large-size transformer units; bus regulation by means of automatic tap changing under load; the elimination of 4-kv feeders to circuit areas; and the use of factory-built unit-type equipment.

2. Reliable service is illustrated by means of an 18-year performance record of a primary network system.

3. Operating economy and convenience results from less prearranged switching for transfer of load during maintenance periods and reduced need for mobile substa-

tion unit. Two-way feed to all loads permits removal from service of any 4-kv circuit breaker or unit without interruption of service to customers. Faulted cable sections in tie mains can be isolated and service restored without extended interruption.

4. Improved voltage regulation and reduced flicker is inherent in the network system as a result of the 2-way feed to load and branches connected to the network mains.

Conditions Favoring Primary-Network Applications

While primary networks have not been used extensively on the Duquesne Light Company system, the advantages listed above warrant further consideration of this type of system for other areas. It is interesting to note, therefore, some of the conditions that favor the installation of such a system:

1. High rate of load growth.
2. Substantial overload relief requirements.
3. Areas of reasonably uniform load density with sufficient total load to warrant three or more network units. Scattered high-density areas with intervening parks, rivers, lakes, or undeveloped sections are not in general adaptable to network service.
4. Expanding urban areas that are in need of a flexible distribution system and a high degree of reliable service.
5. Areas supplied by comparatively long 4-kv feeders. When overload relief is required, a network installation can release such long feeders to serve load close to substations where feeders originate, and to share load of other feeders also in need of overload relief.

In areas where future primary networks are contemplated, the initial unit installation may be arranged for radial operation of 4-kv circuits. At such time that additional units are needed for further overload relief or voltage improvement, the primary network system can be established.

It should be noted, however, that certain radial systems, which are supplied by substation units that do not require duplicate transmission connections with automatic service-restoring features, may be lower in cost than network installations.

In urban areas, on the other hand, where it has been customary to provide radial service from 2-bank tie circuit-breaker substations, or 1-, 2-, and 3-bank automatic loop substations, as well as other similar types for a high degree of reliable service, the primary network will be preferable on a cost basis and also will provide important operating advantages.

References

1. The Primary Network, R. M. Stanley, C. T. Sinclair. *AIEE Transactions*, volume 50, number 3, September 1931, pages 871–84.

2. Year of Experience Solves Primary Network Problems, R. J. Salsbury, H. S. Moore. *Electrical World* (New York, N. Y.), volume 100, November 5, 1932, pages 624–6.

3. Primary Network Stations—Vault, Building, Outdoors, R. J. Salsbury, H. S. Moore. *Electrical World* (New York, N. Y.), volume 100, September 3, 1932, pages 304–7.

4. Short-Circuit Tests Prove Primary Network, R. J. Salsbury, H. S. Moore. *Electrical World* (New York, N. Y.), volume 100, December 24, 1932, pages 849, 851.

5. 4-Kv Network Saves 20 Per Cent, A. H. Sweetnam. *Electrical World* (New York, N. Y.), volume 97, March 14, 1931, pages 500–3.

6. Fundamentals of the Medium-Voltage Network, D. K. Blake. *General Electric Review* (Schenectady, N. Y.), volume 34, April 1931, pages 210–16.

7. Protecting a Medium-Voltage Network, John S. Parsons. *Electric Journal* (East Pittsburgh, Pa.), volume 28, September 1931, pages 520–5.

8. The Primary Network System, H. Richter. *Electric Journal* (East Pittsburgh, Pa.), volume 28, December 1931, pages 661–4.

9. Primary Network Economical for Medium-Load Densities, John S. Parsons, Leonard M. Olmsted. *Electrical World* (New York, N. Y.), volume 101, June 24, 1933, pages 835–8.

10. Theory of Primary Networks, Parts I and II, F. M. Starr. *Electrical Engineering*, volume 53, February 1934, pages 310–17, and March 1934, pages 426–31.

11. Primary Network Proves Advantageous in Boston, St. George T. Arnold. *Electrical World* (New York, N. Y.), volume 112, August 26, 1939, pages 590–92 and 648.

12. Simplified Primary Network Saves $110,-160 on Investment, F. W. Floyd. *Electric Light and Power* (Chicago, Ill.), volume 18, November 1940, pages 47–9.

Discussion

Leonard M. Olmsted (Duquesne Light Company, Pittsburgh, Pa.): Even though one primary network described in this paper has been in service approximately 18 years, the system must still be regarded as new when compared with other methods of distributing electric power. New methods usually have new problems, and it is my intention to discuss some of these new problems here. It is necessary to keep clearly in mind certain distinct differences between network and radial distribution. Whereas the load pickup on a radial system in case of transmission or substation trouble either is manually controlled and placed where it can be carried or picked up automatically on the original distribution feeder at the substation, the load on a network system is picked up instantaneously by redistribution among the remaining sources of power. This redistribution in the network may be totally different from the normal distribution of load, and is governed solely by the characteristics of the various components. This means that any tie circuit between network units may be required at any time to operate supplied from one end only with emergency loading 200 per cent or more of the normal load. Under such conditions, the safe rating of the entire system may well be limited not by the units themselves, or even by the normal ratings of the circuits, but by the emergency ratings of the tie circuits between the units. It is not likely that such an emergency condition will be detected in the field with the metering equipment usually provided, and it is essential, therefore, that it be predetermined either by staged field tests or by calculating board analyses.

Another consideration worthy of note is the effect of network operation upon the clearing of faults. On radial circuits it is becoming recognized that the circuit breakers cannot be expected to protect the smaller sizes of overhead wire. There has been continual compromise between the desire for increased sensitivity and extended reach of the protective equipment, and the requirements for adequate co-ordination with circuit fuses and other protective devices.

On networks, it becomes necessary to clear a fault at two circuit breakers, each with a setting substantially similar to those used on a radial circuit; the resulting level of protection may well cause an increase in the extent of damage caused by faults on the open wire plant.

It has been the practice to install cutouts on radial circuits with interrupting capacity suitable for the duty which can be encountered on the radial circuit. On primary networks, particularly those with larger units, the interrupting duty may be increased substantially, which may cause less satisfactory performance of the fused cutouts on the distribution transformers.

Several of the papers presented here have shown little or no primary circuit switching in or between network mains, or to adjacent radial circuits. It is our opinion that this switching should be eliminated, with the definite objective of reducing hazard to personnel and equipment by discouraging improper switching. It should be kept in mind that the load connected to a primary network may well be on the order of 5,000 to 10,000 kva and, if the network were de-energized, closing one set of switches to an energized radial circuit would pick up this block of load. Obviously the switches are not adequate for this service, and the result would be undesirable, to say the least.

The original literature about primary networks was based upon units generally of 1,500-kva capacity, and a number of networks with such units have been giving very satisfactory service. It is interesting to note that all of the papers presented at this meeting describe larger units, on the order of 3,000 to 4,000 kva, which appears to be a distinct change in the thinking about primary networks. This change in size appears desirable, and it is my opinion that the systems now being installed should render good service to distribution customers for a long time.

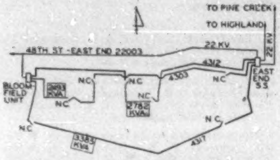
TO PINE CREEK
TO HIGHLAND
22 KV
48TH ST - EAST END 22003
22 KV
4312
4303
BLOOMFIELD UNIT
N.C
N.C
N.C
N.C
N.C
N.C
N.C
KVA
2782 KVA
3383 KVA
4317
EAST END S.S

Figure 1. Schematic diagram of Bloomfield network

D. E. Nesbit (Duquesne Light Company, Pittsburgh, Pa.): As a result of the successful use of the 4-kv primary network type of distribution system in the Pittsburgh area, it is proposed to install a modified type of primary network application on the Duquesne Light Company system which will provide operating experience in the field of special network applications.

It is the purpose of this discussion to describe briefly the Bloomfield network which is a special network application using one 3,750-kva unit of a future 3-unit network system operated temporarily in conjunction with radial circuits from an existing substation.

This project has been authorized to provide overload relief for the Lawrence and East End Substations and 4-kv circuits originating at these substations. The initial network load to be served is 6,000 kva in an area of two square miles and the average load density is 3,000 kva per square mile. Service to this area is now provided by three radial circuits from East End Substation, and partially by a radial circuit from Lawrence Substation.

Some of the conditions which favor the installation of this special application of a primary network are:

1. A single-tap 22-kv supply will be used, thus eliminating 22-kv switching normally required for a loop connection to a radial substation, and resulting in lower first cost and minimum retirement when the customary network is established.
2. The area is one of reasonably uniform load density with a high rate of load growth sufficient to warrant the future installation of one or more additional units.
3. Operating experience will be provided with a special type of network that can be used as an intermediate step in other locations, if found satisfactory.

Figures 1 and 2 of the discussion show 22-kv transmission connections, arrangement of the 4-kv network mains, network unit location, and connected loads of the proposed network. The network area is to be served from one 3,750-kva 22/4-kv unit substation (Bloomfield) and three 4-kv circuits from East End Substation. Nine remaining 4-kv circuits from East End Substation, which serve adjacent areas, will continue to be served from that location.

The 4-kv network mains consist of overhead 1/0 and 4/0 open wire lines and 350,000-circular-mil multiple conductor underground cable lines. For the 4-kv connections to the network unit circuit breakers, single-conductor 500,000-circular-mil cables with oil base rubber insulation, neoprene jacket, and lead sheath will be used to avoid potheads in circuit breaker cubicles.

The 3,750-kva unit type network substation at Bloomfield is similar to and includes the equipment listed in the discussion of the Squirrel Hill primary network. Tap changing underload facilities with inverse reactive compensation will supply the regulation requirements for the network unit at Bloomfield while at East End Substation, three existing single-phase induction regulators reconnected for inverse reactive compensation for each network feeder will be used for this purpose. It is planned to operate the single-phase induction regulators independently of common phase control pending operational experience.

The installation of the 3,750-kva unit at Bloomfield has been completed. Cut-in for network operation is expected to follow within two months. After the load on the Bloomfield network passes 7,500 kva, a review of operating experience, rate of load growth, general area requirements, together with service reliability required for the network area will determine the best time for the installation of the second network unit.

There will be a temporary deficiency in the emergency rating of the network with a unit out of service. Manual transfer switching may be required under some conditions. After the installation of the second unit, the deficiency in automatic load capability will be corrected.

G. N. Hoffman (Duquesne Light Company, Pittsburgh, Pa.): The purpose of the board study of the Squirrel Hill Network was to determine the loads and voltages on the substations and tie circuits under normal, abnormal, and future load conditions. The network consists of three 3,750-kva 22/4-kv unit substations interconnected with five

Table I. Squirrel Hill Network Substations and 4-Kv Circuit Loads

Present 4-Kv load of 7,500 Kva and 22-Kv load of 46,700 Kva

	Shady	Squirrel Hill	Wightman	Total Kva
All Units in Service				
Transformer	2,530	2,320	2,740	7,590
Circuit 4320	225	1,020		
Circuit 4321		350	1,565	
Circuit 4322		950	220	
Circuit 4323	1,130		320	
Circuit 4324	1,180		580	
Shady Unit Out of Service				
Transformer	0	3,670	3,950	7,620
Circuit 4320	(1,230)*	2,480		
Circuit 4321		290	1,650	
Circuit 4322		910	360	
Circuit 4323	445		1,020	
Circuit 4324	815		1,000	
Squirrel Hill Unit Out of Service				
Transformer	3,780	0	3,980	7,760
Circuit 4320	1,440	(125)		
Circuit 4321		(340)	2,280	
Circuit 4322		450	725	
Circuit 4323	1,140		310	
Circuit 4324	1,180		625	
Wightman Unit Out of Service				
Transformer	3,900	3,500	0	7,400
Circuit 4320	390	905		
Circuit 4321		1,269	640	
Circuit 4322		1,630	(450)	
Circuit 4323	1,940		(460)	
Circuit 4324	1,550		270	

* Loads shown in parentheses are into the station bus. All loads are kilovolt-amperes.

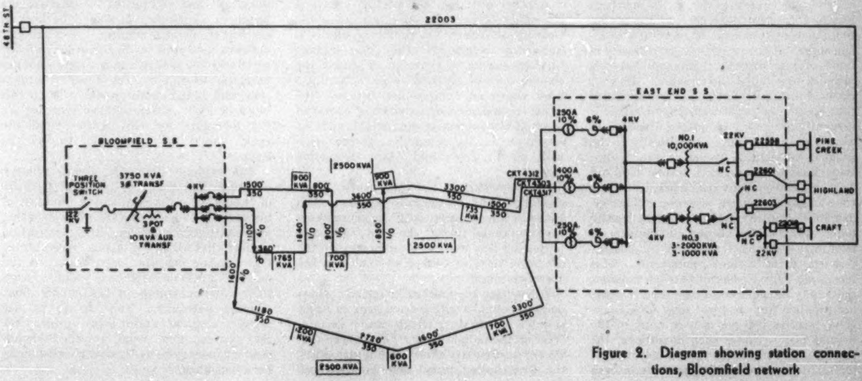
48TH ST
22003
BLOOMFIELD S S
THREE POSITION SWITCH
22 KV
3750 KVA 3Ø TRANSF
3 POT & 10 KVA AUX TRANSF
4 KV
1500' 350
900 KVA
800' 350
2500 KVA
900 KVA
3600' 350
3300' 350
735 KVA
1500' 350
1100' 4/0
380' 1/0
1765 KVA
1840' 1/0
800' 1/0
700 KVA
850' 1/0
2500 KVA
1600' 4/0
1180 350
1200 KVA
2720' 350
600 KVA
2500 KVA
1600' 350
700 KVA
3300' 350
CKT 4312
CKT 4303
CKT 4317
EAST END S S
250A 10%
6%
4 KV
400A 10%
6%
250A 10%
6%
NO.1 10,000 KVA
N C
22 KV
22208
PINE CREEK
22601
HIGHLAND
N C
22603
4 KV
NO.3 3-2000 KVA 3-1000 KVA
N C
N C
22209
CRAFT
22 KV

Figure 2. Diagram showing station connections, Bloomfield network

Table II. Squirrel Hill Network Substations and 4-Kv Circuit Loads

Ultimate 4-Kv Load of 12,500 Kva (167 per cent of Present Load) and 22-Kv Load of 51,500 Kva (110 per cent of Present Load)

	Shady	Squirrel Hill	Wightman	Total Kva
All Units in Service				
Transformer	4,380	4,200	4,350	12,930
Circuit 4320	410	690		
Circuit 4321		1,740	1,160	
Circuit 4322		1,770	1,720	
Circuit 4323	1,940		460	
Circuit 4324	1,980		1,050	
Shady Unit Out of Service				
Transformer	0	6,300	6,700	13,000
Circuit 4320	(1,920)	3,200		
Circuit 4321		1,510	1,380	
Circuit 4322		1,600	1,870	
Circuit 4323	640		1,760	
Circuit 4324	1,320		1,730	
Squirrel Hill Unit Out of Service				
Transformer	6,100	0	6,700	12,800
Circuit 4320	2,400	(1,210)		
Circuit 4321		490	2,430	
Circuit 4322		730	2,610	
Circuit 4323	1,830		545	
Circuit 4324	1,910		1,140	
Wightman Unit Out of Service				
Transformer	6,420	6,500	0	12,920
Circuit 4320	710	520	(290)	
Circuit 4321		3,200	610	
Circuit 4322		2,820	(750)	
Circuit 4323	3,160		460	
Circuit 4324	2,410			

tie circuits. The 22-kv circuits feeding the substations and their loads were set up on the a-c calculating board in addition to the 4-kv network tie circuits and loads. Readings were taken with all substations in service and with each substation out of service for present loads and for the maximum load capability of the network. The effect of inverse reactance was simulated by maintaining the same 4-kv bus voltage at the network substations. The ultimate load capability of the network and the elimination of two bottlenecks in the circuit design were the results obtained from the board study.

The present network load is approximately 7,500 kva distributed on the five tie circuits. The board readings showed this load to be well within the ratings of the substations and tie circuits with all substations in service and with any one substation out of service. The results are shown in Table I of the discussion.

In order to ascertain the ultimate load capability of the network for the present circuit and substation ratings, the 4-kv loads were increased 80 per cent and the 22-kv loads 10 per cent. The previous tests were repeated with the increased loads and in several instances the data showed substation and circuit loads in excess of emergency ratings. The test showing the maximum substation load having been set up again on the board, all 4-kv loads were reduced proportionately until the load was within the rating of the substation. This showed the load capability to be approximately 167 per cent of the initial 7,500 kva load, or approximately 12,500 kva.

Examination of the data showed cable loads exceeded cable ratings at two locations when the network was carrying 12,500 kva. Circuit 4321, Figure 7 of the paper, was carrying 3,700 kva at Wightman Substation when Squirrel Hill Substation was out of service, and circuit 4320 was carrying 4,200 kva at Squirrel Hill Substation when Shady Substation was out of service.

The loads of these two circuits were brought within their ratings by making two changes in the network circuit design. A load of 1,200 kva (167 per cent of 720 kva, west of Wightman Substation) was connected to 4322 instead of 4321, (see Figure 7) whose maximum load at Wightman Substation from all tests was 1,400 kva. This change did not require any additional material or expense, as both circuits were available for this load. In addition, 1,000 kva (167 per cent of 600 kva) was transferred from circuit 4320 to circuit 4321 whose maximum load at Squirrel Hill Substation was 2070 kva. This change involved the installation of a small amount of number 1/0 wire.

The substation and circuit loadings after these changes are shown in Table II of the discussion.

W. P. Holben: The discussion on the results of the calculating board study of the Squirrel Hill Network by G. N. Hoffman is an important and helpful contribution to the subject of Primary Networks. His brief review of the procedure, the statement of the technical problems relating to voltage and division of load for various operating conditions, the tabulated summary of results, and the adjustments in the design of the network as a result of the board analysis provide specific information on an interesting phase of the engineering work associated with primary networks. This discussion demonstrates that adequate design can be assured by the calculating board method. In fact, network design cannot be completed reliably without such an analysis.

The outline of the principal features of the Bloomfield 4,000-volt network in the discussion by D. E. Nesbit provides information that was not available when the paper was prepared. This type, which utilizes a 3,750-kva 3-circuit unit networked with three radial circuits from the existing East End Substation, was suggested by R. J. Salsbury of the Duquesne Light Company.

After a review of the Philadelphia Electric Company experience and an engineering analysis of the Bloomfield area facilities, existing loads, and operating requirements, this installation was recommended and authorized on an experimental basis. Preliminary calculations and the a-c board study indicated the need for three tie mains of approximately the same impedance, in order to avoid circuit overloading with the Bloomfield unit out of service during peak load periods. Minor circuit rearrangements provided these circuit characteristics, and proper allocation of connected load is expected to produce satisfactory operating results.

The problems relating to primary networks as outlined in the discussion by L. M. Olmsted are important considerations for the network design engineer. The problems are not new since most of them also relate to radial systems although possibly to a different degree. The reference to calculating board studies in the previous paragraphs indicates necessary consideration for emergency loading with a unit out of service. An open circuit breaker at one end of a tie main imposes the load of that main on the other end of the circuit. If the load on each tie main is kept within the emergency rating of the conductors at both ends there is no overload problem resulting from an open circuit breaker. The network load capability can be definitely established by means of proper design and the usual check by the calculating board method.

The co-ordinated relay settings for the Verona-Oakmont network have produced excellent operating results. Equally satisfactory experience is anticipated for the Squirrel Hill network. Trees and storms have produced some wire burn-downs. These were usually found on number 6 or number 3 conductors of radial branches from tie mains. The operating men have expressed the opinion that this type of fault is just as frequent on radial circuits. However remedies have been proposed and may be applied whenever the cost can be justified.

The fuse cutouts in use on radial circuits, which have since been converted to form the network, have been left in service. The interrupting duty imposed in most locations is similar to that of heavy duty radial circuits that extend only short distances from large substations. The favorable experience in these cases justifies the continued use of existing cutouts on the network until replacements are made as part of a general betterment program.

The discussion at the Swampscott meeting of sectionalizing and tie switching on primary networks indicated a divided opinion among engineers and operators relative to the hazards of operational errors. It is believed however that ties between network mains are unnecessary, and if left closed inadvertently will mean loss of relay protection. Sectionalizing facilities in the mains should be kept to a minimum in order to avoid maintenance of switches that are rarely used, especially if emergency sectionalizing can be accomplished by other satisfactory methods. The primary network does not require the support of emergency ties to adjacent radial circuits. In some cases such adjacent radial circuits however will be without adequate emergency ties, if the switching is removed. It therefore becomes a matter of weighing the risk of improper operation during an emergency as compared with the disadvantages of inadequate tie facilities, or the additional expense of establishing new ties with other radial circuits. Operating experience and success in providing satisfactory switching procedures will indicate the best choice in most cases.

It is recognized that the primary network has a few limitations and that it may be difficult to justify economically in certain locations. Unit substations to supply radial circuits can be used successfully and economically in many locations. Some of these will probably become a part of a primary network system at a later date. The primary network, however, offers outstanding advantages as outlined in the paper, and favorable operating experience will encourage use of the primary network more extensively in the future.

Design and Experience With 4-Kv Primary Network Systems in the Washington Area

W. J. LANK
FELLOW AIEE

IN THE territory served by the Potomac Electric Power Company, a large part of the area formerly served by k4-v radial stations has been converted to a primary network. This development has been in progress since 1939. Under the particular conditions encountered, it has proved to give better reliability, less congestion on poles or in conduit lines, and more flexible operation than the radial system. Although this paper does not give details of the comparison of cost, the primary network system originally was adopted to reduce the additional investment required for increased loads, and all subsequent extensions have been justified on this basis.

Description of the Types of Distribution Used

The territory served by the Potomac Electric Power Company and its subsidiary, the Braddock Light and Power Company, Incorporated, includes the Washington, D. C., metropolitan area and covers 631 square miles. The maximum 1-hour integrated demand is 449,000 kw. Approximately 91 square miles, having a peak load in 1948 of 139,000 kva, is fed by 4-kv radial feeders and stations. Average load density for this area is 1,530 kva per square mile, and the majority of the distribution is underground. An area of 512 square miles, having a peak load of 120,000 kva, or a load density of 234 kva per square mile, is fed by 4-kv primary network. The greater part of the distribution is overhead; load is uniformly distributed. The 4-kv radial stations, serving both the underground and overhead system, were established twenty to twenty-five years ago and have not been permitted to expand for the last ten years. These radial stations are located in the older urban areas that are fairly well built up, where residential and small commercial load is growing at not more than 5 per cent per year. The network area is in the outlying urban, suburban, and rural areas, where bulk of new housing is being built and where the load is growing at the rate of 25 per cent per year. Customers of 300 kva and over usually are supplied directly from 13.8-kv lines.

Development of the Primary Network System

In 1938 it was realized that a large new 4-kv substation, to provide for increased load in an overhead area remote from existing stations, or equivalent facilities, would be needed. The standards of service for the particular area would require the following:

1. Sufficient 13.8-kv feeder emergency capacity to carry the peak load with any one feeder out of service
2. Sufficient substation-transformer emergency capacity to carry the peak load with one transformer out of service
3. Provision for field switching to transfer the load on any 4-kv feeder to another feeder in case of failure between the substation and the feeding point

Studies were made of a primary network system of three stations as an alternate. Cost of this system was estimated to be 66 per cent of that for a 4-kv radial system to supply the same load. A visit by company engineers to Philadelphia, Boston, Pittsfield, and Pittsburgh utilities, early in 1939, furnished valuable information on operation and performance of primary network systems. Decision was made in favor of the network. Figure 1 shows this network as it exists in 1948. Kearney, Bunker Hill, and Dakota stations were installed initially; Ivy was added in 1946. These stations are spaced about $1^1/_2$ miles apart.

The same problem existed in the outlying areas, but the cost of feeder circuit breakers, necessary for a primary network, was considered excessive for the kilovolt-amperes per feeder. To reduce this cost, 3-shot reclosing fuses were substituted.

In an older section of the city, it was necessary to abandon a large 4-kv radial station, serving an underground area, because the land was condemned for a proposed government building. Studies showed the most economical replacement

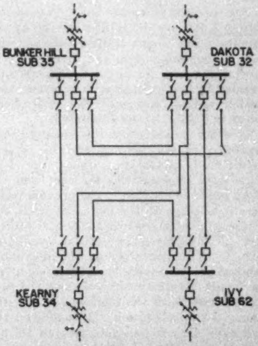

Figure 1. One-line diagram of primary network system supply, Brookland area

---

Paper 49-180, recommended by the AIEE Transmission and Distribution Committee and approved by the AIEE Technical Program Committee for presentation at the AIEE Summer General Meeting, Swampscott, Mass., June 20–24, 1949. Manuscript submitted November 17, 1948; made available for printing May 3, 1949.

W. J. LANK is with the Potomac Electric Power Company, Washington, D. C.

Figure 2. Building for Kearney primary network station

to be an underground 4-kv primary network. This system was installed in 1941.

As the load on any one of the 4-kv radial stations grows to such an extent that the load approaches the maximum permissible for the transformers or feeders, either the low-voltage network is extended from the downtown area, or the primary network is extended from the outlying areas to prevent replacements or additions to the 4-kv radial stations. By this policy, the service in both areas is improved by cutting back the length of the radial feeders to a smaller area, as well as rendering an improved service in the area that is cut over to the secondary-network or primary-network stations. Since the load almost invariably grows at the most rapid rate at the extremities of the areas fed from a given radial station, it usually follows that a small network station located at the point of load growth is also the most economical solution.

Primary Network Design

Consideration of service interruptions and voltage has resulted in the adoption of a maximum of 4,500 kva miles per feeder under normal conditions. In the outlying area, stations are spaced about five miles apart and located at strategic road intersections. Using the limit of 4,500 kva miles, this permits a distributed load of 900 kva per feeder. The average station will have four feeders, each having another terminal in some other station, and approximately 1/2 of each feeder's load will be carried by each station. Therefore, the normal station peak load will be $4\times(900/2)=1{,}800$ kva. In case of the loss of high-voltage supply to one station, the load of each 4-kv feeder into this station is carried from the opposite end. Therefore, the station emergency loading would be 2,250 or 2,700 kva, depending upon whether one or two feeders actually supported the station which has been lost. Studies of load factors have shown that transformers will safely carry 50 per cent in excess of their self-cooled nameplate rating in emergencies, under winter ambient conditions, without undue loss of life. Stations of the type described usually have 2,000-kva transformers. Admittedly the above is not an exact analysis since, with the loss of high-voltage supply, some energy is transferred from one 4-kv feeder to another through the station bus. In actual planning, this fact is taken into consideration.

In suburban areas, the stations are located about three miles apart, and the feeders are loaded to 1,500 kva. This gives a normal station loading of 3,000 kva and an emergency loading of 3,750 or 4,500 kva under the conditions outlined. All new transformers purchased are 3,000-kva self-cooled and 3,900 kva with forced-air cooling. Maximum emergency loading of 5,400 kva is permitted.

Maximum 4-kv feeder loading is limited to 1,800 kva. In urban areas, the stations are placed correspondingly closer, in some cases about one mile apart, to keep within this limit and to provide sufficient station capacity for the load density.

Use of Capacitors

The 4,500 kva miles of distributed load, with 1/0 overhead line, gives approximately 2.5 per cent primary drop between the first customer and the lowest voltage point on the feeder. This is the maximum permissible normal drop on the primary to stay within the limits of customer voltage tolerated upon this system. Under emergency conditions with one end open, or for loss of one station, a maximum drop of 11 per cent is permitted.

By the use of fixed capacitors in the center of the tie, the kva miles can be raised 50 per cent without exceeding the above limitations, or the maximum permissible voltage of 102.5 per cent at the center of the line off peak. Where the load is concentrated near one end, the emergency voltage at peak time with this end open may limit the load upon the feeder. In this case, the permissible load may be increased 80 per cent by the use of capacitors located near this end. Such installations have been used extensively on this system. Fixed capacitors also are used at the extremities of long single-phase taps off network ties, to improve voltages and to reduce the man-hours and copper required for load growth, or to avoid installation of more expensive regulators. Banks of fixed and switched capacitors are installed in some outlying substations to assist the regulators in maintaining normal voltage, and to maintain the voltage at not less than 89 per cent of normal upon the loss of the 13.8-kv supply.

Indoor-Type Primary-Network Station

Figures 2 and 3 show typical station-building designs for the urban and suburban areas where zoning laws require an indoor type of station. These stations purposely are made to resemble the typical $1^1/_2$-story residence. In the Washington area, it usually is necessary to acquire residential property for the strategic location of substations. The limited industrial and commercial property is so expensive that it generally is more economical to acquire residential property and install the necessary building. In this type of installation, appearance and quietness of operation are emphasized. It has been found this policy pays dividends in public relations, which are so necessary when application is made for nonconforming use for a proposed substation site. The photographs show the typical pole-line construction adjacent to the station. In this case, the cable is routed from several terminal poles to the station as unobtrusively as possible, so as to avoid a nest of poles or equipment.

Building Plan and Equipment Layout

The building is 23 by 37 feet in plan and contains the standard 3,000/3,900-kva network-type regulating transformer. In a number of locations, older 1,000- and 2,000-kva transformers banked, together with three 50-kva induction regulators connected for plus or minus 5 per cent range, are used to obtain a normal rating of 3,000 kva or an emergency rating of 4,500 kva. Switching consists of a 100,000-kva truck-type circuit breaker

Figure 3. Building for Blair primary network station

mounted in a structural iron and Transite compartment, together with disconnects, current and potential transformers. The transformer is separated from the room containing the switchgear by a fire barrier wall. The chimney on the house is a ventilating duct for exhaust of hot air. Louvers provide air intake.

Figure 4 shows a typical schematic control diagram. The transformer secondary will trip on instantaneous reverse current or over-or-under voltage on a potential transformer connected from one phase to ground on the high-voltage side. This later protection is necessary because the high-tension feeder is grounded only at the source end, and the line might remain energized from the delta side of the substation transformer on a single phase-to-ground fault. In case the transformer clears by overcurrent, indicating a fault which cannot be cleared by the feeder circuit breakers, all circuit breakers are tripped and locked open. The transformer circuit-breaker reclosing is initiated either by a network-type or by a phase-rotation and voltage-checking relay. Negative reactance compensation is used for control of voltage at all network stations.

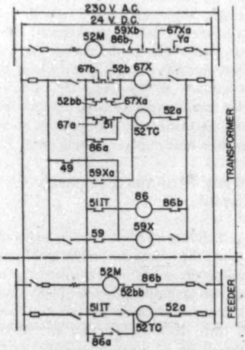

Figure 4. Schematic diagram of typical primary network station showing relay protection and automatic reclosing of transformers and a typical feeder

49	Thermal relays incorporated in the transformer
51	Instantaneous overcurrent relay
51 IT	Very-inverse-time overcurrent relays
52 M	Motor-operated mechanism. Later stations use rectifier and solenoid for closing
52 TC	Circuit breaker trip coil
52 bb	Auxiliary switch closed until circuit breaker latches
59	Over and undervoltage relay operated from one line-to-ground high-voltage potential transformer
59 X	Auxiliary relay for voltage relay
67 X	Auxiliary relay for closing
86	Auxiliary lockout relay to trip all circuits
Y a	Interlock with high-voltage switch

Figure 5. Outdoor primary network station with reclosing fuses

Outdoor Type of Station

Figure 5 shows a typical outdoor network station of the type usually located in the outlying areas. Wherever zoning permits, the outdoor design is employed, consisting of the 2,000-kva transformer, induction regulator, and an automatic oil circuit breaker for transformer secondary located in cubicles. The 13.8-kv side of the transformer is protected by primary fuses. The 4-kv feeder protection consists of 100- or 200-ampere reclosing fuses. These are mounted, as part of the station, on a steel structure, but with wood cross arms to prevent flashover to ground. Each feeder position occupies 10 feet of space, so that a structure 20 by 10 feet may contain five feeders. Fuses may be replaced from the ground to avoid climbing of poles. A gunpowder-type link is used to obtain effective clearing on light faults.

Experience with the reclosing fuse for this type of primary-network service is satisfactory. The advantages of using the reclosing fuse are the low first cost and the fact that a fuse will blow only on the particular phase affected and can always be depended to blow to clear the fault. The reclosing fuse may at times fail to reclose, but this has never caused an interruption to the network service since the fuse at the other end reclosed if the fault was temporary or all three fuses were blown for a permanent fault. These fuses, in a 200-ampere holder, are rated 4,000 amperes interrupting capacity, which is sufficient for a 2,000-kva transformer station. In one station where the transformer capacity is 4,000 kva, a heavy-duty borax reclosing fuse, rated 12,000-ampere interrupting capacity, has been used with equally good results.

Disadvantages of Large Radial Stations

Figure 6 shows typical pole-line congestion which may exist in the vicinity of large radial substations. This condition results when there are only one or two clear routes from a given station and lines cannot be rerouted because there are no through streets or the streets are blocked by trees. Such congestion causes difficulty in maintaining safe working conditions, unsightliness, and a reduced security of supply to the customer. For example, a pole knocked down, lightning, or a tree falling on the wires results in a serious outage to a large area. Requests are made by civic organizations for such lines to be placed underground, and, in some cases, this has been necessary. The cost of such underground construction is difficult to support, since there is no corresponding increase in revenue.

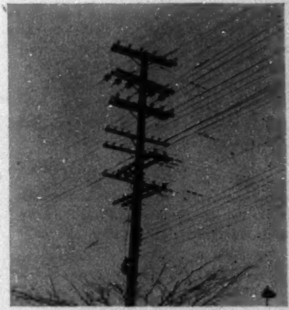

Figure 6. Congested pole line near a large 4-kv radial station

Studies of this situation have shown that, in some cases, it is more economical to break up larger radial stations into three or four network stations spaced at strategic centers and thereby avoid the more expensive underground construction Figure 7 shows the resulting pole line.

During the past year, because of certain highway improvements, there was considerable demand for underground construction through an entire community. By relocating a portion of the older radial station into a new network station and by

Figure 7. Typical pole line of a primary network system

Note the cable riser

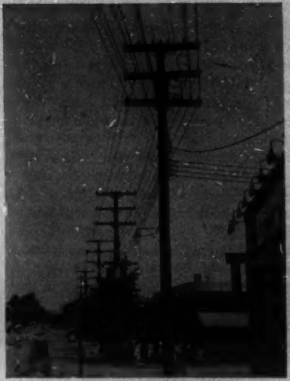

Figure 8. The main street of Silver Spring before rearrangement

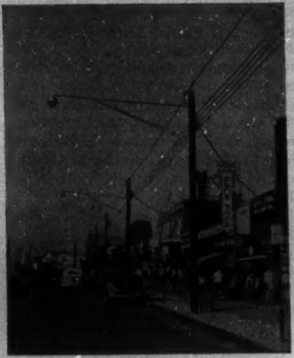

Figure 9. Improvement in the main street of Silver Spring as a result of distribution rearrangement

partial conversion to underground, partial disposal of lines and retaining poles for street lights, traffic signals, overhead secondary mains and services, it was possible to accomplish the desired improvement for $250,000. Complete underground construction would have cost $500,000. Figures 8 and 9 show this area before and after the changes.

Existing large radial stations contain from 30 to 60 feeder regulators which are a potential fire hazard. Several cases of major service interruptions experienced by other companies show this hazard must be given consideration. In a new station supplying an underground area, this hazard can be eliminated by using tap changing under load transformers, with some sacrifice in control of customer voltages. In any event, large concentrations of power give more opportunity for the spread of trouble to cause a major interruption to a large area.

In all of the large radial stations, it is necessary to operate with only one 4,000-kva transformer per bus section and with bus ties open. This type of operation is necessary to reduce the circuit breaker interrupting duty and voltage-regulator short-circuit current duty to approximately 8,000 amperes. Even this reduction is beyond the 5,000-ampere rating of a 50-kva regulator connected for 10 per cent voltage boost.

Sometimes difficulty is experienced in balancing loads between transformers. Short-time interruptions have occurred as a result of tripping transformer circuit breakers either because of trouble or accidentally.

Operating Experience—Stations

On April 17, 1948, a cable connection to a bus selector disconnect failed in one of our older radial stations. The resultant fire, smoke, and copper dust caused a flashover on insulators of both bus connections. Transformer circuit breakers supplying both busses tripped automatically, interrupting 4-kv radial service to the entire Chevy Chase, Md., area for several hours. It was necessary to await clearance of the smoke, determine the extent of the damage, and make emergency repairs before restoring the busses and radial feeders to service.

A network type of station had been built to relieve this radial station and four ties were established to one bus in this station. When the transformer circuit breaker tripped, it automatically opened and locked out the network-tie circuit breakers at this end, thereby permitting the entire network feeder load to be supplied from the other station. All of the radial feeder load was dropped when the radial bus was de-energized. This type of fault is rare, but when it does occur a considerable area is affected.

On September 7, 1948, a primary network cable failed in the Southeast–Southwest underground area. The circuit breaker connected to this cable at the near station failed to open after reclosing, due to a defective mechanism. This caused melting of contacts and subsequent arcover of the circuit breaker. The resulting fault was cleared by the transformer overcurrent relays, which tripped and locked all operable circuit breakers at this

Table I. Comparison of Operating Performance

4-Kv Radial Versus Network Feeders

Location	Years	Miles	Number of Tripouts	Number of Interruptions	Per Mile-Year Tripouts	Per Mile-Year Interruptions
OVERHEAD AREA						
Radial: Tenleytown	1.	11.6	13	3	1.1	0.26
Network: Tenleytown–Wesley	1.0	8.9	5	3	0.56	0.34
Radial: Brightwood–Brooklyn	3.0	29.4	75	30	0.85	0.34
Network: Brooklyn	3.0	12.4	11	7	0.29	0.19
Radial: Riverdale	3.0	25.7	95	41	1.23	0.53
Network: Riverdale–Sunnyside	3.0	15.8	0	2	0	0.04
Radial: Anacostia	3.0	4.7	9	0	0.64	0
Network: Anacostia–Hillcrest	3.0	10.6	13	4	0.40	0.13
Average: Radial Overhead	3.0	71.4	218	80	1.02	0.37
Average: Network Overhead	3.0	47.6	39	22	0.27	0.15
Advantage Factor Favoring Overhead Network					3.8	2.4
UNDERGROUND AREA						
Radial: Eastern	3.0	18.6	12	31	0.21	0.55
Network: Southeast–Southwest	3.0	23.2	11	6	0.16	0.09
Advantage Factor Favoring Underground Network					1.3	6.1

station. The circuit breaker connected to the opposite end of the faulty cable at the other station cleared properly. Aside from the feeder in trouble, no other service was affected, since the other network feeders continued to carry their load. In this case, a sectionalizing circuit breaker was opened in the manhole, and, except for one or two transformer banks, service was promptly restored to the balance of this faulted feeder.

It is quite evident from the two cases cited, as well as others, that the network-type station has a decided advantage over the radial type, since an entire network station may be lost without affecting service.

Operating Experience—Feeders

It is difficult to make an exact comparison of service reliability between the primary network system and the radial-type system, since the primary network is located in the outlying area that has more exposure to lightning, high-speed traffic, tree conditions, and so forth. To reduce the effect of these variables, several different radial areas have been compared with primary-network areas of similar characteristics. Results are given in Table I. This summary averages 71 miles of radial feeders against 47 miles of network feeders for the past three years. This comparison tends to favor the radial type of system, since there is usually more mileage of radial feeder exposure to cover a given area than would be required if converted to the network. The table shows that momentary faults per mile of overhead radial system for a three year period averaged 1.02 and, for network system, averaged 0.27—an advantage factor of 3.8 favoring the network. Permanent faults on the radial system averaged 0.37 per mile and the network, 0.15, or an advantage factor favoring the network type of 2.4. It is interesting to note that, in the underground system, the primary network has an advantage factor of 6.1. This improvement is probably due to use of newer single-conductor paper-leaded cable, lighter normal loading of the network cable, and less heating, due to the absence of congestion of cables in underground conduit system.

It is reasonable to expect some improvement in service for the overhead type of primary network, as compared to the radial system. The reduced congestion, already explained, results in wider spacing of wires, reducing outages due to tree limbs and wires whipping together. The elimination of parallel mains and reduced spacing between stations decreases the total wire miles. There are a minimum of supply or distribution circuits on the same pole line.

Summary

The 10 years of experience with the primary network upon the Potomac Electric Power Company system serving the metropolitan area of Washington, D. C., have resulted in the following conclusions:

1. A primary network system can be installed at a lower cost than new large radial 4-kv stations where load distribution is uniform and reserve facilities against loss of equipment would be supplied for the radial system.
2. Construction to supply new loads is simpler and more flexible with the primary network system, since it tends to avoid overhead wire congestion and the need for underground construction.
3. Operating reliability is improved.
4. Voltage regulation is improved.

Since the start of the war period, the primary network system has grown from 25,000 to 106,000 kva. It was able to pick up large loads with only small increments of new materials during this period, and expected investment economies have been realized.

Discussion

V. A. Rydbeck (General Electric Company, Schenectady, N. Y.): The author's experience with the primary network system confirms our thoughts on its flexibility, reliability, and economics. Its comparative operating performance is particularly impressive.

With reference to his adoption of a maximum of 4,500 kva miles per feeder, this should be a helpful practice in planning the number and location of substations. With a given conductor size, system power factor, and load arrangement, voltage drop is in direct proportion to the product of load times distance. For a given voltage drop, the feeder length can be increased as load is decreased and conversely. A 2.5 per cent primary drop between the first customer and the lowest voltage point on the tie feeder agrees with our thinking of good design practice for providing satisfactory voltage.

The application of shunt capacitors to primary networks, so far as is known, has not been widely practiced. When these capacitors are connected at the mid-point of the respective tie feeders, then a maximum amount of normal voltage improvement is achieved. The 50 per cent improvement in voltage brought about by these capacitors means that primary networks may prove practical in areas of light load density or that existing networks which have excessive voltage drop may be improved at moderate cost.

A capacitor bank connected at the midpoint of a network tie feeder would normally draw one-half of its leading current from each end of the tie feeder. In time of emergency with the transformer at one end of the tie feeder out of service, the leading current of the capacitor would all be supplied from the end in service and hence the voltage improvement effected by the capacitor is doubled. The ability of the capacitor to improve voltage during times of emergency should prove helpful in many cases as a means of deferring additional system investment to take care of emergency conditions.

G. B. Dodds and **R. S. Smithley** (Duquesne Light Company, Pittsburgh, Pa): In Table I of the paper is given a comparison of operating performance of several 4-kv radial areas versus primary network areas. There are several points in connection with the table that are not clear.

1. In the paragraph dealing with operating experience it states that the momentary faults per mile of overhead radial system for a 3-year period averaged 1.02 and for the network system averaged 0.27 which the author claimed is an advantage factor of 3.8 favoring the network. It is not clear that the figures indicate an advantage in favor of the network since it is usually assumed that the greater the percentage of temporary faults, the better the continuity of service provided. On this basis it would appear that the radial system had 1.02/1.39 or 73.37 per cent temporary faults while the network system had 0.27/0.42 or 64.37 per cent temporary faults. This is an advantage factor of 73.3/64.3 or 1.14 in favor of the radial system.

It may be that our understanding of the figures on the table are not correct and if this is so we would appreciate further explanation of the figures.

2. It would be of interest to know whether the columns dealing with number of interruptions (which we interpret as permanent faults) in Table I apply only to faults causing circuit breaker tripouts or whether partial circuit interruptions also are included.

It also would be of interest to have a comparison for the two systems, of the current pick-up of relays on the circuits, the time setting of the relays, as well as information concerning size of conductors, whether bare or covered, and so forth.

It was mentioned in a recent paper by Bryce Brady[1] that somewhat better service continuity might be expected on radial circuits which have co-ordinated sectionalizing fuses, reclosers, and circuit breakers than on primary networks where this coordination does not seem possible. The discussers agree with this feeling.

The discussers recently made studies of the time required to clear faults on primary network feeders as compared to times for radial feeders in which the radial feeders were equipped with instantaneous relays for the first tripout, these instantaneous relays being cutout on recloser. The use of instantaneous low set relays on primary network feeders does not seem to be practical because of overreaching and tripping out for faults on other feeders.

Table I of the discussion shows that on the radial circuit all faults above 850 amperes will cause relay operation in two cycles or less, while on the network feeders sequential operation of the circuit breakers at the two ends often occurs and total relay times are as high as 1.3 seconds at 10,000 amperes. For lower values of current, times will probably be longer. The longer time required to clear faults on network systems will result in a greater percentage of faults becoming permanent. The higher values of fault currents also will increase damage.

The discussers agree that there may be advantages in economics and in operation in favor of primary networks, but they also feel it desirable to recognize the disadvantages of higher fault currents and longer clearing times of faults that usually result from network operation.

Table I. Comparison of Operating Time of Relays on a 4-kv Primary Network Versus 4-kv Radial Circuits

	Network Circuits	Radial Circuits	
	Time Delay	Time Delay	Instantaneous
Relay pick-up in primary amperes	560	480	560
Time	0.4 second at 1,000% of pick up	0.15 second at 1,000%	

	Fault Current				
Condition	Total	Each Relay	Relay Time	Fault Current	Relay Time
Fault at center of circuit	10,000*	5,000	0.43 second	**	1 to 3 cycles at all currents above 850 amperes

		Total Time for Both Relays Operating Sequentially
Fault at end of circuit	10,000 amperes	1.3 second

The above times for the network will increase as fault currents decrease.

* The 10,000-ampere fault current is based on 3—3,750-kva unit substations connected in a 4-kv network.

** Maximum fault current from a 2,000-kva unit substation is 3,000 amperes at 4 kv.

REFERENCE

1. IMPROVEMENTS TO OKLAHOMA CITY PRIMARY NETWORK, Bryce Brady. *AIEE Transactions*, Part I, volume 68, 1949, pages 701–03.

W. J. Lank: Mr. Rydbeck has concisely expressed the argument for capacitors upon primary network ties. One additional use of capacitors is to hold up the voltage on a lateral near the center of a long tie feeder. As Mr. Rydbeck says, the capacitors have been particularly useful in holding up voltage under emergency conditions.

Mr. Dodds and Mr. Smithley have raised the point that the ratio of temporary to permanent faults is slightly better for the radial system than for the network system. Part of this may be due to the more congested pole lines causing more tree limbs to get across lines with the radial system. So far as is possible, the areas compared have about the same exposure and tree conditions. The ratios given in the paper compare the number of "trip-outs" per mile year and the number of "interruptions" per mile year of the radial with the primary network feeders. Under the conditions existing, it is believed that this is a much better indication of the reliability than the ratio of temporary to permanent faults used by them.

By a "tripout" is meant an operation of the circuit breaker or fuse, followed by successful reclosure and restoration of load along the main feeder up to branch line fuses. In the case of a primary network feeder, simultaneous operations at both ends are treated as one tripout. If a circuit reclosed successfully and supplied the major part of the load, but part of the main line had burned clear, it was treated as an interruption.

They have raised some questions about current and time settings and details of construction. The current settings are usually from 240 to 480 amperes, depending upon the load and length of the feeder. Time is usually 20 cycles for the circuit breaker contacts to part at 600 per cent of minimum trip current. In some cases, instantaneous trip attachments set for approximately twice the fault current at the opposite end of the primary network feeder are used in addition to the time delay relays to assist co-ordination. All new construction uses bare wire but most of the older lines have weatherproof wire.

The author agrees with the statement that careful sectionalizing, co-ordinating fuses, and strategic location of reclosers will do much to improve service. The only difficulty found in this respect with the primary network is that it is not practical to use an instantaneous trip at the substation to protect branch line fuses. If service to the branch line is of sufficient importance, the fuses may be omitted if the frequency of trouble is low or a recloser or reclosing fuses used if it is high.

On bare copper wire comparatively few faults become permanent unless confined to a given location by a cause such as a tree limb. Many staged tests using fine wire to initiate the fault have not burned down a circuit. In the case of the comparatively slow blowing reclosing fuses used in some locations, there probably is a slight increase in the percentage of permanent faults, due to the long clearing time of the fuses. Experience cited in Table I of the paper shows that this is more than over-balanced by the reduced number of faults.

In the example of relay settings given by Mr. Dodds and Mr. Smithley, they use a greater time delay for a network feeder. If the relay time delay is sufficient to co-ordinate with the large branch line fuses which are required in order not to blow on the first instantaneous trip on a radial feeder, it will be sufficient for proper selection on a network feeder. The network does lose the advantage of a first instantaneous trip to protect the fuse, as discussed before.

To summarize, we feel the final criterion of reliability is service to the customer, which we have found to be better with network operation.

Reduction of Interference from Radio-Frequency Heating Equipment

G. W. KLINGAMAN
ASSOCIATE AIEE

AS A RESULT of regulations adopted recently by the Federal Communications Commission which govern radiation from radio-frequency heating equipment,[1] there has arisen a need for information on practical methods of dealing with this problem. Since it occurs in a relatively new field of application for electric power, industrial users may find themselves unfamiliar with the necessary techniques for dealing with it. In order to make such information available to industry, committees of the AIEE and the Institute of Radio Engineers have undertaken an investigation of good engineering practices which will minimize or reduce radiation from radio-frequency heating equipment. It is the purpose of this paper to summarize recommended procedures which have been developed through the work of The Committee to Formulate Procedures of Good Engineering Practices in Instances Where Interference is Encountered (sponsored by the AIEE), The Industrial Electronics Committee (sponsored by the Institute of Radio Engineers), and the Engineering Committee of the Induction and Dielectric Heating Section (sponsored by the National Electrical Manufacturers' Association).

The Need for Shielding

High-frequency electric power sometimes appears to behave quite differently from the familiar 60-cycle version. Actually, there is no fundamental difference. The difficulty lies only in the fact that effects which were negligible at 60 cycles become very important as the frequency is raised. It becomes increasingly harder to confine electric currents to desired circuits. Dangerous potentials may exist between apparatus cases which can cause burns to operators. High-frequency currents may circulate in control devices and make them inoperative, or otherwise impair their functions. Circuits and apparatus, which are not associated with the equipment in any way, may pick up high-frequency currents. The ability of high-frequency power to propagate itself through free space without conventional guides, such as wires, leads to interference with apparatus at great distances. The energy may travel along the earth's surface, or it may be reflected from the ionosphere to be returned to earth at tremendous distances from its source. On the other hand, it may be conducted on wires directly to the remote point. The solution to all such hazards is the use of adequate shielding about the high-frequency apparatus, to confine the currents to safe channels.

The Nature of Radiation

The oldest type of generating equipment is the rotating machine. However, this device is not generally used above 10 kc per second. In the range 10 kc per second to 500 kc per second, a common power source is the spark gap. Interference from spark equipment is distributed over a very wide frequency range. For example, a 20-kc per second generator will radiate a continuous spectrum of noise, very similar to automobile ignition interference, which may extend well into the very-high-frequency regions. Vacuum-tube oscillators are used extensively between 200 kc per second and 200 megacycles per second. The frequency spectrum of such generators consists of a fundamental and other frequencies which may be detected with varying amounts of intensity up to and beyond the 300th harmonics.

Essentially, the generation of frequencies other than the fundamental is a result of wave-form and modulation effects. These produce frequencies which are harmonics, plus sideband frequencies which bear no harmonic relation to the fundamental. At times, such phenomena as moding and parasites cause trouble. Moding is manifested as a sudden frequency shift or "skip" of the generator during the loading procedure. Parasites are spurious frequencies generated in a path other than the normal oscillator circuit in the generator. Moding, on the other hand, is a normal oscillator characteristic which is present when a tuned load is tightly coupled to the tank (coil–capacitor) circuit in the generator.

It has been pointed out that high-frequency energy leaks readily into stray paths, where it may produce undesirable local and remote effects unless it is confined to proper circuits. High-frequency electric currents cause radiation when they flow along unshielded conductors having dimensions which are an appreciable fraction of the wave length of the current. The total power loss by radiation from a conductor can be represented at any selected point along its length as the product of an effective radiation resistance and the square of the current at that point. The total impedance measured at the point contains additional components, due to the self-resistance and reactance of the conductor. It often is possible to calculate the effective impedance such a stray path will offer to a radio-frequency voltage source and to reduce it to a simple electric circuit.

An alternative to this "circuit concept" is the "wave concept," which pictures the flow of electric energy in terms of electric and magnetic fields. This view is more fundamental, but more difficult to visual-

---

Paper 49-182, recommended by the AIEE Electric Heating Committee and approved by the AIEE Technical Program Committee for presentation at the AIEE Summer General Meeting, Swampscott, Mass., June 20–24, 1949. Manuscript submitted March 21, 1949; made available for printing May 3, 1949.

G. W. Klingaman is an Industrial Products Engineer with the RCA Victor Division of the Radio Corporation of America, Camden, N. J.

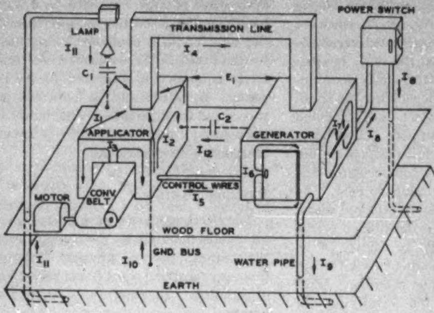

Figure 1. Stray currents which will result in radiation from an installation

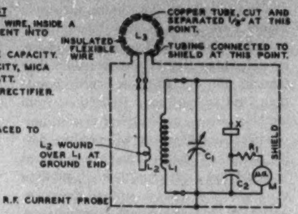
COPPER TUBE, CUT AND SEPARATED 1/8" AT THIS POINT.
L_3
INSULATED FLEXIBLE WIRE
TUBING CONNECTED TO SHIELD AT THIS POINT.
L_2 WOUND OVER L_1 AT GROUND END
L_2
L_1
C_1
X
R_1
C_2
M
SHIELD
R.F. CURRENT PROBE

PARTS LIST

L_3-ONE TURN INSULATED WIRE, INSIDE A 5/16 DIA. COPPER TUBE BENT INTO A 3" I.D. CIRCLE.

C_1-15-200 mmf VARIABLE CAPACITY.

C_2-005 mf FIXED CAPACITY, MICA

R_1-10,000 OHMS, 1/2 WATT.

X-TYPE IN34 CRYSTAL RECTIFIER.

M-0-200 μa METER.

L_1,L_2-SEE TABLE.

BARE, TINNED WIRE, SPACED TO PROPER LENGTH.

COIL TABLE

FREQ. RANGE	L_1				L_2			
	TURNS	COIL DIA.	COIL LG.	WIRE	TURNS	COIL DIA.	COIL LG.	WIRE
13-42 MC.	5	1 1/4	1 1/4	#16	1	1 1/2	—	#16
6.5-20 MC.	12	1 1/2	2	#16	3	1 3/4	3/16	#18
4-12 MC.	20	1 1/2	2 1/8	#18	5	1 3/4	3/8	#18
2.5-8 MC.	34	1 1/2	2 1/8	#18	5	1 3/4	3/8	#18
1.6-5 MC.	54	1 1/2	2 1/8	#22	6	1 3/4	5/8	#18

Figure 3. Design data for a sensitive high-frequency current probe

ize and more complicated mathematically.

Frame currents along the edges and over the surfaces of metallic enclosures surrounding the apparatus are serious sources of radiation. For example, in Figure 1 the necessity for shielding has been recognized by the designer, but due to faulty construction, the shielding is far from perfect. At the applicator, the shielding has been made of large-mesh iron screen, having a high surface reactance and a high resistance because of the characteristics of the iron. This produces excessive leakage of the radio-frequency flux from the inside face of the screen to the outside faces, and results in current I_1 and I_2. A large opening to admit a conveyor belt gives rise to current I_3 around the periphery of the opening. The thickness and conductivity of the generator shield are adequate, but poor contact around the door causes current I_6. Similarly, a slit in the side panel results in an external current I_7. Some additional leaks might be poorly screened windows, open floors, and poor joints around panels.

Currents on power and control wires occur in two ways. Figure 2(A) shows a transverse (wire-to-wire) current wave. Figure 2(B) shows a longitudinal (wire-to-ground) wave. Both waves are transmitted on the inside of a shielding conduit, from the installation to a point where the wires may be exposed to free space and cause radiation. The magnitude of radiation per ampere is apt to be much greater for longitudinal current than for transverse current. On the other hand, currents such as I_4, I_5, I_8, and I_{11} in Figure 1 may be induced on the outside of power conduits due to shielding leaks. A similar current I_9 can occur on the outside of pipes connected to the unit for supplying water, gas, or air to the installation.

A common fallacy is the belief that connecting the apparatus to ground is a convenient cure for high-frequency troubles. Some installers have gone to great pains only to discover that no improvement has been obtained. Such a connection with current I_{10} is shown. It usually has considerable radiation resistance and may actually increase interference instead of reducing it.

Finally, an installation that initially may have been satisfactory eventually may start to leak high-frequency power. Factors contributing to this condition are corrosion of metal parts and carelessness on the part of the operators. A poor choice of metals, from an electrochemical standpoint, may weaken a joint or contact in time.

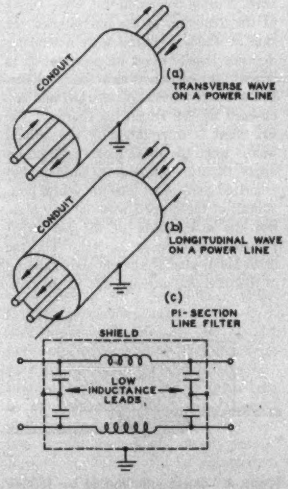

Figure 2. Stray currents on a power line and a filter for eliminating them

The various paths in Figure 1 may be reduced to simple electric circuits as previously discussed. Voltages are induced across the equivalent impedances by direct conduction, by capacity coupling (for example, stray capacities C_1 and C_2), by inductive coupling, or by direct radiation. One such voltage is E_1 between the generator and applicator, due to the impedance of various current paths between them. In the case of spark generators, the complex form of such interference may shock-excite a number of paths at their resonant lengths. This may result in radiation peaks at certain frequencies which are higher than the general level of interference.

Once the high-frequency energy leaves its conventional circuits, it enters free space, where it continues to travel outward by a sort of self-propagation. In this medium, the wave concept is useful. It is found that the electromagnetic field has two components—an induction field which attenuates very rapidly (within one or two wave lengths), to leave only a radiation field which continues to great distances, depending on its intensity. The radiation field may further be separated into a ground wave, which follows the surface of the earth, and a sky wave which is reflected from the ionosphere. The ground wave is greatly affected by the conductivity and dielectric properties of the earth and attenuates rather rapidly. The sky wave attenuates only slowly.

The multiplicity of radiation sources in Figure 1 are found to have different relative phases at the various points in space, in such a way that at certain points they tend to add, and at other nearby points they tend to subtract. Reflections from metallic objects or electrical discontinuities in the neighborhood will produce similar effects. This gives rise to pronounced "interference patterns" or "standing wave patterns," that is, up and down variations of the field strength over relatively short distances.

The ability of a conductor to radiate energy from its surface increases with increasing frequency, up to a certain point. This is entirely due to its increasing electrical length (length in terms of a fraction of the wave length of the current it carries), and its increasing electrical spacing from a ground or other reflecting plane. At frequencies used for induction heating, electrical lengths are short and radiation is not a serious problem. Design practices which would be intolerable at dielectric heating frequencies may cause little trouble at lower frequencies. However, the possibility of harmonic or spark interference makes such practices questionable, in general. At lower frequencies, the conduction of currents along power lines is a considerable source of interference at a distance from the equipment.

LOCATION AND MEASUREMENT OF RADIATION

The rules adopted by the FCC are given in Part 18, a copy of which may be obtained from the United States Government Printing Office.[1] The measurements made to determine whether the limits for industrial heating equipment are met consist essentially of first obtaining a polar plot of the field intensity at 1,000 feet, for example, around the equipment. Following this, readings are taken along a radial in the direction of the strongest lobe of radiation, as determined from the polar plot, to determine the maximum intensity at one mile. The strongest field reading at that distance (antenna vertical or horizontal), at a height of 12 feet, will show whether the limit of 10 microvolts per meter at one mile specified in the rules is complied with. The rules should be referred to for the detailed measurements in any particular case. This limitation applies to all fundamental, harmonic, and spurious emissions. Radiation from a power line must be less than 10 microvolts per meter, one mile from the equipment and 50 feet from the line.

Various devices have been designed to assist in the measurement and location of high-frequency radiation. Chief among these are field intensity meters, which are merely refined and calibrated receivers. Below 18 megacycles, the FCC specifies that such meters shall employ loop antennas. Above 18 megacycles, the specified antenna is a doublet (rod), mounted on an appropriate support. Data taken with such meters at close spacings (within one wave length) should recognize the presence of a strong induction field. The weakest field that may be explored with a field intensity meter is determined by the natural noise level in the vicinity of the meter. Such noise tends to mask the signal and give erroneous readings. Additional instruments for identifying the frequencies of interfering sources, locating leaks in shields, and so forth, include interference locators, radio-noise meters with rod antenna, a loop probe, and others. A very simple type of current probe, using shielded inductive coupling to the circuit is shown in Figure 3.

FCC regulations are concerned with the radiated field. Stray energy also may travel along metallic paths (wires, and so forth) to a remote point where it may cause interference with the operation of other apparatus. This is known as conducted interference. FCC regulations recognize conducted interference indirectly by specifying radiation field measurements along power lines at one mile distance.

When the height above ground of the receiving antenna and of the radiating wires is small compared to a wave length at the frequency of the interference, the rate at which a ground wave attenuates depends largely upon its polarization in space. The earth acts as a "lossy" dielectric which is alternately charged and discharged by the advancing energy. The net effect is attenuation of the ground wave; when the above height restrictions apply, the attenuation of the horizontally-polarized component (electric vector horizontal) of the ground wave is very high, but the attenuation of the vertically-polarized component is less. On the other hand, when the height above ground of the receiving antenna and of the radiating wires is large compared to a wave length at the frequency of interference, the received field component controlled by the losses in the earth becomes relatively unimportant compared to the resultant of direct and ground-reflected waves, and the difference in attenuation of horizontally and vertically polarized components becomes small.

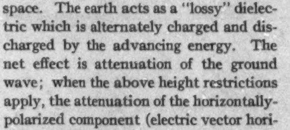

Figure 4. Shield joint formed by locking two metal sheets and attaching them to the supporting frame

REMEDIAL METHODS

The electromagnetic wave in free space attenuates inversely as the distance from the source. Hence, physical isolation from any receiving point is one method of attenuation. In most cases, it is not practical.

When electric apparatus radiates interference over a wide range of frequencies due to the nature of its construction, it may be modified to reduce its bandwidth in some instances. An example of this would be the replacement of spark generators with tube equipment. Another example would be the substitution of a filtered d-c supply in self-rectified vacuum-tube generators.

A third principle of suppression is to cancel approximately one field with another of equal amplitude and opposite phase. This is what occurs when a current-carrying conductor is brought close to a parallel nodal plane (reflecting surface). Similarly, when a conductor carrying an equal and opposite return current is brought close to the transmitting conductor, approximate cancellation takes place. Open-wire transmission lines use this principle. The radiation efficiency of a closed loop may be reduced, in general, by reducing the enclosed area or volume. As another example, the balanced operation of a tuned circuit may, in some instances, reduce its effect on other circuits by cancellation.

An effective and recommended method of reducing radiation is by means of reflection. One very efficient reflector is a shield, made of a good conductor, about the radiation source. The lower the surface resistance and reactance of such a shield, the more efficient it becomes as a reflector. Such shields form a nodal surface which completely surrounds the high-frequency circuit. Single shields often produce sufficiently satisfactory attenuation to meet FCC regulations. A second shield, surrounding the first and insulated from it, gives approximately twice the attenuation (in decibels) of a single shield. When the shields are placed in parallel by a systematic short-circuiting device such as cell-type construction, the attenuation is somewhat reduced but still higher than for a single shield. Attenuation may be impaired by slits, poor joints, excessive flux leakage due to the use of iron wire, too large a mesh of screen, high shield currents due to undue proximity of internal circuits, too small a shield size, or unscreened openings of one sort or another.

As pointed out previously, an attempt often is made to use the earth as an equipotential plane, by connecting each piece of apparatus to a good earth ground (multiple grounding). At best, this yields only mediocre results, since, in practice, it generally is impossible to place apparatus cases at true ground potential because of ground bus and shield impedances.

Nodal (reflection) points in wire conductors may be obtained by line filters or shielded transformers. Figure 2(C) shows a low-pass π-section filter, which is effective against the transmission of both longitudinal and transverse current waves.

It is desirable to choose the image impedance of such a filter as low as possible. The cut-off frequency should be well below the lowest frequency present in the generator output. Low-loss impedances should be used. Additional precautions, to insure high attenuation at fundamental and harmonic frequencies, include low capacitor inductance, low ground-wire impedances, low capacity between input and output terminals, shielded assembly, and mounting of the filter shield directly on the wall of the main apparatus shield, at the point where the filtered wires leave the main shield. Such line filters generally are used in wire circuits which eventually reach open space where they can radiate energy. In place of a line filter, it often is possible to insert a transformer with a grounded electrostatic shield between primary and secondary, in series with a wire circuit. The ground return from this shield should have negligible impedance.

A considerable amount of attenuation may be introduced by surrounding an interference source with an absorbing material.

Iron, with its high resistance, is fairly effective for this purpose. A laminated shield consisting of sheet steel with a copper plating impedes the progress of a radio wave in two ways:

1. The copper surface reflects electric energy.
2. The steel core attenuates by absorption any energy which may penetrate the copper barrier.

However, if possible, the copper coating should be thicker than the depth of current penetration, so that power losses in the underlying steel will not be excessive.

Good Engineering Practice

DESIGN OF EQUIPMENT

First choice of frequency for dielectric heating and some induction heating processes should be the assigned FCC bands. Among the channels to be avoided in all cases are those assigned to distress, navigation, and domestic sound and television broadcasting. The possibility of harmonics, sidebands, or spark noise occurring in these bands should be considered particularly. Well-known engineering practices should be followed to avoid harmonics, parasites and moding. Reduction of the bandwidth through the use of filtered d-c plate supplies with tube equipment is advocated. The wave form of the generated frequency should be as undistorted as is consistent with economical design. In the case of spark equipment, very little can be done along these lines.

The generator should be housed in an effective shield. Louvers, windows, or other openings should be screened, the edges of such screening being securely bonded to the main shield. Plating to improve the conductivity of shielding and to improve the corrosion resistance of joints is advisable. Sufficient thickness of metal should be used to avoid current penetration. Contacting surfaces should be free of paint, dirt, or corrosion. Doors should be continuously bonded to the main shield around their entire periphery by contacting fingers or other suitable means. Door interlocks should be incorporated to prevent operation of the set when opened, as well as for reasons of safety.

It is good practice to protect internal components not associated with the generating circuits from high-frequency currents. This applies to control wires, meters, relays, low-frequency and d-c supply circuits, and so forth. Shielding and filtering of the generator often is simplified by the use of a separate internal shield, containing the high-frequency circuits only.

Where generators require transmission lines, it is recommended that they be designed for use with coaxial line. Other types of lines are a single shielded pair, 2-wire individually-shielded pair, 2-wire open line. In cases where the work circuit must be unshielded (as in some induction-heating installations), such circuits should be as compact as possible and located close to the generator. Open-wire feed lines should be short and closely spaced. If possible, they should be balanced to ground. When practicable, the work area should be enclosed in a screened booth.

A power-line filter should be incorporated in the generator; unshielded auxiliary circuits should be avoided, or else be effectively filtered. All metal pipes associated with water cooling, power supply, grounding, and similar connections should enter the installation at a single point. If this is not done, potentials across the shield surfaces, due to various small leaks, will cause currents such as I_8, I_9, and I_{10} to flow, see Figure 1. Such piping should be bonded to the shielding at the point of entry, in order that high-frequency currents will be effectively short-circuited and will not be conducted from the inside to the outside of the shield. Preferably such connections should approach from underground.

Finally, before a design is released for production, one of the performance tests should be a thorough check for high-frequency leakage with a sensitive probe, such as is shown in Figure 3. Such tests should be made over as wide a frequency range as possible, in order to locate harmonic or other spurious frequency radiation. If possible, the life expectancy and reliability of shielding devices should be checked. If appreciable radiation or poor design is discovered by such tests, every effort should be made at improvement, since this will lessen the problem of interference reduction for every installation that is made.

INSTALLATION

A preferred location for high-frequency equipment is on the first floor or in the basement of a building. The equipment should be as remote as possible from metallic ducts and flues, steam pipes, or power circuits which may pick up energy by capacitive or inductive coupling. It is very desirable to have the entire apparatus housed in a shielded room, although this is seldom practical. In any case, the installation should be as compact as possible, with emphasis on short, direct connections between units. Placing components of an installation on a large metal sheet is helpful.

The transmission line should be of the concentric or shielded-duct type. The outer conductor may be fabricated of copper, copper-plated steel, or aluminum. It is essential that the outer conductor be continuous, for example, where two sections of fabricated sheet-metal outer conductor are bolted together. Such joints and access covers must be fastened with screws, spaced not more than 3-to-4 inches apart. Large, radiating loop circuits may be avoided by running the line between units along the metal base of the installation.

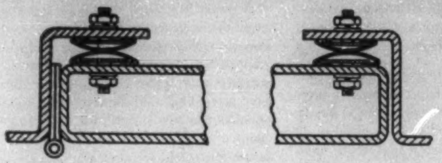

Figure 5. Spring contacting device with clamping strip for bonding doors

If the generator has been designed properly, the major source of interference will be the applicator, for the radio-frequency current and voltage here are apt to be quite large. Therefore, extreme care must be taken in its shielding. The applicator shield may be fabricated from copper, copper-plated steel, or aluminum, copper, or bronze screening (16-mesh). If the latter is used, a double-wall shield will give better results than a single-wall shield. However, adequate shielding frequently can be attained with a single shield at a lower cost if proper attention is paid to the details of construction. Shield currents usually can be reduced greatly by an internal partial shield. This appears to be particularly useful where the electrodes are large and stray capacities set up excessive shield currents. If possible, tuned circuits inside the shield should be attached to it at a single point only, to avoid circulating tank currents in the walls.

The applicator, wherever physically possible, must be completely enclosed by the shield with no openings or discontinuities in the bonding. Paint must be removed at all surfaces of contact, and these surfaces should be inspected at monthly intervals and any corrosion removed. Joints in the metal shield material may be made as in Figure 4. Typical door construction is shown in Figure 5, with continuous bonding around the entire periphery. The spring-like bonding strips are of beryllium-copper or phosphor-bronze construction. Brass or bronze weather stripping, or resilient metal mesh may be substituted for the construction shown. The shield should be as large as space and cost will permit. Under no conditions should the electrodes be spaced less than one foot from any part of the shield for powers in excess of 5 kw (output) and proportionately less for lower powers. For the megacycle range of industrial heating, generous overlap of metal sheeting is helpful in cases where hooked joints, or closely spaced fasteners, are impractical.

In some installations, mainly conveyor-belt operations, it becomes essential that openings be provided. In these cases, it is necessary to construct "vestibules" or "corridors" as shown in Figure 6. With a rectangular cross section as shown, the length *L* must be at least equal to the larger of the two dimensions *A* and *B*. Furthermore, the larger of the dimensions *A* and *B* should not exceed approximately 1/3 the wave length of the highest frequency to be suppressed. Such vestibules should not be located in wall surfaces carrying high currents, or in close proximity to a strong electric field.

Shielding of the applicator floor should not be overlooked. It is important that it be a continuous part of the whole shield, running underneath each of various enclosed components.

Control wiring must be kept out of the applicator wherever possible. If internal wiring becomes necessary, as large a proportion of the circuit as possible should be run externally and metal conduit employed throughout. Conduit should be terminated at both ends in a metal enclosure, junction box, or other shield fitting. Unfiltered wires should not be extended into the open. It has been recommended that the main power supply to the equipment pass through a line filter before leaving a conduit. This applies also to auxiliary power lines which may by-pass the main filter. The use of solid metal conduit or flexible metallic braid is to be preferred to spirally-wrapped metal sheathing (*BX*), due to eventual corrosion and poor contact between turns which will result in high-frequency leakage.

If shielding has been done properly, there is no necessity for grounding, other than for safety. For this purpose, a Standard Underwriters Safety Ground may be installed, or the conduit return to the main entrance switch may be used as a 60-cycle or d-c ground.

Certification of radio-frequency heating equipment is required by Part 18 of the FCC Rules and Regulations.[1] Limitations and test procedures are prescribed therein. Further information pertaining to these measurements may be found in "IRE Standards on Radio Wave Propagation–Measuring Methods, 1942,"[8] and "Measurement of Interference from Radio Frequency Heating Equipment."[9] If tests show the need for improved shielding, the location of trouble sources is facilitated greatly by a current probe, such as previously described. Methods of suppression as recommended in this report should be followed. It is pointed out that prevention by proper design is a much better policy than an extended series of cures after the installation is complete.

USE AND MAINTENANCE

The equipment always should be operated within its ratings as to power, electrode voltage, and frequency. Access panels, doors, and shields always should be in place when the unit is operating. Installers or manufacturers instructions should be observed. Warning notices to this effect may be posted near the equipment. Any changes in operation or repairs should be made in accordance with good engineering practices, and the user should ascertain that such changes have not nullified the results of initial tests for FCC certification.

A regular maintenance schedule should be followed to insure the proper operations of shielding devices. All contacts and bonding strips used in conjunction with openings should be cleaned whenever they show evidence of corrosion. Atmospheres corrosive to copper, bronze, aluminum, and so forth, are often prevalent in factories and may quickly reduce the

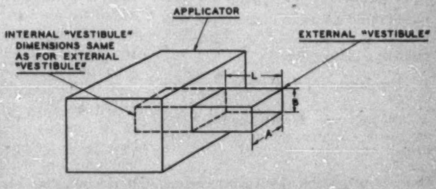
APPLICATOR
INTERNAL "VESTIBULE" DIMENSIONS SAME AS FOR EXTERNAL "VESTIBULE"
EXTERNAL "VESTIBULE"
L
B
A

NOTE: SHIELDING CHARACTERISTICS OF THE INTERNAL OR EXTERNAL "VESTIBULES" ARE THE SAME. SELECTION OF EITHER FOR A SPECIFIC APPLICATION IS MAINLY BASED ON PHYSICAL CONSIDERATIONS.

Figure 6. Shield extensions for attenuation of radiation from openings

The length L must be greater than either A or B. A and B should be less than 1/3 the wave length of the highest frequency present efficiency of a shield by attacking bonding surfaces. Latches, screws, or other devices joining these surfaces should be tightened periodically. Such precautions may be incorporated as part of the regular maintenance schedule for the equipment.

Procedures where Interference Is Encountered

Faulty shielding, poor design, or other factors often cause leakage currents and excessive radiation from an installation after it is completed. Reduction to FCC limits is necessary. On the other hand, even though the field intensity from an installation may comply with the rules, it still is possible that interference with nearby communication services may occur under abnormal circumstances; this must be avoided.

Certain other circumstances may make an investigation of the radiation from high-frequency heating equipment necessary. Among these is the case of equipment, existing prior to the adoption of rules and regulations by the FCC, which does not comply with these rules and which must be modified before a specified date. In the meantime, if such equipment is found to interfere with any authorized radio services, steps to eliminate the interference must be taken. Another case is where the FCC has reason to believe that operation of a previously certified installation no longer meets regulations, and requires that the user renew his certification data.

Preliminary Checks

Where interference and/or excessive radiation is reported and a field intensity meter is not readily available, it often is possible to obtain temporarily a fixed or portable receiver of the communications type, which can give a relative indication of the field strength level (in comparison with other signals) and the nature of the transmission causing the interference. The following observations are recommended:

1. Does the interfering signal have the same frequency as, or bear a harmonic relationship with, the suspected generator frequency?
2. Does the interfering signal fade, indicating a location remote from the receiving point, or is it steady, suggesting a local signal?
3. Does the interfering signal have a characteristic tone or noise which is identifiable with the suspected source?
4. Does the interfering signal have a sequence of operation which is identifiable with the suspected source?

It often is possible to arrange an identifiable schedule of operation for the suspected generator, such as "2 minutes on—30 seconds off" during a known test period.

For a very approximate check on the interference level and to observe the effect of any steps taken as corrective measures, it is possible to use the "*S* meter" on the communications receiver. Roughly, such a meter is calibrated in steps of 6 decibels between successive *S* points, with a signal of 50–100 microvolts at the receiver terminals, corresponding to *S*9. This method should be used only as a temporary expedient. Calibration varies between manufacturers, and there is no way of correcting for the antenna length, current distribution, directional characteristics, matching, and height above ground, or the variation of receiver gain with frequency. These factors must be known in order to calculate the actual field strength in space.

A more accurate method of making field strength observations or noise measurements is with a field-intensity or noise meter. The various factors affecting calibration have been evaluated carefully for such meters, so that readings indicate the true intensity of the field arriving at the surface of the antenna. When the meters are used properly and their readings properly interpreted, they give good results.

Location of Sources

Having ascertained that interference and/or excessive radiation exists, the first step is to determine which unit is at fault, if several are suspected. Careful observations of frequency, operating sequences, or other characteristics may solve the problem quickly. They mav be supplemented through the use of direction-finding loop antennas, such as are incorporated on field-strength meters. Loops frequently are utilized by rotating them until a minimum reading is obtained. The direction from which the radiation is coming is then perpendicular to the plane of the loop. By taking a directional reading at each of two known points, the interference source may be determined by triangulation. Loop direction finders are subject to a 180-degree error because two minima appear as they are rotated through 360 degrees. They also may be inaccurate because of reflections from nearby conductors or other reflecting media, such as the ionosphere. It has been suggested that the errors due to reflection from local objects can be made small by orienting the loop for a maximum reading, as opposed to the method of minima described. In this case, the source of the radiation will be in the plane of the loop. In order to determine the maximum accurately, the loop may be turned both right and left from the maximum position to obtain equal small reductions in the reading. The average of the directions so obtained is the true direction of the source (with 180-degree sense ambiguity). In trying to triangulate the location of sources which are intermittent in operation, it is important to take simultaneous bearings from two points and to be sure that the same signal is being observed at both positions. Otherwise, large errors can easily result.

Dipole antennas may be similarly used to indicate direction of arrival. They are subject to ground, polarization, and reflection errors. The addition of a director or reflector (double dipole) to eliminate the 180-degree error, combined with the tuning procedure as described for loops, has been recommended to improve the accuracy of this type of direction finder. At frequencies above 18 megacycles, dipole antennas are the most effective means of receiving radiated energy.

Another search procedure is by a process of "homing" with a portable receiver. The radiating generator is "tracked down" by following along the direction in which the signal increases. The method is again handicapped to some extent by reflection, unless suitable precautions are taken.

Once the installation causing the interference has been spotted, the problem of reducing leakage is greatly simplified by locating faults in shielding with a current probe, as previously suggested. When the pickup loop L_2 of Figure 3 is brought close to a current leak in the shielding or filtering, a voltage is transmitted to the tuned circuit L_1C_1 and thence to the rectifier circuit, consisting of the crystal X, a filter R_1C_2, and a microammeter M. The rectifier converts the high-frequency current to direct current for deflecting the meter M. The tuned circuit functions both as a variable sensitivity and selectivity control. Leakage currents induce voltages in the pick-up loop by mutual induction. The entire unit is shielded in order to minimize body-capacity effects. Such a probe also has directional characteristics which are useful in plotting the main current paths, illustrated in Figure 1. This feature is best utilized by turning the loop for a minimum reading of the meter. The path of stray current then will be perpendicular to the plane of the loop. When available, noise meters and interference locators may be used for locating shield faults. More accurate quantitative data is obtainable in this way, but it often will be found that the simple probe described is entirely adequate.

Corrective Measures

Where the radiation is within FCC limitations, the interference to a service sometimes may be eliminated quickly by merely changing the frequency sufficiently to avoid any possibility of operation in the service channel. In some instances, it may be possible to place the frequency accurately in the channels assigned for industrial equipment by incorporating an automatic frequency-control device into the generator. When this is done, no special shielding is necessary other than for safety reasons. However, in a great many cases improved shielding, filtering, and bonding of the equipment are the only practical solution to a problem. The steps to be followed are similar to those discussed in previous sections of this paper.

Conclusion

Rules and regulations by the Federal Communications Commission governing radiation from industrial radio-frequency heating equipment have created a need for information on methods and practices which will minimize or reduce interference. Radiation is the result of currents flowing in unshielded conductors, which include equipment, shielding, metal frames, power feeders, and plumbing or other fixtures attached to the installation. The most practical method of locating sources of radiation is with a radio-frequency current probe. The magnitude of the radiation may be measured by means of a field-intensity meter. Among the devices suggested for eliminating interference are shields and filters. Shields should be continuous without gaps, poor joints, or unshielded openings. They should be made of a good conductor, although copper or bronze screen is effective, if care is used in the construction. Double shields provide extra protection but are not necessary in most cases. Filters are installed in unshielded wire circuits. In order that they be effective at high frequencies, the image impedance arrangement of components, and grounding must be selected with care. Principles of good engineering practice should be incorporated in the manufacture, installation, and use of radio-frequency heating equipment.

References

1. **Rules and Regulations Relating to Industrial Scientific and Medical Service.** *Rules and Regulations*, Federal Communications Commission (Washington, D. C.), Title 47, Telecommunication, chapter I, part 18.

2. **Shielding High-Frequency Interference, Albert F. Murray.** *Electronic Industries* (New York, N. Y.), August 1945, page 108.

3. **VHF Ignition Noise, Gilbert Sonbergh.** *Electronic Industries* (New York, N. Y.), November 1944, page 94.

4. **Shielding of Dielectric Heating Installations, G. W. Klingaman, G. H. Williams.** *Electronics* (New York, N. Y.), May 1945, page 106.

5. **Abatement of Radio Interference from Electromedical and Industrial Radio-Frequency Equipment.** *British Standard Code of Practice CP 1002:1947*, British Standards Institution (London, England), 1947.

6. **Abatement of Radio Interference Caused by Motor Vehicles and Internal Combustion Engines.** *British Standard Code of Practice, CP 1001:1947*, British Standards Institution (London, England), 1947.

7. **Electromagnetic Waves (book), S. A. Schelkunoff.** D. Van Nostrand Company, New York, N. Y., first edition, 1943, page 303.

8. **Standards on Radio Wave Propagation—Measuring Methods.** *Proceedings Supplement*, Institute of Radio Engineers (New York, N. Y.), volume 30, number 7, part 2, 1942.

9. **Measurement of Interference from Radio-Frequency Heating Equipment, George H. Brown.** *AIEE Transactions*, volume 67, part 2, 1948, pages 1102–6.

10. **Ignition Interference, W. Nethercot.** *Wireless World and Radio Review* (London, England), October 1947, page 352.

11. **Shielding for Diathermy, Warren C. Stoker, William W. Seifert.** *Docket 6651*, Federal Communications Commission (Washington, D. C.), October 1943. (Final report on contract OEMsr-225-Project C-31, Rensselaer Polytechnic Institute, Troy, N. Y.)

12. **Survey of High Frequency Heating, Raymond W. Wilmotte, Inc.** *Report 667*, Naval Office, Bureau of Ships (Washington, D. C.), Contract 34227 Task Order 2, June 1947.

13. **Report on Radio Interference from Electro-Therapeutic Apparatus.** *Section 12, Inter-American Arrangement Concerning Radio-Communications*, Federal Communications Commission (Washington, D. C.), December 1937.

14. **Radio Propagation at Frequencies Above 30 Megacycles, K. Bullington.** *Proceedings*, Institute of Radio Engineers (New York, N. Y.), volume 35, October 1947, pages 1122–36.

Discussion

C. W. Frick (General Electric Company, Schenectady, N. Y.): Mr. Klingaman's paper is a very good summary of the activities of committees set up by AIEE and the Institute of Radio Engineers and I have been very pleased to have participated in this work. Since such suggestions as I have had are in most cases already incorporated in this resume, I will take this opportunity to make a few comments on the general problem which is presented when new equipment is developed requiring for best performance the use of frequency extending into the radio spectrum. The problem is to operate such equipment without affecting radio communications adversely.

In the present paper the problem is treated largely from the standpoint of shielding. Dielectric heating lends itself very well to such treatment since in many cases the heating operations can be performed inside a shielded enclosure. In most cases of induction heating, even when the work coil is not well shielded, the radiation has been small because the exposed parts are poor radiators.

The AIEE Subcommittee on Induction and Dielectric Heating has been keeping track of interference complaints for induction and dielectric heating equipment. As compared with the total number of installations in service, the number of interference complaints has been very small.

Prior to the development of high frequency equipment for industrial heating, interference problems were encountered with other devices such as "wireless" record players and "gadgets" for the remote control of receivers by radio. The Federal Communications Commission adopted the "low-power rule" which limits the radio field intensity to a specified value at a distance proportional to the wave length used. This rule did not work for industrial heating and different limits were developed as referred to in the paper. Also, neither the "low-power" rule nor the industrial heating rules were suitable for diathermy equipment since that type of apparatus cannot ordinarily be shielded effectively. After considerable study some few frequency bands were assigned for this purpose. These bands also may be used for equipment in industrial and scientific service.

It may be noted that each time problems have come up an individual solution has been worked out. Because of the developments likely to occur in the future, thought should be given to a more general program. Since we cannot forsee what these future developments will be, it has been suggested that the radio spectrum be studied with a view to determining a series of frequency bands, spaced at reasonable intervals on the frequency scale which, if left free for industry to use, would meet the needs reasonably well over a period of years.

G. W. Klingaman: Mr. Frick has presented some of the background of the interference problem and emphasized several interesting points, which were somewhat neglected in the paper. The whole field of radio-frequency heating is still developing. Devices and techniques are constantly being improved and radiation from high-frequency heating equipment, which at first appeared formidably serious has been reduced to a satisfactory degree by standard engineering methods. The material presented in the paper summarizes the work of a number of groups (AIEE, Institute of Radio Engineers, and the National Electrical Manufacturers Association) on the interference problem, which it is hoped will be added to and improved in the future.

Measurements of Erythemal Energy

HOYT S. SCOTT
MEMBER AIEE

ATTENDANT to the growing popularity of solaria and increasing public acceptance of sources generating erythemal ultraviolet, there is a definite need in the field for a rugged, compact direct-reading meter that will measure the E-Vitons* per square foot in quite the same way that a footcandle meter measures lumens per square foot. The design of such a meter is discussed in this paper.

An accurate and accepted method of measuring erythemal ultraviolet is with a monochromator. The basic principle of operation is to pass the energy beam through an optical system, separating the energy into its spectral bands. The band desired is then passed through a slit and measured with a sensitive recorder. For the highest accuracy, warranted only in laboratory work, a double monochromator is needed. The double monochromator makes use of additional sets of optics and slits.[2] The advantage is its large energy-gathering powers, resulting in relatively large amounts of energy in any given wave length at the exit slit. Quartz optics are necessary for the transmission of erythemal ultraviolet. The weight of either single or double monochromators may be in the order of several hundred pounds.

When lower orders of accuracy are desired, the generally accepted practice is to use an instrument employing a special phototube. This may consist of a spectrally selective phototube without special filters, or a more general phototube with special filters. In either case heavy batteries and amplifiers are necessary. The fragility of phototubes, the weight of the batteries, and the instability of phototube calibration limit these instruments to nonportable operation.

From the foregoing, the disadvantages for field use are obvious, and a compromise was considered between a reasonable degree of accuracy for commercial application, and a light compact instrument that could be carried in the pocket.

In a solarium where only a partial degree of portability is desired and moderate weight and bulk is not a factor and where general commercial accuracy is sufficient, an amplifier and galvanometer-type moving element may be used. The best application for this is in conjunction with an optical system for projection on a screen.

In searching for such a device, the use of phototubes was considered to be practical only where portability was relatively unimportant. To this end it is believed that selenium light cells with suitable filters present a more practical approach.

---

*E-Viton: A unit employed to express the health and erythema value of radiations above 2,800 Angstrom units, such as found in natural sunlight, while erythemal flux is that quantity of radiant energy which produces as much temporary reddening as 10 microwatts of energy at 2,967 Angstroms. One E-Viton per square foot is the same as 0.01 erythemally-weighted milliwatts per square foot or 0.01076 erythemally-weighted microwatts per square centimeter.

Paper 49-186, recommended by the AIEE Production and Application of Light Committee and approved by the AIEE Technical Program Committee for presentation at the AIEE Summer General Meeting, Swampscott, Mass., June 20–24, 1949. Manuscript submitted March 21, 1949; made available for printing May 16, 1949.

Hoyt S. Scott is in the Engineering Division, Lamp Department, General Electric Company, Cleveland, Ohio.

The author gratefully acknowledges the assistance of L. J. Buttolph, George Inman, B. T. Barnes, J. B. Hopperton, J. Holloptre, H. C. Froelich, W. H. Eberle, and Harry Billet.

Figure 1. Microammeter and explorer

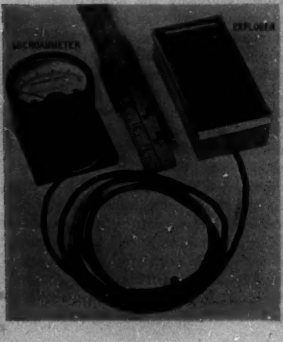

Figure 2. Meter components completely assembled in carrying case

Figure 3. Prefilter, phosphor, post filter, and cells

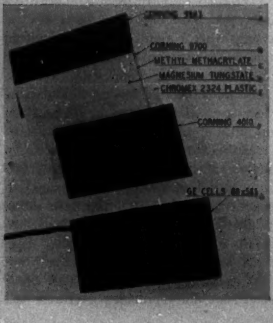

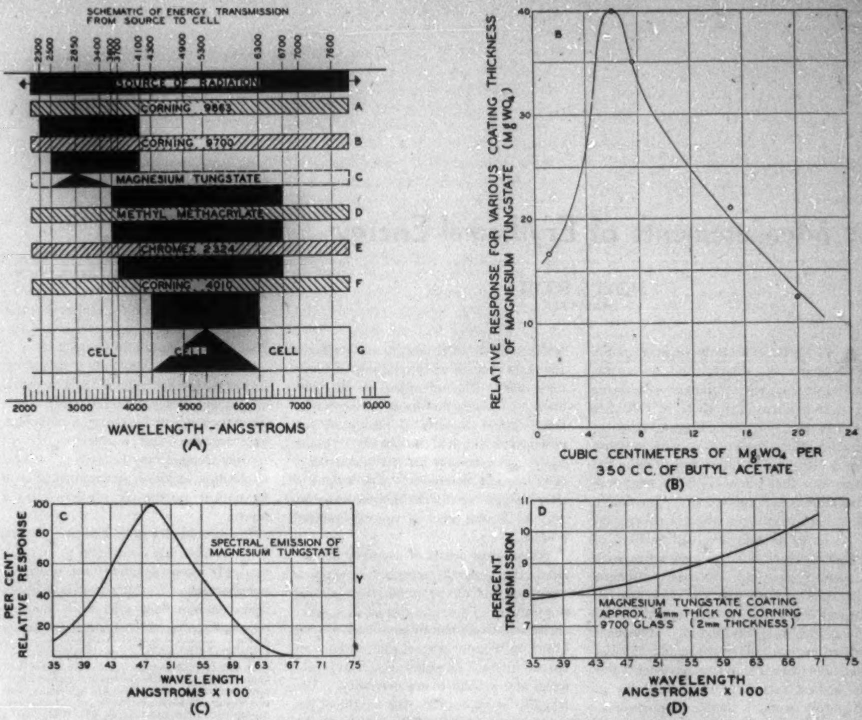

Figure 4.(A) Schematic of energy transmission from source to cell. (B) Relative response of various coating of thickness of magnesium tungstate in butyl acetate.* (C) Spectral response of magnesium tungstate. (D) Neutral-filter action magnesium tungstate

Several very fine types of meters are described by Luckiesh,[2] but for various reasons did not meet the author's requirements.

The barrier-layer type of light-sensitive cells, which become sources of electric energy when activated by energy within their sensitivity range, offer the attractive possibility of dispensing with batteries. They are subject only to the limitation of their spectral sensitivity range and the magnitude of their electric output. Available barrier-layer cells are sensitive to radiant energy from 2,800 to 8,000 Angstrom units, with a maximum response at about 5,800 Angstrom units. While theoretically they could be used to measure directly the 2,800–3,200 Angstrom-unit erythemal energy, their tenfold greater sensitivity at 5,200–6,000 Angstrom units provides a greater cell output even after very selective filtration and a wave length conversion by fluorescence. It has been found possible to connect barrier-layer cells in a series–multiple arrangement to provide sufficient output to give a full-scale deflection of a 0–1 microammeter with such incident energy as is transmitted by the combination of filters and fluorescent phosphors described hereafter.

The primary design problem was that of a combination of filters and a light-sensitive material simulating closely, in over-all response to radiant energy, the skin's erythemal sensitivity, which is considered an index of its beneficial and tanning reaction.

The secondary problem was that of measuring the output of the above filters and fluorescent phosphor with a combination of filters and light-sensitive cells, transmitting and sensitive only to the energy output of the primary filters and phosphor and not responsive to any ultraviolet, especially the 3,200–3,800 Angstrom-units region, or to any visible and infrared of wave length longer than 6,300 Angstrom units, which may have originated from the same source being measured and may have been transmitted by the primary filters and phosphor.

The meter consists essentially of light-sensitive barrier-layer-type cells, with proper correction filters, and a microammeter, as shown in Figure 1. In order to obviate possible solarization of the various filters, the entire device, consisting of explorer unit, leads, and microammeter, is contained in a convenient opaque carrying case, as shown in Figure 2. The combination of light-sensitive cells, similar to those used in the ordinary light meter, and

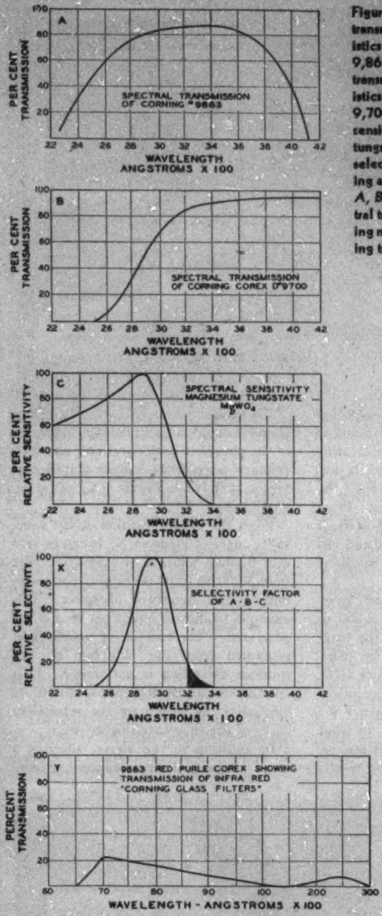

Figure 5.(A) Spectral transmission characteristics of Corning number 9,863. (B) Spectral transmission characteristics of Corning number 9,700. (C) Spectral sensitivity of magnesium tungstate. (X) Relative selectivity factor resulting as product of Curves A, B, and C. (Y) Spectral transmission of Corning number 9,863 showing transmission of infrared

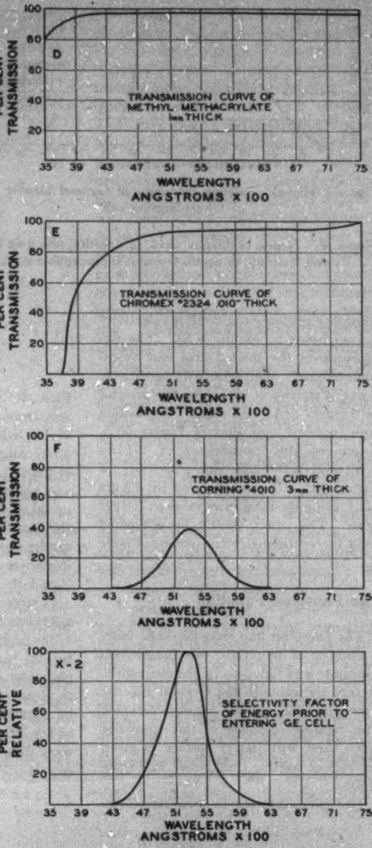

Figure 6.(D) Spectral transmission characteristic of 1-millimeter thickness of methyl methacrylate. (E) Spectral transmission characteristic of plastic Chromex number 2,324—0.010-inch thick. (X-2) Selectivity factor of energy prior to entering light cell

the filters used in conjunction with them are shown in Figure 3. The filters when assembled form a compact package. A diagrammatic sketch of these elements and their functions is shown in Figure 4(A). The details of each element are hereinafter described.

Prefilter

The selective filtering is accomplished by the use of a first filter, red-purple Corning number *9,863*,[3] which absorbs energy above 4,100 Angstrom units and transmits near ultraviolet and visible violet below 4,100 Angstrom units. The transmission characteristics of this first filter is shown in Figure 5(A). Unfortunately, this filter does transmit a slight amount of energy in the near infrared which must be absorbed by the other filters. See Figure 5(Y).

The second filter in the prefilter is Corex *D* Corning number *9,700*.[3] This transmits wave lengths above 2,500 Angstrom units (extremely small amount at 2,537 Angstrom units), but absorbs those below 2,500 Angstrom units. See Figure 5(B).

The prefilter group, in combination with the magnesium tungstate (Figure 5(C)), phosphor transmits the greater part of the energy between 2,800 and 3,200 Angstrom units, a small amount as low as 2,500 and as high as 3,400 Angstrom units plus the small amount of infrared mentioned above.

The net result of the two filters and the

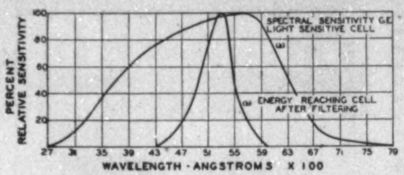

Figure 7 (above). Relative sensitivity of General Electric Company light-sensitive cell

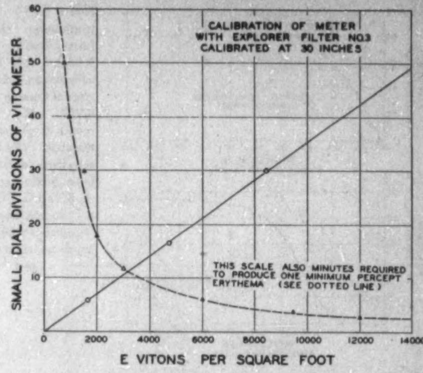

Figure 9. Typical calibration showing linearity, also time in minutes versus intensity, to obtain 1 minimum perceptible erythema

phosphor response is a relative selectivity curve shown in Figure 5(X). The significance of the shaded area will be explained later. This selectivity-sensitivity curve is arrived at by taking the product of Figures 5(A) and 5(B) transmission superimposed over that of Figure 5(C), combining the transmission of Figures 5(A) and 5(B) and the sensitivity of Figure 5(C), then multiplying by Figure 5(C), using the maximum value as 100 per cent. The result should be compared with the erythemal effect curves, Figure 8.

The Phosphor Function

The phosphor unit may be made using a number of materials, but magnesium tungstate was found to be the most satisfactory for use with the General Electric Company cell, catalog number *88X565*. The relative response of this phosphor when used with butyl acetate is given for various coating thicknesses in Figure 4(B).

The phosphor serves two functions. First, it is most sensitive in the 2,850 Angstrom-unit band, thereby generating visible light from approximately 3,600 to 6,700 Angstrom units for the activating of the cell, Figure 4(C). Second, it acts as a nonselective neutral filter from 3,400 up through 7,600 Angstrom units. From the curves in Figures 5(A) and 5(B), it can be seen that near ultraviolet and visible energy will be transmitted by filters *A* and *B*.

Figures 5(A) and 5(B) shows transmitted energy in the range of 2,500 to 4,100 Angstrom units to excite the magnesium tungstate phosphor. This phosphor acts as a neutral filter, Figure 4(D), to absorb whatever visible energy might be transmitted by filters numbers *9,863* and *9,700*. Figure 5(C) shows to what wave lengths magnesium tungstate responds. Figure 4(C) shows the resultant visible wave lengths generated.

The combined filtering action of filters *A* and *B*, in addition to the filtering action of the phosphor itself, over and above its primary purpose as a wave-length convertor, is shown in Figure 5(X) as a selectivity factor.

From the shaded portion of the selectivity curve of Figure 5(X), it can be seen that a small amount of near ultraviolet from 3,200 to 3,400 Angstrom units does fall on the tungstate phosphor. This amounts to slightly over 2 per cent of the generated. The amount of visible light generated from the phosphor by this spurious excitation is not shown. It is felt that it can be disregarded due to its low order, as shown on the sensitivity curve of the tungstate, Figure 4(C).

In addition to the above, there is a small amount of near infrared, Figure

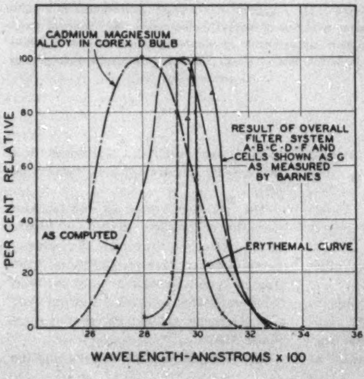

Figure 8 (left). Over-all spectral response of meter to erythemal curve. For comparison, response of cadmium magnesium alloy phototube is shown[5]

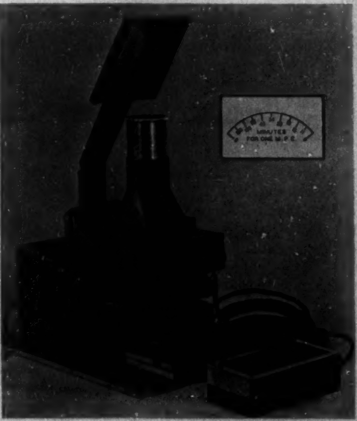

Figure 10 (right). Optical projector and calibration in minutes for minimum perceptible erythema, for use in solarium

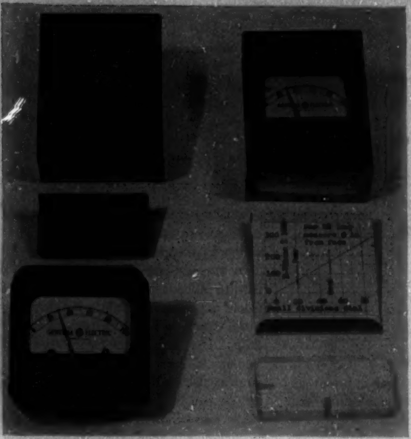

Figure 11. Small-size lower-sensitivity erythemal meter for measuring outputs at short distances

5(A). This infrared, originally transmitted by filters *A* and *B*, also is transmitted by the phosphor. See Figure 4(D).

Because of the infrared energy transmission of the prefilter and phosphor, as well as the transmission down to 2,500 Angstrom units, Figure 5(X), two additional filters are required. These are described as post filters.

Post Filter

The first element in the post filter, Figure 6(D), is a thin film of methyl methacrylate and serves the major purpose of protecting the phosphor coating, and secondarily offers free passage above 3,600 Angstrom units in the visible range. Because of the energy remaining in the range from approximately 2,500 to 2,800 Angstrom units as indicated in Figure 5(X), it is necessary to provide a second filter, Chromex number *2,324*. This is a plastic of British manufacture. The transmission characteristics of Chromex number *2,324* are shown as Figure 6(E). Because the previous filters have not absorbed the incident infrared energy, the third post filter is used with transmission characteristics shown in Figure 6(F). This is Corning number *4,010* sextant green.[3] The net result of the post-filter arrangement is to give energy transmission in the visible range from approximately 4,300 to 6,300 Angstrom units, and is shown in Figure 6(X-2). It is only this energy that activates the light-sensitive cell. Figure 7 shows how the curve in Figure 6(X-2) compares with the spectral sensitivity of the General Electric cell.[4]

Comparing the over-all spectral characteristic of the combined prefilter phosphor and post filter with the erythemal curve, Figure 8, it can be seen that weighting factors can be disregarded, as the meter follows the erythemal curve closely enough for practical purposes even though the sensitivity factor is slightly greater at 3,050 Angstrom units than theoretically would be desirable. Ultraviolet at that wave length is effective in producing dark tanning and hence may be included properly in the measurement of effective energy from a sunlamp.

Cells

In one of the meters, Figure 3, four standard General Electric cells, catalog number *88X565*, are used. The cells are connected in series-parallel in order to obtain the optimum energy transfer, as it is important to match the impedance of the cells to the impedance of the meter.

Moving Element (Meter)

The current delivered is in the order of a microampere. Many difficulties present themselves in the selection of a moving element that is sufficiently sensitive but still rugged enough to be carried in a portable manner. In view of the usual transportation handling problems, a double-suspension meter was selected. The meter used in the original prototype had 0–3-microampere full-scale deflection. One of the unique features in this meter is two push buttons, one to eliminate damping, bringing the pointer quickly to zero; the other "push to read." See Figure 1. A typical calibration curve, Figure 9, shows the linear characteristics. Superimposed on this curve is a curve indicating the minutes necessary for one minimum perceptible erythema for a given intensity. The foregoing statements cover the assembly of a filter exploring pad with its accompanying moving element. It is desired to show how a sensitive meter for field use might be constructed that would follow reasonably close the erythemal curve and measure the erythemal viton intensities without use of weighting factors.

For the measurement of erythemal intensities of commercial sunlamps at close distances (30 inches), a much lesser degree of sensitivity can be tolerated. A single light cell and a 0–8 microammeter with the above filter has been found to be satisfactory. See Figure 11.

A practical example of the use of the meter is in the "sun and star room (Sky Cabana)" of the Senator Hotel, Atlantic City, N. J., where the guest determines the duration of exposure of erythemal ultraviolet for minimum perceptible erythema in the various basking locations. The exploring pad is connected to a cord and plug associated with various convenient outlet jacks along the wall. An optical system, Figure 10, is used to project a scale calibrated in minutes on a screen at the end of the solarium.

References

1. Review of Scientific Instruments, Forsythe and Barnes. American Institute of Physics (New York, N. Y.), May, 1933.

2. Applications of Germicidal Erythemal and Infrared Energy, Matthew Luckiesh. D. Van Nostrand Company, Inc., New York, N. Y., page 70, 1946.

3. Glass Color Filters. Corning Glass Company, Corning, N. Y., 1948.

4. Illumination Measurements with Light Sensitive Cells, C. L. Dows. Illuminating Engineering Society (New York, N. Y.), 1942.

5. Cadmium Magnesium Alloy Phototubes. *Journal*, Optical Society of America, American Institute of Physics (New York, N. Y.), volume 25, 1935, page 184.

No Discussion

Saving Time in Testing Life of Incandescent Lamps

W. R. PURCELL
NONMEMBER AIEE

THE heart of any technique of controlling quality during manufacture is skillful and scientific trouble shooting. To be scientific, the trouble shooting procedure should: leave the process alone when there is no trouble; apply corrective action when there is trouble; and apply such corrective action promptly while the trouble still exists and before many units of substandard quality have been manufactured.

One of the most useful techniques for determining whether there is trouble to shoot is the Shewhart control chart for measurements. In this technique, limits are set for the average and range of the measurements on periodically drawn samples. As long as the statistics continue to fall within the limits, it is presumed that there is no trouble and that the process should be left alone. As soon as a statistic falls outside the limits, there is strong evidence of trouble and corrective action should be applied. How promptly the corrective action can be applied depends on how quickly the measurements can be made and the statistics computed.

In most applications of this control chart technique, measurements can be made promptly. Thus the third element of scientific trouble shooting, prompt action, usually can be made a part of the procedure. In certain cases, however, this is not so, and the time required to make the measurements substantially reduces the value of the technique. An outstanding example is the test of life, in which neither the average nor the range can be computed until the last unit of the sample has reached the end of its life.

In many cases, this difficulty has been partially overcome by increasing the severity of the life test. A classic example is the shortening of the life of incandescent lamps from 1,000 hours to about five hours by burning them at 150 per cent of rated voltage. Even at this acceleration, however, it often requires seven or eight hours to burn out the last lamp of a sample; yet the final result might yield an average so small or a range so great that need of corrective action is indicated. Attempts to accelerate the life test further cause abnormal arcs and do not give a true picture of normal life. Since the test cannot be further accelerated, it is necessary to accelerate the statistics.

Symbols

UCL_m = upper control limit for medians
CL_m = central line for medians
LCL_m = lower control limit for medians
UCL_s = upper control limit for shortest
CL_s = central line for shortest
LCL_s = lower control limit for shortest
M = average of medians
S = average shortest
n = sample size
σ_m = standard deviation of medians
σ_s = standard deviation of shortest
σ' = standard deviation of population
K = constant relating mean first statistic to population standard deviation
C_s = constant relating σ_s to σ'
C_m = constant relating σ_m to σ' in odd-size samples
$\sigma_{n/2}$ = standard deviation of (1/2) nth statistic
C = constant relating $\sigma_{n/2}$ to σ'
$\sigma_{\{1/2\}\{[n/2]+[(n/2)+1]\}}$ = standard deviation of mean of (1/2) nth and $[(n/2+1]$ statistics
$r_{[n/2],[(n/2)+1]}$ = correlation coefficient between (1/2) nth and $[(n/2)+1]$ statistics
T_1 = constant relating $3\sigma_m$ to $(M-S)$
T_2 = constant relating $3\sigma_s$ to $(M-S)$

In conventional statistics, average is used to indicate a shift in the level of the whole population; range is used to indicate a change in population dispersion. A shift in level also can be indicated by the median life, or central failure in the sample; a shift in level or change in dispersion can be indicated by the shortest life, or first failure in the sample. The use of median and shortest as statistics substantially accelerates the results. A tendency toward short life which is indicated by the sample is indicated quickly. It is not necessary to continue the test beyond the median, and corrective action can be started promptly.

Before adopting these new statistics a preliminary study of the inherent frequency distribution of incandescent lamp life was made. Table I is a typical set of data accumulated before control was established. The data indicate the following conclusions:

1. In the long run the average of the medians coincides with the average of the averages.
2. Both of these statistics are about half way between the average shortest life and average longest life.
3. The differences between median and average in individual samples are not significant.*

From these conclusions the assumption was made that the inherent frequency distribution of incandescent lamp life is substantially normal.

In control charts there is a central line about which the statistics are expected to scatter in random fashion just as long as there are no shifts in population center or dispersion.

This central line is located at the long-term average of the statistic. Extending this technique to these new statistics, the central line for medians is located at the average median, and the

---

Paper 49-187, recommended by the AIEE Committee on Production and Application of Light and approved by the AIEE Technical Program Committee for presentation at the AIEE Summer General Meeting, Swampscott, Mass., June 20–24, 1949. Manuscript submitted November 10, 1948; made available for printing May 3, 1949.

W. R. PURCELL is with Sylvania Electric Products, Inc., Salem, Mass.

*Average of the range is 410 hours. From this, the standard deviation of units (σ') is about 176; standard deviation of averages (σ_a) about 80. The average of the absolute differences (40) is only one-half of one standard deviation of averages; the greatest difference (130 in sample 19) is only 1.62 standard deviations of averages.

central line for shortest is located at the average shortest.

Conventional limits allow for variations in the statistics which are not significant. These insignificant variations are due to the constant system of chance causes in the process and operation of chance in sample selection. The control limits are placed at three standard deviations of the statistic above and below the central line of the statistic. A statistic beyond the control limits is then very unlikely if chance is operating alone, and is therefore considered conclusive evidence that some other dominant cause is affecting the process.

Using this same procedure, control limits for medians are placed thus

$$UCL_m = M + 3\sigma_m \tag{1}$$

$$CL_m = M \tag{2}$$

$$LCL_m = M - 3\sigma_m \tag{3}$$

and control limits for shortest life are placed thus

$$UCL_s = S + 3\sigma_s \tag{4}$$

$$CL_s = S \tag{5}$$

$$LCL_s = S - 3\sigma_s \tag{6}$$

To compute the values of σ_m and σ_s, reference was made to a table of order statistics.[1] This table gives the means and standard deviations of the first, second, third, and so forth, statistics of small samples, with reference to the mean and standard deviation of the population.

Confining our attention to the normal distribution, these tables yield, first, a constant (here called K) relating the average of the first statistic (shortest life) to the population standard deviation thus

$$S = M - K\sigma' \tag{7}$$

Thus the population standard deviation is given by

$$\sigma' = (M - S)/K \tag{8}$$

Second, the tables yield another constant (here called C_s) relating the standard deviation of the first statistic (shortest life) to the population standard deviation thus

$$\sigma_s = C_s\sigma' \tag{9}$$

Combining equations 8 and 9 we have

$$\sigma_s = (C_s/K)(M - S) \tag{10}$$

For odd-size samples, the tables yield another constant (here called C_m) relating the standard deviation of the median to the population standard deviation thus

$$\sigma_m = C_m\sigma' \tag{11}$$

Combining equations 8 and 11 we have, for odd-size samples

$$\sigma_m = (C_m/K)(M - S) \tag{12}$$

For even-size samples, the tables yield another constant (here called C) relating the standard deviation of the (1/2) nth statistic to the population standard deviation thus

$$\sigma_{(n/2)} = C\sigma' \tag{13}$$

Combining equations 8 and 13 we have

$$\sigma_{(n/2)} = (C/K)(M - S) \tag{14}$$

In this case, however, it is preferable, in order to avoid confusion, to consider the median as the mean of the $n/2$ and $(n/2) + 1$ statistics, thus retaining the same central line. We have, then, for even-size samples

Table I. Typical Data for Life of Incandescent Lamps in Hours before Establishment of Control

Each sample contains 5 lamps

Sample Number	Shortest	Longest	Range	Median	Average	Difference Between Median and Average
1	270	740	470	580	600	20
2	810	1,140	330	970	1,020	50
3	1,180	1,310	130	1,200	1,260	60
4	860	1,110	250	930	940	10
5	380	1,090	710	1,010	960	50
6	990	1,370	380	1,300	1,260	40
7	850	900	50	850	870	20
8	870	1,740	870	1,300	1,300	0
9	720	1,260	540	1,020	1,110	90
10	740	1,340	600	1,040	1,010	30
11	830	1,140	310	980	1,050	70
12	1,700	2,070	370	1,930	1,840	90
13	680	1,020	340	880	860	20
14	650	1,110	460	970	980	10
15	940	1,070	130	1,020	1,040	20
16	1,160	1,680	520	1,250	1,250	0
17	1,190	1,480	290	1,250	1,340	90
18	1,340	1,490	150	1,420	1,380	40
19	1,180	1,730	550	1,410	1,280	130
20	340	880	540	670	610	60
21	1,100	1,240	140	1,170	1,170	0
22	800	1,550	750	920	970	50
23	930	1,200	270	1,200	1,140	60
24	1,020	1,560	540	1,240	1,210	30
25	690	1,240	550	1,000	980	20
Averages	890	1,300	410	1,100	1,100	40

Table II. Means, Standard Deviations, and Correlation Coefficients for Certain Order Statistics

n	K	C_s	C_m	C	$r_{[n/2],[(n/2)+1]}$
3	0.8463	0.7480	0.6698		
4	1.0294	0.7012		0.6004	0.65
5	1.1630	0.6690	0.5356		
6	1.2672	0.6449		0.4962	0.74
7	1.3522	0.6260	0.4587		
8	1.4236	0.6107		0.4326	0.80
9	1.4850	0.5978	0.4075		
10	1.5388	0.5868		0.3886	0.83

$$\sigma_m = \sigma_{(1/2)\{[n/2]+[(n/2)+1]\}} \tag{15}$$

Now the variance of the sum of two statistics a and b is given by

$$\sigma^2_{a+b} = \sigma_a^2 + \sigma_b^2 + 2r_{a,b}\sigma_a\sigma_b \tag{16}$$

In our case our two statistics are the $n/2$ and $(n/2) + 1$ values. Since the distribution is normal, we know by symmetry that these two variances are equal. Therefore

$$\sigma^2_{[n/2]+[(n/2)+1]} = 2\sigma^2_{(n/2)}[1 + r_{(n/2),(n/2)+1}] \tag{17}$$

Since we want the variance of the mean of $n/2$ and $(n/2) + 1$, and since the variance of a half-statistic is one quarter of the variance of the whole statistic, we have

$$\sigma^2_{(1/2)\{[n/2]+[(n/2)+1]\}} = \sigma^2_{(n/2)}\{1 + r_{(n/2),[(n/2)+1]}\}/2 \tag{18}$$

or, in terms of standard deviations

$$\sigma_{(1/2)\{[n/2]+[(n/2)+1]\}} = \sigma_{(n/2)}\sqrt{\{1 + r_{[n/2],[(n/2)+1]}\}/2} \tag{19}$$

Combining equations 14, 15, and 19, we have, for even-size samples

$$\sigma_m = (C/K)\sqrt{\{1 + r_{[n/2],[(n/2)+1]}\}/2} \times (M - S) \tag{20}$$

Table III. Values for Computation of Median Life and Shortest Life Control Limits

For Substitution In:
$UCL_m = M + T_1(M - S)$
$LCL_m = M - T_1(M - S)$
$UCL_s = S + T_2(M - S)$
$LCL_s = S - T_2(M - S)$

Sample Size n	T_1	T_2
3	2.38	2.65
4	1.50	2.04
5	1.38	1.72
6	1.10	1.53
7	1.02	1.39
8	0.87	1.29
9	0.82	1.21
10	0.73	1.14

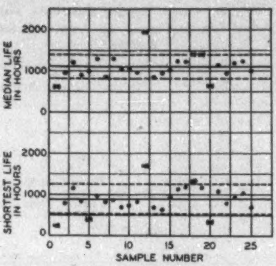

Figure 1. Control chart of data in Table I—control not established

Values of K, C_s, C_m, C, and $r_{[n/2],[(n/2)+1]}$; reproduced from the paper cited, are given in Table II.

For simplicity, we establish new constants T_1 and T_2 such that

$$T_1(M-S)=3\sigma_m \tag{21}$$

and

$$T_2(M-S)=3\sigma_s \tag{22}$$

Combining equations 21 and 12, we have, for odd-size samples

$$T_1=3C_m/K \tag{23}$$

and combining equations 21 with 20, we have, for even-size samples

$$T_1=(3C/K)\sqrt{\{1+r_{[n/2],[(n/2)+1]}\}/2} \tag{24}$$

Combining equations 22 with 10, we have, for any sample size

$$T_2=3C_s/K \tag{25}$$

Values of T_1 and T_2 have been calculated, using equations 23, 24, and 25 and constants in Table II, and are tabulated in Table III for sample sizes from 3 to 10.

The final equations for central lines and control limits are

$$UCL_m=M+T_1(M-S) \tag{26}$$

$$CL_m=M \tag{2}$$

$$LCL_m=M-T_1(M-S) \tag{27}$$

$$UCL_s=S+T_2(M-S) \tag{28}$$

$$CL_s=S \tag{5}$$

$$LCL_s=S-T_2(M-S) \tag{29}$$

Example from the data in Table I

$M=1{,}100$

$S=890$

$n=5$

from Table III, for $n = 5$

$T_1=1.38$

$T_2=1.72$

The control limits and central lines are

$UCL_m=1{,}100+(1.38)(1{,}100-890)=1{,}390$

$CL_m=1{,}100$

$LCL_m=1{,}100-(1.38)(1{,}100-890)=810$

$UCL_s=890+(1.72)(1{,}100-890)=1{,}250$

$CL_s=890$

$LCL_s=890-(1.72)(1{,}100-890)=530$

Another most interesting application of order statistics is destructive tests has been developed elsewhere.[2]

The statistics of median and shortest have been in use at Sylvania for incandescent lamp life test since 1945.

One advantage in the use of these statistics is the saving in time and facilities required for test. A second advantage is the elimination of the calculation of averages and ranges. There is one disadvantage. For the same sample size, median is 10 per cent to 25 per cent less stable, and therefore as a control statistic less sensitive, than the average.

The great advantage is the speed of the corrective action, which is the very purpose of the whole testing procedure. Furthermore, the fastest action is taken when most needed; that is, when life is short.

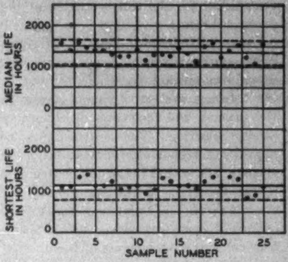

Figure 2. Control chart—control established

Figure 1 (control chart of the data in Table I) illustrates this especially for samples 1, 5, and 20. Action on these statistics was possible in the accelerated equivalent of 270, 380, and 340 hours (that is, slightly over $1^1/_2$ hours). Action on conventional statistics would have been delayed until the accelerated equivalent of 740, 1,090, and 880 hours, respectively, or about $4^1/_2$ hours.

Figure 2 illustrates the appearance of charts based on these statistics after control has been established. The increase in average life and improvement in uniformity have been very gratifying.

References

1. LOW MOMENTS FOR SMALL SAMPLES: A COMPARATIVE STUDY OF ORDER STATISTICS, Hastings, Mosteller, Tukey, Winsor. *The Annals of Mathematical Statistics*, volume XVIII, number 3, September, 1947, pages 413–26.

2. THE RELATIVE POWER OF THREE STATISTICS FOR SMALL SAMPLE DESTRUCTIVE TESTS, Paul H. Jacobson. *Journal*, American Statistical Association, December, 1947.

No Discussion

Economic Loading of a Transformer System

D. L. LEVINE
MEMBER AIEE

H. E. SMITH
MEMBER AIEE

Synopsis: Loading of transformers must be guided by both economic and thermal limitations. For economic limitations, the costs of installation and operation must be evaluated for each type of transformer. Thermal limitations should be in accordance with the present ASA Loading Guide.[1] Transformers subject to both normal and emergency operating conditions should have thermal limitations established for both conditions. Transformer loading must be within the thermal limitations of connected equipment. Voltage regulation requirements may limit the loading of distribution transformers.

IN 1942 the first AIEE operating guide for transformers was issued. This guide grew out of all the knowledge of the industry on the life characteristics of transformer insulation. It was based on everything from laboratory tests on insulation to successful operating experience with large numbers of transformers over as many years as transformers have been used. Since 1942 there has been more intensified study of insulation aging under laboratory conditions. Also, there has been operating experience with transformers at ever-increasing load levels. In 1948 the operating guide was reissued in its second revision since 1942 as the ASA C57.32 "Guide for Loading Oil-Immersed Distribution and Power Transformers."[1] The guide represents the best that is available in the industry and it can serve as a sound basis for thermal loading of transformers of any operating system.

But actual application to an existing system is a problem that the guide cannot cover. That is an individual problem that each company must take upon itself, if it is to make the best use of its own transformers. It is the purpose of this paper to set forth how one large operating company effectively increased the loading on its transformer system by application of the principles of the ASA operating guide to its own needs and conditions.

Economic Study

The entire program was based on the acceptance of the guide as the criterion for thermal loading. However, before instituting such a program it was necessary to show that it was economically proper to do so. Somewhere there had to be a balance between thermal loading and economic loading and it was necessary to find that balance before making any drastic change in loading practices.

For a large system, an economic study must be made applicable to many varying conditions. To do this, the study must be general and cover a range of all the important variables in the problem. For the study as made, the following major variables were considered:

1. Installed cost per kilovolt-ampere.
2. Life of equipment.
3. Annual fixed charges.
4. Operating efficiency.
5. Ratio of copper losses to core losses.
6. Cost of losses.
7. Load cycle.

Installed Costs per Kilovolt-ampere

The installed cost per kilovolt-ampere in the light of present rapid change in construction costs can be almost anything depending on what is considered to be included in the transformer installation. To the bare transformer cost must be added the cost of installation with all associated equipment. Also, for substation transformers, the structural, building and land costs must be added to give the total cost per kilovolt-ampere. In comparative studies it is best to use incremental cost, that is, the cost per kilovolt-ampere of the increase from one standard size to the next. Because of the wide range of such costs, this study covers the general case, with the present average incremental cost per kilovolt-ampere as unity.

Life of Equipment

The question of average life of equipment had to be considered in order to answer the obvious question of what change a policy of increased loading would make. Did transformers wear out or were they discarded because of obsolescence under the existing loading policy? A statistical survey showed that no exact answer could be given to this question. The equipment being dealt with is generally considered to have an average normal life of 30 years or more, and the age of most of the system is less than that, so that statistically no accurate conclusions can be drawn from our own experience.

Rate of Annual Fixed Charges

The rate of annual fixed charges varies over different portions of a power system. Since combinations of associated equipment were being worked with, it was necessary to use a combination of various figures. This includes an annual depreciation charge. If a loading level beyond that for normal thermal life is chosen, then this annual depreciation rate will increase accordingly. An annual unit fixed charge rate was used, to apply only to loading for normal total life.

Operating Efficiency

The operating efficiency of the transformer is a controlling factor in an economic study. For newer large-size power transformers, the efficiency at nameplate rating is better than 99 per cent. For

---

Paper 49-188, recommended by the AIEE Transformer Committee and approved by the AIEE Technical Program Committee for presentation at the AIEE Summer General Meeting, Swampscott, Mass., June 20–24, 1949. Manuscript submitted March 17, 1949; made available for printing May 4, 1949.

D. L. Levine is Senior Engineer and H. E. Smith is Distribution Planning Engineer, Commonwealth Edison Company, Chicago, Ill.

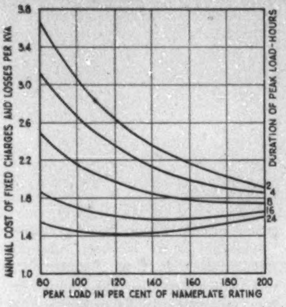

Figure 1. Effect of peak load and peak duration on cost of operation

older units and for distribution transformers the efficiency will run closer to 98 per cent. A range of efficiencies was covered in the study, but for the general case an efficiency of 99 per cent was used.

Ratio of Copper Losses to Core Losses

For variable loading of transformers, the ratio of copper losses to core losses fixes the rate of change of efficiency with load.

This ratio varies with size, type, and year of manufacture of transformers. The study includes a range of ratios from 4/1 to 1/1. For the general case, the loss ratio 2/1 as applicable to newer power transformers was used.

Cost of Losses

It is difficult to fix a reasonable total cost of losses on electric equipment. The coal cost, which may be ascertained without much difficulty, is but a part of the total cost. Base load station cost per kilowatt-hour can be calculated by using total kilowatt-hour output per year and total annual cost of operation, including fixed charges. It is necessary to add to this the fixed charges and the operating cost of that part of the total system which supplies the losses at any particular point on the system. The cost varies for core losses and load losses and for location on the system.

Also, the practice of shutting down portions of large power banks during low-load periods complicates the handling of core losses.

Here again the study was put on a unit basis with a general average cost of losses taken as unity. A range of costs from 0.4 to 1.6 times unity was considered.

Load Cycle

Load cycle is a variable which cannot very well be averaged. In our study it was assumed for purposes of simplification that all load cycles were of the rectangular block form and that the peak occurred once a day. A range of peak duration from two hours for residential lighting load, to 24 hours for base load station transmission transformers was considered. Off-peak load was assumed to be steady at 25 per cent of peak. With rectangular load cycles, this fixed both load factor and loss factor as functions of duration of peak load during a 24-hour period. Results from this method checked with a reasonable degree of accuracy with detailed summaries on an annual basis made on various types of loads on our system.

Overloading with Less than Normal Life

One obvious question that had to be answered was whether or not loading with less than normal life was justifiable. Simply stated the question is this: "To obtain one per cent additional load beyond the limits for normal life from an installation, is it better to overload one per cent or to buy one per cent additional equipment?" A simple answer is obtainable by balancing the increased depreciation charge of the first method against the increased installed cost of the second method. Based on the accepted thermal data of the operating guide, a one per cent increase in load gives a one degree centigrade increase in maximum temperature. Also, a one degree centigrade increase in temperature indicates about nine per cent decrease in life. This would mean a corresponding increase in depreciation charges and in annual fixed charges. The cost of one per cent added capacity to serve one per cent added load will usually be less than the added cost due to shortened life of the existing capacity for one per cent load beyond the load for normal life.

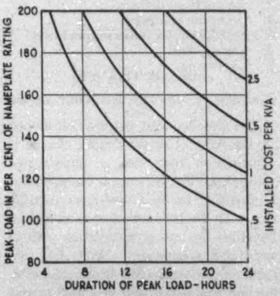

Figure 2. Effect of installed cost on economic peak load

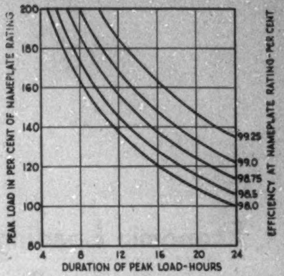

Figure 3. Effect of transformer efficiency on economic peak load

However, where the end of space capacity for a substation, for example, has been reached and increment cost for added kilovolt-ampere capacity must include building costs, daily loading for less than normal life may be cheaper than adding capacity.

It should be noted that these limitations of loading for normal life apply only to normal loading. Emergency loading with some sacrifice of normal life must be analyzed separately.

General

In order to take care of the many possible conditions of cost and loading, the basis of comparison was taken as the average total cost of losses and fixed charges for a kilowatt-year of output. The range of such costs as affected by duration and magnitude of peak load with all other factors constant is shown by Figure 1. It can be seen that the cost curves are quite flat where there is a point of minimum cost. This indicates that, for practical purposes, maximum economy may be obtained over a load range of 20 to 30 per cent.

For a complete study it is necessary to consider the effect of variation in the constants which have been fixed for the average condition shown by Figure 1. To lessen the total data to be compiled, all other curves were drawn to show only the maximum economic load for each set of governing conditions. Method of calculation of the curves is given in the Appendix.

As has been stated previously, all data were considered for a range of hours' duration of peak load, since this could not well be averaged.

Figure 2 shows the effect of installed cost per kilovolt-ampere on economic peak load with other factors remaining constant. This is a most significant set of curves showing as it does the effect of increased installation costs of the last few years on economic peak load.

Figure 3 shows the effect of transformer efficiency on economic peak load. Even at 98 per cent efficiency, economic loads are all above 100 per cent of nameplate rating.

Figure 4 shows the effect of change in ratio of losses on economic peak load. This effect should be given special attention where small transformers with high forced-cooled ratings are being used for normal high loads.

Figure 5 shows the effect of variations in cost of losses on economic peak load. Again, the loads are higher than practical thermal limits, but the figure shows what an increase in cost of losses to match present costs would do in the way of bringing down economic loads.

Figure 6 shows how daily loading with some sacrifice of normal life may be justified where installed cost for added capacity would be considerably higher than the installed cost per kilovolt-ampere of existing equipment.

Obviously these curves cover only a few of the average conditions of variables involved. For any specific case the formulas given in the Appendix may be applied.

These curves bear out the main point that the magnitude of losses and cost of losses are important factors in economic loading but that with present construction costs, installed cost is the main controlling factor. Unless cost of losses is much higher than normal or installed cost is lower than average, economic loading is higher than thermal limitations.

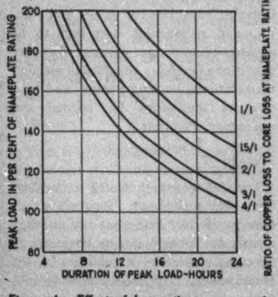

Figure 4. Effect of loss ratio on economic peak load

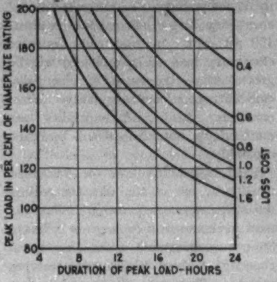

Figure 5. Effect of loss cost on economic peak load

THERMAL LOADING

The acceptance of the ASA "Guide for Loading Oil-Immersed Distribution and Power Transformers" C57.32—1948[1] as the criterion for safe thermal limitations of a transformer still leaves the interpretation and application to the user.

For thermal loading transformers must be divided into two groups. On the Commonwealth Edison Company system most station and substation transformers are operated in parallel banks. Maximum load on a bank is limited to that load which can be carried with the largest unit out of service because of an equipment failure. Failures are infrequent and such operation is treated as a rare emergency that justifies operation with moderate sacrifice of life expectancy. Since either the normal or the emergency condition may be the limit, both conditions must be studied.

For all distribution transformers and for power transformers that are not banked, there is only the normal operating condition to consider. Also, the total number of such transformers is much larger than the number of substation transformers. For this reason, the thermal loading will be covered in two parts, large power transformers and distribution transformers, although much of the data applies to both groups.

Power Transformers

NORMAL LOADING

For normal loading for normal life expectancy, the guide gives definite consideration to actual temperature rise of the transformer, ambient and load cycle.

For practical operation all large power transformers are assumed to have a 65 degree centigrade hottest spot copper temperature rise at nameplate rated load unless test data shows otherwise. Test data may be factory heat runs showing a rise less than 65 degree centigrade or they may be tests of an installed transformer showing a temperature rise greater or less than 65 degree centigrade because of cooling conditions other than those of the original design. Such changes may be a limited supply of air or water to give poorer cooling, or the addition of radiators, fans or other cooling facilities which make the transformer better thermally than its original design. For large power transformers not already fan-cooled, the use of auxiliary fans for added cooling should be a first step in increasing transformer capabilities.

Ambient temperature is always a subject for discussion. Theoretically, load ratings should vary through the year with ambient temperature. Practically, too many ratings complicate operation of a large system. It was found best to limit capabilities to winter and summer operation. For summer operation, a temperature of 30 degree centigrade was chosen as outdoor ambient. Actually this is the normal average maximum temperature for midsummer. On a life basis 30 degree centigrade can be considered conservative for both normal and emergency use without any special higher ambients for hot summer weather. For winter it was necessary to use an ambient that would allow for higher temperatures at both ends of the winter season. Also, for substation transformers it was necessary to allow for partial enclosures. A seasonal winter ambient of 10 degree centigrade was accepted, with lower ambients recognized for specific Christmas peaks. Comparably, cooling-water temperatures of 25 degrees centigrade for summer and 5 degrees centigrade for winter are used, based on 20-year water supply records.

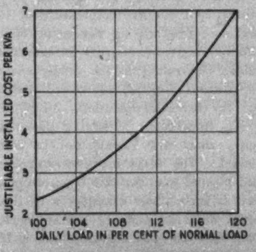

Figure 6. Justifiable installed cost per kilovolt-ampere where daily load exceeds load for normal life

For indoor installations, ambients are based as nearly as possible on actual records. Accepted policy is to ventilate indoor installations in summer, and to heat them in winter for personnel comfort. Where equipment is operated without attending personnel, ventilation is provided when necessary, but summer ambients are allowed to go to 40 degrees centigrade. Such temperatures may necessitate derating indoor transformers, but cooling below a summer maximum of 40 degrees centigrade is not usually economical.

LOAD CYCLE

Daily load cycle is based on measured data. For practical application most loads are either industrial or residential. Only for base load stations and other special applications is it necessary to use other load cycles. For general use ratings for eight-hour and four-hour loads cover all conditions closely enough.

EMERGENCY OPERATION

The loading guide gives elaborate curves for "Short-Time Loading with Moderate Sacrifice of Life Expectancy." Acceptance of these curves is not enough. They present the user with a choice of "Loss of Life" for which he may load, and it is up to the user to justify some specific level of short-time loading before he can apply the guide to his own system.

For the substation system to which the guide is being applied, large power transformers are normally operated in parallel banks of two to five transformers. Total load per bank is limited to that which can be carried with the largest unit out of service. Replacement time for any unit with available spares is from two to five days. Maximum emergency loading will occur only during an outage of the largest unit of a bank at the time of heavy load on the group. On the basis of such infrequent occurrence, emergency short-time loading was limited by a hottest-spot copper temperature of 140 degrees centigrade for residential loads, and 135 degrees centigrade for industrial loads. According to the guide, loss of life of insulation will not exceed two per cent for each such operation.

The importance of setting the emergency limit first should not be overlooked. The ratio between emergency and normal load for this type of operation is high. For example, with three equal units in parallel, the emergency load with one unit out of service is 150 per cent of the normal load. Parallel units are frequently of different size. For about 1,000,000 kva of installed capacity in 55 substations, the average ratio of emergency load to normal load is about 150 per cent. In most cases, ratio of emergency load to normal load will be greater than the ratio of emergency capability to normal capability. When emergency load and capability are matched up, normal load will be below capability.

Load capability can be increased usually by use of auxiliary fan cooling during emergency operation. The fans used for emergency cooling are ordinary 30-inch commercial units, having a capacity of about 10,000 cubic feet per minute. They were chosen, when first used, because they were readily available, portable, and inexpensive. Tests showed that for temporary use, four such fans would give satisfactory forced-air cooling on a 7,500-kva self-cooled transformer.

For the group of substations mentioned before, increased capability in emergencies up to about 25 per cent have been obtained by use of such fans. For the 55 substations, two complete sets of fans are available for emergency use. In this way, the ratio of emergency capability to normal capability has been brought closer to the ratio of emergency load to normal load.

CONNECTED EQUIPMENT

Load ratings for direct application to existing plant or their use in design of new plant must apply as well to the connected equipment that goes with the transformers.

A large group of transformers with some as much as 40 years old presents a variety of problems. But when connected equipment in the form of circuit breakers, disconnects, instrument transformers, cables, bus, and even meters, which had been installed over the same period must be considered also, the problem is just that much greater.

For this part of the problem there is no loading guide such as that available for transformers. A firm foundation for normal and emergency operation of such equipment had to be established from all laboratory and field data that could be found in the entire industry.

OIL CIRCUIT BREAKERS

There are no established overload ratings for oil circuit breakers. Reasonably, such a device can be operated at loads higher than nameplate if it is recognized that such operation will be at higher-than-normal temperatures and may require increased maintenance. The capacity gain economically justifies such operation as an emergency measure. Emergency operation at a maximum temperature up to 100 degrees centigrade was considered acceptable.

Where circuit breakers were not frequently operated, oxidation of copper contacts necessitated derating of older circuit breakers. On newer circuit breakers with silver contacts, condition was found to remain constant even though the circuit breaker might not be operated for long periods of time.

DISCONNECTING SWITCHES

Most old disconnecting switches had low-pressure copper contacts. Also, many were installed in flashproof housings. It was necessary to derate for condition of contacts and for temperature rise within the housing. However, for rare emergency operation, temperatures on such devices were allowed to go as high as 115 degrees centigrade.

Thermal conditions on many older switches have been improved by silver-plating the contact surfaces.

INSTRUMENT TRANSFORMERS

Instrument transformers were covered by the transformer guide. In application of the guide it was necessary to make proper allowance for ambients and enclosures. The co-ordination between nameplate ratings of instrument transformers and their application ratings in metalclad switchgear is being studied now by an AIEE committee.

CONDUCTORS

Cable ratings for specific applications have long been in use in the Commonwealth Edison Company. Most of these ratings were, however, for cables installed in conduit outdoors. The problem here was to evaluate the operating conditions of cables in air, cables in fireproof compartments, and cables in every kind of an environment that 40 years of progressive substation design could create. Carrying capability of copper rod, tubing, and rectangular bars had to be evaluated in a similar manner. In every case it was necessary to establish ambient temperatures, housing factors, and temperature limitations for normal and emergency operation.

METERS

Even ammeters presented a problem. Since their scales were a function of current transformer nameplate ratings, they usually did not have a range large enough to cover emergency capabilities of the transformers. The most economic solution to the problem was to use portable, multiple-range meters for emergency operation. The same meters were designed for use on other types of system equipment also, wherever emergency loads were off-scale on standard meters.

APPLICATION

Emergency load capabilities must be applied from two different points of view, system planning and system operation.

For planning, the load capabilities are furnished in detail. The transformer is the major unit, but all limitations of connected equipment are considered. The lowest limitation becomes the rating of the transformer. Ratings for each group of transformers supplying a common load are matched up with present and future load requirements. Group capabilities can then be increased by replacing limiting equipment up to the transformer capabilities. If a transformer is replaced with one of larger capacity, only those portions of the connected equipment which would limit the new transformer need be replaced. These procedures serve to develop a co-ordinated record of all equipment on a load capability basis, rather than on a nameplate basis, for planning future transformer requirements.

For operating, capabilities of the transformers are issued twice each year, giving only the limiting capability in each case for normal and emergency operation. Indicators are placed on the ammeters for each transformer showing these limitations.

The operator uses these indicators as the guide for safe loading of the transformer and all equipment directly connected to it.

Frequently the immediate result of these load capability surveys has been a temporary decrease in rating below the nameplate of the transformer until such time as a limiting piece of connected equipment could be removed. Quite often elimination of a minor bottleneck will increase the total safe capability 20 or 30 per cent. For both system planning and operating the analysis of load capabilities serves as a complete working guide.

RESULTS

First of all, the careful analysis of load capabilities of substation transformers has resulted in increased average loading of the transformer system. In the past five years, for the million kilovolt-amperes of substation transformers, the maximum loads have increased about 30 per cent. During that time only 3.7 per cent of actual transformer capacity has been added.

In other words, our normal maximum loading has increased about 26 per cent.

Effective capacity for the same installed kilovolt-amperes has been increased by acceptance of higher emergency loading conditions, with auxiliary emergency cooling, and by elimination of bottlenecks in connected equipment to permit the over-all use of these higher transformer loads.

Comparable gains have been made in loading of power transformers in applications other than the substation group on which the primary study was made.

Distribution Transformers

MASS PRODUCTION PROBLEM

The loading of distribution transformers in a large utility system differs from the problem of loading substation transformers, as discussed in the previous section of this paper, primarily in the number of units involved. In a city the size of Chicago, for example, approximately 40,000 transformer units are involved on the distribution system. Since these transformers serve relatively small loads involving small groups of customers, or, in some cases, only one customer, various load cycles will be involved. These may range from refrigeration loads having a summer maximum with long-hour use, to decorative holiday lighting in residential areas involving use for only a few hours each day for about ten days of the year.

Although transformer characteristics will vary considerably, each unit cannot be treated individually in the loading analysis. New transformers purchased during the past ten years vary as much as 15 degrees centigrade in the average copper temperature rise at full load, and as much as 20 degrees centigrade in the copper-to-oil temperature gradient at full load. Transformers removed from the line for reinstallation elsewhere on the system show varying degrees of sludging and blocked oil ducts. Some have shown extremely high copper temperature rise on full load test.

These variations would theoretically make it desirable to have a very large number of classifications in loading practice, depending upon type of load and transformer characteristics. However, it is obvious that a practical solution requires a certain amount of uniformity in the approach to the loading problem.

BASIS OF LOADING POLICY

Several limitations enter into the determination of a desirable loading policy for distribution transformers. Obviously economics would be a major consideration if other limitations were not lower than the economic limit. As indicated in the first part of this paper, calculations based only on transformer losses and fixed charges would indicate a desirable loading well in excess of practical limits.

Voltage regulation is an important factor in this problem. In a large distribution system it is common practice to adjust voltage regulating equipment supplying 4,000-volt distribution feeders to compensate for voltage drop in the primary feeder and drop in the average-loaded distribution transformers supplied through the regulators. This means that the heavily loaded distribution transformers will have a terminal voltage lower than standard, and lightly loaded transformers will have a terminal voltage higher than standard. Since there is considerable diversity in loading cycles of various transformers, the higher the maximum loading adopted for the system, the greater will be the spread between loads on individual transformers at any time, and the greater will be the voltage range. This situation can be somewhat alleviated, but not avoided, by the use of low-impedance transformers. Another factor of importance in the consideration of maximum loading is service continuity. Obviously any approach to the loading problem which results in a relatively short life of the distribution transformer increases the failure rate of transformers in service, with a corresponding detrimental effect upon the quality of service rendered.

Consideration of the factors mentioned before has led to the adoption of the ASA "Guide for Loading Oil-Immersed Distribution and Power Transformers," as a basis for determining practical limits to be applied on the large distribution system with which the writer is associated.

APPLICATION

In the application of this Guide to distribution transformers, load cycles are classified primarily as residential (short-hour, winter maximum), commercial (medium short-hour, winter or summer maximum). and industrial (relatively long-hour use, winter or summer maximum).

The residential transformers, in general, are permitted to carry 140 per cent of nameplate rating during the normal winter maximum load period, with a special allowance of 170 per cent during the holiday season. Transformers supplying commercial and industrial lighting and small power loads are given more individual attention. Demands on these installations usually are of somewhat longer duration than for residential transformers, and are usually higher in the winter than in the summer. Although sometimes limited by summer conditions, a maximum demand, in most cases, of 125 per cent of nameplate rating is permitted. Installations with a summer maximum, and installations enclosed in vault structures where limited ventilation may result in a relatively high ambient temperature, may be restricted to a demand of 100 per cent to 110 per cent of nameplate rating. Transformers supplying industrial power load are given individual attention in most cases, with resulting permissible loads varying from 100 per cent to 125 per cent of nameplate rating, depending upon the time of maximum demand and the load cycle involved. The average installation in this class is permitted to carry a maximum load of approximately 120 per cent of nameplate rating.

At the time of installation of a transformer in any of the classifications mentioned before, the probability of future load increase is studied and a transformer installed which is believed adequate to handle the load at that installation for at least six years before replacing. Load supervision over all transformers is maintained through a periodic check of connected loads in the case of residences and small commercial customers (from card records), maximum demand information from meter records in the case of larger installations, and from a regular program of field measurements of approximately ten per cent of all transformers each year. These measurements not only provide accurate data on the immediate loading of the installation tested, but also provide basic data for estimating demands on transformers not tested.

RESULTS

The average loading reached on a large transformer system will depend upon maximum load permitted, available sizes of transformers, rate of growth, and replacement labor costs. Distribution transformer loads on radial systems are not affected as a rule by emergency ratings, as is the case for substation transformers.

At the present time, the average loading of the distribution transformers in the system referred to is estimated at 95 per cent of nameplate rating. This loading has increased gradually over the past years from approximately 73 per cent, the figure which applied in 1939 under a less severe loading policy. This increased loading represents a saving of over 400,000 kva in transformer capacity, or approximately 19 per cent in investment in transformers installed. This improvement in transformer loading and saving in investment have been effected with relatively small increase in service interruptions. Although the rate of interruptions has risen slightly since 1939, it is still well below acceptable limits. Some further increase is anticipated over a period of years, but the present margin between failure rate and satisfactory service is considered adequate to allow for this trend.

CONCLUSIONS

Present high costs of electric plant have raised the economic limits of transformer loading far beyond the practical thermal limitations of loading for a reasonable life of the equipment.

Proper application of the ASA Guide for Loading Oil-Immersed Distribution and Power Transformers[1] can raise the average loading of most transformer systems.

For daily loading it is not usually economical to load transformers for less than normal life.

For infrequent emergency use, operation with some sacrifice of normal life is justified. Where emergency and normal loading must be coordinated, use of auxiliary cooling during emergencies will permit increased emergency loads and in turn may raise the permissible normal loads.

Transformers are only part of any electrical circuit. Wherever transformers are loaded according to thermal limitations, full consideration must be given to the thermal and electrical limitations of all other parts of the circuit.

Appendix. Formulas for Curves

In Figure 1

$$A = \frac{LN^2CS + LF + RD}{NT}$$

where

A = Total annual cost of fixed charges and losses, per kilovolt-ampere

L = annual cost of losses per per cent load per kilovolt-ampere

N = economic peak load in per cent of nameplate rated full load

C = copper loss in per cent at nameplate rated full load

F = core loss in per cent of nameplate rated full load

R = rate of annual fixed charges in per cent $\times 10^{-2}$

D = installed cost per kilovolt-ampere of nameplate rated full load

S = loss factor

$= \frac{H+P^2(24-H)}{24}$ for a rectangular load cycle

T = load factor

$= \frac{H+P(24-H)}{24}$ for a rectangular load cycle

H = duration of peak load in hours

P = off-peak load in per cent of peak load $\times 10^{-2}$

In Figures 2, 3, 4, and 5

$$N = \sqrt{\frac{LF+RD}{LCS}}$$

In Figure 6

$$J = \frac{DK(\epsilon^{0.0865t} - 1)}{Rt}$$

J = justifiable installed cost per added kilovolt-ampere

K = annual depreciation charge

t = load in per cent above normal full load

Reference

1. GUIDE FOR LOADING OIL-IMMERSED DISTRIBUTION AND POWER TRANSFORMERS, *C57.32–1948*. American Standards Association (New York, N.Y.), 1948.

Discussion

W. R. Brownlee and **J. A. Elzi** (The Commonwealth and Southern Corporation, Jackson, Mich.): So many factors enter into the economic loading of transformers that each general type of application usually will justify specific analysis. Therefore, the authors have been especially helpful in providing a series of curves showing the range of influence on economic loading of the various important elements.

The authors conclude that economic considerations, other than transformer life, would dictate loadings considerably in excess of present practices, but that the extra depreciation charges would make it uneconomical to load units beyond the point where the normal expected life begins to be reduced. This might naturally lead to speculation on the desirability of transformer designs of smaller physical size and correspondingly higher losses, but with means for more rapid heat dissipation, along the lines of some of the forced cooled varieties of transformers now available. Comparisons of such units for a specific application, such as a base load generating plant may show that the larger transformer is not necessarily the higher cost unit.

The comparison given in Table I of the discussion is based on a conservative value of

Table I. Comparison of 3-Phase Oil-Immersed Transformers

75,000 Kva, 138-14 Kv, 55 Degree Centigrade Average Rise, 65 Degree Centigrade Hot Spot Rise

	Self-Cooled	Forced Air Cooled	Forced Oil and Forced Air Cooled
Per cent IZ	8	10	12
Iron loss, kw	142	122	111
Copper loss, kw	233	308	400
Auxiliaries, kw		9	26
Total loss, kw	375	439	537
Cost	$186,000	$167,000	$131,000
Evaluation of losses			
Capacity charge, kw	0	6,400	16,200
Energy charge, kw	0	15,360	38,880
Cost plus kw loss charges	$186,000	$188,760	$186,080
Capacity charge, kvar	0	15,000	30,000
Total comparative costs	$186,000	$203,760	$216,080

$100 per incremental kilowatt of generating capacity, an average weighted energy charge of 3 mills per kilowatt hour and on full load operation of 8,000 hours per year with operating costs capitalized at 10 per cent. In addition to the value of the kilowatt losses, account should be taken of changes in transformer reactance with reductions in physical size and corresponding increases in kilovar losses. In overhead transmission systems, especially if the generating station is in a load area, the extra kilovar loss may be evaluated at, say, $10 per kilovar. The table compares a self-cooled, forced air cooled, and forced oil-forced air cooled version of a 75,000-kva 3-phase 138-kv transformer on the basis of cost (transformer alone), evaluation of kilowatt losses and adjustment for kilovar losses.

It is seen that the first cost of the self-cooled transformer is $55,000 or 42 per cent greater than that of the forced oil-forced air cooled unit. However, with proper evaluation of the differences in kilowatt losses (including auxiliaries), there is little difference in the combined cost, and if a reasonable value is assigned to the extra kilovar losses in the smaller forced oil-forced air unit, the self-cooled transformer is $30,000 or 14 per cent lower in over-all cost than the forced oil-forced air unit. Where cooling water is required for other purposes, such as generator cooling, the application of a water-cooled transformer at a generating station may show rather startling over-all economies which will overshadow the increased operating attention which they may require.

Even in the case of this specific example of a generating unit transformer, the individual circumstances must govern, especially where 3-phase units of the larger sizes cannot be built economically except in the forced-cooled (or water-cooled) type. In view of present trends in construction costs and the costs of electric power on an integrated system, a review of basic transformer designs seems in order to provide a better economic balance of fixed and operating charges without encroaching on transformer life.

D. L. Levine and **H. E. Smith:** W. R. Brownlee and J. A. Elzi have examined the case of the base load station where the transformer carries almost a continuous steady load. They show that the higher initial cost self-cooled transformer with low operating cost has a lower annual cost than the lower priced forced-air or forced-oil cooled transformers with their higher operating costs.

This case could be examined by the methods of the paper. The transformers having forced cooling can be considered as smaller transformers operating at overloads thermally permissible because of added cooling.

Cost curves for these transformers would show that, for continuous loading, such overloads would not be economical.

Transformer Audio Noise Problems on an Electric Power System

C. S. MURRAY
ASSOCIATE AIEE

Synopsis: Since the end of the war, increased load demands, together with the location of housing developments in the vicinity of the power station, tend to make the electric power company more susceptible to noise complaints than ever before. Power companies which had not been concerned with the noise problem in the past now have become involved. The various factors of noise are covered and explained insofar as they apply to a transformer, one of the most common sources of noise. It is hoped that the review and discussion of the problems which exist may be of value to those interested in transformer noise, particularly to the transformer manufacturers and those responsible for transformer noise standards. The experience and views of others, which have been reported elsewhere, are discussed, and a list of references is given for those who care to go into the problem in more detail.

BEFORE the last war the general public was becoming noise conscious and was insistent that all types of objectionable noises be eliminated. During the war, however, the public realized that it could not conscientiously make the same demands of their power company, that had been called upon by the government to supply as much power as possible with the equipment which was available. It was realized in a number of cases, that equipment had been pressed into service that normally would have been used for standby service only. In other cases, equipment could not be removed from service in order to make improvements, or materials for making improvements were not available.

After the war, the public picked up where it had left off prior to it. However, in addition to the revived interest of the public, there are other factors which tend to make the power company more susceptible to noise complaints than at any time in the past. There was a time when generating stations and substations were located in nonresidential areas, but since the war, housing developments have been built adjacent to these stations. Because of the increased load demand, it has become necessary to increase the capacity of the existing stations. Economics demands that the additional power transformers be of the larger sizes and be installed outdoors. Then again, due to load increases, it has been found economical and sometimes necessary to locate unit substations at the load centers, which are in inhabited districts. In many cases the capacity of the power transformers for the packaged unit can create sufficient noise to make their presence in the area objectionable unless proper precautions are taken in the design of the transformer. The distribution system located in a metropolitan area also enters into the transformer noise problem. Because of the nature of the system, it is necessary to install transformers in vaults beneath the streets and in the basements of various buildings. In many of the taller buildings, vertical networks are used; the transformers are located on the upper floors, sometimes with offices on floors both above and below the transformer vaults.

One would surmise that the power company located in a metropolitan area is more concerned than any other with the noise problem. This is true, but when the foregoing factors are considered, any company with outdoor transformer installations, except those in areas remote from residential buildings, is susceptible. As the power demands increase, the transformer noise problem undoubtedly will become increasingly important.

There is very little information in the technical literature to aid the power engineer in obtaining a clear understanding of the transformer noise problem. What information there is available is scattered over many articles. Most of the literature covers the entire audio band, whereas in transformer noise problems the band usually is restricted to frequencies below 500 cycles which are multiples of the power frequency. Very little has been published concerning outdoor noises of this type. The problem is a complex one and is far removed from the problem that the sound engineer has in the laboratory or at indoor locations. It is hoped that the following material, much of which is considered in detail in the references, may be beneficial to those concerned with the problem. It is an attempt at bringing into a single article the highlights of transformer noise as it concerns the power engineer.

The Cause of Transformer Noise

It has been fairly well established that the audio noise of a transformer is caused mainly by the change in dimensions produced in the steel core when it is magnetized. This has been termed magnetostriction. The alternating magnetizing force sets the core in vibration. This vibration is transmitted with small attenuation through the oil and tank to the surrounding air. This results in the characteristic hum emitted by transformers. The amount of noise emitted and its frequency depend on the induction, magnetostriction, and nature of the iron, and on the weight and linear dimensions of the core.[1,2]

If the supply frequency is considered as 60 cycles, the frequency assumed throughout this paper, the noise emitted will have a fundamental tone of 120 cycles per second and harmonics of this frequency. In general, the outstanding noise from distribution transformers is

---

Paper 49-191, recommended by the AIEE Transformers Committee and approved by the AIEE Technical Program Committee for presentation at the AIEE Summer General Meeting, Swampscott, Mass., June 20–24, 1949. Manuscript submitted March 21, 1949; made available for printing May 5, 1949.

C. S. MURRAY is in the Electrical Engineering Department, Consolidated Edison Company of New York, Inc., New York, N. Y.

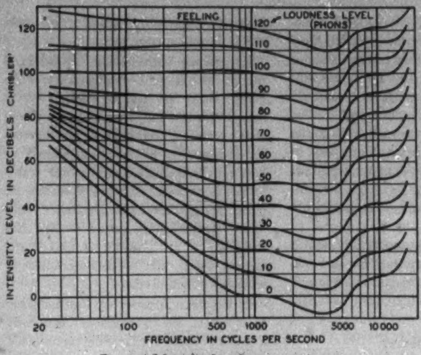

Figure 1 (above). Loudness contours

Reproduced from ASA Standard Number Z 24.2—1942

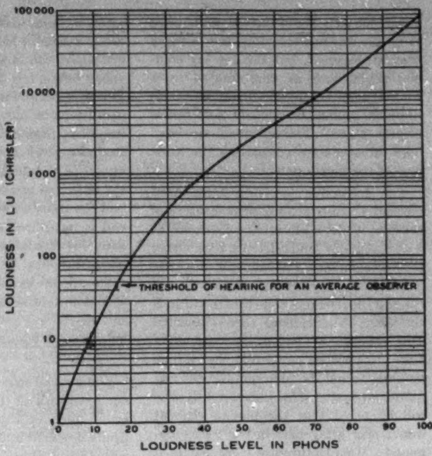

Figure 2 (right). Relation between loudness and loudness level

Reproduced from ASA Standard Number Z 24.2—1942

usually of a frequency of 120 cycles, while for the larger power transformers the outstanding noise may have a frequency of either 120 cycles or 360 cycles. Occasionally, the 240- and 480-cycle components may be outstanding. Therefore, it may be said that, in general, only that range of frequencies between 120 and 480 cycles need be considered here.

Response Characteristics of the Human Ear

Before any equipment can be designed to measure the noise, or before the noise from the transformer can be evaluated properly, we must have some knowledge concerning the characteristics of the ear. It is the ear which dictates whether a sound is objectionable; it is the final judge or arbiter.

Probably the most important aids in understanding the ear are given in ASA Noise Measurement Standard[3] in the form of curves. Figures 1 and 2 are reproductions from that standard, and the power engineer should become acquainted with them.

Figure 1 shows the equal loudness contours for pure tones. The ordinate for the curves is the intensity level, a measure of the amount of noise emitted. For these curves and in most practical sound work the unit is the decibel. The decibel is actually the measure of the ratio of two amounts of power, one being the intensity of the sound under consideration, and the other a reference intensity which, at the present time is 10^{-16} watts per square centimeter. Expressed mathematically

$$\text{Intensity Level} = 10 \log_{10} (I/I_0) \text{ decibels} \quad (1)$$

The ear responds to intensities from minute values to values 10^{12} times as much. The use of decibels provides a practical scale to cover the enormous range. It will be noted that increasing the intensity 10 times results in a change of 10 decibels; doubling the intensity results in a change of 3 decibels. An inspection of the contours shows that the response of the ear depends both on intensity level and frequency of the tone. All pure tones having intensity levels and frequencies on the same contour are equally loud. A 360-cycle note having an intensity level of only 54 decibels is just as loud as a 120-cycle note having an intensity level of 65 decibels, both being on the *50* contour. Both of these tones have a loudness level of 50 phons. The loudness level in phons (phons to distinguish from decibels) of a sound is equal to the intensity level in decibels of the equally loud 1,000-cycle-per-second tone. For these contours various tones were compared with the equally loud 1,000-cycle tone used as a reference.

Figure 2 shows the loudness as a function of loudness level. The loudness scale is such that the ratio of any two loudness values indicates the relative loudness between two tones. For example, a tone having a loudness of 8,000 loudness units is twice as loud as one having 4,000 loudness units.

The use of the two curves gives us a means of determining how much louder one noise is than another. Knowing the intensity level and frequencies of both noises, we can obtain their loudness levels from Figure 1 and their relative loudness from Figure 2.

Figures 1 and 2 are based on pure tones and are obtained under conditions where the background noise or ambient noise is small so as not to interfere with the pure tone heard by the members of the sound jury, who used their ears in the determination of the curves. The presence of other tones would alter the curves, since these other tones might mask (raise the threshold of hearing for a tone to some higher value) the tone under study. Investigations have been carried out whereby the curves may be used for complex tones, that is, those of more than one frequency.[4]

Objective and Subjective Principles of Noise Measurement

The objective principle of noise measurement is employed generally in transformer-noise measurements in the United States. The sound level meter is based on this principle of measurement and is discussed below. In order to evaluate the noise from a transformer, one must understand the limitations of his equipment for measuring that noise.

Obviously, the ideal noise measuring instrument would be one in which a single meter would indicate the loudness of a noise of any type in terms of a primary standard. In order to design this meter, the response of the ear would have to be known, not only for pure tones as given in Figure 1, but also for any complex sound such as that emitted by a transformer. The response of the ear to complex sounds is still in the experimental stage, although methods have been advanced for calculating the loudness of complex sounds.[4]

The subjective or aural comparison method of noise measurement, consists of comparing the noise under measurement with an equally loud reference tone, either pure or complex. For example, the noise under study may be listened to with one ear and the reference tone listened to with the other. The reference tone is adjusted until it is equally loud to the noise under study. It will be noted that the relative loudness could be determined for any sound no matter how complex. It also will be noted that the human element would play a big part in the values obtained. Manufacturers of noise meters in the United States have concentrated on the objective noise meter.

The objective principle consists in having a meter with a response based on the equal loudness contours given in Figure 1. When a pure tone of any frequency is being measured, and assuming the meter is equipped with means to follow all the equal loudness contours of the ear, the meter will indicate the equivalent 1,000-cycle-per-second value. This type of meter, equipped with all the equal loudness contours given in Figure 1, can be used to obtain the loudness of a pure tone. However, when a complex sound is being measured, the meter operates to sum up the energy in the equivalent 1,000-cycle values and indicates this energy sum in a decibel value. This assumes that a given pure tone of the complex sound will be just as loud regardless of the presence of other tones. Measurements made by various investigators show that the ear is not responsive to an equivalent energy summation.[4,5] In the case of transformer noise the summed equivalent energy sometimes is practically equal to the energy of the largest component. The objective meter would indicate a value practically equal to that of the largest component. However, the investigators[4,5] show that the presence of harmonics might make the noise much louder, even though its contribution to the total equivalent energy is negligible. In one case,[5] in tests on ring cores of transformer steel, the objective meter indicated a loudness level of 58 phons and the subjective meter a value of 87 phons. Referring to Figure 2 it will be noted that the objective meter indicated a value about 1/8 as loud as actually existed. Many have found, however, that the objective meter indicates values only a few decibels below the subjective method for sounds not predominantly harmonic in character.[5,10] The American Standards recognize that the loudness level indications may be in error.[6] The sound level meter based on the objective principle has been a useful tool for transformer noise measurements and is recognized as the best means, to date, for obtaining a quantitative noise measurement. Its limitations and the assumptions based on its indications should be kept in mind.

The Sound Level Meter

Commercial sound level meters are not equipped with all the equal loudness contours given in Figure 1. Most of the available sound level meters are equipped with three scales, one approximating the *40* equal-loudness contour, another the *70* equal-loudness contour; the third has a "flat" responsive characteristic. The meter, with its weighted scales (*40* and *70*), is the result of an attempt to duplicate the action of the ear for complex sounds in a practical manner. The response and tolerances for sound level meters have been specified by the American Standards Association.[6]

The sound level meter indicates the sound level of the total noise, a frequency analyzer being necessary for measurement of the components of the noise.

The question often arises as to which scale or weighting network should be used for a particular noise measurement. A chart showing the loudness that would be indicated by each of the three scales for various intensity levels as compared to the loudness as would be interpreted by the ear is given in Figure 3. Pure tones of the frequencies most often met with in transformer audio-noise measurements are given. A 1,000-cycle tone also is given for comparison and shows that the scales all indicate the same value for this frequency. The charts are based on Figures 1 and 2 and the design objective of the ASA Standard for Sound Level Meters.[6] If it is desired to obtain a measurement of the noise that will approximate the loudness indicated by the human ear, the chart will indicate which scale should be used. For instance, the chart shows that for an emitted noise (intensity level) of 80 decibels, having a frequency of 120 cycles, the 70-decibel scale should be used. In transformer audio noise measurements the 40-decibel scale usually is specified regardless of intensity level or frequency. This practice is discussed later.

Experience with various sound level meters of different manufacture while being used in making sound level measurements on transformers shows that certain precautions and procedures must be followed. It should be borne in mind that nearly all transformer noise measurements on an electric power system are made outdoors. Ambient temperatures, stray fields, and varying ambient sound levels (background noise) offer problems not met in laboratory measurements.

It has been found that low temperatures affect the microphone, especially if it is a crystal type, and the meter itself. In tests at temperatures near freezing, with battery operated meter and a crystal microphone, the value of sound level may be in the order of 10 decibels below the value it would indicate at normal room temperature. The major part of this difference is attributed to the crystal microphone. This experience indicates the necessity of using a standard source of sound for over-all calibration of the microphone and meter. It is an accepted practice by many not to make any measurements until after the equipment, both meter and microphone, has been exposed to the existing temperatures for an hour or so.

It also has been found that most sound level meters are not sufficiently shielded against stray fields that may exist in the field. The crystal microphone generally is not affected, but experience with dynamic microphones of the moving-coil type shows that large errors may result from stray magnetic fields. Usually any effect on the equipment can be detected by orienting and moving it with respect to the field. Generally, the meter is placed at some distance from the transformer, the microphone being connected to the meter through shielded leads.

Ambient sound levels of high intensity and varying magnitude exist during the day; this usually demands that the sound level measurements be made during the early morning hours. Sound level measurements should be made when the ambient sound level (sound level when the transformer noise is turned off) is at least 10 decibels below the transformer noise.[7,8] There are methods of correcting for the transformer sound levels if the 10-decibel difference cannot be attained.[8,9] Even when measurements are made at night, street traffic, whistles, trains, chirping of birds, and many other noises interrupt the measurement. There also is another reason for making tests during the early morning hours, especially when measurements at locations remote from the transformer are desired. It is during this period that the transformer noise is most audible and the likely time when this noise will be most objectionable.

Experience shows that the use of the sound level meter by itself is not sufficient in most measurements made at locations remote from the transformer. The sound analyzer used in conjunction with the sound level meter is almost a necessity, in order to evaluate the noise. Many times tests are made to detect the magnitude of improvements made to eliminate objectionable noise. The improvement often does not show up in the indication of the total noise value but in the value of the component frequency only.

Tests often are made to check the measurements made by others. The ASA response characteristics[6] allow a tolerance for sound level meters such that two different meters could indicate values differing by 5 decibels for a noise having a frequency of 120 cycles. This is a considerable difference when it is kept in mind that two equal sources of noise when sounded together will only produce a sound level value of 3 decibels above that value when either is sounded alone. Many users have their meters calibrated by a standardizing sound laboratory to obtain the correction that must be applied to their meter to place its indications at the "design objective."

Objectionable Noise

The problem of determining whether a noise is objectionable is a complex one. A noise which is loud may not be objectionable, although there are many who feel that until the limit of objectionable noise is arrived at, loudness should be the criterion. A noise that is objectionable in one case may not be objectionable in another. The existing ambient noise plays a large part in this determination. In general, unpitched noises, that is, noises which do not have any particular component frequencies, are not objectionable if from 15 to 20 decibels below the total noise at the location considered. Masking of these noises by the existing ambient noise may make them unnoticeable. Pitched noises, those having a single outstanding frequency, are extremely objectionable, and it may be necessary for them to be more than 20 decibels below the total noise in order not to be objectionable.

Noises of the higher frequencies are more objectionable than equally loud low-frequency noises. Noise which is varying continually in intensity or frequency is particularly objectionable. There have been low-frequency noises, caused by extremely large objects in vibration, which were barely audible but gave a feeling of uneasiness. There are no definite ranges of sound levels and frequencies to define an objectionable noise. The power engineer must use experience to estimate whether the noise emitted by his transformer is objectionable.

Transformer Noise Standards

The National Electrical Manufacturers Association Standards for Transformers[7] specify the procedure for obtaining the "average" sound level of a transformer. These standards also specify the average

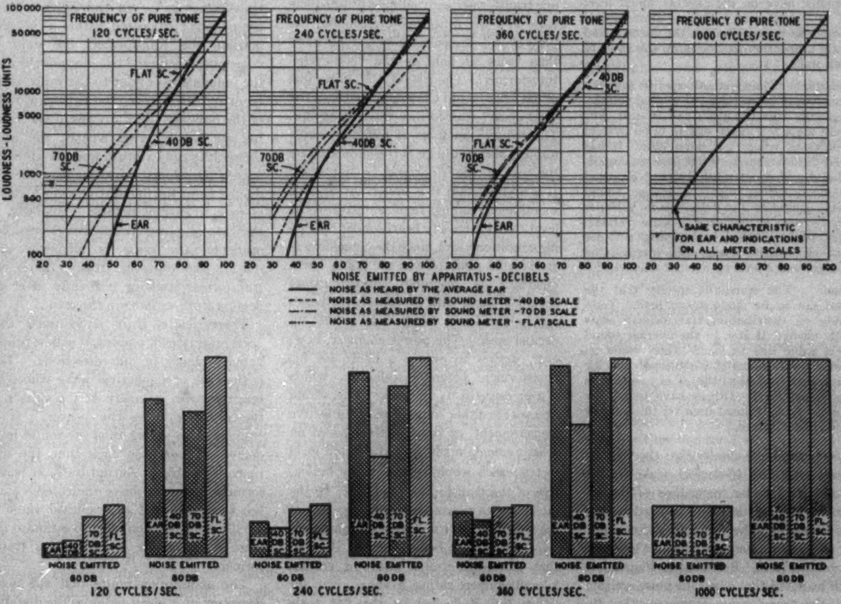

Figure 3. Comparison of sound level meter scales with the human ear for different pure tones

(Above) Apparatus noise measurement; (below) direct comparison of loudness sound level values of the total noise that distribution and power transformers should not exceed.

Briefly, the average sound level value is determined by averaging the readings obtained at a number of points around the transformer, at specified heights and at a distance of one foot from the major sound-producing surfaces. There are other specified conditions of making the tests, and the power engineer may not be able to comply with some of them. He is then left with the problem of determining what effect these conditions have on any measurements he may make.

Some of the conditions are as follows:

Location of Transformer. The standards specify that the transformer be located so that there is no acoustically reflecting surface, other than the floor or ground, within 10 feet of the transformer. This presents no problem where distribution transformers are concerned, since they could be removed to the laboratory where a supply is available to energize them. However, with power transformers, the manufacturer himself may find it difficult to obtain an adequate supply and space for factory tests. Once installed, the transformer is separated from other electric apparatus by means of fire walls. There is very little information as to what effect the fire walls, which are acoustically reflecting surfaces and less than 10 feet from the transformers, have on the average sound level of a transformer. Power transformers should be noise-tested at the factory and again at location to determine the effect of such walls.

Voltage. The standards specify that the transformer be energized at normal voltage. Generally this condition can be met, but there are a few cases, due to other system conditions, when it is impossible. It has been found from tests on 3-phase liquid-filled distribution transformers of 500- and 1,000-kva rating, that the average sound level changes by 2 to 3 decibels for a 10 per cent change in balanced 3-phase voltage. Tests made by others indicate that a 10 per cent increase in voltage will increase the average sound level by about 2 decibels.[10,11]

Load. The standards specify that the tests are to be made at no load. Tests made on distribution transformers show little change, if any, in the average sound level value due to load. Tests made on power transformers of 60,000-kva capacity show that load has little, if any, effect on the sound level. Others have found the same.[12,13] Additional data on this subject should be obtained.

The standards specify that the tests be made with the 40-decibel scale on the sound level meter, regardless of the intensity level of the noise emitted by the transformer. The component frequency or frequencies, loudness level, or loudness is not specified. Referring to Figure 3 it will be noted that when the noise emitted by the transformer increases, the 40-decibel scale ceases to give an approximate picture of the loudness, and that either the 70-decibel or the flat scale would indicate the loudness better for the higher intensity levels.

In general, distribution transformers of 500- and 1,000-kva rating emit noise of such values on the 40-decibel scale as to approximate loudness level. However, above a given kilovolt-ampere rating, the amount of noise emitted is of such a value that the 40-decibel scale indicates a value much below the loudness level. For example, the NEMA standards specify a sound level of 80 decibels for a 50,000-kva transformer. Assuming the noise emitted has a frequency of 120 cycles, this is equivalent to an intensity level of 96 decibels. The loudness level in phons indicated by Figure 1 would be about 96. Referring to Figure 2 and comparing loudness units for 80 and 96, it will be noted that the transformer actually will be over three times louder than indicated by the meters. Others have pointed this out too.[13] Looking into the matter further, and still considering the 50,000-kva transformer above, the standards specify 80 decibels sound level.[9] Two manufacturers could each supply a transformer having an average sound level of 80 decibels on the 40-decibel scale. Yet if one transformer emitted mostly 120-cycle noise and the other 360-cycle noise, the "120-cycle" transformer would be more than twice as loud as the "360-cycle" transformer. The use of the 70-decibel or flat scale would have indicated that the "120-cycle" transformer was the louder. The relative loudness of different transformers also would be better indicated by the use of the 70-decibel or flat scale. It is argued[8] that it is important to have sound level readings representative of the level that is actually heard under operating conditions, and, since the transformers are located remote from the point where quietness is desirable, measurements should be made with the scale corresponding to the lower level, that is the 40-decibel scale. The power engineer, however, desires to obtain a figure for his transformer, before installation, which is a measure of its loudness. This would necessitate either some form of subjective measurement, or some method based on measurements made with the sound level meter which would offer a value indicative of the transformer loudness. In the interim, with measurements being made at the 1-foot distance and with a single sound level meter value being specified, it is felt that for transformers above a certain kilovolt-ampere rating, a value given for either the 70-decibel or the flat scale would be more indicative of the transformer loudness than a value for the 40-decibel scale. The matter should be reviewed by those responsible for transformer audio noise standards.

Tests have been made on a 60,000-kva transformer having an average sound level closely approximating that specified by the National Electrical Manufacturers' Association. The 360-cycle component of the transformer noise, at a point 1,400 feet distant, was about 5 decibels below the total noise at that point. The transformer noise was audible and in the objectionable range. Power transformers supplied in accordance with the National Electrical Manufacturers' Association recommended sound levels have caused and will cause, in many cases, noise complaints. It is felt that a more realistic approach to this problem is required on the part of the manufacturers and bodies responsible for standardization of sound levels.

Transformer Noise at Locations Remote from a Transformer

The noise reaching an observer who is located remote from the transformer is either air-borne or transmitted to him through rigid connections joined to the transformer case. In the latter case, if the observer is located within a building housing the transformer, the noise is transmitted from the transformer through the foundation or floor to the walls of the room and thence over the structural work of the building. If the walls of the housing are not of great weight, the walls themselves may vibrate and set up other noises. Outdoors, the noise may be conducted from the foundation over a strata of rock to distant points. Generally, in the case of power transformers installed outdoors, the noise is air-borne and reaches the observer directly from the transformer itself or indirectly after reflection from surfaces in the area.

Theoretically, if it is assumed that noise originates at a point, it will be propagated radially in all directions. This is the case of a spherical wave whose intensity varies inversely as the square of the distance from the source. It is equivalent to saying that the sound level decreases 6 decibels each time the distance is doubled. Actual tests on transformers in service have indicated values less than this, and an empirical value of 4.5 decibels has been used to estimate the noise at a remote point from a transformer.

The assumption made that the noise decreases at a given value as the distance from the source is increased does not hold if the phenomenon known as interference exists. Sound waves of the same frequency are emitted from different areas, resulting in the effects of the individual waves adding at some points and subtracting at others. In this case, for a range of distances from the transformer, the intensity of the sound goes through a series of maximum and minimum before reaching a distance where the intensity decreases as indicated without interference. The indirect sound from reflecting surfaces such as nearby walls or ground will interfere with the direct noise. The indirect noise may come from some other area of the transformer itself, especially if the dimensions of the source are large compared to the wave length of the sound, which might be the case. Interference may be set up by noises from adjacent transformers. Tests have been made by others[14] which show that the transformer noise at 150 feet from the transformer was as much as the noise 10 feet away; at certain points remote from the source, the transformer noise was more than at positions much closer.

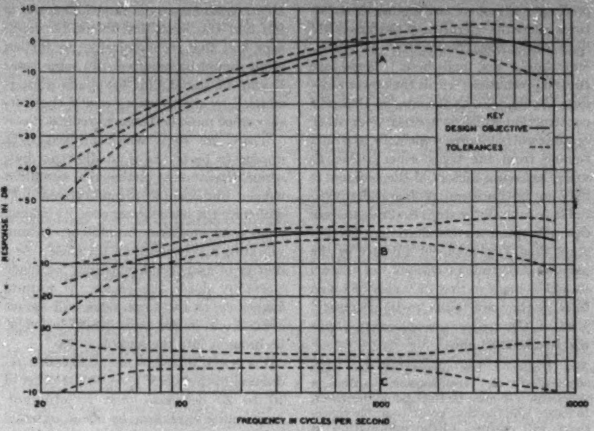

Figure 4. Over-all free-field response-frequency characteristics and tolerances for sound level meters

Reproduced from ASA Standard Number Z 24.3—1944

When measurements are made at the transformer within one foot of the case, the indication of the sound level meter, which is the total noise, remains fairly steady at any one point, assuming that the ambient sound level is at least 10 decibels less than the transformer noise. At any one point there may be a variation of the individual components, depending on the frequency of the component being measured, physical size of the transformer, and nearby reflecting surfaces. At some remote point, assuming that the ambient noise remains at a fixed level, the indication of the sound level meter varies over a small range, usually not more than 1 or 2 decibels. However, the variation of the individual components of the noise may be considerable. The variation is caused by slight variations in the system frequency, variations of wind velocity and direction, and any movement in space of large reflecting areas, such as trucks or trains. Any of these variations may change the existing wave pattern. The amount of observed variation depends considerably on the wave length of the component being measured and the sharpness of the tuning of the sound analyzer. Generally, the components are measured over a period to note the variation and to arrive at minimum, maximum, and average values. It is the maximum transformer noise which exists over a period with which we are concerned. The human element plays a big part when using indicating instruments. Some prefer a recording of the various component noises on a chart. It would be necessary, then, to mark the chart during those periods when extraneous noises occur in the vicinity.

For large power transformers the components of the noise from point to point around the periphery of the transformer differ in magnitude and in relative value with respect to each other. To obtain the average sound level of a given component would necessitate measurement of it in the same manner as when determining the average total sound level. Generally, when the components of a transformer are desired, the noise at some distance from the transformer is analyzed.

Distribution Transformer

When the average sound level of a distribution transformer is desired, sound level measurements must be made even though data are available on a similar one. The results of sound level measurements, made on 25 transformers of different manufacture, show that the average sound level may differ by 15 decibels. Transformers of the same type and manufacture may differ by as much as 6 decibels, a variation which can be the difference between a noisy and a quiet transformer.

In general, when complaints arise from transformers located beneath the streets, the complaint is due to air-borne noise. If a complaint arises from a transformer installed in the basement or other floor of a building housing the complainant, the complaint may be due to either or both air-borne noise and noise transmitted through the floor and other structure of the building. When the latter is the cause, improvements can be obtained by placing vibration dampeners beneath the transformer and between any cable hangers and the transformer connections. There should be no rigid connection between the transformer and the structure of the building. The application of sound absorbing material to the vault walls and ceiling to decrease the noise due to multiple reflections is seldom found to be necessary. Every reasonable precaution should be taken to prevent installation of a noisy transformer in a quiet neighborhood.

Power Transformers

When large power transformers are to be installed in areas adjacent to which are residences, the noise emitted by the transformer may prove costly unless proper consideration is given to this problem as early as the purchase stage.

The transformer manufacturers should be made acquainted with the problem at hand and impressed with the fact that quiet transformers are necessary. This means that noise must be considered in the design stage, since it is practically impossible to decrease the noise level of the equipment itself once it has been built. Consideration also must be given to the design of any fans that may be used for cooling, since there are known installations where the operation of the fans could have caused noise complaints. The problem should not end here. There are certain precautions which the power engineer should take at the site, so that any construction which is necessary for other reasons will not increase the noise at points remote from the transformer. Due to many unknown factors of the problem it may not be considered economically justifiable to take all the steps that might seem desirable prior to installation. Certain steps should be taken in advance of the installation, and provisions for others should be made so that they may be taken later, if they are found to be necessary. Two of the major precautionary items will be discussed now.

Fire Walls. The placing of fire walls adjacent to the transformer is often a necessity. It may be impossible, however, to locate walls so that no undesirable reflections will result. Little information is available which shows the effect of such walls on the noise. Tests made at the factory, with the transformer located at least 10 feet from the nearest reflecting surface, and again after installation with the walls in place, will afford some information. Such a procedure would require data for a considerable number of cases; years might be required to obtain it. There is a possibility that small scale models can be used to study the subject in general, so that the power engineer could obtain a clearer understanding of the subject.

In some instances the application of sound-absorbent materials on the side of the walls facing the transformer has been considered as a means of decreasing the reflection of the noise from them. Unfortunately, there are no known absorbent materials that are suitable for outdoor use which have good absorption coefficients for the 120- to 360-cycle frequency range. Recently, in Denmark, Helmholtz resonators were built into the interior walls of various buildings, resulting in good absorption coefficients for the lower frequencies.[16] In one case, the resonators were made up of regular enclosures in the brick walls together with special tiles with circular openings. At present there are no known similar installations in this country. The possibilities of applying the idea here should be considered by those concerned with sound-absorbent materials and methods.

Transformer Foundation. Placing the transformer on a foundation on which adjacent walls also are mounted is not good practice, because vibrations from the transformer may be transmitted through the foundation to the walls and thus set them in vibration, increasing the noise. There is a possibility that the transformer foundation may rest on a strata of rock running beneath the foundation to a nearby residence. In this case, and for other similar conditions, it might be found necessary to plan on placing the transformer on cork, rubber pads, or other resilient mounting.

Let us assume that the transformer has been installed outdoors and that reasonable precautions have been taken. It is felt that this is all that should be necessary and that, economically, no further steps should be required. In some cases it may be found that too much noise is emitted by the transformer and that further steps must be taken to reduce it.

There are steps which at first sight appear to be in the right direction but, when tried, may make the condition worse. For example, it would appear that stiffening the transformer case, by adding angle or channel iron, would keep it from vibrating and thus reduce the noise. As a matter of fact, conditions may be made worse by doing this, since the natural frequency of the tank sides will be increased and noises, once inaudible, might be brought into the audible range.

For some installations appreciable reduction in the sound level, in the order of 10 to 20 decibels, must be obtained. Appreciable reduction, by means external to the transformer, has been obtained in each of the following methods:

Barriers. The method of placing a simple wall between the source of sound, the transformer, and the point where quietness is desirable, has possibilities and should be considered. The reduction immediately behind the wall is great, but the magnitude of the improvement falls off as the distance increases because of diffusion of the sound around the edges. In general, the results obtained from a simple wall have been disappointing, but there are cases where this wall was effective in decreasing the amount of noise that was being reflected towards a residence by another wall behind the transformer. Care should be exercised in placing the wall so that it will not reflect noise in another direction equally important as the direction under immediate consideration.

It often has been said that a simple wall would never be as effective as it would be if it were one side of a total enclosure. To increase its effectiveness, the wall should be extended at right angles to itself on either or both ends so as to cut down the diffusion. The attenuation of the sound due to a barrier depends on a number of factors such as the effective height of the barrier above the line joining the source of sound and the point of desired quietness, wavelength of the sound, distance between the wall and the sound source, and distance from the barrier to the point of desired quietness. The effect of walls used as sound barriers may be an expensive cut-and-try method, unless the barrier walls can be used later as part of a total enclosure if this is found to be necessary.

Tests already made using small scale models to study a particular outdoor transformer installation show that barriers properly placed will offer substantial noise reduction in a particular direction from the sound source. If the surfaces of the barriers facing the transformer can be made sound absorbing, further reduction is possible.

Total Enclosure. This method usually is considered as the last resort. The power engineer now finds himself at a point where he must house his transformer whether he wishes to or not.

In some instances, notably in England,[15] the radiators have been separated from the tank and the tank enclosed in a sound-proof enclosure. Reductions up to 30 phons have been obtained, and it is claimed that up to 50 phons reduction is possible. The transformer tank is insulated from the floor by mounting it on suitable cork or rubber blocks. All rigid connections between the tank and radiators were avoided so that vibrations of the tank would not be transmitted to the radiators, although some question the necessity for doing this. In order for a surface to radiate sound efficiently, its dimensions must be large compared to the wave length of the sound to be radiated. Most of the noise emitted by a transformer is radiated from the transformer tank. In the case of the larger power transformers, it often is not possible to enclose the tank only, and housing of both the tank and the radiators becomes necessary. Means must be provided for additional cooling, entrance of transformer connections, and removal of transformer in case of failure. Any necessary openings, such as doors and cooling-air ductwork, should be located on the side of the enclosure away from the residences, if possible. It is the soundproofing of these openings which limits the possible value of noise reduction. The walls of the enclosure, if of single-wall construction, must resist vibration, which means that they must have great weight. High efficiency without great weight can be obtained with double-wall enclosure, but bracing of these walls may become a problem in walls of large dimensions.

Any time a transformer is enclosed in a room, reflection of the sound due to the walls, ceiling, and floor increases the sound level measured around the transformer. A 75,000-kva transformer was installed within a brick enclosure in England.[13] The enclosure was designed to give a noise reduction of 45 to 50 phons. The average sound level, at one meter, was measured at the factory and found to be 79 phons, yet after installation in the enclosure, the average sound level was 96 phons. This build-up of noise amounted to 17 phons; if full benefit of the enclosure had been desired, reflection would have had to be minimized within the enclosure by application of sound-absorbing materials to the interior walls and ceiling.

Summary

1. Increased power demands and the location of housing adjacent to power stations and substations are factors which make the transformer noise problem more important than in the past.

2. The measurement of outdoor noise offers problems which do not exist in the laboratory.

3. Present transformer audio noise standards are not adequate, especially for power transformers. An average sound level value obtained at a distance of one foot from the transformer and using the 40-decibel scale of the sound level meter is not indicative of the transformer loud-

ness. Until an improved method can be devised, the use of either the 70-decibel or the flat scale is suggested.

4. Noise reduction by means external to the transformer is costly. The necessity for doing so should be avoided.

5. Power transformers built with sound levels in accordance with existing NEMA standards emit too much noise and they have caused and will cause complaints. The situation is critical; it is felt that more realistic standards are needed. The manufacturers and bodies responsible for the noise standards should co-operate toward this end.

References

1. A Study of Sound Levels of Transformers, **H. Fahnoe.** *Electrical Engineering* (*AIEE Transactions*), volume 60, 1941, pages 277–83.

2. The Audio Noise of Transformers, **W. C. Sealey.** *Electrical Engineering* (*AIEE Transactions*), volume 60, 1941, pages 109–12.

3. Noise Measurement, ASA Z24.2-1942. American Standards Association (New York, N.Y.), 1942.

4. Loudness, Its Definition, Measurement and Calculation, **Fletcher, Munson.** *Journal*, Acoustical Society of America (New York, N. Y.), volume 5, October 1933, pages 89–108.

5. Noise Measurements for Engineering Purposes, **B. G. Churcher.** *Electrical Engineering* (*AIEE Transactions*), volume 54, January 1935, pages 55–65.

6. Sound Level Meters for Measurement of Noise and Other Sounds, ASA Z-24.3-1944. American Standards Association (New York, N.Y.), 1944.

7. Standards for Transformers, National Electrical Manufacturers Association (New York, N. Y.), 48-132, section TR3-130, September 1948.

8. Test Code for Apparatus Noise Measurement, *AIEE Standard number 520*, March 1939.

9. Noise Levels—How to Figure Them, **William Goodman.** *Heating, Piping and Air Conditioning* (Chicago, Ill.), volume 13, December 1941, pages 737–39.

10. The Emission of Noise from Transformers and Regulators, **J. S. Forrest.** Pamphlet number 129, International Conference on Large High Voltage Electric Systems (Paris, France), 1946.

11. Quantitative Survey of Noise Characteristics of Large Transformers, **J. S. Forrest.** *Beama Journal* (London, England), volume 44, number 20, February 1939, pages 51–54.

12. Noise in Power Transformers, **E. T. Norris.** *The Engineer* (London, England), May 5, 1933, pages 446–47.

13. Limitation of Transformer Noise, **Churcher, King.** *Journal*, Institution of Electrical Engineers (London, England), volume 87, number 527, November 1940, pages 539–54.

14. Quieting Substation Equipment, **E. J. Abbott.** *Electrical Engineering*, volume 54, 1935, pages 20–26.

15. The Reduction of Noise From Transformer Substations, **C. A. Mason.** *Beama Journal* (London, England), volume 43, July–December 1938.

16. The Application of Helmholtz Resonators to Sound-Absorbing Structures, **Vilhelm L. Jordan.** *Journal*, Acoustical Society of America (New York, N. Y.), volume 19, number 6, November 1947, pages 972–81.

17. Acoustical Terminology, American Standards Association (New York, N. Y.), February 1949.

18. Measurement of Noise From Power Transformers, **A. P. Fugill.** *Electrical Engineering* (*AIEE Transactions*), volume 53, December 1934, pages 1603–8.

19. Noise Measurements for Engineering Purposes, **B. G. Churcher.** *Electrical Engineering* (*AIEE Transactions*), volume 54, 1935. *Discussion*, A. P. Fugill, April 1935, pages 439–40.

Discussion

E. A. Blomqvist (Consolidated Edison Company of New York Inc., New York, N. Y.): In Figure 1 of Mr. Murray's paper he showed the relationship between sound intensity, loudness level, and frequency. Briefly, these curves show that at low levels of sound intensity, the ear becomes insensitive to low frequency sounds. Due to this characteristic of the ear, all transformers emitting the same amount of sound power may not be equally noisy, depending upon the frequency distribution of the sound.

Perhaps the simplest way to see the effect of the frequency distribution of the sound is to take a few examples of noisy equipment with various frequency distributions and see how noisy they will sound to the ear. For this purpose, four transformers have been assumed, each emitting 160 milliwatts of sound power, but having different frequency distributions. In Figure 1 of the discussion, the loudness level in phons is plotted as a function of distance from the transformer for these transformers. The frequency components of the sound from each transformer are indicated. It will be seen that, right next to the transformers, the loudness level in phons is 85 to 88 for all units, and they will sound equally noisy. As we move away from the transformers, the loudness level decreases, and at a distance of 1,000 feet, transformers *A* and *B* produce loudness levels of about 47 phons, transformer *C* produces 41 phons and transformer *D* produces only 25 phons. Thus there is a very considerable difference in the "noiseness" of these transformers except immediately adjacent to the transformers (where it is unlikely that any one would be living).

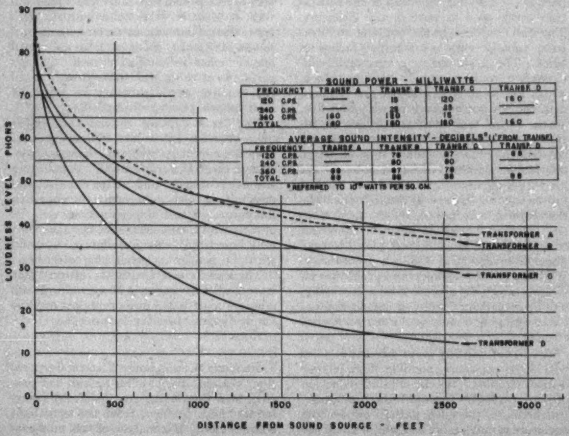

SOUND POWER - MILLIWATTS

FREQUENCY	TRANSF. A	TRANSF. B	TRANSF. C	TRANSF. D
120 C.P.S.	—	15	120	160
240 C.P.S.	—	25	25	—
360 C.P.S.	160	120	15	—
TOTAL	160	160	160	160

AVERAGE SOUND INTENSITY - DECIBELS* (1' FROM TRANSF.)

FREQUENCY	TRANSF. A	TRANSF. B	TRANSF. C	TRANSF. D
120 C.P.S.	—	76	87	88
240 C.P.S.	—	80	80	—
360 C.P.S.	88	87	76	—
TOTAL	88	88	88	88

*REFERRED TO 10^{-16} WATTS PER SQ. CM.

Figure 1. Loudness level versus distance for transformers with various frequency characteristics

Looking at it another way, the number of feet away from the transformers that it is necessary to go before the loudness level drops to 40 phons is as follows: transformer *A*, 2,150; transformer *B*, 1,900; transformer *C*, 1,100; and transformer *D*, 450. This shows a very great difference. The level of 40 phons was selected for this comparison merely because it approximates the loudness level in residential areas.

These curves suggest a further method of obtaining quieter transformers in addition to reducing the total sound power to a minimum, and that is by throwing the sound power into the low frequency range. Thus, a transformer designed for a minimum amount of sound power can be further improved if that sound power can be made predominantly 120 cycles.

A. P. Fugill (The Detroit Edison Company, Detroit, Mich.): This paper by Mr. Murray is most timely, and should be of vital interest to all of us in the electrical industry. Noise reduction in all its phases has had to take a back seat during the last few years, but the time has certainly arrived when we must consider it again whether we want to or not.

To those of us who had something to do with the drafting of the original noise standards, there is a familiar ring to Mr. Murray's perfectly valid objections. When the various standards were first adopted, they were recognized as being far from perfect, as indicated by the several revisions which have already been made, but they represented the best compromise obtainable at the time. About 1930, when we at Detroit Edison first became actively interested in reducing transformer noise at our residential substations, there were no accepted methods of measuring transformer noise. Several reference levels were being used; the units in which results were expressed depended on the individual doing the work; there was no complete agreement on the response of the human ear; and the noise meter was usually designed, built, and calibrated in the laboratory responsible for the measurement. If noise limits were included in purchase specifications, they were so general as to be meaningless. Most users have little, if any, idea of how quiet a transformer should be to prevent complaints. In a word, there was almost no common ground on which manufacturer and user could get together to discuss transformer noise. Today, with our existing standards, at least, we can all talk the same language. We have measuring equipment, which, despite its limitations, does a good practical job of classifying transformers as to noise. The transformer designers have sufficient factual data to predict, with fair accuracy, the degree of quietness to be expected in a transformer before it is actually built and measured. And the user has a much better idea of what he needs to prevent noise complaints. Though we have accomplished a lot in the last 20 years, we must not be complacent and close our eyes to improvement. The points which Mr. Murray has raised about measuring equipment and methods of measurement should certainly be given very careful consideration.

Mr. Murray's contention that the present permissible sound levels for transformers are too high deserves considerable discussion. From the application viewpoint, we agree that quieter transformers are desirable. Any power transformer, 1,000 kva and above, which just falls within the present standards, may result in complaints if located outdoors in a residential neighborhood, particularly if there are several banks at the same location. Again, however, when these values were originally accepted, they were the best compromise between what the manufacturers were willing to accept, without appreciable cost increase, and what the user would like. At that time, many of the transformers we were buying were falling considerably below the limits. With the growing public consciousness of noise, improved materials and construction methods, and more attention by both manufacturer and the user to the subject of noise, we had a secret hope that these limits could be lowered as time went on without undue hardship on anyone. That has not been the case. The war intervened, and in its wake came the stress for more production in the face of material shortages and increasing labor costs. The result was that the average power transformer today is noisier than its counterpart was just before the war. In fact, particularly in the sizes from 1,000 to 4,000 kva, we have received some transformers recently which measured so far above the present specification values that we were forced to reject them. The majority of power transformers of all sizes which we are receiving currently are just about meeting the present exceedingly liberal specification values or even exceeding them slightly.

The answer, however, is not to reduce the limits arbitrarily by 5 or 10 decibels. It is quite likely that would result in an increase in transformer cost for the whole industry. There are still many transformer applications where noise is no problem and if these cases constitute a large percentage of the total transformer business, it would not be wise to raise the cost of all transformers to meet the requirements of a few applications. On the other hand, if the limits can be lowered a certain amount without appreciable increase in cost, and we are not sure that is impossible, it should most certainly be done.

Our present solution to the problem of reducing noise in residential areas where some of our distribution substations are located may be of interest. The transformers involved are rated 6,000 to 15,000 kva, with a specification noise limit of around 70 decibels. We know from experience that a 70-decibel transformer located outdoors in this kind of neighborhood may result in noise complaints. If we buy a 60-decibel transformer, and this can be done without an unreasonable increase in cost, there is a fair chance that we may still have complaints because the noise is still distinctly audible at an adjacent residence, particularly in the middle of the night. With a 50-decibel transformer, which might be built in this rating, but certainly would be expensive, we have very little chance of receiving complaints, unless the noise pattern built up by several units and various reflective surfaces happens to give a noisy spot on the adjoining premises. With a 40-decibel transformer, which probably could not even be obtained in this rating, we would be perfectly safe.

With these facts in mind, we have decided that the best solution is to buy the quietest transformer we can get without an increase in cost, and then enclose it on all sides by a wall about the height of the transformer. In our present design of this type of distribution substation, the enclosure is an integral part of the building, one wall of the substation being used as part of the enclosure. The wall conforms to the building architecture, usually with an external facing of brick. The inside surface is a reasonably inexpensive rough-textured, building block, which has some absorption at low frequencies, though not as much as we would like. There is no roof over the enclosure, although we are using a screen cover for safety reasons. We have not found it necessary to provide mechanical ventilation to move the air within enclosure. Originally we bricked up the opening in the wall through which the transformer was moved, on the basis that the transformer would be changed so infrequently that we could well afford to take down this section of wall when necessary. We are now developing a removable panel, which, though not quite as good acoustically, will be satisfactory and will make the process of changing out a transformer somewhat cheaper.

We do not find any great increase in noise within the enclosure, possibly three or four decibels at most. We can obtain a reduction of 20 decibels through the enclosure. Furthermore, the noise pattern outside the enclosure is much more uniform, with all the local noisy spots eliminated. Considerable noise does go over the top of the wall, but this is dissipated by the time it reaches the level where it may cause annoyance. Possibly, if there were a large apartment building adjacent to the substation, extra precautions would have to be taken. In addition to the acoustical advantages of the enclosures, the appearance is improved and the danger of interference with equipment reduced.

Our success with the transformer enclosure does not mean that we have lost all interest in quiet transformers. Even with the enclosure, we would like a transformer which measures about 60 decibels and a 70-decibel transformer is about the limit which we could tolerate with this arrangement.

In conclusion we would suggest that this whole noise problem be given industry-wide consideration. Perhaps this is the time for a co-operative effort sponsored by the electrical societies, to determine the best way to reduce the effect of noise, not only from transformers but from all electric equipment. The problem cannot be solved by any one section of the industry but must be viewed from all angles.

J. Q. Wray, Jr. (Pennsylvania Water and Power Company, Baltimore, Md.): Mr. Murray is to be congratulated for making available to the industry such a complete analysis of transformer audio noise. This problem will increase in importance as more installations are required in congested areas.

His paper aptly points out the difficulties encountered in eliminating objectionable transformer noise once the transformer is installed. The only really effective method of cutting down appreciable noise is to build a soundproofing wall or enclosure. Such construction is expensive and for large power transformers, will prove impractical more often than not.

In the case of a new installation, the engineer will usually have some selection as to location, and he can also take precautionary measures toward minimizing noise by the several methods mentioned in the paper. However, the man who must find a practical way of lessening the noise emitted from transformers already in service has a real job on his hands. Each job is an individual one and must be handled as such. The experiences of those who have already faced the problem would probably be helpful if such information was compiled.

The final solution to the transformer noise problem is, as Mr. Murray says, to keep the noise to a minimum during the design of the transformer itself. It occurs to the writer that in addition to the electrical design being such as to reduce the noise to a minimum, considerable reduction could be obtained by the development of an acoustic tank liner suitable for installation in oil and with the proper dielectric characteristics.

The writer concurs with Mr. Murray that more realistic standards of noise levels are required and that a more practical method for measuring these levels is needed.

S. Bennon (Westinghouse Electric Corporation, Sharon, Pa.): The author has presented an interesting survey of the transformer noise problem from the operator's point of view. His analysis of field measurement techniques and available methods of noise reduction external to the transformer provides a valuable complement to earlier

Institute papers[1,2] analyzing the problems of internal noise reduction in transformers.

Recognition of the importance of the transformer noise problem has led to a determined effort on the part of manufacturers to reduce over-all transformer levels. A significant step in this direction has been the elimination of resonances[1] which may raise the basic level of the core. The basic sound level produced by a core of fixed material and dimensions is determined primarily by its operating induction. Mr. Murray's figure, which agrees with our experience, shows that a 10 per cent change in induction will produce a sound level change between 2 and 3 decibels. Because of this relatively slow change it is apparent that a large expense is involved in any major sound level reduction secured by a reduction in the operating induction alone. On the other hand, external noise reduction secured by barriers of varying degrees of completeness, as described by Mr. Murray, also represent additional investment to achieve desired results. Under these conditions the practical solution, when unusually low noise levels are required, would appear to involve a comparative cost study of external and internal sound level reduction or possibly a combination of both.

As a result of the almost universal use of sound meters for commercial measurements there is a tendency to consider weighted sound levels as identical with loudness levels. Actually as the author has illustrated in his paper there may be considerable deviation for pure tones. The situation becomes more complex for sounds composed of harmonically related components such as exist in transformer noise. Nevertheless weighted sound levels have been found to be reasonably reliable when used to compare the loudness of transformers. This is fortunate since the essential requirement for standardization is that the method of measurement chosen yield a reliable index of loudness and not necessarily the loudness level. A considerable measure of the success of sound level comparison is due probably to the similarity in frequency spectrum and relative component intensity in the noise produced by the majority of transformers. For these transformers, standards could be formulated in terms of either 40 or 70 weighting. A particular standard on the 70 weighting will be higher than that on the 40 weighting, but each will correspond to approximately the same loudness level.

Any change in weighting at higher levels, such as suggested by Mr. Murray, would stem from a desire to bring the numerical value of the standards closer to loudness levels. Refinements of this type involve analytical problems such as the masking effect of harmonically related components as well as application problems, that is, whether the standards should reflect the loudness at the transformer or at points at which the disturbing effect may be felt. These problems are still in the stage where differences of opinion exist. It is well to realize, however, that if we confine our attention to the fundamental requirement, namely that the weighting provide a generally reliable index of loudness, the problem is less difficult. From this point of view, the present 40 weighting is probably the natural choice for its simplicity.

The evaluation of the resultant transformer level at large distances in terms of the standard 1-foot measurements represents an important field problem. Mr. Murray has presented useful empirical data on the rate of variation of level at considerable distances. One of the factors entering into the resultant level which is frequently overlooked is the physical size of the transformer. Although the actual sound fields in the vicinity of a transformer are rather complex, it is possible to draw some general conclusions by considering a spherical source. The average sound intensity I_d produced at a distance d by a large sphere of radius R whose surface is pulsating with a velocity amplitude v at a frequency of wave length λ is given by

$$I_d=\frac{\rho c v^2}{2}\left(\frac{R^2}{d^2}\right)\left[\frac{\left(\frac{2\pi R}{\lambda}\right)^2}{1+\left(\frac{2\pi R}{\lambda}\right)^2}\right] \qquad (1)$$

where ρ is the density and c the velocity of sound in air. In order to express I_d in terms of the average intensity I_t measured one foot from the transformer some assumption must be made about the form of the wave at this distance. If we assume the wave to be spherical our standard pressure responsive sound meters would indicate an intensity

$$I_t=\frac{\rho c v^2}{2}\left(\frac{R^2}{R_1^2}\right)\left[\frac{\left(\frac{2\pi R}{\lambda}\right)^2}{1+\left(\frac{2\pi R}{\lambda}\right)^2}\right] \qquad (2)$$

where R_1 is one foot greater than the radius R. Substituting equation 2 into equation 1

$$I_d=\frac{R_1^2}{d^2}I_t \qquad (3)$$

On the other hand if we assume the wave at one foot is effectively plane

$$I_t=\rho c v^2/2 \qquad (4)$$

and equation 1 can be written

$$I_d=\frac{R^2}{d^2}\left[\frac{\left(\frac{2\pi R}{\lambda}\right)^2}{1+\left(\frac{2\pi R}{\lambda}\right)^2}\right]I_t \qquad (5)$$

For frequencies whose wave lengths in air are small compared with $2\pi R$ both equation 5 and equation 3 indicate a variation of intensity approximately as the square of the radius. For wave lengths that are of the same order of magnitude as $2\pi R$, equation 5 indicates a higher rate of variation which approaches the fourth power of the radius for wave lengths large compared with $2\pi R$. At a frequency of 120 cycles per second the wave length in air is approximately ten feet, so that if equation 5 is valid it may be possible to observe a fourth power variation for smaller power transformers. For larger power transformers the rate of variation will probably be close to the second power of the linear dimensions.

Based on the foregoing reasoning, we would expect the relative size of two transformers to produce, at a remote point, a difference in level given by

$$\text{Decibel difference}=10\log_{10}\left(\frac{L_1}{L_2}\right)^n \qquad (6)$$

where L_1/L_2 is the ratio of the linear dimensions of the two transformers and n may vary from two to four. If, for example, one transformer has twice the linear dimensions of another, then, even though they have identical levels measured at one foot, the smaller transformer may still be from 6 to 12 decibels lower than the larger transformer at say 200 feet.

Because of the simplifying assumptions involved in the analysis, the exact effect of size on resultant level will have to be established by field tests. The analysis presented is intended to call attention to the influence of transformer size. In this connection it is interesting to note that major advances[3] have been made in recent years in size reduction. The introduction of oriented steel,[4] the formfit construction[5] for shell form power transformers and forced oil cooling[6] all have tended to markedly reduce the size of modern transformers and thus decrease the effective level at large distances.

REFERENCES

1. See reference 1 of the paper.
2. See reference 2 of the paper.
3. HIGH VOLTAGE POWER TRANSFORMER PROGRESS, F. L. Snyder. *Westinghouse Engineer* (East Pittsburgh, Pa.), March 1948, pages 46–51.
4. HIPERSIL, A NEW MAGNETIC STEEL AND ITS USE IN TRANSFORMERS, J. K. Hodnette, C. C. Horstman. *Westinghouse Engineer* (East Pittsburgh, Pa.), August 1941, pages 52–56.
5. FITTED TANKS FOR TRANSFORMERS. *Westinghouse Engineer* (East Pittsburgh, Pa.), August 1943, pages 74–75.
6. A NEW TRANSFORMER FOR BASE-LOAD SUBSTATIONS, Philip Sporn, H. V. Putnam. *Electrical Engineering* (*AIEE Transactions*), volume 60, October 1941, pages 916–18.

J. A. Adams (Philadelphia Electric Company, Philadelphia, Pa.): The subject paper is of considerable interest to the Philadelphia Electric Company, not only because some of the conclusions parallel our experience but due to the comprehensive and informative treatment of the problem. We feel that the author has produced a useful summary in a readable manner of the major factors involved in transformer noise from an operating point of view. We concur that the present noise level standards are too high and that the present standards for noise level determination should be revised to more accurately stimulate the response of the human ear.

The Philadelphia Electric Company has been becoming increasingly aware of the transformer noise problem, not only in connection with the reaction of nearby residents but also in generating stations, particularly where noise emission of large power banks located near offices of superintending personnel could become a disturbing and annoying factor. In this connection, in order to establish an acceptable noise level for the 100,000-kva 66–13.2-kv forced-oil cooled transformer banks at one of our generating stations, measurements were made in 1945 on existing large power transformer installations on our system. At that time, it was recognized that frequency and relative intensities would affect the human ear in a manner different from the response of a decibel meter. Throughout these tests, the transformer noise frequency differences between installations were clearly noticeable. Based on the combined reaction of the listeners, it was concluded that a design level of approximately 85 decibels without fans and 90 decibels with fans would be acceptable. It is interesting to note that the present NEMA Standard establishes an audible sound level of 83 decibels for a transformer of this type and rating.

The following example of the noise problem in residential areas appears to substantiate the conclusions reached by the author of the paper. The substation involved, located in a quiet residential section, is constructed with two 7,000-kva 13,200–2,545-volt, 3-phase to 2-phase, 60-cycle oil-insulated self-cooled outdoor transformers located in outdoor courts. These courts extend from the west wall of the building proper and are bounded on the rear by the building wall, on the sides by brick walls and originally on the front by Transite covered removable framework with an air space of approximately two feet at the ground level. Wall clearance at back and sides of the transformers is 9$^1/_2$ feet and to the front (removable wall) is 6 feet. The transformers involved have a NEMA test noise level of 64 decibels (40-decibel scale), 5 decibels below allowable.

Almost coincident with the initial energizing of these banks, a noise complaint was received from a resident located approximately 200 feet distant diagonally opposite the west wall of the substation. Of particular interest, from the noise frequency point of view, is the fact that the complainant stated that his dogs were made restless and nervous by the transformer noise.

Check sound level measurements (on 70-decibel scale) made in the transformer courts gave an average of 86.6 decibels. Measurements made external to the substation varied from 58 decibels on east side to 75 decibels along the west wall. Twenty feet out from the west wall, the noise level measured 70 decibels. While it was considered from these measurements that the noise level of the installation was not excessive, the final solution of the problem consisted of completely closing up the west wall of the transformer courts.

J. H. Mahoney (Boston Edison Company, Boston, Mass.): Representing the Boston Edison Company, I would like to present a few of our experiences with transformer noise problems.

1. In the transformer yard adjacent to one of our generating stations, we recently installed a 35,000-kva 110/14-kv transformer. Although noise level is no particular problem at this location, it was found that the doors of the control cabinets vibrated excessively. These doors were made of thin metal which actually chattered due to the transformer vibration. This noise was eliminated by the installation of angle-iron braces across the back of the doors.

2. At one of our recent outdoor substations we installed a 7,500-kva 66/14-kv transformer. In this case the inert-air equipment vibrated so seriously that the gauges were broken. This condition was corrected by constructing a separate foundation for the gas equipment. Our laboratory made audio sound level tests at this location, using a General Radio type *759* sound level meter, and as recommended by the NEMA Standards for Transformers in the section covering Audio Sound Levels for Distribution and Power Transformers.[1] The maximum sound level was 75 decibels; the arithmetical mean was 67.2 decibels (for 34 readings). The NEMA standard for this transformer is 72 decibels. A substantial part of the noise level, on the side of the transformer where the nitrogen apparatus is located, was caused by vibration of that cabinet and the apparatus therein. Readings taken one foot in front of this cabinet, with the cabinet door open, gave 84 and 77 decibels at one-third and two-thirds height of the transformer.

3. In one of our strictly residential areas, we have a new unit substation which has two 5,000-kva 14/4-kv transformers. These transformers are approximately 42 feet apart. Using the same methods and instruments as above, the maximum sound level was found to be 73 decibels; the arithmetical mean for 30 readings was 64.7 decibels for one transformer, and 62.8 for the other. The NEMA standard for these transformers is 68 decibels. Sound level measurements were then taken at two other locations with the microphone on a tripod at a level of about five feet.

With the microphone on the sidewalk across the street from the station, approximately 83 feet from the nearest transformer, the following readings were taken:

	Decibels
No traffic	44
Light traffic	56
Heavy traffic	65
Diesel train (20 feet from rear of station) with light traffic	62
Bus accelerating	71

With the microphone at the rear of the station yard approximately 20 feet from the rear transformer and approximately 20 feet from the railroad tracks:

	Decibels
Normal	52–56
Steam engine passing	88
Remainder of train	83
Diesel engine passing	90
Remainder of train (express)	88

4. At one of our 110-kv Ring Stations we recently installed an 18,000-kva 110/14-kv transformer, and again using the same instruments and methods as above, we found the maximum sound level to be 76 decibels; the arithmetical mean for 60 readings was 71.25 decibels. The NEMA standard for this transformer is 77 decibels.

I have talked with several of our operating personnel and it seems to be a general opinion that although the various sizes of transformers meet the NEMA requirements, these requirements are much too lenient. They would like to see the standard values reduced to at least 60 decibels, and possibly lower.

We are now considering seriously the necessity of including noise-level limits in our specifications for the transformers, particularly for residential areas.

The transformers which I have reported on were not made by any one manufacturer. In fact, there were three different manufacturers' equipment involved. We, therefore, feel justified in saying to all transformer manufacturers that more attention should be given to design characteristics to reduce noise and to the mounting of accessories, the fabrication of boxes and the bracing of radiators.

REFERENCE

1. See reference 7 of the paper, pages 33–34.

T. D. Gordy (General Electric Company, Pittsfield, Mass.): Mr. Murray is to be commended for gathering into one paper so much information that has been published previously in many wide and varied papers. In so doing, he has brought into one place the important factors dealing with measurement and evaluation of noise levels and, at the same time, has pointed out the importance of the noise problem to the power system engineer.

One important factor which was stressed is that in evaluating noise, so far as the ear is concerned, component frequencies as well as component intensity levels must be known. These frequencies and intensity levels are necessary if relative loudness is to be evaluated. This same idea of obtaining frequencies as well as intensity levels has been carried over into his recommendation of determining component frequencies along with sound level meter readings of transformer installations.

It is quite true that magnetostriction is one of the driving forces contributing to noise emitted by transformers. However, it is not necessarily the magnitude of the magnetostriction that is so important as it is the shape of the a-c magnetostriction versus flux density curve. It is the shape of this curve that determines the harmonic content of the vibrations caused by magnetostriction. Since the human ear and the sound level meter discriminate between frequencies, it is obvious that the shape of this curve is what determines predominating frequencies in transformer noise, such as 120, 240, 360, and 480 cycles. These are not necessarily the predominant frequencies in all transformers as we have found from our tests. In some cases, the predominant frequency may be as high as 1,200 cycles. Other sources of noise in the transformer are gaps and joints, resonating parts, coils, and vibration from interaction between core and coils. The importance of these sources varies with the design and transformer characteristics.

Mr. Murray has brought out another very important consideration in making noise tests in the field. Such items as temperature, background of the ambient sound level, stray fields, reflecting walls, buildings, or other transformers cannot be overlooked in field testing. Even if the installation is out of town, annoying factors such as airplanes, chirping crickets, barking dogs, and quacking ducks must be tolerated. Evaluation of the transformer noise without considering these bothersome background noises is meaningless.

We check Mr. Murray's change in sound level of 2 to 3 decibels for a 10 per cent change in voltage. This, of course, varies some from design to design, but the figure of two to three is an over-all average which we have found. As Mr. Murray points out, some investigators have found that noise level is independent of load of the transformer. This is true under certain conditions; but depending on the size, type of windings and core, and the winding that is excited, the noise level may be a function of the load. Not only is it a function of the magnitude of the load but also of the load power factor.

The question of which weighting network should be used in evaluating transformer sound levels is one which must be studied thoroughly before present practices are changed. It is true that the 40-decibel weighting network does tend to give low readings when high sound levels are being measured, but it is doubtful if these high sound levels exist at the point where complaints may arise. They do exist one foot out from the transformer contour, but they fall off in accordance with the 4.5-decibel rule obtained by Mr. Murray. Therefore, at some distance from a transformer, the level is no longer so high that the 40-decibel weighting response would be too inaccurate. In order to evaluate transformer noise, a set of standards must be written that will enable all transformers to be tested under very nearly the same conditions. This automatically requires testing at distances from one to a few feet from the transformer contour. Since this level will be diminished when it gets to the observer, it is questionable as to whether or not it is desirable to go to a 70-decibel or flat weighting network for measurements one foot out from the transformer. This whole problem of weighting, microphone location, and distance from the transformer to the microphone should be thoroughly studied by both system engineers and manufacturers in order to arrive at a method of evaluating transformer noise that will be more satisfactory than present standards.

The manufacturer has not overlooked the noise problem in designing large power transformers. He does have other problems, however, that must be considered along with the noise problem. Measures which would reduce noise level cannot always be incorporated in the design because of other characteristics or functions of the design. As a result, at the present state of the art, any decrease in noise level which is built into the transformer will result in a more expensive unit. For example, in one design that was studied, to obtain a reduction in noise level of 10 decibels weight of the transformer was increased 58 per cent which resulted in an increase of 25 per cent in cost. The problem then arises as to whether the extra cost should be put into the transformer itself, or put into buildings or enclosures surrounding a transformer having standard noise levels. There are certain installations which must have exceptionally low noise levels. Manufacturers are well aware that such conditions do arise, but it does not appear advisable to handicap all transformer lines by increasing cost in order to obtain the low noise levels required for these special installations. Systems operating in thickly populated areas are much more aware of the noise problem than those operating in less thickly populated districts, and it is only reasonable that these operators who have unique noise problems may have to pay premiums for obtaining low-noise-level transformer designs.

What noise levels at installations will be acceptable in these metropolitan areas must be determined by the operating companies. Once these satisfactory installation noise levels have been determined, it may properly become a question of economic balance as to whether it is practical to actually design for these levels in the transformer, or whether external means such as various types of enclosures have to be resorted to. At the present time, any method to reduce transformer noise level will be expensive, and this excessive expense must be recognized by operating companies.

F. Von Voigtlander (The Commonwealth and Southern Corporation, Jackson, Mich.): The use of the loudness scale instead of the decibel scale has been explored quite extensively by the signaling apparatus industry with which the writer was formerly connected for some ten years. Experience there indicates that those who work in acoustics prefer decibels for noise level measurement. They reason and calibrate in decibels and the loudness unit requires translation when it is used. In its earlier application to sound signal output rating, the loudness unit was favored because it was thought the customer, usually being nontechnically trained, could evaluate more easily the difference in output between two signals, say one of 88,000 loudness units output level and another of 215,000 loudness units, than if the output level were rated as 100 and 110 decibels respectively. Several years' experience however showed that those who were concerned at all about loudness levels preferred the decibel unit in their work and the loudness unit did not have the popular appeal that was expected of it. The extent to which noise is disturbing depends on so many other factors than the loudness level of the source itself that the introduction of loudness units seems merely to add confusion to the problem.

Whether the 40-decibel, 70-decibel or the flat scale of the sound level meter should be used for transformer noise measurement could become the subject for considerable discussion but it would be of no practical value. There does not appear to be any good reason for not using the flat scale for this particular application. In the frequency ranges of interest the flat scale will give the more accurate results as pointed out by the author. The flat scale is used widely in other applications of the sound level meters for this same reason. The writer agrees with the author that the specifications should be changed to use the flat scale rather than the 40-decibel scale.

Exception must be taken to the author's statement that the 5-decibel tolerance allowed by the ASA standard for sound level meter readings[1] is considerable, and to the statement that two equal sources of noise when sounded together would give a reading 3 decibels higher than when one is sounded alone.

Noise measurements are not exact in the usual sense of electrical measurement accuracy. However, this is of very little practical consequence as the human ear is hardly able to distinguish a level difference as great as 3 decibels. For this reason a variation of 2 to 5 decibels between instruments is not as bad as it may seem. Standardizing instruments to obtain a correction within these limits is frequently of little value as the more popular types of instruments will not hold their calibration that closely under ordinary conditions of use.

Sounding two equal sources of noise together will not give anything near 3 decibels more than the sound level of one sounded alone. In fact with ordinary sound level meters the difference between both and one would not be measurable.

The author states that only the frequency range from 120 to 480 cycles needs to be considered in transformer noises. This is surprising and it is presumed that it is due to the low natural response frequency of the relatively large sections found in power transformers even though the human ear is very much more sensitive to noises in the 1,000-cycle range than to those in the 120-to-480-cycle range.

While low level of transformer noise can be very important in those few cases where transformers are located in quiet residential neighborhoods, it would not seem economically justified to increase the cost of standard transformers for the sake of getting them all down to an ideal noise level. The usual compromise of as good a job as we can get without appreciable increase in cost would seem to be in order here just as it has been in so many other engineering matters. Where very low levels of noise are required the extra cost of such provisions would have to be justified by the particular circumstances. Excessive transformer noise just as excessive noise from any other equipment, may properly lead one to question the adequacy of the design or construction, so that reasonable noise levels may well be taken as an attribute of product quality.

REFERENCE

1. See reference 6 of the paper.

C. S. Murray: Mr. Wray suggests the use of an acoustic tank liner to obtain reduction in the transformer noise. In reference 11 of the paper, Mr. Forrest discusses a liner which may be similar to that which Mr. Wray has in mind. In Mr. Forrest's case, a 20,000-kva transformer was built with a double steel tank, the inner tank being resiliently supported from the other. A reduction of 10 decibels was claimed for this construction. In reference 13 of the paper, Mr. Churcher and Mr. King discuss a similar construction for distribution transformers. The reduction in this case amounted to about 2 to 4 decibels.

Mr. Blomqvist points out that an appreciable reduction in transformer noise will result at points remote from the transformer if the sound power can be made predominantly of a frequency of 120 cycles per second. This is fundamentally sound and the possibilities of doing this should be reviewed by transformer designers. It is interesting to note from Figure 1 of the discussion that transformer *B* emits a noise which at a distance of 500 feet from the transformer has a calculated loudness level value of 57 phons. The intensity levels given for transformer *B* approximate what might be obtained from a 138-kv 60,000-kva transformer designed in accordance with NEMA specified sound levels. There is little doubt that such a transformer would cause a noise complaint at residences located up to distances somewhat beyond 500 feet from such a transformer.

Mr. Fugill's comments on the status of transformer noise around 1930 is very interesting and certainly points out how far we have come since that time. Mr. Fugill's comment that several reference levels were being used is worthy of further comment. Even as late as 1935 there was great confusion as to what reference level should be used. At that time a tentative reference pressure of 0.0002 dyne per square centimeter (same as the reference in use today) was being considered. Many had been using a reference pressure of 0.001 dyne per square centimeter. The adoption of the 0.0002 value resulted in obtaining sound levels 14 decibels above what had been obtained in the past. It took a few years to discuss noise values using the different reference level. Considerable noise data around 1930 to 1935 failed to indicate the reference level and as a result it becomes of little value.

I agree with Mr. Fugill that the answer to lowering the permissible noise levels is not to reduce the limits arbitrarily. It is felt that manufacturers should give this subject considerable study and arrive at means by which transformers can be built at low noise levels economically. I further agree with Mr. Fugill that the whole noise problem be given industry-wide consideration. More and more manufacturers of other electric and mechanical equipment are beginning to believe that something can be done about this noise problem and have begun to take steps in connection with it. It demands the co-operation of all concerned.

Mr. Bennon has pointed out that even though two transformers have identical sound levels when measured at the 1-foot distance, the smaller physical size of transformer may be from 6 to 12 decibels lower than the larger transformer at the 200-foot distance. Power engineers experienced in the noise emitted by distribution and the smaller power transformers should consider this when buying the larger power transformers. This point should also be considered by those responsible for transformer noise standards.

Mr. Bennon states that a considerable measure of the success of sound level comparison is probably due to the similarity in frequency spectrum and relative component intensity in the noise produced by the majority of transformers. A few tests made on six power transformers, of two different manufacturers and ranging from 25,000 to 70,000 kva rating, does not support this statement. A frequency analysis was made at a number of points around each transformer and the values obtained at the different points for each frequency were averaged. It was found that for one transformer the 120- and 240 cycle components predominated; for another transformer the 120- and 360-cycle components predominated; for the remaining four either the 120-, the 240- or the 360-cycle component predominated. Further tests made on four 75,000-kva transformers, at a point about 30 feet distant from each, showed that for two of these transformers of one manufacturer the 120-cycle component predominated. For the other two transformers of a different manufacturer the 360-cycle component predominated. Data obtained by others are similar.

Mr. Bennon brings in the question of simplicity for the noise measurement. The power engineer also is looking for simplicity, but if that simplicity is not going to give him the proper information and allows him to install a transformer that is too loud for a given neighborhood, he is going to abandon the idea and look for something better. It must be borne in mind that once a transformer is purchased for a given sound level and that value of sound level is proved by test, the cost of quieting it, if necessary, becomes the sole problem of the power engineer. The value or values quoted must give the power engineer sufficient information so that he can be fairly sure, without guesswork on his part, how loud his transformer is going to be in the neighborhood where it will be installed.

Mr. Adams' experience with transformer noise levels is interesting. In regard to the noise emitted by the 100,000-kva bank, Mr. Adams states that based on the combined reaction of the listeners, it was concluded that a design level of approximately 85 decibels, without fans, would be acceptable. Mr. Adams does not give the frequency components of the noise nor whether there are any walls or other buildings between the transformer and the offices of superintending personnel. Therefore, it is somewhat difficult to evaluate the noise at the offices. It is assumed that the listeners were company personnel. I question if the same results would have been obtained from noncompany residents, if any, say within an unobstructed distance of less than 1,000 feet. In the case of the 7,000-kva transformer banks, I assume that after the west wall was constructed, no additional cooling for the transformer banks was needed since no mention was made of it. This would agree with the findings of Mr. Fugill.

Mr. Mahoney's experience is valuable information for both the power engineer and the transformer designer. In case 3, where tests were made remote from the transformer, much more valuable information would have resulted if a sound analyzer had been used to measure the components of the transformer noise.

Mr. Gordy brings out that the noise level of a transformer may not be independent of load, but may be a function of the magnitude of the load and the load power factor. The results of a small number of tests on power transformers have indicated that there may be a change in the component frequencies of the noise due to load even though the average sound level remained about the same. Knowing this, it was stated in the paper that additional data on this subject should be obtained.

Mr. Gordy's views on the present use of the 40-decibel weighting response is not surprising. There are bound to be differences of opinion on such a subject as was pointed out by Mr. Fugill in his discussion. Such differences of opinion can best be solved by a co-operative effort of the electrical societies and it is gratifying to know that a working group in the AIEE Transformer Committee will study the transformer noise problem.

Mr. Voigtlander takes exception to my statement that the 5-decibel tolerance allowed for sound level meters is considerable. Distribution transformers have been removed from service due to noise complaints and have been replaced by others from which no further complaints have been received. Average sound level measurements made on the original and also the replacement transformer in the laboratory show that 5 decibels could be the difference between a quiet and a noisy transformer. The American Standards for Sound Level Meters, reference 6 in the paper, recognizes that differences of practical importance may be expected between the results obtained with different meters unless corrections are applied to take into account deviations of the individual meters from the design objective. As a result a method for calibration of the individual meter is given in Appendix "C" of that Standard.

Mr. Voigtlander also takes exception to the statement that two equal sources of noise increase the sound level by 3 decibels over that value when either is sounded alone. Theoretically, if the sources are equal, each source would emit the same amount of sound energy. Therefore, if we double the sound energy, we should, from the definition of a decibel, get an increase of 3 decibels. Appendix "B," of the Standard gives a test for the rms addition. Assuming that Mr. Voigtlander's meter does meet the test for addition, it may be that he is basing his findings on actual transformer tests. It is possible that a point can be selected between transformers where the 3-decibel law would not appear to hold. It is possible to have two similar transformers with equal average sound level values and each of which could have sound level values opposite a point which differed by 10 decibels. The transformer with the lower sound level opposite that point would not materially add to the sound level indicated by the other.

Mr. Voigtlander believes that there are only a few cases where transformers are located in quiet residential neighborhoods. I question this. There are an increasing number of unit substations being installed at load centers with housing fairly close. There is an increase in low-cost housing being located adjacent to generating and substations having large power transformer installations. There was a time when locations such as this were not desirable for housing but today it often happens that it is the only available land in that area. Any power company which is expanding its existing station and installing power transformers out-of-doors, is susceptible to noise complaints. The company may not have a problem today but, unless it owns considerable land about the station or the land is not suitable for housing, it may have a problem in the near future. There are known cases of power companies now having their first transformer noise complaints. The residence does not necessarily have to be adjacent to the station. I mentioned in the paper a case where the complainant was located over a quarter of a mile from the transformer installation. No company can afford even one noise complaint because it has been my experience that as soon as one complaint is registered the public begins to listen for other noises and a series of complaints arise due to operation of other equipment.

Controlled Temperature and Insulation Protection in the Operation Of Power Transformers

W. W. SATTERLEE
MEMBER AIEE

R. D. REED
ASSOCIATE AIEE

MOISTURE and oxygen in varying amounts are the ever-present enemies to the satisfactory and continued operation of liquid immersed transformers. The life of the oil and insulation in a transformer cannot be determined accurately by laboratory tests since it is difficult, if not impossible, to make such tests so as to duplicate operating conditions.

When transformers are operated with the oil in them exposed to the atmosphere, objectionable products are formed from the combination of the oxygen present with the oil. These harmful products are largely water, organic acids which may be water soluble or water insoluble, neutral products and solid precipitates commonly known as sludge. Thus heat, oxygen, and the products of oxidation of oil account for the slow decomposition of cellulose materials. The result is a mechanical weakening of the solid insulation in a transformer and an addition of impurities to those already in the oil.

This deterioration of transformer oil and cellulose insulating materials can be reduced appreciably, if not almost eliminated, depending upon the methods used to prevent the entrance of moisture and oxygen into transformers.

Oxygen is probably responsible for the greatest amount of deterioration; although, as far as oil and insulating structures in transformers are concerned, water is undoubtedly the most objectionable impurity whether it be present as moisture from the inbreathing of air or formed as a by-product of oxidation. Water, directly or indirectly, is the cause of more electrical breakdowns or other types of unsatisfactory operation of transformers than any other impurity.

Protection of the oil and cellulose insulation used in transformers is afforded in varying degrees by what are termed free-breathing, restricted or controlled breathing and completely sealed-tank construction. Thus, in order to determine under actual operating conditions the effects of different forms of protection to oil immersed transformers, a group of small transformers has been under life test operation for more than five years.

Fourteen transformers, representative of power transformer design, were started on life test in May 1943. The operation of these transformers is being continued indefinitely. Physically, all of these transformers are of the same design, each using a round tank, cover-mounted bushings, and containing the same amount of oil, see Figure 1. Their low-voltage windings are of the cylindrical or barrel type construction, while the high-voltage windings are of the continuous-wound pancake-section design. In order that samples of the conductor insulation used in the windings of these transformers can be had for test purposes, a small coil of the same design as the high-voltage windings is mounted in the top oil of each transformer and connected in series with its high-voltage winding.

All 14 transformers are installed and operated under outdoor service conditions. The identification of each transformer under test, including a set of pilot-windings sealed in a tank of oil and operating only at ambient temperatures, is as follows:

Transformer Number 1—Sealed-tank, equipped with activated clay filter.

Transformer Number 2—Sealed-tank, equipped with aluminum oxide filter.

Transformer Number 3—Sealed-tank.

Transformer Number 4—Open air breathing, equipped with aluminum oxide filter.

Transformer Number 5—Open air breathing. Low- and high-voltage windings were treated with varnish.

Transformer Number 6—Open air breathing.

Transformer Number 7—Sealed-tank, equipped with breathing regulator.

Transformer Number 8—Expansion tank, 2-compartment type.

Transformer Number 9—Expansion tank, conventional type.

Transformer Number 10—Inertaire. Low- and high-voltage windings were treated with varnish.

Transformer Number 11—Inertaire.

Transformer Number 12—Inertaire, equipped with aluminum oxide filter.

Transformer Number 13—Inertaire—125 degrees centigrade hottest-spot.

Transformer Number 14—Inertaire—105 degrees centigrade hottest-spot.

Tank Number 15—Pilot windings, sealed in a tank of oil.

All transformers are subjected to identical loading and operating conditions, except that transformers number 13 and number 14 are arranged to operate at hottest-spot winding temperatures of approximately 125 and 105 degrees centigrade, respectively, and the tank of pilot coils number 15 operates at ambient temperatures. Transformers number 1 to number 12, inclusive, operate at a hottest-spot winding temperature of about 115 degrees centigrade.

Paper 49-193, recommended by the AIEE Transformer Committee and approved by the AIEE Technical Program Committee for presentation at the AIEE Summer General Meeting, Swampscott, Mass., June 20–24, 1949. Manuscript submitted November 15, 1948; made available for printing May 2, 1949.

W. W. SATTERLEE is Division Engineer and R. D. REED is Design Engineer, both with the Westinghouse Electric Corporation, Sharon, Pa.

The authors express their appreciation to their associates in the Westinghouse Electric Corporation, E. W. Tipton and J. G. Ford, who contributed to the preparation of this paper.

Description of Installation

The 14 transformers and the tank of pilot coils were installed outdoors and arranged according to the plan view shown in Figure 2. The transformers were platform-mounted which raised them about two feet above the ground level, making their lower drain valves easily accessible for the removal of samples of oil. Figure 3 shows the complete installation.

The transformers were connected for loading by the familiar load-back method which is commonly used in making temperature tests. All of the transformers were magnetized by connecting their high-voltage windings in parallel, thus insuring that all units always operate with essentially the same no-load losses. The secondaries of all transformers are supplied with a load current from an adjustable source of sufficient capacity to get a hot oil temperature of about 95 degrees centigrade with an ambient temperature of 25 degrees. The higher temperature of transformer number 13 was obtained by blanketing its tank and a series reactor was used to get the lower temperature of transformer number 14.

On May 17, 1943, the transformers were started on life test with the following load cycle:

Load on 8:00 a.m. Monday, load off 3:00 p.m. Tuesday.

Load on 8:00 a.m. Wednesday, load off 3:00 p.m. Thursday.

Load on 8:00 a.m. Friday, load off 3:00 p.m. Saturday.

Each transformer is equipped with a thermometer to indicate its hottest oil temperature. Oil temperature and ambient temperature readings were taken and recorded at the beginning of each loading period and after the completion of each 31 hours of operation. This record of oil and ambient temperatures serves to show the extent to which each transformer was loaded during operating periods.

In order to accommodate the servicing of these transformers to factory working hours, the loading cycle was changed; first, after $6^1/_2$ months' operation, to two 55-hour periods per week and then, changed slightly again, $2^1/_2$ years later to have load on at 8:00 a.m. Monday, load off at 3:00 p.m. Tuesday; load on at 8:00 a.m. Thursday, load off at 3:00 p.m. Friday; load on at 8:00 a.m. Monday and so on. This loading is being continued.

Record of the Data Obtained

The object of this life test is to observe and to determine the changes in the condition of the oil and the insulating materials in these transformers over a long period of time and, insofar as possible, under actual operating conditions.

Table I. Oil and Insulation Power Factor

Transformer Number	Description of Transformer	Power Factor High to Low and Iron*	Oil Power Factor
1	Sealed clay filter	0.35	0.03
2	Sealed aluminum oxide filter	2.78	4.17**
3	Sealed	1.48	0.28
4	Open air aluminum oxide filter	2.34	2.83
5	Open air varnished coils	0.88	0.38
6	Open air	2.13	2.29
7	Breathing regulator	0.58	0.28
8	Two compartment expansion tank	1.17	0.29
9	Conventional expansion tank	0.87	0.79
10	Inertaire varnished coils	0.43	0.235
11	Inertaire	0.60	0.375
12	Inertaire aluminum oxide filter	0.26	0.045
13	Inertaire—125 degrees centigrade hottest spot	3.26	0.295
14	Inertaire—105 degrees centigrade hottest spot	2.00	0.265
15	Pilot coils		0.20

* Insulation power factor data taken at a temperature of approximately 25 degrees centigrade for all transformers. Transformer had been on test 1,446 days (3.96 years).

** Open valve—see text.

Table II. Color of Oil

	Days on Test	44	80	187	348	701	819	1,446
	Years on Test	0.12	0.22	0.51	0.95	1.92	2.24	3.96
Transformer Number	Description of Transformer							
1	Sealed clay filter	1	1	1	1	1	1	1.5
2	Sealed aluminum oxide filter	1	1−	1−	1−	1−	1	3.5
3	Sealed	1.25	1.5	1.5+	1.5+	1.5+	1.5+	2.5
4	Open air aluminum oxide filter	1	1	1+	1.5	2	2	3.5+
5	Open air varnished coils	1.25	1.5+	2.5	3.5+	5	5−	5+
6	Open air	1.5	2−	2	3.5	5−	5	5+
7	Breathing regulator	1.25	2.5	3−	4−	5	5	2.0
8	Two compartment expansion tank	1.25	1.5+	1.5+	1.5+	2−	2	2+
9	Conventional expansion tank	1.25	2−	2	2.5	4.5	4	4+
10	Inertaire varnish coils	1.25	2+	2	2.5−	3	2.5+	3+
11	Inertaire	1.5	2	2.5	2.5−	3	2.5	3−
12	Inertaire aluminum oxide filter	1.5	2	2.5	2.5−	3	2.5	3−
13	Inertaire—125 degrees centigrade hottest spot	1.25	1.5+	1.5+	2−	2.5	2	2.5+
14	Inertaire—105 degrees centigrade hottest spot	1.25	1.5−	1.5+	1.5	1.5+	1.5+	2−
15	Pilot coils	1	1	1	1	1	1	1

The initial condition of the oil was checked just before the start of the life test. Samples of oil taken from each transformer were tested for color, neutralization number, water soluble acids, dielectric strength, and interfacial tension.

A complete temperature record has been kept on the operation of each transformer during the entire life test to date. Oil and ambient temperatures were recorded at the beginning and at the end of each loading period. Since hottest-spot winding temperatures could not be recorded, they had to be determined and with relation to hottest-oil temperatures from data which were obtained from temperature tests made on two of the transformers prior to the start of the life test. For example, test data obtained on transformer number 6 are:

No load loss, watts	219
Copper loss, watts	570
Total loss, watts	789
Top oil temperature rise, degrees centigrade	64
High voltage winding average temperature rise, degrees centigrade	70.5
Gradient, degrees centigrade	6.5
Load in kilovolt-amperes	13.

When the transformers were started on life test, it was found that operating conditions made it necessary to excite them at a voltage slightly lower than that at which the original temperature tests were made. Correcting the losses to the lower voltage changed the data as follows:

No load loss, watts	182
Copper loss, watts	570
Total loss, *P*, watts	752
Top oil temperature rise, degrees centigrade	61.6
High voltage winding average temperature rise, degrees centigrade	68.1
Gradient, degrees centigrade	6.5
Load, *P*, in kilovolt-amperes	12

Table III. Total Acids

Milligram of Potassium Hydroxide per Gram to Neutralize

Transformers Number	Description of Transformer	44	80	187	348	701	819	1,446
	Years on Test	0.12	0.22	0.51	0.95	1.92	2.24	3.96
1	Sealed clay filter	0.025	0.023	0.035	0.023	0.022	0.022	0.044
2	Sealed aluminum oxide filter	0.025	0.023	0.035	0.023	0.022	0.022	0.706
3	Sealed	0.037	0.046	0.081	0.046	0.067	0.056	0.055*
4	Open air aluminum oxide filter	0.025	0.035	0.035	0.046	0.067	0.078	0.526
5	Open air varnished coils	0.05	0.081	0.185	0.289	0.576	0.444	0.706
6	Open air	0.05	0.058	0.046	0.185	0.633	0.523	0.896
7	Breathing regulator	0.037	0.092	0.185	0.323	0.644	0.544	0.044
8	Two compartment expansion tank	0.037	0.046	0.058	0.069	0.067	0.067	0.055
9	Conventional expansion tank	0.05	0.070	0.104	0.173	0.300	0.244	0.269
10	Inertaire varnished coils	0.05	0.081	0.185	0.289	0.576	0.444	0.706
11	Inertaire	0.05	0.046	0.058	0.058	0.078	0.067	0.055
12	Inertaire aluminum oxide filter	0.025	0.023	0.023	0.023	0.033	0.044	0.022
13	Inertaire—125 degrees centigrade hottest spot	0.037	0.046	0.058	0.069	0.067	0.078	0.067
14	Inertaire—105 degrees centigrade hottest spot	0.037	0.046	0.058	0.058	0.055	0.056	0.044
15	Pilot coils	0.025	0.035				0.022	0.022

Days on Test heads the columns 44 to 1,446.

*Open valve—see text.

Table IV. Breakdown of Oil

Kilovolts in Standard Test Cup

Transformer Number	Description of Transformer	44	80	187	349	701	819	1,446
	Years on Test	0.12	0.22	0.51	0.95	1.92	2.24	3.96
1	Sealed clay filter	33.2	27.2	33.1	24.2	34.9	32.6	37.8
2	Sealed aluminum oxide filter	35.4	27.4	32.7	28.8	31.4	36.5	38.5
3	Sealed	27.6	18.5	20.3	24.5	25.7	28.5	39.5
4	Open air aluminum oxide filter	32.2	25.1	32.3	28.5	29.1	29.8	35.3
5	Open air varnished coils	34.8	18.1	29.2	17.5	28.7	28.1	32.3
6	Open air	31.6	18.0	32.4	15.6	27.5	28.1	36.0
7	Breathing regulator	31.8	26.2	28.3	23.7	28.7	28.2	38.5
8	Two compartment expansion tank	35.8	27.1	24.6	23.3	33.1	31.5	37.5
9	Conventional expansion tank	32.6	21.6	25.2	26.6	15.2	22.9	38.5
10	Inertaire varnished coils	35.0	26.2	31.7	24.5	27.0	32.0	41.8
11	Inertaire	29.8	25.9	32.4	21.8	26.4	26.5	38.8
12	Inertaire aluminum oxide filter	36.8	30.9	35.2	23.4	30.9	35.8	36.8
13	Inertaire—125 degrees centigrade hottest spot	35.0	22.9	26.8	23.2	31.4	33.0	38.8
14	Inertaire—105 degrees centigrade hottest spot	36.0	29.6	34.3	25.0	34.1	33.8	34.5
15	Pilot coils	35.2	29.0				29.6	36.5

Days on Test heads the columns 44 to 1,446.

A winding hottest-spot gradient of 16.5 degrees centigrade was determined by adding 10 degrees, the conventional allowance used for liquid immersed transformers, to the average winding gradient of 6.5 degrees. Then, after making the following assumptions, it was possible to calculate the hottest-spot winding temperatures and hottest-oil temperatures for any loading desired.

1. Ambient 25 degrees centigrade.
2. Oil temperature rise varies as $L^{0.8}$.
3. Hottest-spot gradient varies as $P^{1.6}$.

On this basis the following equations apply to transformer number 6, and thus to all of the other transformers subjected to the life test:

$$\text{Hottest-oil temperatures} = 25 \text{ degrees} + 61.6\frac{L^{0.8}}{752}$$

$$\text{Hottest-spot temperature} = 25 \text{ degrees} + 61.6\frac{L^{0.8}}{752} + 16.5\frac{P^{1.6}}{12}$$

L = total loss in watts
P = load in kilovolt amperes

Curves are plotted as shown by Figure 4 from which the hottest-oil temperatures, corresponding to the hottest-spot winding temperatures, may be obtained for all of the transformers. For example:

Hottest-Spot Winding Temperature, Degrees Centigrade	Hottest-Oil Temperature, Degrees Centigrade	Ambient Temperature, Degrees Centigrade	Oil Temperature Rise, Degrees Centigrade
105	88	25	63
115	95	25	70
125	103	25	78

The desired hottest-spot winding temperatures were obtained by loading and by blanketing the transformers to give the required hottest-oil temperatures. It is recognized that there may be some difference between the relation of the hottest oil and the hottest winding temperatures of the transformers which are blanketed and of those which are not blanketed.

Obviously, a continued change in ambient temperature resulted in a change of the oil and winding temperatures. A temperature record, typical of that kept on all of the transformers since the start of the life test, is shown in Figure 5 for transformer number 6. It may be noted that the oil temperature reaches the required value at an ambient temperature close to 25 degrees centigrade and that the oil temperatures rise and fall with changes in ambient temperatures.

Power Factor

The power factor of the transformers was measured by applying the bridge

Figure 1 (left). Life test transformers

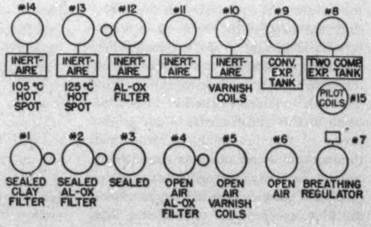

Figure 2 (right). Identification of life test transformers

Figure 3. Life test transformers. View of complete installation

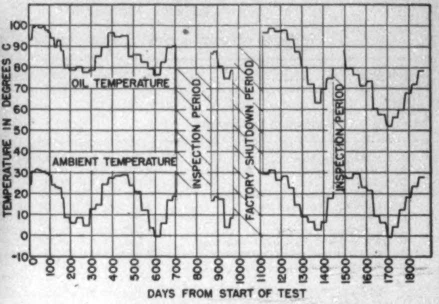

Figure 5. Temperature-time curve for transformer number three

connections from the bushing terminals to ground. The results are shown in Table I for measurements made four years after the start of the life test. In order that the power factor would not be affected by leakage paths over the surface of the bushings, they were cleaned before the measurements were made. The results are rather variable, but it is noticeable that, in general, the transformers with controlled breathing have the lowest power factor. The power factor of the oil in each transformer also was measured after four years of operation and the results are given in Table I. The values of power factor obtained for transformer number 2 and for the oil in it must be discounted, because a valve connecting to the gas space above the oil in the transformer was found open, causing free breathing operation of this unit over a considerable period of time.

Color of Oil

Samples of oil were taken from each transformer at different intervals of time throughout the life test. The changes in color of the oil as the test progressed are shown in Table II. The tabulation clearly indicates the beneficial effects to the sealed units equipped with the filters, since the color of the oil in these transformers is nearest to the original value. The abrupt change in the color of the oil in transformer number 2, as indicated by the value obtained at the last inspection of all of the transformers, is due to the period of free breathing operation and thus a rapid deterioration of the filtering agent. Similarly, the oil in transformer number 7 shows a decided improvement in color as the test proceeded. The reason for this is that a defect was found in the operation of the breathing regulator and the original oil in this transformer was replaced with new oil following 819 days operation.

Acidity of Oil

The total acids measured by the milligrams of potassium hydroxide per gram of oil to neutralize are given in Table III. The acidity should be kept low since oil with too high an acid content is more likely to sludge and to cause rapid corrosion of steel parts. It is evident that the oil in transformer number 1, which is sealed and equipped with a clay filter, has remained low in acid content throughout the life test. Transformer number 2, which was sealed and equipped with an aluminum oxide filter, also contained oil which remained low in acids until free breathing occurred as a result of the open valve. It may also be noted that transformer number 12 contains oil which has low acidity. It is obvious from the results of the test that open or free breathing contributes to the production of acids.

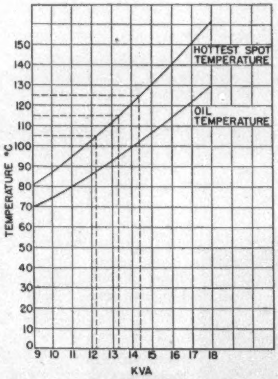

Figure 4. Relation of hottest-spot temperature to oil temperature

Dielectric Strength of Oil

The dielectric strength was measured on samples of oil removed from the top and the bottom of each transformer at seven different intervals during the life test. Five test shots were made on each sample of oil, or a total of ten tests per transformer. Table IV gives the average results of the ten tests made on the oil from each transformer. Although a few values of relatively low dielectric strength were obtained on samples of oil taken from transformers 3, 5, and 6, all other values were high, including those after four years of operation, as indicated in Table IV.

Interfacial Tension of Oil

Tests to determine the interfacial tension of the oil in each transformer were made after four years of operation. Interfacial tension is determined by carefully pouring the sample of oil under test into a beaker of water and measuring, after the oil and water have separated into two layers, the force in dynes per centimeter of length required to pull a planar ring of platinum wire from the water through the interfaces of the water and the oil. The device used to measure interfacial tension is known as a surface tensiometer. The measurement is made under rigidly standardized equilibrium conditions which have been shown in

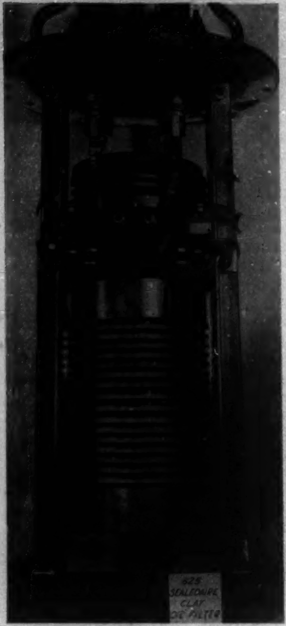

Figure 6. Interior view—life test transformer equipped with clay oil filter

practice to give a reliable indication of the presence of hydrophilic compounds. The interfacial tension data of the oils in these transformers are given in Table V. A high value of interfacial tension is indicative of a satisfactory condition of an oil. A value of 18 is considered by some operators as satisfactory. It may be observed that the transformers, which remained sealed or were operated with controlled breathing, contain an oil having the highest values of interfacial tension.

Mechanical Strength of Paper Insulation

Pieces of the paper insulation were removed from the conductors of the sample coils in each transformer and tested for mechanical strength. In order to make the paper samples suitable for testing, the oil was extracted from them and they were softened with water to facilitate straightening-out the paper samples without breaking them. The paper samples were then dried and tested for tensile strength using a one-quarter inch separation of the jaws of the testing machine. The results of the tests are given in Table VI.

There are many designers and operators who wonder just what correlation there is between the tensile strength of insulating materials and transformer life. In order to obtain some data on this matter, short circuit tests were made on transformer number 5, an open breathing unit, since, as indicated in Table VI, the greatest decrease in tensile strength of the conductor insulation had occurred in this unit. This transformer withstood 5-second short circuits of $2^{1}/_{2}$, 5, and 10 times full load current under sustained voltage without showing any signs of mechanical or electrical failure. Following the short-circuit tests, the transformer was satisfactorily subjected to the disruptive and induced AIEE overpotential tests. Short-circuit tests of the same magnitude will be repeated on this transformer at the next inspection period.

Period Inspections of Transformers

At intervals of approximately two years, the transformers were taken out of service and given a thorough inspection, and a series of tests were made on each transformer to determine its condition.

Insulation power factor and capacity measurements were made immediately after the transformers were shut down so as to obtain values while the transformers were still hot. After the transformers had cooled to the ambient air temperature, the insulation power factor and capacity measurements were repeated. The transformers were then moved indoors where a series of tests were made on each unit, and all units were opened and thoroughly inspected.

The first test made was a disruptive 60-cycle test at the original value of 10,000 volts from high to low and ground, and at 10,000 volts from low to ground. This was followed by an induced voltage test of two times normal voltage for 60 seconds.

Next, each sealed transformer was pressure tested with nitrogen at seven pounds per square inch for one hour to check for leaks which might have developed during the 2-year period of operation. It is interesting to note that no leaks were found.

Following completion of the pressure tests, each transformer was opened for inspection. A view of the core and coil assembly of one of the transformers, as supported from the cover of the tank, is shown in Figure 6. The pancake coil construction of the high-voltage winding is clearly shown in the illustration. While the low-voltage coil is not visible it is of the well-known cylindrical or barrel type design.

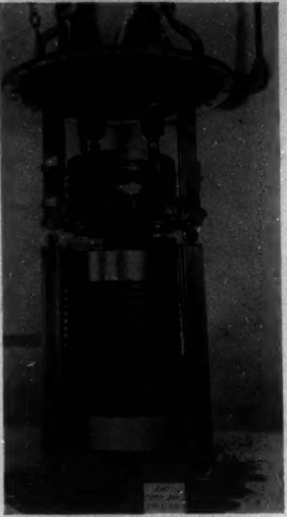

Figure 7. Interior view—life test transformer equipped with open air breather

Resting on top of the core and coil assembly is the sample coil which consists of two sections of the high-voltage winding. The sample coil is connected in series with the high-voltage winding and is thus subjected to essentially the same operation conditions. The purpose of the sample coil is to provide a convenient means of obtaining pieces of the conductor insulation for test purposes by removing one or two turns from the coil at each inspection period.

Photographs of the core and coil assembly of each transformer were made at each 2-year inspection period in order to provide a visual record of the internal condition of each unit. The excellent condition of the sealed-tank unit equipped with the clay filter, transformer number 1, is clearly visible in Figure 6. On the other hand, the effects of moisture and oxygen are very evident in the open-breathing unit, transformer number 6, as shown in Figure 7.

As a part of each 2-year inspection, samples of oil taken from each transformer and a sample of new oil were sealed in glass test tubes. These samples of oil

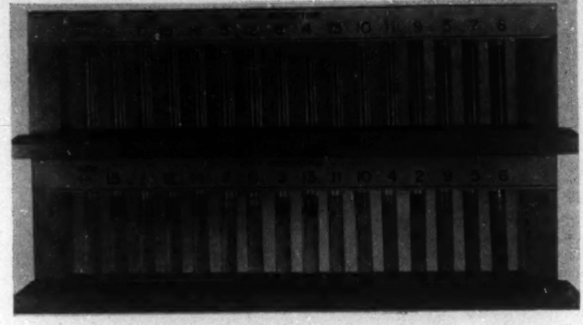

Figure 8. Oil samples taken from life test transformers

were arranged in the order of their color and photographs were made of them, Figure 8. After each inspection of all of the transformers was completed, they were retanked using new gaskets. The transformers were then returned to their outdoor location, and the sealed-tank units with their auxiliary equipment connected were pressure tested for leaks at seven pounds per square inch for six hours. Following this, they were again subjected to the life test load cycle. At present, it is the plan to make the next inspection of the condition of these transformers during the summer of 1949, or after about six years of operation.

Conclusions

Many tests on the aging of oils and insulation have been conducted under carefully controlled laboratory conditions. This type of test is usually accelerated and, although it does show a degree of deterioration of the materials under test, the results are of much less practical value since they are not indicative of actual operating conditions. For instance, W. G. Horsch[1] points out that accelerated laboratory oxidation tests show no correlation with the performance of oils in transformers under controlled test conditions. Therefore, life tests on model transformers, such as described in this paper, are believed to be representative of service conditions and to take into account all of the factors which cause deterioration of oil and insulating materials, and consequently, lead to a reduction in the operating life of transformers.

Table V. Interfacial Tension of Oil

Dynes Per Centimeter

Transformer Number	Description of Transformer	
	Days on Test	1,446
	Years on Test	3.96
1	Sealed clay filter	44.6
2	Sealed aluminum oxide filter	13.8
3	Sealed	20.8
4	Open air aluminum oxide filter	14.9
5	Open air varnished coils	14.2
6	Open air	14.9
7	Breathing regulator	20.8
8	Two compartment expansion tank	21.6
9	Conventional expansion tank	17.1
10	Inertaire varnished coils	16.4
11	Inertaire	20.7
12	Inertaire aluminum oxide filter	39.2
13	Inertaire—125 degrees centigrade hottest spot	21.7
14	Inertaire—105 degrees centigrade hottest spot	23.7
15	Pilot coils	25.9

As with most practical test setups, especially of the magnitude of the one covered in this paper, unforeseen difficulties usually arise as the tests proceed. Thus, it is difficult and sometimes impossible to draw satisfactory conclusions from some of the data obtained. For example, in those tests, the value of the data on power factor is questionable since the transformers operate at very low voltage and, perhaps, the number of measurements made to data are too few.

A review of the characteristics of oil and insulation usually considered in evaluating the condition of oil immersed transformers clearly indicates that the units which are operating under controlled conditions are in the best condition, and thus one may expect a much longer life from these transformers as compared to the probable life of the units which are exposed to restricted or to the free breathing of moisture and oxygen.

For instance, the data on the color of the oil, the acidity of the oil, its interfacial tension, even the power factor of the transformers and of the oil in them, indicate the sealed-tank units, especially those equipped with clay or aluminum oxide filters, to be in the best condition. As with all transformers in service, a relatively high value of dielectric strength of the oil cannot be taken alone as conclusive evidence of good oil and insulation. While the results of the tests for the tensile strength of the conductor insulation show that, generally, the material in the sealed-units is in the best condition, particularly is this true of the filter equipped sealed transformers, the data also indicate the uncertainty of evaluating the operating life of a transformer by the mechanical strength of the conductor insulation. This conclusion is borne out by the fact that transformers which have given uninterrupted service for many years have been found to contain conductor insulation of very low tensile strength, yet the dielectric strength between conductors in the windings of such transformers would be high.

Data from tests of the kind described in this paper, when continued over long periods of time, are of more use than other types of tests in evaluating the condition of transformer oil and insulation or in comparing different methods of oil and insulation preservation now in common use.

Reference

1. OXIDATION TESTING OF TRANSFORMER OILS, W. G. Horsch. *Electrical World* (New York, N. Y.), volume 126, 1946, pages 54, 56, 72.

Table VI. Tensile Strength of Conductor Insulation

Pounds Per Inch of Width

Transformer Number	Description of Transformer	
	Days on Test	1,446
	Years on Test	3.96
1	Sealed clay filter	7.2
2	Sealed aluminum oxide filter	4.0
3	Sealed	2.0
4	Open air aluminum oxide filter	3.1
5	Open air varnished coils	Too Brittle
6	Open air	2.2
7	Breathing regulator	3.9
8	Two compartment expansion tank	2.4
9	Conventional expansion tank	5.3
10	Inertaire varnished coils	3.7
11	Inertaire	3.9
12	Inertaire aluminum filter	6.8
13	Inertaire—125 degrees centigrade hottest spot	Too Brittle
14	Inertaire—105 degrees centigrade hottest spot	3.4
15	Pilot coils	11.5
	New conductor insulation	39.0

Discussion

F. J. Vogel (Illinois Institute of Technology, Chicago, Ill.): I remember when this series of tests was started, and I have been quite curious as to the results obtained. The result expected, when the tests were started, was a real evaluation of the worth of various methods of oil protection, so that controversial opinions might be settled by test data. Naturally, I believe that this is a real service to the industry. I note that the hottest spot was determined by calculation from an assumption of the conventional hot-spot allowance. It seems to me that actual values could either have been measured, or calculated from the actual watts per square inch (or gradient) and the hot oil temperature.

Discussing the results, it would have been desirable had power factor measurements been taken at the start of the tests. However, power factors of less than 0.5 of a per cent for the insulation and of 0.03 or 0.04 per cent for the oil are as low as could be expected for new and well-dried transformers. This would indicate that the sealed transformers with filters had not measurably deteriorated, so far as these properties are concerned. As concluded by the authors, the tests do not indicate much deterioration for the units protected from oxygen, either by sealing or use of inert gas.

The test tube tests made a short time ago entirely sealed in the deterioration products and I believe they showed much more deterioration than the tensile tests reported here. In these tests other materials besides manila paper are present and also in some cases filters were used. The deterioration products then were either diluted or removed. I hope that the presence of these deleterious products might be an explanation of some of the previous vagaries in the experimental data. However, transformer insulation is generally under compression, and hence tensile tests do not prove anything directly as to life. They were chosen rather as giving more reliable test measurements rather than as a direct criterion. I would have liked to have seen results of short circuit tests on transformer Number 13, giving a comparison between varnished and unvarnished coils, with some idea as to the maximum compressive forces in the structure. Still another thing in this respect would be data as to whether there was any shrinkage in the column heights, or loosening of the pressure on the coil clamps. Elaborate means with springs to maintain coil pressure have been used in past practice, although their use now is generally obsolete.

V. M. Montsinger (Pittsfield, Mass.): The authors are to be congratulated for carrying out such a comprehensive set of tests on the protection of oil in transformers. It requires a lot of work to construct and carry out a series of tests as described in the paper. I wish to discuss four of their conclusions.

I agree with some but not all of their conclusions.

Let's consider two statements made in the first paragraph of the authors' conclusion. I agree that tests made on oil at normal temperatures or near normal temperatures are preferable to accelerated laboratory tests. I feel however that there is some question as to whether the use of such extreme cooling and heating cycles represent operating conditions and therefore may lead to erroneous conclusions as to the acceptability of equally good methods of oil preservation. For the conservator and open-type units this method of operation is extremely severe, drawing in more fresh oxygen than would ever happen in power transformers that have core loss and some load loss on all the time. For these units the tests are in effect accelerated tests while for the inertaire and sealed units there is no similar acceleration.

In the second paragraph of their conclusion, I do not understand why the data on power factor is questionable because of the low voltage used. I would ask the authors to explain this.

In paragraph three, I think that all of us will agree that transformers under controlled conditions will have a longer life than transformers exposed to restricted or free breathing of oxygen. In the fourth paragraph the statement that the color, acidity, interfacial tension, and even power factor of the sealed tank units to be in the best condition, in general is true but there are some contradictions in the tables. For example tank number 14, inertaire, has a high power factor. Tank number 11, inertaire, has a fairly low interfacial tension value and tank number 10, inertaire varnished coils, has a high acid content.

My principal objection is to the fifth paragraph namely that because transformers which have very low mechanical strength do not always fail indicates that tensile strength is a poor criterion for evaluating the life of a transformer.

I agree that transformers often operate for extended periods after the mechanical strength is gone provided they are not subjected to severe surges either mechanical or electrical.

I strongly feel that the true life of a transformer is reflected by the mechanical condition of its insulation, especially of its turn insulation. If it cannot resist a surge its true life has been used up. It's really living on borrowed time, and should be removed from service. The trouble is we do not know when it reaches this stage.

P. L. Bellaschi (Sharon, Pa.): This discussion has reference to the economics of power transformers, especially from the application end.

Having been closely connected with and, in fact, instrumental in a good measure to the development reported in this paper, certain comments on the significance of these tests should be in order. In the first place, as I have maintained in previous discussions on the aging and preservation of insulation, tests on miniature transformers are useful in filling in the gap which long since has existed between the results of research tests on insulation as such and the inherently slow-process development resulting from experience on actual equipment in service.

One may justifiably question the significance of some of the results in the tabulations and in the figures and, in fact, their correctness. This is the case in regard to: the mechanical strength tests on the paper insulation, due to probable damage upon its removal from the conductor; the power factor measurements; as well as some of the other data. Therefore, a word of caution in drawing final conclusions is in order, but this should not detract in any manner from the general value of the investigation and from the positive results hereto attained.

Another point one may question is in connection with the true significance of the hottest-spot copper temperatures designated as 105, 115, and 125 degrees centigrade in the tests. These should be considered as nominal reference values and hardly to be taken as equivalent sustained temperatures in the sense we associate continuous temperatures in the standards.

A conclusion of practical significance that can be drawn from these tests is in connection with the relative effectiveness of the various methods of preservation and protection of the insulation. Providing that deterioration of the oil and insulation can be forestalled, as through the use of inert gas (preclusion of air and moisture) and deleterious products eliminated or removed through the use of activated clay, the life of the insulation can accordingly be prolonged materially. In fact, a more effective use of the insulation through higher operating temperatures than was otherwise possible in the past seems possible by a proper utilization of these means. It is an established fact, however, that for prolonged or continuous duty, even with the foregoing protective measures at our disposal, cellulose insulation still has a top hot-spot temperature of about 110 or 115 degrees centigrade that must be recognized. That is, permanent chemical decomposition and damage to the insulation will result if a sustained temperature of about 115 degrees centigrade is maintained.

These tests, as well as other investigations of a similar character and field experience in general, all bear out and further substantiate the inherent conservatism embodied in present standards. Here then we find ourselves face to face with still another opportunity to better utilize present station equipment, to greater economic advantage. A parallel process of rationalization as now is being effected through the application of reduced insulation (see discussion)[1] can be effected through a fuller utilization of the thermal capabilities of oil-immersed transformers and through suitable means of insulation preservation that inherently enhance the life expectancy of the insulation and permit possibly higher operating temperatures.

REFERENCE

1. EXTREMES IN THE INSULATION CO-ORDINATION OF OIL-INSULATED TRANSFORMERS, F. J. Vogel. *AIEE Transactions*, volume 68, part II, 1949 (*Proceedings* T9195). Discussion by P. L. Bellaschi.

W. W. Satterlee: In reply to Mr. Vogel's discussion, we wish to state that before the life test of these transformers was started, the hottest-spot temperatures of two of the transformers were obtained by use of thermocouples in their windings and during load—back run made at different kilovolt-ampere ratings. In other words, we attempted to check actual hottest-spot temperatures against calculated temperatures. In general, the calculated hottest-spot temperatures exceeded the measured temperatures by a few degrees.

We agree that more tests on the transformers for power factor would have been desirable. Also, power factor tests of the oil in the transformers were not made until the 1947, or second 2-year inspection period. It is probable that short-circuit tests will be made on unit number 13 at the next inspection period.

We did find evidence of slight column shrinkage during the recent 1949 inspection of these transformers.

We are quite in agreement with Mr. Montsinger as to the amount of work involved in carrying out this life test program and series of tests on the transformers.

It seems questionable that the operating cycles under which the life test on these transformers is being conducted are especially severe, even if one considers the test as being unfair to restricted and to open breathing units.

The results do show that the transformers with sealed construction or those in which breathing is controlled are afforded the best protection. If a system of protecting the oil and insulation is good under severe operating conditions, then certainly it should be good under conditions less severe, or those which might be called more normal conditions.

The idea in connection with the statement in the paper of questionable data on power factor was intended to mean that had more data on the power factor of the transformers been obtained, and had the transformers under life test been of a relatively high voltage class, then the results on power factor might have been of more interest and perhaps more representative of power transformer operation. It was not intended to convey the idea that the low-voltage transformers used made the results questionable.

We believe one should expect some contradictory results in a series of tests of the kind the paper describes. In fact, this condition or possibility is pointed out in the conclusions.

Whether or not short circuit tests prove the mechanical stability of the insulation in a transformer, or whether the mechanical strength of the turn insulation is any criterion in the length of the operating life of a transformer, it is our belief that continued operation of the life test transformers and periodic inspection and detail tests on all of them will provide much data by which the operating characteristics and life of a transformer may be more fully evaluated.

Our answer to Mr. Bellaschi is that it is difficult to remove insulation from copper conductors without the possibility of some mechanical damage to it. However, extreme care was exercised in obtaining the samples of insulation for test purposes and in making the tests. Comments have been made regarding the power factor tests for one of the previous discussions.

It is not understood exactly what Mr. Bellaschi means by "the true significance of the hottest-spot copper temperatures." The transformers are operated in such a manner that during the loading cycles their windings reach, at least closely, the temperatures given in the paper. However, the transformers do not operate at the specified temperatures continuously. In fact, few power transformers do in actual service.

It is expected that the continued operation of these transformers will provide additional valuable data which will be of much practical use in determining the effects of various methods of protecting oil and insulation in the operation of power transformers.

A Small High-Voltage Bushing Design for High Altitudes

F. J. VOGEL
MEMBER AIEE

H. A. HART
ASSOCIATE AIEE

TRANSFORMERS as component parts for radio service and for fairly high voltages of the order of 10,000 volts occasionally have been required. When in turn they were required to operate at the equivalent of 3.4 inches of mercury pressure and to be corona free, a design problem was presented immediately. There have been several papers written about the problem, with no concrete design procedure given. In this paper, a design procedure for the shape of the porcelain and parts is given, with some test results verifying the design.

A particular transformer design was required to supply 8.6 kv with the midpoint grounded. The porcelains for such a design would have to stand 9.6 kv rms for one minute at atmospheric pressure. Also, they were to be free from corona or radio disturbance at voltages at least up to 25 per cent over rated voltage, or 5.4 kv to ground at a pressure of 3.4 inches of mercury.

In the solution of this problem, the law of similitude was applied directly. This law states that in cases where the parts are in the same proportion and the dielectric field has the same shape, the breakdown voltage will remain constant provided the sizes of the parts vary inversely as the gas pressure. Paschen's law is merely a special case, inasmuch as it refers to uniform fields. This law applies directly to corona rather than breakdown, so that it means that if corona is to be avoided, fundamental data on corona formation is necessary.

Several designs of porcelain were considered, and the bushing, as dimensioned in Figure 1, was the final design. The apparent advantages in the design are:

1. There is no concentration of stress at the edge of the metal parts of the flange or container in air, as in the design shown in Figure 2.
2. There is no concentration of stress in the air at the terminal parts, as in the design shown in Figure 2. The diameter of the terminal rod is the chief factor in the strength, rather than a square edge or point as in Figure 2.

The interior of the assembly required oil filling; therefore, the porcelain was mounted on the bottom of the case, so that the transformer oil filled the porcelain shells. If this were not done the bushing design would have been complicated further.

The advantages cited lead to the big advantage that the design might be corona free up to nearly the breakdown voltage, and hence could be of small dimensions relative to its voltage strength.

To check this, the porcelain according to dimensions shown in Figure 3 was tested. Corona occurred at the edge of the washer on the terminal next to the porcelain at 12 kv. Flashover occurred at 22 kv. These tests were made in air at room temperature and pressure. The assembly then was modified to be similar to the selected design, by adding a fibre washer 1/4-inch long and a metal pipe terminal approximately 0.72 inch in diameter, as shown in Figure 4. Corona then formed on the pipe just above the fibre at 25 kv. Flashover occurred from the pipe to the plate at 26 to 28 kv. Corona also formed on the washer at the extreme end of the pipe at about 18 kv.

In order to determine the voltage at which corona would occur at the flange, the fibre washer length was increased to 7/16 inch and the bushing tested again. Corona occurred at the flange at 29 kv, and flashover at 32 kv. The amount of corona at the flange grew with increased voltage.

The next step was to replace the pipe terminal with one more likely to be the final design. It was made 1/2 inch in diameter, 7/8-inch long, and hemispherical at the end, with provision for a wire to be clamped inside the terminal as shown in Figure 1. Upon test at reduced pressure, 3.15 inches of mercury, corona at the hemispherical end occurred at 5.1 kv, and just above the fibre at 7.9 kv. With number *10* wire extending from the terminal, corona was eliminated except at the end of the wire. The corona voltage at the terminal above the fibre was 7.7 kv. Corona and flashover occurred at about the same time for both the 7.9 kv and 7.7 kv values as given. The string distance from the flange to the terminal was about two inches.

The modified bushing previously described also was tested at room temperature and pressure. Corona at the hemispherical end occurred at 24.5 kv, and at the flange next to the bushing at 32.5 kv. When the number *10* wire was added, corona was eliminated at the cap except at the wire termination, but was observed at the flange at 29 kv.

It is difficult to analyze these data exactly. In the case of the tests at full pressure, it is interesting to estimate the strength of the tube terminal to the plate. For the first tests, the tube was 0.72 inch in diameter, and the string distance from it to the plate was two inches. It might be estimated that the strength of this assembly would be about the same as for a 0.72-inch cylinder inside a 4 + 0.72 or 4.72-inch cylinder. A graph showing the relationship between the corona voltage and separation for concentric cylinders is shown in Figure 5. To estimate the strength, the ratio of outside to inside diameter must be found to locate on a line of constant ratio. This ratio is 6.6 for the preceding case. The voltage corresponding to this ratio and a separation of two

---

Paper 49-194, recommended by the AIEE Transformer Committee and approved by the AIEE Technical Program Committee for presentation at the AIEE Summer General Meeting, Swampscott, Mass., June 20–24, 1949. Manuscript submitted November 15, 1948; made available for printing May 2, 1949.

F. J. VOGEL is with the Illinois Institute of Technology, Chicago, Ill., and H. A. HART is with the Armour Research Foundation, Chicago, Ill.

inches would be about 50 kv. The low corona voltages obtained from the washer at the end of the tube and from the hemispherical end emphasize the importance of the terminal design. Although the data do not permit a definite statement, it would seem that the conditions at the flange still determined the performance with the 0.72-inch terminal. Corona at that point prior to flashover confirms this.

In the case of the 1/2-inch terminal, the string distance was still two inches. By extrapolation of the curve for 1/2-inch diameter and 2-inch distance, the expected corona voltage would be of the order of 36 kv.

In applying the law of similitude, it is easiest to calculate new bushing dimensions, smaller by the ratio of the pressures. In other words, if the bushing dimensions were multiplied by 3.4/30, the 2-inch dimension would become 0.225 inch and the rod diameter of 0.5 inch would become 0.057 inch. The corona voltage of this imaginary small bushing at atmospheric pressure, should be the same as that of the full-sized bushing at 3.4 inches of pressure. It is readily seen that the value noted of 7.7 kv is within the range of probability.

The final bushing design was as shown in Figure 1. The terminal was 0.5 inch in diameter and 7/8-inch long. The bushing, for test purposes, was mounted in a container so that the small end could be covered with oil. All possible precautions were taken to eliminate corona on the leads to the bushing. At room temperature and pressure, 23 degrees centigrade and 744 millimeters of mercury, occasional streamers started at the flange at 27 kv, and flashover occurred at 28.5 kv. At room temperature and 3.4-inch mercury pressure, corresponding to 50,000 feet altitude, corona and breakdown occurred simultaneously at about 6.3 kv. This bushing is satisfactory then, since it only had to meet a 5.4 kv test value.

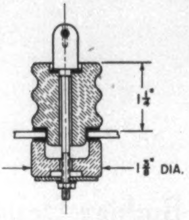

Figure 1. Final bushing design

It would appear at first that there is not too much to gain by electrode design for the low-pressure conditions. This is not quite true. The corona voltage was greatly increased by the addition of a lead from the terminal, as compared to the corona voltage for the terminal alone. Shielding of the flange increases the bushing corona voltage, since it avoids a concentration of stress in air at the edge of the metal. This means that the final bushing design should be a balance between the strength at the terminal and at the flange.

In these tests, the flange or bushing container was connected to ground through a 70-millihenry air-core inductor with a Triumph oscilloscope (sensitivity is 0.09 volts per inch) across the inductor. No additional capacity was used, so that any bushing disturbance would be impressed entirely on the inductance. The question of the point of visual corona against disturbance as noted on an oscilloscope was answered by careful observation in total darkness. It was found that whenever disturbance was present on the oscilloscope, it was possible to see corona at some place in the circuit. The two always occurred simultaneously. However, corona can be hidden behind parts so that it cannot be seen easily, and the oscilloscope then is much more reliable. For example, local corona in the space between the cylindrical terminal and the porcelain occurred when the neoprene gasket was not forced up in that space. This corona showed clearly on the oscilloscope, but could be seen by careful observation only in complete darkness.

Table I. Corona and Breakdown Voltage for Various Bushings and Modifications

Bushing	Corona Voltage		Breakdown Voltage	
	Normal Pressure	Reduced Pressure	Normal Pressure	Reduced Pressure
(Figure 3)	12 kv at terminal washer		22 kv	
(Figure 4) Recessed fibre washer $^1/_4$ inch long. Pipe extension $1^1/_8$ inches long.	25 kv at pipe terminal above fibre washer. 18 kv at metal washer on end of pipe terminal		26–28 kv	
(Figure 4) Fibre washer increased to $^7/_{16}$ inch	29 kv at flange (or container)		32 kv	
(Figure 1) With $^7/_{16}$-inch recessed fibre washer	24.5 kv at hemispherical end. 32.5 kv at flange	3.15 inches mercury. 5.1 kv at hemispherical end. 7.9 kv above fibre washer		3.15 inches mercury. 7.9 kv
(Figure 1) With $^7/_{16}$-inch recessed fibre washer and 1-inch length of number 10 wire extending from terminal	29 kv at flange	3.15 inches mercury. 7.7 kv at terminal above fibre washer		3.15 inches mercury. 7.7 kv
(Figure 1) Final bushing. $^1/_2$-inch diameter, $^7/_8$-inch long hemispherically-ended terminal recessed in porcelain as shown	27 kv at flange	3.4 inches mercury. 6.3 kv. Streamers from terminal to flange	28.5 kv	3.4 inches mercury. 6.3 kv

Figure 5 represents corona or breakdown voltages for concentric cylinders in air, plotted as a function of inner-electrode diameter and separation between electrodes. The four curves, *1/4"D* to *2"D*, represent the inner-electrode diameter, the data having been taken from several sources. As an example of how these curves might be used, suppose one assumes a 1-inch inner-diameter cylinder and a 3-inch outer-diameter cylinder. The corona or breakdown value for this configuration may be found from the intersection of the *1"D* line and a separation of one inch. This value is seen to be approximately 38 kv.

Also shown in Figure 5 are lines of constant ratio of outer diameter to inner diameter. The usefulness of these lines lies in their giving similar fields along any one constant ratio line which complies with the law of similitude. An example of their use might be as follows:

> Assume that two cylinders have a ratio of outer diameter to inner diameter equal to three, but that these cylinders were large and were tested at the upper region of the curve, say 80 kv. In application it might be necessary to determine the dimensions

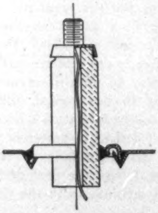

Figure 2. Typical bushing

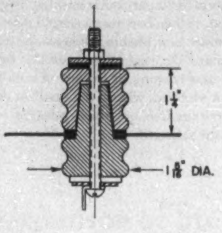

Figure 3. Original bushing design

of concentric cylinders whose field would be the same as the test setup, but whose corona or breakdown value should be about 20 kv. To determine the new cylinder diameters, one travels down the *3/1* constant-ratio line to where it intersects the 20-kv value. From Figure 5 it may be determined that a 0.5-inch inner-diameter cylinder and a separation of 0.5 inch would give the desired breakdown value. The outer cylinder would have a diameter of 1.5 inches.

Another use of the constant-ratio outer-diameter–inner-diameter lines is in applying the law of similitude for reduced-pressure application. Suppose in this example we assume a *4/1* constant-ratio line and a separation of three inches. From Figure 5 this would correspond to a corona or breakdown voltage of 90 kv. If it then is required to find the corona or breakdown voltage of the assumed system at 15 inches of mercury, we may use the *4/1* constant-ratio line, since it automatically gives the same field configuration. At 15 inches of mercury, the 3-inch separation acts the same as a 15/30 × 3 or 1.5-inch separation at 30 inches of mercury. Therefore, if we use the *4/1* line and 1.5-inch separation, we see the new value to be about 45 kv.

Also in Figure 5 are plotted the breakdown curve in air for plane surfaces and the breakdown for an edge of a parallel plate to a plane. It was found that for large spacings, the constant-ratio lines were parallel to the breakdown curve between planes at atmospheric pressure. Of interest is the curve for breakdown of a thin edge to a plane. As may be seen, at some separation less than 0.1 inch, the breakdown of an edge to a plane is about the same as from plane to plane. The dotted portion of the constant ratio lines was not determined experimentally; however, it is expected that the lower portion of these curves must turn up and end finally in the curve for breakdown between planes. The curves are approximately correct for design use.

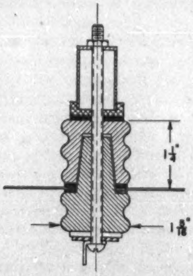

Figure 4. Modified bushing for test

In Figure 5 the experimentally-determined points of corona and breakdown at atmospheric and reduced pressure were used to construct a line of constant ratio for the final bushing design shown in Figure 1. If the values obtained on the final bushing are taken, a line whose constant-ratio value is 8 may be drawn. This can be determined from the string distance of 1.75 inches and the terminal diameter of 0.5 inch; the ratio (2 × 1.75 +0.5)/0.5 follows. Because corona and breakdown occur at approximately the same voltage, the ratio represents a bushing design that is about the smallest obtainable for any given voltage.

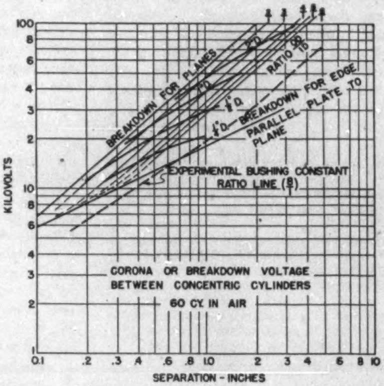

Figure 5. 60-cycle corona voltage for concentric cylinders and final bushing constant ratio line

Having established a ratio line to give a very satisfactory bushing, it is possible, using the law of similitude, to establish the proper bushing dimensions to meet any specified voltage. As an example of the use of the bushing constant-ratio line, we will take a hypothetical problem. A bushing must be corona free at 10 kv rms and at 50,000 feet altitude. From the experimental bushing 8-to-1 ratio line, the separation corresponding to 10 kv is approximately 0.4 inch at normal pressure. Using the law of similitude to find a string distance such that when this new distance is operated at 3.4 inches of mercury it acts as if it were 0.4 inch at normal pressure, we find the equivalent spacing to be 0.4 × 30/3.4, or a 3.5-inch string distance. For a ratio of 8-to-1 the terminal would be one inch in diameter. The ratio of new terminal to old terminal diameter yields the factor by which all bushing dimensions must be multiplied. The final hypothetical bushing dimensions then would be 2.75 inches diameter and 2.5 inches high. A rough sketch of this bushing will show a resulting string distance of about 3.5 inches. The corona voltage of this bushing at atmospheric pressure may be found from the intersection of the bushing constant-ratio (*8/1*) line and a 3.5-inch separation. The voltage corresponding to this point may be seen to be about 55 kv.

In order to apply the law of similitude it must be remembered that the field configuration of the new bushing design must be the same as the one for which the original curve is drawn. To comply with this requirement, the terminal stud and lower portion of the bushing also must be increased in size in the same proportion as the rest of the bushing. Small departure from the original porcelain design should not affect the results too quickly; however, any radical departures in porcelain configuration will affect the field distribution, and expected results may not be met.

From the results of data it may be said that, using Figure 5 as a first approximation, a means of bushing design to avoid corona at either atmospheric or reduced pressure has been presented. It must be realized that the fields associated with a bushing only approach those of concentric cylinders, and as is evident from the final bushing design, the values to be expected for a bushing will be below those for corresponding cylinders. The conditions at the flange are seen to be severe, and it is elimination of stress at this point, especially at atmospheric pressure, that is necessary. By proper proportions it is possible to design a bushing to be corona free up to breakdown. This is borne out by the experimental results stated earlier. If the proper ratio of diameters for a particular bushing is established, it then becomes a simple matter to calculate new bushing dimensions and to estimate the performance of the design. The new bushing, if the law of similitude is not violated, will be the smallest design for corona-free operation relative to its voltage strength.

No Discussion

Comparison of Steady-State and Transient Performance of Servomechanisms

HAROLD CHESTNUT
MEMBER AIEE

ROBERT W. MAYER
NONMEMBER AIEE

A SERIES of charts has been prepared which permit the servo designer to determine readily the kind of servo open-loop transfer function which will yield a desired closed-loop steady-state frequency response or transient response to a step-position input. The open-loop transfer function is expressed in terms of single-gain 2-frequency (or time constant) ratios, and the intermediate attenuation rates so that the servo characteristics are directly interpreted in a form convenient for design purposes.

Study of these charts has indicated to what extent the steady-state and transient characteristics of linear servos may be compared. A number of significant relationships between steady-state and transient performance are discussed.

The performance data which are represented include: the magnitude and frequency at which the maximum of the steady-state response occurs; the magnitude and time at which the peak transient response to a step-function position input occurs; and the settling time and the natural frequency of oscillation of the transient response.

Examples are used to illustrate how the nondimensionalized charts may be employed for synthesizing or analyzing typical servo designs.

Many books and articles have discussed the means whereby a servomechanism system with a known open-loop attenuation characteristic may be analyzed to determine the steady-state frequency response, or to determine the transient response to a step-function input.[1] The converse of this problem, namely, to determine an open-loop attenuation characteristic which will produce a desired frequency response or a transient response to a step function input has been covered only to a limited extent in the literature.[2] However, it is the latter problem which generally confronts the servo designer. He is given a set of specifications involving the steady-state frequency response and/or the transient response to a step input. His problem is to determine the approximate form of the open-loop attenuation characteristic which will provide the desired performance. With this he is in a position to start his more detailed design and to have a fairly definite, although not an absolute, goal toward which to point his design. With the present servo synthesis and design techniques,[3] it is possible for the designer to determine the servo components which will produce the necessary open-loop characteristic.

Since such practical limitations as nonideal components, cost, and weight will probably necessitate deviations from the theoretical open-loop attenuation characteristic initially chosen, it is not essential that the open-loop characteristic be determined with particularly great precision.

It is essential, however to have this open-loop characteristic be reasonably close to the necessary form. In addition, the quantitative effect of changes in the various parameters in terms of the steady-state and transient performance should be understood, so as to indicate a method of refining system design to meet the exact specification requirements.

As a means for meeting the needs just outlined, a series of charts has been prepared which show the steady-state and transient response of ideal linear servomechanisms in terms of the open-loop attenuation characteristics which are necessary to obtain the response. The system parameters which are used to define the open-loop characteristic are described in the next section. The performance characteristics shown on the charts are the following:

$[\theta/D]_m$ = the maximum ratio of output to input of the frequency response

$[\theta/D]_p$ = the peak value of the ratio of output to input for a step function input

ω_m/ω_c = the ratio of the frequency ω_m at which $[\theta/D]_m$ occurs to the frequency ω_c at which the straight line approximation of the open-loop response is zero decibels

ω_t/ω_c = the ratio of ω_t, the lowest frequency of oscillation for a step input to ω_c, the frequency at which the straight line approximation of the open-loop response is zero decibels

$\omega_c t_p = t_p$, the response time from the start of the step function until when $[\theta/D]_p$ occurs, times ω_c, the frequency at which the straight line approximation of the open-loop response is zero decibels

$\omega_c t_s = t_s$, the settling time from the start of the step function until the ouput continues to differ from the input by less than 5 per cent, times ω_c, the frequency at which the straight line approximation of the open-loop response is zero decibels

Indicated in Figures 1(A), (B), and (C) are these various characteristics in terms of the familiar curves of the open-loop transfer function, the frequency response, and the transient response to a step input. In Figure 1(D) are shown how the same characteristics are indicated on the charts merely as a function of the ratio ω_1/ω_c and μ_1. Instead of the more customary curves of Figures 1(A), (B), and (C), only significant performance parameters have been plotted and these

---

Paper 49-196, recommended by the AIEE Joint Subcommittee on Servomechanisms and approved by the AIEE Technical Program Committee for presentation at the AIEE Summer General Meeting, Swampscott, Mass., June 20–24, 1949. Manuscript submitted March 24, 1949; made available for printing May 6, 1949.

Harold Chestnut and Robert W. Mayer are with the General Electric Company, Schenectady, N. Y.

The authors wish to acknowledge the interest and assistance of Dr. C. F. Green, Mrs. Cecile Lester, Dean Wheeler, and members of the Advanced Engineering Program of General Electric Company in making possible the preparation of this material.

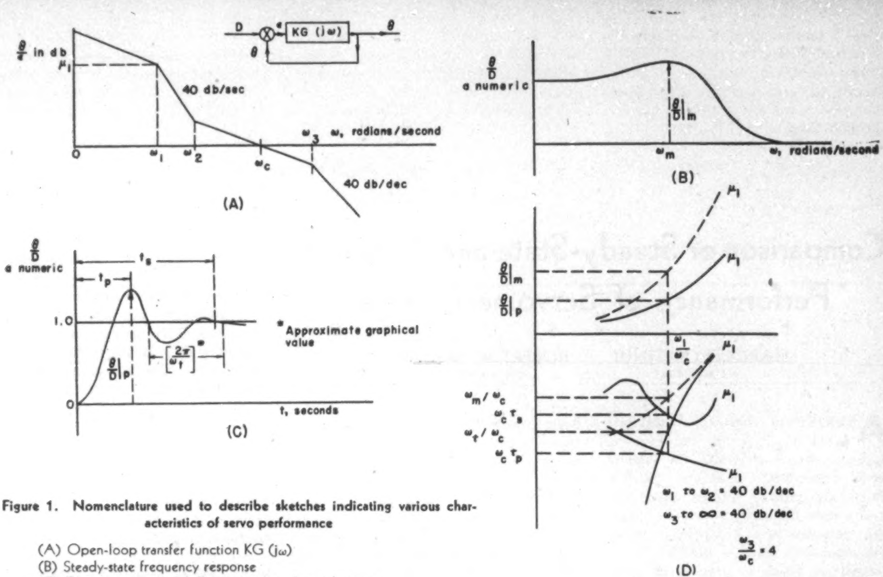
D
ε
KG (jω)
θ
θ
θ/ε in db
μ1
40 db/sec
ω3
ω, radians/second
0
ω1
ω2
ωc
40 db/dec
(A)
θ/D
a numeric
|θ/D|m
ωm
ω, radians/second
(B)
θ/D
a numeric
ts
tp
1.0
0
|θ/D|p
[2π/ωt]*
*Approximate graphical value
t, seconds
(C)
μ1
|θ/D|m
|θ/D|p
ω1/ωc
ωm/ωc
ωc τs
ωt/ωc
ωc τp
ω1 TO ω2 = 40 db/dec
ω3 TO ∞ = 40 db/dec
ω3/ωc = 4
(D)

Figure 1. Nomenclature used to describe sketches indicating various characteristics of servo performance

(A) Open-loop transfer function KG ($j\omega$)
(B) Steady-state frequency response
(C) Transient response following a step-function input
(D) Representation of servo performance characteristics in chart form

in terms of the open-loop attenuation characteristic which will produce them.

The charts have been prepared on the basis that the system contains a single integrating element so that at very low frequencies the open-loop attenuation characteristic has a slope of 20 decibels per decade. However, as is discussed later, the major factor influencing the performance of the system is the attenuation characteristic in the vicinity of 0 decibels. Hence the charts also may be used to provide worthwhile information on the performance of regulating systems which have zero attenuation rate at low frequencies, as well as torque-motor type systems which have an attenuation rate of 40 decibels per decade at low frequencies, providing the attenuation-frequency characteristics of these systems in the vicinity of zero decibels are comparable to the attenuation characteristic of the system shown on the chart which has the desired performance.

Figure 2. Straight line approximation to open-loop attenuation characteristics showing significant values of gain, time constants, and frequencies of attenuation slope breaks

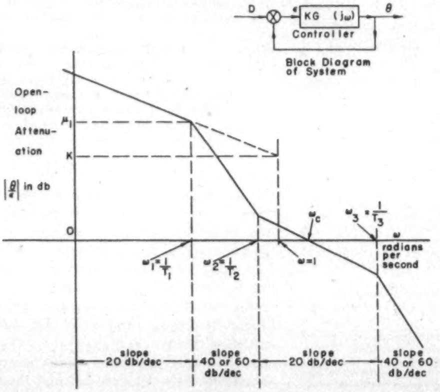
D
ε
KG (jω)
Controller
θ
Block Diagram of System
Open-loop Attenuation
|θ/ε| in db
μ1
K
0
ω1 = 1/T1
ω2 = 1/T2
ω=1
ωc
ω3 = 1/T3
ω radians per second
slope 20 db/dec
slope 40 or 60 db/dec
slope 20 db/dec
slope 40 or 60 db/dec

Figure 3. Comparison of two servo systems having attenuation-frequency characteristics of similar shape but shifted in frequency by the ratio ω_c'/ω_c

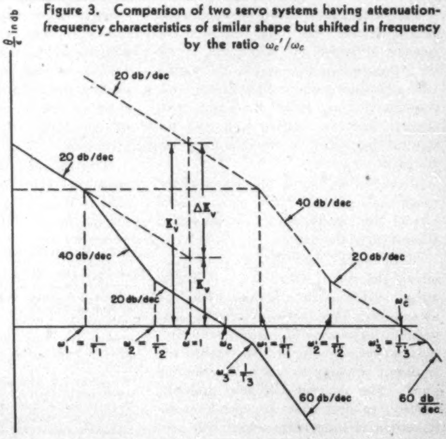
θ/ε in db
20 db/dec
20 db/dec
40 db/dec
ΔKv
K'v
Kv
40 db/dec
20 db/dec
20 db/dec
ω'c
ω1 = 1/T1
ω2 = 1/T2
ω=1
ωc
ω'1 = 1/T'1
ω'2 = 1/T'2
ω'3 = 1/T'3
ω3 = 1/T3
60 db/dec
60 db/dec

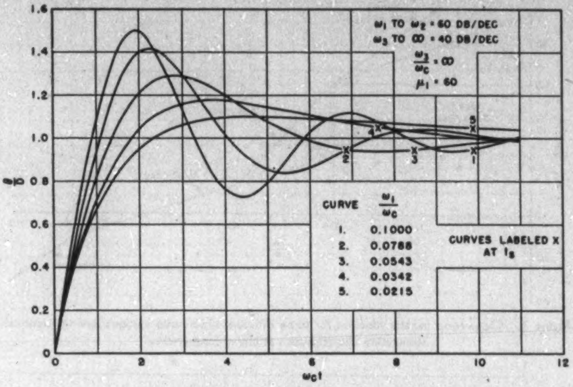

Figure 5. Transient response following step function position input disturbance

Description of Attenuation-Frequency Characteristics Considered

In Figure 2 are shown the significant parameters which have been used to define the idealized attenuation diagrams for which the steady-state and transient performance have been determined. Although the attenuation characteristic and the block diagram of the system indicate that only series elements have been considered as making up the control system, it is apparent that feed-back loops may be included within the control, providing the resultant attenuation characteristic approaches that for an equivalent system containing only series elements. Basically the attenuation diagram considered is one in which:

1. The attenuation slope is 20 decibels per decade in the vicinity of 0 decibels which gain occurs at the frequency ω_c. This type attenuation characteristic is desirable from the standpoint of providing adequate stability.

2. The attenuation slope increases to 40 or 60 decibels per decade at some higher frequency ω_3 for which the equivalent time constant is T_3, that is, $T_3 = 1/\omega_3$. This may correspond to the presence of the power element time constant or to the condition that is obtained when the loop gain around a feed-back loop falls below unity. In addition, this characteristic may be deliberately inserted to help attenuate undesirable higher frequency input signals.

3. The attenuation rate is 40 to 60 decibels per decade in the region of frequencies from ω_1 to ω_2 for which the equivalent time constants are T_1 and T_2 respectively. Thus,

$$T_1 = \frac{1}{\omega_1} \quad \text{and} \quad T_2 = \frac{1}{\omega_2}$$

4. The attenuation rate is 20 decibels per decade from zero frequency to the frequency ω_1. The system gain at ω_1 is defined as μ_1 on the straight line approximation to the attenuation diagram. The actual gain will be 3 or 6 decibels lower at this frequency, depending on whether the attenuation rate from ω_1 to ω_2 is 40 or 60 decibels per decade.

In some cases, certain of the time constants take on limiting values so that the attenuation diagram appears to have a different form from that shown in Figure 2.

For example, if $T_1 = T_2$, then the slope of 20 decibels per decade extending from low frequencies continues constant until the frequency ω_3. This case is represented on the charts by the data at $\omega_1/\omega_c = 0.1$ and $\mu_1 = 20$ decibels. As another example, consider the case where $T_3 = 0$ so that the 20 decibel-per-decade slope at ω_c is maintained from ω_c on out to infinity. These data are contained on these charts where $\omega_3/\omega_c = \infty$.

Referring to Figure 2, it can be seen that μ_1 in general is not the same as the system gain K which is the value of the gain obtained at $\omega = 1$ if the initial slope from 0 to ω_1 were to be maintained at 20 decibels per decade.

The method which has been employed on the charts to define a given attenuation characteristic is to indicate the nature of the slope between ω_1 and ω_2 as 40 or 60 decibels per decade, and also to indicate the slope between ω_3 and infinity as 40 or 60 decibels per decade. Each chart is then drawn up for a constant value of the ratio ω_3/ω_c. The other parameters used to define uniquely the specific attenuation characteristic are the gain μ_1 in decibels, and the frequency ratio ω_1/ω_c. Since μ_1 and ω_1 are definitely related to the servomechanism specification requirements of a certain maximum error at a specific signal frequency, these are particularly significant parameters from

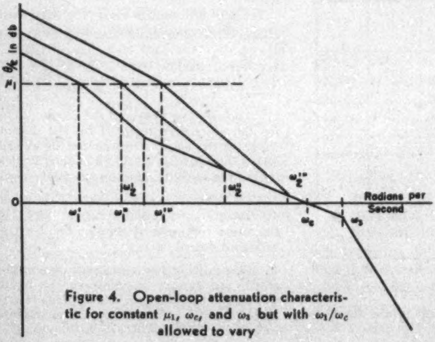

Figure 4. Open-loop attenuation characteristic for constant μ_1, ω_c, and ω_3 but with ω_1/ω_c allowed to vary

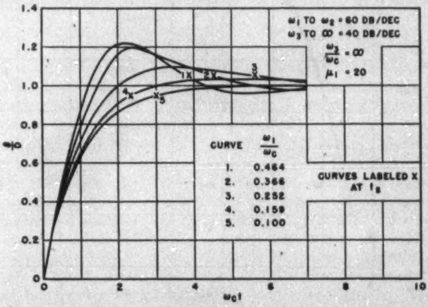

Figure 6. Transient response following step function position input disturbance

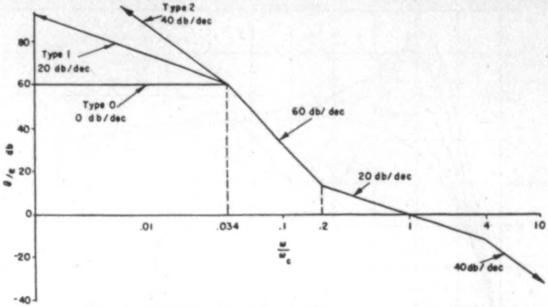

Figure 7. Open-loop transfer function for three different type servo systems having identical attenuation characteristics at higher frequencies

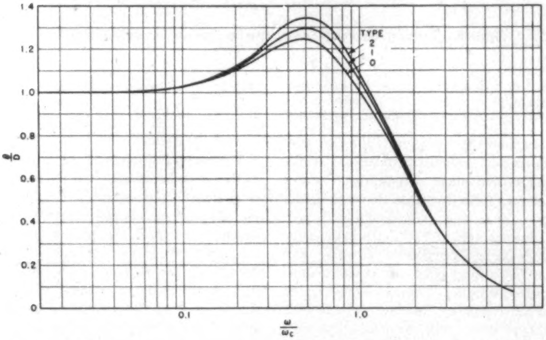

Figure 8. Steady state frequency response for servos with open-loop transfer functions shown in Figure 7

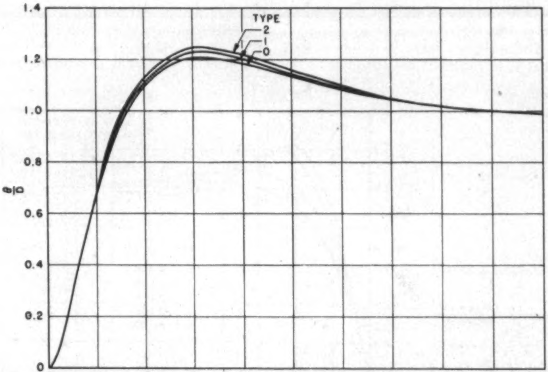

Figure 9. Transient response to a step function for servos with open-loop transfer functions shown in Figure 7

the viewpoint of system needs as well as of their usefulness to the designer.

The use of the dimensionless ratio ω_1/ω_c as the abscissa serves to broaden the utility of the data while permitting the designer to determine the performance if the system if ω_1/ω_c is already established, or to determine the ω_1/ω_c ratio if the performance of the system is selected as the independent condition for system design.

Although it might appear that broad increments of μ_1 have been chosen for the family of curves plotted against ω_1/ω_c, there are sufficient curves shown to permit fairly straightforward interpolation in most cases.

It should be pointed out that although for convenience purposes the attenuation characteristics are represented by their straight-line approximations, the exact attenuation characteristic has been used in the calculations for the charts.

EFFECT OF VALUE OF ω_c ON FREQUENCY RESPONSE AND TRANSIENT RESPONSE

The preceding section has served to emphasize the importance of the shape of the attenuation-frequency diagram in the vicinity of zero decibels. Although Bode's work has pointed out the importance of this characteristic on stability considerations, its effect on the steady-state and transient response of a servomechanism has not been so clearly emphasized.

Consider the case shown in Figure 3 where two similar attenuation-frequency characteristics are drawn. Both have the same value of μ_1 and both have the same rate of change of attenuation with frequency in the region near 0 decibels; however, the values of the frequencies ω_c', ω_1', ω_2' and ω_3' on the dotted curve are ω_c'/ω_c times higher than the comparable ω_c, ω_1, ω_2 and ω_3 for the solid curve.

It can be shown that for the two characteristics described by Figure 3:

1. The velocity error coefficient for the dotted curve is ω_c'/ω_c times that for the solid curve.

2. The response time and the settling time for the system represented by the dotted curve to the same step-function input are altered by the ratio ω_c/ω_c' times their values for the system illustrated by the solid curve.

3. The ratio of the magnitude of the peak overshoot to the initial transient input is the same for systems represented by the solid and dotted curves.

4. The ratio of the maximum magnitude of the steady-state response to the input sinusoid is the same for the systems represented by the solid and dotted characteristics.

Figure 10. Open-loop transfer function and frequency response for low gain system of Case 1 example

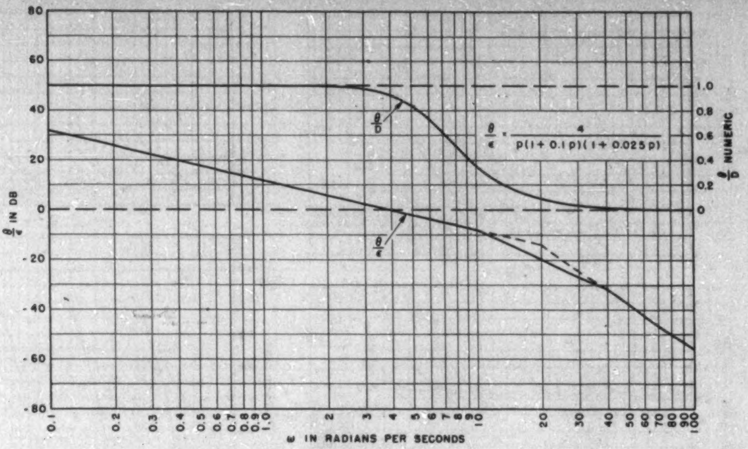

5. The ratio of the frequencies at which maximum output to input ratio of the steady-state response occurs and the frequency at which zero decibels is obtained is the same for systems having the solid and dotted characteristics.

Discussion of Results

From study of the results presented in Figures 12–29, as well as other thoughts which were stimulated by this study, a number of significant relationships were revealed.

EFFECT OF USING PARAMETER ω_1/ω_c FOR ABSCISSA

In Figure 4 are shown a number of open-loop attenuation characteristics in which μ_1, ω_c, and ω_2 are held constant and the ratio ω_1/ω_c is allowed to vary. It is evident that as the frequency ω_1 is increased, the frequency ω_2 also must be increased and therefore is more nearly equal to ω_c. For the increased ω_2, the section of 20 decibel-per-decade slope in the vicinity of 0 decibels is reduced and it would appear from a qualitative point of view that a less stable system would result, that is, one having a higher value of $[\theta/D]_m$ (steady-state) and a higher value of $[\theta/D]_p$ (transient). This result is indicated quantitatively in the curves of $[\theta/D]_m$ and $[\theta/D]_p$ as a function of ω_1/ω_c for μ_1 and ω_c constant.

It might appear that fairly broad interpolation would be required to obtain performance figures at values of μ_1 other than those specifically calculated. Actually the θ/D values for values of μ_1 greater than 40 seem to be determined largely by the values of ω_2, so that the effect of going to higher values of μ_1 has the effect of reducing ω_1/ω_c to a lower value for the corresponding servo performance.

Reference to Figure 29 which has the same ordinates as Figure 24 but which has ω_2/ω_c as its abscissa, indicates that there can be a close dependence of the transient and steady-state on ω_2/ω_c, and that there may be a relatively small effect on the system performance for changes of μ_1 as long as the value of μ_1 is large, say 60 decibels or greater.

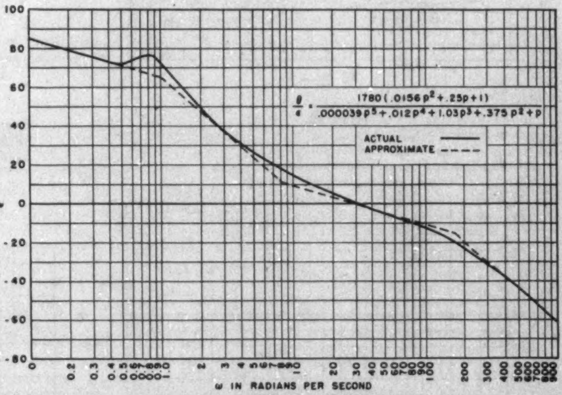

Figure 11. Actual and approximate open-loop transfer function for high gain system of Case 2 example

COMPARISON OF MAXIMUM STEADY-STATE VALUE OF OUTPUT-INPUT RATIO $[\theta/D]_m$ TO PEAK VALUE OF TRANSIENT OUTPUT-INPUT RATIO $[\theta/D]_p$

Study of the data presented on the upper portions of Figures 12 to 29 reveals that the maximum steady-state value $[\theta/D]_m$ generally exceeds the peak value of the transient $[\theta/D]_p$ or most values of ω_1/ω_c although this is not universally true. It is only for systems which have a low value $[\theta/D]_m$ that is, less than 1.25 that $[\theta/D]_p$ may exceed $[\theta/D]_m$. For these systems the maximum value of both the steady-state or transient is low, and

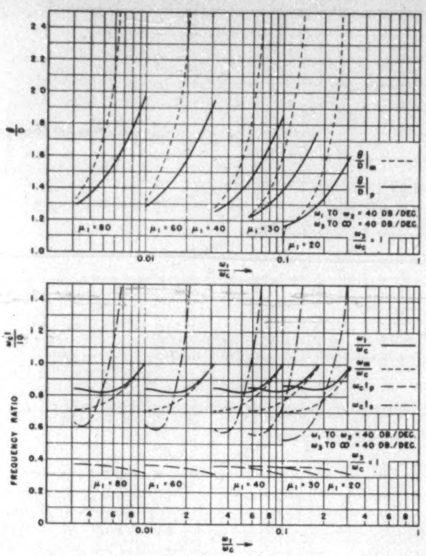

Figure 12

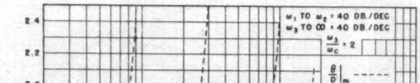

Figure 13

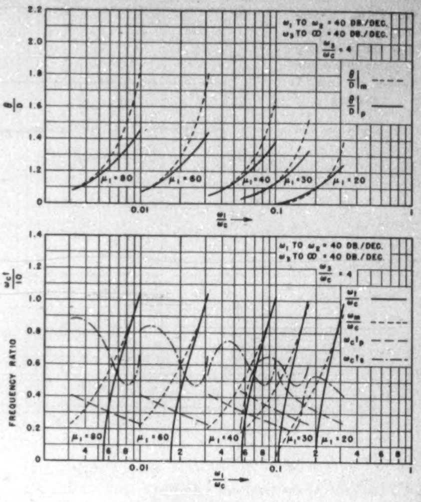

Figure 14

Figures 12 to 21. Comparison of steady-state frequency response characteristics and transient response following a step-function of input as a function of ω_1/ω_c

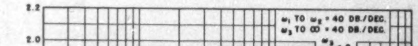

Figure 15

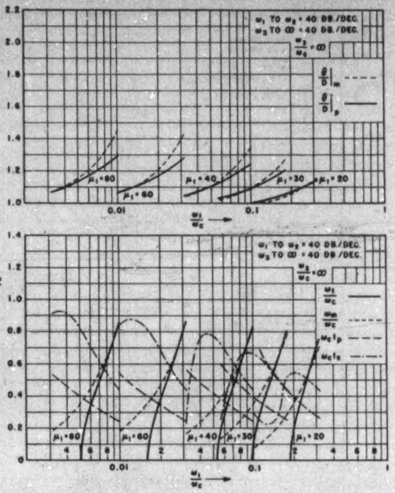

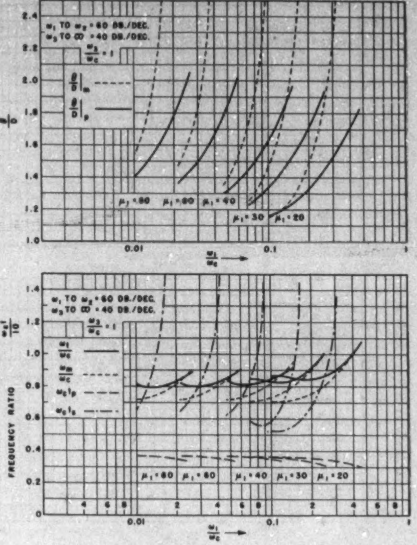

Figure 16 (above), Figure 17 (right). Comparison of steady-state frequency response characteristics and transient response following a step-function of input as a function of ω_1/ω_c

the transient peak seems not to exceed the steady-state maximum by more than 5 per cent of the input in any case. Systems such as these are exceptionally stable ones for which the degree of damping is fairly high although the systems are not quite critically damped. It will be recalled that a highly damped quadratic system of this sort is capable of some overshoot to a step-function transient although the steady-state frequency response has a maximum value of 1.0 or only slightly greater.

The value of $[\theta/D]_m = 1.25$ appears to be one at which $[\theta/D]_m$ for a system is equal to or somewhat in excess of $[\theta/D]_t$. Since $[\theta/D]_m = 1.3$ is a design figure which is frequently used, it is convenient to know that $[\theta/D]_p$ will be less than this amount for this case. Although by proper choice of design the value of $[\theta/D]_p$ may be reduced with the value of $[\theta/D]_m$ held constant at 1.3, the improvement possible is limited to a few per cent.

This comparison of the maximum steady-state and transient magnitudes has revealed quantitatively a condition long realized qualitatively by practical designers, namely, the use of the steady-state rather than the transient basis for design is quite satisfactory since a system having a low maximum value for its steady-state response also will have a low overshoot for its transient response.

COMPARISON OF FREQUENCY ω_m AT WHICH $[\theta/D]_m$ OCCURS TO ω_t, THE LOWEST FREQUENCY OSCILLATORY TERM OF THE TRANSIENT RESPONSE

The figures presented on the lower portion of Figures 12 to 28 compare plots of ω_m/ω_c and ω_t/ω_c for the systems having the $[\theta/D]_m$ and $[\theta/D]_p$ values shown in the upper portion of these figures.

As such these data may be used for the purpose of rapidly determining the frequency characteristics of a contemplated design. Since, as is generally the case, the actual frequency of ω_m is given as a specification requirement, the ω_m/ω_c ratio is useful in establishing the frequency ω_c which will be required to obtain the value of ω_m desired.

In addition these frequency data presented in the charts can be used to indicate certain trends in performance which result from the selection of one or another design, both of which may have comparable values for $[\theta/D]_m$ or $[\theta/D]_p$. If ω_m/ω_c and ω_t/ω_c be compared for the same system, then a direct comparison of ω_m and ω_t can be made. From such a comparison the following generalities are indicated:

Effect of ω_3/ω_c

Systems in which $1<\omega_3/\omega_c<4$ correspond to fairly oscillatory systems with little damping. For these systems the lowest frequency of transient oscillation ω_t is greater than the frequency ω_m at which the steady-state response is a maximum. The variation of the values of ω_t/ω_c and ω_m/ω_c is fairly small and the values of each are about 1.0. For systems having higher values of the ω_3/ω_c ratio, that is, $\omega_3/\omega_c>4$, ω_m exceeds ω_t. There can be a wide variation of both the values of ω_t and ω_m as ω_1/ω_c is changed. The values range from about one for each when ω_1/ω_c is large for a given μ_1, that is, fairly oscillatory systems, to zero for ω_t at low values of ω_1/ω_c when the systems are so stable as to have all real roots. The oscillatory and stable systems correspond to values of ω_2/ω_c which are near 1.0 and near 0.1 respectively.

Effect of Change in μ_1

The shape of the ω_t/ω_c and ω_m/ω_c curves for a constant μ_1 and over a range of ω_1/ω_c bears a close resemblance to these same curves for a different μ_1 but the same ω_3/ω_c. This tends to indicate that if ω_3/ω_c and ω_2/ω_c are fixed and μ_1 and ω_1 alone are changed, the changes in ω_m/ω_c and ω_t/ω_c are not great. However, it is evident from the curves that the effect of reducing the gain μ_1 is to increase the ω_m/ω_c and ω_t/ω_c ratio.

Effect of Attenuation Slope ω_3 to Infinity

For systems in which the attenuation slope from ω_3 to infinite frequency is 60 decibels per decade rather than 40 decibels per decade, the values of ω_m/ω_c are higher. That is, the frequency at the steady-state maximum is more nearly that of ω_c when a 60 decibel-per-decade slope at the higher frequencies is employed. From the point of view of decreasing the transmission of the system at higher frequencies, this appears

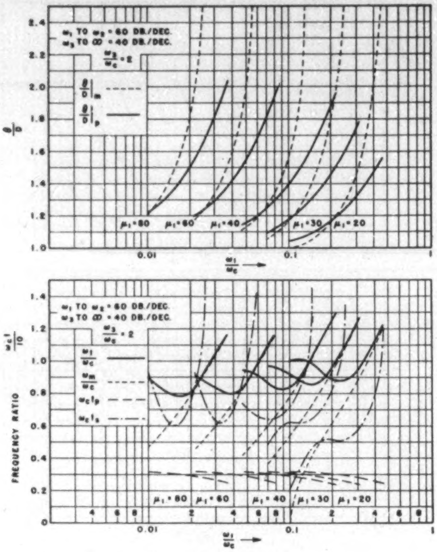

Figure 18

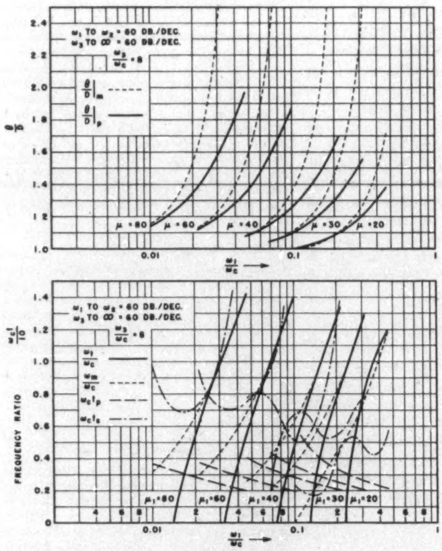

Figure 19

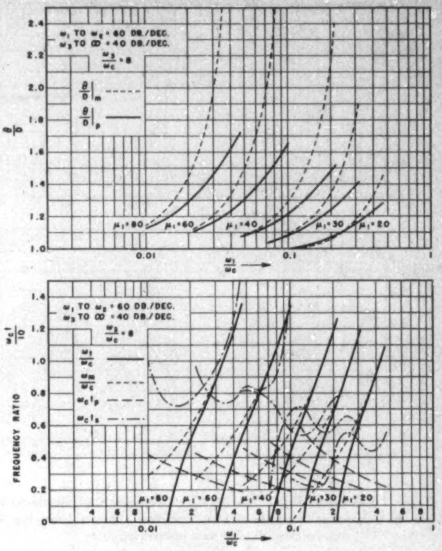

Figure 20

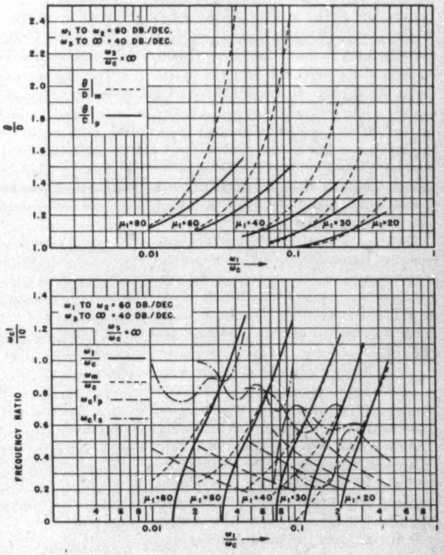

Figure 21

Figures 12 to 21. Comparison of steady-state frequency response characteristics and transient response following a step-function of input as a function of ω_1/ω_c

desirable but transient considerations which are discussed in the following section may be of greater importance.

TIME AT WHICH PEAK OVERSHOOT OCCURS

Reference to Figures 12 to 28 indicates that for the lower values of ω_2/ω_c, in the range from $1 < \omega_2/\omega_c < 4$, $\omega_c t_p$ is approximately equal to three and is relatively unaffected by changes in μ_1 or ω_1/ω_c for a constant value of ω_c. However, since the ordinate of these curves is $\omega_c t_p$ the value of t_p, the elapsed time from the application of a step function until the peak overshoot, is inversely proportional to ω_c. Therefore, it is primarily by increasing ω_c that the time t_p can be reduced.

When $\omega_2/\omega_c \leq 8$, $\omega_c t_p$ tends to vary over a wider range and to decrease as ω_1/ω_c takes on larger values with μ_1, ω_c, and ω_2 constant. This may be verified in a qualitative way by reference to Figure 4 where as ω_1 takes on increasing values, the actual gain of the system is increased for the frequencies lower than ω_2 and a shorter time should be required for the initial step displacement to be reduced to zero. Figures 5 and 6 comparing the actual transient response as a function of time for constant values of μ_1, ω_c and ω_2 indicate in a quantitative fashion the decrease in time required for the higher gain, lower ω_1/ω_c systems to reach their transient peak although the peak attained is higher.

SETTLING TIME AFTER WHICH TRANSIENT OVERSHOOT REMAINS LESS THAN 5 PER CENT OF ORIGINAL DISTURBANCE, t_s

If the magnitude of the peak overshoot can be made less than the allowable limit, then the time t_p alone is of interest. However, when the initial overshoot exceeds the desirable operating value of the output, the performance may still be satisfactory if the succeeding overshoots can be brought within acceptable limits within an allowable length of time.

The acceptable error limit which was selected for purposes of this study is ±5 per cent from the desired step input. Since most high performance servo systems tend not to be linear for large displacements, the step input for which this analysis is valid is likewise small. Consequently 5 per cent of this magnitude is probably a small enough error to be acceptable.

No simple over-all statement can be made concerning the shape of the $t_s\omega_c$ characteristics. There are certain trends which are present that are worthy of mention however, and can be readily appreciated by reference to Figures 5 and 6. It will be noted that as the values of ω_1/ω_c decrease, the amplitude and the apparent frequency of oscillation also decrease. The decrement rate of the exponentially decaying term also changes with ω_1/ω_c so that the time at which the overshoot is 5 per cent is subject to rather large fluctuations of the order of one-half the period of oscillation.

It should be noted that only five data points were used to construct each curve on the charts so that it was not possible to determine the exact value of ω_1/ω_c where the transient no longer exceeded 1.050 to 0.950. Since the ±5 per cent figure represents an arbitrary value, and since slight changes in the system parameters will alter the actual transient response somewhat, smooth curves were drawn to indicate the $\omega_c t_s$ function. These tend to minimize the abruptness of the transition of the $t_s\omega_c$ response from one-half cycle to the next half cycle of oscillation.

Figure 5 shows the transient response of a system in which the initial peak in all cases is greater than 5 per cent. As ω_1/ω_c is decreased from its highest value, $\omega_c t_s$ first decreases as the peak overshoot decreases and the decrement rate remains fairly high. As ω_1/ω_c further decreases, the frequency of oscillation is lowered and the decrement rate is also decreased; hence, the initial overshoot is maintained for a longer period. Therefore $\omega_c t_s$ is increased again as ω_1/ω_c is further reduced.

Curves 1, 2, and 3 of Figure 6 indicate a continuation of the trend noticed in Figure 5 toward higher values of $\omega_c t_s$ as ω_1/ω_c is decreased. However as ω_1/ω_c is further decreased, the peak overshoot falls below 1.05, and for curve 4 the output remains within 5 per cent of the input after it reaches $\theta/D = 0.95$ at $\omega_c t = 2.35$. A further decrease in the ω_1/ω_c ratio as shown by curve 5 causes the system to be more heavily damped and the time required to get to $\theta/D = 0.95$ is again increased.

For a system having μ_1, ω_c, and ω_2 fixed, the time after which the error to a step-position input remains less than a small amount can be decreased only so far by decreasing ω_1. A further decrease in ω_1 merely causes the system to become too sluggish. Quantitative data are provided by Figures 12 to 28 which indicate whether an improvement in system performance will be realized by such a decrease in ω_1/ω_c.

The beneficial effect of increasing the frequency ω_c mentioned in conjunction with t_p also is realized for t_s since the time ordinates on Figures 12 to 28 are $\omega_c t$.

USE OF FIGURES 12 TO 28 FOR SYSTEMS OTHER THAN THOSE HAVING A SINGLE INTEGRATING ELEMENT IN THE CONTROLLER

Although the results presented in Figures 12 to 28 are valid only for systems having the attenuation diagrams specified, they are also of considerable use for predicting the performance of systems having quite different attenuation-frequency characteristics at low frequencies, but which have identical attenuation characteristics for frequencies for which the open-loop characteristic is in the vicinity of zero decibels and for all higher frequencies. Figure 7 shows three such systems while Figure 8 indicates the frequency response of each. Type "0" indicates a system which requires an error to obtain a constant output position and is characteristic of regulating systems. Type "1" indicates a system in which a constant error produces a constant output velocity and represents the type of system used extensively for high performance position controls. Type "2" indicates a system in which a constant error produces a constant output acceleration and represents a type system less frequently employed. It is evident that for these three systems there is little to choose from as far as the frequency response is concerned. The type "0" system has a slightly lower maximum value than that of the type "1" system, while the type "2" system has a slightly higher maximum value than the type "1" system. It would appear that this relationship between the magnitude of the response of systems of these various types is fairly general although it is not probable that the frequency of the maximum of the frequence response will be the same for each in the general case.

Figure 9, in comparing the transient response to a step function of these three seemingly different systems also reveals that there is a close comparison between them. It is doubtful that this close a comparison will be obtained for the more general case, where the attenuation characteristics are dissimilar until the gain is lower than that for the three systems considered. However, the possibilities of the performance results for a type "1" system in providing a ceiling indication for the type "0" system and a lower limit value for the type "2" system is apparent.

For type "2" systems in which the initial attenuation rate is 40 decibels per decade at very low frequencies followed by a section of 20 decibel-per-decade attenuation rate in the region of ω_c, the question arises as to which values of

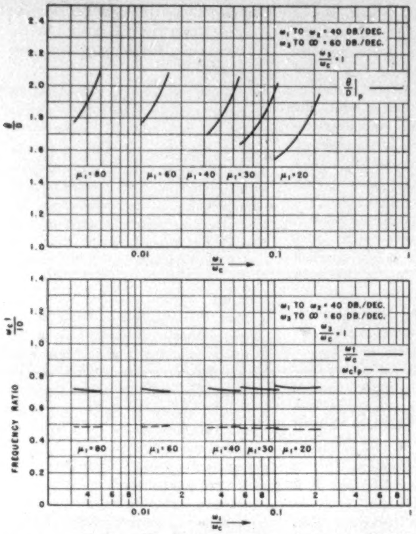

Figure 22. Transient response following a step-function of input as a function of ω_1/ω_c

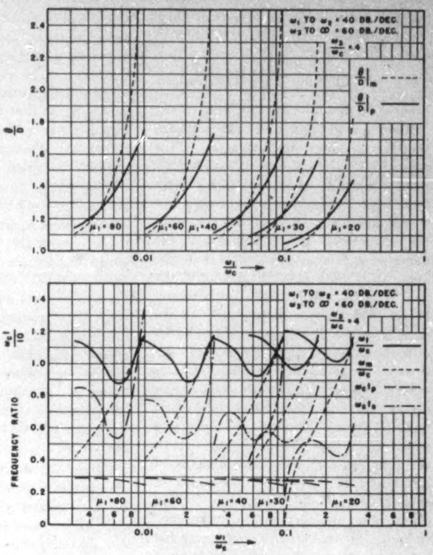

Figure 24

Figures 23 to 28. Comparison of steady-state frequency response characteristics and transient response following a step-function of input as a function of ω_1/ω_c

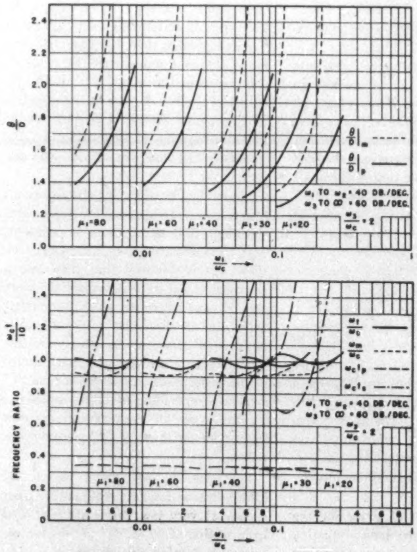

Figure 23

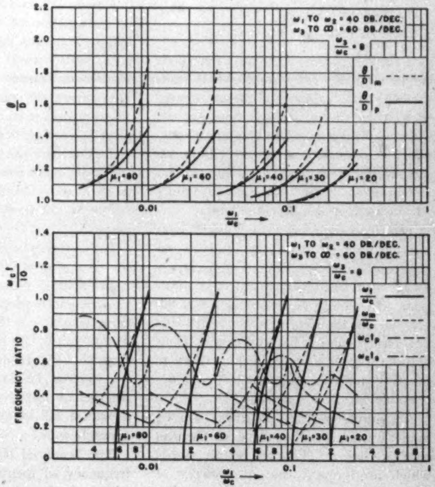

Figure 25

μ_1 and ω_1/ω_c should be used with which charts. The charts to be used are those for which the attenuation rate from ω_1 to ω_2 is 40 decibels per decade and those for which the proper value of ω_3/ω_c and attenuation rate from ω_3 to infinity are obtained. Select the $\mu_1=80$ decibels characteristics and use the value of ω_1 determined at $\mu_1=80$ decibels for the actual transfer function attenuation characteristic; the values of the performance parameters indicated should most closely approximate those actually obtained for the 40 decibels per decade, type "2" system.

EFFECT OF HAVING NONMULTIPLE BREAKS TO OPEN-LOOP ATTENUATION CHARACTERISTICS

In the interest of presenting a fairly complete picture of the performance of representative servo systems with a limited number of charts, it was considered necessary not to include systems in which there are intermediate breaks in the attenuation diagram. For example, the ideal cases represented in the charts by multiple breaks where in the open-loop diagram the attenuation rates change abruptly from 20 to 60 decibels per decade or vice versa are generally realized in practice by two adjacent breaks so that there is an intermediate section of 40 decibels per decade. Fortunately design methods are such that frequently this 40 decibel-per-decade attenuation section is limited to a short range of frequencies. In this way the attenuation and phase shift of the system at some frequency remote from this range of frequencies is essentially the same whether multiple breaks occur for example, at the frequency ω_1, or two separate breaks occur at somewhat higher and somewhat lower frequencies than ω_1. As a general rule,[3] two different but neighboring time constants T_a and T_b may be replaced by two equal time constants of value T_{ab} which are defined as

$$T_{ab}=\sqrt{T_aT_b}$$

This approximation may be verified in a qualitative fashion by a comparison of the terms

$$(1+T_ap)(1+T_bp)=1+(T_a+T_b)p+T_aT_bp^2$$

and

$$(1+T_{ab}p)^2=1+2\sqrt{T_aT_b}p+T_aT_bp^2$$

The difference between the two is that the coefficients of the p term are T_a+T_b and $2\sqrt{T_aT_b}$ respectively. When $T_a=T_b$ the ratio of $(T_a+T_b)/2\sqrt{T_aT_b}$ is 1.0; when T_a is as much as four T_b, the ratio of $(T_a+T_b)/2\sqrt{T_{ab}}$ is only $5/4=1.25$ and the maximum variation between the two amplitude characteristics is only about 2 decibels.

The intermediate frequency ω_{ab} corresponding to the intermediate time constant T_{ab} can be located graphically merely by extending, until they intersect, the sections of 20 and 60 decibel-per-decade slope on either side of the 40 decibel-per-decade slope noting the frequency at the intersection. If this frequency is used for an equivalent ω_1, ω_2 or ω_3 as the case requires, reasonably good agreement should be realized between the actual results and those indicated by the charts.

It is of interest to note that transfer functions having quadratic terms with complex factors also may be represented by two equal factors for purposes of using the charts. Thus, approximately

$$(1+2\zeta T_p+T^2p^2)\simeq(1+T_p)(1+T_p)$$

which yields the same value as that given by T_{ab} in the preceding discussion.

CHOICE OF ATTENUATION RATES BETWEEN ω_1 AND ω_2, AND ω_3 AND INFINITY

For systems in which the parameters μ_1, ω_1, and ω_3 are fixed and the attenuation rate from ω_1 to ω_2 alone is a design choice to be made, the use of a steeper slope (60 decibels per decade) produces lower values of $[\theta/D]_m$ and $[\theta/D]_p$ than use of the less steep (40 decibels per decade) slope. However, it will be noticed that despite the lower initial transient peak for the 60 decibel-per-decade slope, the time required for the transient to settle to 5 per cent of the magnitude of the step input is generally somewhat greater for this case. Hence the choice is not clearcut for all cases and the relative importance of maximum magnitude of transient or setting time must be considered.

In the case where all other system parameters are chosen but the slope of the open-loop attenuation characteristic between ω_3 and infinity, the use of an attenuation rate of 60 decibels per decade rather than 40 decibels per decade increases $[\theta/D]_m$ and $[\theta/D]_p$. In addition the time for the transient error to settle to 5 per cent of its original value also is increased somewhat by use of the steeper slope.

It should be noted however that use of the higher attenuation rate may be advantageous in eliminating undesirable noise signals in the higher frequency region of the spectrum. In a sense the inability of the 60 decibel-per-decade system to respond rapidly to transient inputs may not be a liability for, in so doing, the system also is made insensitive to the extraneous high frequency nois signals as well.

Examples

The information presented in Figures 12 to 28 is useful either for purposes of analysis, that is, determining the response of systems already designed or for purposes of synthesis, such as determining what sort of system will be required to do a specified job. Typical examples of each of these uses are shown in the following:

CASE 1. CHARTS USED FOR SYSTEM ANALYSIS

Determine approximately the value of the maximum value of θ/D and the frequency at which it occurs, and the magnitude of the peak overshoot to a step-function input and the time when it occurs for a system having the transfer function.

$$\frac{\theta}{\epsilon}=\frac{4}{p(1+0.1p)(1+0.025p)}$$

which is drawn on Figure 10. Also drawn on Figure 10 for purposes of check is the frequency response from which $[\theta/D]_m$ and ω_m/ω_c are found to be 1.00 and 0 respectively.

From Figure 10 the information necessary to specify the various parameters for use of the charts can be obtained. Thus

$\omega_c=4$
$\mu_1=20$ decibels
$\omega_1=0.4\quad(=\omega_2);\quad \frac{\omega_1}{\omega_c}=0.1$
$\omega_3=10$ and $\omega_3/\omega_c=2.5$ if slope is 40 decibels per decade, ω_3 to infinity

or

$\omega_3=20$ and $\omega_3/\omega_c=5.0$ if slope is 60 decibels per decade, ω_3 to infinity

Since no section of either 40 or 60 decibels per decade occurs before zero decibels, the charts for which the attenuation rate from ω_1 to ω_2 is 40 decibels per decade may be used with the data obtained at $\mu_1=20$ and $\omega_1/\omega_c=0.1$.

Two alternatives present themselves for selecting the attenuation rate from ω_3/ω_c to infinity. By choosing this rate to be 40 decibels per decade and $\omega_3/\omega_c=2.5$, a system performance somewhat more optimistic than will be actually realized will be determined. By choosing the attenuation rate to be 60 decibels per decade and using a value of $T_3=T_{ab}$, then $\omega_3/\omega_c=5$ and more realistic values of system performance should be determined. Table I is a comparison of the values of the desired performance quanti-

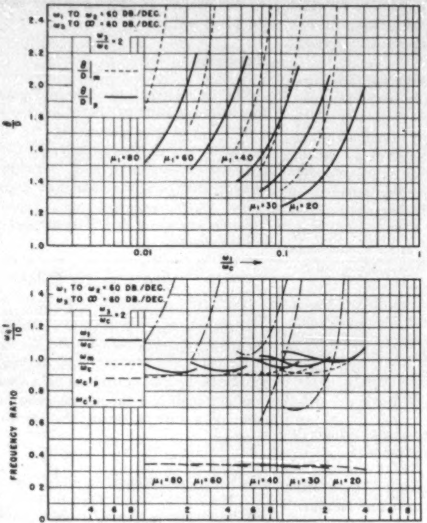

Figure 26 (above), Figure 27 (below)

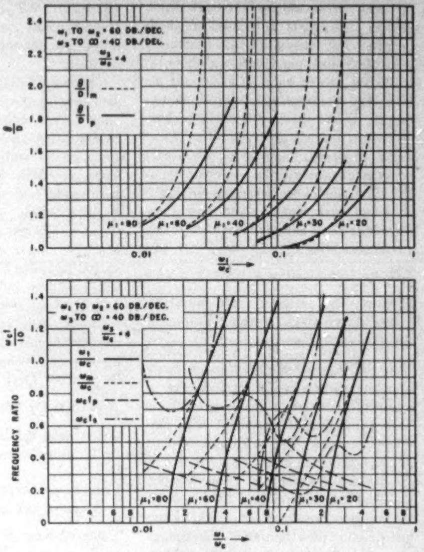

Figure 28

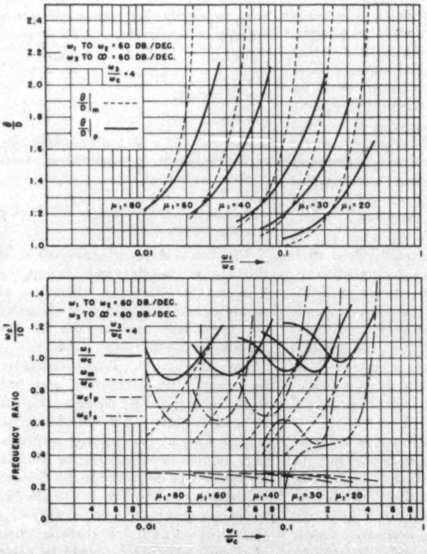

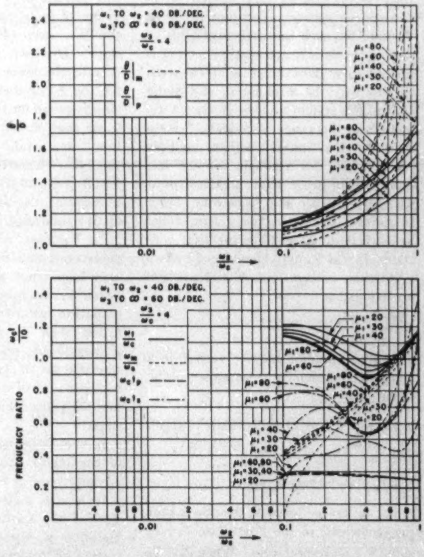

Figures 23 to 28. Comparison of steady-state frequency response characteristics and transient response following a step-function of input as a function of ω_1/ω_c

Figure 29. Comparison of steady-state frequency response characteristics and transient response following a step-function of input as a function of ω_2/ω_c

Table I

	$\frac{\omega_3}{\omega_c}=2.5$ Figures 13, 14	$\frac{\omega_3}{\omega_c}=5.0$ Figures 24, 25	Actual System Performance
$[\theta/D]_m$	1.00	1.00	1.00
ω_m	0	0	0
$[\theta/D]_p$	1.02	1.02	1.04
t_p	0.75	0.75	0.74

ties based on these two assumptions as well as the actual values obtained by direct calculation. It is evident that these results are essentially independent of the method used to obtain them, that is, whether the 40 or 60 decibels-per-decade charts are used.

Case 2. Comparison of System Performance Obtained From Charts and Actual System Calculations

For the high gain system shown in Figure 11 in which the solid line indicates the actual open loop transfer function and the dotted lines indicate the straight line approximations to this transfer function, find the values of $[\theta/D]_m$, $[\theta/D]_p$, ω_m, and t_p.

The information necessary to determine the proper charts and performance is found from Figure 11 to be

$\omega_c=28$ radians per second
$\omega_1=1$ radian per second
$\mu_1=65$ decibels
$\omega_3'=168$ radians per second
ω_1 to $\omega_2=60$ decibels per decade
ω_3' to $\infty=60$ decibels per decade
$\frac{\omega_1}{\omega_c}=0.035$
$\frac{\omega_3'}{\omega_c}=6.00$

It will be noted that the value of ω_3' is an equivalent value and is obtained by use of approximate methods described previously. Hence Figures 27 and 28 must be used. In Table II is a comparison of the desired performance quantities as obtained from the charts with the actual values obtained by direct calculation.

Charts Used for System Synthesis

It is desired to determine an open-loop attenuation frequency characteristic for which the maximum value of the frequency response is 1.4 or less and occurs at frequency greater than 3 cycles per second. The ratio of output to error for a sinusoidal input of 1 radian per second should be at least 500. The attenuation rate for frequencies in excess of 120 radians per second will probably be 60 decibels per decade.

From the foregoing data, the following preliminary values of design parameters may be selected:

$\omega_m=3\times 2\pi=18.8$ radians per second
$\mu_1=60$ decibels (which produces the proper actual gain at ω_1)
$\omega_1=1$ radian per second
$\omega_3=120$ radians per second

Since the attenuation rate from ω_3 to infinity is to be 60 decibels per decade and since high system performance is desired, Figures 26 to 28 will be used. Figure 27 for which $\omega_3/\omega_c=4$, shows that for $\mu_1=60$ and $[\theta/D]_m=1.4$, $\omega_1/\omega_c=0.033$ and $\omega_m/\omega_c=0.68$. For these conditions then, $\omega_c=18.8/0.68=27.6$ radians per second. This indicates that a value of $\omega_c=30$ can be used and the values of ω_1 and ω_3 above are satisfactory. The value of ω_m obtained is $0.68\times 30/2\pi=3.25$ cycles per second and is greater than the minimum allowable value. From this it appears that the specifications have been met.

Table II. Comparison of System Performance Obtained From Charts and Actual System Calculations

	Performance from Figures 27, 28	Actual System Performance
$[\theta/D]_m$	1.56	1.57
ω_m	20	20
$[\theta/D]_p$	1.42	1.40
t_p	0.1	0.1

Therefore, an open-loop attenuation characteristic for which the system performance is satisfactory is

$$\frac{\theta}{\epsilon}=\frac{1{,}000\,(1+0.17p)^2}{p(1+p)^2(1+0.0083p)^2}$$

Since the most convenient means for obtaining this transfer function practically may not be such that the exact time constants indicated before are realized, it is probably not worthwhile to determine the transfer function more precisely from the charts.

References

1. Principles of Servomechanisms (book), Brown and Campbell. John Wiley and Sons Book Company, New York, N. Y., 1948.

2. The Analysis and Optimum Synthesis of Linear Servomechanisms, Donald Herr, Irving Gerst. *AIEE Transactions*, volume 66, 1947, pages 959–70.

3. Theory of Servomechanisms (book), James, Nichols, Phillips. McGraw-Hill Book Company, New York, N. Y., 1947.

No Discussion

Instrument Inaccuracies in Feed-Back Control Systems with Particular Reference to Backlash

H. TYLER MARCY
ASSOCIATE AIEE

MORRIS YACHTER
NONMEMBER AIEE

JEROME ZAUDERER
NONMEMBER AIEE

ALTHOUGH the techniques of analysis and synthesis of feed-back control systems have been developed to a high degree of usefulness, there is continuing need for expanding and improving them. It is the object of this paper to investigate some of the problems of component specification within the feed-back control system. It is obvious that there is a direct relation between most economical component procurement, or production, and optimum specification of their required physical characteristics. But just how good, or how powerful, the components must be is not often simply determined from the requirements of over-all system performance. This problem is particularly important in designing feed-back control systems because of the large percentage of high quality, expensive equipment.

In feed-back control systems, the components may be thought of as a part of the direct, or forward path, the feed-back path, or the comparator as illustrated in Figure 1. Broadly speaking, the function of components in the direct path is amplification of signal level and power with selected frequency response characteristics. On the other hand, the function of the components in the feed-back path and in the comparator is primarily measurement.

The problems of specification of these two general types of components are likely to differ. In more complicated systems, having multiple feed-back paths and cascades of assemblies which themselves employ feed-back techniques, there exist a function of the component in its own local environment and a function of the assembly in which it is incorporated.

A study of measuring equipment as used in feed-back control systems is the primary concern of this paper. The nature of instrument inaccuracies will be considered and cataloged according to type. An attempt will then be made to determine the effect of the specific instrument inaccuracies on the accuracy of the regulating system.

Unfortunately, in considering those threshold operating points of components which determine just how good they are, the problem of analysis does not always remain mathematically simple and clear-cut. Here, use is made of analog techniques in obtaining solutions from an electronic differential analyzer and use is made of mathematical techniques for nonlinear mechanisms.

General Discussion of Instrument Characteristics

When an instrument is applied to an experiment or a process for purely measuring purposes, the resulting data are evaluated differently than when the same instrument is used as a part of a regulating system. The accuracy of an experimental determination of, say, an explicit relation between two variables is more often obtained by a "fairing" of the data[1] through the device of measuring for an appropriate number of settings of the independent variable. In experiments, accuracy of measurement can be improved sometimes by such techniques as unidirectional approach of the measuring point with the variable setting mechanism and by the use of check calibration. When an instrument is used in a regulating system, its ability to command cannot necessarily be compared with its ability to measure in an experiment, because it will be making continuous determinations without special attention from an operator.

The exact effect of an instrument inaccuracy upon the regulating system of which it is a part is observed to be dependent upon the cause of the inaccuracy. For example, the effect of backlash in a position indicator results in a different sort of system error than the effect of random noise in the same indication. It would seem, therefore, that an organization of instrument inaccuracies into types would be prerequisite to a study of their effect of regulating systems.

If the controlled quantity of an automatically regulated process be assigned the mathematical symbol θ_0, then this symbol has a particular physical meaning such as temperature, angle, and so forth. Almost without exception, the controlled quantity is measured, and an equivalent but not like quantity is used to initiate the control action. The instrument used to obtain such an equivalent quantity, such as volts for temperature, is characterized by its ability to produce a known correspondence between its actuating quantity and its output quantity. These characteristics may be classified briefly as describing either internal characteristics in the instrument (such as sensitivity, static and dynamic accuracy, internal passive parameters, or internal active sources) or environmental conditions (such as the relative loading of instrument on the actuating quantity or vice versa, and other physical effects

---

Paper 49-197, recommended by the AIEE Joint Subcommittee on Servomechanisms and approved by the AIEE Technical Program Committee for presentation at the AIEE Summer General Meeting, Swampscott, Mass., June 20–24, 1949. Manuscript submitted April 4, 1949; made available for printing May 23, 1949.

H. Tyler Marcy, Morris Yachter, and Jerome Zauderer are with the Special Projects Department of The M. W. Kellogg Company, Jersey City, N. J.

The authors wish to thank D. B. Rossheim of The M. W. Kellogg Company for his encouragement in this work and for making available laboratory equipment.

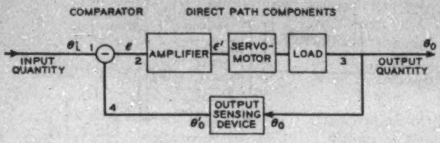

Figure 1. Block diagram of a simple feed-back control system

which the instrument sees in addition to the real actuating quantity).

For the subject at hand the classical separation of instrument characteristics into sensitivity and accuracy is expanded to include sensitiveness to extraneous sources of excitation as additional items measured. The concept of sensitivity is more applicable if associated with that particular part of the instrument which does the converting. In a thermocouple this would be the hot junction itself and would not include the thermocouple well. The cold junction is a second convertor or primary detector within the same instrument.

The prevailing concept of accuracy of instruments needs to be elaborated for the purpose of the present study. The output from a measuring instrument has a value corresponding to the measured quantity.[2] The output may be in the form of a scale reading, a pen position, or any other quantity such as a voltage. There may be, in fact, more than one output in a multi-purpose instrument which indicates and controls. A functional division of an elementary instrument is sketched in Figure 2 after the manner of Kinnard.[3]

A classification of types of instrument inaccuracies which was helpful in the present study of their effect on feed-back control systems is given in Table I. Some common sources of inaccuracy are itemized as examples. A distinction is made between mechanism errors,[4] which are the subject of Table I, and theoretical errors in the primary element, which are not considered here. Since the effect of an energy source on a feed-back control system is different from the effect of a passive circuit, a distinction is made in Table I between these two types of inaccuracy. Another major division is whether the inaccuracy cause is self-contained in the instrument or is environmental.

That the linear analytical techniques thus far developed for feed-back control systems can be widely used in a study of instrument inaccuracies is shown by the number of items of Table I which can be studied by these means, provided none of the nonlinear causes of error are also present. There are preferred techniques of analysis for certain of the items. Whereas the effect of cascaded impedance with the instrument source causes difficulties that can be studied by transient analysis or frequency response methods, on the other hand the random source of the inaccuracy must be treated by statistical means and probably can best be studied by determinations of the rms of regulating error for typical input conditions.[6] An attempt has been made to indicate the technique best applicable.

It is the nonlinear problem that plagues the designer because of his relative inability to assess the importance of such effects. In order to predict how a given system is going to work, at the present state of the art, it is seemingly necessary to either build an experimental prototype of the regulated equipment, use analog or other simulating devices, or just hope for the best. While these procedures always may be used, it would be well to ascertain by some other means what approximate conditions can be expected. It would seem to the authors that the proper job of the professional society is to encourage systematic collection of data and distribution of this information. In this pres-

Table I. An Organization of Instrument Inaccuracies and Suggested Means of Analyzing Their Effect

Examples of Specific Inaccuracies	Suggested Means of Analysis
Passive Sources of Error Due to Internal Defects	
Nonideal transfer function of linear networks	
Band-pass of electronic or other amplifier used as intermediate means	Added element to conventional servo theory
Presence of energy storage elements in cascade with the primary detector	Added element to conventional servo theory
Impedance loading on primary detector or other elements of system	Alters element characteristics in way predictable by circuit theory
Nonlinearities in elements	
Backlash Spring or magnetic hysteresis	Prototype, analogy computer or by approximate analysis.[6]
Breakaway and coulomb friction (or dimensional equivalent)	Analysis by phase plane techniques[8]
Variation from linearity of springs, bridge circuit, and so forth	Incremental treatment, analogy computer or prototype, point by point numerical solution
Saturation	Analysis by phase plane techniques[8]
Nonideal viewing of measured quantity by primary detector	
Measurement at discrete intervals	Analysis of pulsed data systems
Equivalent of scanning time function with square instead of unit impulse	Superposition
Passive Sources of Error Due to Environment	
Effect on measured system by primary detector	
Catalytic effects (accelerating and deterrent)	Experimental
Impedance loading	Circuit theory
Alteration of process as, for example, change of fluid flow from laminar to turbulent in the vicinity of a probe	Experimental
Effect of measured system on primary detector	
Contamination, as for example a gradual destruction of platinum-rhodium thermocouple	Long-time change of system characteristics
Impedance loading on primary detector, such as conduction errors in thermocouple installation, and shielding	Experiment or circuit theory
Internal Active Sources of Error	
Purely random signals	
Thermal noise due to molecular agitation	Statistical analysis of variable, autocorrelation functions
Atmospheric fading as in radar systems	
Quadratic and Harmonic signals	
Minimum transfer signals	Spurious input in conventional servomechanism theory[7]
Imperfect optical transmission	
External Active Sources of Error	
Environmental	
Thermal effect on parameter constants and on contact potentials	Can probably be treated as long-time change of system characteristics; alternatively involves nonlinear analysis or resort to analog techniques
Pressure effect on primary detector and on parameters	
Inertial reactions	
Secondary sensitivities of primary element	
Stray fields	Spurious input in conventional servomechanism theory,[7] except when saturation effects are introduced[8]
Cross-talk as in quadrature sensitivity of linear accelerometer	

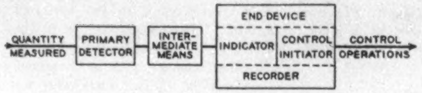

Figure 2 (above). Functional division of an elementary instrument

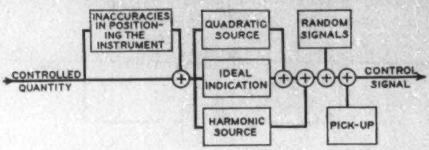

Figure 3 (right). Representation of some inaccuracies of a null instrument

ent study, backlash in the instrument has been a principal object of experimental study. Other investigators have touched on this and some of the remaining problems.[10]

Nonlinear systems which can be described to within reasonable accuracy by a single degree of freedom, can be studied by the so-called phase-plane method of analysis, first introduced by Poincare.[12] This is particularly true for an on-off system with, say, constant displacement or constant velocity input; that is, for a system which is described by a linear differential equation but with discontinuous coefficients, the discontinuities occurring along certain curves in the phase plane, usually not known explicitly. Such a system, with idealized backlash in output measurement, is analyzed in Appendix II in considerable mathematical detail. The major part of such an analysis centers around the investigation of the existence, uniqueness, and stability of limit cycles (hunting in the steady state).

If the input is of a more complex nature, the analysis in the phase plane becomes more cumbersome, but not altogether impossible. On the other hand, if the system cannot be described by a single degree of freedom, then the motion no longer can be represented in a plane. If, then, the analogy to the one-degree-of-freedom case is to be extended, the motion must be represented in spaces of higher dimensions. Accordingly, the geometric picture breaks down altogether and the analysis becomes far more complex.

Minimum Signals from Null Devices

In many types of feed-back control systems the primary control action is to balance two signals in a null. A servomechanism used to indicate the out-of-balance of a resistance strain gage by comparing the bridge unbalance with a voltage-divider position is a good example. Here the signal will be a remote positioning servomechanism with synchro data transmission. Here the error measuring device is fundamentally a variable ratio transformer.

In practice it is well known that none of these voltage-sensing null systems are ideal. Their departure from the ideal is the most important aspect in their consideration. As the regulating system moves toward balance, let us consider the approach of the error-sensing device to zero signal.

1. It may be very possible for some unwanted source to produce an effect on the true error signal, in addition to the motion of the regulated quantity. The stepwise characteristics of a potentiometer produce a step effect which is of this sort. The winding inaccuracies in synchros produce an effect which may be thought of in this light.
2. There may be, in a-c systems, a quadrature voltage. Although small compared to a large error signal, it may predominate when balance is near.
3. There may be harmonic voltages in a-c systems.
4. There may be "pick-up" resulting in a voltage of indefinite relation to the true error signal.
5. There may be a purely random signal caused by thermal agitation in resistive elements or an equivalent phenomenon. An attempt has been made to represent these elements in a circuit as a part of Figure 3.

The designer of regulating systems can do something about most of the items of Figure 3. If the positioning inaccuracies are troublesome, an attempt is made to make unit motion of the regulated quantity cause more motion of the null indicating system. High-speed synchro systems are examples of this technique. If the quadrature voltage is high, a phase-sensitive rectifier not sensitive to quadrature signals may be used to interpret the signals,[10] or, alternatively, a bucking voltage can be inserted. If the harmonics are high, the iron structure of transformer instruments may be saturating. If this cannot be avoided then null networks of the bridged-T type may be cascaded with the error signal to eliminate the harmonics. An example of this latter technique is found in some conical-scanning automatic-tracking radar sets. When random signals play an important role, the basic requirements of the system are analyzed very carefully, and its performance is optimized by filter circuits which cut out all the overcapacity in the system frequency response.

All this is to say that the nonideal signals are not wanted. It might well be asked what would result from their transmission. To study this it will be presumed that a small amount of each is present and cannot be eliminated. The results of such consideration are shown in Table II.

In presenting the information in Table II, the authors are quoting from a limited experience. Free discussion is encouraged among the readers to improve the accuracy of the statements made.

Table II. Consideration of Inaccuracies of Null Instruments, with Quiescent Regulating Input

Source of Inaccuracy in Null Instrument	Effect on Regulator (Input Quiescent)	Remedy
Inaccuracy of positioning instrument	1-to-1 error in positioning regulated quantity	Increase speed of data transmission
Harmonic source	Causes partial saturation in error channel, thus limiting gain allowable. Causes no error in positioning regulated quantity	Selective filters in cascade with instrument
Quadrature source	Causes partial saturation in error channel, thus limiting gain allowable. Causes no error in positioning regulated quantity	Selective phase sensitive detector Buckling voltage
Pick-up	Causes some error in output, some saturation of error channel, sometimes unpredictable jumps and jitters in output	Shielding and grounding. (System is often sensitive to which side of a transformer coil is grounded.) Eliminate excessive adding of signals with high impedance source Reduce source impedance
Random signals with spectral density $G_N(f)$	Random motion of output result	Optimum design of filter Reduce impedance of instrument Redesign instrument to minimize cause of random signal

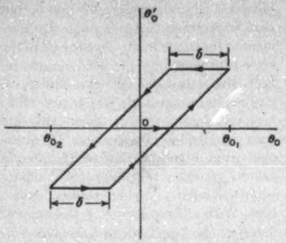

Figure 4. Relationship between angular position of two gears between which backlash exists

Examination of Table II will show that the major difficulty in a null-balancing system is to minimize the unwanted parts of the signal, so that high gain can be used most effectively. The usual mathematics of regulating systems do not include the fact that saturation can occur in the system (at different parts depending on the particular components). Hurewicz and Nichols[8,9] have described analytical means of studying the effect of saturation by means of the phase plane. In these studies the desired quantity, θ_i, was caused to suddenly move at a constant rate. Resulting trajectories for the system were plotted in a plane whose abscissa is the regulated quantity and whose ordinate is the rate of change of the regulated quantity. Tendencies toward instability which may result from saturation thus could be studied. In high performance regulating systems, however, the partial saturation caused by unwanted signals should be kept to a few per cent for reasons other than instability. But when the range of proportional signal is restricted, such an analysis is important to determine the recovery from large disturbances.

Description of System in Which Effect of Backlash Is Described

For the purpose of investigating the effects of backlash, a simple feed-back control system is assumed as shown in Figure 1. The backlash occurs in the instrument whose function it is to sense the output of the control system and feed-back to the comparator a signal proportional to this output. The comparator is assumed ideal here in its function of sending to the controller the difference between input signal and output of the output-sensing device. The input to the system is a shaft rotation, designated θ_i in Figure 1. The output is a shaft rotation, θ_o. The output-sensing device, whose output is θ_o', is assumed ideal in all respects except for the presence of backlash. The backlash is of such character as to result in a relationship between θ_o and θ_o' described by the graph of Figure 4. This figure shows values assumed by θ_o' as the output shaft moves with finite velocity from a position $\theta_o=0$ to a position where θ_o has some positive value, θ_{o1}, greater than 1/2 the backlash angle; then reverses direction of rotation so that θ_o decreases through zero to some negative value θ_{o2}, greater than 1/2 the backlash angle; then reverses again, returning once more to θ_{o1}. δ is the total backlash angle or dead zone, and it is assumed that the coupled components between which backlash exists are initially at the midpoint of the dead zone.

The type of backlash described in Figure 4 is somewhat idealized. If we suppose that the backlash exists between the teeth of a pair of gears, the characteristic shown in Figure 4 implies that there is no elasticity, slippage, or other condition present that would impair the perfect transmission of motion when the gears are in contact with each other, and, on the other hand, that the driven gear has no motion except such as is imparted to it by the driving gear, and that only while there is contact. It should be noted here that a graph similar to that of Figure 4 was used by Schlink,[4] who discussed backlash as an instrument inaccuracy in 1918.

The comparator subtracts θ_o' from θ_i to obtain the error, ϵ, which is fed to the controller in a form which it can accept. The controller operates on the error to produce a signal capable of driving the servomotor. The effects of backlash are described for five different types of controllers. Designating the output of the controller as ϵ', the five controllers are

$$\frac{\epsilon'}{\epsilon}=K \tag{1}$$

$$\frac{\epsilon'}{\epsilon}=K(1+T_Dp) \tag{2}$$

$$\frac{\epsilon'}{\epsilon}=K\left(1+\frac{1}{T_ip}\right) \tag{3}$$

$$\frac{\epsilon'}{\epsilon}=K\left(1+T_Dp+\frac{1}{T_ip}\right) \tag{4}$$

$$\epsilon'=K\left(1+\frac{1}{T_ip}\right)\epsilon+KT_\theta p\theta_0 \tag{5}$$

where

K = a constant
T_D = a time constant
T_i = a time constant

Linear operation of both motor and controller is assumed. The total load on the output shaft of the servomotor consists of inertia and viscous friction.

A mathematical analysis of the effect of backlash for the controllers of equations 1 and 2 is described in Appendix II.

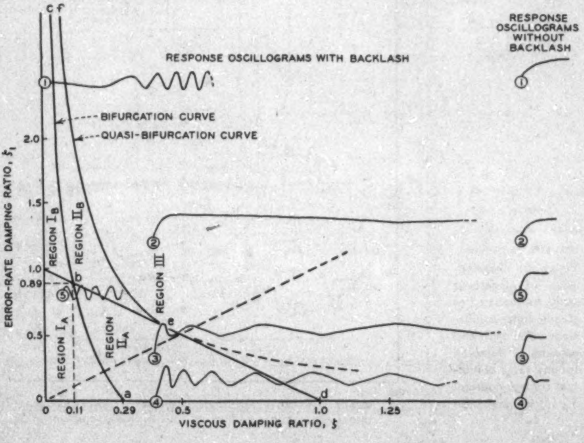

Figure 5. The zeta plane of a single-degree-of-freedom system having backlash in measurement of the output quantity

Region I. Continuous oscillations
- A. For all transient disturbances
- B. For certain transient disturbances

Region II. Quasi-hunting with increasing period
- A. For all transient disturbances
- B. For certain transient disturbances

Region III. Exponential decay

This was used to amplify to and corroborate experimental studies made on an electrical analog of the system described above. The analog is described in Appendix I and follows the techniques described by Ragazzini, Randall, and Russell.[11]

Behavior of Selected Systems in Presence of Backlash

The behavior of feed-back control systems in the presence of backlash is found to be critically dependent upon the type of control action used. The behavior of the single-degree-of-freedom system employing error-rate and/or viscous damping is described in terms of the proportions of these two types of damping. The behavior of the same system with the addition of integral control (see equations 3, 4, and 5) is described in terms of magnitude and frequency of the ever-present oscillations.

Figure 5 summarizes the analytical and experimental data for a single-degree-of-freedom system with backlash. This figure is described as a zeta plane. The abscissa is the damping ratio if only viscous damping were present; the ordinate is defined as the damping ratio if only error-rate damping were present. The sum of these two damping ratios is the total damping ratio of the system. For viscous damping ratios of the order of 0.3 or greater, the response of the computer to a disturbance depends on the total damping and on the relative amount of error-rate damping. If the total damping is less than critical, the response of the system is a transient oscillation of increasing period. The amplitude of the first cycle of the oscillation is greater than it would be in the absence of backlash, by an amount which may be as great as the backlash angle; successive overshoots decrease in amplitude until the output shaft hunts back and forth through an angle equal to that of the dead zone. The period of the oscillation increases, apparently indefinitely. It takes a longer time and a greater number of cycles of oscillation, for the system to settle down to the quasi-steady state of hunting within the limits of the dead zone, than are required by the system without backlash to attain a steady-state condition. If the total damping is greater than critical and the viscous damping ratio is about 0.5 or greater, the transient response of the system will be an exponential asymptotic to one edge of the backlash zone. If the viscous damping ratio is between 0.3 and 0.5, either the exponential response or the quasi-hunting with increasing period may occur depending on the amount of error-rate damping.

For viscous damping ratios below 0.3, the system may exhibit any one of three modes of behavior. It may oscillate continuously in the steady-state with an amplitude which is in general greater than the backlash angle and an inverse function of the total damping; or it may exhibit the quasi-hunting response with increasing period; or it may respond in the exponential manner. Which of these three modes of behavior takes place will depend on the amount of viscous damping and the total damping in the system.

The addition of an integral term in the control function, equations 3, 4, and 5, renders the system at all times oscillatory in the presence of backlash. The amplitude and frequency of the steady-state oscillation are functions of the total damping, the relative amounts of viscous, error-rate, and tachometric damping, and to a lesser extent, of the magnitude of the integral term in the control function.

Figure 6 illustrates this relationship for a single value of integral control constant, $T_i = 1/8$ and a single value of $\omega_n = 24$. The small figures placed at points along each of the curves of Figure 6 indicate the kind of oscillogram that is obtained of the motion of the output shaft in response to a step-angle displacement of the input shaft. In the case of the error-rate damping, the oscillograms reflect the saturation of the derivative channel in response to a step input. This however, does not affect the steady-state data described by the curves. It can be seen from Figure 6 that, with integral control, the effect of tachometric damping is quite similar to that of viscous damping. With either viscous or tachometric damping the amplitude and frequency of the steady-state oscillation can be many times the magnitude of the backlash. It would seem, then, that the design requirement is for much more than usual damping with integral control in the presence of backlash. In the case of error-rate damping, the behavior of the system under conditions of low total damping approaches that of the system under comparable conditions of viscous or tachometric damping. However, for large amounts of error-rate damping the system exhibits two modes of behavior, depending on the amount of viscous damping present. The experienced servomechanism engineer will recognize the high-frequency chatter so often observed with error-rate damping. It is interesting to note that this can occur for zero coulomb friction loads.

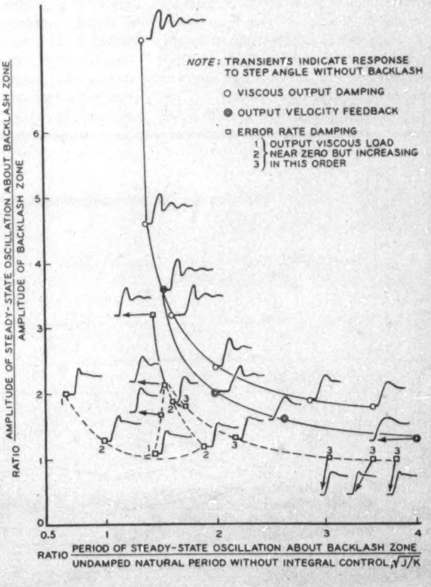

Figure 6. Dependence of magnitude and frequency of steady-state oscillations upon type and amount of damping for one value of integral control constant $T_i = 1/8$ and for $\omega_n = 24$

Summary Discussion of the Effects of Backlash in Feed-Back Control Systems

It would appear from analyzer data and analysis of Appendix II that it may be practical to devise a qualitative picture of steady-state behavior of feed-back control mechanisms in the presence of backlash. The backlash zone may be considered as bounded on either side by barriers having special resilient or energy-giving properties dependent upon the type of control. Pure gain seems analogous to a resilient barrier with the stiffness proportional to gain. Here the penetration of the barrier by the mechanism is a function of the energy at the time of entry, and the energy gained is a function of the time and penetration into the barrier region. With integral control the energy flow aiding the oscillation continues even after the mass has been repulsed from the barrier. Here the rate of energy flow to the mechanism during its next sweep across the dead space is determined by the penetration and the time in the barrier. The effects of various kinds of damping can be seen as primarily determining the speed of the sweep across the backlash zone and thus the energy at the time of entry into the barrier region. The action of error-rate damping is different from the others in the barrier region in that additional repulsive force is developed, giving an artificial stiffness to the barrier. It already has been shown how this effect can become dominant, giving rise to a high-frequency chatter so often associated with error-rate damping in the presence of backlash. Although the authors have not yet studied the effects of coulomb friction and stiction, it would appear from the foregoing reasoning that a difference between coulomb friction and stiction would aggravate the tendency toward large oscillations.

The general effects of backlash of the type studied are to introduce an inaccuracy of magnitude greater than the actual backlash and to destabilize the system. Under some conditions a disturbance in the system may lead to complete uncontrolled instability, whereas if the backlash were absent, the effects of the disturbance would have damped out. Where the effects of a disturbance in the system with backlash do damp out, it takes a longer time for them to be reduced to near-steady-state conditions. This indicates that much high speed of response performance may be lost due to the presence of backlash. Under other conditions of parameter adjustment than the conditions of complete instability or damping out of transients, there can be continuous oscillations of magnitude several times the backlash.

The assumption made in this study—that the backlash was confined to one point in the system—was, of course, an arbitrary one. It was dictated partly by the main topic of this paper, which is a discussion of instrument inaccuracies, and partly by the necessity of simplifying the problem. It would be of considerable value to study further the effects of backlash at other points, or combinations of points, in the system. In addition, it is desirable to extend the study to more complicated systems, to study the effects of coulomb friction and stiction, and possibly, to apply statistical methods to the case where there are numerous sources of backlash.

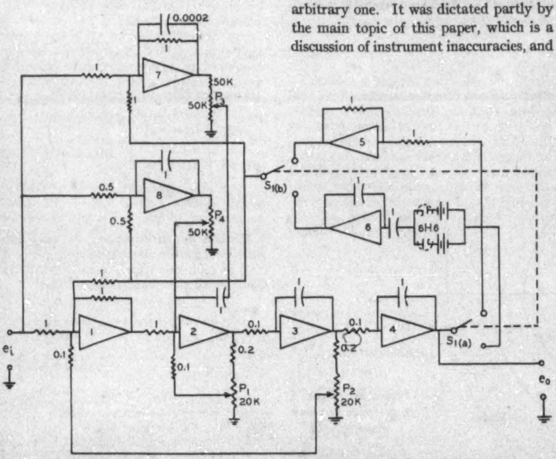

Figure 7. Electrical analog based on d-c amplifier technique as used to study effects of backlash

Unless otherwise noted resistances are given in megohms, and capacitances are given in microfarads

Appendix I. The Analog Computer

Analog studies and mathematical analysis constitute a powerful and fruitful combination in the investigation of nonlinear phenomena. Besides serving as a check, each method produces results which give meaning and direction to the investigations carried out by the other method. Thus, the appearance of a peculiar mode of behavior as observed in the analog study suggests to the mathematician engaged in a phase-plane analysis that he should look for the existence of a limit cycle of which he might not otherwise have been aware; the mathematician's verifying the existence of this limit cycle is assurance that the observed mode of behavior was not due to a concealed imperfection in the analog representation of the system under study. On the other hand, the mathematician may predict from his analysis that the mode of behavior of the system will change for a certain combination of parameters, a fact which the analog investigator might not have discovered except by accident or the application of an infinite amount of patience in setting into the analog all possible combinations of parameters. The manner in which these two methods complement each other is especially felicitous in the investigation of nonlinear systems, since changes in mode, athough expected, may be very difficult to predict, and extrapolation from one set of system conditions to another can seldom be made with assurance.

The electrical analog used in this study is shown in Figure 7. Amplifier *6*, together with its input and feed-back capacitors, the dual diode, and the batteries, constitute the backlash analog. By means of switch S_1 backlash can be inserted into or removed from the analog. The undamped natural frequency of the system is set by means of potentiometer P_1, and the viscous damping by means of potentiometer P_3. Potentiometer P_2 sets the error-rate damping coefficient, T_d, and potentiometer P_4 sets the integral-control coefficient, T_i. The small capacitor placed between the output and input of amplifier *7* was inserted to stabilize one of the loops in the analog. It will be recognized, of course, that the analog is inexact for a suddenly applied displacement of the servomechanism input shaft, since such a disturbance results in an infinite pulse in the derivative of the error, a condition which cannot be realized by any physical analog. In the study of the single-degree-of-freedom system in which a derivative term was inserted in the control function, the transient response of the system was studied by simulating the sudden application of a constant-load torque applied to the output shaft. In all other cases, the system was disturbed by application of a step angle to the input shaft, in some cases, then, reflecting saturation of the derivative circuits.

To obtain data for the tachometric case an additional loop was added to the analog of Figure 7. The coupling between output shafts and tachometer is assumed free of backlash, since this is usually the case in practice. A brief examination will show that, as far as the analog is concerned, tachometric and viscous damping are identical for the single-degree-of-freedom system but not for the integral-control system. The component of output rate is integrated as well as directly transmitted when there is integral control.

Appendix II. Phase-Plane Analysis of Single-Degree-of-Freedom Feed-Back Control System with Backlash in Measurement of Controlled Quantity (Constant Displacement Input)

Symbols

J = mass moment of inertia
C = coefficient of viscous damping
k = spring constant
$C_1 = kT_D$ = effective derivative control damping
t = time
θ_i = input
θ_0 = output
θ_0' = backlash output
Other symbols are defined as they occur in the text.

It is assumed that backlash gears are free and have no inertia and an arbitrarily small amount of damping (say, dry friction).

General

From Figure 1, the differential equation of the system is

$$J\frac{d^2\theta_o}{dt^2}+C\frac{d\theta_o}{dt}=k\epsilon+C_1\frac{d\epsilon}{dt} \tag{1}$$

where $\epsilon=\theta_i-\theta_0'$ is the "error," while for a constant displacement input $\theta_i(t)=\theta_i^{(0)}=$ constant. Equation 1 can-be written

$$\frac{d^2\theta_o}{d\tau^2}+2\left(\zeta\frac{d\theta_o}{d\tau}+\zeta_1\frac{d\theta_o'}{d\tau}\right)+\theta_o'=\theta_i^{(0)} \tag{2}$$

where

$$\left.\begin{aligned}
&\tau=\text{nondimensional time}=\omega_n t\\
&\omega_n=\sqrt{\frac{k}{J}}\\
&\zeta=\frac{C}{C_c}=\frac{1}{2}\frac{C\omega_n}{k}\\
&\zeta_1=\frac{C_1}{C_c}=\frac{1}{2}T_D\omega_n\\
&C_c=2J\omega_n
\end{aligned}\right\} \tag{3}$$

As will appear presently, the introduction of ζ_1 and, in particular, the introduction of a "damping" plane, (ζ, ζ_1), turns out to be of real advantage in the analysis. In general

$$\theta_o'=a+b\theta_o$$

Let the backlash angular gap be δ; we may assume, without loss of generality, that the output gear starts from a position just midway between the teeth of the backlash gear, so that when the two gears are in contact, θ_o' either lags or leads θ_o by an angle of amount $(1/2)\delta$. This convention is introduced merely for purposes of symmetry. If the relative position of the gears at starting is different, that means merely a shift of the $d\theta_o/dt$ axis in the phase plane. All results derived in following paragraphs are invariant with respect to any co-ordinate transformation. We have the following:

When the gears are in contact

$$b=1 \tag{4}$$

and by convention

$$a=-\frac{1}{2}\delta \text{ for } \frac{d\theta_o}{dt}\geq 0$$

$$=+\frac{1}{2}\delta \text{ for } \frac{d\theta_o}{dt}\leq 0$$

When the gears are unmeshed

$$b=0$$

and by convention

$$a=\theta_o^{(0)}+\frac{1}{2}\delta \text{ for } \frac{d\theta_o}{dt}\geq 0$$

$$=\theta_o^{(0)}-\frac{1}{2}\delta \text{ for } \frac{d\theta_o}{dt}\leq 0$$

where

$$\theta_o^{(0)}=\theta_o \text{ at } \frac{d\theta_o}{dt}=0 \tag{5}$$

Equation 5 is true in general, except for a part of the very first cycle.

Finally, let $\zeta_2=\zeta+\zeta_1$ = total effective (nondimensional) damping. As in the ordinary case, the trajectories in the phase-plane $(\theta_o, d\theta_o/dt)$ assume different forms according as $\zeta_2 \lessgtr 1$, that is, according as the system is effectively under- or overdamped.

$\zeta_2 \leq 1$, Underdamped Systems

Gears Meshed. Let

$$\xi=\frac{\theta_o}{\theta_i^{(0)}}-1 \quad \alpha=\frac{1}{2}\frac{\delta}{\theta_i^{(0)}} \quad W=\frac{d\xi}{d\tau} \tag{6}$$

Then the differential equation is

$$\frac{d^2\xi}{d\tau^2}+2\zeta_2\frac{d\xi}{d\tau}+\xi=\pm\alpha\begin{pmatrix}+\alpha \text{ for } W\geq 0\\ -\alpha \text{ for } W\leq 0\end{pmatrix}$$

Let

$$\xi=\xi(0) \text{ at } W=\frac{d\xi}{d\tau}=0$$

Without loss of generality, we may also write $\tau=0$ for the above conditions. For if $\tau\neq 0$ at $\xi(0)$, this merely entails a shift in time. With these conditions, we find

$$\frac{\xi\mp\alpha}{\xi(0)\mp\alpha}=\epsilon^{-\zeta_2\tau}\left(\cos\sqrt{1-\zeta_2^2}\,\tau+\frac{\zeta_2}{\sqrt{1-\zeta_2^2}}\times \sin\sqrt{1-\zeta_2^2}\,\tau\right)$$

$$\frac{W}{\xi(0)\mp\alpha}=-\frac{\epsilon^{-\zeta_2\tau}}{\sqrt{1-\zeta_2^2}}\sin\sqrt{1-\zeta_2^2}\,\tau$$

$$\tau=\frac{1}{\sqrt{1-\zeta_2^2}}\tan^{-1}\left(\frac{-\sqrt{1-\zeta_2^2}\,W}{\xi\mp\alpha+\zeta_2 W}\right)= -\frac{1}{2\zeta_2}\log_\epsilon\left[\frac{(\xi\mp\alpha)^2+2\zeta_2(\xi\mp\alpha)W+W^2}{(\xi(0)\mp\alpha)^2}\right] \tag{7}$$

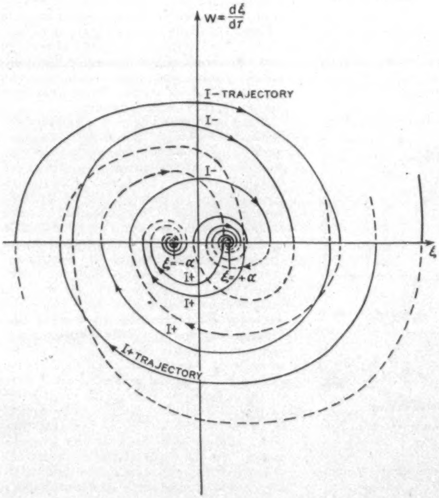

Figure 8. Type I trajectories in phase plane ($\zeta_2<1$)

Arrows indicate increasing time. Singular (focal) points at $\xi=\pm\alpha$; $W=0$. Curves are not drawn to scale

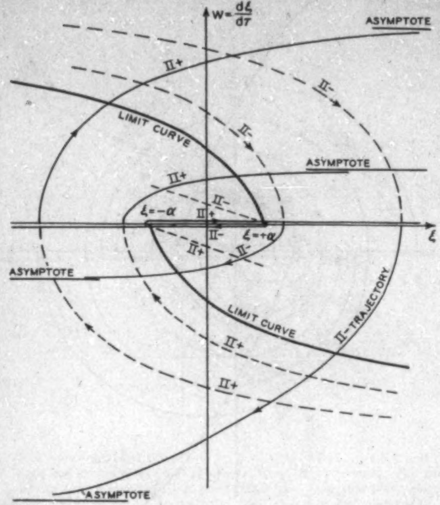

Figure 9. Type II trajectories and limit curves in phase plane ($\zeta_2<1$)

Arrows indicate increasing time. Singular (focal) points at $\xi=\pm\alpha$; $W=0$. Curves are not drawn to scale

Equation 7 is the equation for the trajectories in the phase plane. These trajectories are general spirals and are shown in Figure 8. These curves are marked I_+, I_- according as $+\alpha$ or $-\alpha$ is written in the equations. In accordance with our convention time increases along the trajectories in a clockwise direction, as indicated by the arrows.

The I_+ trajectories tend to $\xi=-\alpha$, $W=0$ as $\tau\to+\infty$. As will be seen soon, only the lower parts of trajectories I_+ and the upper parts of trajectories I_- will come into consideration. Hence the other parts have been drawn with dotted lines in Figure 8. On the lower part of any I_+ trajectory (except the "last" one, that is, a point) we have

$$0\geq\tau\geq-\infty\,;\,0\geq\tan^{-1}\left(\frac{-\sqrt{1-\zeta_2^2}W}{\xi+\alpha+\zeta_2W}\right)\geq-\pi$$

The zero value of the arc tangent is to be taken at $\xi=\xi(0)<-\alpha$; $W=0$. The minima of the lower part of I_+ occur at $\xi+\alpha=-2\zeta_2W>0$, that is, on the other side of $\xi=-\alpha$. Analogous results hold, of course, for the I_- curves.

Gears Unmeshed. The differential equation is

$$\frac{d^2\xi}{d\tau^2}+2\zeta\frac{d\xi}{d\tau}=-(\xi(0)\pm\alpha)\begin{pmatrix}+\alpha \text{ for } W\geq0\\ -\alpha \text{ for } W\leq0\end{pmatrix}$$

From which

$$\tau=-\frac{W+2\zeta[\xi-\xi(0)]}{\xi(0)\pm\alpha}$$

and the trajectories in the phase plane are given by

$$W+2\zeta[\xi-\xi(0)]=\frac{\xi(0)\pm\alpha}{2\zeta}\times \log_e\left[1+2\zeta\frac{W}{\xi(0)\pm\alpha}\right] \qquad (8)$$

For $+\alpha$ only the upper parts and for $-\alpha$ only the lower parts of the curves are of interest.

TYPE II_+ CURVES ($+\alpha$)

$\xi(0)+\alpha\leq0$; τ increases with W; W(at $\tau\to\infty)\to-(\xi(0)+\alpha)/2\zeta$ that is, $W=-(\xi(0)+\alpha)/2\zeta\geq0$ is horizontal asymptote; $\xi\geq\xi(0)$. Analogous results hold for the II_- curves; these curves are shown in Figure 9.

LIMIT CURVES

Consider a typical curve of, say, Type II_-; $W\leq0$; this curve which passes through $\xi=\xi(0)$, $W=0$, $\tau=0$ will not apply after ξ has been decreased by 2α, for then the gears which were unmeshed at $\xi=\xi(0)$ will mesh again, and the motion will resume on a trajectory of Type I_+. The locus of the points where the motion passes from trajectories II_- to trajectories I_+ will be designated as a limit curve. It can be easily verified that its equation is

$$W-\frac{\xi+\alpha}{2\zeta}\log_e\left(1+2\zeta\frac{W}{\xi+\alpha}\right)=4\zeta\alpha$$

$$W\leq0 \quad \xi+\alpha\geq0 \quad 0\leq-\frac{W}{\xi+\alpha}\leq\frac{1}{2\zeta} \qquad (9)$$

It can be verified that

$$\lim_{\substack{\xi+\alpha\to0\\ -W\to0}}\left(-\frac{W}{\xi+\alpha}\right)\to\frac{1}{2\zeta}$$

$$\lim_{\substack{\xi+\alpha\to\infty\\ -W\to\infty}}\left(-\frac{W}{\xi+\alpha}\right)\to0$$

$$\lim_{\substack{\xi+\alpha\to0\\ -W\to0}}\left(-\frac{dW}{d\xi}\right)\to\frac{1}{2\zeta}$$

$$\lim_{\substack{\xi+\alpha\to\infty\\ -W\to\infty}}\left(-\frac{dW}{d\xi}\right)\to0$$

and finally that both $-W/(\xi+\alpha)$ and $(-dW/d\xi)$ decrease monotonically as $\xi+\alpha$ increases from 0 to ∞. Analogous results hold for the upper limit curve which starts at $\xi=\alpha$ and proceeds to the left with $W\geq0$. These limit curves are shown in Figure 9.

LIMIT POINTS AND LIMIT CYCLE

Consider Figure 10. The upper parts of the I_- and II_+ trajectories, the lower parts of the I_+ and II_- trajectories, and the upper and lower limit curves are shown.

Now suppose that at a certain instant the motion of the system is characterized by a point on a I_- trajectory, say between points *2'* and *1*. Then, at $W=0$, $\xi=\xi(0)$, the motion will leave the I_- trajectory and will proceed on a II_- trajectory up to point *2* on the limit curve. Thence the motion will proceed on a I_+ trajectory up to point *1'* at $W=0$, $\xi=-\xi'(0)$. Three alternatives are possible

$$\left|\xi'(0)\right|\substack{<\\=\\>}\left|\xi(0)\right|$$

If the equality sign holds, then, because of symmetry, the motion will proceed from *1'* to *2'* on trajectory II_+ and, finally, from *2'*, along trajectory I_-, back to point *1*. In this case a limit cycle exists, that is, there exists the possibility of hunting in the steady state with an amplitude greater than the reduced backlash gap 2α.

It is now necessary to investigate:

1. **What is the criterion for the existence of such a limit cycle?**
2. **Can there exist more than one such limit cycle?**
3. **Is such a limit cycle stable? That is, will the motion tend towards the limit cycle or away from it?**
4. **If the limit cycle is stable, is it stable only relative to a certain region (or regions) in the phase plane, or stable relative to all trajectories in the phase plane? If the first alternative is true, then only transients that originate in a certain defined region in the phase plane tend to hunting, while the others do not. In the second case, however, all transients, no matter where they might originate in the phase plane, must end up in hunting in the steady state.**

The following can be proved:

1. Let x satisfy the equation

$$(1+2\zeta_2x+x^2)\,\exp\left[\frac{2\zeta_2}{\sqrt{1-\zeta_2^2}}\tan^{-1}\left(\frac{-\sqrt{1-\zeta_2^2}\,x}{1+\zeta_2x}\right)\right]=1$$

$$0<-x<\infty \quad 0<\zeta_2<1 \quad x=\frac{W}{\xi+\alpha}\text{(for lower limit curve)} \qquad (10)$$

Then, if $-x<1/2\zeta$, a limit cycle exists. Substituting $-x=1/2\zeta$ into equation 10 and remembering that $\zeta_2=\zeta+\zeta_1$, there results an equation which represents a curve in the damping (ζ, ζ_1) plane. This equation is valid, of course, only in the region $\zeta_2=\zeta+\zeta_1\leq1$. This curve is shown in Figure 5, passing through points *a* and *b*, and, for reasons that will become clear later, marked "Bifurcation curve."

2. There always exists one, but only one, value of x which satisfies equation 10. From this, it follows that there cannot exist more than one limit cycle.

3. If a limit cycle exists, then if a point crosses the $+\xi$ axis at $\xi_1>\xi(0)$ (see Figure

10), it will cross the $-\xi$ axis at $\xi=-\xi_3$ such that $\xi(0)<\xi_3<\xi_1$ and, conversely, if $\xi_1<\xi(0)$ then $\xi_1<\xi_3<\xi(0)$. Hence trajectories in the phase plane approach the limit cycle monotonically either from within or from without. That is, the hunting cycle is approached either with constantly increasing amplitude and decreasing period or in the opposite manner.

4. This is true for all trajectories in the phase plane. Hence the limit cycle is stable in the large, that is, with respect to the entire phase plane, and all transients must end up in hunting in the steady state, with a fixed period and amplitude greater than the reduced backlash gap $2\alpha=\delta/\theta_i^{(0)}$.

Finally, if $-x>1/2\zeta$, the limit points *2* and *2'*, Figure 10, coalesce into the singular points $\xi=\mp\alpha$ respectively, while the limit cycle degenerates into the ξ axis strip

$$-\alpha\leq\xi\leq\alpha \quad W=0$$

This degenerate limit cycle is a limit case of hunting in the steady state with an amplitude equal to the reduced backlash amplitude 2α, and with zero frequency. All trajectories approach this degenerate limit cycle from without with decreasing amplitude tending to 2α and with ever-increasing period. The designation quasi-hunting seems to be appropriate.

Thus the curve given by equation 10 with $-x=1/2\zeta$ and shown in Figure 5 (bifurcation curve through points *a* and *b*) divides the region $\zeta+\zeta_1=1$, $(\zeta_2>0, \zeta_1>0)$ into two regions marked I_A and II_A. In region I_A all transients end up in hunting in the steady state, while in region II_A all transients end up in what was defined above as quasi-hunting. This holds true so long as there is any finite amount of backlash. The backlash gap enters, of course, in the quantitative values of amplitude, ratio of successively increasing periods in the case of quasi-hunting, and so forth.

Since detailed proofs of the above statements would unduly enlarge this paper, they have been omitted.

$\zeta_2=\zeta+\zeta_1>1$, Effectively Overdamped System

Gears in Contact. The differential equation is

$$\frac{d^2\xi}{d\tau^2}+2\zeta_2\frac{d\xi}{d\tau}+\xi=\pm\alpha$$

where, as already defined

$$\xi=\frac{\theta_0-\theta_i^{(0)}}{\theta_i^{(0)}} \quad \alpha=\frac{1}{2}\frac{\delta}{\theta_i^{(0)}}$$

Again, if $\xi=\xi(0)$ at $W=0$, $\tau=0$, then

$$\frac{\xi\mp\alpha}{\xi(0)\mp\alpha}=\epsilon^{-\zeta_2\tau}\left(\cosh\sqrt{\zeta_2^2-1}\,\tau+\frac{\zeta_2}{\sqrt{\zeta_2^2-1}}\sinh\sqrt{\zeta_2^2-1}\,\tau\right)$$

$$\frac{W}{\xi(0)\mp\alpha}=-\frac{1}{\sqrt{\zeta_2^2-1}}\epsilon^{-\zeta_2\tau}\sinh\sqrt{\zeta_2^2-1}\,\tau \tag{11}$$

$$\tau=-\frac{1}{2\zeta_2}\log_\epsilon\left[\frac{(\xi\mp\alpha)^2+2\zeta_2(\xi\mp\alpha)W+W^2}{(\xi(0)\mp\alpha)^2}\right] \tag{12}$$

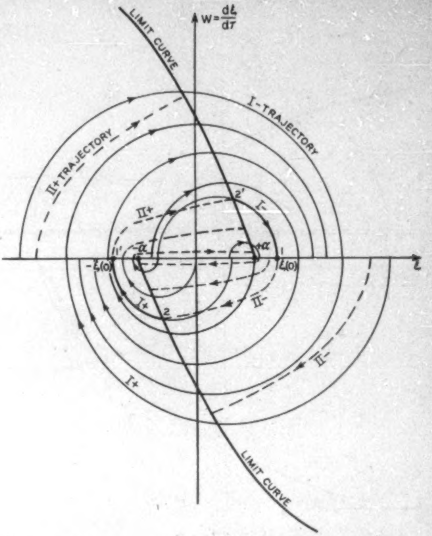

Figure 10. Types I and II trajectories, limit curves, and limit cycle in phase plane ($\zeta_2<1$) limit points: 2 and 2', limit cycle: 1-2-1'-2'-1

Arrows indicate increasing time. Singular (focal) points at $\xi=\pm\alpha$; $W=0$. Curves are not drawn to scale

After eliminating τ we get the equation of the trajectories in the phase plane

$$a_1\log\left(\frac{\frac{W}{a_1}+\xi\pm\alpha}{\xi(0)\pm\alpha}\right)=a_2\log\left(\frac{\frac{W}{a_2}+\xi\pm\alpha}{\xi(0)\pm\alpha}\right) \tag{13}$$

where

$$a_1=\zeta_2+\sqrt{\zeta_2^2-1}\geq1$$

$$a_2=\zeta_2-\sqrt{\zeta_2^2-1}=\frac{1}{a_1}$$

$$0\leq a_2\leq1$$

These curves are shown in Figure 11; curves III_{A+} for $+\alpha$ and curves III_{A-} for $-\alpha$; at $\tau\rightarrow-\infty$ these curves tend to become parallel to the line $W=-a_1(\xi\pm\alpha)$, and at $\tau\rightarrow+\infty$ they become asymptotic to the line $W=-a_2(\xi\pm\alpha)$. These asymptotes will be designated accordingly as asymptotes $1_\pm$, $2_\pm$. It will be seen that the curves so far discussed do not enter the space between the two pairs of asymptotes, that is, between asymptotes 1_+ and 2_+ and between 1_- and 2_-. To determine the equations of the trajectories in these regions, we proceed as follows:

We may consider $\alpha=0$ since this merely means a shift in the W axis. Then the differential equation is

$$\frac{d^2\xi}{d\tau^2}+2\zeta_2\frac{d\xi}{d\tau}+\xi=0$$

Now suppose that the initial conditions are

$$\text{at } \tau=0 \quad \xi=x \quad W=\frac{d\xi}{d\tau}=-kx \quad k>0$$

Then we find

$$\xi=\frac{x}{2\sqrt{\zeta_2^2-1}}\epsilon^{-\zeta_2\tau}[(a_1-k)\epsilon^{\sqrt{\zeta_2^2-1}\,\tau}-(a_2-k)\epsilon^{-\sqrt{\zeta_2^2-1}\,\tau}]$$

$$W=-\frac{x}{2\sqrt{\zeta_2^2-1}}\left[\frac{a_1-k}{a_1}\epsilon^{\sqrt{\zeta_2^2-1}\,\tau}-\frac{a_2-k}{a_2}\epsilon^{-\sqrt{\zeta_2^2-1}\,\tau}\right] \tag{14}$$

and

$$-\frac{W}{\xi}=a_1\left[1-\frac{1-\frac{a_2}{a_1}}{1+\frac{k-a_2}{a_1-k}\epsilon^{-(a_1-a_2)\tau}}\right]$$

$$=a_2\left[1+\frac{\frac{a_1}{a_2}-1}{1+\frac{a_1-k}{k-a_2}\epsilon^{(a_1-a_2)\tau}}\right] \tag{15}$$

Since

$$a_1\geq1, \quad a_2\geq0, \quad 0\leq\frac{a_2}{a_1}\leq1, \quad \epsilon^{a_1\tau}\geq0, \quad \epsilon^{a_2\tau}\geq0$$

It can be seen from the foregoing equations that if

$$a_2\leq k\leq a_1$$

then

$$a_2\leq\left(-\frac{W}{\xi}\right)\leq a_1$$

That is, the trajectories given by equation 14 never pass out of the regions between the asymptotes once they have started in those regions. Furthermore, it is easy to verify

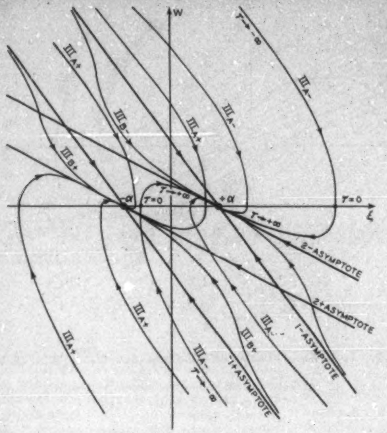

Figure 11. Type III trajectories and asymptotes in phase plane $(\zeta_2>1)$

Arrows indicate increasing time. Singular (nodal) points at $\xi=\pm\alpha$, $W=0$. Curves are not drawn to scale

from equations 15 that as $\tau\to-\infty$, $(-W/\xi)\to a_1$, and as $\tau\to+\infty$, $(-W/\xi)\to a_2$. These curves are marked III_{B+} and III_{B-} in Figure 11.

It is seen from equations 15 that, except for the asymptotes themselves which are also trajectories ($k=a_1$ or $k=a_2$), these trajectories are not straight lines. In pages 19 and 76 of reference 13, these curves are shown as straight lines, apparently by an oversight.

Gears Unmeshed. Since ξ_1 does not enter into the differential equation, the type II_+ and II_- trajectories and the limit curves that have been discussed already in the underdamped case apply without any change in this case too.

Limit Points and Limit Cycles

In contradistinction to the underdamped case, the situation is now different according as $a_1 \gtrless 1/2\zeta$.

$a_1>1/2\zeta$ means that the slope of the limiting curve (upper or lower) at $W=0$ is less than the slope of the 1_+ or 1_- asymptote. This case is shown in Figure 12; a study of this figure shows that in this case all transients damp out exponentially, with no, or at most one, overshoot, except possibly an additional overshoot due to the initial disturbance. All trajectories tend to either of the two singular (nodal) points $\xi=\pm\alpha$, $W=0$, either from within or from without the region $-\alpha\leq\xi\leq\alpha$. The inequality $a_1<1/2\zeta$ or $\zeta+\zeta_1+\sqrt{(\zeta+\zeta_1)^2-1}<1/2\zeta$ represents the region in the damping plane, Figure 5, which is above the line $\zeta_1=\zeta$ and below the hyperbola $\zeta\zeta_1=1/4$. This region is marked I_B and II_B; regions I_A and II_A correspond to the underdamped case. Hence the region outside of regions I_A, I_B, II_A, and II_B which is marked as region III in the damping plane, corresponds to the region of exponential decay of all transients, and no limit cycles exist.

Depending on how the transient starts, it may approach the singular points along different trajectories. Thus, in Figure 12, if a transient starts at, say, points *1*, *2*, or *3* the motion will proceed as indicated and eventually will proceed towards the $-\alpha$ singular point along those trajectories III_{A+} which eventually are asymptotic to the lower part of asymptote 2_+, as shown. On the other hand, a transient starting at point *4* will eventually proceed to the singular point $-\alpha$ along a trajectory III_{B+} which also becomes asymptotic to asymptote 2_+. In other cases the motion will proceed to the singular point $+\alpha$ along a trajectory which ultimately becomes asymptotic to the asymptote 2_-.

It may be well to point out that the transients we are discussing are supposed to be of such a nature as to conform to the conventions we have assumed in writing the differential equations. Other types of transients may occur. Thus a transient may occur in which, although represented by a point in the phase plane, such as *2* in Figure 12 in which case the gears are supposed to be meshed, actually the gears may be unmeshed at that instant. What this means is that initially the motion will proceed along an extension of a trajectory of type II (not shown in Figure 12). However, eventually the motion must go over on a trajectory of type III, and so the essential result of exponential decay still holds.

$a_1<1/2\zeta$ is represented in Figure 13. A closer study of this figure indicates beyond doubt at least the possible existence of a limit cycle. The condition and detailed proofs of the existence, uniqueness, and (relative) stability of the limit cycle are, in this case, even lengthier than in the underdamped case. Hence the detailed proofs again will be omitted. However, the following results can be proved:

Let x satisfy the equation

$$\frac{\log\left(\dfrac{x}{a_1}-1\right)}{\log(a_1x-1)}=\frac{1}{a_1^2};\ a_1=\zeta+\zeta_1+\sqrt{(\zeta+\zeta_1)^2-1} \tag{16}$$

$$\left.0<x<-\frac{W}{\xi+\alpha}\quad\text{For lower limit curve}\right)$$

Then, if $x<1/2\zeta$, a limit cycle exists. Substituting $x=1/2\zeta$ in equation 16 results in a curve in the damping (ζ, ζ_1) plane. It can be shown that this curve is an analytic continuation of the bifurcation curve in the underdamped region between points *a* and *b* of Figure 5.

Accordingly, the region marked I_B, to the left of the bifurcation curve, Figure 5, is a region of hunting in the steady state. However, in contradistinction to the underdamped case, not all transients will end up in hunting. Only those transients which originate in the following regions in the phase plane, as shown in Figure 13, will end up in hunting:

1. The region between the lower boundary curve, the lower part of the 1_+ asymptote and the ξ axis.
2. The left boundary curve ending at intersection of upper limit curve with upper part of 1_- asymptote this upper part of the 1_- asymptote and the ξ axis.
3. The corresponding two regions above and to the right. Again it is understood that the nature of the transients should be limited according to the conventions assumed. All transients originating in regions outside those enumerated above damp out exponentially. Whether the initial transient falls in either region depends upon how it is started.

There is only one value of x which satisfies equation 16, and from this it follows that only one limit cycle can exist.

As in the underdamped case, all transients in the regions enumerated approach the limit cycle either monotonically from without, that is, with constantly increasing period and decreasing amplitude, or vice versa. Again, the amplitude of the limit cycle is greater than the reduced backlash gap 2α.

From preceding paragraphs it follows that the limit cycle is now only relatively stable, that is, with respect to trajectories in a region in the phase plane, and not with respect to all trajectories.

Finally if $x>1/2\zeta$, the limit points *2* and *2′* coalesce with the singular points $\xi=\pm\alpha$; $W=0$, and the limit cycle degenerates into the ξ-axis strip, $-\alpha\leq\xi\leq\alpha$, and, as in the underdamped case, the limit case of hunting or quasi-hunting results. This corresponds to the region marked II_B in the damping plane, that is, the region between the bifurcation curve, the hyperbola $\zeta\zeta_1=1/4$, and the line $\zeta+\zeta_1=1$ in Figure 5. The essential significance of a point on the bifurcation curve to which correspond a pair of values ζ, ζ_1 is that for these values there occurs a fundamental transition which can be illustrated thus:

$$\begin{tikzcd}
\text{stable singularity} \arrow[r] \arrow[dr] & \text{unstable singularity} \\
& \text{stable limit cycle} \\
\text{stable singularity} \arrow[r] \arrow[ur] & \text{unstable singularity}
\end{tikzcd}$$

Poincare, in studying the case:

$$\begin{tikzcd}
& \text{unstable singularity} \\
\text{stable singularity} \arrow[ur] \arrow[dr] & \\
& \text{stable limit cycle}
\end{tikzcd}$$

for a certain critical value of a parameter λ, has designated this phenomenon by the term "bifurcation." In our case, we are dealing with two critical parameters instead of one, and accordingly, it seems appropriate to designate, after Poincare, the curve separating regions I from II as a "bifurcation curve." Likewise, the curve, part hyperbola and part straight line, which separates the regions II and III may be designated as a quasi-bifurcation curve.

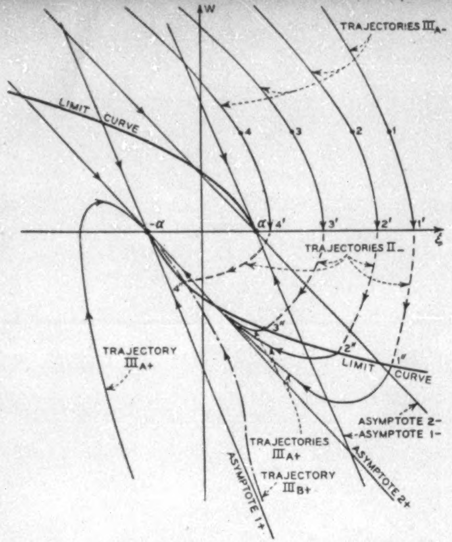

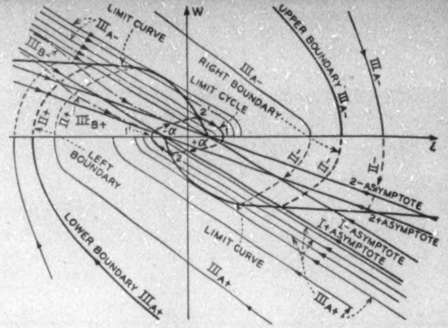

Figure 12. Types II and III trajectories in phase plane ($\zeta_1>1$, $a_1>1/2\zeta$)

Arrows indicate increasing time. Singular (nodal) points $\xi=\pm\alpha$, $W=0$. Curves are not drawn to scale

Figure 13. Trajectories and limit cycle in plane ($\zeta_1>1$, $a_1<1/2\zeta$). Limit points: 2 and 2′, limit cycle: 1–2–1′–2′–1

Arrows indicate increasing time. Singular (nodal) points at $\xi=\pm\alpha$, $W=0$. Curves are not drawn to scale

Incidentally, in the limit as $\zeta\to 0$, $\zeta_1\to\infty$, the bifurcation curve tends to the hyperbola $\zeta\zeta_1=1/8$.

Summary

The damping plane, Figure 5, may be divided into three regions, the first two of which are further subdivided, as follows:

Region I. To left of bifurcation curve; hunting in the steady state

A. For all transients.

B. For transients originating in regions in the phase plane as discussed previously.

Region II. Between bifurcation and quasi-bifurcation curve; quasi-hunting

A.
B. } As for Region I

Region III. To right of quasi-bifurcation curve All transients damp out exponentially.

Again, all of the above results hold so long as there is any finite amount of backlash. The actual value of the backlash gap enters merely in determining the amplitude of hunting, the ratio of successive increasing periods in the case of quasi-hunting, and so forth as in the under-damped case.

Perhaps the most outstanding result of this study is that in the case when a finite amount of backlash is present, viscous damping is absolutely necessary to stabilize the system. Indeed, with no viscous damping at all, the amplitude of the steady-state hunting tends to infinity, no matter how much effective error-rate damping may be present, provided only that this amount is finite.

In other words, the system cannot be stabilized with pure error-derivative control. This is not at all the case for a system without backlash.

If hunting is to be avoided at all, the (ζ, ζ_1) point, Figure 5, must be to the right of region I. If, in addition, the seemingly new phenomenon of quasi-hunting is also to be avoided, the (ζ, ζ_1) point must be situated in region III.

It should be remarked that while theoretically exponential decay in regions I_B and II_B is possible if the transient originates in certain regions of the phase plane, this is only true if no other disturbances occur until the transient damps out completely. However, as the transient is just about to be damped out, any small disturbance may throw it into the region in the phase plane which is characterized by hunting or quasi-hunting. Since the limit cycle is stable relative to all other trajectories, it will take relatively larger disturbances to produce the opposite effect. Practically, this means that if the damping ratios ζ and ζ_1 correspond to any point in regions I and II, all transients will generally end up in hunting and quasi-hunting respectively in the steady state.

Finally, it may be added that all of these purely theoretical results were confirmed completely by the results of the electronic analyzer, as was discussed elsewhere in this paper.

References

1. Experimental Mechanical Engineering, Volume I, Engineering Instruments (book), H. Diedricks, W. C. Andrae. John Wiley and Sons, New York, N. Y., 1930.

2. General Principles of Instrument Analysis, C. S. Draper, G. V. Schliestett. *Instruments* (Pittsburgh, Pa.), May 1939, page 137.

3. Functional Analysis of Measurements, I. F. Kinnard. *AIEE Transactions*, volume 65, 1946, pages 987–95.

4. Variance of Measuring Instruments and Its Relation to Accuracy and Sensitivity, F. J. Schlink. *Paper 328*, National Bureau of Standards (Washington, D. C.), 1918.

5. Advanced Electrical Measurements (book), W. C. Michels. Second edition, 1941, D. Van Nostrand Company, Inc., New York, N. Y.

6. Theory of Servomechanisms (book), H. M. James, N. B. Nichols, R. S. Phillips. McGraw-Hill Book Company, New York, N. Y., 1947.

7. Parallel Circuits in Servomechanisms, H. T. Marcy. *Electrical Engineering* (*AIEE Transactions*), volume 65, August-September 1946, pages 521–9.

8. Servos with Torque Saturation, W. Hurewicz, N. B. Nichols. *Radiation Laboratory Report 555*, Library of Congress (Washington, D. C.), May 1944.

9. Servos with Torque Saturation, Part II, W. Hurewicz, N. B. Nichols. *Radiation Laboratory Report 592*, Library of Congress (Washington, D. C.), September 1944.

10. The Effects of Backlash and Speed-Dependent Friction on the Stability of Closed-Cycle Control Systems, A. Tustin. *Journal*, Institution of Electrical Engineers (London, England), volume 94, part IIA, number 1, May 1947, page 143.

11. Analysis of Problems in Dynamics by Electric Circuits, J. R. Ragazzini, R. H. Randall, F. A. Russell. *Proceedings*, Institute of Radio Engineers (New York, N. Y.), May 1947, pages 444–52.

12. Les Methods Nouvelles de la Mecanique Celeste (book), H. Poincare. Paris, France, 1892.

13. Lectures on Non-Linear Mechanics, K. O. Friedrichs, P. Le Corbeiller, N. Levinson, J. J. Stoker. *Advanced Instruction and Research in Mechanics*, Brown University (Providence, R. I.), Winter 1942–43.

14. Introduction to Non-Linear Mechanics (book), N. Minorsky. Ann Arbor, Mich., 1947.

15. Fundamental Theory of Servo-Mechanisms (book), L. A. Mac Coll. New York, N. Y., 1945.

16. Analysis of Relay Servo-Mechanisms, H. K. Weiss. *Journal of the Aeronautical Sciences* (New York, N. Y.), July 1946.

No Discussion

A Wide-Range Adjustable-Speed Drive

A. G. CONRAD
MEMBER AIEE

E. R. TRIBKEN
STUDENT MEMBER AIEE

Synopsis: This paper describes the theory and characteristics of a drive which provides a wide range of adjustable speeds. The ratio of the maximum to minimum useful speeds attainable is approximately 20-to-1. The system provides high starting-torque, relatively high efficiencies and rapid deceleration through regenerative braking. The drive uses d-c series motors and generators and it can be assembled from standard equipment.

Principle of Operation

WHEN a series motor is supplied with a voltage which is proportional to its current, its speed is essentially constant for various values of output power. The operating speed is determined by the rate of change of the applied voltage with change of input current. A circuit for supplying such voltages to a series motor is shown in Figure 1. The two series machines 1 and 2 are driven at constant speed. Their combined output is used to drive the series motor 3 which provides constant adjustable-speed for the load. If the ratio of the field strengths of the series machines 1 and 2 can be held constant, and the polarities of these machines are unaltered, the voltage supplied to the series motor 3 will vary with load such that the speed of this motor will be kept essentially constant for different values of developed torque. The magnitude of this ratio is determined by the adjustment of the rheostat R_c. The setting of the switch S_1 can be used to change the polarity of the machine 2—thus converting it from a generator to a motor or vice versa.

The voltage applied to the motor 3 can be made equal to either the sum or the difference of the terminal voltages produced by machines 1 and 2. High speeds are obtained by setting the switch S_1 so that the voltages produced in the machines 1 and 2 are aiding. For low speeds the field of machine 2 is adjusted so that it behaves as a motor, thereby reducing the voltage supplied to the motor 3. Minimum speed is obtained when the machines 1 and 2 are producing voltages which are essentially equal and opposite. Maximum speed is obtained when the fields of machines 1 and 2 are fully excited and their voltages are aiding. Intermediate speeds are obtained by proper setting of the rheostat R_c and the switch S_1.

For a given direction of rotation of the motor a reversal of the field of machine 3 through the switch S_2 will change the behavior of this machine from motor action to generator action and vice versa. Regenerative braking can be accomplished if the field strengths of machines 1 and 2 are adjusted so that the power received by machine 2 from machine 3 exceeds that which is delivered by machine 1 to machine 3.

Characteristics

The speed characteristics of this drive are attainable from an analysis of the circuit shown in Figure 1. The constants shown in Table I will be used in the analysis.

The sum of the voltages around the circuit is

$$Eg_1 \pm Eg_2 - I\left(Ra_1+Ra_2+Rf_1+\frac{Rf_2R_c}{Rf_2+R_c}\right) = Eg_3+I(Ra_3+Rf_3) \quad (1)$$

Let $(Ra_1+Ra_2+Rf_1+Ra_3+Rf_3)=R$

$$\therefore\ Eg_1 \pm Eg_2 - I\left(R+\frac{Rf_2R_c}{Rf_2+R_c}\right) = Eg_3 \quad (2)$$

$$Eg_1 = K_1'\phi_1 Ng = K_1 I Ng \quad (3)$$

$$Eg_2 = K_2'\phi_2 Ng = K_2(I-I')Ng \quad (4)$$

$$I-I' = \frac{IR_c}{Rf_2+R_c} \quad (5)$$

$$Eg_2 = K_2\frac{R_c}{Rf_2+R_c}\ INg \quad (6)$$

$$Eg_3 = K_3'\phi_3 N_3 = K_3 I N_3 \quad (7)$$

Substituting equations 3, 6, and 7 in equation 2

$$K_1 I Ng \pm K_2\frac{R_c}{Rf_2+R_c} INg - I\left(R+\frac{Rf_2R_c}{Rf_2+R_c}\right) = K_3 I N_3 \quad (8)$$

Solving for N_3

$$N_3 = \frac{Ng\left(K_1 \pm K_2\frac{R_c}{Rf_2+R_c}\right) - R - \frac{Rf_2R_c}{Rf_2+R_c}}{K_3}$$

$$= K - \frac{R_c}{Rf_2+R_c}\left(Rf_2 \pm \frac{K_2}{K_3}Ng\right) \quad (9)$$

when

$$K = \frac{K_1}{K_3}Ng - \frac{R}{K_3}$$

It is evident from equation 9 that for a given setting of the rheostat R_c the speed of the motor 3 is constant and it is independent of current and therefore independent of the torque developed. Equation 9 also shows that the motor has a definite speed for each setting of R_c and consequently it is an adjustable-speed drive.

The preceding analysis did not take into account the effects of nonlinearities

Table I

	Machine 1, Generator	Machine 2, Motor or Generator	Machine 3, Motor
Armature resistance..	Ra_1	Ra_2	Ra_3
Field resistance......	Rf_1	Rf_2	Rf_3
Generated voltage...	Eg_1	Eg_2	Eg_3
Total flux...........	ϕ_1	ϕ_2	ϕ_3
Speed................	Ng	Ng	N_3
Armature constants..	K_1, K_1'	K_2, K_2'	K_3, K_3'
Armature Current...	I	I	I
Field Current.......	I	$I-I'$	I

Paper 49-199, recommended by the AIEE Rotating Machinery Committee and approved by the AIEE Technical Program Committee for presentation at the AIEE Summer General Meeting, Swampscott, Mass., June 20–24, 1949. Manuscript submitted March 21, 1949; made available for printing May 9, 1949.

A. G. CONRAD, Professor and Chairman of Electrical Engineering Department, and E. R. TRIBKEN are both with Yale University, New Haven, Conn.

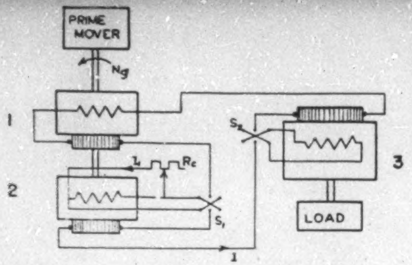

Figure 1. Circuit for wide-range adjustable speed drive

1. Series generator
2. Series motor or generator
3. Series motor

of the machines involved. Some nonlinear effects will result from residual magnetism for low values of power output. Saturation also will produce nonlinear effects when the current in any of the three machines is large. These effects are predictable from relations defined in equation 2 as follows:

1. The voltages Eg_1 and Eg_2 have components which are caused by the residual magnetism of their respective machines. These components are essentially constant and become significant parts of the generated voltages of machines 1 and 2 at low values of current. For the case when Eg_2 opposes Eg_1 and Eg_2 is smaller than Eg_1, the total output voltage will decrease with a decrease of current at a greater rate than it would for linear conditions. This results in a reduction of speed as the current decreases. For high-speed settings of switch S_1, machines 1 and 2 will tend to act like a constant-voltage supply at low values of current. Therefore in the low-torque high-speed range a decrease in load results in a slight increase in speed.

2. The iron of machines 1 and 2 will saturate at high values of current. This produces a lower rate of increase of the total voltage output with an increase in current and thereby causes the speed of the motor to decrease with an increase of load.

3. The generated voltage of machine 3 will possess some degree of nonlinearity. Generally, this tends to counteract the speed changes due to the nonlinearities of the generated voltage of machine 1 and 2.

4. Brush resistances increase with a decrease of current causing a small change in the total resistance of the circuit. The effects of this slight increase in resistance are negligible except when the output voltage of machines 1 and 2 is small. For this condition the motor speed will decrease slightly with a decrease of current.

The reasons for a variation in the speed as the load is changed indicate several counteracting factors. The net result of these factors can be quite different for different machines. The optimum characteristics of this system are obtained only through a design such that the nonlinear effects are minimized. While linear units are desirable, considerable nonlinearity is tolerable if it is properly controlled.

The analysis of this unit thus far has dealt with only conditions of steady-state operation. A complete study of the transient characteristics of the unit is beyond the scope of this paper and is unnecessary since experimental results show that the system is stable. Under certain conditions of operation with generators which are not identical, the total output voltage of machines 1 and 2 may attain certain values such that an increase of current produces a decrease in output voltage and then further increases in current may produce an increase in the voltage. This condition can cause instability in the motor. Generally, an increase in the values of the series resistances will add stability.

Typical ratings for a suitable drive are:

	Horsepower	Volts
Motor—3	10	220
Generator number 1	5	110
Generator number 2	5	110
Prime mover	10	
Total	30	

Performance and Conclusions

The performance of this drive is revealed in Figure 2. This unit has a useful speed range of 20-to-1. Speed regulation for various speed adjustments is:

Speed, Rpm	Speed Regulation, Per Cent
100	13.3
1,000	0
1,800	9.7

These data were taken on standard equipment available in Dunham Laboratory of Electrical Engineering at Yale University. Machines 1 and 2 had similar ratings, but they did not have suitable ratings to match exactly those of machine 3. No attempt was made to compensate for the nonlinearities present in the machines.

The departures from constant speed in the characteristics shown in Figure 2 are caused by the nonlinearities in the machines. With suitable compensation, it should be possible to build a drive which will have less speed variation throughout the entire range of speed adjustment. Such provisions could extend the range.

If the resistance Rf_3 is small, R_c must have a low ohmic value. The design of such a rheostat may, under certain conditions, be difficult. This undesirable feature could, in some cases, limit the application of the drive.

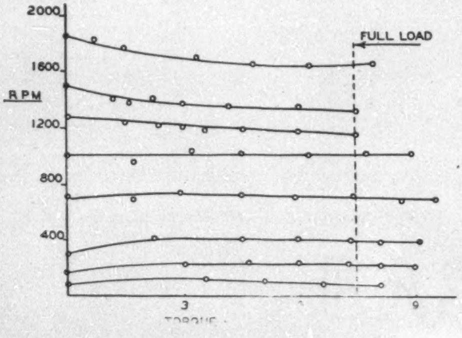

Figure 2. Characteristics of the motor 3 when operating in the circuit of Figure 1

No Discussion

AIEE Transactions Index for Part I, Volume 68, 1949

1. Technical-Subject Index

A-C Generators, A Semiempirical Approach to Voltage Dip—with Suddenly Applied Loads on. Rosenberg..........160–6; disc. 166
A-C Voltmeter, A New Expanded Scale. Millar..641–3
Adjustable-Speed Drive, A Wide-Range. Conrad, Tribken..........789–90
Adjusting Radiosonde Recorder, Automatic Range-. Beggs..........602–07
Advances in Technique of Lightning Measurements. Brownlee..........515–19
Air Circuit Breaker, A New 69-Kv Compressed-. Baker, Frisch..........363–8; disc. 369
Air-Core Reactors as Fault Limiting Means on High Interrupting Capacity Controllers, The Use of. Leitch..........469–74; disc. 474
Alarm and Control System for Remote Control of Coaxial Cable Stations, B-1. Hearn, Weber...622–6
Altitudes, A Small High-Voltage Bushing Design for High. Vogel, Hart..........761–4
Ampere Demand Meter, A New Thermal Volt-. Douglass, Morong..........79–83; disc. 83
Amplifiers with Feedback, Analytical Determination of Characteristics of Magnetic. VerPlanck, Finzi, Beaumariage..........565–70
Analog Computer to Nonlinear Mechanics and Servomechanisms, Application of the California Institute of Technology Electric. McCann, Wilts, Locanthi..........652–60
Analog Computers, Comparison of Long-Time and Short-Time. Paschkis..........70–3
Analogs of Linear Vibration Problems, Summary of Transformations Useful in Constructing. Corbett..........661–4
Analogy, The Transient Behavior of the Two-Stage Rototrol Main Exciter Voltage Regulating System as Determined by Electrical. Carleton....59–63
Analysis of Results to Research Problems in Magnetic Recording, Application of Experimental Test Procedures and Methods of. Thompson......407–17
Analytical Determination of Characteristics of Magnetic Amplifiers with Feedback. VerPlanck, Finzi, Beaumariage..........565–70
Analyzer, A New Fourier Coefficient Harmonic. Charp..........644–9; disc. 639
Application Engineering on Diesel-Electric Locomotives in Railroad Service. Bevan..........125–31
Application of the California Institute of Technology Electric Analog Computer to Nonlinear Mechanics and Servomechanisms. McCann, Wilts, Locanthi..........652–60
Application of Experimental Test Procedures and Methods of Analysis of Results to Research Problems in Magnetic Recording. Thompson..407–17
Application of Multifrequency Pulsing in Switching. Dahlbom, Horton, Moody..........392–6
Applications, Mircowave Channels for Power System (Committee Report)..........40–2; disc. 42
Applications, Two Gas Turbines for Power Generation and Other. Howard..........461–5; disc. 465
Arc, Instrumentation for the Evaluation of the Stability of the Welding. Winsor, Schetky, Wyant..525–33
Armature Iron Losses in Series Motors. Chang, Karr.. ....262–4; disc. 264
Aspects of Relay Circuits, Sequential. Ritchie..577–81
Audio Noise Problems on an Electric Power System, Transformer. Murray..........740–7; disc. 747
Automatic Range-Adjusting Radiosonde Recorder. Beggs..........602–07

B

B-1 Alarm and Control System for Remote Control of Coaxial Cable Stations. Hearn, Weber....622–6
Backlash, Instrument Inaccuracies in Feed-Back Control Systems with Particular Reference to. Marcy, Yachter, Zauderer..........778–88
Bandwidths, The Distinction Between Effective and Circuit. Kessler..........98–9
Bank, The Temperature Rise of Cables in a Duct. Neher..........540–6; disc. 546
(Basic Sciences) Formulas and Tables for the Calculation of the Magnetic Field Components of Circular Filaments and Solenoids. Grover........665–75
(Basic Sciences) Nonharmonic Oscillations as Caused by Magnetic Saturation. Rudenberg..........676–85
(Basic Sciences) The Vector Power Factor of Unbalanced Sinusoidal 3-Phase Circuits. Lamb, Brandt... 507–09
Behavior of the Two-Stage Rototrol Main Exciter Voltage Regulating System as Determined by Electrical Analogy, The Transient. Carleton... 59–63
Boilers and of Hydro Units, Outage Rates of Steam Turbines and. (Committee Report)..........450–7
Bolometer, Detection of Overheated Transmission Line Joints by Means of a. Leslie, Wait..64–8; disc. 68
Braking Control of D-C Series Motors—Experimental Study of Speed-Torque Curves, Dynamic. Heumann..........560–4
Breaker, A New 69-Kv Compressed-Air Circuit. Baker, Frisch..........363–8; disc. 369
Breakers, A Manually-Operated Spring Mechanism for Medium Voltage Oilless Circuit. Wyman, Casey..........357–61; disc. 361
Bushing Design for High Altitudes, A Small High-Voltage. Vogel, Hart..........761–4
Busses, Trolley Coaches Replace. McMillon...403–06

C

Cable Circuits in Philadelphia, 69-Kv Pipe-Type. Kidder, Van Antwerp..........550–6; disc. 556
Cable for Carrier Current Installation on Power Lines, Line Tuning Equipment Used With Coaxial. Sutton..........44–8; disc. 48
Cable Impregnated with Extra-High-Viscosity Oil, High-Pressure Gas-Filled. Sticher, Doan, Atkinson, Meyerhoff..........336–45; disc. 345
Cable Overhead-Conductor 132-Kv Transmission Line at Carrier Current Frequencies, Loss Measurements Made on Underground-. Cornelius, Storer.... 597–601
Cable Stations, B-1 Alarm and Control System for Remote Control of Coaxial. Hearn, Weber...622–6
Cables and Pipes, The Temperature Rise of Buried. Neher..........9–17; disc. 17
Cables, Heating of Radio-Frequency. Macalpine... 283–8
Cables in a Duct Bank, The Temperature Rise of. Neher..........540–6; disc. 546
Cables, The Power Rating of Radio-Frequency. Mildner..........289–98; disc. 298
Calculation of the Magnetic Field Components of Circular Filaments and Solenoids, Formulas and Tables for the. Grover..........665–75
California Institute of Technology Electric Analog Computer to Nonlinear Mechanics and Servomechanisms, Application of the. McCann, Wilts, Locanthi..........652–60
Capacity Controllers, The Use of Air-Core Reactors as Fault Limiting Means on High Interrupting. Leitch..........469–74; disc. 474
Carrier Current Frequencies, Loss Measurements Made on Underground-Cable Overhead-Conductor 132-Kv Transmission Line at. Cornelius, Storer.... 597–601
Carrier Current Installation on Power Lines, Line Tuning Equipment Used With Coaxial Cable for. Sutton..........44–8; disc. 48
(Carrier Current) Microwave Channels for Power System Applications. (Committee Report).......... ....40–2; disc. 42
Changing Temperature, The Measurement of Dielectric Loss at High Frequencies and Under. Whitehead, Rueggeberg..........520–4
Channels for Power System Applications, Microwave. (Committee Report)..........40–2; disc. 42
Characteristics of Distribution Systems, Voltage-Recovery. Witzke..........172–80; disc. 180
Characteristics of Magnetic Amplifiers with Feedback, Analytical Determination of. VerPlanck, Finzi, Beaumariage..........565–70
Characteristics of Two-Phase Servomotors, Operating. Koopman..........319–27; disc. 327
Charged Dust in Rooms, Electrically. Penney, Hewitt.. 278–82
Chart Methods Applied to Frequency Response Curves, Control. Mundel..........424–7
Chesapeake and Ohio Railway Company Steam Turbine-Electric Locomotives, Electric Equipment for. Atwell, Baston..........145–8
Circuit Bandwidths, The Distinction Between Effective and. Kessler..........98–9
Circuit Breaker, A New 69-Kv Compressed-Air. Baker, Frisch..........363–8; disc. 369
Circuit Breakers, A Manually-Operated Spring Mechanism for Medium Voltage Oilless. Wyman, Casey..........357–61; idsc. 361
Circuit of D-C Motors and Generators, Solid Short. Linville, Ward..........119–23; disc. 123
Circuits for Power-Flow Studies, Equivalent. Ward... ....373–80; disc. 380
Circuits in Philadelphia, 69-Kv Pipe-Type Cable. Kidder, Van Antwerp..........550–6; disc. 556
Circuits, Relay "Trees" and Symmetric. Washburn... 582–6
Circuits, Sequential Aspects of Relay. Ritchie..577–81
Circuits, The Logic of Relay. Keister..........571–6
Circuits, The Vector Power Factor of Unbalanced Sinusoidal 3-Phase. Lamb, Brandt......507–09
Circular Filaments and Solenoids, Formulas and Tables for the Calculation of the Magnetic Field Components of. Grover..........665–75
Coaches Replace Busses, Trolley. McMillon...403–06
Coaxial Cable for Carrier Current Installation on Power Lines, Line Tuning Equipment Used With. Sutton..........44–8; disc. 48
Coaxial Cable Stations, B-1 Alarm and Control System for Remote Control of. Hearn, Weber....622–6
Coaxial Systems, Power Supplies for. Spencer..627–30
Codes and Translations. Myers..........592–7
Coefficient Harmonic Analyzer, A New Fourier. Charp..........644–9; disc. 649
(Committee Report) Microwave Channels for Power System Applications..........40–2; disc. 42
(Committee Report) Outage Rates of Steam Turbines and Boilers and of Hydro Units..........450–7
(Committee Report) Protection of Stations Without High-Voltage Switching........226–31; disc. 231
(Committee Report) Stray Load Losses Measured in D-C Motors..........219–23; disc. 223
(Committee Report) Temperature Rise Values for D-C Machines..........206–12; disc. 212
(Communication) A Time Division Multiplexing System. Boothroyd, Creamer..........92–7
(Communication) Application of Experimetal Tests Procedures and Methods of Analysis of Results to Research Problems in Magnetic Recording. Thompson..........407–17
(Communication) Application of Multifrequency Pulsing in Switching. Dahlbom, Horton, Moody...392–6
(Communication) B-1 Alarm and Control System for Remote Control of Coaxial Cable Stations. Hearn, Weber..........622–6
(Communication) Codes and Translations. Myers... 592–7
(Communication) Considerations on Facsimile Transmission Speed. Burkhard......418–23; disc. 423
(Communication) Control Chart Methods Applied to Frequency Response Curves. Mundel......424–7
(Communication) Counting with Relays. Frost..587–91
(Communication) Power Supplies for Coaxial Systems. Spencer..........627–30
(Communication) Power Supplies for Microwave Relay Systems. Ward..........631–6
(Communication) Radio Influence from High-Voltage Corona. Slemon..........198–204; disc. 204
Communication Relay System, A Microwave. Boothroyd, Churchill..........637–41
(Communication) Relay "Trees" and Symmetric Circuits. Washburn..........582–6
(Communication) Rubber Insulators for Pole Lines. Wheeler, Markley..........195–7
(Communication) Sequential Aspects of Relay Circuits. Ritchie..........577–81
(Communication) The Distinction Between Effective and Circuit Bandwidths. Kessler..........98–9
(Communication) The Logic of Relay Circuits. Keister 571–6
(Communication) Vibrating Reed Selective Signaling System for Mobile Telephone Use. Pruden, Hoth..........387–91
(Communication) Vibrating Reed Selectors for Mobile Radio Systems. Keller, Bostwick.........383–6
Commutation of D-C Machines and Its Effects on Radio Influence Voltage Generation. Motter.......... ....491–5; disc. 495
Commutation, Oscillographing. Baldwin.......... ....100–05; disc. 105

Commutator Surface Film Conditions on Commutation, Effects of. Lynn, Elsey........106–112; disc. 112
Comparative Performance Records—Steel and Wood Transmission Lines. Booker......686–9; disc. 689
Comparison of Long-Time and Short-Time Analog Computers. Paschkis........................70–3
Comparison of Steady-State and Transient Performance of Servomechanisms. Chestnut, Mayer....765–77
Components and Systems, Graphical Determination of Transfer Function Loci for Servomechanism. Thomas, Easton................307–14; disc. 314
Components of Circular Filaments and Solenoids, Formulas and Tables for the Calculation of the Magnetic Field. Grover..................665–75
Compressed-Air Circuit Breaker, A New 69-Kv. Baker, Frisch...........................363–8; disc. 369
Computer to Nonlinear Mechanics and Servomechanisms, Application of the California Institute of Technology Electric Analog. McCann, Wilts, Locanthi.................................652–60
Computers, Comparison of Long-Time and Short-Time Analog. Paschkis..........................70–3
(Computing Devices) Summary of Transformations Useful in Constructing Analogs of Linear Vibration Problems. Corbett.............................661–4
Conditions, Fundamental Theory of Inherent-Overheating Protection Under Running Overload. Veinott, Schaefer....................266–70; disc. 270
Conditions on Commutation, Effects of Commutator Surface Film. Lynn, Elsey......106–12; disc. 112
Conductor 132-Kv Transmission Line at Carrier Current Frequencies, Loss Measurements Made on Underground-Cable Overhead-. Cornelius, Storer..597–601
Conductor Economics, Distribution Transformer and Secondary. Brady..............483–6; disc. 486
Conductor, Hy-Therm Copper—An Improved Overhead-Line. Hickernell, Jones, Snyder..22–7; disc. 27
Considerations on Facsimile Transmission Speed. Burkhard........................418–23; disc. 423
Contaminants on Electrical Insulation, Methods for Determining the Effects of. Mathes, Sieffert, Walker, Lindsey................113–18; disc. 118
Control Chart Methods Applied to Frequency Response Curves. Mundel...........................424–7
Control of D-C Series Motors—Experimental Study of Speed-Torque Curves, Dynamic Braking. Heumann...................................560–4
Control System for Remote Control of Coaxial Cable Stations, B-1 Alarm and. Hearn, Weber...622–6
Control Systems with Particular Reference to Backlash Instrument Inaccuracies in Feed-Back. Marcy, Yachter, Zauderer.......................778–88
Controllable Reactors, Universal Curves for D-C. Johnson, Merrell, Alley.............31–7; disc. 37
Controlled Reactors with Resistive Load, Some Fundamentals of D-C. Storm.........188–94; disc. 194
Controlled Temperature and Insulation Protection in the Operation of Power Transformers. Satterlee, Reed..........................753–8; disc. 759
Controllers, The Use of Air-Core Reactors as Fault Limiting Means on High Interrupting Capacity. Leitch.......................469–74; disc. 474
Copper—An Improved Overhead-Line Conductor, Hy-Therm. Hickernell, Jones, Snyder..22–7; disc. 27
Corona, Radio Influence from High-Voltage. Slemon..........................198–204; disc. 204
Counting with Relays. Frost.....................587–91
Current Frequencies, Loss Measurements Made on Underground-Cable Overhead-Conductor 132-Kv Transmission Line at Carrier. Cornelius, Storer..597–601
Current Installation on Power Lines, Line Tuning Equipment Used With Coaxial Cable for Carrier. Sutton...........................44–8; disc. 48
Currents, Rectifier Fault—II. Herskind, Schmidt, Rettig..........................243–51; disc. 251
Curves, Control Chart Methods Applied to Frequency Response. Mundel.......................424–7
Curves, Dynamic Braking Control of D-C Series Motors —Experimental Study of Speed-Torque. Heumann..................................560–4
Curves for D-C Controllable Reactors, Universal. Johnson, Merrell, Alley.............31–7; disc. 37

D

Damper Stabilized Instrument Servomechanisms. Hall.........................299–306; disc. 306
D-C Controllable Reactors, Universal Curves for. Johnson, Merrell, Alley............31–7; disc. 37
D-C Controlled Reactors with Resistive Load, Some Fundamentals of. Storm.......188–94; disc. 194
D-C Machines and Its Effects on Radio Influence Voltage Generation, Communication of. Motter..491–5; disc. 495
D-C Machines, Temperature Rise Values for. (Committee Report)..................206–12; disc. 212
D-C Motors and Generators, Solid Short Circuit of. Linville, Ward.................119–23; disc. 123
D-C Motors, Stray Load Losses Measured in. (Committee Report).................219–23; disc. 223
D-C Series Motors—Experimental Study of Speed-Torque Curves, Dynamic Braking Control of. Heumann..................................560–4
Demand Meter, A New Thermal Volt-Ampere. Douglass, Morong.....................79–83; disc. 83
Design and Experience with 4-Kv Primary Network Systems in the Washington Area. Lank..712–16; disc. 716
Design and Performance Based on Direct Lightning Strokes, Transmission Line. Harder, Clayton..439–46; disc. 447
Design and Ventilation, Transformer Manholes and Vaults: Porter...........................534–9
Design for High Altitudes, A Small High-Voltage Bushing. Vogel, Hart......................761–4
Design of Traction Motors, Twenty-Five Years Progress in the. Baldwin...................132–7
Detection of Overheated Transmission Line Joints by Means of a Bolometer. Leslie, Wait..64–8; disc. 68
Determination of Characteristics of Magnetic Amplifiers with Feedback, Analytical. VerPlanck, Finzi, Beaumariage.............................565–70
Determination of Transfer Function Loci for Servomechanism Components and Systems, Graphical. Thomas, Easton..............307–14; disc. 314
Determining the Effects of Contaminants on Electrical Insulation, Methods for. Mathes, Sieffert, Walker, Lindsey.......................113–18; disc. 118
Developments, Electronic Relay. Loving..233–40; disc. 240
(Devices) A New Fourier Coefficient Harmonic Analyzer. Charp................644–9; disc. 649
(Devices) Comparison of Long-Time and Short-Time Analog Computers. Paschkis...............70–3
Die-Cast Rotors for Induction Motors. Packer..253–60; disc. 260
Dielectric Loss at High Frequencies and Under Changing Temperature, The Measurement of. Whitehead, Rueggeberg..............................520–4
Diesel-Electric Locomotives in Railroad Service, Application Engineering on. Bevan............125–31
Diesel-Electric Rig for Deep-Well Drilling, Performance of. Clark, Moore....................497–506
Diesel-Electric Switching Locomotives, Industrial Plants Prefer. Woods.......................697–700
Dip—with Suddenly Applied Loads on A-C Generators, A Semiempirical Approach to Voltage. Rosenberg........................160–6; disc. 166
Direct Lightning Strokes, Transmission Line Design and Performance Based on. Harder, Clayton..439–46; disc. 447
Distance Relays During Faults and Power Swings, Graphical Method for Estimating the Performance of. Warrington..............608–20; disc. 620
Distinction Between Effective and Circuit Bandwidths, The. Kessler..........................98–9
Distribution System, Lightning Investigation on a Rural. MacCarthy, Stann, Edge, McKinley..428–37; disc. 437
Distribution Systems, Voltage-Recovery Characteristics of. Witzke....................172–80; disc. 180
Distribution Transformer and Secondary Conductor Economics. Brady..............483–6; disc. 486
Division Multiplexing System, A Time. Boothroyd, Creamer..................................92–7
(Domestic) The Heat Pump—Its Significance as a Potential Residential Electric Load. Bary......1–8
Drilling, Performance of Diesel-Electric Rig for Deep-Well. Clark, Moore..................497–506
Drive, A Wide-Range Adjustable-Speed. Conrad, Tribken.................................789–90
Drives for Looms, Selection of Electric. Demartini, Lukens..................................349–56
Duct, Bank, The Temperature Rise of Cables in a. Neher........................540–6; disc. 546
Duquesne Light Company System, Primary Networks on the. Holben, Lange.........704–09; disc. 709
Dust in Rooms, Electrically Charged. Penney, Hewitt..278–82
Dynamic Braking Control of D-C Series Motors—Experimental Study of Speed-Torque Curves. Heumann..................................560–4

E

Economic Loading of a Transformer System. Levine, Smith........................733–8; disc. 738
Economics, Distribution Transformer and Secondary Conductor. Brady..............483–6; disc. 486
Effective and Circuit Bandwiths, The Distinction Between. Kessler...........................98–9
Effects of Commutator Surface Film Conditions on Commutation. Lynn, Elsey.....106–12; disc. 112
Effects of Contaminants on Electrical Insulation, Methods for Determining the. Mathes, Sieffert, Walker, Lindsey...............113–18; disc. 118
Electric Analog Computer to Nonlinear Mechanics and Servomechanisms, Application of the California Institute of Technology. McCann, Wilts, Locanthi..652–60
(Electric Heating) The Measurement of Dielectric Loss at High Frequencies and Under Changing Temperature. Whitehead, Rueggeberg.........520–4
Electric Power System, Transformer Audio Noise Problems on an. Murray............740–7; disc. 747
Electrical Analogy, The Transient Behavior of the Two-Stage Rototrol Main Exciter Voltage Regulating System as Determined by. Carleton......59–63
Electrical Insulation, Methods for Determining the Effects of Contaminants on. Mathes, Sieffert, Walker, Lindsey...............113–18; disc. 118
Electrically Charged Dust in Rooms. Penney, Hewitt..278–82
Electric Drives for Looms, Selection of. Demartini, Lukens..................................349–56
Electric Equipment for Chesapeake and Ohio Railway Company Steam Turbine-Electric Locomotives. Atwell, Baston..............................145–8
Electric Load, The Heat Pump—Its Significance as a Potential Residential. Bary..................1–8
Electric Locomotives in Railroad Service, Application Engineering on Diesel-. Bevan...........125–31
Electric Motive Power, The Renaissance of. Candee..138–44
Electric Rig for Deep-Well Drilling, Performance of Diesel-. Clark, Moore..................497–506
(Electronic Instruments) A Square-Law Power-Level Recorder. Clark, Turner, Williams.......476–82
(Electronic Power Converter) Rectifier Fault Currents—II. Herskind, Schmidt, Rettig...243–51; disc. 251
Electronic Relay Developments. Loving..233–40; disc. 240
(Electronics) Analytical Determination of Characteristics of Magnetic Amplifiers with Feedback. VerPlanck, Finzi, Beaumariage.........................565–70
(Electronics) Electrically Charged Dust in Rooms. Penney, Hewitt...........................278–82
(Electronics) Heating of Radio-Frequency Cables. Macalpine..................................283–8
(Electronics) The Power Rating of Radio-Frequency Cables. Mildner..............289–98; disc. 298
Electro-Optical Shutter for Photographic Purposes, An. Zarem, Marshall, Poole.............84–91
Energy, Measurements of Erythemal. Scott....725–29
Engineering on Diesel-Electric Locomotives in Railroad Service, Application. Bevan..............125–31
Equipment for Chesapeake and Ohio Railway Company Steam Turbine-Electric Locomotives, Electric. Atwell, Baston..............................145–8
Equipment, Reduction of Interference from Radio-Frequency Heating. Klingaman..718–24; disc. 724
Equipment Used With Coaxial Cable for Carrier Current Installation on Power Lines, Line Tuning. Sutton...........................44–8; disc. 48
Equivalent Circuits for Power-Flow Studies. Ward..373–80; disc. 380
Erythemal Energy, Measurements of. Scott....725–29
Evaluation of the Stability of the Welding Arc, Instrumentation for the. Winsor, Schetky, Wyant..525–33
Exciter Voltage Regulating System as Determined by Electrical Analogy, The Transient Behavior of the Two-Stage Rototrol Main. Carleton.......59–63
Expanded Scale A-C Voltmeter, A New. Millar..641–3
Experience With 4-Kv Primary Network Systems in the Washington Area, Design and. Lank..712–16; disc. 716
Experimental Study of Speed-Torque Curves, Dynamic Braking Control of D-C Series Motors—. Heumann..................................560–4
Experimental Test Procedures and Methods of Analysis of Results to Research Problems in Magnetic Recording, Application of. Thompson.......407–17

F

Facsimile Transmission Speed, Considerations on. Burkhard.......................418–23; disc. 423
Factor of Unbalanced Sinusoidal 3-Phase Circuits, The Vector Power. Lamb, Brandt.............507–09
Fault Currents, Rectifier—II. Herskind, Schmidt, Rettig..........................242–51; disc. 251
Fault Limiting Means on High Interrupting Capacity Controllers, The Use of Air-Core Reactors as. Leitch.......................469–74; disc. 474
Faults and Power Swings, Graphical Method for Estimating the Performance of Distance Relays During. Warrington..................608–20; disc. 620
Feedback, Analytical Determination of Characteristics of Magnetic Amplifiers with. VerPlanck, Finzi, Beaumariage.............................565–70

Feed-Back Control Systems with Particular Reference to Backlash, Instrument Inaccuracies in. Marcy, Xachter, Zauderer........................778–88
Field Components of Circular Filaments and Solenoids, Formulas and Tables for the Calculation of the Magnetic. Grover........................665–75
Field Fluxes of the Shaded-Pole Motor, The. Kimberly........................273–7
Filaments and Solenoids, Formulas and Tables for the Calculation of the Magnetic Field Components of Circular. Grover........................665–75
Film Conditions on Commutation, Effects of Commutator Surface. Lynn, Elsey.....106–12; disc. 112
Fluxes of the Shaded-Pole Motor, The Field. Kimberly........................273–7
Formulas and Tables for the Calculation of the Magnetic Field Components of Circular Filaments and Solenoids. Grover........................665–75
Fourier Coefficient Harmonic Analyzer, A New. Charp........................644–9; disc. 649
Frames, Stationary Networks and Transmission Lines Along Uniformly Rotating Reference. Kron........................690–6
Frequencies and Under Changing Temperature, The Measurement of Dielectric Loss at High. Whitehead, Rueggeberg........................520–4
Frequencies, Loss Measurements Made on Underground-Cable Overhead-Conductor 132-Kv Transmission Line at Carrier Current. Cornelius, Storer........................597–601
Frequency Cables, Heating of Radio-. Macalpine........................283–8
Frequency Cables, The Power Rating of Radio-. Mildner........................289–98; disc. 298
Frequency Heating Equipment, Reduction of Interference from Radio-. Klingaman.718–24; disc. 724
Frequency Response Curves, Control Chart Methods Applied to. Mundel........................424–7
Function Loci for Servomechanism Components and Systems, Graphical Determination of Transfer. Thomas, Easton...............307–14; disc. 314
Fundamental Theory of Inherent-Overheating Protection Under Running Overload Conditions. Veinott, Schaefer........................266–70; disc. 270
Fundamentals of D-C Controlled Reactors with Resistive Load, Some. Storm............188–94; disc. 194

G

Gas-Filled Cable Impregnated with Extra-High-Viscosity Oil, High-Pressure. Sticher, Doan, Atkinson, Meyerhoff...............336–45; disc. 345
Gas Turbine Power Plant, A 3,000-Horsepower. Haverstick........................458–60
Gas Turbines for Power Generation and Other Applications, Two. Howard............461–5; disc. 465
Gas Turbines in Stationary Power Generation. Hague........................467–8
Generation and Other Applications, Two Gas Turbines for Power. Howard............461–5; disc. 465
Generation, Commutation of D-C Machines and Its Effects on Radio Influence Voltage. Motter........................491–5; disc. 495
Generation, Gas Turbines in Stationary Power. Hague........................467–8
Generators, A Semiempirical Approach to Voltage Dip—with Suddenly Applied Loads on A-C. Rosenberg........................160–6; disc. 166
Generators, Solid Short Circuit of D-C Motors and. Linville, Ward...............119–23; disc. 123
Geometric Loci of the Synchronous Tie, The. Finzi, Wellard........................168–71
Graphical Determination of Transfer Function Loci for Servomechanism Components and Systems. Thomas, Easton...............307–14; disc. 314
Graphical Method for Estimating the Performance of Distance Relays During Faults and Power Swings. Warrington...............608–20; disc. 620

H

Harmonic Analyzer, A New Fourier Coefficient. Charp........................644–9; disc. 649
Heat Pump—Its Significance as a Potential Residential Electric Load, The. Bary........................1–8
Heating Equipment, Reduction of Interference from Radio-Frequency. Klingaman..718–24; disc. 724
Heating of Radio-Frequency Cables. Macalpine........................283–8
High Frequencies and Under Changing Temperature, The Measurement of Dielectric Loss at. Whitehead, Rueggeberg........................520–4
High-Pressure Gas-Filled Cable Impregnated with Extra-High-Viscosity Oil. Sticher, Doan, Atkinson, Meyerhoff...............336–45; disc. 345
High-Voltage Bushing Design for High Altitudes, A Small. Vogel, Hart........................761–4
High-Voltage Corona, Radio Influence from. Slemon........................198–204; disc. 204
High-Voltage Switching, Protection of Stations Without. (Committee Report)............226–31; disc. 231
Horsepower Gas Turbine Power Plant, A 3,000-. Haverstick........................458–60
Hydro Units, Outage Rates of Steam Turbines and Boilers and of. (Committee Report)......450–7
Hy-Therm Copper—An Improved Overhead-Line Conductor. Hickernell, Jones, Snyder..22–7; disc. 27

I

Impregnated with Extra-High-Viscosity Oil, High-Pressure Gas-Filled Cable. Sticher, Doan, Atkinson, Meyerhoff...............336–45; disc. 345
Improvements to Oklahoma City Primary Network. Brady...............701–02; disc. 702
Incandescent Lamps, Saving Time in Testing Life of. Purcell........................730–2
Indicator, Polar Vector. Walker, Waynick, Sulzer........................154–9
Induction Motors, Die-Cast Rotors for. Packer........................253–60; disc. 260
(Industrial Control) The Use of Air-Core Reactors as Fault Limiting Means on High Interrupting Capacity Controllers. Leitch......469–74; disc. 474
(Industrial) Dynamic Braking Control of D-C Series Motors—Experimental Study of Speed-Torque Curves. Heumann........................560–4
Industrial Plants Prefer Diesel-Electric Switching Locomotives. Woods........................697–700
(Industry) Selection of Electric Drives for Looms. Demartini, Lukens........................349–56
Influence from High-Voltage Corona, Radio. Slemon........................198–204; disc. 204
Influence Voltage Generation, Commutation of D-C Machines and Its Effects on Radio. Motter........................491–5; disc. 495
Inherent-Overheating Protection Under Running Overload Conditions, Fundamental Theory of. Veinott, Schaefer........................266–70; disc. 270
Installation on Power Lines, Line Tuning Equipment Used With Coaxial Cable for Carrier Current. Sutton........................44–8; disc. 48
Instrument Inaccuracies in Feed-Back Control Systems with Particular Reference to Backlash. Marcy, Yachter, Zauderer........................778–88
Instrument Servomechanisms, Damper Stabilized. Hall........................299–306; disc. 306
Instrumentation for the Evaluation of the Stability of the Welding Arc. Winsor, Schetky, Wyant....525–33
(Instruments) A New Expanded Scale A-C Voltmeter. Millar........................641–3
(Instruments) A New Thermal Volt-Ampere Demand Meter. Douglass, Morong.........79–83; disc. 83
(Instruments) An Electro-Optical Shutter for Photographic Purposes. Zarem, Marshall, Poole..84–91
(Instruments) Automatic Range-Adjusting Radiosonde Recorder. Beggs........................602–07
(Instruments) Polar Vector Indicator. Walker, Waynick, Sulzer........................154–9
(Instruments) Surge Protection in a Modern Watt-Hour Meter. Busch, Williams......74–7; disc. 77
(Insulated Conductor) High-Pressure Gas-Filled Cable Impregnated with Extra-High-Viscosity Oil. Sticher, Doan, Atkinson, Meyerhoff........................336–45; disc. 345
(Insulated Conductor) The Thermal Movement of Moisture in Soil. Mickley........330–3; disc. 333
(Insulated Conductors) Transformer Manholes and Vaults: Design and Ventilation. Porter...534–9
Insulation, Methods for Determining the Effects of Contaminants on Electrical. Mathes, Sieffert, Walker, Lindsey...............113–18; disc. 118
Insulation Protection in the Operation of Power Transformers, Controlled Temperature and. Satterlee, Reed........................753–8; disc. 759
Insulators for Pole Lines, Rubber. Wheeler, Markley........................195–7
Interference from Radio-Frequency Heating Equipment, Reduction of. Klingaman..718–24; disc. 724
Interrupting Capacity Controllers, The Use of Air-Core Reactors as Fault Limiting Means on High-. Leitch........................469–74; disc. 474
Investigation on a Rural Distribution System, Lightning. MacCarthy, Stann, Edge, McKinley........................428–37; disc. 437
Iron Losses in Series Motors, Armature. Chang, Karr........................262–4; disc. 264

J

Joints by Means of a Bolometer, Detection of Overheated Transmission Line. Leslie, Wait........................64–8; disc. 68

L

Lamps, Saving Time in Testing Life of Incandescent. Purcell........................730–2
(Land Transportation) Application Engineering on Diesel-Electric Locomotives in Railroad Service. Bevan........................125–31
(Land Transportation) Electric Equipment for Chesapeake and Ohio Railway Company Steam Turbine-Electric Locomotives. Atwell, Baston.......145–8
(Land Transportation) Industrial Plants Prefer Diesel-Electric Switching Locomotives. Woods...697–700
(Land Transportation) The Renaissance of Electric Motive Power. Candee........................138–44
(Land Transportation) Selenium Rectifiers in Motor Vehicle Power Systems. Ramsey........................149–53; disc. 153
(Land Transportation) Trackless Trolley Operation in Rhode Island. Blomquist...............397–402
(Land Transportation) Trolley Coaches Replace Busses. McMillon........................403–06
(Land Transportation) Twenty-Five Years Progress in the Design of Traction Motors. Baldwin....132–7
Law Power-Level Recorder, A Square. Clark, Turner, Williams........................476–82
Level Recorder, A Square-Law Power-. Clark, Turner, Williams........................476–82
Life of Incandescent Lamps, Saving Time in Testing. Purcell........................730–2
(Light) Measurements of Erythemal Energy. Scott........................725–9
(Light) Saving Time in Testing Life of Incandescent Lamps. Purcell........................730–2
Lightning Investigation on a Rural Distribution System. MacCarthy, Stann, Edge, McKinley........................428–37; disc. 437
Lightning Measurements, Advances in Technique of. Brownlee........................515–19
Lightning Strokes, Transmission Line Design and Performance Based on Direct. Harder, Clayton........................439–46; disc. 447
Limiting Means on High Interrupting Capacity Controllers, The Use of Air-Core Reactors as Fault. Leitch........................469–74; disc. 474
Line at Carrier Current Frequencies, Loss Measurements Made on Underground-Cable Overhead-Conductor 132-Kv Transmission. Cornelius, Storer........................597–601
Line Conductor, Hy-Therm Copper—An Improved Overhead-. Hickernell, Jones, Snyder........................22–7; disc. 27
Line Design and Performance Based on Direct Lightning Strokes, Transmission. Harder, Clayton........................439–46; disc. 447
Line Joints by Means of a Bolometer, Detection of Overheated Transmission. Leslie, Wait........................64–8; disc. 68
Line Tuning Equipment Used With Coaxial Cable for Carrier Current Installation on Power Lines. Sutton........................44–8; disc. 48
Linear Vibration Problems, Summary of Transformations Useful in Constructing Analogs of. Corbett........................661–4
Lines Along Uniformly Rotating Reference Frames, Stationary Networks and Transmission. Kron........................690–6
Lines, Comparative Performance Records—Steel and Wood Transmission. Booker.....686–9; disc. 689
Lines, Rubber Insulators for Pole. Wheeler, Markley........................195–7
Load Losses Measured in D-C Motors, Stray. (Committee Report)...............219–23; disc. 223
Load, Some Fundamentals of D-C Controlled Reactors with Resistive. Storm..........188–94; disc. 194
Load, The Heat Pump—Its Significance as a Potential Residential Electric. Bary........................1–8
Loading of a Transformer System, Economic. Levine, Smith........................733–8; disc. 738
Loads on A-C Generators, A Semiempirical Approach to Voltage Dip—with Suddenly Applied. Rosenberg........................160–6; disc. 166
Loci for Servomechanism Components and Systems, Graphical Determination of Transfer Function. Thomas, Easton...............307–14; disc. 314
Loci of the Synchronous Tie, The Geometric. Finzi, Wellard........................168–71
Locomotives, Electric Equipment for Chesapeake and Ohio Railway Company Steam Turbine-Electric. Atwell, Baston........................145–8
Locomotives in Railroad Service, Application Engineering on Diesel-Electric. Bevan............125–31
Locomotives, Industrial Plants Prefer Diesel-Electric Switching. Woods........................697–700
Logic of Relay Circuits, The. Keister..........571–6
Long-Time and Short-Time Analog Computers, Comparison of. Paschkis........................70–3
Looms, Selection of Electric Drives for. Demartini, Lukens........................349–56
Loss at High Frequencies and Under Changing Temperature, The Measurement of Dielectric. Whitehead, Rueggeberg........................520–4

Loss Measurements Made on Underground-Cable Overhead-Conductor 132-Kv Transmission Line at Carrier Current Frequencies. Cornelius, Storer......597–601

Losses in Series Motors, Armature Iron. Chang, Karr......262–4; disc. 264

Losses Measured in D-C Motors, Stray Load. (Committee Report)......219–23; disc. 223

M

Machine, The Negative-Sequence Reactances of an Ideal Synchronous. Duesterhoeft......510–13; disc. 513

Machines and Its Effects on Radio Influence Voltage Generation, Commutation of D-C. Motter......491–5; disc. 495

Machines, Temperature Rise Values for D-C. (Committee Report)......206–12; disc. 212

Magnetic Amplifiers with Feedback, Analytical Determination of Characteristics of. VerPlanck, Finzi, Beaumariage......565–70

Magnetic Field Components of Circular Filaments and Solenoids, Formulas and Tables for the Calculation of the. Grover......665–75

Magnetic Recording, Application of Experimental Test Procedures and Methods of Analysis of Results to Research Problems in. Thompson......407–17

Magnetic Saturation, Nonharmonic Oscillations as Caused by. Rudenberg......676–85

Manholes and Vaults: Design and Ventilation, Transformer. Porter......534–9

Manually-Operated Spring Mechanism for Medium Voltage Oilless Circuit Breakers, A. Wyman, Casey......357–61; disc. 361

Means on High Interrupting Capacity Controllers, The Use of Air-Core Reactors as Fault Limiting. Leitch......469–74; disc. 474

Measurement of Dielectric Loss at High Frequencies and Under Changing Temperature, The. Whitehead, Rueggeberg......520–4

Measurements, Advances in Technique of Lightning. Brownlee......515–19

Measurements Made on Underground-Cable Overhead-Conductor 132-Kv Transmission Line at Carrier Current Frequencies, Loss. Cornelius, Storer......597–601

Measurements of Erythemal Energy. Scott....725–9

Mechanics and Servomechanisms, Application of the California Institute of Technology Electric Analog Computer to Nonlinear. McCann, Wilts, Locanthi......652–60

Mechanism for Medium Voltage Oilless Circuit Breakers, A Manually-Operated Spring. Wyman, Casey......357–61; disc. 361

Meter, A New Thermal Volt-Ampere Demand. Douglass, Morong......79–83; disc. 83

Meter, Surge Protection in a Modern Watt-Hour. Busch, Williams......74–7; disc. 77

Method for Estimating the Performance of Distance Relays During Faults and Power Swings, Graphical. Warrington......608–20; disc. 620

Methods Applied to Frequency Response Curves, Control Chart. Mundel......424–7

Methods for Determining the Effects of Contaminants on Electrical Insulation. Mathes, Sieffert, Walker, Lindsey......113–18; disc. 118

Methods of Analysis of Results to Research Problems in Magnetic Recording, Application of Experimental Test Procedures and. Thompson..407–17

Microwave Channels for Power System Applications. (Committee Report)......40–2; disc. 42

Microwave Communication Relay System, A. Boothroyd, Churchill......637–41

Microwave Relay Systems, Power Supplies for. Ward......631–6

Mobile Radio Systems, Vibrating Reed Selectors for. Keller, Bostwick......383–6

Mobile Telephone Use, Vibrating Reed Selective Signaling System for. Pruden, Hoth......387–91

Modern Watt-Hour Meter, Surge Protection in a. Busch, Williams......74–7; disc. 77

Moisture in Soil, The Thermal Movement of. Mickley......330–3; disc. 333

Motive Power, The Renaissance of Electric. Candee......138–44

Motor, The Field Fluxes of the Shaded-Pole. Kimberly......273–7

Motor Vehicle Power Systems, Selenium Rectifiers in. Ramsey......149–53; disc. 153

Motors and Generators, Solid Short Circuit of D-C. Linville, Ward......119–23; disc. 123

Motors, Armature Iron Losses in Series. Chang, Karr......262–4; disc. 264

Motors, Die-Cast Rotors for Induction. Packer......253–60; disc. 260

Motors—Experimental Study of Speed-Torque Curves, Dynamic Braking Control of D-C Series. Heumann......560–4

Motors, Stray Load Losses Measured in D-C. (Committee Report)......219–23; disc. 223

Motors, Twenty-Five Years Progress in the Design of Traction. Baldwin......132–7

Movement of Moisture in Soil, The Thermal. Mickley......330–3; disc. 333

Multifrequency Pulsing in Switching, Application of. Dahlbom, Horton, Moody......392–6

Multiplexing System, A Time Division. Boothroyd, Creamer......92–7

N

Negative-Sequence Reactances of an Ideal Synchronous Machine, The. Duesterhoeft...510–13; disc. 513

Network, Improvements to Oklahoma City Primary. Brady......701–02; disc. 702

Network Systems in the Washington Area, Design and Experience With 4-Kv Primary. Lank......712–16; disc. 716

Networks and Transmission Lines Along Uniformly Rotating Reference Frames. Kron......690–6

Networks on the Duquesne Light Company System, Primary. Holben, Lange......704–09; disc. 709

New 69-Kv Compressed-Air Circuit Breaker, A. Baker, Frisch......363–8; disc. 369

New Expanded Scale A-C Voltmeter, A. Millar..641–3

Noise Problems on an Electric Power System, Transformer Audio. Murray......740–7; disc. 747

Nonharmonic Oscillations as Caused by Magnetic Saturation. Rudenberg......676–85

Nonlinear Mechanics and Servomechanisms, Application of the California Institute of Technology Electric Analog Computer to. McCann, Wilts, Locanthi......652–60

O

Oil, High-Pressure Gas-Filled Cable Impregnated with Extra-High-Viscosity. Sticher, Doan, Atkinson, Meyerhoff......336–45; disc. 345

Oilless Circuit Breakers, A Manually-Operated Spring Mechanism for Medium Voltage. Wyman, Casey......357–61; disc. 361

Oklahoma City Primary Network, Improvements to. Brady......701–02; disc. 702

Operated Spring Mechanism for Medium Voltage Oilless Circuit Breakers, A Manually-. Wyman, Casey......357–61; disc. 361

Operating Characteristics of Two-Phase Servomotors. Koopman......319–27; disc. 327

Operation in Rhode Island, Trackless Trolley. Blomquist......397–402

Optical Shutter for Photographic Purposes, An Electro-. Zarem, Marshall, Poole......84–91

Oscillations as Caused by Magnetic Saturation, Nonharmonic. Rudenberg......676–85

Oscillographing Commutation. Baldwin......100–05; disc. 105

Outage Rates of Steam Turbines and Boilers and of Hydro Units. (Committee Report)......450–7

Overhead-Conductor 132-Kv Transmission Line at Carrier Current Frequencies, Loss Measurements Made on Underground-Cable. Cornelius, Storer......597–601

Overhead-Line Conductor, Hy-Therm Copper—An Improved. Hickernell, Jones, Snyder......22–7; disc. 27

Overheated Transmission Line Joints by Means of a Bolometer, Detection of. Leslie, Wait......64–8; disc. 68

Overheating Protection Under Running Overload Conditions, Fundamental Theory of Inherent-. Veinott, Schaefer......266–70; disc. 270

Overload Conditions, Fundamental Theory of Inherent-Overheating Protection Under Running. Veinott, Schaefer......266–70; disc. 270

P

Performance Based on Direct Lightning Strokes, Transmission Line Design and. Harder, Clayton......439–46; disc. 447

Performance of Diesel-Electric Rig for Deep-Well Drilling. Clark, Moore......497–506

Performance of Distance Relays During Faults and Power Swings, Graphical Method for Estimating the. Warrington......608–20; disc. 620

Performance of Servomechanisms, Comparison of Steady-State and Transient. Chestnut, Mayer......765–77

Performance Records—Steel and Wood Transmission Lines, Comparative. Booker......686–9; disc. 689

Philadelphia, 69-Kv Pipe-Type Cable Circuits in. Kidder, Van Antwerp......550–6; disc. 556

Photographic Purposes, An Electro-Optical Shutter for. Zarem, Marshall, Poole......84–91

Pipe-Type Cable Circuits in Philadelphia, 69-Kv. Kidder, Van Antwerp......550–6; disc. 556

Pipes, The Temperature Rise of Buried Cables and. Neher......9–17; disc. 17

Plant, A 3,000-Horsepower Gas Turbine Power. Haverstick......458–60

Plants Prefer Diesel-Electric Switching Locomotives, Industrial. Woods......697–700

Polar Vector Indicator. Walker, Waynick, Sulzer......154–9

Pole Lines, Rubber Insulators for. Wheeler, Markley......195–7

Pole Motor, The Field Fluxes of the Shaded-. Kimberly......273–7

Potential Residential Electric Load, The Heat Pump—Its Significance as a. Bary......1–8

Power Factor of Unbalanced Sinusoidal 3-Phase Circuits, The Vector. Lamb, Brandt......507–09

Power-Flow Studies, Equivalent Circuits for. Ward......373–80; disc. 380

Power Generation and Other Applications, Two Gas Turbines for. Howard......461–5; disc. 465

Power Generation, Gas Turbines in Stationary. Hague......467–8

(Power Generation) Outage Rates of Steam Turbines and Boilers and of Hydro Units. (Committee Report)......450–7

(Power Generation) The Transient Behavior of the Two-Stage Rototrol Main Exciter Voltage Regulating System as Determined by Electrical Analogy. Carleton......59–63

Power-Level Recorder, A Square-Law. Clark, Turner, Williams......476–82

Power Lines, Line Tuning Equipment Used With Coaxial Cable for Carrier Current Installation on. Sutton......44–8; disc. 48

Power Plant, A 3,000-Horsepower Gas Turbine. Haverstick......458–60

Power Rating of Radio-Frequency Cables, The. Mildner......289–98; disc. 298

Power Supplies for Coaxial Systems. Spencer..627–30

Power Supplies for Microwave Relay Systems. Ward......631–6

Power Swings, Graphical Method for Estimating the Performance of Distance Relays During Faults and. Warrington......608–20; disc. 620

Power System Applications, Microwave Channels for. (Committee Report)......40–2; disc. 42

Power System, Transformer Audio Noise Problems on an Electric. Murray......740–7; disc. 747

Power Systems, Selenium Rectifiers in Motor Vehicle. Ramsey......149–53; disc. 153

Power, The Renaissance of Electric Motive. Candee......138–44

Power Transformers, Controlled Temperature and Insulation Protection in the Operation of. Satterlee, Reed......753–8; disc. 759

Pressure Gas-Filled Cable Impregnated with Extra-High-Viscosity Oil, High-. Sticher, Doan, Atkinson, Meyerhoff......336–45; disc. 345

Primary Network, Improvements to Oklahoma City. Brady......701–02; disc. 702

Primary Network Systems in the Washington Area, Design and Experience With 4-Kv. Lank......712–16; disc. 716

Primary Networks on the Duquesne Light Company System. Holben, Lange......704–09; disc. 709

Problems in Magnetic Recording, Application of Experimental Test Procedures and Methods of Analysis of Results to Research. Thompson......407–17

Problems on an Electric Power System, Transformer Audio Noise. Murray......740–7; disc. 747

Problems, Summary of Transformations Useful in Constructing Analogs of Linear Vibration. Corbett......661–4

Procedures and Methods of Analysis of Results to Research Problems in Magnetic Recording, Application of Experimental Test. Thompson....407–17

Progress in the Design of Traction Motors, Twenty-Five Years. Baldwin......132–7

Protection in a Modern Watt-Hour Meter, Surge. Busch, Williams......74–7; disc. 77

Protection in the Operation of Power Transformers, Controlled Temperature and Insulation. Satterlee, Reed......753–8; disc. 759

Protection of Stations Without High-Voltage Switching. (Committee Report)......226–31; disc. 231

Protection, Shipshaw Relay. Madill, Duffy......50–5; disc. 55

Protection Under Running Overload Conditions, Fundamental Theory of Inherent-Overheating. Veinott, Schaefer......266–70; disc. 270

(Protective Devices) Lightning Investigation on a Rural Distribution System. MacCarthy, Stann, Edge, McKinley......428–37; disc. 437

(Protective Devices) Voltage-Recovery Characteristics of Distribution Systems. Witzke......172–80; disc. 180

Pulsing in Switching, Application of Multifrequency. Dahlbom, Horton, Moody......392–6

Pump—Its Significance as a Potential Residential Electric Load, The Heat. Bary..........1–8

R

Radio-Frequency Cables, Heating of. Macalpine..........283–8
Radio-Frequency Cables, The Power Rating of. Mildner..........289–98; disc. 298
Radio-Frequency Heating Equipment, Reduction of Interference from. Klingaman..718–24; disc. 724
Radio Influence from High-Voltage Corona. Slemon..........198–204; disc. 204
Radio Influence Voltage Generation, Commutation of D-C Machines and Its Effects on. Motter..........491–5; disc. 495
Radio Systems, Vibrating Reed Selectors for Mobile. Keller, Bostwick..........383–6
Radiosonde Recorder, Automatic Range-Adjusting. Beggs..........602–07
Railroad Service, Application Engineering on Diesel-Electric Locomotives in. Bevan..........125–31
Railway Company Steam Turbine-Electric Locomotives, Electric Equipment for Chesapeake and Ohio. Atwell, Baston..........145–8
Range Adjustable-Speed Drive, A Wide-. Conrad, Tribken..........789–90
Range-Adjusting Radiosonde Recorder, Automatic. Beggs..........602–07
Rates of Steam Turbines and Boilers and of Hydro Units, Outage. (Committee Report)..........450–7
Rating of Radio-Frequency Cables, The Power. Mildner..........289–98; disc. 298
Reactances of an Ideal Synchronous Machine, The Negative-Sequence. Duesterhoeft.510–13; disc. 513
Reactors as Fault Limiting Means on High Interrupting Capacity Controllers, The Use of Air-Core. Leitch..........469–74; disc. 474
Reactors, Universal Curves for D-C Controllable. Johnson, Merrell, Alley..........31–7; disc. 37
Reactors with Resistive Load, Some Fundamentals of D-C Controlled. Storm..........188–94; disc. 194
Recorder, A Square-Law Power-Level. Clark, Turner, Williams..........476–82
Recorder, Automatic Range-Adjusting Radiosonde. Beggs..........602–07
Recording, Application of Experimental Test Procedures and Methods of Analysis of Results to Research Problems in Magnetic. Thompson..........407–17
Records—Steel and Wood Transmission Lines, Comparative Performance. Booker....686–9; disc. 689
Recovery Characteristics of Distribution Systems, Voltage-. Witzke..........172–80; disc. 180
Rectifier Fault Currents—II. Herskind, Schmidt, Rettig..........243–51; disc. 251
Rectifiers in Motor Vehicle Power Systems, Selenium. Ramsey..........149–53; disc. 153
Reduction of Interference from Radio-Frequency Heating Equipment. Klingaman....718–24; disc. 724
Reed Selective Signaling System for Mobile Telephone Use, Vibrating. Pruden, Hoth..........387–91
Reed Selectors for Mobile Radio Systems, Vibrating. Keller, Bostwick..........383–6
Reference Frames, Stationary Networks and Transmission Lines Along Uniformly Rotating. Kron..........690–6
Regulating System as Determined by Electrical Analogy, The Transient Behavior of the Two-Stage Rototrol Main Exciter Voltage. Carleton..........59–63
Relay Circuits, Sequential Aspects of. Ritchie..577–81
Relay Circuits, The Logic of. Keister..........571–6
Relay Developments, Electronic. Loving..........233–40; disc. 240
Relay Protection, Shipshaw. Madill, Duffy..........50–5; disc. 55
Relay System, A Microwave Communication. Boothroyd, Churchill..........637–41
Relay Systems, Power Supplies for Microwave. Ward..........631–6
Relay "Trees" and Symmetric Circuits. Washburn..........582–6
Relays, Counting with. Frost..........587–91
Relays During Faults and Power Swings, Graphical Method for Estimating the Performance of Distance. Warrington..........608–20; disc. 620
Remote Control of Coaxial Cable Stations, B-1 Alarm and Control System for. Hearn, Weber....622–6
Renaissance of Electric Motive Power, The. Candee..........138–44
Research Problems in Magnetic Recording, Application of Experimental Test Procedures and Methods of Analysis of Results to. Thompson..........407–17
Residential Electric Load, The Heat Pump—Its Significance as a Potential. Bary..........1–8
Resistive Load, Some Fundamentals of D-C Controlled Reactors with. Storm..........188–94; disc. 194
Response Curves, Control Chart Methods Applied to Frequency. Mundel..........424–7
Results to Research Problems in Magnetic Recording, Application of Experimental Test Procedures and Methods of Analysis of. Thompson..........407–17
Rhode Island, Trackless Trolley Operation in. Blomquist..........397–402
Rig for Deep-Well Drilling, Performance of Diesel-Electric. Clark, Moore..........497–506
Rise of Buried Cables and Pipes, The Temperature. Neher..........9–17; disc. 17
Rise of Cables in a Duct Bank, The Temperature. Neher..........540–6; disc. 546
Rise Values for D-C Machines, Temperature. (Committee Report)..........206–12; disc. 212
Rooms, Electrically Charged Dust in. Penney, Hewitt..........278–82
(Rotating Machinery) A Semiempirical Approach to Voltage Dip—with Suddenly Applied Loads on A-C Generators. Rosenberg......160–6; disc. 166
(Rotating Machinery) A Wide-Range Adjustable-Speed Drive. Conrad, Tribken..........789–90
(Rotating Machinery) Armature Iron Losses in Series Motors. Chang, Karr..........262–4; disc. 264
(Rotating Machinery) Die-Cast Rotors for Induction Motors. Packer..........253–60; disc. 260
(Rotating Machinery) Effects of Commutator Surface Film Conditions on Commutation. Lynn, Elsey..........106–12; disc. 112
(Rotating Machinery) Fundamental Theory of Inherent-Overheating Protection Under Running Overload Conditions. Veinott, Schaefer..........266–70; disc. 270
(Rotating Machinery) Methods for Determining the Effects of Contaminants on Electrical Insulation. Mathes, Sieffert, Walker, Lindsey..........113–18; disc. 118
(Rotating Machinery) Operating Characteristics of Two-Phase Servomotors. Koopman..........319–27; disc. 327
(Rotating Machinery) Oscillographing Commutation. Baldwin..........100–05; disc. 105
(Rotating Machinery) Solid Short Circuit of D-C Motors and Generators. Linville, Ward..119–23; disc. 123
(Rotating Machinery) Stray Load Losses Measured in D-C Motors. (Committee Report)..........219–23; disc. 223
(Rotating Machinery) The Field Fluxes of the Shaded-Pole Motor. Kimberly..........273–7
(Rotating Machinery) The Geometric Loci of the Synchronous tie. Finzi, Wellard..........168–71
(Rotating Machinery) The Negative-Sequence Reactances of an Ideal Synchronous Machine. Duesterhoeft..........510–13; disc. 513
Rotating Reference Frames, Stationary Networks and Transmission Lines Along Uniformly. Kron..........690–6
Rotors for Induction Motors, Die-Cast. Packer..........253–60; disc. 260
Rototrol Main Exciter Voltage Regulating System as Determined by Electrical Analogy, The Transient Behavior of the Two-Stage. Carleton......59–63
Rubber Insulators for Pole Lines, Wheeler, Markley..........195–7
Running Overload Conditions, Fundamental Theory of Inherent-Overheating Protection Under. Veinott, Schaefer..........266–70; disc. 270
Rural Distribution System, Lightning Investigation on a. MacCarthy, Stann, Edge, McKinley..........428–37; disc. 437

S

Saturation, Nonharmonic Oscillations as Caused by Magnetic. Rudenberg..........676–85
Saving Time in Testing Life of Incandescent Lamps. Purcell..........730–2
Scale A-C Voltmeter, A New Expanded. Millar..641–3
Secondary Conductor Economics, Distribution Transformer and. Brady..........483–6; disc. 486
Selection of Electric Drives for Looms. Demartini, Lukens..........349–56
Selective Signaling System for Mobile Telephone Use, Vibrating Reed. Pruden, Hoth..........387–91
Selectors for Mobile Radio Systems, Vibrating Reed. Keller, Bostwick..........383–6
Selenium Rectifiers in Motor Vehicle Power Systems. Ramsey..........149–53; disc. 153
Semiempirical Approach to Voltage Dip—with Suddenly Applied Loads on A-C Generators, A. Rosenberg..........160–6; disc. 166
Sequence Reactances of an Ideal Synchronous Machine, The Negative-. Duesterhoeft....510–13; disc. 513
Sequential Aspects of Relay Circuits. Ritchie...577–81
Series Motors, Armature Iron Losses in. Chang, Karr..........262–4; disc. 264
Series Motors—Experimental Study of Speed-Torque Curves, Dynamic Braking Control of D-C. Heumann..........560–4
Servomechanisms, Application of the California Institute of Technology Electric Analog Computer to Nonlinear Mechanics and. McCann, Wilts, Locanthi..........652–60
Servomechanisms, Comparison of Steady-State and Transient Performance of. Chestnut, Mayer..........765–77
Servomechanism Components and Systems, Graphical Determination of Transfer Function Loci for. Thomas, Easton..........307–14; disc. 314
Servomechanisms, Damper Stabilized Instrument. Hall..........299–306; disc. 306
(Servomechanisms) Instrument Inaccuracies in Feed-Back Control Systems with Particular Reference to Backlash. Marcy, Yachter, Zauderer......778–88
Servomotors, Operating Characteristics of Two-Phase. Koopman..........319–27; disc. 327
Shaded-Pole Motor, The Field Fluxes of the. Kimberly..........273–7
Shipshaw Relay Protection. Madill, Duffy..........50–5; disc. 55
Short Circuit of D-C Motors and Generators, Solid. Linville, Ward..........119–23; disc. 123
Short-Time Analog Computers, Comparison of Long-Time and. Paschkis..........70–3
Shutter for Photographic Purposes, An Electro-Optical. Zarem, Marshall, Poole..........84–91
Signaling System for Mobile Telephone Use, Vibrating Reed Selective. Pruden, Hoth..........387–91
Sinusoidal 3-Phase Circuits, The Vector Power Factor of Unbalanced. Lamb, Brandt..........507–09
Soil, The Thermal Movement of Moisture in. Mickley..........330–3; disc. 333
Solenoids, Formulas and Tables for the Calculation of the Magnetic Field Components of Circular Filaments and. Grover..........665–75
Solid Short Circuit of D-C Motors and Generators. Linville, Ward..........119–23; disc. 123
Some Fundamentals of D-C Controlled Reactors with Resistive Load. Storm..........188–94; disc. 194
Speed, Considerations on Facsimile Transmission. Burkhard..........418–23; disc. 423
Speed Drive, A Wide-Range Adjustable-. Conrad, Tribken..........789–90
Speed-Torque Curves, Dynamic Braking Control of D-C Series Motors—Experimental Study of. Heumann..........560–4
Spring Mechanism for Medium Voltage Oilless Circuit Breakers, A Manually-Operated. Wyman, Casey..........357–61; disc. 361
Square-Law Power-Level Recorder, A. Clark, Turner, Williams..........476–82
Stability of the Welding Arc, Instrumentation for the Evaluation of the. Winsor, Schetky, Wyant..........525–33
Stabilized Instrument Servomechanisms, Damper. Hall..........299–306; disc. 306
Stationary Networks and Transmission Lines Along Uniformly Rotating Reference Frames. Kron..........690–6
Stationary Power Generation, Gas Turbines in. Hague..........467–8
Stations, B-1 Alarm and Control System for Remote Control of Coaxial Cable. Hearn, Weber..622–6
Stations Without High-Voltage Switching, Protection of. (Committee Report)..........226–31; disc. 231
Steady-State and Transient Performance of Servomechanisms, Comparison of. Chestnut, Mayer..........765–77
Steam Turbine-Electric Locomotives, Electric Equipment for Chesapeake and Ohio Railway Company. Atwell, Baston..........145–8
Steam Turbines and Boilers and of Hydro Units, Outage Rates of. (Committee Report)..........450–7
Steel and Wood Transmission Lines, Comparative Performance Records—. Booker.....686–9; disc. 689
Stray Load Losses Measured in D-C Motors. (Committee Report)..........219–23; disc. 223
Strokes, Transmission Line Design and Performance Based on Direct Lightning. Harder, Clayton..........439–46; disc. 447
Studies, Equivalent Circuits for Power-Flow. Ward..........373–80; disc. 380
Suddenly Applied Loads on A-C Generators, A Semiempirical Approach to Voltage Dip—with. Rosenberg..........160–6; disc. 166
Summary of Transformations Useful in Constructing Analogs of Linear Vibration Problems. Corbett..........661–4
Supplies for Coaxial Systems, Power. Spencer..627–30
Supplies for Microwave Relay Systems, Power. Ward..........631–6
Surface Film Conditions on Commutation, Effects of Commutator. Lynn, Elsey......106–12; disc. 112
Surge Protection in a Modern Watt-Hour Meter. Busch, Williams..........74–7; disc. 77
Swings, Graphical Method for Estimating the Performance of Distance Relays During Faults and Power. Warrington..........608–20; disc. 620
(Switchgear) A Manually-Operated Spring Mechanism for Medium Voltage Oilless Circuit Breakers. Wyman, Casey..........357–61; disc. 361

(Switchgear) A New 69-Kv Compressed-Air Circuit Breaker. Baker, Frisch..........363-8; disc. 369
Switching, Application of Multifrequency Pulsing in. Dahlbom, Horton, Moody..........392-6
Switching Locomotives, Industrial Plants Prefer Diesel-Electric. Woods..........697-700
Switching, Protection Stations Without High-Voltage. (Committee Report)..........226-31; disc. 231
Symmetric Circuits, Relays "Trees" and. Washburn..........582-6
Synchronous Machine, The Negative-Sequence Reactances of an Ideal. Duesterhoeft..........510-13; disc. 513
Synchronous Tie, The Geometric Loci of the. Finzi, Wellard..........168-71
System, A Microwave Communication Relay. Boothroyd, Churchill..........637-41
System, A Time Division Multiplexing. Boothroyd, Creamer..........92-7
System Applications, Microwave Channels for Power. (Committee Report)..........40-2; disc. 42
System as Determined by Electrical Analogy, The Transient Behavior of the Two-Stage Rototrol Main Exciter Voltage Regulating. Carleton..........59-63
System, Economic Loading of a Transformer. Levine, Smith..........733-8; disc. 738
System for Mobile Telephone Use, Vibrating Reed Selective Signaling. Pruden, Hoth..........387-91
System for Remote Control of Coaxial Cable Stations, B-1 Alarm and Control. Hearn, Weber..........622-6
System, Lightning Investigation on a Rural Distribution. MacCarthy, Stann, Edge, McKinley..........428-37; disc. 437
System, Primary Networks on the Duquesne Light Company. Holben, Lange..........704-09; disc. 709
System, Transformer Audio Noise Problems on an Electric Power. Murray..........740-7; disc. 747
Systems, Graphical Determination of Transfer Function Loci for Servomechanism Components and. Thomas, Easton..........307-14; disc. 314
Systems in the Washington Area, Design and Experience with 4-Kv Primary Network. Lank..........712-16; disc. 716
Systems, Power Supplies for Coaxial. Spencer..........627-30
Systems, Power Supplies for Microwave Relay. Ward..........631-6
Systems, Slenium Rectifiers in Motor Vehicle Power. Ramsey..........149-53; disc. 153
Systems, Vibrating Reed Selectors for Mobile Radio. Keller, Bostwick..........383-6
Systems, Voltage-Recovery Characteristics of Distribution. Witzke..........172-80; disc. 180
Systems with Particular Reference to Backlash, Instrument Inaccuracies in Feed-Back Control. Marcy, Yachter, Zauderer..........778-88

T

Tables for the Calculation of the Magnetic Field Components of Circular Filaments and Solenoids, Formulas and. Grover..........665-75
Technique of Lightning Measurements, Advances in. Brownlee..........515-19
Telephone Use, Vibrating Reed Selective Signaling System, for Mobile. Pruden, Hoth..........387-91
Temperature and Insulation Protection in the Operation of Power Transformers, Controlled. Satterlee, Reed..........753-8; disc. 759
Temperature Rise of Buried Cables and Pipes, The. Neher..........9-17; disc. 17
Temperature Rise of Cables in a Duct Bank, The. Neher..........540-6; disc. 546
Temperature Rise Values for D-C Machines. (Committee Report)..........206-12; disc. 212
Temperature, The Measurement of Dielectric Loss at High Frequencies and Under Changing. Whitehead, Rueggeberg..........520-4
Test Procedures and Methods of Analysis of Results to Research Problems in Magnetic Recording, Application of Experimental. Thompson..........407-17
Theory of Inherent-Overheating Protection Under Running Overload Conditions, Fundamental. Veinott, Schaefer..........266-70; disc. 270
Thermal Movement of Moisture in Soil, The. Mickley..........330-3; disc. 333
Thermal Volt-Ampere Demand Meter, A New. Douglass, Morong..........79-83; disc. 83
Three-Phase Circuits, The Vector Power Factor of Unbalanced Sinusoidal. Lamb, Brandt..........507-09
Tie, The Geometric Loci of the Synchronous. Finzi, Wellard..........168-71
Time Division Multiplexing System, A. Boothroyd, Creamer..........92-7
Time in Testing Life of Incandescent Lamps, Saving. Purcell..........730-2
Torque Curves, Dynamic Braking Control of D-C Series Motors—Experimental Study of Speed-. Heumann..........560-4
Trackless Trolly Operation in Rhode Island. Blomquist..........397-402
Traction Motors, Twenty-Five Years Progress in the Design of. Baldwin..........132-7
Transfer Function Loci for Servomechanism Components and Systems, Graphical Determination of. Thomas, Easton..........307-14; disc. 314
Transformations Useful in Constructing Analogs of Linear Vibration Problems, Summary of. Corbett..........661-4
Transformer and Secondary Conductor Economics, Distribution. Brady..........483-6; disc. 486
Transformer Audio Noise Problems on an Electric Power System. Murray..........740-7; disc. 747
Transformer Manholes and Vaults: Design and Ventilation. Porter..........534-9
(Transformer) Some Fundamentals of D-C Controlled Reactors with Resistive Load. Storm..........188-94; disc. 194
Transformer System, Economic Loading of a. Levine, Smith..........733-8; disc. 738
(Transformer) Universal Curves for D-C Controllable Reactors. Johnson, Merrell, Alley..........31-7; disc. 37
(Transformers) A Small High-Voltage Bushing Design for High Altitudes. Vogel, Hart..........761-4
Transformers, Controlled Temperature and Insulation Protection in the Operation of Power. Satterlee, Reed..........753-8; disc. 759
Transient Behavior of the Two-Stage Rototrol Main Exciter Voltage Regulating System as Determined by Electrical Analogy, The. Carleton..........59-63
Transient Performance of Servomechanisms, Comparison of Steady-State and. Chestnut, Mayer..........765-77
Translations, Codes and. Myers..........592-7
(Transmission) Design and Experience With 4-Kv Primary Network Systems in the Washington Area. Lank..........712-16; disc. 716
(Transmission) Hy-Therm Copper—An Improved Overhead-Line Conductor. Hickernell, Jones, Snyder..........22-7; disc. 27
(Transmission) Improvements to Oklahoma City Primary Network. Brady..........701-02; disc. 702
Transmission Line at Carrier Current Frequencies, Loss Measurements Made on Underground-Cable Overhead-Conductor 132-Kv. Cornelius, Storer..........597-601
Transmission Line Design and Performance Based on Direct Lightning Strokes. Harder, Clayton..........439-46; disc. 447
Transmission Line Joints by Means of a Bolometer, Detection of Overheated. Leslie, Wait..........64-8; disc. 68
Transmission Lines Along Uniformly Rotating Reference Frames, Stationary Networks and. Kron..........690-6
Transmission Lines, Comparative Performance Records—Steel and Wood. Booker..........686-9; disc. 689
(Transmission) Primary Networks on the Duquesne Light Company System. Holben, Lange..........704-09; disc. 709
Transmission Speed, Considerations on Facsimile. Burkhard..........418-23; disc. 423
(Transportation, Land) Application Engineering on Diesel-Electric Locomotives in Railroad Service. Bevan..........125-31
(Transportation, Land) Electric Equipment for Chesapeake and Ohio Railway Company Steam Turbine-Electric Locomotives. Atwell, Baston..........145-8
(Transportation, Land) Industrial Plants Prefer Diesel-Electric Switching Locomotives. Woods..........697-700
(Transportation, Land) Selenium Rectifiers in Motor Vehicle Power Systems. Ramsey, 149-53; disc. 153
(Transportation, Land) The Renaissance of Electric Motive Power. Candee..........138-44
(Transportation, Land) Trackless Trolley Operation in Rhode Island. Blomquist..........397-402
(Transportation, Land) Trolley Coaches Replace Busses. McMillon..........403-06
(Transportation, Land) Twenty-Five Years Progress in the Design of Traction Motors. Baldwin..........132-7
"Trees" and Symmetric Circuits, Relay. Washburn..........582-6
Trolley Coaches Replace Busses. McMillon..........403-06
Trolley Operation in Rhode Island, Trackless. Blomquist..........397-402
Tuning Equipment Used With Coaxial Cable for Carrier Current Installation on Power Lines, Line. Sutton..........44-8; disc. 48
Turbines and Boilers and of Hydro Units, Outage Rates of Steam. (Committee Report)..........450-7
Turbine-Electric Locomotives, Electric Equipment for Chesapeake and Ohio Railway Company Steam. Atwell, Baston..........145-8
Turbine Power Plant, A 3,000-Horsepower Gas. Haverstick..........458-60
Turbines for Power Generation and Other Applications, Two Gas. Howard..........461-5; disc. 465
Turbines in Stationary Power Generation, Gas. Hague..........467-8
Twenty-Five Years Progress in the Design of Traction Motors. Baldwin..........132-7
Two Gas Turbines for Power Generation and Other Applications. Howard..........461-5; disc. 465
Two-Phase Servomotors, Operating Characteristics of. Koopman..........319-27; disc. 327
Two-Stage Rototrol Main Exciter Voltage Regulating System as Determined by Electrical Analogy, The Transient Behavior of the. Carleton..........59-63

U

Unbalanced Sinusoidal 3-Phase Circuits, The Vector Power Factor of. Lamb, Brandt..........507-09
Underground-Cable Overhead-Conductor 132-Kv Transmission Line at Carrier Current Frequencies, Loss Measurements Made on. Cornelius, Storer..........597-601
Universal Curves for D-C Controllable Reactors. Johnson, Merrell, Alley..........31-7; disc. 37
Use of Air-Core Reactors as Fault Limiting Means on High Interrupting Capacity Controllers, The. Leitch..........469-74; disc. 474

V

Values for D-C Machines, Temperature Rise. (Committee Report)..........206-12; disc. 212
Vaults: Design and Ventilation, Transformer Manholes and. Porter..........534-9
Vector Indicator, Polar. Walker, Waynick, Sulzer..........154-9
Vector Power Factor of Unbalanced Sinusoidal 3-Phase Circuits, The. Lamb, Brandt..........507-09
Vehicle Power Systems, Selenium Rectifiers in Motor. Ramsey..........149-53; disc. 153
Ventilation, Transformer Manholes and Vaults: Design and. Porter..........534-9
Vibrating Reed Selective Signaling System for Mobile Telephone Use. Pruden, Hoth..........387-91
Vibrating Reed Selectors for Mobile Radio Systems. Keller, Bostwick..........383-6
Vibration Problems, Summary of Transformations Useful in Constructing Analogs of Linear. Corbett..........661-4
Viscosity Oil, High-Pressure Gas-Filled Cable Impregnated with Extra-High-. Sticher, Doan, Atkinson, Meyerhoff..........336-45; disc. 345
Voltage Dip—with Suddenly Applied Loads on A-C Generators, A Semiempirical Approach to. Rosenberg..........160-6; disc. 166
Voltage Generation, Commutation of D-C Machines and Its Effects on Radio Influence. Motter..........491-5; disc. 495
Voltage Oilless Circuit Breakers, A Manually-Operated Spring Mechanism for Medium. Wyman, Casey..........357-61; disc. 361
Voltage Recovery Characteristics of Distribution Systems. Witzke..........172-80; disc. 180
Voltage Regulating System as Determined by Electrical Analogy, The Transient Behavior of the Two-Stage Rototrol Main Exciter. Carleton..........59-63
Volt-Ampere Demand Meter, A New Thermal. Douglass, Morong..........79-83; disc. 83
Voltmeter, A New Expanded Scale A-C. Millar..........641-3

W

Washington Area, Design and Experience With 4-Kv Primary Network Systems in the. Lank..........712-16; disc. 716
Watt-Hour Meter, Surge Protection in a Modern. Busch, Williams..........74-7; disc. 77
Welding Arc, Instrumentation for the Evaluation of the Stability of the. Winsor, Schetky, Wyant..........525-33
Well Drilling, Performance of Diesel-Electric Rig for Deep. Clark, Moore..........497-506
Wide-Range Adjustable-Speed Drive, A. Conrad, Tribken..........789-90
Wood Transmission Lines, Comparative Performance Records—Steel and. Booker..........686-9; disc. 689

2. Author Index

Adams, J. A. Disc..........749
Alexander, E. H. Disc..........474
Alger, P. L. Disc..........214
Alley, R. E., Jr.; W. C. Johnson, B. C. Merrell. Universal Curves for D-C Controllable Reactors..........31-7; disc. 39
Andrews, F. E. Disc..........447
Atkinson, R. W. Disc..........557

Atkinson, R. W.; Joseph Sucher, G. H. Doan, Louis Meyerhoff. High-Pressure Gas-Filled Cable Impregnated with Extra-High Viscosity Oil.........336–45; disc. 347
Atwell, C. A.; C. E. Baston. Electric Equipment for Cheasapeake and Ohio Railway Company Steam Turbine-Electric Locomotives.........145–8

B

Baker, B. P.; E. Frisch. A New 69-Kv Compressed-Air Circuit Breaker.........363–8; disc. 371
Baker, M. A. Disc.........215
Baldwin, M. J. Oscillographing Commutation.........100–05; disc. 105
Baldwin, M. J. Twenty-Five Years Progress in the Design of Traction Motors.........132–7
Bary, Constantine. The Heat Pump—Its Significance as a Potential Residential Electric Load.........1–8
Baston, C. E.; C. A. Atwell. Electric Equipment for Cheasapeake and Ohio Railway Company Steam Turbine-Electric Locomotives.........145–8
Beaumariage, D. C.; D. W. VerPlanck, L. A. Finzi. Analytical Determination of Characteristics of Magnetic Amplifiers with Feedback.........565–70
Beck, E. Disc.........185
Beggs, George E., Jr. Automatic Range-Adjusting Radiosonde Recorder.........602–07
Behn, Eric R. Disc.........306
Bellaschi, P. L. Disc.........447, 759
Bennet, W. R. Disc.........260
Bennon, S. Disc.........748
Berkowitz, R. Disc.........649
Bevan, G. T. Application Engineering on Diesel-Electric Locomotives in Railroad Service.........125–31
Bewley, L. V. Disc.........447
Bills, Glenn W. Disc.........381
Blomquist, E. A. Disc.........747
Blomquist, H. R. Trackless Trolley Operation in Rhode Island.........397–402
Bonneville Power Administration, Engineers of. Disc.........27, 69
Booker, C. A. Comparative Performance Records—Steel and Wood Transmission Lines.........686–9; disc. 689
Boothroyd, Wilson P.; H. J. Churchill. A Microwave Communication Relay System.........637–41
Boothroyd, W. P.; E. M. Creamer, Jr. A Time Division Multiplexing System.........92–7
Bostwick, L. G.; A. C. Keller. Vibrating Reed Selectors for Mobile Radio Systems.........383–6
Brady, Bryce. Distribution Transformer and Secondary Conductor Economics.........483–6; disc. 489
Brady, Bryce. Improvements to Oklahoma City Primary Network.........701–02; disc. 703
Brandt, D. B.; J. F. Lamb. The Vector Power Factor of Unbalanced Sinusoidal 3-Phase Circuits.........507–09
Brown, J. Stanley. Disc.........361
Brown, W. T. Disc.........488
Brownlee, Theodore. Advances in Technique of Lightning Measurements.........515–19
Brownlee, W. R.; J. A. Elzi. Disc.........738
Buckland, Mrs. B. O.; T. M. Linville. Disc.........218
Buller, F. H. Disc.........546
Burkhard, Henry F. Considerations on Facsimile Transmission Speed.........418–23; disc. 423
Busch, F. H.; G. D. Williams. Surge Protection in a Modern Watt-Hour Meter.........74–7; disc. 78
Butler, F. H. Disc.........17

C

Cahen, Francois. Disc.........204
Caldwell, B. H. Disc.........223
Caldwell, B. H.; G. H. Gunnoe. Disc.........212
Campbell, H. E. Disc.........486, 702
Candee, A. H. The Renaissance of Electric Motive Power.........138–44
Carlisle, R. W. Disc.........423
Carleton, James T. The Transient Behavior of the Two-Stage Rototrol Main Exciter Voltage Regulating System as Determined by Electrical Analogy.........59–63
Casey, E. J.; B. W. Wyman. A Manually Operated Spring Mechanism for Medium Voltage Oilless Circuit Breakers.........357–61; disc. 362
Chang, S. S. L. Disc.........327
Chang, Sheldon, S. L.; J. H. Karr. Armature Iron Losses in Series Motors.........262–4; disc. 265
Charp, S. A New Fourier Coefficient Harmonic Analyzer.........644–9; disc. 649
Chestnut, Harold; R. W. Mayer. Comparison of Steady-State and Transient Performance of Servomechanisms.........765–77
Churchill, Harold J.; W. P. Boothroyd. A Microwave Communication Relay System.........637–41
Clark, E. C.; B. I. Moore. Performance of Diesel-Electric Rig for Deep Well Drilling.........497–506
Clark, W. R.; W. R. Turner, A. J. Williams, Jr. A Square-Law Power-Level Recorder.........476–82
Clayton, J. M.; E. L. Harder. Transmission Line Design and Performance Based on Direct Lightning Strokes.........439–46; disc. 448
Cole, Harold. Disc.........487
Concordia, C. Disc.........166
Conrad, A. G.; E. R. Tribken. A Wide-Range Adjustable-Speed Drive.........789–90
Corbett, James P. Summary of Transformations Useful in Constructing Analogs of Linear Vibration Problems.........661–4
Cornelius, H. A.; B. W. Storer. Loss Measurements Made on Underground-Cable Overhead-Conductor 132-Kv Transmission Line at Carrier Current Frequencies.........597–601
Creamer, E. M., Jr.; W. P. Boothroyd. A Time Division Multiplexing System.........92–7

D

Dahlbom, C. A.; A. W. Horton, Jr., D. L. Moody. Application of Multifrequency Pulsing in Switching.........392–6
Davis, S. Disc.........327
deBellis, A. M. Disc.........370
DePuy, S. M. Disc.........270
Del Mar, W. A. Disc.........17
Demartini, R. J.; A. F. Lukens. Selection of Electric Drives for Looms.........349–56
Doan, G. H.; Joseph Sticher, R. W. Atkinson, Louis Meyerhoff. High-Pressure Gas-Filled Cable Impregnated with Extra-High-Viscosity Oil.........336–45; disc. 347
Dodds, G. B.; R. S. Smithley. Disc.........716
Douglass, M. E.; W. H. Morong. A New Thermal Volt-Ampere Demand Meter.........79–83; disc. 83
Duesterhoeft, William C. The Negative-Sequence Reactances of an Ideal Synchronous Machine.........510–13; disc. 513
Duffy, F. H.; J. T. Madill. Shipshaw Relay Protection.........50–5; disc. 57
Dunn, Charles. Disc.........489
Dupuis, H. P. Disc.........620
Dupuis, H. P.; D. C. Harker. Disc.........57
Dwight, H. B. Disc.........20

E

Earle, R. H. Disc.........187
Easton, E. C.; C. H. Thomas. Graphical Determination of Transfer Function Loci for Servomechanism Components and Systems.........307–14; disc. 318
Edge, D. R.; D. D. MacCarthy, D. A. Stann, W. C. McKinley. Lightning Investigation on a Rural Distribution System.........428–37; disc. 437
Elsey, H. M.; C. Lynn. Effects of Commutator Surface Film Conditions on Commutation.........106–12; disc. 112
Elton, M. B. Disc.........489
Elzi, J. A. Disc.........231
Elzi, J. A.; W. R. Brownlee. Disc.........738

F

Falck, Knute. Disc.........361
Finzi, L. A. Disc.........39
Finzi, L. A.; D. W. VerPlanck, D. C. Beaumariage. Analytical Determination of Characteristics of Magnetic Amplifiers with Feedback.........565–70
Finzi, L. A.; L. C. Wellard. The Geometric Loci of the Synchronous Tie.........168–71
Frick, C. W. Disc.........495, 724
Frisch, E.; B. P. Baker. A New 69-Kv Compressed-Air Circuit Breaker.........363–8; disc. 371
Frost, G. R. Counting with Relays.........587–91
Fugill, A. P. Disc.........747
Fuller, John L. Disc.........214

G

Gilchrist, A. D. Disc.........153
Gmeiner, John B. Disc.........241
Goodrich, R. D., Jr. Disc.........380
Gordy, T. D. Disc.........750
Grant, George. Disc.........216
Grover, Frederick W. Formulas and Tables for the Calculation of the Magnetic Field Components of Circular Filaments and Solenoids.........665–75
Guess, I. T. Disc.........487
Gunnoe, G. H.; B. H. Caldwell. Disc.........212

H

Hadley, W. A. Disc.........20, 334
Hague, F. T. Gas Turbines in Stationary Power Generation.........467–8
Halfmann, E. S. Disc.........346
Hall, Albert C. Damper Stabilized Instrument Servomechanisms.........299–306; disc. 306
Halperin, Herman. Disc.........19, 333
Harder, E. L.; J. M. Clayton. Transmission Line Design and Performance Based on Direct Lightning Strokes.........439–46; disc. 448
Harker, D. C.; H. P. Dupuis. Disc.........57
Hart, H. A.; F. J. Vogel. A Small High-Voltage Bushing Design for High Altitudes.........761–4
Hart, Stephen V. Disc.........241
Hatcher, C. T. Disc.........558
Hathaway, C. B. Disc.........217, 224
Haverstick, J. S. A 3,000-Horsepower Gas Turbine Power Plant.........458–60
Hayes, V. J. Disc.........231
Hearn, R. B.; L. A. Weber. B-1 Alarm and Control System for Remote Control of Coaxial Cable Stations.........622–6.
Herskind, C. C.; A. Schmidt, Jr.; C. E. Rettig. Rectifier Fault Currents—II.........243–51; disc. 252
Heumann, G. W. Dynamic Braking Control of D-C Series Motors—Experimental Study of Speed-Torque Curves.........560–4
Hewitt, G. W.; G. W. Penney. Electrically Charged Dust in Rooms.........278–82
Hickernell, L. F.; A. A. Jones, C. J. Snyder. Hy-Therm Copper—An Improved Overhead-Line Conductor.........22–7; disc. 29
Holben, W. P.; J. E. Lange. Primary Networks on the Duquesne Light Company System.........704–09; disc. 711
Holtz, F. C. Disc.........77
Hoover, D. B. Disc.........105
Horton, A. W., Jr.; C. A. Dahlbom, D. L. Moody. Application of Multifrequency Pulsing in Switching.........392–6
Hoth, Daniel F.; Harold M. Pruden. Vibrating Reed Selective Signaling System for Mobile Telephone Use.........387–91
Howard, Alan. Two Gas Turbines for Power Generation and Other Applications.........461–5
Hull, Francis M.; W. A. Sinclair. Disc.........558
Hutchinson, Chase. Disc.........489

J

Johnson, I. B.; J. W. Kalb. Disc.........181
Johnson, Walter C. Disc.........194, 649
Johnson, Walter C.; B. C. Merrell, R. E. Alley, Jr. Universal Curves for D-C Controllable Reactors.........31–7; disc. 39
Jones, A. A.; L. F. Hickernell, C. J. Snyder. Hy-Therm-Copper—An Improved Overhead-Line Conductor.........22–7; disc. 29

K

Kalb, J. W.; I. B. Johnson. Disc.........181
Karr, J. H.; S. S. L. Chang. Armature Iron Losses in Series Motors.........262–4; disc. 265
Keister, W. M. The Logic of Relay Circuits.........571–6
Keller, A. C.; L. G. Bostwick. Vibrating Reed Selectors for Mobile Radio Systems.........383–6
Kessler, William J. The Distinction Between Effective and Circuit Bandwidths.........98–9
Kidder, A. H.; G. S. Van Antwerp. 69-Kv Pipe-Type Cable Circuits in Philadelphia.........550–6; disc. 559
Kierstead, F. H. Disc.........475
Kimbark, Edward W. Disc.........382
Kimberly, E. E. The Field Fluxes of the Shaded-Pole Motor.........273–7
Klingaman, G. W. Reduction of Interference from Radio-Frequency Heating Equipment.........718–24; disc. 724
Koopman, R. J. W. Operating Characteristics of Two-Phase Servomotors.........319–27; disc. 328
Kron, Gabriel. Stationary Networks and Transmission Lines Along Uniformly Rotating Reference Frames.........690–6
Kusters, N. L. Disc.........68

L

Lamb, J. F.; D. B. Brandt. The Vector Power Factor of Unbalanced Sinusoidal 3-Phase Circuits.........507–09
Lange, J. E.; W. P. Holben. Primary Networks on the Duquesne Light Company System.........704–09; disc. 711
Lank, W. J. Design and Experience with 4-Kv Primary Network Systems in the Washington Area.........712–16; disc. 716

Lawton, F. L. Disc. 56
Leitch, John D. The Use of Air-Core Reactors as Fault Limiting Means on High Interrupting Capacity Controllers.......469–74; disc. 475
Lensner, H. W. Disc. 48, 240
Leonard, M. G. Disc. 488
Leslie, J. R.; J. R. Wait. Detection of Overheated Transmission Line Joints by Means of a Bolometer.......64–8; disc. 69
Levine, D. L.; H. E. Smith. Economic Loading of a Transformer System.......733–8; disc. 739
Lewis, W. A. Disc. 513
Lindsey, R. H.; K. N. Mathes, L. E. Sieffert, H. P. Walker. Methods for Determining the Effects of Contaminants on Electrical Insulation.......113–18; disc. 118
Linville, T. M. Disc. 225
Linville, T. M.; H. C. Ward, Jr. Solid Short Circuit of D-C Motors and Generators.......119–23; disc. 123
Linville, T. M.; Mrs. B. O. Buckland. Disc. 218
Locanthi, B. N.; G. D. McCann, C. H. Wilts. Application of the California Institute of Technology Electric Analog Computer to Nonlinear Mechanics and Servomechanisms.......652–60
Loving, James J., Jr. Electronic Relay Developments.......233–40; disc. 242
Lukens, A. F.; R. J. Demartini. Selection of Electric Drives for Looms.......349–56
Lynn, C. Disc. 224
Lynn, C.; H. M. Elsey. Effects of Commutator Surface Film Conditions on Commutation.......102–12; disc. 112

M

Macalpine, William W. Heating of Radio-Frequency Cables.......283–8
MacCarthy, D. D.; D. A. Stann, D. R. Edge, W. C. McKinley. Lightning Investigation on a Rural Distribution System.......428–37; disc. 437
Madill, J. T.; F. H. Duffy. Shipshaw Relay Protection.......50–5; disc. 57
Mahoney, J. H. Disc. 750
Mansfield, C. G. Disc. 333
Marcy, H. Tyler; M. Yachter, J. Zauderer. Instrument Inaccuracies in Feed-Back Control Systems with Particular Reference to Backlash.......778–88
Markley, W. F.; H. H. Wheeler. Rubber Insulators for Pole Lines.......195–7
Marshall, F. R.; A. M. Zarem, F. L. Poole. An Electro-Optical Shutter for Photographic Purposes.......84–91
Maslin, A. J. Disc. 251
Mathes, K. N.; L. E. Sieffert, H. P. Walker, R. H. Lindsey. Methods for Determining the Effects of Contaminants on Electrical Insulation.......113–18; disc. 118
Mayer, Robert W.; H. Chestnut. Comparison of Steady-State and Transient Performance of Servomechanisms.......765–77
McCann, G. D.; C. H. Wilts, B. N. Locanthi. Application of the California Institute of Technology Electric Analog Computer to Nonlinear Mechanics and Servomechanisms.......652–60
McClinton, A. T. Disc. 118
McGrath, M. H. Disc. 18
McKenzie, D. A. Disc. 55
McKinley, W. C.; D. D. MacCarthy, D. A. Stann, D. R. Edge. Lightning Investigation on a Rural Distribution System.......428–37; disc. 437
McMillon, A. B. Trolley Coaches Replace Busses.......403–06
Merrell, B. C.; W. C. Johnson, R. E. Alley, Jr. Universal Curves for D-C Controllable Reactors.......31–7; disc. 39
Merrell, Edwin J. Disc. 345
Meyerhoff, Louis; Joseph Sticher, G. H. Doan, R. W. Atkinson. High-Pressure Gas-Filled Cable Impregnated with Extra-High-Viscosity Oil.......336–45; disc. 347
Michelson, E. L. Disc. 232
Mickley, A. S. The Thermal Movement of Moisture in Soil.......330–3; disc. 334
Mildner, R. C. The Power Rating of Radio-Frequency Cables.......289–98; disc. 298
Millar, N. P. A New Expanded Scale A-C Voltmeter.......641–3
Montgomery, T. B. Disc. 166
Montsinger, V. M. Disc. 759
Moody, D. L.; C. A. Dahlbom, A. W. Horton, Jr. Application of Multifrequency Pulsing in Switching.......392–6
Moore, B. L.; E. C. Clark. Performance of Diesel-Electric Rig for Deep Well Drilling.......497–506
Morong, W. H.; M. E. Douglass. A New Thermal Volt-Ampere Demand Meter.......79–83; disc. 83
Motter, D. P. Commutation of D-C Machines and Its Effects on Radio Influence Voltage Generation.......491–5; disc. 495
Mundel, A. B. Control Chart Methods Applied to Frequency Response Curves.......424–7
Murray, C. S. Transformer Audio Noise Problems on an Electric Power System.......740–7; disc. 751
Murray, C. S. Disc. 751
Myers, E. H. Disc. 495
Myers, Oscar. Codes and Translations.......592–7

N

Nau, Robert H. Disc. 361, 369
Neher, J. H. The Temperature Rise of Buried Cables and Pipes.......9–17; disc. 20
Neher, J. H. The Temperature Rise of Cables in a Duct Bank.......540–6; disc. 548
Nesbit, D. E. Disc. 710
Nye, H. V. Disc. 362, 370

O

Olmsted, Leonard M. Disc. 28, 69, 183, 709
Opsahl, A. M. Disc. 181, 437

P

Packer, L. C. Die-Cast Rotors for Induction Motors.......253–60; disc. 261
Packer, L. C. Disc. 264, 271
Parks, C. E. Disc. 381
Paschkis, Victor. Comparison of Long-Time and Short Time Analog Computers.......70–3
Pease, W. M. Disc. 306
Penney, G. W.; G. W. Hewitt. Electrically Charged Dust in Rooms.......278–82
Poole, F. L.; A. M. Zarem, F. R. Marshall. An Electro-Optical Shutter for Photographic Purposes.......84–91
Porter, L. F. Transformer Manholes and Vaults: Design and Ventilation.......534–9
Pruden, Harold M.; Daniel F. Hoth. Vibrating Reed Selective Signaling System for Mobile Telephone Use.......387–91
Puchstein, A. F. Disc. 264
Purcell, W. R. Saving Time in Testing Life of Incandescent Lamps.......730–2

R

Ramsey, Glen. Selenium Rectifiers in Motor Vehicle Power Systems.......149–53; disc. 153
Rauth, A. W. Disc. 56
Reed, R. D.; W. W. Satterlee. Controlled Temperature and Insulation Protection in the Operation of Power Transformers.......753–8; disc. 759
Rehberg, Charles F. Disc. 314
Rettig, C. E.; C. C. Herskind, A. Schmidt, Jr. Rectifier Fault Currents—II.......243–51; disc. 252
Ritchie, A. E. Sequential Aspects of Relay Circuits.......577–81
Roehmann, L. F. Disc. 298
Rorden, Harold L. Disc. 204
Rosenberg, L. T. A Semiempirical Approach to Voltage Dip—with Suddenly Applied Loads on A-C Generators.......160–6; disc. 167
Rudenberg, Reinhold. Nonharmonic Oscillations as Caused by Magnetic Saturation.......676–85
Rueggeberg, W.; J. B. Whitehead. The Measurement of Dielectric Loss at High Frequencies and Under Changing Temperature.......520–4
Runciman, A. S. Disc. 68
Rydbeck, V. A. Disc. 716

S

Sand, Edward. Disc. 224
Satterlee, W. W.; R. D. Reed. Controlled Temperature and Insulation Protection in the Operation of Power Transformers.......753–8; disc. 759
Schaefer, L. C.; C. G. Veinott. Fundamental Theory of Inherent-Overheating Protection Under Running Overload Conditions.......266–70; disc. 272
Schetky, L. McDonald; L. P. Winsor, R. A. Wyant. Instrumentation for the Evaluation of the Stability of the Welding Arc.......525–33
Schmidt, A., Jr.; C. C. Herskind, C. E. Rettig. Rectifier Fault Currents—II.......243–51; disc. 252
Scott, F. M. Disc. 112, 123, 216
Scott, Hoyt S. Measurements of Erythemal Energy.......725–29
Seely, R. E. Disc. 271
Seelye, Howard P. Disc. 487
Shanklin, G. B. Disc. 346, 558
Shores, R. B. Disc. 369
Sieffert, L. E.; K. N. Mathes, H. P. Walker, R. H. Lindsey. Methods for Determining the Effects of Contaminants on Electrical Insulation.......113–18; disc. 118
Sinclair, W. Allistair; F. M. Hull. Disc. 558
Skeats, W. F. Disc. 370
Slemon, Gordon R. Radio Influence from High-Voltage Corona.......198–204; disc. 205
Smith, Frank V. Disc. 19, 547
Smith, H. E.; D. L. Levine. Economic Loading of a Transformer System.......733–8; disc. 739
Smithley, R. S.; G. B. Dodds. Disc. 716
Snyder, C. J.; L. F. Hickernell, A. A. Jones. Hy-Therm Copper—An Improved Overhead-Line Conductor.......22–7; disc. 29
Specht, T. R.; E. C. Wentz. Disc. 38
Spencer, H. H. Power Supplies for Coaxial Systems.......627–30
Sporn, Philip. Disc. 466
Staats, G. W. Disc. 166
Stann, D. A.; D. D. MacCarthy, D. R. Edge, W. C. McKinley. Lightning Investigation on a Rural Distribution System.......428–37; disc. 437
Stevens, R. F. Disc. 42
Sticher, Joseph; G. H. Doan, R. W. Atkinson, Louis Meyerhoff. High-Pressure Gas-Filled Cable Impregnated with Extra-High-Viscosity Oil.......336–45; disc. 347
Stoelting, H. O. Disc. 186
Stokes, H. E. Disc. 215
Storer, B. Wade; H. A. Cornelius. Loss Measurements Made on Underground-Cable Overhead-Conductor 132-Kv Transmission Line at Carrier Current Frequencies.......597–601
Storm, H. F. Some Fundamentals of D-C Controlled Reactors with Resistive Load.......188–94
Storm, H. F. Disc. 37
Streiff, A. Disc. 489
Sulzer, P. G.; E. A. Walker, A. H. Waynick. Polar Vector Indicator.......154–9
Sutton, Howard J. Line Tuning Equipment Used With Coaxial Cable for Carrier Current Installation on Power Lines.......44–8; disc. 49

T

Tallent, R. J. Disc. 381
Taylor, P. L. Disc. 369
Terrant, F. R. Disc. 214
Terwilliger, D. D. Disc. 318
Thomas, C. H.; E. C. Easton. Graphical Determination of Transfer Function Loci for Servomechanism Components and Systems.......307–14; disc. 318
Thompson, C. S. Application of Experimental Test Procedures and Methods of Analysis of Results to Research Problems in Magnetic Recording.......407–17
Tomlinson, H. R. Disc. 181
Travers, Paul. Disc. 315
Tribken, E. R.; A. G. Conrad. A Wide-Range Adjustable-Speed Drive.......789–90
Turner, W. R.; W. R. Clark, A. J. Williams, Jr. A Square-Law Power-Level Recorder.......476–82

V

Van Antwerp, G. S.; A. H. Kidder. 69-Kv Pipe-Type Cable Circuits in Philadelphia.......550–6; disc. 559
Veinott, C. G.; L. C. Schaefer. Fundamental Theory of Inherent-Overheating Protection Under Running Overload Conditions.......266–70; disc. 272
VerPlanck, D. W.; L. A. Finzi, D. C. Beaumariage. Analytical Determination of Characteristics of Magnetic Amplifiers with Feedback.......565–70
Vikoren, O. B. Disc. 371
Vogel, F. J. Disc. 759
Vogel, F. J.; H. A. Hart. A Small High-Voltage Bushing Design for High Altitudes.......761–4
Von Voigtlander, F. Disc. 153, 751

W

Wait, J. R.; J. R. Leslie. Detection of Overheated Transmission Line Joints by Means of a Bolometer.......64–8; disc. 69
Waite, C. G. Disc. 77, 83
Walker, E. A.; A. H. Waynick, P. G. Sulzer. Polar Vector Indicator.......154–9
Walker, H. P.; K. N. Mathes, L. E. Sieffert, R. H. Lindsey. Methods for Determining the Effects of Contaminants on Electrical Insulation.......113–18; disc. 118
Ward, H. C., Jr.; T. M. Linville. Solid Short Circuit on D-C Motors and Generators.......119–23; disc. 123
Ward, H. M. Power Supplies for Microwave Relay Systems.......631–6
Ward, J. B. Equivalent Circuits for Power-Flow Studies.......373–80; disc. 382
Warrington, A. R. Van C. Graphical Method for Estimating the Performance of Distance Relays During Faults and Power Swings.......608–20; disc. 621
Washburn, S. H. Relay "Trees" and Symmetric Circuits.......582–6

Waynick, A. H.; E. A. Walker, P. G. Sulzer. Polar Vector Indicator..........154–9
Weber, Laurance A.; R. B. Hearn. B-1 Alarm and Control System for Remote Control of Coaxial Cable Stations..........622–6
Wellard, L. C.; L. A. Finzi. The Geometric Loci of the Synchronous Tie..........168–71
Wentz, E. C.; T. R. Specht. Disc..........38
Wheeler, H. H.; W. F. Markley. Rubber Insulators for Pole Lines..........195–7
Whitehead, J. B.; W. Rueggeberg. The Measurement of Dielectric Loss at High Frequencies and Under Changing Temperature..........520–4
Wild, Earle. Disc..........689
Williams, A. J., Jr.; W. R. Clark, W. R. Turner. A Square-Law Power-Level Recorder..........476–82
Williams, G. D.; F. H. Busch. Surge Protection in a Modern Watt-Hour Meter..........74–7; disc. 78
Wilson, W. A. Disc..........465
Wilts, C. H.; G. D. McCann, B. N. Locanthi. Application of the California Institute of Technology Electric Analog Computer to Nonlinear Mechanics and Servomechanisms..........652–60
Winegartner, C. E. Disc..........362
Winsor, Lauriston P.; L. M. Schetky, R. A. Wyant. Instrumentation for the Evaluation of the Stability of the Welding Arc..........525–33
Wiseman, Robert J. Disc..........546, 556
Witzke, R. L. Voltage-Recovery Characteristics of Distribution Systems..........172–80; disc. 187
Woods, Thomas J. Industrial Plants Prefer Diesel-Electric Switching Locomotives..........697–700
World, Richard W. Disc..........620
Wray, G., Jr. Disc..........748
Wyant, Robert A.; L. P. Winsor, L. M. Schetky. Instrumentation for the Evaluation of the Stability of the Welding Arc..........525–33
Wyatt, K. S. Disc..........29
Wyman, B. W.; E. J. Casey. A Manually-Operated Spring Mechanism for Medium Voltage Oilless Circuit Breakers..........357–61; disc. 362

Y

Yachter, M. Disc..........315
Yachter, Morris; H. T. Marcy, J. Zauderer. Instrument Inaccuracies in Feed-Back Control Systems with Particular Reference to Backlash..........778–88

Z

Zarem, A. M.; F. R. Marshall, F. L. Poole. An Electro-Optical Shutter for Photographic Purposes..84–91
Zauderer, Jerome; H. T. Marcy, M. Yachter. Instrument Inaccuracies in Feed-Back Control Systems with Particular Reference to Backlash..........778–88

Blank

Page

Field Tests of Oil Circuit Recloser Substantiate Analytical Co-ordination Method

G. G. AUER
ASSOCIATE AIEE

R. A. BRANFLICK
ASSOCIATE AIEE

L. J. WOODWARD
ASSOCIATE AIEE

W. C. McKINLEY
NONMEMBER AIEE

DEPENDABLE electric service in suburban and rural areas is of increasing importance because of the addition of many new electrical appliances to the home and the continued expansion of farm electrification. Power outages seriously inconvenience the residential consumer and may cause heavy loss of produce on the farm. Moreover, rising labor and automotive costs have increased utility operating expenses to a point where an excessive number of service trips no longer can be tolerated. It is, therefore, of vital importance that overcurrent protection for suburban and rural circuits be applied properly to yield the greatest possible reduction in the number and extent of outages.

In recent years, much emphasis has been placed on the application of automatic reclosers and distribution fuse cutouts for overcurrent protection of outlying distribution circuits. This paper discusses an analytical method for determining co-ordination of reclosers with series fuses and presents field test data which substantiate this method.

Analysis of Recloser-Fuse Co-ordination

The primary function of any recloser in a distribution circuit is to clear, by instantaneous opening, all temporary faults before fuses blow and, by time-delay opening, to provide for clearing all permanent faults occurring in its zone of protection.

A recloser, in order to accomplish this function, must have reliable characteristics capable of providing proper recloser-fuse co-ordination irrespective of ambient temperature changes, and of providing co-ordination with adjacent ratings of reclosers in series.

It is realized that with a recloser and a fuse in series with a fault, each operation of the recloser will cause heating and cooling of the fuse, with the result that the total heat input required to melt the fuse link during successive recloser operations cannot be determined directly from the published melting time–current characteristics of the fuse link.

In preparing a circuit co-ordination study, the effective heating and cooling of the fusible element must be evaluated properly in order to prevent unnecessary fuse blowing or misperformance by recloser lockout.

The following is a procedure that has been established for determining the fuse ratings that will co-ordinate with a particular rating of recloser. This basic procedure is applicable to all types of reclosers to be operated in series with fuses

This procedure includes operating and manufacturing variables of each device:

1. Total variation in recloser tripping characteristics.
2. Total heat input to a fuse link during the time required for the recloser to open and interrupt the fault current.
3. Twenty-five per cent allowance in melting time–current characteristics of fuse to factor operating variables, such as preloading, and progressive melting of fusible element and strain wire.
4. Cooling of the fuse link during intervals that the recloser is open.

Each of the foregoing factors will be considered separately to show how it applies.

Total Variation in Recloser Tripping Characteristics

Referring to Figure 1, it will be noted that the instantaneous characteristic *A* of the recloser is plotted to maximum test points. Hence, all instantaneous opening operations of the recloser will fall either on or below this curve. It serves as a basis, therefore, for determining the co-ordination of the recloser to the melting time–current characteristics of fuses and, hence, for assuring protection of load-side fuses during the first and second (instantaneous) opening operations.

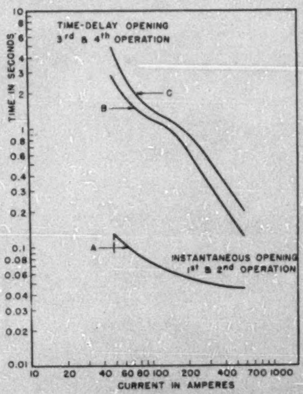

Figure 1. Characteristics of 25-ampere *FR-1* recloser

Paper 49-128, recommended by the AIEE Switchgear Committee and approved by the AIEE Technical Program Committee for presentation at the AIEE Summer General Meeting, Swampscott, Mass., June 20–24, 1949. Manuscript submitted March 22, 1949; made available for printing May 2, 1949.

G. G. AUER is located in Schenectady, N. Y., R. A. BRANFLICK is located in Pittsfield, Mass., and L. J. WOODWARD is located in Philadelphia, Pa.; all with the General Electric Company. W. C. McKINLEY is with the Central Electric Cooperative, Inc., Parkers Landing, Pa.

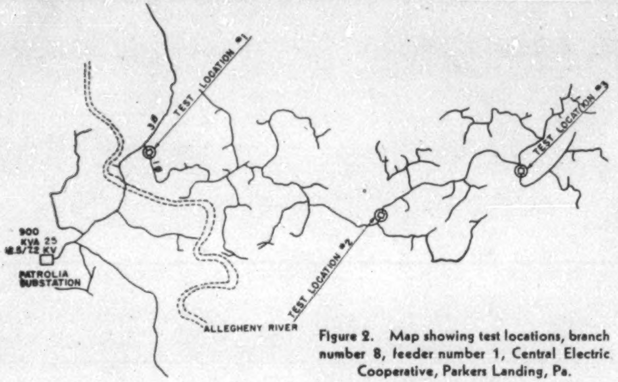
TEST LOCATION #1
3Ø
#8
TEST LOCATION #3
TEST LOCATION #2
900 KVA 25 12.5/7.2 KV
PATROLIA SUBSTATION
ALLEGHENY RIVER

Figure 2. Map showing test locations, branch number 8, feeder number 1, Central Electric Cooperative, Parkers Landing, Pa.

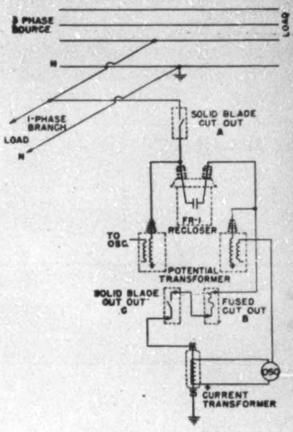
3 PHASE SOURCE
LOAD
N
1-PHASE BRANCH
LOAD
N
SOLID BLADE CUT OUT A
FR-1 RECLOSER
TO OSC.
POTENTIAL TRANSFORMER
SOLID BLADE CUT OUT C
FUSED CUT OUT B
OSC
CURRENT TRANSFORMER

Figure 3. Test circuit diagram

The time-delay characteristic *B* and *C* of the recloser is plotted to both minimum and maximum test points, and, hence, all time-delay opening operations of the recloser will fall within the band of variations.

The minimum time-delay curve *B* serves as a basis for determining the co-ordination of the recloser to the total-clearing characteristics of fuses, to assure that permanent faults will be cleared by load-side fuses during the third or fourth (time-delay) opening operation before the recloser locks open.

The maximum time-delay curve *C* serves as the basis for determining the ability of the recloser to prevent operation of overcurrent relays or fuses on the source side of the recloser during its third and fourth (time-delay) opening operations to lock open.

Total Heat Input to a Fuse Link During the Time Required for the Recloser to Open and Interrupt the Fault Current

The time–current characteristic curves of a recloser can be factored to include heating of a fuse link when comparing with time–current characteristics of fuses.

Let us assume that we wish to prevent a fuse from blowing during two instantaneous openings of the recloser when clearing temporary faults. We must consider the total amount of heat received by the fuse during these two instantaneous openings of the recloser. By doubling each time value on the instantaneous characteristic curve *A*, we arrive at a modified curve which represents the total length of time that short-circuit current flows through the fuse link during the first two recloser openings.

Assuming a permanent fault beyond the fuse, proper co-ordination requires that the fuse melt before the recloser locks open. In this case, we must determine the minimum heat input to the fuse link during the two instantaneous plus two time-delay openings of the recloser, to be sure that it is sufficient to melt the fuse before the recloser locks open. By doubling the time values on both the instantaneous characteristic curve *A* and the minimum time-delay characteristic curve *B* and adding the two together, we arrive at a modified curve which represents the minimum length of time that short-circuit current flows through the fuse link during four recloser operations.

In co-ordinating the recloser with a source-side fuse, it is necessary that the four operations of the recloser to lock open will not cause partial melting of the fuse. In this case, our modified curve would be equal to the sum of two instantaneous openings, curve *A*, plus two time-delay openings, curve *C*. This final curve then represents the maximum or total length of time that short-circuit current is permitted to flow through the fuse link.

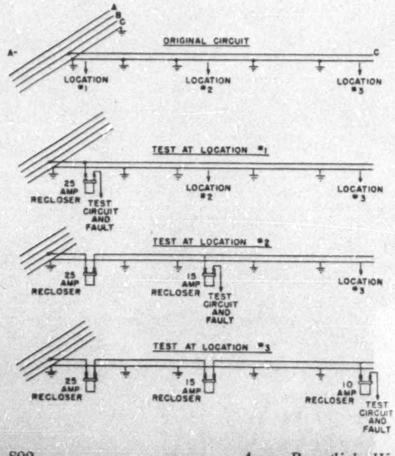
A
B
C
ORIGINAL CIRCUIT
A-
C
LOCATION #1
LOCATION #2
LOCATION #3
TEST AT LOCATION #1
25 AMP RECLOSER
TEST CIRCUIT AND FAULT
LOCATION #2
LOCATION #3
TEST AT LOCATION #2
25 AMP RECLOSER
15 AMP RECLOSER
TEST CIRCUIT AND FAULT
LOCATION #3
TEST AT LOCATION #3
25 AMP RECLOSER
15 AMP RECLOSER
10 AMP RECLOSER
TEST CIRCUIT AND FAULT

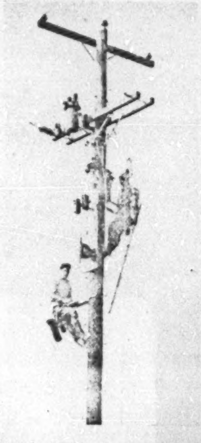

Figure 3(A). (left) Circuit diagrams for each test location

Figure 3(B). (right) Test location number 1

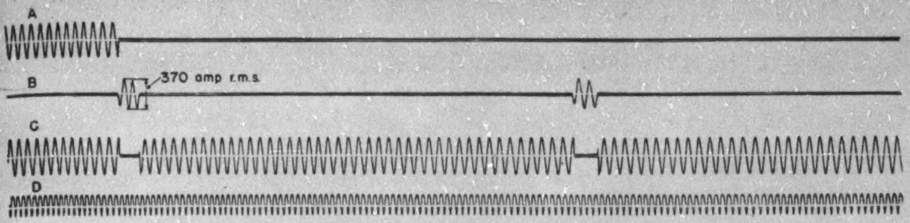

Figure 4. Oscillogram (in two parts) showing co-ordination of 25-ampere recloser with 50-ampere fuse

Curve A—Recloser load side voltage, 120 volts
Curve B—Short-circuit current, 370 rms amperes
Curve C—Recloser source side voltage, 120 volts
Curve D—Timing wave, 100 cycles

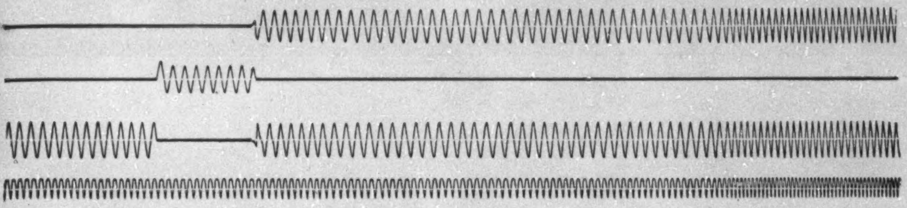

Allowance of 25 Per Cent in Melting Time–Current Characteristics of Fuses to Factor Operating Variables

The time–current characteristic curves of fuse links are based upon no initial load. Whenever fuses are preheated by load current, a 15 per cent reduction in melting time should be taken into consideration. An additional reduction of 10 per cent must also be included to take into account the progressive melting of the fusible element and the strain wire.[1] Therefore, the over-all factor of safety should be a 25 per cent reduction of the melting time–current characteristic of the fuse to assure that the fuse will not be

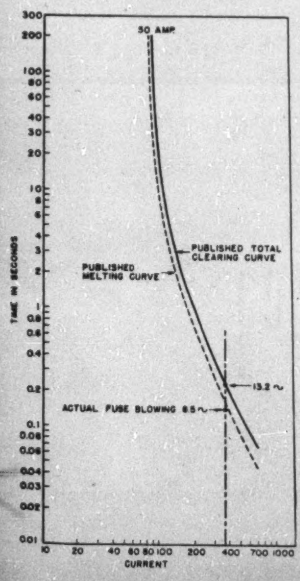

Figure 5 (left). Time-current characteristics of 50-ampere fuse link

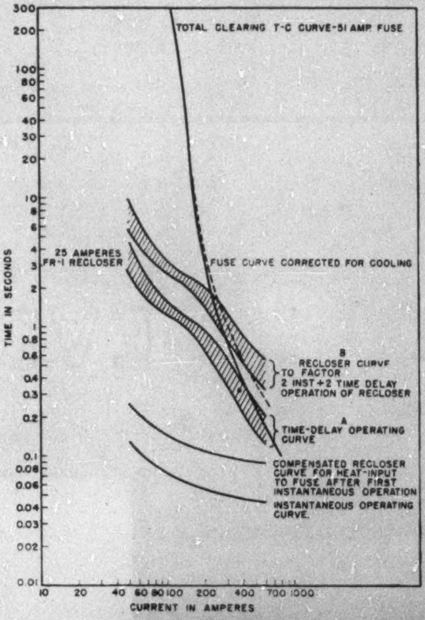

Figure 6 (right). Analytical co-ordination method of comparing characteristics of reclosers and fuses partially melted by the fault current during any instantaneous openings of the recloser.

Cooling of the Fuse Link During Intervals that the Recloser is Open

Each successive opening of the recloser is followed by an interval of approximately 40 cycles before reclosing. During this interval there is no current flowing through the fuse, and, consequently, the fusible element has an opportunity to cool. As a result, the fuse will be somewhat slower in melting than in the case where no cooling is permitted. The additional increment of time for cooling, which can be calculated, must be added to the melting and total clearing time–current characteristics of the fuse.

Test Circuit

This basic procedure for recloser-fuse co-ordination was substantiated by a series of field tests performed on a typical rural distribution circuit located on the Central Electric Cooperative System at Parkers Landing, Pa.

The circuit selected for these tests, Figure 2, was a 7,200-volt single-phase branch line approximately 25 miles long with three sectionalizing points. The first sectionalizing point, where the single-phase line tapped off the main 3-phase line, was six miles from a 900-kva substation. The maximum calculated fault current at this location was 430 amperes line-to-neutral. The second sectionalizing point was 12 miles from the first location; the calculated fault current was 140 amperes. The third and last sectionalizing point was eight miles from the second location, and the calculated fault current at this point was 90 amperes.

To perform these tests in daylight hours under maximum generation on the system and under normal voltage and load conditions, a test circuit was used, as shown in Figure 3. This permitted application of faults with a solid-blade enclosed cut-out and clearance of fault by fuse, or by recloser operation without any prolonged service interruption.

This test-circuit equipment was portable and was moved from one location to another.

Figure 3(B) shows the two enclosed-type cutouts of Figure 3 mounted side by side on the test board at location *1*, Figure 3(A).

One cutout was fused for the purpose of testing the operation of fuses in series with the recloser. The other cutout with the solid disconnecting blade was used as a switch to apply the fault.

A 300/5-ampere current transformer, mounted on the test board below the cutouts, was used to energize the current element in the oscillograph.

Two standard distribution transformers, 7,200/120-240 volts, were used to provide voltage traces on the oscillogram for sequential operation study; one was connected on the source side of the re-

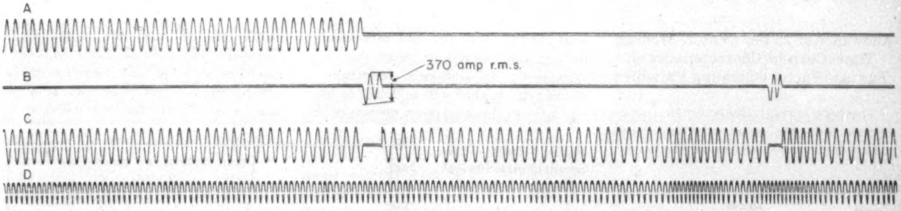

Figure 7. Oscillogram (in three parts) showing co-ordination of 25-ampere recloser with 51-ampere co-ordinating fuse link (equivalent to 75N fuse link)

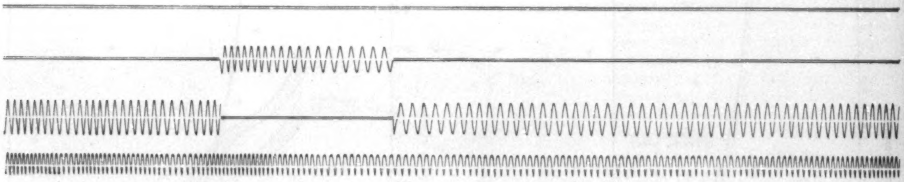

Curve A—Recloser load side voltage, 120 volts
Curve B—Short-circuit current, 370 rms amperes
Curve C—Recloser source side voltage, 120 volts
Curve D—Timing wave, 100 cycles

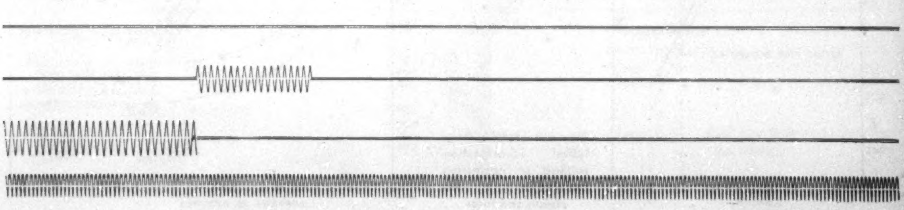

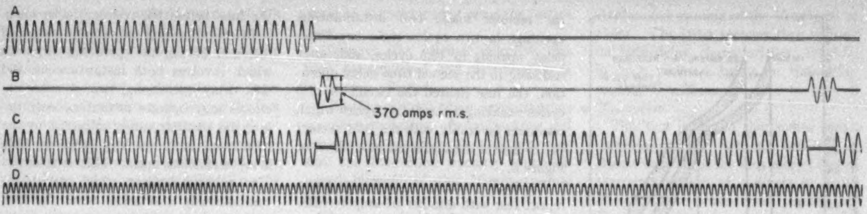

Figure 8. Oscillogram (in three parts) showing second test on co-ordination of 25-ampere recloser with 51-ampere co-ordinating fuse link

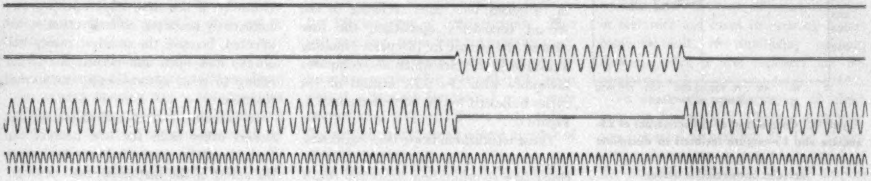

Curve A—Recloser load side voltage, 120 volts
Curve B—Short-circuit current, 370 rms amperes
Curve C—Recloser source side voltage, 120 volts
Curve D—Timing wave, 100 cycles

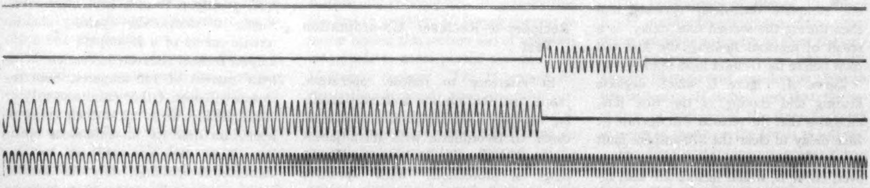

closer, and the other was connected to the load side of the recloser. Because of congestion on the pole and also to improve safety to the linemen, these transformers were omitted from the tests at locations *2* and *3*. A 100-cycle tuning fork was used to record the reference trace at these latter locations.

The ratings of the reclosers used at test locations *1*, *2*, and *3* were selected on the basis of the fault current and load current, resulting in a 25-ampere recloser at location *1*, a 15-ampere recloser at location *2*, and a 10-ampere recloser at location *3*.

The ratings of fuses used in these tests were selected on the basis of the procedure previously described for recloser-fuse co-ordination which took into consideration heating and cooling of the fuse link.

At location *1*, with the test circuit as shown in Figures 3 and 3(A), a 50-ampere fuse link was installed in cutout *B*, to be tested for co-ordinated series operation with the 25-ampere recloser.

Recloser-Fuse Co-ordination Test

At a predetermined time established by the oscillographer, cutout *C* was closed to apply a permanent fault from line-to-neutral on the test circuit.

The oscillogram in Figure 4 shows the magnitude of fault current, the sequence of operation, and the cycle timing.

The measured fault current was 370 amperes. The 25-ampere recloser made its first instantaneous opening in 2.5 cycles; reclosed after 44 cycles; made a second instantaneous opening in 2.5 cycles; and reclosed after 41 cycles for its first time-delay operation. This first time delay of the recloser allowed the 50-ampere fuse to blow in 8.5 cycles, thereby clearing the permanent fault from the circuit.

Referring to Figure 5, the standard published total clearing time–current characteristic of the 50-ampere fuse shows that 370 amperes would melt this link in a maximum time of 13.2 cycles. However, because heat was applied for two instantaneous openings of 2.5 cycles each with 44- and 41-cycle cooling intervals, the fuse cleared the circuit in 8.5 cycles instead of 13.2 cycles during the third (time-delay) operation of the recloser.

This test was repeated twice more at this location using the same rating fuse. The results substantiated the first tests; that is, the final duration of fault current to blow the fuse was 8.5 cycles and 8 cycles, respectively.

This approximately 36-per-cent difference in fuse curve time and actual fuse blowing time emphasizes the importance of the basic procedure in evaluating the heating of a fuse link when co-ordinating reclosers to fuses.

To go a step further in this study of fuse heating plus cooling with respect to its clearing time, a 51-ampere co-ordinating link (equivalent to a *75N* fuse) was selected for the next test at location 1. Taking into consideration the heating and cooling of this link, it should blow during the second time-delay operation of the

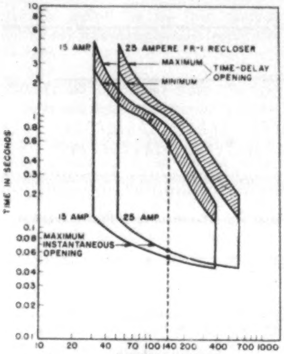

Figure 9. Comparison of characteristics of 25-ampere and 15-ampere reclosers to determine co-ordination between adjacent ratings of reclosers connected in series

25-ampere recloser; that is, the recloser should make two instantaneous openings, one complete time-delay opening, and then during the second time delay, as a result of previous heating, the fuse will blow before the recloser locks open.

Curve *A*, Figure 6, which neglects heating and cooling of the fuse link, indicates that the recloser will operate on time delay to clear the 370-ampere fault before the 51-ampere fuse blows. However, curve *B*, which factors the heat input to the fuse, indicates that before the recloser can complete its second time-delay opening, the fuse will melt and clear the fault.

The oscillogram shown in Figure 7 substantiates this latter analysis; that is, the recloser made two instantaneous openings in two cycles each, one time-delay opening in 19.5 cycles, and, after reclosing to the second time-delay operation, the fuse cleared the circuit in 17.5 cycles—making a total of 41 cycles which compares favorably with the 0.73 second (44 cycles) of the corrected fuse curve of Figure 6.

The oscillogram shown in Figure 8 is a repeat test with another 51-ampere fuse. The recloser made two instantaneous openings in two cycles and 2.5 cycles respectively, plus one time-delay opening in 19 cycles, and, after reclosing to the second time-delay operation, the fuse cleared the circuit in 16 cycles—making a total of 39.5 cycles which also compares favorably with the 0.73 second or 44 cycles indicated by the corrected curve in Figure 6.

These tests also indicate that neglecting the heating and cooling factors in a recloser-fuse co-ordination study can result in misperformances on actual installations which will cause unnecessary and prolonged circuit outages.

Recloser-to-Recloser Co-ordination Test

In reference to recloser operation, proper distribution-line fault sectionalizing depends upon the ability of one recloser to co-ordinate with its adjacent rating and all other reclosers within its range of protection. With repetitive operation of each recloser, the smallest rating adjacent to a permanent fault always must lock open to isolate the fault, just as with recloser-fuse co-ordination, a permanent fault on the load side of the fuse must always blow the fuse before the recloser locks open.

In co-ordinating adjacent ratings of reclosers having an operating sequence which involves both instantaneous and time-delay operations, two or more reclosers may operate instantaneously before the smallest rating adjacent to the permanent fault operates twice on time delay and locks open. This is inherent in all types of reclosers which operate instantaneously and arises from the fact that the instantaneous openings of the larger ratings may be faster than the time-delay opening of the smallest rating. However, if the time-delay openings are sufficiently accurate, co-ordination is not affected, because the smallest rating will always lock open and permit the larger rating to reset automatically to normal position.

It is evident that operations of reclosers other than the one nearest the fault could be prevented by decreasing the speed of the instantaneous openings. However, this seriously limits the ability of the recloser to prevent fuse blowing and conductor or apparatus damage and, therefore, greatly reduces its protective value. Figure 9 shows the opening characteristic curves of a 25-ampere and a 15-ampere recloser connected in series. With fault current of 140 amperes, both reclosers will open, either simultaneously or consecutively, at or below their curve of maximum time for instantaneous opening. After each has made its two instantaneous openings, only the smaller rating recloser will operate twice more on its time-delay characteristics to lock open. The oscillogram shown in Figure 10 shows the proper co-ordination of 25-ampere and 15-ampere reclosers connected in the circuit at locations *1* and *2*

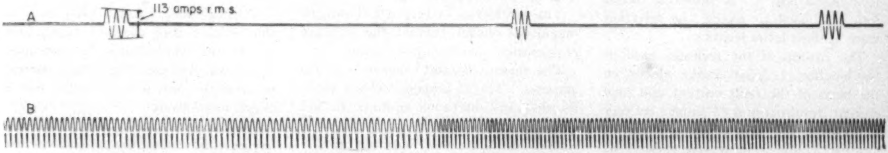

Figure 10. Oscillogram (in two parts) showing proper co-ordination of 25-ampere and 15-ampere reclosers connected in series

Curve A—Short-circuit current, 133 rms amperes

Curve B—Timing wave, 100 cycles

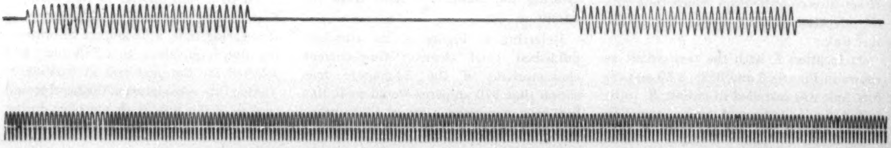

respectively, with a fault current of 133 amperes on the load side of location *2*. The circuit diagram is shown in Figure 3(A).

It is not possible to determine the exact sequence of operations, in view of the fact that the potential transformers could not be installed at location *2*. However, three instantaneous openings and two time-delay openings were indicated on the film.

Bearing in mind that neither recloser can operate on its time-delay characteristic until it has previously made two instantaneous openings, the five openings shown on the film might be analyzed as follows:

The first opening was made by the smaller rating (15-ampere) recloser alone; the second opening was a simultaneous opening of both 15-ampere and 25-ampere reclosers; the third opening was made by the 25-ampere recloser alone; and the fourth and fifth openings were time-delay openings of the 15-ampere recloser which locked open. The co-ordination between reclosers is accomplished during time-delay operation, and, to be successful, reliable characteristics must be inherent in the design.

The oscillogram shown in Figure 11 shows the test results with the 25-ampere recloser at location *1* in series with a 15-ampere recloser and a 30-ampere fuse at location *2*, and a fault applied on the load side of the fuse. The fault current was 133 amperes at this location. This is a typical application for a fused branch line beyond two reclosers in series. The objective, in this case, is to protect the branch fuse during the two instantaneous openings of the source-side recloser nearest this fuse and to blow the fuse before the recloser locks open. After the nearest recloser has completed two operations, instantaneous openings of other reclosers closer to the source may cause the fuse to blow.

However, the original objective has been accomplished and co-ordination is in no way affected.

This film shows three instantaneous openings, indicative of simultaneous and consecutive openings of both reclosers, and one time-delay opening which allowed blowing of the 30-ampere fuse link.

The second instantaneous opening shows clearance of the fault in one cycle, which is considerably faster than characteristic curves of either recloser indicate for 133 amperes of fault current. This fast opening, upon further investigation, was believed to have been influenced by inrush current after the 40-cycle open period. Between locations *1* and *2* were several large strip coal mines and a pumping station, each having a large number of motors in operation.

In analyzing this film, there is indication that the 25- and 15-ampere reclosers opened simultaneously when the 133-ampere fault was first applied. The 25-ampere unit reclosed first, thus energizing the line to location *2*. Inrush current to motor load in this section was of sufficient magnitude to cause partial pickup of the 25-ampere recloser. The 15-ampere recloser then reclosed; thus, the fault current added to the inrush current through the 25-ampere recloser, which was in partial pickup position, tripped in the first cycle of fault current. The 15-ampere recloser did not open in this second operation shown on the film. After this fast opening, the 25-ampere recloser had completed two instantaneous openings and would reclose on its time-delay characteristic. The 15-ampere recloser had made only one instantaneous opening; therefore the third instantaneous opening on the film was the second instantaneous opening of the 15-ampere recloser. The latter recloser then reclosed on time-delay characteristics, resulting in both reclosers being on time-delay, causing the 30-ampere fuse to blow in 25.5 cycles.

This test indicated that motor inrush currents on line sections between reclosers may affect the sequence of instantaneous openings of reclosers in series. This test also proved that possible difference in the instantaneous opening speed and variation in instantaneous opening sequence, will not affect proper co-ordination between adjacent reclosers or reclosers and fuses in clearing a permanent fault, if time-delay opening characteristics of the reclosers are dependable.

To study the performance of three reclosers in series, a 10-ampere recloser was installed at location *3*. The 15-ampere recloser was connected in series in the line at location *2;* the 25-ampere recloser was, as in the previous tests, at location *1*. Figure 3(A) shows the series connections in the 20-mile section of line.

The oscillogram of Figure 12 shows five instantaneous openings and two time-delay openings necessary to clear the permanent fault from the circuit when a 92-ampere fault current was flowing through the recloser. It is believed that the sequence of opening of the three reclosers in series as shown on the film is as follows:

The first instantaneous opening was made by the 10-ampere recloser alone; the second opening is simultaneous instantaneous operation of the 10- and the 15-ampere reclosers; the third opening is the second instantaneous operation of the 15-ampere recloser; the fourth opening is the first instantaneous operation of the 25-ampere recloser; the fifth opening is the second instantaneous operation of the 25-ampere recloser; and the sixth and

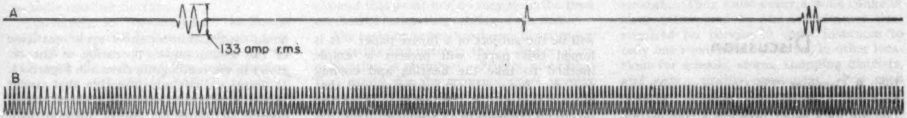

Figure 11. Oscillogram (in two parts) showing test results with 25-ampere recloser in series with a 15-ampere recloser and a 30-ampere fuse during a fault on the load side of the fuse

Curve A—Short-circuit current, 133 rms amperes

Curve B—Timing wave, 100 cycles

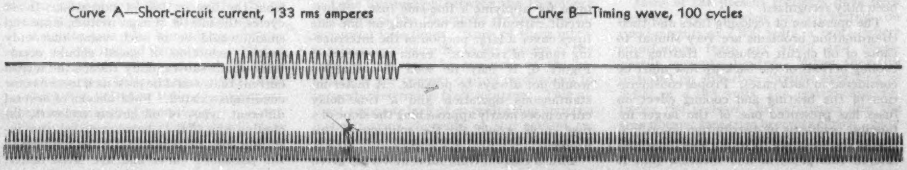

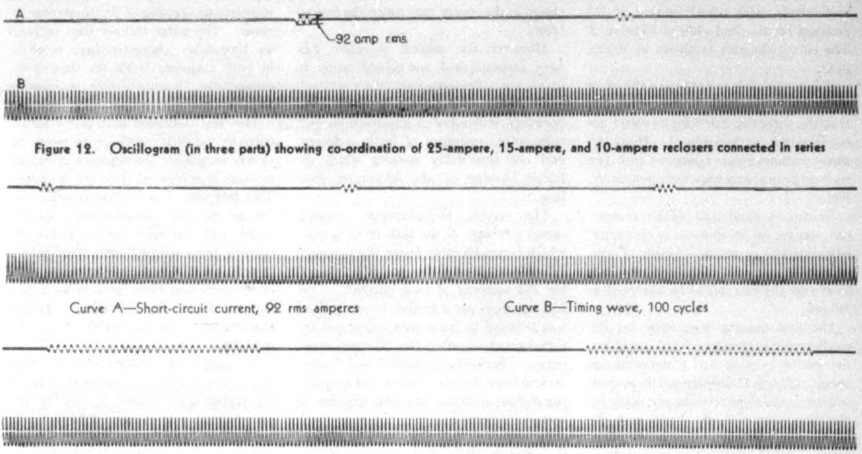

Figure 12. Oscillogram (in three parts) showing co-ordination of 25-ampere, 15-ampere, and 10-ampere reclosers connected in series

Curve A—Short-circuit current, 92 rms amperes

Curve B—Timing wave, 100 cycles

seventh openings are time-delay operations of the 10-ampere recloser which locked open.

This test proved that after each recloser had completed two instantaneous openings, it advanced to time-delay position, but only the smaller rating recloser adjacent to the fault opened on time delay and locked open to sectionalize the fault.

Discussion of Results

The data obtained in the field test show that co-ordination of reclosers with series fuses cannot be determined from direct comparison of the published characteristics of each device. However, a comparison of the test results with those obtained by the analytical co-ordination method set forth in this paper indicates that this method will provide adequate allowances for all manufacturing and operating variables to assure successful co-ordination.

Tests involving co-ordination of two or more reclosers in series show that several reclosers may perform instantaneous operations before the smallest rating of recloser adjacent to the fault locks open to sectionalize the fault. However, if the time-delay characteristics of the recloser are sufficiently accurate, dependable co-ordination of series reclosers can be obtained.

The field tests disclose that motor inrush currents on line sections between reclosers may affect the sequence of instantaneous operations of the reclosers.

Where reclosers and fuses are operated in series, the appreciable difference between published fuse characteristic curves and actual fuse clearing time, which results from intervals of heating and cooling of the fuse link during successive recloser operations, must be evaluated if successful operation is to be obtained. The analytical co-ordination method described affords a reliable means of factoring heating and cooling effect on the fuse link together with all other manufacturing and operating variables which affect co-ordination.

Reference

1. Modern Distribution Fuse Links, G. F. Lincks. *Power Plant Engineering* (Chicago, Ill.), volume 46, number 8, August 1942, pages 55–7.

Discussion

John B. Gmeiner (The Commonwealth and Southern Corporation, Jackson, Mich.): The author's paper presents a compilation of knowledge gained over the past few years in the application of oil circuit reclosers and brings out some facts that have not always been fully recognized.

The operation of reclosing fuses and their co-ordination problems are very similar to those of oil circuit reclosers. Heating and cooling periods of the back-up fuse must be considered in both cases. Proper consideration of the heating and cooling effect on fuses has presented one of the larger intangible problems in distribution co-ordination in recent years. The authors have considered this problem and mention that it will be the subject of a future paper. It is hoped this paper will present a simple method to take the heating and cooling period of fuses into consideration and that the method will be applicable to fuses and oil circuit reclosers of all manufacturers.

It is to be noted from Figure 6 of the paper when consideration is given to all the co-ordination factors, a rather small space is open for applying a line-side fuse. Short-circuit currents often occurring on line-side fuses cover a large portion of the interrupting range of reclosers. From inspection of Figure 6, it may be seen co-ordination would not always be possible. A faster instantaneous operation and a time-delay curve more nearly approaching the slope of a fuse curve would aid the solution of this problem.

Inrush current from mine motors is given as an explanation for the 1-cycle operation of the instantaneous operation of the recloser in the oscillogram shown in Figure 11. It seems a little unreasonable that under proper application where a recloser size is chosen to allow for future load growth, inrush current from motors would cause the fast operation pictured. Many motors have undervoltage controls that remove them from the line on loss of potential. In 40 cycles, the inertia of most motors, large and small, would be of such value that only partial reduction of speed should occur. This would substantially reduce the inrush current that would be present if locked rotor conditions existed. Field checks of several different types of oil circuit reclosers, including the *FR-1*, have revealed the instantaneous shots do not always conform to the published curve and are often faster.

Our field tests would indicate the 1-cycle operation is more likely the result of oil circuit recloser timing inaccuracies rather than motor inrush current. It would have been interesting to have observed one or two more tests performed under the conditions stated for Figure 11. It is agreed that, in any event, proper co-ordination will still be obtained.

The co-ordinated application of reclosers with fuses has been somewhat haphazard in the past. Operation engineers are realizing the need for analytical co-ordination studies before the applications of reclosers are made. For the application engineer this paper should provide a good summary of present-day recloser co-ordination methods.

S. R. Smith, Jr. (General Electric Company, Pittsfield, Mass.): Referring to the section on Cooling of the Fuse Link During Intervals That the Recloser is Open of the author's paper, the additional increment which is added to the fuse curves to factor fuse cooling during the open intervals of the recloser is

$$\frac{I_{300}^2}{i^2}\,T_d$$

where

I_{300} = 300-second current value from the fuse curve being used (or where the curve is asymptotic with the time axis)

T_d = total time the recloser is open for the operating cycle involved

i = circuit current.

To further explain the method of using this cooling correction, consider first the case where it is desired that the recloser go through a given sequence of operations without partial melting of a particular fuse. To ascertain the limit of co-ordination we start with the published fuse melting time curve and add $(I_{300}^2/i^2)\,T_d$ to points along the curve, simultaneously subtracting 25 per cent of the melting time to allow for operating variables (as explained in the paper) so as to arrive at a corrected fuse melting curve. This curve is superimposed on the curve of total opening time of the recloser for the sequence involved (sum of all instantaneous, or instantaneous plus time-delay opening times as determined from the published recloser curves). The point where these curves intersect indicates the current limit to which recloser will function without partially melting the fuse.

Conversely, for the case where the fuse is to clear the circuit before the recloser goes through a given operating sequence, we start with the published fuse total clearing time curve and add $(I_{300}^2/i^2)\,T_d$ to points along the curve so as to arrive at a corrected fuse clearing time curve (conservatism dictates omission of the minus 25 per cent factor for operating variables in this case). This curve is superimposed on the curve of total opening time of the recloser for the sequence involved (sum of all instantaneous, or instantaneous plus time-delay opening times as determined from the published recloser curves). The point where these curves intersect indicates the current limit to which fuse will clear before recloser completes its sequence of operations.

Study of the foregoing methods will show that the same results can be achieved by changing the sign of the corrections and applying them to the recloser curve instead of to the fuse curve.

The cooling correction given before derives from the fuse heat balance equations and we have used it for a number of years in applying reclosing fuses. The point of caution is on very fast fuses, for example where the 0.1-second melting current is only five times the 300-second melting current, in which case the correction may be too large if the individual reclosing intervals are longer than approximately 1.5 seconds.

Chase Hutchinson (Ebasco Services, Incorporated, New York, N. Y.): The benefits of selective operation between circuit breakers or reclosers and fuses has become recognized generally throughout the industry. On overhead distribution lines these benefits are usually manifest by improved service continuity and reduced operating cost. Maximum benefits from a given sequence of operations can be secured by use of accurate application procedures for devices having definite and known operating characteristics. Thus the application procedure described by the authors and checked by field tests should be helpful in obtaining a closer approach to perfect operation of reclosers.

When a fuse is exposed to fault current the heat input is I^2Kt where t is time. For several pulses of fault current of equal magnitude the heat input is

$$I^2K(t_1+t_2+t_3\ldots tn)$$

If no cooling occurs between the several pulses or if the amount of cooling is small the accumulated heat in the fuse may be taken as the heat produced by I amperes flowing for

$$T=(t_1+t_2+t_3\ldots tn) \text{ seconds}$$

The oscillogram of Figure 4 of the paper seems to bear out this reasoning in that (2.5 + 2.5 + 8.5) = 13.5 cycles was required to blow the fuse which apparently checks the 13.2 cycle value given by the authors as published clearing time.

From this reasoning and the test results it appears for practical applications involving a complete cycle of operations occurring in about two seconds, cooling of the fuse link is a negligible factor while heating of the link is substantially the sum of the several pulses of heat. Unfortunately the authors do not expand this point nor do they describe their method of estimating cooling of the link.

The tests on several reclosers in series are interesting and indicate that a degree of co-ordination is obtained. Perfect co-ordination would, for the sequence used, involve three or four recloser operations as contrasted to the eight recloser operations required to isolate the trouble. In the Figure 12 case the line section between the 25- and 15-ampere recloser was interrupted twice and the line section between the 15-ampere recloser and the 10-ampere recloser was interrupted four times. None of these interruptions were essential to the success of the scheme, but were by-products of the inability of the recloser control mechanism to properly determine fault location. This almost complete lack of co-ordination between instantaneous elements of the several reclosers is a characteristic which the writer feels should receive greater attention in future design.

Leonard M. Olmsted (Duquesne Light Company, Pittsburgh, Pa.): The authors have made a commendable effort to evaluate co-ordination between fuses and oil circuit reclosers, giving consideration to the effect of the fuses cooling partially during the open time of the reclosers. It is interesting to see, however, how much error is introduced if this correction is neglected and the time to melt the fuse taken as a summation of the times during each closed period. Taking the first 370-ampere case, the authors report 2.5 cycles during the first opening of the recloser, 2.5 cycles during the second opening of the recloser, and the fuse blowing in 8.5 cycles during the first time delay period of the recloser. If we add these three, we have a total of 13.5 cycles at 370 amperes to blow the 50-ampere fuse, which compares very favorably with its published time of 13.2 cycles. For this case, then, correction of the fuse curve to allow for cooling time does not appear essential. Applying similar reasoning to the case of the 51-ampere fuse which is intended to blow between the first and second time delay operations of the recloser, Figure 6 of the paper indicates that the fuse requires approximately 28 cycles at 370 amperes to clear. If we deduct from this value the two instantaneous openings at 2 cycles each and the first time delay operation in 19.5 cycles, a total of 23.5 cycles, we would expect the fuse to clear during the second time delay operation in approximately 4.5 cycles. The authors' tests show clearing in 17.5 cycles of the second time delay operation, which is longer than the predicted time but still gives the predicted co-ordination. From these two cases, it would seem reasonable to conclude that correction for cooling time in the fuse link may be desirable but that the error introduced by neglecting it should not be of great importance.

In discussing oil circuit reclosers, it should be kept clearly in mind that the requirements are distinctly different from those applying to most other types of switchgear. Whereas station-type switchgear is installed permanently and with protective characteristics more or less matched to the circuit as a whole, it must be anticipated that pole-mounted reclosers will be subject to frequent relocation as the requirements of the distribution circuits change. Co-ordination with only a single fuse size is not enough. They must cover a wide range of sizes determined by the transformer sizes required for service in some instances to only one residential customer, in other locations for schools, stores, shopping districts, and other sizable consumers. For such applications, it is still desirable that the instantaneous tripping of the recloser be fast enough to protect the smallest fuse link, and that the accumulated time before lockout be sufficient to blow the largest fuse link.

Most of the present reclosers have been designed with a view to application on rural circuits at 7,200 volts or more, where transformer fuses are small and short-circuit currents, limited. When they are installed on suburban circuits operating at 2,400 or 4,160 volts, the relationship between the recloser characteristics and the transformer fuse sizes becomes closer. Suburban service requirements are rigid, in many cases indicating the need for automatic sectionalizing equipment, but most of the reclosers now available only partially meet the requirements. The authors appear to have recognized this situation in their proposal that the recloser lock closed on its final operation, thereby throwing the final clearing of a fault on a line fuse which can be of whatever size is required for co-ordination in the circuit.

This feature seems to be distinctly different from previous thought on the matter, but it is my opinion that it is only a compromise until the designers find a way to incorporate sufficient time delay in the recloser mechanism itself. Considerable improvement has been accomplished during the past ten years in this type of equipment, and it is hoped that this improvement will continue until reclosers become available which fully meet all the requirements of suburban distribution.

G. G. Auer, R. A. Branflick, L. J. Woodward, and W. C. McKinley: The discussions of Mr. Olmsted, Mr. Hutchinson, and Mr. Gmeiner confirm the authors' opinion that maximum benefits in co-ordination can be expected when heating and cooling of fuse links is considered during recloser operation. There is general agreement that the heating factor is predominant while the cooling factor is not of too great importance to achieve co-ordination.

Mr. Gmeiner pointed out that by the necessity of adding the required correction factors, limitations were imposed on the application of line-side fuses. This limitation is determined by the characteristics of the overcurrent device on the source side. If this device is an overcurrent relay, the current tap setting based upon short circuit current values rather than load currents will provide room for co-ordination.

It also was pointed out that the instantaneous operations of the reclosers did not conform to the published curves. The published instantaneous curve only indicates the maximum time required for opening of the recloser. A unit might operate in accordance with this curve but, as tests have shown, they usually open faster than indicated. In a co-ordination study or fuse–recloser curve comparison, it is the maximum time in which recloser instantaneous operation can be expected that determines co-ordination possibilities. Faster time of operation is a definite assurance that co-ordination between fuse and recloser will be obtained.

Mr. Chase Hutchinson's thoughts on future design of reclosers which would provide co-ordination during instantaneous operation would be a big improvement from the standpoint of service continuity and elimination of momentary outages on the main line due to branch circuit faults, but to accomplish this, some sacrifice would have to be made in temporary fault protection on the main circuit or else expensive auxiliary equipment would have to be employed.

Mr. S. R. Smith's discussion of the formula to calculate the cooling increment of the fuse link was a great contribution to this paper and did furnish the necessary information to make the analytical procedure complete. Omission of the mathematical procedure and significance of the cooling factor was pointed out by Mr. Gmeiner, Mr. Hutchinson, and Mr. Olmsted.

Wide-Band D-C Amplifier Stabilized for Gain and for Zero

A. J. WILLIAMS, Jr.
MEMBER AIEE

W. G. AMEY
ASSOCIATE AIEE

WILL McADAM
ASSOCIATE AIEE

Synopsis: Previous technical literature has described direct-coupled d-c amplifiers having a wide frequency pass band but with appreciable zero drift,[1,2] and also has described contact-modulated d-c amplifiers having a relatively stable zero but with a narrow pass band.[3] This paper describes an arrangement of a direct-coupled amplifier together with a contact-modulated amplifier. This arrangement retains the wide band of the former and the zero stability of the latter. Block diagrams are used for explanation, and schematic circuits are given for an experimental setup. Records from a fast recorder and from an oscillograph disclose the results achieved, such as rapid response to a step input and greatly reduced, nonpermanent output disturbances following large, unbalanced changes of heater voltage.

ALMOST any electron tube is fundamentally a d-c amplifier having a wide pass band but, in practice, when it is used simply as a "direct-coupled" d-c amplifier, precautions must be taken to retain stability in the face of changes in supply voltage, cathode temperature, cathode emission characteristics, and contact potentials of the tube electrodes, especially of the control grid.[1,2]

A sufficiently stable gain generally can be obtained by the use of negative feedback.[4]

A sufficiently stable zero (zero output for zero input) is more difficult to obtain, some of the precautions being:

1. Stabilized *B* supply for anodes, screens, and so forth.[5]
2. Balanced, bridge, or push-pull arrangement of tubes.[6,7]
3. Stabilized heater (or filament) supply.[5]
4. Adjustable compensation for changes in supply voltage (or for changes in thermionic emission).[8–18]

Because of these zero-stability difficulties with direct-coupled d-c amplifiers, contact-modulated d-c amplifiers have been found useful, first in systems using a mechanical link in the feed-back loop,[19–22] subsequently without a mechanical link and without feedback,[23,24] and eventually without a mechanical link but with feedback (to stabilize gain).[3] The contact-modulated d-c amplifier is useful because its zero is stable to a fraction of a microvolt.[3] Unfortunately, its frequency pass band is limited by the modulation frequency, for instance, with 60 cycle per second modulation and with gain stabilized to about one part in 1,000, the pass band is only about one cycle per second.

This one cycle per second band width (approximately one second response time) applies equally well to the system with the mechanical link (the self-balancing recorder) and to the system without the mechanical link (the contact-modulate d-c amplifier).

Figure 1 shows that the recorder responds completely in less than one second to a step change in input.[22] With the contact-modulated d-c amplifier (narrow-band)[3] ahead of the recorder, the amplifier response time together with the response time of the recorder results in an over-all response time somewhat greater than a second.

The third curve of Figure 1 was taken with the wide-band amplifier which is the subject of this paper. The response time for the third curve is again less than a second, and is essentially the same as for the recorder alone; hence, the amplifier response time is indicated to be small compared with a second. Figure 2 shows a cathode-ray oscillogram of the response of the wide-band zero-stabilized amplifier alone. Since the time markers at the bottom are spaced by 0.01 second, the reponse time can be conservatively stated as less than 0.005 second. In round numbers, therefore, the response time has been reduced by a factor of 200; hence, the band width has been increased by a factor of 200. At this point it should be stated that the particular amplifier used for these tests is only experimental and is not comparable in gain with the more conventional narrow-band amplifier.[3] The

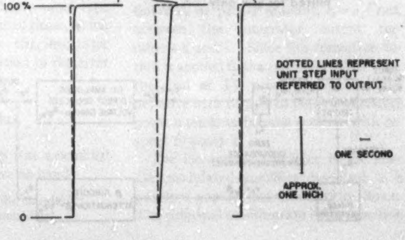

Figure 1. Time response of recorder without and with preamplifiers

Wide-band preamplifier does not contribute appreciable delay

Paper 49-132, recommended by the AIEE Joint Subcommittee on Electronic Instruments and approved by the AIEE Technical Program Committee for presentation at the AIEE Summer General Meeting, Swampscott, Mass., June 20–24, 1949. Manuscript submitted March 21, 1949; made available for printing May 4, 1949.

A. J. Williams, Jr., W. G. Amey, and Will McAdam are all in the Research Department, Leeds and Northrup Company, Philadelphia, Pa.

The authors are grateful to I. M. Stein, Director of Research, Leeds and Northrup Company, for the general support of amplifier development, and for the specific encouragement resulting in the presentation of these results.

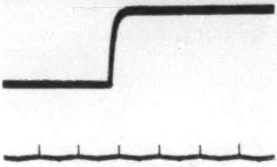

Figure 2. Response of wide-band zero-stabilized amplifier alone

Time markers at bottom are spaced by 0.01 second; hence response is seen to be complete in 0.005 second

principle, however, appears to be applicable to amplifiers of high gain, working down to the natural limits of noise. The discussion which follows is an attempt to explain that principle.

The Problem and the Principle Used for Its Solution

In a simple direct-coupled d-c amplifier, the presence of zero drift cannot be detected (and hence cannot be corrected for) readily without temporarily taking the amplifier out of service, as by shorting the input and observing the output.[25] However, in a direct-coupled amplifier with gain stabilized to a considerable degree (as by feedback), a comparison of input with output divided by gain tells of the presence of zero disturbance at any and all times, with or without signal. The zero stabilization is made on the basis of this comparison.

Figure 3 gives in block form a conventional direct-coupled amplifier with gain stabilized by feedback. The zero drift or disturbance is symbolized by an equivalent voltage e_d entering in an additive way, symbolized by the small block Σ_2. e_x is the input, and e_o is the output. μ is the forward gain, and β is the attenuation in the feed-back circuit. We may write for this circuit

$$\text{Input} = \text{feedback} + \text{error} \tag{1}$$

$$e_x = e_f + e_r \tag{2}$$

$$e_x = e_o\beta + e_r \tag{3}$$

$$e_x = e_o\beta + e_i - ed \tag{4}$$

$$e_x = e_o\beta + e_o/\mu - ed \tag{5}$$

The performance is most apparent when referred to the input, as indicated by equations 1, 2, 3, 4, and 5. The two right-hand terms in equation 5 are the error terms. e_o/μ is the result of limited forward gain and can be reduced below any assigned quantity by increasing the forward gain, μ. The term $-e_d$ represents the troublesome zero disturbance, the effect of which cannot be reduced by increasing the forward gain.

Figure 3 and equation 3 show that the error e_r, which comes from the summing circuit Σ_1, is the result of comparison of input, e_x, with output divided by gain, $e_o\beta$. The error e_r, therefore, should be used to correct for the zero disturbance, as shown in Figure 4.

It is futile to attempt to detect this error with another direct-coupled d-c amplifier (itself subject to zero disturbance), but a contact-modulated d-c amplifier is well suited to this service because of its freedom from zero disturbance. As shown in Figure 4, such an amplifier is employed and is followed by an integrator whose output may be injected at any convenient point, to the right or to the left of the injection of e_d, but, of course, not to the left of the "take off" for the contact-modulated amplifier. Thus, the action will be the same for a zero disturbance occurring at any point between the take off for the contact-moduated amplifier and the output. For the circuit of Figure 4 we may write

$$e_r = e_x - e_f \tag{6}$$

$$= e_x - e_o\beta \tag{7}$$

$$= e_x - e_i\mu\beta = e_x - (e_r + e_d + e_g)\mu\beta = e_x - (e_r + e_d + \alpha \textstyle\int e_r dt)\mu\beta \tag{8}$$

$$= e_x - e_r\mu\beta - e_d\mu\beta - \mu\beta\alpha \textstyle\int e_r dt \tag{9}$$

$$e_r + \mu\beta e_r + \mu\beta\alpha \textstyle\int e_r dt = e_x - \mu\beta e_d \tag{10}$$

For Figure 4 equations 6, 7, 8, 9, and 10 are developed about the error e_r, since it is the error and its reduction with which we are concerned. Equation 10 gives a clue to the performance because of the presence of the integral term, $\mu\beta\alpha\int e_r\, dt$. The nature of this term and the simplicity of the other terms suggest that the error cannot be very large for very long.

Theoretical Performance

Equation 10 provides a basis for computation of the theoretical performance corresponding to prescribed time forms of e_x and e_d.

For convenient manipulation, equation 10 may be rewritten as

$$e_r + K\alpha \int_0^t e_r dt = \frac{K}{\mu\beta} e_x - Ke_d \tag{11}$$

where e_r, e_x, and e_d are functions of time, t, and are assumed to have zero value for all times prior to the reference time $t = 0$; K is equal to $\mu\beta/(1+\mu\beta)$ and μ, β, and α are constants of the system. The Laplace transform of equation 11 then may be written

$$E_r + K\alpha\frac{E_r}{s} = \frac{K}{\mu\beta} E_x - KE_d \tag{12}$$

where E_r, E_x, and E_d are the Laplace transforms of e_r, e_x, and e_c respectively, as functions of the complex variable, s. Solving this equation for the error voltage

$$E_r = \frac{K}{\mu\beta}\left(\frac{s}{s+K\alpha}\right)E_x - K\left(\frac{s}{s+K\alpha}\right)E_d \tag{13}$$

As one of the interesting prescribed time forms, let e_x and e_d be step functions having values of zero, for t less than zero, and constant values $|e_x|$ and $|e_d|$ respectively for t equal to or greater than zero. The Laplace transforms of e_x and e_d are then

$$E_x = \frac{|e_x|}{s}$$

and

$$E_d = \frac{|e_d|}{s} \tag{14}$$

Figure 3. Direct-coupled d-c amplifier stabilized for gain only

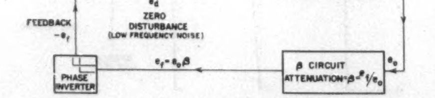
INPUT
(SIGNAL)
$e_x = e_f + e_r$
Σ_1
SUMMING
CIRCUIT
ERROR
$e_r = e_i - e_d$
Σ_2
e_d
ZERO
DISTURBANCE
(LOW FREQUENCY NOISE)
$e_i = e_o/\mu$
D.C. AMPLIFIER
(DIRECT COUPLED)
VOLTAGE GAIN = $\mu = e_o/e_i$
OUTPUT
e_o
e_o
e_o
β CIRCUIT
ATTENUATION = $\beta = e_f/e_o$
$e_f = e_o\beta$
FEEDBACK
$-e_f$
PHASE
INVERTER

Figure 4. Direct-coupled d-c amplifier stabilized for gain and for zero

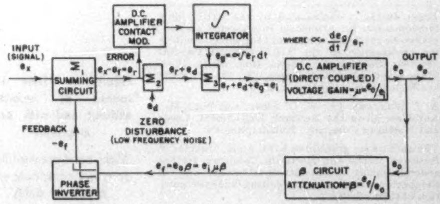
INPUT
(SIGNAL)
e_x
Σ_1
SUMMING
CIRCUIT
ERROR
$e_x - e_f = e_r$
D.C.
AMPLIFIER
CONTACT
MOD.
INTEGRATOR
WHERE $\alpha = \frac{de_g}{dt}/e_r$
$e_g = \alpha\int e_r\, dt$
Σ_2
$e_r + e_d$
Σ_3
$e_r + e_d + e_g = e_i$
e_d
ZERO
DISTURBANCE
(LOW FREQUENCY NOISE)
D.C. AMPLIFIER
(DIRECT COUPLED)
VOLTAGE GAIN = $\mu = e_o/e_i$
OUTPUT
e_o
e_o
e_o
β CIRCUIT
ATTENUATION = $\beta = e_f/e_o$
$e_f = e_o\beta = e_i\mu\beta$
FEEDBACK
$-e_f$
PHASE
INVERTER

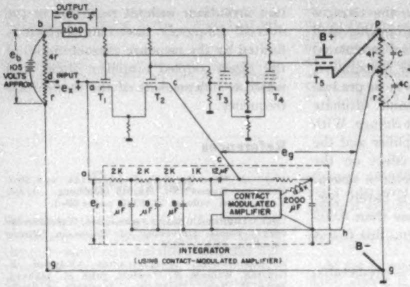

Figure 5. Circuit for experimental setup

respectively, and equation 13 becomes

$$E_r=\frac{K}{\mu\beta}|e_x|\left(\frac{1}{s+K\alpha}\right)-K|e_d|\left(\frac{1}{s+K\alpha}\right) \quad (15)$$

Returning now to the time plane

$$e_r=\frac{K}{\mu\beta}|e_x|\epsilon^{-K\alpha t}K-|e_d|\epsilon^{-K\alpha t} \quad (16)$$

Since the principle of this amplifier is based on the product $\mu\beta$ being large compared with unity, K is nearly equal to unity, and a convenient approximation of equation 16 may be written as

$$e_r=\frac{|e_x|}{\mu\beta}\epsilon^{-\alpha t}-|e_d|\epsilon^{-\alpha t} \quad (17)$$

From equation 16, and more readily from equation 17, it can be seen that the error resulting from an abrupt change of signal is small compared with the signal. Initially it is neither greater nor less than that without the zero stabilizing components; it does, however, vanish with time as a result of the stabilizing components. Again from equation 16, and more readily from equation 17, it can be seen that the error resulting from an abrupt application of a zero disturbance is initially equal to the zero disturbance. If zero disturbances of this abrupt nature were common in practice, the stabilizing components would be of little value, even though the effect of a single such disturbance ultimately would vanish. Fortunately, the more common forms of zero disturbance develop slowly, and the stabilizing components are effective. This can be seen from analysis of the response to uniformly changing or "ramp" functions for e_x and e_d.

In this case, e_x and e_d have values of zero for t less than zero, and values expressed by

$$e_x=a_xt$$

and

$$e_d=a_dt \quad (18)$$

for t equal to, or greater than, zero. The Laplace transforms of e_x and e_d are

$$E_x=\frac{a_x}{s^2}$$

and

$$E_d=\frac{a_d}{s^2} \quad (19)$$

respectively, and equation 13 becomes

$$E_r=\frac{K}{\mu\beta}a_x\frac{1}{s(s+K\alpha)}-Ka_d\frac{1}{s(s+K\alpha)} \quad (20)$$

Returning to the time plane

$$e_r=\frac{K}{\mu\beta}\frac{a_x}{\alpha}\left(1-\epsilon^{-K\alpha t}\right)-K\frac{a_d}{\alpha}\left(1-\epsilon^{-K\alpha t}\right) \quad (21)$$

Since K is nearly equal to unity (as before), a convenient approximation for equation 21 is

$$e_r=\frac{1}{\mu\beta}\frac{a_x}{\alpha}\left(1-\epsilon^{-\alpha t}\right)-\frac{a_d}{\alpha}\left(1-\epsilon^{-\alpha t}\right) \quad (22)$$

From equation 21, and more readily from equation 22, it can be seen that the error resulting from a uniformly changing or ramp-type signal is, at all times, quite small.

Again, from equation 21 and more readily from equation 22, if a ramp-type zero disturbance has a rate of rise a_d which is small compared with the integrator coefficient α, its contribution to the error will, at all times, be small.

Experimental Apparatus

An experimental setup was assembled from two items which were on hand:

1. A contact-modulated d-c amplifier[3]
2. A direct-coupled d-c amplifier

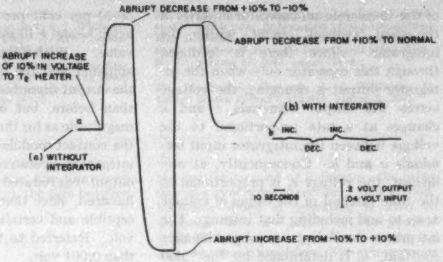

Figure 6. Response to abrupt changes in one heater voltage

The one heater is that of 1/2 of the input stage of the direct-coupled amplifier

Figure 5 shows the direct-coupled voltage amplifier in tube sections T_1, T_2, T_3, T_4, and T_5. The rectifier-filter elements, (which are not shown), supply about 400 direct volts across the B+ and B− terminals.

The principal negative feedback is from the point p through the 5-to-1 voltage divider p-h-g, through the low impedance output of the integrator to the control grid of T_2. More exactly, the feedback is from both terminals of the output load, using both voltage dividers to the two grids of the differential input stage comprising T_1 and T_2. T_1 and T_2 are direct-coupled to T_4 and T_3 respectively to provide effective differential action.

It will be noted that the input signal e_x is connected in series with the grid of T_1 from the divider point d as shown. The integrator output, on the other hand, is connected in series with the grid of T_2 from the other divider point h. Since the voltage dividers p-h-g and b-d-g have exactly the same ratios, the output load voltage bears the proper relation to the input signal (that is, $e_o=e_x/\beta$) only if points a and h are at the same potential. The integrator input terminals are connected to points a and h to measure the error voltage, $e_r=e_x-e_o\beta$, and to effect corrective action by modifying grid potential of T_2 in proper amount, $e_g=\alpha\int e_r dt$, between the integrator output terminals h and c. Since the corrective action is applied to the grid of T_2 rather than the grid of T_1, point c must become negative with respect to point h whenever point a tends to become positive with respect to point h.

The integrating amplifier is the contact-modulated amplifier described in a previous paper,[3] and modified as shown. The principal modification is the insertion of the 12-microfarad capacitor in series in the local feedback circuit, within the integrator. Since there is feedback through this capacitor only when the integrator output is changing, the voltage across the output terminals *c* and *h* changes at a rate proportional to the voltage between the integrator input terminals *a* and *h*. Consequently, at any instant, the voltage e_g is proportional to the time integral of the values of voltage e_r up to and including that instant. The integrator coefficient or proportionality constant, α, is determined by the 7,000 ohms of resistance in the input filter, and the 12 microfarads of capacitance in the feed-back circuit. The determining relation is $\alpha = 1/RC$, so that

$$\frac{1}{\alpha} = RC = 7{,}000 \times 12 \times 10^{-6} = 0.08 \text{ second}$$

for the integrator shown.

Observed Performance

The experimental setup of Figure 5 was used to obtain the third curve of Figure 1 and the oscillogram of Figure 2.

Since changes of cathode temperature are known to produce zero disturbances, the heater voltage of T_2 was varied abruptly ±10 per cent from the rated value, while that of T_1 was held constant at rated value. Figure 6 shows a record of the output voltage. With the contact-modulated amplifier and the integrator inoperative, the output swung more than 1.6 volts. The effect persisted as long as the heater voltage was held off normal. With the contact-modulated amplifier and the integrator operative, the output voltage swing was only 0.03 volt, or a reduction of 50-to-1; moreover, after about 10 seconds, the output disturbance had vanished.

Figure 7 shows the effect of changing the heater voltage of T_2 at a uniform rate of 20 per cent per minute, the changes again being ±10 per cent from the rated value. With the contact-modulated amplifier and the integrator inoperative, the output disturbance was more gradual than before, but of the same ultimate magnitude as for the abrupt change. With the contact-modulated amplifier and the integrator operative, the effect on the output was reduced by a factor of several hundred, since that effect is barely perceptible and certainly is less than 0.005 volt. Referred to the input, this is less than 0.001 volt.

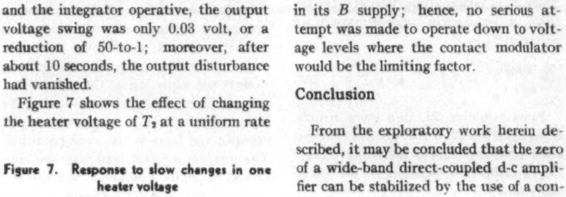

Figure 7. Response to slow changes in one heater voltage

This small order of error is predictable from equation 22. The first curve of Figure 7, with the contact-modulated amplifier and the integrator inoperative, shows the output voltage changing at about 0.04 volt per second, which is 0.008 volt per second when referred to the input. That is, $a_d = 0.008$ volt per second. $1/\alpha$, as determined by the resistance and capacitance constants of the experimental apparatus, was previously calculated as 0.08 second. Extracting from equation 22 the term applicable to the maximum error from a ramp-type zero disturbance

$$e_{r_{max}} = \frac{a_d}{\alpha} = a_d \frac{1}{\alpha}$$

$$= (0.008 \text{ volt per second})\,(0.08 \text{ second})$$

$$\cong 0.0006 \text{ volt}$$

Hence the calculated value of error checks the observed value, in that both are less than 0.001 volt.

The direct-coupled amplifier with which this experimental work was done had definite limitations, such as fluctuations in its *B* supply; hence, no serious attempt was made to operate down to voltage levels where the contact modulator would be the limiting factor.

Conclusion

From the exploratory work herein described, it may be concluded that the zero of a wide-band direct-coupled d-c amplifier can be stabilized by the use of a contact modulator without reduction of the over-all frequency pass band, which is limited by the response characteristics of the direct-coupled amplifier alone, and which is independent of the modulation frequency.

References

1(a). A High-Gain D-C Amplifier for Bio-Electric Recording, **Harold Goldberg.** *AIEE Transactions*, volume 59, 1940, pages 60–4.

1(b). Direct-Coupled Amplifiers, **Harold Goldberg.** *Thesis*, University of Wisconsin Library (Madison, Wisc.), 1936.

2. Distributed Amplification, **Edward L. Ginzton, William R. Hewlett, John H. Jasburg, Jerre D. Noe.** *Proceedings*, Institute of Radio Engineers (New York, N. Y.), volume 36, 1948, pages 956–69.

3. D-C Amplifier Stabilized for Zero and Gain, **A. J. Williams, Jr., R. E. Tarpley, W. R. Clark.** *AIEE Transactions*, volume 67, 1948, pages 47–57.

4. An Improved Vacuum Tube Microammeter, **A. W. Vance.** *Review of Scientific Instruments* (New York, N. Y.), volume 7, 1936, pages 489–93.

5. The "Speedomax" Power-Level Recorder, **William Russell Clark.** *AIEE Transactions*, volume 59, 1940, pages 957–64.

6. The Measurement of Ionization Currents by Three-Electrode Valves, **J. Bretano.** *Nature* (London, England), volume 108, 1921, page 532.

7. A Valve-Amplifier for Ionization Currents, **C. E. Wynn-Williams.** *Proceedings*, Cambridge Philosophical Society (London, England), volume 23, 1927, pages 811–28.

8. The Application of a Valve Amplifier to the Measurement of X-Ray and Photo-Electric Effects, **C. E. Wynn-Williams.** *Philosophical Magazine* (London, England), volume 6, 1928, pages 324–34.

9. A Triode Amplifier for Small Direct Currents, **Alexander Marcus.** *Physical Review* (New York, N. Y.), volume 31, 1928, pages 302–3.

10. The Application of a Valve Amplifier to the Measurement of X-Ray and Photo-Electric Effects, **J. Bretano.** *Philosophical Magazine* (London, England), volume 7, 1929, pages 685–91.

11. A Bridge Grid Resistor Amplifier, **Joseph Razek, Peter J. Mulder.** *Journal*, Optical Society of America (New York, N. Y.), volume 19, 1929, pages 390–403.

12. Measurement of Small D-C Potentials and Currents in High Resistance Circuits by Using Vacuum Tubes, **W. B. Nottingham.** *Journal*, Franklin Institute (Philadelphia, Pa.), volume 209, 1930, pages 287–348.

13. 1-Tube Balanced Circuit for D-C Vacuum Tube Amplifiers of Very Small Current, **Walter Soller.** *Review of Scientific Instruments* (New York, N. Y.), volume 3, 1932, pages 416–22.

14. An Improved D-C Amplifying Circuit, **Lee A. DuBridge, Hart Brown.** *Review of Scientific Instruments* (New York, N. Y.), volume 4, 1933, pages 532–6.

15. Uber ein neuartiges Rohrengalvanometer, **G. Barth.** *Zeitschrift fur Physik* (Berlin, Germany), volume 87, 1934, pages 399–408.

16. Direct-Current Amplifier Circuits for Use with Electrometer Tube, **D. B. Penick.** *Review of Scientific Instruments* (New York, N. Y.), volume 6, 1935, pages 115–20.

17. The Measurement of Small Potential Differences by Means of a Double Triode Valve in a Bridge Circuit, **J. C. M. Bretano, P. Ingleby.** *Journal of Scientific Instruments* (London, England), volume 16, 1939, pages 81–4.

18. Improvements in the Stability of the *FP-54* Electrometer Tube, **J. M. Lafferty, K. H. Kingdon.** *Journal of Applied Physics* (New York, N. Y.), volume 17, 1946, pages 894–900.

19. New Instruments: "Speedomax," **Leeds and Northrup Company.** *Instruments* (New York, N. Y.), volume 6, 1933, page 211.

20. Recorder and Control Circuits, A. J. Williams, Jr. United States Patent 2,113,164, April 5, 1938.

21. Combined Thyratron and Tachometer Speed Control of Small Motors, A. J. Williams, Jr. *AIEE Transactions*, volume 57, 1938, pages 565–8.

22. Electronically Balanced Recorder for Flight Testing and Spectroscopy, A. J. Williams, Jr., W. R. Clark, R. E. Tarpley. *AIEE Transactions*, volume 65, 1946, pages 205–8.

23. Some Experiments on the Amplification of Thermocouple Electromotive Forces, Ross Gunn. *Review of Scientific Instruments* (New York, N. Y.), volume 9, 1938, pages 267–9.

24. A Contact Modulated Amplifier to Replace Sensitive Suspension Galvanometers, Max D. Liston, C. E. Quinn, W. E. Sargeant, G. G. Scott. *Review of Scientific Instruments* (New York, N. Y.), volume 17, 1946, pages 194–8.

25. Measuring Systems, A. J. Williams, Jr. United States Patent 2,312,945, March 2, 1943.

Discussion

Edwin A. Goldberg (RCA Laboratories, Princeton, New Jersey): The principle of the wide-band zero-stabilized amplifier disclosed by Mr. Williams has been employed for quite some time in amplifiers developed under a government contract at the RCA Laboratories for the Special Devices Center, Office of Naval Research for computing purposes. This development was declassified on June 15, 1949. It is also used by the Reeves Instrument Company in amplifiers employed in some models of the *REAC* analog computer. Figure 1 of the discussion is a block diagram of the version used. It utilizes current-summation feedback rather than voltage-summation feedback, and provides for both a grounded input and grounded output without utilizing any floating power sources. The d-c amplifier portion is quite conventional. A is the input grid terminal of the first tube, B is the amplifier output terminal, and C is a point within the amplifier where a zero setting voltage normally is applied. Z_f is the feedback impedance, and Z_i the input impedance. A sample of the voltage at A is chopped, amplified by an a-c amplifier, rectified by a synchronous rectifier, filtered, and applied to point C. If the d-c amplifier has the same gain, $G_1(\omega)$, for signals applied at either point A or point C, and the gain of the chopper, amplifier, rectifier, and filter from point A to point C is $G_2(\omega)$, the gain between points A and B is

$$G_{AB}(\omega)=G_1(\omega)G_2(\omega)+G_1(\omega)$$

At d-c ($\omega=0$), $G_1(0)=50{,}000$ and $G_2(0)=3{,}000$ giving a value for the forward gain $G_{AB}(0)$ of 150×10^6 in a typical computing amplifier, and making possible very high feed-back loop gain to stabilize net over-all gain with feedback against variations in gain within the amplifier itself.

As the frequency increases from direct current, $G_2(\omega)$ decreases about six decibels per octave due to the time constant of 10 seconds for the filter. At 50 cycles, the $G_2(\omega)$ is about unity while $G_1(\omega)$ is still about 50,000, resulting in a forward gain of 100,000. Thus, it can be seen that in addition to minimizing zero offset and drift, the stabilizer also increases the net forward gain even for low a-c frequencies. At high frequencies, $G_2(\omega)$ becomes negligible, and the forward gain is the same as the gain of the d-c amplifier without the stabilizer. The tube complement of this amplifier consists of a *5692*, a *6SH7*, and a *6V6* in the d-c amplifier, and two *5693*'s in the a-c amplifier.

The mechanical chopper is an unpolarized vibrating-reed device which is driven from a 193-cycle source and vibrates at 386 cycles. It has two pairs of contacts, one pair being used as a chopper, the other pair as a synchronous rectifier. The second-harmonic mode of operation is used to minimize false d-c offset due to possible stray 193-cycle pickup from the vibrator drive in the a-c amplifier. The synchronous rectifier is insensitive to frequencies other than 386 cycles.

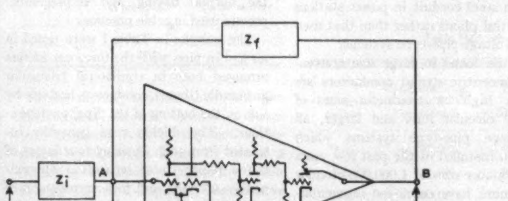

Figure 1. Block diagram of wide-band amplifier

The gain of the amplifier with feedback is the ratio Z_f/Z_i. If Z_f and Z_i are both resistors, the amplifier has a flat frequency response. By supplying several inputs through separate resistors, the amplifier becomes an adding device. If Z_f is made a capacitor and Z_i a resistor, the device becomes an integrator which has an extremely low inherent drift rate. If Z_i is made a capacitor and Z_f a resistor, the device becomes an excellent differentiator with a negligible d-c offset.

The magnitude of d-c offset referred to input grid of the stabilized amplifier depends on three factors:

1. **The inherent effective d-c offset of the chopper itself and associated circuits**
2. **The value of $G_2(0)$**
3. **The voltage e_d which would normally have to be applied at C to zero the amplifier.**

The offset due to (1) is normally negligible, provided the chopper is carefully made and utilized. The offset due to (2) and (3) to first order approximation is $e_d/G_2(0)$. Offsets of about 50 microvolts or less may be obtained fairly easily in computing amplifiers utilizing input and feed-back resistors in the megohm range.

This principle of zero drift elimination may be applied to extremely broad band amplifiers such as video amplifiers with flat response from direct current to extremely high frequencies. The response characteristics of the computing amplifiers used by RCA Laboratories depends on the nature of Z_f and Z_i; however, if both Z_f and Z_i are resistors, the response is extremely flat from direct current to 100 kc.

The accuracy, utility, and ease of operation of d-c-type analog computers have been increased by a large factor through the incorporation of these amplifiers, because the frequent manual adjustments of the amplifier d-c zeros have been eliminated entirely.

A. J. Williams, Jr.: It is gratifying to learn from Mr. Goldberg that he and others have found utility in a wide-band zero-stabilized amplifier similar in principle to the amplifier we have described. Over 20 years of experience with chopper amplifiers at Leeds and Northrup Company have given us considerable confidence in them; hence we are inclined to think up new ways to use them and are pleased that others find new ways to use them too.

A-C Resistance of Segmental Cables in Steel Pipe

L. MEYERHOFF
MEMBER AIEE

G. S. EAGER, JR.
ASSOCIATE AIEE

Synopsis: In recent years, there has been a very great increase in the use of pipe-type systems for long, high-voltage impregnated-paper transmission feeders. Thus, a detailed knowledge of the factors influencing the a-c losses of large size conductors with relatively low skin-proximity effect characteristics is of value to all cable and operating engineers. This paper reports the results of a study of the effective a-c resistance of a compact type of segmental conductor in sizes from 1,000,000 to 2,000,000 circular mils, in air and in steel pipe, with equilateral triangular and cradle configurations. From analysis of the data, an approximate separation is made of losses occurring in the conductor, the outer shield structure and the steel pipe. These component losses are compared with accepted and derived formulas, and application of the data is thus broadened by use of mathematical methods. Based upon the suggested methods of computation, tables are given of losses of cables in steel pipe over a range of conductor sizes and voltage ratings.

SINCE the war there has been a great increase in the use of impregnated paper insulation under high oil or gas-pressure in steel pipe for long high-voltage transmission feeders. Thus, the need for reliable data on carrying capacities of such systems has been greatly enhanced.

The data here presented are not claimed or believed to constitute a complete answer to the problem and are submitted with the hope that they will be found useful to the industry and serve to stimulate other investigators in the accumulation of further data. In presenting this paper, the authors do so with a full appreciation of the benefits accruing to the entire industry from a free discussion of the design factors involved. Sufficient operating and test data have not been and are not available to justify the making of warranties.

While considerable data on the purely thermal elements of the problem have been given in a previous publication[10] only very meager data are available in the technical literature on the a-c loss aspect of cable assemblies of practical interest in pipe-type systems.

Wiseman[1] has made available to the industry data on conventional concentric strand conductors in steel pipe, and also has presented measurements on a single size of segmental conductor. However, in all cases the cable assembly employed was designed primarily to simulate that used in practice on nonleaded low-voltage rubber or varnished cambric cables installed in steel conduit in power stations or industrial plants rather than that used on high-voltage pipe-type systems.

Since the losses in large size conventional concentric strand conductors are relatively high for conductor sizes of 1,000,000 circular mils and larger, all high-voltage pipe-type systems which have been installed in the past few years with conductor sizes of 1,000,000 circular mils or more have employed segmental-type conductors to obtain lower a-c losses.

In the construction of high-voltage pipe-type cables it has been the invariable practice to provide mechanical protection over the individual cables in the form of helically applied, D-shaped copper wires, sometimes termed skid wires. These are usually applied over a surface wrapping consisting of one or more copper tapes intercalated with nonconducting tapes. In some constructions, the nonconducting tape has been a heavy cotton, duck, or paper tape. In others, a polyethylene tape has been used because of its nonhygroscopic nature. In some cable which has been manufactured the surface wrapping has been comprised of two intercalated copper tapes. (None of these cables had a permanent lead sheath.) The protective covering just described, which will be termed the "shield" in what follows, contributes a significant fraction of the total a-c loss of the system, largely because of the circulating currents set up by the induced voltage.

Cables Tested

The cable samples tested and their construction were those shown in Table I. All conductors consisted of four segments, three of which were insulated (insulation consisted of three paper tapes), bound together by a slightly overlapped bronze tape of about 40 per cent conductivity. The individual 90-degree segments were of the Compack type, the essential characteristic of which is that all layers are stranded in one direction, each layer being rolled as applied. In all cases the cable samples were subjected to the normal drying and impregnating process used in cable practice.

The samples in Table I were tested in air and in pipe, with the three conductors arranged both in equilateral triangular and cradle (that is, conductors laid side by side on the bottom of the pipe) configurations. The shields were generally insulated from each other by four layers of heavy paper (total separation approximately 40 mils) and measurements were made both with the shields electrically connected together at the ends, and with the shields not connected together.

For samples *1A*, *1B*, *3A* and *3B*, the pipe used was a length of electrically-welded steel pipe 20 feet 6 inches long having an internal diameter of 6.10 inches and a wall thickness of 0.28 inch and having electrical characteristics as shown in Table II. The cable lengths

---

Paper 49-135, recommended by the AIEE Insulated Conductors Committee and approved by the AIEE Technical Program Committee for presentation at the AIEE Summer General Meeting, Swampscott, Mass., June 20–24, 1949. Manuscript submitted November 16, 1948; made available for printing April 26, 1949.

L. MEYERHOFF and G. S. EAGER, JR. are both with the General Cable Corporation, Bayonne, N. J.

Table I. Cables With Segmental Conductors

Designation	Conductor Size, Circular Mils	Conductor Diameter, Inches	Insulation Wall, Inches	Type of Shield	Dimensions of Skid or D-Wires, Inches
1A	1,000,000	1.12	0.500	HR*	0.070×0.200
1B	1,000,000	1.12	0.500	LR†	0.070×0.200
2A	1,500,000	1.36	0.600	HR**	0.100×0.200
2B	1,500,000	1.36	0.600	LR†	0.100×0.200
3A	2,000,000	1.58	0.315	HR**	0.100×0.200
3B	2,000,000	1.58	0.315	LR†	0.100×0.200

HR = high resistance. LR = low resistance.

* Consists of three 3-mil copper tapes, each intercalated with a 7-mil polyethylene tape. Thereover two skid wires, double start, spaced 1 to 1¹/₄ inches.

** Consists of two 3-mil copper tapes, each intercalated with a 7-mil polyethylene tape. Thereover two skid wires, double start, spaced 1 to 1¹/₄ inches.

† Consists of one 3-mil copper tape, intercalated with a 7-mil polyethylene tape and two 3-mil copper tapes intercalated with each other. Thereover two skid wires, double start, spaced 1 to 1¹/₄ inches.

Table II. Electrical Characteristics of Steel Pipes at 30 Degrees Centigrade

Pipe, Inside Diameter, Inches	Wall Thickness, Inches	D-C Resistance, Microhms Per Foot	Resistivity, Microhm Inches	A-C Resistance, Microhms Per Foot at Various Currents (Amperes) 50	100	150	200	250	300
6.10	0.28	12.2	5.62	72	108	149	158	159	157
8.02	0.32	7.65	5.15	90	144	152	149	143	137

Return conductor inside of pipe for a-c measurements.

Table III. Skin Effect (Y_o) Measurements 9-Inch Spacing

Cable Designation	Conductor Size, Circular Mils, (Segmental)	Type of Shield	D-C Resistance at 30 Degrees Centigrade, Microhms Per Foot	Skin Effect (Y_o) Measured	Computed
1A	1,000,000	HR	10.75	0.02	0.02
1B	1,000,000	LR	10.75	0.02	0.02
2A	1,500,000	HR	7.30	0.03	0.04
3A	2,000,000	HR	5.32	0.07	0.07

Table IV. A-C Losses in Air—Triangular Configuration

Designation	Conductor Size, Circular Mils (Segmental)	Type of Shield	S, Inches	Shields Insulated (SI) or Shields Short Circuited (SS)	R_{ac}/R_{dc} Measured	Computed*
1A	1,000,000	HR	2.38	SI	1.03	1.03
				SS	1.04	1.06
1B	1,000,000	LR	2.38	SI	1.05	1.06
				SS	1.15	1.17
2A	1,500,000	HR	2.83	SI	1.04	1.06
				SS	1.07	1.11
2B	1,500,000	LR	2.80	SI	1.12	1.10
				SS	1.28	1.27
3A	2,000,000	HR	2.42	SI	1.14	1.13
				SS	1.19	1.20
3B	2,000,000	LR	2.46	SI	1.17	1.19
				SS	1.41	1.46

S = center-to-center spacing of adjacent conductor in inches.

* On the basis of mathematical and empirical equations offered here under Development of Method for Computation of Losses. For proximity loss, $K = 3.8$.

used were 25 feet, potential points being placed 20 feet apart.

For samples *2A* and *2B*, the pipe used was a length of lap-welded steel pipe 15 feet 6 inches long having an internal diameter of 8.02 inches and a wall thickness of 0.32 inch and having electrical characteristics as shown in Table II. The cable lengths used were 20 feet, potential points being placed 15 feet apart.

Copper lugs were soldered to each end of each cable length. At each potential point the insulation, the outer shield, the binder, and the segment insulation were removed for a longitudinal distance of one inch. Potential leads were soldered to the conductor, and the segments tied together at the potential points by binding wire.

Measurements—Methods and Accuracy

The apparatus and methods of measurement are described in detail in Appendix I. This Appendix also discusses the accuracy of the resistance measurements and gives results of comparative tests with other laboratories or equipment.

Cable 3A, together with the 6-inch pipe used in the present series of measurements was sent to the Electrical Testing Laboratories (ETL) for comparative measurements. A-c to d-c ratios compared as follows:

	Cable in Air	Cable in Pipe
Authors	1.19	1.63
ETL	1.205	1.65

While making a joint study with the Philadelphia Electric Company, losses were measured both by the method described in Appendix I and by use of a deflecting wattmeter supplied by Philadelphia Electric Company. Comparative values of watts loss were as follows:

	At Room Temperature	At 68.5 Degrees Centigrade
Authors	714	732
Philadelphia Electric Company	713	736

These comparisons are described in greater detail in Appendix I.

Results of Experimental Work

Measurements were made for each size and configuration of cable, at five currents—160, 320, 480, 640 and 800 amperes. Temperatures during the measurements were in the range of 26 to 32 degrees centigrade. The results reported in the following tables, unless otherwise noted, are at ambient temperature somewhere in this range, and at a conductor current of 800 amperes for 1,500,000 and 2,000,000-circular-mil conductor sizes, and 640 amperes for the smaller sizes.

Single-Phase Measurements—Skin Effect

In Table III are listed measured skin effect values of the various cables tested, in comparison with values computed on the basis that the skin effect of a segmental conductor is equal to that of a round conductor having 2.3 times the d-c resistance of the segmental.

THREE-PHASE MEASUREMENTS—IN AIR AND IN PIPE

Measured loss ratios for triangular configuration in air are given in Table IV; for triangular configuration in steel pipe in Table V; and for cradle configuration in steel pipe in Table VI. In each table there are shown for comparison values computed as later explained.

CALORIMETRIC MEASUREMENTS OF PIPE LOSS (Y_t)

Five calorimetric measurements of pipe loss were made by a method paralleling that used by Salter[2] but with certain refinements to give greater assurance of accuracy. The method used is described in detail in Appendix I. The results of these measurements are shown in Table VII.

Table VII. Pipe Loss (Y_t)—Calorimetric Measurements

Designation	Conductor Size, Circular Mils	Configuration	S, Inches	p, Inches	Measured Pipe Loss†	Computed K_1 for Equation 15
2A	1,500,000	Triangular*	2.83	8.02	0.19	0.0178
2A	1,500,000	Cradle*	2.83	8.02	0.28	0.0162
3A	2,000,000	Triangular*	2.42	6.10	0.25	0.0191
Special**	1,500,000	Triangular	2.07	6.10	0.16	0.0208
Special**	1,500,000	Cradle	2.07	6.10	0.26	0.0202

Average K_1 for 8.02-inch pipe—0.017
Average K_1 for 6.10-inch pipe—0.020

* With shields insulated.

** Uninsulated conductors (segmental), assembled with desired spacing and configuration by means of mechanical separators.

† In terms of d-c conductor loss.

INDUCED VOLTAGE IN SHIELD

Induced shield voltage was measured on one type of cable in air and in pipe to establish the ratio between the two. The measured value in air agreed very satisfactorily with the value computed from the equation

$$e = 0.0529\ I\ \log_{10}\frac{S}{c} \qquad (1)$$

where

e = induced voltage, volts to neutral, per 1,000 feet
S = center-to-center spacing of conductors, inches
c = mean shield radius, inches
I = current in amperes

The ratio between the induced voltages in pipe and in air was found to be 1.35 and this value has been used in the computations of shield circulating current. It is interesting to note in this connection, though not directly pertinent, that Del Mar[9] reports a ratio of 1.3 between the reactance of cables in pipe and in air. Results are shown in Table VIII.

SHIELD RESISTANCE

Resistance of some of the shields and components was measured and values obtained as in Table IX. These measured values were used as a basis for calculating the shield and component resistances of the various shields.

Determination of Component Losses from the Data

Measurements having been made in air and in pipe, with shields insulated and with shields short circuited, on cables with low-resistance shields and on similar cables with high-resistance shields, it is possible to arrive by differences at reasonable approximations of the component losses in air and in pipe. For the separation of the losses in pipe it was necessary first to calculate the pipe loss itself, which was done by use of semi-empirical equation 15, with $K_1 = 0.020$ for the 6.10-inch inside diameter pipe and 0.017 for the 8.02-inch inside diameter pipe, determination of which is shown in Table VII.

The results of the separation of losses for the six segmental cables here reported are shown in Table X, together with the method used in arriving at the various values.

Table V. A-C Losses in Pipe—Triangular Configuration

Designation	Conductor Size, Circular Mils (Segmental)	Type of Shield	S, Inches	p, Inches	Shields Insulated (SI) or Shields Short Circuited (SS)	R_{ac}/R_{dc} Measured	R_{ac}/R_{dc} Computed*
1A	1,000,000	HR	2.38	6.10	SI	1.19	1.19
					SS	1.25	1.24
1B	1,000,000	LR	2.38	6.10	SI	1.22	1.26
					SS	1.46	1.46
2A	1,500,000	HR	2.83	8.02	SI	1.26	1.29
					SS	1.33	1.37
2B	1,500,000	LR	2.80	8.02	SI	1.34	1.39
					SS	1.65	1.69
3A	2,000,000	HR	2.42	6.10	SI	1.53	1.51
					SS	1.62	1.63
3B	2,000,000	LR	2.46	6.10	SI	1.68	1.66
					SS	2.20	2.16

p = Inside diameter of pipe in inches.

* On the basis of mathematical and empirical equations here offered under Development of Method for Computation of Losses. For proximity loss, $K = 3.8$. For pipe loss, $K_1 = 0.020$ for 6-inch pipe and $K_1 = 0.017$ for 8-inch pipe.

Table VI. A-C Losses in Pipe—Cradle Configuration

Designation	Conductor Size, Circular Mils (Segmental)	Type of Shield	S, Inches	p, Inches	Shields Insulated (SI) or Shields Short Circuited (SS)	R_{ac}/R_{dc} Measured	R_{ac}/R_{dc} Computed*
2A	1,500,000	HR	2.83	8.02	SI	1.38	1.40
					SS	1.50	1.53
2B	1,500,000	LR	2.80	8.02	SI	1.45	1.49
					SS	2.01	1.96
3A	2,000,000	HR	2.42	6.10	SI	1.69	1.63
					SS	1.82	1.79
3B	2,000,000	LR	2.46	6.10	SI	1.79	1.78
					SS	2.37	2.42

* On the basis of mathematical and empirical equations here offered under Development of Method for Computation of Losses. For proximity loss, $K = 3.8$. For pipe loss, $K_1 = 0.020$ for 6-inch pipe and $K_1 = 0.017$ for 8-inch pipe.

Table VIII. Induced Shield 3-Phase 60-Cycle Voltage

Cable Used–number 2B–1,500,000–circular-mil Segmental, Low-Resistance Shield; Configuraton–triangular; Center-to-Center Spacing–S=2.83 inches; Mean Shield Radius (less skid wires) c=1.31 inches; Conductor Current, I=802 amperes

	Volts Per 1,000 Feet
Measured shield voltage in air (average of three cables)	—14.0
Calculated shield voltage (by Equation (1))	—14.2
Measured shield voltage in 8.02-inch pipe (average of three cables)	—19.0
Ratio of voltage in pipe to voltage in air, 1.35	

Development of Method for Computation of Losses

Based upon accepted equations for computation of the component losses in air, modified formulas have been developed for the computation of corresponding component losses in pipe, the modifications being those indicated by the data. Additionally, a formula for pipe loss in nonmagnetic pipe has been developed and this also has been modified, as indicated by the data, for magnetic pipe.

In a 3-phase system of the type here discussed, with current, I, flowing through the conductors, the a-c loss may be expressed as I^2R_{ac}, where R_{ac} is the effective a-c resistance. R_{ac} may be regarded as consisting of several components and may be expressed for convenience in terms of R_{dc}, the d-c resistance, as

$$\frac{R_{ac}}{R_{dc}}=1+Y_c+Y_s+Y_i \qquad (2)$$

where

Y_c = increment in ratio due to increased losses in the conductor

Y_s = increment in ratio due to losses in the shield

Y_i = increment in ratio due to losses in the pipe

Y_c and Y_s may be further subdivided as follows

$$Y_c=Y_o+Y_{cp} \qquad (3)$$

and

$$Y_s=Y_{sc}+Y_{sp} \qquad (4)$$

where

Y_o = increment in ratio due to skin effect in the conductors

Y_{cp} = increment in ratio due to proximity effect in the conductors

Y_{sc} = increment in ratio due to circulating current in the shield

Y_{sp} = increment in ratio due to proximity effect in the shield

If the system is operated in air instead of in pipe, Y_i vanishes. To avoid confusion, the symbols for component losses in air will be shown, respectively, as Y_c', Y_s', and so forth.

Each of the foregoing components must be evaluated separately, and may be evaluated in the manner given below. It should be noted that absolute accuracy for each component is not claimed, as there is doubtless some influence of each component on each of the others. However, the total loss as calculated fits satisfactorily the total losses determined on the samples actually measured, and there is also fairly satisfactory correlation between calculated component losses and corresponding component losses as measured directly or as derived from measurements. It is believed that the scheme of evaluation here given provides a rational basis for evaluation of losses within the practical range of segmental high-voltage cables in pipe.

Inasmuch as all measurements were made at 26 to 32 degrees centigrade, the values obtained in the below calculations are on the basis of a temperature of 30 degrees centigrade. Later it will be indicated how the results may be translated to other temperatures.

The forms of the equation used in the following are, as far as possible, based on those of equations generally accepted, but the constants are in general obtained empirically on the basis of component losses derived from the data.

CONDUCTOR SKIN EFFECT (Y_o)

Skin effect of segmental conductors may be evaluated reasonably closely by use of the more or less generally accepted rule that it is equal to the skin effect of a round solid conductor having 2.3 times the d-c resistance of the segmental conductor. For convenience, the values for conductors from 1,000,000 to 2,000,000 circular mils are given in Table XI.

CONDUCTOR PROXIMITY EFFECT (Y_{cp} AND Y_{cp}')

The proximity effect, resulting from superposition of the magnetic fields due to the individual currents in the three conductors, has been worked out for round solid conductors by various in-

Table IX. Resistance of Shield and Components

Cable Designation	Conductor Size, Circular Mils	Type of Shield	Approximate Over-all Diameter, Inches	Resistance, Microhms Per Foot of Cable: Entire Shield R_s	Resistance, Microhms Per Foot of Cable: Skid Wires	Resistance, Microhms Per Foot of Cable: Calculated* for Shield Less Skid Wires R_s'
1A	1,000,000	HR	2.36	955		
1B	1,000,000	LR	2.36	240	1,310	295
2A	1,500,000	HR	2.78	845		
2B	1,500,000	LR	2.78	242	1,010	318
3A	2,000,000	HR	2.40	890		
3B	2,000,000	LR	2.40	217	880	289

* Calculated on basis of parallel resistances.

Table X. Separation of Losses

	Cable Designations: *1A*	*1B*	*2A*	*2B*	*3A*	*3B*
Triangular Configuration in Air (Table IV)						
Measured R_{ac}/R_{dc}—shields insulated (RSI)	*1.03*	*1.06*	*1.04*	*1.12*	*1.14*	*1.17*
Measured R_{ac}/R_{dc}—shields short circuited (RSS)	*1.04*	*1.15*	*1.07*	*1.28*	*1.19*	*1.41*
Skin plus proximity effect in conductor (Y_c')	0.03	0.03	0.04	0.04	0.14	0.14
Shield circulating current loss (Y_{sc}')	0.01	0.10	0.03	0.16	0.05	0.24
Shield proximity loss (Y_{sp}')	0.	0.02	0.	0.08	0.	0.03
Triangular Configuration in Pipe (Table V)						
Measured R_{ac}/R_{dc}—shields insulated (RSI)	*1.19*	*1.22*	*1.26*	*1.34*	*1.53*	*1.68*
Measured R_{ac}/R_{dc}—shields short circuited (RSS)	*1.25*	*1.46*	*1.33*	*1.65*	*1.62*	*2.20*
Pipe loss (Y_i) (by equation 15)	0.13	0.13	0.18	0.18	0.26	0.26
Skin plus proximity effect in conductor (Y_c)	0.06	0.06	0.08	0.08	0.27	0.27
Shield circulating current loss (Y_{sc})	0.06	0.24	0.07	0.31	0.09	0.52
Shield proximity loss (Y_{sp})	0.	0.03	0.	0.08	0.	0.15
Cradle Configuration in Pipe (Table VI)						
Measured R_{ac}/R_{dc}—shields insulated (RSI)			*1.38*	*1.45*	*1.69*	*1.79*
Measured R_{ac}/R_{dc}—shields short circuited (RSS)			*1.50*	*2.01*	*1.82*	*2.37*
Pipe loss (Y_i) (by equation 15)			0.29	0.29	0.37	0.37
Skin plus proximity effect in conductor (Y_c)			0.09	0.09	0.32	0.32
Shield circulating current loss (Y_{sc})			0.12	0.56	0.13	0.58
Shield proximity loss (Y_{sp})			0.	0.07	0.	0.10

$Y_c' = RSI$ (A sample) − 1. Assumed the same for B sample.
$Y_c = RSI$ (A sample)—Y_i—1. Assumed the same for B sample.
Y_{sc}' and $Y_{sc} = RSS—RSI$.
Y_{sp}' and $Y_{sp} = RSI$ (B sample)—RSI (A sample). Assumed 0 for A sample.

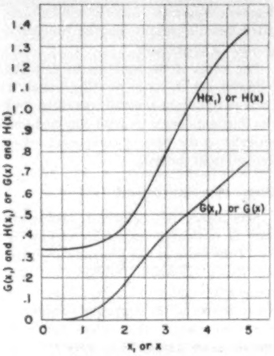

Figure 1. *G* and *H* functions to be used with equation 6 for determination of conductor proximity effect (Y_{cp}')

vestigators and is expressed by the following equation, as given by Arnold[4] for the 3-phase case in air for balanced 3-phase currents, the conductors being in equilateral triangular configuration.

$$Y_{cp}' = \frac{1.5\alpha^2 G(x)}{1-0.208\alpha^2 H(x)} \qquad (5)$$

where

$\alpha = d/S$
d = diameter of the conductor in inches
S = center-to-center spacing of the conductors in inches
$G(x)$ and $H(x)$ are Bessel functions, which are given in the curves of Figure 1
$x = 6.80/\sqrt{R_{dc}}$ at 60 cycles
R_{dc} is the d-c resistance of each conductor in microhms per foot

For segmental conductors Arnold's equation has been modified as follows

$$Y_{cp}' = \frac{1.5\alpha^2 G(x_1)}{1-0.208\alpha^2 H(x_1)} \qquad (6)$$

where all symbols are as in equation 5 and

$x_1 = K/\sqrt{R_{dc}}$

where K is a factor having a value of 3.8 for segmental conductors with three insulated segments, such as used in the cables here reported.

Limited data on other segmental cables, not here reported, indicate that K is influenced considerably by whether or not the conductors were "treated" (that is, had received the drying and saturating treatment usual for impregnated paper cables), by whether two or three of the segments were insulated and by the type of binder holding the segments together.

Table XI. Skin Effect of Segmental Conductors at 30 Degrees Centigrade

Circular Mils	Y_o
1,000,000	0.017
1,250,000	0.026
1,500,000	0.038
1,750,000	0.050
2,000,000	0.065

Based on d-c resistance values as given in Table XVI-A of Reference 3,* adjusted to 30 degrees centigrade. Skin effect = that of round solid conductor having 2.3 times the d-c resistance of the segmental conductor.
* See References at end of paper.

With three segments insulated these variables have little effect. With two segments insulated, however, a K value as high as 6.0 was obtained for an untreated conductor having a bronze binder applied with a slight lap. It may be of interest to note that on the 2,500,000-circular-mil segmental cable, measurements on which were reported by Wiseman,[1] the reported proximity effect in air corresponds to a K value of 5.4. These values compare with a K value of 6.80 for solid conductors.

For $K = 3.8$ proximity effect in air may be obtained from Table XII. For other values of K, equation 6 and Figure 1 may be used.

TOTAL CONDUCTOR LOSS INCREMENT (Y_c AND Y_c')

The total conductor loss increment in air (Y_c') is the sum of Y_o and Y_{cp}'. From all the data on segmental conductors which were available to the authors it appears that the conductor loss increment in pipe (Y_c) bears the following empirical relation to Y'_c

$$\frac{Y_c}{Y_c'} = 1 + \frac{28d(S-d)}{p^2} \qquad (7)$$

The data given by Wiseman[1] for the 2,500,000-circular-mil segmental cable also fit equation 7. This equation also applies with fair accuracy to the data given by Wiseman for concentric conductors in triangular configuration in conduit, but not in steel pipe.

In practical cables Y_c/Y_c' generally will be found to have a value of about two.

With cradle configuration in pipe it is conservative to use the same Y_c value as for triangular configuration.

SHIELD CIRCULATING CURRENT LOSS (Y_{sc} AND Y_{sc}')

A well accepted equation,[7] for the losses in the shield, in air, due to circulating current is

$$Y_{sc}' = \frac{R_s}{R_c}\,\frac{X_s^2}{R_s^2+X_s^2} \qquad (8)$$

where

R_s = longitudinal resistance of the shield including skid wires in microhms per foot
R_c = conductor resistance in microhms per foot
X_s = reactance of the shield in microhms per foot
= 52.9 $\log_{10}(S/c)$ at 60 cycles
c = mean shield radius in inches

For the usual case of cables bunched together and equipped with skid wires, S/c is about 2.20, whose logarithm to base 10 is 0.343, and $X_s = 18.2$.

It may also be noted that X_s for close spacing is small compared to R_s and may be neglected in the denominator. Thus, for close equilateral spacing, equation 8 may be rewritten as

$$Y_{sc}' = \frac{X_s^2}{R_s R_c} = \frac{330}{R_s R_c} \qquad (9)$$

In practical cases the value of R_s is approximately 300 microhms per inch of diameter over the skid wires, per foot of cable, where the shield is of the construction which we have designated as "high resistance" with two 100 by 200 mil copper D-wires applied double start with about 1-inch longitudinal spacing. The value of R_s is approximately one-quarter of the above value where the shield consists of two intercalated 3-mil copper tapes, with skid wires as above.

Table XII. Proximity Effect of Segmental Conductors in Air, Triangular Configuration, Three Segments Insulated, Lapped Bronze Binder

Calculated by Equation 6 with K = 3.8

	Proximity Effect (Y_{cp}') Circular Mils				
S, Inches	1,000,000	1,250,000	1,500,000	1,750,000	2,000,000
1.8	0.016				
2.0	0.013	0.025			
2.2	0.011	0.021	0.034	0.053	
2.4	0.009	0.017	0.029	0.045	0.064
2.6	0.008	0.015	0.024	0.038	0.054
2.8	0.007	0.013	0.021	0.033	0.047
3.0			0.018	0.028	0.040
3.2				0.025	0.035

For equilateral triangular spacing in pipe our data show that X_s is 1.35 times its value in air, see Table VIII. Thus, for equilateral triangular spacing in pipe, equation 9 becomes

$$Y_{sc}=\frac{600}{R_sR_c}\text{ (triangular)}. \tag{10}$$

For cradle configuration, the spacing may be taken as

$$S'=\sqrt[3]{S_1S_2S_3}$$

where S_1, S_2 and S_3 are the respective separations between each pair of conductors.

The ratio of S' to S is in general equal to about 1.16.

Thus

$$Y_{sc}=\frac{850}{R_sR_c}\text{ (cradle)} \tag{10A}$$

However, for low resistance shield it is important to obtain the actual value of S' and evaluate the constant in equation 10(A) directly.

SHIELD PROXIMITY LOSS (Y_{sp} AND Y_{sp}')

The shield proximity loss is due to eddy currents induced in the shield by the main currents. The equation for this loss, based on an equation given by Wedmore,[6] is

$$Y_{sp}'=\frac{398}{R_s'R_c}\left(\frac{c}{S}\right)^2 \tag{11}$$

in which c, S and R_c have the same meaning as in equation 8, and R_s' is the resistance of the shield minus skid wires, in microhms per foot.

For shields in which the copper tapes are intercalated with nonmetallic tapes R_s' is so high (order of 5,000) that Y_{sp} and Y_{sp}' are negligible. For shields in which two copper tapes are intercalated with each other, however, R_s' is only of the order of 300 microhms per foot and Y_{sp}' may be quite large.

Equation 11 may be simplified by substituting in place of c/S its usual value of about 0.46. With this substitution, equation 11 becomes

$$Y_{sp}'=\frac{84}{R_s'R_c}\text{ (triangular)} \tag{12}$$

For triangular configuration in pipe the shield proximity loss Y_{sp} is about 2.5 times Y_{sp}'.

For cradle configuration it may be taken as the same as for triangular configuration.

Thus

$$Y_{sp}=\frac{210}{R_s'R_c}\text{ (triangular or cradle)} \tag{13}$$

PIPE LOSS (Y_t)

An equation for the loss in nonmagnetic pipe, under 3-phase operation, has been derived by one of the authors upon the assumption that the conductor currents may be considered as concentrated at the centers of the conductors and that the various circulating and eddy currents existing in the system do not affect the pipe loss. The derivation of this equation is indicated in Appendix II.

The equation for loss in nonmagnetic pipe, as derived, is

$$Y_t\begin{pmatrix}\text{nonmagnetic}\\ \text{at 60 cycles}\end{pmatrix}=\frac{1.51p't\,(CI)\,Q}{\rho\rho_c} \tag{14}$$

where

p' = mean pipe diameter in inches

t = pipe thickness in inches

(CI) = area of one conductor in circular inches

ρ = resistivity of pipe in microhm-inches

ρ_c = resistivity of conductor in microhm-inches

$$Q=\sum_{n=1}^{\infty}\frac{a^{2n}+b^{2n}+c^{2n}-a^nb^n\cos n\underline{|AB}-b^nc^n\cos n\underline{|BC}-c^na^n\cos n\underline{|CA}}{n^2}$$

$a=2A/p'$; $b=2B/p'$; $c=2C/p'$

A, B, C = distances in inches between the center of the pipe and the respective centers of the three conductors

$\underline{|AB}$, $\underline{|BC}$, $\underline{|CA}$ = the angles formed between the respective lines joining the center of the pipe and the centers of the three conductors

For magnetic pipe it is assumed that the equation can be used with an empirical modification of the term in front of the summation. It has been determined that the following applies for the several cases in which pipe loss was measured with the cables in triangular and cradled configurations.

$$Y_t\begin{pmatrix}\text{magnetic}\\ \text{at 60 cycles}\end{pmatrix}=K_1p(CI)Q \tag{15}$$

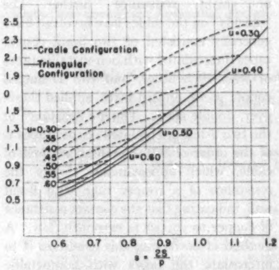

Figure 2. Factor Q to be used with pipe loss equation 16 for triangular and cradle configurations

S = center-to-center conductor spacing in inches

p = inside diameter of pipe in inches

$u=2U/p$ where U = distance between inner pipe surface and center of contiguous conductor in inches

In equation 15 all notations are as in equation 14 except that p' is replaced by p, the inside diameter of the magnetic pipe, and K_1 is a constant depending on the material of the pipe.

K_1 has been determined empirically as 0.020 for the 6-inch pipe used in the measurements, and as 0.017 for the 8-inch pipe, see Table VII. It is recommended in the interest of conservatism that for estimating purposes a value of 0.020 for K_1 be used.

Thus, for estimating purposes equation 15 becomes simply

$$Y_t\begin{pmatrix}\text{magnetic}\\ \text{at 60 cycles}\end{pmatrix}=0.020\,p(CI)Q \tag{16}$$

where

Q = a series having values shown in Table XIII for most practical cases and in Figure 2 for more general application.

Table XIII. Values of Q for Equation 16

$s=\frac{2S}{p}$	Triangular Configuration	Cradle Configuration
0.65	0.78	1.36
0.70	0.87	1.43
0.75	0.97	1.47
0.80	1.08	1.51
0.85	1.20	1.50
0.90	1.32	1.46

EVALUATION FOR TEMPERATURES OTHER THAN 30 DEGREES CENTIGRADE

As stated previously, all the data in the present series were obtained at temperatures in the neighborhood of 30 degrees centigrade. Thus, the ratio of a-c to d-c resistance as evaluated above is at 30 degrees centigrade.

Table XIV gives data for calculation of skin effect of round conductors at 60, 65, 70, and 75 degrees centigrade if the skin effect at 30 degrees centigrade is known. It has been found convenient to use these data for estimation of all a-c losses. Wiseman[1] has found that this method may be used with good accuracy in connection with the data reported by him. One isolated check which we have made indicates that using the table to evaluate the ratio at a higher temperature from the ratio at a lower temperature is conservative. The evaluation may be carried out for the entire loss or for the loss up to any desired point. For example, assume the 30 degree ratios of a-c to d-c resistance to be 1.10 at the conductor, 1.20 at the shield and 1.40 at the pipe. From Table XIV, the ratios at 70 degrees centigrade conductor temperature will be 1.08 at the conductor, 1.16 at the shield and 1.33 at the pipe.

Table XIV. R_{ac}/R_{ac}

Temperature, Degrees Centigrade 30	60	65	70	75
1.000	1.000	1.000	1.000	1.000
1.100	1.083	1.081	1.079	1.077
1.200	1.168	1.164	1.160	1.156
1.300	1.255	1.349	1.243	1.237
1.400	1.344	1.336	1.328	1.320
1.500	1.435	1.425	1.415	1.405
1.600	1.528	1.516	1.504	1.492
1.700	1.622	1.608	1.595	1.582
1.800	1.717	1.702	1.688	1.674
1.900	1.813	1.798	1.783	1.768
2.000	1.91	1.895	1.88	1.865

BRIEF SUMMARY OF COMPUTATION OF LOSSES

1. Obtain Y_o from Table XI.
2. Obtain Y_{cp}' from Table XII.
3. Add Y_o and Y_{cp}' to obtain Y_c'.
4. Multiply Y_c', by factor from equation 7 to obtain Y_c for both triangular and cradle configurations.
5. Calculate Y_{sc} by equation 10 for triangular configuration, or by equation 10(A) for cradle configuration.
6. Calculate Y_{sp} by equation 13. This is negligible for cable with high-resistance shield.
7. Add Y_{sc} and Y_{sp} to obtain Y_s.
8. Obtain Y_t from Table XIII and equation 16.
9. $1+Y_c+Y_s+Y_t$ = ratio of a-c to d-c resistance at 30 degrees centigrade.
10. Obtain ratio at desired temperature from Table XIV.

Attention is called to the fact that in making computations to compare "computed" loss values with measured values, as shown in Tables IV, V, and VI, the short-cut methods indicated in the equations given in this section were generally not used, but rather the more exact values determined from actual measured dimensions. Thus, the computed values shown in the tables will in some instances be slightly different than would be obtained from the short-cut equations. In all cases the short-cut equations give the more conservative values.

SAMPLE COMPUTATION OF LOSS RATIO

Given a 2,000,000 circular mil segmental in 6.10-inch (inside diameter) pipe, triangular configuration, $d=1.58$, $p=6.10$, $S=2.42$, $s=2S/p=0.794$, $R_c=5.5$, $R_s=890$.

From Table XI, $Y_o=0.065$. From Table XII, $Y_{cp}=0.064$, and, combining $Y_c'=Y_o+Y_{cp}'=0.129$. From equation 7, $Y_c/Y_c'=1+[(28\times1.58\times0.84)/37.2]=2.00$. Therefore $Y_c=2.00\times0.13=0.26$.

From equation 10, $Y_{sc}=600/(890\times5.5)=0.12$. As Y_{sp} is negligible for this cable, $Y_s=0.12$. From Table XIII, $Q=1.07$, and therefore, from equation 16, $Y_t=0.02\times6.10\times2\times1.07=0.26$.

Adding, $Y_c+Y_s+Y_t=0.64$. Thus, R_{ac}/R_{dc} at 30 degrees centigrade = 1.64. Consulting Table XIV, we see that R_{ac}/R_{dc} at 75 degrees centigrade = 1.53.

Discussion of Results

It is evident from the data that the construction of the protective covering, which for convenience we have called the "shield," may have a large effect on the losses. With a shield of very low resistance, the losses due to circulating currents and proximity effect in the shield may constitute 30 per cent of the total loss, or 50 per cent of the excess of a-c over d-c loss in the case of a 2,000,000-circular mil conductor. With smaller conductors this effect is much smaller, but is still of an important magnitude. Ordinarily, there is no justification in using a shield of resistance low enough to contribute to the losses to so large an extent. However, there are conditions, such as for example, to provide a path for carrier currents, which might make a continuous low resistance shield highly desirable and warrant acceptance of the resulting higher loss.

It is appropriate to develop the matter of shield resistance further. The "shields" on the cables here involved have generally consisted of two 3-mil copper tapes intercalated with non-metallic tapes or with each other, and two D-shaped copper wires, or skid wires, applied thereover, double start. The d-c resistance of the two 3-mil intercalated copper tapes is of the order of 300 microhms per foot of cable, which approximates closely the resistance of a copper tube with 6-mil wall, indicating that the contact resistance of copper to copper is extremely low. A method of correcting this condition is to intercalate the tapes with nonmetallic tapes, which results in producing a resistance in the two 3-mil copper tapes alone of about 5,000 microhms per foot of cable. However, the two skid wires (100 by 200 mils), which form a parallel path to the copper tapes, have a resistance of about 1,000 microhms per foot of cable, and the over-all resistance becomes about 250 microhms per foot of cable for the lower resistance shield and about 835 microhms per foot of cable for the higher resistance shield. In other words, in the case of the lower resistance shield the copper tapes are the main factor in determining the over-all resistance, whereas in the case of the higher resistance shield the skid wires are the main factor.

The matter of contact resistance between metal surfaces has not, in the opinion of the authors, received the attention that it merits. From limited experimental data not reported here, it appears that while two bright copper tapes intercalated with each other have very low contact resistance, two oxidized copper tapes have so high a contact resistance that the resistance of two such tapes intercalated with each other is no different than if they were separately intercalated with nonmetallic tapes. These data indicate further that there also is a satisfactorily high-contact resistance between bright copper and bright aluminum and between two bright aluminum tapes. Thus, if an entirely metallic shield is desired, any one of the last three mentioned alternatives is probably practical. Still another alternative would be to use tapes of higher resistivity, such as a high-resistance bronze or one of the nickel alloys, with attendant higher cost, however.

With any of the arrangements just mentioned, paralleled by two 100 by 200 mil copper skid wires, the resistance would be no higher than of the order of 850 microhms per foot of cable, because, as stated already, the skid wires are the chief determining factor of the resistance. In the case of the 2,000,000-circular-mil cable (number *3A*) the circulating current loss with a shield of this resistance is about 12 per cent of the d-c conductor loss. Suppose that with the same skid wire arrangement only one copper tape, with suitable intercalation, were used, the circulating loss would be reduced by only about 1 per cent in the case cited. Suppose that instead of using two skid wires, double start, only one skid wire were used, with one-half the lay (that is, the same separation between successive convolutions), the skid wire resistance would then be about 4,000 microhms per foot of cable and the parallel resistance with a tape structure having a resistance of 5,000 microhms per foot of cable would be about 2,200 microhms per foot of cable and the circulating current loss would be reduced from 12 per cent to about 4.5 per cent of the d-c conductor loss. One might go further and substitute skid wires of smaller cross-section or higher resistivity, but it should be noted that the largest gain possible is that represented by the loss due to the shield circulating current, which, with the higher resistance shields used in the measurements, is a relatively small portion of the total loss.

Mention has been made of the proximity effect loss in the shield. This is important only in the case of the low-resistance shields and is entirely negligible with those of higher resistance. It should be noted that there is no proximity loss in the skid wire portion of the shield because of the open spiral application.

The tests on segmental conductors reported here have been confined to treated segmental strand having three insulated segments and a bronze binder of about 40 per cent conductivity applied with a slight lap. A limited amount of experimental work also has been done on "treated" and "untreated" segmental strand, with various type binders and with both 2-segment and 3-segment insulation. The indications from these limited data are that with three insulated segments the conductor losses are affected very little by the foregoing variables, whereas when only two segments are insulated the effect of some of the variables on the conductor loss may be important. In this connection, it may be noted that the 2,500,000-circular mil segmental conductor reported by Wiseman,[1] which has two segments insulated and is untreated, has very much higher losses than would be obtained on treated strand with three insulated segments, based on data reported here. It is hoped that further study along the lines indicated in this paragraph can be pursued at an early date. However, segmental strand with three insulated segments is an effective means of keeping down conductor proximity losses.

It also may be stated that some measurements have been made on experimental segmental strand in which an insulating tape is inserted between the outer layer of wires in each segment and the inner layers. Preliminary measurements indicate that it may be possible by this means to reduce the conductor skin and proximity effect losses by a very material amount even from that obtainable with ordinary 3-segment insulation. Further work will have to be done before a definite report can be made. It is well to note, however, that in pipe-type cables the loss in the pipe itself is so large a part of the total loss that it is questionable whether there would be sufficient practical value in obtaining losses in the conductors much below what is obtainable with treated normal segmental strand having three insulated segments.

Consideration also might be given to the use of concentric conductors stranded with enamelled wires, which should have no proximity effect. With conductor proximity loss eliminated, the over-all loss in steel pipe may approach that with segmental conductors. The cost of such a conductor may be reduced by omitting the enamel on alternate wires of alternate layers, thereby still retaining at least one layer of enamel at every junction of adjacent wires.

At times the question has been raised as to the effect of short circuits occurring between segments of a segmental conductor. Theoretical considerations indicate that a single short circuit can have no effect on the losses, and multiple short circuits on the same segments, if spaced several lay lengths from each other, can have but inappreciable effect. The worst condition should theoretically occur if the short circuits are exactly one-half lay length apart, but even with such a condition the increased loss would occur only in the few feet between short circuits and would be insignificant with respect to the over-all loss. The matter was investigated with results shown in Appendix III. In these measurements, short circuits were deliberately inserted at each half-lay point of the entire 20-foot section of one of the conductors under test, and under this condition a maximum increase of 1.5 per cent of the d-c loss was noted with the cable in pipe. The short circuits were of a very low order of resistance. It may be concluded from these data that accidental short circuits between segments of segmental strand are of no practical consequence.

Data are given in Appendix IV of losses of pipe-type cable with 800,000-circular-mil Compack round conductors. Compack is a trade name describing a conductor in which all strands are applied with the same direction of lay and heavily rolled at each layer to produce a very compact assembly of wires. Analysis of the data indicates that the over-all losses are somewhat lower than would be indicated by Wiseman's[1] data. The measured ratio of a-c to d-c resistance in 6-inch pipe with closed triangular configuration is 1.23 at 30 degrees centigrade. Computation from Wiseman's formulas yields a value of 1.28 after addition of 0.033 for shield circulating current loss which Wiseman's cables did not have. Further analysis of the data shows that the indicated proximity loss in pipe is about the same as in air for this cable, instead of being nine times as great by Wiseman's formula. It will doubtless be desirable to investigate this matter further. Theoretical considerations indicate that proximity loss in a unidirectional strand should be much lower than in the usual construction of alternating direction of lay for successive layers of strand.

On the basis of the data and equations presented a tabulation has been prepared of losses in pipe of segmental conductor cables ranging from 1,000,000 to 2,000,000-circular mil in steps of 250,000 circular-mil, with insulation thicknesses of 315, 480 and 560 mils and the following construction details:

1. Number of insulated segments—3.
2. Binder—5-mil 40 per cent or lower conductivity bronze tape intercalated with a paper tape.
3. Shield—one or two copper tapes, each

Table XV. Estimated Losses of Segmental Cables in Steel Pipe

Triangular Configuration—At 70 Degrees Centigrade

Conductor** Size, Circular Mils	Insulation Wall Thickness, Inches	Pipe, Inside Diameter, Inches	R_{ac}/R_{dc}		
			At Conductor	At Shield	At Pipe
1,000,000*	0.315	5.047	1.05	1.11	1.20
1,000,000	0.480	6.125	1.05	1.10	1.19
1,000,000	0.560	6.125	1.05	1.11	1.22
1,000,000	0.560	8.125	1.03	1.10	1.19
1,250,000*	0.315	6.125	1.07	1.13	1.24
1,250,000	0.480	6.125	1.07	1.14	1.29
1,250,000	0.480	8.125	1.06	1.14	1.25
1,250,000	0.560	8.125	1.06	1.14	1.26
1,500,000*	0.315	6.125	1.10	1.21	1.35
1,500,000	0.480	8.125	1.08	1.17	1.33
1,500,000	0.560	8.125	1.09	1.17	1.34
1,750,000*	0.315	6.125	1.14	1.25	1.44
1,750,000	0.480	8.125	1.11	1.21	1.42
1,750,000	0.560	8.125	1.12	1.21	1.43
2,000,000*	0.315	6.125	1.20	1.31	1.56
2,000,000*	0.315	8.125	1.15	1.28	1.48
2,000,000	0.480	8.125	1.16	1.27	1.51
2,000,000	0.560	8.125	1.17	1.27	1.54

* The ratio R_{ac}/R_{dc} for the wall thickness of 315 mils is given at 75 degrees centigrade.

** Conductor diameter assumed to be the same as for conventional concentric strand and conductor resistance values based on those given in Table XVI-A of Reference 3.

Table XVI. Estimated Losses of Segmental Cables in Steel Pipe

Cradle Configuration—At 70 Degrees Centigrade

Conductor** Size, Circular Mils	Insulation Wall Thickness, Inches	Pipe, Inside Diameter, Inches	R_{ac}/R_{dc} At Conductor	R_{ac}/R_{dc} At Shield	R_{ac}/R_{dc} At Pipe
1,000,000*	0.315	5.047	1.05	1.15	1.28
1,000,000	0.480	6.125	1.05	1.14	1.29
1,000,000	0.560	6.125	1.05	1.12	1.27
1,000,000	0.560	8.125	1.03	1.12	1.30
1,250,000*	0.315	6.125	1.07	1.20	1.39
1,250,000	0.480	6.125	1.07	1.17	1.36
1,250,000	0.480	8.125	1.06	1.17	1.40
1,250,000	0.560	8.125	1.06	1.16	1.39
1,500,000*	0.315	6.125	1.10	1.25	1.48
1,500,000	0.480	8.125	1.08	1.21	1.50
1,500,000	0.560	8.125	1.09	1.20	1.50
1,750,000*	0.315	6.125	1.14	1.29	1.57
1,750,000	0.480	8.125	1.11	1.26	1.60
1,750,000	0.560	8.125	1.12	1.24	1.60
2,000,000*	0.315	6.125	1.20	1.37	1.69
2,000,000*	0.315	8.125	1.15	1.32	1.70
2,000,000	0.480	8.125	1.16	1.31	1.73
2,000,000	0.560	8.125	1.17	1.31	1.74

* The ratio R_{ac}/R_{dc} for the wall thickness of 315 mils is given at 75 degrees centigrade.

** Conductor diameter assumed to be the same as for conventional concentric strand and conductor resistance values based on those given in Table XVI-A of Reference 3.

intercalated with a nonmetallic tape.

4. Skid wires—D-shaped copper 200 by 100 mils, applied double start with spacing of 1 to $1^1/_4$ inches between successive convolutions.

The losses have been computed with $K=3.8$ for conductor proximity loss and $K_1=0.02$ for pipe loss and are shown for 75 degree centigrade copper temperature for 315-mil insulation and 70 degrees centigrade for 480- and 560-mil insulation. These values are given in Table XV for triangular configuration and Table XVI for cradle configuration.

Analysis of the losses as shown in Tables XV and XVI shows that the overall losses for a given conductor size and configuration are surprisingly alike for the different insulation thicknesses. However, there are small, but perhaps important differences in the distribution of the losses.

Appendix I. Measurements—Methods and Accuracy

Apparatus and Methods

D-C Measurements

A standard Kelvin Bridge was employed for making all d-c resistance measurements.

A-C Measurements

A null a-c potentiometer method was employed for measuring the a-c resistance of the cables. The circuit is shown in Figure 3. The conductors under test were connected in a wye for 3-phase measurements and in series for single-phase measurements. The power was received from a bank of three single-phase transformers with secondaries connected in delta. The primaries of these transformers were connected through Variacs to a 3-phase step-type voltage regulator, the regulator being used for relatively coarse adjustments of current and the Variacs for fine adjustments. Currents in the three phases were accurately balanced. However, even a relatively large unbalance has generally been found not to affect the average a-c to d-c resistance ratio to any significant extent.

For both single-phase and 3-phase measurements, the reactive components of the conductor voltage drops are balanced out by means of astatic mutual inductors with primaries carrying the full conductor current. The resistance component is balanced with a resistance potentiometer carrying current from the secondary of a 160-to-1 current transformer, the primary of which carries the conductor current. The detector employed is an a-c galvanometer. The galvanometer field is energized by a phase shifter which permits a balance to be obtained first with the field in quadrature to the main current (inductance balance) and then with a field in phase with the main current (resistance balance). The standard resistances used with the potentiometer are noninductive. In the measurements reported here, three different standard resistances, of approximately 0.035, 0.065 and 0.10 ohm were used. In making the resistance determinations, the apparent a-c resistance was measured for each conductor, the average of the two or three measurements being taken as the average a-c resistance of the conductors.

The a-c potentiometer reads in steps of 0.1 per cent, but there is ample sensitivity, especially at the higher currents, to interpolate to one-fifth of this value. As the potentiometer readings were generally in the middle third of the scale, the over-all sensitivity was of the order of 0.04 per cent.

At the balance of the potentiometer, the following expression holds for the a-c resistance of the conductor

$$R_{ac}=\frac{Mr}{v}\cos\delta$$

where

R_{ac} = apparent a-c resistance of conductor under test
M = potentiometer setting, expressed as a decimal of the standard resistance
r = resistance of potentiometer in ohms
v = current transformer ratio
δ = phase angle of current transformer. This is about one degree at 160 amperes and about 30 minutes at 800 amperes in the transformers used. Thus, $\cos\delta=1$ for all practical purposes

A simplified vector diagram for the balanced condition is shown in Figure 4.

Skin effect measurements were made single-phase with two conductors placed parallel to one another and spaced nine inches between opposing surfaces. For 3-phase measurements, three test conductors were employed, the operation of the circuit being substantially the same as in the single phase case. The three conductors were placed in triangular or cradle configuration as desired.

A typical set of 3-phase data is given in Table XVII.

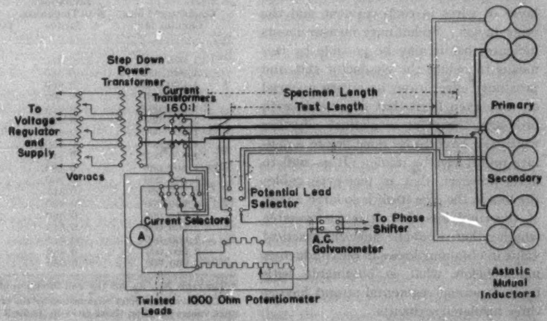

Figure 3. Schematic diagram of connections for a-c resistance measurements under 3-phase load

For single-phase measurements, one conductor and one mutual inductor are omitted

Table XVII. A-C Resistance Determinations of Cable 2A 1,500,000-Circular-Mil Segments in 8.02 Inch Inside Diameter Steel Pipe, Triangular Configuration

Resistance of Standard—0.0658 Ohm; Current Transformer Ratio—160.1; Temperature—30 Degrees Centigrade

A-C Measurements

Shields Short Circuited. Distance between Potential Points, 15 Feet

Current, Amperes	Potentiometer Settings at Balance Phase *A*	Phase *B*	Phase *C*	Average	Average Resistance, Microhms	Average Ratio, R_{ac}/R_{dc}
160	0.343	0.275	0.475	0.364	149.5	1.37
320	0.318	0.252	0.495	0.355	146.0	1.34
480	0.318	0.252	0.495	0.355	146.0	1.34
640	0.320	0.262	0.479	0.354	145.7	1.34
800	0.325	0.268	0.462	0.352	144.8	1.33

D-C Measurements

D-c Resistance of Conductors in Microhms

Immediately Before A-C Run Phase A	Phase B	Phase C	Immediately After A-C Run Phase A	Phase B	Phase C
109.1	109.3	108.6	109.4	109.5	108.8

The wide variation in the apparent resistance of the three conductors has been observed whenever 3-phase measurements have been made. Indeed, with cradle configuration one of the readings is often negative. This has been observed by other investigators[3] and is due to dissymmetry of conductor and lead arrangement. However, while the individual readings do not truly reflect the division of losses in the individual conductors, the average value is the true average a-c resistance as in any other 3-wattmeter method of 3-phase measurement. Heat runs with triangular configuration have shown no significant differences in the temperature rise of the three conductors, indicating no large differences in loss actually generated in the individual conductors.

For single-phase measurements, potential leads from the east potential points were carried along the tops of the north and south conductors and contiguous thereto, to the west potential points, where they were twisted together and carried to the measuring circuit. This method of carrying the potential leads to the measuring circuit was found to give true skin effect indication in cases where these could be checked against accepted theoretical values.

Salter[2] in his recent paper discusses in detail the accuracy of various methods of disposing the potential leads. Our experience over a period of some 13 years has paralleled Salter's and we have arrived independently at the same solution.

For 3-phase measurements in air, the potential leads from the three potential points at the east end were twisted together, and carried perpendicularly to a point $1^1/_2$ feet above the cables. From there they were carried parallel to the cables to a point perpendicularly above the west end potential points where they were joined by the three twisted leads from the west end potential points. From this point, all six leads were twisted together and carried to the measuring circuit.

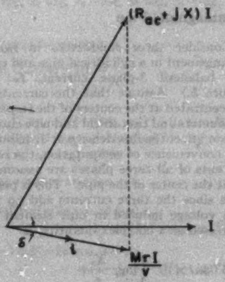

Figure 4. Vector diagram of a-c potentiometer circuit at balance

X = reactance of conductor, ohms
R_{ac} = a-c resistance of conductor, ohms
r = resistance of potentiometer, ohms
M = potentiometer setting expressed as a decimal
I = conductor current, amperes
i = current in current transformer secondary, amperes
v = current transformer ratio I/i
δ = phase angle of current transformer
At Balance: $R_{ac}I = Mr\,i\cos\delta$. $\cos\delta \cong 1$

When the cables were placed in the pipe, the potential leads from the three potential points at each end were twisted together and carried away perpendicularly from the cables through holes in the pipe opposite the potential points. They were then carried to the measuring circuit in the manner described for 3-phase measurements in air.

Calorimetric Determination of Pipe Loss

The portion of increase in the a-c resistance due to the pipe loss was determined by a calorimetric method.

The three cables were placed in the pipe, which was in a closed area, free of air currents. With the desired configuration of conductors, and shields insulated from one another, 3-phase current was passed through the conductors for a period of 10 minutes. By means of the Kelvin Bridge, the pipe resistance was measured each minute for a period of 10 minutes before the current was turned on; and each minute for a period of 10 minutes after the current was turned off. From these readings, the rise in the pipe resistance during the 10-minute period that the current was on, was determined.

After a suitable rest period there was passed through the pipe for 10 minutes direct current of such magnitude as to produce substantially the same resistance increase as was produced during the a-c run. In order to predetermine the necessary magnitude of this current it was usually necessary to make one or more trial runs. As in the case of the a-c run, pipe resistance was measured by means of the Kelvin Bridge each minute during the 10-minute period immediately preceding and that immediately following the current run, and from these measurements the resistance increase determined.

During the a-c run, heat was being generated in the conductors as well as in the pipe and some of the heat from the conductors was being transferred to the pipe. Thus, the increase in pipe resistance was due to both the heat generated in the pipe and (to a small extent) that transferred to the pipe from the conductors. In order to reproduce this condition during the d-c run, while direct current was being passed through the pipe, a direct current of a different magnitude was simultaneously passed through the three conductors in series. The magnitude of the conductor current was such as to produce substantially the same heating effect in the conductors as did the alternating current. From previous a-c resistance measurements, an estimate of the skin-proximity loss of the conductors, sufficiently accurate for this purpose, can be made, and the necessary value of direct current to be passed through the conductors calculated. Thus, estimating 10 per cent skin-proximity effect in a given case, the direct current which must be passed through the conductors should be $\sqrt{1.10}$ times the current used during the a-c run.

The watts fed into the pipe during the d-c run being known, the watts generated in the pipe during the a-c run can be calculated readily by multiplying the d-c value by the ratio of the pipe resistance increase during the a-c run to that during the d-c run.

The probable accuracy of this calorimetic method is believed to be about 3 per cent of the pipe loss.

A set of data and a sample calculation for the determination of pipe loss are given in the example below.

Example

Given three 1,500,000-circular-mil segmental conductors in 6.10-inch inside diameter steel pipe; triangular configuration; 2.09 inch center-to-center spacing.

A-c Run. 783 amperes, 3-phase, through conductors for 10 minutes. Average d-c conductor resistance during run—106.9 microhms.

D-c conductor watts $=3\times783^2\times106.9\times10^{-6}=197$ watts. Increase in pipe resistance in 10 minutes—0.29 microhm.

D-c Run. 430 amperes, direct current, through pipe for ten minutes. (Simultaneously 840 amperes were passed through the three conductors in series on the basis of estimated 15 per cent skin-proximity loss, that is, $783\times\sqrt{1.15}=840$.)

Average pipe resistance during d-c run—183.2 microhms, and therefore watts fed into pipe during d-c run $=430^2\times183.2\times10^{-6}$, or 33.8 watts. The increase in pipe resistance in 10 minutes was 0.32 microhm. Calculating, the loss in pipe during a-c run $=33.8\times(0.29/0.32)$, or 30.6 watts. D-c conductor loss during a-c run equals 197 watts, and therefore pipe loss equals 30.6/197 or 0.16 in terms of d-c resistance of the conductor.

Accuracy of Resistance Measurements

D-C Measurements

A Leeds and Northrup standard Kelvin Bridge, with a suitable d-c galvanometer and scale, was employed for making the d-c resistance measurements. Numerous checks against known laboratory resistances established the accuracy of these measurements to be better than ±0.1 per cent.

A-C Measurements

Possible sources of error in the a-c measurements and how they are taken care of will be indicated.

1. The out-of-phase component of the conductor voltage drop is balanced out by voltage from the secondary of a mutual inductor, the primary of which carries the full conductor current. The primary lead and the primary coil are made of a cable employing a litz-wire construction. Thus, quadrature between the secondary voltage and conductor current is assured. Both the primary and secondary windings are astatic, thus assuring a minimum of interference from stray fields.

The use of a mutual inductor taking its primary current directly from the line is believed to be unique. Salter,[3] following common practice, takes the primary current for his mutual inductor from the secondary of a current transformer with primary carrying the full conductor current. With such an arrangement, correction must be made for the phase angle of the current transformer, and the phase angle must be known very accurately.

2. The in-phase component of the conductor voltage drop is balanced by a resistance potentiometer which takes its current from a current transformer, the primary of which is in series with the conductor. The cosine of the phase angle of this current transformer appears in the resistance balance formula as a multiplying factor. However, the phase angle of the current transformer used is no greater than one degree under the conditions of the test, and thus the cosine is 0.9998 or higher and may be regarded as unity for all practical purposes. The ratio of the current transformers, as calibrated recently, ranges from 160.0 to 160.2 over the range of currents used in the measurements and a ratio of 160.1 has been used for computing resistances at all currents, introducing a maximum error of ±0.06 per cent.

The standard resistances used with the potentiometer are essentially noninductive and are calibrated by means of the same Kelvin Bridge as was used for the d-c measurements. It should be noted that a small phase angle in the standard resistance is unimportant for the same reason as given for the phase angle of the current transformers.

3. A possible source of error is variation in the temperature of the conductors between the start and finish of a series of measurements. A technique was developed whereby the current was turned on only momentarily for each adjustment of the potentiometer or of the mutual inductor when balancing, thus heating up the conductor to an insignificant extent during a given series of measurements. D-c resistance measurements were made just before and just after each series of a-c measurements and, as illustrated in Table XVII, changed by only a small fraction of 1 per cent.

Several checks and comparative measurements with other laboratories were made for greater assurance of accuracy of the a-c resistance measurements, as detailed later.

When the equipment used in the present tests was first assembled, about ten years ago, a calibration measurement was made on copper tubes of 1.90 inch outside diameter and 1.49 inch inside diameter. A-c to d-c resistance ratio was measured with 30-inch separation at 20 degrees centigrade. The measured values were 1.005 and 1.006 for the two conductors, as compared with a theoretical skin effect value of 1.010.

The conductors were then brought together to a center-to-center separation of 2.26 inches. Two determinations of the ratio gave values of 1.307 and 1.310, respectively, at 400 amperes. The computed ratio from accepted theory[5] is 1.310.

In the foregoing measurements the distance between potential points was 18 feet.

During the course of the present series of measurements cable *3A* (2,000,000 circular mils) together with the 6-inch (nominal) inside diameter steel pipe were sent to the Electrical Testing Laboratories for comparative measurements with their equipment. Comparative values are given in Table XVIII.

Table XVIII. Comparative Tests with ETL 2,000,000-Circular-Mil Segmental Cable
Spacing 2.42 Inches, Center-to-Center, Shields Short Circuited

	A-c to D-c Resistance Ratio Authors	ETL
Triangular configuration, in air, 3-phase measurement	1.19	1.205
Triangular configuration, in 6-inch inside diameter steel pipe, 3-phase measurement	1.63	1.65

The ETL measurements in pipe were made with 15 feet between potential points, according to their standard method. Our measurements were made with 20 feet between potential points. The ETL measurements were at about 600 amperes, while ours were at 640 amperes. The agreement is satisfactory considering that the measurements were made with two separate setups.

Another check on our apparatus was obtained while making joint studies with Philadelphia Electric Company. An electrodynamometer-type wattmeter was supplied by Philadelphia Electric Company and connected into the circuit so as to measure the watts loss in each conductor simultaneous to measurement by the a-c potentiometer. The cable was installed in a 6-inch inside diameter steel pipe, in equilateral triangular formation. The shields, including skid wires, were touching throughout the test length. Comparative values between the wattmeter and the potentiometer method are shown in Table XIX. It is to be observed that the two methods checked each other extremely well. The watts loss listed under the a-c potentiometer column were calculated from the measured value of the a-c resistance, by using the measured value of conductor current.

Table XIX. Comparative Wattmeter and Potentiometer Readings

	Total Watts Loss Wattmeter	A-c Potentiometer
Room temperature (31 degrees centigrade)	713	714
At final conductor temperature (68.5 degrees centigrade)	732	736

Note also the measurement of skin effect of a round conductor reported in Appendix IV, on which the measured value was 1.056, as compared with a theoretical value of 1.057.

The check measurements given appear to give an excellent check on the a-c measurements. It is believed that the probable accuracy of these measurements is within ±0.5 per cent or better in all cases.

Appendix II. Pipe Loss in a Balanced 3-Phase Pipe-Type System

Nonmagnetic Pipe

Consider three conductors in random arrangement in a cylindrical pipe and carrying balanced 3-phase current, I. (See Figure 5.) Assume that the currents are concentrated at the centers of the respective conductors and that shield and pipe currents do not affect the flux density or distribution. For convenience of computation, the return currents of all three phases are assumed to be at the center of the pipe. This is permissible since the three currents add up to 0. The voltage induced in pipe element $r\,t\,d\theta$, expressed as a complex quantity, is

$$e=5.08\omega I\times10^{-9}\left(\log_e\frac{X_1}{r}+\frac{-1+j\sqrt{3}}{2}\log_e\frac{X_2}{r}+\frac{-1-j\sqrt{3}}{2}\log_e\frac{X_3}{r}\right)$$

$$=5.08\omega I\times10^{-9}\left(\log_e x_1+\frac{-1+j\sqrt{3}}{2}\log_e x_2+\frac{-1-j\sqrt{3}}{2}\log_e x_3\right) \quad (17)$$

or

$$e=5.08\omega I\times10^{-9}\times\sqrt{\begin{matrix}(\log_e x_1)^2+(\log_e x_2)^2+(\log_e x_3)^2-\\ \log_e x_1\log_e x_2-\log_e x_2\log_e x_3-\log_e x_3\log x_{1e}\end{matrix}} \quad (18)$$

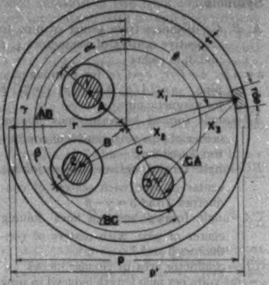

Figure 5. Graphic representation of notation in deriving pipe loss formula

$a=A/r_1$ $b=B/r_1$ $c=C/r_1$ $x_1=X_1/r_1$ $x_2=X_2/r_1$
$x_3=X_3/r$

The resistance of pipe element $rtd\theta$, in ohms per inch length, being $\rho\times10^{-6}/rtd\theta$, the watts loss per inch length in the element $rtd\theta$ is

$$dw=\frac{e^2rtd\theta}{\rho\times10^{-6}}=\frac{25.8\omega^2I^2rt\times10^{-12}}{\rho}\times\\ [(\log_e x_1)^2+(\log_e x_2)^2+(\log_e x_3)^2-\log_e x_1\\ \log_e x_2-\log_e x_2\log_e x_3-\log_e x_3\log_e x_1]d\theta \qquad (19)$$

and

$$w=\frac{25.8\omega^2I^2rt\times10^{-12}}{\rho}\times\\ \int_0^{2\pi}[(\log_e x_1)^2+(\log_e x_2)^2+(\log_e x_3)^2-\\ \log_e x_1\log_e x_2-\log_e x_2\log_e x_3-\log_e x_3\times\\ \log_e x_1]d\theta \qquad (20)$$

This may be written as

$$w=\frac{6.45\omega^2I^2rt\times10^{-12}}{\rho}\times\\ \int_0^{2\pi}[(\log_e x_1^2)^2+(\log_e x_2^2)^2+(\log_e x_3^2)^2-\\ \log_e x_1^2\log_e x_2^2-\log_e x_2^2\log_e x_3^2-\\ \log_e x_3^2\log_e x_1^2]d\theta \qquad (21)$$

By the law of cosines

$$x_1^2=1+a^2-2a\cos(\theta+\alpha)\\ =[1-a\epsilon^{j(\theta+\alpha)}][1-a\epsilon^{-j(\theta+\alpha)}]$$

$$x_2^2=1+b^2-2b\cos(\theta+\beta)\\ =[1-b\epsilon^{j(\theta+\beta)}][1-b\epsilon^{-j(\theta+\beta)}]$$

$$x_3^2=1+c^2-2c\cos(\theta+\gamma)\\ =[1-c\epsilon^{j(\theta+\gamma)}][1-c\epsilon^{-j(\theta+\gamma)}] \qquad (22)$$

Substituting these values of x_1^2, x_2^2 and x_3^2 in equation 21 we have

$$w=\frac{6.45\omega^2I^2rt\times10^{-12}}{\rho}\times\\ \int^{2\pi}[g_1^2+2g_1g_2+g_2^2+h_1^2+2h_1h_2+h_2^2+\\ m_1^2+2m_1m_2+m_2^2-g_1h_1-g_2h_2-\\ g_2h_1-g_1h_2-g_1m_1-g_1m_2-g_2m_1-\\ g_2m_2-h_1m_1-h_1m_2-h_2m_1-h_2m_2]d\theta \qquad (23)$$

The 21 terms of equation 23 may be integrated separately and will yield

$$w=\frac{25.8\pi\omega^2I^2rt\times10^{-12}}{\rho}\times\\ \sum_{n=1}^{\infty}\frac{a^{2n}+b^{2n}+c^{2n}-a^nb^n\cos n\underline{|AB}-b^nc^n\cos n\underline{|BC}-c^na^n\cos n\underline{|CA}}{n^2}$$

or

$$w=\frac{25.8\pi\omega^2I^2rt\times10^{-12}}{\rho}Q \qquad (24)$$

Now

$$Y_t=\frac{w}{w_c}$$

and

$$w_c=\frac{3I^2\rho_c\times10^{-6}}{0.25\pi(CI)}=\frac{3.82I^2\rho_c\times10^{-6}}{(CI)}$$

Therefore

$$Y_t=\frac{25.8\pi\omega^2rt(CI)Q\times10^{-6}}{3.82\rho\rho_c}$$

or

$$Y_t(\text{nonmagnetic})=\frac{1.51p't(CI)Q}{\rho\rho_c}\quad\text{at 60 cycles} \qquad (14)$$

Magnetic Pipe

If the pipe material is magnetic, only the inner portion of the wall thickness of the pipe will carry induced current. As a first approximation it may be assumed that the portion of wall thickness carrying the current is the same as the depth of penetration. From the data in Table II the depth of penetration at the current giving the highest a-c resistance is 12.2×0.28/159=0.0215 inch for the 6-inch pipe, and 7.65×0.32/152 =0.0161 inch for the 8-inch pipe. Substituting in equation 14 the above depths of penetration for t, the values given in Table II for ρ and 0.72 for ρ_c (resistivity of copper at 30 degrees centigrade, adding 2 per cent for stranding and cabling of segments), and replacing p' by p, the right-hand member of equation 14 becomes 0.0079 p (CI) Q for the 6-inch pipe and 0.0066 p (CI) Q for the 8-inch pipe, as first approximations.

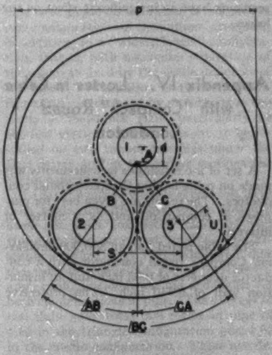

Figure 6. Cables in equilateral triangular configuration in magnetic pipe

$a=2A/p_1$ $b=2B/p_1$ $c=2C/p_1$ $s=2S/p_1$
$u=2U/p$
$b=c=1-u$

$$a=\sqrt{b^2-s^2/4}-\sqrt{\frac{3}{2}}s$$

$\underline{|AB}=\underline{|CA}=\sin^{-1}s/2b$
$\underline{|BC}=2\sin^{-1}s/2b$

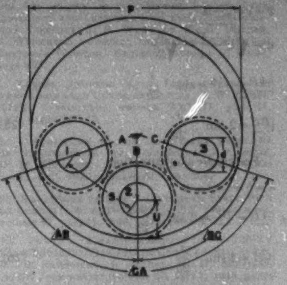

Figure 7. Cables in cradle configuration in magnetic pipe

$a=2A/p_1$ $b=2B/p_1$ $c=2C/p_1$ $s=2S/p_1$
$u=2U/p$
$a=b=c=1-u$
$\underline{|AB}=\underline{BC}=2\sin^{-1}s/2b$
$\underline{|CA}=4\sin^{-1}s/2b$

However, the presence of the magnetic material not only increases the flux but also tends to concentrate the flux in the material of the pipe, thus producing higher losses than calculated with the foregoing assumptions.

Calorimetric determinations of the loss in the two steel pipes used in the measurements reported in the paper (see Table VII) have indicated that the numerical factors in these expressions are about 2.6 times the values indicated, that is to say, 0.020 for the 6-inch pipe and 0.017 for the 8-inch pipe. For conservatism, and because the 6-inch pipe more nearly represents the type of pipe likely to be used in pipe installations, it is recommended that 0.020 be used. Thus,

$$Y_t\begin{pmatrix}\text{magnetic}\\\text{60 cycles}\end{pmatrix}=0.020p(CI)Q\text{ at 30 degrees centigrade} \qquad (16)$$

Evaluation of Q for Practical Cases

The evaluation of Q for random distribution of the cables in the pipe is a time-consuming process. Generally, however, cables are considered to be arranged either in equilateral triangular configuration or in cradle configuration, as shown graphically in Figures 6 and 7. For these cases the various distance ratios and angles involved are subject to considerable simplification.

Thus, for equilateral triangular configuration

$$b=c=1-u$$

$$a=\sqrt{b^2-\frac{s^2}{4}}-\sqrt{\frac{3}{2}}s$$

$$\underline{|AB}=\underline{|CA}=\sin^{-1}\frac{s}{2b}$$

$$\underline{|BC}=2\sin^{-1}\frac{s}{2b} \qquad (25)$$

For cradle configuration

$$a=b=c=1-u$$

$$\underline{|AB}=\underline{|BC}=2\sin^{-1}\frac{s}{2b}$$

$$\underline{|CA}=4\sin^{-1}\frac{s}{2b} \qquad (26)$$

Note that $\cos\phi=\cos(-\phi)$.

Thus, in evaluating say $\underline{|AB}$ for the purposes of the equation for Q it is immaterial whether α is subtracted from β or β is subtracted from α. It will be most convenient to subtract in a manner which will produce a positive angle.

It should be noted further that equations 25 apply to any equilateral triangular arrangement, regardless of whether or not the cables touch the inner pipe surface; also that equations 26 apply to any arrangement wherein all conductors are equally distant from the center of the pipe and the two outside cables are symmetrical with respect to the center cable.

Where adjacent cables are touching, as they are normally considered to be, u for both equilateral and cradle configurations will be equal to the over-all radius of the cables and very nearly equal to $s/2$. Table XIII gives the values of Q for this condition. The values of Q for both the equilateral triangular and cradle configurations in the broad sense explained before are given graphically in Figure 2.

Appendix III. Effect of Accidental Short Circuits Between Segments

A series of tests was performed to determine the effect of accidental short circuits between segments. In order to accentuate the effect, the measurements were made with short circuits deliberately imposed at frequent intervals. The results of these tests are given in Table XX.

The short circuits were placed in the top conductor only. Copper wedges, driven between adjacent segments, served as the short circuits for these determinations. The effective resistance of these short circuits was 65±20 microhms. Short circuits between bare and opposite segments were obtained by removing the segment insulation from the segment opposite the bare segment. Copper wedges were driven between the bronze binder tape and the insulated opposite segment at the place where the insulation was removed. The effective resistance of these short circuits was 345±50 microhms.

From the results, it is evident that the short circuiting of the bare segment with either an adjacent or the opposite insulated segment by means of several low-resistance short circuits spaced one-half lay length apart has no measurable effect on the a-c resistance of a segmental cable system in air. Similar short circuits have measurable but slight effect on the a-c resistance of cables in steel pipe. It may be concluded that occasional accidental short circuits between segments have an insignificant effect on the losses.

Table XX. Effect of Short Circuits

Cable 1B with Shield Removed—Triangular Configuration (S=2.35 Inches)

	Three-Phase A-c to D-c Resistance Ratio
Short Circuits Between Bare and Adjacent Segments	
Cable in Air	
No short circuits	1.022*
Short circuits at each lay length	1.023
Short circuits at each one-half lay length	1.023
Short circuits at each one-half lay length, but top conductor rotated 90 degrees	1.023
Cable in 6.10-Inch Inside diameter Steel Pipe	
No short circuits	1.178
Short circuits at each one-half lay length	1.188
Short circuits at each one-half lay length, but top conductor rotated 90 degrees	1.194
Short Circuits Between Bare and Opposite Segments	
Cable in Air	
No short circuits	1.027*
Short circuits at each lay length	1.027
Short circuits at each one-half lay length	1.027
Cable in 6.10-Inch Inside Diameter Steel Pipe	
No short circuits	1.180
Short circuits at each one-half lay length	1.186

* Difference between these two values probably due to some difference in separation.

Appendix IV. Losses in Cable with "Compack" Round Conductors

A set of a-c resistance measurements was made on cable having Compack round conductors. The results are given here for purposes of comparison and as a matter of interest.

The cable tested had an 800,000-circular-mil Compack round conductor with a conductor diameter of 0.95 inch and an insulation wall of 0.540 inch. The protective

Symbols

A, B, C = distances from center of pipe to respective centers of conductors 1, 2 and 3, in inches

$a=A/r$; $b=B/r$; $c=C/r$ for nonmagnetic pipe. $a=2A/p$; $b=2B/p$; $c=2C/p$ for magnetic pipe

$\underline{AB}$ = angle formed between lines joining center of pipe with centers of conductors 1 and $2=\beta-\alpha$

$\underline{BC}$ = angle formed between lines joining center of pipe with centers of conductors 2 and $3=\gamma-\beta$

$\underline{CA}$ = angle formed between lines joining center of pipe with centers of conductors 3 and $1=\alpha-\gamma$

(CI) = conductor area in circular inches

e = rms volts per inch length induced in pipe element $rtd\theta$

f = frequency in cycles per second

$g_1=\log_\epsilon[1-a\epsilon^{j(\theta+\alpha)}]$ $g_2=\log_\epsilon[1-a\epsilon^{-j(\theta+\alpha)}]$

$h_1=\log_\epsilon[1-b\epsilon^{j(\theta+\beta)}]$ $h_2=\log_\epsilon[1-b\epsilon^{-j(\theta+\beta)}]$

$m_1=\log_\epsilon[1-c\epsilon^{j(\theta+\gamma)}]$ $m_2=\log_\epsilon[1-c\epsilon^{-j(\theta+\gamma)}]$

I = current per phase in rms amperes

p = internal pipe diameter in inches

p' = mean pipe diameter in inches

$$Q=\sum_{n=1}^{\infty}\frac{a^{2n}+b^{2n}+c^{2n}-a^nb^n\cos n\underline{|AB}-b^nc^n\cos n\underline{|BC}-c^na^n\cos n\underline{|CA}}{n^2}$$

r = mean pipe radius in inches

S = distance between centers of adjoining conductors in inches

$s=2S/p$

t = wall thickness of pipe in inches

U = distance from inner periphery of pipe to center of contiguous conductor in inches

$u=2U/p$

w = watts loss per inch length of pipe

w_c = d-c watts loss per inch length in the three conductors

X_1, X_2, X_3 = distances from center of pipe element $rtd\theta$ and respective centers of conductors 1, 2, and 3, in inches

$x_1=X_1/r$; $x_2=X_2/r$; $x_3=X_3/r$

Y_t = loss in pipe expressed as a decimal of w_c

α, β, γ = angles formed between reference line and lines joining center of pipe to respective centers of conductors 1, 2, and 3

ϵ = Naperian base of logarithms

θ = angle formed between reference line and line joining center of pipe to center of pipe element $rtd\theta$

ρ = resistivity of pipe material, in microhm-inches

ρ_c = resistivity of conductor material, in microhm-inches

ω = angular velocity $=2\pi f$

Table XXI. Losses of 800,000 Circular Mils Compack Round

Air or Pipe	Configuration	S, Inches	p, Inches	R_{ac}/R_{dc} Shields Insulated	R_{ac}/R_{dc} Shields Short Circuited
Air	Triangular	2.25		1.07	1.09
Air	Triangular	3.10		1.06	1.11
Air	Cradle	2.25		1.07	1.10
Pipe	Triangular	2.25	6.10		1.23
Pipe	Triangular	3.10	6.10		1.34
Pipe	Cradle	2.25	6.10		1.32

shield consisted of two 3-mil copper tapes, each intercalated with a 7-mil polyethylene tape, with two 0.100- by 0.200-inch skid wires, applied double start, with a spacing of $1^1/_4$ inches between successive convolutions.

Measurement of skin effect produced a value of 1.056. This compared with a value of 1.057 as calculated from accepted formulas for round homogeneous conductors.

Results of 3-phase measurements in air and in steel pipe are given in Table XXI.

References

1. A-C Resistance of Large Size Conductors in Steel Pipe or Conduit, **R. J. Wiseman.** *AIEE Transactions*, volume 67, part II, 1948, pages 1745–57.

2. Problems in the Measurement of A-C Resistance and Reactance of Large Conductors, **E. H. Salter.** *AIEE Transactions*, volume 67, part II, 1948, pages 1390–96.

3. Specifications for Varnished-Cambric Insulated Cables for the Transmission and Distribution of Electrical Energy. Insulated Power Cable Engineers Association, fifth edition, July 1946.

4. Eddy Current Losses in Multi-Core Paper-Insulated Lead-Covered Cables, Armoured and Unarmoured Carrying Balanced 3-Phase Currents. **A. H. M. Arnold.** *Journal*, Institution of Electrical Engineers (London, England), volume 88, part II, number 1, February 1941.

5. Proximity Effect in Solid and Hollow Round Conductors, **A. H. M. Arnold.** *Journal*, Institution of Electrical Engineers (London, England), volume 88, part II, number 4, August 1941, page 349.

6. A Critical Study of a Three-Phase System of Unarmored Single-Conductor Cables, from the Standpoint of the Power Losses, Line Constants and Interference with Communication Circuits, **E. B. Wedmore, P. D. Morgan, S. Whitehead.** *Journal*, Institution of Electrical Engineers (London, England), volume 67, 1929, page 359.

7. Losses, Induced Volts and Amperes in Armor and Lead Cover of Cables, **H. W. Fisher.** *AIEE Transactions*, volume XXVIII, part II, 1909, pages 747–65.

8. Calculation of the Electrical Problems of Transmission by Underground Cables, **D. M. Simmons.** *Electric Journal* (East Pittsburgh, Pa.), 1925, volume 22, page 366.

9. Reactance of Large Cables in Steel Pipe or Conduit, **W. A. DelMar.** *AIEE Transactions*, volume 67, part II, 1948, pages 1409–15.

10. Thermal Characteristics of a 120-Kv High-Pressure, Gas-Filled Cable Installation, **W. D. Sanderson, J. Sticher, M. H. McGrath.** *AIEE Transactions*, volume 67, part I, 1948, pages 487–502.

Discussion

C. T. Hatcher (Consolidated Edison Company of New York, Inc., New York, N. Y.): Proper selection of cable size to meet carrying capacity requirements has been a troublesome phase in the engineering of pipe cable lines, especially in the case of the heavier circuits installed during the past few years. Basic technical data were limited with respect to vital factors involved in the rating of these systems—namely, component a-c losses and thermal resistance of the soil.

Considerable research has been carried on during that time on both of these subjects and the situation today is considerably improved. Basic data are being obtained, and the underlying theory governing effect is being developed.

This paper is a major contribution to our knowledge of the behavior of a-c losses in pipe cable systems and a very necessary supplement to Mr. Wiseman's Insulated Power Cable Engineers Association[1] report. As a result of these two studies, the general theory has been more adequately developed and, with the more complete understanding now furnished of the component sources of a-c losses in pipe, the direction of attack towards reduction of these losses becomes apparent.

The authors have not claimed to offer a complete answer to the problem and, because of the number of variables involved, further tests are deemed desirable. The need for additional test data has been recognized generally by the industry. Some months ago the Consolidated Edison Company was confronted with the need for specific data in order to evaluate properly design features proposed by cable manufacturers for several projected 138-kv pipe cable lines. A research program, to be conducted by Electrical Testing Laboratories, was authorized for study of the component losses in cables of 1,500,000-circular-mil size. Because of the concurrent interest of other utilities, an Association of Edison Illuminating Companies—Edison Electric Institute Working Group was appointed to sponsor further research on this subject. In setting up the Consolidated Edison Company research program, the cable manufacturers and members of the AEIC—EEI Working Group were invited to participate in a series of discussions with a view to formulating a comprehensive program of research which might be correlated with possible further research under AEIC—EEI sponsorship.

The test program as set up at joint conferences was patterned very much after the lines pursued by Mr. Meyerhoff and Mr. Eager. Basic tests were to be made to determine: conductor loss; loss in shield and skid wires; and loss in pipe. Tests have been in progress for some months and a number of measurements of a-c/d-c resistance ratio have been made in air and in pipe on various samples of 1,500,000-circular-mil 138-kv cable from different manufacturers. All of these samples are of the "high resistance shield" type, corresponding approximately to sample 2*A* of the authors' tests. Three-phase measurements in air and in pipe were made on a number of samples in two configurations of the authors' tests and, in addition, in a "wide triangle" configuration, that is, with maximum separation of the cables as fixed by the inside diameter of the pipe. The addition of the latter configuration was dictated by an interest in the limits of resistance ratio, particularly as 300 feet vertical riser sections are to be installed on two tunnel crossings under the East River and in these riser sections the cables hang free.

To date no measurements of pipe loss have been made, and the data so far obtained have not been completely analyzed yet. However, the measured total a-c/d-c resistance ratios check reasonably well with the authors' computed values for the triangle configuration in air, but are higher for both configurations in pipe. The average of test data gave total loss ratios in pipe of 1.40 in the triangle configuration and 1.62 in the cradle configuration. These are dependent somewhat on details of construction.

The test results obtained in the "wide triangle" configuration indicate that values greater than those of the cradle formation may result with random lay in the field and this has been borne out by field test measurements made on two existing lines.

In their discussion of results, the authors have pointed out the line of attack in reducing the "shield" circulating current loss by increasing skid wire circuit resistance. Some tests have been made on samples with modified skid wire design which bear out this point, reductions of two-thirds or more in the "shield" circulating current loss having been obtained.

In the majority of tests made, measurements were obtained of the induced voltages in the "shield" circuits in air and in pipe. Measurements also were made, with tong ammeter, of the currents flowing under short circuit conditions in component parts of the "shield" assembly, insofar as these were separable. The indicated ratios varied considerably but on the average an increased loss in pipe over values in air of the order of 2.1 times for the close triangle configuration and 2.5 times for the cradle configuration was indicated. The over-all average ratio for all three configurations measured is 2.3.

Extra a-c losses are inherent in pipe-type construction. It is obvious however, that these losses can be reduced, some of them considerably so, by the use of proper techniques or choice of material. A number of steps in this direction are already underway and further improvement can be expected. The authors' paper illuminates the field for further research.

Losses in the conductors are considerably improved by the use of segmental construction in the larger sizes and it is possible that conductor loss can be still further reduced by insulating individual strands with some type of high resistance film which will suppress proximity effect.

Reductions of losses in shields and skid wire circuits were effected by the use of high resistance materials. As indicated by test data, increasing the circuit resistance by the use of low conductivity alloys and/or reducing the number and pitch of skid wires, can, for all practical purposes, eliminate the greater part of this seat of loss.

The authors and the General Cable Corporation are to be commended for carrying on this extremely valuable research which, when correlated with data now being obtained or planned by other manufacturers and utilities, will establish the necessary understanding for most economical design of the complete pipe cable system.

Reference

1. See reference 1 of the paper.

F. H. Buller (General Electric Company, Schenectady, N. Y.): For several years there has been a real need of data on the a-c/d-c ratio of cables in steel pipe and conduit. A good start was made on this problem in the paper on the Electrical Testing Laboratories tests on cables in steel pipe, presented by R. J. Wiseman before the AIEE in 1948. It was recognized at the time that additional information was badly needed especially on segmental conductors, and on the effect of losses in the shield and skid wire.

Mr. Meyerhoff and Mr. Eager appear to have made a substantial contribution along these lines. While the data they have presented are valuable and are badly needed, a few comments are in order.

Referring to Table III* and Table XI of the paper covering skin effect (Y_0), we have summarized the results given in those tables, in Table I of the discussion together with the calculated skin effect using multipliers of 2.0 and 2.3. It is evident from this table that the results given by the authors in their Table III and Table XI do not agree, and that on the 1,000,000- and 2,000,000-circular-mil sizes these results are appreciably lower than the test results, whereas on the 1,500,000-circular-mil size they are considerably higher than the tests. We are inclined to wonder if the test result on this size is not somewhat low. Furthermore, it is quite evident that the 2.3 multiplier is too high; the true multiplier should be around 2.1. This agrees with Mr. Wiseman's results presented in his paper.

Next with regard to Table IV of the paper, the computed results appear to agree with the test results within about 20 per cent (that is 20 per cent of the extra a-c loss, not 20 per cent of the a-c/d-c ratio) except in two cases. The two cases in question are designation *1A* short-circuited shield where the computed result is 50 per cent high and designation *2A* where the computed results are 50 per cent high on the insulated shield and 57 per cent high on the short-circuited shield.

It seems likely that the discrepancy in designation *1A* and designation *2A*, insulated shield, may be due largely to the difficulty in measuring small increments of loss, and possibly to the rounding off of the various figures involved. This is not true of designation *2A* short-circuited shield where the extra a-c loss is 7 per cent measured and 11 per cent computed. A series of tests now in progress on a conductor of this size appears to give 11 per cent for the extra a-c loss which agrees well with the calculation given in the paper. It would seem likely therefore that the test result of 7 per cent is low in this instance.

Table I. Skin Effect Y_0

Conductor Size, Circular Mils	Calculated Skin Effect 2.0 Multiplier	Calculated Skin Effect 2.3 Multiplier	Reported Skin Effect Calculated Table III	Reported Skin Effect Calculated Table XI	Reported Skin Effect Test
1,000,000	0.023	0.018	0.014	0.017	0.020
1,500,000	0.048	0.039	0.039	0.038	0.032
2,000,000	0.091	0.069	0.072	0.065	0.072

Table II. Values of Y_{sp} and Y_{sp} from Equations 12, 13, and Test

Conductor Size, Circular Mils	R_{cm}	R_s'	Cable in Air—Y_{sp}' Calc.	Cable in Air—Y_{sp}' Test	Cable in Pipe—Y_{sp} Calc.	Cable in Pipe—Y_{sp} Test
1,000,000	10.75	240	0.033	0.020	0.081	0.030
1,500,000	7.31	242	0.047	0.080	0.118	0.080
2,000,000	5.32	217	0.073	0.030	0.182	0.150

Incidentally, while 20 per cent is reasonably good agreement for cables in magnetic pipe between calculation and test, it does seem like a rather large discrepancy for cables in air. Possibly it might be well to refine the method of calculation to bring this discrepancy down, if this can be done.

An estimate of proximity loss in the shield Y_{sp} and Y_{sp}' in pipes and in air can be obtained from Table IV and Table V of the paper by comparing a-c/d-c ratio as measured on high-resistance shields where it is negligible and low-resistance shield where it is appreciable. Table II of the discussion compares the results obtained in this way with the calculations and equations 12 and 13 of the paper. It is evident from this table not only that the test results are somewhat erratic (probably a matter of taking the difference between small quantities), but that the equations do not agree with the test results at all. In our opinion much better agreement is needed before equations 12 and 13 can be used with any confidence.

The over-all discrepancy in a-c/d-c ratio in Table V of the paper ranges from −4 per cent to +18 per cent. This is probably about as good as could be expected in a magnetic pipe. The agreement in Table VI is even better, from −9 per cent to +9 per cent. This indicates that an empirical correction factor of from 10 to 20 per cent should be added to the losses calculated by the authors' equations if they are to be applied for practical use with a reasonable factor of safety. Incidentally, tests now in progress give a figure of 1.39 rather than 1.33, as in Table V of the paper, designation *2A*, shield short-circuited. It would seem therefore that Mr. Meyerhoff and Mr. Eager are running somewhat lower on their test results both in pipe and in air than other investigators. This is another reason which would justify the empirical correction factor just suggested.

In the paper there appears equation 6 for the quantity Y_{cp}' (conductor proximity effect) with segmental conductors. This equation and the subsidiary equation for X_1 with its coefficient $K=3.8$ for three insulated segments and 6.0 for two insulated segments, make it appear that proximity effect is very much less with three insulated segments than with two. The only possible cause of this difference is the short circuiting effect of the binder tape on the two uninsulated segments, and since this short circuiting effect is necessarily not very large it is very surprising that there should be such a difference in proximity effect between the two cases. We believe that the authors should support these *K* constants with extensive test data before they may be safely considered authoritative.

Appendix II involves a nice piece of mathematical work resulting in formulas for pipe loss in nonmagnetic pipes. As might be expected when it is attempted to apply these formulas to magnetic pipe, certain approximations as to depth of penetration are necessary, and rather large empirical multipliers are involved. Here again extensive test data are desirable to support these multipliers and this approximation before the results can be considered authoritative. We believe it would be of value to the industry if the authors saw fit to present these test data, and also the test data on which the *K* factor is based either before the AIEE or somewhere else in the technical press.

Finally, it is clear from the data presented in this paper that a nonintercalated shield is a bad business, and that much lower losses are obtained by intercalating the shielding tape.

J. H. Neher (Philadelphia Electric Company, Philadelphia, Pa.): It is in large measure due to the efforts of Mr. Meyerhoff and Mr. Eager as embodied in their excellent paper, that we are rapidly approaching the point where we can stop guessing and commence to calculate the loss components in a pipe-type cable system with reasonable assurance of coming somewhere near the right answers. And this process will be materially simplified if we look carefully at the fundamentals involved and in so doing discard a few cumbersome practices which have been dragged along from the past.

I refer specifically to the continued use of the a-c/d-c ratio concept. Fundamentally the losses consist of d-c losses and extra a-c losses. The former depend upon the temperature of the conductor, but the extra a-c losses originating outside of the conductor in the shielding tapes and pipe depend upon their respective temperatures which are only indirectly related to the conductor temperature. Furthermore the extra a-c losses originating in the conductors have such a slight dependence on conductor temperature that they may be considered as being independent of this temperature. This was noted by E. H. Salter in the Electrical Testing Laboratories tests[1] and is confirmed by the Arnold Theory of Skin and Proximity Effects.[2]

From a practical standpoint, therefore, a given problem is more conveniently solved by calculating the extra a-c losses at representative temperatures and expressing them in terms of an equivalent extra conductor resistance, since it is a value of resistance which we ultimately use, and then adding this resistance to the d-c resistance of the conductor at its operating temperature. The a-c/d-c ratio which changes with conductor temperature need not enter the calculation, but the net result is the same as that obtained by use of the formulas given in the paper.

---

* Editor's Note: The figures in Table III referred to by Mr. Buller appeared in the preprint of the author's paper, but were revised as noted in the author's closure before publication.

The authors choose to calculate the skin and proximity effects in air separately, although they are combined when calculating the net effect within the pipe. Actually they may be calculated together just as simply by using the particular version of the Arnold Theory cited in Mr. Wiseman's paper.[2] The relationship between the additional conductor loss in pipe and the loss in triangular configuration in air is given as an empirical equation, 7, in the paper but its development is not indicated. I have examined this relationship for all of the tests given in the paper and also the tests of the Electrical Testing Laboratories[1,2] and find that within the limits of expected accuracy this ratio is 1.5 for triangular configuration in conduit, 2.0 for triangular configuration in steel pipe, 1.7 for cradled configuration in conduit, and 2.3 for cradled configuration in steel pipe. In all cases these ratios are based on a triangular configuration in air of the given adjacent conductor separation.

In the case of segmental conductors, and also theoretically in the case of stranded conductors, the Arnold Theory employs a modification factor in formulating the argument used in the Bessel Functions (equation 6 of the paper) to determine the skin and proximity effects. This factor may be introduced in several different ways, and the authors' K is not the same as Arnold's K. It seems more desirable to effect this modification by introducing a factor F as a multiplier of the d-c resistance. Thus

$$x_1 = \frac{6.80}{\sqrt{FR_{dc}}} \tag{1}$$

For a solid conductor $F=1$ and this also applies for the concentric stranded conductor in the Electrical Testing Laboratories' tests. For the conductors covered in the paper, F is equal to 3.2, which is in effect the factor of merit of the conductor construction, since the higher the value of F, the lower the additional conductor losses for a given size of conductor.

The authors are to be commended on their mathematical persistence in solving for Q in equation 16 which represents the pipe loss component, but Q also can be obtained somewhat more simply by graphical integration. It would seem, however, that equation 16 may be improved by using R_e in preference to (CI). Thus

$$Y_t\left(\begin{matrix}\text{magnetic at}\\ \text{60 cycles}\end{matrix}\right) = 0.21\frac{pQ}{R_e} \tag{2}$$

The numerical constant in this equation applies to steel pipe. Based on the Electrical Testing Laboratories' tests,[1] the corresponding constant is 0.18 for conduit.

REFERENCES

1. See reference 2 of the paper.
2. See reference 1 of the paper.

A. H. Kidder (Philadelphia Electric Company, Philadelphia, Pa.): The authors are to be commended for presenting so thorough a description of their recent tests on certain segmental cable constructions, together with approximate quantitative illustrations of relationships which become increasingly important in the design of heavy-duty pipe-type cable circuits. Their observations of total losses are thought to have sufficient accuracy to permit an approximate appraisal of the basic problem, which is to identify and control the factors which determine the efficiency of heavy-duty pipe-type cable designs.

The authors present over-all ac-dc ratios which bring us near but not quite to a complete qualitative understanding of the problem.

Designers of pipe-type circuits are confronted with the need to provide paths for transmitting loads of 1,000 amperes or more, through environments having heat dissipating characteristics which determine the maximum permissible watts losses, and in turn the maximum permissible resistance, or required conductance, of each such path. The cable designer then must select the particular cable construction and the conductor size which will provide the required conductance. The ratios which the authors have presented permit ready analysis from which it will become apparent that the conductance of a pipe-type circuit, however, may have little or no relation to the conductor size.

For example, consider Figure 1 of the discussion which has been constructed to illustrate the effects of steel pipe and cable configuration on 69-kv conductor size, using the information given in Tables X, XV, and XVI of the paper. If a resistance of 0.0125 ohm per 1,000 conductor feet will satisfy the given conditions, the corresponding conductance would be 80 mhos per 1,000 conductor feet. From the illustration it will be seen that the minimum conductor size would be 1,060,000 circular mils for use in nonmetallic pipe. For installations in steel pipe, the conductor size would be 1,300,000 circular mils if the three cables were to be triplexed, or 1,560,000 circular mils if the cables were to be cradled as in present conventional practice. Conversely, it is apparent that adoption of a triplexed construction would save 260,000 circular mils of copper cross-section in this particular case and that the use of a nonmetallic pipe would save an additional 240,000 circular mils. The cost of cables is very sensitive to conductor size. The opportunities for copper economy are substantially greater under conditions which require conductances in the order of 90 to 100 mhos, and could be converted into substantial cash savings by proper design, if there were some degree of consistency between identical tests on cables of apparently identical construction. A practical substitute for magnetic steel pipe apparently would solve the whole problem, or at least reduce considerably the need for improved cable designs. For the present, however, steel pipe must be included in the analysis.

The large uncertain effects of apparently trivial variations in cable design and inconsistencies between successive tests on cables of identical manufacture, suggest that a good bit of thought can be given profitably to consideration of methods for increasing the conductor efficiency in steel pipe installations. In Figure 2 of the discussion, for instance, I have plotted conductor size against 75-degree-centigrade conductance in triangular formation for several 69-kv pipe-type cable sizes. The heavy curve represents the construction for which the authors have estimated R_{ac}/R_{dc} in Table XV. Also shown and identified for

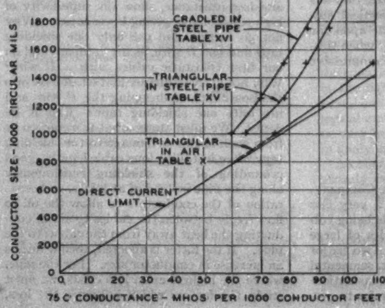

Figure 1. (left) Effects of steel pipe and cable configuration on 69-kv conductor size

Figure 2. (right) Relation between 75 degree centigrade conductance and 69-kv pipe-type cable size for triangular configuration in steel pipe

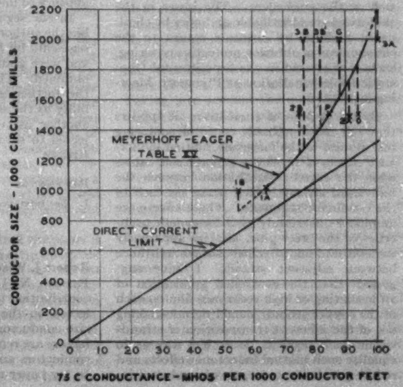

comparison are tests reported by the authors in Table X for samples 1*A*, 2*A*, 3*A*, 1*B*, 2*B*, and 3*B*, together with corresponding data from four manufacturers' tests, 3*B'*, *G*, *O*, and *P*, made in conformity with certain purchase specifications with which I am familiar. Several significant observations become apparent from a study of these data:

1. The four, 2,000,000-circular-mil constructions have conductances the same as analysis of Table XV would indicate to be expected of conductors whose sizes range from 1,250,000 to 2,200,000 circular mils.

2. Similarly, the four 1,500,000-circular-mil constructions have conductances respectively the same as would be expected from Table XV for conductors whose sizes range from 1,200,000 to 1,850,000 circular mils.

3. The extra copper required to offset the higher losses in the authors' "low resistance shield" type of construction appears far out of proportion to any possible advantages that might be gained by its possible use as a path for carrying currents.

4. The fact that constructions 3*B* and 3*B'* may be considered to be identical and were tested in the same laboratory, suggests that slight variations in manufacture and perhaps even in handling the cables may have substantial effect upon their efficiency as conductors. The extra polyethylene-intercalated 3-mil copper tape of sample 3*B* hardly would account for its 5 per cent lower conductance.

The 1,500,000 circular mil sample *O* was probably the first on which a full-scale a-c loss test was made. The results were far better than had been expected, giving a conductance in the order of 94 mhos per 1,000 conductor feet. Test accuracy may have been less dependable than in later tests. It is therefore possible that this considerably older cable design had no higher conductance than the authors' sample 2*A* at 91 mhos.

The wide dispersion of test results suggests, however, that the respective constructions probably include some important indeterminate which should be brought under control before additional tests or increased test accuracy can have much value.

The inefficiency of the authors' novel "low resistance shield" construction can be avoided very conveniently by returning to the conventional use of intercalated insulation or the equivalent. The losses in the skid wires are identifiable and may be eliminated perhaps by eventual return to the canvas-type of abrasion protective covering, such as was used in the experimental Oilostatic cable installation at Plymouth Meeting in 1933.

By the process of elimination, it appears that the most probable cause of confusing test results is the uncertain mutual inductance effects of nearby segments and cables upon the current distribution between the individual strands which make up each of the conductor segments. These effects are amplified uncertainly by the magnetic properties of the steel pipe, also by apparently variable and uncontrolled contact resistance between adjacent strands. I have suggested[1] that the controlled application of an insulating or high-resistance film on each of the copper strands should permit making use of the inherent transposition of strands within each segment, in such a way as to equalize such mutual inductance effects and reduce proximity as a cause of conductor inefficiency. The authors' suggested possible use of enameled wires should not be nearly so effective with untransposed strands in concentric conductors, as with the transposition inherent in segmental construction, and I am not convinced that enamel is the answer. The authors' reference to the high contact resistance for aluminum suggests that aluminum strands might be more efficient than copper for large cables, despite the lower specific conductivity. A practical alternative may be the application of a very thin (possibly oxidized) aluminum film on the copper strands before the segments are stranded and compacted. Still another possibility is use of the conventional oxidized lead-coated copper strand, although it appears likely that the compacting pressures might make it less effective than aluminum. The use of a copper oxide or copper sulphide film might have similar advantages, but such films are thought to be more active catalysts than lead, aluminum, or their oxides. The method of joining conductors would, of course, have to be correlated with such a modification of the conductor strand.

Reference

1. 69-Kv Pipe-Type Cable Circuits in Philadelphia, A. H. Kidder, G. S. Van Antwerp. *AIEE Transactions*, volume 68, part I, 1949, pages 550–59.

W. A. Del Mar (Phelps Dodge Copper Products Corporation, Yonkers, N. Y.): This paper is of great value to the industry both for the wealth of experimental data and for the mathematical analysis which has required not only a knowledge of the physics involved, but even more, a well-balanced judgment in evaluating the many necessary assumptions and approximations.

That the authors have used these qualifications and have made the best use of Arnold's work is clear to me because I have been able to check values of a-c/d-c resistance ratio calculated by their method against laboratory test data and, using reasonable assumptions, find a very close agreement.

The practical use of the method would be helped if Figure 5 of the paper were supplemented either by a table from which large scale curves could be made, or by reference to Arnold's Table I[1] from which Figure 5 appears to have been plotted.

In our segmental compression cables we, like the authors, have avoided short circuiting segments by having only one bare segment and were gratified to find the low resistance obtained. The 3-segment construction has the further advantage of mechanical stability as the segments cannot slide upon one another as in a 4-segment cable, when subjected to severe longitudinally compressive stresses.

Reference

1. See reference 4 of the paper.

Robert J. Wiseman (The Okonite Company, Passaic, N. J.): This paper is a very fine contribution to the data which is being collected on the electrical properties of large size conductors in steel pipes. Two major factors are reported in this paper, segmental conductors and shielding of the insulation. In my paper which the authors refer to we, that is, the Insulated Power Cable Engineer's Association reported on concentric conductors and only one segmental conductor and also on nonshielded cables. As the authors state our results are more applicable to low-voltage rubber or varnished cambric cables and not high-voltage cables, yet they can be used for heavy-wall nonshielded cables in pipes.

I like very much the detailed information which the authors report and the development of the theoretical aspects of the various factors. It is good that they have given curves and tables for some of the terms used in the formulas. Otherwise some of us would not want to go through the calculations each time we had to determine a conductor size to carry a given current. It is desirable, if possible, to use as simple formulas as possible. Therefore, as a matter of interest I took the pipe loss as given in Table XV of the paper and computed it by the formula given in my paper, namely, $PL = 0.00150\ S^2/p$ ohm per 1,000 feet, where S is the spacing, center to center, for triangular spacing and p is inside diameter of pipe. Table III of the discussion compares the values given by the authors, column 3, with the above calculations, column 4. Likewise for the cradle configuration, I took the geometric mean spacing, that is $S' = \sqrt{S_1S_2S_3}$ and $PL = 0.00180\ S'^2/p$ ohm per 1,000 feet obtained the values shown in column 6 as compared to column 5 for the authors. The agreement is good considering that we are making assumptions which involve approximation.

I hope that time will be available later to see what can be done with proximity effect.

There is considerable information given in the paper which affords us a means for studying what is the order of magnitude of each of the factors which contribute to the extra a-c losses and how can they be reduced. For example, the authors use a 4-segment conductor and insulate three of the four segments. It is customary to insulate the two opposite segments. If we assume, as the authors do, that the skin effect of a 4-segment conductor is the same as that for a round conductor having 44 per cent of the area of the segmental conductor, then nothing appears to be gained by insulating three segments over two segments, as the Insulated Power Cable Engineer's Association tests made on a 2,500,000-circular-mil conductor gave the same result and two of these segments were insulated. Perhaps this could be investigated further.

The results on shielding losses, both high and low resistance, show the superiority of high resistance in giving lower losses. Why not go further and use only one shielding tape and one *D* wire, as my company did on our first Oilostatic cables with a *D* wire? Why not go even further and let us look into the possibility of dropping the *D* wire and use only one shielding tape? Can it be done? We must study what it means to us from such angles as damage to the shielding tape when installing long cable lengths, good grounding of the shielding continuously along the pipe instead of at joints, and separation of the conductors to allow the oil to flow freely between the cables to aid in conducting the heat away from the cables to the pipe. If the latter is affected, then it means an increase in conductor size. For the pipe, where the highest extra loss exists, we must study the factors which influence the loss,

Table III. Pipe Losses

Conductor Size, Circular Mils	Insulation Thickness, Inches	Table XV Meyerhoff and Eager	Table XV Computed A*	Table XVI Meyerhoff and Eager	Table XVI Computed B**
1,000,000	0.315	0.09	0.09	0.13	0.15
	0.480	0.09	0.10	0.15	0.17
	0.560	0.11	0.12	0.15	0.18
	0.560	0.09	0.09	0.18	0.16
1,250,000	0.315	0.09	0.11	0.19	0.19
	0.480	0.15	0.15	0.19	0.23
	0.480	0.11	0.11	0.23	0.20
	0.560	0.12	0.13	0.23	0.21
1,500,000	0.315	0.14	0.14	0.23	0.24
	0.480	0.16	0.15	0.29	0.26
	0.560	0.17	0.16	0.30	0.29
1,750,000	0.315	0.19	0.19	0.28	0.30
	0.480	0.21	0.19	0.34	0.32
	0.560	0.22	0.21	0.36	0.35
2,000,000	0.315	0.25	0.23	0.32	0.36
	0.315	0.20	0.17	0.38	0.32
	0.480	0.24	0.23	0.42	0.39
	0.560	0.27	0.26	0.43	0.43

* $PL = 0.00150\, S^2/\rho$ $\quad A = 1 - PL/R_{dc}$
** $PL' = 0.00180\, S'^2/\rho$ $\quad B = 1 - PL'/R_{dc}$

namely, spacing of the conductors, pipe diameter, and pipe material. Increase in the spacing between the conductors increases the loss for a given pipe size. Increasing the pipe size decreases the loss for both triangular and cradle configuration. As cradle configuration gives a higher loss than triangular formation, we should endeavor to keep the cables in triangular configuration. The nature of the pipe material is the major factor. Perhaps a nonmagnetic pipe of high resistance would be best, but its cost may be prohibitive. A magnetic pipe of low permeability may be helpful, but Dr. Hutchings of the British Electrical and Allied Industries Research Association has made calculations to show that using a steel of permeability of $\mu = 300$ and $\mu = 1{,}700$ gives about the same loss. Therefore, we would have to go under $\mu = 300$.

Table IV of the discussion gives total a-c/d-c ratios for some cables that we have tested.

Table IV

Cable	Ratio R_{ac}/R_{dc}	Temperature, Degrees Centigrade
3 single conductor, 1,500,000 circular mil, segmental $t = 0.315$ inch; $6^5/_8$ inch OD pipe	1.38	27.4
	1.27	65.8
3 single conductor, 500,000 circular mil, compact $t = 0.500$ inch, 6 inch OD pipe	1.19	32.3
3 single conductor, 350,000 circular mil compact	1.13	78.0
$t = 0.465$ inch; $5^9/_{16}$ inch OD pipe	1.08	68.2
3 single conductor, 500,000 circular mil $t = 0.560$ inch; number 10 American wire gauge	1.47	38.2
copper armor over insulation;	1.41	107.0
$6^5/_8$ inch OD pipe	1.45	46.0

The values for the 350,000-circular-mil circuit and the 500,000-circular-mil circuit (nonarmor) are the same as the Insulated Power Cable Engineer's Association[1] have set up for 3-conductor cables.

The results reported in this paper and the investigation now being made by the Electrical Testing Laboratories for the Association of Edison Illuminating Companies will supply us with plenty of data to analyze carefully and draw conclusions from, with the hope that we will arrive eventually at a construction that will give us an optimum value of extra a-c losses at a reasonable cost.

REFERENCE

1. CURRENT CARRYING CAPACITY OF IMPREGNATED PAPER, RUBBER AND VARNISHED CAMBRIC INSULATED CABLE FOR THE TRANSMISSION AND DISTRIBUTION OF ELECTRICAL ENERGY. *Publication P29-226*, Insulated Power Cable Engineers Association (New York, N. Y.), December 1943, Table A, page 9.

L. Meyerhoff and G. S. Eager, Jr.: The reception of the paper, as evidenced by the various discussions submitted, is highly gratifying. In general, there is agreement that the methods of computation given in the paper give a reasonably close approximation to losses measured by other observers. One of the discussors points out discrepancies between observed and calculated values and suggests that modifications of certain equations are in order for greater reliability. Another intimates that since there is so wide a range of losses with apparently identical constructions, too close correlation should not be expected.

All of the foregoing is in line with the statement in the early part of the paper that the data presented are not claimed or believed by us to constitute a complete answer to the problem. We concede that there are discrepancies among the data and between the data and calculations and that some of the equations may be subject to modification in the light of later information. We believe, however, that we have presented a logical mathematical approach which should be very helpful in planning future work and in analyzing other data.

A concrete accomplishment of the paper is already evident in the apparently complete acceptance that shield circulating current losses vary substantially according to equations 9 and 10 of the paper. Various lines of approach which were mentioned and analyzed in the paper have received attention, such as using shielding materials of higher resistance and using one *D*-wire instead of two, and the shield losses, within experimental error, have been found to vary inversely as the shield resistance, as the equations indicate. Mr. Hatcher's data indicate, however, that the ratio between shield loss in pipe and that in air may be greater than indicated by the paper.

Mr. Hatcher, Mr. Kidder, and Mr. Wiseman discuss further the matter of reduction of conductor losses by use of various devices which would increase contact resistance between the individual wires making up the strand. Enamel, copper oxide, copper sulphide, or aluminum coatings on the wires, if the coatings are not broken up too much in compacting, may all be very effective in reducing the proximity effect and probably also, to a lesser extent, the skin effect of segmental conductors. The scheme mentioned in the paper, where the outer layer of wires in each segment is separated from the other layers by an insulating tape, also might be effective to a somewhat smaller extent but would probably be less expensive and easier to splice. The use of enamelled concentric strand was suggested in the paper as a possible way of obtaining the same conductor losses as with ordinary segmental conductors, but with a possible cost saving. We agree with Mr. Kidder that concentric strand made with enamelled wires would have higher losses than segmental strand made with enamelled wires, provided, of course, that in the latter the integrity of the enamel coating is not seriously impaired by compacting.

Mr. Kidder's suggestion that aluminum conductors might be used in place of copper is interesting. Aside from possible reduction in conductor losses, there may, in fact, be conditions where the use of aluminum conductors will result in a lower cost installation, as, for example, where the diameter of the pipe used with copper conductors is sufficiently large to accommodate aluminum conductors having a conductance about equal to that of the copper conductors.

The matter of reduction of pipe losses is touched on by Mr. Kidder and Mr. Wiseman. Of course, a suitable nonmetallic pipe, if such were available, would be the most satisfactory answer. A metallic, nonmagnetic pipe would be a satisfactory answer only if the resistivity of the pipe material is extremely high. It is evident from equation 14 that, within the assumptions used, the loss in nonmagnetic pipe is proportional to the thickness of the pipe and inversely proportional to its resistivity. For magnetic pipe actual thickness is replaced by the "depth of penetration," which is of the order of 5 to 10 per cent of the thickness. Taking into account the multiplying factor of 2.6 for magnetic pipe, the resistivity of nonmagnetic pipe must be of the order of 4 to 8 times that of steel, that is, 30 to 60 times that of copper, to produce the same loss as steel pipe, assuming the same wall thickness. To obtain lower losses than with steel pipe, the resistivity of the nonmagnetic pipe would have to be still higher. It may be expected, however, that the use of nonmagnetic pipe will reduce the conductor and shield losses somewhat.

Regarding the losses in magnetic pipe, it should be pointed out that the losses are high primarily because the conductance is high and not because the pipe is magnetic. The common impression, reflected in Mr. Wiseman's comment, is that the way to reduce losses in magnetic pipe is to reduce the permeability. On the contrary, the evidence is that reducing the permeability will increase the losses. Thus, the two lines of attack are to increase the resistivity and to increase the permeability. From the data in Table II of the paper it appears that, with the currents used in the tests, the permeability of the 8-inch pipe is about 50 per cent higher than that of the 6-inch pipe, yet the pipe loss factor is about 15 per cent lower for the 8-inch pipe than for the 6-inch pipe, in spite of the fact that the resistivity of the 8-inch pipe is 10 per cent lower. Similarly, the data in Mr. Wiseman's Table XIII indicate lower permeability and higher resistivity for the steel pipe than for the various conduits, but the loss data indicate higher losses for the steel pipe. Deduction from equation 14 leads to the same conclusion, bearing in mind that, for magnetic pipe, t must be replaced by "depth of penetration," which is inversely proportional to the square root of the permeability.

The excellent agreement between pipe losses as calculated by the simple formulas used by Mr. Wiseman and as calculated by equation 15 is interesting and suggests that for purposes of rough approximation, simple approximations of some of the other equations in the paper also may be found useful.

In Table IV of the discussion Mr. Wiseman gives loss data on four additional cables. It is assumed that these were tested with close triangular configuration. It is to be regretted that construction details have not been given, as these would add greatly to the value of the data.

In Figure 2 of the discussion, Mr. Kidder points out the large spread of effective conductance with conductors of the same size. The reduced effective conductance was produced in most cases by low resistance shields but in one case perhaps by low contact resistance in the strand. It should be noted that Mr. Kidder's comparison of different constructions on the basis of conductance alone, as derived from over-all a-c/d-c ratio, is an oversimplification of the actual design problem and one that could readily lead to erroneous conclusions concerning carrying capacity. In addition to the over-all a-c/d-c ratio one must of necessity give proper weight to the point in the thermal circuit at which the various losses are generated. It is obvious, for example, that a given degree of extra loss developed in the conductors will produce more rise in temperature than an equal amount of extra loss originating in the shielding assembly or in the pipe.

Again referring to Mr. Kidder's Figure 2, it will be noted that our samples 2*A* and 2*B* fall below the line drawn from the approximate calculated losses as given in Table XV of the paper. The reason for this is that the actual conductor diameters, and hence the conductor separations, were somewhat smaller than for conventional concentric strand, which were used in calculating Tables XV and XVI, resulting in lower actual than calculated losses. The loss values as given in Tables XV and XVI were intended to be conservative.

Table V. The Functions $G(x)$ and $H(x)$

x	$G(x)$	$H(x)$	x	$G(x)$	$H(x)$
1.1	0.022	0.345	2.6	0.318	0.630
1.2	0.031	0.350	2.7	0.341	0.667
1.3	0.041	0.356	2.8	0.363	0.705
1.4	0.054	0.364	2.9	0.384	0.745
1.5	0.069	0.373	3.0	0.405	0.785
1.6	0.086	0.385	3.1	0.425	0.826
1.7	0.106	0.399	3.2	0.444	0.867
1.8	0.126	0.414	3.3	0.463	0.908
1.9	0.149	0.433	3.4	0.481	0.948
2.0	0.172	0.454	3.5	0.499	0.987
2.1	0.197	0.477	3.6	0.516	1.025
2.2	0.221	0.503	3.7	0.533	1.061
2.3	0.246	0.531	3.8	0.550	1.096
2.4	0.271	0.562	3.9	0.567	1.129
2.5	0.295	0.595	4.0	0.584	1.160

Mr. Buller points out various discrepancies between measured and computed values. The measured skin effect values as given in the original Table III of the preprint of this paper are indeed somewhat higher than the corresponding values in Table XI. However, the skin effect values given in Table III are based on measured resistances at temperatures somewhat lower than 30 degrees centigrade, whereas in Table XI they are based on calculated resistances at a specific temperature. Since there is no particular point in showing the values of skin effect to the third decimal, as was originally done, the values in the revised Table III are shown only to the second decimal.

The discrepancies in shield proximity losses pointed out by Mr. Buller must be attributed to sample variability. These losses constitute a minor part of the total losses and are entirely negligible for the more common cable constructions. Moreover, the results obtained from the equations, as given, appear to be conservative for most cases. Until further data show it to be desirable, there does not appear to be much need for revision of these equations or any of the others given in the paper.

Regarding the value of 6.0 for K, which was indicated for one case of strand with two insulated segments, this was obtained on one specific sample which had a low resistance path between the two bare segments, produced by a lapped bronze binder, and in which the contact resistance between individual wires might be expected to be low by reason of the fact that it received no drying treatment at all. As also pointed out in the paper, the data for a segmental cable reported by Mr. Wiseman show a K value of 5.4. However, it was not intended to convey the impression that all segmental strand with two insulated segments have so high a K factor. Indeed, tests performed since the presentation of the paper have shown that a K factor of 3.8 applies not only to strand having three insulated segments, but also to strand having two insulated segments, provided that the cable with two insulated segments is dried with access of air for part of the time and the conductor binder consists of a bronze tape, intercalated with a paper tape, or is of some other construction having sufficiently high resistance.

We agree with Mr. Buller on the desirability of supporting the K_1 factor for loss in magnetic pipe with extensive data. However, we believe the data given in Table VII are sufficient for a good start in that direction. Perhaps other investigators will supply additional data.

Mr. Neher suggests that a better method of approach toward the evaluation of extra a-c losses is on the basis of apparent resistance increment rather than ratio of a-c to d-c resistance. From the operating man's standpoint his suggestion has much merit. However, the use of the ratio lends itself more readily to the accumulation and evaluation of laboratory data. We believe that this is largely a matter of personal preference, as is also the choice between the K factor as used in the paper and the F factor suggested by Mr. Neher, and the use of conductor resistance instead of conductor size in the pipe loss formula.

Regarding Mr. Neher's suggestion of evaluating skin and proximity effect in air together instead of separately, we believe that separate evaluation has certain advantages, especially because in segmental conductors different K factors apply for the two, K being about 4.5 for skin effect and 3.8 for proximity effect.

It is interesting to note that Mr. Neher has found from available data more or less definite multiplying factors between excess a-c conductor loss in pipe and in air.

Empirical equation 7 given in the paper was an attempt to correlate all available data. Perhaps there is not adequate justification to go beyond establishing constants for the various broad conditions as Mr. Neher has done.

In compliance with Mr. Del Mar's suggestion, there are given in Table V of the discussion, $G(x)$ and $H(x)$ values for the range of x values required in the present connection for equations 5 and 6. These were taken from Table I of reference 4 of the paper.

Self-Saturation in Magnetic Amplifiers

W. J. DORNHOEFER
ASSOCIATE AIEE

THE PURPOSE of this paper is to describe self-saturation in magnetic amplifier circuits and to propose a simplified but approximate method of calculating the performance of this type of circuit. To illustrate the simplified method, the calculated performance for a particular case is compared with the measured performance.

Saturable Reactors

The literature is replete with references to the elementary magnetic amplifiers known as saturable reactors.[1] A saturable reactor, as is known, is a device having an a-c impedance which can be adjusted by means of d-c premagnetization. Simple saturable reactors, in general, are of slightly larger size than 2-winding transformers of the same kilovolt-ampere rating. They are commonly made in one of two styles—3-legged or 4-legged. In the 3-legged reactor, the a-c windings embrace the outer legs of a shell-type transformer structure, while the control, or d-c winding, embraces the inner leg. The a-c windings are so connected in series or in parallel that the fundamental magnetic flux path is through the outer legs and yokes, giving no fundamental component of power-frequency voltage in the control winding. In the 4-legged reactor, a-c windings are wound on each of the two inner legs, while the d-c winding embraces both. In this case also, no fundamental component of power-frequency voltage is induced in the control winding. With respect to static performance, the two constructions yield reactors with similar characteristics. While differences exist between them with respect to leakage flux conditions and even-harmonic pick-up in the control coil, the 3- and 4-legged reactors operate in much the same way.

The reactance of the a-c windings is adjusted by varying the value of d-c premagnetization in the a-c magnetic path, by passing direct current through the control winding. The reactance is an inverse function of the control current, so that it is maximum at zero direct current and falls to relatively low values at high values of premagnetization. Obtaining optimum utilization of the reactor structure involves supplying a premagnetization with the d-c winding at least equal to the peak magnetomotive force developed by the a-c coils plus the amount necessary to saturate the magnetic circuit of the reactor. Generally, the d-c increment is from 25 to 100 ampere-turns per inch of mean magnetic path. As the result of the excess of d-c over a-c ampere-turns, saturable reactors usually are made with more of the window space devoted to control-winding copper than to power-winding copper. For this reason, a reactor of a given rating is generally slightly larger in size than its analogous 2-winding transformer.

However, assuming that the same window space will be used by both the a-c and d-c windings gives a simplified and not-inaccurate idea of saturable reactor sizes and amplifications. For example, if the copper losses of a moderate sized transformer constitute approximately 2 per cent of the rating of the transformer, the copper losses of each winding are the equivalent of 1 per cent of the rating. The a-c winding of a reactor resembles the secondary winding of the transformer in that the current and voltage ratings are equivalent if each has the same amount of iron and secondary copper. For equal d-c and a-c window space and ampere-turns, copper losses in the d-c and a-c reactor windings are equal, both being 1 per cent of the reactor rating for this example. Thus the effective power gain realized through decoupling the d-c winding from the a-c winding is of the order of 100. In practice, because of the use of more than 50 per cent of the window by the d-c coil, gains of approximately 250 can be realized in 50-kva saturable reactors, while gains of approximately 50 are obtained in 2-kva reactors. Of course, the gains mentioned are realized partly at the expense of apparatus efficiency; that is, a larger amount of iron and copper must be provided in the reactor than in a transformer of equivalent rating.

Saturable Reactor Limitations

The simple saturable reactors described have several limitations. The control windings require a great many turns of small wire, in which the induced voltages become extremely high if one of the two a-c coils becomes inoperative. Because of the many turns used in the d-c coils, all of which link the entire magnetic circuit, the time delay (or effective time constant) of the d-c coil is generally long. The delay is reduced if the d-c winding is controlled from a high-resistance source or if resistance is inserted in series with the control coil. This method of reducing the time constant of the control circuit is not economical of control power, and the gain in dynamic response is accomplished only at the expense of the power amplification of the saturable-reactor circuit.

Reactors with Feedback

In simple saturable reactors, a considerable portion of the control power is required to equilibrate the peak a-c magnetomotive force. By making use of feedback or compensation, this portion may be reduced. The use of feedback permits the same range of control of the output as is available in simple reactors. The d-c coil supplies only the magneto-

---

Paper 49-140, recommended by the AIEE Electronics and Basic Sciences Committees, and approved by the AIEE Technical Program Committee for presentation at the AIEE Summer General Meeting, Swampscott, Mass., June 20-24, 1949. Manuscript submitted December 1, 1948; made available for printing May 16, 1949.

W. J. Dornhoefer is with the Vickers Electric Division of Vickers, Incorporated, St. Louis, Missouri.

motive force required to saturate the magnetic circuit of the reactor, while the feed-back means supplies sufficient magnetomotive force to equilibrate that of the a-c coils. Several investigators have reported on a method of feedback known as self-excitation or external feedback.[2,3,4] External feed-back circuits are shown in Figures 1 and 2. In these circuits, the alternating current flowing in the main windings is rectified and caused to flow in additional windings on the reactors in such a way that in one reactor the d-c magnetomotive force assists the a-c magnetomotive force at a given instant; while in the other, the d-c ampere-turns oppose the a-c ampere-turns. Of course, on the succeeding alternation of current, the assistance and opposition alter in sense, so that, at any instant, either one or the other of the a-c windings exerts no net magnetomotive force on the core, providing the feedback winding turns are made approximately equal to the a-c winding turns. As a result, saturation of the magnetic core material by means of the d-c control winding can be accomplished by supplying only sufficient magnetomotive force to saturate the magnetic circuit.

External feed-back circuits offer considerable improvement in sensitivity over the simple saturable-reactor arrangement. It is possible, by adjusting the turns in the feed-back winding, to compensate exactly, to over-compensate, or to under-compensate for the power-winding magnetomotive force. Overcompensation corresponds to feedback reactors having feedback turn ratios of greater than unity. It has the effect of reducing the control ampere-turns required by the reactor and accentuating nonlinearities in the output versus d-c premagnetization, or transfer, curve. Under-compensation gives opposite effects.

Several important considerations which enter the design and evaluation of such circuits involve the precision of the equilibrium which can be obtained between the magnetomotive forces of the a-c and feed-back windings. In general, it is not only desirable but absolutely necessary to reduce the leakage flux between the a-c power winding and the feed-back winding to a minimum. This is often done by winding both at the same time, that is, two-in-hand. Moreover, it is necessary to be certain that the current conversion ratio of the rectifier does not change. This, of course, means that back-current leakage in the rectifier must be minimized. The considerations involved in equilibrating the feed-back and a-c winding magnetomotive forces are particularly important with reactors using high quality magnetic materials in gapless magnetic circuits.

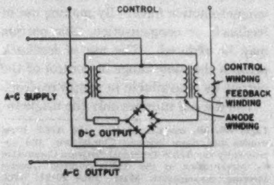

Figure 1. Circuit diagram of a d-c premagnetized reactor having external feedback and parallel connection of the a-c windings

Symbols

N = anode winding turns
ϕ = flux linking anode winding, maxwells
i = anode circuit current, amperes
R = anode circuit resistance, ohms
E_m = maximum value of sinusoidal supply voltage, volts
e_R = forward voltage drop on rectifier, volts
e_L = instantaneous value of load voltage, volts
$e_{L(Avg)}$ or $\bar{e}_L$ = average value of load voltage, volts
E_f = a defined critical voltage for firing $= B_f \omega NA \times 10^{-8}$ volts
A = effective area of magnetic core, square centimeters
l = effective mean length of magnetic path in core, centimeters
f = supply frequency, cycles per second
ω = angular supply frequency, radians per second
θ = angular argument of supply frequency, radians
B = instantaneous magnetic flux density in core, gausses
B_0 = initial magnetic flux density, gausses
B_m = maximum value of alternating magnetic flux density associated with supply voltage $= E_m \times 10^8 / \omega NA$, gausses
B_f = critical value of magnetic flux density for firing, gausses
$H(B)$ = instantaneous magnetizing force indicated as a function of B, oersteds
H_i = magnetizing force due to anode current, oersteds
H_0 = initial magnetizing force, oersteds
H_f = critical value of magnetizing force, oersteds
t_f = instant at which firing occurs, seconds
θ_f = angular argument at which firing occurs, radians

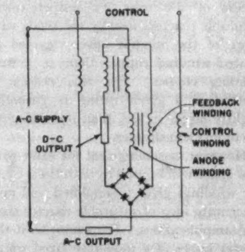

Figure 2. Circuit diagram of a d-c premagnetized reactor having external feedback and series connection of a-c windings

One investigator[5] has reported a 4 to 1 change in the output versus input characteristics of a magnetic amplifier using external feedback when the turns in the feed-back winding were changed from 100 per cent of the power winding turns to 100.1 per cent of power-winding turns.

These results, as might be expected, were found using high quality core material with a gapless structure. Variations of magnetic amplifier characteristics to be expected with reactor core structures built up of conventional *E-I*, *E-E*, or *F*-type laminations, and the adverse effect of slight unbalances in feed-back turns, would not be as great.

Self-Saturation

Another method of balancing the power-winding magnetomotive force involves the use of self-saturation of the type found in the circuit given in schematic form in Figure 3.[6,7]

The schematic circuit drawing of Figure 3, while not that of a practical self-saturating magnetic amplifier, will serve to illustrate the form of feedback which is the principal topic of this discussion. In this circuit an electric valve is connected in series with the power winding of a reactor. Ideally, the current flowing in the power winding is pulsating and unidirectional, and causes pulsating, unidirectional magnetic flux in the core of the reactor, which flux never falls below a minimum value. This value depends on the maximum flux density and magnetizing force achieved during the forward alternation of supply voltage and positive pulsation of anode-winding current. It depends also on the magnetomotive force of the control winding.

In order that the effect upon the output of premagnetization supplied by the control winding may be appreciated, a

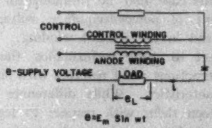

Figure 3. Circuit diagram of the basic half-wave magnetic amplifier with self-saturation

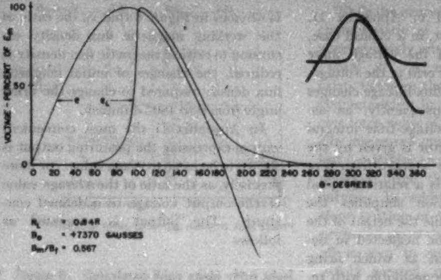

Figure 4. Calculated wave form, see Appendix I, of output voltage of a half-wave magnetic amplifier circuit and oscillogram for corresponding conditions

Calculated	Oscillogram
$B_m/B_f=0.57$	$B_m/B_f=0.57$
$R_L/R=1.0$	$R_L/R=0.94$

typical reactor with self-saturation is analyzed in Appendix I. Briefly, this appendix treats a half-wave magnetic amplifier, with a sufficiently high impedance connected in control circuit so that the voltage induced in the control winding causes no fundamental-frequency current. (In the case of the practical magnetic amplifier circuits, the induced voltage of fundamental frequency which appears in each control coil is balanced by an equal voltage in another coil; these are so connected that no fundamental voltage appears at the control-circuit terminals.) It is shown in Appendix I that the calculated output-voltage wave resembles the output of a gas-filled grid-controlled electronic tube. See Figure 4. The output-voltage wave form contains a portion with very great slope, which is associated with "firing" of the magnetic amplifier. The time at which firing occurs depends on the magnetomotive force H_0 of the control winding, and in particular, upon the initial magnetic flux density B_0 associated with this magnetomotive force. For purposes of comparison, an oscillogram of the measured output-voltage wave form for the same conditions and values used for the calculation is shown also in Figure 4. A recalculated output-voltage wave form, which is more nearly in accordance with the test conditions of the oscillogram, is shown in Figure 5.

The labor involved in the step-by-step calculations of Appendix I makes it an inconvenient method either for gaining a general understanding of the circuit or for predicting performance.

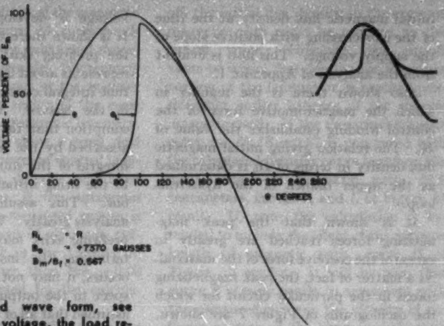

Figure 5. Recalculated wave form, see Appendix I, of output voltage, the load resistance comprising only 94 per cent of the total circuit resistance

Calculated	Oscillogram
$B_m/B_f=0.57$	$B_m/B_f=0.57$
$R_L/R=0.94$	$R_L/R=0.94$

Effect of Control Premagnetization

The effect of control premagnetization upon the output can be seen in the oscillograms of Figures 6 and 7. As the values of H_0 and B_0 are adjusted, the point of firing varies along the angular time base from 180 degrees towards 0 degrees. Before firing, virtually all the supply voltage is absorbed as a voltage-time integral (flux-linkage change) by the coil. After firing the core is saturated, and almost all of the supply voltage appears on the load resistor. This is particularly evident in the oscillograms of Figure 6. Corresponding oscillograms showing magnetic conditions in the core are given in Figure 7.

The operation of the circuit can be considered in a simplified way as being of this nature:

> The anode winding is capable of developing a large electromotive force due to magnetic flux changes with small changes and small values of anode current, since the reactor for which the oscillograms are shown has a high-permeability gapless core structure. Consequently, from $t=0$, when the supply voltage becomes positive with positive slope, until some later time, all of the supply voltage appears across the anode winding of the reactor, which may be thought of as absorbing a voltage-time integral. The absorption of a voltage-time integral by the reactor must be associated with a change of magnetic flux in the reactor core. When the change of flux from the initial value is such that the magnetic flux density reaches a certain critical value B_f, firing occurs. At firing, the reactor no longer can readily change its flux linkages, and the current increases abruptly from a small value to a value sufficient so that the iR drop is approximately equal to the supply voltage. Figure 4 shows that the iR drop is actually in excess of the supply voltage by the small amount associated with the low rate of discharge of the reactor flux linkages as the magnetic flux is dropping below its maximum value.

The B versus $H(B)$ oscillograms of Figure 7 will serve to illustrate the operation of the self-saturating magnetic amplifier circuit somewhat more clearly. They represent the operating minor hysteresis loops existing in the circuit for which the supply-voltage and load-voltage oscillograms of Figure 6 were taken. The oscillograms are shown in the same order as in Figure 6 from minimum output to a maximum output. The outputs are given in a convenient form developed in Appendix II.

Effect of Hysteresis

The oscillograms of Figure 7 give an insight into the principal factor involved in control of the output. When the minimum flux density, which is the flux density in the core at the time of the axis-crossing with positive slope of the supply voltage, is adjusted to a minimum value ($B_0=-5,300$ gausses in Figure 7), the excursion of flux density associated with the supply voltage, the anode turns, and the core area, is not sufficient to cause saturation of the reactor, so that the anode current remains at a small value corresponding to a normal alternating exciting current of the reactor. As the initial flux density B_0 is adjusted upward, firing occurs. As B_0 is increased, firing occurs earlier in time phase and results in larger peak and average values of a-c magnetizing force H_t and output voltage. From these oscillograms, it is evident that the fundamental consideration involved in controlling a self-saturating reactor output is the matter of adjusting the initial magnetic flux density at the time of the axis-crossing with positive slope of the supply voltage. This also is evident from the analysis of Appendix I.

Also shown there is the manner in which the magnetomotive force of the control winding establishes the value of B_0. The relation giving initial magnetic flux density in terms of H_0 is determined as the upper branch of the hysteresis loop.

It is shown that the peak magnetizing forces reached are greatly in excess of the coercive force of the material. As a matter of fact, the peak magnetizing forces in the particular circuit for which the oscillograms of Figure 7 are shown, amount to more than 1,000 times the coercive force of the material. Consequently, operation corresponding to the decay of flux is on the upper branch of the first, second, and third quadrant hysteresis loop, with maximum induction at saturation.

As a result of the saturation caused by the anode current on each half cycle, during the next half cycle when no anode current flows, the magnetic core is in a condition somewhere along the upper branch of the hysteresis loop. Thus, control is obtained along this portion of the magnetization curve, rather than on the normal magnetization curve.

Output, Firing Angle

A method of calculation giving the approximate firing angle and output voltage is developed in Appendix II. It is shown there that, in a typical case, the prefiring skirt of the voltage wave represents about 3 per cent of the voltage-time integral causing flux-linkage changes in the reactor. Consequently, an assumption that the voltage-time integral absorbed by the reactor is given by the integral of the supply voltage from zero to the firing instant is a relatively good one. This assumption simplifies the analysis greatly. While the height of the prefiring skirt may be neglected in determining the instant at which firing occurs, it may not be negligible with respect to the output. Furthermore, it is assumed that all of the circuit resistance is in the load, and that no extraneous effects, such as eddy-current shielding occur. What the assumptions amount to then is this: Before firing all of the supply voltage appears across the coil, while after firing all of the supply voltage appears across the load. This is obviously a rather naive assumption, but it will be seen that the results are in fair agreement with the approximations developed on this basis. Following Appendix II, the firing angle is given by

$$\theta_f = \cos^{-1}\left(\frac{B_m+B_0-B_f}{B_m}\right) \quad 0\leq\theta_f\leq\pi \qquad (11)$$

Figure 6. Oscillograms of supply voltage and load voltage of the half-wave magnetic amplifier shown in Figure 3. For increased values of B_0, "firing"—the abrupt rise in output voltage—occurs at earlier instants; that is, at smaller firing angles

$B_m/B_f=0.57$ $R_L/R=0.94$

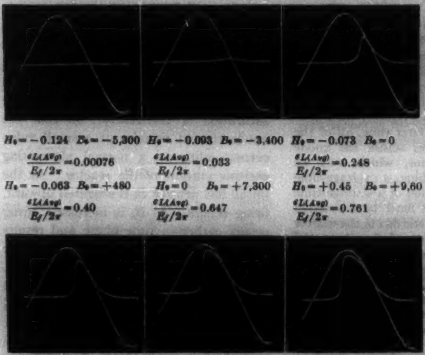

This relation giving the firing angle is plotted in Figure 8. Several features of the relation are of interest. In the first place, if the working magnetic flux density B_m exceeds the critical magnetic flux density at which firing occurs, then regardless of the value of B_0, firing cannot be prevented. Consequently, one of the elementary principles of self-saturating magnetic amplifiers is operation of the reactor core material at magnetic flux densities below the critical value. It also is obvious in Figure 8 that as the ratio of the working magnetic flux density excursion to critical magnetic flux density is reduced, the changes of initial magnetic flux density required to change the firing angle from 0 to 180° diminish.

In Appendix II the most convenient way of expressing the postfiring output is shown to be as an average value—or more precisely, as the ratio of the average value of the output voltage to a defined constant. The output is expressed as follows

$$\frac{e_{L(avg)}\Big|_{\theta_f}^{\pi}}{E_f/2\pi}=\frac{2B_m}{B}+\frac{B_0}{B_f}-1$$

$$-1\leq\frac{B_0}{B_f}\leq+1 \qquad (14)$$

A chart of this relation is shown in Figure 9, which is the so-called transfer or static characteristic of an ideal half-wave magnetic amplifier circuit. The postfiring output ratio is plotted as the ordinate while the ratio of initial to critical magnetic flux density is shown as abscissa. The transfer curves in these co-ordinate systems are straight lines. The effect of changing the ratio of working magnetic flux density excursion to the critical magnetic flux density value is shown for several values of the ratio.

Experimental Results

In order to indicate the nature and magnitude of the errors introduced by the

Figure 7. Oscillograms of the minor hysteresis loops associated with operation of the half-wave magnetic amplifier circuit of Figure 3. Circuit conditions correspond with those in Figure 6

$B_m/B_f=0.57$ $R_L/R=0.94$

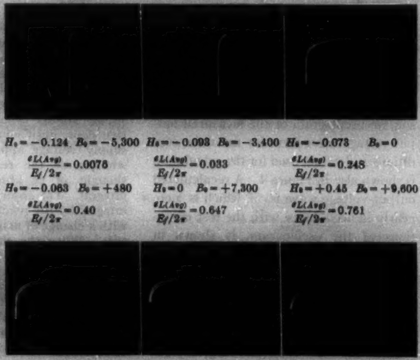

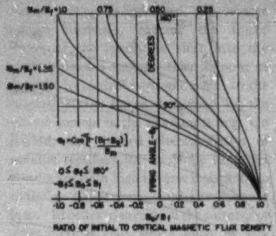

Figure 8. Calculated firing angle of an ideal half-wave magnetic amplifier as a function of the ratio of initial magnetic flux density of a defined critical magnetic flux density. The firing relation is shown for several values of B_m/B_f as parameter

idealizing assumptions of Appendixes I and II, a magnetic amplifier circuit using a core as shown in Figure 10 was constructed and tested. Oscillograms of supply voltage, load voltage, and B versus $H(B)$ have been shown for stated conditions in Figures 6 and 7. Evaluation of oscillograms, several of which are given in Figure 6, serve to determine the firing angle, yielding the experimental points shown in Figure 12. Data and the calculated firing angle curve are for $B_m/B_f=0.57$. Correspondence between the measured values of firing angle and the theoretical values is no better than fair, because the oscillograms of Figure 6 were taken on small 35-millimeter film, making the firing angles rather difficult to measure accurately.

A calculated transfer characteristic, with the initial premagnetization in terms of a magnetizing force rather than a ratio of initial to critical magnetic flux density, is shown in Figure 13. The abscissas are given in oersteds, while the ordinate is shown as the output factor of equation 14. As a result of the shape of the hysteresis loop, the straight lines of Figure 9 are reflected in Figure 13 as shown, with large slope in the vicinity of the coercive force value of the magnetizing force and with small slope in the vicinity of the flat portions of the hysteresis loop of Figure 11.

A set of measured transfer characteristics for a half-wave magnetic amplifier circuit of the sort which has been under discussion is shown in Figure 14. The ordinate has been reduced to the normalized units of equation 14, and the abscissas have been calculated on the basis of the known control magnetomotive force and the arithmetic mean length of magnetic path in the core.

While the general shape of the measured characteristic of Figure 14 corresponds approximately with the calculated shape, Figure 13, a noticeable discrepancy exists between the slopes of the transfer characteristics in the region of the coercive force value of the magnetic intensity. The measured curves show a great deal less sensitivity to changes of control magnetizing force than do the calculated curves. In addition, if the maximum slope portion of the measured curves is projected upon the axis of abscissas, cut-off is seen to occur in the vicinity of −0.12 oersted, rather than the −0.08 oersted value predicted by the calculations.

Several explanations of this departure from expected behavior are possible. Two are considered most likely. They are: eddy-current shielding of the laminated core structure and consequent broadening of the hysteresis loop; and the effect of the distributed parameters of the magnetic circuit of the test core. It is shown in Appendix II that the reason for the discrepancy between the calculated and measured results probably is concerned with the radial depth of the toroidal magnetic core. Careful consideration of the conditions in the core during the time when control is obtained, that is, during the negative alternation of the supply voltage, indicates that for complete cut-off, the initial flux density in the extreme magnetic path must be reduced to the cut-off value. However, the cut-off value of initial flux density for the inner portion of the lamination is reached considerably earlier because of the shorter magnetic path. If the measured transfer curve for $B_m/B_f=0.57$ is compared with the calculated transfer curve based on the mean length of magnetic path, 21.9 centimeters, curves *A* and *C* of Figure 15 result. If, now, the calculation is extended to include the effect of the extreme length of magnetic path, curve *B* of Figure 15 results. It will be seen that curve *B* is more nearly in agreement with the measured curve in the vicinity of the linear portion of the characteristic than is the curve calculated on the basis of mean length of magnetic path, curve *A*. While no further work has been done to determine the exact effect of the radial depth of the magnetic core and to confirm what may be inferred from Figure 15, it is felt that the radial depth consideration offers a reasonable explanation of the departure of the calculation, using only the mean length of magnetic path, from the measured performance.

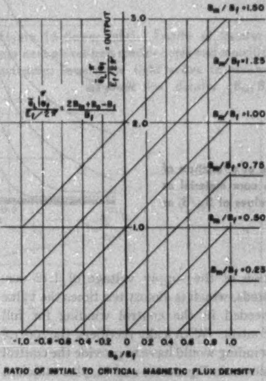

Figure 9. Integrated average output voltage of an ideal half-wave magnetic amplifier plotted as a function of the ratio of initial magnetic flux density to the defined critical magnetic flux density

Initial Induction, B_0

The value of magnetic flux density B_0 in the core at the start of the forward alternation of supply voltage plays a major role in determining the subsequent values of maximum, rms, and average output current and voltage. The changes in value of B_0 which result in changes of

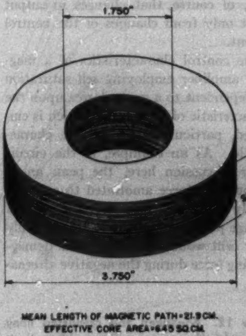
1.750"
1.00" NET STACK
3.750"
MEAN LENGTH OF MAGNETIC PATH=21.9CM.
EFFECTIVE CORE AREA=6.45 SQ.CM.

Figure 10. Reactor core used for purpose of demonstrating the sample calculations. Core is a composite structure using stacked laminations of 0.0066 inch (0.0167 centimeter) thickness

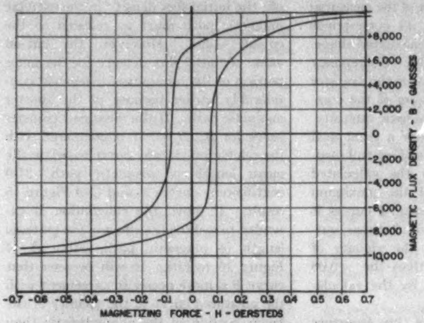

Figure 11 (above). Hysteresis loop of core material employed in reactor for which the oscillograms in Figures 6 and 7 and the measured transfer characteristic of Figure 14 are shown

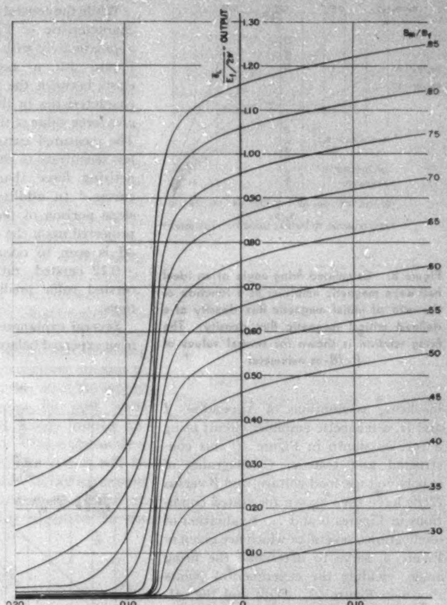

Figure 13 (right). Calculated average load voltage as a function of the control premagnetizing force for reactors with core material as in Figure 11. Characteristics shown with several values of B_m/B_f as parameter

output may occur as a result of the operation of several factors, of which the control current, anode current, operating hysteresis loop, and magnetic circuit configuration are most obvious. It is desired, of course, that changes in output result only from changes of the control current.

The control characteristics of a magnetic amplifier employing self-saturation are dependent to a great degree upon the characteristic of the rectifier which is employed, particularly the reverse characteristic. As an example, in the circuit under discussion here, the peak anode magnetizing force amounted to approximately 112 oersteds. Reverse current leakage permitted by the rectifier of only 1 per cent would cause an anode demagnetizing force during the negative alternation of the supply voltage of 1.12 oersteds, which is almost ten times the value needed in the control winding for full control. With leaky rectifiers, the control winding would have to provide the control shown in Figures 13 and 14, plus sufficient magnetizing force to compensate for leakage of the rectifiers. Consequently, rectifiers for use in magnetic amplifier circuits must have high values of reverse resistance, particularly where high-permeability cores with gapless construction are employed.

Figure 12. Measured and calculated firing angles of half-wave magnetic amplifier circuit consisting of a reactor with core as shown in Figure 10 and magnetization curve as shown in Figure 11. The measured values of firing angle are from oscillograms, several of which are shown in Figure 6

$B_m/B_f = 0.57$

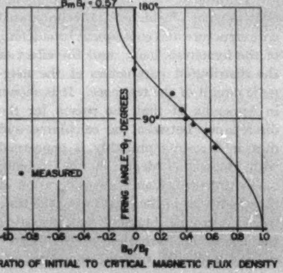

The rectifiers used most commonly in the magnetic amplifier practice are of the metallic type. Metallic rectifiers, of course, have limited values of inverse resistance, which means simply that the reverse current associated with rectifier leakage causes an increase of control ampere-turns required for a given change of magnetic amplifier output. The effect of leakage currents in magnetic amplifiers is an upward shift of the control characteristics of the amplifier, by an amount which depends on the leakage. If the inverse resistance of the rectifiers were constant, the amount of shift would, of course, be proportional to the supply voltage. This general effect is seen in the family of magnetic amplifier transfer curves shown in Figure 16. These transfer curves were taken with a magnetic core material of even higher permeability than the medium-nickel-iron alloy for which the curves thus far have been shown, and with particularly unsuitable rectifiers, in order to bring out the effect of reverse current. For small applied voltages, leakage in the rectifier causes little shift of the characteristic. As the ratio to working flux density to critical flux density is increased, that is, as the supply voltage is increased, the reverse current increases, causing the upper curves of the family to shift into the positive control region. The amount of the shift in control is proportional to the magnetomotive forces developed by the reverse current in the anode winding. In general, the desired characteristics of metallic rectifiers for magnetic amplifier circuits are both high inverse resistance to minimize the leakage, and low forward drop. In order to minimize the number of series rectifier cells which must be employed in the stack, it also is desirable that the allowable working voltage per cell be as high as possible. Good practice dictates, for instance, that, with commercial selenium rectifier plates normally rated at 18 volts rms per cell, working voltages for magnetic amplifier circuits be of the order of 8 to 12 volts per cell, which means about 10 series plates per leg for

Figure 15. Calculated and measured average output voltage of a half-wave magnetic amplifier circuit as a function of the control magnetizing force, with the radial depth of the core of Figure 10 taken into consideration

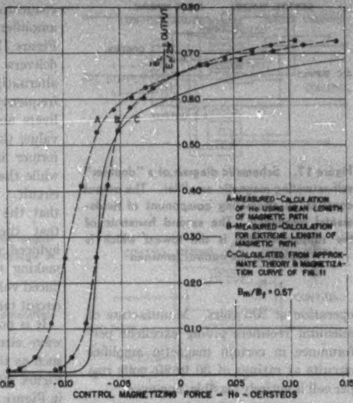

Figure 16 (lower right). Family of transfer characteristics of a magnetic amplifier with 80 per cent nickel-iron reactor cores and metallic rectifiers. The shift of similar portions of the characteristics toward the right is due to reverse current leakage of the rectifiers as the working magnetic flux density (B_m/B_f) and applied voltage increase

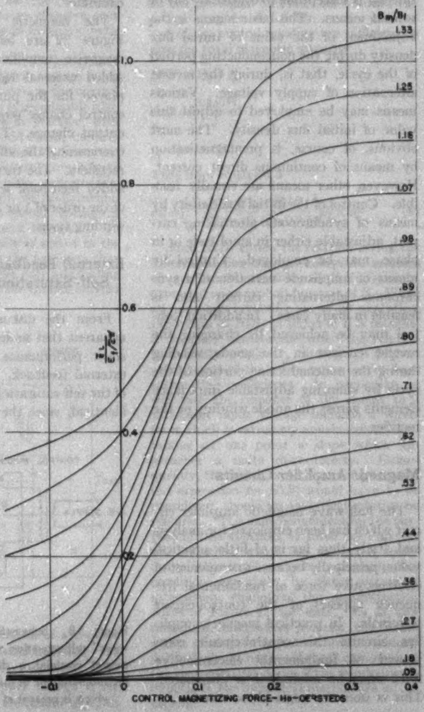

Figure 14. Measured average output voltage of half-wave magnetic amplifier circuit with cores as in Figure 10 and magnetization characteristics as in Figure 11, with several values of the ratio of working magnetic flux density to critical magnetic flux density

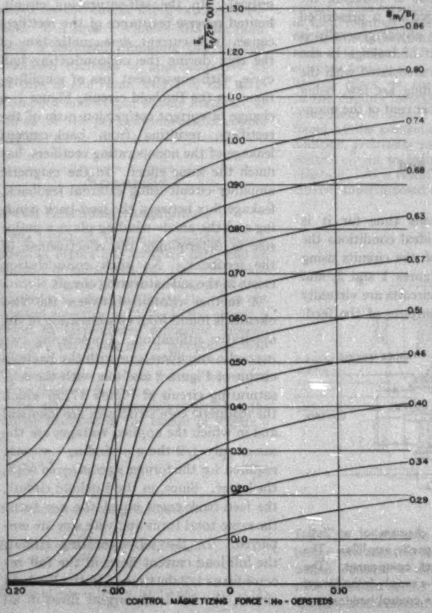

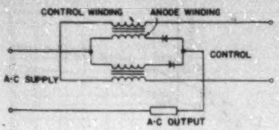

Figure 17. Schematic diagram of a "doubler" self-saturating magnetic amplifier. The output contains an alternating component of fundamental frequency. The second harmonic of the supply voltage is the lowest which is present at the control terminals

operation at 100 volts. Manufacture of selenium rectifiers giving excellent performance in certain magnetic amplifier circuits at ratings of 30 to 40 volts rms per cell is entirely feasible, however.

Control Means

The half-wave self-saturating magnetic amplifier circuit which has been discussed thus far is susceptible to control by any of several means. The basic means is the adjustment of the value of initial flux density during the nonconducting portion of the cycle, that is, during the reverse alternation of supply voltage. Various means may be employed to adjust this value of initial flux density. The most obvious, of course, is premagnetization by means of continuous direct current. However, other means are equally feasible. Control of the initial flux density by means of synchronous alternating current, adjustable either in amplitude or in phase, may be employed. Control by means of amplitude variation of a synchronous alternating current also is feasible in many cases. In addition, control may be achieved by changing the reverse current in the anode winding during the nonconducting portion of the cycle by shunting adjustable impedance elements across the anode winding or the rectifier.

Magnetic Amplifier Circuits

The half-wave magnetic amplifier circuit which has been employed for analysis and study thus far is of little practical value, principally because a component of electromotive force of fundamental frequency appears at the control-circuit terminals. In practical magnetic amplifier circuits this control-circuit component of fundamental electromotive force must be minimized or eliminated. This is done in single-phase circuits by connecting a second half-wave magnetic amplifier circuit to the first, as shown in Figure 17 or 18. The circuit of Figure 17 delivers an output which contains an alternating component of fundamental frequency, while that of Figure 18 delivers an output which has an average value, that is, a direct component. The former is called the "doubler" circuit, while the latter is called the "full-wave" circuit. It will be noted in these figures that the control coils are so connected that the fundamental components of induced voltage in the coils are opposed, making the lowest harmonic of the induced voltage that appears at the control-circuit terminals the second.

It is possible to connect the basic half-wave circuit in polyphase arrangements such as the 3-phase wye circuit shown in Figure 19, the 6-phase star circuit shown in Figure 20, or the 3-phase bridge circuit shown in Figure 21. In general, the polyphase circuits are used where particularly fast response is required and where output ripple requirements are difficult to meet with the single-phase circuits.

The magnetic amplifier circuits of Figure 22 are basically self-saturating magnetic amplifier circuits, in which added external feedback has been employed for the purpose of reducing the control change required for a prescribed output change. The object generally is overcoming the effect of leakage in the rectifiers. The turns associated with the added feed-back winding are few, being of the order of 1 or 2 per cent of the main-winding turns.

External Feedback and Self-Saturation

From the discussions thus far it is apparent that under ideal conditions the static performance of the circuits using external feedback, Figures 1 and 2, and of the self-saturating circuits are virtually identical, since the purpose of the feedback in both cases is to balance the magnetomotive force of the anode windings and thus permit control of the magnetic amplifier output with an amount of signal power equal to that required for saturation of the magnetic core material. A recent analysis has indicated excellent correspondence both for calculated and for measured static performance of the two circuits for the case of built-up laminated cores with air gaps.[12]

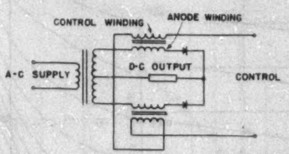

Figure 18. Schematic diagram of a "full-wave" self-saturating magnetic amplifier. The output contains a direct component. The second harmonic of the a-c supply is the lowest which is present at the control terminals

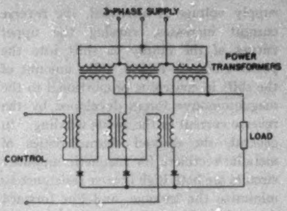

Figure 19. Schematic diagram of a "3-phase half-wave" self-saturating magnetic amplifier. The output contains a direct component. The third harmonic of the supply voltage is the lowest which is present at the control terminals

In both circuits, the characteristics of the rectifiers are quite important, if not critical. In the self-saturating circuit, limited reverse resistance of the rectifiers causes back-current demagnetization of the core during the nonconducting half cycle, with consequent loss of amplification. In the Buchold circuit, Figure 1, a change of current conversion ratio of the rectifiers, resulting from back-current leakage of the nonoperating rectifiers, has much the same effect. In the magnetic amplifier circuit using external feedback, leakage flux between the feed-back winding and the anode winding plays a major role in determining the effectiveness of the feedback. No such consideration exists in the self-saturating circuit.

A further relation between the two circuits is found from consideration of the apparatus utilization. Considering two magnetic amplifiers, one with the Buchold circuit of Figure 2 and one with the self-saturating circuit of Figure 17, in which the magnetic core structures are identical and in which the applied voltages are the same, only 1/2 the a-c winding turns are required for the former as compared with, the latter. Since, in the Buchold circuit, the feed-back turns equal the a-c turns the same total turns and wire size are employed. In the self-saturating circuit, the full load current flows in the full reactor turns 1/2 the time. In the Buchold circuit, the full load current flows in all

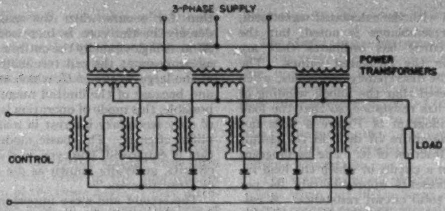

Figure 20 (above). Schematic diagram of a "6-phase diametrical" self-saturating magnetic amplifier. The output contains a direct component. The sixth harmonic of the supply voltage is the lowest which is present at the control terminals

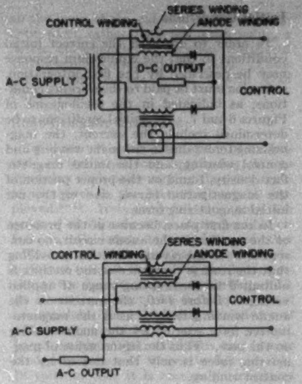

Figure 22 (right). Schematic diagrams of doubler and full-wave self-saturating magnetic amplifiers with added external feedback to compensate for rectifier leakage current

windings during the entire cycle, and the power dissipation in the circuit with external feedback is twice that in the self-saturating circuit. Conversely, for the same temperature rise, the output of the Buchold circuit must be limited to 50 per cent of that allowable in the self-saturating circuit using the same weight of copper and iron. To reach the same output with the Buchold circuit with operation on the same voltage, the copper section must be approximately doubled. Thus, twice the window area will be required for the circuit using external feedback. If a square window and the same stack is assumed, doubling the window means an increase of approximately 41 per cent in the mean length of the magnetic path and weight of core material, as well as the 100 per cent increase of copper weight.

Appendix I

Circuit Relations, Assumptions

The half-wave magnetic amplifier circuit shown in Figure 3 is analyzed here, and an example is calculated for the core shape shown in Figure 10, with core material characteristics as given in Figure 11. The differential equation applying to the circuit is solved by step-by-step numerical integration for a particular set of operating conditions and circuit parameters, in order to find the waveform of the voltage appearing across the load resistor e_L.

The differential equation describing the voltage relations in the circuit of Figure 3 is

$$e = N\frac{d\phi}{dt}\times 10^{-8}+iR+e_R \qquad (1)$$

If the applied voltage is sinusoidal

$$E_m \sin \omega t = N\frac{d\phi}{dt}\times 10^{-8}+iR+e_R$$

$$E_m \sin \omega t - e_R = N\frac{d\phi}{dt}\times 10^{-8}+iR \qquad (2)$$

If $E_m >> e_r$, it is approximately true that

$$E_m \sin \omega t = N\frac{d\phi}{dt}\times 10^{-8}+iR$$

$$d\phi = \frac{(E_m \sin \omega t - iR)}{N}dt\times 10^{8} \qquad (3)$$

For the present, it is assumed that the distributed parameters of the magnetic circuit may be lumped to an effective area A and an arithmetical mean magnetic path length l.

Further, it is assumed that the impedance of the control circuit is of large enough value to suppress harmonic currents in the control circuit. This assumption is permissible and, in fact, required because in practice, with high-permeability cores and circuit connections as in Figures 17 through 21, harmonic currents flowing in the control circuit have limited effect on the static performance. In the circuits mentioned, no fundamental component of supply-frequency voltage is found at the control-circuit terminals. In addition, resistance usually is added in the control circuit to reduce the amplifier time constant. As a result, the only alternating current superimposed on the control current is a higher harmonic of small amplitude. To make the calculated response of the half-wave circuit resemble conditions actually found in the conventional self-saturating amplifier, it will be assumed that the control circuit impedance is sufficient to suppress all but the signal current. As a result, the magnetizing forces of the anode winding and of the control winding are sufficient to give the total magnetic intensity

$$H(B) = H_0 + H_i$$

$$H_i = \frac{0.4\pi Ni}{l}$$

$$d\phi = A\,dB$$

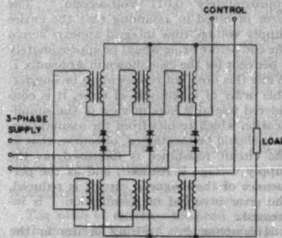

Figure 21. Schematic diagram of a 3-phase bridge self-saturating magnetic amplifier. The output contains a direct component. The sixth harmonic of the supply voltage is the lowest which is present at the control terminals

Then from equation 3

$$dB = \left(\frac{E_m \sin \omega t}{NA} - \frac{H_i l R}{0.4\pi N^2 A}\right)dt\times 10^{8} \qquad (4)$$

Since $H(B)$ enters the relation giving the differential flux change, analytical solution of equation 4 is possible only if $H(B)$ can be expressed as an explicit function of B. While an approach involving use of an analytical expression of $H(B)$ in terms of B is feasible, it becomes burdensome when the relation is radically nonlinear, causing the higher-order terms of the series expansion to have substantial coefficients. In particular, in this case the response of the circuit to a sinusoidal input voltage includes a waveform which is extremely nonsinusoidal, containing at one point a slope which approaches a finite discontinuity. Consequently, the higher-order terms of an analytical expression for $H(B)$ would have to be considered, should an analytical solution be required. It is more convenient for the purpose of this appendix to solve the differential equation, which has numerical coefficients if the circuit parameters and operating conditions are given, by direct numerical integration, employing the magnetization curve of Figure 11 for data. As in any numerical integration process, the increments of angular argument must be small, particularly in regions of sharp curvature of the characteristic curve, if the requirements implicit in the numerical method are to be satisfied.

Initial Conditions

In order to establish the correct initial conditions so that the equilibrium response may be described by the first integration, attention must be paid to the working conditions, as indicated in the oscillograms of Figures 6 and 7. The initial conditions to be determined include the current, the magnetizing forces due to the main winding and control winding, and the initial magnetic flux density, found on the proper portion of the magnetization curve, due to the net initial magnetizing force.

In the first place, because of the presence of the rectifier in the anode circuit, no current flows in the reverse direction, providing that the reverse resistance of the rectifier is unlimited in the working range of applied voltage. Before $t=0$, the current in the anode winding is zero, as is the magnetomotive force exerted by the main winding on the core. Thus the initial value of magnetizing force is only that caused by the control winding.

Secondly, in order to determine the initial magnetic flux density, it is necessary to note in the oscillograms that the forward current during the positive alternation of the supply voltage causes magnetic intensities greatly in excess of the coercivity of the material. This may be verified by observing in the B versus $H(B)$ oscillograms of Figure 7 that the right-hand portion of the magnetization curve is essentially flat, indicating that the core material becomes thoroughly saturated during the forward alternation of the supply voltage. Following saturation, the decaying value of anode-winding magnetizing force approaches zero along the upper branch of the hysteresis loop, indicating that during the succeeding negative alternation, the magnetic condition of the core is defined by that branch of the loop. The value of initial magnetic flux density B_0 then may be found, for a given value of initial premagnetization H_0 exerted by the control winding, by referring to the upper branch of the hysteresis loop.

Sample Wave Form Calculation

Following determination of the initial conditions, numerical integration according to equation 4 is carried out. A particular set of values has been chosen for illustration; a calculated load voltage wave form is shown in Figure 4. The illustrative values are:

$E_m=141.4$ volts
$l=21.9$ centimeters
$R=50.3$ ohms
$N=650$ turns
$\omega=377$ radians per second
$A=6.45$ square centimeters
$H_0=0$ oersteds
$B_0=7{,}300$ gausses
Magnetization data as given in Figure 11

The working equation is

$$dB=\left(E_m\sin\theta-\frac{H_i lR}{0.4\pi N}\right)\frac{d\theta}{\omega NA}\times 10^8 \qquad (5)$$

The calculated wave form of the total iR drop in the anode circuit is shown in Figure 4. Also shown is an oscillogram of e_L taken in a half-wave circuit with values as enumerated, core as in Figure 10, and magnetization curve as in Figure 11. When this is compared with the calculated wave form, a general resemblance is noted, but the calculated curve has ordinates that are greater than the measured values. The reason for the discrepancy is obvious, when it is considered that the anode winding of the reactor has resistance, so that the load voltage oscillogram of Figure 4 does not represent the entire iR drop in the circuit but only a fraction of it. The oscillogram was taken in a circuit in which the load resistance represents approximately 94 per cent of the total circuit resistance. A calculated wave form of load voltage with this factor considered is shown in Figure 5, together with another oscillogram of the measured wave form with the same conditions.

Appendix II

While the method of numerical integration illustrated in Appendix I serves to predict approximately the wave form of the output voltage, from which the effective and average values may be found, it is not convenient to use in predicting the static performance characteristic of the amplifier, principally because of the labor involved. It is the purpose of this appendix to point out how the performance curves may be simply approximated, and to indicate the magnitude of the errors introduced by the simplifying assumptions made in the course of the approximation.

Firing Angle

Assumption 1. Firing of a half-wave self-saturating magnetic amplifier circuit employing a high-permeability gapless core occurs abruptly enough so that the iR drop before firing may be neglected in determining the angular argument at which firing occurs.

In evaluating this assumption, it is revealing to consider the calculated response of the circuit given in Appendix I. In Figure 5, firing occurs at approximately 90 degrees. The voltage-time integral (flux-linkage change) absorbed by the anode winding during the prefiring interval is 0.375 volt-second, less the value of voltage-time integral associated with the voltage drop in the circuit resistance during that interval—approximately 0.011 volt-second. The error involved in assuming that the entire supply voltage-time integral appears across the coil before firing would be approximately 3 per cent for the case shown in Appendix I. While this does not represent an inconsiderable order of magnitude of error, it is considered tolerable here in view of the simplification which results from the assumption.

It should be mentioned, of course, that as the circuit resistance is increased, as the supply voltage is reduced, and as the permeance of the magnetic circuit is reduced, the error involved in Assumption 1 is increased.

Assumption 2. Firing occurs in the mode shown in Appendix I. This limitation rejects one of the two possible modes of firing. The rejected mode obtains when the core is premagnetized beyond negative saturation in a negative direction ($B_0<-B_f$). If this condition exists, then, following $t=0$, the entire supply voltage appears initially as a drop on the circuit resistance. Firing in a reverse sense from that illustrated thus far occurs when the magnetic flux density in the core is increased to $-B_f$. After firing, virtually the entire supply voltage appears at the coil terminals. Because of the large values of H_0 which are required and because of the limited range of control possible, this mode of operation is at present of only secondary interest in magnetic amplifier circuits. This basic mode of operation is employed, however, in d-c metering circuits, generally known as d-c converters or "transformers."[18]

The second and more important mode of firing, for magnetic amplifiers at any rate, is the type illustrated in Appendix I. The restriction $-B_f\leq B_0\leq +B_f$ is sufficient to include this mode and exclude the d-c "transformer" mode.

On the basis of these assumptions and those of Appendix I, a simple relation for the firing angle may be set down, following equation 3. Since the prefiring skirt is neglected, and $d\phi=AdB$, equation 3 becomes

$$dB=\frac{E_m\sin\omega t}{NA}dt\times 10^8 \qquad (6)$$

$$B=B_0+\int\frac{E_m\sin\omega t}{NA}dt\times 10^8 \qquad (7)$$

Firing occurs when the instantaneous magnetic flux density reaches the critical value B_f

$$B_f=B_0+\int_0^{t_f}\frac{E_m\sin\omega t}{NA}dt\times 10^8 \qquad (8)$$

$$B_f-B_0=\frac{E_m\times 10^8}{\omega NA}(1-\cos\omega t_f)$$

$$\theta_f=\cos^{-1}\left(1-\frac{(B_f-B_0)\omega NA}{E_m\times 10^8}\right) \qquad (9)$$

where

$$\theta_f=\omega\times t_f$$

But the maximum value of flux density associated with the supply voltage is

$$B_m=\frac{E_m\times 10^8}{\omega NA}$$

so that

$$\theta_f=\cos^{-1}\left(1-\frac{B_f-B_0}{B_m}\right) \qquad (10)$$

The values of the angular argument at which firing occurs are given by equation 10. Restrictions of the value of θ_f exist and should be recognized. Because of the rectifier

$$\theta_f\leq\pi$$

Because of the limitation of Assumption 2 that is, $-B_f\leq B_0\leq +B_f$

$$\theta_f\geq 0$$

Thus a complete statement giving the firing angle in convenient form is

$$\theta_f=\cos^{-1}\left(\frac{B_m+B_0-B_f}{B_m}\right);\ 0\leq\theta_f\leq\pi \qquad (11)$$

It is most convenient to plot equation 11 by showing θ_f as a function of B_0/B_f with B_m/B_f as parameter. This is done in Figure 8. As an experimental check, a set of load-voltage oscillograms, several of which are shown in Figure 6, were taken with the circuit parameters and conditions as in Appendix I and with the core of Figure 10. The calculated firing-angle curve, together with the experimental points, are shown in Figure 12.

Output

Assumption 3. While ignoring the prefiring skirt of the output-voltage wave form introduces small error in the approximate calculation of the firing angle, it may introduce serious error in the approximation of output.

As is obvious in the first two oscillograms of Figure 6, for values of B_0 near cut-off there may be measurable output, even though sharp firing never occurs. As an approximation to be evaluated later by comparison of calculated and measured static characteristic or transfer curves, let the alternating exciting current corresponding to the value of working flux density B_m be added to the postfiring output to represent the contribution of the prefiring skirt. Comparison of transfer curves will indicate whether this approximation is justified.

To find the output current and voltage after firing, it is convenient to express the output voltage as an integrated average value. To be consistent with the assumptions made thus far, if all the circuit resistance is in the load

$$e_L=E_m \sin\theta;\ \theta_f\leq\theta\leq\pi$$

Expressing the postfiring output voltage as an integrated average value

$$e_{L(Avg)}\Big|_{\theta_f}^{\pi}=\frac{1}{2\pi}\int_{\theta_f}^{\pi}E_m \sin\theta d\theta \tag{12}$$

$$e_{L(Avg)}\Big|_{\theta_f}^{\pi}=\frac{E_m}{2\pi}(1+\cos\theta_f) \tag{13}$$

From equation 11

$$e_{L(Avg)}\Big|_{\theta_f}^{\pi}=\frac{E_m}{2\pi}\left(1+\frac{B_m+B_0-B_f}{B_m}\right)$$

A more convenient form of output relation results if a critical maximum voltage is defined as

$$E_f=\omega NAB_f\times10^{-8}$$

Thus

$$e_{L(Avg)}\Big|_{\theta_f}^{\pi}=\frac{\omega NA}{2\pi}(2B_m+B_0-B_f)\times10^{-8}$$

And finally

$$\frac{e_{L(Avg)}\Big|_{\theta_f}^{\pi}}{E_f/2\pi}=\frac{2B_m}{B_f}+\frac{B_0}{B_f}-1 \tag{14}$$

Since

$$0\leq\theta_f\leq\pi$$

The output is restricted

$$0\leq\frac{e_{L(Avg)}\Big|_{\theta_f}^{\pi}}{E_f/2\pi}\leq\frac{2E_m}{E_f}$$

The ideal postfiring average output of the half-wave magnetic amplifier circuit is shown in Figure 9 as a function of B_0/B_f, with B_m/B_f as parameter.

Transfer Characteristic

The ideal transfer characteristic of Figure 9 shows several features of magnetic amplifier operation. For values of maximum working magnetic flux density in excess of the critical value $B_m/B_f>1.0$, the output can never be reduced to zero, regardless of the premagnetization. For lower values of B_m/B_f, the characteristic shows both cut-off and saturation.

The transfer curves of Figure 9 are more useful when put in the form of an output versus control magnetic intensity chart with B_m/B_f as parameter, as in Figure 13.

The calculated transfer curves are shown with the H_0 magnetic intensity value found from the upper branch of the hysteresis loop of Figure 11, and with several values of B_m/B_f as parameter. It should be noted that the calculation gives $e_{L(Avg)}/(E_f/2\pi)$ as a function of H_0 without regard for the particular values of circuit parameters. Further, the alternating exciting currents are added to the postfiring output to account for the effect of the prefiring skirt, which is particularly evident near cut-off and below.

A set of measured transfer curves for magnetic and electric circuit parameters as in Appendix I and Figure 10, is shown in Figure 14. In order to simplify comparison, the output has been reduced to the general form given in equation 14. Values of control H_0 given in Figure 14 were calculated from the data by making use of the known control winding turns and current and an arithmetic mean value of magnetic path length (21.9 centimeters).

The general shapes of the calculated and measured curves show certain resemblances. The calculated effects of saturation for positive values of H_0 are seen to occur in the measured curves, and the nature of the effect of the working value of flux density (B_m/B_f) on the value of H_0 for cut-off is seen to be predicted correctly by the calculation. There is one notable difference between the calculated and measured curves—the slope and location of the linear, sensitive portion of the transfer curve.

In order that this discrepancy between the calculated approximate performance may be seen more clearly, the measured transfer curve for $B_m/B_f=0.57$ and a transfer curve for that value calculated by making use of the approximations are shown in Figure 15. The measured transfer curve *A* is plotted as before, with H_0 found by the calculation from the known magnetomotive force and the arithmetic mean magnetic path length. It is obvious that the linear portion corresponds neither in slope nor in location with the calculated curve.

Possible explanations of the discrepancy involve the effect of distributed magnetic circuit of test core and eddy-current shielding of the core laminations.

MAGNETIC CIRCUIT

The ratio of extreme to mean magnetic path length of the core structure of Figure 10 is 1.36, while the ratio of longest to shortest path length is 2.14. In view of these values, it might be questioned whether calculations of the sort thus far outlined, which are based on a lumped magnetic circuit with a fixed path length, properly apply to such a core.

It is of interest to note that if the experimental data are reduced to fundamental units on the basis of the extreme length of magnetic path, rather than the mean value, a better correspondence between calculated and measured performance is found. (Compare transfer curves *B* and *C* with *A* of Figure 15.)

EDDY-CURRENT SHIELDING

In order to evaluate the order of magnitude of hysteresis loop broadening due to operation with time-varying flux, the techniques given in the literature may be employed.[9–11] It is intended that only the order of magnitude of the worst possible effect be calculated, to determine whether eddy-current demagnetization might be sufficient to cause the shift of the linear portion of the transfer curve noted in Figure 15. As a matter of fact, the techniques which are available for calculating the effects of eddy-current shielding are, in general, based on sinusoidal conditions and low or moderate values of magnetic flux density. In spite of this, it is reasonable to expect that at least the order of magnitude of the effect can be predicted in this case.

In order to determine the maximum broadening to be expected, for the 47.5 per cent nickel-iron alloy used, take:

$\rho=51\times10^{-6}$ ohm-centimeters
$\mu=50{,}000$ centimeter-gram-second electromagnetic units
$f=60$ cycles per second
$a=0.0084$ centimeter–half lamination thickness

Then, following the procedure of reference 10:

$$\frac{L}{L_0}=\frac{s}{2a}\frac{\sinh\left(\frac{2a}{s}\right)+\sin\left(\frac{2a}{s}\right)}{\cosh\left(\frac{2a}{s}\right)+\cos\left(\frac{2a}{s}\right)}$$

where s is the skin depth and is given by

$$s=\frac{5{,}030}{\sqrt{\frac{\mu f}{\rho}}}=0.0208 \text{ centimeter}$$

The ratio of lamination thickness to skin depth is

$$\frac{2a}{s}=0.804$$

Solving

$$\frac{L}{L_0}=0.96$$

At this frequency, the greatest broadening of the hysteresis loop which might be expected is of the order of 4 per cent, a value insufficient to resolve the discrepancy between curves *A* and *C* of Figure 15. Consequently, it is inferred that the effect is probably due principally to the radial depth of the test core.

References

1. Bibliography on Transductors, Magnetic Amplifiers, H. B. Rex. *Instruments* (Pittsburgh, Pa.), volume 21, number 4, 1948, page 332.

2. Uber gleichstrom vormagnetisierte Wechselstrom drosselspulen und deren Ruckkopplung, Th. Buchold. *Archiv für Elektrotechnik* (Berlin, Germany), volume 36, 1942, pages 221–37.

3. UNITED STATES PATENT 1,730,254, **Phillips Thomas.** October 1, 1929.

4. UNITED STATES PATENT 1,328,797, **Ernest F. Alexanderson.** January 20, 1920.

5. INFLUENCE OF CORE MATERIAL ON MAGNETIC AMPLIFIER DESIGN, **A. O. Black.** *Proceedings*, National Electronics Conference, (Chicago, Ill.) volume 4, 1948, pages 427–35.

6. UNITED STATES PATENT 1,997,179, **Frank G. Logan.** Issued April 9, 1935.

7. THE TRANSDUCTOR, D. C. PRE-SATURATED REACTOR, WITH SPECIAL REFERENCE TO TRANSDUCTOR CONTROL OF RECTIFIERS, **U. Lamm.** *Esselte Aktiebolag* (Stockholm, Sweden), 1943.

8. WIRKSAME PERMEABILITAT UND EISENVERLUSTE IN BLECHEN UND DRAHTEN BEI SCHWACHEN MAGNETISCHEN FELDERN, **W. Cauer.** *Archiv für Elektrotechnik* (Berlin, Germany), volume 15, number 4, 1925, page 308.

9. A BRAUN TUBE HYSTERESIGRAPH, **J. B. Johnson.** *Bell System Technical Journal* (New York, N. Y.), volume 8, 1929, pages 286–308.

10. VARIATION OF THE INDUCTANCE OF COILS DUE TO THE MAGNETIC SHIELDING EFFECT OF EDDY CURRENTS IN THE CORES, **K. L. Scott.** *Proceedings*, Institute of Radio Engineers (New York, N. Y.), volume 18, 1930, pages 1750–64.

11. EDDY CURRENTS IN COMPOSITE LAMINATIONS, **E. Peterson, L. R. Wrathall.** *Proceedings*, Institute of Radio Engineers (New York, N. Y.), volume 24, 1936, pages 275–86.

12. AN ANALYSIS OF MAGNETIC AMPLIFIERS WITH FEEDBACK, **D. W. VerPlanck.** *Proceedings*, National Electronics Conference, (Chicago Ill.) volume 4, 1948, page 426.

13. EIN EINFACHER GLEICHSTROMMESSWANDLER MIT ECHTEN STROMWANDLEREIGENSCHAFTEN, **W. Kramer.** *Elektrotechnische Zeitschrift* (Berlin, Germany), volume 58, 1937, pages 1309–13.

14. EIN NEUER GLEICHSPANNUNGSMESSWANDLER ZUR MESSUNG HOHER GLEICHSPANNUNGEN, **W. Kramer.** *Elektrotechnische Zeitschrift*, volume 59, 1938, pages 1295–8.

Discussion

L. A. Finzi, D. W. VerPlanck, D. C. Beaumariage (Carnegie Institute of Technology, Pittsburgh, Pa.):

Mr. Dornhoefer is to be congratulated for an analysis of a half-wave magnetic amplifier circuit which is very interesting and thought provoking, and which appears to throw further light on the behavior of practically useful circuits having two or more elements. It would be of interest to know more about how the author uses his results as obtained for the single-element case in predicting the performance of actual amplifiers.

Comparing Mr. Dornhoefer's analysis with that given by the writers in a paper presented at the same session,[1] it is seen that there are two basic differences in the underlying assumptions:

1. Mr. Dornhoefer assumes that his control circuit has infinite impedance to harmonic currents, while the writers' analysis[1] takes the opposite extreme and assumes that harmonic currents may circulate freely there.

In other terms the writers have dealt with a case which has been called unconstrained or natural magnetization[2] while Mr. Dornhoefer assumes totally constrained conditions.

2. Mr. Dornhoefer treats a case where the magnetization curve has a relatively sharp knee and then becomes essentially horizontal permitting no further increase in flux. The writers, on the other hand, treat the case of a core which never reaches complete saturation.

It appears thus that by other combinations of the alternatives under each of the preceding statements, one may have two additional extreme types of treatment, making a total of four. It is conceivable that practical conditions might arise making anyone of these four the best approach.

REFERENCES

1. ANALYTICAL DETERMINATION OF CHARACTERISTICS OF MAGNETIC AMPLIFIERS WITH FEEDBACK, **D. W. VerPlanck, L. A. Finzi, D. C. Beaumariage.** *AIEE Transactions*, volume 68, part I, 1949, pages 565–70.

2. THE TRANSDUCTOR, **H. B. Rex.** *Instruments*, (Pittsburgh, Pa.) volume 20, 1947, page 1104.

S. B. Cohen (Sperry Gyroscope Company, Great Neck, N. Y.): The assumptions used for the determination of θ_f are valid for most of the magnetic materials used, including cores made up of EI^-, EE^-, or F-type laminations. We have been able to reproduce Figure 12 of the paper with about the same degree of correlation using EI and EE cores.

The determination of the output (voltage or current) is, however, a more difficult problem and depends upon the assumptions used and the type of core construction and material.

In Appendix I, the step-by-step solution of the differential equation 5 of the paper yields a current or voltage output across the load as is shown in Figures 4 and 5 of the paper. The angle at which conduction ceases can be called the conduction angle θ_t. In Figure 4 of the paper the conduction angle is about 260 degrees. This conduction angle is a function of the material and core structure if the core is made up of EI- or EE-type laminations. However, in Appendix II, the angle of conduction was assumed to be 180 degrees. This assumption is valid if:

1. Most of the resistance of the circuit is assumed to be in the load.
2. The material and core used present an extremely low effective impedance when saturated, that is, the B-H characteristic is almost a horizontal line after saturation.

These assumptions are essentially valid for the particular examples in Appendix II. However, in those cases where core structure (that is, EI-type), and material do not have the characteristic as mentioned previously in assumption 2 (for example, silicon iron for higher power work), and where the load resistance is comparable to the rectifier impedance, which may be the case when matching for maximum power into the load, the assumptions are not quite valid.

If equation 2 of the paper were solved for the current

$$E_m \sin \omega t = N\frac{d\phi}{dt}10^{-8} + iR_T + e_R$$

or

$$E_m \sin \omega t = L\frac{di}{dt} + iR_T + e_R$$

where

$L(di/dt)$ is the equivalent of $N(d\phi/dt)10^{-8}$

The value of L is the equivalent value of inductance of the core when saturated, because we are interested in the current during the conduction period. If assumption 2 were valid, then L would be zero.

For some value of θ_f; say $\theta_f = 0$ degrees, the solution of equation 2

$$i(t) = I_m\left[\sin(\theta-\omega t) + \frac{\sigma}{\cos\theta} - \left(\sin\theta + \frac{\sigma}{\cos\theta}\right)\epsilon^{\frac{-R_T}{\omega L}\omega t}\right]$$

where

$$I_m = \frac{E_m}{\sqrt{R_T^2 + (\omega L)^2}}$$

$$\theta = \tan^{-1}\frac{\omega L}{R_T}$$

$$\sigma = \frac{e_R}{E_m}$$

to solve for θ_t, set $i(t) = 0$

$$\sin(\theta-\theta_t) + \frac{\sigma}{\cos\theta} = \left(\sin\theta + \frac{\sigma}{\cos\theta}\right)\epsilon^{\frac{-R_T}{\omega L}\theta}$$

This equation is solved empirically for θ_t.

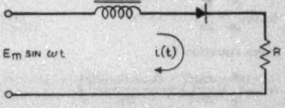

Figure 1. Self-saturable magnetic amplifier circuit

The solution for θ_t as a function of $\omega L/R_T$ is plotted in Figure 2 of this discussion with σ as a parameter. From this plot, we can see that for $\sigma = 0$ assuming $e_R = 0$ and rectifier is constant resistance lumped in R_T, the conduction angle is 180 degrees as $\omega L/R_T$ approaches zero. It is possible to obtain large values of θ_t if $\omega L/R_T$ increases as is shown. It also is interesting to note that for finite values of σ, the conduction angle can be less than 180 degrees.

The use of material in cores other than those mentioned in assumption 2 introduces finite values of $\omega L/R_T$ which can be large enough to yield values of θ_t, which are appreciably higher than 180 degrees. The errors introduced in the calculation of power output by using 180 degrees instead of the θ_t from Figure 2 of the discussion may be as high as 25 per cent in some cases.

Since in many applications power is the primary interest, a plot of power as a function of $\omega L/R_T$ is shown in Figure 3 of the discussion for various values of σ. If E_m were 37 volts (26 volts rms) and the drop across a typical rectifier were 2 volts, then $\sigma = 2/37 = 0.054$. This would mean a loss

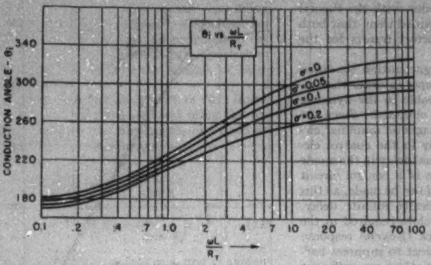

Figure 2. Conduction angle (θ_i) as a function of $\omega L/R_T$

of about 20 per cent in power at optimum conditions.

It is interesting to note that the optimum value of $\omega L/R_T$ for maximum power is about 2.4 for $\sigma = 0$. This means that $R_T = \omega L/2.4$ for maximum transfer of power to R_T.

Another set of curves, Figure 4 of the discussion, indicates the effect of the rectifier resistance in the power transferred to the load. These curves were calculated for $\sigma = 0$, but assuming the rectifier to be a resistance equal to R_T. This means that e_R actually exists and varies, but according to the method used in the setting up of the equation, we have $\sigma = 0$. As can be seen from these curves, the point of maximum power varies with variations in λ.

The type of calculation and curves presented in this discussion can be used to obtain a step-by-step determination of the transfer curves in the self-saturable amplifier. We have used the curves drawn for various values of θ_f, σ, and θ_i to obtain end design figures for various types of amplifier applications.

The experimental results yield fairly close correlations using the design values so obtained. The use of *EI*-type laminations yield inferior results with respect to gain per unit time constant as compared to the solid stamping or ribbon-wound type cores. However, the maximum power obtained is almost the same for a given size core, and the stability obtained as far as reproducibility is concerned is quite good.

In many applications, the lower performance can be tolerated, but the reproducibility is very desirable.

It may be of interest, therefore, to include in the theory of calculating procedure methods for handling cores which do not exhibit the ideal characteristics, and also conditions in which the forward characteristics of the rectifiers used are not negligible in comparison to the load and anode winding.

H. F. Storm (General Electric Company, Schenectady, New York): In his very interesting paper Mr. Dornhoefer presents several transfer characteristics of magnetic amplifiers, such as those shown in Figures 13–16 of the paper. These characteristics demonstrate the performance of magnetic amplifiers in the region of high gain; that is, between the lower and the upper right knee, but they do not indicate the trend beyond the two knees. In Appendix II, Mr. Dornhoefer mentions correctly that the operation beyond the lower knee is related to the mode of operation of d-c metering circuits, and then lists references 13 and 14. While Mr. Dornhoefer's paper deals with regenerative circuits, the aforementioned reference does not include such circuits; hence the reader may remain in doubt as to the performance of magnetic amplifiers beyond the lower knee. Inspecting Figures 13–16 of Mr. Dornhoefer's paper, the reader may conclude that for large negative control currents the transfer characteristics approach zero output current. This, however, is not so; on application of large negative control currents the load current again increases as shown in Figures 5 and 6 of the discussion. It is the object of the following discussion to describe the transfer characteristic beyond the region shown in Mr. Dornhoefer's paper.

Figure 5 of the discussion demonstrates a transfer characteristic of a magnetic amplifier which Mr. Dornhoefer calls "full-wave" self-saturating connection, Figure 18 of the paper; more specifically, it relates to a circuit where the impedance of the source of control current is small in comparison with the resistance of the control winding. In that region of the transfer characteristic which is located to the right of the lower knee, a change of control current I_c in a negative direction will cause a reduction of the load current I_L, both currents being measured in average values. However, if the control current is made more negative than the value corresponding to the lower knee, that is, in this case, more negative than —5 milliamperes, the load current again increases. In order to demonstrate the full range of negative control currents, Figure 6 of the discussion utilizes a much larger scale for the control-current scale. It can be seen from this figure that the load current I_L first increases almost linearly with negatively increasing control current I_c, and finally approaches a horizontal asymptote at the same level as for very large positive control current (Figure 5 of the discussion). It is an important conclusion that increasing the negative control current causes a reduction of load current when operating to the right of the lower knee, but an increase of load current when operating to the left of the lower knee.

In automatic-control and regulator engineering an error signal often is used to excite the control winding of a magnetic amplifier. This error signal normally operates on the steep section of the transfer characteristic, that is, to the right of the lower knee. The magnetic amplifier usually is connected into the regulated system in such manner as to reduce the error signal and thus tends to keep the regulated quantity constant. If now a large disturbance occurs in the regulated system, the error signal suddenly may become so large as to operate on that part of the transfer characteristic which is to the left of the lower knee. Hence, the load current instead of becoming smaller actually may increase instead and thus produce a still larger error signal. As a result

Figure 3. Power coefficient (ξ) as a function of $\omega L/R_T$ with σ as a parameter

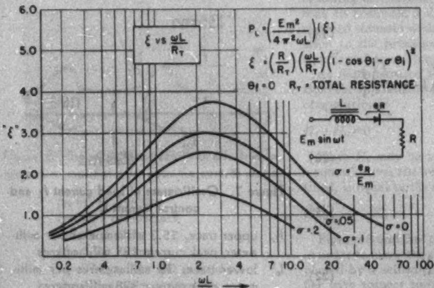

Figure 4. Power coefficient (ξ) as a function of $\omega L/R_T$ with λ as a parameter

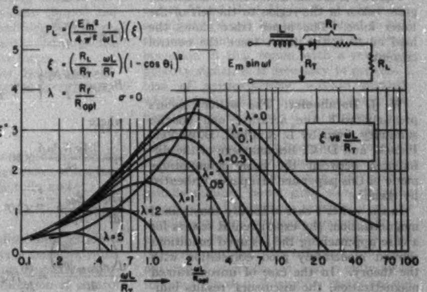

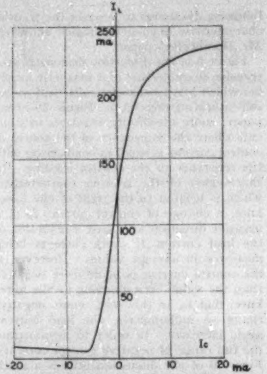

Figure 5. Transfer characteristic of magnetic amplifier in the region of highest gain

the system will no longer operate as a regulator but may drive itself into a ceiling condition. Such occurrence obviously should be avoided, and in order to evaluate the possibility of loss of control, it is necessary to know the transfer characteristic to the left of the lower knee.

There are theoretical reasons why this transfer characteristic should approach a straight line throughout a considerable range of negative control currents as demonstrated by Figure 6 of the discussion. While space does not permit dwelling on these reasons in this discussion, the resulting equation for the straight line approximation can be stated simply.

$$I_L = -I_c \frac{N_c}{N_L}$$

where I_L is the average current in the load resistor (see Figure 18 of the paper), I_c the average current in the control winding, N_c the number of turns of the control winding, and N_L the number of turns of the anode winding.

This equation gives a good approximation when the reactor material is operated at magnetic flux densities at or below the critical value, as defined in Mr. Dornhoefer's paper.

Figure 7 of the discussion shows an oscillogram taken in the region to the left of the lower knee. The upper trace shows the load current, the lower trace the control current.

W. J. Dornhoefer: The writer concurs precisely with the accurate and concise summary given by L. A. Finzi, D. W. VerPlanck, and D. C. Beaumariage of the differences between the basic assumptions made in this paper and in a paper presented by them.[1]

In the writer's case of totally constrained magnetization, the experimental results for a case approaching the assumed conditions showed moderately good correlation with the theory. In the case of unconstrained magnetization, the discussors' results indicated excellent correlation with the theory. It may be taken for granted then, that both approaches lead to correct results for the assumed conditions.

The constrained magnetization condition was assumed in this paper in order that results ultimately applicable to the dynamic performance might be obtained. Since the time delay found in magnetic amplifier circuits resides principally in the control circuit, with a small residual delay in the anode circuit, the assumption of a control circuit lacking resistance could not be made, as this would involve theoretically infinite delay. While the resistance values required in the control circuit for quick (1-cycle) response are generally not sufficient to suppress harmonic currents entirely, they are sufficient to make the assumption quite reasonable.

The dependence of the transient response of saturable reactors upon the control circuit resistance was given in an unpublished paper by Mr. Finzi, Mr. VerPlanck and Mr. Beaumariage. In this paper, the assumption of zero control circuit impedance would have led to trivial results and could therefore not be made as it was before. Rather, the significant time-delay factor was shown to be of the nature

$$\tau_s = \frac{2N_1A}{\mu R_1 I_1 \infty}$$

where

N_1 = control turns
A = core area
R_1 = proportional to control circuit resistance
μ = magnetization curve-fitting argument
$I_1\infty$ = ultimate value of control circuit current

A similar relation can be shown for the self-saturating case with small changes of output for which an effective permeability can be defined. Following equation 14 of the paper

$$\frac{d\left(e_{L(avg)}\Big|_{\theta_f}^{\pi}\right)}{dt} = \frac{d}{dt}\left\{\frac{\omega NA}{2\pi}(2B_m + B_0 - B_f) \times 10^{-8}\right\} \qquad (15)$$

$$\frac{d\left(e_{L(avg)}\Big|_{\theta_f}^{\pi}\right)}{dt} = fNA\frac{dB_0}{dt} \times 10^{-8} \qquad (16)$$

$$i_0 = i_{00} + \frac{E_{dc}}{R_1}\left(1 - \epsilon^{-\frac{t}{\tau_1}}\right) \qquad (17)$$

$$B_0 = \mu\frac{0.4\pi N_1}{l}i_0 \qquad (18)$$

$$B_0 = \mu\frac{0.4\pi N_1}{l}\left\{i_{00} + \frac{dc}{R_1}\left(1 - \epsilon^{-\frac{t}{\tau_1}}\right)\right\} \qquad (19)$$

where

$$\tau_1 = \frac{0.4\pi N_1^2 \mu A}{lR_1} \times 10^{-8} \qquad (20)$$

$$\frac{dB_0}{dt} = \frac{E_{dc}}{N_1A}\epsilon^{-\frac{t}{\tau_1}} \times 10^8 \qquad (21)$$

$$\frac{d\left(e_{L(avg)}\Big|_{\theta_f}^{\pi}\right)}{dt} = \frac{N}{N_1}fE_{dc}\epsilon^{-\frac{t}{\tau_1}} \qquad (22)$$

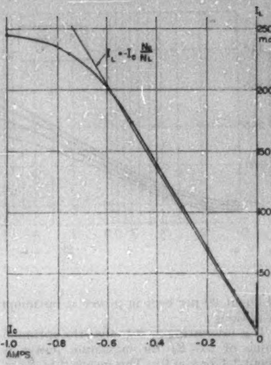

Figure 6. Transfer characteristic of magnetic amplifier for negative control currents

Anode winding: 592 turns each, control winding: 200 turns

where

i_{00} = initial control current
E_{dc} = amplitude of step-function input voltage change
R_1 = control circuit resistance
τ_1 = control circuit time constant (approximate)
N_1 = control winding turns

and the remainder of the nomenclature is as given in the paper.

Again, as in the results cited previously, the control circuit resistance is an important quantity insofar as transient response is concerned. The values of R_1 for fast response were felt to be such that the case of zero harmonic currents in the control circuit would be the more generally useful one, particularly where transient response might be an important consideration.

Mr. Cohen's discussion, giving the calculation of self-saturating magnetic amplifier output for the completely saturated condition, is a useful contribution to the calculation methods for this type of circuit. The assumption of a constant post-firing inductance adds to the difficulty of literal solution but leads to extremely interesting results.

Essentially the method given by Mr.

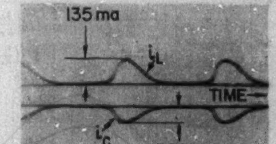

Figure 7. Oscillogram of load current I_L and control current I_c

I_L: upper trace, 15.3 milliamperes per millimeter, peak current 135 milliamperes
I_c: lower trace, 75 milliamperes per millimeter, peak current 398 milliamperes

Cohen involves an assumption resembling Mr. Boyajian's "2-zone" magnetization curve,[2] as does the method proposed in the paper. In Mr. Cohen's case, particular attention was paid to the second, or saturated, zone.

Adapting equations 21–24 of Mr. Boyajian's paper to this case, and using the nomenclature of the discussion, one finds an expression for the current

$$i_{(t)}=I_m\left\{\sin(\omega t-\theta)-\frac{\sigma}{\cos\theta}+\left(\sin\theta+\frac{\sigma}{\cos\theta}\right)\epsilon^{-\frac{R_T}{L}}\right\}\qquad(23)$$

As Mr. Boyajian points out, and is evident in his Figures 5 and 6, the exponential decay of current after the axis-crossing with negative slope of the supply voltage is principally a zone *1*, or unsaturated, variation. Examination of a numerical integration schedule, or of Figures 6 and 7 of the paper, seems to confirm this. Of course, by his assumption $\theta_f=0$, Mr. Cohen has excluded all unsaturated operation of the reactor and has given a useful calculation method for the saturated output. It would be interesting to see a general "2-zone" treatment in which θ_f was not so restricted.

The treatment of the effect of nonideal rectifiers on the saturated output also is of considerable interest, particularly in view of the indication given in Figure 2 of the discussion that assumption 3 of the paper would be very poor for large values of $\omega L/R_T$ and small values of σ.

The discussion of the shape of the transfer characteristic of a self-saturating magnetic amplifier in the range of extreme negative premagnetization beyond the cutoff point, or lower knee, which Mr. Storm has prepared, represents an important addition to the material contained in the paper. The mode of firing involved in operation in this region has been described[3,4] and is presented briefly: Due to saturation, the reactor cannot initially change its flux linkages and thus can introduce no voltage drop in the anode circuit. As a result, the anode current, following the axis-crossing with positive slope of the supply voltage, increases sinusoidally, as in a resistive circuit, until it has reached a value sufficient so that the anode magnetomotive force equilibrates the premagnetizing magnetomotive force. When this condition prevails, the reactor core becomes unsaturated and is capable of developing an inductive voltage in the anode winding. This voltage assumes a value so that the load current is constant and gives rise to an anode-winding magnetomotive force which remains equal to the premagnetizing magnetomotive force during the remainder of the alternation. Similar events occur in the other anode circuit during the following alternation, causing the load current to resemble a drastically clipped and rectified sinusoid with amplitude directly related to the premagnetization through the equality of magnetomotive forces.

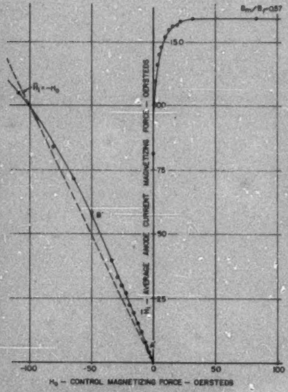

Figure 8. Transfer characteristic of a full-wave magnetic amplifier over extreme control range

E_m=141.4 volts
l=20.1 centimeters
R=40.5 ohms
N=1,200 turns
ω=377 radians per second
A=3.5 square centimeters

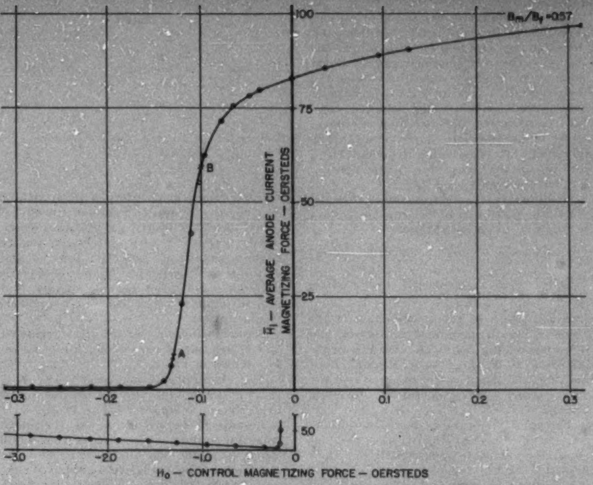

Figure 9. Transfer characteristics of a full-wave magnetic amplifier over normal control range

As demonstrated in Mr. Storm's discussion, the fundamental relation for this mode of operation is

$$H_t+H_o=0\qquad(15)$$

Since H_t may be taken approximately as a square wave, the average value, when rectified, is equal to the amplitude, and

$$H_{t(avg)}=-H_o\qquad(16)$$

Figures 8 and 9 of the discussion are given in order to show the extreme anisotropy displayed by a self-saturating magnetic amplifier with respect to the direction of control premagnetization on opposite sides of cut-off. They are quite similar to Figures 5 and 6 of Mr. Storm's discussion, referring as they do to the same type of circuit, and are presented to illustrate the effect of extreme negative premagnetization for conditions similar to those of the illustrative example given in the paper. While the saturable-core reactors employed were not identical with those described in Appendix I, they were gapless and consisted of the same material, and had magnetization data similar to Figure 11.

The increase of output on either side of the cut-off point, which has been pointed out by Mr. Storm with particular reference to automatic control and regulator applications, is evident in Figure 8 of the discussion, and in the inset of Figure 9 of the discussion. In order to determine the importance of the loss of signal polarity sense in automatic control work, the orders of magnitude of the effects must be considered. As an example, in regulator applications, it is generally desirable to limit the range of operation of the amplifier to that portion of the characteristic between points A and B of Figure 9, at which the sensitivity (slope) has been reduced to half the maximum value. In order to permit operation in this region with a reversible polarity signal, it is necessary to provide a bias of approximately −0.115 oersted; while a single polarity signal would require a negative bias of at least 0.130 oersted.

Generally, the use of extreme negative bias on a single-ended amplifier, together with signal values of commensurate magnitude, is to be avoided, since the result is usually reduced power gain, slow dynamic response, and inordinate sensitivity of the amplifier to supply voltage changes. In the case of a push-pull amplifier, bias is used only to establish the balanced quiescent outputs of each channel, and is quite small in value. Push-pull amplifier stages are not subject to complete loss of signal polarity sense under extreme signal conditions, and are thus excluded from this discussion. Actually, the only amplifiers subject to this possibility are single-ended units operating with reversible polarity signals or with extreme negative bias. In addition, good practice dictates the matching of impedances of intermediate stages of multistage amplifiers, thus precluding the possibility of loss of polarity sense due to overdrive in any but the lowest-level stage.

In automatic control work, then, the cases where the possibility of loss of polarity sense is a significant consideration are:

1. Input stage, single-ended, reversible polarity signal.

2. Input stage, single-ended, extreme single-polarity signal and bias values.

Examination of the co-ordinates of the points A and B mentioned previously, and of corresponding points (A′ and B′) on the left portion of the transfer characteristic indicates the signal values required to cause "transformer" mode operation, shown in Table I.

The sensitivity ratio is seen to be $(49.4-5.5)/(0.130-0.0098)=1{,}370$, while the bias ratio, or permissible signal overdrive ratio is $5.5/0.13=42.3$.

As indicated above and in Figures 8 and 9 of the discussion, a difference of sensitivity of more than three orders of magnitude is seen to exist on opposite sides of cut-off. A signal overdrive of at least 40 times is evidently permissible as well. As the quality of the magnetic core material is lowered, and as the reverse resistance of the rectifiers is reduced, these ratios become smaller, and may ultimately reach values that would be troublesome.

Table I

Point	$H_{i(avg)}$ Oersteds	H_0 Oersteds
A	6.75	− 0.130
A′	6.75	− 5.5
B	57.8	− 0.098
B′	57.8	−49.4

Table II

Point	I_1 Milliamperes	I_0 Milliamperes
A	25	− 3.9
A′	25	− 75
B	180	+ 2.5
B′	180	−550

Similar ratios for Mr. Storm's Figures 1 and 2, locating the operating limits as before shown in Table II.

The sensitivity ratio equals $(550-25)/(2.5+3.9)=82$, and the permissible signal overdrive ratio equals $75/3.9=19.2$.

Providing the overdrive on the input stage due to the extreme value of a push-pull signal, or of the bias alone with zero value of extreme single-polarity signal, is maintained within the foregoing limits (20 to 40), little difficulty is encountered with the "transformer" mode of operation. It also should be mentioned that optimum gain and speed of response considerations in high-performance regulators and servomechanisms generally limit the operating levels to maximum overdrive ratios of approximately three to five.

REFERENCES

1. ANALYTICAL DETERMINATION OF CHARACTERISTICS OF MAGNETIC AMPLIFIERS WITH FEEDBACK, **D. W. VerPlanck, L. A. Finzi, D. C. Beaumariage.** *AIEE Transactions*, volume 68, part I, 1949, pages 565–70.

2. MATHEMATICAL ANALYSIS OF NON-LINEAR CIRCUITS, **A. Boyajian.** *General Electric Review* (Schenectady, N. Y.) volume 34, September 1931, pages 531–37.

3. UNITED STATES PATENTS 2,137,878, 2,153,377, and 2,153,378. **W. Kramer.** November 22, 1938 and April 4, 1939.

4. See references 13 and 14 of the paper.

Automatic Grounding and Air-Break Switches for Protection of Transformer Stations

E. A. RICKER
MEMBER AIEE

A COMBINATION of an automatic-grounding switch with an automatic-opening air-break switch can be used as a substitute for a 110-kv circuit breaker. Although customers, who are supplied from a small transformer station tapped to a 110-kv line, would have an occasional interruption in service, they are receiving electric energy at a lower rate per kilowatt-hour because of the lower capital cost of the transformer station. Since each 110-kv circuit breaker requires two isolating disconnecting switches, the capital reduction for each combination of automatic switches is almost equal to the installed cost of one circuit breaker. With proper installation and maintenance, the switches will give reliable protection for small transformer stations.

The following paragraphs give a discussion of the preferred station diagrams, ways of mounting these switches, and reviews of experience since 1930 with several types of automatic switches operated by spring and motor-driven mechanisms amounting to a total of 260 switch years. The favorable operating experience with automatic disconnecting switches has resulted in their adaptation for use in other parts of transformer stations.

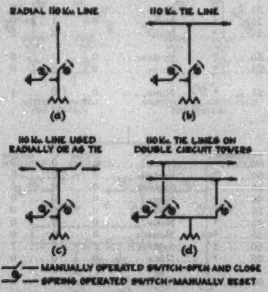
RADIAL 110 Kv. LINE
110 Kv. TIE LINE
(a)
(b)
110 Kv. LINE USED RADIALLY OR AS TIE
110 Kv. TIE LINES ON DOUBLE CIRCUIT TOWERS
(c)
(d)
MANUALLY OPERATED SWITCH-OPEN AND CLOSE
SPRING OPERATED SWITCH-MANUALLY RESET

Figure 1. Small transformer stations without 110-kv circuit breakers

Sequence of Operation

When automatic grounding and air-break switches are used at transformer stations, the circuit breakers at distant stations are given the double duty of protecting both the transmission line and the distant transformer. An automatic single-phase grounding switch, located on the 110-kv switching structure of a transformer station, is used to apply a solid line-to-ground fault on a transmission line whenever the protective relays of a transformer have detected a fault. The artificial line-to-ground fault is detected by ground relays at distant stations, causing circuit breakers to operate and disconnect the sources of energy from the faulted line. After the line is de-energized, an automatic 3-pole air-break switch is opened on the 110-kv side of the defective transformer to disconnect from the line both the transformer bank and the single-pole grounding switch. This combination of automatic switches allows a small transformer station to be supplied from a high-voltage transmission line without using an expensive 110-kv circuit breaker.

Since the trip circuit of the air-break switch is controlled by a pallet switch on the automatic grounding switch, a timer is usually put into the circuit to delay the tripping of the 3-pole automatic air-break switch by a time interval ranging from 0.5 to 3.0 seconds. During this interval, the distant circuit breakers will have time to interrupt the flow of fault current, and the automatic air-break switch can be opened with safety. With the faulted transformer removed from the system, automatic reclosing relays can close the circuit breakers after a time delay and restore the line to service.

General System Conditions Permitting the Use of Automatic Switches

Automatic grounding switches are not recommended for stations which supply part of a load along with local generation, because the artificial fault will cause a disturbance to both the system and local generation. For the same reason, they should not be used with transformers which are a tie between two parts of a large system where power might be transferred in either direction. This objection is reduced if the low-voltage circuit breakers are made to operate first, and the artificial ground fault is applied after a time delay. However, the distant circuit breakers are tripped after a longer delay, thereby giving slower clearance of the faulted transformer. In Table I, there are at least five installations which are exceptions to the above preferred system conditions. When the local station is connected to a source of generation on the low-voltage side, the 110-kv windings of the transformer should be star-connected with the neutral solidly grounded, to prevent damaging the insulation on the high-voltage winding.

Paper 49-143, recommended by the AIEE Substations Committee and approved by the AIEE Technical Program Committee for presentation at the AIEE Summer General Meeting, Swampscott, Mass., June 20–24, 1949. Manuscript submitted March 22, 1949; made available for printing May 4, 1949.

E. A. RICKER is an Assistant Relay Engineer with The Hydro-Electric Power Commission of Ontario, Toronto, Ontario, Canada.

Another factor which must be considered before deciding whether the high-voltage circuit breaker can be eliminated by the substitution of automatic switches, is the class of service that is required by the customers supplied from the station. Whenever any grounding switch operates at a station, the power supply for all customers is interrupted. If a station has two or more transformer banks with as many high-voltage circuit breakers, customers are not affected by faults in one transformer. If there is only one transformer bank at the station, service is not improved by using a circuit breaker in place of automatic switches. If the station has two banks of transformers, both equipped with automatic switches, and if the distant circuit breakers have automatic reclosing equipment, the local station has only a short interruption for a fault in one transformer, because the supply of energy to the load is restored as soon as the distant circuit breaker has been reclosed automatically.

Mounting of Automatic Switches

The single-pole automatic grounding switch usually is mounted near the automatic air-break switch. The steel structure might be used to support both. The grounding switch often is used to produce a circuit to ground across the insulator stack at the hinge end of the air-break switch, an extra contact jaw for the grounding switch being attached to the top casting on the stack of insulators.

The spring operated mechanism for the single-pole grounding switch usually is mounted near the hinge of the grounding switch; linkages extend the manual control to the ground level. Energy is stored in the springs by moving a lever through an angle which ranges from 90 to 180 degrees.

The box containing the spring-operated mechanism for the automatic 3-pole air-break switch usually is mounted nearer the base of the steel structure. The box is heavier and contains stronger springs which must be capable of breaking three contacts rated at 600 amperes each, and of moving the linkages and arms of three switches to the open position. Springs of different strength are combined to give extra force at the beginning of the travel and to overcome excess friction caused by corrosion of the contacts or obstructions such as ice formation. Energy is stored in the springs by operating a lever manually. The second movement of the lever returns the arms of the air-break switch to the closed position. Motor-operated mechanisms are available for winding up the springs. When the mechanism has been latched in the loaded condition, the lever can be used for opening or closing the switch manually to energize or isolate

Table I. Installations of Automatic Grounding Switches

	Grounding Switch			Air Break Switch			Transformer Bank Data				Generation	Number of Troubles Reported		
Station	Date in Service	Years	Months	Number	Mechanism	Battery Voltage	Kva Capacity	Voltage (kv)	Frequency	Connection	Kva on Low Voltage Side	Ground Switch	Air Break	Control
Hanover	Oct. '30	13	3		None	125	6,750 8,000	110/6.6 110/14.2	25	*	10,000	2		4
St. Clair	Oct. '32	16	5		None	125	15,000	110/26.4	25	*	None	2		2
Ontario Paper (S)	Feb. '33	10	8	3	Motor	24	67,500	121/6.6	25	*	None	0	0	2
Matachewan	Apr. '34	14	11	1	Spring	24	4,500	121/27.7	25	*	None	0	0	0
Kirkland Lake	July '34 Apr. '39	12 7	3 11	2	Motor	125	28,500 28,500	117.5/12	25	**	4,250	1	1	1
Smooth Rock Falls	Aug. '34	14	8	2	Motor	24	39,000	121/6.6	25	*	None	0	0	8
Cornwall (H.S-S)	Aug. '34	11	7	1	Spring	24	20,000	105/6.6	60	*	None	0	0	0
Falconbridge	Nov. '35 (Oct. '45)	3	8	1	Spring	24	4,500	121/27.7	25	†	None	0	3	2
Larder Lake	Dec. '35 May '40	13 8	4 10	2	Spring	24	4,500 4,500	121/27.7	25	†	None	0	1	2
Timmins	Nov. '35 Oct. '37	4 2	2 3	2	Spring	125	4,500 4,500	121/27.7	25	†	None	0	0	0
Pamour	Dec. '36 July '40	12 8	3 8	2	Spring	(24) 110	4,500 4,500	121/27.7	25	†	None	0	0	0
Long Lac	June '38	10	9	1	Spring	24	9,000	110/44	60	†	None	0	0	0
Crow River	Sept. '39	8	5	1	Hand	48	3,750	66/23	60	**	3,500	0		0
Allanburg	Dec. '39	8	3	3	Motor	125	67,500	121/12	25	*	None	0	0	0
Norfolk	Jan. '40	9	2	1	Spring	(110) 125	8,000	110/28.4	25	*	None	0	0	1
Crystal Falls	Mar. '40	9	0	1	Spring	125	8,000	110/22	60	**	8,500	0	0	0
Coniston	Mar. '40 Feb. '49	9	0	1	Spring	125	8,000 8,000	110/22	60	**	11,400	1	0	0
Ramore	Apr. '40	8	11	1	Spring	24	4,500	121/27.7	25	†	None	0	0	0
Shiningtree	Apr. '41	7	11	1	Spring	24	4,500	121/27.7	25	†	None	0	1	0
Palmerston	Dec. '41	8	3	1	Spring	(110) 125	8,000	110/26.4	25	*	None	5	5	3
Oshawa	Feb. '42	4	4	1	Spring	125	15,000	110/44/4	60	‡	System	0	1	0
St. Catharines	May '42	6	11	1	Spring	24	8,000 8,000	110/28.4	25	*	None	0	0	0
Thorold	Oct. '42	6	6	4	Spring (then motor–'42)	(24) 125	15,000 ('29) 15,000 ('36) 15,000 ('37)	121/13.2	25	*	None	0	0	1
Fort William	Apr. '45	4	2	1	Hand	125	15,000	110/22	60	*	None	0	0	0
Barrie	June '46	1	11	1	Spring	125	15,000	110/44/4	60	‡	System	0	2	0
Schumacher	Feb. '47	2	0	1	Spring	125	9,000	110/12	25	*	System	0	0	0
Cornwall (CIL)	Feb. '47	2	1	1	Spring	125	15,000	110/13.2	60	*	None	0	0	0
Caledonia	Apr. '47	1	11	2	Spring	125	8,000	110/28.4	25	*	None	0	0	0
Kerr-Addison	June '48	0	9	2	Spring	125	15,000	121/27.7	25	*	None	0	0	0
Kingsville	July '48	0	8	1	Spring	125	8,000	110/28.4	25	*	None	0	0	0
Owen Sound	July '48	0	8	1	Spring	125	15,000	110/44/4	60	‡	System	2	0	1
Wallaceburg	Aug. '48	0	7	1	Spring	125	8,000	115/28.4	25	*	None	0	0	0
Stewartsville	Sept. '48 Sept. '48 Oct. '48	0 0 0	6 6 5	3	Motor	125	27,000 27,000 27,000	115/13.2	60	**	72,000	0	0	0
											Total	13	14	22

Note: The following symbols are used to denote connections of windings in transformer banks: * Star/delta, † Delta/delta, ** Grounded-star/delta. ‡ Star/grounded-star/delta.

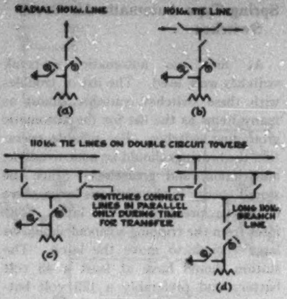
RADIAL 110Kv. LINE
110Kv. TIE LINE
(a)
(b)
110Kv. TIE LINES ON DOUBLE CIRCUIT TOWERS
SWITCHES CONNECT LINES IN PARALLEL ONLY DURING TIME FOR TRANSFER
LONG 110Kv. BRANCH LINE
(c)
(d)

Figure 2. Modifications which permit easy testing of automatic switches

a transformer while it is off load. Arcing horns are added to the switch to prevent burning the main contacts.

Both kinds of automatic switches have solenoids which are energized from the station battery for moving the trip-latch or moving a linkage through a neutral position. Both types of mechanism boxes contain pallet switches for opening circuits to trip coils and controlling other circuits to relays and lamps.

Since automatic switches are used at stations during the earlier stages of their growth, the supporting structure should be designed for the addition of a circuit breaker with the least modification. A 3-pole automatic air-break switch and a 3-pole disconnecting switch might be mounted on a steel structure above the place where the circuit breaker could be installed. The function of the extra disconnecting switch will be discussed later

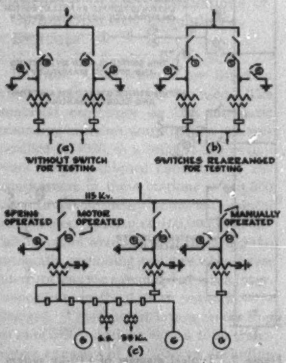
(a)
WITHOUT SWITCH FOR TESTING
(b)
SWITCHES REARRANGED FOR TESTING
115 Kv.
SPRING OPERATED
MOTOR OPERATED
MANUALLY OPERATED
6.6
33 Kv.
(c)

Figure 3. Stations with two and three banks of transformers

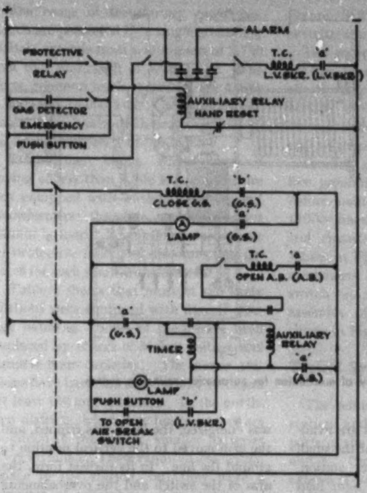
+
−
ALARM
PROTECTIVE RELAY
T.C.
'a'
L.V.BKR. (L.V.BKR.)
AUXILIARY RELAY HAND RESET
GAS DETECTOR
EMERGENCY PUSH BUTTON
T.C.
'b'
CLOSE G.S.
(G.S.)
'a'
LAMP
(G.S.)
T.C.
'a'
OPEN A.B.
(A.B.)
'a'
(G.S.)
TIMER
AUXILIARY RELAY
'a'
(A.B.)
LAMP
PUSH BUTTON
TO OPEN AIR-BREAK SWITCH
'b'
(L.V.BKR.)

Figure 4. Diagram of control circuits for automatic switches

with the procedure for tests. The foundations for the steel structure should be well made, so that wind and frost will not force the structure out of line and cause excessive friction in the bearings of the switches. Wood poles are not recommended as supports since they are more likely to be heaved by the frost, causing misalignment.

Arrangement of Equipment on Diagrams of Stations

In the simplest station having only one transformer, the low-voltage breaker might be omitted and fuses used. When the load includes synchronous motors or local generation, a circuit breaker is required to remove the source of fault current and to reduce interruptions to the high-voltage line by the operation of the overload protection on the transformer. When two or more banks are in parallel, low-voltage breakers are required to isolate the faulted bank. The breaker usually is tripped a short time before the artificial line-to-ground fault is applied to the high-voltage side of the faulted bank.

When two transformers are installed for reducing the duration of interruptions, the overload relays for each transformer should have settings which are greater than the combined loads of both banks, or else the second bank would be lost due to overload whenever the first bank develops an internal fault.

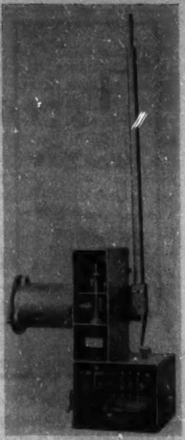

Figure 5. Automatic grounding switch with cover removed from mechanism box

Resistance of Station Ground

For successful operation of a scheme which includes automatic grounding switches, the protective equipment with the circuit breakers at the distant ends of the transmission line must include relays which are capable of detecting ground faults caused by automatic grounding switches. At some stations the resistance through ground might reduce the current to a value that cannot be detected by the relays at the distant station, as well as causing dangerous voltages in the local station. Considerable expense might be involved in installing numerous ground rods, in burying long bare-copper cables as counterpoise, or in extending a solid connection from the station to the nearest wet location. The alternatives are installation of high-voltage fuses or circuit breakers.

Testing Routine

Experience has shown that some installations of automatic switches are unreliable and require frequent testing. Since many of the troubles have developed in control circuits rather than in the switches themselves, the tests should be a complete check of the whole clearing process, from the closing of a contact at the panel to the final opening of the air-break switch. A push button usually is installed as a means of initiating the process. When

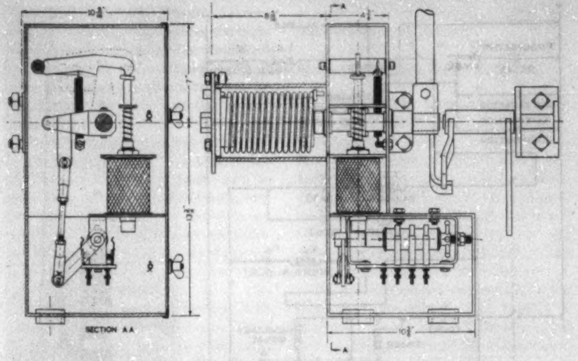

Figure 6. Assembly of mechanism for automatic grounding switch

low-voltage lines and switches are available for transferring the load of the small transformer station to another station, the test can be made during light load periods. When the station is in an isolated location, the tests are made during prearranged interruptions.

Tests on a station having a single transformer involve a complete interruption of the station. Load is removed from the transformer by tripping the low-voltage breaker. The exciting current of the transformer is broken by the air-break switch. A 3-pole disconnecting switch should be installed on the line side of the automatic air-break switch to permit the test being made without operating the breakers at the distant ends of the line. When the automatic switches have been isolated, the air-break switch should be reset to its normal operating position. Then the emergency push button on the control panel should be operated to trip the grounding switch and the air-break switch in their normal sequence. This test should be repeated once or twice to clean the contacts. The present practice is to make these tests monthly wherever possible. Whenever an automatic operation from one of the protective relays has occurred during a month, the routine monthly test can be omitted.

Gravity-Type Automatic Grounding Switch

The first installation of an automatic grounding switch was placed in service in 1930. A weight was added to one phase of an ordinary manually-operated line-grounding switch. The arm of the switch remained horizontal while in the normally open position. When the coil was energized, the latch was tripped, and the arm moved to the vertical position to ground the line. In its earliest form, the arm of the switch and the overbalancing counterweight were in a straight line. Experience showed that the angle of 180 degrees should be reduced by 30 or 45 degrees to produce a force which would keep the contact closed. Rebounding of the arm was reduced by using a resilient material in the jaw. Guides for the jaw and arcing horns were added.

There were only two installations of gravity-type switches, and no automatic air-break switch was used with them.

The mechanical design of the switch was the cause of failure to operate in four cases; troubles in control circuits prevented operation in six other cases. All failures except two occurred during routine tests.

Spring-Type Automatic Grounding Switch

This type of switch with its method of mounting already has been described. The stored energy is limited by the adjustments of the spring mechanism. Some looseness in the mechanism will allow a mechanical impact to break a coating of ice. Excessive spring pressures might cause damage at the jaw of the switch.

Troubles were recorded on 10 installations out of a total of 35, the auxiliary equipment being the cause of many of them. Nine cases of failure were caused by the mechanical parts not functioning properly; in 11 cases the operations of control circuits were incomplete or faulty. Only three of all these failures occurred during service; the others occurred during routine tests.

Spring-Type Automatic Air-Break Switches

At first, no automatic air-break switches were used. The list of troubles with these switches contains almost as many items as the list for the automatic grounding switches. For reliable operation the bearings should be noncorrodible, antifriction, and greaseless. Since the stored energy in the spring is large, there is greater pressure on the latch. The force from the tripping solenoid should be large enough to move the latch. The station should have at least a 48 volt battery and preferably a 125 volt battery. The higher voltage will avoid troubles caused by resistance in contacts and control wiring. The design should be chosen so that ice formation does not prevent operation to either the open or closed positions.

Among 32 installations, seven switches were the subject of 13 reports on troubles. Eight failures were caused by mechanical troubles and three, by control circuits. The cause of five other failures could not be determined. One failure occurred while the switch was in service; the others occurred during routine tests.

Motor-Operated Air-Break Switches

Due to slower operating speed of air-break switches with motor-operated mechanisms, the timer controlling the trip coil is often omitted. The motor usually is rated at one-quarter horsepower, and the full capacity of the station

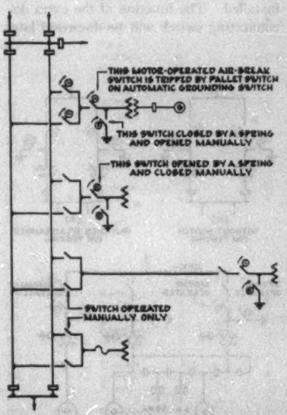
THIS MOTOR-OPERATED AIR-BREAK SWITCH IS TRIPPED BY PALLET SWITCH ON AUTOMATIC GROUNDING SWITCH
THIS SWITCH CLOSED BY A SPRING AND OPENED MANUALLY
THIS SWITCH OPENED BY A SPRING AND CLOSED MANUALLY
SWITCH OPERATED MANUALLY ONLY

Figure 7. Typical diagram of 110-kv system showing manual disconnecting switches which permit testing of automatic air-break switches

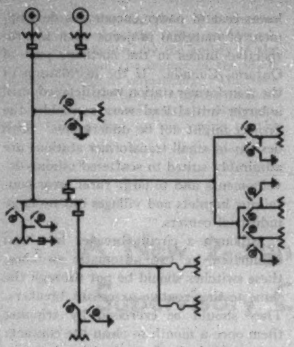

Figure 8. Growth by extension of branch circuits

battery is the stored energy available to operate it. In a total of over 16 installations, three of them were the subject of trouble reports.

One long interruption in service was caused by failure of lamps to indicate that a switch at a distant station had remained in the closed position. Other failures were found during routine tests. In one case the bevel gears had been broken by a person moving the lever for hand operation in the wrong direction. Another motor-driven switch had been operated by the controller to the open position, but it failed to close when the controller was turned to the close position. This failure might have been caused by ice or snow, as the temperature was −50 degrees Fahrenheit.

Experience with 39 Installations of Spring-Operated Grounding Switches

In Table I, 33 stations are listed in which automatic switches are used. The combined experience on the automatic grounding switches since the first one was installed in 1930, is a total of 260 switch years. The combined capacities of the transformers in these stations is 643,500 kva. In five of these stations with a total transformer capacity of 150,000 kva, circuit breakers were installed replacing the automatic grounding switches when fewer interruptions were required or when interconnections in the 110-kv network were changed. Construction is now proceeding on nine other stations with a total transformer capacity of 96,000 kva, including 11 automatic grounding switches and 13 air-break switches.

The range of transformer capacities, which are protected by a single grounding switch, extends from a minimum of 3,750 kva to a maximum of 67,500 kva. The three common bank capacities are 4,500, 8,000, and 15,000 kva. One station contains three banks with separate 110-kv air-break switches for each bank.

Transformer banks which have a rating of less than 3,000 kva usually are not equipped with bushing-type current transformers; therefore, protective relays cannot be used. High-voltage fuses serve as protective links and disconnecting devices for such small transformers.

Table I shows that most of the early stations were equipped with 24-volt storage batteries. Some of these have been replaced by others of higher voltage and ampere-hour capacity. The newer stations have batteries rated at 125 volts and at least 160 ampere-hours. In the northern districts, where low temperatures are common in the winter, smaller batteries were installed. These required less heated space in the station, but they were a sacrifice of reliability. The number of low-voltage circuit breakers in a station, the frequency of tripping and closing them, and the amount of other motor-operated station equipment will be factors in deciding the size of the station battery.

Typical Installations of Automatic Switches in Stations

Small transformers stations can be supplied from a radial line, or a single tie line, or from either of two tie lines supported on double-circuit towers. These connections are illustrated in Figure 1. When a single-circuit line is intended for use as either a tie line or a radial feeder, additional manually-operated disconnecting switches are installed, as illustrated in Figure 1(C). Figure 1(D) shows how a small station can be connected to either of two parallel tie lines. Except when the tapped station is being transferred from one circuit to the other, the high-voltage lines are never connected in parallel.

None of these diagrams shows any method for testing the automatic switches. Figure 2 shows how manually-operated switches can be added to the stations in Figure 1, so that the automatic switches can be given a complete test without tripping circuit breakers on the 110-kv supply lines.

A station with two banks of transformers is shown in Figure 3(A). One manually-operated disconnecting switch can be added to this diagram, as shown in Figure 3(B), so that the automatic switches can be tested easily.

The equipment which is not essential for this discussion has been omitted from all of these diagrams, such as disconnecting switches associated with high-voltage circuit breakers, line sectionalizing switches and transfer switches, coordinating gaps, lightning arresters, and line grounding switches that are closed before maintenance work is done on the 110-kv lines. A typical diagram of control circuits for automatic switches is shown in Figure 4. Figure 5 shows the mechanism and blade of the grounding switch in the tripped position. The assembly of the tripping mechanism is shown in Figure 6.

Typical System Connections

The relation of the small transformer stations and the tapped lines to the other parts of the system is shown in Figures 7 and 8. The latter shows growth by the extension of branch circuits with the addition of two circuit breakers in the

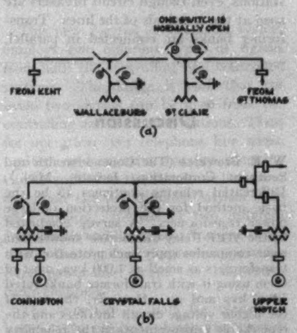

Figure 9. Tapped stations on loop lines in a 110-kv system

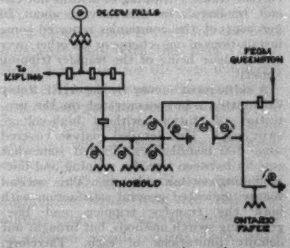

Figure 10. Motor-operated switches in tie lines

main branches. The main disadvantage is that faults which occur on the main supply line cause an interruption to stations on the branch lines as well. A total of seven stations is illustrated in Figure 8.

Figures 9 and 10 show loop lines which supply tapped stations. The loop in Figure 9(A) is closed only during an emergency or to transfer load, because the terminal stations are connected by other transmission lines. In Figure 9(B) no other lines connect these stations; all disconnecting switches remain in the closed position for normal operation. Under these conditions, the loop lines are actually single-circuit tie lines. Figure 10 shows two stations which are operated with tie lines closed through automatic motor-operated disconnecting switches.

Economy by Use of Automatic Disconnecting Switches

The infrequent occurrence of faults in transformers has resulted in the elimination of high-voltage circuit breakers for transformers from nearly all transformer stations, even though circuit breakers are used at the terminals of the lines. Transformer banks are connected in parallel, and automatic motor-operated disconnecting switches on the high-voltage side and low-voltage circuit breakers are used to isolate the faulted bank after the auxiliary tripping relay has operated to disconnect all sources of fault current.

Low-voltage windings on transformers usually are delta-connected, and zig-zag grounding reactors are used as sources of ground current to the feeders. Since faults in grounding reactors do not occur frequently, 3-phase circuit breakers between the terminals of the reactor and the station bus usually are omitted. An automatic motor-operated disconnecting switch is used in place of the circuit breaker to disconnect the zig-zag grounding reactor after all sources of fault current flowing into the low-voltage bus have been removed by operation of the circuit breakers.

Conclusions

Omitting high-voltage circuit breakers from a station gives a considerable saving in capital, but it is accompanied by more interruptions of the power supply to the customers. The reduced carrying charges permit lower rates for electric energy being charged to the customer. The lower cost of power encourages development of marginal projects, such as prospective mines in the northern part of Ontario, Canada. If the installation of the transformer station were delayed until a larger initial load were available, the project might not be undertaken. Such designs of small transformer stations are admirably suited to scattered mining developments and to large rural areas containing hamlets and villages but no large industrial centers.

Although a circuit breaker has been eliminated by two automatic switches, these switches should be put through the same testing routine as circuit breakers. They should be exercised by tripping them once a month to clean the contacts and to check the control wiring for open or short circuits. The stored-energy source for operating the automatic switches should be effective through the whole travel of the switch with a safe margin.

Energy stored in springs appears to be sufficient for single-pole grounding switches. The larger amount of stored energy in the station batteries and motor-operated mechanisms would be preferred for opening the 3-pole air-break switches.

Discussion

W. R. Brownlee (The Commonwealth and Southern Corporation, Jackson, Mich.): Differential relaying continues to be the basic method for the protection of large power transformers. A survey conducted by the AIEE Relay Committee[1] showed that some companies apply such protection with transformers as small as 1,000 kva, most of them using it with transformer banks rated 5,000 kva and up. However, the cost of the higher voltage circuit breakers and the remarkable improvements in the reliability of modern power transformers have led to the substantial application of local differential relaying, either with automatic line grounding switches or with pilot wire or carrier current transfer tripping of distant line circuit breakers. In this survey, about 75 per cent of the companies reported some installations of one scheme or the other, over half of these being of the transfer tripping variety.

A subsequent survey by the AIEE Relay Committee was concentrated on the protection of stations without high-voltage switching.[2] This detailed analysis covered some 100 installations, divided somewhat equally between transfer tripping and line-grounding switch schemes. This second survey indicated general satisfaction with both the transfer tripping and line-grounding switch methods, but brought out definite limitations of each. Therefore, this detailed analysis of application and performance presented by the author is most timely and should assist in a more accurate evaluation of the proper field for automatic grounding switches. It would be interesting to learn what consideration the author gave to the use of transfer tripping schemes, and the reasons for preferring the automatic grounding switch method.

Speed of operation of the automatic grounding switch is rather important, since its operating time plus that of the ground relays at remote stations adds directly to the total time of fault clearing, when comparing this scheme with either a local circuit breaker or transfer tripping arrangement. The time of operation of the type of spring-operated grounding switches described by the author would be of interest (from energizing the trip coil until the contacts touch).

In view of the relative infrequency of faults in modern power transformers, it seems unfortunate that the grounding switch scheme requires interrupting the load for test purposes, in the case of single transformer installations, as often as once a month. Consideration might be given to additional disconnecting and by-pass facilities to avoid interruptions during tests, but it is doubtful if this added complication and expense would be justified.

Increased speed of operation of automatic grounding switches and improved reliability of the entire scheme seems highly desirable. Accordingly, designs based on a straight line motion might be preferable for line grounding switches.

REFERENCES

1. RELAY PROTECTION OF POWER TRANSFORMERS, **AIEE Relay Subcommittee.** *AIEE Transactions*, volume 66, 1947, pages 911–16.

2. PROTECTION OF STATIONS WITHOUT HIGH-VOLTAGE SWITCHING, **AIEE Committee Report.** *AIEE Transactions*, volume 68, part I, 1949, pages 226–32.

E. A. Ricker: The discussion of the automatic grounding switch would not have been complete without references to surveys by the AIEE Relay Committee and reports which were published in AIEE Transactions for 1948 and 1949. For this favor, grateful acknowledgment is given to W. R. Brownlee.

Although the second general survey by the Relay Committee showed that both the transfer tripping and line grounding switch methods of opening circuit breakers in remote locations will perform correctly in the majority of operations, automatic grounding switches have been preferred by the Hydro-Electric Power Commission for several reasons. Carrier equipment for transferring tripping signals has been shown by tests to be not always effective and reliable. Carrier transmitters and receivers require more maintenance and adjustment by specially-trained personnel. The cost of a complete installation of carrier equipment is higher than the cost of installing additional supports and switches associated with the automatic grounding device. No power is required by the automatic switch during the standby condition.

The time delay in operation of the grounding switch was made small by using light materials in the blade to reduce its inertia and co-ordinating designs for the spring, trip latch, and jaw. The amount of energy stored in the spring can be adjusted. It is limited by the ability of the jaw to withstand the impact of the blade without damage or rebounding. The force caused by current in the tripping solenoid must be several times greater than the opposite force caused by the spring on the trip latch even after months without an operation. Automatic grounding switches are normally adjusted so that the time delay is less than 0.5 second from the time the trip coil is energized until the blade makes contact with the jaw of the switch.

To all employees of the Hydro-Electric Power Commission of Ontario who gave assistance by providing opportunities to review records of operating conditions, who passed on their knowledge of early developments, who gave suggestions on the contents of this paper, and to those who prepared the drawings, the first copies of the text and checked the material, the author acknowledges a debt of gratitude.

A New 2-Signal Synchronous Supervisory Control System

W. A. DERR
MEMBER AIEE

THERE are two fundamental methods of selecting a desired unit in a supervisory control system. The one method, known as direct selection, is based on applying signals which are different for each unit. The other method, known as synchronous selection, is based on having both the controlling and controlled station equipment connect to each unit in sequence until the desired unit is reached.

Two different types of direct selection systems have been manufactured. One of these types uses a different code of pulses to select each desired unit, with the station receiving the selection pulses returning a similar code of pulses to verify the correctness of selection.[1] The other type also employs a different code of pulses to select each desired unit, but the coding is made so that only the correct unit can be selected. With this latter type it is necessary only to verify that a selection has been made and not that a particular selection has been made.[2]

In a synchronous system there is no specific code or signal associated with each individual unit which must be selected. Instead, signals are transmitted which cause the controlling and controlled station equipment to step through each unit in sequence and in synchronism. The equipment stops when the desired unit is reached. A new system based on synchronous selection will be described in this paper.

All supervisory control systems require signal responsive elements at the controlling station and at the controlled station. Direct selection systems are available which require only a single type of signal and hence a single signal responsive element at each location.[1,2] However, a minimum of two different types of signals must be employed to provide a reliable synchronous system.

When different signal responsive elements are employed at the controlling station and at the controlled station for each station controlled, it is known as single station operation. This is the basic arrangement for which either direct selection or synchronous selection systems are applicable.

The control of several stations employing common signaling means at the controlled stations as well as at the controlling station is known as multistation operation. Direct selection systems using a single signal responsive element at each location are the only systems which are practical to use for multistation operation. Multistation operation is advantageous when only a single pair of wires or a single power-line carrier channel is available for the control of several stations since only one type of signal must be provided.

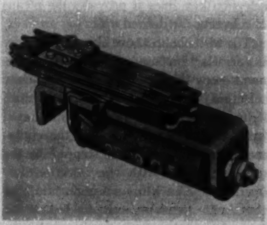

Figure 1. Type of relay employed in new system

Since a reliable synchronous system must employ a minimum of two different signals, multistation operation is not practical.

The synchronous principle provides for rapid checking of the position of devices supervised. A synchronous system also is advantageous where functions must be performed consecutively, since it is only necessary to step to each unit in turn, thus reducing the operating time.

Principle of Operation

This new 2-signal synchronous system employs two different types of signals from both the controlling and controlled stations. The design is such that the same two signals can be used from the controlling and controlled stations. Thus, for operation over telephone line wires, positive and negative battery potential can be applied to the telephone line wires to obtain the two different signals from each station. Signals of two different frequencies can be used from each station as the signaling means for operation over power-line carrier or microwave radio channels.

The selection of units for control is based on the principle of stepping through each unit in turn until the desired unit is reached. A single pulse is used for each step, with all stepping pulses originating from the controlling station. One of the two types of signals employed at the controlling station is used for the odd-numbered steps with the other type of signal being used for the even-numbered steps. Thus the same signal never repeats itself for consecutive steps. This prevents the possibility of the controlling and controlled stations ever operating out of step.

The controlling station waits for a supervision signal from the controlled station after each stepping pulse. The supervision signal consists of a single pulse of either of the two types of signals used at the controlled station. Thus, the

---

Paper 49-144, recommended by the AIEE Substations Committee and approved by the AIEE Technical Program Committee for presentation at the AIEE Summer General Meeting, Swampscott, Mass., June 20-24, 1949. Manuscript submitted March 21, 1949; made available for printing April 28, 1949.

W. A. DERR is Supervisory Control Supervising Engineer with the Westinghouse Electric Corporation, East Pittsburgh, Pa.

Table I. Indication of Signal Pulses

Controlling Station Signal Number		Controlled Station Signal Number
1	→ Step No. 1	
	Supervision ←	1
2	→ Step No. 2	
	Supervision ←	1
1	→ Step No. 3	
	Supervision ←	1
2	→ Step No. 4	
	Supervision ←	1
1	→ Step No. 5	
	Supervision ←	1
2	→ Step No. 6	
	Supervision ←	2
1	→ Step No. 7	
	Supervision ←	2
2	→ Step No. 8	
	Supervision ←	2
1	→ Step No. 9	
	Supervision ←	2
2	→ Step No. 10	
	Supervision ←	2

supervision pulse verifies or changes the lamp indication for the particular unit and also provides the signal that the stepping can continue.

A better picture of the stepping arrangement just described can perhaps be obtained by referring to Table I. This table indicates the signal pulses which would be employed for a supervisory control system providing control and supervision of ten units (for example, circuit breakers), with the first five units being in one position (open) and the last five units being in the other position (closed).

When the stepping is started by the operation of a selection key, the stepping stops when the unit associated with that particular key is reached. Such selection of a desired unit is referred to usually as point selection. When a unit or point has been thus selected, it is possible to initiate the control signals. Signal number 2 is used for both control functions which can be performed, with the number of pulses of this signal determining the control function. For example, two short pulses constitute the control code for closing a circuit breaker and three short pulses constitute the control code for tripping a circuit breaker.

A long pulse of signal number 1 is transmitted from the controlling station to prepare for stepping from the normal at rest condition or for stepping after a unit has been selected. The use of a long pulse eliminates the possibility of unwanted stepping from any extraneous disturbing voltages to which the signal receiver elements may be subjected.

A long pulse of signal number 2 is transmitted from the controlled station if any supervised device changes position automatically. Receipt of this signal at the controlling station results in a long pulse of signal number 1 being transmitted from the controlling station to initiate stepping. When stepping is thus initiated due to an automatic operation at the controlled station, and position of all devices supervised is checked in sequence.

Following is a list of the different signaling means employed in the operation of this system, as just described:

From Controlling Station	
Start	Long pulse, signal number 1
Odd steps	Short pulse, signal number 1
Even steps	Short pulse, signal number 2
Close control	Two short pulses, signal number 2
Trip control	Three short pulses, signal number 2
From Controlled Station	
Alarm	Long pulse, signal number 2
Close supervision	Short pulse, signal number 1
Trip supervision	Short pulse, signal number 2

Operating Features

The supervisory control system described in this paper is an all-relay system employing telephone-type relays as shown in Figure 1.

An escutcheon or key and lamp plate as shown in Figure 2 is used at the controlling location for any of the following functions which may be performed:

1. Control and supervision of any device. (For example, a circuit breaker.)
2. Supervision and alarm of any device. (For example, indication of high transformer temperature.)
3. Telemetering of any quantity. (For example, telemetering of kilowatt load.)
4. Control of any device with simultaneous telemetering of quantity controlled. (For example, control of tap changer with simultaneous telemetering of tap changer position.)

The key at the bottom of the escutcheon shown in Figure 2 is a pull-type key which is operated to initiate stepping of the equipment. This key is called a selection key since it provides the means of selecting the desired unit.

The white lamp above the selection key is the selection lamp. When the equipment steps through each unit, the white selection lamps associated with each unit, light in turn. If the stepping is initiated by operating a selection key the equipment stops when it has stepped to the unit associated with the selection key operated. The white selection lamp for that unit then remains lighted. The desired operation on that unit can then be performed after which the pull-type selection key should be restored. When the key is thus restored, the equipment proceeds to step through the rest of the units.

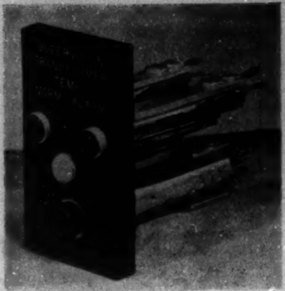

Figure 2. Escutcheon used in new system for each unit controlled and supervised

The two upper lamps on the escutcheon shown in Figure 2 are for indicating the position of the device supervised. If the device supervised is a circuit breaker, these would of course be red and green lamps to indicate whether the circuit breaker was closed or open. If the escutcheon is used for a telemetered indication or for control and simultaneous telemetering, these position indicating lamps are omitted.

To indicate the automatic change of position of a device, the associated position indicating lamp on the escutcheon is flashed. For example, if a circuit breaker is tripped by a protective relay, the green lamp on the escutcheon for that circuit breaker is flashed in addition to an alarm bell being sounded. If a circuit breaker which is equipped with an automatic recloser, trips and is reclosed successfully, the green lamp on the associated escutcheon at the controlling station is first momentarily flashed, after which the red lamp is flashed.

There are five common push-type keys used at the controlling station in the operation of this system. Two of these keys are the control keys which are operated after a unit is selected to change the position of the device controlled. For example, considering a circuit breaker, one of these keys would be operated after selection to close the circuit breaker. The other key would be operated after selection to trip the circuit breaker.

The third common key is designated as the reset key. Operation of this key causes the system to step through all of the points. Thus, it performs the function of checking the position of all of the devices supervised since the position indicating lamps are checked on every step. Operation of this key also restores the equipment to normal in the event that it is off normal for any reason.

The fourth common key is operated to silence the audible alarm which is initiated when any supervised device changes position other than by operation of the supervisory control equipment.

The fifth common key is operated to cause any position indicating lamp or lamps which may be flashing as a result of automatic change of position of the devices supervised to be lighted continuously.

The system is suitable for use with any of the commonly employed types of telemetering equipment. Voltage or current magnitude types as well as impulse types can be used when operation is over telephone line wires. For operation over power-line carrier or microwave radio channels, impulse-type telemetering equipment must be used. It is possible to have the telemetering circuits arranged so that any telemetered indication can be continuously received while the equipment is at rest, without interfering with any other operations. This can be done regardless of the channel means employed.

Communication can be provided readily over the same pair of wires used for operation of the supervisory control equipment. It is customary to have the telephone ringing function provided by the supervisory control equipment.

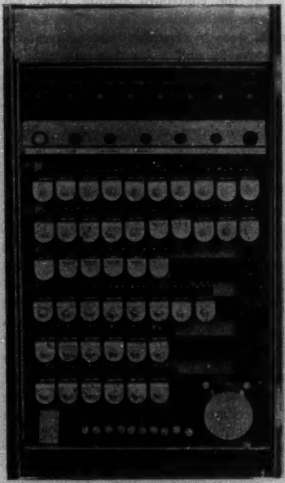

Figure 3 (A). Controlling station end of 2-signal model

When several units are to be controlled or several telemetered readings taken, it is not necessary to step through all of the units for each selection to be made. The selection keys of all of the desired units may be operated one after another. When this is done the equipment will step as far as the unit associated with the first selection key. Then, when this key is restored the equipment will only step to the next unit for which the selection key had been operated. This arrangement is particularly advantageous when there are a number of telemetered readings which must be checked at frequent intervals, since a large number of readings can be obtained very rapidly.

Whenever any supervised device changes position automatically at the controlled station, all points are stepped through with the lamp indications being changed for the unit or units which changed position. If any supervised unit changes position after it has been stepped past, the equipment immediately steps through all of the points a second time as soon as the first cycle of stepping has been completed. Thus, no changes of indication will be missed.

Approximately ten points are stepped through in a second. Thus, if fifty circuit breakers are controlled and supervised, the position of all of the circuit breakers can be checked in five seconds.

Figure 3 shows the controlling and controlled station equipment of a model of this new supervisory control system which is being used in microwave operation on the property of the Pennsylvania Electric Company. This model is designed for the control and supervision of six circuit breakers and two selective telemetered indications.

Detailed Description of Operation

To describe the operation of this new system, partial schematic diagrams only showing the particular elements involved in the operation being described are presented. Only those circuits necessary to obtain an understanding of the circuit arrangements which can be used to provide for operation on the principle of operation described previously are presented.

On the diagrams to be described, only those coil circuits are shown which were deemed necessary. In some cases only the contacts of relays are shown. For such cases, the time at which the coils of these relays would be energized and de-energized is described.

Following is a description of the elements shown on the partial schematic diagrams of Figures 4 to 10 inclusive:

	Contact of relay which closes when relay is energized or operated.
	Contact of relay which is closed when relay is de-energized or released.
	Fast type telephone relay.
	Telephone relay with copper sleeve around core to delay release when it is de-energized.
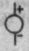	Polarized telephone type relay.
	One coil of two coil telephone relay. Relay will operate when either coil is energized.
	Resistor.

CHANNEL ELEMENTS

Figure 4 indicates how signals are applied and received on the basis of positive and negative d-c pulses being used for signaling. It will be noted from this figure that a single polarized relay (LR) is connected to the line wires at both the controlling and controlled stations through break contacts of all of the relays which can apply potential to the line wires.

Figure 5 indicates how signals are ap-

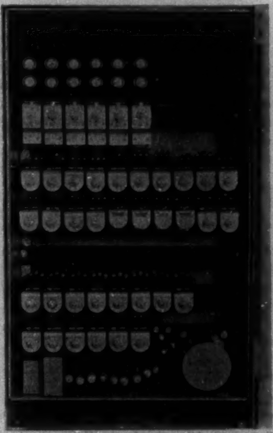

Figure 3 (B). Controlled station end of 2-signal model

plied and received on the basis of two different frequencies being used for signaling, instead of positive and negative d-c pulses with the same two frequencies being used from each station. This necessitates the use of break contacts of the signaling relays in the receiver relay circuits. If two different frequencies are used from each station these break contacts are not required.

With reference to both Figures 4 and 5, the relay contacts shown in the signaling circuit at the controlling station are operated to transmit signals as indicated below:

Relay 1—Transmits odd stepping pulses to controlled station and steps odd point relays at controlling station.

Relay 2—Transmits even stepping pulses to controlled station and steps even point relays at controlling station.

Relay 3—Transmits starting pulse.

Relay 4—Transmits operation control pulses. ("Trip" and "close" pulses in the case of circuit breakers.)

At the controlled station, relay 1 operates after each step to send the supervision pulse. Relay 1 also operates to transmit the alarm signal. Relay 2 determines which of the two supervision pulses is transmitted. In the description which follows, these will concern the indication of circuit breaker positions and will be referred to as "close" and "trip" supervision pulses. When relay 2 is energized a close supervision pulse is transmitted and when relay 2 is de-energized a trip supervision pulse is transmitted.

STEPPING CIRCUIT

Figure 6 shows the essentials for stepping at the controlling station. Figure 7 shows the essentials for stepping at the controlled station. The stepping pulses are all transmitted from the controlling station.

With reference to Figure 6, the relays shown which were not mentioned previously, perform the following functions at the controlling station:

Relay 5—Energized when stepping stops and a point is selected.

Relay 6—Energized to start stepping pulses and released at end of first step.

Relay 7—Operates from contact LR1 on receipt of "close" supervision.

Relay 8—Operates in series with odd-numbered point selection relays.

Relay 10—Operates in series with even-numbered point selection relay

Relays A1, A2, and so forth—Point selection relays.

With reference to Figure 7, the relays shown which were not mentioned, previously, perform the following functions at the controlled station:

Relay 3—Energized by starting pulse which precedes stepping pulses and remains energized until stepping pulses from controlling station stop.

Relay 4—Operates in series with odd-numbered point selection relays.

Relay 5—Operates in series with even-numbered point selection relays.

Relay 6—Operated by starting pulse which precedes stepping pulses. Releases at end of first stepping pulse.

Relays F1, F2, and so forth—Point selection relays.

Relays G1, G2, and so forth—Point indication relays. Each *G* relay is operated if the associated circuit breaker is closed.

Stepping is started from the controlling station as a result of operation of a point selection key, operation of the reset key or receipt of an alarm signal from the controlled station resulting from the automatic operation of a supervised device.

To start the stepping, relay 6 is energized at the controlling station. A contact of relay 6 completes a circuit for energizing relay 1. Contacts of relay 1 transmit the first stepping pulse to the controlled station as shown in Figures 4 and 5. Another contact of relay 1 energizes A1 and 9 in series at the controlling station. When relay 9 is thus energized it opens the energizing circuit of relay 1. When relay 1 releases it removes the first stepping pulse from the channel and opens the energizing circuit for relays A1 and 9. However, these two relays remain energized through a make contact of relay A1 and break contacts of relays 2 and 10 in parallel. The controlling station then waits for the first supervision pulse from the controlled station. It is to be noted that relay 6 releases at the controlling station after the first stepping pulse is transmitted.

When the first stepping pulse is received at the controlled station, relay LR is energized and contact LR1 closes. Relays F1 and 4 are energized then in series. When relay 4 is energized it completes a circuit to energize relay 2 providing relay G1 is energized as a result of the associated circuit breaker being closed. Assume that relay 2 is energized as a result of relay G1 being energized.

When the first stepping pulse is removed from the channel, contact LR1 opens at the controlled station, which results in relay 1 being energized in series with relays F1 and 4. When relay 1 is energized the supervision pulse is transmitted to the controlling station. Which of the two supervision signals is transmitted is dependent on whether or not relay 2 is energized at the time. The energizing of relay 1 releases relay 6, which allows relay F1 to remain energized but releases relays 1 and 4. The supervision pulse is removed from the channel when relay 1 releases.

Receipt of the close supervision pulse at the controlling station results in relay LR being energized, contact LR1 in turn energizing relay 7. The energizing of relay 7 results in the lamp indication on point number 1 being changed to red if it was not already red. The red and green position indicating lamp circuits will be discussed later.

When the supervision pulse is removed from the channel, relay 2 is energized in series with relay 7. Contacts of relay 2 transmit the second stepping pulse to the controlled station. Another contact of relay 2 energizes relays A2 and 10 in series. At the controlling station, when relay 10 is thus energized it de-energizes relays A1 and 9 and also opens the energizing circuit of relay 2. When relay 2 releases it removes the second stepping pulse from the channel and opens the energizing circuit for relays A2 and 10. However, these two relays remain energized through a make contact of relay A2 and break contacts of relays 1 and 9 in parallel. The controlling station then waits for the second supervision pulse from the controlled station.

At the controlled station, relay LR is energized and contact LR2 closes when the second stepping pulse is received. Relays F2 and 5 are then energized in series. When relay 5 is energized it completes a circuit to energize relay 2 providing relay G2 is energized as a result of the associated circuit breaker being closed. Assume that relay G2 is not energized, thus leaving relay 2 de-energized.

When the second stepping pulse is removed from the channel, contact LR2 opens at the controlled station, which results in relay 1 being energized in series with relays F2 and 5. When relay 1 is energized, the second supervision pulse is transmitted to the controlling station. The energizing of relay 1 also releases relay F1. When relay F1 releases, relays 1 and 5 are de-energized but relay F2 remains energized.

Receipt of the trip supervision pulse at the controlling station results in relay LR being energized, contact LR2 then energizing relay 8. The energizing of relay 8 results in the lamp indication on point number 2 being changed to green if it was not already green.

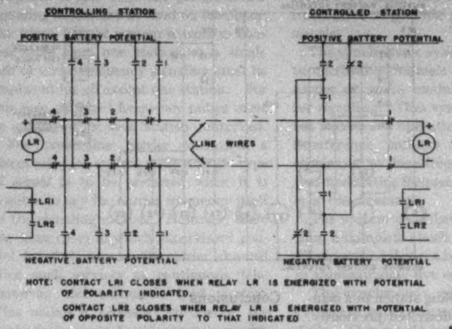
CONTROLLING STATION
CONTROLLED STATION
POSITIVE BATTERY POTENTIAL
NEGATIVE BATTERY POTENTIAL
LINE WIRES
LR
LR1
LR2
NOTE: CONTACT LR1 CLOSES WHEN RELAY LR IS ENERGIZED WITH POTENTIAL OF POLARITY INDICATED.
CONTACT LR2 CLOSES WHEN RELAY LR IS ENERGIZED WITH POTENTIAL OF OPPOSITE POLARITY TO THAT INDICATED

Figure 4. Diagram of essential transmitting and receiving elements using d-c pulses for signaling

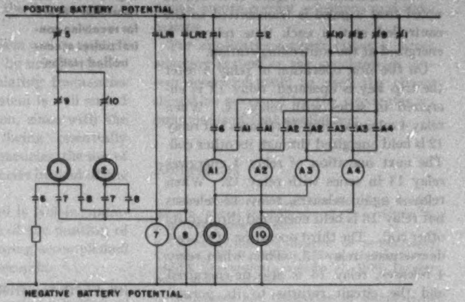
POSITIVE BATTERY POTENTIAL
NEGATIVE BATTERY POTENTIAL
LR1
LR2
A1
A2
A3
A4

Figure 6. Fundamental circuits for controlling station stepping and supervision

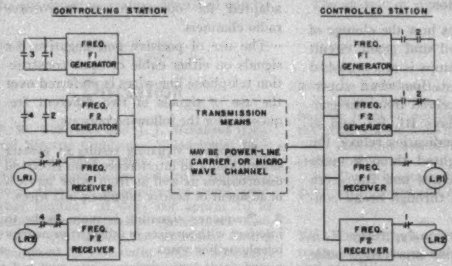
CONTROLLING STATION
CONTROLLED STATION
FREQ. F1 GENERATOR
FREQ. F2 GENERATOR
FREQ. F1 RECEIVER
FREQ. F2 RECEIVER
TRANSMISSION MEANS
MAY BE POWER-LINE CARRIER, OR MICRO-WAVE CHANNEL
LR1
LR2

Figure 5. Diagram of essential transmitting and receiving elements using two different frequency pulses for signaling

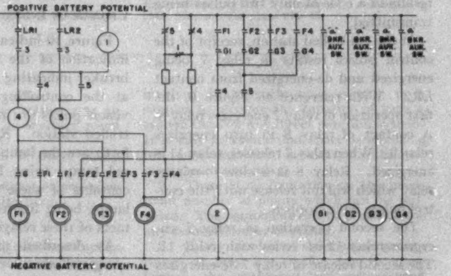
POSITIVE BATTERY POTENTIAL
NEGATIVE BATTERY POTENTIAL
LR1
LR2
F1
F2
F3
F4
G1
G2
G3
G4
BKR. AUX. SW.

Figure 7. Fundamental circuits for controlled station stepping and supervision

When the supervision pulse is removed from the channel, relay 1 is energized in series with relay 8. Contacts of relay 1 transmit the third stepping pulse to the controlled station.

In a similar manner, stepping is continued through all of the points. If the stepping is started by the operation of a selection key, relay 5 is energized when the A relay associated with the selection key operated is energized. Thus, the stepping stops with the proper A relay energized at the controlling station and the proper F relay energized at the controlled station.

If the stepping is started from an alarm signal or the reset key, the stepping continues through all of the points.

Control Sending and Receiving

Figure 8 shows the essentials for transmitting the control pulses. After a unit has been selected by operation of a selection key, the desired control code is initiated at the controlling station by operation of the close key or the trip key. The close code consists of two pulses and and trip code consists of three pulses. Figure 9 shows the essentials for receiving the control pulses at the controlled station.

With reference to Figure 8, the relays indicated which were not mentioned previously, perform the following functions at the controlling station:

Relays 11, 12 and 13—Control counting chain relays. Count trip and close pulses.

Relay 14—Operates in conjunction with relay 4 to transmit control pulses.

With reference to Figure 9, the relays which were not mentioned previously perform the following functions at the controlled station:

Relay 7—Operates from contact LR2 on receipt of control pulses. Energizing circuit not completed until after point selection.

Relay 8—Slow-to-release relay associated with control counting chain. Remains energized during receipt of trip or close pulses and releases when pulsing stops.

Relay 9—Slow-to-release relay which maintains control circuit closed long enough to allow circuit breaker to operate.

Relays 11, 12, and 13—Control counting chain relays. Count trip and close pulses.

Relays C1, C2, and so forth—Close interposing relays which complete circuits to circuit breaker closing relays.

Relays T1, T2, and so forth—Trip interposing relays which complete circuits to circuit breaker trip coils.

If the trip key is operated at the controlling station after a point is selected, relay 11 is energized. Relay 4 is then energized through a make contact of relay 11 and relay 4 in turn energizes relay 14. A break contact of relay 14 then opens the coil circuit of relay 4. Relays 4 and 14 then continue to operate each other as long as any of the relays 11, 12, or 13 are energized.

With reference to Figure 4, it will be noted that a pulse is transmitted to the controlled station each time relay 4 is energized at the controlling station.

On the first operation of relay 4 after the trip key is operated, relay 12 is energized in series with relay 11. When relay 4 releases, relay 11 releases but relay 12 is held energized through its other coil. The next operation of relay 4 energizes relay 13 in series with relay 12. When relay 4 again releases, relay 12 releases but relay 13 is held energized through its other coil. The third operation of relay 4 de-energizes relay 13. Then when relay 4 releases, relay 14 is also de-energized and the circuit returns to its normal position.

The operation is similar when the close key is operated except that relay 12 is energized rather than relay 11. This results in a code of only two pulses being transmitted.

At the controlled station, receipt of the control pulses results in relay 7 being energized and de-energized from contact LR2. With reference to Figure 9, the first operation of relay 7 energizes relay 8. A contact of relay 8 in turn energizes relay 9. When relay 7 releases, relay 11 is energized. Relay 8 is a slow-to-release relay which will not release until the control pulses have stopped.

The second operation of relay 7 energizes relay 12 in series with relay 11. The second release of relay 7 de-energizes relay 11 but relay 12 is held energized through its other coil. Similarly, on the third control pulse relay 13 is energized in series with relay 12 and relay 12 is de-energized when relay 7 again releases.

When the pulsing stops relay 8 releases, completing a circuit to the T or the C relay of the point previously selected depending on whether relay 12 or 13 is energized. Relay 12 or 13 releases when slow-to-release relay 9 releases.

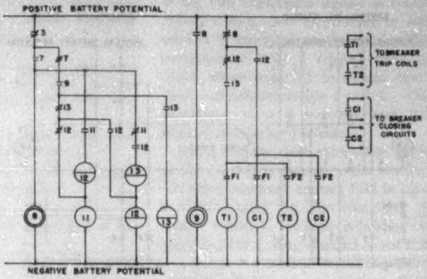
POSITIVE BATTERY POTENTIAL
NEGATIVE BATTERY POTENTIAL
3
7
9
13
12
11
8
T1
T2
C1
C2
F1
F2
TO BREAKER TRIP COILS
TO BREAKER CLOSING CIRCUITS

Figure 9. Fundamental circuits for receiving control pulses at controlled station

The supervision pulse is then transmitted to the controlling station in a manner similar to that described previously. The circuits for transmitting the supervision pulse at the end of a control operation are not shown.

Change of Indication

Figure 10 indicates how the change of indication of the red and green circuit breaker indicating lamps is accomplished at the controlling station when supervision pulses are received from the controlled station. Relays B1, B2, and so forth are the lamp indication relays, the red lamps being lighted through make contacts of these relays and the green lamps being lighted through break contacts of these relays.

As described previously, relay 7 is energized when a close supervision pulse is received and relay 8 is energized when a trip supervision pulse is received. The B relays are connected to make contacts of relays 7 and 8 through contacts of the associated A point selection relays as shown in Figure 10. The contact of relay 7 completes a circuit to energize the particular B relay. When a B relay is thus energized it seals itself in through a resistor. The contact of relay 8 shunts the particular B relay and causes it to release.

Conclusions

The 2-signal synchronous supervisory control system described is well adapted for the control of any size single station on telephone line wires and also is well adapted for operation on microwave radio channels.

The use of positive and negative d-c signals on either cable or open construction telephone line wires is preferred over the use of signals of two different frequencies for the following reasons.

1. Frequency signaling results in greater susceptibility to interference from electrical disturbances as well as from other services in adjacent or nearby telephone line wires.

2. Frequency signaling is more likely to interfere with services in adjacent or nearby telephone line wires

3. Frequency signaling necessitates the use of expendable parts such as tubes.

4. For operation over long distances of cable wires, repeaters may be necessary with frequency signaling. D-c signaling has been employed over cable wire lengths in excess of 100 miles.

It is to be noted that open construction telephone line wires can be adequately protected for d-c signaling.[3]

The fact that positive and negative pulses can be employed in the system

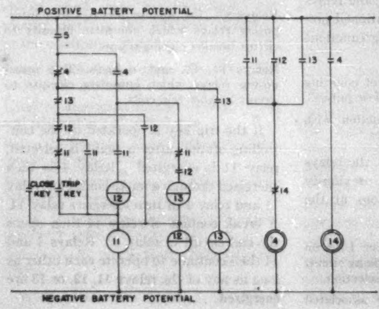

Figure 8 (left). Fundamental circuits for transmitting control pulses from controlling station

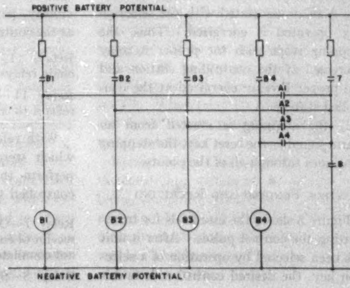

Figure 10 (right). Position indicating relay circuits at controlled station described means that the preferred d-c signaling means can be used on telephone line wires. If the system is used to control more than one station on a single pair of wires, frequency signaling must be employed for all except one station. For this case, different frequency pulses must be employed for each station controlled.

For power-line carrier operation, a direct selection system using a single type of signal is to be preferred when it is feasible to key the carrier frequency itself as the signaling means.[4] However, there are some cases in which supervisory control must share a single carrier channel with such services as continuous telemetering and automatic load control. This makes it necessary to operate the supervisory control equipment on modulating audio frequencies regardless of the signal requirements of the supervisory control equipment. For such applications the synchronous system described can be applied by using two modulating audiofrequencies to provide the two necessary signals.

The synchronous system can be applied to microwave channels by using two subcarrier or audio modulating frequencies for signaling. This system is well suited for microwave operation, since with the interference problem being essentially eliminated at these frequencies, the use of two modulating frequencies instead of one is no disadvantage.

The system described is fast in operation, a complete check of the position of 50 supervised devices being accomplished in approximately five seconds.

The synchronous system provides for extremely rapid consecutive selection of units. This is a desirable feature when a number of selective telemetered indications must be checked at frequent intervals.

The system of signaling and the check and guard features incorporated in the design assure correct selections and indications.

For applications where either a direct selection system or the synchronous system described could be used, the choice should be governed by the particular requirements of that application.

References

1. Viscode Supervisory Control, **L. J. Cissna.** *Electric Journal* (East Pittsburgh, Pa.), volume 28, July 1931, pages 424–30.

2. A Self-Checking System of Supervisory Control, **M. E. Reagan.** *Electrical Engineering* (*AIEE Transactions*), volume 57, 1938, October Section, pages 600–605.

3. Channels for Operation of Supervisory Control Equipment, **W. A. Derr, M. J. Brown.** *AIEE Transactions*, volume 67, 1948, pages 1654–60.

4. The Combination of Supervisory Control with Other Functions on Power-Line Carrier Channels, **R. C. Cheek, W. A. Derr.** *Electrical Engineering* (*AIEE Transactions*), volume 64, 1945, May section, pages 241–46.

Discussion

P. W. Schirmer and **J. J. Winsness** (General Electric Company, Philadelphia, Pa.): The supervisory system described in this paper has some design and circuit simplifications. However, its application seems somewhat limited. It does not appear to be suitable for multistation application. Also, if used with carrier the additional cost of equipment for two audio tones is necessary. It has been our experience that there have been objections to the use of locking pull key for selection, because if the operator neglects to reset the key after completing an operation, the equipment remains tied up to the selected point and cannot transmit changes of indication from the remote to the control station.

In addition to these comments, there are certain questions, the answers to which are not clearly brought out in the paper. These are as follows:

1. What would be involved in expanding an equipment with a given number of points to one with a greater number of points after installation?
2. What is the maximum number of points available in a standard equipment and in what steps or groupings can these points be furnished?
3. What happens if one station gets an impulse from an outside interference when the other station does not?
4. Are unit assemblies of relays easily removable?
5. Can telemetering be put on the same point with control and indication?

W. A. Derr: The following comments apply to the discussion submitted by Mr. Schirmer and Mr. Winsness.

The types of applications for which this new system is most suitable are outlined in the conclusion of the paper. As stated in the seventh paragraph of the paper, the new system is not suitable for multistation applications.

Both locking-type pull keys and spring-return push keys have been used on supervisory control systems. Which type is preferable is a matter of personal opinion. The system as described in the paper is based on the use of pull-type keys. However, push-type keys could be used with a small additional amount of equipment.

The following answers apply to the numbered questions of the discussion submitted by Mr. Schirmer and Mr. Winsness.

1. Since no individual selection codes are involved in a synchronous system, it is simpler to increase the capacity of such a system than for any direct selection system. It is only necessary that space be available for mounting the necessary additional escutcheons and relays.
2. There is no limitation on the maximum number of points which can be provided. The equipment can be provided for any desired number of points.
3. If any number of short pulses are received at only one station due to interference, the equipment will not respond since long pulses are involved in starting the equipment. If a long pulse of the proper signal is received due to interference, the equipment will master check. Interference will not result in selection of an individual point.
4. The method of relay assembly is a construction feature. The paper has presented the principles and operation details of a new system and has not discussed construction features. However, this new system is as readily adaptable to various types of assembly and relay groupings as any other all-relay system.
5. Telemetering can be provided on the same point with control and indication with the new synchronous system just as can be done with direct selection systems.

Power Line Carrier for Relaying and Joint Usage—Part I

G. W. HAMPE
MEMBER AIEE

B. WADE STORER
ASSOCIATE AIEE

THIS is offered as the first of a pair of papers which are intended to summarize a number of principles and ideas that are in line with standard practices in carrier and related fields, to emphasize points of uncertainty and controversy, and to explore a number of ideas, both new and old, that are not necessarily standard, but do not deviate widely from what is, or potentially could be, done with existing equipment.

The second part of this paper will deal with these potentialities, and will show that more efficient use may be made of modern power line carrier channels, resulting in substantial economies and in conservation of the carrier frequency spectrum.

Need for Evolution in Carrier Usage

As the title indicates, the point of view is that relaying is a primary carrier function, even though the emphasis on specialized forms of relaying, singly and in combination with other specific functions, is reserved for the second paper under the same title. There are several reasons why carrier relaying is useful in place of, or in addition to, other relay schemes. Until recently, the principal one has been that any system of speedy and reasonably adaptable relaying for *ground* faults has been a pilot scheme, whether by wire, power line carrier, or (quite recently) by space radio. If the recently-developed ground distance relays prove effective[1] they will probably be adapted to work with carrier, resulting in decreased complexity and greater reliability in the control of carrier for ground fault relaying on those systems where the neutrals are essentially solidly grounded. Not all systems are of this type, and even on such systems faults-to-ground range from severe to quite limited, hence other means, perhaps electronic,[2] for simplified carrier control also would be desirable. Statements that limited faults to ground do not need quick clearing are to be discounted for the following reasons:

1. An extended fault arc frequently involves another phase conductor, and occasionally another line.
2. If longitudinal motion of the arc is limited by ice, a static (ground) wire, or even a conductor, may be burned in two.
3. If a static wire has its steel core exposed by an arc, and the burn is not located and repaired, corrosion will cause eventual breakage, probably under ice loading. This danger, which is greater for some types of static wire than others, also may apply to line conductors to some extent.

The newer factors which make it necessary that carrier relaying continue to evolve are immediate automatic reclosing, and the multiterminal line.[3] Economic pressure is forcing power system designers to adopt these, sometimes both on the same line, and means of efficient relaying must be found. The writers predict that such relaying will involve pilot channels, many with carrier as a pilot medium, and that some of them will involve hybrid combinations of relaying principles such as are to be set forth in the second paper.

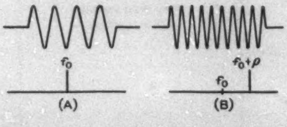

Figure 1. (A) Unmodulated carrier which might be keyed on and off. (B) A side frequency of a suppressed carrier, resulting from a single tone modulation (s-s-b)

(B) Also could be set up by a keyed frequency shift (n-b-f-s)

Joint Usage Considerations

Power line carrier is used widely for services other than relaying, and most carrier relay schemes have certain provisions for limited nonrelaying usages. This paper will point out that these limited provisions lead to inefficient use of carrier energy and spectrum space, and have some hazards which are not recognized by all users. It would therefore seem desirable to examine the joint usage problem.

At present, with separate usages, economic compromise usually results in a communication channel which is not reliable when needed most, as in bad weather. At the same time, high grade equipment is used on relatively short distances to provide relaying channels which are in active use only a few seconds a year, while the nonrelaying usages tend to be frequent or continuous. (The economics of joint usage tend to become increasingly obvious as the number of needed functions increases.) These conditions point toward joint usage of carrier channels and equipment.

Carrier channels and equipment can be shared in varying degrees. Thus two or more functions, such as relaying and voice communication, might be combined, all utilizing the same frequencies and the same carrier receivers, transmitters, and so forth. These same functions might be combined by utilizing jointly the same "yard" equipment such as traps, coupling and tuning units, but using separate electronic equipment all on the same or separate carrier frequencies. Arrangements of the latter type would possibly

---

Paper 49-151, recommended by the AIEE Carrier Current Committee and approved by the AIEE Technical Program Committee for presentation at the AIEE Summer General Meeting, Swampscott, Mass., June 20–24, 1949. Manuscript submitted March 21, 1949; made available for printing April 28, 1949.

G. W. HAMPE is with the Relay Settings Section, and B. WADE STORER is with the Electronics and Communications Division, both with the Commonwealth Edison Company, Chicago, Ill.

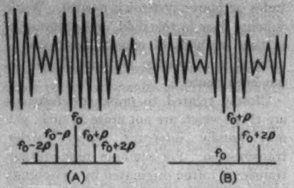

Figure 2. (A) Two methods of representing a carrier, amplitude modulated by two tones of frequency ρ and 2ρ are shown. (B) The modulation components remaining when the carrier and one side band have been suppressed are indicated

overcome special problems that sometimes arise, as in servicing equipment for unlike functions.

In general, every carrier application presents somewhat different requirements, and one form of joint usage or choice of apparatus is not necessarily the best solution to all problems. Hence it is necessary to study the various forms of carrier signals available, as to their particular advantages and limitations.

Carrier Channel Building Blocks

Carrier signals may be classified as to types of signal control or modulation or, the combination of the two. The direct form of control is that of keying the carrier frequency itself after the manner of a telegraph signal. Putting a carrier on (Figure 1) or taking it off, or both, is common in relaying practice. Keying, shifting a frequency, and coding the impulses produced by such controls also can be applied to carrier modulations. Descriptions of methods of transmitting modulated signals are given in subsequent paragraphs.

Carrier signals may be modulated in amplitude (a-m) after the pattern of the original form of broadcast radio. That is, the carrier frequency cycles may be compressed or enlarged in magnitude inside the envelope determined by the modulating frequency or set of modulating frequencies, Figure 2. The modulating frequencies are usually audio tones, that is, in or near the frequencies of audible sound. Such a signal at the receiving end is put through the process of detection, which is essentially rectification. This eliminates the carrier frequency, and the modulating (audio) frequency is reconstituted.

The modulating frequency also may be used to advance or retard the carrier waves in time phase. This is called phase modulation (p-m) as a general term. Since the changes of phase also are instantaneous changes of frequency, one form of phase modulation has been designated as frequency modulation (f-m). A frequency modulated signal when received is converted by a discriminator back to the original modulating signal.

When a carrier signal is modulated it tends to be spread over an appreciable portion of the carrier spectrum. This is true for all forms of modulation, not merely for f-m where it is obvious. (One special exception is indicated in Figure 1.) The resultant signal can be analyzed into the components which are the unmodulated carrier, and side frequencies, which, if modulation is done by a complex of frequencies, become side bands. The manner in which side bands originate can be found in several recent references.[4,5]

It can be seen that if carrier is modulated, the modulation as contained in at least one side band is essential. There are two variations of a-m which are intended to accentuate side-band energy. One involves the transmitter only, and is known as the Taylor[6] or "supermodulation" principle. In this system radio frequency power is supplied to the output circuit during the positive half of the modulation cycle by an auxiliary audio-pulse controlled power amplifier tube. Greater over-all efficiency with compressed carrier and emphasized side-band operation is claimed. In the second, one side band and the carrier are suppressed in the low energy stages of the transmitter, so that the entire transmitted energy is concentrated in one side band.[6] In the nomenclature of this and the sequel paper, the abbreviation s-s-b (single side band) indicates the suppression of both one side band and the carrier. For s-s-b the carrier must be reintroduced at the receiver as part of the process of detection.

For s-s-b, if a single modulating frequency is used, a single-side frequency is transmitted. The result, in wave form and frequency, is the same as if the carrier had been given a keyed shift, Figure 1. In Figure 2 complex modulation by two tones is shown for double side-band a-m, and the same with one side band and carrier suppressed as in s-s-b.

The modulating frequencies as well as the carrier itself can be keyed on and off. For f-m and a-m, the termination of all modulation restores unmodulated carrier. For s-s-b it terminates transmission.

A fourth carrier channel building block is equipment which operates on the narrow band frequency shift (n-b-f-s) principle. Here, instead of a modulation or an on-off keying, the carrier undergoes a keyed frequency shift. The frequency shift transmitter operates on such a narrow band that a number of such channels, each with its own transmitter and receiver, can be operated on line tuning and coupling equipment and traps which are tuned for one conventional broad-band carrier frequency.[7] The frequency shift is small, on the order of 60 cycles (on carrier of 100 kc). The receiver includes crystal filters and a discriminator, (f-m type, see Figure 3) and offers high selectivity with respect to spurious signals. It is stated in the foregoing reference that the spacing between these narrow channels, with frequencies stabilized by crystals need be only 0.5 per cent of the average carrier frequency. This applies to channels with the same direction of transmission. For transmission versus reception at the some terminal, the spacing required is stated to be approximately 5 per cent. Such transmission is useless for voice, but for other services, including some forms of relaying, it offers an alternative to audio tones superimposed on carrier.

Any of the foregoing principles may be used to transmit pulsed signals which may vary in frequency (pulsing rate), or which may be coded, that is, varied in amplitude, duration, spacing, or combinations of the foregoing to form code signals. Such pulses, pulsing rates, and pulse codes may be used for telemetering, supervisory control, and load control. All the forms of transmission are not equally adaptable to all uses, as the pulses may approach too closely to modulating frequencies, or be too rapid for the transitions required between states. As a rule, the narrower the spectrum in which the transmitted energy is confined, the more sluggish it is in changing states. This is a consequence of the energy stored and released by the filter elements. Given

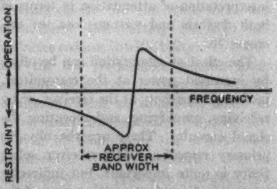

Figure 3. Characteristic of a discriminator (essentially an f-m type) as used for n-b-f-s signal reception

enough spectrum space, as in short-wave radio, even voice can be changed to coded pulses, transmitted as such, and changed back to voice[8,9] sounds. On a much slower basis similar principles might be used in the carrier field.

Carrier Channel Limitations

ATTENUATIONS

The energy impressed on a carrier transmission link is dissipated in various ways, so that the power at the receiving end is considerably less than at the sending end. This loss of energy or decrease of power is called attenuation. If there are irregularities of structure along the conductor paths, the response throughout the frequency spectrum may be quite irregular, limiting the choice of suitable frequencies. Sections of underground cable may have very high attenuation at all frequencies, but this varies considerably with the type of construction. For some types the means of bonding sheath sections is a critical factor. A paper on carrier attentuation measurements was recently presented.[10]

On some lines, particularly those with irregular frequency response, switching conditions may cause wide variations in attenuation. This indicates that in some cases terminal equipment beyond the line section has considerable bearing on carrier transmission—a factor which will be reconsidered in regard to the application of traps. If the extraneous influences are coupled to the line by other wires on the same right-of-way, the choice of a suitable frequency to meet all contingencies may involve a considerable number of test measurements.

Bad weather conditions, such as ice formation, greatly increase attenuation at a time when good relaying and communication are at a premium. Dirty insulators combined with fog, rain, or ice also may cause increased attenuation. The attenuation, as a function of the ratio of transmitted to received power, is expressed usually in decibels.[21] For an interpretation of attenuation in terms of both decibels and wattage loss, see reference 10.

The effect of attenuation can be offset by increased power at the transmitter, increased sensitivity at the receiver, or by receiving, amplifying, and repeating the signal enroute. These are the obvious primary remedies. The receiver selectivity is quite important, but indirectly so, as it is dependent on the nature of the desired signal. This is discussed in detail later. The amount of attenuation can be reduced by other means, such as changing the route of transmission, the frequency of the carrier, the form of coupling, and so forth.

For voice transmission over longer distances, the joint usage of relay channels may be made practical by the use of audio by-passes at intermediate switching stations. Audio by-passes introduce distortion, however, so that the number of links that can be thus placed in tandem is limited. Such by-passes, by reception and repeated transmission into the succeeding line section, make the amplification of the nonrelaying (communication) signals possible. This large gain in signal strength makes practical transmission over much greater distances. Such by-passes are essentially independent of switching conditions, probably to a greater degree than conventional by-passes on yard equipment, and further permit passing the through-type communication signal on to a succeeding carrier relay channel.

SIGNAL VERSUS INTERFERENCES

The principal limitation on receiver sensitivity is that type of interference known generally as noise. Noise, which for present purposes is not defined as being limited to audible range, may be fairly constant for appreciable time intervals (that due to corona for example), or may come in random pulses, or be tied in, more or less predictably, with reproducible phenomena on the line or in its proximity. In interpreting the effects of noise, it is often combined with signal strength values and referred to as the signal-noise ratio. Some functions can tolerate a lower signal noise ratio than others. Although the transmitters and receivers for communication and conventional relay carrier are similar, the communication receiver can usually be adapted to work through a greater attenuation than the relay signal, hence the latter channel must be limited in attenuation or bolstered to meet relay standards. Under average conditions this is logical, as signals too weak or too noise-ridden for relaying may be quite intelligible to experienced personnel. In bad weather when communication is at a premium, the weak and noisy signals become worse, which may be unfair to those depending on them under those conditions. The signal-noise ratio can fall off due to increased attenuation, increased noise, or both, and during bad weather conditions both limiting factors usually become worse, and a simple listening test is not a very reliable indication as to which effect predominates. Greater knowledge of signal-to-noise ratios, and of noise amplitudes on power systems is needed. Work is being done in this field, and progress in getting methods of measurement standardized into readily comparable forms has been made.[11]

Closely related to noise interferences are those which are not noise as such, yet may totally interrupt proper carrier transmission. For example, high-voltage transients (often originated by switching) may flashover safety devices on the carrier apparatus. Interference also may take the form of spurious signals which are essentially indistinguishable from the functional ones. Total signal suppression and spurious signals may result from the same or similar causes.

This brings up a very interesting and important observation. One would expect that fault arcs might set up spurious signals. This they probably do, but experience and staged fault tests indicate that sufficient spurious signal to interfere with relaying is quite rare.

Circuit breaker arcs have been observed to cause considerable interference, and the question arises as to whether automatic circuit breaker operations on one line can suppress (or falsely initiate) signals on an adjacent line. Further evidence on this point should be gathered. One manufacturer has provided relay circuit controls for over-riding a transient of this type. Experience indicates that the most pronounced interferences, both as to suppression of signal and spurious signal, result from low-power arcs in circuit breakers and on disconnect switches in, and adjacent to, carrier terminals.

Signal transmission may be interrupted by short circuits or open circuits on the transmission line. Just what constitutes an effective short circuit or open circuit is questionable, however, where carrier is concerned. The deliberate use of alternate paths has been proposed.[12]

AVAILABILITY OF CHANNEL SPACE

Another class of interferences might be likened to the problem of cross-talk in the field of audio communication over metallic channels. In a given locality the carrier spectrum (bearing in mind that some frequencies may be found unusable because of excess attenuation) often rapidly becomes congested. Each power line is of course closely coupled to the other lines paralleling its path so that frequency separation is necessary. Interference with other line sections is limited by geographical distance and frequency separation, that is, by keeping adjacent frequencies at remote parts of the power system. In special cases, more expensive arrangements, such as trapping every phase of every line beyond a certain bus, may be found expedient. There also are interferences with respect to other power companies and other utilities outside the field of electric service.

It was mentioned before that receiver selectivity is an important factor in limiting interference from random noise. With regard to adjacent channel interference it is even more important. The narrower the acceptance band of the receiver, the less interference it will pick up, and, other things being equal, the closer it can be placed to its neighbors, both in geographical and spectrum space.[20] The acceptance band width will depend on the nature and content of the transmitted signal, and will in general tend to be at least somewhat wider than that covered by the signal. This is due in part to the need for some tolerance in regard to the stability of transmitting and receiving equipment, and partly due to the inherent nature of reception. For example, for some applications there is monofrequency transmission, but there is no way of providing reception that will accept only one frequency. Furthermore, an acceptance band whether narrow or wide, Figure 4, never has perfectly straight sides, hence signals of considerable frequency deviation will be received if they are strong enough. This puts a considerable handicap on close spectrum spacing of a receiver and transmitter at the same terminal.

The f-m discriminator used with the n-b-f-s receiver has a characteristic as shown in Figure 3. It offers a sharp and stabilized point in the frequency spectrum at which the carrier crosses over from restraint to operation and vice versa, hence the narrow band effect is accentuated. Noise covers a wide band, in general, hence cancels itself in the discriminator circuit. Adjacent channel interference may be limited considerably by crystal filters, but placing the n-b-f-s channel so that adjacent carrier tends to produce restraint may be an added factor of safety.

For a-m, f-m, or s-s-b a wide band tone receiver can be used to provide restraint if spurious signals are received. In one proposal[15] everything (so far as practical) outside the narrow band required for the desired signal is to be received and applied through appropriate circuits as a restraint.

Another principle in guarding against interference is to transmit a continuous nonoperating or restraint signal which must be removed or shifted before an operation can be transmitted. By automatic volume control action, such a restraint signal reduces the sensitivity of the receiver to noise and unwanted signals, in addition to whatever direct holding effect the signal provides. The objection is that a continuous transmission of carrier, or a tone modulation thereof, furnishes a constant source of possible interference. This applies both as to the fundamental transmitted frequency and possible harmonics. In some cases a constant source may be worse than an intermittent one as regards other channels. It is questionable whether this is really a valid objection, and data are needed to substantiate it. In other applications provision is made for reception of a restraint signal, but it is deliberately transmitted only when conditions become abnormal.

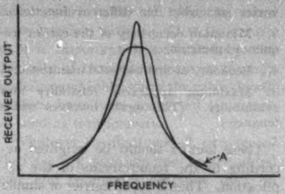

Figure 4. A typical acceptance band of a receiver

A signal impressed at A, if sufficiently strong, will cause interference

For any type of carrier transmission the acceptance band of the receiver should fit the transmitted signal fairly closely, but in trying to cover a variety of standard applications with a minimum variety of apparatus, this is not consistently followed. For example much relaying is done with a monofrequency, keyed carrier, but the receiver is wide band. This permits reception of the side bands which are added to the carrier when test or emergency communication is used, but the receiver also is wide open for noise and for interference from other signals. If a narrow-band receiver were used for relaying, transmitters of present wattage ratings would provide for operation through considerably increased attenuation ranges. If the transmitter wattage should be reduced to cover any but the most exceptional conditions, more relay channels could be fitted into a given spectrum space, both because of increased discrimination against unwanted signals, and the reduction in power of those signals.

For example, if there are four carrier relay channels between two terminals, test and emergency communication is hardly necessary for all of them. Similar logic applies where specific provision for communication has been made. Note that if the relay carrier receiver band can be narrowed only moderately, as for phase comparison relaying, the foregoing still applies, but to a reduced extent. Other considerations may outweigh the saving in spectrum space, and other adaptations, as offered in the second paper, may be more advantageous.

Carrier channels normally operate at frequencies between 50 and 150 kc, with the band between 150 and 300 kc being used mainly because of congestion in the lower band. The higher frequencies will tolerate a more rapid keying or pulsing rate, which is an advantage, but the carrier attenuation tends to be somewhat greater than for the lower band.

DISTORTION

Transmission also is limited by signal distortion, that is, by differences in quality of the input and received signal existing even in the absence of extraneous disturbance. When the signal is produced by keying carrier the transients of the apparatus, which determine the time required for the carrier to go from one steady state to another, are the principal distortion. The same type of distortion occurs when an audio tone is keyed. If an audio tone is keyed at a rate approaching its own frequency, distortion of signal naturally results.

Audio tones, including the voice frequencies, are subject to harmonic distortion, frequency distortion, phase distortion (usually not serious) and cross modulation. All of these forms tend to originate from, or be augmented by, the nonlinear characteristics of carrier apparatus. Such nonlinearities may be the result of imperfections or deliberate design. For example, a flat frequency characteristic from 200 to 3,000 cycles is considered necessary if voice is to be transmitted naturally and intelligibly. Cutting off the low end tends to reduce naturalness, but cutting the high frequencies reduces intelligibility. To transmit the low frequencies requires large amounts of energy, tending to overload equipment such as amplifiers, hence in some cases intelligibility may be improved by eliminating the lowest voice frequencies. This is particularly true on equipment not primarily designed for communication. It is a matter of general observation that test and emergency communication over carrier relay channels is usually better on the lines with weaker signals, as strong signals saturate the receiving apparatus.

Another cause of distortion is overmodulation. For amplitude modulation including single side band, this means the modulating tone or combination of tones is more than sufficient to bring the carrier wave down to zero amplitude. The "super-modulation" principle is an interesting attack on this problem.[6] For f-m transmission, over-modulation means a frequency shift beyond the channel width for which the equipment is designed. For any conventional type of modulation it is evident that elimination of portions of the low audio spectrum, which involve high energy levels, tends to prevent that form of distortion which results from overloading and overmodulation.

Cross modulation arises in various ways, but becomes a particular problem when part of the audio spectrum is set aside for tone signals, as for telephone ringing or for relaying. To avoid it, audio tones which exist simultaneously must not have frequencies which when added or subtracted will give rise to tones where they are not wanted, in the voice band for example. This becomes an interference problem.

Another source of distortion as well as loss of signal strength may be apparatus instability, that is, the tendency of the apparatus components to drift out of line with age or changing atmospheric conditions. This involves problems of detail design and maintenance.

Choice of Carrier Channel Building Blocks

At present, the available carrier channel building blocks are: (1) keyed carrier, (2) modulations transmitted by (a) conventional (a-m) (with "super-modulation" as a possible variation), (b) single side band, (c) frequency modulation, and (3) the narrow band frequency shift. Each has distinctive properties which should be considered for a given set of functions in a given installation. Combining functions in joint usage in varying degrees gives quite a variety of possible combinations, and it is quite possible that more than one building block can be used to an advantage.

The choice of building blocks should be guided according to the following factors:

1. Suitability for the desired function. (There are usually several means of obtaining the same result.)
2. Operating range sufficient to work through the maximum attenuation and interferences. (The pressure in this respect varies somewhat for different functions.)
3. Minimum occupancy of the carrier frequency spectrum.
4. Economy of first cost and maintenance.
5. Maximum apparatus reliability and availability. (This again involves maintenance.)

These factors should be weighted according to the requirements of the application. Thus if keyed carrier or simple a-m will suffice, that is what should be used. Unfortunately, particularly in regard to line characteristics, the necessary data are often lacking, so that an installation may prove to be inadequate in use, or may be made much more than adequate at excess cost, to allow for unknown factors. To avoid misapplications sufficient test data should be taken in advance.

SPECIAL PROPERTIES

Some special properties have already been discussed under the limiting factors of attenuation, noise, cross-talk, and distortion, but there are others which were not emphasized. Thus n-b-f-s can be used for telemetering, and so forth, and some kinds of relaying. It cannot be used for communication, but can be superposed on an a-m communication channel.[7] The s-s-b type of transmission makes possible a minimum acceptance band for voice. As an example of limited joint usage, n-b-f-s could share common yard equipment with s-s-b. The n-b-f-s channels can be placed in the spectrum space on either side of the s-s-b signal.

Conventional a-m and f-m occupy approximately twice the channel width of s-s-b. Where channel width is not a final determining factor, it should be pointed out that f-m transmission (with limiters to eliminate amplitude variations) provides an excellent automatic volume control characteristic that is quite advantageous.

There are many carrier applications where it is desired to accomplish a number of separate functions such as transferred tripping, load control, and so forth. These functions may be accomplished by either tone modulations of a-m, f-m, or s-s-b transmitters or by n-b-f-s transmissions, with possible pulse coding in any case for greater adaptability. A tone carries only a portion of the total energy of the modulated carrier, but it also picks up only a portion of the total interference suffered by that carrier, hence, within limits, tone signals are quite reliable. The greater the number of simultaneous tones, the more the total signal energy must be subdivided. With n-b-f-s channels there is a similar limitation. The greater the number of n-b-f-s channels using common yard equipment at a given terminal, and transmitting signals simultaneously in a given direction, the less the range of each.[7]

For reasons stated previously, the present-day relay practice of using a wide band carrier channel exclusively to transmit a simple on-off signal will in the future meet increasing resistance from economic considerations and spectrum crowding.

Terminal Equipment

Carrier transmitters and receivers are coupled to the power line by capacitors connected between one phase conductor and ground, or between two phase conductors of the same 3-phase circuit (interphase coupling) or between two conductors on different circuits (intercircuit coupling). The same equipment may be used jointly for separate channels on more than one type of coupling. For example, the coupling capacitors (and traps) of two conductors coupled to ground on two circuits with the same station destinations also may be used for intercircuit coupling by the addition of line tuning units for added frequencies.

One advantage of interphase, or better still, intercircuit coupling is that certain types of line work can be done without interrupting the channel. Also it is claimed that the channel can be balanced so as to minimize interference to and from it. The counterclaim is that this balance is too hard to maintain to have any practical value. For some types of relaying, phase-to-ground coupling is not considered acceptable as will be discussed in the second paper. The disadvantages of interphase or intercircuit coupling are greater cost (unless in combination as above) and increased coupling loss (attenuation). The coupling loss is generally a minor factor however.

By the introduction into the power line conductor of an inductance in parallel with a capacitor, a carrier frequency or a band of frequencies with a spread of up to about 12 per cent can be substantially prevented from passing a certain point in that conductor.[18] Such devices are called traps, and may be tuned to block more than one frequency band. Tuning one trap to resonate for more than two frequencies is considered highly impractical, however.

Carrier for relaying is usually blocked by a trap at the end from which a signal is to be transmitted, so that the signal is projected, initially at least, in only one direction. The trap can be omitted if some other device such as a power transformer serves the same purposes, or if 2-way projection is admissible. The principal purpose of trapping relay carrier is to prevent the transmission of carrier energy from being short circuited or seriously attenuated by a fault or switching condition exterior to the protected line at the transmitting terminal. If intercircuit coupling is so arranged that no fault or special system operating setup can reduce the carrier energy to an unsafe level, trapping may be omitted in some cases. Also, if a signal is only received at a terminal, trapping for that signal at that terminal may not be necessary. A trap that is tuned for one or two frequencies offers considerable impedance to other frequencies, particularly the adjacent ones in the spectrum. Often a dead short circuit beyond a protected line section would still leave sufficient signal transmission for satisfactory relaying because a trap that is not resonant to a certain frequency still offers considerable impedance. For relaying, this is not often trusted, however, because the off-resonance value of a trap is either inductive or capacitive, and there may be some condition beyond the line terminal which will reduce the effective value of that inductance or capacitance to practically zero. In particular cases, as when the trap is backed up by a piece of power apparatus that blocks all frequencies, operating more than one frequency on a single tuned trap may be just as efficient as double tuning, or when compared to coupling to additional phases, there may be considerable economy. Limited trapping should be considered for minimum cost installations on low-voltage lines.

The other functions of trapping are to decrease attenuation by largely confining signal energy to a given line section, and to decrease the cross-talk type of interference with other carrier channels. In some exceptional cases all three conductors of a line (sending or receiving or both) may be trapped, as the natural coupling between phase wires tends to put the signal on to conductors from which it can propagate into other sections. How effective this is depends on what other conductors are on the same right-of-way or adjacent to it (and for what distance), and how much is propagated over static wires.

Whether multiconductor trapping with phase-to-ground coupling decreases the effectiveness of transmission is at present disputed. It has been stated that the noncoupled conductors, in parallel with the earth and static wire, form part of the signal return path, and that the extra traps interfere with it. That the return path is important is evidenced by the difficulty of transmitting carrier through underground cable where the cable sheath sections have been connected by means of bonding transformers.

Whatever the final answer on some of the foregoing questions may be, the added care and equipment generally used on relay carrier channels, as compared to carrier channels for other services, becomes available to increase the reliability of those services under joint usage.

Performance Requirements

Power line carrier performance requirements may be classified into three groups according to functions, as relaying, communication, and miscellaneous services.

CARRIER RELAYING

Relaying by carrier requires a high degree of transmission reliability and availability. This means a good received signal even under adverse conditions and means of readily checking and maintaining the over-all carrier and relay performance. Other things being equal, carrier relay equipment which can be checked and maintained independently of the noncarrier relay elements (which may be either first line or back-up relay elements) is preferable. With respect to joint use of carrier relaying equipment for nonrelaying purposes, there are advantages and disadvantages. As most of the other services are constantly in use they automatically monitor the carrier equipment which otherwise functions only during system disturbances.

Maintenance of a jointly-used carrier channel may run into difficulties where separate groups of personnel, communication and relay sections of the same organization, for example, are both handling carrier transmission equipment. Fundamentally there is little difference in this equipment whether it be for relay carrier or communication carrier. Since power line carrier is a highly specialized field it would seem that the simplest solution to this maintenance problem would be to have a separate carrier section responsible for all types of carrier equipments. If such an arrangement cannot be worked out, the problem must be recognized, and the carrier equipment for joint use be laid out so that the functions may be separated satisfactorily. In some cases separation of the functions into separate cabinets is a satisfactory solution for maintenance under divided authority with joint usage.

CARRIER COMMUNICATION

Communication by carrier can be classified into three functional grades. The lowest is for testing and emergencies. The next is for operating, that is, switching orders, load dispatching, and possibly work dispatching. This calls for a high degree of reliability and availability, quite similar to that for relaying, but high voice quality (for example, personal voice recognition) is not so essential. It is surprising how much distortion and noise can be tolerated by experienced personnel. The highest grade is administrative communication, which in addition to high reliability and availability needs fairly good tone quality. Those who use the channels regularly will accept distortions which others will not. Good quality requires a band 2,500 to 3,000 cycles wide, hence uses a considerable slice of the carrier spectrum.

Communication also may be classified as point-to-point, push-to-talk, party-line, selective ringing, duplex, and so forth, which are not all equally suitable for the three functional grades mentioned before. Signaling (as by tones) is required for some of the above functions.

MISCELLANEOUS SERVICES

The miscellaneous services follow:

Glaze (ice) Detection. This is essentially a by-product of received signal strength measurements, but may justify equipment designed for the purpose.

Supervisory Control. This includes remote control of switching and remote indications of system conditions—usually on an on-off or alarm basis. It is accomplished usually by coded signals. High reliability is desirable, but the signals are merely keyed pulses.[19]

Automatic or Semiautomatic Load Control. This is similar to supervisory control, but reliability under adverse conditions is not at a high premium.

Telemetering. Next to voice and some forms of relaying this may be the hardest form of signal to transmit, but reliability requirements are much like those for load control.

A Fundamental Relay Control Problem with Joint Usage of a Single Signal

TYPES OF CARRIER RELAYING

There are at present three standard types of carrier relaying. These are:

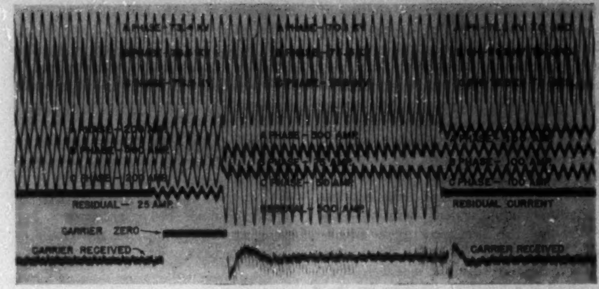

Figure 5. A record of a fault in which relay control of carrier was lost when the line opened at one end

(a) transferred tripping; (b) directional comparison; and (c) phase comparison.

Type (a) is usually used to protect terminal apparatus.[3] It is limited to special cases and is not often combined with types (b) and (c). A continuous carrier blocking tone is sometimes used to prevent false trip-outs. To date, the most important applications of (a) have been on two terminal lines, but multiterminal applications show promise.

In types (b) and (c) carrier signals are not normally transmitted continuously for relaying. Standard relay equipment provides for the use, or ready adaptation, of the carrier frequency for test and emergency communication and for keyed signal functions such as telemetering. One disadvantage in having relay carrier (or a tone) held on for relaying or any other purpose, such as signal strength tests, or measurements for sleet detection, is that on-off control of the signal by relay elements must be provided at both terminals when a fault occurs.[16]

If at a given terminal there is a firm source of fault current, present equipment is designed to accomplish this purpose. If there is no fault current source for a terminal, or if the path of that fault current is interrupted, there are no standard provisions for the relay elements to secure control. With the types (b) and (c) if a steady signal is transmitted (as under joint usage) from a terminal which does not supply fault current, carrier relaying at the terminal which does supply fault current is suspended.

The cases in which no effective fault current can flow from a given terminal are as follows:

1. No source of positive phase sequence current. The failure to open where there is no source is not generally serious, but the carrier restraint at the supply end may be objectionable. Generally noncarrier relays must function at the source terminal.

2. A feeble or transient positive sequence current source. If there is no immediate automatic reclosure, this may be viewed the same as (1), but with such reclosure, immediate opening at both ends may be required to prevent the feeble source, motor regeneration for example, from sustaining an arc which would cause retripping.

3. A positive sequence source, but no effective source of zero sequence current at a terminal. In this case a fault to ground (even though cleared from one end by noncarrier relays) may lead to continued abnormal voltage stresses, possibly augmented by an arcing ground at the point of fault.

4. The circuit breaker being initially open, or open pending automatic reclosure. During glaze storms lines may be open at one end for several minutes, and occasionally, to shift load to other lines for glaze prevention, single end excitation (called "holding a line alive on back feed") may extend to hours.

5. Sequential operations. Occasionally, because of system or fault conditions, a line opens quickly at one end only. The open end relays then have lost control of the carrier, and the remaining end is still to be opened, Figure 5.

6. A breakage of one or more phase conductors. This interrupts the path of the fault current from one terminal in many instances.

An Example of Loss of Relay Control

The oscillogram of Figure 5 shows an example of (5). Carrier had been placed on at the remote terminal for glaze detection and was received as shown on the oscillograph trace. A fault-to-ground occurred and the remote end circuit breaker opened promptly from the instantaneous (noncarrier) ground relay. For unexplained reasons the local end did not furnish enough ground current to actuate the carrier control relays. The received carrier ceased momentarily, but as soon as the remote circuit breaker opened the carrier stopping relay at that end reset and carrier was again transmitted from the remote terminal and received as shown. The local circuit breaker would have been opened by the ground backup relay, but meanwhile the arc extinguished of its own accord as shown by the neutral current trace. The local circuit breaker did not open.

The same difficulties can be encountered if carrier is transmitted from the no-source end for telemetering, communication, or even push-button tests. Inquiries have revealed that in some utilities that use carrier for relaying, this aspect of joint usage on standard equipment is not recognized, or at least not fully evaluated.

If deliberate, not incidental, joint usages of carrier relay channels become common, as economics and spectrum crowding already dictate, the problems of relay control must be solved so that carrier relaying is not handicapped under any system conditions. Solutions of this fundamental carrier control problem under joint usage will be presented in the second paper.

Summary

1. Carrier relaying according to the present practice, or the equivalent, is needed, particularly, but not exclusively, for ground faults, and will be increasingly needed with adaptations for automatic reclosing and multiterminal lines.

2. Joint usages, which may be adopted in various degrees, will alleviate spectrum crowding, and for many installations such usages will provide either reductions in installation and maintenance costs, or improved performance, or both.

3. Various types of carrier control and modulation are available.

4. The problems of carrier transmission and reception can be discussed qualitatively, but quantitative knowledge is meager.

5. In comparing carrier types or systems there are distinctive characteristics in each, both as to function and performance, which may be advantageous.

6. The choice between the available systems will depend largely on the functional characteristics desired, but it appears that there are undeveloped potentialities in each, and possibilities of making combinations.

7. The nonrelay usages vary in their requirements, making each application a distinct problem.

8. Present standard relaying equipment provides for limited joint usages of a single carrier signal with possible consequences which do not seem to be generally recognized, namely, the wide receiver acceptance band, with corresponding inefficient use of carrier energy and spectrum space, and in-

complete carrier control by primary relays.

9. Carrier relaying needs to evolve to meet new problems. Suggestions along that line, including solutions to the primary relay control problem, will be offered in the second paper.

References

1. A New Distance Ground Relay, S. L. Goldsborough. *AIEE Transactions*, volume 67, part II, 1948, pages 1442–46. (Digest in *Electrical Engineering*, January 1949, page 27.)

2. Electronic Relay Developments, James J. Loving. *AIEE Transactions*, volume 68, part I, 1949, pages, 233–40.

3. Protection of Stations Without High-Voltage Switching, Project Committee. *AIEE Transactions*, volume 68, part I, 1949, pages 226–31.

4. Comparison of the Amplitude-Modulation, Frequency-Modulation, and Single-Side-Band Systems for Power Line Carrier Transmissions, R. C. Cheek. *Electrical Engineering* (*AIEE Transactions*), volume 64, May 1945, pages 215–20.

5. A New Single-Side-Band Carrier System, B. E. Lenehan. *AIEE Transactions*, volume 66, 1947, pages 626–30.

6. The Taylor 'Super-modulation' Principle, R. E. Taylor. *Radio and Television News*, (Chicago, Ill.) volume 40, number 3, September 1948, pages 42–44, 96–102; also number 4, October 1948, pages 44–46, 192–195.

7. The Characteristics of New Carrier-Current Equipment for Telemetering and Load Control, R. W. Beckwith. *AIEE Transactions*, volume 67, part II, 1948, pages 1649–53.

8. Coded Pulse Modulation Minimizes Noise, "F.R." *Electronics* (New York, N. Y.), volume 20, December 1947, pages 126–31.

9. PCM Equipment, H. S. Black, J. O. Edson. *AIEE Transactions*, volume 66, 1947, pages 895–99.

10. Loss Measurements Made on Underground-Cable Overhead-Conductor 132 kv Transmission Line at Carrier Current Frequencies, H. A. Cornelius, B. Wade Storer. *AIEE Transactions*, volume 68, part I, 1949, pages 597–601.

11. Report on Method of Measurements at Carrier-Current Frequencies, Carrier Current Committee. *AIEE Transactions*, volume 67, part II, 1948, pages 1429–32.

12. United States Patent Number 2,387,146, H. W. Haberl.

13. Symposium on Operation of the Boulder Dam Transmission Line—Transmission Line Relay Protection, L. L. Draper. *Electrical Engineering* (*AIEE Transactions*), volume 58, April 1939, pages 151–56.

14. Bandwidth vs. Noise in Communication Systems, "D.G.F." *Electronics* (New York, N. Y.), volume 21, January 1948, pages 72–75.

15. United States Patent Number 2,307,771, W. T. Denton, et al.

16. Possibilities and Methods of Extending a Carrier Current Relay Channel to Other Uses, R. M. Smith, S. L. Goldsborough. *Electrical Engineering* (*AIEE Transactions*), volume 60, January 1941, pages 23–7; Discussion page 645.

17. Field Tests on Power-Line Carrier-Current Equipment, R. H. Miller, E. S. Prud'homme. *Electrical Engineering* (*AIEE Transactions*), volume 65, December 1946, pages 824–27; Discussion page 1177.

18. Application of Carrier to Power Lines, F. M. Rives. *AIEE Transactions*, volume 62, 1943, pages 835–44, Discussion page 945.

19. The Combination of Supervisory Control With Other Functions on Power-Line Carrier Channels, R. C. Cheek, W. A. Derr. *Electrical Engineering* (*AIEE Transactions*), volume 64, May 1945, pages 241–6.

20. The Distinction Between Effective and Circuit Bandwidths, Wm. S. Kessler. *AIEE Transactions*, volume 68, part I, 1949, pages 98–99.

21. Power-Line Carrier Channels, M. J. Brown. *Electrical Engineering* (*AIEE Transactions*), volume 64, May 1945, pages 246–51.

Discussion

C. E. Asbury (The Commonwealth and Southern Corporation, Jackson, Mich.): This paper gives quite a complete outline of the present-day equipment available, conventional methods of application and summarizes the present problems and limitations of carrier relay applications.

We agree with the authors that there is need for evolution in present-day carrier usage which will extend its application and usefulness. These developments should extend carrier relaying for protection of modern systems being built up to include multiterminal lines, lines supplying tap loads and lines terminated in transformer banks without high-voltage circuit breakers.

One of the major factors leading to joint usage of carrier channels is that of economics. Most of this joint usage is brought about in order to justify the installation of the carrier relay equipment and is not chosen just to accommodate other services. Much of the cost of a carrier installation is in the terminal equipment, such as coupling capacitors and wave traps. If these devices could be eliminated and a more economical method found to perform their functions, it is quite probable that there would be much less need for joint usage especially on carrier relay channels. There are a number of disadvantages of joint usage on carrier relay channels when using present-day practices. The authors apparently have studied all of these various objections and plan to outline methods of solution in their following paper on the subject. Such information should be helpful and welcomed by the industry. Some of the problems that need to be considered are:

1. Any additional equipment which may key the carrier is likely to block carrier relaying with that line terminal open when the line is being tested from the opposite end. It is not always desirable to block these additional functions while the circuit breakers are open. This loss of relaying control is very undesirable, and some provision should be made to avoid it where joint usage of carrier relay channels is to be utilized.

2. In a number of applications, joint usage is made of the coupling capacitors and occasionally of the wave traps. Such joint use results in the installation of filters to block one carrier frequency from the other. Not only are these filters expensive, but they complicate the maintenance of the equipment and are a potential source of trouble due to failure or possible shifting of frequency, requiring frequent checks on tuning.

3. Additional functions often are performed over a given carrier relaying channel by the use of audio tone equipment. Where such applications are used, it is necessary that provisions be made to avoid the loss of relay control, especially for conditions of one circuit breaker being open. The amount of carrier energy available for each tone channel is reduced as the number of tones is increased. Thus there is a limitation as to the decibel range of such equipment and to the number of tones that may be applied successfully.

4. There is a limitation to the number of frequencies that may be passed through a given coupling capacitor. Usually no more than two such frequencies can be utilized successfully on one coupling capacitor where amplitude modulation equipment, such as carrier relaying, is utilized.

It appears that considerable advantage could be realized in carrier current relay applications if the band width occupied in the frequency spectrum could be reduced. With present design carrier relay sets, it usually is considered necessary to separate frequencies on adjacent lines or on parallel lines by as much as 15 to 20 per cent. It is interesting to note that crystal control transmitters are available for metering; 15 or 20 of these channels can be worked successfully through a coupling capacitor. The decibel range of these metering carrier equipments is approximately two times that of the conventional carrier used for relaying and yet the cost of carrier relaying transmitters and receivers is approximately twice as much as that of the metering equipments.

Even with the present broad-band frequency required for carrier relaying and communication, little real difficulty is experienced with interference between channels. Regional committees have been appointed by various power groups to study and to assign frequencies in the regions to avoid interference. However, there is a dire need for 150–300 kc frequency band to extend the use of power line carrier equipment. With continued co-operation among the power companies in wisely utilizing the frequencies available in the 50–300 kc band for metering communication, supervisory control, relaying, and other similar functions, it is believed that with the continued co-operation of the carrier current equipment manufacturers in reducing the amount of frequency spectrum required per channel that little difficulty should be experienced due to interference between channels for the next several years. In the application of carrier relaying, it usually is possible to utilize the same frequency for a number of channels since each channel is trapped. Usually one intervening line section operating on a different frequency is all that is required for proper separation of lines having carrier relay channels operating at the same frequency.

H. W. Lensner (Westinghouse Electric Corporation, Newark, N. J.): In the development of power line carrier equipment for relaying, simplicity always has been one of the main factors. The transmitter usually is a conventional oscillator-amplifier combination using a stable oscillator which is adjustable over the carrier-frequency band. The amplifier increases the output power to a reasonable level. The relaying receiver has been kept as simple as possible consistent with good engineering practice. More than 20 years of experience has shown that a transmitter-receiver combination capable of working through an attenuation of 30 decibels is satisfactory for very nearly all carrier relaying applications. A 10-watt transmitter and a single tube receiver will provide this operating range, which is sufficient for most overhead line sections.

A single tube receiver will have a response curve several kilocycles wide, but its limited sensitivity makes it possible to use a frequency only a few kilocycles away at a remote point on the power system without interference. A more selective receiver will of necessity be more complex, and if the transmitted power is reduced to lessen interference in other channels, the increased sensitivity of the receiver makes it more susceptible to line noise, although this may be somewhat offset by the increased selectivity. Up to the present time, the simple relaying receiver has been adequate, but with the limited frequency spectrum available, the increased use of carrier in the future well may require the use of more selective receivers.

One subject briefly discussed in the paper is the unfortunate situation (which usually exists) that line characteristics are often lacking in the negotiation stage of a carrier application. This lack of information is a great handicap, particularly in considering a carrier communication channel running through several hundred miles of power lines with their taps, busses, parallel lines, and re-entrant circuits. It would be very desirable to have frequency-attenuation data on a power system in advance of the purchase and installation of suitable equipment. Such data would be of value to the manufacturer in determining what equipment was necessary, and to the user in putting the channel in operation. Unfortunately, in most cases suitable test apparatus is not available, and it is necessary to wait until the equipment is installed to check the characteristics of the power system. At the present time, there is no known method of calculating with any degree of accuracy the frequency-attenuation relation of a complex power network, so field tests are necessary to obtain this information which is needed to assure a dependable channel with various conditions of weather and system switching.

Another subject discussed is the carrier relaying of a line in which no effective fault current can flow from one terminal. When such a condition exists, some means must be provided at that terminal for on-off control of the carrier signal, so that if a fault occurs during communication, proper relaying can take place. The requirement has been met in several installations by using high-speed undervoltage relays, with their contacts in the communication carrier-start circuit. Upon the occurrence of an internal fault, at least one of the undervoltage elements will drop out, thus stopping carrier and allowing the other terminal to trip. An extension of this idea has been used to provide high-speed tripping of both ends of a line section with little or no source of fault current at one end. A continuous carrier signal is transmitted from the terminal which has a firm source of fault current. At the opposite terminal, the received carrier signal energizes a relay element to hold its contact open. This contact is in series with the paralleled contacts of three undervoltage elements to complete the trip circuit. Upon the occurrence of an internal fault, carrier is stopped by normal relay operation at the terminal with a firm source, and the loss of carrier plus a reduction in voltage on at least one phase completes the trip circuit at the opposite terminal. While this system requires a continuous carrier signal, it does solve a rather difficult relaying problem and allows the use of normal carrier relays at both line terminals with a few additional relay elements to provide complete protection.

G. W. Hampe and **B. Wade Storer:** We agree readily with Mr. Lensner's desire to keep power line carrier equipment as simple as practical. Compared with some equipment designed to compete with power line carrier, it is simplicity itself.

Specifically, where a wide band receiver and a transmitter in a combination capable of working through 30 decibels is satisfactory, that is what should be used. There have been and probably will be a number of lines where the application is not in question.

However, our present knowledge of the effect of weather conditions and line irregularities, such as taps and cable sections, is meager. The makeup of some present line installations is such that the attenuations and noise levels are high normally and go still higher under abnormal conditions. The newer lines, and the older lines with added taps, need high standard relaying, such as only carrier can offer at the present stage of the art. Thus we find ourselves attempting to solve carrier problems of progressively increasing difficulty. One of our several needs is for increased operating ranges, in which is included a good signal-to-noise ratio.

One way to improve this situation seems to be to increase receiver selectivity. This fortunately falls in line with the need for conserving spectrum space, as Mr. Lensner agrees. Considering the great improvements in receiver component parts made possible during and since the war, a more complex receiver may well be more reliable than the present ones.

Mr. Lensner mentioned the handicap of not having beforehand knowledge of transmission characteristics on long communication channels. The AIEE Carrier Committee is gathering data which should be of substantial benefit in such cases. The writers question, however, whether long hauls at a single carrier frequency are really necessary. Under joint usage the problem can be simplified. By utilizing the well trapped carrier relay channels with repeater points at the ends of the line sections, the effects of attenuation and varying system operating conditions can be greatly reduced. The repeater points can use audio by-passes, provided the number in tandem is not excessive. An application of this type, with one audio by-pass, is now in service on the Commonwealth Edison System, and a second application using two such by-passes has been planned for future use.

Another similar solution has been proposed which would use a nondemodulating carrier repeater (so called for lack of better name). This would repeat the communication signal at a different carrier frequency in the next line section without descending to the audio-frequency level.

In reference to the use of undervoltage relays to remove auxiliary services during fault conditions:

This is quite feasible in some applications, but to do so for the open circuit breaker condition requires an adequate set of potential transformers or potential devices on the line itself. In many cases bus, not line, potential transformers are used. In such cases there may be only a single-phase potential device for synchronizing and back-feed indication. In other cases, the line potential transformers are "VV" connected, and their secondary output gives no clear-cut indication of the existence of a single line-to-ground fault.

If the auxiliary services are at all important, it is desirable to continue them past an open circuit breaker or even with the line dead. This means that an additional device, such as a fixed time relay, must be used to restore the auxiliary services. It would be desirable to have a solution to the control problem which would be more generally applicable and simpler. One should not lose sight of the voltage variation principle in setting up carrier relay schemes, however, as Mr. Lensner indicates.

Mr. Asbury indicates that much of the cost of a carrier installation is in the terminal equipment such as coupling capacitors and traps. There is no generally accepted way of dispensing with the coupling capacitor, but it can, of course, be used jointly for various services.

In regard to trap requirements it is necessary to consider the type and location of the line itself, the attenuation and interference problem, and the number and nature of the desired services. On trunk lines, for example, adequate trapping is essential. Economies in trapping should be obtained, not by eliminating traps, but by making greater use of each trap that is required. For example a wide band of frequencies might be trapped by utilizing the trap as a band elimination filter. Likewise, utilization of the coupling capacitor as a wide band-pass filter will provide joint usage with the resulting economies that both the authors and Mr. Asbury feel are necessary. A proposal covering this use of traps and coupling capacitors is presented in a paper scheduled for the AIEE Pacific General Meeting.[1]

On subtransmission lines there may be few desired services other than relaying, and costs must be cut. Traps should be used sparingly. Just how sparingly depends largely on the interference and attenuation problems.

In restating the problems presented in our paper, Mr. Asbury also mentioned cost and maintenance difficulties of filters. To the extent that we have dealt with filters to date, we have found them simple to maintain and quite stable. The objection should be made more explicit.

Mr. Asbury points out that the power companies have generally worked out their interference problems. He states that they can continue to do so, if the band now available between 50 and 300 kc is used. To this we heartily agree.

Mr. Asbury also agreed to the main premise of our paper, which was that power line carrier needs to evolve to extend its application and usefulness. From the relaying standpoint, this includes protection for multiterminal lines, lines supplying tap loads, and lines terminating without high-voltage circuit breakers. The factor of immediate automatic reclosing should be included.

Reference

1. A Proposal for Broad-Band Coupling of Power-Line Carrier Equipment. R. H. Miller. *AIEE Transactions*, volume 68, part II, 1949, pages 1028–31.

Relaying of Transmission Lines from the New Sunbury Generating Station

H. H. GREEN
NONMEMBER AIEE

J. A. G. OEWEL
MEMBER AIEE

O. RAMSAUR
MEMBER AIEE

IN PLANNING the development of the transmission facilities needed for the output of the new Sunbury plant of Pennsylvania Power and Light Company, provision of spare lines has been avoided by placing full dependence on the ability of modern line protective and restorative relaying to reduce to short durations all outages except those caused by relatively rare persistent faults. As a result, the number of lines is being held to those already in existence in close proximity and those required for carrying capacity to certain regional loads.

This paper deals with the functional requirements of relaying in the development of the transmission outlet for the initial 150-megawatt installation at Sunbury, some of the special problems encountered, and the kinds of relaying selected to meet these requirements and to solve these problems. Circuit and elementary diagrams are omitted, on the assumption that relay engineers are familiar with the common types of protective and reclosing relay methods being used.

A brief discussion of the new generating station and the transmission system will provide background for the discussion on relaying.

The New Plant

The new plant is situated on the west bank of the Susquehanna River, about two miles below Sunbury, Pa. The site was acquired many years ago because of its central location in the western part of the system, which was the logical point of the next large power source, and because of the availability of sufficient water, proximity of fuel sources, and so forth. Its ultimate installation has been kept continually in mind in the planning of all new major facilities in that vicinity.

The initial installation comprises two 75,000-kw units, each connected through a 13.8–69-kv step-up transformer bank directly to one of the two sections of the 66-kv double bus, as indicated schematically in Figure 1. These first two units are expected to go in regular service in 1949. A third unit of 100,000-kw capacity is already under way, to be completed in 1951.

Transmission System

The major transmission system is shown in map form in Figure 2. Basically, it consists of a 66-kv network which is fed at dispersed points by generating stations of various sizes, a 220-kv interconnection, and several 66-kv interconnections. Transformer neutrals are solidly grounded at main supply points. This 66-kv network plays the dual role of distribution system as well as transmission system, being tapped at will to supply power to lower-voltage distribution systems and large industrial plants.[1]

All but two of the 66-kv lines tying into Sunbury already existed in the general proximity and are simply being extended into Sunbury from other terminations. New 66-kv lines have been built, however, to Lock Haven and to Millersburg, tying in with existing lines to provide additional capacity required by increasing load. The 132-kv line between Sunbury and the large 220–66-kv substation at Siegfried forms a bulk-power channel between these two major supply points, terminating on the 66-kv bus at each end through a 50,000-kva 132/66-kv autotransformer. The 132-kv line initially is made up of a new section of 220-kv construction and an existing section of 132-kv construction. Later on, as required by the need for more capacity, the 220-kv construction will be completed all the way and the line then will be operated at that voltage.

Requirements of Transmission System

Basically, of course, the function of a transmission system is to transport power, for which it must have adequate capacity from the standpoint of conductor loading and voltage drop. In this case, the transmission is mainly to two regions: the main part of the system, lying eastward from Sunbury; and the northwestern portion, the load in which will be taken over largely by Sunbury. The one 66-kv line to the south will not only take over the load en route, but will bolster supply to the southern region.

All of the connections to Sunbury shown in Figure 2 have been governed either by the proximity of existing lines and the ease of tying them in, or by the need for additional transmission capacity to carry normal peak-load requirements in the regions to be served.

As to reliability, every reasonable effort is being made to provide lines that will stay out of trouble. New lines and extensions are of modern construction, resistant to lightning and sleet and located on private rights of way remote from highway and other such hazards. The older lines are being reinforced to improve their resistance to lightning and sleet.

The record of experience with lines of these types shows predomination though infrequent occurrence of inherently nonpersistent faults and a very rare occurrence on peak of persistent faults due to mechanical damage of some sort. The grouping of lines is such that momentary outage of any one line will not affect

---

Paper 49-153, recommended by the AIEE Relay Committee and approved by the AIEE Technical Program Committee for presentation at the AIEE Summer General Meeting, Swampscott, Mass., June 20–24, 1949. Manuscript submitted February 18, 1949; made available for printing May 23, 1949.

H. H. Green, J. A. G. Oewel, and O. Ramsaur are all with Pennsylvania Power and Light Company, Allentown, Pa.

appreciably any but those customers fed directly from the line itself. The cost of providing spare lines to avoid possible drastic measures for those extremely rare occasions when a long outage occurs on peak is not justified.

Functional Requirements of Relaying

Recognizing that no over-all line relaying can alleviate situations arising from persistent faults, the functional requirements of relaying for these lines are:

1. To clear all nonpersistent faults due to lightning and other transient causes quickly enough to avoid their becoming persistent because of arc damage at the point of fault. Experience has indicated that this can be accomplished with standard 8-cycle circuit breakers and fast protective relaying.

2. To reclose the terminal breakers quickly enough to give reasonable assurance that the faulted line will have been restored to service before another of its group is faulted. Experience with other 66-kv tie lines, including double-circuit lines, indicates that, in practically all cases where the faults were not simultaneous at the start, a reclosing time of two to three seconds is adequate. Even when outages are simultaneous, at least one line usually is restored successfully. An additional objective, of course, is quick restoration of service to loads tapped off the lines.

From the standpoint of channel reliability, it is recognized that persistent faults caused by mechanical damage are very infrequent and that they seldom result in simultaneous outage of two lines in a group, because their cause usually is localized. On the other hand, nonpersistent faults usually are caused by lightning, which occurs during a relatively few hours a year, so that outages of two lines are more apt to occur close together. It is for the latter type that relaying achieves its real aim.

The problem of stability does not enter into the need for fast relaying in this case, as the ties to the main network are stiff enough to give adequate synchronizing power under the assumed conditions.

Based on past experience on 66-kv tie lines with fairly fast protective relays and sequential reclosure of the 2 terminal circuit breakers within 3 seconds, it is reasonably certain that the transmission requirements enumerated will be satisfactorily met with the medium-speed protective and reclosing relaying about to be described, because:

1. There are comparatively few trip-outs of modern or modernized lines.

2. Most faults are transient in nature, so that reasonably fast clearing will keep the line ready for successful reclosure.

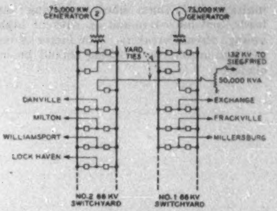

Figure 1. One-line diagram of initial installation at Sunbury

3. Since there are no double-circuit lines around Sunbury, there is little chance of simultaneous outages.

4. Even though two lines should go out together, it can be expected that at least one will be successfully restored within a short enough time to prevent serious results.

It is pointed out that fast tripping and reclosing of lines also gives improved service to tapped loads, which include some important customers and distribution supply substations.

Line Protective Relays

As might be surmised from what has been said about fast clearing of all faults, carrier-pilot relays are a practical requirement for all the lines leaving Sunbury. Only pilot relays can meet the requirements of simultaneous tripping of both terminal circuit breakers (or at least instantaneous sequential tripping, as may be encountered on two lines to be mentioned later), to minimize fault damage and to permit faster reclosure than would be possible with conventional relays. In fact, pilot relays are inherently fast enough to meet the requirements of fast clearing with circuit breakers of normal speed. This is especially important at the terminals away from Sunbury, where some of the circuit breakers are already in existence. The carrier pilot also provides a channel for emergency telephone communication.

Having decided upon carrier-pilot control of the relays as an essential requirement, there remained only the choice of basic relay types to suit the conditions imposed by the various lines. In this connection, the policy of tapping lines introduced some problems not found on untapped tie lines:

1. The difficulty of reaching faults at the ends of the taps, because of the increase in the apparent impedance seen by the relays at one terminal by current flowing over the tap from the other terminal. The permissible lengths of taps are limited by the fact that relay settings must be high enough, in terms of distance, to reach the tap ends with adequate margin, but, at the same time, must be low enough to permit carrying the maximum expected loads. Where the two limits of settings approach each other, there is also danger that a fault will produce enough current in one terminal to operate a carrier-starting element and send a blocking signal, but not enough current to operate the tripping element at the same terminal and stop the signal. This condition can be overcome by making the carrier-starting element directional, so that it will start carrier only for a fault in the nontripping direction at its terminal, thus establishing the condition that the tripping relays are free to trip the circuit breaker at the terminal where the fault on the tap is recognized, after which the other terminal will trip immediately. In no case encountered is it necessary to protect a tapped transformer, as fuses are used for this purpose.

2. The desirability of avoiding overtripping for faults on the low-voltage feeders from the tapped step-down substations. For very large transformers, a carrier terminal often is required for this, but for the lines covered by this paper, there are no tapped transformers large enough to require it for the type of relaying chosen. (Phase-comparison relays were rejected because certain transformers tapped to the lines were of sufficient capacity to require carrier blocking terminals with this type of relaying.) Consequently, no line has more than two carrier terminals. In this connection, it is pointed out that no attempt is made to avoid tripping the line for faults on the high-tension side of a tapped transformer, because it is expected that the transformer fuse will blow during the tripping time and thus disconnect the fault from the line and permit its immediate reclosure. These faults are so rare that special equipment to prevent line tripping is not warranted.

3. The necessity for opening low-voltage circuit breakers on transformers tapped off the lines, the low-voltage sides of which tie in to other transformers tapped off other lines. This back-feed into 66-kv line faults requires slowing up line reclosure long enough to open the ties, in addition to creating the problem of when and how to open the low-voltage circuit breakers. The problem is further aggravated by the fact that all of the tapped transformers have delta primaries, so that the only current flowing for a ground fault after the terminal circuit breakers trip is that caused by the unbalance in line-charging current.

For clearing phase-to-phase faults, review of the above and other conditions and restrictions imposed by the line connections and their maximum loads led to the conclusion that the relays best suited were the 3-element 3-zone impedance type *HZM*, with modified (offset) characteristics.[3] These relays offer a wide range of choice of settings and characteristics, and appear adaptable to any condition likely to arise. Also, the offset characteristic facilitates directional carrier starting.

As is customary for carrier-controlled

relays, all three elements will trip independently of carrier control, after their respective time settings. Zone *1* will be set to cover about 80 per cent of the line and will trip instantaneously through a directional element for faults in this range. Zone 2 will be set to cover the entire line and the taps, plus adequate margin, to trip through a directional element for faults in the far-end zone after a suitable co-ordinating time delay. Zone *3* will have its impedance characteristic almost completely offset, to make it largely directional and thus operative only for faults behind the bus and within a short distance out on the protected line; it will be set to outreach the second-zone element at the far end and will trip after a time delay longer than that of the second-zone element. It should be noted that the third-zone element will trip the circuit breaker at the terminal nearest a prolonged external fault, thus keeping the protected line in service to carry its tapped load.

For carrier-controlled tripping, the second-zone time element will be by-passed in the usual manner by the carrier auxiliary relay, to permit instantaneous tripping for faults within reach of the second-zone impedance and directional elements that are not blocked by a carrier signal. Operation of the third-zone element will start the carrier signal, and, being largely directional, it usually will start carrier only for faults requiring blocking, thus avoiding the condition of a blind terminal mentioned previously. Operation of the second-zone elements to trip will stop any carrier signal originating at the same terminal. While the third-zone element will also start carrier for faults within a short distance on the protected line, the second-zone element will definitely overreach it and stop carrier.

The scheme of operation outlined in preceding paragraphs assures instantaneous tripping of both terminal circuit breakers simultaneously for nearly all phase-to-phase faults anywhere on the protected lines. For those few cases where a fault on a tap will not operate the second-zone tripping relay at one end until the other end has tripped, at least instantaneous sequential clearing is assured.

Separate back-up relays for phase-to-phase faults are not being provided, because the relays on each phase operate as conventional 3-zone elements independently of the carrier pilot control, and because the phase relays will be taken out of service only one at a time for test. This is acceptable because full ground fault protection will be maintained at all times, because the phase relays remaining on the other two phases still offer limited back-up for the removed relay, and because relay testing is restricted to conditions of good weather, and so forth, when the probability of a pure phase-to-phase fault on the particular phase with limited protection is extremely low.

For phase-to-ground faults, the carrier-pilot protection is provided by two sets of zero-sequence directional and instantaneous overcurrent elements, one for tripping and one for starting the carrier blocking signal. As in the case of the phase relays, the starting combination operates only for the flow of zero-sequence current away from the line, so that the carrier blocking signal is transmitted only when required to prevent overtripping by the relays at the far terminal and is not transmitted for faults on the protected line.

The directional carrier-start feature is particularly valuable on the lines to Lock Haven and Williamsport, where there are no grounded-neutral transformers and where the main source of zero-sequence current is over the lines from Sunbury itself. For ground faults near Sunbury, there is practically no zero-sequence current in the Lock Haven and Williamsport terminals until after the Sunbury circuit breaker opens. This leads to the existence, at the Sunbury end of each of these lines, of a long zone in which a ground fault would operate a nondirectional starting element at the far end but would not operate the higher-set tripping element, thus blocking tripping by the carrier-controlled relays. With a directional starting element, this condition is avoided; instantaneous sequential tripping of the two terminal circuit breakers will result. While the back-up ground relay also should trip instantaneously for such a fault, it is desirable that the carrier-controlled elements stand on their own feet as far as possible.

Back-up protection for phase-to-ground faults is provided at Sunbury by simple inverse-time induction overcurrent relays with instantaneous attachments. At all terminals away from Sunbury, except at Siegfried, it was necessary to make these relays directional; one direction element was used to supervise both the inverse-time and instantaneous overcurrent elements.

The ground back-up relays are entirely independent of the carrier-controlled relays, so that either can be taken out of service for calibration and maintenance without losing full coverage for ground faults.

All directional relay elements are potential polarized, except the ground relays on the Siegfried line. Current polarization of the ground relays at Sunbury would have been unduly complicated by the double-bus arrangement, which would require special safeguards to insure that relays always would be polarized by a proper source of zero-sequence current. To insure correct potential for polarization of all relays and for other purposes, each line at Sunbury is being equipped

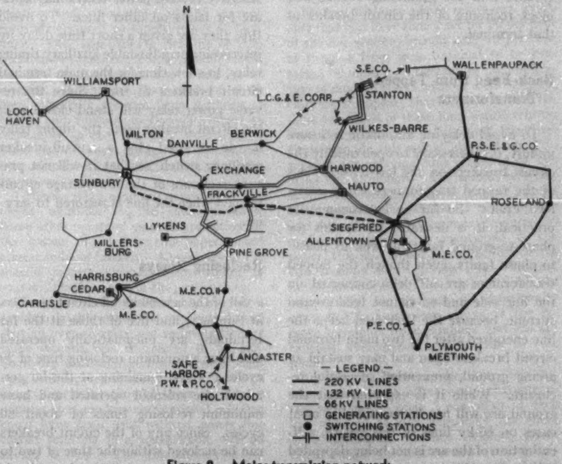

Figure 2. Major transmission network

with a complete set of three 66-kv potential transformers, connected Y-Y with neutral grounded, to supply all required potentials directly from the line itself. This cost little more than other methods, because it eliminates bus potential transformers. Each line does have a manually-operated switch for transferring the relays to another potential source whenever it is necessary to take the normal source out of service. In most cases, the relays on the terminals remote from Sunbury receive potential from bus potential transformers, as none of the adjacent stations except Siegfried has a double bus. The ground relays on the Siegfried line are current polarized. The current is supplied from a current transformer within the delta tertiary winding of the 132/66-kv autotransformer.

Since the 132-kv line to Siegfried is terminated by 66-kv circuit breakers only and a 132/66-kv autotransformer with solidly-grounded neutral at each end, the protective relaying is complicated a little by the necessity of providing complete protection of the terminal transformers. Because the protection offered by the line relays was not considered adequate under all conditions, differential protection for each transformer is provided in addition to the line relays. For this purpose, the transformers are equipped with bushing-type current transformers on the 132-kv side; a single-pole 132-kv grounding switch is provided at each terminal to force tripping of the far terminal. The transformer differential relays trip both the terminal circuit breaker and the grounding switch, and block reclosure of the circuit breaker at that terminal.

Back-Feed from Tapped Transformers

To avoid delaying automatic reclosure unduly, it is necessary to open quickly the circuit breakers on the low-tension sides of the tapped transformers where cross-feed exists. So far as is economically practical, it is desirable to do this for phase-to-ground faults as well as phase-to-phase faults, even though the tapped transformers are all delta-connected on the line side and so cannot feed ground current, because the back-feed keeps the line energized after the two main-terminal circuit breakers open and may sustain an arcing ground, preventing successful reclosure. While it is expected that the ground arc will not be sustained in most cases on 66-kv lines of this length, self-extinction of the arc is not being depended upon. For this reason, it is considered good practice to interrupt the back-feed, if it is possible to do so without resorting to expensive equipment for this purpose.

Remote tripping of the back-feed points over the carrier channels may have been practical but would have been expensive, so, after consideration of several other schemes, sensitive reverse-power relays were adopted.

Taking a tip from network relays, sensitive high-speed polyphase directional relays with watt characteristics are being used for this purpose. These relays are given a slight spring bias in the "reverse" direction, so that the contact will stand closed with full potential and zero current. Under normal conditions, there always will be enough load current toward the low-voltage bus to keep the relay open. With the line circuit breakers open, however, the presence of the spring bias, transformer core loss, and, in some cases, other load tapped off the line, will insure prompt closing of the relay as soon as the line circuit breakers open, if it has not closed already because of flow of positive- and negative-sequence currents into the fault.

The watt characteristic of the relay was selected because the wattless component of the reverse current may be either lagging because of transformer magnetizing current or tapped-load current, or leading because of line-charging current. The watt component is therefore the only one that can be depended upon for the proper direction.

For faults near Sunbury, some of these sensitive reverse power relays may operate for faults on other lines. To avoid this, they are given a short time delay by interposing an adjustable auxiliary timing relay, to allow time for the main-terminal circuit breakers to trip. Since the reverse power relay will stand closed with the circuit breaker open, the timing relay is de-energized by a circuit-breaker auxiliary switch, so that it will not prevent reclosure of the low-voltage circuit breaker when the line is restored to service.

Reclosing Relays

All of the new 66-kv oil circuit breakers at Sunbury, and five of those at the far terminals, are pneumatically operated and have a minimum reclosing time of 20 cycles. Those remaining at the far terminals are solenoid operated and have minimum reclosing times of about 60 cycles. Since any of the circuit breakers can be reclosed within the time of two to three seconds set as a limit, the policy is to reclose as quickly as possible with existing circuit breakers and under the particular conditions on each line. This means that reclosure will be fast enough if it is done as soon as it can be certain that the line is de-energized. On the other hand, reclosure is being speeded as much as possible without resorting to special equipment to do so. Therefore, the reclosing time of any circuit breaker is determined by the expected clearing time of the circuit breaker at the other terminal and on any low-voltage ties, plus time for arc deionization.

For reclosing the Sunbury circuit breakers, time is being allowed for sequential tripping of the far circuit breakers, because it is not certain that ground faults near Sunbury always will result in sufficient ground current at the far end to trip properly until after the Sunbury circuit breaker opens. In fact, as mentioned before, sequential tripping is almost a certainty for ground faults near Sunbury on the lines to Lock Haven and Williamsport. A time of only about 10 cycles is allowed for this, which is of little consequence.

Time is being allowed for tripping of the circuit breakers feeding back from low-voltage cross ties after the main-terminal circuit breakers trip, because of the time delay purposely introduced, as mentioned before, and because it is not certain that they will even start timing out before the terminal circuit breakers open. This adds some 35 cycles.

The result is that it is expected that both terminal circuit breakers will be reclosed within 30 cycles on the lines to Millersburg, Lock Haven, and Siegfried, which have no back-feed from low-voltage ties, and within about 65 cycles on all others except the line to Exchange, which will be about 100 cycles because it has two back-feeds that may trip sequentially with respect to each other as well as to the 66-kv circuit breakers.

The reclosing time is varied by setting up the reclosing circuit as for one-shot instantaneous reclosure, but delaying it with an auxiliary relay with adjustable time delay.

Because each line is terminated on two circuit breakers at Sunbury, a selector switch is provided to select the circuit breaker that will be reclosed automatically. If reclosure is successful, the other circuit breaker will be reclosed manually. If the one automatic reclosure is not successful, any further tests also will be manual.

Automatic reclosure of any circuit breaker is blocked by the manual switch that removes carrier control of tripping

It is also blocked by operation of bus differential relays or by manual tripping of the circuit breaker by the control switch. Manual reclosing restores the automatic reclosing feature.

On the low-voltage ties, circuit breaker reclosure will take place after a time delay following restoration of the 66-kv line to service. As on a secondary network, proper conditions for reclosure are indicated by a directional relay so connected that it acts as a phasing relay.

Bus Protection

While bus protection does not come under the heading of line relaying, a brief description of the Sunbury bus protection may be of interest.

Linear couplers were selected for differential protection of each of the four 66-kv bus sections because of their superiority over other conventional methods considered.[3] This method eliminates any possibility of bushing current transformer saturation by the heavy currents to be expected for nearby line faults, and, at the same time, retains the simplicity of a straight differential scheme. Simplicity is highly valued.

The linear couplers are connected by multiconductor control cable, without benefit of shielding, because calculations of induced voltages in the relay circuits for ground faults in the vicinity of the switchyard were reassuring, even when based on pessimistic assumptions such as no spiraling. Actually the cable is spiralled about every 15 inches, so that induced voltage between conductors should be practically zero. Voltages induced along the conductors are equal in all conductors and hence produce no relay current.

Considerable thought was given to the selection of a satisfactory method of supervising or checking the linear coupler circuits. The method adopted was suggested by the manufacturer. Absence of short circuits is checked by switching high-resistance low-reading voltmeters in parallel with the relays to test for abnormal differential voltages, such as would be caused by short-circuited linear couplers. Continuity of the circuits is checked by introducing about 0.5 volt from an external source. This is done, without opening the circuits, by applying the voltage across a resistor of low ohmic value which is left permanently in the circuit. Correct readings of the voltmeters, which are in parallel with the relays, indicate continuous circuits.

The yard tie circuits are protected by percentage differential relays. Since both yard tie circuits are tapped, 3-way differential circuits are employed. The 66–132-kv autotransformer in the Siegfried line at Sunbury is included in the yard-tie differential relay zone of protection. The operation of the differential relays trips the two 66-kv circuit breakers and closes a single-phase 132-kv grounding switch which insures tripping the Siegfried terminal. A similar arrangement is provided for the transformer protection at Siegfried substation. The line relays receive current from the 66-kv current transformers and thus provide limited back-up protection for transformer failures.

References

1. Power System Voltage Control without Feeder Voltage Regulators, N. N. Smeloff. *AIEE Transactions*, volume 67, part II, 1948, pages 1462–6.

2. A Distance Relay with Adjustable Phase-Angle Discrimination, S. L. Goldsborough. *Electrical Engineering* (*AIEE Transactions*) volume 63, November 1944, pages 835–8.

3. Linear Couplers for Bus Protection, E. L. Harder, E. H. Klemmer, W. K. Sonnemann, E. C. Wentz. *Electrical Engineering* (*AIEE Transactions*) volume 61, May 1942, pages 241–8.

4. Linear Couplers, Field Tests and Experience at York and Middletown, Pa., E. L. Harder, E. H. Klemmer, R. E. Neidig. *Electrical Engineering* (*AIEE Transactions*) volume 65, March 1946, pages 107–113.

Discussion

C. E. Asbury (The Commonwealth and Southern Corporation, Jackson, Mich.): This paper describes some interesting relay applications and is perhaps typical of some modern trends in system planning such as tapping high-voltage transmission lines to serve load without the use of high-voltage circuit breakers. This particular plant is perhaps unusual in one respect, in that it has eight major ties into the transmission system. Often in the initial installation of one or two units at a new plant site, only two or three transmission lines connect between the plant and system, and often these are quite long electrically. Such conditions, of course, are brought about because of the availability of plant sites and their location relative to the existing transmission system and load centers.

It is noted that the switching arrangement used at Sunbury consists of two sets of double 66-kv busses, one for each generator. It would be interesting if the authors would point out the advantages of the two sets of double busses with two yard tie circuit breakers between them, over that of one double bus often used for installations similar to this. It also would be interesting to know how future generators will connect to these busses.

This switching arrangement includes two circuit breakers for each line connection, and it is not clear in the paper whether these are normally operated both closed or with one normally open. It would be interesting to know the method of operation and the location and connections of the current transformers used to supply relays at Sunbury. The approximate length of the transmission lines connecting Sunbury with the rest of the system also would be of interest. It appears that some of these lines, especially the two from Sunbury to Milton and Sunbury to Danville, might be reasonably short. We were wondering if these lines are short enough for the application of pilot-wire relays, and if pilot-wire relays were considered.

Different relay engineers would have different solutions to the same problem. Some other points of view on protection for the system outlined in this paper would appear to be of interest. Knowledge of the specific system characteristics would, of course, influence some of the applications.

The paper states that stability was not a problem in this particular application, and that an over-all relay and reclosing time of three seconds was considered to be adequate for transmission lines between Sunbury and the rest of the system. Based on a total reclosing time of three seconds, it appears that modern conventional relaying could have been used without power line carrier resulting in a considerable over-all saving in cost. The communication requirements mentioned could be satisfied with a much more economical power-line carrier of the Simplex multistation type. Such a communication channel probably would not require the use of line traps at a number of points where they were required for relaying.

Modern distance phase relays are available that can have zone *1* set for 90 per cent of the line section, leaving only 10 per cent of the line from each terminal to be protected by zone *2*. Considering the application of modern relays without a carrier pilot channel, it appears that at least one of the main terminals of these lines would trip by zone *1* step distance relays, and, based on three seconds this would leave about $2^{8}/_{10}$ seconds for relaying and reclosing of the other two terminals. The second terminal should trip sequentially on zone *2*, which could probably be set for 15 or 20 cycles, and even if the third terminal required 35 cycles for tripping as mentioned in the paper, this still would leave approximately two seconds for reclosing time. Ground faults probably could be cleared similarly sequentially, by the use of directionally controlled instantaneous relays at the remote terminals from Sunbury and instantaneous overcurrent attachments at the plant.

In this particular application, step distance relays with offset circle characteristics were used. Zone *3* was offset at each line terminal to give essentially the effect of a directional distance element, directional out of the line section at each terminal. It must, of course, be realized that where this arrangement is used about the only function of zone *3* is for carrier starting and that zone *3* provides little back-up protection. One reason for being limited as back-up protection is the interposed feed of short-circuit current from other transmission lines terminating on the same bus. This infeed at each line terminal limits considerably the reach of zone *3* as a back-up element. This would be especially true for all lines terminating at Sunbury Plant. Such limitation is not placed on zone *3* when it is set to provide back-up protection of its associated line section. Another reason for the limitation of zone *3* as back-up protection, where this method is applied in a system equipped with other distance relays applied in the conventional manner, is that zone *3* of all lines which are set for back-up protection on its particular line section and, therefore, any additional back-up protection such as provided from adjacent carrier having zone *3* set looking out of its line section, is of little benefit. Such an arrangement would provide double back-up protection for some lines and will probably result in zone *3* having the same time delay setting for two or more zone *3* settings at the same substation. If this arrangement is used and a fault occurs in a line section requiring the operation of zone *3* back-up relays, then two lines will be opened at the same substation instead of one. It would be interesting if the authors would point out how zone *3* time delay was co-ordinated with zone *3* of adjacent line sections which may have been equipped with conventional distance relays.

Apparently, the zone *3* elements were offset to look out of the line section at each terminal to avoid starting carrier due to load currents, assuming zone *3* elements had been set to cover the line section, including tapped spurs to loads. It is apparent that with the settings as described in the paper, it is not necessary to start carrier by zone *3* before tripping the line by zone *2*, since zone *3* covers only a small portion of the protected section. With this type of operation, a standard impedance element could have been used at each line terminal to start carrier as long as it was set to reach farther out of the line section than zone *2* at the opposite end of the line. Since it is only necessary to cover the line plus a small margin by zone *2*, such an impedance starting element could have a short setting and can be less susceptible to pick-up on load than zone *2* at the opposite end of the line. This arrangement would permit the use of zone *3* as back-up protection for its own line section.

The paper describes the use of ground relays where one directional element was used to supervise both the inverse and the instantaneous over-current element. It would be interesting to know what type of relays were used for this arrangement and whether or not the instantaneous elements were directionally controlled.

Mention is made of T-tap loads on a number of 66-kv lines which have back-feed from other low-voltage lines. Apparently the other low-voltage sources of these loads are sufficient to carry the loads with the 66-kv line out of service, since high-speed tripping and reclosing is not utilized. It appears that if the load had been such that the emergency supplies were inadequate with the 66-kv line open, which probably will be true in the future as the load increases, it may be desirable to add additional terminals of carrier to provide high-speed tripping and reclosing of these terminals. Application of reverse power relays biased with spring tension to trip on full voltage with no incoming power is an interesting application. Apparently, the system loading and supply is such that there is no back-feed at any of these terminals from low-voltage ties during light-load conditions.

O. Ramsaur: Mr. Asbury asks a number of questions that are quite pertinent to the subject and have probably arisen in the minds of other readers of the paper.

The two sets of 66-kv busses were adopted for physical reasons. This arrangement provides the greatest number of future bays in the available space, greatly facilitates connections to the generators and get-away of the east and west lines without having circuits crossing each other, and minimizes the distance from the switchyard to the control house, which is located between the two sets of busses. It should be noted that the amount of switchyard equipment is practically the same as for one long double bus, because the yard ties serve dual purposes (at present they are used for the 66/132-kv transformer and a 66/4-kv stand-by auxiliary supply transformer; in the future they will be used to terminate two 220/66-kv transformer banks).

The double-bus arrangement, together with the automatic sectionalizing afforded by the yard ties, is required for reliability and for flexibility of operation. Initially all circuit breakers shown in Figure 1 of the paper will be operated closed. As the station grows in capacity, however, it will be necessary to "split" the 66-kv bus to limit short-circuit currents. The double-bus arrangement facilitates a flexible mixture of east and west lines on each of two independent busses, by opening the proper circuit breakers, with provision for transferring to the other bus for outage of any bus section.

Future generation will be connected to a 220-kv bus, which will be tied to the 66-kv busses through transformers, as mentioned before. The current transformers for the line and yard-tie relays at Sunbury are bushing type, located in the bus sides of the circuit breakers. The two sets associated with each circuit are paralleled. The linear couplers for bus protection are located in the line sides of the circuit breakers.

The line lengths vary from 15 miles for the line to Milton to 75 miles for the 132-kv line to Siegfried. Pilot-wire relays were considered for the Milton line; but the carrier-current pilot was selected for its greater reliability, there being no great difference in over-all cost.

Speed of fault clearing is usually dictated by the lesser of two times: (1) that required to avoid instability and (2) that required to avoid line damage. It was the intention of the authors to bring out in the paper that, since there is no problem of instability, the aim of fast fault clearing is to prevent line damage. Also, since the allowable outage time of two or three seconds is comparatively long, there is plenty of time left for reclosure, even after waiting to disconnect the line from sources of feedback.

Considering co-ordination with existing relays on adjacent circuits, neither conventional nor impedance relaying would have been fast enough for safety from line damage, especially for faults in the end zones away from Sunbury. Instantaneous ground relays would not operate sequentially, because there is practically no increase in current at Sunbury after the far-end circuit breaker opens. Carrier-current relaying was required, therefore, to avoid line damage; and emergency communication was mentioned only as a by-product, although it is considered quite valuable.

It is true that the reversed zone *3* elements offer only partial back-up protection for faults on either the protected line or other lines, because of the interposed currents mentioned. For back-up coverage of the protected line, it is believed that little would be gained by using zone *3* in the conventional manner, however, because failure of the zone *1* and zone *2* elements to trip is almost always due to failure of something common to all three elements—open trip coils, open current circuits, loss of polarizing potential, loss of tripping potential, stuck timers, faulty auxiliary switches, and so forth. Rarely can failure to trip be attributed to something associated only with a particular relay element. Also, it is seldom that a fault does not involve ground current; so that the ground relays usually back up the phase relays anyhow. There is little chance that a pure phase-to-phase fault will occur at the same time that failure to trip is due to something peculiar to one relay element. And back-up coverage of adjacent lines by the reversed zone *3* is greater for the same setting than a conventional zone *3*. This is important where coverage is limited by ability to carry load.

Since the coverage of the reversed zone *3* elements is less than that of the instantaneous relays on adjacent line sections employing conventional relays, there is no problem of co-ordination. Nor would there be any if zone *3* were used in the conventional manner, for the same reason. Where adjacent lines have distance relays, it is assumed that if an adjacent zone *2* does not trip, then zone *3* also will not, for the reasons mentioned; and again there is no need for co-ordination. The use of a standard impedance relay to start carrier in the manner described by Mr. Asbury should be satisfactory, although it would add three impedance elements at each terminal.

Directional supervision of both instantaneous and inverse-time ground relays is accomplished with two standard relays. One is a combination of a high-speed directional element and a directionally controlled inverse-time element in one case. The other is an instantaneous plunger-type relay, which trips through the directional element in the first relay, an extra stud having been provided for this purpose. The instantaneous element is not directionally controlled. Each of the low-voltage sources of loads with backfeed is able to carry the load alone, the backfeed resulting from 2-way supply to these important loads. As the loads increase, additional transformer capacity will be provided; but this capacity is not expected to be large enough to require carrier-current terminals. No backfeed under light-load conditions is expected. Should it occur unexpectedly, the reclosing relay set-up inherently provides for holding the circuit breaker open until voltage of the proper magnitude and phase angle to carry load is again established; and, if the other source fails, the load will be transferred.

A Thermal Converter for Telemetering and Totalizing

WILLIAM C. DOWNING, JR.
MEMBER AIEE

JUST 20 years ago, Professor Paul M. Lincoln described a "thermal converter" for use in the telemetering and totalizing of large power loads.[1] At that time the installations employing this instrument were less than a dozen in number. Today the thermal converter is generally accepted as an important primary element in the measurement and control of a large portion of the power systems of this country. A number of these installations have been described in *Electrical Engineering* and elsewhere.[2-8]

The thermal converter may be described briefly as an instrument which generates a direct electromotive force accurately proportional to the power flowing in the a-c circuit which it is connected to measure. The voltage so generated may be transmitted readily over considerable distances and recorded or indicated on a potentiometer for telemetering; the output circuits of two or more converters may be connected in series to totalize the power from a number of sources. Since only the series addition of direct voltages is involved, the circuits totalized may differ in types or frequencies, and loads may be subtracted, as well as added, in attaining a record of total load.

In principle, the thermal converter comprises an electric circuit in which the difference of the power generated in two heaters is proportional to the power measured. The temperature difference so produced is measured by thermocouples, the voltage from which is thus a measure of power. In addition to the measurement of power, the thermal converter may be adapted to the measurement of reactive power, power factor, current, or voltage.

Types of Thermal Converters

The two types of converters commercially available may be classified according to the means by which heat is transferred from the heaters to the thermocouple junctions. In the "indirectly-heated" type,[1] the a-c heater circuit is insulated electrically from the thermocouple circuit but is in close thermal contact with it. In the "directly-heated" type,[9] a common circuit is provided for heaters and thermocouples, separation of the a-c and d-c components being obtained by a bridge circuit which, properly balanced, eliminates the alternating voltage from the output circuit.

In the indirectly-heated type, the interposing of electrical insulation inevitably results in some temperature drop between heater and thermocouple junction and in a delay in the response of the thermocouple temperature to a rapidly changing load. Nevertheless, the time of response of the commercial thermal converter of this type, defined, in the usual manner for thermal meters, as the time required for the output to reach 90 per cent of its ultimate value, is approximately 4 seconds. In the directly-heated type of thermal converter, on the other hand, where the heat is generated directly in the thermocouple circuit, the speed of response depends chiefly upon the dimensions and material of the wires composing the thermocouples; a response time of less than 1/2 second readily is obtainable.

In the majority of installations it may be questioned whether the faster speed of response is of more than academic interest, since, where load changes occur only as small increments of the total load, the difference in the record obtained may be barely discernible, but, in control applications, the faster response does have marked advantages. This means, in general, that a high-speed electronically-balanced potentiometer recorder is required to take full advantage of the faster response of the directly-heated-type thermal converter.

Against the disadvantage of the indirectly-heated type of converter in response speed, there may be considered its advantage of complete freedom from a-c component in its d-c output circuit, due to the electrical insulation between circuits. In the directly-heated type described, however, alternating voltages exist simultaneously with the direct voltages in the thermocouple circuit, and precise balancing must be attained to reduce the alternating voltage component to a value which can be tolerated by the receiving equipment. While the functioning of a mechanically-balanced potentiometer is not adversely affected by a considerable a-c component, the electronically-balanced potentiometer, in which the advantage of faster converter response is best realized, may be rendered sluggish in its action by an alternating voltage component of only a few per cent of the magnitude of the direct voltage output.

In order to combine the advantages of efficiency and speed of response of the directly-heated type of converter with the freedom from a-c component of the indirectly-heated type, and at the same time to provide facility of adjustment and manufacturing control of characteristics, a new thermal converter recently has been developed.

In this converter each thermocouple junction is in direct contact with its associated heater, but each heater circuit is isolated by means of multiple-winding potential and current transformers; since but one point of contact exists between the thermocouple circuit and each of these isolated heater circuits, the development of an alternating voltage in

---

Paper 49-159, recommended by the AIEE Joint Subcommittee on Telemetering and approved by the AIEE Technical Program Committee for presentation at the AIEE Summer General Meeting, Swampscott, Mass., June 20-24, 1949. Manuscript submitted March 18, 1949; made available for printing April 29, 1949.

WILLIAM C. DOWNING, JR. is with the Sangamo Electric Company, Springfield, Ill.

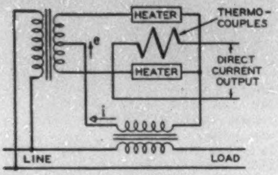

Figure 1. Basic thermal converter circuit

the output circuit is effectively eliminated.

Basic Circuit of New Converter

The basic circuit of any thermal wattmeter is illustrated, for the case of an indirectly-heated converter, in one of its simpler forms in Figure 1 (for simplicity only two thermocouples are shown). Two heaters of equal resistance, R, are supplied in series from the low-voltage secondary of a potential transformer whose primary is excited from the line, so that, due to voltage, e, alone, a current, $e/2R$, circulates through the heaters. A current transformer, excited by line current, is connected through a center tap in the potential-transformer secondary to supply the heaters in parallel so that, due to current, i, alone, current $i/2$ passes through each heater. In one heater these currents are additive and, in the other, subtractive; one heater, accordingly, develops heat at a rate proportional to $(e/2R+i/2)^2R$ and the other heater, $(e/2R-i/2)^2R$. The difference in the power developed in the two heaters is ei, or is proportional to the instantaneous power of the circuit measured; the temperature difference, measured by the thermocouples associated with these heaters, is thus a measure of the average power.

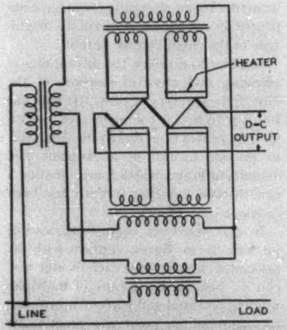

Figure 2. Basic thermal converter circuit with isolating transformers to permit direct contact between heaters and thermocouples

In the foregoing example it is obviously impossible to connect the thermocouple circuit directly to the heater circuit at more than one point. If, however, each heater is replaced by an isolating transformer with as many separate secondaries and heaters as there are thermocouples, an equivalent circuit is obtained, as shown in Figure 2, in which each thermocouple junction may be in direct contact with its associated heater.

In the new thermal converter, the two extra transformers introduced in Figure 2 are eliminated by the use of multiple-winding potential and current transformers, as shown in Figure 3. For each thermocouple junction there is an associated heater and a completely isolated secondary winding on both the potential transformer and the current transformer. Each heater circuit consists of a heater in series with a potential-transformer secondary coil and a current-transformer secondary coil; in half of the heater circuits, the polarity of the connection between the potential- and current-transformer secondary windings is such that the effects of line voltage and line current are additive, while in the other half the polarity is reversed to provide a subtractive effect. The general condition, then, that one set of heaters is heated proportionally to $(e/R+i)^2$ and the other to $(e/R-i)^2$ is met as before.

It will be noted that the series interconnection of potential- and current-transformer secondary coils of Figure 3 introduces no adverse inductive effects, such as might produce appreciable phase-angle errors in the resultant measurement, since the current transformer represents a noninductive burden to the potential-transformer output, and, conversely, the potential transformer appears noninductive to the current-transformer output. For example, if potential only is applied to the converter, all circuit constants being equal, the magnetomotive force resulting in the current transformer due to the circulating current flowing through the coils of additive connection will be exactly balanced by the circulating current flowing in the opposite direction through the subtractively-connected coils.

The single thermocouple, with each of its junctions in contact with a heater, also may be replaced, without affecting the principle of measurement, by two opposing thermocouples, each measuring the temperature difference between a heater and some common reference point. The use of opposing thermocouples in pairs, instead of the single thermocouple, offers structural advantages and reduces the thermocouple junction temperatures without affecting the temperature difference between junctions.

Thermocouple Construction and Characteristics

The construction of the basic thermocouple-heater unit is illustrated in Figure 4. The thermocouple consists of #38 molybdenum wire butt-welded to #33 constantan wire. The heater, of #33 constantan wire also, is welded at right angles to the thermocouple wire on the constantan component close to the thermocouple junction. The cross thus formed is in turn welded to four terminals, so located that the distance from junction to terminal is 0.125 inch for the constantan wires and 0.225 inch for the molybdenum wire. The terminals are in intimate thermal contact with, but electrically insulated from, the plate in which they are mounted; the plate, in turn, being of high thermal conductivity, insures that all terminals are maintained at substantially the same temperature and functions as a "heat sink."

To avoid conductive pickup of alternating voltage from the heater circuit by the thermocouple, the ideal junction between heater and thermocouple should be a point contact. Such a contact obviously would be undesirable from the point of heat transfer, as well as unattainable, but it follows that the cross weld between heater and thermocouple, and the butt weld between the components of the thermocouple, must be symmetrical to prevent any component of alternating voltage along the path of the d-c circuit, By careful control of these welds, it has been found entirely practical to keep this a-c component well within the allowable limits.

When current is passed through the heater, the temperature rises until the

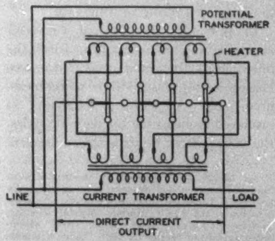

Figure 3. Basic circuit of new thermal converter

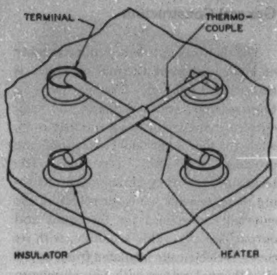

Figure 4. Heater-thermocouple unit

heat loss by conduction and by convection (radiation being negligible) balances the heat input. The "cold junctions" of the thermocouple at the terminals are held, by their close thermal association with the heat sink, at the reference temperature, while the "hot junction" approaches the maximum temperature of the heater.

The rate at which the temperature of the thermocouple junction rises—and, therefore, the speed of response of the converter—depends in general upon the ratio of heat storage capacity of the system to the rate of heat loss from it. If only the heat loss by conduction, which constitutes the major portion of the total heat loss, is considered, it will be seen that for any given materials the lengths of the heater and thermocouple wires become the most important factor in speed of response, since both the heat storage capacity and the conductive heat loss vary directly with the cross section of the wire. Faster response means shorter lengths; this in turn involves either a smaller cross section or higher conductive losses. Practical design, then, indicates a compromise between losses and speed of response such that the response is limited to that which is necessary to, and which can be utilized by, the equipment operating from the thermal converter. With the thermocouple unit described above, the output voltage follows closely an exponential curve, reaching 90 per cent of its ultimate deflection in approximately one second; with this response speed, the potential loss at rated voltage is limited to 2.4 watts and the current circuit loss at rated current to 0.9 watt per element.

Since the accuracy of the thermal converter requires that the output voltage must vary proportionally with the load measured, the electromotive force developed in any thermocouple pair must be proportional to the difference of power input to the heaters associated with that pair. It also may be shown that, if this proportionality is to be maintained for all conditions of voltage, power factor, and load (including reversal of load), each individual couple must generate a voltage proportional to the power developed in its associated heater.

The proportionality of power input to voltage generated in a thermocouple-heater unit depends upon the relation between the power input and the temperature difference between thermocouple junctions, and upon the relation between this temperature difference and the thermocouple voltage. If either of these relations varies from strict proportionality, the other relation must vary in the same degree, but in the opposite manner, if the output voltage is to vary directly with the power input.

In a constantan-molybdenum thermocouple the electromotive force increases more rapidly than the temperature difference. This factor is compensated, however, by the tendency for the temperature difference to increase less rapidly than the heat input. This latter factor is the combination of several effects: the heat loss by conduction through the constantan and the heat loss by convection both increase more rapidly than the temperature difference, whereas the heat loss by conduction through the molybdenum rises less rapidly than the temperature difference.

The temperature coefficient of thermal conductivity of molybdenum, as for most pure metals, is negative (that is, the conductivity decreases with rising temperature), but the coefficient is positive for constantan, as is characteristic of alloys in general. This difference provides a means for controlling the over-all relation between heat loss and temperature difference, by so varying the dimensions of the two materials as to change the proportion of heat flow through them. With the present dimensions, for example, the conductive heat loss through the molybdenum is roughly 1/2 that through the constantan, and the resultant load curve of the thermal converter is linear within ±1/4 per cent. If the diameter of the molybdenum thermocouple wire were increased and the diameter of the constantan wire decreased, the net heat loss might be left unchanged, but the proportion of heat flow through the two materials would be altered; in such an example, then, the increase in proportion of heat flow through the molybdenum would cause the converter output voltage to rise more rapidly than the measured load.

Adjustments

A schematic diagram of a complete, single-element, thermal converter is shown in Figure 5. Each such unit is complete in itself, and as many identical units are employed as are necessary for the type of circuit to be metered. For the measurement of 3-phase, 3-wire circuits for example, two single-element units are provided in a single enclosure.

Where a number of thermal converters are connected in series for totalizing, if the instrument transformer ratios of the various circuits to be totalized differ, the maximum output ratio is specified for the circuit having the highest instrument-transformer ratio. The output ratios of all other converters are reduced propor-

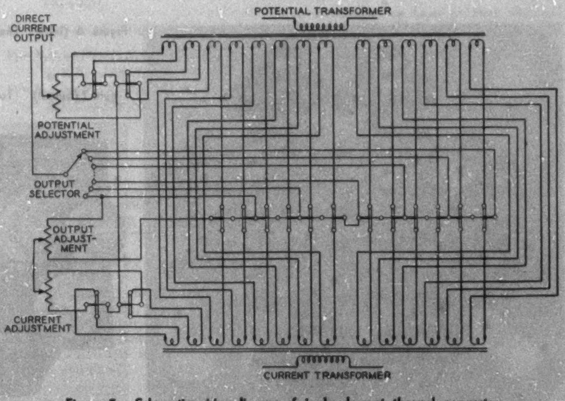

Figure 5. Schematic wiring diagram of single-element thermal converter

tionally to the ratios of the instrument transformers with which they are used, so that the millivolt output per kilowatt of primary power will be the same for each converter. Means should be provided, therefore, for the continuous adjustment of the output ratio from zero to the maximum output of the instrument.

Each converter element includes, for the measurement of power, six thermocouple pairs permanently connected in series. The external circuit is connected into this string of thermocouple pairs through a selector switch, in such manner that any number of thermocouple pairs, from six to one, may be included in the output circuit. A small voltage divider, permanently connected across the final thermocouple pair, provides for fine adjustment of the output ratio over a range of 1/6 of the maximum output ratio; this, in conjunction with the selector switch, permits continuous adjustment of the output ratio to any value up to the maximum rating of 60 millivolts per kilowatt for a 120-volt 5-ampere converter.

In addition, means must be provided for balancing out any errors which may exist due to dissymmetry of the input or output circuits. It may be shown (see the Appendix) that differences of heater resistances, or of the "efficiency" with which heat is translated into voltage in various thermocouples, result in an equation of the form

$$\text{Output voltage} = \Delta V = KEI \cos\theta + K_eE^2 + K_iI^2 \qquad (1)$$

The E^2 and I^2 terms, while small compared to the power term $EI \cos\theta$, nevertheless represent errors for which correction must be made if accuracy is to be attained. At no load, but rated voltage, for example, an appreciable E^2 term would cause an incorrect zero indication on the potentiometer.

The corresponding condition, of current but no voltage on the converter, would of itself be of no practical significance; however, when superimposed upon the main term, $EI \cos\theta$, of the expression for electromotive force, an appreciable I^2 term would result in load-curve distortion, power-factor errors, and inequality of output ratio on forward and reverse power flow.

These errors may be corrected readily by the inclusion, in series with the output circuit, of adjustable sources of direct voltage, proportional, respectively, to E^2 and I^2, which may be set to be exactly equal and opposite to the error terms. Two thermocouples, with heaters supplied from the potential transformer, are additively connected in series, across a small adjustable resistor connected as a voltage divider; by varying the position of the resistor brush, the voltage between it and the connection between the two thermocouples may be caused to vary in either direction from zero. A similar voltage divider and pair of thermocouples, heated by the current transformer only, provides a voltage proportional to I^2 which can be adjusted in either direction. In adjusting the thermal converter, then, the E^2 voltage divider is adjusted until, with rated voltage but no load, the output of the converter is zero, and the I^2 voltage divider is adjusted until the output at some load is the same in magnitude as, but of opposite polarity to, the voltage obtained when the same load is applied in the opposite direction.

General Construction

The thermocouple and heater assembly of a single-element thermal converter is shown in Figure 6. The six pairs of thermocouples which comprise the main output circuit are in the two center rows, while the four additional couple units are provided for E^2 and I^2 correction. The terminals, extending through the mounting plate, provide studs for soldering the external connections for the input and output circuits. This assembly, with its cover, is electrically insulated from, but in close thermal contact with, four aluminum studs which support it in the base. By providing this additional insulation between the output circuits and ground, the level of the insulation between the thermocouple terminals and their mounting plate may be reduced to that necessary to insulate between parts of the thermocouple and heater circuit.

The potential transformer is of conventional shell-type design, with 12 2-turn secondary coils for supplying heaters of the power group of couples and two 1-turn secondary coils for supplying the E^2 thermocouple heaters. The current transformer is of the core type and is made of a high permeability alloy in order to provide adequate ratio and phase-angle characteristics. In order to take full advantage of the high permeability of the core material, solid laminations (without gaps) are employed, and the primary and secondary coils are wound on the assembled core. Twelve 8-turn secondary coils provide for supplying heaters of the power group of thermocouples; two 6-turn secondary coils, for the I^2 heaters. The primary coil is wound on

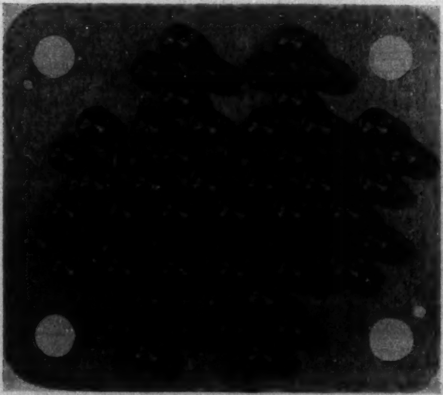

Figure 6 (left). Thermocouple assembly of single-element thermal converter

Figure 7 (below). Two-element thermal converter, with cover removed

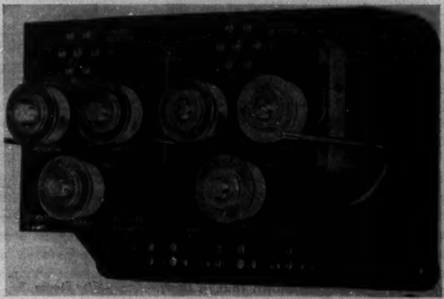

Figure 8. Two-element thermal converter

one end section. The secondary windings are disposed along each leg of the rectangular core. The interconnections between potential-transformer and current-transformer secondary coils are arranged so that the magnetizing effect of current due to potential cancels in adjacent coils of the current transformer. The combined phase angle of both transformers thus may be kept within ±15 minutes throughout the operating range of the instrument, a feature which is of importance in the case of a tie-line application where the power transferred may be largely or wholly reactive.

The voltage dividers for adjustment of potential balance, current balance, and output ratio, consist of six turns of manganin wire supported by a spirally-grooved steatite spool; an adjustment knob, operating on a thread of the same pitch as that of the spool, carries the brush which makes contact, under heavy pressure, with the manganin wire. A knurled locking nut is provided to secure the adjustment. These three resistors, together with a link and studs for selection of the output range, are mounted on a panel in the front of the converter element.

A dust-tight case and cover, with molded-melamine terminal-block construction, encloses the thermal converter. A 2-element converter, complete except for cover, is illustrated in Figure 7, and, with cover in place, in Figure 8.

Conclusion

In output ratio, speed of response, and freedom from a-c component, this new converter represents a compromise between the characteristics of existing converter types, which, it is felt, is distinctly practical in its application to present-day receiving instruments. Early tests indicate that its accuracy under all conditions of load, voltage, or temperature equals or exceeds that of existing converters. Its characteristics are controllable in manufacture and its adjustment facilities permit full advantage to be taken of its inherent accuracy. The design is, in general, adaptable to the measurement of any type of circuit of commercial voltage, current, and frequency rating.

Appendix. Derivation and Illustration of Equation 1

In Figure 9:

e, E = line voltage
i, I = line current
i_1, i_2 = heater currents
R_1, R_2 = heater resistances
p_1, p_2 = instantaneous heater power
P_1, P_2 = average heater power
θ = phase angle between E and I
V_1, V_2 = output voltages
N_1, N_2 = "efficiency" of conversion from power to thermocouple voltage
ΔV = net output voltage
K, K_e, K_i = constants

By Kirchhoff's laws

$$e = i_1R_1 - i_2R_2$$
$$i = i_1 + i_2$$

From which the heater currents are

$$i_1 = (iR_2 + e)/(R_1 + R_2)$$
$$i_2 = (iR_1 - e)/(R_1 + R_2)$$

The instantaneous heater inputs are

$$p_1 = i_1^2R_1 = (iR_2 + e)^2R_1/(R_1 + R_2)^2$$
$$p_2 = i_2^2R_2 = (iR_1 - e)^2R_2/(R_1 + R_2)^2$$

The average heater inputs are

$$P_1 = [(I^2R_2^2R_1) + 2EI\cos\theta \times R_2R_1 + E^2R_1)]/(R_1 + R_2)^2$$
$$P_2 = [(I^2R_2R_1^2) - 2EI\cos\theta \times R_2R_1 + E^2R_2)]/(R_1 + R_2)^2$$

The thermocouple outputs are

$$V_1 = N_1P_1 = (I^2R_2^2R_1N_1 + 2EI\cos\theta \times R_2R_1N_1 + E^2R_1N_1)/(R_1 + R_2)^2$$
$$V_2 = N_2P_2 = (I^2R_2R_1^2N_2 - 2EI\cos\theta \times R_2R_1N_2 + E^2R_2N_2)/(R_1 + R_2)^2$$

The net output is

$$\Delta V = V_1 - V_2$$
$$= I^2 \times \frac{R_1R_2(R_2N_1 - R_1N_2)}{(R_1 + R_2)^2} + EI\cos\theta \times \frac{2R_2R_1(N_1 + N_2)}{(R_1 + R_2)^2} + E^2 \times \frac{(R_1N_1 - R_2N_2)}{(R_1 + R_2)^2}$$
$$= I^2K_i + EI\cos\theta \times K + E^2 \times K_e \qquad (1)$$

To illustrate the effect of the I^2 term in load-curve distortion, power-factor errors, and difference of output ratio on forward and reverse power flow, let $K = 0.1$ millivolt per watt, $K_i = 0.04$ millivolt per ampere squared, and $K_e = 0$.

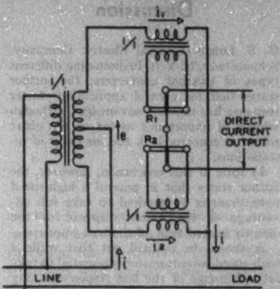

Figure 9. Basic thermal converter circuit for illustrating effect of unequal resistance and conversion efficiency

Case I. $E = 100$ volts, $I = 10$ amperes, $\cos\theta = 1.0$

$\Delta V = 100 + 4 = 104$ millivolts

Case II. $E = 100$ volts, $I = 5$ amperes, $\cos\theta = 1.0$

$\Delta V = 50 + 1 = 51$ millivolts

(ΔV should be 52 millivolts.)

Case III. $E = 100$ volts, $I = 10$ amperes, $\cos\theta = 0.5$

$\Delta V = 50 + 4 = 54$ millivolts

(ΔV should be 52 millivolts.)

Case IV. $E = 100$ volts, $I = -10$ amperes, $\cos\theta = 1.0$

$\Delta V = -100 + 4 = -90$ millivolts

(ΔV should be -104 millivolts.)

References

1. Totalizing of Electric System Loads, **P. M. Lincoln.** *AIEE Transactions*, volume 48, July 1929, pages 775–82.

2. Totalizing the Load of Four Stations, **Perry A. Borden.** *Electrical News* (Toronto, Ont., Canada), volume 35, December 1, 1926.

3. Load Totalizing in the New York Area, **F. Zogbaum.** *Electrical Engineering*, volume 53, June 1934, pages 886–89.

4. Interconnection Economies Through Telemeter Totalizing, **W. J. Lank.** *Electrical World* (New York, N. Y.), volume 103, June 30, 1934, pages 948–9.

5. Power Telemetered on Pennsylvania Line, **E. H. Brown.** *Electrical World* (New York, N. Y.), February 29, 1936.

6. Tie-line Control and Telemetering Essential in Power Interchange, **N. C. Pearcy.** *Electric Light and Power* (Chicago, Ill), May 1947.

7. Telemetering Proves Invaluable System Operating Tool, **R. G. Meyerand.** *Electric Light and Power* (Chicago, Ill.), volume 26, number 4, April 1948, pages 82–8.

8. Telemetering—Fundamentals for Power System Applications, **N. Cohn.** *Electric Light and Power* (Chicago, Ill.), volume 26, number 8, August 1948, page 72.

9. A High-Speed Thermal Wattmeter, **J. H. Miller.** *Electrical Engineering* (*AIEE Transactions*), volume 60, January 1941, pages 37–40.

Discussion

G. S. Lunge (General Electric Company, Schenectady, N. Y.): In discussing different types of thermal converters, the author states that for control applications faster response has marked advantages, although seldom of importance as far as the chart record is concerned, in the majority of installations.

In spite of this conclusion, however, the author states that in general a high-speed potentiometer is required to take full advantage of the faster response of the directly heated type of thermal converter.

It should be pointed out that while a high-speed potentiometer is essential to take full advantage of the fast response of any high-speed thermal converter, this potentiometer need not necessarily include recording features.

High-speed response in a recorder for rapidly varying measured quantities will simply result in producing a wide band of ink and hence a less legible chart record if ordinary chart speeds such as 1, 2 or 3 inches per hour are used, as is customary in measurement of electric power, for instance.

Consequently, it is suggested that consideration be given to using normal-speed recorders rather than high-speed recorders, in the interest of producing a more legible and considerably less expensive record than could be secured by the use, for instance, of exceptionally high chart speeds so as to resolve the record sufficiently to make its rapid variations clearly legible.

Wherever possible, the signal required for control purposes should be transmitted directly to the controller, without having to be retransmitted from a recorder. The recorders then are used only for their usual functions, namely, producing legible and continuous records of the quantities measured.

Perry A. Borden (The Bristol Company, Waterbury, Conn.): Although the combination of the thermal wattmeter network with differentially connected thermocouples to obtain a d-c effect proportional to a-c power has been known for 60 years, it is interesting to note that the device described by Mr. Downing represents only the third embodiment of this principle to have been developed to what may be called a practical form for the measurement of commercial power. The earlier two, both mentioned in this paper, were introduced in 1926 and 1940 respectively. In fact, the latter of these was first publicly described by Mr. J. H. Miller in his classical paper[1] at the Summer Meeting of the Institute, held in this place just nine years ago. Despite the wide and important application which has been made of the thermal wattmeter principle in telemetering and totalizing, as well as in demand measurement, our textbooks have given it little attention; and in the most recent (1946) edition of Encyclopedia Britannica the subject is dismissed with a scant two lines.

The Lincoln thermal converter, as pointed out by Mr. Downing, is characterized by a relatively long time interval of response, this being due both to the mass of material whose temperature must follow each variation in the measured magnitude and to the unavoidable thermal insulation between heaters and thermocouples. Also, this device is known to have a high internal resistance, with a correspondingly low power output and consequent limitation of practical measurement of its d-c potential to null methods.

The "Thermoverter," described in Mr. Miller's 1940 paper, is characterized by a rapid response—of the order of 1/2 second for 90 per cent of the final reading—and also by a reasonably high power output, making possible under some conditions the determination of output potentials with a direct-deflecting millivoltmeter of the switchboard type. Since the temperature rise of the heaters tends to be proportional to the square of the current which they carry, instruments of the thermal type are especially subject to damage by abnormal currents, as would result from short circuits or other faults in the line under measurement.

While the high thermal inertia of the Lincoln converter tends to offset this susceptibility to damage, it has been found necessary in the low-inertia unit described by Mr. Miller to meet such conditions "artificially," by designing the current transformers which form a part of the instrument in such a manner that their cores become saturated at a current value somewhat above the working range of the device, thus eliminating from the heaters the flow of a secondary current of objectionable magnitude.

In the light of the foregoing comments, we should have further information on the following two points:

1. As a criterion of practical application under normal conditions of use with a null-type recorder, and also as an indication of its adaptability to use with direct-deflecting instruments, it would be of interest to know the resistance value of the output circuit of the new converter, and also the maximum milliwatts available when supplying a matched external impedance.
2. What provision, if any, is made for protection of the heating elements against damage by abnormal currents?

Reference

1. See reference 9 of the paper.

William C. Downing, Jr.: In reply to Mr Borden's question as to the d-c circuit resistance of this thermal converter, the major portion of the resistance is in the potential dividers provided for the adjustments and therefore is dependent upon the position of these adjustments. For a single thermal converter element, with output ratio of approximately 30 millivolts for 500-watts input, the resistance of the d-c output circuit would be between 1 ohm and 7 ohms.

This converter is designed primarily for use with recording or indicating potentiometers. For use with indicating instruments of the d'Arsonval type, where a somewhat lower degree of accuracy might be acceptable than with the potentiometer, the E^2 and I^2 adjustments may be omitted and the output ratio adjustment modified so that the d-c circuit resistance might be of the order of 2 ohms.

It is quite true, as Mr. Borden states, that the older type Lincoln thermal converter obtained some degree of protection on heavy overloads of short duration due to its thermal inertia. However, where it has been necessary to meet specifications of ability to withstand 35 times rated current for 1/2 second, we have for a good many years supplied these converters with a saturable reactor shunted across the current element. In this new thermal converter, the saturable reactor is unnecessary as the design requirements of the current transformer, to give adequate phase angle accuracy, automatically give protection to the converter through saturation of the current transformer core. Incidentally, it may be shown, I believe, that the best that either an ideal saturable reactor or saturable current transformer can accomplish is to reduce the heating effect so that it approaches the first power, rather than the square, of the line current.

Heat Flow Ratio as a Design Parameter in Thermal Demand Meters

J. S. NELSON
ASSOCIATE AIEE

THE time of response of demand meters is of critical importance wherever a demand charge is made for electricity. In demand meters of the mechanical, block-interval type the demand interval is usually governed by a gear train and resetting mechanism connected with some synchronous device, such as a clock motor, and response time presents no special problems in design. The response time of thermal meters depends upon less-easily evaluated constants and coefficients. This paper examines these factors and presents equations from which the time of response may be calculated.

Specifically, these equations pertain to a thermal meter designed with opposed, self-heated, bimetallic spirals connected by a shaft. The effect of relative heat flow from the two opposing bimetallic actuators upon the time constant of a thermal demand meter is explored. To accomplish this, the time equation for a device responding to the difference in temperature of two similar bodies connected by a thermal shunt and each supplied with constant heat input is derived for the general case wherein the heat flow from one of the bodies is not equal to that from the other, that is, heat flow ratio other than unity.

This approach has yielded valuable information pertaining to the effect of differential heat escape upon response time. By making use of these equations, a linear-scale meter (for watt demand) and a square-law scale meter (volt-ampere demand) have been designed for the same response time to meet the same meter code requirement without the necessity for different designs of bimetallic spirals. The significance of this becomes clear when it is recalled that response time is defined in the Code for Electricity Meters[1] as time to reach 90 per cent of ultimate indication (in watts or volt amperes). Hence if two meters having different scale distribution are to meet the same code requirements, their physical response times, in terms of angular deflection, must differ correspondingly.

It is hoped that these equations may find application also to the design of integrating or indicating instruments employing thermal storage such as I^2T indicators for welding energy, small panel instruments of the bimetallic spiral variety, and differential thermometers composed of pairs of resistance-temperature detectors, bourdon tubes, thermocouples, or bimetallic actuators.

Although the effects described may be appreciated intuitively, mathematical equations are developed concurrently with the text for precision and clarity. A complete listing of the symbols used in this analysis, together with their relationships, is shown in Appendix I.

While it is not the purpose of this paper to examine electrical rates and metering methods, it is felt that a brief explanation of the purpose and operation of demand meters will be helpful in orienting the general reader with respect to the device serving as the subject for this analysis.

The demand of an installation or system is the load at the receiving terminals averaged over a specified interval of time.[2] This average may be a simple arithmetic average such as obtained with mechanical, block-interval meters or it may be a continuous logarithmic average[3] as obtained with a thermal demand meter of suitable design. In either type of metering, the information used for billing purposes is usually the maximum demand recorded between meter readings, which is combined with the kilowatt-hour consumption in a formula determined by the particular rate structure in effect. Rate structures with penalty clauses based on demand are used in many localities, in an effort to apportion more equitably the cost of providing generating and distributing capacity adequate for peak loads on the system.

The demand interval is usually made generous in length to avoid penalizing a customer unduly for normal heavy starting loads and other momentary peaks. A typical demand interval is 15 minutes.

Registration of maximum demand is accomplished normally by means of a pointer which can be driven only in the upscale direction by the action of the meter. The position of this pointer at the end of the month (or other billing period) is noted by the meter reader, who then resets it to zero or to the current position of the driving means. The driver, or pointer pusher, is itself a pointer, indicating the demand on a system at any instant (averaged over the current demand interval) for the convenience of the customer and for use in checking the operation of the meter.

Watt-demand and volt-ampere demand are frequently the basis for demand charges. The present paper deals with an assembly, the thermal unit, which may be used as the primary detector for measuring either quantity. The associated electrical circuit is designed to supply this unit with electric currents which are functions of the quantity measured.[3,4] The thermal unit combines the heating effects of these currents and translates these effects into a pointer position that is the proper function of the current flowing and the time during which it flows. It is

---

Paper 49-160, recommended by the AIEE Instruments and Measurements Committee and approved by the AIEE Technical Program Committee for presentation at the AIEE Summer General Meeting, Swampscott, Mass., June 20–24, 1949. Manuscript submitted March 21, 1949; made available for printing April 29, 1949.

J. S. Nelson is with the Meter and Instrument Divisions, General Electric Company, West Lynn, Mass.

The author is indebted to the authors of references 3 and 5, shown at the end of the paper, whose analyses have been extended to the more general case of unequal heat escape from the two bodies.

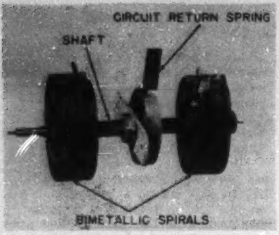

Figure 1. Basic thermal mechanism for demand metering

the purpose of this paper to demonstrate how small changes in thermal geometry may be used to effect differing time functions for this thermal unit and analogous thermal systems.

Analysis

The analysis presented is based on the performance of the thermal unit, Figure 1, which is used for thermal watt demand[3] and thermal volt-ampere demand metering.[4] This unit is composed essentially of two bimetallic spirals mounted on the same shaft in such a manner that increasing temperature in the two spirals produces opposing torques on the shaft. The angular position of the shaft at any time is therefore a function of the difference in temperature of the two spirals. The circuit is such that the current in spiral number 1 is greater than the current in spiral number 2 for up-scale deflection of the associated pointer. The shaft is of thermally conductive material and at a point between the two active spirals is a circuit-return spring connected to a copper lead whose thermal conductance accounts for a significant portion of the total heat loss from the assembly. If this spring is not located at the center point, it will conduct away relatively more heat from the nearer spiral. Similar differences in heat flow may be effected by varying the sizes of the wires connected to the spirals or the characteristics of the insulating shrouds. This relative heat flow, or, more precisely, the relative heat escape, expressed as a ratio, is a useful design parameter.

The utility of heat-escape ratio as a design parameter is not limited to cases of bodies of equal mass, but to avoid complication, M, the heat stored per degree of temperature, is assumed to be the same for the two bodies (bimetallic spirals). The thermal conductance from spiral number 1 to the ambient is denoted by h_1,[*] and h_2 represents the thermal conductance from spiral number 2. H_1 and H_2[*] are the rates of heat developed in (or supplied to) the two spirals, respectively, and Q is the thermal conductance of the connecting means (principally the shaft). θ_1 and θ_2 are temperature increments in the spirals resulting from the application of current to the meter. θ_{01} and θ_{02} are the initial temperatures at the beginning of the period under study, expressed in degrees above ambient temperature.

The heat input to spiral number 1, less the heat being lost down the shaft and by other means to spiral number 2, must at any instant equal the heat escaping to ambient added to the heat being stored in the spiral. In symbols

$$H_1dt-Q(\theta_1-\theta_2+\theta_{01}-\theta_{02})dt \\ =h_1(\theta_{01}+\theta_1)dt+Md\theta_1 \qquad (1)$$

and similarly,

$$H_2dt+Q(\theta_1-\theta_2+\theta_{01}-\theta_{02})dt \\ =h_2(\theta_{02}+\theta_2)dt+Md\theta_2 \qquad (2)$$

At some loss in generality, the solution to this pair of equations may be simplified by letting $\theta_{01}=\theta_{02}=\theta_0$. This limits the specific analysis to the case of initial equilibrium of the thermal unit, with pointer indicating zero, and with ambient temperature constant.

$$H_1dt-Q(\theta_1-\theta_2)dt=h_1(\theta_0+\theta_1)dt+Md\theta_1 \qquad (1a)$$

$$H_2dt+Q(\theta_1-\theta_2)dt=h_2(\theta_0+\theta_2)dt+Md\theta_2 \qquad (2a)$$

The substitution in equation 2a of the value of θ_2 and its derivative from equation 1a yields a second-order differential equation in θ_1

$$\frac{d^2}{dt^2}\theta_1+A\frac{d}{dt}\theta_1+B\theta_1=C-B\theta_0 \qquad (3)$$

wherein A, B, and C are shorthand for combinations of the primary design constants of the system (see Appendix I). By primary design constants are meant those constants such as mass, conductivity, thermal capacity, and so forth, which are controllable in design. The general solution may be obtained by the method of Euler and d'Alembert as follows

Let m be such that $\theta_1=\epsilon^{mt}$.

Substituting

$$m^2\epsilon^{mt}+Am\epsilon^{mt}+B\epsilon^{mt}=C-B\theta_0$$

from which is obtained the auxiliary or characteristic equation

$$m^2+Am+B=0$$

from which, by the quadratic formula

$$m=\frac{-A\pm\sqrt{A^2-4B}}{2}$$

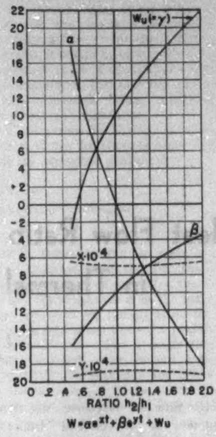

Figure 2. Effect of heat-escape ratio on thermal-unit coefficients

and the general solution may be written

$$\theta_1=c_1\epsilon^{\frac{-A+\sqrt{A^2-4B}}{2}t}+c_2\epsilon^{\frac{-A-\sqrt{A^2-4B}}{2}t}+c_3 \qquad (4)$$

wherein c_1, c_2, and c_3 are constants of integration.

An exactly analogous process yields the solution for θ_2:

$$\theta_2=c_1{}'\epsilon^{\frac{-A+\sqrt{A^2-4B}}{2}t}+c'_2\epsilon^{\frac{-A-\sqrt{A^2-4B}}{2}t}+c_3{}' \qquad (5)$$

It will be recalled that the angular position of the shaft and pointer is a function of the temperature difference, W, of the two spirals. Defining W as $\theta_1-\theta_2$, performing the subtraction, and introducing more shorthand to combine the integration constants

$$W=\alpha\epsilon^{\frac{-A+\sqrt{A^2-4B}}{2}t}+\beta\epsilon^{\frac{-A-\sqrt{A^2-4B}}{2}t}+\gamma \qquad (6)$$

rewritten for convenience.

$$W=\alpha\epsilon^{xt}+\beta\epsilon^{yt}+\gamma \qquad (7)$$

The only variables in equation 7 are W and t. This then is an expression for instantaneous temperature difference as a function of time. It remains to evaluate the constants α, β, and γ in terms of primary design constants.

Evaluation of Constants

The Constant γ

In equation 7, the exponent of ϵ may be

---

[*] See Appendix I for definition.

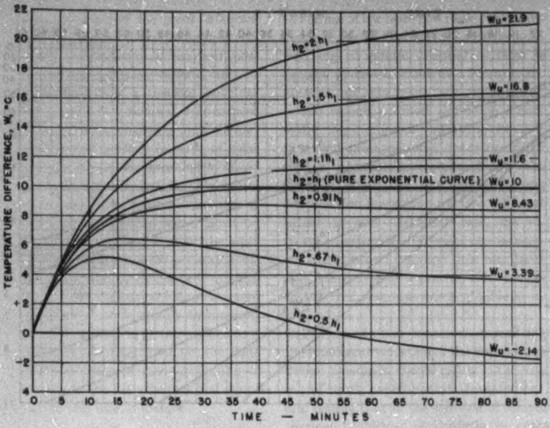

Figure 3. Calculated effect of heat-escape ratio on thermal unit time-performance curve

demonstrated negative for all real values. Hence at $t=\infty$, $W=\alpha\epsilon^{-\infty}+\beta\epsilon^{-\infty}+\gamma,=\gamma$; or, $W_{t=\infty}=\gamma=$(by definition) W_u, ultimate temperature difference.

From equation 3 and the analogous equation in θ_2, it is easy to find the ultimate values of θ_1 and θ_2, their difference, W_u, being rendered as

$$W_u=\frac{h_2H_1-h_1H_2}{Q(h_1+h_2)+h_1h_2} \tag{8}$$

In the special case where $h_1=h_2=h$

$$W_u=\frac{H_1-H_2}{2Q+h} \tag{9}$$

the same equation derived directly for this case in the literature.[4,5]

THE CONSTANTS α AND β

A new boundary condition is needed for the evaluation of the constants α and β. Before any heat can be lost from a body at room temperature, a temperature gradient must be established. If this hypothetical body has a finite heat capacity and a sudden input is applied, these two factors will, as t approaches zero, govern the rate of temperature rise.

This line of reasoning gives the equations

$$\left.\frac{d\theta_1}{dt}\right|_{t=0}=\frac{H_1}{M} \text{ and} \tag{10}$$

$$\left.\frac{d\theta_2}{dt}\right|_{t=0}=\frac{H_2}{M} \tag{11}$$

from which

$$\left.\frac{dW}{dt}\right|_{t=0}=\frac{H_1-H_2}{M} \tag{12}$$

Letting $W=0$ at $t=0$, from equation 7 is derived

$$\alpha+\beta=-\gamma \tag{13}$$

Differentiating equation 7 yields

$$\frac{dW}{dt}=x\alpha\epsilon^{xt}+y\beta\epsilon^{yt} \tag{14}$$

At $t=0$,

$$\left.\frac{dW}{dt}\right|_{t=0}=x\alpha+y\beta \tag{15}$$

Equating equations 12 and 15 and solving simultaneously with equation 13 yields β and α

$$\beta=\frac{h_2H_1-h_1H_2}{Q(h_1+h_2)+h_1h_2}\times\left(\frac{h_1+h_2+2Q-\sqrt{(h_1-h_2)^2+(2Q)^2}}{2\sqrt{(h_1-h_2)^2+(2Q)^2}}\right)-\frac{H_1-H_2}{\sqrt{(h_1-h_2)^2+(2Q)^2}} \tag{16}$$

$$\alpha=-\frac{h_2H_1-h_1H_2}{Q(h_1+h_2)+h_1h_2}-\frac{h_2H_1-h_1H_2}{Q(h_1+h_2)+h_1h_2}\times\left(\frac{h_1+h_2+2Q-\sqrt{(h_1-h_2)^2+(2Q)^2}}{2\sqrt{(h_1-h_2)^2+(2Q)^2}}\right)+\frac{H_1-H_2}{\sqrt{(h_1-h_2)^2+(2Q)^2}} \tag{17}$$

The exponents x and y were developed previously and their expanded forms are listed in Appendix I.

The fundamental equation of the thermal unit, equation 7, may now be expressed in terms of primary design constants. These constants, namely heat input, heat escape, thermal conductance, and thermal capacity, are all under the control of the designer and when these values are known thermal unit response may be predicted. As has been pointed out, when the heat-escapes from the two spirals are made equal a well-known result is obtained, equation 9, and when the thermal conductance between the bodies is reduced to zero, equation 7 reduces to an expression wherein the terms involving body 1 and body 2 are separated, as would be expected.

Interpretation of Results

The coefficients in the expression for temperature difference are presented graphically in Figure 2, and the performance of thermal units designed with such coefficients is illustrated in the succeeding figures. The shape and disposition of these curves is of greater interest than the numerical values, which are arbitrary.

The Ideal Design Parameter

The ideal design parameter, academically speaking, is one which influences only one characteristic of the device. The designer or experimenter can vary this parameter to produce a desired result with no effect on any other characteristic, and such a parameter is a very effective tool.

At first glance the parameter M, heat capacity, appears to fulfill the requirements for an ideal parameter. It appears only in the exponential terms and not in the expression for ultimate value. This appearance is illusory, at least with regard to the thermal mechanism of Figure 1, for practically it would be very difficult to change the heat capacity without affecting also the heat-escape properties, the electrical resistivity, or the thermal deflection properties of the bimetallic spirals.

On the other hand, the construction of Figure 1 affords a ready means of varying another parameter, namely heat-escape ratio, with relatively small effect upon the other design constants of the thermal unit, provided the changes in heat escape ratio are kept small. Quite significant changes in performance may be effected simply by placing the circuit return spring a short distance to left or right of the midpoint of the shaft. In order to appreciate the advantages and limitations of this parameter as a design tool, it is well to examine the effects of wide variations in h_2/h_1.

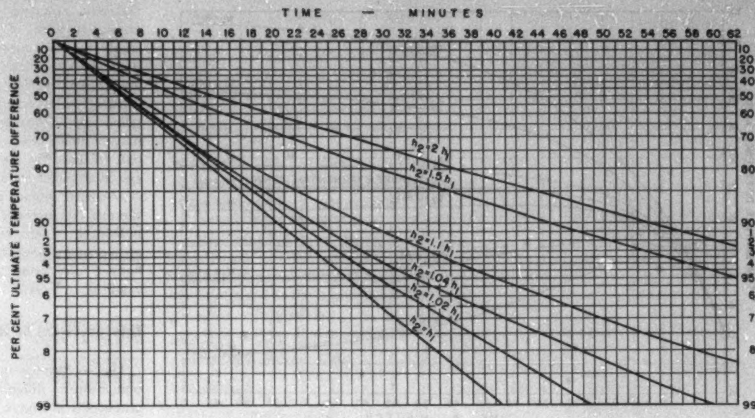

Figure 4. Per cent ultimate temperature difference as a function of time

Effects of Varying the Heat-Escape Ratio

The major effect of changing the design parameter h_2/h_1 is to operate upon the coefficients of the equation, the exponents x and y being very little affected by large changes in heat-escape ratio, Figure 2.

Referring again to Figure 2, it may be seen that selecting a heat-escape ratio other than unity is, to a first approximation, equivalent to adding or subtracting a definite fraction of a temperature increment that follows a different exponential curve from that at unity ratio. By adjusting the proportions of the two exponential terms through appropriate selection of the heat-escape ratio, various overall times of response may be attained, Figure 5. In cases of systems not required to approximate a simple exponential curve, a range of response times varying by a factor of ten or more may be achieved by doubling the heat-escape ratio.

Four categories of heat escape ratio are of interest and will be commented upon:

Ratio unity: A simple logarithmic curve results.

Ratio small: Temperature difference will lessen or reverse with time.

Ratio large: Response time is increased, but time constant is rendered complex.

Ratio slightly larger than unity: Response time may be controlled with the least effect upon other characteristics.

UNITY RATIO

Referring to Figure 2, the coefficient, α, of the first term has become zero and the coefficient, β, of the second term is equal numerically, but opposite in sign, to W_u, the ultimate temperature difference. A thermal unit designed with these coefficients will approach the value shown in equation 9 along a simple exponential curve with time (see Figure 3, curve labeled $h_2=h_1$). This performance curve is ideal for a demand meter indicating a continuous logarithmic average.[3]

SMALL RATIO

At values of heat-escape ratio less than unity the performance curve will overshoot, Figure 3, or dip, a condition to be avoided particularly in demand meters which contain maximum demand pointers. In indicating instruments such a condition is analogous to underdamping and is less serious the shorter the time required to reach the designed indication.

At very small values of h_2/h_1, W_u becomes negative, corresponding to an ultimate deflection in the direction governed by the spiral receiving the less input.

LARGE RATIO

A thermal mechanism designed with heat-escape ratio equal to or greater than unity will not overshoot, Figure 3. The response time increases with increasing ratio as depicted in Figure 5, which was plotted from the intersection of the curves in Figure 4 with the 90 per cent line. The ultimate difference also increases with h_2/h_1, as shown in Figures 3 and 5, so that no independent adjustment of response time is possible. At values greater than unity the performance does not follow a simple exponential curve, for two exponential functions are involved. In this connection note the departure from linearity of the response curves plotted on semilogarithmic co-ordinates, Figure 4, at ratios other than unity. If this "trailing off" is great enough, the result is known as "creeping"[3] which is, of course, objectionable in measuring devices.

RATIO SLIGHTLY LARGER THAN UNITY

The region between 1.0 and 1.1 or less is the useful area for demand meter thermal-unit design. In this region, a wide variation in response time may be obtained without the objectionable creep that results from the introduction of too large a portion of a second exponential term. As noted before, the unit cannot overshoot when h_2/h_1 is greater than unity. The value of deflection response time is very sensitive to variations in heat-escape ratio near unity, Figure 5, and it is in this region that heat-escape ratio partakes to the greatest extent of the characteristics of an ideal parameter. The change in heat-escape ratio necessary to produce a 10 per cent change in response time from the value at unity ratio will produce only a 4 per cent change in ultimate deflection or sensitivity of the thermal unit. As the thermal conduction path from a spiral through the shaft to the circuit return spring, Figure 1, is an important source of heat escape, a dislocation of the circuit return spring will cause a significant change in heat-escape ratio without materially affecting total heat escape. It may be seen from equation 8 that any change in the material or cross-section of the shaft which reduces h_1 and h_2 will increase the sensitivity or ultimate deflection of the thermal unit. This effect is made more pronounced by the reduction in Q accompanying such a modification. Because of the great influence of shaft design upon the response time and thermal unit sensitivity, it has been possible to adapt one basic thermal unit to the requirements of a thermal watt demand meter and a thermal volt-ampere demand meter by changing only the design of the shaft, which is made of solid brass in the former instance and of stainless steel tubing in the latter. The inherent or angular deflection response time of the volt-ampere demand meter must be materially greater than that of the watt demand meter, because 90 per cent indication occurs at only 81 per cent angular deflection when indication follows a square law. The bimetallic spirals themselves, the circuit return springs, the cups, covers, shrouds, and end shields remain the same for the two units, a standardization of great value in the manufacture and maintenance of this line of meters.

Summary

The role of heat-escape ratio in the performance of thermal units for demand metering has been illustrated. The curves presented were calculated with the use of arbitrary, although reasonable values for the design constants and do not in all cases agree with values chosen for the final designs of the thermal unit. The actual ratio of h_2 to h_1 also is affected by the lower temperature-rise-per-watt at higher temperatures, a radiation phenomenon neglected in the computation of these curves. These curves do, however, give a qualitative picture of the effect of varying the heat-escape ratio.

The use of the heat-flow ratio parameter in the design of thermal units for demand metering or similar thermal systems is subject to two limitations: First, it influences not only response time but also, to less extent, ultimate deflection. Secondly, this method of controlling response time will produce some departure from simple exponential response. In the example cited, one thermal unit was adapted for measuring at two different rates. In this particular case, the increase in ultimate deflection accompanying the increased response time was desirable and the small departure from simple exponential response was negligible in its effect.

The use of these equations, permitting the intelligent variation of the appropriate design constants, should result in the saving of much experimental, development, and testing time in the solution of related thermal problems, particularly in cases where it is desired to adapt one basic assembly to different times of response.

Appendix I. Definitions of Symbols and Their Relationships

H_1 = rate of heat applied to spiral number 1, in gram-calories per second

H_2 = rate of heat applied to spiral number 2 (exclusive of that received by conduction from spiral number 1), in gram-calories per second

h_1 = thermal conductance from spiral number 1 by all paths to ambient (exclusive of the path from spiral number 1 through the connecting means to spiral number 2) (gram-calories per second per degree centigrade)

h_2 = thermal conductance by all paths from spiral number 2 to ambient (gram-calories per second per degree centigrade)

Q = thermal transfer coefficient of shaft, or rigorously, heat transferred from one spiral to the other by all paths (gram-calories per second per degree centigrade)

θ_{01} = initial temperature of spiral number 1, degrees centigrade above ambient

θ_{02} = initial temperature of spiral number 2, degrees centigrade above ambient

θ_1 = instantaneous temperature of spiral number 1 above θ_{01} (degrees centigrade)

θ_2 = instantaneous temperature of spiral number 2 above θ_{02} (degrees centigrade)

M = thermal capacity of each spiral (assumed equal) (gram-calories per degree centigrade)

$$A=\frac{h_1+h_2+2Q}{M}$$

$$B=\frac{Q(h_1+h_2)+h_1h_2}{M^2}$$

$$C=\frac{Q(H_1+H_2)+h_2H_1}{M^2}$$

$$C'=\frac{Q(H_1+H_2)+h_1H_2}{M^2}$$

c_1, c_2, c_3 and c_1', c_2', c_3': integration constants evolving α, β, and γ

W = instantaneous temperature difference = $(\theta_1+\theta_{01})-(\theta_2+\theta_{02})$

$\gamma=c_3-c_3'$, a constant of integration, evaluated as W_u

ϵ = base of Napierian logarithms

$$x=\frac{-A+\sqrt{A^2-4B}}{2}$$

$$=-\frac{h_1+h_2+2Q-\sqrt{(h_1-h_2)^2+(2Q)^2}}{2M}$$

$$y=\frac{-A-\sqrt{A^2-4B}}{2}$$

$$=-\frac{h_1+h_2+2Q+\sqrt{(h_1-h_2)^2+(2Q)^2}}{2M}$$

t = time measured from application of load (seconds)

$\beta=c_2-c_2'$, a constant of integration evaluated as follows:

$$\beta=\frac{h_2H_1-h_1H_2}{Q(h_1+h_2)+h_1h_2}\times\left(\frac{h_1+h_2+2Q-\sqrt{(h_1-h_2)^2+(2Q)^2}}{2\sqrt{(h_1-h_2)^2+(2Q)^2}}\right)-\frac{H_1-H_2}{\sqrt{(h_1-h_2)^2+(2Q)^2}}$$

In special cases

$$\beta\Big|_{h1=h2=h}=-\frac{H_1-H_2}{2Q+h}$$ (value at unity heat-escape ratio)

$$\beta\Big|_{Q=0}=-\frac{H_1}{h_1}$$ (value for an isolated spiral)

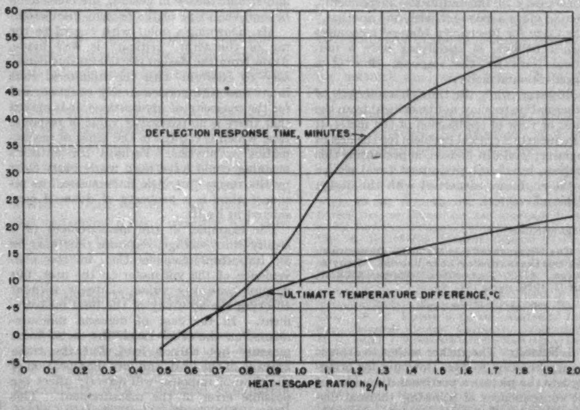

Figure 5. Response time and ultimate temperature difference as functions of heat-escape ratio

$\alpha = c_1 - c_1'$, a constant of integration evaluated as follows:

$$\alpha = -\frac{h_2H_1 - h_1H_2}{Q(h_1+h_2)+h_1h_2} - \frac{h_2H_1 - h_1H_2}{Q(h_1+h_2)+h_1h_2} \times \left(\frac{h_1+h_2+2Q-\sqrt{(h_1-h_2)^2+(2Q)^2}}{2\sqrt{(h_1-h_2)^2+(2Q)^2}}\right) + \frac{H_1-H_2}{\sqrt{(h_1-h_2)^2+(2Q)^2}}$$

In special cases

$$\alpha\Big|_{h_1=h_2=h} = 0 \text{ (value at unity heat-escape ratio)}$$

$$\alpha\Big|_{Q=0} = \frac{H_2}{h_2} \text{ (value for an isolated spiral)}$$

The fundamental equation 7:

$$\left.\begin{aligned} W &= \alpha\epsilon^{xt}+\beta\epsilon^{yt}+W_u \\ &\text{or,} \\ W &= -\alpha(1-\epsilon^{xt}) - \beta(1-\epsilon^{yt}) \end{aligned}\right\} \text{(Where } x \text{ and } y \text{ are; negative constants the only variables, } W \text{ and } t)$$

The ultimate temperature difference (full-scale value)

$$W_u = \gamma = -(\alpha+\beta) = \frac{h_2H_1 - h_1H_2}{Q(h_1+h_2)+h_1h_2}$$

References

1. Code for Electricity Meters. *C*-12-1941, American Standards Association (New York, N. Y.) 1941.

2. American Standard Definitions of Electrical Terms. AIEE, August 1941, section 35.20.-075, page 121.

3. Theoretical Possibilities of an Internally Heated Bi-Metal Type of Thermal Watt Demand Meter, E. E. Lynch. *Electrical Engineering (AIEE Transactions)*, volume 61, October 1942, pages 760–70.

4. A New Thermal Volt-Ampere Demand Meter, M. E. Douglass, W. H. Morong. *AIEE Transactions*, volume 68, part I, 1949, pages 79–83.

5. Rates and Rate Making, Paul M. Lincoln. *AIEE Transactions*, volume 34, part II, October 1915, pages 2279–2318.

Discussion

Wm. C. Downing, Jr. (Sangamo Electric Company, Springfield, Ill.): In presenting his excellent analysis of the effects of thermal dissymmetry on the time of response of thermal demand meters, Mr. Nelson has made a worthwhile contribution to the literature on this subject. While these general principles have been appreciated, in the past, and have been employed to control the response time characteristics of thermal meters, there has not been available, to my knowledge, any such quantitative analysis. This paper, therefore, should provide a valuable reference for future work in this field.

While the heat flow ratio has been selected as the parameter for this analysis, it is inferred that a comparable set of equations might be developed based upon the thermal capacity ratio as a parameter, the heat flow ratio being unity. In other words, the time of response also may be controlled by unbalancing the heat storage factors instead of the heat flow. Practical considerations, based on constructional features, normally determine the choice of one of these methods, or a combination of them; for, while it is quite true that it is difficult in general to unbalance the thermal capacity without disturbing the heat flow ratio, unbalancing of the heat flow ratio must be used with caution to avoid the introduction of errors which may be of much more importance than the time characteristic. As this latter point is not considered in this paper, it may be well to amplify it.

Let us assume, for example, a thermal watt demand meter in which the heat flow ratio is 1.1. If for a certain load, H_1 is 3 watts and H_2 is 1 watt, the numerator of the expression for W_u, equation 8, is $3.3-1$, or 2.3. For the same power measured, but at a different power factor, for example, H_1 might be 4 watts and H_2 2 watts, since the electrical circuit provides only that the difference between H_1 and H_2 remains proportional to the power measured; however, in this latter case, the numerator of equation 8 becomes $4.4 - 2$, or 2.4. As W_u should be alike in these two cases, the introduction of a heat flow ratio other than unity has introduced an error in meter registration. This would appear to be a more serious limitation to the use of heat flow ratio as a parameter than either of those mentioned in the paper.

Actually, of course, some such "error" may be desirable to compensate for the tendency of the temperature-rise-per-watt to decrease when the total power input is increased as in the foregoing example, and watt demand meters have been built for years with a heat flow ratio slightly greater than unity for this reason. Nevertheless, it may be argued that the importance of the heat flow ratio in minimizing power factor, voltage, or balance errors should dominate, in design, its effect on time of response.

In only one respect, however, would I question Mr. Nelson's paper and that is in reference to the opening statement that "the time of response of demand meters is of critical importance." Insofar as the timing accuracy of a demand register is concerned, this is quite true; but I believe it has been rather well established by a number of independent surveys that whether the time interval is 15 minutes or, say, 20 minutes, for either a demand register or a thermal demand meter, makes negligible difference in the billing of the great majority of demand loads. For one such reference, refer to P. A. Borden's paper presented before the Institute in 1920[1]; "Except upon the most fluctuating loads, the demand meters of one type, and of differing time periods give indications which, generally, within the limits of accuracy of the individual instruments, were in close agreement with one another." The Code for Electricity Meters[2] recognizes this, I believe, in specifying only a unilateral limit for the response time of a lagged-demand meter.

However, while the time characteristic of a thermal meter may not be critical from the point of view of application of the meter, it is frequently a critical problem for the design engineer; and Mr. Nelson, in presenting this analysis, has, I feel, performed a real service to the engineers concerned with the design of thermal meters.

References

1. The Measurement of Maximum Demand and The Determination of Load Factor. Perry A. Borden. *AIEE Transactions*, volume XXXIX, part II, 1920, pages 1847–94.

2. See reference 1 of the paper.

J. S. Nelson: The author wishes to express his appreciation to Mr. Downing for bringing into the picture a pertinent discussion of the consequences of allowing thermal dissymmetry to affect ultimate deflection. He states that "the electrical circuit provides only that the difference between H_1 and H_2 remain proportional to the power measured," and deduces therefrom certain errors in registration at different levels of spiral energization. In this connection it is well to point out that, in certain instances, circuit elements may be provided with resistance characteristics such that the expression proportional to the quantity measured is not $H_1 - H_2$, but $kH_1 - H_2$, where k is a constant containing the parameter h_2/h_1. A circuit designed for such proportionality in the measurement of volt ampere demand has been described in a previous paper before the Institute by Douglass and Morong.[1]

Mr. Downing's reservation may therefore be regarded as particular, rather than general, specifically applying to the use of unbalanced heat escape in thermal watt demand meters, and with this reservation the writer is in full agreement. In a family of meters using the same basic thermal motor, the watt demand meter should be assigned the position at or nearest unity ratio. Power factor errors still present may be compensated successfully by the appropriate relationship between the resistances of the upscale and downscale bimetallic spirals, which resistances are themselves functions of temperature and current. The design criteria for accomplishing this compensation, and circuit theory in general, are considered beyond the scope of the present discussion.

Mr. Downing's point with regard to the use of the term "critical" is well made. Aside from the design considerations necessary to conform with the unilateral code limits and with good metering practice, and for the majority of applications, it is agreed that there is no particular value of response time which is critical in the sense of mathematics or physics. Perhaps the author's meaning could have been made more clear by the terms "intrinsic importance," as response time is a property of demand considered in itself.

For example, in the measurement of a steady-state voltage, response time may be an important consideration in the convenience of the voltmeter to the user, but it may have any value whatever without effecting the accuracy of the final measurement. In the case of demand measurements, on the other hand, the meter must measure not only a load, but the time-average of the load, and any modification of the time of response will directly affect the possible error of the measurement. This means that, in the ideal, the time of response is just as critical as the demand measurement itself (but no more so). If a 15-minute demand interval meter produces the same maximum reading as a 20-minute demand interval meter connected to the same terminals, it must be due to the fortuitous circumstance that the system had equal 15-minute and 20-minute maximum demands during the period of the test. Happily, as Mr. Downing points out, this ordinarily will be the case, and this fact should be recognized in the application of thermal demand meters.

Reference

1. See reference 4 of the paper.

An Improved A-C Network Analyzer

W. A. MORGAN
MEMBER AIEE

F. S. ROTHE
MEMBER AIEE

J. J. WINSNESS
NONMEMBER AIEE

SINCE the first a-c network analyzer was installed in 1929 at the Massachusetts Institute of Technology,[1] it has become the accepted tool for the solution of the complex circuit problems involved in the design, planning, and operation of power systems. There are now over 20 a-c network analyzers in the United States[2] and several more built or planned in Canada, England, Europe, South America, and India. Many of these analyzers are used by a number of different groups on a rental or co-operative basis. The improvements in design and performance of the analyzer which are described in this paper will thus be of interest to a large number of users of such equipment. These improvements include: master instruments which read power and reactive flows directly in megawatts and megavars for any one of three system megavolt-ampere bases and on any one of six current scales; a complete set of generator instruments which allows volts, megawatts, and megavars to be preset; load-adjusting autotransformers with voltmeters, which permit the system loads to be held constant without reference to the master instruments; a flexible method for the exact representation of a transmission line by means of an equivalent circuit; push button selection of circuits to be metered, either singly or in groups; and complete factory wiring, assembly, and testing. An analyzer of this improved design recently has been installed at the United States Bureau of Reclamation in Denver, Colorado.

Value of the A-C Network Analyzer

There are several reasons for the acceptance of the a-c network analyzer as a tool in solving power-system problems. In contrast with numerical calculating machines, it uses voltage, current, and impedances to solve the problem. Thus a power system covering several states can be represented realistically on an analyzer in a medium-sized room by simply replacing the elements of the power system with electric circuits. The power engineer is familiar with the use of equivalent circuits for such elements as synchronous machines, transformers, and transmission lines. By the use of equivalent circuits a variety of problems in electromagnetic fields, vibration, heat flow, and other subjects also have been solved on network analyzers.[3]

The modern a-c network analyzer is a very flexible device. System changes such as a load increase, a line outage, a change in transformer taps, or a change in the supply of reactive power, can be simulated rapidly and their effect found immediately. Since power-system design is based on the collective judgment of several persons, the problem is not one of specifying a set of initial conditions and obtaining a result correct to four decimals but rather a determination by trial and error of the best design based on a number of initial assumptions. The a-c network analyzer is essential for the expeditious study of complicated networks under variable conditions; even on simpler systems the accuracy of a numerical calculator is not necessary.

The first cost of a modern analyzer might seem high, but is actually low in comparison with possible savings in system design. A recent study made on the analyzer of the United States Bureau of Reclamation resulted in the substitution of a single-circuit 115-kv line for over 15 miles of 2-circuit line which had been previously thought necessary. Another saving resulted when it was determined that a synchronous condenser was not needed at an extension of the power system as originally planned.

Perhaps the greatest savings in power-system design, resulting from the use of the a-c network analyzer by the Bureau of Reclamation has been in power-system transient stability studies. Wherever practicable, and where the nature of the load justifies it, it is the policy of the Bureau of Reclamation to design its power systems to be stable for the most severe probable fault conditions. This becomes a determining factor because the Bureau's hydroelectric generation is usually at a long distance from the load centers.

Low generator transient reactance is an important factor in transient stability. However, due to their slow speed, hydroelectric generators normally do not have as low a reactance as steam-turbine generators, and special low reactances are obtained at extra cost. The a-c network analyzer is the best means available to evaluate this extra cost, which would be considerable for a plant such as Grand Coulee with an installed capacity of over 2,000,000 kva.

The value of rapid reclosing of circuit-breakers (12–20 cycle) on transient stability of a power system can be determined accurately in advance only by analyzer studies. Such studies, made in 1944 by the Bureau of Reclamation demonstrated that two 161-kv transmission lines, 140 miles long, with 20-cycle reclosing circuit breakers, were the practical equivalent of three lines without 20-cycle reclosing circuit breakers for the loads involved.[4] Subsequent operation through two complete years of this system, in lightning-active country, proved that the calculating-board studies were accurate. In the future, the important

---

Paper 49-164, recommended by the AIEE Computing Devices Committee and approved by the AIEE Technical Program Committee for presentation at the AIEE Summer General Meeting, Swampscott, Mass., June 20–24, 1949. Manuscript submitted March 7, 1949; made available for printing April 29, 1949.

W. A. Morgan is in charge of the Power System Technical Section, Bureau of Reclamation, Denver, Colo.; F. S. Rothe is in the Analytical Division, General Electric Company, Schenectady, N. Y.; and J. J. Winsness is in the Switchgear Divisions, General Electric Company, Philadelphia, Pa.

The authors wish to acknowledge the important contribution from H. A. Peterson of the University of Wisconsin, formerly with the General Electric Company, to the general design of the analyzer, and from H. P. Kuehni of the General Electric Company to the design of the master instrument system.

load served by these two transmission lines will be supplied principally from a different direction as new hydroelectric generation sources are developed. At that time the two initial lines are all that are required from a power-flow or stability standpoint from the present source of generation even without dependence upon reclosing circuit breakers. Thus, the application of reclosing circuit breakers for the initial system saved building a 140-mile 161-kv line that would not be required in the ultimate system. It is Bureau of Reclamation practice, in the design of practically all its power systems of 115 kv and above, to utilize to the fullest extent the advantage of ultra-rapid reclosing circuit breakers in transient stability, with the result that the a-c network analyzer will help the Bureau to save many hundreds of miles of transmission lines.

For some important loads an interruption of any kind is a serious matter. Such loads could not tolerate the instability that would result if reclosing on a permanent fault occurred. Thus, in areas where the faults are less likely to be due to lightning and faults due to airplanes and similar hazards are more probable, rapidly reclosing circuit breakers may not be so essential. In these cases, the a-c network analyzer is used to investigate stability of the power system for the condition of faulting and clearing, without reclosing, the most heavily-loaded transmission line section. If rapid reclosing circuit breakers are used on such a system to restore the faulted line section to service as soon as possible, then the a-c network analyzer would be used to determine what must be done to the system to make it stable for the condition of reclosing on a permanent fault and clearing the faulted line a second time.

These are but a few specific examples that show how the a-c network analyzer installed at the Bureau of Reclamation already has paid for itself in design savings.

General Design Features

The best design of an a-c network analyzer should satisfy the requirements of accuracy, flexibility, and reliability at reasonable cost. The choice of the base electrical quantities of voltage, current, and frequency on which the per-unit representation of the power system is made is very important. A small current base and high impedance base result in freedom from heating and contact problems, allow the use of the very reliable telephone-type cords, plugs, and jacks, and permit a wide range in the operation of the units. The first analyzer employing a base current less than 1 ampere was built in 1938.[5] This analyzer used a base voltage of 50 volts, a base current of 50 milliamperes, and a base frequency of 480 cycles. This analyzer has been in continuous use since that date. During the war it was in operation 16 hours a day for two years; since the war it has been operating 60 hours a week until recently. This experience and the small amount of maintenance has shown that the choice of base quantities was sound, and that the design of the board was such as to make it very reliable. The stray capacitances associated with the high impedance base have not been found to be important in system studies. The new analyzer, shown in Figure 1, makes use of such techniques as careful arrangement of wiring and use of low-capacitance switches and relays to make this effect negligible. Therefore, the use of these same base quantities has been continued in the improved analyzer.

Table I shows the number, range, and ratings of the different types of circuit units in the Bureau of Reclamation analyzer. The ranges of units are such that, in the majority of cases, one unit will cover the range required. All of the impedance and transformer units are rated 1.25 per unit volts and 5 per unit current. Their thermal ratings are such that no damage will be done to them at 10 per unit current. Low flux densities and air-gap construction utilized in the reactors results in very little variation in impedance up to 10 per unit current and 1.25 per unit volts. The generator units are rated 2.5 per unit volts and have 2 per cent regulation at 10 per unit current. They are capable of delivering 20 per unit current with slightly higher regulation. These wide operating limits make it possible to handle most problems such as load and short-circuit studies with ease, without spending a considerable amount of time in setting up the system between narrow limits. For extreme conditions, it is possible to reduce the analyzer input voltage to $^1/_2$ or $^1/_4$ normal. With 25 per cent input voltage to the analyzer and 20 times normal current from a generator,

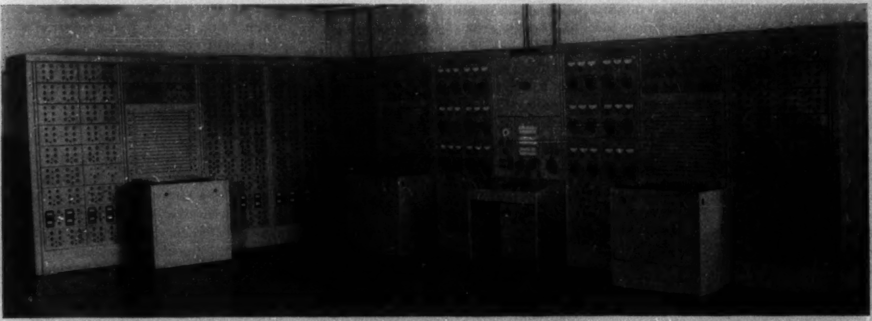

Figure 1. A typical modern a-c network analyzer

The center cabinet of the front section contains the master instruments and associated voltage, current, and push-button selector switches. Adjacent to and on each side of the instrument cabinet is a unit cabinet containing six generator units and six synchronous impedance units. Cabinets 2, 6, and 10 (numbered from left end) are plug-and-jack cabinets in which the terminals of circuit units in two or three adjacent cabinets are brought out for interconnection. The remaining cabinets are unit cabinets containing line, load, autotransformer, capacitor, and mutual transformer units. This analyzer has the front section and left wing with provisions for future addition of a right wing

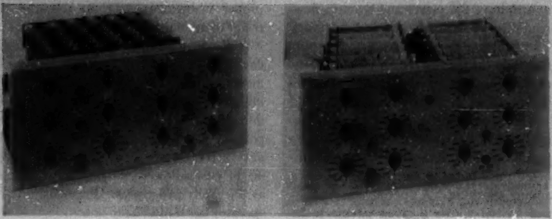

Figure 2. Capacitor-unit and line-unit drawout tray

Line unit with Pi-line switches

a fault current of 80 times the system base can be supplied from any generator unit. This large current range has proved to be very valuable in making system studies.

Tapped resistors, reactors, and capacitors are used in all units, except for the 0 to 0.1 per unit resistance in the load unit, in order to obtain definite fixed values of impedance. The accuracy on all taps down to 0.02 per unit at a specified current is ± 1 per cent, and ± 2 per cent at 0.01 and 0.02 per unit. The change in reactance of the reactors is less than ± 2 per cent over the full current range at any setting.

The impedance and transformer units are mounted on standard 8-inch high by 16-inch wide by 18-inch deep drawout trays. Figure 2 shows typical line-unit and capacitor-unit trays. Two line units or six capacitor units are mounted on one tray as shown. The generator unit is mounted on a double-height drawout tray, as shown in Figure 3. This standardization in tray size permits a standard unit cabinet size and maximum flexibility in arrangement of units and cabinets.

Load Units and Load Adjusters

The load units have individual voltmeters with manually-set pointers, and are connected to the system through individual autotransformers so that the voltage impressed on each unit can be kept constant regardless of changes in system voltage. This is especially helpful during the initial adjustment period, before the transmission line voltage opposite a given load substation has stabilized. The settings of the resistance and reactance values of the load units are calculated previously on the basis of one per unit voltage. If voltages other than one per unit prevail, then the loads would be different from what they are supposed to be, with no change in the load unit settings. The individual voltmeters allow the adjuster to monitor these load units and to keep the voltage at one per unit by adjustment of the one per cent taps of the autotransformer, without reference to the master instruments. It has been found that this feature saves considerable time in making load studies where it is desired to keep the system load constant during variations in the system design.[6]

Generator Units

Each generator unit consists of two selsyns, one for controlling phase angle and the other for controlling voltage magnitude. In addition, each generator unit has its own instrumentation, including a voltmeter, varmeter, and wattmeter, as shown in Figure 3. These instruments have red hand-set pointers that may be used to indicate the conditions under which the generator is expected to operate. A varmeter has been substituted for the ammeter usually found on generator units because watts and vars are of primary interest in adjusting a generator unit during a system study. In order to minimize the load imposed by the instruments on the generator and to decrease their effect on regulation, a current amplifier is used to feed the wattmeter and varmeter. The voltmeter can be connected either at the generator terminals or at any desired bus on the system.

Equivalent Pi-Line Units

Pi-line units have been found to be very useful in making system studies. It is desirable to be able to meter both ends of a pi-line unit and also, if possible, to use the capacitors and line unit individually. The equivalent pi-line unit consists of two standard capacitor units and one standard line unit, with a toggle switch on the line unit to connect a capacitor unit to each end of the line unit. Figure 4 shows the equivalent pi-line circuit. By plugging the capacitor-unit cords for units *300* and *301*, it is possible to read power flow at both ends of the line. Opening the toggle switch permits free and independent use of the line-unit and capacitor-unit sections in any manner desired. This permits having pi-line units without incurring restrictions in flexibility.

Instrument System

The master-instrument system is probably the most important part of a network analyzer. Figure 5 shows the master-instrument control panel, including the master instruments, scale selector switches, voltage and current selector switches, motor-generator-set control switches, reference phase shifter, and push-button selector panel. The master instruments include a voltmeter, ammeter, and wattmeter-varmeter of the light-beam-type, with 8-inch scales having 150 divisions. These instruments have an extremely fast rate of response and are well damped, making possible rapid reading. The burden imposed on the network by these instruments is minimized by the use of current and voltage feedback amplifiers. For the nominal

Table I. Number and Range of Circuit Units

Number	Units	Per Unit Range	Steps	Rating: Per Unit Volts	Rating: Per Unit Amperes
12	Generator unit	V 0—2.5	Continuous	2.5	10.0
		ϕ 0 ± 180 degrees	Continuous		
12	Synchronous impedance	R 0—0.11	0.001	1.25	5.0
	(Series $R + jX$)	X 0—1.11	0.001		
108	Line units	R 0—0.51	0.001	1.25	5.0
	(Series $R + jX$)	X 0—0.81	0.001		
32	Load units	R 0—16.1	Continuous	1.25	5.0
	(Series or parallel $R + jX$)	X 0—16.05	0.05		
32	Load unit autotransformer	V 0— ±15 per cent	1 per cent	1.25	5.0
42	Capacitor units (Susceptance)	0—1.1	0.01	1.25	
4	Large capacitor units (Susceptance)	0—50.0	1.0	1.25	
18	Autotransformer units	V 0— ±30.5 per cent	0.5 per cent	1.25	5.0
12	Mutual transformer units	1:1 Ratio		1.25	5.0

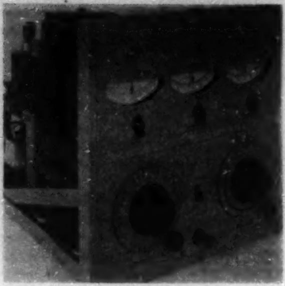

Figure 3. Generator unit

analyzer voltage and current of 50 volts and 50 milliamperes, a maximum potential drop of 0.01 volts (0.02 per cent) across the current shunts and a potential current of 0.1 milliamperes (0.2 per cent) was set as limits of instrument burden. The accuracy of the master-instrument system is within ± 0.5 per cent of full scale.

The scales on the master ammeter and wattmeter are arranged so that the digits appearing at the large scale divisions change with the scale multipliers. The current shunts of the instruments also are changed simultaneously by the knurled-handled scale-selector switch. Thus, the ammeter is direct reading in per unit for any of the six available current multipliers, and the wattmeter is made direct reading either in per unit, or on a 20-megavolt-ampere, 50-megavolt-ampere, or 100-megavolt-ampere base for any of the available current multipliers. This feature is a big improvement, as it allows the operator to change the multiplier readily, for successive metered points if he wishes, so as to get the reading at a favored location on the instrument scale and to have the power and reactive flows read directly in megawatts and megavars. The operator does not have to multiply mentally the reading by a factor to get the actual reading, or remember which of several scales to read.

The master instruments may be connected to meter any circuit selected by means of a 3-column keyboard of numbered push buttons, similar to that of an adding machine. A special master control switch allows a given circuit to be selected by the push buttons while the previous circuit, indicated by the numbered lights adjacent to the push-buttons, is still being metered. This saves time as, while the recorder is putting down the previous reading and the instruments are kept on the previous circuit in case a question should arise, the operator can refer to the plugging diagram, select the next circuit he wishes to meter, and push down the corresponding selector push buttons. Then, when the recorder is ready, the operator pushes the master control switch which connects the instruments to the new circuit and lights the adjacent numbered lights corresponding to the numbered push-buttons, and the operator announces to the recorder which circuit is being metered. While the recorder is locating the new circuit on the diagram, the operator has selected the proper instrument scale to use and is ready to announce the readings.

A special connection of the metering circuit allows the watt and var measurements to be of the proper sign when looking away from a bus, whether the given unit is metered from its polarity or nonpolarity jack plug end. This feature permits faster recording and simplifies checking of power-flow readings around a bus as the study progresses. Previously, the operator has had to keep in mind whether he was metering the polarity or nonpolarity jack plug end of a unit and mentally reverse the sign of the watts or vars from that indicated by the instruments and switches, when appropriate.

The Bureau of Reclamation has taken full advantage of this feature in originating a new method of indicating polarity sign of watt and var readings on power-flow diagrams. This is illustrated in Figure 6. The arrows are made up initially as part of the basic single-line diagram and are for reference only, to show the direction the instruments were looking when the readings were taken. The plus and minus signs in front of the watts (above the line) and vars (below the line) are then the actual signs indicated to be used by the master instruments and polarity switches, referred to the reference arrow direction, which is always away

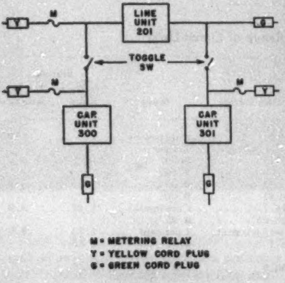

Figure 4. Schematic diagram of equivalent pi-line unit

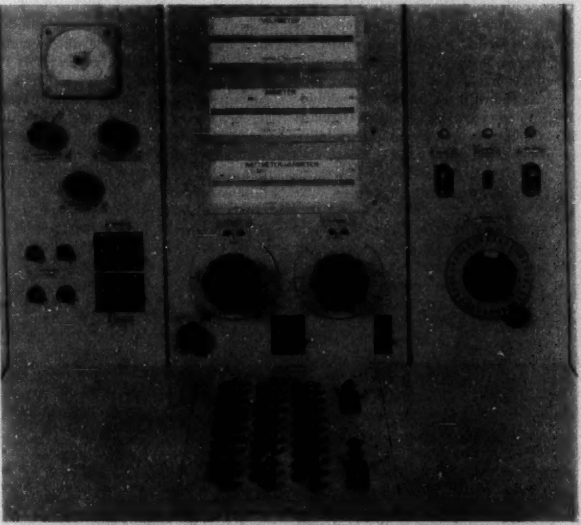

Figure 5. Master-instrument and control panel showing master instruments, scale-selector switches, metering switches, push-button keyboard, and other controls

from the bus. An analyzer unit with jack plug ends on two different busses would read plus power at one end and minus power at the other end, corresponding to the flow of power out of one bus and into the second bus. By having the plus and minus signs in front of the watt and var readings, the recorder readily can add algebraically the power and reactive-power flows over the circuits connecting to each bus to see that they total zero. This may be done conveniently by a third person without delaying the recording process. These checks make it possible to correct errors in reading or recording before conditions on the analyzer have been changed.

Construction and Wiring

Each of the circuit units terminates in plugs in one of the plug and jack cabinets. Because of the large number of circuit units in the analyzer, precautions were taken to minimize the length of interconnecting wires. There is a plug and jack cabinet for every three unit cabinets, with provisions made for interconnecting some of the jacks on each of the cabinets as required by the system connection diagram. The metering bus for each plug and jack cabinet is further subdivided into two sections; only one section is connected to the instrument system at any time. The wiring is carried in a 9-inch high subbase of the analyzer, and all wires are spaced on 1/2-inch centers and away from the steel to minimize the stray effects. This construction permits the complete wiring and testing of the equipment in the factory. The analyzer is built and shipped in sections comprising several cabinets, and relatively few interconnections are required at installation.

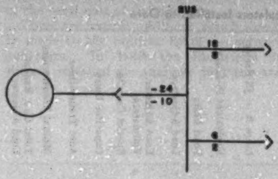

Figure 6. Example of method of representing polarity of watts and vars on a power-flow diagram

Summary

This type of a-c network analyzer with its low volt-ampere base has proved to be of reliable design over a number of years of actual operating experience. The improved analyzer described in this paper incorporates many new features, including direct-reading master instruments, a fuller complement of generator instruments, push-button selection for meter readings, and complete factory assembly and testing. These features should further increase the usefulness of this tool in power-system design.

References

1. The M.I.T. Network Analyzer, **H. L. Hazen, O. R. Schurig, M. F. Gardner.** *AIEE Transactions*, volume 49, July 1930, pages 1102–14.

2. Use of A-C Network Calculator in Planning and Operating Electric Power Systems, **P. O. Bobo, H. A. Travers, E. E. George.** *Report 328*, International Conference on Large High-Voltage Electric Systems (Paris, France), June 24–July 3, 1948.

3. Analyzers, **C. Concordia, H. A. Peterson.** *General Electric Review* (Schenectady, N. Y.), September 1945, pages 29–37.

4. Power System Stability Requirements Determined by A-C Calculating Board Study, and Operating Performance Proved by Staged Fault Tests, **W. A. Morgan, Byron Evans.** *Report 319*, International Conference on Large High-Voltage Electric Systems (Paris, France), June 24–July 3, 1948.

5. A New A-C Network Analyzer, **H. P. Kuehni, R. G. Lorraine.** *Electrical Engineering* (*AIEE Transactions*), volume 57, February 1938, pages 67–73.

6. Auxiliary Equipment Facilitates Network Calculator Operation, **L. B. LeVesconte.** *Electric Light and Power* (Chicago, Ill.), volume 24, October 1946, page 50.

Discussion

R. B. Squires (Westinghouse Electric Corporation, East Pittsburgh, Pa.): The author's paper is valuable primarily because it gives definite examples of how a large power system can benefit through the use of a network calculator or analyzer. Savings in system design such as is given in the paper have demonstrated the value of the network calculator to an increasing number of utility groups. This has resulted in the installation of a number of calculators throughout the country.

The increase in facilities has been especially rapid since the end of the war. Six network calculators or analyzers have been installed in the last three years, an increase of about 30 per cent over the total prewar figure.

Although the peak has probably passed, the average use of each installation continues at a higher level than before the war, demonstrating that the use expands as more companies have easy access to these devices.

Table I of the discussion has been prepared to summarize the various installations and show their essential features. There is a possibility that on some of the calculators additional facilities have been installed with which we are not familiar.

The network calculators are listed in Table I in the order of their original installation. For example, the second installation was at Westinghouse in East Pittsburgh in 1929. This was reinstalled at Purdue University, with some additions, in 1942. The present Westinghouse calculator dates from that year.

The power supply frequency is usually between 400 and 500 cycles, depending on the design of the manufacturer. For instance, the unit described in this paper uses 480 cycles; the units with which the writer is most familiar use 440 cycles.

The remaining columns show the number of units of each type, such as generators, instruments per generator, load adjusters, load adjuster voltmeters, and how the circuits are selected and metered.

The units listed as pi-line circuits also can be used as regular lines in all cases. The capacitor units listed are those in addition to the capacitors used with the pi-lines. The latter are equal in number to twice the pi-lines, but are not listed in the table.

As can be seen from the table, the majority of the features presented as new in this paper have been incorporated in all calculators manufactured during the past several years. The owners of the more modern equipments appreciate from experience the value of these features.

The network analyzer described in this paper represents an interesting adaptation of up-to-date features, (such as direct reading master instruments, more generator instruments, push button metering, and load adjusting voltmeters) to their high impedance level design. It has been the experience of the writer over the past several years that these features have been great time savers and conveniences on all the modern network calculators. The Bureau of Reclamation will no doubt find them of equal and continuing use in the future.

Edward W. Kimbark (Northwestern University, Evanston, Ill.): The network analyzer described in the paper differs from the one built by the same manufacturer in 1937 with respect to several rather minor details. (Incidentally, the date 1938 given in the present paper is not correct. The analyzer was in full operation in Schenectady by June 1937.) The paper would be more valuable to persons familiar with the earlier models of analyzers if it had specifically listed the features of the new model differing from the 1937 model. These features, as nearly as I can gather them from the paper, are the following:

1. Addition of load adjusters (autotransformers) and voltmeters to the load units.

2. Pi-lines.

3. Decentralization of cord and jack panels.

4. Push-button selector switch of adding-machine style and relays for connecting master instruments to the selected network unit.

5. Automatic change of ammeter and wattmeter scales when range-selector switch is moved.

6. Light-colored paint.

7. Addition of current amplifier to the watt-varmeter on each generator unit.

Table I. A-C Network Calculators Installed to Date

Owner	Year Installed	Frequency Cycles	Generator Units	Generator Imp. (Z)	Inst. Per Generator	Circ. Select.	Lines R + JX Series	Equivalent Pi-Lines	Load Units	Load Adjusters	Load Adjuster Voltmeters	Special Circuits	Capacitor Units	Auto Transformer	Mutual Transformer	Total Circ. Except Load Adjuster
Massachusetts Inst. Technology	29	60	16	0	3	R	80	0	40	0	0	6	55	12	0	209
Purdue University*	42	440	16	0	3	R	160	0	40	40	0	38	60	36	33	383
Pennsylvania Railroad	32	440	6	0	3	S	168	0	40	0	0	40	12	14	16	296
Commonwealth Edison Company	32	440	6	0	3	S	72	0	48	0	0	12	24	18	6	186
General Electric Company	37	480	12	0	2	S	150	0	50	0	0	2	64	20	15	313
Public Service Electric and Gas Co.	38	480	8	0	2	S	85	0	30	0	0	0	18	10	12	163
Tennessee Valley Authority	38	440	18	0	3	S	120	0	44	24	0	8	34	24	22	270
Bonneville Power Administration	39	480	18	0	2	R	130	0	70	0	0	12	60	20	16	326
Sao Paulo Tramway Light and Power Company	40	440	6	0	3	S	32	0	16	16	0	0	12	6	12	98
Potomac Electric Power Company	41	440	6	0	3	S	52	0	18	18	0	0	12	6	8	120
Hydro Electric Power Commission	41	440	15	0	3	R	98	0	32	32	0	49	36	18	11	259
Public Service Co. of Oklahoma	41	60	7	0	2	S	87	0	30	0	0	21	26	14	0	185
Westinghouse Electric Corporation	42	440	22	22	4	R	152	24	48	48	48	0	48	36	36	384
Illinois Institute of Technology	45	440	12	12	3	R	100	0	40	40	40	0	36	18	18	236
Iowa State College	46	10^4	4	4	3	R	0	24	12	12	0	0	12	4	4	64
Texas A and M College	47	440	18	18	3	R	134	16	56	56	56	0	54	24	24	344
City of Los Angeles	47	440	18	18	3	R	120	0	40	40	0	0	36	16	18	266
University of Kansas	47	60	8	0	2	S	56	0	32	32	0	11	12	8	6	133
Associated Electrical Industries, Ltd.	47	500	12	0	2	R	120	0	30	0	0	4	60	36	12	274
Georgia School of Technology	47	440	18	18	3	R	88	72	60	60	0	0	24	24	18	322
Pacific Gas and Electric Company	48	440	14	14	3	R	132	32	48	48	0	0	48	24	12	324
Consolidated Gas, Electric Light and Power Co. of Baltimore	48	440	16	16	3	R	122	0	44	44	44	0	10	20	12	240
United States Bureau of Reclamation	48	480	12	12	3	R	87	21	32	32	32	0	4	18	12	240

S = Circuit selection by switches or plugs

R = Circuit selection by remote selector & relays

* First installed in 1929, reinstalled in 1942

8. New convention on relative signs of watts and vars at the two ends of a circuit element.

Will the authors please correct me if I have omitted any important changes from this list?

Actually features 1 to 6 are not new, having been included previously in analyzers built by another manufacturer. Thus the present paper offers very little that is really new in network analyzer design or operation.

A network analyzer incorporating at least one important novel feature has been designed by Professor E. B. Phillips and is in operation at the University of Kansas. The novel feature is that impedances set up on the analyzer are shifted by a constant angle of $\cos^{-1} 0.85$ from the corresponding impedances of the power system represented. This feature enables reactors of relatively low Q to be used to represent pure reactance, thus making possible the use of small 60-cycle reactors. The use of 60 cycles eliminates the need of a motor-generator set, which is one of the expensive components of conventional network analyzers. (The expense arises not only from the cost of the motor-generator set itself but also from the fact that, because of its noise, the set must be installed in a separate room and conduits must be installed connecting the two rooms.) It is to be hoped that the appropriate AIEE technical committee will prevail upon Professor Phillips to present to the Institute a complete technical description of his new and very carefully worked-out design.

More innovations such as those on the Phillips analyzer are needed to decrease the cost of network analyzers enough so that every power company can afford to have one. However, even with the present costs, power companies cannot afford not to use network analyzers for studying important changes in their systems. The authors perform a valuable service by citing new examples of possible savings in construction costs without sacrifice of reliability. They also present some interesting thoughts on the pros and cons of rapid-reclosing circuit breakers where the utmost reliability is sought.

Eric T. B. Gross (Illinois Institute of Technology, Chicago, Ill.) This paper is a most valuable contribution since it brings us up to date by the description of a modern analyzer, a tool which simplifies greatly most of the work of the power systems engineers.

It is of interest that in this improved a-c network analyzer nearly all the modifications are incorporated which have been developed in recent years by different users of such calculating boards at various locations. At the Illinois Institute of Technology, we have found the recording table (described in reference 6 of the paper) of great advantage since the work is speeded up considerably, possible errors are checked, and the operating engineer is able to visualize quickly how kilowatts and kilovars are distributed in the whole system. This recording table is of the most help in load studies, and I would say that 20 to 25 per cent more work can be done in the same time with the aid of this tool. I understand that similar recording tables now are in use at some other institutions.

F. S. Rothe: The authors wish to thank the discussors of this paper for their remarks. There is general agreement that the improvements in network analyzers as described in the paper will benefit a large number of users through increased efficiency of operation.

There was criticism of the paper because some of the features described were not new. However, we believe it is fair to say that the features described in general represent definite improvements over existing designs. The method described in the paper for reading megawatts and megavars with the correct sign directly on the master instruments is an example of this.

In connection with the novel analyzer of Professor Phillips, Professor Kimbark cites the saving of a motor generator set as

Table II

Owner	Year Installed	Frequency	Generator Units	Low $\frac{R}{X}$ Units	Pi Line Units	Line Units	Load Units	Load Adjusters	Load Adjuster Voltmeters	Capacitor Units	Large Capacitor Units	Auto-transformer	Mutual Transformer
General Electric Company Number 1	1937	480	12	2	0	150	50	0	0	60	0	20	15
Public Service Electric and Gas Company of New Jersey	1938	480	10	0	0	121	40	10	0	30	0	18	22
Bonneville Power Administration	1939	480	18	12	0	130	70	0	0	60	0	20	16
Bureau of Reclamation	1948	480	12	12	21	87	32	32	32	42	4	18	12
General Electric Company Number 2	1949	480	12	12	50	96	56	56	56	100	4	16	15
University of California	1949	480	6	6	0	50	16	0	0	35	0	8	4
India Institute of Science		480	16	16	24	76	50	50	50	48	0	32	8

eliminating an expensive component from the analyzer. We do not find this to be the case for the low volt ampere base analyzer described in the paper, since the cost of the set, including wiring, is but a small fraction of the total cost of the analyzer.

There are several additions which should be made to Mr. Squires' list of a-c network analyzers. In 1948 the Electricité de France installed an analyzer in Paris and there have been references in the literature to a-c network analyzers in Russia. An up-to-date list of analyzers built by the General Electric Company is given in Table II of this discussion.

General Theory, and Experimental Confirmation, of the Moving Coil Fluxmeter

THOMAS JAMES HIGGINS
MEMBER AIEE

GLENN ROBERTSON
STUDENT MEMBER AIEE

THE moving coil fluxmeter is an instrument for the measurement of magnetic flux. Essentially, the mechanism is that of a D'Arsonval galvanometer so designed that the net restoring torque due to the suspension (if used) and the spiral leads to the moving coil is held to a minimum. Usually, the search coil connected to the fluxmeter is of low resistance. The combination of minimum restoring torque and low search-coil resistance results in a preferred operating characteristic: namely, if under certain conditions the flux ϕ linking the N-turn search coil experiences an incremental change $\Delta\phi$, the deflection D of the pointer of the fluxmeter is proportional to the corresponding incremental change $\Delta\lambda$ in the flux linkages λ associated with the search coil.*

The theory of the fluxmeter has been developed in various degrees of completeness by several writers.[1–9] Study of their papers, epitomized in Appendix I, reveals that in the course of formulating a differential equation which approximately characterizes the deflection D, each writer introduces certain simplifying assumptions. For the most part these assumptions are tantamount to discarding, as negligible by comparison with those remaining, certain terms in the general differential equation which accurately characterizes the deflection D. The approximate differential equation stemming from these assumptions, when solved subject to a prescribed simple set of boundary conditions, has the solution $D=\Delta\lambda/C$; or equivalently

$$\Delta\lambda = CD \tag{1}$$

where C is a constant, fixed by the design of the instrument.

If, as is commonly the case in practice, the same flux ϕ links each of the N_{sc} turns of the search coil, $\Delta\lambda=N_{sc}\Delta\phi$. Substituting this expression in equation 1 and solving for $\Delta\phi$ gives

$$\Delta\phi = CD/N_{sc} \tag{2}$$

One or the other of equations 1 or 2 is the equation implied by the information printed on the scale of a commercial fluxmeter or cited in accounts of the fluxmeter contained in various reference sources: textbooks on electrical measurements or on principles of electrical engineering, handbooks of electrical engineering, instruction manuals for fluxmeters, and elsewhere. In practice, however, it frequently occurs that the actual circuit conditions are such that the terms discarded in formulating the approximate differential equation of which equation 1 is the solution are not negligible. In consequence, calculation by equations 1 or 2 is not valid; depending on the conditions at hand, the calculated values will be either smaller or larger than the actual existing values. Yet accounts of the fluxmeter to be found in available reference sources do not cite the restrictions under which equations 1 and 2 are valid (except that some instruction manuals specify the maximum allowable value of search-coil resistance, a bit of information that often goes unheeded); nor, more generally, do these reference sources discuss how a fluxmeter can be used for accurate measurement under any set of circuit conditions that are likely to occur in practice.

Now, if the general equation relating $\Delta\lambda$ to D were known, analysis of this equation would enable:

1. Determination of the correct use of the fluxmeter under any set of circuit conditions that occur in practice.
2. Establishment of various approximate equations especially convenient for calculation in those situations that most often arise in practice and of the corresponding restrictions limiting use of these approximate equations.
3. Estimate of the error to be expected from use of a given approximate equation.
4. Ascertainment of other factors of interest and value.

Obviously, this information is precisely that which is desired by one who has occasion to make extensive use of the fluxmeter in practice. It is, therefore, the purpose of this paper to provide this desired information for both the unshunted (single-range) and the shunted (multiple-range) fluxmeter.

It happens that the study of each of these two types of fluxmeter falls naturally into three parts:

1. Derivation of the general equation relating $\Delta\lambda$ to D.
2. Deduction from this equation of useful approximate equations, of the corresponding restrictions limiting their use, and of the approximate magnitude of inherent error.
3. Advance of experimental data confirming the correctness of this theory.

---

* This is actually the case, although the information printed on the scale of a commercial fluxmeter usually results in the inexperienced user inferring that deflection is proportional to the change in flux $\Delta\phi$. Again, some textbook accounts of the fluxmeter state, incorrectly, that deflection is proportional to change in flux. Note, however, equation 16. This confusion stems primarily from the fact that, in the sources mentioned, discussion is based on a 1-turn search coil, for which $\Delta\phi$ is numerically equal to $\Delta\lambda$.

Paper 49-168, recommended by the AIEE Basic Sciences Committee and approved by the AIEE Technical Program Committee for presentation at the AIEE Summer General Meeting, Swampscott, Mass., June 20–24, 1949. Manuscript submitted January 14, 1949; made available for printing May 6, 1949.

THOMAS JAMES HIGGINS is Professor of Electrical Engineering, University of Wisconsin, Madison, Wis. GLENN ROBERTSON is an instructor at Illinois Institute of Technology, Chicago, Ill.

This paper is based upon a thesis supervised by Professor Higgins and submitted by Mr. Robertson to the faculty of Illinois Institute of Technology in January, 1949, in partial fulfillment of the requirements for the degree of Master of Science in Electrical Engineering.

Derivation of the General Equation for the Unshunted Fluxmeter

In the circuit of Figure 1 let e_{sc} be the (instantaneous) voltage generated in the search coil, e_f the voltage generated in the moving coil of the fluxmeter, i the circuit current, R the total resistance, and L the total inductance of the circuit. Then, by Kirchhoff's voltage law

$$e_{sc}=iR+Ldi/dt-e_f \qquad (3)$$

Inasmuch as the fluxmeter is a D'Arsonval galvanometer (with particularly chosen design parameters) its moving coil rotates in a radial magnetic field. Let B be the magnitude of the radial flux density, h and b the vertical height and horizontal breadth of the rectangular moving coil of area $A=hb$ and of N turns, θ the (instantaneous) angular position of the plane of the coil measured from a conveniently chosen reference position $\theta=0$, $w=d\theta/dt$ the angular velocity of the coil, and $v=bw/2$ the linear velocity of the vertical side of the coil angularly located at θ (the other vertical side is located at $\theta+\pi$). Then the voltage generated in one turn of this vertical side of the fluxmeter coil is $-Bhv=-Bhbw/2=-(BA/2)(d\theta/dt)$; whence the voltage generated in the coil is $e_f=-BAN(d\theta/dt)=-Gd\theta/dt$, where $G=BAN$ is a design constant commonly termed the "winding area."

The voltage generated in the search coil is $e_{sc}=d\lambda/dt$, where λ is the negative of the instantaneous flux linkages associated with the search coil.

Substituting for e_{sc} and e_f in equation 3 yields

$$d\lambda/dt=iR+Ldi/dt+Gd\theta/dt \qquad (4)$$

The electrodynamic force acting on a vertical side of one turn of the fluxmeter coil is Bhi; whence the total electrodynamic torque t_e acting to increase θ is $t_e=(Bhi)(bN)=Gi$. The torques acting to prevent increase of θ are: the inertia torque $t_i=Jd^2\theta/dt^2$, the air friction torque $t_f=k_fd\theta/dt$, the electromagnetic checking torque due to eddy currents induced in the metal frame (if any) on which the coil is wound, $t_c=k_cd\theta/dt$, and the restoring torque $t_r=U\theta$, which expression indicates that the reference position $\theta=0$ of the plane of the coil has been chosen to coincide with the position of zero restoring torque—a choice which imposes no limitation on the generality of treatment, yet simplifies the subsequent analysis. Herein, J is the polar moment of inertia of the coil about its vertical axis; k_f and k_c are damping constants (that in moving-coil instruments the friction and electromagnetic checking torques are essentially proportional to the angular velocity of the moving coil has been verified by numerous experiments.[10]); U is the sum of the torsion constant of the suspension if used and the effective spring constant of the spiral or other type of leads to the moving coil.

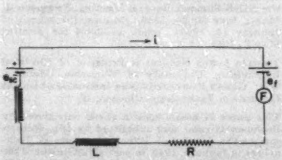

Figure 1. Circuit of unshunted fluxmeter

Equating driving torque to the sum of the opposing torques yields the general differential equation characterizing the mechanical motion of the fluxmeter coil, namely

$$Gi=Jd^2\theta/dt^2+Kd\theta/dt+U\theta \qquad (5)$$

where $K=(k_f+k_c)$.

Solving equation 5 for i, substituting the resulting expression in the term iR of equation 4, and collecting like terms gives

$$d\lambda/dt=(JR/G)d^2\theta/dt^2+[(RK/G)+G]d\theta/dt+Ldi/dt+(UR/G)\theta \qquad (6)$$

Integrating each side of equation 6 between $t=t_1$ and $t=t_2$, where t_1 and t_2 are arbitrary except for the condition $t_2>t_1\geq 0$, yields

$$[\lambda]_{t_1}^{t_2}=(JR/G)[d\theta/dt]_{t_1}^{t_2}+[(RK/G)+G][\theta]_{t_1}^{t_2}+L[i]_{t_1}^{t_2}+(UR/G)\int_{t_1}^{t_2}\theta\,dt \qquad (7)$$

Designating the values of λ, i, θ, and $w=d\theta/dt$ at $t=t_1$ and $t=t_2$ by corresponding subscripts and evaluating equation 7 yields

$$\lambda_2-\lambda_1=(JR/G)(w_2-w_1)+[(RK/G)+G](\theta_2-\theta_1)+L(i_2-i_1)+(UR/G)\int_{t_1}^{t_2}\theta\,dt \qquad (8)$$

Equation 8 is the desired general equation relating change in flux linkages associated with the search coil to the corresponding change in coil position.

Approximations for the Conditions Commonly Encountered in Practice

At $t_1=0$, with the fluxmeter coil at rest ($w_1=0$) at $\theta=\theta_1$, and with zero current ($i_1=0$) through it, let a quick change in the flux linkages associated with the search coil be initiated. The driving torque stemming from the generated current sets the coil in motion. Let $t_2=T$ be the time at which it acquires maximum angular displacement. At this instant $\theta=\theta_2$, $w_2=0$, and $i=i_2$. For the stated boundary conditions, equation 8 reduces to

$$\lambda_2-\lambda_1=[(RK/G)+G](\theta_2-\theta_1)+Li_2+(UR/G)\int_0^T\theta\,dt \qquad (9)$$

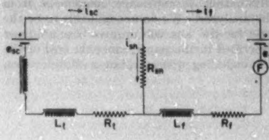

Figure 2. Circuit of shunted fluxmeter

It is commonly the case, in practice, that L is small in comparison with R; that is, the circuit is substantially noninductive.* In such case the circuit current is substantially in phase with the net generated voltage in the circuit. Now the term "quick" implies that the total change in flux linkages has been completed before maximum displacement is attained. If so, at $t=T$ the flux through the search coil is not changing, whence the generated voltage in the search coil is zero. Again, at $t=T$ the fluxmeter coil is stationary ($w_2=0$); whence the generated voltage in the coil is zero, and, as the circuit current is substantially in phase with the net generated voltage, $i_2\cong 0$. Accordingly, for $R>>L$ equation 9 reduces to

$$\lambda_2-\lambda_1=[(RK/G)+G](\theta_2-\theta_1)+(UR/G)\int_0^T\theta\,dt \qquad (10)$$

Thus, unless L is commensurate with R—a case usually encountered in practice only when heavy iron-cored inductors are in series with the fluxmeter—the magnitude of a quick change in flux linkages associated with the search coil is to be calculated, in general, from equation 10. It is to be noted that the restriction to a quick change in flux linkages imposes no essential limitation, for, as discussed below, it is only quick changes that actually are utilized in practice.

Evaluation of the Integral Term in Equation 10

The integral in equation 10 cannot be evaluated explicitly, for θ is an unknown function of t. However, an upper limit to its actual value is established easily by use of a well-known equality in the elementary calculus

$$\left|\int_a^b f(x)dx\right|\leqq\int_a^b|f(x)|dx\leqq|f_m(x)|(b-a) \qquad (11)$$

---

* For detailed discussion of the essential meaning and implications of this statement, see Appendix II.

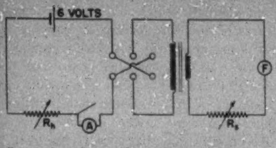

Figure 3. Circuit for studying variation of deflection with circuit resistance

(R_f and R_{sc}) in series with R_s is not shown

wherein $b>a$, and $|f_m(x)|$ designates the maximum magnitude of $f(x)$ in the interval $a \leqq x \leqq b$. Accordingly, it follows from equation 11 that

$$(UR/G)\left|\int_0^T \theta\, dt\right| \leqq (UR/G)T|\theta_m| \tag{12}$$

wherein $|\theta_m|$ designates the maximum magnitude of θ over the time interval $0 \leqq t \leqq T$.

Obviously, $|\theta_m| \geq |\theta_2-\theta_1|$. Usually a fluxmeter is so adjusted and so used in practice that $\theta_1=0$. In this case, $|\theta_m| \equiv |\theta_2|$.

The Case When Both $R>>L$ and $[(RK/G)+G]>>URT/G$

The magnitude of the first term of the right-hand member of equation 10 is $[(RK/G)+G]|\theta_2-\theta_1|$. The magnitude of the second term is, by equation 12, less than or equal to $(URT/G)|\theta_m|$. Accordingly, it follows that if

$$[(RK/G)+G]|\theta_2-\theta_1| >> (URT/G)|\theta_m| \tag{13}$$

equation 10 is well approximated by

$$\lambda_2-\lambda_1 = [(RK/G)+G](\theta_2-\theta_1) \tag{14}$$

Now, it is to be noted that the right-hand side of equation 13 is directly proportional to R, whereas the left-hand side is positively biased by the constant term G. Accordingly, it follows: that for R sufficiently near zero, the right-hand side is very small by comparison with the left-hand side; that as R increases from zero, the right-hand side increases faster than does the left-hand side, thus weakening the inequality; and that possibly (the actual variation depends on the relative values of the other parameters) for sufficiently large R, the two sides become commensurate and the inequality no longer holds.

Accordingly, whether or not this last possibility occurs, there is a range of R for which equation 13 holds. Further, it follows from equation 13 that the upper limit of this range increases as G increases in magnitude and U decreases in magnitude. Now the gain through increasing G, say through using more turns on the fluxmeter coil, tends to be offset by the increased value of T resulting from the more sluggish action of the moving coil because of the increased moment of inertia J. On the other hand, decreasing U also tends to decrease T because of decrease in the restoring torque opposing motion, and decrease of T also tends to extend the maximum value of R for which equation 13 is applicable.

Now, equation 14 is a preferred operating characteristic for a commercial fluxmeter. For if a given fluxmeter is always used with search coils having a specified resistance, the circuit resistance R is substantially constant, and it follows from equation 14 that $(\lambda_2-\lambda_1)$ is of constant proportionality to $(\theta_2-\theta_1)$; whence the scale of the fluxmeter can be calibrated directly in terms of $(\lambda_2-\lambda_1)$. To attain this desired operating characteristic, a commercial fluxmeter is so designed that the moving coil is made as light as is feasible, the winding area as large as is feasible, and the restoring torque is reduced to a minimum. Then G, U, and T are of such magnitudes that the maximum value of R for which equation 13 holds is several times greater than the least value to which R can actually be reduced when using the instrument, namely, R equal to the internal resistance of the fluxmeter. Inasmuch as the bracketed term in equation 14 is positive, it follows that

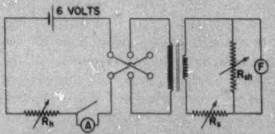

Figure 4. Circuit for studying variation of deflection with shunting resistance

R_f and R_{sc} are not shown

$$|\lambda_2-\lambda_1| = [(RK/G)+G]|\theta_2-\theta_1| \tag{15}$$

The bracketed term in equation 15 is a constant, of specific value determined by the pertinent values of R, K, and G. Thus, it is convenient to write

$$\Delta\lambda = C'D \tag{16}$$

wherein: $\Delta\lambda = |\lambda_2-\lambda_1|$ is the magnitude of the change in flux linkages; $D = |\theta_2-\theta_1|$ is the magnitude of the angular deflection of the moving coil, expressed in scale divisions of angular deflection of the fluxmeter pointer; and

$$C' - [(RK/G)+G] \tag{17}$$

flux linkages/scale division of pointer deflection, is the "working constant" of the instrument.

Accordingly, it follows from equations 16 and 17 that a fluxmeter can be employed in a circuit containing arbitrary total resistance R, and that the change in flux linkages $\Delta\lambda$ associated with the search coil can be calculated with accuracy from equation 16, provided that the corresponding value of C' is known or can be determined, that the specified boundary conditions $w_1=w_2=i_1=0$ are observed, and that the restrictions $R>>L$ and $[(RK/G)+G]D>>(URT/G)|\theta_m|$ are satisfied. Now, as mentioned above, the fluxmeter is usually so adjusted and so used that $\theta_1=0$, whence $|\theta_m| \equiv |\theta_2| \equiv D$. If so, the latter restriction reduces to $[(RK/G)+G]>>(URT/G)$.

Determination of Flux

If $\Delta\lambda$ is written as $\Delta\lambda = N\Delta\phi$ where $\Delta\phi$ is the change in a flux ϕ linking each of the N_{sc} turns of a search coil, equation 16 can be written in the form $\Delta\phi = C'D/N_{sc}$. (This equation implies not only that the same flux ϕ links each of the N_{sc} turns but, further, that the diameter of the wire comprising the search coil is negligible by comparison with the diameter of the cross section of the search coil; whence essentially no flux passes through the wire of the coil. Though these conditions commonly are satisfied in a well-designed search coil, they often are not satisfied if a search coil is constructed by one lacking knowledge of the principles involved.) Obviously, if the change in flux is produced by reversal of a flux ϕ from ϕ to $-\phi$, then $\Delta\phi = 2\phi$, whence $\phi = C'D/2N_{sc}$. Again, if the flux is changed from 0 to ϕ, or from ϕ to zero, then $\Delta\phi = \phi$, whence $\phi = C'D/N_{sc}$.

The Permissible Value of R

It obviously is desirable, for facility of general use, that the scale of a fluxmeter be calibrated directly in terms of the desired quantity $\Delta\lambda$. Inspection of equations 16 and 17 indicates that this can be done, providing R is held constant at

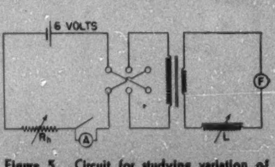

Figure 5. Circuit for studying variation of deflection with circuit inductance

(R_f+R_{sc}) is not shown

some convenient fixed value, say R_m. If R is not constant, calibration still can be essentially accomplished, provided R is allowed to vary only within limits such that $[(RK/G)+G] \cong [(R_m K/G)+G]$. As, in practice, the total resistances of different circuits tend to vary because of differences in the resistances of the leads and search coils utilized, fluxmeters are designed on this latter basis.

Thus, as purchased, the fluxmeter is direct reading for $\Delta\lambda$ and, thus, for $N_{sc}\Delta\phi$, providing it is used in a circuit where R is as specified by the manufacturer. (Usually, this specification is stated in the cover or on the scale of the instrument.) Thus, in Rawson fluxmeters the manufacturer specifies that the resistance of the search coil and associated leads shall not be greater than one ohm. This implies a permissible variation in R over the range $R_f \leqq R \leqq (R_f+1)$, where R_f is the internal resistance of the fluxmeter. Similarly, the early model of Sensitive Research Instrument fluxmeter has a value of R_f of about the same magnitude as that of the Rawson instrument, and the same restriction is stated.

Obviously, then, if R differs from the value R_m for which the scale is calibrated, the user must determine the appropriate value of C', for example, from a calibration curve prepared as discussed in the following section. This restriction on the permissible value of R if the fluxmeter is to be direct reading is an important point in the correct use of a fluxmeter; it is not emphasized or clearly stated in most textbook discussions of the instrument, and is frequently violated in practice if the user is without knowledge of the restriction. Commonly, this violation occurs through use of search coils comprised of many turns of fine wire, and thus of high resistance.

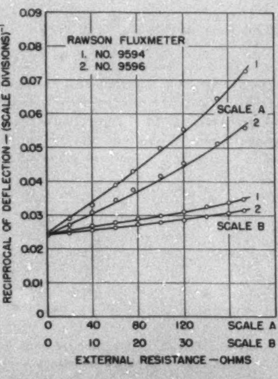

Figure 6. D^{-1} **versus** R_{ex}**: Rawson fluxmeters**

Determination of C'

For $R=R_m$, equation 17 can be written in the form

$$\Delta\lambda = CD \tag{18}$$

where

$$C=[(R_m K/G)+G] \tag{19}$$

Commonly, fluxmeters are designed so that, as received new from the manufacturer, the value of C is

$$\begin{aligned} C &= 10^4 \text{ maxwell-turns/scale division} \\ &\quad \text{(centimeter-gram-second units)} \\ &= 10^{-4} \text{ weber-turns/scale division} \\ &\quad \text{(meter-kilogram-second units)} \end{aligned} \tag{20}$$

Manufacturers print this value of C (usually in centimeter-gram-second units) on the scale of the instrument. However, it commonly happens that with use, or through repair, unless done by the manufacturer, the characteristics of the fluxmeter change somewhat, thus necessitating redetermination of C. Accordingly, when using a fluxmeter it is wise to ascertain whether or not such a redetermined value is to be used; if so, it is commonly to be found recorded in the cover of the instrument.

Occasionally a fluxmeter must be used in a circuit where R is appreciably larger than R_m. For such use it is convenient to have available a calibration curve of C' versus R or R_{ex}. The co-ordinates for such a curve can be obtained in several ways. Thus, for various values of R or R_{ex} the deflections corresponding to a known fixed change in flux linkages $\Delta\lambda$ can be noted and the values of C' calculated from equation 17. The fixed value of flux linkages can be ascertained by initial measurement with $R=R_m$, whence $C'=C$, and $\Delta\lambda$ can be calculated from equation 18; or else a fixed known value can be obtained by reversing a known current passed through a standard mutual inductor or a standard solenoid; or still other artifices can be employed. Again, the values of (K/G) and G can be determined experimentally as discussed in following paragraphs, and values of C', corresponding to various assumed values of R, can be calculated from equation 17.

Extending the Range of a Fluxmeter

The possibility of easy determination of C' enables use of a fluxmeter in a circuit where the value of R is substantially greater than R_m: for example, in a circuit where the search coil, wound of many turns of fine wire for use in mapping a weak magnetic field, is of high resistance. In this case, it follows from equations 17 and 19 that $C'>C$. If so, it follows from equation 16 that a greater change in flux linkages $\Delta\lambda$ is required to produce a given deflection D, now that $C'>C$ is the working constant of the instrument. In turn, this analysis suggests that the range of a fluxmeter can be extended by inserting resistance in series with the fluxmeter. However, this method of extending the range of a fluxmeter is less preferable than that of shunting the fluxmeter coil with a low resistance, for, as is shown below, shunting a fluxmeter, rather than inserting series resistance, enables a greater deflection for the same change in flux linkages, and hence provides greater sensitivity of measurement. In consequence, commercial multiple-range fluxmeters are multiranged by use of shunts.

Incorrect Use of Equations 16 and 18

In conclusion, it is to be noted that use of equations 16 and 18 is subject to the restrictions: $w_2=w_1=\dot{i}_1=0$, $R>>L$, $[(RK/G)+G]|\theta_2-\theta_1|>>|\theta_m|URT/G$. If an of these conditions are substantially departed from, correspondingly modified equations must be used. As a particular example, a student inexperienced in the use of a fluxmeter, having obtained a deflection by reversal of a flux ϕ, and being desirous of obtaining a check through re-reversing the flux to its original value and direction, often does so while the pointer is returning towards its initial position with appreciable velocity

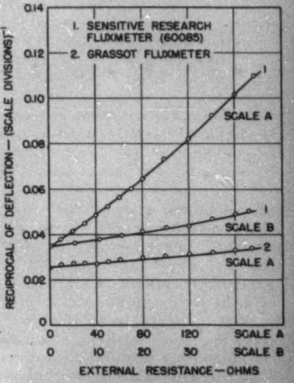

Figure 7. D^{-1} **versus** R_{ex}**: Grassot and Sensitive Research Instrument fluxmeters**

w. At the instant t_1 of re-reversal, however, $w_1>0$; whence it follows from equation 8 that, because of the resulting smaller values of $(JR/G)(w_2-w_1)$ a given change in flux linkages $(\lambda_2-\lambda_1)$ results in a greater value of $(\theta_2-\theta_1)$, and hence a greater pointer deflection D, than would have resulted if w_1 were equal to zero. In consequence, if equation 16 or 18 is, incorrectly, used to calculate $\Delta\lambda$, the larger value of D results in a calculated value of $\Delta\lambda$ greater than the actual value. Obviously, the magnitude of error increases as w_1 increases. In consequence, if through damage and poor repair a fluxmeter coil tends to return rather rapidly towards its initial position, a substantial error easily can result if the fluxmeter is so used.

Derivation of the General Equation for the Shunted Fluxmeter

In the circuit of Figure 2 let $e_{sc}=d\lambda/dt$ be the voltage generated in the search coil, $e_f=-Gd\theta/dt$ the voltage generated in the moving coil of the fluxmeter, i_{sc} the current through the search coil, i_{sh} the current through the shunt, i_f the current through the fluxmeter, L_t and $R_t=(R_{sc}+R_s)$ the total inductance and total resistance of the branch containing the search coil, R_{sh} the resistance, including leads of the shunt, and L_f and R_f the total inductance and total resistance of the branch containing the fluxmeter coil.

Applying Kirchhoff's voltage law to the right-hand loop of Figure 2 yields

$$d\lambda/dt=(i_{sh}+i_f)R_t+L_td(i_{sh}+i_f)/dt+i_{sh}R_{sh} \quad (21)$$

Applying Kirchhoff's voltage law around the outside of the circuit of Figure 2 yields

$$d\lambda/dt=(i_{sh}+i_f)R_t+L_td(i_{sh}+i_f)/dt+i_fR_f+L_f(di_f/dt)+Gd\theta/dt \quad (22)$$

By analogy with equation 5, the differential equation characterizing the mechanical motion of the fluxmeter coil is

$$Gi_f=Jd^2\theta/dt^2+Kd\theta/dt+U\theta \quad (23)$$

Subtracting equation 21 from equation 22 and solving for i_{sh} yields

$$i_{sh}=R_{sh}^{-1}[i_fR_f+L_fdi_f/dt+Gd\theta/dt] \quad (24)$$

Solving equation 23 for i_f and substituting in equation 24 yields

$$i_{sh}=R_{sh}^{-1}G^{-1}[R_fJd^2\theta/dt^2+R_fKd\theta/dt+R_fU\theta]+R_{sh}^{-1}L_fdi_f/dt+R_{sh}^{-1}Gd\theta/dt \quad (25)$$

Integrating equation 21 between t_1 and t_2 gives

$$\int_{t_1}^{t_2}d\lambda=(R_t+R_{sh})\int_{t_1}^{t_2}i_{sh}dt+R_t\times\int_{t_1}^{t_2}i_fdt+L_t[i_{sh}+i_f]_{t_1}^{t_2} \quad (26)$$

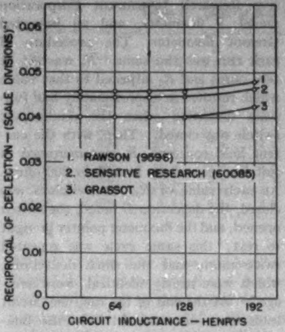

Figure 8. D^{-1} versus circuit inductance L

Substituting from equations 23 and 25 in equation 26 as indicated, performing the indicated integration, and collecting coefficients of like terms yields

$$\lambda_2-\lambda_1=[R_t+R_f(1+R_tR_{sh}^{-1})]JG^{-1}(w_2-w_1)+\{[R_t+R_f(1+R_tR_{sh}^{-1})]KG^{-1}+(1+R_tR_{sh}^{-1})G\}(\theta_2-\theta_1)+(1+R_tR_{sh}^{-1})L_f(i_{f2}-i_{f1})+L_t(i_{sh2}+i_{f2}-i_{sh1}-i_{f1})+[R_t+R_f(1+R_tR_{sh}^{-1})]\times UG^{-1}\int_{t_1}^{t_2}\theta dt \quad (27)$$

Equation 27 can be recast in a form more convenient to analyze; namely

$$\lambda_2-\lambda_1=(R_p+R_f)R_tR_p^{-1}JG^{-1}(w_2-w_1)+[(R_p+R_f)KG^{-1}+G]R_tR_p^{-1}(\theta_2-\theta_1)+R_tR_p^{-1}L_f(i_{f2}-i_{f1})+L_t(i_{sh2}+i_{f2}-i_{sh1}-i_{f1})+(R_p+R_f)R_tR_p^{-1}UG^{-1}\times\int_{t_2}^{t_1}\theta dt \quad (28)$$

where $R_p=R_tR_{sh}/(R_t+R_{sh})$.

Equation 28 is the desired general equation relating change in flux linkages associated with the search coil to the corresponding change in coil position.

The General Equation for the Conditions Usually Encountered in Practice

At $t_1=0$, with the fluxmeter coil at rest $(w_1=0)$ at $\theta=\theta_1$ and with zero current $(i_1=0)$ through it, let a quick change in the flux linkages associated with the search coil be initiated. Let $t_2=T$ be the time at which the fluxmeter pointer attains maximum deflection. At this instant $\theta=\theta_2$, $w_2=0$ and $i=i_2$.

Under these conditions equation 28 yields

$$\lambda_2-\lambda_1=[(R_p+R_f)KG^{-1}+G]R_tR_p^{-1}(\theta_2-\theta_1)+[R_tR_p^{-1}L_fi_{f2}+L_t(i_{sh2}+i_{f2})]+(R_p+R_f)R_tR_p^{-1}UG^{-1}\int_0^T\theta dt \quad (29)$$

As discussed previously, it is commonly true in practice that L_t and L_f are small against the corresponding values of R_t and R_f; whence, as before, $i_{sh2}=i_{f2}\cong 0$. In such case the second term of the right-hand member of equation 29 vanishes. Again, in fashion analogous to the evaluation of the integral term of equation 10, it is to be deduced that the magnitude of the integral term is small by comparison with the magnitude of the first term for a range of (R_p+R_f) such that

$$[(R_p+R_f)KG^{-1}+G]|\theta_2-\theta_1|>>(R_p+R_f)UTG^{-1}|\theta_m| \quad (30)$$

This inequality is the same as the inequality of equation 13, except that R now is replaced by (R_p+R_f). Accordingly, the analysis and remarks developed previously for the unshunted fluxmeter are applicable in obvious fashion to the shunted fluxmeter under discussion here.

In particular, it follows that there is a range of (R_p+R_f) for which the inequality of equation 30 is valid, and that over this range equation 29 is well approximated by

$$\lambda_2-\lambda_1=[(R_p+R_f)KG^{-1}+G]R_tR_p^{-1}(\theta_2-\theta_1) \quad (31)$$

subject to the stated boundary conditions and the restrictions $R_t>>L_t$ and $R_f>>L_f$.

The coefficient of $(\theta_2-\theta_1)$ in equation 31 is a constant of specific value determined by the pertinent values of (R_p+R_f), R_t, K, and G. Thus, again it is convenient to write equation 31 in the form

$$\Delta\lambda=C'D \quad (32)$$

where now

$$C'=[(R_p+R_f)KG^{-1}+G]R_tR_p^{-1} \quad (33)$$

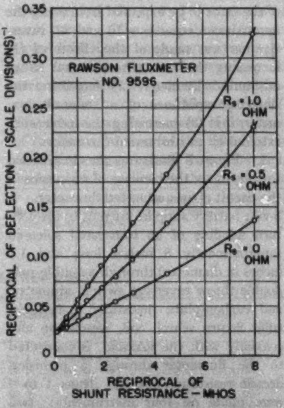

Figure 9. D^{-1} versus R_{sh}^{-1}: Rawson fluxmeter

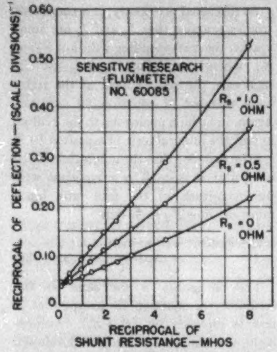

Figure 10. D^{-1} versus R_{sh}^{-1}: Sensitive Research Instrument fluxmeter

Thus, for a given fluxmeter in a given circuit, the coefficient C' in equation 32 is fixed in value. Hence, providing the same precautions are observed as discussed at length for the unshunted fluxmeter, the scale of the instrument can be calibrated in terms of the changes in flux linkages associated with the search coil $\Delta\lambda$. Moreover, as the value of C' depends on the assigned value of $R_p = R_{sh}R_t/(R_{sh}+R_t)$, multiple-range instruments can be obtained by use of several different fixed values of R_{sh}.

Experimental Apparatus and Procedure

To obtain experimental confirmation of the correctness of the theory developed above and to obtain quantitative measure of the error to be expected from using the approximate equations 16 and 32, investigation was made of the effects of (1) increasing the resistance external to an unshunted fluxmeter, (2) decreasing the shunting resistance of a shunted fluxmeter, and (3) increasing the inductance external to an unshunted fluxmeter.

1. Figure 3 illustrates the circuit used to investigate the increase of resistance in the circuit of an unshunted fluxmeter. A 6-volt battery supplies current to the 485-turn winding of an iron-cored solenoid (approximately 8 inches long and 1.5 inches in diameter) through a double-pole double-throw reversing switch, ammeter, and carbon-plate rheostat. A flat circular 8-turn search coil, wound on and coaxially with the solenoid, is connected to the fluxmeter through a precision decade resistance box R_s. Runs 1 to 4 were made on four instruments: two Rawson model 504 fluxmeters, a Sensitive Research Instrument Corporation model *F* fluxmeter, and an imported Grassot fluxmeter. The procedure of each run was the same. R_s was set at zero ohms and R_h adjusted to that value which resulted in approximately half full-scale deflection when the double-pole switch was closed. Then, with the current held constant, R_s was increased in suitable increments from 0 to 200 ohms. At each value of R_s, the switch *S* was closed, the deflection *D* noted, the switch opened, and the fluxmeter pointer brought to rest; this same cycle was repeated twice more, and the three deflections, which were nearly identical, were averaged. At the end of the run, the circuit leads were disconnected from the fluxmeter and connected to a precision 4-decade d-c resistance bridge; the decade resistance box R_s was set in turn to each of the values used during the run, and the total external-circuit resistance R_{ex} was measured. The resistance measured when the decade box is set at zero ohms yields the resistance of the search coil plus circuit leads. Table I comprises a typical set of data—that of run 1.

2. Figure 4 illustrates the circuit used to investigate the effect of decreasing the shunting resistance R_{sh} of a shunted fluxmeter. The circuit derives from that of Figure 3 through the addition of a shunting precision decade resistance box R_{sh}. Runs 5 to 8 were made on four fluxmeters, one of the Rawson instruments noted above being replaced by a General Electric catalog number *32C24764* fluxmeter. Three sets of data were taken for each instrument. For fixed values of R_s equal, in turn, to 0, 0.5, and 1 ohm, R_{sh} was decreased in suitable decrements for infinity (open circuit) to a value yielding a pointer deflection of only several divisions. Data were taken as described above. Finally, the total resistance R_t of the series combination of search coil, resistance box, and leads and the resistance R_{sh} of the shunting resistance box and its leads, were accurately measured with the resistance bridge. Table II comprises a typical set of data—that of Run 5.

3. Figure 5 illustrates the circuit used to investigate the effect of increasing the total inductance *L* relative to the total circuit resistance *R* of an unshunted fluxmeter. The circuit is that of Figure 3 with the precision decade resistance box R_s replaced by a variable heavy iron-cored inductor. Runs 9 to 11 were made on the three fluxmeters used in runs 2, 3, and 4. For a fixed circuit resistance of 26 ohms external to the fluxmeter, *L* was increased in suitable increments from zero to the maximum obtainable value. Data were taken as previously described. The utilized values of *L* then were calculated from measured values of 60-cycle impedance and resistance. Table III comprises the data of runs 9 to 11.

Experimental Confirmation of the Theory of the Unshunted Fluxmeter

If C' from equation 17 is substituted in equation 16 and the resulting expression solved for $D^{-1}(\equiv 1/D)$ we obtain

$$D^{-1} = (K/G\Delta\lambda)R + G/\Delta\lambda \qquad (34)$$

Inasmuch as $R = (R_{ex}+R_f)$, equation 34 can be recast in the form

$$D^{-1} = (K/G\Delta\lambda)R_{ex} + (KG^{-1}R_f + G)/\Delta\lambda \qquad (35)$$

In equation 34 let $\Delta\lambda$ be of fixed value and the equation be interpreted as expressing D^{-1} as a function of *R*. Then equation 34 is that of a straight line, where $(K/G\Delta\lambda)$ is the slope and $(G/\Delta\lambda)$ is the ordinate intercept. Obviously, equation 35 can be similarly analyzed.

Accordingly, if for $R >> L$ and a fixed value of $\Delta\lambda$, *D* is observed as a function of *R*, and if, from these data, D^{-1} is plotted as a function of *R* or R_{ex}, it is to be expected that the resulting curve will be a straight line over that range of *R* for which equations 34 and 35 are valid, namely, the range of *R* for which equation 13 holds.

The curves of Figures 6 and 7, plotted from the data of runs 1 to 4, are precisely such curves. It is to be noted that the

Table I. Data of Run 1 on the Grassot Fluxmeter

R_s	D	D^{-1}	R_s	D	D^{-1}
0.590	38.5	2.60 × 10^{-2}	60.6	35.2	2.84 × 10^{-2}
5.580	38.0	2.63	65.6	35.0	2.86
10.6	37.9	2.64	75.6	43.3	2.92
15.6	37.8	2.65	90.6	33.9	2.95
20.6	37.2	2.69	100.6	33.0	3.03
25.6	37.0	2.70	120.6	32.0	3.12
35.6	36.3	2.76	135.6	31.3	3.20
40.6	36.1	2.77	150.6	30.2	3.31
45.6	36.0	2.78	175.6	29.5	3.39
55.6	35.4	2.80	200.6	28.8	3.57

Table II. Data of Run 5 on the Grassot Fluxmeter

R_{sh}	R_{sh}^{-1}	D $R_s=0$	D $R_s=0.5$	D $R_s=1$	D^{-1} $R_s=0$	D^{-1} $R_s=0.5$	D^{-1} $R_s=1$
∞	0.000	44.0	44.0	44.0	2.27×10^{-2}	2.27×10^{-2}	2.27×10^{-2}
10.02	0.100	41.9	40.0	38.0	2.49	2.50	2.63
2.02	0.495	33.7	28.0	24.0	2.96	3.57	4.16
1.02	0.980	27.5	21.0	17.0	3.64	4.75	5.88
0.72	1.385	24.0	17.1	13.4	4.16	5.85	7.45
0.52	1.915	20.1	13.9	11.0	4.98	7.20	9.10
0.42	2.470	18.0	12.0	9.0	5.55	8.33	11.10
0.32	3.090	15.1	9.6	7.4	6.62	10.40	13.50
0.22	4.500	11.8	7.0	5.4	8.47	14.80	18.50
0.13	8.000	7.1	4.1	2.8	14.10	24.40	35.70

curves for the Rawson and Sensitive Research fluxmeters are linear over essentially the same range of external circuit resistance—about 45 ohms—whereas the Grassot fluxmeter is linear up to about 180 ohms. The greater range of linearity of the Grassot fluxmeter is due to the very delicate system of suspension and spiral connections employed by the moving coil. In consequence, the Grassot fluxmeter has a much smaller value of U. In turn, this smaller value of U enables satisfaction of equation 13 over a range of R several times greater than that of the other instruments.

It is to be noted that beyond the range of linearity the curves of Figures 6 and 7 bend upwards, thus indicating that for a given value of R the value of D^{-1} is greater than would have been obtained if the linear law had persisted over these values of R. This also is to be expected, for the linear characteristic is that which stems from equation 10 when the integral term can be neglected. If it cannot be neglected, it follows that for a given change in flux linkages $(\lambda_2-\lambda_1)$ at a given value of R, the first term of the right-hand member of equation 10 and, therefore, the actual value of $(\theta_2-\theta_1)$, must be smaller than it would be if the integral term were absent. Accordingly, the actual value of $D\equiv|\theta_2-\theta_1|$ will be less and, therefore, the actual value of D^{-1} greater than that calculated on the basis of the linear characteristic stemming from neglect of the integral term. This is precisely what the curves of Figures 6 and 7 evidence.

The curves of Figure 8 are plotted from the data of runs 9 to 11, as tabulated in Table III. In these runs R and $\Delta\lambda$ are held constant; D is determined for increasingly large values of L. Figure 8 evidences that, as L increases, D^{-1} increases; equivalently, as L increases, D decreases—which is to be expected, for, in equation 10, the integral term can be neglected—in which case $(\theta_2-\theta_1)$ will be constant for a constant change in flux linkages $(\lambda_2-\lambda_1)$—only if equation 13 is satisfied. In the experimental work, $\theta_1=0$; whence $|\theta_2-\theta_1|=|\theta_2|\equiv|\theta_m|$ and the inequality equation 13 reduces to $[(RK/G)+G]>>URT/G$. As L increases, however, the motion of the moving coil becomes increasingly more sluggish because of the slower rate of increase of the induced current in the circuit and, as was actually found in the experimental work, T increases substantially with L. Thus, the right-hand side of the inequality increases with L, and the left-hand side is constant; the inequality weakens as L increases. Eventually a value of L is reached for which the integral term in equation 10 cannot be neglected. Since this term increases in magnitude relative to the preceding term as L increases, since $(\lambda_2-\lambda_1)$ is constant, and since the coefficient $[(RK/G)+G]$ is constant, it follows that $(\theta_2-\theta_1)$ must decrease as L increases. Thus, $|\theta_2-\theta_1|=D^{-1}$ increases with L—in precise agreement with the curves of Figure 8. As before, the slower increase of D^{-1} manifest for the Grassot fluxmeter stems from its value of U being much smaller than those of the other two fluxmeters.

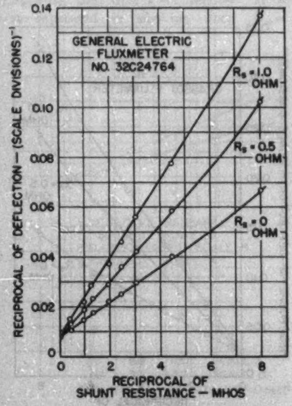

Figure 11. D^{-1} versus R_{sh}^{-1}: General Electric fluxmeter

Obviously, Figure 8 confirms Golding's[6] conjecture that a substantial value of inductance can be inserted in a fluxmeter circuit without appreciable change in the working constant of the fluxmeter.

Experimental Confirmation of the Theory of the Shunted Fluxmeter

If C' from equation 33 is substituted in equation 32, R_p^{-1} replaced by its value $(R_t+R_{sh})/R_tR_{sh}$, and the resulting expression solved for D^{-1}, we obtain

$$D^{-1}=[(1/\Delta\lambda)(R_fKG^{-1}+G)R_t]R_{sh}^{-1}+(1/\Delta\lambda)[(R_t+R_f)KG^{-1}+G] \quad (34)$$

In equation 34 let $\Delta\lambda$ and R_t be of fixed value and let the equation be interpreted as expressing D^{-1} as a function of R_{sh}^{-1}. Then equation 34 is that of a straight line where $(1/\Delta\lambda)(R_fKG^{-1}+G)R_t$ is the slope and $(1/\Delta\lambda)[(R_t+R_f)KG^{-1}+G]$ is the ordinate intercept. Accordingly, if for $R_t>>L_t$ and $R_f>>L_f$ and for fixed values of $\Delta\lambda$ and R_t, D is observed as a function of R_{sh}^{-1}, it is to be expected that the resulting curve will be a straight line over the range of R_{sh}^{-1} for which equations 32 and 34 are valid, namely, the range of R_{sh}^{-1} for which equation 30 holds.

The curves* of Figures 9 to 12, plotted from the data of runs 5 to 8, are precisely such curves. The curves bend upwards beyond the linear range, for reason analogous to that discussed previously in accounting for the corresponding phenomenon in the curves of Figures 6 and 7. The increase, as R_s increases, of the slopes of the linear portions of the three curves of a given figure stems from the fact, evidenced in equation 34, that the slope is

Table III. Data for Runs 9 to 11

L Henrys	R_{ex}	Rawson D	Rawson D^{-1}	Sensitive Research D	Sensitive Research D^{-1}	Grassot D	Grassot D^{-1}
0	26	22	4.55×10^{-2}	22.5	4.45×10^{-2}	25.0	4.00×10^{-2}
32	26	22	4.55	22.5	4.45	25.0	4.00
64	26	22	4.55	22.5	4.45	25.0	4.00
96	26	22	4.55	22.5	4.45	25.0	4.00
128	26	22	4.55	22.5	4.45	25.0	4.00
192	26	21	4.76	21.0	4.65	23.5	4.25

---

* In examining these curves, it is to be recalled that R_s is the resistance of only the variable decade resistor R_s of Figure 4.

Table IV. Co-ordinates for Figures 13 and 14 for Grassot Fluxmeter

R_{ex}	R	D	C'/C	R_{ex}	R	D	C'/C
0	100	38.5	1.00	50	150	35.8	1.08
10.0	110	37.9	1.02	80	180	34.2	1.13
20.0	120	37.4	1.03	120	220	32.1	1.20
30.0	130	36.8	1.05	160	260	30.0	1.28
40.0	140	36.2	1.06	200	300	27.9	1.38

directly proportional to R_t, increasing with R_t and thus with R_s, since $R_t=(R_s+R_{sc})$. A corresponding increase in the ordinate intercept $(1/\Delta\lambda)[(R_t+R_f)\times KG^{-1}+G]$ actually occurs as R_s increases from 0 to 0.5 to 1 ohm, but because of the relative magnitudes of the parameters in this expression, the increases are too small to be detected on the curves. Accordingly, all three curves appear to have the same ordinate intercept.

Determination of C'

The various excellent agreements between theory and experiment as previously set forth substantiate in general the correctness of the theory developed for the unshunted and the shunted fluxmeters. In particular, it follows that a fluxmeter can be used for accurate measurement in a circuit where the resistance external to the fluxmeter is any arbitrary value within the linear range of the instrument, providing the corresponding value of C' is used in working equation 16 or 32.

For an unshunted fluxmeter it follows from equation 16 that, if $\Delta\lambda$ is of constant value, then $C'D'=CD_C$, or, equivalently

$$(C'/C)=(D')^{-1}/D_C^{-1} \qquad (35)$$

where C' and $(D')^{-1}$ are corresponding values for an arbitrary value of total circuit resistance R, and C and D_C^{-1} are corresponding values for $R=R_m$. R_m and C are stated by the manufacturer; D_C^{-1} and $(D')^{-1}$ can be obtained from a constant $\Delta\lambda$ curve of D^{-1} versus R or a constant $\Delta\lambda$ curve of D^{-1} versus R_{ex}, as in Figures 6 and 7. If, with values so obtained, the corresponding values of C' versus R or R_{ex} are plotted, the resulting calibration curve furnishes ready determination of the working constant C' for any value of R or R_{ex} that can be utilized in practice.

For convenience of use it usually is preferable to plot a calibration curve of C'/C versus $R_{ex}=R-R_f$. The curves of Figure 13 are precisely such curves. These curves are plotted from data typified by that of Table IV for the Grassot fluxmeter. The values therein are calculated, as just outlined, from smoothed data taken from the pertinent curve of Figure 6. For each of the three fluxmeters, $C'=C$ when $R=R_m=R_f$, for the manufacturer's injunction that the external resistance R_{ex} be kept below one ohm implies that the working constant is C when $R_{ex}=0$. Accordingly, a value of C'/C corresponding to a given value of R_{ex} is to be calculated by dividing the corresponding value of D^{-1} by the value of $D^{-1}\equiv D_C^{-1}$ for $R_{ex}=0$.

Figure 14 comprises a calibration curve of C'/C versus R, and is included for use with the material which follows.

The linearity of the curves of Figures 13 and 14 is to be expected, for over the linear range of R, the constant C' is defined by equation 17. This can be written in the form

$$(C'/C)=(K/GC)R+(G/C) \qquad (36)$$

Since $R=R_{ex}+R_f$ equation 36 can be written in the form

$$(C'/C)=(K/GC)R_{ex}+(K/GC)R_f+(G/C) \qquad (37)$$

For the fluxmeters under discussion, $R_m=R_f$. Accordingly, it follows from equation 19 that equation 37 can be written in the form

$$C'/C=(K/GC)R_{ex}+1 \qquad (38)$$

If equation 36 be interpreted as expressing C'/C as a function of R, it is the equation of a straight line of slope K/GC and ordinate intercept G/C. Similarly, equation 38 is that of a straight line of slope K/GC and ordinate intercept one. Accordingly, if, over the linear range of R, experimentally determined values of C'/C be plotted as a function of R or R_{ex}, it is to be expected that the resulting curve will be a straight line—as in Figures 13 and 14.

The values of C for the fluxmeters of Figures 13 and 14 are encompassed in Table V. As purchased new, each fluxmeter had a working constant of $C=10^4$ maxwell-turns. But because of student use, with resulting damage and repair in the school's instrument shop, the present values of C are as tabulated. These values were determined by use of a Cenco Standard Variable Magnetic Inductor. Interestingly, the C of the Grassot instrument, maintained as the laboratory standard, has not changed appreciably since purchase several decades ago. This indicates that if a fluxmeter has been used only by those experienced and careful in use of it, C can be taken as the new value; it is not necessary to make a separate determination of C prior to using the calibration curve of C'/C versus R or R_{ex}.

Determination of the Parameters of a Fluxmeter

As discussed immediately after equation 38, the curves of Figure 14 are straight lines of slope K/GC and ordinate intercept G/C. Accordingly, the values of K/GC and G/C can be scaled from the curves of Figure 14. From these values and the values of C in Table V, K/G, G, and K can be calculated. The corresponding numerical values are tabulated in Table V.

The units of the tabulated values are: R_f in ohms; C and G in maxwell-turns per scale-division; K/G in maxwell-turns per ohm scale-division; K in maxwell-turns^2 per ohm scale-division^2; and U_m in maxwell-turns^2 per ohm second scale-division.^{2}

To determine U we note that equation 10 can be written in the form

$$D^{-1}=(K/G\Delta\lambda)(R_{ex}+R_f)+(G/\Delta\lambda)+(URD^{-1}/G\Delta\lambda)\int^{T}\beta dt \qquad (39)$$

This equation is the over-all characteristic of the curves of Figures 6 and 7. Omission of the integral term yields equation 34, the equation of the linear portion of the curves of Figures 6 and 7, hence also the equation of the straight lines obtained by extending the linear portions. Accordingly, it follows that, for a given

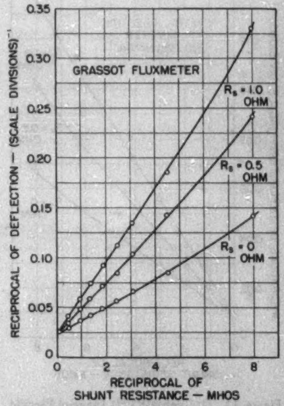

Figure 12. D^{-1} versus R_{sh}^{-1}; Grassot fluxmeter

value of R_{ex}, hence of $(R_{ex}+R_f)$, the integral term is the magnitude of the difference between the actual ordinate of the curve D^{-1} and the ordinate of the linear portion extended d^{-1}. Now as discussed previously, $\left|\int_0^T \theta dt\right| = T\left|(\theta_2-\theta_1)_m\right|$. All experimental data were taken for $\theta_1=0$, whence $\left|(\theta_2-\theta_1)_m\right| = \left|\theta_2\right| \equiv D$. Accordingly for the case at hand, $(D^{-1}-d^{-1}) \equiv (URD^{-1}/G\Delta\lambda)\int_0^T \theta dt \leqq URT/G\Delta\lambda$. In consequence, $(D^{-1}-d^{-1})G\Delta\lambda/RT \leqq U$, or since $\Delta\lambda = CD_C$

$$(D^{-1}-d_1^{-1})GCD_C/RT \leqq U \qquad (40)$$

Equation 40 yields a minimum value of U. Actual observation of θ as a function of t indicates that the two are approximately linearly related over a considerable portion of the deflection. In consequence, the actual value of U is approximately twice the minimum value of equation 40. But although equation 40 thus does not yield the actual value of U, it furnishes information sufficient to ascertain the order of magnitude of U for the fluxmeters of Table V and also the relative sizes of the parameters of the three instruments—all that is desired for the purpose at hand.

Minimum values of U, calculated from equation 40, are tabulated in Table V. The necessary values of the ordinates have been scaled from the curves of Figures 6 and 7 for $R_{ex}=200$. Calculation is typified by that for the Sensitive Research Instrument fluxmeter: $(D^{-1}-d^{-1}) = 1.44\times10^{-2}$, $U_m = [(1.44\times10^{-2})(8.9\times10^{-3})(1.13\times10^4)(28.8)/(211)\times(1)] = 1.97\times10^5$.

It is to be recalled that D_C is the deflection corresponding to $R_{ex}=0$, $R=R_{ex}+R_f$; and that $T=1$ second. If R is expressed in abohms, then $U_m = 1.97\times10^{-4}$ dyne-centimeter per scale division.

The small value of the U_m of the Grassot fluxmeter stems from the previously mentioned very delicate system of suspension and spiral connection employed with the moving coil.

Table V. Parameters of Fluxmeters*

Fluxmeter	R_f	C	K/G	G	K	U_m
Rawson	16.5	1.08×10^4	83.5	8.7×10^3	72.7×10^4	0.57×10^5
Sensitive Research Instrument	11.0	1.13×10^4	107.0	8.9×10^3	95.0×10^4	1.94×10^5
Grassot	100.0	1.00×10^4	16.3	8.4×10^3	13.7×10^4	0.10×10^5

* See text for statement of units of tabulated values.

Misstatements in Textbooks

The fact that some textbooks state, incorrectly, that the deflection of a fluxmeter is proportional to the change in flux, rather than—correctly—to the change in flux linkages, has been mentioned in the introduction. Again, in developing a theory of the fluxmeter, some textbooks assume that the "RI drop" can be neglected. Commonly, this term is considered negligible because the current is small, whence also the RI drop is small. The resulting analysis yields a working constant equivalent to that defined by equation 14 where $R=0$. As evidenced by Figure 14, however, the working constant of the Grassot fluxmeter, for example, would be 0.834×10^4 for $R=0$, as compared with the actual value of 10^4 for $R=R_f=100$ ohms; or, again, that of the Rawson fluxmeter would be 0.838×10^4 for $R=0$, as compared with the actual value of 1.08×10^4 for $R=R_f=16.5$ ohms.

Obviously, it is most desirable that a textbook development of the theory of the fluxmeter should retain the iR term of equation 4, obtain the actual linear-range working constant C' of equation 14, and therefrom stress the significance of maintaining the resistance of the fluxmeter circuit at substantially the manufacturer's value of R if his value of C is to be used as the working constant. As an example of the practical importance of such a discussion, it is to be noted that the working constant $C=10^4$ of the multiple-range fluxmeter manufactured by the Sensitive Research Instrument Corporation is based on using the fluxmeter with a special 15-ohm search coil. If some other search coil of small resistance is used, as may be necessary for a particular measurement, it is imperative that additional series resistance be added to make $R_{ex}=15$ ohms if $C=10^4$ is still to be the working constant. The necessity of adding the additional series resistance is obvious if the dependence of C' on R is known to the user, but otherwise the necessity is not evident.

Summary

1. An inclusive mathematical theory of the operation of the unshunted fluxmeter is developed. Previously published accounts of the theory of the unshunted fluxmeter are analyzed and found to be encompassed as special subcases of the theory developed in this paper.

2. From the general equation of operation a simple approximate equation is deduced which can be utilized for accurate calculation, provided the stated pertinent boundary conditions and restrictions are observed.

3. Experimental data are advanced which confirm the correctness of the general theory and make clear the necessity of observing the stated boundary conditions and restrictions.

4. Analysis and experimental confirmation analogous to that outlined in the three preceding paragraphs is advanced for the shunted fluxmeter.

5. Experiment reveals that a considerable amount of inductance can be inserted in series with a fluxmeter without substantially changing the working constant of the instrument.

6. Experiment indicated that a fluxmeter can be used in a search-coil circuit of arbitrary resistance up to, in general, several times its internal resistance, provided that the corresponding numerical value of the working constant C' is selected from the

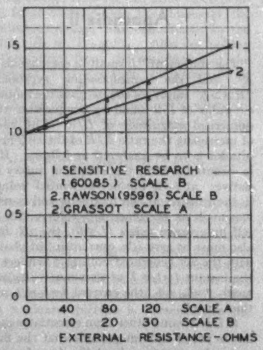

Figure 13. Calibration curves of C' versus external resistance R_{ex}

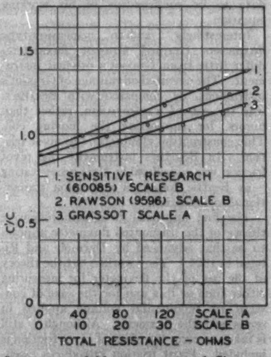

Figure 14. Calibration curves of C' versus total circuit resistance R

calibration curve of C' versus circuit resistance. A combined numerical-experimental procedure for effecting this calibration curve is advanced. This procedure is illustrated by effecting the calibration curves of several fluxmeters.

7. A procedure for determining the mechanical and electrical parameters of a fluxmeter is advanced and illustrated by calculation of the parameters of several different fluxmeters.

8. Several misstatements commonly found in reference sources are mentioned and suggestion advanced as to how to correct these inaccurate statements.

Appendix I

In 1902 Beattie[1] suggested that a pivot-type D'Arsonval galvanometer designed with minimum restoring torque and used in a circuit of low resistance could be employed for determination of the flux in an iron specimen on which a hysteresis loop was being run. Taking R, L, and U as zero enabled Beattie to deduce an equation relating D to Q, the total charge passed through the fluxmeter by the voltage generated in the search coil. From knowledge of Q the change in flux $\Delta\phi$ is then determined as when using a ballistic galvanometer for flux determination. Beattie constructed an instrument, tested it, and found experimental data to be confirmative of his working equation.

Thus, Beattie proposed the instrument now termed the pivot-type fluxmeter, but it is to be noted that he used it as a charge meter—hence his name of quantometer for the instrument. In 1904 Grassot[2] suggested that a suspension-type D'Arsonval galvanometer designed with minimum restoring torque and used in a circuit of low resistance could be used for the direct measurement of flux. Taking R, L, and U as zero yielded a working constant $C'=G$, to be obtained from equation 17 by setting $R=0$. As deflection is directly proportional to change in "flux," Grassot termed the instrument a fluxmeter. Grassot constructed an instrument, tested it, and found experimental data to be confirmative of his working equation.

Interestingly, modern suspension-type fluxmeters (termed Grassot fluxmeters) differ little from Grassot's original instrument. The essential advantage of Grassot's instrument, as compared with Beattie's, was the use of a suspension, rather than pivots, for supporting the moving coil. This construction eliminates the pivot friction. In Beattie's instrument the pivot friction was considerable, thus necessitating —as Beattie found—a correction proportional to deflection.

The first approach to a comprehensive theory of the unshunted fluxmeter appears to be that advanced by Darmois and Ribaud in 1924.[3] They worked out the theory of the use of the fluxmeter for measuring either time or flux and for the case of constant or exponential voltage applied in series with the fluxmeter. Although U still is taken as zero, the effect of pivot friction is included. Pivot friction introduces essentially a Coulomb friction force: that is, the pivot friction torque is a constant F, independent of the angular position of the moving coil. Pivot friction torque was neglected in formulating the theory of this paper as it is negligible in modern fluxmeters. However, it is easily introduced. Thus adding the opposing pivot friction torque F to the right-hand side of equation 5 results in an additional term FR/G in equation 6, an additional term $FR(t_2-t_1)/G$ in equations 7 and 8, and an additional term FRT/G in equations 9 and 10. If in this resulting equation 10, the integral term is taken as zero through assuming $U=0$, we obtain Darmois and Ribaud's working equation. In modern instruments, however, it is the restoring torque and not the pivot torque which results in departure from linear operation—except, of course, in a pivot-type fluxmeter where long continued use or careless handling has resulted in deterioration of the jewels or pivots.

Table VI. Maximum and Final Deflections in Run 9

L Henrys	D_m	D_f
0	22	22
32	25	22
64	26	22
96	27	22
128	26	22
192	25	21

Darmois and Ribaud effect, for certain conditions, the equation for the deflection as a function of time. In so doing they find that if $L>JR^2/4G$, the motion of the moving coil in taking up its final position is a highly damped oscillation. This phenomenon was observed during the experimental work of runs 9, 10, and 11. As indicated by the data in Table VI for the Rawson fluxmeter, for values of L other than $L=0$, the pointer swung up to a maximum deflection, then dropped back several divisions to the final steady-state value. It may be noted that as L increases from 0 to larger values, R being constant, the inequality $L>(JR^2/4G)$ strengthens. Correspondingly, the degree of oscillation increases at first; whence the greater difference between D_m and D_f with increase of L, as tabulated in Table VI. But as L is increased, the effect of the integral term in equation 8, neglected in Darmois and Ribaud's analysis, also increases. The effect of this term is such that at a certain value of L the value of D_m is a maximum and thereafter decreases as L increases—as is manifest in Table VI.

The effect of restoring torque was first considered by Surugue.[4] In 1935 he worked out a theory wherein F, L, and U are taken as zero. The resulting working constant is identical with equation 17. The effect of restoring torque is then introduced through use of an additional semiempirically-determined factor multiplying C'.

In reviewing the theory pertinent to use of the fluxmeter as a device for the integration of current or voltage over a long period of time, Dunn[5] (1939) points out that neglect of the integral term of equation 10 introduces a substantial error in the measured quantity; he names this term the "drift error" because after deflection the pointer drifts back towards zero under the influence of $U\neq 0$, and finds its maximum value to be URT/G—in agreement with the value found in the more comprehensive discussion of this paper. This reference contains statement of experimental methods, different from those used herein, for obtaining the parameters of a fluxmeter.

In 1933 Golding[6,7] advanced theory for both the unshunted and the shunted fluxmeter. In the first instance R, L, F, and U are taken as zero, whence the working constant obtained is $C'=G$, to be obtained from equation 17 by setting $R=0$. Corresponding approximate treatment of the shunted fluxmeter results in a working constant $C'=G(R_{sh}+R_t)/R_{sh}=GR_tR_p{}^{-1}$. This differs from the accurate working constant of equation 33 in that the first term of the latter is missing—a consequence of approximations introduced in effecting the theory. Golding's theory is encompassed in his book,[12] and in a survey paper by Miller.[8]

A more accurate theory of the shunted fluxmeter was worked out by Tagg[9] in 1945, in the course of formulating the general theory of the time–deflection characteristics of moving-coil instruments. Taking F and U as zero yields working constants for the unshunted and shunted fluxmeters which are identical with those of equations 17 and 33.

To conclude, although the following are not concerned with general theory, they encompass information on fluxmeters which is of particular interest.

1. Haworth[13] has described use of a fluxmeter with feedback applied through a phototube which results in counterbalance of the restoring torque, thus eliminating the drift toward zero after attainment of deflection.

2. As evidenced by the curves of Figures 6, 7, 13, and 14, the sensitivity of a moving-coil fluxmeter decreases as circuit resistance increases. In consequence, if the search-coil resistance is high (as may be the case in mapping rapidly-varying weak magnetic fields), the deflection may be too small for accurate measurement. Dicke[14] has described an electronic fluxmeter which possesses among other advantages both zero drift and the possibility of use of search coils of resistance up to 10,000 ohms.

3. The remarks of Salisbury[15] on calibration of moving-coil fluxmeters are of general interest and utility.

Appendix II

The statement "L small in comparison to R" and the corresponding symbolism "$R>>L$" imply, of course, that the numerical value of L is small by comparison with numerical magnitude of L/R. The effect of increasing the ratio L/R of the two magnitudes is to be analyzed as follows. If L is essentially zero, the circuit is purely resistive; at $t=t_2$ the net generated voltage in the search coil and fluxmeter coil is zero; inasmuch as no generated voltage due to self inductance exists ($L\cong 0$), the iR drop also must be zero (the current is "in phase" with the net generated voltage); whence at the instant $t=t_2=T$ of maximum displacement, $\theta=\theta_m=\theta_2$, the current $i=i_2=0$, and thus $Li_2=0$.

If L is a value other than essentially zero, but is yet of such magnitude that the fluxmeter does not overshoot the "steady-state deflection" (defined below), it still is true that, at $t_2=T$, the net generated voltage in the circuit is zero, but it does not now follow that $i_2=0$. For inasmuch as the circuit is not purely resistive, an electromotive force generated by change of current in the self-inductance of the circuit can support an equal i_2R drop at $t=t_2$. All that now can be said is that at $t=t_2$ the combined mechanical and electrical torque is zero. However, it is obviously true that, if L does not differ too much from zero (whence for arbitrary but fixed R, the ratio L/R is still small), it is to be expected that circuit conditions at $t=t_2$ are approximated by those holding for $L=0$, whence i_2 and thus Li_2 are substantially zero.

However, in a well-adjusted fluxmeter, the drift is extremely slow, whence the reading is taken at steady-state deflection. Accordingly, it must be that in such a fluxmeter $i_2=0$. (Otherwise an electromagnetic torque exists and steady-state deflection is not the case) Accordingly, if $t_2=T$ is taken, more generally, as the time of attainment of steady-state deflection, $i_2=0$, and the analysis is yet as given, except now θ_2 is the position of steady-state deflection. This position may or may not be that of maximum deflection for if L is sufficiently large, the fluxmeter will overshoot as evidenced in Table VI and discussed in Appendix I. If it is, $|\theta_2|=|\theta_m|$; if not, $|\theta_2|<|\theta_m|$.

From the practical point of view, the experimental curves of Figure 5 evidence that the self-inductance of the circuit must be considerable before steady-state deflection is influenced; whence it could be deduced directly from experiment that analysis based on neglect in equation 9 not only of Li_2, but of the influence of L on the value of

$$(UR/G)\int_0^T\theta/dt$$

as well, is valid up to very large values of L.

References

1. An Electric Quantometer, **R. Beattie.** *The Electrician* (London, England), volume 50, 1902, pages 383–5.

2. Fluxmètre, **M. E. Grassot.** *Journal de Physique Théorique et Appliques* (Paris, France), series 4, volume 3, 1904, pages 696–700.

3. Etude Théorique et Expérimentale du fluxmètre, **G. Darmois, G. Ribaud.** *Annales de Physique* (Paris, France), series 10, volume 1, 1924, pages 172–212.

4. Sur la Théorie du Fluxmètre Grassot, **J. Surugue.** *Journal de Physique et le Radium*, series 7, volume 6, 1935, pages 486–8.

5. The Grassot Fluxmeter as a Quantity Meter, **H. K. Dunn.** *Review of Scientific Instruments* (New York, N. Y.), volume 10, 1939, pages 368–70.

6. The Grassot Fluxmeter, **E. W. Golding.** *The Electrician* (London, England), volume 111, 1933, pages 503–5.

7. The Use of the Grassot Fluxmeter as a Quantity Meter, **E. W. Golding.** *Journal*, Institution of Electrical Engineers (London, England), volume 76, 1935, pages 113–17.

8. Fluxmeter Method of Measurement, **H. A. Miller.** *The Electrician* (London, England), volume 136, 1946, pages 1577–9.

9. Time-Deflection Characteristics of Moving Coil Instruments, **G. F. Tagg.** *Journal*, Institution of Electrical Engineers (London, England), volume 92, part II, 1945, pages 214–25.

10. Electrical Measuring Instruments (book), **C. V. Drysdale, A. C. Jolley.** E. Benn, Ltd., London, England, 1924.

11. Elements of Electrical Engineering (book), **W. J. Creamer.** McGraw-Hill Book Company, New York, N. Y., 1948, page 273.

12. Electrical Measurements and Measuring Instruments (book), **E. W. Golding.** Sir Isaac Pitman and Sons, Ltd., London, England, edition 3, 1940, page 348.

13. A Fluxmeter with Counter-Balanced Restoring Torque, **F. E. Haworth.** *Review of Scientific Instruments* (New York, N. Y.), volume 2, 1931, pages 125–8.

14. Electronic Fluxmeter, **R. H. Dicke.** *Review of Scientific Instruments* (New York, N. Y.), volume 19, 1948, pages 533–4.

15. Note on Calibration of Grassot Fluxmeters, **R. S. J. Salisbury.** *Journal of Scientific Instruments* (London, England), volume 22, 1945, pages 213–15.

Discussion

Frank Wenner (Consulting Physicist, Washington, D. C.): Obviously the authors have arrived at a very much better understanding of the actions of a fluxmeter (that is, a heavily overdamped galvanometer when used ballistically) than that apparently possessed by most of those who have written on the subject. There are, however, a number of points which might be explained in such a way as to ease the requirements on the part of the reader. One only, and scarcely the most important of these, is selected for discussion here. It is the transition from equation 15 to equation 31.

Keeping in mind equation 15 and applying the principle of the potential divider, it follows from an inspection of Figure 2 (neglecting L_t, L_f) that for the same electromotive force impulse into the fluxmeter the flux-linkage change must be increased by the factor $(R_t + R_{sh})/R_{sh}$. Also on looking at the circuit from the standpoint of the fluxmeter it follows from an inspection of Figure 2 that the resistance $R = R_f + R_{sh}R_t/R_{sh} + R_t$. Consequently when the fluxmeter is shunted, equation 15 takes the form

$$\lambda_2-\lambda_1=[(R_t+R_{sh}/R_{sh})]\{[R_f+R_{sh}R_t/(R_{sh}+R_t)]K/G+G\}(\theta_2-\theta_1)$$

This is equivalent to equation 31 provided the typographical error in the equation defining R_p is taken into account. Thus by using relations well-known to most of those skilled in electrical measurements instead of one of Kirchhoff's laws, not only is a considerable amount of algebra avoided but a clearer picture is presented to the reader.

Morley J. Lush (Rawson Electrical Instrument Company, Cambridge, Mass.): The authors are to be congratulated for finally bringing together, in one equation and discussion, all the error-producing factors which can influence the results when using regular commercial models of the fluxmeter.

Recent experiments by this writer have shown that values of both K and U can be reduced considerably without making the instrument as delicate as the old Grassot type.

It should be noted that the results in the paper were obtained with a circuit giving practically instantaneous changes of flux linkage. If hand-operated search-coils are used, with time intervals up to one-half second, it is not possible to use search-coil resistances as high as those mentioned. Under these conditions, the integral term in equation 10 due to spiral torque is sufficient to cause an error which is variable unless the time interval can be standardized in some way. The Rawson Company has always recommended a search-coil resistance under one ohm whenever possible, practically eliminating all errors, or a maximum value of 10 ohms if corrections can be made.

It is possible to invert equation 15 using the first two terms of a series expansion, and put it into the form

$$S=S_0\left[1-\frac{S_0KR_{sc}}{G}\right]$$

where S is the general sensitivity, and S_0 is the scale calibration sensitivity ($R_{sc}=O$). Both S and S_0 are in divisions per flux linkage. The equation is within one-half of 1 per cent if the second term is less than 5 per cent. To one further degree of approximation

$$S=S_0\left[1-\frac{S_0^2KR_{sc}}{10^9}\right]$$

This form of the equation is interesting because it shows that the variation in calibration constant with search-coil resistance depends upon air damping constant K and the square of the sensitivity. If a deflection sensitivity higher than that of the old Grassot instrument is attempted, the calibration constant becomes very dependent upon the search-coil resistance (unless the air damping can be reduced in some way). This explains why some makers have adopted the practice of requiring all search-coils to be adjusted to a particular value of resistance.

Thomas James Higgins and **Glenn Robertson:** Mr. Lush's equation neatly exhibits the dependence of sensitivity on search coil resistance and very well complements the author's discussion thereof.

With respect to Dr. Wenner's remark that "there are a number of points which might have been explained in such a way as to ease the requirements on the part of the reader" the authors would point out that Dr. Wenner's purported derivation of their equation 31 is invalidated by his remark "neglecting L_t, L_f".

If the authors had chosen to neglect terms *a priori* they could have shortened the over-all analysis of the paper considerably. Rather, it was their stated intention, to carefully and completely consider the influence of all pertinent factors and to establish definitely under what conditions certain approximations could be introduced, that necessitated the approach through Kirchhoff's laws. Thus, it is clearly established in the paper under what conditions terms involving inductances drop out, thus resulting in equation 31. On the other hand, Dr. Wenner merely "neglects L_t, L_f" whence (on the basis of Dr. Wenner's derivation) no specific condition results as to when his resulting equation is valid.

Further, it was not the intention of the authors that their paper would be intelligible merely "to most of those skilled in electrical measurements" but rather to so write that the paper as a whole would be clear to any reader with an ordinary undergraduate training in circuit analysis and electrical measurements. For it is the engineer with only an average training in electrical measurements who commonly falls into error in using a fluxmeter, not the highly-skilled worker in electrical measurements.

A 66-Kv Subtransmission Plan for a Metropolitan Area

K. M. SMITH
MEMBER AIEE

E. L. MICHELSON
MEMBER AIEE

THE planning of the subtransmission system to deliver power from the power supply station to the substation represents a fertile field for the activities of the system planning engineer. Many different possibilities present themselves in any particular system, and there are numerous factors that require consideration before the most desirable plan can be determined. The basic conditions change from time to time, so that it is necessary to review the problem periodically to take into account new developments that affect the economics of the subtransmission system.

In Chicago a new arrangement was adopted recently to provide for the expansion in load which is being experienced. This arrangement utilizes as a subtransmission voltage 66 kv, formerly used only at transmission levels. In this paper the basic reasons for the adoption of the new system are described, and some of the details of the system are discussed from the viewpoint of the system planning engineer. In order to provide a background for this discussion, the history of the Chicago system is reviewed briefly.

History of the Chicago Power System

In the early development of the power system in the city of Chicago, all the generators were located inside the city and relatively close to the load. The subtransmission for the 60-cycle load consisted of lines at the generated voltage (12 kv) direct from the generating station to the distribution substations, and the various generating stations were sometimes interconnected by these same 12-kv lines. The complexity of this arrangement caused difficulties in operation and protection, and led to the separation of the 12-kv system into various subtransmission zones, supplied from major 12-kv switchhouses originally located exclusively at the sites of generation. These zones were then interconnected by a 66-kv transmission system.

Figure 1 shows in detail the connections of one of these generating station switchhouses and a typical arrangement of 12-kv lines and substations. Several substations are combined into a group, which operates independently of other groups. In this manner a highly reliable system has been developed, which is relatively simple to operate and protect.

A further development in the subtransmission arrangement occurred in the late 1920's and early 1930's, when two large distributing stations were constructed along the route of the 66-kv interconnections, midway between generating stations. These distributing stations were supplied by 66/12-kv transformers from the 66-kv transmission system, and served as a source of supply for the subtransmission lines in their vicinities. The length of 12-kv lines required for subtransmission was thereby reduced. The 12-kv switching structures at these stations are similar in size and construction to the switchhouses at generating stations.

The system as it existed previous to the current development under discussion is shown in simplified form in Figure 2. At this time there was a total of 275 12-kv lines supplied from seven switchhouses located on six sites. These lines are usually 3-conductor 500,000-circular-mil underground cable.

With a closely interconnected high capacity system, it is obvious that potentially high fault currents are available. The switchhouses built since 1921 have therefore been of isolated-phase construction. This design is carried through the 66-kv transmission system by the use of single phase transformers and single conductor cable, so that the possibility of a phase-to-phase fault on these elements of the system was practically eliminated. Neutral grounding resistors are used on the 66-kv system and in the 12-kv generating stations to limit the phase-to-ground fault currents, and reactors are installed on the 12-kv lines at the switchhouses to reduce the effect of phase-to-phase faults on the 3-conductor subtransmission cables. As a result of this design, it has been possible to operate the phase-isolated 12-kv switchhouses and 66-kv terminals with circuit breakers rated below the calculated 3-phase fault current. Normal or automatic sectionalization of busses has effected a further reduction of fault current.

Recent Developments

While the design of switchhouse construction and the subtransmission arrangement described have been quite successful and reliable, certain recent developments, as outlined in the following, have stimulated consideration of an alternative plan:

1. In recent years it has been necessary to develop generating sites outside the city. Power from these sites is transmitted into Chicago at high voltage, and is made available to the 66-kv interconnecting system in the city. This situation has a considerable effect on the economics of the subtransmission system, because it makes more favorable the use of 66 kv as a subtransmission voltage to deliver the power closer to the point of utilization. Present indications are that the trend towards power being made available in the city at a higher voltage will continue.

Paper 49-172, recommended by the AIEE System Engineering and Transmission and Distribution Committees and approved by the AIEE Technical Program Committee for presentation at the AIEE Summer General Meeting, Swampscott, Mass., June 20-24, 1949. Manuscript submitted March 2, 1949; made available for printing April 29, 1949.

K. M. SMITH is System Planning Engineer and E. L. MICHELSON is Section Engineer, both with the Commonwealth Edison Company, Chicago, Ill.

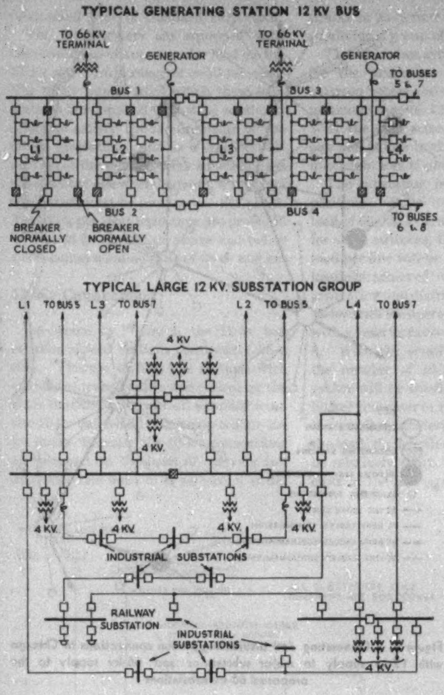

Figure 1. Generating station 12-kv bus and 12-kv substation connections

2. The present 12-kv lines average about four miles in length, and the longest lines extend eight to ten miles from the switchhouse. With rapidly increasing load density, particularly in areas remote from the present switchhouse sites, continued subtransmission from these sites at 12 kv involves considerable costs, and the need for a higher voltage is indicated.

3. In recent years there has been an extensive development of factory assembled switchgear, which has many attractive features. Switchgear of this type, in a price class which makes it suitable for substation use at 12 kv, has been made available in interrupting capacities as high as 500,000 kva. A plan which would permit the integration of this type equipment into the system appeared desirable.

In the light of these developments, and as the need for 12-kv switch positions for subtransmission purposes has increased, various studies have been made of the economies of extending the 66-kv system for subtransmission purposes. Instead of constructing additional large switchhouses, or extending present ones, consideration was given to the use of smaller 66/12-kv substations of simplified construction which would be supplied from 66-kv lines and be superimposed on the existing pattern of 12-kv subtransmission. Investigation disclosed the following advantages for the use of the smaller type of 66/12-kv installations:

1. It has been the experience that the large switchhouses designed for 40 to 60 line positions have a costly development period due to the necessity for constructing the station in large increments. As a result, it may take many years to obtain full utilization of the capacity of the switchhouse. The use of smaller substations permits a closer match between system requirements and actual construction.

2. The use of 66-kv reduces the amount and cost of cable required for subtransmission purposes. The small 66/12-kv substation permits extending the 66-kv lines close to the center of the load, with the result that the lines between the 66-kv substation and other substations requiring 12 kv in the vicinity are relatively short. In addition, if the 66/12-kv substation can be located adjacent to an existing major 12/4 kv-substation, 12-kv lines for the latter are eliminated completely.

3. With the larger switchhouses, involving as many as 60 12-kv cables and the various 66 kv, and possibly 4 kv, cables required for the station, the problem of cable congestion in the streets adjoining the station can become a serious problem. In some cases the number of possible conduit runs is rather limited, and the cable congestion may lead to excessive heating with resultant reduction of cable capacities.

4. Smaller installations inherently will have a lower value of short-circuit current. While the calculated value of fault current at the larger 12-kv switchhouses ranges from 1,000,000 to 2,000,000 kva, it was found that an economical size of 66/12-kv substation could be selected which would easily restrict fault current values to 500,000 kva. This makes possible the use of low interrupting capacity switchgear. It also makes possible the elimination to a large extent of 12-kv line reactors which are required on lines emanating from the larger switchhouses.

5. Substations are more adaptable to supervisory control than large switchhouses due to the simplicity of the layout and the smaller amount of load being supplied from the station. As a result, the operating costs for a 66/12-kv substation of relatively small size can be kept to a minimum.

6. The smaller 66/12-kv substations provide improved reliability for the 12-kv system by reducing the number of 12-kv lines to one location. To the extent that a switchhouse is subject to complete outage from fire, explosion, and other similar occurrences, the reduction in the number of 12-kv lines originating at one location should reduce the severity of any one case of trouble.

New 66/12-Kv Substations

The growth of load in Chicago during the recent war and postwar period resulted in prospective full utilization of some 12-kv switchhouses. The general advantages of 66 kv for subtransmission purposes using small 66-kv substations, appeared to make the use of this voltage very attractive. Also, general economic studies, which are discussed in a later section of this paper, showed considerable savings for the 66-kv system. After a review of conditions in each specific case, it was decided to provide expansion of the subtransmission system by the construction of 66/12-kv substations, rather than by enlarging the existing switchhouses or constructing additional large switchhouses.

The installation of several small 66/12-kv substations is planned, and one of these stations was placed in service in the latter part of 1948. Figure 3 shows the existing subtransmission system with the new 66-kv lines and substations superimposed. In each case, the new 66-kv substation supplements the existing system by supplying load on the fringes of the present zones. In this manner, the great-

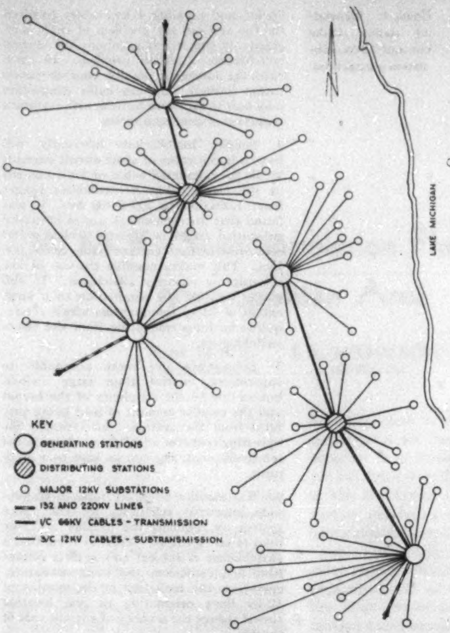
LAKE MICHIGAN
KEY
GENERATING STATIONS
DISTRIBUTING STATIONS
MAJOR 12KV SUBSTATIONS
132 AND 220KV LINES
1/C 66KV CABLES - TRANSMISSION
3/C 12KV CABLES - SUBTRANSMISSION

Figure 2. Generating and distributing station connections in Chicago with 12-kv supply to major substations

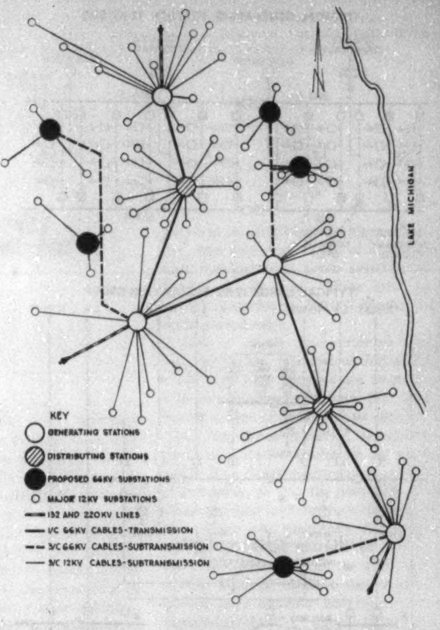
LAKE MICHIGAN
KEY
GENERATING STATIONS
DISTRIBUTING STATIONS
PROPOSED 66KV SUBSTATIONS
MAJOR 12KV SUBSTATIONS
132 AND 220KV LINES
1/C 66KV CABLES-TRANSMISSION
3/C 66KV CABLES-SUBTRANSMISSION
3/C 12KV CABLES-SUBTRANSMISSION

Figure 3. Generating and distributing station connections in Chicago with 12-kv supply to major substations and 66-kv supply to the proposed 66-kv substations

est reduction in the length of 12-kv lines is effected, and the maximum economy is obtained.

The following is a description of the elements of these subtransmission systems which concern the planning engineer. The general layout for one of these systems is shown in Figure 4.

Basic Capacity Elements

From a planning point of view, an important problem was the co-ordination of capacity of the various components of the system. As the 66-kv substation lines will operate as a radial system not interconnecting 66-kv transmission terminals and without 66-kv bussing at the substations, it is possible to co-ordinate line and transformer capacity on an individual line basis. The maximum size of 3-conductor 66-kv cable which may be installed in the existing duct system is 650,000 circular mils, which will have a normal summer rating of 49,000 kva, and an emergency rating of 66,000 kva. To match this line capacity, a transformer size was selected which permits the connection of two transformers per line, that is, a 3-phase unit with a 25,000 kva forced-air rating and an emergency rating of 33,000 kva. Thus, a 3-line subtransmission group will supply two substations, each with three transformers, and each having a firm capacity of 66,000 kva so that the total load will match the emergency line and transformer capacity with one line out of service. The cable between the two substations is, of course, smaller as it must serve only one transformer. Cable of 250,000 circular mils was selected for this purpose.

66-Kv Lines

All 66-kv cable is 3-conductor oil filled. At or near the first substation at the termination of the 650,000-circular-mil cable, a 3-position disconnect device is installed from which will be taken the tap to a transformer in the first substation and the 250,000-circular-mil cable supplying a transformer in the second substation. This device will permit disconnection of either outgoing tap and restoration of service to the other.

At the supply point, each of the 66-kv subtransmission lines is connected to a different bus section for maximum reliability. The use of 3-conductor cable makes it necessary to provide line reactors at this point. The reactors have a value of 3.5 ohms, which will reduce the value of fault current imposed upon the 66-kv phase isolated terminal, by a multiphase fault on the 3-conductor cable, to less than 1,000,000 kva.

Transformers

The 3-phase 66/12-kv transformers will have an impedance value of 11 per cent, based on the self-cooled 20,000-kva rating. This is the maximum impedance value available without special design. Here again, the factor of co-ordination appears, as with three transformers of the size and impedance selected, the 3-phase fault current on the 12-kv side is somewhat less than 500,000 kva, the value corresponding to the interrupting capacity of an economical type of standard switchgear.

The transformers are equipped with automatic tap changers under load on the 12-kv side with a range of ±10 per cent. The 66-kv busses from which these substations are supplied cannot be regulated solely to satisfy the requirements of the 66-kv substations, and as a considerable portion of the load on these substations is unregulated elsewhere, adequate range of regulation must be provided at this point. Two $2^1/_2$ per cent fixed taps are provided on the 66-kv windings above and below the nominal winding ratio of 66 to 12.6 kv.

12-Kv Connections

As shown in Figure 4, the 12-kv bus consists of four sections connected into a ring. The use of four bus sections with only three transformers was chosen on the basis that the units of load supplied from the 12-kv bus would require up to four 12-kv lines. Because the 12-kv connections are planned on the basis of carrying full load with one line out of service, it is desirable to have four separate bus sections supplying a group of four lines.

The 12-kv bus arrangement is designed for the maximum electrical separation between busses and transformers with the minimum use of 12-kv circuit breakers. With the arrangement shown in Figure 4, any one failure in the station will cause a maximum loss of one transformer.

The substation includes 16 12-kv line positions. Based on a maximum 12-kv load of 66,000 kva, and without allowance for spare switches, the average coincident load per line will be lower than the actual loadings achieved on existing lines from generating and distributing stations where 12-kv lines are operated in groups of eight, with a reserve ratio of approximately 1 to 8. With the smaller 66-kv substations, the number of 12-kv lines grouped together will be smaller, with consequently higher line reserve ratio. However, with the smaller substations located closer to the load, the length of each 12-kv line will be relatively short, and as the increment costs of the line circuit breakers in these substations is relatively low, the lesser line loading does not adversely influence the economics of the 66-kv subtransmission system to a serious extent.

Since the maximum possible fault current is below the capacity of the 500,000-kva circuit breakers, reactors are not required on outgoing lines to protect the substation equipment. However, line reactors will be required in a few cases to protect lower capacity circuit breakers at customer substations supplied at 12 kv from 66-kv substations.

System Grounding

The substation transformers will be delta connected on the 66-kv side, and star connected on the 12-kv side. The 12-kv winding neutral is grounded through a 3-ohm resistor, principally for the purpose of limiting the value of phase-to-ground fault current which will be imposed on the lead sheaths of the 12-kv underground cables. Resistance is used in the neutral rather than reactance

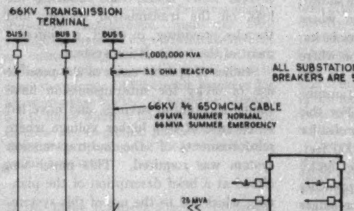

Figure 4. 66-kv supply to the new 66 kv/12-kv substations and substation bus connections

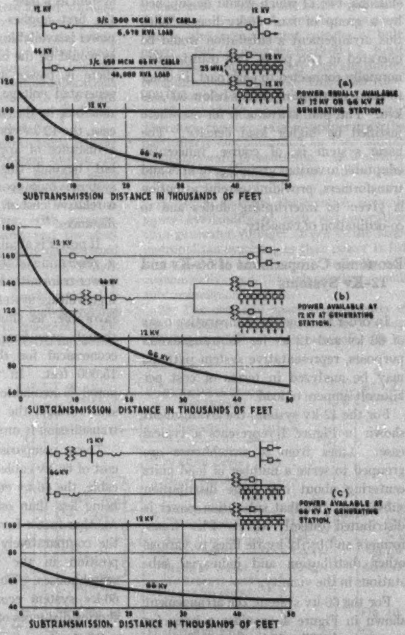

Figure 5. Comparative costs per kilovolt-ampere load 12-kv versus 66-kv subtransmission

to limit transient overvoltages in the 12-kv system.

Relay Protection

The relay protection provided for the new subtransmission system is conventional in most respects. Over-current relaying is provided on the 66-kv and 12-kv lines, and differential protection is provided for the transformers and busses. Because the substation transformers are connected to the lines without 66-kv circuit breakers, the transformer differential relays actuate a remote trip circuit to clear the remote ends of the lines. This trip circuit is incorporated at small additional cost in the pilot wire cable which is required for the oil-pressure alarm system for practically the entire length of the 66-kv cable.

Other Possible Arrangements

It is possible, with satisfactory co-ordination, to use the same units of capacity to develop 4-transformer substations, two of which would be supplied by a group of four 66-kv lines. With this arrangement a substation would be operated in two parts, two transformers normally connected to each part, in order to keep interrupting duties below 500,000 kva. This plan is available for use where justified by higher load density. The basic system is, of course, inherently adaptable to various groupings of lines and transformers, providing careful attention is given to interrupting duties and to co-ordination of capacity.

Economic Comparisons of 66-Kv and 12-Kv Systems

In order to show the comparative costs of 66 kv and 12 kv for subtransmission purposes, representative system patterns may be analyzed in terms of cost per kilovolt-ampere of load.

For the 12-kv system, the arrangement shown in Figure 1 represents a typical case. Lines from a switchhouse are grouped to serve a number of load units centering about one large distribution substation. At that substation power is distributed directly to its 4-kv transformers and by 12-kv tie lines to various other distribution and industrial substations in the vicinity.

For the 66-kv system, the arrangement shown in Figure 4 provides a basis for comparison. The 66-kv lines and transformers, in effect, replace the 12-kv lines between generating station and the load center of the group substation.

Figure 5 shows the results of the economic comparison. The 12-kv system costs include the switch position in the generating station, the 12-kv cable, and a total of three circuit breakers at the substation. The latter allocation is based on actual experience and takes into account all the circuit breakers, at each large substation, including bus ties, transformer circuit breakers, and tie lines to other substations. Since the 66-kv substation supplants all of these circuit breakers, a credit is taken for them in the cost comparison. The average maximum load per line of 6,670 kva is based on actual experience with the Chicago system. The comparable 66-kv system consists of one 66-kv line position, the 650-000- and 250,000-circular-mil 3-conductor cable, and the transformers and 12-kv circuit breakers supplied by this line. For convenience the 66-kv line is evaluated in terms of equivalent length of the larger size. The expected maximum line loading is 40,000 kva.

Figure 5 shows the relative costs of the two systems using the cost of the 12-kv system as a base. Three cases are shown; the first applies to a condition where power is available either at 12 kv or 66 kv, as would be the case at a location where there is power available either at the generated voltage or from the transmission bus in the same station. For this case, the 12-kv system has a lower cost for a distance of approximately 3,000 feet, but beyond this distance, the 66-kv system is more economical and approaches a relative cost of 50 per cent for longer distances.

If power is available only at 12 kv, as at a generating station where there is no power transmitted to the station from the high-voltage system, the 66-kv plan is less favorable, as shown by curve (b); although, even here, 66 kv would be more economical for distances greater than 15,000 feet. In the third case, where power is available only at the transmission voltage, the use of 66 kv for subtransmission is most advantageous.

These comparisons reflect the lower cost of 66-kv cable, as compared to 12-kv cable, the 66-kv cost per kilovolt-ampere being less than one-half the 12-kv cost. Another factor favoring the 66-kv plan is the comparatively high cost per switch position in the isolated phase 12-kv switchhouses. This tends to make the 66-kv system economical even for the shorter distances of subtransmission.

While these comparative studies provide a general basis for appraising the economy of the higher voltage system, there are various other practical considerations that affect the final answer. For instance, the general comparison is based on the installed cost of the 12-kv or 66-kv lines, while in actual practice any existing 12-kv lines released by the introduction of the 66-kv system will yield only salvage value. Fortunately, however, portions of such 12-kv cables can, within a short period of time, be used in place to provide for load growth in the area closer to the switchhouse. Thus, to a great extent, the actual salvage value approaches their cost in place.

The general comparison also is based on average 12-kv subtransmission line loadings. In areas remote from the switchhouse, this may not always be achieved due to the necessity for a somewhat lower loading to meet the requirements of voltage regulation. In such cases the 66-kv system has an economic advantage.

Another practical factor is the interrelationship between 66-kv subtransmission and transmission. Where the 66-kv subtransmission parallels the transmission system in the direction of power flow upon the latter, it may serve load taken from several 12-kv zones, thus reducing the load on the transmission system, and thereby providing, in effect, a reinforcement of the transmission system.

Studies of specific cases of the possible use of 66-kv for subtransmission have shown substantial savings, and have led to the use of this higher voltage where reinforcement of the subtransmission system was required. This paper has aimed at a brief description of the planning which led to the use of this system. Higher load densities, increased transmission of power into the city from outside stations, comparative costs of construction for extending existing facilities, and the availability of economical factory-assembled switchgear are primary factors which have been considered.

The gain in economy and reliability resulting from the use of the system described is evidence that time which is devoted to the planning of the subtransmission portion of a system may be well justified.

Discussion

H. R. Wall (The Commonwealth and Southern Corporation, Jackson, Mich.): The authors' interesting description of the use of higher voltage for subtransmission extensions in their territory presents a convincing demonstration of the benefits which can be obtained in this manner. Their use of radial 69-kv subtransmission supply to step-down substations, without 69-kv automatic switching at those substations, presents an economically attractive subtransmission plan.

It is noticed that the paper mentions the new extensions as "supplying load on the fringes of the present zones." It is assumed that even "fringe" territory in this location is so congested that it is not feasible to use 69-kv wood pole lines. In less congested territory where overhead lines can be used the use of higher subtransmission voltage, such as 69 kv, offers material economic advantages, since the voltage drop in the lower voltage (overhead) subtransmission circuits also is a serious consideration, as well as the thermal capacity limitations found in cable circuits. Higher voltage subtransmission might be indicated to avoid additional crowding of city streets by a greater number of low-voltage subtransmission lines.

The necessity for restricting maximum fault current on these subtransmission systems, as pointed out by the authors, with the intentional introduction of additional impedances in order to achieve that purpose, leads to a question regarding the possible use of switched capacitors for voltage control instead of, or supplementing, the tap changing underload apparatus, in order to reduce the additional losses associated with the intentionally added impedances.

The authors have mentioned the simplified relaying applied in their plan. No mention is made of the means of clearing 69-kv faults by the 12-kv circuit breakers of the step-down transformers. Since the low-voltage busses of the step-down transformers are operated in parallel, it is assumed that directional overcurrent relays are used to open the proper 12-kv circuit breakers for phase-to-phase faults. It would be interesting to know whether any provision is made to clear line-to-ground faults on the 69-kv circuits by opening the 12-kv transformer circuit breakers.

D. K. Blake (General Electric Company, Schenectady, N. Y.): It was a pleasure to read this paper for three reasons. First it is well written. I want to commend the authors for their brief and clear presentation of the pertinent factors. Second, it is encouraging and refreshing to see this departure from complications towards simplification. Third, it is a confirmation and illustration of the same economic principles that determine substation sizes whether they are for transformation from 69 kv to 12 kv or from 12 kv to 4 kv.

Some perhaps will be startled, after reading the authors' "the small 66/12-kv substation," to find they are 66,000 kva firm rating. In many other systems this would be considered "large" and would be large for those areas.

Whether a substation is large or small is not defined on economic grounds by its kilovolt-ampere rating. It is defined more properly and accurately by the area in square miles, or if one prefers, by the number and average length of the feeders departing from it. As the area decreases in size, with increasing load density, the feeder lengths to cover the area eventually become so short that a point of diminishing return is reached. There is not much left to save in 12-kv lines to offset the added substation and 66-kv extension cost inherent in diminishing substation size. Increases in load density from thereon are met by increasing the number of feeders until line or duct congestion impose their limits.

The concept of separating the load supplying function from the transmitting function in system design is a very sound procedure in my opinion and should be more widely adopted. The load supplying function is what distinguishes "distribution" from "transmission." Do the authors propose to eliminate 12-kv transformation and step from 66 to 4 kv in areas where applicable? All that is needed is enough load to economically load the 66-kv circuits and after that it becomes possible to save money by eliminating a transformation.

V. E. Hill (Duquesne Light Company, Pittsburgh, Pa.): This is a very interesting paper that has been well organized and which was easy to follow. The authors describe a principle that has become quite necessary in recent years, that is, the use of much higher transmission voltages for the distribution of power to large load centers. The plan adopted certainly has the merits of simplicity and economy. However, while going through the paper, a few questions arose.

In the reference to the use of higher voltages (that is above 66 kv) to bring power into the Chicago area from the more distant generating systems, has any consideration been given to stepping these higher voltages directly down to 12 kv? Likewise, was there any consideration given to the establishment of direct 66/4-kv substations? The latter statement assumes the installation of high capacity distribution substations in one locality. There seems to be a tendency to get away from this type of station with the use of the unit substation.

Use of 12 kv as a subtransmission voltage was, of course, quite common during the early days of the industry, because loads were light and because this was the generator voltage and it avoided the step-up transformation. However, with modern, heavily concentrated loads, and the duct congestion which is frequently encountered near generating stations or bulk supply stations, such as are described here, it is wondered whether any consideration has been given to the use of higher voltage cables, such as 22 kv in place of 12 kv.

We were very much interested in the fact that these new 66/12-kv transformers are being acquired with automatic tap changing under load. We have been checking the need of this additional control device on our 66/22-kv bulk supply stations for some years, but have not yet quite justified the cost except at one station where the voltage regulation is rather extreme. In this connection we are wondering what the regulation would be on the 12-kv busses without the tap changing under load. Are you maintaining a flat 12-kv voltage or are you adjusting it automatically by means of load compensators?

In reference to the use of four 12-kv bus sections, it was mentioned that this number was chosen because the size of the (load) units required four 12-kv lines and provision is made for one line out of service. How large are the "units" that are referred to here? That raises the question of whether there are any customers so large that they are supplied directly from the 66-kv system. The latter voltage also may be dictated by flicker limitation.

The economic comparisons in Figure 5 of the paper are very interesting and demonstrate that it is very essential to consider at what voltage the power is available.

C. A. Woodrow (General Electric Company, Schenectady, N. Y.): Any subtransmission investigation can easily become extremely complicated. Subtransmission generally includes a simple transmission function; that is, the point-to-point transfer of bulk power. But, it must go further! It must reach down and adequately feed the underlying distribution system. This latter function involves an area concept and all the ramifications of varying load density. Therefore, the authors of this paper are to be particularly complimented on their simple straightforward presentation. They clearly make two particular points which seem widely significant:

1. As in Chicago, the trend is towards power availability at high voltage rather than generator voltage. Even in the large metropolitan systems, as that power is fed down into the load areas, it logically and economically clears through relatively small subtransmission stations.

2. The cost and space requirements of the modern metalclad, 13.8-kv oil-less switch-gear (indoor and outdoor) are so

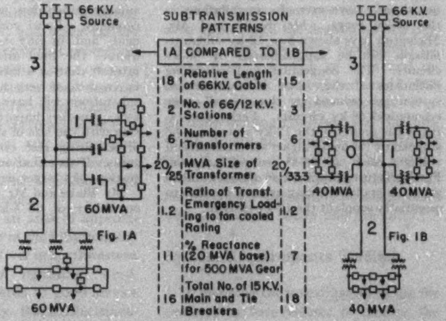

1A	COMPARED TO	1B
18	Relative Length of 66K.V. Cable	15
2	No. of 66/12 K.V. Stations	3
6	Number of Transformers	6
20/25	MVA Size of Transformer	20/33.3
1.2	Ratio of Transf. Emergency Loading to fan cooled Rating	1.2
11	% Reactance (20 MVA base) for 500 MVA Gear	7
16	Total No. of 15K.V. Main and Tie Breakers	18

Figure 1. Alternative subtransmission patterns

attractive that they dictate subtransmission patterns which limit the 12- and 13.8-kv short circuits to 500,000 kva or less.

Though the authors have made an important contribution, a note of caution seems justified. The firm capacity of 60 to 66 megavolt-amperes may be small for 66/12-kv stations in Chicago but it is large for a great many urban areas. Quite often, considerable expense in 12- or 13-kv circuits can be saved if much smaller stations can economically and judiciously be provided within the load area. Figure 1(B) of the discussion illustrates a possible step in that direction. It provides three 40-megavolt-ampere stations as an alternate to the Chicago plan, Figure 1(A) with two 60-megavolt-ampere stations. A 2-source rather than a 3-source station is used for two reasons:

1. To reduce the number of transformers and 66-kv cable T taps.
2. It is much less costly to run two, rather than three, 66-kv laterals out into the load area to supply 40 megavolt-amperes.

As is indicated by the comparison chart of Figure 1, the principal difference in substation apparatus cost is the use of high velocity fans (or equivalent), Figure 1(B), rather than low velocity fans, Figure 1(A), on the 20-mva 3-phase transformers. However, as is illustrated by the relative cable length shown, this extra cost can often be largely eliminated. If load ratio control transformers are used, the two patterns appear to break even (real estate and underlying 12-kv cable *not* included) when the 66-kv 3-conductor cable saving of Figure 1(B) is equivalent to about two miles of cable. Without load ratio control, they break even with about one mile of cable saving.

Where the additional substation site can be made available, subtransmission pattern Figure 1(B) often warrants a serious consideration. In many cases the same pattern can be economically used to serve a total load of 80 to 90 megavolt-amperes. Correspondingly smaller subtransmission stations and smaller 3-conductor 66-kv cable would be used in these cases.

H. G. Barnett and **D. F. Shankle** (Westinghouse Electric Corporation, East Pittsburgh, Pa.): Voltages in the 15-kv class are frequently too low for subtransmission in present-day metropolitan distribution systems. Many utilities probably would adopt a higher subtransmission voltage if they did not already have extensive installations in the 15-kv range. Mr. Smith and Mr. Michelson have shown how 12-kv subtransmission can be supplemented by 66-kv circuits. The congestion and operating difficulties of the 12-kv subtransmission system are reduced by the over-all more economical 66-kv circuits. Perhaps eventually the growth of the 12-kv system can be stopped by the use of higher subtransmission voltages such as 66-kv subtransmission. Further future simplification of 66-kv underground installations may make it possible to essentially supplant the 12-kv system.

It is interesting to note that the 66-kv circuits are treated as subtransmission circuits and not as parts of the transmission system. This simplifies the operation of the system and improves the over-all economy of both the subtransmission and transmission systems.

Eric T. B. Gross (Illinois Institute of Technology, Chicago, Ill.): The authors state that it is planned to ground the 12-kv neutrals of the transformers through 3-ohm resistors, principally for limiting single-line-to-ground fault currents.

I am wondering if resonant neutral grounding has been considered. It seems to me that ground fault neutralizers would bring additional advantages; they have been used in this country in underground cable systems when no other solution promised power supply to the consumers as free from disturbances as resonant grounding.[1] The experiences have been very satisfactory.

I do not underestimate the importance of transient overvoltages, but the differences between their values at various kinds of neutral grounding are small, and should be negligible in a 12-kv system. Resonant neutral grounding has proved successful in underground cable systems at much higher voltages. Relaying of ground faults in resonant grounded systems can be done easily by means of sensitive single-phase directional relays which are activated by the residual feeder current, and polarized by the neutral displacement (zero sequence) voltage. If such relays are installed, any voltage dips are eliminated which are otherwise unavoidable on single-line-to-ground faults.

REFERENCE

1. RESONANT GROUNDING OF DISTRIBUTION SYSTEMS, E. Herzog, *Proceedings*, Midwest Power Conference, Illinois Institute of Technology, Chicago, Ill., volume 11, 1949.

K. M. Smith and **E. L. Michelson:** The authors appreciate very much the interest in their paper and the various discussions which have been offered.

Mr. Woodrow has provided an excellent example showing that in some cases it would be more economical to use a smaller substation than the one being used in Chicago. It is very possible that with lighter load densities than those existing in Chicago, the smaller substation would provide greater economy. Local conditions vary a great deal, and in any economic study these dictate the final answer. It may be of interest that in a later project in Chicago, in an area of very high load density, the substations will have a capacity of 100,000 kva. Another important factor in connection with the size of station is the difficulty of acquiring real estate in crowded city areas. This situation tends to favor substations of a larger size.

Mr. Blake and Mr. Hill both mention the possibility of 66/4-kv substations. This arrangement has been investigated, but for various reasons it has not appeared to be advantageous for the Chicago conditions. It seems that a more logical development would be the use of 12-kv for distribution purposes to replace the existing 4-kv system.

While this possibility has been seriously considered, many difficult design and operating problems for the conditions existing in the Chicago system have prevented the adoption of the higher distribution voltage.

Mr. Wall is correct in his assumption that the fringe territories referred to in the paper are sufficiently congested that it is not feasible to use overhead construction. He refers to the use of switched capacitors for voltage control, but this method is not being used in Chicago due, principally, to the disadvantages of locating these capacitors in crowded alleys. In connection with the relay protection for the 66-kv lines, directional relays are used to open the 12-kv circuit breaker for a phase-to-phase fault on the 66-kv line. In the case of a phase-to-ground fault, the ground relays at the supply end of the line energize the same remote-trip wires that are used for transformer protection, and in this manner all terminals of the line are opened for all types of line and transformer faults.

In answer to Mr. Hill's questions, the power brought into Chicago from distant generating systems now is being supplied to the 12-kv busses of the generating and large distributing stations. In the new development the only change is that the 66-kv system is carried closer to the ultimate load. The advantages gained by the use of 22-kv instead of 12-kv do not appear to be sufficient to justify a major change in the subtransmission system, due to the relatively small increase in voltage. In effect, the new system in Chicago has increased the subtransmission voltage from 12-kv to 66-kv. The 12-kv cables which are required with the new arrangement are relatively short and are not an important factor in the over-all economy. With regard to the 12-kv bus voltage at the new substations, the voltage is compensated for load, with the result that the bus voltage varies from 12-kv at minimum load to approximately 12.4-kv at maximum load. In Chicago there are a few customers supplied directly from the 66-kv system. The units of loads supplied from the new 66-kv substations in some cases may be a single customer, but in most cases consist of small substation groups which require a maximum of four 12-kv lines.

Resonant neutral grounding is not being used in Chicago at the present time. Dr. Gross' suggestion for its use in the new 66-kv substations is a very logical one, and consideration should be given to its use. However, it does not appear that this type of grounding offers any over-all advantage compared to resistance grounding when it is considered that reserve capacity is provided for all substations and 12-kv customers, and, therefore, there is practically no need to operate a cable while it is faulted.

Overcurrent Investigation on a Rural Distribution System

G. F. LINCKS
MEMBER AIEE

D. R. EDGE
ASSOCIATE AIEE

W. C. McKINLEY
NONMEMBER AIEE

J. H. LEH
NONMEMBER AIEE

GOOD service continuity with the least possible outlay is a major problem on every rural distribution system. To make the rural line pay, the farmer must use electric power for milking machines, hay drying, water pumping, and many other tasks about the farm which affect his livelihood. With such industrialization of the farm, the average monthly consumption per consumer approaches 150 or 200 kilowatt-hours at present and is expected to reach as high as 400 or 500 in some areas in the future. Loads of these magnitudes make provision for high quality service more economically practicable.

Experience has shown that distribution primary line faults are the major cause of power service outages. Sectionalizing the line with overcurrent protective devices is an accepted procedure for economically reducing the number and duration of outages caused by primary line faults. The problem now is to evaluate numerically the benefits with different types of equipment and better protective methods.

Objective of Investigation

The objectives of the overcurrent investigation on the Central Electric Co-operative's system at Parkers Landing, Pa., during the years 1944, 1945, 1946, and 1947, were to:

1. Obtain a measure of the quality of service continuity provided to consumers.
2. Evaluate the effect of tree trimming on service continuity.
3. Gain experience with, and measure the effectiveness of, a new protective method employing overlapping operation of fuses and oil circuit reclosers to improve service continuity and to reduce restoration expense.
4. Study the effect of line length on service continuity.
5. Obtain operating data on the overcurrent protection problems at individual transformers.
6. Obtain fundamental data on overcurrents on rural circuits.

The Rural System

Characteristics of the Central Electric Cooperative's 7,200/12,470-volt 4-wire multigrounded wye rural-distribution system included long radial circuits, penetration into less densely populated areas resulting in wider separation of lightning protective equipment, and other factors which magnify the overcurrent protection problem. The Cooperative's management recognized the imperative need for improving service continuity and made the system available for experimentation in a combined overvoltage[1] and overcurrent investigation. It was believed that the data obtained would be of value to all operators of rural systems.

This system feeds an area of approximately 40 by 60 miles in the hilly country along the Allegheny River in northwestern Pennsylvania, where lightning, wind, trees, and other hazards to good service are of typical severity. Rural Electrification Administration type of line construction is employed, using practically only one make of electric equipment. In 1944, there were 1,015 miles of primary line ($87^{1}/_{2}$ per cent single phase line-to-neutral) feeding 4,178 consumers through 3,100 transformers. East and west sections of the system were fed by separate 900-kva transformer banks, supplied from the West Penn Power Company's 25-kv line. There were two feeders on each section, as shown in Figure 1. Tables I and II show the growth of the system during the period of the investigation.

The Overcurrent Protective Equipment History

As on many rural distribution systems, originally fuses alone were used to sectionalize the main feeder and to isolate faults to branches, and sub-branches. However, fuses are not capable of differentiating between nonpersistent faults, which can be cleared with only a momentary outage, and persistent faults which require the service of a line crew. The high percentage of nonpersistent faults prevalent on rural systems caused too many unnecessary outages and service trips. This led to the substitution of reclosers in the main line and on long branches. Most branches were not protected, as shown in Figure 1, since in 1944 available reclosers did not provide for coordination with fuses and to use reclosers in each branch was too costly.

Neither fuses alone nor reclosers alone even approached the desired service continuity. The need was recognized[2] for co-operative operation of fuses and reclosers in which the recloser would clear all nonpersistent faults without even partially melting the fuses, and the fuses would isolate all persistent faults to the faulted section of the line. This system, referred to as "overlapping protection," has been used successfully for many years with substation relays and line fuses.[3-4]

System Requirements Studied

In planning the investigation to use the overlapping fuse-recloser protection, the

---

Paper 49-175, recommended by the AIEE Transmission and Distribution Committee and approved by the AIEE Technical Program Committee for presentation at the AIEE Summer General Meeting, Swampscott, Mass., June 20–24, 1949. Manuscript submitted November 15, 1948; made available for printing May 2, 1949.

G. F. LINCKS is with the General Electric Company, Pittsfield, Mass.; D. R. EDGE is with the Graybar Electric Company, Inc., Chicago, Ill.; W. C. MCKINLEY is with the Central Electric Cooperative, Inc., Parkers Landing, Pa.; and J. H. LEH is with the General Electric Company, Pittsburgh, Pa.

The authors wish to express their appreciation to the Board of Directors of the Central Electric Cooperative Inc., and to the line crew of the same company, as well as D. D. MacCarthy, J. W. Kalb, W. H. Eason, D. A. Stann and to Mrs. M. C. Lovejoy.

Figure 1. System map showing location of overcurrent protective equipment January 1944 to May 1945

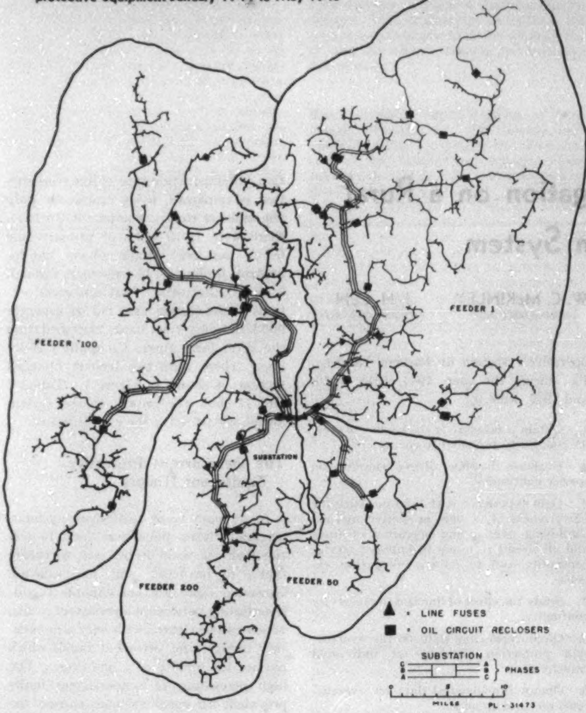

following system requirements were apparent:

1. The overlapping protection must include the entire system from the substation to the ends of feeders and all branches. Otherwise the maximum improvements in service continuity and in reduction of restoration expense can not be realized.

2. For economical use of reclosers, each recloser should clear nonpersistent faults on as much of the feeder and connected branches as it is capable of protecting.

3. Generally reclosers, applied as in (2) will protect from 15 to 25 miles, or more, of line. Such distances are too great for quick location of faults and, at times, for the physical endurance of the crews. Thus additional sectionalizing is necessary between reclosers to isolate persistent faults. Fuses are most economical for achieving this additional sectionalizing.

4. Overcurrent protective means must be provided for the isolation of persistent faults to the faulted branch or sub-branch. Again fuses are the most economical devices.

5. All reclosers and fuses in the line must co-ordinate properly with both external and internal primary fuses at the individual distribution transformer installations. Self-protected transformers of pre-1939 manufacture, with the larger internal fuses,[5–6] were scattered all over the system. Since determination of pre- or post-1939 manufacture was not considered practicable, a minimum primary line fusing of 15 or 20 amperes for $1^1/_2$- and 3-kva transformers and 20 or 25 amperes for $5–7^1/_2$- and 10-kva ratings was necessary.

6. The same 100 per cent successful co-ordination, which has been proved practicable between fuses, must be provided in the co-ordinated overlapping protection using reclosers with line sectionalizing fuses, branch fuses, sub-branch fuses, and internal transformer fuses, all connected in series for sequential operation.

Table I. System Growth During Investigation—Miles of Line and Number of Consumers

Approximately 10 Per Cent is Three-Phase, $2^1/_2$ Per Cent is Two-Phase and $87^1/_2$ Per Cent is Single Line-to-Neutral Construction

Feeder and Phase	Exposure in Miles* 1944	1945	1946	1947	Number of Consumers 1944	1945	1946	1947
Feeder number 1	(437)†	(455)	(476)	(476)				
	510	528	549	567.5	1,841	1,938	1,950	2,476
A	180	186	187	196	633	666	670	832
B	80	84	169	172	299	315	610	755
C	250	258	193	199.5	909	957	670	889
Feeder number 50	(72)	(74)	(88)	(88)				
	90	92	106	112.5	310	339	337	490
A	44	45	54	59	101	110	110	176
B	32	33	33	34.5	118	128	127	140
C	14	14	19	19	91	101	100	174
Feeder number 100	(319)	(334)	(335)	(339.5)				
	423	438	440	451	1,230	1,245	1,240	1,520
A	77	80	149	158.5	170	175	406	579
B	264	273	158	159	725	730	496	593
C	82	85	133	133.5	335	340	338	348
Feeder number 200	(187)	(202)	(208)	(208)				
	221	236	242	254	797	866	861	1,100
A	48	53	71	72	125	148	222	344
B	81	86	74	77	321	344	267	322
C	92	97	97	105	351	374	372	434
	(1,015)	(1,065)	(1,107)	(1,111.5)				
	1,244	1,294	1,337	1,385	4,178	4,388	4,388	5,586

* Changes due to growth and rephasing.

† Mileage values shown in parentheses treat three-phase and two-phase as one line. Other mileage totals add three lengths for three-phase and two for two-phase.

Overcurrent Protective Methods and Equipment

Three co-ordinated overlapping fuse-recloser protective methods were analyzed by making actual co-ordination studies on the Central Electric Cooperative system, the findings are shown in Table III.

This analysis showed the co-ordinated fuse-lock-closed recloser method (number 3) to be best. Therefore, a mechanism, Figure 2, was designed to modify the type *FP-119* reclosers in use on this rural system so the reclosers opened instantaneously twice and then they locked closed.

Because of lack of energy to reset this mechanism, it had to be reset manually after the properly co-ordinated fuse blew. This was neither as efficient nor error-proof as the reclosers designed later for automatic resetting.[9]

Co-ordination Study

It was decided to make the study on the feeder on which the lightning investigation[1] was being conducted, thus making possible the co-operative use of an automatic oscillograph, to be described later. The proper rating of reclosers and fuses were determined by a co-ordination study.

All branches from each of the main feeders were numbered using series starting with 1, 50, 100, and 200 and the feeders became known by these numerals, as shown in Figure 1. All of the subbranches were lettered on each of the main branches.

The map, Figure 3, shows the location of the reclosers and fuses and Table IV gives a history of the installations of protective equipment during 1944, 1945, 1946, and 1947.

Table II. System Growth During Investigation —Distribution Transformers and Load

Year	Average Number of Transformers	Average Kilowatt-Hours Consumed Per Consumer Per Month
1944	3,100*	81.6
1945	3,100*	91.1
1946	3,225*	100.5
1947	3,410*	150 (approx.)

* Approximately 950 of these were the conventional distribution transformers with external fuse cutouts and lightning arresters (on the first 400 miles.) All other transformers were the self-protected type with internal primary fuses and secondary circuit breakers.

Original system: 400 miles energized in August 1938 with 1,200 consumers; 400 miles energized in June 1940 with 1,200 consumers; and 300 miles energized in February 1941 with 1,600 consumers.

During this 4-year period the load increased to 184 per cent of its original value. In doing so it greatly exceeded the ultimate load for which the system was designed.

The maximum and minimum (40-ohm fault resistance) short-circuit currents were calculated using the General Electric simplified template method of calculation,[10] and were checked independently within 2 per cent by graphical calculation.[11] When checked later against oscillograph data, the calculated values proved to be slightly high. Field tests showed this to result from not factoring sufficient reductions in fault current at the substation during light load generation.[12]

The co-ordination of the reclosers and fuses was determined as follows:

1. Reclosers were located on the main feeder at, or on the source side of, the point where the calculated minimum fault current equalled the minimum pick-up current of the next recloser on the source side. Reclosers were located at the branch junction points of long branches which the main line recloser would not protect to the ends.

2. Charts were made for the overlapping fuse-recloser co-ordination, which included a correction for the cooling of the fuse link during the period between the first opening and reclosing of the recloser.

3. Existing charts[13] were used for fuse-to-fuse co-ordination.

Obtaining the Data

System Operating Data

The data originated from individual job reports of the linemen and trouble crews which were recorded in a log book

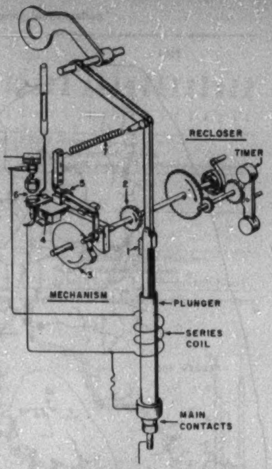

Figure 2. Mechanism modifying *FP-119* reclosers to provide two instantaneous openings to lock closed

Operation:—Fault current through series coil moves plunger up opening main contacts. When plunger resets to reclose contacts, rack 1 engages pinion 2, rotating eccentric cam 3. Second reclosing moves cam 3, so armature 4 is picked up by alnico magnet 5, closing auxiliary contacts 6, which shunt series coil and lock recloser closed. Spring 7 moves magnet 5 away from armature 4 for manually resetting mechanism

Table III

Method Number	Nonpersistent Faults Cleared Without Partially Melting Fuses by:	Sectionalizing or Branch Fuse Caused to Isolate Faulted Section by:	Findings
1	Three instantaneous openings by recloser	Going to recloser location and manually shunting the recloser with a fuse after the recloser locks open	(a) Does not save travel time and expense. Does aid in locating fault (b) Required line fuses too small (below 15 amperes) to co-ordinate with internal transformer fuses
2*	Two instantaneous openings by recloser	Two time delayed openings of recloser (lock-out of recloser clears a section of feeder on the load side)	(a) Presented a problem of co-ordination with fuse on source side (b) Sectionalizing between reclosers generally must be done with more costly reclosers. If fuses are used, it increases the number of cases under (c) (c) In some cases required line fuses too small to co-ordinate with internal transformer fuses
3*	Two instantaneous openings by recloser	Recloser locks closed until fuse blows, then resets automatically (fuse at recloser location clears a section of feeder on the load side after recloser locks closed)	(a) Co-ordination with source side fuse is no problem (b) Meets all of the system requirements outlined previously

* No commercial reclosers available when investigated. Findings were rechecked later when they became available.[7,8,9]

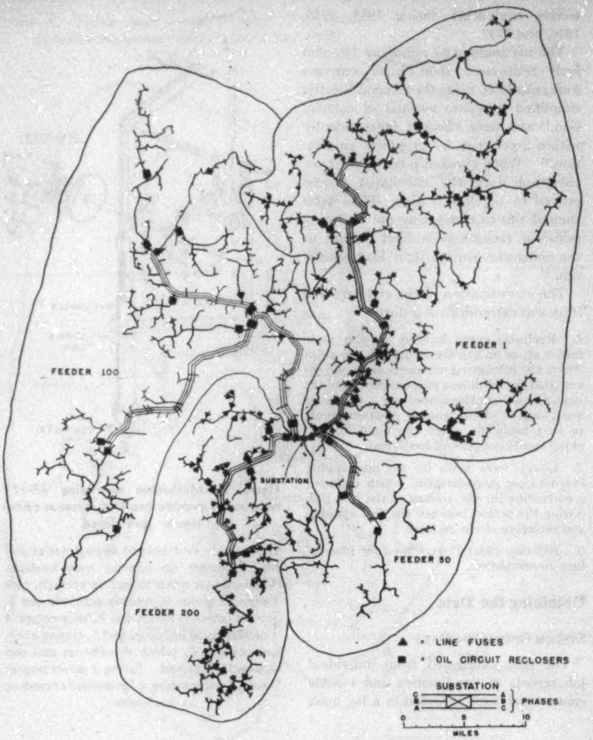

Figure 3 (left). System map showing location of overcurrent protective equipment for 1947

See Table III for dates of installation of coordinated fuses and recloser on feeders 1 and 200

and on line and distribution transformer outage reports, Figure 4.

FUNDAMENTAL DATA ON OVERCURRENTS

Information on overcurrents were obtained from *GE-PM-13* automatic electromagnetic oscillographs,[14] which were in operation on feeder number 1 during the periods from April to November of the years 1945, 1946, and 1947, and on feeder number 200 from July to November 1946 and April to November 1947. Each oscillograph tripped automatically within one-half cycle and recorded all 60-cycle fault currents beyond the oscillograph in each of the 3-phase conductors, and the system neutral, as well as *A* and *C* phase voltages. Its operation was checked by periodic calibration and daily inspection and also by periodically short circuiting the ends of the line.

The System Operating Data Obtained on Primary Lines

The data, presented in a series of charts, cover persistent faults, which caused prolonged outage and required the attention of trouble crews. All parts of feeders 1, 50, 100, and 200 were protected by reclosers and thus nonpersistent faults were cleared with only a momentary outage. They were not recorded, except by the oscillographs, since the services of the trouble crews were not required. In order to interpret these results in terms of total faults, the percentage of nonpersistent faults on feeders 1 and 200 are given in Table V, as obtained from oscillograph records.

CAUSES OF PERSISTENT LINE FAULTS, FIGURE 5

The causes of persistent line faults are compared on the basis of the number per mile of line, in order to factor differences in exposure. A chart plotted on the basis of the number of faults is similar to Figure 5. Note the relatively wide variations for different years which indicates the value of several years' experience in obtaining good average data.

A comparison with other published data, on the basis of the number of faults and the percentage of the total number of faults, is given in Table VI using the terminology for causes of Gilkeson, Jenne, and Davenport.[3]

A relatively low percentage of flash-

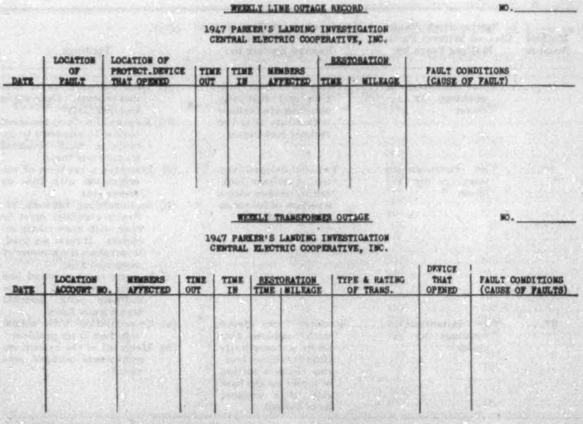

WEEKLY LINE OUTAGE RECORD NO.________

1947 PARKER'S LANDING INVESTIGATION
CENTRAL ELECTRIC COOPERATIVE, INC.

DATE	LOCATION OF FAULT	LOCATION OF PROTECT. DEVICE THAT OPENED	TIME OUT	TIME IN	MEMBERS AFFECTED	RESTORATION		FAULT CONDITIONS (CAUSE OF FAULT)
						TIME	MILEAGE	

WEEKLY TRANSFORMER OUTAGE NO.________

1947 PARKER'S LANDING INVESTIGATION
CENTRAL ELECTRIC COOPERATIVE, INC.

DATE	LOCATION ACCOUNT NO.	MEMBERS AFFECTED	TIME OUT	TIME IN	RESTORATION		TYPE & RATING OF TRANS.	DEVICE THAT OPENED	FAULT CONDITIONS (CAUSE OF FAULTS)
					TIME	MILEAGE			

Figure 4. Samples of weekly line and transformer outage reports

Table IV. History of Installation of Overcurrent Protective Equipment During Investigation*

1944: Jan. Feb. Mar. Apr. May June July Aug. Sept. Oct. Nov. Dec.
1945: Jan. Feb. Mar. Apr. May June July Aug. Sept. Oct. Nov. Dec.
1946: Jan. Feb. Mar. Apr. May June July Aug. Sept. Oct. Nov. Dec.
1947: Jan. Feb. Mar. Apr. May June July Aug. Sept. Oct. Nov. Dec.

Feeder Number 1	16—*FP119* reclosers 1—section fuse 5—branch fuses	May 11	5—fused section points 125—branch fuses	19—Modified *FP119* reclosers** 6—fused section points 151—branch fuses†	171—branch fuses†
Feeder Number 50	6—*FP119* reclosers 0—fused section point 2—branch fuses				
Feeder Number 100	18—*FP119* reclosers 1—fused section point 2—branch fuses (3 element)				
Feeder Number 200	9—*FP119* reclosers 0—fused section point 2—branch fuses (3 element)	Sept. 1		16—modified *FP119* reclosers 5—fuses section point 71—branch fuses	90—branch fuses†

* See Maps, Figures 1 and 3. ** See Figure 2. † Extra fusing found to be advisable through operating experience.

overs were recorded as causing persistent faults, see investigation number 1, Table VI. A majority of flashovers, all whipping conductors, some tree limbs on line, and so forth, were nonpersistent faults, being cleared with only a momentary outage. Conversely, in investigation 9, Table VI, the fuses in reclosing cutouts probably were blown by some of these faults. Thus the comparison of values in investigations 1 and 9 may indicate the margin of benefit of co-ordinated fuses and reclosers versus reclosing fuse cutouts. A similar condition is indicated in Table IX showing 0.12 and 0.28 persistent faults per mile per year respectively for investigations 1 and 9. These differences would indicate an additional margin in benefits for overlapping fuse-lock-closed recloser co-ordination versus 3-shot reclosing cutouts over that shown later for overlapping fuse-lock-closed recloser co-ordination versus reclosers only.

Section 10 on "impulse blowing of fuses," Table VI, (lightning storm-blown fuses, Figure 5) is analyzed in more detail in Table VII. Fuses were considered to have been blown by lightning currents passing through the fuse to ground where there were no oscillograph records of 60-cycle current corresponding to the blowing of a line fuse during a lightning storm. If lightning arresters had been installed on each side of the line fuse, the impulse currents might have gone to ground without passing through the fuse. Thus Table VII in showing lightning blowing of fuses to be about 5.2 per cent for all the fuses on the line, represents the most severe condition.

The section on "insulator or conductor breakage," Figure 5, resulted almost entirely from irresponsible shooting by hunters.

The sections on "acts of man" in Table VI and "Trees—man, and motorized equipment" in Figure 5 are high because of extensive right-of-way clearing on the entire system in 1945, heavy logging operations along the right-of-way in 1947, and the strip coal mining carried on in the area.

"Wires down" were recorded under other causes in Figure 5 and thus is left blank in Table VI. The 78 cases of wires down are analyzed in Table VIII showing that quicker fuse blowing might have prevented burndown in only 12 cases (15 per cent). Mechanical breakage occurred in 67 per cent of the cases and may have in 18 per cent more.

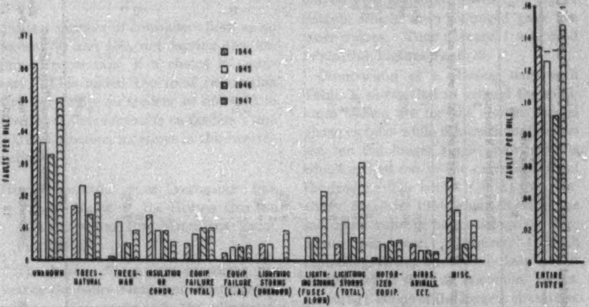

Figure 5. Causes of persistent line faults

Faults per mile of line

Exposure—Number of Persistent Faults, per Mile of Line, Figure 6

The exposure, expressed in terms of the number of faults per mile, affords a measure of the severity of overcurrent protection problems. Direct comparisons of exposure can be made for different periods on the same system or between systems provided causes of unusual numbers of nonpersistent faults are taken into consideration or only persistent faults are included, as is done in this investigation.

Note, in Figure 6, the wide variation in the exposure on different phases (single-phase circuits) of the same feeder during the same year. This shows the value of making the analysis on the basis of 12 single-phase circuits rather than just four feeders where loads and branches are predominantly single phase. This is also shown in Figures 7, 9, and 10. In the lightning investigation,[1] spot checks covering a large area on this rural system,

Table V. Nonpersistent Faults in Per Cent of Total Faults (From Oscillograph Data)

Feeder Number	1944	1945	1946	1947
1	*	84.8%**	80.4%†	82.9%†
200	*	*	88.1%‡	89.0%†
1 and 200	*	*	84.3%	85.9%

* No oscillograph data. ** May to November. † April to November. ‡ July to November.

Table VI. Comparison of Causes of Persistent Line Faults, Figure 5 with Other Published Data

Causes of Persistent Line Faults*	Investigation 1	2	3	4	5	6	7	8	9	10
Bibliographical Reference	Figure 6	3	3	3	3	3	3	2	15	16
	Number of Faults Per Percent of Total Number of Faults									
1. Flashover (lightning storm unknown)	20 3.7%	26 87%	146 76%	62 52%	670 96.3%	1 5%	260 88%		495 43.5%	104 52%
2. Insulator or bushing failure (insulation of conductor)	40 7.7%						1 0.3%		28 2.5%	
3. Wires down	Included in other causes		15 90%	41 35%	2 0.3%	3 14%	15 5%	10.1%	11 1%	
4. Birds or animals	14 2.8%		1 0.5%		3 0.5%	8 36%				11 5.6%
5. Poles broken or blown down		1 3%	2 1%	2 2%				1.9%		
6. Whipping conductors	Not recorded			5 4%	1 0.2%				63 5.6%	
7. Crossed wires			7 3.5%		1 0.2%					
8. Trees or limbs on line (trees natural)	80 15.3%	1 3%	5 2%	1 1%		1 5%	7 2.7%	25.5%	212 18.3%	47 23.6%
9. Acts of man (trees-man and motorized equipment)	49 9.3%								55 4.8%	
10. Impulse blowing of fuses (lightning storms fuses blown)	39 7.4%									
11. Under fused									4 0.4%	
12. Equipment failures	26 5.0%		17 9%	7 6%	16 2.5%		12 4%	11%	77 6.8%	5 2.6%
13. Miscellaneous	62 11.8%							18.5%	20 1.8%	
14. Cause unknown	194 37%	2 7%				9 40%		21.2%	165 14.5%	32 16.2%

Data on Systems Investigated	1	2	3	4	5	6	7	8	9	10
Type of Circuit	Rural 5 Per Mile	Urban	Rural Suburban	Urban	Rural Suburban	Urban	Rural 7 Per Mile	Rural	Rural	Rural
Voltage, kilovolts	7.2/12.5	4	4	6.9	12	13.8	13.8	7.2	2.3, 4, 7.2, 12.5	6.9
Lightning protection	Expulsion and valve lightning arresters	Lightning arresters	Lightning arresters	Lightning arresters	Spill gaps	Spill gaps expulsion lightning arresters	Spill gaps	¹/₂ spill gaps ¹/₂ lightning arresters		Lightning arresters
Tree condition	Bad	Bad-Good	Good-Fair	Average	Average	Light	Light			
Protective equipment	Reclosers and fuses	Station Circuit Breaker**	Station Circuit Breaker**	Station Circuit Breaker**	Station Circuit Breaker**	Station Circuit Breaker**	Station Circuit Breaker**	Reclosers	Single and reclosing fuses	Reclosers and reclosing fuses
Length of circuit in miles	1015 to 1111	43	193	118	633	22	55,238	369	35	295
Period of investigation	1-1-44 to 12-31-47	6-14-34 to 1-1-36	10-25-33 and 6-8-34 to 5-12-38	7-19-34 to 10-13-38	5-20-36 to 3-7-39	3-10-38 to 7-11-38	5-26-36 to 7-11-38	4-1-42 to 10-1-42	1943 to 1947	Summer 1945
Type of faults†	*a*	*b*	*b*	*b*	*b*	*b*	*b*	*c*	*d*	*a*

* Terminology in parentheses is that for Figure 5.

** Instantaneous ground relays and immediate reclosure locking out after initial operation and inverse time delay phase relays. Fuses and reclosers used in branches.

† Type of fault included in data.

a Persistent faults only, requiring trouble crew.

b Persistent and nonpersistent faults recorded by oscillograph.

c Persistent and nonpersistent faults determined by counter readings on reclosers which may be high because often successive recordings are made for individual faults.

d Persistent faults only. Blowing the third fuse of reclosing cutouts by temporary faults caused recorded outages.

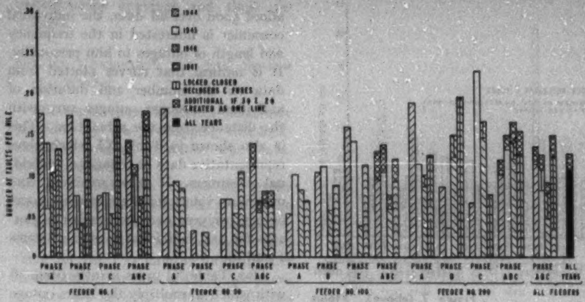

Figure 6. Exposure—Number of persistent faults per mile per year

showed wide variations in the number and severity of lightning storms even for distances of 10 or 15 miles.

The comparison of exposure with other published data, in Table IX, indicates about equal conditions to that for other systems where comparable lightning protection was employed. The "spill gaps" used for lightning protection in investigations 5, 6, and 7 naturally increased the number of faults per mile. The data in investigation 7 may be high since it is prorated to a yearly basis from data taken during the lightning period and by counter readings on reclosers which do not take into consideration successive recordings of the counter on the same fault in some cases.

Hours Out Per Outage, Figure 7

The hours out per outage for any year or period are influenced largely by whether or not there were any long outages, as shown by spot checking the data. Most of these long outages result either from long repair jobs or a fault which was difficult to locate, such as a damaged insulator. Therefore Figure 7 is not usable to compare the benefits from the use of different types of protective equipment. However, since it does show the prevalence or absence of long outages, the data in Figure 7, when combined with the exposure data in Figure 6, are extremely valuable to check the severity of fault conditions in making other comparisons.

The average restoration time curves, Figure 8, show that the "fault location time" is the only portion of the total hours out per outage affected by different types of overcurrent protection. However, when the overcurrent protection on one portion of a system markedly reduces the number of consumers affected by faults such as on feeders 1 and 200, it is natural to send the crew to take care of greatest number of consumers first, as on feeders 50 and 100, not having the improved protection, if a choice is necessary. This added the total restoration time for faults on feeders 50 and 100 to the travel time for faults on feeders 1 and 200 on numerous occasions in this investigation.

Hours Outage per Consumer Per Year, Figure 9, or Hours Outage Per Consumer Per Mile Per Year, Figure 10

The hours outage per consumer per year or the hours outage per consumer per mile per year appear to be the only measures which will define the quality of service rendered either the individual consumer or all the consumers on a circuit or system.

They are determined as follows:

$$\text{Hours Outage Per Consumer Per Year} = \frac{\text{Yearly sum of (no. of consumers affected) by (number hours out) for each outage}}{\text{Total number of consumers on circuit}}$$

$$\text{Hours Outage Per Consumer Per Mile Per Year} = \frac{\text{Hours outage per consumer per year}}{\text{Total number miles of line in circuit}}$$

The number of consumers and length of circuit existing at the first of the year were used throughout the year regardless of growth.

The only known published data using hours outage per consumer per year are those presented by W. J. Lyman[16] and a mathematical study made on a hypothetical circuit in 1941.[17] Other data, such as in references 2, 3, 16, 19 and 20 have measured the effectiveness of automatic reclosing protection by the number of momentary circuit interruptions versus the number of lockouts.

A study of Figures 9 and 10 shows the minimum and maximum hours outage per consumer per year (or per mile per year) for the 12 circuits to vary as shown in Table X.

Note that the minimum and maximum values were obtained on the same feeder and phase for both the hours outage per consumer per year and the hours outage per consumer per mile per year, except for the maximum in 1944, the minimum in 1946 and the maximum in 1947.

Average 1 in Table X, based on averaging the hours outage per consumer per year (or per mile per year) for the 12 single-phase circuits, differs considerably from average 2 (or $2'$), in which the system is treated as a unit. This difference was shown for each of the four 3-phase feeders. In average 1 only the actual number of consumers (and mileage) involved were employed for each of the 12 circuits which when averaged gave the truer values. Thus average 1 was used in plotting Figures 9 and 10.

Comparison of a phasing map with Table X shows that in general the minimum values are for the shorter single-phase circuits while the maximum values are for the longer single-phase circuits which extend out to the extreme ends of the feeder. The circuit (100A) was relatively short in 1944 when showing the minimum value of hours outage per consumer per year. However, through rephasing, it was a relatively long circuit in 1947 when showing maximum values. Circuit *1C* is one of the longest circuits on the system, but had the overlapping fuse-lock-closed recloser protection when showing the minimum hours outage per consumer per mile per year in 1946. Circuit *50A*, the maximum in 1947, while a relatively short circuit is the longest of feeder 50 and did not have the improved protection.

Some urban circuits are reported to have 1.25 hours outage per consumer per year. W. J. Lyman[20] gives the service continuity standards for his company as one hour for urban systems and two hours for rural systems. These values are well below most of those shown in Figure 9 for the early years of the investigation. This indicated considerable margin for improvement by the use of co-ordinated fuses and lock-closed reclosers if such a continuity standard was to be provided.

Outages for Individual Consumer

While studies of relative service continuity applied to the system as a whole afford good over-all data, the individual consumer is interested in the frequency and length of outages to him personally. It is natural that curves plotted from data on the number and duration of individual consumer outages vary with the distance from the substation. This is also shown in Table XI which gives representative data on outages of individual consumers. It shows minimum and maximum values for the maximum hours outage per year and the number of outages for any individual consumer (items 1 and 6).

Also, Table XI gives a ratio (item 9) with which to multiply the hours outage per consumer per year for the whole circuit to determine the maximum hours outage per year for any individual consumer. The average ratio for all four years was 3.18, with a minimum of 1 and a maximum of 9.8.

Restoration Expense, Figure 11

The manhours and mileage traveled given in Figure 11, as obtained from the weekly reports during 1947, show reductions of maintenance expense which are vitally important today. The fact that 61.5 per cent of the total line mileage for the system had the overlapping fuse-lock-closed recloser protection while only 38.5 per cent was without this improved protection, tends to make comparisons more conservative. Also, in figuring the actual costs, the assumptions of $1.25 per hour average pay for the trouble crew and the 6 cents per mile for transportation probably are low in most cases.

Determination of Benefits Obtained with Fuse-Lock-Closed Recloser Co-ordination

Hours Out Per Outage

Figure 8 shows that 1/2 hour was required to locate faults with the co-ordinated fuses and reclosers as against 1.25 hours with only the reclosers having four

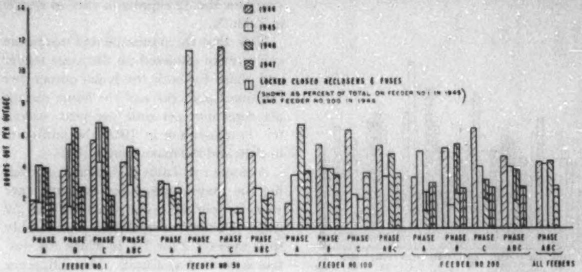

Figure 7 (above). Hours out per outage

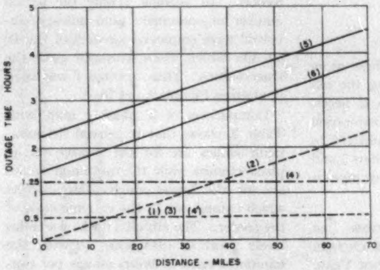

Figure 8 (left). Average restoration time curves based on approximately 480 outages 1944–1947

The total restoration time (5) with reclosers only or (6) with improved fuse and recloser protection = (1) Time elapsed before outages report + (2) travel time + (3) repair time + (4) fault location time with reclosers only or (4') with improved fuse recloser protection

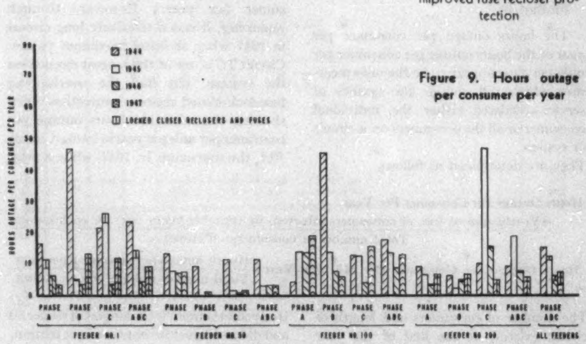

Figure 9. Hours outage per consumer per year

Table VII. Lightning Blowing of Line Fuses

Determined From Oscillograph Records Where No Fault Current Was Recorded When a Fuse Link Blew During a Lightning Storm

Rating of Fuse	1945* Number Blown	1945* Number in Circuit	1945* Per Cent Blown	1946** Number Blown	1946** Number in Circuit	1946** Per Cent Blown	1947† Number Blown	1947† Number in Circuit	1947† Per Cent Blown	Average Number Blown	Average Number in Circuit	Other Data‡ Per Cent Blown	Other Data‡ Number in Circuit
15	4	28	14.3	3	56	5.35	6	73	8.2	13	157	8.3	72
20	2	27	7.4	2	33	6.0	3	52	5.8	7	112	6.2	78
25	0	18	0.0	1	45	2.2	3	58	5.2	4	121	3.3	No Data
30	0	19	0.0	1	12	8.3	2	23	8.7	3	54	5.5	No Data
40	1	12	8.3	0	16	0.0	2	28	7.1	3	56	5.4	No Data
15 to 40	7	104	6.7	7	161	4.3	16	234	6.8	30	500	6.0	No Data
All Rating	7	128	5.5	7	181	3.9	16	261	6.1	30	670	5.2	No Data

* On feeder number 1 May to November.

** On feeder number 1 May to November and feeder number 200, July to November.

† On feeders number 1 and 200, April to November

‡ Three years data on another system.

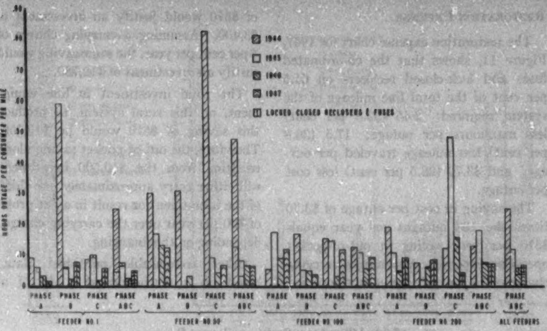

Figure 10. Hours outage per consumer per mile per year

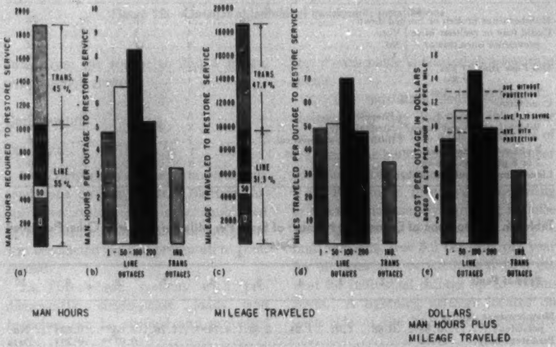

Figure 11. Restoration expense

instantaneous openings and three reclosures.

Service Continuity for the System as a Whole

The improvement in service continuity provided by the overlapping fuse-lock-closed recloser co-ordination was evaluated as follows:

1. In 1945, the results on feeder number 1 for the $4^1/_2$ months prior to the installation of the fuse-lock-closed recloser co-ordination were compared with those for the $7^1/_2$ months following the installation. On each of the single-phase circuits the severity of fault conditions measured in the number of outages per mile, Figure 6, and the hours out per outage, Figure 7, were slightly greater during the period with the fuse-recloser co-ordination than without it. Thus the comparison of the values for each period in Figure 10 is conservative in showing the following very substantial reductions in hours outage per consumer per mile per year: on *A* phase—64.6 per cent; on *B* phase—88.8 per cent; on *C* phase—85.5 per cent; and *ABC* phases—80.0 per cent.

2. In 1946 and 1947, the operating data were compared for the portions of the system having each type of protection (feeders 1 and 200 versus feeders 50 and 100), since comparisons could not be made on one circuit. As pointed out, feeders 50 and 100 benefited indirectly from the overlapping fuse-lock-closed recloser protection on feeders 1 and 200, so these comparisons are conservative. The consumer hours outage per mile were reduced 67.5 per cent in 1946 with slightly more severe fault conditions indicated by Figures 6 and 7.

In 1947, 70.5 per cent of the faults per mile, shown in Figure 6, were on the portion of the system with the co-ordinated fuses and reclosers. The hours per outage, Figure 7, were approximately the same (2.5 versus 2.8). Even under these conditions there were 21 per cent less hours outage per consumer per mile per year. If the faults per mile had been approximately equal on the two portions of the system, this saving would have been about 66 per cent.

A mathematical study of a hypothetical circuit in 1941[17] showed a possible saving of 88 per cent with overlapping line protection versus no line protection.

R. O. Askey and C. V. Miller reported[21] that benefits were obtained during $1^1/_2$ years operating experience with fuses and lock-closed reclosers co-ordinated for overlapping operation on a 17-mile 7.2-kv line. They also discussed other advantages of this method of protection.

Ability to Meet Desired Service Continuity

The hours outage per consumer per year on the portion of the system with the overlapping fuse-lock-closed recloser protection in Figure 9 varied as follows on the single-phase circuits.

Feeder Number	Year	Hours Outage	Average
1	1946	3.29 to 5.9	4.2
1	1947	3.1 to 13.0	9.2
200	1947	4.5 to 6.6	5.9

These values indicate that even with the best overcurrent protection it may not be possible to meet a service continuity standard of 2 hours outage per consumer per year on all single-phase circuits or a whole 3-phase rural feeder having extremities from 45 to 60 miles from the substation.

Since feeder 50 has a maximum length of only 25 miles and received a slight benefit from quicker handling of faults, because of the improved service continuity from the protection on feeders 1 and 200, its hours outage per consumer per year was much lower, as follows:

Year	Outage	Average
1946	0.8 to 8.0	3.0
1947	0 to 7.3	2.9

With the overlapping fuse-lock-closed recloser protection, it is probable that the service continuity on this feeder would have approached a standard of two hours outage per consumer per year.

Restoration Expense

The restoration expense chart for 1947, Figure 11, shows that the co-ordinated fuses and lock-closed reclosers on 61.5 per cent of the total line mileage of the system required: 2.45 (32.8 per cent) less manhours per outage; 17.5 (26.8 per cent) less mileage traveled per outage; and $3.70 (28.5 per cent) less cost per outage.

The saving in cost per outage of $3.70 times the 138 outages per year equals $510 per year saving in out-of-pocket operating expense. Assuming a carrying charge of 15 per cent per year, the saving of $510 would justify an investment of $3,400. Assuming a carrying charge of 4 per cent per year, the same saving would justify an investment of $12,750.

The total investment in line equipment, on this rural system, to produce this saving of $510 would be $10,500. Therefore, the out-of-pocket saving alone resulting from the $10,500 investment will either carry approximately one-third of the investment or result in a net profit of $90 per year over the carrying charge, depending on the financing.

Other comparable published data, based on a mathematical study of a hypothetical circuit,[31] showed possible savings of 60 to 70 per cent in manhours and also in mileage traveled when comparing overlapping line protection with no line protection.

Table VIII. Lines Broken or Burned Down

		1944	1945	1946	1947	Total
Number lines broken or burned down		16	17	15	30	78
Could fuse or recloser have prevented burn down?	Yes	0	4	1	7	12
	No	12	9	11	20	52
	?	4	4	3	3	14
Did Fuse Blow?	Yes	12	12	10	16	50
	No	0	4	5	5	14
Recloser opened	Yes	4	1	0	9	14
Conductor						
Which 1 phase was down?	Phase only	3	3	3	6	15
	Neutral only	0	3	0	3	6
	Both phase and neutral	8	7	7	16	38
3 phase—all four lines down		2	1	0	0	3
1 or 3 phase lines down		3	3	5	5	16
Lines damaged but not broken		2	3	0	3	8

Table IX. Comparison of Exposure in Number of Faults Per Mile Per Year with Other Published Data*

Type of Fault	1	2	3	4	5	6	7	8	9	10
Nonpersistent and persistent	0.88*	0.88	1.01	1.24	2.56	4.71**	1.76	3.65**	0.63†	No Data
Persistent only	0.12							0.07**	0.28†	

* For bibliographical reference and data on system see Table VI.

** Actual data based on period of less than a year. Values prorated to yearly basis and thus are only approximately correct.

† Based on 944 "cases of trouble" which are persistent faults. The nonpersistent and persistent value is based on the 2,314 fuses reported as blown assuming that these were blown by nonpersistent faults which blew fuses in the three shot cutouts and cleared the fault with only a momentary outage.

Table X

Hours Outage Per Consumer Per Year	1944	1945	1946	1947
Minimum	4.0 (100A)*	0 (50B)	0.8 (50C)	0 (50B)
Maximum	46.9 (1B)	46.5 (200C)	15.3 (200C)	19.0 (100A)
For All Four Feeders				
Average 1**	17.3	12.2	5.8	7.8
Average 2†	22.1	16.3	6.4	9.2
Hours Outage Per Consumer Per Mile Per Year				
Minimum	0.053 (100A)	0.0 (50B)	0.018 (1C)	0.0 (50B)
Maximum	0.082 (50C)	0.48 (200C)	0.158 (200C)	0.125 (50A)
For All Four Feeders				
Average 1	0.248	0.118	0.059	0.069
Average 2′‡	0.018	0.012	0.005	0.0075

* Figures in parentheses are single-phase circuits.

** Average 1 is based on averaging the hours outage per consumer per year (or per mile per year) for the 12 single-phase circuits.

† Average 2 is based on the total hours outage for all faults on the systems divided by the total number of consumers on the system.

‡ Average 2′ is average 2 divided by the total mileage on all the feeders.

The Operating Data on Outages at Individual Transformers

Outages at individual transformer installations accounted for 0.23 and 0.20 hours outage for every consumer on the system in 1946 and 1947 respectively. These values would be about 10 per cent of an over-all rural system performance of two hours outage per consumer per year and thus are significant. The restoration expense for outages at transformer installations, Figure 11(A) and (C) is nearly 50 per cent of the total.

Figure 12(A) shows the relationship in per cent of the total number of faults for each type of outage at individual transformer installations. Figure 12(B) shows the frequency of fuse blowings per 1,000 installations of external primary fuses at 950 conventional transformers; the blowing of internal primary fuses and the operations of secondary circuit breakers in 2,150 to 2,260 self-protected transformers.

Consumer faults or overloads on the load side of the service entrance fuses, caused the greatest number of outages; generally by opening the secondary circuit breaker. It is believed that a large percentage of the outages from unknown causes resulted from consumer faults. Probably the inability to make replacements influenced the 1946 and 1947 figures.

Lightning caused about an equal number of outages with both types of transformers. The blowing of 2-ampere fuse links at $1^1/_2$- and 3-kva and 3-ampere fuse links at 5-kva conventional transformers during lightning storms (when protected by interconnected lightning arresters located on the line side of the fuse), varied as follows:

	1944	1945	1946	1947	Average
Fuses blown by lightning in per cent of fuses installed	0	0.12	0.06	0.34	0.13

Generally 1 per cent fuse blowing during lightning storms is considered normal under similar conditions of lightning protection.

Open circuit causes resulted from mechanical breakage of secondary service wires or wires pulling loose at connection points.

Fundamental Data Obtained on Overcurrents

FAULT RESISTANCE

The data in Figure 13 should aid in determining the assumed fault resistance to be included when calculating minimum fault currents. To obtain the full protective ability of reclosers they should be located where the minimum fault current is equal to, or greater than, the minimum pickup current of the recloser on its source side. An assumed fault resistance of 40 ohms was used in the calculations for the investigation.

Figure 13 takes into consideration the lower short-circuit currents at the substation during periods of light load generation. This affects minimum fault currents and thus must be included in the calculations.[13]

INRUSH CURRENTS FOLLOWING PROLONGED OUTAGES

Inrush currents to start a high percentage of the appliance motors on a circuit can make it very troublesome in getting a circuit re-energized following a prolonged outage. The inrush currents on feeders 1 and 200 did not exceed two and one half to three times the load current and thus were not of sufficient magnitude to be troublesome. However, on several occasions it was impossible to re-energize feeder 100 through reclosers with four instantaneous openings.

Unfortunately there was no oscillograph on feeder 100 to record the currents, but undoubtedly they were higher than those recorded on feeders 1 and 200. The reclosers tripped open and, in order to establish service, had to be shunted by fuses of equivalent ratings to that used at similar points with the lock-closed recloser on feeders 1 and 200.

DIVISION OF FAULT CURRENTS IN NEUTRAL AND GROUND ON MULTIGROUNDED CIRCUITS

A study of many oscillograms of single-phase faults showed that 40 per cent of the fault current in the phase wire returned in the neutral conductor and 60 per cent through the ground. This was generally true regardless of the magnitude of the fault current except near the substation. A fault about a mile from the substation on the source side of the oscillograph initiated the oscillograph and recorded current traveling in the neutral away from the source to find a return path through ground.

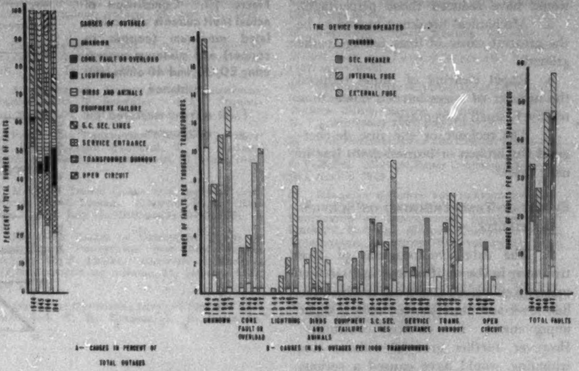

Figure 12. Outages at individual transformer installations

Conclusions

GENERAL

1. Comparison of the data on circuit conditions on the Central Electric Cooperative system with other published data indicates that this investigation was conducted on a representative rural system.

2. Three-phase systems with predominantly single-phase loads and branches can be studied and protected best if each phase is treated as a separate circuit.

3. The maximum hours outage experienced by any individual consumer varied from 1.0 to 9.8, with an average of 3.2, times the hours outage per consumer per year for that phase.

4. Blowing of primary sectionalizing or branch line fuses by lightning impulse currents, not accompanied by 60-cycle fault currents, was 5.2 per cent per year for all fuses and varied from 5 to 8 per cent for individual ratings up to 40 amperes. A lightning arrester located on each side of the line fuse undoubtedly

Table XI. Data on Number and Duration of Outages to Individual Consumers

Item	1944		1945		1946		1947	
	Min.	Max.	Min.	Max.	Min.	Max.	Min.	Max.
	Data to Show Minimum and Maximum Values for Maximum Hours Outage Per Year to Individual Consumers. (With Corresponding Values for Other Items)							
1. Maximum hours outage per year to individual consumer	8.5^1	104.7	17.8	94.8^2	1.0^3	40.0^5	9.2^6	56.9
2. Hours outage per consumer per year	4.1	45.2	1.8	46.5	1.0	5.9	4.5	15.6
3. Ratio $\frac{\text{Item 1}}{\text{Item 2}}$	2.18	2.31	9.80^4	2.02	1.0	6.78	2.05	3.65
4. Number outages per year to individual consumer	3^1	11	4	23^2	1^3	10^5	4^6	7
5. Miles from substation	16^1	47	4	38^2	8^3	32^5	42^6	36
	Data to Show Minimum and Maximum Number of Outages (With Corresponding Values for Other Items)							
6. Number outages per year to individual consumer	3^1	12	3	23^2	1^3	10^5	4^6	11
7. Maximum hours outage per year to individual consumer	8.5^1	93.3	24.0 18.7	94.8^2	1.0^3	40^5	14.4 11.7 9.2^6	56.8
8. Miles from substation	16^1	61	12 18	38^2	8^3	32^5	12 12 42^6	62
	Data to Show Minimum, Maximum and Average Ratios Item 1 to Item 2							
9. Ratio $\frac{\text{Item 1 Maximum}}{\text{Item 2 Average}}$	1.34	4.38	1.51	9.80^4	1.00^3	6.96	1.61^6	7.31
	2.45		3.64		3.14		3.31	

Superscripts 1, 2, 3, 4, 5 and 6 following items in any one year indicate that they are values for the same single-phase circuit.

would have reduced those percentages.

5. Mechanical breakage proved to be the greatest cause of lines falling to the ground.

6. Rapid clearing of faults reduced the number of wires burned down to a relatively small percentage.

7. The recloser or the fuse de-energized the broken or burned down line in most cases.

Effect of Tree Trimming on Service Continuity

8. The extensive program of tree trimming in the right-of-way in 1945 was undertaken before the trees reached the line level and thus showed only a slight improvement in service continuity. However, further growth, without this trimming, would have caused a serious increase in outages.

Effect on Service Continuity of Fuses and Lock-Closed Reclosers Co-ordinated for Overlapping Protection

9. The lock-closed recloser was shown to provide the most advantages for co-ordinated overlapping operation with several fuses in series (a) at sectionalizing points between recloser, (b) at branch junctions, (c) at sub-branch junctions and (d) at transformer installations especially of the self-protected type.

10. Such co-ordinated overlapping protection was shown to be necessary on the entire circuit in order to even approach adequate service continuity on rural distribution systems.

11. The investigation showed that fuses and lock-closed reclosers co-ordinated for overlapping protection, when applied to the entire feeder, will provide the following benefits over lines protected by reclosers only:

a. The average time to locate faults was reduced three-quarters of an hour per fault, or 60 per cent.

b. The hours outage per consumer per mile per year was reduced 70 to 90 per cent below that provided by reclosers alone.

c. The savings in restoration expense is 32.8 per cent in manhours, 26.8 per cent in mileage traveled, and 28.5 per cent in cost.

d. This conservative estimate of average yearly cost saving for restoring service will justify an investment in reclosers and fuse cutouts of $3,400 with an annual charge of 15 per cent or $12,750 with a 4 per cent charge.

This will either carry one-third of the investment, or result in a net saving of $90 per year, depending on the financing.

e. A comparison with unprotected lines or lines protected with reclosing fuse cutouts would show even greater benefits.

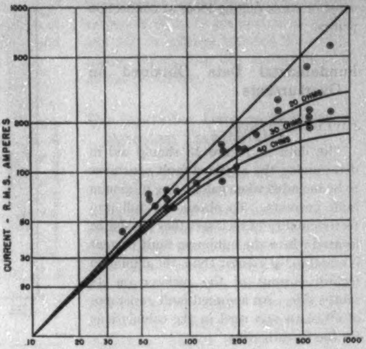

Figure 13. Comparison of actual fault currents with calculated maximum (copper to copper) and minimum currents using 20, 30, and 40 ohms fault resistance

⊙ Fault current measured on oscillogram

12. A service continuity standard of two hours outage per consumer per year does not appear to be possible, even with the fuse-lock-closed recloser overlapping co-ordination, where rural circuits extend 45 to 60 miles from the substation.

13. Such a standard appears to be possible where the greatest length of line is 25 miles and the overlapping fuse-lock-closed recloser co-ordination is employed.

14. Inrush currents following outages is not a problem with the co-ordinated fuses and lock-closed reclosers since the fusing can be high enough to prevent fuse blowing on inrush currents even if the recloser is locked closed. The recloser with four instantaneous openings did lock open and had to be shunted by fuses in order to restore service.

Effect of Outages at Individual Transformer

15. The reduction of the hours outage per consumer per year, as caused by outages at individual transformer installations is very important with both conventional and self-protected types. It can be as much as 10 per cent of the total for the system when the primary line is adequately protected.

16. Outages caused by faults on the consumers premises which cause the internal secondary circuit breakers to open or primary fuses to blow, instead of being cleared by the service entrance fuses, deserve further study as this was the largest cause of transformer outages. Such a study would weigh the increased outage time and restoration costs against the effect of better protection.

17. Blowing of 2- and 3-ampere external primary fuse links at transformer installations during lightning storms varied from 0.06 to 0.34 per cent per year, with an average of 0.13 per cent.

Fundamental Data on Overcurrents

18. The nonpersistent faults varied from 80 to 89 per cent of the total faults with an average of 84.6 per cent.

19. The assumed 40-ohms fault resistance used in this investigation, proved to be more than ample for determining minimum fault currents and might have been reduced to 30 ohms.

20. The decrease in short-circuit currents available at the substation during periods of light load generation should be factored in calculating minimum fault currents.

21. On this multigrounded neutral circuit 40 per cent of the current returns in the neutral conductor and 60 per cent in the ground. Oscillograph data showed that the ground current travels in the neutral for several pole spans in both directions from the fault, seeking a path to ground.

References

1. Lightning Investigation on a Rural Distribution System, **D. D. MacCarthy, D. A. Stann, D. R. Edge, W. C. McKinley.** *AIEE Transactions*, volume 68, part I, 1949, pages 428–38.

2. Experience with Oil Circuit Reclosers on REA Systems, **Lee M. Moore, Bruce O. Watkins.** *Electrical Engineering* (*AIEE Transactions*), volume 62, December 1943, pages 531–35.

3. Performance of Ground Relayed Distribution Circuits During Faults to Ground, **C. L. Gilkeson, P. A. Jenne, J. C. Davenport.** *AIEE Transactions*, volume 61, 1942, pages 40–48.

Positive Disconnection of Distribution Circuits During Faults to Ground, *Engineering Report Number 47*. Joint Sub-Committee on Development and Research, Edison Electric Institute and Bell Telephone System (New York, N. Y.), July 24, 1941.

4. Trend in Distribution Overcurrent Protection, **G. F. Lincks, P. E. Benner.** *Electrical Engineering* (*AIEE Transactions*), volume 56, January 1937, pages 138–52.

5. Sectionalizing and Internal Transformer Fusing on Rural Power Circuits, **B. O. Watkins.** *AIEE Transactions*, volume 66, 1947, pages 383–88.

6. Line Sectionalizing with Internally Fused

Transformers, G. F. Lincks. *Distribution* (Schenectady, N. Y.), January, 1945, pages 14–16.

7. Improved Fault Protection for Rural Distribution Systems, A. Van Ryan. *Electrical Engineering* (*AIEE Transactions*), volume 64, May 1945, pages 261–63.

8. An Improved Automatic Circuit Recloser, J. M. Wallace. *AIEE Transactions*, volume 66, 1947, pages 255–58.

9. A New Relayed Automatic Oil Circuit Recloser, E. J. Casey, E. T. McCurry. *Distribution* (Schenectady, N. Y.), April 1948, pages 3–7.

10. Quicker Way of Computing Distribution Short Circuits, J. D. Sauter, G. F. Lincks. *Electrical World* (New York, N.Y.), March 21, 1942, pages 70–72.

11. Graphical Method of Calculating Fault Currents on Rural Distribution Systems, F. W. Linder. *Electrical Engineering* (*AIEE Transactions*), volume 64, January 1944, pages 16–19.

12. Short Circuit Currents and Recovery Voltages on Rural Distribution System, W. H. Bason, I. B. Johnson, J. W. Kalb, H. A. Peterson. *AIEE Transactions*, volume 68, part II, 1949, pages 930–38.

13. Coordinating Fuses for Distribution Reliability, G. F. Lincks. *Electrical World* (New York, N. Y.), July 29, 1933, pages 140–43.

14. Advances in Technique of Lightning Measurements, T. Brownlee. *AIEE Transactions*, volume 68, part I, 1949, pages 515–19.

15. Farm Line Protection Presents a Difficult Coordination Problem, C. F. Dodson. *Electric Light and Power* (Chicago, Ill.), June 1946, pages 80–82.

16. Keeping Down Costs for Service Continuity, W. J. Lyman. *Electrical World* (New York, N. Y.), July 13, 1940, pages 50–53, 106.

17. Relative Value of Different Types of Overcurrent Protection for Distribution Circuits, G. F. Lincks. *Electrical Engineering* (*AIEE Transactions*), volume 61, January 1942, pages 19–26.

18. One-Shot Reclosers Improve Service Stop Complaints, T. H. Kinnear, L. R. Patterson. *Electrical West* (San Francisco, Ill.), September 1937, pages 63–64.

19. Reclosing Fuses Reduce Outages on Rural Lines 61 Per Cent, C. C. Cornelius. *Electric Light and Power* (Chicago, Ill.), February 1937, pages 32–33.

20. Service Continuity Standards Aid Economical Distribution Planning, W. J. Lyman. *Bulletin* Edison Electric Institute (New York, N. Y.), September 1947, pages 325–29.

21. The Application of Oil Circuit Reclosers to Rural Distribution Systems, R. O. Askey, C. V. Miller. Midwest Power Conference (Chicago, Ill.), April 8, 1948.

22. Relative Expense for Service Restoration with Different Types of Overcurrent Protection on Distribution Systems, G. F. Lincks, C. R. Craig. *Electrical Engineering* (*AIEE Transactions*), December 1942, volume 61, pages 821–31.

23. Field Tests of Oil Circuit Recloser Substantiate Analytical Coordination Method, G. G. Auer, R. A. Branflick, L. J. Woodward, W. C. McKinley. *AIEE Transactions*, volume 68, part II, 1949, pages 801–10.

Discussion

C. E. Asbury (The Commonwealth and Southern Corporation, Jackson, Mich.): This paper tabulates and summarizes some very useful data for rural systems such as outage times per customer per year, the ratio of persistent to nonpersistent faults, the number of transformer failures, classification of various types of faults experienced, and so forth.

The necessity of good service continuity to rural systems is being realized more and more since the agriculturist of today depends very heavily upon his electrical servant to do many of his farm chores. The paper mentions average consumption per consumer for rural areas in that region to be in the order of 2,000 to 2,500 kilowatthours per year. Recent reports from some midwestern states with rather large rural areas show annual energy consumption in the order of 3,000 to 4,000 kilowatthours per farm customer. It is obvious that loads of these magnitudes must be given dependable service.

It should be kept in mind that all comparisons made for automatic circuit recloser performance are based on four instantaneous trips versus two instantaneous plus locked-closed operation with co-ordinated fuses.

Three overcurrent protective methods were considered for this particular application:

1. Use of automatic circuit reclosers having three instantaneous openings. We have shared the findings of the authors in attempting such applications and also find it is practically impossible to obtain any degree of co-ordination between such devices and fuses.

2. Reclosers having two instantaneous openings followed by two time-delay openings to lockout were considered but were not used for three reasons listed in the paper:

(a) It presented a problem of co-ordination with fuses on the source side. This difficulty is especially troublesome with certain makes of reclosers and fuses and emphasizes the desirability of recloser and fuse characteristics being co-ordinated in design to parallel each other. The so-called fast type of fuse having steep slope on the time current characteristics are especially troublesome in this co-ordination problem. Also, in general, fuses which are designed to melt in five minutes with current of 150 per cent rating do not co-ordinate as well with reclosers and fuses having a melting time of five minutes at the 200 per cent rating. Using fuses with different ampere ratings in the two designs to give equivalent time current characteristics is not always satisfactory because these fuses do not have the same load ability.

(b) It is not clear just what the authors mean by item 2(b) of Table III of the paper when they say sectionalizing between reclosers generally must be done with more costly reclosers. It does not appear to be good practice to consider inserting fuses between reclosers for sectionalizing in the main trunk line. In most applications, reclosers are used out on the rural line away from the substation and a station circuit breaker is used in the substation with fuses on the high side of the transformer. In the smaller rural stations, reclosers especially in the larger capacities are being used in place of the conventional circuit breakers for line protection. In such applications it is, of course, necessary to allow for the cumulative heating on the high side fuse due to recloser operations before lockout. This problem is not particularly new in co-ordination since a similar co-ordination factor must be taken into consideration where automatic reclosing conventional circuit breakers are to be co-ordinated with high side fuses.

(c) Item 2(c) in Table III states that in some cases the line fuses were too small to co-ordinate with internal transformer fuses for reclosers when two instantaneous and two time-delay shots were used. As pointed out in another section of the paper, some transformers using internal fuses are fused with rather large fuses in the order of 15 to 20 amperes which provides no protection for the transformers and such fuses are so large that it places a very definite handicap on applying sectionalizing fuses in a rural system. This is one of the disadvantages of using transformers with internal fuses. This is especially true on systems which may be electrically long where the short-circuit current may be low at the remote end of the line. With ordinary 3-kva transformers having internal fuses it is necessary that a minimum sectionalizing fuse of 25 or 30 amperes be used near the end of the circuit. Obviously, this limits the number of sectionalizing points that may be used on such a circuit and it also results in very large fuses near the station. Where conventional external fuses are used for transformers a minimum sectionalizing fuse of 15 amperes can be utilized which co-ordinates nicely with recloser applications especially when reclosers and fuses are selected having similar slopes in their time current characteristics.

Mention was made in the paper of sectionalizing fuses as well as two or three ampere transformer fuses blowing on lightning surges. It would be helpful if the authors would point out the type and characteristics of the fuses used in this particular application. Apparently, the transformer fuses were not of the newer design known as the high-surge type. Fuses classified as "fast" type are more susceptible to this type of operation than the so-called "slow" fuses. Fuses designed to have a melting time of 300 seconds with 150 per cent of rated current have much less surge ability for the same ampere ratings than do fuses designed to operate at the same time with 200 per cent of rated current. The proposed Edison Electric Institute–National Electrical Manufacturers Association (EEI–NEMA) Standard for universal fuse links is based upon all fuses being designed to have a melting time of 300 seconds at 200 per cent of rating. This should reduce considerably fuse blowing on lightning surges. Fuses designed to have characteristics within the limit described by the proposed EEI-NEMA Standard Curve *T* should present much less difficulty in blowing due to lightning surges than the so-called fast fuses described as *K* by the Standard.

The paper tabulates some comparative savings in outage time, replacement costs, traveling time, and man-hours. Again, it must be kept in mind that these comparisons are based on recloser operation with two instantaneous and locked closed performance. It is not clear in the paper on just what basis this comparison is made. Apparently, it is a comparison between two instantaneous and locked-closed recloser operations as compared with four instantaneous recloser operations or with the circuit being protected by single shot or possibly reclosing fuses. It would be helpful if the authors would state with which of the three possible comparisons the locked-closed recloser operation was compared. It must be kept in mind that such a comparison does not reflect what might be expected when using reclosers having one or two instantaneous operations followed by two time-delay operations.

The curves in Figure 13 showing the comparison of actual fault currents as compared to the calculated values with various values of resistance supplies interesting information. It is not clear just what unit the abscissa of the curve represents. How was the actual fault location for these plotted points established? It is very important that the actual location be known quite accurately in order that a misinterpretation as to fault impedance not be obtained.

It is difficult to arrive at a reasonable value of fault impedance for calculations on lower voltage systems. If too high a value of fault impedance is used, the application of protective equipment is made particularly difficult and is likely to result in applying a large number of sectionalizing devices. This is especially true as the system voltage is decreased. A fault resistance of 40 ohms was assumed for this particular investigation. If 40-ohms fault impedance is applied to systems having line-to-line voltages of 7,200 volts and less, the reach of protective devices is very short. It appears that in order to make reasonable applications of overcurrent protective devices a sliding scale needs to be used in the selection of fault impedances with lower values of fault impedance being selected for the lower voltages. It would be interesting if the authors would point out their practice in this respect and state the value of fault impedance used in lower voltage systems, such as 7.2, 4.16, and 2.4 kv.

It appears that feeders number 1 and number 200 shown in Figure 3 of the paper are considerably overburdened with sectionalizing devices. Not only does this represent an appreciable investment but is entirely too many sectionalizing devices to be co-ordinated adequately in series. On some of these feeders it appears necessary to co-ordinate 10 to 12 sectionalizing devices in series between the substations and the end of the feeders.

The information outlined in this paper on performance of reclosers having four instantaneous trips or two instantaneous trips and locked-closed operation with the particular fuses used in the application should be useful to the industry in making applications of similar equipment. It would be helpful if further data could be obtained from similar studies where modern reclosers having one or two instantaneous followed by one or two time-delay openings were co-ordinated with fuses having characteristics similar to the proposed EEI-NEMA Standard, especially with transformers being fused with external primary fuses of the high-surge type or with links having similar characteristics to that used for sectionalizing purposes.

G. F. Lincks, D. R. Edge, W. C. McKinley, J. H. Leh: Mr. Asbury has presented some interesting and helpful comments on our paper. As he points out, it is important to keep in mind that all comparisons of both the service continuity and the restoration expense data, were based on reclosers having four instantaneous openings with no fuse sectionalizing versus fuses co-ordinated with reclosers having two instantaneous plus a locked (or hold)-closed operation. However, it should be appreciated that equal improvements in service continuity and in reduction in restoration expense would be obtained if it were economically and technically practical to install reclosers having four instantaneous openings at all the locations where fuses and reclosers were employed in the investigation. This would hold true for any overcurrent protective equipment or combination of equipments (such as co-ordinated fuses and reclosers with two instantaneous plus two time-delay operations or reclosers with isolators or sectionalizers), provided that in themselves or co-operatively, they clear a majority of all temporary faults with only a momentary outage and isolate all persistent faults to equally short sections of the lines. The savings discussed in our paper show economic justification for the co-ordinated fuse-lock-closed recloser combination. However, these savings did not provide much margin for substituting more costly equipment, for the low cost fuses. If, for economical or technical reasons, fewer sectionalizing points are protected than we employed, the benefits in improved service continuity and in restoration expense shown by this investigation will be decreased proportionately, as is shown superlatively by the comparisons made in the investigation. As pointed out in our paper, technical difficulties would have necessitated fewer sectionalizing points with the instantaneous plus time-delay reclosers. This led to the choice of the instantaneous plus lock-closed reclosers.

If the co-ordinated fuse-lock-closed recloser combination had been compared with fuses alone (no reclosers) even greater benefits would have been shown over those given in the paper. The mathematical studies in references 17 and 22 of our paper indicate such a comparison would show only a slight change in the service continuity, but a very marked change in the restoration expense. Without the recloser to protect the fuses, they would be blown by both temporary and permanent faults causing outages to only a few customers on each branch, but necessitating many extra trips to restore service. Reclosing fuses would approach the advantages of the fuse-lock-closed recloser combination to the extent that manual replacement of fuses blown by temporary faults approaches the automatic resetting of the recloser in eliminating prolonged outages. Maintenance cost, however, probably would be prohibitive.

Mr. Asbury questions the use of fuses between reclosers for sectionalizing main trunk lines or long branches. Again this is an economic consideration. The orbit of protection (or "reach") of a recloser is bounded by the points on the main line and connected branches where the minimum fault current (limited by line impedance and fault resistance at the time of minimum generation on the system supplying the distribution circuit) equals the minimum pick-up (or tripping) current of the recloser. On a 7.2/12.5-kv multigrounded Y-circuit, the orbit can reach out 15 to 25 miles. Obviously, sectionalizing is necessary between reclosers located 15 to 25 miles apart. The function of a recloser or a fuse at this additional sectionalizing point is to isolate persistent faults. An additional recloser located within the orbit of protection of another recloser offers practically no additional benefits in clearing non-persistent faults. Thus, why pay for a recloser when a fuse will do the job equally well at one-tenth the cost. The lock-closed recloser permits the use of a fuse whereas the instantaneous plus time-delay recloser necessitates the use of a recloser. With the instantaneous-time-delay reclosers, a fuse at this additional point, which would have the correct rating to co-ordinate for the overlapping function with the recloser on its source side, would be too large to permit the recloser on its load side to lock open before the fuse was partially melted.

As to the overburdening of feeders 1 and 200 with sectionalizing devices, nearly five years operating experience has proved that:

1. The system functions successfully,
2. Any less number of devices would not provide the same improvement in service continuity or savings in restoration expense, and
3. These savings will pay from one-third to more than all the yearly carrying charges on the investment depending on the financing. To this would be added the savings from loss of revenue while the circuit is out, plus those chargeable to consumer good will.

There were a maximum of nine primary line sectionalizing devices connected in series. Seven of these installations are normal. Two installations are abnormal; one because the two main feeders branch off from a common feeder a mile from the substation, and the other, because an inaccessible portion of the line had to have a device at each end to save unnecessary hunting for troubles on snow shoes during $4^1/_2$ months each year. The furthest transformer was 67-line miles from the substation so the normal sectionalizing was approximately only one installation every ten miles of line. Shortening the lines, as suggested in our conclusions, would reduce the number of sectionalizing devices in series while permitting the same coverage.

Mr. Asbury suggests that fuse links on the source side of reclosers which melt at 200 per cent rated current in five minutes co-ordinate better with the reclosers than do fuse links which melt at 150 per cent rated current, such as were used in our investigation. Also, he indicates benefits would be obtained in reducing unnecessary lightning blowing. He is correct in these statements if he compares the fuse links only on the basis of the ratings, since then the 200 per cent rated links have a larger physical size and melt at higher currents throughout the whole range of time-current characteristics. However, they will not provide as good protection to connected apparatus. The 5-minute (300-second) melting current of a fuse link governs the overcurrent protection it affords connected apparatus and thus should be the basis of comparison between different fuse links. The rating is the maximum current the fuse link will carry continuously without causing excessive heating of the fuse cutout in which it is installed. The speed ratio (0.1 to 300 second melting currents) of fuse links having similar 300 second melting currents, governs the ability to co-ordinate with relays, reclosers, and other fuse links. This is true regardless of whether the fuse link is rated to carry continuously, say for example 25 amperes with the 200 per cent basis of rating or 40 amperes with the 150 per cent basis of rating. It may not be possible to apply the 25-ampere link where the 40-ampere link is applicable unless the 25-ampere link can carry that much more current than its rating. Similarly, the speed ratio, and not the basis of rating, affects the relative lightning blowing characteristics of different fuse links since such blowing involves high currents and short times. The speed ratio is a product of the physical design of the fuse link. It is not affected by the basis of rating except where higher melting temperature fusible metals, requiring the 200 per cent basis of rating, may handicap the designer in providing a desired higher speed ratio; the slow time-current characteristic which Mr. Asbury states, and we agree, may be beneficial.

The fuse links employed in our investigation have a speed ratio of from six to seven. The standard for universal fuse links currently being proposed by the Edison Electric Institute Subcommittee on Distribution Fuse Standardization, to which Mr. Asbury refers, have a speed ratio of six to eight for the *K* fast fuse links, and 10 to 13 for the *T* slow fuse links. Thus, the fuse links used in this investigation have practically the same ability, to co-ordinate with reclosers and the same lightning blowing characteristics as the *K* fast fuse links currently being proposed by the Edison Electric Institute, if compared on the basis of the 300-second melting currents. The fuse links, employing a tin fusible element as used in our investigation, are rated to carry more current continuously than it is possible to rate fuse links in the proposed standard, which also must include fuse links employing the higher melting temperature silver and copper fusible elements.

The lightning blowing of the 2- and 3-ampere fuse links used at conventional transformer installations in our investigation never exceeded one-tenth of one per cent of those installed, in any one of the four years. One to two per cent fuse blowing during lightning storms is considered normal on most systems having the lightning arrester ground interconnected with the secondary neutral. Thus, the margin of possible benefit was too small to warrant including Hi-Surge type of fuse link in our investigation.

Time-delay, time-current characteristics paralleling fuses would be desirable in reclosers, as suggested by Mr. Asbury, if co-ordination with source side fuses was the only problem. Also, it would be beneficial in co-ordinating the instantaneous opening of reclosers so as to prevent partial melting of load side fuses by non-persistent faults. However, parallel fuse and time-delay recloser characteristics starting directly from the minimum pick-up current permit co-ordination with only one or two adjacent ratings of load side fuses that also could be protected by the instantaneous opening of the recloser. A wider range of ratings was found necessary in order to fuse sectionalizing points between reclosers, branches, and sub-branches connected in service. Thus the time-delay characteristics of reclosers having two instantaneous plus two time-delay operations to lock out must be a compromise between the opposing characteristics which are desirable for co-ordination with source side and with load side fuses. The ability of the lock-closed recloser to eliminate the time-delay characteristic and all the co-ordination problems entailed therewith led to its choice as the best recloser function for our investigation.

With reference to the questions on Figure 13, the abscissa is the calculated maximum (copper to copper) fault current. The automatic oscillographs recorded the date and time each record was made so the reading could be related to the faults as reported by the trouble crews. The data were included only when the fault location was determined accurately. We know of no similar data which is available for other systems. However, it would appear that the fault resistance would be a function of the type of line construction or fault conditions rather than the voltage, except possibly as voltage effects the length of the short circuit path between conductors. Additional field data on this subject are very desirable, both on 7.2-kv and lower voltage circuits.

Short-Circuit Currents and Recovery Voltages on Rural Distribution Systems

W. H. EASON
MEMBER AIEE

I. B. JOHNSON
MEMBER AIEE

J. W. KALB
ASSOCIATE AIEE

H. A. PETERSON
FELLOW AIEE

THIS paper deals with the nature of short-circuit currents and of the recovery voltages that can occur on multigrounded neutral rural distribution systems. This information is useful in the design, application, and preparation of test standards of lightning arresters, fuse cutouts, oil circuit reclosers, and other protective devices for these rural systems.

The results were obtained from field tests made on an actual system and from calculations and analysis using the transient analyzer[1] or miniature system method. The transient analyzer studies were made primarily to analyze the most severe or boundary conditions obtainable. The field studies were necessarily limited in the type of circuit conditions, and represent more typical operating conditions. Several sets of field operating conditions were duplicated on the transient analyzer for purposes of comparison.

In so far as the authors are aware, this paper presents the first published data concerning measured values of recovery transient voltages on a rural distribution system and their correlation with transient analyzer measurements.

Fault currents and recovery voltages were studied on various combinations of single-phase and 3-phase circuits that included the effects of the angle of incidence of the fault on the voltage wave, of the location of the fault on the line, of the length of line, of the transformer rating, and of the type of fault—single line-to-ground or 3-phase.

The results are presented and discussed in three parts: transient analyzer study; field study; and comparison of field investigation with analyzer results and calculations. The analyzer study presents data from a representation in miniature of a multigrounded neutral rural distribution system, and the field study includes data from an actual 7,200/12,470-volt multigrounded-neutral wye rural distribution system.

Summary of Results and Conclusions

Some factors which affect the severity of transient recovery voltages experienced on rural distribution lines are:

1. The length of line remaining connected to the substation after the fault interruption. The rate of voltage rise decreases with increasing length of line. Whereas, in general, the crest recovery voltage appears to be relatively low with no line remaining connected after the fault, it increases to a maximum as line is added and then decreases with further increases in length of line.

2. Distance between substation and fault. For single, unbranched lines the crest recovery voltage generally decreases with increasing distance between substation and fault.

3. X/R ratio of the line between substation and fault. Crest recovery voltage decreases with decreasing X/R ratio of the line.

4. Arc voltage characteristics of the fault clearing device. A sharp rise in arc voltage immediately before arc extinction tends to increase crest recovery voltage of the transient.

5. Complexity of system network. Reflections from branch points and ends of branch lines influence the nature of the transient recovery voltages.

6. Magnitude of system load connected after interruption of fault current. The damping effect of load resistance reduces the magnitude of crest recovery voltages.

7. Kilovolt-ampere rating of substation transformer bank. Rate of voltage rise increases with increasing transformer kilovolt-amperes. Crest recovery voltages tend to decrease with increasing transformer kilovolt-amperes.

8. Lumped capacitance between line and ground such as substation bus structure or power factor capacitors. This will reduce the rate of voltage rise. An increase in capacitance up to certain values is accompanied by an increase in the crest recovery voltage.

The most severe recovery voltages measured on the transient analyzer were obtained on a study involving six miles of unloaded, unbranched line. This length of line was selected because shorter lengths of line, while giving more rapid rates of voltage rise, would generally result in lower crest voltages. Table I lists measurements obtained on this study for various values of substation kilovolt-amperes.

The shortest measured time to 0.9 times normal crest voltage, $T_{0.9}$, for either field or analyzer tests, was 22 microseconds. This was measured during field tests at the 900-kva substation bank with no connected line.

Crest recovery voltage, V_M, was 0.94 times normal.

The highest crest recovery voltage,

Table I

Substation Transformer, 3-phase Kva	V_M Crest Recovery Voltage, Times Normal Crest Voltage	$T_{0.9}$ Time to 0.9 Normal Crest Voltage, Microseconds
50	1.75	280
100	1.70	230
500	1.55	110
1,000	1.43	85
2,000	1.28	80

Paper 49-177, recommended by the AIEE Transmission and Distribution Committee and approved by the AIEE Technical Program Committee for presentation at the AIEE Summer General Meeting, Swampscott, Mass., June 20–24, 1949. Manuscript submitted November 15, 1948; made available for printing May 2, 1949.

W. H. Eason and J. W. Kalb are with the General Electric Company, Pittsfield, Mass., I. B. Johnson is with the General Electric Company, Schenectady, N. Y., and H. A. Peterson is with the University of Wisconsin, Madison, Wis.

The authors desire to acknowledge the work of E. J. Wade, D. D. MacCarthy, G. F. Lincks, P. H. Light and D. Inwood. The field tests were made possible by the co-operation of the personnel of the Central Electric Cooperative, Inc.

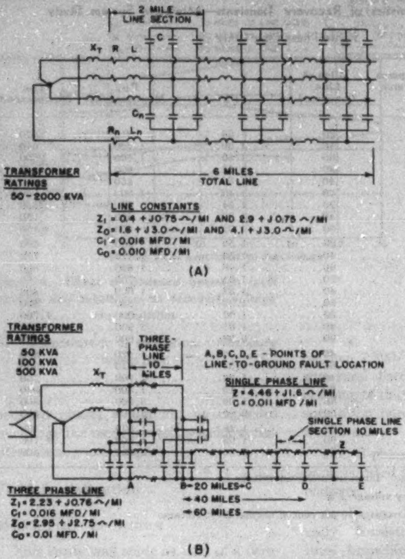
2 MILE
LINE SECTION
X_T
R
L
C
C_n
R_n
L_n
TRANSFORMER RATINGS
50 - 2000 KVA
6 MILES
TOTAL LINE
LINE CONSTANTS
Z_1 = 0.4 + J0.75 ~/MI AND 2.9 + J0.75 ~/MI
Z_0 = 1.6 + J3.0 ~/MI AND 4.1 + J3.0 ~/MI
C_1 = 0.016 MFD/MI
C_0 = 0.010 MFD/MI
(A)
TRANSFORMER RATINGS
50 KVA
100 KVA
500 KVA
X_T
THREE-PHASE LINE 10 MILES
A, B, C, D, E - POINTS OF LINE-TO-GROUND FAULT LOCATION
SINGLE PHASE LINE
Z = 4.46 + J1.6 ~/MI
C = 0.011 MFD/MI
SINGLE PHASE LINE SECTION 10 MILES
Z
A
B
20 MILES
C
D
E
40 MILES
60 MILES
THREE PHASE LINE
Z_1 = 2.23 + J0.76 ~/MI
C_1 = 0.016 MFD/MI
Z_0 = 2.95 + J2.75 ~/MI
C_0 = 0.01 MFD./MI
(B)

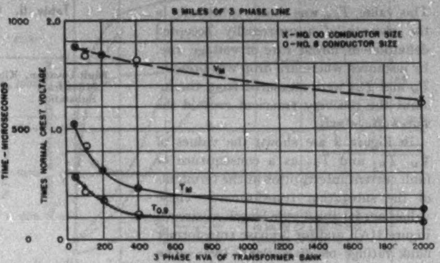

Figure 1 (left). Representative circuits in miniature for 6,900-volt rural distribution systems

Figure 3 (above). Effect of kilovolt-ampere rating of substation transformer on recovery voltage characteristics

Six miles of line connected to substation
Miniature system data

V_M, measured during field tests was 1.33 times normal.

Comparison of field measurements and transient analyzer results for similar circuit conditions show good agreement, demonstrating the accuracy of the transient analyzer in securing data on recovery voltages for rural distribution systems. Its value lies in the ability to extend circuit conditions beyond those found readily in the field.

Short-circuit currents measured in the field agree with values obtained by simplified fault calculators.[3,4]

Transient Analyzer Study

In this study the systems used in miniature represented 6,900-volt multigrounded neutral rural distribution systems. Substation transformer bank ratings of 50 to 2,000 kva were considered with the high voltage side of these transformers assumed connected to an infinite bus. The transformer reactances were taken as 5.5 per cent on their own base. Neither the effect of other transformers than the substation transformer nor the effect of capacitors for power factor correction were investigated. Except for special cases to be discussed later, no system load was represented in the miniature system.

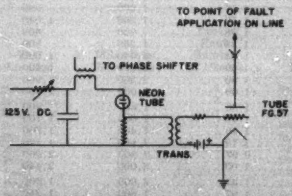
TO POINT OF FAULT APPLICATION ON LINE
TO PHASE SHIFTER
NEON TUBE
125 V. DC.
TUBE FG.57
TRANS.

Figure 2. Circuit for producing fault initiation and fault interruption in miniature system

The systems in miniature used in the analyzer studies were single radial lines—3-phase and/or single-phase—emanating from the substation transformer with no branch lines connected thereto. These circuits are shown in Figure 1. In Figure 1(A) the 3-phase line was built up in 2-mile sections to represent a total of six miles of line. The line constants for this circuit are given in the figure where it is indicated that two values of positive sequence or line resistance were considered, covering a range of line conductor sizes from the order of number 00 to number 8 American wire gauge. In Figure 1(B) the 3-phase and single-phase lines were built up in 10-mile sections to represent line lengths up to 70 miles. The line constants shown in this figure were based on a rural distribution system in which the single-phase lines, as well as the 3-phase lines and the neutral were number 6 copper, and in which spacings of 36 inches between the phase and neutral wires and between the phase wires were assumed.

The device used for the initiation of a fault and the removal of the fault at the first subsequent current zero, simulating the operation of an expulsion lightning arrester or a transformer fuse, is shown in Figure 2. The voltage drop across the *FG-57* tube simulating arc voltage during the period of fault current flow was made approximately zero for the tests made using the circuit of Figure 1(B). For the tests made with the circuit of Figure 1(A) no attempt was made to eliminate tube voltage drop. The device was connected to various points on the distribution lines of Figure 1 wherever it was decided to determine the nature of the recovery voltage as a consequence of the application and removal of a line-to-ground fault at that point.

In the operation of lightning arresters and transformer fuses, the fault current can be initiated at any instant relative to the 60-cycle fundamental frequency voltage. For an analytical treatment of the effect of initiating angle and circuit X/R on recovery transient severity, see Appendix I.

On the transient analyzer the angle of incidence of the fault was varied to give the maximum severity in recovery voltage, and these recovery voltage characteristics were expressed in terms of: (a) the maximum crest recovery voltage, V_M, that appears across the protective device following its operation; (b) the time, T_M, to reach crest of this transient recovery voltage; and (c) the time, $T_{0.9}$, for this recovery voltage to reach 90 per cent normal system crest voltage.

This value, $T_{0.9}$, was chosen arbitrarily in the absence of a universally accepted definition of initial rate of voltage rise. In instances where arc drop was present, T_M and $T_{0.9}$ were measured from the instant the recovery transient crossed the zero voltage axis.

In Figure 3 are shown the values of V_M, T_M, and $T_{0.9}$ as a consequence of fault current interruption at the terminals of the substation transformer. These values are for the 6-mile length of circuit, Figure 1(A), and for 3-phase transformer bank ratings of 50 to 2,000 kva. The condition of a fault at the transformer terminals with short lengths of connected line would be expected to give the most severe transient recovery voltages. These results indicate that V_M decreases with increasing kilovolt-amperes of the transformer bank from 1.75 times normal for a 50-kva bank to 1.28 times normal for a 2,000-kva bank. Values of T_M and $T_{0.9}$ decreased with increasing kilovolt-amperes of the transformer bank and reached values of 140 and 80 microseconds respectively for a 2,000-kilovolt-amperes bank.

To study the effect of longer lengths of line remaining connected after fault clearing and variation in fault locations, the circuit of Figure 1(B) was used. The results are shown in Tables II and III. Some of these results also are presented graphically in the curves of Figures 4, 5, and 6. The data of Tables II and III for remaining connected lines of 10-mile lengths or greater, show the following:

1. Maximum crest voltage, V_M, decreases as the number of miles of remaining connected single-phase line increases. For a fault at the terminals of a 500-kva bank, V_M for 60 miles of connected line is about 84 per cent of that for 20 miles of connected line.

2. Maximum crest voltage, V_M, decreases as the distance between the fault and the substation transformer increases. For a 60-mile line supplied through a 500-kva bank, V_M for a fault at the end of the line is 69 per cent of that for a fault at the transformer terminals.

3. In general, T_M and $T_{0.9}$ increase as the distance between the fault and the step-down transformer is increased. For a 60-mile length of remaining connected line supplied through a 500-kva bank, $T_{0.9}$ for a fault at the end of the line is 1,530 per cent of that for a fault at the substation.

It was found that the addition of single-phase line in the two unfaulted phases had very little effect on the recovery voltage of the faulted phase. This was because the only between-phase mutual coupling in the miniature system studied exists in the short 10-mile section of 3-phase line. Therefore, any unbalance

Table II. Characteristics of Recovery Transients—Miniature System Study

Single-Phase Line Only

Fault Location, Miles from Substation	Kilovolt-Amperes of Transformer Bank	Miles of Line Connected	V_m	T_M, Microseconds	$T_{0.9}$, Microseconds
0	50	20	1.66	810	420
		40	1.60	1,200	610
		60	1.50	1,600	800
	100	20	1.62	600	240
		40	1.50	460	410
		60	1.40	1,000	600
	500	20	1.54	320	150
		40	1.39	600	150
		60	1.32	800	150
20	50	20	1.50	900	500
		40	1.53	1,220	720
		60	1.46	1,600	860
	100	20	1.25	700	460
		40	1.32	1,000	600
		60	1.28	1,280	800
	500	20	1.02	3,000	1,700
		40	1.01	2,900	1,700
		60	0.93	2,600	2,300
40	50	40	1.36	1,420	820
		60	1.39	1,610	950
	100	40	1.22	2,900	760
		60	1.15	1,300	920
	500	40	1.00	3,900	1,800
		60	0.90	2,600	2,500
60	50	60	1.28	1,800	1,100
	100	60	1.02	1,400	1,100
	500	60	0.90	2,600	2,300

V_M = Maximum recovery voltage. Times normal crest voltage.

T_M = Time to maximum recovery voltage V_M.

$T_{0.9}$ = Time for recovery voltage to reach 90 per cent of normal crest voltage.

Table III. Characteristics of Recovery Transients—Miniature System Study

With Ten Miles of 3-Phase Line Between Substation and Single-Phase Line

Fault Location, Miles from Substation	Kilovolt-Amperes of Transformer Bank	Total Miles of Line Connected	V_M	T_M, Microseconds	$T_{0.9}$, Microseconds
6	50	10	1.63	700	400
		30	1.65	1,100	580
		50	1.60	1,400	680
		70	1.52	1,800	960
	100	10	1.58	500	260
		30	1.58	800	400
		50	1.46	1,000	540
		70	1.42	1,200	600
	500	10	1.50	280	140
		30	1.40	440	240
		50	1.35	700	260
		70	1.35	960	270
10	50	10	1.60	640	340
		30	1.61	1,100	540
		50	1.58	1,400	720
		70	1.50	1,800	920
	100	10	1.47	520	280
		30	1.50	900	480
		50	1.46	1,100	600
		70	1.38	1,300	800
	500	10	1.02	2,600	300
		30	1.05	2,400	400
		50	1.02	2,100	640
		70	1.00	2,800	900
30	50	30	1.48	1,300	740
		50	1.50	1,600	900
		70	1.50	1,900	1,040
	100	30	1.18	900	600
		50	1.25	1,260	800
		70	1.25	1,540	1,000
	500	30	1.00	2,500	1,600
		50	1.00	2,200	1,900
		70	1.00	3,000	2,400
50	50	50	1.38	1,600	900
		70	1.40	2,000	1,100
	100	50	1.10	1,400	1,000
		70	1.13	1,600	1,120
	500	50	0.97	2,300	2,000
		70	1.00	3,000	2,440
70	50	70	1.32	2,000	1,200
	100	70	1.07	1,800	1,280
	500	70	1.00	3,000	2,400

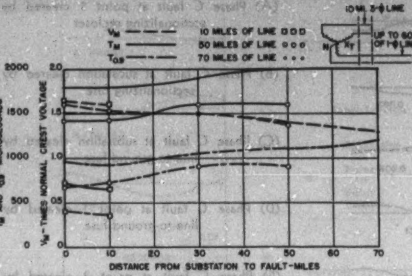

Figure 4. Effect of distance between fault location and substation on recovery voltage characteristics

50-kva transformer at substation. Miniature system data

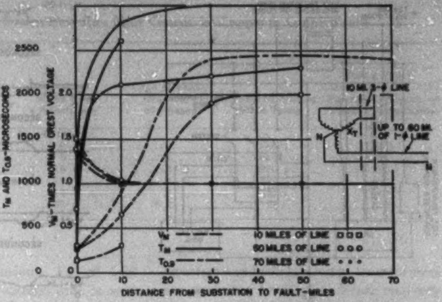

Figure 6. Effect of distance between fault location and substation on recovery voltage characteristics

500-kva transformer at substation. Miniature system data

between phases would not be expected to change the recovery voltage characteristics on any one phase.

Field Investigation

Description of System

This study was made as part of a comprehensive field investigation[5,6] in cooperation with the Central Electric Cooperative, Inc., in western Pennsylvania, on their 7,200/12,470-volt multigrounded wye rural distribution system. Figure 7 is a map of that portion of the system and substation bank upon which these tests were made.

The 3-phase substation transformer bank is rated 900-kva, 4.01 per cent impedance.

As Figure 7 shows, the system basically consists of long single-phase lines branching from 3-phase feeders. Forty-two miles of 3-phase, and 524 miles of single-phase 7,200-volt line were involved.

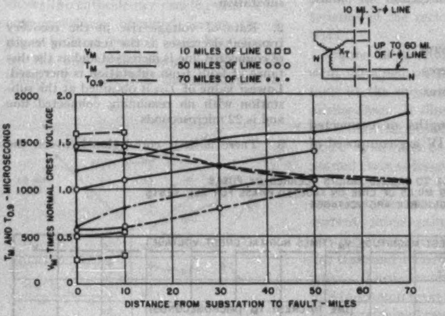

Figure 5 (left). Effect of distance between fault location and substation on recovery voltage characteristics

100-kva transformer at substation. Miniature system data

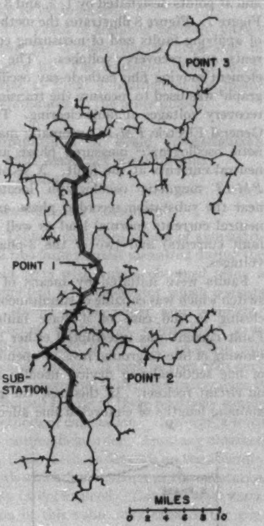

Figure 7 (right). Map of 7.2-kv multigrounded lines upon which field tests were made

Table IV. Characteristics of Recovery Transients Measured During Field Tests

Test Location	Miles from Substation	Type of Fault, Number of Phases	Fault Cleared by	Miles of Line Connected After Fault on Particular Phase Involved	Fault Current, Average Amperes Rms Symmetrical	Characteristics of Most Severe Recovery Transients Recorded			Clearing Angle, Degrees
						V_M	T_M	$T_{0.9}$	
Substation	0	3	Sectionalizing fuse	0	748	0.95	30	28	73
Substation	0	3	Line-to-ground fuse	241	748	1.20	1,000	360	57
Substation	0	1	Sectionalizing fuse	0	817	0.94	25	22	53
Substation	0	1	Line-to-ground fuse	289	817	1.15	1,480	340	55
Point 1	16	3	Sectionalizing recloser	29	270	1.33	550	190	35
Point 1	16	3	Line-to-ground fuse	289	270	1.32	1,520	670	41
Point 1	16	1	Sectionalizing recloser	29	220	1.09	660	260	50
Point 1	16	1	Line-to-ground fuse	289	220	1.10	1,640	880	49
Point 2	18½	1	Line-to-ground fuse	241	130	1.00	570	340	59
Point 3	52½	1	Sectionalizing recloser	215	56	1.03	1,360	980	50
Point 3	52½	1	Line-to-ground fuse	289	56	1.14	1,570	1,030	65

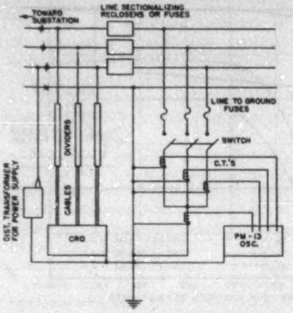

Figure 8. Equipment for making short-circuit current and recovery voltage field tests

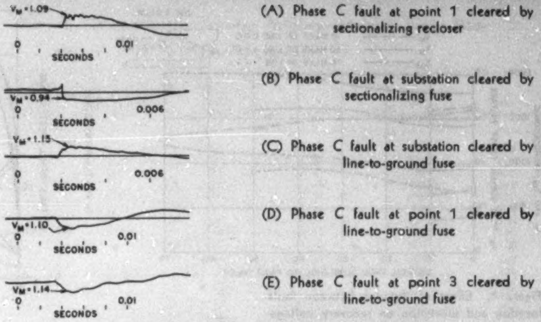

(A) Phase C fault at point 1 cleared by sectionalizing recloser

(B) Phase C fault at substation cleared by sectionalizing fuse

(C) Phase C fault at substation cleared by line-to-ground fuse

(D) Phase C fault at point 1 cleared by line-to-ground fuse

(E) Phase C fault at point 3 cleared by line-to-ground fuse

Figure 10. Oscillograms of voltage transients obtained during field tests

Method of Test

Faults were produced at the substation and at points designated by 1, 2, and 3 on Figure 7. Figure 8 illustrates the method of applying faults and of measuring currents and recovery voltages. The 3-element moving film cathode-ray oscillograph[2] was used to measure the transient recovery voltages at fault clearing. The General Electric *PM-13* automatic magnetic oscillograph[2] measured phase and neutral currents at the fault. A second *PM-13* magnetic oscillograph located near the substation recorded phase and neutral currents (normal load as well as fault currents) and two of the 3-phase voltages.

Faults were initiated by means of a switch which was capable of simultaneous closing in the case of 3-phase faults. Fault current was interrupted either by blowing of line-to-ground fuse, or opening of line sectionalizing device, usually an oil circuit recloser. In this case the remaining lengths of connected line affecting recovery voltages were those on the substation side of the fault location since the line beyond the fault was disconnected by the sectionalizing device.

Test Conditions

At the substation and at Point 1 of Figure 7, both single-phase and 3-phase faults were produced. At Points 2 and 3 only single-phase faults could be produced. Table IV summarizes the conditions associated with each of the field tests.

Approximate load currents at the substation preceding initiation of faults were:

Phase *A:* 23 rms amperes
Phase *B:* 10 rms amperes
Phase *C:* 25 rms amperes

The remaining lengths of connected line shown in Table IV are composed of moderately long branches together with many short spurs as shown on Figure 7. The farthest point from the substation (3-phase + single-phase line) on the lines studied is 68 miles.

Results and Conclusions

Table IV shows the average recorded fault currents and the characteristics of the most severe recorded recovery transients associated with each test condition. These results indicate:

1. Fault current decreases as expected with increase in distance between fault and substation.

2. Rate of voltage rise in the recovery transient decreases as the remaining length of connected line is increased and as the distance of fault from substation is increased. Lowest value of $T_{0.9}$ is obtained at the substation with no remaining connected line and is 22 microseconds.

3. There is little correlation between the

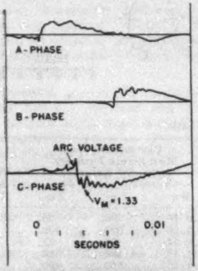

Figure 9. Oscillograms obtained during field tests at point 1

Voltage transients resulting from clearing of 3-phase fault by sectionalizing reclosers

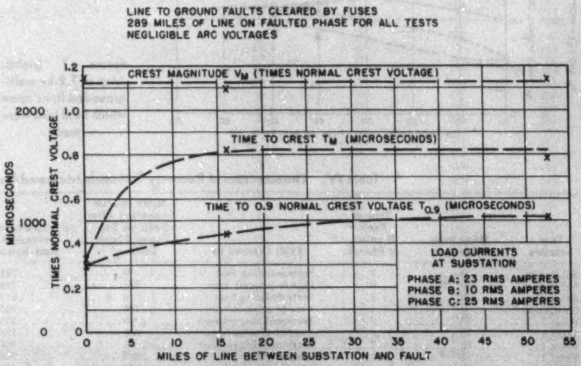

Figure 11. Effect of distance between fault and substation on recovery voltage characteristics. Field test data

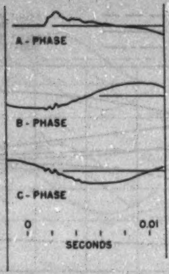

Figure 12. Oscillograms obtained during field tests at point 1. Voltage transients on phase *A* and minor disturbances on phases *B* and *C* due to coupling between phases

crest magnitudes of the most severe recovery transients and the test circuit conditions as will be discussed in a following paragraph.

4. Measured clearing angles for faults at the substation are less than 90 degrees. This results in lower restored circuit voltages and therefore the crest recovery voltages are less than the maximum possible. Clearing angle is defined as the time measured in electrical degrees by which the current zero lags the preceding voltage zero.

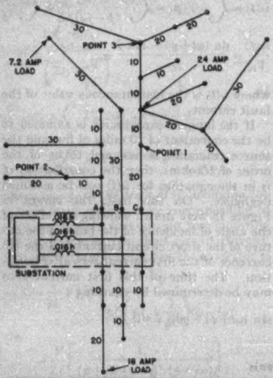

Figure 13. Miniature system used for transient analyzer study of field test conditions

Numbers represent miles of line in a given section

Table V. Symmetrical Rms Fault Current for Copper to Copper Faults

Fault Location	Miles from Substation	Type of Fault, Number of Phases	Fault Current: Measured During Field Tests	Fault Current: Using Fault Calculator *GES-3261* (Based on Measured Values at Substation)
Substation	0	3	748	(748)
	0	1	817	(817)
Point 1	16	3	270	270
	16	1	220	225
Point 2	18 1/2	1	130	140
Point 3	52 1/2	1	52	56

Examination of several of the oscillograms of recovery voltage transients helps explain 3 and 4 above. Figure 9 shows the cathode-ray oscillograms of recovery voltage obtained during the 3-phase fault at Point 1 which was cleared by the line sectionalizing reclosers, see Table IV. This was the maximum recorded recovery transient, V_M, of 1.33 times normal crest voltage and is seen occurring on phase *C*. Its severity is largely due to the final rapid rise in arc voltage of the line sectionalizing recloser just prior to current interruption. During most field tests, the arc voltage characteristics of the fault clearing devices were an important factor in determining magnitude of the recovery voltages. Figure 10(A) shows the oscillogram obtained during the single-phase fault at the same location, Point 1, and cleared by the same (*C*-phase) sectionalizing recloser. In this case the recovery voltage magnitude, V_M, was only 1.09 times normal crest voltage.

The reduction in magnitude, rate of voltage rise, and change in clearing angle shown in Table IV appear to be due to the change in arc voltage characteristics of the recloser between the two tests.

Figure 10(B) shows the recovery transient obtained on clearing a single-phase fault at the substation with the sectionalizing fuse. It illustrates the rapid rate of voltage rise possible under these conditions. The value of V_M is only 0.94 times normal crest voltage.

During a few of the tests, the recovery transients were modified very little by the current interrupting device, thus permitting other circuit conditions to control the transient recovery voltage characteristics. These involved faults cleared by line-to-ground fuses in which the following factors remained relatively constant.

1. Miles of connected line constant at 289.
2. Substantially no final rapid rise in fuse arc drop before current interruption.
3. Low fuse arc drop during current flow.
4. Clearing angles near most severe condition.
5. Load at substation constant at about 25 rms amperes on the faulted phase.

The oscillograms of the recovery transients are shown in Figures 10(C), 10(D) and 10(E). Results are shown on the curves in Figure 11. These results show that devices such as expulsion lightning arresters and fuses located at transformers are subjected to very moderate recovery transients with respect to both crest magnitudes and rates of rise under normal conditions anywhere on the system under study. When short lengths of line remain connected after the fault as in the case of line sectionalizing devices near the substation, more severe recovery transients may be experienced.

The effect of coupling between phases along the 3-phase line is illustrated in Figure 12. The transient voltage on *A*-phase at Point 1 resulted in the minor disturbances on the other phases.

Comparison of Field Investigation with Analyzer Results and Calculations

SHORT-CIRCUIT CURRENTS

Table V compares values of symmetrical rms fault current measured during the field tests with values obtained using a simplified fault calculator which consists of special graph paper and template.[3] Another method of calculation[4] gave values within 2 per cent of these calculated values. It may be seen that very close agreement with measured values is obtained by use of these relatively simple methods of calculation. However, a word of caution is in order. Accuracy obtained by these methods depends on the accuracy with which fault current at the substation bus is determined. Considerable variation in this value may exist as the generating capacity of the system supplying the substation is changed. For example, on the system where the field studies were made, fault current at the substation bus could vary from 509 to 865 symmetrical rms amperes for 3-phase faults and from 613 to 916 amperes for single-phase line-to-ground faults.

It is thus evident that available fault currents near the substation are not constant for a given system. This band of possible values must be considered in coordination studies of overcurrent protective devices. The variations cited are true only for this system and may or may

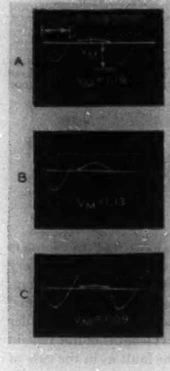

Figure 14 (left). Oscillograms obtained during transient analyzer tests on simulated field system

(A) Fault at point 1 cleared by sectionalizing recloser

(B) Fault at substation, phase C, cleared by line-to-ground fuse

(C) Fault at point 1 cleared by line-to-ground fuse

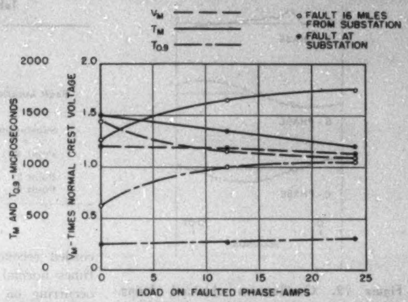

Figure 15 (right). Effect of load on recovery voltage characteristics. Transient analyzer results from simulated field system

not be typical of other rural systems, depending upon their source of power.

RECOVERY VOLTAGES

Comparison of recovery voltage magnitudes, V_M, of Tables II and III with those of Table IV shows that maximum values obtained by the field tests were less than those of the transient analyzer tests. This is to be expected since the analyzer tests were made to show the most severe conditions on a simple, unbranched, unloaded system.

In order to investigate the effect of system loading and system complexity, and to demonstrate the ability of the analyzer to reproduce accurately transient recovery characteristics, additional tests were made. The miniature system of Figure 13 was used. While it is still a considerable simplification of the actual system as shown in Figure 7, it is much more nearly representative of that system than the unbranched lines used in the original analyzer studies. Connected system load was represented as lumped resistances at the points shown on Figure 13. The resistance on the faulted phase was varied to show its effect on system recovery voltage characteristics. The results of this study were:

1. When the miniature system approximates the actual system in complexity of branching and the damping effect of system load is represented, excellent agreement between field and analyzer oscillographic measurement of transient recovery characteristics results. Figure 14 shows three of the oscillograms obtained on the transient analyzer. A tabulation listing corresponding oscillograms from the field tests and comparative measurements are given in Table VI.

2. The damping effect of system load can substantially reduce the magnitude of system recovery voltage. This effect is illustrated by the curves of Figure 15. For example, for a fault at Point 1, 16 miles from the substation, V_M is 33 per cent greater with completely unloaded lines than with a 24-ampere load.

3. Figure 15 indicates that V_M is higher for a fault at Point 1 than for a fault at the substation. In Figures 4, 5, 6 where the complexity of the system was not represented in miniature, the highest values of V_M generally occur for faults at the substation.

These results show that both system complexity and system load are important factors in determining recovery transient characteristics and should be taken into account in transient analyzer studies.

Appendix I

For a simplified representation of recovery voltage, let there be considered the circuit shown in Figure 16, where the line or other capacitance is represented by the lumped capacitance C supplied from a 60-cycle voltage source through a source inductance L. The switch across the capacitor is used to simulate the application and removal of a fault.

Initially with the switch open the current and voltage are in a steady state relationship given by

$$\frac{i(t)}{V_m}=\frac{\cos\left(\omega t+\frac{\pi}{2}\right)}{|x_l-x_c|} \qquad \text{(where } x_c>x_l\text{)}$$

where $i(t)$ is the instantaneous value of current, V_m is the crest value of the source voltage expressed as $V_m \cos \omega t$, and x_l and x_c are inductive and capacitive reactances.

Upon closing the switch and assuming the effect of the discharge of the capacitor C through the shorting switch to be negligible, the equation to be solved is

$$Li_0+\mathcal{L}\,v(t)=(pL)\,Y(p)$$

where i_0 is the initial current in the inductance at the instant of the closing of the switch. If $v(t)=V_m \cos(\omega t+\psi)$ where ψ is the angle of switching, then

$$\mathcal{L}\,v(t)=\mathcal{L}\,Re\,V_m\epsilon^{j(\omega t+\psi)}=\mathcal{L}\,V\epsilon^{j\omega t}$$
$$=\frac{V}{p-j\omega}$$

where

$$V=Re\,V_m\epsilon^{j\psi}$$

Inverting the circuit equation and solving for the current gives

$$i_f(t)=\mathcal{L}^{-1}\,Y(p)=\mathcal{L}^{-1}\frac{V}{(p-j\omega)pL}+\mathcal{L}^{-1}\frac{i_0}{p}$$

$$\frac{i_f(t)}{V_m}=\frac{\sin(\omega t+\psi)-\sin\psi}{x_L}+\frac{i_0}{V_m}$$

where $i_f(t)$ is the instantaneous value of the fault current.

If the lumped capacitance is assumed to be the equivalent of 10 miles of line and the source reactance is assumed to be of the order of 15 ohms, then the contribution of i_0 in the equation for $i_f(t)$ can be assumed negligible. On this basis the curves in Figure 16 were drawn showing the effect of the angle of incidence of the fault in the nature of the short circuit current and the occurrence of the first current zero after initiation. The time of this first current zero may be determined by equating

$$\sin(\omega t+\psi)-\sin\psi=0$$

Table VI. Comparison of Analyzer and Field Measurements

Fault Location	Miles from Substation	Type of Fault	Miles of Line Connected After Fault	Analyzer				Field Test			
				Figure	V_M	T_M	$T_{0.9}$	Figure	V_M	T_M	$T_{0.9}$
Point 1	16	Line sectionalizing	29	14(A)	1.19	1,100	270	10(A)	1.09	660	260
Substation	0	Line to ground	289	14(B)	1.13	1,200	305	10(C)	1.15	1,480	340
Point 1	16	Line to ground	289	14(C)	1.09	1,770	1,070	10(D)	1.10	1,640	880

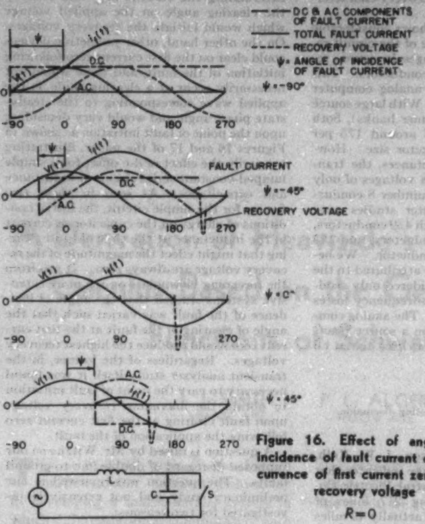

Figure 16. Effect of angle of incidence of fault current on occurrence of first current zero and recovery voltage

$R=0$

This equation is satisfied for one condition with $(\omega t+\psi)=(\pi-\psi)$, or $\omega t=\pi-2\psi$.

If the fault current is assumed to stop at its first current zero, a transient voltage appears across the capacitor. This recovery voltage may be calculated by superimposing the effects of the initial current and voltage in circuit if any upon the results obtained by the closing of a switch connecting the series circuit of L and C upon the voltage source at switching angle on the voltage wave given by the instant the short circuit passes through zero. Thus, for this case of zero initial current and voltage, the spectral equation for the current is

$$Y(p)=\frac{\mathcal{L}\,v(t)}{\left(pL+\frac{1}{pC}\right)}$$

$$\mathcal{L}\,v(t)=\mathcal{L}\,V_m\cos\,(\omega t+\pi-\psi)$$

$$=\mathcal{L}\,Re\,V_m\epsilon^{j(\pi-\psi)}\epsilon^{j\omega t}=\frac{V}{p-j\omega}$$

where $(\pi-\psi)$ is the angle of switching on the voltage wave of the source corresponding to the instant of the first current zero following the initiation of the short-circuit current. The recovery voltage across the capacitor is

$$v_c(p)=\frac{1}{pC}Y(p)=\frac{V}{pC\left(pL+\frac{1}{pC}\right)(p-j\omega)}$$

$$=\frac{V}{LC}\left[\frac{1}{(p+j\Omega)(p-j\Omega)(p-j\omega)}\right]$$

where $\Omega=1/\sqrt{LC}$.

Inverting the equation and solving for the voltage gives

$$v_c(t)=\frac{V_mRe}{LC}\left[-\frac{\epsilon^{-j(\Omega t-\pi+\psi)}}{2(\Omega^2+\Omega\omega)}-\frac{\epsilon^{j(\Omega t+\pi-\psi)}}{2(\Omega^2-\Omega\omega)}-\frac{\epsilon^{j(\omega t+\pi-\psi)}}{\omega^2-\Omega^2}\right]$$

for $\Omega>>\omega$.

$$\frac{v_c(t)}{V_m}=\cos\,(\omega t+\pi-\psi)-\frac{\cos\,(\Omega t-\pi+\psi)}{2}-\frac{\cos\,(\Omega t+\pi-\psi)}{2}$$

$$=\cos\,(\omega t+\pi-\psi)-\cos\,\Omega t\cos\,(\pi-\psi)$$

The voltage at the first peak of the transient will be obtained for $t=\pi/\Omega$. Thus,

$$\frac{v_c(t)}{V_m}=2\cos\,(\pi-\psi)\qquad(t=\pi/\Omega)$$

The maximum recovery voltage in the simplified circuit occurs for the case in which the fault current was initiated at $\psi=0$ or at the crest of the voltage wave. The time to crest voltage is given by $t=\pi/\Omega$ seconds.

If it is assumed that $x_L=15$ ohms and $x_c=25{,}000$ ohms (capacitance of approximately 10 miles of single-phase line) the time to the maximum first peak of the transient of two times normal is 204 microseconds.

The results of the effect of an appreciable resistance ($R=10$ ohms) added in series with the inductance as shown in Figure 17 are given in Figure 17 for various angles of fault application. The curves are based on the fault current equation

$$\frac{i(t)}{V_m}=\frac{1}{Z}\,(\cos\,\omega t+\psi-\theta)-\epsilon^{-\frac{R}{L}t}\cos\,(\psi-\theta)$$

where

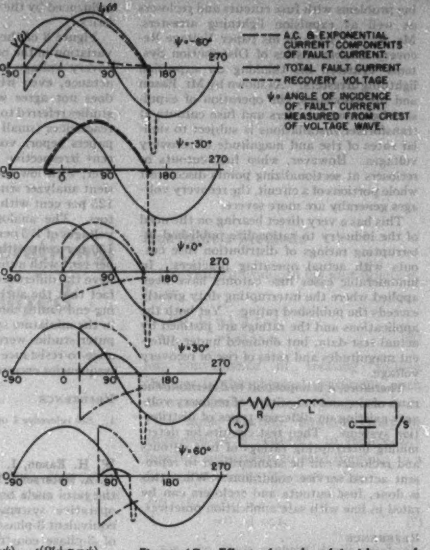

Figure 17. Effect of angle of incidence of fault current on first current zero and recovery voltage

$R=10$ ohms, $X_L=15$ ohms

$Z=R+j\omega L$

$\psi=$angle of switching, measured from crest of voltage wave

$\theta=\tan^{-1}\omega L/R$

References

1. An Electric Circuit Transient Analyzer, H. A. Peterson. *General Electric Review* (Schenectady, N. Y.) volume 42, 1939, pages 394–400.

2. Advances in Technique of Lightning Measurements, T. Brownlee. *AIEE Transactions,* volume 68, part I, 1949, pages 515–19.

3. Quicker Way of Computing Distribution Short Circuits, John D. Sauter, G. F. Lincks. *Electrical World,* (New York, N. Y.) March 21, 1942, pages 70–72.

4. Graphical Method of Calculating Fault Currents in Distribution Circuits, F. W. Linder. *Electrical Engineering* (*AIEE Transactions*), volume 64, January 1945, pages 16–19.

5. Lightning Investigation on a Rural Distribution System, D. D. MacCarthy, D. A. Stann, D. R. Edge, W. C. McKinley. *AIEE Transactions,* volume 68, part I, 1949, pages 428–37.

6. Overcurrent Investigation on a Rural Distribution System, G. F. Lincks, D. R. Edge, W. C. McKinley, J. H. Loh. *AIEE Transactions,* volume 68, part II, 1949, pages 915–29.

Discussion

G. Fred Lincks (General Electric Company, Pittsfield, Mass.): The authors have recognized the broader scope of the problem of recovery voltages as it applies to the interrupting problems with fuse cutouts and reclosers as well as expulsion lightning arresters. Mr. R. L. Witzke in his paper Voltage Recovery Characteristics of Distribution Systems[1] centered his thinking on expulsion lightning arresters. As shown by Mr. Eason and his associates, the operation of expulsion lightning arresters and fuse cutouts at transformer installations is subject to similar rates of rise and magnitude of recovery voltages. However, when fuse cutouts or reclosers at sectionalizing points disconnect whole portions of a circuit, the recovery voltages generally are more severe.

This has a very direct bearing on the need of the industry to rationalize published interrupting ratings of distribution fuse cutouts with actual operating practices. In innumerable cases fuse cutouts have been applied where the interrupting duty greatly exceeds the published rating. Yet both the applications and the ratings are justified by actual test data, but obtained under different magnitudes and rates of rise of recovery voltage.

Therefore, it is important to determine the rates of rise and magnitude of recovery voltages existing on different types of distribution systems. Then test circuits for determining interrupting ratings of fuse cutouts and reclosers can be standardized to represent actual service conditions. When this is done, fuse cutouts and reclosers can be rated in line with safe application practices.

REFERENCE

1. VOLTAGE-RECOVERY CHARACTERISTICS OF DISTRIBUTION SYSTEMS, R. L. Witzke. *AIEE Transactions*, volume 68, part I, 1949, pages 172–87.

R. L. Witzke (Westinghouse Electric Corporation, East Pittsburgh, Pa.): This paper will be useful to the industry because it contains field-test data on distribution-circuit recovery-voltage characteristics. As most recovery-voltage data are obtained from miniature-system studies, it is highly desirable to have field data available for comparative purposes. It was gratifying to see that substantial agreement could be obtained between field and laboratory results.

The Central Electric Cooperative system, on which the tests were made, has 217 miles of equivalent 3-phase circuit. This length of circuit, with its large number of branches, and the small conductor sizes are in a direction to give low recovery voltages, as compared to what might be experienced on a less extensive system. This factor should be kept in mind in the design and application of protective devices.

The transient analyzer studies reported in this paper were made by varying the angle of incidence of the fault. Analog computer studies summarized in the paper "Voltage-Recovery Characteristics of Distribution Systems," neglected this factor as unimportant because of the frequencies involved.[1] In high-frequency circuits the initiating transient usually is damped to a negligible level in a half-cycle of a 60-cycle wave, and consequently cannot contribute appreciably to the recovery transient.

The authors have given no consideration to double line-to-ground faults. As these faults may be more severe than single line-to-ground faults, they should not be neglected in the design and application of protective devices, the performance of which is influenced by the circuit recovery characteristics.

Figure 3 of the paper shows considerable variation in the magnitude of the circuit recovery voltage with changes in source reactance, even with 2/0 conductors. This does not agree with our analog computer studies referred to earlier. With large source reactances (small transformer banks), both papers report voltages of around 175 per cent irrespective of conductor size. However, with low source reactances, the transient analyzer studies show voltages of only 125 per cent with 2/0 or number 8 conductors. The analog computer studies gave voltages of 175 per cent with 4/0 conductors, 150 per cent with 2/0 conductors, and 125 per cent with number 6 conductor. We believe the differences can be attributed to the fact that the authors considered only sending-end faults, and to high-frequency losses in the miniature systems. The analog computer studies were based on a source reactance-to-resistance ratio of at least ten at all frequencies encountered.

REFERENCE

1. See reference 1 of the preceding discussion.

W. H. Eason, I. B. Johnson, J. W. Kalb, H. A. Peterson: Mr. Witzke indicates that the tests made on the Central Electric Cooperative system involving 217 miles of equivalent 3-phase circuit (actually 42 miles of 3-phase construction and 524 miles of single-phase multibranched lines) was such as to give low recovery voltages as compared to what might be experienced on a less extensive system. While, in general, this is true, it is also true that the results obtained for the complete system were lowered somewhat by loads at the time of testing as illustrated in Figure 15 of the paper; it is also true that results also were obtained on this extensive system involving shorter portions subsequent to the clearing of the fault, such as 29 and 0 miles of line connected to the substation transformer as indicated in Table III of the paper. In these tests with less extensive system connections, recovery voltages were also relatively low, particularly for the case of 0 miles of line connected to the transformer where it had been expected that the worse recovery voltages would occur rather than those obtained which did not exceed normal crest line to neutral voltage. For this latter case, a factual evaluation and understanding of the attenuation factors producing these results have not, at present, been accomplished—but are being studied. However, we feel that the system and the results obtained therefrom, both in the field and on the analyzer, are representative of a typical rural distribution system.

Another comment is made regarding the fact that the transient analyzer results were obtained by varying the angle of incidence of the fault which was not done in Mr. Witzke's studies on the analog computer because it was assumed the initiating high-frequency transients would be damped to a negligible value and would not contribute to the recovery transient. In studying recovery transients as related to various protective devices for distribution systems, some of these could clear the fault under relatively steady-state conditions where the phase-angle relationship between current and voltage imposed by the circuit would be the defining factor in determining the current zero and thereby the clearing angle on the applied voltage which would initiate the recovery voltages. On the other hand, other protective devices could clear on the first current zero following initiation of the fault, and these would not necessarily occur at a clearing angle on the applied wave corresponding to the steady-state phase angle and would vary depending upon the point of fault initiation as shown in Figures 16 and 17 of the paper, illustrating primarily the effect of d-c offset for a simple lumped-constant series circuit of inductance and capacitance. As seen in these two figures for the simple circuit, the initial conditions of charge on the capacitor or current in the inductance at the time of fault clearing that might effect the magnitude of the recovery voltage are always zero. It was from the foregoing viewpoints on the more extensive systems studied that the angle of incidence of the fault was varied such that the angle of clearing of the fault at the first current zero would produce the highest recovery voltages. Regardless of the former, in the transient analyzer study itself it was found necessary to vary the point of fault initiation to obtain the maximum recovery voltage upon fault clearing at the first current zero following the application of the fault.

A question is raised by Mr. Witzke on our supposed disregard of double line-to-ground faults. The question was reviewed in our preliminary study and not extensively investigated for two reasons:

1. Rural distribution systems of the type studied are predominantly single-phase except for some short 2-phase and 3-phase sections near the substation.

2. Multigrounded neutral rural distribution systems should have ratios of X_0/X_1 not appreciably greater than one, and it is for those systems where this ratio is appreciably greater than one where double line-to-ground faults become more severe than single line-to-ground faults and should not be neglected.

Lastly, Mr. Witzke mentions a disagreement in the magnitude of the recovery voltages between those obtained on the analog computer and those obtained on the transient analyzer for the conditions of low source reactance and short lengths of line with different size conductors. With low source reactance, the transient analyzer gave results of the order of 125–130 per cent maximum recovery voltages for short lengths of line having conductor sizes ranging from number 8 up to 2/0. Analog computer studies gave results of 125 per cent for number 6 conductor, increasing to 150 per cent for 2/0 conductor. For the smaller size line conductors, the conclusions from the two sets of data appear to be in good agreement. For the larger size conductors approaching 2/0, the disagreement reaches the order of a 15 per cent difference. To the extent to which all the circuit factors actually are known precisely and included, it is a question as to whether or not this difference may not be considered a fair agreement.

In Mr. Lincks' discussion, he has emphasized the applicability of these results to design and test standards for fuse cutouts and reclosers as well as for expulsion-type lightning arresters. The material presented in this paper and in others dealing with other types of distribution systems should be utilized in considering revision of test standards to recognize the important factor of system transient recovery characteristics.

A Derivation of Heaviside's Operational Calculus Based on the Generalized Functions of Schwartz

J. J. SMITH
MEMBER AIEE

P. L. ALGER
FELLOW AIEE

THE RECENT work of the French mathematician Laurent Schwartz,[1] in developing a mathematical system in which differentiation is commutative with integration, is of great practical importance, as it enables the operational methods of Heaviside to be verified and usefully extended. Schwartz has generalized the concept of a "function" by considering it to be represented by a distribution of mass, and he has thus been able to interpret such discontinuous expressions as the Dirac function and its derivatives in ways not previously permitted by classical mathematics. These ideas provide a rigorous mathematical basis for the intuitive methods of Heaviside.

Differentiation and Integration Noncommutative

The beginning student of calculus learns that taking the derivative of a function is a "many-to-one" process. No matter what the value of the constant term, A, is, the derivative of $f(x)—A$ has the same value, $f'(x)$

$$\frac{d}{dx}(f(x)-A)=f'(x) \qquad (1)$$

He also learns that integration between fixed limits is a "one-to-one" process. With a given lower limit of integration, B, the equation

$$\int_B^x f'(x)dx=f(x)-f(B) \qquad (2)$$

is always true.

He thus comes to realize that differentiation is not always commutative with (the inverse of) integration. If we first differentiate $f(x)—A$, and then integrate the result, we get $f(x)—f(B)$

$$\int_B^x dx\frac{d}{dx}(f(x)-A)=\int_B^x f'(x)dx=f(x)-f(B) \qquad (3)$$

If we first integrate $f(x)—A$ and then differentiate the result, we obtain $f(x)—A$ again

$$\frac{d}{dx}\int_B^x(f(x)-A)dx=\frac{d}{dx}\left[\int_B^x f(x)dx-A(x-B)\right]=f(x)-A \qquad (4)$$

One consequence of this state of affairs is that solving the differential equation representing any physical problem requires finding the appropriate integration constants. In complex problems, this sometimes presents real difficulties, besides being a time-consuming process.

A little study of equations 3 and 4 shows that integration will be the reverse of differentiation, if $A=f(B)$. Practically, this requires

$$A=f(B)=0 \qquad (5)$$

It will be found that differentiation and integration are always commutative if the function vanishes at the lower limit of integration.

Heaviside's Methods

Heaviside introduced his unit function, H, or

$$\begin{aligned}1=H(t,\ t_0)&=1 \text{ if } t>t_0\\ &=0 \text{ if } t<t_0\end{aligned} \qquad (6)$$

for convenience in treating sudden changes in the physical conditions, such as a suddenlv applied voltage at $t=t_0$. This same function, however, may be employed as a "cut-off" to reduce any function arbitrarily to zero previous to a desired moment. We may write

$$\begin{aligned}H(t,t_0)f(t)&=f(t) \text{ if } t>t_0\\ &=0 \quad \text{if } t<t_0\end{aligned} \qquad (7)$$

Or, we may assume $t_0=0$, and abbreviate equation 7 to the simple form

$$\begin{aligned}Hf(x)&=f(t) \text{ if } t>0\\ &=0 \quad \text{if } t<0\end{aligned} \qquad (8)$$

Heaviside also denoted the differential operator, d/dt, by p, also using its inverse, p^{-1}, to define the integration process. This we regard as merely a convenience in writing. In this paper, we retain d/dt to emphasize that the substitution of p is purely a matter of convention.

Heaviside[2] states:

> "The reader may have observed . . . . . that we change the order of operators at convenience, as in
>
> $$(p)g(p)1=g(p)f(p)1 \qquad (9)$$
>
> and that it goes. But I do not assert the universal validity of this obviously suggested transformation. It has, however, a very wide application, and transforms functions in a remarkable manner. Reservations should be learned by experience."

The classical objection to this statement of Heaviside is given by the following example.* Let $f(p)=p^m$, representing m successive differentiations, and $g(p)=p^{-n}$, representing n successive integrations.

Then, it is reasoned

$$p^m1=\frac{d^m1}{dt^m}=0 \qquad (10)$$

Paper 49-184, recommended by the AIEE Basic Sciences Committee and approved by the AIEE Technical Program Committee for presentation at the AIEE Summer General Meeting, Swampscott, Mass., June 20-24, 1949. Manuscript submitted March 23, 1949; made available for printing May 3, 1949.

J. J. Smith and P. L. Alger are with the General Electric Company, Schenectady, N. Y.

* It should be noted that in this paper we consider only whole integrations and differentiations. Fractional differentiation will be considered in a subsequent paper.

$$p^{-n}1=\int^{t}\int\int_{n}\int\ldots 1\,dt^{n}=\frac{t^{n}}{(n)!} \qquad (10A)$$

if we consider only values of t greater than zero, for which the unit function is unity.

From equations 10 and 10(A), if $m<n$

$$f(p)g(p)1=p^{-(n-m)}1=\frac{t^{n-m}}{(n-m)!} \qquad (11)$$

Or, if $m>n$

$$f(p)g(p)1=p^{m-n}1=0$$

But, for all values of m and n

$$g(p)f(p)1=0$$

since when the differentiation is performed first, the zero answer of equation 10 is not changed by subsequent operations.

The reply to this objection is that classical mathematics leaves out of consideration the discontinuity of the unit function 1 at $t=0$, on the assumption that the derivative does not exist at such a point.

The discrepancies are cleared up if this derivative is properly interpreted, as will be seen in the discussion following equation 19. Thus, the use of the unit function, while solving the problem of making differentiation and integration generally reversible, introduces the new problem of taking discontinuities into account. Schwartz now has provided the solution for this second problem.

The Contribution of Schwartz

Schwartz states in the introduction of his 1945 paper:

> "Since the introduction of operational calculus, physicists have commonly employed certain concepts, or certain formulas, whose success has been incontestable, even though they were not justified mathematically. Thus, the function $H\ (t)$ of the real variable t, equal to zero for $t<0$, to one for $t>0$, is usually considered as having for its derivative the 'Dirac function,' $H'(t)=\delta(t)$, that is zero for $t\neq 0$, equal to $+\infty$ for $x=0$, and is such that, besides
>
> $$\int_{-\infty}^{\infty}\delta(t)dt=+1 \qquad (12)$$
>
> "Such an 'abuse of language' is entirely incompatible with the usual concept of a function and its derivative! And what should we think of considering successive derivatives of the Dirac function!"

The essence of the Schwartz method lies in considering the Dirac function as being represented by a unit mass placed at the origin, giving it a physical reality in "mass space." By conducting the desired mathematical operations in this mass space, and then transforming the result back into function space, he avoids any direct dealing with infinities.

Schwartz considers a set of continuous infinitely differentiable functions that are zero outside of a finite interval, that is, functions $\phi(t)$, such that

$$\begin{aligned}\phi(t)&=0 \text{ if } t<-k_1\\ &=0 \text{ if } t>+k_2\end{aligned} \qquad (13)$$

He multiplies the function $f(t)$, with which it is desired to deal, by $\phi(t)$, and integrates from $-\infty$ to ∞, calling the result a "functional," $f(\phi)$

$$f(\phi)=\int_{-\infty}^{\infty}f(t)\phi(t)dt \qquad (14)$$

Then $f(\phi)$ is the representation of $f(t)$ in mass space, where $\phi(t)$ is any function satisfying the conditions stated above. Inversely, if the right-hand side is obtained as the representation in mass space, then the function it represents is $f(t)$.

Similarly, replacing f by f', the representation of the derivative in mass space, if f' exists, is

$$f'(\phi)=\int_{-\infty}^{\infty}f'(t)\phi(t)dt \qquad (15)$$

Integrating equation 15 by parts, we obtain

$$\int_{-\infty}^{\infty}f'(t)\phi(t)dt=[f(t)\phi(t)]_{-\infty}^{\infty}-\int_{-\infty}^{\infty}f(t)\phi'(t)dt \qquad (16)$$

By equation 13, however, $\phi(t)=0$ at both ∞ and $-\infty$, so that the first term on the right-hand side of equation 16 drops out, leaving

$$\int_{-\infty}^{\infty}f'(t)\phi(t)dt=-\int_{-\infty}^{\infty}f(t)\phi'(t)dt$$

or

$$f'(\phi)=-f(\phi') \qquad (17)$$

The above is straightforward when $f(t)$ is continuous and $f'(t)$ exists. When $f(t)$ is not continuous, $f'(t)$ "does not exist" at the point of discontinuity. However, $df(t)$ does exist in general at this point and is equal to the jump or "saltus" of $f(t)$ at this point. In such cases Schwartz replaces the Riemann integral in equation 15 by the Stieltjes integral

$$f'(\phi)=\int_{-\infty}^{\infty}\phi(t)df(t) \qquad (18)$$

and, by integrating by parts as before, it is found that

$$f'(\phi)=-f(\phi') \qquad (17)$$

Thus equation 17 holds not only when $f(t)$ is continuous but also when it is discontinuous.

As an example, we may find the representation $\delta(\phi)$ of the Dirac function $\delta(t)$ in mass space. Putting H for $f(t)$ in equation 17 we have

$$\begin{aligned}\delta(\phi)=H'(\phi)=-H(\phi')&=-\int_{-\infty}^{\infty}H(t)\phi'(t)dt\\ &=-\int^{\infty}\phi'(t)dt=\phi(0)\end{aligned} \qquad (19)$$

This is the same result that is obtained if $f(t)$ is put equal to H in equation 18 so that $df(t)=dH$ has the value unity (unit mass) at the origin and zero elsewhere and the integration carried out. Thus the Dirac function is represented in mass space by $\phi(0)$ and it also corresponds to a unit mass dH placed at the origin. Similarly, we find

$$-\delta'(\phi)=\phi'(0)$$

and

$$(-1)^{n}\delta^{(n-1)}\phi=\phi^{(n-1)}(0)$$

Schwartz then shows that $\phi'(0)$ can be interpreted as a unit doublet at the origin and gives similar interpretations for $\phi''(0)\ldots\ldots\phi^{(n)}(0)$.

It now is evident in connection with equation 11 that putting $p^{m-n}1=0$ ignores the discontinuity at $t=0$ and that its representation in mass space is $\phi^{(m-n-1)}(0)$, in which form it is available for subsequent operations.

Since engineers are better acquainted with the Riemann integral, it may be of interest to indicate how Heaviside's use of the impulse function or its equivalent, the Dirac function, would give the same result; subject, of course, to the limitation that some of the steps may not exist in the strict mathematical sense. In this case, we would write $\delta(t)$ for $f(t)$ in equation 14 and obtain

$$\delta(\phi)=\int_{-\infty}^{\infty}\delta(t)\phi(t)dt=\phi(0) \qquad (20)$$

on making the usual assumption that $\delta(t)$ is zero everywhere except at $t=0$ where it is infinite in such a manner that its integral from $0-\epsilon$ to $0+\epsilon$ is equal to unity.

Application to a First-Order Differential Equation

To illustrate the application to differential equations, a simple example will be taken so that the procedure will be clear. The problem will be solved by three methods so that similarities and differences between methods will be apparent:

1. Ordinary mathematical method.
2. Heaviside method.
3. The Schwartz transformation method.

The problem to be solved is:

A voltage E is applied at the time $t=0$ to a circuit containing resistance R and inductance L in series. The current in the circuit is zero when $t<0$. Find the current when $t>0$.

ORDINARY MATHEMATICAL METHOD

In the ordinary method of solution we write

$$L\frac{di}{dt}+Ri=E \tag{21}$$

This is the basic form of a linear differential equation of the first order and first degree. The standard mathematical method gives the following solution, which involves the constants of integration C and C_1 which have to be determined.

$$i=C+C_1\epsilon^{-Rt/L} \tag{22}$$

From this, when $t=\infty$ we reason, that $di/dt=0$ and hence

$$C=E/R \tag{23}$$

It then is reasoned that since energy is stored in the inductance and we cannot have an instantaneous change of energy, which would require infinite voltage, i must be the same immediately before and after $t=0$, and thus, from equation 22 and the initial conditions

$$C=-C_1 \tag{24}$$

From this

$$i=E(1-\epsilon^{-Rt/L})/R \tag{25}$$

when $t>0$

and we were given as one of the conditions of the problem that

$$i=0 \tag{26}$$

when $t<0$

In this method of solution it will be noted that we had to determine the value of i at $t=0+\epsilon$ by an additional fact, such as the energy consideration above, which was not contained in the original statement of the problem. While this may not have been difficult in the above case, it does become a problem for an equation of the nth order, where n constants of integration have to be evaluated.

HEAVISIDE METHOD

In the Heaviside method we note, first, that it is given that the voltage and current are zero when $t<0$. To ensure this we introduce the Heaviside unit function and write the current in the form iH and the voltage in the form EH, where, for convenience in writing, H is the Heaviside unit function whose value is zero when $t<0$ and is equal to unity when $t>0$, equation 8.

We therefore write the equation in the form

$$L\frac{d}{dt}(iH)+RiH=EH \tag{27}$$

and take the solution for this to be

$$iH=(C+C_1\epsilon^{-Rt/L})H \tag{28}$$

where $-\infty<t<\infty$ and the presence of H ensures that the current is zero when $t<0$. Substituting this value of iH in equation 27, two of the terms cancel out, and we obtain

$$CRH+(C+C_1\epsilon^{-Rt/L})LH'=EH \tag{29}$$

where $H'=dH/dt$. This equation is really two separate equations, one including all terms having the factor H and the other including all terms having the factor H'. By equation 12, H' is zero at all values of t except $t=0$. Thus, when $t\neq 0$ equation 29 still must be valid after the terms including H' are removed. Therefore, taking the terms involving H only gives

$$C=E/R \tag{30}$$

and taking the terms involving H' only gives

$$(C+C_1\epsilon^{-Rt/L})H'=0 \tag{31}$$

From this the coefficient of H' must be zero when $t=0$, since for this value of t, H' is not equal to zero. Hence

$$C+C_1\epsilon^{-Rt/L}=0 \tag{32}$$

when $t=0$, or

$$C=-C_1 \tag{33}$$

Substituting equations 30 and 33 in equation 28 we obtain

$$iH=E(1-\epsilon^{-Rt/L})H/R \tag{34}$$

The difficulty with the above method is, of course, that H' is not a function in the accepted sense of the word. $H'=0$ when $t\neq 0$, but when $t=0$ it must be infinite in such a way that its integral

$$\int_{-\epsilon}^{0+\epsilon}H'dt=1$$

For this latter reason, the mathematicians say "it does not exist at $t=0$." This impasse can be overcome readily by the method of Schwartz, by carrying out our operations in mass space where the counterpart of H' remains finite and interpretable. Having thus detoured around the use of H', we transfer back from the mass space to the function space and find the result checks exactly with that given, using the straight Heaviside method, as will be illustrated now.

SCHWARTZ TRANSFORMATION METHOD

Let us now consider the same problem using the methods developed by Schwartz. We start with the same equation

$$L\frac{d}{dt}(iH)+RiH=EH \tag{35}$$

Assume as before a solution of the form

$$iH=(C+C_1\epsilon^{-Rt/L})H \tag{36}$$

Then the representation of iH in mass space is, from equation 14

$$\int_{-\infty}^{\infty}iH\phi(t)dt=\int_{-\infty}^{\infty}(C+C_1\epsilon^{-Rt/L})H\phi(t)dt$$
$$=\int^{\infty}(C+C_1\epsilon^{-Rt/L})\phi(t)dt \tag{37}$$

and from equation 17, $d(iH)/dt$ is represented in mass space by

$$-\int_{-\infty}^{\infty}iH\phi'(t)dt=-\int_{-\infty}^{\infty}(C+C_1\epsilon^{-Rt/L})\times$$
$$H\phi'(t)dt=-\int_0^{\infty}(C+C_1\epsilon^{-Rt/L})\phi'(t)dt \tag{37A}$$

which, by equation 16, reduces to

$$-\int_{-\infty}^{\infty}iH\phi'(t)dt=(C+C_1)\phi(0)-$$
$$\int_0^{\infty}\frac{C_1R}{L}\epsilon^{-Rt/L}\phi(t)dt \tag{38}$$

Similarly, EH is represented in mass space by

$$\int_{-\infty}^{\infty}EH\phi(t)dt=\int_0^{\infty}E\phi(t)dt \tag{39}$$

Substituting these representations in mass space in the differential equation 35 we get

$$L(C+C_1)\phi(0)-\int_0^{\infty}C_1R\epsilon^{-Rt/L}\phi(t)dt+$$
$$\int_0^{\infty}R(C+C_1\epsilon^{-Rt/L})\phi(t)dt=\int_0^{\infty}E\phi(t)dt \tag{40}$$

This gives

$$L(C+C_1)\phi(0)+\int_0^{\infty}(CR-E)\phi(t)dt=0 \tag{41}$$

Now

$$\int_0^{\infty}(CR-E)\phi(t)dt=\int_{-\infty}^{\infty}(CR-E)H\phi(t)dt$$

is the representation in mass space of $(CR-E)H$ for all values of t, while $\phi(0)$ corresponds to a unit mass placed at the origin and zero mass elsewhere, and is the representation in mass space of the derivative of the unit function as shown by Schwartz, equation 19. Thus we have

$$CR-E=0 \tag{42}$$

Substituting this in equation 41, since $\phi(0)$ represents a unit mass at $t=0$

$$C+C_1=0 \tag{43}$$

Substituting the values of C and C_1 from equations 42 and 43 in equation 36, we find as before, in equation 34

$$iH=E(1-\epsilon^{-Rt/L})H/R \tag{44}$$

DISCUSSION OF THREE METHODS

The results obtained in equations 34 and 44 are fundamental in connection with the Heaviside operational calculus. They say that when the equation for the current is written in the form

$$L\frac{d}{dt}(iH)+RiH=EH \tag{45}$$

this equation has one and only one solution given by

$$iH=E(1-\epsilon^{-Rt/L})H/R \tag{46}$$

This comes about by recognizing that when the value of the current is substituted in the differential equation, and considering H as a function of time t, there can be no terms of the form H' or its representation in mass space on the left-hand side of the equation if there are no terms of this form on the right-hand side. This allows us to conclude from equations 29 or 40

$$C=-C_1 \tag{47}$$

In this method of solution it will be noted that it is not necessary to introduce the condition that $i=0$ when $t=0+\epsilon$ as well as when $t=0-\epsilon$, which was required in the solution by the ordinary mathematical method in equations 21 to 26. In view of the emphasis usually placed in standard mathematical procedure on the determination of necessary and sufficient conditions for a problem, it would appear that the Heaviside and Schwartz method of solution are more powerful than the ordinary mathematical method, since they do not require this added condition $i=0$ when $t=0+\epsilon$.

Application to a Second-Order Differential Equation

Before proceeding to an nth order differential equation, it may be of interest to consider a second-order differential equation from a slightly different viewpoint. As an example, we shall consider the well-known Heaviside operational expression

$$\frac{p^2}{p^2+\omega^2}H=\cos\omega tH \tag{48}$$

If we were not given the result, we could evaluate the operational expression on the left-hand side by writing it equal to iH as follows

$$iH=\frac{p^2}{p^2+\omega^2}H \tag{49}$$

This can be written in the form of a differential equation on putting $p=d/dt$

$$\frac{d^2}{dt^2}(iH)+\omega^2iH=\frac{d^2H}{dt^2} \tag{50}$$

Here, of course, we are in trouble immediately because d^2H/dt^2 is not a "function." Let us proceed, however, in the Heaviside method to assume a solution

$$iH=(C_1+C_2\sin\omega t+C_3\cos\omega t)H \tag{51}$$

We then can write formally in the Heaviside manner

$$\frac{d}{dt}(iH)=(\omega C_2\cos\omega t-\omega C_3\sin\omega t)H+(C_1+C_3)H' \tag{52}$$

where the coefficient of H' is the value of $(C_1+C_2\sin\omega t+C_3\cos\omega t)$ at $t=0$. Differentiating again

$$\frac{d^2}{dt^2}(iH)=-\omega^2(C_2\sin\omega t+C_3\cos\omega t)H+\omega C_2H'+(C_1+C_3)H'' \tag{53}$$

where now the coefficient of H' is the value of $(\omega C_2\cos\omega t-\omega C_3\sin\omega t)$ when $t=0$.

Substituting this value in equation 50 we find

$$\omega C_2H'+(C_1+C_3)H''+\omega^2C_1H=H'' \tag{54}$$

Equating the coefficients of H, H', and H'' on both sides of this equation

$$C_1=0 \tag{55}$$

$$C_2=0 \tag{56}$$

and

$$C_3=1 \tag{57}$$

Thus, substituting in equation 51 we find

$$iH=\cos\omega tH \tag{58}$$

as the solution of equation 50, and hence we verify the value of the Heaviside operational expression, equation 48.

Let us now apply the Schwartz method in solving this problem. From equations 14 and 51 the representation of iH in mass space is

$$\int_{-\infty}^{\infty}iH\phi(t)dt=\int_{-\infty}^{\infty}(C_1+C_2\sin\omega t+C_3\cos\omega t)H\phi(t)dt=\int_0^{\infty}(C_1+C_2\times\sin\omega t+C_3\cos\omega t)\phi(t)dt \tag{59}$$

and $\frac{d^2}{dt^2}(iH)$ is represented in mass space by

$$\begin{aligned}\int_{-\infty}^{\infty}iH\phi''(t)dt&=\int_0^{\infty}(C_1+C_2\sin\omega t+C_3\cos\omega t)\phi''(t)dt\\&=-(C_1+C_3)\phi'(0)-\int_0^{\infty}\omega(C_2\cos\omega t-C_3\sin\omega t)\phi'(t)dt\\&=-(C_1+C_3)\phi'(0)+\omega C_2\phi(0)-\int_0^{\infty}\omega^2\times(C_2\sin\omega t+C_3\cos\omega t)\phi(t)dt\end{aligned} \tag{60}$$

where, in the second line, the coefficient of $\phi'(0)$ is the value of $(C_1+C_2\sin\omega t+C_3\cos\omega t)$ at $t=0$, and in the third line, the coefficient of $\phi(0)$ is the value of $(C_2\cos\omega t-C_3\sin\omega t)$ when $t=0$.

Since, as we have already pointed out, d^2H/dt^2 "does not exist as a function," we are in difficulty with the right-hand side of equation 50. However, we may choose to recognize it as the second derivative of the unit function, and although "it does not exist as a function," its representation in mass space does exist and is equal to

$$\int_{-\infty}^{\infty}H\phi''(t)dt=\int_0^{\infty}\phi''(t)dt=-\phi'(0) \tag{61}$$

Now substitute the mass representations given by equations 59, 60, and 61 in the differential equation 50 and obtain

$$-(C_1+C_3)\phi'(0)+\omega C_2\phi(0)-\int_0^{\infty}\omega^2(C_2\sin\omega t+C_3\cos\omega t)\phi(t)dt+\int_0^{\infty}\omega^2(C_1+C_2\sin\omega t+C_3\cos\omega t)\phi(t)dt=-\phi'(0) \tag{62}$$

In this equation we equate the parts under the integral sign and the coefficients* of $\phi(0)$ and $\phi'(0)$ on each side of the equation and obtain

$$\omega^2C_1=0 \tag{63}$$

$$\omega C_2=0 \tag{64}$$

and

$$C_1+C_3=1 \tag{65}$$

Hence

$$C_3=1 \tag{66}$$

as in equation 57 and, substituting in equation 51, we obtain

$$iH=\cos\omega tH \tag{67}$$

as in equation 58.

Application to an nth-Order Differential Equation

We may apply the above method to an nth-order equation

$$\sum_n a_n\frac{d^n}{dt^n}(iH)=EH \tag{68}$$

and assume a solution for it of the form

$$iH=\left(C_0+\sum_n C_n\epsilon^{-\alpha_nt}\right)H \tag{69}$$

where the α_n are determined in the usual manner. Substituting this in equation 68 we obtain $n+1$ equations by equating the coefficients of $H', H'', \ldots .H^{(n)}$ on each side of the equation, and from these the unknown constants can be determined. The difficulties associated with the use of $H', H'', \ldots .H^{(n)}$ can be avoided, of course, by using the Schwartz transformation method.

---

* The reason for equating the coefficients of $\phi(0)$ and $\phi'(0)$ separately is that $\phi(0)$ corresponds to a unit mass at $t=0$ and $\phi'(0)$ corresponds to a doublet at $t=0$.

This becomes a lengthy operation when n even exceeds two, and would involve an infinite set of equations when $n=\infty$, as it does in the solution of partial differential equations. The Heaviside expansion theorem is a very skillful way of getting around this difficulty, as we shall show now.

It has been seen that the values of the unknown constants in equations 28 or 36 can be obtained directly from the differential equations 27 or 35, and that no other assumptions have to be made in order to solve it. Since the information given in equations 27 or 35 by the introduction of H ensures that it has one and only one solution, we can assign a meaning to the equation when written in the form

$$iH=\frac{E}{L\frac{d}{dt}+R}H \tag{70}$$

To evaluate this expression for i, we simply rearrange in the form of equations 27 or 35 and solve this differential equation as shown and arrive at the solution in equations 34 or 44. From this we can write

$$\frac{E}{L\frac{d}{dt}+R}H=E(1-\epsilon^{-Rt/L})H/R \tag{71}$$

We may add n such terms together and get

$$\sum_n \frac{E}{L_n\frac{d}{dt}+R_n}H=\sum_n E(1-\epsilon^{-R_nt/L_n})H/R_n \tag{72}$$

We may add all the quantities on the left-hand side of this equation to get the quotient of two operators acting on H which we may write

$$\frac{\sum_n b_{n-1}\frac{d^{n-1}}{dt^{n-1}}}{\sum_n a_n\frac{d}{dt^n}}EH=\sum_n \frac{E}{L_n\frac{d}{dt}+R_n}H$$
$$=\sum_n E(1-\epsilon^{-R_nt/L_n})H/R_n \tag{73}$$

These three steps, in the order shown, are equivalent in reverse order to those used by Heaviside in the development of his expansion theorem. Using his terminology, replacing d/dt by p, he wrote[3]

$$iH=\frac{Y(p)}{Z(p)}EH=\sum_n \frac{Y(p_n)}{\left[p\frac{dZ}{dp}\right]_{p=p_n}}\frac{1}{p-p_n}H$$
$$=\frac{Y(0)}{Z(0)}H+\sum_n \frac{Y(p_n)\epsilon^{p_nt}}{\left[p\frac{dZ}{dp}\right]_{p=p_n}}H \tag{74}$$

Thus, by expanding in partial fractions we break the solution of a differential equation of the nth order up into the solution of n equations of the first order, whose solution has been found already in equations 34 and 44, and thus we avoid writing a general solution for the nth degree equation and then finding the values of $n+1$ constants in equation 69.

Application to Differential Equations of Infinite Order and Partial Differential Equations

This idea can be extended to differential equations of infinite order such as, for instance, a typical form shown by[4]

$$vH=\frac{\sinh\,(l-x)\sqrt{RS\frac{d}{dt}}}{\sinh\,l\sqrt{RS\frac{d}{dt}}}EH$$
$$=E\left(1-\frac{x}{l}\right)H-\frac{2E}{\pi}\times$$
$$\sum_{n=1}^{n=\infty}\frac{\sin\frac{n\pi x}{l}\epsilon^{-(n^2\pi^2t/RSl^2)}H}{n} \tag{75}$$

Such differential equations of infinite order arise naturally in one method of solution of the partial differential equations of mathematical physics. The introduction of H gives directly the coefficients of the functions in the resulting Fourier series or integrals, without the necessity of assuming a series with an infinite number of unknown constants and later determining these constants by methods similar to those involved in the use of Fourier's theorem. An extensive application employing this method will be found in a paper by one of the authors.[5]

In that paper are derived solutions of the differential equations of mathematical physics corresponding to Poisson's equation, the equation of heat conduction, Maxwell's wave equation, and the wave equation in a dissipative medium. These solutions are given in generalized orthogonal co-ordinates. To use them for a particular problem, it is only necessary to substitute in them the appropriate function, sine or cosine, or the Bessel functions, or the Legendre functions, and so forth, to get the final solution, which has checked in all cases tried with that given in the literature. Tables of such solutions for Green's functions for rectangular co-ordinates were presented at the AIEE winter meeting in 1949.

The method used in the Journal of the Franklin Institute paper[5] is based directly on the use of the impulse function where necessary, since the Schwartz method was not available at that time. It will be found that the use of the impulse function can be avoided by using the Schwartz method, which will lead to the same results given in that paper. Since this application of the Schwartz method is relatively easy, we refer the reader to that paper for more details as to the method of application to partial differential equations.

Application of Method to Given Initial Conditions

Since sometimes it is stated that the Heaviside method cannot be applied to problems where given initial conditions have to be met, it may be well to point out that this is not so and to indicate how such problems can be solved. Many such examples will be found worked out in chapter one of Jeffreys' book[7] using a different notation. To use it in the case of the simple example already discussed, we reformulate the problem stated on page 7 of reference 7 as follows:

> A voltage E is applied at the time $t=0$ to a circuit containing resistance R and inductance L in series. The current in the circuit is zero when $t<0$. At $t=0+\epsilon$ the current is i_0. Find the current when $t>0$.

We can write as before

$$L\frac{d}{dt}(iH)+RiH=EH \tag{76}$$

when $t<0$ and $t>0$. It must be noted that we now restrict the validity of this equation to the region $t<0$ and $t>0$, since the introduction of the terminal condition $i=i_0$ when $t=0+\epsilon$ means that it cannot hold at $t=0$. To introduce the terminal condition $i=i_0$ when $t=0+\epsilon$, integrate from $-\infty$ to t and obtain

$$LiH+R\int_0^t iHd\ =EtH+Li_0H \tag{77}$$

when $-\infty<t<\infty$. Then this equation incorporates all the given conditions of the problem and is valid from $-\infty$ to ∞.

Either the Heaviside or the Schwartz method can be used to solve it along the lines given in the previous example. In both of these methods we start with the solution in equation 28 and substitute in the integro-differential equation 77. It then will be found that by differentiating once, the equation reduces to one involving H and H' in the Heaviside method, and we obtain the values of the constants C_1 and C_2 as before, subject, of course, to the difficulties inherent in the use of H'. In the Schwartz method we get a representation in mass space consisting of two terms, one being an integral from $-\infty$ to ∞ and the other involving $\phi(0)$. By equating the coefficients of these two terms as before, we get the required result

$$iH=\frac{E}{R}(1-\epsilon^{-Rt/L})H+i_0H\epsilon^{-Rt/L} \tag{78}$$

It may be well to point out that in the Heaviside manner we find by differentiating equation 77 that this is the solution of

$$L\frac{d}{dt}(iH)+RiH=EH+Li_0H' \tag{79}$$

when $-\infty<t<\infty$. Thus equation 76 requires the addition of an impulse-function term to make it valid from $-\infty$ to ∞. Furthermore, equation 78 is the only solution of equation 79, just as equation 46 is the only solution of equation 45. There is no conflict between these statements.

Conclusion

In the paper we have emphasized the use of two concepts—the introduction of the Heaviside unit function to ensure that a given expression has the value zero in some parts of the region in which it is defined; the use of the impulse function and its derivatives which arise when we attempt to differentiate the unit function. These seem to the authors to be the ideas which make the operational methods used by Heaviside and others give the results they do.

Some difficulties are encountered in proceeding in this manner, due to the fact that the impulse function and its derivatives are not functions in the accepted mathematical sense of the word. The method of Schwartz is introduced; this permits us to take practically identical steps with those taken in the Heaviside approach. However, since the operations are carried out in mass space, no infinities are encountered and the results are put on a sound mathematical basis.

Some authors view the operational calculus as a method based upon substituting p for d/dt and then treating p as if it were a number. The point of view presented here considers that the substitution of p for d/dt is just a convenience in writing, and in order to emphasize this, no use has been made of p in this paper.

We have endeavored to focus attention on the other concept used by Heaviside, his unit function 1, for which we have used the symbol H. It is, perhaps, unfortunate that Heaviside, after explaining his unit function and its use, then decided that for brevity's sake he would omit it from the equations. If he had written it in the equations continually, its presence would have aroused curiosity, and its importance would have been better understood. In this paper we have tried carefully to be sure that in all the equations where a function of d/dt arises, it acts on an operand which is multiplied by H. If any are found which do not conform to this pattern they are oversights.

Other authors approach the operational calculus from the point of view of the Laplace transformation. In a certain sense the Schwartz method may be regarded as a generalization of the Laplace transform

$$\int_0^\infty \epsilon^{-ax}f(x)dx$$

in which the function $\phi(t)$ replaces the exponential factor and the limits of integration are extended throughout the range of the function $\phi(t)$ rather than from zero to infinity. It goes much further than this, however, as it gives us a method of interpreting the derivative of any order of a discontinuous function. Furthermore, on account of the general character of $\phi(t)$, it can be used with many types of functions—Bessel, Legendre functions, and so forth, and their associated differential equations; whereas the Laplace transform is intimately tied in to the exponential function and its associated linear differential equation with constant coefficients of the first degree and nth order.

By the introduction of H we obtain a system in which integral and differential operations are reversible. This comes about due to the fact that when H is suitably introduced into the differential equations and the differential and integral operations are performed, there results an equation of the form

$$\sum_{n=0}^{n=p}a_n\frac{d^nH}{dt^n}=\sum_{n=0}^{n=p}b_n\frac{d^nH}{dt^n} \tag{80}$$

in the Heaviside method or an equation of the form

$$a_0\int_{-\infty}^{\infty}f(t)\phi(t)dt+\sum_{n=1}^{n=p}a_n\phi^{(n-1)}(0)$$
$$=b_0\int_{-\infty}^{\infty}f(t)\phi(t)dt+\sum_{n=1}^{n=p}b_n\phi^{(n-1)}(0) \tag{81}$$

in the Schwartz method.

From this we can conclude that the coefficients of the nth derivative of H on each side of the equation are equal in the Heaviside method, while in the Schwartz method $a_0=b_0$ and the coefficients of $\phi^n(0)$ on each side of the equation are equal, so that

$$a_0=b_0$$
$$a_1=b_1$$
$$\cdots\cdots$$
$$a_n=b_n \tag{82}$$

This is quite analogous to the case of the complex variable where if x,y,a, and b are real and we are given

$$x+iy=a+ib \tag{83}$$

we can conclude that

$$x=a,\ y=b \tag{84}$$

The methods in this paper follow very closely the ideas expressed by Heaviside in the following quotation,[6] which seems an appropriate one with which to conclude:

> "It may be remembered that I have insisted on the definiteness and fullness of the meaning of an operational solution, and that it contains within itself not only the full statement of the problem, but also its solution. No external aid is therefore required to algebrise it fully; no assumption, for instance, of a special type of solution and that the solution is the sum of a number of that type with subsequent determination of the constants required to complete the matter. The work of satisfying the imposed conditions has been done already."

References

1. Generalization de la Notion de Function, de Derivation, etc., **L. Schwartz.** *Annales*, l'Universite de Grenoble, volume 21, 1945, page 57. Also, *Annales des Telecommunications*, (Grenoble, France) volume 3, number 4, April 1948, pages 1–6.

2. Electromagnetic Theory (book), **Heaviside.** Benn Brothers, Ltd. (London, England), volume 2, 1922, page 59.

3. Electrical Papers (book), **Heaviside.** Copley Publishers (Boston, Mass.), volume 2, page 226, equation 163, 1925.

4. Electromagnetic Theory (book), **Heaviside.** Benn Brothers, Ltd. (London, England), volume 2, page 139, equation 43, 1922.

5. The Extension of the Heaviside Expansion Theorem to the Equations of Engineering and Physics in Curvilinear Orthogonal Coordinates, **J. J. Smith.** *Journal*, Franklin Institute (Philadelphia, Pa.), volume 238, October 1944, page 245.

6. Electromagnetic Theory (book), **Heaviside.** Volume 2, page 122, paragraph 280.

7. Operational Methods in Mathematical Physics (book), **H. Jeffreys.** Cambridge University Press (Cambridge, England), 1927.

Discussion

P. A. Abetti (General Electric Company, Pittsfield, Mass): The authors are to be commended for their derivation of Heaviside's operational calculus which, among the many attempted so far, is mathematically rigorous, physically simple, and closely related throughout to Heaviside's own work. In fact, if we consider the simple applications to first and second order differential equations, we find a complete equivalence of every step of the Schwartz method with every step of the Heaviside method. For instance, in the section in the paper on second order differential equations, the following equations are equivalent: 59 to 51; 60 to 53; 62 to 54; 63 to 55; 64 to 56; 66 to 57; 67 to 58.

It will be recognized, however, that the equations 51 to 54 are simpler in form and easier to manipulate than equations 59 to 62, which contain infinite integrals and the minus signs introduced by equation 17. On the other hand, the Schwartz transformation equations are mathematically rigorous in the mass space, while the derivatives H', H'' of the unit function "do not exist" mathematically at the point of discontinuity and are zero elsewhere, so that the legitimacy of equations 50 to 54 is extremely doubtful.

It appears that a compromise between the rigorousness of the Schwartz method and the simplicity and elegance of the Heaviside would be very useful, especially for those who are concerned with the operational methods as working tools. Such a compromise may be obtained easily by writing all steps of the solution in the Heaviside manner, but adding a special symbol, say Ⓜ or Ⓢ, whenever derivatives of the unit function appear, to indicate that the operations take place in the mass space, or in the field of the Schwartz transform, and are therefore rigorous and legitimate.

Mr. Alger and Mr. Smith also must be commended, for psychological reasons, for having written d/dt instead of p everywhere in their paper. In fact, let us consider the reactions of the layman, practical engineer or student, to the introduction of the operational calculus in his daily work, as specified by Angelini.[1]

1. Some find the operational calculus very useful in its application to practical problems, especially in the electrical field.

2. Others do not believe that it is worthwhile to employ operational methods, either because they find no occasion in which these might be useful, or else because such occasions appear so seldom in their work that they consider the effort necessary to learn these new methods of calculation out of proportion with the limited use they would have for them.

3. Others finally are disappointed and puzzled by the many different aspects under which the operational calculus is presented to them, by the lack of mathematical rigour and ensuing pitfalls of some methods, and sometimes by the opinion of some mathematicians on the subject. They renounce therefore to learn and to employ the operational methods and make use, whenever necessary, of the classical methods of analysis.

Concentrating our attention to the last group, and eventually also to the second, and especially to those who have not yet formed their opinion on the subject, the operational methods may be presented to all these groups with emphasis on either one of the following two points wherein they basically differ from the classical ones:

1. The completeness of the solution which incorporates the initial conditions and eliminates the integration constants of the classical methods.

2. The "symbolic" property of writing p (or any other letter) for the operator d/dt, and treating this symbol as any other algebraic quantity.

Any person who has used the classical methods and wrangled with the calculations of several integration constants, will appreciate the great advantages of point 1 above. Very few engineers or students instead, are favorably impressed with point 2 as such, wherein they see no practical advantages for their work, and which they sometimes distrust as "illegitimate" from the standpoint of mathematical rigour. K. W. Wagner[2] attributes to this reason the fact that the first rigorous approach to operational methods contained in two very remarkable papers[3,4] written by Giorgi as far back as 1904–05, has found such poor reception among engineers.

The only point in the paper Messrs. Alger and Smith wrote which might draw the suspicion of the layman is the appearance of the symbol $\sqrt{RSd/dt}$ in equation 76. However, the introduction of fractional differentiation and integration, as Riemann[5] defined it in 1876, will clear these difficulties and we look forward to the announced paper on this subject.

Giorgi also first realized the great importance of the impulse function, which now, together with its derivatives, finds a legitimate place in the mass space through the transformation of Schwartz.

In view of the fact that the work of Giorgi is little known in this country and was not even quoted among the 84 references of a recent paper[6] on the history of the operational calculus, its accomplishments will be reviewed here.

On the basis of the work of Pincherle[7] and other mathematicians on the properties of distributive operations, Giorgi justifies the application of the algebraic rules to the operator $d/dt = \Delta$ and establishes the limits of their validity.

The operational expression of Giorgi is

$$i(t) = \psi(\Delta)v(t) \tag{1}$$

in which the operator is a function, eventually irrational, of the symbol Δ and $v(t)$ is a "physical" function, that is, which satisfies Dirichlet's conditions. Giorgi interprets equation 1 by resolving the function $v(t)$ in its frequency components by the Fourier integral, applying to each component the operator, and obtains the results by superposition. We arrive thus at a general formula, called "Giorgi's integral," for the evaluation of operational expressions.

For practical applications, instead of using Heaviside's and Carson's "indicial admittance," the response to a unit step function H, Giorgi employs the response to a unit impulse function ΔH, that is, Green's function $g(t)$

$$g(t) = \psi(\Delta)\Delta H \tag{2}$$

The response to the function $v(t)$ is obtained as the sum of the responses to an infinite number of impulse functions in which $v(t)$ has been resolved

$$\psi(\Delta)v(t) = \int_{-\tau}^{+\infty} g(t-\tau)v(\tau)d\tau \tag{3}$$

Changing the variable from $(t - \tau)$ to θ in equation 3 we obtain the equivalent expression

$$\psi(\Delta)v(t) = \int_0^\infty g(\theta v(t-\theta)d\theta \tag{4}$$

Giorgi has proved, even for discontinuous functions, the relation

$$\epsilon^{h\Delta}v(t) = v(t+h) \tag{5}$$

so that equation (4) may be written as

$$\psi(\Delta)v(t) = \int_0^\infty g(\theta)\epsilon^{-\theta\Delta}v(t)d\theta \tag{6}$$

Wherefrom, since equation 6 is valid for any $v(t)$, we obtain

$$\psi(\Delta) = \int_0^\infty g(\theta)\epsilon^{-\theta\Delta}d\theta \tag{7}$$

Under certain conditions, equation 7 expresses the fact that Green's function $g(\theta)$ is the inverse Laplace transform of the operator $\psi(\Delta)$. If instead of Green's function, we write the initial admittance $A(\theta)$ in equation 7 we obtain, since $g(\theta) = \Delta A(\theta)$

$$\frac{1}{\Delta}\psi(\Delta) = \int_0^\infty A(\theta)\epsilon^{-\theta\Delta}d\theta \tag{8}$$

which is the same as the integral used by Carson (1922–26) as the foundation of his approach to operational calculus.

If we consider that these relations which correlate the principal methods of the operational calculus, were obtained as far back as 1905, seven years before Heaviside himself finished his great work and 11 before the appearance of Wagner's and Bronwich's justification of Heaviside's work, we must conclude that Giorgi's work deserves more recognition and study than it has been granted in the past 45 years.

REFERENCES

1. PRINCIPLES AND PRACTICAL VALUE OF THE OPERATIONAL CALCULUS APPLIED TO ELECTRICAL ENGINEERING, **A. M. Angelini**, *Elettrotecnica*, (Milan, Italy), 29 January 1942, pages 1–69.

2. OPERATORENRECHNUNG (OPERATIONAL CALCULUS), **K. W. Wagner**. Johann Ambrosius Barth, (Leipzig, Germany), 1940, page 27.

3. THE SYMBOLIC METHOD IN THE STUDY OF VARIABLE CURRENTS. **G. Giorgi**. *Atti Associazione Elettrotecnica Italiana*, (Milan, Italy) 1904, pages 65–141.

4. ON THE CALCULATION OF FUNCTIONAL SOLUTIONS OF ELECTRODYNAMICAL PROBLEMS. **G. Giorgi**. *Atti Associazione Elettrotecnica Italiana*, (Milan, Italy) 1905, pages 651–99.

5. GESAMMELTE WERKE, **B. Riemann**. (Leipzig, Germany) Edition 1 (1876), page 331; Edition 2 (1892), page 353.

6. THE HISTORY AND PRESENT STATE OF THE OPERATIONAL CALCULUS AS APPLIED IN ELECTRIC CIRCUIT ANALYSIS, **T. J. Higgins**. *Electrical Engineering*, January 1949, pages 42–45.

7. LE OPERAZIONI DISTRIBUTIVE E LE LORO APPLICAZIONI ALL' ANALISI (DISTRIBUTIVE OPERATIONS AND THEIR APPLICATIONS TO ANALYSIS), **S. Pincherle, U. Amaldi**. *U. Zanichelli*, (Bologna, Italy) 1901.

J. J. Smith and **P. L. Alger**: We thank Mr. Abetti for bringing out clearly the equivalence between the equations using the Schwartz method and the Heaviside method.

In writing the paper we started out with the idea of using only the Schwartz method but it became apparent that if this method alone were used the paper would not be easy for engineers accustomed to the Heaviside method to understand. We therefore adopted the compromise of using both the Heaviside method and the Schwartz method on the same problems, so it is hoped the equivalence between the steps in both methods is apparent from this procedure.

While the Schwartz method is simple to use when one is accustomed to it and is more rigorous, nevertheless, it does entail considerably longer expressions than those involved in the Heaviside method. Here, Mr. Abetti makes a good suggestion. He says, why not write, for instance, equation 29 as follows:

$$(C+C_1\epsilon^{-Rt/L})LH'+CRH=EH \qquad Ⓜ \quad (29)$$

$$\text{or} \qquad Ⓢ \quad (29)$$

where the symbol before the number of the equation means (1) the mass space equivalent Ⓜ or (2) the equivalent representation of Schwartz Ⓢ is to be understood. This equation can be translated into the Schwartz terminology by noting that since H' is zero everywhere except when $t=0$, the equation can be written putting $t=0$ in the exponential

$$(C+C_1)LH'+CRH=EH$$

and the mass space representation of this equation is then given by

$$L(C+C_1)\phi(0)+CR\int_{-\infty}^{\infty}H\phi(t)dt=$$

$$E\int_{-\infty}^{\infty}H\phi(t)dt$$

which is equation 41.

In the more general case of the nth order derivative, we have

$$\frac{d^n}{dt^n}(f(t)H)=\sum_{p=0}^{p=n}f^{(p)}(0)H^{(n-p)}$$

in the Heaviside method. Whereas in the Schwartz method taking the representation of $f(t)\ H$ in mass space we have

$$\int_{-\infty}^{\infty}\frac{d^n}{dt^n}\{f(t)H\}\phi(t)dt$$

$$=(-1)^n\int_{-\infty}^{\infty}f(t)H\phi^{(n)}(t)dt$$

$$=(-1)^n\int_{0}^{\infty}f(t)\phi^{(n)}(t)dt$$

$$=\int_{0}^{\infty}f^{(n)}(t)dt+\sum_{p=1}^{p=n}(-1)^{p-1}f^{(p)}(0)$$

$$\phi^{(n-p)}(0) \qquad (9)$$

By comparing these two formulas, any equation written in the Heaviside notation can be rewritten readily in the Schwartz notation by replacing

$f(t)H$ by $\int_{-\infty}^{\infty}f(t)H\phi(t)dt$

$f(0)H'$ by $f(0)\phi(0)$

$f(0)H^{(n)}$ by $(-1)^{n-1}f(0)\phi^{(n)}(0)$

With regard to the symbol $\sqrt{RSd/dt}$ in equation 75, it will be noted that both the numerator and denominator are odd functions of $\sqrt{RSd/dt}$ and thus this term cancels out leaving functions of RSd/dt so that no fractional differentiation is involved in this particular example. However, as mentioned in a footnote, we shall discuss fractional differentiation in a subsequent paper.

With regard to Mr. Abetti's reference to Giorgi's work, there is much to be said in favor of using the response of a system to a unit impulse, rather than the response to a unit function (indicial impedance). The resulting expressions are often much simpler and more symmetrical and in many cases can almost be written down on sight. A close examination of the superposition theorem will show that the differentiation involved in it is really used to derive the response to an impulse function from the indicial impedance and the subsequent integration corresponds to the summation of the effects of a large number of such impulse functions to simulate the given function whose reaction it is required to determine. Of course, the main objection to its use up to now has been the "nonexistence" of the impulse function in the mathematical sense. The introduction of the Schwartz method should rectify this and justify the very elegant derivation of the Laplace integral given by Mr. Abetti. We have given an even simpler derivation in a paper just completed basing it similarly on the properties of the unit function and its derivative.

In connection with this nonexistence in the mathematical sense of H', $H^{(n)}$, and so forth, and which also leads Mr. Abetti to point out "the legitimacy of equations 50 to 54 is extremely doubtful," there may be a possibility of handling such entities in the Heaviside manner without resorting to the Schwartz method. This involves consideration in the Stieltjes manner of the differentials dH, $d^2H, \ldots d^nH$ which exist, rather than the derivatives H', H'', $\ldots$ $H^{(n)}$ which do not exist. It is, perhaps, premature to raise hopes in this respect, although the authors hope to write up some ideas on this in the near future. In the meantime, it might be well if students of engineering were introduced to Stieltjes integrals and functionals so as to be able to study Heaviside's work from these points of view.

Heating of Transformers Under Short-Circuit Conditions

V. M. MONTSINGER
MEMBER AIEE

G. H. HALSEY
ASSOCIATE AIEE

THIS PAPER discusses the effect of turn insulation on the temperature rise and the relative aging of this insulation during the heating and cooling periods. It is shown: that the absorption of heat by the insulation cannot be neglected in accurate calculation of temperature rise; that most of the aging occurs during the cooling period; and that the allowable temperature limit should depend upon the rate of cooling.

This paper gives a formula for calculating temperature rise that allows for the effect of insulation. This formula is easier to use than those given in the ASA C57 Standards for Transformers, Regulators and Reactors.[1] It is pointed out that the present formulas in the standards are cumbersome to use and do not factor the absorption of heat by turn insulation. It is also pointed out that additional work is necessary before any revision of the ASA standards can be undertaken.

General Considerations

For many years, the AIEE transformer standards, and, in more recent years the ASA standards, have specified that short-circuit temperature rises be calculated without allowing for heat storage capacity of the winding insulation. Furthermore, while the standards have made no definite statement about it, it has been the general understanding that the duration of the short-circuit and the ultimate temperature reached are the most important factors to be considered in determining the life of the insulation.

When a short circuit is applied to a winding, all the heat is stored in the copper at the very beginning. As the temperature increases, heat is transferred to the insulation and later to the oil adjacent to the insulation. The insulation may comprise both turn-to-turn and layer-to-layer insulation.

The maximum temperature that is important is that temperature existing in the insulation when the aging starts to be a measurable amount. This is illustrated in Figure 1, in which it is assumed that the temperature of the copper reaches 250 degrees centigrade before any heat is absorbed by the insulation, at which time the short circuit is removed. The cooling takes place in two stages: firstly, the conductor insulation absorbs its share of the heat very rapidly, reducing the temperature of the copper to, say, 220 degrees centigrade in three to five seconds. Secondly, the cooling from this point on takes place by dissipation of the heat to the oil at a relatively slow rate, in terms of minutes instead of seconds, during which time most of the aging takes place. For practical purposes then, the temperature during the slow-cooling period is far more important than the maximum copper temperature attained up to the time when the slow rate of cooling starts in.

The ASA Standards C57.12.050-.051[2] have two limitations under short circuit. One limitation (mechanical) is that the magnitude of the symmetrical current must not exceed 25 times normal current. The other limitation (thermal) is that the maximum copper temperature must not exceed 250 degrees centigrade when using class *A* insulation.

This paper is concerned only with the thermal limitation for transformers using class *A* insulation. The authors will show:

1. That turn-to-turn insulation should be factored when calculating the storage of heat in transformer windings.

2. That, for a given maximum temperature, the aging of the insulation resulting from a short circuit depends on the rate of cooling rather than on the duration of the short circuit.

3. That, to produce the same thermal effect, the maximum temperature should vary with the rate of cooling.

Tests to Determine Temperatures During Heating and Cooling Cycle

To obtain heating and cooling data, many tests were made on transformer windings of the disk-coil type having three sizes of conductors with different amounts of turn insulation, as shown in Table I.

The tests were made with the coils in both horizontal and vertical positions and in oil at temperatures ranging from 24 to 75 degrees centigrade. These tests provided two kinds of data: firstly, a comparison of the tested and calculated rises (based on all heat stored in the copper) during the heating period; and secondly, the thermal capacity of the turn insulation that applied during both the heating and cooling periods, under loads ranging from moderate overloads (run until conditions became constant) to short-circuit conditions until temperature rises as high as 200 degrees centigrade were reached.

HEATING PERIOD

Figure 2 is typical of tests made on the three sizes of conductors. This illustra-

Table I

Test Series Number	Conductor Size, Inches	Turn Insulation—Both Sides, Inches	
		Paper*	Cotton Wrap
1	0.435×0.095	0.012	0.007
2	0.450×0.075	0.024	0.007
3	0.500×0.100	0.066	0.007

* 0.003 Manila paper.

Paper 49-189, recommended by the AIEE Transformer Committee and approved by the AIEE Technical Program Committee for presentation at the AIEE Summer General Meeting, Swampscott, Mass., June 20-24, 1949. Manuscript submitted March 14, 1949; made available for printing May 5, 1949.

V. M. MONTSINGER and G. H. HALSEY are with the General Electric Company, Pittsfield, Mass.

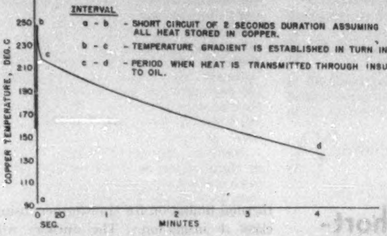

Figure 1 (above). Heating and cooling of typical oil-immersed transformer winding when subjected to short-circuit

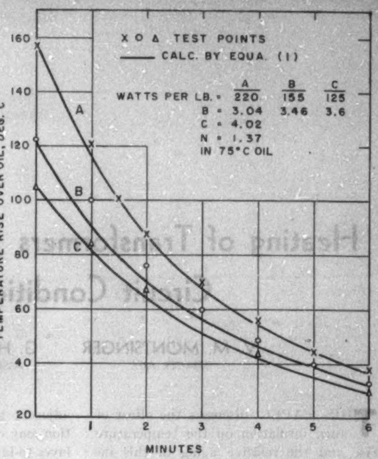

Figure 3 (right). Cooling curves of winding having conductor 0.450 by 0.075 inch, *P.024-C.007*, two sides, insulation

tion shows curves of tested and calculated temperature rises during 40-second short circuits when 400, 500, and 550 amperes were forced through the 0.450- by 0.075-inch conductor with *P.024-C.007* insulation in 30-degree-centigrade oil. It will be noted that the solid lines representing the test values fall below the dashed lines representing the calculated values assuming all the heat stored in the copper. For example, at the end of ten seconds duration, the percentage of generated heat that remained in the copper was as shown in Table II.

Results of similar tests reported in Figures 1 and 2 of reference 4, made on 0.435- by 0.095-inch *P.012-C.007* insulated conductor, are seen in Table III.

It appears safe to assume that at least 20 per cent of the total heat generated will always be stored in the insulation of an average winding.

COOLING PERIOD

Figures 3 and 4 show a comparison of tested and calculated cooling of windings having 0.450- by 0.075-inch *P.024-C.007* conductors in which the temperature rise at the start of the cooling ranges from approximately 100 to 200 degrees centigrade. The cooling was calculated by the following equation

$$\theta=\theta_0\left[1+(n-1)\frac{T}{\tau}\right]^{\frac{-n}{n-1}} \tag{1}$$

where

θ = temperature rise of winding, degrees centigrade, at any time, T
θ_0 = temperature rise of winding at start of cooling period
n = exponential power of ultimate temperature rise (θ_0^n) versus loss
T = time after start of cooling—minutes
$\tau=\frac{\theta_0 C}{W_0}$
C = specific heat of copper plus insulation
W_0 = watts per pound necessary to maintain a steady-state temperature rise of θ_0

After the current density of the copper to maintain the temperature rise, θ_0, is determined, W_0 can be calculated from

$$W_0=KD^2 10^{-6}$$

where

K = 2.16 for copper at 25 degrees centigrade
D = amperes per square inch

Based on the limited data available, the authors have used for several years the thermal capacity of turn insulation by volume as one-half that of copper, that is

$$C=2.96+1.48\frac{A_i}{A_c} \tag{2}$$

where

A_i = cross section of insulation
A_c = cross section of copper

The value of 2.96 for copper corresponds to a specific heat of 0.0935 calorie per gram per degree centigrade. As the specific heat of copper increases slightly with temperatures, the value of 3.04, instead of 2.96, was used in AIEE Standards Number 32.[3] Also, when the Standards for Neutral Grounding Devices, were under preparation, the data at that time indicated that "by volume" the thermal capacity of turn insulation was 86 per cent that of copper. That is,

$$C=3.04+2.62\frac{A_i}{A_c} \tag{3}$$

A thorough study of all tests made on the three different amounts of turn insulation previously mentioned, including both the heating and cooling cycles, indicates that the thermal capacity of turn insulation is by volume approximately 67 per cent (or 2 A_i/A_c) that of copper.

Rounding out the 2.96 and 3.04 values to 3.00 which is easily remembered, the equation which best fits the test results is

$$C=3.00+2.0\frac{A_i}{A_c} \tag{4}$$

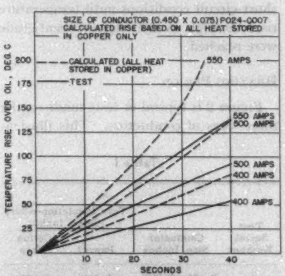

Figure 2. Tested and calculated temperature rises during 40-second duration in 30-degree-centigrade oil

Table II

Amperes	Per Cent Heat Retained in Copper in First Ten Seconds
400	65
500	78
550	80

Table III

Amperes	Per Cent Heat Retained in Copper in First Ten Seconds	
	Figure 1	Figure 2
400	70	60
500	70	72
550	68(500 amperes)	70

which allows 67 per cent "by volume" for the turn insulation. See Table IV for comparison of tested and calculated values of temperature rises using equations 3 and 4.

According to equation 1, the rate of cooling is determined largely by the time constant which ranges from approximately 3 to 15 minutes for most transformer windings at normal operating temperatures. When windings attain short-circuit temperatures, the time constant is reduced, since the steady-state temperature rise does not vary directly with the loss. For example, equation 8 of Appendix II of ASA C57.32[1] states that the time constant varies as the 0.25 power of the ratio of the temperature rise at rated load to any higher rise. That is, if the coil rise over oil at rated load is 20 degrees centigrade when the rise over oil under short circuit reaches (250 degrees–75 degrees oil temperature =) 175 degrees centigrade, the time constant will be decreased to $(20/175)^{0.25} = 0.58$ of that at 20 degrees centigrade rise. Therefore, time constant of 15 minutes at rated load will be 15 by 0.58 = 8.7 minutes, or approximately one-half that at rated load.

Aging of Insulation During Heating and Cooling Periods

Now, having discussed both the heating and cooling during a short-circuit cycle, we can now determine what percentage of the total aging takes place during the heating cycle.

As shown previously,[5] the aging of insulation during an abrupt rise in temperature and slow cooling can be calculated by integrating the area of the heating and cooling curve either by using the equation

$$A = te^{XT_2} \qquad (5)$$

where

A = aging units
t = time expressed in seconds, minutes, or hours
X = constant (0.0865 when the aging doubles for each 8 degrees centigrade increase in temperature)
T_2 = maximum temperature, degrees centigrade

or, by forming a trapezoid the area of which is approximately the same as the temperature area, and using the equation

$$A = t\left[\frac{e^{XT_2} - e^{XT_1}}{X(T_2 - T_1)}\right] \qquad (6)$$

When $X = 0.0865$, equation 6 reduces to

$$A = t\left[\frac{\log_{10}^{-1}(0.0375\ T_2 - 0.0375\ T_1)}{0.0865\ (T_2 - T_1)}\right] \qquad (7)$$

where

T_2 = maximum temperature of trapezoid
T_1 = lower temperature of top line of trapezoid. The values of T_1 should be such that the aging is negligible for T_1 and lower values
t = time corresponding to length of top line of trapezoid

Figure 5 shows curves constructed of two heating periods of five and ten seconds, also, three cooling curves for windings having 2-, 4- and 8-minute time constants (at 250 degrees centigrade).

As the aging with which we are concerned here is the ratio of the aging during the heating period to the aging during the cooling period, time, t, can be expressed in any convenient units. Letting $T_2 = 175$ degrees centigrade and $T_1 = 100$ degrees centigrade for the 5-second heating period, t is approximately 2.1 seconds.

By equation 7

$$A = 2.1\left[\frac{\log_{10}^{-1}(0.0375 \times 175 - 0.0375 \times 100)}{0.0865(175 - 100)}\right] = 1.2 \times 10^6 \text{ units}$$

Since the heating curve is almost a straight line, the aging during the 10-second heating period is approximately 2.4 by 10^6 units.

Referring to Figure 5, it will be seen that the lapse of time from the point on the triangle *a b c*, when the coils having a time constant of two minutes reach 100-degree rise on the 5-second heating period and decrease to 100-degree rise on the cooling period, is 59 seconds. Experience has shown that the integration of triangle *a b c* gives approximately the same results as the integration by parts of the entire heating and cooling area *a b d*. The aging during this complete cycle can also be calculated by equation 7, that is

$$\text{Aging} = 59\left[\frac{3{,}630{,}000 - 5600}{0.0865(175 - 100)}\right] = 32.9 \times 10^6 \text{ units}$$

Therefore, the aging during the 5-second heating period is

$$\frac{1.2 \times 10^6 \times 100}{32.9 \times 10^6} = 3.65 \text{ per cent of the total aging}$$

The percentage of aging for coils with time constants greater than two minutes

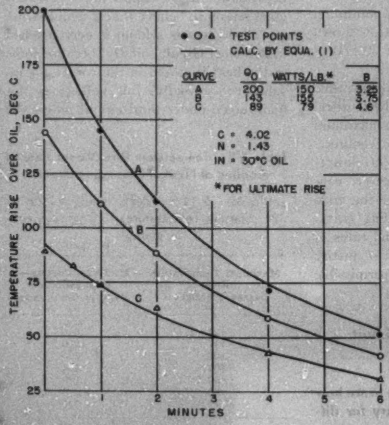

Figure 4 (left). Cooling curves of winding having conductor 0.450 by 0.075 inch, P.024-C.007 insulation

Figure 5 (below). Heating and cooling curves of windings with 2-, 4-, and 8-minute time constants at 250 degrees centigrade or approximately 4, 8, and 15 minutes at 95 degrees centigrade

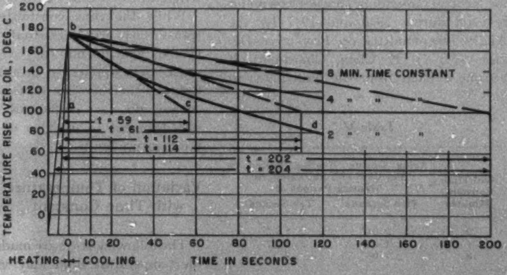

Table IV. Summary of Heating-up Data Taken on Coils Having Three Sizes of Conductors

Conductor	Degrees Centigrade Temperature Rise Versus Time in Minutes									
	2 Minutes		5 Minutes		10 Minutes		Ultimate θ_u		Watts Per Pound at	
0.435 × .095-inch *P.012 C.007*										
Horizontal coils										
Amperes	140	200	140	200	140	200	140	200	140	200
Test	15.0	30.0	27.0	50.5	34.5	63.0	38.0	68.0	31	68
Calculated A* Rise	14.1	29.6	26.1	51.7	34.3	64.1	—	—		
Calculated B**	13.5	28.4	25.3	50.4	33.8	63.5	—	—		
0.450 × .075-inch *P.024–C.007*										
Horizontal coils in 30-degree oil										
Amperes	140	200	140	200	140	200	140	200	140	200
Test	8.0	21.5	18.5	40.0	29.0	55.5	38.0	65.0	23	50
Calculated A* Rise	9.9	20.6	20.1	40.0	29.6	55.4	—	—		
Calculated B**	9.2	19.2	19.0	38.0	28.4	53.8	—	—		
Vertical coils in 25-degree oil										
Amperes	100	140	100	140	100	140	100	140	100	140
Test	8.5	21.0	17.0	34.0	25.0	46.5	30.0	53.0	22	47
Calculated A*	9.2	18.9	17.9	35.4	25.2	47.1	—	—		
Calculated B**	8.5	17.6	17.0	33.7	24.4	46.0	—	—		
0.500 × .100-inch *P.066–C.007*										
Horizontal coils in 70-degree oil										
Amperes	140	250	140	250	140	250	140	250	140	250
Test	8.0	27.5	17.0	53.5	25.0	75.0	31.5	88.0	21.5	80
Calculated A* Rise	7.6	27.0	15.7	52.8	23.5	73.9	—	—		
Calculated B**	6.8	24.3	14.4	48.8	22.2	70.6	—	—		
Vertical coils in 70-degree oil										
Amperes	140	250	140	250	140	250	140	250	140	250
Test	8.5	24.0	17.0	52.5	25.0	72.0	30.5	85.5	22	76
Calculated A* Rise	7.7	25.7	15.8	50.6	23.4	71.3	—	—		
Calculated B**	6.9	23.2	14.5	46.8	22.1	68.0	—	—		

* Based on $C=3.00+2.0\ A_i/A_e$. ** Based on $C=3.04+2.62\ A_i/A_e$.

will, of course, be less than 3.65 per cent because the cooling is at a slower rate.

Using the curves shown in Figure 5 and calculating the aging as illustrated, Table V shows the aging during the heating period in percent of total aging for coils having 2-, 4-, and 8-minute time constants and for 5- and 10-second heating periods.

From Table V, it is seen that for heating periods up to ten seconds practically all the aging under short-circuit conditions occurs during the cooling period, which depends on the time constant of the windings. From a thermal standpoint, the duration of a short-circuit of any reasonable period can therefore be neglected.

Method of Specifying Temperature Limits

When AIEE Standard Number 32 for Neutral Grounding Devices was under revision during 1946 and 1947 by the AIEE Subcommittee on Protective Devices (Mr. J. E. Clem, Chairman), it became evident from the data given in reference 4 that the temperature limits during a fault of one minute's duration or less should be a function of the rate of cooling after the fault had been removed rather than the length of time during the fault. This was especially true for transformers having a wide range of cooling rates and time constants. For example grounding transformers may have either well-ventilated coils and rapid cooling rates with normal time constants or they may have practically no cooling ducts resulting in very slow cooling rates and large time constants.

Table V

Coil Time Constant, Minutes	Aging During Heating Period in Per Cent of Total Aging, for Heating Periods of	
	Five Seconds	Ten Seconds
2	3.65	7.05
4	1.92	3.77
8	1.06	2.1

Based on these considerations, the subcommittee established a table of allowable temperature rises versus minimum cooling rates for the first minute as shown in Table VI taken from Table 32.11B of AIEE Standard Number 32.

So far as is known, this is the first time that the heating period has been disregarded and the permissible maximum temperatures based on rate of cooling.

While the time constants of power-transformer windings that carry continuous load do not vary over the wide range that applies to grounding transformers, the time constants and rates of cooling do vary sufficiently to justify establishment of a range of permissible temperature limits.

Variation of Temperature Limit with Time Constant

The following steps are made to see how the temperature limit may vary for different time constants to produce approximately the same aging during a short circuit.

Table VI

Time Constant, Minutes	Time, *t*, Seconds	Relative Aging
2	59	1.0
4	112	1.9
8	202	3.42

In Figure 5, the relative aging for all three time constants will be proportional to the time, *t*, since T_2 and T_1 have the same values for all three curves.

For the 5-second heating and three cooling periods, the aging is as in Table VI.

Based on the aging doubling for each eight degrees increase in temperature, to produce the same aging in the three coils would require: a difference of 7.5 degrees centigrade between coil number *1* and coil number *2;* and a difference of 14 degrees centigrade between coil number *1* and coil number *3.* For a coil having a time constant of 16 at 250 degrees centigrade, the temperature limit should be approximately 25 degrees centigrade less than for coil number *1.*

Based on these data, if we assume that 250 degrees centigrade is a safe maximum temperature for all windings having a time constant of two minutes or less the figures given in Table VIII can be drawn up.

The temperature limit under short-circuit conditions for power transformers has been 250 degrees for the past 30 or 40 years. As pointed out previously, this temperature has been based on all heat being stored in the copper only. There is good reason to believe that a temperature of 250 degrees is seldom if ever reached under short circuit; firstly, because some of the heat is stored in the conductor insulation; secondly, full voltage is not maintained under short-circuit unless the

Table VII. Temperature Rise Versus Rate of Cooling of Neutral Grounding Devices

Table 32—2.11A—AIEE Standard Number 32. Starting Temperature, 75 Degrees Centigrade

Maximum Temperature Rise, Degrees Centigrade	Minimum Cooling—First Minute, Degrees Centigrade
125	30.0
117	15.0
109	7.5
101	3.8
93	1.9
85	0.9
77	0.5

Table VIII

Approximate Winding Time Constant in Minutes		Maximum Temperature to Produce Approximately Same Aging, Degrees Centigrade
At 250 Degrees Centigrade	At 95 Degrees Centigrade	
2 or less	3.5 or less	250
4	7.0	242.5
8	14.0	236
16	28.0	225

kilovolt-ampere capacity of the transformer in question is small in comparison with the source of power; and thirdly, the protective relay generally comes into action before the time limit is reached. If an allowance is made for the storage of heat in the conductor insulation, the question naturally arises as to whether 250 degrees is the proper value or should it be reduced to obtain approximately the same temperature as has been attained in the past. For example, if we assume that the temperature rise of the windings during short circuit is, say, 80 per cent of the calculated value based on all heat stored in copper only, this means that if the initial temperature is 95 degrees, the actual temperature attained would be (250–95) 0.8+95=219 degrees centigrade instead of 250 degrees centigrade.

Formula for Calculating Storage of Heat

Equations 22.105(a) and (b) given in the ASA Standards C57.22[1] do not include the effect of insulation in the storage of heat. Furthermore, these equations are cumbersome to use, especially 22.105(a).

The equation given in paragraph 32-3.11A of AIEE Standard Number 32 allows for storage of heat by the conductor insulation. This equation, however, expresses the copper loss in watts per pound instead of amperes per square inch which term is more convenient to use. With zero eddy loss and when expressed in amperes per square inch this equation reduces to

$$\theta=T_0\left[\log_{10}^{-1}\left(\frac{6D^2t10^{-11}}{C}\right)-1\right] \qquad (8)$$

where

θ = temperature rise in degrees centigrade
T_0 = starting temperature absolute $(234.5+\theta_0)$
θ_0 = starting temperature in degrees centigrade
D = amperes per square inch
t = time in seconds
C = specific heat of copper plus insulation
$C=3.00+2.0\frac{A_t}{A_c}$
A_t = cross section of turn insulation
A_c = cross section of copper conductor

In equation 32–3.11A of AIEE Standard Number 32 the eddy loss is lumped in with the I^2R loss watts per pound. This assumes that the eddy loss varies directly with the absolute temperature the same as I^2R varies.

In ASA equation 22.105(b), the eddy loss varies inversely with the absolute temperature.

If an empirical eddy-loss factor is put in equation 8, very good agreement is obtained with ASA equation 22.105(b) over a wide range of amperes per square inch and per cent eddy loss. With an eddy-loss factor introduced, equation 8 becomes

$$\theta=T_0\left[\log_{10}^{-1}\left(\frac{6D^2Et10^{-11}}{C}\right)-1\right] \qquad (9)$$

where

$E=\left(1+\frac{e}{100}\right)^{0.8}$
e = eddy loss in per cent of I^2R at 75 degrees centigrade

Table IX. Comparison of Results

Initial Temperature = 95 Degrees Centigrade

Amperes Per Square Inch	Time, Seconds	Eddy Loss, e, Per cent	Comparison of Copper Temperatures Calculated By: AIEE Number 32 Equation 32.3.11A*	Equation 9 in Paper	ASA Equation 22.105(b)
	2	0		123.0	123.0
30,000	2	20		128.1	128.5
	2	40		132.8	133.5
	2	0		147.5	147.5
40,000	2	20		157.1	156.0
	2	40		165.3	164.5
	5	0		127.0	127.0
20,000	5	20		131.8	132.5
	5	40		137.2	137.5
	5	0	170.5	170.5	170.5
30,000	5	20	189.0	184.2	183.5
	5	40	217.0	197.7	195.0
	5	0	241.8	241.8	241.8
40,000	5	20	280.0	270.0	264.5
	5	40	322.0	298.7	284.5
	10	0	161.5	161.5	161.5
20,000	10	20	177.4	173.7	172.5
	10	40	193.8	185.1	182.5
	10	0	264.0	264.0	264.0
30,000	10	20	311.0	297.4	290.5
	10	40	361.0	332.3	315.5

* Using $C=2.96$ instead of 3.04 for copper only.

Table IX gives a comparison of the results obtained by three equations to show the effect of eddy loss without factoring the turn insulation:

1. 32–3.11A from AIEE Standards Number 32.
2. Equation 9 in paper.
3. 22.105(b) from ASA Standard C57.22.

A comparison of the values shown in Table IX shows:

1. With zero eddy loss, the three equations give the same results.
2. With eddy loss present and for temperatures up to 250 degrees centigrade, the values calculated by equation 9 give results quite close to those given by ASA equation 22.105(b).

Since equation 9 is easy to use, it is recommended that it replace ASA equation 22.105(a) which is cumbersome to use and does not allow for the absorption of heat by the insulation.

Effect on Transformer Design of Changing Short-Circuit Temperature Rules

The question naturally arises as to the effect on transformer design of changing the short-circuit temperature rules. The present limiting temperature of 250 degrees centigrade calculated on the basis of all heat stored in the copper is easily met in present-day designs, except in very rare cases. However, if the copper densities are increased as improved methods of cooling are developed or by other design requirements, more accurate calculation of temperatures resulting from short-circuit conditions may be required.

Future Work

The data presented in this paper were obtained on disk types of windings. Other factors which may materially affect the rate of cooling are additional insulations not present in disk windings, such as layer insulations between multiconductor layers and windings wound directly on cylinders. Future investigations also should determine the effect of storing heat in the oil flowing up through tall windings where the oil temperature may be increased greatly for an appreciable time before it leaves the coil stack following a short circuit.

While these factors will probably have a small effect on the storage of heat, they may have a decided effect on the rate of cooling. When these factors have been investigated and reported, the question of revising the ASA standards to put them on a more logical basis, should be considered by the AIEE Transformer Committee.

References

1. American Standards for Transformers, Regulators, and Reactors. American Standards Association (New York, N. Y.), C57, 1948.

2. American Standard for Distribution, Power, and Regulating Transformers, and Reactors Other than Current-Limiting Reactors. American Standards Association (New York, N. Y.), C57.12, 1949.

3. Neutral Grounding Devices. AIEE Standard Number 32, 1947.

4. Temperature Limits and Short-Time Overloads for Oil-Insulated Neutral Grounding Reactors and Transformers—Part II, V. M. Montsinger, J. E. Clem. *AIEE Transactions*, volume 65, 1946, pages 966–73.

5. Temperature Limits for Short-Time Overloads for Oil-Insulated Neutral Grounding Reactors and Transformers, V. M. Montsinger. *Electrical Engineering* (*AIEE Transactions*), volume 57, January 1938, pages 39–44.

Discussion

V. V. Mason (The Hydro-Electric Power Commission of Ontario, Toronto, Ontario, Canada): For estimating the loss of life due to a short time overload the authors give their equation 5

$$A = Ie^{XT_2} \qquad (1)$$

For the more elevated temperature where the rate of loss of life doubles for each rise of 8 degrees centigrade, this formula holds, but only for constant T_2. For varying temperatures, the integral form must be used, namely

$$A = \int e^{XT} dt \qquad (2)$$

In the authors' equation 6, an approximation is made to the above integral by assuming that the cooling curve is a straight line. This approximation, gross as it may seem at first glance, is probably not so bad in most practical cases if cleverly made. However, it is sometimes difficult to decide just how clever an approximation one has made.

The purpose of this discussion is to introduce a new type of graph paper which we call "loss-of-life" paper. Use of this paper avoids the uncertainty attendant upon making the approximation used by the authors. This loss-of-life paper has a linear time scale and a nonlinear temperature scale, such that the distance along the Y-axis is proportional to the rate of loss of life. Thus the area under any curve representing a temperature cycle is proportional to the loss of life for that cycle.

An additional advantage which accrues from the use of this paper is that account may easily be taken of the fact that the rate of deterioration halves for smaller and smaller temperature decrements as the temperature falls towards 95 degrees centigrade. That is, we may take into account the nonlinearity of the curves of per cent loss of life versus hot-spot temperature when plotted on semilog paper as in Figure 4 of Appendix 1 of the American Standards for Transformers, Regulators, and Reactors. It was the rate of loss of life figures calculated from these American Standards Association curves which were used in the preparation of this special graph paper.

Figures 1 and 2 of this discussion show samples of this type of paper. Figure 1 is for moderate overloads going up to a maximum of 131 degrees centigrade, while Figure 2 is for more severe overloads going up to 183 degrees centigrade.

This loss-of-life paper not only avoids the approximations otherwise necessary but also makes the procedure almost entirely graphical. This is especially so if it is used in conjunction with the transient heating and cooling papers which have been described in previous literature.[1,2]

References

1. Simplified Method of Calculating Transformer Temperature Rise Under Variable Loads, W. C. Sealey. *Allis Chalmers Electric Review* (Milwaukee, Wis.), December 1939, pages 11–15.

2. Simplified Graphical Method of Computing Thermal Transients, Paul Narbutovskih. *AIEE Transactions*, volume 66, 1947, pages 78–81.

Figure 1 (below). Transformer loss-of-life paper with moderate overload

Figure 2 (right). Transformer loss-of-life paper with severe overload

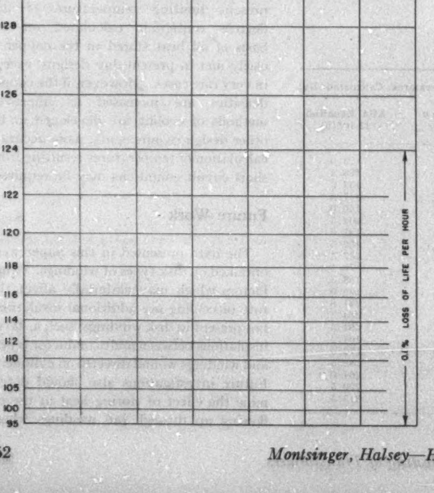

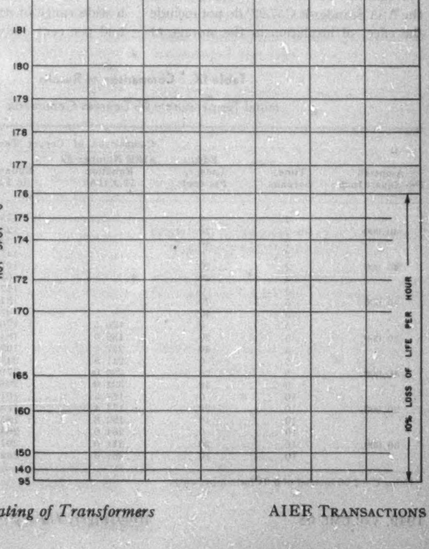

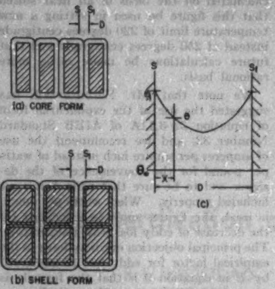

Figure 3. Arrangement of copper and insulation in core and shell form transformers

Paul Narbutovskih (Westinghouse Electric Corporation, Sharon, Pa.): In their paper the authors have brought up for consideration by industry and the utilities a subject which has been maturing for some time. The basic thesis—the relation of the permissible winding temperatures in transformers under very short time overloads to the duration of the cooling period rather than the heating period—is fundamentally sound, and has been recognized for a number of years, although until now it has not been proposed for inclusion into the industry standards for transformers. Our knowledge of the insulation life under exposure to high temperature is still imperfect. So long, however, as the available knowledge has been applied to the formulation of permissible overloads on transformers, it can be applied to the formulation of permissible practices for short circuit conditions. From this point of view the paper is undoubtedly a step in the right direction.

The inclusion of the thermal capacity of insulation into calculation of the windings temperature under short-circuit conditions is likewise entirely sound. The quantitative effect of the insulation, however, may merit further consideration, particularly in view of the fact that on Figure 2 of the paper the calculated temperature rise for 550 amperes appears to be erroneously too high. A correction of this curve will increase the per cent heat stored in copper to about 95 or 97 per cent instead of the 80 per cent quoted in the paper for the first 10 seconds. A further insight into the effect of the insulation upon the final temperature reached by the copper and the insulation can be gained by considering the diffusion of heat from copper into the insulation under transient conditions.

Consider Figure 3 of the discussion, which shows a cross section of a typical conductor and insulation arrangement for core and shell form transformers. Upon occurrence of a short circuit, a certain amount of heat is rapidly imparted into copper, raising its temperature. During the heating period and during the first part of the cooling period the heat from the copper diffuses into the insulation, the rate of this depending upon time, thermal diffusivity, and the thickness of the insulation. Intuitively, one may expect that on extremely rapid temperature rises all heat will be stored in copper alone, the insulation temperature remaining unchanged. In the next moment insulation immediately adjacent to the copper assumes the same temperature as the copper, the temperature of the remaining part of the insulation being unchanged. Then gradually, as the heat diffuses into the insulation, its temperature increases, while that of copper decreases. Simultaneously, the process of heat loss by convection to oil begins.

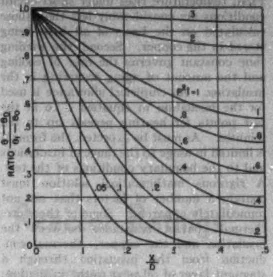

Figure 4. Transient temperature rise in insulation between conductors

When the duration of the short circuit is finite, it appears that the two processes, that of heat generation in the copper, and the heat diffusion into insulation, are simultaneously present, the result of which will be that the copper will never attain the temperature corresponding to all heat stored in copper. However, if the thermal transient in the insulation is of long duration compared to the duration of the short circuit, the insulation will progressively play a decreasingly smaller part as the duration of the short circuit decreases. Hence, in the calculation of the copper temperature the effect of the thermal capacity of insulation must be related to the duration of the short circuit.

The required quantitative relation may be obtained by considering heat diffusion from two parallel surfaces, S and S_1, whose temperature was suddenly changed from θ_0 to θ_1, into a slab of insulation, included between them of thickness D, whose initial temperature is θ_0, Figure 3(C) of the discussion. It can be readily appreciated that this corresponds closely to the insulation included between turns, or between layers in cylindrical windings. Under this condition the transient temperature within the slab is given by a differential equation

$$\frac{\partial\theta}{\partial t}=\alpha\frac{\partial^2\theta}{\partial x^2} \qquad (1)$$

where

θ = temperature at time t minutes and at point distant x inches from surface S

$\alpha=\frac{K}{\rho c}$, is the thermal diffusivity of the insulating material, square inches, divided by minutes

K = thermal conductivity of insulation, $\frac{\text{watts}}{\text{inch}\times\text{degrees centigrade}}$

ρ = density of insulation, pounds per cubic inch

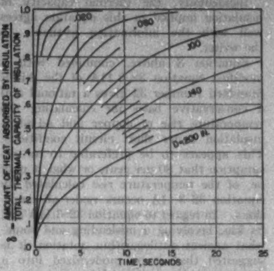

Figure 5. Heat absorbed by conductor insulation under transient conditions

c = thermal capacity, $\frac{\text{watt minutes}}{\text{pounds, degrees centigrade}}$

Solution of equation 1, satisfying the necessary boundary conditions, is

$$\theta=\theta_1-(\theta_1-\theta_0)\frac{4}{\pi}[\epsilon^{-p^2t}\cdot\sin qx+$$
$$\epsilon^{-(3p)^2t}\cdot\sin 3qx+\epsilon^{-(5p)^2t}\cdot\sin 5qx+\ldots \qquad (2)$$

Where

$$p=\frac{\pi\sqrt{\alpha}}{D}, \quad q=\frac{\pi}{D}$$

Equation 2 is presented graphically, on Figure 4 of the discussion, as a family of curves.

Under the transient temperature distribution the effective thermal capacity of insulation is reduced by a factor δ, whose value is equal to the ratio of the mean and the maximum temperatures obtained from any one of the curves, Figure 4. Figure 5 of the discussion gives values of factor δ, as defined above, calculated for the following values of thermal conductivity, capacity, and density which apply reasonably well to oil-soaked manila paper insulation

$$K=0.0042\ \frac{\text{watts}}{\text{inches, degrees centigrade}}$$

$$\rho=0.035\ \frac{\text{pounds}}{\text{cubic inches}}$$

$$c=18\ \frac{\text{watt minutes}}{\text{pounds, degrees centigrade}}$$

As can be seen from the curves of Figure 5 of the discussion, the heat penetration into insulation is quite rapid for relatively thin insulation. Thus for a heating period of five seconds, and for insulation thickness less than 0.050 inch, the insulation is more than 90 per cent effective in absorbing the heat from the copper. This is not so for heavier insulation, for which the time lag in absorbing the heat from the copper may be quite considerable. Curves of Figure 5 may be used in the calculation of the copper temperature rise, if factor δ from Figure 5 is introduced into equation 4 of the paper

$$c=3+2\delta\frac{A_i}{A_c} \qquad (3)$$

Incidentally, the thermal capacity of insulation implied in this equation agrees well with the information available to the writer.

Equation 3 above, combined with a modified equation 32–3.11A of the AIEE Standard Number 32 gives a rational and a conservative basis for calculating the temperature rise of copper and adjacent insulation under short circuit conditions. This appears to be preferable to an assumption that 80 per cent, or what it may be, of the temperature rise calculated by equation 32–3.11A occurs under all conditions. In regard to equation 32–3.11A and its kin, involving a misleading and somewhat ancient antilogarithm notation, it is suggested that it be modernized into a directly usable exponential form

$$\theta = T_0\left[10^{\frac{W_0 t}{mCT_0}} - 1\right]$$

or

$$\theta = T_0\left[\epsilon^{\frac{W_0 t}{CT_0}} - 1\right] \tag{4}$$

for equation 32–3.11A, and

$$\theta = T_0[\epsilon^{At} - 1] \tag{5}$$

with

$$A = (1.38)10^{-10}\,\frac{D^2E}{C} \tag{6}$$

for equation 9 in the paper. In the above ϵ is the base of natural logarithms.

V. M. Montsinger and **G. H. Halsey:** The paper was intended to present two important facts for further consideration. First, temperature rises under short-circuit conditions are considerably less than those calculated on the basis of all heat being stored in the copper. Second, the winding time constant governs the rate of cooling and the amount of aging occurring in the insulation. An empirical allowance is used for the insulation in equation 4 to fit the test points for heating periods up to ten minutes. As must be expected, the formula is limited in usage to the range of insulations and to the boundary conditions of the test. A rigorous mathematical solution must contain a number of factors that are not immediately apparent. Some of these are: thermal contact resistance between the insulation and the copper; thermal conduction from the insulation through a stagnant layer of oil next to the insulation; and heat transfer rates across these two boundaries that are functions of temperature.

A solution embodying some of these features has been made and was thought to be too involved to be easily used. The solution presented by Mr. Narbutovskih may be found in various textbooks[1] for the assumed boundary condition that the inner face of the insulation in contact with the copper reaches ultimate temperature at time $t=0$. As a result of this assumption, one calculates a more rapid heat flow into the insulation than actually exists. The insulation temperature will not rise as fast as indicated in Figures 4 and 5 of his discussion. Effects of the process of heat transfer through the stagnant oil layer and subsequent convective heat transfer to the main body of oil are included in the empirical formula of the paper.

The paper suggests that since most windings with normal turn insulation reach only 80 per cent of the temperature rise calculated on the basis of all heat stored that this figure be used in setting a new temperature limit of 220 degrees centigrade instead of 250 degrees centigrade and that future calculations be made on a more rational basis.

We note that Mr. Narbutovskih has suggested the use of the exponential form of equation 32–3.11A of AIEE Standard Number 32, and we recommend the use of amperes per square inch instead of watts per pound for the convenience of the designer and to be sure that eddy losses are included properly. When watts per pound is used, the figures must be corrected for the decrease of eddy loss with temperature. The principal objection one may have to the empirical factor for eddy loss as expressed by E in equation 9 is that the formula is approximate and not mathematically correct. Reference to Table VIII will show that the results obtained are accurate enough for all practical purposes.

We wish to thank Mr. Narbutovskih for pointing out an error in Figure 2 of the paper. The 550-ampere curves should have been labeled for 600 amperes. References made to 550-ampere tests in Tables II and III should be changed to 600 amperes. The exponent in equation 1 should be changed to $-1/(n-1)$. In Figures 3 and 4, the letter B should be changed to τ and the watts per pound value of 155 in Figure 3 should be changed to 255.

The loss-of-life paper suggested by Mr. Mason should prove helpful in future computations.

REFERENCE

1. HEAT TRANSMISSION, W. H. McAdams. McGraw-Hill Publishing Company, New York, N. Y., second edition, 1942, pages 29–30.

Standardization of Reactor Ratings

F. H. KIERSTEAD
MEMBER AIEE

J. L. THOMASON
MEMBER AIEE

REACTORS are used widely for numerous applications in power and other equipment and they are accepted apparatus for limiting fault currents in power systems. Repetitive manufacturing offers economies which can best be realized in reactors when definite physical sizes are frequently duplicated. Before the physical sizes can be duplicated, it is necessary to standardize the ratings of reactors. There are several items of ratings which normally appear on the nameplates, and some of the most pertinent items such as voltage, current, and inductances will be discussed further. While it is advisable to standardize the ratings of all types of reactors that are made in quantity, for illustrative purposes only current-limiting reactors will be considered here. The advantages obtained from the standardization of other types of electric equipment are largely applicable to reactors.

Voltage Classes

The voltage rating of a current-limiting reactor establishes two features: the insulation strength for voltage stress; and the mechanical strength for short-circuit stress.

The latest issue of the Report of the Joint Committee of the Edison Electric Institute and the National Electrical Manufacturers Association "Preferred Voltage Ratings for A-C Systems and Equipment"[1] establishes the nominal system voltages and their range at substations and on transmission systems. These, then, are the voltages to which reactors are subjected in the general application. Hence, these voltages should establish the voltage ratings of current-limiting reactors as listed in Table I.

Current Classes

The continuous current ratings of current-limiting reactors have been established by past usage. Table II shows the present standards for circuit breakers, current transformers and reactors, and also, the recommended reactor current ratings. Included are current ratings that would be established by the preferred series of numbers, 60 per cent and 25 per cent steps; and it is recommended that the use of the 60 per cent steps be emphasized to reduce the number of standard sizes. It is recommended that current classes other than those tabulated be considered specials. However, it is recommended that the specials be placed in preferred sizes as 12 per cent and 6 per cent steps. The short-time current rating of current-limiting reactors is well established by ASA C57.16–1948[2] by the maximum allowable temperatures of 350 degrees centigrade, class *B*, or 250 degrees centigrade, class *A*, for maximum current for five seconds. For neutral grounding devices AIEE Standard 32[3] gives rated time and temperatures rise for short-time ratings. The rating of current-limiting reactors could be matched with the continuous and 5-second rating of circuit breakers for the minimum cost of this natural combination. Further study will be made on this.

Inductance Unit—The Ohm

The reactor is fundamentally an inductance coil and the fundamental unit of inductance is the henry. However, system engineers like an easier applied unit such as the ohm or per cent IX. For standardization purposes, fractions of the henry would be best as the rating in ohms is directly proportional to the frequency. If the reactor is rated in per cent IX it will have an added variable of circuit volts which may vary from the standard classes. Since a large percentage, possibly 95 per cent, of the current-limiting reactor applications are at 60 cycles, it is recommended that current-limiting reactors be rated in ohms at 60 cycles.

The relation between per cent IX and ohms at 60 cycles is given in Figure 1 which shows the relation

$$\text{Ohms} = \frac{\text{per cent } IX}{100} \times \frac{\text{circuit volts}}{\text{amperes } \sqrt{3}}$$

In Figure 1 the reactor amperes as ordinates and the ohms as abscissas are plotted on log-log paper. Two other variables are needed if the reactor is to be rated as per cent IX; these are shown as circuit volts and per cent IX. Four examples are given on Figure 1. Example 1 calls for 0.100 ohms and 300 amperes and the heavy lines indicate their intersection

Table I. Voltage Classes, Volts 60 Cycle

Nominal System Voltage*	Recommended Reactor Voltage Ratings: Nominal Voltage Rating	Recommended Reactor Voltage Ratings: Maximum Design Voltage Rating
600	600	625
2,400	2,400	2,750
4,160	4,160	4,760
4,800		
7,200	7,200	8,250
12,000		
12,470	12,470	13,700
13,200		
14,400	14,400	15,500
23,000	23,000	25,800
27,600	27,600	31,000
34,500	34,500**	38,000**
46,000	46,000†	48,300†
69,000	69,000	72,500
115,000	115,000	121,000
138,000	138,000	145,000
161,000	161,000	169,000
230,000	230,000	242,000
288,000	288,000	302,000
360,000	360,000	378,000

* From latest issue of Report of Joint Committee of the Edison Electric Institute and the National Electrical Manufacturers Association "Preferred Voltage Ratings of A-C Systems and Equipment"[1] up to and including 230,000 volts.

** Maximum for outdoor air insulated.

† Maximum for enclosed air insulated.

Paper 49-190, recommended by the AIEE Transformers Committee and approved by the AIEE Technical Program Committee for presentation at the AIEE Summer General Meeting, Swampscott, Mass., June 20–24, 1949. Manuscript submitted March 21, 1949; made available for printing May 5, 1949.

F. H. KIERSTEAD and J. L. THOMASON are with the General Electric Company, Pittsfield, Mass.

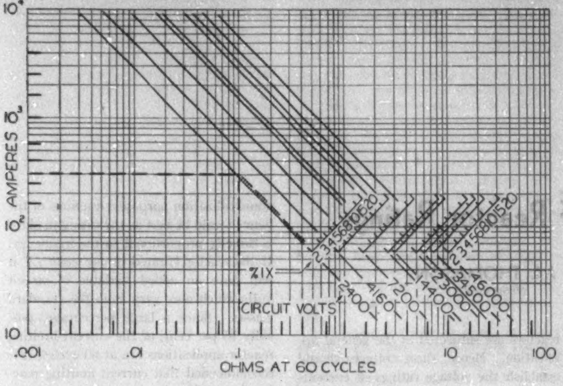

Figure 1. Reactor ratings, ohms and amperes by preferred sizes

$$\text{ohms} = \frac{\text{Per cent IX}}{100} \times \frac{\text{circuit volts}}{\text{amperes } \sqrt{3}}$$

Examples:

	Ohms	Amperes	Circuit Volts	Per cent IX
1.	0.100	300	2,400	2.2
2.	10.00	400	46,000	15.1
3.	0.250	2,000	14,400	6.0
4.	0.100	1,200	7,200	2.9

point. To obtain the per cent *IX* at 2,400 volts project this ohm-ampere intersection point parallel to the voltage line until it intersects the per cent *IX* line—in this case 2.2 per cent *IX*. Other circuit volts and per cent *IX*'s can be secured by interpolation. The kilovolt-ampere per phase is equal to $I^2X/1{,}000$; lines could be placed on Figure 1 to show this relation, but a small graph would become crowded. Figure 1 shows how logically the preferred series of numbers establishes both ohms and amperes.

Inductance Sizes—Preferred Steps in Ohms

It is recommended that the inductance values of current-limiting reactors be expressed in terms of ohms at 60 cycles by sizes according to the preferred series of numbers, ASA-Z-17, 1-1936.[4] Table III shows a range of values which amply cover most applications. The use of the 60 per cent steps should be encouraged. Experienced system engineers would probably find that ratings in the 60 per cent and 25 per cent steps could generally be used and that other ratings could be considered as special cases. However, the special cases should be handled in a logical manner as by 12 per cent and 6 per cent preferred sizes. It might be helpful to note that in the preferred series of numbers, 60 per cent steps means that between two consecutive steps there is a difference of 60 per cent, for example, 100 amperes and 160 amperes. Furthermore, the 60 per cent steps correspond to the five series (that is, 5 steps between decimal units such as 10 and 100), 25 per cent to the 10 series, 12 per cent to the 20, and 6 per cent to the 40.

Table II. Continuous Current Ratings, Amperes 60 Cycles

ASA C37.6–1945[5] Table 3 Circuit Breakers	ASA C57.13–1948[6] Table 13.017 Current Transformers	ASA C57.16–1948[3] Part 16.007 Reactors	ASA Z-17.1-1936[4] Preferred Numbers	Recommended Reactor Ampere Ratings: Preferred Sizes, 60 Per Cent Steps	Recommended Reactor Ampere Ratings: Additional Sizes if Required, 25 Per Cent Steps
	100	100	100*	100	
			125		125
	150	150	160*	160	
	200	200	200		200
		250	250*	250	
	300	300	315		315
400†	400	400	400*	400	
		500	500		500
600	600	600	630*	630	
800	800	800	800		800
			1,000*	1,000	
1,200	1,200	1,200	1,250		1,250
	1,500	1,600	1,600*	1,600	
2,000	2,000	2,000	2,000		2,000
			2,500*	2,500	
3,000	3,000		3,150		3,150
4,000	4,000		4,000*	4,000	

† NEMA 46-116-1946[7] (Part SG6-70) lists the same currents for circuit breakers except omitting the 400 amperes.

* 60 per cent steps (or five series), all are 25 per cent steps (or ten series).

Rating Target

To show the ease with which current-limiting reactors with standard ratings could be applied and ordered, a typical rating target is shown in Table IV. The standard ratings in ohms and amperes are given. The minimum enclosure space required and other data could be tabulated. A separate sheet may be required for each circuit voltage class. This rating target shows that in comparison with an infinite number of special rated (or tailored-made) reactors that with preferred sizes the number of ratings become reasonable in the practical range of per cent *IX* of 3 to 10. On Table IV the X's indicate six ratings of ohms for each current, and for the nine ratings of current a total of 54 standard sizes of reactors for this voltage class. For the 10 voltage classes recommended in Table I for air insulated reactors, there would be 540 standard sizes of reactors. However, the lower and higher ratings are infrequently used, and thus, the number of frequently used standard sizes would probably reduce to 5 by 5 by 5 = 125.

Specifications for Current-Limiting Reactors

Current-limiting reactors should meet the following specifications:

1. Withstand the dielectric test in the rated insulation voltage class.
2. Withstand the short-circuit force in the rated circuit voltage class.
3. Not exceed allowable temperature rise for continuous and short-circuit ratings.
4. Meet the tolerance for variations in in-

Table III. Reactance Classes in Ohms at 60 Cycles by Preferred Numbers 0.001 to 100 Ohms

Per Cent Steps 60	25	60	25	60	25	60	25	60	25
0.00100	0.00100	0.0100	0.0100	0.100	0.100	1.00	1.00	10.0	10.0
	0.00125		0.0125		0.125		1.25		12.5
0.00160	0.00160	0.0160	0.0160	0.160	0.160	1.60	1.60	16.0	16.0
	0.00200		0.0200		0.200		2.00		20.0
0.00250	0.00250	0.0250	0.0250	0.250	0.250	2.50	2.50	25.0	25.0
	0.00315		0.0315		0.315		3.15		31.5
0.00400	0.00400	0.0400	0.0400	0.400	0.400	4.00	4.00	40.0	40.0
	0.00500		0.0500		0.500		5.00		50.0
0.00630	0.00630	0.0630	0.0630	0.630	0.630	6.30	6.30	63.0	63.0
	0.00800		0.0800		0.800		8.00		80.0
0.01000	0.01000	0.1000	0.1000	1.000	1.000	10.00	10.00	100.0	100.0

Table IV. Rating Target for Current-Limiting Reactors

Class: 14,400 Volts, 60-Cycles, 3-Phase, 0.10 to 10.0 Ohms

Ohms 60 Cycles Per Cent Steps 60	25	Amperes 100	160	250	400	630	1,000	1,600	2,500	4,000
0.100	0.100								X	X
	0.125								X	X
0.160	0.160							X	X	X
	0.200							X	X	X
0.250	0.250						X	X	X	
	0.315						X	X	X	
0.400	0.400					X	X	X		
	0.500					X	X	X		
0.630	0.630				X	X	X			
	0.800				X	X	X			
1.00	1.00			X	X	X				
	1.25			X	X	X				
1.60	1.60		X	X	X					
	2.00		X	X	X					
2.50	2.50	X	X	X						
	3.15	X	X	X						
4.00	4.00	X	X							
	5.00	X	X							
6.30	6.30	X								
	8.00	X								
10.0	10.0									

Table V. Reactor—Enclosure Size Combinations

Type of Reactor	Enclosure, Minimum Dimensions Width	Depth	Height	Reactor Nominal Circuit Volts	Reactor, Maximum Kilovolt-Amperes
1. Current-limiting, self-cooled	—	—	—	600	—
	—	—	—	2,400	—
	—	—	—	4,160	—
	—	—	—	7,200	—
	—	—	—	12,470	—
	—	—	—	14,400	—
	—	—	—	23,000	—
	—	—	—	27,600	—
	—	—	—	34,500	—
	—	—	—	46,000	—
2. Current-limiting, fan-cooled	—	—	—	—	—

ductance as established by ASA C 57.16–1948[2] as minus 3 per cent plus 7 per cent, or in effect ±5 per cent. When the standardization is developed so that frequent duplications are manufactured, the actual variations will probably be less.

Standard Physical Sizes of Reactors and Enclosures

After the ratings of reactors have been standardized, the physical sizes should be standardized. Experience should establish the most practical designs to keep at a minimum material, floor space, heating, and so forth for the lowest cost. The definite trend toward the use of enclosures would allow a recommended practice to be set up between enclosure and reactor sizes.

It may be desirable to standardize the reactor enclosure sizes with the sizes of other metal-clad equipment. However, three items should be pointed out. First, in the past, metal-clad enclosure sizes have fluctuated from time to time. Second, if metal-clad enclosures are going to be standardized, the sizes should be established by definite steps (as six inches) in depth, width, and height, or the sizes should be established by the series of preferred numbers. Third, it must not be overlooked that reactors dissipate heat and that clearances must be provided for air circulation.

Enclosure sizes could be established by minimum height and inside dimension for maximum reactor voltage and kilovolt-amperes as suggested in Table V. Adequate strike distance and working space inside should be provided. Special sizes will probably be required occasionally.

Advantages of Reactor Standardization

Some of the advantages of reactor standardization are:

1. Acceptance of preferred ratings should eventually result in: reduced costs; shorter delivery time; better use of materials as tests and service on the same size of reactor will point to improvements.

2. Standardizing on ohms on a 60-cycle basis rather than on per cent *IX* will be very helpful in promoting preferred ratings.

3. The use of preferred sizes (as on a rating target) will allow reactors and enclosures to be designed and used in logical sizes. Enclosure sizes and designs can then be made to harmonize with other metal-clad equipment.

4. Voltage and current ratings will be in agreement with accepted standards.

References

1. Preferred Voltage Ratings for A-C Systems and Equipment. *Report*, Joint Subcommittee of Edison Electric Institute and National Electrical Manufacturers Association (New York, N. Y.), May 1949.

2. Current-Limiting Reactors, *C57.16–1948*. American Standards Association (New York, N. Y.), 1948.

3. Neutral Grounding Devices. *AIEE Standard Number 32*, 1947.

4. Preferred Numbers, *Z17.1–1936*. American Standards Association (New York, N. Y.), 1936.

5. Schedule of Preferred Ratings for Power Circuit Breakers, *C37.6–1945*. American Standards Association (New York, N. Y.), 1945.

6. Instrument Transformers, *C57.13–1948*. American Standards Association (New York, N. Y.), 1948.

7. Power Circuit Breaker Standards. National Electrical Manufacturers Association (New York, N. Y.), *Publication Number 46–116*, 1946.

Discussion

J. A. Elzi (The Commonwealth and Southern Corporation, Jackson, Mich.): There is no question as to the desirability of standardization of certain types of reactors which are used on power systems; particularly those used on distribution circuits to protect feeder voltage regulators, distribution equipment in underground vaults, and those used to limit fault currents and thus reduce shock to the system and circuit breaker duty. However, some of the recommended standard values given in this paper should be given further consideration.

Voltage Classes

It seems that since the EEI-NEMA preferred voltage report[1] stops at 230,000 volts, it is undesirable to include the higher voltages which still have not been standardized. In fact, for the type of standardization discussed in this paper, that is, reactors that are used in quantity, it appears that the standardization should terminate with the 23,000- or 34,500-volt rating.

Current Classes

The authors mention that continuous current ratings of current limiting reactors have been established by past usage and in Table II a comparison is made between present American Standard Association preferred reactor current ratings and the current ratings of circuit breakers and current transformers. It is not felt that the comparison is parallel. The latest ASA circuit breaker tables[2] start with a continuous current rating of 600 amperes and a large number of standard reactor ratings would be below this value. In the case of the current transformers, the current ratings are influenced by the requirements of instruments and relays and do not necessarily indicate the requirements for reactors. The applications where reactors would be used in numbers would be on distribution circuits and the current ratings chosen should be such as to meet the requirements of such circuits. It would seem very important to co-ordinate the reactor current ratings with the preferred current ratings of feeder voltage regulators. There is some evidence that the current ratings of regulators need revision, but it is felt that the current ratings of the regulators and reactors should be co-ordinated.

The authors recommend the use of ratings based on a preferred series of numbers. This is probably a good method of arriving at the steps in general, but from practical considerations it is thought that for purposes of standardization it would be advantageous to avoid such numbers as 160 amperes, 315 amperes, and so forth. For practical purposes these could just as well be 150 amperes, 300 amperes, and so forth.

Inductance Unit

The authors' recommendation that the ohm be used as the standard unit to express inductance would, it seems, be detrimental rather than helpful in promoting preferred ratings. Application engineers are interested in the percentage drop introduced by reactors and in most cases would have to convert ohms into per cent in making their calculations. The per unit or per cent method is widely used for circuits and other apparatus, and we feel that the use of ohms for standard reactors would be very unsatisfactory. It is true that for certain types of reactors the use of ohms is desirable, but these would fall into a minor class and need not affect general standardization.

Standard Physical Sizes

The authors have an excellent point in recommending standardizing of physical size. It appears that this should be entirely practicable and would certainly be welcomed by the users.

REFERENCE

1. See reference 1 of the paper.

2. PREFERRED RATINGS FOR POWER CIRCUIT BREAKERS, *C37-6-1949*. American Standards Association (New York, N. Y.), 1949.

N. E. Dillow (General Electric Company, Schenectady, N. Y.): The authors have shown that there are many advantages to be gained from reactor standardization. However, when the question of standardization is raised in any line of apparatus the question arises as to the limitations in the application of the standardized line. It therefore appears desirable to consider the proposals made by the authors from the application viewpoint.

The nominal voltage ratings for reactors listed in Table I of the paper are chosen from the listings in the EEI-NEMA report. Considering system application, current-limiting reactors will generally be installed where they are subjected to voltages tabulated in the EEI-NEMA report as the range of the tolerable zone for voltages at substations and on transmission systems. The values listed in Table I of the paper as the maximum design voltage rating agree with the maximum of the tolerable zone. Hence, the proposal should adequately meet the application requirements as to voltage ratings.

Current-limiting reactors generally are applied in series with circuit breakers and current transformers. It is for this reason, probably, that the authors have listed the present American Standard Association current ratings for these equipments in addition to the recommended reactor ampere ratings. There is reasonable correspondence among the columns, and from an application viewpoint, the ampere ratings listed in Table II of the paper as the preferred sizes (60 per cent steps) appear to offer sufficient choice of current ratings.

By habit, application engineers have considered the inductive size of a reactor as a per cent reactance. This follows easily from the calculations usually employed to determine the reactance to limit the short-circuit currents or to balance loadings on parallel circuits. However, the conversion of per cent quantities to basic ohmic values also is a step familiar to the application engineer as he must use such conversions in calculations involving wires and cables. Hence, such a proposal to rate reactors in ohms should be acceptable.

Consider an example for the application of the standardized ratings proposed in the paper: assume a 13.2 kv feeder, rated at 5,000-kva capacity. It is desired to limit the 3-phase short-circuit current in the feeder to 100,000 kva maximum. A short circuit on the bus is 250,000 kva. Specify the standardized reactor ratings.

Calculations:

$$\text{Equivalent bus reactance} = \frac{5,000}{250,000} = 2.0 \text{ per cent}$$

(5,000 kva base)

$$\text{Desired feeder reactance} = \frac{5,000}{100,000} = 5 \text{ per cent}$$

Reactor reactance required = 3 per cent
Base ohms (5,000 kva, 13.2 kv) = 34.85 ohms
Reactor ohms = 1.05
Reactor current = 219 amperes

Specify reactor as follows:

Nominal voltage rating = 14.4 kv (Table I)
Continuous current rating = 250 amperes (Table II;
Reactor reactance = 1.00 ohms (Table III)

These ratings are compatible with the application. The reactance specified is actually nearer the calculated value than the accuracy of the usual data justifies. In addition, manufacturing tolerances allowed would permit almost as large a variation as exists between the specified and calculated value.

The proposals of the paper would not place any limitation on the general application of current-limiting reactors.

F. H. Kierstead and **J. L. Thomason:** In also advocating the standardization of reactor ratings but with some controversial suggestions, J. A. Elzi has undoubtedly brought up points which other engineers and members of the AIEE, NEMA, and EEI may wish to consider. The standardization of reactor ratings will be satisfactory to all concerned only if first, there are enough ratings to cover the fields of applications and if second, there are few enough ratings so that economies may be realized.

Regarding circuit voltages, the discusser recommends a top limit of 23,000 or 34,500. Some such limit within a frequently used range would certainly form a practical starting point in the standardization program.

Regarding the current ratings of reactors, the problem again seems to be basically economics:

First, it would appear that if all apparatus carrying the same current had the same current rating, the cost of the whole group would be a minimum. Second, it is undoubtedly more economical to supply certain apparatus with a higher current rating than needed if this rating is a frequently used standard. Third, the use of current ratings based upon the 60 per cent steps by the series of preferred numbers gives a logical and wide choice of ampere ratings. In the future, as standards are changed, it is recommended that all apparatus be given ampere ratings according to the preferred series of numbers; subdivisions then would be logical and orderly. During or before this transition period it will probably be necessary to retain ampere ratings in the well-established "round number" classes; economies will result when sizes are frequently duplicated.

Regarding the inductance unit, the ohm is considered best for the reasons set forth in the paper. All applications can be calculated on a percentage basis. Then the reactor can be ordered on a standard ohm rating.

The standardization of the physical features of reactors is desirable but is largely dependent upon first achieving standardization of the ratings of the reactors.

Mr. Dillow has analyzed the standardization of reactor ratings from the application viewpoint. He has shown that there are several advantages and no limitation by such standardization.

Use of Thyrite in Power Transformers

J. R. MEADOR
MEMBER AIEE

ELECTROSTATIC shielding long has been recognized as an effective means of controlling the impulse-voltage distribution in transformer windings. Under certain conditions, the same, or a better, result can be achieved by the use of Thyrite.*

The development of Thyrite[1] was reported in 1930. This ceramic-bonded inorganic material, strong, stable, and possessing precise electrical characteristics, is characterized by its nonlinear resistance; it passes a current proportional to a relatively high exponent of the applied voltage. Developed as a material for lightning arresters, its versatility is attested by its many important applications. One of these is the part it takes in the internal protection and "shielding" of power-transformer windings.

The increase in complexity of power transformers, particularly from a circuit standpoint, has been so gradual as to be almost imperceptible. A comparison between the modern transformer and its 25-year-old counterpart, however, reveals startling differences. The simple 2-winding machine with a ten per cent tap range, typical of the vast majority of transformers formerly produced, now represents an ever-diminishing share of power-transformer production. On the other hand, the enormous increase in the use of autotransformers, regulating transformers, load-ratio-control transformers, and transformers with complicated winding arrangements and wide tap ranges has introduced to the designer new problems of winding protection against overvoltages. Thyrite, immersed in the transformer oil and shunting portions of the windings, has, in the past ten years, achieved a prominent position in the solution of these problems.

Although the use of Thyrite in transformers, as described in this paper, has proved eminently successful for effectively controlling overvoltages within the transformer, this advance does not eliminate the necessity for normal protection consisting of modern lightning arresters connected from line to ground in the station, and overhead ground wire shielding of the station structure and at least 2,500 feet of connected transmission lines adjacent to the station.

Thyrite Characteristics

Thyrite used in transformers is normally in the form of standardized disks, either $1^1/_2$ inches thick and 3 inches in diameter, or 3/4 inch thick and 6 inches in diameter (Figure 1). Its high mechanical strength, about 23,000 pounds per square inch in compression, and its electrical and thermal stability under pressure or vibration make for trouble-free performance.

The volt-ampere characteristic of transformer Thyrite is

$$I = KE^N$$

where I and E are the instantaneous values of current passed and voltage applied, respectively, and K and N are constants depending on the disk dimensions and constituents. The constant K can be controlled over a wide range of values.

The exponent N is usually of the order of 3.5, so that an elevenfold current increase through the Thyrite causes only a doubling of the voltage across it. Since the volt-ampere relationship is independent of time, it applies equally to alternating, direct, or impulse voltages and currents, as long as instantaneous values are considered.

While Thyrite can be used continuously at 110 degrees centigrade, and for short periods at 150 degrees centigrade, the limit maintained in transformers is the same as the winding hot spot temperature; that is, 95 degrees centigrade.

Application in Transformers

Thyrite is used within transformers to perform one or more of three important functions:

1. To limit the impulse voltage across the portion of the winding to which it is applied
2. To control the impulse-voltage distribution in the portion of winding across which it is connected.
3. To establish and fix the potential of momentarily or continuously "floating" windings. This application is not discussed in this paper.

In the first case, a portion of winding is shunted by a stack of Thyrite disks and the nonlinear character of the material is such that at normal power-frequency operating voltages, its resistance is sufficiently high so as to have no measurable effect on the transformer. When carrying high surge currents, however, its resistance falls and limits the voltage drop across it and across the connected portion of the winding to a predetermined safe level.

In some instances, additional protection is needed, and the Thyrite is called upon to serve its second function. It is a well-known fact that a transformer winding is a rather intricate network of inductances interturn and intercoil capacitances, and capacitances to ground. At normal operating frequencies, the capacitances can be disregarded and the winding considered as a nearly pure inductance with a uniform linear distribution of voltage throughout its length. Under impulse conditions, the capacitances become prominent and alter the voltage distribution. Thus, intermediate parts of the Thyrite-shunted winding may develop high voltage gradients even though the voltage between the ends of the

---

* Registered trade-mark of General Electric Company.

Paper 49-192, recommended by the AIEE Transformers Committee and approved by the AIEE Technical Program Committee for presentation at the AIEE Summer General Meeting, Swampscott, Mass., June 20–24, 1949. Manuscript submitted February 10, 1949; made available for printing May 2, 1949.

J. R. MEADOR is with the General Electric Company, Pittsfield, Mass.

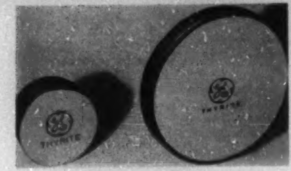

Figure 1. Thyrite disks: 3 inches in diameter and 1 1/2 inches thick; and 6 inches in diameter and 3/4 inch thick

winding is controlled by the Thyrite. If, now, intermediate points of the winding are connected to intermediate points of the Thyrite stack, the voltage distribution in the winding can be made to approach its normal power-frequency linearity. This follows from the fact that the Thyrite stack behaves as a pure resistance which is quite low under high transient voltages compared with the impedance of the shunted winding, and consequently it divides the voltage uniformly along the Thyrite and winding.

Before going on to a detailed examination of some of the applications, it is well to distinguish briefly between the employment of Thyrite in transformers and in lightning arresters. Gaps are not used in series with the Thyrite disks in the transformer; hence, the resistance of the Thyrite must be high enough at normal power-frequency operating voltage to limit the heat loss to a value easily dissipated into the oil. In valve-type lightning arresters, which utilize gaps to seal the power-frequency follow current after discharge of an impulse through the arrester, a lower Thyrite resistance at normal operating power voltage is permissible, since the Thyrite valve element is disconnected from the circuit except during, and immediately following, an impulse discharge.

Thyrite Across Taps in Transformers

Almost all transformers have taps in one or more windings for changing the turn ratio. In a simple 2-winding transformer with, say, four $2^1/_2$ per cent taps, the taps introduce no particular problem to the designer, since the only winding structures that are used are those that can be tapped. A line of standardized ratio adjusters is normally available to cover the usual range. The problem of the number and type of ratio adjusters to provide is a simple question of economics. It is obviously impractical to design a new ratio adjuster for every transformer. It is equally impractical to expect one or two ratio-adjuster designs to fill economically the needs of all transformers.

Ratio adjusters basically must meet two requirements:

1. The insulation between adjacent taps and across the tap range must withstand the continuous voltage to which it is to be subjected.
2. The insulation between adjacent taps and across the tap range must withstand the impulse voltage that appears in the portion of the winding to which it is connected.

Thus, a ratio adjuster normally has a double rating; (a) the voltage at which it can be continuously operated; (b) and a safe withstand impulse strength between its parts.

The method of application of the first rating is obvious. Its selection from the standpoint of the second rating depends on the insulation level of the winding, the percentage of the winding connected across the ratio adjuster, and the impulse-voltage distribution in the winding. Unless these conditions are known and met, there can be no assurance that the adjuster application is correct.

In very-high-voltage transformers or for abnormally large tap ranges, there is often a choice between using a high-voltage ratio adjuster in the normal way or using a lower-voltage ratio adjuster and shunting all or part of the tap range with Thyrite.

The choice is made on the basis of over-all economy. If a certain adjuster meets rating but is inadequate on rating, it is sometimes to advantage to shunt all or part of the taps with Thyrite and thereby bring the tap-range impulse requirements down to the rating of the adjuster.

Sometimes, because of some unusual design requirement, the impulse-voltage distribution in the tap winding may be difficult to calculate with a sufficient degree of accuracy. In such cases, the predictability of the Thyrite-shunted taps may justify the use of Thyrite.

The two usual types of tap connections and the shunting Thyrite are shown in Figure 2(A) and 2(B).

A typical example of the quantitative effect of the Thyrite shunt across the tap range is shown by the test points plotted in Figure 3. The 10.5 per cent tap range is shunted with Thyrite. By changing the number of disks, the impulse voltage across the taps can be held to almost any desired level as shown by the curve. In general, the Thyrite is selected to permit the tap range to have its normal share of the applied impulse voltage (that is a 10 per cent voltage for a 10 per cent tap range).

Autotransformers

Thyrite is particularly useful in autotransformers. To explain these applications, it is necessary to mention briefly some of the rather exacting demands of autotransformer designs. From an insulation standpoint they are as follows (refer to Figure 4):

1. High-voltage (*HV*) taps may be for ten per cent of the terminal voltage, but if the co-ratio is low (such as in a 138-kv grounded wye to 115-kv grounded wye), the taps may be 30 to 50 per cent of the series winding.

Figure 2 (below). Thyrite across transformer taps

Figure 3 (right). Effect of Thyrite shunt on impulse voltage across taps in unshielded winding

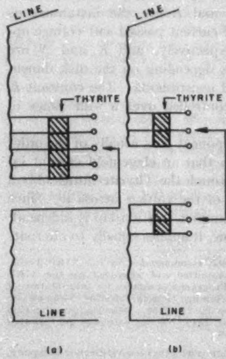

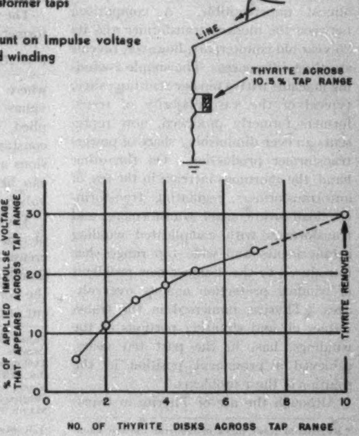

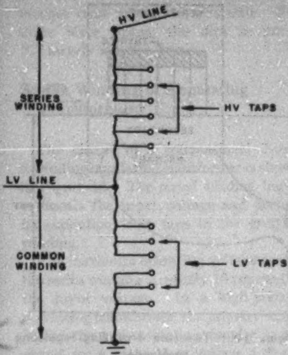

Figure 4. Autotransformer with taps in common and series windings

2. Although only a small percentage of the turns from the high-voltage terminal to ground may be in the series winding, a large percentage of the voltage appears across the series winding when an impulse voltage is applied to the high-voltage terminal. This is caused by the relatively low impedance from the low-voltage (*LV*) terminal to ground which results from connecting the low-voltage terminal to a transmission line or other similar load.

3. It is often desirable to place taps in the common winding immediately adjacent to the low-voltage terminal, rather than in the middle of the common winding as was shown in Figure 4.

4. The series winding may have an impulse voltage applied to either of its terminals. While this condition is the same as that in any delta-connected winding, nevertheless it introduces special problems when it occurs in combination with some or all of the aforementioned requirements.

The role of Thyrite in helping to meet these demands will be discussed in detail.

An example of items 1 and 2 is shown in Figure 5. An autotransformer rated 132-kv grounded wye to 62.7-kv grounded wye has taps for changing the voltage from 115.5 kv to 141.9 kv. While this range is 20 per cent of rated voltage, the taps are 33 per cent of the series winding. Impulse-voltage distribution tests were made for two different conditions: with the low-voltage terminal grounded; and with 630 ohms connected from the low-voltage terminal to ground. In both cases, the ratio adjuster was set on the minimum tap, and the impulse was applied to the high-voltage terminal. Under these conditions, the impulse voltages measured were as follows:

Resistance, Ohms, Low-Voltage Terminal to Ground	Per Cent of Applied Voltage Across Series Winding	Per Cent of Applied Voltage across Ratio Adjuster and Tap "Break"	
		With Thyrite	No Thyrite
630	80	31	51
0	100	29	63

The two conditions of "loading" the low-voltage terminal represent a wide range of service conditions. The Thyrite shunt across the taps holds the tap-range voltage to a relatively constant, normal magnitude. It should be added that the series winding in this case was well shielded electrostatically. The improvement brought about by the Thyrite would have been much greater in an unshielded winding since the tap voltage without Thyrite would have been much greater.

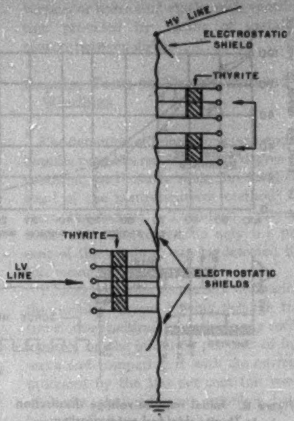

Figure 6. Autotransformer having common-winding taps located at the low-voltage line

Figure 4 shows taps located in the center of the common winding. Placing these taps immediately adjacent to the low-voltage line is a safe procedure if the taps are shunted with Thyrite as shown in Figure 6. Without a Thyrite shunt, this is a hazardous practice because of the high transient voltages that may exist across the tap coils, tap leads, ratio adjusters, and so on.

Furthermore, if the low-voltage line voltage is such that electrostatic shields are used, the Thyrite shunt permits the shields to be fully effective when connected at the extremities of the tap range as shown in Figure 6. When an impulse voltage is applied to the low-voltage terminal, the charging current to the shields is furnished through the Thyrite instead of through the series capacitance of the tap portion of the winding.

An extreme example of autotransformer taps is shown in Figure 7. In this case, two systems of essentially the same voltage were connected by this auto-

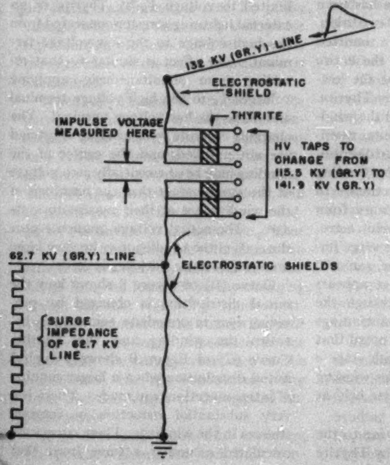
132 KV (GR.Y) LINE
ELECTROSTATIC SHIELD
IMPULSE VOLTAGE MEASURED HERE
THYRITE
HV TAPS TO CHANGE FROM 115.5 KV (GR.Y) TO 141.9 KV (GR.Y)
62.7 KV (GR.Y) LINE
ELECTROSTATIC SHIELDS
SURGE IMPEDANCE OF 62.7 KV LINE

Figure 5. (left). Autotransformer tested for voltage across high-voltage taps with impulse applied to 132-kv line

Figure 7 (right). Autotransformer for equal high-voltage and low-voltage tap range

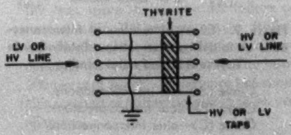

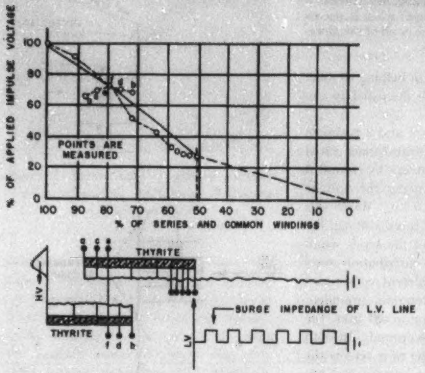

Figure 8. Initial impulse-voltage distribution in Thyrite-shielded series winding

transformer with the expectation that power might flow in either direction. The problem here is similar to that illustrated by Figure 6. With a Thyrite shunt, taps can be placed at any location in a winding without fear of transient-voltage trouble.

Item 4 in the autotransformer design requirements concerns the impulse-voltage distribution in the untapped portion of the series winding. As has been shown, the major portion of the impulse voltage reaching the high-voltage terminal may appear across the series winding. Consequently, in medium- and high-voltage transformers, the series winding usually must be shielded.

In general, an electrostatic shield is used to nullify the ground capacitance of a winding so as to achieve a reasonably uniform impulse-voltage distribution in the winding. In this way, harmful concentrations of voltage are avoided. Shields are very effective and their application is straightforward in transformers of normal proportions.

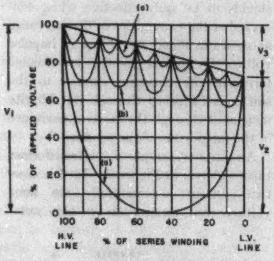

Figure 9. Effect of number of interconnections on initial impulse-voltage distribution in Thyrite-shielded series winding

Curve (A)—no interconnections
Curve (B)—four interconnections
Curve (C)—nine interconnections

Occasionally, the untapped portion of a series winding is so small physically or contains such a small number of turns that conventional electrostatic shielding is inadequate to maintain a reasonable impulse-voltage distribution. This condition is aggravated by an abnormally large tap range. Optimum shielding designed for one tap connection may leave much to be desired for a widely different tap connection.

Figure 8 shows how Thyrite has been used to advantage for such a condition. The conventional shields are omitted from the series winding, and the entire winding (including the taps at the low-voltage terminal) is shunted by Thyrite. By connecting the Thyrite and the winding together at numerous points, essentially straight-line initial voltage distribution is obtained throughout the winding in the circuit for all tap connections. In this case, with a surge impedance from low-voltage terminal to ground corresponding approximately to the surge impedance of the low-voltage line, some 70 per cent of the applied voltage appears across the series winding, although the turns in the series and common windings are about the same. It will be noted that the "overhanging taps" (with tap *e* connected to tap *f*) in the series winding that are not in the circuit all are held at essentially the same potential.

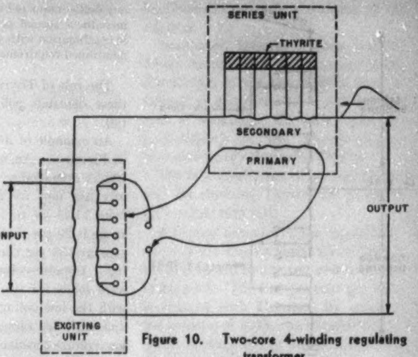

Figure 10. Two-core 4-winding regulating transformer

An interesting problem relating to the "shielding" of series windings by Thyrite concerns the necessity for interconnections between the windings and the Thyrite. It may be asked why the same result can not be obtained using an unshielded series winding and a lightning arrester connected across the terminals of the winding. The arrester will definitely limit the surge voltage appearing between the high-voltage and low-voltage terminals. It may, however, have little, if any, effect on the internal voltages (between turns and coils and between taps) in the winding. Figure 9 shows what happens.

Curve (A) of Figure 9 shows the initial impulse-voltage distribution in a series winding when an impulse voltage V_1 is applied to the high-voltage terminal and the impulse voltage across the winding is limited to voltage V_3 by Thyrite or an external lightning arrester connected from the high-voltage to the low-voltage terminal. The effect is similar to that resulting from simultaneously applying voltages V_1 to the high-voltage terminal and V_2 to the low-voltage terminal. The charging currents from winding to ground are not nullified, and the center of the winding may be at essentially zero voltage at the same instant that the terminals of the winding are at their maximum voltages. The actual voltage gradients near the ends of the winding may be very large if no electrostatic shielding is used.

Curve (B) of Figure 9 shows how the initial distribution is changed by providing four intermediate connections between the winding and the Thyrite. Curve (C) of Figure 9 shows a typical initial distribution when a larger number of interconnections are made. There is a very substantial reduction in internal stresses in the winding. These curves are calculated assuming a wave front that reaches crest voltage in zero time. For finite wave fronts, the dips in curve (C) largely will disappear.

Series Winding of Regulating Transformers

The circuit of a conventional 2-core 4-winding regulating transformer is shown in Figure 10. The series winding bucks or boosts the input voltage and derives its excitation from taps in the exciting winding.

The maximum operating voltage across the series winding is usually 10 per cent of the input voltage. In a high-voltage regulating transformer, the primary winding of the series winding usually is designed for a rather low voltage to keep down the size of the tap-changing equipment. In many cases, the primary and secondary windings of the series transformers have approximately the same number of turns.

As has been pointed out for autotransformers, when an impulse voltage is applied to the high-voltage terminal, the majority of the voltage appears across the series winding. The same phenomenon occurs in a regulating transformer. It is well known that electromagnetic transfer of impulse voltages occurs between transformer windings, the induced voltage being in the ratio of the turns in the two windings in many cases.

Referring again to Figure 10, assume that the input voltage is 115 kv wye and the maximum series-winding voltage is 11.5 kv wye (6.64 kv phase voltage). Also, assume that the primary winding of the series transformer is 6.64 kv phase voltage, which is a reasonable voltage for tap-changing purposes. (In other words, the turn ratio of the series transformer is one to one).

When an impulse is applied to the output terminal of a magnitude consistent with the protective equipment on a 115-kv system, the bulk of the voltage may appear across the series winding. This voltage, under some conditions, will be transferred into the low-voltage winding at the turn ratio of one to one. That is, the bulk of the impulse voltage that can appear on a 115-kv system will be transferred into the low-voltage tap-changing circuit of the regulating transformer. The exact amount of the voltage depends mainly on the surge impedance of the input line, the leakage reactance of the transformer, the tap connections being used, and the length of the applied impulse wave.

It is obviously impractical to design the primary circuit for such high voltages. The solution is to limit the voltage across the series winding by shunting the winding with Thyrite or with an external lightning arrester. In high-voltage circuits, this brings up the same problem as that encountered in autotransformers and illustrated by Figure 9. Thyrite across the winding, connected at a proper number of intermediate points, not only limits the voltage appearing across the winding, but also distributes the surge voltage uniformly across the winding. (Under some conditions it is desirable to use Thyrite across the winding for voltage-distribution purposes, and, in addition, to shunt the winding with an external lightning arrester.)

Precautions Observed in Use of Thyrite

Thousands of Thyrite disks a year are used in power transformers in the manner described in this paper. None has failed to function properly in service. This 100 per cent service record is largely due to the care used in the Thyrite applications.

After manufacture, every Thyrite disk is tested for resistivity and stamped with a marking that is keyed to a volt-ampere curve. The transformer designer selects the disks needed from these curves. Before the disk assembly is mounted in the transformer, it is tested for resistivity. The induced voltage test on the completed transformer provides the final test.

Successful application of Thyrite in transformers requires that the same attention be paid to proper supporting and bracing of the Thyrite as is given to the winding and insulation of the transformer.

When a portion of winding is shunted by Thyrite, three thermal requirements are met: the number of disks in series is such that with continuous operating voltage across the Thyrite a temperature of 95 degrees centigrade is not exceeded; the Thyrite loss during induced voltage test (usually 3.46 times normal voltage or less) is within the heat storage capacity of the disks; and the energy input into the Thyrite is within its heat storage capacity during a system fault, when abnormal voltages may appear across a winding (notably, the series winding of an autotransformer).

All of these requirements are subject to calculation and are the basis for the selection of the disks. The insulation between turns, coils, taps, and so on, of the winding is determined from the expected impulse voltage across the Thyrite. Thyrite disks may be mounted in either vertical or horizontal stacks with ventilation provided by means of metallic spacers between disks.

Impulse Tests on Thyrite Shunted Windings

The detection of failures on commercial impulse tests has reached a high degree of precision, particularly since the development of the neutral-current method[3] of wave comparison. Turn-turn failures, where one turn represents only 0.1 per cent of the winding, can be detected by this means.

Failure detection consists of measuring the impulse current flowing through the transformer neutral, by cathode-ray oscillograph, on the initial 50 per cent of full wave and comparing it with the current produced by the 100 per cent full wave after the chopped wave impulses have been applied.

Failure is indicated by a difference in the wave shape. The wave changes because the failure has short-circuited a portion of the winding, and, consequently, the circuit constants of the winding have changed.

When Thyrite shunts part of a winding, the equivalent circuit of the transformer contains a resistor across that part of the circuit. Thyrite, however, does not have a constant resistance. Consequently, the equivalent circuit of the transformer is different for applied impulses of different crest values. Therefore, the neutral-current wave shape changes slightly for different applied voltages; that is, the initial 50 per cent impulse produces a different wave shape from the final 100 per cent impulse.

A new technique has been developed to handle circuits of this kind. Fortunately, as higher impulse voltages are applied to the line terminal, the change in circuit constants produced by the change in Thyrite resistance is gradual and the change in the neutral-current wave shape is gradual. Thus a trend is observable and departures from this trend show failure.

The test technique consists of applying initial full waves of 50, 70, and 100 per cent followed by the chopped waves and ending with a 100 per cent full wave. Comparison of the first two initial waves of 50 and 70 per cent with the initial 100 per cent wave shows whether failure occurred on the 100 per cent wave. Following the chopped waves, the final 100 per cent full wave is compared with the initial 100 per cent wave. Experience has shown this method of failure detection to be very effective.

Conclusions

Thyrite, a nonlinear resistance material, has many effective uses in power transformers. It is another means for controlling transient voltages in windings. It is used to supplement and in some cases to replace electrostatic shielding.

Thyrite has easily determinable and precise electrical characteristics. Its mechanical properties are excellent. As used in transformers, it has very high surge-current capacity, and since no gaps are used, the problem of interrupting follow current does not exist. The low-frequency loss in the Thyrite has little, if any, measurable effect on the transformer characteristics.

Thyrite is particularly useful in autotransformers and regulating transformers where normally certain insulation and transient-voltage problems are more acute than in simple 2-winding power transformers.

The remarkably good service record of Thyrite, which has been used in hundreds of transformers during the past ten years, is a result of careful electrical and mechanical application.

References

1. THYRITE, A NEW MATERIAL FOR LIGHTNING ARRESTERS, K. B. McEachron. *AIEE Transactions*, volume 49, April section, 1930, pages 411–17.

2. PROGRESS IN IMPULSE TESTING OF TRANSFORMERS, J. H. Hagenguth. *AIEE Transactions*, volume 63, 1944, pages 999–1005.

Discussion

W. H. Eason (General Electric Company, Pittsfield, Mass.): Mr. Meador points out that Thyrite possesses "precise electrical characteristics." Because of its nonlinear resistance characteristics, this material has found many other important applications in the central-station, industrial, and electronics fields, notably as discharge resistors for inductive circuits and in voltage stabilizing circuits. Engineers using Thyrite in these applications generally will find that it is necessary to allow electrical tolerances of ±30 per cent in applied voltage at a given current. Mr. Meador's statement and this fact do not at first glance appear to be in agreement and may require further elaboration.

A specific Thyrite disk does possess precise electrical characteristics and is stable over reasonable ranges of temperature and humidity. There are many variables which enter into the complex manufacturing processes involved in producing Thyrite. Each affects the ultimate electrical characteristics to some degree. Elaborate precautions taken during manufacture reduce these variations to a minimum, but their number is such that it is not possible to predict the ultimate electrical characteristics closer than the ±30 per cent indicated. However, dictates of design in circuits utilizing Thyrite generally permit such tolerances.

Every Thyrite disk is tested during manufacture to determine its electrical characteristic. The tolerance may be considerably narrowed by dividing a given "batch" of disks into narrower classes during production testing.

The use of Thyrite in transformers is large enough and the requirements are sufficiently diversified so that various combinations of classes of disks may be selected to give the required characteristics and still utilize the entire production.

The same procedure has been followed in special Thyrite disks made for other high production applications. A case in point is a discharge resistor for protection of large generator fields, which utilizes 20 disks connected in parallel. During manufacture these disks are segregated into three resistance ranges and designated as class *A*, *B*, or *C*. In assembling the resistor, care is taken to use as many class *A* as class *C* disks, so that the over-all electrical characteristics are those of 20 class *B* disks; the tolerance thus is effectively reduced by 67 per cent.

Extremes in the Insulation Co-ordination of Oil Insulated Transformers

F. J. VOGEL
MEMBER AIEE

THE margins obtained and degree of co-ordination between transformers and other insulation in transmission systems depends largely on the possibilities inherent in the insulation design of the transformer. Recently some units have been designed which take full advantage of the impulse characteristics of insulating materials as compared to their 60-cycle strengths. These designs are core form, or at least have concentric coils, and it is likely that they might be considered to have maximum impulse characteristics compatible with present 60-cycle test requirements. It is believed that these characteristics affect, and should be given consideration, in the setting of future required impulse levels and tests, and perhaps in the 60-cycle tests which are required. The basic insulation levels only include full-wave values and it is believed that this is not sufficient for transformers. This matter affects the cost and the service reliability of transformers. It is believed that besides the basic insulation level, either a steep front or other type of test should be included.

Design Considerations and Test Data, 69-Kv Transformers

To illustrate some of the problems confronting both the system and transformer designer, one important design consideration and the results of some tests made in the development of a possible new line of transformers are described.

It is believed that irrespective of present standards, the major insulation, and the turn-to-turn and coil-to-coil insulation should be about equal in impulse strength.

Present rules do not require this relationship, but investigation shows that the saving using a relatively weak winding is small. The designs referred to in this paper were made so that the winding strength is in excess of the insulation strength to ground. Tests to check the design have been made on a 1,000-kva 34.5-kv transformer, a 667-kva 69-kv transformer, and a 69-kv potential transformer. The results of the tests on the 667-kva transformer, which are representative, are shown in Tables I and II. With the exception of the failure to ground on X_1, no failures were found, as X_2 showed no signs of failure. The tests on the 1,000-kva 34.5-kv unit were somewhat similar except that the gap length and voltages were reduced. The 69-kv potential transformer tests were similar to those above. The 667-kv transformers did not fail to ground with a 60-cycle voltage of 160 kv on the high-voltage winding.

ANALYSIS OF RESULTS

Table III shows the actual demonstrated strengths with present American Standards Association (ASA) and National Electrical Manufacturers Association (NEMA) requirements.

Let us analyze these tests. A margin, so that there will be practically no shop failures, is necessary. The extreme right-hand column would not be safe to use as guaranteed values. Margins used differ and are those deemed reasonable by the manufacturer. The margin ensures freedom from injury on test except for defective materials or assembly.

The chopped wave tests under present circumstances do not prove very much, at least, with these designs. If the bushing is flashed over, it indicates that the windings will stand more than the bushing and this characteristic may be desirable. The full-wave test made with the oversize bushing emphasizes the correlation between 60-cycle strength and impulse strength for the core-type construction. If full-wave co-ordination and tests only were required, it is obvious that a large decrease in insulation would be possible, at least in the ratio of 450/410, or nearly one voltage class.

The steep-front tests indicate a larger margin between test and requirements in terms of voltage than actually exists, due to the effect of time and the fact that to meet 580 kv, considerable variation in test conditions requires designing to meet 620 kv or more, with a margin besides.

The question then arises, is the steep front test and NEMA value desirable? In the case of the design of some bushings, flashover would occur, likely porcelain breakage, and possibly even fire. Other bushings have much higher steep front strength. Unless some type of gap is used which will protect both the transformer and bushing, it may not be desirable. But there are two other points of view.

Suppose the user wishes to depend alone on gap protection. It seems likely that a very good degree of protection to the transformer and bushing can be obtained at the expense of some gap flashovers and outages. One user does.

Suppose also that the operator uses line type lightning arresters. Lines of the above ratings are not always well protected. Several cases of bushing flashover and damage even when lightning arresters and ground wire protection were used have occurred. In one case the lightning arrester and transformer were both badly damaged and the operator was extremely irate over what he felt to be a case of poor transformer design. Hence,

---

Paper 49-195, recommended by the AIEE Transformers Committee and approved by the AIEE Technical Program Committee for presentation at the AIEE Summer General Meeting, Swampscott, Mass., June 20–24, 1949. Manuscript submitted November 15, 1948; made available for printing May 2, 1949.

F. J. VOGEL is Professor of Electrical Engineering, Illinois Institute of Technology, Chicago, Ill.

The test data presented here are by the courtesy of the Allis-Chalmers Manufacturing Company, and were taken in the course of development work done both in their Pittsburgh and West Allis works.

Table I. Impulse Tests on 667-Kva 69-Kv Transformer, High-Voltage Winding

Type of Test	Oscillogram	Rod Gap, Inches	Number of Tests	Average Kilovolts
Reduced front waves			2	181
Steep front waves		14½	3	648
Chopped waves			2	418
Full waves			4	350
Steep front waves	*2393-2*	14½	25	663
Steep front waves	*2408-1a*	15½	25	746
Steep front waves	*2409*	16½	13*	833
Full wave**	*2410-1o*		2	354
Full wave			15	355
Full wave			15	380
Full wave			15	402
Full wave			15	423
Full wave			15	450
Full wave	*2422-12c* *2422-12d*		2†	472

* Bushing porcelain broken.

** Oversize bushing installed.

† Transformer winding failed to ground—no failure found in turns or coils.

Table II. Impulse Tests on 667-Kva 69-Kv Transformer, Low-Voltage Winding, 7.2 Kv/12.470 Kv Star

Type of Test	Oscillogram	Rod Gap, Inches	Number of Tests	Average Kilovolts
Reduced FW	X_2		2	62
Steep front	X_1	3	3	175
Chopped	X_2		2	136
Full wave	X_2		2	117
Steep front	X_2	3	25	178
Steep front	X_2	3½	25	206
Steep front	X_2	4	25	232
Steep front	X_2 *2419-10 B*	4½	25	248
Full wave	X_1		15	110
Full wave	X_1		15	121
Full wave	X_1		15	132
Full wave	X_1 *2412*		3	141
Full wave	X_2		15	107
Full wave	X_2		15	120
Full wave	X_2		15	131
Full wave	X_2		15	140

Table III. Comparison of Actual and Required Strengths

Winding	Type of Test	NEMA or ASA Standard	Kv Required	Kv Withstood
High Voltage	Chopped wave	ASA	410	418*
	Full wave	ASA	350	450
	Steep-front wave	NEMA	580	833**
	60 cycle	ASA	140	160
Low Voltage	Chopped wave	ASA	130	136
	Full wave	ASA	110	140
	Steep-front wave	NEMA	195	248
	60 cycle	ASA	34	

* Not breakdown tests but to ensure standards were met.

** Winding stood up, but bushing flashed over.

Table IV. Steep Front Tests on Model

Number of Tests	Gap Length, Inches	Kilovolts, Average
25	24	800
25	27	850
25	30	1,020
25	33	1,120
25	34½	1,070
50	36	1,100
25	37½	1,100
27	39	1,200
29	40½	1,200

all things equal, it would probably have been better had this transformer been relatively as strong as the one in Table III. In the case of an extremely high rate of current rise, the voltage across a lightning arrester can resemble a steep-front wave, which can be higher at the transformer than at the lightning arrester by as much as 10 to 15 per cent, and will also be longer in time duration. A transformer protected by modern lightning arresters at the terminals, and with strengths in line with Table III would withstand lightning except in extremely rare cases. Further, even in the case of lightning arrester damage or removal, a very considerable margin over most line disturbances would remain, particularly if the gap were added.

If the industry believes that steep front strength is not necessary, the advantages just given may not be obtained. In that case, full advantage of a decrease in insulation within the unit to meet the requirements could not be obtained without decrease in 60-cycle test requirements or destroying the co-ordination within the winding.

To sum up, it would seem desirable, for the 69 kv or lower voltage systems, not to design transformers to depend entirely on the normal published characteristics of lighting arresters, due to the varying degrees of lightning protection on these lines. If this is true, these transformers should have impulse strengths at least in line with present NEMA and ASA rules, both steep front and full wave. It is believed that the use of full waves as a test and standard alone would result in a lower strength of transformers, and there would be some failures, whereas it is understood that practically no lightning failures of transformers designed in the last 15 years now occur.

Design Considerations and Test Data on 138-Kv Transformers

The same design consideration as to major and coil insulation came up with regard to the higher voltage transformers, and it is believed that the windings should be stronger than the insulation to ground. With this in view, tests on some models and on large complete units were made.

Tests on transformer insulation for full and chopped waves have been reported in other papers, and would indicate that 138-kv transformers[1,2] should be able to stand from 810 to 860 kv with a factor of safety, in the order of that for the 60-cycle test. In order to see what values might be obtained with steep-front tests, the tests shown in Table IV were made with a wave rising at a rate of 1,000 kv per microsecond for gap lengths up to 33 inches.

Above 33 inches, some rounding of the applied wave was experienced, and experience shows that the test severity is reduced. No failure, however, occurred on these tests in the winding or to ground, which would indicate that deterioration, due to testing should not be greatly feared in this particular design. The model withstood 25 full waves at both

Figure 1 (left). Impulse tests on 667-kva 69-kv transformer

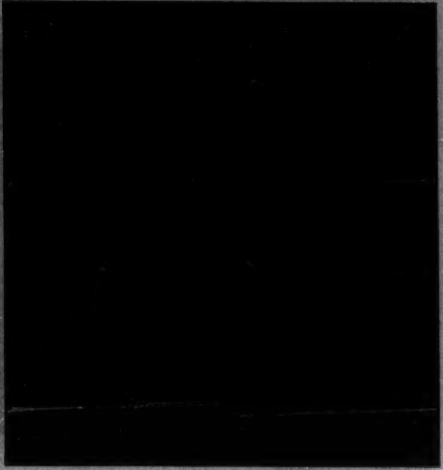

Figure 2 (above). Oscillogram of test on 138-kv transformer insulation

650 and 675 kv after these tests were made. A record of the steep front impulse test at 33 inches gap length on the model is shown on oscillogram *1144-65*.

Tests on a large 138-kv transformer which had to be rebuilt were made. Tests, not to failure, but which were under the "design level" at which failures might be expected were made. The results of these tests are shown in Table V. The required values versus the test values are shown in Table VI. The values given in these tables might be studied as before. If full waves of 650 kv only were required, probably some reduction in 60-cycle test voltage could be made, since it is believed that the 925-kv wave could have been held as a full wave provided the bushing had not flashed over. If a reduction in 60-cycle strength is not made, the winding strength alone could be reduced, and the unit would not be internally co-ordinated. Co-ordination is highly desirable.

If we retain present levels, the user who depends on gap protection alone is reasonably safe. Further, if a lightning arrester is used and is subject to undue currents or rates of rise, some transformer failures will be averted.

Present failure rates are extremely low, which indicates that excessive currents or rates of rise are very seldom met, or that some steep front transformer strength exists. Some years ago, transformers had two thirds their present full-wave levels, no lightning arrester protection and no steep front strength and relatively few failures occurred. Perhaps, therefore, the number of failures would not be changed if the full-wave strength and test of transformers were barely met, when lightning arresters are used.

Lines are now designed where there are practically no lightning failures. Stations can be so well protected that very low currents result. Perhaps the lightning arrester characteristics can be entirely relied upon in transformer design, and then it would seem definite that steep front strength is unnecessary, and reductions in 60-cycle strength and steep front strength could be made provided the standards would permit.

The following proposals might be made:

1. For the full waves now specified, make a new 60-cycle test somewhat lower and drop the chopped-wave test and reduce the steep-front test.
2. Retain approximately the present full-wave and steep-front test.
3. Have a full-wave test only.

Conclusions

Test results have been shown which indicate the impulse strengths of transformers compatible with the 60-cycle insulation strength. This information is useful in considering the highest values obtainable for use in co-ordination studies.

Depending on the degree of co-ordination, it is possible to reduce some of the insulation tests of transformers. It is believed that this subject should be considered in two groups for oil insulated power transformers. These are transformers from 15 to 69 kv and from 115 kv up.

It would be recommended that the standards for the first group be changed as follows: Add the NEMA steep-wave tests to the ASA standards, and eliminate the chopped waves. If acceptance tests were to be required by the standards, like the present 60-cycle tests, only the full-wave tests, consisting of full waves as specified now, might be used. The requirements for the second group are not as clear. It would seem that a reduction in 60-cycle strength, and in the NEMA steep-front test could be made, dropping the chopped-wave test, and retaining the present full-wave tests. Those using gap protection only would require the present higher grade of insulation.

Table V. Tests on Transformer*

Type of Test	Number of Tests	Gap Length, Inches	Oscillogram	Kilovolts
Steep front	7	$30^{1}/_{2}$		
Steep front	10	32	*1144-66*	1,090
Chopped waves	5			875
Chopped waves	4		*1144-68*	925
Full wave	1		*1144-67*	650

* No failures occurred on these tests.

Table VI. Comparison of Required and Test Values, 138-Kv Insulation

Type of Test	NEMA or ASA Standard	Kilovolts Required	Kilovolts Withstood	Gap Length, Inches	
				NEMA	Actual
Steep front	NEMA	960	1,090	29*	32
Chopped wave	ASA	750	925		
Full wave	ASA	650	650		

* The equivalent gap length for 960 kv and 0.96 microsecond is not given, but is estimated to be in the order of 27 to 29 inches.

References

1. Factors Influencing the Insulation Co-ordination of Transformers, F. J. Vogel. *AIEE Transactions*, volume 52, June section, 1933, pages 411–16.

2. Dielectric Strength of Transformer Insulation, P. L. Bellaschi, W. L. Teague. *Electrical Engineering (AIEE Transactions)*, volume 56, 1937, pages 164–77.

Discussion

J. R. Meador (General Electric Company, Pittsfield, Mass.): Mr. Vogel has written a paper on a subject that deserves a great deal of thought and discussion. The question of what types of impulse waves to use in test, and what their relative voltage levels should be, is very important to the industry. It is this importance that leads me to question some of the actual and implied conclusions.

In testing a developmental transformer, coil stack, or insulation structure, it is obviously desirable to get as much data as possible. We have to be careful, however, to distinguish between proof-testing a new proposed design and getting data for a revision of existing standards.

This is exemplified by the maximum voltages applied to the high-voltage winding of the 667-kva transformer, which were as follows:

Full wave, 472 kv—failed
Steep wave, 833 kv—did not fail
Chopped wave, 418 kv—did not fail
60-cycle, 160 kv—did not fail

These tests demonstrate what this particular transformer will withstand on the different types of tests but they certainly do not show what the strength of the transformer is, except on the full wave. Even the full-wave strength may have been affected, for example, by incipient damage during the steep-wave tests.

None of the tests show the 60-cycle breakdown strength. How can it be concluded then that the present ratio of 60-cycle test to full-wave test should be changed? The same applies to all of the other relative voltage levels.

I have one comment on the author's various proposals for possible future tests. It concerns the substitution of steep waves for the present chopped waves. Without discussing the merits of the change so far as stress on the transformer is concerned, there is one argument that should not be overlooked. It is well known that internal winding failures, such as those that might be caused by chopped waves or steep waves, will often regain much of their original strength if permitted to soak in oil for a short period. It is essential therefore that the final full wave (and neutral current) oscillograms be taken as soon as possible after the application of the steep tailed waves. This is easy to do in the case of the chopped wave. When steep waves are applied, a change in connection of the impulse generator is often required before the remaining tests are made. In this case the interval may be long enough to prevent detection of the failure.

E. R. Whitehead (Illinois Institute of Technology, Chicago, Ill.): Mr. Vogel's paper illustrates the feasibility of designing modern power transformers to meet the NEMA steep-front impulse tests with suitable margins, and recommends that future standards for transformers of 69 kv and lower voltage rating include these requirements as design, if not acceptance, tests. For the higher voltage classes of 115 kv and above the possible reduction in winding strength is pointed out.

I should like to comment in support of Mr. Vogel's view that transformers up to and including the 69-kv ratings be designed to meet steep-front tests at or near the present NEMA levels even if the steep-front tests are not included in the standard acceptance tests. I believe it is well understood that factors of line impulse insulation, ground wire protection (or lack of it), structure footing resistances, and the type and location of lightning protective devices are much more variable on the lower voltage than on the higher voltage systems for which the best system design practices are more easily justified economically. Experience indicates that this variability contributes to the relative importance of steep front waves of magnitude substantially greater than that established by the standard tests on lightning arresters.

For the higher voltage classes, perhaps 115 kv and above as suggested, it seems logical to take advantage of the factors of good ground wire protection, low structure footing resistance and transformer-mounted lightning arresters and establish winding strengths more directly dependent upon the protective levels set by the lightning arresters. The cost of providing adequate insulation is a factor of greater importance in the high voltage classes than in the lower.

It has been the writer's experience over many years of association with impulse testing of transformers that defects in material or workmanship are detected much more frequently than are errors in design. Based on this experience, it might be concluded that steep-front design tests should be made to check each new design, and that full-wave tests be employed as the normal acceptance tests.

Wm. L. Teague (Westinghouse Electric Corporation, Sharon, Pa.): In his paper, Mr. Vogel has presented some interesting data. His comparisons of the relative severity of steep-front, chopped-wave, and full-wave tests are based on a few specially designed units. An evaluation of the relative severity of tests with the three types of waves also can be made by considering the results of commercial impulse tests on a large number of transformers.

The results of impulse testing 500 power transformers over a period of 15 months were analyzed. All of these transformers were designed to withstand front-of-wave, chopped-wave, and full-wave tests. Although some of the designs were for special levels and some of the tests varied from standard, these variations were relatively small and kept at a constant proportion for the three types of waves. Of the 500 units tested approximately 300 were given front-of-wave and full-wave tests; 100 were given chopped-wave and full-wave tests; and the remaining 100 were subjected to front-of-wave, chopped-wave and full-wave tests. This would mean that all 500 units were subjected to full-wave tests, 400 to front-of-wave tests, and 100 to chopped-wave tests. The faults revealed by the three types of tests expressed as a percentage of the total units that received the test were essentially the same. Hence, in the commercial impulse testing of power transformers in large numbers the front-of-wave, the chopped-wave, or the full-wave test was equally searching in its effect.

The results of these tests also indicate that the volt-time characteristics of transformer insulation as defined by NEMA front-of-wave tests and ASA chopped- and full-wave tests are approximately correct.

Since both the front-of-wave test and the chopped-wave test stress the turns, coils, and major insulation at the line end of the winding, it is not necessary or economical to apply both types of waves in the commercial testing of transformers. Either type of wave should be sufficient to verify that the windings will withstand flashovers and have the required short-time strength level. Of the three types, the full wave comes nearest to being a complete test. It constitutes a reasonable test on the line end of the winding up to full-wave levels and demonstrates the dielectric strength between interior parts of the winding and to ground where voltage stresses may result from oscillations. Hence, in the commercial impulse testing of transformers some form of chopped wave and the full wave are essential. The trend in impulse testing should be toward simplifying and streamlining the tests.

Philip Sporn and **I. W. Gross** (American Gas and Electric Service Corporation, New York, N. Y.): This paper apparently suggests the reduction of severity of dielectric tests on transformer insulation, and bases the suggestion largely on "results of some tests made in the development of a possible new line of transformers." The author seems to imply that there is a relation between the 60 cycle and impulse strength of transformers. This is a philosophy which we thought was entirely abandoned over 15 years ago based on experience with designs prevalent at that time. The basis for the 60-cycle test values for transformers which has been unchanged for more than 30 years has given such a good account of itself under service conditions, that any attempt to change it at this time should be made only after the fullest consideration of the fundamentals of transformer design and the expected over-voltages in service. Of course, this assumes that impulse requirements will be independently handled.

As to impulse strength and test values, the present basic insulation levels are based on so solid a theoretical foundation and on so much practical experience that no attempt should be made to change them except on clear indication of the soundness of the new course.

When the impulse testing of transformers was being developed nearly 20 years ago on a commercial basis, various ideas were held on the required severity. As fundamental analysis progressed and more became known about the types of impulse surges to which transformers in service could be subjected, and as the impulse design problem in transformers was better understood, the thinking in our own company developed along these lines: It was believed that transformers in service could be subjected to three different types of impulse or surges of lightning origin: first, a full-wave impulse without alteration by reason of gap flashover or lightning arrester action; second, a chopped wave where the chop took place on the wave tail; and third, a chopped wave where the chop took place on the front of the wave. The reasons why such surges could reach a transformer are now too well known to require further comment. The initial impulse testing of transformers used the full wave, supplemented by a chopped wave which was representative of conditions obtaining when the bushing (air gap) flashed over.

For the third condition, that is, flashover on the front of the wave, we requested and received commercial impulse tests on transformers with a steep front in the order of 1,000 kv per microsecond, flashover taking place on the front.

The ability of transformers as far back as 15 years ago to withstand such waves was amply demonstrated by commercial factory tests, and the successful operation of such transformers under impulse conditions, on our own system at least, has given ample justification for continuing these types of tests up to the present time. It is not clear from the author's comments whether he questions the ability of transformers built within the last 15 years or so of withstanding all three types of wave—full wave, chopped wave, and fast front. Neither is it clear why he believes the transformers on which he has reported impulse tests are superior to those which have been built within the past 15 to 18 years.

The general pattern of impulse testing today is for the transformer to be made to withstand a full wave of the basic impulse insulation class together with a chopped wave, the chop taking place on the tail at 115 per cent of the full wave, and a fast front test with the crest value being in the order of 150 to 200 per cent of the full-wave value, depending on the transformer voltage class. As mentioned before, present-day transformers are capable, as demonstrated by commercial tests, of withstanding these test values.

We are in thorough agreement with the author that if we required only a full-wave test on the transformer insulation it would result in a lower impulse strength of transformer insulation. If, as he predicts, and we concur therein, some transformer failures would develop if the impulse tests were limited to full waves, such a proposal should be considered all the more carefully in the light of the over-all economic penalties attendant upon failure. It does not seem to us that with the existing background such a procedure would be at all attractive.

The author states that it is believed "the windings should be stronger than the insulation to ground." Further amplification of this statement is certainly desirable. We consider a transformer as a unit, and whether it fails between turns or to ground is beside the point. A failure is a failure, and if there is a service interruption by reason of a failure, it is of little concern whether that failure took place between turns or sections, or to ground.

There does seem to be some point in eliminating the so-called chopped-wave test and substituting therefor the front-of-wave test. After all, the three tests which are now required on our system transformers merely determine three points on the volt time co-ordinates of the transformer insulation curve. To omit the chopped-wave test (not fast-front test) could probably be tolerated without any appreciable sacrifice of transformer quality.

The proposal of the author that the acceptance test of a transformer so far as impulse is concerned be limited to the full-wave test would leave us in the position where we know nothing about the short time impulse strength of the transformer. We certainly do not want to face this situation now or in the future.

There seems to be some implication in the author's paper that he favors the use of an air gap as a protective device for a transformer. If the transformer is built with insulation sufficiently above the test level of the gap, there certainly is no objection to this, provided the user is willing to live with the service outages that are inherent in such protection. However, we are firmly convinced that the fundamental insulation requirements of a transformer should be such that it will perform successfully without service interruption when protected by the modern lightning arrester which has given such a high degree of reliability as proved by experience obtained in service during recent years.

P. L. Bellaschi (Consulting Engineer, Sharon, Pa.): This discussion has reference to the economics of power transformers, especially from the application end. First, in regard to the insulation: "Does the present structure of tests provide a balanced and economical design in modern transformers?" My answer is "yes." These are the principal reasons. The volt-time characteristics embodied in present ASA impulse tests and NEMA front-of-wave tests are fundamentally sound, economically attainable, and well co-ordinated with available methods of protection. Whether the chopped wave is retained or dropped would not change the picture fundamentally. Presumably if the chopped wave is dropped, the front-of-wave would be substituted in its place in the tests.

On 230-kv stations designed with overhead ground wire over the station structure and extended for at least one-half mile on the line, as is now the practice, the modern lightning arrester provides co-ordinated protection to the full-wave strength of transformer insulation, for lightning arrester discharge current well up to the values so far experienced in these stations. The higher voltage, front-of-wave transformer tests in present standards provide for the necessary strength to withstand the stresses such as can result from short-time effects due to lead drops, and so forth, as are entailed from rapid impulses. Similar conclusions regarding present full-wave and short-time tests apply even more so for the low and medium voltage substations, for in these applications higher discharge currents prevail and lead drops can assume relatively greater importance.

Looking to the future, to the rationalization process in course, we shall soon be dealing with reduced insulation more and more, especially in applications to high-voltage grounded systems. In fact on well-grounded systems at the higher voltages, 230 kv and above for instance, we shall be dealing quite commonly with 75 per cent and even 70 per cent insulation levels.

In speaking of well-grounded systems, I have reference to systems in which dynamic overvoltages to ground on the unfaulted phases do not exceed 65 to 70 per cent line-to-line voltage or even lower. That is, where X_0/X_1 is less than one and R_0/X_1 is under a quarter or thereabout. Equally import, overvoltages resulting from load dropping and runaway of hydro machines, as well as surges due to restrikes of circuit breakers, all are within proper and acceptable limits by design and operation.

Under these conditions on these systems, 75 per cent and possibly 70 per cent lightning arresters can be safely applied. In these applications the basic insulation levels of transformers especially would be proportioned accordingly with corresponding economies, not to mention other advantages such as in the improved electrical characteristics of the equipment proper and relative reduction of physical size. These practices are currently in full course of development and mark another milestone in the economies attainable, in keeping with sound engineering, through the process of rationalization of co-ordination and protection of station insulation.

F. J. Vogel: My paper as written was intended to raise questions regarding present insulation standards in the design of transformers, particularly as to whether; first, the relations of steep-front full-wave and 60-cycle tests are correct; second, if the present levels up to 69-kv class are desirable; third, if steep front values are required; and last, if reductions in the test values for the higher voltage classes are in order.

With respect to the first question, it seemed to be the opinions of both Mr. Teague and Mr. Bellaschi that they are. Mr. Meador questioned it on the basis of lack of test data, referring to the fact that the 60-cycle breakdown value was not given. However, its insulation to ground was very similar to that referred to in many previous papers, where the impulse ratio was about two, which would indicate that the 60-cycle strength would not be greatly in excess of the 160-kv cited. Please note that the value of 472 kv was obtained using oversize bushings and it is apparent that if no 60-cycle tests were required, and full-wave impulse tests only were required, a large decrease in insulation clearances and materials could have been made.

The second question is answered only by Mr. Whitehead, who agrees with me that the present levels for transformer insulation up to the 69-kv class are desirable without change.

The question regarding steep front wave strength is not so directly answered and has a number of ramifications. Both the discussions of Mr. Whitehead and Mr. Sporn and Mr. Gross indicate that that feature is required. I would like to point out that the ability to meet the chopped wave does not imply ability to meet steep front waves, although the converse is likely. This means that the basic insulation levels alone do not ensure an adequate transformer, and that the full waves and steep front waves probably do ensure the maximum values. The questions of difficulty in applying steep front tests, and even failure detection, were brought up by both Mr. Meador and Mr. Teague. I think further discussion of this is necessary.

With respect to the last question, there does seem to be agreement that reductions for the higher classes are possible, on the basis of lightning arrester applications. Mr. Whitehead and Mr. Bellaschi are in agreement, and I know that the practice is being given serious consideration elsewhere.

The discussion by Mr. Sporn and Mr. Gross would seem to merit some further reply. I wish to thank them for a most constructive discussion. My reply to their discussion is as follows: They raised the question as to a relation between 60-cycle and impulse strength of transformers. Fifteen years ago there was no relation between the 60-cycle and impulse strength of transformers. It was just a little bit like the question of the members of the human race. You could say that all men were members of the human race but you could not say that the human race were all men. Likewise transformers are composed of major insulation to ground and winding insulation. The impulse strength to ground was found to bear a fairly definite relation to the 60-cycle strength. If the winding insulation were made equal to it then it also would bear this fixed relation, and this fixed relation would be the best which you could obtain compatible to the 60-cycle strength. I have no objection to the present basic insulation levels as applied to operating voltages, particularly up to 69 kv. I question very much that they are based on a very exact foundation, but they certainly have given a good practical account of themselves.

I am in complete agreement with the discussors' thinking with respect to the three different types of impulse. That there will be full waves is beyond question and that the voltage may be high enough to cause a flashover adjacent to the transformer also seems to be a possibility. This may definitely take place on the wave tail or on the front of the wave.

It is very likely that the paper was not clear with respect to proposals made by me, but the fact is that I intended to raise questions rather than to give my viewpoints. I believe that full-wave and either chopped- or steep front-wave tests should be given to nearly all transformers. It was proposed by some members in the Transformer Committee that chopped waves might be eliminated and full waves be used only. It is clear from the discussion that we both agree that full waves alone are inadequate.

There are a number of other questions which can be lumped together. Were the transformers 15 years ago just as good? Why should the winding be stronger than the insulation to ground? Why favor the use of some form of limiting gap as a possible protection device? The answers to these questions are as follows:

In two papers which I presented recently, methods of obtaining the strength between coils and in determining the difference in effect between steep wave-front tests and chopped-wave tests were derived. So far as I know this is the first line of transformers which were laid out using these data. A study of the values given in the paper show that very high impulse strengths were obtained and that broad gaps sufficiently long to avoid trouble with switching surges could probably be used.

The NEMA steep front tests as at present constituted are less severe than the tests using the gaps specified by one user and which can easily be made based on the performance of these transformers.

It is true that the transformer's insulation strength so far as the user is concerned is a unit. However, if the transformer winding is strong enough, the transformer's maximum strength as determined by the major insulation is obtained. I believe that a slight margin in the winding above this should be taken. Another reason is that there is an additional stress in the coil structure due to the fact that it is excited. Further, there is little or no extra cost in making the winding and major insulations equal.

There are two reasons why the use of a gap as an auxiliary protection device might be desirable. One is that for one reason or another the lightning arrester may not do its duty; or the lightning arrester may not be used for economical or other reasons. Another reason is that tests made by the author on several occasions have shown that with man-made lightning, it is possible to obtain excessive voltages even with lightning arresters present. I do not think that this is any argument against the use of lightning arresters since they prevent outages and possibly give an extra margin of protection. Nevertheless if there is a gap which can ordinarily be protected by the lightning arresters, and will always protect the transformer, I see no objection to it.

A Method for Designing Pulse Transformers

H. S. KIRSCHBAUM
ASSOCIATE AIEE

C. E. WARREN
ASSOCIATE AIEE

THE RAPID development in recent years of circuits and techniques employing short-duration pulses of voltage and current has created considerable interest in the use of transformers as coupling devices under pulsed conditions. The pulse transformer will perform one or more of the following functions with a minimum of distortion to the transmitted pulse:

1. Impedance transformation.
2. Voltage and current transformation.
3. Phase inversion.
4. D-c isolation of two or more circuits.

This paper will describe a method for designing pulse transformers, coupling linear resistive source and load impedances with either step-up or step-down turns ratio, nonphase inverting. The design procedure will be concerned largely with controlling wave form on the front and top of the output pulse. Other features of the wave form, transformer size, rating, and efficiency may be adjusted within certain limitations.

Some Fundamental Considerations

In order to design a pulse transformer to give a specified performance in a particular circuit, it is necessary to determine the transformer parameters which significantly affect the over-all performance of the circuit. Since the pulse transformer is required to transmit wave forms which are essentially transient in character, it is evident that the distributed capacitances of the transformer will play an important part in determining the transformer performance. In fact, a rigorous approach to the problem would involve a consideration of the electric and magnetic fields within the transformer in terms of Maxwell's equations. This approach, however, is much too general and cannot be handled in cases of practical interest. The first step in the simplification of the problem, therefore, is to approximate the fields in terms of lumped circuit parameters.

Figure 1 (A) shows a simplified transformer illustrating the several physical quantities usually considered in pulse transformer theory. These quantities may be classified in terms of the magnetic and electric field energies as follows:

1. Magnetic energy stored in the mutual flux field Φ_m, within the transformer core.

2. Magnetic energy stored in the leakage flux fields Φ_1 and Φ_2. This energy is usually considered as residing in the space between primary and secondary windings.

3. Electrostatic energy stored in the capacitance network of the transformer. The capacitance network illustrated consists of the capacitances of the individual turns to the core, capacitance between adjacent turns on the same winding and capacitance from primary to secondary turns.

The simplified transformer shown in Figure 1 (A) is still too complicated for convenient analysis and is usually simplified by means of the following assumptions:

1. The energy stored in the capacitance between adjacent turns on the same winding is small and therefore these capacitances are usually neglected.

2. The energy stored in the distributed winding-to-core and winding-to-winding capacitances is considered to be stored in equivalent capacitances connected to the coil terminals. See Figure 1(B). A primary and secondary terminal of like polarity are at the core potential either conductively or pulsewise.

In Figure 1 (B), the equivalent capacitances C_{pe} and C_{se} will store the same energies respectively as would be stored in the distributed primary and secondary winding-to-core capacitances of the actual transformer. The capacitance C will store the same energy as would be stored in the distributed primary-to-secondary capacitance of the winding. The equivalent capacitances as defined are usually calculated[1] on the assumption of a linear distribution of voltage along the coil. A detailed analysis of circuits similar to that of Figure 1(A) shows that the assumption of linear voltage distribution is in error during the initial part of the transient period. However, experience has shown that for the usual circuit applications, the higher modes of oscillation in the transformer are well damped and do not affect over-all circuit performance. In some cases the initial nonuniform distribution of potential along the coil may overstress the turn-to-turn insulation of the coil.[2]

A Pulse Transformer Equivalent Circuit

The circuit of Figure 1(B) may be replaced by the equivalent circuit of Figure 2(A) where L is the transformer leakage inductance and the shunt branch is a circuit taking into account the pulse excitation properties of the transformer core. The circuit of Figure 2(A), in turn, may be replaced on a one-to-one, primary basis by the equivalent circuit[3] of Figure 2(B).

The design procedure described in this paper is based on the transformer equivalent circuit of Figure 2(B). This circuit differs from others[1,4] which have been used as a basis for pulse-transformer design in that the capacitance, nC, shunting

---

Paper 49-198, recommended by the AIEE Communication and Electronics Committees and approved by the AIEE Technical Program Committee for presentation at the AIÉE Summer General Meeting, Swampscott, Mass., June 20–24, 1949. Manuscript submitted February 2, 1949; made available for printing May 3, 1949.

H. S. KIRSCHBAUM and C. E. WARREN are with The Ohio State University, Columbus, Ohio.

The work described in this paper was performed under contract between the Air Materiel Command, Watson Laboratories, Cambridge (Mass.) Field Station, Cambridge, and the Ohio State University Research Foundation, Columbus.

The authors wish to acknowledge the assistance of Neal Smith and Leo Botwin in obtaining and preparing the data used in this paper.

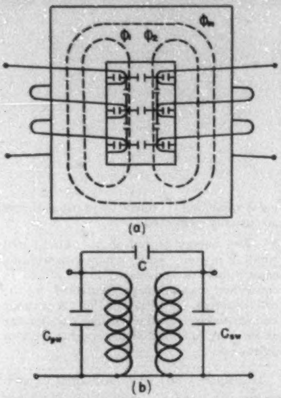

Figure 1. (A) Schematic diagram of transformer showing capacitance network and magnetic fluxes

(B) Simplified transformer circuit showing reduction of capacitance network to equivalent terminal capacitances

the leakage inductance, L, has been retained as an essential part of the circuit. The circuit is not unique or complete, but it has been found to be adequate for the design of transformers with turns ratios, n, in the range of about 1/10 to 10, but not in the vicinity of n equals one. In some cases, the design of unity turns-ratio transformers requires consideration of higher modes of oscillation and, therefore, a more complicated equivalent circuit.

The circuit parameters in the equivalent circuit of Figure 2(B) may be related to the design parameters of the transformer by simple analytic expressions. It has been found that a wide range of practical designs may be realized in terms of a simple 2-layer concentric-coil winding; therefore, only this type of winding design will be described in this paper. The design equations and properties of other types of windings are described in reference 1. The leakage inductance, L, and effective interwinding capacitance, C, of the 2-layer, concentric-coil winding are given in the following equations:

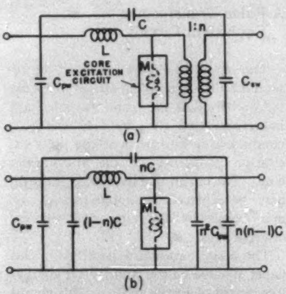

Figure 2. (A) Transformer equivalent circuit before reduction to one-to-one primary basis (B) Transformer equivalent circuit reduced to one-to-one primary basis

$$L=b\frac{4\pi N_p^2U}{d}\left(\Delta+\frac{a_1+a_2}{3}\right)10^{-9}\text{ henries} \qquad (1)$$

$$C=\frac{0.0885\,kdU}{3\Delta}10^{-12}\text{ farads} \qquad (2)$$

The shunt core-excitation circuit shown in Figure 2(B) may assume a variety of forms[5] depending on the problem under consideration. For the purposes of this paper, the core-excitation circuit will be considered as a single shunt inductance, M, related to the design parameters by the following equation:

$$M=\frac{4\pi N_p^2A}{10^9l}\mu_e\text{ henries} \qquad (3)$$

The effective pulse permeability, μ_e, usually is determined experimentally for a particular core material and takes into account eddy-current and hysteresis effects, in addition to the usual excitation ampere-turns. Pulse permeability depends on pulse duration, maximum flux density change, lamination thickness, and the magnetic and resistive properties of the core material. A complete discussion of core-excitation phenomena during pulse excitation is long and involved and the reader is, therefore, referred to reference 1 for a more detailed treatment of this subject.

Equivalent Circuits for the Step-Up Transformer

The complete primary-basis equivalent circuit of the step-up pulse transformer, coupling resistive primary and secondary impedances, and including external, shunt, primary and secondary capacitances, C_p and C_s, is shown in Figure 3(A). The secondary impedance, R_s, and external shunt capacitance, C_s, are secondary parameters referred to the primary by the square of the turns ratio. Examination of the expression for the total primary shunt capacitance, C_3, shows that the transformer introduces a term which is negative for turns ratios greater than one. Unless an abnormal amount of external shunt primary capacitance is present, C_3 is small and may be neglected in the design procedure.

For purposes of analysis, it is practicable to divide the transmitted pulse into three parts, consisting of: the rising front and subsequent damped oscillation, if present; the sloping top of the pulse; and the tail or subsidence transient. This division is based on the assumption of a rectangular pulse input (see Figure 4). The pulse front is represented very well by the equivalent circuit of Figure 3(B), which omits the excitation branch.

Symbols

a, a_1, and a_2 = wire diameter in centimeters
b = empirical correction factor in formula for leakage inductance
d = coil length in centimeters
e, e_0 = input and output voltages, respectively
k = dielectric constant
l = core length magnetic circuit, centimeters
n = turns ratio
p = derivative operator
t_0 = time in seconds for pulse to rise to 90 per cent flat pulse voltage, E
A = net core area, square centimeters
C = effective interwinding capacitance, farads
C_{pw} = effective primary winding-to-ground capacitance, farads
C_{sw} = effective secondary winding-to-ground capacitance, farads
C_p = external primary circuit capacitance, farads
C_s = external secondary-circuit capacitance referred to primary, farads
$C_{op}=C_{pw}+C_p$
$C_{os}=n^2C_{sw}+C_s$
$C_1=nC$
$C_2=n(n-1)C+n^2C_{sw}+C_s$
$C_3=(1-n)C+C_{pw}+C_p$
D = per unit pulse droop
E = basic flat-top pulse in volts
E_m = maximum value of output pulse in volts
E_δ = output pulse voltage at end of pulse duration
L = leakage inductance on primary basis, henrys
M = equivalent magnetizing inductance, henrys
$N_1=C_2/C_1$
$N_2=C_3/C_1$
N_p = primary turns
R_p = primary resistance, ohms
R_s = secondary resistance, referred to primary, ohms
T = base unit of time, $2\pi\sqrt{LC_2}$ for step-up transformer, $2\pi\sqrt{LC_3}$ for step-down transformer
U = mean coil perimeter, centimeters
$Z_0=\sqrt{L/C_2}$ for step-up transformer, $\sqrt{L/C_3}$ for step-down transformer
γ = impedance ratio, R_p/Z_0
Δ = interwinding insulation thickness, centimeters
δ = pulse duration, seconds
τ = per unit pulse rise time, t_0/T
μ_e = effective pulse permeability
λ = derivative operator

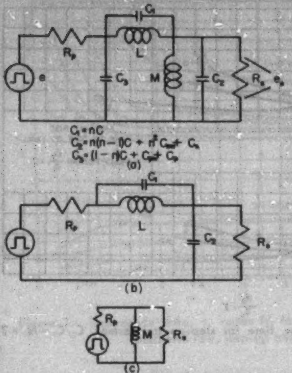

Figure 3. (A) Complete primary-basis equivalent circuit of step-up transformer and terminations
(B) Equivalent circuit for analyzing front of pulse
(C) Equivaent circuit for analyzing top of pulse

For the pulse top, only the excitation branch and terminating impedances are of importance and the transformer may be represented by the equivalent circuit of Figure 3(C). The equivalent circuit for the pulse tail in general involves all the circuit elements, including a more elaborate representation of the excitation circuit. For many practical applications the wave form of the pulse tail is not important or at least the wave forms resulting from the proposed design procedure are tolerable. A detailed discussion of this matter will be found in references 1 and 4.

Design of the Step-Up Transformer

The design procedure which is described in the following paragraphs provides a means for controlling the shape of the transmitted pulse on the front and top of the pulse. The design procedure is based on the assumption that the equivalent circuits of Figure 3 adequately represent the pulse transformer and that the behavior of these circuits, for perfect rectangular pulse input, represents all possible wave forms for the transmitted pulse for a given set of circuit conditions. The design then is carried out in three main steps.

1. For a given set of circuit conditions and turns ratio, to determine the transformer parameters L and C which give a satisfactory wave form, particularly on the pulse front.
2. Construct a transformer with the required turns ratio and the L and C parameters as determined in step one.
3. Adjust the design until proper performance on the top and tail of the pulse is obtained.

Since only a limited range of pulse wave forms may be obtained, with perfect rectangular pulse input, it will be possible to define certain salient features of the transmitted pulse and incorporate these factors into the design procedure. With reference to Figure 4, three features of the pulse wave form are defined as follows:

1. The time t_0 for the pulse to rise to 90 per cent of the flat-top pulse voltage; that is the voltage which would be obtained if the transformer were ideal.
2. Amount of overshoot expressed as a percentage of the flat-top pulse voltage.
3. Amount of droop, D, which is the deficiency in pulse top voltage at the end of the pulse duration, δ, expressed in per unit of the flat-top pulse voltage.

The first two of these wave-form specifications are related to the pulse front and may be determined with the aid of the circuit of Figure 3(B). This circuit contains five independent parameters, and the determination of values of the two performance specifications for all possible combinations of these parameters would be a formidable task. However, consideration of the differential equations of the circuit shows that the performance of the circuit depends on only three dimensionless ratios of the five parameters and the definition of an arbitrary unit of time. These ratios which are derived in Appendix I are listed for reference:

Base unit of time, $T = 2\pi\sqrt{LC_2}$

R_p/R_s

R_p/Z_0 (where $Z_0 = \sqrt{L/C_2}$)

C_2/C_1

The determination of rise time, t_0, and per cent overshoot for a wide range of the above dimensionless parameters was made by means of a transient analyzer.[6,7] A typical set of these data for $C_2/C_1 = 7$ is shown in Figures 5 and 6. It is not possible to include all the data in this form because of space limitations. However, since an output wave form with zero per cent overshoot is desirable in many applications, Figures 7 and 8 have been prepared giving data in terms of per unit rise time, $\tau = t_0/T$ and $R_p/Z_0 = \gamma$ versus the ratio, $C_2/C_1 = N_1$ for several values of R_p/R_s and for zero per cent overshoot. Similar curve sheets for other values of per cent overshoot may be plotted from a complete set of basic data as illustrated by Figures 5 and 6.

It should be noted here that there are two values of the ratio γ for which zero per cent overshoot occurs with particular values of the ratios, R_p/R_s and N_1. These two values of γ will be referred to as zero per cent overshoot, low, or zero per cent overshoot, high, meaning the low or high value of γ for a particular set of values for the ratios, R_p/R_s and N_1. The occurrence of two critically damped points in the response of the circuit of Figure 3(B) is particularly interesting in that it makes possible two alternative designs for a particular set of specifications. This matter will be discussed later in the paper.

At this point, it is possible to find the two winding constants L and C in terms of fundamental specifications of the pulse wave form and external circuit parameters.

The two quantities τ and γ may be written as follows:

$$\tau = t_0/2\pi\sqrt{LC_2} \tag{4}$$

$$\gamma = R_p/\sqrt{L/C_2} \tag{5}$$

where $C_2 = n(n-1)C + C_{os}$ and $C_{os} = C_s + n^2C_{ms}$. From equations 4 and 5

$$L = \frac{t_0R_p}{2\pi\tau\gamma} \tag{6}$$

$$C = \frac{1}{n(n-1)}\left(\frac{\gamma t_0}{2\pi\tau R_p} - C_{os}\right) \tag{7}$$

The leakage inductance, L, and effective interwinding capacitance, C, may be found, provided the quantities in equations 6 and 7 are known. Of the several quantities involved, t_0, R_p, n, and an estimated value of C_{os} will be immediately available. The values of τ and γ may be found from Figures 7 and 8 for zero per cent overshoot, low or high, provided R_p/R_s and N_1 are known. The ratio, R_p/R_s, will be given as part of the fundamental specifications, but the proper value of N_1 remains to be specified. In order to determine N_1 in terms of fundamental specifications of wave form

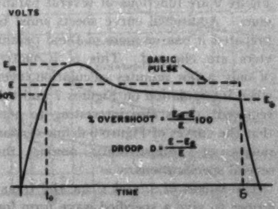

VOLTS
E_m
E
90%
BASIC PULSE
E_δ
% OVERSHOOT $= \frac{E_m - E}{E}100$
DROOP $D = \frac{E - E_\delta}{E}$
t_0
TIME
δ

Figure 4. Specifications of pulse waveform

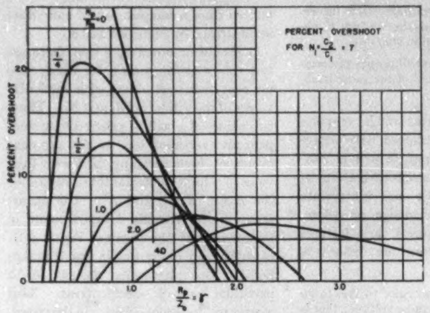

Figure 5. Percentage overshoot for step-up transformer, $C_2/C_1=N_1=7$

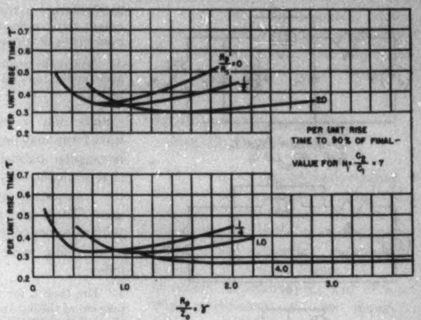

Figure 6. Per unit rise time for step-up transformer, $C_2/C_1=N_1=7$

and circuit parameters, the following calculation is made:

By definition

$$N_1=\frac{C_2}{C_1}=\frac{n(n-1)C+C_{os}}{nC}$$

Solving for C from the foregoing equation and using equation 7, the following equality is found

$$\frac{C_{os}}{nN_1-n(n-1)}=\frac{1}{n(n-1)}\left(\frac{\gamma t_0}{2\pi\tau R_p}-C_{os}\right)$$

When rearranged the foregoing equation becomes

$$\frac{t_0}{R_pC_{os}}=\left[\frac{2\pi\tau}{\gamma}\right]_{N_1}\frac{N_1}{N_1-(n-1)} \tag{8}$$

Equation 8 is implicit in N_1, since τ and γ are functions of N_1. The equation may be solved by assuming values of N_1, evaluating the term in square brackets from Figures 7 and 8, and plotting the left-hand side of the equation as a function of N_1. Figure 9 shows the result of such a calculation for zero and five per cent overshoot, both low and high, with $R_p/R_s=1$ and a turns ratio $n=5$. Data for five per cent overshoot are included to illustrate the relative difficulty of designing for specified overshoot at high and low values of γ.

It should be noted that the curves of Figure 9 are functions of several parameters. Additional curve sheets must be prepared if one or more of these parameters are changed. This is a matter of only a few minutes calculation, even when interpolation on Figures 7 and 8 is required. It is also interesting to note that the curves of Figure 9 define certain ranges of compatibility among the several specifications.

The values of L and C for the transformer to give a specified wave form for specified terminating conditions now may be calculated. For example, if $R_p/R_s=1.0$, $R_p=50$ ohms, $t_0=10^{-7}$ second, $C_{os}=700\times10^{-12}$ farad, zero per cent overshoot, high, then $t_0/R_pC_{os}=2.85$ and from Figure 9, $N_1=6.8$. From Figures 7 and 8, for the derived value of N_1, $\tau=0.38$ and $\gamma=2.10$. From equations 6 and 7, $L=10^{-6}$ henry and $C=50\times10^{-12}$ farad.

The next step in the design procedure is to determine from equations 1 and 2 and the required values of L and C, the significant dimensions of the transformer core and coils. The manner in which this problem is handled will be guided by the following considerations.

1. A lower limit on wire size is set either by current loading or by mechanical strength and ease of winding.

2. A minimum is set on the interwinding insulation thickness Δ by the transformer voltage and the dielectric strength of suitable insulating materials.

3. The mean coil perimeter, U, and coil length, d, must be chosen to fit one of a standard set of cores.

Equations 1 and 2 may be put in the following form

$$N_p^2U^2=\frac{3\times10^{21}}{4\pi\times0.0885}\,\frac{LC}{bk}\,\frac{\Delta}{\left(\Delta+\frac{a_1+a_2}{3}\right)} \tag{9}$$

$$d^2=\frac{12\pi10^3}{0.0885}\,\frac{N_p^2bC\Delta\left(\Delta+\frac{a_1+a_2}{3}\right)}{kL} \tag{10}$$

In one form of the design procedure, it is convenient to start by assuming an appropriate wire size, and a value for Δ at least as large as required by the transformer voltage rating and the dielectric strength of the insulating material to be used.

1. With the chosen values of a_1, a_2, and Δ calculate $N_p^2U^2$ from equation 9.

2. Select a core and its corresponding value of U^2 from Table I and calculate N_p. As a rule of thumb, limiting the ratio E/N_p to about 100 to 150 volts per turn, maximum will give a reasonable design. In Table I, values of U^2 are tabulated for several of the cores in a standard line. The value of U is based on a 1/16-inch clearance from core to mean coil perimeter all around. This clearance usually will prove satisfactory for values of Δ less than 60 mils. Tables of this sort for the standard lines of cores and for several values of clearance are extremely valuable in this design procedure.

3. With the value of N_p calculated previously, determine d from equation 10. The value of d must be such that the coil may be wound on one or both legs of the core with adequate creepage margin at the coil ends and the product of required secondary turns by the wire diameter, a_2, does not exceed d.

4. In case the required value of d is not satisfactory, steps 1, 2 and 3 must be repeated. Perhaps a core with a larger value of U may be used or Δ, a_1 and a_2 may be changed. In some cases, an insulating material with larger dielectric constant k, and dielectric strength must be used. In any event, equations 9 and 10 indicate the

Table I. Significant Dimensions for a Standard Line of Cores

Style Number	Core Leg Width, Inches	Core Leg Depth, Inches	Core Window Width, Inches	Core Window Length, Inches	U Centimeters*	U^2, Square Centimeters	A/l, Centimeters
1356250	1/4	3/16	1/4	5/8	3.49	12.2	0.042
1356254	1/2	1/4	1/4	7/8	5.08	25.8	0.087
1356261	1/2	1/2	1/2	19/16	6.35	40.3	0.111
1356262	5/8	1/2	1/2	19/16	6.99	48.8	0.188

* 1/16-inch clearance from core to mean perimeter all around.

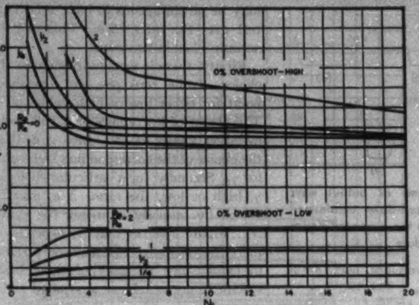

Figure 7. Impedance ratio, γ, versus N_1 for zero per cent overshoot, high and low, step-up transformer

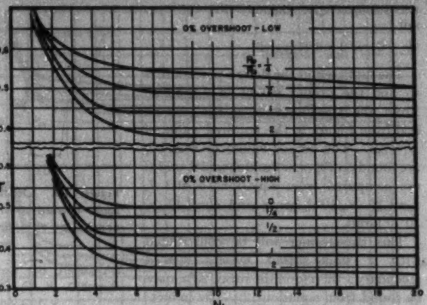

Figure 8. Per unit rise time, τ, versus N_1 for zero per cent overshoot, low and high, step-up transformer

several possibilities for effecting the proper change in design.

In the design procedure just described, a series of cuts and trys will lead to a choice of core, coil dimensions, and coil turns. However, two critical points arise in the design at step 3. The second of these points could be avoided if it were possible to find a relation such that the chosen wire diameter would just fill the required length, d, with the required number of secondary turns. Fortunately, such a relation can be developed. If the secondary and primary wire sizes are assumed to be equal, $a_1=a_2=a$, then equation 10 may be put in the following form

$$\frac{d^2}{a^2n^2N_p^{\,2}}=\frac{12\pi 10^8}{0.0885}\;\frac{\frac{\Delta}{a}\left(\frac{\Delta}{a}+\frac{2}{3}\right)bC}{n^2kL} \tag{11}$$

The denominator of the term on the left of the equal sign is just equal to d^2 if the wire diameter a includes an allowance for the winding space factor. Therefore, equation 11 gives the following relation when solved for Δ/a

$$\frac{\Delta}{a}=-\frac{1}{3}+\sqrt{\frac{1}{9}+\frac{0.0885}{12\pi 10^8}\,\frac{n^2k}{b}\,\frac{L}{C}} \tag{12}$$

Equation 12 determines uniquely the ratio of interwinding insulation thickness to wire diameter so that the secondary always may be wound with a single-strand closely spaced winding in the required coil length, d, with the required number of secondary turns. If the relation of equation 12 is satisfied, it will be necessary in step 3 to satisfy only the first requirement.

Equations 9 and 10 or 9 and 12 provide the starting point for designing a coil with circuit constants required to give a specified rate of rise and overshoot on the pulse wave form. There remains the problem of controlling the amount of droop on the pulse top. This characteristic sloping of the pulse top is due to the transformer exciting current flowing through the primary resistance, R_p. An approximate expression for the amount of droop, D, is derived in Appendix II and is given here for reference.

$$D=\frac{R_sR_p}{R+R_p}\,\frac{\delta}{M} \tag{13}$$

From equation 3 for the equivalent transformer magnetizing inductance and equation 13, it is found that the following inequality must hold if a specified amount of droop, D, is not to be exceeded.

$$N_p^{\,2}\mu_e>\frac{10^9}{4\pi}\,\frac{l}{A}\,\frac{R_pR_s}{(R_s+R_p)}\,\frac{\delta}{D} \tag{14}$$

It has been found convenient to design the transformer by means of equations 9 to 12 and then to check the droop requirements with equation 14. Equation 14 indicates the influence of the various parameters on droop and serves as a guide in altering a preliminary design.

The preceding discussion has described a design procedure for step-up transformers of the iso-type (that is, a transformer with isolated primary and secondary windings). Corresponding design equations for auto-type transformers are given in Appendix III.

Example of Step-Up Transformer Design

Assume the following transformer specifications:

1. Step-up iso-type transformer; $n=5$.
2. Primary resistance, $R_p=200$ ohms.
3. Primary-secondary impedance ratio, $R_p/R_s=1$.
4. Secondary external shunt capacitance, $C_{os}=75\times10^{-12}$ farads.
5. Pulse duration, $\delta=10^{-6}$ seconds.
6. Pulse front, $t_0=1/3\times10^{-7}$ seconds, zero per cent overshoot, high.
7. Pulse top, $D<0.05$.
8. Wire size number *33*; effective diameter, $a=0.0153$ centimeter.
9. Interwinding insulation, Kraft paper and oil; dielectric constant, $k=3.0$; dielec-

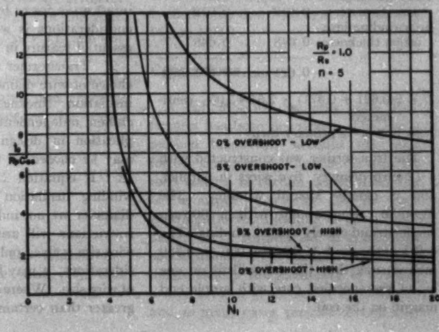

Figure 9. Graph of equation 8 for $R_p/R_s=1$, $n=5$

tric strength approximately 300 volts per mil.

10. Core, 2-mil Hypersil.

The first step in the design procedure is to find the proper values of L and C. From the specifications, $t_0/R_pC_{os}=2.22$, and from Figure 9, the required value of $N_1=8.5$. The proper values of τ and γ are found on Figures 7 and 8, and L and C are computed from equations 6 and 7, $L=1.36\times10^{-6}$ henry and $C=3.40\times10^{-12}$ farad.

This transformer will be constructed with a single-strand closely spaced secondary; therefore, the ratio, Δ/a, may be found from equation 12. The inductance correction factor, b, is assumed equal to one.

$$\frac{\Delta}{a}=-\frac{1}{3}+\sqrt{\frac{1}{9}+\frac{0.0885}{12\pi10^3}\,\frac{25\times3}{1}\,\frac{1.36\times10^{-6}}{3.4\times10^{-12}}}$$

$$\frac{\Delta}{a}=8.07$$

$a=0.0153$ centimeter or 6 mils
$\Delta=0.123$ centimeter or 48.4 mils

From equation 9, the core primary-turns factor, $N_p^2U^2$, is computed as follows

$$N_p^2U^2=\frac{3\times10^{21}}{0.0885\times4\pi}\,\frac{1.36\times3.4\times10^{-18}}{3.0}\,\frac{0.123}{0.133}$$

$$N_p^2U^2=3.85\times10^3$$

At this point, a cut-and-try procedure to select primary turns and core is employed. Only the correct try will be shown here. Use of the values of U from Table I will facilitate this procedure. It is found that core number *1356254* is about right. Allowing 1/32-inch clearance over-all on the core dimensions, so that the coil will slip over the core, an exact value of U is calculated as follows:

Core dimensions:	0.500 inch	0.250 inch
Clearance:	0.031	0.031
Twice primary to core insulation thickness:	0.030	0.030
Twice primary wire diameter:	0.012	0.012
Interwinding insulation thickness:	0.048	0.048
	0.621 inch	0.371 inch

$U=2(0.621+0.371)\times2.54=5.05$ centimeters
$N_p=12.3$ or 12 primary turns

The transformer was constructed with a 12-turn primary, five wires in parallel, and a closely spaced winding. The secondary was wound with a 60-turn single-strand closely spaced winding. The coil length, $d=5\times12\times0.006=0.360$ inch is such that the coil will fit on one leg of the specified core with ample end margin on the coil.

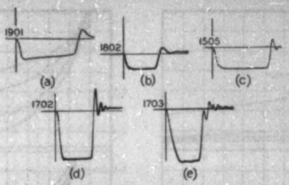

Figure 10. Oscillograms of output wave forms of step-up and step-down transformers constructed according to the proposed design procedure

(A) Zero per cent overshoot, high, $n=5$, $R_p=200$, $R_p/R_s=1$, $C_{os}=75\times10^{-12}$, $t_0=1/3\times10^{-7}$, $\delta=10^{-6}$

(B) Zero per cent overshoot, low, $n=1/5$, $R_p=312$, $R_p/R_s=1/4$, $C_{op}=5\times10^{-12}$, $t_0=10^{-7}$, $\delta=10^{-6}$

(C) Zero per cent overshoot, low, $n=2$, $R_p=50$, $R_p/R_s=1$, $C_{os}=56\times10^{-12}$, $t_0=10^{-7}$, $\delta=10^{-6}$

(D) Zero per cent overshoot, low, $n=5$, $R_p=50$, $R_p/R_s=1$, $C_{os}=175\times10^{-12}$, $t_0=10^{-7}$, $\delta=10^{-6}$

(E) Zero per cent overshoot, low, $n=10$, $R_p=20$, $R_p/R_s=1$, $C_{os}=700\times10^{-12}$, $t_0=2\times10^{-7}$, $\delta=10^{-6}$

The transformer was constructed according to the foregoing design, and bridge measurements of L and C gave $L=1.35\times10^{-6}$ henry and $C=5.8\times10^{-12}$ farad. The output pulse of the transformer is shown in the oscillogram of Figure 10(A).

Further Aspects of the Design Procedure

There are several features of the design procedure which should be emphasized at this point.

1. The method is basically a means for controlling certain features of the output pulse wave form resulting from a perfect rectangular input pulse. The qualitative correlation of response to other types of input wave forms by frequency spectrum considerations is well known and is an essential feature in the design procedure.

2. Transformer rating is fixed by the choice of wire diameter and interwinding insulation thickness. They may be chosen independently, with some complication in design procedure, or they may be chosen on the basis of equation 12. If equation 12 is used the interwinding insulation thickness and wire diameter are not independent and certain restrictions will arise. If, for example, wire size is fixed only by mechanical considerations, Δ may be adjusted by choice of wire size. Where Δ and a must both be greater than certain minimum values, it may be advantageous to have some control over the ratio, Δ/a. This may be accomplished in two ways.

Firstly, there is usually freedom in the choice of the zero per cent overshoot point for either low or high values of γ. The choice of low values of γ will result in larger values of the ratio, Δ/a, than the choice of the corresponding high value for γ. Secondly, for a particular choice of γ, high or low, the ratio, Δ/a, may be varied by properly adjusting the value, N_1. Figure 9 shows that N_1 depends on the ratio, t_0/R_pC_{os}. It may be possible to change one or more of these basic specifications to achieve a required ratio, Δ/a. For example, on the zero per cent overshoot, high, curve of Figure 9, decreasing t_0 results in an increase in the required value of N_1. Calculation will show that this procedure increases the ratio Δ/a, other factors being held constant. It is also true that the Δ/a ratio will be larger for the autotype transformer.

3. The physical size of the transformer is controlled largely by the considerations discussed in part 2. For example, choice of the minimum mechanically or electrically feasible wire size will lead to the smallest possible transformer. However, it should be noted that even for a given wire size there is freedom of choice in the physical proportions of the transformer through the relations of equation 9. For example, a design may be realized for several different values of primary turns N_p, resulting in a choice among several of a given line of cores.

It should be noted that the physical size of the transformer is also related to the pulse duration, δ, through the rise time, t_0. If t_0 is to be a fixed percentage of the pulse duration, reduction of pulse duration requires a corresponding reduction in t_0. Reference to equations 6 and 7 shows that the transformer parameters, L and C, will change in proportion to the change in t_0. A study of equations 9 and 10 shows that as L and C are reduced in magnitude, the physical dimensions of the transformer also must decrease.

4. The primary winding for step-up transformers will be wound with two or more strands in parallel to give a closely spaced winding. This is necessary in order to satisfy the approximations under which the basic formulas for leakage inductance and interwinding capacitance were derived. Because of this requirement, two difficulties arise in practical design.

First, nonuniform distribution of current in the parallel strands, particularly for ratios of Δ/a less than about two,

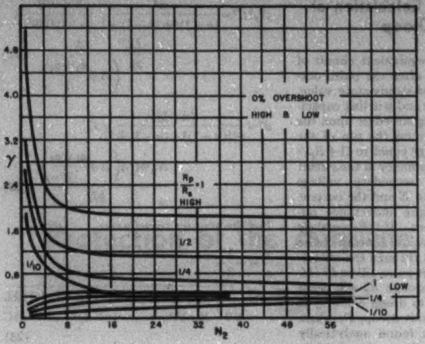

Figure 11. Impedance ratio, γ, versus N_2 for zero per cent overshoot, high and low, step-down transformer

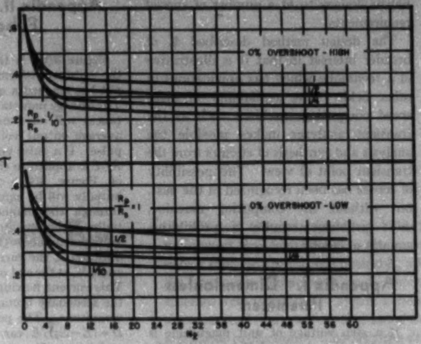

Figure 12. Per unit rise time, τ, versus N_2 for zero per cent overshoot, high and low, step-down transformers

cause the actual leakage inductance to depart from the required design value. This difficulty has been taken care of in the design procedure by introduction of the empirical factor, b, in the inductance formula. This empirical factor will range from one to two in magnitude and must be found by a series of approximating designs.

Secondly, for nonintegral ratios of transformation, it is difficult to obtain closely wound primary and secondary windings of practically equal length with equal primary and secondary wire sizes. With small wire size and low turns ratio, the difference in winding lengths may not be significant, and any small variation in parameters may be corrected by a proper choice of the factor, b. However, for other situations, it may be necessary to use unequal primary and secondary wire sizes. The extension of equations 11 and 12 to cover this situation is required.

Equivalent Circuit for the Step-Down Transformer

The complete primary-basis equivalent circuit of the step-down transformer is the same as that shown in Figure 3(A). All circuit elements shown will have the same interpretation as for the step-up transformer, except the turns ratio, n, will be numerically less than one. For the step-down transformer, the total secondary shunt capacitance, C_3, contains a term which is negative for turns ratios less than one. In many cases, the winding-to-core and external shunt capacitances, n^2C_{sw} and C_s respectively, are such that C_3 is negligibly small and may be assumed to be zero. Considerable data, too extensive to present in this paper, have been taken where C_3 is not small. It has been found that a design procedure based on the assumption, $C_3=0$, leads to satisfactory designs in all but extreme cases.

Therefore, under the assumption $C_3=0$, the dimensionless ratios and base unit time for the step-down transformer are found to be as follows:

Base unit of time, $T=2\pi\sqrt{LC_3}$

R_p/R_s

R_p/Z_0 (where $Z_0=\sqrt{L/C_3}$)

$C_3/C_1=N_2$

Design of the Step-Down Transformer

The design procedure for the step-down transformer is similar to that used for the step-up transformer. The basic pulse-front data giving per unit rise time, τ, and impedance ratio, γ, for zero per cent overshoot, both high and low, are shown in Figures 11 and 12. In these illustrations, the abscissa is the capacitance ratio, $C_3/C_1=N_2$, and curves are given for different values of R_p/R_s. For the step-down transformer, $\tau=l_0/2\pi\sqrt{LC_3}$ and $\gamma=R_p/\sqrt{L/C_3}$.

From the foregoing definitions, the required leakage inductance and effective interwinding capacitance of the transformer may be found.

$$L=\frac{l_0R_p}{2\pi\tau\gamma} \tag{15}$$

$$C=\frac{1}{1-n}\left(\frac{\gamma l_0}{2\pi\tau R_p}-C_{op}\right) \tag{16}$$

where $C_{op}=C_p+C_{wp}$. The relation between the capacitance ratio, N_2, and basic design specifications is found to be

$$\frac{l_0}{R_pC_{op}}=\left[\frac{2\pi\tau}{\gamma}\right]_{N_2}\frac{nN_2}{nN_2-(1-n)} \tag{17}$$

Equation 17 is analogous to equation 8 and is used in the determination of L and C from Equations 15 and 16, exactly as described in the case of the step-up transformer.

Equations 9 and 10 may be used without modification for the design of iso-type step-down transformers. Equations 11 and 12 will be changed because the primary winding is now the high-voltage winding and the coil length, d, for a single-strand close-wound primary is aN_p. Equation 18 gives the ratio, Δ/a, for the iso-type step-down transformer. The corresponding equation for the auto-type step-down transformer will be found in Appendix III.

$$\frac{\Delta}{a}=-\frac{1}{3}+\sqrt{\frac{1}{9}+\frac{0.0885}{12\pi10^3}\frac{k}{b}\frac{L}{C}} \tag{18}$$

Equations 13 and 14 are to be used in checking the top-of-the-pulse characteristics of the design. An oscillogram of a typical step-down design is shown in Figure 10(B).

Conclusions

A technique for designing pulse transformers has been described. This design method takes into account the transformer terminating impedances and permits control of certain specified features of the output wave form. The procedure is straightforward leading to an optimum design for a suitable set of transformer specifications. The design relations indicate clearly the possibility of realizing a design for a given set of specifications and, in many cases, provide several alternative designs to fit a number of special requirements.

The design method described is of broader interest in that it is illustrative of a technique which has applications in other fields. The availability of high-speed computing machines such as the transient analyzer makes possible the analysis and synthesis of circuits from the transient point of view. This possibility of course has been recognized in the past, but without the computing machine, most problems require a prohibitive amount of labor.

Appendix I. Dimensionless Parameters

If a step voltage of unit magnitude is applied to the circuit of Figure 3(B), the operational form of the load voltage, e_0, will be

$$e_0(p)=\frac{R_s(1+p^2LC_1)}{(R_p+R_s)+(L+R_pR_sC_2)p+[R_s(C_1+C_2)+R_pC_1L]p^2+R_pR_sLC_1C_2p^3}$$

Now, instead of using seconds as a unit of time, a new dimensionless time unit will be introduced, $t_1=t/2\pi\sqrt{LC_2}$. In other words, one per unit time is equivalent to $2\pi\sqrt{LC_2}$ seconds. When this change is made in the independent variable, e_0 can be expressed as an operational function of λ where $\lambda=d/dt_1=2\pi\sqrt{LC_2}p$.
The above substitution gives

$$e_0(\lambda)=\frac{2\pi\left(4\pi^2+\frac{C_1}{C_2}\lambda^2\right)}{8\pi^3\left(1+\frac{R_p}{R_s}\right)+4\pi^2\frac{R_p}{Z_0}\times\left[1+\frac{R_p}{R_s}\left(\frac{Z_0}{R_p}\right)^2\right]\lambda+2\pi\left[1+\left(1+\frac{R_p}{R_s}\right)\frac{C_1}{C_2}\right]\lambda^2+\frac{R_pC_1}{Z_0C_2}\lambda^3}$$

where $Z_0=\sqrt{L/C_2}$

From this equation, it can be seen that the time form of the solution for e_0 will depend not upon the magnitudes of the parameters, R_p, R_s, L, C_2, C_1, but upon the dimensionless ratios R_p/R_s, R_p/Z_0, and C_1/C_2. This permits the scaling of a particular problem to fit the frequency and impedance range of the transient analyzer and also permits a more concise presentation of data than would be possible using the actual circuit constants.

Appendix II. Calculation of Pulse Droop

Figure 3(C) is the equivalent circuit of the pulse transformer after the pulse output has reached a quasi-steady-state value. The leakage inductance and winding capacitances will have negligible effect upon the average output voltage on the top of the pulse. If a pulse voltage equal to $(1+R_p/R_s)E$ is applied to the primary of the circuit of Figure 3(C), the secondary voltage initially will be equal to E and the current through the magnetizing inductance initially will be equal to zero. If the secondary voltage remains at the value, E, for the pulse duration, δ, the current through the inductance, M, at the end of the pulse will be $E\delta/M$. This current flowing through R_p will cause the secondary voltage to droop below E in magnitude. The per unit droop, D, where $D=(E-E_\delta)/E$ can be found analytically as follows. If a step voltage of magnitude $(1+R_p/R_s)E$ is applied to the circuit of Figure 3(C), the actual instantaneous secondary voltage as a function of time will be

$$e=E\epsilon^{\frac{-R_pR_s}{M(R_p+R_s)}t}$$

For the usual transformer application δ is much smaller than $M(R_p+R_s)/R_pR_s$ so that at the end of the pulse duration, the secondary voltage will be approximately,

$$E_\delta=E\left[1-\frac{\delta R_pR_s}{M(R_p+R_s)}\right]$$

and

$$D=\frac{\delta R_pR_s}{M(R_p+R_s)}=\frac{\delta R_p}{M(1+R_p/R_s)}$$

Appendix III. Design Equations for Auto-Type Transformers

In the auto-type of pulse transformer, a portion of the secondary turns are closely coupled to the primary turns, either by winding side by side or by having two layers of winding separated by only a few mils of insulation. The closely coupled primary and secondary turns are usually made equal. With this arrangement, the following design equations result:

$$L=\left(\frac{n-1}{n}\right)^2b\frac{4\pi N_p^2U}{d}\left(\Delta+\frac{a_1+a_2}{3}\right)10^{-9} \quad (19)$$

$$C=\frac{(n-1)^2+(n-1)+1}{(n-1)^2}\;\frac{0.0885kUd}{3\Delta}10^{-12} \quad (20)$$

$$N_p^2U^2=\frac{n^2}{(n-1)^2+(n-1)+1}\;\frac{3\times10^{21}}{4\pi\times0.0885}\times\frac{LC}{bk}\;\frac{\Delta}{\left(\Delta+\frac{a_1+a_2}{3}\right)} \quad (21)$$

$$d^2=\frac{(n-1)^4}{n^2[(n-1)^2+(n-1)+1]}\times\frac{N_p^2bC\Delta\left(\Delta+\frac{a_1+a_2}{3}\right)}{kL} \quad (22)$$

For the step-up transformer

$$\frac{\Delta}{a}=-\frac{1}{3}+\sqrt{\frac{1}{9}+\frac{0.0885}{12\pi10^3}\;\frac{n^2[(n-1)^2+(n-1)+1]}{(n-1)^2}\;\frac{kL}{bC}} \quad (23)$$

For the step-down transformer

$$\frac{\Delta}{a}=-\frac{1}{3}+\sqrt{\frac{1}{9}+\frac{0.0885}{12\pi10^3}\;\frac{n^2[(n-1)^2+(n-1)+1]}{(n-1)^4}\;\frac{kL}{bC}} \quad (24)$$

References

1. Pulse Generators (book), **G. N. Glasoe, J. V. Lebacqsz.** Massachusetts Institute of Technology Radiation Laboratory Series, volume 5, McGraw-Hill Book Company, Inc., New York, N. Y., 1948, chapters 12–15.

2. Traveling Waves on Transmission Systems (book), **L. V. Bewley.** John Wiley and Sons, Inc., New York, N. Y., 1933, chapters 12–16.

3. Magnetic Circuits and Transformers (book), **Massachusetts Institute of Technology Staff.** John Wiley and Sons, Inc., New York, N. Y., 1943, pages 489–90.

4. Electronic Transformers and Circuits (book), **Reuben Lee.** John Wiley and Sons, Inc., New York, N. Y., 1947, chapter 9.

5. Equivalent Circuit of a Pulse Transformer Core, **H. L. Rehkof.** Radiation Laboratory Report Number 666, Massachusetts Institute of Technology (Cambridge, Mass.), March 20, 1945.

6. System Recovery Voltage Determination by Analytical and A-C Calculating Board Methods, **R. D. Evans, A. C. Monteith.** *Electrical Engineering* (*AIEE Transactions*), volume 56, June 1937, pages 695–705.

7. A New Device for the Solution of Transient-Vibration Problems by the Method of Electrical-Mechanical Analogy, **H. E. Criner, G. D. McCann, C. E. Warren.** *Journal of Applied Mechanics* (New York, N. Y.), September 1945, pages 135–39.

No Discussion

Protection of the Airplane Main Bus

D. W. EXNER
MEMBER AIEE

INCREASED thought has been directed in recent years toward protection of the airplane electric system so as to improve its reliability and reduce the hazards which result from its failure. Up to and including the early years of World War II, little attention was paid to electric system protection beyond the obvious necessities of reverse-current relaying on the generator circuits and the use of fuses and small circuit breakers on the distribution circuits. During these years the size of the system was growing rapidly and the primary system voltage was advanced from 14 to 28 volts direct current. From the 1,500-watt 14-volt system on a popular pre-war commercial transport, system capacities advanced to 11.2 kw at 28 volts on the early *B-17* bombers and eventually to 50 kw on the *B-29*'s. Because there is little sign of slowing up in the trend toward greater installed capacities, particularly on military airplanes, higher voltage a-c and d-c systems have been in the process of development for the past ten years. Until very recently the greater emphasis has been on the 160-kva 208-volt 3-phase 400-cycle system because of its selection by the Air Force for the *B-35* and *B-36* bombers, and still larger versions of this system are in the offing. After a slow start some years ago, the 115-volt d-c system is finally undergoing a new intensive development for certain military applications.

In view of this growth in size and because greater dependence is placed on electric power on modern airplanes, certain phases of system protection are receiving much attention at the present time.[1,2] This paper will discuss methods for protecting the main bus. To set the stage, a brief history of airplane circuit protection is reviewed first.

Review of Protection History

As the electric systems became larger and operating conditions more severe, the circuit protection deficiencies were demonstrated by a number of cases of fires resulting from ground faults on the generator feeders and main bus. In some cases the generator contactor failed because of insufficient arc rupturing capacity at high altitude or because of contacts welding. Even if the contactor operated correctly, there was no provision for deenergizing the field in the case of a faulted generator or generator feeder. Out of these difficulties better designs of reverse-current contactors appeared,[3] but the need for some form of back-up protection was apparent. Fusible fault limiters designed to blow above normal overload levels proved to be a solution of sorts. Another solution was the use of manually-reset reverse-current circuit breakers located between the bus and the generator contactors and having auxiliary contacts to open the generator field circuit when the circuit breaker tripped. Initial experience with these circuit breakers was unfortunate, to say the least, because their lack of time delay allowed them to trip on normal system reverse-current surges and the necessity of locating them at the nacelles, adjacent to the generator contactors, made them inaccessible for manual resetting. Subsequent provision of some inverse time delay to these circuit breakers minimized the danger of nuisance tripping, and the modern tendency toward the use of a centralized bus in the fuselage permits access for resetting.

In the early stages of development of the 208-volt 400-cycle system in 1943, it was agreed that comprehensive alternator circuit fault protection was desirable, and the necessary equipment and control schemes were developed. Figure 1 shows a representative single-line diagram of the alternator protection. This provides differential current protection against alternator line-to-line and line-to-ground faults and includes the feature of opening the field circuit in case of fault. Alternator feeder faults are cleared by the use of multiple conductors with fusible fault limiters of an improved type[4] in each end of each wire. A form of back-up protection is provided by a thermal delay relay which removes the alternator from the line and opens its field circuit when the alternator excitation is maintained at ceiling level for longer than about six seconds.[5] As this is a nonselective type of protection, it is not intended that it should act except for such severe conditions as a major main bus fault or a bogged-down system caused by heavy motor starting loads when the generating capacity has been abnormally reduced by heavy combat damage.

Within the last two years good progress has been made in the development of integrated generator control and protection equipment for the 28- and 115-volt d-c systems. Up to the present time, the details which constitute the electric system usually have been designed and procured to individual detail specifications which ostensibly cover every requirement and condition of service, including the interaction with other pieces of equipment. With the inevitable different sources of supply, and the practical impossibility of writing a "hole-proof" specification, the result has been that our systems were nonhomogeneous in performance and deficient in protection. Now for the first time the d-c generation system has been studied as a whole by individual equipment manufacturers from the viewpoint of established industrial power practices, with the result that a much higher order of protection is offered with a relatively small increase in over-all weight and with greatly improved facility of maintenance.[1,2] In addition to genera-

---

Paper 48-203, recommended by the AIEE Air Transportation Committee and approved by the AIEE Technical Program Committee for presentation at the AIEE Middle Eastern District Meeting, Washington, D. C., October 5–7, 1948 and at the Pacific General Meeting, San Francisco, Calif., August 23–26, 1949. Manuscript submitted July 28, 1948; made available for printing August 12, 1948.

D. W. Exner is Research Engineer with the Boeing Airplane Company, Seattle, Wash.

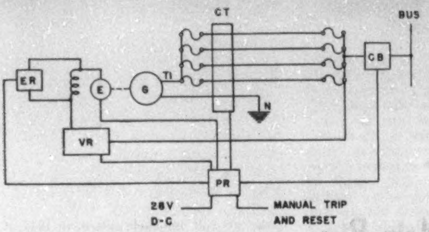

Figure 1. 400-cycle 3-phase alternator protection. Simplified single-line diagram, showing multiple-conductor feeder

G = alternator (phase 1 shown); E = exciter; CB = alternator circuit breaker; CT = differential-current transformer and relay; PR = pilot relay, exciter control; ER = exciter protection relay, thermal delay; VR = voltage regulator

tor and generator feeder fault protection, over-voltage protection is provided.

Since the earliest days of airplane electric systems, distribution circuits have had fuse or circuit breaker protection designed in general to protect the wire against dangerous overload. In many cases this has not been completely successful in preventing damage to the wire but generally has been able to interrupt in time to prevent fires. Particularly in commercial airplanes, but also in military airplanes, because of the adverse psychological effects, it is very desirable to avoid reaching wire temperatures at which the insulation gives off smoke or noisome odors. Distribution circuit breaker design has not fully kept pace with the increased fault current capacity of modern systems. Even the wartime *B-29* system, with armament amplidyne motor-generators in operation, was able to develop a peak fault current in excess of 12,000 amperes for a fault close to the main bus. The inadequate ultimate rupturing rating of small circuit breakers has in some cases required that back-up protection be provided by fusible limiters where it is necessary to tap loads from or near the main bus. Present practice in the 208-volt 400-cycle systems is to use three or more multiple circuits with fault limiter protection at each end of each wire so that a wire which develops a fault will be removed without losing the entire circuit. While this method is effective, the maintenance involved in periodic inspection of the many limiters required is excessive. This same protection may, perhaps be used on the 115-volt d-c system but will require careful study because of the limited sustained fault current capacity of the self-excited system operating without a battery and at a wide range of generator speed. Other methods of load feeder protection have been suggested, using current-balance or combined reverse-current and over-current principles, but to date none of these have been developed to the degree necessary for their use on airplanes. It should be mentioned that any method requiring the use of one or more pilot wires is not looked on with favor because of the added weight and increased vulnerability, particularly under combat conditions. While this feature may be tolerated within reason in generator protection schemes the much greater number of distribution feeder circuits makes it impractical.

The preceding review of the protection situation in airplane electric generation and distribution systems indicates that suitable methods are fairly well in hand with two exceptions:

1. Further work is needed on simpler and more effective methods of load feeder protection.
2. Main bus protection methods have not been developed to a satisfactory stage.

This paper concerns primarily a discussion of main bus protection.

The Need for Main Bus Protection

Practically all of the American multiengine airplanes flying today have an electric system in which two to six d-c generators or alternators are normally paralleled on a main bus from which the various distribution circuits extend, usually in a simple radial configuration.[6] The question of parallel versus isolated operation has been discussed many times in recent years, but it is generally conceded that motor starting and, in some cases, fault clearing requirements are met with minimum total generating capacity in a paralleled system.[7,8] Modern large airplanes have relatively large total motor loads, with a few individual motors approaching in some cases the rating of each generator. On the d-c systems some of the larger motors and a rather high percentage of the total motor load will be shunt or compound wound, so that the motor contribution to peak fault current will be high.[9]

The main bus in the paralleled system constitutes a principal vulnerable point, damage to which can disable the entire electric system. Recognition of this fact influences the designer to devote special attention to design and location of the bus structure so as to reduce the possibility of damage. For commercial airplanes at the present time, this is the best solution and is preferable to the added complication and weight of protective relaying. For combat airplanes such design treatment is, of course, necessary also, but some suitable form of quick-acting automatic protection is needed badly.[10] No amount of care in design, installation, or even armoring can eliminate the chance of missile damage completely. A direct hit on a bus compartment, or a nearby explosion, is almost certain to produce an electric fault either by impact damage to the conductors or by tearing and curling adjacent structure into contact with the bus. Methods for minimizing the results of such damage will be discussed.

Protection by Reducing Exposure

The first principle of bus protection is, naturally, to decrease the exposure area. Most multiengine airplane designs up to and including the war years used a wing-to-wing main d-c bus, shown in Figure 2. This showed weight economy by permitting engine starter and accessory loads to be tapped off in the nacelles instead of running separate feeders back from the center section. Although some postwar designs still use this method, it cannot be considered good practice from the safety standpoint. In such cases, the bus occupies the same general area with hydraulic lines and mechanical control cables and is adjacent to fuel tanks and lines. It is in a hot area when thermal wing de-icing is used. Extra precautions must be taken against abrasion failures of insulation and possible cable damage during maintenance work on other facilities in that area. Under combat conditions, it is extremely vulnerable to missile damage. If the bus itself is concentrated in the center section, the generator feeders which have to run through the wing section can be protected fairly well by present current-balance methods.

Location of the main bus in the fuselage offers maximum reduction in exposure area and incidentally improves the voltage regulation. The effective size of the bus is then determined mainly by the number and size of the generator contactors and load feeders which must be attached to it. It may be beneficial to move many of the secondary load circuits to separate load busses which are fed from the main bus through multiple conductors individually protected at each end by fusible fault limiters. The area around, and particularly above, the main and load busses should be kept clear of fuel, hydraulic, alcohol, and oxygen lines. In a recent case which emphasizes this point, a mechanic was tightening a connection to a circuit breaker at a load point. His screwdriver slipped and made contact with an oxygen line, starting a fire which caused heavy damage to the airplane before it was extinguished.

Much can be done to reduce the vulnerability of a bus by careful attention to arrangement and insulation so that foreign objects such as loose washers or small tools cannot create a fault. During the war, a new *B-29* was lost in Puget Sound because of conditions initiated by a fault which resulted from a loose washer lodging between two terminals of a reverse-current contactor. In this case, the design of the contactor was at fault, offering an example of the need for adequate enclosure and for insulating terminal guards on electric equipment.

Insulated Bus Compartments

At the present time, the use of bus compartments constructed entirely of insulating material is being considered seriously. Present techniques in the use of glass fiber laminates make this attractive and apparently practical. Needless to say, the resin should have nontracking and fire-resistant properties. Attention should be given to the location and shielding of any metallic attachment fittings so as to prevent accidental contact between the bus and those details which are at ground potential. A minor weak point in this arrangement is the need for control circuit ground connections to the coils of the generator contactors located inside the bus compartment. It would seem desirable from a safety standpoint to leave the contactor frames ungrounded and to complete the control ground circuits through number 20 gauge wire leads which can burn clear in the event of an internal breakdown in the contactor.

The construction of an equally safe 3-phase bus compartment presents more difficulty because of the dual danger of phase-to-phase and phase-to-ground faults and because of the unavoidable crossovers resulting from connections to the bus. The use of solid noncombustible insulating barriers between phases and at crossovers is good practice. The crossover problem becomes simpler if the three phases are stacked or staggered in depth.

Mechanical Protection

For protection against missile damage some use has been made of armor plating the bus compartments, although the constant struggle with weight problems on airplanes makes this extremely unattractive if it is made reasonably effective. In some cases it has been possible to obtain a certain degree of flack protection by suitable location with respect to heavy primary structure such as wing spar caps. There is then the probability that a direct explosive hit which would destroy the bus will do enough structural damage that the bus failure will be incidental.

The Sectionalized Bus

If we assume that a means is available for isolating a faulted bus section, it goes without saying that the bus must be arranged in two or more sections in order to obtain any benefit in continuity of service. In a commercial airplane the sections may be all in one compartment with suitable barriers. In a combat airplane, however, it is important to have the sections in separate compartments, well separated to minimize the chance of simultaneous damage. So as to avoid excessive exposure, the bus tie conductors should be run in spaced multiple with fusible limiter protection at each end of each conductor. Additional security is obtained if the bus sections are connected in a ring configuration so that the isolation of a central section will not cause the loss of parallel operation. The ring arrangement makes better use of the remaining generating capacity to blow the limiters to a faulted section and may also justify the use of lighter individual bus tie lines and tie limiters, the latter making easier the matter of clearing a faulted section. Vital loads on an airplane usually are duplicated, in which case they may be distributed over two or more bus sections.

Sectionalizing Through Fusible Limiters

For automatic isolation of a faulted bus section the fusible limiters in the tie lines function reasonably well under generating and load conditions which result in high fault current. This means having all or nearly all generators in operation, well loaded, and preferably with shunt motors on the line to contribute fault current. In the case of a d-c system a more favorable condition is to have the generators operating at speeds somewhat

Figure 2. Typical 28-volt wing-to-wing bus

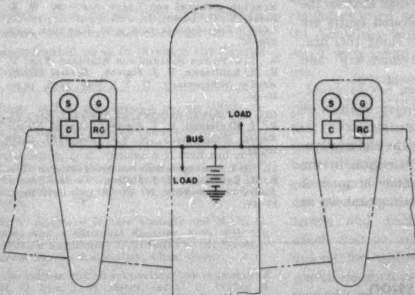

Figure 3. D-c bus section protected by ground-current tripping, with reverse-current and current-balance protection on generator feeder

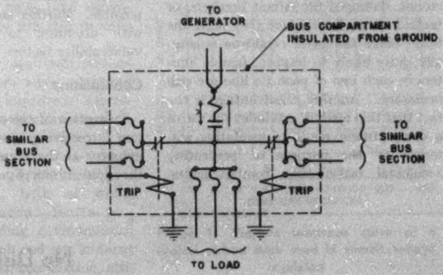

above the minimum. As the system load is reduced or generators are lost from service the short circuit current capacity goes down and limiter blowing time lengthens until eventually it may become excessive. Because of the wide range of possible operating speed, which is a desirable feature of d-c systems, exciters have not been practical and therefore such systems are at present universally self-excited. This limits their sustained fault current capacity. In the 400-cycle system the alternators have individual exciters and, under a solid fault to the main bus, can deliver an ultimate sustained fault current which is appreciably higher than the transient current. On systems having a high percentage of motor loads, nevertheless, one cannot depend on the ultimate fault current for blowing limiters without running into the danger of essentially stalling all motors because of the long time involved. This may leave the system with a heavier starting load than it can pick up, and it may remain stalled until manual supervision removes the major motor loads. Calculations backed up by some tests on the 400-cycle system indicate that a clearing time longer than about 0.1 second may lead to this condition.

Ground-Current Relaying

Because of the imperfect performance of limiters for main bus protection, other faster and more selective means are needed for combat airplane systems. An inherently instantaneous method which has been proposed[11] is shown in Figure 3. Here the metallic bus compartment is insulated from the airplane structure except for a path through the low-impedance trip coils of the circuit breakers. The trip coils must be designed to operate even though they are partially short circuited by a low-impedance fault between box and ground. It is also to be assumed that battle damage to the box has not ruptured the trip coil circuit, damaged the circuit breakers, or faulted the tie lines where they leave the box. Since the latter condition is actually quite likely to happen, fusible limiters in each end of each tie line are still necessary. Another disadvantage is the fact that this method precludes the use of a compartment made of insulating material for the purpose of preventing accidental rather than combat faults, unless a heavier composite construction is used. Because of the difficulty of sensing phase-to-phase faults, and the problems in designing a 400-cycle trip magnet, it would seem that this method is best suited for d-c systems. As far as the author is aware, circuit breakers for this protection method are not yet available for airplane use.

Differential-Current Protection

Although differential-current bus fault protection is used widely in industrial practice, its use on airplane 400-cycle systems, especially under combat conditions, does not appear at all attractive. The difficulty arises principally from the large number of points at which current must be summed, particularly when line-to-line as well as line-to-ground faults are to be detected. Although 400-cycle current transformers are individually small and relatively light, the large number which is required enlarges the bus compartment so much that vulnerability is greatly increased. A broken control wire or a grazing hit on one transformer is sufficient to trip the bus off the line although the bus itself may be undamaged. While use of this method only for ground fault protection will reduce the number of transformers by two-thirds, when using through-type transformers, the lower order of protection obtained offsets the slight improvement in vulnerability. Also the reduction in number of transformers is obtained at the expense of bunching all conductors of all phases at the transformer, and this is a questionable practice. The need for bus-tie circuit breakers in either of the foregoing methods adds to the bus compartment size and vulnerability.

For the d-c systems it is conceivable that an arrangement of directional over-current relays might be devised to detect a bus fault and clear it by means of bus-tie circuit breakers. In some respects the problem appears simpler than that for the a-c case because only ground faults are possible. Further study along this line, with attention to nuisance-trip and vulnerability factors, is suggested.

Conclusions

Protection of the airplane electric system is receiving much attention in the industry at the present time because of the rapid growth of generating capacity in recent years and the greater dependence of airplane safety and performance upon the system reliability. While methods of generator circuit protection are fairly well in hand, the main bus, and to a lesser extent the distribution circuits, are inadequately protected because fully effective methods are not yet available. Although improved bus structure design and installation, such as the use of nonmetallic bus compartments, may afford sufficient protection for noncombat airplanes, more-positive and faster-acting protection is urgently needed in combat systems. At the present time the safest bus is the ring type with dispersed bus sections interconnected by multiple-conductor limiter-protected bus tie lines. The clearing time for a bus fault in this system is dangerously long after partial loss of generating capacity and may result in system collapse because of stalled motor loads. Further work on simple low-vulnerability bus protection methods is needed and there is a possibility that some form of directional over-current relaying would be suitable.

References

1. Control and Protection of Aircraft D-C Power Systems, **B. O. Austin.** *Electrical Engineering (AIEE Transactions)*, volume 65, November 1946, pages 741–45.

2. D-C Aircraft Generator Power Center, **E. L. Bottemiller.** *AIEE Transactions*, volume 66, 1947, pages 1267–70.

3. An Aircraft Differential-Voltage Cutout, **O. C. Walley.** *Electrical Engineering (AIEE Transactions)*, volume 63, September 1944, pages 632–34.

4. A Current-Limiting Fuse for Aircraft Applications, **A. H. Powell.** *Electrical Engineering (AIEE Transactions)*, volume 64, July 1945, pages 541–45.

5. Generator Fault Protection, United States Patent 2,426,005.

6. Paralleling and Regulation of 24–28-Volt D-C Generators in Multiengine Aircraft, **Arthur Siegal, Dennis G. DeCourcey.** *Electrical Engineering (AIEE Transactions)*, volume 63, November 1944, pages 854–57.

7. Parallel Operation of Airplane Alternators, **D. W. Exner.** *Electrical Engineering (AIEE Transactions)*, volume 62, December 1943, pages 755–60, Discussion, page 993.

8. Basic Considerations in Selection of Electric Systems for Large Aircraft, **W. K. Boice, L. G. Levoy, Jr.** *Electrical Engineering (AIEE Transactions)*, volume 63, June 1944, pages 279–87.

9. D-C Power Systems for Aircraft, Part V, **R. H. Kaufmann, H. J. Finison.** *General Electric Review* (Schenectady, N. Y.), May 1946, pages 46–54.

10. D-C Power Systems for Aircraft, Part VI, **R. H. Kaufmann, H. J. Finison.** *General Electric Review* (Schenectady, N. Y.), June 1946, pages 46–52.

11. D-C Power Systems for Aircraft, Part VII, **R. H. Kaufmann, H. J. Finison.** *General Electric Review* (Schenectady, N. Y.), August 1946, pages 41–48.

No Discussion

Aircraft Carbon-Pile Voltage Regulators, Fundamentals, and Design Improvements

B. O. AUSTIN
MEMBER AIEE

H. H. C. RICHARDS
NONMEMBER AIEE

IT HAS been known for many years that mixes of carbon can be processed into plates of various shapes, hardnesses, finishes, and thicknesses. When these plates are stacked and pressure applied at right angles to their surfaces, the resistance of the stack varies with the pressure change. Figure 1 is a typical curve of pressure plotted against resistance for such a carbon stack. This curve shows that the resistance decreases with an increase of pressure. The design of the carbon-pile voltage regulator is based on this fundamental characteristic of carbon surfaces in series under a controlled variable pressure.

D-c generator field strength is one of the determining factors for output voltage. Field strength may be controlled by varying the current with variable series resistance. Stacked carbon plates provide such a resistor when the applied pressure is properly controlled. Many designers in the past several decades have conceived a large variety of electromechanical mechanisms for controlling the pressure on carbon piles. These mechanisms have consisted usually of levers, cams, pivots, dash-pots, springs, rollers, magnets, and electrical dampers co-ordinated so as to produce the desired results.

Generally, the main design objective for carbon-pile voltage regulators is to provide an electromagnet with the necessary mechanisms arranged so that the pull curve of the magnet matches the force curve of the spring throughout the operating travel range of the magnet armature to properly control the pressure on the carbon stack. See Figure 2 for a typical matching curve. This accomplished, the device becomes a servomechanism for automatically regulating the resistance in series with the field winding of the generator to hold constant voltage output when the regulator operating coil senses generator voltage.

Carbon-pile voltage regulators designed for aircraft use appeared in quantity on military aircraft early in World War II. These regulators were similar to the English design by Newton which were of the direct-acting type with many of the mechanical arrangements common to the carbon-pile voltage regulators eliminated. Due to their mechanical ruggedness and ability to withstand momentary overload, they have been more successful than other types of regulators used previously. Even with the difficulties which have been experienced with them, they are still in wide use.

Many of the users of aircraft carbon-pile voltage regulators have suggested that the regulators be improved. Operators want longer life, easier maintenance, better temperature compensation, no creeping, no fluttering, no over-voltage due to stack wear, and minimum hysteresis and friction, both of which affect voltage regulation. Better provisions for withstanding environmental conditions such as high and low ambient temperature, vibration, acceleration, altitude, sand, salt spray, and humidity are further refinements desired.

In further consideration of the improvements in the design of the aircraft carbon-pile voltage regulator, it was found that it is much easier to build satisfactory regulators in model shops than to produce satisfactory regulators of the same design in the production line unless the design is adapted to easy accurate methods in obtaining close tolerances and perfect alignments of vital parts.

Performance Objectives

With the performance data from actual service at hand and with a wealth of information from production experience, it was clear that a complete study of all factors affecting the performance and production of aircraft carbon-pile voltage regulators was long overdue. The first requirement of any voltage regulator is accurate regulation. Regulator performance, as outlined in the *AN-R-la* Specification issued by the United States War and Navy Departments, is required from minimum generator speed to maximum generator speed with generator load varying suddenly or gradually over the load range. The load may be suddenly removed or applied at any time. This operating load condition may repeat at low or high ambient temperatures or under altitude conditions. Regulator

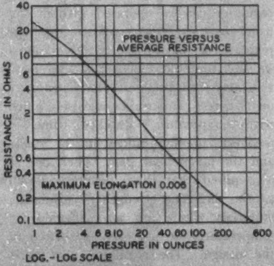

Figure 1. Pressure resistance curve of a typical carbon stack used in aircraft voltage regulators

---

Paper 48-214, recommended by the AIEE Air Transportation Committee and approved by the AIEE Technical Program Committee for presentation at the AIEE Middle Eastern District Meeting, Washington, D. C., October 5-7, 1948, and at the Pacific General Meeting, San Francisco, Calif., August 23-26, 1949. Manuscript submitted July 21, 1948; made available for printing August 25, 1948.

B. O. AUSTIN is Section Manager and H. H. C. RICHARDS is Electrical Engineer, both with the Aviation Engineering Department of the Westinghouse Electric Corporation, Lima, Ohio.

The authors wish to acknowledge the assistance of H. D. Else, J. D. Miner, and O. C. Walley of Westinghouse Electric Corporation.

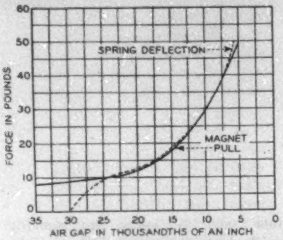

Figure 2. Curve showing matching between spring force and magnet force in the aircraft voltage regulator

performance must be such that minimum stack resistance will permit satisfactory generator output at low speeds. On the other hand, the maximum high resistance values at no-load and maximum speed must be accurate and stable under conditions of vibration. It is further required that the voltage controlled by the carbon-pile voltage regulator during load changes between rated load and no-load shall recover in the order of 0.1 second or less. Regulators are sometimes subjected to full field current through the stack and must carry this overload current for a long period without damage to any operating parts. Carbon-pile voltage regulators in operation on airplanes are subjected to periods of continuous acceleration. This is a severe operating condition which must be met without loss of regulation at high generator speed and high stack resistance, and the regulator must remain stable. Paralleling equalizer coils must be provided in the regulator so that satisfactory load division will be maintained by the generators. See Figure 3 for the diagram of paralleled regulators and generators.

Total temperature produced by watts loss in a carbon-pile voltage regulator determines the watts rating at which the regulator can be operated without unusual wear or damage affecting voltage regulation. Therefore, the design must be such that the regulator will dissipate the rated watts without overheating any of its parts. Endurance is closely allied with temperature, stability, time of recovery, pressure range on the stack, and the magnet air gap. Therefore, it is required that these factors (as well as the dielectric strength of insulating materials which are also affected by temperature) be properly considered in the design. The regulator also must have the ability to withstand sand, dust, salt air or spray, high or low humidity, and resistance to fungus growth.

Design Procedure and Results

There are many factors governing the carbon stack design which must be considered and accounted for if long life and good performance are to be expected. The operating temperature of carbon is limited by disintegration at the surface of the plates and therefore watts loss of these surfaces must be within the temperature limits of the carbon surfaces, which is in the order of 400 degrees centigrade. Resistance per inch of length of the carbon plates or disks must be controlled so as to limit the watts input. Therefore, the total length of the stack is determined largely by how fast the carbons can be cooled and the maximum temperatures that carbon can stand without disintegration. It is not advisable to blow air directly on the carbon stack as the oxygen present accelerates combustion at the hot spots.

Carbon plates in stacks do not make contact uniformly throughout the area of the plates. This is due to very minute high spots, even with the best grinding and polishing methods. Heat is concentrated at the points where high spots first make contact. This may result in glowing or overheating of the carbon at the localized points if the volts and amperes per plate are too high. This is controlled by providing the proper number of plates per inch of stack length. Therefore the permissible watts for each contact surface are a determining factor in the number of disks per inch. There seems to be no known means of cooling these hot spots fast enough to prevent disintegration of the carbon and to permit a reduction in the number of carbon plates and the lengths of stack in a given application.

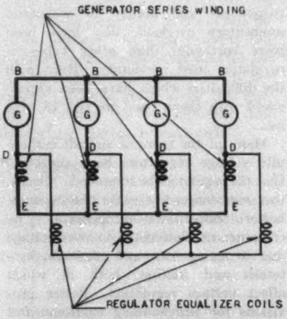

Figure 3. Diagram of equalizer circuits for equalizing generator loads

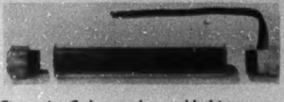

Figure 4. Carbon stack assembled in a pyrex tube and the electrodes for the aircraft carbon-pile voltage regulator described

Two other important factors entering into the stack design are the minimum and maximum resistance to be obtained under operating conditions and the available forces in the magnet and spring. A large number of disks per inch aid in obtaining maximum resistance, reduce arcing between plates and provide stability. On the other hand, a small number of disks aid in obtaining the minimum resistance. The design must be compromised between these two factors and the hardness of the carbon.

Stack sizes or diameters should be kept small provided they can be cooled satisfactorily. This is to minimize the weight of the stack which aids in the solution of vibration and manufacturing problems. The smaller diameter disks are easier to grind flat and they remain flat after heating in the regulator. Large rigid disks are hard to grind and warp easily with temperature. This can seriously affect the performance of the regulator. Very thin disks may be acceptable when they can be produced with sufficient strength. In this case, the surfaces of the carbon disk would adjust themselves to one another by bending. Figure 4 shows the stack used in the improved regulator.

The method of cooling and the necessity for enclosing the carbon stack make it necessary to support the stack with a tube made of such material as Pyrex glass or ceramic. Both of these materials are satisfactory; the ceramic material being a little more difficult to grind and polish to eliminate friction.

Probably the most important structure in the carbon-pile voltage regulator is the armature and its associated parts. The vital parts of this armature consist of an iron disk, an abutment on which the spring rests, a damper, a spring, a spring clamp, insulation, electrode, and hardware.

For the purpose of obtaining quick response and eliminating difficulties due to vibration, the component parts of the armature assembly which move are kept as light as possible. A flat star-shaped spring is used whose ends rest on an outer abutment ring. The ring surface is shaped so that as the spring travels, the forces required to make it travel are nonlinear and match the pull curve of the magnet. For maintaining accuracy of the assembly, this special design uses a star-shaped spring which is flat and is not formed before being included in the armature assembly. During the assembly of the armature an inner and an outer cone-shaped coined washer clamps the spring and forms it to the desired angle. This eliminates the manufacturing difficulties of accurately forming springs. In this same assembly there is a thin, soft, copper diaphragm whose purpose is to air and spring damp the action of the star-shaped spring and control the wear curve of the regulator, minimizing armature flutter and over-voltage due to carbon stack wear.

The problem of excessive heat transfer from the electrode and carbon stack to the star-shaped spring was solved in the regulator shown by using a ceramic bushing support for the electrode which is clamped into the armature assembly. The ceramic was selected for its high heat insulating characteristics. The electrode has a shunt which is attached to the electrode by tamping. The shunt passes through a slot in the side of the ceramic bushing. The electrode can be removed from the ceramic bushing in about the same manner a carbon brush is removed from a generator. This provides an armature which is very stable and is not subject to change or shrinkage such as that experienced with other types of armatures. See Figure 5 illustrating the component parts of the armature assembly.

Magnetic forces to operate the armature are rather simple and are subject to standard calculations. The pull curve is matched to the armature spring as nearly as it is practical to do with such a design. Structural studies of the magnetic circuit were made and the circuit arranged so as to provide the maximum ease in the accuracy of assembly during production and maintenance operations. Hysteresis in the magnetic field is minimized by thoroughly hydrogen annealing all iron in the magnetic circuit. In addition a high grade iron is used to eliminate as many impurities as possible.

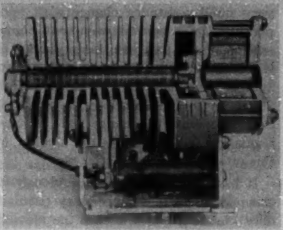

Figure 6. Cut-away view of the aircraft carbon-pile voltage regulator

The stationary electrode is the same as the moving electrode except that it does not have a shunt and is pressed into a metal threaded plug. It is removable and replaceable. Removing the stationary electrode plug permits the removal of the carbon stack without further disassembly. This plug is clamped in place by the support casting being split and closed with a clamp screw.

Heat dissipation and thermal expansion are controlled by the amount of radiating surface and the characteristics of the materials used. The carbon stack which is to be cooled is enclosed in a Pyrex tube which is not a good heat conductor, but is acceptable from this standpoint and is used. This material and a ceramic are about the only ones that will stand the heat shocks and provide the necessary insulation. The stack diameter, the inside and the outside diameter of the Pyrex glass tube are controlled as closely as it is practical to avoid blankets of air which also are very poor conductors of heat. Tolerances between the glass tube and the metal tube of the housing are closely controlled for the same reason.

Heat is finally dissipated by means of cast aluminum fins on an invar steel tube. The number and area of these fins depend on the watts to be dissipated and the maximum allowable total temperature rise of the carbons. An aluminum cast housing for cooling and supporting the structure has been a problem due to the high temperature coefficient of the expansion of aluminum. The problem was solved by casting the aluminum fins separately on an invar tube which has a very low temperature coefficient of expansion. In this manner, the individual aluminum fins can expand, but do not affect the over-all expansion of the housing. Temperature rise of the invar tube is about 135 degrees centigrade for 90 watts dissipation. See Figure 6 for a cut-away view showing this construction.

Carbon stacks and electrodes have not as yet been designed so that they will have an indefinite life. They are an item of wear and must be replaced. The regulator structural design was studied thoroughly and arranged so that any of these parts could be removed and replaced within ten minutes. At the same time, the design also was arranged so that when it was disassembled or reassembled there would be no errors of misalignment which could cause poor voltage regulation due to increased friction of parts being pushed sidewise. See Figure 6.

External to the body of the regulator is a 1-piece mounting bracket or base on which are mounted three resistors and the necessary terminals. The variable re-

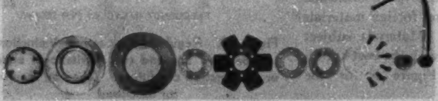

Figure 5 (left). Exploded armature in line of assembly, left to right (1) armature, (2) copper damper, (3) abutment ring, (4) coned washer, (5) star-shaped spring, (6) concave washer, (7) spacer, (8) clamping washer, (9) hardware, (10) ceramic bushing electrode support, (11) graphite electrode and shunt

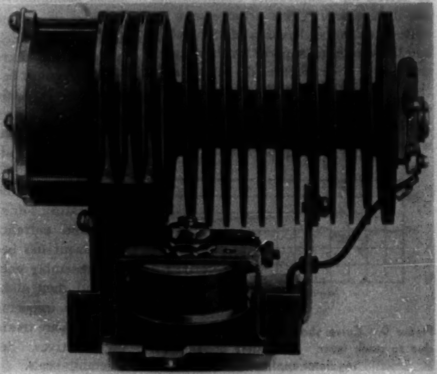

Figure 7 (right). A 90-watt aircraft carbon-pile voltage regulator

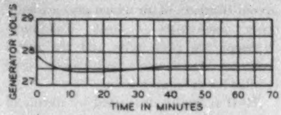

Figure 8. Voltage regulation curve during a 70-minute warmup period from a 25 degree centigrade ambient

sistor is in series with the operating coil of the regulator. The purpose of this is to set the regulator voltage within the established limits. It was felt by the designers that an improvement could be made by providing a locking nut for this adjustment, rather than by using a detent or ratchet mechanism to hold the adjustment in place. The locking nut can not be changed so easily by unauthorized persons and it has, therefore, been provided. The fixed resistor is in series with the operating coil and is for temperature compensation, which will be discussed later. The fixed stabilizing resistor is connected so as to form a feedback to the operating coil, thereby stabilizing the action of the coil in the magnet circuit of the regulator. See Figure 11.

Aircraft carbon-pile voltage regulators are subjected to a very high range of temperatures from ambient sources as well as warm-up due to heat generated within them. For this reason, temperature compensation of the regulator was thoroughly studied and means were provided for correction. Several variations of materials such as steel whose magnetic characteristics change with temperature were tested and evaluated. The design was finally co-ordinated with materials used in the construction of the regulator. With such an arrangement, the adding of details for temperature compensation was unnecessary. This arrangement involved the proper location of invar alloy and the aluminum support for the magnet assembly. (See Figure 6.) Also note that tie rods formerly used have been eliminated. A fixed resistor mounted on the base is connected in series with the winding of the operating coil. It has a very small resistance change with temperature and is used to swamp out a large portion of the total resistance change of the operating coil. The ratio of the resistance of the resistor to that of the coil is about 4.4 to 1. Therefore, the effect of coil temperature change on voltage regulation is reduced by the amount of this ratio.

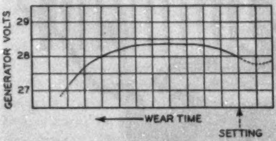

Figure 9. Curve showing voltage regulation due to stack wear. Wear time depends on regulator application

It has been pointed out previously in this paper that it was necessary to minimize the weight and anchor the moving parts of the armature. This was done and proved to be very helpful in the solution of the vibration and centrifugal force problems. The carbon stack also is a free member and is subject to this same service condition. Likewise, its weight, as well as the number of disks in the stack, is important. A small number of disks require less pressure and separate more readily under vibration. Therefore, the number of disks to be used is a compromise between arcing conditions at the disk surfaces and arcing due to vibration.

Endurance or life of an aircraft carbon-pile voltage regulator depends on many factors, some of which have been discussed previously in this paper. Carbon stacks must be operated at or below the recommended temperatures to prevent disintegration. Flutter or unstable action of the armature must be damped out or otherwise excessive arcing and burning will take place at the electrodes and between the disks. Effects of vibration, acceleration, and centrifugal forces on these moving parts must be minimized. Grade or hardness of carbon disks used must be carefully selected and co-ordinated with many other factors in the stack design. Operating stack pressures must be sufficient to prevent arcing under maximum resistance conditions.

There are several environmental conditions, with which many are familiar, under which aircraft carbon-pile voltage regulators must be operated satisfactorily. These are sand, dust, salt air, humidity, and fungus growth. After a thorough study, arrangements were made for the effective sealing of the vital parts against these hazards. Wherever possible, pressure is used at the open joints and high temperature soft synthetic seals are used at cable entrances. Considerable improvement has been made at the armature assembly enclosure where exclusion of sand, dust, and other foreign materials is highly important. Materials subject to fungus are treated with the best known preventatives. See Figure 6 for the assembly seals.

Test Results on 90-Watt 28-Volt Regulator

1. Voltage regulation at 3,500 rpm of a 200-ampere United States Air Force type *P-1* generator varied from 0 to 0.3 volt for three observations, zero load to full load.

2. Voltage regulation at 4,500 rpm of a 200-ampere type *P-1* generator varied from 0.2 to 0.3 volt for three observations, zero load to full load.

3. Voltage regulation at 3,500 rpm of a 200-ampere type *P-1* generator varied from 0.05 to 0.4 volt for three observations, zero load to full load at −55 degrees centigrade ambient.

4. Voltage regulation at 4,500 rpm of a 200-ampere type *P-1* generator varied from 0.1 to 0.4 volt for three observations of zero load to full load at −55 degrees centigrade ambient.

5. Voltage regulation at 3,500 rpm of a 200-ampere type *P-1* generator varied from 0.1 to 0.3 volt for three observations of zero load to full load at +72 degrees centigrade ambient.

6. Voltage regulation at 4,500 rpm of a 200-ampere type *P-1* generator varied from 0.2 to 0.3 volt for three observations of zero load to full load at 72 degrees centigrade ambient. (See Figure 8).

7. Dielectric strength was satisfactory at 500 volts for one minute from live parts to base.

8. With 0.25 volt applied to the equalizer coil, the regulator voltage was lowered 2.35 to 2.50 volts on ten regulators.

9. Minimum resistance varied from 1.17 to 1.22 ohms on the ten regulators tested as per Specification *AN-R-1a*. Resistance of 1.25 ohms or less is acceptable.

10. Maximum resistance of 35 ohms under vibration conditions without producing arcing in the stack is shown by curve in Figure 11.

11. Maximum recovery time tested 0.06

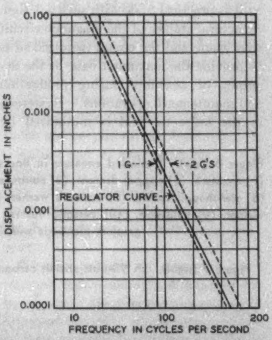

Figure 10. Regulator stack arcing elimination test between one and two gravitational units under vibration conditions. Taken on regulator described

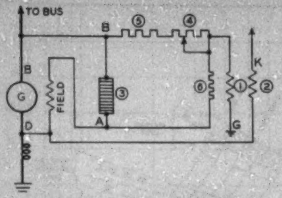

Figure 11. Schematic diagram of connections for the 90-watt aircraft voltage regulator

second. Recovery time of 0.10 second is acceptable.

12. Voltage regulation at 4,500 rpm of a 300-ampere *P-1* generator, 72 degrees centigrade ambient, after 25 hours varied from 0.1 to 0.3 for three observations zero to full load.

13. Carbon stack closed with no voltage on the operating coil. Regulator withstood 15 amperes through the carbon stack for one hour without damage.

14. Maximum increase in ripple, voltage tested to be 0.35 volts, while 0.6 volt is acceptable.

15. Regulator was placed in a centrifuge under the most unfavorable conditions (coil end toward center, stack radial); satisfactory operation was observed up to 6 G's (acceleration due to gravity). 5 G's acceptable to Specification *AN-R-1a*.

16. Regulator was vibrated for two hours in each of three directions making a total of six hours without shock mounts; 10 to 55 cycles at 0.06 total excursion. No damage resulted.

17. At the end of a 200-hour accelerated endurance test the voltage dropped 0.7. The voltage did not change more than 0.3 during any 25-hour period.

18. Regulator was subjected to salt spray for 25 hours, passing regulation requirements afterwards.

19. Regulator was subjected to sand resistance tests for eight hours. At the end of the test, voltage had changed 0.1.

Conclusions

Objectives accomplished in this program of designing and improved aircraft carbon-pile regulator resulted in the following:

1. Better voltage regulation.
2. Lower operating temperatures.
3. Improved acceleration and vibration characteristics which affect life and regulation.
4. Longer life.
5. Sealed protection against salt spray, sand, and other foreign objects.
6. Good temperature compensation without added details.
7. Friction and creep reduced very substantially.
8. Better performance under high and low ambient temperature conditions.
9. Wearing parts made readily accessible and replaceable.
10. Reduction in the number of parts.
11. Disassembly and reassembly without change in alignment.
12. Improved armature construction.
13. Dissipates a maximum of 90 watts.
14. Weight increased about two ounces over regulators of 75-watt rating.
15. Design well adapted to production and maintenance of alignment of parts.

References

1. CARBON-PILE VOLTAGE REGULATORS FOR AIRCRAFT, W. G. Neild. *Electrical Engineering* (*AIEE Transactions*), volume 63, November 1944, pages 839–43.

2. THE APPLICATION OF VOLTAGE REGULATORS TO AIRCRAFT GENERATORS, L. W. Thompson, F. E. Crever. *AIEE Transactions*, volume 61, 1942, pages 363–65.

3. PARALLELING AND REGULATION OF 24–28-VOLT D-C GENERATORS IN MULTIENGINE AIRCRAFT, Arthur Siegal, Dennis G. DeCourcey. *Electrical Engineering* (*AIEE Transactions*), volume 63, November 1944, pages 854–56.

No Discussion

Current Ratings of Aircraft Cable

WADE H. ASKEW
ASSOCIATE AIEE

A. T. McCLINTON
MEMBER AIEE

Synopsis: This paper presents the results of an investigation conducted to determine the continuous and short-time current ratings of copper aircraft cable, using visual indication of smoke as the limiting factor. Tests were made on several wire sizes at various ambient temperatures, using six types of aircraft cable. Curves were obtained showing the highest current which can be carried continuously by each size of cable at different ambient temperatures without evolvement of smoke. Thermal curves, with smoking and delayed smoking values, were obtained for various current overload applications. Procedure is given for interpolating smoking and delayed smoking curves for wire sizes not experimentally obtained. Results of this investigation indicate that present continuous current ratings are too high for most of the cable used during this investigation.

MUCH of the electric equipment in aircraft is used, or draws its greatest current, for short periods of time. When voltage drop is not a restricting item, considerable saving in weight and material can be realized by the use of small size cables to carry, for these short periods, currents much higher than the continuous ratings. If the wiring system is designed on the basis of cables being subjected to overload currents, it is necessary that protective devices be installed to make certain that the interval of application shall not exceed the safe time limit. Proper co-ordination between protective equipment and short-time ratings is necessary to assure that the cable will not be subjected to an excessive overload-time combination.

Tests conducted previously by other laboratories indicate that, for short-time periods, a conductor temperature sufficient to produce light smoke will cause no measurable change in the insulating or physical properties of the cable. However, any trace of such smoke in a plane is psychologically dangerous; therefore, the wiring must be protected from possible smoke evolvement.

Definitions

Certain terms used throughout this report are defined as follows:

Maximum Continuous Current. The highest current which can be carried for an unlimited time by a specified cable at given ambient conditions without producing visible evidence of smoke.

Overload. Any value greater than the maximum continuous current.

Smoking Time. The time required to produce visible evidence of smoke when an overload current is carried by a cable.

Delayed Smoking Time. The longest interval of time an overload current can be carried by a cable without visible evidence of smoke occurring after the current is interrupted.

Methods of Conducting the Investigation

Tests were conducted on single cables in still air, at approximately sea level altitude, in ambient temperatures of 0, 25, and 45 degrees centigrade. Cable sizes *AN* numbers 0, 8, 16, and 20 from various manufacturers were used for the investigation. Data for other ambient temperatures and cable sizes were interpolated from the results experimentally obtained.

The conductor temperature was ascertained at any time during test runs by calculating the change in resistance as indicated by the change in voltage drop across a section of the cable. A submarine battery was used as the source of power; the current was held constant by variable resistors, paralleled as necessary for the various currents used. Tests proved that when only light traces of smoke evolved, the same cable could be used several times without noticeable change in any of the measured results. When the sample was used more than once, subsequent tests were made only after the cable had cooled to room ambient temperature.

Since the appearance of smoke determined the length of time the cable could carry a specified current, it was necessary to have an accurate method of detecting the smoke. Preliminary test runs showed that the best results were obtained in a partially darkened room, using a small desk-type fluorescent lamp secured about three inches above the cable. A piece of photographer's cloth was hung about three feet behind the light, and a small strip of this cloth was suspended just below the light, about two inches in front of the cable. It was found that accumulation of smoke in the lamp shade was particularly helpful in observations where the time at which smoke appeared was not an essential factor, that is, observations for determining continuous current

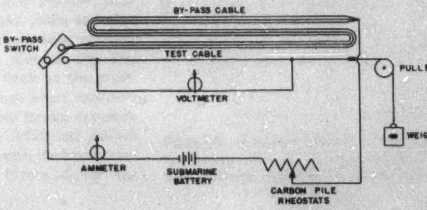

Figure 1. Schematic diagram of test circuit

Paper 49-202, recommended by the AIEE Air Transportation Committee and approved by the AIEE Technical Program Committee for presentation at the AIEE Pacific General Meeting, San Francisco, Calif., August 23–26, 1949. Manuscript submitted September 3, 1948; made available for printing June 28, 1949.

WADE H. ASKEW and A. T. MCCLINTON are both with the Naval Research Laboratory, Washington, D. C.

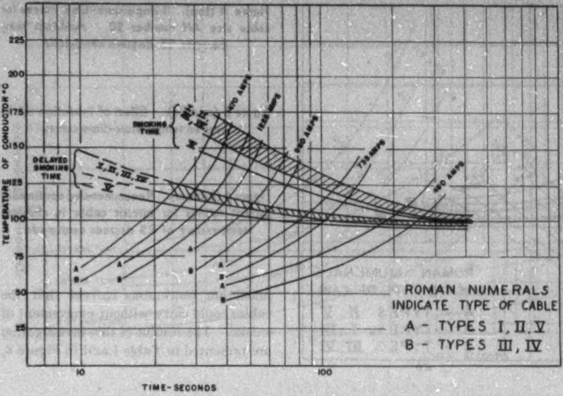

Figure 2. Temperature–time curves for cable size *AN* number 1/0. Ambient temperature 25 degrees centigrade

and delayed smoking values. The best position for observation was found to be 12 to 24 inches directly in front of the light.

Consideration was given to the possibility that different individuals might not detect smoke at the same time under similar conditions. However, data taken from observations made by six persons during a minimum of 20 test runs showed that except for the first five or six observations, the difference is observed time for the various individuals was well within the experimental error.

Figure 1 shows a schematic diagram of the test circuit. The by-pass circuit consisted of three parallel cables, each of the same size as the cable under investigation, but three times its length. This circuit was used for the initial setting of the variable resistors. Carbon piles were used for the variable resistors since their change in resistance partially compensated for the change in resistance of the cable, thus facilitating the maintenance of a constant current. Weights of 20 pounds for size number 0; 5 pounds for size number 8; and one pound for size number 16 and number 20 cable were hung over a pulley with a cord connecting the weight to the cable. Any slack caused by elongation due to temperature rise was taken up by the weight, and the tension was kept constant. These weights were not sufficient to cause stretching of the cable.

Discussion of Results

Figures 2, 3, and 4 show conductor temperature versus time curves for overloads applied to the various types and sizes of cable. The delayed smoking time values shown on these and other curves establish the overload-time values for the cables; but for comparative information, the smoking time values also are shown. It will be noticed that the grouping of thermal, smoking time, and delayed smoking time curves by types is not consistent for the different sizes of cable used during the investigation. This is probably due to different graduated scales used by the manufacturers to determine the relative amounts of primary insulation and braid components for the various sizes of cable. For example, it was found that the weight ratio of primary insulation and/or braid to the total weight of the cable might be nearly equal on one size for cable from four of the manufacturers, whereas when the same type of comparison was made using another size, this weight ratio would be about the same for possibly only two companies; and for a third size, these ratios would be different for all of the manufacturers.

Several tests were made to determine the effect of increase in insulation thickness (outside diameter), the results of which are shown in Figure 5. No attempt was made to determine the thickness of any material added or removed, but attention is directed to the fact that every material added decreased the operating temperature of the conductor, and that the type of outer surface apparently had little effect. Also, this indicates that the heat dissipated from the cable by conduction and convection is large compared to that dissipated by radiation.

In addition to the data mentioned previously on short-time temperature characteristics, data were obtained to show the

Figure 3. Temperature–time curves for cable size *AN* number 8. Ambient temperature 25 degrees centigrade

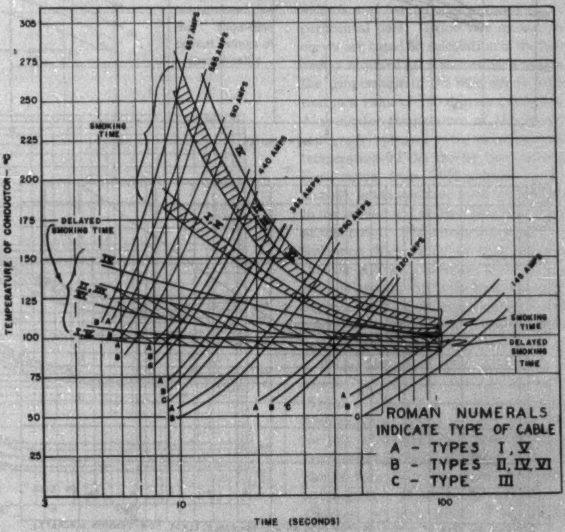

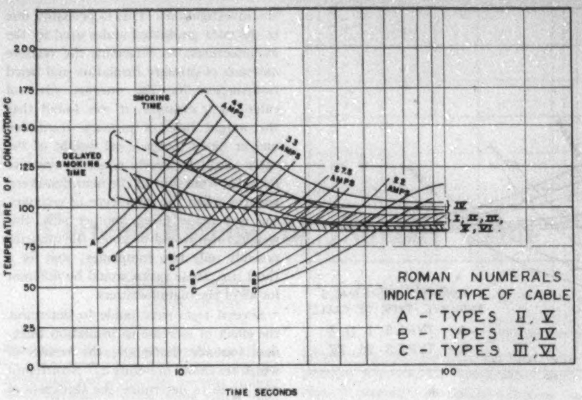

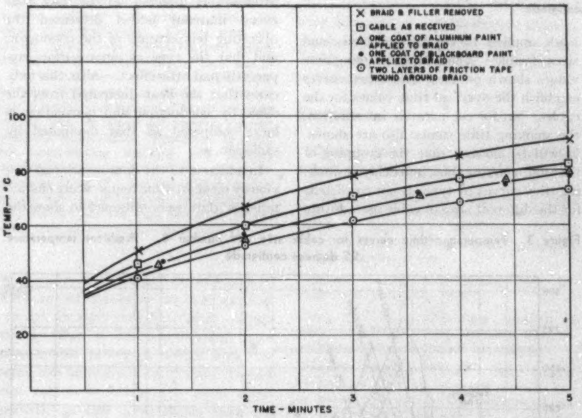

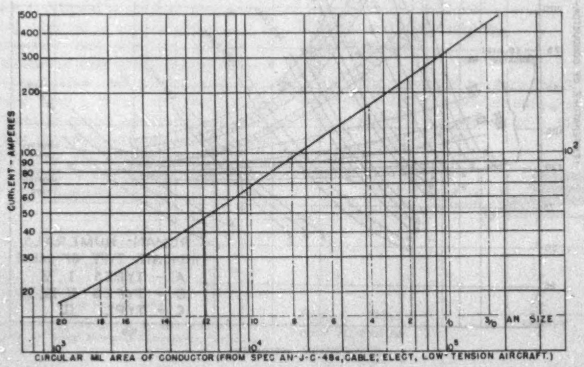

Figure 4 (top). Temperature–time curves for cable size *AN* number 20. Ambient temperature 25 degrees centigrade

Figure 5 (middle). Effect of insulation thickness on temperature–time curves

Figure 6 (bottom). Recommended continuous current ratings for aircraft cable in ambient temperature of 25 degrees centigrade

maximum continuous current that the cables could carry without evolvement of smoke. The results of this investigation are presented in Table I and in Figure 6.

Table I

Cable Type	AN Size Number	Current, Amperes	Temperature* of Conductor When Stabilized, Degrees Centigrade
1	8	92	91.5
3	0	305	89.8
3	8	102.5–107.5	95.4–104.2
3	20	19	93.0
4	0	330	101.4
4	8	102.5–107.5	99.8–107.1
4	20	20	105.2
5	8	92.5–95.0	90.4–92.7
5	20	17	84.5

* Ambient temperature—25 degrees centigrade.

The values shown in Table I are the highest currents that the respective cables could sustain without causing the insulation to smoke while operating in an ambient temperature of 25 degrees centigrade. Those of Figure 6 are the average continuous current values for the six types of cable investigated. It should be noted that most of the conductor temperatures in Table I are lower than the 100 degrees centigrade generally accepted as being satisfactory.

The effect of ambient temperature on short-time and continuous ratings of the various cables also was investigated. Figure 7 shows the thermal curves with smoking time and delayed smoking time values obtained on one type of cable at various ambient temperatures. The average maximum continuous current ratings are shown in Figure 8. It should be noted that the current rating curves will all approach zero current at 95 degrees centigrade.

These tests were extended to show the effects of ambient temperature on the short-time ratings of the various types of

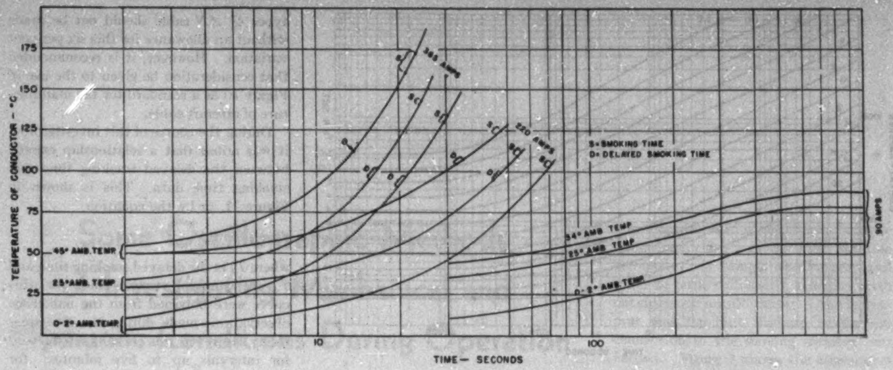

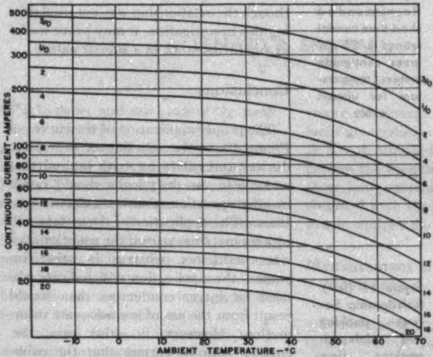

Figure 7 (top). Effect of ambient temperature on temperature–time curves of one type of cable. *AN* size number 8

Figure 8 (left). Effect of ambient temperature on continuous current ratings of aircraft cable

Figure 9 (below). Effect of ambient temperature on the short-time current ratings of aircraft cable

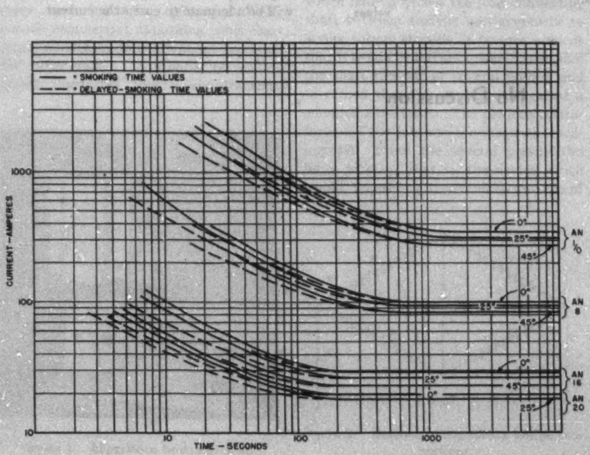

cables. Figure 9 presents the average results of smoking-time and delayed smoking-time as a function of current for various ambient temperatures. Data were not taken for periods of time less than five seconds because of limitations of accuracy in control and measurement.

Using the data of Figures 8 and 9 a set of curves was prepared showing the maximum safe current that a conductor could carry for a given period of time when in an ambient temperature of 25 degrees centigrade. This is shown in Figure 10. The shape of the curves for *AN* sizes numbers 0, 8, 16, and 20 for times between 2,000 seconds and five seconds is based on experimental data. Below one second the curves are based on calculation of the heat energy required on a no-loss basis to raise the temperature of the wire size in question to a value of 150 degrees centigrade. A conductor temperature of 150 degrees centigrade was used as the maximum safe temperature for the shorter time periods. Each curve, from 2,000 seconds to five seconds, is extrapolated from five seconds to one second to join the calculated curve at this point. The curves for other wire sizes were drawn with the same shape as that for *AN* sizes numbers 0, 8, 16, and 20; and asymptotic to the lines representing maximum continuous currents for the respective cable sizes and ambient temperature as found on Figure 8.

It is important that attention be directed to the fact that the curves of Figures 6, 8, 9, and 10 are values averaged from six types of *AN* aircraft cable used for this investigation. These values do not exceed by more than six per cent those obtained for the cables most susceptible to smoking. Therefore, the general application of these curves to all existing

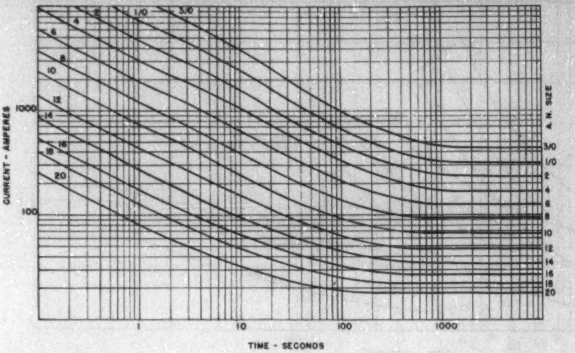

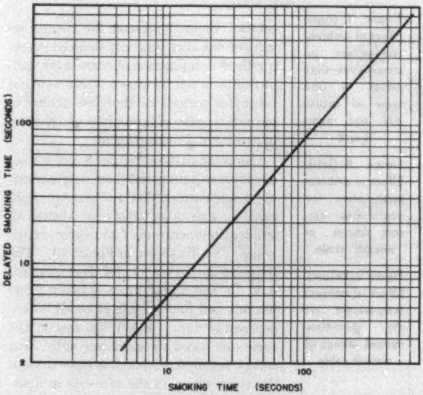

Figure 10 (top). Recommended short-time current ratings in 25 degrees centigrade ambient temperature for aircraft cable

Figure 11 (left). Relationship between smoking and delayed-smoking time values

types of *AN* cable should not be made without an allowance for this six per cent variation. However, it is recommended that consideration be given to the use of Figure 10 as a standard for the manufacture of aircraft cable.

During the course of this investigation, it was noted that a relationship existed between the delayed smoking time and smoking time data. This is shown in Figure 11, or by the equation

$$T_d = 0.46 T_s^{1.12}$$

where T_d is the delayed smoking time and T_s the smoking time. Data for this curve were obtained from the numerous observations made during the investigation. However, this curve is satisfactory for intervals up to five minutes; for longer periods of application the continuous current rating should be used. Although the relationship was not used during this investigation, it may prove useful in any future work of a similar nature.

Conclusions

The proper application of the curves of Figure 10 to the selection of protective devices and cables for both intermittent and continuous duty loads should result in safer operation of aircraft electric systems. The application of these data will in some instances permit the use of smaller size conductors, whereas in other instances the application will indicate the need for larger conductors than would result from the use of less adequate information. However, in either case, the engineer can be certain that the cable will be adequate to carry the current.

No Discussion

Some Oscillographic Methods of Investigating Mechanical and Hydraulic Conditions During Operation of Hydroelectric Units

LENARD R. ENGVALL
ASSOCIATE AIEE

THIS paper outlines some of the methods by which a magnetic oscillograph, with auxiliary equipment, has been used at the Grand Coulee Power Plant, Columbia Basin Project, to obtain and co-ordinate information about hydroelectric units which can not be obtained from ordinary indicating and recording instruments. Quantities measured and recorded include mechanical movement, hydraulic pressures, bearing loads, and turbine vibration and noise.

A special form of impedance bridge was built to measure mechanical movement and hydraulic pressure. Well-known commercial apparatus, plus electronic amplifiers, were adapted to register the other values. A number of oscillograms illustrates how a simultaneous record of several related quantites can facilitate analysis of a particular problem. It is not intended to imply that a new process has been developed, but rather to show how valuable information can be obtained with the help of comparatively simple equipment.

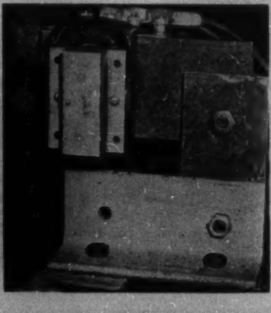

Figure 1. Impedance bridge pick-up

Measurement of Mechanical Movement

While attempting to adjust a Kingsbury thrust bearing, following some trouble which had subjected the long connecting shaft between turbine and generator to severe torque stresses, it became evident that it would be advantageous to measure the shaft run-out at several points, and to record these measurements against a common time base. The obvious instrument for the job was the magnetic oscillograph. From the several possibilities for a pick-up, that is, the device which would transform mechanical movement into electrical quantities, the impedance bridge was chosen as the most suitable because it was simple and rugged, and could be made sufficiently sensitive with out electronic amplification. Also important was the fact that no mechanical connection to the moving member was needed. Figure 1 shows the appearance and physical arrangements of the pick-up, which is shown in position for use in measuring movement of 44-inch diameter steel shaft. Coils are wound on laminated core of one square inch cross section. Two coils on each core are connected electrically in diagonally opposite sides of bridge circuit.

The particular form used consists of four identical coils connected in a bridge circuit and placed in pairs on two iron cores. One core is held firmly on a minutely adjustable support a little less than one-eighth inch from the moving member of which the record is to be taken, so that that member completes the magnetic circuit and varies its reluctance. The other, for convenience, is mounted on the same frame, but its magnetic circuit is entirely independent, and includes a fixed and approximately equal

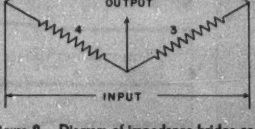

Figure 2. Diagram of impedance bridge connections

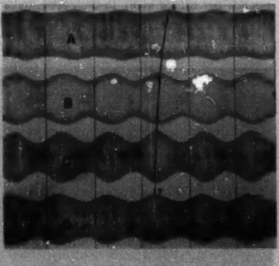

Figure 3. Typical record of large vertical shaft

Paper 49-204, recommended by the AIEE Instruments and Measurements and Power Generation Committees and approved by the AIEE Technical Program Committee for presentation at the AIEE Pacific General Meeting, San Francisco, Calif., August 23-26, 1949. Manuscript submitted May 9, 1949; made available for printing July 14, 1949.

Lenard R. Engvall is with the United States Department of the Interior, Coulee Dam, Wash.

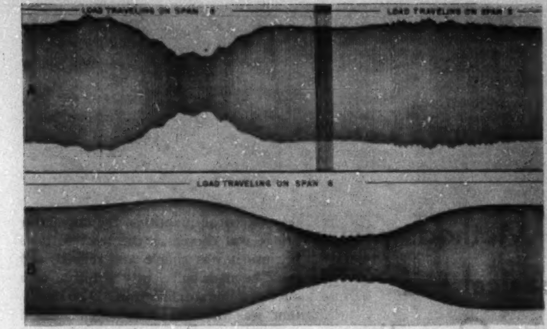

Figure 4. Records of deflection of center of 150-foot span on multiple-arch reinforced-concrete bridge while 35-ton load is passing over

Curve A was taken with load traveling 25 miles per hour. Maximum deflection downward is 0.060 inch; upward 0.017 inch. Curve B was taken with load traveling 5 miles per hour. Maximum deflection downward is 0.069 inch, upward 0.012 inch. Maximum design loading is 40 tons, concentrated. Pick-up located at center of span 6

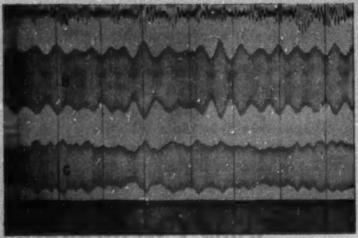

Figure 6. Record of hydraulic conditions in relation to shaft run-out on 150,000-horsepower turbine, 0.40 gate, 50,000-kw load

Maximum pressure change in scroll case, trace B, is 16 pounds per square inch; in draft tube, trace D, 7 pounds. Shaft run-out, trace C, at approximate middle is 0.007 inch

air gap. Electrical connections are shown in Figure 2, showing coils 1 and 3 mounted on one laminated iron core, coils 2 and 4 on the other.

A low, constant, 60-cycle a-c potential is applied to one pair of terminals of the bridge and an oscillograph galvanometer connected to the "neutral," or output, terminals. Actually, the device functions because it is always unbalanced, the adjustment of the variable air gap being made either greater or lesser than the fixed air gap so that the neutral point is not crossed. The galvanometer then indicates the amount of unbalance, and the peak-to-peak deflection of the trace on the record is a measure of the movement being studied.

It should be kept in mind that in the oscillograms shown in this paper which were obtained by the use of an impedance bridge, only a change in envelope width indicates a change in the quantity measured. This relation is calibrated. The actual width of the envelope has little significance. While the relation between movement and deflection is not exactly linear, it is sufficiently close to it so that the error can be disregarded for most purposes. A change of one inch in the width of the envelope on the original record indicates a movement of approximately 0.015 inch

Figure 3 shows a typical record of a shaft in normal operation on 108,000-kw machine turning 120 rpm. The distance between top and bottom pickups is about 62 feet. Trace A shows a horizontal movement of 0.003 inch at a point just below the thrust bearing, that is, a run-out of 0.0015 inch either way from the average position. Trace B is taken at a point just below the rotor and shows a run-out of 0.004 inch; trace C is taken at the intermediate coupling, and trace D just above the turbine bearing, indicating run-outs of 0.0055 and 0.0035 inch respectively.

Figure 5. Record of hydraulic conditions in relation to generator output on 150,000-horsepower turbine, .046 gate, 60,000-kw load

Maximum pressure change in scroll case, trace B, is 15.5 pounds per square inch; in draft tube, trace C, about 10 pounds per square inch. Variation in output, trace D, is about 2 per cent

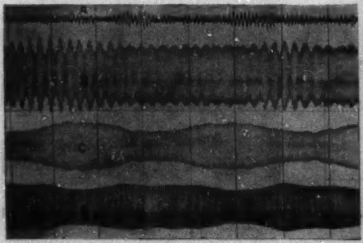

Figure 7. Record of pressure build-up in scroll case of 150,000-horsepower turbine in relation to generator electrical quantities during load rejection test

Pressure increased 38 pounds per square inch. Penstock is 18 feet in diameter and about 340 feet long

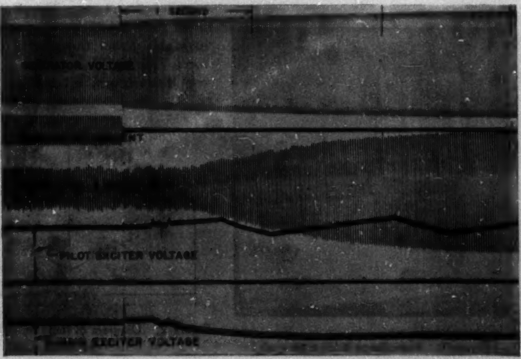

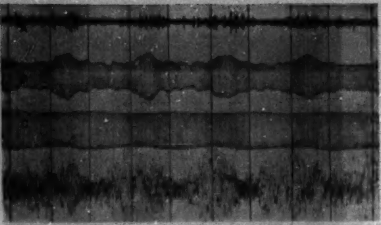

Figure 8. Record of noise and vibration associated with pressure changes in hydraulic turbine

One might logically expect the whole shaft to move in the same direction at the same time. This it does not do, however, as may be seen from the curve *X-Y*, drawn through the maximum point in each trace, which indicates a phase difference of about 120 degrees between the top and bottom. Similar records have been of assistance in balancing the rotors on these slow speed machines.

Another interesting application is the use of this apparatus to check the deflection and vibration of one span of a multiple-arch reinforced-concrete bridge under a rapidly moving load. Figure 4 shows the deflection at the center of the span as a 35-ton load passed over at speeds of 25 and 5 miles per hour, respectively. Maximum deflection from no load was 0.068 inch. Attempts had been made to obtain the same information by reading indicating instruments, but the changes were too rapid to obtain satisfactory results.

Measurement of Hydraulic Pressure

Since there has been reason for considerable curiosity about the performance of the turbines at the Grand Coulee Power Plant, the next logical step was the investigation of hydraulic pressures under various conditions of operation. The impedance bridge also lent itself admirably to this application. To the end of a Bourdon tube, taken from an ordinary pressure gauge, is attached a small piece of sheet steel which becomes the moving member of the bridge. This type of pick-up is somewhat limited in frequency response, the particular ones constructed having a natural frequency of a little over 20 cycles per second. Where much higher frequency measurements are necessary, a diaphragm type of gauge probably would give better results. Such pick-ups connected to show the scroll case and draft tube pressures gave a good picture of how the two varied at different loads, and to what extent disturbances on one side of the turbine runner appeared on the other side. In Figure 5, trace A shows the crown plate vibration, trace B scroll case pressure, trace C draft tube pressure, and trace D generator output. A swing of about two per cent can be detected in the output, but it does not appear to be synchronized with the hydraulic variations.

At certain loads, interesting relations have been found between shaft run-out and draft tube pressures. An example of this appears in Figure 6, where traces C and D represent shaft run-out and draft tube pressure, respectively. It is evident that these pressure changes, which seem to have definite cycles of about three revolutions each, and may be the result of vortex movements, are powerful enough to pull the shaft an appreciable amount out of line.

Figure 7 shows a record of pressure build-up in the scroll case resulting from governor action during a load rejection test when 132 megawatts were dropped.

Measurement of Noise and Vibration

A device which has been adapted to yield additional information is the ordinary radio loud-speaker of the permanent-magnet field type. By weighting and cushion-mounting the frame so that its movement is negligible, and mechanically coupling the moving coil or cone to the member being studied, an alternating current is produced which is generally indicative of its movement. The output is usually sufficient to be easily recorded on a fairly sensitive galvanometer. Unfortunately, it is not readily calibrated, since the output voltage is dependent on frequency as well as amplitude. Nevertheless, it is valuable for comparison. Noise, transmitted by air, can be similarly recorded. An example of a record on which are shown these quantities is given in Figure 8. Trace A indicates vibration of the turbine cover plate, as picked up by the loud-speaker, traces B and C show pressures in the scroll case and draft tube respectively, and trace D represents noise coming from the draft tube.

Measurement of Bearing Loads

Another type of pick-up device has provided considerable information about bearings. On each jack pin supporting a segment of the Kingsbury thrust bearing on the main units at the Grand Coulee Power Plant, are mounted two Baldwin-Southwark type *SR-4* strain gauges. These are used in the initial installation to secure equal loading on all the bearing shoes. However their usefulness does not end there. By connecting each pair in the well-known Wheatstone bridge circuit, and applying an a-c potential, a small output is obtained across the midpoints whenever the bridge is adjusted a little off balance. This output must be amplified before the ordinary oscillograph can record it, and this was done by using a multiple channel electronic amplifier of conventional design. By means of a vacuum tube voltmeter, the over-all response was calibrated, and the change in bearing loading measured.

Examples of the type of records obtained are shown in Figures 9 and 10. It is evident from Figure 9, that in spite of the extreme care with which these bearing runners are finished, this one had two high spots, but it is otherwise typical of normal operation. Figure 10 shows the variation in total loading assumed to be caused by hydraulic disturbances. Measurements indicate a total load change of 192,000 pounds or 96,000 pounds more or

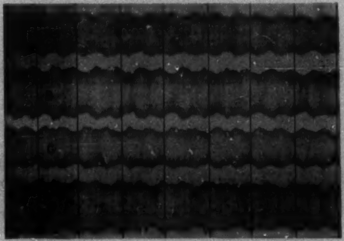

Figure 9. Record of load changes on alternate shoes of a Kingsbury thrust bearing, on a 108,000-kw generator turning 120 rpm, full load. Average load change per shoe is 7,500 pounds

less than the average. This amounts to six per cent of the 1,430,000 pounds rotating weight.

The apparatus also has been used for a determination of the hydraulic thrust, which for the particular unit on which these records were taken amounts to as much as 280,000 pounds upward, reducing the bearing load to 80 per cent of the maximum.

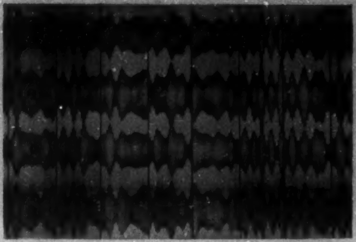

Figure 10 (right). Record of load changes on 4 of 8 shoes of Kingsbury thrust bearing, on a 108-megawatt generator, 25-megawatt load. Trace A indicates maximum load change of 19,000 pounds, trace B 27,000 pounds, traces C and D 25,000 pounds

Conclusion

The foregoing examples have been selected from the files of the United States Bureau of Reclamation, to show the variety of information which can be readily recorded and is likely to be of value at any hydroelectric station. Probably many instances will occur to operating and test engineers where similar data would be helpful. Since the oscillograph first came into general use, its value for testing electrical circuits on all kinds of power equipment has been recognized. The ease with which it can record mechanical conditions as well, such as shaft movements, bearing pressures, hydraulic or steam pressures, vibration, and many others, and the low cost and simplicity of the auxiliary apparatus required should make it of equal value to operating and maintenance personnel.

No Discussion

Deionization Time of High-Voltage Fault-Arc Paths

EVERETT J. HARRINGTON
ASSOCIATE AIEE

E. C. STARR
FELLOW AIEE

AUTOMATIC reclosing of circuit breakers in high-voltage transmission lines can materially increase system transient stability limits provided reclosure can be accomplished very rapidly. In case of temporary faults resulting from lightning, the minimum time in which this reclosure can be accomplished successfully is determined mainly by three factors:

1. Circuit breaker limitations.
2. Total duration of lightning stroke or its multiple components.
3. Deionization time of the fault-arc path and its consequent recovery of dielectric strength.

With regard to the first factor, modern circuit breakers have been developed to the point where minimum reclosing time is not expected to be limited by them. The second factor is one which may very well be the determining item. Inasmuch as this is a natural phenomenon, limitations which it may impose can be determined only by extensive experience with high-speed reclosing combined with field data on lightning-stroke duration. The rather meager data available at present on multiple lightning strokes to lines indicate that approximately 10 per cent persist for more than 0.25 second or 15 cycles (from initiation of fault) on a 60-cycle system.[1]

The third factor is one on which little data are available, particularly in regard to deionization time of fault-arc paths on 115- and 230-kv transmission lines. In order that reclosure be successful, dielectric recovery of the ionized fault-arc path must have proceeded to the point where re-application of system voltage will not produce sufficient current through the arc path to maintain ionization. If for a given recovery voltage and length of arc path the minimum current to maintain ionization is known, the minimum time in which successful reclosure can be accomplished can be determined provided the high-voltage resistance of the arc path in respect to time can be obtained.

Figure 1. Schematic diagram of 115-kv test circuit

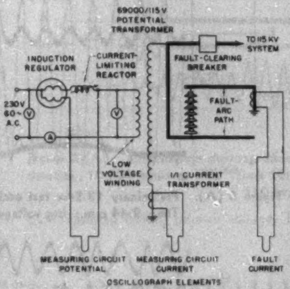

A method has been developed for determining the resistance and dielectric recovery rate of the arc path after fault-current interruption. Field tests on a 115-kv system (at the J. D. Ross Substation of the Bonneville Power Administration) were performed, and data obtained on deionization of fault-arc paths produced by single-phase faults having equivalent 3-phase magnitudes from 750 to 3,000 megavolt-amperes. The effects of fault magnitude and duration are shown, and additional tests are proposed.

Test Circuit

In order to determine the dielectric strength of the fault-arc path during the period subsequent to fault-current interruption, it is essential that the high-voltage measuring circuit have negligible effect upon the resistance of the ionized path and its rate of dielectric recovery.

Figure 1 shows the circuit used in the 115-kv tests. A measuring potential was applied to the arc path from a high-impedance source consisting of a 69,000/-115-volt potential transformer whose low-voltage winding was energized from a 60-cycle a-c source through a current-limit-

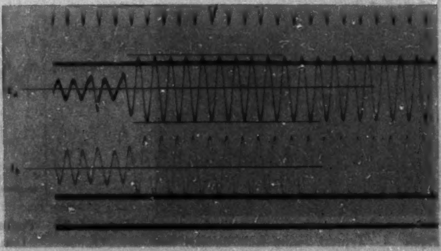

Figure 2. Recovery characteristic of test circuit only. Short circuit on secondary of measuring circuit cleared by opening circuit breaker B26

E_A = measuring circuit, primary voltage

I_A = measuring circuit, secondary current

Paper 49-205, recommended by the AIEE Instruments and Measurements, and Transmission and Distribution Committees and approved by the AIEE Technical Program Committee for presentation at the AIEE Pacific General Meeting, San Francisco, Calif., August 23–26, 1949. Manuscript submitted May 25, 1949; made available for printing June 29, 1949.

EVERETT J. HARRINGTON is with the United States Department of the Interior, Bonneville Power Administration, Portland, Oreg.; and E. C. STARR is Professor of Electrical Engineering at Oregon State College, Corvallis, Oreg.

The authors wish to acknowledge the assistance of George Anderson, Richard Dietrich, and the Pacific Electric Manufacturing Corporation in the preparation of this paper.

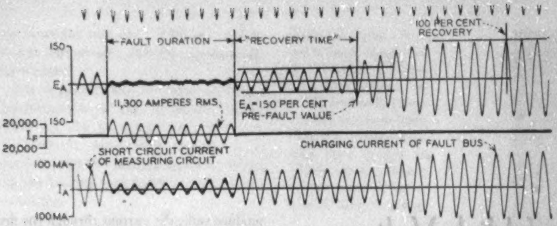

Figure 3. Typical recovery oscillogram 8.5-cycle fault; 11,300 amperes rms. Time, 10:20 p.m.; fault megavolt-amperes, 2,200; bus voltage, 110 kv; arc location, air

E_A=measuring circuit, primary voltage; I_F=fault current; I_A=measuring circuit, secondary current

ing reactor. This reactor was adjusted as follows: with the transformer high-voltage winding open circuited (test bus capacitive excitation load only), the induction regulator was adjusted to give 69 kv across the transformer high-voltage winding. This winding was then short circuited, and the reactor adjusted so as to limit the current in the winding to less than 100 milliamperes. This adjusting procedure was repeated until the desired open-circuit voltage and short-circuited current were obtained.

Establishment of the fault arc short circuits the transformer high-voltage winding, and the oscillograph element across the low-voltage winding indicates a potential essentially equal to the transformer and its supply lead impedance drop. This drop is small compared to that across the current-limiting reactor. After fault-current interruption, deionization of the arc path and consequent increase in its resistance progressively limits the transformer current and the voltage across its terminals rises, reaching normal value when conduction through the arc path ceases. This voltage is then a measure of arc-path conductivity. Under ideal test conditions the current in the transformer high-voltage winding would drop to zero when arc-path conduction ceases, and normal voltage is re-established.

During the tests described herein, cessation of current flow in the arc path did not result in zero current through the transformer high-voltage winding due to the presence of appreciable capacitance in the form of bus work, insulators, and circuit breaker bushings. The charging current at normal voltage to this equipment was actually greater than the short-circuit current; consequently dielectric recovery of the arc path resulted in a rise of measuring-circuit current. This effect plus the fact that the measuring-circuit potential recorded was actually the vector sum of the arc-path resistance and transformer and lead impedance drops prevent simple direct calculation of arc-path resistance from these data. Figure 2 is an oscillogram showing the time of response of the measuring circuit only. This was the tained by opening a short circuit across ob- high-voltage winding of the potential transformer by means of a 115-kv oil circuit breaker. From this it may be seen that the natural recovery period of the measuring circuit was slightly more than one cycle which is less than the recovery time of any of the phenomena investigated.

Another test circuit has been designed which will permit recording of voltage

Figure 4. Typical arcing fault on test bus

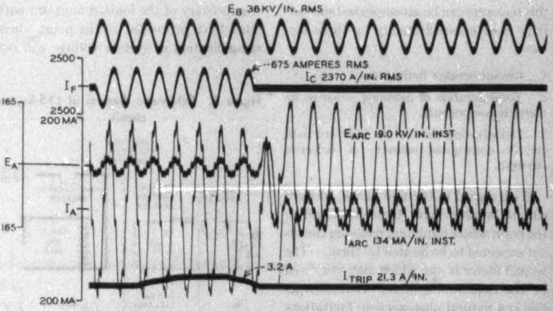

Figure 5 (A). Preliminary 13.8-kv test oscillogram of 7-cycle fault arc; 675 amperes rms. Time, 2:44 p.m.; bus voltage 13.8 kv; arc location, insulator

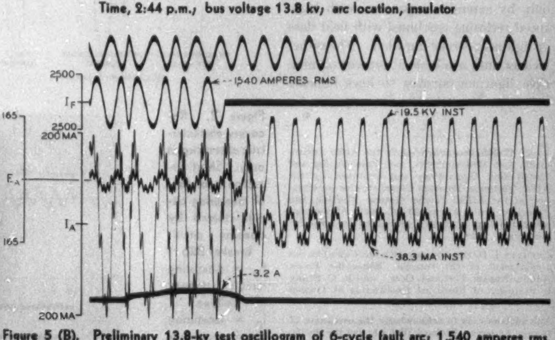

Figure 5 (B). Preliminary 13.8-kv test oscillogram of 6-cycle fault arc; 1,540 amperes rms. Time, 1:39 p.m.; bus voltage 13.8 kv; arc location, insulator

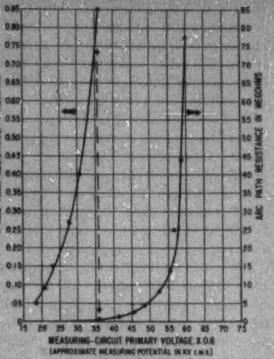

Figure 6. Fault-path resistance during recovery period as a function of measuring circuit primary voltage

Figure 7. Equivalent measuring circuit

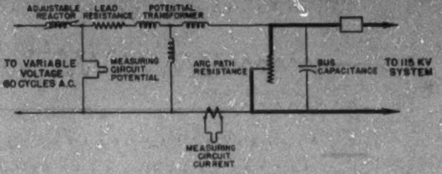

drop across the arc path only and conduction current through this path only. This circuit will be described in subsequent paragraphs. It was not used during these tests, as they were performed in conjunction with a group of scheduled circuit breaker tests, and the time available for preparation did not permit construction of the necessary equipment.

The records obtained, while not ideal do permit dielectric recovery of the arc path to be observed in terms of measuring circuit potential. Figure 3 is typical of these oscillographic records. E_A is the measuring-circuit potential. Prior to application of fault current, the fault bus was grounded by a fuse wire; consequently the amplitude of the trace E_A is proportional to the transformer and lead impedance drops until the fault circuit breaker is closed. At this time the potential E_A drops to a low value due to reduction in station-service voltage combined with a phase difference in fault-producing potential. Immediately after fault interruption this voltage returns to the prefault value and remains so for several cycles, thereby indicating low arc-path resistance. After approximately 7$^1/_4$ cycles in this case, the voltage begins to rise and continues to do so until full voltage is reached. At this point dielectric recovery may be considered nearly complete, as approximately 69 kv is being applied across the arc path with practically no conduction resulting.

Before using the circuit just described, it was first necessary to establish proof that currents in the order of 100 milliamperes or less would not prolong dielectric recovery of the arc path. There also was some question as to the validity of initiating fault arcs by small diameter copper wire. To determine these effects, preliminary tests at 13.8 kv were performed using a very similar circuit except that the current-limiting impedance was in the form of capacitors rather than a reactor. Use of capacitors necessitates precautions to prevent series resonance and ferro-resonant conditions in circuit.

Test Procedure

The 13.8-kv preliminary tests were performed by closing into a fault established by a fuse wire across a 15-kv insulator or a comparable gap with subsequent automatic tripping of the fault circuit breaker and interruption of the arc. Faults were initiated by copper fuse wires varying in size from number 19 to number 33 American wire gauge. Fault currents of 600 and 1,600 amperes were used. Magnitude of the measuring-circuit current was varied from approximately 2 milliamperes to 140 milliamperes. All pertinent currents and voltages were oscillographically recorded.

The 115-kv tests were all single-phase-to-ground faults. All faults were initi-

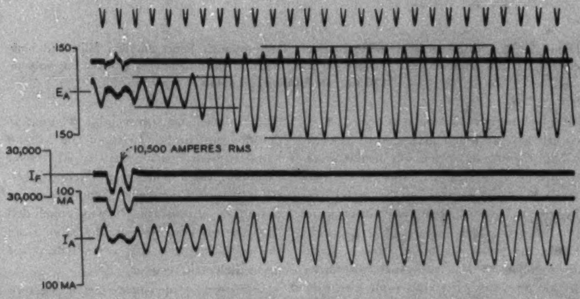

Figure 8 (A). Oscillogram showing effect of fault duration upon recovery time. Short fault duration, 10,500 amperes rms. Time 10:38 a.m., fault megavolt-amperes 2,000, bus voltage 110 kv, arc location, air

E_A = measuring circuit, primary voltage, I_F = fault current, I_A = measuring circuit, secondary current

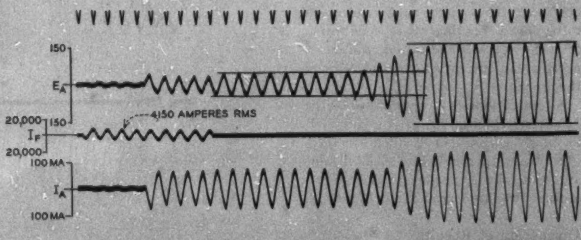

Figure 8 (B). Oscillogram showing effect of fault duration upon recovery time. Long fault duration, 4,150 amperes rms. Time, 2:14 a.m., fault megavolt-amperes 805, bus voltage 110 kv, arc location, air

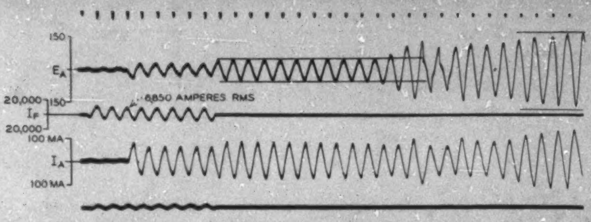

Figure 9 (A). Oscillogram showing recovery interruptions. Long duration fault and relatively low current, 6,850 amperes rms. Time 4:44 a.m., fault megavolt-amperes 1,330, bus voltage 106 kv, arc location, air

E_A = measuring circuit, primary voltage, I_F = fault current, I_A = measuring circuit, secondary current

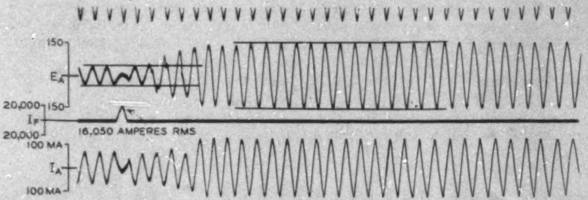

Figure 9 (B). Oscillogram showing recovery interruptions. Short duration fault and high current, 16,050 amperes rms. Time 9:40 p.m., fault megavolt-amperes 3,060, bus voltage 110 kv, arc location, insulators

ated by number 33 American wire gauge, copper wire and were arranged to cascade a 7-unit string of suspension insulators or to bridge a vertical gap formed by two strain busses spaced 46.5 inches apart (see Figure 4), except that two faults were produced between busses 14 feet apart. Fault megavolt-amperes varied from approximately 750 to 3,000 (4,000 to 16,000 amperes rms), and fault duration varied from a fraction of a cycle to a maximum of 10 cycles.

Data Obtained

A total of 28 tests was performed at 13.8 kv from which 21 useful oscillograms were obtained. These data enable conclusions to be drawn regarding effect of initiating faults by fuse wire and the effect of measuring-circuit current upon deionization of the arc path.

A total of 48 tests was performed on the 115-kv system resulting in 41 useful oscillograms. Ultra-rapid motion pictures (3,000 frames per second) of 13 of the fault arcs were taken. Single frames from two of these films are reproduced in Figure 12.

Discussion of Results

The 13.8-kv preliminary tests indicated variation of wire size from number 19 to 33 produced no appreciable change in deionization time. In all of the 13.8-kv tests recovery was very rapid, never exceeding three cycles from current interruption to full recovery of the measuring potential. From this it was concluded that the presence of metallic vapor from the initiating fuse had very little effect upon dielectric recovery.

Variation of measuring-circuit current from 2 to 140 milliamperes during the preliminary tests produced no noticeable change in deionization time. As a result, it was decided to make the 115-kv tests using number 33 copper wire to initiate the fault arc and a measuring-circuit current of approximately 70 milliamperes.

Variation of fault current from approximately 600 amperes to 1,600 amperes produced only a small change in deionization time at 13.8 kv. Figure 5 shows typical oscillograms obtained during these tests. It will be noted in Figure 5(A) that full recovery occurred in approximately 1.25 cycles with a fault current of 675 amperes rms. Figure 5(B) indicates full recovery in approximately two cycles with a fault current of 1,540 amperes. Apparently low-energy faults produce such small quantities of ionized gas that deionization is accomplished in a very brief interval of time.

In interpreting the data obtained during the 115-kv tests, it was necessary to select a time after fault-current interruption as the point where dielectric recovery had progressed sufficiently that re-ignition would not occur upon reapplication of full voltage. This point was arbitrarily chosen as being the point where the measuring-circuit potential had recovered to 150 per cent of the value attained immediately after fault interruption. For the circuit used, this point corresponds to an arc-path resistance of approximately 0.25 megohm. It is believed, however, that system voltage (69 kv to ground) could not maintain ionization through a normal fault path whose resistance is in excess of 50,000 ohms; therefore the foregoing criterion is considered conservative. The time from fault-current interruption to this point is hereafter referred to as

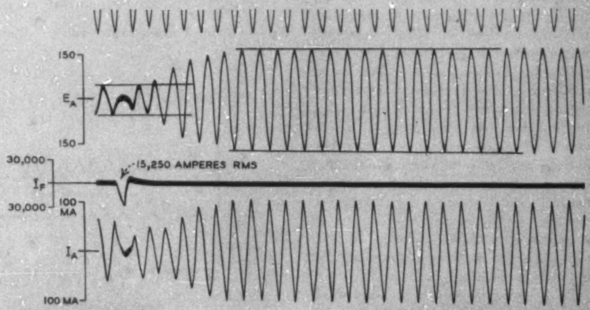

Figure 10. Oscillogram showing very rapid recovery after fault of 0.75-cycle duration, 15,250 amperes rms. Time 3:20 p.m., fault megavolt-amperes 2,920, bus voltage 110.5 kv, arc location, air

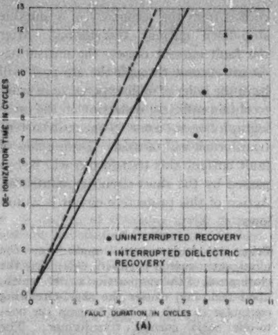

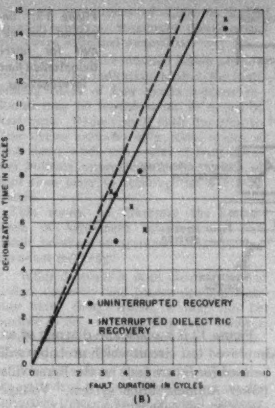

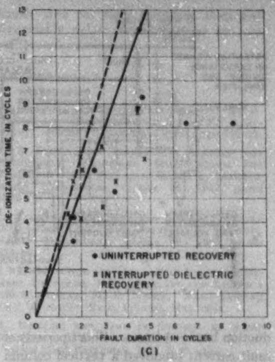

Figure 11. Deionization time as a function of fault duration. Curves drawn through maximum time points

(A) (above) 750-megavolt-ampere faults
(B) (center) 1,200-megavolt-ampere faults
(C) (right) 2,000-megavolt-ampere faults

"recovery time." This recovery time has been selected to give a consistent basis for recovery comparison and does not necessarily represent minimum time for successful reclosure.

Figure 6 is a curve of arc-path resistance shown as a function of measuring-circuit potential. This curve was obtained by setting the equivalent measuring circuit, Figure 7, up on an a-c calculating board. Arc-path resistances necessary to give currents and voltages corresponding to instantaneous values recorded on the oscillogram for test number *PE-4C* throughout the recovery period were determined directly thus eliminating much calculation. This curve shows that the path resistance is approximately 50,000 ohms at the point where the measuring potential first begins to increase. An increase in measuring potential of 150 per cent corresponds to a path resistance of approximately 0.25 megohms.

Figures 8, 9, and 10 are typical of the records obtained during the 115-kv tests. Note that in Figure 8 the measuring-circuit potential indicates a relatively low resistance of the arc path for a period of several cycles after fault interruption, after which a fairly uniform increase in path resistance occurs until conduction ceases and the measuring potential becomes a maximum. Figure 9 indicates somewhat the same conditions except that recovery is interrupted as evidenced by sudden collapse of the measuring potential. These interruptions and subsequent recoveries are probably the result of eddying of gases in the ionized column due to convection currents. Whether such recovery interruptions represent a decrease in resistance sufficient to permit re-ignition is a matter that still has to be determined. It is believed that re-ignition will not occur as a result of such interruptions as may occur after quite a few cycles of dead time; however, in order to be conservative, recovery times here-in were, in the cases where such interruptions occurred, measured from fault-current interruption to the measuring-voltage crest succeeding the last dielectric interruption.

Deionization Time of Arc Path

Figure 11 shows the recovery times obtained for three values of fault megavolt-amperes. Perhaps the most significant fact disclosed by this is that recovery time is to a great extent determined by fault-current duration. Faults greater than 2,000 megavolt-amperes resulted in somewhat greater recovery time, but in all cases a decrease in fault duration shortens the recovery time. Figures 3 and 8(A) serve to illustrate this effect. In Figure 3 a fault current of 11,300 amperes rms lasting for 8.6 cycles gave a recovery time of 8.2 cycles, while in Figure 8 a fault current of approximately the same magnitude but of only 1.6-cycle duration required a recovery time of only 4.2 cycles. In Figures 8(B) and 9(A) it may be seen that relatively low currents of long duration required long recovery times, while in Figures 9(B) and 10, high currents of very short duration resulted in very rapid path deionization. The reason recovery is rapid after very brief fault durations is quite apparent from study of a series of ultra-rapid (3,000 frames per second) motion pictures taken of some of the arcs. In the cases of long fault duration, even at relatively low currents, very large volumes of luminous gases are created which cool and break up relatively slowly; furthermore, magnetic forces caused the arc to progress along the lower fault bus in one direction and along the upper fault bus in the opposite direction, see Figure 12 (left). The hot gases produced along the lower bus rise toward the upper bus as a large billowing mass prolonging con-

Figure 12. High-speed photographs of 115-kv fault arcs

(below) Long duration arc (7,500 amperes rms)
(right) Short duration arc (16,000 amperes rms)

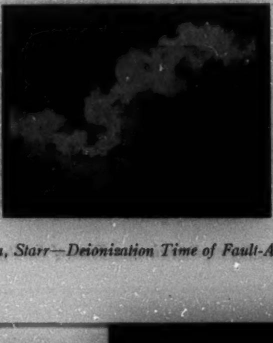

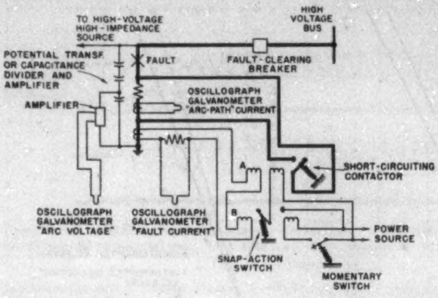
TO HIGH-VOLTAGE HIGH-IMPEDANCE SOURCE
HIGH VOLTAGE BUS
POTENTIAL TRANSF. OR CAPACITANCE DIVIDER AND AMPLIFIER
FAULT
FAULT-CLEARING BREAKER
OSCILLOGRAPH GALVANOMETER "ARC-PATH" CURRENT
AMPLIFIER
A
SHORT-CIRCUITING CONTACTOR
B
OSCILLOGRAPH GALVANOMETER "ARC VOLTAGE"
OSCILLOGRAPH GALVANOMETER "FAULT CURRENT"
POWER SOURCE
SNAP-ACTION SWITCH
MOMENTARY SWITCH

Figure 13. Improved test circuit for future deionization time investigations

duction between buses. Short periods of fault current produced a vertical column of luminous gas, see Figure 12 (right) of relatively small cross section which, upon current interruption, broke into segments as it rose and rapidly disappeared.

Circuit Breaker Reclosing Time

The results of these tests should not be taken as conclusive in respect to absolute minimum time of reclosure in practice. They are considered, however, as being indicative and possibly somewhat conservative as to 3-phase reclosing times applicable to 115-kv grounded-neutral systems. The curves of Figure 11 indicate that large magnitude faults cleared in 4.5 cycles might require as much as 12.5 to 14.5 cycles of dead time for path deionization, thereby permitting reclosure 17 to 19 cycles after inception of the fault. This is, of course, based upon the assumption that no additional lightning strokes occur after or immediately prior to reclosing.

Additional Tests

In order that definite reclosing times may be established, much additional data are necessary. Further tests on the Bonneville Power Administration 115- and 230-kv systems are planned; moreover, it is proposed that manufacturers having suitable facilities incorporate such tests as a part of routine and special high-voltage circuit breaker tests. It is believed that these investigations should be organized to provide more data similar to that presented in this paper. In addition, a series of reclosing tests should be performed in an attempt to establish what arc-path resistance is necessary to permit successful reclosure, and to determine whether the dielectric recovery interruptions discussed previously are of such a nature as to permit re-ignition if reclosure is made during that period.

Figure 13 is a schematic diagram of an improved test circuit which probably will be used for future tests on the Bonneville Power Administration system. Voltage across the arc path will probably be taken from a bushing-capacitance tap and applied to the oscillograph through an amplifier.[2] Fault current will be recorded from the secondary of a suitable step-down current transformer. After the fault current ceases, the measuring-circuit current through the arc path will be in the order of milliamperes, so in order to obtain sufficient deflection on the oscillograph element a one-to-one ratio current transformer will be used. During flow of fault current this transformer will be by-passed by the short-circuiting contactor. Action of this protective circuit is as follows:

> Prior to fault-current application the momentary switch is closed, energizing the closing coil of the snap-action switch which, upon reclosing, causes the short-circuiting contactor to pick up and by-pass the one-to-one ratio current transformer. The momentary switch is then released and the fault applied. Flow of fault current through coil "B" causes the snap-action switch to open, thereby de-energizing the short-circuiting contactor pick-up coil. This contactor is prevented from opening by flow of fault current through holding coil "A." Interruption of fault current permits the short-circuiting contactor to open and thus

Table I. Summary of Results of Deionization Tests at 115-Kv J. D. Ross Substation of the Bonneville Power Administration

Test Number	Fault Mva	Fault Duration in Cycles	Time to Start of Recovery in Cycles	Deionization Time in Cycles*	Alternate Deionization Time in Cycles**	Arc Location
PE-1F	741	4.6	8.2	9.2	10.2	Air
AC-2B	717	5.0	8.2	8.8		Air
PE-1A	745	7.6	6.8	7.2		Air
PE-1E	750	8.0	8.1	9.2		Insulators
PE-1B	792	9.0	8.2	10.8	11.8	Air
PE-1C	792	9.0	9.8	10.2		Air
PE-1D	741	10.1	10.1	11.7		Air
PE-2D	1,272	2.6	2.7	3.8	5.8	Air
PE-2E	1,349	3.4	4.2	4.8	7.3	Insulators
AC-3B	1,262	3.6	3.2	5.2		Insulators
PE-2F	1,336	3.9	6.2	7.2		Air
AC-4B	1,297	4.3	3.2	3.7	6.7	Air
AC-1A	1,241	4.7	7.2	8.2		Insulators
WE-1A	1,380	4.9	3.8	4.2	5.7	Insulators
PE-2C	1,324	8.4	12.8	14.2		Air
PE-2B	1,305	8.4	10.7	11.6	14.6	Air
PE-3F	1,758	1.5	2.2	3.3	5.8	Insulators
PE-3E	1,793	2.9	6.7	7.3		Air
AC-8B	1,980	1.5	2.3	2.8	4.3	Air
PE-4F	1,995	1.6	3.2	4.2		Air
PE-5F	2,290	1.7	2.1	3.1		14-feet long
PE-8E	2,045	1.7	2.7	3.2	5.7	Insulators
AC-7B	1,992	1.7	4.1	4.2		Insulators
PE-4D	2,053	2.0	2.1	2.1	4.1	Air
PE-3D	1,970	2.0	2.3	2.8	6.8	Insulators
PE-3A	1,907	2.1	3.2	3.7	6.2	Insulators
PE-4E	2,016	2.5	3.7	4.7	8.2	Insulators
PE-5B	2,097	2.6	5.7	6.2		Air
AC-2A	1,967	2.9	5.2	5.7	7.2	Air
AC-3A	1,955	2.9	2.1	2.6	4.6	Insulators
AC-9B	1,990	3.5	1.7	2.2	5.7	Air
PE-5D	1,980	3.5	3.3	5.3		Insulators
PE-7E	2,056	4.5	7.7	8.8		14-feet long
AC-6B	1,989	4.5	6.2	6.2	8.7	Insulators
PE-4A	2,157	4.6	10.8	12.2		Air
PE-3C	1,960	4.7	8.2	9.3		Insulators
WE-3A	2,000	4.75	4.7	6.2	6.7	Insulators
WE-4A	2,060	6.6	7.2	8.2		Air
PE-4C	2,166	8.6	7.1	8.2		Air
PE-6F	3,000	0.75	1.6	2.0		Air
PE-5A	3,150	0.8	1.6	2.1	4.1	Insulators

* Taken as the time from interruption of fault current until measuring-circuit potential has recovered to 150 per cent of the value attained immediately after fault interruption.

** In cases where dielectric recovery was characterized by one or more interruptions, this alternate deionization time was taken as the time from interruption of fault current until the first measuring-circuit voltage crest after the last recovery interruption.

energize the oscillograph element recording measuring-circuit current through the arc path during the recovery period.

This circuit should permit recording of the arc-path voltage drop and current from which instantaneous values of arc-path resistance may be computed throughout most of the recovery period.

Conclusions

1. A method of obtaining useful data on fault-arc deionization time has been devised. It is hoped this will lead to the obtaining of additional data which, when summarized, will enable minimum reclosing times for 115- and 230-kv circuits to be established.

2. Deionization time of arc path is principally a function of fault duration.

3. On the 115-kv system variation of fault magnitude from 750 to 1,700 megavolt-amperes had very little influence on maximum deionization times of the arc path. For fault magnitudes of 2,000 to 3,000 megavolt-amperes, maximum deionization times were increased somewhat.

4. Although data contained herein are not conclusive, the indication is that for fault clearing times of four cycles 3-phase reclosure may be feasible after 10 cycles of dead time. Reduction of fault duration to three cycles indicates only seven cycles of dead time; while two cycles of fault duration indicate approximately five cycles of dead time prior to reclosure on a 115-kv system.

This serves to illustrate the importance of high-speed relaying and fast circuit breakers on systems contemplating ultra-fast reclosing.

5. While decrease in fault-clearing time is always desirable and future developments may make this possible, it may not be feasible to decrease reclosing time below a certain limit as determined by multiple-lightning-stroke phenomena.

6. The presence of insulator strings in the arc path does not appreciably decrease deionization time. The use of small diameter copper wire for fault initiation does not appreciably delay deionization of the arc path.

References

1. Multiple Lightning Strokes—II, K. B. McEachron. *Electrical Engineering* (*AIEE Transactions*), volume 57, September 1938, pages 510–12.

2. A Simple and Inexpensive Method for Accurately Measuring Steady-State and Transient High Voltages, Harold L. Levinton. *AIEE Transactions*, volume 66, 1947, pages 1304–11.

3. Lightning and 60-Cycle Power Tests on Wood-Pole Line Insulation, P. L. Bellaschi. *AIEE Transactions*, volume 66, 1947, pages 838–50.

4. L'extinction des Arcs dans le Reenclenchement Ultrapide Monophase sur les Lignes a 220 Kilovolts, M. E. Maury. *Revue Generale De L'Electricite* (Paris, France), May 1944.

5. Keeping the Line in Service by Rapid Reclosing, S. B. Griscom, J. J. Torok. *Electric Journal* (East Pittsburgh, Pa.), May 1933.

6. Systematic Tests with Automatic High-Speed Reclosing in the Gossgen and Laufenburg Power Systems, W. Wagner. *The Brown Boveri Review* (Baden, Switzerland), December 1945.

Discussion

T. E. Browne, Jr. (Westinghouse Research Laboratory, East Pittsburgh, Pa.): This paper describes an interesting experimental study of an important but heretofore little understood phenomenon, the post-arc dielectric recovery of long open-air arc trails, and is to be commended as a pioneering effort. As such, it is understandable that these early results are not entirely satisfactory or conclusive, but they do give some new insight into the behavior of fault-arc paths.

In particular the authors speak of deionization, rise of high-voltage resistance, and dielectric recovery of the fault-arc paths as if these expressions were virtually synonomous. Also, in interpreting their results, the authors appear to overlook significant differences in meaning between the measured arc path resistances and the inferred dielectric strengths of the arc paths. They speak of and plot an arbitrarily defined "recovery time" or "deionization time" based on use of arc resistance, without showing how this is related to the desired practical quantity, time for recovery of sufficient dielectric strength to permit successful circuit breaker reclosure.

The basic concepts involved in the dielectric recovery of a long arc space were discussed rather completely by Dr. Slepian[1] nearly 20 years ago. The long-time scale involved here, many cycles for dielectric recovery of long open-air power arcs compared with a fraction of a half-cycle for circuit breaker arcs, does not really alter the phenomena so long as the arc can be considered to be homogeneous throughout its length. Dr. Slepian pointed out that the stable existence of an arc column depended upon a balance between power loss, *W*, from the hot ionized arc space due to cooling and ion diffusion, and the electric power input e_a times *I*. The dielectric strength of an arc space was defined as the voltage required to maintain this balance and so to hold the conductance of the arc space constant. In terms of the arc resistance, *R*, this can be very simply expressed by the equation

$$\frac{E_d^2}{R}=W_0, \text{ or } E_d=\sqrt{RW_0}$$

when E_d is the dielectric strength corresponding to the arc space resistance, *R*, and also to the existing rate of energy loss from the arc space, W_0. It is clear that E_d is a breakdown voltage, since any sustained increase in applied voltage above E_d will cause the arc space energy to increase, resulting in lowered resistance and cumulatively increasing current flow.

In assuming correspondence between the dielectric strength and the resistance of a long arc space, the authors have treated W_0, the power dissipation from the arc space, as a constant. If, as the writer believes, W_0 also is a variable, it is equally as important as *R* in determining the dielectric strength of the arc space. It is true that effective dielectric recovery of an arc space will accompany a rise of arc space resistance to and above some high value, but the actual magnitude of this critical resistance is entirely dependent upon the existing level of W_0. Therefore, in the absence of knowledge about W_0, the arbitrary selection of some level of arc space resistance as indicating effective "deionization," or dielectric recovery of the arc space would appear to be relatively meaningless. In particular, one would expect W_0 to be quite largely determined by both the magnitude and duration of the fault-arc current preceding the recovery period, since these quantities largely affect the actual arc path length and diameter, the degree of turbulence in the immediately surrounding air, and the related temperature and ion density gradients during the recovery period. Thus, it is not at all surprising that plots versus fault current and fault duration of "deionization time" based on rise of arc resistance alone, Figure 11 of this paper, do not agree with the plots of directly observed dielectric recovery times in the paper by Boisseau, Wyman, and Skeats.[2]

Another consideration which may lessen the practical value of resistance measurements is the observed inhomogeneity of the arc space, especially toward the end of the recovery period, as reported by the authors, and shown in Figures 4(A) and 12(A) in the paper by Boisseau, Wyman, and Skeats. If this apparent "breaking up" of the arc residue should result in virtual loss of conductance by some fraction of the arc path only, this fraction might be too short to sustain the full restored voltage even though the total resistance of the arc path may have already approached infinity. This appears to be the explanation of the so-called "recovery interruptions" reported in the paper and illustrated by the oscillograms of Figure 9. In Figure 9(A) there is clearly a dielectric failure with sudden discharge of the bus capacitance at about 60-kv rms restored voltage somewhat later than the point defined as the end of the deionization time, followed by three other successive breakdowns at still lower voltages. These show that the dielectric recovery was influenced by the measuring circuit and was not accurately indicated by the resistance measurement. In Figure 9(B) the discharges apparently begin much earlier, occurring both before and after the specified deionization time.

In view of these observations, it is the opinion of the writer that resistance rise measurements are interesting and of value in aiding our knowledge of the nature and behavior of post-fault arc trails but that they cannot safely be substituted for actual dielectric tests in determining limits for circuit breaker reclosing times.

A further comment with regard to Figure 11 is that the lines, if drawn through the means of the points instead of through extreme points in the badly scattered groups, would have slopes roughly proportional to the arc current magnitudes, indicating that the resistance rise time may be more accurately said to depend upon the product of fault current and fault duration rather than upon duration alone.

With regard to future studies, the writer wonders whether the authors have considered the use of a direct rather than an alternating source of voltage in the resistance measuring circuit.

REFERENCES

1. Extinction of a Long A-C Arc, J. Slepian. *AIEE Transactions*, volume 49, April 1930, pages 521–30.

2. Insulation Flashover Deionization Times as a Factor in Applying High-Speed Reclosing Circuit Breakers, A. C. Boisseau, B. W. Wyman, W. F. Skeats. *AIEE Transactions*, volume 68, part II, 1949, pages 1058–67.

D. M. Umphrey (Pacific Electric Manufacturing Corporation, San Francisco, Calif): The authors have made a valuable contribution to fundamental knowledge concerning the high-speed reclosing of transmission circuits. It has been difficult in the past to isolate the various factors which control minimum reclosing times. For example, this paper presents the first quantitative information, to my knowledge, regarding the effect of fault arc duration on minimum reclosing time. The minimum permissible de-energized time for successful staged reclosing tests has varied from as low as six to as high as 16 cycles. There was only speculation as to whether the discrepancy was caused by air velocity, influence of metal vapor from fuse wire, humidity, time of arc duration, the proximity of porcelain insulating surfaces, or perhaps capacitively induced currents in the fault arc path during the supposedly de-energized period. In all such cases with which I am familiar, shorter fault arcing time permitted faster reclosing. This would be expected from the information supplied by the authors.

It is interesting also to note that metal vapor from the fuse wire has little effect on deionizing time. This has been a controversial point for some time.

The principle reason in the past for clearing faults in the shortest possible time on high-voltage circuits was to minimize the direct effect on transient stability. However, there now appears to be another reason of nearly equal importance, in that the time consumed by fault clearing equipment such as relays and circuit breakers, can seriously influence the shortest permissible reclosing time. The effect of multiple lightning discharges on high-speed reclosing may present a rather serious problem in addition to that of limiting reclosing speed as indicated by the authors. During the de-energized period in which deionization must take place, circuit breakers at the line terminals will receive an impulse with every repetitive stroke. Thus the circuit breaker arc rupturing equipment will be subjected to a series of impulses throughout its opening and closing strokes. I understand that such repetitive impulses have damaged interrupting equipment during normal opening operations. Furthermore, it is apparent that the circuit breaker dead time should be considered only when the circuit breaker is sufficiently open to withstand such impulses. Otherwise added interrupter arcing time may seriously reduce the interval intended for deionization.

G. Jancke (Swedish State Power Board, Kungl Vattenfallsstyrelsen, Stockholm, Sweden): The length of the dead time at automatic reclosing with regard to system stability is of great interest. The authors state that the minimum dead time is determined mainly by three factors:

1. Circuit breaker limitations. I think that we cannot neglect the spread in the relay protection time and in the electromagnetic or pneumatic-mechanical devices which govern the dead time.

2. Total duration of lightning stroke or its multiple components. The authors state that the data available at present indicate that about 10 per cent of the lightning strokes persist for more than 0.25 second. The experiences of the Swedish State Power Board refer mainly to 22-kv systems. We have statistics from 1,100 high-speed reclosures up to 1947. The system networks are grounded through Petersen coils and thus the experiences refer to 2-phase and 3-phase faults, the single-phase faults being mainly extinguished without line circuit breaker operation. Eighty-two per cent of the high-speed reclosures have been successful, while in 14 per cent of the cases a second delayed reclosure in a couple of minutes has succeeded. The fault duration has been about 0.10 second and the dead time 0.20 to 0.25 second. At first a dead time of 0.10 to 0.15 second was used but then the percentage of unsuccessful reclosures was much higher. The 14 per cent may be caused by multiple strokes, birds, trees, and so forth. On 132- and 220-kv networks we have used 0.25 to 0.30 second dead time interval with good results. Our experiences however, are not sufficient to allow any definite conclusions. In many cases it is very important to use short dead time interval with regard to stability and then we might take the risk of being unsuccessful at the relatively spare multiple strokes of long duration.

3. Deionization time of the fault-arc path and its consequent recovery of dielectric strength. The experiments made by the authors are most valuable and form a good base for the determining of the dead time interval. I am especially interested in the conclusion that high-speed relaying and fast circuit breakers are of an extreme importance. The authors promise that further tests will be performed. I think it would then be valuable to investigate single-phase reclosure and especially the influence from line section length on the minimum dead time. Furthermore many circuit breakers are fitted with resistors. On a common Swedish 220-kv circuit breaker, nonlinear resistors will be inserted to diminish switching surges. The current through the resistors will not be interrupted during the dead time. It is very small but may affect the deionization unfavorably to some extent.

E. J. Harrington and **E. C. Starr:** The comments by Mr. Umphrey relative to the influence of multiple lightning strokes on circuit breaker reclosing performance, and the experience data on high-speed reclosing in Sweden given by Mr. Jancke are valuable additions to the paper. In general, the gain in system stable capacity obtained by high-speed reclosing is very sensitive to fault and reclosure times. Fast clearing and the minimum possible dead time are highly desirable, but unsuccessful reclosures must be kept to an acceptable minimum. The present paper covers an investigation of some of the interrelated variables involved in the problem.

In reply to the excellent discussion by Mr. Browne, it should be emphasized again that the authors were attempting primarily to obtain relative information on the dielectric recovery of fault-arc paths for a limited number of fault conditions. Information was desired and obtained on the actual time required for the arc trail to deionize to such a degree as to permit full voltage to be restored across the space, using a high-impedance source to limit the current to a negligible value.

Since fault-path resistance values were available from the data obtained, and since finite currents are required to re establish such an arc, a resistance value (250,000 ohms), obtained at relatively high voltage, was chosen as a bench mark to indicate a relative state of deionization. As was stated in the paper, it is not known just what per cent of successful reclosures could be obtained at this indicated resistance; that information is yet to be obtained. The very character of the arc, that is, turbulence, looping, and path multiplicity, as vividly shown by high-speed motion pictures taken during the tests, is such as to make the minimum successful-reclosure time a matter of probability; there can be no abrupt threshold between successful and unsuccessful reclosure times.

It was pointed out in the paper that eddying of the hot gases tended to produce voids that probably resulted at times in measured resistances that would infer dielectric strengths greater than actually existed. In some of these cases the rapid rise in measuring potential caused at least partial breakdown of the voids with accompanying decrease in resistance. There is no assurance however, that reapplication of full voltage at the instant of interruption in recovery would have resulted in currents of sufficient magnitude in each case to re-establish the arc. These delays or interruptions in dielectric recovery were taken into account in the curves presented.

The equation given by Mr. Browne for arc voltage, $E_d = \sqrt{RW_0}$, is recognized as applying to stable arcs. Since the voltage drop across a given length of arc is essentially constant and independent of current, it is indicated that the critical resistance is inversely proportional to the energy loss from the path of the arc core. If that core is surrounded by a cloud of incandescent gas resulting from long arc duration at high current, the energy loss will be lower than if the gas cloud is absent or less extensive. Hence the critical resistance for arc reignition should be somewhat lower for short-duration arcs, but there is probably not an order of magnitude difference. Furthermore the short-duration arcs exhibit a much more rapid rise of resistance than the arcs of long duration. See Figures 8(A), 8(B), and 10 of the paper.

The authors cannot agree with Mr. Browne's statement that the dielectric recovery was influenced by the measuring circuit. If this were the case the extremely rapid recovery indicated in Figure 10 following a 1-cycle 15,000-ampere arc would not have occurred.

Future studies are contemplated again in connection with a limited number of circuit breaker capability and acceptance tests. Improved measuring techniques will be employed, but a source of high-voltage direct current will not be available for the measuring circuit at least not for the next tests. Some of the future work may include the influence of charging current in the arc path following fault interruption to simulate the conditions of single-pole switching.

A Transient Fault Locator for High-Voltage Transmission Lines

L. R. SPAULDING
ASSOCIATE AIEE

C. C. DIEMOND
MEMBER AIEE

THE location of high-voltage power line faults by echo-ranging means has received considerable attention during the post-war years. Recent work by the Bonneville Power Administration (BPA) in the development of high-voltage transmission line fault locators, together with a broad review of the problem in general and a rather complete bibliography, has been reported in another paper,[1] therefore, that material will not be repeated here except in brief summary. That paper describes two types of transient fault locators operating on the fault generated surge principle.

In the type *A* system, the surge from the fault travels to a station at one end of the line where it starts a timing device and reflects back toward the fault. From this instant, the device acts in normal echo-ranging sequence as though the surge were generated at the station. The round-trip time to the fault and back again is a measure of the distance to the fault.

In the type *B* system, the surge from the fault travels to a station at one end of the line where it starts a timing device. The reflection of the surge from the station bus is not used. A surge simultaneously travels from the fault to a station at the other end of the line where it is transmitted via a broad-band radio channel to the first end. The elapsed time interval between the arrival of the two surges at the first station provides a measure of the distance to the fault.

Another system also has been proposed[2] for transient fault location in which an echo-ranging type of fault locator continuously pulses the line and makes a photographic record automatically from an oscillograph during fault. This device is permanently coupled to just one phase of a 3-phase line.

Other echo-ranging fault locators of the nontransient type also have been described, or are commercially available. Most of these require that the line be removed from normal service for fault location purposes.

One type,[3] builds up direct voltage on the line to a potential high enough to break down any point of weak insulation. The surge generated by this breakdown is used to start the timing device and to reflect from the line discontinuities in typical echo-ranging sequence.

Another type,[4] requiring metallic connections to the line, applies a repetitive pulse to a permanently faulted phase of the line and gives a visual presentation of the fault location on an oscilloscope screen.

Still another type applies a continuous wave of constant frequency (nonpulsing) to a faulted phase of a line and observes the phase shift of the reflected wave.

It is the purpose of this paper to report further work by the BPA in the study of the problem and in particular to describe the type *C* fault locator which fulfills several additional requirements of an ideal fault locator.

The transient fault locator discussed in this paper permits the location of nonpermanent faults such as are often caused by lightning. These may not remove the line permanently from service, but may cause damage to insulation or conductors. It is highly important that these points of fault be located for inspection and repair.

The type *C* fault locator is designed for use where suitable wide-band communication circuits are not available to carry the intelligence requirements of the type *B* fault locator. It also provides a freedom from spurious pulses; a trace which does not require specially-trained engineering personnel for interpretation when a photographic record is used; a means of operating an electronic counter for a direct reading record; and a freedom from causing interference to closely associated carrier or radio communication facilities.

The difficulty encountered from spurious pulses associated with the surge at the start of a fault which was used as the source of pulse energy for echo-ranging in the type *A* fault locator, together with difficulty in handling the extremely wide ranges of pulse magnitudes encountered in the fault generated surge, lead to investigations of this so-called pulse-radar method of echo-ranging for fault location.

Improved methods of coupling the equipment to a live line through carrier coupling capacitors which are connected during fault by information from a conventional phase selecting relay system, were developed to obtain more pronounced reflections from the fault and a single applied pulse instead of a continuously repeating pulse was selected for simplicity and freedom from causing carrier and radio interference.

Operation of the Type *C* Fault Locator

During the waiting period between faults, the fault locator is not connected to the line. When a single-line-to-ground fault occurs, a simple phase selecting relay system connects the fault locator through a carrier coupling capacitor between the faulted phase and ground. After approximately 33 milliseconds from the

---

Paper 49-206, recommended by the AIEE Instruments and Measurements and Transmission and Distribution Committees and approved by the AIEE Technical Program Committee for presentation at the AIEE Pacific General Meeting, San Francisco, Calif., August 23–26, 1949. Manuscript submitted May 2, 1949; made available for printing June 29, 1949.

L. R. SPAULDING and C. C. DIEMOND are both with the Bonneville Power Administration, Portland, Oregon.

The authors wish to express their appreciation to A. W. Adams, H. L. King, D. E. Smith, T. T. Smith, and T. W. Stringfield for their criticisms and suggestions.

start of the fault, a single unidirectional (d-c*) 1-microsecond pulse from a 10-kv source is applied to the line after which the pulsing unit is disconnected and a receiving unit is actuated. A timing device is started by the initial pulse and the elapsed time before the return of a reflection is recorded. This provides a measure of distance to the fault. In the event of a multiple phase fault such as a phase-to-phase or 2-phase-to-ground fault suitable information from the relay system will connect the fault locator between one of the two or three faulted phases and ground.

Investigation

In the experimental work, the timing device used was a cathode-ray oscilloscope with a linear sweep. The initial pulse started the sweep and the reflected pulse appeared as another "pip" on the sweep at some time later proportional to the fault distance. The permanent record was obtained by photographing each trace on an individual frame with a standard 16-millimeter motion picture camera. This method was particularly suited to the work because of its ability to show the presence of any spurious or undesired pulses which might interfere with the operation of an electronic counter or other direct indicating devices which might be employed.

In the development of the type *C* locator, these questions had to be answered:

1. What pulse magnitude should be used?
2. What interval during the fault should be used for operating the fault locator?
3. Should the pulse be repeated continually at all times; applied on a repetitive basis during fault; or applied just once during fault?
4. What pulse width should be used?
5. Should a d-c or a radio-frequency pulse be used?
6. How should the fault locator be coupled to the line?
7. What type of recording device should be used?
8. What relaying system should be used?

Obviously these questions are all related so the best answer to one might not allow the best answer to the others.

Pulse Magnitude

In seeking an answer to the question of pulse magnitude, a large number of oscillograms were reviewed which were obtained from automatic magnetic oscillograph operations throughout the Bonneville system during a period of several years. Also, cathode-ray oscillograms obtained by photographic means during staged faults were reviewed, paying particular attention to voltage wave distortions existing during the first few cycles after the start of a fault. The information gained from the magnetic oscillograms was limited due to the comparatively low-frequency response of the oscillographs and their related inability to record steep-wave fronts of the order which would provide interference to a fault locator of the type proposed. However, it was the best accumulated source of information available and did give an idea of the frequency of occurrence of low-frequency voltage distortions in the time immediately after the start of a fault. A comparison of the magnetic and cathode-ray oscillograms indicated that it was logical to assume that indicated low-frequency distortions would be related to higher frequency distortions and that an interval free from low-frequency distortions would probably be free from higher frequency distortions. The results of this review, together with a

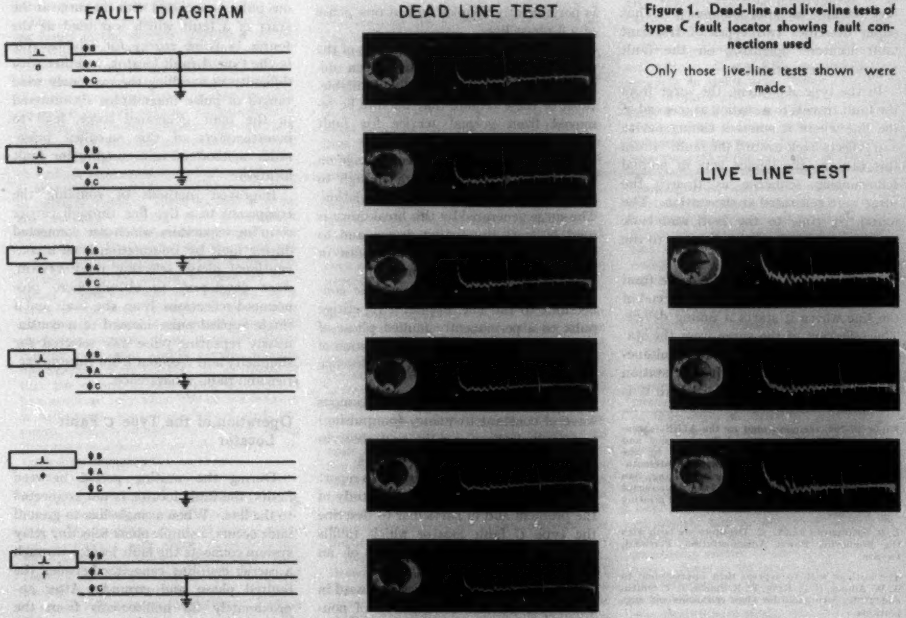

Figure 1. Dead-line and live-line tests of type C fault locator showing fault connections used

Only those live-line tests shown were made limited number of live-line fault tests using a d-c pulse for echo-ranging, disclosed that a pulse from a 10-kv source could be expected to override most interference after the second cycle of fault.

---

* The term "d-c pulse" is used to denote this unidirectional pulse.

Interval During Fault

Since the device must obtain its information before the fault is cleared, yet must wait at least two cycles of 60 cycles, the third cycle of fault was defined as the logical time for its operation.

Pulse Repetition

If a continuously repeating pulse were to be used, the time of most value in obtaining a record, for example, photographing a cathode-ray trace, would be during the third or later cycle of fault. A photograph of multiple traces on one frame might be distorted by spurious pulses if an exposure were started too soon after the start of the fault or continued through the circuit breaker opening time. The number of useful repetitions of the pulsing interval which might be expected during the third cycle of fault depends upon the length of the line being monitored and the recovery time required by the pulse originating equipment. For a 100-mile line, the theoretical maximum number of pulses could not exceed 16 and the actual practical number might not exceed five. In the event an electronic counter were employed, it could only make use of the first transmitted pulse and its reflection, so subsequent pulses would be of no value. Considering the added complications involved in delivering a repetitive pulse of the required magnitude for the benefit of the photographic record, and the questionable advantage to be gained, it was decided to use only one pulse properly placed with respect to time after fault initiation and before fault interruption.

Pulse Width and Type

In the interest of accuracy of measurement, it was desirable to use as narrow a pulse as possible. A d-c pulse of the order of one microsecond could be passed through an ordinary carrier coupling capacitor without undue losses and a d-c pulse was by far the easiest to produce. A radio-frequency pulse could be made longer than one microsecond and of any particular shape desired for easy recognition on a photographic record. However, it was felt that the reflection obtained from the type *C* locator would be pronounced enough so that a special shape of pulse would not be necessary. This fact became evident after improved coupling schemes had been developed. For the operation of the electronic counter, the magnitude of the pulse is of more importance than the shape. Therefore, the 1-microsecond d-c pulse was chosen.

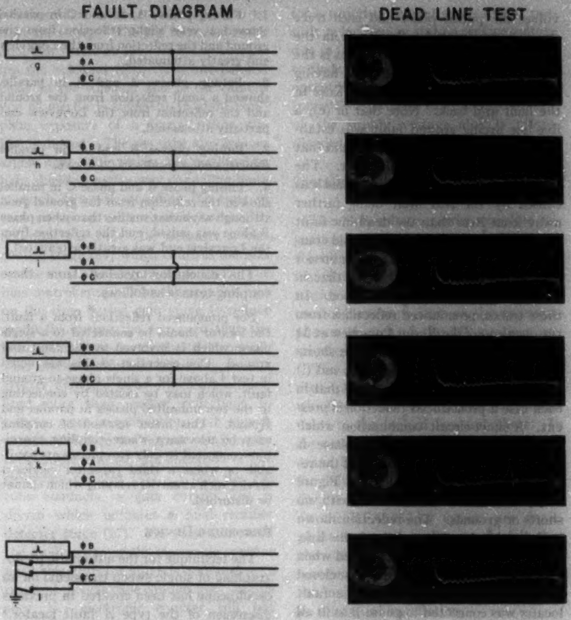

Figure 2. Dead-line tests of type C fault locator showing fault connections used

No live-line tests were made

Coupling

One of the most important factors to be decided was that of coupling to the line. Early experience with the type *A* locator[1] suggested that a loose common coupling to all phases of a station bus would not give best results for all faults regardless of the phase that was faulted. Also it suggested that close coupling to just one phase of a 3-phase line would not give equally good results for faults on the other phases.

Accordingly, a series of tests were arranged on the BPA 230-kv Ross–Longview line in which a series of connections were made at a point 32 miles from the Ross Substation representing various types of faults but with the line dead. Phase B was pulsed through the coupling capacitor at Ross Substation for each condition. In order to verify the assumption that these dead-line connections would appear practically the same to the fault locator as an actual fault, three of the combinations were repeated under arcing line to ground fault conditions. The results of these tests are summarized in Figures 1 and 2. Phasing shown in Figures 1 and 2 is that existing at the point of fault.

In these figures, the left-hand columns show the fault connections for each test. The square attached to the top phase represents the fault locator. The center column shows the photographic record made for each dead-line test. The right-hand column shows the record made for an actual arcing line to ground fault for the condition shown in the left-hand column. In these cases, the fault was produced by pulling a small copper wire into the line with a glass string. The traces shown have been touched up for reproduction purposes by inking over various reflection "pips". The regularly spaced negative "pips" appearing on each trace are range markers indicating each ten miles of line.

Figure 1 shows 3-phase, 2-phase, and single-phase grounds designated as A, B, and C respectively. Each case involves the pulsed phase and each trace shows a pronounced reflection from the ground. The reflection at 64 miles is the second return of the pulse after having completed two round trips from Ross to the fault and back. Note that in (c), a live-line arcing ground fault was established for purposes of comparison and that the two traces check each other. The slight difference in distance indicated was caused by the real fault being farther away from Ross than the dead-line fault connection. Figure 1 shows ground combinations at (d), (e), and (f) which do not involve the pulsed phase. Note that in each case the reflection is not good. In these traces, pronounced reflections from the open end of the line at Longview at 51 miles are present. Figure 2 shows short-circuited combinations at (g), (h), and (i) involving the pulsed phase. Note that in each case a pronounced reflection is present. A short-circuit combination which does not involve the pulsed phase is shown by Figure 2 (j). Note that the reflection from the fault is not good. Figure 2 (k) shows a trace obtained with no shorts or grounds. The reflection shown is from the Longview end of the line. Figure 2 (l) shows a trace obtained when the ground switch at Ross was closed grounding all three phases. The fault locator was connected to phase B as in all the previous tests through a carrier coupling capacitor on the line side of the carrier line traps about 50 feet away from the ground switch. Note that the different shape of the reflection from the Longview end at 51 miles consists of high-frequency oscillations apparently caused by the line connections at Ross.

The fact that every reflection shown extends both above and below the base line indicates that even though the pulse originates as a unidirectional pulse, its characteristics are modified by the system parameters and connection of the circuits through which it feeds and to which it is connected. This might suggest that a radio-frequency pulse would be affected by these reactances and that for greater efficiency, it is desirable to shock-excite these reactances with a d-c pulse.

Additional dead-line tests were made with a ground on B phase 32 miles from Ross, but with the fault locator coupled through carrier coupling capacitors to various combinations of paralleled phases. All parallel connections were made on the fault locator side of the coupling capacitors.

Photographic records of these tests are not reproduced in this paper but the results are as follows:

1. Pulsing phases A, B, and C in parallel showed a very slight reflection from the ground and the reflection from the Longview end greatly attenuated.
2. Pulsing phases A and B in parallel showed a small reflection from the ground and the reflection from the Longview end partially attenuated.
3. Pulsing phases B and C in parallel showed similar results to (2) above.
4. Pulsing phase A and phase C in parallel showed the reflection from the ground good although somewhat smaller than when phase B alone was pulsed, and the reflection from the Longview end was greatly attenuated.

The conclusion reached from these coupling tests is as follows:

> For pronounced reflections from a fault, the locator should be connected to a single phase which is involved in the fault and ground. One exception to this was noted in test 4 above for a single-phase-to-ground fault, which may be located by connecting to the two unfaulted phases in parallel and ground. This latter method of coupling may be necessary where coupling capacitors connected to only two phases are available or where a third capacitor carries a service such as carrier relaying which cannot be disturbed.

RECORDING DEVICE

The technique for the automatic photographing of single sweep transients on an oscilloscope has been covered in previous discussion of the type *A* fault locator.[1] Until the satisfactory operation of an electronic counter as applied to the type *C* locator has been fully confirmed by experience, the use of the oscilloscope and camera will be continued. An electronic counter now on order will later be incorporated in a type *C* fault locator now being constructed for installation at Spokane Substation, together with the oscilloscope photographic recording equipment. In this way, the oscilloscope trace can be used to check the operation of the counter and it is hoped that the photographic recording equipment can eventually be eliminated.

In operation, the initial pulse will start the counter which records the number of 1-microsecond time intervals until it is stopped by a reflected pulse from the fault. The reading appears on a decade bank of lights which hold their indication until manually reset. The time necessary for the pulse to travel one mile and to be reflected back to the point of origination is 10.73 microseconds. The fault distance in miles will be obtained by referring the indicated time interval to a calibrating curve.

RELAYING SYSTEM

Various means for controlling the time of pulse application were considered for the type *C* fault locator. Economy of equipment dictated use of a relaying scheme which would switch the fault locator to one of the faulted phases on either line. Employing relatively inexpensive relaying components allows the use of the more complex and expensive electronic devices in this equipment, such as the oscilloscope, for fault location on more than one 230-kv line.

Limitations of available electro-magnetic relays including inertia, burden, and so forth, should not present too many problems in this application. However, we are hopeful that newer developments possibly in electronic relays will permit closer control of this fault locator.

FUNCTIONAL DETAILS OF THE TYPE *C* FAULT LOCATOR

The functional details of the type *C* fault locator are shown diagrammatically in Figure 3. In this figure are shown a transmission line (1) connecting two substation busses, a fault (2), carrier current coupling capacitors (3) for each phase and coupling capacitor selector relay contacts (4) which are operated by the phase selecting relay system. The connections leading to a typical carrier communication equipment (5) and a conventional protective gap (6) for protection of the line tuning unit are also shown.

When a C-phase-to-ground fault occurs, the phase-C selecting relay operates the related coupling capacitor selector relay so as to first disconnect the carrier communication equipment and second, to connect the fault locator to this phase. Simultaneously, the pulse originating relay which operated contacts (7) is energized. This relay, together with the phase selecting relay, is timed to operate from 2 to $2^1/_2$ cycles after the start of a fault. The coupling capacitor selector relay contacts are timed so as to always close ahead of the pulse originating relay contacts (7). As these pulse originating relay contacts move towards closure, the voltage from the 10-kv power supply breaks down gap (8) and the reduced gap across contacts (7), applying a pulse through the phase C coupling capacitor to the line. Due to the constants of the coupling capacitor, the line, and the supply circuits, current will flow through the coupling capacitor for a time in the order of one microsecond. This completes the transmission of the pulse.

As long as the arc across gap (8) continues, the relatively large output capacitor (9) in the 10-kv power supply provides a shunt path to ground through which any reflection coming back to the station will pass. In order to disconnect this part of the circuit as quickly as possible after the pulse has been originated, an 8-ohm resistor (11) and gap (12) were provided through which the output capacitor will discharge in about ten microseconds. This gap (12) shorts out the 750-ohm resistor (13) during the discharge of the output capacitor so as to reduce the voltage fed to the receiving circuit through coupling condenser (14).

The phase selecting relay system in the fault locator is arranged so that all elements reset when the fault current is cleared. After gap (8) has fired, condenser (9) has discharged, and the arc across gap (8) extinguished, the voltage across condenser (9) is prevented from building up to full value immediately by resistor (33). This gives the pulse originating relay contacts time to reset before gap (8) would break down a second time. In this way, only one pulse is supplied to the line for each fault.

Gaps (12) and (8) extinguish simultaneously leaving the receiving circuit connected to the line through the 8-ohm resistor (11). The 750-ohm resistor (13) provides little shunting effect to the desired incoming signal yet assists in properly terminating the line from the carrier capacitor. Coupling condenser (14) together with coaxial cable (15) acts as a differentiating circuit to discriminate against low-frequency signal components attempting to enter the receiving circuit. The high-pass filter (16) provides proper termination for the coaxial cable and discriminates against all frequencies below 200 kc, in particular the carrier frequencies. In this way, even though the carrier transmitter connected to the line is operating at the time of fault, it will not interfere with the operation of the fault locator through stray coupling which inevitably exists around the coupling capacitor selector relay contacts. The carrier signal is interrupted only during the fault and is restored to normal as soon as the circuit breaker is opened and the relays reset. On a voice circuit, this provides very little more interference than the fault itself together with fault interruption by the circuit breaker.

A limiter amplifier (17) is provided in the receiving circuit which prevents the initial pulse from distorting the trace (in the case where an oscilloscope is used) or from saturating one of the following stages.

Breakdown of gap (8) also results in application of a positive pulse to the grid of a gas tube (18) through coupling condenser (19) and coaxial (20). This causes the gas tube to conduct and to supply a positive pulse to the oscilloscope (29) to start the sweep. The gas tube also racks up a new frame on the camera by operating the solenoid (22). The mechanical delay in the solenoid and in the camera due to inertia is sufficient to allow complete exposure of a frame before the film is moved. The gas tube also fires an argon light (23) within the oscilloscope light shield in such a way as to illuminate a watch face for recording the time of each sweep on each exposed frame. In addition, gas tube (18) actuates a bias control stage (24) which controls the bias on the time varied gain stage (25). The bias control stage allows the negative bias on the time varied gain stage to reduce gradually during the sweep so that the gain will increase during the sweep period. This allows reflections returning from a greater distance away which are attenuated more than earlier reflections to receive more amplification and appear more uniform on the record. Uniformity is desirable also for the operation of the electronic counter (31). When the gas tube conducts, a gate circuit (26) is driven which actuates a final rectifier detector stage (27). No pulse can reach the oscilloscope or the electronic counter until this detector stage is actuated as a result of the gas tube conducting. In this way, the electronic counter will not operate at the wrong time due to spurious pulses feeding into the receiving circuit across the capacitance of coupling capacitor selector relay contacts or through other stray coupling. The d-c plate voltage is removed momentarily by reset circuit (28) after completion of one chain of operation.

The camera (32) is a standard 16-millimeter motion picture camera with the shutter removed. Each frame is continually exposed to the oscilloscope screen but the screen is completely blanked out between operations.

Difficulty was experienced at first from light radiation from the cathode of the cathode-ray tube coming directly through the screen into the camera and clouding the film. After attempts were made to correct the trouble with light filters, this undesirable condition was finally overcome by lowering the camera several inches so that it was out of the direct line from the cathode. In order to prevent small quantities of stray light from eventually clouding the film, the camera is racked up automatically once an hour by a pair of contacts which are operated by a clock motor.

It is desirable in automatic models to use large storage condensers throughout the equipment to sustain the d-c voltages for a period of several cycles during possible reductions in station service voltage due to fault. Use of electron tubes of the cathode type which maintain satisfactory operating temperatures for several cycles (on a 60-cycle basis) after an interruption of the supply voltage also is recommended.

Installation at Spokane Substation

The high-voltage carrier coupling capacitors required for operation of the type *C* locator is a major item of expense. The installation of the device at Spokane Substation has been simplified by the presence of these capacitors on the necessary phases of each of the 230-kv lines terminated there.

The scheme as designed for Spokane uses phase selecting relay equipment which switches the fault locator equipment to the faulted line and phase. In the actual installation as shown in Figures 4 and 5, selecting equipment is provided for only the line-to-ground faults. Since the overwhelming preponderance of faults on the BPA 230-kv system are single-phase-to-ground faults, it was felt that the added complication necessary to recognize and properly switch the locator for multiphase faults was not warranted in this initial installation.

The phase selector relays are high-speed directional elements. In this application, the faulted phase is selected by comparing the direction of power transformer neutral current with phase current. The faulted line is determined by operation of an instantaneous overcurrent relay or by the operation of a directional comparison carrier ground auxiliary relay. The overcurrent relay is set above the maximum through fault current for each line.

Operating experience in this particular application may show the need for a more complex phase selecting scheme. If changes are found necessary, it is planned to use a negative-zero sequence current comparison scheme as in a previously reported system for single pole reclosing.[6]

A modification of the basic relaying scheme is shown for Spokane at the bottom of Figure 5. Here the coupling capacitor on phase A of each line carries the carrier relaying channel. On this channel, the carrier signal cannot be interrupted during fault as can voice channels. In order to avoid filtering the fault locator pulse out of the carrier relay equipment which would be connected in parallel during the fault locator operating period, it was decided to try the connec-

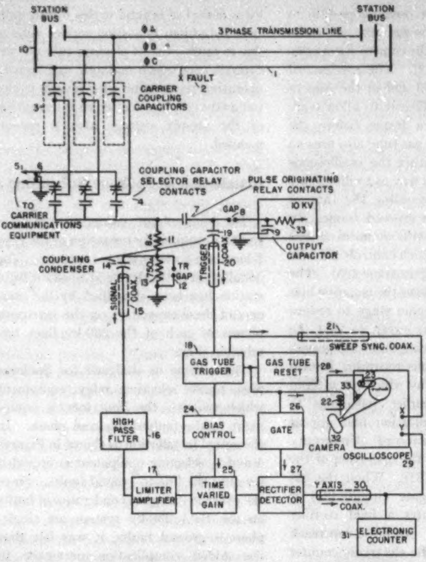
STATION BUS
STATION BUS
ϕA
3 PHASE TRANSMISSION LINE
ϕB
ϕC
10
X FAULT
2
1
3
CARRIER COUPLING CAPACITORS
5_1
6
TO CARRIER COMMUNICATIONS EQUIPMENT
COUPLING CAPACITOR SELECTOR RELAY CONTACTS
4
PULSE ORIGINATING RELAY CONTACTS
7
GAP 8
10 KV
9
33
OUTPUT CAPACITOR
8Ω
11
19
TRIGGER
COAX
20
COUPLING CONDENSER
14
750Ω
13
TR GAP
12
SIGNAL
COAX.
15
21
SWEEP SYNC. COAX.
18
GAS TUBE TRIGGER
GAS TUBE RESET
28
23
33
22
X
Y
32
CAMERA
OSCILLOSCOPE
29
HIGH PASS FILTER
16
24
BIAS CONTROL
26
GATE
17
LIMITER AMPLIFIER
25
TIME VARIED GAIN
27
RECTIFIER DETECTOR
Y AXIS
30
COAX.
31
ELECTRONIC COUNTER

Figure 3. Functional diagram of type fault locator general

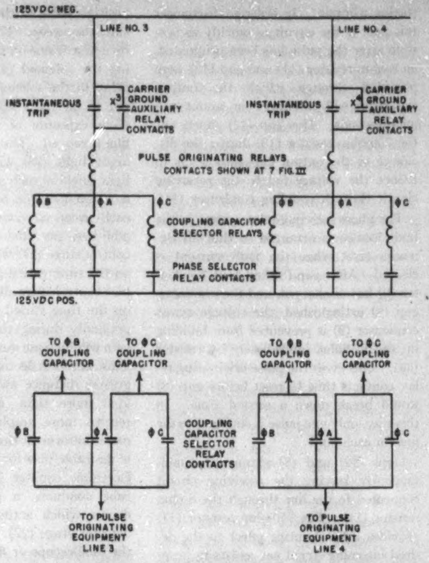
125 VDC NEG.
LINE NO. 3
LINE NO. 4
INSTANTANEOUS TRIP
X^3
CARRIER GROUND AUXILIARY RELAY CONTACTS
INSTANTANEOUS TRIP
X^4
CARRIER GROUND AUXILIARY RELAY CONTACTS
PULSE ORIGINATING RELAYS
CONTACTS SHOWN AT 7 FIG. III
ϕB
ϕA
ϕC
COUPLING CAPACITOR SELECTOR RELAYS
ϕB
ϕA
ϕC
PHASE SELECTOR RELAY CONTACTS
125 VDC POS.
TO ϕB COUPLING CAPACITOR
TO ϕC COUPLING CAPACITOR
TO ϕB COUPLING CAPACITOR
TO ϕC COUPLING CAPACITOR
ϕB
ϕA
ϕC
COUPLING CAPACITOR SELECTOR RELAY CONTACTS
ϕB
ϕA
ϕC
TO PULSE ORIGINATING EQUIPMENT LINE 3
TO PULSE ORIGINATING EQUIPMENT LINE 4

Figure 5. Schematic diagram of Spokane coupling capacitor selecting relay system

Figure 4 (below). Schematic diagram of Spokane phase selecting relay system for single-line-to-ground faults

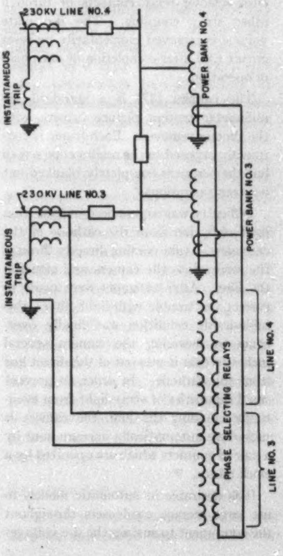
230 KV LINE NO. 4
INSTANTANEOUS TRIP
POWER BANK NO. 4
230 KV LINE NO. 3
INSTANTANEOUS TRIP
POWER BANK NO. 3
LINE NO. 4
PHASE SELECTING RELAYS
LINE NO. 3

tion scheme indicated by test (4) in the section on coupling in which phases B and C are paralleled and pulsed for faults occurring on phase A.

A separate pulsing unit for each of the two 230-kv lines is provided for Spokane, one mounted on each dead end tower. Each unit includes a 10-kv power supply, a pulse originating relay and the associated gaps, three coupling capacitor selector relays, and coaxial fittings for terminating two coaxial cables connecting to the receiving equipment. The corresponding coaxials from these two pulsing units are connected in parallel so that only one receiving unit is required.

In addition to its primary function, the location of power line faults, it is felt that this equipment might prove to be a valuable tool in investigation of phenomena related to traveling waves and line attenuation on high-voltage transmission circuits. We also can see some possibilities for power line relaying with related devices. It also has been suggested that a continuously pulsing device of this kind using a high repetition rate might be used in the investigation of fault arc deionization time and lightning discharge duration.

At the present date, we have made no detailed analysis of the data so far obtained on the BPA system on traveling waves and line attenuation.

References

1. A Transmission Line Fault Locator Using Fault-Generated Surges, **R. F. Stevens, T. W. Stringfield.** *AIEE Transactions*, part II, volume 67, 1948, pages 1168–79.

2. The "Linascope"—An Echo-Ranging Type Fault Locator for High-Voltage Lines, **J. R. Leslie, K. H. Kidd.** *AIEE Transactions*, part II, volume 67, 1948, pages 1162–67.

3. The Localization of Faults on Overhead Lines by Means of Impulse Waves, **S. Margaulies, P. Fourmarier.** *Paper number 307*, International Conference on High Tension Electric Systems (Paris, France) 1948.

4. Fault-Finder, Type FF-1. Radar Engineers, Seattle, Wash.

5. Relays and Breakers for High-Speed Single-Pole Tripping and Reclosing, **S. L. Goldsborough, A. W. Hill.** *Electrical Engineering* (*AIEE Transactions*) volume 61, February 1942, pages 77–81.

Discussion

Y. J. Fujimura (Department of Water and Power, Los Angeles, Calif.): With the ever-increasing installation of high-voltage transmission lines of considerable length, often through territories not easily accessible, the necessity and the value of an improved method for quickly locating transient faults become apparent. The engineers of the Bonneville Power Administration have contributed a great deal toward the ultimate goal of an ideal fault locator[1] and this paper is welcomed as another step forward with possibilities of approaching the ideal requirements.

The Los Angeles Department of Water and Power is interested in some quick means of determining the location of transient faults which may occur on the 250-mile 230-kv Owens Gorge line to be constructed in the near future. Basically, we have considered schemes which depended upon one of the three sources of possible fault indication; by measurement of the fault current, by timing the traveling waves impressed on the line from an external source, and by timing the surge generated by the fault. None of the various schemes in its present state satisfies all the requirements of an ideal fault locator.

The paper indicates that this new method called type *C* is still in the experimental stage. Its two outstanding features are a new improved means of coupling to a live line and the possibility of obtaining records without the use of photographic films. We hope that they will succeed in developing an electronic counter and its auxiliaries which will operate only on the desired pulses. An electronic counter will eliminate film development and the necessity of skilled interpretation, and it will give more accurate indication with respect to distance.

What would happen if the lines were hit by a multiple lightning stroke? There is the possibility that subsequent strokes will generate surges which may interfere with the reflected pulse. It is true that the initial fault surge will have practically disappeared by waiting two cycles, but a lightning stroke may contribute surges which may occur several cycles after the initial stroke. If the authors can separate the reflected d-c pulse from any other pulses by some filter arrangement, the objection to interference will be eliminated.

Their experimental data from tests on the Bonneville Power Administration 230-kv Ross-Longview line are based only on solid faults on dead lines and on arcing faults on live lines. Appreciable reflection resulted by proper coupling to the faulted phases; however, on other types of faults involving high resistance to ground or between phases, the reflection may be too small to be identified on the scope or to operate the electronic counter.

Type *C* method also is limited to faults located more than a mile beyond the point of application of the d-c pulse. As the authors indicate, some ten microseconds are required for the output capacitor to discharge, which will block out the receiver for that period. Possibly a time delay circuit may overcome this difficulty.

REFERENCE

1. A TRANSMISSION LINE FAULT LOCATOR USING FAULT-GENERATED SURGES. **R. F. Stevens, T. W. Stringfield.** *AIEE Transactions*, volume 67, part II, 1948, pages 1168–79.

J. R. Leslie and **K. H. Kidd** (The Hydro-Electric Power Commission of Ontario, Toronto, Ontario, Canada): The pulse technique of fault location on power and telephone lines is receiving a great deal of attention and several groups are pioneering in the development of various instruments which operate on the same basic principle but which differ in detail. The Bonneville Power Administration is to be commended for the thorough manner in which it is investigating several of the possible methods.

The echo-ranging fault locator, utilizing a repetitive short duration d-c pulse, has become well established as an instrument for locating sustained faults.

The Hydro-Electric Power Commission of Ontario now has seven of these instruments located at strategic points in its operating area. These have been used with great success on a wide variety of telephone circuit faults. Operating experience on power lines has been limited, but the instruments have been of use in phasing in new circuits, checking for construction grounds, and in detecting faulty openers. Tests indicate that a variety of faults may be detected including phase-to-phase, phase-to-tower and phase-to-sky-wire short circuits, on open circuited phase conductors, and a phase conductor lying on or near the ground.

The Hydro-Electric Power Commission of Ontario also has in operation an experimental transient fault locator which is similar in principle to that described by Spaulding and Diemond but which differs in a number of details. The authors use a single short duration d-c pulse of about one microsecond duration, whereas The Hydro-Electric Power Commission has been experimenting with a short duration burst lasting about 40 microseconds and containing about ten cycles at a frequency of 250 kc per second. There are theoretical advantages to be claimed for either method and the choice must finally rest on actual operating experience. It is fortunate that the two techniques are being tried simultaneously under roughly similar circumstances, so that their relative merits should be clarified in the near future.

The short duration d-c pulse may be generated more simply than the wave burst and a large amplitude can be obtained much more readily. The wave burst equipment at present produces a voltage of about 500 volts peak to peak as compared to 10 kv utilized by Spaulding and Diemond, a ratio of about 26 decibels. A 1-microsecond pulse also is desirable in preference to a 40-microsecond pulse, in that the accuracy of distance determination is improved accordingly.

The d-c pulse has a much sharper front than has the burst and this is a desirable factor in that it produces a larger reflection from certain types of faults. Thus, a sharp fronted pulse is essential in the sustained fault locator in order to detect a phase conductor lying on high resistivity ground. However, in the case of an arcing fault on an energized line either shape is probably equally acceptable in this respect.

The attenuation along the line is greater for the shorter duration d-c pulse and it also may be more difficult to detect it in the presence of background noise. It is doubtful whether a 200-mile range can be attained with such a short duration pulse.

The main factor which may favor the burst is that the burst energy is confined to a narrower frequency spectrum than that of the d-c pulse. It is very desirable that the transient fault locator be operated without interference to or from carrier equipment on the same transmission line and possibly on the same coupling capacitor. Interference to the carrier receiver is not a problem since both the d-c pulse and wave burst are of such short duration. However, the carrier transmitter may interfere with the fault locator receiver particularly when they use the same capacitor. The present wave burst receiver utilizes a bandpass filter with a pass band of 100 kc centered on 250 kc and an attenuation peaking to 60 decibels at the carrier frequency of 172 kc and also rising to 30 decibels through the broadcast band. Careful attention must be paid to the transient response of the filter to assure short rise time and freedom from ringing.

Of course the simpler approach might be to shut off the carrier equipment for several milliseconds while the pulse is transmitted but it is feared that this would restrict the versatility of the instrument.

The two instruments also differ in a number of minor details. Spaulding and Diemond use a single pulse whereas The Hydro-Electric Power Commission uses a repetitive burst, sending out from five to eight bursts for a transient fault. The first method again gives simplicity and economy of equipment while the latter may be expected to give a clearer photographic record particularly in the presence of noise. The Hydro-Electric Power Commission equipment is used for observing sustained faults visually as well as transient faults photographically and hence the repetitive burst is necessary.

Both groups use a photographic recording technique at present and they appear to be equally anxious to get away from it. The electronic counter will be a most desirable advance but much experience will be needed before a suitable sensitivity is chosen. In some cases, it also may be necessary to render the counter insensitive to large fixed echoes from stations or junctions along the circuit under test.

The Hydro-Electric Power Commission group feel that the photographic technique is satisfactory so far as the operator's ability to interpret the record is concerned, especially as a photograph of the normal appearance of the circuit also is provided him. However, the time and trouble of processing the film is undesirable. Some thought is being given to magnetic tape or smoked chart recording, but the required writing speed may be too high. A magnetic tape record which the operator could play back onto the cathode-ray tube seems inviting.

L. R. Spaulding: In answer to Mr. Fujimura's first question, it is true that a lightning stroke, subsequent to the first one, which started a power arc might fall during the interval of operation of the type *C* fault locator and could cause interference. It would be more difficult to overcome this interference by use of a filter in this sytem than for a system using a radio-frequency or waveburst pulse. This is one thing in favor of the waveburst pulse.

Regarding high resistance faults, it does not appear likely that a high resistance fault will occur under transient or live line conditions on a 230-kv line. As a transient fault locator, the device depends upon a power arc for the reflecting discontinuity, and requires fault currents to accomplish the necessary relaying functions.

If a line fails to go back into service after an outage, a permanent fault may be located on the dead line by manually operating test switches provided for individual phase selection and pulsing. High resistance faults may be located either phase-to-ground or phase-to-phase by this means. The short duration d-c pulse is better for this purpose than a low frequency wave burst pulse.

As noted, the fault locator will not indicate faults in the first mile of line due to the time required to de-energize the transmitter and actuate the receiver. This is considered one of the limitations of the device. However, usually there are other visual indications for faults this close to a station. It was felt that the added complications necessary to overcome this deficiency were not warranted.

The comparison by Mr. Leslie and Mr. Kidd of the advantages and disadvantages of a d-c pulse versus a wave burst for echo ranging describes one difference between the Linascope and the type *C* fault locator. However, the greatest difference in the type *C* is in the use of a phase selecting relay system to connect the fault locator to the faulted phase. This results in a greatly increased reflection from the fault. It also provides a means of monitoring all phases on several lines with one set of equipment. When one conductor of a 3-phase line is pulsed and another conductor is involved in a fault, our tests show that the reflection from the point of fault is apt to be small or unusable, depending upon type of fault and the balance of the line constants.

In the discussion closure of Leslie and Kidds' paper,[1] they have indicated that their transient Linascope is connected to one phase only of a 220-kv bus through which four lines are paralleled. We believe our use of phase-selecting relays to be a distinct improvement in coupling means.

We recognize that the attenuation along the line is greater for a short duration d-c pulse than for a wave burst. However, the maximum line length to which it will be applied is about 136 miles. We do not plan to monitor more than one line section with the device, that is, station-to-station. It is at present temporarily installed at Spokane on the two 230-kv lines between Coulee and Spokane. Their lengths are 83 miles each. Very satisfactory reflections from the far end of these lines is obtained.

We have noted with interest certain advantages reported in favor of a radio-frequency, or wave burst pulse. Should our operating experience indicate the need, we shall give further consideration to this type of pulse.

REFERENCE

1. See reference 2 of the paper.

Electrical Design Features—Steam-Electric Generating Station P of the Pacific Gas and Electric Company

FRANCIS S. BENSON
MEMBER AIEE

A STEAM-ELECTRIC generating station known as Station P (Hunters Point) is located on the west shore of San Francisco Bay within the city of San Francisco, Calif. The original plant was completed during 1930, the installation consisting of one 35,000-kw 12-kv 3-phase 60-cycle condensing turbogenerator and a 3,500-kw turbogenerator (noncondensing and spinning type) for supplying power to the station auxiliary motors. The main generator supplied energy to an outdoor 12-kv bus from which feeders radiated to load areas.

The extension of Station P, completed during the spring of 1949, consists of the installation of two 100,000-kw 0.87-power-factor 13.8-kv condensing turbogenerators, and two 7,500-kw 0.7-power factor 4.16-kv condensing spinning turbogenerators installed in an extension of the turbine room. The new 100,000-kw generators supply electric energy at 13.8 kv to single-phase step-up transformers, the high-voltage terminals of which are directly connected to the 115-kv outdoor ring bus.

The electric energy leaves the 115-kv bus over three underground high-voltage pipe-type high-pressure nitrogen-gas-filled cables, each cable having a rating of 100,000 kva at 120 kv. The insulated conductors in the pipe are maintained at a pressure of 200 pounds per square inch. Two pipe-type cables transmit energy to Station H (Martin Station), and one cable supplies energy to Mission Substation, located in the downtown area of San Francisco.

The terminal position of each high-voltage underground cable at Station P is equipped with a grounding switch, in addition to the usual circuit disconnecting switch. This grounding switch is used to drain the capacitance charge off the cable after it has been disconnected from any source of energy.

115-Kv Ring Bus

The high-voltage (115-kv) ring bus is built outdoors; it consists of a number of steel structures equipped with insulators, disconnecting switches, and oil circuit breakers. Figure 1 is a single-line diagram of the ring bus. Each oil circuit breaker has a current rating of 1,200 amperes at 115 kv and an interrupting rating of 3,500,000 kva. Each circuit breaker also is equipped with six multitap bushing current transformers and two or four capacitor-type potential devices. No 115-kv potential transformers are used.

The ring bus is supplied with energy from two main transformer banks, each having a capacity of 111,750 kva and each consisting of three 37,250-kva 13.8/115-kv single-phase transformers which are outdoor, forced-air rated. The transformer banks are connected delta-Y, and the high-voltage winding neutral is solidly grounded. The transformer installation is equipped with transfer disconnecting switches on both the high- and low-voltage sides for electrically connecting a spare single-phase transformer in the position of any other transformer.

One 50,000 kva 3-phase transformer with $7^1/_2$ per cent plus or minus tap-changing-under-load equipment is installed to interchange energy between the 110-kv and 12-kv systems. This is an outdoor forced-air-cooled transformer rated 110/12 kv, connected Y-Y with a tertiary winding connected in delta.

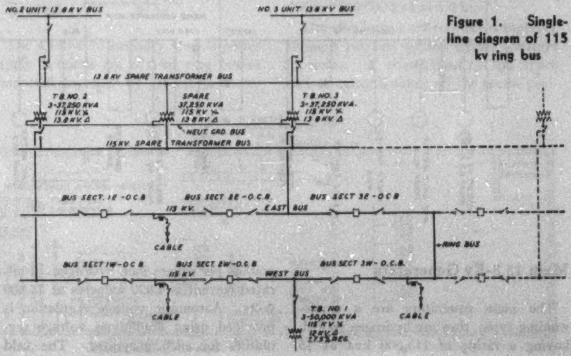

Figure 1. Single-line diagram of 115 kv ring bus

Paper 49-208, recommended by the AIEE Power Generation Committee and approved by the AIEE Technical Program Committee for presentation at the AIEE Pacific General Meeting, San Francisco, Calif., August 23–26, 1949. Manuscript submitted May 23, 1949; made available for printing June 29, 1949.

Francis S. Benson is with the Department of Engineering, Division of Electrical Distribution, Pacific Gas and Electric Company, San Francisco, Calif.

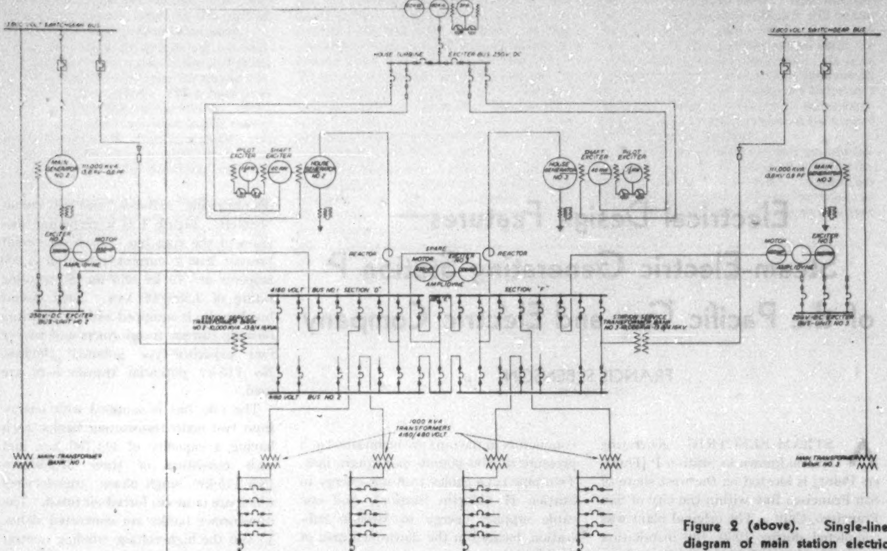
13800 VOLT SWITCHGEAR BUS
MOTOR
EXCITER
PILOT EXCITER
HOUSE TURBINE
EXCITER BUS 250V DC
PILOT EXCITER
SHAFT EXCITER
HOUSE GENERATOR NO 2
HOUSE GENERATOR NO 3
SHAFT EXCITER
PILOT EXCITER
MAIN GENERATOR NO 2
115,000 KVA 13.8KV 0.8 PF
MAIN GENERATOR NO 3
115,000 KVA 13.8KV 0.8 PF
EXCITER NO 2
MOTOR
AMPLIDYNE
REACTOR
SPARE
MOTOR
EXCITER
AMPLIDYNE
REACTOR
MOTOR
EXCITER NO 3
AMPLIDYNE
250V-DC EXCITER BUS-UNIT NO 2
250V-DC EXCITER BUS-UNIT NO 3
4160 VOLT BUS NO 1 SECTION "D"
SECTION "F"
STATION SERVICE TRANSFORMER NO 2 10,000 KVA 13.8/4.16 KV
STATION SERVICE TRANSFORMER NO 3 10,000 KVA 13.8/4.16 KV
4160 VOLT BUS NO 2
1000 KVA TRANSFORMERS 4160/480 VOLT
MAIN TRANSFORMER BANK NO 1
MAIN TRANSFORMER BANK NO 3
LOAD CENTER NO 1
LOAD CENTER NO 2
LOAD CENTER NO 6
LOAD CENTER NO 7

Figure 2 (above). Single-line diagram of main station electric connections

Figure 3 (below). Single-line diagram of 4,160-volt auxiliary power bus

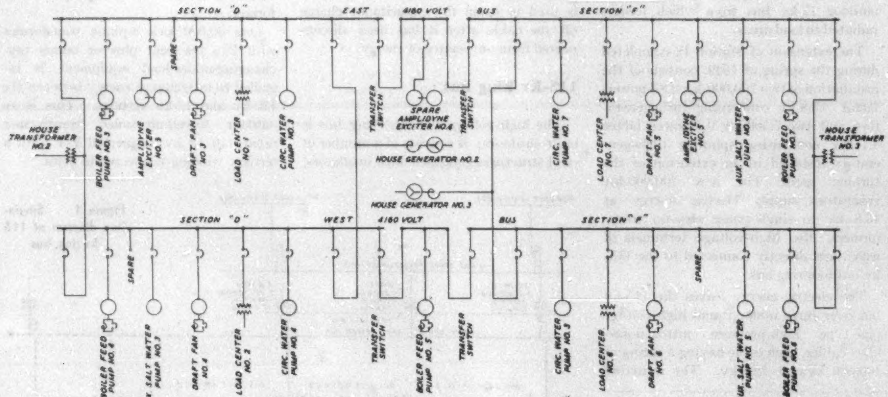
SECTION "D"
EAST
4160 VOLT
BUS
SECTION "F"
HOUSE TRANSFORMER NO.2
BOILER FEED PUMP NO.3
AMPLIDYNE EXCITER NO.3
DRAFT FAN NO.3
LOAD CENTER NO.1
CIRC. WATER PUMP NO.3
TRANSFER SWITCH
SPARE AMPLIDYNE EXCITER NO.6
TRANSFER SWITCH
HOUSE GENERATOR NO.2
HOUSE GENERATOR NO.3
LOAD CENTER NO.7
DRAFT FAN NO.5
AMPLIDYNE EXCITER NO.5
AUX. SALT WATER PUMP NO.4
BOILER FEED PUMP NO.7
HOUSE TRANSFORMER NO.3
CIRC. WATER PUMP NO.7
SECTION "D"
WEST
4160 VOLT
BUS
SECTION "F"
SPARE
BOILER FEED PUMP NO.4
AUX. SALT WATER PUMP NO.3
DRAFT FAN NO.4
LOAD CENTER NO.2
CIRC. WATER PUMP NO.4
TRANSFER SWITCH
BOILER FEED PUMP NO.5
TRANSFER SWITCH
CIRC. WATER PUMP NO.3
LOAD CENTER NO.6
DRAFT FAN NO.6
SPARE
AUX. SALT WATER PUMP NO.5
BOILER FEED PUMP NO.6

Main 13.8-Kv Generators

The main generators are a single-winding type; they are hydrogen cooled, having a rating of 115,000 kva at 15 pounds per square inch hydrogen. Full-rated current is 4,820 amperes at 13,800 volts. Automatic voltage regulation is provided using amplidyne voltage regulators for each generator. The field voltage is 250 direct volts, supplied by a 1,200-rpm 450-horsepower motor-driven exciter of 300-kw capacity, direct connected to a 7.5-kw amplidyne pilot exciter. A complete spare motor exciter

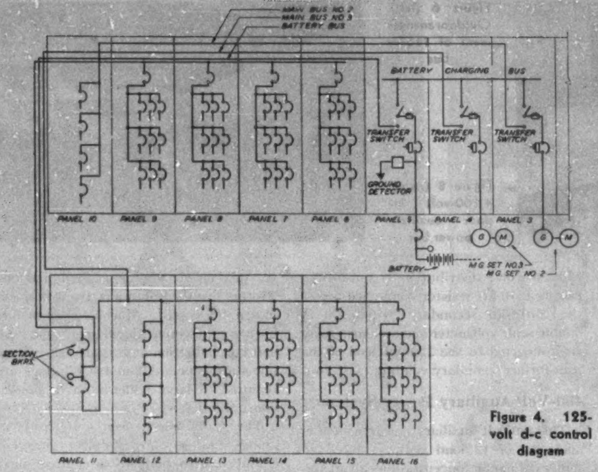
MAIN BUS NO 2
MAIN BUS NO 3
BATTERY BUS
BATTERY CHARGING BUS
TRANSFER SWITCH
TRANSFER SWITCH
TRANSFER SWITCH
GROUND DETECTOR
PANEL 10
PANEL 9
PANEL 8
PANEL 7
PANEL 6
PANEL 5
PANEL 4
PANEL 3
G
M
G
M
BATTERY
M G SET NO.3
M.G. SET NO 2
SECTION BKRS
PANEL 11
PANEL 12
PANEL 13
PANEL 14
PANEL 15
PANEL 16

Figure 4. 125-volt d-c control diagram

including regulator is provided for the generators in case one of the generator motor exciters is out of service. Each exciter unit is equipped with a flywheel to maintain full exciter output for a short period of time if motor power fails. The voltage regulation system is designed for an excitation response of 0.5.

The terminals of the main generators are connected to the step-up transformers through a 13.8-kv 5,000-ampere isolated-phase bus, enclosed in metal ducts. A 5,000-ampere air-blast circuit breaker having an interrupting duty of 2,500,000 kva is installed in the 13.8-kv bus between the step-up transformer bank and the generator terminals. A single-line diagram, Figure 2, shows the main station electric connections. A 10,000-kva station auxiliary power transformer bank is connected to the 13.8-kv bus through a 2,000-ampere air-blast circuit breaker having an interrupting rating of 1,500,000 kva. These circuit breakers operate with an air pressure of 250 pounds per square inch. The 13.8-kv bus connections are such that the station auxiliary power transformers may receive power from the 115-kv bus when the main generator is out of service.

The neutral point of each main generator winding is grounded by elevated neutral equipment consisting of a 50-kva 7,620–120/240-volt single-phase transformer, the 240-volt secondary winding of which is shunted with a 50-kw resistor. An alarm relay and a double-scale voltmeter, one scale indicating 1/10 the value of the other scale, are connected across the 120-volt coil of the transformer secondary.

4,160-Volt Auxiliary Station Power System

The 4,160-volt auxiliary station power supply is made up of two ring busses connected together by circuit breakers. Refer to Figure 3 for the single-line diagram of connections. One 7,500-kw house turbine and one 10,000-kva house bank is connected to each ring bus. Each ring bus is operated normally as a separate auxiliary power system, but the busses may be connected together for emergency operation. The house generator and the house bank each have sufficient capacity to supply the auxiliary power load connected to each ring bus section; one acts as a standby source of power to the other. The house turbines have a rating of 7,500 kw, 0.7 power factor, 10,714 kva, 4,160 volt, three phase, 60 cycles; each house bank has a rating of 10,000 kva, 13.8/4.16 kv, three phase, self-cooled and 13.333 kva, forced-air-cooled; the windings are connected delta-delta. The transformers are single-phase units; their high-voltage and low-voltage terminal connections are arranged with metal links to allow any two single-phase transformers to be quickly reconnected as an open-delta bank having a capacity of 7,600 kva, three phase, forced-air-cooled.

Each house generator has automatic voltage regulation and is equipped with a shaft exciter and pilot exciter, using 250 direct volts as a field voltage. The excitation system has a voltage response of 0.5. A 2,000-ampere 5-per cent metal-enclosed 5-kv indoor current limiting reactor is installed in the house generator lead to the ring bus to reduce the possible short-circuit current on each ring bus.

The 4,160-volt ring bus is made up of 5-kv metal-enclosed lift-up-type electrically-operated air circuit breakers, mounted in steel cells. The circuit breakers have a rating of 1,200 amperes for motors and 480-volt transformers, and 2,000 amperes for the house generators, house transformers, and bus section circuit breakers. They have an interrupting duty of 250,000 kva at 5.0 kv.

The ring busses are connected together through two bus section circuit breakers in series. A connection to the spare exciter motor is taken off the center posi-

Figure 5. Central control room arrangement

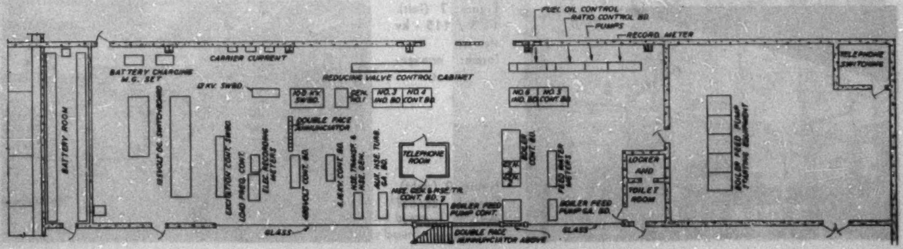
BATTERY ROOM
BATTERY CHARGING M.G. SET
125 VOLT DC SWITCHBOARD
CARRIER CURRENT
13 KV. SWBD.
100 KV SWBD.
GEN. NO.1
NO. 3 IND. BD
NO. 4 CONT. BD.
REDUCING VALVE CONTROL CABINET
DOUBLE FACE ANNUNCIATOR
EXCITATION CONT. SWBD.
LOAD FREQ. CONT.
ELEC. RECORDING METERS
480 VOLT CONT. BD.
4.16 KV. CONT. BD.
HSE. TRANSF. & HSE. GEN.
AUX. HSE. TURB. GA. BD.
TELEPHONE ROOM
HSE. GEN. & HSE. TR. CONT. BD. 7
BOILER FEED PUMP CONT.
DOUBLE FACE ANNUNCIATOR ABOVE
GLASS
FUEL OIL CONTROL
RATIO CONTROL BD.
PUMPS
RECORD. METER
NO. 6 IND. BD.
NO. 5 CONT. BD.
BOILER CONT. BD.
FEED WATER METERS
BOILER FEED PUMP GA. BD.
GLASS
LOCKER AND TOILET ROOM
BOILER FEED PUMP STARTING EQUIPMENT
TELEPHONE SWITCHING

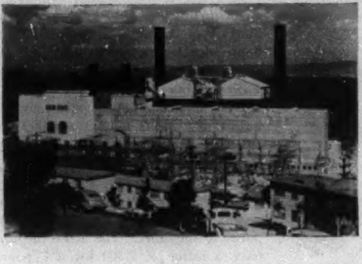

Figure 6 (left). Outdoor arrangement of 115-kv bus

Figure 8 (right). 4,160-volt indoor auxiliary power bus

tion between two bus section circuit breakers, while a connection to boiler feed pump number 5 is taken off the center connection between the other two bus section circuit breakers. Figure 3 indicates this connection.

The following station auxiliary power load is supplied from the 4,160-volt busses:

Four 1,000-kva 3-phase oil-immersed self-cooled 4,160/480-volt transformer banks.

Four 400-horsepower circulating-pump motors (Main generating units).

Three 300-horsepower auxiliary salt-water pump motors (Auxiliary cooling service).

Four 2,000-horsepower boiler fan motors (One per boiler).

Five 2,000-horsepower boiler feed-pump motors.

Three 450-horsepower motor-driven exciters.

The small motors, 300, 400, and 450 horsepower, are started across the line at full voltage. The 2,000-horsepower motors are equipped with starting reactors and a starting circuit breaker connected in the neutral leads of the motor; six leads are brought out of the motor enclosure. These motors start at a reduced line voltage of 50 per cent.

The 4,160-volt auxiliary power supply is delta-connected; however, the house generator windings are Y-connected. The neutral point of the generators is grounded through an elevated neutral connection consisting of a 10-kva 2,400-120/240-volt distribution transformer having a 10-kw resistor connected across the 240-volt secondary winding. A double-scale voltmeter and an alarm relay are connected to the 120-volt coil of the transformer secondary winding.

480-Volt Auxiliary Power System

The 480-volt auxiliary power system is made up of 12 load centers placed at centers of motor concentrations about the plant; they are connected to each other by tie cables. The load centers are supplied with energy from four 1,000-kva 3-phase oil-immersed self-cooled 4,160/480-volt delta-connected transformers. This auxiliary power system consists of load centers which are interconnected as a sectionalized radial system. Each load center is metal enclosed, and is equipped with drawout circuit breakers; each load center bus is sectionalized into two or three sections connected together by bus-section circuit breakers. All air circuit breakers are 3-pole, electrically operated, equipped with thermomagnetic overcurrent protection; they have an interrupting rating of 25,000 amperes for motor and lighting transformer circuits and 50,000 amperes for main load-center tie circuits and bus-section circuit breakers.

Motors

All motors in sizes from 1 to 200 horsepower are 480 volts, and are splash-proof or drip-proof when installed indoors. Motors installed outdoors are totally enclosed, fan-cooled. Machine-shop motors only are the conventional open type. All 480-volt induction motors are full-voltage line-start type. All motor windings are required to have boiler-room or powerhouse treatment.

The 2,000-horsepower 4,160-volt 3-phase motors are totally enclosed, equipped with built-in water-to-air heat exchangers, which are mounted on top of the motor. A moisture detector relay is installed in each motor to indicate excessive moisture within the enclosure, which may be caused by a small leak in the heat exchanger tubes. These motors are equipped with starting reactors and starting circuit breakers connected in the neutral leads.

All motors are induction type, except the fuel-oil pump motors which are wound-rotor type, and are equipped with resistors to give full pump output at three speeds: 1,530, 900, and 450 rpm.

Lighting

Lighting circuits are 3-phase 4-wire supplied with energy from 3-phase indoor dry-type transformers, rated at 25 kva and $37^1/_2$ kva, and are connected 480-120/208 volts, delta-Y. The neutral point of the secondary winding of the transformers is solidly grounded. All lighting circuits are connected between phase wires and neutral; they are pro-

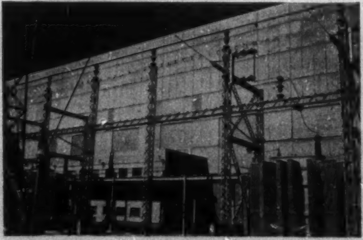

Figure 7 (left). 13.8 / 115 - kv step-up transformer arrangement

Figure 9 (right). Central control room arrangement

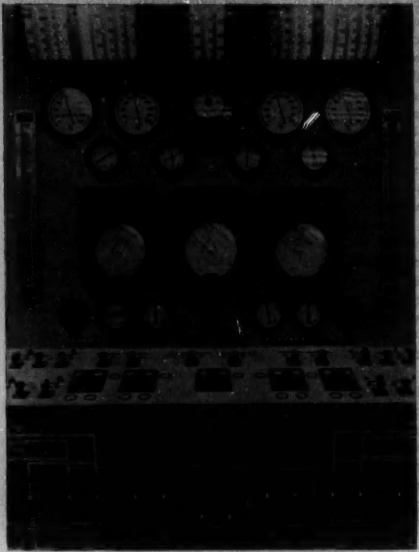

Figure 10. Master control board

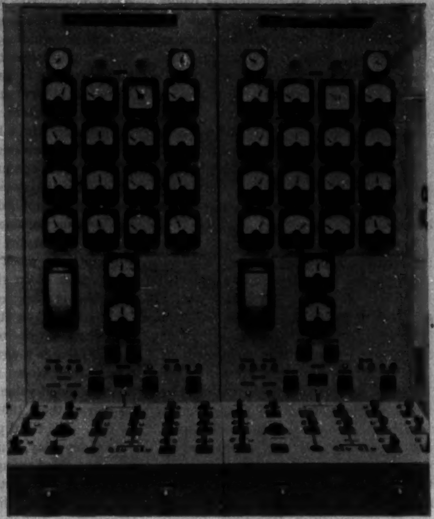

Figure 11. Main generator control panels

tected by single-pole 250-volt a-c thermal circuit breakers. The lighting neutral is carried throughout the plant as an insulated conductor.

The switchboard control room and offices are lighted with surface-mounted fluorescent lighting units enclosed in prismatic glass fixtures, which project some light against the ceiling, eliminating a marked lighting contrast between walls and ceiling. All other lights within the plant area are Mazda lights mounted in prismatic glass fixtures.

An emergency d-c lighting system is installed; certain lighting circuits normally operating on alternating current and using Mazda lamps are switched automatically over to the 125-volt d-c battery system, in case the a-c power supply fails, by double-pole double-throw electrically-operated industrial type contactors. These circuits are returned automatically to the a-c power supply when a-c voltage returns to normal. Small motors, less than 1-horsepower single-phase and 3-phase, are connected to the 208-volt 3-phase power supply.

125-Volt D-C Battery and Control Service

The 125-volt d-c control power system is supplied with power from a 60-cell 640-ampere-hour (8-hour rate) chloride accumulator type storage battery. Two motor-generator battery charging sets are installed; each generator is a diverter pole type with 25-kw capacity, two wire, whose maximum ceiling voltage is 140 direct volts.

The 125-volt d-c switchgear is metal enclosed with sectionalized busses for the control circuits so that all control power is not lost if one bus fails. The battery and charging-set bus connections are such that either battery-charging motor-generator set can be used to trickle charge or gas the battery, while the other set is connected to the control bus.

All 125-volt d-c circuits are protected with thermal circuit breakers or fuses of proper rating. Refer to Figure 4.

Circuit and Equipment Protective Relays

A modern steam plant requires many auxiliary relays in addition to those used for circuit and equipment protection. Each of the three main 110-kv underground cable circuits is protected by three high-speed directional overcurrent relays, one high-speed directional overcurrent ground relay, and pilot carrier-current ground relays.

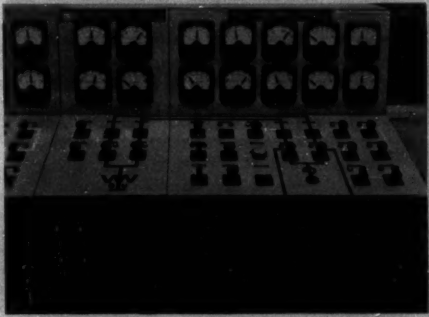

Figure 12. House generator and house transformer board

The main step-up transformer banks, 13.8/115-kv (121,750 kva) are protected with differential relays (10-cycle type) and 4- to 15-ampere overcurrent standard time, inverse relays for back-up protection. The 115/12-kv step-down 3-phase transformer bank (50,000 kva) is protected by differential relays and 4- to 15-ampere overcurrent standard-time inverse relays. The 115-kv outdoor bus is a ring bus; the 115-kv cable and transformer bank protection overlap each other.

The main generators are protected by differential relays (1-cycle type).

The house transformers are protected by differential relays (10-cycle) and 4- to 15-ampere overcurrent standard-time inverse relays for back-up protection. The house generator is protected by differential relays (1-cycle type).

The 4,160-volt ring bus is protected by two sets of bus differential relays, one set for each half of the ring bus overlapping the other; therefore only 1/2 of the ring bus will be lost if a short circuit occurs on the other half of the ring bus. All 4.16-kv motors are protected with 2- to 8-ampere overcurrent long-time inverse relays, and equipped with instantaneous overcurrent elements having a rating of 20 to 80 amperes.

If the 4,160-volt motor protection fails and a short circuit is maintained on the motor feeder because its circuit breaker fails mechanically, certain overcurrent relays (4 to 15 amperes), acting as short-circuit current relays, will close their contacts and trip the house bank, 4.16-kv circuit breakers and one generator circuit breaker supplying power to that half of the ring bus which is in trouble. The other generator circuit breaker remains closed. Therefore, only 1/2 of one ring bus is de-energized when a circuit breaker fails to open due to mechanical trouble.

During normal operation, the 4.16-kv house transformer bank and house generator operate in parallel with the high-voltage (115-kv) transmission system. In case of severe transmission system disturbances, the 4.16-kv auxiliary power bus will be separated from the main 115-kv system and operate as a separate power supply for the station auxiliaries, which then will be supplied with electric energy by the house turbines. The auxiliary bus separates from the transmission system automatically when one of three protective relays close their contacts. The first relay is a frequency relay, adjustable type, set to close its contacts when the frequency drops to 58 cycles. The second relay is a directional over-current type, which closes its contacts when a predetermined value of kilovolts-amperes flows from the 4,160-volt bus to the 13.8-kv bus. The third protective relay is an out-of-step relay, which closes its contacts after the third swing during system disturbances; the function of each relay is to separate the auxiliary bus from the transmission system during abnormal disturbances.

Fire Protection

A modern generating plant requires fire-fighting equipment especially adapted to the fire hazards at hand. In general, the plant fire protection equipment consists of four separate forms of suppression equipment; they are: fixed CO_2 gas, mechanical foam equipment, a standby hydrant and hose system using fixed fog nozzles, and portable first-aid fire equipment.

The portable first-aid equipment consists of 1-quart and 1-gallon carbon tetrachloride extinguishers, stored-pressure type using nitrogen gas at 100 pounds per square inch to project the liquid from the extinguishers, and $2^1/_2$-gallon foam extinguishers located near turbine control-oil storage tanks and around the fuel-pump area.

The lubricating-oil and control-oil tanks for the main turbines and house turbines are protected by a fixed carbon-dioxide system, consisting of piping CO_2 gas tanks, and rate-of-rise thermostats. The thermostats are mounted within the tanks near the top; when their contacts close, CO_2 gas is discharged into the oil tanks in sufficient quantity to maintain a concentration of gas of not less than 25 per cent for 30 minutes.

The main generators are hydrogen-cooled; therefore, no fire protection is required. The house generators are air-cooled and are protected by a fixed system of carbon-dioxide gas consisting of piping, nozzles, CO_2 tanks, a timing device to discharge the gas at regular intervals to maintain a 25 per cent concentration of gas within the generator casings for a time period of not less than 30 minutes. Rate-of-rise thermostats installed within the

Figure 13 (below). Boiler feed-pump motor control board

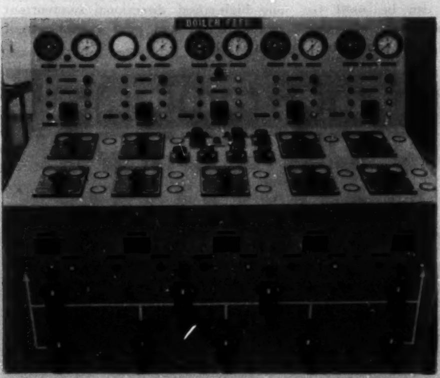

Figure 14 (right). Boiler number 6 control board

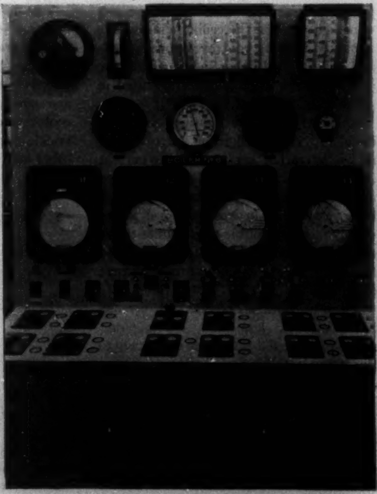

generator casing close the'r contacts when excessive temperature occurs.

A fixed mechanical foam system protects the fuel-oil tanks. The foam is projected on top of the floating roof of each tank through pipes and nozzles installed for that purpose. Additional foam nozzles will project foam around the outside of the tanks within the area surrounded by the levee. The fuel-oil pumps installed under the boilers also are protected by mechanical foam projected from hose lines which are located in that area.

A hydrant and hose system is installed both indoors and outdoors to provide general water-fog fire protection for all installations, including the 115-kv switchyard, 12-kv switchyard, main transformers, and indoor equipment. Each hydrant is equipped with 100 feet of $1^1/_2$-inch rubber-lined cotton-jacketed hose having a fixed-fog nozzle connected thereto. Water pressure at 100 pounds per square inch is maintained by two 1,000-gallon-per-minute pumps, one pump motor-driven and the other steam-turbine driven. The motor-driven pump is started by push button, from the control room.

The warehouse is protected by an automatic sprinkler system, and a flow device mounted in the main water-pipe connection to the warehouse closes an alarm contact if water flows and also starts the fire pump to increase the water pressure.

Central Control Area

The general design of this station is such that it is built around a central control area. The boilers, turbines, boiler feed pumps, fuel pumps, 110-kv feeders, and auxiliary power busses are all controlled from this area. See Figure 5. The central control area is not completely soundproofed but is open to both the boiler firing aisle and the turbine bay, as the operators become sensitive to changes of pitch or intensity of normal generating plant noise and often become aware something is amiss and requires attention before the instruments and gauges give a substantial change in indication. A large glass-enclosed telephone room is placed at the center of the control area near the vitally important switchboards, so that the operator can read the instruments and telephone the information to necessary offices. Vital control boards, such as the master panel (which controls all the boilers), main generator panels, house-generator and house-bank panels, and boiler feed-water control panels are arranged around three sides of an open square with the telephone room in the center. This is a planned arrangement to provide operators with a direct view of the important equipment, boilers, turbines, and boiler feed pumps as well as the control panels; it also provides quick access to the equipment when supervising the automatic functions of the plant. The control panels themselves are designed so that operation of each part of the equipment is logical and is oriented correctly with respect to its actual location about the plant. Instruments, gauges, control handles, and lights are deliberately arranged in unsymmetrical patterns to allow quick visual identification by the operating staff. The arrangement of the master panel is such that the boilers, circulating water pumps, and condensate pumps are controlled here.

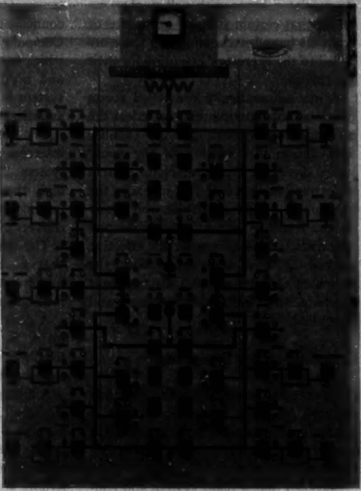

Figure 15. 4,160-volt remote control board

A generating plant using a central control scheme requires the installation of automatic control equipment such as combustion control, boiler feed-water control, fuel control, and automatic transfer equipment for circulating water pumps, condensate pumps, and many others.

Motor-driven pumps also are arranged for automatic transfer to standby pumps fed from other sources in case of loss of power, motor failure, too high or too low a pressure, too high or too low a liquid level, or excessive temperature. Such transfer operations occur automatically when the initiating contacts close, without requiring attention or supervision from the station operators.

Annunciators and Alarm Circuits

A centrally controlled plant requires an extensive alarm system, as the many automatic devices must report their operation to the central control area. Therefore a complete annunciator and alarm system is installed, giving both audible and visual indication. The annunciator boxes are large, giving good visibility from a distance of 30 to 40 feet; their electric circuits are designed so that the audible alarm (horn or bell) may be shut off while the annunciator box remains lighted; the horn or bell are then available to announce other operations. This plant has many transfer devices which also require annunciator boxes whose function is to indicate that a transfer has been initiated and has been completed swiftly and accurately. The operation of some devices requires immediate attention, while others indicate a routine operation; therefore, some annunciator boxes are equipped with colored glass to call attention to the degree of urgency of the alarm. An annunciator box with red glass indicates that immediate attention must be given to the device initiating this alarm. Annunicator boxes with white glass indicate an operation of lesser importance than those indicated by red glass, and attention may be deferred until the general emergency period is over.

Annunciator boxes with yellow glass indicate that certain standby operations or transfers have been completed; these are called to the operators' attention for their information.

A semiautomatically controlled steam plant cannot function reliably unless the personnel understand and are familiar with abnormal operation of the many varied devices. The annunciator system is designed so that each box indicates the function of a separate device which may be the result of a routine or abnormal operation. This serves as an effective method of continually reminding the personnel of the many and diverse plant functions that must be supervised and controlled.

Communication Equipment

An extensive communicating system is required for large steam plants. It is used in conjunction with the annunciator system for plant maintenance and operation.

Station P has a plant system and connections to two outside telephone systems. One installation of telephones is connected to the Pacific Gas and Electric Company's private telephone system, which has a network covering the central and northern part of California. This system is used for both routine business and dispatching requirements.

The company's private system also is interconnected with the plant interphone system. The latter system is automatic, dial type, selective ringing, selective talking, and capable of handling five conversations simultaneously.

The other outside telephone system is that of the local telephone company; four trunks have been installed to handle routine business in San Francisco.

A code call system is installed in the plant, in conjunction with the private telephone system, for calling station personnel to the nearest telephone.

A 2-wire telephone circuit has been installed within the station for maintenance purposes. Many polarized 2-wire outlets have been installed throughout the plant, from the top of the boilers to the remote areas on the first floor of the turbine room. Maintenance personnel plug their telephone hand sets into convenient outlets and thus have a common communication circuit for their use.

Conclusion

The electrical control of this plant is arranged to co-ordinate the general plant design of automatic control of major steam generating and fuel equipment and automatic transfer of many other motor-driven devices. This requires personnel who are adequately trained and resourceful, as they must correctly interpret the function of a device initiating an alarm in relation to other devices about the plant. The central control area design necessitates use of the many advantages of automatic control for equipment functions, and the use of an extensive annunciator system to acquaint the operators and keep them informed of the normal equipment functions, as well as calling attention to abnormal or faulty operation.

The electric installation was designed and installed by the Stone and Webster Engineering Company for the Pacific Gas and Electric Company.

Discussion

V. F. Estcourt (Pacific Gas and Electric Company, San Francisco, Calif.): The author is to be congratulated for having prepared a very comprehensive description of the electrical design features of the Pacific Gas and Electric Company's Station P. I have been asked to comment on this paper with particular reference to some of the automatic control features, and the centralization of a great many of these controls in one control room.

Before discussing the Station P control layout in more detail, it is essential to understand the fundamental operating objectives underlying this type of design. Due to the fact that the Pacific Gas and Electric Company's generating facilities are divided about equally between steam and hydro, seasonal variations in rainfall and water storage make it necessary to operate the steam plants over very wide load ranges, that is, from approximately 10 to 100% of their rated capacity. They also must be prepared to pick up large blocks of load in a matter of seconds in the event of any interruption to the incoming power generated from hydroelectric sources and delivered over long-distance transmission lines.

The first major experience of the Pacific Gas and Electric Company with the application of full automatic decentralized control for steam plant operation dates back to the year 1934 in connection with the 120,000-kw 1,400-pound, 750 degree Fahrenheit—750 degree Fahrenheit reheat Station A in San Francisco. As a result of several years of development and experimental work, this plant operated successfully on full automatic control under operating conditions ranging from base load to wide load range operation at rates of load change in excess of 1,500 kw per second with either natural gas or fuel oil firing. The first plant with a large amount of centralized control was installed in 1940 and subsequent installations such as Station P have followed the same general pattern.

Automatic control, as applied to steam plant operation, is intended to accomplish the following basic objectives:

1. The establishment of uniform operating patterns by incorporating these into the control devices, so that not only is maximum operating efficiency and reliability obtained, but individual operators are prevented from introducing variations from the optimum pattern which has been determined by careful tests.

2. Reduction of psychological stress upon the operator to a minimum so that his mind is free to concentrate upon the overall picture, with particular reference to trouble conditions, rather than have his attention diverted by the need for handling manually numerous operating adjustments and load changes.

3. The final objective is to combine the aforementioned advantages of automatic control into a layout which will permit the centralization of a large proportion of these controls, instruments, and alarm signals in one main control room. By means of carefully planned centralization, the advantages of full automatic control are all the more accentuated and the net result is more reliable operation, less operating errors, and a smaller operating crew, with resultant lower operating costs. In fact, with a decentralized control job, it is doubtful whether as much automatic control can be justified for the reason that more operators are required and their respective duties and responsibilities are correspondingly less. However, the problem of communication and general co-ordination of operating activities is thereby greatly aggravated, particularly during trouble conditions.

As has been pointed out by the author, the major equipment at Station P, which includes the boilers, turbines, and boiler feed pumps, is grouped around the control room; the firing aisle, control room, and turbine deck are at the same elevation, thereby providing the operators in the control room with direct vision of and close access to these major components of the plant.

This has the effect of keeping the operators inherently centralized in one location with a relatively short-radius area to patrol for the purpose of inspecting and handling such equipment. Much of the advantage of a centralized control room will be lost if consideration is not given to the orientation of major equipment with respect to this central control room, for the reason that it will require additional operators stationed around the important items of equipment due to their inaccessibility from the control room. If it is necessary to keep a number of operators in decentralized locations, then it is difficult to justify a highly centralized control layout.

The author has referred to the automatic starting of standby pumps. This has to do particularly with various items of auxiliary equipment located at plant elevations other than the control room, and which are therefore inaccessible to the control operators in the control room. Two or three shift operators are all that are required to patrol and inspect these minor auxiliaries which are located on the lower floor of the turbine room and boiler room and in the yard outside the main building. This would not be possible without a very reliable system for the automatic starting of standby equipment plus an adequate alarm system to warn the operators in the control room as to certain types of operating trouble. Our practice is to use two initiating sources for automatically starting any piece of standby equipment. These sources are usually undervoltage at the motor terminals plus pump discharge pressure or tank level as the case may be.

Bringing most of the controls into a central control room, plus other necessary related features, probably has added approximately 50 per cent to the total investment cost of such a control layout as compared with a completely decentralized job. This additional investment cost is more than offset by the saving in shift operating labor and greater operating reliability. Furthermore, as a result of our operating experience at the Kern Steam Plant and also at Station P, it is believed that we can make an appreciable reduction in the cost of controls in our future installations by eliminating from the control room certain controls and control panels which are in effect a duplication of local controls elsewhere in the plant. We were afraid to do this at either Kern or Station P, due to lack of sufficient experience with the operation of some of these controls under severe operating conditions. Therefore, we were quite generous with respect to the amount of remote controls which were brought into the control room. However, the actual performance of the various automatic features has come up to our most optimistic expectations, and we now are satisfied that some of these remove controls located in the main control room can be eliminated without impairing operating reliability. It is therefore anticipated that the advantages that have been realized through centralized control can be accomplished in the future at a substantially lower investment cost.

There are three control operators stationed on the main operating floor, and they are headquartered in the control room. Due to the fact that the operator has a full view of the firing aisle from the control room and also, due to the visibility and close proximity of the boiler feed pumps and main turbines to the control room, these same three operators are able to take care of patrolling this major equipment. These control operators are trained to handle both the electrical and mechanical equipment. Some of them were originally electrical operators but probably about two-thirds of them were only mechanically trained.

The nucleus of the shift operating organization at Station P was transferred from other centralized control plants where these men had already received a combination electrical and mechanical training. The balance of the organization has been built around this nucleus. Our present practice, in the case of a fairly large job such as Station P, is to assign two full-time instructors for a period of months for the purpose of training the shift operating organization. One of these instructors devotes his entire time to electrical instruction and the other to mechanical instruction; and of course, the operating background of these two instructors makes them particularly qualified to handle their respective assignments, and it also is necessary that they work with each other in order to properly co-ordinate this program instruction.

W. Ridgway (General Electric Company, San Francisco, Calif.): It is immediately evident upon reading this paper that many aspects of this plant show the most modern engineering practices. I should like to elaborate on several features of particular interest.

The unit type main generator excitation system with its high inertia motor driven exciter set provides the most reliable and effective equipment available. The exciter set is designed to meet or exceed the performance characteristics of a direct-connected exciter with maintenance advantages of a separate motor-generator set operating at lower speed.

An amplidyne generator is direct-connected to the shaft of the exciter set and is controlled by a static circuit to provide regulation of the main generator armature voltage. A feature of this static circuit is a lower limit of excitation which is automatically varied proportional to the generator kilowatt loading. This permits under-excited operation of the turbine generator with a reasonable margin of excitation over the steady-state pull-out point for any given loading condition. Local system conditions indicate that this may be a particularly valuable operating tool at this station.

The metal-enclosed isolated phase bus runs and station-type air blast circuit breakers afford fully co-ordinated interconnections between the generator terminals and the house and main transformer banks. Each phase of the bus runs is enclosed in a square aluminum duct. It is dust-tight and watertight and provides complete protection from phase-to-phase faults. Each continuous length of duct is completely sealed and all circulating current paths are broken by insulating joints. Each length is provided with a hinged door for ready access to the interior for inspection.

The station-type air blast circuit breakers are completely metal enclosed and are furnished with a main and stand-by air compressor. Phase isolation is maintained throughout the equipment. Internal illumination of the disconnect switch compartments has been provided for the convenience of the operator. All current transformers are provided with terminal blocks located in a metal-enclosed compartment which is accessible without opening any live compartment. The circuit breaker mechanism is designed for 5-cycle interruption and is provided with complete interlocking for safety of the equipment and operating personnel. Use of 250 pound-per-square-inch air for circuit breaker operation permits smaller air receivers for a given volume of air and results in improved arc interruption.

The hydrogen-cooled turbine generators are rated at 15 pound-per-square-inch hydrogen pressure. Suitable gas seals have been provided for 25 pound-per-square-inch operation should the additional generator capacity available at the higher pressure be desired.

In his discussion, Mr. Whelchel has thoroughly covered the place of house turbines in modern steam plant design. Suffice to say here that in some of the newest plants the house generators and house transformer banks between the generator terminals and the auxiliary station power bus have been omitted entirely. Thus no switching is necessary at generator voltage and the main transformer bank is fed direct from the generator terminals. Power for station auxiliaries is obtained from a transformer bank connected to the high-voltage system.

This simplified construction has permitted considerable economies in steam plant initial investment and may be employed where the integrity of the high-voltage system is unquestioned. As more plants similar to Station P are completed, this integrity should be realized on the Pacific Gas and Electric system.

C. C. Whelchel (Pacific Gas and Electric Company, San Francisco, Calif.): Mr. Benson's paper includes a description of the auxiliary station power supply made up of house turbinegenerators and house transformer banks. Since house turbinegenerators have found their widest application on the West Coast, some additional comments on why they are required, may be of interest.

Primarily the function of the house turbinegenerator is to supply independent 60-cycle full-voltage power to the station auxiliary motors during system disturbances. Their need is therefore dictated by the electrical design and operation of the system.

The Pacific Gas and Electric Company, like some others on the West Coast, has large blocks of hydro-electric generating capacity located at considerable distances from the load. Initially, and to some extent now, this power was brought in over long distance high-voltage lines with an electrical system design which essentially amounted to "synchronizing at the load" with the reliability of generation tied up with its associated transmission line. This form of system design could be and perhaps was carried further in the relatively lightning-free California territory than elsewhere. Although having lower first cost, it was necessary with such a design to take other steps to protect service—one of these being "quick pick-up" main steam generating units with their house turbinegenerators located near the system electrical load center.

The greatest usefulness of house turbinegenerators occurs when the main steam units are operating at light load and due to the loss of a large block of generating capacity elsewhere, it is desired to load the steam units in the shortest possible time. During such disturbances the system voltage and frequency will have fallen to such an extent that the auxiliaries in the steam plant must be transferred to the house unit in order to continue to operate satisfactorily. By this transfer of plant auxiliaries the main unit is in a position to pick up from light load to more than 3/4 load in 30 seconds or less, regardless of low-system voltage and frequency. To the degree that house units contribute to the economical solution of the system electrical problem which has been described, then to that degree it is believed that they are justified.

We recognize that there are power systems in this country that upon the sudden loss of generation automatically reduce load to maintain system frequency at a predetermined minimum on the assumption that the least over-all disturbance occurs when load and generating capacity are approximately matched.

The success of this method of operation plus splitting up the system electrically in case of trouble depends on the characteristics of the particular system under consideration. As conditions permit, this approach to the problem is receiving attention by the Pacific Gas and Electric Company. The objective on any power system is to design the steam stations as simply as possible to meet system requirements. As integration and growth continues, the need for additional "quick pick-up" steam stations with their house turbinegenerators will probably tend to decline. The future trend of steam station design here as well as elsewhere is expected to be in the direction of simplification of equipment and plant layout and still lower station heat rates.

Matching Electrical Characteristics of McNary Generators and Transformers with Bonneville Power Administration Transmission System

B. V. HOARD
MEMBER AIEE

LEWIS WEINER
ASSOCIATE AIEE

CARRYING out the planned orderly development of the Columbia River for power, navigation, reclamation, and flood control purposes, the Federal Government has selected the McNary damsite as the next major project. The site is located on the main stem of the lower Columbia River between the present Bonneville and Grand Coulee dams and near Umatilla, Oreg. The dam will produce slack water approximately 59 miles up the river to a point approximately 32 miles above the mouth of the Snake River. The ultimate installed capacity of the power plant will consist of 14 generating units rated at 73,684 kva each at 95 per cent power factor, thereby permitting the plant to generate 1,127,000 kw at rated power factor, including an overload of 15 per cent which the generating units are being designed to handle. Present plans call for the installation of 10 to 12 of these units with the balance of the machines to await the development of other up-stream plants which will provide sufficient increased storage reservoir capacity to justify installation of the additional units.

The McNary project, being constructed on a navigable stream with important navigation as well as power features, will be under the authority of the Corps of Engineers, United States Army, and hence will be designed, constructed, and operated by that agency. The Bonneville Power Administration (BPA) has the responsibility of transmitting and marketing the power and providing payout of costs of the transmission system and those costs of the generating station chargeable to power purposes for all Federal multipurpose projects within the Columbia River Basin. Hence, the Administration will receive the power generated at McNary and will provide the transmission network necessary to deliver this power to the distant load centers. It is vitally interested in the cost features of the dam and generating plant properly chargeable to power.

The engineers of both Federal agencies recognized that the electrical characteristics which are built into the generating and transformer equipment at McNary would have a great effect upon the overall economy and the operating characteristics of the complete system, and that close co-operation between the two agencies would obtain a combination of generating plant and transmission system which would adequately serve the needs of the area and obtain the least total cost to the Federal Government. Accordingly, the agencies have worked closely together to this end. The Corps of Engineers requested the BPA to study and recommend the characteristics for the generators and transformers to be installed at McNary. This request resulted in the following:

1. The generators should have a transient reactance not greater than 32 per cent on the generator rating of 73,684 kva at 95 per cent power factor.

2. Continuous damper windings should be provided that will give a ratio of X_q''/X_d'' not greater than 1.1, as determined by tests at air-gap excitation corresponding to rated current, power factor, and voltage with X_q'' determined from X_2.

3. The exciter response should be not less than 1.5.

4. The transformers should have a reactance of not more than 8 per cent on the bank rating of 169,500 kva with two generators connected to a bank.

Following these recommendations, cost figures were compiled by the Corps of Engineers which indicated that the transient reactance for minimum-cost machines for the McNary installation would be 44 per cent on a base of 73,684 kva. With an additional installed cost of $1,550,000 for 14 machines, it would be possible to obtain machines having the recommended transient reactances of 32 per cent. Similarly, reactances for minimum cost transformers, each bank of which is designed to carry the output of two generators, would be 13.5 per cent on a base of 169,500 kva, but this value could be reduced to as low as 8 per cent with an additional cost of $590,000 for seven such banks of transformers. Other additional costs would be incurred with low-reactance units because of the greater physical size of such equipment. These costs included greater investment in the powerhouse and crane and an equivalent capitalized value due to lowered generator efficiency. The total increased cost for reduced reactances for both machines and transformers was calculated to be $3,200,000 including all these factors as compared with the cost of minimum-cost equipment. Obviously, a strong justification was needed for the expenditure of $3,200,000 for special characteristics for the McNary generators and transformers; therefore the Corps of Engineers requested the BPA to prepare this justification.

Paper 49-209, recommended by the AIEE Transmission and Distribution Committee and approved by the AIEE Technical Program Committee for presentation at the AIEE Pacific General Meeting, San Francisco, Calif., August 23-26, 1949. Manuscript submitted May 13, 1949; made available for printing June 29, 1949.

B. V. Hoard and Lewis Weiner are both with the Bonneville Power Administration, Portland, Oreg. The authors wish to express their appreciation to R. C. Schuknecht, L. K. Fisher, and E. C. Starr for their assistance in the preparation of this paper.

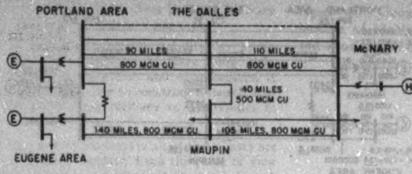

Figure 1. Transmission system for McNary generation

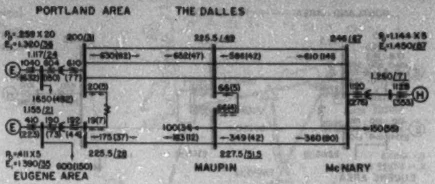

Figure 1(A). Load flow diagram 1

McNary reactances $X_d'=32$ per cent on 73.68-megavolt-ampere base; X of transformer = 8 per cent on 170-megavolt-ampere base; 1,128-megawatt output at McNary; maximum swing—104.5 degrees

System Studied

The most satisfactory measure of the benefits to be gained from lower reactance facilities at McNary is a comparison of the maximum power which can be transmitted over the power system with high- and low-reactance terminal equipment, and a determination of what additional transmission facilities must be installed with high-reactance equipment to obtain the same stability as with low-reactance equipment. These factors were obtained through use of the Administration's a-c network analyzer.

In making the study, a simple 3-machine equivalent system was devised, Figure 1, which could be expected to act reasonably close to the actual system. The major components of this simplified system are indicated geographically in Figure 6; and specific details of assumed reactances and inertia factors are as follows:

McNary Characteristics

Generators*:
- 44 per cent X_d' on 73.68-megavolt-ampere base, $WR^2=186\times10^6$ pound feet squared
- 32 per cent X_d' on 73.68-megavolt-ampere base, $WR^2=219\times10^6$ pound feet squared
- 14 units at 70 megawatts, 73.68 megavolt-ampere, 95 per cent power factor
- Maximum loading, 1,128 megawatts (15 per cent overload)

Transformers:
- 7 units at 170 megavolt-amperes each (for two generators)
- $X=8$ to 13.5 per cent on 170-megavolt-ampere base

Portland Area Characteristics

Generator:
- $X_d'=40$ per cent on 1,500-megavolt-ampere base
- $H=4$

Transformer:
- $X=30$ per cent on 1,500-megavolt-ampere base (includes equivalent system)

Eugene Area Characteristics

Generator:
- $X_d'=40$ per cent on 500-megavolt-ampere base
- $H=4$

Transformer:
- $X=30$ per cent on 500-megavolt-ampere base (includes equivalent system)

---

* WR^2 includes estimated values for generator plus water wheel.

This system consisted of the McNary generators and equivalent receiver-end machines at Portland and Eugene, with the latter two equivalent machines representing the composite effect of all generators in the two areas which experience has shown will act as a group for faults which are far removed from these areas. The transient reactances and inertia factor selected for these receiver-end machines are an approximation of the weighted average for all generators and synchronous condensers considered. The reactances of the receiving-end transformers also were based on average values of all transformers in the area with an allowance for the reactance of the distribution and transmission system between the actual generating plants and the high-voltage receiving-end busses shown in Figure 1. The transmission network consisted of essentially three 200-mile 230-kv lines from McNary to the Portland area, utilizing 800,000 circular-mil copper equivalent conductor, with a sectionalizing station at The Dalles, 110 miles from McNary; two 105-mile 230-kv lines utilizing this same conductor from McNary to Maupin, and one similar line from Maupin to the Eugene area, a distance of 140 miles. A 40-mile 230-kv line connects The Dalles and Maupin, and the equivalent impedance between the Portland and Eugene areas represents the impedance of transformer and 115-kv lines between the 230-kv busses in these areas. From a study of the normal operating power factors of the individual generators in the Portland and Eugene areas and including the effects of synchronous condensers, it was possible to approximate the power factor at which the equivalent generators used in the study should operate.

The power factor of the receiving-end loads was then adjusted so that the proper generator power factors were obtained. This process might be considered comparable to the adding of static capacitors on the system for the purpose of limiting the reactive requirements on the generating plants. Admittedly, the simplified network cannot be expected to perform exactly as the actual system, but, as will be subsequently shown, the net error should be small in view of the comparison method used to obtain results.

In previous studies it had been established that the most severe fault for the system would be near McNary on one of the lines to The Dalles in spite of the fact that the circuits between The Dalles and Portland would be more heavily loaded than those between McNary and The Dalles. Accordingly, a 3-phase fault was assumed at McNary on one of the lines to The Dalles. The faulted line was assumed to be cleared simultaneously at both ends in $3^1/_2$ cycles and reclosed at both ends in 21 cycles through the use of microwave relaying and high-speed reclosing. This clearing and reclosing time is about the ultimate which might reasonably be expected by the time the McNary generation is installed.

Procedure

The first step in the procedure was to obtain a load-flow diagram of the system using low-reactance generators and transformers with the 14 machines at McNary loaded to 1,128 megawatts, including the overload capability of 15 per cent, then to check the transient stability of the system for the fault assumed. The result of this procedure is shown in Figure 1(A) which was transiently stable for the fault assumed with a maximum swing between machines of 104.5 degrees. It will be shown later that this swing was very close to the transient stability limit since an increase in loading of the order of one per cent of the output of McNary would result in instability. In Figure 1(A) the output of McNary was 1,128 megawatts. The three McNary-The Dalles lines carried 610 megawatts and the three lines from The Dalles to Portland carried 652 megawatts. The power factor of the output of the Portland and Eugene area equivalent generators was held at 85 and 88 per cent, respectively, and the voltage at the high-side bus at McNary was held at 246 kv, which value had been established previously by other network analyzer studies.

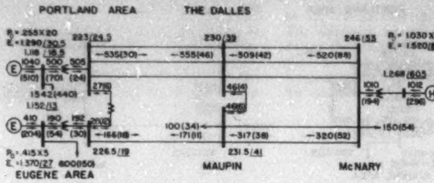
PORTLAND AREA
THE DALLES
223/24.5
230/39
246/55
R₀ = .255X20
E = 1.290/30.5
R₀ = 1.030X5
E = 1.520/82
1.118/16.5
1040
500
505
(510)
(70)
(24)
←535(30)←
←555(46)
←509(42)
←520(88)
1.268/60.5
1010
1012
(194)
(296)
27(6)
46(4)
46(6)
1542(440)
1.152/13
410
190
192
(204)
(54)
(30)
26(12)
100(34)←
→150(54)
←166(18)←
←171(11)
←317(38)
←320(52)
226.5/19
231.5/41
R₀ = .415X5
E = 1.370/27
600(150)
EUGENE AREA
MAUPIN
McNARY
E
H

Figure 2. Load flow diagram 2

McNary reactances $X_d'=44$ per cent on 73.68-megavolt-ampere base; X of transformers = 13.5 per cent on 170-megavolt-ampere base; 1,012-megawatt output at McNary; maximum swing—102.5 degrees

The second step in the procedure, starting with the identical system as used before, was to substitute high-reactance transformers and generators at McNary for the low-reactance equipment used in the preceding study, and determine how far down the loading on McNary must be dropped to gain the same degree of system stability. All local loads and receiver-end generators were held constant except that the local load at the Portland area was varied to control the output of the McNary plant. Assuming the same fault, clearing time, and reclosing as previously, it was found that the output at McNary had to be decreased from 1,128 to 1,012 megawatts if high-reactance equipment is installed at McNary and no new transmission lines are constructed. The loading conditions with high-reactance equipment and the output of McNary reduced to 1,012 megawatts are shown in Figure 2. This loading had a maximum swing of 102.5 degrees, essentially the same as for Figure 1.

Assuming identical transmission systems, the permissible loading of the generating station was decreased 116 megawatts, or 10.3 per cent, by the use of high-reactance equipment as compared to the use of low-reactance equipment. The permissible loading on the transmission system from McNary to Portland and Eugene was decreased from 978 to 862 megawatts by the use of high-reactance equipment, a decrease of 11.9 per cent.

Figure 3. Load flow diagram 3

McNary reactances $X_d'=44$ per cent on 73.68-megavolt-ampere base; X of transformers = 13.5 per cent on 170-megavolt-ampere base; 1,128-megawatt output at McNary; system unstable

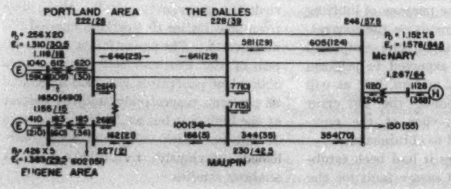
PORTLAND AREA
THE DALLES
222/28
228/39
246/57.5
R₀ = .256X20
E = 1.310/30.5
R₀ = 1.152X5
E = 1.578/84.5
McNARY
1.118/18
1040
612
620
(550)
(109)
(30)
←646(25)←
←661(29)
581(29)
605(124)
1.267/64
1120
1128
(240)
(358)
28(4)
77(0)
77(5)
1650(490)
1.156/15
410
183
185
(210)
(60)
(34)
26(6)
100(34)←
→150(55)
162(21)
166(5)
344(35)
354(70)
227/21
230/42.5
R₀ = .426X5
E = 1.383/29.5
602(151)
EUGENE AREA
MAUPIN
E
H

The next phase of the problem was to determine what additions must be made to the system so that the generating station can be loaded to the 15 per cent overload value of 1,128 megawatts with transient stability if high-reactance equipment is installed.

Accordingly, a fourth line section was assumed installed between The Dalles and Portland, the most heavily loaded portion of the system, and the McNary plant was loaded to 1,128 megawatts by increasing the local load at the Portland area. The resultant loading is given in Figure 3. For the fault, clearing time, and reclosing assumed previously, this system was insufficient as it was unstable.

Then a fourth line was assumed installed between McNary-The Dalles-Portland area, and the system again balanced to 1,128-megawatts output of McNary as shown in Figure 4, using essentially the same substation loads as in Figures 1 and 3. This loading proved to be transiently stable with a maximum swing of 101.5 degrees.

An additional study was made to demonstrate that the differences in the angle of maximum swing obtained for loadings corresponding to Figures 1, 2, and 4 do not represent any significant difference in system stability, and that these loadings are very close to the transient-stability limit. To prove this the system loading shown in Figure 4 was increased by only 20 megawatts in the Portland area to obtain the conditions shown in Figure 5. This load increase amounts to less than 2 per cent of the output of McNary, but this slight addition resulted in a change from a stable condition with an angle of maximum swing of 101.5 degrees to an unstable condition. This indicates that the system loadings in Figures 1, 2, and 4 are such that the system stability is practically identical and very close to the transient stability limit.

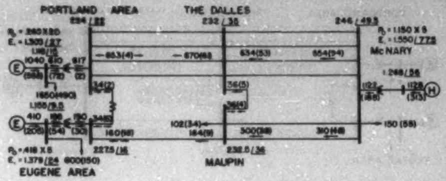
PORTLAND AREA
THE DALLES
224/22
232/35
246/49.5
R₀ = .260X20
E = 1.303/27
R₀ = 1.150X5
E = 1.550/77.5
McNARY
1.118/15
1040
610
617
(568)
(72)
(2)
←653(4)←
←670(68)
634(53)
654(94)
1.268/56
1122
1128
(188)
(313)
34(2)
36(5)
36(4)
1650(490)
1.155/9.5
410
190
190
(206)
(54)
(30)
34(6)
102(34)←
→150(55)
160(18)
164(9)
300(38)
310(48)
227.5/16
232.5/36
R₀ = .418X5
E = 1.379/24
600(150)
EUGENE AREA
MAUPIN
E
H

Figure 4. Load flow diagram 4

McNary reactances $X_d'=44$ per cent on 73.68-megavolt-ampere base; X of transformer = 13.5 per cent on 170-megavolt-ampere base; 1,128-megawatt output at McNary; maximum swing—101.5 degrees

From these load studies it was concluded that if high-reactance equipment is purchased for McNary it will be necessary to build an additional 230-kv line from McNary to The Dalles to the Portland area, a distance of 200 miles.

Summary of Network Analyzer Studies

1. With three 230-kv lines between McNary and the Portland area and low-reactance equipment at the generating station, the system is transiently stable for the full 1,128-megawatt output of McNary including the 15 per cent overload.

2. With the same transmission system as given before, but with high-reactance equipment at the generating station, the output of McNary must be reduced to 1,012 megawatts to assure transient stability, a decrease of 116 megawatts or 10.3 per cent of the total output of the generating station. The corresponding decrease in the permis-

Figure 5. Load flow diagram 5

McNary reactances $X_d'=44$ per cent on 73.68-megavolt-ampere base; X of transformer = 13.5 per cent on 170-megavolt-ampere base; 1,148-megawatt output at McNary; system unstable

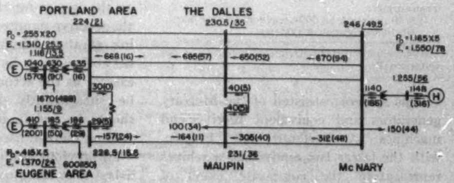
PORTLAND AREA
THE DALLES
224/21
230.5/35
246/49.5
R₀ = .255X20
E = 1.310/25.5
R₀ = 1.165X5
E = 1.550/78
1.118/13.5
1040
630
635
(570)
(90)
(16)
←668(16)←
←685(57)
←650(52)
←670(94)
1.255/56
1140
1148
(166)
(316)
30(0)
40(5)
40(5)
1670(488)
1.155/9
410
185
186
(200)
(50)
(29)
29(5)
100(34)←
→150(44)
←157(24)←
←164(11)
←306(40)
←312(48)
226.5/15.5
231/38
R₀ = .415X5
E = 1.370/24
600(150)
EUGENE AREA
MAUPIN
Mc NARY
E
H

sible loading on the lines between McNary and the coast was 11.9 per cent.

3. To assure system stability for 1,128-megawatt output of McNary using high-reactance generators and transformers, it will be necessary to construct a fourth 200-mile line from McNary to The Dalles to Portland.

4. System loadings in all of these cases are essentially identical from the point of view of transient stability and are very close to the transient-stability limits.

5. While the method used in the individual studies may have inherent error due to over-simplification and inability to get exact equivalents of the receiving-end portion of the system, the conclusions of the study are formed by obtaining incremental capability of the system through comparison of two or more studies; therefore possible inaccuracies should almost all cancel out.

Cost Analysis

A cost analysis of the system was made for two cases, the first having low-reactance equipment and one less transmission line as per Figure 1, the second having reactance corresponding to minimum-cost generators and transformers but with the additional transmission line as per Figure 4. In order to minimize possible inaccuracies, the method of obtaining incremental costs in the transmission system and in the generating station was used to determine the benefit to cost ratio. A summary of this cost study is shown in Table I. Information for costs in the generating station was supplied by the Corps of Engineers and included factors for increased powerhouse and crane cost and capitalized values of energy lost due to reduced machine efficiencies when low-reactance equipment was being considered. For the transmission system a capitalized value for the increased transmission losses with one less line was included.

Figure 6. Geographical location of McNary Dam and associated transmission system

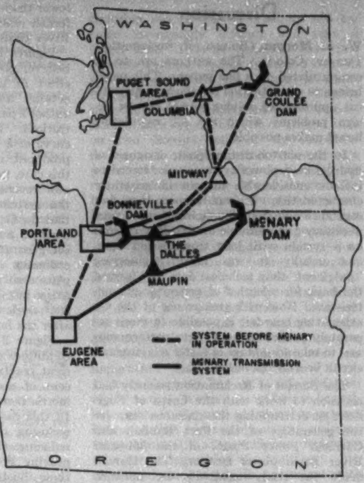

The results of this study indicated a very large saving in the transmission system and a net over-all saving to the government of over $7,000,000 through purchase of low-reactance equipment at McNary even though the value of increased equipment cost would be over $3,000,000. The benefit to cost ratio is of the order of 3.2 which would indicate that from an economic standpoint still lower machine and transformer reactances could be justified. This was considered but the physical size of the equipment became a determining factor. For example, transformers with 8 per cent reactance are the largest which could be conveniently shipped as a unit any larger size would have to be assembled in the field.

There are physical limitations in the generating unit also which resulted in the manufacturers recommending against going to any larger size. However, the high ratio of benefits to cost obtained through lowering the reactances of the McNary generators and transformers does appear to fully justify obtaining low-reactance equipment for this plant.

Table I

Line Cost Analysis		
Cost of additional 230-kv line with four circuit-breaker positions based on 1948 cost values using 800,000 circular-mil equivalent copper conductors:		
McNary-The Dalles section, 110 miles at $48,000 per mile including right-of-way and clearing	$5,280,000	
The Dalles-Portland section, 90 miles at $62,000 per mile, including right-of-way and clearing	5,580,000	
Four 230-kv circuit-breaker positions at $218,000	870,000	
Cost of additional transmission system in lieu of low-reactance powerhouse equipment		$11,730,000
Subtracting capitalized value of additional line losses by having one less line in service. Incremental loss of peak firm and peak secondary power from Figures 1 and 4 = 12,400 kw. Average value per peak kilowatt incremental loss: $5.67 per kilowatt-year. Interest, replacement, and operations and maintenance 4.8 per cent. 12,400×5.67/0.048		1,470,000
Net system savings available for reducing powerhouse equipment reactances		$10,260,000
Powerhouse Equipment Cost Analysis		
Increased cost of 14 generators because of reduced reactance and increased installation cost	$1,550,000	
Increased cost of seven transformers because of reduced reactance and increased installation cost	590,000	
Capitalized value of lower generator efficiency due to low-reactance generators. Estimated reduction in efficiency, 0.4 per cent. Value at $185 per installed kilowatt. $185×70,000×14×0.004	730,000	
Estimate of increased powerhouse and crane cost due to low-reactance equipment	300,000	
Increased cost chargeable to low-reactance equipment		3,170,000
Net Over-All Saving to the Government Through Use of Low-Reactance Units at McNary		$ 7,000,000

Conclusions

It is felt that the results of this study will be of major interest to the industry, for while most engineers agree that low-reactance equipment should be used, the question of justifying such equipment economically nearly always presents a major problem. It is recognized that each project becomes an individual problem to be studied in accordance with the peculiar conditions arising, for it is the combined system, including both transmission and generation, which must be studied. This paper presents, in our opinion, a very satisfactory method of investigating and solving this type of problem. We feel this method can be applied successfully in many cases.

Discussion

W. A. Morgan (Bureau of Reclamation, Denver, Colo.): The authors are to be congratulated on a fine paper. This paper brings to our attention the modern, analytical approach of solving power system design problems which the a-c calculating board makes possible.

In the not-too-distant past, designers of hydroelectric power systems were forced to include considerable margin in generator characteristics. It was known that low reactance and high short-circuit ratio were necessary and desirable for stability reasons on a system with long transmission lines, and usually it was more engineering "judgment" than technical data that formed the basis for selection of generator characteristics. Now with greater use of the a-c calculating board it is possible to more accurately predetermine system performance and to take advantage of faster relaying and circuit breaker operation.

The Bureau of Reclamation recently had occasion to work with the Corps of Engineers in determining the characteristics for the generators of the Fort Randall and Garrison Power Plants of the Missouri River Basin power system. The Bureau made the study using its a-c network analyzer which is located in Denver. The Bureau investigated previously proposed general methods of evaluating incremental system performance improvement and the incremental cost per kilowatt of the increased power limit. However, this general method of approach could not be justified for the Missouri River Basin power system. A study of specific savings in designs similar to that outlined by the authors, was the basis for justifying a certain amount of lower-than-normal generator and transformer reactance in the case of the Missouri River Basin power system.

Figures 1 and 2 of this discussion will, I believe, give you a graphic picture of the effect of lower-than-normal generator reactance and thereby augment both the author's paper and my discussion with illustrations. Figure 1 shows a power-swing curve of a particular fault condition which produced instability on the system. In this case, normal calculated values of generator reactance and inertia were used and the system was *unstable*. You will note that the Garrison generators tend to diverge from or pull out of step from the rest of the generators which swing together. The ordinates represent relative angular displacement in electrical degrees. The time axis is in cycles, and in this case we assumed $20^1/_4$-cycle reclosing of the circuit breakers after the fault.

Figure 2 shows the same fault-and-load conditions except that the generator transient reactance has been lowered to 85 per cent of normal calculated value and the inertia increased to 116 per cent of normal. In this case the system is *stable* with fast reclosing of the breakers. The effect of reducing the generator reactance in improving system stability is apparent from these illustrations.

There are a few questions I would like to ask the authors, because I believe the value of these meetings sometimes is brought out by discussions:

1. It is noted that 800,000 circular-mil copper equivalent conductor is to be used on the McNary-Portland 230-kv transmission lines. This is a larger than usual size and we have been interested in these large sizes. Apparently this choice of size is based upon the most economic design considering losses and initial investment. What average kilovolt-ampere loading, power rate for losses, and installed cost for the conductor were used to obtain this size conductor?

2. A system having a transmission distance of 200 miles with no intermediate loads would appear to be in the range of consideration of voltages higher than 230 kv, or to 230-kv series capacitors. Were these types of transmission line design considered as an alternate to the straight 230-kv transmission system in the economic studies?

3. It is stated that a 3-phase fault was assumed for the studies. The proportion of 3-phase faults to total faults is less for lines without overhead ground-wires than those with overhead ground-wires and, of course, the total number of faults is greater. Studies that the Bureau of Reclamation have made have indicated an appreciable difference in power limit for different kinds of faults, depending upon the clearing time. Was any consideration given to the different types of faults?

4. The reliability of some power systems will not allow consideration of fast reclosing circuit breakers. However, where fast reclosing circuit breakers are used, it would appear that the maximum benefits would be sought. It is appreciated that experience data is not completely available as to the minimum reclosing time allowable from an arc deionized air standpoint. However, studies by the Bureau indicate considerable benefit to system stability by reducing reclosing times below 20 cycles. Were reclosing times faster than 21 cycles considered in the studies by the authors?

The use of the a-c calculating board in analyzing power system problems is very valuable. It is the purpose of these questions to bring out the importance of the assumptions that are made in the studies as they are fundamentally important in getting the proper answers and factual

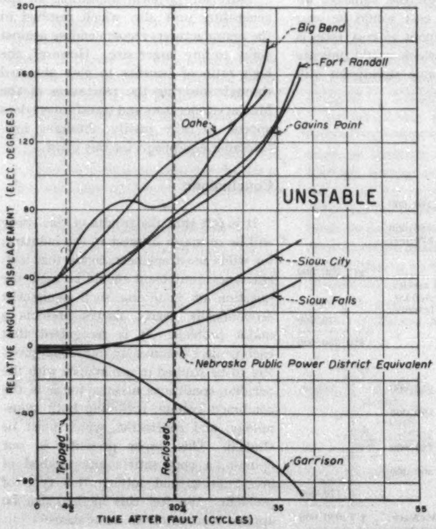

Figure 1 (left). Power system unstable with normal calculated values of generator transient reactance assumed

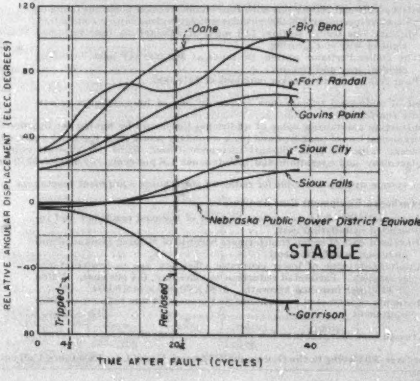

Figure 2 (right). Power system stable for the same fault and load conditions as for Figure 1 except that the generator transient reactance was reduced to 85 per cent of normal calculated value

data upon which to base engineering design decisions.

B. V. Hoard and **Lewis Weiner:** It is of interest to the authors to learn in the case of the Fort Randall and the Garrison Power Plants in the Missouri River Basin that decreasing the transient reactance to 85 per cent of normal values had the effect of making a system which was quite unstable into one which was reasonably stable. They also are pleased to learn that an approach was made to solve that problem, which in several ways was similar to that discussed in the paper.

The very important and timely questions which were raised by Mr. Morgan are taken up in the order in which he listed them.

1. A rather extensive cost comparison was made between 500,000 and 800,000 circular-mil copper equivalent conductors for the McNary-Portland 230-kv transmission lines before selection of the larger conductor was made. The total initial cost of a line utilizing the larger conductor including right-of-way was estimated to be from 15 to 20 per cent greater than for a 500,000 circular-mil copper equivalent conductor, depending to some extent on the terrain, right-of-way and clearing costs. Using this figure and evaluating losses at $15 per kilowatt year, transmission costs were identical for the two conductors at loadings around 140,000 to 150,000 kva. At loadings above this value, cost analyses favor the use of the larger conductor. It is expected that peak loads of 200,000 kw per line at annual load factors of 70 to 80 per cent will be realized. With future addition of other developments to the system, still higher peak loads on these lines are expected.

2. The possibility of utilizing a transmission line voltage of 287 kv for McNary was given some consideration and study. A cost analysis indicates that for distances of 200 miles only a very slight benefit can be gained by use of this higher voltage and then only if no intermediate loads have to be served. Since intermediate loads and eventually a large intermediate generating station at The Dalles had to be considered and since the Bonneville Power Administration system is at present a 230-kv system, it was decided to continue with the level at which we have had experience, as being more economical than the higher voltage. Series capacitors were no longer given serious consideration when it was discovered that this particular 230-kv system could be loaded close to the economic limit without unduly risking instability. On the other hand, several 230-kv series-capacitor installations are being considered elsewhere on the Bonneville Power Administration system, and one experimental installation is expected to be in operation in the latter part of 1950.

3. It is agreed that the transient-stability limit of a system will depend to some extent on the type of fault, and the power limit will be somewhat less for a 3-phase fault than for a double-line-to-ground fault which might have been used as a criterion. However, for the purposes of this study, we feel that the assumption of the more severe fault was proper for the following reasons:

(a) Five years will have elapsed between the time this study was completed and the time the first McNary generator will be energized, and eight or more years will have passed before the station will be essentially completed. Estimates so far in the future of load division in the various areas must necessarily be approximate. For this reason the final details of the transmission system cannot be decided at this time, as there undoubtedly will be some changes in the assumed transmission system.

(b) It follows that the final transmission system was not determined by this preliminary study, but only the pattern of development was selected, that is, low-reactance equipment and fewer transmission lines as compared with high-reactance equipment and more lines. Economically the results were decidedly in favor of low-reactance equipment.

(c) Aside from the simplicity of using 3-phase faults when making the study on the analyzer, it is customary in preliminary studies, where many essential factors are still indeterminate, to use a more severe criterion than might be used for the final design when with elapsed time the load pattern and magnitude have been established. As a matter of necessity, the final plan will be influenced to considerable extent by the development of other future generating stations, but, whatever their influence, we feel that the proper system pattern has been established for the McNary development, and this pattern certainly would not have been changed by assuming a somewhat less severe fault than a 3-phase fault.

From the standpoint of the final design, the McNary plant will be a major source of power in a fairly large and widespread network, and any instability would seriously affect a rather large heavily populated area. Furthermore as the Bonneville Power Administration system increases in scope, restoring service after a break-up will become increasingly difficult and take a longer time. It is not known at this time whether a simple 3-phase fault or a double-line-to-ground fault will be used as a criterion for the final design; or whether something more complicated might be considered, such as a double-line-to-ground fault on two circuits followed by successful reclosure on one circuit and reclosure on a permanent fault and then lockout of the circuit breakers on the second circuit. We have had a considerable number of simultaneous faults on double-circuit lines which makes such a criterion a distinct possibility.

4. The authors did not consider reclosing times faster than 21 cycles, although it is admitted that reclosing time has a considerable effect upon stability where a fault on one of two parallel lines is involved. On the other hand, as the number of parallel circuits is increased, as will be the case for McNary, the outage time becomes less important. Also, in view of the lack of experience along the line of the safe minimum reclosing time, it was deemed best to be realistic in the study until additional experience indicated that appreciably shorter reclosing times would still allow sufficient deionizing time for extinguishing the fault arc. We, of course, are heartily in agreement with most engineers that shorter reclosing times should be tried, and, if proved successful, should be used for system planning.

The authors believe that the system developed for the transmission of the power from McNary meets two very important criteria in that normal loading conditions are near the economic limit, and the system is essentially stable for all but multicircuit faults. While the paper presents a method of evaluating the benefits of lowered generator and transformer reactances, the authors would like to emphasize that each particular situation must be investigated in line with the conditions peculiar to it. For example, in a recent investigation of the future transmission system of another large generating station, it was shown that due to the relatively short transmission distance to the load, plus necessary strong ties to other existing generating stations, the additional stability resulting from low-reactance equipment could not be utilized from a practical standpoint and therefore reactances corresponding to minimum-cost equipment were recommended.

A Proposal for Broad-Band Coupling of Power-Line Carrier Equipment

R. H. MILLER
ASSOCIATE AIEE

Synopsis: This paper proposes the development of broad-band multichannel power-line carrier systems. The particular problem of a band stopping filter, for use in power lines, to make such a system practicable, is discussed, and a possible filter structure for this application is proposed.

THE APPLICATION of carrier equipment to power lines has led to the development of methods of line treatment in order that the effects of station busses, tap lines, and other discontinuities that may exist in the power system will have a minimum effect on the operation of carrier-current equipment that may be applied to such power lines. Early installations of power-line carrier equipment made use of bus coupling, which required a minimum of equipment but resulted in carrier channels which were greatly affected by switching setups on the power system. The ideal circuit for application of line carrier equipment is a single isolated, untapped line. In such a case, the attenuation of a line is relatively uniform and increases almost linearly with frequency. Tap lines or untrapped extensions introduce reflections, which at odd quarter wave lengths appear as low impedance points with correspondingly high attenuation.

Line Traps Used for Blocking Carrier

In order to minimize the effects of busses and tap lines, resonant traps have been developed which are placed in the lines on which carrier is to be applied, between the points of coupling and station busses and in tap lines at the points where they connect to the through line.

The resonant traps in common use on power-line carrier systems consist of air-core inductance coils with conductor sufficiently large to carry line current and tuned with capacitors to parallel resonance at the frequency of operation of the carrier equipment. In the case of 2-frequency duplex carrier systems, the traps are double tuned to give two points of high impedance corresponding to the two frequencies at which the carrier terminals are adjusted to operate. Figure 1 shows schematic diagrams of typical single- and double-frequency line traps.

Line traps of the types presently available are sharply tuned devices and present high impedance to the carrier signals at the points of resonance, but fall off rapidly on either side of the resonant point so that the attenuation to the side bands is much reduced. Figure 2 shows typical resonance curves taken from field tests of both single- and double-frequency traps. It can be seen from these curves that any errors in line-trap tuning reduces the effectiveness of the trap in attenuating the carrier signals in the direction that suppression is desired, and reduces the isolation of the carrier channel from effects of reflections of tap lines, low impedance busses, and so forth.

Blocking Filters

The development of broad-band stopping and broad-band coupling equipment for power-line carrier systems would make possible increased utility of power lines for carrier purposes, making feasible the simultaneous operation of several duplex voice channels, along with relaying and supervisory signals, on one line. Present coupling methods become complicated with a large number of tunable elements which require precise field adjustment when more than one or two carrier frequencies are applied to a line. With more than two frequencies in use, additional line traps are necessary, in series with the line, making a cumbersome and expensive installation.

In proposing broad-band coupling for power-line carrier systems, it is realized that the cost of a band stopping filter, which would block a relatively wide band of frequencies, would be somewhat greater than the present resonant-type traps however, with the possibility of using several simultaneous carrier channels with only one set of blocking filters at each end of the line to which the carrier is applied, an over-all economy seems probable.

In order to investigate the feasibility of designing filters which would block a relatively broad band of carrier frequencies, several filter structures have been studied.

The simplest filter which would have the properties desired is a conventional constant K type of low pass filter,[1] shown in Figure 3. The formulas for element values for a filter of this type are

$$L=\frac{R}{\pi f_c} \qquad (1)$$

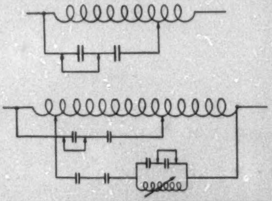

Figure 1. Schematic diagrams of typical power-line carrier line traps

Single-frequency trap above, 2-frequency trap below

Paper 49-210, recommended by the AIEE Carrier Current Committee and approved by the AIEE Technical Program Committee for presentation at the AIEE Pacific General Meeting, San Francisco, Calif., August 23–26, 1949. Manuscript submitted May 24, 1949; made available for printing June 29, 1949.

R. H. MILLER is with the Pacific Gas and Electric Company, San Francisco, Calif.

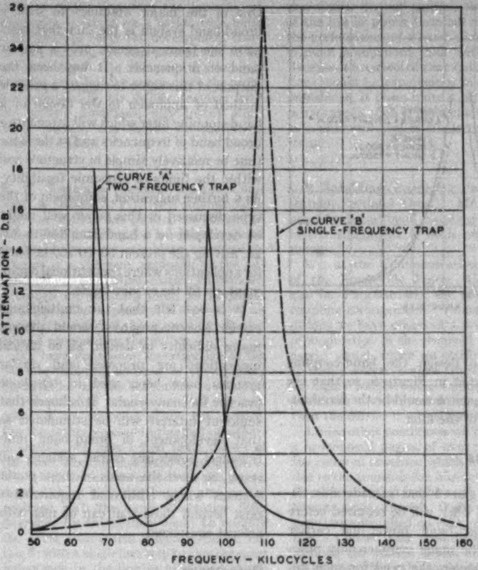

Figure 2. Attenuation characteristics of single and double-frequency carrier line traps

$$C = \frac{1}{\pi f_c R} \tag{2}$$

This type of filter requires components, both series inductance and shunt capacitors, of such magnitudes as to be impractical.

Of the other filter structures, the constant-*K* band elimination filter, Figure 4, seems to present possibilities for practical development. The formulas for element values for this type filter are

$$L_1 = \frac{(f_1 - f_2)R}{\pi f_1 f_2} \tag{3}$$

$$C_1 = \frac{1}{4\pi(f_2 - f_1)R} \tag{4}$$

$$L_2 = \frac{R}{4\pi(f_2 - f_1)} \tag{5}$$

$$C_2 = \frac{f_2 - f_1}{\pi f_1 f_2 R} \tag{6}$$

This type of filter gives an attenuation characteristic as shown in Figure 5, and can be designed to attenuate relatively broad bands with values of C_2 available in present sizes of coupling capacitors.

A practical filter of the band elimination type, used for blocking power-line carrier signals, would take the form shown in Figure 6.

A blocking filter of this type to cut off frequencies from 100 to 150 kc for a 600-ohm line has been calculated from equations 3, 4, 5, and 6 to require the following components: $L_1 = 0.637$ millihenry, $C_1 = 0.00267$ microfarad, $L_2 = 0.956$ millihenry, and $C_2 = 0.00177$ microfarad.

The calculated value of C_2 is higher than that available for 230-kv capacitors commercially available; however, the shunt arm of the filter can be designed for a higher impedance than that of the transmission line with the sacrifice of some attenuation, particularly at the mid-frequency of the rejection band, but without materially altering the properties of the filter otherwise. In this manner the capacitance required in the shunt arm can be reduced. In the practical case, if the term *R* in equations 5 and 6 is doubled, L_2 will be doubled and C_2 halved, which brings the value of C_2 into the range of commercially available components. Doubling the value of L_2 should not present any particular problem in mechanical or electrical design as the power-line current is not carried by this element.

An experimental filter of the type shown in Figure 6 was built to determine its effective attenuation band. This filter was built using the constants given above, for cutoff frequencies of 100 and 150 kc. Facilities were not available to construct such a filter with the current and voltage ratings that would be necessary for power-line carrier work; however, a filter using the same constants should be identical when built for the current and voltage ratings that would be required for power-line carrier applications, with the possible exception that the *Q* of the inductors might be somewhat different than those used in the experimental filter. However, the *Q* of air-core coils used in such power-line filters probably would be of the same order of magnitude as those used in the experimental filter. Figure 7 gives curves showing the rejection band of the experimental band elimination filter, both for 600-ohm shunt impedance, curve *A*, and for 2.5 × 600-ohm shunt impedance, curve *B*. These curves indicate a rejection band approximately 30 kc wide, with attenuation of 15 decibels or greater. This band is of sufficient width for three simultaneous carrier telephone channels, with almost complete blocking in the unwanted direction.

Curves *B* of Figure 7 shows the effect of increasing the shunt-arm impedance in order to reduce the size of shunt capacitors. The effect of such an increase of shunt-arm impedance is primarily a re-

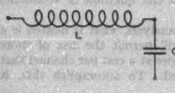

Figure 3 (left). Elementary low-pass filter

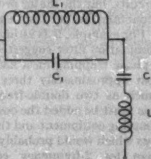

Figure 4 (right). Elementary band-elimination filter

Figure 5. Attenuation characteristics of band-elimination filter (ideal)

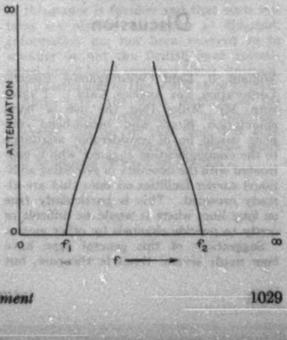

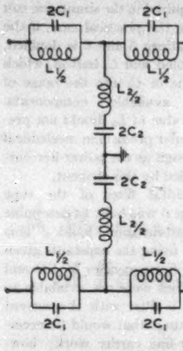

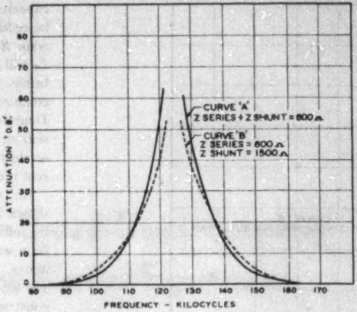

Figure 6 (above). Schematic diagram of practical band-elimination filter

Figure 7 (right). Attenuation characteristics of experimental band-elimination filter

duction of peak attenuation at mid-band, with a slight increase of the attenuation band for values below 20 decibels.

Multichannel Carrier Systems

The development of a broad-band elimination filter would make feasible the use of power lines for multichannel carrier telephony by methods well established in the telephone industry. Group modulation of several low-frequency carrier channels similar to a standard "C" carrier system[2] could be used to translate frequencies upward to the power-line carrier frequency band, and these channels could be coupled by means of a band-coupling filter to the power line. Similarly, the received signals, by means of a group demodulator, would be translated downward in frequency and separated by receiving-band filters into their respective channels. A block diagram of such a proposed multichannel power-line carrier system is given in Figure 8. It would be necessary to design the band-coupling filter, indicated in Figure 8, so that the coupling capacitor would be the terminating element of the filter.

Conclusions

It is recognized that considerable developmental work will be required before such a broad-band power-line carrier system can be made commercially practicable; however, the need for such development exists due to increasing requirements for communication in the operation of power systems, and the impracticability of coupling more than one or two channels of carrier to power lines by means of conventional equipment. One of the major obstacles to such a broad-band system is the fact that resonant line traps attenuate only a narrow band of frequencies. It has been the purpose of this paper to suggest a possible method of approach to the design of a band stopping filter which will attenuate a broad band of frequencies and at the same time be relatively simple in structure and within the limits of economic feasibility. As a further suggestion, equipment of the type discussed in this paper well might be developed for a band from 150 to 300 kc, leaving the present 50- to 150-kc band for applications where conventional equipment can fill the requirements.

It is not felt that the multichannel carrier system proposed would present major difficulty in design, as no radical innovations are proposed and similar systems have been used in telephone practice for many years. It is hoped that sufficient interest will be stimulated so that development of broad-band multichannel power-line carrier systems will result, to meet the needs of those power systems where additional requirements exist beyond those that can be met with present equipment.

References

1. ELECTRICAL ENGINEERS HANDBOOK (book), **Harold Pender, Knox McIlwain.** Third edition, John Wiley and Sons, New York, N. Y., pages 7-46—7-52.

2. ELECTRICAL COMMUNICATION (book), **A. L. Albert.** Second edition, John Wiley and Sons, New York, N. Y., page 449.

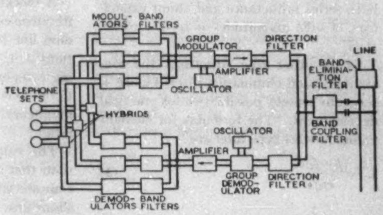

Figure 8. Block diagram of proposed multichannel power-line carrier telephone terminal

---

Discussion

William U. Dent (Westinghouse Electric Corporation, Los Angeles, Calif.): I agree with Mr. Miller that the use of band elimination filters and broad-band coupling would be of considerable assistance to the communication engineer who is confronted with the necessity of providing additional carrier facilities on lines that are already crowded. This is particularly true on long lines where it would be difficult or costly to provide channels by other means.

Suggestions of this general type have been made several times in the past, but each time it has been found that the need for this type of equipment was not sufficient to justify its cost. Today the situation may be different, particularly in some parts of the country, because of the crowding in the carrier spectrum and the need for additional circuits, but the major problem is still one of economics, rather than engineering.

For example, it is estimated that the band elimination filter suggested in this paper for 2-phase trapping on a 230-kv circuit would cost approximately three to four times as much as two double-frequency traps. To this must be added the cost of the band-pass coupling equipment and the coupling capacitors which would probably be slightly higher than for 2-frequency equipment. These figures do not include the necessary development costs which are difficult to estimate at this time.

From this it can be seen that band elimination filters of the type described and band coupling equipment can only be justified if at least four channels can be used on the circuit involved.

The suggestion for a multichannel carrier system may be the answer to this, since the filter circuits would permit such an operation, but again the question of economics arises.

In the final analysis, what is desired is a system that will permit the use of more channels of carrier at a cost per channel that can be justified. To accomplish this, it must be shown first that the quantity of equipment involved on a nation-wide basis is sufficient to cover the development costs without running the cost per channel to an excessive figure. In the past this has not been the case, but the approach to the problem suggested by Mr. Miller, together with the present conditions, may justify additional studies, and should be considered very thoroughly.

E. W. Kenefake (General Electric Company, Syracuse, N. Y.): It is commendable that the author has picked the subject of broad-band blocking for investigation, and it should serve to stimulate considerable interest in a different approach to the application of power-line carrier equipment. Although his blocking filter, as proposed, would be rather expensive, it is probably an essential element of the general application scheme proposed by the author.

We have done some investigating of the blocking problem, and also of the coupling problem, for approaches similar to this, but as yet sufficient information has not been collected to really evaluate the system. For the author's consideration and any others interested, we have noted some phases of the band blocking and band-coupling problem which were not covered in this paper. A quick check indicates that the attenuation achieved with the band elimination filter described by the author would be roughly the same attenuation which could be obtained with a single line trap having the same inductance in the line as employed in the band elimination filter. We would welcome the author's comments on this comparison. If this is true, then effectively the same characteristics could be obtained without the use of a shunt arm which involves a rather expensive coupling capacitor. Using inductances of these values in transmission lines raises some new technical problems which also will require considerable study.

A further problem involved in using a shunt arm to achieve greater attenuation at the edges of the band is the impedance discontinuity at the cutoff frequencies. This is a problem because carrier transmitters and receivers working in conjunction with varying impedances would suffer somewhat performance-wise, so that the full bandwidth might not be useful.

There has been considerable discussion of the need for 3-phase blocking of power lines in order to achieve effective trapping. This logically arises from observing the effect of opening circuit breakers and disconnect switches on the attenuation of carrier-current signals. Some better evaluation of the effectiveness of trapping all three phases or using band elimination filters in all three phases versus one or two phases would be useful information.

It is probably too early to attempt to draw any economical conclusions from this paper, but it would seem that band elimination filters would have to provide considerably better blocking of carrier signals than is possible with line traps to justify the expense of the shunt arm in the band elimination filter. In our studies, the impedance of the bus or power terminal equipment on the performance of a band elimination filter is more pronounced than with line traps. Because it is expected that quite wide variations would be experienced in the terminal impedance, it poses quite a problem for the proper application of band elimination filters as a universal tool in the over-all coupling circuit.

L. R. Spaulding (Bonneville Power Administration, Portland, Oreg.): Mr. Miller's proposal for broad-band coupling of power-line carrier equipment is both interesting and timely.

We, at the Communications Laboratory of the Bonneville Power Administration, also have encountered the need for such a coupling arrangement. Under certain conditions we have observed a pronounced loss of modulation in the received envelope of a carrier signal, which we attributed, in part, to highly selective wave traps and, in part, to highly selective line tuning units. The sidebands are subjected to greater losses than the carrier in these circuits.

Under other conditions we have observed a pronounced degree of over-modulation in the received envelope which was apparently due to the transmission of sidebands directly through a station in the path of the carrier circuit, even though sharply tuned line traps were installed on each side of the station. Under this condition the path through the station would either be much better than the path provided by the station bypass circuits, or would cause a different degree of phase shift in the carrier, or both.

We have considered the use of isolated overcoupled secondaries[1] on existing traps and line tuning units for the purpose of broadening them, and have conducted limited experiments of this kind. The amount of broadening practicable by this means does not appear to be suitable for a wide band of carrier channels but might well be adapted for improved operation of a single channel.

Reference

1. Radio Engineers' Handbook (book), F. E. Terman. McGraw-Hill Book Co., (New York, N. Y.), 1943, page 154.

R. H. Miller: Mr. Dent has given consideration to the economic aspects of the development of a broad-band carrier system, such as proposed in this paper. It is realized that the blocking filters, as proposed would require considerable development expense and would be more expensive than resonant traps. I agree with Mr. Dent that a careful study should be made to determine the economic feasibility of the proposal.

Another factor to be weighed along with the purely economic consideration is the greater utility of the carrier frequency band which should be possible with the proposed system. In many locations, the carrier spectrum is already congested and additional communications requirements will have to be met either by wire, radio, or new development in the power-line carrier art. In such cases, the economic comparison would be with alternate methods of communication rather than with conventional power-line carrier systems. It is agreed that the economy of such a system would be realized where several channels of communication would be required on one line.

Mr. Spaulding's comments are quite pertinent. It is interesting to learn that other operators have experienced limitations due to the use of highly selective wave traps. Although no experimentation with isolated, overcoupled secondaries, as mentioned by Mr. Spaulding, was carried out, this possibility of increasing the rejection band of line traps was considered, and it did not appear that sufficient advantage would result to justify a detailed investigation. Mr. Spaulding's results apparently bear out this conclusion.

Mr. Kenefake suggests that attenuation equal to that obtainable with a band elimination filter can be obtained with a single line trap using the same amount of series inductance as would be required for the band elimination filter. Our experimental results indicated considerably more attenuation with the band elimination filter, and also that a wider band of frequencies were attenuated than were feasible with a single trap. Considerably more work should be done on this problem to determine the most desirable blocking arrangement. The band elimination filter was suggested for this purpose merely because it appeared to be the simplest structure that would provide the required characteristics, but the field was by no means completely explored.

Concerning the impedance discontinuities at cutoff frequencies, mentioned by Mr. Kenefake, these effects can probably be minimized by designing the blocking and coupling filters so that they are complementary. This procedure is commonly employed in designing high- and low-pass line filters for telephone carriers.

I agree that the question of 3-phase blocking should be further investigated, and in some cases it is probably highly desirable.

Subsequent to the presentation of this paper, information was received from Mr. F. J. Bartholomew of Vancouver, B. C., that the British General Electric Company has developed a multichannel power-line carrier system, very similar to that proposed in this paper, and that such systems have been in satisfactory operation for several years, using band filter coupling, and providing up to eight duplex channels over one carrier system. Consequently, it appears that a carrier system such as was proposed in this paper is feasible and that such systems are already in service in England. Information has not been received as to whether or not the British have investigated broad-band stopping filters, however, and information on this would be of interest.

Apparently, the main purpose of the paper has been accomplished, in that considerable interest in this topic has been aroused, and it is hoped that serious study and development work will result.

Magnetic Heating of Transmission Line Clamps

V. L. CRABB
MEMBER AIEE

J. M. SHEADEL
ASSOCIATE AIEE

Synopsis: Magnetic heating of transmission line clamps is reduced by the use of nonmagnetic parts. An economical method is the use of a non-ferrous body. Of the three methods used to measure clamp power loss, the multiturn coil circuit is recommended. The results of tests made with the multiturn coil show the marked difference between the power loss of the all-ferrous clamp and that of the nonferrous-body clamp. If clamp and conductor losses are known, the temperature rise of a conductor inside a clamp can be estimated.

MAGNETIC heating of suspension and strain clamps has received increased design consideration because of higher transmission line currents. The temperature rise of conductors with sustained load currents of several hundred amperes may be excessive inside all-ferrous clamps.[1,2] At these currents, a decrease in clamp magnetic power loss to reduce temperature rise may justify, economically, the purchase of more expensive nonmagnetic clamps. Some purchasing specifications list the maximum power loss which a clamp may have at a given current.

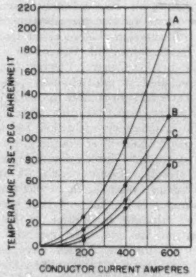

Figure 1. Typical temperature rise above ambient of 1.12-inch seat diameter suspension clamp and 477,000-circular-mil steel-reinforced aluminum cable (ACSR)

Curve A. All-ferrous suspension clamp
Curve B. Ferrous body and nonferrous keeper piece, U-bolts, and nuts
Curve C. Cable alone in air
Curve D. Nonferrous body suspension clamp

Typical temperature-rise and power-loss curves, Figures 1 and 2, show the marked difference between the all-ferrous and the nonferrous-body clamp designs. For the all-ferrous clamp a line current of several hundred amperes is required to produce a significant loss or an appreciable temperature rise.

Power Loss in Clamps

An all-ferrous clamp which surrounds a conductor carrying alternating current has hysteresis and eddy-current losses. Substitution of nonmagnetic material for certain parts of the clamp increases the reluctance to the magnetic force. The resulting decrease of flux in the magnetic loop reduces power loss and heating. Figure 3 shows the application of this method. Measurements on a clamp with a nonmagnetic body show a power loss of about 1/20 of that of the all-ferrous design. Measurements on a clamp with all parts nonmagnetic show no power loss.

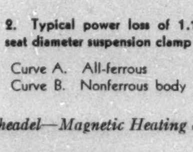

Figure 2. Typical power loss of 1.12-inch seat diameter suspension clamp

Curve A. All-ferrous
Curve B. Nonferrous body

Economic reasons have directed the use of suspension clamps with all ferrous parts or those with nonferrous body and other parts ferrous. Hence, laboratory tests have been made principally on these two types of clamps. Because of galvanic corrosion, it is desirable to have bronze-body clamps with copper conductor and aluminum-alloy-body clamps with aluminum conductor.

Methods of Power-Loss Measurement

CURRENT TRANSFORMER METHOD

High current is passed through a conductor by means of a current transformer. The power loss of a clamp is determined by subtracting the other circuit losses from the total input power. These other circuit losses, which include core loss of the current transformer, I^2R loss in the windings, and I^2R loss of the conductor, are high compared to the small losses in nonferrous clamps; therefore, this method is not accurate when small clamp losses are measured.

An alternative is to use a low power factor wattmeter with its current coil supplied from a current transformer on the conductor and its voltage coil connected across the clamp.[4] This requires a special meter since the voltage usually is less than two volts.

Paper 49-212, recommended by the AIEE Transmission and Distribution Committee and approved by the AIEE Technical Program Committee for presentation at the AIEE Pacific General Meeting, San Francisco, Calif., August 23-26, 1949. Manuscript submitted May 23, 1949; made available for printing June 30, 1949.

V. L. CRABB and J. M. SHEADEL are both with the Ohio Brass Company, Barberton, Ohio.

The authors wish to thank Mr. W. R. Cress of the Ohio Brass Company for his assistance in supervising many of the laboratory tests.

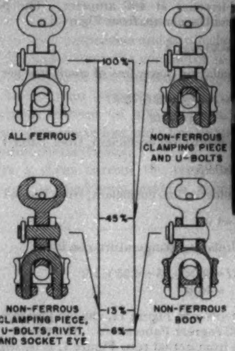
ALL FERROUS
NON-FERROUS CLAMPING PIECE AND U-BOLTS
100%
45%
NON-FERROUS CLAMPING PIECE, U-BOLTS, RIVET, AND SOCKET EYE
13%
6%
NON-FERROUS BODY

Figure 3. Power-loss reduction with nonmagnetic parts for 1.12-inch seat diameter suspension clamp

CALORIMETER METHOD

For this method a conductor is placed in an insulated water bath. With the test current flowing in the conductor, the time to raise the temperature of the known amount of water a given number of degrees is measured. To reduce error caused by heat transfer between the water bath and surrounding air, the temperature of the water is raised from below room temperature to an equal number of degrees above room temperature. From the data obtained, the watts dissipated in the water are calculated. Two tests are made, one with conductor alone and one with the clamps attached; the power loss of the clamps is the difference of the two values. This method is slow and inconvenient, and requires special equipment.

MULTITURN COIL METHOD

In place of a single conductor, a multiturn coil of insulated wire may be used. The schematic diagram of this method is shown in Figure 4. The clamp to be measured is mounted on the coil as illustrated in Figure 5. With the same ampere-turns, a multiturn coil and a single conductor have equal magnetic force. For example, a clamp placed on a coil of 200 turns carrying one ampere per turn and the same clamp mounted on a single conductor carrying 200 amperes have equal magnetic power loss.

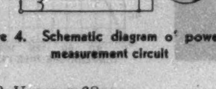

Figure 4. Schematic diagram of power-loss measurement circuit

Figure 5 (above). Power-loss measurement circuit

Figure 6 (right). Power loss of all-ferrous suspension clamps versus seat diameter and conductor current

The power loss of a clamp is determined by subtracting the loss of the coil from the loss of the coil and clamp. The coil shown in Figure 5 is wound on a square form to accommodate four clamps per test.

The testing of several clamps at one time improves accuracy when low-loss clamps are measured, since the ratio of clamp loss to coil loss is increased.

Example: To measure the power loss of a 1.12-inch seat diameter nonferrous-body suspension clamp, place four clamps on 150-turn coil. At four amperes (equivalent to 600-ampere line current):

Total input power	52	watts
Coil power loss	31	
Four clamps power loss (difference)	21	watts
One clamp power loss (21/4)	5.25	watts

The cross-sectional diameter of the coil is determined by the size of the clamp; the number of turns is determined by the power source and required ampere-turns. The coil can be designed for use with a 0–120-volt 60-cycle source, and the shape can be formed to fit the curves of strain clamps.

The power-loss data in this paper were measured with the multiturn coil circuit because of its simplicity and accuracy. The watts loss of other conductor attachments also may be determined by this method. Since normal heating of the line conductor is not present, the multiturn coil is not suitable for temperature-rise measurements.

Power-Loss Values

All power-loss tests were made with 60-cycle current. Figure 6 shows loss measurements of all-ferrous suspension clamps as a function of seat diameter and conductor current. With increasing seat diameter there is a proportional increase in the length of the clamp and the volume of metal; hence, power loss increases.

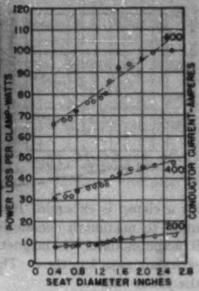

Figure 7 shows loss measurements of nonferrous-body suspension clamps. For this design the magnetic loss occurs primarily in the steel U-bolts and nuts. The flux path for the U-bolts and nuts includes the air gap between the nuts. For larger clamps, this air gap is longer, and the reluctance is greater. Hence, the power loss of nonferrous-body suspension clamps decreases with increasing seat diameter.

Figure 8 shows power-loss measurements of all-ferrous strain clamps. For a given current a strain clamp has more power loss than a suspension clamp with the same seat diameter, because the former has a larger volume of metal.

Figure 9 shows power-loss measurements of nonferrous-body strain clamps. The power loss of these clamps is small and is determined by the number and size of the U-bolts. The 0.46-inch seat diameter strain clamp has two U-bolts, and the 0.68-inch and the 0.84-inch seat diameter strain clamps have four U-bolts. This accounts for the increase in magnetic loss of the two larger sizes.

Measurements on one size of clamp may vary from the average by plus or minus 10 per cent. These variations result from the air gaps and nonmagnetic galvanizing between the ferrous parts

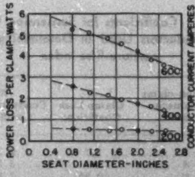

Figure 7. Power loss of nonferrous-body suspension clamps versus seat diameter and conductor current

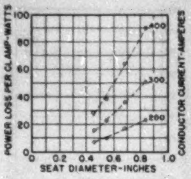

Figure 8 (left). Power loss of all-ferrous strain clamps versus seat diameter and conductor current

Figure 9 (right). Power loss of nonferrous-body strain clamps versus seat diameter and conductor current

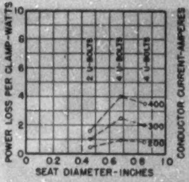

As a clamp is expanded from the minimum to maximum conductor sizes that it accommodates, its magnetic path and series air gaps lengthen. This decreases the power loss.

Temperature-Rise Measurements

Temperature-rise tests were made with both aluminum and copper conductors and both all-ferrous and nonferrous-body clamps. The test conductor formed the secondary loop of a high current transformer, and clamps were placed at least six feet apart, see Figure 10. There was little air movement over the test arrangement. Temperature rise was measured with iron–constantin thermocouples placed between outer strands of the conductor. Values were recorded for both the conductor in air and the conductor inside the clamp. With a constant value of 60-cycle current, several hours were required to reach stable temperature values. Room temperatures were between 70 and 90 degrees Fahrenheit.

As shown in Figure 1, nonmagnetic parts reduce temperature rise. The added heat dissipating area afforded by a nonmagnetic clamp more than compensates for the small clamp power loss; therefore, the temperature of conductor inside the clamp is less than that of the conductor in air. The converse generally is true for the all-ferrous clamps.

Based on test data, a relationship has been developed between clamp and conductor power loss and conductor temperature rise inside the clamp. Temperature rise of a given conductor inside a clamp can be estimated by determining a "Temperature-rise index" for the combination. The temperature-rise index for a given current is calculated from the magnetic power loss of the clamp and the I^2R loss per foot of the conductor by the following equation

$$TRI = K_1 \times P_{cl} + K_2 \times P_{co}$$

where

TRI = Temperature-rise index
K_1 = Clamp loss coefficient
P_{cl} = Magnetic power loss of clamp
K_2 = Conductor loss coefficient
P_{co} = I^2R loss per foot of conductor at 50 degrees centigrade

K_1 and K_2 are given in Table I for seven sizes of suspension clamps. These coefficients apply equally well to magnetic and nonmagnetic clamps and to copper and aluminum conductors.

When armor rods are used, the equivalent resistance of the conductor and armor rod inside the clamp must be calculated. This resistance is used in determining P_{co}.

After TRI is determined, the temperature rise may be obtained from Figure 11. Approximately 85 per cent of our test values lie within 10 per cent of this curve.

Example: To determine the temperature rise of 477,000-circular-mil steel-reinforced aluminum cable (*ACSR*) inside a 1.12-inch seat diameter suspension clamp (all-ferrous) at 400 amperes. The power loss of the clamp, from Figure 6

$P_{cl} = 36$ watts

Calculating power loss of conductor per foot

$$P_{co} = 400^2 \times 0.216/5280$$
$$= 6.55 \text{ watts}$$

The clamp loss coefficient, from Table I

$K_1 = 0.95$

Conductor loss coefficient, from Table I

$K_2 = 1.9$

Calculating temperature-rise index

$$TRI = 36 \times 0.95 + 6.55 \times 1.9$$
$$= 46.6$$

Referring to Figure 11, the temperature rise is 93 degrees Fahrenheit. The temperature rise from actual test, Figure 1, is 96 degrees Fahrenheit.

The estimates by this method for lines in service probably are conservative because of improved radiation factors after weathering and because of air movements over the clamps.

Conclusions

Several methods for measuring power loss in conductor clamps have been compared. The multiturn coil method is recommended for its simplicity and accuracy.

The reduction of magnetic loss in suspension and strain clamps is practicable. The use of a nonferrous body with all other parts iron and steel has proved to be an economical procedure.

Measured power loss values for all-ferrous clamps show that several hundred amperes are required before a significant loss is found. Measured loss values for nonferrous-body clamps show no significant loss.

Because of the magnetic loss characteristics of the clamps, a conductor inside all-ferrous suspension and strain clamps generally will be warmer than the con-

Figure 10 (below). Test arrangement for temperature rise measurements

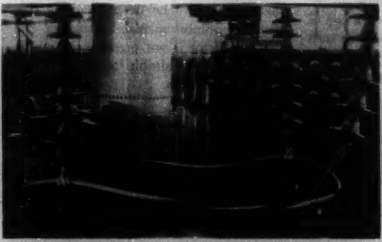

Figure 11 (right). Curve for predicting temperature rise above ambient of suspension clamps

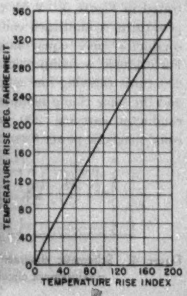

Table I. Coefficients for Suspension Clamps and Conductors Used in Determining Temperature-Rise Index

Suspension-clamp Seat Diameter Inches	K_1 Clamp Loss Coefficient	K_2 Conductor Loss Coefficient
0.7	1.1	2.35
0.8	1.1	2.35
1.0	0.95	1.9
1.12	0.95	1.9
1.4	0.7	1.6
1.8	0.55	1.5
2.25	0.45	1.45

ductor in air; a conductor inside nonferrous-body suspension and strain clamps will be cooler than the conductor in air.

A requirement that the clamp magnetic loss be less than 10 watts per clamp at a conductor current of 400 amperes will assure a low power loss and a low temperature-rise characteristic.

For a given current the temperature rise of the conductor inside a clamp is dependent on the conductor I^2R loss and the clamp magnetic loss. From these losses an empirical method of estimating conductor temperature rise values inside suspension clamps has been developed.

References

1. EFFECT OF MAGNETIC HEATING ON CABLES, W. H. Burleson. *Electrical World* (New York, N. Y.), volume 119, number 12, March 20, 1943, pages 100–102.

2. JOINTS AND HARDWARE LIMIT OVERHEAD CONDUCTOR RATINGS, Leonard M. Olmsted. *Electrical World* (New York, N. Y.), volume 127, number 1, January 4, 1947, pages 42–5.

3. NON-MAGNETIC CLAMPS INCREASE POWER SAVINGS, J. M. Sheadel. *Electrical World* (New York, N. Y.), volume 128, number 25, December 20, 1947, pages 86–90.

4. SUSPENSION CLAMP POWER LOSS TESTS, Alfio Bissiri. *Electrical World* (New York, N. Y.), volume 129, number 1, January 3, 1948, pages 58–62.

No Discussion

Lightning Stroke Damage to Aircraft

J. H. HAGENGUTH
MEMBER AIEE

Synopsis: The paper describes a series of tests made in the period 1938 to 1942 to determine in the laboratory the effects of lightning strokes on the safe operation of aircraft. Due to wartime restrictions, publication was deferred. Investigated were: the burning of holes in the metal skin of planes and other metallic parts of planes; damage to airplane fuel tanks; breaking of safety glass in windshields; the effect of current flow on ball bearings; effect of impulse sparks on the vision of pilots; and tests on nonmetallic airplane parts. The tests showed that the probability of damage from lightning strokes to airplanes of sufficient magnitude to prevent further operation and to result in loss of the airplane is extremely small and can be discounted.

THESE investigations were carried on in collaboration with the National Advisory Committee for Aeronautics under the direction of Dr. K. B. McEachron to determine whether or not lightning strokes represent a danger to airplanes. It was thought at the time that some unexplained airplane accidents may have been caused by lightning. Any conclusions drawn from the tests are those of the author.

From various lightning investigations it is known that lightning strokes essentially consist of two characteristic forms. The so-called current peaks have relatively high peak amplitudes–average: 15,000 amperes; maximum: 200,000 amperes.

There may be as many as 42 current peaks in a lightning stroke; however, the average stroke has only two current peaks. In the interval between current peaks, so-called continuous current flows through the lightning channel with amplitudes ranging from a few thousand amperes to probably less than one ampere. The duration of these continuing discharges may be as long as a second and a half, while the duration of the current peaks is only of the order of between 20 and 100 microseconds. This describes the normal cloud-to-ground stroke.

Many of the lightning discharges, however, occur between clouds or within the clouds. There is very little known about these discharges, but photographic evidence and theoretical considerations seem to indicate that cloud-to-cloud discharges probably are of the continuing-current type only. Any current peaks are expected to be of low amplitude, probably less than 10,000 amperes. The oscillogram of a typical cloud-to-ground stroke to the Empire State Building[1] in New York City is shown in Figure 1.

There were two reasons for selecting certain elements of the plane for study: to gain statistical data from planes actually struck by lightning as to the type of lightning stroke and its characteristics responsible for the damage observed; and to study the possibilities of lightning damage not before encountered.

Figure 1. Composite plot of continuing currents and current peaks of a lightning stroke to the Empire State Building, New York, N. Y.

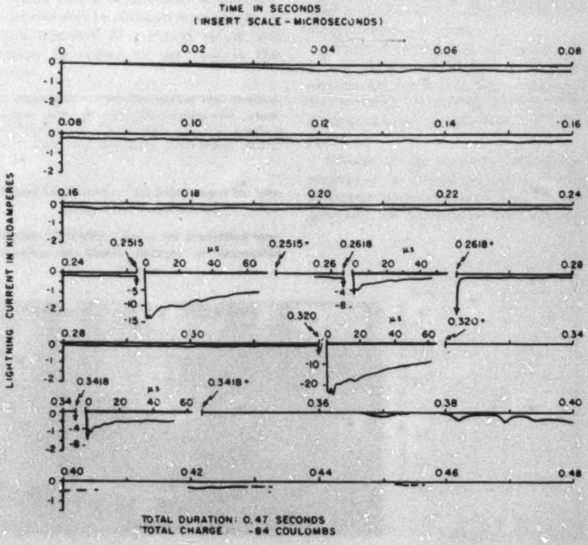

Paper 49-214, recommended by the AIEE Air Transportation, and Transmission and Distribution Committees and approved by the AIEE Technical Program Committee for presentation at the AIEE Pacific General Meeting, San Francisco, Calif., August 23–26, 1949. Manuscript submitted January 21, 1949; made available for printing June 30, 1949.

J. H. Hagenguth is with the General Electric Company, Pittsfield, Mass.

The tests described in this paper were made by the personnel of the High Voltage Engineering Laboratory of the Pittsfield Works, General Electric Company. The author wishes to express his appreciation, in particular to C. R. Craig, W. C. Lesher, C. McIntosh Jr., R. A. Johns, J. W. Flowers, R. B. Gustafson, I. B. Johnson, A. F. Rohlfs, and M. E. Noon.

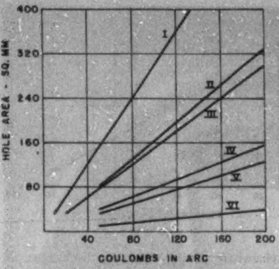

Figure 2. Relation between coulombs in the arc and the size of hole burned in metal sheets. Arc current amplitude ranges between 50 and 1,000 amperes

I. Stainless steel–10 mil
II. Galvanized iron–15 mil
III. Copper–20 mil
IV. Stainless steel–40 mil
V. Aluminum–51 mil
VI. Aluminum–100 mil

Subject to study were the following items:

1. Burning of holes in the skin and other metallic parts of airplanes or distortion of metal parts.
2. Damage to airplane fuel tanks.
3. Breaking of the safety glass in windshields.
4. Effect of current flow through ball bearings of the control system.
5. Effect of the light from a lightning stroke on the vision of a pilot.
6. Effect of exhaust gases.
7. Nonmetallic airplane parts.

Figures 3. Samples of holes burned with long-time laboratory discharges

Top: 20-mil copper sheet
Bottom: 25-mil aluminum sheet

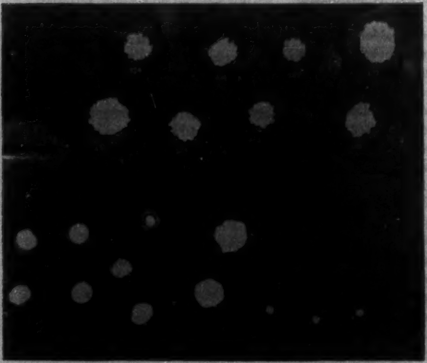

Figure 4 (right). Holes burned in aluminum rudder bow tubing by actual lightning stroke and by laboratory arcs. 25-mil wall thickness, 1-inch tubing

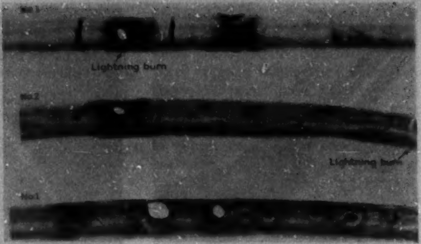

Burning of Holes in Metal Parts of Airplanes

In a previous paper[2] the effect of lightning on metal sheets was discussed for copper and steel sheets. It was shown that the principal effect of lightning on metal sheets is from the continuing type of discharge, the result being a hole burned in the metal. The work was extended to aluminum and steel sheets using the test circuit described previously. Figure 2 shows the results for all metals tested.

The type of metal appears to have very little influence. In every case the size of the hole burned is directly proportional to the coulombs or ampere-second flow of the arc current into the sheet. The size of the hole burned in a sheet of a given thickness can be expressed by two equations which give fairly accurate results

$$A = 25.3 \times C \times t^{-0.8} \text{ for } t = 0 \text{ to } 35$$

$$A = 245 \times C \times t^{-1.44} \text{ for } t = 35 \text{ to } 150$$

where

A = area of hole burned in square millimeters
C = coulombs in arc
t = thickness of sheets in mils

The appearance of the holes burned differs. Copper produces bead-like globules at the edges; also, stainless steel, with a reduced number, while aluminum rarely had any beads. For aluminum, a crater-like partially burned area usually occurred, in addition to a well-defined hole. The area of this crater is approximately 2:1 for 25-mil sheets and about 6:1 for 100-mil sheets. The difference in the appearance of the holes burned is shown in Figure 3.

The more exposed regions in a plane are the relatively sharp edges of control equipment, such as rudders and flaps. The metal at the trailing edges of these devices sometimes is formed with circular tubing or with trapezoidal sections offering a double surface opposite to the lightning stroke.

Typical lightning burns and test burns are shown in Figure 4 on 1-inch diameter aluminum tubing with 25-mil wall thickness. The size of the hole burned in the surface facing the test electrode is approximately equal to that burned in sheets of the same thickness. Up to approximately 50 coulombs, only a single hole is burned. For higher coulombs, holes also are produced on the opposite side of the tubing. The worst type of hole burned by natural lightning is shown in Figure 5. In this case the tubing was almost burned in two. It is estimated that this damage was caused by a lightning stroke conducting approximately 300

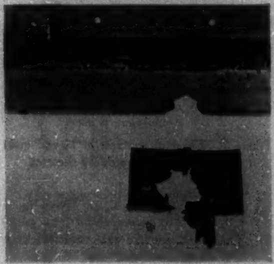

Figure 5 (right). Holes burned in a wing edge (top) and a rudder bow (bottom) by natural lightning. Estimated 300 coulombs in lightning stroke for both cases

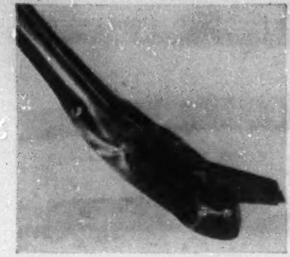

Figure 6. Rudder protector tip damaged by natural lightning stroke consisting of at least one high current peak in excess of 100,000 amperes and a continuing discharge of probably 500 coulombs

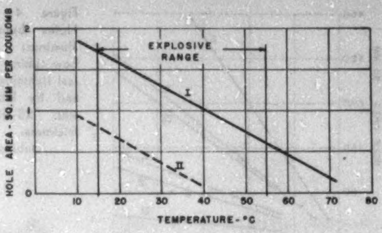

Figure 8 (right). Effect of temperature of liquid on hole size burned by d-c arc in 10-mil quart tin cans

I. Arc above liquid level
II. Arc below liquid level

coulombs. However, even with the severe damage inflicted in this case, the plane remained under control.

Other parts on planes burned by lightning strokes are pitot tubes, used for determining the velocity of the plane. It is conceivable that the accuracy of the measurements made is impaired by holes burned in strategic places of the tubes. This is, however, not considered to have a serious effect on the safety of the plane.

In the cases where holes are burned in the metal sheets, it is impossible to tell whether or not current peaks were involved in the stroke, since current peaks leave only small bead-like marks which would be obliterated by the holes burned with continuing discharges.

In the case of the protector tip, shown in Figure 6, there is evidence that the stroke causing the damage was a combination of high current peaks and continuing discharges. The fact that the metal was burned greatly at the end of the protector tip indicates a continuing discharge of approximately 500 coulombs. The fact that the static mast itself is pinched together and that its support was lifted from the rudder bow, indicates that at least one current peak in excess of 100,000 amperes was involved. Also, the front of this current peak must have been relatively steep to concentrate most of the discharge flow into the plane proper at the tip end of the rudder, where the high current density of the spark between rivets and the structural members of the rudder caused sufficient pressure to rupture the bond between the members and caused the upturn of the edge metal. However, even with such a severe stroke, the damage caused was insufficient to prevent safe operation of the plane.

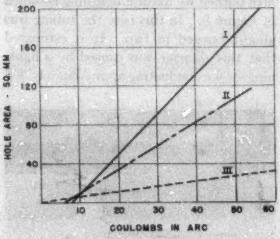

Figure 7. Effect of contents of 10-mil quart tin cans on holes burned by d-c arcs

I. Empty cans
II. Cans filled with Sovasol; arc above liquid level
III. Cans filled with Sovasol or water; arc below liquid level

The type of damage described requires the flow of considerable charges. The smallest hole that could be produced in a 25-mil aluminum sheet in the laboratory was 15 square millimeters, requiring approximately 20 coulombs. Also, in order to burn holes, the heat must be fairly concentrated. If the current in the stroke decreases to too low a value, the same number of coulombs required to burn a hole through the metal for the larger current will only scorch the sheet, because of the much longer time required for the flow of current. Heat can be dissipated more readily to the surrounding areas. It is, therefore, inconceivable that the relatively minute currents involved in corona discharges on planes traveling through highly active lightning-storm regions could cause burning of holes.

One rather interesting fact which follows from the damage on planes as described, is the fact that lightning strokes appear to have a tendency to hang onto the point contacted without materially shifting the point of contact.

For instance, in the case of the protector tip with 500 coulombs of charge, it it estimated that the duration of this stroke was at least of the order of one second. This follows from evidence obtained at the Empire State Building[1] and elsewhere[3] that continuing discharges, at least to ground, are of the order of 500 amperes and less, and there is no evidence that cloud-to-cloud discharges of the continuing kind would carry higher currents of long duration.

A plane traveling at the rate of 200 miles per hour would cover approximately 290 feet in one second. Considering the action of the wind under thunderstorm conditions, it is remarkable that the stroke terminal remained fixed to the one point of the plane.

Damage to Airplane Fuel Tanks

The burning of holes in the metal skin of gasoline tanks was investigated, particularly in view of the added danger of burning of the gas, or even explosion. Ordinary tin cans of 10-mil wall thickness, and small aluminum tanks of 51-mil wall thickness were used. Furthermore, the effect on double-wall tanks was investigated.

Sovasol and sovatone were used for

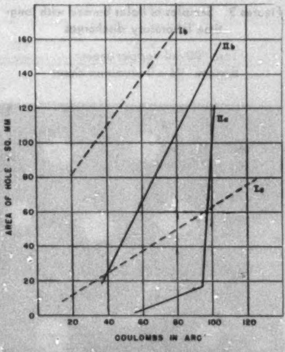

Figure 9. Aluminum alloys may show variations in hole size burned by d-c arcs. Sheet thickness: 51 mils

I. Aluminum alloy *A*
II. Aluminum alloy *B*. Curve (*a*) hole area curve (*b*) hole and surrounding melted area

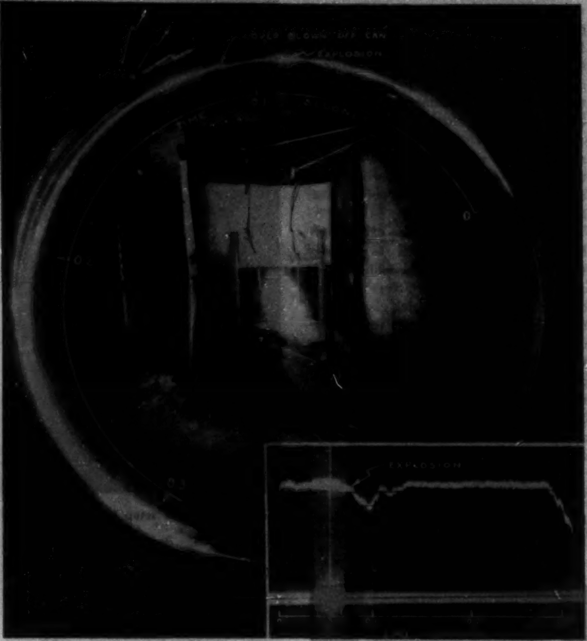

Figure 10. Photograph of arc test on gasoline tanks

Center: still picture. Circle: reproduction of rotating lens photograph showing the arc duration and the flight of the cover blown off by explosion

preliminary tests because their explosive range lies between 15 and 50 degrees centigrade, convenient for outdoor testing at Pittsfield. Since the explosive range of 100-octane gasoline is between −20 and −40 degrees centigrade, artificial cooling of the tanks with dry ice was required previous to the tests.

The results obtained differ considerably from those obtained with sheets previously tested in the following respects:

A marked effect was found on the size of the hole which could be burned in the tin cans, depending on whether the can was empty, partly filled with liquid with an arc applied to the space above the liquid, and completely filled with the arc applied below the liquid level. This is illustrated in Figure 7.

Sufficient data were available from tests with sovasol and tin cans to determine that the holes were largest at the lower end of the explosive range and gradually decreased as the upper range was approached. This is particularly pronounced for the case of the cans where the arc was held below the liquid level, as shown in Figure 8.

Under "Burning of Holes in Metal Parts of Airplanes," it is stated that the hole size is almost independent of the type of metal used. The principal difference for aluminum was that in addition to a hole, a much larger melted area was produced surrounding the hole. With the types of alloys used for the test tanks, however, the relations for the size of hole burned, as well as the melted area, were considerably changed, as shown in Figure 9. The alloy used for the gas-tank tests produced holes of about 1/10 the size previously obtained up to about 60 coulombs, and then rapidly increased to about double size at 100 coulombs. This seems to indicate that certain alloys may be available where even greater values of coulombs may be required to burn holes into the sheet.

However, when the tanks were partially filled with gasoline, at a temperature within the explosive range, holes were burned in some cases of about the same size as the melted area in the empty tanks. In other cases, no holes were produced applying arcs of 73 coulombs well above the point where holes could be produced. These examples show that under such conditions, the holes burned in metal sheets cannot be accurately evaluated as to the coulomb content of the arc causing the damage.

The explosive effects observed during these tests can be summarized as follows:

With tightly closed tin cans, violent explosions could be produced if the arc were struck above the liquid level, resulting in blowing the top off the can, or, in some cases, ripping open the seam. The small aluminum tanks were bulged considerably.

When the gas tanks were vented by even small holes, any explosion which occurred usually would vent itself by means of a violent flame of high intensity without any further visible evidence of structural damage. However, evidence indicates that the vent opening must be of sufficient size. The amount of gas available for the explosion undoubtedly would determine the size of the vent necessary to prevent an explosion.

When the arc was applied to the can or tank below the liquid level, no explosions were observed, although frequently but not always, fires were started.

Photographs were taken with a medium speed Boys camera[4] to show the duration of the arc, supplemented by magnetic oscillograms to determine the coulombs in the arc. A typical picture and oscillogram are shown in Figure 10, which shows the close correlation between arc light and current flow. This picture is of special interest because the cover of the tin can was blown off and can be seen in various positions during its flight in the top left-hand corner.

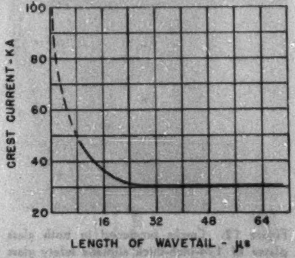

Figure 11. Effect of length of surge current wave tail on amplitude required to break ordinary 1/8-inch-thick window glass

The effectiveness of double walls to prevent arcs coming in contact with the volatile liquids in gasoline tanks was investigated, using stainless steel sheets of various thicknesses and spacings between sheets without the presence of gasoline or other liquids. These tests were made applying an arc of approximately 110 coulombs to one sheet, the other sheet being spaced at varying distances. Tests made with the second sheet grounded or isolated did not show much difference. The results of the tests indicate certain minimum spacings between sheets required to prevent hole burning in the second sheet, as shown in Table I for 110 coulombs flowing in the arc.

For extreme lightning conditions exceeding 110 coulombs, more liberal spacings would be required.

The chances of severe damage to a plane from exploding gasoline caused by a lightning stroke, however, are extremely small because:

1. The fuel tanks usually are mounted in the flat parts of the wings where lightning strokes are not expected to strike.
2. The gasoline tank must be partially empty and the vapor space above the liquid must be at a rather critically low temperature.

Glass Breaking Tests

While it is highly inconceivable that a lightning stroke would occur close to and across the cockpit windows, it was desirable to determine the effect of such strokes on glass. The probability of such an occurrence is very small because the windows are completely enclosed and generally relatively small—of the order of 12 inches high. It is known that corona streamers play on the surface of the glass due to the falling of charged rain drops on the glass. Such streamers may increase the chances of a close stroke across the cockpit window. Recently, a report was received of a windshield so badly shattered that the pilot could not see through the window. The plane, of course, landed safely.

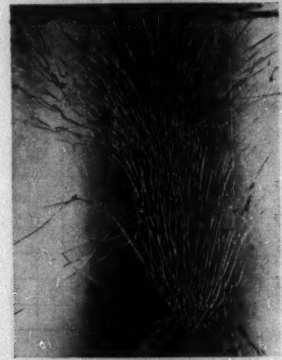

Figure 12. Cracks produced in both glass plates of 1/4-inch-thick airplane safety glass by application of a 235,000-ampere surge across the length of the window; plastic filler intact

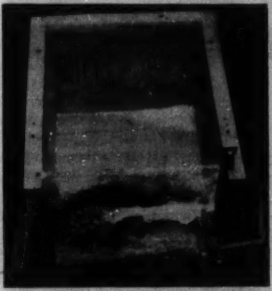

Figure 13. Test box with 1/4-inch-thick auto safety glass shattered by one 235,000-ampere surge; plastic filler intact

Note glass splinters in box and embedded in rear wood panel

Table I. Minimum Distance Between Stainless-Steel Sheets Required to Prevent Hole Burning in Second Sheet when 110-Coulomb Arc is Applied to First Sheet

Thickness of Sheets Mils	Spacing Between Sheets Inches
	Greater than:
16	$1^1/_4$
20	$^3/_4$
30	$^3/_8$
40	$^1/_4$

It quickly was found that exceedingly high currents are needed to damage safety glass. The safety glass–automobile or airplane—used in these tests consisted of two panes of 1/8-inch thick glass, joined by a plastic filler, giving it a total thickness of 1/4 inch. A number of exploratory tests, therefore, were made with ordinary glass, because with the much lower currents required, the flexibility of the surge current generator was sufficiently good to apply waves of various shapes at different amplitudes.

Some of the principal requirements were:

1. The impulse spark had to be relatively long, covering practically the whole pane to produce cracking at low current, while with a short spark of one to two inches in length, currents of about 90,000 amperes were required; with long sparks in the proper position, only 50,000 amperes were required.

Figure 14. Test setup for ball bearings

1. Bearing
2. Pulley
3. Weight Pan
4. Counterweight

2. In order to produce the longer sparks, a fuse wire (0.002-inch manganin) was used to start the spark. The highest voltage of the surge current generator was only 150 kv and sufficient only to spark over a few inches. This wire was mounted at an angle of 30 degrees with respect to the glass to obtain optimum conditions. The top electrode, therefore, was mounted at a distance of less than one inch from the glass. This made it necessary to omit the grounded frame at the top and the sides, and for practically all tests, only the bottom end of the glass plate was laid in a grounded frame.
3. For most tests, the glass plates were mounted in front of a small wooden box to prevent rapid equalization of pressures on the two sides of the glass. It was found that the use of the box as compared to an open glass plate did not result in materially lower crest currents.
4. Although not many tests are available, it appears that current wave shape, particularly the wave tail, has a significant effect on the crest current required to break the glass. This is illustrated in Figure 11. The longer the wave tail of the surge current, the lower is the crest current required to break the glass.

The same criteria probably apply to

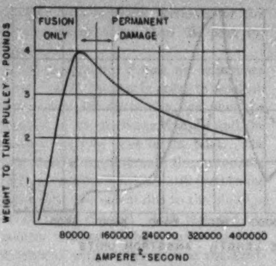

Figure 15. Relation between weight required to free ball bearing after having been subjected to high current discharges as function of amperes-squared seconds

safety glass. However, the strength of this glass with regard to exposure to high surge currents is so great that similar experiments could not be made because the available equipment was not sufficiently flexible, although the surge current generator was capable of producing a crest current of 265,000 amperes during oscillatory discharge.

For safety glass, either airplane or automobile—used because of ready availability—about 170,000 amperes were required to crack the glass on one side; 235,000 amperes to produce cracks on both sides (Figure 12) but the plastic filler remained intact. The mechanical strength of the airplane safety glass appeared superior to that of the automobile glass used.

It required several successive surges of 235,000 amperes to crack the safety glass completely, including the plastic filler. The glass and plastic filler could be broken if the surge current were made to penetrate the window to a grounded point on the side opposite from the origin of this spark.

Lightning currents of this amplitude, if they exist at all—maximum reported 220,000 amperes[5]—would be exceedingly rare. The possibility of repeated surges of this amplitude is believed nonexistent. The direct stroke through the window is inconceivable. Twelve-foot long sparks to a cockpit invariably contacted the metal rim around the window.

Factors, such as the wind stream, action of rain or hail as might be encountered in a plane in flight, were not reproduced, because the threshold current was found to be so high. One possible source of trouble is illustrated in Figure 13, which shows glass splinters embedded in the back part of the wooden box, although the glass itself was not completely ruptured. With modern planes—the automatic pilot and a co-pilot being provided—this should not contribute to destruction of a plane, unless during critical periods the co-pilot should not be available.

Effect of Current Flow Through Ball Bearings of the Control System

Rudders, ailerons, and other control surfaces are hinged to the body of the plane by means of ball bearings of rather small size. Previous tests had shown that fusion could result from d-c arcs, similar to continuous current discharges, on counterpoise gaps described elsewhere[6] (Figure 2b, reference 6). Tests on the bearings showed a complete immunity to continuing discharges, at least up to 300 coulombs, although fusing of the 1/16-inch gap (Figure 2b, reference 6) would occur with only 70 coulombs. On the other hand, high current discharges had effects on the bearings which definitely impeded their operational quality.

The test setup was not elaborate, as shown in Figure 14. The bearing was suspended, fixed at the outer race. A pulley was mounted on the shaft carrying the inner race and held in equilibrium by an empty can and a counterweight. After the test, small pellets were slowly poured into the can to determine the weight required to break the bearing loose, if the current had caused freezing of the balls to the races. The weight of the pellets is, of course, proportional to a steady force required to break the bearing free. The data obtained on 18 bearings can be presented in various forms, such as the effect of coulombs in the arc, which is unsatisfactory because low current discharges of high coulomb value did not harm the gap; or crest current in high current discharges, which results in rather meaningless variations of between 0.1 pound to 3.4 pounds to free the bearing after a 60,000-ampere discharge, depending on whether the surge was unidirectional or oscillatory. The relation which fitted all test results best is the weight required to free the bearing as function of the energy through the bearing expressed in amperes squared seconds, as shown in Figure 15. A maximum weight is required at 90,000 amperes-squared seconds. Further increase in energy increased the physical damage but did not require greater weights.

Current peaks of at least 40,000 am-

Figure 16. Microdensitometer analysis of impulse spark spectrum between brass electrodes

A. Without filter
B. With Burtweld filter

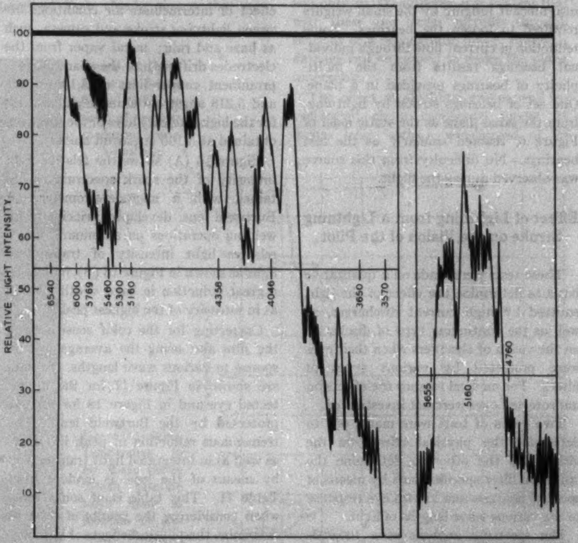

(a) ENTIRE SPARK SPECTRUM

(b) PORTION OF SPECTRUM TRANSMITTED THROUGH BURTWELD LENS

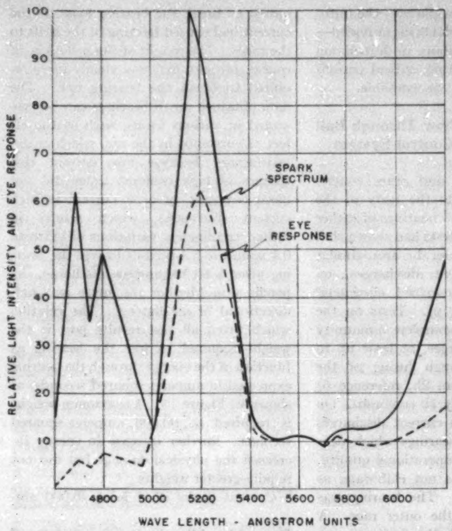

Figure 17 (left). Approximate relative light intensity produced by a 100,000 - ampere crest oscillatory surge current between electrodes at various wave lengths and eye response to spark

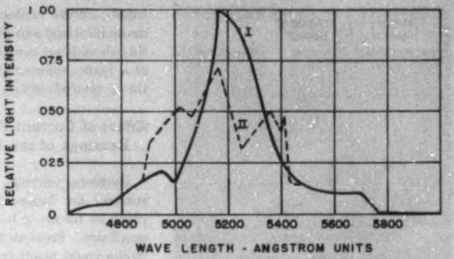

Figure 18. Approximate relative light intensity of same spark as Figure 17, but filtered through Burtweld lens

I. Calculated
II. Test

peres crest are required to prevent free spinning of the bearing. Considering that lever arms are provided, the force required to free frozen bearings would be insignificant judging by the small weights required to loosen the bearings. Some reduction in current flow through individual bearings results from the multiplicity of bearings provided in a plane. One set of bearings struck by lightning, from the same plane as the static mast of Figure 6, reacted similarly as the test bearings. No difficulty from this source was observed during the flight.

Effect of Lightning from a Lightning Stroke on the Vision of the Pilot

These tests were made on a qualitative basis to determine the effect of the light emitted by high current discharges, as well as the continuing type of discharge, on the vision of observers when their eyes were protected by various types of filters. For medical reasons the effects on unprotected eyes were not investigated.

Two types of tests were made, one to determine the physical effects on the vision and the other to determine the optimum filter specifications by means of spectral analysis and known eye response to the various wave lengths of light.

The spectrum analysis of a 100,000-ampere surge current discharge through a 3-inch long gap revealed prominent lines comparing well to Fox's[7] spectrum of an actual lightning stroke. Differences in relative intensity probably are due to: different color sensitivity of the film used; effect of intermediate air conditions between lightning stroke and camera, such as haze and rain; metal vapor from the electrodes drifting into the spark space—prominent copper lines at 5,105, 5,153, and 5,218 angstrom units might account for the high intensity lines of the spectrum obtained at 5,160 angstrom units.

Figure 16 (A) shows the relative light intensity of the spark spectrum as obtained with a microdensitometer. A Burtweld lens, developed principally for welding operations on aluminum, had a relative light intensity of transmitted light as shown in Figure 16 (B), indicating a great reduction in band width, as well as in intensity of the highest peaks.

Correcting for the color sensitivity of the film and using the average eye response to various wave lengths, the data are shown in Figure 17 for the unprotected eye and in Figure 18 for the eye protected by the Burtweld lens. The tremendous reduction in peak intensity, as well as in integrated light transmission by means of the lens, is evident from Table II. This table is of some value when considering the results of tests to determine the physical effects of blinding. In these tests the spark was observed through a filter from a distance of 5.5 and 12 feet. Results showed no fundamental difference in blinding effect for the two distances.

The blinding effect was determined by focusing the eye upon the gap. Immediately after the discharge, an attempt was made to read fine print. The image formed by the spark on the fovea of the eye (the most sensitive part of the eye, located at the center of the retina) generally prevented reading until the image had disappeared. The time required to enable the observer to read was considered a measure of exposure. With the Burtweld lens, a recovery time of between 29 and 47 seconds was required to restore the eye to normal visibility. Considering the great difference in eye response with and without the filter as shown in Table II, it is easily seen that an unprotected eye could be blinded for a considerably longer time. From actual flight experience it has been claimed that complete blindness existed for a period of ten minutes.

The effect of continuous discharges on the visibility was tested with a 1-inch gap consisting of one carbon and one aluminum electrode conducting an arc of 110 coulombs. The blind time with the Burtweld lens was approximately the same as for the 100,000-ampere discharge. This comparison strongly suggests that the in-

Table II. Comparison of Light Intensities

	Maximum	At Angstrom units	Integrated
Spark	100	5,160	100
Eye response	62	5,210	53
Transmitted through Burtweld lens	7.6	5,160	10
Eye response to spark through Burtweld lens	6.5	5,210	4

tegrated light intensity accounts for the blinding effect rather than the peak intensity.

The probability of such an occurrence is very small, because in order to result in momentary blindness, the eye must be focused on the discharge channel and the channel must be close to the pilot. The fact that a co-pilot and the automatic pilot are available reduces still further the possibility of accident due to the blinding effect of the channel. This fact and the greatly reduced visibility under normal conditions with a filter such as the Burtweld lens, made it appear impractical to recommend the use of such lenses.

Effect of Exhaust Gases on Guiding a Stroke to a Plane

Tests using actual exhaust gases were not made. Preliminary investigations on the effect of heat and possible ionization from a gasoline torch gave some interesting results. The test setup is shown in Figure 19, consisting of a line electrode and two identical grounded gasoline torches. Both torches had a 2-inch wire electrode projecting above the torch barrel. The left torch was lighted to produce a 5-inch flame. The large curvature of the impulse spark to the left electrode is evidence of the influence of the heated gases on the sparkover path. By substituting a 7-inch wire extension for the flame, a similar sparkover path was obtained. Temperature measurements above the flame, shown in Figure 20, indicate a temperature of 450 degrees centigrade at seven inches from the torch barrel. As far as the impulse spark is concerned, gas temperatures of 450 degrees centigrade and higher seem to be as effective in spark conduction as a metallic wire.

Further sparkover tests with 60-cycle test voltage indicated a reduction in sparkover voltage to approximately 70 per cent due to the influence of the flame. Most of this reduction can be explained by reduction in breakdown strength due to the temperature of the gas space above the flame on the basis of the influence of relative air density on the breakdown.

Thus, a definite effect of temperature was shown to exist in determining the breakdown path in a gap. The tests are inconclusive as far as planes are concerned because many of the factors are unknown; for instance, heat distribution of exhaust gases behind a plane. The fact that planes ordinarily do not get struck at the exhaust would indicate to some extent that the attractive effect of the exhaust gases is not as predominant as in the case of the tests described.

Nonmetallic Airplane Parts

The investigatory tests previously described have clearly shown that airplanes surrounded by metallic skins were practically immune against lightning strokes. However, wooden planes or planes built up of plastic materials were expected to be rather vulnerable because in these planes, metallic objects, such as engines and electrical and mechanical control wires, would attract the stroke, which then had to penetrate the insulating outer structural parts to reach the metal components.

As expected, the damage which can be caused by heavy current discharges through nonmetallic airplane parts is extensive, as illustrated in Figure 21 which shows the destruction of a plywood wing section due to a 20,000-ampere surge current discharge through the wing. The heavy damage caused is due to the fact that the destroyed section was not vented. Tests on a plastic-impregnated fabric flap with a 20,000-ampere current discharge produced only a few small holes. Most of the discharge in this case occurred over the outside of the flap, and sufficient ventilation was provided to prevent greater structural damage due to the gas expansion from the portion of current flowing internally. When the ventilation holes were plugged up, the fabric pulled away from its supports at the edge, but was not damaged to any greater extent than shown in Figure 22. However since the surge current amplitude was only 20,000 amperes, it is evident that with these and larger currents through sections of a nonmetallic plane, sufficient damage can be caused to make the plane inoperable.

The effect of shielding cables was investigated on a cardboard model 25 inches long, with a wingspread of 28

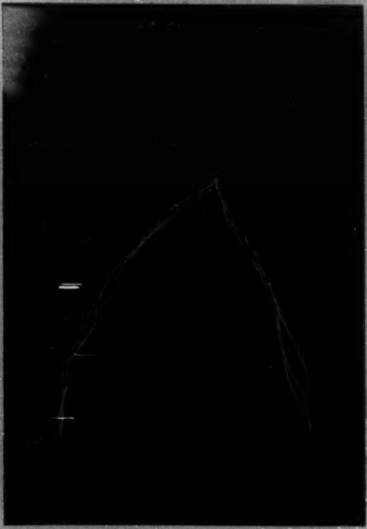

Figure 19 (left). Effect of 5-inch flame (left) on path of impulse sparkover over a 5-foot gap

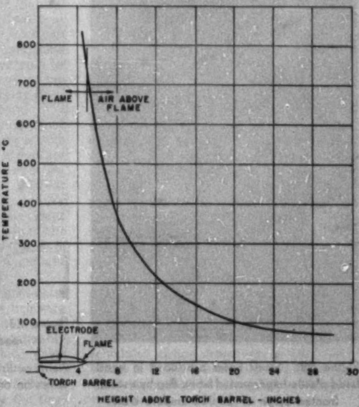

Figure 20 (right). Temperature in air space above 5-inch gasoline torch flame as function of distance. Flame in vertical position. See Figure 19

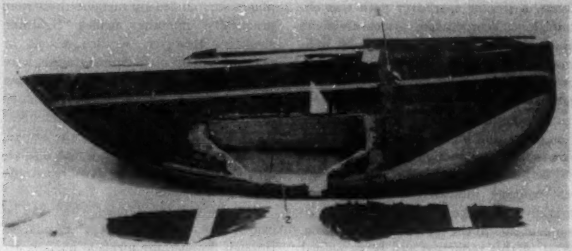

Figure 21. Shattering of plywood wing section by a 20,000-ampere surge between points 1 and 2

inches. Even with shielding wire following the contours of the model and a longitudinal wire through the center on the side facing the line electrode, puncture often occurred when the spark contacted the center of the model, as shown in Figure 23. When both sides of the plane model were wired, punctures did not occur, although the cardboard was scorched at the point of contact.

These tests show that rather elaborate protection must be provided in actual planes to prevent sparking inside the plane proper or sideflashes from the protective wiring to internal metallic parts.

Conclusions

1. This series of tests has shown that although the possibility exists that a lightning stroke may cripple an all-metal plane, the probability that all factors required occur simultaneously is so small that the lightning stroke can be disregarded as a serious potential hazard to a properly protected plane.

2. Evidence obtained from airplane parts struck in flight, when compared with laboratory tests on the same or similar parts, indicates that planes may be subjected to current peaks of strokes to ground of the order of 100,000 amperes and to continuing discharges or the order of 500 coulombs.

3. Nonmetallic planes, unless well shielded with a network of wires or other protective coating, are subject to damage from even minor lightning strokes of the order of 20,000 amperes.

4. Considering the other factors associated with lightning strokes, such as violent air drafts, rain, and icing, it would be considered safe policy to avoid areas of lightning activity.

5. Pilots should well understand the potential dangers as shown in this paper; to be prepared in case the unexpected, rare combination of several of these factors should occur.

IMPULSE
LINE ARC
GROUND
ARC

Figure 22. Small holes produced in ventilated plastic-impregnated fabric flap by a steep-fronted surge of 20,000-ampere crest

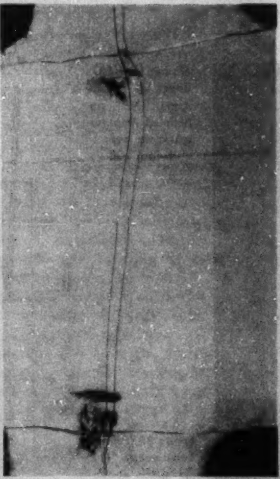

Figure 23. Holes produced in pressboard model plane by surge currents

Plane outline wired. Longitudinal and cross wires on one side only. Plane suspended in center of an 8-foot gap

References

1. Lightning to the Empire State Building, **K. B. McEachron.** *Electrical Engineering* (*AIEE Transactions*), volume 60, September 1941, pages 885–90.

2. Effect of Lightning on Thin Metal Surfaces, **K. B. McEachron, J. H. Hagenguth.** *Electrical Engineering* (*AIEE Transactions*), volume 61, August 1942, pages 559–64.

3. The Measurement of Lightning Currents in Direct Strokes, **G. D. McCann.** *AIEE Transactions*, volume 63, 1944, pages 1157–64.

4. Lightning Recording Instruments, **J. H. Hagenguth.** *General Electric Review* (Schenectady, N. Y.), volume 43, numbers 5 and 6, May and June, 1940, pages 195–201 and 248–55.

5. Lightning Investigation on Transmission Lines—VIII, **W. W. Lewis, C. M. Foust.** *Electrical Engineering* (*AIEE Transactions*), volume 64, March 1945, pages 107–15.

6. Symposium on Operation of the Boulder Dam Transmission Line—Insulation and Lightning Protection, **Bradley Cozzens.** *Electrical Engineering* (*AIEE Transactions*), volume 58, April 1939, pages 140–7.

7. Spectrum of Lightning, **Philip Fox.** *Astrophysical Journal* (Chicago, Ill.), volume 18, 1903, pages 294–5.

Discussion

L. P. Harrison (United States Weather Bureau, Washington, D. C.): Mr. Hagenguth is to be congratulated for his valuable paper summarizing results of tests made principally to determine damage to various aircraft components caused by simulated lightning strokes. These results have been most useful to the aviation industry. To a certain degree they have shown the extent of damage to be expected in cases of natural lightning strokes to aircraft, and they have indicated the nature and degree of protection necessary for aircraft to withstand the effects of such strokes without serious consequences. Conversely, by duplicating natural lightning damage to aircraft parts by employing artificial lightning strokes in the laboratory, the engineer has been enabled to calibrate the natural strokes. This has permitted him in some instances to determine approximately the peak current and the total charge in coulombs of the lightning. The author's findings permit us to give more credence than heretofore to the results of tests made with laboratory-produced lightning.

It is interesting to compare Mr. Hagenguth's data with those secured from the airlines and military services in regard to damage to aircraft caused by natural lightning. A report based on actual cases of lightning strokes to commercial and military aircraft has already been published for the Subcommittee on Lightning Hazards to Aircraft of the National Advisory Committee for Aeronautics.[1]

One of the theories which has been regarded as applying to a significant proportion of such cases is that discharges may be triggered by the intrusion of the aircraft into a region within or adjacent to certain cloud types. According to this theory, the field intensity of a region may be less than the critical breakdown potential gradient before the aircraft enters the region. However, after the aircraft makes its abrupt appearance under the given conditions of intense field, the phenomenon of electrical induction at the convex extremities (such as wing or propeller tips, antennas, and so forth) causes the local gradient to exceed the breakdown value, thus initiating a disruptive discharge.

Unpublished data in the writer's possession, together with those already published,[1] seem to indicate that triggering of disruptive discharges occurs most often when the aircraft is flying in a cloud with moderate or heavy snow or other frozen precipitation at a temperature near 32 degrees Fahrenheit, while presumably the cloud mass at lower levels consists largely of water droplets. These conditions are conducive to development of steep potential gradients.

Inasmuch as the theory of triggering is in harmony with known physical principles, and we have some pilots' reports giving factual information which apparently supports the theory, we can have a considerable degree of confidence in the reality of triggered strokes.

Now, one may wonder whether the characteristics of such strokes are invariably the same as those of natural cloud-to-cloud discharges, which Mr. Hagenguth states "probably are of the continuing-current type only." In a good proportion of the cases in which we believe triggering of a discharge by the aircraft was involved, pilots have reported the accompanying sound as "loud" (in one instance described as similar to a 155-millimeter howitzer going off in the cabin). Since loud thunder is a concomitant of lightning strokes characterized by a steep wave-front, we infer that at least some of the triggered discharges possess this characteristic, which apparently is not typical of natural cloud-to-cloud strokes. While it is possible that a triggered discharge may propagate to the ground and yield a steep-wave front return stroke, the high altitude and attendant meteorological conditions lead this reviewer to incline to the belief that development of such return strokes is not invariant in the cases considered.

In connection with the author's equations giving area of hole burned as a function of coulombs in arc and thickness of sheet, some reservations appear to be necessary to show their limitations. This is suggested because the equations are based on laboratory determinations and do not take into account heat losses under the conditions of low air density, low temperature, rapid relative air movement and often moisture or ice accretion prevalent in the case of an actual aircraft struck during flight through clouds or precipitation.

Mr. Hagenguth refers to the remarkable circumstance of a stroke terminal that remained fixed to one point on a plane even though the aircraft was traveling at the rate of 200 miles per hour. This is readily rationalized by regarding the airspace between the charge centers of the cloud as similar to that between the plates of a giant charged condenser. Under the conditions existing between extensive distributions of charges forming dissimilar charge centers, it is possible for the potential gradient to approach the critical breakdown value over a considerable horizontal extent. The intrusion of the metallic airplane effectively increases the potential gradient, causing the breakdown value to be exceeded progressively over a horizontal distance. Once a disruptive discharge occurs at the metallic surface of the airplane, the arc provides a copious supply of electrons and ions. The branching streamers that feed the main stroke channel in the cloud are distributed in space and vary their currents and paths to conform to the horizontal displacement of the channel as the aircraft moves through the field.

We consider especially noteworthy the author's finding of the marked effect of alloy-type on the relation of area of hole burned to charge in coulombs.

In regard to the tests on models of airplane fuel tanks, one may infer with confidence that double-walled tanks are in themselves much safer against explosive effects than tanks integral with the wing skin. Since the tanks can be partially empty and the temperature of their outer walls may lie in the range −20 to −40 degrees centigrade, following a dive, it is clear that integral tanks or single-walled, droppable, exposed tanks are not absolutely immune from such effects, as lightning occasionally does strike in relatively flat parts.[1]

The author states: "It is known that corona streamers play on the surface of the glass due to the falling of charged rain drops on the glass." We wish to point out that the drops need not be charged initially to produce corona, provided the intensity of the electric field is sufficiently great. Coronas are produced by fields that arise either from charges accumulated on the aircraft or from external distribution of charges, or both, as shown by Gunn, Hall, and Kinzer[2] and Edwards and Brock.[3]

The artificial lightning spectrum studied in the laboratory possessed certain prominent copper lines absent in the natural lightning spectrum, and lacked lines that may occur owing to passage of the discharge through a field containing numerous cloud or rain drops, which is often encountered by a pilot during flight. These differences between simulated and natural lightning spectra might be significant in exact work.

The author also states that the probability of a blinding effect owing to lightning is very small. Reports received from pilots indicate that temporary blinding may sometimes last about three minutes, and in two different reports pilots stated they were blinded for about eight minutes. From this it is evident that as a safety measure at least one of the crew in the cockpit should keep his eyes shielded during flights when lightning might strike.

With reference to the role of exhaust gases in the initiation or conduction of lightning strokes, it seems relevant to point out that the importance of this role is considerably lessened by the diffusion of these gases through the action of air currents induced by wings and propellers. These diffusive transports quickly tend to reduce the temperature and ionization of the gases, thus lessening the probability of breakdown or guidance of a discharge by the stream of ionized particles. However, the fact that the exhaust stack of aircraft is not ordinarily struck should not be used too strongly as an argument that the effect of the exhaust gases is not as predominant as the tests indicate (see paragraph F). It must be recalled that the direction of the potential gradient of the space surrounding the aircraft has a dominant influence on the direction taken by a disruptive discharge, and that the turbulent streak of exhaust gases may not be nearly parallel to the gradient, while other projecting members of the aircraft (such as the tail assembly) afford some protection to the exhaust stack.

With regard to tests on nonmetallic airplane parts, it would have been appropriate for the author to have referred to the more comprehensive investigations of this nature made at the High Voltage Laboratory of the National Bureau of Standards[4] under the general direction of Dr. F. B. Silsbee. One of the outstanding developments in these investigations was the demonstration of the value of protective coatings.

In closing, we may state that the author in his interesting paper has clearly demonstrated the protection against lightning provided by an all-metallic aircraft (as would be expected from the Faraday cage effect). His conclusions, however, do not appear to emphasize sufficiently the optical hazards to pilots and the frequent damage to radio equipment owing to lightning discharges.

REFERENCES

1. LIGHTNING DISCHARGES TO AIRCRAFT AND ASSOCIATED METEOROLOGICAL CONDITIONS, **L. P. Harrison.** *Technical Note Number 1001*, National Advisory Committee for Aeronautics (Washington, D.C.) May 1946.

2. THE PRECIPITATION-STATIC INTERFERENCE PROBLEM AND METHODS FOR ITS INVESTIGATION, **Ross Gunn, Wayne C. Hall, Gilbert D. Kinzer.** *Proceedings*, Institute of Radio Engineers (New York, N.Y.) volume 34, 1946, pages 156P-178P and 234-47.

3. METEOROLOGICAL ASPECTS OF PRECIPITATION STATIC, **R. C. Edwards, G. W. Brock.** *Journal of Meteorology* (Lancaster, Pa.), volume 2, 1945, pages 205-213.

4. PROTECTION OF NONMETALLIC AIRCRAFT FROM LIGHTNING, (four reports) High Voltage Laboratory, National Bureau of Standards (National Advisory Committee for Aeronautics) Washington, D.C., *AAR 3I10*, September 1943; *AAR 3J12*, October 1943; *AAR 4C20*, March 1944; *AAR 4I28*, March 1945.

A. E. Raymond (Douglas Aircraft Company, Inc., Santa Monica, Calif.): We enjoyed reading Mr. Hagenguth's excellent paper on the effects of lightning strike damage to aircraft. We agree that we do not know of any actual accidents or injuries to persons in aircraft due to the effects of lightning. However, the dangers from lightning strikes should not be minimized.

Furthermore, data from the Thunderstorm Project[1,2] Reports indicate that there were 21 lightning strikes in 1,363 thunderstorm missions which amounts to over 1.5 per cent. Another report from the Safety Bureau of the Civil Aeronautics Board[3] shows that there were over 1,800,000 scheduled airline departures in the United States in 1947. We have no way of knowing what percentage of these flights encounter thunderstorm activity enroute.

We were very interested to read the conclusions reached by Mr. Hagenguth concerning the use of ball-bearing bonding jumpers. His data and tests show that the bearing damage from lightning was negligible. Our own tests at the Douglas Aircraft Company have shown that even a properly installed jumper under the best conditions would carry no more than about one-third of the total current traversing the bearing. For both reasons we discontinued the use of jumpers several years ago.

We think there has been one notable omission from the paper with regard to lightning damage. This is the effect of lightning on radio and electronic equipments in aircraft. There have been many cases of lightning strikes interrupting the operation of such equipments due partly at least to blown tubes, fused contacts, burned out wires, and the like.

REFERENCES

1. OPERATION AND ACTIVITY OF THE THUNDERSTORM PROJECT, APRIL 1–OCTOBER 1, 1947. *Report Number 3, U. S. Weather Bureau* (Washington, D. C.), November 1947.

2. A REPORT ON THUNDERSTORM CONDITIONS AFFECTING FLIGHT OPERATIONS. *Report Number 7, U. S. Weather Bureau* (Washington, D. C.), April 1948.

3. FREQUENCY OF ENGINE FAILURES IN SCHEDULED AIR CARRIER OPERATION, **James S. Rice.** *Civil Aeronautics Board* (Washington, D. C.), June 3, 1948.

F. B. Silsbee (National Bureau of Standards, Washington, D. C.): This paper summarizes briefly the results of a very considerable effort given during the war to assist the work of the National Advisory Committee for Aeronautics Subcommittee on Lightning Hazards to Aircraft. It should be of great value both to the aeronautical industry which is directly concerned and which can make good use of the technical findings and to the traveling public which should feel much reassured by the results.

For a long time lightning has been used as a scapegoat to "explain" the cause of otherwise unexplainable accidents. The work of the National Advisory Committee for Aeronautics Subcommittee has gradually eliminated one possible explanation after another until very few remain. As stated in conclusion number 4 of the paper, other features of a thunderstorm such as violent gusts constitute much more serious hazards than does the lightning discharge itself.

Those interested in this field will find further information in the paper by L. P. Harrison[1] in which he summarizes observations on nearly 200 cases of lighting strokes to aircraft and discusses the meteorological conditions under which they occurred.

It is interesting to note the experimental data on the melting of holes in sheet material are so closely concordant with the results reported by P. L. Bellaschi[2] who performed similar tests on pointed conductors. The present results show that approximately 1.6 coulombs are required per cubic millimeter melted while Bellaschi's values ranged from 1.7 to 2.5. The slight difference doubtless results from the radically different shape of the specimens. Presumably the electrode drop is nearly independent of the current and is of the same magnitude in either case. The resultant heat developed is applied somewhat more effectively in the case of sheet material

The fact that the results on ball bearings are best co-ordinated on the basis of the energy dissipated in a fixed resistance (that is, they are a function of $\int i^2dt$) is consistent with the results of tests made in the High Voltage Laboratory of the National Bureau of Standards on the ability of various thin foils and sprayed metal deposits to carry surge currents.[3]

In spite of statements to the contrary by other workers, the author's conclusion that it is inconceivable that the small currents produced by corona discharge alone could burn holes in the aluminum skin would seem to be well founded. However, such corona currents which develop when aircraft are flying near thunderstorms even though no lightning discharge occurs, do cause a serious interference with radio communication. This problem is one for which an entirely satisfactory solution has apparently not yet been developed. Still another hazard from corona discharge arises in the case of a glider towed with the usual nylon towline. Extrapolated estimates from laboratory experiments[4] indicate that such currents might well be sufficient to burn or melt the towline even at a distance of a kilometer or so from an active thunderhead.

The destruction shown in Figure 21 is a fine "horrible example" of what might be expected if an unprotected plywood aircraft, like the British Mosquito Bomber, were struck by lightning. Moreover, the control wires of such airplanes and gliders usually are so located that they would lead current directly to the pilot with fatal results. It appears that a moderate amount of conducting material, which would not be impossibly heavy, can be properly placed on such an aircraft to give reasonable protection.[5] However, even with such protection, and in the case of the usual all-metal airplane, there still remains one remote possibility of danger. If the bulk of the lightning current should be so concentrated as to flow in the metallic structure past one side only of a person his body might function as the secondary circuit of a transformer the primary of which is formed by the current path. If the current is changing at the frequently observed rate of 10^{10} amperes per second, the electromotive force induced in a loop the size of the human heart at a distance of 1 meter would be 80 volts! Of course the duration of such a surge is very short, the chance that it would occur during the sensitive phase of the heart cycle is probably not greater than 1 to 5 and the probability with an all-metal plane that the current path would be so closely concentrated is rather small. Experiments with animals at the National Bureau of Standards under conditions simulating this situation showed no fatal effects although very marked muscular reactions were produced in anaesthetized guinea pigs by such a transformer action.

REFERENCES

1. LIGHTNING DISCHARGE TO AIRCRAFT AND ASSOCIATED METEOROLOGICAL CONDITIONS, **L. P. Harrison.** *Technical Note Number 1001*, National Advisory Committee for Aeronautics (Washington, D.C.) May 1946.

2. LIGHTNING STROKES IN FIELD AND LABORATORY, III, **P. L. Bellaschi.** *AIEE Transactions*, volume 60, 1941, pages 1248–56.

3. LIGHTNING CONDUCTOR MATERIALS, *Wartime Report Number W-60*. National Advisory Committee for Aeronautics (Washington, D. C.).

4. ELECTRICAL EFFECTS IN GLIDER TOWLINES, *Wartime Report Number W-62*. National Advisory Committee for Aeronautics (Washington, D. C.).

5. ELECTROCUTION HAZARDS FROM INDUCTIVE VOLTAGES, *Wartime Report Number W-85*. National Advisory Committee for Aeronautics (Washington, D.C.).

J. H. Hagenguth: The contributions of the discussors to the subject of the paper are gratefully acknowledged. The paper was strictly confined to a report on findings from tests made on various parts of the airplane

It was recognized that effects of corona discharges on radio reception, damage from strokes to the antenna and radio equipment, demagnetization of the magnetic compass, and other potential dangers exist. These effects were not introduced because they were not investigated. Omission did not imply that these factors are not of equal or greater importance than those covered in the paper. The bibliographies included in the discussions cover many of these factors and the investigations reported there are of considerable importance in the field of lightning hazards to airplanes.

The induced voltage effects on the hearts of pilots noted by Dr. Silsbee are an interesting speculation.

Mr. Harrison's comments on the trigger action of the plane probably are correct. It also is possible that charges on the plane may contribute to a steep-wave current; however, of relatively low magnitude. The stroke doing the damage shown in Figure 6 of the paper may have had one such component. It is doubtful that the noise produced would be very loud. I would suspect that loud noise results only when one or several stroke components reach ground. Discharges between clouds, generally speaking, would not be expected to produce return strokes based on experience at the Empire State Building in New York. When the leaders start at the building towards the cloud, no visible or measurable return stroke results.

This indicates that charges within the cloud are not sufficiently concentrated to produce return strokes.

Many factors may contribute to the hanging on of a stroke to a plane. The fact that the discharge does not move, of course, accounts for the large holes burned in the metal.

It was not intended to minimize the blinding effect. With a single pilot this might have disastrous consequences. In the case of air transport where two pilots are available, well acquainted with the possibilities of being blinded, a dangerous condition should not result.

Any conclusions drawn on current magnitude and charges in strokes to airplanes are necessarily approximate, if based on tests in the laboratory. The exact conditions existing at and near the plane are never known. However, such tests give an over-all story on the characteristics of lightning in the upper atmosphere which otherwise would be very difficult to obtain.

Mr. Raymond's statistical figures indicate a rather high incidence of lightning to aircraft. This should make it well worthwhile to educate flight personnel about the possible dangers involved. His remarks about badly damaged aircraft indicate that constant vigilance must be maintained.

Dielectric Strength of Oil with Variations of Pressure and Temperature

W. G. HOOVER
MEMBER AIEE

W. A. HIXSON
STUDENT MEMBER AIEE

THE DIELECTRIC properties of insulating oil under conditions other than those of atmospheric pressure and temperature are of interest in their effects on the performance of switchgear and other apparatus. The relatively small amount of information published on these effects prompted the study reported in this paper. The information to be presented is far from a complete coverage of the subject, but does result in some interesting conclusions and suggests the desirability of further research in this field.

Experimental Procedure and Equipment

The experimental procedure consisted principally of observing the breakdown strength of commercial quality insulating oil with variations of pressure up to 200 pounds per square inch gauge (above atmospheric) and down to −14.3 pounds per square inch gauge (below atmospheric). Samples of different quality, according to the standard 0.1-inch gap test, were tested with 60-cycle sine-wave voltages, long duration unidirectional impulse voltages (100 × 4,000-microsecond wave), and short duration unidirectional impulse voltages ($1^{1}/_{2}$ × 40-microsecond wave). Tests were made also on samples of partially degassed oil. Additional tests were carried out over the above pressure range with temperature variations of from 20 to 100 degrees centigrade.

The oil used for all reported tests was 100 per cent mineral oil, having a viscosity at 25 degrees centigrade of approximately 68 seconds, Saybolt Universal,[1] and a viscosity index of approximately 46.[2] The color of the oil in a small sample was just a shade off water-clear, and was estimated as having a color number of approximately two.[3]

All tests were made with breakdown taking place between 1-inch diameter brass spheres. The test tank was designed to permit an adjustment of the position of one of the spheres by a micrometer device operated through a control extending through the top of the tank. The micrometer setting could be observed through a window in the side of the tank. A small motor submerged in the oil in the tank drove a propeller to circulate the oil while the tests were being carried on. A vitreous enamelled resistor in the tank was used for heating the oil if desired. The power dissipated in the resistor was controlled by supply-voltage variation. The volume of oil contained in the test tank was approximately eight gallons. It was felt that with this relatively large volume and with the forced circulation of the oil, a given breakdown did not appreciably alter conditions under which a succeeding breakdown took place, due either to the presence of a small amount of decomposition products or to any possible clean-up action on impurities. This assumption seemed to be confirmed by the absence of any definite "hysteresis" effect upon reducing the pressure after a test run with increasing pressure.

Pressures above atmospheric were obtained by coupling the test tank through a short length of pipe to an Ashcroft gauge tester. The pressure could be raised by forcing oil into the tank by the piston on the gauge tester. The tank and tester were completely filled with oil, so that a small volume of oil displaced by the piston could vary the pressure over the entire range. The pressure could be adjusted accurately in steps of 5 pounds up to 200 pounds per square inch.

Pressures below atmospheric were obtained with a rotary vacuum pump. By means of a system of valves, the reduced pressure could be placed on the tank without changing any connections. An arrangement of bleeder valves was used to maintain the vacuum at the desired level. This condition was observed by a gauge placed in the line leading from the vacuum pump to the tank. The minimum possible pressure obtainable at the test gap was approximately 0.4 pound per square inch due to the head of oil above the gap.

For positive pressure, the results were influenced by the fact that the amount of air in the oil was limited to the amount contained in the oil when the tank was filled at atmospheric pressure. For negative pressures, air given up by the oil as the pressure was reduced could be drawn off by the vacuum pump until equilibrium was reached for the particular pressure involved.

The partially degassed oil was oil from the same source as tested in normal condition, but sprayed into a small storage tank from which the air was previously removed by a rotary vacuum pump. The process then was effectively repeated by allowing this oil to spray into the test tank under vacuum. However, the removal of all the air from the oil is a difficult process, and even with the above method a small amount of air remained in the oil.

The 60-cycle high voltage was obtained from a 110/65,000-volt test transformer. The primary voltage was controlled by a variable transformer ("Variac"). The Variac control shaft could be driven through a gear reduction train by a small motor to turn the shaft at a con-

---

Paper 49-216, recommended by the AIEE Basic Sciences, and Instruments and Measurements Committees and approved by the AIEE Technical Program Committee for presentation at the AIEE Pacific General Meeting, San Francisco, Calif., August 23–26, 1949. Manuscript submitted May 27, 1949; made available for printing July 18, 1949.

At the time this paper was written, W. G. Hoover and W. A. Hixson were both with Stanford University, Stanford, Calif. Since that time W. A. Hixson has joined the General Electric Company, Pittsfield, Mass.

stant speed, resulting in a uniform rate of voltage application. The rate of voltage rise was set at three kv per second. A 600,000-ohm resistor was placed in the high-voltage lead to limit the current flow at breakdown and to reduce pitting of the surfaces of the spheres.

The impulse voltages were obtained using two 100-kv 0.25-microfarad capacitors in a simple Marx circuit impulse generator. Both of the impulse wave forms previously mentioned were obtained by controlling the circuit resistances and load capacitances of the impulse generator. Wave forms of applied impulse voltages were observed with a cathode-ray oscillograph. Breakdown was noted either by change of wave shape of impulse voltage or by the sound produced by the breakdown in the tank.

Results of Tests

Experimental results are summarized in Figures 1 to 5. The curves were drawn through the averages of a number of breakdown values for each condition tested. Since it was found that some time was required for stabilization of breakdown strength after a change of pressure was made, values of breakdown voltage for the curves plotted as functions of pressure are values obtained after several minutes had been allowed for stabilization.

As is characteristic of breakdown tests of insulating oil, there was a considerable range of variation in individual breakdown voltages for a given test condition. Curves were drawn through what seemed to be the most probable value in each case. Individual points tended to be clustered with greater density near the curves as drawn, with points having larger deviation occurring less frequently. The spread of values was greatest in the 60-cycle tests, with most values lying within the range of ±25 per cent. For the impulse tests the range was more nearly ±15 per cent.

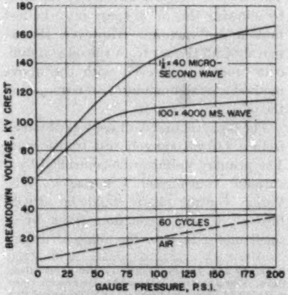

Figure 1. Breakdown of sample of good oil at positive gauge pressures, 0.04-inch gap between 1-inch diameter spheres

Breakdown of air at 60 cycles shown for comparison

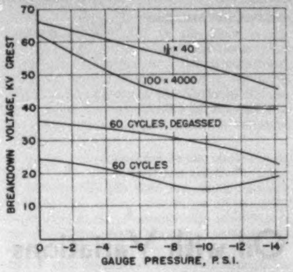

Figure 2. Breakdown of sample of good oil at negative gauge pressures, 0.04-inch gap

It will be observed that in all cases where the pressure was above atmospheric pressure, an increase in pressure resulted in an increase in dielectric strength. The beneficial effects of pressure appear to be greatest in the pressure regions just above atmospheric, with a tendency toward leveling off of the curves at the higher pressures. In all cases, the rate of increase of dielectric strength was considerably less than directly proportional to the total pressure, as is more nearly true for air (Figure 1).[4] The curves for pressures below atmospheric, Figure 2, show in general a continuation of the tendencies exhibited at higher pressures. The distinct minimum shown at less than minimum pressure for curve *A* of Figure 2 is characteristic of results obtained at 60 cycles with oil having the normal amount of air at atmospheric pressure.

The time requirement for stabilization of breakdown values after pressure changes from atmospheric to the limits available in these tests is illustrated in Figure 4. For this test the oil first was allowed to stand at atmospheric pressure to acquire its normal amount of dissolved air. Then the pressure was quickly increased to 200 pounds per square inch and readings taken of breakdown strength as time elapsed. A similar process was followed in obtaining the values corresponding to a rapid decrease of pressure. In this latter case the breakdown was at first reduced to nearly half its final value.

Effects of the duration of applied voltage are shown by the marked differences between curves in Figure 1. At 200 pounds per square inch, the 0.04-inch gap required an average breakdown gradient of about 4,000 volts per mil with the $1^{1}/_{2} \times 40$-microsecond wave. This was more than four times the value required at 60 cycles.

In Figure 3 a comparison of results of tests at 60 cycles is shown. Curve *A* is the same as the curve for 60 cycles in Figure 1 and applies to a sample of good oil, which tested at about 30-kv rms in a standard test cup. Curves *B* and *C* are for another sample of oil, which tested at about 22 kv. Curve *C* is for a gap of 0.15 inch, nearly four times the spacing of 0.04 inch for the other curves. It shows, however, the same characteristic shape. Comparative tests of different samples of oil showed much smaller differences with impulse voltages than at 60 cycles.

Definite improvement in the performance of oil may be effected by degassing, as shown by curves in Figures 2 and 3. Advantage may be taken of this improvement where the oil is in sealed containers, such as in certain types of capacitors, transformers, and so forth.

Theoretical Considerations

The experimental results can be explained to a large degree by considering the apparent influences of gases and impurities in the oil. Oil as ordinarily used contains dissolved gas, generally air, and in addition may have gas in the form of a suspension or emulsion. A certain con-

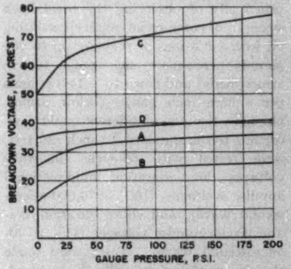

Figure 3. Breakdown for positive gauge pressures at 60 cycles

A. Breakdown of good oil, 0.04-inch gap
B. Breakdown of poor quality oil, 0.04-inch gap
C. Breakdown of same oil as for A, 0.15-inch gap
D. Breakdown of good partially degassed oil, 0.04-inch gap

centration of impurities, such as water and other foreign matter, is usually present.

The effect of gas in liquid dielectrics is known if the gas is present in suspension. Gas in this form makes up part of the volume of the insulating medium and lowers the dielectric strength. Most modern theories concerning the electrical breakdown of liquid dielectrics,[5,6,7] agree in stating that the ionization of gases in suspended form, where such gases can exist, is responsible for the initiation of the breakdown process. Stable gas suspensions do not exist in oil, but it has been shown that such can exist at a liquid–solid interface.[7] Furthermore, the application of an electric field may result in the liberation of gas from the dissolved state into the suspended form.[6,8] The breakdown gradient under these conditions should be a function of the electrical properties of the released gas.

In pure oil, this action of gas evolution no longer holds, and the process of breakdown is changed. All insulating materials have some conductivity[9] and therefore contain charged particles. It has been postulated[9] that the movements of such charged particles under the influence of the applied field results in a space charge which moves toward the electrode of opposite sign. As a portion of this space charge discharges itself, a film of neutral molecules is established, across which a difference of potential exists due to other portions of the space charge and to the applied field. The rupture of this film results in the profuse ionization that causes breakdown of the pure oil. In this case, however, the breakdown voltage is higher than that required if gas is present.

In oil containing gas in suspension, ionization of the gas is usually the dominant factor. It is to be expected that if a change of external conditions, such as pressure or temperature, should effect the availability of gas in the suspended form, the breakdown gradient would be altered. The physical nature of the suspended gas, such as bubble size, number of bubbles per unit volume of oil, density of gas within the bubbles, and so forth, should influence the contribution of the gas to breakdown. Time is required to produce a change in the ratio of dissolved to suspended gas. The breakdown gradient thus should be affected by the duration of the applied voltage and by the amount of time elapsed since a change of external conditions.

It is well known that the presence of water is detrimental to the electric strength of oil. As with gas, water may exist in either the molecular (dissolved) or emulsion phases. Emulsified water is apparently much more effective in reducing the electric strength than is dissolved water.[8,10] In the process of aging, emulsified water becomes more and more concentrated and may act to reduce greatly the breakdown value. The presence of sufficient water or other impurities may mask the effects of gas in the oil.

The solubility of air in oil is nearly directly proportional to pressure over a wide range. As a function of temperature the solubility at atmospheric pressure exhibits an upward trend through zero degrees centigrade to a maximum at about 70 degrees centigrade, beyond which the solubility falls off.

The experimental results show tendencies in agreement with the above theories. For positive pressures, the 60-cycle breakdown curves exhibit a definite rise at first, followed by a nearly horizontal section. The tested oil samples first were allowed to stand at atmospheric pressure until the oil was saturated with dissolved air. As pressure was applied in the sealed tank, the percentage of saturation decreased. Apparently during the rising part of the curve the electric field in the gap was able to extract gas from the dissolved state. The difficulty of liberation of gas and the density of the liberated gas increased with the pressure, causing the upward slope of the curves. Beyond 50 pounds per square inch pressure, the electric field necessary for extracting the gas apparently exceeded the breakdown value for the oil itself; little further increase with pressure occurred. This idea is further confirmed by the tests of partially degassed oil, in which the slope on the initial part of the curve is much less.

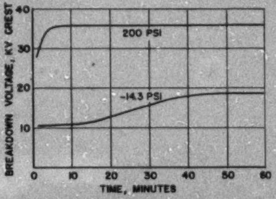

Figure 4. Breakdown voltages at 60 cycles following sudden changes from atmospheric to gauge pressures shown on curves

Initial breakdown at atmospheric pressure, 26 kv

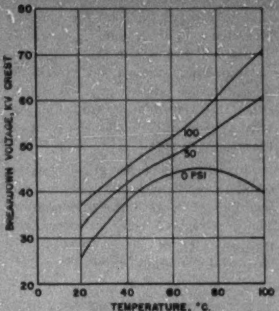

Figure 5. Breakdown of good oil at 60 cycles as functions of temperature

Numbers on curves show gauge pressure

Other contaminants in the oil, such as water, seem to affect the heights of the curves without significantly modifying the shape. This suggests that for the lower pressures, where gas is released, the space in the gap is in the nature of gas bubbles and oil layers in series, with the breakdown voltage for the combination a function of both air and oil.

For impulse voltages, the presence of free gas in the oil apparently plays an important part for the lower pressures. The breakdown values are much higher than for 60 cycles, due perhaps to the smaller sizes of bubbles produced, or to the possible time limitation, especially for the $1^1/_2 \times 40$-microsecond wave, of gas being available only at the electrode-liquid interfaces.[7] Less time is also available for the lining up of impurities in the electric field, so that these should play a relatively unimportant part. The extremely high breakdown gradients at the higher pressures indicate that field emission at the electrodes is probably an important factor in the initiation of breakdown at these pressures.

For negative gauge pressures the excess of air was drawn off by the vacuum pump. The further release of air with the application of voltage to the gap produced bubbles of lower density and consequent easier ionization, resulting in a decrease of breakdown voltage with decrease of pressure. For the curve for 60 cycles, Figure 2, the minimum could be explained as a point beyond which the total amount of air extractable from the oil was insufficient, in spite of its lower density, to provide as adequate a source of ionization as before. In this respect the picture is somewhat like the upward rise of the breakdown voltage for air as the pressure is reduced below the point for minimum breakdown at low pressure. For partially degassed oil and for impulse voltages, the above minimum did not occur within the pressure range covered probably due to either the insufficient amount of air dissolved or the time available for its extraction.

The effects of temperature observed correlate well with the solubility of air as functions of temperature and pressure. The improvement noted at higher temperature is opposite to the effects usually observed for solid insulations.

References

1. Method of Test for Viscosity by Means of the Saybolt Viscometer. *Standard D88-44*, American Society for Testing Materials (Philadelphia, Pa.), 1944.

2. Standard Method for Calculating Viscosity Index. *Standard D567-41*, American Society for Testing Materials (Philadelphia, Pa.), 1941.

3. Method of Test for Color of Lubricating Oil and Petrolatum by Means of A. S. T. M. Union Colorimeter. *Standard D155-45T*, American Society for Testing Materials (Philadelphia, Pa.), 1945.

4. The Electric Strength of Air at High Pressures—II, **H. H. Skilling, W. C. Brenner.** *Electrical Engineering* (*AIEE Transactions*), volume 60, March 1941, pages 112–5.

5. Role of Dissolved Gases in Determining the Behavior of Mineral Insulating Oils, **F. M. Clark.** *Journal*, Franklin Institute (Philadelphia, Pa.), volume 215, 1933, pages 39–67.

6. Electrical Breakdown of Liquid Dielectrics, **F. M. Clark.** *Journal*, Franklin Institute (Philadelphia, Pa.), volume 216, 1933, pages 429–58.

7. Role of Gases in Breakdown of Liquid Dielectrics, **A. Walther, O. Tscheljustkina.** *Technical Physics in the U. S. S.R.*, (Leningrad, Russia) volume 3, 1936, pages 940–6.

8. Influence of Absorbed Air on Dielectric Strength of Liquids, **F. Koppelmann.** *Elektrotechnische Zeitschrift* (Berlin, Germany), volume 52, 1931, pages 1413–6.

9. Space Charge in Liquid Dielectrics, **J. B. Whitehead, E. E. Minor.** *Physics*, (New York, N. Y.) volume 6, 1935, pages 380–8.

10. Hygroscopicity in Liquid Dielectrics, **A. Lazareu.** *Technical Physics of the U. S. S. R.*, (Leningrad, Russia) volume 1, 1934, pages 169–86.

No Discussion

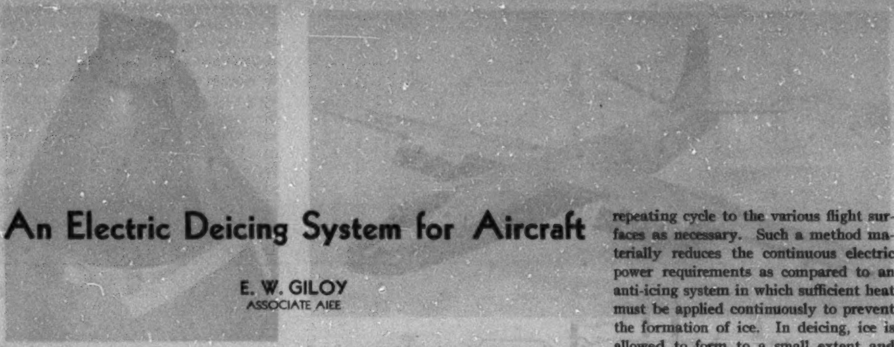

An Electric Deicing System for Aircraft

E. W. GILOY
ASSOCIATE AIEE

Synopsis: This paper covers an electric ice removal system as applied to a recent experimental airplane. The system is described in detail from the power generators to the ice removal blankets and includes such items as extent of ice protection coverage, construction and installation of ice removal blankets, system electric power requirements, and system control. The paper does not treat the subject of ice protection in any of its theoretical aspects. The complete ice protection system installation is believed to be the first of its kind in this country.

THE FORMATION of ice on the flight surfaces of airplanes has been one of the major operational limitations of aircraft since World War I. Early research on the problem attempted a solution by the use of compounds such as soap or glycerin applied to an airfoil section. A successful practical solution by such means was thwarted by the large quantities of fluid and the need for its continual application. Later research along other lines led to the successful removal of ice by means of a rubber boot applied to the leading edge of the wing or airfoil. The rubber boot was periodically inflated by air, thereby cracking and breaking up any ice that was formed and allowing it to be blown away by the air stream. The present ice removal systems[1] used most successfully on today's modern airplanes, both commercial and military, apply heat (hot air) to the inner leading-edge surface of the metal wing skin. The large amounts of hot air required for such thermal ice removal systems usually are obtained from either engine exhaust-gas heat exchangers, combustion heaters, or air bled from the compressor on jet engines. Presently under investigation for flight surface protection is an electrical form of ice removal that is similar to one used for aircraft-propeller ice protection. Electric energy is converted to heat energy for ice removal by means of electrical resistance blankets applied to the inside or outside leading-edge skin of the wing, nacelle, and tail surfaces. It is this electrical method of ice removal that was applied to a recent experimental airplane.

Why Electrical Method

The wing construction of the experimental airplane is characterized by corrugations running spanwise and placed between an inner and outer leading edge skin. This type of wing construction, along with the limitation of a maximum allowable structure temperature of 200 degrees Fahrenheit, complicated the design of a hot-air ice removal system that would effect a heat transfer exceeding 1,500 Btu per hour per square foot through the inner wing skin and corrugation to the outer skin. The electrical method of ice removal offered a solution in that heat could be applied directly to the outer skin by the use of rubber blankets containing embedded resistance elements. The problem of providing sufficient electric power for the resistance blankets presented no undue difficulty since sufficient engine generator drives beyond the requirements of the airplane's 28-volt d-c primary-power system were available. Further, the airplane being an experimental model offered an opportunity to aid and to advance the art of ice removal by electrical methods.

Deicing Versus Anti-Icing

In designing for the removal of ice by electrical means it was felt, based on experience with propeller ice removal and National Advisory Committee for Aeronautics research, that a successful system could be provided by the deicing method in which heat is applied periodically in a repeating cycle to the various flight surfaces as necessary. Such a method materially reduces the continuous electric power requirements as compared to an anti-icing system in which sufficient heat must be applied continuously to prevent the formation of ice. In deicing, ice is allowed to form to a small extent and then is removed by the application of heat.

The ice that has formed acts as an insulator over the heated surface, with the result that only the bond between the airplane and the ice is broken upon application of heat, allowing the bulk of the ice to be removed by the airstream.

Extent of Deicing

The heating blankets are applied to approximately the forward ten per cent of chord, in line with the theory that only the forward portion of the chord of a wing need be heated to provide ice protection for the entire wing. The horizontal stabilizer and vertical fin of the airplane are protected in a similar manner. The blanket area for each surface is forward of the front spar and entirely within each removable leading edge. In the nacelle regions, protection is provided for the leading edge lip of jet-engine diffusers, jet-engine air intakes, and the by-pass tunnels located between engine nacelles. Deicing protection for the jet-engine diffusers covers an area one inch aft of the leading edge on the inner surface to seven inches aft on the outer surface. For the jet-engine air intakes and the by-pass tunnels, the coverage is one inch on the inner surface to approximately 16 inches on the outer surface. Figure 1 provides an overall view of the airplane's heated areas.

Paper 49-218, recommended by the AIEE Air Transportation Committee and approved by the AIEE Technical Program Committee for presentation at the AIEE Pacific General Meeting, San Francisco, Calif., August 23–26, 1949. Manuscript submitted July 30, 1948; made available for printing June 30, 1949.

E. W. Giloy is in the Electrical Design Engineering Section, The Glenn L. Martin Company, Baltimore, Md.

The author takes this opportunity to thank E. W. Colehower and other individuals of The Glenn L. Martin Company for their assistance in the preparation of this paper.

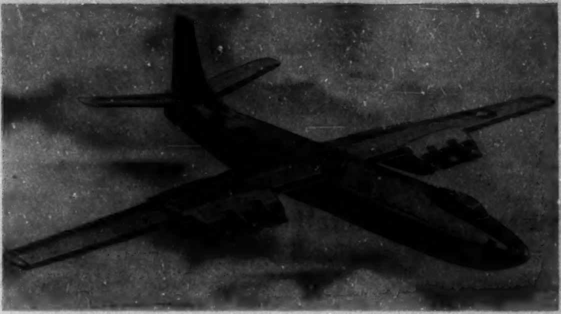

Figure 1. Artist's conception of airplane with deicing blankets

Means of Deicing

The heat necessary to effect ice removal for the areas outlined is obtained by means of the aforementioned electrical resistance blankets applied to the outside of the airplane skin. The blankets are of a laminated-vulcanized construction with electrical resistance wiring providing the heating element sandwiched between two thicknesses of black neoprene rubber. The finished product is 0.060 -inch thick with length and width as necessary. The wire elements of a blanket are spaced approximately 1/8 inch apart and run between braided internal bus bars, located at opposite edges of the blanket. For each blanket, heat is distributed evenly over its electrical area by the numerous parallel heating circuits contained therein. The electric connections to a blanket are made at each bus bar by an insulated conductor pigtail which is molded into the blanket normal to its surface. The directly heated or electric section is less than the total area of a blanket by the area occupied by the imbedded bus bars and a dead rubber area approximately 3/8-inch wide surrounding the electric section. This unheated area of each blanket varies the deicing protection slightly from the theoretical ten per cent of chord coverage for wing and tail surfaces.

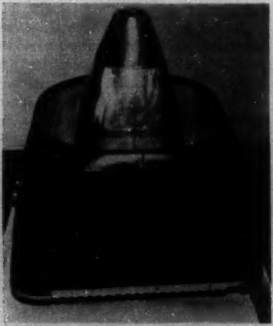

Figure 2. Deicing blankets installed on engine air intake and engine diffuser (center)

Installation of Blankets

The leading edge of wing, tail, and nacelle areas to receive icing protection are recessed 0.060 inch, the thickness of the deicing rubber blanket, from the desired final surface contour to provide a smooth contoured installation. For this particular installation the heating blankets are installed on the flight surfaces with the resistance wires contained therein running chordwise and the bus bars falling spanwise at the two aft edges of the blanket. The blankets as manufactured provide extra dead rubber in excess of the aforementioned 3/8 inch around the electrical section and are trimmed as necessary at installation to provide a butt joint between adjacent blankets and the airplane skin edge at the chordwise extremities of the recessed area. The installation is similar to that of fitting and laying inlaid linoleum to a table or floor provided with an edging strip. The rubber blankets are bonded to the metal surfaces of the airplane with a synthetic resin neoprene cement. Air that is advertently trapped under a blanket at various locations during installation is removed by piercing the rubber blanket with a hypodermic needle at each of the air pockets or blisters. Holes for the electric conductor pigtails are provided in the airplane skin at blanket locations and dimensionally match the conductor pigtails on each blanket. The molded-in conductor pigtails of the blankets pass through these holes and are connected to the airplane's wiring as the various circuits dictate. A terminal strip disconnect is provided in the circuit of each blanket and is located between each blanket and the airplane's wiring to facilitate the removal of a particular leading edge surface. Sufficient slack is provided in the wiring such that a leading edge section of wing, tail, and so forth, can be removed sufficiently to provide access to the terminal disconnects. For general ease of handling and installation, any individual deicing blanket is limited to a maximum length of about six feet, although it may contain more than one electric section as necessary to bring about a more satisfactory load division between blanket power sources.

Figure 3. Partial installation of engine diffuser blankets

Note electric connection to blanket and indication of blanket heating wires

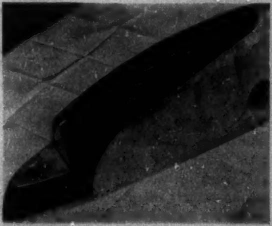

Figure 4. Installation of deicing blanket on airplane wing tip

Note cutout in blanket for wing tip light

It can be pointed out that with blankets installed side by side on a surface, there is a dead or unheated strip of rubber approximately 3/8 inch times two or 3/4-inch wide between the electric sections of adjacent blankets on which ice may tend to form and remain, but it is anticipated that sufficient heat will flow from the directly heated area of each blanket to this so-called dead area and effect a removal of ice under all but the more severe icing conditions. Figures 2, 3, and 4 show the installation of several of the deicing blankets.

Power Requirements

The rate of heat generation required by the deicing blankets for ice removal amounts to nearly 4,000 Btu per hour per square foot or an electric power consumption of eight watts per square inch. The total area covered by deicing blankets on the airplane amounts to approximately 400 square feet and is composed of 81 individual blankets with a total of 105 individual electric sections. The total connected deicing load of these blankets amounts to 452 kw with the average maximum, continuous load from the standpoint of generator capacity (due to deicing cycling, which will be covered later) amounting to 113 kw. In addition to this deicing load, variable-frequency a-c power is required for radar equipment, amounting to a maximum continuous demand of 7.8 kw plus *NESA** windshield anti-icing requirements as high as 2.5 kw.[2] An a-c system was elected to power the deicing loads based on the light weight per kilowatt and the individual capacities of recent a-c generators as well as the a-c needs of the radar and *NESA* loads. The deicing and *NESA* loads normally are supplied power by three engine-driven 208-volt 3-phase alternators with a normal rating each of 40 kva at 0.75 power factor. A fourth machine is provided as a deicing spare in event of an alternator failure and is normally used only as a primary power source for the radar load. These four alternators do not operate in parallel but are connected individually to their respective loads. Manual switching is provided to connect the fourth alternator to any one of the other three alternator deicing loads as may be necessary in event of failure of one of the three normally used machines. The load per alternator normally averages around 40 kw, as itemized in Table I.

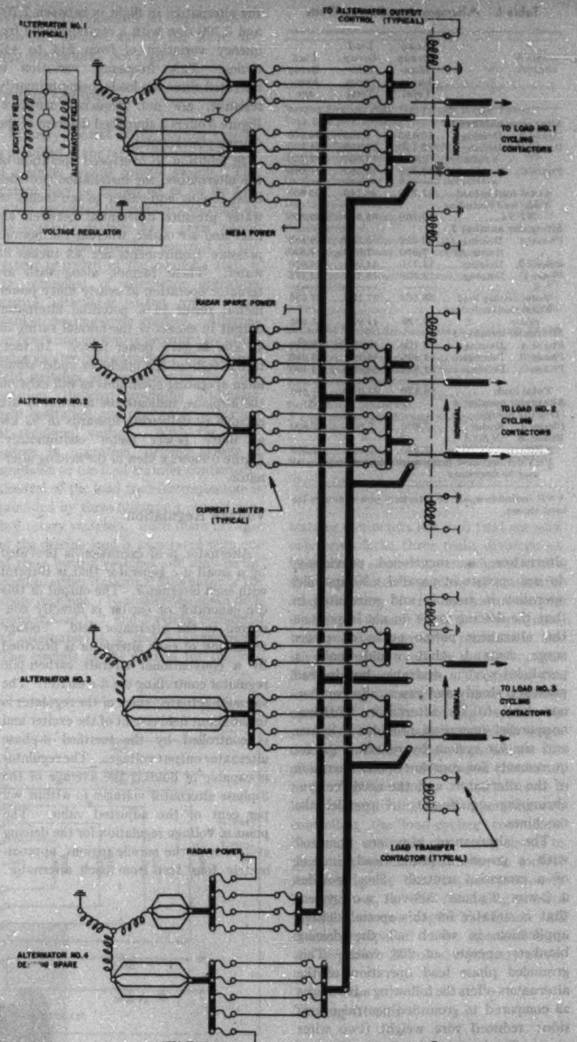
TO ALTERNATOR OUTPUT CONTROL (TYPICAL)
ALTERNATOR NO. 1 (TYPICAL)
EXCITER FIELD
ALTERNATOR FIELD
VOLTAGE REGULATOR
NESA POWER
NORMAL
TO LOAD NO. 1 CYCLING CONTACTORS
RADAR SPARE POWER
ALTERNATOR NO. 2
NORMAL
TO LOAD NO. 2 CYCLING CONTACTORS
CURRENT LIMITER (TYPICAL)
ALTERNATOR NO. 3
NORMAL
TO LOAD NO. 3 CYCLING CONTACTORS
LOAD TRANSFER CONTACTOR (TYPICAL)
RADAR POWER
ALTERNATOR NO. 4 DEICING SPARE
NESA SPARE POWER

Figure 5. Diagram of deicing power system

Alternator Operation

The four alternators[3] used here for deicing power are a type developed for the Army Air Force and are normally intended for use as primary power sources for 120/208-volt 3-phase 400-cycle a-c systems. The alternators are Y-connected 8-pole machines, and in a normal paralleled a-c system are operated with grounded neutrals, thereby providing a line-to-line voltage of 208 volts and a line-to-ground voltage of 120 volts. However, for this deicing application the

---

* *NESA* denotes a conducting coating applied to windshields for electrical anti-icing.

Table I. Alternator Loading in Watts

	Load Group Maximum Total	Load Group Minimum Total	Load Group Average
Alternator number 1			
Phase *A*. Deicing	10,380	9,460	10,070
Phase *B*. Deicing	12,110	12,120	11,770
NESA	2,500	2,500	2,500
Phase *C*. Deicing	15,230	14,560	15,040
Total deicing load	37,720	36,140	36,880
Total load including *NESA*	40,200	38,640	39,380
Alternator number 2			
Phase *A*. Deicing	10,320	8,880	9,500
Radar *SP**	7,800	7,800	7,800
Phase *B*. Deicing	14,316	14,000	14,010
Phase *C*. Deicing	13,730	14,316	14,175
Total deicing load	38,366	37,196	37,685
Total load including radar	46,166	44,996	45,485
Alternator number 3			
Phase *A*. Deicing	10,160	10,520	9,850
Phase *B*. Deicing	14,170	14,100	14,365
Phase *C*. Deicing	14,500	13,390	14,190
Total load	38,830	38,010	38,405
Alternator number 4 (Deicing Spare)			
Phase *A*. Radar	7,800	7,800	7,800
Phase *B*. *NESA* *SP**	2,500	2,500	2,500
Plus deicing load from any other alternator as may be necessary			

* *SP* indicates spare or alternate power source for load shown.

alternators, as mentioned previously, do not operate in parallel. Nonparallel operation is feasible and warranted in that the deicing loads do not impose on the alternator power peaks or power surge demands that would make a paralleled system desirable, but instead present a steady and practically continuous load to the alternator. Further, nonparallel operation provides a lighter and simpler system by relieving the requirements for constant-speed operation of the alternators and the need for synchronizing equipment to parallel the machines.

The alternators also are operated with a grounded phase lead instead of a grounded neutral. This provides a 2-wire 3-phase 208-volt a-c system that is suitable for this special deicing application in which all the deicing blankets operate at 208 volts. This grounded phase lead operation of the alternators offers the following advantages as compared to grounded neutral operation: reduced wire weight (two wires versus three), and reduced quantity and thereby weight of circuit protective devices in the ratio of two to three. In operation, the alternators do not operate at their synchronous speed of 6,000 rpm, but rather at jet-engine speeds since they are directly driven by these engines through an extended shaft at the nose, without the bulk and weight of constant-speed drives.[4] The operating speed of the alternators in flight is between 7,700 and 6,700 rpm with a corresponding frequency variation of from 514 to 447 cycles. This frequency variation is tolerated since the loads, being primarily resistive, are not frequency sensitive. Figure 5 offers a simplified diagram of the deicing power system.

In addition to overspeed operation of the alternators, the installation provides blast cooling equivalent to ten inches of water pressure differential between air inlet and air outlet, whereas the normal pressure requirements are six inches of water. These factors, along with alternator operation at nearly unity power factor, result in a potential alternator output in excess of the normal rating of 40 kva at 0.75 power factor. In fact, recent tests of the machines under simulated operating conditions as will exist on the airplane, indicate the alternators are capable of delivering upwards of 52 kw at unity power factor continuously. Figure 6 shows a view of the deicing alternator.

Voltage Regulation

Alternator field excitation is provided by a small d-c generator that is integral with each alternator. The output of this d-c generator or exciter is directly connected to the alternator field. Voltage regulation of each alternator is provided by a conventional aircraft carbon-pile regulator controlling the d-c exciter. The solenoid-actuated stack of the regulator is in the shunt field circuit of the exciter and is controlled by the rectified 3-phase alternator output voltages. The regulator is capable of holding the average of the 3-phase alternator voltages to within ±2 per cent of the adjusted value. The point of voltage regulation for the deicing system is in the nacelle regions, approximately four feet from each alternator. The regulators are set to a nominal voltage of 208 volts and are installed in the flight area of the airplane, accessible for servicing in flight as may be necessary.

Cycling of Load

The electric load as represented by the deicing blankets is divided into three nearly equal divisions, with each division supplied power by one of the aforementioned 3-phase variable-frequency alternators. Each alternator's load is again divided into four basic 3-phase load groups, each group being composed of single-phase deicing blankets connected in delta. These load groups are supplied with electric power successively in a cyclic fashion, such that any one deicing blanket may receive power for a maximum of 1/4 of the total time in which the deicing system is in operation. Since the cycling time required for effective deicing is somewhat uncertain at the present stage of the art, a variable heating cycle control is provided. The "on" time for each blanket is continuously variable from a period of 26 seconds to 160 seconds, with the "off" time normally being three times the selected "on" time. Control also is provided for an increased "off" time greater than that mentioned. This additional "off" time, when used, is continuously variable from 40 to 240 seconds. For example, if the heating cycle control is set for 30 seconds and the additional time "off" control is set for 60 seconds, each alternator will supply power to its four basic load groups, one at a time, in succession for 30 seconds each and then will "rest" for 60 seconds before starting the cycle over again. If no additional time "off" is selected, the alternator "rest" period is eliminated, and the alternators will continuously cycle their four load groups one at a time in succession every 30 seconds. A diagram of a

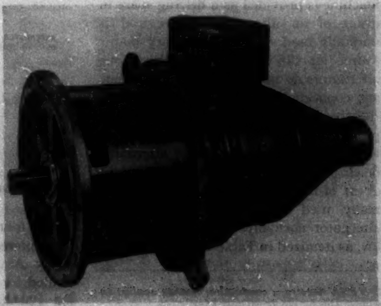

Figure 6. Deicing alternator. Alternator envelope is approximately 19 by 12 inches

typical deicing load on one alternator is provided in Figure 7.

Grouping of Blankets

In subdividing the deicing blankets into electric load units and connecting these units to the various alternators, care has been exercised to insure that corresponding blanket areas which are symmetrical about the center line of the airplane (namely areas on the wing and horizontal stabilizer) are connected in parallel so as to derive power through a common circuit protector from the same phase of a particular alternator. This arrangement insures that the ice which forms on the airplane between heating periods will be deposited in a symmetrical manner with the least disturbance to the airplane's balance and aerodynamic characteristics. Thus, under normal operation in icing conditions, ice will be forming on 3/4 of the ice-protected areas in a symmetrical pattern while ice removal is being effected on the remaining 1/4 of the area. Further, unforeseen power failures on various loads, as well as open-circuit protectors resulting from faulted wiring or blankets, still will provide a nearly balanced airplane as regards ice load. The subdivision of blankets applied to the nacelles is based on each deicing alternator being assigned the task of protecting its own particular jet-engine air intake system. The remaining jet-engine nacelle areas are divided among the three deicing alternators. See Figure 8.

System Control

Primary control of the deicing system is provided at the pilot's station by means of a single deicing control switch. The system may be turned off or on by this switch, provided the auxiliary controls at the copilot's station have been preset properly. The auxiliary controls of the system provided at the copilot's station are composed of alternator operation control, alternator output control, and blanket heating-cycle control. Alternator operation control is provided by alternator exciter-field switches. The exciter-field switches are normally in the "on" position, thereby providing alternator field excitation and alternator operation at regulated voltage. With the alternators in operation, deicing power is available to the load transfer contactors.[1] Control of the load transfer contactors is provided by three alternator output control rotary switches. Each main division of the deicing load is associated with one of these control switches and may be applied to either its normal alternator or the spare machine. Normally the main divisions of load 1, 2, and 3 will be connected to alternators 1, 2, and 3, respectively. The circuits of the control for the load transfer contactors are such that one and only one of the three main divisions of load can be electrically transferred to the spare alternator regardless of accidental mispositioning of the alternator, output control switches. With the output control switches correctly positioned, deicing power is available to the various load-cycling contactors. Control of the load-cycling contactors and thereby operation of the deicing system is provided by the aforementioned single deicing control switch located at the pilot's station. Positioning of the switch to the "on" position provides power to a load-cycling timing circuit operating and controlling the load-cycling contactors. Necessary control of the timing circuit to provide a variable heating-cycle control for the deicing blankets, as previously brought out, is the remaining control provided at the copilot's station. All control equipment is d-c operated from the airplane's 28-volt d-c primary power system.

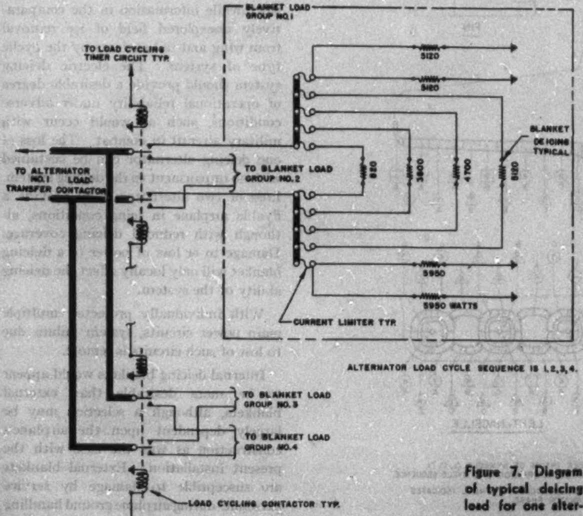
BLANKET LOAD GROUP NO. 1
TO LOAD CYCLING TIMER CIRCUIT TYP.
5120
5120
BLANKET DEICING TYPICAL
TO ALTERNATOR NO. 1 LOAD TRANSFER CONTACTOR
TO BLANKET LOAD GROUP NO. 2
820
3800
4700
5120
5950
5950 WATTS
CURRENT LIMITER TYP.
ALTERNATOR LOAD CYCLE SEQUENCE IS 1,2,3,4.
TO BLANKET LOAD GROUP NO. 3
TO BLANKET LOAD GROUP NO. 4
LOAD CYCLING CONTACTOR TYP.

Figure 7. Diagram of typical deicing load for one alternator

Table II

	Weight, Pounds
Deicing System Plus *NESA* and Radar Power	
Four 40-kva alternators with exciter at 79 pounds	316
Four regulators at 12.5 pounds	50
Four alternator mounting provisions	60
Deicing power wiring and switches	35.3
Deicing blankets at 1/2 pound per square foot	200.4
Deicing contactors	59.7
Deicing wiring, fuses	160.2
Deicing control	18.9
Miscellaneous deicing provisions	28
Radar power transformer and power provisions	26.5
NESA power transformer and power provisions	8.7
Total	960.7
Estimated Weight for Separate *NESA* and Radar Power System	
Two 8-kva alternators at 48 pounds	96
Two exciter-regulators at 22 pounds	44
Two alternator mounting provisions at 15 pounds	30
Radar power provisions	15
NESA power transformer and power provisions	15.7
Total	200.7
Net weight increase for deicing system	760

Timing Circuit

The timing circuit controlling the load-cycling contactors consists of a motor-driven cam and a low travel limit switch controlling the coil of a stepping relay. The stepping relay advances with each operation of the limit switch, and completes the control circuits to the various load-cycling contactors of each alternator in sequence. Variations in the timing cycle are obtained through speed control of the motor-driven cam. The increased "off" or rest period control of the heating cycle is obtained by the stepping relay progressing through several "dead" or unused contact positions at a controlled rate before again picking up the various cycling contactor circuits. When the increased time "off" cycle is not desired the stepping relay is stepped quickly through its unused contact positions such that a continuous and steady series of power intervals are supplied simultaneously to each alternator's load cycling contactors in a 1, 2, 3, 4,—1, 2, 3, 4 sequence.

Visual indication of the operation of the timing circuit and cycling contactors as well as alternator operation is provided in the form of four heating-cycle lights controlled by a load-check selector switch located at the copilot's station. Each light is connected to a pole of its respective cycling contactor and receives energy from the alternator supplying power to the particular load selected. With the load-check switch set for one of the three main divisions of load and with the system in operation, the four heating-cycle lights will operate in sequence and in step with their cycling contactor as each cycle of the load is energized. An "off" position is provided for the load-check selector switch so that the airplane crew need not contend with the load-cycling lights continuously during operation of the deicing system.

Circuit Protection

Protection of alternators, main power wiring, and blanket circuits is provided by single-phase aircraft limiters,[8] developed specifically for the 120/208-volt a-c system. The limiters are fusible metal links, similar to the common fuse, with an inverse-time–current characteristic particularly suitable for the protection of aircraft circuits. In the selection of limiter sizes the melting characteristics of the limiters were co-ordinated with the time–current smoking characteristics of the various gauge wires to provide protection against faulted or otherwise overloaded wiring.

The limiters for main power feeder protection are mounted in the nacelle regions near the alternators, while the bulk of the limiters associated with individual blanket circuit protection are installed at the power distribution center located in the fuselage in the bomb-bay area. Those limiters associated with individual tail surface blankets are installed in the aft section of the fuselage. None of the limiters are accessible in flight.

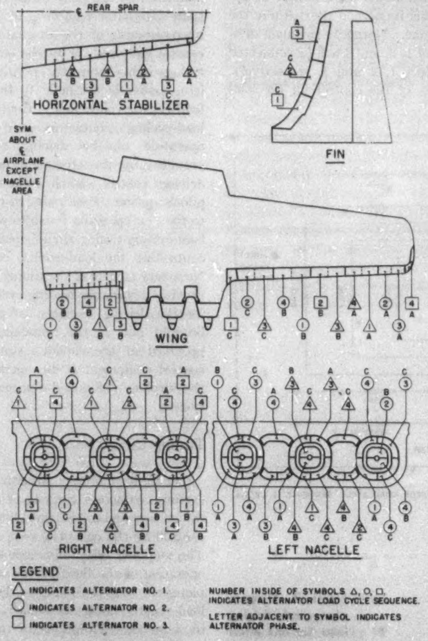
℄ REAR SPAR
HORIZONTAL STABILIZER
FIN
SYM ABOUT ℄ AIRPLANE EXCEPT NACELLE AREA
WING
RIGHT NACELLE
LEFT NACELLE
LEGEND
△ INDICATES ALTERNATOR NO. 1.
○ INDICATES ALTERNATOR NO. 2.
□ INDICATES ALTERNATOR NO. 3.
NUMBER INSIDE OF SYMBOLS △, ○, □, INDICATES ALTERNATOR LOAD CYCLE SEQUENCE.
LETTER ADJACENT TO SYMBOL INDICATES ALTERNATOR PHASE.

Figure 8. Electrical breakdown of deicing blankets for alternator load

Weight

The net weight increase to the airplane for the electric deicing system amounts to 760 pounds, as indicated in Table II. This table in one part itemizes the total weight of the deicing system together with the power-system equipment necessary for the radar and *NESA* windshield loads. Also indicated is a weight total that would have been incurred for a radar and *NESA* power supply system alone if the airplane had not been electrically deiced. The difference between these two subtotals (760 pounds) is therefore the net weight incurred by the airplane for the electric deicing system. The deicing system weight falls within the generally accepted allowance of one per cent of airplane gross weight for ice protection systems.

Conclusions

Operational data and evaluation of the deicing system is not available at the present time. Regardless of the final findings, the installation will provide worthwhile information in the comparatively unexplored field of ice removal from wing and tail surfaces by the cyclic type of system. The electric deicing system should provide a desirable degree of operational reliability under adverse conditions, such as would occur with military aircraft in combat. The loss of one deicing alternator can be sustained with no impairment to the deicing system. Loss of two alternators may provide a flyable airplane in icing conditions, although with reduced deicing coverage. Damage to or loss of power to a deicing blanket will only locally affect the deicing ability of the system.

With individually protected multiple main power circuits, system failure due to loss of such circuits is remote.

Internal deicing blankets would appear to be more desirable than external blankets, although a selection may be largely dependent upon the airplane's construction as was the case with the present installation. External blankets are susceptible to damage by service personnel during airplane ground handling and by stones, and so forth, kicked up during take-off and landing. In flight the external blanket also is subject to wear from the impact of rain and sand.

On the other hand, internal blankets would be protected by the airplane metal skin with a resulting longer normal service life. Internal blankets would, however, require an increased power input and a longer cycle time due to the additional material between the blanket heating element and the ice.

The electrical method of ice protection may or may not provide the optimum in ice removal systems, but it does possess the highly desirable feature of flexibility and is certain to remain as a useful ice removal means in a capacity that will be determined by time alone.

References

1. N. A. C. A. Research Ends Ice Hazard, Robert McLarren. *Aviation Week*, (New York, N. Y.), December 22, 1947, page 24.

2. Electric Anti-Icing of Aircraft Windshields, J. D. McCrumm. *Electrical Engineering* (*AIEE Transactions*), volume 65, December 1946, pages 786–91.

3. A 40-Kva 400-Cycle Aircraft Alternator, H. E. Keneipp, C. G. Veinott. *Electrical Engineering* (*AIEE Transactions*), volume 63, November 1944, pages 816–21.

4. Constant-Speed Drives for Aircraft Alternators, C. J. Breitwieser. *Electrical Engineering* (*AIEE Transactions*), volume 64, November 1945, pages 763–7.

5. Alternating-Current Contactors for Aircraft, F. J. Russell, A. P. Charbonneau. *Electrical Engineering* (*AIEE Transactions*), volume 63, September 1944, pages 613–6.

6. A Current-Limiting Fuse for Aircraft Applications, A. H. Powell. *Electrical Engineering* (*AIEE Transactions*), volume 64, July 1945, pages 541–5.

No Discussion

Insulator Flashover Deionization Times as a Factor in Applying High-Speed Reclosing Circuit Breakers

A. C. BOISSEAU
ASSOCIATE AIEE

B. W. WYMAN
MEMBER AIEE

W. F. SKEATS
FELLOW AIEE

SINCE the initial tests and trial application of high-speed reclosing to high-voltage tie-line circuit breakers a little over 13 years ago by Philip Sporn and D. C. Prince,[1] high-speed reclosing of such circuit breakers has become standard practice on most modern American transmission systems. Today, when capital investment and operating costs are more important than ever before, high-speed reclosing is almost universally recognized by transmission engineers in this country as one of the most economical methods of:

1. Increasing the maximum power which can be transmitted over long high-voltage tie-lines without loss of synchronism following a short-circuit tripout. This is shown graphically for a typical system in Figure 1.
2. Reducing system disturbance and shock at the instant of reclosing by reconnecting the two parts of the system before they have swung too far apart. Figure 2 shows how the angular displacement between the two ends of a typical system increases with reclosing time.
3. Reducing line outage time and improving service to customers.

When Sporn and Prince made their original investigation of high-speed reclosing, the primary limitation was the operating speed of available circuit breakers which, in comparison with present-day circuit-breaker speeds, was relatively slow. The interrupting time from energizing of the circuit-breaker trip coil to interruption on standard high-voltage circuit breakers was eight cycles. The time required after interruption to again reclose contacts was 27 cycles. By definition, the reclosing time of a circuit breaker is the sum of these two values, or 35 cycles from the energizing of the circuit-breaker trip coil to the recontacting of the arcing contacts. This time was sufficiently long to permit loss of synchronism on many long, heavily loaded tie-lines. Stability studies showed that much heavier loads could be transmitted without loss of synchronism if the reclosing time could be reduced.

With a given circuit-breaker interrupting time, the minimum deenergized time for successful reclosure is the time required for the flashover arc path to deionize sufficiently to prevent arc reignition when the line is reenergized. Sporn and Prince first studied this time for 132-kv insulator flashovers, both in the high-power laboratory and on an operating transmission line. Although their studies showed considerable variation, they found that if the fault current lasted eight cycles, 12 cycles of deenergized time was generally adequate to prevent arc reignition upon reclosure. This gave 20 cycles as the total necessary reclosing time. Special high-speed mechanisms were then developed for 138-kv circuit breakers capable of 20-cycle reclosure and were installed on the 132-kv line between Marion, Ohio and Ft. Wayne, Ind. The results obtained on the initial installation were so promising that manufacturers immediately embarked on a program of developing standard high-voltage circuit breakers with pneumatic mechanisms which could be reclosed in 20 cycles or less. As the interrupting time of the circuit breaker

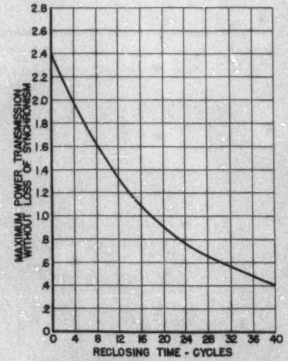

Figure 1. Maximum per unit power which may be transmitted without loss of synchronism during transient faults as a function of total circuit breaker reclosing time for a typical system

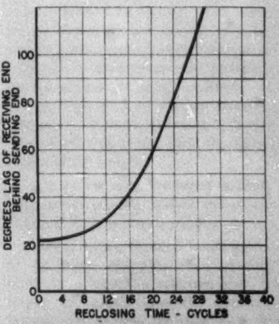

Figure 2. Angular displacement in degrees of system at receiving end of a tie-line behind system at sending end at instant of reclosing as a function of reclosing time

---

Paper 49-221, recommended by the AIEE Switchgear Committee and approved by the AIEE Technical Program Committee for presentation at the AIEE Pacific General Meeting, San Francisco, Calif., August 23-26, 1949. Manuscript submitted May 25, 1949; made available for printing July 9, 1949.

A. C. BOISSEAU, B. W. WYMAN and W. F. SKEATS are all with the General Electric Company, Philadelphia, Pa.

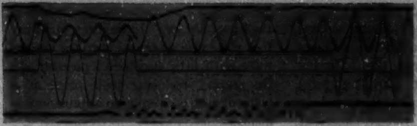

Figure 3(A) (upper left). Oscillogram of typical reclosing test with reclosing occurring at voltage zero showing absence of overvoltage oscillation at instant of reclosing

Figure 3(B) (upper right). Oscillogram of typical reclosing test on 230-kv suspension insulator with reclosing taking place at voltage crest showing double overvoltage oscillation at instant of reclosing

Figure 4(B) (lower left). Oscillogram of 8,000-ampere flashover shown in Figure 4(A) showing interruption of fault current in 2.3 cycles followed by reclosing operation eight cycles later at a voltage crest resulting in immediate reignition

Trace 1—trip coil current
Trace 2—generator voltage
Trace 3—arc voltage
Trace 4—short-circuit current
Trace 5—circuit breaker travel

also is important in increasing the maximum power which can be transmitted without loss of synchronism, the interrupting times of standard circuit breakers were subsequently reduced to five and three cycles. The results of nearly nine years operating experience with 20-cycle reclosing on the American Gas and Electric Company system have been outstanding and have shown that nearly 90 per cent of all faults of any type have been successfully reclosed at this speed.

Purpose of Present Investigation

Until recently, 15 to 20 cycles represented the minimum reclosing time which could be obtained with most high-voltage circuit breakers. However, recent developments in high-speed reclosing impulse circuit breakers effected such a drastic reduction in the time for the circuit breaker to reclose its contacts after interruption, that it became evident that the limitation on over-all reclosing time would most likely be the time required to deionize the fault arc, rather than the circuit breaker reclosing speed. Tests at Grand Coulee Dam last year on a modern high-speed impulse circuit breaker showed it capable of reclosing 8,700,000-kva faults in 8.6 cycles. The only remaining limitation, therefore, is the required deionization time of the flashover path around the insulator string. With circuit-breaker reclosing times adjusted down to the maximum flashover deionization time, maximum power transmission can be achieved without danger of loss of synchronism. There are a number of factors which will cause this to vary between systems. Several investigations have been made both here and abroad to study the effect of some of these factors at a particular voltage which was of interest to the investigator. Unfortunately, however, much of the information obtained has not been published, and that which has been published has not been sufficiently well co-ordinated to make a ready reference.

A general investigation was, therefore, undertaken to determine the minimum necessary deionization times for insulator flashovers on 69-kv to 230-kv circuits under various conditions which would be encountered in actual service.

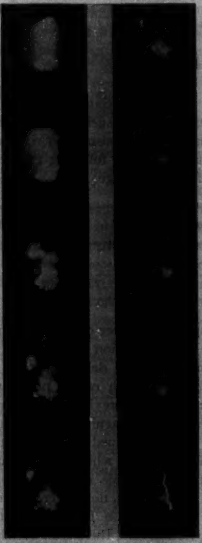

Figure 4(A). Pictures from 4,000-frame-per-second film of an 8,000-ampere flashover interrupted in 2.3 cycles and reclosed eight cycles later at a voltage crest with arc reignition taking place. (Only one picture per cycle shown)

Variable Factors in Determining Necessary Deionizing Time

Some of the more important factors in determining necessary deionization time for insulator flashovers are:

1. Magnitude of short-circuit current. The higher the fault current, the larger the amount of ionized gas which will be generated. This will tend to be offset somewhat by the greater amount of turbulence initiated in the surrounding air causing greater swirling and mixing with cool air. Also the magnetic blowout action increases with higher currents tending to loop the arc away from the insulator and lengthen it. Maximum short-circuit currents at high-voltage have increased several-fold since earlier investigations were made.

2. Duration of short-circuit current. The longer the fault current flows, the greater the total heat energy liberated. This will tend to be offset somewhat by greater turbulence. Also longer magnetic blowout action with the longer current duration may loop the arc out farther away from the insulator before the current is interrupted. When the initial 132-kv tests were made, standard circuit breaker interrupting times were eight cycles and tests were conducted with fault currents of this duration. Since that time standard circuit breaker interrupting times have been reduced to five and three cycles which besides reducing the total reclosing time by a corresponding amount, may have some effect on the necessary de-energized time.

3. Magnitude and duration of capacitive coupling follow-current which may flow due to induced voltage on de-energized conductor if adjacent conductors remain energized. This assumes particular importance when single-phase reclosing circuit breakers are used.

4. Magnitude and duration of resistance follow-current which may flow momentarily through shunting resistors with some types

of circuit breakers which are equipped with shunting resistors in parallel with the main interrupting contacts. This was not considered in the original investigation by Sporn and Prince since no high-voltage circuit breakers used in this country at that time were equipped with resistors.

5. Magnitude of re-energization voltage applied.

6. Point on voltage wave at which circuit is re-energized. This determines the magnitude of the surge. If re-energized at a zero point, no surge will be present. If energized at a crest voltage, a surge approaching twice crest voltage will occur. This was not considered in previous investigations and is believed to account for much of the randomness in the results obtained.

7. Configuration of the current path at the terminals of the arc. If the current path forms right angles at either end of the arc, magnetic forces will tend to loop the arc away from the insulator string.

8. Length of insulator string which determines the minimum length of flashover path.

9. Weather conditions. A strong wind will tend to lengthen the arc prior to interruption and also tend to carry the ionized gas column bodily away from the insulator string after interruption. The tendency of wind to lengthen the arc prior to interruption will be minimized with fast tripping circuit breakers.

10. Shape of grading rings and other parts at the end of the suspension insulator which determine the distribution of dielectric stress when voltage is reapplied.

The first six items were considered to be of the greatest importance in determining the necessary de-energization time for deionization. Tests were therefore made to determine the effect of each of these. These tests were made in the high-power testing laboratory rather than an actual power system for the following reasons:

1. A very large number of tests would be required to complete the investigation. These tests could be scheduled with greater ease in the laboratory than on an actual system.

2. A much wider range of conditions could be obtained in the laboratory.

3. Previous experience had shown that previous flashover tests made in the high-power laboratory had given results very comparable to those obtained on field tests.

Tests Made

In order to cover the range of fault currents normally encountered at the present time or anticipated in the near future, insulator flashover tests were made at approximately 1,000, 8,000, and 25,000 amperes with re-energization potentials equal to the phase voltages of 69, 138, and 230 kv. This range can be obtained readily in the high-power testing laboratory by supplying the fault current from one voltage source and the re-energization potential from a second voltage source. This combination of voltages and currents represents the following range of short circuit kilovolt-amperes which cover the range encountered in most systems of these voltage classes at the present time.

Kilovolts	Amperes	Kilovolt-Amperes
69	1,000	120,000
69	8,000	950,000
69	25,000	3,000,000
138	1,000	240,000
138	8,000	1,900,000
138	25,000	6,000,000
230	1,000	400,000
230	8,000	3,200,000
230	25,000	10,000,000

To be able to apply high-speed reclosing circuit breakers to all types of systems, flashover deionizing data were desired under conditions which would simulate the following types of circuits:

1. Single-circuit transmission line protected with triple-pole circuit breakers.

2. Double-circuit transmission line with both lines on same tower, each circuit being protected by triple-pole circuit breakers.

3. Single- or double-circuit transmission line protected by single-pole reclosing circuit breakers.

Test Procedure

All arcs were initiated by a fine fuse wire tied over the surface of the string. Standard Locke suspension insulators were used with the following number of units for each voltage:

Kilovolts	Units
69	5
138	10
230	15

A sufficient number of tests were made under each condition to establish the maximum probable deionizing time. It was felt that much of the randomness encountered by previous investigators was due to the magnitude of the surge which was determined by the point on the voltage wave at which re-energization took place, for while no voltage appreciably higher than normal crest occurs when re-energization takes place at or near a voltage zero, there is an overshoot almost to double when re-energization takes place at the crest. This is well illustrated in the two oscillograms of Figure 3. Both of these films represent successful reclosures after an 8,000-ampere flashover on a 230-kv insulator string with a reclosing voltage equal to the leg of 230 kv. In the first, reclosing took place near a zero point on the voltage wave with little oscillation present. In the second, reclosing took place at a voltage crest, oscillating to approximately double.

A synchronous closing switch capable of accurately selecting the closing angle was therefore used to re-establish the circuit throughout the tests. Test series made under the two conditions with this switch gave no restrikes after a de-energized interval above $6\frac{1}{4}$ cycles when reclosing at the voltage zero, although four tests were made with reclosing times between $6\frac{3}{4}$ and $7\frac{3}{4}$ cycles; when closing on the voltage peak on the other hand, restrikes were obtained at $7\frac{1}{2}$, 8, $8\frac{1}{2}$ and $9\frac{1}{2}$ cycles, with only one successful reclosure at an interval less than $9\frac{1}{2}$ cycles. There is thus a difference of about three cycles between the deionizing times for the two conditions while the

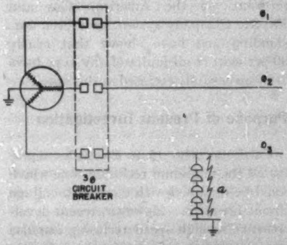

Figure 5(A). Single-circuit transmission line protected with triple-pole high-speed reclosing circuit breaker with single-line-to-ground flashover at point a on phase 3

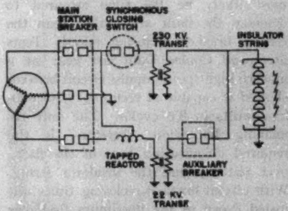

Figure 5(B). High-power laboratory circuit used to simulate flashover on single-circuit transmission line showing main station protective circuit breaker, tapped reactor for varying the magnitude of short-circuit current, 22-kv transformer for supplying fault current to the flashover, auxiliary circuit breaker for interrupting fault current, and synchronous switch for closing the high-voltage transformer for supplying the recovery voltage at the desired point on the wave

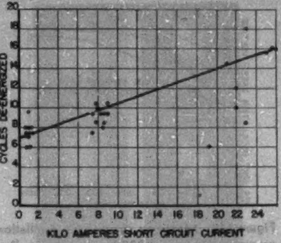

Figure 6. Results of high-speed reclosing tests after flashover on 230-kv suspension insulator with various values of short-circuit current

Black circles represent restrikes; open circles represent successful reclosure. Dividing line just above maximum restriking points represents absolute minimum de-energization time to prevent restrikes

data for each condition are quite consistent. It therefore appears certain that much of the randomness reported by previous investigators was due to lack of control of the closing point on the reclosing voltage wave. After proving the effect of this variable, all subsequent tests were made reclosing at a voltage crest to simulate the most severe conditions. This reduced considerably the number of tests necessary at each voltage and current condition to establish necessary deionizing times.

A 4,000-frame-per-second camera was used to photograph the tests to determine how and where arc re-establishment took place if encountered. A 60-cycle neon bulb exposure was printed on the side of the film to aid in correlating with oscillographic data. Figure 4 (A) shows every 66th picture (one picture from each cycle) of an 8,500-ampere flashover test on a 230-kv insulator string with a fault duration of 2.3 cycles followed by a de-energized time of 8.0 cycles with re-energization at crest voltage causing arc reignition. Figure 4(B) shows the oscillogram of this same test. Examination of each picture during the arcing period shows that the diameter and brilliance of the ionized gaseous arc column increased and decreased with the instantaneous current. This conforms with the well-known fact that the arc resistance varies inversely with current so that the voltage drop along the length of the arc is practically constant. The several thousand degree centigrade temperature core at the center of the arc sets up considerable turbulence and eddies in the surrounding air. Each small loop which is originated by turbulence then tends to be magnified by magnetic action. When the current flow is interrupted, the turbulence set up in the surrounding air aids in deionizing and cooling the column as can be seen from picture 3 to 9 in Figure 4 (A). When the insulator was re-energized from a 132-kv source at a voltage crest, an oscillation having a peak of 360 kv occurred which caused breakdown, as can be seen in the last picture.

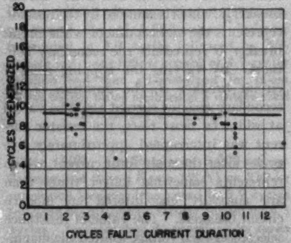

Figure 7. Results of tests varying the duration of fault current prior to interruption showing its effect upon necessary time to deionize arc

Tests made on 230-kv suspension insulator with recovery voltage equal to phase voltage of 230 kv. Fault current in all tests equals 8,000 amperes. Black circles represent restrikes, and open circles represent successful reclosures

Triple-Pole Reclosing—Single-Circuit Transmission Line

Figure 5 (A) represents a single circuit transmission line protected by a triple-pole high-speed reclosing circuit breaker without shunting resistors with a flashover from phase-3 to-ground over an insulator. A tie-line between two systems would have a similar high-speed reclosing circuit breaker at the other end also, but since both circuit breakers would normally be tripped and reclosed simultaneously, the other end may be disregarded in determining the deionizing time of the flashover path *A*. As phases 1 and 2 are opened with phase 3, they may be neglected when simulating this circuit in the high-power laboratory.

Figure 5 (B) shows the laboratory circuit used to determine the required deionization time of a flashover arc under this condition. The high-current short circuit was supplied from a 22-kv transformer connected to one phase of the high-power generator with the fault being interrupted by auxiliary circuit breaker. Re-energization potential equal to the phase voltage of 69-, 138-, and 230-kv circuits was supplied from a second transformer connected to the same phase.

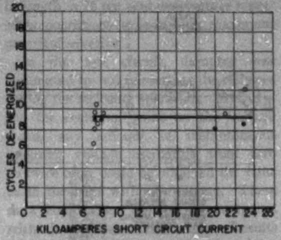

Figure 8. Results of high-speed reclosing tests after flashover on 138-kv suspension insulator with various values of short-circuit current

Black circles represent restrikes; open circles represent successful reclosures. Dividing line just above maximum restriking points represents absolute minimum de-energization time to prevent restrikes

Any desired number of cycles, as well as the point on the voltage wave, could be selected for re-energization by closing this circuit through the synchronous closing switch in the primary of the high-voltage transformer circuit.

Figure 6 shows a plot of results obtained following 1,000-, 8,000-, and 25,000-ampere flashovers on a 15-unit insulator string with 3-cycle fault duration and 132-kv re-energization voltage, which corresponds to the phase voltage of a 230-kv system. The open circles represent successful reclosures while the solid circles represent restrikes. By plotting the longest unsuccessful reclosing time as the necessary deionization time for that current, it will be noted that the necessary deionization time for 230-kv systems increases linearly with the short-circuit

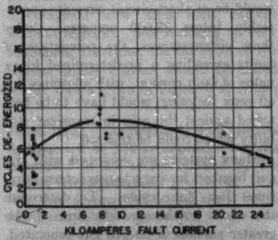

Figure 9. Results of high-speed reclosing tests after flashover on 69-kv suspension insulator with various values of short-circuit current

Black circles represent restrikes; open circles represent successful reclosures. Dividing line just above maximum restriking points represents absolute minimum de-energization time to prevent restrikes

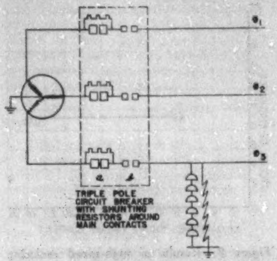
φ1
φ2
φ3
a
b
TRIPLE POLE CIRCUIT BREAKER WITH SHUNTING RESISTORS AROUND MAIN CONTACTS

Figure 10(A). Single-circuit transmission line equipped with triple-pole circuit breakers having shunting resistors with insulator flashover on phase 3

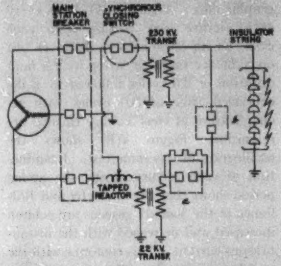

Figure 10(B). High-power laboratory circuit used to simulate reclosing with various de-energization times after interruption of fault current and 5-cycle resistor follow current

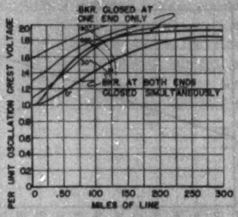

Figure 11. Maximum overvoltage oscillation on various lengths of 230-kv transmission line when reclosed at crest voltage by circuit breaker equipped with shunting resistors of 2,700 ohms per pole

current. By adding three cycles for arc interruption to each of these values for the circuit breaker to interrupt, the minimum total reclosing time for 3-cycle circuit breakers is obtained. For example, if high-speed reclosing 3-cycle circuit breakers were used on a 230-kv system where the maximum fault current was 9,000 amperes, a de-energized time of 10 cycles would be required. This added to the 3-cycle interrupting time results in a total minimum reclosing time of 13 cycles. If applied on a system with possible fault currents up to 25,000 amperes, the total reclosing time would have to be increased to 16 plus 3, or 19 cycles. If system studies on an actual transmission system having possible fault current of 25,000 amperes showed a considerable gain in transient stability by using a slightly shorter reclosing time than 19 cycles, the transmission engineer might decide to use the shorter time on the basis that most of the faults on the system would be at short-circuit currents appreciably below 25,000 amperes. Under these circumstances, the percentage of faults exceeding a predetermined lower value of fault current, with allowance for off-peak reclosing, would have to be balanced against the gain in transient stability which could be realized.

Many systems are equipped with circuit breakers having a longer interrupting time than three cycles. To determine the effect on deionization time of the greater amount of ionized gas generated, a series of tests were made with 10-cycle fault durations and approximately 8,000 amperes. Figure 7 shows the results of these tests as compared with 3-cycle fault durations. This figure shows that the maximum deionization times for 10-cycle faults are approximately equal to those of 3-cycle faults. This may indicate that the larger amount of ionized gas was offset by the greater amount of turbulence and looping due to magnetic blowout action, which does not agree completely with previous investigations.

Figure 8 is a plot of tests taken on a 10-unit insulator string with a re-energization potential of 80 kv, representing phase voltage of 132-kv systems. It will be noted that instead of increasing with higher currents as it did at 230 kv, the deionization time remains approximately constant up to 25,000 amperes.

Figure 9 is a similar plot of tests taken on a 5-unit insulator string re-energized with 44 kv, corresponding to phase voltage of a 69-kv system. It will be noted that for such short insulator strings, the extra magnetic blowout action more than offsets the extra amount of ionized gas generated at high currents. Although Figure 9 shows the results only up to approximately 25,000 amperes, successful reclosure was obtained in 2.3 cycles after 43,000 amperes which indicates this decreasing trend continues at even higher currents.

By adding these deionizing times to the circuit breaker interrupting time, the minimum possible total reclosing time will be obtained. How near these points circuit breakers should be adjusted will depend upon the stability margins of the particular system under consideration. If the stability margin is large, no advantage would be gained by adjusting for the absolute minimum reclosing time. Under this condition, an appreciable margin of safety would normally be added to these values to allow for the most unfavorable combination of circumstances. On the other hand, if the stability margin is small, the reclosing time at which it would be desirable to operate is as close to the minimum as possible.

Triple-Pole Reclosing by Circuit Breaker Equipped with Shunting Resistors—Single-Circuit Transmission Line

Many modern high-voltage circuit breakers are equipped with shunting resistors to eliminate overvoltages when interrupting the charging current of long unloaded transmission lines. When interrupting fault currents, the contacts of this type of circuit breaker interrupt the main fault current in either three or five cycles. The shunting resistor current in most such circuit breakers does not exceed 50 amperes and is interrupted by secondary contacts a few cycles later. Figure 10 (A) represents a single-circuit transmission line protected by triple-pole circuit breakers equipped with shunting resistors. Figure 10 (B) shows the laboratory circuit to simulate insulator flashovers under these conditions. Two separate circuit breakers were used to simulate the two sets of contacts. Circuit breaker *A*, which is shunted by the resistor, represents the main contacts, while circuit breaker *B* represents the secondary contacts. By varying the tripping time of circuit breaker *B*, the duration of the secondary resistor current could be varied at will. In most tests, the resistor current was interrupted approximately five cycles after the main fault current, which represents somewhat longer times than are normally encountered on modern circuit breakers. The value of resistance selected at each voltage limited the magnitude of the resistor current to 50 amperes.

Figure 12 (A) shows a series of pictures obtained on a test made on this circuit. In this figure, every 66th frame taken with the 4,000-frame-per-second camera (1 picture per cycle) is shown. In the test a 230-kv insulator string was flashed over by an 8,000-ampere arc, interrupted in 3.9 cycles, after which there was a

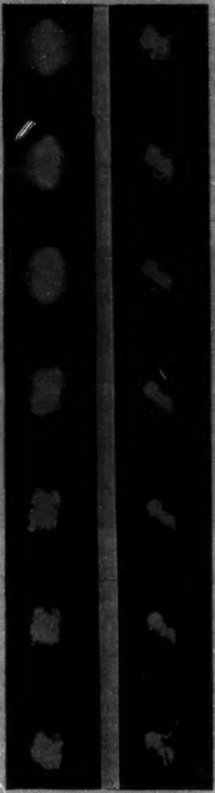

Figure 12(A). Pictures from 4,000-frame-per-second film of 8,000-ampere flashover interrupted in 3.9 cycles followed by 50-ampere resistance follow current of 4.7-cycles duration and then de-energized for seven cycles before being reclosed at a voltage crest with restriking taking place

50-ampere resistance follow current for 4.7 cycles. The circuit was then de-energized for seven cycles and re-energized at a voltage crest with arc reignition taking place. Figure 12 (B) shows the oscillogram of the same test showing restriking after seven cycles. Figure 12 (C) is an oscillogram of the same current but with a de-energized time of 8.3 cycles after which reclosure was successful at a voltage crest.

In reclosing, a resistance shunted circuit breaker will first connect the circuit through a resistor and then short out the resistor. When reclosure on a transmission line takes place through a resistor of 2,700 ohms, which is a typical value, the oscillation is completely damped out for transmission line lengths of a mile or more, so that even though this reclosure may take place at a voltage crest, restriking of the fault arc would correspond to voltage zero conditions. Under this condition, tests at 8,000 amperes at a re-established voltage corresponding to 230 kv indicated that only $2^1/_2$ cycles of dead time are required.

When the resistance is finally shorted out, an oscillation takes place with an amplitude equal to the instantaneous voltage across the resistor just before it is shorted. The corresponding overvoltage increases with the length of the line as shown in the curves of Figure 11, which shows the overvoltage corresponding to shorting the resistor at the worst point on the voltage wave for the following conditions:

1. Circuit breaker at one end of the line fully closed before the circuit is closed through the resistor at the other end.
2. Both ends of line connected through resistors before either resistance is shorted out. Under this condition the amount of overshoot will vary with the phase angle between the two ends of the line at the time of reclosure. Curves are shown for angles of 0, 30, 60, and 90 degrees.

The overvoltage is greater for long than for short lines. For lines up to 100 miles in length, a 75 per cent overvoltage represents conditions approaching maximum practical severity.

In the test circuit, damping was eliminated by not reinserting the resistors during the reclosing operation. By varying the reclosing point on the voltage wave, any amount of instantaneous reclosing voltage oscillation from zero to twice crest could be obtained the same as in the tests without resistors. These data could then be directly compared with the previous tests made. Results similar to reclosing a short line with resistance-shunted circuit breakers could therefore be obtained by closing near a voltage zero where no overvoltage oscillation would occur. Results similar to reclosing a long line with resistance shunted circuit breakers could be obtained by closing at the crest of the voltage wave which gave twice crest oscillations. These tests showed that when a resistance-shunted circuit breaker which had a 5-cycle 50-ampere resistance follow current interrupted an 8,000-ampere flashover on a 230-kv insulator string, successful reclosure could always be obtained when reclosed at a voltage zero after a de-energized time of four cycles. Added to the five cycles of resistor current, this makes a total of nine cycles after the main interruption of the fault current for successful reclosure on a short transmission line. This agrees closely with the necessary de-energized time shown in Figure 6 without resistor follow current. When this test circuit was re-energized at crest voltage after an 8,000-ampere flashover to simulate long-line reclosing where overvoltage oscillation might be encountered, several cycles extra time were required. In some cases, the necessary de-energized time after resistor current was almost equal to the necessary de-energized time after fault current without resistors. For reclosing on very long lines, therefore, the duration of the resistor follow current should be added to the values given in Figure 6 to obtain

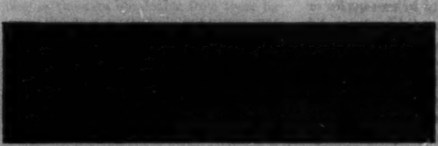

Figure 12(B). Oscillogram of 8,000-ampere flashover test shown Figure 12(A) on 230-kv suspension insulator interrupted in 3.9 cycles followed by 50-ampere resistor current for 4.7 cycles. Insulator then de-energized for seven cycles before being reclosed at a voltage crest causing arc reignition

Trace 1—trip coil current-circuit breaker *B*
Trace 2—generator voltage
Trace 3—arc voltage
Trace 4—short-circuit current
Trace 5—trip coil current-circuit breaker *A*
Trace 6—resistor current
Trace 7—travel-circuit breaker *B*

Figure 12(C). Oscillogram of 8,000-ampere flashover test on 230-kv suspension insulator interrupted in 3.5 cycles followed by 50-ampere resistor current for five cycles. Insulator then de-energized for 8.3 cycles before being successfully reclosed at a voltage crest

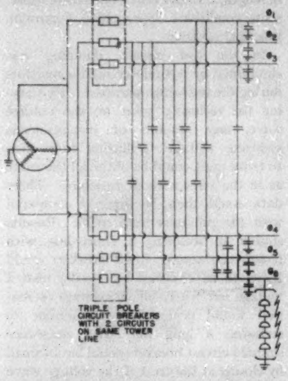
φ1
φ2
φ3
φ4
φ5
φ6
TRIPLE POLE CIRCUIT BREAKERS WITH 2 CIRCUITS ON SAME TOWER LINE

Figure 13(A). Double-circuit transmission line with both circuits mounted on the same towers and with each circuit protected by its own triple-pole high-speed reclosing circuit breaker with insulator flashover on phase 6

Figure 14(right). Three-phase transmission line protected by high-speed single-pole reclosing circuit breakers with insulator flashover on phase 3

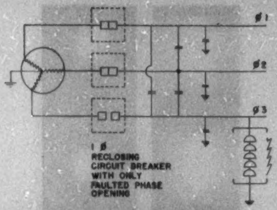
φ1
φ2
φ3
1 φ RECLOSING CIRCUIT BREAKER WITH ONLY FAULTED PHASE OPENING

Figure 15 (lower right). Oscillogram of 7,100-ampere flashover on 230-kv suspension insulator interrupted in 3 cycles with capacitive coupling voltage of 22 kv. Capacitance current from 4.5 microfarads coupling representing 300 miles of line is interrupted only after 22 cycles

Trace 1—trip coil current
Trace 2—generator voltage
Trace 3—capacitor current
Trace 4—arc voltage
Trace 5—short circuit current
Trace 6—circuit breaker travel

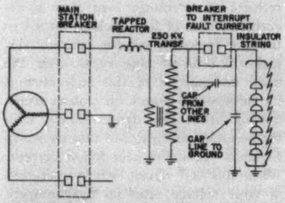

Figure 13(B). High-power laboratory circuit used to determine the length of time required for interruption of capacitive follow current with various values of capacitive coupling voltage tending to sustain arc

the minimum possible reclosing time.

Most systems will fall somewhere between the short-line and long-line case. For these systems, an intermediate value of resistor current duration based upon the relative overvoltage obtainable in Figure 11 may be added to determine the minimum possible reclosing time.

Triple-Pole Reclosing—Double-Circuit Transmission Line

Figure 13 (A) represents a double-circuit transmission line with both circuits mounted on the same towers and with each circuit protected by its own reclosing circuit breaker. When a fault occurs on one circuit, only the circuit breaker on that circuit will open. The capacitive coupling between the isolated line and the energized line causes the isolated conductors to float at some intermediate voltage. This voltage, if high enough, will feed current through the flashover path as long as it is still partially ionized. If the voltage and current are small enough, this capacitive follow arc will interrupt itself as the ionized flashover path cools. On the other hand, if this capacitive coupling arc is supplied by a high enough voltage and current, it will represent a new stable arcing condition and would arc indefinitely so that the circuit can never be successfully reclosed.

Figure 13 (B) shows the test circuit used to simulate the capacitive coupling conditions to determine the length of time required for final interruption of this capacitive arc. The voltage at which the unenergized conductors tend to float is determined by the ratio of the circuit-to-circuit capacitance to the circuit-to-ground capacitance. The current which will flow is determined by the values of the capacitances. These tests showed that capacitive currents were interrupted successfully in two cycles or less as long as the coupling voltage did not exceed 10 kv with short initial short-circuit durations. Considerable randomness was encountered in the length of time required for interruption, but this is to be expected in such a nonstable arc. The magnitude of the coupling voltage appeared to be much more important than the current in the arc, for 5-ampere arcs required as long to interrupt as 50-ampere arcs.

Fortunately capacitive coupling voltages at which one circuit of a double-circuit transmission line tends to float with normal transposition are appreciably below 10 kv. As shown in Appendix I, about 5 kv may be expected on a 220-kv circuit without transposition, and less than 3 kv with reverse transposition. With the normal values of capacitance coupling encountered from such operation, therefore, the follow current will not generally continue for more than one or two cycles. Triple-pole reclosing may, therefore, be used on 230-kv double-circuit transmission lines by allowing one or two cycles extra time in the reclosing cycle for interruption of capacitive follow current. This agrees with previous experience and with operating data on 132-kv systems.

Single-Pole Reclosing—Single- or Double-Circuit Transmission Line

Figure 14 represents a 3-phase transmission line protected with single-pole reclosing circuit breakers. When a flashover occurs on such a system and the circuit breaker in the faulted phase opens, capacitive coupling current will flow as in the previous case. The magnitude of

Table I. Tests to Determine Duration of Capacitive Follow Current after Interruption of Main Fault Current on 230-kv Suspension Insulator

Capacitive Recovery Voltage	Voltage Supplying Main Fault Current	Fault, Amperes	Fault Duration, Cycles	Ratio C_1/C_2 Microfarads	Equivalent Miles 230-kv Line	Capacitance Follow Current,* Amperes	Duration Capacitive Follow Current Cycles
10,000	22,000	7,700	5.0	0.68/0.82	100	2.3	0.7
10,000	22,000	930	2.0	0.68/0.82	100	2.0	2.2
10,000	22,000	900	2.0	0.68/0.82	100	2.0	0.6
10,000	22,000	870	9.5	0.68/0.82	100	2.0	0.6
10,000	22,000	870	9.0	0.68/0.82	100	2.0	5.5
10,000	22,000	6,800	10.5	0.68/0.82	100	3.0	6.5
10,000	22,000	6,600	10.5	0.68/0.82	100	3.0	0.1
10,000	22,000	6,800	11	0.68/0.82	100	2.0	0.5
10,000	22,000	6,600	10.5	0.68/0.82	100	2.8	1.6
10,000	22,000	6,800	11	0.68/0.82	100	3.3	0.5
10,000	22,000	6,800	8.5	2.04/2.46	300	25	1.2
10,000	22,000	6,800	9.0	2.04/2.46	300	22	2.1
10,000	22,000	6,800	9.5	2.04/2.46	300	20	1.7
12,000	22,000	8,100	3.7	0.82/0.68	100	2.6	0.6
12,000	22,000	8,000	2.9	0.82/0.68	100	2.1	0.8
12,000	22,000	880	2.4	0.82/0.68	100	2.0	3.6
12,000	22,000	890	1.9	0.82/0.68	100	2.0	4.3
12,000	22,000	6,800	10.5	0.82/0.68	100	2.0	2.5
12,000	14,500	16,200	2.8	3.72/0.78	300	17.5	0.2
12,000	14,500	18,100	2.8	3.72/0.78	300	17.5	0.7
14,500	14,500	17,700	3.8	4.5/open	300		0.3
15,000	22,000	7,600	3.0	1.02/0.48	100	2.5	0.7
15,000	22,000	7,600	3.5	1.02/0.48	100	5.1	7.0
15,000	22,000	8,000	2.4	1.02/0.48	100	5.5	1.8
15,000	22,000	6,900	8.5	3.07/1.43	300	39	3.7
15,000	22,000	6,900	9.0	3.07/1.43	300	16	0.9
15,000	22,000	7,300	4.4	3.07/1.43	300	40	3.1
15,000	22,000	7,700	2.0	3.07/1.43	300	22	0.6
15,000	22,000	7,600	3.0	1.02/0.48	100	11	2.6
15,000	22,000	7,600	3.5	1.02/0.48	100	37	2.2
22,000	22,000	7,100	3.0	4.5/open	300	100	22
22,000	22,000	7,200	3.0	4.5/open	300	120	26
22,000	22,000	7,500	3.1	1.5/open	100	35	32†
22,000	22,000	7,200	3.0	1.5/open	100	35	18
33,000	44,000	4,200	1.5	1.13/0.376	100	50	10†
33,000	44,000	4,100	2.0	1.13/0.376	100	35	23
33,000	44,000	3,600	4.0	1.13/0.376	100	35	28†
33,000	44,000	3,700	3.5	1.13/0.376	100	105	24
33,000	44,000	3,800	3.0	3.37/1.12	300	105	31†
44,000	44,000	3,900	2.9	1.5/0	100	44	31†
44,000	44,000	3,800	4.0	1.5/0	100	44	31†

*Current magnitudes in the column may be subject to error from difficulties in reading films due to poor wave shapes and short current durations.

†Did not clear.

the capacitance coupling voltage sustaining this current flow will be much higher in this case, however. This increase is due to (a) the field from the two phases not being as well balanced as the transposed 3-phase field from an adjacent circuit in the double-circuit triple-pole reclosing case, and (b) the closer spacing normally employed between the three conductors of one circuit as compared with the spacing between two circuits. The appendix shows calculations for determining the values of these voltages.

The test circuit for this condition is similar to the circuit used for the previous series, except for the magnitudes of the capacitances and the transformer voltages. Tests were made with capacitive coupling voltages ranging from 10 kv to 44 kv. Capacitances were varied to give the equivalent of 100 and 300 miles of 230-kv transmission lines. All tests were carried out on a standard 15-unit insulator string. The data from these tests are given in Table I. It will be seen from this table that when capacitive coupling voltages equal or exceed 22 kv, the necessary deionizing time becomes very long and in many of the tests interruption did not occur at all in the half-second or more after fault current interruption. Whether interruption would have subsequently occurred is extremely doubtful. As shown in the appendix, however, capacitive coupling voltages will be frequently encountered in this range with single-pole reclosing on 230-kv lines. Despite the gains that may be shown in transient stability under some conditions on 230-kv systems with single-pole reclosing circuit breakers, these data do not indicate that such operation will always be feasible. Similar data were not taken in this investigation using shorter insulator strings to simulate lower voltages.

Conclusions

The following conclusions may be drawn from this investigation:

1. When capacitive coupling is not present, the de-energization time after insulator flashover necessary to prevent arc reignition upon reclosure of the line increases linearly with the fault current on 230-kv systems is practically constant for 132-kv systems, and decreases at high current on 69-kv systems. By adding the circuit breaker interrupting time to the data obtainable from these figures, the minimum reclosing times permissible on various systems may be obtained.

2. On systems with small stability margins, gains in the maximum power transmission without loss of synchronism during transient faults may be obtained by using circuit breakers with reclosing time much less than the present standard of 20 cycles.

3. Triple-pole reclosing on double-circuit transmission lines may be accomplished by adding one or two cycles extra de-energized time. This will still fall well under the present standard of 20 cycles in most cases.

4. Shunting resistors do not tend to increase the minimum total reclosing time on circuit breakers applied on short lines. On long lines they may increase it up to the duration of the resistor follow current.

5. The capacitive coupling associated with single-pole reclosing appears to make single-pole reclosing infeasible under many conditions on 230-kv systems unless excessive de-energization times are allowed.

Appendix I. Calculation of Voltages Electrostatically Induced on Unconnected Transmission Line Conductors

The voltage induced on one of two long parallel conductors by a charge on the second when their spacing is large in comparison with their diameter and with the effect of the ground plane taken into account is given very closely by the equation

$$e=25{,}740\,q\log\frac{a'}{a} \qquad (1)$$

where

e = voltage induced on first conductor, in kilovolts
q = charge on second conductor, coulombs per mile
a = distance between the two conductors
a' = distance from one conductor to the reflection of the other in the ground plane

The voltage induced on a conductor by its own charge is given by the same equation with a set equal to the conductor radius.

By setting up a system of equations like equation 1 and solving simultaneously, it is possible to determine the charge on each of a system of conductors connected either to ground or to a voltage source of moderately low impedance. Then the voltage on nearby unconnected conductors may be determined as the sum of the effects of all charges on the connected conductors.

Thus for a system of two ground wires, a and b, and 3-phase conductors, 1, 2, and 3, the following system of equations would be used to determine the charges, the quantities in the fractions representing the distances between the indicated conductors or reflections

$$e_a=25{,}740\left(q_a\log\frac{aa'}{aa}+q_b\log\frac{ab^1}{ab}+\right.$$
$$\left.q_1\log\frac{a1'}{a1}+q_2\log\frac{a2'}{a2}+q_3\log\frac{a3'}{a3}\right)=0$$
$$e_b=25{,}740\left(q_a\log\frac{ba'}{ba}+q_b\log\frac{bb'}{bb}+\right.$$
$$\left.q_1\log\frac{b1'}{b1}+q_2\log\frac{b2'}{b2}+q_3\log\frac{b3'}{b3}\right)=0$$
$$e_1=25{,}740\left(q_a\log\frac{1a'}{1a}+q_b\log\frac{1b'}{1b}+\dots\right)=E$$
$$e_2=25{,}740\left(q_a\log\frac{2a'}{2a}+\dots\dots\right.=E\underline{/120^\circ}$$
$$e_3=25{,}740\left(q_a\log\frac{3a'}{3a}+\dots\dots\right)=E\overline{\diagdown 120^\circ}\qquad(2)$$

One of the 220-kv transmission lines in this country has two circuits carried on the same towers with flat vertical spacing and the following dimensions:

Distance between conductors of the same circuit, feet	16.5
Average height of lowest conductor above ground, feet	100
Distance from center line of tower to conductors, feet	14.5
Average vertical distance from conductors to ground wires, feet	20.7
Distance from center line of towers to ground wires, feet	8.67
Effective conductor radius, inches	0.52
Effective ground wire radius, inches	0.19

Calculating interconductor distances from these values, substituting in equations 2, and solving for the charges when one circuit only is energized, the other being disconnected, gives the following values

$$\left.\begin{aligned}q_a&=-1.2-0.4j\\q_b&=-0.7-0.3j\\q_1&=14.4-1.2j\\q_2&=-7.6+13.2j\\q_3&=-6.2-13.1j\end{aligned}\right\}\times10^{-6}E\qquad(3)$$

Table II

	Induced Voltages		
	Per Unit	Kv at 220 Kv	Amperes Per Mile at 220 Kv
Top conductor	$0.035+0.022j=\lvert0.041\rvert$	5.2	0.024
Center conductor	$-0.006+0.011j=\lvert0.013\rvert$	1.6	0.007
Bottom conductor	$-0.037-0.019j=\lvert0.042\rvert$	5.3	0.024
Similarly transposed	$0.028+0j=\lvert0.028\rvert$	3.6	0.016
Reverse transposed	$0.010+0.018j=\lvert0.021\rvert$	2.7	0.012

Table III

	Induced Voltages		
	Per Unit	Kv at 220 Kv	Amperes Per Mile at 220 Kv
Top conductor	$-0.15+0.06j=0.16$	20	0.097
Center conductor	$-0.20j+0.01j=0.20$	25	0.120
Bottom conductor	$-0.15-0.09j=0.17$	22	0.102
Transposed	$0.17+0.02j=0.17$	22	0.102

The voltages of the unconnected conductors are then as shown in Table II. The effective capacitance of one conductor under these conditions is 0.012 microfarad per mile and currents that would flow in a connection to ground also are shown.

These lines are transposed on the same towers, but in opposite rotation. Because of asymmetry with respect to the ground circuits, this would not completely balance out the induced voltage even if the transposition were otherwise perfect. The residual voltage is somewhat less than if the lines were similarly transposed.

Current measurements were made on the three phases, grounded individually, of a 58.5-mile length of one circuit of this line, the other circuit being energized, and the two circuits being transposed in sections of 18.88, 22.84, and 16.80 miles. These measurements correspond with calculated values as follows:

	Amperes		
Calculated values	0.70	0.74	0.58
Measured values	0.60	0.63	0.52

These voltages and currents tend to increase with greater conductor diameter and greater spacing between conductors in the same circuit; they tend to decrease with greater height above ground, greater separation from the ground wires and between circuits. Complete elimination of the ground wires, however, increases the voltages of the two upper phases by 70 and 60 per cent, but decreases the voltage of the bottom phase by 25 per cent. Transposed values are increased about 20 per cent.

Single-Phase Switching

For single-phase switching, the voltage induced on one unconnected phase of a single circuit when the other two phases are energized is of interest. These values have been calculated by the method indicated above, and are shown in Table III. The values are for one circuit of the line described with the other circuit de-energized, and for phase rotation 1, 2, 3. With the other circuit energized, the values will be modified somewhat by induction from the other circuit.

These values tend to increase with greater conductor diameter, more height above ground, and greater separation from the ground wire. They tend to decrease with greater phase spacing.

Reference

1. Ultrahigh-Speed Reclosing of High-Voltage Transmission Lines, Philip Sporn, D. C. Prince. *Electrical Engineering (AIEE Transactions)* volume 56, January 1937, pages 81–90.

Discussion

W. M. Leeds (Westinghouse Electric Corporation, East Pittsburgh, Pa.): These test results on the deionization times of fault arcs flashing over insulator strings will undoubtedly be of assistance in establishing minimum reclosing intervals for the rapid reclosing of high-voltage circuit breakers. The conclusions drawn are of considerable interest even though some points may require more data for complete confirmation.

For instance, a superposition of the curves of Figures 6, 8, and 9 would indicate that the minimum de-energization time is approximately independent of voltage over the range from 69 kv to 230 kv for fault currents up to 8,000 amperes. While the curves obviously diverge for higher currents, the data hardly substantiates the statement that the minimum times at 132 kv are constant over a wide range of current, particularly below 8,000 amperes.

In the section Triple-Pole Reclosing by a Circuit Breaker Equipped with Shunting Resistors, it is stated in the third paragraph that reclosing tests at 8,000 amperes at a reestablished voltage corresponding to 230 kv indicated only $2^1/_2$ cycles of dead time to be required. Adding 5 cycles of resistor current flow after fault interruption gives a total of $7^1/_2$ cycles which, astonishingly enough, is appreciably shorter than the 9 cycles deenergized time indicated by Figure 6 for a circuit breaker without any resistor at all.

The fifth conclusion suggests that single pole reclosing at 230 kv may not be feasible, in many instances, because of the small current maintained in the fault path due to capacitive coupling from the unfaulted phases. Since 3-pole reclosing will be required in the majority of high-voltage applications where rapid reclosing is to be applied, it would appear advantageous to design the circuit breakers for operation of all three poles by a single mechanism whenever possible to avoid the expense of maintaining three operating mechanisms instead of one.

In recent years considerable design and development work has been applied to the mechanical operation of high-speed reclosing circuit breakers for 115 kv and above. The pneumatic type of operating mechanism has proved to be more flexible than the solenoid for this purpose, and has been equipped with quick-acting air inlet valves and trip-free links for maximum operating speed. As an indication of the progress that has been made, it should be mentioned that high power fault interruptions were made at Grand Coulee Dam in March 1947 at 230 kv with successful reclosure in 12 cycles. These results were reported by Killgore and Clagett.[1]

Still more recently, by utilizing a number of design improvements including antifriction roller bearings at the most heavily loaded pivots in the pole unit linkage, all three poles of the largest 230-kv oil circuit breaker rated 10,000,000 kva have been reclosed in less than 9 cycles with a single pneumatic mechanism. Still shorter reclosing times are possible with separate mechanisms to operate each pole, although flashover deionization times appear to set a lower limit for practical application at 12 to 15 cycles.

As indicated by the test results reported in this paper, circuit breakers which are capable of functioning satisfactorily without low value resistors have an advantage for reclosing duty since the effect of the residual resistor current in delaying the flashover deionization is thus avoided. The necessity for such resistors can be eliminated by incorporating into the interrupting units of conventional circuit breaker designs spring-driven oil pistons of moderate size which will provide substantially restrike-free performance during the interruption of transmission line charging current.

There are thus available to the industry simple steel-tank high-voltage circuit breakers of the dependable downward break type with an isolating oil gap below highly effective interrupting units which provide high speed arc clearing in less than 3 cycles, actually approaching 2 cycles under normal system voltage recovery rates, over the entire range of line-charging, magnetizing or fault currents up to 10,000,000 kva or even higher. Furthermore, mechanically trip-free pneumatic operating mechanisms which require no air or external assistance during the tripping function can provide high-speed reclosing within time intervals shorter than any practical service requirement.

REFERENCE

1. FIELD TESTS FOR DEVELOPMENT OF 10,000,000-KVA 230-KV OIL CIRCUIT BREAKERS FOR GRAND COULEE POWER PLANT, C. L. Killgore, W. H. Clagett. *AIEE Transactions*, volume 67, part I, 1948, pages 271–87.

•

Philip Sporn (American Gas and Electric Service Corporation, New York, N. Y.): The work on ultra-rapid reclosing of high-voltage lines, initially carried out by D. C. Prince and myself more than 13 years ago, foreshadowed a good many of the results indicated here. It is most gratifying, however, not only to have all of that definitely confirmed, but to have available the results of the complete job the authors have done. Of much greater importance is that we now have the benefit of the work carried out by the authors as a further stimulus to the development of the idea of ultra-rapid reclosure as a major tool in the exploration of the maximum economy at which high tension transmission of electric power and energy can be carried out.

It is particularly gratifying to have available the technical basis for speeding up ultra-rapid reclosure to a considerably lower elapsed time interval than 20 cycles; to have a clarification of the fundamentals of, and particularly the difficulties and limitations inherent in, the use of single-pole reclosing; and to know the effect of shunting resistors on successful reclosure. With this information application of ultra-rapid reclosure to lines of 220 kv and higher voltage should not only be possible to the same degree that has been successfully applied at 132,000 volts, but the degree of successful functioning should be further increased at 132,000 volts and the higher voltages beyond present experience.

The authors are to be congratulated on this outstanding contribution toward the development of a major tool in the art of transmission of power and energy at high voltages.

Harry P. St. Clair (American Gas and Electric Service Corporation, New York, N. Y.): This paper is of particular value in throwing light on two important questions, first, the effect of resistors on circuit breaker deionization time and second, the feasibility of single-pole reclosing on long high-voltage lines.

Resistors appear to be necessary on many types of circuit breakers to enable them to handle the charging current of long lines without excessive restriking and resulting overvoltage transients. One of the important results of the authors' test is that these resistors are no help in cutting down deionizing time and reducing the reclosing cycle, since resistor current time must be added to the reclosing time. This would affect both 3-pole and single-pole reclosing.

As to relative merits of single-pole and 3-pole reclosing and the theoretical improvement in stability offered by single-pole reclosing, we are particularly indebted to the authors for a realistic analysis and tests. It seems quite conclusive that for higher voltage lines, even where distances are moderate, such as 100 to 200 miles, the mutual coupling effect may not only offset the theoretical gain from single-pole reclosing, but as the authors state, make it entirely impossible.

Finally, it also may be concluded that any proposed combination of single-pole reclosing with resistor-equipped circuit breakers would encounter especially hard going and it may well be that at least for higher voltage lines, neither can be used.

The work done by the authors as reported in this paper is a job that has been badly needed and constitutes another important milestone in the transmission art. In discussion with the authors, I was told that time did not permit carrying out the test program to the extent that would be desirable. We sincerely hope that such tests will be continued and further results made available. Also, the differences shown between 138-kv and 230-kv results indicate the desirability of exploring high-speed reclosing at voltages even higher than 230 kv.

A. C. Boisseau, B. W. Wyman and W. F. Skeats: In an investigation of this nature, the interest and encouragement for continuation from such pioneers in the high-speed reclosing field as Mr. Sporn and Mr. St. Clair are sincerely appreciated.

In this investigation of the fundamental considerations involved in high-speed triple-pole and single-pole reclosing, the authors did not confine their data to any particular type of circuit breaker. The data presented are applicable to either impulse-type low oil content circuit breakers or to tank-type circuit breakers either with or without resistors, as most of these types have been developed to the point where they will either exceed or approach the minimum practical reclosing times which can be applied on high-voltage systems. Mr. Leeds suggests, in addition, a tank-type circuit breaker equipped with auxiliary spring-driven pistons to provide "substantially" restrike-free performance during the interruption of transmission line charging current. The blast of oil furnished by such a piston is in principle similar to that used for many years in the impulse-type circuit breaker. In the experience of the authors, such a piston, if properly designed, should not only "substantially" eliminate but should completely eliminate restrikes, as no restrikes have ever been obtained with the impulse type circuit breaker. The authors feel that by putting the piston-type interrupter inside a tank-type circuit breaker, as Mr. Leeds suggests, the biggest advantage of the piston is being lost, namely, the elimination of the large tank and thousands of gallons of oil which the impulse-type circuit breaker accomplishes automatically.

The authors agree with Mr. Leeds that deionization may be expected to be substantially independent of voltage over the range from 69 to 230 kv for fault currents up to 8,000 amperes.

As stated in the paper, when shunting resistors are used, reclosure takes place in two steps: first, through the resistor, and finally, by shunting out the resistor. So far as the first step is concerned, the overshoot associated with reclosure is completely damped out with a resistance of the order of 3,000 ohms and transmission line lengths of a mile or more. For this condition, the tests indicate, as Mr. Leeds points out, that at 230 kv and 8,000 amperes, the shortening of the necessary dead time caused by elimination of the overshoot is greater than the increase caused by the flow of resistor current. Thus, considering the first step only, there is a net gain from the use of resistors. However, the second step must be considered also, and here, as indicated in Figure 11, the overshoot is dependent to a considerable extent on switching conditions and the necessary dead time may be expected to vary accordingly over a range from $2^1/_2$ cycles with favorable conditions on very short lines to nine cycles with unfavorable conditions on long lines.

Development and Application of Electric Heating to Deicing of Aircraft Propellers

JACK H. SHEETS
NONMEMBER AIEE

EDWARD J. SAND
NONMEMBER AIEE

THE use of heat for protecting aircraft propellers against ice formation is considered as one of the most positive approaches to the problem. Electric energy is a very convenient means for obtaining necessary heating on the propeller blades under adverse installation conditions. This paper discusses the development of the electric heating system and design practices being used on current commercial and military aircraft. In view of design problems with respect to power supply and application probable future trends also are discussed.

Propeller Icing Problem

Ice formation on the propeller is a potential hazard to flight safety because of the serious effects it can have on the aerodynamic, balance and structural characteristics of the propeller and the airplane. Available data are very meager with respect to a quantitative evaluation of these factors. Difficulties in applying widely varying meteorological conditions to propeller icing have been a major stumbling block to adequate definition of the problem. Flight test data taken in the past under natural icing conditions have not been reliable because of difficulties in separating performance losses caused by ice accretion on other parts of the airplane structure from the aerodynamic characteristics of the propeller under icing conditions.

The most reliable data on the reduction of propeller efficiency caused by icing are believed to be those presented by the National Advisory Committee for Aeronautics at a recent conference on aircraft ice prevention[1] where it was indicated that in a total of 42 ice encounters, approximately 37 per cent of the encounters showed a loss in propeller efficiency of 0 to 5 per cent; 50 per cent of the encounters showed a loss of 5 to 10 per cent; 5 per cent of the encounters showed a loss of 10 to 15 per cent; and 8 per cent of the encounters showed a loss of 15 to 20 per cent. These data were taken in actual flight on an airplane with very complete ice protection equipment and instrumentation in order to isolate as closely as possible the aerodynamic effects of ice accretion on the propeller and other parts of the airplane.

Nonuniform build-up or shedding of propeller ice will cause propeller unbalance which can result in objectionable propeller and engine vibration. It is doubtful that propeller unbalance would be sufficient to cause structural damage even under severe icing conditions on installations using dynamic engine mounting. On installations with rigid engine mounting, continued operation under vibratory conditions resulting from nonuniform ice build-up might cause structural damage. In either case the resulting unbalance could be sufficiently objectionable to require feathering the propeller.

The amount of ice that will build-up on the propeller blade depends upon many factors and will vary widely with the type and severity of icing conditions encountered. Pieces of ice will be thrown from the rotating propeller even when no ice prevention methods are employed. Experience has shown that these pieces of ice thrown from the rotating propeller can be large enough to cause structural damage to the fuselage, windows, stabilizer, and other components of the airplane. Likewise the noise from the impact of ice thrown from the propeller on the fuselage is objectionable for commercial operations because of passenger discomfort and annoyance even though the ice particles may not be of sufficient size to be harmful structurally.

While there is still much discussion on the quantitative effects of propeller icing which will not be resolved until further studies are made, it is generally conceded that the best possible propeller icing protection should be provided for both commercial and military operations. This is particularly true since improvements in icing protection being made available for other airplane components will make it practical to schedule operations through more severe icing conditions with adequate flight safety.

Early Methods of Ice Protection

Early methods for protecting the propeller in icing conditions included the use of fluids which acted to lower the freezing point at the blade surface sufficiently to provide a liquid interface between the blade surface and any ice layer which forms. The adhesion of the ice to the blade is lowered sufficiently under this condition to allow pieces of ice to be thrown off under normal centrifugal forces. Chemical paints and pastes also have been applied to the blade surface to accomplish the same purpose.

With the fluid system a slinger ring is mounted on the propeller hub. Fluid is pumped from a supply tank in the airplane into an annular channel in the slinger ring through a stationary feeder tube mounted on the engine nose. Fluid is discharged along the leading edge of the blade at the shank by the centrifugal forces on the fluid through suitable dis-

---

Paper 49-222, recommended by the AIEE Air Transportation Committee and approved by the AIEE Technical Program Committee for presentation at the AIEE Pacific General Meeting, San Francisco, Calif., August 23–26, 1949. Manuscript submitted August 15, 1947; made available for printing June 30, 1949.

JACK H. SHEETS and EDWARD J. SAND are both with the Curtiss-Wright Corporation, Caldwell, N. J.

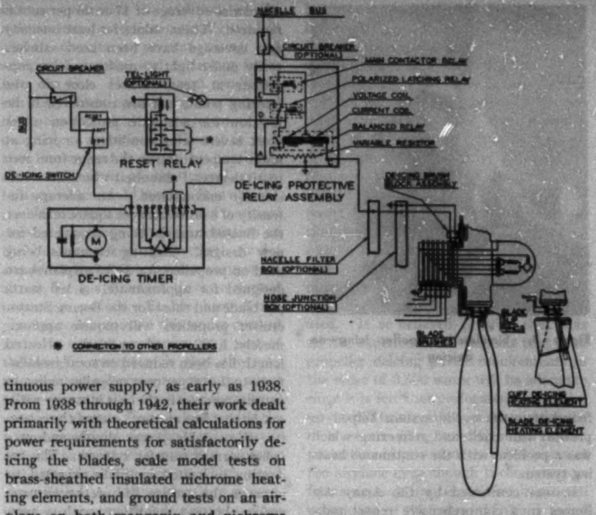
NACELLE BUS
CIRCUIT BREAKER (OPTIONAL)
MAIN CONTACTOR RELAY
POLARIZED LATCHING RELAY
VOLTAGE COIL
CURRENT COIL
BALANCED RELAY
VARIABLE RESISTOR
CIRCUIT BREAKER
TEL-LIGHT (OPTIONAL)
BUS
RESET
OFF
ON
RESET RELAY
DE-ICING SWITCH
DE-ICING PROTECTIVE RELAY ASSEMBLY
DE-ICING TIMER
DEICING BRUSH BLOCK ASSEMBLY
NACELLE FILTER BOX (OPTIONAL)
NOSE JUNCTION BOX (OPTIONAL)
BLADE BRUSHES
CUFF DE-ICING HEATING ELEMENT
BLADE DE-ICING HEATING ELEMENT
* CONNECTION TO OTHER PROPELLERS

Figure 2. Propeller deicing wiring diagram

charge tubes connected to the slinger ring. A series of grooves molded in a thin strip of synthetic rubber cemented to the leading edge of the blade is used usually to assist in fluid distribution over the entire length of the blade. The fluid normally used is isopropyl alcohol.

While the fluid system has given reasonably satisfactory results under light icing conditions, the trend toward larger diameter propellers with lower rotational speeds, together with general increases in operating air speeds, has made it much more difficult to obtain satisfactory fluid distribution over the blade. Increased blade angle ranges being used on controllable pitch propellers providing feathering and reverse pitch also complicate the problem of providing a satisfactory fluid discharge on the blade leading edge. On long-range multiengine aircraft, the weight of fluid which must be carried is also significant. It is very doubtful that fluid anti-icing performance would be considered acceptable under the more severe icing conditions for which icing protection is expected to be required.

The chemical agents of the anti-icing paints and pastes are used up under icing conditions to such an extent that they maintain their effectiveness for only a limited time. Operation in rain has the same effect on using up their effective period even though icing conditions are not encountered. Because of these characteristics it has been considered that the various chemical pastes and paints are not suitable for long-range operation. Satisfactory protection for shorter range operation can be maintained only by reapplication after operation in rain or icing conditions. Reapplication is quite time-consuming because of the care and drying time usually required to maintain satisfactory coverage under air and centrifugal forces. While these anti-icing pastes and paints have been shown to give reasonably satisfactory icing protection for short periods, application time requirements make their use undesirable for even short range flights on scheduled operation.

Electric Heating Development

The National Research Council of Canada had started development work on an electric anti-icing system, using a continuous power supply, as early as 1938. From 1938 through 1942, their work dealt primarily with theoretical calculations for power requirements for satisfactorily de-icing the blades, scale model tests on brass-sheathed insulated nichrome heating elements, and ground tests on an airplane on both manganin and nichrome wire elements covered with sprayed aluminum and rubber respectively. By this time, the National Research Council had done sufficient background testing to recommend flight testing as a means of checking the heat intensities they had calculated and to determine the extent of heating element coverage required. Under conditions of the tests, they had concluded that a heat intensity of 1.25 watts per square inch provided satisfactory de-icing performance.

A continuous heating system using a generator mounted on the rear of the propeller hub for the power source, together with suitable blade heating elements was designed in 1940 for use by the Army Air Forces. The generator was rated at 750 watts and the design heat intensity on the elements was 2.5 watts per square inch. Flight tests conducted on these units under natural and simulated icing conditions indicated the necessity for higher heat intensities with an indication that 4 watts per square inch along the leading edge and 2.5 watts per square inch over the remainder of the heated area would be required. These tests indicated the significance of providing an adequate thermal insulating layer between the heating element and the blade to reduce conducted heat losses.

Changes in design requirements requiring use of larger diameter, lower rpm propellers resulted in hub generator designs which were not too practical even for the power requirements then being considered because of increases in size and weight necessary to obtain the required output. A cyclic-heating system was investigated by the Army Air Forces where heat is applied on the propeller blades for a relatively short period. It was found that an energization time of approximately 12 seconds would be sufficient to reduce the surface adhesion of the ice by establishing a liquid interface so that the normal centrifugal force would throw off the ice. With this cyclic system it was shown that the over-all power requirements could be reduced by successive energization of propellers or groups of blades on multiengine aircraft. This reduction in over-all power requirements made it practical to consider the possibility of using the airplane power supply for propeller de-icing even though it was found that somewhat higher heat intensities would be required than those necessary to give equivalent results with the continuous heating system. It also was

Figure 1. Heating element installed on blade and cuff

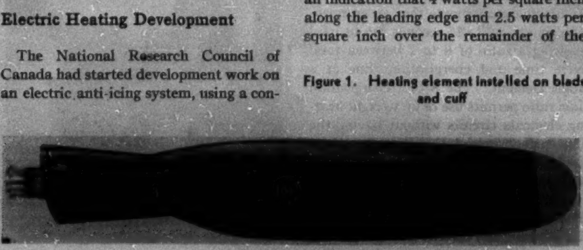

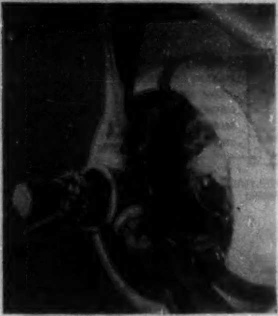

Figure 3. Simulated propeller icing—no deicing

found that the cyclic system helped to prevent run back and refreezing which was a problem with the continuous heating system.

It was concluded by the Army Air Forces in a comprehensive report published in 1944[2] that the cyclic-heating system should be adopted because of improvements in propeller ice protection, together with the advantages in weight and power saving over the continuous heating systems considered previously.

Present Design Practice

Electric deicing systems on current production propellers utilize heating elements cemented to the leading edge of the propeller blades which are connected to slip rings rotating with the propeller. Brushes mounted on the engine nose are used to transfer current to the rotating propeller through these slip rings. The normal power supply system which is the conventional 28-volt d-c system on installations being made at this time is used for propeller deicing. A timing mechanism operates remotely controlled contactors to give successive energization to the several propeller deicing circuits. A propeller deicing power connection is generally made at the nacelle bus in order to reduce wiring weight although a separate deicing bus could be used from a main load center. A typical installation and wiring diagram are shown in Figures 1 and 2.

Army Air Forces Specification *29542*, which was the original basis for design of present propeller electric deicing systems, requires 5.72 watts per square inch at the leading edge and 2.86 watts per square inch over the remaining heated area for a cyclic system. Heating element coverage of 75 per cent of the exposed length with a chordwise coverage of 17 to 25 per cent is required. These values for heat intensity and coverage have been used satisfactorily under light to moderate icing conditions at temperatures close to the freezing point, but are considered to be too low for adequate protection under more severe icing conditions or icing at lower temperatures in the range from zero to 10 degrees Fahrenheit which are occasionally encountered. An average intensity of 8 or 9 watts per square inch over the heated area is being considered for new designs. Heating elements being used on propellers for *DC-6* airplanes are designed for approximately 1,100 watts per blade and those for the Boeing Stratocruiser propellers will require approximately 1,600 watts per blade. Heated length has been reduced on some installations to the 60 per cent propeller radius to permit increases in the heat intensity without having line currents exceed the capacity of available power supply and propeller current transfer systems. This reduction in heated length is expected to improve the service life of the element under abrasion conditions with a negligible reduction, if any, in deicing effectiveness at the tip.

The total cycle time between successive energization periods of a given element is limited by the amount of ice which can be allowed to build up on the blade. The amount of ice build up must be kept below that which could cause structural damage when thrown off. This condition is considered to be more severe than the aerodynamic effects of propeller icing. Another requirement for airline operation, which is in turn more limiting than that of no structural damage, is that ice thrown from the propeller blades should not cause noise inside the cabin from strikes against the fuselage which would be objectionable from the passenger standpoint. Some investigations have indicated that total cycle times between successive energization can be 200 seconds or more, but it is felt that total cycle times in the order of 100 to 150 seconds will be the highest which will be generally acceptable under cabin noise limitations. Available data indicate that an energization time of 12 to 15 seconds can be used allowing a ratio of 8 to 1 between total cycle time and energization time of a single element. The 8 to 1 energization time ratio permits use of up to eight heating elements circuits without having the line current exceed that required for a single circuit. This is an important factor in determining power requirements. The cyclic energization of elements also is significant in reducing the temperature rise in wiring and current transfer brushes. Energization times between 20 and 30 seconds with a 4 to 1 energization ratio are being used on some installations, but it is felt that a total cycle time of 120 seconds with an 8 to 1 ratio giving 15 seconds energization to individual elements will be found entirely adequate.

Two types of heating element constructions are in general use. Both of these types are molded from synthetic rubber compounds, usually neoprene. A laminated construction is used with an external layer of material approximately 0.020-inch thick for abrasion protection and a layer of material approximately 0.030-inch thick on the side of the element that is bonded to the blade for thermal and electrical insulation. One of these types has a grid of resistance wires embedded between the cover layers, and the other an intermediate layer of conductive rubber. With either construction suitable lead terminations and internal connections are incorporated as a part of the molding process. Conductive rubber elements were used in early hub generator systems operating at approximately 50 volts. The resistance wire elements appeared to be more suitable for use with 28-volt systems, although earlier difficulties with conductive rubber elements having resistance values suitable for this system voltage have been resolved, and both types are currently being furnished in production. It is not felt that sufficient service experience has been accumulated to date to indicate a superiority for either type of element.

Current transfer to the rotating propeller imposes definite design problems because of space limitations and high vibration levels in addition to brush difficulties at altitude which require special measures to obtain satisfactory results. Experience gained in the design of brushes

Figure 4. Typical electric deicing under simulated icing conditions

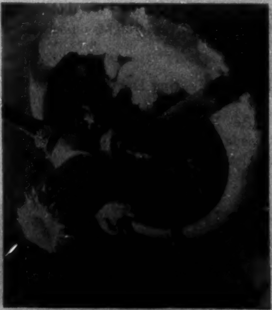

and slip rings used in the pitch changing circuits of conventional propellers using an electric motor for pitch changing power has been helpful in solving this problem, although the higher current required for electric deicing accentuates brush voltage drop and heating problems. High altitude treated carbon brushes with high copper content are currently being operated with current densities of 500 amperes per square inch with spring pressures of approximately 8 pounds per square inch on bronze slip rings at a surface speed of 2,000 feet per minute. It is believed that a current density of 750 amperes per square inch will be a limiting value for these conditions. It must be noted that these values are for cyclic energization and probably would not be satisfactory for continuous duty because of excessive heating. Relative motion between the blades and the hub structure also complicates current transfer, but this is not so great a design problem because the movement is limited to approximately 120 degrees at a relatively slow rate. An additional set of brushes and slip rings has been considered desirable at this point, although propellers are being operated with a pig-tail connection between the hub and the blade element with careful attention to the design details to eliminate service difficulties resulting from centrifugal forces, vibration, and handling damage. Figures 5 and 6 show current transfer brushes and slip rings being used on production propellers.

Electric deicing circuits require under-current protection in addition to the over-current protection normally used in aircraft circuits to prevent wiring and equipment damage and to isolate faults from the bus. Under-current conditions can result from open circuits or internal short circuits within the system. This condition is undesirable when it is such that low current is drawn by one blade element because of the propeller unbalance which could result. It is also desirable to receive an indication of marginal deicing protection through actuation of the under-current protective device should blade elements or other parts of the circuit become damaged prior to normal inspection periods. It has been found possible to incorporate this under-current and over-current protection as a part of the nacelle contactor so that the contactor circuit will remain open in the event of line currents above or below the normal operating range. Since a device with the proper sensitivity for this application is difficult to build with sufficient capacity to handle high fault currents which could occur with a solid short circuit to ground, it is customary to provide circuit breakers or limitors for this type of protection.

It has been difficult to establish design specifications for power requirements of blade heating elements because of the problem in defining adequately the limiting meteorological conditions under which operation is expected with propeller deicing equipment. Airplane operation under more severe icing conditions has been made possible by improvements in anti-icing protection for other parts of the airplane. Available data have indicated that earlier estimates as to power requirements for propeller electric deicing systems are lower than desirable to provide complete propeller deicing under some of the more extreme conditions. Since some propeller deicing systems currently in use have been designed with definite restrictions on the amount of power available, it is considered essential that definite attention be paid to the performance of these existing systems in actual operation in order that the extent of compromise, if any, with theoretical performance requirements can be evaluated. It is believed possible that this service experience will indicate that total propeller deicing power requirements in the order of 3,500 watts will be adequate since it is felt that performance with this power will insure safe operation under the most severe icing conditions for which protection is provided on other parts of the airplane even though theoretical performance may not be satisfied in a small percentage of the cases. If this is found possible, a practical compromise will have been achieved without requiring the power increases to approximately 4,500 watts indicated by some recent data. It is recommended, however, that the value of 4,500 watts for propeller deicing power be used as a basis for new designs with three blade propellers up to 13 feet basic diameter and four blade propellers up to 15

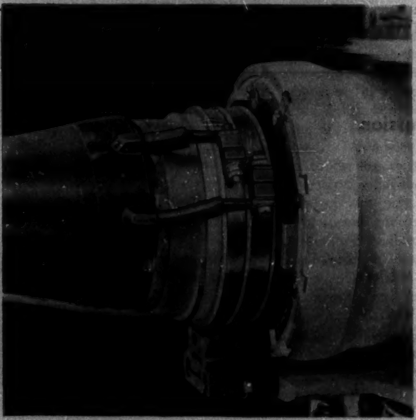

Figure 5. (below) Blade deicing brushes and slip rings—protective cover removed

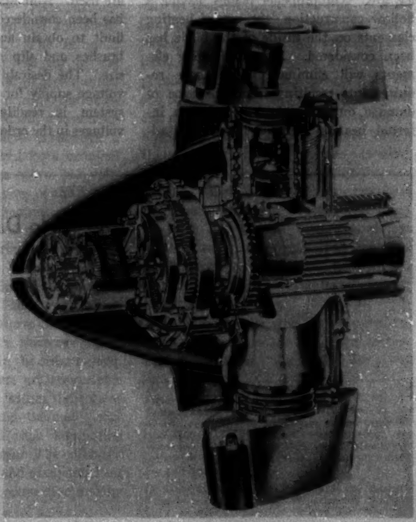

Figure 6. (right) Propeller section showing hub slip rings

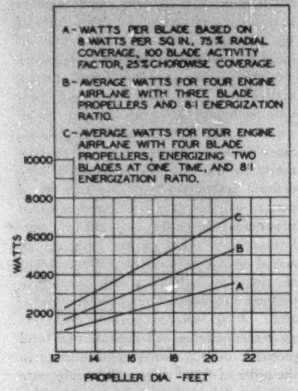

Figure 7. Recommended maximum power requirements for propellers with external heating elements

feet basic diameter until actual operating requirements are better established.

Probable Future Trends

Heating elements mounted on the blade leading edges are susceptible to damage from stones picked up on runways as well as wear from water and sand abrasion. Changes in materials and methods of fabrication for external elements will probably be desirable to improve service life. On propeller blades having a hollow construction, the use of heating elements on the inside of the blade has been considered. Internal heating elements will eliminate maintenance requirements resulting from this type of damage on external elements. An internal heating element has the disadvantage of requiring additional power input and an increase in the cyclic energization time as a result of the thermal lag of the increased material thickness between the heating element and the layer of ice. In addition to the power increase required per blade, this will have the effect of doubling airplane power requirements on installations where energization of two deicing circuits is required simultaneously in view of limits on the allowable icing build-up between successive energizations. Power requirements for internal elements are not as well established as those for external elements and more work will be required to permit a better definition of these requirements.

Available data indicate that an average of 8 watts per square inch should be used on new designs until the service experience discussed previously has been obtained. This will require 2,300 watts per blade on a 16 foot 6-inch diameter blade having heating element coverage to 75 per cent radius and a cordwise coverage of 25 per cent. On a 4-engine airplane with four blade propellers this will require 4,600 watts from the airplane power system with two blades being energized at a single time at an 8 to 1 energization ratio. A more general indication of these power requirements is given in Figure 7.

It can be seen that line currents in the order of 200 amperes are required with the normal 28-volt d-c power system to provide propeller deicing if heating intensities and coverage of the type described are used. A line current of 250 amperes has been considered as a practical upper limit to obtain acceptable service with brushes and slip rings of a reasonable size. The desirability of using a higher voltage supply for the propeller deicing system is readily apparent. Supply voltages in the order of 110 volts alternating or direct current would be very desirable for this application. These higher voltages would permit an appreciable reduction in wire weight and would make the system less sensitive to variations in element resistance through reduction in the percentage of the system voltage lost through wiring and brush-slip ring drops.

The electric deicing system for propellers has found favor because of its flexibility and the ease with which it could be adapted to existing propeller designs. Another system for deicing propellers using blades of hollow construction by means of heated air passed through the inside of the blade is being developed. This system in its present form requires an appreciably greater power input to the propeller than with the electric system, although the use of exhaust heat exchangers or relatively simple combustion heaters make this power much more readily available than that required from the airplane electric system. It is believed that the heated air propeller anti-icing system will be improved through further development to a point where the deicing performance will be as good as or better than that provided by the electric system with lower installation weight and reduced maintenance requirements. Until this development is completed electric deicing systems for propellers will continue to play an important part in insuring the safety of all-weather operation of aircraft.

References

1. EFFECT OF ICE FORMATIONS ON AIRPLANE PERFORMANCE, C. Merritt Preston, W. V. Gough, Jr. National Advisory Committee for Aeronautics Conference on Aircraft Ice Prevention, June 26–27, 1947 (To be published).

2. PROPELLER ELECTRICAL ANTI-ICING SYSTEMS. Army Air Forces (Washington, D. C.) *Memorandum Report Number TSELA-3C-581-144-6*, September 25, 1944.

No Discussion

Lightweight Aircraft Transformers

D. S. STEPHENS
ASSOCIATE AIEE

Synopsis: The purpose of this paper is to discuss characteristics and construction of lightweight aircraft transformers. It is intended primarily to be of interest to those members of industry who design and service electric systems of aircraft. Topics covered are construction, materials, standard ratings, window heating transformers, operating characteristics, and estimated life.

THE higher voltages of the a-c system are required to handle economically the ever-expanding electrical loads of large commercial and military airplanes. Modern aircraft require approximately 1 kw of electric power for each ton of gross weight and with such electrical loading increasing applications are found for transformers. Transformers are required for applications such as lighting, instruments, control, rectification, and window deicing. The development of a laminated glass which can be heated by the passage of current through a conductive layer[1] has increased the demand for larger aircraft transformers capable of supplying loads of 1,000 to 8,000 watts. Transformers are relatively heavy electric apparatus and the weight problem requires consideration from both the aircraft and transformer industry. Weight reduction is a permanent contribution to the increased range or pay load of the aircraft. As the lower nominal frequency of aircraft generators is fixed at 400 cycles per second, transformer size and weight are fundamentally determined by the quality of the magnetic circuit and temperature limits of the insulation. It is assumed that copper is the most practical current conductor and that established limits on regulation and efficiency must be met. Therefore, increased core and copper losses are the prices to be paid for size reduction. This requires magnetic materials of high flux carrying capacity, heat stable insulation, and abnormally high operating temperatures in proper combination to result in minimum size transformers.

General Features

United States Air Force Specification *32450* provides a general pattern of performance and construction although only 12 ratings are covered in the tabulated section of the specification. The construction of a medium size auto-connected transformer is shown in Figure 1. The design is proportioned to take advantage of the 200 degree centigrade rise permitted on aircraft transformers. The construction features an exposed coil and shell-type magnetic circuit. The terminal studs are located near the top of the unit and close to the coil to give a minimum over-all size. Locating terminals close to the coil is, in itself, a manufacturing problem as there is always a minimum length required for a terminal connection. In ratings below 350 volt-amperes the space saving of the 2-loop core design becomes unappreciable and the single core-single coil arrangement is used. Over a wide variation in the ratio of copper loss to iron loss the inside of the winding has the highest temperature rise of any part of the transformer. The operating temperatures are gradually lower for the coil surface, the core surface, and the frame surface in the order named. It is unlikely that there are appreciable temperature gradients within the core as it is comprised of good thermally conductive material and each lamination reaches two core surfaces. The coil has a small surface exposed and dissipates heat loss by radiation and convection and by conduction to the core.

Core Frames

The frame which holds the type *C* Hipersil cores is typified by the vertical side pieces and base being an integral piece of sheet steel for rigidity. The cores are cradled in horizontal and vertical channels welded to the inside of the inside of the U-shaped steel part. Refer to Figure 1 for this type of construction. Variation of this construction is found on small single-phase transformers and 3-phase transformers. The arrangement gives a low center of gravity with respect to the mounting plane. The cores on the larger transformers, those weighing approximately three pounds and over, are positively held by means of a screw through the center of the top and bottom channel. The screws are tightened to bring pressure to bear on the core. On small units the cores are held by packing tightly into a rigid top and bottom channel.

Fishpaper channels are placed between the edge of the core and the metal channels to prevent short circuiting of core laminations. It would appear that fishpaper, being a class *A* insulating material, is unsatisfactory for such an application. However, the temperature of the core is much lower than that of the coil upon which allowable temperature is based, and fishpaper stands up well under this service. The paper receives a coating of silicone varnish at transformer assembly which imparts heat resistant qualities. It has been found that mica tends to disintegrate when placed between two metal parts that undergo varying compressive forces. Such would be the condition in an aircraft transformer in actual service.

After fabrication the frame parts receive a cadmium plate for protection against corrosion. The frames are given

---

Paper 49-223, recommended by the AIEE Air Transportation Committee and approved by the AIEE Technical Program Committee for presentation at the AIEE Pacific General Meeting, San Francisco, Calif., August 23–26, 1949. Manuscript submitted May 23, 1949; made available for printing July 1, 1949.

D. S. STEPHENS is Design Engineer in the Specialty Transformer Engineering Department, Westinghouse Electric Corporation, Sharon, Pa.

a heat resistant black enamel finish which improves the appearance of the completed unit and increases the radiation constant. The high temperature enamel has a silicone base and was developed originally for finish of space heaters and similar equipment.

Cores—Magnetic Circuit

The cores are of type *C* construction which consists of a continuous strip of lamination, wound to size on a mandrel, annealed, bonded solidly, and cut at the center.[2] The resulting air gap is of the order of 0.002 inch total, and in combination with the high quality steel gives an unusually small exciting current in a 400-cycle transformer. There is no overlap of laminations in a type *C* core which results in saving of space and weight, again an important contribution to light-weight aircraft transformers.

The core material is 0.005-inch thick Hipersil.[2] Hipersil is silicon steel of high permeability wherein the grain orientation is controlled during processing. The elementary pattern of crystals in the steel is arranged so that their axes of easiest magnetization are nearly parallel and aligned in the direction of rolling. As the 400-cycle flux travels in the direction of rolling, very high densities are possible. A common core density for single-phase cores is 15,000 gauss which still permits an over-voltage of 10 per cent without exciting current difficulties. The apparent watts loss (product of exciting current and applied voltage) per pound of core is 10.0 at 15,000 gauss while *TW* (true watts iron loss) is 8.0 at 15,000 gauss. Thus it can be recognized that 5-mil Hipersil is an important contribution to lightweight aircraft transformers.

The top and bottom *C*-shaped sections of the core are held together by steel bands. The steel bands are in definite tension and the ends of the bands are locked together in a crimped seal. A soldered seal is used to hold the bands on small cores when the temperature rise is insufficient to loosen high temperature solder. A film of thermosetting joint compound is placed on the core faces at core assembly and immediately baked. The joint compound is effective in reducing magnetostriction noise.

Coil Materials

The coil insulating materials are chosen to withstand an average temperature rise of 200 degrees centigrade at 25 degrees centigrade ambient. A flexible mica wrapper lines the inside of the coil. Glass-insulated copper wire or strap is used as a current conductor. Silicone impregnated fiber glass serves as layer insulation, end turn sleeving, and coil side wrapper.[3] Glass tape is used where applicable. As the maximum voltage of most designs is below 500 volts, relatively little insulation is required between core and coil. Common test voltages to ground are 1,500 and 2,500 volts. With a minimum of insulation a very solid coil results. A solid coil has two advantages; first it can be wedged solidly on the core and secondly good heat conduction from within the interior results. An ordinary solder joint cannot be used for attaching leads in the coil because of the operating temperature. Leads are incandescent brazed to wire of coil. If the coil wire is very small brazing is difficult to perform without embrittling the copper and in those cases, a high temperature solder joint is made. Stranded copper leads are used to prevent lead breakage arising from vibration. The leads are insulated with a silicone impregnated glass sleeving.

Designs have been made wherein vertical coil ventilating ducts were formed between layers of the coil during winding, as shown in Figure 2. The ducts are effective in permitting high current densities in the copper but lose their advantage with low air densities. Disregarding high altitude performance, a transformer with coil ducts can be made lighter than a transformer without ducts but the decrease in weight tends to be offset by the increase in the long dimension of the coil. Some objection is made to ventilated coils from an appearance and sturdiness viewpoint. A coil with ducts is quite difficult to wind and has multiple openings for penetration of moisture and salt laden air. Experience indicates that the solid coil is more practical.

Core—Coil Assembly

Stiff mica plate is used to wedge the coil on the core and to space the coil sides centrally in the core window. The coil is wedged securely in order to withstand vibration. The core-coil assembly is vacuum impregnated with silicone varnish. A feature of this varnish is that it neither becomes fluid nor brittle over a wide range of temperature. It is "tacky" and penetrates the coil crevices and aids in holding the insulating materials together. Also the conduction of heat from within the coil is improved. Thus, because of their insulating qualities and ability to withstand higher temperatures, mica, glass, and the silicones definitely contribute to lightweight aircraft transformers.

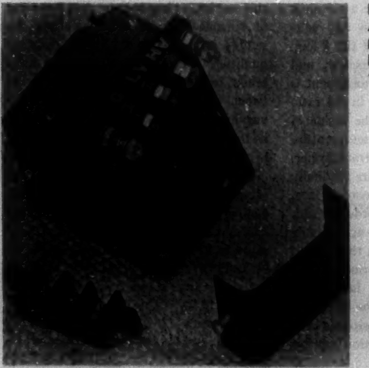

Figure 1 (left). Aircraft transformer of 0.75 kva, voltage ratio 115 to 28, autoconnected

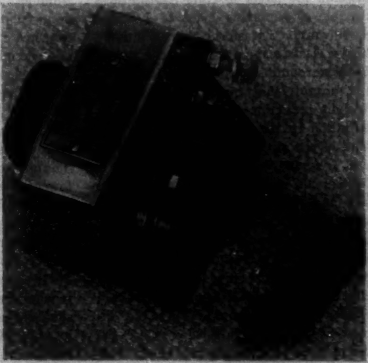

Figure 2 (right). 1.3-kva deicing transformer with ventilating ducts in coil

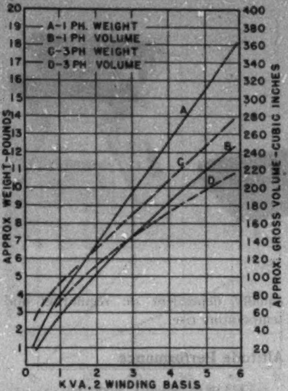

Figure 3. Weight and volume of aircraft transformers, 3-phase and single-phase

Standard Aircraft Transformers

The standard single-phase ratings in United States Air Force Specification *32450* cover a range from 0.005 to 5.0 kva and are auto-connected for an open circuit ratio of 115 to 28 volts. Table I contains the electrical characteristics of standard designs. Figure 3 illustrates weight and volume of high temperature aircraft transformers. In referring auto-connected transformers to this curve the relation shown in the following equations must be considered.

$$\text{Equivalent 2-winding kva} = \frac{E_1 - E_2}{E_1} \times \text{load kva}$$

where

E_1 = high-voltage line voltage
E_2 = low-voltage line voltage

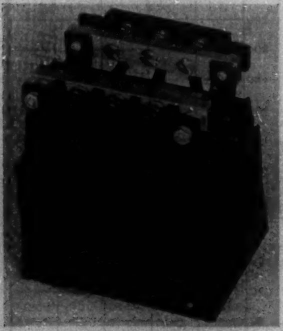

Figure 4. Three-phase aircraft transformer, 0.25 kva, 208 volts wye to 120 volts delta

The volume is maximum space occupied that is, the product of the maximum dimensions along the three axes. Spot checks have shown that the net volume is approximately 45 per cent of the gross volume. A line of standard ratings is very useful in estimating the size of special or new designs. In using Figure 3 consideration must be given to factors other than equivalent kilovolt-amperes which affect the size of a transformer. These factors are ratio, number and position of terminals, current capacity of terminals, terminal protective covers, test voltages, coil guards, and mounting arrangement.

Three-Phase Transformers

Weights and volumes are contained in Figure 3 and typical construction is illustrated by Figure 4. Three-phase 2-winding designs are used for supplying 3-phase loads and approximately balanced single-phase loads from 208-volt generators. A few applications exist for 3-phase deicing transformers which are either auto-connected or extended delta connected. Three-phase transformers use the same materials and construction as single-phase transformers. Three-phase type *C* cores are formed by placing two core loops side by side on a face plate and winding around them a build-up of lamination equal to the build-up of the individual core loops, as shown by Figure 5. This method permits available single-phase core mandrels to be used and results in a wide choice of size. Three-phase cores have higher core loss and exciting current than single-phase cores operated at the same induction because a portion of the flux must travel across rather than along the laminations.

Window Heating Transformers

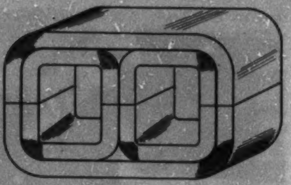

Figure 5. Sketch of 3-phase type *C* core construction

Standard load and voltage ratings are impractical on deicing transformers. The heat requirements to prevent formation of ice on windows is based on a certain watts per square inch of window surface.[1] The current and voltage requirements can be found by Ohms Law wherein the resistance is a function of unit area resistivity of conductive film and proportions. The window shape and number of windows vary with each type of airplane and a special transformer is necessary. Ratings of single-phase deicing transformers range from 1,000 to 8,000 watts output. It is apparent that such ratings will be quite heavy even at 400 cycles and high temperature limits, and the auto-connection is used for minimum weight. Figure 6 shows a high production window deicing transformer. Load voltages vary from 250 to 500 volts and dual simultaneous loads are common. Plus or minus taps are usually required on the nominal load voltage to adjust for variations in glass resistance. Primary taps are used to reduce the load voltage during a warm-up period to prevent cracking of glass due to heat shock.

The aircraft industry specifies 1 per cent to 2 per cent tolerances on load voltages. By comparison, 2 per cent tolerance is customary on filament transformers for radio application. This tolerance becomes a difficult design problem whenever 4- to 16-load voltages are specified. The volts per turn on large deicing transformers will be approximately 3 to 4 volts and adjusting one load voltage by a change of turns may place another load

Table I. Electrical Characteristics of Standard Aircraft Transformers

Army Air Force Specification *32450* Reference Item Number	Load, Kva	No-Load Current as Per Cent of Full-Load Current	Voltage Regulation, Per Cent	Efficiency, Per Cent
1*	0.30	45	5.0	90
2	0.005	60	7.0	80
3	0.05	25	6.0	90
4	0.100	20	6.0	88
5	0.200	10	7.0	90
6	0.50	10	5.0	94
7	0.75	15	6.5	92
8	1.0	13	6.5	92
9	1.5	10	6.0	92
10	2.0	8	5.5	95
11	3.0	6	4.5	95
12	5.0	3.5	5.3	96

* 3-Phase.

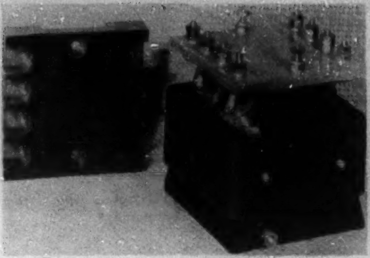

Figure 6 (left). Single-phase de-icing transformer of 3.5-kva load. Voltage ratio 115 to 282 maximum

Figure 7 (right). Aircraft transformer with Fosterite treatment

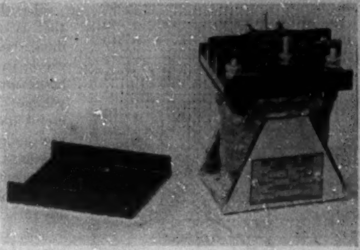

voltage out of tolerance. In general, the more voltages required and the larger the transformer, the more difficult becomes the fixing of the turns ratio. It would be helpful if the aircraft industry would permit 3 to 4 per cent tolerances where more than 4-load voltages are specified.

Insulation of Small Aircraft Transformers

The problem arises as to the best method of insulating and processing the small aircraft transformers which have operating temperatures not requiring high temperature insulation. In order to reduce size it is desirable to eliminate a case and use an open-type core-coil assembly. A resin developed during the last war, is ideal for impregnating and coating open-type core-coil assemblies which have an ultimate temperature rise below 120 degrees centigrade. The resin (named Fosterite after the inventor, Newton C. Foster) changes by heat polymerization from a liquid to a solid state with only a slight change in volume. It has very low viscosity, in the liquid state, requires no solvent, and with care, can be made to produce complete filling of the coil. A resin of higher viscosity can be prepared to form a protective coating over the parts. Fosterite serves a 2-fold purpose by protecting the windings against moisture penetration and by improving the transfer of heat from within the coil. As the units utilizing this resin would normally have small wire sizes it is all the more important that they be protected against moisture penetration and fungus attack. The following example illustrates how Fosterite improves thermal conductivity. A 450 volt-ampere transformer had a 156 degree centigrade rise with high temperature insulation and silicone varnish impregnation. The same design when Fosterite impregnated (see Figure 7) had a temperature rise of 117 degrees centigrade, a 25 per cent decrease. This illustrates that use of Fosterite on certain designs will permit a change to less expensive insulation and give better moisture resistance.

Frequency and Regulation

The present aircraft a-c nominal frequency is 400 cycles ± 10 per cent. The minimum frequency is 380 cycles which determines the size because maximum induction in the core and maximum core losses occur at minimum frequency for constant applied voltage. Operating frequencies higher than 440 cycles are limited by the effect of transformer reactance on voltage regulation as reactance is proportional to frequency. The ratio of per cent reactance to per cent resistance increases with size for similar transformers. Designs 2 kva and above have acceptable regulation up to 800 cycles while smaller ratings have acceptable regulation to 1,600 cycles.

Military specifications require the voltage regulation to be not more than 8.0 per cent for transformers of less than 1-kva rating, and not more than 6 per cent for transformers of 1 kva or larger at 0.8 power factor at normal operating temperatures in a 25 degree centigrade ambient. The regulation of 200 volt-ampere transformers and smaller is predominantly caused by the resistive drop in the windings and is proportional to copper loss. Hence, their size is fixed by the permissible regulation and not necessarily by temperature rise. For example it is possible for the temperature rise of a small transformer to be only 50 degrees centigrade and just meet the regulation limit. For such a transformer class *B* insulation would be unnecessary. By contrast the size of a 1.5-kva transformer and larger ratings is dependent on temperature rise while their regulation is low and efficiency high in comparison to normally specified values. The size of ratings between 200 volt-amperes and 1.0 kva is approximately equally dependent on regulation and temperature rise.

Altitude Performance

It should be noted how the heat loss in a transformer is affected by altitude. The heat transmitted by conduction is a function of the mounting surface contact area, temperature difference between frame and surface, and the thermal conductivity of adjoining materials. Radiation loss is proportional to the fourth power of the absolute temperature and the surface area of the unit. Cooling by convection is a function of the air density and hence decreases rapidly with altitude. As convection decreases with altitude the temperature rise is such as to offset the decrease in cooling by convection with increased conduction and radiation.

Figure 8. Variation of transformer temperature with altitude

Curve A—coil temperature by resistance
Curve B—coil surface
Curve C—core surface

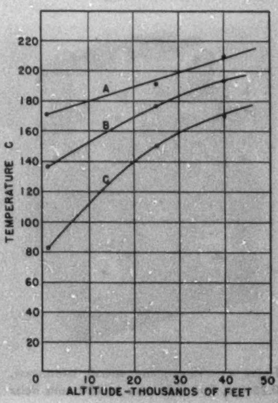

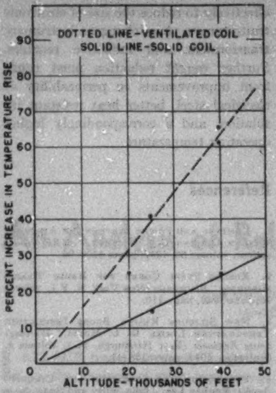

Figure 9. Comparison of solid coil and ventilated coil temperature increase with increased altitude

Load tests have been made at simulated altitudes. Figure 8 indicates the temperature rise on a 3.5-kva autotransformer. The average coil temperature rise and coil surface rise have approximately straight line variation with altitude. However the core surface temperature rise flattens out with higher elevation. As the frame surface closely encloses the core and is large compared to the coil surface it can radiate more heat than the coil. As the temperature of the transformer increases, due to loss of convection cooling, more watts are dissipated by radiation and the core tends to have less rise than the coil.

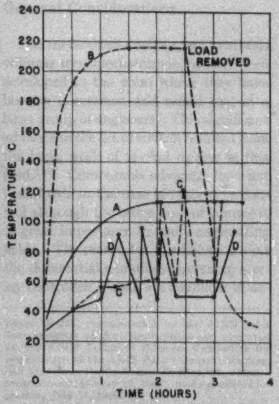

Figure 10. Transformer coil temperature (by thermocouple) at normal load and overloads

Curve A—normal load
Curve B—150 per cent load continuous
Curve C—150 per cent load, 5 minutes on—15 minutes off
Curve D—250 per cent load, 1 minute on—19 minutes off

Figure 9 compares the temperature rise of a transformer of ventilated coil construction with one of solid-coil construction. The ventilated coil design had a 65 per cent increase in temperature rise at 40,000 feet altitude over the sea level temperature rise. The solid coil design has only a 25 per cent increase in temperature rise at 40,000 feet. Ventilated coils can dissipate more watts, at near sea level conditions, than a solid coil of the same cross section but become ineffective with altitude.

United States Air Force Specification *32450* recognizes the effect of altitude by permitting a temperature rise of 225 degrees centigrade at zero degree ambient at 50,000 feet pressure altitude conditions. The specification also stipulates that the temperature rise shall not exceed 200 degrees centigrade at sea level conditions. Hence, Specification *32450* assumes that the transformer has a 112.5 per cent increase in rise in going from sea level to 50,000 feet altitude. Tests, as stated in the preceding paragraph, have shown the increase to be more of the order of 130 per cent. The altitude condition then governs the design by fixing the sea level rise at 225 degrees centigrade divided by 1.3 which equals 170 degrees centigrade. Thus the transformer must be designed for a 170 degree centigrade rise at near sea level conditions and not 200 degrees centigrade as at first might be assumed.

Tests shown in Figures 8 and 9 were made with the transformer mounted on wood in accord with United States Air Force Specification *32450*. Such mounting prevents heat transfer by conduction. In actual use the transformer would be bolted to metal which would promote good heat transfer. If the transformer was bolted to a metal surface that became very cold with altitude, a lower transformer temperature would result. However it is unwise to assume that the temperature of ambient air and adjoining parts will decrease with altitude and offset the effect of decreased air density.

Overload Ratings

The heat storage capacity of a transformer permits intermittent overloads.[4] It must be recognized that the increase in voltage regulation will be proportional to the amount of overload. An overload of 50 per cent can be delivered for five minutes if followed by an off period of 15 minutes in a cyclical manner for a long period of time. Similarly a 250 per cent load can be delivered on a 1-minute-on and 19-minute-off cycle. If the overload temperature exceeds normal temperatures only for a short period of time no measurable damage to the insulation results. Figure 10 shows coil temperatures at various loadings. At 150 per cent load the highest recorded temperatures exceeds the normal load temperature by less than 10 degrees centigrade. The 250 per cent load cycle results in still lower maximum temperature. The transformer of Figure 10 weighed $1^1/_2$ pounds. A heavier unit would have lower temperature peaks during overload because it wou'd have more capacity to store heat and the temperature would rise more slowly. The overload capacity of aircraft transformers increases their dependability and permits the load of one transformer to be shifted to another loaded unit under emergency conditions.

Estimated Life

Temperature is a more important factor in the life of a transformer than in many other types of electric apparatus. Since a transformer is a static device, not subject to wear or mechanical failure, its life depends on the life of its insulation.

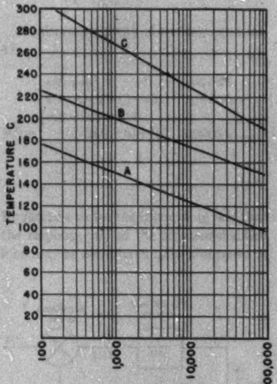

Figure 11. Estimated life

Curve A—class *A* insulation
Curve B—class *B* insulation, varnish treatment, 10 per cent duty cycle
Curve C—silicone insulation and silicone impregnation

As insulation deterioration is a function of temperature, the importance of using operating temperature to predict transformer life becomes evident. Very little data is available which is based on actual life tests on aircraft transformers and a comparison method must be used to estimate life. The transformer industry has accumulated volumes of data on life of class *A* insulation (organic material such as paper and cloth) which can be accepted as valid because it has stood the test of time. The life of class *A* insulation is shown by curve A of Figure 11. It should be noted that life is halved by an 8 degree centigrade increase in temperature. Curve B illustrates the life of class *B* insulation (inorganic materials such as mica and glass) with common varnish impregnation. Curve B is based on a 10 per cent duty cycle but meager data exist for its proof. Curve C* of Figure 11 gives the estimated life of silicone insulation (includes mica) impregnated with silicone varnish. Curve C is based on tests made on electric motors[5] operating continuously, and is believed to be sufficiently accurate in predicting the life of aircraft transformer insulation because of the similarity of motor and transformer insulation. This curve has a slope such that a 12 degree centigrade increase in operating temperature halves the life. After giving due consideration to variations in manufacture it is reasonable to expect a continuous duty life of 2,000 to 5,000 hours for a silicone insulated aircraft transformer operating at 225 degrees centigrade.

Conclusion

Thin gauge Hipersil, type *C* cores, class *B* insulation, silicone materials, and high operating temperature reduce the volume and weight of aircraft transformers to a minimum value. The same materials and methods also can be used effectively to reduce the size of electronic transformers, phase-changers, instrument transformers, and inductive reactors. Further weight reduction must result from improvements in permeability of electrical steel, better heat resistant insulation, and a correspondingly higher operating temperature.

---

* Curve C courtesy of *Westinghouse Engineer.*

References

1. Control and Power Systems for Aircraft Window Deicing, C. L. Mershon. *AIEE Transactions,* volume 66, 1947, pages 1400–06.

2. Rolled Steel Cores for Radio Transformers. *Electronics* (New York, N. Y.), volume 16, June 1943, page 110.

3. New Silicone Resins Boost Insulation Temperature Limits, G. L. Moses. *Westinghouse Engineer* (East Pittsburgh, Pa.), volume 4, September 1944, pages 138–41.

4. Electronic Transformers and Circuits (book), Reuben Lee. John Wiley and Sons, New York, N. Y., 1947, pages 41–44.

5. Silicone Insulation Proved by Test, T. A. Kauppi, G. Grant, G. L. Moses, R. F. Horrell. *Westinghouse Engineer* (East Pittsburgh, Pa.), volume 5, September 1945, pages 135–40.

No Discussion

An Analysis of Relay Servomechanisms

DAVID A. KAHN
MEMBER AIEE

LAPLACE transform theory is applied to the analysis of relay-type servomechanisms. Transient and periodic behavior is analyzed, and a method established for determining whether a given system is stable or unstable. The method is not restricted to cases of intermittently applied constant torque as in previous treatments, but is applicable to any controlled object whose unilateral transfer function can be written, as for example, a motor, a vacuum-tube circuit, or a complete servomechanism loop. This method of analysis is directly applicable to problems of missile guidance, torpedo direction, and gun tracking.

General Considerations

The methods of analysis and synthesis of linear servomechanism loops have been developed to the point where they have become a common and useful tool of a large group of engineers. This significant advance in the art of control resulted from the basic work of several writers in this field.[1-3] Comparable advances have not been made in the case of relay-type control although the latter kind of control is of great importance in many engineering fields. The reason for this failure is that the differential equations governing a relay controlled system are nonlinear in nature and cannot be solved by conventional means. In an excellent paper,[4] H. K. Weiss has applied the methods of phase-space to this problem with gratifying results. In the present treatment the system response is analyzed by accepting something less than a finite analytic expression for the solution of the governing differential equation. In the following development, the response of relay-controlled systems will be expressed as a series of terms, either finite or infinite in number, and by the proper use of this series the behavior of the system can be found.

Basic Relations

In this section a semigraphical method of solution is developed which is applied to second-order differential equations where the driving function is a step displacement or step velocity. Solution of higher order equations with arbitrary driving function is treated in a later section.

Figure 1 represents a conventional relay servomechanism loop. The differential equation governing the system is

$$Z(p)y(t)=\Gamma(x-y) \tag{1A}$$

where

$$\Gamma(x-y)=\begin{cases}+E & (x-y)>\varepsilon\\ 0 & -\varepsilon<(x-y)<+\varepsilon\\ -E & (x-y)<-\varepsilon\end{cases} \tag{1B}$$

Figure 2 illustrates three typical system responses, $y_i(t)$, and a plot of $\Gamma(x-y_1)$.

In order to introduce the method of obtaining a solution, consider the case wherein $\varepsilon=0$. The unilateral Laplace transform[5] of equation 1 is

$$Z(s)Y(s)-I(s)=\frac{E}{s}(1-2e^{-t_1s}+2e^{-t_2s}-2e^{-t_3s}+\ldots) \tag{2}$$

where

$Y(s)=\mathcal{L}[y(t)]$

$I(s)=$ a term containing the initial conditions

$t_1, t_2, t_3, \ldots$ are roots of the equation $x(t)-y(t)=0$

From equation 2 is obtained

$$Y(s)=\frac{E}{sZ(s)}(1-2e^{-t_1s}+2e^{-t_2s}-2e^{-t_3s}+\ldots)+\frac{I(s)}{Z(s)} \tag{3}$$

and the inverse transform of equation 3 is

$$y(t)=\eta(t)u(t)-2\eta(t-t_1)u(t-t_1)+2\eta(t-t_2)u(t-t_2)-\ldots+i(t) \tag{4}$$

where

$$\eta(t)=\mathcal{L}^{-1}\left[\frac{E}{sZ(s)}\right]$$

$$i(t)=\mathcal{L}^{-1}\left[\frac{I(s)}{Z(s)}\right]$$

$$u(t-t_k)=\begin{cases}0 & t<t_k\\ 1 & t\geq t_k\end{cases}$$

An alternative way of writing equation 4 is

$$y(t)=\begin{cases}\eta(t)+i(t) & 0\leq t\leq t_1\\ \eta(t)-2\eta(t-t_1)+i(t) & t_1\leq t\leq t_2\\ \eta(t)-2\eta(t-t_1)+\\ \qquad 2\eta(t-t_2)+i(t) & t_2\leq t\leq t_3\\ \vdots & \vdots\end{cases} \tag{4A}$$

Equation 4 states the interesting fact that the response $y(t)$ of the servomechanism loop may be considered to be composed of

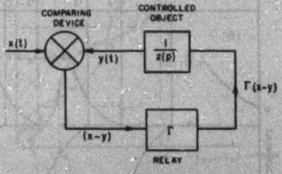

Figure 1. Block diagram of a relay servomechanism loop

Paper 49-224, recommended by the AIEE Joint Subcommittee on Servomechanisms and approved by the AIEE Technical Program Committee for presentation at the AIEE Pacific General Meeting, San Francisco, Calif., August 23–26, 1949. Manuscript submitted May 10, 1949; made available for printing July 11, 1949.

DR. DAVID A. KAHN is with the Cornell Aeronautical Laboratory, Inc., Buffalo, N. Y., formerly with the Curtiss-Wright Corporation, Columbus, Ohio.

This paper is a condensation of a dissertation presented in partial fulfillment of the requirements for the degree, Doctor of Philosophy, in the Graduate School of The Ohio State University.

The author is indebted to Professor C. E. Warren of The Ohio State University for suggestions and criticisms in carrying out this work.

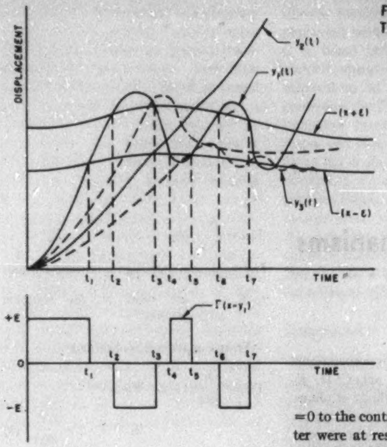

Figure 2 (left). Typical system responses

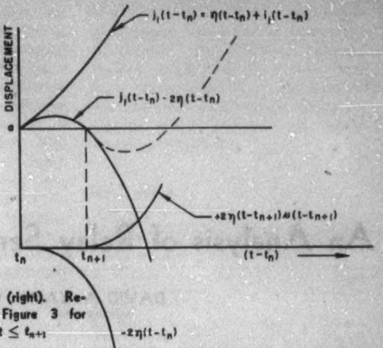

Figure 4(A) (right). Response of Figure 3 for $t_n \leq t \leq t_{n+1}$

a series of terms, each term after the first being of the form $2\eta(t-t_i)u(t-t_i)$.

Figure 3 illustrates equation 4, showing a typical response, $y(t)$, and the components from which it may be synthesized.

The basic quantity $\eta(t)$ which will play an important part in the analysis to follow, has this simple physical significance. It is the output of the controlled object which results from steady application of the input signal $+E$ when the controlled object is initially at rest. That is, if the relay were blocked closed so that its output remained at the constant value $+E$, and if this relay output were applied at $t=0$ to the controlled object when the latter were at rest, then the output of the controlled object would be just $\eta(t)$.

Referring to Figure 3, consider the form the response would take if the relay were blocked so that after some number of operations it remained closed in such direction as to continuously apply $+E$ to the controlled object. Suppose, for example, that this occurred at some value of t between t_{n-1} and t_n. Instead of continuing to oscillate (for illustrative purposes an oscillating response has been assumed) the system output will generate a curve shown qualitatively by the dashed line. If a co-ordinate system were set up with origin at $(t_n, 0)$, then calling the abscissa τ, the dashed curve would be

$$\eta(\tau)+i_1(\tau)$$

where $i_1(\tau)$ represents appropriate initial conditions.

Let

$$j(\tau)=\eta(\tau)+i_1(\tau) \tag{5}$$

All of the preceding remarks apply to a general system subject to the assumptions which were made concerning the form of $\Gamma(x-y)$. Next, however, consider the specific case of a motor having moment of inertia J and velocity friction f, and assume that the relay output appears as a constant torque of magnitude E intermittently applied to the motor shaft. Assume further that the input signal is a step displacement $au(t)$.

Then

$$Z(p)=Jp^2+fp \tag{6}$$

where

$p=d/dt$

and

$$\eta(t)=\mathcal{L}^{-1}\left[\frac{\frac{E}{J}}{s^2(s+\alpha)}\right]=\frac{E}{\alpha^2J}(\epsilon^{-\alpha t}+\alpha t-1) \tag{7}$$

where

$\alpha=f/J$

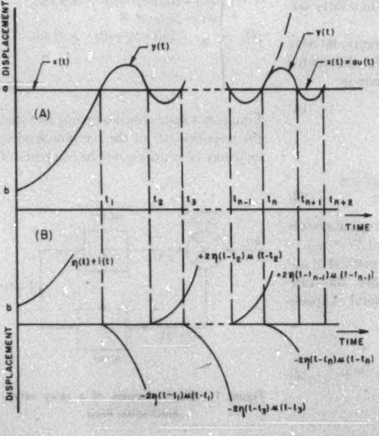

Figure 3 (left). Synthesis of a typical response

Figure 4(B) (right). Response of Figure 3 for $t_{n+1}\leq t\leq t_{n+2}$

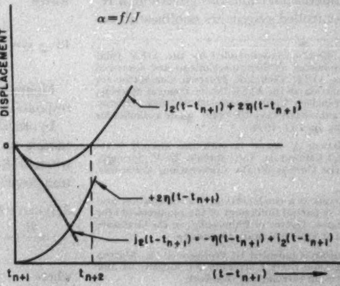

By equation 4

$$i_1(t)=\mathcal{L}^{-1}\left[\frac{I(s)}{Z(s)}\right]$$

The form of $I(s)$ is given directly by the process of taking the transform of $Z(p)y(t)$

$$I(s)=Js\text{ (initial displacement)}+J\text{ (initial slope)}+f\text{ (initial displacement)}$$

and

$$i_1(t)=\mathcal{L}^{-1}\left[\frac{\text{initial slope}}{s(s+\alpha)}+\frac{\text{initial displacement}}{s}\right]$$

therefore

$$i_1(t)=\frac{\text{initial slope}}{\alpha}(1-\epsilon^{-\alpha t})+\text{initial displacement} \qquad (8)$$

By "initial slope" and "initial displacement" is meant the slope and displacement, respectively, when the argument of i_1 is zero.

Figure 4(A) is a plot of the portion of Figure 3(A) for which $t \geq t_n$. Since the intersection at $t=t_n$ was arbitrarily selected, the relations qualitatively illustrated are representative of what happens at any intersection of x and y at which y' is positive. The response of the system for $(t-t_n)>0$ can be constructed by adding the terms $j_1(t-t_n)-2\eta(t-t_n)+2\eta(t-t_{n+1})-\ldots$.

It should be noted by reference to Figure 3 and Figure 4(A) that

$$y(t)\equiv j_1(t-t_n)-2\eta(t-t_n) \quad t_n \leq t \leq t_{n+1} \qquad (9)$$

Thus by inspection of Figures 3 and 4(A) one can write

$$i_1(t_{n+1}-t_n)-2\eta(t_{n+1}-t_n)=a$$

$$y'(t_{n+1})=j_1'(t_{n+1}-t_n)-2\eta'(t_{n+1}-t_n) \qquad (10)$$

Substitution of equations 7 and 8 in equation 10 leads to

$$y'(t_n)=\frac{E}{\alpha J}\left[\frac{\epsilon^{-\alpha(t_{n+1}-t_n)}+\alpha(t_{n+1}-t_n)-1}{1-\epsilon^{-\alpha(t_{n+1}-t_n)}}\right] \qquad (11A)$$

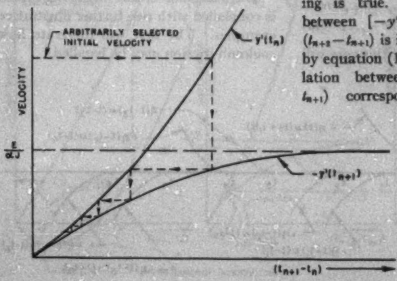

Figure 5. Plot of equations 11 showing the geometry for obtaining the system response

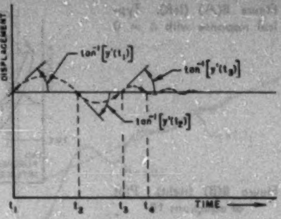

Figure 6. Plot of the information available from Figure 5

$$y'(t_{n+1})=\frac{E}{\alpha J}\times\left[\frac{\epsilon^{-\alpha(t_{n+1}-t_n)}+\alpha(t_{n+1}-t_n)\epsilon^{-\alpha(t_{n+1}-t_n)}-1}{1-\epsilon^{-\alpha(t_{n+1}-t_n)}}\right] \qquad (11B)$$

Equations 11 may be qualitatively plotted by inspection and are shown in Figure 5. The two curves represent a functional relation between the velocities at successive intersections of x and y and the interval of time between intersections.

As the reader may have already deduced by observation of the directed dashed line of Figure 5, the solution of the problem is available directly from the two curves. The reason that this is true and the interpretation of the results are as follows.

Since t_n represents any intersection of x and y at which y' is positive, assume that $n=1$. For any arbitrarily selected velocity assumed to exist at $t=t_1$ enter the curve of $y'(t_n)$ at this value. The abscissa thus determined is the interval (t_2-t_1), and associated with it is the velocity of the response at the end of the interval, namely, $y'(t_2)$; this is directly obtainable from the curve of $-y'(t_{n+1})$.

Because of certain symmetries in the particular problem selected, it may be shown from physical reasoning or by starting with Figure 4(B) and proceeding as in equations 10 and 11 that the following is true. The functional relation between $[-y'(t_{n+1})]$ and the interval $(t_{n+2}-t_{n+1})$ is identical to that expressed by equation (11A), and similarly, the relation between $[y'(t_{n+2})]$ and $(t_{n+2}-t_{n+1})$ corresponds to equation 11B. Therefore, if the curve of $y'(t_n)$ is reentered at value of velocity $[-y'(t_2)]$, one may proceed, as illustrated in Figure 5, to find all of the succeeding intervals and the velocities at each intersection.

The information obtainable from Figure 5 is plotted in Figure 6. This is ordinarily ample for engineering design purposes.

Figure 7 illustrates a few typical solutions characteristic of those systems representable by one pair of curves. It will subsequently be shown that for most complex systems two or more pairs of curves are necessary to obtain the system response.

Figure 7(A) clearly indicates instabil-

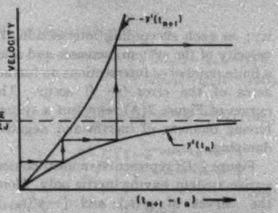

Figure 7(A). An unstable response

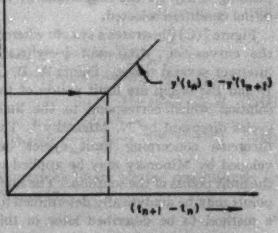

Figure 7(B). A conservative system

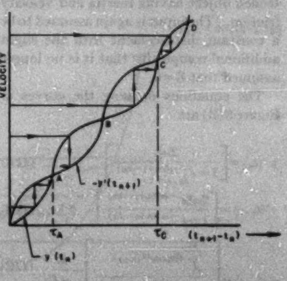

Figure 7(C). A system with limit points

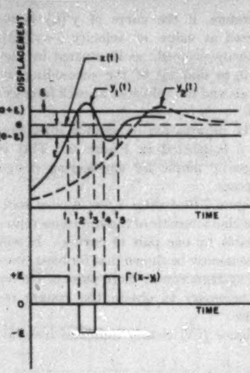

Figure 8(A) (left). Typical response with ε ≠ 0

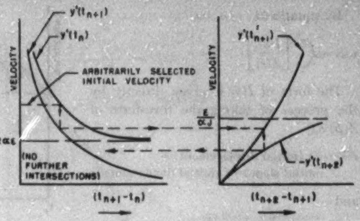

Figure 8(B) (right). Plot of equations 12

ity; at each succeeding intersection the velocity of the system increases and after a finite number of intersections no further zeros of the error $(x-y)$ occur. The curves of Figure 7(A) represent a system having moment of inertia and negative damping.

Figure 7(B) represents an ideal conservative system having inertia only. Here, the curves of $y'(t_n)$ and $[-y'(t_{n+1})]$ degenerate into the same straight line indicating that periodic motion occurs for any initial condition with period depending solely on the magnitude of the initial condition selected.

Figure 7(C) illustrates a system wherein the curves of $y'(t_n)$ and $[-y'(t_{n+1})]$ intersect several times. Points A, B, C, D and the origin are limit points of the solution which correspond to the limit cycles discussed by N. Minorsky.[6] The theorems concerning limit cycles developed by Minorsky may be applied to the limit points of the solution. The limit points may be analytically determined by a method to be described later in this paper.

Figure 8 illustrates the case of a controlled object having inertia and velocity friction. The input is again assumed to be a constant displacement with the slight additional complexity that it is no longer assumed that $\mathcal{E}=0$.

The equations defining the curves of Figure 8(B) are

$$y'(t_n)=\left[\frac{2\alpha\mathcal{E}}{1-\epsilon^{-\alpha(t_{n+1}-t_n)}}\right] \tag{12A}$$

$$y'(t_{n+1})=\left[\frac{2\alpha\mathcal{E}\epsilon^{-\alpha(t_{n+1}-t_n)}}{1-\epsilon^{-\alpha(t_{n+1}-t_n)}}\right] \tag{12B}$$

$$y'(t_{n+1})=\left[\frac{\frac{E}{J}(t_{n+2}-t_{n+1})}{1-\epsilon^{-\alpha(t_{n+2}-t_{n+1})}}\right]-\frac{E}{\alpha J} \tag{12C}$$

$$y'(t_{n+2})=\left[\frac{\frac{E}{J}(t_{n+2}-t_{n+1})\epsilon^{-\alpha(t_{n+2}-t_{n+1})}}{1-\epsilon^{-\alpha(t_{n+2}-t_{n+1})}}\right]-\frac{E}{\alpha J} \tag{12D}$$

The number of excursions across the band formed by $(a-\mathcal{E})$ and $(a+\mathcal{E})$ is determined by the initial conditions and the system parameters. It is readily shown that the system response is obtainable as follows. Enter the curve of $y'(t_n)$ at some arbitrarily selected initial velocity and proceed to determine $(t_{n+1}-t_n)$ and $y'(t_{n+1})$ as in the previous case. At the value of $y'(t_{n+1})$ thus found, enter the second pair of curves to determine $(t_{n+2}-t_{n+1})$ and $-y'(t_{n+2})$. Re-enter the curve of $y'(t_n)$ with this value, and repeat the above procedure. Inspection of Figure 8(B) indicates that there will always be a finite number of crossings of the band. The solution indicated by the directed dashed line of Figure 8(B) corresponds to one crossing of the band as illustrated by $y_2(t)$ of Figure 8(A).

In the derivation of equations 12 the method described previously may be followed in detail except for two minor variations. Firstly, the relay output is now assumed to be given by equation 1B with $\mathcal{E}\neq 0$, so that

$$\mathcal{L}[\Gamma(x-y)]=\int_0^{t_1}E\epsilon^{-st}dt-\int_{t_2}^{t_3}E\epsilon^{-st}dt+\int_{t_4}^{t_5}E\epsilon^{-st}dt\ldots$$
$$=\frac{E}{s}(1-\epsilon^{-t_1s}-\epsilon^{-t_2s}+\epsilon^{-t_3s}+\epsilon^{-t_4s}-\epsilon^{-t_5s}-\ldots) \tag{13}$$

Solution of equation 1 for this case will indicate that the system output $y(t)$ may be considered to be the sum of a series of terms identical in form and disposed along the time axis in the manner indicated in Figure 9. Since only a finite number of oscillations take place under the assumptions leading to equations 12, the series will actually possess a finite number of terms.

The second variation from the previous solution is that the form of $j_1(t)$ and of $j_2(t)$ is not precisely the same as in the derivation leading to equation 11. The form of $j_t(t)$ for any system can be found by physical reasoning, but this is frequently difficult to do. For this reason, the following simple rule for finding j is much preferable. Write down qualitatively the distribution of components comprising the total solution in similar manner to that illustrated in Figure 9. Then $j(t)$ at any instant may be found by summing the components all written with the same argument from $t=0$ up to but not including the instant under consideration and adding the undetermined initial condition.

For example, for the case illustrated by Figure 9

$$\begin{aligned}
j_1(t)&=\eta(t)+i_1(t) && 0<t\leq t_1\\
j_2(t)&=\phantom{-\eta(t)+{}}i_2(t) && t_1<t\leq t_2\\
j_3(t)&=-\eta(t)+i_3(t) && t_2<t\leq t_3\\
j_4(t)&=\phantom{-\eta(t)+{}}i_4(t) && t_3<t\leq t_4
\end{aligned} \tag{14}$$

The form of $i(t)$ is automatically determined in taking the transform of equation 1.

The discussion of this method of attack is concluded with two further illustrative examples. The first will illustrate how coulomb friction may be handled.

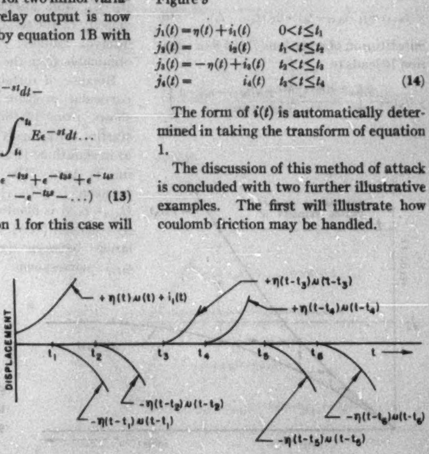

Figure 9. Components comprising the response indicated by Figure 12

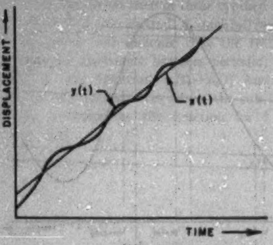

Figure 10(A). Response wherein y′(t) has no reversals of sign

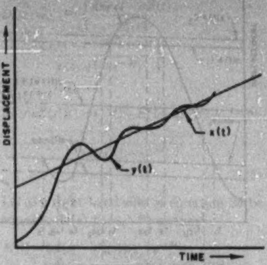

Figure 10(B). Response wherein y′(t) has a finite number of reversals of sign

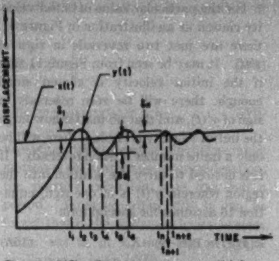

Figure 10(C). Response wherein y′(t) has a large number of reversals of sign

Consider a system having moment of inertia and velocity friction, and suppose that the input $x(t)$ is a velocity step; that is, $x(t) = btu(t)$. Let $C(t)$ = torque due to coulomb friction, and assume that the relay output provides constant torque control. For this example again let $\mathcal{E}=0$.

The system response is qualitatively shown in Figure 10. Depending on the system parameters the output velocity $y'(t)$ may reverse its sign zero times as in Figure 10(A) or a small number of times as in Figure 10(B) or a large number of times as in Figure 10(C). The equations of the system will be set up to describe a response of the form (C), and the solution will indicate just how many reversals in sign of $y'(t)$ occur.

Let

$$C(t)=\begin{cases}+K & y'(t)<0\\ -K & y'(t)>0\end{cases} \tag{15}$$

and let $t_2, t_4, t_6, \ldots$ be roots of $y'(t) = 0$, as shown in Figure 10(C).

Equation 1 now must be replaced by

$$Z(p)y(t) = \Gamma(x-y)+C(t) \tag{16}$$

The transform of equation 16 when solved for $Y(s)$ is

$$Y(s)=\frac{E-K}{sZ(s)}(1-\epsilon^{-t_1s}-\epsilon^{-t_2s}+\epsilon^{-t_3s}+\epsilon^{-t_4s}-\ldots)-\frac{E+K}{sZ(s)}(\epsilon^{-t_1s}-\epsilon^{-t_2s}-\epsilon^{-t_3s}+\ldots)+I(s) \tag{17}$$

and therefore

$$y(t)=(E-K)\eta(t)-2E\eta(t-t_1)u(t-t_1)+2K\eta(t-t_2)u(t-t_2)+2E\eta(t-t_3)u(t-t_3)-2K\eta(t-t_4)u(t-t_4)-2E\eta(t-t_5)u(t-t_5)-\ldots+i(t) \tag{18}$$

where

$$\eta(t)=\frac{1}{\alpha^2J}(\epsilon^{-\alpha t}+\alpha t-1)$$

$$\alpha=\frac{f}{J}$$

$$i(t)=\frac{\text{initial velocity}}{\alpha}(1-\epsilon^{-\alpha t})+\text{(initial displacement)}$$

By following the procedure described previously, the following system of equations results

$$y'(t_n)=\frac{E+K}{\alpha J}\left[\frac{1-\epsilon^{-\alpha(t_{n+1}-t_n)}}{\epsilon^{-\alpha(t_{n+1}-t_n)}}\right] \tag{19A}$$

$$[\delta n-a(t_{n+1}-t_n)]=\frac{E+K}{\alpha^2J}\times\left[\frac{1-\epsilon^{-\alpha(t_{n+1}-t_n)}}{\epsilon^{-\alpha(t_{n+1}-t_n)}}\right]-\left[\frac{E+K}{\alpha J}+a\right](t_{n+1}-t_n) \tag{19B}$$

$$[\delta_n-a(t_{n+1}-t_n)]=\frac{E-K}{\alpha^2J}\times[\epsilon^{-\alpha(t_{n+2}-t_{n+1})}+\alpha(t_{n+2}-t_{n+1})-1]+a(t_{n+2}-t_{n+1}) \tag{19C}$$

$$y'(t_{n+2})=-\frac{E-K}{\alpha J}[1-\epsilon^{-\alpha(t_{n+2}-t_{n+1})}] \tag{19D}$$

$$y'(t_{n+3})=-\frac{E+K}{\alpha J}\left[\frac{1-\epsilon^{-\alpha(t_{n+3}-t_{n+2})}}{\epsilon^{-\alpha(t_{n+3}-t_{n+2})}}\right] \tag{19E}$$

$$[\delta_{n+1}+a(t_{n+3}-t_{n+2})]=\frac{E+K}{\alpha^2J}\times\left[\frac{1-\epsilon^{-\alpha(t_{n+3}-t_{n+2})}}{\epsilon^{-\alpha(t_{n+3}-t_{n+2})}}-\alpha(t_{n+3}-t_{n+2})\right]+a(t_{n+3}-t_{n+2}) \tag{19F}$$

$$[\delta_{n+1}+a(t_{n+3}-t_{n+2})]=\frac{E-K}{\alpha^2J}\times[\epsilon^{-\alpha(t_{n+4}-t_{n+3})}+\alpha(t_{n+4}-t_{n+3})-1]-a(t_{n+4}-t_{n+3}) \tag{19G}$$

$$y'(t_{n+4})=\frac{E-K}{\alpha J}[1-\epsilon^{-\alpha(t_{n+4}-t_{n+3})}] \tag{19H}$$

Equations 19 are plotted qualitatively in Figure 11.

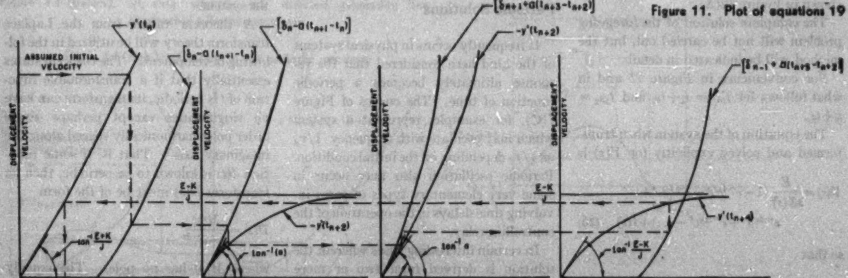

Figure 11. Plot of equations 19

For the particular value of initial velocity chosen as an illustration in Figure 11, there are just two reversals in sign of $y'(t)$. It may be seen from Figure 11 that if the initial velocity is chosen small enough, there will be zero reversals in sign of $y'(t)$, and that no matter how large the initial velocity is chosen, there will be only a finite number of such reversals. If it is desired to carry the solution into the region wherein $y'(t)$ is of one sign, equation 16 assumes the special form

$$Z(p)y(t)=\Gamma(x-y)-K \tag{16A}$$

The solution of equation 16A follows the same pattern as equation 16 and will not be carried out here.

As a concluding example before proceeding to a discussion of periodic solutions, consider the following case. Suppose that the electromechanical unilateral transfer function of the controlled object is $Z(s)$; that is, $Z(s)$ is the ratio of input to output of the controlled object expressed as a function of the complex frequency s. Let the relay output be given by equation 1B and suppose that due to the physical nature of the circuit there is a time delay t_{d_1} associated with the relay operation; that is, t_{d_1} is the time interval between the instant at which the relay receives the signal and the instant at which the voltage appears at the relay output. Similarly, let t_{d_2} be the time delay associated with the relay release; that is, t_{d_2} is the time interval between the instant at which the signal to the relay is removed and the instant at which the relay contacts open. Assume further that the input signal is $x(t)=at+b$.

In dealing with an actual relay, the voltage differential of the relay may not be negligible. The relay voltage differential results in the relay closing at one value of error and reopening at some lower value. In this example voltage differential is taken into account and its effect is shown in Figure 12(A).

The complete solution of the foregoing problem will not be carried out, but the method will be indicated in detail.

For convenience in Figure 12 and in what follows let $t_{id_1}=t_i+t_{d_1}$ and $t_{jd_2}=t_j+t_{d_2}$.

The equation of the system when transformed and solved explicitly for $Y(s)$ is

$$Y(s)=\frac{E}{sZ(s)}\left(1-\epsilon^{-t_{1d_2}s}-\epsilon^{-t_{2d_1}s}+\epsilon^{-t_{3d_2}s}+\epsilon^{-t_{4d_1}s}-\ldots\right)+I(s) \tag{20}$$

so that

$$y(t)=\eta(t)u(t)-\eta(t-t_{1d_2})u(t-t_{1d_2})-\eta(t-t_{2d_1})u(t-t_{2d_1})+\eta(t-t_{3d_2})u(t-t_{3d_2})+\ldots+i(t) \tag{21}$$

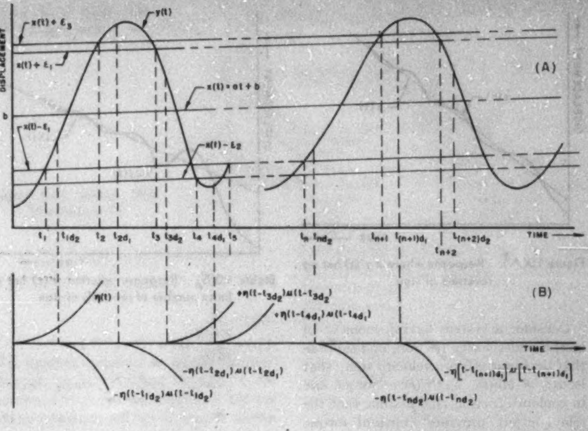

Figure 12. System response showing the components from which it may be generated

The components of which $y(t)$ is comprised are shown in Figure 12(B). The solution for $y(t)$ is available by drawing the eight pairs of curves

$y'(t_n)$ and δ_n versus $(t_{nd_2}-t_n)$
δ_n and $y'(t_{n+1})$ versus $(t_{n+1}-t_{nd_2})$
$y'(t_{n+1})$ and δ_{n+1} versus $(t_{(n+1)d_1}-t_{n+1})$
δ_{n+1} and $y'(t_{n+2})$ versus $(t_{n+2}-t_{(n+1)d_1})$
$y'(t_{n+2})$ and δ_{n+2} versus $(t_{(n+2)d_2}-t_{n+2})$
δ_{n+2} and $y'(t_{n+3})$ versus $(t_{n+3}-t_{(n+2)d_2})$
$y'(t_{n+3})$ and δ_{n+3} versus $(t_{(n+3)d_1}-t_{n+3})$
δ_{n+3} and $y'(t_{n+4})$ versus $(t_{n+4}-t_{(n+3)d_1})$ (22)

This concludes the presentation of the basic method for obtaining the desired solutions. A large amount of work can be done in expanding this analysis to cover cases of increasingly complicated transfer functions. An investigation also is in order to determine the possibility of generating the curves typified by Figure 11 in nondimensional form.

Periodic Solutions

It frequently occurs in physical systems of the kind here considered that the response ultimately becomes a periodic function of time. The curves of Figure 7(C), for example, represent a system which may oscillate with frequency $1/\tau_A$ or $1/\tau_C$ depending on the initial condition. Periodic oscillation also may occur in some very elementary types of cases involving time delays in the operation of the controlling relay.

In certain interesting cases wherein the solution is derived from two or more pairs of curves, the period of oscillation may not be apparent by inspection. For example, the system illustrated in Figure 13 ultimately oscillates with periodic motion as indicated by the fact that the directed line will ultimately approach a limiting rectangle. Figure 13 in fact represents the motion of a torsion pendulum having moment of inertia, viscous friction, and a restoring torque proportional to its displacement. In obtaining the solution of the problem one can readily draw the curves of Figure 13 in a qualitative way, thus determining that the system response does become periodic. In order to graphically determine the limiting rectangle the curves must be quantitatively correct and careful geometric plotting of the directed line must be accomplished. Instead of proceeding in such a manner, a much shorter procedure will be described which leads to analytic information concerning the periodic behavior of the system.

A theorem taken from the Laplace transform theory will be utilized in the following development. The theorem states essentially that if a transformable function of t is periodic, its transform can have no singularities except perhaps single order poles harmonically spaced along the imaginary axis.[7] That is, if some function $d(t)$ is known to be periodic, then its transform $D(s)$ must be of the form

$$D(s)=\frac{M(s)}{1-\epsilon^{-\delta s}}$$

where $M(s)$ has no poles. The equally spaced single order poles along the imaginary axis as required by the theorem are all contained in factor $1/(1-\epsilon^{-\delta s})$.

When the curves such as those typified by Figure 13 are plotted, a qualitative investigation will indicate that the response $y(t)$ ultimately becomes periodic; that is, the function $y_u(t)-x_u(t)$ has periodically spaced zeros where the subscript u designates the function for t large. Let

$$d_u(t)=y_u(t)-x_u(t) \tag{23}$$

and let

$$\mathcal{L}[d_u(t)]=D_u(s)$$

By $\mathcal{L}[d_u(t)]$ is meant the transform of a function having the form of $d_u(t)$ for all t. Then according to the theorem $D_u(s)=M(s)/(1-\epsilon^{-\delta s})$ where $M(s)$ is everywhere analytic. Just how this information is to be applied may be made clear by the following example.

Assume that the system response, when transformed, is given by equation 3 and that the input giving rise to equation 3 is $x(t)=au(t)$, so that $X(s)=a/s$.

It is assumed that $y_u(t)-x_u(t)$ is periodic with one positive excursion and one negative excursion comprising a period. For $t \geq t_n$, that is, after n intersections

$$\begin{aligned} D_u(s)&=Y_u(s)-X_u(s)\\ &=\left[\frac{E\epsilon^{-t_n s}}{sZ(s)}+\frac{I(s)\epsilon^{-t_n s}}{Z(s)}-\frac{a}{s}\epsilon^{-t_n s}\right]-\\ &\quad 2\frac{E}{sZ(s)}(\epsilon^{-t_n s}-\epsilon^{-t_{n+1}s}+\\ &\quad \epsilon^{-(t_n+\delta)s}-\epsilon^{-(\delta+t_{n+1})s}+\dots) \end{aligned} \tag{24}$$

Write

$$\epsilon^{-t_n s}(1-\epsilon^{-(t_{n+1}-t_n)s}+\epsilon^{-\delta s}-\epsilon^{-(\delta+t_{n+1}-t_n)s}+\dots)=\frac{1-\epsilon^{-(t_{n+1}-t_n)s}}{1-\epsilon^{-\delta s}}$$

This is true for $Re(s)>0$ since the expression on the left is a geometric progression. Therefore

$$D_u(s)=\epsilon^{-t_n s}\left\{\frac{E+sI-aZ(s)}{sZ(s)}-\frac{2E(1-\epsilon^{-(t_{n+1}-t_n)s})}{sZ(s)(1-\epsilon^{-\delta s})}\right\}$$

$$D_u(s)=\epsilon^{-t_n s}\,\frac{[sI-aZ(s)](1-\epsilon^{-\delta s})-E(1-2\epsilon^{-(t_{n+1}-t_n)s}+\epsilon^{-\delta s})}{sZ(s)(1-\epsilon^{-\delta s})} \tag{25}$$

Let the right-hand side of equation 25 be equal to $M(s)/(1-\epsilon^{-\delta s})$ so that

$$M(s)=\frac{[sI(s)-aZ(s)](1-\epsilon^{-\delta s})-E(1-2\epsilon^{-(t_{n+1}-t_n)s}+\epsilon^{-\delta s})\epsilon^{-t_n s}}{sZ(s)} \tag{26}$$

In accordance with the theorem, $M(s)$ can have no poles. To illustrate how this requirement may be utilized, consider the case of a conservative system having moment of inertia J, so that $Z(s)$ is simply Js^2 and $I(s)=Jsa+Jy'(t_n)$. Equation 26 therefore becomes

$$M(s)=\frac{sy'(t_n)(1-\epsilon^{-\delta s})-\frac{E}{J}(1-2\epsilon^{-(t_{n+1}-t_n)s}+\epsilon^{-\delta s})}{s^2} \tag{27}$$

Let $M(s)=N(s)/(s^2)$ and expand $N(s)$ in a MacLaurin series. Then

$$M(s)=\frac{N(0)+sN'(0)+\frac{s^2N''(0)}{2!}+\frac{s^3N'''(0)}{3!}+\dots}{s^2}$$

and if $M(s)$ is to have no poles, then

$$\begin{aligned} N(0)&=0\\ N'(0)&=0\\ N''(0)&=0 \end{aligned} \tag{28}$$

Since

$$N(s)=sy'(t_n)(1-\epsilon^{-\delta s})-\frac{E}{J}(1-2\epsilon^{-(t_{n+1}-t_n)s}+\epsilon^{-\delta s})$$

therefore the conditions in equation 28 lead to

$$(t_{n+1}-t_n)=\frac{\delta}{2} \tag{29A}$$

$$y'(t_n)=\frac{E}{2J}(t_{n+1}-t_n)=\frac{E}{4J}\delta \tag{29B}$$

Equation 29A states that during periodic motion of the system under consideration, the positive excursion lasts one half a period. From equation 29B it can be found that if the system velocity is some value, say v_0, at t_n, then the period of oscillation, δ, is $4v_0J/(E)$.

Consider one further illustrative example. Suppose the input is of the form $x(t)=bt$ and let the transfer function of the controlled object $Z(s)$ be unspecified. Assume $\mathcal{E}\neq 0$ so that $\Gamma\ (x-y)$ is given by equation 1B and assume further that a time delay t_{d_1} is associated with relay "make" and that t_{d_2} is associated with "break". Then

$$\begin{aligned} D_{un}(s)=\epsilon^{-t_n s}\Bigg\{&\left(\frac{E}{sZ(s)}+\frac{I_n(s)}{Z(s)}-\frac{a}{s}\right)-\\ &\frac{E}{sZ(s)}\left(\frac{\epsilon^{-t_{d_1}s}+\epsilon^{-(t_{n+1}+t_{d_2}-t_n)s}}{1-\epsilon^{-\delta s}}-\right.\\ &\left.\frac{+\epsilon^{-(t_{n+2}+t_{d_1}-t_n)s}+\epsilon^{-(t_{n+3}+t_{d_2}-t_n)s}}{1-\epsilon^{-\delta s}}\right)\Bigg\} \end{aligned} \tag{30}$$

Equation 30 was obtained by writing the initial conditions with respect to t_n; that is, $I_n(s)$ will be a function of $y'(t_n)$. Equations similar to 30 may be written based on conditions at t_{n+1}, t_{n+2}, and t_{n+3}. The resulting equations can be put in the form

$$D_{uk}(s)=\frac{M_k(s)}{1-\epsilon^{-\delta s}} \quad k=1,2,3,4 \tag{31}$$

$M_k(s)$ may be treated in the manner just described for the conservative system. The resulting equations will determine a

Figure 13 (below). A case wherein the directed generating line approaches a limiting rectangle

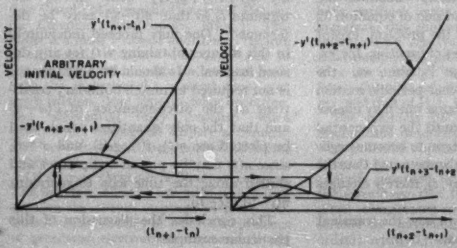

Figure 14 (right). One cycle of a periodic response

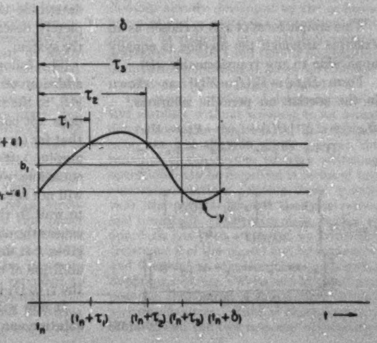

set of relations among the circuit parameters that must hold when the system oscillates with periodic motion.

Solution of Higher Order Equations

In order to summarize the methods described before, a particular equation now will be treated and information about its behavior obtained.

Consider as an example the equation

$$a_6\frac{d^6y}{dt^6}+a_5\frac{d^5y}{dt^5}+a_4\frac{d^4y}{dt^4}+a_3\frac{d^3y}{dt^3}+a_2\frac{d^2y}{dt^2}+a_1\frac{dy}{dt}+a_0y=\Gamma(x-y) \quad (32)$$

where the a_i are real, and

$$\Gamma(x-y)=\begin{cases}+E & (x-y)>\mathcal{E}\\ 0 & -\mathcal{E}\leqq(x-y)\leqq+\mathcal{E}\\ -E & (x-y)<-\mathcal{E}\end{cases}$$

When transformed, equation 32 becomes

$$Y(s)=\frac{\left(\frac{E}{a_6}\right)(1-\epsilon^{-t_1s}-\epsilon^{-t_2s}+\epsilon^{-t_3s}+\epsilon^{-t_4s}-\ldots)}{s\left(s^6+\frac{a_5}{a_6}s^5+\frac{a_4}{a_6}s^4+\frac{a_3}{a_6}s^3+\frac{a_2}{a_6}s^2+\frac{a_1}{a_6}s+\frac{a_0}{a_6}\right)}+\frac{\frac{1}{a_6}I_0[s,y(0^+),y'(0^+),\ldots y^{(5)}(0^+)]}{\left(s^6+\frac{a_5}{a_6}s^5+\ldots+\frac{a_0}{a_6}\right)} \quad (33)$$

where I_0 is determined in routine manner and contains the initial conditions. The t_i are as defined by Figure 2.

The expression

$$\left(s^6+\frac{a_5}{a_6}s^5+\ldots+\frac{a_0}{a_6}\right)$$

now must be written as

$$Q(s)=(s+\alpha_1)(s+\alpha_2)(s+\alpha_3)\ldots(s+\alpha_6)$$

Suppose that first one inquires as to the periodic behavior of the system when the driving function is

$$x(t)=b_1u(t) \quad (34)$$

This simple form of $x(t)$ is chosen as an example although the method is equally applicable to any transformable $x(t)$.

Form $D_u(s)=Y_u(s)-X(s)$ as shown in the section on periodic solutions.

$$D_{u_1}(s)=\epsilon^{-t_ns}\{H(s)+I_1(s)-X(s)-H(s)(1+\epsilon^{-\tau_1s})-\epsilon^{-\tau_2s}-\epsilon^{-\tau_3s}+\epsilon^{-\delta s}+\epsilon^{-(\delta-\tau_1)}+\ldots\}$$

$$D_{u_1}(s)=\left\{\frac{(1-\epsilon^{-\delta s})\left[s\frac{1}{a_6}I_1-b_1Q(s)\right]}{sQ(s)(1-\epsilon^{-\delta s})}-\frac{\frac{E}{a_6}\left[\epsilon^{-\tau_1s}-\epsilon^{-\tau_2s}-\epsilon^{-\tau_3s}+\epsilon^{-\delta s}\right]}{sQ(s)(1-\epsilon^{-\delta s})}\right\}\times\epsilon^{-t_ns} \quad (35)$$

$$D_{u_1}(s)=\left\{\frac{\left[\frac{N_1(s)}{s(s+\alpha_1)(s+\alpha_2)\ldots(s+\alpha_6)}\right]}{(1-\epsilon^{-\delta s})}\right\}\epsilon^{-t_ns}=\frac{M_1(s)\epsilon^{-t_ns}}{(1-\epsilon^{-\delta s})} \quad (36)$$

The τ_i are defined by Figure 14.

In order to describe the periodic state, the following 28 quantities must be determined.

$$y(t_n),y'(t_n),\ldots y^{(5)}(t_n),y(t_{n+1}),y'(t_{n+1}),\ldots y^{(5)}(t_{n+1}),y(t_{n+2}),\ldots y(t_{n+3}),\ldots,\tau_1,\tau_2,\tau_3,\delta$$

It may be observed by reference to Figure 14 that

$$y(t_n)=y(t_{n+3})=b_1-\mathcal{E}$$
$$y(t_{n+1})=y(t_{n+2})=b_1+\mathcal{E}$$

so that there remain 24 undetermined quantities.

From the requirement that $M_1(s)$ be analytic, one can obtain the six conditions

$$N_1(-\alpha_i)=0 \qquad i=1,2,\ldots 6 \quad (37)$$

By exactly the same procedure one may write the requirement that $D_{u_2}(s)$, $D_{u_3}(s)$, and $D_{u_4}(s)$ be periodic. The initial condition term for these cases will contain derivatives evaluated at (t_{n+1}), (t_{n+2}), and (t_{n+3}).

The form of $D_{u_2}(s)$, $D_{u_3}(s)$ and $D_{u_4}(s)$ may be found by reference to equations 24 and 13. The $D_{u_i}(s)$ are

$$D_{u_2}(s)=\epsilon^{-t_ns}\{I_2(s)-X(s)-H(s)[\epsilon^{-\tau_1s}-\epsilon^{-(\tau_2-\tau_1)s}-\epsilon^{-(\tau_3-\tau_1)s}+\epsilon^{-(\delta-\tau_1)s}]\}$$

$$D_{u_3}(s)=\epsilon^{-t_ns}\{-H(s)+I_3(s)-X(s)+H(s)[\epsilon^{-\tau_2s}+\epsilon^{-(\tau_3-\tau_2)s}-\epsilon^{-(\delta-\tau_2)s}-\epsilon^{-(\delta+\tau_1-\tau_2)s}]\}$$

$$D_{u_4}(s)=\epsilon^{-t_ns}\{I_4(s)-X(s)+H(s)\times[\epsilon^{-\tau_3s}-\epsilon^{-(\delta-\tau_3)s}-\epsilon^{-(\delta+\tau_1-\tau_3)s}+\epsilon^{-(\delta+\tau_2-\tau_3)s}]\} \quad (38)$$

Each of these three equations will yield six conditions. These together with the six relations expressed by equation 37 will determine the 24 quantities which completely describe the periodic behavior of the system.

The following should be noted. The addition of an arbitrary function, say $g(t)$, to the right-hand side of equation 32 does not complicate the problem, except that for certain classes of function, for example, $g(t)=c_1t+c_2\epsilon^{-\gamma t}\sin\omega t$, the equations will show that periodic motion will not occur. Of course one may choose to wait in this case until the exponential causes the offending term to become negligible. It should further be noted that the addition of time delay, t_d, merely changes the τ_i to (τ_i+t_d).

It now will be shown how the transient solution can be found.

In treating higher order differential equations, the method of inspecting the first derivative to determine the system behavior is no longer directly applicable since corresponding inspection of all derivatives would require portrayal in some manner in multidimensional space. However, the more general aspects of this paper may be applied as follows.

Consider again equation 32 and to increase its generality slightly add a transformable but otherwise arbitrary function $G(t)$ to its right-hand side. Then the transformed equation is

$$Y(s)=H(s)(1-\epsilon^{-t_1s}-\epsilon^{-t_2s}+\epsilon^{-t_3s}+\epsilon^{-t_4s}-\ldots)+I(s)+G_1(s) \quad (39)$$

where

$$H(s)=\frac{\frac{E}{a_6}}{s(s+\alpha_1)(s+\alpha_2)\ldots(s+\alpha_6)}$$

$$I(s)=\frac{\frac{1}{a_6}I_0(s,y(0),y'(0)\ldots y^{(5)}(0)}{(s+\alpha_1)(s+\alpha_2)\ldots(s+\alpha_6)}$$

$$G_1(s)=\frac{\frac{1}{a_6}G(s)}{(s+\alpha_1)(s+\alpha_2)\ldots(s+\alpha_6)}$$

The inverse transform of equation 39 is

$$y(t)=\eta(t)-\eta(t-t_1)u(t-t_1)-\eta(t-t_2)u(t-t_2)+\eta(t-t_3)u(t-t_3)+\ldots+i(t)+g_1(t) \quad (40)$$

where

$$\eta(t)=\mathcal{L}^{-1}[H(s)]$$
$$i(t)=\mathcal{L}^{-1}[I(s)]$$
$$g_1(t)=\mathcal{L}^{-1}[G_1(s)]$$

Next assume some $x(t)$ for purposes of illustration. The $x(t)$ may be completely arbitrary; in fact, let it be assumed that $x(t)$ is available only as a graphical plot. Then from equation 40 one proceeds as follows:

Plot $\eta(t)$, $i(t)$, $g_1(t)$, $(x+\mathcal{E})$, and $(x-\mathcal{E})$. The intersection of $[\eta(t)+i(t)+g_1(t)]$ with $(x-\mathcal{E})$ determines t_1. Having thus obtained t_1, plot $\eta(t-t_1)$ $u(t-t_1)$. Then the intersection of $[\eta(t)-\eta(t-t_1)u(t-t_1)+i(t)+g_1(t)]$ with $(x+\mathcal{E})$ determines t_2 so that $\eta(t-t_2)$ may be determined. One may proceed indefinitely in this manner obtaining $y(t)$ for any desired interval. It should be noted that it is not required to match boundary conditions at the discontinuities of $\Gamma(x-y)$ and that the only quantities which need be plotted are $\eta(t)$, $i(t)$, $g_1(t)$ and $x\pm\mathcal{E}$, since $\eta(t)$ may be put on a slip sheet and shifted along the time axis to represent $\eta(t-t_j)$ $u(t-t_j)$.

This concludes the discussion of this particular example.

Conclusions

The method of attack described in this paper is applicable to a wide variety of on-off type problems. This method should be particularly useful to designers of control systems for turrets, pilotless aircraft, torpedoes, and to designers in certain industrial fields. The examples chosen to illustrate certain typical behaviors were all taken from the field of mechanics in order that a simple physical picture could be associated with the mathematical manipulation. In the examples discussed moment of inertia, friction, and torque were taken as parameters. These parameters could instead have been chosen as inductance, resistance, and voltage, for example.

References

1. THE ANALYSIS AND SYNTHESIS OF LINEAR SERVOMECHANISMS (book), **Albert C. Hall.** The Technology Press, Massachusetts Institute of Technology (Cambridge, Mass.) 1943.

2. FUNDAMENTAL THEORY OF SERVOMECHANISMS (book), **LeRoy A. MacColl.** D. Van Nostrand Co. Inc., New York, N. Y., 1945.

3. BEHAVIOR AND DESIGN OF SERVOMECHANISMS, **Gordon S. Brown.** Printed November, 1940, under auspices of Fire Control Committee (Sec. D-2) of National Defense Research Committee.

4. ANALYSIS OF RELAY SERVOMECHANISMS, **H. K. Weiss.** *Journal*, Aeronautical Sciences (New York, N. Y.), volume 13, July 1946, page 364.

5. TRANSIENTS IN LINEAR SYSTEMS (book), **M. F. Gardner, J. L. Barnes.** John Wiley and Sons, Inc., New York, N. Y., 1942.

6. INTRODUCTION TO NON-LINEAR MECHANICS (book), **N. Minorsky.** J. W. Edwards, Ann Arbor, Mich., 1947.

7. THE LAPLACE TRANSFORM (book), **D. V. Widder.** Princeton University Press, Princeton, N. J., 1946.

Discussion

W. J. Schart (Consolidated Vultee Aircraft Corporation, San Diego, Calif.): All in all the paper is a very good presentation of a new technique, especially the concept portrayed in its simplest form by Figure 5. I did have a little trouble, however, in following the author's development and hope that my suggestions will be of help to the author.

The essence of the technique of finding the size of the successive time intervals is based on the fact that $y'(t_n)$and $y'(t_{n+1})$ can be expressed in terms of the known quantities E, J, α, and the interval $T_{n+1}=t_{n+1}-t_n$. In other words $y'(t_n)$ and $y'(t_{n+1})$ are known functions of T_{n+1}.

Once this is known, then the use of Figure 5 shows how these known functions can be used to determine the intervals under discussion.

Having shown the essence of the technique for the simple case, I would suggest that the author point out, that for $x(t)=au(t)$, we have $y(t_n)=y(t_{n+1})$, and that under these circumstances it is possible to express $y'(t_n)$ and $y'(t_{n+1})$ in terms of known quantities and the interval T_{n+1}. It also could be mentioned at this point that the technique readily generalizes to the case where $x(t)=bt\,u(t)$, for under this condition $y(t_n)-y(t_{n+1})=x(t_n)-x(t_{n+1})$.

From these remarks the technique is readily generalized to the other systems discussed by the author.

These comments are necessarily quite brief, since technically there is nothing to criticise in the paper, and very little to be added since it is very complete and thorough in its presentation. My comments are merely concerned with the psychology of its presentation.

Ben Ciscel (Minneapolis-Honeywell Regulator Company, Minneapolis, Minn.): This paper is a most welcome addition to the lore of automatic control. The exposition of the simple system with no neutral zone, then the inclusion of a neutral zone, coulomb friction, dead time in relay operation, and differential relay response when opening and closing, all display a remarkable awareness of the practical problems in the field.

Of course, there are still other enigmas. The first that came to my mind was that of defining the output response with the controlled object initially at rest. The presence of generated electromotive forces will add another element of nonlinearity in many systems. There are other controls which have a narrow band of proportionality whose dynamic performance could be analyzed by the methods outlined in Dr. Kahn's paper. These include clutch servos and some amplifier-servo combinations which reach torque saturation with very small error signals.

As a personal note, I would like to raise one slight criticism. The practicing engineer is engrossed in a dual problem—one is that of doing his work and the other is that of keeping up with the technical advances of his field. The latter job could be made much easier if the technical papers were more consistent in their use of symbols, letters, and terminology. The little things that slow down the reading and assimilation of a paper such as this were: the use of t for roots and time, the use of E for voltage and for torque, the use of j in a nonimaginary sense, (especially when it has no relationship to capital J, nor any other apparent reason for its choice), the use of x for displacement and as a multiplication sign, and the inexplicable use of p as a differential operator in equation 6. These do not detract from the value of a paper, but they do prolong the reading time.

I am looking forward to the opportunity of applying some of this relay control theory to some of our systems, and appreciate this opportunity to offer a few comments on the paper.

R. J. Kochenburger (Massachusetts Institute of Technology, Cambridge, Mass.): Dr. Kahn's paper represents a timely treatment of a subject possessing considerable importance from the standpoint of engineering application, but which has been generally neglected as far as the development of methods of analysis and synthesis are concerned. Unlike continuous servomechanisms, which have received extensive treatment in the literature, this subject has been given consideration by relatively few authors. The most outstanding previous contributions to date are probably those of MacColl and Weiss shown as references 2 and 4 of the paper, and that of H. L. Hazen in 1939.[1]

The methods for treating relay servomechanisms described prior to this paper were generally applicable to only the simpler forms of such systems. The basic method of analysis proposed by Dr. Kahn possesses the advantage that it can be extended to more complicated systems (systems described by differential equations of higher order); naturally, the labor of computation would increase under such circumstances. The ability to treat more complicated systems is an important consideration in any method of analysis because servomechanisms including even the simpler forms of servomotors can involve complicated dynamics when suitable compensating or "computer" networks are introduced.

In view of the varied forms of treatment proposed for the analysis of relay servomechanisms, some review may be advisable. Three basic problems are considered by the contributors in the field. The first involves a method for determining the transient response of the system to various disturbances and obtaining the output or error response as a function of time. The second involves a method for determining the "relative stability" or damping of such oscillations by graphical methods without involving the necessity of computing the actual time response. The third involves the determination of conditions under which self-sustained oscillations may arise.

Dr. Hazen treats the first problem by means of the classical differential equation approach. Weiss and MacColl do not treat it directly but indicate how the time response may be determined by means of auxiliary constructions associated with the "phase-plane" method of approach. Dr. Kahn suggests a means of analysis whereby it is merely necessary to determine the system response to a step-function disturbance initiated by the relay. Each time that a new relay switching operation takes place, it may be taken into account by adding or subtracting this new step-function response, with a translated time axis, from the response relationship already developed by the accumulation of earlier switching operations. The process is reduced to a relatively simple graphical procedure and there is no apparent limit to its application as far as the complexity of system dynamics is concerned.

The second problem of determining relative stability without recourse to an actual determination of the time response depends upon the fact that, in simple systems, the response of the system to relay switching operations may be described in terms of two algebraic equations relating three quantities: the output, its first time derivative, and time itself. The phase plane method of approach has been employed by Minorsky (reference 6 of the paper) and by Andronow and Chaikin[3] in other problems concerning nonlinear systems. Weiss and MacColl propose the application of this method to relay servomechanisms. Time is eliminated as a variable and the two response relationships result in one simple relationship relating the output and its first time derivative. These are plotted against each other, the plane of this plot being called the "phase plane." Weiss and MacColl show how the response of the servomechanism may be determined by a simple graphical construction of the "trajectory paths" in the phase plane. Dr. Kahn eliminates a different variable, the output, and obtains plots of the output's time derivative versus time itself. This method also results in a simple graphical construction which enables the relative stability of the system to be determined. When the discusser handled several typical problems by both the phase plane method and by the method proposed by Dr. Kahn it did appear that the latter entailed less computational and graphical labor. The phase plane method is definitely restricted to systems of simple dynamics; possibly Dr. Kahn's method could be extended to more involved systems although his paper does not illustrate how this might be done.

The third problem of determining conditions of self-sustained oscillations also is handled in a novel fashion. Hazen handled this problem by means of the transient response relationships. He assumed that such oscillations occurred by specifying that the responses at the beginning and end of some given period were identical and then solved for the conditions necessary to satisfy the assumed periodicity. Weiss used essentially the same approach although he employed the equations describing the phase-plane trajectory. Dr. Kahn's method for treating this problem, described in the last two sections of his paper, appears somewhat more complicated at the outset, but has the advantage that is more readily extended to systems having complicated dynamics. An interesting phenomenon encountered by both Weiss and Kahn is the existence of both convergent and divergent equilibrium operating points when the conditions leading to the self-sustained oscillations are determined. Only the convergent points correspond to true oscillations in a physical system. Dr. Kahn's Figure 7C is an example, where intersection points A and C represent convergent equilibrium while the origin and points B and D represent divergent equilibrium. This phenomenon is peculiar to nonlinear systems. Dr. Kahn's discussion of this was necessarily brief and an interested reader is referred to Andronow and Chaikin[2] for further consideration of this effect.

As the title of the paper implies, the treatment described here is chiefly intended for purposes of analysis. In the case where a system is to be synthesized and appropriate compensating networks are to be selected, the method could be applied only by performing repeated analyses with various trial values of design constants. This is not mentioned as a defect of the treatment, which is adequate within itself, but as a suggestion for further work in the field.

In the case of continuous servomechanisms, the frequency response method has proved very applicable for this purpose. This method is described in references 1, 2, and 3 of the paper. A corresponding method of treatment applied to relay servomechanisms would be of considerable aid to designers in this field.

In the past, relay servomechanisms have frequently been avoided in instances where they could have provided the most suitable answer to an engineering problem for the simple reason that they were not readily subject to analysis. It is believed that papers such as the one discussed should do much to correct this situation. Dr. Kahn is to be congratulated on his treatment and presentation of the subject.

1. THEORY OF SERVOMECHANISMS, Harold L. Hazen. *Journal*, Franklin Institute (Philadelphia, Pa.) volume 218, number 3, September 1934, pages 279–330.

2. THEORY OF OSCILLATIONS, A. A. Andronow, C. E. Chaikin. Moscow, 1937. English edition, Solomon Lefschitz, Princeton University Press, Princeton, N. J., 1949.

David A. Kahn: The writer wishes to thank Dr. Kochenburger and Mr. Ciscel and Mr. Schart for their comments. As pointed out by Dr. Kochenburger, the treatment of the relay servomechanism problem described in the paper is chiefly intended for purposes of analysis. The writer has done a small amount of investigation of the application of these methods to the problem of synthesis of compensating networks. It appears that in a large number of cases, the sign of $\eta''(t)$ serves as a useful criterion of over-all performance. Networks that change the form of $\eta(t)$ in such manner that $\eta''(t)$ becomes negative improve the system stability. However, much additional work on this problem is needed.

The Design of D-C Motors for Use in Automatic Control Systems

PAUL LEBENBAUM, JR.
MEMBER AIEE

THE increased use and accuracy of automatic control systems for industrial and military applications has made it essential that system components be reexamined in terms of over-all system operation. It is the purpose of this paper to study the application of d-c motors in these systems in order to: determine the motor constants which affect system performance; convert the important motor system constants into design factors, such as armature diameter and length, flux and copper densities, and so forth; and to determine the motor design which will give optimum over-all system performance.

Summary of Conclusions

When a separately excited shunt-wound d-c motor is used as the output member of a closed-cycle automatic control system, the motor time constant is the motor constant which the system designer uses in calculating the stability, allowable amplification, accuracy, and speed of response of the system. It is defined as the time in seconds to accelerate the motor and load inertia to 63.2 per cent of its final speed when a d-c voltage of constant magnitude is suddenly applied to the motor terminals. Optimum system design requires that this factor be as small as possible.

The motor time constant is a function of the motor armature circuit resistance, the inertia of the motor and the load, and the torque and generated voltage constants of the motor. (The armature circuit inductance and steady-state load and friction torques have been neglected in this derivation. These assumptions are discussed in the section on The D-C Motor as an Output Member of a Closed-Cycle Automatic Control System.)

$$T_e = \frac{RJ}{K_T K_V} \text{ seconds} \tag{1}$$

When this equation is converted to design terms, it is found that the time constant is directly proportional to functions of the ratios of armature diameter to armature length, load inertia to motor inertia, and commutating field conductor copper density to armature conductor copper density; and inversely proportional to functions of the pole face flux density, and the ratios of pole pitch to pole arc, armature slot depth to armature diameter, and pole face flux density to armature tooth flux density at the tooth root. Equation 8 gives the mathematical relations between the various factors.

If these design factors and ratios are given optimum values which make the time constant a minimum, the following equation is obtained

$$(T_e)_{\min} = 1.25\times10^{-3}\,\frac{K_J}{K_e}\left(1+\frac{J_L}{J_M}\right)\times \left[1+\frac{\pi}{P_M\cos\theta}+(1.2K_C)\left(\frac{B_{CCP}}{B_{CA}}\right)\left(\frac{P_c}{P_M}\right)\right] \text{ seconds at 75 degrees centigrade} \tag{2}$$

Equation 2 shows that the minimum possible motor time constant is fundamentally a function of the armature diameter to length ratio and is not a function of the machine rating. Figure 1 is a plot of this equation for a line of 4-pole 1,750-rpm motors, ranging in size from 5 to 60 horsepower, having negligible load inertia.

A study of the equations derived in this paper reveals that the following points should be considered in designing a motor with a minimum time constant:

1. The flux density at the root of the armature tooth should be high.
2. The pole face flux density should have a value of about one-half the flux density at the root of the armature tooth.
3. The armature slot depth should have a value as close to one-eighth of the armature diameter as possible.
4. The ratio of pole arc to pole pitch should be large.
5. The armature slot activity should be high.
6. The ratio of commutating field to

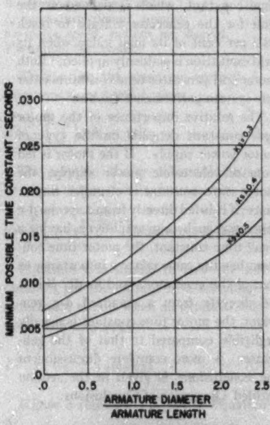

Figure 1. Minimum possible motor time constant as a function of the ratio of armature diameter to length, for a line of four pole, commutating pole, 1,750 rpm motors, ranging in size from 5 to 60 horsepower

Negligible load inertia, one commutating field circuit, commutating field to armature copper density ratio of one-half, and 1.15 compensation

---

Paper 49-225, recommended by the AIEE Rotating Machinery and approved by the AIEE Technical Program Committee for presentation at the AIEE Fall General Meeting, Cincinnati, Ohio, October 17–21, 1949. Manuscript submitted November 17, 1948; made available for printing September 1, 1949.

PAUL LEBENBAUM, JR., is with the Motor Engineering Department of the General Electric Company, West Lynn, Mass.

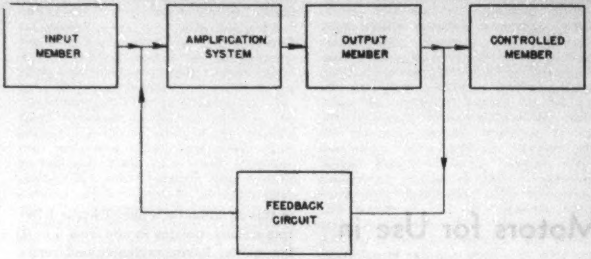

Figure 2. Components of a closed-cycle automatic control system

armature conductor copper density should be small.

7. The ratio of armature diameter to length should be small, when the load inertia is negligible. When the load inertia is not negligible, an increase in this ratio may actually give a smaller motor time constant. Under this condition, a larger value of the ratio may result in a greater decrease in armature circuit resistance than the corresponding increase in motor and load inertia.

The motor time constant is only one of several time constants found in automatic control systems. Another important time constant is the generator time constant, which is defined as the time for the generator voltage to reach 63.2 per cent of its final value when its field excitation is suddenly applied. Both motor and generator time constants enter into system performance studies.

The relative importance of the motor time constant depends on the type of motor power supply. If the motor is fed from an electronic power supply, the motor time constant is of major importance; if it is fed directly from a special d-c generator, such as an amplidyne, having a small time constant, the motor time constant has the same relative importance as that of the generator; and finally if it is fed directly from a standard d-c generator, the motor time constant is usually negligible compared to that of the generator. A more complete discussion of the conclusions is given in the section entitled Discussion of Conclusions.

Automatic Control Systems

An automatic control system is a device or combination of devices which controls the output of the system without the use of a human operator. Systems of this type are of two principal kinds: "open-cycle" and "closed-cycle". In an open-cycle system, the output is a function of an independent parameter; in a closed-cycle system, the output is a function not only of an independent parameter but also of the output itself. An example of the first type is the time-operated traffic signal control where the output is solely a function of an independent time setting. The second type can be represented by the common house heating system in which the sensitive element of a thermostat controls the amount of heat supplied, which in turn effects the indication of the thermostat in such a manner that the temperature of the house is held at an approximately constant value. The difference between open-cycle and closed-cycle automatic control is, therefore, that in the latter an indication of the output is fed back so as to modify the input to the device.

The term servomechanism is often applied to a closed-cycle system in which the output element is so actuated that the difference between the output and input indications tends to approach zero.

Common applications of closed-cycle systems are in continuous industrial processes such as steel, paper, and textile mills, where the speed of the material being processed must be accurately held; side register control, where the position of a moving material must be accurately held in a direction perpendicular to its motion; gun positioning, and target locating and tracking devices in the military field; and automatic steering devices for ships and airplanes, where the direction of the line of travel is held by comparing the actual direction with a compass setting.

In general the components of a closed-cycle system are those shown in Figure 2.

In order to demonstrate the functions of the various components, a system used to control the speed of an output shaft, shown in Figure 3, will be explained.

The input member in this case is a potentiometer supplying a constant d-c voltage input to the system. The amplifier, amplidyne, and d-c generator act as an amplification system to increase the power input from the input member and the feed-back circuit to a level sufficient

Nomenclature

A_A = number of armature circuits

A_{CF} = number of commutating field circuits

A_{CA} = area of armature conductor, square inches

A_{CCP} = area of commutating field conductor, square inches

B_{CA} = armature conductor copper density, amperes per square inch

B_{CCP} = commutating field conductor copper density, amperes per square inch

B_{PF} = pole face flux density, lines per square inch

B_t = armature tooth flux density at root, lines per square inch

d = armature slot depth, inches

D = armature core diameter, inches

g = gravitational constant, 32.2 feet per second squared

I_a = armature current, amperes

J = total motor armature and load inertia, referred to motor shaft speed, pound feet per second squared

J_L = load inertia, referred to motor shaft speed, pound feet per second squared

J_M = motor armature inertia, referred to motor shaft speed, pound feet per second squared

K_C = commutation compensation, per unit

K_i = iron stacking factor

K_J = motor armature inertia factor (Figure 6)

K_s = armature slot activity = $\dfrac{\text{armature slot copper area}}{\text{armature slot area}}$

K_T = motor torque constant, foot pounds per ampere

K_V = motor generated voltage constant, volts per radian per second

L = armature core length (iron only), inches

MLT_A = mean length of turn of armature conductor, inches

MLT_{CP} = mean length of turn of commutating field conductor, inches

N = number of armature slots

θ = angle between armature winding end turns and armature end punchings, degrees

ϕ_P = flux per pole, lines

P_c = number of commutating poles

P_M = number of main poles

R = total motor armature circuit resistance, ohms

R_A = armature resistance, ohms

R_{CP} = commutating field resistance, ohms

ρ = specific resistance of copper $= 0.825 \times 10^{-6}$ ohms per inch per square inch at 75 degrees centigrade

$\tau = \dfrac{\text{pole arc}}{\text{pole pitch}}$

T_0 = motor time constant, seconds

w = armature slot width, inches

Z = total number of armature conductors to drive the output member, which is a d-c motor. The motor in turn drives the controlled member or load, which might be the roll of a paper machine, steel mill, printing press, and so forth, whose speed is to be held constant at some preset value. The feedback, in this example, is the output voltage of a tachometer generator driven by the same shaft as the load. This voltage, proportional to the load speed, is fed back to the input of the amplifier in such a manner that the net voltage applied to the amplifier is the difference between it and the voltage supplied from the potentiometer. Thus if the speed of the load decreases, the input to the amplifier is increased, the voltage applied to the motor is increased, and the load speed increases to its normal value; similarly, if the load speed increases, the input to the amplifier is decreased, the voltage applied to the motor is decreased, and the load speed decreases to its normal value. The speed setting may be varied by an adjustment of the potentiometer of the input member.

The problem of the servomechanism designer, then, is to design a system which will be accurate and at the same time stable. In the example given of the speed control system, it is necessary that the deviation from the preset speed be as small as possible with all changes in load, and, if the speed does change, that it be returned to its preset value as rapidly as possible with a minimum of oscillation about the mean speed.

The two factors which affect the stability of the system are the amplification of the system, and the phase displacement between a signal caused by a disturbance at some point in the system and the correction signal which returns to that point through the feed-back circuit. If the phase displacement is 180 degrees, the connections of the feed-back circuit are such that the correction signal will add directly to the initial signal. If at the same time the system amplification is such that the correction signal is greater than the initial signal, then the signals will continually increase in magnitude and the system will be unstable. To correct the situation either the amplification must be reduced until the correction is less than the disturbing signal so that the oscillations will eventually die out, or the phase displacement must be decreased. Reduction in amplification will make the system less accurate. Therefore, methods of keeping the phase displacement small must be investigated.

The over-all system phase displacement is a function of the phase displacement between the input and output of each individual system component. Since the d-c motor is used as the output member of many closed-cycle control systems, the relation between its input (armature voltage) and output (shaft speed) is important in determining the performance of these systems. The slower the response of shaft speed to a change in armature voltage, the greater is the over-all system phase displacement and the greater is the tendency of the system to be unstable. The relation between input and output for a d-c motor and methods of reducing the time delay between the two quantities will now be investigated.

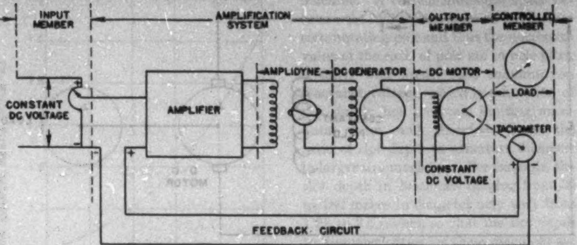

Figure 3. Closed-cycle automatic control system for controlling the speed of an output shaft

The D-C Motor as an Output Member of a Closed-Cycle Automatic Control System

Consider a separately-excited shunt-wound d-c motor and its load suddenly connected to a source of constant voltage, E, as shown in Figure 4.

The voltage impressed across the motor terminals is equal to the sum of the armature circuit resistance drop and the motor generated voltage, neglecting the effect of armature circuit inductance. Also, the motor electrical torque must equal the mechanical shaft torque, which is the torque required to accelerate the motor and load inertia, if steady-state load and friction torques are neglected.

The validity of the assumptions concerning armature circuit inductance and steady-state load and friction torques should be checked for each specific case. In general, the armature circuit resistance inductance time constant is small compared to the motor time constant, especially where compensated d-c motors are used. Also the accelerating torques are usually large compared to the steady-state load and friction torques. If these assumptions cannot be made, the effects which have been neglected must be taken into account in the analysis, and resulting equations will be more complex.

It also is assumed that the torque and generated voltage constants, K_T and K_V, are not changed by demagnetizing effects of the load current. D-c motors for automatic control systems are usually designed in this manner. If normal designs are not satisfactory from this standpoint, compensated designs are used.

In mathematical form, the foregoing statements become

$$E=I_aR+K_Vn \text{ volts} \quad (3)$$

$$T=J\left(\frac{dn}{dt}\right)=K_TI_a \text{ foot pounds} \quad (4)$$

where

E = applied voltage, volts
I_a = armature current, amperes
n = motor speed, radians per second
T = torque, foot pounds

Eliminating the armature current, I_a, from equations 3 and 4, gives

$$E=\frac{RJ}{K_T}\left(\frac{dn}{dt}\right)+K_Vn \text{ volts} \quad (5)$$

The solution of this differential equation for a motor starting from rest is

$$n=\frac{E}{K_V}\left(1-\epsilon^{-\frac{K_TK_V}{RJ}t}\right) \text{radians per second} \quad (6)$$

Equation 6 is similar in form to that obtained for the current in a resistance-inductance circuit when an external voltage is suddenly applied.

$$I=\frac{E}{R}\left(1-\epsilon^{-\frac{R}{L}t}\right) \text{ amperes} \quad (7)$$

Figure 5 represents a plot of equation 6.

The time required for the speed to reach 63.2 per cent of its final value is equal to RJ/K_TK_V, and this time is defined as the motor time constant, in a manner similar to the familiar time constant of the resistance-inductance circuit.

$$T_\theta=\frac{RJ}{K_TK_V} \text{ seconds}$$

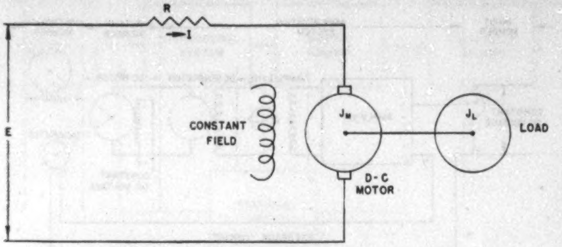

Figure 4. Diagram of a d-c motor and load supplied from constant voltage source, *E*

Thus, the smaller the motor time constant, the more rapidly does the motor speed reach its final value, and the smaller is the phase displacement between input voltage and output shaft speed.

The problem of the motor designer is to make this time constant as small as possible. The system designer will then be given a component which will not force him to lower the system amplification, and thus the system accuracy, in order to gain stability.

The Motor Time Constant in Design Terms

To design a motor for minimum time constant, it is necessary for the motor designer to convert the motor time constant equation, as defined in equation 7, into design terms, such as dimensions, flux and copper densities, and so forth. Knowing the limitations of these various factors, he can then vary them in such a manner so as to obtain a motor design having the smallest possible time constant.

The conversion is made for a commutating pole, noncompensated d-c motor in Appendix I and the resulting equation is

$$T_o=\frac{8.5\times10^4K_J\left(1+\frac{J_L}{J_M}\right)\times\left[1+\frac{\pi}{P_M\cos\theta}\left(\frac{D}{L}\right)+(1.2K_C)\left(\frac{B_{CCP}}{B_{CA}}\right)\left(\frac{P_C}{P_M}\right)\right]}{K_SB_{PF}{}^2\tau^2\left(\frac{d}{D}\right)\left[1-2\left(\frac{d}{D}\right)-\frac{B_{PF}}{K_tB_t}\right]}$$

seconds at 75 degrees centigrade (8)

The two assumptions involved in this conversion are:

1. The armature and commutating field mean lengths of turns are

$$MLT_A=2L+\frac{2\pi D}{P_M\cos\theta} \qquad (9)$$

$$MLT_{CP}=2.4L \qquad (10)$$

Equation 10 gives an approximate value for the mean length of turn of a machine with commutating poles only. If motors having compensating windings are used, the numerical factor should be increased accordingly.

2. The motor armature inertia is given by the equation

$$J_M=6\times10^{-6}K_JD^4L$$

K_J is an empirical constant, greater than unity, which takes into account the fact that the end windings, commutator, armature leads, shaft extensions, fans, and so forth, make the inertia of the armature greater than the value calculated from the D^4L value of the core portion alone. Figure 6 shows the variation of K_J with the ratio of armature core diameter to length for a line of 1,750-rpm 4-pole motors, ranging in size from 5 to 60 horsepower.

The two main variables which affect the value of the denominator are the pole face density, B_{PF}, and the ratio of armature slot depth to armature diameter, d/D.

The values of these variables which make the denominator a maximum, and, therefore, the time constant a minimum, are

$$B_{PF}=\frac{1}{2}K_tB_t \qquad (11)$$

$$\frac{d}{D}=\frac{1}{8} \qquad (12)$$

Optimum use of material requires that the tooth flux density be kept as high as possible. For the limiting value of this density of 140,000 lines per square inch, the pole face density will be about 66,500 lines per square inch, which is high by normal design standards, but which is theoretically possible.

With a sufficient number of armature slots the ratio of pole arc to pole pitch can be made equal to 0.7.

The substitution of these values and equations 11 and 12 into equation 7 gives a minimum value of time constant at 75 degrees centigrade of

$$(T_o)_{\min}=1.25\times10^{-8}\frac{K_J}{K_S}\left(1+\frac{J_L}{J_M}\right)\times\left[1+\frac{\pi}{P_M\cos\theta}\left(\frac{D}{L}\right)+(1.2K_C)\left(\frac{B_{CCP}}{B_{CA}}\right)\left(\frac{P_C}{P_M}\right)\right]\text{ seconds} \qquad (13)$$

Discussion of Conclusions

The results of this study were summarized previously where it was shown what factors must be considered in the design of a d-c motor in orderto obtain the smallest motor time constant.

Before discussing the results and the factors which limit the minimum value of the motor time constant, it may be well to review the assumptions on which this analysis has been based. The following assumptions have been made:

Figure 5. Speed-time curve for a d-c motor and load started from a constant voltage source

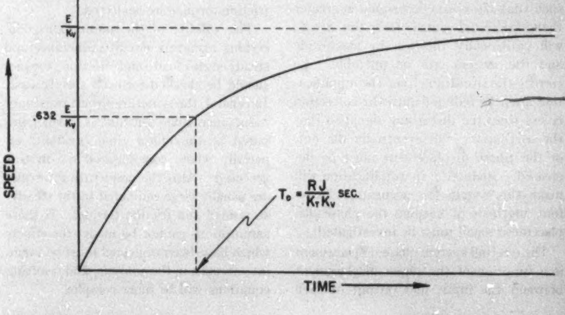

1. The effects of armature circuit inductance have been neglected.

2. The steady-state load and friction torques have been considered negligible compared to accelerating torques.

3. The torque and generated voltage constants are not affected by the demagnetizing effects of load current.

The validity of these assumptions was discussed in a previous section.

An inspection of equation 13 for the minimum possible motor time constant indicates that its value is mainly dependent on the ratio of armature diameter to length. The reason for this can best be explained by studying the original motor time constant equation

$$T_o = \frac{RJ}{K_T K_V} \text{ seconds}$$

The values of the generated voltage and torque constants are fixed by the motor speed and voltage. Therefore, the motor time constant is only changed by a variation in the armature circuit resistance and total motor and load inertia. Both of these factors are functions of the ratio of armature diameter to length. As this ratio is increased (or decreased), while motor speed and voltage, pole face density, and the ratio of armature slot depth to diameter are held constant, it is found that the armature circuit resistance decreases (or increases) by approximately the same amount as the motor armature inertia increases (or decreases). Thus their product, except for secondary effects, remains constant and the motor time constant is independent of the ratio.

The secondary effects result from the presence of commutators, fans, end windings, and so forth, on the armatures. These "nonuseful" electromagnetic parts result in a more complex variation of motor armature inertia and armature circuit resistance with the ratio of armature diameter to length. The secondary effects tend to increase the motor time constant as the ratio is increased. Thus, when the motor has negligible load inertia, the ratio should be kept as small as possible.

When the load inertia is not negligible, it may be advantageous to use a larger value of the ratio. If the motor time constant equation is rewritten as

$$T_o = \frac{1}{K_T K_V}(RJ_M + RJ_L) \text{ seconds}$$

it can be seen that while the first term in the bracketed expression increases with increase in the ratio, as in the case for a motor with negligible load inertia, the second term decreases. Therefore, at some point, the motor time constant will reach a minimum value as the armature-diameter-to-length ratio is increased. It should be noted, however, that an increased ratio may result in larger motors as well as larger generators, so that cost, size, and weight considerations must be weighed against motor time constant requirements.

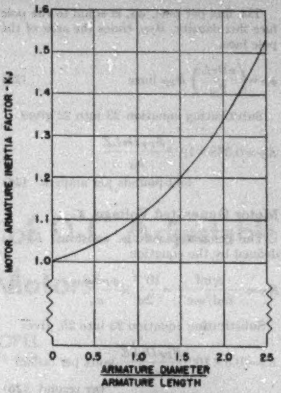

Figure 6. Motor armature inertia factor as a function of the ratio of armature diameter to length, for a line of four pole, commutating pole, 1,750 rpm motors, ranging in size from 5 to 60 horsepower

The factors which limit the minimum value of the time constant are the maximum possible values of the flux density at the root of the armature tooth, the slot activity factor, the ratio of pole arc to pole pitch, and, for larger size machines, the armature slot depth which can be used. Of these limitations, the first two depend mainly on the materials used in the machine, and the second two involve the commutating ability of the machine.

The maximum flux density which present-day magnetic materials can carry is limited to about 140,000 lines per square inch. The slot activity is a function of the insulation materials which can be used. Thinner insulation will give higher slot activities and thus lower time constants. Another decrease in time constant can be obtained from an increase in this factor by the use of comparatively low voltage machines having fewer turns per coil and requiring less insulation. However, the size of commutators, number of brushes, and size of line cables all limit the minimum value of voltage which can be used.

The third and fourth limitations involve the commutating ability of the machine. A certain minimum space between the main poles must be left for the commutating pole and thus the maximum value of the ratio of pole arc to pole pitch is fairly well fixed. Also commutation reactance voltage, which is a function of slot depth, has a certain limiting maximum value, and, therefore, limits the ratio of slot depth to armature diameter in larger size machines. For example, the slot depth in machines ranging from 30 to 180 inches in diameter may vary from 1.25 to 2.5 inches, so that the slot depth to diameter ratios for these machines are far from the optimum value of one-eighth. Hence, improvements in design, which will raise the maximum allowable commutation reactance voltage, also will lead to lower time constants.

The results of this paper can be effectively used in the design of d-c motors for closed-cycle automatic control systems, when the motor time constant is found to be an important consideration. Reductions in motor time constant of considerable magnitude over the time constants of the usual general purpose design are indicated. The main reduction is made by increasing the pole face flux density to a value equal to approximately one-half of the flux density at the root of the armature tooth. The motor designer can, therefore, give the system designer a component, when necessary, which will enable him to design systems of greater accuracy and stability.

Appendix I. Derivation of the Equation for Time Constant in Design Terms

Starting with the general expression for the time constant of a d-c motor

$$T_o = \frac{RJ}{K_T K_V} \text{ seconds} \qquad (14)$$

each of the terms in this equation will be considered separately and expressed as a function of design factors.

Total Motor Armature Circuit Resistance, *R*

The resistance of any winding is equal to the specific resistance of copper, ρ, divided by the area of copper times the length of the winding, or

$$R_A = \frac{\rho}{A_{CA}}\left(\frac{MLT_A \times Z}{2a_A^2}\right) = \frac{\rho B_{CA}(MLT_A)Z}{2I_a a_A} \text{ ohms} \qquad (15)$$

$$R_{CP} = \frac{\rho}{A_{CCP}}\left(\frac{P_C K_C \times MLT_{CP} \times Z}{2P_M a_A a_{CP}}\right) = \frac{\rho B_{CCP} P_C K_C (MLT_{CP})Z}{2I_a P_M a_A} \text{ ohms} \qquad (16)$$

Using the approximations

$$MLT_A = 2L + \frac{2\pi D}{P_M \cos\theta} \text{ inches} \qquad (17)$$

$$MLT_{CA} = 2.4L \text{ inches} \qquad (18)$$

and substituting these into equations 15 and 16, and adding, gives the total motor armature circuit resistance, R.

$$R = \frac{\rho LZB_{CA}}{I_a a_A}\left[1 + \frac{\pi}{P_M \cos\theta}\left(\frac{D}{L}\right) + (1.2K_C)\left(\frac{B_{CCP}}{B_{CA}}\right)\left(\frac{P_C}{P_M}\right)\right] \text{ ohms} \qquad (19)$$

Total Motor Armature and Load Inertia

The moment of inertia of a cylinder is given by the equation

$$J = \frac{W}{g}\frac{D_c^2}{8} \text{ pounds feet per second squared} \qquad (20)$$

where

D_c = diameter of cylinder, inches
W = weight of cylinder, pounds

Assuming that the inertia of a motor armature is equal to some constant times the inertia of the core portion, and taking the average specific gravity of iron, copper, and insulation, as 0.28 pound per cubic inch

$$J_M = 6\times10^{-6}K_J D^4 L \text{ pound feet per second squared}$$

$$J = J_M + J_L = 6\times10^{-6}K_J D^4 L\left(1 + \frac{J_L}{J_M}\right) \text{ pound feet per second squared} \qquad (21)$$

where J_M and J_L are motor armature and load inertias referred to the motor shaft speed.

Motor Torque Constant, K_T

The torque constant, K_T, the torque per ampere of the motor, is given by the equation

$$K_T = \frac{T}{I_a} = \frac{\phi_P Z P_M}{8.52\times10^8 a_A} \text{ foot pounds per ampere} \qquad (22)$$

The flux per pole, ϕ_P, is equal to the pole face flux density, B_{PF}, times the area of the pole face.

$$\phi_P = \left(\frac{\pi D_\tau L}{P_M}\right) B_{PF} \text{ lines} \qquad (23)$$

Substituting equation 23 into 22 gives

$$K_T = 0.368\times10^{-8}\frac{B_{PF}D_\tau LZ}{a_A} \text{ foot-pounds per ampere} \qquad (24)$$

Motor Generated Voltage, K_V

The generated voltage constant, K_V, is defined by the equation

$$K_V = \frac{\text{cemf}}{\text{rad/sec}} = \frac{10^{-8}}{2\pi}\times\frac{\phi_P Z P_M}{a_A} \qquad (25)$$

Substituting equation 23 into 25, gives

$$K_V = 0.5\times10^{-8}\frac{B_{PF}D_\tau LZ}{a_A} \text{ volts per radian per second} \qquad (26)$$

Motor Time Constant, T_o

If the equations for R, J, K_T, and K_V (equations 19, 21, 24, and 26) and the value for the resistivity of copper, ρ, at 75 degrees centigrade are substituted into equation 14, there results

$$T_o = \frac{26.9\times10^4 K_J D^2\left(1 + \frac{J_L}{J_M}\right)\times\left[1 + \frac{\pi}{P_M\cos\theta}\left(\frac{D}{L}\right) + (1.2K_C)\left(\frac{B_{CCP}}{B_{CA}}\right)\left(\frac{P_C}{P_M}\right)\right]}{B^2{}_{PF}\tau^2\left(\frac{ZI_a}{a_A B_{CA}}\right)} \text{ seconds} \qquad (27)$$

The term $ZI_a/a_A B_{CA}$ in the denominator of equation 27 represents the total copper conductor area of the armature, since Z is the total number of conductors and $I_a/a_A B_{CA}$ is the area of each conductor. This expression also can be written as

$$\left(\frac{ZI_a}{a_A B_{CA}}\right) = K_s \times \text{total slot area} \qquad (28)$$

The "total slot area" of an armature having rectangular slots is given by the equation

$$\text{Total slot area} = Nwd \text{ square inch} \qquad (29)$$

However, the flux density at the base of the armature teeth is

$$B_t = \frac{\text{Flux per pole}}{\text{Teeth per pole}\times\text{core length}\times K_t\times\text{tooth width at bottom of slot}}$$

$$= \frac{B_{PF}\left(\frac{\tau\pi DL}{P_M}\right)}{\left(\frac{N_\tau}{P_M}\right)(L)(K_t)\left[\frac{\pi}{N}(D-2d) - w\right]} \qquad (30)$$

Eliminating the armature slot width, w, from equations 29 and 30 and solving for "total slot area" gives

$$\text{Total slot area} = \pi dD\left[1 - 2\left(\frac{d}{D}\right) - \frac{B_{PF}}{K_t B_t}\right]\times \text{square inch} \qquad (31)$$

If equations 28 and 31 are substituted into equation 27, the motor time constant becomes

$$T_o = \frac{8.5\times10^4 K_J\left(1 + \frac{J_L}{J_M}\right)\times\left[1 + \frac{\pi}{P_M\cos\theta}\left(\frac{D}{L}\right) + (1.2K_C)\left(\frac{B_{CCP}}{B_{CA}}\right)\left(\frac{P_C}{P_M}\right)\right]}{K_S B^2{}_{PF}\tau^2\left(\frac{d}{D}\right)\left[1 - 2\left(\frac{d}{D}\right) - \frac{B_{PF}}{K_t B_t}\right]} \text{ seconds at 75 degrees centigrade} \qquad (32)$$

References

1. DYNAMIC BEHAVIOR AND DESIGN OF SERVOMECHANISMS, G. S. Brown, A. C. Hall. *Transactions*, American Society of Mechanical Engineers (New York, N. Y.), volume 68, 1946, pages 503–24.

2. THEORY OF SERVOMECHANISMS, H. L. Hazen. *Journal*, Franklin Institute (Philadelphia, Pa.), volume 218, 1934, pages 279–331.

3. PRINCIPLES OF SERVOMECHANISMS (book), G. S. Brown, A. C. Hall. John Wiley and Sons, New York, N. Y., 1948.

4. FUNDAMENTAL PRINCIPLES OF AMPLIDYNE APPLICATIONS, F. E. Crever. *Electrical Engineering* (*AIEE Transactions*), volume 62, September 1943, pages 603–06.

5. PROCEEDINGS AT THE CONVENTION ON AUTOMATIC REGULATORS AND SERVOMECHANISMS. *Journal*, Institution of Electrical Engineers (London, England), volume 92, part IIA, numbers 1 and 2, 1947, pages 1–307.

No Discussion

Limitations in Design of D-C Adjustable Speed Motors

L. G. OPEL
ASSOCIATE AIEE

A d-c adjustable speed motor is one in which its speed is varied by changing the value of current in its shunt field. The speed of the motor can be varied over a wide range in this manner with a very small amount of power. It is a very popular motor and has many applications where variable speed is required, such as machine tools, reel drives, fans, and others. These motors have been built successfully with speeds adjustable over as high as an eight-to-one range.

There are many factors to consider when designing an adjustable speed motor. The same factors exist when designing any d-c machine, but usually they are well below the critical values. The four main factors which limit the design of adjustable speed motors are commutation, speed regulation, heating, and the maximum safe speed of the motor. Each factor will be discussed in this paper.

Commutation

All data given pertaining to the reactance voltage are based on values calculated by Lamme's equations[1] and have been proved in tests on actual motors.

Commutation becomes a serious problem in adjustable speed motors. The greater the speed range the more difficult commutation becomes. For a motor supplying a constant or increasing horsepower load, the maximum operating speed will be the limiting condition and the commutation factors should be calculated for this condition.

Table I gives the limiting values for the reactance voltage per coil and the reactance voltage per brush. These values are based on tests of a large number of motors and successful commutation can be obtained if they are not exceeded. These two factors should always be calculated on a new design. It is also necessary to calculate the voltage which will be obtained between commutator bars. If this voltage becomes too great, there is danger of a flashover between commutator bars and between brush arms.

An analysis of Lamme's equation for calculating the reactance voltage of the armature coils undergoing commutation indicates how this voltage varies with the machine constants and how by careful design we can minimize this voltage by proportioning the machine constants properly.

The reactance voltage is proportional to speed, current in armature conductor, total armature conductors, and the equivalent number of armature turns per coil

$$E_c = \frac{K(W_t I_c T_c R_s \pi)}{10^8}$$

For a 2-circuit winding

$$T_c = \frac{T_{ca} P}{2}$$

For a multiple-wound armature

$$T_c = T_{ca}$$

The reactance voltage can then be kept to a minimum by using as few armature turns per coil as economical. For example, a 4-pole 2-circuit winding would have double the reactance voltage for a 2-turn coil than it would have for a 1-turn armature coil. Of course, a 1-turn armature coil requires that twice the number of commutator bars be used than with a 2-turn coil. For a given diameter of commutator we are physically limited to the maximum number of commutator bars that we can use.

Increasing the armature core length or diameter permits the use of fewer armature turns for a given rating. This is equivalent to increasing the frame size.

The constant K in the equation is a flux which is the sum of the interpolar, armature end windings, and slot fluxes of the motor. Each of these factors is discussed in detail in the following paragraphs.

The interpolar flux is kept to a minimum by using the same number of commutating poles as main poles. This factor becomes zero with the same number of interpoles as main poles when the interpoles are as long as the core length. When using half the number of interpoles as main poles, the length of interpole has to be divided by two when applying the equation

$$\text{Interpolar Flux} = \frac{2PD(L-L_1)C_1}{(0.25P+0.5)(\pi D - PW_p)}$$

The armature end turn flux varies directly with the armature diameter and inversely with the number of poles. N_1 is the number of slots spanned by the coil pitch and increases as the total number of slots increase.

$$\text{Armature End Flux} = \frac{4D}{P}(0.9+0.035\ N_1)C_2$$

Table I. Maximum Values of Reactance Voltage Per Coil and Voltage Per Brush When Using a High Quality Electrographitic Grade of Brush*

Type of Brush	Voltage Per Coil	Voltage Per Brush
Solid brush	5	16
Double brush with a single finger	7	23
Double brush with two fingers	8	27

* Values given apply to industrial size motors ranging from 1 to 250 horsepower at 1,200 rpm.

Paper 49-226, recommended by the AIEE Rotating Machinery Committee and approved by the AIEE Technical Program Committee for presentation at the AIEE Fall General Meeting, Cincinnati, Ohio, October 17–21, 1949. Manuscript submitted November 16, 1948; made available for printing September 21, 1949.

L. G. OPEL is with the Westinghouse Electric Corporation, Buffalo, N. Y.

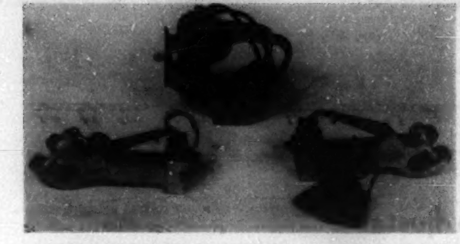

Figure 1. Left to right: a solid brush, a double brush in a double holder, and a double brush in a single holder

The slot flux is directly proportional to armature core length and is influenced by the ratio of slot depth to width. The greater the ratio, the greater the slot flux and the reactance voltage. The tooth pitch decreases with an increase in the total number of slots which reduces the slot flux.

$$\text{Slot Flux}=\frac{L}{b_s}(4/3\ d_s+0.52+P_t)C_3$$

For a normal design of three commutator bars per slot, a maximum slot ratio of 5/1 is desirable.

The type, grade, and thickness of the carbon brush used affects commutation. The thickness of the brush determines the number of commutator bars undergoing commutation. The reactance voltage per brush is the product of the volts per coil and the number of bars per brush. Increasing the brush thickness will then increase the reactance voltage per brush. However, increasing the thickness will also reduce the reactance voltage per coil, therefore, the increase in voltage per brush is not proportional to the brush thickness. The constant C_3 for the slot flux is influenced by brush thickness.

$$C_3=\frac{\text{Bars per slot}}{\text{Commutating Zone in Bars}}$$

The commutating zone increases as the number of bars per brush increase.

The magnitude of the reactance voltage per armature coil and the reactance voltage per brush are two factors which are very important in determining whether the motor will commutate successfully. They are related to each other and both have to be kept within the limits as given in Table I, with the brushes being used today.

The ordinary carbon brush will commutate $2^1/_2$ volts, as a limit, per brush without any visible signs of sparking. Therefore, if we can adjust our interpole compensation to compensate for all but $2^1/_2$ volts per brush, good commutation will be obtained. If the motor were compensated to within 90 per cent of perfect compensation, we would be able to commutate 25 volts per brush.

It is not too difficult to adjust a motor to be within 25 per cent of being perfectly compensated, but it is next to impossible to adjust to 100 per cent compensation. Therefore, it becomes necessary to set up limits for the reactance voltage per brush as given in Table I.

It should be recognized that an improvement in commutation cannot always be made by merely changing the type of brush used. The commutating pole air gap may require a different adjustment, or if the current loading of the motor is increased, interpole saturation may be encountered.

The normal voltages and speed ranges over which adjustable speed motors operate are:

115- and 230-volt motors—four to one
440-volt motors—three to one
550-volt motors—two to one

Motors have been designed and built which operate over greater speed ranges. You will notice that the speed range becomes less as the voltage is increased. The reason for this is that the upper limit of the commutation factors is reached at lower speeds. For a given rating and speed the number of armature conductors, increases as the voltage increases. The voltage conversion factor, therefore, increases. For example: A 10-horsepower 230-volt 38-ampere motor has 135 bars, a 1-turn armature coil, four poles, and a 2-circuit winding.

$$E_c=\frac{k(135\times1\times2\times19\times2\times rpm)}{10^8\qquad 60}$$

A 10-horsepower, 460-volt motor would have a current of 19 amperes and 135 commutator bars, a 2-turn armature coil, four poles and a 2-circuit winding. Its factor would be

$$E_c=\frac{k(135\times2\times2\times9.5\times4\times rpm)}{10^8\qquad 60}$$

This motor has twice the reactance voltage of the 230-volt motor for the same speed.

Therefore, its speed range will be one-half that of the 230-volt motor. The speed range of the higher voltage motors can be increased by increasing the size per rating. Increasing its armature dimensions decreases the number of armature conductors required for the same speed and therefore increases the speed at which the motor can be operated and still commutate successfully.

Another factor to be considered is the voltage between commutator bars. This voltage has to be kept below certain values in order to build a motor which will not flash over under normal operating conditions. The limit of the flashover voltage is influenced by the resistance of the armature. High resistance armature windings permit greater voltages to be used between commutator bars. The thickness of the mica insulation between bars limits the maximum voltage per bar permitted. A factor of 1.10 volts per mil thickness of mica is used to determine the permissible value of voltage that should be used between commutator bars. The following values are for 25-mil thick mica and motor sizes ranging from 1 to 250 horsepower at 1,200 rpm:

1. The average voltage between bars $=(EP)/B$ maximum $=15$ volts.
2. The maximum voltage under the

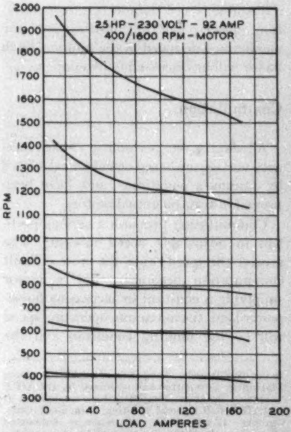

Figure 2. Typical speed regulation curves of adjustable speed motors

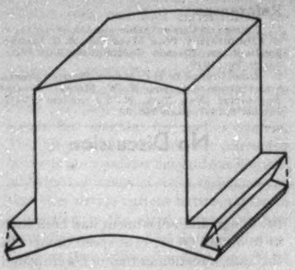

Figure 3. A type of pole tip notch

poles at no load = $(EP)/(Bk)$ maximum = 23 volts.

$$k=\frac{\text{Pole Circumference }(P)}{\text{Armature Circumference}}\cong 0.65$$

3. The maximum voltage under load = $(EP)/(Bk)\ \phi_1/\phi_2$, maximum equal to 35 volts per bar.

Where

ϕ_1 = flux at value of ampere turns equal to the ampere turns required to give ϕ_2 plus the armature distortion ampere turns

ϕ_2 = flux at maximum operating rpm

Speed Regulation

The speed regulation of standard adjustable speed motors varies over the operating speed ranges. At low speeds the regulation is low, and at top speeds the regulation becomes high. See Figure 2 for typical regulation curves.

The armature distortion effects the regulation as it does not reduce the flux the same amount at all values of operating fluxes. Because of the reduced flux under load, it becomes necessary to add a series field to the motor to compensate for the reduced flux in order to obtain a drooping speed characteristic with load. Since the saturation curve is not linear over its range of operation, the flux changes and speed changes with load and will be very high at high speeds.

The speed regulation can be improved by special notching of the field poles as shown in Figure 3. The pole tip notch causes the main pole tip to become saturated at low values of ampere turns on the main poles. Since the pole tip is saturated, the flux through it will not change appreciably as the armature distortion ampere turns add and subtract from the main field ampere turns. Therefore, there will not be as much reduction in the flux under load as there was before the pole tips were notched, and the motor will require less series field ampere turns to stabilize it. Less series ampere turns means that the motor will have a smaller variation in speed between no load and full load at the high speeds.

By designing machines with compensating windings (or pole face windings) the speed regulation of adjustable speed motors can be made more uniform over their range of operation. This is accomplished because the armature distortion effect is greatly reduced when compensating windings are used. This also reduces the maximum voltage between commutator bars and the danger of flashovers. Compensating windings are not used very frequently on the smaller size motors because of the high cost involved.

Other methods involving special windings and circuits on the main field poles have been devised which give improved speed regulation and some improvement in commutation. One such method is used on the eight-to-one speed range motor.[2]

Maximum Safe Speed

The maximum safe speed the motor armature can safely operate at and not fail mechanically has to be considered in the design. The excessive speed regulation at weak fields, or high speeds at no-load, determine the maximum speed the armature has to be made safe for. This means special mechanical designs for very high speed motors.

Heating

Since the adjustable speed motor operates over a wide range in speed, the amount of ventilating air through the motor will vary as the speed changes. At the low speeds very little air circulation is obtained relative to that which is obtained at the higher speeds. Figure 4 shows how the watts dissipated from an armature rotating in free air varies with its peripheral velocity. Note that it is a straight line variation until a critical velocity A is reached, after which it increases very slowly.

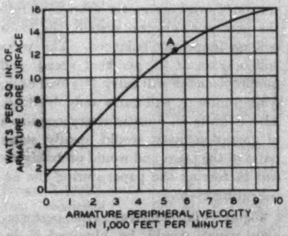

Figure 4. A typical armature heat transfer curve

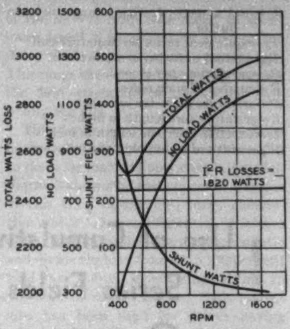

Figure 5. Variation in watts loss with rpm of a 25-horsepower 230-volt 400/1,600-rpm motor

The losses of the motor do not vary proportionally to the speed. Figure 5 shows how the losses of a constant horsepower motor vary with the speed. The losses at the low speed are even greater than the losses at intermediate speeds.

A comparison of the losses against the amount of air circulation obtained at various speeds clearly indicates that the motor will have the highest temperature rise at the lower speeds. If the motor were designed to meet its temperature rise at its lowest speed, it would be larger than necessary to meet the temperature rise at the higher speeds. The fact must not be overlooked that it is possible to operate the motor at a sufficiently high speed so that the increase in losses will be greater than the increase in the ventilation. The motor will then have a greater rise at these high speeds than at some lower speed.

It is recognized that in most adjustable speed motor applications, the motor will not operate at its base speed continually. A standard has been set up so that the motor will be designed to meet its specified temperature rise at 150 per cent of its base speed. It is felt that this condition is a good average of the operating range of the motor.

Nomenclature

E_c = commutating volts

W_t = total conductors on armature

I_c = load amperes flowing in armature conductor
T_c = equivalent turns per armature coil
T_{ca} = actual turns per armature coil
R_s = revolutions per second
P = number of main poles
D = armature diameter in inches
L = armature core length in inches
L_i = effective interpole length in inches
W_p = width of main pole body in inches
N_1 = slots spanned by one coil pitch
b_s = width of slot in inches
d_s = depth of slot in inches
P_t = tooth pitch in inches
C_1, C_2, C_3 = constants
k = constant
B = number of commutator bars
E = induced armature voltage
K = constant
ϕ = flux

References

1. Theory of Commutation and Its Application to Commutating Pole Machines, B. G. Lamme. Westinghouse Electric Corporation, East Pittsburgh, Pa., 1919.

2. Dual Fields in D-C Motor Provide Simple 8-to-1 Speed Control, R. W. Moore. *Product Engineering* (New York, N. Y.) volume XVIII, number 8, 1947, pages 166–69.

No Discussion

Use of Cumulative and Differential Series Fields in the Parallel Operation of D-C Motors

A. W. KIMBALL
ASSOCIATE AIEE

D-C MOTORS are used in parallel on a large number of applications. In some of these, the division of load is of relatively minor importance. However, in others it is essential if the best performance is to be obtained.

An example of this is the sectional printing press used in printing newspapers. In this case, the press sections and motors are so designed that the total inertia load and horsepower rating of the motors are balanced. The press then can be accelerated or decelerated at the maximum rate with a resulting minimum loss of time for change of rolls of paper, and so forth. Also, one or more sections can be dropped from operation without affecting the performance of the press as a whole. However, the torque produced by each motor must match that of each of the others within close limits throughout the complete cycle of operation in order that best performance can be obtained without overstressing any part of the press or tearing the paper. The use of cumulative and differential series fields accomplishes this with simplicity and a minimum of control elements.

Motors with One Series Field

The manner in which two or more motors, when operated from the same power source and connected to the same load, will divide it between them is determined by their regulation curves. Figure 1(A) shows such a system using normal standard motors. Assume the series fields have been set to give 10 per cent regulation in each case and the shunt field rheostats have been set so that all units carry 100 per cent load at 100 per cent speed. The regulation curves then will be as shown by the solid line curves in Figure 1(B). This system then is set up for parallel operation and it will function with good load division until some change takes place to upset the adjustment.

To take an extreme case, suppose that motors *A* and *B* have been operating continuously and are up to temperature, but motor *C* has been idle and is therefore cold. In addition to this, assume that the effect of this temperature difference is such that its speed load curve is lowered 10 per cent. This is shown by the dash curve for this motor. Now if additional pages are to be added to the paper and section *C* with its motor connected into the press and electric system, the loads will no longer be balanced. The press will operate at 97 per cent speed, and motors *A* and *B* will carry $1^1/_3$ load each, while motor *C* will carry only $^1/_3$ load. This is quite an unsatisfactory condition of operation, as it would unduly stress parts of the press and would probably result in tearing the paper during the accelerating cycle.

Figure 1(C) illustrates the performance which would be obtained if, instead of adjusting the series field for 10 per cent regulation no load to full load, the design and adjustment had been such as to obtain 60 per cent speed droop. In this case, if section and motor *C* were added to the system cold, then the load division would be much better. Motors *A* and *B* would each carry 105.5 per cent load and motor *C* would carry 89 per cent load. The press again would operate at 97 per cent speed. This would be good parallel operation. However, a regulation of 60 per cent is impossible to obtain if the motors are to be operated over a wide speed range by field control. This range is usually 4-to-1. Regulations of approximately 5 per cent at full field and 15 to 20 per cent at weak field are obtainable in shunt wound motors and result in good maintenance of speed with changes in load.

Motors with Two Series Fields

The problem then becomes one of obtaining heavily compounded motor performance for parallel operation while preserving the shunt wound motor characteristic for over-all performance. This is obtained by using two series fields in each motor. If one series turn per pole is required to give the desired shunt motor

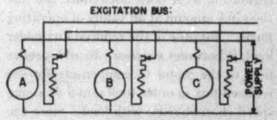

FIGURE I (a) CONNECTION DIAGRAM

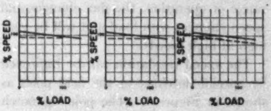

FIGURE I (b) REGULATION CURVES WITH 10% DROOP

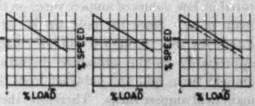

FIGURE I (c) REGULATION CURVES WITH 60% DROOP.

Figure 1. System with only cumulative series

Paper 49-227, recommended by the AIEE Rotating Machinery Committee and approved by the AIEE Technical Program Committee for presentation at the AIEE Fall General Meeting, Cincinnati, Ohio, October 17–21, 1949. Manuscript submitted November 16, 1948; made available for printing September 22, 1949.

A. W. Kimball is with the Westinghouse Electric Corporation, Buffalo, N. Y.

characteristic and four series turns required to give the compound motor characteristic, then the motor is built having a cumulative series of four turns per pole and a differential series of three turns per pole. Figure 2(A) shows the connection diagram for such a system. The differential series coils are connected between the equalizer bus and one line and adjusted by means of series resistances so that they divide current between them in proportion to the rated current of their respective motors. The shunt field rheostats are then adjusted so that the motors divide the load in proportion to their respective ratings.

Any variation in the current division between the differential series fields is compensated by the adjustment of the shunt field rheostat. It, therefore, of course, influences the matching of the characteristics of the motors, but division within ±5 per cent is generally satisfactory and not particularly difficult to obtain. Since the voltage drops are low, it is sometimes found desirable to solder all connections to prevent change.

The system then will operate as a combined unit as though each motor had a regulation curve as shown by the solid lines in Figure 2(B). However, the motors will divide the load (assuming operation at 100 per cent load) as though each had a regulation curve as shown by the dash lines. This is true because, for a given operating condition, the power required to drive the press is practically constant. Therefore, current drawn from the power source also is practically constant. The differential series fields will divide this current between them in proportion to the rating of their respective motors. This was a condition of the adjustment and since we have assumed 100 per cent load operation, this will be rated current in each case.

The equalizer connection isolates the differential series portion of the circuit from that of the motor armatures and cumulative series fields and permits the current to divide in this part of the circuit according to the resulting regulation curve for each unit. Since the differential series field is constant, the combined effect of it and the shunt field is such that, if the motor were uncoupled, it would operate at 160 per cent of full load speed.

However, at full load current the cumulative series is such that the field is strengthened and the motor will operate at 100 per cent speed. The motor armatures will, therefore, divide the load in accordance with the regulation curves shown by the dash lines. If the power requirements are reduced so that the total load is only 50 per cent of the sum of the ratings of all the motors, then the resulting regulation curves for load division will be as shown by the dot-dash lines.

The control required for this system is quite simple. Usually a resistance-type starter is provided for each motor to bring it up to base speed. The steps of these starters are so matched that the same voltage is applied to each motor on corresponding steps. The step contactors are then operated from the master control at the same time. This permits acceleration of any group or combination of motors as desired by simply opening or closing a given motor circuit. The control of the motors from base speed to maximum speed is simplified by exciting the shunt fields from a variable voltage bus. This range then can be covered by varying the field excitation of the exciter supplying the bus.

This design has been used for systems having as many as six motors connected to the same load and operating in parallel. Figure 3 shows the test curves of a motor of this type having $3^{1}/_{2}$ turns cumulative and $2^{1}/_{2}$ turns differential series per pole. These motors operate consistently and divide the load from 40 to 100 per cent load over a 4-to-1 speed range within 10 per cent of rated current. This system also has been used for drives having mixed horsepower rating. Care must be used, in such cases, to match the saturation curves, regulation curves with and without the differential series, and the shunt field design. When this is done, satisfactory performance is obtained.

Designs having cumulative and differential series fields also have been used in the parallel operation of generators with very good results. They can be made with under-, flat-, or over-compounded machines with equally good results. The only undesirable features of the system are the necessity of an equalizer, and that the adjustment of the differential series field circuit be made accurately and in such fashion that it will not change appreciably with time.

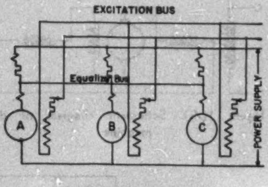

FIGURE 2(a) CONNECTION DIAGRAM

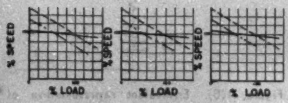

FIGURE 2(b) REGULATION CURVES

Figure 2 (left). System with cumulative and differential series fields

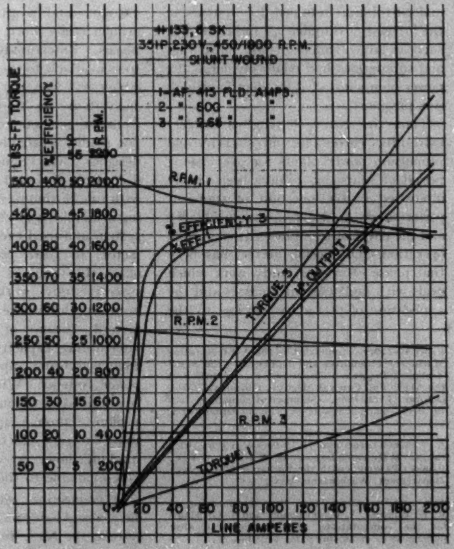

Figure 3 (right). Test regulation curves with both series fields excited by line current

Conclusions

Motors built with this type of winding provide shunt motor regulation characteristics over a wide speed range with good division of load. This permits sectionalizing of mill or press drives with the resulting simplification of design. It also permits operation at full efficiency when sections of the mill or press are not required for the particular operation being performed.

No Discussion

Transient Characteristics of D-C Motors and Generators

A. T. McCLINTON
MEMBER AIEE

E. L. BRANCATO
MEMBER AIEE

ROBERT PANOFF
ASSOCIATE AIEE

SINCE the first installation of electric power on board the *USS Trenton* in 1883, the United States Navy has always been a major user of d-c power. After the introduction of 440-volt alternating current into the Navy with installations on the Farragut-class destroyers in 1932 there was still a continued use of a sizable amount of direct current. All vessels having a-c systems required some direct current for powering excitation supplies, searchlights, battery chargers, and interior communications. Although alternating current had become the accepted standard, smaller vessels such as landing craft and patrol craft retained d-c systems in the interest of simplicity. Other vessels, such as large tenders, repair ships, tugs and submarines had relatively large d-c power plants installed for electric propulsion purposes.

Thus the Navy, having extensively used direct current for ship's service and propulsion power plants for over a long period of years, has always been vitally interested in the question of transient performance of d-c rotating machinery and the effect of the transients on system operation. Of special interest has been that phase of system study work which deals with fault current analysis and the application of protective devices to the power plant. In the early days of small capacity plants, fault current analysis was not of major importance since the available amount of short-circuit current in the system was relatively small and most of the protective devices, which had been primarily designed for shore station use, had more than adequate interrupting capacity to meet the application requirements. Thus accurate knowledge of fault currents that could be obtained was inconsequential. As the electric loads on Naval vessels started to increase at a great rate shortly before World War II, with the resultant increase in generating capacity and available fault currents, system study work received a new emphasis. Unfortunately, the mathematical tools available to the a-c system designer, which give him the ability to calculate such items as subtransient reactances from the geometry of the machines, are not readily available to the d-c system designer. The engineers concerned with d-c system work had to satisfy themselves with rule-of-thumb methods for calculating available short-circuit currents in the system and used excessively large safety factors in their protective devices to offset the probable inaccuracy in their system study work. In most cases, however, this worked out entirely satisfactorily because of the fact that high-interrupting capacity protective equipment was being applied to low-capacity power systems. Where test data could be obtained on the machinery to be used, a more thorough and accurate system study design could be made. Generally speaking, however, very little test data were available to the system designer.

In connection with the design of a naval vessel having a large d-c propulsion system, the Navy initiated the development of completely new design rotating machinery. Machines of new voltage ranges, speeds, and ratings were designed. Associated with this machinery development program was the design of new fuses, circuit breakers, and contactors. Thus the application engineer was faced with the problem of setting up design and performance specifications for this new protective equipment without accurate knowledge of the conditions under which the equipment might have to operate. In the case of shipboard d-c systems where freedom from commutator flashover and reliable circuit breaker operation are extremely important, consideration of the performance of d-c machinery under fault conditions is extremely significant. This is especially true in the larger capacity systems, where excessive fault currents cause commutator flashover and extremely low-fault currents make the attainment of circuit breaker selectivity extremely difficult. In order to successfully set up design specifications for protective devices that will operate reliably with the rotating machinery, the application engineer should have the following information:

1. The maximum short-circuit current of motors and generators in the system.
2. The rate of rise and decrement of the short-circuit current of the motors and generators.

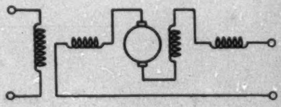

Figure 1(A). Schematic diagram of d-c machine

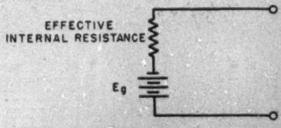

Figure 1(B). Equivalent representation of d-c machine

Paper 49-229, recommended by the AIEE Rotating Machinery Committee and approved by the AIEE Technical Program Committee for presentation at the AIEE Fall General Meeting, Cincinnati, Ohio, October 17-21, 1949. Manuscript submitted July 19, 1949; made available for printing September 1, 1949.

A. T. McClinton and E. L. Brancato are with the Naval Research Laboratory, Washington, D. C. Robert Panoff is with the Bureau of Ships, Navy Department, Washington, D. C.

The authors acknowledge the contributions of R. E. Whipple, J. P. O'Connor, and J. G. Allard for the computations and experimental work performed to make this paper possible.

3. Information relative to the flashover characteristics of the rotating machinery.

4. Information relative to the effect of changes in voltage, speed, and machine loading on the short-circuit characteristics of the machinery.

In attempting to set up design specifications for this particular power plant which would result in the smallest possible size of protective equipment, an investigation was made into the various methods of calculating the transient performance of d-c machinery. Some theoretical treatises on this subject were available; however, most of these were conflicting in theory and results, and generally all were too unwieldy to be of use to the application engineer. In this instance where the machine design work was paralleling the protective device development, the system engineer was hampered by the fact that there was not a thoroughly reliable mathematical tool available with which he could calculate the transient performance of the rotating equipment. It was immediately apparent that if the Navy was to continue using d-c systems, and in some cases this could not be avoided, some means must be established for the accurate calculation of the transient performance of d-c machinery from the geometry of the machines concerned.

After a complete review of the various technical papers on this subject and many discussions with manufacturers of Navy d-c rotating machinery, three technical papers,[1,2,3] were investigated for application to shipboard system analysis. Using certain methods prescribed in these papers for the d-c calculations, various sizes of this newly designed rotating machinery were calculated to determine the peak short-circuit current. In all cases, the results obtained appeared excessive.

Table I. Short-Circuit Constants of Machines for Operation at Normal Full Load Ratings

Machine	Rated Voltage, Volts	Rated Speed, Rpm	Rated Current, Amperes	Current Rise Amps/Sec. $\times 10^6$	Effective Internal Resistance, Ohms	Zero Resistance Short-Circuit Current, Per Unit, Calculated
Generator	415	750	2,650	2.0	0.019	8.5
Generator	345	1,200	870	1.43	0.0355	12.0
Motor	415	1,300	2,600	2.5	0.021	7.5
Motor	415	280	2,650	2.5	0.032	5.0
Motor	250	1,750	298	0.2	0.085	10.0
Motor	250	550	176	0.04	0.170	8.5
Motor	250	1,600	73	0.04	0.360	9.5

Since these machines had not as yet been built, there were no means available for checking these calculations. Accordingly, it was deemed necessary at that time that the theoretical considerations set forth in the foregoing papers should be checked with test data on Navy-type equipment. In order that enough test data could be obtained to completely evaluate the theoretical considerations, a mock ship's system was set up, complete with propulsion motors, propulsion generators, and auxiliary motors in various horsepower ranges. Instrumentation was installed in this system for a twofold purpose:

1. To measure the peak short-circuit current and rate of rise and decrement of short-circuit current under various conditions of loading, speed, voltage, and external fault resistance.

2. Instrumentation to determine the internal phenomena under fault conditions. This involved measuring the change in flux in various portions of the machine.

It was anticipated that the first phase of this test program would result in data which could easily be checked against values obtained by calculation. The second phase of the program regarding the internal phenomena of the machines is a longer range program, the results of which are expected to simplify present theory or evolve new theory.

The purpose of the following discussion is to demonstrate the scope of these tests and their relationship to the theoretical considerations of the problem. The data described herein merely covers the highlights of the test work performed and is presented to the extent that it assists in an understanding of the factors involved in the transient characteristics of d-c machines.

Equivalent Circuit

The selection of a suitable equivalent circuit for adequate representation of the

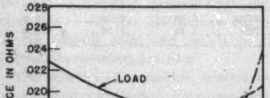

Figure 2. Effect of initial operating conditions on effective internal resistance, 1,100-kw 415-volt 750-rpm generator

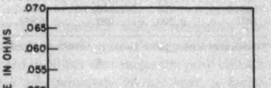

Figure 3. Effect of initial operating conditions on effective internal resistance, 300-kw 345-volt 1,200-rpm generator

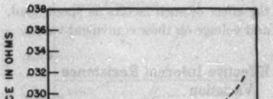

Figure 4. Effect of initial operating conditions on effective internal resistance, 1,375-horsepower 415-volt 280-rpm motor

d-c machine presented schematically in Figure 1 (A) will depend upon the application of the circuit in later studies. One form of simplified representation is found in Figure 1 (B). The effective internal resistance represents all factors tending to restrict the flow of current from the generator. These factors are armature circuit ohmic resistance, brush contact drop, reactance voltage, and flux reduction and distortion. The voltage E_q represents the generated voltage prior to short circuit which is assumed to remain constant during the short circuit whereas the flux reduction and distortion are treated as ohmic resistance.[1]

It should be noted that this circuit is applicable only for the computation of peak values of short-circuit current for individual machines or for the total value of several in a system. Reasonable accuracy can be expected in a system calculation if the time to reach peak current is essentially equal for all machines on the system and if the effective internal resistance is accurately known. Where the transient of the current is desired, a more nearly complete representation of the machines with an equivalent circuit will be required. Such a circuit would require resistance and inductances to represent the armature and field circuits. However, the required accuracy of calculations would have to justify such elaborate computations as this would imply.

Table I presents values of effective internal resistance and generated voltage that have been found for several machines by laboratory tests. The values shown in this table are for operation at rated conditions prior to application of the fault. Discussion to follow will indicate the effect of such factors as speed, load, and voltage on these equivalent values.

Table II. Generator—1,100 Kw, 415 Volts, 2,650 Amperes, 750 Rpm

Volts Generated	Load	Speed	r_e	r_d'	$I_{\text{Calc.}}$	I_{Test}	Percentage
428.8	2,300	715	0.2407	0.3557	2.91	3.09	94.2
427.3	2,000	715	0.01450	0.13085	7.86	7.02	112.0
415	0	715	0.01213	0.12667	7.89	7.74	102.0
214.1	2,600	715	0.01448	0.12657	5.97	5.70	104.7
214.2	2,400	715	0.01453	0.12407	4.15	3.92	105.6
116.9	850	619	0.0152	0.1126	2.50	2.41	103.7
116.7	800	428	0.0150	0.0936	3.00	3.02	99.5
206.6	1,200	715	0.0142	0.1258	3.96	3.77	105.0
204.8	600	715	0.0148	0.1241	3.98	3.47	104.5

Table III. Generator—300 Kw, 345 Volts, 870 Amperes, 1,200 Rpm

Volts Generated	Load	Speed	r_e	r_d'	$I_{\text{Calc.}}$	I_{Test}	Percentage
270	0	1,200	0.02172	0.21261	4.88	5.07	96.4
283	1,045	1,200	0.02172	0.21241	5.125	6.71	76.4
345	0	1,200	0.01238	0.1315	7.6	8.45	90.0
365	1,028	1,200	0.01238	0.1325	7.96	10.52	76.0

Table IV. Motor—1,375 Horsepower, 415 Volts, 2,600 Amperes, 1,300 Rpm

Volts Generated	Load	Speed	r_e	r_d'	$I_{\text{Calc.}}$	I_{Test}	Percentage
209	1,900	950	0.01235	0.09753	5.17	6.30	82.1
205	1,700	1,240	0.01229	0.11409	4.34	5.70	76.2
134	1,800	718	0.01450	0.0696	4.63	4.71	98.3
133	1,720	418	0.01430	0.0714	4.52	4.97	91.1
122	1,600	718	0.01203	0.06714	4.36	5.70	76.5
122	1,800	450	0.01197	0.06026	4.87	5.20	93.6
230*	2,470	1,300	0.01660	0.1221	4.53	3.65	124.2
247*	100	1,300	0.01490	0.1205	4.95	4.88	101.4
256	1,725	1,300	0.01415	0.1055	5.16	5.64	91.6

* Motor action during pre-short condition.

Table V. Motor—1,375 Horsepower, 415 Volts, 2,650 Amperes, 280 Rpm

Volts Generated	Load	Speed	r_e	r_d'	$I_{\text{Calc.}}$	I_{Test}	Percentage
394	2,600	270	1.065	1.2101	0.785	0.679	115.5
390	2,700	267	0.0231	0.1672	5.62	4.15	135.4
279	2,400	267	0.02304	0.16277	4.13	3.43	120.3
173	2,400	267	0.02375	0.15918	2.62	2.15	121.8
148	2,450	91	0.02546	0.11984	1.82	1.25	145.5
88	2,650	92	0.02529	0.10307	2.06	1.64	125.5
253*	1,745	280	0.02323	0.1659	3.68	4.0	92.0
247.4	100	280	0.0249	0.16738	3.56	3.23	110.0
237	2,300	280	0.02874	0.1709	3.34	2.15	155.0

* Generator action prior to short circuit.

Effective Internal Resistance Variation

The experimentally obtained transient resistances are plotted in Figures 2 through 4 against the parameters of load, speed, and voltage. Referring to Figures 2 and 3, it is noted that the magnitude of load prior to short circuit has a sizable influence on the resulting peak short-circuit currents or effective internal resistance, and that the peak current increases and resistance decreases with increasing load. The reason for this behavior is not evident, although it is suspected that higher resistance in the field circuit at lower loads may result in a faster deterioration of flux linkages which may augment the reduction in air gap flux beyond that anticipated from the increase of leakage flux during transient loading. A comparison of the percentage decrease in internal resistance between a lightly differentially compounded machine of Figure 2 and a more heavily differentially compounded machine of Figure 3 tends to verify the inference, namely the percentage increase in field circuit resistance, between full load and no load, and in the transient field current, due to transformer action of the armature circuit during a short circuit, is smaller for a lightly than a heavily differentially compounded machine. Thus the change in the rate of destruction of flux linkages for a change of load from full load is percentagewise higher in the heavily differentially compounded machine. By this token, it is expected that the magnitude of short-circuit currents from a cumulatively compounded machine would not be unduly influenced by the initial load.

The speed also influences the machine effective resistance. The speed characteristics were obtained for the two large machines and are graphed on Figures 2 and 4. The effect of speed change is consistent for all units, that is, the internal resistance rises and the peak current correspondingly decreases with increasing speed. This trend is expected for the speed proportionally affects the

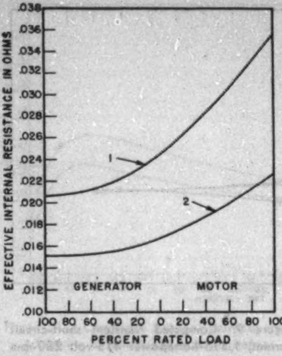

Figure 5. Effect of change from motor to generator action as initial condition on effective internal resistance

(1) 1,375-horsepower 415-volt 1,300-rpm motor

(2) 1,375-horsepower 415-volt 280-rpm motor

reactance voltage which, appearing as an equivalent brush drop, contributes to the magnitude of machine effective resistance.

If the machine effective resistance were constant, then the peak current would increase with the generated voltage. However, it is observed in Figures 2, 3, and 4, that this resistance is constant up to 50 per cent voltage but above this voltage the machine resistance rises. It is inferred that this effect is due to an increase in leakage flux owing to increased saturation of the pole iron. In addition, there is an accompanying increase in reactance voltage since the crowding of the flux in the pole tips increases the steepness of the flux distribution curve at the neutral point and results in a decrease in commutation time.

The behavior of a machine, relative to short-circuit contribution, when operating as a motor or as a generator, is of practical interest. Two motors were operated, each as generator and as motor, at similar load, voltage, and speed conditions. Referring to Figure 5, it is noted that the peak short-circuit current is less for motor action than for generator action; and that this difference in current decreases as the initial load is decreased.

Peak Short-Circuit Current

In an attempt to verify the validity of existing theory relating to short-circuit characteristics of d-c machines, calculations of peak short-circuit currents were made for the fault conditions to which these machines have been subjected. The method of calculation is outlined in Appendix I. The results of these computations are embodied in Tables II through V. These tables outline the pertinent conditions and resistances and compare the calculated values to the actual test results. A review of this comparison convinces one that the relations employed in Appendix I merit further improvements.

These improvements may result only from the acquisition of a more fundamental knowledge of the machine internal transient phenomena. Hence this work is being continued along the theoretical approach with this objective in mind. The factors of internal and external ohmic resistance, decay in air gap flux, and the development of a reactance voltage opposing the generated electromotive forces are considered to be all the variables that enter into the calculation of short-circuit currents. However, the weighting of these effects in the proportions occurring in a d-c machine may not be accurately expressed by the existing relations.

This observation is illustrated by a set of experimental characteristics on the 1,100-kw generator which are plotted in Figure 6 and compared with a corresponding set of computed characteristics. These curves attempt to demonstrate graphically the relation of peak short-circuit currents developed with variations of operating conditions of load, speed, and generated voltage.

Focusing the attention on the curves showing the effect of load, it is observed that the peak short-circuit current is a function of preshort-circuit current while the calculated values are entirely independent of initial load. There is no factor in the equations which recognizes the effect of load, yet a change in load from zero to 50 per cent raises the peak current by approximately 20 per cent, a factor that cannot be neglected even in an approximation.

Referring to the effect of voltage, it will be recalled that the effective resistance of a machine is independent of generated voltage for voltages below 50 per cent and rises appreciably beyond it. The equations involve the voltage only in the flux reduction factors, r_x', for uncompensated or partially compensated machines. Although the increase in the effective resistance of this machine, from half to full voltage, is 30 per cent, the calculated rise in value for r_x' over the same region is only 10 per cent. As r_x' is one of the three factors embraced by the effective internal resistance, r_a', while the other two are independent of voltage, it is evident that the effective resistance is inadequately influenced by the change in the calculated r_x' with voltage.

In comparing the experimental to the calculated curves showing the effect of speed, it is observed that the calculated values describe a nearly straight line relation; the experimental values, although following the same trends, indicate a sharper decrease in peak current with speed, at the larger magnitudes of speed. The calculated effect of speed is apparently insufficiently descriptive of the physical behavior of the machine. The speed enters in the calculations of the reactance voltage factor, r_b', and the flux reduction factor r_x', as a linear function, except at very low speeds where the correction factor for distribution of current in the brush face becomes appreciable when calculating r_b'.

Transient Armature Current

A second consideration, and of equal importance with computation of peak short-circuit current, is the prediction of rate of rise and decrement of the transient current. The accuracy with which the rate of rise can be predicted has been demonstrated by test and calculation to be as accurate as the computation of armature inductance for conditions prior to the short circuit. Curves 1 and 6 of Figures 7 and 8, and curves 1 and 5 of

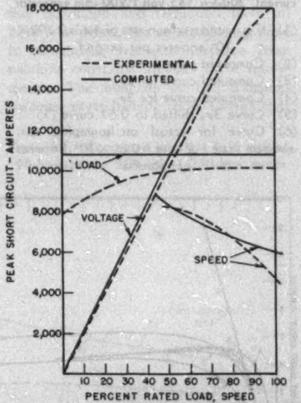

Figure 6. Comparison of computed and experimental data on peak short-circuit current

1,100-kw 415-volt 750-rpm generator

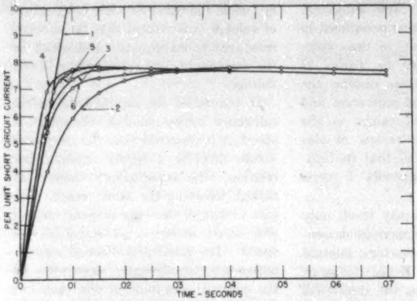

Figure 7. Computed transient short-circuit current, 1,100-kw 415-volt 750-rpm generator

(1) Computed maximum rate of rise—2.95×10^6 amperes per second
(2) Computed curve for σ_a
(3) Computed curve for $2\sigma_a$
(4) Computed curve for $3\sigma_a$
(5) Curve $3\sigma_a$ shifted to 0.67 curve (1)
(6) Curve for actual oscillographic test. Maximum rate of rise—4.18×10^6 amperes per second

Figures 9 and 10 indicate the agreement between computed and experimental data.

The calculation of the complete transient build-up is difficult to achieve due to the effect of saturation, change of flux linkages, and reduction in generated voltage during the current rise. It has been proposed that the assumption should be made that the time constant of the armature circuit be decreased by two-thirds as the armature current reaches its peak values.[1] Experimental evidence indicates that this represents too great a decrease in inductance. Results presented in Figures 7 and 8 show that for these machines the inductance decreased approximately 50 per cent as indicated by curve 3, whereas data shown in Figures 9 and 10 indicate that the oscillographic trace can be more nearly duplicated with a curve representing a fixed value of armature inductance. However, such an assumption is basically incorrect since the rate of rise at any point on the curve is influenced by the voltage as well as the inductance at the corresponding interval. Thus a procedure which recognizes only an inductance change is incomplete.

The remaining portion of the transient, that is the decay of current after peak value, is associated with the shunt field circuit and its time constant. Accurate measurement of this time constant is difficult to achieve because of the necessity of duplicating the saturation of the armature and pole faces and distortion of field flux that accompany the high-armature currents under short-circuit conditions. Therefore the shunt field inductance was computed on the basis of complete saturation of the armature teeth. This reduces the inductance to approximately one-tenth the base value at no load. Although the results of the

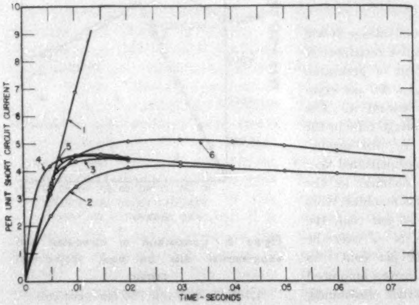

Figure 8. Computed transient short-circuit current, 300-kw 345-volt 1,200-rpm generator

(1) Computed maximum rate of rise $=0.792\times10^6$ amperes per second
(2) Computed curve for σ_a
(3) Computed curve for $2\sigma_a$
(4) Computed curve for $3\sigma_a$
(5) Curve $3\sigma_a$ shifted to 0.67 curve (1)
(6) Curve for actual oscillographic test, maximum rate of rise $=0.80\times10^6$ amperes per second

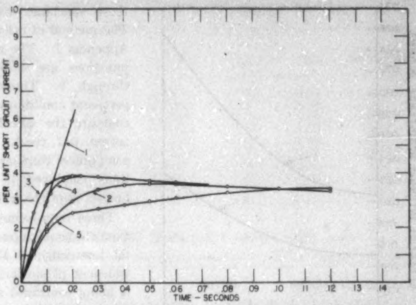

Figure 9. Computed transient short-circuit current, 1,375-horsepower 415-volt 280-rpm motor

(1) Computed maximum rate of rise $=0.79\times10^6$ amperes per second
(2) Computed curve for σ_a
(3) Computed curve for $3\sigma_a$
(4) Curve $3\sigma_a$ shifted to 0.67 curve (1)
(5) Curve for actual oscillographic test—2 rates of rise noted. First $=1.14\times10^6$ amperes per second. Second $=0.53\times10^6$ amperes per second

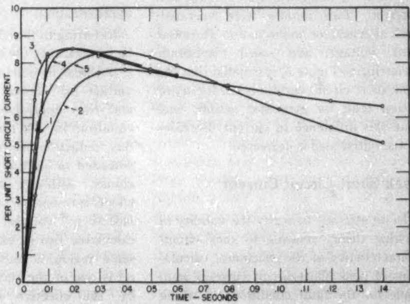

Figure 10. Computed transient short-circuit current, 90-horsepower 250-volt 1,750-rpm motor

(1) Computed maximum rate of rise $=0.248\times10^6$ amperes per second
(2) Computed curve for σ_a
(3) Computed curve for $3\sigma_a$
(4) Curve $3\sigma_a$ shifted to 0.67 curve (1)
(5) Curve for actual oscillographic test, maximum rate of rise $=0.29\times10^6$ amperes per second

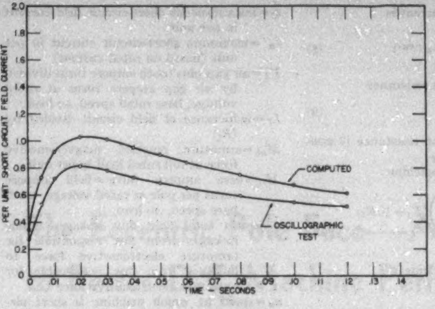

Figure 11. Computed transient field current, 1,100-kw 415-volt 750-rpm generator

approximations are fairly close to test data, there are additional factors such as mutual inductance and compensation which must be considered. It is important that accurate predictions of the shunt field inductance be possible since it can materially influence the peak value of short-circuit current as evidenced from Figure 10. The computed value of peak current without giving consideration to this decrement is 9.27 per unit, whereas this becomes 7.74 per unit when the decay of the shunt field is considered. Thus it becomes evident that the influence of the shunt field on the peak fault current cannot be ignored.

Transient Shunt Field Current

Computations of the shunt field current traces compare favorably with observed data for rate of rise and decrement. However, considerable difference is observed for the peak value as can be seen in Figures 11 through 14.

Figure 12. Computed transient field current, 300-kw 345-volt 1,200-rpm generator

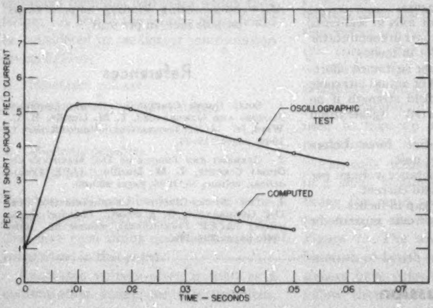

An examination of equation 8, in Appendix I, for transient field current will show that an approximation of the change in current from steady state will be

$$i_f \text{ (transient)} = \frac{r_z'}{r_d'} \frac{e_0}{n_0 n_f} \text{ per unit} \qquad (1)$$

Where e_0 is the per unit armature voltage before short circuit, n_0 is the per unit speed, n_f is the flux leakage coefficient, r_z' is a per unit value of resistance which indicates the effect of fault currents on field flux producing the generated electromotive force, and r_d' represents the total transient resistance. Thus equation 1 shows that the per unit increase in field current is a function of the reduction in net air gap flux.

Consideration of the term r_d' used in computing the curves of Figures 11 through 14 shows that it is in error by no more than 20 per cent, whereas the oscillograph trace of field current is approximately 230 per cent of the computed value. This leads to the observation that the possible flux change is greater than that predicted by r_z'. As has been noted previously, proper application of the constant flux linkage theorem may increase this term to a larger value. A second factor that may require consideration is the coupling between the series and shunt field. This is not adequately covered by equation 1.

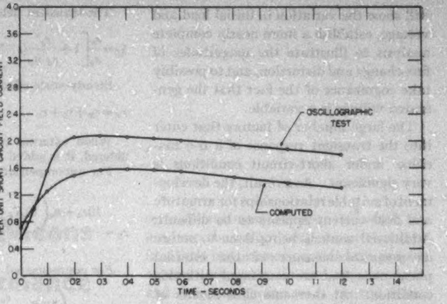

Figure 13. Computed transient field current, 1,375-horsepower 415-volt 280-rpm motor

Conclusions

In view of the difference between experimental and computed values of short-circuit currents using present techniques, it is necessary that the theory of transient characteristics of d-c machines be extended to provide the accuracy necessary for attaining the optimum in shipboard system design. Although the factors contributing to the limitations of short-circuit current, namely, armature and external circuit ohmic resistance, brush contact drop, reactance voltage and flux distortion and reduction have all been considered, the application of these in calculating transient response from machine constants appears to be inadequate. The analysis of the transient response must include those factors that

Figure 14. Computed transient field current, 90-horsepower 250-volt 1,750-rpm motor

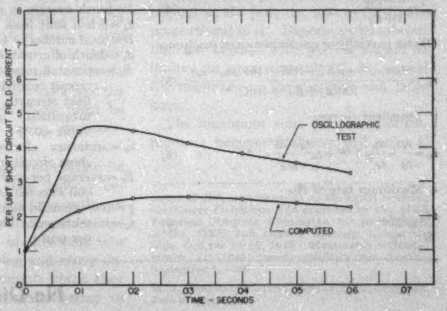

will show the variation in initial load and voltage, establish a more nearly complete analysis to illustrate the magnitudes of flux change and distortion, and to possibly take cognizance of the fact that the generated voltage is a variable.

The large number of factors that enter into the transient response of a d-c machine under short-circuit conditions is very significant. As a result, the development of suitable relationships for armature and field current appears to be difficult. Additional work is being done to secure an accurate measure of the internal phenomena that are associated with this condition. At the same time results of the study are being correlated with system performance studies to assure completion of a theoretical approach that will be applicable to this over-all problem of system analysis under transient conditions.

Appendix I. Equations for Short-Circuit Calculations

The relations which were derived by Linville[1] and employed in making the calculations of transient current are as follows.

Peak short-circuit current

$$I_a'=\frac{e_0}{r_d'} \tag{1}$$

Effective internal resistance

$$r_d'=r_w+r_b'+r_x' \tag{2}$$

When external circuit resistance is considered, it is added to r_d'.

Reactance voltage and brush drop factor

$$r_b'=n_0E_rb\left(\frac{\epsilon^x+1}{\epsilon^x-1}\right)+V_c \tag{3}$$

where

$$x=\frac{n_0E_rb}{V_c}$$

Flux reduction factor
(A) for fully compensated machines

$$r_x'=\frac{K_3n_fn_0}{1+n_f} \tag{4}$$

(B) for partially or uncompensated machines

$$r_x'=\frac{10n_fe_0+n_f(K_1+10K_2)(10K_3n_0-e_0)}{100(n_f+K_2)+10K_1} \tag{5}$$

Transient current

$$i_a=\frac{e_0}{r_d}-\frac{e_0}{r_d'}\epsilon^{-\sigma_at}+e_0\frac{r_d-r_d'}{r_dr_d'}\epsilon^{-\sigma_ft} \tag{6}$$

Maximum rate of rise

$$\frac{di_a}{dt}=\frac{e_0\sigma_a}{r_d'} \tag{7}$$

The transient field current is

$$i_f=\frac{e_0}{n_0}\left[1+\frac{r_x'}{r_d'n_f}(\epsilon^{-\sigma_ft}-\epsilon^{-\sigma_at})\right. \tag{8}$$

Steady-state effective resistance

$$r_d=r_w+r_b+r_x \tag{9}$$

When external circuit resistance is considered, it is added to r_d.

For uncompensated machine

$$r_x=\frac{10e_0+n_0\left(10K_3-\frac{e_0}{n_0}\right)(K_1+10K_2)}{100} \tag{10A}$$

For compensated machine

$$r_x=\frac{e_0+n_0\left(10K_3-\frac{e_0}{n_0}\right)}{10} \tag{10B}$$

where

$$K_1=\frac{P_p\phi_t}{P_aM_{al}C_c}$$

$$K_2=\frac{1.25gK_t}{g+d_s}$$

$$K_3=\frac{(b\pm2b_s)PM_{al}}{B}\pm C_sM_s$$

Use $+2b_s$ for brush shift in direction of rotation and $+C_sM_s$ for differential field.

Partial compensation factor

$$C_c=1-\frac{P_p}{P_a}\ \frac{M_{bl}}{M_{al}}$$

$$r_b=E_r(1-E_c)b\left(\frac{\epsilon^x+1}{\epsilon^x-1}\right)+V_c \tag{11}$$

where

$$x=\frac{E_r(1-E_c)b}{V_c}$$

Decrement factors

$$\sigma_a=\frac{r_d'}{L_a} \tag{12}$$

$$\sigma_f=\frac{r_f}{L_f} \tag{13}$$

Nomenclature

b = brush overlap in segments
b_s = brush shift from polar axis in segments
B = total number of segments in commutator
d_s = depth of armature slot in inches
E_c = estimated ratio (under sustained short-circuit conditions) of actual interpole field strength to field strength if no saturation occurred (generalized value = 0.3)
e_0 = armature electromotive force before short circuit in per unit
E_r = average per-unit reactance voltage per coil at rated full load current
g = average main pole air gap in inches
i_a = instantaneous short-circuit current in per unit
i_f = instantaneous short-circuit field current in per unit
I_a' = maximum short-circuit current in per unit (based on rated current)
K_t = air gap plus tooth ampere turns divided by air gap ampere turns at rated voltage, base rated speed, no load
L_f = inductance of field circuit divided by (R_1)
M_{al} = armature reaction magnetomotive force at full rated load in per unit
M_{fl} = base ampere turns = field ampere turns per pole at rated voltage, rated base speed, no load
n_f = ratio total field flux linkages minus linkages from flux responsible for armature electromotive force to linkages from flux responsible for armature electromotive force
n_0 = speed at which machine is short circuited in per unit
p_a = pole arc in inches
p_b = pole pitch in inches
P = number of poles
r_b = steady-state resistance equivalent to reactance voltage and brush contact in per unit
r_b' = transient resistance equivalent to reactance voltage and brush contact in per unit
r_d = steady-state effective total resistance of machine under short circuit in per unit
r_d' = transient effective total resistance of machine under short circuit in per unit
r_e = external resistance in per unit
r_f = resistance of field circuit in per unit
r_x = steady-state resistance equivalent to flux reduction in per unit
r_x' = transient resistance equivalent to flux reduction in per unit
r_w = total resistance of windings in armature circuit in per unit
R_1 = base ohms = V_1/I_{al}
V_1 = base volts = rated voltage in volts
V_c = normal brush contact drop at full load in per unit
ϕ_1 = base flux = flux per pole in maxwells at rated voltage, rated base speed, no load
ϕ_t = iron flux per pole in per unit = average section of armature tooth in square inch times number of teeth in pole arc by 123,000 lines per square inch divided by ϕ_1
σ_a = armature circuit decrement factor
σ_f = field circuit decrement factor
C_s = series field coupling factor
M_s = series field ampere turns, in per unit
M_{bl} = compensating winding ampere turns on pole face, in per unit

References

1. Solid Short Circuit of Direct Current Motors and Generators, T. M. Linville, H. C. Ward, Jr. *AIEE Transactions*, volume 68, part I, 1949, pages 119–24.

2. Current and Torque of D-C Machines on Short Circuit, T. M. Linville. *AIEE Transactions*, volume 65, 1946, pages 956–65.

3. The Short-Circuit Characteristics of D-C Generators, G. E. Frost. *Electrical Engineering (AIEE Transactions)*, volume 65, June 1946, pages 394–402.

No Discussion

The Eccentric Pole Face—A Means to Better D-C Machine Performance

M. A. BAKER
MEMBER AIEE

NO ONE factor, calculation, or design constant will tell the designer whether or not his design will commutate satisfactorily. Many factors must be considered simultaneously, and in the end judgment and experience must be used in interpreting the calculations and predicting commutation. It is beyond the scope of this paper to attempt an analysis of all factors affecting commutation, but some of the more common design guides will be discussed briefly. The primary purpose of this paper is to show how the flaring main pole gap improves the commutation and performance of d-c motors and generators. While this is not new, recent studies of eccentric pole face design may be of interest to d-c designers. While much of the following discussion applies equally well to all d-c motors and generators, the flaring air gap is of special importance on adjustable speed motor designs.

Commutation Guides

Predicting commutation is not an exact science, and designers have certain empirical formulas and rules which they follow. A few of the factors that should be considered in predicting commutation are as follows:

1. Reactance voltage.
2. Commutating pole dimensions.
3. Neutral or clearance zone.
4. Magnetic densities.
5. Volts per bar.

Brushes and brushholders are not discussed here; good brushes and holders that give good riding qualities are taken for granted in this paper.

Reactance voltage often is used as a commutation index on d-c machines. Many formulas are available for calculating this, and each designer has one that he follows. Experience tells him what the maximum practical values are. On noncommutating pole machines this is probably the most important commutation guide. However, reactance voltage does not, in itself, cause sparking on machines equipped with commutating poles. It is the uncompensated reactance voltage, or the difference between reactance voltage and the voltage induced by the commutating poles, that causes sparking. If reactance voltage could be perfectly compensated for, it would not be a limiting factor of commutation. Since there is a practical limit in the accuracy to which we can neutralize reactance voltage, it is one of the standard yardsticks by which designers predict commutation. However, as progress in the art continues and we learn how to better compensate for reactance voltage, we should be able to increase the limit.

The design of the commutating pole is, of course, of utmost importance in the commutation of a d-c machine. The proper tip width must be used to adequately cover the commutating zone, and the correct air gap must be used to give the correct flux pattern. Pole body width must be great enough to avoid saturation at all anticipated loads and the proper amount of brass shims must be used to take up any excess over-compensation.

The coils undergoing commutation lie in a small stationary zone midway between the main pole tips frequently referred to as the commutating zone, see Figure 1. The width of this zone is a function of brush overlap and many designers have rules of thumb which they follow that limit the brush overlap to certain maximum values. However, it has been the author's experience that this is of little importance provided the proper commutating pole tip and gap are used and sufficient clearance, or neutral zone, is provided between the edge of the commutating zone and the main pole tip. Experience indicates that one slot pitch margin should be provided between each side of the commutating zone and the main pole tip. This is of great importance in the design of adjustable speed motors, but satisfactory performance of constant speed motors and generators often can be obtained with slightly less clearance.

Magnetic densities in the magnet frame and armature core may affect the commutation since these parts carry both main and commutating pole flux. In adjustable speed motors it is of prime importance to keep the densities in these two parts below the knee of the saturation curve in order to obtain satisfactory commutation at both base and top speeds. On constant speed motors or constant voltage generators, some saturation in the magnet frame and armature core parts can be accommodated by increasing the strength of the commutating field.

If there is any one factor that all d-c designers calculate on their designs, it is probably volts per bar, in some form or other, and most designers have rules which they follow to a certain degree. The average volts per bar of a given design gives little insight as to its commutating ability. It is of importance only in that the maximum volts per bar, volts per bar at the pole tip, and so forth, are proportional to it. Experience has shown that the average volts per bar should be limited to approximately 20 in normal d-c machines in the medium and large sizes.

The maximum volts per bar is of importance because flashover will occur if

---

Paper 49-230, recommended by the AIEE Rotating Machinery Committee and approved by the AIEE Technical Program Committee for presentation at the AIEE Fall General Meeting, Cincinnati, Ohio, October 17–21, 1949. Manuscript submitted March 21, 1949; made available for printing September 1, 1949.

M. A. Baker is with the General Electric Company, Fort Wayne, Ind.

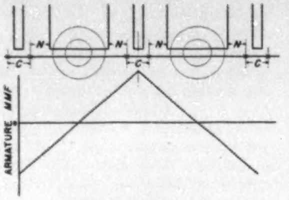

Figure 1. Armature flux

C = commutating zone
N = neutral or clearance zone

this becomes too great. Experience has shown that flashover is liable to occur if the maximum volts per bar exceeds approximately 45 on large machines with 30–40 mil mica. However, on medium-sized and smaller machines this value can often be exceeded without danger of flashover. The maximum volts per bar under load will occur at the main pole tip on uncompensated machines with concentric or uniform air gaps. If the pole face is chamfered or flared the maximum volts per bar will occur under the pole face, see Figure 4.

The author's experience on adjustable speed motor designs leads him to believe that one of the most important factors in the commutation of these machines is the volts per bar at the leading edge of the main pole tip (trailing edge of a generator). This factor is a measure of the flux concentration at the pole tip near the commutating zone and if this is too great, leakage flux from the main pole will fringe into the commutating zone causing poor commutation and speed instability. Experience has shown that if the volts per bar at the pole tip is limited to approximately 30, and one slot pitch margin is provided between the main pole tip from the commutating zone, good commutation and speed regulation can be obtained. Because of the importance of tip volts per bar on adjustable speed motors, a study of several pole arc shapes has been made to determine their effect on this important factor.

Calculation of Flux Distribution at Weak Field

When load is applied to a d-c machine, the armature sets up a stationary magnetic field that is a maximum underneath the commutating pole and zero under the center of the main pole. Since the armature magnetomotive force is of opposite polarity under each half of the main pole, a circulating flux is set up in the main pole face as shown in Figure 1. This adds to the magnetic densities at one half of the pole and subtracts on the other. In case of motors the flux density is increased on the leading half and reduced on the trailing half. In a generator the converse is true. The armature magnetomotive force is superimposed on the main field excitation, and under weak field conditions, such as top speed on an adjustable speed motor, the flux under part of the pole may be reversed.

Since the voltage induced in the armature coils is directly proportional to the flux, at constant speed, the induced volts per bar under the main pole arc gives a direct measurement of the flux distribution under the main pole. The average volts per bar is calculated from the following simple equation

$$V_{b_{\text{avg}}} = \frac{(V)(P)}{S} \tag{1}$$

where

$V_{b_{\text{avg}}}$ = average volts per bar
V = rated voltage
P = number of poles
S = number of commutator segments

However, since voltage is induced only in the active conductors under the main pole arc (plus fringe area), the average volts per bar under the main pole is appreciably higher than the average volts per bar calculated by equation 1. The average volts per bar under the main pole arc can be readily calculated from the following equation

$$V_{b_p} = \frac{(V)(P)}{(S)(\tau)}K \tag{2}$$

where

V_{b_p} = average volts per bar under main pole arc
τ = per cent pole arc = pole arc divided by pole pitch
K = fringing factor = $\dfrac{\text{flux entering armature directly under main pole arc}}{\text{total armature flux per pole}}$

Under weak field condition, saturation can be neglected and the flux can be assumed to be directly proportional to the magnetomotive force and inversely proportional to the air gap. Thus the volts per bar at any point under the pole arc can be expressed as follows

$$V_b = \frac{(V)(P)}{(S)(\tau)}K\frac{G}{g}\,\frac{(NI+a)}{NI} = \left[\frac{(V)(P)(K)(G)}{(S)\,(\tau)(NI)}\right]\left[\frac{NI+a}{g}\right] \tag{3}$$

where

V_b = volts per bar at point under consideration
G = average air gap
g = air gap at point under consideration
NI = air gap ampere turns
a = armature reaction at point under consideration.

To calculate the volt per bar curve across the main pole face, it is necessary to either calculate the air gap at several points or scale it off an accurate layout. The armature reaction at any point can be calculated readily since it is uniformly distributed and is zero under the center of the main pole and a maximum midway between the main pole tips. A simple equation for this calculation is

$$a = \frac{(A)(2)(d)}{PP} \tag{4}$$

where

A = maximum armature reaction in ampere turns per pole
d = distance of point in question from center of main pole arc
PP = pole pitch

If it is desired to know the volts per bar at the main pole tip without calculating the entire curve, this can be done from the following equation.

$$V_{bt} = \left[\frac{(V)(P)(K)(G)}{(S)\,(\tau)(G_t)}\right]\left[\frac{NI+(\tau)(A)}{NI}\right] \tag{5}$$

where

V_{bt} = volts per bar at main pole tip
G_t = air gap at main pole tip (other terms defined previously)

To check the validity of the foregoing equations, several volts per bar tests were made on a 30/40-horsepower 400/1,600 rpm 230-volt shunt-wound-motor operating at maximum speed. The test procedure used consisted of the following. Small holes were carefully punched ex-

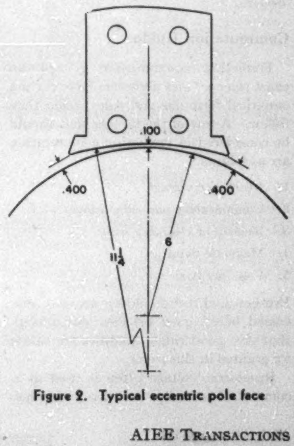

Figure 2. Typical eccentric pole face

actly one commutator bar pitch apart in a narrow strip of tough kraft paper. This strip was then laid on the commutator between two adjacent brush studs and secured to the holders to prevent movement. With the machine running at top speed, normal voltage, voltage readings were taken from a brushholder stud to each hole in succession with a pencil sticker. The data were carefully plotted and a smooth curve drawn through the points. The difference in voltage between any two adjacent points was read off the curve and plotted to give the volts per bar curve; this is a direct measure of the flux distribution. An attempt was made to read volts per bar directly by placing pencil stickers in two adjacent holes, but accurate readings were difficult to obtain and it was felt that the stud-to-bar method gave more accurate results since errors could be detected and minimized by plotting a stud-to-bar voltage curve. Data were taken with the machine operating both at no load and at full load. The machine tested had an eccentric pole face with a 2.8:1 flare. The test and the calculated data are plotted in Figure 3.

The accuracy of the calculations is to a great extent dependent upon the accuracy with which the fringing flux can be estimated. Approximate checks have indicated this to be in the order of magnitude of 10 per cent, so K was assumed to be 0.9 in making the calculations plotted in Figures 3 and 4. The increased error at the pole tip is due, in part at least, to the fact that the actual pole tip had a liberal radius at the corner of the pole arc while this was assumed to be a sharp corner in making the calculation.

Figure 3 clearly indicates the accuracy which can be expected of equations 3 and 5. While not extremely accurate, they do give approximate values of sufficient accuracy to aid in predicting commutation and to be of value in studying various pole arc shapes.

Effect of Pole Arc Shape on Tip and Maximum Volts Per Bar

The fact that increasing the main pole gap reduces the circulating flux and minimizes flux distortion is well known to d-c designers. This is obvious by inspection of Figure 1 and can be evaluated for weak field condition by equations 3 and 5. However, increasing the main pole air gap has the disadvantage of increasing the excitation and is therefore subject to certain limitations. By reducing the center gap slightly and chamfering the pole tips to give a larger tip gap, the circulating flux can be reduced without increasing the excitation. This is commonly done but has the disadvantage of concentrating the flux at a point where the chamfer starts and causing high maximum volts per bar at this point. By designing a main pole arc with a constant radius which is considerably greater than the air gap radius, a gradually flaring gap is obtained without the disadvantage of the chamfered tip. Figure 2 is typical of the eccentric pole face design. This pole was designed for a 12-inch diameter armature. The $11\frac{1}{4}$-inch pole face radius gives a tip gap of approximately 0.400 with a center gap of 0.100 or a 4:1 flare with approximately 60 per cent pole arc.

In an attempt to evaluate several different shapes of main pole arcs, the flux distribution or volt per bar curve was calculated for several assumed pole arc shapes for a standard 25/30-horsepower 400/1,600 rpm 230-volt motor. Calculations were made for 1,600 rpm full load with equation 3. These calculated data are plotted in Figure 4. The air gap data for these curves are given in Table I.

Discussion of Results

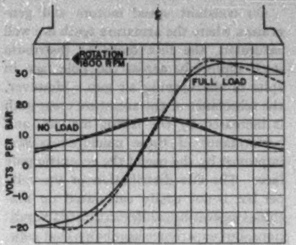

Figure 3. Comparison of test and calculated volts per bar CD 1138-4-30/40 HP-400/1600 RPM-230 volt

——Calculated
- - - - -Test

Attention is called to the fact that the average air gap and hence excitation was maintained constant for all conditions shown in Figure 4. These curves clearly show that the tip and maximum volts per bar can be appreciably reduced, on adjustable speed motors, by increasing the tip gap and reducing the center gap to maintain constant excitation. Curve A is for a uniform gap and the volts per bar increases linearly from the center line on the leading half of the pole and decreases in a similar manner in the trailing half. The volts per bar at the leading edge are very high and it is doubtful that satisfactory performance could be obtained with this design. Curve B shows how the tip volts per bar are reduced approximately 50 per cent by using a 2.8 : 1 flare with an eccentric pole face. Curves C and D show still further reductions by the use of a 4 : 1 and 6.2 : 1 eccentric gap. Curves E and F show that chamfering the main pole face (concentric center gap) materially reduces the volts per bar at the pole tip but results in very high maximum volts per bar under the pole. For this reason curve B, C, or D is preferable. There is no sharply defined optimum ratio of maximum to minimum air gap. Increasing this ratio reduces the volts per bar at the main pole tip. However, the author feels that a 4 : 1 ratio is a good compromise for adjustable speed motors since greater ratios result in a very small center gap.

It is interesting to note that regardless of the main pole arc shape, all the full load volts per bar curves go through zero at the point where the armature reaction equals the air ampere turns. While not illustrated in Figure 4, increasing the air gap moves the crossover point farther to the left. If the same ratio of minimum to maximum air gap is maintained and the average is increased, the curve is rotated about the point where it crosses the main pole center line.

Numerous adjustable speed motors ranging from 25 horsepower to 200 horsepower have been built with 4 : 1 eccentric air gap. Exceptionally good performance was obtained and the motors had a drooping speed characteristic throughout the speed range without the use of a series stabilizing field. Similar motors with less flare required the use of a stabilizing field.

Table I

Curve	Type	Flare	Air Gap (Inches) Minimum	Air Gap (Inches) Maximum	Average
A	Concentric gap	1:1	0.130	0.130	0.130
B	Eccentric pole face	2.8:1	0.090	0.250	0.130
C	Eccentric pole face	4:1	0.078	0.312	0.130
D	Eccentric pole face	6.2:1	0.066	0.408	0.130
E	Chamfered tip	2.9:1	0.108	0.312	0.130
F	Chamfered tip	4:1	0.102	0.408	0.130

On constant speed motors and generators where the armature teeth are well saturated, the flux tends to distribute itself uniformly across the pole face in spite of the varying air gap. However, the reluctance of the armature cross path is increased by the flaring air gap, and performance of these machines is also improved by the use of the eccentric pole face. The flux distribution or tip volts per bar is not easily calculated on machines operating under saturated conditions, but experience has shown that commutation is materially improved by using the eccentric pole face on all machines.

The tendency of the eccentric pole face to crowd the flux toward the center of the pole increases the noload core loss slightly. This would tend to increase the heating and reduce the conventional efficiencies slightly. However, the eccentric pole face will reduce the load loss by minimizing the field distortion and the resulting double frequency core loss at weak fields.

Thus the actual efficiency and heating on adjustable motors is not seriously affected. On constant speed motors and high speed generators, the core loss is a larger percentage of the total armature loss than it is on adjustable speed motors and therefore has more effect on heating. On these machines the increased no load core loss resulting from the eccentric pole arc may present a more serious problem. No direct comparative data are available.

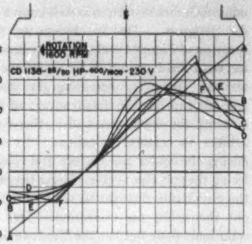

Figure 4. Effect of pole arc shape on unsaturated flux distributed at full load

A—concentric air gap .... 1 : 1 flare
B—eccentric pole face .... 2.8 : 1 flare
C—eccentric pole face .... 4 : 1 flare
D—eccentric pole face .... 6.2 : 1 flare
E—chamfered tip .... 2.9 1 flare
F—chamfered tip .... 4 : 1 flare

Crowding the main pole flux towards the center of the pole is of definite advantage in exciters and generators that must operate self-excited over a wide range of voltage. Concentrating the flux at the center of the pole tends to saturate the armature teeth at this point and increases the voltage stability. This effect is not great enough to produce a visible effect in the saturation curve, but experience indicates that it has a definite effect on stability. Self-excited generators have been built for operation at 25 per cent voltage with an eccentric pole face. No pole slots or partial shims were used to bend the saturation curve.

Conclusion

The eccentric pole face offers the designer a means of reducing the tip volts per bar and improving commutation and speed regulation on adjustable speed motors. A 4:1 ratio of maximum to minimum gap has given excellent performance on motors and generators as well. While no optimum ratio can be derived, this appears to be a good compromise.

The eccentric pole face has been used to advantage on constant speed motors and generators to improve voltage regulation, and on variable voltage generators and exciters the eccentric gap improves the voltage stability. The need for the eccentric pole face does not exist on fully compensated machines, but a slightly flaring gap may be of advantage on partially compensated machines.

One of the disadvantages of the eccentric pole face is the reduced center gap for a given excitation. However, this is not serious if a reasonable ratio of maximum to minimum gap is adhered to. The most serious disadvantage is the increased no load core loss. This is offset partially by reduced load loss and presents no serious problem on adjustable speed motors. On constant speed motors and generators this must be taken into consideration in deciding on the amount of flare to use.

No Discussion

An Analysis of Rotating Amplifiers

BERNARD LITMAN
MEMBER AIEE

ELECTRICAL amplifying devices exist in a number of distinct forms such as electronic, magnetic, and rotating amplifiers, each with a distinct field of usefulness. The rotating amplifier is the most prominent in those applications where relatively large power outputs are required. However, even rotating amplifiers have been used in the past only as small exciters to excite the fields of larger machines. This paper considers the incorporation of amplification in large sized generators where questions previously neglected must be considered.

These machines take advantage of the fact that it is possible to produce voltage between selected pairs of brush arms on a multipolar commutator machine by exciting particular poles and to utilize these voltages to excite other sets of poles so that amplification can be obtained. The presence of amplification enables these machines to be used for regulation of their output voltage or any other desired quantity.

In order to make complete use of its capacity as a power generator, all the brush arms will be required to carry their normal share of the output load current as they would in a standard machine and, in addition, any required internal circulating currents. It is necessary to have a multiplicity of windings on the poles, arranged to produce the required fluxes and to neutralize the demagnetizing effects of any one stage of amplification upon the other stages.

To illustrate how amplification is added to a standard generator, one may take as an illustration the simplest case of the 4-pole machine. It is well known that a relatively small amount of power in the field winding of a standard generator will control a much larger amount of power in the armature. Therefore a field winding is placed on two diametrically opposite poles as if they alone formed a 2-pole machine. This will generate a voltage between the two corresponding brushes and if they are joined together, a current will flow. Hence these brushes are joined with a heavy copper winding which is wound on all the poles to excite them as a standard machine. Since the internal currents give rise to other (undesirable) fields, still other field windings must be added to neutralize these fields. Thus in the most complex case, the lead coming from each brush arm may pass through windings on all the poles before it reaches the external load.

Thus several magnetic and electrical circuits have been superimposed on one physical structure. As treated in detail later the stator windings for any machine will be designated by a matrix which tabulates all the windings which each brush lead must pass through. This matrix characterizes the machine and from it the machine properties can be determined. Typical dimensionless curves of machine characteristics will be obtained and performance under various conditions will be considered.

Notation, Units, and Sign Conventions

In order to study these machines, expressions will be set up for all the reactions within the machine when subjected to any unbalanced set of currents, magnetomotive forces, and so forth.

The system consists of a structure containing N main poles and N commutating poles. To designate the various poles, currents and so forth, an index notation is used throughout. See Figure 1.

The various air gaps may in general be unequal. The air gap reluctance of the i'th main pole is represented by R_i and the reluctance of the i'th commutating pole by r_i. The i'th commutating pole is the one immediately clockwise of the i'th main pole, while the i'th brush arm is directly under main pole i. There is a leakage reluctance between adjacent poles which is the same for all poles and is represented by A. There also is a reluctance path from the rotor through the shaft and back to the stator, which is designated by B.

A per-unit system is used throughout so as to eliminate most numerical constants and make numerical values fall within a narrow range for all sizes of machines. Unit voltage is taken as rated output voltage and unit flux is that existing in one main pole when unit output voltage exists at no load. Unit magnetomotive force is that across the main pole air gap when it carries unit flux. One unit of magnetic reluctance is that in one main pole air gap when it has its nominal design value. A special time unit is used to make induced voltages and speed voltages compare, without any factor depending on rotor speed. This time unit, of course, depends on rotor speed and is given by $1/4\,f$ seconds where f is the rotor frequency in cycles per second.

The following sign conventions are employed: positive fluxes and magnetomotive forces point from the pole to the rotor; positive currents point outward from each brush arm and internal armature currents are positive when traveling from one arm to the next clockwise arm. Voltages between arms are positive when the potential increases as one travels clockwise. Thus a balanced machine will have alternately positive and negative values.

Fluxes Due to Stator and Rotor Excitations

For convenience in analysis our magnetic structure is replaced by the equivalent electrical circuit of Figure 1.

To determine the effects of a complex

Paper 49-231, recommended by the AIEE Rotating Machinery Committee and approved by the AIEE Technical Program Committee for presentation at the AIEE Fall General Meeting, Cincinnati, Ohio, October 17–21, 1949. Manuscript submitted June 7, 1949; made available for printing September 9, 1949.

BERNARD LITMAN is with the Arma Corporation, Brooklyn, N. Y.

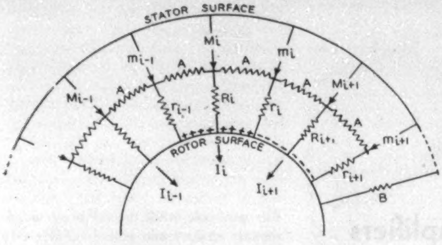

Figure 1. Diagrammatic representation of the machine

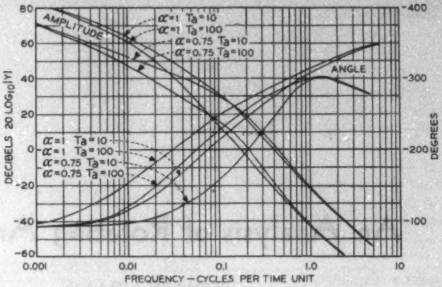

Figure 3. Transfer curves—magnitude and angle of the transfer function

pattern of magnetomotive force, an arbitrary magnetomotive force, M_i, is applied to the i'th main pole only and the fluxes are determined. By inspection of Figure 1 it is seen that all the leakage paths are short circuited except for the two paths adjacent to M_i. Similarly all the resistances which remain (except for R_i) are effectively in parallel and this parallel group is in series with R_i. The flux in pole i is then given by

$$F_i=\frac{M_i}{R_i+\dfrac{1}{\left[\Sigma_i\dfrac{1}{r_i}+\Sigma_i\dfrac{1}{R_i}-\dfrac{1}{R_i}+\dfrac{1}{B}\right]}} \qquad (1)$$

The flux F_i returns through the other paths in inverse proportion to their reluctances so that the other fluxes are given by

$$F_{k\,(k\neq 1)}=-\frac{F_i}{\left[\Sigma_i\dfrac{1}{r_i}+\Sigma_i\dfrac{1}{R_i}-\dfrac{1}{R_i}+\dfrac{1}{B}\right]+R_k}$$

$$=-\frac{M_i}{R_iR_k\left[\Sigma_i\dfrac{1}{r_i}+\Sigma_i\dfrac{1}{R_i}-\dfrac{1}{R_i}+\dfrac{1}{B}\right]+R_k} \qquad (2)$$

and

$${}_k=-\frac{M_i}{R_ir_k\left[\Sigma_i\dfrac{1}{r_i}+\Sigma_i\dfrac{1}{R_i}-\dfrac{1}{R_i}+\dfrac{1}{B}\right]+r_k} \qquad (3)$$

If arbitrary magnetomotive forces now are applied to each main pole, the flux in pole i will be given by a term of the form (1) due to M_i plus terms of the form (2) (with the indices i and k interchanged) due to the other magnetomotive forces and the total effect can be obtained by suitable summation. In order to select the right term to use as the summation is performed, each equation is multiplied by a suitable selection symbol so that the addition becomes a routine algebraic procedure.

Thus equation 1 should be multiplied by a symbol, δ_{ik} defined by $\delta_{ik}=1$ for $i=k$ and $=0$ for $i\neq k$. This assures that this term will appear only once in the summation, namely when $i=k$. (This is recognized as the Kronecker delta symbol.) Similarly, equation 2 should be multiplied by a symbol which is written as η_{ik} and defined as $\eta_{ik}=0$ for $i=k$ and $=1$ for $i\neq k$. Hence it is seen that $\delta_{ik}+\eta_{ik}=1$ for all i's and k's. Using these symbols, our total flux bebecomes

$$F_i=\Sigma_k\left(\frac{M_k\delta_{ik}}{R_k+\dfrac{1}{\left[\Sigma_i\dfrac{1}{r_i}+\Sigma_i\dfrac{1}{R_i}+\dfrac{1}{B}-\dfrac{1}{R_k}\right]}}-\frac{M_kn_{ik}}{R_kR_i\left[\Sigma_i\dfrac{1}{r_i}+\Sigma_i\dfrac{1}{R_i}+\dfrac{1}{B}-\dfrac{1}{R_k}\right]+R_i}\right) \qquad (4)$$

The quantity

$$\Sigma_i\frac{1}{r_i}+\Sigma_i\frac{1}{R_i}+\frac{1}{B}$$

has a fixed value, independent of the indices k or i and it is designated by C.

$$C=\Sigma_i\frac{1}{r_i}+\Sigma_i\frac{1}{R_i}+\frac{1}{B} \qquad (4A)$$

Hence F_i becomes

$$F_i=\Sigma_k\left(\frac{M_k(CR_k-1)\delta_{ik}}{CR_k^2}-\frac{M_k\eta_{ik}}{CR_iR_k}\right) \qquad (5)$$

POLE	1	2	3	4	5	6
ARM 1	$\frac{1}{3}$	1	$\frac{1}{3}$	$-\frac{2}{3}$	$-\frac{1}{3}$	$-\frac{2}{3}$
3	$-\frac{2}{3}$	$\frac{1}{3}$	$-\frac{2}{3}$	$\frac{2}{3}$	$-\frac{1}{3}$	$\frac{2}{3}$
5	$-\frac{1}{3}$	$-\frac{2}{3}$	$-\frac{1}{3}$	$\frac{2}{3}$	$\pm\frac{1}{3}$	$\frac{2}{3}$

6 POLE

POLE	1	2	3	4
ARM 1	$\frac{1}{2}$	$1-\frac{1}{2}$	$\frac{1}{2}$	$-\frac{1}{2}$
2		$\frac{1}{4}$	1	$-\frac{1}{4}$
3	$-\frac{1}{2}$	$\frac{1}{2}$	$-\frac{1}{2}$	$1+\frac{1}{2}$
4	1	$-\frac{1}{4}$		$\frac{1}{4}$

4 POLE

Figure 2. Winding matrices of the 4-pole and 6-pole structures

Then, adding and subtracting $M_k\delta_{ik}/$-$CR_iR_k)$ one obtains

$$F_i=\Sigma_k\left(\frac{M_k}{CR_k}\left(\frac{1}{R_i}+C-\frac{1}{R_k}\right)\delta_{ik}-\frac{M_k}{CR_iR_k}(\delta_{ik}+\eta_{ik})\right) \qquad (5A)$$

Remembering that $\delta_{ik}+\eta_{ik}=1$ as well as the obvious property of δ_{ik} that $\Sigma_k\psi_k\delta_{ik}=\psi_i$ for any expression, ψ, the summation reduces immediately to

$$F_i=\frac{M_i}{R_i}-\frac{1}{CR_i}\Sigma_k\frac{M_k}{R_k} \qquad (6)$$

Equation 6 should be extended to include commutating pole magnetomotive forces and proceeding in the same manner, it becomes

$$F_i=\frac{M_i}{R_i}-\frac{1}{CR_i}\Sigma_{kk}\frac{M_k}{R_k} \qquad (7)$$

Here Σ_{kk} represents a summation for both the main and commutating poles. An analogous procedure for the commutating pole fluxes gives

$$f_i=\frac{m_i}{r_i}-\frac{1}{Cr_i}\Sigma_{kk}\frac{M_k}{R_k} \qquad (8)$$

The summation term in equations 7 and 8 will ordinarily drop out. This is due to the fact that the machines normally dealt with have equal gaps, and the magnetomotive forces, though unequal, will (as seen later) add up to zero. Thus the flux in each pole may be obtained from the excitation on that pole and is independent of the other excitations. Moreover, if unequal air gaps give a nonzero summation, the quantity within the summation sign will no longer have any indices after being summed. Hence this summation needs to be calculated just once and will apply to all the poles in the machine.

Figure 1 also shows a rotor current in

that branch of the winding from arm i to arm $i+1$. The fluxes set up by this current may be determined in a manner analogous to what has just been done for stator excitations and then the effect of more complicated current patterns is determined by superposition.

The rotor current linked in any one of the loops in Figure 1 is given by $\rho i_i/2$. Here ρ is a quantity which ties in the per-unit systems between rotor and stator. This is numerically the same as the ratio of armature magnetomotive force at rated balanced load to unit main pole magnetomotive force. ρ will be of the order of magnitude of 1 for most machines.

Equations for the various loops now may be written in order to solve for the fluxes set up by this rotor current. Then an expression for the fluxes set up by a compound set of rotor currents may be obtained

$$F_i=\frac{\rho}{2R_i}(i_i+i_{i-1})-\frac{\rho}{2CR_i}\Sigma i_{kk}\left(\frac{2}{r_k}+\frac{1}{R_k}+\frac{1}{R_{k+1}}\right) \qquad (9)$$

Similarly, for the commutating pole, the expression takes the form:

$$f_i=\frac{\rho}{r_i}i_i-\frac{\rho}{2Cr_i}\Sigma_k i_k\left(\frac{2}{r_k}+\frac{1}{R_k}+\frac{1}{R_{k+1}}\right) \qquad (10)$$

As with equations 7 and 8, it is seen that for a machine with balanced air gaps, the summation terms will drop out.

Rotor Voltages

General expressions now may be obtained for rotor voltages due to speed and inductive effects under unbalanced conditions. One of the rotor coils is taken in an arbitrary position and its flux linkage expressed as a function of position and the flux in the stator poles. The coil voltage is then proportional to the total derivative of this expression; the position change giving the speed voltage while the stator flux change gives the induced voltage. By using the special time unit, rotor speed is eliminated from this expression and the equation reduces to

$$E_i=\frac{F_i-F_{i+1}}{2}-P\left(\frac{F_i+F_{i+1}}{2}\right) \qquad (11)$$

where P is the differential operator with respect to the unit of time.

The voltage between any two nonadjacent terminals will be designated as E_{ij} where i and j refer to the two terminals between which voltage is measured. This value can be obtained by direct summation from equation 11, giving

$$E_{ij}=\sum_{i=1}^{i=j-1}E_i=\frac{F_i-F_j}{2}-P\left(\sum_i^j F_i-\left(\frac{F_i+F_j}{2}\right)\right) \qquad (12)$$

Equation 12 is rather simple in form since it depends only on the total flux under each pole and not on the distribution of this flux along the pole face. A more careful analysis shows that arbitrary variation of air gap reluctance and magnetomotive force along the pole face will cause some error in the expression. However, this error affects only the transient term and for any variations that might be encountered, this error is found to be small enough to neglect.

Commutation

Commutation is a matter of prime importance on a large machine. In contrast to small generators, where little attention need be paid to this question, satisfactory commutation must be assured in order to have a successful device. The machine presents the problem of a very large current collecting surface traveling at high peripheral speed. Even minor imperfections will cause serious interruption of the contact surface between brush and commutator. Hence it is important to provide proper electrical conditions for commutation of any unbalanced combination of rotor currents.

To determine the required stator commutating windings, an arbitrary coil undergoing commutation is considered. A coil short circuited by brush i undergoes a change of current from i_{i-1} to i_i during its short-circuit period and there is a corresponding reactance voltage designated by $\gamma(i_i-i_{i-1})$. The factor γ includes inductance and time of commutation.

There also will be an appreciable mutual effect due to coils short circuited by the adjacent brushes on either side. Thus the over-all voltage can be written as

$$E_c=\gamma(i_i-i_{i-1})-\mu(i_{i-1}-i_{i-2})-\mu(i_{i+1}-i_i) \qquad (13)$$

Here μ is similar to γ except that it accounts for the mutual effects. In order to have satisfactory commutation, it is necessary that this voltage be completely neutralized by the fluxes f_i and f_{i-1} of the two commutating poles through the fields of which the coil is passing. The desired opposing voltage is then proportional to $f_{i-1}-f_i$ and can be calculated by using equations 8 and 10 which give the commutating pole fluxes due to both the armature currents and the stator excitations. Application of these two equations yields

$$f_{i-1}-f_i=\rho\left(\frac{i_{i-1}}{r_{i-1}}-\frac{i_i}{r_i}\right)+\frac{m_{i-1}}{r_{i-1}}-\frac{m_i}{r_i}+\left(\frac{1}{r_i}-\frac{1}{r_{i-1}}\right)\left[\frac{\rho}{2C}\Sigma_k i_k\left(\frac{2}{r_k}+\frac{1}{R_k}+\frac{1}{R_{k+1}}\right)+\frac{1}{C}\Sigma_{kk}\frac{M_k}{R_k}\right] \qquad (14)$$

This flux, $f_{i-1}-f_i$, must (except for an appropriate multiplying constant) be equal to equation 13 and the terms m_i, must be chosen so as to accomplish this.

It is seen that the term $\Sigma_{kk}M_k/R_k$ of equation 14 also includes main pole magnetomotive forces so that the commutating pole windings must correct for main pole excitations. This undesirable requirement can be eliminated if r_i is made equal to r_{i-1}, which is easily done by making all commutating gaps equal. (This still has put no restriction on main pole air gaps.) Equation 14 now reduces to

$$f_{i-1}-f_i=\frac{\rho}{r}(i_{i-1}-i_i)+\frac{1}{r}(m_{i-1}-m_i) \qquad (15)$$

Equations 13 and 15 now are equated and at the same time a new set of currents, the external currents leaving each brush arm, are introduced. These currents, which are the only ones directly available for use in the stator windings are defined by

$$I_i=\frac{1}{2}(i_{i-1}-i_i) \qquad (16)$$

The factor of 1/2 has been chosen so that with normal balanced load, I_i also will equal 1. This gives

$$\frac{1}{2r}(m_i-m_{i-1})=\frac{\rho}{r}I_i+\gamma I_i-\mu(I_{i-1}+I_{i+1}) \qquad (17)$$

To determine the required pattern of commutating pole exciting windings it is assumed that each pole may need separate windings from each brush arm so that

$$m_i=A_iI_i+A_{i+1}I_{i+1}+A_{i+2}I_{i+2}+\ldots\ldots A_{i-1}I_{i-1} \qquad (18)$$

Because of the symmetry of the machine, the sequence of windings on the next adjacent pole must be the same except for a change of one unit in the index of m and the I's, giving a similar expression for m_{i-1}. If all the currents were independent variables, one could take m_i-m_{i-1} and equate coefficients of the various I's to the corresponding terms on the right side of equation 17. However, use must be made of the fact that all the currents are not independent, for the sum of the currents leaving the rotor must equal zero. Using this relation, one of the currents is eliminated and the coefficients of the remaining currents are equated. It is possible to solve this set of $(N-1)$ equations in N unknowns if one more requirement is added and this requirement is that the sum of the absolute values of all the A's is a minimum, thus giving a minimum amount of copper in the machine. Proceeding on this basis, the final result obtained is

$$\left.\begin{aligned} A_i &= \frac{N}{2}D+2r\mu \\ A_{i+1} &= -\left(\frac{N}{2}-1\right)D-2r\mu \\ A_{i-1} &= \left(\frac{N}{2}-1\right)D \end{aligned}\right\} \quad (19)$$

and for the others,

$$A_{i+k}=\left(k-\frac{N}{2}\right)D$$

where

$$D=\frac{2\rho+2r\gamma-4r\mu}{N}$$

It should be noted that these values are not in actual turns but in per-unit magnetomotive force for unit current. This may be compared with the amount of winding on a normal balanced machine and it is found that the ratio of the two is approximately $0.4N+0.2$.

This formula brings out a practical limitation to the number of independent poles to be used on a machine, since the amount of copper increases undesirably when the number of poles increases. However, as pointed out later, there is no need for a very large number of amplification stages, and hence the number of truly independent poles in the structure need not be very large. Thus an 8-pole machine might be built as two 4-pole machines and the commutating windings would then be designed for a 4-pole structure. A 6-pole machine cannot be further broken down and it would be necessary to treat it as a 6-pole structure.

Stator Winding Arrangements and Selection

The problem of selecting the most effective pattern of stator windings to accomplish a given purpose now may be considered. Various arrangements will be discussed and where possible windings will be made to serve multiple purposes. It is necessary to become somewhat specific in discussing these winding arrangements but the treatment will demonstrate the general technique to be used on any structure.

In a typical application, all the positive brush arms are connected together at one point, after first going through the required commutating coils and such main pole coils as are required. The resistances from brush arm to common junction should be equal on all arms so that the main load current will divide equally in the steady state. Similar connections are made for the negative brush arms.

Normally, the main pole air gaps will be made equal so that at steady state the currents will divide nearly equally and the machine will operate at greatest efficiency. However, the formulas will permit calculating the effects when the gaps are unequal.

Previous attempts to consider possible internal amplification stages have visualized patterns which were similar to standard machines. Thus an 8-pole machine might use every other pole as a 4-pole structure. This procedure is inapplicable to machines whose total number of poles divided by an even integer fails to yield an even integer for a quotient. An example is the 6-pole or 10-pole machine, for here one cannot pick out a normal 2-pole or 4-pole machine pattern, by using arms which are normally at the same potential. Therefore the present treatment also will consider circulating paths between arms which are not symmetrically spaced. This in turn will set up unsymmetrical current and flux patterns but these can be used to obtain amplification.

For clarity in illustration, a particular case of a 6-pole machine is taken. This will demonstrate all the features to be brought out and also require the use of unsymmetrical paths in the machine. Initially a control field is placed on two poles which have the same polarity for the output stage. Thus poles 1 and 3 are picked and excited so that $M_1=1$ and $M_3=-1$. With balanced air gaps the resultant fluxes are then very simply given by equation 7 as: $F_1=-F_3=1, F_k=0_{k\neq 1 \text{ or } 3}$. The steady-state generated voltages now are determined from equation 12 giving: $E_{13}=1$ and $E_{15}=1/2$. It is seen that there is no current flow from 5 but only from terminal 1 to terminal 3. This current may be used to excite the normal 6-pole machine or, if desired, to provide another internal stage of amplification. The first possibility is chosen here since this provides sufficient amplification for most practical cases. Hence windings are placed in the circuit 1–3 to neutralize the armature reaction effects set up by this current and in addition to excite the 6-pole structure. The armature reaction fluxes should not be cancelled completely since these fluxes may alter the machine characteristics in a desirable manner.

If the current from 3 to 1 is called I_{31}, the current in the short path through the armature from arm 1 to arm 3 is $2/3\, I_{31}$ and that in the long path is $1/3\, I_{31}$. Equation 9 is then applied, giving

$$F_1=F_3=\frac{1}{3}\rho I_{31};\quad F_2=\frac{4}{3}\rho I_{31};$$
$$F_4=F_5=F_6=-\frac{2}{3}\rho I_{31} \quad (20)$$

To neutralize these armature reaction fluxes, the following compensating windings are placed in the 3 to 1 path

$$N_1=-\frac{1}{3}\alpha\rho;\quad N_2=-\frac{4}{3}\alpha\rho;\quad N_3=-\frac{1}{3}\alpha\rho;$$
$$N_4=N_5=N_6=\frac{2}{3}\alpha\rho \quad (21)$$

Here the polarities are given for circulating current from arm 3 to arm 1. After specifying on which side of the common junction point to place the windings, the polarities may be specified in terms of our standard notation. α is a number which indicates how effectively the armature reaction is compensated for. It would be equal to 1 for 100 per cent compensation and will be some number close to 1 in practice. In addition to these windings, there are also windings (called the forcing windings) to excite all six poles as a normal machine. These need not be a set of separate windings but may be combined with the compensating windings.

For the moment, neglecting these windings and taking the windings already present, a decision is made on how to divide them on each side of the junction. These windings not only supply the excitations desired but also provide excitation when normal balanced load is supplied. To avoid these additional excitations, each coil must be split into two half coils, one on each side of the junction point, so that they neutralize each other for balanced load. A better procedure is to use these additional excitations and thus have the coils serve a double purpose. These excitations will be used for the self-excited "tuned series field" for the final 6-pole stage of the machine. This amounts to a positive feedback for this stage and will be used to make the steady-stage amplification infinite so that in the steady state the machine can regulate very accurately and the unbalanced currents of the preliminary stages are very small. By this procedure one also avoids splitting the compensating coils into two parts, thus saving many coil interconnections.

The first step in splitting these windings is to place them so that for normal load they provide excitation in the proper

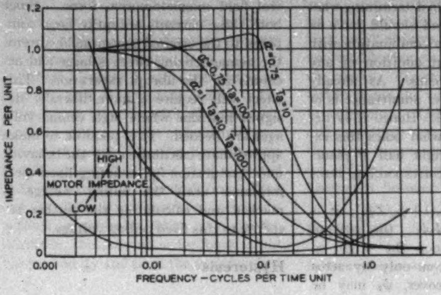

Figure 4. Minimum load impedance for stability

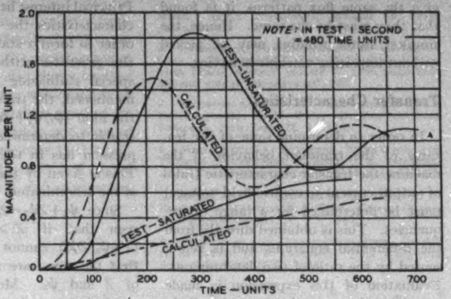

Figure 5. Transient response of machine—calculated and test values

direction for the series field excitation of the output stage. This can be done by inspection. In these two arms our forcing windings also must be placed. Rather than place them here as completely independent windings, an economy of coil connections may be effected by combining them with the existing coils. The total amount of excitation to be provided by the forcing windings is not critical. The more used, the more effective is the excitation of the final output stage. However, the use of too much excitation involves an excessive winding and corresponding copper loss. A suitable compromise is one unit of magnetomotive force per pole for unit circulating current.

The forcing winding has an equal number of turns on each pole and since the most desirable way to split these windings on each side of the junction point is not known, they are tentatively split into two parts; one in arm 1 of magnitude $a\alpha p$ and one in arm 3 of magnitude $b\alpha p$. Since αp is approximately equal to 1 or a bit larger, $a+b$ will be made roughly equal to 1. These quantities are added to what is already present on these poles and then expressions for the absolute values of the windings in these arms are written. Curves for these absolute values can be plotted and any horizontal line on these curves will pick out a pair of values for a and b which gives equal resistance in arms 1 and 3. By inspection, a convenient combination can be selected which does not give rise to a large number of odd coil sizes.

The result finally obtained is shown in the pattern of Figure 2 which is called the stator winding matrix. The total turns in each arm is now 10/3 and an equal amount is placed in arm 5 to balance the resistances. These extra turns are selected by inspection and are used to correct the excitations on all the poles so that they are proper for normal load. The winding matrix, made up of pure numbers, characterizes the machine independently of its size or rating and may be used to determine the performance of the machine.

Similar winding matrices may be developed for other variant types of this class of machine. In particular, a matrix for a 4-pole structure is of interest in order to get some data for comparison with machines that have already been built. The same techniques are used as illustrated above, and the matrix is built up in systematic fashion. This 4-pole matrix also is shown in Figure 2.

Differential Equations

It is desired to set up the differential equations of the machine and use them to determine some of the features of the machine behavior. Since the machine has a great many windings, the procedure is lengthy but can be carried out in a systematic manner.

In the case of the 6-pole structure, there are five degrees of freedom for the six arm currents (since the sum of these currents is zero) and an additional current for the control field. Thus the over-all current pattern will require six components and any six current patterns may be chosen as the basic currents provided they are all independent. Similarly, for any structure involving N poles, there are N independent current patterns.

The choice of the actual patterns to use is largely a matter of convenience. There are those patterns which are intentionally set up for purposes of amplification. For example, in the 6-pole machine there are the internal circulating current I_{31} and the control field current. In addition, the normal load current, I_L, and any three other patterns are used. For these the fluxes through the machine are determined and then the effects of these fluxes in both stator and rotor. Eventually all the currents will be eliminated except the control current and load current which are the two of interest.

In determining the voltages around the various loops equation 12 is used for that part of the voltage between rotor terminals. The voltage induced to any of the stator windings is proportional to the magnitude of the winding and the rate of flux change through the winding. These voltages can be obtained in a systematic fashion by writing the fluxes as a column vector of N elements (each element being the flux under one pole) and then multiplying from the left by the stator winding matrix. The result of this matrix product is a column vector whose elements represent the induced voltages in each of the arms. When combined with the voltages in the rotor windings and the resistance drops, the complete expressions for the differential equations are obtained as a set of self and mutual factors between the currents.

Invariance of Machine Behavior to Matrix Changes

The previous work discussed various arrangements of stator windings to produce the required flux patterns. The windings were altered freely to obtain the most economical arrangement and no attention was paid to possible changes in machine behavior.

Actually it can be shown that if two radically different windings set up the same flux patterns, they also will have the same induced voltages in all the loops and thus give rise to the same machine behavior. This can be done by taking the winding matrix and using it to express the induced voltage as a matrix product. Examining the elements of this matrix product for any two arrangements which give the same flux patterns, it is found that they must be the same. Hence, the simplest stator winding may be picked without impairing machine behavior.

Transfer Characteristics

In order to determine some of the features of the transient behavior of the machine the transfer characteristic (ratio of output current to control field voltage) must be determined for a range of frequencies. This is obtained directly from the differential equations and is represented by the ratio of two determinants. Evaluation of this expression is made practicable by expressing it graphically in terms of only a few parameters. This can be done since the per-unit notation gives approximate numerical values for many quantities such as rotor resistances which fall within a narrow range of values. The expression, when evaluated, is of the form $\psi_1/(\psi_2+Z\psi_3)$. Here ψ_1, ψ_2, ψ_3 are integral functions of the frequency and contain as parameters the control field time constant, T_a, and the amount of machine compensation, α. Z is the load impedance and it is seen that the transfer expression depends on type of load used.

The type of load most commonly encountered is one which at zero frequency has unit resistance drop (to balance the unit terminal voltage) and at other frequencies presents an inductive impedance. This load may therefore be written as $1+LP$. L will ordinarily be very large in the per-unit system since loads usually encountered will have moderately large time constants. For this case it can be shown that L may be removed as a separate factor with little inaccuracy and the transfer expression reduces to the form

$$\frac{I_L}{E_a}=\frac{H}{R_aL}Y(P,\alpha,T_a) \qquad (22)$$

where $Y(P,\alpha,T_a)$ is a function of frequency with α and T_a as parameters. H represents the magnitude and R_a the resistance of the control field winding. Curves for $Y(P,\alpha,T_a)$ are plotted for both amplitude and phase angle in Figure 3. These data are given for the matrix of the 4-pole structure and will be used for comparison with actual tests. A similar set of curves can be prepared for the 6-pole structure and when this is done it is found to be very similar in form and even in fair quantitative agreement over a large portion of the frequency range.

Limitations on Load Impedance

The properties of the transfer expression may be considered for any load, Z. Principal interest lies in determining what characteristics the load should have in order to form a stable combination with the generator without addition of any special stabilizing means. As already mentioned, the transfer admittance is of the form $(\psi_1/\psi_2+Z\psi_3)$. Hence it is desirable to determine what poles this expression has in the right half P plane. This is given by the corresponding zeros of the denominator.

Since $\psi_2+Z\psi_3=Z\psi_3(1+\psi_2/Z\psi_3)$; it is seen that if $|Z|>|\psi_2\psi_3|$, the plot of $(1+\psi_2/Z\psi_3)$ cannot loop the origin so that the zeros are given only by zeros of Z and ψ_3. Moreover, ψ_3 may be checked separately and it is found that it has no zeros. Hence a sufficient (though not necessary) condition for a stable load has been set up. This limiting value of Z is plotted as a set of curves over the frequency spectrum in Figure 4. Again the values for the 4-pole structure are used although the curves for the 6-pole structure are quite similar. Here it is seen that a serious restriction has not been imposed since $|Z|$ stays close to 1 and soon drops to zero. Any Z used will usually start at 1 and rise as the frequency increases, so that it will meet this condition.

There is one possible type of load which will fall below these curves over part of the frequency range. This is a load which contains very large capacitance elements which make their effect felt at low frequencies. Such a load is represented by the impedance of a motor.

The range of values which the motor impedance may take can be obtained by considering possible per-unit values of the motor constants and the differential equation of the motor. This has been done and curves plotted in Figure 4. It is seen that the motor impedance definitely lies below the required limit over part of the frequency range, so that instability would be expected. A more complete check verifies that this does give rise to an unstable combination.

Saturation

As soon as the point is reached where saturation in the iron becomes noticeable, it is found that the effect does not appear gradually, but occurs abruptly enough so that it may be described in terms of a ceiling voltage which the machine has reached. This behavior can be accounted for by examining the armature reaction magnetomotive forces due to internal circulating current and to output current. These currents combine to produce saturation under one control field pole and not the other. The loss in flux due to this saturation is such as to require more control field magnetomotive force. Since both these currents are quite large compared to the original control field current, the demagnetizing effect is large and accounts for the abrupt saturation. This effect will require a more liberally designed machine where high ceiling voltages are needed. It is possible to make approximate calculations for the behavior under saturation by assuming linear performance until the ceiling voltage is reached and calculating the further response to this fixed ceiling voltage.

Hysteresis

Hysteresis, although small enough so that the transient behavior is not greatly affected, will prevent the machine from providing perfect accuracy of regulation in the steady state. An approximate investigation of this error shows that the only magnetic path which contributes an important term to this error is the control field path. The other paths have sufficiently large currents and magnetomotive forces so that the hysteresis is small by comparison.

An approximate formula may then be set up for the hysteresis error as

$$\text{error}=\frac{\Delta M}{\dfrac{H}{R_a}K_o} \qquad (23)$$

Here ΔM is the width of the hysteresis loop and K_o is the amount of feedback from the error detecting device in whatever regulating system the generator is being used. As expected, the error is reduced by larger values of K_o since the error detecting device attempts to reduce whatever error appears.

Comparison With Test Results

The transfer curves for the 4-pole structure may be employed to determine transient behavior for comparison with test data.

The regulating generator as tested, was used in the voltage regulation of a turbo alternator whose field winding constitutes the load of the regulating generator. The output voltage (assumed proportional to alternator field current) is rectified and a fraction of it, K, is compared with a reference standard, E_o. The difference, if any, is applied to the control field which then corrects the voltage as needed. Thus $E_a=E_o-KI_L$ and there results for transfer expression with feedback present

$$I_L=\frac{E_o}{K}\cdot\frac{1}{\left(1+\dfrac{LR_a}{HYK}\right)} \qquad (24)$$

This frequency curve may then be transformed to the corresponding time response for various input voltages.

Figure 5 shows a calculated time response to unit step voltage change in the control field together with an actual test curve for this case. The agreement is seen to be fairly good. The fact that the error is still moderately large is to be expected from the nature of the calculation. Thus the data for this machine have been interpolated graphically from the curves. Similarly, the amount of feedback is not known exactly and since the system is not far away from the critical value of feedback, small changes in feedback will cause appreciable changes in the overshooting of the curves. Figure 5 also shows another test in which the voltage was raised close to saturation. The machine reached its ceiling voltage very quickly and most of the curve represents response to this ceiling voltage. Again there is fairly good agreement between test and calculation.

References

1. THE MULTISTAGE ROTOTROL, M. M. Liwschitz. *AIEE Transactions*, volume 66, 1947, pages 564–8.

2. THEORIE DU FONCTIONNEMENT DE LA METADYNE, J. M. Pestarini. *Revue Generale de L'Electricite* (Paris, France), volume 27, 1930, pages 355, 395 and volume 28, pages 227, 260.

3. NETWORK ANALYSIS AND FEEDBACK AMPLIFIER DESIGN (book), H. W. Bode. D. Van Nostrand Company, New York, N. Y., 1945.

4. MAIN EXCITER ROTOTROL EXCITATION FOR TURBINE GENERATORS, C. Lynn, C. E. Valentine. *AIEE Transactions*, volume 67, 1948, pages 535–39.

5. APPLICATION OF TENSORS TO THE ANALYSIS OF ELECTRICAL MACHINERY, G. Kron. *General Electric Review* (Schenectady, N. Y.), 1942.

6. PRINCIPLES OF SERVOMECHANISMS (book), G. S. Brown, D. P. Campbell. John Wiley and Sons, New York, N. Y., 1948.

No Discussion

Temperature Rise Values for D-C Machines—II

AN AIEE COMMITTEE REPORT

THE results of heat run tests made jointly by the Allis-Chalmers Manufacturing Company, Century Electric Company, General Electric Company, Reliance Electric and Engineering Company, and Westinghouse Electric Corporation on a motor exchange program involving motors at 1,750 rpm, 40 degrees centigrade open, from 1/2 to 50 horsepower, were reported in a previous paper.[1]

It was recommended that Table I of the American Standards Association C-50[2] be expanded, using values derived from the results of tests, to cover short-time rated motors and to include limiting values of temperature rise by the resistance method corresponding to existing values for the thermometer method for all windings. An expanded table was given as a conclusion and it was recommended that after due discussion and verification it be used to replace the present standard. Use of the resistance method for windings of less than 1-ohm resistance was considered only as an alternative test procedure of practical value in occasional instances, but not usable without determination and public recognition of temperature rise values corresponding to standard values for the thermometer method.

In publishing the previous paper the committee recognized the need for similar data on a sufficient number and variety of machines to make the results representative of d-c machines generally. An exchange motor test program on large machines was not practical, but the same companies offered from their engineering data files, test results on a large number of machines of all sizes. These results are reported in this paper giving a new expanded table with values suitable for a general standard covering integral-horsepower d-c machines.

It is recommended that this table supersede the one of the previous paper and that expansion of Table I of ASA Standard C-50 be made accordingly. For reasons of accuracy, reliability, and economy in the testing procedure of d-c machines, in general, the committee recommends the thermometer method as the preferred or standard test procedure. These reasons are elaborated with substantiating data later in the paper. In lieu of expansion of the ASA Standard, the committee recommends the use of the table given herein in cases where the alternative use of the resistance method is desirable.

Method

Although the test procedure used by the different manufacturers varied in details, the following procedure is sufficiently representative to show what was done by each.

Hot- and cold-resistance readings were taken on shunt field and armature windings.

For the field winding the hot resistance was determined by reading the field volts V and the amperes A just previous to shutdown taking the ratio V/A. This was done to avoid the error possible in correcting the measured resistance to the instant of shutdown. When measuring V and A, it is necessary that the true field volts and amperes are read excluding the current taken by the low-voltage relay usually connected across the field circuit.

For the armature winding the resistance is measured between two segments on the commutator. This measurement is taken when the armature is cold and again after the machine is operated under normal conditions of load and ventilation until the temperature of the stationary parts becomes constant. For the latter, the machine is shutdown quickly maintaining the load current until nearly stopped. Quickly after the machine stops the resistance is read between the same segments or at the most accessible spot on the commutator. If the same segments are not used, contact is made with two segments the same distance apart as for the cold reading. The resistance and the elapsed time from the start of the shutdown are recorded together at intervals of about one minute for 15 or 20 minutes. The exact position at which the hot resistance was read is marked on the commutator and after the machine has cooled to room temperature a cold-resistance check is made at this same position.

The resistance measurements are taken using a double bridge connected as shown in Figure 8. A special bridge for low resistance is used with a very sensitive external galvanometer. Current is fed into the armature through leads or through the brush rigging of the machine. Voltage drop is taken off the commutator segments. Care is exercised to allow the readings to be taken without effect from the equalizing winding and with negligible effect from the resistance of the commutator segments and risers to which the voltage contacts are connected. This means that the temperatures indicated by the changes in resistance are for the armature windings alone and are not affected by the temperature changes of the risers, commutator, and equalizer winding.

Temperature rise by thermometer

Paper 49-232, recommended by the AIEE Rotating Machinery Committee and approved by the AIEE Technical Program Committee for presentation at the AIEE Fall General Meeting, Cincinnati, Ohio, October 17-21, 1949. Manuscript submitted July 20, 1949; made available for printing September 16, 1949.

Prepared by the AIEE Subcommittee on D-C Machines of the Rotating Machinery Committee. Committee personnel: T. M. Linville, *Chairman*, Mrs. B. O. Buckland, W. B. Clancy, F. A. Compton, Jr., Lanier Greer, L. N. Grier, J. L. Hamilton, C. B. Hathaway, V. P. Hessler, V. B. Honsinger, W. R. Hough, P. Lebenbaum, C. Lynn, L. G. Opel, D. Ramadanoff, J. F. Sellers, B. H. Caldwell, Jr., W. H. Fifer, D. E. Fritz, and A. T. McClinton.

Table I. Present Table ASA-C50-1943

Item	The temperature rises in degrees centigrade in this table apply to the several classes of machines as given at the heads of the respective columns. Machine Part	Method of Temperature Determination to Be Employed	General Purpose Generators and Motors Class A Insulation Col. 1	Totally Enclosed, Totally Enclosed Fan-Cooled, Explosion-proof, Waterproof, Dust-tight, and Submersible Motors Class A Insulation Col. 2	Totally Enclosed, Totally Enclosed Fan-Cooled, Explosion-proof, Waterproof, Dust-tight, and Submersible Motors Class B Insulation Col. 3	Generators Having a Nominal Rating At End of 2-Hour Overload Class A Insulation Col. 4	Generators Having a Nominal Rating At End of 2-Hour Overload Class B Insulation Col. 5	Generators Having a 2-Hour 25 Per Cent Overload Rating At Continuous Load Class A Insulation Col. 6	Generators Having a 2-Hour 25 Per Cent Overload Rating At Continuous Load Class B Insulation Col. 7	At End of Two-Hour Overload Class A Insulation Col. 8	At End of Two-Hour Overload Class B Insulation Col. 9	Motors and Generators Other Than Col. 1–9 Inclusive Class A Insulation Col. 10	Motors and Generators Other Than Col. 1–9 Inclusive Class B Insulation Col. 11
1	Armature windings, and all windings other than 2 and 3	Thermometer See 2.054	40	55	75	55	75	40	60	55	75	50	70
2	Shunt field windings	Thermometer See 2.054	40*			55*	75*	40*	60*	55*	75*	50*	70*
		Resistance See 2.055	50*	60	80	65*	85*	50*	70*	65*	85*	60*	80*
3	Single-layer field windings with exposed uninsulated surfaces and bare copper windings	Thermometer See 2.054	50	65	85	65	85	50	70	65	85	60	80
4	Cores and mechanical parts in contact with or adjacent to insulation	Thermometer See 2.054	40			55	75	40	60	55	75	50	70
5	Commutators and collector rings**	Thermometer See 2.054	55†	65	85	65	85	55	70	65	85	65	85
6	Miscellaneous parts (such as brush holders, brushes, pole tips, etc.) may attain such temperatures as will not injure the machine in any respect.												

* The method of temperature determination to be used shall be optional with the manufacturer unless otherwise agreed upon. Only one method of temperature determination shall be required in any particular case.

** The class of insulation refers to insulation affected by the heat from the commutator, which insulation is employed in the construction of the commutator or is adjacent thereto.

† The limiting observable temperature rise for commutators of generators for electrolytic service shall be 50 degrees centigrade.

Proposed New Table

Item	The temperature rises in degrees centigrade in this table apply to the several classes of machines as given at the heads of the respective columns. Machine Part	Method of Temperature Determination	General Purpose Generators and Motors Class A Insulation Col. 1	General Purpose Generators and Motors Class B Insulation Col. 2	Totally Enclosed, Totally Enclosed Fan-cooled, Explosion-proof, Waterproof, Dust-tight, and Submersible Motors Continuous Rated Class A Insulation Col. 3	Totally Enclosed, Totally Enclosed Fan-cooled, Explosion-proof, Waterproof, Dust-tight, and Submersible Motors Continuous Rated Class B Insulation Col. 4	Motor and Generators Rated 30 Minutes to 2 Hours Inclusive Class A Insulation Col. 5	Motor and Generators Rated 30 Minutes to 2 Hours Inclusive Class B Insulation Col. 6	Motors and Generators Rated 15 Minutes or less Class A Insulation Col. 7	Motors and Generators Rated 15 Minutes or less Class B Insulation Col. 8	Generators Having a 2-Hour 25 Per Cent Overload Rating at Continuous Load Class A Insulation Col. 9	Generators Having a 2-Hour 25 Per Cent Overload Rating at Continuous Load Class B Insulation Col. 10	Generators Having A 2-Hour 25 Per Cent Overload Rating and Generators Having a Nominal Rating at End of 2-Hour Overload Class A Insulation Col. 11	Generators Having A 2-Hour 25 Per Cent Overload Rating and Generators Having a Nominal Rating at End of 2-Hour Overload Class B Insulation Col. 12	Special Purpose Drip-proof and All Motors and Generators Other Than Col. 1–12 Inclusive Continuous Rated Class A Insulation Col. 13	Special Purpose Drip-proof and All Motors and Generators Other Than Col. 1–12 Inclusive Continuous Rated Class B Insulation Col. 14
1	Armature windings and all windings other than 2 and 3	Resistance See 2.055	60		70	100	80	110	90	125	60	90	80	110	70	100
		Thermometer See 2.054	40		55	75	55	75	55	75	40	60	55	75	50	70
2	Shunt Field Windings	Thermometer See 2.054	40				55	75	55	75	40	60	55	75	50	70
		Resistance See 2.055	60		70	90	70	90	70	100	60	90	75	105	70	90
3	Single-layer field windings with exposed uninsulated surfaces and bare copper windings	Resistance See 2.055	60		70	100	80	110	90	120	60	90	80	110	70	90
		Thermometer See 2.054	50		65	85	65	85	65	85	50	70	65	85	60	80
4	Cores and mechanical parts in contact with or adjacent to insulation	Thermometer See 2.054	40				55	75	55	75	40	60	55	75	50	70
5	Commutators and collector rings	Thermometer See 2.054	55	75	65	85	65	85	65	85	55	70	65	85	65	85
		Pyrometer	65	85	75	100	75	100	75	100	65	85	75	100	75	100
6	Miscellaneous parts (such as brush holders, brushes, pole tips, and so forth) may attain such temperatures as will not injure the machine in any respect.															

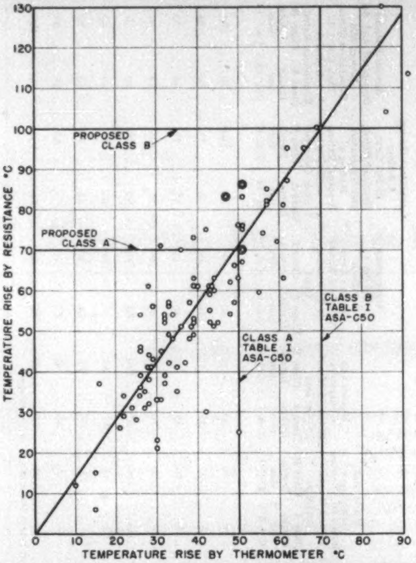

Figure 1. Armature temperature rise by resistance versus rise by thermometer. Composite curve, data from all participating companies

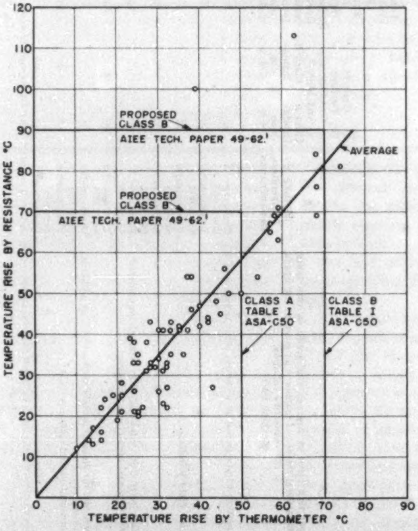

Figure 2. Shunt field temperature rise by resistance versus rise by thermometer. Composite curve, data from all participating companies

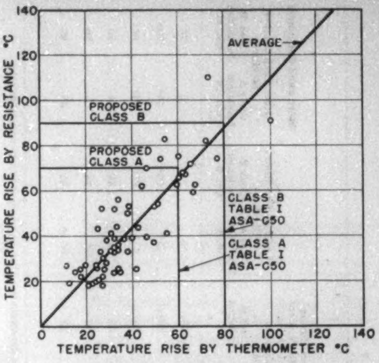

Figure 3. Commutating field temperature rise by resistance versus rise by thermometer. Data reported by company A

method was determined in accordance with AIEE Test Code 501.[3]

Plotting Data and Correcting to Instant of Shutdown

The hot-resistance readings minus the cold resistance are plotted on semilog graph paper against the elapsed time from the start of the shutdown. The resulting graph can be extended back to the instant when shutdown was begun showing approximately the temperature at this instant. In general the temperature decreases exponentially from the initial hot value to the final cold value. There are some relatively quick changes immediately after shutdown and the true curve

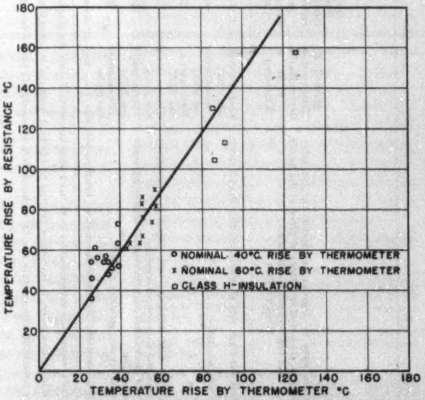

Figure 4. Typical plot of data covering armatures with mica insulation having nominal rise by thermometer of 40, 60, and 95 degrees centigrade

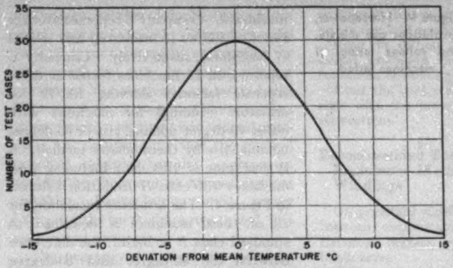

Figure 5 (above). Probability curve for armature temperature rise by resistance method. Results of tests on 413 machines. Mean temperature rise = 76.5 degrees centigrade

Figure 7 (right). Per cent error in measured temperature rise resulting from a given error in measured resistance as a function of the magnitude of the temperature rise to be measured

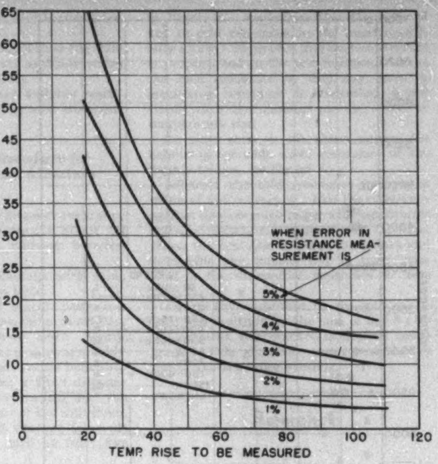

contains several components with different exponentials. If only one long-time component exists, the data will plot on semilog paper as a line which can be continued readily back to the initial instant of shutdown. It has been generally acceptable to plot the data on semilog paper and to draw a line through the points, extending this line back to the initial instant. This averages out the error in individual readings and, therefore, gives a more accurate reading for temperature at the initial instant assuming the quick initial changes of temperature to be negligibly small.

To obtain a correct line using semilog paper and as a matter of fact whenever semilog paper is used, only the difference between the temperature reading and the final cold temperature (room temperature) should be plotted for each instant of time. Otherwise a straight line cannot be drawn through the points and the temperature at the initial instant will not be correct. The resistance readings should never be plotted directly. The true conditions are

$$T_x = T_C + (T_H - T_C)\epsilon^{-\sigma t} \text{ (by assumption)}$$

where

T_x = temperature at any instant
T_C = temperature cold
T_H = temperature hot
t = time in seconds
σ = reciprocal of thermal time constant

T_x plotted against time will be a curved line on either linear or semilog paper. A similar plot of $T_x - T_C$ on semilog graph

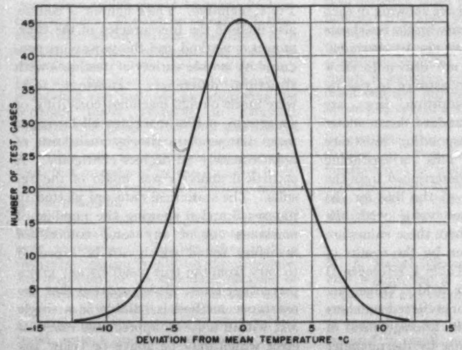

Figure 6. Probability curve for shunt field temperature rise by resistance method. Results of tests on 420 machines. Mean temperature rise = 49.7 degrees centigrade

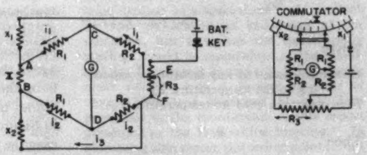

X = RESISTANCE TO BE MEASURED
x_1 = LEAD, BRUSH, AND PART WINDING RES.
x_3 = LEAD, BRUSH, AND PART WINDING RES.
R_1 = BRIDGE RATIO RES.
R_2 = BRIDGE RATIO RES.
R_3 = KNOWN VARIABLE RES.

$R_1 = KR_2$ WHERE K = BRIDGE RATIO SET BY SWITCH WHEN BRIDGE IS BALANCED:

POINTS C AND D ARE AT SAME POTENTIAL.

$$R_2 i_1 = R_3(i_2+i_3) + R_2 i_2$$
$$R_1 i_2 + X(i_2+i_3) = R_1 i_1$$

THEN:

$$R_1 i_2 + X(i_2+i_3) = KR_3(i_1+i_3) + KR_2 i_2$$
$$KR_2 i_2 + X(i_2+i_3) = KR_3(i_2+i_3) + KR_2 i_2$$

OR:

$$X = KR_3$$

THE SAME CURRENT MUST FLOW THROUGH X AS FLOWS THROUGH R_3. THEREFORE, THERE MUST NOT BE A SHUNT AROUND R_3 UNLESS IT IS CONNECTED FROM E TO F AND THE COMBINED RESISTANCE USED AS THE VALUE OF R_3.

Figure 8. Double-bridge connections

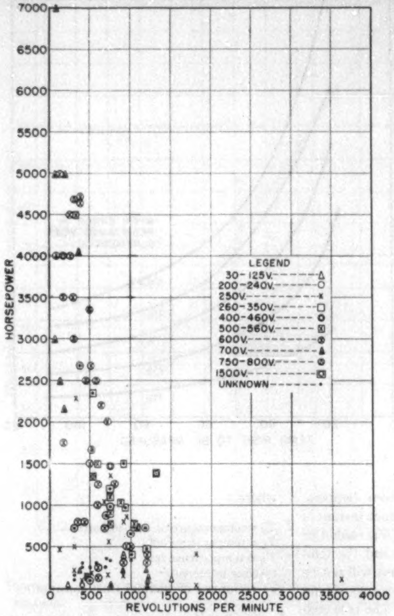

Figure 9. Horsepower, revolutions per minute, and voltage ratings of machines tested

paper will be a straight line. Furthermore

$$T_x - T_C = \frac{r-R_C}{R_C}(234.5+T_C) = (T_H - T_C)\epsilon^{-\sigma t}$$

where

r = the resistance at any instant corresponding to the temperature T_x

R_C = resistance cold at temperature T_C

Then

$$r - R_C = \frac{R_C(T_H - T_C)}{234.5+T_C}\epsilon^{-\sigma t} = K\epsilon^{-\sigma t}$$

Therefore, if from each resistance reading the cold resistance is subtracted and the remainder plotted at each instant of time on semilog paper, a straight line may be drawn through the points and continued back to the initial instant of shutdown. Other ways of plotting the resistance-time data are likely to lead to an appreciable error resulting in an amplified error in the calculated temperature rise.

A straight line must not be taken for granted as curvature will be caused by a complex thermal time constant. For this reason there should be as little time as possible between shutdown and the first reading of hot resistance.

Results

Tests on 116 machines from about 4 horsepower to 7,000 horsepower and from about 100 to 1,200 rpm are reported. The horsepower, root-mean-square, and voltage of these machines are plotted in Figure 9 to show clearly the ratings of the machines tested. Results of tests are given in Figures 1 to 3 inclusive showing in each case the temperature rise by the resistance method plotted against rise by thermometer method. Lines are drawn to show the ratio of rise by resistance to rise by thermometer. In addition, lines are drawn to show the standard thermometer value and the corresponding resistance value for Table I. This corresponding value in each case is determined from the point of intersection of the line for the standard thermometer value with the line for the ratio. Where these values are lower than those given by the results of the earlier tests (see Table 1, reference 1) the former values are held. Values are rounded off to nearest preferred numbers in each instance. The average ratio of rise by resistance to rise by thermometer reported by company *A* was 100/74 for the armature winding (11 machines) and 100/84 for the shunt field winding (55 machines). Company *B* reported average ratios of 100/89 (5 machines) and 100/84 (7 machines), respectively. Company *C* reported on 72 machines tested at three separate factories showing 100/70 for armature windings for machines with either 40-degree nominal rise or 60-degree nominal rise by thermometer method. A typical plot of this data including four machines with class-*H* insulation is shown in Figure 4. The armature insulation for all of these machines is described as standard class *B* or better, the difference between the 40-degree and 60-degree machines being chiefly in the heat generated in the parts. The ratio for the shunt field winding reported by company *C* is 100/89 from tests on six machines. Company *D* reported 100/85 for armature windings as the average for 12 machines. The ratio for the commutating field was reported by company *A* only showing 100/91 for the average of 61 machines plotted in Figure 3.

It should be kept in mind that substantially all of the data was taken from the records of the companies and, therefore, are not the results of a preplanned test program with carefully followed uniform procedure. Hence, some of the data possibly have relative errors especially because of the correction of the results to the instant of shutdown. It follows that the data should be looked at in the aggregate. In the case of each company the range of results is broad as can be seen from the nature of the composite data of Figures 1, 2, and 3.

Values for short-time ratings are repeated from the previous paper.[1]

The combined reliability and accuracy of the resistance method is indicated by the spread of the data shown on Figures 1 to 4, inclusive. These figures, of course, also include the inaccuracies of the thermometer method and the variations produced by a wide variety of machines with structural differences. However, tests were made on 420 machines consisting of six groups of like machines all having a mean temperature rise by resistance of approximately 80 degrees centigrade. A statistical analysis was made of the results. The statistical data are plotted in Figures 5 and 6 showing the number of machines out of any total number of machines tested which can be expected to vary from the true result by any given percentage error. It is apparent that the resistance method is reliable in a single test within only an appreciable range of error which may be above or below the true result. Thus, a number of repeated heat run tests must be made for any single machine using the resistance method or a number of duplicate machines must each be tested. Therefore, the method is not generally appropriate or economical but may be useful when a number of like machines are being built. Factories making groups of like machines where special equipment and trained operators are justified may find the method practical, whereas for d-c machines in general the thermometer method is more suitable. Nevertheless, until proper values for the method are recognized, it is useful in no instances.

The necessity for especially accurate measurement when using the method is clearly shown by Figure 7.

Class H is omitted from Table I as the basic thermometer values are not yet established. When these are established the corresponding values for the resistance method will be given by multiplying the thermometer values by the same ratios as used to determine class-A and -B values.

Appendix

Recommended Test Procedure for Resistance Method for Field Windings

On field windings, read the true current in the field coils excluding low-voltage relay or other devices or current shunts connected across the field winding.

Read the voltage directly across the field circuit excluding rheostats and any series connected devices and cables.

Read the cold resistance and hot resistance with the same meters and the same connections.

Recommended Test Procedure for Resistance Method for Armature Windings

On armature windings measure resistance between commutator segments about 90 electrical degrees apart midway between brush arms.

Take cold and hot readings with same instruments, leads, and so forth.

After temperature of stator parts has become constant, shut machine down fast maintaining load current until nearly stopped. Start resistance readings as quickly as possible. Have contact points built into a yoke which holds them a fixed distance apart. Record resistance reading and the elapsed time from the start of the shutdown.

Record resistance and time at intervals of about two minutes until at least five readings are obtained.

Mark the exact position at which the hot resistance was taken and after the machine has cooled to room temperature measure the cold resistance with the contacts in the same position with the same instruments, leads, and so forth.

Use a double bridge with very sensitive external galvanometer connected as shown in Figure 8. Remember that the ratio of hot to cold resistance in the usual case is only 1.12 to 1.25 per cent and the temperature is proportional to the hot resistance minus the cold resistance so that any error in measuring resistance is multiplied 4-to-8 times when the readings are converted to temperature rise.

Be sure there is no shunt across the balancing (or slide wire) resistance of the double bridge, see Figure 8.

Subtract the cold resistance from each value of hot resistance. Plot the difference against time on graph paper with logarithmic scale for resistance and linear scale for time. Draw the best line through the points and determine the intersection at time zero. This is the differential resistance at zero time.

Divide this resistance by the cold resistance and multiply by the sum of 234.5 plus the ambient temperature in degrees centigrade. This gives the mean temperature rise of the armature winding.

References

1. TEMPERATURE RISE VALUES FOR D-C MACHINES. An AIEE Committee Report. *AIEE Transactions*, volume 68, part I, 1949, pages 206–18.

2. ROTATING ELECTRICAL MACHINERY, C50. American Standards Association (New York, N.Y.), 1943.

3. TEST CODE FOR D-C MACHINES. *AIEE Standard Number 501*, 1941.

Discussion

A. T. McClinton (Naval Research Laboratory, Washington, D. C.): This report states that the change in resistance method of measuring temperature is unreliable and inaccurate, and thus preference is given the thermometer method. Unfortunately, little is said concerning the reasons for this inaccuracy nor are precautions given which should be taken in overcoming them. It must be recognized, however, that under certain conditions it is almost mandatory to employ the change in resistance method for measuring temperature, and therefore its limitation should be recognized and methods for improving the accuracy made available to everyone through this paper. Our own experiences at this Laboratory have shown that there are other sources of error in its use other than that introduced by the equation itself. If these are corrected, satisfactory results can be obtained.

On small machines it has been found highly desirable, and in certain cases necessary, to remove the brushes before making resistance measurements on the armature. An inspection of the schematic diagram of the armature circuit will reveal that under some conditions it is possible to have the armature circuit resistance paralleled by brush contact and lead resistance. Naturally the presence of these in the circuit will introduce error. It is recognized that in larger machines it will be impractical to remove the large number of brushes and therefore this precaution cannot be taken. However, it should also be noted that in the larger machines such a precaution is not necessary to provide the necessary accuracy.

A second source of error to be considered in making these measurements is the introduction of voltages in the galvanometer circuit through thermocouple action at the junction of the probes and commutator surface. Our experience has shown that probes, although supposedly made of identical material, when placed on the hot commutator will give voltages that are high enough in magnitude to seriously unbalance the measuring circuit. If we recognize the sensitivity required for the galvanometer circuit it becomes quite obvious that only small voltages introduced by thermocouple action can create a sizable error as well as erratic error in the measurement. It is believed that this source of error may overshadow any other that may enter into the measurement of temperature by change in resistance measurement, and that extreme care should be taken to assure that this thermocouple action does not exist.

M. A. Baker (General Electric Company, Fort Wayne, Ind.): One of the conclusions reached in this report was that the resistance method is not generally appropriate or economical for use on machines manufactured in small quantities. In the Fort Wayne Large Motor and Generator Division of the General Electric Company, we build a great variety of machines in small quantity manufacture, usually in lots of one or two. We agree thoroughly with the conclusion of this Subcommittee based on our own experience with temperature rise by resistance measurements over a period of about eight years. We look at the resistance method as a specialized tool by which we can get additional knowledge of our machines, but feel that the thermometer method should be maintained as the standard for guarantees because it is inherently more reliable with a limited number of tests. This was observed in the data presented in the counterpart of this report presented at the 1949 winter meeting.[1] In discussing this report the writer pointed out that in spite of the unusual care and laboratory equipment used in making these tests, the per cent variation between the two independent tests was greater for resistance rise than for the thermometer rise, on armatures and commutating fields. This should not be surprising when we realize, as was pointed out in this report, that errors made in measuring resistances are magnified many times when converted to temperature rise. On shunt fields where resistance is much higher, and where it can be determined prior to shut down, it is much easier to obtain accurate data, and rise by resistance is a practical test for main field coils.

The data presented in the report[1] shows that the ratio of thermometer rise to hot spot is just as definite as the ratio of resistance rise to hot spot, so with proper allowances set up, the thermometer method is a reliable measure of hot-spot temperature. In view of this, the simplicity of the test and its greater reliability (at least in

Table I. Proposed New Table

The temperature rises in degrees centigrade in this table apply to the several classes of machines as given at the heads of the respective columns Item	Machine Part	Method of Temperature Determination	General Purpose Generators and Motors		Totally Enclosed, Totally Enclosed Fan-Cooled, Explosion-proof, Waterproof, Dust-tight, and Submersible Motors Continuous Rated		Motor and Generators Rated 30 Minutes to 2 Hours Inclusive		Motors and Generators Rated 15 Minutes or less		Generators Having a 2-Hour 25 Per Cent Overload Rating at Continuous Load		Generators Having A 2-Hour 25 Per Cent Overload Rating and Generators Having a Nominal Rating at End of 2-Hour Overload		Special Purpose Drip-proof and A Motors and Generators Other Than Col. 1–12 Inclusive Continuous Rated	
			Class A Insulation Col. 1	Class B Insulation Col. 2	Class A Insulation Col. 3	Class B Insulation Col. 4	Class A Insulation Col. 5	Class B Insulation Col. 6	Class A Insulation Col. 7	Class B Insulation Col. 8	Class A Insulation Col. 9	Class B Insulation Col. 10	Class A Insulation Col. 11	Class B Insulation Col. 12	Class A Insulation Col. 13	Class B Insulation Col. 14
1	Armature windings and all windings other than 2 and 3	Thermometer See 2.054	40		55	75	55	75	55	75	40	60	55	75	50	70
		Resistance See 2.055			70	100	80	110	90	125		90		110	70	100
2	Shunt field windings	Thermometer See 2.054	40				55	75	55	75	40	60	55	75	50	70
		Resistance See 2.055	60		70	100	80	110	90	125	60	90	80	110	70	100
3	Single-layer field windings with exposed uninsulated surfaces and bare copper windings	Thermometer See 2.054	50		65	85	65	85	65	85	50	70	65	85	60	80
		Resistance See 2.055			70	100	80	110	90	120		90		110	70	90
4	Cores and mechanical parts in contact with or adjacent to insulation	Thermometer See 2.054	40				55	75	55	75	40	60	55	75	50	70
5	Commutators and collector rings	Thermometer See 2.054	55	75	65	85	65	85	65	85	55	70	65	85	65	85
6	Miscellaneous parts (such as brush holders, brushes, pole tips, and so forth) may attain such temperatures as will not injure the machine in any respect.															

cases when only one or two runs are available) we in the Large Motor and Generator Division, Fort Wayne, heartily endorse the recommendation that the thermometer method be considered as the preferred or standard test procedure.

We have had a double standard (optional with manufacturer) for some time on main field temperature rating. Since rise by resistance is a practical test on main field coils we do not seriously object to this as long as proper limits are established. Based on our experience and data presented we concur with the proposed increased values of rise by resistance for shunt fields as long as the method of test is optional with the manufacturer. However, since resistance tests are not practical for production tests on low-resistance circuits, we recommend deleting the rise by resistance values for armatures and single layer field windings. Dual standards tend to cause trouble and misunderstanding, and we can see no benefits to be gained by leaving rise by resistance as an optional standard for general-purpose d-c machines. If rise by resistance is desirable on specialized lines of machines, a special standard should be prepared to cover these lines.

The temperature rise of any part of a machine should correspond to the insulation on that particular part. Most commutators are class-*B* insulated, and we recommend that class-*B* temperatures be allowed on all class-*B* commutators even when used in class-*A* insulated machines.

In concluding I would like to make a few remarks regarding the calculation of rise by resistance. I think this report overemphasizes the straight line relationship between the differential resistance and time. It has been our experience on a wide variety of d-c machines that the slope of the cooling curve during the first two or three minutes is appreciably different from the slope after this time. In fact, if we do not get at least two, or preferably three, points in the first two minutes, we do not consider the test satisfactory. The computation method given in this report gives the temperature rise above the ambient at which the cold resistance was measured. If the ambient has increased during the heat run, the results should be corrected by subtracting the difference between the final and initial ambient. If the final ambient is lower, the difference should be added to the calculated temperature rise

REFERENCE

1. TEMPERATURE RISE VALUES FOR D-C MACHINES, AIEE Committee Report. *AIEE Transactions*, volume 68, part I, 1949, pages 206–18.

B. H. Caldwell, Jr.: The AIEE Subcommittee on D-C Machines met immediately following the presentation and discussion of the report.

It was decided that the Proposed New Table should be modified. See Table I of the discussion.

The principal changes are:

Rise by Resistance for Armature Windings

Measurement of temperature rise by resistance for armature and single layer field windings is not recommended for d-c machines having a guarantee of 40-degree centigrade rise by thermometer for continuous load. This means that the temperature rise by resistance values will be omitted in columns 1, 9, and 11 for items 1 and 3.

It is for the low temperature rise that the percentage error in measured rise is greatest for a given error in the measured resistance, see Figure 7 of the paper. It is felt that the resistance method is not practical at this time for 40-degree centigrade rise machines. This change in the table removes most of the objections to use of the resistance method.

It was decided that the remaining resistance values should be included in the table as an alternate method.

Rise by Resistance for Shunt Windings

Since the shunt field is relatively a high-resistance winding, use of the resistance method meets with essentially unanimous approval. The table proposed in the report specified values of rise by resistance consistent with data obtained from the test program as being equivalent to the present limit as measured by thermometer method. This results in lower rise by resistance for the shunt field than for the armature. Since the shunt field winding is not subject to mechanical stress nor to as severe overloads as the armature winding, it is logical to establish the limits for the shunt field winding at least as high as for the armature winding. It is, therefore, recommended that the limits for temperature rise by resistance for the shunt field winding be made the same as for the armature winding.

Machines with Two or More Classes of Insulation

At least for the larger machines most modern commutators are insulated with class-*B* materials. A liberal interpretation of American Standards Association *C50*, 1943,[1] would seem to permit class-*B* temperature rise for such commutators even though they are connected to an otherwise class-*A* machine. It is recommended that this be made clear in the next revision of ASA *C50*. The same principle applies to other components having different classes of insulation.

In all cases it should be made clear that the temperature limits here proposed are intended to represent only the safe limit for satisfactory insulation life. It is quite possible that other considerations will impose a lower limit. For example, it would not in general be safe to attempt to operate an existing commutator, which was built for a temperature rise of 55 degrees centigrade, at a higher temperature rise, since adequate provision for the increased thermal expansion may not have been made in the original design and construction. In general other parts of a machine may have similar limitations.

It remains the manufacturer's responsibility to construct the machine so that not only is satisfactory insulation life obtained, but also that other factors which influence satisfactory operation are kept within safe limits. The user must recognize that insulation temperature is only one of the load limiting factors, and should consider all important factors before making a decision to operate a machine beyond its original rating.

The Proposed New Table as modified in this discussion is recommended as a basis for revision of Table A, ASA *C50*, 1943, page 10. Favorable action on this proposal by the Standards Committee is requested.

Reference

1. See reference 2 of the report.

Progress Report on AIEE Test Code for Electric Brushes

AN AIEE COMMITTEE REPORT

Synopsis: This report presents material which the Joint Subcommittee recommends for inclusion in a test code for electric brushes. It is presented to secure general discussion preliminary to formulation of a trial test code. The material presented generally represents the viewpoint and agreement of the AIEE Joint Subcommittee. Items which the Subcommittee agrees are desirable for inclusion in the test code but upon which further work must be done are indicated.

THE AIEE Committee on Electric Brushes, a joint subcommittee of the Power Rotating Machinery Committee and the Air Transportation Committee has for its major assignment the development of a test code for electric brushes. The personnel of the committee includes members of the technical group of the carbon section of the National Electrical Manufacturers Association (NEMA) so there has been continuous liaison with the electric brush manufacturers. It is the intention of both groups to bring their standards into agreement in those areas in which both groups are interested. The committee has adhered to the principle that an AIEE test code on electric brushes should define standard procedures for making tests and not be concerned with specifications concerning acceptable test results.

Much experimental work remains to be done before a complete and satisfactory test code on electric brushes can be written. The material of this progress report includes those items upon which there is general agreement and suggests additional items for which standard procedures should be prepared, but of which insufficient knowledge is available for standardization at the present time. The committee will procede with the study of these additional items.

Table of Contents

1.000 Purpose
2.000 Measurements on Material Specimens
  2.100 Sampling Schedule for Material Specimen Tests
  2.200 Material Specimen Test Procedure
    2.210 Specific Resistance
      2.211 Voltmeter-Ammeter Method (Standard Method)
      2.212 Kelvin Bridge Method (Alternate Method)
    2.220 Density
      2.221 Apparent Density
      2.222 Immersion Method (Alternate)
      2.223 Real Density—Oil Absorption Method
    2.230 Porosity
    2.240 Scleroscope Hardness
    2.250 Transverse Strength
    2.260 Percentage Ash
3.000 Tests on Brush Assemblies
  3.100 Shunt connection millivolt drop
  3.200 Vibration Test on Shunt Connection
4.000 Sliding Contact Operating Characteristics
  4.100 Test Equipment
    4.110 Slip Ring
    4.120 Brush Holders
    4.130 Test Brushes
    4.140 Equipment for Friction Measurement
    4.150 Equipment for Ring Surfacing
    4.160 Air Conditioning Equipment
  4.200 Preparation for Tests
    4.210 Preparation of Ring Surface
    4.220 Method of Seating Brushes
  4.300 Tests
    4.310 Contact Drop
    4.320 Coefficient of Friction
  4.400 Test Schedule
5.000 Life Tests
6.000 Commutating Ability Tests
7.000 Altitude Tests
  7.100 Standard Test Conditions
    7.110 Temperature
    7.120 Air Pressure

1.000 Purpose

It is the purpose of this brush test code to define procedures for measuring the physical properties of electric brush materials, for determining the quality of brush assemblies, and to test the performance of brushes as part of the sliding contact. Since some of the tests are empirical, and since the test results vary with many test conditions, it is desirable to standardize test procedures to reduce these variables to a minimum. Test data based on standard procedure should facilitate comparison of various brush grades and assist designers in the selection of the most satisfactory brush for the machine application and operating condition involved.

2.000 Measurements on Material Specimens

Tests of the physical properties of brush materials are made primarily for the purpose of checking manufacturing processes to obtain a uniform product since it is not yet possible to correlate closely the physical properties of brush materials with the operating characteristics of the brush.

Paper 49-234, recommended by the AIEE Rotating Machinery Committee and approved by the AIEE Technical Program Committee for presentation at the AIEE Fall General Meeting, Cincinnati, Ohio, October 17–21, 1949. Manuscript submitted November 15, 1948; made available for printing September 21, 1949.

Personnel of the AIEE Joint Subcommittee on Electric Brushes: V. P. Hessler, *Chairman;* W. H. Austry, H. R. Brown, W. E. Clancy, J. V. Dobson, H. M. Elsey, C. J. Herman, L. H. Hildebrandt, H. E. Keneipp, E. A. Lapham, T. M. Linville, D. Ramadanoff, Orrin Rutledge, S. D. Summers, A. L. Van Emden.

2.100 SAMPLING SCHEDULE FOR MATERIAL SPECIMEN TESTS

Table I

Number of Specimens in Lot	Number of Samples
1– 39	1
40–109	2
110–179	3
180–299	5
300–499	7
500–799	10

2.200 MATERIAL SPECIMEN TEST PROCEDURE

2.210 *Specific Resistance*

2.211 *Voltmeter-Ammeter Method* (*Standard Method*). Test specimens shall have, where practicable, a length of not less than four times the width or thickness. Direct current shall be passed through the specimen from end to end through contact plates which make contact across the entire area of both ends of the specimen. A good electrical contact with the carbon may be obtained with contact plates of silver-plated copper gauze, having a backing of 1/4-inch thick neoprene, or similar resilient material. The magnitude of the current shall be sufficient to give a satisfactory millivolt reading without overheating the specimen. A current of 2.5 amperes is satisfactory for a 1/2-inch square specimen. Sharp potential pointers shall be used, and the distance between the points shall not be less than either the width or thickness dimensions or greater than 50 per cent of the length of the specimen. The voltage or millivolt drop shall be taken by means of a potentiometer-type meter or a relatively high resistance voltmeter. The specimen should be tested at a temperature of 30 degrees centigrade, ±5 degrees centigrade.

The resistivity in ohm-inches shall be calculated by the use of the following equation:

$$\rho=\frac{Ewt}{Il}$$

where

ρ = resistivity in ohm-inches
E = voltage drop in volts
w = width of the specimen in inches
t = thickness of the specimen in inches
I = current in amperes
l = length between potential pointers in inches

2.212 *Kelvin Bridge Method* (*Alternate Method*). A Kelvin Bridge may be used to determine the resistance of the specimen instead of using the voltmeter-ammeter method. Care must be taken to avoid overheating the specimen. Follow the procedure outlined for the voltmeter-ammeter method and calculate the resistivity by the following equation:

$$\rho=\frac{Rwt}{l}$$

where R is the resistance in ohms measured between the potential pointers and the other quantities correspond with those of the voltmeter-ammeter method.

2.220 *Density*

Manufactured carbon is inherently a porous material and therefore both real and apparent density tests are useful for purposes of quality control.

2.221 *Apparent Density.* Finish the specimen to a shape such that the dimensions can be measured accurately with a micrometer. Weigh the specimen in grams to four significant figures. Calculate the volume in cubic centimeters and determine the apparent density by dividing the weight in grams by the volume in cubic centimeters.

2.222 *Immersion Method* (*Alternate*). Since this method of determining apparent density involves the determination of volume by water displacement, an irregularly shaped sample may be used. No preparation is necessary other than observing that the sample is clean, dry, and free from metal or other foreign material. Weigh the sample to four significant figures. Then coat the sample with thin grease or other waterproof masking material to prevent absorption of water. Suspend the sample in water from a balance with a number 40 thread. The sample must be completely immersed and all air bubbles must be removed from the surface of the sample. Weigh the sample to four significant figures while immersed. Calculate the apparent density as follows:

$$\text{Apparent density}=\frac{\text{Weight in air}}{\text{Weight in air—Weight in Water}}$$

2.223 *Real Density—Oil Absorption Method.* Real density is defined as the ratio of the weight of the specimen in grams to the real volume of the specimen material, that is, to the total volume less the volume of the interstices. The volume of the interstices is determined from the weight of oil of measured density which is absorbed by the specimen.

The following equipment is needed:

1. Micrometer.
2. Scale or balance with range of about 100 grams and sensitivity of 0.01 gram.
3. Hydrometer having a range of 0.800 to 0.900 at 20 degrees centigrade and graduated to 0.001.
4. Hydrometer cylinder 40 millimeters in diameter and 300 millimeters long.
5. Thermometer with range of zero to 100 degrees centigrade.
6. Vacuum flask of 1,000 cubic centimeter capacity.
7. Vacuum pump capable of producing a vacuum equivalent to 740 millimeters of mercury.
8. Water bath held below 20 degrees centigrade.
9. Petroleum oil grade *SAE-10*, *Texaco Regal B*, or equivalent.

Finish the specimen to a shape such that its dimensions can be determined accurately with a micrometer. Measure the specimen and calculate its total volume in cubic centimeters. Record this volume as V_t. Weigh the specimen in grams to four significant figures. Record this weight as W_1. Place the specimen in the vacuum flask and cover completely with oil. Place thermometer in the flask with its bulb immersed in the oil. Apply heat with care to heat the oil slowly to 70 degrees centigrade. While heat is being applied, connect the pump to the flask and increase the vacuum gradually to a value equivalent to about 740 millimeters of mercury. Care must be used to avoid undue foaming in applying the vacuum. Maintain the 70 degrees centigrade and vacuum until the specimen stops emitting bubbles. Three to five hours are usually required. Release the vacuum and cool the flask and contents to room temperature, and then to below 20 degrees centigrade in the water bath. Remove the flask from the water bath and allow the temperature to rise to 20 degrees centigrade. Remove the specimen from the oil, wipe dry, and weigh. Record this weight as W_2. Pour the oil from the flask into the hydrometer cylinder, cool to 20 degrees centigrade if the temperature has risen above this value and read its specific gravity. Record this figure as d.

Calculation of real density

Weight of oil absorbed $= W_0 = W_2 - W_1$
Volume of oil absorbed $= V_0 = W_0/d$ cubic centimeters

$$\text{Real density}=\frac{W_1}{V_t-V_0}$$

If desired the total volume V_t may be determined as in the immersion method by weighing the specimen submerged immediately following the weighing to determine W_2. Record this weight as W_3. Then

$$V_t=W_2-W_3$$

and

$$\text{Real Density} = \frac{W_1}{W_2 - W_3 - V_0}$$

2.230 *Porosity*

The porosity of carbon is defined as the ratio of the volume of the interstices in a given specimen to the total volume of the specimen. The per cent porosity is calculated by the following equation where P represents the percentage porosity, RD the real density, and AD the apparent density:

$$P = \frac{(RD - AD)100}{AD}$$

2.240 *Scleroscope Hardness*

This measurement is made with the Shore, *Model C-2,* Scleroscope, equipped by the manufacturer with a special type of hammer for carbon. In making the tests, the instrument is mounted on a firm support and levelled by means of levelling screws so that the plumb rod is in the center of the ring. The anvil of the instrument must be kept clean. When round pieces are to be tested, a Vee block is used. All specimens must be surface ground before testing. Test pieces are placed in the instrument so that the hammer impact is applied in the direction of molding compression in the case of brush plate materials and perpendicular to the axis of extrusion for extruded materials. To make the test, the specimen is placed on the anvil or in the Vee block and the tube is lowered firmly against the specimen. Release the hammer and read the height of rebound. Take at least six readings at various spots on each side of a rectangular block and record the average as the scleroscope hardness. On round pieces take at least six readings at various places and record the average as the scleroscope hardness.

2.250 *Transverse Strength*

The transverse strength test is made by applying the breaking force in the direction of molding pressure in the case of specimens cut from plate stock and at right angles to the axis of extrusion in the case of extruded stock. For carbon, electrographitic, and graphite grades the specimen should be $1^5/_8$ inches long by 0.200 inch by 0.200 inch (+0.000 inch − 0.002 inch). For metal graphite grades the specimen should be $1^5/_8$ inches long by 0.125 inch by 0.125 inch (+0.000 inch − 0.002 inch). The direction in which the breaking force is to be applied must be clearly marked on the ends of the specimen at the time of machining.

To make the test on the 0.200 inch by 0.200 inch specimen, support it on two knife edges of 0.010 inch radius spaced 1.2 inches apart and apply the breaking force at a point midway between the two knife edges with a third knife edge of 0.010 inch radius. The force shall be applied at a steady rate not exceeding 500 pounds per minute. Note and record the total force in pounds at which the specimen ruptures.

To make the test on the 0.125 inch by 0.125 inch specimen, adjust the supporting knife edges to a spacing of 0.6 inch and apply the breaking force at a point midway between the supporting knife edges. The force shall be applied at a rate not exceeding 250 pounds per minute. Note and record the force in pounds at which the specimen ruptures.

The transverse strength is calculated with the following equation:

$$\text{Transverse strength} = \frac{3lF}{2Wt^2}$$

where

l = distance between supporting knife edges in inches
F = rupturing force in pounds
W = width of the specimen in inches
t = thickness of the specimen in inches

2.260 *Percentage Ash*

The basic procedure is to heat a representative sample of the material in an oxidizing atmosphere until complete incineration takes place. The remaining ash is then weighed and expressed as a per cent of the initial weight of the sample. Since the ash content of some electrographitic materials may be less than 0.1 per cent, special precautions must be taken to prevent errors in weight.

The apparatus should consist of a small muffle or tube furnace capable of maintaining a controlled temperature of 750 to 850 degrees centigrade and with an inlet for air or oxygen, an analytical balance, a dessicator if the ash is not to be weighed soon after removal from the furnace, and a platinum crucible of such size that the sample does not more than half fill the crucible. A glazed porcelain or equivalent crucible may be substituted for the platinum if a sample two or three times as large is used to minimize error due to change of weight of the crucible.

The sample should be cut from a representative section of plate or brush stock in such a manner that all surfaces of the sample are newly cut. The sample should contain 15 to 25 grams of material, but in any case the residue should not be less than five milligrams. The sample may be crushed to reduce the incineration time but extreme care must be used to exclude foreign matter.

Fire the crucible at red heat, cool and weigh. Place the sample in the crucible and weigh again. Place the crucible in the furnace and maintain the temperature between 750 and 850 degrees centigrade until the carbon is completely incinerated. Air or oxygen should be admitted to the furnace in such a manner that no ash is blown from the crucible. Remove crucible from furnace, cool to room temperature and weigh. If weighing is delayed, place crucible in desiccator.

$$\text{Percentage ash} = \frac{\text{Weight of residue}}{\text{Weight of sample}} \times 100$$

Sections 3.000 to 7.400 as shown in the Table of Contents are considered essential to a complete code and are being worked out. A trial test program is to be planned and carried out jointly with a committee of NEMA. It is hoped that the AIEE and NEMA committees will be combined officially to form a single operating group and that the final code can be issued for general trial within a year.

No Discussion

Differential Leakage of the Different Patterns of a Fractional Slot Winding

M. M. LIWSCHITZ
MEMBER AIEE

WHEN the conditions for balance are satisfied, a fractional-slot lap winding can be laid out in many different patterns all of which are balanced. The usual pattern is that for maximum distribution factor of the main wave. If this pattern is called the "basic," all other patterns can be derived from this one by cyclic shifts of coils from one phase to the other within the same repeatable group.[1] The distribution factor of the main wave of the derived patterns, that is, of the patterns with cyclic shift of coils, is always smaller than that of the basic layout. As regards the distribution factors of the harmonics of the derived patterns some are smaller, and some larger than those of the basic pattern.

The use of the patterns with cyclic shift of coils, which reduce the main wave, is justified, when it becomes necessary to reduce one or several electromotive force or magnetomotive force harmonics. However, it is generally assumed that the patterns with cyclic shift of coils have a smaller differential leakage than the basic pattern.

The aim of this paper is to show that this assumption is not correct and that the use of patterns with cyclic shift of coils, in order to reduce the differential leakage, cannot be justified.

Differential Leakage of Different Patterns

It has been shown in a previous paper[2] that the differential leakage of a 3-phase fractional-slot winding is given by the equation

$$X_d=\frac{4}{\pi^2}mf_1N_{ph}^2\frac{\tau l_e}{pgk_ck_s}10^{-7}\times C \text{ ohms per phase} \qquad (1)$$

where

$$C=\frac{\beta^2}{4}\sum_{\nu\neq\beta/2}\left(\frac{k_{d\nu n}'}{\nu}\right)^2 \qquad \nu=1,2,4,5,7\ldots \qquad (2)$$

when β is an even number, and

$$C=\beta^2\sum_{\neq\beta}\left(\frac{k_{d\nu n}'}{\nu}\right)^2 \qquad \nu=1,5,7,11\ldots \qquad (3)$$

when β is an odd number.

The cyclic shift of coils does not introduce new harmonics nor does it change the pitch factors of the winding. It changes only the distribution factors $k_{d\nu}'$.

Therefore, for a comparison of the differential leakage of the different patterns, it is sufficient to compare their magnitudes of C.

A method of calculating the distribution factors for the basic pattern and for the patterns with cyclic shift of coils is given in Appendix 1. Here the results will be given for three 3-phase windings with $2^3/_8$, $1^{11}/_{13}$, and $2^6/_{11}$ slots per pole per phase.

Winding with $q = 2^3/_8$. The coil grouping of phase A for the basic layout is, in 8 poles:

3 2 2 2 2 2 3 3

The calculations were made for the basic layout and for three cyclic shifts of coils which yield the following coil grouping for phase A in 8 poles:

3 2 2 3 2 2 2 3 cyclic shift 1
3 2 3 2 2 2 3 2 cyclic shift 2
3 2 2 2 2 3 2 3 cyclic shift 3

The distribution factors of the harmonics $k_{d\nu}'$, up to the slot harmonics of first order, are given in Table I. It can be seen from this table that all cyclic shifts of coils increase the distribution factors of the subharmonics while some of the distribution factors of the har-

Table I. Distribution Factors of a 3-phase Winding with $q=2^3/_8$ for Different Layout-Patterns

ν	Basic Layout	Cyclic Shift 1	Cyclic Shift 2	Cyclic Shift 3	ν	Basic Layout	Cyclic Shift 1	Cyclic Shift 2	Cyclic Shift 3
1	0.0284	0.0773	0.0727	0.0585	32	0.0269	0.0500	0.0813	0.0970
2	0.0366	0.0868	0.0301	0.0410	34	0.0308	0.0743	0.0544	0.1145
4	0.9560	0.9480	0.9530	0.9250	35	0.0444	0.0742	0.0239	0.0383
5	0.0740	0.0234	0.3760	0.0417	37	0.1916	0.1320	0.1625	0.1260
7	0.0290	0.0776	0.6750	0.1002	38	0.0526	0.0460	0.0003	0.0554
8	0.0260	0.0142	0.0767	0.0316	40	0.0274	0.0637	0.0702	0.0992
10	0.0348	0.0728	0.0455	0.0478	41	0.0264	0.0334	0.0817	0.0577
11	0.0582	0.0391	0.0095	0.0537	43	0.0414	0.0676	0.0235	0.0264
13	0.0882	0.0372	0.0600	0.0317	44	0.0882	0.0372	0.0600	0.0317
14	0.0414	0.0676	0.0235	0.0264	46	0.0582	0.0391	0.0095	0.0537
16	0.0264	0.0334	0.0817	0.0577	47	0.0348	0.0728	0.0445	0.0478
17	0.0274	0.0637	0.0702	0.0992	49	0.0264	0.0142	0.0767	0.0316
19	0.0526	0.0460	0.0003	0.0554	50	0.0290	0.0776	0.0675	0.1002
20	0.1916	0.1320	0.1625	0.1260	52	0.0740	0.0234	0.0376	0.0417
22	0.0444	0.0742	0.0239	0.0383	53	0.9560	0.9480	0.9530	0.9250
23	0.0308	0.0743	0.0544	0.1145	55	0.0366	0.0868	0.0301	0.0410
25	0.0269	0.0500	0.0813	0.0970	56	0.0284	0.0773	0.0727	0.0858
26	0.0320	0.1395	0.1050	0.1890	58	0.0284	0.0773	0.0727	0.0858
28	0.1370	0.0918	0.1140	0.0602	59	0.0366	0.0868	0.0301	0.0410
29	0.1370	0.0918	0.1140	0.0602	61	0.9560	0.9480	0.9530	0.9250
31	0.0320	0.1395	0.1050	0.1890					

Paper 49-235, recommended by the AIEE Rotating Machinery Committee and approved by the AIEE Technical Program Committee for presentation at the AIEE Fall General Meeting, Cincinnati, Ohio, October 17–21, 1949. Manuscript submitted November 8, 1948; made available for printing September 1, 1949.

M. M. Liwschitz is a professor with the Polytechnic Institute of Brooklyn, Brooklyn, N. Y., and also is connected with the Westinghouse Electric Corporation, East Pittsburgh, Pa., as consulting engineer.

The author gratefully acknowledges the assistance in calculating Tables I to IV by Mr. I. A. S. Bokhari, which were a part of his Master Thesis, worked out under the guidance of the author.

Table II. Quantity $C=16\sum_{\nu\neq 4}\left(\frac{k_{dp\nu}'}{\nu}\right)^2$ of a 3-phase Winding with $q=2^3/_4$ for Different Layout-Patterns

W/τ	Basic Layout	Cyclic Shift 1	Cyclic Shift 2	Cyclic Shift 3
Without Subharmonics				
0.983	0.0218	0.0176	0.0182	0.0176
0.842	0.0186	0.0165	0.0170	0.0176
0.701	0.0175	0.0155	0.0172	0.0172
With Subharmonics				
0.983	0.0263	0.0458	0.0320	0.0286
0.842	0.0224	0.0374	0.0278	0.0259
0.701	0.0199	0.0307	0.0244	0.0241

List of Symbols

A_n' = magnitude of the electromotive force or magnetomotive force of a phase part
d = difference between two adjacent vectors of the slot star
D = distance between the axes of the phase parts
f_1 = line frequency
g = air gap
k_c = Carter factor
k_s = saturation factor
k_{dn}' = distribution factor of the n'th harmonic
k_{dpn}' = distribution times pitch factor of the n'th harmonic
l_e = effective core length
m = number of phases
n' = order of the harmonic with respect to a fundamental, the wave length of which is equal to $2p\tau$
N_{ph} = number of turns per phase
N = numerator of the fraction which fixes the number of slots per pole per phase = number of slots per phase in β poles
N' = number of slots in a phase part
p = number of pole pairs
P = smallest integer which makes d an integer
q = number of slots per pole per phase
W = coil width measured in units of τ
x_d = differential leakage
α_m = angle between two vectors of the slot star for the main wave
α_n' = angle between two vectors of the slot star for the n'th harmonic
β = denominator of the fraction which fixes the number of slots per pole per phase = number of poles in a repeatable winding part
θ_n' = angle between the axes of the phase parts for the n'th harmonic

monics of higher order than the main wave are smaller, and others larger than those of the basic layout.

Table II shows the quantity

$$C=16\sum_{\nu\neq 4}\left(\frac{k_{dp\nu}'}{\nu}\right)^2$$

that is, the relative differential leakage, for the four different layout patterns at three different coil pitches W/τ. It can be seen from this table that, with the subharmonics neglected, the differential leakage of the patterns with cyclic shift of coils is somewhat smaller than that of the basic layout and that, with the subharmonics taken into account, the differential leakage of the patterns with cyclic shift of coils is larger than that of the basic layout. It is true that the harmonics of low order and especially the subharmonics, are more damped by a squirrel-cage rotor or by eddy currents than the harmonics of higher order. However, very little gain, if any, with respect to the differential leakage can be expected from the cyclic shift of coils for the winding considered.

Table III shows the quantity C for a 3-phase winding with $q = 1^{11}/_{13}$ at three values of W/τ. The first column refers to the basic layout, the second column to a pattern with a cyclic shift. The coil grouping of phase A is in 13 poles:

2 2 1 2 1 2 2 2 2 2 2 2 2

for the basic layout and:

2 2 1 2 2 2 2 2 1 2 2 2 2

for the pattern with cyclic shift. For this winding, the differential leakage of the pattern with cyclic shift is larger than that of the basic layout even when the subharmonics are neglected.

Table IV shows the relative differential leakage C for a 3-phase winding with $q = 2^5/_{11}$ at three different values of W/τ. The first column refers to the basic layout, the second column to a pattern with a cyclic shift. The coil grouping of phase A in 11 poles is:

3 2 3 2 2 3 2 2 3 2 3

for the basic layout and

2 3 2 3 2 3 2 3 2 3 2

for the pattern with cyclic shift. It can also be seen from this table that no reduction of the differential leakage is to be expected from the pattern with cyclic shift of coils.

Appendix I. Determination of the Distribution Factors for the Basic Pattern and for the Patterns with Cyclic Shift of Coils

Basic pattern. In this case the N slots which belong to each phase in β poles lie in the slot star together and the distribution factor of the n'th harmonic is[3]

$$k_{dn'}=\frac{\sin N(\alpha_{n'}/2)}{N\sin(\alpha_{n'}/2)} \tag{4}$$

The vectors of the slot star follow the series 1, 1+d, 1+2d, 1+3d..., where

$$d=\frac{mNP+1}{\beta} \tag{5}$$

and P is the smallest integer which makes d an integer. With the quantities d and P and

$$\alpha_m=\frac{180°}{mN} \tag{6}$$

$$\alpha_{n'}=n'd\alpha_m\frac{\beta}{p}\text{ when } P \text{ is an even number}$$

$$\alpha_{n'}=n'd\alpha_m\frac{\beta}{p}+180°\text{ when } P \text{ is odd and } \beta \text{ is even}$$

$$\alpha_{n'}=n'(d\alpha_m+180°)\frac{\beta}{p}\text{ when } P \text{ is odd and } \beta \text{ is odd} \tag{7}$$

Patterns with cyclic shift of coils. In this case the N slots which belong to each phase in β poles do not lie together in the slot star but are divided into several parts. If the number of slots of a part is denoted by N', then the distribution factor of that part is

$$k_{dn'}=\frac{\sin N'(\alpha_{n'}/2)}{N'\sin(\alpha_{n'}/2)} \tag{8}$$

Assuming that the magnitude of the electromotive force or magnetomotive force of one coil side is equal to 1, the magnitude of the electromotive force or magnetomotive force of that part is

$$A_{n'}=\frac{\sin N'(\alpha_{n'}/2)}{\sin(\alpha_{n'}/2)} \tag{9}$$

If D is the distance between the axes of the parts, measured in angles α_n', then the angle between the vectors A_n' is

$$\theta_n'=D\times\alpha_n' \tag{10}$$

The resultant vector of the whole phase is

$$A_n'\text{res}=\sqrt{\Sigma(A_n'\cos\theta_n')^2+\Sigma(A_n'\sin\theta_n')^2} \tag{11}$$

and the resultant distribution factor of the phase

$$k_{dn'}=\frac{A_n'\text{res}}{\Sigma N'} \tag{12}$$

This procedure will be demonstrated on

Table III. Quantity $C=169\sum_{\nu\neq 13}\left(\frac{k_{dp\nu}'}{\nu}\right)^2$ of a 3-phase Winding with $q=1^{11}/_{13}$ for Different Layout-Patterns

W/τ	Basic Layout	Pattern with Cyclic Shift
0.903	0.0270	0.0285
0.723	0.0244	0.0285
0.542	0.0186	0.0265
0.903	0.0462	0.0492
0.723	0.0372	0.0424
0.542	0.0259	0.0340

the 3-phase winding with $q=2^3/_8$, considered previously. For this winding, $N=19$, $\beta=8$, and $d=50$ with $P=7$. The d-series yields for the basic pattern, the following slots for the three phases in a repeatable group (8 poles):

																			Phase
1	51	44	37	30	23	16	9	2	52	45	38	31	24	17	10	3	53	46	A
39	32	25	18	11	4	54	47	40	33	26	19	12	5	55	48	41	34	27	C
20	13	6	56	49	42	35	28	21	14	7	57	50	43	36	29	22	15	8	B

If a cyclic shift is made in such a manner that slot 15 of phase B is assigned to phase A, slot 53 of phase A is assigned to phase C, and slot 34 of phase C is assigned to phase B, then phase A consists of 3 parts

$N_0'=17$ (slots 1 to 3), $N_1'=1$ (slot 46)
$N_2'=1$ (slot 15)

The axis of the first part lies over slot 2. Taking this axis as reference and considering the angles in clockwise direction as being positive, the distance D_1 for slot 46 is equal to $+10$. The distance of slot 15 from the axis through slot 2 is $+47$ or -10. The smaller distance is to be chosen, because the larger distance will yield a smaller main wave, that is, coil 15 must be connected in a proper manner with the other coils of phase A. Thus, $D_2=-10$.

References

1. Doubly Chorded or Doubly Shifted Fractional-Slot Lap and Wave Windings, M. M. Liwschitz. *AIEE Transactions*, volume 67, 1948, pages 684–86.

2. Differential Leakage of a Fractional-Slot Winding. M. M. Liwschitz. *AIEE Transactions* volume 65, 1946, pages 314–20.

3. Distribution Factors and Pitch Factors of the Harmonics of a Fractional-Slot Winding, M. M. Liwschitz. *AIEE Transactions*, volume 62, 1943, pages 664–66.

Table IV. Quantity $C=121\sum_{\nu\neq 11}\left(\frac{k_{d\nu}'}{\nu}\right)^2$ of a 3-phase Winding with $q=2^4/_{11}$ for Different Layout-Patterns

W/τ	Basic Layout	Pattern with Cyclic Shift
0.950	0.0176	0.0158
0.815	0.0155	0.0155
0.679	0.0158	0.0152
0.950	0.0214	0.0502
0.815	0.0184	0.0416
0.679	0.0179	0.0332

Discussion

P. L. Alger (General Electric Company, Schenectady, N. Y.): Dr. Liwschitz has added one more to the list of valuable papers he has contributed to the Institute. His present topic of the harmonic fields produced by irregular windings is one of peculiar fascination to the designer, but of little practical interest to the user. This is because every good designer makes sure that the harmonics of his machines are not large enough to be noticed by the customer.

However, speaking as one who has always been interested in design problems, I concur in Dr. Liwschitz' conclusions as now presented, and should like to add the following comments.

First, I know of no one who has stated a belief that the winding of maximum distribution factor is not the one of lowest reactance, as might be inferred from Dr. Liwschitz' statements. All the calculations of which I know have indicated that under the ideal assumptions made by Dr. Liwschitz the winding of minimum differential leakage reactance is the same as that for maximum distribution factor; but the conclusion has been reached because all of the examples studied have come out that way, rather than because of any satisfactory generalized proof.

Second, I question the accuracy of some of the harmonic field and reactance values given in the paper, for the reason that the method of summation of individual harmonics the author has employed is very difficult to check.

Gabriel Kron, in his very interesting book, Tensor Analysis of Networks,[1] has presented a method of calculation of these differential reactances that is entirely general, and, in my opinion, a good deal shorter than the method of summing all the individual harmonics, as presented by Dr. Liwschitz. In fact, the method of summing all the harmonic terms that he has used generally gives reactance values on the low side, because the series converges slowly, and one's patience is exhausted before he has calculated the terms out to a high enough order of harmonics. For example, the value of 3-phase differential leakage for the basic pattern of the $2^3/_8$ slot winding with 0.842 pitch calculated by Kron's exact method is 0.0267, instead of the 0.0224 value given by Dr. Liwschitz. Also, the fundamental distribution factor for this grouping is 0.95504, instead of 0.9560.

The actual reactance that will be observed in a particular machine departs from the ideal in two respects. First, the presence of slot openings, or of a large air gap, markedly reduces the higher harmonics as compared with the fundamental as shown in a recent Institute paper by H. R. West and me entitled The Air Gap Reactance of Polyphase Machines.[2] In the second place, the squirrel cage or other secondary winding of the machine has an admittance that is different for each harmonic field, and which is highly selective in the case of a few of the harmonics. For these reasons, the lowest reactance in practice may not coincide with the winding for maximum distribution factor.

The designer's wish to minimize noise and vibration leads him to prefer a winding arrangement that will minimize the fields with numbers of poles close to the fundamental. For example, in the case of the $2^3/_8$ slot per pole per phase winding considered by Dr. Liwschitz, the winding that gives minimum vibration has a coil grouping in phase A of

3 2 3 2 2 3 2 2.

This particular case is the only one of the five possible groupings of this winding that was omitted by Dr. Liwschitz from his analysis. For the least noise winding, the differential leakage is 0.0883, and the fundamental distribution factor is 0.9320. On the other hand, the worst grouping of this winding, from the point of view of vibration, is the cyclic shift 2, since Table I of the paper indicates that for this grouping the $\gamma=5$ field has a distribution factor of 0.376. In practice, this field, combined with the fundamental $\gamma=4$ field would give severe vibration.

Calculations made by my associates using the Kron method, for the case of a $2^4/_7$ slot per pole per phase winding, give differential leakage reactances of 0.0215, 0.0336, 0.0407, and 0.0675, for the four possible distributions of phase A, all for 0.907 pitch.

3 3 2 2 3 3 2,
3 3 2 2 2 3 3,
3 2 2 3 2 3 3, and
3 3 2 3 2 3 2.

The first of these has the best distribution factor and also the lowest ideal differential leakage. The last one has the lowest vibration but also the highest reactance. However, in many other cases, the lowest vibration winding has one of the lowest reactances as well.

REFERENCES

1. Tensor Analysis of Networks (book), Gabriel Kron. John Wiley and Sons, New York, N. Y., chapter 12, 1939.

2. The Air Gap Reactance of Polyphase Machines, P. L. Alger, H. R. West. *AIEE Transactions*, volume 66, 1947, pages 1331–43.

J. S. Gault (University of Michigan, Ann Arbor, Mich.): In paragraph 3, column 3, of page 1129 of the paper, the three shift patterns are apparently chosen quite at random. The only one explained in detail is shift 2, which is obtained by substituting coil 15 for coil 53 in phase A, and so forth. Since this presents the simplest shift pattern, 1-17-1, and also since the value of K_{d4} is least affected, it would seem as though this should be called shift 1. In Table I of the paper, the value of K_{d2} for shift 2 is given as 0.0301. I computed 0.0388, which also would be the value for K_{d16} and K_{d18}.

Shift 1 is apparently obtained by substituting coil 25 for coil 44 in phase A, and so forth. This gives a pattern, 2-16--1. I tried to check his value for K_{d4}, but computed 0.0839 instead of the value 0.0868 given.

Shift 3 might be obtained by substituting coils 25, 4, and 39 for coils 44, 23, and 1 respectively or by substituting 29, 36, 50, 8 and 15 for 10, 17, 31, 46 and 53 respectively. Either gives a shift pattern, 1-2-14-1--1. For this I computed $K_{d4}=0.944$, instead of the value 0.925 given in the paper, but checked his figure of 0.041 for K_{d2}.

The author is to be commended for his brevity and the tabular display of data to prove his point. The sampling of six values in Table I, however, indicates that 50 per cent of the values given may only be correct to the first significant figure.

M. M. Liwschitz: I wish to thank Mr. Alger, who has done fundamental work on the differential leakage of electric machines, for his comments on my paper, and I was glad to learn that he concurs in my conclusions with respect to the differential leakage of the fractional-slot windings. However, I do not agree with some of his statements.

Mr. Alger mentions that all the calculations of which he knows "have indicated that under the ideal assumptions made by Dr. Liwschitz the winding of minimum differential leakage reactance is the same as that for maximum distribution factor." I have not seen any published calculations of differential leakage of fractional-slot windings except my own paper, Differential Leakage of a Fractional-Slot Winding,[1] in which the influence of the slot-openings as well as of the damping by a squirrel-cage rotor is considered. The paper by Mr. Alger and Mr. H. R. West, The Air Gap Reactance of Polyphase Windings,[2] does not treat the fractional-slot windings.

Mr. Alger questions the accuracy of some of my results "for the reason that the method of summation of individual harmonics the author has employed is very difficult to check. . . the series converges slowly and one's patience is exhausted before he has calculated the terms out to a high enough order of harmonics." Mr. Alger has overlooked equations 22 and 23 of my paper mentioned above. They give a simple formula for the sum of all slot harmonics so that only the harmonics of low order have to be considered individually. The consideration of the individual harmonics is necessary if the damping by a squirrel-cage rotor is to be considered. Mr. Alger did not try to do this in his paper mentioned above, otherwise he would be forced to consider the harmonics individually and not in lumps.

Mr. Alger apparently had in mind only the 120-cycle noise due to stator harmonics. It is different when one considers the noise produced by stator and rotor harmonics together, which is usually much more disturbing than the 120-cycle noise. There it may become necessary to reduce one specific stator harmonic, which yields an inadequate number of force pole-pairs, and a coil grouping which reduces to a certain degree several stator harmonics may not be satisfactory.

The coil grouping depends upon the individual case and there exists no coil grouping which is the best for all cases.

Mr. Gault has overlooked the practical aspect of the paper. The shift patterns chosen are not at random. They are all of the same importance, one pattern being the right one for one machine, the other pattern being the right one for another machine. The practical engineer reduces the distribution factor of the main wave, if it is necessary to avoid noise, and thus it depends upon the individual case to decide which pattern should be called the best and given the first place.

Mr. Gault overlooks further the fact that it is not the first or second or third significant figure which counts here but the decimal place of the significant figure. A harmonic, the first significant figure of which starts in the third decimal place, is of no importance no matter how large the significant figure is. The values of all tables of the paper have been calculated using the slide-rule because no greater accuracy is necessary for the practical engineer. It is impossible that two engineers using the slide-rule will get exactly the same results in complicated calculations of the kind made for the tables. I am not sure whether Mr. Gault or the graduate student mentioned in my paper has made errors in the third decimal place and in one case even in the second decimal place. It is not worthwhile to check this because it has no practical value. Table I contains about 160 figures. Mr. Gault made calculations for five of them. Overlooking the important fact that not the significant figures but the decimal places are of importance, he states that "50 per cent of the values given may only be correct to the first significant figure." A reader who is not familiar with the problem of harmonics may get the wrong impression that the paper is incorrect. Mr. Gault neither acknowledges the fact that his calculations are based on formulas derived for the first time in my paper nor does he comment on the substance of the paper.

References

1. See reference 2 of the paper.
2. The Air Gap Reactance of Polyphase Machines, P. L. Alger, H. R. West. *AIEE Transactions*, volume 66, 1947, pages 1331–43.

Motor Tests Evaluate Thermal Endurance of Class-H Insulation and Silicone Varnish

GEORGE GRANT, III
MEMBER AIEE

T. A. KAUPPI
ASSOCIATE AIEE

GRAHAM LEE MOSES
MEMBER AIEE

G. P. GIBSON
MEMBER AIEE

The thermal endurance of silicone resins was first evaluated by laboratory tests. Subsequently, accelerated tests were made on insulation specimens and then a few isolated machines were tested.[1,2] It was recognized, however, that a comprehensive test program involving a number of machines operated at various temperatures would have to be completed before the life expectancy of this new class of insulation could be evaluated properly. In October 1943, Dow Corning Corporation set up a motor testing laboratory at Midland, Mich., where such a program was carried out in co-operation with the Westinghouse Electric Corporation. Progress reports have been made on part of the results.[3,4] This program is now complete enough to be summarized and reported as a completed project. It is believed that the results will prove of interest and value in the further application of class-H insulation.

Objectives

The motor test program was planned originally to determine the thermal endurance of silicone-insulated motors at several different temperatures. The objective was to obtain a scattering of thermal life end points over a sufficiently wide temperature range to permit extrapolation of life expectancy to lower temperatures. It was further desired to obtain a comparison between the behavior of class-B insulation and class-H insulation under the same test conditions. A further purpose was to attempt some correlation between laboratory tests on insulation components and the behavior of the components in motors.

The fundamental concept followed in this test program is that appreciable decrease in the insulation resistance of the windings after exposure to excessive humidity is a criterion of minimum insulation life. Ultimate or maximum life is taken to be the point at which the insulation deteriorates mechanically to such an extent that the motor fails to operate.

Apparatus Tested

The results reported in this paper include the original six induction motors with class-H insulation treated with *DC 993* silicone varnish, and two class-B induction motors of similar design. One traction motor with class-H insulation treated with *DC 993* silicone varnish also is included. All of the induction motors were wound on standard *284* frames and rated at 10 horsepower. A complete description of the motors tested is given in Appendix I.

Test Procedure

The test cycle started with a period of operation at the test temperature followed by cooling to room temperature and exposure of the windings to 100 per cent relative humidity for a 24-hour period. The period of running was determined by dividing the estimated life by 25 so that each motor would experience approximately the same number of cycles before failure. The precise test procedure is given in Appendix II.

Results

Typical data on three units have been plotted in Figures 1 through 8. Figures 1 through 6 show how aging alters the insulation resistance and dissipation factor as determined just before humidification, and after humidification. Per cent change in the winding resistance (at 25 degrees centigrade) as a function of aging also is shown on these graphs. Capacitance was not plotted since it showed no significant change as a result of aging.

In general the same pattern is obtained on each unit. The humidified insulation resistance and dissipation factor show little change for a period. Then suddenly insulation resistance decreases and dissipation factor increases indicating a major change in the condition of the insulation. This is the point at which moisture begins to penetrate the winding. It is considered to be a minimum life point. Coincident with the loss of moisture resistance, fine crazing of the resin became very noticeable.

Insulation resistance and dissipation factor are not affected by ambient conditions until the minimum life point has been reached. Thereafter, they become dependent on ambient conditions. This interdependence is indicated by data given in Figures 7 and 8. The insulation resistance cooling curves in Figure 7 show an increase in moisture absorption after aging at high temperature. Line A, taken before minimum life was reached, shows no moisture pickup on cooling. However, both B and C which were taken

---

Paper 49-237, recommended by the AIEE Rotating Machinery Committee and approved by the AIEE Technical Program Committee for presentation at the AIEE Fall General Meeting, Cincinnati, Ohio, October 17-21, 1949. Manuscript submitted March 10, 1949; made available for printing September 1, 1949.

George Grant, III, is an electrical engineer and T. A. Kauppi is Manager, Product Engineering, both with the Dow Corning Corporation, Midland, Mich. Graham Lee Moses is Manager, Development Insulation Section, Westinghouse Electric Corporation, East Pittsburgh, Pa., and G. P. Gibson is design engineer with Westinghouse Electric Corporation at Buffalo, N. Y.

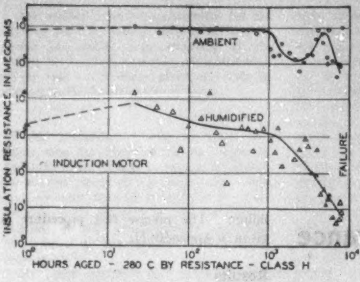

Figure 1 (left). Effect of aging at 280 degrees centigrade and periodic humidification on insulation resistance of class-H induction motor winding

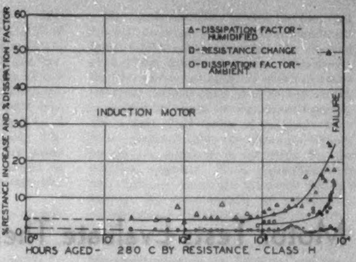

Figure 2 (above). Changes in dissipation factor of insulation and cold resistance of the winding as a function of hours aging at 280 degrees centigrade on class-H induction motor

after minimum life, show definite moisture pickup. Line B with less aging than C, shows much more pickup due to the greater humidity. The curves in Figure 8 show that a new unit is relatively unaffected by ambient humidity while a unit that has passed the minimum life point could almost be used as an indicator of humidity.

Insulation resistance readings on a motor under ambient conditions, therefore, gives no positive indication of the condition of the insulation unless ambient conditions are known. Under low humidity conditions, insulation resistance readings will be high regardless of the extent to which the windings have been aged. Under high humidity conditions, however, high-insulation resistance indicates that the minimum life point has not been reached.

Figure 2 also shows the change in cold winding resistance as a result of aging. Very little change is noted until the minimum life point has been reached. The cold copper resistance then tends to increase at an accelerating rate due to oxidation of the conductors.

This trend occurred in each of the four silicone units which have failed so far. Failure occurred during the heat run and was caused by the fusing of the conductors. This fusion was the result of localized reduction in the cross-sectional area of the wires due to oxidation of the copper. Oxidation started to take place when crazing of the insulation at minimum life permitted air to penetrate the voids to the hot copper. Thus, localized oxidation took place resulting in a local increase in resistance of sufficient magnitude to be reflected by an increase in cold winding resistance. With the load current flowing, the heating and consequently the temperature in these high-resistance spots increased. This increase in temperature accelerated the rate of oxidation and the rate of increase in resistance. This cumulative condition progressed until fusing of the conductor took place.

At the time of failure no fire was encountered on these four units. The windings were firm though the resin was brittle. Failure of the class-B units took place during the 5-minute no-load run after humidification. Failures were due to short circuits within the winding caused by moisture penetration. Both units caught fire. The windings were very loose at the failure point and there was little visible resin left on the winding.

Had much vibration been present, the class-B units probably would have failed much sooner because of the lack of resin bonding of the windings. However, since the silicone windings were still firmly bonded, they probably would not have failed much sooner under vibration conditions.

Discussion

As background for this discussion, the points at which minimum life and failure took place are listed in Table I. Except for two of the units for which the test procedure was altered, the number of cycles required to reach minimum life and to reach failure are very nearly the same from unit to unit. This indicates good reproducibility of results.

It is agreed generally that the thermal life of insulation is reduced by one-half for each increase of 8 to 12 degrees centigrade in temperature. Thus, if life is plotted logarithmically and temperature linearly, a straight line results. The minimum life points of the silicone units are so plotted in Figure 9. The two lowest points through which a straight line can be drawn are 950 hours at 280 degrees centigrade and 9,750 hours at 240 degrees centigrade. These points were taken to determine the slope of the life line. The line through these points is taken to be the minimum time to be expected to reach minimum life. It shows a rule of half life for increments of 11.6 degrees centigrade which, for practical purposes, may be considered to be 12 degrees centigrade. Similarly, a line parallel to this was drawn through the point (1,000 hours at 300 degrees centigrade) that produced the greatest spread. This line represents the maximum time to be expected to reach minimum life. These two lines represent the probable spread in minimum life.

After minimum life has been reached, failure would be determined largely by external factors and might be expected anywhere up to the points found in this testing. It is believed that there is little

Table I. Summary of Motor Test Results

Motor Number	Insulation Class	Temperature Degree Centigrade by Resistance	Minimum Life Hours	Minimum Life Cycles	Time to Breakdown Hours	Time to Breakdown Cycles	Type Motor	Figure Number
1	H	310	500	25	5,131	47	Induction	
2	H	300	1,000	8	5,179	45	Induction	
3	H	300	500	22	6,888	50	Induction	
4	H	285	800	26	1,610*	42*	Traction	5, 6
5	H	280	950	17	8,548	41	Induction	1, 2
6	H	240	10,750	28	13,950*	35*	Induction	
7	H	240	9,750	26	13,450*	34*	Induction	
8	B	275	20	9	1,056	33	Induction	3, 4
9	B	200	200	16	3,760	40	Induction	

* These motors were still operating in January 1949.

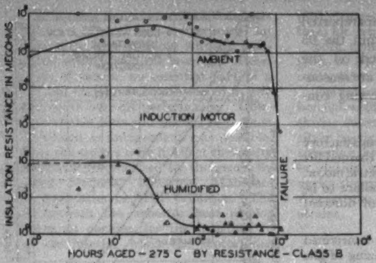

Figure 3 (left). Effect of aging at 275 degrees centigrade and periodic humidification on insulation resistance of class-B induction motor winding

chance that units built like these will run much beyond the failure points in this testing. The actual failure points and the originally estimated life line for *DC 990A* also are plotted for reference.

Tinned or cadmium-plated wire probably would reduce or eliminate the oxidation of the copper conductors and increase the time to failure. However, chemical action, severe vibration, moisture, or other factors encountered by many motors in service, probably would cause failure to take place within the limits of minimum life and the plotted failure points.

At the beginning of the testing of the second and eighth units listed in Table 1, longer heat runs than those called for by dividing the estimated life by 25, were used. Hence, more aging was obtained during each cycle and fewer cycles were required to reach minimum life. Further, the relative minimum life of the second unit was double the average of the other silicone motors and determined the line for maximum time to minimum life as plotted in Figure 9. It therefore appears that the number of times a motor is cooled is a factor in these tests. More frequent cooling produces shorter minimum life because the thermal expansion differences which tend to damage the insulation are encountered more often.

Another minimum life line based on the method suggested by Dakin[8] was drawn in Figure 9. According to this theory the insulation life as a function of temperature can be considered as a first order chemical reaction. The logarithm of the life then is a function of the inverse absolute temperature. In the zone of temperatures used in this testing, little difference between the two life lines is noticeable. Outside this zone some divergence is noted and life as predicted by the inverse absolute temperature is always greater than that obtained by extrapolation based on the 12-degree centigrade rule. For general purposes the 11.6- or 12-degree centigrade rule should prove satisfactory and Dakin's method simply offers greater assurance in selecting safe operating temperatures.

The hottest-spot temperatures as measured by thermocouples were found to be not more than 10 degrees centigrade above the temperatures measured by resistance. Hence, 10 degrees centigrade were added to the temperature shown in Figure 9 and the resulting minimum life lines were plotted in Figure 10. Also plotted in Figure 10 are the minimum life points found on the class-B units and minimum life data on classes A and B as presented by other investigators.[6,7] It will be noted that all of the class-A and -B data are closely grouped and in a much lower temperature zone. A life of seven years (61,300 hours) has been used to represent a typical life for these classes of insulation at their respective permissible temperatures.[8] According to the 12-degree centigrade line for class H, a life of approximately ten times this could be expected at the 180-degree-centigrade hottest-spot temperature now set for class H. For a 7-year life, a temperature of 220 degrees centigrade should be permissible. Comparing the class-H line with the top class-B line at 180 degrees centigrade, it will be seen that class H should have 430 times the life of class B.

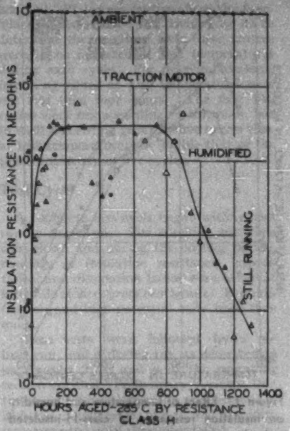

Figure 5. Dry and humidified insulation resistance data for class-H-insulated traction motor as a function of hours aged at 285 degrees centigrade

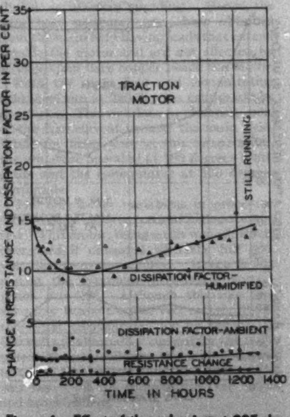

Figure 6. Effect of thermal aging at 285 degrees centigrade on dissipation factor and cold resistance of the winding of class-H-insulated traction motor

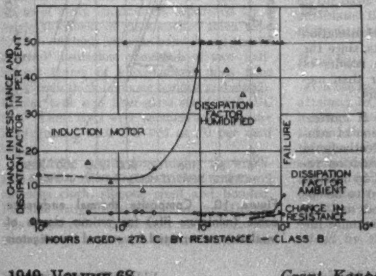

Figure 4 (left). Changes in dissipation factor of insulation and cold resistance of the winding as a function of hours aging at 275 degrees centigrade on class-B induction motor

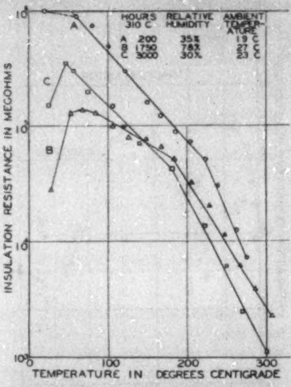

Figure 7. Effect of temperature and humidity on insulation resistance of class-H-insulated induction motor at various degrees of aging at 310 degrees centigrade

Conclusions

The conclusions reached concern thermal aging and moisture resistance of insulations. Therefore, other design considerations are disregarded in these conclusions.

A number of motors were tested at different temperatures, but there were not a sufficient number at any one test condition to permit statistical analysis of the results. However, the points reported can be considered to fall within the 95 per cent failure zone. Based on the knowledge that the test points are reasonable approximations, the following conclusions were reached:

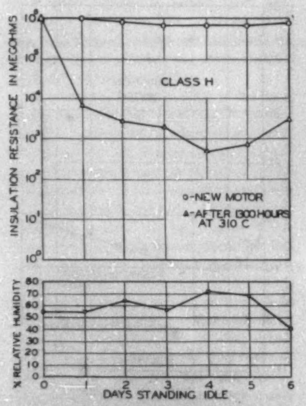

Figure 8. Change in insulation resistance of a class-H-insulated induction motor while standing idle-new and after aging 1,300 hours at 310 degrees centigrade

1. This method of testing is a satisfactory way to determine the minimum thermal life expectancy of insulation in an electric motor. It also determines the type of failure to be expected from thermal aging of different kinds of insulation.

2. The minimum life points as determined by this method and serious crazing of the resin occur after the same amount of aging.

3. Failure of the windings of silicone insulated motors has been found to occur before the bonding of the resin is seriously weakened and was due to copper conductor failure.

4. Silicone insulation presents less fire hazard than do other classes of insulation as shown by these tests and other independent flammability tests.

5. When motors of this size operate at temperatures near 280 degrees centigrade, the number of times they are cooled will affect the minimum life. More frequent thermal cycling may reduce the minimum life.

6. The minimum thermal life of class-H-insulated equipment using *DC 993* varnish is approximately twice that of equipment made with *DC 990A* varnish.[4]

7. The results of these tests indicate about a 100-degree-centigrade temperature advantage for class-H insulation compared with class-B insulation. If current concepts of thermal aging are correct, the class-H insulation could be expected to operate as much as several hundred times as long as class-B equipment, where thermal aging is the primary factor in establishing insulation life.

8. At least seven years of continuous operation at a hottest-spot temperature of 220 degrees centigrade will be required to reach the minimum thermal life of class-H-insulated equipment.

9. The thermal life of class-H silicone insulated motors closely follows a 12-degree-centigrade rule. It is possible that the life of class-H-insulated equipment, employing *DC 993* silicone resin, may follow the more optimistic rule

$$\text{Log}_e\,(\text{hours life}) = \frac{16{,}520}{\text{Absolute Temperature}} - 23$$

10. The maximum life of class-H insulation was not determined by these tests, since the ultimate end points were the results of copper conductor failure rather than mechanical disintegration of the resin.

11. In silicone varnished class-H motors, insulation resistance as a function of relative humidity can be used effectively in maintenance work. If the insulation resistance is not seriously affected by humidity, the motor may be presumed to be entirely satisfactory for continued use. If dependent on humidity, the minimum life point has been reached.

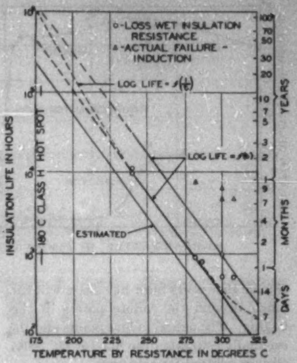

Figure 9. Thermal aging curve indicating the minimum life zone of class-H-insulated windings

Appendix I. Description of the Motors Tested

Induction Motors

The induction motors selected for test were rated at 10 horsepower, 60 cycles, 1,140 rpm, 440 volts. The frame (number *284*) was a totally-enclosed type and the end brackets were the wound-rotor type of open construction. Each bracket carried a 1-inch thick asbestos heat shield instead of the normal air shields. Matching heat shields were mounted on the shaft and rotated with it. With this and special bearing cooling construction a temperature of 450 degrees centigrade in the winding was required to

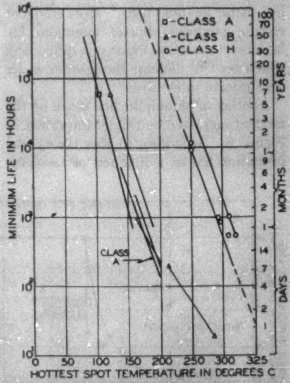

Figure 10. Composite thermal endurance curve (minimum life) for various classes of insulation as reported by several investigators

raise the bearing temperature to 100 degrees centigrade. Thus, high-temperature insulation tests were possible without complications arising from the bearings. Bearings are, of course, an essential part of a motor, and they must be considered in any prediction of over-all performance. However, insulation tests and bearing tests must be performed as independently as possible.

Thus, the motors were in effect thermally enclosed but not enclosed by the generally accepted National Electrical Manufacturers Association or AIEE definition. The space between the asbestos heat shields provided an opening for the moisture to leave the interior when the motor was dried.

The silicone class-H stators were wound with mush coils using double glass covered wire treated with silicone resin *DC 993*. A combination of glass cloth and mica 0.026-inch thick treated and bonded with *DC 993* resin was used for the slot cells and center wedges. Similar material 0.010-inch thick was used for phase insulation. Since suitable silicone materials were not available at the time these motors were built, an asbestos phenolic laminate served for the top wedges. Untreated glass tape was applied from iron to iron on the end turns. All connections were taped with a silicone bonded flexible glass and mica tape over which untreated glass tape was applied. After winding, the stators were prebaked then vacuum-and pressure-impregnated with *DC 993* silicone resin, followed by multiple dips in the resin. Each dip was followed by a bake at 250 degrees centigrade.

The class-B motors were identical to the silicone units in all details except that synthetic organic class-B varnishes were used in place of the silicone resin and appropriate baking temperatures were used.

Traction Motor

The railway motor was the same as those used on standardized PCC (President's Conference Car) streetcars (Westinghouse type *1432*). The general motor design was identical to the standard production models except that class-H silicone insulation was applied as follows:

Armature coil conductors were glass-covered wire treated with silicone varnish *DC 993*. Ground insulation consisted of $2^{1}/_{2}$ turns of glass-backed mica wrapper 0.008-inch thick. The glass cloth was silicone-varnish sized and a silicone bond was used. Binder tape was fiber-glass, sized with silicone varnish *DC 993*. The coils were impregnated with silicone varnish *DC 993*.

Main and commutating field coils were made of strap conductors, separated by a single thickness of glass-backed mica tape 0.007-inch thick (silicone bonded and sized). Ground insulation consisted of two half-lapped layers of glass-backed mica tape 0.007-inch thick (silicone bonded and sized). Binder tape was fiber-glass sized with *DC 993*. These coils were vacuum and pressure impregnated with *DC 993* at 70 per cent solids.

Insulation details for winding the armature were made of glass-backed mica and asbestos cloth, silicone sized and bonded. For slot wedges asbestos-melamine Micarta was employed. Coils were soldered in the commutator necks with high melting solder (304 degrees centigrade solidus temperature) for extra protection.

Both armature and stator were dipped twice in *DC 993* silicone varnish at 50 per cent solids.

The commutator was insulated with mica bonded with a high-temperature synthetic shellac substitute. The bars were made of silver-bearing hard-drawn copper to avoid softening during the high-temperature bake or during operation. During all baking cycles the commutator nut was loosened to relieve the vee binding from pressure strains.

Appendix II. Details of Test Procedure

Preliminary

1. A low-temperature standardizing run of 48 hours at 130 to 140 degrees centigrade was made to arrive at a dry condition. While cooling from this run, the insulation resistance, capacitance, and dissipation factor were taken at intervals of 20 degrees centigrade.

2. Upon reaching room temperature, the motor with the end bracket removed, was placed under humidification for a period of one week. Daily readings of insulation resistance, capacitance, and dissipation factor were made and a high-potential test of rated voltage 60 cycle was applied for five minutes between windings and frame.

3. Within five minutes after humidification the three quantities were again read and the high potential test again was applied. Within 15 minutes after humidification, the end bracket was replaced and the motor was run at full rated voltage, no load, for five minutes. Following this, insulation resistance, capacitance, and dissipation factor were measured and the standard high-potential test was repeated once more.

4. The motor was then put on a drying run in which the temperature rose to 100 degrees centigrade in the first $1^{1}/_{2}$ hours and to 130 to 140 degrees centigrade in six hours. This temperature was maintained for eight to twelve hours.

5. If the test temperature exceeded the baking temperature of 250 degrees centigrade, a break-in run was made. This consisted of taking the motor up to 250 degrees centigrade by overloading and then setting load so that the temperature increased at the rate of 10 degrees centigrade per hour till the test temperature was reached. The break-in time was evaluated on the basis of the 12-degree rule. This accumulated time was counted in on the time of the first heat run.

Heat Run

On the heat run, the test temperature was attained as quickly as possible by overloading. In the interests of test standardization, the duration of heat runs was determined from the estimated life. The estimated life was based on the premise that the life of silicone insulation *DC 990A* was 5,000 hours when operated at a temperature of 240 degrees centigrade. The estimated life at any other temperature was determined by the 12-degree rule using 5,000 hours at 240 degrees centigrade as the base. This calculated time was divided by 25 to determine the length of time these motors were to be operated at test temperatures during each cycle. For practical reasons, operating times at test temperature were not less then four hours. The first five cycles were run according to this plan, but in each succeeding group of five cycles time at test temperature was double that of the preceding group of five cycles.

Test Cycle

A complete test cycle began with a heat run as described. The machine was then shut down and during the cooling period, readings of insulation resistance, capacitance, and dissipation factor were taken at intervals of 20 degrees centigrade. Humidification and high-potential tests were then made.

These tests were followed by a no-load run, and a drying run as described in paragraphs 2, 3, and 4 in the preceding section entitled "Preliminary," except that the period of humidification was reduced to 24 hours. Such cycles of heat and humidity were repeated until the motor failed

Traction Motor-Test Procedure

The traction motor, being a d-c machine, required some slight variations in the general procedure outlined before. It was planned originally that the insulation resistance, capacitance, and dissipation factor of the main field, commutating field, and armature should all be studied. However, it was soon found, because of the noninsulated lead ends, brush rigging, commutator, and other unavoidable bare copper, that the severe humidification caused insulation resistance, capacitance, and dissipation factor values of the commutating field and armature to reach magnitudes that could not be measured with the equipment at hand.

The complexity of the circuits precluded satisfactory guarding. Hence, the data here presented are those obtained from the main field having leads that extend outside the motor and are not affected by leakage from bare copper inside the motor.

Both the main field and commutating field were run at 285 degrees centigrade by resistance. This was done by shunting some of the line current around the main field. While the fields were at this temperature, the armature operated at 180 degrees centigrade and the commutator at 150 degrees centigrade.

The only other variations in procedure were in the 5-minute run and high-potential test. This motor, being series wound, would overspeed if unloaded with the full 300-volt direct current applied. Hence it was run at the maximum permissible voltage which was 125. Although this was considerably below the 300-volt rating, it was somewhat compensated for by the use of 500 volts of alternating current for the high-potential tests. Before the high-potential test and the no-load run the excess water was blown off the commutator, vee rings, and brushholders.

Methods of Measurement

1. Temperature by resistance was calculated from the value of resistance ob-

tained by projecting to zero time the resistance curve of the windings while cooling.

2. Insulation resistance values are 1-minute readings obtained with a 500-volt d-c megohm bridge. They are corrected to a temperature of 25 degrees centigrade from temperature-insulation resistance data.

3. Capacitance values were measured between windings and frame by means of a 60-cycle low-voltage bridge. They are corrected to 25 degrees centigrade.

4. Dissipation factor of the insulation was evaluated on the capacitance bridge and was obtained concurrently with the capacitance.

References

1. Organo-Silicon Compounds for Insulating Electric Machines, T. A. Kauppi, G. L. Moses. *Electrical Engineering* (*AIEE Transactions*) volume 64, March 1945, pages 90–93.

2. The Application of Silicone Resins to Insulation for Electric Machinery, J. DeKiep, L. R. Hill, G. L. Moses. *Electrical Engineering* (*AIEE Transactions*) volume 64, March 1945, pages 94–98.

3. Silicone Insulation Proved by Test, T. A. Kauppi, George Grant, G. L. Moses, R. P. Horrell. *Westinghouse Engineer* (East Pittsburgh, Pa.) September 1945, pages 135–40.

4. Investigation of Silicone Insulation on High-Temperature Railway Motor, George Grant, III, T. A. Kauppi, Graham Lee Moses. *AIEE Transactions*, volume 66, 1947, pages 305–11.

5. Electrical Insulation Deterioration Treated as a Chemical Rate Phenomenon, Thomas W. Dakin. *AIEE Transactions*, volume 67, 1948, pages 113–22.

6. Synthetic Insulation and the 10-Degree Rule, G. L. Moses. *Westinghouse Engineer* (East Pittsburgh, Pa.) July 1945.

7. Temperature-Aging Tests on Class-A-Insulated Fractional-Horsepower Motor Stators, J. A. Scott, B. H. Thompson. *Electrical Engineering* (*AIEE Transactions*) volume 61, July 1942, pages 499–501.

8. Predicting Insulation Performance by Statistical Analysis, Graham Lee Moses. *Electrical Manufacturing* (New York, N. Y.) volume 43, April 1949, pages 108–12.

No Discussion

General Theory of Multiple Cage Induction Motors

SHELDON S. L. CHANG
ASSOCIATE AIEE

IN designing the rotor lamination of a multiple cage motor, a designer usually feels the double difficulties of too many variables and too many demands. The slots can be of any shape, any multiplicity, and the same lamination may be used for motors of different speed and horsepower to give, under all circumstances, the best possible performances which nobody knows. In this paper, an attempt is made to simplify this problem:

1. By deriving a quantitative relationship between torque at all values of slip and current at all values of slip with no restriction whatsoever on the rotor construction.
2. By defining a basic leakage factor $k_{r\infty}$ which is a quantitative measure of the "circumstance" which limits the performance of the motor in general.
3. By determining the combinations of full load slip, power factor, and starting kilovolt-amperes per horsepower which can be obtained without reduced accelerating torque for motors with a given value of $k_{r\infty}$.
4. By showing a design method which gives the slot areas and over-all slot constants, and the apparent rotor impedance at various slip frequencies for any selected possible combination of slip, power factor, and starting current.

The analysis is based upon three assumptions:

1. The saturation effect on the leakage reactance is negligible.
2. The stator resistance is negligible.
3. The iron loss does not have any appreciable effect on torque and current.

Of these three assumptions, the third is always true. The first assumption is common in most machinery analysis. The second assumption is justified by the following considerations:

1. In larger induction motors of 30 horsepower and above, the ratio of stator resistance to leakage reactance is usually so low that the stator resistance is smaller in magnitude compared to the change in leakage reactance due to saturation effect.
2. By neglecting these two effects, the possible performance derived in this paper fixes the upper limit for induction motors.
3. The combined effect of these two factors introduces an approximately constant voltage drop. This voltage drop can be corrected in actual motor design without much difficulty.

Derivation of General Equations Between Torque and Current

The conventional equivalent circuit of an induction motor is in stator terms. The frequency and voltage are always the line frequency and voltage. Both the primary and secondary reactances are assumed constant and the conductivity of rotor material is multiplied by the slip.

The equivalent circuit in rotor terms is just as true and easy to prove. In such an equivalent circuit, the line frequency and voltage are multiplied by the slip.

The inductances instead of the reactances are now constant. The conductivity of the rotor material is constant while that of the stator material is divided by s.

Under the assumption of negligible stator resistance, this equivalent circuit is exactly the same circuit of the motor under locked rotor condition while a voltage of variable frequency is applied to its terminals, since throughout the circuit, the inductances and conductivity are constant. With stator resistance neglected, an equivalence is established between a running motor at constant frequency and voltage and a locked motor tested under a test frequency and voltage in proportion to slip.

Suppose $Y = G - jB$ is the admittance per phase of the locked motor measured at angular frequency ω, where $\omega = \omega_1 \times s$, ω_1 is the line frequency. The phase current I of the motor running at a slip s is

$$I = sYV \tag{1}$$

The stator input watts per phase is

$$W = sV^2G \tag{2}$$

Under the assumed conditions, the total stator input is equal to the total secondary input which is the torque in synchronous watts.
Therefore

$$T = snV^2G \tag{3}$$

The total reactance volt amperes is

$$U = snV^2B \tag{4}$$

The performance of the motor, such as power factor, speed at different load, starting torque, starting current, and accelerating characteristic are completely described by T and U as functions of the slip. From equations 3 and 4, we see that T and U are not completely independent but they are the imaginary and real components of a single function F, namely

$$F = U + jT \tag{5}$$

From equations 3, 4, and 5

$$F = \frac{nV^2}{\omega_1} \times j\omega Y \tag{6}$$

F is called the performance function, because once F is known, the complete performance of the motor is known.

We have shown that the torque in synchronous watts and the total reactive volt amperes are respectively the imaginary and real components of a complex function F. This function F is a constant times $j\omega$ times an admittance function Y of a stationary electric circuit, since a

---

Paper 49-238, recommended by the AIEE Rotating Machinery Committee and approved by the AIEE Technical Program Committee for presentation at the AIEE Fall General Meeting, Cincinnati, Ohio, October 17–21, 1949. Manuscript submitted March 23, 1949; made available for printing September 2, 1949.

SHELDON S. L. CHANG is with Robbins and Myers, Inc., Springfield, Ohio.

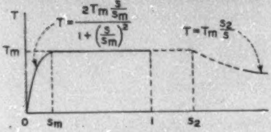

Figure 1. The speed torque curve of a constant torque motor

motor with rotor locked is not different in anyway from an ordinary electric circuit. Network theorems show that the real and imaginary components of F do not vary with frequency independently, and that they are tied together by the following equations[1]

$$\int_{-\infty}^{\infty} T du = \frac{\pi}{2}(U_\infty - U_0) \tag{7}$$

$$U_c - U_0 = -\frac{2\omega_c^2}{\pi}\int_0^\infty \frac{\frac{T}{\omega} - \frac{T_c}{\omega_c}}{\omega^2-\omega_c^2}d\omega \tag{8}$$

$$T_c = \frac{2\omega_c}{\pi}\int_0^\infty \frac{U-U_c}{\omega^2-\omega_c^2}d\omega \tag{9}$$

In equations 7 through 9, $U=\ln s$, U_c and T_c are values of U and T at a slip frequency ω_c, U_0, and U_∞ are the total reactive voltamperes at $s=0$ and $s=\infty$ respectively.

Equation 7 states that the total torque area is equal to $\pi/2$ times the difference between the reactive volt amperes at infinite slip frequency and zero slip frequency. Once these two values are fixed, any variation in the shape and conductivity of rotor cages shifts the location of torque on the speed axis but does not change the total torque area. At $s=0$

$$U_0 = n\frac{V^2}{X_0} \tag{10}$$

where X_0 is the total reactance which is the sum of the primary leakage reactance, and magnetizing reactance. At infinite slip frequency, the rotor bars are equivalent to short circuits, and

$$U_\infty = n\frac{V^2}{X_\infty} \tag{11}$$

where X_∞ is the total leakage reactance at infinite slip frequency. Since at high slip frequency all the induced current is concentrated at the rotor bar surface, the total leakage reactance X_∞ does not include any rotor slot leakage permeance except that of the slot opening only. If the skin effect of the outer cage is neglected in calculating the performance, the value of X_∞ should include the leakage permeance of the outer cage correspondingly. In any case, X_∞ is quite independent of the shape of the rotor slot, or the inner cage.

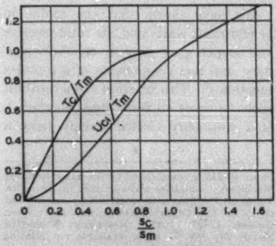

Figure 2. Reactive current of a constant torque motor

Substituting equations 10 and 11 in equation 7, it becomes

$$\int_{-\infty}^{\infty} T du = \frac{\pi}{2}\left(\frac{nV^2}{X_\infty} - \frac{nV^2}{X_0}\right) = \frac{\pi}{2}\frac{nV^2}{X_\infty}k_{r\infty} \tag{12}$$

An equation for U_0 can be derived from equation 12 as follows

$$U_0 = \frac{nV^2}{X_0} = \frac{nV^2}{X_\infty}\frac{X_\infty}{X_0} = \frac{nV^2}{X_\infty}(1-k_{r\infty}) \tag{13}$$

Combining equations 12 and 13, a relation between the no load current and torque area is obtained; it is

$$U_0 = \frac{2}{\pi}\frac{1-k_{r\infty}}{k_{r\infty}}\int_{-\infty}^{\infty} T du \tag{14}$$

These equations give the necessary conditions which the torque and current of induction motors must follow. They are very general conditions in that most arbitrarily assigned torque curves do not lead to a motor that can be actually built. However, most commercially desirable speed torque curves can be approximated with that of an actual motor. This point will be illustrated in an example later.

Constant Torque Motors

To illustrate the application of equations 8 and 12 to actual motor design, a motor with the speed torque curve of Figure 1 is studied. This particular speed torque curve is chosen because it is simple and is satisfactory for general application. For slip less than one, we are interested in keeping the torque at its maximum value. At very high slip frequencies the torque is inversely proportional to the slip if the skin effect of the outermost cage is neglected. There is a transitional region between the constant torque characteristic and the declining torque characteristic. We do not know what the torque curve looks like in this region, and it would make the design job simpler if we leave this region flexible. However, in calculating the current curve for a slip equal to one or less, very slight error is introduced in assuming the dotted curve which is an extension of the two torque curves which meet at a slip s_2. $s_2>1$ and can be arbitrarily chosen, but it has to be large enough to allow an adequate transition region.

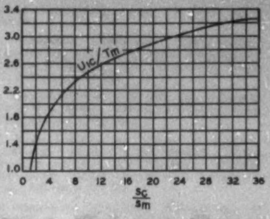

Figure 3. Reactive current of a constant torque motor

Since the skin effect of the outermost cage is neglected, its leakage reactance should be included in X_∞.

For deep bar motors, the skin effect is not negligible, and the motor torque is inversely proportional to the square root of slip for large values of slip. X_∞ does not include any of the rotor slot leakage except at the slot opening.

For the torque curve of Figure 1, the corresponding reactive power can be calculated from equation 8. First, equation 8 is written in terms of the slip s and s_c instead of the angular frequency. $s=\omega/\omega_1$, $s_c=\omega_c/\omega_1$.

Equation 8 becomes

$$U_c - U_0 = -\frac{2s_c^2}{\pi}\int_0^\infty \frac{\frac{T}{s} - \frac{T_c}{s_c}}{s^2-s_c^2}ds \tag{15}$$

Since the values of T and T_c are described by different functions in different ranges

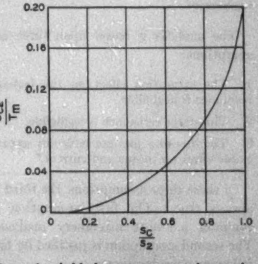

Figure 4. Added reactive current due to the declining torque characteristics at high slip frequency

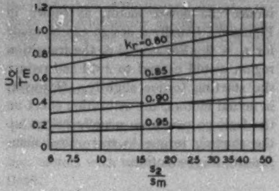

Figure 5. No load current as a function of the range of maximum torque

of s and s_e, it is necessary to separate the integral into three parts and integrate separately. Finally we obtain

$$U_e=U_0+U_{e1}+U_{e2} \tag{16}$$

where, for

$s_e<s_m$:

$$U_{e1}=\frac{s_e^2T_m}{s_e^2+s_m^2}+\frac{2T_m}{\pi}\frac{s_es_m}{s_e^2+s_m^2}\ln\frac{s_m+s_e}{s_m-s_e}+\frac{T_m}{\pi}\ln\left[1-\left(\frac{s_e}{s_m}\right)^2\right] \tag{17}$$

for

$s_m<s_e<s_2$:

$$U_{e1}=\frac{s_e^2T_m}{s_e^2+s_m^2}+\frac{2T_m}{\pi}\ln\left(1+\frac{s_e}{s_m}\right)-\frac{T_m}{\pi}\frac{(s_e-s_m)^2}{s_e^2+s_m^2}\ln\frac{s_e+s_m}{s_e-s_m} \tag{18}$$

and for all values of $s_e<s_2$:

$$U_{e2}=\frac{2T_m}{\pi}\left[1-\frac{s_2}{2s_e}\ln\left(\frac{s_2+s_e}{s_2-s_e}\right)-\frac{1}{2}\ln\left(1-\frac{s_e^2}{s_2^2}\right)\right] \tag{19}$$

for $s_e=s_2$:

$$U_{e2}=\frac{2T_m}{\pi}(1-\ln 2) \tag{20}$$

The no load volt amperes U_0 can be evaluated from equation 14 which gives

$$U_0=\frac{2T_m}{\pi}\frac{1-k_{r\infty}}{k_{r\infty}}\left(2.57+\ln\frac{s_2}{s_m}\right) \tag{21}$$

Equations 17–21 are plotted into curves in Figures 2, 3, 4, 5. These curves, together with equation 16, allow the current at any value of slip to be readily calculated.

Example

As an example to illustrate the application of these curves, suppose a motor has the following constants and requirements: $k_{r\infty}=0.95$; full load slip $s_e=0.02$; $s_2=1.50$; and maximum torque=starting torque=2 times full load torque.

From Figure 2, we see that for a load point of $T_e=0.5\ T_m$; $s_e=0.268s_m$; $U_{e1}=0.13\ T_m$.

Then calculate

$s_m=0.02+0.268=0.0746$

$\frac{s_2}{s_m}=20.1 \qquad \frac{s_e}{s_2}=0.0133$

From Figures 4 and 5, we have

$U_{e2}=0.000019T_m$

$U_0=0.187T_m$

From equation 16

$U_e=(0.187+0.130+0.000019)T_m=0.317T_m$

The full load power factor is

$$P.F.=\frac{T_e}{\sqrt{T_e^2+U_e^2}}=\frac{0.5}{\sqrt{0.5^2+0.317^2}}=84.5 \text{ per cent}$$

For the locked rotor condition

$s_e=1, \qquad \frac{s_e}{s_m}=13.4, \qquad \frac{s_e}{s_2}=0.667$

From Figures 3 and 4 we have

$U_{e1}=2.65T_m \qquad U_{e2}=0.054\ T_m$

$U_e=(0.187+2.65+0.054)T_m=2.89\ T_m$

The starting kilovolt-amperes per horsepower is

$$\sqrt{1+2.89^2}\times2\times0.746\times\frac{1}{0.98}=4.66$$

Curves of Power Factor and Starting Kilovolt-amperes Per Horsepower

The above example can be repeated for different values of $k_{r\infty}$ and full load slip, with fixed values of s_2 and of maximum torque to full load torque ratio. The result is plotted in Figures 6 and 7. These curves give the values of full load power factor and starting current for given values of full load slip and $k_{r\infty}$. Conversely, knowing $k_{r\infty}$ and starting current, the minimum full load slip without low accelerating torque can also be determined.

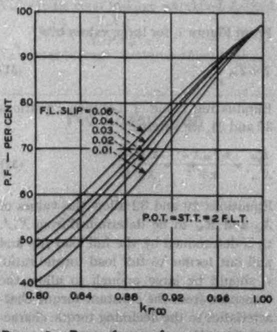

Figure 6. Power factor of a constant torque motor

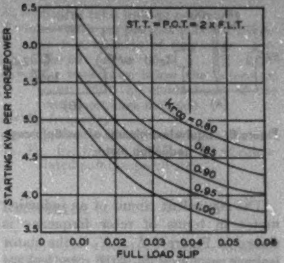

Figure 7. Starting current of a constant torque motor

The significance of these curves lies in that $k_{r\infty}$ is determined as soon as the stator slots, air gap, and the number of rotor slots of the external cage are given. These curves allow a pair of values of full load slip and starting current to be chosen which represent the best compromise under the given conditions. Then the inner cage can be designed accordingly.

Because of the saturation effect of the leakage reactance and the stator resistance, the starting current values of actual motors are about 10 to 20 per cent higher than the curve values. They nevertheless give a fairly close idea of what the starting currents are like for various values of full load slip and leakage factor

Leakage Reactance and Effective Rotor Resistance as a Function of Slip Frequency

The foregoing analysis explores the possible performances of a multiple cage induction motor. No attention is paid to the rotor itself. In the following, the same method will be employed to determine the rotor constants which would give the desired performance.

It is generally assumed that the magnetizing current can be represented by a reactance directly across the voltage source. In that case, the rotor current can be obtained by subtracting U_0 from U. However, such a method is subject to error, as the actual magnetizing current varies with the slip. A more rigorous analysis arrives at essentially the same result with slight modification on the motor constants.

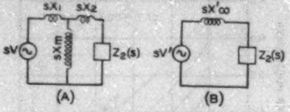

Figure 8. Equivalent circuits of multiple-cage induction motor

The equivalent circuit of an induction motor in terms of rotor frequency is shown in Figure 8(A). X_1 is the stator leakage reactance, X_2 is the rotor leakage reactance without including any leakage flux below the outermost cage. X_m is the magnetizing reactance. Z_2 is a function of the slip and

$$\lim_{s\to\infty}\left(\frac{Z_2}{s}\right)=0$$

The reactances X_∞ and X_0 are

$$X_\infty=X_1+\frac{X_2X_m}{X_2+X_m}$$

$$X_0=X_1+X_m$$

The admittance Y is the admittance looking into the circuit from the voltage source.

As far as the rotor current is concerned, the circuit of Figure 8(A) is equivalent to that of Figure 8(B) as a result of Thevenin's Theorem. In Figure 8(B)

$$X_\infty'=X_2+\frac{X_1X_m}{X_1+X_m}$$

$$V'=V\frac{X_m}{X_0}$$

Let Y' be the admittance looking into the circuit from the voltage source V' and $F'=jsnV'^2Y'$. The same analysis can be applied to show the relationship between the torque and the reactive components of the rotor current. The same set of equations is obtained except that in the new equations

$$U_0'=0 \qquad {}_{r\infty}'=1$$

and X_∞', V' take the places of X_∞, V. From the values of U' and T', the effective total leakage reactance X_e and rotor resistance R_e can be calculated. Since these values are stated in terms of line frequency, they are related to Y' by the following equation

$$R_e+jsX_e=\frac{1}{Y'} \tag{22}$$

By definition of F', it can be easily verified that

$$R_e=\frac{nV'^2T's}{U'^2+T'^2} \tag{23}$$

$$X_e=\frac{nV'^2U'}{U'^2+T'^2} \tag{24}$$

The d-c rotor resistance R_d and the total leakage reactance at no load X_d are approximately

$$X_d=\frac{nV'^2}{2T_m} \qquad R_d=X_ds_m \tag{25}$$

Substituting these expressions in equations 23 and 24 we obtain

$$\frac{R_e}{R_d}=\frac{2\left(\frac{T'}{T_m}\right)\frac{s}{s_m}}{\left(\frac{U'}{T_m}\right)^2+\left(\frac{T'}{T_m}\right)^2} \tag{26}$$

$$\frac{X_e}{X_d}=\frac{2\left(\frac{U'}{T_m}\right)}{\left(\frac{U'}{T_m}\right)^2+\left(\frac{T'}{T_m}\right)^2} \tag{27}$$

Since $U_0 = 0$ and U_{c2} is negligible for values of $s_c<0.5s_2$, equation 16 shows that U'/T_m is approximately U_{c1}/T_m over the working range of $s_c<1$. The values of U'/T_m and T'/T_m are read from Figure 2 and 3 as a function of s/s_m. The values of R_e/R_d and X_e/X_d are calculated and plotted in Figure 9.

Since $k_{r\infty}' = 1$, equation 12 becomes

$$\frac{nV'^2}{2X_\infty'}=\frac{1}{\pi}\int_{-\infty}^{\infty}Tdu=\frac{T_m}{\pi}\left(2.57+\ln\frac{s_2}{s_m}\right) \tag{28}$$

Substituting equation 25 in 28 we obtain

$$\frac{X_d}{X_\infty'}=\frac{1}{\pi}\left(2.57+\ln\frac{s_2}{s_m}\right) \tag{29}$$

Let R_∞ be the resistance of the outermost cage. At very high slip frequency, the effective rotor resistance is equal to R_∞ and the rotor current is equal to V'/X_∞', therefore the torque is

$$T=n\left(\frac{V'}{X_\infty'}\right)^2\frac{R_\infty}{s} \tag{30}$$

From Figure 1, for large values of s

$$T=T_m\frac{s_2}{s} \tag{31}$$

Eliminating s and T between equations 30 and 31, we obtain

$$\frac{R_\infty}{X_\infty'}=\frac{s_2T_mX_\infty'}{nV'^2}=\frac{X_\infty'}{X_d}\frac{s_2}{2} \tag{32}$$

Equations 29 and 32 allow the values of X_d and R_∞ to be determined from X_∞'. s_m is determined by the full load slip and pull out torque to full load torque ratio. s_2 should be large enough to allow the transition from the constant torque characteristics to the declining torque characteristics. However, too large a value of s_2 would increase the no load current and reduce the power factor, as shown in Figure 6. Usually a design can be made for $s_2 = 2$. For $s_2 = 1.5$, the transition region would extend to $s<1$ and reduce the starting torque slightly. However, in actual motors, the saturation effect on the leakage reactance usually brings up the starting torque to more than compensate this reduction.

A Direct Design Procedure

The analysis given above allows a multiple cage motor to be designed without very much trial and error. Usually the rotor lamination design is the most difficult and important. After the stator lamination, air gap, and the number of slots of the outermost cage are assumed, we can proceed in accordance with the following procedure:

1. Calculate X_1, X_2, X_m, X_∞, X_∞', X_0, $k_{r\infty}$ for the worst case. This is usually the motor with a maximum number of poles and shortest stack.

2. Choose a satisfactory performance point from Figures 6 and 7 or any other similar curves. If $k_{r\infty}$ is too low to obtain a satisfactory performance, means for increasing X_0 or reducing X_∞ must be used to improve $k_{r\infty}$.

3. After a satisfactory selection is made, determine

$\frac{X_d}{X_\infty'}$ from equation 29

$\frac{R_\infty}{X_\infty'}$ from equation 32

$$\frac{R_d}{X_\infty'}=\frac{X_d}{X_\infty'}s_m$$

These ratios determine the over-all slot constant, the slot area of the outermost cage, and the total slot area respectively.

4. Approximate the actual R_e and X_e to

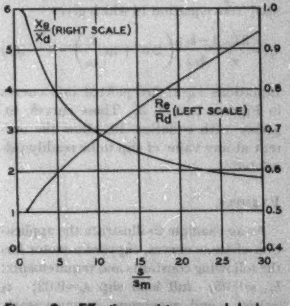

Figure 9. Effective resistance and leakage reactance of a constant torque motor as functions of slip frequency

the ideal values of Figure 9 by changing the shape and multiplicity of the inner cages while keeping the total area and slot constant to the predetermined values.

Conclusion

In the foregoing analysis, we have established the following facts about induction motors with multiple cage constructions:

1. By varying the shape and number of rotor slots, we can control either the torque or the reactive current as a function of slip. However, as soon as one of the two is fixed for all values of slip, the other component is automatically determined, see equation 8.

2. While in single-cage motors the total leakage reactance is determined by the maximum torque, a corresponding leakage reactance, in the more general case, is fixed by the torque area, equation 12. Therefore, in designing multiple cage induction motors, the torque area takes the same place as the maximum torque takes in single-phase motors.

3. Figures 6 and 7 show the starting torque, current, and full load power factor as a function of full load slip and $k_{r\infty}$. As the value of $k_{r\infty}$ does not depend on the inner cage construction, these curves fix the best performances that can be expected from multiple cage motors without bad accelerating characteristics. It also establishes $k_{r\infty}$, the leakage factor, as the most important single factor which determines the motor performance.

4. A direct design approach is shown which gives the values of slot areas and motors constants at different values of slip for any chosen, possible, performance.

5. Last, and perhaps most important of all, is that this general analysis tells where to look for improvements on cage construction. For example, most double-cage motors have trouble with poor power factor.

It would appear that the inner cage is the place to look for such improvements. However, since the basic leakage factor $k_{r\infty}$ is independent of the inner cage construction, any improvement on the power factor by modifying the inner cage is necessarily accompanied by undesirable effects on the full load slip, or starting and accelerating characteristics. The only effective way to improve motor performance in general is to increase the leakage factor $k_{r\infty}$. It can be accomplished by increasing the number of stator slots, or the number of slots in the outer cage, or any other effective measures. If the leakage factor is improved, and the necessary change is made on the inner cage to restore the desired speed torque characteristic, the improvement on full load power factor follows as a natural consequence.

List of Symbols

B = alternating current susceptance per phase of a locked motor
F = performance function, defined as $U+jT$
F' = performance function, defined as $U'+jT'$
G = alternating current conductance per phase of a locked motor
I = phase current of a running motor at line frequency and voltage
$k_{r\infty}$ = basic leakage factor, defined as $1-\frac{X_\infty}{X_0}$
n = number of phases
R_d = rotor resistance at very low slip
R_e = effective rotor resistance
s = slip
s_c = slip at calculated point
s_m = smallest slip, to which maximum torque is maintained
s_1 = slip at which the constant torque curve and the declining torque curve meet
T, T' = torque in synchronous watts
U = total reactive volt-ampere input to stator
U' = total reactive voltampere input to rotor
V = line voltage
V' = air gap voltage at no load
X_0 = total reactance per phase $=X_1+X_m$
X_1 = stator leakage reactance
X_2 = rotor leakage reactance, which does not include any slot leakage below the outermost cage
X_m = magnetizing reactance
X_∞ = basic total leakage reactance, defined as $X_1+\frac{X_2X_m}{X_2+X_m}$
X_∞' = basic total leakage reactance, defined as $X_2+\frac{X_1X_m}{X_1+X_m}$
X_d = total leakage reactance at no load
X_e = effective total leakage reactance
Y = admittance per phase of a locked motor. Y is a function of frequency. $Y=G-jB$
Z_2 = rotor impedance below the outermost cage, with the conductance of the outermost cage included
ω = slip frequency
ω_c = slip frequency of the calculated point
T_c, T_c', U_c, U_c' are T, T', U, U' at calculated point respectively

References

1. Network Analysis and Feedback Amplifier Design (book), **H. W. Bode.** D. Van Nostrand Company, New York, N. Y., 1945, pages 276–336.

2. Heat Losses in the Conductors of A-C Machines, **W. V. Lyon.** *AIEE Transactions*, volume 40, part II, 1921, pages 398–410.

3. Development of Low Starting Current Induction Motor, **P. L. Alger.** *General Electric Review* (Schenectady, N. Y.), volume 28, 1925, pages 499–508.

4. Theory of the Double Squirrel-Cage Motor, **H. Lund.** *Archiv fuer Elektrotechnik* (Berlin, Germany), volume 15, 1925, pages 121–37.

5. Boucherot Motors, **H. Lund.** *AEG Progress* (London, England), volume 2, May 1926, pages 87–91.

6. Polyphase Induction Motors with Double Squirrel-Cage Windings, **C. W. Kincaid, D. F. Alexander.** *Electric Journal* (East Pittsburgh, Pa.), volume 23, 1926, pages 15–19.

7. Squirrel Cage Induction Motors for High Starting Torque and Low Starting Current, **M. Liwschitz.** *Siemens-Schuckert Review* (Berlin, Germany), volume 2, 1926, pages 60–66, 87–95.

8. Double Squirrel Cage Motor, **R. Baffrey.** *Elektrotechnik und Maschinenbau* (Vienna, Austria), volume 46, 1928, pages 749–54.

9. Squirrel Cage Induction Motors, **D. B. Hoseason.** *Institution of Electrical Engineers, Journal* (London, England), volume 66, 1928, pages 410–42.

10. Line-Start Induction Motors, **C. J. Koch.** *AIEE Transactions*, volume 48, part I, 1929, pages 282–35.

11. Circle Diagram of Boucherot Motor, **M. Krondl.** *Elektrotechnik und Maschinenbau* (Vienna, Austria), volume 49, 1931, pages 161–67.

12. Modern Polyphase Induction Motors (book), **F. Punga, O. Raydt,** translated by **H. M. Hobart.** Sir Isaac Pitman & Sons, London, 1933.

13. Influence of Mutual Inductance between Starting and Operating of a Double Squirrel Cage Motor, **W. Moenning.** *Electrotechnik und Maschinenbau* (Vienna, Austria), volume 57, 1939, pages 450–53.

14. Practical Design of Double Squirrel Cage Motors, **D. Oerlel, G. Jekelialussy.** *Engineers' Digest* (New York, N. Y.), volume 4, 1947, pages 253–56.

No Discussion

Saturation Effect of Leakage Reactance

SHELDON S. L. CHANG
ASSOCIATE AIEE

T. C. LLOYD
MEMBER AIEE

IT HAS long been an observed fact that the leakage reactance of an induction motor is not a constant, but varies with the saturation. Locked rotor tests at full voltage reveal reactances which are too low for correct running performance. On the other hand, calculated values of leakage reactance, useful for running performance, need adjustment downward before they can be used for calculating locked rotor conditions accurately. The need for this adjustment in polyphase induction motors is especially acute with attention centered through National Electrical Manufacturers Association and other Standards, upon starting current limitations and starting torque requirements.

It is the purpose of this paper to discuss the nature of the saturated leakage reactance and to show a practicable though somewhat empirical method of obtaining useful results.

What Causes Saturation?

The leakage reactance of an induction motor is considered to consist of the components discussed briefly in the following:

END LEAKAGE

This is usually not saturable because the flux paths are non-magnetic for a relatively great distance.

SLOT LEAKAGE

This flux system can be separated into two parts, the first of which includes the yoke and the sides of the teeth. At standstill the flux density in this part is about equal to, or less, than the running densities and hence this major portion of the slot leakage path is not saturable.

The part of the slot leakage flux which travels across the tooth tip shows saturation and calculations must take into account the areas of the tips.

SKEW LEAKAGE

This component causes saturation effects because of the excessive magnetizing currents at the ends of the motor. Under locked rotor conditions, the stator and rotor currents at the center of the motor are about equal and opposite. At the two ends there is a phase shift in these currents of $\theta_k/2$. In this case, θ_k is the angle of skew in electrical radians.

The vector sum of the stator and rotor currents at the two ends is approximately equal to $I_s\theta_k/2$. This current would magnetize the motor at the two ends. Approximately

$$I_s=\frac{V}{X}$$

and

$$\theta_k=\frac{\pi k}{S}$$

Then the magnetizing current at the two ends is approximately

$$I_{me}=\frac{V}{X}\frac{\pi k}{2S}$$

where

S = number of stator slots per pole
k = rotor skew in stator slot pitch
V = volts per leg
X = leakage reactance

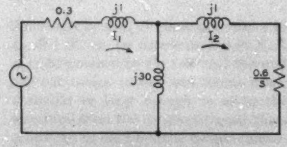

Figure 1. An equivalent circuit for one phase of the polyphase motor

Consider a typical example of a motor with nine slots per pole and a leakage reactance of 5 per cent of the magnetizing reactance, X_m. Then

$$I_{me}=\frac{V}{X_m}\times 20\times\frac{\pi k}{18}$$

$$=3.5k\frac{V}{X_m}$$

Now with a rotor bar skew of one stator tooth pitch, the "end" magnetizing current is 3.5 times the normal magnetizing current. When it fails to produce the proportional air gap flux, the skew leakage reactance is effectively saturated. This effect is greater if $k>1$; but it is not so dependent upon the number of slots per pole as the equation indicates, because the ratio X/X_m is usually reduced with the increase in the number of slots.

ZIGZAG AND BELT LEAKAGE

These are both of the same general nature, the former being caused by tooth harmonics. Belt leakage involves harmonics of a lower order. Since the stator and rotor harmonic magnetomotive forces usually do not cancel each other as the fundamental magnetomotive forces do, the resultant harmonic magnetomotive forces reach very high values under locked rotor conditions. As they saturate the tooth faces and fail to induce a proportional air gap harmonic flux, the zigzag and belt leakage reactances show the effects of saturation.

Example. Assume a typical squirrel cage induction motor has an equivalent circuit as shown in Figure 1. Assume that stator and rotor slots, under locked rotor conditions, are lined up as shown in Figure 2, which also indicates the stator coil positions.

In Figure 1 we know

$$\frac{I_2}{I_1}=\frac{j30}{j31+0.6}\text{ or }0.967\underline{/1.1}\text{ degrees}$$

Paper 49-240, recommended by the AIEE Rotating Machinery Committee and approved by the AIEE Technical Program Committee for presentation at the AIEE Fall General Meeting, Cincinnati, Ohio, October 17-21, 1949. Manuscript submitted July 20, 1949; made available for printing September 22, 1949.

SHELDON S. L. CHANG and T. C. LLOYD are with Robbins and Myers, Inc., Springfield, Ohio.

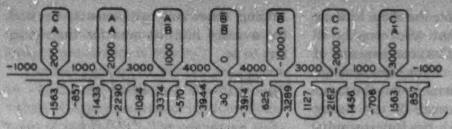

Figure 2 (above). Comparative values of the magnetomotive forces effective at the various tooth and slot positions

The bar notations over A, B, C indicate reversed polarity of the coil sides of the respective phases

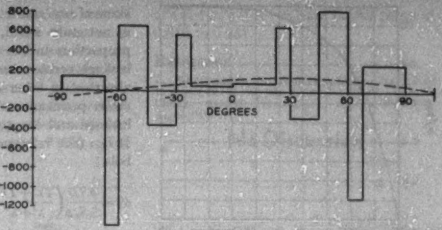

Figure 3 (right). The magnetomotive forces in the air gap

Consider the instant when phase A = 1,000-ampere conductors per coil side; phase B = 0; and phase C = 1,000-ampere conductors per coil side

The instantaneous ampere conductors in each stator slot are shown by the numbers in the slots. The magnetomotive force of the teeth also are shown by the numbers on the teeth of Figure 2.

The maximum rotor conductor current is

$$M \times K_w \times \frac{S \times 2}{S'} \frac{I_2}{I_1}$$

where

M = peak stator ampere conductors per coil side
K_w = the winding factor
S = stator slots per pole
S' = rotor slots per pole

Then for the example

$$\frac{1{,}000}{0.866} \times 0.933 \times \frac{6 \times 2}{8} \times 0.967 = 1{,}616 \times 0.967 = 1{,}563 \text{ amperes (1 conductor)}$$

Because of the phase difference between the stator and rotor currents, the rotor bar in the center has a current of 1,563 sin 1.1 degrees, and the currents in the other slots are calculated by adding $\pm n \times 22.5$ degrees to the angle 1.1 degrees. The rotor bar currents are shown as numbers in the rotor slots. The magnetomotive forces of the rotor teeth are calculated and shown on the rotor teeth, Figure 2.

The sum of the stator and rotor magnetomotive force's gives the net magnetomotive force in the air gap. This is plotted in Figure 3. While it exhibits a variable pattern, its magnitude should be compared to the fundamental component of the air gap magnetomotive force. Such a comparison is quite difficult from examination of the actual magnetomotive force of Figure 3, but can be made by calculating the magnetizing current and then the peak value of the ampere-turns. From the circuit we know

$$\frac{I_m}{I_1} = \frac{j1+0.6}{j31+0.6} = \frac{1.168\underline{/59} \text{ degrees}}{31\underline{/88.9} \text{ degrees}} \text{ or } 0.0376\underline{/-29.9} \text{ degrees}$$

The peak value of the fundamental component of the air gap magnetomotive force is

$$\frac{1{,}000}{0.866} \times 0.0376 \times 2 \times 0.933 \times 1.5 \times \frac{4}{\pi} = 154 \text{ ampere-turns}$$

This is plotted in Figure 3 as the dotted line.

At running load, the maximum value of the air gap magnetomotive force is about 250 ampere turns. Figure 3 shows that the maximum value of the harmonic magnetomotive force at locked rotor condition is about five times this value. Since the stator and rotor tooth faces are saturated to a reasonable degree with normal magnetizing current, this large harmonic magnetomotive force evidently cannot induce a harmonic flux in proportion. Consequently the zigzag leakage reactance is reduced at locked rotor and pull out conditions.

Generally the zigzag leakage permeance and its degree of saturation can both be reduced by increasing the number of stator and rotor slots. However, between motors of different speeds with the same punchings, there is no conspicuous difference in the saturation factor. This fact is justifiable theoretically because with the total number of slots and ampere conductors per slot kept constant, both the harmonic magnetomotive force and the fundamental magnetizing magnetomotive force increase in proportion with the number of poles.

A Semiempirical Method of Determining Saturated Leakage Reactance

Though the physical picture of the saturation effect on leakage reactance is not difficult to see, to calculate it rigorously is nearly impossible. It would be necessary to solve nonlinear partial differential equations for the magnetic circuit. The boundary conditions are more complicated than anything that has ever been solved in mathematical physics. In addition, it would be necessary to solve scores of these differential equations for one motor, corresponding to different stator and rotor slot positions and different stator and rotor currents.

A semiempirical method will be shown to obtain a simple and useful solution.

The leakage permeance will be separated into two parts. The unsaturable leakage permeance consists of the end leakage and the main portion of the slot leakage. The saturable leakage permeance consists of the tooth tip, zigzag, skew, and belt leakage permeances. Suppose we plot the leakage flux due to these saturable permeances as a function of winding current. At low values of current, the flux increases with current linearly, with a slope determined by the unsaturated value of the saturable leakage permeance. At high values of current, the flux levels off and approaches a maximum value ϕ_m which can be determined in terms of the dimensions and multiplicity of the stator and rotor slots. The following flux values are in lines per pole (peak value):

ϕ = actual value of the saturable leakage flux
ϕ_m = maximum value of the saturable leakage flux
ϕ_o = the value of the saturable leakage flux if it were not saturable

The actual space distribution of the saturable portion of the leakage flux depends to a great extent upon the primary winding current and the relative position between the rotor and the stator. Its effect is to produce a reactive voltage drop in the stator winding, either by direct linking with the stator winding or by reflecting into the stator through the rotor circuit. The sum total of this effect can be expressed as the equivalence of a sinusoidally distributed flux ϕ linking the stator alone. This equivalence is useful in determining the maximum value ϕ_M from actual lamination dimensions.

Evidently ϕ_o is proportional to the winding current. If we plot ϕ/ϕ_m against ϕ_o/ϕ_m instead of ϕ against winding current, a universal saturation curve would be obtained. At low values of ϕ_o/ϕ_m the curve is a straight line with unity slope

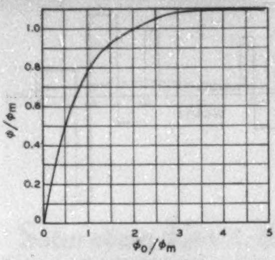

Figure 4. A universal saturation curve for determining the saturable leakage reactance

because ϕ and ϕ_o are then equal. At high values of ϕ_o/ϕ_m; ϕ/ϕ_m approaches unity, as shown in Figure 4. Theoretically the curves for different motors should agree only at the high and low ranges of ϕ_o/ϕ_m, however, the curve of Figure 4 was found to be applicable to all the 31 motors analyzed.

One difficulty which prevents the making of a direct determination of this curve is that of separating the saturable components from the unsaturable components of leakage reactance. To make an analysis of a motor having slot shapes which are easy to calculate is unreliable, because any empirical result has to be based on the data of a large number of normal and representative samples. The data obtained on a particularly shaped sample motor may deviate materially from that of average motors.

Let $\mathcal{P}_2$ and $\mathcal{P}_2'$, denote the unsaturated and saturated values of the saturable leakage permeance. Then

$$\mathcal{P}_2' = \mathcal{P}_2 \times \frac{\phi}{\phi_m} \div \frac{\phi_0}{\phi_m} \tag{1}$$

This semiempirical universal saturation curve method of determining the saturable leakage reactance can be applied readily to any design procedure an engineering office happens to be using. It is necessary to determine the proportional constant between ϕ_0 and I, and the maximum saturated leakage flux ϕ_m. These values have to be determined in line with the traditional method of calculating leakage reactance. It is believed that improvements on existing methods should prove more useful than attempting an entirely new approach.

In an earlier paper[1], the writers have explained a method used in calculating leakage reactance of squirrel cage induction motors. In this analysis, the skew leakage reactance was not calculated, but the slot, zigzag, and end leakage reactances were multiplied by experience factors. Generally, with standard rotor skew of one stator slot, the skew leakage is not only small, but also roughly in proportion to the other components of leakage permeances. With skew leakage absorbed in other components, the saturable permeance consists of the zigzag leakage and the tooth tip leakage only. It is: (See reference for additional symbols.)

$$\mathcal{P}_2 = \frac{9.7D}{S_1S_2\Delta}\left(\frac{Tc'+Tc''}{\lambda'+\lambda''}-0.5\right)^2(0.8_p+0.2)L+$$
$$4.1\left(\frac{d'}{e'S_1}+\frac{d''}{e''S_2}\right)(0.625_p+0.375)L \tag{2}$$

The unsaturable permeance consists of the slot and end leakages. It is

$$\mathcal{P}_1 = 4.1\left(\frac{K_{sc}'}{S_1}+\frac{K_{sc}''}{S_2}\right)(0.625_p+0.375)L+$$
$$\frac{\lambda}{q}K_e(1.25p-0.25)$$

$$K_{sc}' = K_s' - \frac{d'}{e'} \qquad K_{sc}'' = K_s'' - \frac{d''}{e''} \tag{3}$$

The constants given in the foregoing equations are larger than those in the earlier paper, because the unsaturated values are larger than the compromise values which the original equations are intended for. The saturable leakage inductance per phase is $C^2n\mathcal{P}_2$. ϕ_0 is obtained by multiplying the inductance by the peak value of stator current and then divided by the effective turns per phase. It is

$$\phi_0 = C^2n\mathcal{P}_2 \times \sqrt{2}I \div \frac{CKw}{2}$$
$$= 2\sqrt{2}\left(\frac{n\mathcal{P}_2}{K^2{}_w}\right)(CIK_w) \tag{4}$$

The maximum flux ϕ_m consists of the maximum zigzag and tooth tip flux. The maximum zigzag flux can be determined by the overlap method. Consider the zigzag flux that links the rotor slot S in Figure 5. Its value is determined by the smaller one of the two overlapping areas on the left and right of S. The relative position repeats itself as slot S moves one stator tooth pitch. The average value of the smaller overlapping area is

$$A_2 = \frac{2L}{\lambda'}\int_0^{\frac{1}{2}(t'-e'')} xdx = L\,\frac{(t'-e'')^2}{4\lambda'}$$
$$= \frac{L\,\lambda'-(e'+e'')^2}{4\lambda'} \tag{5}$$

Similiarly the zigzag flux linking a stator slot has an average value of the smaller overlapping area of

$$A_1 = \frac{2L}{\lambda''}\int_0^{\frac{1}{2}(t''-e')} xdx = L\,\frac{[\lambda''-(e'=e'')]^2}{4\lambda''} \tag{6}$$

Adding these two components, we find the average limiting area for the zigzag flux to be

$$A_{zz} = \frac{L}{4}\left[\lambda'-2(e'+e'')+\frac{(e'+e'')^2}{\lambda'}+\right.$$
$$\left.\lambda'-2(e'+e'')+\frac{(e'+e'')^2}{\lambda}\right]$$
$$= \frac{L}{4}\left\{\frac{[\lambda'+\lambda''-2(e'+e'')]^2}{\lambda'+\lambda''}+\right.$$
$$\left.(e'+e'')^2\left[\frac{1}{\lambda'}+\frac{1}{\lambda''}-\frac{4}{\lambda'+\lambda''}\right]\right\}$$
$$= \frac{L}{4}\left\{\frac{[\lambda'+\lambda''-2(e'+e'')]^2}{\lambda'+\lambda''}+\right.$$
$$\left.\frac{(e'+e'')^2(\lambda'-\lambda'')^2}{\lambda'\lambda''(\lambda'+\lambda'')}\right\} \tag{7}$$

In an average motor the second term is negligible compared to the first term. Therefore

$$A_{zz} = \frac{L}{4(\lambda'+\lambda'')}(\lambda'+\lambda''-2e'-2e'')^2 \tag{8}$$

The tooth tips furnish another passage for the saturable leakage flux. Its area is $(d'+d'')L$. The maximum saturable leakage flux per pole should be proportional to the total area. The proportionality constant is determined from test data to be 160,000. Therefore

$$\phi_m = 160{,}000L\left[\frac{(\lambda'+\lambda''-2e'-2e'')^2}{4(\lambda'+\lambda'')}+\right.$$
$$\left.d'+d''\right] \tag{9}$$

Besides neglecting the second term in equation 7, another source of error is due to the fact that A_1 and A_2 have considerable portion in common. However, it is quite difficult to separate this common portion. Equation 9 is derived to determine how the maximum flux depends on the various slot dimensions. The errors are absorbed partially in the experimental constant 160,000.

The above example illustrates how the universal saturation curve method can be merged into an established design method. From equations 4 and 9, the values of ϕ_0 and ϕ_m can be calculated. Then the value of ϕ/ϕ_m is determined from Figure 4. The saturated value of the

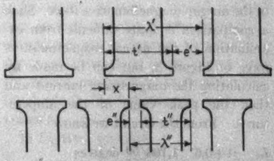

Figure 5. An analysis of the zigzag leakage flux

zigzag and tooth tip permeance then is calculated from equation 1. The total leakage permeance is $\mathcal{P}_1+\mathcal{P}_2'$.

The test data on 31 motors were taken to check the method. There are 61 values of leakage reactance in different degrees of saturation. The calculated leakage reactance agrees with test within 5 per cent in 39 cases, between 5 per cent to 10 per cent in 21 cases. The deviation is 11 per cent in one case. However, most of the deviation is introduced in calculating the value of unsaturated permeances $\mathcal{P}_1$ and $\mathcal{P}_2$. The agreements of saturation factors are all within 5 per cent, with but one exception of 6 per cent. The ratios of $(\mathcal{P}_1+\mathcal{P}_2')/(\mathcal{P}_1+\mathcal{P}_2)$ are in the range of 0.616 to 0.951.

Reference

1. Reactances of Squirrel-Cage Induction Motors, T. C. Lloyd, Victor F. Giusti, S. S. L. Chang. *AIEE Transactions*, volume 66, 1947, pages 1349–55.

No Discussion

The Torques of the Synchronous Tie—A Steady-State Analysis

L. A. FINZI
ASSOCIATE AIEE

H. M. McCONNELL
ASSOCIATE AIEE

IN A previous paper[1] methods have been given to determine the current loci and thus the performance of synchronous ties consisting of two identical polyphase induction machines with interconnected rotors and with additional secondary impedance networks. The stator currents of both induction machines are functions of their common slip s and of the phase angle δ between voltages induced in corresponding rotor windings. It was found that the vectors representing these currents at any given slip describe a circular locus (called delta-circle) when δ varies; these circles are constructed easily from the two loci obtained for the stator currents by varying s and keeping $\delta=0$ and $\delta=\pi$ respectively. A torque axis can be drawn for each delta-circle.

In this paper the operation of synchronized drives of this kind is examined further in terms of the torque requirements which occur in practical applications.

Motor Torques and Synchronizing Torques

The torques impressed upon the rotors of the machines of the tie by their revolving air gap fields are functions of s and δ. As derived in the Appendix for any given slip these torques can be written in the form

$$\tau_{\text{leader}}=\tau_0+(\tau_\pi-\tau_0)\sin^2\frac{\delta}{2}+\tau_k\sin\delta \qquad (1)$$

$$\tau_{\text{lagger}}=\tau_0+(\tau_\pi-\tau_0)\sin^2\frac{\delta}{2}-\tau_k\sin\delta \qquad (2)$$

Torques acting in the direction of field rotation are positive. Consistently with the notations used in reference 1 the subscript "leader" applies to the machine whose induced rotor voltages lead in time the corresponding rotor voltages of the other machine, for which the subscript "lagger" is used. As should be expected, 1 and 2 are of the same type as those for the power flow in a general impedance circuit with two voltage sources.[2] τ_0 and τ_π are the torques acting upon either rotor at $\delta=0$ or respectively at $\delta=\pi$. At any other angle τ_{leader} and τ_{lagger} differ, their difference being largest (and equal to $2\tau_k$) at $\delta=\pi/2$.

The notations introduced are illustrated in Figure 1. Analytical expressions also are derived in the Appendix for τ_0, τ_π, and τ_k in terms of the design data of the tie and of the slip in equations 11, 12, and 13. Equations 1 and 2 can be rewritten in the form

$$\tau_{\text{leader}}=\tau_m+\tau_s \qquad (3)$$

and

$$\tau_{\text{lagger}}=\tau_m-\tau_s \qquad (4)$$

where

$$\tau_m=\text{motor torque}=\frac{1}{2}(\tau_{\text{leader}}+\tau_{\text{lagger}})$$

$$=\tau_0+(\tau_\pi-\tau_0)\sin^2\frac{\delta}{2} \qquad (5)$$

and

$$\tau_s=\text{synchronizing torque}=\frac{1}{2}(\tau_{\text{leader}}-\tau_{\text{lagger}})$$

$$=\tau_k\sin\delta \qquad (6)$$

as also illustrated in Figure 1, for $\delta=65$ degrees.

When $s>0$, τ_{leader} is also positive, thus positive power is transferred through the air gap of the leader into its rotor, and the a-c line supplies this power and the stator losses. Moreover if $\tau_m>\tau_s$, τ_{lagger} is also positive, so that positive power is transmitted through the air gap of the second machine into its rotor and again the sum of this power and of the stator losses is supplied from the line. On the other hand if $\tau_m<\tau_s$, power is transmitted from the rotor of the lagger into its stator and given back to the line after deduction of the stator losses. In this case the machine called lagger, seen from its stator terminals, behaves as an electric generator. If the slip is negative, the situation reverses as one or both machines act as induction generators; operation of the tie in the negative slip region however is practically unlikely, as will be discussed later.

Assuming as unit power the rated mechanical output of one machine and as unit torque this power divided by rated rotor speed, it also is seen that $2\tau_m$ represents the total per-unit power transmitted from both stators through the air gaps. This power is positive for positive slips and negative for $s<0$. The over-all per-unit mechanical power delivered by both induction machines (if friction and windage are considered part of the mechanical loads) is $2\tau_m(1-s)$ while $2\tau_m s$ represents the losses in the resistances of the rotor windings and external rotor network.

Values of τ_0, τ_π, and τ_k, obtained from equations 11, 12, and 13, are plotted in per-unit in Figure 2 as functions of s for a synchronous tie consisting of two 10-horsepower 1,120-rpm 60-cycle 3-phase induction motors. Assuming as unit voltage the rated stator phase voltage and as unit current the rated mechanical output per phase in watts divided by rated stator phase voltage, the impedances of each machine are in per-unit: stator resistance $R_1=0.033$; stator leakage reactance (at rated frequency) $X_1=0.124$; rotor resistance $R_2=0.05$; rotor leakage reactance $X_2=0.124$ (both reduced to primary terms.) Moreover, for a representation of the magnetizing branches as

---

Paper 49-241, recommended by the AIEE Rotating Machinery Committee and approved by the AIEE Technical Program Committee for presentation at the AIEE Fall General Meeting, Cincinnati, Ohio, October 17–21, 1949. Manuscript submitted July 19, 1949; made available for printing September 14, 1949.

L. A. Finzi and H. M. McConnell are both with the Carnegie Institute of Technology, Pittsburgh, Pa.

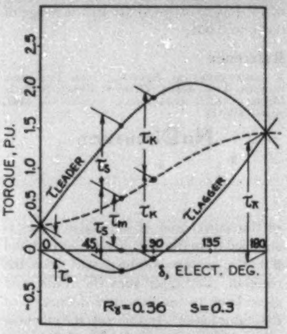

Figure 1. Example of torque-angle characteristics at constant speed

used in the top of Figure 8, Appendix, it is $R_0=19.40$ and $X_0=2.15$. Figure 2(A) gives curves calculated for a simple tie with direct rotor connection without external impedances in full lines, while the dotted lines refer to the addition of shunt inductances ($X_{\gamma L}=0.36$ per phase). Figure 2(B) refers to additional shunt resistors ($R_\gamma=0.36$ in full lines and $R_\gamma=0.09$ in dotted lines). In all these cases τ_π is represented by the same curve, since the presence of shunt impedances of any kind is not felt in the operation at $\delta=\pi$. In fact this curve coincides with the torque-slip characteristic of a machine operating singly with short-circuited slip rings. It also may be noted that in Figure 2(A) for the case of $R_\gamma=\infty$, τ_0 is always zero since for $\delta=0$ no currents flow in the rotor at any slip, while for finite values of R_γ the curve expressing τ_0 in Figure 2(B) can be obtained from the τ_π curve simply by changes of the slip scale; in fact at $\delta=0$ each machine behaves as a conventional induction machine having an external rotor rheostat with phase resistance $2R_\gamma$.

The use of shunt capacitors seems less advisable in view of limitations imposed by the danger of excessive magnetic saturation for the machines or by the size of capacitors needed, although combinations of capacitors with other network elements may be of interest. More elaborate rotor networks including series and shunt branches in symmetrical T in each phase also may be investigated by means of equations 11, 12, and 13.

Operation of the Synchronous Tie Under Load

The general arrangement of a synchronized drive is shown in Figure 3. The two remote stations A and B each consist of a driver D (prime mover or motor of any kind) driving a mechanical load L and coupled to one of the induction machines of the synchronous tie.

For any given situation it is presumed that the torque-speed characteristics of loads and drivers are known; thus the resultant mechanical torque, obtained by algebraic summation of the torques of driver and load, is a known function of speed for each station. (Some obvious care is needed to co-ordinate this information with the previous analysis[1] in which units of power and torque have been established on the basis of the name plate data of the induction machines and in which definite sign conventions already have been set for speed and torque in terms of the revolving air-gap fields). Figure 4(A) indicates with self-explanatory subscripts the torque-speed characteristics of drivers and loads as well as the resultant torques T_a and T_b of the two mechanical systems, plotted as functions of speed or slip for a hypothetical case in which "operation with the field" is intended; here driver torques act in the same direction as positive air-gap torques of the induction machines, and therefore are positive quantities. It also is conceivable and common, however, to operate the synchronous tie with fields revolving in the direction opposite to the torques of the drivers; for this type of "operation against the field" the resultant torque-speed characteristics of the mechanical systems have been redrawn in Figure 4(B) in order to avoid conflicts of sign conventions.

If the synchronous tie were removed, each station would operate independently at some speed n_a and n_b respectively, for which the equilibrium conditions $T_a=0$ and $T_b=0$ are satisfied. It is the task of the machines M_a and M_b of the tie to supply synchronizing torques, acting in opposite directions at the two stations, so as to obtain operation synchronized at a common speed. At the same time, however, M_a and M_b also supply motor torques acting in the same direction at both stations. In steady-state synchronized operation the speed (or the slip s) and the angle δ adjust themselves so as to satisfy simultaneously for each station the condition that the sum of all torques be zero, the summation including now the torques of the mechanical system and the air-gap torque as well. These equilibrium equations can be written

$$T_{\text{leader}}+\tau_{\text{leader}}=0 \tag{7}$$

and

$$T_{\text{lagger}}+\tau_{\text{lagger}}=0 \tag{8}$$

where τ_{leader} and τ_{lagger} are given by equations 1 and 2 respectively while T_{leader} and T_{lagger} are the resultant torques of the mechanical systems at the station whose machine is respectively the electrical leader or lagger. It may be noticed that the rotor of the station with algebraically larger mechanical torque is more advanced in the direction of positive field rotation; thus for $s>0$ its induced phase voltages lag in time behind the voltages induced in the corresponding rotor phase windings of the other machine; this consideration establishes to which station the subscript leader or lagger applies. (In the example of Figure 4(A) station A is the leader, while it is the lagger in Figure 4(B).)

The equilibrium conditions can also be written as

$$T_m+\tau_m=0 \tag{9}$$

and

$$T_s+\tau_s=0 \tag{10}$$

where τ_m and τ_s are given by equations 5 and 6, while the further notations $T_m=1/2\,(T_{\text{leader}}+T_{\text{lagger}})$ and $T_s=1/2(T_{\text{leader}}-$

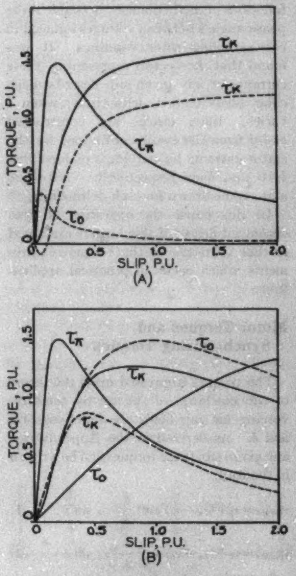

Figure 2. Plots of functions τ_0, τ_π, τ_k

A ——— simple tie without networks
- - - - shunt reactors $X_{\gamma L}=0.36$
B ——— shunt resistors $R_\gamma=0.36$
- - - - shunt resistors $R_\gamma=0.09$

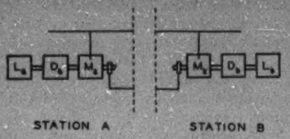

Figure 3. General type of synchronized drive

T_{lagger}) are introduced now. (Thus in the example of Figure 4(A) $T_s = 1/2\,(T_a - T_b)$ while in Figure 4(B) $T_s = 1/2\,(T_b - T_a)$.) The physical meaning of equations 9 and 10 is evident: if condition 9 is not met, both stations are going to accelerate or decelerate; on the other hand the relative angular displacement of the two shafts is going to increase or decrease if condition 10 is not satisfied.

A direct determination of s and δ from equation 7 and 8 or 9 and 10 is hardly possible by algebraic means, even if the torques of drivers and loads are assigned in the form of simple functions of the speed. A convenient procedure is suggested by the chart in Figure 5 in which families of curves τ_m = constant and τ_s = constant are drawn in terms of the two independent variables s and δ; the synchronous tie for which this chart applies consists of the two induction machines described previously with additional resistors $R_\gamma = 0.09$ in shunt to the rotor interconnections. For the mechanical situation represented by the graphs of Figure 4(A), $-T_m$ and $-T_s$, which are known functions of s, have been plotted on the chart, by scanning the families of curves τ_m = constant and τ_s = constant. Thus, the plot of $-T_m$ gives values of s and δ satisfying equation 9, and likewise the plot of $-T_s$ satisfies equation 10. Hence the slip s and the rotor voltage angle δ for synchronized operation are determined by the intersection of the two plots. The situation represented in Figure 4(B) could be examined similarly, extending the chart to values of higher positive slips and plotting on it the functions $-T_m$ and $-T_s$ obtained in Figure 4(B) for the assumption of operation against the field.

Different situations arising from conceivable changes of drivers' or loads' characteristics can be investigated likewise and limits of steady-state stability can be determined, the synchronized operation becoming impossible when the plots of $-T_m$ and $-T_s$ no longer cross on the chart. A number of somewhat less general situations, for which these graphical procedures simplify or even become unnecessary, will be discussed later.

If factors of design are changed, for example by variation of the chosen impedances of the rotor network, the chart obviously needs redrawing. But the calculations required are easy, at least for commonly simple types of networks, if one assigns values for s and solves equations 5 and 6 for δ. Moreover, some preliminary insight on the influence of changes of parameters is gained if one considers, for example, that the intersections of the family of curves τ_m = constant with the horizontal at $\delta = \pi$ do not vary for any changes of impedances in the shunt branch. The intersections of the same family of curves with the horizontal at $\delta = 0$ also are found by linear readjustments of the slip scale, if in a simply resistive shunt network R_γ is changed. The family τ_s = constant is symmetrical about the horizontal at $\delta = \pi/2$ and has kernels corresponding to maximum values of τ_s which are obtained at $\delta = \pi/2$ and at a slip which maximized τ_k. For the simply resistive shunt network considered, there is only one such kernel in the region of positive slips, which wanders towards higher slips if R_γ increases and goes to s = infinity in the limiting case of R_γ = infinity.

For the sake of completion some remarks can be made on the performance of the drive at negative slips. Since for $s < 0$, τ_m is negative and over-all electric power is delivered through the air gaps to the a-c line at the expense of the mechanical systems, operation of this kind is not generally wanted. This situation may arise accidentally, however, when a reversal of the load torques unduly accelerates systems originally operating with the field. In this case, while both stations speed up into the region of negative slips, the machine with the largest acceleration gradually becomes more advanced in the direction of the revolving field; this however is slower than the rotors so that the machine considered is the electric leader. For s negative, τ_k remains generally positive and therefore, for $0 < \delta < \pi$, $\tau_{\text{leader}} > \tau_{\text{lagger}}$; that is, the more advanced machine is pushed further ahead by its air-gap torque and the angle of the rotors increases to 180 electrical degrees and beyond; when this new condition is reached the machine considered becomes the electric lagger and synchronizing action in regenerative operation can take place. However, the transition through $s = 0$ implies a temporary loss of synchronizing action and the two stations most likely will fall out of step at this point. Similar considerations apply to a tie operating at $s > 0$ for which, however, τ_k over a region of slips happens to be negative, as is the case at small values of s for the inductive shunt network of Figure 2(A).

Types of Applications

THE LOAD DIVIDER

In many practical instances the synchronous tie is required to act as a load divider or equalizer, helping the driver of the more heavily loaded station and passing a share of its burden to the driver of the less loaded station. In such cases there is often no intention or need to obtain any over-all contribution of power from the a-c line supplying the stators of the machines of the tie which is therefore designed primarily to develop adequate

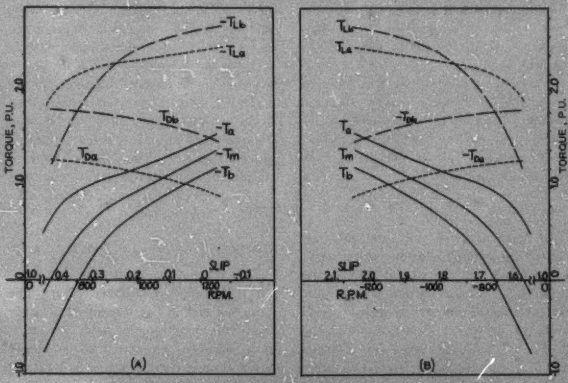

Figure 4. Examples of assigned torque-speed characteristics

A—operation with the field

B—operation against the field

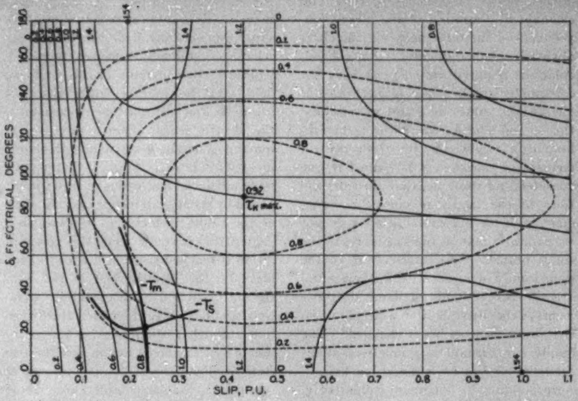

Figure 5. Chart for the determination of s and δ

synchronizing torque. Hence straight rotor connections, without external rotor networks, are commonly used. Then $\tau_0=0$, and τ_m can be assumed negligible if δ is not large. Hence in first approximation the synchronized speed of the stations is obtained directly from equation 7 as the speed for which $T_m=0$, that is, $T_a=-T_b$; thus τ_k is determined and finally δ results from equations 6 and 10.

Operation either with or against the field is practical and the latter often is preferred, in view of the larger values obtainable for τ_k, which make possible the equalization of load differences over a wider range. It also is seen that for operation against the field τ_k does not vary greatly for varying s; it is this consideration that makes it possible to some extent to elaborate on the steady-state stability of the system[3] in terms of the variable δ only.

Somewhat larger values of τ_k may be obtainable for rotation against the field if shunt capacitors are used, but tentative calculations for the machines in the example indicate then the close risk of excessive saturation.

The Follow-up Drive

In applications of this type only one station (for example, station A in Figure 3) has a driver. If the tie has no external networks, the main burden of supplying the mechanical power of both loads rests upon this driver. For operation with the field and $T_a>T_b$ the station B is retarded and M_b is the electrical leader. Operation against the field also is practical (and has the same advantage of larger τ_k mentioned in the section the Load Divider), but for the same mechanical situation, M_b is the electric lagger. Again external networks may be used if motor torques are needed to satisfy equation 9; for operation with the field then some of the burden is shifted from the driver upon the a-c line.

A simple analysis applies if the driver is provided with a governor fixing its speed at a constant value. In this case the angle δ results immediately from the equilibrium condition for station B, that is from equation 7 for operation with the field and from equation 8 for operation against the field, while the governor intervenes to satisfy the equilibrium condition of station A in any event. The angle at which pull-out occurs is then $\delta=\tan^{-1}(-\tau_k/\tau_\pi-\tau_0)$ for rotation with the field since this angle maximizes τ_{leader}, while it is $\delta=\tan^{-1}(\tau_k/\tau_\pi-\tau_0)$ for rotation against the field since this angle maximizes τ_{lagger}. Further simplifications occur if the tie has no mutuals and if the stator resistance and magnetizing current are neglected, since the problem reduces then to the analysis of the power flow between two voltage sources connected through a series impedance. The pull-out torque of station B is given then by equation 12, chapter 1, of reference 2, the leader being the sending end.

The Self-Synchronous Drive

This type of application is characterized by the absence of either driver. The induction machines are required not only to provide synchronizing torques keeping both shafts in step, but also to deliver motor torques corresponding to the total power requirements of the loads. Thus only operation with the field is intended (although reversal of speed and operation at $s>1$ may occur for excessive loads) and external rotor networks are needed. Shunt resistors are used commonly, although suggestions have been made recently[4] to substitute these resistors by reactances with the intent of reducing rotor losses; actually the question of network design is more comprehensive as it involves basic compromises between the motor and synchronizing actions obtainable. In any event for given τ_m the rotor losses are expressed by $2\tau_m s$ regardless of the type of rotor circuit used. For the example considered in Figure 2(A) it appears that inductive shunt reactances for certain sets of τ_m and τ_s values give lower s values than the shunt resistors $R_\gamma=0.09$ of Figure 2(B) and therefore lower rotor losses, but the over-all disadvantages of smaller τ_k and the likely loss of synchronism at $s=0.1$ are evident. On the other hand capacitive reactances do not seem practical in view of the low values of rotor frequencies.

At any given speed the pull-out occurs for the value $\delta_{\max}=\tan^{-1}(\tau_k/\tau_\pi-\tau_0)$ which maximizes the smaller of the two air-gap torques, that is τ_{lagger}; some information may be gained calculating the expression $\Delta=(\tau_s/\tau_m)$ at $\delta=\delta_{\max}$, which has been called "ratio of inequality" by some authors.[5,6,7] But Δ is a function of the slip, which here is not a preassigned variable, and the immediate usefulness of this concept seems to be limited. In fact the simultaneous determination of both s and δ for the self-synchronous drive for any load situation results from the solution of equations 7 and 8 or 9 and 10 as discussed already in general.

It may be of some practical interest to evaluate the upper and lower values of T_b which limit the range of possible synchronized operation, at positive slip, for any given value of T_a. These limits are plotted, in Figure 6, which has been ob-

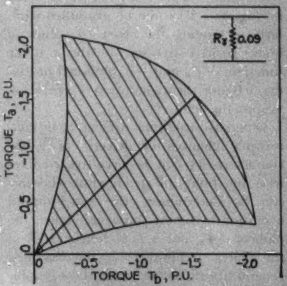

Figure 6. Limits of operation of a self-synchronous tie

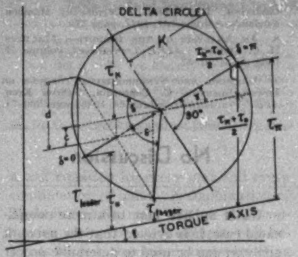

Figure 7 (left). Delta-circle and torque axis

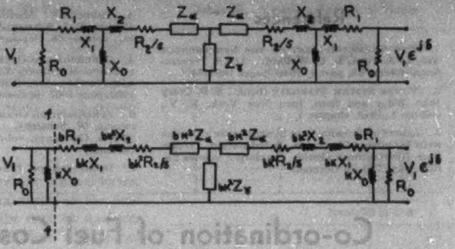

Figure 8 (right). Equivalent circuits of the synchronous tie

tained from the chart of Figure 5 by searching for the largest values of τ_π which are compatible with preassigned values of τ_m. Synchronized operation is possible for points within shaded area.

Conclusions

The torques of the induction machines of the synchronous tie have been obtained in forms which evidence the synchronizing and motor action of the drive, and expressions have been derived for the calculations of these torques at any speed and angular displacement in terms of design data.

The operation of the tie has been analyzed for general mechanical situations and methods have been suggested for the solution of the equilibrium equations of the system. Thus speed and angular displacement are obtained and currents, losses, and so forth, also can be evaluated with the procedures developed already in reference 1. Typical synchronized drives of this type have been discussed in particular.

The analysis presented is limited to the steady-state operation; the use of the derived torque expressions in differential equations describing mechanical transients may be acceptable as approximations for those transients in which speed and angular readjustments are sufficiently slow. In such cases some information concerning the influence of design of machines and rotor networks on the mechanical transient response may be gained in elementary fashion. More comprehensive analyses are available in the literature.[8,9]

Appendix

The air-gap torques of the two induction machines can be obtained graphically, for constant s and varying δ, from the delta-circle described by the vectors of the stator currents, by use of its torque axis.[1] As seen in Figure 7, simple geometrical considerations yield for these torques

$$\tau_{\text{leader}}=(\tau_\pi+\tau_0)/2-c+d$$

$$\tau_{\text{lagger}}=(\tau_\pi+\tau_0)/2-c-d$$

where

$$c=K\frac{\sin\gamma}{\cos\xi}\cos\delta,\ d=K\frac{\cos\gamma}{\cos\xi}\sin\delta$$

Also, by the law of sines

$$K\cos\gamma/\cos\xi=\tau_k,\ K\sin\gamma/\cos\xi=(\tau_\pi-\tau_0)/2$$

Hence

$$\tau_{\text{leader}}=\tau_0+(\tau_\pi-\tau_0)\sin^2\delta/2+\tau_k\sin\delta \quad (1)$$

$$\tau_{\text{lagger}}=\tau_0+(\tau_\pi-\tau_0)\sin^2\delta/2-\tau_k\sin\delta \quad (2)$$

τ_0, τ_π, and τ_k depend on the parameters of the equivalent circuit of the synchronous tie and on the slip. In order to derive usable expressions in analytical form, it has been found convenient to modify the original equivalent circuit transferring the magnetizing admittances at the stator terminals and correcting for this the remaining impedances of the circuit as indicated in the two steps of Figure 8. This transformation, which does not affect the general properties of the loci discussed in reference 1, has been suggested independently by Professor J. F. H. Douglas of Marquette University and by Professor G. F. Tracy of the University of Toronto in their unpublished lectures on induction machines. It implies the multiplication of the stator reactances by a factor $k=1+x_1/x_0$ and the rotor circuit impedances by k^2 and also the further multiplication of all impedances, with exception of those of the magnetizing branches by a factor $b=\epsilon^{j\theta}$ where $\theta=2R_1/kx_0$.

Then, by usual procedures of circuit analysis it is found, in per-units,

$$\tau_0=V_1^2(1-s_r)\frac{R^0-R_1}{(R^0)^2+(X^0)^2} \quad (11)$$

$$\tau_\pi=V_1^2(1-s_r)\frac{R^\pi-R_1}{(R^\pi)^2+(X^\pi)^2} \quad (12)$$

$$\tau_k=V_1^2(1-s_r)\left(\frac{1}{2}\frac{X^\pi}{(R^\pi)^2+(X^\pi)^2}-\right.$$
$$\frac{1}{2}\frac{X^0}{(R^0)^2+(X^0)^2}-$$
$$\left.R_1\frac{X^\pi R^0-X^0R^\pi}{[(R^0)^2+(X^0)^2][(R^\pi)^2+(X^\pi)^2]}\right) \quad (13)$$

Here V_1 is the per-unit stator phase voltage and s_r is the slip corresponding to the rated name plate speed of the induction machines, the factor $(1-s_r)$ appearing throughout in view of the choice of unit torque made in the text. R^0 and X^0 and respectively R^π and X^π are the resistances and the reactances of the input impedance at the terminals *ff* of the modified equivalent circuit for operation at respectively $\delta=0$ and $\delta=\pi$, having set $b=1$. For instance if, for the sake of generality, it is assumed that the external T rotor network of the original equivalent circuit consists of series impedances $Z_\alpha=R_\alpha/s+jX_{\alpha L}-jX_{\alpha c}/s^2$ and of a shunt impedance $Z_\gamma=R_\gamma/s+jX_{\gamma L}-jX_{\gamma c}/s^2$ (where $X_{\alpha L}$ and $X_{\gamma L}$ are inductive reactances and $X_{\alpha c}$ and $X_{\gamma c}$ are capacitive reactances, all at line frequency and reduced to primary terms) it is

$$R^0=R_1+k^2(R_2+R_\alpha+2R_\gamma)/s,$$

$$X^0=kX_1+k^2(X_2+X_{\alpha L}-X_{\alpha c}/s^2+2X_{\gamma L}-$$
$$2X_{\gamma c}/s^2)$$

$$R^\pi=R_1+k^2(R_2+R_\alpha)/s$$

$$X^\pi=kX_1+k^2(X_2+X_{\alpha L}-X_{\alpha c}/s^2)$$

as seen also applying the modification discussed above to the circuits of Figures 3(B) and 3(A) of reference 1. In practical cases the external rotor networks are of a less general nature and the equations 11, 12, and 13 are easier to calculate. Considerable simplifications are obtained if the machines of the tie are such as to make acceptable the simplifying assumptions $R_1=0$ and $X_0=\infty$. For instance, for the comparatively simple, but practically very important, case of a synchronous tie whose external rotor network consists of shunt resistors only, it is then

$$\tau_0=V_1^2(1-s_r)\frac{(R_2+2R_\gamma)/s}{[(R_2+2R_\gamma)/s]^2+(X_1+X_2)^2}$$

$$\tau_\pi=V_1^2(1-s_r)\frac{R_2/s}{(R_2/s)^2+(X_1+X_2)^2}$$

$$\tau_k=V_1^2(1-s_r)\frac{X_1+X_2}{2}\times$$
$$\left(\frac{1}{(R_2/s)^2+(X_1+X_2)^2}-\right.$$
$$\left.\frac{1}{[(R_2+2R\ )/s]^2+(X_1+X_2)^2}\right)$$

which simplifies even further, obviously, in the case of straight rotor connections $(R_\gamma=\infty)$.

References

1. The Geometric Loci of the Synchronous Tie, L. A. Finzi, L. C. Wellard. *AIEE Transactions*, volume 68, part I, 1949, pages 168–171.

2. Power System Stability (book), S. B. Crary John Wiley and Sons, Inc., New York, N. Y., volume 1, 1945, chapter 1.

3. Limits of Stability of Synchronized Drives with Induction Machines, E. Scharstein. *Archiv Fuer Elektrotechnik* (Berlin, Germany), volume 28, 1934, page 770 (in German).

4. Induction Motors for Synchronized Drives, E. L. Schwarz-Kast. *Electrical Engineering*, volume 68, October 1949, page 856.

5. Synchronized Operation of Polyphase Induction Machines, L. Dreyfus. *Elektrotechnik und Maschinenbau*, (Vienna, Austria) volume 48, 1930, page 1007 (in German).

6. Synchronized Operation of Induction Machines, W. Schuisky. *Archiv Fuer Elektrotechnik* (Berlin, Germany), volume 28, 1934, page 601 (in German).

7. Operation of Induction Motors in Synchronism, T. F. Wall. *Engineering* (London, England), volume 164, 1947, page 579.

8. An Analysis of the Induction Machine, H. C. Stanley. *AIEE Transactions*, volume 57, 1938, pages 751–57.

9. Damping and Synchronizing Torques on Power Selsyns, C. Concordia, Gabriel Kron. *AIEE Transactions*, volume 64, 1945, pages 366–71.

No Discussion

Co-ordination of Fuel Cost and Transmission Loss by Use of the Network Analyzer to Determine Plant Loading Schedules

E. E. GEORGE
FELLOW AIEE

H. W. PAGE
NONMEMBER AIEE

J. B. WARD
MEMBER AIEE

DETERMINATION of the most economical division of load between generating plants is of considerable importance on large interconnected systems, as a small percentage gain in plant or transmission efficiency will result in savings of considerable magnitude. The theory and practical application of incremental heat rates have been known and practiced for years in the preparation of loading schedules,[1] but such schedules have usually been based on principal consideration of total and incremental fuel costs.

Generally, little or no attempt has been made to allocate generation to reduce transmission losses, except in isolated cases where the losses were obviously very great and the fuel penalty relatively light. Where transmission losses have been considered, it has usually been on basis of a simple tie connection between two plants; where more complex arrangements were studied, trial and error calculations were so involved and time-consuming that satisfactory analysis was difficult.

No practical method of determining transmission network losses for routine operating purposes was known to the authors until the loss formula method was developed by one of them in 1942.[2] This method was greatly simplified in 1945 by J. B. Ward who developed a procedure for using the network analyzer to replace the tedious trial and error determinations of power flows from each generating plant and interconnection previously needed in setting up the loss coefficients.

The transmission loss formula was combined with total and incremental fuel costs by two of the authors in 1946 in the preparation of loading schedules for a large system. The method involved a large amount of trial and error calculations, but its possibilities were apparent. As a result, work was started to determine whether or not the network analyzer could be used to solve simultaneously the variables of incremental fuel cost and incremental transmission loss. Results were successful and were applied in the preparation of loading schedules for a large system.

This new time saving method forms the basis of this paper, which has for its purpose the description of how total and incremental transmission losses for a given system may be determined and combined with the incremental heat rates of the several plants of the system and a loading schedule determined that will give minimum delivered cost.

While applied here to a more complicated case, it is evident that the network analyzer can be used to determine proper loading of units, plants, and systems, considering incremental fuel costs alone or in conjunction with transmission losses. It opens up new possibilities for quick determination of proper loading, and the time may come when a simplified network analyzer will be an essential part of the load dispatcher's equipment.

Description and Application of Method

Following is a brief description of the method as applied to a system having eight interconnected plants, the plants having various economies and fuel costs.

To convert the system data into a form suitable for the solution of loading problems on the network analyzer (or by any other means), it is necessary to have a formula for total system transmission loss in terms of megawatt generation at each plant and a formula or curve for each plant showing total fuel cost at that plant in terms of its generation (preferably net). The total transmission loss formula is best determined on the network analyzer, using the method outlined in Appendix II. The formulas or curves of total fuel cost at each plant may be obtained by conventional methods.[3]

The first step is to convert the formula for total transmission loss into a set of equations for incremental transmission loss. This is done by taking the first partial derivative with respect to each plant in turn, using methods of calculus. Table I shows the total transmission loss formula for the system. Table II shows equations of incremental transmission loss for the system.

It will be noted that the incremental-loss equations are symmetrical about the diagonal (from upper left to lower right). This symmetry is essential for electrical solution.

The next step is to convert the formulas or curves of total fuel cost into incremental-cost equations, such as those shown in Table IV. There will be at least one incremental-cost equation for each plant. Plants with more than one unit will have

---

Paper 49-242, recommended by the AIEE System Engineering Committee and approved by the AIEE Technical Program Committee for presentation at the AIEE Fall General Meeting, Cincinnati, Ohio, October 17–21, 1949. Manuscript submitted July 18, 1949; made available for printing September 12, 1949.

E. E. George is an Electrical Engineer and H. W. Page is a Mechanical Engineer with Ebasco Services, Inc., New York, N. Y. J. B. Ward is Analyzer Engineer with Purdue University, Lafayette, Ind.

The authors wish to acknowledge the assistance of associates and others in the preparation of this paper, with especial credit to Professor L. M. Haupt, A. W. Lotz, and Professor J. R. Eaton.

Table I. Total Transmission Loss in Kilowatts—Sum of Following 36 Terms

$1.53G_a^2$	$+1.26G_b^2$	$+1.57G_c^2$	$+0.98G_d^2$	$+2.18G_e^2$	$+8.73G_f^2$
$+15.22G_g^2$	$+11.33G_h^2$	$+2.12G_aG_b$	$+1.64G_aG_c$	$+0.82G_aG_d$	$-0.78G_aG_e$
$-4.18G_aG_f$	$-5.36G_aG_g$	$-2.80G_aG_h$	$+1.93G_bG_c$	$+0.82G_bG_d$	$-0.78G_bG_e$
$-4.18G_bG_f$	$-5.36G_bG_g$	$-2.80G_bG_h$	$+0.82G_cG_d$	$-0.78G_cG_e$	$-4.18G_cG_f$
$-5.36G_cG_g$	$-2.80G_cG_h$	$+0.36G_dG_e$	$-3.04G_dG_f$	$-4.23G_dG_g$	$-1.69G_dG_h$
$-0.02G_eG_f$	$-1.20G_eG_g$	$-0.58G_eG_h$	$+16.28G_fG_g$	$-0.58G_fG_h$	$-1.69G_gG_h$

G_a, G_b, G_c, and so forth equal net generation in megawatts at plants *a*, *b*, *c*, and so forth.

Table III. Loading Ranges of Plants

Plant	Unit	Minimum and Maximum Loads, Megawatts
a	3	10 to 44
b	8	10 to 45
c	4	8 to 30
d	3	8 to 30
e	1	10 to 44
f	1 and 2	8 to 30
g	1	10 to 44
h	1	6 to 18
	Total	70 to 285

a cost equation for every unit and every combination of units. A combination of dissimilar units may involve a discontinuity where the most efficient unit becomes loaded, thus requiring intersecting or offset cost curves.

The incremental-cost equation may be derived from the total-cost curve graphically, or by arithmetic, or by calculus. When the graphic method is used, the resulting curve should be converted to an equation. A linear equation provides adequate accuracy and is much simpler to use than an equation with square terms. Approximation may be made by drawing a straight line through the points of minimum and maximum loading, and a parallel line tangent to the convex intermediate portion, and then a final line parallel and halfway between the first two. The intercept (at zero load on the plant) and the slope of this final line will determine the incremental-cost equation. Figures 4, 5, and 6 show typical incremental-cost curves, with the linear approximation.

Table III lists the practical minimum and maximum loads of the plants and units under consideration. These limits must be taken into consideration in operating the network analyzer, as explained in the section on the Use of the Network Analyzer in Solving Numerical Co-ordination Equations.

Table IV shows the incremental fuel cost equations of the plants, and units under consideration. It will be noted that, unlike the incremental-loss equations, the incremental fuel cost equations include constant terms and do not involve other plants. This latter condition means that they do not have any mutual terms. Therefore, the mutual terms in the final equations set up on the network analyzer involve only loss coefficients and do not change with availability of plant units. This greatly simplifies the solution.

The next step is to combine incremental transmission loss and incremental fuel cost, but before doing so it is necessary to reduce both of these to dollars or to kilowatts. The latter has the advantage that the incremental loss terms remain in their usual form and are of convenient magnitude for calculation. To make this conversion from dollars to kilowatts, it is necessary to use a factor. This factor β is the weighted average fuel cost of the plants under consideration. The use of this average as a constant throughout the range of loading is an approximation, which has little effect on accuracy of the results, as shown in Table IX.

Table V shows incremental fuel cost terms thus obtained from Table IV.

Table VI is the final group of equations with detached coefficients. This table is obtained from Tables II and V by combining fuel and loss coefficients, placing known terms and constants on the right, and setting variables as column headings. The two constants are combined into a single one, denoted by ϕ. For convenience, the plant symbols are shown at the left to indicate the partial derivative represented. This facilitates preparation of a wiring diagram for the equations. Plant *f* is omitted in this and further steps, because it was not needed in the range of system loads under consideration.

The wiring diagram, Figure 3, is prepared from Table VI, (using simplifications described later). The same diagram of connections is used for loading schedules involving other combinations of units. The only changes from Table VI for such other loading schedules are in the diagonal terms and in the constant terms on the right-hand side of the equality sign. These diagonal terms affect only the values of the series impedances and do not change any circuit connections. The constant terms affect only generator voltages and do not change any circuit connections.

Network analyzer readings are then obtained. Typical readings are plotted in Figure 7, which shows the proper loading for one particular combination of plants and units. Table X shows the accuracy of the results obtained with the network analyzer as compared with results obtained from algebraic calculations.

Proper loading for other combinations is determined in the same manner until all desired combinations have been investigated. Since total fuel cost data are available for all plants, it is a simple matter to prepare total cost curves for each combination of plants or units. Comparison of the total cost curves will indicate what combination of plants should be used to carry a given load, and when additional units or plants should be started or taken off the line. The total cost curves and data, such as that shown in Figure 7, are used in the preparation of the usual tabulated loading schedules.

Table II. Incremental Transmission Loss in Kilowatts Per Megawatt of Generation

With Station Below as Variable									
a	$+3.06G_a$	$+2.12G_b$	$+1.64G_c$	$+0.82G_d$	$-0.78G_e$	$-4.18G_f$	$-5.36G_g$	$-2.80G_h$	$= K_1$
b	$+2.12G_a$	$+2.52G_b$	$+1.93G_c$	$+0.82G_d$	$-0.78G_e$	$-4.18G_f$	$-5.36G_g$	$-2.80G_h$	$= K_1$
c	$+1.64G_a$	$+1.93G_b$	$+3.14G_c$	$+0.82G_d$	$-0.78G_e$	$-4.18G_f$	$-5.36G_g$	$-2.80G_h$	$= K_1$
d	$+0.82G_a$	$+0.82G_b$	$+0.82G_c$	$+1.96G_d$	$+0.36G_e$	$-3.04G_f$	$-4.23G_g$	$-1.69G_h$	$= K_1$
e	$-0.78G_a$	$-0.78G_b$	$-0.78G_c$	$+0.36G_d$	$+4.36G_e$	$-0.02G_f$	$-1.20G_g$	$-0.58G_h$	$= K_1$
f	$-4.18G_a$	$-4.18G_b$	$-4.18G_c$	$-3.04G_d$	$-0.02G_e$	$+17.46G_f$	$+16.28G_g$	$-0.58G_h$	$= K_1$
g	$-5.36G_a$	$-5.36G_b$	$-5.36G_c$	$-4.23G_d$	$-1.20G_e$	$+16.28G_f$	$+30.44G_g$	$-1.69G_h$	$= K_1$
h	$-2.80G_a$	$-2.80G_b$	$-2.80G_c$	$-1.69G_d$	$-0.58G_e$	$-0.58G_f$	$-1.69G_g$	$+22.66G_h$	$= K_1$

Note: G_a, G_b, G_c, and so forth equal net generation in megawatts at plants *a*, *b*, *c*, and so forth.

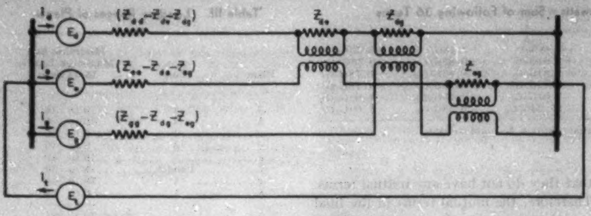

Figure 1. Electric circuit analog for 3-plant optimum loading equations. Coupling transformers are 1 to 1 ratio

Table V. Incremental Fuel Cost Terms of Plants

Plant	Unit	Variable	Constant
a	3	$4.80G_a$	.805
b	8	$3.12G_b$	.885
c	4	$12.80G_c$	.770
d	3	$12.80G_d$	.740
e	1	$3.00G_e$	.905
f	1 and 2	$27.70G_f$	.824
g	1	$2.80G_g$	.885
h	1	$11.00G_h$	.955

Note: G_a, G_b, G_c, and so forth equal net generation in megawatts at plants a, b, c, and so forth.

The Mathematical Derivation of the General Co-ordination Equation

MATHEMATICAL BASIS

The determination of allocation of generation between plants to give minimum total cost of delivered energy presents a problem in calculus, of the type usually discussed under the heading Determination of Maxima and Minima with Subsidiary Conditions. A very clear treatment of this subject may be found in volume II of Differential and Integral Calculus by R. Courant.[4] The desired allocation of generation between plants to give minimum total cost (with due recognition of fuel prices, heat rates, and transmission losses) is obtained when

$$\frac{\delta D_t}{\delta G_n}=\phi \tag{1}$$

where

D_t = total system fuel cost of delivered energy in dollars per hour
G_n = generation in megawatts at any plant n
ϕ = a constant, known in calculus as Lagrange's multiplier

Equation 1 expresses the fact that the total delivered cost of power will be a minimum when the incremental delivered cost is the same for every plant. This fact is known from cut-and-try determinations of total delivered cost, as well as from the principles of calculus.

The problem in hand is to break down the preceding general equation into components involving available plant and line data, and suitable for use on the network analyzer (a-c calculating board).

Because transmission losses are measured in megawatts or kilowatts and fuel costs are measured in dollars per megawatt-hour (or mills per kilowatt-hour), it is not immediately apparent how the two quantities should be combined. Even if they were in the same terms, a constant (Lagrange's multiplier) would be needed to relate them in a single general equation of minimum total delivered cost.

At the optimum allocation (minimum delivered cost), any difference in incremental fuel cost between any two given plants a and b must be offset by an equal and opposite difference in incremental transmission loss, priced appropriately in terms of incremental fuel cost.

$$\frac{\delta F_t}{\delta G_a}-\frac{\delta F_t}{\delta G_b}=\frac{\beta}{1{,}000}\left[\frac{\delta L_t}{\delta G_b}-\frac{\delta L_t}{\delta G_a}\right] \tag{2}$$

where

F_t = total system generated fuel cost in dollars per hour
L_t = total system transmission loss in kilowatts
G_a = generation in megawatts at plant a
G_b = generation in megawatts at plant b
β = weighted average system incremental fuel cost in dollars per megawatt-hour or mills per kilowatt-hour

Incremental fuel costs for plants can be calculated by conventional methods. The total system transmission loss can be expressed in terms of plant loading by means of a loss formula,[2] and from this formula the incremental loss terms appearing in equation 2 can be obtained by differentiation. The coefficients representing plant loading are in megawatts, but the formula is solved for loss in kilowatts, hence the average incremental fuel cost β must be divided by 1,000.

Equation 3 is derived from Equation 2 by the following steps:

1. Divide through by β.
2. Replace β by an estimated weighted average incremental fuel cost.
3. Multiply through by 1,000.
4. Transpose to collect a and b terms.
5. Set either half of the equation equal to ϕ instead of equal to the other half.

Because equation 2 applies to each pair of plants, the expression for any single plant may be equated to ϕ instead of equating two expressions to each other.

$$1{,}000\,\frac{\delta G_t}{\delta F_t}\,\frac{\delta F_t}{\delta G_n}+\frac{\delta L_t}{\delta G_n}=\phi \tag{3}$$

where

G_t = total system generation in megawatts
G_n = generation in megawatts at any plant n
$\frac{\delta G_t}{\delta F_t}$ = reciprocal of β
$\frac{\delta F_t}{\delta G_n}$ = incremental fuel cost in dollars per megawatt-hour at plant n with net generation G_n
$\frac{\delta L_t}{\delta G_n}$ = incremental transmission loss in kilowatts for one megawatt change in net generation at plant n

From the form of equation 3 it may be

Table IV. Incremental Fuel Costs of Plants

Plant	Unit	Incremental Fuel Costs
a	3	$4.025+0.0240\,G_a=K_2$
b	8	$4.425+0.0156\,G_b=K_2$
c	4	$3.850+0.0640\,G_c=K_2$
d	3	$3.700+0.0640\,G_d=K_2$
e	1	$4.525+0.0150\,G_e=K_2$
f	1 and 2	$4.120+0.1385\,G_f=K_2$
g	1	$4.425+0.0140\,G_g=K_2$
h	1	$4.775+0.0550\,G_h=K$

Note: Incremental fuel costs are in dollars per megawatt hour. G_a, G_b, G_c, and so forth equal net generation in megawatts at plants a, b, c, and so forth.

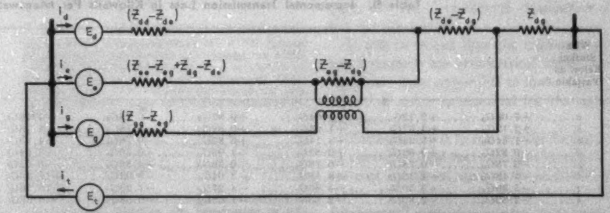

Figure 2. Modified circuit requiring fewer coupling transformers

Table VI. Final Equations for Solution on Network Analyser

Combined Incremental Fuel Cost and Incremental Transmission Loss

	G_a	G_b	G_c	G_d	G_e	G_g	G_h	
a	+7.86	+2.12	+1.64	+0.82	−0.78	−5.36	−2.80	$=\phi-805$
b	+2.12	+5.64	+1.93	+0.82	−0.78	−5.36	−2.80	$=\phi-885$
c	+1.64	+1.93	+15.94	+0.82	−0.78	−5.36	−2.80	$=\phi-770$
d	+0.82	+0.82	+0.82	+14.76	+0.36	−4.23	−1.69	$=\phi-740$
e	−0.78	−0.78	−0.78	+0.36	+7.36	−1.20	−0.58	$=\phi-905$
g	−5.36	−5.36	−5.36	−4.23	−1.20	+33.24	−1.69	$=\phi-885$
h	−2.80	−2.80	−2.80	−1.69	−0.58	−1.69	+33.66	$=\phi-955$

Note: *f* row and G_f column were omitted because plant *f* was not used in the schedule used for illustration. See note for Table V.

seen that β and ϕ qualify as Lagrange's multipliers, and accordingly have physical meanings which become apparent at later stages in the solution. From actual solution of problems by means of equation 3, it has been found that β is equal to the weighted average incremental fuel cost. ϕ may be eliminated in either algebraic or analyzer solutions, but its value is useful in checking analyzer circuits and in verifying either algebraic or analyzer solutions. The value of ϕ is discussed in a later paragraph.

For simplification it can be assumed that the weighted average incremental fuel cost is constant. This is very nearly true, as the rate changes very slowly near the point of optimum allocation between plants. This minor approximation makes all the partial derivative equations linear, provided further that all incremental fuel cost curves can be approximated by straight lines. The problem is soluble without these simplifying assumptions, but the extra work entailed is not justified by the added precision of the results.

The same value may be used for β throughout an individual study of a particular combination of units or for all comparative combinations without serious loss of accuracy. The relatively small error introduced by making this approximation for β is shown in Table IX.

Equation 3 (applied to every plant) is the basic equation for determining the optimum allocation between plants for minimum total cost. Beginning in the next paragraph this equation is expanded into a set of simultaneous equations for a system having three plants. Tables I to VI illustrate a more general expansion for a system of eight plants.

EQUATIONS FOR A 3-PLANT SYSTEM

In order to illustrate the application of the method, assume that only plants *d*, *e*, and *g* are operating in the system referred to in Tables I to VI.

The loss formula will be of the form

$$L_t = G_d^2K_{dd}+G_e^2K_{ee}+G_g^2K_{gg}+ G_dG_eK_{de}+G_dG_gK_{dg}+G_eG_gK_{eg} \qquad (4)$$

where the *K*'s are coefficients in kilowatts loss per megawatt per megawatt of load, and the *G*'s are the plant loadings in megawatts (see Appendix II).

Taking the partial derivative of equation 4, first with respect to G_d, then with respect to G_e, and finally G_g

$$\frac{\delta L_t}{\delta G_d} = 2K_{dd}G_d+K_{de}G_e+K_{dg}G_g \qquad (5)$$

$$\frac{\delta L_t}{\delta G_e} = K_{de}G_d+2K_{ee}G_e+K_{eg}G_g \qquad (6)$$

$$\frac{\delta L_t}{\delta G_g} = K_{dg}G_d+K_{eg}G_e+2K_{gg}G_g \qquad (7)$$

Using approximate linear incremental fuel costs, the first term of equation 3 for each plant will be

$$\frac{1,000}{\beta}[I_d+S_dG_d] \text{ and } \frac{1,000}{\beta}[I_e+S_eG_e] \text{ and } \frac{1,000}{\beta}[I_g+S_gG_g]$$

In the above equation, *I* is the intercept of the linear incremental fuel cost line, in dollars per megawatt-hour, and *S* is the slope of the line in dollars per megawatt-hour per megawatt of load. β is the average system incremental fuel cost in dollars per megawatt-hour. Combining these fuel cost terms with the corresponding incremental transmission loss equations, as indicated in equation 3

$$\left[\frac{1,000}{\beta}S_d+2K_{dd}\right]G_d+K_{de}G_e+K_{dg}G_g = \phi-\frac{1,000}{\beta}I_d \qquad (8)$$

$$K_{de}G_d+\left[\frac{1,000}{\beta}S_e+2K_{ee}\right]G_e+K_{eg}G_g = \phi-\frac{1,000}{\beta}I_e \qquad (9)$$

$$K_{dg}G_d+K_{eg}G_e+\left[\frac{1,000}{\beta}S_g+2K_{gg}\right]G_g = \phi-\frac{1,000}{\beta}I_g \qquad (10)$$

Taking numerical values from Tables I and IV and using a value for β of $5.00 per megawatt-hour, these loading equations become

$$14.76G_d+0.36G_e-4.23G_g=\phi-740 \qquad (8A)$$

$$0.36G_d+7.36G_e-1.20G_g=\phi-905 \qquad (9A)$$

$$-4.23G_d-1.20G_e+33.24G_g=\phi-885 \qquad (10A)$$

Writing the coefficients in matrix form

$$\begin{array}{ccc} d & e & g \end{array}$$
$$\begin{array}{|ccc|}\hline 14.76 & 0.36 & -4.23 \\ 0.36 & 7.36 & -1.20 \\ -4.23 & -1.20 & 33.24 \\ \hline\end{array} \cdot \begin{array}{|c|}\hline G_d \\ G_e \\ G_g \\ \hline\end{array} = \begin{array}{|c|}\hline \phi-740 \\ \phi-905 \\ \phi-885 \\ \hline\end{array}$$

The allocation of total generation between plants *d*, *e*, and *g* in such a manner that these equations are satisfied yields the minimum total fuel cost. The complete set of optimum-loading equations for the system is given in Table VI.

VALUE OF TOTALIZING VOLTAGE

In equation 3 the term on the right, designated by ϕ, is a quantity the value of which is not needed in the solution of

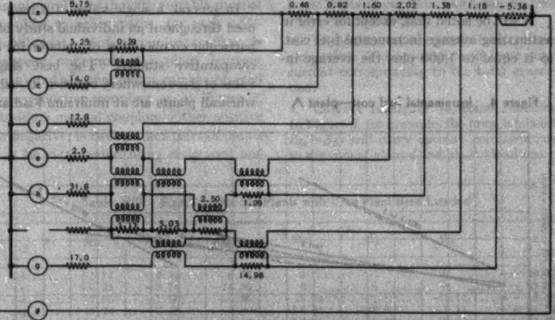

Figure 3. Circuit for equations of Table VI

Numbers correspond to actual coefficients. Analyzer resistances were set at ten times these values

Table VII. Equations for Seven Plants for Algebraic Solution

	G_a	G_b	G_c	G_d	G_e	G_g	G_h	
a-b	+5.74	−3.52	−0.29	0	0	0	0	= + 80
a-c	+6.22	+0.19	−14.30	0	0	0	0	= − 35
a-d	+7.04	+1.30	+0.82	−13.94	−1.14	−1.13	−1.11	= − 65
a-e	+8.64	+2.90	+2.42	+0.46	−8.14	−4.16	−2.22	= +100
a-g	+13.22	+7.48	+7.00	+5.05	+0.42	−38.60	−1.11	= + 80
a-h	+10.66	+4.92	+4.44	+2.51	−0.20	−3.67	−36.46	= +150
	+1.00	+1.00	+1.00	+1.00	+1.00	+1.00	+1.00	= +200

the equation by algebraic methods, because it can be eliminated by subtraction after equation 3 is expanded in matrix form as per Table VI.

When the matrix of Table VI is solved on the network analyzer, ϕ becomes the external voltage of the generator in the common return or totalizing circuit. This voltage is varied to get the proper current in the return circuit—corresponding to total system generation. Even in this case, calculation or measurement of the totalizing voltage is not essential to solution. In selecting a voltage and current base for the analyzer set-up, it is helpful to know the range of values of ϕ. This quantity varies with total system load, but not over a wide range. It also varies with the availability of units and with other factors controlling incremental fuel cost or incremental transmission loss. The value of ϕ may be calculated from the data for any individual plant or from the data for the entire system. In either case, the optimum allocation of generation must first be determined.

For any individual plant n, the value of ϕ may be calculated from equation 3. This amounts to substitution of the optimum loading values in any row in Table VI. Substitution in every row of Table VI should always be done for one system load as a check study. If the same value of ϕ is obtained for every row of Table VI, the calculations based thereon, the analyzer connections and the analyzer readings may be considered correct.

As it is difficult to estimate allocation accurately in advance of solution, a preliminary value of ϕ may be calculated from system averages, if needed.

$$\phi=\left[1{,}000+\frac{\delta L_t}{\delta G_t}\right]\left[\text{actual}\,\frac{\delta F_t}{\delta G_t}\right]+\left[\text{estimated}\,\frac{\delta F_t}{\delta G_t}\right] \qquad (11)$$

It will be noted that, except for error in estimating average incremental fuel cost, ϕ is equal to 1,000 plus the average incremental transmission loss (in kilowatts of loss per megawatt of added generation).

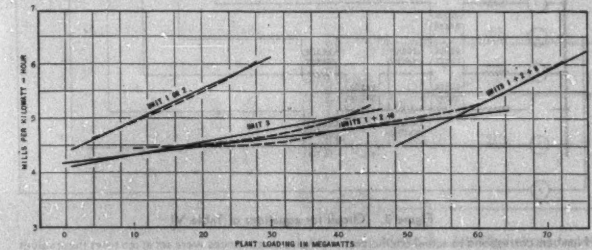
Figure 4. Incremental fuel cost—plant A

The average incremental transmission loss in kilowatts per megawatt can be shown to be 20 times the total transmission loss in per cent at the same system load. The value of ϕ usually lies between 1,025 and 1,125. It tends to increase with total system generation and to decrease with the number of plants available. It tends to increase as more and more plants reach maximum or minimum load. It also varies in opposite direction to the error in estimating average incremental fuel cost.

The physical meaning of ϕ is that it is a linear multiple of the incremental delivered cost of power from any plant, and that if it has the same value for every plant, the optimum allocation of generation has been found.

Value of Average Incremental Fuel Cost β

In equation 2 the average incremental fuel cost is designated by β. In equation 3, β is replaced by a derivative more clearly setting forth its meaning. Although β is technically a function of the solution of the equation, the allocation of generation is so little affected by the choice of the value of β that the latter is recommended to be estimated.

In general, a single value of β may be used throughout an individual study of a particular combination of units or for all comparative studies. The best single value of β is somewhere between its value when all plants are at minimum load and its value when all plants are at maximum load. These values are easily determined prior to solution of the allocation equations (Table VI). A value about halfway between minimum and maximum values is bound to be exact at some value of total generation where all (or most all) plants are "within range."

β operates on all factors on both sides of equation 3 except incremental transmission loss. Therefore, an error in estimating β produces an error in average allocation reduced in the ratio of total generation to twice total transmission loss. For instance, with a total transmission loss of five per cent, and an incremental transmission loss of ten per cent, an error of twenty per cent in estimating average incremental fuel cost would affect allocation only about two per cent.

Table IX shows a comparison of allocations, using three different estimated average incremental fuel costs: 4.64, 5.00 and 5.40 mills. It may be seen that the allocation is affected only slightly by the variation in estimated average incremental fuel costs.

Use of the Network Analyzer in Solving Numerical Co-ordination Equations

Solution by Network Analyzer

Simultaneous equations such as those given in Table VI, or equations 8(A), 9(A), and 10(A) which define the optimum loading schedule can be solved readily by establishing an electric-circuit analog; that is, by designing an electric circuit whose equations of performance are identical in form with the given equations, and reproducing this circuit on a network analyzer. In this circuit, impedances represent the coefficients of the equations, current represents megawatt loading, and voltage represents the known and undetermined constants on the right-hand side of the equations. Solution for the desired loading schedules requires the following steps.

1. Determination of a suitable equivalent circuit.

2. Choice of suitable current, impedance and voltage multipliers.

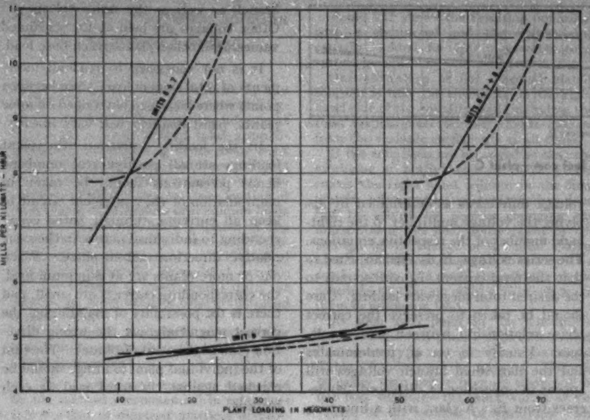

Figure 5. Incremental fuel cost—plant B

3. Adjustment of the analyzer set-up to represent a given combination of machines, fuel costs and total system generation.
4. Measurement of currents in the network and interpretation of the results in terms of plant loading schedule.

The establishment of an electric-circuit analog can be illustrated conveniently with the simple 3-plant system used previously.

Several circuits might be devised which would yield a set of equations similar in form to equations 8(A), 9(A), and 10(A), but one particular circuit which has the advantage of being easily extended to the general case of any given number of plants is shown in Figure 1. The following equations may be written describing the performance of this network, and the desired analogy established by a term-by-term comparison with the above equations.

$$Z_{dd}i_d+Z_{de}i_e+Z_{dg}i_g=E_t-E_d \qquad (12)$$

$$Z_{de}i_d+Z_{ee}i_e+Z_{eg}i_g=E_t-E_e \qquad (13)$$

$$Z_{dg}i_d+Z_{eg}i_e+Z_{gg}i_g=E_t-E_g \qquad (14)$$

Examining the requirements of the circuit which must duplicate the optimum-loading equations, currents, and voltages will be in-phase because of the scalar nature of the corresponding quantities in the loading equations. The loss formula may give rise to negative coefficients, hence the coefficients above have either positive or negative real values. Since negative coefficients appear only in the mutual terms it has been found most convenient to use resistance and to represent negative mutual terms by reversing the polarity of the corresponding coupling transformers.

An alternative circuit for the 3-plant system under discussion is shown in Figure 2. If the order of the equations and variables is chosen so that Z_{dg} in Figure 2 is the largest negative coefficient and Z_{de} is the next-largest negative coefficient (or smallest positive coefficient), the likelihood of encountering negative residual resistance in series with the voltage sources is reduced.

The resistance Z_{dg} in the modified circuit, Figure 2, need not be set up in the process of obtaining the analyzer solution. Since the total current, corresponding to total system load, flows through this branch the resulting voltage drop can be combined with the series voltage source E_t.

The circuit of Figure 1 can be extended to larger systems by providing an additional parallel path, with suitable mutual coupling to other paths, for each additional plant. Mutual coupling coefficients between one particular plant (current path) and all other plants can be obtained by conductive coupling as in Figure 2. Residual mutual coupling, either positive or negative, between other pairs of plants can be represented using resistance and 1:1 coupling transformers. Some further simplification of the network can be accomplished when several mutual coefficients are equal. As an illustration, the circuit used in the solution of the equations of Table VI is shown in Figure 3.

In more simple cases involving few equations, it may be possible to eliminate coupling transformers altogether. Equivalent circuits for parallel transmission lines presented by Starr[8] accomplish this under certain conditions. Such circuits that only involve negative resistance in series with E_t can be solved on a d-c board.

Choice of Multipliers

The quantities of interest in the equivalent circuit are current, voltage, and impedance or resistance. Three multipliers or scale factors are involved in the correlation of the information embodied in the original equations with the equivalent circuit quantities. These are:

1. Ratio of analyzer resistance in ohms to unit value of loading-equation coefficient.
2. Ratio of analyzer current in amperes or per unit to megawatt loading.
3. Ratio of analyzer voltage in volts (or per unit) to unit value of expression on the right-hand side of the loading equations.

When any two of these multipliers are selected arbitrarily, the third is uniquely determined by Ohms Law. The choice of multipliers requires consideration of the following factors:

1. Range of magnitude of coefficients in the original equations, and comparison with range of resistance values which can be set accurately on the analyzer. Consideration should be given to the magnitude of coupling transformer leakage and exciting impedance in choosing a suitable multiplier.
2. Range of variation in individual plant loading, as compared with the upper and lower limits of currents which can be read on the analyzer meters.
3. Minimum and maximum total system generation. The series source E_t must carry current corresponding to the total generation.
4. Current rating of resistance circuits. In Figure 2, for example, the branch labeled $Z_{de}-Z_{dg}$ will carry current corresponding to the sum of plant *d* and plant *e* loadings.

Table VIII. Equations for Six Plants with One Plant Base-Loaded

	G_a	G_b	G_c	G_d	G_g	G_h	
a-b	+5.74	−3.52	−0.20	0	0	0	= + 30.00
a-c	+6.22	+0.19	−14.30	0	0	0	= − 35.00
a-d	+7.04	+1.30	+0.82	−13.94	−1.13	−1.11	= − 14.84
a-g	+13.22	+7.48	+7.00	+5.05	−38.60	−1.11	= + 61.52
a-h	+10.66	+4.92	+4.44	+2.51	−3.67	−36.46	= +158.80
	+1.00	+1.00	+1.00	+1.00	+1.00	+1.00	= +256.00

Note: Plant *e* base-loaded at 44 megawatts with 300-megawatt system load. Arranged for algebraic solution.

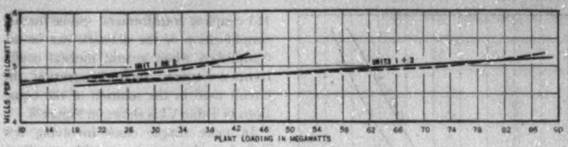

Figure 6. Incremental fuel cost—plant C

5. Voltage range required in the sources of the equivalent circuit, particularly the series source E_t. It is to be noted that the division of current among the several branches in Figure 1, that is, the desired optimum plant load division, depends primarily on voltage differences impressed across the several paths, and on the impedances of the network. Hence, it is permissible to add a fixed voltage to E_d, E_e, and E_g if the same amount is added to E_t.

The choice of multipliers will ultimately depend on the system characteristics and the type of analyzer being used. It may be necessary to use two different voltage multipliers to cover the desired range in system loading. If the current multiplier is modified inversely at the same time, it will not be necessary to reset the resistances.

The two sets of multipliers used in the solution of the sample problem, Table VI, are:

1 ampere = 100 megawatts (or 200 megawatts)
0.1 volt = unit value of RHS (or $^1/_2$ unit value of RHS)*
10 ohms = unit value of coefficient (not changed)

Adjusting, Checking, and Reading the Equivalent Circuit

After the network has been designed and the multipliers selected, the analyzer set-up can be made. It is desirable to check the set-up and this can be done easily, remembering that the impedance coefficients in equation 8, for example, represent "volts per ampere." That is, Z_{eg} is the voltage in circuit e per ampere in circuit g with all paths except g open. For a check, source E_t may be suppressed, all other sources but one opened, and unit current, or some fraction thereof, forced through the one branch or path which is energized. The voltages in all paths measured across the open source terminals will yield the coefficients in the row (or column) of the matrix corresponding to the energized source.

In adjustment of the set-up for obtaining the desired plant loading schedules, the sources are adjusted to the proper voltage differences as determined by applying the voltage multiplier to the right-hand member of the respective equations. The series voltage, E_t, is then adjusted so that the total current, I_t, corresponds to the desired total megawatt loading. Care should be taken to preserve the correct phase relationship between source voltages. Usually E_t (or ϕ) predominates and the individual branch voltages will appear in opposition or displaced 180 degrees from E_t. A plant with a linear incremental cost curve having a negative intercept may call for an individual voltage source in an aiding or additive relationship with E_t. Also, the shifting of a constant component voltage from E_t to all the individual voltages may produce such a condition.

It is desirable to adjust initially for some intermediate total system load which will not result in any plant operating at maximum or minimum load. The division of current among the several paths in the network, as read in the individual sources, gives the optimum division of loading among the plants. A new value of total system load is established by varying the source voltage, E_t, until the total current reaches the desired value.

If an individual plant reaches base load, the corresponding branch current is subsequently held constant by adjusting the individual source voltage in that branch as well as the series voltage E_t. Other voltages are held at the scheduled values until other plants reach base load.

It is not necessary to read all increments of total system load, since between points where base load is attained on some plants, plant loadings will vary linearly.

In the loading equations, the plant loadings are all positive real numbers, hence precautions should be taken in manipulation of the equivalent circuit to keep all currents, through paths corresponding to individual plants, in the same relative direction and in-phase. When one or more plants are at minimum load, the corresponding currents are small, and there is the possibility of maintaining the correct magnitude but the wrong direction (180 degrees out of phase). The sum of the individual plant loadings should be checked against the total load at each reading.

Another situation which may occur frequently in the course of running the loading schedules is the starting up of an additional unit in some plant at an intermediate point between minimum and maximum total system load. This changes the linear incremental fuel cost curve of the plant in question and requires a corresponding change in the voltage and series resistance of that path in the network. If the added unit has widely different characteristics, a discontinuity in the curve may appear in the form of a corner or offset (see Figure 5). The point of change can usually be predicted quite accurately by extrapolating the linear loading curves through points already plotted from lower values of total load. At this predicted value of total load the circuit is changed to conform to the new section of incremental fuel cost curve, and a new minimum-maximum loading bracket established for this plant.

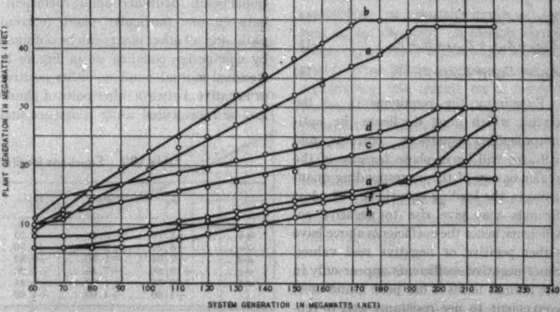

Figure 7. Typical loading chart as plotted from network analyzer readings

---

* Where RHS stands for "right-hand side" of equations 8, 9, or 10 or $[\phi - 1{,}000/\beta I]$.

Appendix I. Algebraic Solution for Optimum Loading

The solution of loading equations by any algebraic method is not recommended except for check studies or for other infrequent use. The algebraic method takes approximately ten times as long as the same work done on the network analyzer if seven plants are involved. The time required with the algebraic method is due to: base loading of some plants at maximum or minimum loads near the upper and lower portions of the schedule; time required to locate and correct the almost inevitable errors in arithmetical operations (generally procedural errors); and the absence of check results until the solution for some value of total system load is completed.

The algebraic method is practical (for occasional use) only where the following procedure is observed:

1. The simultaneous equations are solved by the method recommended in references 5 or 6—that of diagonal matrices or post-multiplication of determinants. See also references 3 and 7.

2. A motor-driven calculating machine is available.

3. All calculations (except the basic data) are carried to five significant figures (this will result in accuracy to tenth megawatts in the answer).

4. The first answer is checked by calculating ϕ in two or more equations.

5. All answers are plotted on a chart showing plant loads against total system load (this is an excellent check against errors as well as an indication of where base-loading will occur).

In the range where no plants are base-loaded the increment of load for any plant is constant for uniform changes in total system generation. This means that the plant loads are straight lines on the chart referred to in (5) above, until any plant reaches maximum or minimum load. Three or more loads are sufficient to determine (and check) the plant load lines in the linear portion.

If the solution of the equations is to be done algebraically, it is preferable to eliminate ϕ. This may be done by subtracting each of the last six equations from the first in Table VI. The necessary seventh equation is as follows

$$1.00G_a+1.00G_b+1.00G_c+1.00G_d+1.00G_e+1.00G_g+1.00G_h=G$$

Table IX. Effect of Changing Estimated Value of β on Allocation of Generation

Plant	$\beta=4.63$	$\beta=5.00$	$\beta=5.40$
a	40.1	39.9	39.8
b	40.8	40.7	40.6
c	20.2	20.4	20.5
d	23.6	23.7	23.9
e	34.8	34.7	34.6
g	26.4	26.3	26.1
h	14.1	14.3	14.5
Total	200.0	200.0	200.0

Notes: Values of β are in dollars per megawatt hour. Loading is given in megawatts.

Table VII shows the resulting equations with ϕ eliminated and the constraining equation added for 200 megawatts total system generation.

One advantage of the diagonal matrix solution is that the constants on the right hand side of the equality sign (including the total system generation) are kept separate from the variable coefficients at all times.

If the equations are arranged so that the totalizing or bottom row in Table VI becomes the right hand column in the final matrix, other values of total system load can be solved by merely changing the numerator in the final determinant by the amount of the change in the total system load. It is always desirable to start with a total system load near the middle of the schedule, so that no plant will be at maximum or minimum load.

As soon as a point in the schedule is reached where any plant will be base-loaded, it is necessary to rearrange the equations of Table VI and repeat the solution. This will be easier than before because there will be one less variable—the work varies as the square of the number of variables. The equations are rearranged by substituting in the proper column in Table VI the base load of the plant in question, moving the resulting numerical quantities to the right-hand side of the equality sign, and eliminating the row corresponding to the base-loaded plant, see Table VIII.

Appendix II. Determination of Transmission Loss Formulas

1. The following procedure for the determination of transmission losses in a power system is based upon the derivation of a loss formula by means of readings on the network analyzer and the application of this loss formula to a variety of generating conditions. Although the simplified method described here involves several approximations it is reasonably accurate for operating conditions where the normal operating angles between generator busses are not too great and where the power factor and geographic distribution of substation loads do not change too greatly. The method described is a combination of those presented in an AIEE paper by E. E. George[3] and in an unpublished paper by J. B. Ward.

2. Set up the system loads and lines for the loss condition expected to be most representative, remembering that losses vary as the square of the system load. Include station use as a load on the bus and use gross generation, or omit station use and use net generation.

3. Set up the generating plants and interconnections for number 2, giving preference to typical loading of major plants and interconnections. Small plants and minor interconnections should be netted, if practicable, as each additional source complicates the loss formula.

4. Read and record megawatts and megavars for the system of number 2 and number 3 including generators, lines, loads, capacitors, and so forth. Read and record all generator voltages and phase angles. Read vector load currents referred to some generator bus.

Table X. Accuracy of Analyzer Method

Plant	Loading in Megawatts Calculated by Algebraic Method	Loading in Megawatts Read on Network Analyzer
a	31.73	31.5
b	27.57	27.7
c	16.61	16.3
d	19.82	19.6
e	24.43	25.0
f		
g	19.70	19.5
h	10.14	10.0
Total	150.00	149.6

Notes: Accuracy of analyzer readings could be improved by pro-rating to total 150.0, preferably with help of graphic plot of adjacent readings (140 and 160 megawatts).

Plant *f* was not used in this study.

5. Supply the system of number 2 and number 3 from one of the major generating plants with all other sources disconnected. Adjust the plant output to any round value giving nearly full scale on the board ammeter, preferably 100 per cent current. Set the meter reference voltage in phase with the generator current, so that the vector reading of generator amperes has a zero reactive component. Using the vector ammeter, read and record the generator current and the current in every line. These readings should be in complex form. Watch and record signs carefully. There is less chance of error if the plugging diagram provides continuity of polarity throughout the system (See number 16).

6. Repeat number 5 for each remaining generator and each active interconnection, one at a time. This will give as many vector current flow diagrams as there are active generating plants and interconnections. Steps 2 to 6 include all the work that has to be done at the analyzer board.

7. Set up tabulation A, listing in the first column each line by the names of its two terminals, followed in the second column by the resistance of the line in per cent ohms, using any convenient base, preferably the one used in number 2. Horizontally opposite each line set down (from the flow diagrams of number 5 and number 6) per unit vector amperes with the real and reactive components in adjacent vertical columns for each of the sources. This provides a basic tabulation from which all of the loss coefficients are derived.

8. Set up tabulation B with the same two columns for line names and line resistances, followed by scalar I, I squared and I squared R for each line, using three vertical columns for each source. Total each IIR column, multiply by ten, and divide by the base in megavolt-amperes (used in number 7).

Except for later correction for voltage and power factor, this total figure provides the K constant for each source.

Tabulation B takes care of the square terms in the loss formula.

9. Set up tabulation C of per unit vector products as follows: In two columns at the left set up the name of each line and its per unit resistance as in previous tabulations A and B. To the right set up three columns for each pair of sources. (This may require

more than one page). In the first of the three columns, set up the product of the two real per unit components of current for the two sources in question. In the second column, enter the product of the corresponding reactive components. These components are given in tabulation B. In the third column enter the algebraic sum of the two components multiplied by the corresponding line resistance. Total each product column, multiply by 20, and divide by the base in megavolt-amperes (used in number 7). Tabulation C takes care of the product terms in the loss formula.

10. The square term constants derived in number 8 and the product term constants derived in number 9 require correction for voltage and power factor, so that plant loadings in megawatts squared may be converted to amperes squared. In number 11 this correction is made by using individual per cent voltage and individual per cent power factor for each source.

11. For voltage correction the totals referred to above in number 8 and number 9 should be divided by the square or product of the respective per unit voltages, prevailing for the typical load flow condition as read in number 4. Divide the above totals corrected for voltages by the square or product of the respective power factors (expressed as decimals).

12. The expression for total 3-phase transmission loss in kilowatts on a system consists of addition of the above terms after multiplying each square term by the square of the megawatts loading at its source and multiplying each product term by the product of the megawatts loadings of its two sources.

13. On systems where angles between sources are excessive and likely to affect superposition in the network, it is possible to make the readings of number 5 and number 6 reflect the normal angular condition by setting up a common reference voltage for all sources, maintaining the same angles found in number 4.

14. Losses can be studied separately on two or more portions of system, if there are one or more busses between portions.

15. Excessive losses (due to a single distant source) will distort relative loads and voltages in number 5. On most transmission systems, this effect should be minimized by trimming load impedances to get the normal vector load currents of number 4. Methods have been developed recently to facilitate this operation.

References

1. Economic Loading of Steam Power Plants, and Electric Systems (book), **M. J. Steinberg, J. H. Smith.** McGraw-Hill Book Company, New York, N. Y., 1935.

2. Intrasystem Transmission Losses, **E. E. George.** *Electrical Engineering* (*AIEE Transactions*) March 1943, volume 62, pages 153–58.

3. Four Methods for the Solution of Simultaneous Linear Equations, **R. H. Scanlan, M. G. Harrison.** *Product Engineering* (New York, N. Y.), June 1946, pages 513–15.

4. Differential and Integral Calculus (book), **R. Courant.** Interscience Publishers, New York, N. Y., volume II, 1936, pages 188–211.

5. The Mathematics of Physics and Chemistry (book), **H. Margenau, G. M. Murphy.** D. Van Nostrand Company, New York, N. Y., 1943, pages 480–82.

6. Elementary Matrices (book), **R. A. Frazer, W. J. Duncan, A. R. Collar.** MacMillan Company, New York, N. Y., 1946, pages 125–33.

7. The Marginal Efficiency, **A. Meldahl.** *Brown Boveri Review* (Baden, Switzerland), August, September 1947, pages 180–83.

8. Equivalent Circuits, **F. M. Starr.** *AIEE Transactions*, volume 51, part II, 1932, pages 287–98.

Discussion

H. P. St. Clair and **C. A. Imburgia** (American Gas and Electric Service Corporation, New York, N. Y.): The job of determining the most economical division of load between generating plants is a complicated one and requires a great deal of hard work, not the least of which is the determination of incremental heat rates for each individual unit or type of unit and for each of the several generating plants on the system. The authors referred to the book by Steinberg and Smith[1] in which there was described a special type of slide rule for a ready determination of the most economical division of load between units on the basis of incremental fuel costs only. The authors have pointed out that until recently little attempt has been made to tie in with such determination of economical plant loading the effect of transmission losses.

On the American Gas and Electric Company system a great deal of work has been done in determining incremental heat rates, and this part of the job may be said to be very well in hand. In the application of this data to economical plant loading, we have made use of the Steinberg and Smith incremental slide rule. The question of transmission losses is obviously a very important one on the widespread transmission system which we operate, and from the beginning we have attempted to take into account transmission losses, at least in a rough way wherever they appear to be important. At the present time, however, we are in the midst of a serious study of this problem and have already made considerable progress in devising more accurate means of taking into account transmission losses as a penalty against fuel costs in various stations on the system under different station and system loading conditions. A considerable number of a-c board studies have already been made to serve as a basis for determining quantitative values of fuel cost penalties under different plant loading schedules and at different points on the system load curve.

Obviously, all of this is to a considerable extent a trial and error method. In order to take into account a large number of variations and system operating conditions, a more direct method, such as that described by the authors, if it can be worked out and applied to our problem, will be most welcome. For this reason we are glad to see the interest being taken in this problem as shown by the work of the authors and others who have contributed to this subject.

We hope that this interest will continue and that not only the authors but others will pursue such studies further.

Reference

1. See reference 1 of the paper.

M. J. Steinberg (Consolidated Edison Company of New York Inc., New York, N. Y.): This paper describes the application of a simplified network analyzer for determination of economy loading of generating stations with correction for the effect of transmission line losses. Because of the complex nature of the problem, solution along theoretical lines has been impractical making it necessary to resort to arbitrary and approximate methods. The promise of a relatively simple solution makes desirable the careful study and analysis of the paper, and for this purpose it would be helpful to have available a single-line diagram of the system to which the procedure described in the paper was applied by the authors, together with circuit impedance values. It is hoped, therefore, that this information will be supplied with the authors' written closure. The value of the paper for analytical purposes also would be enhanced if an appendix had

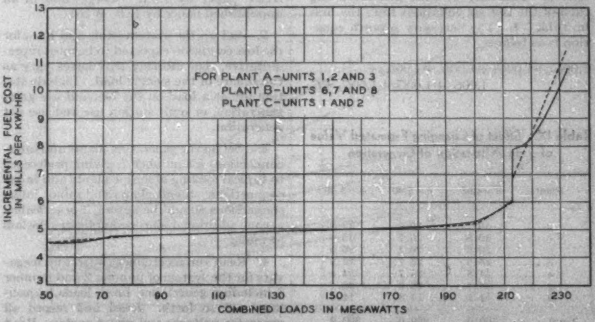

Figure 1. Comparison of incremental costs for plants a, b, and c combined, by using exponential and linear incremental cost curves for individual plants

been included showing the calculation of the K terms which are indicated as the coefficients of the G terms in Table I of the paper, so as to make it unnecessary to refer to other papers for this information.

The writer is impressed by the simplifying assumption which replaces exponential-type incremental cost curves with linear curves, because of its possible application to effect considerable reduction in the computations required to establish performance curves for the various generating stations of the writer's system. To ascertain the variation which might be expected, incremental cost curves were computed for plants a, b, and c combined using both types of cost curves. The results are shown in Figure 1 of this discussion. The variation in the range of load from a minimum value to the value corresponding to the discontinuity in the cost curve for plant b is so small as to be negligible. For combined loads above 213 megawatts the variation shown could be reduced considerably by a more judicious location of the linear curve approximating the performance of plant b for loads above 51 megawatts. It would appear from a preliminary study that the use of linear relations between incremental fuel costs and load will not introduce appreciable error.

Another simplification is introduced by the use of an average value for β. As indicated in the second paragraph following equation 8, this value is a weighted average and, as subsequently stated in the paper, lies about halfway between minimum and maximum values corresponding respectively to the minimum and maximum generated loads when all plants are in service. A sample calculation illustrating the method of weighting employed would be most welcome as clarifying information.

The authors and those associated with them in the analytical studies described in the paper are to be congratulated for their originality of approach and for a valuable contribution to the art. It may well be, as stated in the introduction, "that a simplified network analyzer will be an essential part of the load dispatcher's equipment."

H. B. Smith (Buffalo Niagara Electric Corporation, Buffalo, N. Y.): The material presented in this paper is very interesting and represents a valuable contribution to the techniques for handling power systems.

At the AIEE Fall General Meeting, it was stated that several persons had informed the authors that they had found the paper hard to understand. This was interesting, and perhaps comforting, to me because my reactions were the same. Because of this I feel that a few comments on various parts of the paper might be helpful to some who had difficulty getting through the material:

1. The authors state that: "Table I shows the total transmission loss formula for the system." What system? Evidently it is for a system having eight sources. A 1-line diagram of this system would help.

2. Re ninth paragraph under the section on Description and Application Method: Incremental transmission loss is in kilowatts per megawatt change in generation at some particular plant. Or, for a one hour period, incremental transmission loss is in kilowatt-hours per megawatt change in generation at some particular plant.

Incremental fuel cost is in dollars per megawatt-hour. Thus the conversion to be made is from dollars to kilowatt-hours (or megawatt-hours), and not dollars to kilowatts.

Then the factor β (which might have seemed less mysterious if Greek letters had been avoided) is the average of the increment fuel costs for all generators operating in dollars per kilowatt-hour.

The reciprocal of β is the number of megawatt-hours that could be produced on the average in the rest of the system for each dollar that might be saved in fuel costs due to swapping a megawatt of load from plant a to plant b, and so forth.

3. I believe the title of Table II of the paper is more correctly Incremental Transmission Loss in Kilowatts Per Megawatt Change in Generation (For Small Changes in Generation).

Then, with station a as the variable

$$\frac{\Delta L_t}{\Delta G_a} \doteq \frac{\delta L_t}{\delta G_a} = 3.06\ G_a + 2.12\ G_b + 1.64\ G_c + \ldots\ldots 2.8\ G_h = K_1$$

All the equations in Table II ($\delta L_t/\delta G_a$, $\delta L_t/\delta G_b$, $\delta L_t/\delta G_c$, and so forth) are equal to each other and thus equal to a constant K_1 only when the plants are loaded so that total transmission loss is a minimum.

4. In equation 2, F_t is total system fuel cost of generated energy. It follows then that $\delta F_t/\delta G_a$ is the incremental fuel cost for the entire system for a change in generation at plant a.

Under equation 3, it is stated that $\delta F_t/\delta G_n$ is the incremental fuel cost at plant n for a change in generation at plant n. Why, then, should not this be $\delta F_n/\delta G_n$? The inconsistency is removed if it is pointed out that, for a change in generation at plant $a\ \delta F_t/\delta G_a = \delta F_a/\delta G_a$.

5. A check of the units used in equation 2 may be helpful

$$\left(\frac{\delta F_t}{\delta G_a} - \frac{\delta F_t}{\delta G_b}\right) = \frac{\beta}{1{,}000}\left(\frac{\delta L_t}{\delta G_b} - \frac{\delta L_t}{\delta G_a}\right) \qquad (2)$$

F_t in \$/hr
L_t in kw
G_a and G_b in mw
β in \$/mw hr (not in mills/kwhr)

Substituting in equation 2

$$\frac{\$/\text{hr}}{\text{mw}} = \frac{\$/\text{mw hr}}{1{,}000}\ \frac{\text{kw}}{\text{mw}} = \frac{\$}{\text{kwhr}}\ \frac{\text{kw}}{\text{mw}} = \frac{\$}{\text{hr mw}}$$
$$= \frac{\$/\text{hr}}{\text{mw}}$$

Numerically dollars per megawatt-hour is equal to mills per kilowatt-hour. However, from the above it can be seen that β in mills per kilowatt-hour would not yield a "units" check for equation 2. Things like this, though clear to the authors, may be confusing to the reader.

6. The authors refer to E. E. George's paper Intrasystem Transmission Losses[1] for the method of determining the loss formulas.

In Appendix I of this paper, "per cent" appears three times, once in the reading and twice in the equations. This is in error and "per cent" should be struck out in these three places.

Reference

1. See reference 2 of the paper.

S. B. Crary (General Electric Company, Schenectady, N. Y.): The authors have made a very important contribution which can be expected to have a significant influence on system design and operation.

As is often the case in the solution of what is considered to be an overwhelming problem, the authors have been forced to make many simplifying engineering assumptions. Herein lies an opportunity for them to materially improve the understanding of their paper. I would like to suggest that they put down in one place the development of their method step-by-step with all of the necessary simplifying assumptions clearly stated.

Readers also will be interested in their evaluation of some of these approximations. We have found the transmission loss formula to be quite accurate for a relatively simple check case. It would help materially in the understanding of the method if more details concerning the system benefits in design and operation were presented. For example, it would be desirable to know what advantages accrue from considering line losses in addition to fuel costs for an actual system.

This comparison, if possible, should be made both for a solution based on the assumptions made in the paper and for a method without the approximations. This would more clearly show the desirability of further refinements in the method.

The line loss formula used by the authors, although approximate, appears to be quite accurate. Its accuracy is questionable only at loadings that are considerably higher than normal loadings and more in the region of emergency operation.

Undoubtedly improvements in the method will develop with use. Even in its present state it appears to be a long step in the direction of improved economy and should re-emphasize in a very understandable and practical way the need for lower loss transmission systems.

C. W. Watchorn (Pennsylvania Water Power Company, Baltimore, Md.): I have only general knowledge as to the operation of a so-called a-c calculating board and consequently, I am in no position to pass expert judgment on the facility with which such computing devices may be used for handling problems of this nature. My general impression is that unless the suggested computations are greatly simplified they would be impractical to use directly for operating purposes. However, it may be possible that general calculations along the line suggested by the authors could possibly be used to great advantage as a basis for judgment in modifying the incremental rates to allow for transmission losses. In this sense, such computations could be quite useful. However, there would still be the difficulty of determining the rates to be used for interchange billing where several systems are interconnected. Another difficulty would be encountered in connection with changing conditions that would result, more generally where several systems are interconnected, when there would be tendencies, under varying and

Table I. Effect of Changing Estimated Value of β

(On Allocation of Generation)

Plant	Light Load $\beta = 5.00$	Light Load $\beta = 4.81$	Medium Load $\beta = 5.00$	Medium Load $\beta = 5.25$	Heavy Load $\beta = 5.00$	Heavy Load $\beta = 5.99$
a	22	22	38	39	71	73
b	14	16	41	42	44*	44*
c	13	13	21	21	30*	30*
d	16	16	25	24	50	48
e	18	17	43	41	44*	44*
f	8	8	14	15	30*	30*
h	7	6	16	16	18*	18*
Total	98	98	198	198	287	287

*Base loaded.

Notes: Values of β are in dollars per megawatt-hour. Loading is given in megawatts.

generally unforeseeable conditions, to interchange large blocks of power in one direction under one set of conditions and in other directions under other sets of conditions.

It is believed that the simplifying assumption used by the authors of using straight lines to represent the input-output curves may lead, in many instances, to rather erroneous results, particularly where the curvature for the actual curves is fairly large. This condition would be more generally encountered where several units in the various stations are combined and especially for the higher loads thereon, as shown by the right-hand portion of Figure 5 of the paper, unless such conditions are represented by numerous short straight lines, which may become rather cumbersome to handle.

There are several specific comments I wish to make relating to the section on The Mathematical Derivation of the General Co-ordination Equation. I believe that the significance of equation 2 would be somewhat more apparent on its face if β therein were replaced by $\delta F_t/\delta G_t$, the reciprocal of which is shown under equation 3, and with the appropriate modifications in the explanation of the symbols under equation 2. β could then be substituted in equation 3 as the reciprocal of $\delta G_t/\delta F_t$ which is shown therein, and which, of itself, has no useful significance as related to the problem at hand. This presentation would then logically result in the expression, $1000/\beta$, as shown below equation 7 and also in equations 8, 9, and 10 in the paper. It also is believed that the significance of equation 3 would be more readily appreciated if equated first to $\delta D_t/\delta G_n$ and then ϕ, or equation 1. Equation 3 would then be written as

$$\frac{1{,}000}{\beta}\cdot\frac{\delta F_t}{\delta G_n}+\frac{\delta L_t}{\delta G_n}=\frac{\delta D_t}{\delta G_n}=\phi$$

It also is believed that the statement following equation 10 should read "Taking numerical values from Tables I or II and Table IV, . . ." rather than "Taking numerical values from Tables I and IV, . . ."

It also is believed that it would help the reader if it were stated under Description and Application of Method as related to the description of Table I that this table shows coefficients, K_{nn} and K_{nm}, as for equation 4, and if the heading of or a footnote on Table I stated that the numerical values were the coefficients as for equation 4. It also would be helpful to state in this portion, and also on Table I that the coefficients were derived in the manner described in Appendix II. In somewhat the same way, the description of Table II, would be clearer if explained as showing the coefficients $2K_{nn}$ and K_{nm} as for equations 5, 6, and 7 and that the numerical values shown on the diagonal, from the upper right to the lower left, were the coefficients $2K_{nn}$.

It is further believed that it is possible the numerical solution may very well be carried out with greater facility by means of automatic digital calculators, such as the *IBM 602A* or *604* calculators, along the general lines described in Appendix I, rather than by means of an analogue calculator such as a network analyzer in the manner described in the paper. Such calculations could then be carried out en masse, practically on a full automatic basis, for any reasonable number of desired conditions, essentially as one group of computations. This should be a large time saver in making the necessary calculations for large systems and interconnected systems. However, this method of solution also would be impractical to use directly for operation purposes and the results again be useful only for judgment modification of the incremental rates to allow for transmission losses.

It might be misleading if it is not pointed out in the paper the approximate value of 5.00 mills per kilowatt-hour used for β therein applies satisfactorily to the example illustrated and that it might be considerably different for other situations. This caution is particularly desirable since ϕ is but slightly greater than 1,000 regardless of conditions and the reader may be left with the impression that β is similarly approximately independent of conditions.

It is suggested that all through the paper, where the expression "fuel cost" or "fuel costs" is used, including the title, that this be changed to recognize the fact that other costs than fuel are involved in the cost of production with changes in generation. The term "variable generating costs" might be appropriate for this purpose.

I have followed through the remaining portions of the paper in so far as I am able (limited as stated, to my meager knowledge of a-c calculating boards) and find everything else to appear to be all right.

E. E. George, H. W. Page and J. B. Ward: The authors wish to thank those who have contributed verbal or written discussions of this paper. The interest shown in the subject and the recognition of the possibilities of the described procedures are extremely gratifying.

A number of simplifying approximations

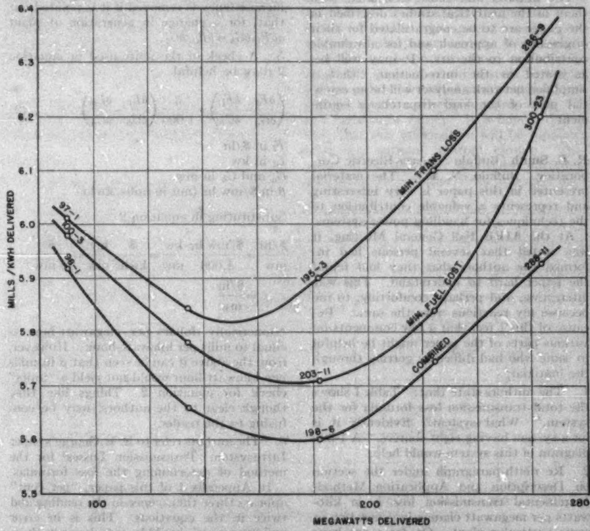

Figure 2. Relative cost of delivered energy for one combination of units

were used in the derivation of the incremental transmission loss formulas and their combination with incremental fuel costs. For the system illustrated and for which loading schedules were derived by the new method, the approximations can be considered to have little effect on the results and, in general, the discussion has borne out their acceptability. It must be recognized that electric generating systems vary in their separate descriptions and characteristics. The approximations made in the paper may have to be modified or supplemented by additional simplifying approximations in applying the method to a particular system. It is felt however, that the basic procedures can find wide application in the derivation of system loading schedules and in system planning. The extent to which the details of the method are applied will depend on the system itself and on the results that are desired.

Comments by H. B. Smith on symbols, units, and definitions are appropriate and should be helpful to many readers. F_t and F_n are synonymous because the total and the partial differentials of F are equal. This results from the fact that the incremental fuel costs of the various plants are independent of one another.

With regard to E. E. George's paper on Intrasystem Transmission Losses, the authors are unable to agree with Mr. Smith on his comment. The confusion probably arises from the fact that line flows were expressed in per cent in George's paper, whereas they are expressed in per unit in the present paper.

M. J. Steinberg suggested that the calculation of the K terms be included in the closure. This is not being done because an improved method of determining the loss coefficients has been developed. It is hoped that this new procedure will be presented to the AIEE in the near future. Steinberg also requested information on the effect of varying β. Table I of the discussion shows that this approximation does not have any great effect on the determination of proper loading providing that the value of β is properly chosen. The weighted average value of β used in the paper is an approximation obtained by taking a load for each plant, halfway between minimum and maximum capabilities, multiplying this load by the incremental fuel cost at that load, adding the products and dividing the sum by the total of the individual loads. This approximate value was found to be satisfactory for the particular system under consideration. For other systems, it may be found desirable to use more than one value of β, each value being applied for conditions approximating those for which it was developed.

A 1-line diagram of the system under consideration was requested by Steinberg and Smith. This is not included herewith for lack of space but copies are available on request to the authors.

H. P. St. Clair and C. A. Imburgia have expressed their interest in the application of the new method and their comments are appreciated. Their interest in the matter of incremental losses has already resulted in the development of a more direct method of measuring incremental loss coefficients on the network analyzer.

In answer to S. B. Crary's question regarding system benefits, it must be pointed out that savings which can be made depend on the fuel costs and other characteristics of the particular system. It is believed that Figure 2 of the discussion will serve to illustrate the savings that are being obtained on the system discussed in this paper.

The three curves shown indicate respectively delivered energy costs obtaining (1) when plants are loaded for minimum transmission loss, (2) when plants are loaded for minimum fuel cost and (3) when fuel costs and transmission losses are combined to give minimum delivered cost. The percentage figures at top of figure indicate the savings effected by considering transmission losses. The figures on the curves represent the megawatts of generation required and the megawatts of transmission loss sustained in each case to result in megawatt delivery shown on the abscissa of the chart. In this particular case, system demand can be met with 12 megawatts less generating capacity when plants are loaded according to condition 3. This serves to illustrate the use of the method in system planning. By analyzing the system on the network analyzer, the location for new generating capacity can be determined which will result in proper compromise between transmission losses and fuel costs. The lowered transmission losses can be reflected in reduced capital investment in generating capacity.

C. W. Watchorn questions use of straight lines to represent incremental cost curves. The authors suggest that wherever an extreme case of curvature is found, the curve can be approximated by two or three intersecting straight lines. Experience on the network analyzer has shown that such a combination of straight line equations is not difficult to handle. Watchorn makes some helpful suggestions relating to symbols and notation. Although the text has not been revised to incorporate these suggestions, they may improve the clarity of the mathematical derivation.

The authors have not had actual experience with automatic calculators such as the International Business Machine tabulating machine and cannot comment in detail on the suggestion to use such equipment, although inclined to doubt that there is any mechanism more suitable than the network analyzer for making plant loading schedules on the average system. This statement is influenced by the fact that practically every power system has engineers familiar with the use of the network analyzer.

As Watchorn states it should be noted that the value of β varies widely on various different systems, and might be as low as one mill or as high as ten mills. Experience in fuel cost studies leads the authors to feel that fuel costs only should be considered when dealing with incremental production costs for the purpose of making loading schedules on the network analyzer, although there is nothing in the methods recommended which would preclude the addition of other factors, if desired.

Prediction of Ultimate Temperature Rise from Early Heat Run Data

J. E. RYAN
MEMBER AIEE

Synopsis: When temperature-time data from heat runs departs markedly from a simple exponential form, existing methods of predicting the ultimate rise from early data may be inaccurate. This paper presents a graphical method for doing this which, although widely applicable, is especially useful on electromagnets. Substantial savings in testing time result from its use.

THE experimental determination of the steady-state temperature rise of electric apparatus is a tedious matter, particularly when the apparatus is large. In such cases, hours may be spent waiting for equilibrium to be reached. Obviously, great economies in testing time could be made if an accurate method for extrapolating early heat run data were available.

Several authors[1,2,3] have set forth methods for doing this when the temperature rise of the body being measured is of the form

$$\theta = A(1-\epsilon^{-\alpha t}) \qquad (1)$$

throughout the heating period. However, this simple relation is followed only when the device under test acts at all times as a single body at uniform temperature throughout. Mr. V. Karapetoff[4] pointed out that the temperature rise of a particular part of a device, such as the winding, is more accurately expressed by

$$\theta = A(1-\epsilon^{-\alpha t}) \pm B(1-\epsilon^{-\beta t}) \pm C(1-\epsilon^{-\gamma t}) \pm \ldots \qquad (2)$$

The number of exponential terms required depends upon the number of heat sources and heat-absorbing masses, as well as the thermal resistances connecting the latter. For a great number of devices such as tractive magnets, which contain only two major masses and heat sources, two terms are sufficient.

Cooney,[5] and later Jeffrey and Osborn,[6] took account of the double-exponential nature of temperature rise when developing their methods for predicting winding temperature as loads varied, but at least one complete heat run was required as a preliminary for their considerations.

This paper presents a method by which early heat run data on 2-mass devices can be extrapolated to find the steady-state temperature of the mass (for example, the winding) being measured.

Nomenclature

θ = temperature rise of the part of the device being measured, degrees centigrade
t = time from start of heat run, minutes
α, β, γ = reciprocals of thermal time constants, minutes^{-1}
A, B, C = steady-state temperature rise components, degrees centigrade
$Y_a = A\alpha\epsilon^{-\alpha t}$
$Y_b = B\beta\epsilon^{-\beta t}$
$Y_c = A\alpha\epsilon^{-\alpha t} + B\beta\epsilon^{-\beta t}$
$Y_d = A\alpha\epsilon^{-\alpha t} - B\beta\epsilon^{-\beta t}$

Subscripts and superscripts

1 and 2 refer to arbitrary times
a, b, c, d refer to corresponding curves
u refers to ultimate rise
Primes denote values at the time when ultimate rise prediction is made

Derivation

If the 2-term form of the winding temperature equation 2 be differentiated, there results

$$\frac{d\theta}{dt} = A\alpha\epsilon^{-\alpha t} \pm B\beta\epsilon^{-\beta t} \qquad (3)$$

Either of the terms on the right-hand side of equation 3 will plot as a straight line on semilog paper when the co-ordinates are chosen as in Figure 1. For the first term (curve "A"), the scale value at the Y-axis intercept is $A\alpha$, and the slope is

$$-\alpha = \frac{\log_\epsilon Y_{a2} - \log_\epsilon Y_{a1}}{t_2 - t_1} \qquad (4)$$

For the second term (curve "B"), the Y-axis intercept is at $B\beta$ (or $-B\beta$) and the slope is

$$-\beta = \frac{\log_\epsilon Y_{b2} - \log_\epsilon Y_{b1}}{t_2 - t_1} \qquad (5)$$

In general, one of the exponentials will decay faster than the others as time proceeds, due to having a larger coefficient of t in the exponent. Therefore, let β be substantially greater than α. Values of A and B used in Figure 1 are arbitrary but typical.

Adding the ordinate scale values of curves "A" and "B," Figure 1, at each of a number of values of t and plotting these sums on the same graph, the $d\theta/dt$ versus t relation defined by equation 3 is obtained (curve "C"). The shape of this curve is typical for the coil of a d-c magnet wherein the copper loss of the coil causes a

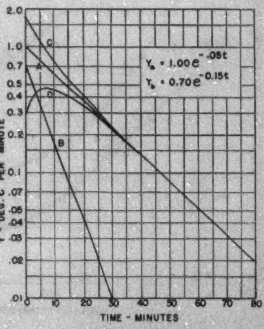

Figure 1. Typical forms of rate-of-rise curves

Paper 49-244, recommended by the AIEE Industrial Control Committee and approved by the AIEE Technical Program Committee for presentation at the AIEE Fall General Meeting, Cincinnati, Ohio, October 17-21, 1949. Manuscript submitted November 16, 1948; made available for printing September 2, 1949.

J. E. Ryan is with the General Electric Company, Schenectady, N. Y.

Table I. Determination of Rate of Rise for Large D-C Magnet

t	θ	2Δθ	2Δt	Δθ/Δt
0	0			
10		48.0	20	2.40
20	48.0			
30		15.5	20	0.78
40	63.5			
50		9.0	20	0.45
60	72.5			
70		6.3	20	0.31
80	78.8			
90		5.2	20	0.26
100	83.0			
110		3.0	20	0.15
120	86.0			
130		2.8	20	0.14
140	88.8			
150		2.1	20	0.10
160	90.9			

relatively rapid rise of coil temperature at first, decreasing as the heat conducts into and gradually raises the temperature of the iron.

By subtracting the curve "B" ordinates from those of curve "A" instead of adding, the second typical form of the $d\theta/dt$ versus t curve is obtained (curve "D"). This represents the condition in a large a-c magnet coil which receives heat from the iron.

Now, if the earlier parts of either curve "C" or "D," Figure 1, were given in the first place, the two component curves "A" and "B" could be found by trial, knowing that both of the latter have to be straight lines. This is particularly easy if β is much larger than α, for then curve "C" or "D" becomes a straight line relatively early in the run. In any case, however, a few trials will locate two straight lines whose Y values, when added or subtracted as the case may require, will closely approximate the corresponding $d\theta/dt$ values.

Having found these component lines, $A\alpha$, α, $B\beta$, and β may be found from the intercepts and slopes. Hence, A and B become known. Theoretically, this is all that is necessary to find θ_u since, from equation 2

$$\theta_u=A\pm B \tag{6}$$

However, it is more accurate to extrapolate from the last experimental value of θ as follows

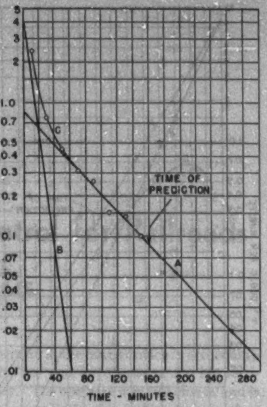

Figure 3. Rate-of-rise curves of a large d-c magnet

$$\theta_u=\theta_{t'}+\int_{t'}^{\infty}\left(\frac{d\theta}{dt}\right)dt=$$

$$\theta_{t'}+A\alpha\int_{t'}^{\infty}\epsilon^{-\alpha t}dt\pm B\beta\int_{t'}^{\infty}\epsilon^{-\beta t}dt$$

$$=\theta_{t'}+A\epsilon^{-\alpha t'}\pm B\epsilon^{-\beta t'} \tag{7}$$

Since, at time t', the ordinates of the component lines are, respectively

$$Y_a'=A\alpha\epsilon^{-\alpha t'} \tag{8}$$

$$Y_b'=B\beta\epsilon^{-\beta t'} \tag{9}$$

equation 7 may be written as

$$\theta_u=\theta_{t'}+\frac{Y_a'}{\alpha}\pm\frac{Y_b'}{\beta} \tag{10}$$

For finding from experimental data the values of $d\theta/dt$ required for the preceding analysis, the approximation

$$\frac{d\theta}{dt}\cong\frac{\Delta\theta}{\Delta t}=\frac{\theta_{t+\Delta t}-\theta_{t-\Delta t}}{2\Delta t} \tag{11}$$

Table II. Determination of Rate of Rise for Large A-C Solenoid

t	θ	2Δθ	2Δt	Δθ/Δt
0	0			
2.5		1.4	5	0.28
5	1.4			
10		3.6	10	0.36
15	5.0			
20		5.5	10	0.55
25	9.5			
30		5.9	10	0.59
35	15.4			
40		6.0	10	0.60
45	21.4			
50		5.6	10	0.56
55	27.0			
60		5.2	10	0.52
65	32.2			
70		5.6	10	0.56
75	37.8			
80		5.3	10	0.53
85	43.1			
90		5.1	10	0.51
95	48.2			
100		4.3	10	0.43
105	52.5			
110		3.7	10	0.37
115	56.2			
120		3.7	10	0.37
125	59.9			
130		2.6	10	0.26
135	62.5			
140		2.4	10	0.24
145	64.9			
150		2.1	10	0.21
155	67.0			
160		1.5	10	0.15
165	68.5			

is used, Δt being a reasonably small time interval. It is usually desirable to smooth the θ versus t data before differentiating.

Application

Figure 2 is the smoothed temperature-time curve of a large d-c magnet, energized at constant voltage. In Table I, values taken from the curve at 10-minute intervals are used in equation 11 to find $\Delta\theta/\Delta t$. The latter are then plotted as curve "C," Figure 3.

In this case, the curve becomes substantially straight as early as $t=80$ but the time of prediction is delayed until $t=130$ to be more certain.

By trial, lines "A" and "B" are located

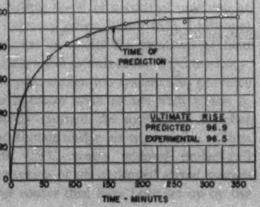

Figure 2 (left). Temperature rise of a large d-c magnet

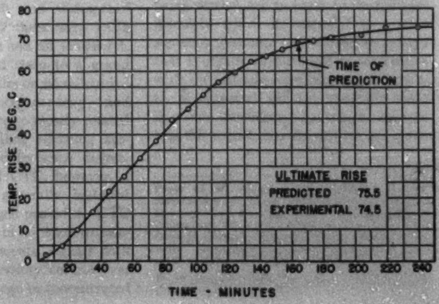

Figure 4 (right). Temperature rise of a large a-c solenoid so that their Y values add to give a close approximation to the known portion of curve "C". Using equations 4 and 5

$$\alpha = 0.0144$$
$$\beta = 0.100 \qquad (12)$$

Then, from the curves of Figures 2 and 3 at $t' = 160$

$$\theta_{t'} = 90.9$$
$$Y_a' = 0.086$$
$$Y_b' \cong 0 \qquad (13)$$

Substituting these into equation 10, the predicted ultimate temperature rise is

$$\theta_u = 90.9 + \frac{0.086}{0.0144} = 96.9 \qquad (14)$$

This is practically identical with the experimental value obtained later. Figure 4 is the smoothed temperature rise curve of a large a-c solenoid, energized at constant voltage.

Following the same procedure as before, the $\Delta\theta/\Delta t$ values for Figure 5 are obtained in Table II. When plotted, these do not indicate early convergence to a straight line so, by trial, lines "A" and "B" are located so that the difference of their ordinates gives curve "D". These yield

$$\alpha = 0.0218$$
$$\beta = 0.0274 \qquad (15)$$

Further, from Figures 4 and 5,

$$\theta_{t'} = 68.5$$
$$Y_a' = 0.220$$
$$Y_b' = 0.086 \qquad (16)$$

Substituting these into equation 10, it is predicted that

$$\theta_u = 68.5 + \frac{0.220}{0.0218} - \frac{0.086}{0.0274} = 75.5 \qquad (17)$$

If a line were drawn through the last six or seven experimental points of Figure 5, assuming incorrectly that this represents the $A\alpha\epsilon^{-\alpha t}$ asymptote and that the $B\beta\epsilon^{-\beta t}$, term has already become negligible, the prediction made on this basis is still within a degree of the correct value.

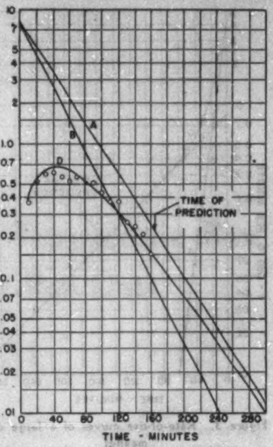

Figure 5. Rate-of-rise curves of a large a-c solenoid

Discussion

The second example above is more difficult than usual since α and β are fairly close together. It was used because it illustrates the complete method. Quite often the third term on the right side of equation 10 can be neglected when the estimate is undertaken, as was true in the first case.

Great accuracy in determining the component lines "A" and "B" of Figures 3 and 5 is not required. For example, an error of 10 per cent in slope will cause about the same per cent error in the estimate of the remaining rise, but if the rise at the estimate time is already 80 per cent of the ultimate, this will result in only (1.0—0.80)(0.10) = 0.02 or 2 per cent error in the final figure.

If the predicted rise is not the one desired, a readjustment of the voltage (or current) is made, causing the temperature to approach a new equilibrium. The $d\theta/dt$ versus t plot is continued without interruption. It will deviate from its original locus, but will still be of the form of equation 3; hence, the new θ_u may be estimated in the regular manner, confining the determination of component lines to the period after readjustment.

Although the procedure presented in this paper is applicable to devices of all sizes, it is most useful for large, slow heating ones where the possible time saving justifies the tabular and graphical work. This is frequently more than 50 per cent of the time otherwise required.

References

1. The Thermal Time Constants of Dynamo-Electric Machines, A. E. Kennelly. *AIEE Transactions*, volume 44, February 1925, pages 137–54.

2. Predicting Heat Rise on Electrical Machinery, A. F. Puchstein, T. C. Lloyd. *Product Engineering* (New York, N. Y.) volume 8, August 1937, pages 305–06.

3. Production Temperature Rise Tests on Transformers, H. S. Holbrook. *Journal*, Institution of Electrical Engineers (London, England) volume 88, part II, number 3, June 1941.

4. Parameters of Heating Curves of Electrical Machinery, Vladimir Karapetoff. *AIEE Transactions*, volume 45, February 1926, pages 349–54.

5. Predetermination of Self-Cooled Oil-Immersed Transformer Temperatures Before Conditions Are Constant, W. H. Cooney. *AIEE Transactions*, volume 44, May 1925, pages 611–18.

6. Interpretation of Time-Temperature Curves of Rotating Machines, F. Jeffrey, R. M. Osborn. *Allis-Chalmers Review* (Milwaukee, Wis.) volume 6, number 2, June 1941, pages 20–29.

No Discussion

Centralized Traffic Control for Railroads

W. D. HAILES
MEMBER AIEE

Synopsis: Railroads have installed many thousands of miles of a control system that retains all the time-tested safety features of railway signaling and centralizes the control of traffic on long sections of railroad. Special code type communication circuits and equipment have been perfected to furnish the remote control demanded by this system. The new communication facilities can be combined with other services on the same line wires and the range of control can be extended by the use of carrier current equipment. This centralized form of control has proved to be a dependable source of additional traffic capacity and increased earning ability.

CENTRALIZED Traffic Control (CTC) stands for an improved system of railroad operation as well as the organization of equipment and circuits by which it is accomplished.

Under this system of operation, train movements over a railroad division or major portion thereof are directed by supervised signal indications without the use of train orders or train superiority.

CTC combines an underlying railway signaling system with a supervisory communication system to concentrate the control of railroad traffic at a strategic point called the Control Office. The communication system automatically furnishes the operator at the control office with essential information concerning the constantly changing positions of the trains in his territory.

This information is displayed on the operating panel of a control machine at the control office, along with additional information about the positions of field switches and signals in the CTC territory. The communication system also provides the operator with means with which to quickly control the motorized switches and signals under his supervision. Thus with CTC, trains proceed under full protection of an approved signal system over routes that have been set up by the operator at the control office in accordance with his plan of operation for his territory. The operator is in full charge and is able to quickly change his plan of operation to meet unexpected changes in operating conditions and thus avoid long and costly delays that occur without CTC under these circumstances.

Train operation by signal indication only without the use of train orders was first instituted on the St. Louis—San Francisco Railway in 1914; however, previous to July 25, 1927, every installation of any appreciable extent, or requiring the operation of switches, necessitated operators at intermediate points. In these installations a train director coordinated the activities of operators who threw certain switches, cleared certain signals, and reported time of passage of the trains.

On July 25, 1927, the New York Central, Ohio Central Lines, completed the first installation of a new system. This installation covered 40 miles, extending from Stanley to Berwick, Ohio. It was called centralized traffic control and was the first system that made it possible for the train director to do all of the foregoing operations by himself.

Since this first installation, CTC has had a steady growth and widespread application. By 1937 there were 1,975 track miles in service and on January 1, 1948, this figure had risen to a grand total of 9,972 track miles on 65 railroads.[1]

Safety, speed, track capacity, and operating economy are so closely related and interdependent that signaling systems affect each one to some degree. Before the advent of CTC, however, a signal system was generally installed primarily for the safety it provided. CTC has changed this for, in addition to safeguarding train movements, signals with CTC provide a supervisory control over train movements that can be concentrated at a strategic point from which the traffic of a whole railroad division, or more, can be regulated and co-ordinated so as to effect large savings in time and money.

To accomplish this it was necessary to discover a way of controlling switches and signals many miles away and do it safely. It was not until the idea of decentralizing the safety features while centralizing control facilities was conceived that CTC became feasible. It was this contribution that made it possible to design a system that would conform to the "fail safe" principle and still provide supervisory control of remote switches and signals. The switches can be moved and signals cleared to give a "proceed" indication only if the local safety circuits at the remote point in the field permit them to do so. These local circuits associated with each field layout insure that no switch will move if there is a train moving across it or permit it to move if a train has been given a signal to proceed over it. Neither will a signal give a proceed indication unless the local safety circuits show that it is safe for the train to proceed. The operator at the control office might send a control to move a switch or clear a signal when it was not safe to move the switch or clear the signal; or the communication portion of the CTC system might fail to deliver the control exactly as intended because of some detailed failure along the CTC line circuit, but the switch would not move and the signal would not clear. The local safety circuits would prevent the control from being carried out and satisfy the fail-safe principle which is essential to proper signaling systems. In a device or system that is organized and built in accordance with the fail-safe principle, any failure in the system itself will automatically result in a safe condition. In a signaling system this means that the system will auto-

---

Paper 49-245, recommended by the AIEE Communications and Land Transportation Committees and approved by the AIEE Technical Program Committee for presentation at the AIEE Fall General Meeting, Cincinnati, Ohio, October 17–21, 1949. Manuscript submitted February 21, 1949; made available for printing September 2, 1949.

W. D. Hailes is with the General Railway Signal Company, Rochester, N. Y.

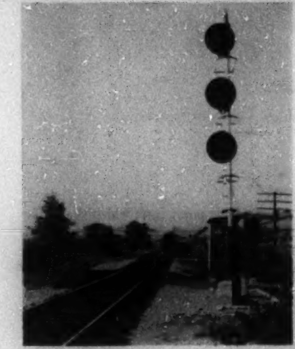

Figure 1. A typical field location

matically display or enforce a restrictive signal or restrictive control in case of a failure of the system itself.

Salient Characteristics

The principles of CTC are applicable to any track layout whether it be single track, multiple track, or a combination thereof. In fact, a CTC installation is basically a series of layouts or plants rather widely separated from each other but co-ordinated and controlled remotely from the CTC control office. The layout at the end of a passing siding on single-track railroad is a very common layout and will be used as the typical example in explaining CTC.

A siding end has a single switch and a group of associated signals. It has a short track circuit, which includes the switch, that is known as the detector or "OS" track circuit, plus two "approach" track circuits extending in each direction away from the switch on the main track. Frequently the side track also is equipped with a track circuit. The track circuit is probably the most important single element on which modern signaling systems are built. To obtain a track circuit a section of track is insulated from the track at either end by insulated rail joints placed in each rail. A source of electric energy (direct or alternating current) is connected between the rails at one end of this insulated section of track and an electric relay is connected across the rails at the opposite end of the section. A closed circuit is thus set up over which the relay receives electric energy to pick it up only so long as there are no broken rails and the rails of the section are not shunted by the wheels and axles of a train or car. These track circuits provide the primary or basic safety features. For example, unless a track section is unoccupied and the track relay is picked up to its energized position, the signals governing train movements over that section can not display a proceed indication. In a similar manner the other necessary safeguards are derived from the local signaling circuits including the interlocking of each remote layout with the next one. This is frequently done by signal line circuits extending from one layout to the next.

Figure 3. Portion of a control machine on the Boston and Maine Railroad with the operator sending out a control code

Figure 2. Signal relays and code equipment inside a field cabin on the Boston and Maine Railroad

Figure 4. Rear of a control machine having a slide type of support for code relay units

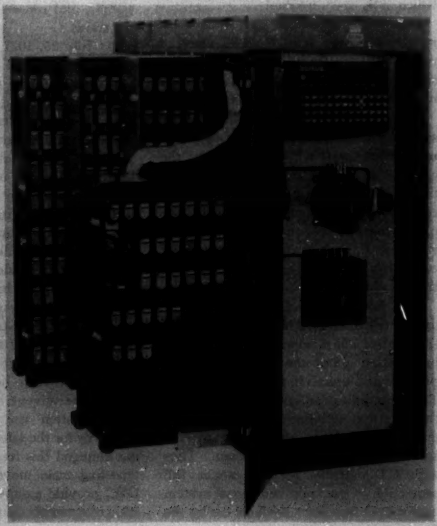

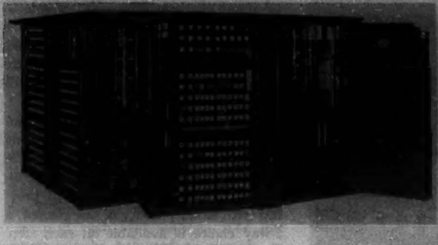

Figure 5. Rear of a control machine on the Union Pacific Railroad having a hinged type of support for code relay units

Recently there have been developed schemes by which this control can be obtained by means of special track circuits known as "coded" track circuits. These circuits can transmit "vital" controls in addition to performing their primary vital function of detecting occupancy or a broken rail.

A vital control is one on which the safe operation of trains depends and it must be given in accordance with the fail-safe principle described previously.

A coded track circuit is one in which the energy can be supplied to the track circuit in a series of pulses which on arrival at the other end of the track circuit cause the track relay to alternately pick up and release in conformity with the code pattern used in applying energy to the circuit. Either steady energy or coded energy will serve to show unoccupancy and therefore the choice of steady or coded energy can be used for a control.

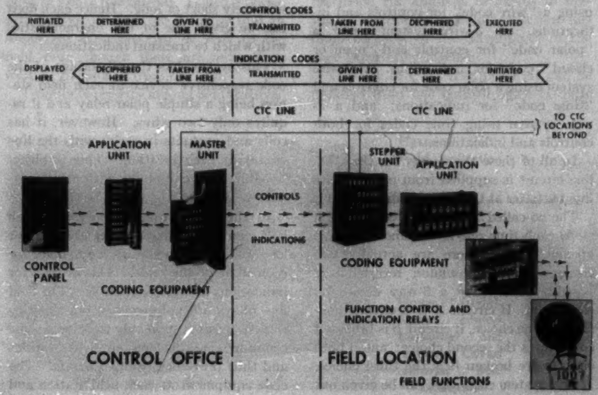
CONTROL CODES
INITIATED HERE
DETERMINED HERE
GIVEN TO LINE HERE
TRANSMITTED
TAKEN FROM LINE HERE
DECIPHERED HERE
EXECUTED HERE
INDICATION CODES
DISPLAYED HERE
DECIPHERED HERE
TAKEN FROM LINE HERE
TRANSMITTED
GIVEN TO LINE HERE
DETERMINED HERE
INITIATED HERE
CTC LINE
CTC LINE
TO CTC LOCATIONS BEYOND
APPLICATION UNIT
MASTER UNIT
STEPPER UNIT
APPLICATION UNIT
CONTROLS
INDICATIONS
CONTROL PANEL
CODING EQUIPMENT
CODING EQUIPMENT
FUNCTION CONTROL AND INDICATION RELAYS
CONTROL OFFICE
FIELD LOCATION
FIELD FUNCTIONS

Figure 6. Organization of a coded CTC system

With full CTC control the track switch and signals at a layout are motorized so that they can be operated from local energy by remote control. Also the local signal circuits automatically select the appropriate signal unit when the switch is moved from one position to the other. For example, when a switch is moved to the "reverse" position, the local signal circuits select the signal unit that governs train movements over the switch when it is set for the side track. When a switch is moved to the "normal" position, the local signal circuits select the signal unit that governs train movements over the switch when it is set for the main track. These are some of the more important and simple acts that are performed automatically by the local circuits and equipment of the signaling system to guarantee safe conduct of trains. The signal circuits and equipment, particularly relays, are also the sources of information from which the communication portion of a CTC system automatically reports the movement of trains and the positions occupied by switches and signals. It is the movement of a track relay from its picked-up to its released position that momentarily opens the starting circuit of the CTC communication system and causes it to report that a train has just entered the track section associated with the relay that released as the train shunted the rails of the section. Certain other relays are the means by which the supervisory controls are introduced into the signal system.

Figure 7. Automatic train recorder, with transparent cover raised, installed in desk of control machine

CTC requires a very special kind of communication system and a great deal of development has gone into the present-day circuits and equipment. The chief requisites for this communication system are as follows:

It shall automatically and quickly transmit essential information called "indications" concerning movement of trains and other information from a series of points in the field called "field locations" to the operator at the control office.

It shall quickly transmit directives called "controls" from the operator to any one of the field locations to produce the action he desires to accomplish there.

It shall perform its functions on the fewest number of line wires and at least cost for equipment and maintenance.

It shall perform with a nearly faultless reliability; for, notwithstanding the fact that vital controls are not entrusted to it, the communication system of a CTC system must be reliable if the value of CTC is to be realized.

It shall be capable of operation from local energy sources in case of failure of commercial power sources.

It should permit the superposition of other communication facilities on the CTC wires and be capable of application to existing line circuits carrying other services without causing mutual interference.

It shall be readily adaptable to remote control over a carrier current link circuit

At first a relatively large number of line wires were used to effect the control desired. Some of the early installations used one line wire from the control office to each of the outlying field locations, plus a common return wire made up in the form of a cable supported by a steel messenger wire. However, it soon became evident that the cost for so many line wires would become prohibitive, particularly since CTC was being contemplated for long stretches of territory. It thus became necessary to develop systems that required only a few wires. This meant that schemes would have to be found to use the same line wires successively for all field locations for controls as well as indications.

Two general solutions for dividing line time among the several field locations have been used. One of these solutions distributed the CTC line time by scanning all locations, one after another, every time even one indication or one control was to be transmitted. In this way a complete set of indications and controls could be sent on one trip of the scanning operation, but there is rarely, if ever, a need for this facility and it became costly in line time and scanning equipment when contemplated for large installations.

The other solution is based on a selective use of the CTC line circuit. In this scheme the line is used to serve one location at a time and only when needed to report a change at the location or to deliver a control to the location. The result of this approach to the problem is the coded CTC communication system. Practically all CTC installations today are controlled by some form of the coded CTC communication system.

The name comes from the fact that controls and indications are transmitted in the form of coded messages that can be sent over the CTC line circuit or circuits. Each code consists of a series of digits whose characteristics comprise the message. The first part of a control code contains the digits that select the particular location and station and the last part contains the digits that deliver a complete set of controls to the field station. It will be well at this point to define location and station.

A point in the field at which one or more switches and signals are grouped and handled by one field code unit is called a CTC field location. If a location is complex, there will be two or more subdivisions within the location in order to facilitate communication to and from the location. These subdivisions are called CTC stations. If a location has only one station, the terms station and location stand for the same thing and station is usually used. In fact, station is the fundamental unit and will be used hereafter.

Figure 8. Field stepper unit

Similarly, the first part of an indication code contains the digits that register, in the control office, the identity of the station that is transmitting, and the second part contains the digits that completely describe the field conditions at the field station.

When a CTC code system is not required to transmit either controls or indications, it automatically goes into a period of rest and remains quiescent but sensitized to detect any change that would call for its operation. When set into operation it goes through a prescribed series of steps called a cycle. Step by step, synchronism is maintained by the CTC line circuit between the control office and field stations and each step carries a part of the coded message.

Among the coded CTC systems in operation today are: a 3-wire system using a "wire code" for controls and indications. A 3-wire system using a "polar code" for controls and "open or closed" code for indications. A 2-wire system using a polar code for controls and "time code" for indications; and a 2-wire system using time codes for both controls and indications.

In all of these the energy for the CTC line circuit is supplied from one or more line batteries at the control office.

The so-called 3-wire wire code system steps each time one of the line circuits is opened. Since there are actually two circuits using a common return, it is possible to exercise a 3-way choice on each step. If circuit *A* is broken it constitutes one choice, if circuit *B* is broken it constitutes the second choice; and if both circuits are broken it is the third choice. In this system each digit can be given one of three characteristics with which to transmit controls or indications. This system is fast acting and relatively simple, but it requires three line wires, and there are important considerations that favor a 2-wire line circuit.

The 3-wire polar code system has a control circuit and an indication circuit using a common return wire. The stepping is done by interrupting the control circuit. However, since the stepping will progress with either polarity of line current, a 2-way choice is available on each step. The control wire may be made positive or negative with respect to common and the field polar line relays will detect this difference. Thus each digit can be given one of two characteristics with which to transmit a control.

This system uses the third wire to transmit indications. During each step the intervals when the control line is de-energized and when it is energized provide two opportunities to send an indication digit. There is a 2-way choice for each digit since the indication circuit can be closed or opened during each interval to give character to each digit. This system is fast acting and relatively simple and is capable of transmitting controls and indications simultaneously. However, it has the handicap of requiring three line wires and does not lend itself readily to combination with other services on the same line wires.

The 2-wire polar code system uses the same scheme that is used in the 3-wire polar code system for transmitting controls. But in this system indications are transmitted by a time code. During an indication cycle the rate of stepping is determined by the field station that is transmitting and each step provides half-step intervals, each of which can be made relatively short or long. Hence each digit can be given one of two characteristics with which to transmit indications.

This system has the advantage of the code responsive device at each field station being a simple polar relay and it requires only two wires. However, it has coils and contacts in series with the line circuit at each location. This is objectionable when combining with other services.

In the 2-wire time code system each half step can be made relatively short or long and thus provide a 2-way choice for each digit of the code. This is true for indications as well as controls. The field line relays are polar relays, but polarity is used in this system only to enforce some common condition on all field stations and thus prevent unwanted action. The code equipment at each field station and the control office must provide means for transmitting short and long intervals and means for detecting the difference between short and long intervals of time in order to send and receive time codes. This tends to make the time code system somewhat more complex than the polar code or the wire code systems, but the advantages of this system outweigh these objections. The time code system can be operated on two line wires without the use of relay coils or contacts in the line circuit at each field station. The line circuit can be balanced to provide an acceptable circuit for voice or carrier communication and it can be more readily superposed on existing line circuits than the other types of CTC line circuits.[2,3] The first 2-wire time code system was placed in service on September 17, 1929, on the Chicago, Burlington and Quincy Railroad, and the first 2-wire time code system having field stations in multiple went into service on July 31, 1940, on the Pennsylvania Railroad.

In developing coded CTC systems it was found that there were a relatively large number of schemes that could be used to transmit controls at the will of the operator to any one of several field stations, but there are very few schemes that can automatically transmit indications from each field station to the control office. The difficulty arises from the fact that trains moving at various points along the CTC territory set up indications at random intervals, each one demanding a share of the CTC line circuit time for transmission to the control office.

It is necessary therefore to enforce some form of superiority among field stations so that they will transmit their information in an orderly fashion instead of interfering with one another with the resultant garbling or loss of indications. It also is necessary to give priority to controls so that an important directive can be sent to the field even though there are indications waiting to come in from the field.

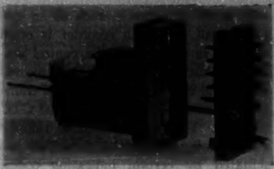

Figure 10. Typical code relay

To enforce priority among field stations, two schemes have been used in various ways. One scheme is based on the relative geographic positions of the field stations with respect to the control office where the line battery is located. The other employs a principle called "code superiority". In the geographic scheme each station is inferior to all those that are nearer the control office and superior to all those beyond it. This superiority resides in the ability of a station to deprive more distant stations of line battery energy by opening or shunting the CTC line circuit.

Referring now to the code superiority method, it is possible to arrange the code responsive circuits so that a station with a particular arrangement of code digits can force other field stations to retire from the line temporarily. The various codes can be arranged in order, with respect to superiority, and they can be assigned without regard to relative geographic locations of the field stations. The advantage of this code superiority method is that any field station can be given first priority, so it could always take the line to report its indications even though there were other stations nearer the control office ready to transmit.

However, the geographic scheme is simpler and is used more widely. Furthermore, the addition of means to prevent a location from holding the line has removed most of the advantages of the code superiority scheme.

The size of CTC territory that can be handled from one control office is quite unlimited and it has probably not yet been reached, although some of the longer installations probably approach a practical limit beyond which it may not pay to extend the territory.

There are, however, rather definite limits on the size of CTC installations that can be handled by one CTC section as defined by the length of its CTC line circuit. There are two factors: line attenuation of the CTC code impulses; and capacity to transmit codes rapidly enough to keep up with field changes. The first depends on the size and kind of line wires used and the second depends on the number of field stations in the territory and the number of trains that are on the section at the same time. It is therefore difficult and rather meaningless to attempt to give a value for the maximum distance or the largest number of stations that can be controlled by one CTC section. However, there are many CTC sections 75 to 100 miles long with from 30 to 35 stations per section that are successfully handling 20 to 40 trains a day.

This brings us to a consideration of ways and means of extending CTC beyond the capacity of one CTC code section. One way is to start out from the control office with a second pair of line wires extending to a second more remote code section and thus provide a second path over which to transmit codes independently of the first section. This has been done in several installations. It is costly, however, and would probably not be used today except for special circumstances. The present method is to employ carrier currents superposed on the line wires of the first CTC code section to control a second CTC code section extending beyond the first section. This principle of extension can be used to control several additional sections by using additional carrier frequencies.

Each carrier circuit acts as a link between its CTC code section and the control office and provides a separate communication path over which information

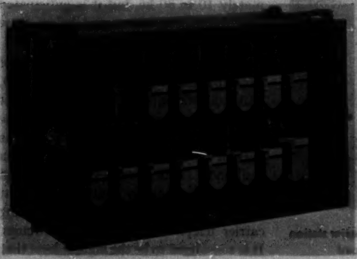

Figure 9 (left). Field application unit

Figure 11 (right). Carrier control transmitter and receiver. Covers removed from transmitter can be transmitted independently of the other sections. The full application of this principle of extension by carrier link entails the use of carrier repeaters to overcome the attenuation encountered in traversing long line circuits. It also requires the use of various kinds of filters to block and pass the several frequencies involved. The first carrier-controlled section of centralized traffic control extended from Delta to Redding on the Southern Pacific Railway and it was controlled from Dunsmuir, Calif. Carrier control has proved to be an important development in CTC and a great many installations have one or more carrier-controlled sections.

Equipment

The equipment of a CTC system falls into two main classifications: signal equipment; and code equipment. The principal units in the former class are the switch machine, the signal mechanism, and signal relays of many kinds. These devices have been brought to a very high degree of perfection and reliability over a period of years. They are not new, although some new features have been added since the advent of CTC. The functions of these devices have been discussed previously but a discussion of the devices themselves is beyond the scope of this paper.

The second division of CTC equipment, namely, the code equipment, is in reality a special form of communication system that has been developed to meet the needs of CTC. Figures 1 through 12 show some of the equipment that has been developed for this service.

At a typical control office the CTC communication equipment will include a control machine, a code relay unit called a master unit, and several CTC relay units called application units. These code relay units are used to transmit and receive CTC codes. Frequently the code relay units are housed in the control machine behind the control panel which carries a track diagram of the CTC territory, indication lights, control levers, and pushbuttons.

A control code is initiated on the control panel, its code characteristics are determined in the application unit and it is given to the line by the master unit. An indication code is taken from the line at the control office by the master unit, deciphered in the application unit and displayed on the control panel.[2] Figure 6 illustrates this procedure; it shows the organization of a coded CTC system.

The control machine is often equipped with auxiliary controls, such as an employee call. A train recorder is often mounted in the desk of the control machine. This device automatically records the arrival and departure times of trains as they pass field locations in the CTC territory. The record is made on a slowly moving roll of paper by pens that are actuated by certain indication codes. These records show the delays that each train may have encountered in its run through the CTC territory and where they occurred. The record is taken from the CTC machine each day and it is studied by the railroad operating department in order to discover how to improve the operation under CTC.

At a typical field location the CTC communication equipment will consist of a code relay unit called a stepper unit and one or more CTC relay units called application units. This apparatus, plus the signal relays, local batteries, and chargers, is usually housed in a small steel cabin. The cabin is frequently equipped with a telephone booth for use by the train crews in talking with the control office as well as for the use of the maintenance forces. This booth is arranged so that the telephone can be used without going into the main portion of the cabin where the signal and code equipment is located.

An indication code is initiated by the operation of a field function relay, its code characteristics are determined in the field application unit and it is given to the line by the stepper unit. A control is taken from the line at a field location by the stepper unit, deciphered in the field application unit and delivered to the field functions that are to be controlled,[2] as shown in Figure 6.

Figure 12. Interior of a carrier repeater station on the Union Pacific Railroad

The relays used in the CTC coding equipment are the result of intensive development and long experience. They are designed to operate for years and for millions of operations without the need for servicing or overhaul. Special care in design and manufacture is responsible for their very high degree of reliability. Contacts are carefully made, cleaned and adjusted, and protected from dust and dirt by enclosing the relays in cabinets. Arc suppressors are used to protect nearly all contacts except those that operate only occasionally. Arc suppressors also are required to prevent CTC code systems from interfering with radio reception. Many of the relays employed in CTC are equipped with quick-detachable connections. This feature also is used on many small relay units to assure easy and quick replacement for inspection and to clear trouble promptly.

Several pieces of equipment for combining CTC with other services have been developed. These include chokes, blocking condensers, matching transformers, and a group of filters. Low pass, high pass, band pass, and band elimination filters have been employed and their use is increasing as CTC is extended to longer distances and more complex line circuits.

The basic equipment used in carrier control consists of a carrier transmitter, a carrier receiver, and a code converter unit. The transmitter and receiver are electronic units; the code converter is a code relay unit, resembling a field stepper, in which a code arriving by carrier is converted into a CTC line code and vice versa. The transmitters and receivers can be obtained for operation directly from the 24-volt CTC battery or from the 110-volt 60-cycle power supply. In one design, the transmitter and receiver are built around the *26A6* and *26A7GT* tubes which can be operated directly from the local 24-volt CTC battery without the use of any other power supply. The transmitter and receiver are designed for operation on frequencies ranging from approximately 10 to 30 kc, but it is anticipated that frequencies above and below these values will be used in the future.

The transmitter has an output level of 18 decibels above one milliwatt (+18dbm), 63.1 milliwatts, which is the highest power level that is permitted under the recommendations of the Communications Section of the Association of American Railroads. This power level was selected several years ago by mutual agreement among the various companies operating carrier telephone and telegraph circuits. It is considered to be the highest level that can be used and still permit interference between circuits to be reduced to acceptable limits by practicable measures. It is equivalent to 6.15 volts when applied to a 600-ohm open type line. The transmitter is equipped with facilities for measuring the current in each tube and to control the output.

The receiver is capable of operation at 12 decibels below one milliwatt (−12 dbm) which is equivalent to 0.19 volt across a 600-ohm open type line. It has an output of 250 milliwatts and is equipped with facilities with which to measure the current in each tube and to control the gain.

Benefits derived from CTC

Railroads benefit by the use of CTC[4] because it:

1. Saves train hours.
2. Reduces overtime hours.
3. Increases availability and productivity of locomotives.
4. Expedites movement of freight traffic, thereby increasing the utilization of freight cars.
5. Eliminates train order or block offices and makes these employees available for other important work.
6. Increases safety of operations.
7. Provides broken rail protection where automatic block signals are not now in use.
8. Often permits increased train tonnage.
9. Eliminates train stops, thereby saving fuel, and reduces the possibilities of break-in-two's.
10. Assists in obtaining minimum unit cost of operation.

CTC is the only satisfactory substitute for additional trackage when the capacity of existing facilities has become saturated, and it may be provided for a fraction of the investment cost for an additional main track. Conversely, it also represents a satisfactory means of eliminating multiple tracks with the attendant savings in maintenance expenditures.

Conclusion

CTC has shown itself to be a dependable source of additional traffic capacity and earning ability.[1] CTC with cab signals extends the system all the way from the operator at the control office to the engineman riding in his cab. It is expected that its use will continue to grow. It is believed that new uses will be developed for CTC and that the system will be modified to suit the new uses. Development work is being carried out on faster communication systems in anticipation of some of the new uses that are expected.

References

1. Tabulation of Statistics. Interstate Commerce Commission (Washington, D. C.) January 1, 1948.

2. Centralized Traffic Control, Type K Class M Coded System. *Handbook Number 30*, General Railway Signal Company (Rochester, N. Y.) 1948.

3. Centralized Traffic Control Manuals Number 506A and Number 507. Union Switch and Signal Company (Swissvale, Pa.) 1947.

4. Operating Advantages and Possible Modifications in Rules in CTC Territory. *Report of Committee Number 2*, American Association of Railroad Superintendents (Chicago, Ill.) page 21, 1948.

5. American Railway Signaling Principles and Practices. American Association of Railroads (Washington, D. C.) 1946, chapter III, pages 54–66.

No Discussion

Attenuation and Delay Equalizers for Coaxial Lines

W. R. LUNDRY
NONMEMBER AIEE

Synopsis: This paper describes the theoretical and practical aspects of a series of attenuation and delay equalizers developed for the *L-1* coaxial system. Attention is focused on the adjustable attenuation equalizers and the delay equalizers. An indication is given of the precision required in manufacture in order to meet the close tolerances of television or long telephone circuits.

THE general problem of equalization is discussed in a companion paper.[1] The fixed or basic equalizers used at auxiliary and main repeaters are of conventional types and will not be discussed here. Instead attention will be directed to the equalizers located at main stations. These comprise the delay equalizers used on television circuits only and the adjustable attenuation equalizers, usually designated the *A* and *B* equalizers used on both telephone and television circuits.

Adjustable Attenuation Equalizers

The adjustable loss characteristics obtained in the *A* and *B* equalizers are shown by the curves of Figure 4. These curves show the maximum adjustment range above and below a reference loss which is approximately 40 decibels in each equalizer. Pairs of curves are identified by a number corresponding to the line-up frequency in kilocycles. The loss can be adjusted continuously or in small steps to fall on curves intermediate to those shown. All intermediate curves are proportional, to a high degree of approximation, to the limiting cases shown.

THEORY OF DESIGN

The *A* and *B* equalizers are complex assemblies of adjustable networks which may be derived from a simple prototype developed by Bode.[2]

In its simplest form, this structure may be represented and used as shown in Figure 1. Here, a 2-terminal network is used to adjust the transmission of a circuit containing a sending impedance R_s and a receiving impedance R_r. The structure and behavior of this 2-terminal network are our immediate concern. It consists of a 4-terminal network, N, associated with two resistances R_1 and R_a.

The 4-terminal network N is one having constant resistance image impedances at the pairs of terminals connected to the resistances R_1 and R_a, and an image transfer constant, φ_a. If the image impedances are equal and have the value R_o, then it is apparent that when $R_a = R_o$ the insertion loss of the complete structure is independent of frequency. Let the insertion loss of the structure be called θ and the value assumed when $R_a = R_o$ be θ_o. Then there is a value of R_1 such that

$$\tanh\frac{1}{2}(\theta-\theta_o)=\frac{K}{2}\,\rho_a\epsilon^{-2\varphi_a} \qquad (1)$$

where

$$\rho_a=-\frac{R_o-R_a}{R_o+R_a},\; K=2\,\tanh\frac{\theta_o}{2}$$

$$\theta-\theta_o=2\,\tanh^{-1}\frac{K}{2}\,\rho_a\epsilon^{-2\varphi_a}=K\rho_a\epsilon^{-2\varphi_a}+\frac{1}{12}(K\rho_a\epsilon^{-2\varphi_a})^3+\frac{1}{80}(K\rho_a\epsilon^{-2\varphi_a})^5+\ldots \qquad (2)$$

In most practical cases the first term of this series gives an adequate representation of the performance. The design problem then becomes one of choosing a structure for N whose image transfer constant, φ_a, will give the desired value of $\theta-\theta_o$ as a function of frequency when substituted in equation 2. Since we are interested only in the loss characteristics of the structure we may write

$$\alpha-\alpha_o\cong Re[K\rho_a\epsilon^{-2\varphi_a}] \qquad (3)$$

This structure can be designed to give any of the adjustable loss characteristics required in the *L-1* system. However, another structure giving identical characteristics has some practical advantages.

Consider a network N of Figure 1 in which the first section is a bridged-T loss equalizer as shown in Figure 2(A), with $R_b = R_c = R_o$ and $Z_1Z_2 = R_o^2$. Now φ_a as used in equation 3 is given by

$$\epsilon^{\varphi_a}=\left(1+\frac{Z_1}{R_o}\right)\epsilon^{\varphi_a'} \qquad (4)$$

The section having an image transfer constant, φ_a' has been called a "building out" section.

Suppose the network of Figure 2(A) is redrawn as in Figure 2(B). Then when $R_a = R_c = R_o$ the structure may be used as an adjustable network with R_b as the control resistance. Moreover, the circuit may be opened at the left of R_b and a building-out section having image impedance R_o may be inserted. If this section has an image transfer constant φ_b' then θ_b, obtained from

$$\epsilon^{\varphi_b}=\left(1+\frac{Z_1}{R_o}\right)\epsilon^{\varphi_b'} \qquad (5)$$

may be used instead of φ_a in equation 3 to give the performance of the structure.

This structure with the added building-out section becomes particularly interesting when we use both R_a and R_b as adjustable controls. It can be shown that

$$\theta-\theta_0=2\,\tanh^{-1}\frac{K}{2}(\rho_a\epsilon^{-2\varphi_a}+\rho_b\epsilon^{-2\varphi_b})$$

$$=2\,\tanh^{-1}\frac{\varphi_{ab}}{2}$$

$$=\varphi_{ab}+\frac{1}{12}(\varphi_{ab})^3+\frac{1}{80}(\varphi_{ab})^5+\ldots \qquad (6)$$

Paper 49-246, recommended by the AIEE Communication Committee and approved by the AIEE Technical Program Committee for presentation at the AIEE Fall General Meeting, Cincinnati, Ohio, October 17–22, 1949. Manuscript submitted July 18, 1949; made available for printing September 2, 1949.

W. R. LUNDRY is with the Bell Telephone Laboratories, Inc., Murray Hill, N. J.

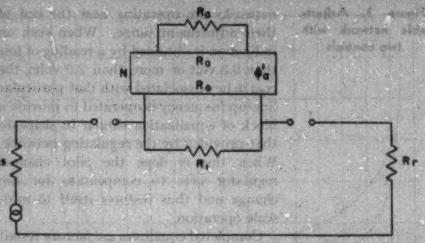

Figure 1. Adjustable network—prototype

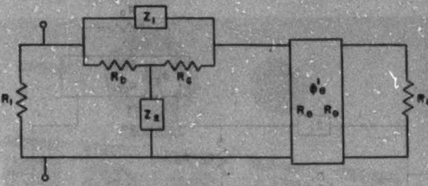

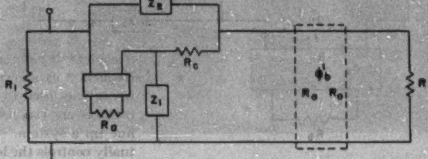

Figure 2(A) (top right). Prototype network with building-out section

Figure 2(B) (right). Inverted prototype with building-out sections

Here again the first term of the series is an adequate approximation, so that

$$\alpha-\alpha_0 \cong R_e\varphi_{ab}=Re[K(\rho_a\epsilon^{-2\varphi_a}+\rho_b\epsilon^{-2\varphi_b})] \quad (7)$$

This would make it appear that adjustment of the control resistances R_a and R_b, which vary the values of ρ_a and ρ_b respectively between −1 and +1, would produce independent changes of the insertion loss, α. This, of course, is not strictly true in view of equation 6. Moreover, φ_a and φ_b are not completely independent as will be evident from a study of equations 4 and 5. Since $Z_1Z_2=R_o^2$, small values of Z_1 give large values of Z_2. At frequencies where ρ_a must produce large changes in loss then ρ_b can at best produce only small changes. Practically, this leads to designs in which ρ_a and ρ_b are used to control the loss in distinct parts of the frequency range.

Both the *A* and *B* equalizers consist principally of combinations of 2-terminal impedances similar to Figure 3 or its inverse. The use of the network of Figure 3 as the series arm and of its inverse as the shunt arm of a constant-resistance bridged-T equalizer is a fairly obvious application. By using rheostats in which both R_a and its inverse are ganged to a single shaft and similarly for R_b and its inverse, a 4-terminal network is obtained which gives two adjustable loss characteristics while always presenting a constant-resistance impedance to the through circuit. Any number of such networks may be connected in tandem with complete independence of the adjustable controls in successive 4-terminal networks. One such section is indicated in Figure 5, the second section from the left. Sections of this type may be used when it is necessary to provide independent controls working in overlapping frequency ranges.

When practical considerations prevent the use of this type of section the configuration shown by the third section from the left in Figure 5 may be used. While this does not achieve complete independence of the adjustable characteristics, careful design will make the loss changes produced by one of the adjustable resistances tolerably independent of the values at which the other resistances may be setting. The theory of this configuration is quite involved and beyond the scope of this paper.

Another structure which has proved particularly useful is one which uses networks of the type shown by Figure 3 as series arms and its inverse as the shunt arms of a ladder network as shown by Figure 6. To understand the operation of this network, consider again Figure 3. When φ_a' has a large real component, that is, a high attenuation, the impedance z_a is very nearly R_o for all values of R_a. Similarly, Z_b equals, very nearly, R_o for all values of R_b. But, this is the condition for the impedance of the complete 2-terminal structure to be equal to R_o. (This condition also is achieved if the real parts of φ_a and φ_b are large, regardless of the values of φ_a' and φ_b'.) Thus, when R_a and R_b are required to produce loss changes over small portions of the frequency band there is left a large part of the band over which the impedance of the 2-terminal network is essentially a pure resistance. By taking advantage of this fact and giving careful attention to the frequency behavior of adjacent series and shunt branches a configuration may be found in which the loss variation produced by any one control is substantially independent of the settings of all other controls.

Design and Performance of the *A* Equalizer

The configurations described above and exhibited as block schematics in Figure 5 form the backbone of the *A* equalizer. There are other features which deserve more than passing mention. Loss adjustments which are required in large steps are obtained by switching in whole equalizer sections, by changing the element values of the individual arms of such section or by modifying the configuration of the arms by adding additional groups of elements. Switching of this type is accomplished by means of standard telephone switchboard keys.

Three of the loss adjustments are frequently made by means of pilot frequency regulators. In order to implement this, thermistors are used as the control element (resistance R_a or R_b of Figure 3). By controlling a small amount of power to a heater winding in the thermistor, its temperature may be changed to give a large change in the resistance of the thermistor element. This in turn controls the loss. For locations where pilot regulation is not used, provision is made to supply regulated direct-current to the thermistor heaters through manually adjusted potentiometers. In such cases it is necessary to protect the thermistors against ambient temperature changes. This is accomplished by placing the thermistors in an oven having a thermostatically controlled heater element operating from 110-volt a-c power.

In addition to its adjustable sections, the *A* equalizer also contains a series of fixed loss sections which serve to equalize the accumulated fixed errors of 11 auxiliary repeater sections. These are simple configurations of familiar equalizer types. In some cases they are associated with adjustable sections in order to reduce the over-all *A* equalizer loss to tolerable values.

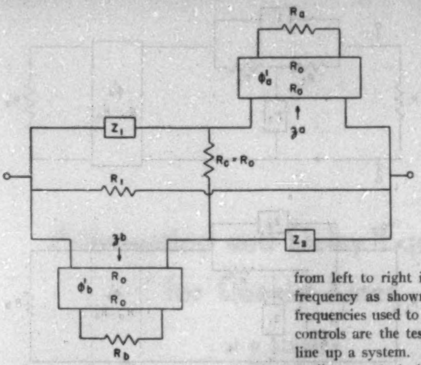

Figure 3. Adjustable network with two controls

The assembled *A* equalizer occupies $12^{1}/_{4}$ inches of relay rack space. All controls are accessible from the front panel and are arranged in two rows reading from left to right in order of ascending frequency as shown on Figure 9. The frequencies used to designate the various controls are the test frequencies used to line up a system. Each dial or key actually controls the loss characteristic over a moderately wide frequency range. The meter is provided to enable the operating force to check the thermistor voltages in order to determine when the regulating networks are operating near the end of their adjustment range. When such an indication is obtained by a reading of less than 0.3 volt or more than 2.0 volts, the coarse key associated with that particular line-up frequency is operated to provide a block of equalization similar in shape to that provided by the regulating network. When this is done the pilot channel regulator acts to compensate for the change and thus restores itself to mid-scale operation.

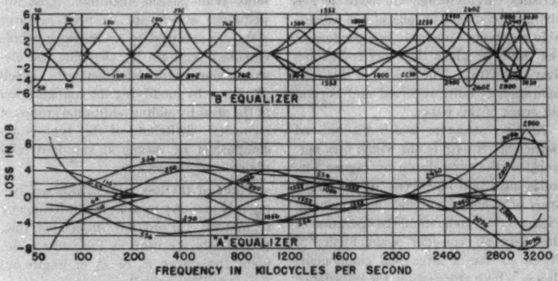

Figure 4. Adjustable loss characteristics of *A* and *B* equalizers

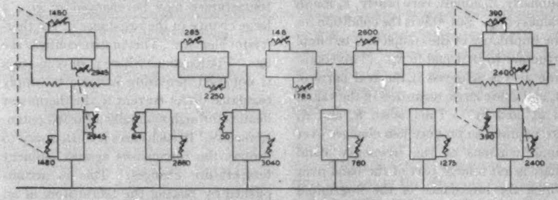

Figure 5. Adjustable sections of *A* equalizer

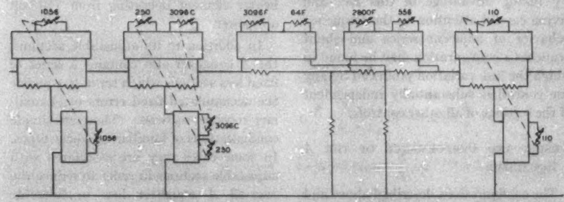

Figure 6. Adjustable sections of *B* equalizer

Completed equalizers are factory tested to insure a product uniformity of ±0.13 decibel. This check is made for the nominal, minimum, and maximum positions of each dial and key individually. This test is made by comparing each equalizer with a reference standard equalizer on a recording loss circuit. A continuous curve of the loss over the frequency range 50 to 3,150 kc is plotted in three minutes with this circuit. Twenty-four curves are taken on each completed equalizer.

In order to meet these extremely close end-product limits, careful control is exercised at each step in the manufacturing process. The individual capacitors used in the equalizer are manufactured to limits of ±1/2 or ±1 per cent, depending on the type of loss section. All resistors are manufactured to ±1 per cent tolerance. The inductors are manufactured in most cases to ±1 per cent and to ±2 per cent wherever these limits are tolerable. In many cases, however, closer limits are required on the inductance-capacitance product of coil-capacitor combinations. In these cases adjustable inductors are used. The adjustment is obtained by use of a magnetic core in the center of the solenoidal winding. The core and the winding form are threaded so that rotation of the core moves it longitudinally inside the winding. When such coils are used the resonant frequency of a coil-capacitor combination is adjusted to ±0.5 per cent. In some cases the coils being adjusted may be as low as 0.2 microhenry. Thus the adjustment requires setting the effective inductance to ±0.002 microhenry. Careful attention to details are required in setting up and adjusting the sections to this precision.

Design and Performance of the *B* Equalizer

The "B" equalizer has 15 adjustable loss characteristics shown at the top of Figure 4, obtained by using the configuration shown in Figure 6. The equalizer itself is shown in Figure 10. All adjustments are made by dials having 20 uniform loss steps. These are arranged on

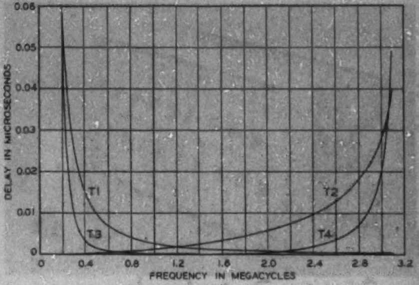

Figure 7. Basic delay characteristics of system

Figure 9 (right). *A* equalizer

the face of the equalizer in three rows reading from left to right in order of ascending frequency, except for the three dials which provide small steps duplicating the performance of coarse keys in the *A* equalizer. In order to simplify the line-up procedure these three dials are located at the upper left, to facilitate their adjustment before beginning the routine adjustment of the *B* equalizer controls.

The sections of the *B* equalizer are associated in unit assemblies in order to break up the assembly into parts which may be manufactured and tested conveniently. Typical unit assemblies are shown in Figure 11. The individual components in this assembly are mounted on fibre strips which individually form a subassembly to which requirements may be assigned for purposes of checking or trouble shooting.

In general, the loss characteristics of the *B* equalizer tend to be narrower and hence, to require a more precise setting of the resonant frequency of coil-capacitor combinations. For example, one of the *B* equalizer characteristics adjusts the loss over a band 200 kc wide centered at 3,030 kc where the resonant frequency must be adjusted to ±6 kc or ±0.2 per cent. This circuit is so sensitive to the parasitic capacities of the surrounding metal container that it is necessary to assemble the network completely and then to make the adjustment through holes in the can. The adjusting holes are later closed by soldering on a metal disk.

Figure 8. Delay characteristics of typical equalizers

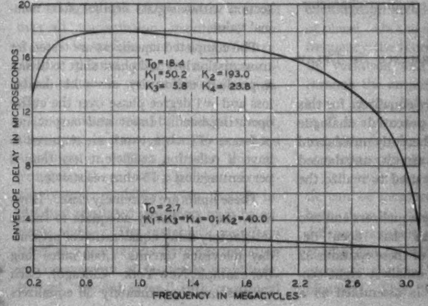

Since *B* equalizers are used less frequently in the circuit, wider end product limits are tolerable. The performance of the completed equalizer is checked by comparing its loss to that of a standard equalizer at the maximum and minimum settings of each of the 15 controls on a recording loss circuit. Limits of ±0.25 decibels are set on these characteristics.

Delay Equalizers

LINE AND EQUALIZER CHARACTERISTICS

The delay characteristics encountered in the *L-1* system are comparatively simple to describe. They consist principally of the delay arising from the minimum phase associated with the gain cutoffs of the system. For a detailed discussion of the minimum-phase concept, see H. W. Bode, Network Analysis and Feedback Amplifier Design.[8] The four types of amplifier (auxiliary, receiving, transmitting, and flat-gain) used in the system have different cut-off characteristics so that it is necessary to provide a flexible system of equalizers which will allow for different numbers and proportions of these types in any one circuit.

A satisfactory description of the delay of a circuit is obtained by using four delay characteristics, two to describe the behavior at the higher frequencies and two at the lower frequencies, that is

$$T = T_0 + K_1T_1 + K_2T_2 + K_3T_3 + K_4T_4$$

where T is the envelope delay of the system, T_1,—, T_4 are delay characteristics (shown in Figure 7) and K_1,—, K_4 are constants. The constant delay represented by T_0 arises principally from the finite transmission time of the cable but includes any other effects which introduce linear phase.

Figure 10. *B* equalizer

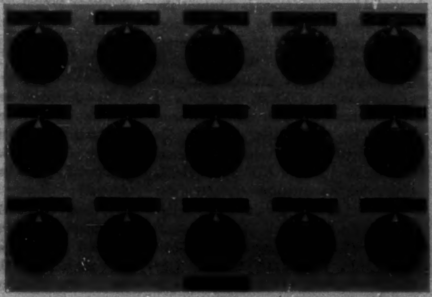

Figure 11. Typical units of *B* equalizer

Figure 12. Assembly and components of typical delay equalizer

From a study of several short systems the most frequently occurring values of K_1, —, K_4 were determined and a series of equalizers was designed. The larger units in this series are designed to equalize an average system and have a delay characteristic which is a composite of the functions T_1, —, T_4. Smaller units are used to permit trimming the equalization to specific circuits. These usually have characteristics which are defined by one of the T_1, —, T_4.

Delay equalizers consist of a series of "all-pass" or "nonminimum phase" sections. Physical restrictions limit these to positive delay, that is to a phase characteristic which is a monotonic, increasing function of frequency. This means that the equalizers must be designed to have a delay complementary to that of the unequalized system so that the sum of equalizer plus system delay is constant with frequency at a value equal to or greater than the maximum delay of the unequalized system. Thus the delay of the equalizers is expressible in the form

$$T_e = T_0 - K_1T_1 - K_2T_2 - K_3T_3 - K_4T_4$$

Practically, the minimum value of T_e in the useful frequency range is substantially greater than zero in order to permit adequate design control of the delay characteristic near the edges of the band. This requires that T_0 be greater than the maximum value of ΣK_iT_i, regardless of the frequency at which this maximum occurs. Thus, an equalizer equalizing for T_2 alone would have a value of T_0 determined by the value of K_2T_2 at 3.1 megacycles, while an equalizer correcting for T_1 alone would have a value of T_0 determined by the value of K_1T_1 at 0.2 megacycle. On the other hand, an equalizer compensating for both of these distortions would have a T_0 determined by the larger of them (since $T_2=0$ at 0.2 megacycle and $T_1=0$ at 3.1 megacycles). For equal distortion at the two ends of the band, the delay level (T_0) would be half as much in the combination equalizer as in the case where two independent equalizers are used.

The delay level is not particularly important from an operational point of view. However, the fact that this level must be built up by means of all-pass sections is important economically. The equal distortion case just cited would require at least twice as many sections in the individual equalizers as in a combination design.

The delay characteristics of one equalizer of each type are shown on Figure 8.

Small adjustment of delay must be made periodically to compensate variations in the system, due to temperature changes, aging, and similar effects. It proves more economical to make these adjustments by adding small increments of delay simulating the delay of the system. This requires that the equalizers used in a circuit shall be chosen to equalize the maximum distortion ever expected in the line. Then, most of the time, the delay is built up by the adjustable networks to match the equalizer characteristics.

Design and Performance of Delay Equalizers

The designs of delay equalizers for this system follow the potential analogue method.[4] To fit the inherently unbalanced nature of the coaxial circuit, unbalanced bridged-T sections are used to realize the design.

A family of six delay equalizers and two building-out networks has been developed. The largest of these contains 52 all-pass sections, the smallest eight sections. Each section is assembled as a completely shielded unit to simplify adjusting, testing, and handling.

An exploded view of one of these equalizers is shown in Figure 12. Each of the 52 all-pass sections is assembled in its individual shield. Most of these contain two inductances and three capacitances arranged in conventional bridged-T configuration. The capacitances are manufactured to close tolerances—usually 1/2 per cent. The inductors contain threaded magnetic plugs which are used to adjust the inductance to resonate with the associated capacitors.

The critical frequencies of the sections, corresponding to the resonant frequencies of the series and shunt arms, are adjusted to an accuracy of ±0.5 kc. At 3,000 kc this corresponds to a frequency accuracy of 0.017 per cent, or, in terms of the adjustable element, an inductance accuracy of 0.008 per cent.

The comparatively wide manufacturing variations encountered in the dissipation factor of the inductors makes it necessary to provide means for adjusting each one individually. This is done by adding two resistances external to the unit assembly at the time the resonance frequency adjustments are made. Selected resistance values are used to hold the loss of each section within ±0.03 decibel of its nominal value.

The completed equalizers are tested for transmission loss and phase shift to insure a product uniformity of ±0.1 decibel loss and ±1 degree phase over the entire operating band. Input and output impedances of each network are required to have a reflection coefficient less than 5 per cent against a 75-ohm resistance.

These limits are extremely close. However, they are barely adequate to insure satisfactory delay equalization of present-day television circuits, 1,000 miles long (for example, New York—Chicago). Such circuits use approximately 30 equalizers distributed along the line and the cumulative effect of such manufacturing deviations is large compared to the tolerances acceptable for present-day television transmission. For circuits of transcontinental length further refinement of the equalization method will be required.

References

1. Equalization of Coaxial Lines, K. E. Gould, *AIEE Transactions*, volume 68, part II, 1949, pages 1187–92.
2. Variable Equalizers, H. W. Bode. *Bell System Technical Journal* (New York, N. Y.), volume XVII, April 1938.
3. Network Analysis and Feedback Amplifier Design (book), H. W. Bode. D. Van Nostrand and Company (New York, N. Y.), chapters 14 and 15, 1945
4. Delay Equalization of Eight Kilocycle Program Circuits, C. H. Dagnall, P. W. Rounds. *Bell System Technical Journal* (New York, N. Y.), volume XXVIII, April 1949.

No Discussion

Stability of Tandem Regulators in the L-1 Carrier System

J. P. KINZER
NONMEMBER AIEE

Synopsis: The *L-1* coaxial carrier system, with its dynamically-regulated amplifiers, has envelope gain in the vicinity of two cycles per second. With a large number of such amplifiers in tandem, the transient response to an input step function has a peak-to-peak amplitude, or oscillation, many times greater than the size of the initial step. It therefore is necessary to insure that the over-all envelope gain is not so great that small input disturbances normally occurring in system operation are magnified to a point where transmission is impaired.

Calculated effects agree with experimental observations with small steps.

THE *L-1* carrier system[1] transmits a band from 64 to 3,096 kc over coaxial conductors with repeater stations at about 8-mile intervals for $^3/_8$-inch coaxial, and $5^1/_2$-mile intervals for the older $^1/_4$-inch coaxial. A pilot frequency of 2,064 kc is supplied at the transmitting terminal. Somewhat more than half the repeater stations are equipped with pilot regulators, which operate on their associated amplifiers to maintain a constant level of pilot at the amplifier outputs. By this means, variations in the loss of the coaxial (caused by temperature changes, for example) are compensated, and the over-all transmission maintained constant. At stations not having pilot regulators, manual gain controls are supplied and these are readjusted occasionally.

In a transcontinental coaxial circuit, there may be more than 200 regulated amplifiers in tandem. Under this circumstance there arises a problem of over-all dynamic stability, even though individual regulated amplifiers may be entirely stable. The instability manifests itself as a continuous irregular variation in transmission of moderate amplitude, termed "normal jitter," with occasional large excursions or "hits" of perhaps several decibels (db).

Figure 1 shows a block schematic of a line amplifier with its associated regulator. The 2,064-kc pilot frequency is picked off by a crystal filter, amplified and rectified. The rectified direct current is used to control the bias on an oscillator tube and thus control its 2,000-cycle output. This output heats the thermistor, which is in the feed-back path of the line amplifier and controls its gain. The circuit is so arranged that a drop in pilot level results in an increase in amplifier gain which restores the pilot level to almost its original value. Thus a change in the pilot level at the input of the amplifier appears at the output greatly reduced in magnitude.

Any variation, or amplitude modulation of the pilot level, is usualy spoken of as the envelope. If the pilot-frequency amplitude modulation is sinusoidal, one speaks of the envelope frequency.

If the envelope frequency is relatively high, say more than 100 cycles per second, the thermistor is unable to follow because of thermal lag, and the pilot variation is passed through the amplifier-regulator combination without change of amplitude or phase. On the other hand, at very low frequency the thermistor is able to follow the variation, and it suffers a loss going through the amplifier-regulator combination. In the *L-1* system, this loss is 20 to 30 db at zero frequency. The combination therefore has an envelope transmission-frequency characteristic.

The envelope transmission characteristic can be measured directly. This has been done in the field on lines with different numbers of regulators in tandem. It also can be calculated from measurements on the feed-back loop of the combination. This "backward-acting" amplifier-regulator combination is a feed-back circuit with a rather well-defined feed-back loop, and general principles of feed-back-amplifier design apply.[2,3] A convenient place to break the feed-back loop for measurement of low-frequency complex $\mu\beta$ (notation is that of Bode)[2] is at the grid of *V-3* (line designated D-C Bias in Figure 1). The envelope transmission ET, is then given by

$$ET=\frac{1}{1-\mu\beta}$$

The two methods of determining the envelope transmission characteristic agree well. Figure 2 shows a representative characteristic. Note that there is actually an envelope gain of about 0.3 db at 2.5 cycles per second. This adds directly for tandem regulators, so that 130 regulators would have an over-all envelope gain of some 40 db.

This means that if the 2,064-kc pilot at the input of a 130-db regulator system has 1/10 per cent modulation with 2.5 cycles per second (for example), at the output of this system the pilot would have 100 times as much modulation, that is, 10 per cent. Of course, this situation normally does not exist, as the pilot frequency supplies are exceptionally well stabilized. However, it might occur as a trouble condition in a station with an abnormal cross-talk path between two independent nonsynchronized pilot supplies.

Input disturbances more likely to occur in service are sudden changes, called hits, caused, for example, by bridging a high-impedance transmission measuring set across the line to make a maintenance measurement, or by switching from one line to another. This type of input transient is easy to create and lends itself as well as any to mathematical analysis.

Paper 49-247, recommended by the AIEE Communication Committee and approved by the AIEE Technical Program Committee for presentation at the AIEE Fall General Meeting, Cincinnati, Ohio, October 17–21, 1949. Manuscript submitted July 20, 1949; made available for printing September 2, 1949.

J. P. Kinzer is with the Bell Telephone Laboratories, Inc., New York, N. Y.

The results summarized herein include the contributions of many other members of the technical staff of the Bell Telephone Laboratories. To these, appropriate appreciation is extended herewith.

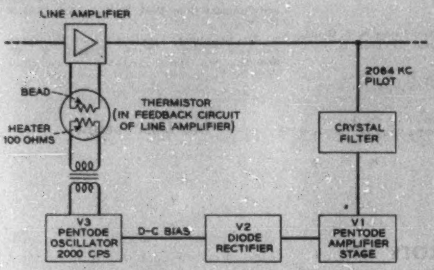
LINE AMPLIFIER
BEAD
THERMISTOR (IN FEEDBACK CIRCUIT OF LINE AMPLIFIER)
HEATER 100 OHMS
2064 KC PILOT
CRYSTAL FILTER
V3 PENTODE OSCILLATOR 2000 CPS
D-C BIAS
V2 DIODE RECTIFIER
V1 PENTODE AMPLIFIER STAGE

Figure 1 (above). Block schematic of pilot regulator and line amplifier

Figure 3 (right). Transient response to 0.2-db step-up, of loops with 10, 20, 30, and 40 regulators

Oscillograms were retouched to show the initial step plainly

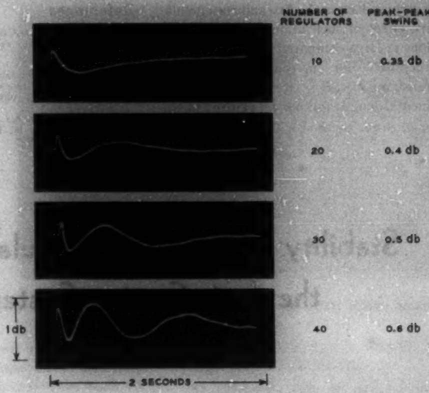

Figure 3 shows a typical transient produced by 0.2-db stepup in pilot level. The circuits were so arranged that the pilot could be observed simultaneously after passing through 10, 20, 30, and 40 regulators. Note that as the number of regulators in tandem, and hence the overall envelope gain, increases, the magnitude of the transient increases. When the envelope gain is large, the magnitude of the transient may be much greater than the initial disturbance. The ratio of the peak-to-peak magnitude of the transient to the size of the original step is called the magnification.

Figure 4 shows the relation between total envelope gain and magnification. Various field measurements on the *L-1* system are indicated by dots, circles, and so forth. The heavy line thus represents the experimentally observed relation between total envelope gain and magnification, and the dashed line a reasonable extrapolation. The light line shows a mathematically derived relation. The agreement between theory and observation is good.

Large transients represent one type of difficulty resulting from excessive envelope gain. Another, called normal jitter, is shown on Figure 5. This is believed to be the end result of the summation of a large number of transients caused by tiny disturbances all along the system. It is believed that the major source of these disturbances is power supply fluctuation, changing the operating points of vacuum tubes in regulators and amplifiers. Normal jitter is very erratic in nature and its magnitude varies greatly from time to time. The oscillogram shows about $^1/_2$-db peak-to-peak normal jitter; it was taken on a system that had almost 40-db envelope gain, or about 0.5 db per regulator. The system of Figure 3 had about 0.4-db envelope gain per regulator. Since these oscillograms were made, design changes in the regulator have reduced the envelope gain to about 0.3 db maximum, as shown in Figure 2. The envelope gain also de-

Figure 4. Transient performance of cascaded regulated amplifiers

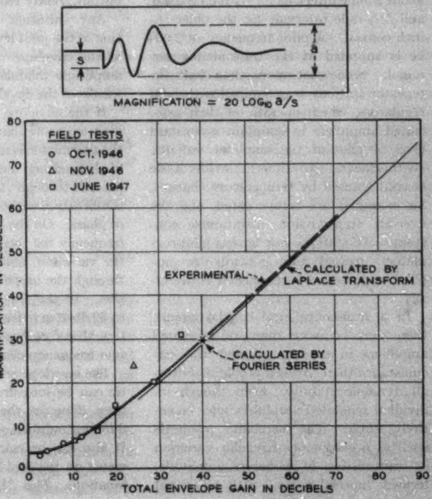

Figure 2 (below). Envelope transmission of line amplifier with pilot regulator

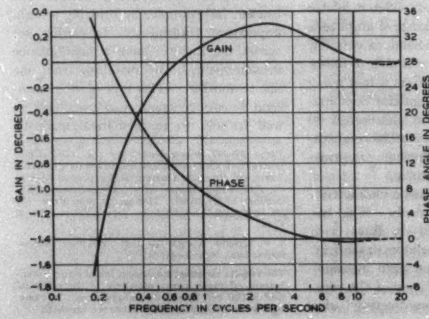

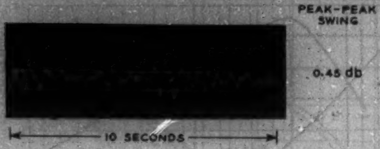

Figure 5. Normal jitter on loop with 86 regulators

pends on the portion of the regulation range which is in use, and thus on the time of the year.

Calculation of Transient Response to Step Input

It is desirable to be able to calculate the transient response of a system, before it is available for test, from the known envelope transmission characteristic. Two methods of doing this are by the Fourier Series and the Laplace Transform. In principle, these are essentially equivalent, but the techniques of working out the final result differ greatly.

By the Fourier Series method, the steady-state response of a system to a square wave input is calculated. If the period of the square wave is large compared to the duration of the transient response to a step function, the steady-state response to the square wave is then very closely a repetition of the transient responses to steps in alternate directions. The method is simple enough in principle, but rather tedious in operation because extensive computations are necessary. Briefly, each component of the (input) spectrum of the square wave is modified by the transmission characteristic (amplitude and phase) of the system and the modified (output) components combined to give the response. This must be done for each instant of time, and to achieve any accuracy, a considerable number of components must be taken.[4] The method is, however, well adapted to machine computation.

As a verification of the validity of the method, the transient response was calculated for a system on which experimental data were available. The comparison of computed and measured response is shown in Figure 6; it is seen that the agreement is good. On this figure, the solid lines represent the limits of a strip within which fall all of six experimental characteristics. The dotted line represents the calculated response. The zero of time has been taken at the instant of the first peak. The start of the transient is not well defined on the oscillograms, and the Fourier Series method gives poor results near the origin, as is well known.

The definition of the first peak is better than that of the later ones, which tend to be broader. For clarity, Figure 6 has been drawn to a larger scale than is justified by the accuracy of the measurements.

The calculated response of a system with 40-db envelope gain is shown in Figure 7. The response was first calculated by a relay computer using harmonics up to the 139th, and in steps of 2 degrees. This was to determine the region of maximum oscillation, and was followed by a fine structure determination in this region using steps of 0.5 degree.

As shown in Figure 7, the initial step is lost in the inaccuracy of the method near the origin, and the dotted line has been drawn to show the probable response near the origin. From this curve the magnification ratio is 32, that is, 30 db. The value is shown as the star in Figure 4 and has been used as a guide in the drawing of the curve.

By the Laplace Transform method, the response to a unit step function is computed by analytic methods. An analytic expression is fitted to the experimental envelope transmission characteristic. The direct Laplace Transform of the unit step is multiplied by this expression, and an inverse Laplace Transform made to obtain the result. Analytic methods are necessary because this is the only feasible way to carry out the necessary integrations in the complex plane.

The technique used is to assume a rather simple expression for a single regulator, and raise it to *n*th power for *n* regulators in tandem. This method is the one by which the theoretical curve of Figure 4 has been calculated. Details are given in Appendix I. An alternative procedure is to fit an analytic expression, say a power series, to the experimental overall envelope transmission characteristic, and proceed from this point. This attack has not been attempted here.

Experimental Results

The theoretical approaches discussed above of necessity imply a linear system. However, it has been observed that as the size of step is increased, nonlinearity effects in the system operate to reduce the magnification rather rapidly and to produce differences between steps up and steps down in pilot level. See Figure 8.

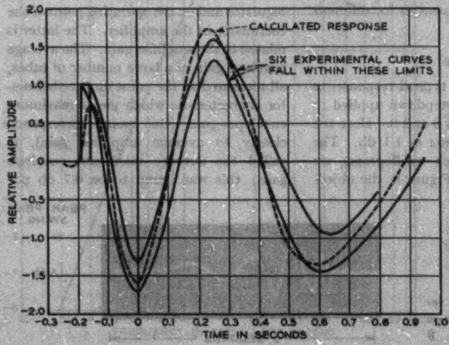

Figure 6 (left). Comparison of calculated and experimental transient response of system with 16-db envelope gain

Figure 7 (below). Calculated transient response of system with 40-db envelope gain

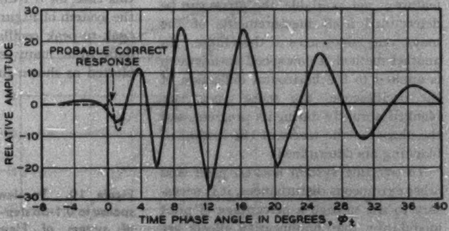

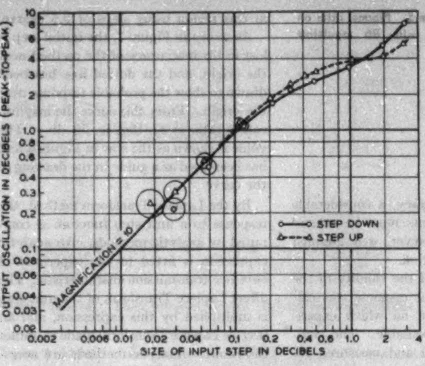

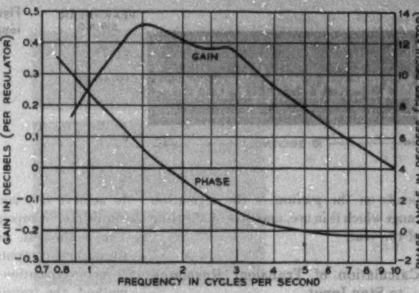

Figure 8 (left). Transient performance of system with 28-db envelope gain

Figure 9 (above). Envelope transmission of the system of Figure 8. This loop had 62 regulators

Over-All System Envelope Transmission

System envelope transmission characteristics are measured on a loop by applying a small percentage of low-frequency sinusoidal modulation to the outgoing 2,064-kc pilot, and comparing this in magnitude and phase with the modulation of the received pilot. The low-frequency oscillator has two outputs, whose relative phase can be varied over 360 degrees and read directly from a phase dial. One output is connected to the horizontal drive of a long persistence oscilloscope (*P-7* screen), and the other used to modulate the pilot. An attenuator is provided in this output to permit variation of the amount of pilot modulation. The pilot envelope is applied to the vertical deflection of the oscilloscope. Rotation of the phase dial collapses an ellipse on the scope screen into a straight line. Two scopes are used, one at the output of the transmitting amplifier, the second at the output of the receiving amplifier. The procedure is to adjust the phase dial and attenuator to obtain reference traces on the two scopes in turn, and take the difference between readings. If a low-frequency oscillator with the variable phase feature is not available, the phase can be determined from measurements of the major and minor axes of the ellipse. In another method, a slow speed linear sweep is applied to the horizontal deflection of the oscilloscope, the scope spots are blanked abruptly during its progress, and the phases of the traces at the instant of blanking are determined.

To override system normal jitter and other extraneous disturbances, it is necessary to use so high a percentage of pilot modulation that nonlinearity effects are appreciable. Also, at frequencies below the peak of envelope transmission, harmonics in the oscillator become troublesome as they are amplified with respect to the fundamental in going through the system. Both these effects result in considerable distortion of the ellipses and make measurements at envelope frequencies below one cycle per second very uncertain.

Typical results on a loop with 62 regulators, reduced to a per regulator basis, are shown in Figure 9. It is found that the general shape and magnitude of these gain and phase curves are in agreement with those for a single regulated amplifier under similar working conditions. This indicates that there probably is no large error in the measurements and that the regulators probably do not differ greatly from typical specimens. It has been noted that there is a decided flattening of the gain characteristic for many regulators in tandem. This may be a consequence of the peak in envelope gain coming at slightly different frequencies for different regulators.

Transient Response

Figure 10 shows a typical response, in this case for 0.1-db stepdown applied to the system of Figures 8 and 9. Here the peak-to-peak oscillation is 1.1 db. The data from many such oscillograms are plotted as shown in Figure 8, the object being to get the best possible extrapolation back to the small step case. The magnitude of the oscillation in db is plotted against the step size on log-log paper, and a 45-degree asymptote drawn that best fits the plotted points. The intercept of this asymptote with the 1-db abscissa gives the magnification ratio. On Figure 8, the size of each circle gives an indication of the estimated accuracy of the respective plotted point. It is evident that the magnification can be determined only roughly.

All the magnifications determined in this way have been plotted on Figure 4, which represents the best presently available experimental relation between the envelope gain and magnification.

Reduction of Envelope Gain

The envelope gain of a particular regulator-amplifier combination varies widely; it depends largely upon the characteristics of the oscillator tube in the regulator and on the operating point of the thermistor in the amplifier. The latter is related to the amplifier gain. The average envelope gain of a large number of tubes, all measured at the point on the thermistor characteristic which yields maximum envelope gain (this point corresponds closely to average amplifier gain), is called the average maximum envelope gain; this was found to be 0.7 db per

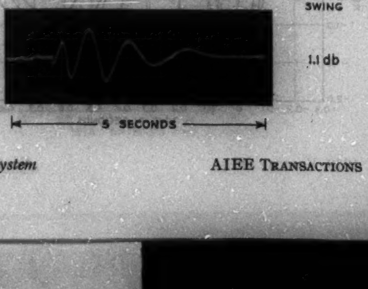

Figure 10. Transient response to 0.1-db step-down of system of Figure 8

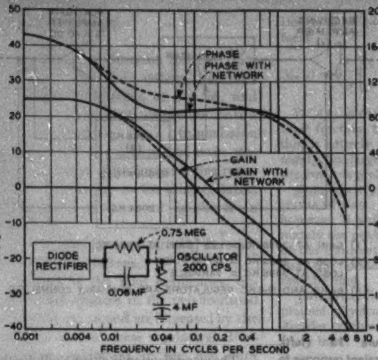

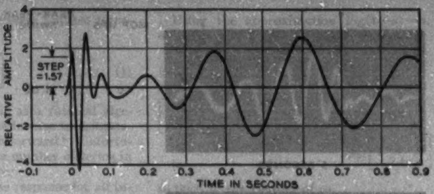

Figure 11 (left). Feed-back loop (μβ) characteristic of regulator and amplifier, with and without corrective network

Figure 13 (above). Calculated transient response of system with mop-up regulators, in which the envelope transmission characteristic has two peaks, each of 20-db gain

regulator for the regulators as used in the field tests. With an arbitrary limit of, say, 40 db on the envelope gain, the maximum number of regulators in tandem would be limited to about 60. This limit can be met readily on message facilities because traffic flexibility considerations dictate the termination of the coaxial system and the supply of fresh pilot frequency at least this often. Furthermore, field experience indicates that the maximum value of 0.7 db is not likely to be reached on all regulators. Nevertheless, methods for the reduction of envelope gain were explored.

It is not particularly difficult to design a completely new amplifier-regulator combination with a large reduction in envelope gain. It is quite a different problem, however, to devise a method for practical modification of large numbers of existing equipments. A number of methods were tried and found unsuitable for one reason or another. The modification finally adopted is the addition of a corrective network in the feed-back circuit, inserted at the oscillator grid (lead labelled D-C Bias in Figure 1). The network configuration and its effect on μβ of a particular regulator are shown in Figure 11. This network is of a type, well known in feed-back amplifier design, in which phase is transferred from a region (0.05 cycle per second) where it is in excess to a region (5 cycles per second) where it is needed. This network gives somewhat more than 2 to 1 reduction in envelope gain and results in a regulator-amplifier combination whose average maximum envelope transmission is shown in Figure 2.

Use of a larger capacitor in a network like that of Figure 11 gives more reduction in envelope gain. A network using 30 microfarads was field tested and found to yield a reduction of 6 to 1 in envelope gain. However, the 4-microfarad capacitor is the largest that can be included in the regulator case; an electrolytic capacitor cannot be used because of leakage requirements.

MOP-UP REGULATOR

If further reduction of the envelope gain should be required, this can be supplied by the use, at infrequent intervals, of mop-up regulators, whose function is to supply envelope loss at the frequency where the other regulators have envelope gain. This regulator is similar in principle to the other 2,064-kc regulators but its circuit details are quite different and it operates in conjunction with a different thermistor in its associated amplifier. Trial models have been built which are externally similar and mechanically interchangeable with the standard regulator and mount in the same position in the office as the ordinary regulator which they replace.

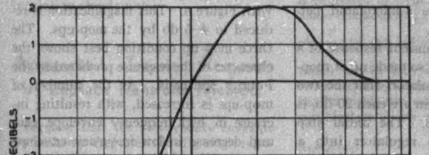

Figure 12 (left). Average envelope gain of six experimental mop-up regulators

Figure 14. Envelope gain of 2,000-mile circuit with mop-up regulators

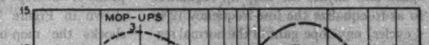

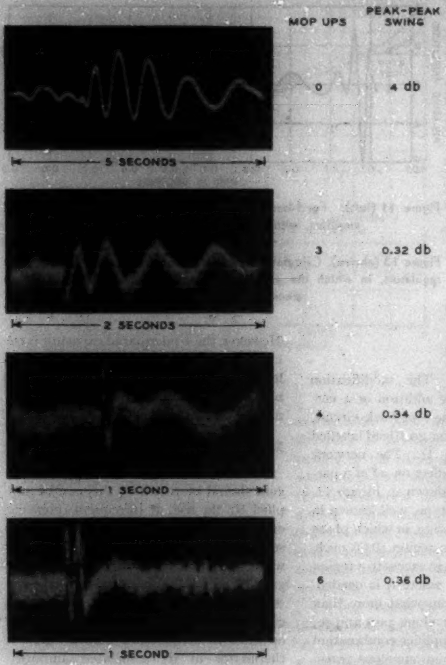

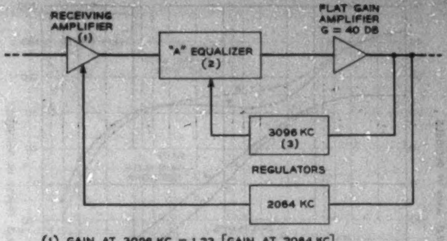

(1) GAIN AT 3096 KC = 1.23 [GAIN AT 2064 KC]
(2) LOSS AT 2064 KC = 40 DB FIXED
LOSS AT 3096 KC = VARIABLE
(3) 64 KC AND 556 KC REGULATORS ARE SIMILARLY CONNECTED

Figure 15 (left). Transient response to 0.2-db step-up, of 2,000-mile loop with mop-up regulators

Figure 16 (above). Simplified block schematic of regulators at a main station

Figure 12 shows the average envelope transmission of six trial model mop-up amplifier-regulator combinations. Note that considerable envelope gain exists in the vicinity of 25 cycles per second.

The determination of the correct spacing for the mop-up regulators is quite complex as it depends on a large number of factors, some of which are not too well known. If only over-all envelope gain is considered, it is in principle possible to space and adjust the mop-up regulators so as to equalize the low-frequency (2 to 4 cycles) envelope gain of the normal regulators and the higher frequency envelope gain of the mop-up units.

Naturally, it is to be expected that the characteristics of the transient response (to a step input) of such a system will be different than that observed on systems with only a single peak of envelope gain. Calculation of the transient response by Fourier synthesis was therefore made with punched card equipment.

The calculated transient response of 67 tandem regulators with the 4-microfarad network (20-db peak envelope gain) gives a value for the magnification of 14 db, which agrees well with the previous experimental result of 13.5 db, as shown in Figure 4. This indicates that for the same total peak envelope gain, the slight difference in shape of the envelope transmission characteristics of the regulator with or without the 4-microfarad network is unimportant.

The calculated transient response of a hypothetical system, so made up of mop-up and ordinary regulators that the two peaks of envelope gain are each 20 db, is shown in Figure 13. The initial step shocks the mop-up regulators into a transient response whose chief component is about 25 cycles per second. This transient dies out in about 0.1 second, during which time the other regulators change relatively little. The mop-up regulators now are ready to go to work on the transient introduced by the line regulators. Without the mop-ups this would build up to a tremendous amount (to ordinates of more than ±400 on the scale of Figure 13) but the mop-ups are successful in holding the swings to the extent shown. The transient is substantially over in about two seconds.

The magnification is about 13 db for the high-frequency part, and 10 db for the low-frequency part, of the transient. This is slightly more favorable than the result for a single-peaked characteristic.

A field test of the mop-up regulator was made on a circuit equipped with 134 ordinary regulators. The envelope gain of the normal circuit was 40 db, or 0.3 db per regulator. Over-all envelope gain measurements of the circuit with three, four, five and six mop-ups are shown in Figure 14. One might interpret these as showing that something between three and four mop-ups would be the optimum number for this line.

Transient tests showed the mop-up regulators to give the expected improvement. Figure 15 shows the response to a 0.2 db step upward. The peak-to-peak swing of 4 db for the no mop-up condition is seen to be reduced by a factor of about 12 to 1. The no mop-up case shows a magnification of 28 db which, for 40-db envelope gain, is in good agreement with Figure 4. This magnification is reduced to 4–5 db by the mop-ups. The three mop-up condition best shows the character of the response predicted by the Fourier synthesis. As the number of mop-ups is increased, with resulting increase in high-frequency envelope gain and decrease in low-frequency envelope gain, the initial higher frequency transient is enhanced and the lower frequency transient is decreased. This results in a reduction of the duration of the transient. The mop-up regulators also give a marked reduction in line jitter. The addition of one mop-up shows an improvement of 3 to 1, and three mop-ups give an improvement of 6.5 to 1. For the six mop-up case it is difficult to determine the amount of additional improvement as the jitter is masked by 120-cycle noise, which appears as the fuzzy broad trace on the four and six mop-up cases of Figure 15.

Office Regulators

In addition to the main 2,064-kc pilot frequency, the *L-1* system transmits other pilot frequencies, at 64, 556, and 3,096 kc. These pilots are used to control the characteristic of a transmission equalizer (the *A* equalizer) at main stations by means of backward acting regulators very similar to the line regulator. The general arrangement is shown in Figure 16.

In a transcontinental circuit, there are about 40 such stations.

At each of the pilot frequencies, envelope disturbances in the neighborhood of 2 cycles per second are increased by the envelope gain of these regulators. Furthermore, variations in the line pilot (2,064 kc) react on the office pilots, because a change in the line amplifier gain affects all frequencies. The design of the line amplifier is such that the change in gain in db is proportional to $\sqrt{\text{frequency}}$. The networks in the *A* equalizer are such that the loss at line pilot stays fixed, so there is no reaction of the office pilots on the line pilot.

The simplified analysis of Appendix II indicates that because of the $\sqrt{f}$ factor, the transient performance at 3,096 kc will always tend to be worse than at 2,064 kc. Similarly, conditions are likely to be more favorable at 64 and 556 kc. The equipment arrangements of the office regulators differ from those of the line regulator, and considerable difficulty would be experienced in incorporating the 4-microfarad network. For these, a reduction of envelope gain to 0.3 db is obtained by a cathode resistor in oscillator tube *V-3*. This leaves these regulators with 20-db d-c feedback which is adequate from a regulation standpoint.

Appendix I. Transient Response by Laplace Transform Method

Suppose that the steady-state envelope transmission characteristic of a single regulated amplifier can be considered as that of a 4-terminal linear invariant unilateral network.

Let $p=\sigma+j\omega$ be the complex frequency, and let $y(j\omega)$ be the envelope transfer ratio, that is

$$y(j\omega)=\frac{M_o}{M_i}=\frac{\text{per cent modulation of output pilot frequency}}{\text{per cent modulation of input pilot frequency}}$$

If transit time between amplifiers is neglected, the envelope transfer ratio of n similar tandem regulated amplifiers is $[y(j\omega)]^n$. The transfer function is then $[y(p)]^n$ and the response to a unit step function is given by the inverse Laplace transform

$$M_n(t)=\mathcal{L}^{-1}\left[\frac{1}{p}y^n(p)\right] \qquad (1)$$

If $y(p)$ is expressible as a rational algebraic fraction, then the inverse transformation is entirely straightforward.[5] Unfortunately, for large n, the number of terms in the result is prohibitive.

Equation 1 gives the response for all instants of time. For engineering purposes, however, it suffices to determine approximately the peak-to-peak swing (oscillation) of the transient and its duration. To this end, the "principle of stationary phase"[6,7] may be used.

This principle is perhaps most clearly explained physically in connection with the Fourier synthesis of the response to a square wave input

$$M_n(t)=\sum_{h=1}^{\infty}A_h^{(n)}\sin(n\varphi_h+h\varphi_t);\quad (h\text{ odd})$$

in which

$A_h^{(n)}$ = the amplitude of the hth harmonic of the fundamental after traversing n regulated amplifiers

φ_h = its phase shift in traversing a single amplifier

φ_t = the time-phase, that is, the phase of the fundamental at the instant under consideration

The principal contribution to M_n comes from those components having the largest values of A_h^n. If these are all clustered around the largest, say A_m, then they all add directly when the phase angle $(n\varphi_h+h\varphi_t)$ is nearly the same for all. This occurs at the time, t_m, when the phase is stationary with respect to h in the neighborhood of $h=m$, that is, when

$$\varphi_{t_m}=-n\left[\frac{\Delta\varphi_h}{\Delta h}\right]_{h=m} \qquad (2)$$

This addition is very clearly seen in the course of calculation of a Fourier synthesis.

To apply the principle, the transfer ratio is expressed in terms of its amplitude and phase characteristics

$$y(\omega)=A(\omega)\exp[jB(\omega)]$$

which are in turn expanded in Taylor's series about ω_0, the frequency at which $A(\omega)$ has its maximum value, $A(\omega_0)$. For typographical simplicity, write

$$A_0=A(\omega_0)$$

$$A_0'=\left[\frac{d}{d\omega}A(\omega)\right]_{\omega=\omega_0}\text{, and so forth}$$

$$\delta=(\omega-\omega_0)$$

Then the Taylor's series are

$$A(\omega)=A_0+\frac{{}_0''}{2}\delta^2+\ldots$$

$$B(\omega)=B_0+B_a\delta'+\frac{B_0''}{2}\delta^2+\ldots$$

At the maximum of $A(\omega)$, $A_0'=0$, it also is assumed here that $A_0''<0$ (this is necessary for a maximum) and that the other terms of the series can be neglected.

Using the approximation $\log(1+a)=a$, one has

$$\log\left[\frac{A(\omega)}{A_0}\right]=\frac{A_0''}{2A_0}\delta^2$$

$$\left[\frac{A(\omega)}{A_0}\right]^n=\exp\left[n\log\frac{A(\omega)}{A_0}\right]=\exp\left[n\frac{A_0''}{2A_0}\delta^2\right]$$

so that, in the vicinity of ω_0,

$$y^n(\omega)=A_0^n\exp\left[n\frac{A_0''}{2A_0}\delta^2+jn\times\left(B_0+B_0'\delta+\frac{B_0''}{2}\delta^2\right)\right] \qquad (3)$$

The further approximation now is made that, in the important range of ω, the spectrum of the step function is sufficiently constant so that it is given by $1/j\omega_0$.

The foregoing now are substituted in the Fourier integral

$$M_n(t)=\Re_e\left[\frac{1}{\pi}\int_0^{\infty}S(\omega)\exp(j\omega t)d\omega\right] \qquad (4)$$

in which $S(\omega)$ is the spectrum of the response to the unit step. This form is used because the physical network has equal transfer ratios for positive and negative values of ω, whereas the approximation, equation 3, is valid only for values of ω in the vicinity of positive ω_0. Furthermore, because the value of equation 3 is negligible for negative values of ω, the lower limit of integration in equation 4 can be made $-\infty$.

With the following additional substitutions made in equations 3 and 4

$$p=j\omega,\ p_0=j\omega_0,\ \omega=2\pi f$$

$$\delta=-j(p-j\omega_0)$$

$$\rho=-\frac{n}{2}\left(\frac{A_0''}{A_0}+jB_0''\right)$$

$$\lambda=nB_0'$$

equation 4 becomes

$$M_n(t)=\Re_e\left[\frac{2A_0^n\exp(jnB_0)}{j\omega_0}\times\int_{-\infty}^{+\infty}\exp[\rho(p-p_0)^2+\lambda(p-p_0)]\exp(pt)df\right.$$

in which the integral is of the exact form given in the Campbell and Foster[8] tables. Application of pairs 206 and 729 of the tables yields

$$M_n(t)=\Re_e\left(\frac{A_0^n}{j\omega_0\sqrt{\pi\rho}}\exp(jnB_0+j\omega_0 t)\times\exp\left[-\frac{(t+\lambda)^2}{4\rho}\right]\right)$$

The magnitude of the oscillation now is quickly determined. The second exponential has its largest value, unity, when

$$t=-\lambda=-nB_0'$$

which is the exact analog of equation 2. The complex factor $\sqrt{\rho}$ can be expressed in terms of its magnitude and phase. This phase and the factor $1/j$ are combined with the first exponential, which is recognized as a rotating unit vector; it therefore assumes the extreme values ±1.

Thus, the peak-to-peak swing of $M_n(t)$ is given by

$$M_n \text{ (peak-peak)} = \frac{2A_0^n}{\omega_0\sqrt{\pi\rho}}$$

or, in a somewhat different form

$$M_n \text{ (peak-peak)} = \sqrt{\frac{8}{\pi}}\,\frac{A_0^n}{\omega_0\sqrt{n}}\,G_0 \qquad (5)$$

in which

$$G_0 = \left[\left(\frac{A_0'}{A_0}\right)^2 + (B_0'')^2\right]^{-1/4}$$

To introduce envelope gain and magnification, there now is defined

E = envelope gain = 20 $\log_{10} A_0^n$ decibels
M = magnification = 20 $\log_{10} M_n$ (peak-peak) decibels

whereupon equation 5 can be thrown into the form

$$M = E - 10\log_{10} E + 17 + 20\log_{10} F_0 \text{ decibels}$$

$$F_0 = \frac{G_0\sqrt{\log_{10} A_0}}{\omega_0}$$

If F_0 were a constant, the magnification would depend only upon the total maximum envelope gain and not upon the shape of the envelope gain-frequency characteristic. The term in F_0 is therefore a measure of the effect of this characteristic.

A good fit to the experimental envelope characteristic of a single regulated amplifier with 0.7-db maximum envelope gain is obtained with a transfer function of the form

$$y(p) = \frac{p(p+1)}{(p+\alpha)(p+\beta)}$$

For $\alpha = 0.1$, $\beta = 0.87$, it is found that $A_0 = 0.78$ db, $F_0 = -10.7$ db. Hence, the theoretical relation between envelope gain and magnification is given by

$$M = E - 10\log_{10} E + 6 \text{ decibels}$$

This is plotted as the theoretical curve in Figure 4; the agreement between theory and experiment is quite satisfactory.

Appendix II. Envelope Modulation of 3,096-kc Pilot

Attention is here confined to single-frequency sine wave modulation of the pilot frequencies.

Symbols

A_a = amplitude modulation ratio of 2,064-kc pilot entering line
$A_a^{(n)}$ = amplitude modulation ratio of 2,064 kc leaving nth main station
A_b = amplitude modulation ratio of 3,096-kc pilot entering line
$A_b^{(n)}$ = amplitude modulation ratio of 3,096 kc leaving nth main station
R_a = voltage ratio corresponding to the envelope gain of the 2,064-kc regulators in one main section (that is, of six 2,064-kc regulators on the average)
R_b = voltage ratio corresponding to the envelope gain of a 3,096-kc regulator
n = number of main sections
K_a = normal level of 2,064-kc pilot, volts
K_b = normal level of 3,096-kc pilot, volts

Analysis

The maximum voltage at 2,064 kc entering the section is $K_a(1+A_a)$ and leaving the section is $K_a(1+R_aA_a)$. Hence the maximum "instantaneous" gain is

$$IG_a = 20\log\frac{1+R_aA_a}{1+A_a} \text{ decibels}$$

There is a phase angle associated with the envelope gain and a more exact treatment would take this into account.

For small x, 20 log $(1+x) = 8.68x$, and $IG_a = 8.68\,A_a(R_a-1)$ decibels. Since variations in system equivalent in decibels follow a $\sqrt{f}$ law, at 3,096 kc the gain is

$$IG_b = \sqrt{\frac{3{,}096}{2{,}064}}\,(IG_a) = 1.225(IG_a) \text{ decibels}$$

If the 3,096 kc enters the section at a constant level of K_b volts, its maximum level at the end is

$$K_b[1+1.225A_a(R_a-1)] \text{ volts}$$

That is, the 3,096-kc pilot has an amplitude modulation at the end of the section, although it had none entering the section. On the basis of the usual definition of envelope gain, then, at 3,096 kc it is infinite; some modification is therefore necessary.

Suppose now the 3,096-kc pilot entering the section has an amplitude modulation A_b in phase with A_a, that is, its maximum level is $K_b(1+A_b)$. Then the corresponding level at the output of the section is $K_b(1+A_b)[1+1.225\,A_a(R_a-1)]$; neglecting the term in A_aA_b, the 3,096 kc at the output has an amplitude modulation of $[A_b+1.225\,A_b(R_a-1)]$.

So far no 3,096-kc regulator has been assumed. At a main station, the arrangements are as shown on Figure 16. We assume that the A equalizer has a fixed 40-db loss at 2,064 kc, regardless of its loss variations at 3,096 kc. At the input to the A equalizer, the 3,096-kc pilot has the amplitude modulation given above. The 3,096-kc regulator sees this modulation and tries to compensate for it, but because the A equalizer-regulator combination has envelope gain, instead it increases the amplitude by the factor R_b. At the input to the next line section, the amplitude variations are therefore

$$A_a^{(1)} = A_aR_a$$
$$A_b^{(1)} = R_b[A_b + 1.225\,A_a(R_a-1)]$$

If subsequent sections are similar to the first, at the output of the nth section the modulations are

$$A_a^{(n)} = A_aR_a^n$$

$$A_b^{(n)} = R_b^n\left(A_b + 1.225\,A_a(R_a-1)\times\left[\frac{\left(\frac{R_a}{R_b}\right)^n - 1}{\frac{R_a}{R_b}-1}\right]\right)$$

If R_a is larger than R_b, and if A_a is comparable with A_b (both suppositions are valid for the *L-1* system), then for n large enough, the above reduces to

$$A_b^{(n)} = 1.225\,A_a^{(n)}\,\frac{(R_a-1)R_b}{(R_a-R_b)} \text{ approximately}$$

For $R_a = 1.23$ (1.8 db) and $R_b = 1.035$ (0.3 db), $A_b^{(n)} = 1.5\,A_a^{(n)}$.

This gives the interesting result that (for more than about 12 sections for the assumed values of envelope gain) the modulation of the 3,096-kc pilot is only about 3.5 db greater than that of the 2,064 kc and that the input modulation on the 3,096 kc is of little importance.

If the envelope gain of the line regulators is considerably less than that of the office regulators, so that R_a and R_b are nearly the same, then the effect of A_b predominates.

This simplified analysis indicates that the transient performance at 3,096 kc will always tend to be worse than at 2,064 kc. However, conditions are likely to be more favorable at 64 and 556 kc because the $\sqrt{f}$ factor (1.225 for 3,096 kc) is less than unity for these frequencies.

References

1. PROGRESS IN COAXIAL TELEPHONE AND TELEVISION SYSTEMS, L. G. Abraham. *AIEE Transactions*, volume 67, part II, 1948, pages 1520–27.

2. NETWORK ANALYSIS AND FEEDBACK AMPLIFIER (book), H. W. Bode. D. Van Nostrand and Company, New York, N. Y., 1945.

3. AUTOMATIC VOLUME CONTROL AS A FEEDBACK PROBLEM, B. M. Oliver. *Proceedings*, Institute of Radio Engineers (New York, N. Y.) volume 36, 1948, pages 466–73.

4. ANALYSIS OF SYSTEMS WITH KNOWN TRANSMISSION-FREQUENCY CHARACTERISTICS BY FOURIER INTEGRALS, W. L. Sullivan. *Electrical Engineering*, volume 61, May 1942, pages 248–56.

5. TRANSIENTS IN LINEAR SYSTEMS (book), M. F. Gardner, J. L. Barnes. John Wiley and Sons, New York, N. Y., volume 1, 1942, chapter VI.

6. HYDRODYNAMICS (book), Sir Horace Lamb. Sixth edition, Dover Publishing Company, New York, N. Y., 1945.

7. FREQUENCY ANALYSIS, MODULATION AND NOISE (book), S. Goldman. D. Van Nostrand and Company, New York, N. Y., 1948, section 4.14.

8. FOURIER INTEGRALS FOR PRACTICAL APPLICATIONS (book), G. A. Campbell, R. M. Foster. D. Van Nostrand and Company, New York, N. Y., 1942.

No Discussion

Equalization of Coaxial Lines

K. E. GOULD
ASSOCIATE AIEE

EQUALIZATION of coaxial lines has been discussed in a general way in a number of previous papers.[1,2,3] The present paper is intended to describe in somewhat more detail the equalization methods used in the Bell System's coaxial lines now in operation.

For telephone service, the requirements on equalization are fairly modest in terms of the capabilities of the present coaxial system. In the first place, the misalignment (that is, the variation in level from the nominal value) must not exceed a few decibels at any point in the system, throughout the transmission band, in order to avoid excessive noise because of low levels, or excessive modulation products because of high levels. Secondly, at the receiving end of each switching section (nominally 100 miles or so in length) the difference in level between working line and spare must not exceed perhaps 1/2 decibel over the band, in order that disturbances in individual channels be kept within tolerable limits at the time of manual switches made in the course of normal maintenance routines.

For television service, the equalization requirements are more severe, and are much less readily expressed in terms of simple transmission measurements. Misalignment is important, of course, because of its effect on signal-to-noise ratio and modulation, and similarity of working line and spare in each switching section must be maintained within reason. However, a much more serious problem is that of providing satisfactory equalization on long television circuits, both over-all and for intermediate dropping points.

For telephone service, delay distortion requirements for the broad-band system are extremely lenient and present no serious problem, but delay equalization must, of couse, be provided for television service. Delay distortion within the transmitted band arises primarily from gain cut-off at the ends of the band, and thus for the most part is of a broad nature. Nevertheless, the magnitudes are such that a high degree of precision is needed to meet television requirements.

Repeaters and Line

Auxiliary Repeaters

From an equalization standpoint, the performance of the line repeater (herein called the auxiliary repeater) is of paramount importance. The coaxial line itself provides a transmission medium which is uniform to a high degree and stable in its transmission characteristics. The principal variation is a predictable one due to temperature changes. Since the cable is essentially all underground, even these changes are relatively slow. Thus, if the repeater could be made to compensate the loss characteristics of the cable with reasonable precision, and the deviations from a flat gain characteristic for the combination of repeater and associated line, including the effects of all variables, were known to a high degree of precision, the gain equalization of the system would be straightforward.

The magnitudes of the quantities involved in gain equalization are, however, rather large, since the variation in cable loss across the frequency band employed is some 45 decibels per repeater section and the corresponding seasonal variation at the upper end of the band is as much as 5 decibels. In terms of a 4,000-mile circuit, these figures represent an equalization across the band of over 20,000 decibels and a seasonal correction of perhaps 2,500 decibels.

The auxiliary repeater for the present coaxial system is shown in block form for one direction of transmission by Figure 1. Since our interest here is primarily in transmission features of the repeater, the power supply is shown in rather incomplete form, for the sake of simplicity. At the input and at the output, next to the line itself, power separation filters isolate the 60-cycle power from the signal band, which extends roughly from 60 to 3,100 kc. These filters, incidentally, provide some gain equalization at the lower end of the band. Between the power separation filter and the input of the amplifier is an equalizer, known as the "basic equalizer," which compensates for a substantial part of the loss-frequency characteristic of the cable. At the input and at the output of the amplifier, a variable capacity is provided which is adjusted to offset approximately the variations in impedance seen by the amplifier due to connecting cable, splices, and so forth.

The circuit diagram of the auxiliary amplifier itself is shown in Figure 2. This is a 3-stage cathode-feed-back amplifier in which the beta circuit has been designed to perform two important functions: (1) compensation for a considerable part of the loss-frequency characteristic of the cable, and (2) variation of the gain-frequency characteristic in a manner closely matching the change in cable loss with temperature. Since this latter change is approximately equivalent to a change in length of the cable, this regulating network is used also to take care of minor variations in cable length. More substantial variations in length, which are inevitable in any system layout, are roughly compensated by the introduction of a line building-out network ahead of the basic equalizer.

Two vacuum tubes are used in parallel in each stage for the sake of improved reliability, the failure of a single tube in any stage resulting only in somewhat impaired performance, particularly as to modulation, but not to such a degree as to seriously affect the coaxial system. An

---

Paper 49-248, recommended by the AIEE Communications Committee and approved by the AIEE Technical Program Committee for presentation at the AIEE Fall General Meeting, Cincinnati, Ohio October 17–21, 1949. Manuscript submitted July 15, 1949; made available for printing September 6, 1949.

K. E. Gould is with the Bell Telephone Laboratories, Inc., New York, N. Y.

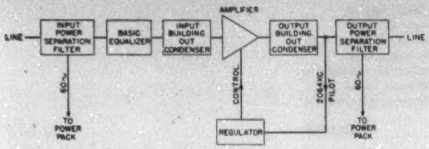
LINE
INPUT POWER SEPARATION FILTER
BASIC EQUALIZER
INPUT BUILDING OUT CONDENSER
AMPLIFIER
OUTPUT BUILDING OUT CONDENSER
OUTPUT POWER SEPARATION FILTER
LINE
60~
TO POWER PACK
CONTROL
2064KC PILOT
60~
TO POWER PACK
REGULATOR

Figure 1. Block diagram of auxiliary repeater

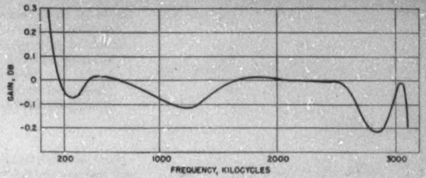

Figure 3. Gain of auxiliary amplifier section

additional cathode-feed-back network is incorporated in the output stage to improve the modulation performance of the high-level vacuum tubes.

The regulation of amplifier gain is accomplished by varying the impedance of the beta circuit, an indirectly-heated thermistor being incorporated for this purpose. At alternate repeaters, automatic regulation of gain is provided, which maintains the 2064-kc pilot at a prescribed power. This arrangement is shown in Figure 1. The behavior of this feed-back regulator system is described in a companion paper[4] and will be discussed here only insofar as it bears on the equalization problem.

The precision with which the over-all repeater gain should be made to match the cable loss is largely a question of economics. As long as the misalignment can be made small enough that signal-to-noise ratio and modulation performance are not jeopardized, it is obviously uneconomical to incorporate a large number of elements in the individual repeater to meet equalization requirements for a long system. A more economical arrangement would provide, at rather widely spaced intervals, equalizers to take care of accumulated gain deviations. Thus the gain of an "auxiliary repeater section" (auxiliary repeater combined with its associated length of cable) has been made only as flat as a modest number of circuit elements in the repeater will permit. The result is shown in Figure 3.

In manufacture and in the repair of the amplifier, the insertion gain is controlled to provide the auxiliary section gain of Figure 3 to within a few tenths of a decibel for individual amplifiers, with an average value for any considerable group of amplifiers within perhaps 0.05 decibel over-all of the transmitted band except the extreme upper frequencies, where the deviations may be two or three times as great. A high degree of manufacturing control must be maintained to obtain such performance, not only in the adjustment of the assembled amplifier, but also with regard to individual components, particularly in the input and output coupling networks. The gain deviations associated with changes in various elements must be known with considerable precision, not only in order to establish manufacturing requirements but also to guide the design of the adjustable features which are incorporated in the rather widely spaced gain equalizers mentioned previously. Figure 4 shows the amplifier gain-deviation characteristics for small changes in the most critical elements, leakage inductance of the input and output transformers, and inductance

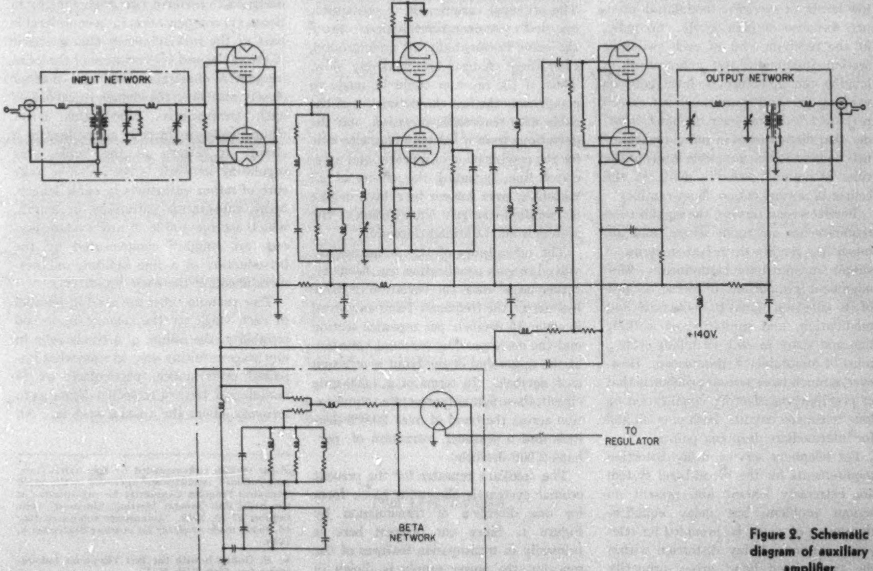

Figure 2. Schematic diagram of auxiliary amplifier

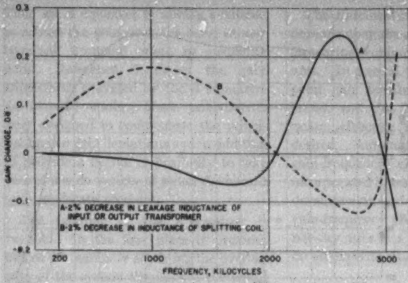

Figure 4. Effect of element deviations on amplifier gain

of the "splitting" coils in the input and output coupling networks.

For control of repeater insertion gain to the accuracy objectives adopted here, precise control of repeater panel impedances (that is, the impedances faced by the amplifier) is necessary. Figure 5 shows the effect on gain of 1 per cent changes in conductance and susceptance across the amplifier input and output respectively. For small changes, these effects are nearly independent, and represent gain-frequency characteristics which must be accommodated by the adjustable equalizers.

The general objective in establishing manufacturing control of the repeaters was to reduce uncertainties in the behavior of the repeater under operating conditions to the point where variations in circuit elements, made as small as good manufacturing practice will permit, are controlling. The reliability of repeater insertion gain as measured in the shop (or at amplifier maintenance points in the field) was checked by installing a group of carefully measured repeaters in a line and measuring the over-all transmission characteristics. This was done successively in various sections involving the several types of installed cable, and the degree of precision involved is probably best illustrated by the measures required to assure adequate accuracy with respect to cable loss as a function of frequency.

Figure 5. Change in gain due to one per cent increase in admittances facing auxiliary amplifier

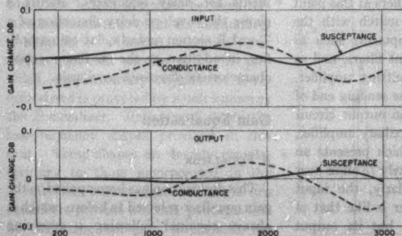

CABLE LOSS

There are four principal types of cable now in the plant: (1) rubber disk insulation, outer conductor 0.27-inch in diameter, (2) polyethylene disk insulation, outer conductor 0.27-inch in diameter, (3) similar to (2) but with outer conductor 0.375-inch in diameter, and (4) similar to (3) but slightly thicker outer conductor, 0.012 inch rather than the previous 0.010 inch. The last of these types is the present standard, and on the basis of appropriate choice of repeater spacing differences in performance of all but the rubber-disk type are very slight.

The most precise direct measurements of cable loss were made on the polyethylene-disk insulated cable with an outer conductor 0.375 inch in diameter and 0.010-inch thick. Even these measurements could profitably be smoothed by computing the loss as a function of frequency, using constants chosen to give a good general fit with the measured loss.

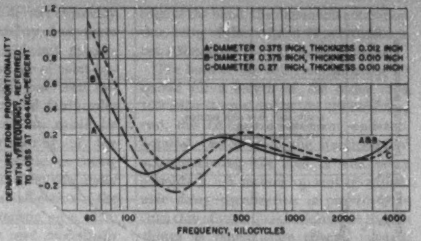

Figure 6. Cable loss—polyethylene disk insulation with various outer conductors

The result is shown in Figure 6 as departure from proportionality with the square root of the frequency. The refinement of these computations, which are due to J. P. Kinzer, is illustrated by the fact that it was necessary to consider the inner conductor as a soft copper core surrounded by a 0.00045-inch shell with a resistivity 4 per cent higher than that of the core, an hypothesis reasonably consistent with the method used in making the inner conductor.

Differences in loss due to changing the cable structure from that considered above to either of the other two with polyethylene disks can be computed with considerable precision, and Figure 6 shows the loss for these other two types of cable. It might be mentioned that the effect of temperature variation on cable loss can also be computed with precision, and correlated with measured temperature coefficients, to provide a high degree of accuracy in determining regulation error for the system. With regard to the loss of rubber-disk insulated cable, which is installed in present plant only in a few

Figure 7. Change in gain of auxiliary repeater section due to temperature effects and aging

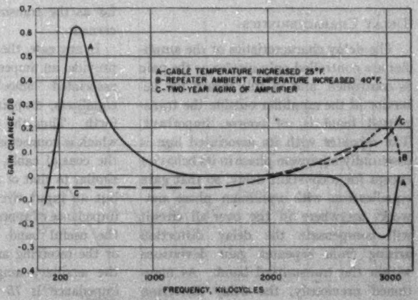

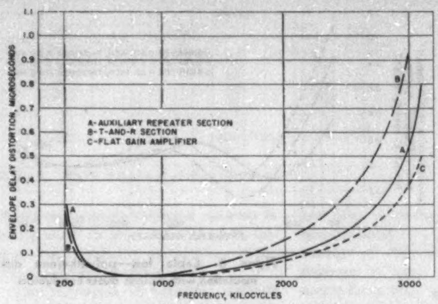

Figure 8. Envelope delay distortion

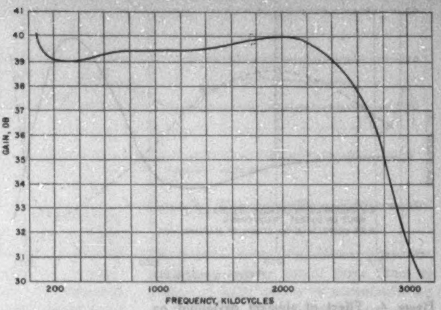

Figure 9. T-and-R section gain

sections, the loss is sufficiently different from that of cable with polyethylene insulation that even the basic equalizer must be different to avoid serious misalignment.

Systematic Deviations

There are three principal sources for systematic deviations in auxiliary repeater section gain under operating conditions: (1) regulation error, (2) aging of vacuum tubes, and (3) repeater temperature effects. These gain changes must, of course, be taken care of by means of the adjustable equalizer, but since these changes occur slowly, they are readily handled by routine procedures. Regulation error is due to the lack of precise matching of the beta circuit gain control to change in cable loss. Aging of vacuum tubes results generally in a gradual reduction in transconductance, which in turn affects the gain most seriously where the feedback is lowest, that is, toward the upper end of the useful band. Repeater temperature effects, while a composite of many factors, are reasonably systematic. Figure 7 shows curves of these three effects for an auxiliary repeater section.

Delay Characteristics

The delay characteristics of the amplifier are controlled only insofar as the gain is controlled, and in this regard the behavior of the amplifier outside the transmitted band is, of course, important. The repeater with its associated line is essentially minimum phase in its behavior except for a constant delay, so that gain equalization with minimum phase networks anywhere in the over-all circuit will compensate the delay distortion arising from repeater gain deviations within the transmitted band. As mentioned previously, the delay distortion appearing in the transmitted band due to the gain characteristic outside the band, is quite broad. The envelope delay distortion for one auxiliary repeater section is shown in Figure 8. A companion paper[8] describes the method of analysis employed to match such a delay characteristic with an equalizer having an essentially constant loss over the entire transmitted band.

Office Repeaters

At spacings of perhaps 50 to 100 miles, gain equalization must be provided as mentioned previously, to restore the levels across the transmitted band. In highly built-up areas, the spacing may be dictated by the need for dropping circuits, but in other areas, equalization may be provided even though no circuits are dropped. This equalization may be a part of a main station, where power is supplied to the coaxial system, whether switching facilities are provided or not, or may appear in an equalizing auxiliary station, which replaces an ordinary auxiliary station in a long power feed section requiring additional equalization. Figure 2 of reference 3 shows these arrangements except for the equalizing auxiliary station, which is essentially the same as a nonswitching main station as far as the transmission circuits are concerned.

In any case, the amplifiers at this point provide an impedance match with the associated "office" equipment, such as equalizers, dropping-point filters, and so forth. Thus the transmitting amplifier, which is connected to the sending end of the coaxial cable, has an output circuit similar to that of the auxiliary amplifier, but an input circuit which presents an impedance of approximately 75 ohms over the useful band. Similarly, the input of the receiving amplifier is like that of the auxiliary amplifier, but its output impedance is 75 ohms. The receiving amplifier includes a variable beta circuit like that in the auxiliary amplifier, so that variations in loss of the cable associated with the combination of transmitting and receiving amplifiers may be compensated.

It is convenient to consider this combination of transmitting amplifier, receiving amplifier, and associated section of coaxial cable as a unit, and this has been designated a T-and-R section. Figure 9 shows the gain of a T-and-R section. The droop in this gain characteristic at the upper end of the frequency range is an incidental result of level allocation in the system for optimum modulation performance, and is not important from the standpoint of the present paper. In brief, it is more economical to incorporate the equalization of this characteristic in the *A* equalizer, which will be discussed later, than to design the receiving repeater with the additional gain at the upper frequencies.

To offset the losses of such equipment as the *A* equalizer, one or more flat-gain amplifiers are provided. These amplifiers have a gain of approximately 40 decibels, and contribute but little to the gain equalization problem. They do introduce appreciable delay distortion, which must be included in the requirements for delay equalizers. Figure 8 shows the envelope delay distortion of a T-and-R section and of a flat-gain amplifier, in addition to the auxiliary-section characteristic discussed previously.

Gain Equalization

A Equalizer

This designation has been applied to the gain equalizer referred to before, which is always required following a receiving amplifier, to equalize a T-and-R section.

Thus an *A* equalizer is always available to adjust the gain over the band at any terminal, dropping point, or switching point. Reference 5 shows the gain adjustment provided by the *A* equalizer. As implied earlier, these adjustments were designed to compensate the principal known gain deviations and in addition to provide a degree of flexibility to take care of a wide variety of minor deviations with moderate precision.

The function of the *A* equalizer is twofold. In the first place it provides means for manually adjusting the over-all gain of the system throughout the useful band. In addition, three automatically regulated loss-frequency characteristics are provided to reduce the gain deviations arising in the course of time, thus permitting less frequent manual realignment. These automatic controls are in some respects similar to the regulation facilities, described earlier, for equalizing the major change in the system, variation of cable loss with temperature. In each case a pilot signal is employed, the level of this pilot being controlled by a regulator. In the *A* equalizer, thermistors are supplied with heater current from regulators operating from pilots at frequencies of 64, 556 and 3,096 kc, respectively. These thermistors produce loss-frequency characteristics, as described in reference 5, with a maximum in each case in the vicinity of the pilot frequency. For television transmission, the 556-kc pilot control is particularly important since it tends to stabilize the level of the 311-kc television carrier.[6]

For telephone service, the *A* equalizer provides adequate performance for all but the very longest spans between terminals, that is, between points at which all channels are brought down to voice frequencies.[7] For television service, it is generally necessary to provide additional equalization, which will be described in the following section.

B EQUALIZER

As mentioned in the preceding section, where the length of system between terminals exceeds that which the *A* equalizer is capable of adjusting adequately, or where television service is to be provided, supplementary adjustment is required and is provided by a unit known as the *B* equalizer. Reference 5 shows the loss-frequency shapes provided in this unit. These shapes are largely complementary to those incorporated in the *A* equalizer, and in combination the two equalizers provide a rather powerful tool for adjusting the gain throughout the entire band.

The usefulness of such devices obviously depends upon the availability of adequate measuring equipment and test procedures. In general, a schedule of point-by-point gain measurements has been followed, and this has proved fairly adequate, although slower than would be desired. Automatic recording of the gain-frequency characteristic is being incorporated in test equipment now under development, and visual indication of the gain-frequency characteristic on a cathode-ray tube has been used successfully on an experimental basis.

Delay Equalization

The envelope delay distortion of an auxiliary repeater section, of a T-and-R section and of a flat-gain amplifier are shown in Figure 8. A representative television link, say 100 miles in length, might include 12 auxiliary repeater sections, one T-and-R section, and two flat-gain amplifiers. Thus the envelope delay distortion for this section would be perhaps 4 microseconds at the lower end of the television band[6] and some 13 microseconds at the upper end. Delay equalization must, of course, be provided by increasing the delay at other parts of the band to the system delay at the upper edge of the band, the maximum correction thus being of the order of 13 microseconds per 100 miles.

The bulk of the delay equalization required for a length of the order of a 100 miles is provided at the transmitting end, this being a convenient and economical choice from the standpoint of accommodating the loss of the delay equalizers. A certain amount of adjustable delay equalization is provided, to take care of variations in delay due to such things as temperature effects, vacuum tube aging, and deviations in amplifier performance, the adjustable units being placed at the receiving end for ease of establishing the correct settings. Since adjustable delay is more easily provided in this form, the variable units have delay characteristics roughly like those of a section of line. The receiving end also includes some smaller delay equalizers, particularly those associated with dropping point equipment and thus needed at only one point in any over-all television circuit.

Since the system layout varies from place to place, so that various numbers of repeater sections and so forth must be accommodated, considerable flexibility is required in the delay equalizers available. This has been accomplished by

Figure 10. Transmission characteristics—Washington-Chicago circuit

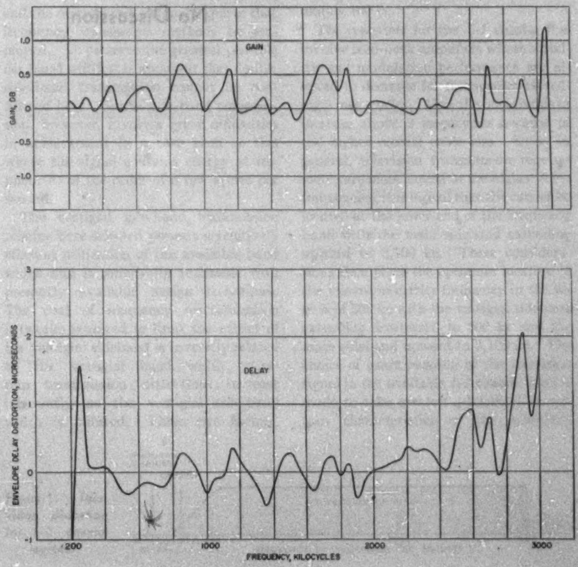

providing a series of "building blocks" of delay equalization beginning with a large unit which will equalize a representative long section between television dropping points and progressing through successively smaller units until the residual interpolation can be made with adjustable units. With this approach the latter type of phase equalizer thus performs a dual purpose, and reduces the number of types of fixed units required. Since there are moderate variations in the proportions of auxiliary repeater sections, T-and-R sections and flat gain amplifiers, for each of which the delay distortion characteristic is different, additional flexibility is required in delay equalizers beyond simply a scale-factor change. This is accomplished by incorporating minor changes in the delay-frequency characteristics of some of the smaller units, and more particularly by providing supplementary units which bridge the gaps between the various system layouts, that is, between the various extremes in proportions of the several components which contribute to delay distortion. The design features incorporated in the delay equalizers are described in reference 5.

As mentioned before, adjustable delay equalization has been provided not only to ease the problem of accommodating various system layouts but also to take care of gradual changes in the system. As described in reference 5, adjustments may be made independently at each end of the band. So far, a single shape has been provided on keys, with merely an adjustable scale factor, but there is no reason why a more flexible arrangement could not be adopted if this should be needed.

As in the case of gain equalization, adjustments must be based on transmission measurements, and this calls for adequate test equipment. Two types of delay measuring equipment are being made available, one involving point-by-point measurements of envelope delay distortion with a rather wide frequency interval and the other automatic recording simultaneously with the gain, using a narrow interval for measuring envelope delay distortion. Further experience with television transmission on coaxial systems will be required before a sound decision can be made on the choice of delay measuring equipment for this system.

System Performance

As an example of coaxial system equalization for television transmission, Figure 10 has been prepared showing the measured gain and envelope delay distortion for a circuit from Washington to Chicago. This is representative of the performance presently obtainable with these facilities, although perhaps not as good as that which might be realized from an installation incorporating recent improvements introduced specifically because of television requirements.

References

1. Television Transmission Over Wire Lines, **M. E. Strieby, J. F. Wentz.** *Bell System Technical Journal* (New York, N. Y.) volume XX, January 1941, pages 62–81.

2. Television Network Facilities, **L. G. Abraham, H. I. Romnes.** *AIEE Transactions*, volume 66, 1947, pages 541–48.

3. Progress in Coaxial Telephone and Television Systems, **L. G. Abraham.** *AIEE Transactions*, volume 67, part II, 1948, pages 1520–27.

4. Stability of Tandem Regulators in the L-1 Carrier System, **J. P. Kinzer.** *AIEE Transactions*, volume 68, part II, 1949, pages 1179–86.

5. Attenuation and Delay Equalizers for Coaxial Lines, **W. R. Lundry.** *AIEE Transactions*, volume 68, part II, 1949, pages 1174–79.

6. Television Terminals for Coaxial Systems **L. W. Morrison, Jr.** *AIEE Transactions*, volume 68, part II, 1949, pages 1193–99.

7. Frequency Division Techniques for a Coaxial Cable Network, **R. E. Crane, J. T. Dixon, G. H. Huber.** *AIEE Transactions*, volume 66, 1947, pages 1451–59.

No Discussion

Television Terminals for Coaxial Systems

L. W. MORRISON, JR.
NONMEMBER AIEE

THE broad features of operation of the *L-1* coaxial system for the transmission of television have been discussed in a recent paper.[1] It is the purpose of this paper to describe in somewhat more detail the factors influencing the design of the coaxial television terminals and the features of the equipment now in service in the Bell Systems' television network. The television terminals here described were placed into network service in 1947, but in basic form are similar to experimental models developed prior to the war and used in early television transmission studies over the coaxial cable.[2,3]

Frequency Allocation Considerations

The nominal transmission band of the *L-1* coaxial line extends from 64 to 3,100 kc. In contrast to this available band, the television video signal nominally occupies the frequency region extending from a few cycles per second upwards to 4 megacycles. It is the function of the television terminals to properly translate this video band of frequencies upward into the transmission region of the coaxial line and, after transmission over the system, to restore the television signal to its original video form for use by the broadcaster.

In addition to the necessity for frequency translation of the video signal, it is apparent that the over-all available band width for television transmission is somewhat less than 3 megacycles. Numerous experiments have been conducted with a view toward evaluating the subjective loss of sharpness of a television image with restricted transmission bands.[4] It is sufficient to say here that a definite visible effect requires a change in band width somewhat in excess of 1 megacycle in a 4-megacycle system, which is the increment we are here concerned with. The practical operation of the *L-1* coaxial system for television service during the past several years appears to confirm this conclusion.

The relative positions of the transmission band of the *L-1* coaxial system and the original video signal requires that frequency translation methods be employed. To preserve the greatest possible net band width it is apparent that double side-band transmission cannot be considered here. Single side-band transmission, however, involves great difficulties in achievement in a case such as this where the signal contains energy at frequencies of the order of a few cycles per second.

The vestigial side-band transmission scheme here selected permits a relatively efficient utilization of the available band width and is practically realizable with presently available design techniques. The cost of frequency discrimination networks required to limit the extent of the vestigial sideband is inversely related to the vestigial band width. Certain transmission distortions increase inherently as the vestigial side-band width is reduced. These two factors, which will be discussed in more detail later, must be balanced against the desirability of utilizing the available band width to the fullest extent to achieve optimum transmission performance consistent with economic considerations. A vestigial-to-main side-band width ratio of approximately 4 per cent is here selected as representing a satisfactory condition for the *L-1* coaxial system.

The delay distortion of a long coaxial system tends to increase rapidly at frequencies approaching the lower cut-off. While this is unimportant for telephone application, for television use precise delay equalization over the entire band is required. A study of the *L-1* coaxial system indicates that in consideration of the extent of delay equalization required for television a lower practical limit of 200 kc is advisable. This and the preceding considerations result in a main side-band width of approximately 2,800 kc with the vestigial sideband occupying approximately 100 kc.

The repeaters for the *L-1* coaxial line involve feed-back amplifiers whose stability and modulation performance are allowed to decrease for frequencies exceeding 2 megacycles. Also, the noise tends to increase above 2 megacycles because of the higher coaxial cable loss. Since, in general, television transmission requirements are more lenient at the higher video frequencies, it is logical that the carrier be located at the lower end of the frequency band with the main sideband extending upward to 3,100 kc. These considerations then place the optimum location of the television carrier frequency in the region of 300 kc with the vestigial sideband extending downward to 200 kc and the main sideband upward to 3,100 kc. The choice of exact location of the television signal in the available *L-1* coaxial band is made to take greatest advantage of certain characteristics of the television

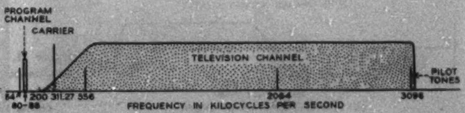

Figure 1. Television allocation for *L-1* coaxial system

Paper 49-249, recommended by the AIEE Communication Committee and approved by the AIEE Technical Program Committee for presentation at the AIEE Fall General Meeting, Cincinnati, Ohio, October 17–21, 1949. Manuscript submitted July 19, 1949; made available for printing September 6, 1949.

L. W. MORRISON, JR., is with the Bell Telephone Laboratories, Inc., New York, N. Y.

The design and development of the television terminals for the *L-1* coaxial system represents the contributions and efforts of a considerable number of individuals at the Bell Telephone Laboratories. The author has been privileged to represent them in this presentation.

Figure 2. Modulation diagram for television carrier terminals

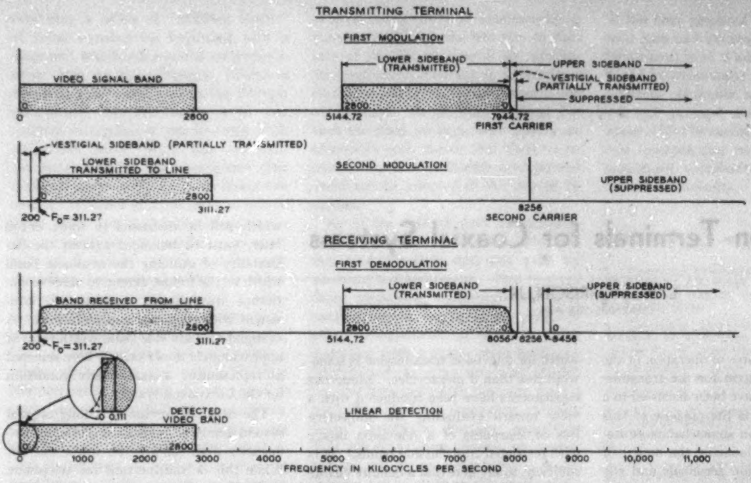
TRANSMITTING TERMINAL
FIRST MODULATION
VIDEO SIGNAL BAND
0
2800
LOWER SIDEBAND (TRANSMITTED)
UPPER SIDEBAND
VESTIGIAL SIDEBAND (PARTIALLY TRANSMITTED)
SUPPRESSED
2800
0
5144.72
7944.72
FIRST CARRIER
VESTIGIAL SIDEBAND (PARTIALLY TRANSMITTED)
LOWER SIDEBAND TRANSMITTED TO LINE
SECOND MODULATION
UPPER SIDEBAND (SUPPRESSED)
0
2800
200
F0= 311.27
3111.27
8256
SECOND CARRIER
RECEIVING TERMINAL
FIRST DEMODULATION
BAND RECEIVED FROM LINE
LOWER SIDEBAND (TRANSMITTED)
UPPER SIDEBAND (SUPPRESSED)
0
2800
200
F0= 311.27
3111.27
2800
0
5144.72
8056
8256
8456
0
0.111
DETECTED VIDEO BAND
2800
LINEAR DETECTION
0
1000
2000
3000
4000
5000
6000
7000
8000
9000
10,000
11,000
FREQUENCY IN KILOCYCLES PER SECOND

signal, the transmission properties of the coaxial line, and to permit simplification of operating and maintenance practices.

As described in a previous paper,[5] the television signal produced by scanning is composed of concentrations of energy located in frequency regions related to the line and field scanning frequencies and harmonics thereof. The alternate regions of low energy content may be considered as related to specific forms of complex detail rarely present in television scenes. In a converse fashion, the introduction of extraneous energy into these idle regions has been found to produce complex visual effects of which, in general, the viewer is very tolerant. In the television terminal designed for the *L-1* coaxial system, this phenomenon is utilized where possible by locating the exact position of the transmitted television band so that existing unavoidable interferences fall within these regions of comparative insensitivity. For example, three of the pilot frequencies employed for gain equalization purposes are located at 556, 2,064, and 3,096 kc.[6] The effective interference produced by these control tones with the transmitted television carrier signal is reduced in this manner.

Another characteristic of the energy-frequency distribution of the television signal which is of importance here is the relatively high concentration of energy at the lower video frequencies and the usual diminution at the higher frequencies. It is possible to encounter variations in this characteristic when unusual specific scenes or test patterns are considered, but in the large majority of cases a considerable reduction of energy with frequency is the rule. By means of predistorting methods this broad energy-frequency characteristic is altered for transmission over the coaxial line resulting in improved transmission performance as discussed in more detail later.

Another factor which influences the exact position of the transmitted television signal on the coaxial line is the practical problem of maintenance of these precise carrier frequencies over a nationwide network. In the terminal design which will be described later, the highly stable coaxial line pilot frequencies which are always available are used as frequency reference standards in maintenance of this equipment.

The exact location of the modulated

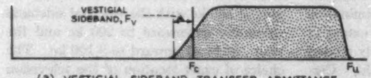
VESTIGIAL SIDEBAND, FV
Fc
Fu

(a) VESTIGIAL SIDEBAND TRANSFER ADMITTANCE

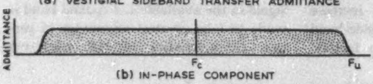
ADMITTANCE
Fc
Fu

(b) IN-PHASE COMPONENT

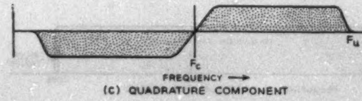
Fc
Fu
FREQUENCY →

(c) QUADRATURE COMPONENT

Figure 3. Transfer admittance of a vestigial sideband carrier system

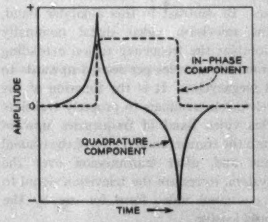

Figure 4. In-phase and quadrature components of a rectangular pulse

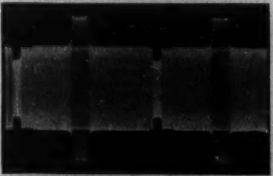

Figure 5. Modulated television carrier signal prior to detection

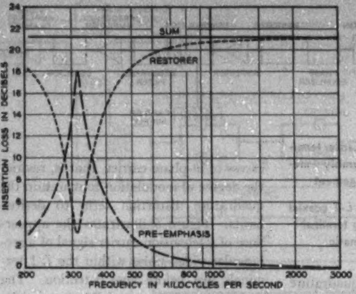

Figure 6 (left). Pre-emphasis and restorer characteristics

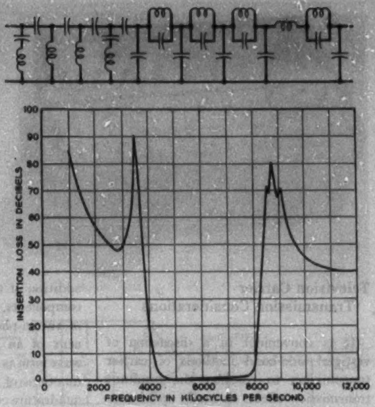

Figure 9 (right). Band-pass filter—configuration and loss characteristics

television carrier signal as transmitted over the *L-1* coaxial system is shown in Figure 1. The television carrier is located at 311.27 kc. Provision also is made for transmission of the accompanying sound program by single side-band carrier means in the region of 80–88 kc. The equipment and methods employed here have been described recently.[7]

The Terminal Modulation Process

To achieve the translation of a band of frequencies by an amount small as compared to the band width, multiple modulation steps must be employed. Figure 2 illustrates the features of the double modulation process employed here.

The original video signal extending from a few cycles per second upwards to 3 megacycles is modulated with a carrier frequency of 7.944 megacycles. The resultant lower sideband together with a vestige of the upper sideband as selected by the following band filter is then modulated again, this time with a carrier located at 8.256 megacycles. The lower sideband of this second modulation step is selected by a following low-pass filter and now lies between 200 and 3,100 kc with the original zero video frequency now located at 311.27 kc. This frequency position is the one desired for transmission over the coaxial line. It should be noted that the vestigial shaping process is only partially completed in the transmitting terminal, the remainder of this process being provided within the receiving terminal.

After transmission over the *L-1* coaxial line, a similar double-demodulation process is employed to restore the signal to its original video form. The incoming carrier signal at the receiving terminal first is modulated with a carrier frequency of 8.256 kc. Following this, a band filter similar to that in the transmitting terminal selects the lower sideband and introduces the remainder of the vestigial side-band shaping. The resulting television carrier signal now falls in the region of 5 to 8 megacycles and at this point envelope detection is employed to recover the video signal for transmission to the broadcaster.

The choice of final demodulation by envelope detection rather than through the use of a local carrier demodulator results in a considerable simplification of the terminal equipment. For satisfactory operation of product demodulation in a television system such as this, it has been found necessary to maintain the relative phase between the incoming carrier of the television signal and the local demodulating carrier to within one degree for satisfactory transmission performance. The realization of such phase precision throughout a nation-wide network would require extremely costly and complex terminal equipment. The satisfactory operation of a carrier television system which employs envelope detection, however, necessitates certain restrictions as to the form of the modulated signal envelope. However, in this system it was considered advantageous to accept these restrictions and employ envelope detection.

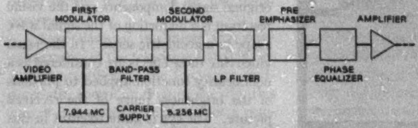

Figure 7 (left). *L-1* coaxial television transmitting terminal—block schematic

Figure 8 (below). First modulator—equipment layout

Figure 10 (right). Typical equalizer section—mechanical arrangement

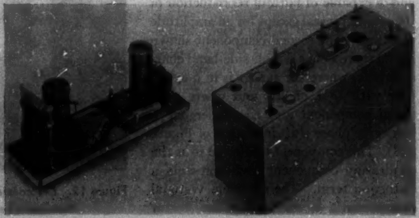

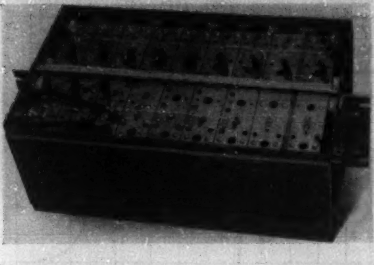

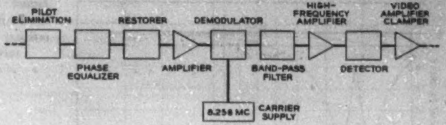

Figure 11 (left). Carrier terminal network assembly—mechanical arrangement

Figure 13 (right). *L-1* coaxial television receiving terminal—block schematic

Television Carrier Transmission Considerations

It is convenient in a discussion of vestigial side-band methods of carrier transmission to consider the resultant transmission effects as made up of contributions from two components, an inphase or real component and a quadrature or distortion component. This method of analysis was described originally by Nyquist.[8] The process is illustrated in Figure 3. Here the transfer admittance shown in (A) represents the idealized conditions for vestigial side-band transmission. The main side band is shown extending from the carrier frequency location F_c upwards to F_u, the cut-off of the system. A vestige of the lower sideband extends from F_c downward as shown. In the region $F_c \pm F_v$ the admittance characteristic is so chosen that the sum of the admittances offered to any upper sideband frequency and the corresponding lower side-band frequency is a constant. In this idealized view a linear phase with frequency characteristic over the entire frequency band, that is, constant envelope delay, is assumed.

The vestigial side-band system admittance function shown in Figure 3 (A) may be considered to be equivalent to the sum of two other admittance forms illustrated in (B) and (C). Both of the latter functions are of a double side-band form and may be treated as such. The admittance component shown in (B) represents a double side-band characteristic, where the carrier is in phase with the original signal and is capable of faithful reproduction of the original signal except for an amplitude constant. The second component shown in (C) represents a double side-band characteristic, where the carrier is in quadrature with that of (B) and where each signal component also has undergone a 90-degree phase shift from that of Figure 3(B). This component is referred to as the quadrature component and represents a distortion term. The complete vestigial characteristic is formed by the vector addition of the in-phase and quadrature components. Figure 4 illustrates the form of the in-phase and quadrature component of an idealized rectangular video wave form as obtained with the admittance functions of Figure 3. The form of the quadrature component is a function of the band width of the vestigial sideband, and its peak amplitude is inversely related to this band width. The contribution of this distortion term to the resultant output of a vestigial transmission system can be made as small as desired by providing an excess of in-phase carrier, supplied by either local generators or contained in the transmitted carrier signal.

As discussed previously, the *L-1* television terminals employ envelope detection and here it is required to transmit an excess of in-phase carrier, that is, restrict the degree of modulation to maintain the quadrature distortion term to desired limits. Figure 5 illustrates the appearance of a television carrier signal of a rectangular video pulse within the *L-1* terminals just before final detection. The quadrature effects are visible here in the envelope.

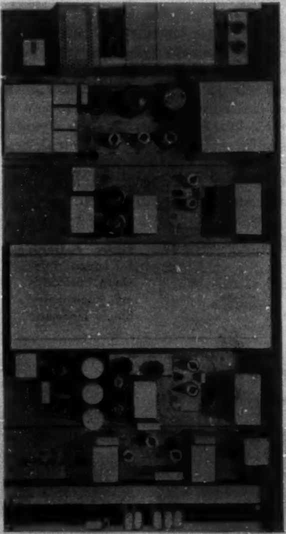

Figure 12. *L-1* coaxial television transmitting terminal—bay arrangement

The signal-to-noise performance of a carrier transmission system is directly proportional to the modulated amplitude of the transmitted signal. Given an upper peak amplitude limit which may be transmitted satisfactorily over such a system, it follows that an increase in the excess carrier ratio must be accompanied by a reduction in the signal modulation with a resultant poorer signal-to-noise performance. The excess carrier condition shown in Figure 5 is employed presently in the *L-1* system and represents an economical balance between quadrature distortion and signal-to-noise performance.

It is of interest to consider the resultant effects of unwanted modulation distortion of the *L-1* carrier television signal introduced during transmission over the coaxial line amplifiers. In the case of transmission of a television signal in the original video form, all important energy components of the signal are harmonically related to the scanning frequencies. Under these conditions, the introduction of modulation distortions also of a harmonic nature results only in a modification of the amplitude and phase of the original signal components and the visual resultant is a distortion of the signal wave shape in a geometric sense. In the usual video case these effects are considered as a nonlinearity function applied to portions of the brightness range of the received picture. The eye is quite tolerant in this respect so that quite lenient video signal modulation requirements result.

In the case of carrier transmission of television signals, the regions of concentrated energy are not harmonically related by virtue of their displaced frequency position. Harmonic modulation products of this carrier signal are no longer simply related to the original signal components and extraneous frequency components are produced. As might be expected, the modulation requirements

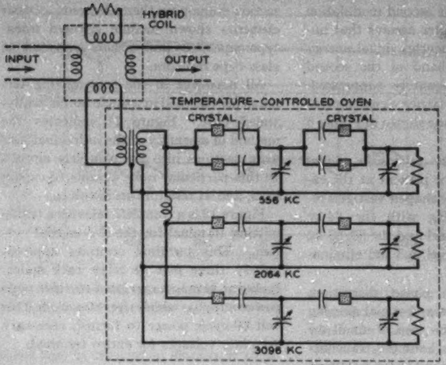

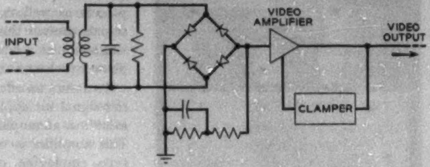

Figure 14 (above). Pilot elimination filter—simplified schematic

Figure 15 (top right). Pilot elimination filter—details of construction

Figure 16 (right). Envelope detector and video amplifier-clamper—simplified schematic

under these conditions of carrier transmission are considerably more severe than in the case of the video form of transmission.

In the present system the greatest amplitude modulation products are of a second and third harmonic nature and are formed by the carrier frequency and the high energy signal components in the immediate vicinity of the carrier frequency. The second harmonic of the carrier frequency will fall at 622 kc and the third harmonic at 933 kc. After final detection these extraneous distortion products will appear in the 311 and 622 kc regions respectively, where they produce extremely objectionable visual effects. There is, however, an advantage obtained in arrangement of the allocation as mentioned previously such that these products occur in the idle regions of the signal spectrum.

Pre-emphasis of the upper frequency components of the television signal is employed according to the frequency characteristic shown in Figure 6. By this means it is possible to introduce a complementary restoring characteristic as indicated in the receiving terminal which effectively reduces any extraneous interference, including modulation effects, above 400 or 500 kc on the coaxial line. Since the restorer characteristic is the exact complement of the pre-emphasis characteristic, the over-all transmission characteristic is unaffected. In this manner a theoretical reduction of 16 decibels of the second harmonic and 17 decibels of the third harmonic is effected. It should be noted here that in the process of pre-emphasis, the peak factor of the carrier television signal is altered and therefore the extent of modulation improvement indicated is not completely realized in practice.

Transmitting Terminal Equipment

A block schematic of the elements of the *L-1* coaxial television transmitting terminal is shown in Figure 7. This terminal provides for the translation of the video signal upward into the transmission band of the *L-1* coaxial line. The double-modulation method has been shown previously in Figure 2.

The video signal to be transmitted over the *L-1* coaxial system is received from the network operating center over a balanced 110-ohm video transmission circuit. The first modulator unit consists of a video amplifier, d-c inserter, modulator, and associated carrier supply.

The d-c inserter consists of a germanium crystal element connected so that, in conjunction with the coupling capacitors, the extremes of the standard television synchronizing pulses are always maintained at zero potential with respect to the modulator grids regardless of the picture content of the video signal. In this manner the peaks of the synchronizing pulses correspond to a fixed amplitude of excess carrier which, as discussed previously, is desirable when envelope detection is employed.

The video signal, which now contains the d-c component, is impressed upon the grids of a balanced modulator while the carrier voltage is introduced in a conjugate manner into the cathode circuit. The excess carrier to be transmitted is provided by unbalancing the modulator by differentially varying the screen voltage of each modulator tube by the desired amount. To assure that this excess carrier component is in exact phase relation with that modulated by the input video signal, an additional phase or quadrature balance control is provided. This circuit arrangement allows any carrier leak which may be present in the modulator plate circuit, due to transmission through the tube elements or other parasitic reactances, to be independently balanced out.

The carrier frequency of 7.944 megacycles is generated in a crystal-controlled oscillator and provides, through a buffer amplifier stage, approximately 5 volts of carrier to the modulator proper.

Figure 8 is a first modulator unit as mounted on the transmitting terminal equipment bay. The video amplifier, d-c inserter, modulator, and carrier supply oscillator are included on this panel. The carrier balance controls may be noted.

Figure 9 indicates the network configuration and the frequency-loss characteristic of the band filter which selects the lower and vestigial sideband of the first modulation step. This network is formed of low-pass and high-pass sections. The particular configuration here results in an economy of coils, desirable because of the

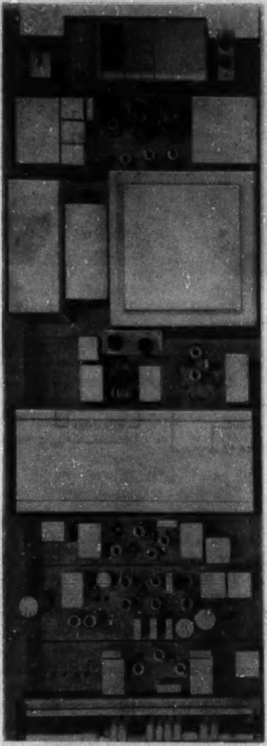

Figure 17. *L-1* coaxial television receiving terminal—bay arrangement

practical difficulties of such elements with respect to parasitic capacities. Small compact assemblies also result with this design as well as certain advantages in control of cut-off characteristics in design and manufacture. At this point only partial shaping of the vestigial sideband is accomplished. Further networks in the transmitting and receiving terminals also contribute to this total shaping.

The second step of modulation follows the band filter selection of the signal in the 5- to 8-megacycle region. The second modulator is supplied with a carrier frequency of 8.256 megacycles. The balanced modulator and carrier supply oscillator is similar in circuit form to that described for the first modulation step. By the use of a balanced modulator, certain second order unwanted modulation products are reduced to noninterfering levels. Following the second modulation process, a low-pass filter assures that unwanted 5- to 8-megacycles signal energy and the upper sideband of the second modulation are adequately suppressed. Pre-emphasis of the carrier signal according to the characteristic shown in Figure 6 now is introduced.

To guard against television signal energy, which may be present at the extreme of the partially shaped vestigial region, from interfering with the 64-kc pilot regulation channel and the 80–88-kc sound program channel, a band elimination filter is provided.

The considerable phase distortion, which is inherent in the vestigial shaping process as well as the sum of small residuals present throughout the transmitting terminal, is equalized in the following phase equalizer as indicated.

To assure an adequate level of the carrier signal for application to the *L-1* coaxial line, an amplifier finally is provided. This amplifier is of a 3-stage feed-back type employing common cathode impedance of a form such that the feedback is maintained at a high value for the lower frequencies where the higher signal energy condition obtains. This type of feed-back amplifier design exhibits improved stability under conditions of variations in internal gain, such as caused by aging of vacuum tubes and variation of other elements.

The networks previously referred to, that is, band-filter, low-pass filter, pre-emphasis network, band elimination filter, and phase and attenuation equalizers, represent the major contribution to the shaping and control of the transmission band characteristic of this vestigial sideband carrier terminal. Accordingly, to adequately meet the severe television transmission requirements, these networks must embody not only precise design techniques but also must be capable of exact control and adjustment during manufacture and must maintain their performance over the normal life of the terminal equipment under all operating conditions. To achieve this exacting performance standard, it has been found necessary to develop some new type network elements as well as more precise methods of construction and assembly. A new series of retardation coil types is employed, featuring metallic slugs for inductance adjustment. These elements are available in a continuous range of inductance from 0.22 to 220 microhenries. The form of these coils is designed for ease in mechanical assembly, and to assure a minimum of parasitic effects. Figure 10 shows the mechanical features of a typical constant resistance equalizer section employing these elements. Other elements shown include silvered mica-type capacitors and carbon deposited on glass-type resistors.

All networks in the transmitting terminal are enclosed in a single hermetically-sealed case. Figure 11 indicates the method of assembly of the individual network sections into the complete circuit. In this particular unit, 43 coils, 68 capacitors, and 41 resistors are involved.

Figure 12 is a complete television transmitting terminal for the *L-1* coaxial system. This terminal occupies approximately three feet of relay rack space. Included here is a regulated rectifier-type power supply, which operates from 115-volt 60-cycle power to furnish necessary d-c plate voltages for entire terminal.

Receiving Terminal Equipment

A block schematic of the elements of the *L-1* coaxial television receiving terminal is shown in Figure 13. The receiving terminal recovers the video signal from the received carrier signal as transmitted over the coaxial line. The modulation methods involved were discussed previously and are shown in Figure 2.

The pilot frequencies at 556, 2,064, and 3,096 kc which are transmitted over the coaxial line for gain regulation purposes

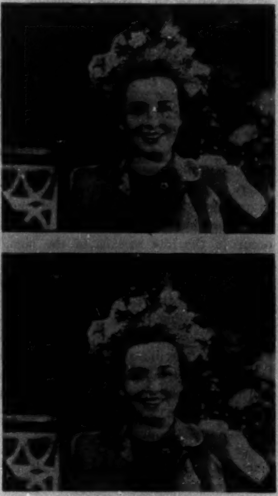

Figure 18. Television transmission performance of *L-1* carrier terminals

Top—Video Transmission
Bottom—Terminal Transmission

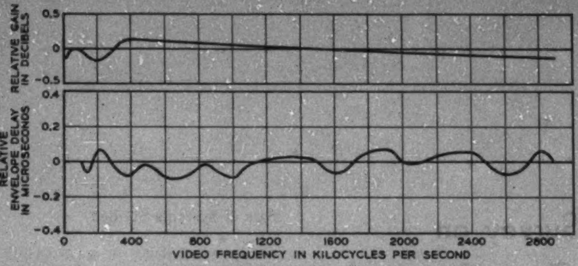

Figure 19. Over-all transmission characteristic for *L-1* coaxial television carrier terminals

must here be reduced in amplitude to assure noninterference with the television signal. A simplified schematic of the pilot elimination network is given in Figure 14. The operation of this circuit is based upon the condition of infinite attenuation presented between two windings of a hybrid coil when the remaining two windings are terminated in equal impedances. In this instance, one winding of the hybrid coil is terminated in a resistance. The associated winding is terminated by a transformer and three crystal filter networks as shown. At the resonance frequency of each crystal network, the impedance of the array, as presented at the terminals of the hybrid coil, is adjusted to be equal to the resistance termination of the associated winding. In these three very narrow frequency regions, located to coincide with the pilot tones, high attenuation is introduced within the signal branch of the hybrid coil. To assure coincidence of the resultant attenuation band and the pilot tone, the elements of the crystal networks are maintained at a constant temperature by means of a thermostatically controlled oven. The effective band elimination width is approximately 20 cycles at 556 kc, 60 cycles at 2,064 kc, and 100 cycles at 3,096 kc. Figure 15 shows some of the constructional features of the pilot elimination network.

The function of the phase equalizer following the pilot elimination network as shown in Figure 13 is similar to that discussed previously in the transmitting terminal. The band elimination filter here provides the necessary discrimination to the 64-kc pilot tone and to the 80–88-kc carrier sound channel. The restorer network characteristic has been previously indicated in Figure 6.

The following amplifier is identical to that described in the transmitting terminal. The demodulator which follows is supplied with a carrier frequency of 8.256 megacycles and provides the method by which the carrier signal as received from the coaxial line is again modulated into the 5- to 8- megacycle region. This demodulator is of the balanced type with conjugate carrier excitation as in the transmitting terminal. This is required to reduce the carrier leak and unwanted second order modulation products to noninterfering levels.

The lower sideband of this modulation process is selected by the following band filter where the remainder of the vestigial sideband shaping is accomplished. This filter is identical to the band filter similarly employed in the transmitting terminal. To provide an adequate level of this carrier signal for final envelope detection, an amplifier is provided furnishing approximately 31 decibels of gain in the 5- to 8-megacycle frequency band. This amplifier is of a 3-stage feed-back type.

The simplified schematic of the envelope detection circuit is shown in Figure 16. The modulated carrier signal with the carrier located at 7.944 megacycles, with the main sideband extending downward to approximately 5.1 megacycles, and with the vestigial sideband extending upward to approximately 8.056 megacycles, is impressed upon a bridge rectifier circuit. The nonlinear elements of this detector are germanium crystals. The rectified video signal output then is amplified and clamped prior to delivery to the receiving network operating center.

The theory of design and operation of clampers in television transmission has been presented recently. It is sufficient here to relate that the clamper, as employed in television transmission, periodically restores the video signal to a desired constant reference value. In this case, this is done upon the arrival of each horizontal synchronizing pulse. In this manner very low-frequency distortion or interference is effectively attenuated, the amount of attenuation being directly related to the ratio of the fundamental horizontal synchronizing frequency to the distortion frequency. A theoretical reduction of 31 decibels in a 60-cycle interference voltage may be obtained by this means. In the case of the *L-1* coaxial system, this clamping action reduces the effects of any power frequency modulation of the carrier which may have been introduced during transmission over the line. The arrangement of the equipment comprising an *L-1* coaxial television receiving terminal is shown in Figure 17. This terminal equipment occupies approximately 4 feet of relay rack space and operates from 115-volt 60-cycle power.

The *L-1* coaxial television terminal equipment which has been described here developed following basic design principles established in connection with experimental television transmission studies over the coaxial cable prior to the last war. The present type of equipment was first placed in commercial service in 1947, and at this time approximately 30 transmitting and 40 receiving terminals are in daily operation in the Bell System's television network.

Figure 18 presents a comparison between television signals before and after transmission through these *L-1* coaxial television terminals. The video circuit employed had a band width in excess of 4 megacycles, while in the case of the terminal transmission a low-pass filter simulating the cut-off characteristics of the coaxial line was included. The phase and attenuation characteristic for this back-to-back condition is shown in Figure 19.

References

1. PROGRESS IN COAXIAL TELEPHONE AND TELEVISION SYSTEMS, L. G. Abraham. *AIEE Transactions*, volume 67, part II, 1948, pages 1520–27.

2. COAXIAL CABLE SYSTEM FOR TELEVISION TRANSMISSION, M. E. Strieby. *Bell System Technical Journal* (New York, N. Y.), volume 17, July 1938, pages 438–59.

3. TELEVISION TRANSMISSION, M. E. Strieby, C. L. Weis. *Proceedings*, Institute of Radio Engineers (New York, N. Y.), volume 29, July 1941, pages 371–81.

4. SUBJECTIVE SHARPNESS OF SIMULATED TELEVISION IMAGES, M. W. Baldwin, Jr. *Proceedings*, Institute of Radio Engineers (New York, N. Y.). volume 28, October 1940, pages 458–68.

5. THEORY OF SCANNING, Pierre Mertz, Frank Gray. *Bell System Technical Journal* (New York, N. Y.), volume 13, July 1934, pages 464–515.

6. EQUALIZATION OF COAXIAL LINES, K. E. Gould. *AIEE Transactions*, volume 68, part II, 1949, pages 1187–92.

7. A CARRIER SYSTEM FOR 8,000-CYCLE PROGRAM TRANSMISSION, R. A. Leconte, D. B. Penick, C. W. Schramm, A. J. Wier. *Bell System Technical Journal* (New York, N. Y.), volume 28, April 1949, pages 165–80.

8. CERTAIN TOPICS IN TELEGRAPH TRANSMISSION THEORY, H. Nyquist. *AIEE Transactions*, volume 47, February 1928, pages 617–44.

No Discussion

Report of a Survey on the Performance of Shunt Capacitors

AN AIEE COMMITTEE REPORT

IN November 1947, a Capacitor Subcommittee was formed under the AIEE Transmission and Distribution Committee. This Subcommittee was charged with the responsibility of studying capacitor performance, revising existing capacitor standards, and so forth.

A project, suggested at the first meeting of the newly formed Subcommittee, was that of accumulating operational information on the application of shunt capacitors to power systems, with particular regard to capacitor unit failures or operating difficulties experienced by operating engineers. A working group was formed to study the problem. It was soon realized that this subject was very broad in scope and the decision was made to invite the Transmission and Distribution Committee of the Edison Electric Institute (EEI) to participate in the study.

The report as presented is therefore the result of close co-operation between working groups appointed by the AIEE and the EEI and represents the results of the accumulation of considerable data by members of both organizations.

In order to obtain information to prepare a report on experience with the operation of shunt capacitors, a questionnaire was formulated and sent to electric operating companies in this country and Canada.

A copy of the questionnaire is included in this report. Interest in the work of the two subcommittees was evidenced by the excellent response to the questionnaires.

The application of shunt capacitors on power systems received great impetus shortly preceding and during the war years. Added current carrying capacity of lines, transformer banks, and other equipment was to be gained by their use and power system operating personnel became acutely aware that the application of capacitors was a great boon to the industry at a time when other electric equipment was extremely difficult to obtain in time to meet rapidly growing demands for power.

With the shunt capacitor now firmly established as a valuable tool of the industry, it became evident, through miscellaneous but minor difficulties experienced in capacitor use, that there existed a need for accumulation of information pertaining to the operation of this equipment. This report endeavors to present this information in a concise and impartial form, without embarrassing any manufacturer or utility.

Scope of Distribution of the Questionnaire

The questionnaire forms were sent to 118 operating utilities in all portions of the United States and Canada. All companies represented on the EEI Transmission and Distribution Committee received a copy and all other operating companies not associated with EEI but having a maximum system load peak of at least 50,000 kw for 1947 were included in the mailing.

A total of 88 replies was received from those companies contacted. In that some companies contacted had few or no capacitors installed, the replies of 83 companies (42 replies from companies represented on the EEI Transmission and Distribution Committee and 41 replies from other companies) were included in the data for the report.

Of the 83 companies returning the questionnaire, 66 classified themselves as supplying energy to urban and rural load, while 17 classified themselves as supplying predominantly metropolitan areas.

Size of Systems Studied

The total combined 1947 peak loads of all companies responding with data was 28,147.2 megawatts. It is felt that these companies represent a very fair segment of the power industry in the country. The size of individual systems reporting varied from 24.0 megawatt demand to 1,455.0 megawatt demand. One larger utility answered the questionnaire but its ratio of capacitor capacity installed was so small compared to the system size that the statistical data furnished was not included in the report since it was considered as not being representative of the group.

Capacitor Installations—Total

The total capacity of the shunt capacitor installations on the systems reported was 2,849.7 megavars (mvar). This figure represents 10.1 per cent of the total system demand of all reporting. Thus, for each 1,000 kw of system demand, the reporting companies had installed an approximate 101 kilovars (kvar) of capacitors as an average.

Type of Capacitor Installations

Most capacitor installations fall under four general classes with regard to mounting or housing. The questionnaire listed these, and the resulting replies are shown in Table I.

Paper 49-251, recommended by the AIEE Transmission and Distribution Committee and approved by the AIEE Technical Program Committee for presentation at the AIEE Fall General Meeting, Cincinnati, Ohio, October 17–21, 1949. Manuscript submitted July 26, 1949; made available for printing September 6, 1949.

Prepared by the Joint Working Groups of the Capacitor Subcommittee of the AIEE Transmission and Distribution Committee and the Edison Electric Institute Transmission and Distribution Committee.

Personnel of the AIEE Capacitor Subcommittee Working Group: C. B. Baugh, B. W. Dillard, K. E. Hapgood, E. R. Hendrickson, R. B. Miller, C. E. Parks (Co-Sponsor).

Personnel of the EEI Transmission and Distribution Committee Working Group: H. E. Stites (Co-Sponsor).

Table I

Type of Mounting	Megavars Installed	Per Cent of Total Installed Megavars
Pole-type installations of outdoor units	1,738.3	61.0
Open rack installations of outdoor units	410.0	14.4
Pole-type housed installations	110.8	3.9
Substation housed installations	590.6	20.7

Voltage Rating of Installed Capacitors

In order to obtain data on the voltage class of the systems to which capacitors were applied, the questionnaire listed four general ranges of system voltages. Data furnished by those answering questionnaire is summarized in Table II.

Table II

Voltage Rating	Megavars Installed	Per Cent of Total Installed Megavars
600 volts or less	49.1	1.7
2.3–4.8 kv	2,165.5	76.1
6.9–12.5 kv	519.7	18.2
Over 12.5 kv	115.4	4.0

Method of Control of Capacitors or Capacitor Banks

To determine the method by which capacitors or capacitor banks were placed in service or removed from service, the questionnaire requested a breakdown of information on the installations. Data was requested for a summary of the equipment which was normally switched by one method or another. It is assumed that the individual company's capacitors which are not switched by the methods listed remain on the systems permanently a majority of the time. The results of the data obtained from information furnished are as follows: capacitors regularly switched, either manual or automatic, total 1,002.9 mvar or 35.2 per cent of all capacitors installed, see Table III. Capacitors not regularly switched total 1,846.8 mvar or 64.8 per cent of all units installed.

Table III

Method of Control	Capacitors Controlled, Megavars	Per Cent of Total of Switched Units
Voltage control	330.5	33.0
Kilovar control	7.4	0.7
Current control	11.1	1.1
Time-switch control	110.9	11.0
Manual control	509.1	50.8
Other methods	33.9	3.4

Type of Protection of Capacitor Units

In order to determine present practices in the application of protection to capacitor installations, data was secured on the several present methods of protection employed. Since in numerous cases, the protection was overlapping, the total megavars of units protected is greater than the total installed capacity. The results of data secured are shown in Table IV.

Table IV

Method of Protection	Megavars of Units Thus Protected	Per Cent of Total Installed Capacitor Megavars
Individual unit fusing	493.0	17.3
Group fusing	714.2	25.1
Total bank fusing	1,269.9	44.5
Relay protection on oil circuit breaker	715.2	25.0
Other types of protection	8.2	0.3
	3,200.5*	112.2

* Thus, approximately 350.8 mvar of capacitor installations were protected by overlapping of the several methods listed. This represents 12.2 per cent of total installed capacitor units.

Lightning Arrester Protection of Capacitors

The question was asked concerning lightning arrester application in connection with capacitor installations. The results obtained are as follows:

65 companies out of 83 generally use lightning arrester protection. This represents 78 per cent of all companies reporting.
18 companies did not apply lightning arrester protection. This represents 22 per cent of all companies reporting.

Choice of Protection of Capacitors

Data was further requested as to whether voltage class of system determined the type of fuse or relay protection of capacitors or capacitor banks.

58 companies reported that voltage class did not determine type of protection—70 per cent.
5 companies reported that voltage class determined type of protection—6 per cent.
20 companies did not report on the question—24 per cent.

Capacitor Failures

The primary purpose of this investigation was the determination of the cause for capacitor failures that have occurred within the past several years with the hope that this information will serve as a guide to those contemplating additional installations of such equipment. The subject of capacitor failures on the questionnaire was treated in two ways. Several of the most common causes for failure were listed and it was asked that these failures be further differentiated as to the period within the last several years in which they occurred. It is realized that many more capacitors have been installed in the last six years than were installed previously, hence it would be reasonable to conclude that more failures should have taken place in this period. The collected data bears out this conclusion.

The tabulation of the data reported is made in several different manners for purposes of comparison of one type of failure against another, one voltage class of capacitor against another class, one period of failure against another, and so forth.

Of the 2,849.7 mvar of capacitors installed, 34.160 mvar have failed or had to be removed from service for one reason or another. This represents a failure of only 1.2 per cent of all installed units.

Reported causes of failure for any reason are shown in Table V.

Table V

Cause	Kilovars of Units Removed from Service	Per Cent of Total Kilovars of Units Removed from Service
Internal failure	20,735	60.7
Bushing failure or breakage*	1,600	4.7
Leaks in case or bushing seal	1,235	3.6
Mechanical defects or damage	5,540	16.2
Misapplication		
Overvoltage	150	0.4
Bad waveform	30	0.1
High ambient (lack of ventilation)	385	1.1
Low ambient (units de-energized)	815	2.4
Lack of adequate lightning protection*	1,225	3.6
Other causes**	2,445	7.2

* Some failures listed in these two classifications were attributed to direct lightning strokes.

** Under this classification were listed manufacturers' construction difficulties, wrong connections upon installation, gun shot, switching, and so forth.

A breakdown of the capacitor failures from all causes into number of years in service before failure is as follows:

8,610 kvar or 25.2 per cent failed within one year after installation.
18,215 kvar or 53.3 per cent failed after having been installed 1 to 5 years.
7,335 kvar or 20.5 per cent failed after having been installed over 5 years.

A further breakdown of total capacitor failures by voltage class is as follows:

3,525 kvar or 10.3 per cent were in the

6.9-kv class or higher, representing 0.55 per cent of total installed in this class.
30,575 kvar or 89.5 per cent were in the 2.3–6.8-kv class, representing 1.41 per cent of total installed in this class.
60 kvar or 0.2 per cent were in the 600 volts or less class, representing 0.12 per cent of total installed in this class.

There follows a listing by the particular cause of trouble experienced which caused the capacitor units to be removed from service. Each of these causes is tabulated in the same manner as were the total failures.

INTERNAL FAILURES

Failures from this cause may be attributed to many reasons. Usually the evidence of the cause was destroyed in the resulting failure.

Of the total of 20,735 kvar of internal failures:

5,235 kvar or 25.2 per cent were caused to units in service 1 year or less.
9,630 kvar or 46.5 per cent were caused to units in service 1 to 5 years.
5,870 kvar or 28.3 per cent were caused to units in service over 5 years.

Of the 5,235 kvar of units failing during the first year of service:

1,025 kvar or 19.6 per cent were in the 6.9-kv class or higher.
4,180 kvar or 79.8 per cent were in the 2.3–6.8-kv class.
30 kvar or 0.6 per cent were in the 600 volts or less class.

Of the 9,630 kvar of units failing during 1 to 5 years of service:

905 kvar or 9.4 per cent were in the 6.9-kv class or higher.
8,725 kvar or 90.6 per cent were in the 2.3–6.8-kv class.

Of the 5,870 kvar of units failing after service over 5 years:

90 kvar or 1.5 per cent were in the 6.9-kv class or higher.
5,780 kvar or 98.5 per cent were in the 2.3–6.8-kv class

Of the total of 20,735 kvar of internal failures:

2,020 kvar or 9.7 per cent were in the 6.9-kv class or higher.
18,685 kvar or 90.2 per cent were in the 2.3–6.8-kv class.
30 kvar or 0.1 per cent were in the 600 volt or less class.

BUSHING FAILURES OR BREAKAGE

Failures from this cause may have been caused by lightning, bad porcelain, poor handling, or poor packing at the factory.

Of the total of 1,600 kvar of units failing due to bushing failures or breakage:

445 kvar or 27.8 per cent were caused to units in service 1 year or less.
870 kvar or 54.3 per cent were caused to units in service 1 to 5 years.
285 kvar or 17.7 per cent were caused to units in service over 5 years.

Of the 445 kvar of units which failed during the first year of service:

230 kvar or 51.7 per cent were in the 6.9-kv class or higher.
215 kvar or 48.3 per cent were in the 2.3–6.8-kv class.

Of the 870 kvar of units after 1 to 5 years of service:

240 kvar or 27.6 per cent were in the 6.9-kv class or higher.
630 kvar or 72.4 per cent were in the 2.3–6.8-kv class.

Of the 285 kvar of units failing after having been in service over 5 years:

285 kvar or 100 per cent were in the 2.3-6.8-kv class.

Of the total of 1,600 kvar of units failing because of bushing trouble:

470 kvar or 29.4 per cent were in the 6.9-kv class or higher.
1,130 kvar or 70.6 per cent were in the 2.3–6.8-kv class.

LEAKS IN CASE OR AROUND BUSHINGS

Failures attributed to "leaks" were described as seam welding defects in the case, bushing gasket difficulty, and so forth:

Of the total of 1,235 kvar of units failing because of leaks:

360 kvar or 29.1 per cent were caused to units in service 1 year or less.
550 kvar or 44.6 per cent were caused to units in service 1 to 5 years.
325 kvar or 26.3 per cent were caused to units in service over 5 years.

Of the 360 kvar of units failing during the first year of service:

15 kvar or 4.2 per cent were in the 6.9-kv class or higher.
345 kvar or 95.8 per cent were in the 2.3–6.8-kv class.

Of the 550 kvar of units failing during 1 to 5 years of service:

30 kvar or 5.5 per cent were in the 6.9-kv class or higher.
490 kvar or 89.0 per cent were in the 2.3–6.8-kv class.
30 kvar or 5.5 per cent were in the 600-volt class or less.

Of the 325 kvar of units failing after over 5 years of service:

325 kvar or 100 per cent were in the 2.3–6.8-kv class.

Of the total of 1,235 kvar of units failing because of leaks:

45 kvar or 3.6 per cent were in the 6.9-kv class or higher.
1,160 kvar or 94.0 per cent were in the 2.3–6.8-kv class.
30 kvar or 2.4 per cent were in the 600-volt or less class.

MECHANICAL DEFECTS OR DAMAGE

Failures falling under this heading were attributed to hangar welding breakage, case damage in shipment, and so forth.

Of the total of 5,540 kvar of unit failures caused by mechanical defects or damage:

1,030 kvar or 18.6 per cent were caused to units in service 1 year or less.
4,330 kvar or 78.2 per cent were caused to units in service 1 to 5 years.
180 kvar or 3.2 per cent were caused to units in service over 5 years.

Of the 1,030 kvar of units failing during the 1st year of service:

120 kvar or 11.7 per cent were in the 6.9-kv class or higher.
910 kvar or 88.3 per cent were in the 2.3–6.8-kv class.

Of the 4,300 kvar of units failing during 1 to 5 years of service:

540 kvar or 12.5 per cent were in the 6.9-kv class or higher.
3,790 kvar or 87.5 per cent were in the 2.3–6.8-kv class.

Of the 180 kvar of units failing in service over 5 years:

180 kvar or 100 per cent were in the 2.3-6.8-kv class.

Of the total of 5,540 kvar of units failing because of mechanical defects or damage:

660 kvar or 11.9 per cent were in the 6.9-kv class or higher.
4,880 kvar or 88.1 per cent were in the 2.3–6.8-kv class.

Numerous failures were attributed to "misapplication" of the units. Under the following headings will be discussed the results of replies received covering these difficulties.

OVERVOLTAGE

Failures which were caused by applying units on systems which were operated at voltages above the permissible voltage ratings on the capacitor units are described in this category:

Of the total of 150 kvar of units failing because of overvoltage:

90 kvar or 60.0 per cent were caused to units in service 1 year or less.
60 kvar or 40.0 per cent were caused to units in service over 5 years.

Of the total of 150 kvar of units failing because of overvoltage:

150 kvar or 100 per cent were in the 2.3–6.8-kv class.

Questionnaire on Shunt Capacitor Operation and Experienced Failures or Difficulties

Joint Working Group on Performance of Shunt Capacitors of the AIEE and EEI Transmission and Distribution Committees

---

Please answer the following questions regarding troubles experienced with shunt capacitors installed or maintained by your company:

1. Size of system on which capacitors are installed in terms of peak megawatts for 1947 .... Megawatts
   (a) System predominantly metropolitan.........or integrated urban and rural..........
2. Approximate total shunt capacitors installed on December 31, 1947 .... Megavars
   (a) Pole-type installations of outdoor units .... Megavars
   (b) Open rack installations of outdoor units .... Megavars
   (c) Pole-type housed installations .... Megavars
   (d) Substation housed installations .... Megavars
3. Total megavars of capacitors installed by voltage class on December 31, 1947
   (a) On systems rated 600 volts or lower .... Per Cent
   (b) On systems rated 4.1 kv or 2.3 kv .... Per Cent
   (c) On systems rated 11 kv or 6.9 kv .... Per Cent
   (d) On systems rated over 11 kv .... Per Cent
4. Automatically or manually switched per cent of total megavars .... Per Cent
   (a) Voltage controlled ....% of total megavars
   (b) Kilovars controlled ....% of total megavars
   (c) Current controlled ....% of total megavars
   (d) Time-switch controlled ....% of total megavars
   (e) Manually controlled ....% of total megavars
   (f) Controlled otherwise ....% of total megavars. Explain:
   ....
   ....
   ....
5. Type of protection generally used for capacitors in per cent of total megavars:
   (a) Fused individually ....%, by groups ....%, or by total banks ....%
   (b) Protected by circuit breakers with overcurrent relays ....%
   (c) Is lightning arrester protection generally used? .... If method of connection of capacitors or grounding of capacitor unit cases governs this, please explain: ....
   ....
   ....
   (d) Other methods of protection, explain: ....
   ....
   (e) Does voltage class determine type of protection? Explain: ....
   ....
6. How many capacitor units (or what total megavars of units) have been removed from service because of any failure or defect, approximately how many years were the units in service before removal, what voltage class were units which were removed? Explain in following tabulation.

	Years Service					
	Under 1 Year		1 to 5 Years		Over 5 Years	
	Mvar	Kv	Mvar	Kv	Mvar	Kv
(a) Due to internal failure	......	......	......	......	......	......
(b) Due to bushing failure or breakage	......	......	......	......	......	......
(c) Due to leaks	......	......	......	......	......	......
(d) Due to mechanical defects of damage	......	......	......	......	......	......
(e) Due to misapplication:						
(1) Overvoltage	......	......	......	......	......	......
(2) Bad Waveform	......	......	......	......	......	......
(3) High ambient temperature or lack of ventilation	......	......	......	......	......	......
(4) Low ambient temperature with units de-energized	......	......	......	......	......	......
(5) Lack of adequate lightning protection	......	......	......	......	......	......
(6) Other reasons (explain)	......	......	......	......	......	......

   ....
   ....
   (f) Other reasons for failure which are not described above (explain in detail) ....
   ....

   Note: The Committee would appreciate detailed reports on each case of failure to the extent available.

7. In the application of capacitors to the system, have any of the following troubles been experienced? If these difficulties have beencorrected by changes in connection of capacitor units or by other methods, please explain remedial measures taken.
   (a) Due to telephone interference ....
   (b) Due to harmonic overcurrent ....
   (c) Due to carrier current interference ....
   (d) Due to radio interference ....
   (e) Due to inrush or discharge current ....
   (f) Other causes, describe. ....
8. Inspection and Maintenance.

	Pole Type Outdoor	Open Rack Outdoor	Pole Type Housed	Substation Housed
(a) Do you have periodic inspection?	......	......	......	......
(b) If so, at what intervals	......	......	......	......

   (c) Describe procedure of inspection and maintenance..............................
   ....

General Remarks and Recommendations: ....
....
....
....
....
Signed.......................................
Name of Company .... Location ....

Bad Waveform

Failures attributed to bad waveform were described as mostly caused by prevalent fifth harmonics in fundamental frequency on the system to which the capacitors were applied.

Of the total of 30 kvar of units failing due to bad waveform:

30 kvar or 100 per cent failed during the first year of service. These units were all in the 2.3–6.8-kv class.

High Ambient Temperature (Lack of Ventilation)

Units which failed due to high ambient temperature were described as being located where ventilation was poor.

Of the total of 385 kvar of units failing because of high ambient temperature:

325 kvar or 84.5 per cent failed during the first year of service.

60 kvar or 15.5 per cent failed after 1 to 5 years of service.

Of the total of 385 kvar of units failing because of high ambient temperature:

385 kvar or 100 per cent were in the 2.3–6.8-kv class.

Low Ambient (Units De-energized)

Failures for this reason were attributed to the low temperatures producing lowered dielectric strength of insulating medium or production of voids in units which punctured when units were energized after having been out of service for some time during low temperature periods.

Of the total of 815 kvar of units failing because of low temperature:

215 kvar or 26.4 per cent were caused to units in service 1 year or less.

540 kvar or 66.3 per cent were caused to units in service 1 to 5 years.

60 kvar or 7.3 per cent were caused to units in service over 5 years.

Of the total of 815 kvar of units failing in all years of service:

815 kvar or 100 per cent were in the 2.3–6.8-kv class.

Lack of Adequate Lightning Protection

Failures attributed to this cause were described as either being brought about by direct lightning strokes or by the fact that no lightning arresters were applied on installation.

Of the total of 1,225 kvar of units failing due to lack of adequate lightning protection:

220 kvar or 17.9 per cent were caused to units in service 1 year or less.

720 kvar or 58.8 per cent were caused to units in service 1 to 5 years.

285 kvar or 23.3 per cent were caused to units in service over 5 years.

Of the 220 kvar of units failing during the first year of service:

220 kvar or 100 per cent were in the 2.3–6.8-kv class.

Of the 720 kvar of units failing during 1 to 5 years service:

105 kvar or 14.6 per cent were in the 6.9-kv class or higher.
615 kvar or 85.4 per cent were in the 2.3–6.8-kv class.

Of the 285 kvar of units failing after being in service over 5 years:

285 kvar or 100 per cent were in the 2.3–6.8-kv class.

Of the total of 1,225 kvar of units failing due to lack of adequate lightning arrester protection:

105 kvar or 8.6 per cent were in the 6.9-kv class or higher.
1,120 kvar or 91.4 per cent were in the 2.3–6.8-kv class.

Other Causes for Failure

Under this classification are grouped those failures which occurred from miscellaneous causes such as wrong connections of units at time of installation, gun shot damage, improper switching which caused failure, and so forth.

Of the total of 2,445 kvar of units which failed from other causes:

690 kvar or 28.2 per cent were caused to units in service 1 year or less.
1,485 kvar or 60.7 per cent were caused to units in service 1 to 5 years.
270 kvar or 11.1 per cent were caused to units in service over 5 years.

Of the 690 kvar of units failing during the first year of service:

180 kvar or 26.1 per cent were in the 6.9-kv class or higher.
510 kvar or 73.9 per cent were in the 2.3–6.8-kv class.

Of the 1,485 kvar of units failing after being in service 1 to 5 years:

30 kvar or 2.0 per cent were in the 6.9-kv class or higher.
1,455 kvar or 98.0 per cent were in the 2.3–6.8-kv class.

Of the 270 kvar of units failing after being in service over 5 years:

270 kvar or 100 per cent were in the 2.3–6.8-kv class.

Of the total of 2,445 kvar of units which failed from other causes:

210 kvar or 8.6 per cent were in the 6.9-kv class or higher.
2,235 kvar or 91.4 per cent were in the 2.3–6.8-kv class.

Application Difficulties

In the application of capacitors, numerous troubles of minor nature have been encountered. The questionnaire listed the most prevalent causes of such difficulty and the information below summarizes the data furnished.

Telephone Interference

Out of the 83 companies reporting, 41 stated that trouble had been experienced with telephone interference caused by capacitor installations and 42 replied that no trouble had been encountered.

This trouble had generally been corrected by proper transposition, by the moving of the capacitor bank, by removing grounds on Y-connected capacitor banks, by relocating distribution lines, by installing filters, by using neutral reactor in capacitor bank neutral, by solidly grounding capacitor cases, and by the telephone company making changes in their installations.

Harmonic Overcurrent

Fourteen companies reported difficulty due to harmonic overcurrent on capacitor installations and 69 reported no trouble.

This trouble generally was corrected by reducing size of capacitor banks, switching banks out during off-peak conditions, removing Y-ground, changing system set-up, and so forth. It was noted that this is a condition which must be closely checked, particularly at times system load is light. On one remote installation, a recording ammeter installed indicated a serious harmonic condition existing which was not appreciated and units had to be removed from service to correct this.

Carrier Current Interference

Only one company reported having any difficulty which was credited to this condition. No information was supplied but it was stated that interference was caused to "carrier telephone and telegraph."

Radio Interference

Five companies indicated that they had experienced radio interference upon the installation of capacitors. By relocating the capacitor banks or removing pole grounds, this trouble was usually corrected.

Inrush Current

A total of 6 companies indicated that trouble had been encountered due to the heavy inrush currents experienced by the energizing of capacitor banks. Usually this resulted in the blowing of fuses. Such difficulty was corrected by the installation of a larger fuse.

It was reported that the paralleling of large banks of capacitors on the same bus aggravates this condition under some conditions.

Other Reasons

Five companies reported miscellaneous troubles encountered, not listed above. Resonance was caused in one case and the removing of the capacitor bank Y-ground corrected it. Serious system unbalance resulted when capacitors were connected to a circuit supplied by an open-delta bank. The closing of the bank delta corrected this trouble.

Inspection and Maintenance

Questions were asked to determine the extent of inspection and maintenance which is being carried out by the companies reporting.

Periodic Inspection

About 60 per cent of the reporting companies indicated that they maintain periodic inspection on their capacitor installations. The extent of this inspection varied greatly, but most companies reported only a visual check of case condition, fuse position, and general over-all appearance.

Interval Inspection

The answers to this question also were widely divergent, varying from three per day (for substation installations) to every five years. The average period was from one to three months, inspection made by line maintenance, service, substation maintenance, and line patrol personnel.

Procedure on Inspection and Maintenance

The standard procedure for inspection is by visual means only. Numerous companies reported that split-core ammeter checks were made occasionally. Inspections of paint, connections, mounting, and so forth, were reported by some, and one company reported that it regularly had the bushings cleaned. Evidently the maintenance problem of capacitor units must not be serious in that no reports were received of an extensive maintenance program being required to maintain good capacitor performance.

By far the most interesting aspect of this report, in the minds of the working group, were the comments given by the reporting companies regarding their experience with capacitor installations. It is felt that much good information, from an operating engineers' standpoint, is contained in the remarks made. For this reason, the reporting of the data received from the utilities will be in the most part as taken directly from the letters received and from comments noted on the questionnaire. These comments follow:

Two companies report failure of gas-filled capacitors. One company reports that of 720 kva of gas-filled capacitors installed in 1937 and 1938, only 45 kva remain in service.

Several companies report large capacitor installation programs just starting.

Several companies report a power factor clause in their rate schedule and for this reason the majority of their larger customers have installed their own power factor correction.

Company number 1 reports that their substation housed capacitors are power-factor tested once a year.

Company number 2 reports difficulty in correctly adjusting feeder voltage regulators on 4-kv circuits having capacitors.

Company number 3 has a mobile capacitor trailer of 1,080 kva capacity. One-half of its capacity is controlled manually and the other half, either manually or automatically by voltage. Each 15-kva single-phase unit is fused individually.

Company number 4 reports that they found it impossible to install capacitors on circuits supplying resonant relay controlled street lamps due to improper relay operation.

Company number 5 reports: "Two cases of trouble were experienced in the same location where 2 180-kvar capacitor banks were located on the load side of sectionalizing fuses in a branch circuit. The capacitor units were 4.16-kv units, delta connected, on a 4.0-kv Y primary system with a 120/240-volt delta secondary system. Both open delta and closed delta transformer banks are in service, serving an area predominately industrial. On two occasions, the blowing of one of the sectionalizing fuses caused the capacitors to be fed back through rotating equipment and distribution transformers, which in turn, it is thought, caused saturation of the iron cores, and nonlinear resonance with resulting extremely high voltages. On both occasions, failure of both line and transformer lightning arresters occurred, transformer fuses in the area blew and the failure of one transformer is thought attributable to this. In this case, it was not desirable to remove sectionalizing fuses, so the capacitors were relocated, but as a general rule, when capacitors are installed, any single pole disconnects or fuses are removed or relocated beyond the capacitors."

Company number 6 reports: "The individual capacitors in the station-type installations are 2,400-volt units connected in parallel, and these parallel groups are connected in series from line to line to make a 3-phase delta bank. This makes possible the use of moderate capacity fuses for individual fuse protection, even though the bank may be connected to a bus with high fault duty."

Company number 7 reports that where pole-type housed units were used, the cases were made of ordinary steel and have rusted badly and require frequent painting.

Company number 8 reports: "Failure of 180 kvar (12–15-kvar capacitors) 2,400-volt automatically-switched capacitor units which were in service on a part of our system where long periods of 0 degrees Fahrenheit to −40 degrees Fahrenheit ambient temperatures are not unusual. These units are voltage controlled and are normally in service five days a week from 7:00 a.m. to 11:00 a.m. and from 12:00 noon to 4:00 p.m. Investigation revealed that failure was caused by solidification of thin columns of insulating liquid between layers in the capacitor unit; this solidification occasionally caused separation of the column and on energizing resulted in a phase-to-phase internal failure across the void. The manufacturer has developed a unit filled with "low temperature" liquid and we are in the process of replacing all individual capacitors in switched service which are subject to these extreme low ambient temperatures for long periods."

Company number 9 reports voltage relays in ungrounded neutral ties between groups of a switched capacitor bank. These relays protect against over-voltage on units in series-parallel combinations of 2,400-and 460-volt units making up Y-connected groups on an ungrounded 13.8-kv system.

Company number 10 reports failure of some ten units last February during very cold weather: "By this time you may be familiar with the cause of this trouble. We were just informed of it by the manufacturer last week. We are told that the insulating medium used in these capacitors, and in fact all capacitors up to the present time is found to be not suitable for cold weather. During temperatures in the order of 10 to 15 degrees below zero we can expect failures. The failures occur when the capacitor has been disconnected and is, therefore, cold and is energized under those circumstances.

"We have put in service three other 2,520-kvar banks of the same type, and we can expect the same kind of trouble on these if something is not done. The manufacturer has proposed as a remedy that heaters be installed in the housings. If they could be kept energized at all times during extremely cold weather we would expect to avoid trouble because the internal heat generated by the losses in the capacitor are sufficient to prevent a drop in temperature low enough to cause trouble."

Company number 11 has used relay protection for capacitor bursting protection on those large capacitor banks of 1,200 kvar and greater where capacitors are Y-connected. "The capacitor bank is divided into two equal kilovar sections and the Y points of the two sections are connected together through either a current or a potential transformer and the secondaries connected to an appropriate relay. Although both methods of relaying have proved satisfactory, the current protection is preferred as this allows enough time in case of fault in a capacitor for the case to bulge and to find it on a visual inspection."

Company number 12 reports that they have had a comparatively great number of failures of 15-kva 2,400-volt capacitor units due, the manufacturer believes, to accidental breaks in vacuum during the process of installing the bushings and terminals, and not due to electrical operating conditions.

"We have already recommended to manufacturers that, in capacitor assemblies, greater current carrying capacity be provided throughout to permit these assemblies to operate satisfactorily on rated voltage containing a 10 per cent fifth harmonic voltage. On our system troubles arising from this source have been met by switching the capacitors out of service during period of light load when our system operated with a maximum fifth harmonic voltage. Furthermore, we recommend that the units themselves be designed to operate at the standard temperature rise with this order of fifth harmonic voltage."

Company number 13 reports that all units are power-factor tested and most defects have been located by this test. Any units having power factor over 1 per cent are considered defective.

Company number 14 reports: "Our capacitor units are really doing a job in giving dependable automatic corrective. Our capacitors, along with a 20,000-kva synchronous condenser give a very flexible corrective arrangement."

Company number 15 reports: "All failures from leaks were new capacitors."

Company number 16 reports: "Prior to 1939, we had installed a few of the gas-filled type on which we have had some trouble due to loss of gas."

Company number 17 reports: "High voltage resulted when one line fuse blew ahead of a line section having a 4,160-volt delta capacitor bank and several transformer banks connected. Condition corrected by moving line fuses to load side of the capacitor bank."

Company number 18 reports: "From what information we have, it appears that the great majority of failures have been during electrical storms."

Company number 19 reports: "We recently experienced a failure of 13 units constituting one of the groups in a bank of 4,000-volt units connected directly to the 22-kv system. No cause has been found for the failure. The unbalanced voltage protection was out of service at the time of failure and it is felt that had this been in service, the bank would have been taken off the line with the damage confined to fewer units.

Company number 20 reports: "Resonance causing high voltage has resulted at light load when primary fuse opened toward source. Remedy is to use units connected solidly from phase to neutral. Capacitor units are failing at a much higher rate than transformers. One manufacturer used inadequate internal clearances and excessive volts per mil stress on paper resulting in high percentage of failure in first five years."

Company number 21 reports: "Capacitor cases of units located near water front and subjected to salt spray rusted out in one year."

Company number 22 reports: "On distribution system being supplied from substation transformer banks connected open-delta, capacitors caused serious unbalance in system voltages. Adding third transformer to substation remedied this condition."

Company number 23 reports: "Defective welding of the seams or repairing by welding of a leak was the primary cause of several failures. Upon opening the capacitor cases on several occasions, hair-like projections, due to improper welding, were found to be the cause of insulation failure."

Company number 24 reports: "Due to inrush currents arcing at current transformer secondary links at time of circuit breaker closing. Corrected by shunting current transformer primaries with 1/10-ohm resistor. The manufacturer investigated some units which failed and suggested that the trouble was due to the improper storage of the paper used in their manufacture."

Company number 25 reports: "The 11.5 mvar of pole-type installations were mostly installed in 1941–42. Of these, a total of 0.036 mvar or 0.314 per cent have failed in service in 6 or 7 years. As none are protected by lightning arresters, this indicates no need for such protection."

Company number 26 reports: "On the 12-kv system, we have two Y-connected banks of 153-2.4-kv units each. Difference in potential between the floating neutral points of the two banks of capacitors is depended upon to trip the main oil circuit breaker in event of failure of any one unit. A problem in connection with low-voltage industrial installations is matter of exceeding the allowable voltage limits of the 230- and 460-volt rated units on the nominal 240-and 480-volt secondaries."

Conclusion

It is hoped by all members of the working group, both EEI and AIEE, that the analysis of the reports given on the questionnaire forms received will be enlightening and helpful to all in their application problems in connection with the installation of capacitors. Certainly, individual ideas of the engineers answering the questionnaire are to be expected. These ideas must be weighed in light of the fact that systems vary widely, both in scope and location.

It is quite evident that the manufacturers of capacitor units are continually striving to improve their product through the use of new materials, new designs and by profiting from the operational experience of utilities who use their products. The steadily improving performance of capacitors over the past two decades is indicative that the capacitor art is advancing rapidly.

Discussion

I. W. Gross (American Gas and Electric Company, New York, N. Y.): This is an excellent report on the field performance of shunt capacitors and represents a vast amount of work by the Subcommittee which prepared it, not only in obtaining information, but in summarizing it in condensed and usable form to bring out the major points of significance in capacitor operation.

I am particularly interested in the lightning protection aspects where these capacitor banks are used in large sizes. The report states that 65 companies use lightning arrester protection for the capacitor and 18 companies do not. Some 20 years ago the theory was advanced that the capacitance of high-voltage bushings, as a sort of lightning arrester, should supply some degree of lightning protection to equipment. The capacitance of such bushings was in the order of 0.0003 microfarads. As more was learned about natural lightning phenomena, this theory was soon exploded as the capacitance was too small to be at all significant. However, the capacitor banks dealt with in this report range in the general order of up to 12 microfarads, and therefore present a different picture.

In the protection of d-c equipment, capacitance elements only are used as so-called lightning arresters and have capacitance in the order of 5 microfarads. The question therefore arises, are not capacitor banks of the larger sizes mentioned in the report self-protecting against lightning due to their inherent high capacitance?

We encountered a problem of this type recently in the installation of a 10,000-kva capacitor bank on a 44-kv system. The conclusion we reached was that the inherent capacitance of the capacitors supplied the required protection. As this bank was installed at a substation, the question arose as to how other equipment would be protected against lightning, in view of the fact that this bank was of a switched type (on and off during periods of heavy and light load). The station already had lightning protection before the capacitors were installed, and we questioned the thermal ability of the lightning arresters to function properly with the capacitor bank connected. For example, when a lightning arrester on a transmission line is required to function, it may be called on to discharge the entire stored energy of the line, 1/2 CE^2. When a lightning arrester at a large capacitor bank functions, it may be called upon to discharge, in addition, a large part of the stored energy of the capacitor bank at an elevated voltage of perhaps double-line voltage. Since the lightning arrester when operating is essentially a resistance, there is an energy dissipation in the lightning arrester blocks proportional to the square of the current through the lightning arrester and its time duration. This may exceed the ability of even modern lightning arresters to function properly without overheating and failing. The grounding of transformer neutrals in the station, if feasible, is, of course, helpful in reducing the thermal duty on the lightning arrester, but this grounding condition cannot always be assumed.

In the case cited in the previous paragraph, we have left the lightning arresters in service at the station and equipped them with surge crest ammeter links to measure lightning arrester discharge currents in normal operation. Since this installation is comparatively new, we have no information to report at this time. We now are attempting to learn by experience what it has so far been impossible to predict by theory, that is, whether the lightning arresters are capable of performing satisfactorily where large capacitor banks are located.

Two questions are offered for consideration: 1. Are large capacitor banks self-protecting against lightning? 2. Does the use of large capacitor banks impose a higher duty on present-day lightning arresters than they can safely discharge, and if so, what is to be done about it?

M. E. Scoville (General Electric Company, Pittsfield, Mass.): The Subcommittee is to be commended for such a factual report on the service experience with shunt capacitors. The report is valuable to the user, pointing up the effects of abnormal service conditions and establishing a normal of experience for individual comparison. It is valuable to the manufacturer, pointing up opportunity for improvements and establishing more accurate data on service conditions.

The report arbitrarily divides time into three periods with a breakdown of failures divided; 25.2 per cent in one year or less, 53.3 per cent in one to five years, and 20.5 per cent after five years. At first glance these percentages seem to indicate about 1/4 of the failures the first year and about 1/10 or less per year for the next four years A more detailed consideration of the basis

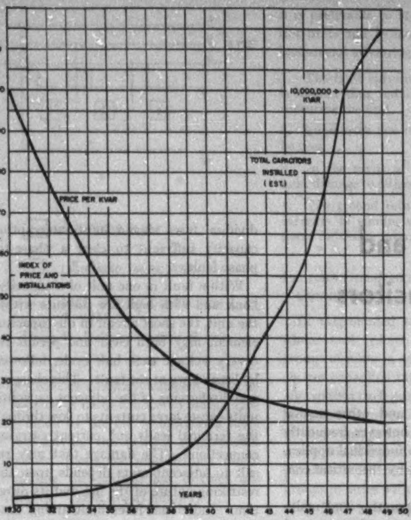

Figure 1. Curves showing price reduction on individual 2,400-volt capacitor units versus years since the introduction of Pyranol and the estimated total reactive kilovolt-amperes of installed capacitors for power factor correction in the United States

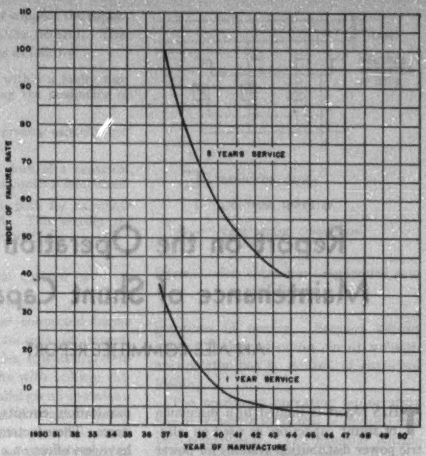

Figure 2. Median curves showing one- and five-year accumulated internal dielectric failure rates for outdoor pole-type capacitors. The number of failures in five years from 1937 installations is assigned an index figure of 100 and the records for the succeeding ten years are plotted in relative values to show a significant trend

for these percentages is interesting. The data from the questionnaire does not disclose the time of installation, thus permitting us to determine the effect of time on the percentage of failures. The report indicates that the rate of installations has increased in the last six years. This indication may be amplified by showing the yearly increase in installations for the period since 1930 as shown by Figure 1 of the discussion. Note that about 3,300,000 reactive kilovolt-amperes was installed by the end of 1942 and 7,500,000 reactive kilovolt-amperes by the end of 1946. If we can assume a corresponding increase in installations for the utilities reporting to the Subcommittee, then the total reactive kilovolt-amperes from which the 1-year failures occurred was in the order of twice that from which the 1- to 5-year failures occurred. I suggest, therefore, that these 1-year and 5-year failure percentages may not be rigorously applied to a single given installation.

Also, another factor adds complexity to our consideration because the record of failures probably was accumulated over an extended period of time. We know the rate of failures is decreasing in recent years. Supporting this fact I have accumulated detail records on internal dielectric failures in outdoor pole-type capacitor units since their introduction in 1937. For each year of manufacture and assumed installation I have plotted curves to show the relationship of failure rate trends as shown by Figure 2 of the discussion. We note that the failure rate within a year after installation has decreased by ten-to-one in ten years. The failure rate within five years has decreased at a slower rate. The fact that failure rates are undoubtedly decreasing with time indicates futility in using a past record of failure rates to predict future trends.

Comparing the slope of these failure rate trends to the price trend in Figure 1 of the discussion, it is interesting to note that the relative decrease in failure rates exceeds that of price trend. Although prices have been decreased, the quality has been increased to insure less and less failures. I agree enthusiastically with the second conclusion in the Subcommittee report, that the manufacturers are striving to improve their product and that the capacitor art is advancing rapidly.

C. E. Parks: The members of the Working Groups who assembled the information included in the report wish to express their appreciation for the fine response and interest which the report promoted. This interest indicated the evident need for such a survey and justifies the Capacitor Subcommittee's decision to proceed with the project.

It was the intent of the Working Groups to obtain information on the subject in a form as complete as possible in order that the data could be further analyzed, segregated, and studied with the thought that those who were interested in certain phases of the problem would be in a position to separate the data required and to draw upon this data for conclusions. It was not the intent of the Working Groups to analyze the collected data further than that required to place it in convenient table form.

Discussions presented at the time of the report's presentation generally indicated the availability of the necessary information in the report and the several discussors added greatly to its value by elaborating on certain portions of the collected data. Of particular interest were the discussions given by Mr. Scoville and Mr. Gross.

With the present rapid development in the field, it is likely that another such survey will be made in the future, possibly within five years.

Report on the Operation and Maintenance of Shunt Capacitors

AN AIEE COMMITTEE REPORT

THIS report is limited to a discussion of shunt capacitors as used on electric power distribution systems for power factor correction and/or voltage improvement. It was the objective of the committee to provide a résumé of the experience and investigational work on this subject which has been made available through various published articles. They hope that this will be helpful to the users of such capacitors in providing them with a relatively short pamphlet giving the pertinent factors which should be considered in their operation and maintenance.

This is intended to be a continuation of a report on shunt capacitors prepared by the General Systems Subcommittee of the AIEE Committee on Power Transmission and Distribution,[1] presented in 1943. It describes the use of shunt capacitors as a means of providing increased capacity of transmission and distribution facilities. The economics of shunt capacitors versus synchronous condensers is explained. For these phases of the problem, the reader is referred to this previous report.

It is intended that this present report provide a résumé of the best current practice in the industry with respect to the operation and maintenance of shunt capacitors. It is not intended to provide sufficient information to properly design and apply capacitor installations. It outlines the basic considerations in operating and maintaining such installations and points the way to other items which the user may wish to investigate in detail.

Many of the problems arising out of capacitor operation are functions of local conditions; such as, the characteristics of the circuits, specific location of the capacitors, proximity and type of communication circuits, and other similar items. These factors, however, frequently have less effect on an individual application than is indicated by theoretical considerations.

Where a specific operating and maintenance practice appears to have general acceptance, this fact has been mentioned. Where there is a clear divergence of opinion among substantial numbers of capacitor users regarding any specific practice, this difference has been stated, and the relative advantages and disadvantages discussed.

This report does not replace instructions and other information provided by capacitor manufacturers. It is suggested that users obtain such information.

Type of Connection

Capacitor units may be installed in 3-phase banks connected in delta or star. For a balanced 3-phase load either connection may be used. The choice usually is determined by other factors, such as size of bank, wave form, and so forth. The relative installed costs of capacitor units and their relative kilovar ratings also will influence the type of connection used.

DELTA CONNECTION

Capacitor units for 2,400-volt circuits are generally delta connected, see Figure 5. Lower voltage units for star connection on 2,400-volt circuits are not standard.

When capacitor units are connected in delta, a faulted unit may be subjected to a high fault current. This may generate sufficient gas to rupture the case before the arc is interrupted. Case rupture usually is prevented when capacitor units are individually fused. Such individual fuses should have interrupting capacity sufficient to clear a phase-to-phase fault.

With a fault in one unit of a capacitor bank and with high arc currents within the unit, the short circuit in the capacitor element may burn clear and permit recovery voltage each half cycle, followed by breakdown at the fault. This charging and discharging of the adjacent capacitor units causes large currents to flow through the terminal leads and current carrying connections. The damage that may result to adjacent units depends upon the restriking nature of the arc and its duration. Individual fuses limit arcing time in the faulty unit thus minimizing the probability of damage to other units in the bank.

In high-voltage delta banks, where each phase is made up of several groups of capacitors in series, the fault currents associated with a unit failure are limited. The use of individual fuses is desirable. The number of units in parallel in a single group should be such as to give satisfactory operation of fuses and avoid excessive voltage across any capacitor unit following the operation of a fuse. This is accomplished by selecting capacitor units with a voltage rating such that there will be a minimum number of groups in series and a maximum number of units in parallel.

STAR CONNECTION

For circuits of 4,160 volts and above, it is usually possible and desirable to star connect the capacitor units, see Figure 6. This permits using capacitor units with the same voltage rating in 3-phase banks and in single-phase installations.

When the neutral of a bank of capacitors is effectively grounded and fault currents are large, restriking arcs within a

---

Paper 49-252, recommended by the AIEE Transmission and Distribution Committee and approved by the AIEE Technical Program Committee for presentation at the AIEE Fall General Meeting, Cincinnati, Ohio, October 17–21, 1949. Manuscript submitted July 26, 1949; made available for printing September 6, 1949.

Personnel of the working group of the AIEE Subcommittee on Capacitors: E. R. Hendrickson, *Chairman;* Glen Appleman, R. E. Marbury, R. B. Miller, M. E. Scoville, R. A. Wood.

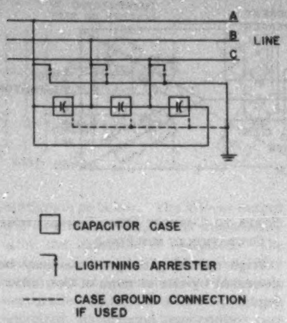

Figure 1. Delta connection diagram

faulty unit can damage adjacent units, as in the case of delta-connected units. This is avoided by the use of individual fuses or by leaving the neutral ungrounded. However, there are installations where grounding the neutral has distinct advantages. These are as follows:

1. In small banks, individual fuses are usually not used. If the neutral is not grounded, a fault in a capacitor unit would not blow the main bank fuses and the resulting unbalanced voltages would be excessive.
2. Capacitor units are designed to be operated with a grounded neutral when star connected. This frequently permits using units having a lower insulation level than that corresponding to the circuit voltage. When the neutral is not grounded the insulation level of the capacitor units should correspond to the circuit voltage.
3. The operation of an individual fuse in one phase of small bank will not cause a serious voltage unbalance when the neutral is solidly grounded.
4. In some cases it is desirable to provide a low impedance path for the control of harmonic voltage levels on the system. A capacitor bank with neutral grounded provides this path.

If the number of units per phase in a large capacitor bank is sufficient to insure satisfactory operation of individual fuses, it is preferable to star connect the capacitor units and isolate the neutral. This has several advantages as follows:

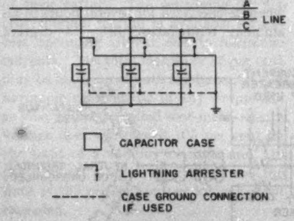

Figure 2. Star connection-floating neutral diagram

1. The fault current within a faulty unit is limited thus reducing the possibility of rupturing the unit.
2. Fuses with low rupturing capacity can be used.
3. In the event of failure of a capacitor unit, damage to adjacent units is minimized.
4. The ground return path for harmonic currents is eliminated. This usually reduces inductive interference.

FACTORS INFLUENCING CHOICE OF CONNECTION

In ungrounded star connected banks where each phase consists of several groups of units in series, it is desirable to choose capacitor units with voltage ratings so that each parallel group contains a large number of units. A bank consisting of three groups in series per phase, each group consisting of 18 7,200-volt units in parallel, is far more desirable than nine groups in series with each group consisting of 6 2,400-volt units in parallel. The latter arrangement results in too few units in parallel for proper functioning of individual fuses. Also the voltage across the remaining units of a group in which a fuse has blown will become excessive. These relations are more completely covered under Protection of Distribution Systems Against Capacitor Failures.

Operating and Ambient Temperatures

EFFECT OF TEMPERATURE ON CAPACITOR RATINGS

Capacitors have exceptionally low losses when compared with other electric equipment with equal kilovolt-ampere rating. The losses of modern capacitors do not exceed 3.3 watts per kilovar of rating. Low losses give low operating temperatures, which are desirable for the following reasons:

1. Life in service is a function of temperature and voltage stress.
2. Capacitors when energized at rated voltage are always operating at full load. System load cycles have no effect on capacitor losses.
3. Capacitors are designed to operate with a maximum internal temperature near their temperature stability limit. It is imperative that there be no occasional conditions of operation above this internal temperature stability limit.

Capacitor units differ from most other electric equipment in that the container is permanently sealed and there is no easy way of measuring internal operating temperatures in service. Because kilovar loading is dependent on circuit voltage, an operator has no control of capacitor loading.

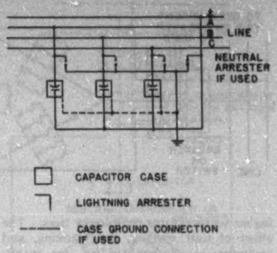

Figure 3. Star connection-ungrounded neutral diagram

The maximum operating temperature rise of capacitor units can be divided into two components. The external surface of the container operates with a rise above ambient which can be measured readily in service. The internal dielectric operates with a temperature rise above case surface. This cannot be measured in service. The dissipation of losses through a large number of layers of paper and foil is slow. Therefore there is an appreciable temperature gradient between the internal parts of a unit and the case.

Following are several of the factors which affect operating temperatures:

1. The maximum allowable kilovar loading (AIEE Standard) is 135 per cent of rating, including the effects of both fundamental and harmonic voltages. Temperature rise increases with kilovar loading.
2. Mounting arrangements and spacings between capacitor units affect their temperature rise. When units are mounted in rows, side by side, the heat dissipation is restricted, thus causing an increase in the temperature rise. When rows of units are mounted one over another, the air from a lower tier is heated before passing into an upper tier. Even with unrestricted natural circulation of air higher tiers will operate at

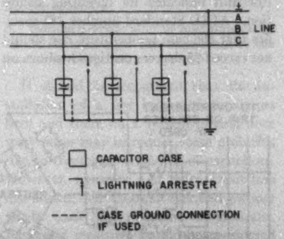

Figure 4. Star connection-multigrounded neutral diagram

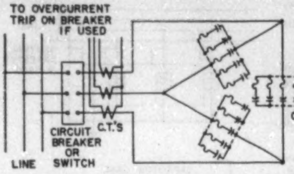

Figure 5 (left). Capacitor protection by individual fuses-delta connection

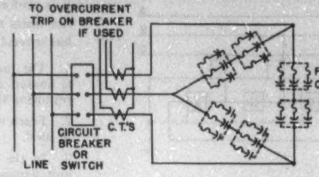

Figure 7 (right). Series banks of capacitor units protected by individual fuses-delta connection

higher temperatures than lower tiers. The effect of unit spacing, tier stacking, and enclosures as determined by one manufacturer is shown in Table I. These values are in terms of per cent case temperature rise. The 100 per cent case is a single isolated unit operating at nominal rating in a large room. The arrangement assumes three tiers of units, two rows wide in a sheet-metal enclosure with top and bottom ventilation openings to provide natural circulation of air.

Table I

Spacing Between Case Sides, Inches	Per Cent Case Temperature Rise of Units		
	Bottom Tier	Middle Tier	Top Tier
0.5	191	216	233
1	161	181	198
2	136	155	170
4	123	140	153
8	118	135	148

3. Radiation from the sun and other bodies operating at higher temperatures than the surrounding ambient increases the temperature rise in a capacitor. For example, one manufacturer has determined that the internal temperature of a single isolated capacitor unit is increased three degrees centigrade when it is subjected to the direct rays of a bright sun.

4. Enclosures such as housings or vaults may increase the temperature rise over that obtained with open-type installations due to reduction in radiant heat dissipation.

5. Restriction of natural circulation of air such as by housings increase the capacitor unit temperature rise.

Normally the maximum surface temperature rise above ambient of a capacitor unit indicates its operating condition. AIEE Standard number 18[2] specifies that the case temperature rise should not exceed 25 degrees centigrade above an ambient of 40 degrees centigrade thus giving a maximum permissible case temperature of 65 degrees centigrade. For the usual operating conditions it is ordinarily desirable that the maximum case temperature does not exceed 55 degrees centigrade and for abnormal or emergency conditions that it does not exceed 70 degrees centigrade.

Experience as reported by one manufacturer indicates that capacitor units may be operated at the maximum ambient temperatures shown in Table II without incurring an inordinate decrease in capacitor life.

Table II

Arrangement	Maximum Ambient Temperature, Degrees Centigrade	
	15 Kvar Units	25 Kvar Units
Outdoor, single row, single tier, unrestricted ventilation	50	46
Outdoor, two rows, two or three tiers, unrestricted ventilation	46	40
Indoor, two rows, single tier, unrestricted ventilation	40	40
Indoor or enclosed, two rows, two or three tiers, unrestricted ventilation	40	40*
Enclosed outdoor or indoor, multiple rows and tiers with forced ventilation and forced circulation about units**	46	40

* Forced circulation of air about unit surfaces is necessary.

** The forced ventilation is considered to be eight cubic feet per minute, per kilovar, per degree centigrade rise with a 50 degree centigrade maximum air outlet temperature.

These ambient temperatures are based on a minimum center to center horizontal spacing between units of approximately $7^1/_2$ inches.

Steps to Correct Over-Temperature Operation in the Field

High operating temperatures may be decreased by one or more of the following:

1. Increase spacing between units.
2. Reduce operating voltage.
3. Reduce harmonic voltages.
4. Use forced air cooling.
5. Move capacitor bank to a location of lower ambient temperature.
6. Install capacitor units having a higher ambient rating.

Extremely Low Ambient Temperatures

It is important to recognize that the electrical and mechanical properties of capacitor materials may change at low temperatures. The synthetic liquids commonly used in capacitors at the present time become practically solid at temperatures below approximately −10 degrees centigrade. The solid state alone does not adversely affect the electrical properties. However, very recent experience has shown that such liquids do become brittle enough to fracture at temperatures in the range of −20 degrees centigrade, and below. Low temperatures combined with mechanical shock and stress increases the probability of electrical failure. Experience has shown that a few failures have occurred soon after the capacitors were energized after being out of service overnight, or extended periods, at low ambient temperatures.

A synthetic liquid-filled capacitor has a capacitance about 70 per cent of normal when de-energized for several hours in an ambient temperature of −15 degrees

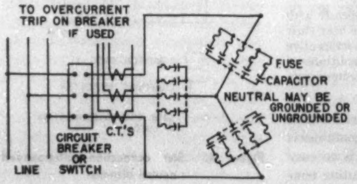

Figure 6 (left). Capacitor protection by individual fuses-star connection

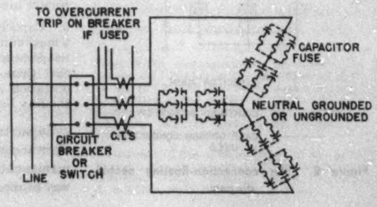

Figure 8 (right). Series banks of capacitor units protected by individual fuses-star connection

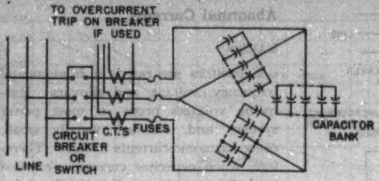
TO OVERCURRENT TRIP ON BREAKER IF USED
CIRCUIT BREAKER OR SWITCH
LINE
C.T.'S
FUSES
CAPACITOR BANK

Figure 9 (left). Capacitor protection by group fuses-delta connection

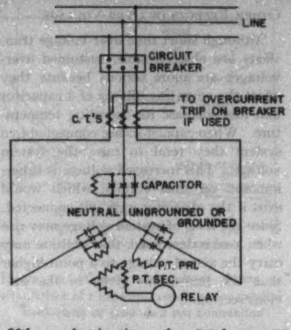
LINE
CIRCUIT BREAKER
TO OVERCURRENT TRIP ON BREAKER IF USED
C.T'S
CAPACITOR
NEUTRAL UNGROUNDED OR GROUNDED
P.T. PRI.
P.T. SEC.
RELAY

Figure 11 (right). Capacitor protection by voltage unbalance between phases

centigrade or below. The kilovar output will be correspondingly low immediately after the capacitor is energized. The losses of a capacitor go through a very sharp peak at approximately −4 degrees centigrade. As soon as a cold capacitor is energized, its internal temperature rises rapidly until it reaches a stable value corresponding to some point on the downward slope of the loss curve as shown by Figure 18. The capacitance and kilovar output are normal at this stabilized operating point. The kilovar output will not drop below the rated value when the capacitor is in continuous operation at temperatures as low as −40 degrees centigrade.

It is, therefore, to be noted that continuous operation at low temperatures is not objectionable. However, intermittent operation in which capacitors are frequently energized at temperatures below −20 degrees centigrade may give trouble unless special precautions are taken.

Maximum Voltage Limitations

Effect of Over-Voltage Wave Form

Standard capacitor units are designed with a 35 per cent thermal margin. Thus the maximum allowable kilovar loading is 135 per cent of nameplate rating. The operating kilovar of a capacitor increases as the square of the voltage and directly with frequency.

Capacitor units are designed to operate at an average voltage (over any 24-hour period) not exceeding 105 per cent of their rating. The average operating kilovar on this basis will not be over 110 per cent of their rating. The remaining 25 per cent thermal margin is available for excess operating kilovar due to harmonic currents. The total margin of 35 per cent may be made up of both fundamental and harmonic components in any proportion so long as the measured root-mean-square voltage does not exceed 105 per cent on the basis of a 24-hour average, and 110 per cent on a short time basis and the limit of 135 per cent output kilovar is not exceeded.

Since capacitor current depends upon frequency as well as voltage, merely measuring the line voltage and current with commercial instruments and multiplying these values together may not give the actual operating kilovar unless the voltage follows a sine wave.

Where the voltage contains one or more harmonic components, the actual kilovar at which the capacitor is operating must be calculated separately for each harmonic, and these kilovar values added to obtain the total operating kilovar.

Applications of most concern are those where resonance does exist for some particular harmonic. If the apparent kilovar determined by multiplying the total voltage and current is within the 135 per cent limit, and the average voltage is within 105 per cent, it may safely be concluded that the capacitor is not overloaded thermally because such a procedure is in error in the conservative direction. Where thermal overload is indicated, it then is advisable to actually determine the current and voltage for the predominating harmonic, and actually compute the operating kilovars at both the harmonic and fundamental frequency, and determine the total operating kilovars.

The harmonic frequencies usually encountered are the third and fifth. It can be shown that when the operating voltage is 105 per cent and the third harmonic is present and predominating, the total current may reach 145 per cent of normal before exceeding the 135 per cent thermal limit. On the same basis with the fifth predominating, the total current may reach 160 per cent of normal before exceeding the 135 per cent thermal limit.

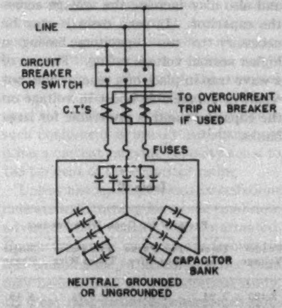
LINE
CIRCUIT BREAKER OR SWITCH
C.T.'S
TO OVERCURRENT TRIP ON BREAKER IF USED
FUSES
CAPACITOR BANK
NEUTRAL GROUNDED OR UNGROUNDED

Figure 10. Capacitor protection by group fuses-star connection

There are relatively few cases where harmonic currents interfere with the use of shunt capacitors. It is the usual practice to ignore these currents when installing capacitors, taking corrective steps only if trouble is encountered. When it is known that the wave form is bad, care must be taken in planning the location of the capacitor units on the system, and in choosing the size of bank for a given location. A particular capacitor bank may be deliberately planned to operate in a predetermined manner with respect to harmonics so as to bring about a change in the level of harmonic voltage components on the system. A superimposed high-frequency current on the system is sometimes used to operate relays which control street lighting circuits, water heaters, and so forth. While this current is not harmful to the capacitors due to its short duration, it may occasionally blow capacitor fuses.

When a particular installation of capacitors is overloaded due to harmonic currents, the overload can be reduced by:

1. **Changing the size or relocating the bank to offer increased impedance to the flow of the harmonic currents.**

2. **Adding reactance to the circuit supplying the capacitor.**

3. **Adding a device offering high impedance to the harmonic, yet low impedance to the fundamental such as a wave trap.**

It should be recognized that the installation of a few banks of capacitors here and there on a system having poor wave form may introduce some problems due to thermal overloading of capacitors. However, as more and more capacitors are added, the thermal overload on any single bank may become insignificant. Remedial measures should be considered only in connection with the entire capacitor program.

OTHER EFFECTS OF OVER-VOLTAGE

Although short time over-voltage transients are objectionable, sustained over-voltages are more serious because they affect the operating kilovar of a capacitor unit and increase its operating temperature. When capacitors are connected to a system they tend to raise the system voltage. This increased voltage is superimposed on that voltage which would exist if the capacitor were not connected. Since the level of system voltage may rise when load is decreased, this addition may carry the actual voltage to a point higher than the limitations given in the previous section.

EFFECT OF CAPACITORS ON SYSTEM VOLTAGE

The rise in circuit voltage when a capacitor is connected to a circuit is dependent on the capacitor kilovar and the circuit reactance. The rise through each transformer may be computed by multiplying the transformer per cent reactance by the ratio of capacitor kilovar to transformer kilovolt-amperes.

The rise in circuit voltage due to feeder reactance on ordinary types of open-wire distribution can be approximated as follows:

$$\text{Per cent rise in voltage} = \frac{CKVAR \times FT \times F}{1{,}000{,}000}$$

$CKVAR$ = total capacitor kilovar in bank
FT = feet distance from substation bus to point on the feeder where the capacitor is connected
F = factor shown in Table III which is based on average circuit characteristics.

When capacitors are installed with a total kilovar equal to the minimum reactive requirements, it usually is practical to leave them permanently connected without encountering objectionable light load voltages. When maximum possible benefits are being obtained and sufficient kilovar of capacitors is being used to meet heavy load reactive requirements, it usually is necessary to switch the capacitors in relation to changes in load conditions or system voltage. In some cases, the voltage on the system is controlled by switching capacitors. It may be necessary to switch a large bank of capacitors in two or three steps with changing load to prevent excessive voltage variation.

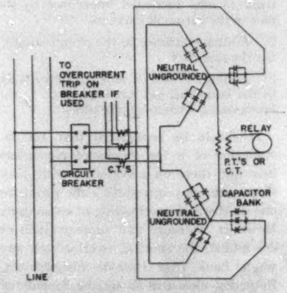

Figure 12. Capacitor protection by unbalance between neutrals

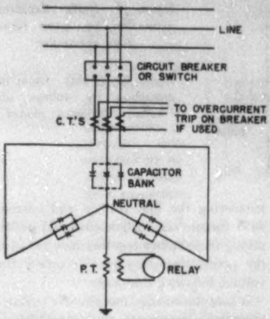
LINE
CIRCUIT BREAKER OR SWITCH
TO OVERCURRENT TRIP ON BREAKER IF USED
C.T.'S
CAPACITOR BANK
NEUTRAL
P.T.
RELAY

Figure 13. Capacitor protection by voltage unbalance between neutral and ground

When the circuit load follows a definite cycle each day, time- or manually-operated switches are frequently used to switch capacitors. For automatic switching of capacitors, voltage sensitive devices are usually used, although current and kilovar sensitive devices also are used.

With carrier current in a circuit, reactors must be used in series with shunt capacitors. These reactors limit the flow of carrier current through the capacitors and also may increase the voltage across the capacitor. In such cases it may be necessary to use capacitors having a higher normal voltage rating. The use of a wave trap in place of a reactor does not result in appreciable boost in voltage on the capacitors and is preferable for large banks.

Table III

	Factor F for Open Wire Feeders			
Feeder Voltage	Three Phase	Two Phase Four Wire	Two Phase Three Wire	Single Phase
2,400	2.24	2.24	2.24	4.48
4,160	0.75	0.75	0.75	1.50
4,800	0.56	0.56	0.56	1.12
7,200	0.25	0.25	0.25	0.50

Abnormal Currents

CAUSES

Capacitors are rated in fundamental frequency, voltage, and kilovars. Harmonic voltages occur in most power systems and, although usually small, cause harmonic currents to flow. Therefore, when capacitor currents are measured under service conditions, the value read is usually in excess of the nominal value obtained from rated kilovar and rated voltage. The excess current may be due to:

1. The plus capacitance tolerance provided by the manufacturer.
2. Application of more than rated voltage at fundamental frequency.
3. Harmonic voltages.
4. Over-currents such as those caused by switching, arcing in supply circuit, and other system disturbances.

REMEDIAL MEASURES

1. Plus capacitance tolerance provided by the manufacturer will produce over-currents. Although there are no remedial measures, these over-currents are usually small enough to be of little consequence.

2. The application of more than rated voltage at fundamental frequency will result in over-currents which will not be excessive if established limits for over-voltage operation are followed (see Maximum Voltage Limitation). Excessive over-voltage at fundamental frequency is generally the result of improper setting of transformer taps or voltage regulators. Remedial measures include adjustment of transformer taps or voltage regulator settings. If the capacitors themselves are contributing to the over-voltage due to the rise at light load, it may be necessary to switch part or all of the capacitors. Relocation of a capacitor bank also may alleviate over-voltage conditions where the system will permit such relocation.

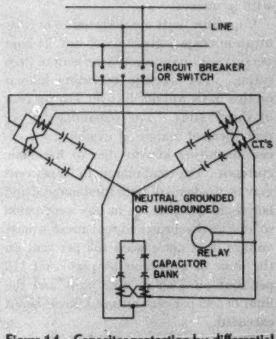

Figure 14. Capacitor protection by differential current transformers in parallel

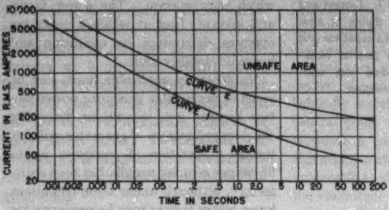

Figure 15. Current versus time for a short-circuited capacitor unit to rupture due to gas pressure after an internal short circuit occurs

Area below curve 1 is safe with no damage expected beyond slight swelling of case. Area between curve 1 and curve 2 is safe practically for many conditions of installation, although occasional crack in a seam or bushing seal may occur. Area above curve 2 is unsafe due to rupture occurring frequently with sufficient violence to damage the adjacent units

3. Harmonic voltages produce harmonic over-currents. Several things may cause harmonic voltages. Their order of importance, with suggested remedies where applicable, is as follows:

(a). Transformer magnetizing currents cause a distortion of the impressed voltage wave due to the saturation of the magnetic core. The third harmonic is the predominant component in this magnetizing current. Delta-connected transformer windings circulate these third harmonic currents and prevent them from getting out on the system. These delta windings also reduce the multiples of the third harmonics such as the 9th, 15th, and so forth. Therefore, odd harmonics such as the 5th, 7th, 11th, and so forth, are usually those which appear on the system. The harmonic currents flowing through the circuit reactance produce harmonic voltages on the line. The voltages are equal to the harmonic current times the circuit reactance at the frequency of the harmonic current. These harmonic voltages appear at various parts of the system, depending on the system reactance and magnitude of current flowing. The most direct and simple method of reducing harmonic voltages arising from transformer magnetizing current is to reduce any over-excitation of the transformers in the affected areas.

(b). Rectifiers cause harmonic voltages and currents to appear in the supply circuit. They usually cause inductive interference with communication circuits instead of overloading capacitors. Resonant shunts usually will eliminate these harmonic currents.

(c). Generators and motors do not generate a perfect sine voltage wave. This source of trouble is not serious in rotating equipment of modern design. It has been encountered with very old equipment, particularly water wheel generators.

(d). Insulator leakage and corona causes intermittent currents to flow to ground. This intermittent flow of current distorts the voltage and current waves of the circuit and is manifested as harmonics.

(e). Arc lamps and arc furnaces may distort the voltage wave shape due to their change in impedance during various parts of the voltage cycle.

(f). Transformer banks operated in conjunction with capacitors may cause harmonic resonance. The capacitor kilovar which will produce this condition when operated with transformer banks of equal rating is three times as large for delta as for open delta transformer banks. Therefore, it may be necessary to limit the size of capacitor banks operated adjacent to open delta transformer banks.

Harmonic over-currents due to resonance or partial resonance to a harmonic frequency, irrespective of cause, can be reduced by relocation of the capacitors to eliminate or reduce the resonant condition.

When harmonic over-currents exist at light load periods, they can be eliminated by switching the capacitors.

Harmonic over-currents which cannot be satisfactorily reduced by other means may require suppression with reactors or wave traps. Since harmonic voltages rarely overstress a capacitor, it is only necessary to slightly alter the circuit constants to disturb the resonant condition. This may be done by adding reactors in series with part or all of the capacitor bank. The frequency and magnitude of the offending harmonic must be known in order to apply the proper remedial measures.

4. The arcs resulting from switching or other system disturbances may produce over-currents at frequencies above the fundamental. If the circuit is resonant at this frequency capacitor over-currents may result. These usually may be reduced by moving the capacitors to eliminate the resonant condition.

Ability of Capacitors to Carry Over-Currents

Capacitor units are designed with ample latitude for over-currents encountered in service consistent with the over-voltage limitations. (See section on Maximum Voltage Limitations.) Since capacitor impedance varies inversely with frequency, the allowable current may be comparatively large at higher harmonics. Circuit breakers, current transformers, and other equipment in series with capacitors must therefore have a current carrying capacity in excess of the nominal capacitor current. Experience has shown that for ordinary operating conditions such equipment is usually satisfactory if it has a current carrying capacity equal to 135 per cent of the capacitor rating.

Unless history of previous installations indicate a disturbing harmonic condition, advance study usually is not warranted. Excess harmonic currents are frequently less troublesome in actual practice than may be indicated by a theoretical study. In those rare instances where such difficulties are encountered, the trouble usually can be readily corrected.

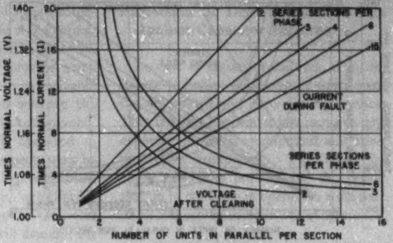

Figure 16. Current and voltage during or after failure of a capacitor unit in series parallel bank-delta or grounded star connection

Inductive Co-ordination

Causes of Inductive Interference

Shunt capacitors usually are installed in balanced 3-phase banks. The connection may be line-to-ground, line-to-line, or ungrounded star. Capacitors connected line-to-line or in ungrounded star can in no way affect any residual (neutral to ground) voltage that may be on the system. They can only affect the balanced harmonics, and these are less important.

When capacitors are connected line-to-ground, the capacitive and inductive reactances for the existing residual voltage may amplify the residual voltage and current. Even this condition may not cause trouble for the following reasons:

1. Modern communication equipment is not sensitive to 180-cycle current which is the third harmonic residual current of the usual power system. The telephone interference factor for 180 cycles is 15, compared with 205 for 300 cycles and 4,400 for 1,500 cycles.

2. Even though circuit constants are such as to produce resonance, the third harmonic voltages usually existing in a system are so small that trouble would not result.

The approximate computed rise of the fundamental voltage when capacitors produce resonance are as follows:

Order of Harmonic	Approximate Per Cent Voltage Rise
3	5.0
5	4.0
7	2.0
9	0.6
11	0.8

The capacitors applied usually will give at least a 2 per cent voltage rise which corresponds to a resonant" condition for the seventh harmonic. This is a balanced component and rarely causes trouble.

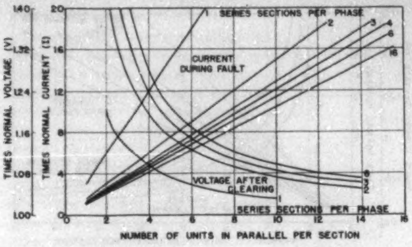

Figure 17. Current and voltage during or after failure of a capacitor unit in series parallel bank-ungrounded star connection

The ninth harmonic current circulates in the transformer delta windings and therefore does not cause trouble. The amplitudes of higher harmonic voltages are small and may be neglected.

When capacitors are connected line-to-ground on a 4-wire 3-phase distribution system, the fifth harmonic voltage is usually responsible for the few instances where inductive interference is experienced. This is caused by unequal amount of transformer kilovolt-amperes per phase which allows some residual fifth harmonic magnetizing current to appear. Since residual currents cause most telephone interference, resonance with the fifth harmonic current is a potential source of trouble.

The communication industry has co-operated in solving these problems and they recognize that capacitors represent an advance in the art of power distribution. In the last decade, the communication equipment has been improved so that it is very insensitive to the lower harmonics. This has further minimized inductive interference.

Remedial Measures

The general solution of inductive interference is one of co-ordination between the types of circuits and equipment involved.

Some of the more common remedial measures for solving these problems are as follows:

1. Relocate the capacitors.
2. On a multigrounded system where the neutrals of the capacitor banks are normally connected to ground, some of these ground connections may be removed and the capacitor neutrals allowed to float. This reduces the magnitude of the residual ground return current.
3. Capacitor banks may be connected delta in place of star on multigrounded circuits, thereby limiting the flow of harmonic current in the ground return.
4. Gaps or reactors may be placed between the neutral connection of the capacitor bank and ground to prevent the flow of harmonic ground return currents.
5. Wave traps or filters may be used to block residual harmonic currents. The nature of exposure, source and magnitude of the harmonic current, and type of power circuit must be considered in the design of the filter or wave trap.
6. The type of construction of communication circuits determines their susceptibility to inductive interference. Cables with grounded sheaths are practically free from interference. Two-wire communication circuits are very much less susceptible to interference than those using one wire and a ground return. Communication circuits with high-impedance ringers are much less susceptible to interference than are those with low-impedance ringers.

The probability of capacitors increasing the inductive interference on communication circuits is small and if it occurs, well-known remedial measures can be taken. Full co-operation with communication groups is recommended. Communication engineers are well informed on the best methods of minimizing inductive interference.

System Stability

Usually shunt capacitors may be added to a system without affecting system stability. When capacitors supply kilovars they reduce the excitation required on the system generators to maintain the voltage level. The system stability margin is reduced with lower generator excitation. This usually happens during periods of light load especially when large numbers of capacitors have been gradually added to the system.

The number of fixed capacitors which may be applied to a system is limited by other capacitive kilovar on the system and the minimum allowable excitation of the generators. Other sources of capacitive kilovar may be shunt capacitors already in use, synchronous condensers and motors, and high-voltage circuits of the system.

The algebraic difference between inductive and capacitive kilovars in conjunction with the kilowatt load on the generators determines the power factor at which they operate. The power factor and kilowatt load at which a generator operates determines its excitation and hence its stability limit.

No generally applicable limits can be given of permissible generator power factors because local conditions determine the required margin of generator pull-out torque. Operation of machines up to 95–98 per cent lag usually has been satisfactory, although under some conditions lower power factors may be necessary for stable operation. However, higher power factors may be feasible on some systems.

All generators should be operated with a pull-out torque margin sufficient to allow them to pick up their share of sudden load increases, such as might occur when a major source of power is lost. The pull-out torque margins also must be large enough to maintain stability during reductions in system voltage produced by large increases in reactive requirements. This might be caused by the loss of excitation on a large generator unless "loss of field" relays are provided. Reasonably fast automatic regulation of the excitation will in many cases act to increase generator pull-out torque during emergency conditions.

Generators of old design may be subject to an excessive temperature rise in the end structure of the stator if operated with approximately rated stator current and low field current. Most modern gen-

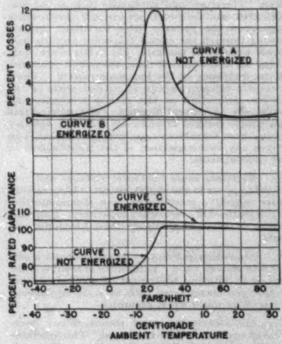

Figure 18. Typical loss and capacitance variations in synthetic liquid filled capacitors

Curve A shows the per cent losses of a capacitor upon energizing after being out of operation for an extended period. Curve B shows the per cent losses of a capacitor unit in continuous operation. Curve C shows the per cent of rated capacitance of a capacitor in continuous operation. Curve D shows the per cent of rated capacitance of a capacitor not energized for an extended period erators may be operated without excessive heating of stator iron at loads of approximately 60 per cent rated kilovolt-amperes at 0 per cent leading power factor; 93 per cent rated kilovolt-amperes at 90 per cent leading power factor; and 100 per cent rated kilovolt-amperes at unity power factor. If operation near these limits is expected, it is advisable to check the characteristics of the individual generators.

On some systems it may be necessary to switch part of the capacitors off at light load to maintain the required margin of system stability. Usually when shunt capacitors introduce a stability problem, other problems, such as high voltage on station busses or circuits, will be encountered. The solution of these other problems will usually correct the stability problem.

Protection

LIGHTNING

Capacitor units are vulnerable to lightning disturbances. These disturbances may cause bushing flashover or breakdown the insulation between the internal elements and the case. Lightning arresters are usually installed when capacitor units are connected phase-to-phase; line-to-ungrounded-neutral; and line-to-unigrounded-neutral. If the case is grounded, the lightning arrester ground should be connected to the case with the shortest possible lead.

Capacitor units connected line-to-neutral on a multigrounded neutral system provide a low impedance path for lightning surge current and some protection from over-voltage due to lightning. Star connected capacitor banks with the neutral point ungrounded provide some degree of protection when a suitable lightning arrester is placed between the neutral point of the bank and ground. However a capacitor unit operated in either of the above arrangements may be vulnerable to damage by lightning when the magnitude and duration of lightning surge is sufficient to charge the capacitor to a high voltage which will damage the insulation, or when a steep front high magnitude voltage wave is not absorbed by the capacitor in sufficient time to prevent damage to the insulation.

Therefore, it is good practice to install lightning arresters on capacitors connected phase-to-multigrounded-neutral. However, advantage is taken of this inherent self-protective feature and capacitors connected phase to multigrounded neutral are sometimes operated without lightning arresters.

Diagrams of typical connections are shown in Figures 1, 2, 3, and 4.

TRANSIENT OVER-VOLTAGE

Transient over-voltages may be caused by switching operations, arcing grounds, discharge of lightning arresters, resonance or near resonance caused by motors while starting, and other similar causes. Such voltage disturbances are of short duration and usually are of lower magnitude than those caused by lightning. Lightning arresters will ordinarily provide adequate protection against such transient disturbances. Unusual cases may require special remedies.

Protection of Distribution Systems Against Capacitor Failures

In case of capacitor failures, it is desirable to isolate the damaged units from the circuit without interrupting service. This requires co-ordination between the capacitor protective equipment and other protective equipment. For most installations, it is possible for the power system to continue in operation with part or all of a capacitor bank out of service.

CIRCUITS PROTECTION REQUIREMENTS AGAINST CAPACITOR FAILURES

Properly co-ordinated protective device will:

1. Disconnect a short-circuited capacitor before the case ruptures, damaging adjacent equipment or causing personal injury.
2. Disconnect a damaged capacitor without causing operation of other circuit protective devices.
3. Disconnect a damaged capacitor unit or group of units with minimum loss of kilovars.
4. Not disconnect a capacitor when subjected to non-damaging system disturbances.
5. Indicate the location of a failed unit in a large bank.
6. Disconnect a capacitor unit which is arcing internally in order to minimize damage to adjacent units due to their repetitive charging and discharging.

TYPES OF PROTECTION

The more common types of protection in approximate order of their importance are:

1. Fuses for individual units, see Figures 5, 6, 7, and 8.

Table IV. Summary of the Discussion of the Types of System Protection Against Capacitor Failures

Type of Protection	Figure Number	Function of Type of Protection May Prevent Case Rupture*	No Affect on Other System Prot. Devices	Limits Kvar Loss	Requires Immediate Maintenance	Insensitive to External Disturbances	Indicated Failed Unit Location
1. Individual fuses	5–6–7–8	Yes	Yes	Yes	No	Yes	Yes
2. Group or bank fuses	9–10	Yes	Yes	Yes	Yes	Yes	No†
3. Line current transformers and overcurrent relays		Yes	Yes	No	Yes	Yes	No
4. Voltage unbalance between phases	11	Yes	Yes	No	Yes	Yes**	No
5. Voltage unbalance between neutrals of double star bank	12	Yes	Yes	No	Yes	Yes	No
6. Voltage unbalance between ungrounded neutral of star bank and ground (usually permissible only on grounded system)	13	Yes	Yes	No	Yes	No	No
7. Differential current transformers in parallel	14	Yes	Yes	No	Yes	Yes	No
8. Reduced conductor size—limited to 240 volts maximum		No	No‡	Yes	Yes§	Yes	No

* Depends on time current curve of protective device which should be co-ordinated with the curve of Figure 15.

† Group fusing will not indicate individual unit failure.

‡ Depends on co-ordination with other system protective equipment.

§ Depends on extent of damage if any due to case rupture.

** Except when neutral is grounded.

2. Fuses for groups or banks of units, see Figures 9 and 10.

3. Line current transformers operating direct trip coils or over-current relays to trip circuit breaker.

4. Potential transformers connected across each phase or part of each phase to trip a circuit breaker on phase voltage unbalance, see Figure 11 for star ungrounded neutral banks. This arrangement also may be used for delta or star grounded neutral banks which contain two or more series sections per phase.

5. Potential or current transformers connected between ungrounded neutrals of two star banks operating a relay to trip a circuit breaker, see Figure 12.

6. Potential transformer connected between neutral and ground of a star ungrounded neutral bank operating a relay to trip a circuit breaker, see Figure 13.

7. Differentially-connected current transformers in parallel capacitor groups, operating a relay to trip a circuit breaker.

8. Reduced conductor section to burn open with over-current.

COMPARISON OF VARIOUS TYPES OF PROTECTION

Table IV is a summary comparing the eight types of protection previously mentioned. A detailed discussion of each follows:

1. Fuses on individual units are used most extensively because they provide the maximum number of desirable features. When fault currents through shorted capacitors are excessive, individual fuses are desirable to avoid case rupture and also to avoid possible damage to adjacent units due to their repetitive charging and discharging.

In addition to the normal considerations followed in the general application of fuses (see section on Abnormal Currents) they should have a time current characteristic to successfully withstand the high charge and discharge currents associated with switching transients.

The interrupting duty of individual fuses may be reduced by the use of parallel groups of capacitor units connected in series between lines or the use of star connected units with the bank neutral ungrounded. In case of unit failure, these arrangements provide other units in series with the faulted unit and thereby limit the fault current. Properly selected capacitor units with individual fuses may be connected in series providing the following conditions are met.

(a). The number of capacitor units in parallel contribute to the fault current which will flow through a fuse connected to a shorted unit. Sufficient units should be used to provide a fault current which will clear the fuse before the case ruptures. This will usually require a fault current several times the current rating of the fuse. Figure 15 shows the relationship between current and the time required to rupture the case as determined by one manufacturer. The number of units in each parallel group must be increased when the number of parallel groups in series is increased. Figures 16 and 17 show the fault current through a failed unit for various series parallel combinations. These curves also show the maximum voltage that will exist across the remaining units of a parallel group after a failure in this group.

(b). When one unit of a parallel group fails the remaining units of this group will be subjected to an over-voltage due to the change in circuit impedance. A sufficient number of units must be operated in parallel to limit this voltage to 110 per cent of rated capacitor voltage until the unbalance is corrected.

Table V, which was prepared from Figures 16 and 17, shows the minimum number of units which may be operated in parallel after the operation of an individual fuse without exceeding 110 per cent of operating voltage. This is based upon normal voltage at the time of fuse operation. For this type of protection, it is assumed that not more than one unit in a series group will fail at one time and that it will be cleared by its individual fuse before the backup protective equipment operates. On the rare possibility of two simultaneous series failures, it is expected that some damage might occur before the backup protection for the circuit could clear the fault. Experience has shown this assumption to be valid. Generally, more units connected in parallel give a greater factor of safety for the operation of fuses, and minimum over-voltage after a fuse has blown. Capacitor banks for circuit voltages above 15 kv are usually built up in series parallel connected groups.

2. Fuses for banks or groups of capacitor units are subjected to the same limitations in application as are those for individual units. The fusing of banks or groups requires larger fuses. This limits their use since a fuse of high current carrying capacity allows considerable energy to be dissipated in the fault before circuit interruption. The fuse must clear the circuit before the energy dissipated in the fault can cause case rupture, see Figure 15.

3. Line current transformers used with auxiliary equipment to trip circuit breakers can be used for capacitor bank protection. The time required to clear a faulted capacitor unit by over-current tripping of a circuit breaker is approximately 1/10 of a second. This may cause case rupture if the fault current exceeds a few hundred amperes. Therefore, this arrangement is usually used as backup protection to group or individual fuses.

4. The use of unbalanced phase voltages on a capacitor bank to tip a circuit breaker as shown in Figure 11 is applicable where the possible loss of the entire bank is permissible in case of a unit failure.

5. Circuit breakers tripped by voltage or current sensitive relays connected between the ungrounded neutrals of two star banks as shown in Figure 12 is an inexpensive means of protection. Failure of a unit allows current to flow between the neutral points, operating the relay and circuit breaker. This type of protection may be used when the loss of the banks, in case of a unit failure, is not serious. The use of this arrangement is limited by the time required for circuit breaker operation.

6. Potential or current transformers may be connected between the neutral and ground of an ungrounded neutral star connected bank as shown in Figure 13. Failure of a capacitor unit causes bank unbalance and shifts the neutral. The resulting current flow to ground or voltage between neutral and ground operates the relay and circuit breaker. This type of protection has the same limitations as the arrangement described previously. Circuit disturbances, external to this capacitor bank, also may cause this protective equipment to operate. This may usually be prevented by incorporating time delay equipment. This type of protection usually can be used only on a grounded system.

7. When banks of equal parallel groups of capacitor units are used, they may be protected by circuit breakers operated by differentially connected current transformers as shown in Figure 14. Failure of a capacitor unit causes a current unbalance between the parallel group of the phase involved. This means of protection has the same limitations as described in paragraph 4 (Figure 11). It may be used when the fault current is not sufficient to rupture the capacitor case. Because the normal relay current is zero this arrangement is very sensitive to capacitor unit failures.

8. Reduced conductor sections that are melted and burned open by fault currents may be used to protect capacitors. Their use is limited to circuits of 240 volts and below where sufficient fault current is available. This means of protection may be used when capacitor units are in housings or vaults where case rupture is not objectionable. This means of protection is not considered satisfactory for circuits above 240 volts, since the melting of conductor section may be followed by continued arcing and much damage before fault is cleared.

Table V

Grounded Star Banks			Ungrounded Star Banks		
Number of Groups in Series	Minimum Units Per Group	Total Units Per Phase	Number of Goups in Series	Minimum Units Per Group	Total Units Per Phase
2	6	12	2	8	16
3	8	24	3	9	27
4	9	36	4	9	36
5	9	45	5	10	50
6	9	54	6	10	60
7	10	70	7	10	70
8	10	80	8	10	80
9	11	99	9	11	99
10	11	110	10	11	110
11	11	121	11	11	121
12	11	132	12	11	132
13	11	143	13	11	143
14	11	154	14	11	154
15	11	165	15	11	165
16	11	176	16	11	176

The foregoing discussion applies to methods of protection which operate after capacitor unit failures. It is more important to prevent failure of a unit by protecting it against abnormal operating conditions. A more complete discussion of some of the means used to help mitigate these abnormal operating conditions is given in other sections of this report.

Grounding Cases of Capacitor Units

GENERAL

Single-phase capacitor units are built with either one or two bushings. In the former, one of the terminals is a stud electrically-connected to the case.

The 2-bushing unit may be used for any type of connection. Its case may be grounded, provided it has sufficient terminal to case insulation. Two bushing units have approximately 0.002 microfarad capacitance between terminals and case. This allows a few milliamperes of charging current to flow to ground when a case to ground connection is made.

Single bushing units have the case grounded when connected to a circuit having one conductor grounded, such as a 3-phase 4-wire multigrounded neutral system. When the terminal common to the case cannot be connected to ground, the capacitor case must be insulated from ground. Under this condition the case floats at some potential above ground and may become a hazard. Therefore barriers are usually provided.

Economics determine whether the cases should be insulated from ground or whether this insulation should be built into the capacitor unit. When capacitor units are installed on ungrounded systems of 12 kv and above, and on all systems where units are connected in series, it is usually more economical to insulate the cases from ground. On lower voltage circuits, it is usually more economical to standardize on two bushing units having the insulation built into the capacitor. These have a more universal application.

POLE MOUNTED CAPACITOR UNITS

Two-bushing units may be mounted on poles without cases being grounded. Under this condition the wood poles or structures provide some insulation between case and ground. Two bushing units must be used on multigrounded neutral systems when necessary to operate with cases ungrounded. Pole mounted single bushing units should only be used on multigrounded neutral systems with the case connected to the neutral. Single bushing units are not usually used for installations where wood supports furnish the full line-to-ground insulation.

The advantages of grounding cases of pole mounted units are:

1. Prevents the case from becoming a hazard by providing a path to ground for terminal to case charging current thus keeping the case at ground potential.
2. Prevents the case from becoming a hazard by keeping it at ground potential in event of a terminal to case insulation failure.
3. Makes it possible to improve lightning protection by interconnecting the capacitor case and lightning arrester ground.

The disadvantages of the grounding cases of pole mounted units are:

1. The necessity of obtaining a satisfactory ground.
2. The expense of providing ground leads.
3. The capacitor unit is more vulnerable to lightning damage when the lightning arresters are not used.
4. The hazard of a large grounded surface on the pole.

This subject is closely related to the general subject of transformer and other case grounding on poles. It has been the object of considerable controversy for several years.

GROUND LEVEL CAPACITOR INSTALLATIONS

Unless cases are grounded, ground installations without housings usually will require barriers or other means of preventing accidental contact. Single bushing capacitor units should be connected to the multigrounded neutral unless they are mounted on insulators. When ground connections are used, they must be adequate to dissipate fault current with no hazardous rise of voltage.

Article 460 of the National Electrical Code[3] outlines the code requirements for indoor capacitor installations. Among these are those on grounding and isolation which state that "capacitor cases shall be grounded in accordance with Article 250" and "all live parts of capacitors which are connected to circuits of more than 600 volts between conductors and are accessible to unqualified persons, shall be enclosed or isolated."

The relative advantages and disadvantages of grounding cases and housings for ground level installations are similar to those for pole mounted installations.

Safety Precautions in Handling Capacitor Units

The same precautions must be taken with capacitor units as with other electric equipment when they are taken out of service for repair or maintenance. A capacitor is unique in that it may retain a hazardous charge for an indefinite period after being disconnected. This requires extra precaution.

Generally, discharge resistors are built into each capacitor unit. When a unit is disconnected from its power supply, these discharge devices will reduce the terminal voltage of the unit to 50 volts or less in one minute for units rated at 600 volts and lower, and in five minutes for units rated above 600 volts. It is not advisable to put complete dependence on such devices.

Before capacitor units are handled, it is good practice to short circuit and ground the terminals. As a precaution, these short circuit and grounding provisions should be left intact until all work on an installation is finished. Capacitors not equipped with discharge resistors may build up a small charge after having been discharged. Therefore it is considered good practice to connect all capacitor terminals together and to ground before making bodily contact with such parts.

Short circuiting and grounding equipment may be temporary portable conductors and clamps, or built-in short circuiting devices, depending on how often they may be used.

Capacitor cases, unless grounded, may pick up a residual charge. Although this is not dangerous, it can cause discomfort when the case is contacted. This creates a hazard and might cause an accident.

When cases are operated grounded, special attention should be given to the condition of the ground before working on the equipment. The same precaution should be followed as those for working near any other large grounded surface.

Maintenance and Periodic Inspection of Capacitor Installations

GENERAL

The maintenance requirements of a capacitor installation are relatively few and, for that reason, are frequently overlooked. However, certain phases of capacitor installations do require attention. Since all modern capacitors have sealed cases, the only parts requiring physical maintenance are the bushings, terminals, and the case.

ITEMS TO BE CHECKED

The following items should be periodically checked:

1. Bushings for contamination and breakage.

2. Case for rust and leaks.
3. Terminals for corrosion and breakage.
4. Ambient operating temperature.
5. Operating voltage.
6. Protective and other auxiliary equipment.

Frequency of Inspections

The frequency with which inspections are made depends upon local conditions and past experience. Manufacturers recommend that the voltage on the capacitor units be checked during light system load within 24 hours after installation.

Small Installations

Small capacitor banks installed on distribution circuits can be inspected along with the routine checking of other equipment during periodic load checks. Experience has shown that line crews and servicemen can check capacitors for blown fuses and other troubles, while they are in the area. This check will usually be adequate. Periodic customer voltage checks will usually indicate the maximum voltage appearing on the capacitors.

Large Installations—Indoor and Outdoor

Large capacitor banks installed near substations or other terminal points will require more frequent inspection. In these installations, the failure of capacitor units may affect the system voltage and current flow. A sustained fault in one unit may damage adjacent units and cause additional failures later. The use of individual fuses will usually minimize this hazard.

Inspection of large installations for capacitor unit failures, blowing of fuses, and so forth, may be put on the same schedule as similar work for other substation or terminal equipment. The frequency of such inspections should be more frequent than for small installations.

Voltage and ambient temperature should be checked periodically, as well as when the installation is made. The season of the year, addition of other equipment adjacent to the capacitor installations and similar factors may affect the ambient temperature. Checks should be made at times when the maximum ambient operating temperature is expected.

Similar checks should be made on indoor installations, particularly for contamination of the insulators and ambient temperature. Industrial plant atmospheres may carry contamination which will collect on bushings and cause bushing flashover. The ambient temperature in indoor installations may change due to the addition of other equipment, building alterations, and so forth.

The frequency of inspection for indoor installations should be on a schedule similar to the maintenance of other indoor electric equipment. Initially inspections at short intervals are desirable. These can be lengthened as experience indicates.

References

1. Shunt Capacitors, **AIEE Committee Report.** *Electrical Engineering* (*AIEE Transactions*) volume 62, May 1943, pages 222–30. (Since the present report is a continuation of the above item, the references listed at the end of that report are not repeated below.)

2. Capacitors. AIEE Standard Number 18, June 1934.

3. National Electrical Code, *C-1-1947*. American Standards Association (New York, N. Y.) 1947.

4. Shunt Capacitors. *Publication Number 45-100*, National Electrical Manufacturers Association (New York, N. Y.). August 1945.

5. Performance of Shunt Capacitors, **AIEE Committee Report.** *AIEE Transactions*, volume 68, part II, 1949, pages 1200–07.

6. Power Capacitors (book), **R. E. Marbury.** McGraw-Hill Book Company, Inc., New York, N. Y., 1949.

7. The Why of a 25 Kvar Capacitor, **M. E. Scoville.** *General Electric Review* (Schenectady, N. Y.) May 1949.

8. Switched Capacitor Control Voltage and Improved System Loading, **N. N. Smelloff, O. Ramsaur.** *Electrical World* (New York, N. Y.) December 4, 1948, page 85.

9. Practical Aspects of Applying Static Capacitors, **V. R. Parrack.** *Electric Light and Power* (Chicago, Ill.) December 1948, pages 70–73.

10. Capacitors Why and Where to Use, **H. Brooks.** *Factory Management and Maintenance* (New York, N. Y.) September 1948, pages 100–02; October 1948, pages 122–25.

11. Pole-Mounted Automatically Switched Capacitors Prove Economical, **C. F. Myers.** *Electric Light and Power* (Chicago, Ill.) September 1948, pages 64–66.

12. Why, When, and Where to Install Capacitors, **J. W. Butler.** *Industry and Power* (St. Joseph, Mich.) March 1948, pages 77–79.

13. Underexcited Operation of Turbogenerators, **C. G. Adams, J. B. McClure.** *AIEE Transactions*, volume 67, part I, 1948, pages 521–28.

14. New Kraft Capacitor Paper, **H. F. Miller, R. J. Hopkins.** *General Electric Review* (Schenectady, N. Y.) December 1947, pages 20–24.

15. Why not Bury the Capacitor Ghosts? **J. W. Butler.** *Electric Light and Power* (Chicago, Ill.) November 1946, pages 40–41; December 1946, pages 72–74; January 1947, pages 66–68.

16. Selection of Control Equipment for Automatic Switching of Capacitors, **W. C. Bloomquist.** *Electrical World* (New York, N. Y.) November 22, 1947, pages 88–91.

17. The Use of Capacitors in Industrial Plants, **W. C. Bloomquist.** *Electrical Construction and Maintenance*, (New York, N. Y.) part I, October 1947, pages 149–52; part II, November 1947, pages 129–32; part III, December 1947, pages 81–86.

18. The Probable Breakdown Voltage of Paper Dielectric Capacitors, **H. Brooks.** *AIEE Transactions*, volume 66, 1947, pages 1137–45.

19. Automatic Switching Schemes for Capacitors, **W. H. Cuttino.** *AIEE Transactions*, volume 66, 1947, pages 311–14.

20. Telephone Influence Factor and What to Do About It, **G. L. Oscarson.** *Petroleum Engineering* (Dallas, Texas), volume 18, August 1947, page 100.

21. Telephone Interference from Power Systems, **P. B. Frost, E. H. Gould.** *Electrical World* (New York, N. Y.) February 1, 1947, page 82.

22. Inductive Co-ordination of Rural Power and Telephone Systems. *Engineering Report Number 40*, Edison Electric Institute (New York, N. Y.) 1938.

23. Selective Devices for Reducing Harmonics in Power Systems—Part II, A-C Systems, *Engineering Report Number 34*, Edison Electric Institute (New York, N. Y.) 1937.

24. Banks of Capacitors Reinforce 132 kv Grid, **L. F. Ferri, C. S. Dayton.** *Electrical World* (New York, N. Y.) March 29, 1947, pages 66–69.

25. The Economies of Using Capacitors in Amounts to Require Automatic Switching, **J. W. Butler.** *AIEE Transactions*, volume 66, 1947, pages 322–28.

26. Capacitors Can Cause Motors to Reverse, **H. Van Horn.** *Electrical World* (New York, N. Y.) March 15, 1947, pages 127–36.

27. Safe Discharge of A-C Power Capacitors, **R. L. Fancher.** *Electrical World* (New York, N. Y.) April 13, 1946, pages 105–07.

28. Switched Capacitors Retrieve Line Loading Capacity, **R. O. Loomis, E. J. Archbold.** *Electrical World* (New York, N. Y.) April 27, 1946, pages 46–48.

29. Shunt Capacitors Reduce Costs and Increase Power Capacity, **W. H. Cuttino.** *Buildings and Building Management* (Cedar Rapids, Iowa) April 1946.

30. Selection and Application of Automatic Control for Capacitors, **T. W. Schroeder, W. C. Bloomquist.** *General Electric Review* (Schenectady, N. Y.) part I, October 1945, pages 7–11; part II, December 1945, pages 22–31; part III, March 1946, pages 37–41.

31. How Kilovars Are Related to System Design and Operation, **J. W. Butler.** *General Electric Review* (Schenectady, N. Y.) volume 48, September 1945, pages 51–57.

32. Application of Capacitors for Power-Factor Improvement of Induction Motors, **W. C. Bloomquist, W. K. Boice.** *Electrical Engineering* (*AIEE Transactions*) volume 64, May 1945, pages 274–78.

33. Use the Right Capacitor with Induction Motors, **J. B. Owens.** *Factory Management and Maintenance* (New York, N. Y.) May 1945, pages 144–46.

34. Power Supply for A-C Arc Welding, **A. U. Welch, R. F. Wyer.** *Electrical Engineering* (*AIEE Transactions*), volume 64, March 1945, pages 116–20.

35. Industrial Capacitor Application Calculation, **J. S. Francis, S. Freeman, Jr.** *Electrical World* (New York, N. Y.) February 3, 1945, pages 85–87.

36. Characteristics of Chlorinated Impregnants in D-C Paper Capacitors, **L. J. Berberich, C. V. Fields, R. E. Marbury.** *AIEE Transactions*, volume 63, 1944, pages 1173–79.

37. Capacitor Installation at Newport News, **V. R. Parrack, E. L. Harder.** *AIEE Transactions*, volume 63, 1944, pages 1165–72.

38. Automatic Control and Switching Equipment for Capacitor Banks and Its Application, **T. W. Schroeder, W. C. Bloomquist.** *Electrical Engineering* (*AIEE Transactions*) volume 63, September 1944, pages 649–54.

39. Extending the Use of Shunt Capacitors by Means of Automatic Switching, **W. H. Cuttino.** *Electrical Engineering* (*AIEE Transactions*), volume 63, September 1944, pages 674–78.

40. The Cause and Control of Some Types of Switching Surges, **T. W. Schroeder.** *Electrical Engineering* (*AIEE Transactions*) volume 62, November 1943, pages 696–700.

41. Safe Capacitor Selection for Power Factor Improvement, **J. E. Barkle.** *Power* (New York, N. Y.) April 1943.

42. Reactive Power Metered as In-Out Magnetizing, **G. S. Lunge.** *Electrical World*

(New York, N. Y.) April 18, 1942, pages 58–59.

43. Harmonics and Power Factor, G. W. Stubbings. *Electrical Review* (London, England) volume 130, June 5, 1942, pages 726–27.

44. Paper Dielectric Containing Chlorinated Impregnants, D. A. McLean, L. Egerton, G. T. Kohman, M. Brotherton. *Industrial and Engineering Chemistry* (Easton, Pa.) volume 34, 1942, pages 101–09. Also articles in January 1945, May and November 1946, and November 1947.

45. Power Factor Improvement, M. I. Alimansky, Insley. *Paper Trade Journal* (New York, N. Y.), December 1941, pages 37–38.

46. Important Properties of Electrical Insulating Papers, H. H. Race, R. J. Hemphill, H. S. Endicott. *General Electric Review* (Schenectady, N. Y.), volume 43, 1940, pages 491–99.

47. Impregnated Paper Insulation (book), J. B. Whitehead. John Wiley and Sons, Inc., New York, N. Y., 1935.

48. Dielectric Properties of Chlorinated Diphenyls, A. H. White, S. O. Morgan. *Journal, Franklin Institute* (Philadelphia, Pa.), volume 216, 1933, pages 633–34.

49. Lectures on Dielectric Theory and Insulation (book), J. B. Whitehead. McGraw-Hill Book Company, Inc., New York, N. Y., 1927.

No Discussion

The Calculated Risk of Operating Capacitors Without Individual Fuses

HAMILTON BROOKS
MEMBER AIEE

Synopsis: The development of power capacitors has proceeded along the line of relatively small individual units for sound engineering reasons, and the performance of capacitor units as individuals has been very satisfactory. When capacitors are grouped in banks, this individuality or independence may be retained by fusing each unit. When group protection only is supplied, as by the use of bank fuses or circuit breakers the installation is no longer a collection of individuals but a consolidated group whose performance may be decidedly different. It is shown in this paper how the performance characteristic of the individual unit changes with the size of the group. Since the selection of protective methods and equipment may be dictated largely by economical considerations, the risk of operating groups of capacitors without individual fuses is evaluated.

THE USE of shunt capacitors for power factor correction on distribution circuits has developed in a large way only during the past 15 years. Many papers have been written concerning the advantages, economics, and satisfactory performance of shunt capacitors[1] and they are accepted by the distribution engineer as an established item of distribution apparatus of proven worth. Capacitors differ from other distribution apparatus, however, in certain unique ways that are not always properly taken into account in the application. This sometimes influences the performance of the capacitor installation. One of the unique characteristics in the use of power capacitors is the installation of large blocks of corrective capacity which are composed of a large number of relatively small units. One does not, for example, make a 2,500-kva transformer installation by using 100 small transformers in parallel. The reason that capacitors are built in this manner is, of course, because it is the practical and economical way to do it.[2] It is perfectly possible to build a large tank-type capacitor, but when the thermal, mechanical, and insulation requirements are adequately handled, the resulting capacitor has no practical usefulness because of the cost.

It is fortunate that the unit construction is the economical way to build power capacitors. The advantages in standardization, diversity of application, and ease of handling and installation are important factors in the choice of capacitors to do a particular job as compared to other alternates. In addition, the reliability of operation that may be obtained by individualization cannot be achieved in a large consolidated unit, whether it be a capacitor or something else. It is a mathematical fact which is intuitively recognized that the life, strength, and reliability of a group of independent individuals tends toward the average, whereas that of a consolidated group is represented by the most unfortunate individual in the group.

The means of maintaining unit independence in the performance of groups of capacitor units is readily provided by special-purpose individual fuses that may be mounted on or near each unit. Sometimes it may appear that such protection is inconvenient or unjustifiable and uneconomical, and such may well be the case. Under many circumstances, however, omissions of individual fuses are indefensible. Capacitors have been particularly advantageous in that they may be economically installed in small groups distributed over a system, and a majority of capacitors have been applied in this way. Here the individuality of the capacitor unit does not play an important part in the performance. The application of larger and higher voltage banks is developing, however, and in these installations the influence of individuality on performance may not be neglected.

It seems appropriate, therefore, to discuss the manner in which life and reliability may be expected to be influenced by grouping and by the size of capacitor groups. It is proposed to show in a general way how fault conditions and protective measures govern the severity of contingent damage following the failure of a capacitor unit. Finally, it is the purpose of this paper to illustrate how a numerical value may be derived to represent the risk incurred in economizing on or in providing inadequate protective measures.

The Life Expectancy of Power Capacitors

The mortality curve of capacitor units is similar in many respects to the human mortality curve, the typical shape of which is shown by Figure 1. In this curve can be seen the hazards of infancy, the culling out of weak individuals, the continuous influence of accident and disease, and the inevitable aging or wearing out of the individuals. Such a curve, however, is only representative of a population as a whole. It does not reflect the benefits of infant care or the result of gross neglect. It does not distinguish between occupational hazards, nor does it show the effects of abuse as compared to that of careful living. Clearly only a part of the life expectancy thus represented is due to unavoidable factors in the individual make-up. A great deal depends on the individual's environment or lies within his control.

Accurate performance records of apparatus are difficult to obtain. No doubt all capacitor manufacturers maintain

---

Paper 49-253, recommended by the AIEE Transmission and Distribution Committee and approved by the AIEE Technical Program Committee for presentation at the AIEE Fall General Meeting, Cincinnati, Ohio, October 17–21, 1949. Manuscript submitted July 18, 1949; made available for printing September 9, 1949.

Hamilton Brooks is with the Westinghouse Electric Corporation, East Pittsburgh, Pa.

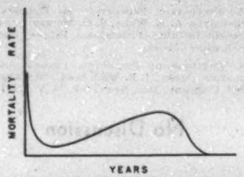

Figure 1. The shape of a human mortality curve showing the probability of death at a given age

careful service records, but these at best are incomplete and difficult of interpretation, and tend to greater inaccuracy with increasing age of the capacitor. The demise of a capacitor, unfortunately, usually takes the form of a short circuit of the insulation, regardless of whether it comes at the end of a long and useful life or at a premature age. The result of internal mechanical damage, or electrical and thermal abuse, is often the same, and the cause must be assigned from the circumstantial evidence. Unlike mechanical devices, there is no visual evidence of wearing out. Furthermore, insulation tests such as resistance and power factor measurements cannot be depended upon to indicate approaching failure, because capacitors as a class are very effectively sealed against entrance of moisture and other contaminants, and such chemical deterioration as may take place is highly localized and its effect is masked. Obviously then, the natural termination of the useful career of a capacitor unit is a short circuit unless it should be retired beforehand. Individual fuses are designed for this eventuality.

The AIEE-EEI Joint Subcommittee on Capacitors has recently made an extensive survey of the operation of shunt capacitors on electric power systems.[3] Valuable information is contained in this survey with respect to the mortality of capacitors in their early years of service. Such records, however, are representative in the same sense as the human mortality curve of Figure 1. The early years of a capacitor mortality curve are shown by Figure 2. This was derived from the AIEE-EEI data supplemented by other records. It is evident that aging or wearing out has not begun within the period covered by the curve and that the capacitors are still young. The difference in the initial shape of the curve reflects the effect of factory tests; the defective human individual is not killed at birth. As with the human mortality curve, however, the effects of care or abuse and hazards or protection are buried in the averaging. Using the terminology of the quality control engineer, one would expect rational subgroups from such a heterogeneous population as represented by all kinds of capacitors operated under all sorts of conditions to exhibit lack of control. More simply, the difference in performance between one set of capacitors and another is likely to be greater than can be accounted for by chance.

In economic studies, and in the analysis that follows, it is necessary to assign some value to the probability of failure within some given period. In any practical situation such a value must be largely arbitrary and dependent upon the amount of information and experience available. It is certainly desirable, however, to fit it as well as possible to the conditions at hand. Curve *A* of Figure 3 gives the cumulative mortality of capacitors from year to year corresponding to the yearly mortality of Figure 2. For the present purpose one may call this the probability of failure within the indicated period of usefulness. As pointed out, however, this is representative only in a broad way. Curves *B* and *C* illustrate how much a particular situation may depart from the average. There are distribution systems that use many small groups of capacitors dispersed over the system, and this application is of great benefit in relieving circuits of excess burden by applying the correction close to the load. Such capacitors are often exposed to lightning disturbance without protection and to mechanical damage in outlying districts and rural locations. Under these conditions and in view of the benefits, a performance as indicated by Curve *B* has been considered economical and satisfactory. With large installations continuity of service becomes important, and the investment warrants careful attention to operating conditions and protective devices. Equipment as received from the transportation agency is carefully inspected and tested for damage before installation. Records of these installations show a performance as typified by Curve *C*, if not better.

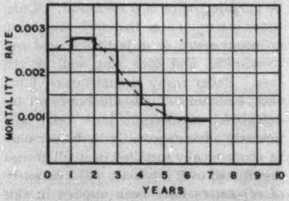

Figure 2. The shape of a capacitor mortality curve showing the probability of failure at a given age (derived from AIEE-EEI data)

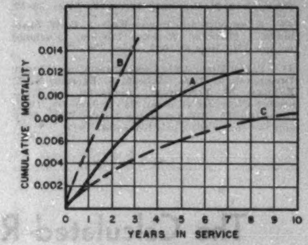

Figure 3. The cumulative mortality of capacitor units with years of service as shunt capacitors on distribution circuits

A—Consolidation for all conditions of service as derived from AIEE-EEI data

B—Severe and unprotected service. Applies to many small banks

C—Protected from severe and abnormal conditions. Applies to most large installations

The life expectancy of capacitors under practical conditions is therefore not so much a quality inherent in the capacitor unit as it is of the installation. It is accordingly determined to a considerable degree by circumstances within the control of the user. The capacitors may be deemed expendable as in the case for Curve *B*, or the importance of the installation may demand the best of care and protection. A value for the probability of failure, or the life expectancy, should then be chosen to fit the application. A reasonable way out of this difficulty is to select a convenient figure for the probability of failure and allow the age to vary to fit the circumstances. With reference to Figure 3, one may say that for the probability of unit failure within five years, $p=0.01$ is representative. For the hazardous conditions of curve *B* the loss of one out of a hundred units within two years may be expected. And finally, for the conditions applying to curve *C* it appears that 0.01 is a fair representation of the chance of an individual failure within a useful life span of 10 to 15 years. In what follows, a probability $p=0.01$, for the chance of a capacitor unit failure will be used in this sense, and the years may be selected to fit the application.

The Probability of Failure in a Group

The failure rate of capacitor units, from an economic standpoint, may be viewed as the rate of wearing out and incorporated in the cost of the installation. With industrial applications, where the monetary benefits are more sharply defined, capacitors almost always pay for themselves within $2^1/_2$ years or twice in five years. Thus, if the representative rate of one per cent failure in five years is used, the cost of wearing out over this period is only one-half of one per cent of the value received. As capacitors are grouped into banks, however, the interest shifts more or less from the probability of failure of a capacitor unit to the probability of failure in a group. The point of interest may be the cost of maintenance, the possibility of outage, or the matter of contingent damage resulting from the capacitor short circuit. It becomes of value, therefore, to investigate the probability of failure in groups.

Formally, the problem presents itself as follows: What is the probability of at least one failure in a group of n capacitors if the probability of failure of an individual is p? For small groups, say from one to ten units, the answer for all practical purposes is np, so for a group of ten units and a probability of unit failure $p=0.01$, the probability is that one group out of ten will experience a unit failure within the appropriate period. For larger groups it becomes necessary to calculate more precisely. This is conveniently done with the Poisson summation formula, and letting $P(A)$ stand for the probability of at least one failure, the answer is given by

$$P(A)=1-\epsilon^{-np}$$

extensive tables of which are available.[4] Figure 4 shows the probability of at least one failure in groups of size n when the probability of failure per unit is $p=0.01$. For a bank of 100 units, the probability turns out to be 0.63, meaning that a failure in two out of three such banks is to be expected within the arbitrary service period that is chosen. When $n=1{,}000$, a failure within the corresponding period is almost certain.

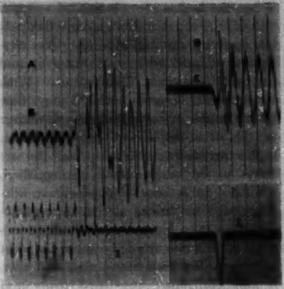

Figure 5. Capacitor unit fault currents

Oscillogram A shows a 250-ampere current that cleared after 26 cycles

Oscillogram B shows a 3,500-ampere current that produced violent rupture in 1/2-cycle

Figure 4. The probability of at least one failure in a group of *n* capacitors if the probability of failure per unit is 0.01

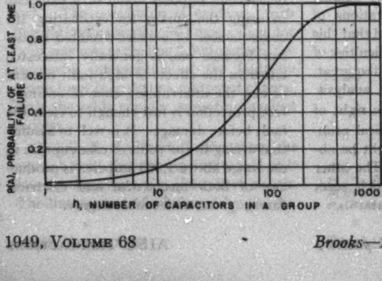

It is often desired to compare the degree of conformity of actual experience to statistical hypothesis, and a method of doing this may be mentioned. In any group of size n and probability of failure p, the expectation of failure is np, which should match with the average number obtained if an infinity of groups could be observed. Any experience with chance, however, is sufficient to demonstrate that a considerable departure from expectation is not unusual, even in matching coins. In the Poisson distribution, the standard deviation from expectation is the square root of the expectation, and it is an experimental fact that individual observations will very seldom depart more than three standard deviations from expectation through chance alone. To illustrate, if in a bank of 100 units one failure is expected, that is, $np=1$, the actual experience of no failure or four failures would fall within the bounds of chance, since $np \pm 3\sqrt{np}=0$ or 4. A minus probability has no meaning. The occurrence of five failures would merit investigation or a re-evaluation of p, as would also be true if the average for a number of such installations were much different from the expected value. A considerable refinement in this process is theoretically possible but hardly justified by the necessary generality of assumptions. It should be noted that the expected number of failures, np, is not the same as the probability of at least one failure, $P(A)$.

One other observation may be made before passing on, although it should be somewhat obvious. It is not often that outage is a factor of prime importance in small- and medium-size capacitor banks but it becomes of increasing importance with larger installations. In such cases the individually-fused unit provides the means for obtaining great reliability. It is inconceivable that more than a very few units should fail within any short interval even in the event of extremely severe disturbances. It is truly surprising how much abuse is required to break a capacitor when one sets out to do it. If the loss of a small portion of the units would not adversely affect the operation of the circuit, and such would surely be the case, it requires no mathematical manipulation to show the improbability of losing the benefit of the capacitor. Therefore, individual fuses for each capacitor unit should always be used when continuity of service is important and bank outage is to be prevented.

The Consequences of a Short-Circuited Capacitor

A short-circuited capacitor unit may produce mechanical and electrical disturbances, the nature of which is somewhat peculiar to capacitors because of their characteristics. These disturbances are of concern mainly because of the possibility of damage to other units in the bank. If a faulted capacitor unit can be automatically disconnected without damage to the remaining units, then concern is limited to the loss of a unit or the outage of a bank, depending on whether individual fuses are used or bank fuses. If

Figure 6 (right). The probability of capacitor case rupture with consequential damage for various durations of fault current

The dash curve represents a hypothetical probability distribution

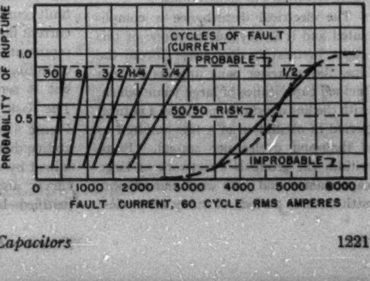

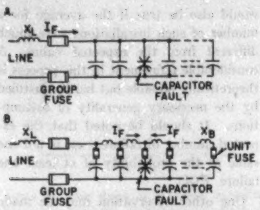

Figure 7. A simplified diagram showing the flow of fusing current to a capacitor fault

A—Capacitor group with main fuses only
B—Capacitor group with individual unit fuses

damage to other units in the group is likely to ensue, then this becomes the contingency of utmost importance.

Organic insulating materials in the presence of an arc decompose into large volumes of gases. In the case of modern capacitors, these gases are noninflammable and nonexplosive and no hazard occurs in this respect. The gases seek to escape the small confines of a compact capacitor unit, however, and if generated in sufficient quantity the pressure eventually forces a rupture of the capacitor case. In most apparatus employing fibrous and liquid dielectrics the proportion of metallic conductor is large compared to dielectric, at least in the neighborhood of the arc, and the conductors often fuse together, extinguishing the arc. The opposite is true in the capacitor, the conductor being light gauge foil finely laminated with the paper insulation in between. The arc, therefore, tends to eat away the conductor and grow larger. A greater production of gas at a faster rate is then to be expected in a capacitor fault. If the fault current is limited to a few hundred amperes, the pressure builds up slowly and many cycles of current flow may be endured before case rupture takes place. When the short circuit current exceeds 5,000 amperes, a violent rupture is generally produced within a half-cycle. Violent rupture results in mechanical damage to adjacent units and often in short-circuited bus connections.

The electrical disturbance is complicated and it is beyond the scope of this paper to treat it rigorously. From the line, the capacitor bank appears to be a lumped capacitance of large value which, with the line constants, produces a natural period of oscillation of a few hundred to a thousand cycles per second. From within, the group is a network of large capacitances and very small inductances with natural periods of many kilocycles. When the fault current is limited to small values, the arc in a short-circuited capacitor sputters along in a more or less continuous manner with small arc drop and no great electrical disturbance. With larger fault currents, which may flow from the line or come from the discharge of the other capacitors into the fault, higher arc voltages develop and the arc tends to be momentarily extinguished, resulting in a series of repetitive discharges. Oscillations at five to ten kilocycles, or even higher, then circulate currents of high magnitude between the fault and the other capacitor units, and this, if long continued, may fuse leads and spark internal connections or produce other incipient damage to the remaining capacitors which culminate in additional failures at some later time. When very large short-circuit currents are available from the line, the development of gas pressure takes place with great rapidity and in proportion to some power of the rise of current. Complete rupture of the capacitor case may then be expected at an instant of high current value, and the reaction of the sudden cessation of current flow may result in voltages severe enough to puncture insulation and flashover insulators and busses. Figure 5 serves to illustrate two of these conditions. Oscillogram *A* shows the moment of interruption of a 250-ampere current which has lasted for over 20 cycles and which ended in temporary clearing without the faulty unit being disconnected. Oscillogram *B* shows a 3,500-ampere current which caused violent rupture within the first half-cycle.

It can be seen from this discussion that for a certain range of fault currents and durations there is a probability or a risk of contingent damage which may be either mechanical or electrical. For conditions on either side of this region, there is either almost no risk in the case of small values or there is almost certain damage in the case of large values. It is of help in the selection of protective means to measure this region of probability in a numerical way insofar as practical. Such is the purpose of Figure 6, which shows the probability of case rupture against fault current for various durations of current flow. It is not presumed that this representation is exact, the difficulties of collecting sufficient data being too great, but it serves for the present analysis. The dash curve at the extreme right of Figure 6 represents a hypothetical probability distribution such as might be obtained by exhaustive testing. The other curves are approximations which seem justified by the available data.

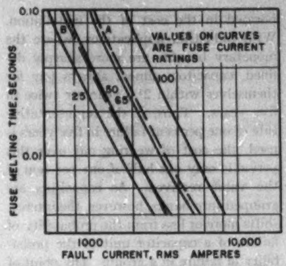

Figure 8. Average melting time—current characteristic curves for a representative type of fuse

Capacitor case rupture characteristics are superimposed, (A) showing probable case rupture and (B) improbable case rupture

The words probable and improbable are indefinite and unsatisfactory in an analysis unless some numerical value is attached. Accordingly, probable is defined as a probability of the order of 0.9 and improbable is a probability of the order of 0.1. These two boundaries are indicated by dash lines on the figure. Several things of importance may be perceived at once from this set of curves. For one, the inadequacy of circuit breaker protection to prevent case rupture is obvious from the low current values which fall within the limits of the 8-cycle distribution. More striking perhaps is the evident impossibility of preventing rupture at moderate short-circuit currents by means of conventional fuse operation. A dependence on 1/2-cycle fuse interruption would be most optimistic.

Figure 6 is deficient in that no graduation in the violence of case rupture is shown. A capacitor case is not a pressure vessel and a slowly accumulating gas pressure forces the seams to give way in a far less violent manner than when the pressure is built up quickly. Also, no measure of electrical damage is indicated by the curves. Actually, neither of these deficiencies imposes much of a handicap in using the curves for estimating the consequences of a short-circuited capacitor because one is generally interested either in the effects of high fault current or else the interrupting time of ordinary fuse protection is fast enough to clear the fault before damage. It is well to assume that arcing to the point of case rupture in the range above 1,500 amperes is productive of both mechanical and electrical damage to an undesirable degree.

The Effectiveness of Fuse Protection

Fuse protection is applied to capacitor installations for the purpose of clearing a fault. The possibility of some harmonic current and the low impedance of the capacitor to transient currents necessitate a liberal margin between the fuse rating and the normal capacitor current, so that close overload protection could not be achieved even though it were necessary. Faults between busses and over insulators are of much the same nature as in any other piece of equipment and may be cleared by circuit breaker or fuses in the conventional manner. The result of a short circuit within a capacitor unit, however, may be additionally guarded against by an individual fuse connected to the unit. The effectiveness of group fuses and of individual fuses for this contingency is now to be examined.

Figure 7 illustrates the flow of fault current to a short-circuited capacitor unit in an elementary manner. Circuit *A* is a capacitor group protected by group fuses. A fault developing in a capacitor unit is followed by the flow of an abnormal current from the line through the group fuse. With reference to the curves of Figure 6, a race takes place between the fuse and the capacitor unit to see if the one melts and interrupts before the other ruptures and causes damage. The odds on this race are portrayed by Figure 8, which shows a set of melting time-current curves for a representative type of power fuse. The capacitor rupture time-current characteristic is superimposed, the dash line *A* being the boundary of probable rupture, that is, the 0.9 probability level, and line *B* the improbable boundary or 0.1 level. The parallelism between fuse melting time and capacitor rupture time is remarkable and it is at once evident that no ordinary fuse of a higher current rating than 50 amperes may be depended upon to clear the fault before case rupture. Moreover, as higher fault currents are considered, a point is reached where the fuse must melt and interrupt within one-half cycle, a dubious situation, and then even the 50-ampere fuse ceases to protect. The conclusion is evident: with fuse ratings exceeding 50 amperes and for fault currents exceeding 3,500 amperes the successful interruption of the fault by group fuses is entirely a matter of chance, with the odds rapidly mounting against success.

Circuit *B* of Figure 7 illustrates the current flow through an individual unit fuse in the event of a unit short circuit. The line current is reinforced by the discharge of the other capacitor units into the fault. In fact, the line fault current is generally of little consequence and the individual fuse performs far beyond its apparent capability. Several things contribute to this effectiveness. For one, the current rating of the individual fuse is small, usually 15 to 25 amperes, the importance of which has been demonstrated by Figure 8. For another, the individual fuse is often blown entirely by the discharge of the other capacitors if the group is large and if the instant of short circuit occurs near the crest of the voltage wave when the capacitors are fully charged, and this is usually the case. With capacitors charged to 2,400 volts root mean square, the discharge current may be expected to attain a value of 10,000 amperes within 1/2,000th of a normal cycle. The greatest contribution to success, however, seems to be the effect of the natural period of oscillation within the group of capacitors which may range from five to 50-kc depending on the size of the group and the unit rating. This, along with the high discharge current, melts the fuse and forces a current zero sufficient to complete interruption before the line current has time to build up to a dangerous value. Thus, the individual fuse performs the apparent impossibility of clearing a fault in times far less than one-half cycle.

The Risk of Operating Capacitors Without Individual Fuses

Individual capacitor unit fuses are undesirable to the extent by which their use may increase installation cost, maintenance or space requirements, and there are many occasions where their need may be legitimately questioned. The curves of Figures 4 and 6 are useful in deciding this point. First, there are several situations that may be disposed of quickly. It should be clear that the magnitude of the available fault current has a large bearing on the probability of case rupture and contingent damage. The fault current may be satisfactorily limited by the circuit, as is sometimes the case with small capacitor installations. The fault current may be limited by the manner of connection, as with ungrounded star connection or where there is resistance in the neutral. Then the fault current through a short-circuited capacitor unit in one phase is limited to the current that may flow through the capacitor units in the other two phases. Large high-voltage installations are conveniently made by using a series of parallel groups of lower voltage rating units, and the fault current through a short-circuited capacitor unit is limited by the other series groups. Here much care must be used in proportioning the series and parallel groups to insure sufficient fault current to give reliable fuse operation.[8] In this case the choice of individual fuses is dictated by other considerations than the possibility of contingent damage.

Many capacitor installations are connected in delta or in star with grounded neutral at points where the fault current is large enough to cause damage. These installations may be large or small, and it is on this basis that a risk may be profitable or unprofitable. It will be presumed that individual unit fuses prac-

Table I. The Probability of Failure Accompanied by Contingent Damage and Group Outage for Capacitors Protected Only by Group Fuses

Based on 25-Kvar Units and a Unit Failure Probability $p = 0.01$ Within an Arbitrary Period of Usefulness

Circuit Voltage	Number of Units in Group	3-Phase Kvar	Fuse Rating, Amperes	P(A)	Capacitor Fault Current, Rms Amperes					
					<3500		≈4500		>5500	
					P(B)	P_A(B)	P(B)	P_A(B)	P(B)	P_A(B)
4,160	3	75	30	0.03	0.1	0.003	0.5	0.015	0.9	0.027
	6	150	50	0.06	0.1	0.006	0.5	0.030	0.9	0.054
	9	225	65	0.09	0.9	0.08	0.9	0.08	0.9	0.08
	12	300	85	0.11	1.0	0.11	1.0	0.11	1.0	0.11
	18	450	125	0.16	1.0	0.16	1.0	0.16	1.0	0.16
	24	600	175	0.21	1.0	0.21	1.0	0.21	1.0	0.21
	48	1,200	300	0.38	1.0	0.38	1.0	0.38	1.0	0.38
13,800	3	75	10	0.03	0.1	0.003	0.5	0.015	0.9	0.027
	6	150	20	0.06	0.1	0.006	0.5	0.030	0.9	0.054
	9	225	25	0.09	0.1	0.009	0.5	0.045	0.9	0.08
	12	300	40	0.11	0.1	0.011	0.5	0.055	0.9	0.10
	18	450	50	0.16	0.1	0.016	0.5	0.08	0.9	0.14
	24	600	60	0.21	0.1	0.021	0.5	0.11	0.9	0.19
	48	1,200	100	0.38	1.0	0.38	1.0	0.38	1.0	0.38

P(A) is the probability of one or more unit failures per group.
P(B) is the probability of contingent damage *if* a unit fails.
$P_A(B)$ is the total probability of damage $= P(A) \cdot P(B)$.

tically always clear a short-circuited capacitor before other damage occurs and this is well justified by experience. Group fuses may or may not be successful and this constitutes part of the gamble. The other element of chance lies, of course, in the probability that a short circuit will take place. Let the event of at least one unit failure in a group of n capacitor units be denoted by A. Also, let the probability of an individual unit failure within X years of service be set at $p = 0.01$, the value of X being appropriate to the service conditions or experience as has been previously outlined. Then the probability $P(A)$ of at least one failure in a group of n units within the X year period is given by Figure 4. Now, if a short circuit does take place, material damage may occur and this is denoted by event B.

The probability $P(B)$, once a short circuit exists, may be estimated from Figure 6, taking into account the fuse characteristics. For practical purposes it seems well to say that damage is either probable, $P(B) = 0.9$, or improbable for which $P(B) = 0.1$. The total probability of damage is then conditional upon a short circuit happening in the first place, or

$$P_A(B) = P(A) \cdot P(B)$$

The total probability of damage has been calculated for some examples where the capacitors are protected only by group fuses. These examples are listed in Table I. With groups of capacitors, such as three or six units, the probability $P(A)$ of failure of at least one of the units in the group is small. If the available fault current is less than 3,500 amperes, the probability $P(B)$ of damage before fault interruption is estimated from Figures 6 and 8 to be 0.1, since the fuse rating can be 50 amperes or less. The total probability $P_A(B)$ being the product of $P(A)$ and $P(B)$, the risk of damage is very slight. If the fault current is approximately 4,500 amperes, Figure 6 shows the chance of damage to be about 50/50 if a short circuit occurs, because one must count on very quick interruption to avoid damage. Here again the total probability is small. For fault currents exceeding 5,500 amperes, the 50 ampere fuse may occasionally interrupt successfully if it melts fast enough, and a value of 0.9 is indicated for $P(B)$. Even in this case, however, the risk of damage may be reasonably incurred because the probability of a faulty capacitor is small and the corresponding product $P(A) \cdot P(B)$ does not have a very great value.

For groups of capacitors of intermediate size, such as for example 12 or 18 25-kilovar units, a fuse of the necessary current rating may not be capable of melting fast enough and so there is little chance of interruption before case rupture and damage occurs. Such is the case for the 4,160-volt groups and thus a probability of 1.0 is assigned to $P(B)$ even for fault currents less than 3,500 amperes. Now the total probability is identical with the probability of a short circuit in the group of units, and this may or may not be a reasonable risk depending on the economic factors affecting the particular instance. In the case of still larger installations, illustrated by the 48-unit group, $P(A)$ takes on such values as have been shown by Figure 4, and with $P(B)$ fixed at 1.0 because damage is almost certain if a short circuit occurs, the risk becomes a matter no longer to be decided by economic considerations. Large groups require individual fuse protection for satisfactory performance.

The absolute values of probabilities arrived at in this manner naturally should not be taken too seriously, although they can be as good as the data on which they are based. The real advantage is that the numerical values carry a significance that cannot be attached to a verbal description or arrived at by a mental weighing. In addition, the important factors, and the trend of their influence, can be clearly demonstrated.

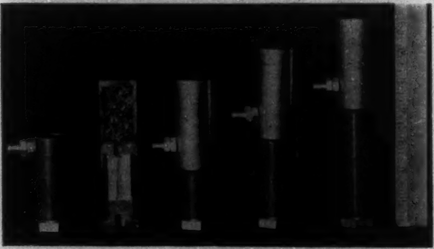

Figure 9. Some individual fuses for indoor use

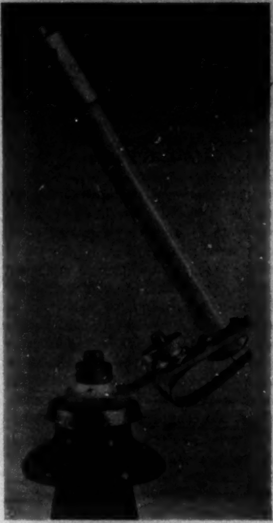

Figure 10. An expulsion-type outdoor individual fuse

Conclusions

The important place that power capacitors have attained in the economics of power distribution demands a better understanding of the problem of fault protection, and this is of increasing importance as the trend grows toward larger installations of capacitors. Capacitors are a reliable component and the fact that they are inexpensive enough to be expendable in many instances does not alter the inherent reliability that is possible when the individuality is properly maintained in large groups by the means of individual fuses.

The economic evaluation of different methods of protection requires a statistical treatment as well as a consideration of what is to be accomplished by the protection. The requirements of fuse protection have been outlined only briefly, but it should be evident that success hinges on the ability of the fuse to disconnect a faulty capacitor unit before rupture or electrical damage can take place. This is practically assured with individual fuses but is dictated by chance when group fuses alone are used if the fuse rating exceeds 50 amperes or if the fault current exceeds some 3,000 amperes. It has been shown that with small banks of 3 to 12 units this risk may be profitable depending on particular considerations, but that with large groups of capacitors the omission of individual fuses can be none other than costly if large fault currents can flow into the capacitor unit. A method has been outlined by which such risks may be evaluated.

The development of special purpose capacitor fuses has progressed along with capacitor unit development, and proven designs are available which meet the requirements of inexpensiveness and convenience. Figure 9 shows one such fuse intended for indoor use, the fuse being screwed directly on a terminal stud of the capacitor unit. A fuse suitable for outdoor use is shown in Figure 10 and also this may be mounted directly on the capacitor terminal or on the bus. The means of successfully disconnecting a short-circuited capacitor unit is therefore available and, by methods demonstrated in this paper, the conditions demanding individual fuses can be determined in a logical manner.

References

1. Shunt Capacitors, AIEE Committee Report. *Electrical Engineering* (*AIEE Transactions*), volume 62, May 1943, pages 222–30.

2. The Why of a 25-Kvar Capacitor, M. E. Scoville. *General Electric Review* (Schenectady, N. Y.) volume 52, May 1949, page 19.

3. Report of a Survey on the Performance of Shunt Capacitors, AIEE Committee Report. *AIEE Transactions*, volume 68, part II, 1949, pages 1200–07.

4. Poisson's Exponential Binomial Limit (book), E. C. Molina. D. Van Nostrand Company, Inc., New York, N. Y., 1947.

5. Power Capacitors (book), R. E. Marbury. McGraw-Hill Book Company, Inc., New York, N. Y., 1949, page 113.

Discussion

Glenn W. Bills (Bonneville Power Administration, Portland, Oreg.): The author has clearly presented the protection problem facing power system engineers who are responsible for the installation of capacitors. Since power-factor correction by use of shunt capacitors is now commonplace because of overloaded system conditions, a solution such as outlined is particularly invaluable at this time.

In the Bonneville Power Administration system, over 300,000 reactive kilovolt amperes of shunt capacitors are installed, and many more are scheduled for installation, including 115-kv groups as well as 230-kv series capacitors. Initial experience over a period of seven years indicated that fuse failures occurred, although very few capacitors failed and then mostly due to the failure of fuses to open. It was felt that the individual fuses were more of a hazard to normal system operation than were capacitor failures. However, our capacitors are installed in banks as large as 60,000 reactive kilovolt amperes, and the large short circuits which could occur required individual fuses for capacitors. Since newer, more appropriate fuses have been developed, our natural desire to avoid or to minimize their use is less pronounced.

Not only has the author given a lucid physical picture of the action that occurs when a capacitor unit fails, but he has provided a method of determining when to use individual capacitor fuses. It is pleasing to note that probability theory has been used to achieve numerical results rather than use of some "rule of thumb" method which may not produce the most economic solution. The majority of engineers shy from the use of probability mathematics, and papers such as this have the merit of bringing to their attention the ease with which fairly complex problems can be solved with the aid of simple probability methods.

Connection Arrangements and Protective Practices for Shunt Capacitor Banks

N. R. CLARK
ASSOCIATE AIEE

S. B. FARNHAM
MEMBER AIEE

THE FACT that capacitors are commonly built in units of 25 or 15 kilovars for power circuits makes possible a wide variety of groupings of these convenient "building blocks" to form large banks. The particular arrangement in which the individual capacitor units are connected in a 3-phase bank, and the type of protective arrangement used, may influence the cost of the installation and these factors certainly will have an important bearing on its operation and on the operation of its associated protective devices under fault conditions. Since a number of different connection and protective arrangements are possible, all resulting in banks having substantially the same kilovar and voltage ratings, it is in order to review briefly the commonly used arrangements and to outline their salient characteristics.

This paper is intended as an indorsement of, and a supplement to, certain sections of the AIEE Committee Report on the Operation and Maintenance of Shunt Capacitors,[1] herein referred to as the AIEE report.

Connection Arrangements

Consider first the simple delta and Y connections with all units in each phase connected in parallel. Here the voltage rating of each individual capacitor unit is equal to the system line-to-line voltage for the delta connection, or to the system line-to-neutral voltage for the Y connection. For systems in the 11—13.8-kv class the Y connection is generally used, since it takes advantage of the economical capacitor designs up to approximately 8 kv. For systems in the 2.4—7.2-kv group, however, either the delta or the Y connection may be employed at substantially equal cost. Here the gradual changeover of many 2.4-kv systems to 4.16-kv operation has resulted in the general acceptance of 2.4-kv capacitor units for both systems. Similarly, 7.2-kv capacitor units are often used on both the 7.2 and 12.5-kv systems. This practice offers obvious advantages with respect to standardization and stocking.

Capacitor banks for use on systems 23 kv and higher are almost invariably composed of two or more groups of parallel-connected capacitor units in series per phase.

The choice between delta and Y connection is generally determined by whichever arrangement will permit the fuller utilization of standard voltage rated capacitors. It frequently happens that the user has a preference for capacitor units of some particular voltage rating, especially if units of that same rating are already being used on his lower voltage distribution circuits. On the other hand, since the kilovars delivered by capacitors are proportional to the square of the applied voltage, there is a disproportionate reduction in the realizable kilovar capacity if capacitors are not operated at their full voltage rating. Hence, it may be advantageous in some cases to resort to special voltage rated capacitors, which will be more expensive per kilovar of rating, but which can be fully utilized. A practical expedient may be to use capacitor units of two different voltage ratings in different series groups of the same phase. Here the majority of the units can be of the desired standard rating, while the remainder may be either of a different standard rating or special. This is an entirely acceptable procedure so long as the ratios of the rated kilovars of the series groups are the same as the ratios of the rated voltages of the parallel-connected capacitor units in the series groups. For example, if a phase includes a series group of 2,400-volt units and a series group of 4,800-volt units, the 4,800-volt group should consist of twice the kilovars of the 2,400-volt group.

When the Y connection is selected, the question often arises as to whether the neutral should be grounded, or insulated and allowed to "float". Normally, only the floating neutral arrangement is employed on ungrounded neutral systems, or those protected by ground fault neutralizers. On grounded systems, either arrangement may be used. The floating neutral, however, does afford certain advantages to the capacitor equipment, including its protective devices, and generally is preferred as the standard arrangement. The advantages of the floating neutral are:

1. The capacitors are not subjected to the abnormal line-to-ground voltage stresses which may appear on the system as a result of lightning, switching transients, ground faults, or phase voltage unbalance.
2. For banks installed on ungrounded systems, the rack upon which the capacitors are mounted may conveniently and economically be insulated from ground, and allowed to float at a potential above ground. With such an arrangement, the terminal-to-case insulation provided in the individual units need correspond only to the voltage across the unit rather than the line-to-line voltage, and usually results in a saving in cost of the banks, particularly if the circuit voltage is 12 kv or higher.
3. When fuses are used for protection, the floating neutral arrangement limits the interrupting duty and makes it independent of the system short-circuit capacity, as will be explained later. This allows the use of economical fuse rating.
4. The floating neutral arrangement permits the use of "balanced" relay protection. This is covered more fully in a later section.

Paper 49-254, recommended by the AIEE Transmission and Distribution Committee and approved by the AIEE Technical Program Committee for presentation at the AIEE Fall General Meeting, Cincinnati, Ohio, October 17–21, 1949. Manuscript submitted July 21, 1949; made available for printing September 6, 1949.

N. R. CLARK is with the General Electric Company, Pittsfield, Mass., and S. B. FARNHAM is with the General Electric Company, Schenectady, N. Y.

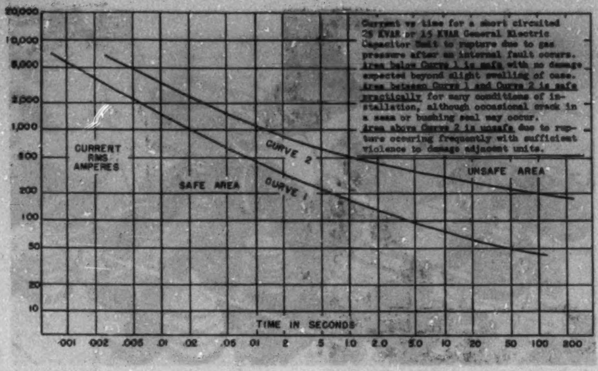

Figure 1. Current versus time for short-circuited capacitor units

Functions Desired of the Protective System

In order to secure maximum benefits, shunt capacitor banks used for kilovar supply are usually located on the distribution circuits, as near the load as practicable. As indicated previously, they may also be installed on subtransmission circuits above 15 kv if the particular case so dictates. Wherever located, they require adequate protection, in common with other system equipment, to provide the highest practicable degree of continuity of service to the users of electric power. Protective requirements for shunt capacitor banks differ from those for series-connected equipment such as transformers, in that for most installations it is possible for the power circuit to remain in operation with part or all of a capacitor bank out of service. Hence, in the event of capacitor failure, it is desirable to isolate the failure from the power system and minimize damage, without interruption in service.

Basically, protection is provided for the circuit, and not the capacitor. When an internal short circuit occurs in a capacitor unit, the arcing generates gases which can ultimately rupture the case, and danger to life and equipment is possible. A capacitor unit has a current-time characteristic similar to that of a fuse link; it should be disconnected from the circuit before sufficient energy has been delivered to the capacitor under short-circuit conditions to cause its case to rupture.

More than 100 tests have been made to establish the time-current characteristics of the modern capacitor manufactured by the company with which the authors are associated. Empirical curves plotted from the test data to show practical limits are shown in Figure 1. The test units were intentionally short circuited in all internal series sections by driving nails through the case and into the rolls, removing the nails, and soldering the holes in the case. The test capacitors were connected in series with suitable fuses, and short-circuit currents of various magnitudes were applied for various times under controlled conditions. Oscillograms were taken to record the voltage, current, and time. Figures 2 and 3 are a few of the capacitors used in these tests; they are typical of the test results from which the curve in Figure 1 was prepared.

For example, the first unit on the left, see Figure 2, received 400 amperes rms for 12 seconds, which is in the unsafe area above the upper curve, Figure 1.

The fifth unit from the left, Figure 2, received 3,700 amperes peak for 0.0083 second. This corresponds to approximately 2,600 amperes rms, and falls in the area between the two curves in Figure 1. The first unit on the left, Figure 3, received 600 amperes rms for 1/2 second, which is approximately on the upper curve, Figure 1. Figure 4 shows the damage which occurred when a capacitor unit failed in a 4,275-kilovar 2,400-volt 3-phase outdoor installation for which proper protection had not been provided. This represents a point in the high current area above the upper curve, Figure 1.

It is not intended to present the curves in Figure 1 as absolutely accurate for all types of installations for all fault conditions. They do, however, represent the pattern which resulted from the large number of tests made, and may be used as a guide in the selection of protective arrangements.

Listed here are a number of functions a capacitor protective arrangement may perform, all of which are generally desirable, and any of which may be considered mandatory by the particular system operator.

1. **Protection against rupture of container.**
2. **Avoidance of system outage.**
3. **Indication of failure location.**
4. **Prevention of overvoltage.**
5. **Immunity to false operation.**
6. **Avoidance of overtemperature operation.**
7. **Limitation of kilovar loss to minimum.**

How the Desired Functions Are Provided

The protective functions required for an individual capacitor bank are dependent upon operating conditions; and the selection of means to perform these functions is determined by economics and the policy of the operating company. No single protective device will perform all the functions listed, and ordinarily two or more devices are combined to attain the desired degree of protection. On the other hand, it generally is not necessary to provide an arrangement for any particular bank which will perform all the possible protective functions. The importance of a particular function will vary with the conditions of capacitor operation and the purpose the installation is intended to serve in the operation of the system.

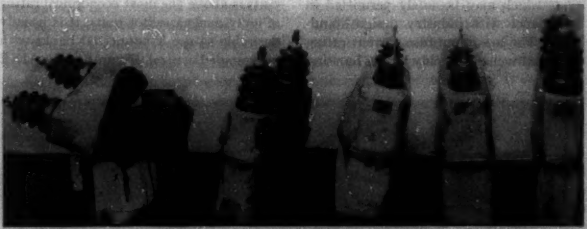

Figure 2. General Electric Pyranol capacitors shown after short-circuit tests

Fuses

In the early days of capacitor application as far back as 1910, capacitor fusing was recommended. Experience today with greatly improved fuses substantiates this early recommendation. Fusing provides the maximum number of desirable features and has been used most extensively for capacitor application. It is generally recommended as the best and most economical means of accomplishing the desired results for most installations.

INDIVIDUAL FUSES

For indoor installations and for housed outdoor installations, indoor-type current-limiting fuses of the indicating type are ordinarily used. Figure 5 shows a typical arrangement of this type. For outdoor installations without protection from the weather, expulsion-type outdoor fuses, as shown in Figure 6, are available.

The voltage rating of an individual fuse should be not less than the rated voltage of the capacitor unit with which it is used, and its maximum current-interrupting capacity should be not less than the current which will flow in the event the capacitor unit is short circuited.

Standard capacitors are designed with a zero to +15 per cent tolerance in microfarads, and must be capable of carrying 135 per cent of rated reactive kilovolt-amperes continuously. They are further required to withstand a maximum of 110 per cent of rated voltage, and 105 per cent of rated voltage average over a 24-hour period. Combining all these factors, it will be seen that a rms current of some value above 110 per cent of nominal can flow continuously in the capacitor. Therefore, as a general practice, fuses which have a 300-second melting time of the order of 5 to 10 times the rated capacitor current should be used. The purpose is to avoid unnecessary fuse blowing caused by the previously mentioned factors, by short time disturbances which do not adversely affect the operation of the capacitor bank, or by harmonic currents which may be safely permitted in accordance with industry design standards. The maximum fuse current rating is limited technically only by the bursting characteristics of the capacitor itself, although for economic reasons the upper limit is usually selected in the neighborhood of 250 per cent of nominal capacitor current.

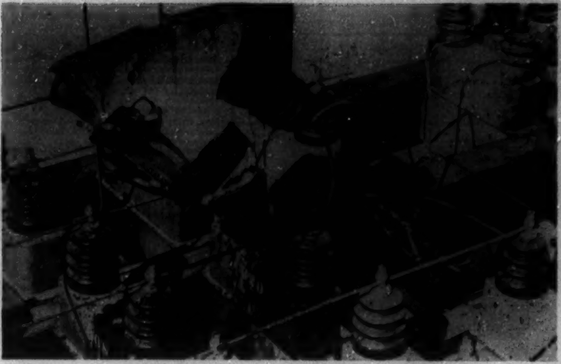

Figure 4. Damage resulting from improper protection

Since a dielectric failure in a capacitor unit does not always result in a low impedance fault, the current which will flow may vary from the full short-circuit current available down to a value which may approximate the 5-minute melting current of the fuse. Thus, individual fuses which will operate satisfactorily at the minimum as well as the maximum current should be selected.

Fuses of appropriate voltage ratings and time-current characteristics are available to meet the requirements of most circuits for delta-connected capacitor banks as shown in Figure 5 of the AIEE report, or similar banks Y-connected with grounded neutral.

Fuses so applied to delta-connected banks must be capable of interrupting system line-to-line fault currents; fuses for grounded Y-connected capacitors must be suitable for handling the system line-to-ground short-circuit currents. Where exceptionally high interrupting capacity requirements are encountered, or where line-to-line voltage of the circuits is above the most economical rating of individual capacitor units, it is usually desirable to use Y-connected banks with ungrounded neutral (Figure 6 of the AIEE report), thus limiting the fault current in case of a unit failure, and consequently duty on the fuse, by virtue of the impedance of the capacitors in the two unfaulted phases. It can be shown readily that the fault current is thus limited to a maximum of three times the continuous current which flowed in the faulted phase before the fault occurred. For line-to-line voltages above 13,800 volts, a delta-connected bank consisting of two or more series groups per phase (see Figure 7 of the AIEE report), or similar Y-connected bank, is appropriate. In either case, the fault current is limited by the impedance of the capacitors in series, which will withstand the momentary overvoltage resulting from a unit failure until the fault is cleared.

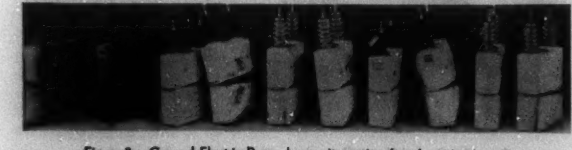

Figure 3. General Electric Pyranol capacitor units after short-circuit tests

GROUP FUSES

Group fusing of capacitor banks may be considered as a special case of individual fusing, and in general the same advantages and limitations apply. Connections for group fusing of a complete bank are shown in Figures 9 and 10 of the AIEE report. These are the arrangements used extensively in small banks on distribution feeders, where fuse cutouts may be used both as a means of protection and for switching. For larger banks, groups of two or more capacitor units with a single fuse may be connected in parallel or in series-parallel combinations.

Fusing of groups of units involves the use of fuses with relatively high continuous current ratings, which necessarily allow more energy to flow into a fault before interruption occurs than would be the case with individual fuses. Thus, in order to prevent rupture of the container of a

Table I

Number of Parallel Groups in Series	Minimum Number of Units Per Group for Capacitor Bank-connected: Ungrounded Y	Delta or Grounded Y
1	4	1
2	8	6
3	9	8
4	9	9
5, 6	10	9
7, 8	10	10
9 through 16	11	11

failed capacitor, group fuses should have a characteristic which falls below the time-current characteristics indicated in Figure 1.

LIMITATIONS

Although individual or group fuses perform the majority of the functions desired of a protective system in the usual case, they have limitations of which the operator should be aware, and which may be important in specific installations.

Individual unit fuses will not, of course, give protection in case of a line-to-ground or a line-to-line fault in the bus or connections external to the capacitor units, and current transformers arranged to trip a circuit breaker and disconnect the bank are desirable to provide protection for this condition. Group fuses provide protection against such faults only when one fuse is used in each line for the entire bank.

For the Y-ungrounded-neutral connection, and for either delta or Y connection when two or more series groups are used in each phase, the following considerations apply:

1. The number of capacitor units, or groups of units connected to a single fuse, in parallel contribute to the fault current which will flow through a fuse connected to a short-circuited unit, and this number should be sufficient to provide enough fault current to cause the fuse to clear in time to prevent rupture of the capacitor container.

2. The number of capacitor units, or groups of units connected to a single fuse, in parallel affects the distribution of voltage among the remaining units after one or more fuses have blown. The minimum number of units or groups which should be connected in parallel is determined by the permissible overvoltage operating limits of capacitors.

Table I indicates the minimum number of units which should be connected in parallel to insure sufficient current for proper fuse blowing in the event of a fault, and to maintain overvoltage on the remaining units within 110 per cent of the voltage prior to the fault. Where group fusing is used, a group with a single fuse should be considered as a single unit for purposes of applying the table.

Although capacitors are guaranteed for a maximum average of 105 per cent of rated voltage over a 24-hour period, the short time maximum allowable voltage of 110 per cent of rating was selected in making up the table, since it was assumed that the blown fuse would be located, its cause corrected, and the fuse replaced promptly.

Relays

Overcurrent or overvoltage relays used in conjunction with suitable instrument transformers to detect a fault and trip a circuit breaker may be used either alone or as a supplement to fuses. This means of protection cannot, as a general rule, be arranged to indicate the defective unit when failure occurs, and therefore usually is employed as a supplementary measure.

Overcurrent relays connected in the secondary circuit of current transformers in the capacitor line connections may be used to provide minimum protection, but are generally used to supplement fuses. Since the minimum time required for disconnecting a capacitor bank from the line with a circuit breaker and relays is of the order of 1/10 second or more, considerable damage may occur if fault currents exceed a few hundred amperes.

Except for limited bank sizes connected Y-ungrounded-neutral, or banks connected either Y or delta with two or more series groups per phase, wherein the current is limited, this method does not prevent rupture of a container, because of the inherent time required for circuit breaker operation.

Because of the considerable magnitude of the transient charging current which flows when a capacitor bank is energized, the use of instantaneous relays connected to line current transformers may under certain conditions result in immediate tripping of the circuit breaker when it is closed to energize the bank. The magnitude and frequency of the transient charging current is determined by the circuit voltage, the size of the bank, and the inductance of the circuit between the capacitor bank and the source. When a bank is energized adjacent to a second bank which is already energized, the second bank will discharge into the first, increasing the possibility of operating instantaneous relays. Time delay current relays which will "ride-out" the transient inrush, used in conjunction with fuses, provide a satisfactory arrangement for such a situation.

Figure 5. Housed outdoor capacitor bank with individual current-limiting fuses

A relay connected in the secondary of a transformer between capacitor bank neutral and ground is sometimes used as shown in Figure 13 of the AIEE report. Failure of a capacitor unit destroys the symmetry of the arrangement, and results in a neutral-to-ground voltage if a potential transformer is used, or the flow of current from neutral to ground if a current transformer is used. The relay is of the voltage type or current type, as appropriate to the transformer employed. Ordinarily the relay is of the time delay type, since an instantaneous relay may be susceptible to false operation on system line-to-ground faults external to the capacitor bank. Because of its relatively slow speed of operation, due to the necessity of using time delay relays co-ordinated with other system relays, and to the inherent time required for circuit breaker operation, this arrangement does not usually afford protection against capacitor case rupture. It is ordinarily used only as a supplement to fuses, and is normally employed only on grounded systems.

It is sometimes desirable to connect a capacitor bank in double-Y with neutrals of the two parts of the bank ungrounded but connected together through a transformer, with a relay in the transformer secondary to trip a circuit breaker and de-energize the bank in the event of failure of a capacitor unit (Figure 12 of the AIEE report). This arrangement operates on the unbalance between the neutral points of the two Y sections which results in a flow of current if a current transformer is used, and a voltage differential if a potential transformer is used. For large banks which have all capacitor units in each leg connected in parallel, it is not possible to obtain breaker operation in time to prevent case rupture even with an instantaneous re-

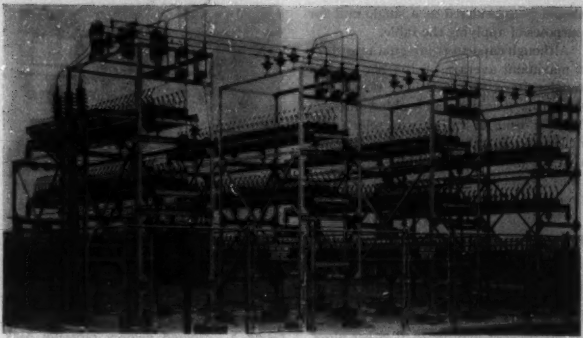

Figure 6. Outdoor open capacitor bank with individual expulsion-type fuses

lay, and in such cases this type of protection is sometimes used as a supplement to fuses. Since this arrangement does not protect against a line-to-line or a line-to-ground fault, line current transformers are also ordinarily used.

A differential current protective arrangement which may be used is that shown in Figure 14 of the AIEE report. Each phase is divided into two sections, and current transformers are differentially connected in each section so that under balanced conditions no current flows in the relay coil. When a unit failure occurs, the resulting current unbalance flows through the relay coil, picking up the relay and tripping the circuit breaker. This arrangement offers no appreciable advantage over that described in the previous paragraph, and since it is usually more expensive it is little used.

Still another transformer and relay protective arrangement uses voltage unbalance between phases as the operating signal; a sketch is included as Figure 11 of the AIEE report. The primary winding of a potential transformer is connected in parallel with the capacitors in each phase of the bank, and the secondary windings are connected in broken delta, with a voltage relay connected across the break in the delta. Failure of a capacitor unit results in a voltage unbalance across the relay coil, causing the relay to operate and trip the circuit breaker. In common with other relay-transformer arrangements, this means of protection requires de-energizing the entire bank when a single unit fails. Often, tripping of the circuit breaker cannot be attained prior to container rupture, and fuses are required if such protection is desired. However, this arrangement will trip the circuit breaker if a line-to-line fault occurs in the capacitor bank, and also in the event of a line-to-ground fault if the system neutral is grounded.

Thermal relays are occasionally used, as a supplement to other types of protective arrangements, to detect abnormal operating temperatures and initiate corrective action before damage is done. Thermal relays are used extensively to control operation of forced cooling equipment, such as fans, permitting intermittent operation only as required to meet operating conditions.

Lightning Protection

In common with other apparatus connected to a power system, capacitors should be protected by lightning arresters. Here the primary function is protection of the capacitor bank, and not the system itself. The choice between lightning arresters rated for grounded neutral service or ungrounded neutral service should be in accordance with established industry practices. The rating of the lightning arrester (line-to-ground) is determined by the system grounding, and is not related to the grounding, or lack thereof, of the capacitors themselves.

Occasionally the suggestion is made that lightning arresters are unnecessary for capacitor banks which are Y-connected with grounded neutral. It is true that capacitors so connected do have some ability both to slope off the steep front of an incoming wave and to reduce its crest value. However, this ability is limited by the size of the capacitor bank, while the amount of energy to be expected in a given surge or lightning stroke is indeterminate. Hence, granting that the grounded capacitor tends to help protect itself, this ordinarily should only be regarded as a fortuitous circumstance, and not as a justification for omitting the lightning arresters. Also, there are generally switches or circuit breakers associated with the capacitor installation which require lightning arresters. Their need for protection is greatest when in the open position, with the capacitor bank de-energized. Hence, the lightning arresters should be connected on the line side of any circuit-interrupting or isolating devices at the capacitor installation.

A related voltage-stress problem is whether or not the capacitor cases should be grounded. This decision is usually based on the operator's safety practices. Some operating groups require that the frameworks, tanks, and cases of all apparatus be grounded for safety, while others require that they be ungrounded for the same reason. Let it suffice, therefore, to point out that if the capacitor case is grounded, the full voltage-to-ground appears across one bushing in parallel with the terminal-to-case insulation inside the capacitor. If the case is not grounded, the voltage-to-ground will divide across the bushing, the internal insulation, and the insulation of the supports. Obviously this division in any given bank will depend on the size and connection arrangement of the bank and on the details of its supporting structure.

Conclusions

1. Capacitor units in standard voltage and kilovar ratings may be used as convenient "building blocks" to make up practically any size bank desired, for practically any circuit voltage.

2. Like other system equipment, capacitor banks require adequate protection in order to maintain a high degree of continuity of service to power purchasers.

3. There are several protective functions to be performed, and a variety of protective arrangements to perform the desired functions.

4. Engineering data obtained from tests and presented in this paper permit correlation of the time-current characteristics of the protective arrangement with the time-current characteristics of the individual capacitor unit under fault conditions.

5. For specific cases, it may be desirable to supplement fuses, or to use an alternative arrangement, at the discretion of the operator or the manufacturer; however, fuses are the most common, and the generally recommended means for obtaining system protection against capacitor unit failure.

Reference

1. REPORT ON THE OPERATION AND MAINTENANCE OF SHUNT CAPACITORS, AIEE Committee Report. *AIEE Transactions*, volume 68, part II, 1949, pages 1208–19.

Discussion

A. E. Peltosalo (General Electric Company, Pittsfield, Mass.): The authors have presented an excellent paper outlining the parameters involved in protective practices and connection arrangements for shunt capacitor banks. The time-current characteristic curves contained in Figure 1 of the paper are worthy of close scrutiny.

The safe limits of capacitor behavior under fault conditions are subject to many different interpretations. A capacitor failure which results in even a small crack in the container, but allows leakage of the dielectric liquid may be intolerable, as in locations where the general public has access to the area below the capacitor installation. However, in many locations, such as a substation, temporary dripping of liquid may not be regarded as very serious. Similar considerations must be given to the degrees of damage which may result from rupture of the capacitor container. The authors' paper has shown that, if sufficient energy is put into the unit, the container may rupture with sufficient violence to damage adjacent units and to endanger any personnel in the immediate vicinity. There are, however, many locations where the rupture of a container might not be objectionable, for example, a capacitor bank completely enclosed by a wire fence in an isolated location.

To assist system operators in the fusing of capacitor units, the curves of Figure 1 include both a safe and unsafe area with a band between. Experience has shown that this intermediate band is usually safe for most conditions of installation, although an occasional crack in a seam or bushing may occur. These curves might well be called damage curves, because by means of these curves the operator is able to predict the damage resulting from particular values of fault current and time.

It is the usual practice to group-fuse pole-type unit installations (approximately 60 per cent of all power factor capacitors are installed in this manner). If, for instance, it is acceptable to fuse up to curve 2, rather than curve 1, the cost per kilovar of the larger capacitor bank (made necessary by this arrangement) may be smaller. This is due, of course, to the allocation of the installation cost (line crew's time, lightning arresters, hangers, and cutouts) to the larger bank. For these installations it now is common practice to use fuse links which have a total clearing time-current characteristic below curve 2 (it may or may not be below curve 1). For example, a plot of the time-current characteristics of General Electric universal fast-blowing cable-type fuse links will show it possible to use fuse ratings up to and including a 75-ampere size and still remain below curve 2. These time-current characteristics will fall below curve 2 and provide satisfactory protection in most cases. A similar comparison can be shown for the fuse links of any manufacturer, as long as the total clearing time-versus-current characteristic is known. By means of this type of comparison the operator is able to predict the possible damage resulting from a capacitor failure and can therefore set the limits of fuse sizes for any particular application. Occasionally operators have used fuses with characteristics above curve 2. Experience has shown that some damage to adjacent units may result from this manner of fusing. Some operators have even made a practice of omitting fuses entirely, since the chance of capacitor failure is quite small, and since the damage resulting from failure would not be seriously objectionable. Thus, there are wide variations in fusing practice, reflecting different evaluations of the possible degree of damage by different operators.

To obtain the minimum cost of installation consistent with safety it is well for eacy capacitor user to verify the amount of damage tolerable in case of a capacitor failure in any particular location. To this end the curves of Figure 1 should prove very useful.

Harry P. St. Clair (American Gas and Electric Service Corporation, New York, N. Y.): In connection with this paper on connection arrangements for shunt capacitors, it may be of interest to describe briefly the recent program carried out on the American Gas and Electric Company system in the application of high-voltage capacitors. Following an investigation which disclosed the favorable economics of high-voltage shunt capacitor banks in fairly large sizes, several installations were undertaken at 44 kv, followed by several more at 33 kv and one at 22 kv. A partial list of these installations already in service or authorized is shown on Table I of the discussion.

Table I

Location	Capacity, Kva	Voltage, Kv	Control
Logan	10,000	44	Manual
Sprigg	10,000	44	Time Clock
Allen	6,600	44	
Mike Grady	6,600	44	
Scarbro	13,200	44	
Bellefonte	12,000	33	
Fremont	6,000	33	
Fieldale	6,000	33	
Kenton	3,300	22	

In all of these installations the entire capacitor block is controlled by a single switch, and the voltage boost produced by the capacitor varies from three or four volts to six or seven volts. With a voltage change of this magnitude automatic control by voltage relay is not considered feasible and time clock control, arranged to switch the capacitor on over the normal load period of the day, is used instead. It is considered that a large voltage change occurring only twice a day, once in the morning and once in the evening, will not be as objectionable as more frequent voltage changes, even of smaller magnitudes. For the most part, the 44-kv capacitor installations are in coal mining territory where close voltage regulation is not as critical as in urban areas.

In several instances, these large high-voltage capacitor installations have been applied at locations where a synchronous condenser or even generators are available for voltage regulation so that the capacitors provide a supplemental boost, leaving the job of fine regulation to the condenser. This has worked out very well, and it is expected that the practice will be followed even more extensively in the future.

The problem of switching at first appeared to limit the size of a single 44-kv step to about 10,000 kva, but further tests carried out by the switch manufacturers showed that a much larger block, up to 30,000 kva, could be handled by one switch. It also now appears that large capacitor blocks can be installed and operated at 69 kv at about the same unit cost as those already installed at 44 kv. The switching problem up to blocks of 30,000 kva appears to offer no difficulty and it is expected that fairly early use of this technique will be made.

In one case, which may be of interest, a large saving was realized by installing a 20,000-kva 11-kv capacitor bank on the tertiary winding of a 37,500-kva transformer bank, originally designed to accommodate a 20,000-kva synchronous condenser. With a 15,000-kva condenser already in operation at this station, the control problem offered no difficulty and the capacitors provided the needed additional correction.

N. R. Clark and S. B. Farnham: Mr. Peltosalo's discussion is a welcome amplification of the considerations which apply in using the time-current characteristic curves included in Figure 1 of the paper.

The use of capacitors in comparatively large banks on circuits above 15 kv, as mentioned by Mr. St. Clair in his discussion, is an application which is gaining increasing acceptance. While one of the basic principles of capacitor application is that they be located as near the load as possible, it is sometimes desirable to locate banks to supply bulk kilovars on the subtransmission system. This has been done in many cases by connecting the capacitor bank to the low-voltage tertiary winding of an existing transformer. When such a connection is not possible, it is quite feasible in many cases to take advantage of the flexibility of capacitors and utilize a high-voltage bank connected, with a suitable switching means, directly to the power line.

Design of Mobile Radio Communication Equipment for Land-Mobile Services Operating on Frequencies Between 152–174 Megacycles

R. A. BEERS
NONMEMBER AIEE

W. A. HARRIS
NONMEMBER AIEE

A. D. ZAPPACOSTA
NONMEMBER AIEE

Synopsis: The rapid growth of the relatively new 152–174 megacycle mobile communications band and the resultant problems are discussed briefly. Equipment has been designed to double the number of usable channels in the same locality for most applications. A description of the equipment and its performance is presented.

SINCE the opening of the 152–162 megacycle band on an experimental basis to the land-mobile services in 1945, its utilization has been so rapid that available channels for assignment to certain types of services have about reached the exhaustion point in many localities. This band was set up on the basis of 60-kc channels and a block of continuous channels was designated for each type of service. Actual assignments have been on an alternate channel basis in the same locality.

With alternate channel operation in the same locality, it was not long until considerable interference between stations was encountered. Some of this interference was caused by insufficient alternate channel selectivity in the intermediate frequency portion of the receiver. In other instances where the intermediate frequency selectivity was adequate, the receiver front end selectivity was insufficient and the receiver became desensitized by a strong alternate channel signal and hence could not receive the desired signal.

In areas where three or more alternate channel services were simultaneously in operation, a type of interference was encountered which was not anticipated. The alternate and next alternate channel signals mixed in the receiver front end, and produced a third signal whose frequency was exactly the same as that to which the receiver was tuned.

Example:

Desired signal frequency = 152.00 megacycles
First alternate signal frequency = 152.120 megacycles
Second alternate signal frequency = 152.240 megacycles

$$\begin{array}{rl} 2\times 152.120 = & 304.240 \\ & 152.240 \\ \hline & 152.000 \text{ megacycles the desired frequency} \end{array}$$

The same condition also exists if the two unwanted signals are 120 and 240 kc respectively, below the desired signal frequency.

Mathematical exploration showed that this condition, which now is generally called intermodulation interference, existed because of third-order plate characteristic curvature of the receiver radio-frequency amplifier tubes and fourth-order plate characteristic curvature of the mixer tube, and laboratory work pointed to the fact that the mixer tube was the worst offender. It was found that two transmitters located closely together and separated by 120 kc in frequency also would produce and reradiate off-frequency signals, both above and below their actual frequency, whose frequency would be their carrier frequency plus or minus the frequency difference between the two transmitters. Transmitter intermodulation usually is much less serious than receiver intermodulation, unless the two transmitter antennae are located very closely together.

As the use of the service grew beyond expectations, it was soon apparent that more channels would become a necessity, particularly in the metropolitan areas. Adjacent channel operation in the same locality would double the number of channels, but was considered impractical by many for one or more of the following reasons:

1. Difficulty of obtaining the required selectivity and over-all stability.
2. Transmitter modulation products and spurious radiations must be materially reduced.
3. Receiver intermodulation.
4. Size of mobile equipment to give desired performance.
5. Equipment cost.

Before adjacent channel operation was

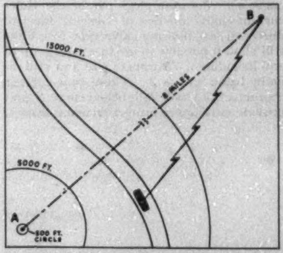

Figure 1. 2-signal adjacent channel test

Paper 49-256, recommended by the AIEE Communications Committee and approved by the AIEE Technical Program Committee for presentation at the AIEE Fall General Meeting, Cincinnati, Ohio, October 17–21, 1949. Manuscript submitted July 19, 1949; made available for printing September 13, 1949.

R. A. Beers, W. A. Harris, and A. D. Zappacosta are all with the Radio Corporation of America, Camden, N. J.

The authors wish to acknowledge the assistance of B. F. Zimmerman and W. W. Coxe.

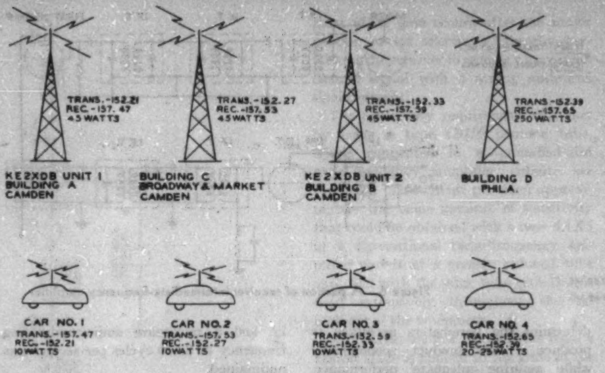
TRANS.-152.21
REC.-157.47
45 WATTS
KE2XDB UNIT 1
BUILDING A
CAMDEN
TRANS.-152.27
REC.-157.53
45 WATTS
BUILDING C
BROADWAY & MARKET
CAMDEN
TRANS.-152.33
REC.-157.59
45 WATTS
KE2XDB UNIT 2
BUILDING B
CAMDEN
TRANS-152.39
REC.-157.65
250 WATTS
BUILDING D
PHILA.
CAR NO. 1
TRANS.-157.47
REC.-152.21
10 WATTS
CAR NO. 2
TRANS.-157.53
REC.-152.27
10 WATTS
CAR NO. 3
TRANS.-152.59
REC.-152.33
10 WATTS
CAR NO. 4
TRANS.-152.65
REC.-152.39
20-25 WATTS

Figure 2. 4-signal adjacent channel test

discarded as impractical, a thorough investigation of the matter was undertaken to determine if the problems involved could be adequately solved.

Field Tests

Preliminary Operational Tests

Extensive field tests were carried out with transmitters of various power rating from 2 to 30 watts under conditions of favorable terrain and in various industrial sections such as Philadelphia, Pa., and Camden, N. J., to determine what power was needed in the transmitter and what sensitivity was required of the receiver. Data collected on the Radio Manufacturers Association's recommendation was gathered on the maximum temperature and humidity conditions to be expected anywhere in North America. Calculations and some field tests were made to determine the maximum adjacent channel signal strength to be expected from a land station of 250-watt power in a mobile receiver to determine the required receiver adjacent channel selectivity. This was necessary so that the mobile receiver would be able to receive a weak desired signal when located very close to a powerful land transmitter. Adjacent channel field tests were run using a very selective receiver to determine the degree of modulation control required to allow practical adjacent channel systems. Tests were run with a number of different persons, both male and female voices, under widely varying conditions of ambient noise with abrupt changes in sound level to evaluate the performance of various modulation limiters for the transmitter.

Two Adjacent Channel Tests

Two 45-watt land station transmitters, designated as *A* and *B*, with a carrier separation of 60 kc, were operated simultaneously, see Figure 1. The 1/4 wavelength ground-plane antennae for both stations were approximately 100-feet high.

Using mobile equipment available in late 1948, the mobile receiver was interfered with to such an extent that the desired signal was "captured" by the nondesired signal whenever the mobile car was within one to three miles of the adjacent channel 45-watt land station transmitters.

The new mobile receiver was able to listen to the desired frequency without interference until it was within 250 feet or less of the adjacent channel 45-watt transmitter.

Four Adjacent Channel Tests

In order to best simulate normal operating conditions, the tests were run in conjunction with two commercial services that were already in operation. These services were the Yellow Cab Company of Camden, N. J., and the Bell Telephone Company of Pennsylvania.

The equipment in building *C* was operating on 152.27 megacycles and 157.53 megacycles, while building *D* was on 152.39 and 157.65 megacycles. Experimental transmitters were placed in operation on 152.21, 152.33, 157.47, and 157.59 megacycles. This resulted in four adjacent channel systems, each having two frequencies. The arrangement is shown in Figure 2.

In the first test that was run, the four mobile units were parked in front of building *A* which housed one of the transmitters. The four land station transmitters were separated from the mobile receivers by 100 feet, 1 1/2 blocks, 7 blocks, and 2 1/2 miles respectively. All four of the mobile receivers responded with clear and interference-free reception. A sketch of this test is shown in Figure 3.

In the second test the procedure was reversed and the mobile transmitters were put on the air. The equipment in building *B* was remote controlled so that the signals could be heard in building *A*, and station receivers were installed on the two commercial channels with antennae

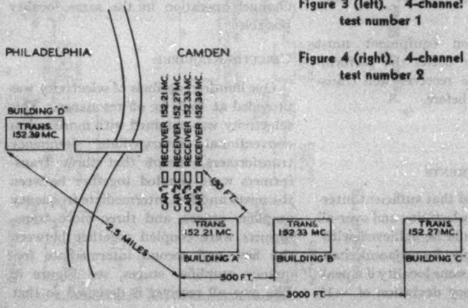
TEST-1
PHILADELPHIA
CAMDEN
BUILDING "D"
TRANS.
152.39 MC.
CAR 1 RECEIVER 152.21 MC.
CAR 2 RECEIVER 152.27 MC.
CAR 3 RECEIVER 152.33 MC.
CAR 4 RECEIVER 152.39 MC.
100 FT.
2.5 MILES
TRANS.
152.21 MC.
BUILDING "A"
TRANS.
152.33 MC.
BUILDING "B"
TRANS.
152.27 MC.
BUILDING "C"
500 FT.
3000 FT.

Figure 3 (left). 4-channel test number 1

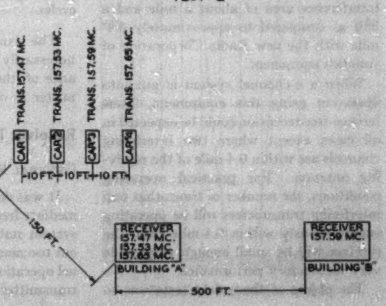
TEST-2
TRANS. 157.47 MC.
TRANS. 157.53 MC.
TRANS. 157.59 MC.
TRANS. 157.65 MC.
CAR 1
CAR 2
CAR 3
CAR 4
10 FT.
10 FT.
10 FT.
150 FT.
RECEIVER
157.47 MC.
157.53 MC.
157.65 MC.
BUILDING "A"
RECEIVER
157.59 MC.
BUILDING "B"
500 FT.

Figure 4 (right). 4-channel test number 2

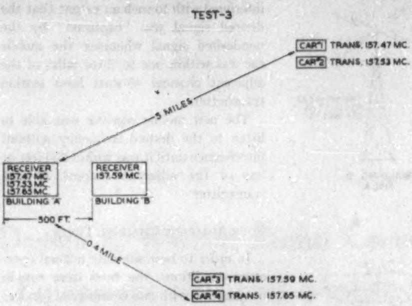

Figure 5. 4-channel test number 3

on building *A*. In this way all of the mobile transmitters could be heard from one building. The second test was as successful as the first in that signals heard in each receiver were free from interference. The sketch of this test is shown in Figure 4.

The outstanding improvements in intermodulation response of these receivers were observed in the third test of the series. Mobile units numbers 2 and 3 were placed 0.4-mile from building *A* and mobile units numbers 1 and 4 were placed 5 miles away.

The two nearby mobile transmitters produced intermodulation products in the receivers tuned to the distant transmitters, as shown in the preceding section. However, the distant mobile transmitters, were able to call in from a distance of 5 miles with no interference, as shown in Figure 5.

If the mobile units that were producing the interference were brought in nearer, some intermodulation response would have been noted, but they could come very close before they would block out the transmitters which were 5 miles away. This represents a remarkable improvement over the older designs which have an interference area of about a mile and a half as compared to approximately 0.4-mile with the new Radio Corporation of America equipment.

When a 4-channel system is put into operation using this equipment, interference-free reception could be expected in all cases except where two interfering channels are within 0.4-mile of the receiving antenna. For practical operating conditions, the number of times that two interfering transmitters will be operating simultaneously within 0.4-mile from the receiver will be small enough to provide very satisfactory performance.

The object of these field tests was to determine the parameters necessary to produce a new product economically while assuring adequate performance. The following decisions were made in order to provide adjacent channel operation in a low cost mobile system:

Mobile Receiver

1. Sensitivity—0.5 microvolt for 20-decibel quieting.
2. Adjacent channel selectivity—100-decibel attenuation at ±60 kc.
3. All spurious responses to the attenuated 85 decibels.
4. Frequency stability—0.003 per cent from −30 to +60 degrees centigrade, ambient.
5. Frequency range—152 to 174 megacycles.

Mobile Transmitter

1. Power output of 12 to 14 watts.
2. Modulation limiter which produces a high average modulation on sudden increase of speech energy. The limiter should prevent overmodulation and introduce no distortion or microphonics.
3. All spurious emissions to be attenuated at least 60 decibels.
4. Frequency stability—0.003 per cent from −30 to +60 degrees centigrade, ambient.
5. Frequency range—152 to 174 megacycles.

The land station equipment must necessarily equal or better the performance of the mobile receiver and transmitter as outlined before.

Receiver Design

General Requirements

It was determined that sufficient intermediate frequency selectivity and over-all system stability could be achieved without too much difficulty for adjacent channel operation in the same locality if a peak transmitter frequency deviation of ±15 kc and a maximum audio-modulating frequency of 3,500 cycles per second was maintained.

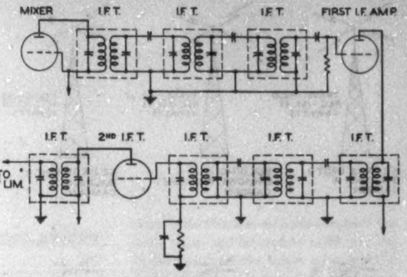

Figure 6. A portion of receiver intermediate-frequency amplifier

Measurements and tests indicated that the receiver should have a sensitivity in the order of 0.5 microvolt input for 20 decibels of noise quieting, because the ambient noise level was found to be low enough in a number of areas where the equipment may be used to provide reliable communication on a 0.5-microvolt signal if the receiver had the required sensitivity.

As far as the intermodulation problem is concerned, it was reasoned that intermodulation should be very little more severe with adjacent channel operation than with alternate channel operation. Little radio-frequency selectivity can be achieved with components that will fit into a mobile receiver at either 60 or 120 kc off resonance. Anything that could be done to improve the receiver's susceptibility to intermodulation interference and desensitization by improvements in circuit design, aside from increased radio-frequency selectivity, should therefore be equally effective for adjacent or alternate channel operation. From results of these early calculations and tests, a receiver was designed incorporating the features believed necessary to make adjacent channel operation in the same locality possible.

Circuits Required

One hundred decibels of selectivity was provided at 45-55 kc off resonance. This selectivity was obtained with more or less conventional intermediate frequency transformers, except that three transformers were coupled together between the mixer and first intermediate frequency amplifier stages, and three more transformers were coupled together between the first and second intermediate frequency amplifier stages, see Figure 6. The over-all receiver is designed so that most of its gain occurs after the major portion of its selectivity, thereby permitting the receiver to receive a very weak desired signal with a strong undesired signal present.

The sensitivity requirement was met by using a type *6BH6* pentode tube, triode connected in a grounded-grid radio-frequency amplifier circuit, see Figure 8. This circuit provided approximately the same amount of sensitivity that could be obtained with a type *6AK5* in a conventional radio-frequency amplifier circuit at a greatly reduced tube cost, and with the same tube type that is used extensively throughout the remainder of the equipment.

Automatic volume control bias from a limiter stage is applied to the grids of the radio-frequency amplifier tubes. This, along with some refinements in the radio-frequency amplifier and first mixer design, considerably improve the intermodulation rejection performance, because the desired signal will bias off the radio-frequency amplifier stages and reduce the amplitude of the undesired signals at the first mixer grid. Since the selectivity to the automatic volume control takeoff point is in the order of 100 decibels, the undesired signal can never produce a control voltage.

Performance of the Receiver

The series of curves illustrated in Figures 9-14 show the performance of the new receiver. Figure 9 shows the noise quieting selectivity of the receiver. The information for this curve was obtained by inserting sufficient radio-frequency signal input to the antenna at the receiver's resonant frequency to produce 20 decibels of noise quieting. The signal generator was then detuned above and below resonance to 60 kc, the adjacent channel in steps of 10 kc, and the signal generator output increased until 20 decibels of noise quieting was obtained.

Figure 10 shows the receiver sensitivity in terms of signal-to-noise plus distortion ratio versus input microvolts in series with a 50-ohm dummy antenna. The input signal was modulated ±10 kc at 1,000 cycles per second.

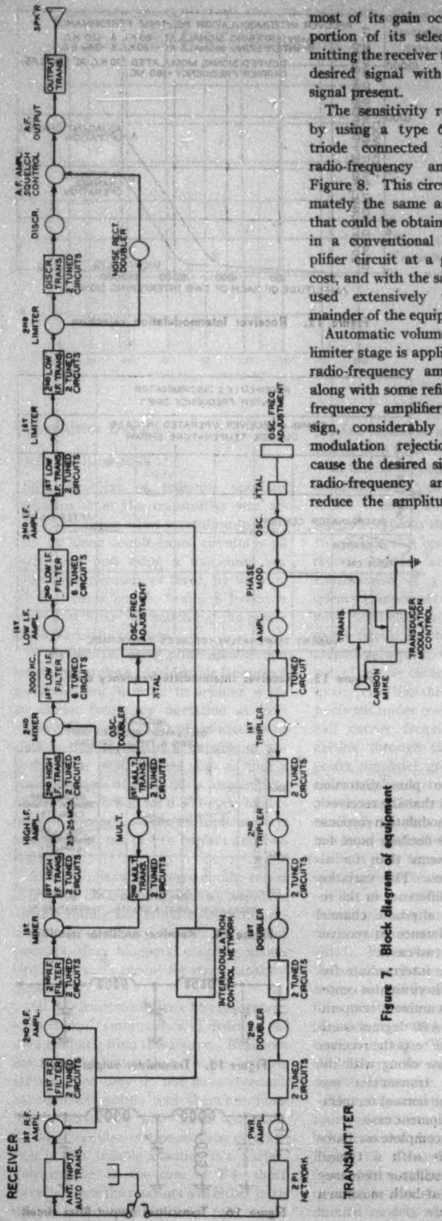
RECEIVER
ANT. INPUT AUTO TRANS.
1ST R.F. AMPL.
1ST R.F. FILTER
2 TUNED CIRCUITS
2ND R.F. AMPL.
2ND R.F. FILTER
2 TUNED CIRCUITS
1ST MIXER
1ST HIGH I.F. TRANS.
2 TUNED CIRCUITS
HIGH I.F. AMPL.
23-25 MCS.
2ND HIGH I.F. TRANS.
2 TUNED CIRCUITS
2ND MIXER
2000 KC.
1ST LOW I.F. FILTER
6 TUNED CIRCUITS
1ST LOW I.F. AMPL.
2ND LOW I.F. FILTER
8 TUNED CIRCUITS
2ND I.F. AMPL.
1ST LOW I.F. TRANS.
2 TUNED CIRCUITS
1ST LIMITER
2ND LOW I.F. TRANS.
2 TUNED CIRCUITS
2ND LIMITER
DISCR. TRANS.
2 TUNED CIRCUITS
DISCR.
A.F. AMPL. SQUELCH CONTROL
A.F. OUTPUT
OUTPUT TRANS.
SPK'R
NOISE RECT. DOUBLER
INTERMODULATION CONTROL NETWORK
2ND MULT. TRANS.
2 TUNED CIRCUITS
MULT.
1ST MULT. TRANS.
2 TUNED CIRCUITS
OSC. DOUBLER
XTAL
OSC. FREQ. ADJUSTMENT
TRANSMITTER
2 PI NETWORK
PWR. AMPL.
2 TUNED CIRCUITS
2ND DOUBLER
2 TUNED CIRCUITS
1ST DOUBLER
2 TUNED CIRCUITS
2ND TRIPLER
2 TUNED CIRCUITS
1ST TRIPLER
1 TUNED CIRCUIT
AMPL.
PHASE MOD.
OSC.
XTAL
OSC. FREQ. ADJUSTMENT
TRANS.
TRANSDUCER MODULATION CONTROL
CARBON MIKE

Figure 7. Block diagram of equipment

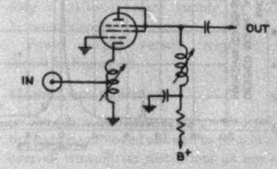

Figure 8. Receiver first radio-frequency amplifier

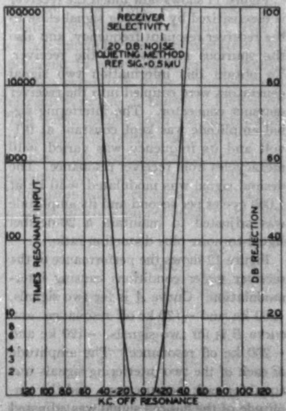

Figure 9. Receiver selectivity

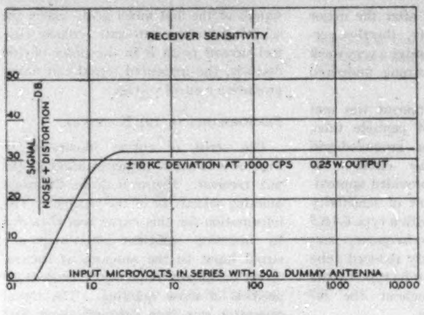

Figure 10. Receiver sensitivity

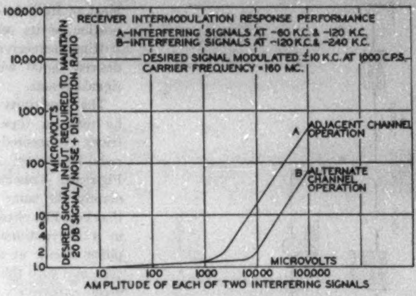

Figure 12. Receiver intermodulation rejection

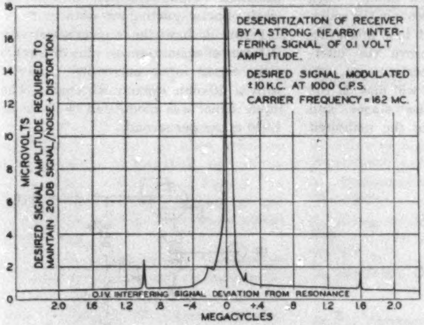

Figure 11. Receiver spurious response rejection

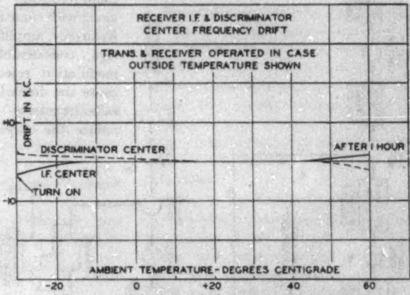

Figure 13. Receiver intermediate-frequency drift

Figure 11 shows how much the receiver is desensitized by a strong signal close to the receiver resonant frequency, and also the spurious responses of the receiver. To obtain this information two signal generators were coupled into the receiver antenna connector. The interfering signal amplitude was kept constant at 0.1-volt and its frequency was varied ±10 megacycles from receiver resonance. The desired signal was modulated ±10 kc at 1,000 cycles per second and its amplitude was adjusted to maintain a 20-decibel signal-to-noise plus distortion ratio.

Figure 12 shows the performance of the receiver under conditions causing intermodulation. Curve *A* is for two signals, −60 kc and −120 kc off resonance, and curve *B* is for two signals, −120 kc and −250 kc off resonance. The amplitude of each of the two interfering signals was equal for each measurement, and the amplitude of the desired signal was adjusted for each measurement to produce a 20-decibel signal-to-noise plus distortion ratio. It will be noted that the receiver's susceptibility to intermodulation response averages only about 9 decibels more for adjacent channel systems than for alternate channel systems. This variation is largely due to the difference in the receiver's adjacent and alternate channel rejection plus the difference in receiver desensitization for the two cases.

Figure 13 shows the intermediate frequency amplifier and discriminator center frequency drift over an ambient temperature range of −30 to +60 degrees centigrade. In making these tests the receiver was operated in its case along with the transmitter, and the transmitter was operated to produce the normal temperature rise inside the equipment case.

Figure 14 shows the complete oscillator circuit frequency drift with a typical crystal and with the oscillator frequency trimmer capacitor set at both maximum and minimum capacity.

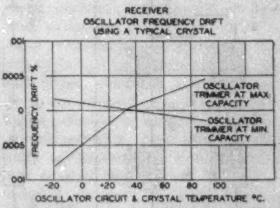

Figure 14. Receiver oscillator stability

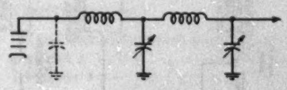

Figure 15. Transmitter output circuit

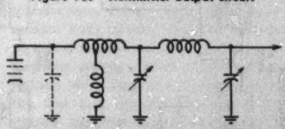

Figure 16. Transmitter output filter circuit

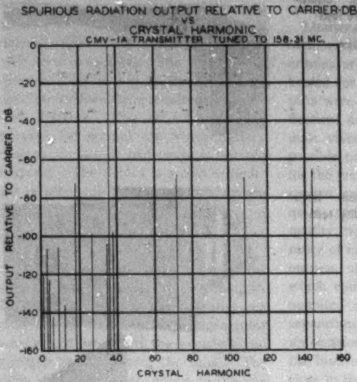

Figure 17 (left). Transmitter spurious emission

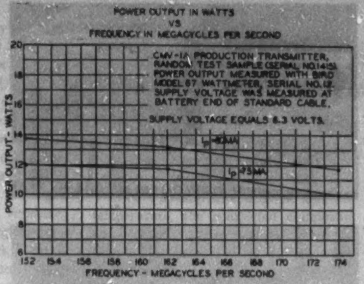

Figure 18 (right). Transmitter power output

Transmitter Design

Spurious Emissions

The problem of reducing spurious emissions from the transmitter was attacked by using a low crystal multiplication, by using double-tuned circuits in all multipliers and using a maximum per stage multiplication of three, by filtering all *B*+ leads and by using a 2-section band-pass filter for matching the power amplifier to the antenna.

A transmitter using phase modulation normally employs considerable frequency multiplication in order to achieve ±15-kc carrier frequency deviation at low-audio frequencies. The phase modulator used in this apparatus is capable of approximately ±90 degrees shift so that a multiplication of only 36 is required to allow full deviation for a 300-cycle modulating frequency. This multiplication is arrived at by use of two triplers and two doublers.

All multiplier stages were double tuned in order to obtain the selectivity required. Double tuning also is quite helpful in reduction of difficulty caused by ground currents, since magnetic coupling allows circuit isolation except for stray capacity coupling.

All *B*+ leads were filtered by resistance-capacitance combinations in order to reduce coupling from this source. Resistors are actually better than chokes for this service since they do not have resonant transmission points and therefore filter over an extremely wide band. An additional advantage of this method of isolation is that trouble shooting is considerably simpler in the case of *B*+ short circuits, since the resistors will either burn up and act as a visible blown fuse or will provide isolation so that an ohmmeter can be used to detect the bad circuit.

In the initial design work of the power amplifier output circuits, we had planned to use a simple 2-section network of the low-pass type as shown in Figures 7 and 15. While this operated as predicted to reduce carrier harmonics, it allowed transmission of a one-half carrier frequency component which would normally have been eliminated by a parallel resonant circuit in the plate of the power amplifier; a parallel resonant circuit does not, of course, eliminate carrier harmonics to anything like the extent of the low pass *pi* circuit under consideration. This one-half carrier frequency component was getting through the doubler plate and power amplifier grid circuits with sufficient amplitude to be amplified by the power amplifier and cause trouble. Accordingly the first *pi* circuit was changed to a band-pass network by the addition of a shunt coil tapped on the first series inductance, as shown in Figure 16.

Care was taken in circuit layout, shielding, and grounding in order to prevent coupling around the circuits provided. Particular attention was paid to the antenna changeover relay, which is of a type proved by many years of successful aircraft service to give less trouble than has been encountered with available coaxial types. The relay is carefully shielded, yet the contacts are readily accessible for service.

The engineering model showed no spurious emission in excess of 70 decibels below carrier frequency, as shown in Figure 17. Measurements were carried from 4.2 megacycles (the crystal frequency) to about 800 megacycles. Production models which have been tested have shown variations of about ±6 decibels from the values given in Figure 18.

Power Output

The total power amplifier plate network efficiency is slightly better than that which is obtained by use of a more conventional parallel tuned circuit, thus allowing a power amplifier efficiency of approximately 50 per cent. This efficiency is quite good for a *2E26* tube with only a 310-volt plate supply at 152-174 megacycles.

Power output versus frequency is shown in Figure 18.

Modulation Control

The phase modulator design and multiplication employed allowed us to achieve over-all transmitter distortions as low as 2 to 5 per cent.

To control deviation without adding distortion or microphonics, a transducer modulation control (TMC) system was devised. The TMC system takes advantage of the fact that output from a carbon microphone is approximately proportional to microphone button current below a saturation value. The circuit is extremely simple, as shown in Figure 19. The audio output from the microphone transformer is differentiated by *C-1*, *R-1* to give a pre-emphasis characteristic and applied to the amplifier rectifier tube *V-1*. Thus from this rectifier a d-c voltage is derived which is proportional to the fre-

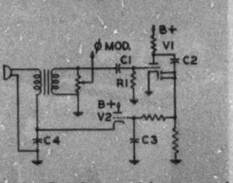

Figure 19. Transducer modulation control circuit

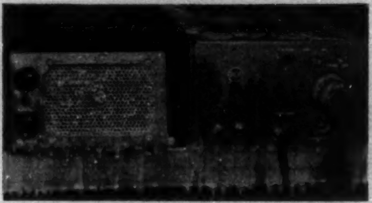

Figure 20 (top left). Equipment temperature tests

Figure 21 (bottom left). Equipment humidity tests

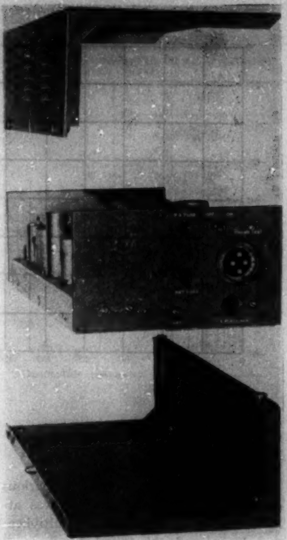

Figure 23 (right). Equipment mounting versatility

quency deviation given by the phase modulator. This control voltage is fed to *V-2* with proper polarity so as to reduce the microphone current should the deviation be increasing above a certain threshold; this reduction in current then reduces the audio input to the phase modulator. The time constants of the resistance-capacitance networks in the d-c line are arranged so that the microphone current is reduced quickly to control deviation and released slowly to prevent appearance of excessive noise between words.

The control range is 20 to 30 decibels; such a wide control range is especially desirable when a carbon microphone is employed, since output from the carbon microphone is quite variable depending on position.

It can be seen from Figure 19 that the audio signal circuit does not go through the limiter tubes at all, thus no distortion or microphonic products are added. Any noise produced by *V-2* is by-passed by capacitor *C-4* and does not affect the signal circuit. Also, it will be observed that the modulation control circuit in no way affects the phase-modulated waves emitted by the transmitter. The increase in frequency deviation with modulation frequency is compensated for by a de-emphasis network in the receiver.

POWER SUPPLY

Two power supplies are used for the transmitter. A small power supply is used for either the receiver or for the transmitter low level and audio circuits. A larger supply is used for the doubler-driver and power amplifier stages only.

The small power supply utilizes a self-rectifying vibrator and delivers 50 milliamperes at 200 volts. This supply runs continuously when the equipment is turned on and is switched from receiver to transmitter by contacts on the antenna relay.

The larger power supply delivers 135 milliamperes at 325 volts, using an interrupter-type vibrator and a separate full-wave rectifier. The vibrator has two sets of interrupter contacts which are wired separately to individual primary

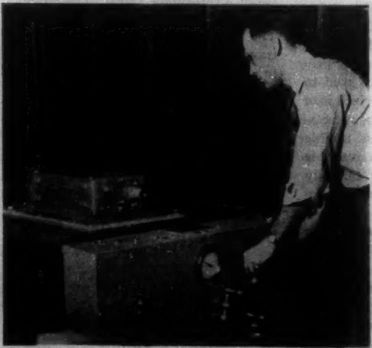

Figure 22 (left). Equipment vibration tests

Figure 24 (right). Equipment mounted in car

windings on the power transformer to obtain good contact life. The rectifier is either a single *OZ4-A* or two *6X5GT* tubes connected in parallel. The two *6X5GT* tubes may be used in applications where maximum reliability is required on much-used systems. The *OZ4-A* is recommended for normal use where battery drain is important and usage is not too frequent. The *OZ4-A* is a cold cathode-gas rectifier and its life is limited to approximately 15,000 to 45,000 starts.

TRANSMITTER TESTS

Spurious emissions were tested on the antenna line by a substitution method. Each crystal harmonic was measured on a receiver. A calibrated signal generator was then adjusted until the receiver signal strength readings were the same. The ratio of the generator output to the line voltage existing at the carrier frequency was taken as the ratio of spurious signal to desired carrier. It was necessary to trap out a portion of the fundamental carrier frequency to prevent its reaching the receiver; it was found that the receivers used would produce harmonics of their own if fed a very strong signal.

Actual field intensity measurements also were made with equipment installed in an automobile. In this case, field intensities were obtained for the carrier and the various crystal harmonics, and were compared directly. The automobile itself was rotated for maximum pickup and both the horizontal and vertical components of radiation were obtained.

Limiter action was checked by use of an oscillograph connected across the discriminator of a suitable receiver and calibrated for deviation. Normal voice inputs were used with widely varying inflections and levels. Both male and female voices were tried. It was found possible to overmodulate the equipment for the first portion of certain syllables if spoken very loudly after a prolonged quiet period; however, as expected, quality was very good throughout the range of inputs used. To check the seriousness of the occasional short burst which could get through, systems were operated on adjacent channels (60 kc separation) and it was found that while an occasional burst could be heard when the interfering signal was very loud and close to the receiver, it was of such short duration that no intelligence was lost.

System Design Considerations

EXACT FREQUENCY ADJUSTMENT

Simplicity in adjusting the mobile receiver to the land station transmitter was accomplished by providing a vernier capacity in the crystal oscillator circuit to give a frequency adjusting range of ±0.01 per cent. This vernier capacity is adjusted to give zero discriminator voltage when receiving the desired signal. It is not necessary to change the adjustment of the discriminator or intermediate frequency amplifier circuit. The mobile transmitter crystal-controlled oscillator circuit also is provided with a vernier capacitor which is adjusted to give zero discriminator voltage at the land station receiver.

TEMPERATURE, HUMIDITY, AND VIBRATION

To insure optimum performance under extreme temperature variations from −30 to +60 degrees centigrade ambient temperature, the completed equipment was carefully tested and measured as shown by Figures 13, 14, and 20. The equipment was tested for several days at 90 per cent humidity and 60 degrees centigrade, as shown by Figure 21. The mobile equipment was designed to operate at optimum performance while subjected to several hours of vibration in three planes with an amplitude of ±1/32 inch and a frequency variation from 5 to 55 cycles per second, see Figure 22.

MOUNTING AND SERVICING

The mounting base of the mobile equipment becomes one-half of the case. The cover becomes the top of the case, see Figure 23. The chassis is reversible 180 degrees without changing the position of the base plate or of the cover. Also, the equipment can be mounted in two planes. The chassis is removed from the case without requiring any headroom as in a drawer-type case. One main battery cable connects the equipment to the battery and control unit.

No Discussion

A New Loss-of-Excitation Relay for Synchronous Generators

C. R. MASON
MEMBER AIEE

INTEREST in loss-of-excitation protection for synchronous generators has been increasing, judging by the number of AIEE and other papers that have been presented and by the number of inquiries that have been received. Perhaps the principal reason for this increasing interest is that the time-honored use of field-undercurrent and undervoltage relays for loss-of-excitation protection is receiving critical examination, particularly because of the increasing practice of operating generators under-excited during light-load periods.[1,2] It has been reported from several sources that such relaying cannot be adjusted to differentiate between purposely reduced excitation during light-load periods and accidental loss of excitation.[3] It also may be that the increasing size of generators and reductions in reserve capacity are causing growing concern of the possible harm to a machine that may follow loss of excitation.

The consequences that may attend loss of excitation are severe system-voltage reductions, and overheating of the generator rotor. Not only is voltage reduction undesirable in itself, but it also reduces the pull-out limits of other machines.[1] The likelihood of undesirable reduction in system voltage can be determined analytically; systems where automatic generator-voltage regulation is not used are most apt to experience such a difficulty. Concern with rotor overheating is chiefly limited to round-rotor generators without amortisseur windings, but the likely degree of damage is most difficult to determine. A need for further investigation in this direction seems to be indicated. The experience of some electrical utilities would seem to indicate that an alert and skillful operator can recognize a loss-of-excitation condition and take the necessary steps to correct the situation in time to avoid obvious damage to a machine. A relay that could indicate which of several machines was in trouble would be very useful in such cases. Others prefer to rely on automatic protective relaying.[3] It is generally agreed, however, that if excitation is lost and cannot be restored quickly, the generator should be disconnected promptly from the system.

Perhaps the first occasion where the difficulty (of selecting between purposely reduced excitation and accidental loss of excitation) received serious consideration was that which produced the reactive-current relay.[3] This relay uses the a-c quantities at the terminals of the generator, and is capable of greater selectivity than field-undercurrent and undervoltage relays.

Further study of the characteristics of loss of excitation as compared with power swings and loss of synchronism, coupled with new relay developments,[4] has led to simpler relaying equipment having still greater selectivity. A single-phase distance-type relay, commonly called a mho relay, is arranged to respond only to certain relations between the alternating current and voltage at the terminals of a generator. How these relations vary after excitation is lost, and how the relay can distinguish between loss of excitation and other normal or abnormal operating conditions, is described in this paper.

The Loss-of-Excitation Relay

The loss-of-excitation relay, Figure 1, is a single-phase single-element high-speed distance-type relay of the so-called mho family.[4] It is arranged to operate from the voltage between two phases, and the difference between the currents of the two phases, at the terminals of the generator to be protected. The operating element is fundamentally the same as that employed in distance relays, but its operating characteristic is shifted from the position used for distance relaying.

Figure 2 shows the operating characteristic plotted on an R-X diagram, where the co-ordinates are positive-phase-sequence per-unit ohms based on the full load rating of the generator. The center of the circle is on the $-X$ axis. For reasons to be given later, the offset OC is shown to be approximately equal to half of the direct-axis transient reactance of the generator, and OD is approximately its direct-axis synchronous reactance. However, both the offset and the diameter are adjustable. The relay will operate to close its contacts for any impedance vector, such as $\mathbf{Z}$, which terminates within the circular operating characteristic.

In terms of phase-to-neutral secondary ohms under balanced 3-phase conditions (positive-phase-sequence ohms), the offset is adjustable to be 0, 1, 2, 3, or 4 ohms. The diameter of the circle is adjustable between 3 and 30 ohms in 1 per cent steps. Assuming that generator current transformers, having standard 5-ampere secondaries, are chosen so that rated full-load current of the generator is 75 per cent of the current-transformer rating, and that the potential source at rated voltage provides 120 secondary volts phase-to-phase, the offset steps in per-unit ohms become approximately 0, 0.054, 0.11, 0.16, and 0.22. Similarly, the range of diameter adjustment is approximately 0.16 to 1.6 per unit.

Paper 49-260, recommended by the AIEE Relays Committee and approved by the AIEE Technical Program Committee for presentation at the AIEE Fall General Meeting, Cincinnati, Ohio, October 17–21, 1949. Manuscript submitted July 19, 1949; made available for printing September 6, 1949.

C. R. Mason is with the General Electric Company, Schenectady, N. Y.

The author wishes to take this opportunity to acknowledge the work of Mr. M. Temoshok, who supervised the differential analyzer studies and coordinated the results, and also to thank other of his associates who helped in the planning of the material for this paper.

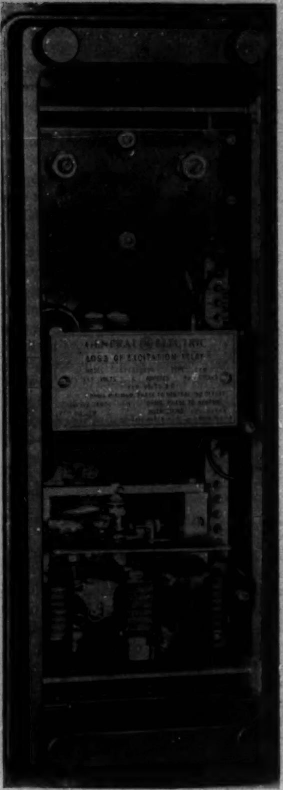

Figure 1. Loss-of-excitation relay

The conventions employed in the use of the *R-X* diagram are as follows. In terms of per-unit ohms at the terminals of the generator under balanced 3-phase conditions, the diagram shows the resistance and reactance components of an impedance which is the ratio of a phase-to-neutral voltage to the corresponding phase current. Positive *R* means that the generator is supplying power to the system, and negative *R* means that the generator is receiving power from the system. Likewise, positive *X* means that the generator is supplying reactive power to the system, as when it operates with high excitation; and negative *X* means that the generator is receiving reactive power from the system as when it operates with low excitation.

In other words, by the use of the *R-X* diagram, there can be shown all possible relations between a given combination of generator current and voltage, as well as a particular area in which these relations will operate a relay which is energized by the same current-and-voltage combination. It remains, therefore, to show the loss-of-excitation characteristic on the *R-X* diagram in order to show how the relay will respond. Then, other normal or abnormal system-operating characteristics will be shown for which the relay should not operate.

The Loss-of-Excitation Characteristic

Differential-analyzer studies have been made of the loss-of-excitation characteristic under various conditions, taking into account the important variables. The technique of these studies was the same as that described in reference 5, and will not be described here; instead, only the pertinent results will be given.

Figure 3 shows typical loss-of-excitation characteristics for the various conditions studied, plotted on the *R-X* diagram together with the suggested relay characteristic of Figure 2. The values of *R* and *X* corresponding to the initial generator loading at the instant before the excitation was affected (or in other words, at zero time) determine one end (labelled zero) of each characteristic. The time in seconds after the excitation was affected is shown at various points along each curve. Each characteristic is terminated at the instant just before the generator first reaches 180 degrees out of phase with the equivalent generator back of the system.

The characteristics do not actually end at those points, but from then on the changes in impedance become so erratic that it is not feasible to try to plot them. Nor do they have any further significance in so far as relay operation is concerned because the relay has already had ample opportunity to operate. If the slip is relatively high, as for heavy initial generator loading, the impedance varies within a restricted area centered approximately on the last plotted point of the characteristic. If the slip is low, as for light initial generator loading, the impedance varies for a while about the last point, then swings entirely outside of the relay characteristic, and then retraces the same loss-of-excitation characteristic until the next pole is slipped, and so forth.

The reason for the erratic changes in impedance is the effect on the generator impedance of erratic changes in rate and direction of slip as poles are approached and passed, as shown in Figure 4. The curves of Figure 3 end at the equivalent impedance of the generator, but as each pole is slipped, there is a change in generator impedance from direct-axis to quadrature-axis values, and these values themselves vary with rate of slip. At very slow slip, as for operation below the knee of the generator slip-torque curve, the variations of impedance are large in comparison with the average and are obtainable only from a differential-analyzer study. But if the machine is operating beyond the knee of the slip-torque curve, the variations in slip are small in comparison with the average value, and the direct- and quadrature-axis impedances can be calculated with fairly good accuracy using the average value of slip. There will still be variation from direct- to quadrature-axis impedance as each pole is slipped, but the region within which the end of the loss-of-excitation characteristic will lie can be fairly well located.

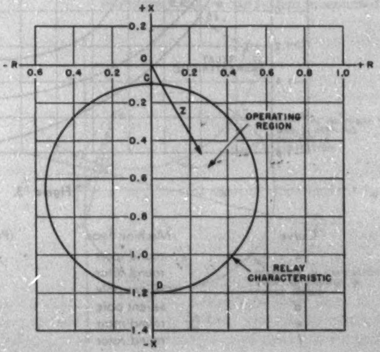

Figure 2. Operating characteristic of loss-of-excitation relay

Figure 5 shows a curve of the average of the calculated direct- and quadrature-axis impedances about which the end of the loss-of-excitation characteristic varies for all possible values of slip of a generator having certain constants. The average impedance is low at high slip, approaching the average of the direct-axis and quadrature-axis subtransient impedances of the generator. At very low slip, the average impedance approaches the average of the direct-axis and quadrature-axis synchronous impedances. Neither extremes are ever actually reached, however.

The foregoing considerations will serve to show that the suggested operating characteristic of the loss-of-excitation relay encompasses an area into which all loss-of-excitation characteristics will enter prior to the generator slipping its first pole. The size of machine, initial loading, governor and voltage-regulator action, and so forth, all affect the final rate of slip which, together with the machine constants, determines where the characteristic ends. In comparison with the relatively slow change in impedance of the loss-of-excitation characteristic, the relay may be assumed to operate immediately its operating region is entered.

Relation Between Loss-of-Excitation and Loss-of-Synchronism Characteristics

A differential-analyzer study is necessary to take into account certain variables and to show how certain quantities vary with time; however, much valuable analytical work has been done in connection with loss of synchronism and its effect on relays, in which certain simplifying assumptions have been made, and the finding of such studies can be applied to this problem. Reference 6 gives loss-of-synchronism characteristics for all possible values of excitation. Since loss of excitation involves both changes in excitation and loss of synchronism, an examination of that paper will provide an excellent insight into the mechanism of loss of excitation.

The essential information to be gained from reference 6 is shown in Figure 6. The line *OA* is the equivalent impedance of the generator, assumed to be the direct-axis transient impedance. The line *OB* is the equivalent impedance of the rest of the system to which the generator is connected, including the direct-axis transient impedance of an equivalent generator back of the system impedance. Three loss-of-synchronism characteristics are shown for three different conditions of the voltage *E* back of transient reactance of the generator in question (which we shall call *A*) relative to the generator back of the system (which we shall call *B*). These three curves are actually arcs of circles centered on extensions of the straight line *AB*. The curve for $E_A/E_B=1$ is a straight line (a circle of infinite radius) and is the perpendicular bisector of the straight line *AB*. There is an infinite number of

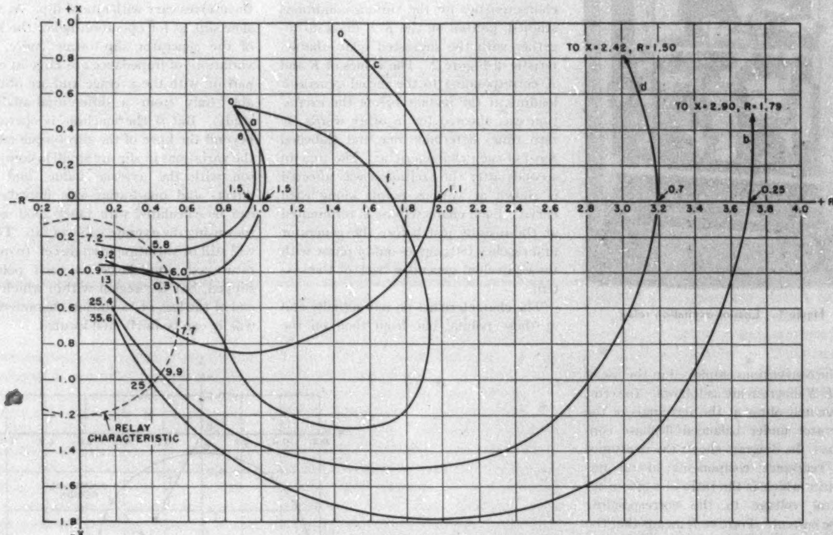

Figure 3. Loss-of-excitation characteristics

Curve	Machine Type	Initial Load (Per Cent of Rated)	System Impedance, Per Unit	Type of Field Failure
a	round rotor	100	0.015+j0.1	short circuit
b	round rotor	29.4	0.015+j0.1	short circuit
c	salient pole	58.8	0.015+j0.1	short circuit
d	salient pole	35.3	0.015+j0.1	short circuit
e	round rotor	100	0.03 +j0.2	short circuit
f	round rotor	100	0.015+j0.1	open circuit

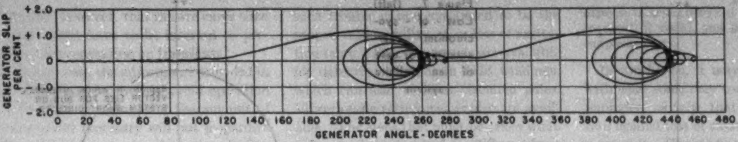

Figure 4. Generator slip versus phase angle by which the generator leads the equivalent system generator

such curves for all possible values of E_A/E_B. For values of E_A/E_B progressively greater than unity, the circles become smaller, their centers move in toward *B*, and finally the circles shrink to the point *B*. Similarly, for values of E_A/E_B progressively smaller than unity, the circles shrink to point *A*.

The arc *PA* of Figure 6 is part of a circle, the rest of which is shown dotted, which passes through *A*, *B*, and *P*, and whose center is on the $E_A/E_B=1$ line. This is the circle for a certain phase angle between the generator at *A* and the equivalent generator at *B*, with generator *A* leading generator *B*. There is an infinite number of such circles for all possible angular relations between the generators, and all of these circles pass through *A* and *B*. As the phase angle increases, the diameter of the circle decreases until its center is at *M* and its diameter is *AB*. At this point, generator *A* is 90 degrees ahead of generator *B*. Further advance in phase angle is represented by circles of increasing diameter with their centers farther and farther to the left of *M*.

As indicated on Figure 6, starting from an initial point *P*, the impedance vector will trace curve *PX* for an increase in phase angle with no change in excitation, and curve *PA* for a decrease in excitation with no change in phase angle. Since loss of excitation involves both types of change simultaneously, it follows that the actual curve lies between the boundary arcs *PX* and *PA*. For rapid decrease in excitation with relatively little advance in angle, as for the case of an open-circuited generator field under light-load conditions, the characteristic lies close to the arc *PA*. But for a short-circuited field having a long time constant, the characteristic lies farther away from *PA*.

The foregoing considerations lead to the question of what happens to the left-hand end of the characteristic. With the simplifying assumptions of this approach to the problem, the characteristic must ultimately terminate at *A*. Whether it would follow the arc *PA* directly to *A*, or would cross the line *AB* between *A* and *X*, and then spiral in a counterclockwise direction around *A*, finally ending at *A*, would depend on the relative rate of change of phase angle and of excitation.

We have obviously reached the point where further speculation is useless. Actually, owing to induction, the effective excitation is never completely lost; the nearest approach is for an open circuit in the field of a generator having no amortisseur. Also, the point *A* is fictitious because the generator impedance is not a constant value equal to the direct-axis transient impedance, as has been previously pointed out. However, this method of analysis has served to provide a better concept of the loss-of-excitation characteristic than could be obtained from the results of a differential-analyzer study alone.

It also has provided a good introduction to the next subject to be considered, which is the effect of power swings or loss of synchronism on the loss-of-excitation relay.

Effect of Power Swings or Loss of Synchronism on the Loss-of-Excitation Relay

The loss-of-synchronism characteristic has been shown already in Figure 6 and explained in the foregoing text. It remains to examine this characteristic for the purpose of determining whether or not the loss-of-excitation relay might operate undesirably during such conditions.

It is probably evident that since these loss-of-synchronism characteristics completely blanket the *R-X* diagram, if the excitation of the generator is sufficiently reduced there is no area in which a loss-of-excitation relay could operate without operating also for power swings or loss of synchronism. Prolonged out-of-step operation of a generator may reduce the machine excitation, even though the source of normal excitation voltage is unaffected, to a point where relay operation would occur. This, however, generally would be advantageous. In fact, Figure 6 does not show the condition that most seriously restricts the location of the loss-of-excitation characteristic, which is when the generator in question is small in comparison with the rest of the system. This condition is shown in an exaggerated way in Figure 7, where the system is assumed

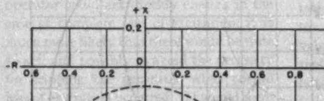

Figure 5 (left). Average of direct- and quadrature-axis impedances for all values of slip

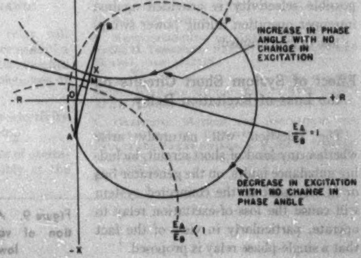
+X
-X
-R
+R
B
P
X
M
O
A
$\frac{E_A}{E_B} > 1$
$\frac{E_A}{E_B} = 1$
$\frac{E_A}{E_B} < 1$
INCREASE IN PHASE ANGLE WITH NO CHANGE IN EXCITATION
DECREASE IN EXCITATION WITH NO CHANGE IN PHASE ANGLE

Figure 6 (right). Loss - of - synchronism characteristics

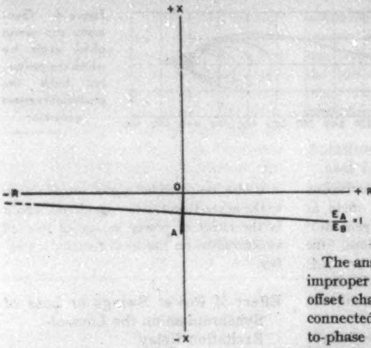

Figure 7. (left) Loss-of-synchronism characteristic for case of an infinite system

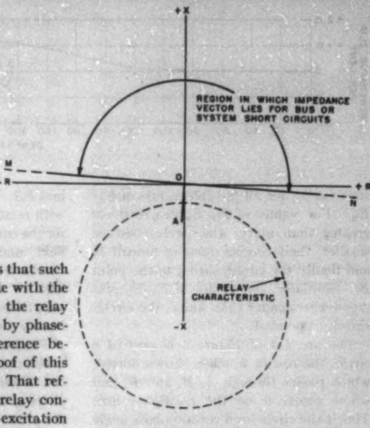
+X
REGION IN WHICH IMPEDANCE VECTOR LIES FOR BUS OR SYSTEM SHORT CIRCUITS
M
-R
O
+R
N
A
RELAY CHARACTERISTIC
-X

Figure 8. (right) External fault impedance region

to be infinitely large, relative to the generator in question.

It will be observed that the system impedance *OB* of Figure 6 has been reduced to zero in Figure 7. The loss-of-synchronism characteristic for $E_A/E_B=1$ is still the perpendicular bisector of the total impedance, which now is reduced to the generator impedance *AO*. Since such a condition of excitation is not at all unusual, it is reasonable to conclude that in the general case the operating area of the relay should lie no closer to *O* than one half of *OA* (or approximately one half of the direct-axis transient reactance of the generator). However, it will be evident that one need not assume an infinite system to see that the operating area of the relay in general should be somewhat below the *R* axis if operation during severe power swings or loss of synchronism is to be avoided.

Thus, while it will be evident that the relay characteristic need not be offset from the origin in those cases where the generator is large with respect to the rest of the system (*AO* is small with respect to *OB*), it has been shown that for general application the offset is necessary. But principally, it has been shown that the proposed shape and location of the relay characteristic is such that the greatest possible selectivity is provided against improper operation during power swings or loss of synchronism.

Effect of System Short Circuits on the Loss-of-Excitation Relay

The question will naturally arise whether any kind of short circuit, including unbalance faults, on the generator bus or in any part of the connected system will cause the loss-of-excitation relay to operate, particularly in view of the fact that a single-phase relay is proposed.

The answer to this question is that such improper operation is impossible with the offset characteristic, and with the relay connected so as to be operated by phase-to-phase voltage and the difference between the phase currents. Proof of this will be found in reference 7. That reference paper proves that for a relay connected the same as the loss-of-excitation relay, the region in which the impedance vector will lie for any kind of fault involving any combination of phases is substantially that indicated on Figure 8 for nonarcing short circuits. The line *MN* is perpendicular to the generator impedance *AO*. For an arcing fault on the generator bus, the impedance can lie slightly below *MN*, but it will be well outside of the dotted relay characteristic.

If the relay were not connected as it is, or if its characteristic were not offset, it could operate for a bus fault, which is another reason for offsetting the characteristic and limiting its size.

The relay can operate for a fault in its generator, but this is of no consequence since the generator would be removed from service anyway by other protective relays.

Effect of Line-Charging Current on the Loss-of-Excitation Relay

The value of *OD* in the relay characteristic of Figure 2 was said to be approximately equal to the direct-axis synchronous reactance of the generator. Actually, under extreme line-charging conditions, this value should be the quadrature-axis synchronous reactance in order to avoid relay operation. If the reduction had to be much more, the line-charging capacity of the generator would be exceeded. It is

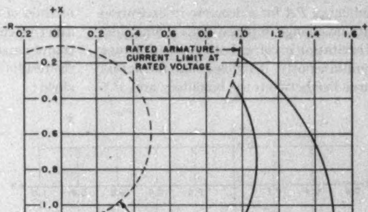

Figure 9. Area of operation of voltage-regulator low limit

possible, however, that in rare cases time delay might have to be inserted to prevent relay operation on transients.

In any case, the adjustment provided in the relay can be used to avoid operation during line charging, and the amount of adjustment necessary will not jeopardize the operation under loss-of-excitation conditions.

Effect of Partial Loss of Excitation on the Loss-of-Excitation Relay

The statement has been made that "field protective relays should be sensitive to any reduction of excitation that will, at any generator load, become unsatisfactory for continued operation of the machine."[4] The question will arise whether the loss-of-excitation relay will fulfill this broad requirement.

Reference 2 establishes suggested lower limits of excitation for normal operation for a turbogenerator which, when converted to the *R-X* diagram, are shown in Figure 9, together with the loss-of-excitation-relay characteristic for the generator involved. It is immediately evident that excitation can be reduced below the suggested limit without benefit of protection by the relay if the proposed relay adjustments are used.

The important point to remember is that the choice of the adjustment of the relay was made on the basis of preventing improper operation under certain conditions. It is possible that, for some applications, the diameter of the circle and its offset could be adjusted to provide protection against partial loss of excitation without the risk of improper operation under any of the other conditions.

A second point to consider is whether immediate tripping of a generator is desirable under such conditions. While there may be some question whether an operator could act quickly enough in the case of complete loss of excitation, it is much more likely that there would be time to act, and possibly to avoid the necessity for tripping the generator when partial loss of excitation occurred. It would seem reasonable to conclude, therefore, that protection against partial loss of excitation might better be provided by a separate relay arranged to sound an alarm.

One type of partial loss of excitation that would require immediate action is complete short circuiting of part of the generator-field poles. This may cause serious vibration. Protection against such trouble is not considered to be the proper responsibility of a loss-of-excitation relay. Relaying means are available for detecting grounds in field windings, which can lead to short-circuited poles. Vibration-detecting means also are available. The steps that must be taken when poles are short circuited are different from those when the entire source of excitation is affected. Consequently, other relaying means should be employed which can differentiate between this type of trouble and any other.

The Reactive-Current Relay

It is interesting to examine the characteristic of the reactive-current relay of reference 3 on the basis of the *R-X* diagram. This relay is a directional type having maximum torque at 90 degree lead. Ordinarily, the operating characteristic of such a relay on the *R-X* diagram would be an infinite number of circles, all passing through the origin and all centered on the *X*-axis, the diameter of each circle being directly proportional to the square of the applied voltage. Through the use of a voltage regulator which maintains substantially constant voltage at the relay over a wide range of supply-voltage variation, a single circular characteristic through the origin is obtained. Adjustment of its diameter is made by means of a tapped coil.

The adjustment chosen for the relay was such that the diameter of its characteristic circle is between 2.0 and 3.0 per-unit ohms. This provides good protection against partial loss of excitation, which is one of the stated objects of the originators of the relay.

Conclusions

While the principal purpose of this paper was to describe a new loss-of-excitation relay, much space has been allotted to other related considerations. The value of the *R-X* diagram as a powerful tool for the analysis of problems of this nature will be particularly evident. The following conclusions may be drawn:

1. The new loss-of-excitation relay will operate before the angular displacement of a generator with respect to its system reaches 180 degrees for any case of complete loss of excitation.

2. The relay will provide greater selectivity than has heretofore been available.

3. Protection against partial loss of excitation can be obtained, but possibly at the expense of selectivity; if such protection is required, it could, and perhaps should, be supplementary.

In conclusion, it may be well to close with what some may consider an obvious reminder, namely, that the best protection against loss of excitation is to try to prevent it. Having to trip a generator is apt to be embarrassing at any time, and it is especially aggravating when made necessary by failure of an auxiliary service. Should more than one generator be affected, the consequences might be far worse. The fact that reliable protective relaying is available should not overshadow the primary importance of a thoroughly reliable excitation system and of personnel well versed in its care and use.

Appendix I. Determination of *R* and *X* for Constructing *R-X* Diagrams for Balanced 3-Phase Conditions

$$R=\frac{V^2W}{VAR^2+W^2}$$

$$X=\frac{V^2VAR}{VAR^2+W^2}$$

where all quantities are actual or per-unit values, and where

R = line-to-neutral (positive-phase-sequence) resistance
X = line-to-neutral (positive-phase-sequence reactance)
V = phase-to-phase voltage
W = 3-phase power (supplied by generator to system)
VAR = 3-phase reactive power (supplied by generator to system)

References

1. GENERATOR STABILITY AT LOW EXCITATION, E. L. Michelson, L. F. Lischer. *AIEE Transactions*, volume 67, part I, 1948, pages 1–9.

2. UNDEREXCITED OPERATION OF TURBOGENERATORS, C. G. Adams, J. B. McClure. *AIEE Transactions*, volume 67, part 1, 1948, pages 521–28.

3. LOSS-OF-FIELD PROTECTION FOR GENERATORS, G. C. Crossman, H. F. Lindemuth, R. L. Webb. *Electrical Engineering* (*AIEE Transactions*), volume 61, May 1942, pages 261–66.

4. THE MHO DISTANCE RELAY, R. M. Hutchinson. *Electrical Engineering* (*AIEE Transactions*), volume 65, June 1946, pages 353–59.

5. RESYNCHRONIZING OF GENERATORS, C. Concordia, M. Temoshok. *AIEE Transactions*, volume 66, 1947, pages 1512–18.

6. IMPEDANCES SEEN BY RELAYS DURING POWER SWINGS WITH AND WITHOUT FAULTS, Edith Clarke. *AIEE Transactions*, volume 64, 1945, pages 372–84.

7. GRAPHICAL METHOD FOR ESTIMATING THE PERFORMANCE OF DISTANCE RELAYS DURING FAULTS AND POWER SWINGS, A. R. van C. Warrington. *AIEE Transactions*, volume 68, part I, 1949, pages 608–21.

No Discussion

One Slip Cycle Out-of-Step Relay Equipment

W. C. MORRIS
ASSOCIATE AIEE

WHEN the out-of-step condition develops on a power system, the resulting disturbance may result in a major loss of load. It is, therefore, desirable to be able to recognize such a condition promptly and to take corrective measures to minimize the disturbance. This paper describes a new relay equipment which is capable of recognizing an out-of-step condition before the completion of the first slip cycle, whereas earlier forms of out-of-step relays did not usually give an indication until after the third slip cycle.

Such a relay may be used in a number of different ways:

1. The separation of a system into two or more sections at preselected points so that each section may have sufficient generation to meet its own load requirement.[1]
2. To disconnect a machine which is out-of-step from the system in order to avoid damage to the machine.[2,3]
3. To correct an out-of-step condition in the case of a generator by controlling the input to the prime mover so as to either slow down or speed up the particular machine.[4]

This new relay equipment in addition to recognizing an out-of-step condition more quickly than previous relays, has the further feature that it is capable of determining the relative direction of slip, thus permitting application for case 3 above.

One previous type of out-of-step relay uses three reversals of power as an indication of an out-of-step condition. An overcurrent relay is used as a fault detector so that it is necessary to have higher than normal current and also a power reversal before the reversal is counted. When a fault occurs the current is high and the power may reverse. Then while the fault is still on, one circuit breaker may open and change the conditions so that the power reverses again. Since it is possible to have two power reversals accompanied by high current during a fault, it is necessary to block the relay from operating on the first two power reversals. As there is only one power reversal accompanied by high current each slip cycle, this relay cannot trip on out-of-step until the third slip cycle.

Other previous out-of-step relays use voltage dips or current surges to indicate the out-of-step condition. These types of out-of-step relays also have to be blocked for the first two voltage dips or current surges to prevent them from tripping incorrectly during faults not involving an out-of-step condition.

A new relay scheme that will trip correctly for an out-of-step condition during the first slip cycle and will not trip incorrectly during a fault is based on establishing three areas as shown in Figure 1. During an out-of-step condition the impedance seen by the relays located at *O* will always pass through each of the three areas in sequence and will be in each area for a time determined by the rate of slip. The out-of-step condition is recognized by the relay equipment through a chain of auxiliary relays which must be picked up in proper sequence and with a certain minimum time required for each step.

By establishing the three areas it is possible for this relay scheme to determine the relative direction of slip. If the slip is in one direction the impedance vector will go through area number 1, then area number 2, and finally area number 3. If the slip is in the opposite direction it will go through the areas in the sequence, area number 3, area number 2, and then area number 1. How these two sequences can be used to set up different circuits is described later.

The relay equipment is composed of two relays. One relay, known as the angle impedance relay, Figure 3, is composed of two induction cup units, one with characteristic *AA*, Figure 1, and the other with characteristic *BB*.

These units are similar to standard reactance units, differing only in that their characteristics have been shifted so they are parallel to the system impedance. These same units have been used as blinders for long line applications.[5]

Each unit has two contacts. The *A* unit has a contact A_1 which is closed for all impedances to the left of characteristic *AA* and a contact A_2 that is closed for all impedances to the right of characteristic *AA*. The *B* unit has a contact B_1 which is closed for all impedances to the left of characteristic *BB* and a contact B_2 that is closed for all impedances to the right of characteristic *BB*.

The other relay, known as the "overcurrent and time-delay relay," is composed of one plunger-type overcurrent unit and six telephone-type time-delay auxiliary relays. The overcurrent relay characteristic is shown as a circle in Figure 1 although it is really a family of circles depending on the voltage, because it has a fixed pickup in amperes.

The telephone-type auxiliary relays are used to set up the trip circuit or control circuits when they are picked up in the proper sequence.

How the Two Relays Operate

The contact circuits of the two angle impedance units and the contact and coil circuit of the overcurrent and telephone-type relays are shown in Figure 2. Contacts on the angle impedance units which are closed in each area is shown in Figure 1.

Paper 49-261, recommended by the AIEE Committee on Relays and approved by the AIEE Technical Program Committee for presentation at the AIEE Fall General Meeting, Cincinnati, Ohio, October 17–21, 1949. Manuscript submitted July 19, 1949; made available for printing September 7, 1949.

W. C. Morris is with the General Electric Company, Philadelphia, Pa.

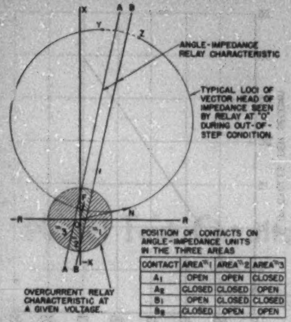
X
A
B
Y
Z
ANGLE-IMPEDANCE RELAY CHARACTERISTIC
TYPICAL LOCI OF VECTOR HEAD OF IMPEDANCE SEEN BY RELAY AT "O" DURING OUT-OF-STEP CONDITION.
F
N
-R
R
O
3
2
1
-X
A
B
OVERCURRENT RELAY CHARACTERISTIC AT A GIVEN VOLTAGE.
POSITION OF CONTACTS ON ANGLE-IMPEDANCE UNITS IN THE THREE AREAS

CONTACT	AREA № 1	AREA № 2	AREA № 3
A_1	OPEN	OPEN	CLOSED
A_2	CLOSED	CLOSED	OPEN
B_1	OPEN	CLOSED	CLOSED
B_2	CLOSED	OPEN	OPEN

Figure 1. Impedance characteristic of out-of-step relay scheme

Under normal conditions the impedance seen by the angle impedance units at location *O* will be to the right of characteristic *BB* but outside the overcurrent relay characteristic. When an out-of-step condition appears the impedance vector will move to the left. When it crosses into area number 1, the overcurrent unit will close its contacts. As contact B_2 is closed in this area the telephone-type relay X_1 will be energized and will pick-up providing contact B_2 stays closed for 0.005 second after the contacts of the overcurrent unit closes. When the impedance vector crosses into area number 2, contact B_2 will open and de-energize coil X_1 and contact B_1 will close. As contact A_2 is closed in area number 2 the coil of X_2 will be energized providing X_1 has had time to pick-up while the vector was crossing area number 1. When X_2 picks up it seals in around the contact of X_1 in its coil circuit. When the impedance vector crosses into area number 3, contact A_2 opens and de-energizes X_2 and contact A_1 closes and energizes X_4. The contact of X_4 energizes X_3 providing X_2 had time to pick-up while the impedance vector was crossing area number 2. When X_3 picks up it closes its contacts (studs 2-12) and also seals in around the contact of X_2. When the impedance vector passes out of area number 3 by crossing the overcurrent units characteristic, the contacts of the overcurrent unit will open and de-energize X_3. However X_3 has an adjustable time delay drop-out from 0.5 to 3 seconds. Therefore if the time of one slip cycle is less than the drop-out time setting of X_3, then X_3 will be re-energized before it can drop-out and will remain picked up. If the time of one slip cycle is more than the drop-out time setting of X_3, then X_3 will drop-out after the time delay has expired, but will be picked up again on the next slip cycle. The above cycle was based on one part of the system having fallen behind the other. If this same part of the system starts to go out-of-step by pulling ahead of the other, the impedance vector will go through the three areas in the sequence of area number 3, area number 2, and finally area number 1. This reversed sequence will cause relays X_4, X_5, X_1, and X_6 to operate and the contacts of X_6 (studs 1 and 11) will close.

When a fault occurs the impedance vector changes instantly from some value to the right of characteristic *BB* and outside the overcurrent characteristic, such as *ON*, to a new value in area number 2 such as *OF*. As this change is made instantly neither auxiliary X_1 nor X_4 have a chance to pick-up before the contacts of A_1 and B_2 are both open.

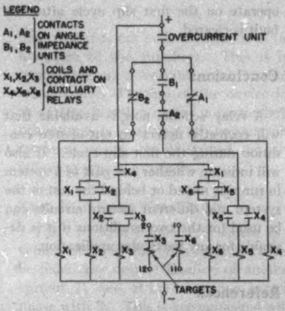
LEGEND
A1, A2 / B1, B2 CONTACTS ON ANGLE IMPEDANCE UNITS
X1,X2,X3 / X4,X5,X6 COILS AND CONTACT ON AUXILIARY RELAYS
+
OVERCURRENT UNIT
B1
B2
A1
A2
X6
X1
X1
X2
X6
X5
X2
X3
X5
X4
2
10
X3
X6
X1
X2
X3
X6
X5
X4
12
11
TARGETS
−

Figure 2. Control circuit of out-of-step relay scheme

The purpose of the overcurrent unit is to prevent operation on normal oscillations such as caused by the generator hunting. The loci of the vector heads will oscillate back and forth along some line such as *YZ*, Figure 1. Even though the impedance vector crosses the *AA* and *BB* characteristics in the proper sequence, it cannot cause the auxiliary relays to set up the trip or control circuits because this is blocked by the contacts of the overcurrent unit remaining open.

The distance between the two impedance angle relay characteristics *BB* and *AA* determines the maximum slip cycles per second at which the relay scheme will operate. The maximum slip cycles per second is determined by the pick-up time of the time delay relays. These relays will pick-up in approximately 0.005 second.

If the impedance vector crosses between *BB* and *AA* in less than 0.005 second, the auxiliary relays will not pick up and the relay scheme will not operate. The time required for the impedance vector to cross between the *BB* and *AA* characteristic is related to the number of slip cycles per second and the number of electrical degrees between the characteristic by the following equation

$$t=\frac{1}{S}\times\frac{\theta}{360} \tag{1}$$

Where *S* is the number of slip cycles per second, and θ is the change in the angle of the impedance vector, as seen by the relay, as the vector crosses between the two characteristics. By substituting the pick-up time of the time delay relays (0.005) in this equation, the maximum slip cycles (S_{max}) can be found

$$S_{max}=\frac{\theta}{1.8}\text{ cycles per second} \tag{2}$$

It is necessary to change θ from electrical degrees to relay ohms in order to set the relay. In Figure 4, line *R-S* is the impedance of the total circuit and point *O* is the electrical center. β is the angle

Figure 3. Angle-impedance relay

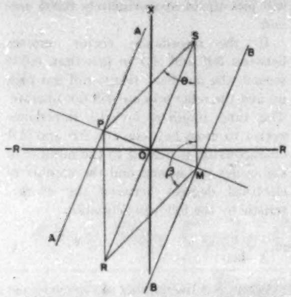

Figure 4. Relation of angle-impedance relay characteristics to impedance seen by relay

between the two ends of the system. The ohm setting of the B angle impedance unit is OM and ohm setting of the A angle impedance unit is OP. As both units are set the same $OM=OP$, and $OR=OM \tan \beta/2$. From this equation and equations 1 and 2, it is possible to obtain the curve shown in Figure 5. This shows the maximum slip cycles per second at which the relay scheme will work. By knowing the total ohms of the system and the maximum slip cycles at which the relay must operate, it is possible to determine the relay setting. The relay is adjustable from 0.25 to 2.5 ohms phase-to-neutral in 1 per cent steps.

Limitations

When a generator loses excitation, it will lose synchronism but the impedance values as seen by a relay at the generator terminals do not follow the typical loci of Figure 1. Hence, this out-of-step relay may not operate in the case of loss-of-excitation. To protect the generator against out-of-step due to loss-of-excitation it is necessary to use a different relay known as a loss-of-excitation relay.[6]

This relay scheme will not operate while a fault is on the phases associated with the relay because the impedance vector crosses only one of the two relay characteristics. However, this relay will operate on the first slip cycle after the fault is cleared.

Conclusions

A relay scheme now is available that will correctly detect an out-of-step condition during the first slip cycle. It also will indicate whether one part of a system in running ahead or behind the rest of the system and different control circuits can be used for the two conditions if it is desirable for any particular application.

References

1. Relay Operation During System Oscillations, C. R. Mason. *Electrical Engineering*, July 1937, pages 823–32.

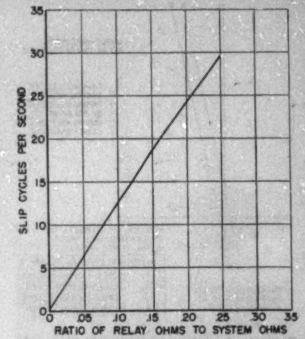

Figure 5. Curve showing maximum slip cycles at which relay will operate relative to relay setting

2. Power System Stability (book), S. B. Crary. John Wiley and Son, Inc., New York, N. Y., 1947, page 239.

3. A System Out of Step and Its Relay Requirements, L. N. Crichton. *Electrical Engineering*, October 1937, pages 1261–7.

4. Governor Performance During System Disturbance, R. C. Buell, R. J. Caughey, E. M. Hunter, V. M. Marquis. *AIEE Transactions*, volume 50, March 1931, pages 354–69.

5. Protective Relaying for Long Transmission Lines, A. R. van C. Warrington. *Electrical Engineering* (*AIEE Transactions*), volume 62, June 1943, pages 261–68.

6. A New Loss-of-Excitation Relay for Synchronous Generators, C. R. Mason. *AIEE Transactions*, volume 68, part II, 1949, pages 1240–45.

No Discussion

Novel Test Circuits for Protective Relays

W. K. SONNEMANN
MEMBER AIEE

IN THE test, calibration, checking, and setting of protective relays, and in the determination of their characteristic operating curves, it is of course necessary to apply to the relays the quantity or quantities which are expected to operate them. When the quantities are rather simple, such as a single variable current value, there is no special problem, particularly in the laboratory. When two or more variable a-c quantities are involved, the problem becomes more complex, particularly when the phase angle between these quantities must be either known or controlled. The solution to such problems may generally be obtained in the laboratory by special circuits and equipment. It is the purpose of this paper to discuss certain of these circuits and the capabilities of certain equipment which the author believes are not common knowledge. As a related item, methods of checking an over-all installation in the field by means of load current and voltage as delivered to the relay from the instrument transformers will be discussed for a particular case which involves sequence components not normally present under load conditions.

Versatility and Limitations of a Variable Ratio Autotransformer

The variable ratio autotransformer,* as a very convenient device for varying a voltage, has received considerable attention and, accordingly, it has enjoyed widespread acceptance. One of its capabilities, however, seems quite generally to have been overlooked; so much so, in fact, that it is not even mentioned in the literature of the suppliers. This is its possibilities as a variable ratio current transformer. The use of the device for this latter function makes it particularly convenient in the test of certain differential relays, as illustrated by the following typical examples.

TYPE *HCB* PILOT WIRE RELAY

The circuit of Figure 1 is shown as a typical example wherein a current, I_F, can be made any desired fraction of another current, I_N, and, at the same time, kept in phase with it. This is accomplished with only one load bank which represents another advantage, since, ordinarily, two loads are required to control two currents.

Figure 1 is purely schematic insofar as the pilot wire circuit is concerned, the principal point to the diagram being to illustrate the control of two currents relative to each other. The current circuit is complete, however, and it should be noted that the current I_N flowing in the near relay is given the reference polarity from *A* to *N* (phase *A* to neutral). In the far relay, the corresponding current, I_F, is shown flowing from *N* to *A*. This is the correct polarity to simulate an external phase-to-ground fault on phase *A*. Thus, a set-up is made whereby typical operating characteristic curves, as shown in Figure 2, may be obtained.

The terminals of the variable ratio autotransformer have been numbered for convenience in Figure 1. Terminals *1* and *2* are the normal input terminals, and *3* and *4* are the normal output terminals. Note that the total circuit current, I_N, enters at terminal *3*, which is associated with the moving contact, or brush. If this is adjusted to make contact with the same turn as terminal *1*, then the ratio between I_N and I_F will be substantially 1-to-1, and $I_F = I_N$, the far relay being merely paralleled by the magnetizing impedance of the autotransformer. This would correspond with a dial setting on the device of 100 per cent voltage. For the other extreme, consider the moving contact in the position normally associated with zero voltage output, wherein the moving contact makes contact with the start turn of the winding associated with terminals *2* and *4*. In this case, the current, I_N, passes through a short circuit between terminals *3* and *4*, and I_F must equal zero.

The extremes of $I_F = 1 \times I_N$ and $I_F = 0 \times I_N$ have thus been covered. At any intermediate position, such as actually illustrated in Figure 1, the total current, I_N, must divide into two component parts, I_P and I_S, wherein the subscripts *P* and *S* denote primary and secondary, and wherein I_S is identical with I_F. These currents must satisfy the balance of ampere turns between primary and secondary windings, just as in any transformer when magnetizing current is neglected. Thus, I_S times the number of turns between terminals *1* and *3* must be substantially equal to I_P times the number of turns between terminals *3* and *4*. Since the number of turns is adjustable by moving the dial or pointer of the device, a smooth control of I_F with respect to I_N is obtained between the limits of multi-

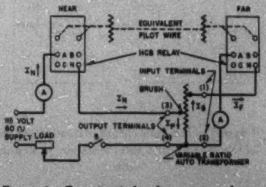

Figure 1. Test circuit for determining characteristic curve for external faults for *HCB* relays

---

* This device is marketed by at least three suppliers. The General Radio Company, Cambridge, Mass., supplies it under the trade name of Variac, and the Superior Electric Company, Bristol, Conn., supplies it under the trade name of Powerstat. The General Electric Company, Schenectady, N. Y., supplies it under the name of Variable Voltage Autotransformer. The author knows of no other manufacturer supplying similar equipment.

Paper 49-262, recommended by the AIEE Relays Committee and approved by the AIEE Technical Program Committee for presentation at the AIEE Fall General Meeting, Cincinnati, Ohio, October 17–21, 1949. Manuscript submitted July 11, 1949; made available for printing September 7, 1949.

W. K. SONNEMANN is with the Westinghouse Electric Corporation, Newark, N. J.

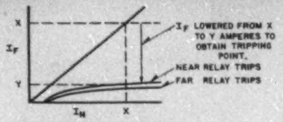

Figure 2. Typical characteristic curve obtained with test set-up of Figure 1

pliers of 1 and zero. Some of these devices have extended windings as illustrated so that, actually, a ratio of I_F to I_N of somewhat more than unity can be obtained.

As the brush contact is moved over the winding, it will short circuit a turn when passing from one turn to the next. If the contact is left in a position where one turn is short circuited, it is theoretically true that the phase-angle error of the device will be affected. However, one turn is so small a percentage of the total winding, and the circulating or short-circuit current in it is so small, that there is no material effect.

Switch *S* is shown to represent schematically a means of throwing the circuit on and off, although a contactor having a contact in each side of the supply line will generally be used. This is desirable because in running curves similar to Figure 2, the higher current values will greatly exceed the continuous current-carrying capacity of the relay and the autotransformer and it is desirable to leave the current on for only the time required to obtain an observation. In this connection, ammeters with an adjustment for presetting the pointer, as in ammeters for measuring inrush currents, are particularly convenient.

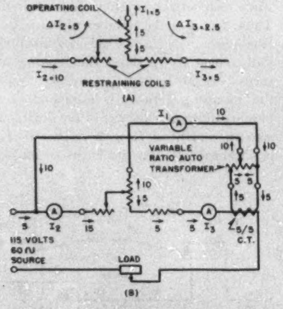

Figure 3. Test connections illustrating the use of the variable ratio autotransformer in step-up ratio

A. Schematic diagram of *CA* relay
B. Connections to develop $\Delta I_2 + I_1$ of (A)

In taking the curve of Figure 2, it is convenient to start with a point wherein the currents are equal, such as $I_N = I_F = X$. This checks a point on the true balance line, wherein neither relay should trip. With this preset value of $I_N = X$, the far relay current is then lowered until a tripping point is reached at $I_F = Y$, this being found by observing the relay action on successive short applications of current. The number of trials necessary will generally be small in number if, after a point or two is obtained, the shape of the curve is predicted and the adjustment for the expected value of $I_F = Y$ is made prior to throwing the current on.

In making any circuit set-up such as in Figure 1, the adequacy of the variable ratio autotransformer should be considered from the standpoint of both voltage and current rating. Considering voltage first, other tests on the type *HCB* relay, for example, have shown that the voltage required to pass up to 80 amperes, 60 cycles, through it from phase *A* to neutral requires from 20 to 40 volts, depending upon the relay taps in use. This is much less than the normal value of 115 volts which a device rated at 115 volts can develop as a counter voltage between the normal input terminals *1* and *2*. The voltage capacity of the device is therefore adequate for the test of type *HCB* relays as per Figure 1, and it can be assumed with safety that the magnetizing current drawn will not be high enough to introduce a material phase-angle error.

The second consideration of current rating should be viewed in the light of the momentary duty required for the test at hand. Information obtained from one manufacturer of these devices indicates that they should not be operated at momentary currents higher than five times the normal rating. One such device rated at 18 amperes continuous has been in use in the laboratory in circuits similar to Figure 1 and to as high a current as 80 amperes, and has been so used for a number of years without showing any signs of distress. Based on the supplier's recommendation of a five times figure, the 18-ampere device could have been used to 90 amperes, so that the actual testing left a margin of safety of 10 amperes. For current values higher than 80 amperes, the author uses a device rated at 40 amperes continuous.

TYPE *CA* PERCENTAGE DIFFERENTIAL RELAY

Figure 3 illustrates an application wherein the variable ratio autotransformer is used to step up the current which it controls. Figure 3(A) illustrates the basic problem in the test of a 50 per cent differential transformer type *CA* relay in use on the 5/10 auto-balance taps. Thus, the particular current values of $I_2 = 10$, $I_3 = 5$, and $I_1 = 5$ amperes represents a true balance for normal operation. To check the percentage characteristics on one side, the current, $\Delta I_2 = 5$ amperes, must be added to I_2, representing a 50 per cent increase in I_2. To check the percentage characteristics on the other side, the current, $\Delta I_3 = 2.5$ amperes, must be added to I_3, representing a 50 per cent increase in I_3. Either of these increments must be added into the original balanced condition, requiring the splitting of the current $I_2 = 10$ amperes into two equal parts. The solution to the first problem only, that of adding $\Delta I_2 = 5$ amperes to the initial condition, is illustrated in Figure 3 (B).

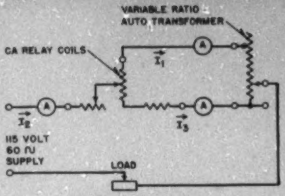

Figure 4. Circuit diagram for arrangement alternate to Figure 3(B)

In Figure 3(B), the 5/5 current transformer is used for insulating purposes, as a separate controllable current is thereby obtained for reintroduction into the relay circuit. In this case, the capacity of the autotransformer and the current transformer to develop the necessary voltage should not be overlooked. In general, the limits of satisfactory operation will be reached at much lower current values than when a step-down ratio is used, as in Figure 1.

An alternate method of accomplishing the same results as in Figure 3(B) is

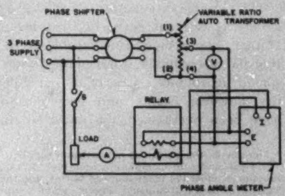

Figure 5. Circuit for determining the phase-angle characteristic of a relay in terms of current and voltage

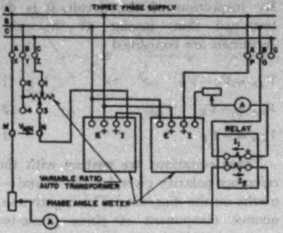

Figure 6. Circuit for the determination of the phase-angle curve of a relay operating on two currents

shown in Figure 4. It is simpler through the omission of the 5/5 current transformer, but it is more difficult to use for those readings when I_3 is the reference current. This is because an adjustment to raise the value of I_1 must necessarily decrease the value of I_3, thus requiring a readjustment of the load. On the other hand, the circuit is convenient when the relay is to be checked for its characteristic involving ΔI_3, Figure 3 (A), for I_2 is then the reference current and is not materially disturbed by an adjustment in the variable ratio autotransformer.

PHASE-ANGLE CURVES

The circuit of Figure 5 shows a set-up for determining the phase-angle characteristic of a relay in terms of the current leading or lagging a reference voltage. It is probably well known in the art, but a trouble spot not so well known is the possibility of distortion of the voltage wave, which, in some cases, leads to erroneous data. The variable ratio autotransformer is shown as a means to adjust the reference voltage to the desired value. Since it has an iron core, there are, of necessity, harmonics in its exciting current. These harmonic components must flow through the impedance of the phase shifter, thereby introducing a harmonic voltage drop in the phase shifter. It follows, therefore, that even with perfect sine wave supply at the input terminals of the phase shifter, the output voltage used at terminals *1* and *2* of the variable ratio autotransformer must contain harmonics, and these will correspondingly show up at the same percentage value at terminals *3* and *4* of the autotransformer. These harmonics affect the instrument indications and may affect the operation of the relay, leading to erroneous data.

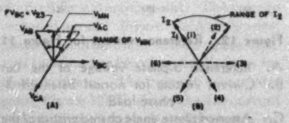

Figure 7. Vector diagrams for Figure 6

The problem of harmonics just discussed occurs in varying degrees. Some phase shifters have more internal impedance than others, and the exciting current of the variable ratio autotransformers depends upon size and rating. In many cases, provided the phase shifter is adequate, the harmonics may be reduced to a negligible factor by using a 230-volt variable ratio autotransformer with a phase shifter having nominal voltage output of 115 volts. By this means, the exciting current is greatly reduced through working the iron core at one-half its normal flux density. In any case, it is desirable to check the wave form of the voltage with an oscilloscope to see if the problem exists. In the more difficult cases, it becomes necessary to replace the variable ratio autotransformer with the old-fashioned potentiometer.

PHASE-ANGLE CURVES BETWEEN TWO CURRENTS

If it is desired to take a phase-angle curve on a relay which operates on two currents, the usual voltage phase shifter, as shown in Figure 5, is generally inadequate because of its limited current rating. The variable ratio autotransformer comes to the rescue through providing a means of getting a current at any desired phase angle from a 3-phase source, as shown in Figure 6. If of adequate rating, say 18 or 20 amperes continuous, its ability to furnish much larger currents momentarily makes it possible to take data to the higher values of current usually encountered in relay work.

Two phase-angle meters are shown in Figure 6 because the author knows of no commercially available instrument which will measure the angle between two currents directly. It is necessary, therefore, to obtain the value of the phase angle between the two currents by taking the difference between their phase angles read with respect to a common reference voltage. An alternate method to the use of two phase-angle meters as indicated is to use a single instrument in connection with a switching arrangement so that the phase angles of the two currents may be read one at a time.

As shown connected in Figure 6, the variable ratio autotransformer acts as a voltage divider on phase *BC*. As the brush contact is moved over the winding, the potential of the brush contact, corresponding to output terminal *3* and reference terminal *N*, can be made to assume any potential on a straight line between phase terminals *B* and *C*, or even beyond, with the extended winding as shown. Thus, the voltage, V_{23}, between terminals *2* and *3* is some function of V_{BC}, and may be expressed as $V_{23}=FV_{BC}$. The circuit voltage, V_{MN}, between terminals *M* and *N* used to supply the relay current, I_2, may be determined by inspection of the circuit as follows

$$V_{MN}=V_{AB}+V_{23}$$

$$=V_{AB}+FV_{BC}$$

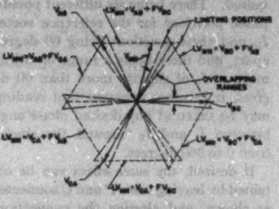

Figure 8. Vector diagram showing control of V_{MN} by separately interchanging *X*, *Y*, *Z* leads, and *M*, *N* terminals of Figure 6

Figure 7 shows the vector diagrams for the circuit of Figure 6. The voltages V_{AB}, V_{BC}, and V_{CA} are the three phase-to-phase voltages of the supply. The locus or range of adjustment of V_{MN} is shown in Figure 7(A), wherein it is shown that a range of slightly more than 60 degrees may be obtained by using the extended winding of the autotransformer. The corresponding range of I_2 is shown in Figure 7(B), assuming substantially unity power factor for the current circuits.

Figure 7(B) also shows six different possible positions for the reference vector, I_1. As shown solid for position (1), it is drawn for the connections as shown in Figure 6, where lead *P* is connected to terminal *A* and lead *Q* is connected to terminal *B*. There being two circuit leads *P* and *Q*, and three supply terminals *A*, *B*, and *C*, there are, of course, six combinations possible, remembering that *P* and *Q* may be interchanged when re-

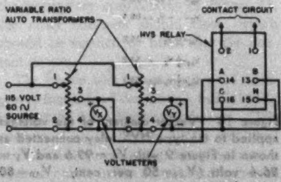

Figure 9. Test diagram for *HVS* relay

quired. There being six different possible phase positions for the reference vector, I_1, and these positions being 60 degrees apart, and there being a range of adjustment of I_2 of slightly more than 60 degrees, it becomes apparent that readings may be taken at any desired phase angle between I_1 and I_2 "around the clock," from 0 to 360 degrees.

If desired, the same effect can be obtained by leaving leads *P* and *Q* connected as shown, and altering the connections with leads *X*, *Y*, and *Z*, and interchanging the connections to terminals *M* and *N* as required. A vector diagram showing the control thus obtained on V_{MN} is shown in Figure 8 wherein LV_{MN} indicates the locus of the extremity of the V_{MN} vector. In this diagram the range of V_{MN} is extended both ways from the central 60-degree sector, remembering that the connections to terminals *1* and *2* of the autotransformer may be reversed, thus placing the extended winding "on the other end." There are six sectors indicated, and to obtain any one of them, the connections to be used are determined from a consideration of the subscripts appearing in the equation given for LV_{MN} for that sector.

The vector diagram of Figure 8 also suggests that, in the event a voltage phase shifter of the usual type is not available, tests may be made on any relay using voltage and current at any desired phase angle by using terminals *M* and *N* of Figure 6 to energize the voltage coil of the relay. This requires reconnecting and using only one phase-angle meter, of course, and will require a separate device for control of the magnitude of the voltage to be applied to the relay potential coil.

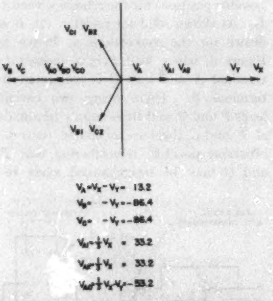

Figure 10. Vector diagram of the voltages applied to the type *HVS* relay connected as shown in Figure 9 with $V_X = 99.6$ and $V_Y = 86.4$ volts ($V_{A2} = 50$ per cent, $V_{A0} = 80$ per cent)

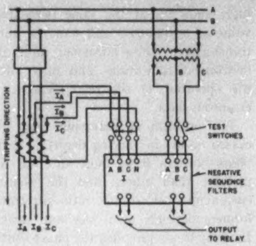

Figure 11. Abbreviated diagram of negative sequence filter and relay connections showing operation of test switches for checking purposes

TYPE *HVS* RELAY

Appropriate methods and circuits for testing relays which operate on sequence components are rather generally "not in the book," except as brought out in instruction leaflets. An interesting case where sequence components are made to order for test purposes is illustrated by the type *HVS* relay. This relay, a single phase-to-ground fault-detecting relay, operates in response to a restraining force from negative sequence voltage, and an operating force from zero sequence voltage, neither of which are present under normal system conditions. Furthermore, the relay has only four voltage terminals, for phases *A*, *B*, *C*, and neutral terminal *N*, so that, somehow, separately controllable negative sequence and zero sequence voltages must be applied to these four terminals if the relay is to be calibrated. Figure 9 shows how this may be done with a single-phase supply.

It is apparent that on a normal 3-phase system, if a solid short circuit occurs on two terminals, such as *B* and *C*, that, at the point of fault, one of the three phase-to-phase voltages disappears, and the other two collapse. The end result is that, to all practical purposes, there is at the point of fault one single-phase voltage between terminal *A* and short-circuited terminals *B-C*. Note that in Figure 9, relay terminals *B* and *C* have been short-circuited together, and a single-phase voltage, V_X, applied between terminal *A* and short-circuited terminals *B-C*, thus simulating a solid phase-to-phase fault. This condition furnishes the required negative sequence voltage to the relay accompanied by positive sequence voltage to which latter voltage the relay does not respond. It is independent of the potential of the neutral terminal, *N*, which is proved by the following analysis in terms of phase-to-neutral quantities. By inspection of the circuit, it is determined that, insofar as the relay terminals are concerned

$$V_{AN} = V_X - V_Y \tag{1}$$

$$V_{BN} = -V_Y \tag{2}$$

$$V_{CN} = -V_Y \tag{3}$$

These equations are written with the reference polarity given by the + and − marks on the diagram. The negative sequence component of these phase-to-neutral voltages is determined in the usual way.

$$\begin{aligned} V_{A2} &= {}^1/_3[V_{AN} + a^2V_{BN} + aV_{CN}] \\ &= {}^1/_3[V_X - V_Y + a^2(-V_Y) + a(-V_Y)] \\ &= {}^1/_3[V_X - V_Y(1 + a + a^2)] \end{aligned}$$

$$V_{A2} = {}^1/_3 V_X \tag{4}$$

Equation 4 shows that the desired value of negative sequence voltage can be obtained by setting the voltage, V_X, to a value of $3V_{A2}$.

The zero sequence voltage is determined by adding equations 1, 2, and 3, from which

$$3V_{A0} = V_X - 3V_Y$$

$$V_{A0} = {}^1/_3 V_X - V_Y \tag{5}$$

Equation 5 shows that if V_Y is made zero, V_{A0}, being then equal to $1/3V_X$, also is equal to V_{A2}, and a top limit is reached for a positive value of V_{A0}, using the circuit shown. If V_Y is made equal to $1/3V_X$, then $V_{A0} = 0$ and the neutral is not displaced with respect to the collapsed voltage triangle. If V_Y now is further increased, equation 5 gives a negative value for V_{A0}, which simply means that V_{A0} and V_{A2} will be 180 degrees out of phase. The 180 degree phase relationship is of no consequence for this particular relay, and does not thereby spoil the desired end result of being able to make V_{A0} greater than V_{A2}.

Numerical values are given in Figure 10 for a particular calibrating point, together with appropriate vector diagram.

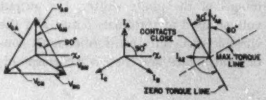

Figure 12. Reference vectors for Figure 11

A. Reference 3-phase voltage of the bus
B. Current vectors for normal balanced 3-phase load
C. Assumed phase-angle characteristics of the negative sequence relay

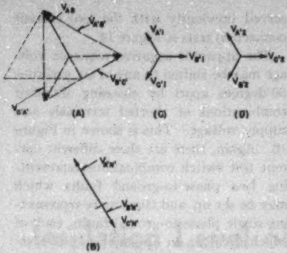

Figure 13. Vector analysis of the voltage conditions of Figure 11

FIELD TESTING WITH LOAD CURRENT AND VOLTAGE

The last test circuit discussed covered means of establishing negative and zero sequence components of voltage in what is essentially a laboratory setup. Going a step beyond this, it is certainly desirable to have some means of checking the overall installation of a relay of the sequence type in order to make sure that the relay and all its external connections are correct. When the relay ignores positive sequence, an illustrative example being the type *CRS* negative sequence directional relay, the fact that it has no response to normal load is inconclusive. Temporary alterations in the external connections can be made, however, as shown in Figure 11, so that sequence components artificially produced from the load currents and voltages are presented to the relay. Since these are derived from the primary quantities, the external connections are thereby checked. In making a test as illustrated in Figure 11, it is necessary to have available instruments not shown in the diagram to determine the magnitude and relative phase angle of the load current flowing at the time of the test. These instruments may be switchboard instruments already installed and connected to the same or other instrument transformers if properly located in the primary circuit. The important thing is that the phase angle, and preferably also the magnitude, of the current I_A, I_B, and I_C flowing in the line must be known, as will be shown from the following diagrams.

Figure 12 gives the basic information required for a starting point. The voltage vector diagram, Figure 12(A), showing phase-to-neutral and phase-to-phase voltages is taken as the reference diagram for phase position. The current vector diagram, Figure 12(B), shows the line current vectors in their proper position with respect to the given voltages for assumed balanced unity power factor load current flowing away from the bus and out over the line in question. This diagram is drawn separately from the voltage diagram in order to keep from having too many vectors in the same picture. It is tied in with the voltage vector diagram, however, through the 90-degree angle which I_A and V_{AN} each make with the X-axis as shown. Figure 12(C) shows the inherent phase-angle characteristics of the relay, wherein V_{A2} and I_{A2} are the negative sequence voltage, in terms of phase-to-neutral quantities, and the negative sequence current applied to the input terminals of the filter. This picture shows the zero torque line leading the voltage by 30 degrees, a typical characteristic. Note that the 180-degree zone in which the current may lie and close the relay contacts is substantially on the out-of-phase side. This makes the characteristic opposite in nature to the usual directional element characteristic. This is necessary because negative sequence power flows away from the fault rather than toward it.

Figure 13(A) shows the voltages involved with the temporary connections of Figure 11. The dotted voltage triangle comes from Figure 12(A), but only V_{AB} is in use. Since terminals B and C are shorted together, this voltage also is V_{AC}, or $-V_{CA}$ insofar as the filter is concerned. The identity of $V_{AB}=V_{AC}$ corresponds to the collapse of the dashed line triangle $V_{A'B'}$, $V_{B'C'}$, $V_{C'A'}$ which would occur with a solid phase-B′ to phase-C′ fault on such a system. The phase-to-neutral voltages which correspond to this collapse are shown in Figure 13(B) wherein $V_{A'N'}={}^2/_3V_{AB}$ and $V_{B'N'}=V_{C'N'}={}^1/_3(-V_{AB})$. These voltages are analyzed into positive and negative sequence components as shown in Figure 13(C) and (D), wherein $V_{A'2}={}^1/_2V_{A'N'}={}^1/_3V_{AB}$. The apparent negative sequence voltage presented to the filter now is determined, and as soon as the apparent negative sequence current is determined, operation of the relay can be predicted.

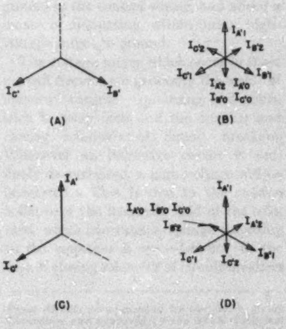

Figure 14. Vector analysis of currents applied to filter

A. Load currents, I_B and I_C, applied
B. Sequence components for (A)
C. Load currents, I_A and I_C, applied
D. Sequence components for (C)

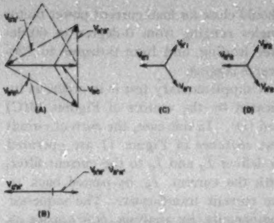

Figure 15. Vector analysis of voltage V_{BC} applied from terminals *A*, *B* to terminal C

The currents, $I_{B'}$ and $I_{C'}$ of Figure 14(A), which were taken from Figure 12(B), are the only two currents flowing into the current filter, and must come out of the box at the neutral terminal. Insofar as the filter is concerned, it appears that the system is experiencing a two phase-to-ground fault. An analysis by means of symmetrical components resolves the currents into the sequence components as shown in Figure 14(B). It will be found that $I_{A'2}$ occupies a position 180 degrees out of phase with the actual current I_A, and is $^1/_3$ of the magnitude of I_A. The vectors for the sequence components have been drawn accordingly.

All the vector diagrams were drawn with respect to the *X*-axis as a reference. It is therefore determined by inspection that $I_{A'2}$ of figure 14(B) leads $V_{A'2}$ of Figure 13(D) by 150 degrees. Referring to Figure 12(C), it is seen that when I_{A2} leads V_{A2} by any angle from 30-degrees leading to 210-degrees leading, the contacts will close. The angle of 150 degrees being within this range, it is concluded that with unity power factor load as depicted by Figure 12(A) and (B) and with the temporary connections of Figure 11, the relay contacts should close, which should be verified by observing the contact action.

The above test is not limited to unity power factor load conditions, but is easily interpreted for other power factors. The current, $I_{A'2}$, of Figure 14(B) will shift in the leading or lagging direction in step with any shift in the actual load currents, Figure 12(B). It follows that the contacts should close for load current power factor angles ranging from 0-degree to 60-degree leading, and from 0-degree to 120-degree lagging.

A supplementary test is in order, as indicated by the vectors of Figures 14(C) and (D). In this case, the current circuit test switches of Figure 11 are operated to deliver I_A and I_C to the current filter, with the current, I_B, by-passed back to the current transformer. The sequence components, by analysis, now appear as shown in Figure 14(D), and it is found that $I_{A'2}$ now lags $V_{A'2}$ by 90 degrees. This is a contact opening condition as determined from Figure 12(C), and the relay contacts should open.

The connections at the voltage filter now may be changed to short-circuit A and B terminals together with switch A open and switch B and C closed. The apparent voltages are analyzed in a manner similar to Figure 13, the results being shown in Figure 15. In this case, the negative sequence voltage, $V_{A'2}$ of Figure 14(D) is 180 degrees out of phase with its former position shown in Figure 13(D). The relay contacts should therefore operate in reverse to the action observed previously with the two current connection tests of Figure 14.

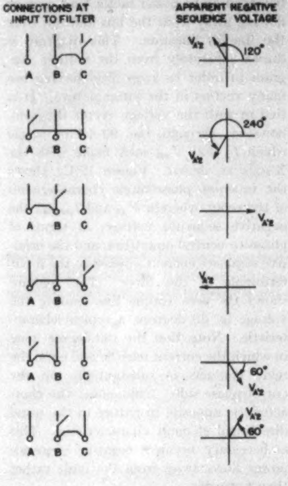
CONNECTIONS AT INPUT TO FILTER
APPARENT NEGATIVE SEQUENCE VOLTAGE
A
B
C
$V_{A'2}$
120°
240°
60°

Figure 16. The apparent negative sequence may be obtained in any of six phase-angle positions with the connections as shown

The apparent negative sequence voltage may be shifted to any of six positions 60 degrees apart by choosing different combinations of shorted terminals and supply voltage. This is shown in Figure 16. Again, there are three different current test switch combinations representing two phase-to-ground faults which may be set up, and three more representing single phase-to-ground faults, each of which involves an apparent negative sequence current. By utilizing several of these combinations, so that each phase of the current and voltage supply is used at least once, the over-all installation can be checked quite satisfactorily.

Summary

It was not the intent of this paper to try to cover the entire subject of relay testing in complete detail, but, rather, to present some new material on the subject. It is hoped that the circuits here presented, together with the analytical methods used therewith, will lead to further new and useful circuits and test methods.

No Discussion

Insulation Level of Relay and Control Circuits

AN AIEE COMMITTEE REPORT

THIS is a report of a Project Committee of the AIEE Relay Committee which was established to study the insulation level of relay and control circuits. Various discussions disclosed that there have been experienced a number of flashovers of relay circuits, which have caused unnecessary interruptions of service. There also have been experiences with over-voltages on control circuits, which have damaged equipment and subjected personnel to hazardous conditions. These discussions indicated the need for determining a suitable standard of permissible voltages on relay and control circuits.

In considering this subject, the circuits can be subdivided into current circuits and control circuits.

Current Circuits

In the case of these circuits it is necessary to consider both the voltages which can be imposed upon the circuits by the current transformers under normal conditions, and under conditions of open circuit. In the former case, the voltages are generally limited to less than a few hundred volts and do not represent an insulation problem. On the other hand, the open circuit voltage of current transformers may reach a value of several thousand volts. Under this condition, it is expected that the operation of any relays associated with that particular current transformer may be improper or incomplete. The general opinion appears to be that it is not practical to design the current circuits to withstand the open circuit voltage of all current transformers, and special means must be used where this protection is desired. The usual method of providing this type of protection is to install a spark-gap across the current transformer secondary terminals. The flashover of these gaps must be sufficiently higher than the maximum voltage expected during system troubles to prevent these gaps from short-circuiting the current transformer and causing incomplete or erroneous relay operations.

Control Circuits

The insulation of control circuits, such as the tripping circuits of protective relays, presents a different type of problem. These control circuits are generally operated from a battery of 120 or 240 volts which is ungrounded. The voltage to ground of this battery is often stabilized by the use of small lamps connected from each terminal to ground. These lamps give visual indication of any accidental ground in the control wiring, and afford a means of dissipating, within limits, high-voltage surges to ground.

The voltage surges which occur in these control circuits are generally the result of opening circuits containing solenoids, such as relay coils and the opening and closing solenoids of circuit breakers. Whenever an inductive circuit is suddenly de-energized, a high-voltage will be generated. This is due to the sudden collapse of the magnetic field of the solenoid, which generates a voltage according to the equation $E = -Ldi/dt$. In the case of closing solenoids of circuit breakers considerable energy is available, with the result that the opening of such a coil circuit may produce severe surge voltages. Following are the principle troubles which may be caused by these surge voltages:

1. The destruction of the grounding lamps.
2. The breakdown to ground of the trip wire or trip coil of another circuit breaker, resulting in an unwanted opening.
3. Where bus protective schemes using instantaneous overcurrent relays are employed, the breakdown between a control circuit and relay coil circuit may permit the solenoid to discharge through the relay coils to the current transformer ground and cause all of the circuit breakers on the bus to open.
4. Operating and maintenance personnel may receive an electric shock.

It has been the experience that the voltages generated by inductive circuits are sufficiently high to cause difficulties in control circuits. At the same time relatively simple means are available to limit the magnitude of these voltages. It, therefore, becomes necessary to determine a standard which can be followed in the design of a control circuit. In order to obtain information on the experience of various power companies, a questionnaire was circulated among several companies. Following is a summary of this questionnaire and the answers received:

Question number 1. What standard test voltage should be used in relaying associated with power switchgear?

Of the 14 companies reporting, 13 indicated that a manufacturer's test voltage of 1,500 volts rms would be sufficiently high. The other company suggested a level of 2,500 volts.

Question number 2. Should different test levels be specified for different circuits?

With only one exception, the companies indicated that it would not be practical to apply different test voltages to different circuits, so that it appears to be reasonable to design all circuits of the relay for the same level.

Question number 3. What is the preferred method for taking care of surge voltages in the control battery circuits?

Paper 49-263, recommended by the AIEE Relay Committee and approved by the AIEE Technical Program Committee for presentation at the AIEE Fall General Meeting, Cincinnati, Ohio, October 17–21, 1949. Manuscript submitted July 18, 1949; made available for printing September 7, 1949.

Personnel of the AIEE Project Committee on Insulation Level of Relay and Control Circuits: B. L. Michelson, *Chairman;* R. E. Cordray, S. Goldsmith, T. R. Halman, V. J. Hayes, W. K. Sonnemann.

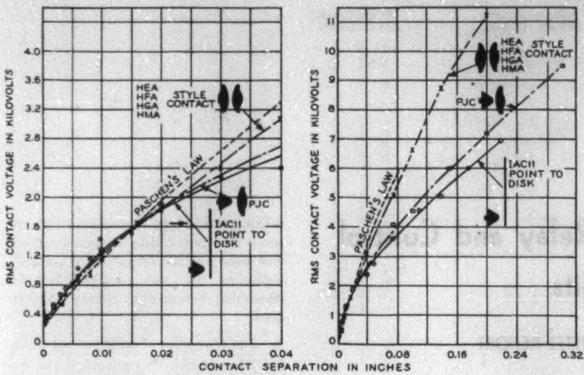

Figure 1. Spark-over voltage of relay contacts for General Electric relays

Note that below 0.1 mil the voltage breakdown increases. This is due to the separation being of the order of the "mean free path" of the electrons and hence an increase in field gradient to produce ionization by collision

All companies indicated that surge voltages should be controlled at their source rather than by designing relays for high insulation levels.

Question number 4. What test voltage is used during maintenance periods on equipment which has been in service?

The test voltages used vary considerably with the different companies. The 500-volt megger test is the most widely used. Some companies use a 1,000-volt megger, others, 220-volt, 1,000-volt or 1,500-volt alternating current.

As indicated under Question number 3 it was the consensus that surge voltages on the d-c control circuits should be limited by the use of special equipment on the solenoids, which are the source of these high voltages. Various methods are available to reduce the magnitude of the voltage, as for example, by installing a resistor across the solenoid to provide a discharge path when the circuit is opened. Discussions within the Project Committee disclosed that Mr. T. R. Halman, of the Detroit Edison Company, had done considerable work along this line. This resulted in the presentation of a paper given before the AIEE in 1948.[1] The paper describes in detail the source of high voltages in control circuits, the troubles caused by these voltages, and methods of their suppression. Following are the conclusions which are stated in the Halman-Harris paper:

"1. There is a high voltage produced by the decay of flux when an inductive device is de-energized. Uncontrolled, it may injure personnel, interrupt service, and damage equipment.

"2. The magnitude of this voltage depends on the value of the energizing voltage, the size, shape, and material of the magnetic circuit, the number of coil turns, and the speed of de-energizing. The discharge voltage of a small relay is often higher than that of a large circuit breaker closing solenoid.

"3. The energy stored in the inductive circuit varies approximately with the size of the device.

"4. A dry-plate rectifier paralleling the coil of each inductive device holds the discharge voltage to a safe value. A slow acting switch, a small capacitor (1 to 4 microfarads), a small resistor, or a gaseous discharge rectifier performs well when used with small low-energy devices such as control relays.

"5. A dry-plate rectifier connected across the control battery with its mid-point grounded prevents the communication of high discharge voltage between circuits.

"6. All these methods of reducing the surge voltage involve slowing the transfer of stored magnetic energy to the electric circuit, which in turn delays the dropout of relays or solenoids. This delay usually is not objectionable but must be evaluated carefully."

Arcing Across Relay Contacts

One of the vulnerable points in the d-c system is the gap between contacts, particularly those in high-speed relays. In order to obtain high-speed operation, it becomes necessary to use very small spacing between contacts. Discussions within the Project Committee indicated that it was not certain whether a 1,500-volt standard would be sufficiently high to prevent the possibility of contacts flashing-over due to surge voltages. Test data prepared by the General Electric Company and Westinghouse Electric Corporation, as shown in Figures 1 and 2, gives relationships between contact separation and voltage required to cause flashover.

Figure 2 shows the results of several tests made by the Westinghouse Electric Corporation on typical relay contacts in different mounting arrangements. The curve numbers, from 1 to 4 are identified with suitable sketches, drawn approximately to scale, to show the contacts and the method of supporting the contacts.

The results for the contacts of curves 3

Figure 2. Curves prepared by Westinghouse Electric Corporation showing spark-over voltage of relay contacts

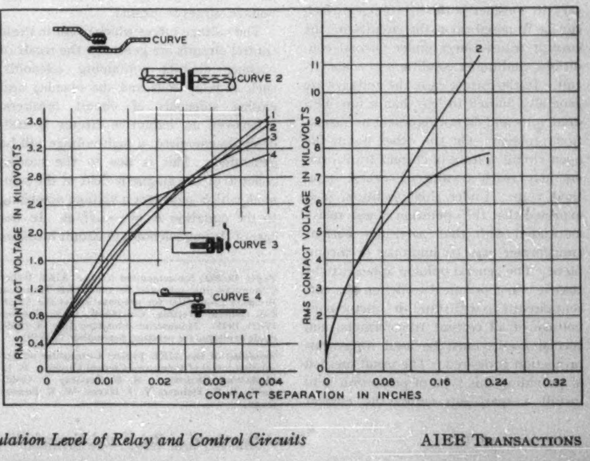

and 4 are not shown on the right-hand side of the curve sheet because, at the higher values of spacing and voltage involved, the arc path was frequently between points on the metallic supports rather than straight through the air between contacts. This phenomenon was observed at about 5.6 kv, (0.10-inch separation) for the contacts of curve 3, and about 3.1 kv, (0.04-inch separation) for contacts of curve 4.

Consideration of these curves indicates that there is not a great amount of difference in the arc-over voltage of different forms of relay contacts at the separations used in high-speed relays. However, it should be noted that the form of the contact support and the connections thereto definitely have a bearing on the results. This is particularly noticeable at the high values of curves 1 and 2.

These curves have been drawn through points which deviate from a smooth curve. The amount of deviation seemed to depend upon air currents and temperature of the contacts more than anything else, although no definite data was obtained to prove this.

Relative humidity of the air also was found to be a factor in the results.

An investigation of recommended settings for high-speed relays indicated that 1,500 volts would not be sufficient to cause flashover of these contacts. The recommended gap settings for high-speed relays which operate in approximately 1 cycle varies from 0.015 inch to as much as 0.050 inch.

It can be seen from reference to Figures 1 and 2 that these gaps are sufficient to prevent flashover by a voltage of 1,500 volts.

Other Sources of Surge Voltages

While the principle source of surge voltages in control circuits is the opening of the inductive circuits, other types of surge voltages have been experienced. One case which was reported in the Project Committee was caused by the capacitive coupling between 66-kv cables and the control wiring. Sudden application of voltage to the 66-kv cables caused sufficient transient voltage to flashover the contacts of a protective relay and cause a transmission line to be opened. In this case the condition was corrected by the installation of capacitors in the control circuit.

Standards for Insulation Levels

At the present time, the ASA Standard on Power Relays[2] is being revised. The test voltage for relay circuits, as determined by this standard, will be a factory test voltage of 1,500 volts rms, and a field test equal to 75 per cent of the factory test, which amounts to 1,125 volts rms, or approximately 1,600 volts crest.

The Association of Edison Illuminating Companies specifies for oil circuit breakers that "the inductive kick caused by interrupting the closing currents shall be less than 1,500 volts crest." While the present AIEE Standard on switchgear does not cover this point, it is expected that future revisions will include some limitation on transient voltages.

References

1. **VOLTAGE SURGES IN RELAY CONTROL CIRCUITS, T. R. Halman, L. K. Harris.** ***AIEE Transactions*** **volume 67, 1948, pages 1693–1701.**

2. **RELAYS ASSOCIATED WITH POWER SWITCHGEAR,** ***C37.1-1937.*** **American Standards Association (New York, N. Y.) 1937.**

No Discussion

A New Technique in the Manufacture of Soldered Porcelain Potheads

A. E. PAPP
MEMBER AIEE

J. H. NICHOLAS
ASSOCIATE AIEE

WITH the development of the art of making metal to ceramic seals during the past two decades, there has been an ever-increasing interest by the public utilities of this country in the use of soldered porcelain potheads for terminating important cables. The advantages of bonded metal-to-porcelain seals over the more common gasketed seals in the manufacture of potheads are:

1. Permanent factory assembly and test of all joints between metal and porcelain.
2. Greatly increased resistance to aging, cold-flow, and permanent set.
3. Complete resistance to the chemical action of filling compounds and cable oils.
4. Greater stability through time and range of temperature.

The disadvantages are:

1. High initial cost due to the complicated technique required in manufacture.
2. Limited application due to mechanical and size restrictions.

Soldered porcelain potheads, properly installed, form a hermetic seal on the ends of cables so necessary for the satisfactory performance of paper-insulated cables.

Our earliest Soldertite potheads of about 12 years ago used a solder sealing process developed by a large porcelain manufacturer. The process was found to be satisfactory but rather hard to handle. It also was extremely expensive and limited our procurement of porcelain to one source. Because of these factors we decided to develop our own metal-to-porcelain solder seal.

This new process, we felt, should be adaptable to a wide range of sizes and shapes of porcelain required by the users of our equipment. It should be so devised that it could be used on porcelain produced by any porcelain manufacturer. It should be as simple as possible and more rugged than the other then-known methods. It should be less expensive than the other contemporary processes.

We finally did develop a new process and are using it today. Briefly, the process consists of coating certain areas of a heated, chemically clean glazed porcelain with molten copper sprayed from a metalizing gun; tinning those areas with solder; and then soldering to a metal part. The completed seal consists, really, of three bonds or joints in series. The copper-to-porcelain bond is the most difficult to make and requires a great deal of consistency and control. The copper-to-solder bond is the easiest to make and requires only ordinary care. The solder-to-metal bond is not very difficult to make but it does require manual dexterity and skill that come only with long practice.

Because the initial copper-to-porcelain bond is of the adhesion-cohesion type, it is highly dependent upon the absolute chemical cleanliness of the porcelain. The porcelain is cleaned with detergents and carbon tetrachloride and given a final cleansing in a vapor degreaser. After this cleaning treatment nothing is permitted to touch the bond surfaces until they are sprayed with molten copper. The porcelain then is heated in a chemically clean atmosphere to drive off all of

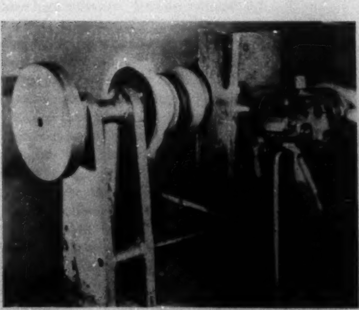

Figure 1 (left). The spray fixture facilitates rapid adjustment of gun-to-porcelain spacing, masking with transite shield and rotation of porcelain

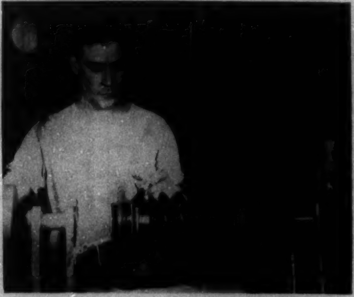

Figure 2 (right). Metalized areas are scrubbed with soldering flux prior to tinning

---

Paper 49-264, recommended by the AIEE Insulated Conductors Committee and approved by the AIEE Technical Program Committee for presentation at the AIEE Fall General Meeting, Cincinnati, Ohio, October 17–21, 1949. Manuscript submitted November 18, 1948; made available for printing September 20, 1949.

A. E. PAPP and J. H. NICHOLAS are both with the G and W Electric Specialty Company, Chicago, Ill.

Figure 3. Openings of the porcelain tube are plugged and the metalized areas tinned in a solder pot

the surface moisture and to raise the temperature to such a point that it will withstand the thermal shock of the oxygen acetylene flame of the metalizing gun.

The heating is done in an electric oven that permits close control and recording of temperature. The proper temperature and time cycle for this oven was determined experimentally by testing a large number of units to destruction to establish the optimum conditions for obtaining the best copper-to-porcelain bond. After the heating cycle is completed, the porcelain is placed into a special spraying fixture that exposes only the areas to be metalized to the flame and molten metal spray of the metalizing gun, see Figure 1. The spraying of molten copper onto certain areas of porcelain is done very rapidly and under closely controlled conditions. When the spraying is completed, the porcelain is quickly placed into another oven whose temperature is somewhat lower than that of the first oven and allowed to cool slowly to soldering temperature.

Every step of this metalizing process, from oven to oven, must be rigidly controlled in time, temperature, and technique. The porcelain must be heated gradually and evenly to the proper spraying temperature. The movement of the porcelain from the first oven, to spraying fixture, to the second holding oven must be done rapidly in order to keep the ceramic from fracturing due to the thermal shock of room temperature. The total allowable oven-to-oven time is about 15 or 20 seconds. Because of the short period of time available for molten metal spraying, every bit of equipment that is used is especially designed and arranged so that the operation is done swiftly.

After the metalized porcelain has cooled gradually to a predetermined temperature in the holding oven, the pieces are removed individually, the metalized surfaces are cleaned with soldering flux, see Figure 2, and tinned with molten 50-50 solder of a closely regulated temperature, see Figure 3. Then, before the insulator has a chance to cool, it is immediately soldered to freshly tinned metal parts that are heated to a certain critical temperature. The soldering is done by placing the insulator on end into a tinned metal hood, with a preformed asbestos gasket forming a gap and solder dam, and filling the gap between the tinned porcelain and the tinned hood with molten solder. As this molten ring of solder cools and solidifies, a large soldering iron is used in contact with the top of the molten solder to keep it in a liquid state as the ring solidifies from the bottom up. This same procedure is used for making the solder joint at the wiping sleeve, Figures 4 and 5.

When the soldered porcelain assembly has cooled to room temperature, it is carefully washed and cleaned and given a "bump" test. This test is rather rough and crude but it tells us what we want to know. Essentially it consists of taking the whole soldered assembly and bouncing it from a height of about two feet onto a wooden table about ten times with the axis of the terminal parallel to the table.

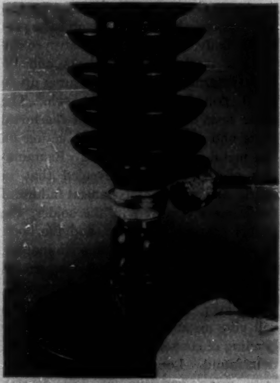

Figure 4. Solder is poured into the gap formed by the asbestos gasket between the hood and porcelain

Figure 5. Wiping sleeve is soldered to porcelain as table is rotated

Following the bump test, the pothead is tested for leaks with 30 pounds per square inch air pressure while it is submerged in hot water at about 170 degrees Fahrenheit. The final test is an electrical test in which the inside bore of the porcelain is explored with a grounded probe while the wiping sleeve and conduction glaze area is energized at 20-kv 60-cycle alternating current. We have found that if the potheads withstand the leak test and the electrical test after being bumped, they will perform without difficulty in the field.

The hood and the wiping sleeve are made from copper spinnings and machined bar stock brazed together with silver solder. No castings are used, thus eliminating trouble due to porous castings. The pothead is designed to reduce the amount of heat and time necessary to make a good tight soldering job in the field. The electric connection at the top is made by crushing the hood thimble tightly against the internal cable ferrule by means of the pressure exerted by clamping the aerial lug onto the hood thimble. The internal cable ferrule has several grooves along its surface to permit free venting of the pothead through a small hole at the top of the hood while filling. This small vent hole is closed by a tinned machine screw and can be soldered shut with a soldering iron with no danger of damaging the soldered joint between the metal hood and the porcelain. The wiping sleeve is quite long and thoroughly tinned so that with ordinary care and attention to solder temperature there is little danger of damaging the joint between the wiping

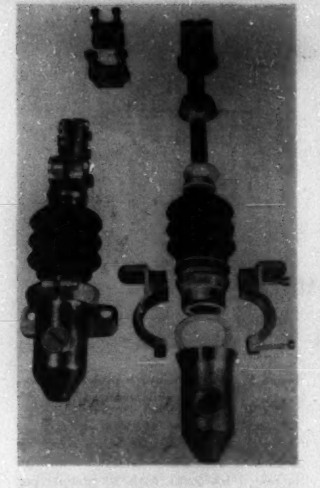

Figure 6. Component parts to complete the Soldertite pothead installed on paper-insulated lead-covered cable

sleeve and the porcelain due to the heat from the wiping operation, Figure 6.

The Soldertite method of attaching metal parts to porcelain is the result of a large number of experiments and tests undertaken to establish a metal-to-porcelain soldered joint that would be hermetically tight under all known service conditions.

The electrical design criteria we established for this new pothead were rather easy to meet even though there were some new principles involved, such as conductive glaze shielding along the lower external cylinder of the bushing terminating under the lowest petticoat. This new principle (for potheads) has the effect of reducing the electrical stress at the terminus of the grading cone on the inside of the pothead porcelain. The mechanical design criteria were something else again and were quite complex in their solution. It was decided that the pothead should remain mechanically perfect and free from leaks at 30 pounds per square inch and vacuum under the following conditions:

1. Repeated instantaneous thermal shocks from 250 degrees Fahrenheit to −10 degrees Fahrenheit.

2. A frigid test for about four hours at −70 degrees Fahrenheit.

3. Abnormal vibration of aerial conductors and pothead mounting structures.

4. Severe shock such as is used in the bump test.

To eliminate "pinch-off" or cracking of the porcelain under the low temperature −70 degrees Fahrenheit test, we had to proportion our metal sections and our tapered sections of porcelain so that the metal parts could contract elastically without rupturing the soldered joint or crushing the porcelain. Then too, these same structures had to be elastic enough to "take" repeated flexings as occur when the pothead is subjected to repeated thermal shocks from 250 degrees Fahrenheit to −10 degrees Fahrenheit. We found that even the shape, size, and condition of the asbestos gaskets affected the performance of the pothead under the rigid requirements that were established.

During the first year of development it was not uncommon to lose nine out of ten insulators during various stages of manufacture and test. We found that too rapid initial heating developed cracks in the porcelain. When the hot porcelain was exposed to room temperature too long, cracking and splitting occurred. A mechanically weak conductive glaze caused cracking. Because it was easier to clean, we found that metalizing adhered to glazed surfaces better than to unglazed ones. We found that in periods of high humidity we were getting porous soldered joints because of the moisture absorbed by the asbestos gaskets turning to steam when hot solder was poured into the joint. We found that to get the perfect solder joint all parts must be hot and freshly tinned to eliminate the oxide film.

Tests to destruction indicate that the soldered metal-to-porcelain joint of Soldertite potheads equals or exceeds the tensile strength of the glaze and the porcelain body. Joints were destroyed by straight mechanical pull tests and by using internal hydraulic pressures up to 1,500 pounds per square inch. The latter tests caused bloating of the metal parts and a resultant peeling action on the metal-to-porcelain joint. Examination of the fractures revealed that in nearly all cases the mechanical failure of good joints occurred in the solder, the copper coating, the glaze, and the body of the porcelain rather indiscriminately, indicating that the various components of the joint were of about equal strength.

However, a nondestructive test that will give an absolute indication of poor bonding of copper particle to glaze is yet to be found. Long time internal pressure tests using kerosene at 180 degrees Fahrenheit and 30 pounds per square inch and hydraulic tests at 300 degrees Fahrenheit with pressure surges of 60 pounds per square inch do not positively reveal poor bonding in all cases. X-ray examination and high-frequency dielectric tests have failed to discriminate between good and bad joints and little hope is held for test results with a Sperry Reflectascope using supersonic vibrations.

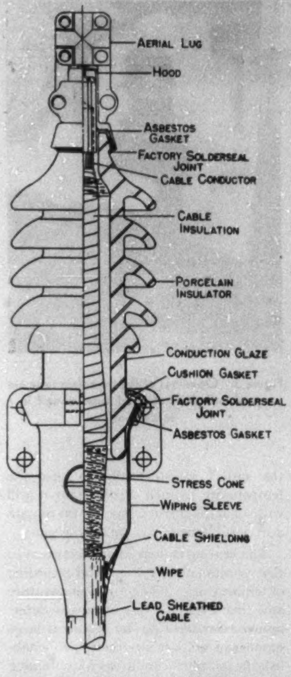

Figure 7. Details of a 15-kv 500,000 circular mils Soldertite pothead installed on paper-insulated, lead-covered cable

So far all that can be done is to test joints to destruction periodically as a check on the process and at the same time rigidly adhere to established procedure and technique.

Soldertite potheads, see Figure 7, using the described method of soldered porcelain technique have been in actual service since 1940 and many of them are installed on gas-filled cables. To date, the service record of this type of construction is excellent. Industry-wide approval is indicated by the more and more general use on all types of cable and by complete standardization on this type of pothead by several large utilities in this country.

Discussion

L. I. Komives (The Detroit Edison Company, Detroit, Mich.): This discussion presents the thinking of engineers of The Detroit Edison Company concerning potheads in general and soldered potheads in particular. We would like to commend the G & W Electric Specialty Company for their progressiveness in working out problems pertaining to potheads especially in trying to eliminate true gaskets.

The G & W design also should be complimented on the electric connection between the ferrule and the terminal connector. This connection is made by crushing the hood against the ferrule when the clamp-type terminal connector is tightened in place. On the pothead we are using, this type of connection also is provided when a clamp-type terminal connector is used.

We believe the paper is very complete in describing the meticulous processes of manufacture, but it seems to us that the importance of control during manufacture, places too much responsibility on the dexterity of the workmen. The illustrations included in the paper show that the manufacturing process is vulnerable to many variables which are independent of the dexterity of the workmen. For instance, the amount of metal sprayed on the porcelain is not accurately controlled, the temperature of the solder, even though controlled, can vary beyond the desired limits after being placed in the ladle, and there are no safeguards against the inclusion of dross in the solder which would result in an inferior seal. In other words detrimental variables can enter the manufacture without being obvious to the workmen.

The ideal type of metal for metal-to-porcelain application is one which has the same thermal coefficient of expansion as the porcelain. We then could expect the two materials to expand in unison, without placing stresses on the metal or the porcelain.

It is recognized that seals-in-series, where one seal depends upon the behavior of another, is not desirous in such a terminal, the sealing ability of which is of greatest importance. The three materials used in the three seals in series have different coefficients of expansion, and in order to evaluate the resulting effects of temperature changes in the range of −10 degrees Fahrenheit to 250 degrees Fahrenheit, we have calculated the dimensional changes of the materials if these materials are unrestrained. We have estimated the outside diameter of the porcelain at the metallization point to be seven inches.

Table I

Material	Circumferential Increase, Inches	Diameter Increase, Inches
Porcelain	0.0114	0.0036
Copper Spray	0.0530	0.0168
Lead-Tin	0.0825	0.0262
Copper Sleeve	0.0554	0.0176

Table I of the discussion shows the copper-spray tends to pull away from the porcelain, the lead-tin tends to pull away from the copper-spray, and the copper sleeve is stressed to contain the lead-tin. We cannot visualize the action of the solder during temperature cycles, but we do know that on a cooling condition the solder will not revert to its original shape after being forcibly deformed during the previous heating, but rather the solder will necessarily be forcibly reshaped or the solder will pull away from the copper sleeve. We believe that a combination, such as this, is conducive to poor sealing and for that reason should be avoided. Inasmuch as we question the life of the seal, we believe it will be a comparative short time when one or the other metal will pull apart to produce an opening for leaking. The life of the seal should be infinite.

There is no provision in the G & W design for determining the level of the compound during filling. We believe that the field workman will either under-fill or over-fill the compound. In the case of over-filling, the overflow will flow out the venting hole, thereby making it very difficult to produce a good soldering job to seal the screw in the venting hole. Over-filling also will cause the compound to coat the ferrule and certain types of compounds will interfere with making good electrical contact when the hood is crushed against the ferrule when the aerial lug is tightened in place. On a well designed pothead of this type, the venting hole should be large enough to determine the level of the compound, and should be located at the level to which the hot compound is poured, filling of course from the bottom upwards. The proper pouring level is thus indicated by the issuance of compound at the venting hole. The venting hole can then be closed and the natural shrinkage of the compound during cooling will provide expansion space for service operation.

Inasmuch as the metal, having the same thermal coefficient of expansion as porcelain is not available for this application, the next best is to seal between the porcelain and the metal with resilient material, such as synthetic rubber, thereby preventing the possibility of overstressing either the porcelain or the metal. Such an assembly makes for a semiflexible joint wherein mechanical shock to the metal is not transferred to the porcelain. Such an assembly also provides for relieving the porcelain of the mechanical loading at the terminal, especially when the porcelain is not truly round at the hardware point. Under heavy loading, the resilient sealing material will conform to the shape of the porcelain, without harmfully spot-loading the porcelain.

The pothead we are using is constructed to provide seals which are dependable, and which are easily tested to insure tightness. The seal between the porcelain and the hardware is effected by the rolled-on process which dependably seals and at the same time provides a joint which inherently is resilient. The seal at the terminal end has been 100 per cent reliable in the field when simple rules of applying are followed. The metal-to-metal joint, between the hooded-type terminal connector and the metal cap, in effect is a ground joint although it is not produced by any special machining. This metal-to-metal joint also acts as the stop to determine the compression of the copper-asbestos gasket which is in parallel sealing relationship with the metal-to-metal joint. To check on the sealing of the metal-to-metal joint, a few months ago, five potheads were drawn at random from stock and tested for seal without the copper-asbestos gasket. All five potheads tested tight.

The metal-to-metal joint also provides additional current carrying ability at this point.

These potheads have means for readily determining the level of the compound during filling or for later inspection. The hole in the top cap is used for this purpose as well as to vent during filling. This hole is sealed with a copper-asbestos gasket and a metal-to-metal ground joint between the plug and the cap.

A. E. Papp: Admittedly, there are operations in the technique that do not entirely eliminate the human element—what operation does? In our opinion, one of the factors that is producing almost 100 per cent satisfactory soldered porcelain seals in our process is the fact that we have given men a pride in their job to do a good job, and have given them a full realization of their responsiblities so that the job content really becomes a psychological factor in maintaining a good spirit and morale.

In the first place, we see no way in making all of the processes involved in the procedure automatic because of the large variation in size and shape of the different types of porcelain, and because of the inspection necessary between each operation. We could go on and on in a long discussion of this subject, but in our opinion we have mechanized as far as we want to go until we come to a point where we are making thousands of exactly the same type and size of soldered porcelain potheads, and then perhaps we can put some automatic machinery to work.

We feel that ladle temperature control is entirely unnecessary, since the ladle is constantly floated in the molten solder bath and is maintained at that temperature. It is removed only from the solder bath to pour the joint between the porcelain and the metal fittings, and the pouring period takes only about three to five seconds. In our opinion we would rather not complicate this very simple and satisfactory operation. Under the temperature limits that we use, very little dross accumulates at the top of the solder pot and the dross that does accumulate is skinned back every time a ladle full of solder is used.

Admittedly, the ideal type of metal to porcelain application is one which has the same thermal coefficient for the metal as that for the porcelain. However, that is over simplifying the problem. With the new metals coming into use we should imagine that such a joint could eventually be produced, but we rather suspect at a cost somewhat out of reason. We have a series of seals between porcelain, copper, solder and then copper again in which thermal coefficients of expansion vary considerably and theoretically to the disadvantage of the joint. But, as usual, the proof of the pudding being the eating thereof, the actual practical experience indicates that we have had not one whit of trouble from this source. What troubles we have experienced have been in the improper cleaning of the porcelain and its preparation for metal spraying. We rather suspect that the seal works in spite of the disadvantageous thermal coefficient of expansion because the pothead in actual service never reaches the temperature at which the solder itself solidifies, namely about 350 degrees Fahrenheit. Mr. Komives' observations regarding the differences in coefficients of expansion and diameter increases of the various materials making up the joint are correct. However we believe the seal works well because the porcelain which changes diameter the least is on the inside of the combination of the series of joints. Because this is true, we believe that regardless of the differences in coefficient of expansion between the copper spray the solder and the copper sleeve and the apparent disruptive force between the copper sleeve and the solder, the sum total stress in the joint, in fact, is entirely compression. The porcelain in effect stays where it is and the metals try to close in on it. However, because the porcelain will not move, all of the metals we believe end up at operating temperatures being in compression, that is, we are convinced that the copper spray, the solder and copper sleeve are all in compression in a radial direction, although admittedly they are in tension circumferentially. Because this is true we make the copper sleeve very light in construction so that it can be deformed as it cools.

We agree with Mr. Komives that the rolled-on type of seal that he speaks of is very effective and efficient. However, we see no particular advantage to it over any other good gasketed type of pothead construction. Gasketed potheads are still very much in the picture and with reasonable installation care, give excellent results.

Design Fundamentals of Potheads 69,000 Volts and Below

J. H. NICHOLAS
ASSOCIATE AIEE

PROPER selection, installation, and utilization of electric equipment for transmission and distribution systems requires a knowledge of the basic functions and design fundamentals of each component.

There has been considerable information published in American technical journals on the theory, design, test, and application of underground cables and cable joints. On the other hand, very little information is available on the termination of these cables in potheads and, therefore, some discussion on this subject seems warranted.

Potheads are usually employed where cables of moderate or high voltage are connected to generators, switchgear, transformers, overhead lines, or sectionalizing equipment. They are designed to provide:

1. A hermetic seal of the cable end to prevent contamination of the cable insulation by moisture or liquid dielectrics used in equipment to which the cables are connected.
2. A protection of the cable insulation against weather and adverse contaminating atmospheric conditions.
3. Physical protection and mechanical support of the cable conductors, insulation sheath, armor, and so forth.
4. Means for making external electric connections with the cable conductors within the pothead housing.
5. Adequate external dielectric strength commensurate with the desired insulation level of the cable system and an internal dielectric strength (including that of the cable end) a safe margin above this level.

Years of development work and operating experience have resulted in improvements in the design of potheads and an understanding of their electrical characteristics. New gasket materials now are in use which apparently have excellent aging characteristics, low percentage of set and cold flow, and high resistance to oils, asphalt compounds, and synthetic dielectrics. The design of the metal parts and methods of making the gasketed joints have been improved and permit easier and more reliable assembly in the field. Potheads having metal parts soldered to the porcelain insulator and requiring no gaskets also have been developed. A discussion of the various types of potheads and the design of their component parts would be quite long; however, some of the factors influencing the design of a pothead for the desired dielectric strength of a cable termination can be generalized and, therefore, the scope of this paper has been limited to this subject.

It is hoped that the following test data and electric field patterns will clearly indicate that the over-all dielectric strength of a pothead installation is not merely a function of creepage distances between live parts and ground or oversized porcelain insulators, but rather a function of proper pothead selection for a given size and type of cable and coordination of the dimensions and location of the stress relief cone with respect to its metal parts.

A basic cable termination has the conductor bared for several inches to permit electric connection to equipment and the conducting jacket, cable shielding or sheath removed for a given distance to provide surface insulation between the live conductor and the grounded sheath. The approximate electric field pattern for this type of termination, indicating the voltage distribution in and along the surface of the insulation when the cable is energized, is shown by Figure 1 (A).

The lines which begin coaxially with the conductor within the conducting sheath are equipotential lines that is, (1/2 and 1/4 equal 50 and 25 per cent respectively of the conductor to sheath voltage.) The lines which extend from the conductor to the sheath are flux lines. These two groups of lines provide a means of visualizing electric fields and when carefully constructed, permit relatively accurate estimates of capacitance and voltage gradients. High concentration of the flux lines upon a small area of a conductor and close grouping of the equipotential lines near this area indicate zones of high electric stress and possible points of insulation failure.

The electric field patterns included in this paper were developed graphically. Although the effect of the different dielectric constants (specific inductive capacitance) of the various insulating materials has not been included, these patterns are quite sufficient to indicate the high-potential gradients possible at cable terminations. They also emphasize the importance of good stress relief cone construction and pothead selection.

Figure 1(A) indicates that the potential gradients within and along the surface of the cable insulation are not uniform and in this case, approximately 75 per cent of the conductor to sheath voltage appears across the first inch of surface insulation. In the design of cable terminations it is important to realize that the electric field and potential gradients are not a function of the exposed length of cable insulation but mainly the shape, size, and separation of the electrodes.

Figure 2 indicates 60-cycle surface flashover values for various lengths of exposed cables in air. Ionization of the air (corona) begins at the sheath end at the same potential (for a given size and type of cable) regardless of the length of

---

Paper 49-265, recommended by the AIEE Insulated Conductors Committee and approved by the AIEE Technical Program Committee for presentation at the AIEE Fall General Meeting, Cincinnati, Ohio, October 17-21, 1949. Manuscript submitted July 1, 1949; made available for printing September 12, 1949.

J. H. NICHOLAS is with the G & W Electric Specialty Company, Chicago, Ill.

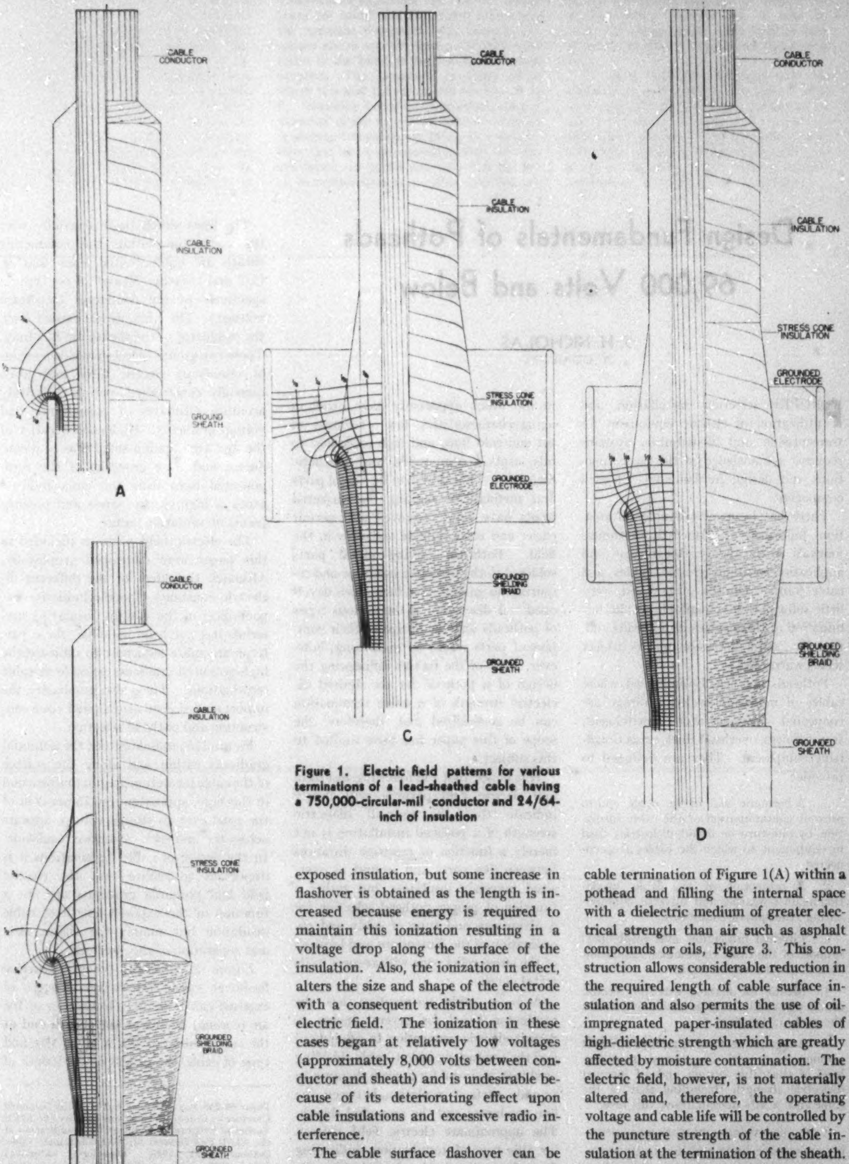
CABLE CONDUCTOR
CABLE INSULATION
GROUND SHEATH
A
CABLE CONDUCTOR
CABLE INSULATION
STRESS CONE INSULATION
GROUNDED SHIELDING BRAID
GROUNDED SHEATH
B
CABLE CONDUCTOR
CABLE INSULATION
STRESS CONE INSULATION
GROUNDED ELECTRODE
GROUNDED SHIELDING BRAID
GROUNDED SHEATH
C
CABLE CONDUCTOR
CABLE INSULATION
STRESS CONE INSULATION
GROUNDED ELECTRODE
GROUNDED SHIELDING BRAID
GROUNDED SHEATH
D

Figure 1. Electric field patterns for various terminations of a lead-sheathed cable having a 750,000-circular-mil conductor and 24/64-inch of insulation

exposed insulation, but some increase in flashover is obtained as the length is increased because energy is required to maintain this ionization resulting in a voltage drop along the surface of the insulation. Also, the ionization in effect, alters the size and shape of the electrode with a consequent redistribution of the electric field. The ionization in these cases began at relatively low voltages (approximately 8,000 volts between conductor and sheath) and is undesirable because of its deteriorating effect upon cable insulations and excessive radio interference.

The cable surface flashover can be materially increased and the effects of weather and atmospheric contamination practically eliminated by enclosing the cable termination of Figure 1(A) within a pothead and filling the internal space with a dielectric medium of greater electrical strength than air such as asphalt compounds or oils, Figure 3. This construction allows considerable reduction in the required length of cable surface insulation and also permits the use of oil-impregnated paper-insulated cables of high-dielectric strength which are greatly affected by moisture contamination. The electric field, however, is not materially altered and, therefore, the operating voltage and cable life will be controlled by the puncture strength of the cable insulation at the termination of the sheath. This value is generally much lower than the puncture strength of the cable proper, see Table I.

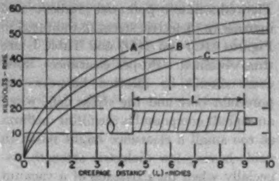

Figure 2. 60-cycle dry flashover values of various length cable ends in air

A. 2/0, 15-kv 22/64-inch rubber-insulated cable
B. 750,000-circular-mil 15-kv 16/64-inch varnish cambric insulated cable
C. 2/0, 15-kv 13/64-inch paper-insulated cable

The high-potential gradients at the sheath end which produce the low puncture values may be reduced by applying to the cable additional insulation in the form of a double cone with a conducting braid electrically and physically connected to the sheath or cable shielding tape, wrapped up the cone and terminated at a diameter greater than that of the cable insulation. This construction is called a stress relief cone and the associated electric field, increase in dielectric strength and the reduction in potential gradients are evident in Figure 1(B) and Table 1.

Unfortunately, the effectively electrical strength of wrapped insulation in the axial direction is considerably less than in the radial direction, so it is important that the hand-applied insulation of the stress relief cone be carefully applied to form a logarithmic or, more practically, a gradual taper (4 to 7 degrees) since too steep a cone may produce high axial potential gradients with consequent failure within the cone insulation again resulting in low puncture strength. Stress cones for paper- or varnish-cambric insulated cables are generally constructed of tightly-wrapped half-lapped layers of oil-packed *VC* tape. Stress cones for rubber-insulated cables are made with rubber or moisture-free, dry *VC* tape. The resultant puncture strengths are a function of the diameters of the stress cone. See Table 1.

It has been the general practice to make the maximum thickness of stress relief cones for rubber, varnish cambric or solid-type, paper-insulated cables the same as that of the applied cable insulation. In view of the improvement in the quality of cable insulation with consequent reduction in thickness for a given voltage, this practice might result in inadequate stress relief cone design. Stress relief cones for gas- and oil-filled paper cables require special consideration owing to the relatively thin walls of insulation employed.

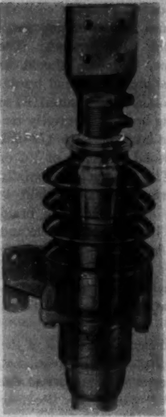

Figure 3 (left). Gasketed-type 15,000-volt pothead for compound-filled single-conductor cable terminations

The electrical stresses at the stress relief cone are not a function of the radial dielectric strength of the cable but of the electrode separation. This being the case each pothead installation should be given proper consideration in order to obtain maximum internal dielectric strength.

It is impractical to establish general rules for stress relief cone design because of the great number of sizes and types of cables which may be used with a given pothead and it is, therefore, desirable to follow the recommendations of the pothead manufacturer.

Some pothead metal parts at sheath potential can be employed to advantage in reducing the axial potential gradients as well as the puncture gradients. Figures 1(C) and 1(D) illustrate the proximity effect of another grounded electrode upon the electric field of figure 1(B). This electrode can be part of the pothead body, a conducting glaze on the external porcelain surface, or an insulated shield mounted about the stress relief cone within the pothead and electrically connected to the sheath. The maximum longitudinal gradients in Figures 1(C) and 1(D) are about one-half and one-quarter, respectively, of the gradients in Figure 1(B). Sixty-cycle voltage-time tests were conducted on carefully insulated test mandrels with different thicknesses of stress cone insulation and various shielding electrodes. The results are tabulated in Table 1 and details of the test mandrels are indicated on Figure 4. All tests were made with the test mandrels immersed in cable oil having a viscosity of 100 Saybolt at 100 degrees Fahrenheit and a

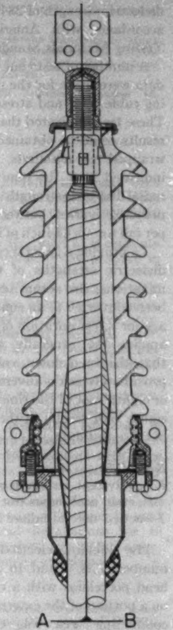

Figure 5 (right). Gasketed-type 34,500-volt pothead with two cable terminations. *A* is preferred because the use of maximum thickness of cone insulation and effective shielding by the pothead metal body results in minimum internal dielectric stresses

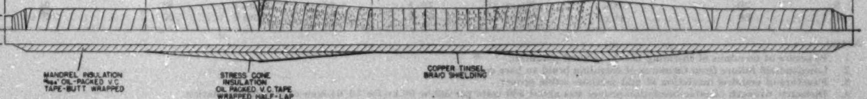
30"
5"
4"
4"
4"
MANDREL INSULATION
OIL-PACKED V.C TAPE-BUTT WRAPPED
STRESS CONE INSULATION
OIL PACKED V.C TAPE WRAPPED HALF-LAP
COPPER TINSEL BRAID SHIELDING

Figure 4. Details of insulated mandrels prepared for tests listed in Table I

dielectric strength of 28 kv when tested in accordance with American Society for Testing Materials Standards *D117-33*.[1]

A number of tests not included in these data were made for the purpose of checking cable joint and stress cone materials. These tests indicated that very consistent results could be obtained with the hand-wrapped test mandrels. Also these tests indicated that the equivalent one hour radial dielectric strength of these insulated mandrels varied between 360-370 volts per mil for 16/64-inch of insulation.

To provide a general comparison of the dielectric strengths of the various terminations, the actual test voltages have been converted to an equivalent test voltage for a test duration of one hour. This applies the generally accepted theory that the breakdown voltage varies approximately as the inverse sixth, seventh, or eighth root of the time to failure. The eighth root results in the best agreement of these test data.

$E = V\sqrt[8]{T}$

E = equivalent test voltage for 1 hour
V = actual continuous test voltage
T = actual time to failure in hours

The shielding electrodes used in tests numbers 7, 8, 9, and 10 consisted of pothead porcelains with a conducting glaze on a portion of the external surface. The conducting area was electrically connected to the shielding braid and mounted coaxially with the test mandrels as indicated in Figures 1(C) and (D).

The use of gas-filled cables introduces an additional problem in the termination of the cable ends since it is generally desirable to fill the pothead with nitrogen at 12 to 15 pounds per square inch pressure. This low-pressure gas does not have the high dielectric strength of asphaltic compounds or oil and, therefore, it is possible that the internal surface dielectric strength may not be adequate to withstand the impulse and switching surge conditions of the cable system. The stress relief cone, therefore, should be modified by wrapping additional insulation over the stress cone of Figure 1(B) so that the shielding braid is effectively terminated within a layer (1/8- to 1/4-inch thick) of a semisolid dielectric of *VC* or paper and oil. This treatment materially increases the surface ionization point at the termination of the shielding braid with consequent increase in 60-cycle and impulse-surface flashover values as much as 25 to 30 per cent. The proximity effect of the shielding electrode can increase the surface flashover an additional 30 to 40 per cent.

The external dielectric strength of the pothead can be affected by the location of the stress relief cone with respect to the external grounded parts. By locating the stress relief cone well up in the porcelain, the external grounded parts can be effectively shielded so that an increase in external flashover value will be obtained. This principle is applied to some high-voltage bushings.[2] With this location in a pothead Figure 5(B) however, the electric field at the stress cone will assume that of Figure 1(B) with possible high-potential gradients at the braid termination. For maximum dielectric reliability of the cable termination, any effective electric shielding should be applied so that the potential gradients of the cable insulation and stress relief cone will be as low as possible since considerable variation in the quality of the hand-applied insulation and stress cone construction must be expected. The preferred location of the stress cone is, therefore, where the shielding braid is terminated below the top of the grounded external parts and as close to them (in a radial direction) as possible (Figure 5(A)). The reduction in potential gradients and increase in dielectric strength indicated in Figures 1(C) and 1(D) and Table I, are thus obtained. Proper clearances, however, should be allotted between the porcelain bore and the stress cone when an asphalt compound is the filling medium as too small a clearance might result in voids having low dielectric strength, especially when the existence of a vacuum in these voids is possible.

It is impossible to have an individual pothead design for each type and size of cable; therefore, they must be designed to handle a range of conductor sizes and different types of insulation. Variation in conductor size can affect the external dielectric strength (flashover) as much as 15 per cent. This effect is subject to considerable variation depending upon the length of the porcelain tube and the size and shape of the pothead electrodes. Flashover values obtained from tests made on potheads without conductors may be as much as 30 per cent above the values obtained when the pothead is assembled with the cable for which it was designed. Because of this fact, it is important that the flashover characteristics be determined with the pothead completely assembled on the size and type of cable for which it was designed. AIEE Pothead Standards Number 48[3] specifies that the electrical design tests be made in this manner. The older practice of using simulated electrodes and no internal conductors has, therefore, been eliminated.

Like cable joints, the actual construction of the cable termination and assembly of the pothead must generally be done in the field under unfavorable working conditions. Therefore, the dielectric strength and hermetic seals of the complete pothead termination are directly dependent upon the assembly procedure and skill of the personnel responsible for making the

Table I. Comparison of Dielectric Strengths of Various Cable Terminations Under 60-Cycle Long-Time Test Conditions

Test Number	Maximum Thickness of Stress Cone Insulation, 64ths Inch	Shielding Electrode Diameter, Inches	Electric Field Pattern	Test Voltage, Kilovolts	Duration of Test, Hours	Test Results	Equivalent Test Voltage on 1 Hour Basis, Kilovolts	Apparent Dielectric Strength Ratio of Termination to Cable Proper (Per Cent)—Note 4
1	None used	None used	Figure 1A	62.5	0.083	Note 1	45.7	51
2	None used	None used	Figure 1A	42.5	2.0	Note 1	47.0	52
3	16	None used	Figure 1B	62.5	1.5	Note 1	65.5	73
4	16	None used	Figure 1B	65.0	0.9	Note 1	62.5	70
5	22	None used	Figure 1B	62.5	3.5	Note 2	73.0	80
6	22	None used	Figure 1B	72.5	0.8	Note 1	70.5	78
7	20	$4^1/_8$	Figure 1C	72.5	0.8	Note 1	70.5	78
8	20	$3^5/_8$	Figure 1C	62.5	7.0	No failure	80+	89+
9	20	$3^5/_8$	Figure 1C	72.5	4.0	Note 1	82	91
10	28	$4^1/_8$	Figure 1C	67.5	7.5	Note 3	90	100+

Notes:

1. Puncture at terminus of shielding braid—ground potential.
2. Longitudinal failure from terminus of shielding braid to bare conductor.
3. Puncture of mandrel insulation at mid-section—cable proper.
4. Dielectric strength of cable insulation proper was about 360 volts per mil or 90 kv for 16/64-inch of mandrel insulation.

actual installation. A knowledge of the pothead design fundamentals given above plus the use of insulating materials of the highest grade and good installation technique should result in better cable terminations and a more reliable transmission of electric power by means of underground cables.

References

1. ASTM STANDARDS ON ELECTRICAL INSULATING MATERIALS. *Standard Number D117-33.* American Society for Testing Materials (Philadelphia, Pa), September 1933.
2. HIGH-VOLTAGE BUSHINGS DESIGNED TO MEET MODERN SERVICE, T. F. Brandt, H. L. Rorden. *Electric Engineering (AIEE Transactions)* volume 60, June 1941, pages 255–60.
3. POTHEADS. AIEE Standard Number 48, January 1948.

Discussion

L. I. Komives (Detroit Edison Company, Detroit, Mich.): The following questions were asked during the discussion period of this paper:

1. The author states that "There has been considerable information published in American technical journals on the theory, design, test, and application of underground cables and cable joints." This is not in agreement with Short's paper[1] in which he says that there is very little information available in this field. Would Mr. Nicholas be good enough to cite articles on which to base the above statement?
2. There are no tests shown in Table I to indicate differences between constructions shown in Figures 1(C) and 1(D). It seems to be desirable to have such test results.
3. We like the construction of the paragraph in which the author mentions that the stress relief cone is buried within a layer of semisolid dielectric of varnished cambric or paper and oil. This in our estimation is a very good construction not only for gas-filled cables as the author seems to think, but also for oil-filled cables and terminals, especially at higher voltages.

REFERENCE

1. A THEORETICAL AND PRACTICAL APPROACH TO THE DESIGN OF HIGH-VOLTAGE CABLE JOINTS, H. D. Short. *AIEE Transactions*, volume 68, part II, 1949, pages 1275–83.

A. L. McKean (Phelps Dodge Copper Products Corporation, Yonkers, N. Y.): The author has given an excellent and interesting summary of basic principles. It should be pointed out that these fundamentals of stress cone termination and auxiliary shielding can be safely carried to much higher voltage levels. For example, extensive testing on compression cable at potentials up to 200 kv to ground have been carried on successfully, employing simple stress cones and auxiliary shielding as demonstrated in Mr. Nicholas' paper. At higher voltage levels, more comprehensive capacitor-type designs appear mandatory.

J. H. Nicholas: Mr. Komives is probably justified in questioning the statement that considerable information has been published upon the theory, design, and test of cable joints.

The treatment of cable joint design fundamentals, detailed installation and construction information on a number of typical joints and the relatively large number of references (compared to potheads) included in the Underground Systems Reference Book[1] published by the National Electric Light Association in 1931, may have been somewhat misleading. Especially, since this material dates back to the 1916–1930 period.

A paper, such as Mr. Short's,[2] is certainly needed to indicate present-day practice in joint design.

The electric field pattern of Figure 1(D) was not included for quantitative evaluation but for illustrating the relative proximity effect of a shielding electrode. Pothead designs for 69 kv and below generally do not employ internal shielding electrodes and the tests reported in Table I are intended to illustrate the improvement possible within this voltage classification.

The degree of proximity indicated in Figure 1(D) has been utilized in pothead designs of higher voltage ratings with very encouraging results. This is confirmed by Mr. McKean's comments.

We have been recommending that the embedded type of stress relief cones be used on oil-filled pothead installations for 10 years, and we, therefore, are in full agreement with Mr. Komives on this point.

REFERENCES

1. UNDERGROUND SYSTEMS REFERENCE BOOK. Edison Electric Institute (New York, N. Y.) 1931.
2. A THEORETICAL AND PRACTICAL APPROACH TO THE DESIGN OF HIGH-VOLTAGE CABLE JOINTS, H. D. Short. *AIEE Transactions*, volume 68, part II, 1949, pages 1275–83.

Cable Accessory Design Utilizing New Laboratory Techniques

PHILLIPS N. BOSWORTH
MEMBER AIEE

HAROLD K. FARR
NONMEMBER AIEE

Synopsis: Cable joints and potheads are a vital link in the high-voltage cable circuit for power transmission. Some recent designs of joints and potheads are described with emphasis on the use of the electrolytic field-analyzer for electric stress analysis and of ultrasonic transmission for controlling manufacturing quality.

IN RECENT years the introduction of high-pressure fluid-filled cable systems for power transmission and the trend toward higher voltages have posed new problems in the design and construction of cable joints and potheads. Certain laboratory techniques have contributed much to the solution of these problems by providing the designer with accurate information and the producer with dependable test methods.

Adequate mechanical strength and easy field assembly must be achieved without sacrificing economy. Joints in particular must be designed to the smallest possible dimensions since they are the principal factor in determining costs of manholes in underground installations. The proper electrical strength must be obtained by good stress control and the use of modern dielectric materials. Laboratory methods have helped particularly to satisfy the electrical requirements although these, in turn, stem largely from mechanical considerations.

Before discussing methods of testing and development of cable accessories, a general description will be given of certain modern high-voltage cable accessories.

Joints and Potheads for Modern Cable Systems

Cable systems may be classified according to the operating pressure of the filling medium as low, medium, intermediate, or high pressure. Oil-filled systems may be either low-pressure or high-pressure systems. Gas-filled systems may be any of these classes. Nominal pressure ranges which apply in each case are as follows:

	Pounds Per Square Inch Gauge
Low pressure	0–15
Medium pressure	35–45
Intermediate pressure	100–150
High pressure	180–225

In addition to being either gas- or oil-filled, high-pressure systems may be referred to as self-contained and pipe-cable systems.

The difference in these two types of high-pressure systems basically rests with the fact that the self-contained cable contains a filling medium under pressure from the time it leaves the factory. The pipe-cable is shipped from the factory with a protective jacket and is pressurized after it has been pulled into the steel pipe and the pipe is filled with the filling medium.

CABLE POTHEADS AND JOINTS

A pothead is a device for terminating the end of a cable so that it can be used for power transmission.

Joints in a cable system are used to join together two lengths of cable. The simplest type of joint is the normal joint. Special conditions require variations and complications in jointing procedure. Low-pressure oil-filled cable lines often follow a profile with considerable variations in elevation along its length. Static oil pressures may develop which will expand or burst the lead sheath due to these differences in elevation. Stop joints then may be furnished to sectionalize the cable oil supply so that excessive static pressures do not appear. A stop joint connects two cable ends together but at the same time contains an oil barrier to separate the oil supplies of the two cable ends being joined.

In high-pressure systems the static pressure problem is not present. Stop joints may be used, however, to help control the filling medium and prevent large oil or gas losses under fault or repair conditions. Occasionally it is necessary to join a high-pressure system to a low-pressure system and this requires separation of the two pressure mediums.

In general, stop joints are not common on gas-filled systems. Each layout must be considered on its own merits.

POTHEADS FOR HIGH-PRESSURE SYSTEMS

Figure 1 shows representative potheads for a 115-kv high-pressure cable system. Figure 1(A) shows the pothead as used for a self-contained cable system with an outer lead sheath over the re-enforcing tapes. The pothead design is a practical correlation of three sections, the high-pressure section, the low-pressure section, and the electrical stress control section which physically involves portions of the other two sections.

The high-pressure section includes the high-pressure self-contained cable entrance with a double re-enforced wipe shown at *A*, the nonmagnetic support casting *B* and the stop tube *C*. This last unit is a cylinder made by laminating paper impregnated with resin. It is characterized by high mechanical as well as electrical strength and is used here to seal the high-pressure fluid from the porcelain.

The low-pressure section consists of the compartment outside the pressure cylinder and inside the enclosing porcelain

---

Paper 49-266, recommended by the AIEE Insulated Conductors Committee and approved by the AIEE Technical Program Committee for presentation at the AIEE Fall General Meeting, Cincinnati, Ohio, October 17–21, 1949. Manuscript submitted July 22, 1949; made available for printing September 8, 1949.

PHILLIPS N. BOSWORTH and HAROLD K. FARR are both with the General Electric Company, Pittsfield, Mass.

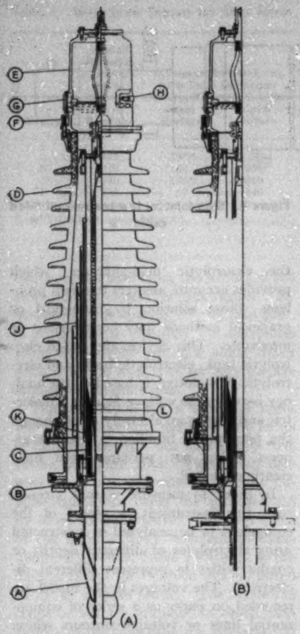

Figure 1. Pothead for high-pressure high-voltage cable termination

A—For self-contained cable
B—For pipe cable

shell *D* and the dome *E*. This section is designed to operate at a gauge pressure which would equal 10 pounds per square inch at a temperature of 75 degrees centigrade and in any case would not exceed 100 pounds per square inch. A pressure relief feature is afforded by the use of the springs *F* to maintain pressure on the gasket seal between the dome and the top of the porcelain. The whole dome will lift at some pressure between 50 and 100 pounds per square inch and reseal when the pressure returns to its normal range. This is provided to protect the low-pressure section from a leak in the high-pressure section. Pressure changes due to normal temperature variations in the low-pressure section are accommodated, without lifting the seal, by an expansion chamber in the dome. The dome also contains an oil-level gauge *G* and an outlet *H* for treating and filling.

The large oil volume in the low-pressure section is broken up as shown at *J* by cylindrical barriers spaced around the stop tube to increase the electrical strength.

This description has been given on the basis of a pothead being installed on a high-pressure self-contained cable. When the pothead is used on a high-pressure pipe cable system, the double wipe at *A* and the wiping sleeve are omitted and the pothead is adapted for mounting directly to a plate on the pipe riser. This construction is shown in Figure 1(B). Except for this mounting provision, the pothead may be the same for both applications.

The function of the stress control section is the termination of the cable ground shield in a way which will avoid setting up dangerous electrical stresses. In the cable proper a high voltage is supported across a relatively narrow insulation space between the conductor and shield because the electric field is uniform and radial, that is, at right angles to the paper layers. At the pothead the ground shield is tapered out gradually in region *K* in Figure 1(A) to the inner surface of the stop tube so as to keep the longitudinal stresses small. This insulation is built up by means of taping applied by hand over the regular cable insulation up to the inside of the ground shield and the stop tube.

Its maximum diameter is made as large as is consistent with easy assembly to insure a tight fit against the inside of the stop tube. This is done to decrease the width and thus increase the electrical strength of the oil channel between the taped section and the tube.

At the line *L* where the ground shield meets the stop tube, the ground circuit is continued into the wall of the tube by means of a conducting impregnant. This is a conducting material which is sprayed on the paper as the tube is manufactured and which hardens so as to produce a tube with a built-in shield. It is shaped so as to terminate the ground shield in the wall of the stop tube where the electrical strength is high. The conducting impregnant is very useful in controlling stresses where properly applied. Its proper use is, however, greatly dependent on experience and improper application can do more harm than good. In this connection, as in any stress control problem, the electrolytic field-analyzer discussed later is of considerable help.

It is apparent that the stop tube is a critical component of the pothead assembly subjected to high stresses both mechanical and electrical. Its manufacture is carefully supervised and checked by electrical and ultrasonic tests as described later.

Potheads for Low-Pressure Systems

A new low-pressure high-voltage power cable pothead of the solder seal[1] design is shown in Figure 2. A solder seal is made at each end of the porcelain to the metal parts at the factory. There are no gaskets in the complete pothead assembly, therefore there can be no leaks in service from that source. The mounting clamp location *B* is adjustable up and down the wiping sleeve assembly to compensate for variations in cable cut-off length and mounting heights.

This pothead differs further from the high-pressure pothead described previously in that the stop tube is eliminated and the pressure of the cable fluid is retained by the porcelain shell. The ground shield is tapered outward and the cable insulation built up as in the previous design.

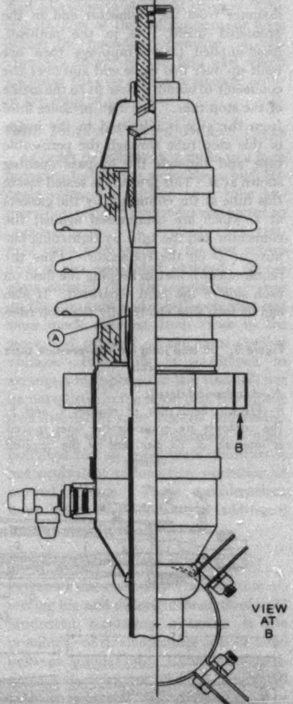

Figure 2. Solder seal pothead for low-pressure high-voltage cable system

Since the stop tube is not used, the end of the ground shield is protected by a semiconducting cloth, *A* in Figure 2, whose resistance is chosen to cause a gradual voltage drop in an axial direction along the cloth and thereby reduce the stress at the end of the ground shield at both 60 cycles and impulse voltages.

JOINTS FOR HIGH-PRESSURE SYSTEMS

For the purposes of this paper the discussion of joints for high-pressure pipe cable systems will be limited to stop joints. A representative design of such a joint is shown in Figure 3(A).

As mentioned previously, the stop joint separates the cable fluid in either side of the joint. This is accomplished by the use of a stop tube similar to that described in the discussion of the pothead. The two cable ends are brought in from either end of the joint to the connector at the center. The cable shield is cut back to the end of the ferrules, as shown at *A*, to give the required electrical creepage distance from the connector end to the grounded shield. As in the pothead, hand-applied tape wrappings then are built up over this cable end and over the connector to obtain a close fit to the inside of the stop tube. The high-pressure fluid from the pipe is admitted to the inside of this stop tube through the permeable tape and through the by-pass opening shown at *B*. This pressure is sealed inside this tube at the connector by the gaskets at *C* which are compressed against the connector and the tube by tightening the nuts at *D* on the connector. Thus the requirement is met in keeping the fluid on each side of the joint separated. It also can be seen that electrically the stop tube occupies the same critical position that it does in the pothead.

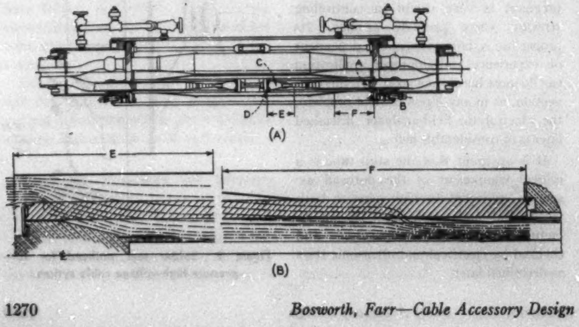

Figure 3. A stop joint for high-pressure pipe cable

A—Mechanical details

B—Electric field plot of regions E and F. The contours are equipotential lines spaced at intervals of 10 per cent of the applied voltage

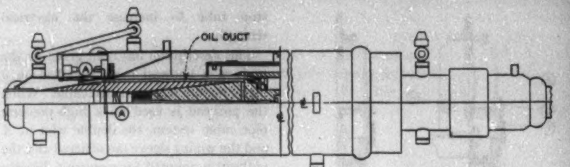

Figure 4. Stop joint for low-pressure oil-filled cable

The stress control problem is somewhat simpler in the stop joint than in the pothead because the ground circuit is not terminated but is carried completely around the joint.

JOINTS FOR LOW-PRESSURE SYSTEMS

A new design stop joint for low-pressure oil-filled cable systems is shown in Figure 4. The principal feature in this new design is the stop tube which replaces the molded cone-shape barrier used in older designs. A good quality tube made from resin-impregnated paper laminant is strong mechanically and electrically and permits cylindrical taping contours which are easily made during field assembly. This component is like that discussed for the high-pressure joint. However, this low-pressure joint is designed for 15 pounds per square inch gauge pressure, which means lighter-weight parts throughout. It also is for use with hollow-core oil-filled cable so that provision is made for oil flow from the cable core up through radial holes in the connector half, and back through the longitudinal ducts under the stop tube. A discussion of the electric stresses in this duct area is given later in this paper.

Laboratory Techniques

THE ELECTROLYTIC FIELD-ANALYZER

An instrument of great help to the designer of high-voltage cable accessories is the electrolytic field-analyzer, which provides accurate answers to stress problems whose solution by numerical or graphical methods may be laborious or unreliable. This device, also called electrolytic tank, electrolytic bath, and electrolytic flux plotter, is based on the analogy between the voltage field in a dielectric and that in an electrolyte. Although the principle is familiar to many engineers it has not, perhaps, been sufficiently exploited.

In order to measure voltage stresses with this instrument, a model of the equipment to be analyzed is constructed using electrolytes of different depths or conductivities to represent different dielectrics. The voltages in the model are recorded on paper as a series of equipotential lines or voltage contours whose spacing determines the electrical stress or gradient in each region. Field plots obtained in this way have been applied to the design of high-voltage cable accessories to improve construction, to predict the voltage level and location of insulation failure, to assess the value of high-voltage tests, and as an educational aid.

ANALYSIS OF ELECTRIC FIELDS IN CABLE JOINTS

Figure 3(B) is a field plot, made by means of an electrolytic field-analyzer, which shows the voltage distribution in a high-voltage high-pressure cable stop joint. The contour lines are traces of surfaces of constant voltage drawn at intervals of 10 per cent of the total voltage. As all the insulating materials are laminated cylindrically, the electrical strength is high in a radial direction. The important quantity is, therefore, the component of stress in the direction of the cable axis, because this stress acts to cause failure along the laminations in which direction the electrical strength is lowest. It would be expected, for example, that failure would occur first along the outer surface of the laminated stop tube in region *G* of Figure 3(B) since the spacing of the

Table I. Breakdown Stresses for Stop Joints

Design	Applied Potential at Failure under Impulse Test, Kilovolts	Maximum Stress Along Stop Tube Surface at Failure, Kilovolts Per Inch	
		Inner Surface	Outer Surface
A	325	139*	33
B	210	160	680*
C	350	140*	350
D	above 700	above 49	above 140

* Indicates location of failure.

equipotential lines along the surface of the stop tube is closest in this region. By measuring this spacing on the field plot, it is possible to calculate the maximum stress in kilovolts per inch along either surface of the stop tube for any voltage applied to the cable joint.

This was done for a series of high-voltage high-pressure gas-filled stop joints of different designs, one of which is that shown in Figure 3(A). These units also were given high potential tests under impulse conditions using the standard 1.5 by 40 microsecond wave. The crest value of the impulse wave sufficient to cause failure is given in Table I for each of the designs except for *D* which was subjected to 700 kv without failure. The maximum stress or voltage gradient to which each surface of the stop tube was subjected at the crest of the wave also is listed in the table.

It will be seen that two of the joints failed along the inner surface when the stress in that region reached about 140 kv per inch. The other two did not fail along the inner surface but were subjected to 49 and 160 kv per inch respectively. This implies that the average electrical creepage strength along the inner surface of all four stop tubes is about 150 kv per inch. Failure occurred along the outer stop-tube surface in only one joint and this was at a stress of 680 kv per inch. None of the other stop tubes were subjected to this stress although the outer surface of one reached 350 kv per inch without failure. Thus, the outer surface of the stop tube appears to be at least four times as strong for creepage as the inner surface. This may be explained by the fact that it is possible to wrap the tape much closer to the outer surface. In any case, the designer must take particular care to keep the stresses small along the inner surface of the stop tube. Design *D*, which shows very low stresses even at 700 kv, was developed after a study of field plots and high potential tests on units *A*, *B*, and *C*. This illustrates what can be accomplished by careful design guided by results obtained from the field-analyzer.

Field Stresses in Oil Ducts

The electrolytic field-analyzer also has been applied to the study of electrical stresses in the ducts used in cable stop joints to introduce the cable fluid. As indicated in Figure 4, these ducts run parallel to the cable axis between the inside of the stop tube and the outside of the built-up taping. They are formed by pressboard spacers which also run lengthwise along the inside of the stop tube. Figure 5 shows a field plot and the mechanical arrangement of the ducts at section *AA* of Figure 4. The field plot indicates that the maximum stress appears across the center of the duct. The voltage drop across this space is plotted in Figure 6 for joints with ducts of constant height but varying in number and width. The solid curve was obtained with four ducts by varying the width of the individual ducts. For the dotted curve the total duct area was varied by adding spacers of constant one-half inch width so as to change both the size and the number of ducts.

These curves show that the stress increases with the duct area. Comparison of the ordinates of the two curves taken at the same abscissa, however, shows the decrease in stress obtained, for a given total duct area, by breaking this area up into a number of smaller ducts.

This oil duct study illustrates the value of the field-analyzer as an educational device. Before the field plots were obtained, a fear was expressed that the abrupt change in dielectric constant across the radial wall of the duct might lead to excessive electrical stresses. The smooth flow of the voltage contour lines across the boundary, however, is convincingly shown by the field plot which indicates that no excessive stresses occur at the walls of the duct.

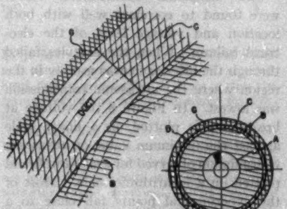

Figure 5. Fluid ducts in a stop joint. Field plot in region of one duct (left). Mechanical details (right)

A—Cable conductor
B—Paper insulation
C—Pressboard spacer
D—Fluid duct
G—Ground shield formed by conducting portion of stop tube

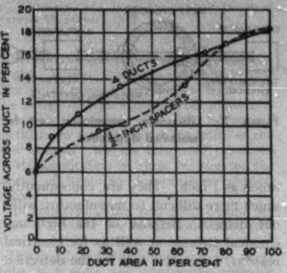

Figure 6. Electrical stresses in oil ducts, a résumé of data obtained from field plots like that of Figure 5

Ordinate is the voltage across the duct expressed in per cent of the total voltage applied to the stop joint. Abscissa is the actual duct area expressed as per cent of the total available annular area for fixed duct height

High-Voltage Testing of Stop Tubes

In order to subject stop tubes to a high potential test before assembly, a high 60-cycle voltage is applied to a tube immersed in oil with electrodes connected to opposite ends. To evaluate this test, field plots were made of the test set-up and of the assembled pothead. These plots showed that the electrical stresses on the stop tube under high-potential test were much different from those in the assembled pothead at the same applied voltage. Practically, it is difficult to arrange a high-potential test that will not be unrealistic in the sense that the tube is overstressed in some regions and understressed in others. Furthermore, a high-potential test of one-minute duration is not equivalent to long-time operation at normal voltage. These considerations have led to the adoption of additional tests on stop tubes.

The Ultrasonic Transmission Test

One of the most important factors affecting life and dielectric strength of solid laminated insulating materials is the possibility of small openings or poor bond between laminations. Cylinders of moderate wall thickness can be fabricated with considerable assurance that they will be free of such defects. Stop tubes used in high-pressure cable systems, however, may have a wall thickness of as

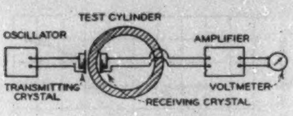

Figure 7. Ultrasonic transmission test for laminated stop tubes

much as 1 inch. They are, consequently, much more difficult to manufacture without defects. Because of the high mechanical stresses as well as for electrical reasons, a sensitive test for the detection of poorly bonded areas in such cylinders is particularly desirable. Such a test makes it possible to reject weak materials before assembly and aids in the development of improved materials.

The measurement of the transmission characteristics of a material for ultrasonic waves constitutes one such test. When a very high frequency sound wave is sent through a homogeneous material of moderate thickness in a direction perpendicular to the plane of the laminations, it emerges from the far side with little decrease in amplitude. In a region where any laminations are not well impregnated or well bonded, however, the transmitted amplitude will drop sharply. This so-called ultrasonic transmission test is one of several familiar techniques[2] for applying ultrasonic waves to the examination of the interior of opaque materials. Its present interest lies in its use as an indication of dielectric strength.

The ultrasonic transmission test has been applied to pressure stop tubes used in cable joints and potheads. To insure that the material will be free of interior corona, this test seems to be superior to any other applicable to these units. A stop tube is subjected during operation to full line-to-ground voltage from end to end.

Because poorly bonded laminations result in a weakness to voltage stress applied parallel to the laminations, their detection is more important in stop tubes than in materials subjected to purely radial stresses.

The test set-up is shown schematically in Figure 7. An electric oscillator of frequency approximately one megacycle per second is used to drive a crystal transducer which converts electric into mechanical vibrations. After the waves pass through the wall of the test cylinder, a second transducer converts the energy back to electric oscillations that are amplified and read on an output meter. Transducers and test piece are immersed in ordinary transil oil, which is an efficient sound transmission medium and which obviates the necessity of direct contact between transducer and test cylinder. The use of high frequency and small crystals (about 5/8-inch square) results in a narrow beam of energy which permits the detection of flaws covering only small areas.

The equipment is arranged to read transmitted amplitude as per cent of the value obtained when the beam passes directly through the oil with no test material in place. Paper laminates of good quality up to 1 inch in thickness made with a resin binder show transmissions in the range of 20 to 50 per cent of that for oil alone. Where there are any cracks or openings, however, the transmission usually falls to a value below 1 per cent. The cylinder may be scanned by dropping it 1 inch at a time and rotating it 1 revolution at each stop.

In order to establish the significance of the ultrasonic readings for dielectric materials, tests were made comparing dielectric strength with ultrasonic transmission. One-inch-long sections were cut from rejected stop tubes at interesting points where a careful ultrasonic check had been made. The resulting ring-shaped sections were given a 60-cycle voltage breakdown test between 12-inch diameter parallel plate electrodes in transil oil at room temperature with voltage increasing at the rate of 3 kv per second. A uniform stress was applied parallel to the laminations of the sample so as to induce breakdown along any openings between laminations. The end surfaces of the sample were given a thin coat of grease to exclude oil from such openings and maintain the conditions under which the ultrasonic test was made.

The ultrasonic transmission values were found to correlate well with both location and voltage level of the electrical failure. When the samples failed through the interior, it was usually in the region where the ultrasonic transmission was lowest. In Figure 8 the voltage at breakdown is plotted on a linear scale against the minimum value of ultrasonic transmission observed for each sample and plotted on a logarithmic scale. Most of the experimental points fall close to a curve which represents a constant dielectric strength of 53 kv rms per inch for ultrasonic transmission values in the range of 0.005 per cent to 1 per cent and then rises to about 110 kv per inch. At transmission readings around 10 per cent and above, the strength of the material is actually higher than that shown because the samples failed by flashover along the surface instead of through the interior.

The flat portion of the curve corresponding to very low transmission values represents breakdown through the air in an interior crack. The voltage of 53 kv per inch agrees with Peek's values[3] for breakdown in air between large spheres 1 inch apart. Those experimental points which are far from the curve probably represent samples in which the crack was not continuous from one side to the other.

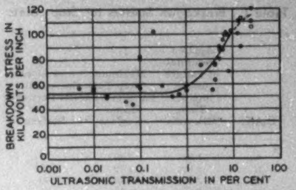

Figure 8. Experimental correlation between ultrasonic transmission through laminated stop tubes and electrical strength for breakdown parallel to the lamination

It is evident that the ultrasonic transmission test can be very valuable as an indication of the dielectric strength of certain materials. The equipment is rather simple and involves no high-voltage hazard. The test is nondestructive and gives a localized reading for every region of a sample. Its principal disadvantage is that its application and interpretation are simple only for samples of simple shape such as cylinders and plate stock. For more complicated shapes the test may be impractical.

Conclusion

The foregoing discussion has indicated some of the mechanical problems of high-voltage high-pressure design of cable accessories and certain electrical problems which arise from the mechanical requirements and from the high voltage. Some of the laboratory techniques which help to solve the electrical problems were seen to be: the electrolytic field-analyzer which helps the engineer to design apparatus with the lowest possible electrical stresses on the insulation and gives quantitative information as to the actual stresses that will exist in the completed equipment; and the ultrasonic transmission test which provides a sensitive indication of the presence of flaws that would affect the dielectric strength of solid insulating materials.

It is felt that the engineer must be prepared to take advantage of such modern techniques in order to build high-voltage cable accessories which will be reliable and economical.

References

1. Soldered Ceramic-to-Metal Seals, A. L. Jenny. *Product Engineering* (New York, N. Y.), December 1947, pages 154–57.

2. Ultrasonics (book), Benson Carlin. McGraw-Hill Book Company, New York, N. Y., 1949.

3. Dielectric Phenomena in High Voltage Engineering (book), F. W. Peek. McGraw-Hill Book Company, New York, N. Y., third edition, table XXIII, 1929, page 121.

Discussion

L. I. Komives (The Detroit Edison Company, Detroit, Mich.): The methods proposed by the authors to test high-voltage cable accessories are very interesting and should be very useful. Both the electrolytic field analyzer and the ultrasonic transmission test should help the terminal designer in designing trouble-free terminals for higher voltage cables. The following questions were brought up in connection with this paper:

1. In Figure 1 a very interesting spring-loaded gasketing *F* is shown. Why not carry this idea further and have the porcelain itself supported by spring loading to carry high pressure inside of the porcelain? Such terminals have been used by The Detroit Edison Company experimentally for four or five years and in actual service for nearly a year.

2. In text and in Figure 2 when discussing potheads for low-pressure systems, the authors mention that "There are no gaskets in the complete pothead assembly, therefore there can be no leaks in service from that source." This is a very admirable construction and we like this feature very much.

As a matter of fact, in Detroit we apply this same principle to the high-pressure cable systems and we eliminate gaskets shown halfway between *B* and *A*. The two other gaskets shown at *B* and at the top of the terminal under *F* are spring loaded. We would like to know how does one assemble the pothead shown in Figure 2? Does the wiping sleeve slide over the stress cone? If so, should not the opening in the wiping sleeve be larger? This is not quite clear from the drawing and description.

3. We are very interested in the ultrasonic transmission problem. It is felt that in order to be useful, ultrasonic transmission values should be obtained or established transwise (not radially and not exactly longitudinally) across the plastic tubes. We also feel that such tests should be made on the complete stop tube assembly ready to use, not on the plastic tube alone, as we have had sad experiences with such constructions where weaknesses did not show up until the stop tube was completely assembled.

4. In Figure 5 the constant stress lines showing an increase in the oil duct would indicate that the authors are right when they say that a better distribution is obtained if one breaks this area up into a number of smaller ducts. We are wondering whether one would have to make these ducts so small as to impede oil flow in order to produce a decided decrease in stress.

E. R. Thomas (Consolidated Edison Company of N. Y., Inc., New York, N. Y.): The use of electrodes in electrolytes has been used by other experimenters to map the equivalent electric fields in the dielectric for cable and joint configuration where only a single permittivity of dielectric was being considered. The authors are to be complimented on extending this technique to explore equivalent electrical stresses in complex insulation made up of different permittivities. The authors state a model is constructed using electrolytes of different depths or conductivities to represent the different dielectrics. It is obvious that different depths of the same unit conductivity of electrolyte could represent differences in permittivity, but it is not very clear how use can be made of different unit conductivities of electrolyte to represent different permittivities, as this would seem to introduce retaining boundaries. The resistivity of these boundaries would affect the measurements. I would appreciate if the authors would more fully explain the details of the actual laboratory equipment utilized.

The measurement of ultrasonic transmission through laminated insulation to determine the presence or absence of voids seems to be a very useful method of nondestructive testing. For the record, it would seem desirable to indicate whether the percentage indications on the output meter are in terms of the percentage energy transmitted, or whether it reads in percentage of amplitude of the wave transmitted. The statement that laminates of good quality showed transmission ranges of from 20 to 50 per cent of that for oil alone seems to be a rather broad range of values. Is it not true that the percentage of transmission through a particular laminate will be a function of its thickness compared to the length of the path through oil, as well as the relative density of the laminate compared to the density of oil? This latter would to a large extent determine the amount of energy which would be reflected at the oil-laminate boundary. In order to equate this mechanical measurement, it would seem desirable to include the terms regarding density of the material under test and the length of paths through oil and the material under test.

E. J. Merrell (Phelps Dodge Copper Products Corporation, Yonkers, N. Y.): Pothead design presumably is done within the framework of the AIEE Standard for Potheads.[1]

I should like to ask Mr. Bosworth and Mr. Farr whether, in view of their findings, the test voltages included in this standard are applicable without reservation to pressure-tube type terminals. The voltages specified, it seems, might introduce maximum tangential stresses in such terminal structures of a magnitude greatly in excess of those found in low-pressure designs without pressure tubes, possibly of an order closely approaching the intrinsic dielectric strength of the materials employed.

We have been unable to find specific information relative to the safe direct voltage which may be applied to potheads during routine field tests on cable. I wonder if the authors could enlighten us. Also, would d-c testing of potheads perhaps possess an advantage over customary a-c tests?

1. Standards for Potheads. AIEE Standard Number 48, January 1948.

E. H. Grosser and H. L. Pedley, (Commonwealth Edison Company, Chicago, Ill.): This paper presents certain new features in the design of high-voltage cable joints and terminals, together with the laboratory methods for establishing the validity of the new designs. We are interested primarily in the application of these features to the design of joints for low-pressure oil-filled cable.

In considering the stop joint design, we believe that the use of the conducting material applied to the surface of the paper, which is subsequently formed into the paper tube, is a novel and apparently workable method of controlling the ground potential. It also permits fastenings for the clamping ring to extend into the end of the stop tube without distorting the electric field.

The study of closely spaced pressboard spacers between tape and stop tube shows that improved control of stresses in this critical region is possible. It may increase the difficulty of assembling the tube over the cable end on large conductors.

The new oil-filled stop joints with cylindrical stop tubes are longer and larger in diameter than stop joints previously made with the conical tubes. While the joint is easier to tape uniformly, the cost of the manhole to accommodate these larger joints is increased.

In the low-pressure pothead illustrated in Figure 2, the soldering of the solder-sealed top cap directly to the terminal stud as shown entails a large amount of heating, particularly for studs on large conductors, with the consequent risk of damaging the solder seal at the top of the procelain. We have such troubles on potheads which were similarly solder-sealed between stud and cap. Perhaps this trouble would not occur in this design with the thinner and longer spun cap.

C. S. Schifreen (Philadelphia Electric Company, Philadelphia, Pa.): This paper is a very instructive disclosure of the types of techniques so far developed as aids for proving the designs and constructions of joints and potheads for high-voltage cable systems. The ultrasonic test goes farther than the electrolytic field analyzer since the former permits a quality check of the finished manufactured component while the latter is at best an auxiliary tool to assist in preliminary design. The paper, unfortunately, is very vague in its reference to the technical features of the field analyzer. From the authors' example summarized in Table I, however, it does appear possible to use an analog at extremely low voltages to analyze stresses at levels many times higher than the values used in the analyzer itself. It would be most instructive to see the results of similar comparisons between impulse breakdown tests and stresses based on the analyzer when applied to potheads and stop joints in the same voltage class but in which conducting materials were incorporated in the stop tube to produce a built-in shield.

It is desirable, of course, to secure the most economical cable installations consistent with reliable performance. There is danger, however, that the manufacturer's effort to design for the "smallest possible dimensions" may encroach upon essential factors of safety which generally are related to the length of the joint. Never in my experience has the length of the manhole been a design limit of any consequence. Accordingly, I suggest that the manufacturer determine the dimensions needed to provide electrical strength at least equal to that of the cable. The application engineer then will provide the required structure. After all, the cost of the joint and pothead materials and manholes is only about 5 per cent of the installed cost of the cable system.

P. N. Bosworth and **H. K. Farr:** The discussions presented indicate sincere thought and interest in the problems of accessory design and manufacture. Like the paper, the discussions naturally divide themselves between considerations of design and of laboratory techniques. This closure will deal with the various points in that order.

D-c testing of power cable has been used for many years and has proved valuable in uncovering high resistance incipient faults before actual failure occurs under alternating voltage. In a cable the stress is essentially radial so that a direct voltage will search the fault without the disadvantages of large capacity effects experienced with alternating voltage. The situation in a joint or pothead is entirely different. The important consideration in these devices is the field distribution due to capacitive voltage division. The direct-voltage pattern is one of a pure resistance divider and does not stress the device in a manner similar to alternating voltage. For this reason a d-c test is not as realistic in a joint or pothead as it is in a cable.

It is, therefore, difficult to assign definite values of test voltage to a device without first carefully taking account of all influential factors in the design with seasoned judgment.

In joints or potheads utilizing annular fluid duct spaces for fluid flow, definite improvement in electrical strength can be realized if these channels are kept small as indicated by Figure 6 in the paper. However, for a construction of the type shown in Figures 4 and 5, the improvement cannot be more than 12 per cent. The correct design is in the direction of the smallest fluid space consistent with adequate fluid flow. Assembly will present no problem if the proper design is made.

Solder seals are the future goal of progressive designers. There is no reason why they cannot be applied to large devices after the technique and field experience has been gained on the smaller equipments. Figure 2 is an example of one application by one manufacturer on a line of potheads through 69 kv. For assembly, the stud is first soldered or pressure-attached to the cable end. The wipe sleeve containing the treating fitting then is passed over the cable end and wiped to its proper position on the cable sheath. After the cable end has been reinforced, the procelain assembly is lowered on to the wipe sleeve and two soldering operations are performed, one to the wipe sleeve at the bottom and one to the stud at the top. The parts are so proportioned that these soldering operations do not endanger the solder seals to the procelain if usual care is taken to protect them.

Center clamping of procelain parts to gasketing surfaces has many advantages worth considering. Much work is being done at present in this and other directions to produce a suitable high-pressure high-voltage pothead that is economical and simple to assemble in the field.

A detailed discussion of the technique of the electrolytic field analyzer falls outside the scope of the present paper. Another paper covering this subject is planned for future presentation.

A method of accurately representing controlled resistance material in the model has not yet been developed. Shields made of conducting materials incorporated in the stop tubes are, of course, represented in the electrolytic model as full conductors. Design *D* in Table I does include a tapered ground circuit which is carried through the stop tubes by means of a conducting impregnant. The use of ultrasonic vibrations as a test for the dielectric strength of resin-impregnated laminates is sufficiently new that much data is still needed. There would seem, however, to be little value in a test with transmission in a direction other than that normal to the laminations, because flaws never develop in the radial direction. Because of the complexity of the structure, it is not possible at present to interpret transmission readings taken on completed joints or potheads.

The authors neglected to mention in the paper that the ultrasonic transmission values reported were expressed in terms of amplitude of the vibrations transmitted through the cylinder under test. The transmitted energy is, therefore, proportional to the square of these readings.

The data presented in connection with the ultrasonic transmission test apply only to material of one type and to structures whose shape and thickness fall within a certain range. Because of the effect of reflections at the surfaces and of losses in the interior of the material, additional data might be needed if the tests were to be extended to other shapes or materials. In spite of rather wide variations in the transmission through normal materials the test is significant because a delaminated area usually results in such a large change in transmission as to be unmistakable.

The authors wish to thank those presenting discussions for their interest and for the useful suggestions made.

A Theoretical and Practical Approach to the Design of High-Voltage Cable Joints

H. D. SHORT
MEMBER AIEE

THE design of high-voltage cable joints on a theoretically rigorous basis has not hitherto been published in a full or comprehensive manner, as a search of the literature on the science of cable making reveals. In contradistinction there exists a wealth of recorded information by many eminent authorities on the theory, design, behavior, and performance in duty of high-voltage cables per se. Indeed it would seem, at least for the lower working voltages, that the designs of cable joints have not always been granted the consolatory devices of scientific theory; and that precedent and empirical rule and rote have in some respects governed their construction and usage.

As an example, there is today a great deal of well-deserved consideration given to the breakdown strength of cables under internal transient surges and assimilated atmospheric transient surges (more commonly referred to as impulse tests). But the effects of a joint on the isotropic nature of the distributed transmission characteristics of the cable system have not received much attention. Notwithstanding this fact, most cable engineers are well aware of the influence of a discontinuity on the propagation of electromagnetic waves; and of how reflections do occur at these discontinuities, which are really localities having innate characteristics at variance with those of the main portion of the line.

A change in the over-all attenuation constant of the cable line at such a juncture consequent upon the joint having, let us say, a smaller capacity (owing to its diameter being greater than that of the adjacent cable) could alter not only the transmission characteristics but also the current rating.[7] Just how important or how great are the magnitudes of these phenomena would have to be ascertained from a mathematical investigation of the general case, and the adaptation of the related results to particular events.

To the author's knowledge no one has put these matters under observation in investigating the behavior of joints in service, or their impulse voltage breakdown strength properties. Nonetheless a study in these directions has by intent been omitted; leaving it, as is probably best, to be dealt with at some later time by way of a separate contribution to the whole question.

The more immediate phase of the subject is a formal design method for the joint proper and in this respect the present paper is more distinctly concerned. And in being so concerned the author has not overlooked the fact that sensory preceptions and old customs are sometimes better than logical reasoning. A rigid analytical approach has been followed and as a consequence formulas have been developed for several types of joints. While no claim is made for the originality of most of the formulas, two of them (for example, that for a joint design composed of heterogeneous materials), are novel to the art and have been found useful in practical applications.

Symbols

d = diameter over the conductor
d_f = diameter over ferrule (assumed herein $>d$)
$r = d/2$
$r_f = d_f/2$
D_t = diameter over cable insulant
D_j = diameter over joint insulant
$R_j = D_j/2$
$R_t = D_t/2$
k = dielectric constant, with subscripts to correspond to the different dielectrics referred to
E = operating voltage to neutral, or radial potential drop
C = electrostatic capacity, with subscripts to correspond to the different dielectrics referred to
g_c = radial stress at surface of conductor in the cable
g_p = longitudinal stress along the stress control cone profile
g_f = radial stress at surface of ferrule
g_t = longitudinal stress along the stepping profile

The Design Problem

The jointing of a single-conductor paper-insulated cable presents the simplest introduction to the problem while at the same time distinctly exposing the principal characteristics of design to be studied. These characteristics are fundamental and germane to all types of joints; and form the criterions of successful performance in duty. We will therefore, in what follows, confine our thinking to the single-conductor joint.

A cable joint is made up of three elemental components. First, there is the ferrule (or connector) which joins together electrically and mechanically the conductors of the two cable ends, see Figure 1. Secondly, there is the tapering down of the insulant on each cable (called

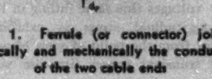

Figure 1. Ferrule (or connector) joining electrically and mechanically the conductors of the two cable ends

---

Paper 49-267, recommended by the AIEE Insulated Conductors Committee and approved by the AIEE Technical Program Committee for presentation at the AIEE Fall General Meeting, Cincinnati, Ohio, October 17–21, 1949. Manuscript submitted July 18, 1949; made available for printing September 15, 1949.

H. D. SHORT is with the Canada Wire and Cable Company, Toronto, Ontario, Canada.

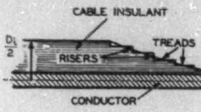

Figure 2. The "stepping" of the cable insulant of one of the cable ends in the joint adjacent to the ferrule

the cable insulant) to some predetermined dimensions. This is called the "stepping" of the insulant; a term derived from the usual practice, with an insulant composed of helically-wrapped tapes, of achieving the taper by removing individual tapes to form (in the plane of this piece of paper) a set of steps having "risers" and "treads" from the level of the conductor surface to that of the cable insulant surface, see Figure 2. In applying the insulant over the ferrule (called the joint insulant) it is paramount that it be well blended into the cable insulant in order that the over-all distribution of the system insulant is maintained as homogeneous as possible; stepping of the cable insulant is one of the most common ways of accomplishing this result. One other scheme[1,2] has been employed abroad but to the author's knowledge has not been followed here; its main feature emphasizes the blending of the cable and joint insulants.

Some degree of discontinuity must, of course, occur along the stepping (and also at the ends of the ferrule, on the assumption that $d_f > d$), distorting the otherwise uniform radial electric field between the conductor and its zero potential electrode (or the ground electrode of the field). As a consequence, the electric field is no longer everywhere radial (as would obtain at the center of two concentric cylinders) but has components some of which are longitudinal to the cable axis and therefore parallel to the plane of the paper tapes (that is, to the plane in which the paper fibers lie). This brings to bear the fact that the long-time voltage breakdown strength of impregnated papers in cable form, normal to the paper, and at atmospheric pressure, is 15 times greater than that in the longitudinal plane of the paper.[3,5] Thus it becomes a desideratum to so portion the stepping that the longitudinal component of the electric field (called the longitudinal stress) along the treads (and at the ferrule ends) is well below the 1/15th value. Under transient surge voltages this same failing in regard to longitudinal stress is exhibited,[2,6] so that from the point of view of assimilated transient surges (impulse voltage strength) the longitudinal stress, particularly along the treads (g_t), must not be overlooked (as Brazier, Halperin, and Shanklin have shown).[2,6]

In the third place, but by no means the least, comes the stress control cone, see Figure 3. Jointing is almost always carried on in the field which, together with the foregoing stress consideration in respect of the weakness of the tapes in the longitudinal direction, necessitates the building up of the joint insulant to some diameter greater than that of the cable insulant. The well-known exponential distribution of the electric stress between two concentric cylinders illustrates the point to those familiar with the proposals in hand. Additionally it may be stated that tapes hand-applied in the field are not susceptible to being wrapped with the tension and degree of uniformity feasible under cable-making practice. The resultant joint insulant diameter makes necessary a transition between this diameter and the cable insulant diameter as Figure 3 shows, the bounding curve of which is called the stress control cone. Here again, as along the stepping treads, the radial consistency of the electric field is disturbed and longitudinal stresses come into play. So once again they must be accommodated and limited to a value at which incipient deterioration[4] to the insulating tapes along and within the transitional boundary A-B, Figure 3, is amply prevented. In all high-voltage engineering it is an ineluctable rule that ionization must not be allowed to become malignant.

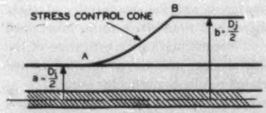

Figure 3. The stress control cone profile (the transitional bounding curve between the cable insulant diameter and the joint insulant diameter)

Having arrived at a conception of the physical nature of the problem, it remains to determine the proper profile and relative dimensions of the two transitional boundaries (or curvatures), namely, the stepping and the stress control cone. As in both instances the longitudinal stress is the criterion, then the corollary follows that these profiles will be functions of the longitudinal stress along them. It, of course, will be comprehended readily that any longitudinal stress within the confines of these profiles must, from the laws of electrostatics, be less than that at any point lying on the profile.

The Development of the Formulas for the Longitudinal Stress Along the Stress Control Cone

In Figure 4 there is depicted one-half of a joint, symmetrical about its (transverse) center-line axis. The electric field throughout the transitional curve A-B of the zero potential electrode (or ground electrode of the field) in passing from the cable insulant diameter D_i to the joint insulant diameter D_j is in reality three dimensional. However, it is a very difficult matter to handle the three dimensions of this field relation simultaneously as extreme rigor would demand. By taking any two dimensions of the field together at one time renders a resolution of the electric field to be more readily attained, and leads to sufficiently accurate results for all practical purposes. Then in any plane containing the longitudinal axis of the joint, the electric field may be ascertained by the ordinary exponential formulas that obtain from a consideration of the radial attributes of concentric circles in a second plane normal to the former. Two particular cases, in respect of the stress control cone, now present themselves, which collectively represent all the variables to be encountered in this phase of the design problem. These two propositions are treated separately as the homogeneous case and the heterogeneous case; and in such the meaning of the chosen terminology is clearly revealed.

The Homogeneous Case

Under the predetermined conditions of homogeneity it is implied that the cable insulant and the joint insulant are of identical materials, and have, therefore, the same dielectric constant. A cross section of the joint in the plane containing the longitudinal axis of the joint is seen in Figure 4 relative to the arbitrarily

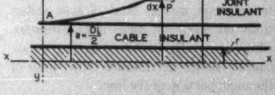

Figure 4. One half of a joint proper symmetrical about its longitudinal and transverse axes (minus the stepping), having identical materials for the joint insulant and the cable insulant—the homogeneous case

chosen x, y axis of the Cartesian co-ordinate system. In this picture the stepping of the cable insulant is omitted, as it is to be assumed that the stress control cone does not overlap the cable insulant; which, at least theoretically, is the right order of things.

The conductor will be at some potential relative to the zero potential electrode, and hence the radial potential drop between the conductor and the zero potential electrode will be the same value throughout the joint and the cable. Then we may proceed as in the following if the profile surface of the stress control cone is maintained at zero potential, by means of the usual shielding; the profile surface thereby becoming a part of the zero potential electrode.

Let

E = the radial potential drop between the conductor and the zero potential electrode

k = dielectric constant of the cable and joint insulant

At the point A in Figure 4

g_c = the radial stress at the conductor surface in the cable.

$$=\frac{E}{r\log_e\frac{D_i}{d}}$$ volts per unit of length (radially through the insulant)

Point P of Figure 4 is any point close to the transitional curve A-B within the joint insulant. A cross section of the stress control cone through this point in the plane normal to that containing the joint longitudinal axis is shown in Figure 5.

C_1 = capacity of layer 1, that is between the conductor and the cylindrical surface through the point P

$$=\frac{k}{2\log_e\frac{y}{r}}$$ statfarads per wire unit of length (or to neutral)

C_2 = capacity of layer 2, that is, between the cylindrical surface through the point P and the cylindrical surface of the stress control cone profile

$$=\frac{k}{2\log_e\frac{Y}{y}}$$ statfarads per wire unit of length (or to neutral)

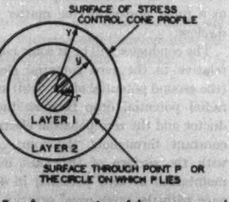
SURFACE OF STRESS CONTROL CONE PROFILE
Y
y
r
LAYER 1
LAYER 2
SURFACE THROUGH POINT P OR THE CIRCLE ON WHICH P LIES

Figure 5. A cross section of the stress control cone (in the plane normal to the cable or joint longitudinal axis) through the point P shown in Figure 4

It can be shown that the potential drop across layer 2 is some portion of E the magnitude of which is inversely proportional to its capacity and the reciprocal sum of both capacities C_1 and C_2. That is

$$E_2=\frac{1/C_2}{1/C_1+1/C_2}E$$

$$=\frac{1/k\log_e Y/y}{1/k\left(\log_e\frac{y}{r}+\log_e\frac{Y}{y}\right)}$$

$$=\frac{\log_e Y/y}{\log_e Y/r}E$$

If P is infinitely close to the stress control cone profile then g_p = longitudinal stress at the point P along the elemental longitudinal distance $dx=dE_2/dx$ (that is, rate of change of E_2 with respect to x).

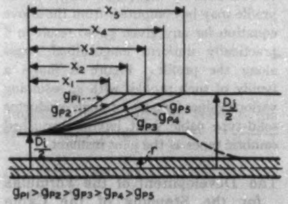

Figure 6. A family of stress control cone profiles for various values of g_p in arbitrary units, showing the practical significance of g_p in determining the over-all length of the joint

Hence we can write

$$g_p=\frac{dE_2}{dY}\frac{dY}{dx}$$

$$=\frac{d}{dY}\left(\frac{E\log_e Y/y}{\log_e Y/r}\right)\frac{dY}{dx}$$

$$=E\frac{d}{dY}\left(\frac{\log_e Y/y}{\log_e Y/r}\right)\frac{dY}{dx}$$

$$=E\left(\frac{\log_e Y/r\dfrac{d}{dY}(\log_e Y/y)-\log_e Y/y\dfrac{d}{dY}(\log_e Y/r)}{(\log_e Y/r)^2}\right)\frac{dY}{dx}$$

$$=\frac{E}{Y}\left(\frac{\log_e y/r}{(\log_e Y/r)^2}\right)\frac{dY}{dx}$$

Now if P actually lies on the profile

$$y=Y$$

and we have

$$g_p=\frac{E}{Y}\frac{1}{\log_e\frac{Y}{r}}\frac{dY}{dx}$$

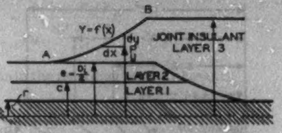

Figure 7. One half of a joint proper symmetrical about its longitudinal and transverse axes, having a variety of materials for the joint insulant and the cable insulant—the heterogeneous case

An integration of this expression between the limits of $D_i/2$ and Y yields the following equation for g_p

$$g_p=\frac{E}{x}\log_e\left(\frac{\log_e Y/r}{\log_e D_i/2r}\right)$$

Knowing r, D_i and E, and choosing a suitable value for g_p, the x and y co-ordinates of the stress control cone may be computed from this equation and its curve drawn to reveal the proper profile at the transitional region. The curve is, obviously, exponential and for different values of g_p a series of curves may be developed having A as the origin. Such a series is shown in Figure 6, from which it is evident that the lower the value of g_p the longer the stress control cone profile becomes and consequently the longer the joint must be. This is certainly a fact of practical significance.

HETEROGENEOUS CASE

Secondly under this heading we shall study the case where the cable insulant is graded with two layers of dielectric material having the usual difference in their dielectric constants, and the joint insulation is of a still foreign type of material, as shown in Figure 7. As in the preceding case it will be assumed that the stress control cone does not overlap the stepping of the cable insulant.

Again as in the section on the Homogeneous Case we have P as any point close to the transitional curve A-B, and

E = the radial potential drop between the conductor and the zero potential electrode
k_1 = dielectric constant of layer 1
k_2 = dielectric constant of layer 2
k_3 = dielectric constant of layer 3
C_1 = capacity of layer 1

$$=\frac{k_1}{2\log_e\frac{c}{r}}$$ statfarads per wire unit of length or to neutral

C_2 = capacity of layer 2

$$=\frac{k_2}{2\log_e\frac{R_i}{c}}$$ statfarads per wire unit of length

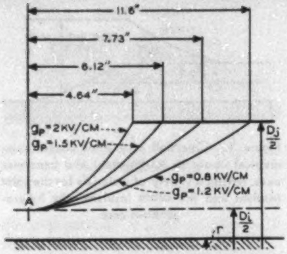

Figure 8. A family of stress control cone profiles for a particular joint design for a 1-conductor 350,000-circular mil concentric-stranded paper-insulated lead-covered 69-kv grounded-neutral solid-type cable of conventional design having a graded paper insulant thickness of 0.750 inch and varnished cambric joint insulant in a direct buried installation (Winnipeg, Canada, direct buried installation)

C_3 = capacity of layer 3

$$= \frac{k_3}{2 \log_e \frac{y}{R_i}} \text{ statfarads per wire unit of length}$$

C_4 = capacity of layer 4 (the hypothetical layer above the point P)

$$= \frac{k_4}{2 \log_e \frac{Y}{y}} \text{ statfarads per wire unit of length}$$

E_4 = potential drop across layer 4

$$= \frac{1/C_4}{1/C_1 + 1/C_2 + 1/C_3 + 1/C_4} E$$

Letting

$1/k_1 = \gamma$
$1/k_2 = \alpha$
$1/k_3 = \beta$
and $k_3 = k_4$

we have

$$E_4 = \frac{\beta \log_e Y/y}{\gamma \log_e \frac{c}{r} + \alpha \log_e R_i + \beta \log_e \frac{Y}{R_i}} E$$

$$= \frac{\beta \log_e Y/y}{\log_e \frac{(c^{\gamma-\alpha} R_i^{\alpha-\beta} Y^{\beta})}{r^{\gamma}}} E$$

Now letting

$$\frac{1}{c^{\gamma-\alpha} R_i^{\alpha-\beta}} = \rho$$

we find

$$E_4 = \frac{\beta \log_e Y/y}{\log_e \frac{Y^{\beta}}{\rho r^{\gamma}}} E$$

As in the preceding case we can write

$$g_p = \frac{dE_4}{dY} \frac{dY}{dx}$$

$$= \frac{d}{dY}\left(\beta E \frac{\log_e Y/y}{\log_e Y^{\beta}/\rho r^{\gamma}}\right)\frac{dY}{dx}$$

$$= E \frac{d}{dY}\left(\frac{\log_e (Y/y)^{\beta}}{\log_e Y^{\beta}/\rho r^{\gamma}}\right)\frac{dY}{dx}$$

$$= \frac{E\beta}{Y}\left(\frac{\log_e (y^{\beta}/\rho r^{\gamma})^{\beta}}{(\log_e Y^{\beta}/\rho r^{\gamma})^2}\right)\frac{dY}{dx}$$

if P actually lies on the profile y = Y and hence

$$g_p = \frac{E\beta}{Y} \frac{1}{\log_e Y^{\beta}/\rho r^{\gamma}} \frac{dY}{dx}$$

which upon rationalizing becomes

$$g_p = E \frac{1}{Y \log_e \frac{Y^{\beta}}{(\rho r^{\gamma})^{1/\beta}}} \frac{dY}{dx}$$

Integrating both sides of this expression yields

$$g_p = \frac{E}{x} \log_e \left(\frac{\log_e Y/(\rho r^{\gamma})^{1/\beta}}{\log_e R_i/(\rho r^{\gamma})^{1/\beta}}\right)$$

For the heterogeneous case the x and y co-ordinates of the stress control cone profile may be computed, from the above equation for any given g_p, to result in a practically uniform longitudinal stress along the profile. Figure 8 shows a family of such profiles with g_p assuming various values for a 69-kv single conductor solid-type cable joint having varnished cambric tapes as the joint insulant.

The Development of the Formulas for the Stepping of the Cable Insulant

In essence the cable insulant stepping is but a stress control cone in reverse as it were—this is logical because the physical aspects of the two propositions are alike in all respects. They do, nonetheless, differ in the magnitude of the dimensional quantities and of the stresses involved. Here one is confronted more directly with the stresses at the surface of the conductor and the ferrule; whereas in the case of the stress control cone one has to deal more with the stresses at the surface of the cable and joint insulants, which are however of much smaller consequence. Because of these circumstances the ferrule stress and the concomitant conductor stress, must be taken into account, as will be subsequently done.

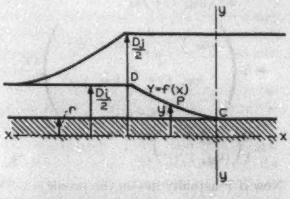

Figure 9. One half of a joint proper symmetrical about its longitudinal and transverse axes showing the transitional bounding curve C-D (the stepping profile) between the cable insulant diameter and the conductor diameter to which the actual stepping should conform within certain limits

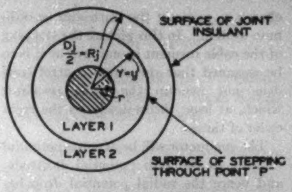
SURFACE OF JOINT INSULANT
$\frac{D_j}{2}$=Rj
Y=y
r
LAYER 1
LAYER 2
SURFACE OF STEPPING THROUGH POINT "P"

Figure 10. A cross section of the stepping profile (in the plane normal to the cable or joint longitudinal axis) through the point P shown on Figure 9

As before the three dimensional aspects of the electric field throughout the transitional curve *C-D* of Figure 9 in passing from the conductor diameter *d* to the cable insulant diameter D_i is, once again, determinable more readily by working with any two dimensions at a time. Figure 9 shows one-half of a symmetrical joint in the plane containing the longitudinal axis of the joint, wherein the cable insulant is considered to be of all the same grade of paper and thence homogeneous in respect of the dielectric constant. The material composing the joint insulant may however be such as to have the same or different dielectric constant as the cable insulant. That the presumption of a homogeneous cable insulant is warranted for all practical intents may be discerned in the following formula development. Here it will be observed that the radial potential drop between the stepping pattern and the zero potential electrode is the main determinant of the longitudinal stress along the treads. Grading of the cable insulant has no serious influence on this potential drop, as a fuller pursuit of the matter would disclose.

The conductor will be at some potential relative to the zero potential electrode (the ground potential of the field) and the radial potential drop between the conductor and the zero potential electrode is constant throughout the joint. Then with the surface of the joint insulant maintained at zero potential in accordance with the more usual practice (commonly referred to as full shielding of the joint, or a fully shielded joint) the following obtains.

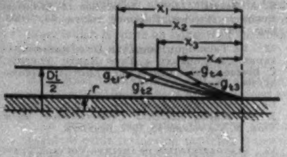

Figure 11. A family of stepping profiles for various values of g_t in arbitrary units showing the practical significance of g_t in determining the over-all length of the joint

E = radial potential drop between the conductor and the zero potential electrode
k_1 = dielectric constant of the cable insulant
k_2 = dielectric constant of the joint insulant
g_c = stress at the surface of the conductor in the joint

$$= \frac{E}{r \log_e \frac{D_j}{d}} \text{ volts per unit of length}$$

Point P in Figure 9 is any point on the transitional curve, C-D. A cross section of the stepping profile through this point, in the plane normal to that containing the joint longitudinal axis, is given in Figure 10.

k_1 = dielectric constant of cable insulant (and that of layer 1)
k_2 = dielectric constant of joint insulant (and that of layer 2)
E = potential drop between the conductor and the zero potential electrode
C_1 = capacity of layer 1

$$= \frac{k_1}{2 \log_e \frac{Y}{r}} \text{ statfarads per wire unit of length or to neutral}$$

C_2 = capacity of layer 2

$$= \frac{k_2}{2 \log_e \frac{R_j}{Y}} \text{ statfarads per wire unit of length or to neutral}$$

E_2 = potential drop across layer 2

$$= \frac{1/C_2}{1/C_1 + 1/C_2} E$$

$$= \frac{1/k_2 \log_e R_j/Y}{1/k_1 \log_e Y/r + 1/k_2 \log_e R_j/Y} E$$

THE HOMOGENEOUS CASE

Here the joint and cable insulants are identical materials and therefore have the same dielectric constant. Hence, $k_1 = k_2$ and we can write

$$E_2 = \frac{\log_e R_j/Y}{\log_e Y/r + \log_e R_j/Y} E$$

$$= \frac{\log_e R_j/Y}{\log_e \frac{Y}{r} \frac{R_j}{Y}} E$$

$$= \frac{\log_e R_j/Y}{\log_e \frac{R_j}{r}} E$$

Now

g_t = the longitudinal stress at the point P for the elemental distance dx, or the longitudinal stress along the elemental distance dx of the tread at P

$$= \frac{dE_2}{dx}$$

from which it follows that

$$g_t = \frac{dE_2}{dY} \frac{dY}{dx}$$

$$= \frac{d}{dY} \left(\frac{\log_e R_j/Y}{\log_e \frac{R_j}{r}} \right) \frac{dY}{dx} E$$

$$= \frac{E}{\log_e \frac{R_j}{r}} \frac{d}{dY} \left(\log_e \frac{R_j}{Y} \right) \frac{dY}{dx}$$

$$= \frac{E}{\log_e \frac{R_j}{r}} \frac{d}{dY} (\log_e R_j - \log_e Y) \frac{dY}{dx}$$

$$= \frac{E}{\log_e \frac{R_j}{r}} \left(-\frac{1}{Y} \frac{dY}{dY} \right) \frac{dY}{dx}$$

$$= \frac{-E}{\log_e \frac{R_j}{r}} \frac{1}{Y} \frac{dY}{dx}$$

integrating this expression between the limits Y and r yields

$$g_t = \frac{-E}{x \log_e \frac{R_j}{r}} \left(\log_e \frac{Y}{r} \right)$$

THE HETEROGENEOUS CASE

In this instance the joint and cable insulants are of different materials having unequal dielectric constants.

Letting

$1/k_1 = \gamma$
$1/k_2 = \alpha$

we may write

$$E_2 = \frac{\alpha \log_e R_j/Y}{\gamma \log_e Y/r + \alpha \log_e R_j/Y} E$$

$$= \frac{\alpha \log_e R_j/Y}{\log_e \left(\frac{Y}{r} \right)^{\gamma} \gamma + \log_e \left(\frac{R_j}{Y} \right)^{\alpha}} E$$

$$= \frac{\alpha \log_e R_j/Y}{\log_e \left(\frac{Y}{r} \right)^{\gamma} \left(\frac{R_j}{Y} \right)^{\alpha}} E$$

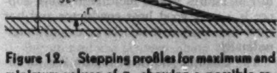

Figure 12. Stepping profiles for maximum and minimum values of g_t, showing a possible relationship to the actual stepping

$$= \frac{\alpha \log_e R_j/Y}{\log_e \frac{R_j^{\alpha} Y^{\gamma - \alpha}}{r^{\gamma}}} E$$

As in the preceding section above

$$g_t = \frac{dE_2}{dY} \frac{dY}{dx}$$

$$= \frac{d}{dY} \left(\frac{\alpha \log_e R_j/Y}{\log_e \frac{R_j^{\alpha} Y^{\gamma - \alpha}}{r^{\gamma}}} \right) E \frac{dY}{dx}$$

$$= \alpha E \log_e \left(\frac{R_j}{r} \right)^{-\gamma} \times \left(\frac{1}{Y} \frac{1}{\left(\log_e \frac{R_j^{\alpha} Y^{\gamma - \alpha}}{r^{\gamma}} \right)^2} \right) \frac{dY}{dx}$$

Now letting

$$\left(\frac{R_j}{r} \right)^{-\gamma} = \left(\frac{r}{R_j} \right)^{\gamma} = a$$

and

$$\frac{(R_j^{\alpha})}{(r^{\gamma})} = b$$

we may write

$$g_t = \alpha E \log_e a \left(\frac{1}{Y} \left(\frac{1}{\log_e b\, Y^{\gamma - \alpha}} \right)^2 \right) \frac{dY}{dx}$$

integrating this expression between the limits Y and r yields

$$g_t = \frac{\alpha E \log_e a}{x(\gamma - \alpha)} \left(\frac{1}{\log_e b r^{\gamma - \alpha}} - \frac{1}{\log_e b Y^{\gamma - \alpha}} \right)$$

Using either of these equations for g_t, depending upon the conditions in hand, and by choosing suitable values for g_t a family of exponential curves (having C as origin) can be produced depicting several possible stepping profiles. Such a family of curves is shown in Figure 11 from which it is evident that the greater g_t is, the steeper the slope of the curve, and hence the shorter the stepping. This means that with higher values of g_t the joint length is reduced.

Now by electing a maximum and minimum value of g_t two curves will result, for any given joint design. Between these two curves the actual risers and treads can be disposed to produce the proper stepping. Such a procedure is shown in Figure 12, wherein it is seen tht the juncture of the risers and treads are points on the curve of minimum g_t. They, of course, do not need to be on this curve, but could be displaced somewhere between the two curves, or below the minimum curve. However, as the stresses at these points, in respect of impulse strength especially, are the most onerous, it would seem best to position them on or below the curve of minimum g_t.

The practical significance of this

method of determining the stepping profiles lies in the fact that a relatively constant longitudinal stress along the treads may be accomplished, and hence a shorter stepping profile employed than if designed upon other principles.

The Determination of the Joint Diameter

The diameter over the joint insulant (D_j) is a comparatively simple parameter to calculate if a value has been assigned to the stress at the surface of the ferrule, g_f. In terms of this value of g_f this diameter may be found from the following long established equations

$$g_f = \frac{E}{r_f \log_e \frac{D_j}{d_f}} \text{ volts per unit of length, (radially through the insulant)}$$

then

$$\log_e \frac{D_j}{d_f} = \frac{E}{r_f g_f}$$

Since r_f, d_f, g_f, and E are known the value of D_j may be calculated. To determine the proper value of g_f compatible with sound design is, however, a matter of some burden. For, as we have seen in the preceding discussions, the length of stress control cone profile, the length, and the shape of the stepping profile are all indirect functions of g_f.

Intermingled with these considerations is the radial impulse voltage time-to-breakdown strength characteristics of the joint which also must be taken into account in arriving at the proper value of g_f. Conventional practice seems to be based upon a value of g_f varying from 40 to 70 per cent of the stress at the surface of the conductor in the cable, g_c; the actual value depending upon the circumstances involved.

Having decided upon the proper g_f all other features of the joint design become readily computable by use of the formulas already developed herein.

References

1. Uber Abrundungen Bei Muffen Und Endverschlussen Metallisierter Kabel Und Die Hier Auftretende Langsbeanspruchung Der Geshichteten Isolation, **F. Loebner.** *Archiv fur Electrotechnik* (Berlin, Germany), volume 17, number 2, 1926.

2. Manufacture and Installation of a 33,000 Volt Type H.S.L. Submarine Cable, **K. Takalashi.** *International Conference on Large High Voltage Electric Systems* (Paris, France) volume II, 1931, page 505.

3. Joints, Sealing Ends and Accessories for Pressure Cable, **L. G. Brazier.** *Journal*, Institution of Electrical Engineers (London, England) volume 93, part II, October 1946.

4. The Breakdown Mechanism of Impregnated Paper Cables, **D. M. Robinson.** *Journal*, Institution of Electrical Engineers (London, England) volume 77, 1935, page 90.

5. Modern Supertension Cables, **C. C. Barnes.** *The Electrician* (London, England) July 18, 1947.

6. Impulse Strength of Insulated-Power-Cable Circuits, **H. Halperin, G. B. Shanklin.** *AIEE Transactions*, volume 63, 1944, pages 1190–97.

7. Investigation of High-Tension Cable Joints, **E. W. Davis, G. J. Crowdes.** *AIEE Transactions*, volume 44, 1925, pages 600–11.

8. Esterified Styrenated Insulation in the Power Field, **T. R. Scott.** *International Conference on Large High Voltage Electric Systems* (Paris, France) 1939.

9. The Jointing and Terminating of High Voltage Cables, **W. Holttum.** *Journal*, Institution of Electrical Engineers (London, England) volume 80, 1937, page 517.

10. Cable Terminations, **D. B. Irving.** *Journal*, Institution of Electrical Engineers (London, England) volume 92, part II, number 26, April 1945, page 73.

11. Some Developments in the Routine Pressure-Testing of High Voltage Cables, **E. A. Beavis.** *Journal*, Institution of Electrical Engineers (London, England) volume 66, 1928, page 1086.

12. La Technique Actuelle Des Transformateurs De Courant a Tres Haute Tension, **C. Breson.** *Revue Generale de l'Electricite*, volume 54, 1945, page 326.

13. Condenser Cones for Cable Testing, **J. K. Webb.** *Electrical Communication* (New York, N. Y.) volume 15, 1937, page 354.

14. Standardization of Impulse-Voltage Testing, **T. E. Allibone, F. R. Perry.** *Journal*, Institution of Electrical Engineers (London, England) volume 78, 1936, page 257.

15. The High-Pressure Gas-Filled Cable, **C. J. Beaver, E. L. Davey.** *Journal*, Institution of Electrical Engineers (London, England) volume 91, part II, 1944, page 35.

16. The Impulse Electric Strength of High-Voltage Cables, **R. Davis.** *Journal*, Institution of Electrical Engineers (London, England) volume 89, number 7, part II, February 1942.

17. A Problem in 33 Kv Jointing, **W. Hill.** *Proceedings*, Institution of Electrical Engineers (London, England) volume 96, part I, number 97, January 1949, page 25.

18. The Cleveland 66 Kv Cable Joint, **H. L. Wallan.** *Electrical World* (New York, N. Y.) volume 82, 1923, page 1058.

19. A New 132,000 Volt Cable Joint, **D. M. Simmons.** *AIEE Transactions*, volume 46, 1927, pages 240–47.

20. Joints in High Voltage Multi-Conductor Cable, **T. F. Peterson.** *AIEE Transactions*, volume 46, 1927, pages 963–74.

21. The 60,000 Volt Underground Network of the Union d'Electricite, **E. Mercier.** *Journal*, Institution of Electrical Engineers (London, England) volume 65, 1927, page 499.

22. Nomogram for the Calculation of Condenser Bushings, **F. Cerovsky.** *Elektrotechnicky Obsor* (Czechoslovakia) volume 36, number 16, August 1947, page 298.

23. Condenser Type of Insulation for High-Tension Terminals, **A. B. Reynders,** *AIEE Transactions*, volume XXVIII, part 1, 1909, pages 209–68.

24. N.E.L.A. Underground Systems Reference Book. *Edison Electric Institute* (New York, N. Y.) Chapter V, Section EEE, 1931, page 143.

25. The Impulse Strength of High Tension Cable Installations, **C. Held, H. W. Leichsenring.** *International Conference on Large High Voltage Electric Systems* (Paris, France) Paper number 207, 1939.

Discussion

L. I. Komives (The Detroit Edison Company, Detroit, Mich).: Mr. Short's remark that there is a scarcity of impulse test data on joints is well taken. I would like to remind him that we have done considerable work in Detroit in this respect and this data was given to Mr. Halperin and Mr. Shanklin who presented it to the Institute in May 1944.[1] We hope that others who have similar data will come forward and tell us where this data is available.

In the paper, the author says that "reflections do occur at these discontinuities which are really localities having innate characteristics at variance with those of the main portion of the line." We think that joints can be made to resemble adjacent cable quite closely. We are using such joints in our 120—138-kv gas pressure cables as well as in duct splices made for lower potentials. In duct splices we use very thin connectors and build the insulation up to only slightly larger than the cable insulation and we know that Cleveland goes a step further and by brazing the copper conductor they get the diameter down to even less than we do. However, it must be kept in mind that the discontinuities which Mr. Short is talking about are much more important at higher potentials.

The connector diameter shown in Figure 1 is an example of the use of too large connectors. It seems that a revision of National Electric Light Association connectors should be made very soon in the light of more recent developments. We feel that sector connectors should be designed for mechanical forces rather than electrical properties (conductivity) and the same applies to round connectors. If there is a local heating due to insufficient conductivity across the connector, it is not as bad as figures would indicate because copper is a very good heat conductor and hot spots are dissipated to a large extent longitudinally.

The example shown in Figure 2 is an indication that a thickly insulated conductor should be stepped with a larger number of steps than shown on the example. We think that radial and longitudinal breakdown should be about even on tests, and for design purposes impulse testing can be used which shortens the time considerably. In order not to arrive at erroneous conclusions, one should take into account the experience of the General Cable Corporation as described by Mr. Atkinson and Dr. Simmons in a paper entitled Oil-Filled Cables and Accessories,[2] in which it is said: "As a result, tests involving both radial and longitudinal stresses are more likely to produce longitudinal failure when made at very high voltages for short time and radial failures when made as long-time tests at lower voltages."

The ratio between insulation thickness and longitudinal leakage distance in high-voltage joints in use at Detroit at the present time is 1/28.

Mr. Short mentions "that tapes hand-applied in the field are not susceptible to being wrapped with the tension and degree of uniformity feasible under cable making practice." When talking about hand-applied insulation not being equivalent to factory insulation, one must not forget the exposure to moisture during field operations which is quite as important as tension or degree of uniformity.

In Figure 3, the profile shown may be very good theoretically, but in practice a straight line from *B* to *A* is just as good and easier to obtain in field.

In practice one finds that the starting point of cable insulation tapering is usually under the stress control cone, not outside as shown in Figures 6 & 7. This could be shown in this manner so as not to be misleading, especially on Figure 6 where various lengths of stress control cone are shown.

Referring to Figure 12, approach to logarithmic profile may be achieved by the use of thinner tapes near the conductor and removing the same number of tapes for each step. The removal of the same number of tapes for each step may be quite a bit easier on the splicer. It is very difficult to specify diameters, especially with sector-shape conductors.

High-voltage joints with a value of g_f equal to 86 per cent of the stress at the surface of the conductor are giving satisfactory service.

REFERENCES

1. IMPULSE STRENGTH OF INSULATED-POWER-CABLE CIRCUITS. **Herman Halperin, G. B. Shanklin.** *AIEE Transactions*, volume 63, 1944, pages 1190–97.

2. OIL-FILLED CABLE AND ACCESSORIES, **R. W. Atkinson, D. M. Simmons.** *AIEE Transactions*, volume 50, December 1931, pages 1421–29.

E. R. Thomas (Consolidated Edison Company, New York, N. Y.): I am very glad that Mr. Short has raised the question of changes in surge impedance introduced by cable joints used on cable systems. This, to me, is a relatively important matter which has been overlooked to a large extent in the usual designs of high-voltage cable joints. I cannot agree with Mr. Atkinson that because the lengths of power cable usually used on 60-cycle systems are but a very small fraction of a wave length corresponding to that frequency, that the matter of discontinuity in surge impedance is of small importance. Mr. Atkinson's statement would be true if we were concerned with only steady-state operating conditions insofar as they would affect terminal conditions, but the propagation of an electric wave along a cable conductor is essentially at the same velocity whether you are talking about 60-cycle frequency or about many thousands of cycles of frequency. Therefore, discontinuity will always produce an electric field distortion at the point of discontinuity, and this will alter the stresses at this point to a value different than would be calculated by theory which neglects traveling waves. When we consider the superposition of transient waves traveling along the cable system due either to sudden changes in the values of current being carried or to sudden application of a voltage transient, then we deal with wave fronts having components of frequency a great many times higher than the normal power frequency. This is one of the reasons why many of the operating companies are turning more and more to the use of surge testing of components of the system as providing a better index of the suitability of that component to function under the operating conditions normally imposed on it in such a system.

It would seem to me axiomatic that in the design of any cable joint that if means are taken to preserve the surge impedance of the connection through the joint, a fundamentally better operating component will result.

A. L. McKean (Phelps Dodge Copper Products Corporation, Yonkers, N. Y.): Mr. Short's paper is a welcome contribution to the electric cable field and helps bridge the gap between experience and theory. The logarithmic formula which Mr. Short has amplified so extensively has been a basic design tool for many years in our own high-voltage research and development on cable joints and terminals, and we should like to testify briefly to its practical significance in such work.

It has been found, for example, that proper design, with careful attention to selection of gradient and length of stress cone, permitted the use of a thin wall terminal made of varnished cambric tape and Oil Stop compound, which may be slipped over the end of the cable, and used over and over again. These terminals have proved of special value in our long-time load cycle aging tests of 17-kv paper cable which we test at 57 kv over a period of time varying from a few weeks to a year. Before the logarithmic stress relief cone was adopted, a comparatively heavy or large diameter stress cone had consistently failed to withstand the severe stress concentrations incurred by poor basic design.

E. H. Grosser (Commonwealth Edison Company, Chicago, Ill.): The author presents an interesting analysis of longitudinal stresses in cable joints. Basically, he shows a means of controlling such stresses adjacent to the surface of the shielding cone by adjusting the shape of the cone to produce uniform longitudinal stresses. He thus arrives at a cone of exponential shape.

In actual practice, using ordinary construction methods with either varnished cambric or crepe-paper tapes, it is not feasible to construct stress cones having the desired theoretical shape. We arrive at either a single straight line slope or, at best, a so-called double slope. Recognizing this practical limitation it has been our practice in Chicago, in the design of high voltage cable accessories, to design for a known maximum value of longitudinal stress at the point where the stress cone begins, and to adjust the angle of the stress cone accordingly. This approach takes into consideration the probability that the weakest path longitudinally within a cable joint is the junction of the factory-applied cable insulation and the hand-applied tape. If this method of design is followed, it imposes a limitation on longitudinal stresses at the point where they are likely to do the most harm. Obviously, average longitudinal stresses also must be taken into consideration by proper dimensioning of the leakage distance.

A method is shown in the paper of arriving at uniform stresses along the steps by a control of the stepping profile. This appears to be a refinement which is not justified practically except in extreme cases. An exponential type of stepping was used on one of our 66,000-volt duct splices where a rigid control of diameter was necessary because of space limitations. Even here, the value of this refinement appears doubtful.

The British practice, referred to in the paper, of designing joints for radial stresses as high as 70 per cent of maximum radial stresses in cables, appears to be less conservative than American joint design practice. The latter, however, is based largely, if not almost wholly, on the use of varnished cambric tape for joints on paper-insulated cable, whereas the British practice refers to joints insulated with the same kind of paper tape that is used in the cable. It is possible, of course, that our joints can be operated satisfactorily under higher stresses than are customarily used. It appears that more data need to be accumulated on this subject.

R. W. Atkinson (General Cable Corporation, Bayonne, N. J.): The general method used by Mr. Short for calculating stresses in a joint and for determining its dimensions are simple and adequately accurate and have been effectively used in designing many of the high-voltage joints that are in service.

Mr. Short says that it is "assumed that the stress control cone does not overlap the cable insulant; which, at least theoretically, is the right order of things." Reading this statement in terms of the figures, it is understood that the thought is that the stress control cone should not overlap the stepping of the factory insulation. If correctly interpreted, this idea cannot be taken as generally true. Indeed, in many of the joints in service, the stress control cone does overlap the steps of the cable insulant by a major portion of its length. A requirement that there be no such overlap would greatly weaken, or lengthen, these joints.

Mr. Short quotes authorities giving a factor of 15 for the relative strength of tape insulation normally and longitudinally of its plane. For tapes hand-applied over stepped insulation, as shown in his designs, and in terms of average stress, this figure is quite acceptable. In terms of the strength of the factory insulation the value will be 30 or more. Thus, where full benefit is to be taken of taping methods which permit obtaining in the field-applied insulation a radial strength comparable to that of the factory insulation, the corresponding much higher ratio must be used in determining the permissible longitudinal stresses.

At the beginning of his paper Mr. Short introduces some incidental remarks indicating that electrical reflections may occur at a joint as a result of the discontinuity of the electrical properties at the joint. He says that the magnitude of such phenomena would have to be investigated from a mathematical standpoint. Fortunately this has already been done. The classic work of Professor M. I. Pupin[1,2] on the famous Pupin loading coils for telephone circuits showed that a circuit will pass a wave with no significant reflection providing the spacing between coils does not exceed about 10 per cent of the wave length. And, of course, the discontinuity due to having nearly all of the line inductance lumped in wound coils is very great compared with some local variation in capacitance per unit length. We are thus conservative in applying Pupin's data to a joint in a power line. The wave lengths to be considered are for the power frequency and for surges. At 60 cycles, the wave length is about 1,500 miles. For a standard surge we may take the wave front of $1\,^{1}/_{2}$ microseconds as approximately equivalent to a wave length of about 3 microseconds or 1,500 feet. Ten per cent of even this latter figure is 150 feet which is the length below which discontinuities would not cause reflections at frequencies significant in power work. It is thus completely adequate to do as the author has done, namely, to design the joint (very short compared with 150 feet) purely on the basis of electric stresses, radial and longitudinal. The discontinuities are important only as they affect these stresses, especially the latter.

To be sure, electrical discontinuities made in cable sheaths at joints for the purpose of controlling sheath losses may be troublesome for carrier current use. Also for a cable to be used for transmitting radar frequencies in the range of centimeter lengths, irregularities even in the internal structure of the joint would be significant. However, these things are another story and not related to the subject at hand.

The question has arisen many times concerning the possible effect of reflections in power cable joints and thus it seems desirable to point out with emphasis that this is not a practical problem in determining dimensions and insulation of such a joint.

REFERENCES

1. PROPAGATION OF LONG ELECTRICAL WAVES, M. I. Pupin. *AIEE Transactions*, volume XVI, 1899, pages 93–142.

2. WAVE TRANSMISSION OVER NON-UNIFORM CABLES AND LONG DISTANCE AIR-LINES, M. I. Pupin. *AIEE Transactions*, volume XVII, 1900, pages 445–512.

H. D. Short: Mr. Komives has suggested the disclosure of impulse test data in relation to high-voltage cable joints. Such information would be extremely useful in joint design. I would like to see such data correlated specifically with the full physical dimensions and constructional details of the particular joint designs, including, for example, the stress control cone and stepping profiles and their relation to one another in the joint proper. To say that a joint withstood a certain test voltage either on an impulse test or a voltage-time-to-breakdown test does not mean very much to one concerned with high-voltage joint design unless the complete details of the joint's dimensions and construction are at hand.

I agree with Mr. Komives that it is possible to make joints which possess characteristics closely resembling those of the adjacent cable. However, I think this matter is worthy of more study and the disclosure of impulse data mentioned above would be of material help in these directions.

Figure 2 of the paper is intended only to illustrate what is meant by the term "stepping"; it has been drawn to an arbitrary scale and does not reveal the author's opinions in regard to the number of steps or the optimum dimensions of the risers and treads in any particular instance. The formula of g_t given in the paper clearly shows that the cable insulant thickness is one of the criterions of the stepping profile. Mr. Komives also refers to Figure 12, and I am completely in conformity with his thoughts in regard to the practice of removing an equal number of tapes at each step. Indeed, the use of short treads and risers of heights equal to the thickness of one tape (that is, one paper tape of the cable insulant) permits closer adherence to a given stepping profile as determined by the paper's formula for some specific value of g_t.

In reference to Mr. Komives' remarks concerning Figures 6 and 7, there is no question but that the stress control cone should not overlap the stepping profile from a theoretical aspect. As Mr. Komives says, very often in practice one does not find this theory accepted; however, this practice does not invalidate the theory nor a contention that it is better to avoid this overlapping in an actual joint. I am of the opinion that a more economical joint for any predetermined set of conditions can be made by not overlapping the stepping profile, but this can only be proved by test data on comparative designs and I know of no one who has such data. Glovers and Enfield[1,2] in England do not allow the stress control cone to overlap the stepping profile in their high-voltage designs, and there is at least one of the highest voltage installations in the United States wherein this practice is followed.

Mr. Komives cites a statement ascribed to Mr. Atkinson and Dr. Simmons. I am very glad that Mr. Komives has inserted this reference as it serves to corroborate some of the premises which prompted the publication of the paper. However, I think it should be stated here that it is not tractable with available data to infer that there exists an established or empirically authenticated relationship between short-time tests at high voltages and long-time tests at low voltages in respect of high-voltage joints. Mr. Komives mentions a ratio of longitudinal leakage distance to joint insulant thickness of 28. Assuming that the correct interpretation has been put on this ratio, it is difficult to accept such "in puris naturalibus" as a design criterion. It is nonetheless interesting information and no doubt based upon experience in service and test. I should like to know if it is related to any flashover value; for example, so many centimeters per kilovolt to neutral. The value of g_f equal to 86 per cent of g_c quoted by Mr. Komives appears to be much higher than is conventional here or abroad for high-voltage cable joints. But then any specific value of such must be interpreted in the light of the joint design, the type of joint insulant and degree of jointing skill employed, and last but by no means least, the desired factors of safety relative to atmospheric and internal surges. As pointed out in the paper, the determination of the proper or most suitable value of g_f is a matter of some burden. The factors involved are many and need more clarification and emphasis from experimental data; meanwhile, to achieve the impulse voltage breakdown strength usually dictated by present trends, a value more closely akin to 50 per cent of g_c seems to be indicated.

I am indeed grateful to Mr. Thomas for his remarks confirming my postulations in regard to the importance of the characteristic (or surge) impedance of joints introduced into a cable system. His able amplification of the thoughts I had in mind when preparing the paper is a most salutary contribution. I too find it difficult to agree entirely with Mr. Atkinson's discussion in these respects. Mr. Atkinson refers to the "classic work" of Professor Pupin; surely he is not overlooking the mathematical "locus classicus" of Oliver Heaviside.[3,4] He did the classic work which permitted Pupin to reduce to practice the distortionless line. It seldom, if ever, happens in a high-voltage cable line that the joints are as close as Mr. Atkinson says is required for the spacing of loading coils towards assimilating Pupin's uniform distribution of the inductance parameter. If what he says is correct, then his later deductions militate against his premise since joints are nearly always spaced more than 10 per cent of a wave length of 1,500 feet apart, and the length of the discontinuity is not significant in this argument. Indeed, using Mr. Atkinson's example and spacing the joints 375 to 400 feet apart results in a 1/4 wave length between joints which, of course, is an ideal condition for complete reflection. Simple calculations show, assuming a joint characteristic impedance twice that of the cable, a not too unrealistic value, that at a junction of a cable and joint and transmitted or refracted portion of the voltage wave could under the worst conditions be of the order of 30 per cent greater than the incident wave. In the case of a cable connected to an overhead line there is no question but that the cable will flatten the wave front and increase the peak value of the wave; and the shorter the cable the greater the peak value of the wave becomes in comparison to the incident wave.

In reference to Mr. Atkinson's mention of the relation of the ultimate breakdown strength of paper in the normal direction to that in the plane of the fibers, I am not too sure that I comprehend his meaning. If he means that the diameter of the joint insulant and the longitudinal stresses should be such as to allow greater factors of safety than obtain in the adjacent cable then I am in agreement with him; but I cannot categorically agree that the factors of safety in the joint should be twice that in the cable as circumstances alter cases. I must also take the opposite point of view to Mr. Atkinson when he says "a requirement that there be no such overlap would greatly weaken, or lengthen, these joints." My related remarks on Mr. Komives' discussion are appropriate here.

Mr. Grosser refers to their method of attaining the stress control cone profile using varnished cambric and crepe-paper joint insulation. With such hand-applied insulation it is not easy to arrive at the true exponential profile consequent upon some chosen value of g_p. Nonetheless it is quite feasible to very closely approach this boundary curve by means of a succession of straight lines; not more than three straight lines will most always reproduce very closely the exponential profile to within practical application, it being all too obvious how this can be achieved when one recalls that a curve is but a series of straight lines. Mr. McKean's experience is pertinent to this matter and emphasizes the author's opinions of the desirability of achieving as nearly as possible the theoretically correct control cone profile. With preformed preimpregnated paper rolls it is a simple matter to arrive at the actual exponential profile that the theory predicts. I am wondering if Mr. Grosser has any data to substantiate his reflection that the "exponential type of stepping" used on their 66-kv duct splices appears to doubtful value. Mr. Grosser opines that a value of g_f equal to 70 per cent of g_o appears to be less conservative than American design practice. This is interesting in view of Mr. Komives' remarks in these respects; I presume though that Mr. Grosser is not including the 66-kv duct splices he mentioned earlier. Undoubtedly the use of paper-joint insulation in contradistinction to varnished cambric permits the use of higher values of g_f and concomitantly smaller joint diameters; but here again more experimental data would seem worthwhile, as Mr. Grosser has suggested.

I appreciate Mr. McKean's remarks in substantiation of the practical significance of the work embodied in the paper.

REFERENCES

1. THE HIGH-PRESSURE GAS-FILLED CABLE, C. J. Beaver, E. L. Davey. *Journal*, Institution of Electrical Engineers (London, England), volume 91, part II, number 10, February 1944.

2. GAS COMPRESSION CABLE, F. W. Main. British Electrical Industry Overseas Manual (Benn Brothers, Ltd., London, England), 1949, page 61.

3. ELECTROMAGNETIC THEORY, Oliver Heaviside. Ernest Benn Ltd., London, England, volume 1 1893.

4. THE ELECTRICIAN, Oliver Heaviside. Ernest Benn Ltd., London, England, June 17, 1887.

Transient Temperature Phenomena of 3-Conductor Cables

F. O. WOLLASTON
MEMBER AIEE

TRANSIENT temperature phenomena are of fundamental importance in two fields of cable engineering, namely the calculation of short-time overload ratings and the design of oil-filled cable lines. Sufficient fundamental theory has been published to cover the subject quite adequately. However, much remains to be done in developing practical methods of applying rigorous solutions to common problems and in making the methods available to engineers generally. The solution of transient problems, although inherently difficult, is capable of much simplification through methods which are familiar in other technical fields. For example, in transmission line engineering, the laborious task of calculating the electrical performance of long lines has been greatly simplified by the production of accurate performance charts.

In the field of cable engineering, the calculation of steady-state ratings has received considerable attention and several convenient handbooks on the subject are available. Unfortunately similar work has not been undertaken for short-time ratings of cables and for oil demands of oil-filled cables. Consequently, very few utilities have engineers on their staffs who are capable of handling these problems. The oil demands of oil-filled cables might seem to be a subject of little interest to most utilities. However, a surprisingly large number of utilities have had occasion to consider seriously the installation of oil-filled lines. In such lines the size of the hollow core in the conductor, the number and location of stop joints, and the type and location of reservoirs are major factors in design which are dependent wholly or partially on the oil demand of the cable. Where engineering competence in oil-demand calculations is lacking, the utility must perforce rely entirely on the cable manufacturing companies to carry out its design studies. This situation must surely be rather unsatisfactory to the utility and also places a considerable burden on the engineering staff of the manufacturer.

Where engineering competence is lacking in the calculation of short-time ratings for cables, the utility cannot take full advantage of the substantial economies which can be achieved by the intelligent use of the short-time overload capabilities of underground lines. The overloads which cables can carry for one or two hours are frequently quite large and can be made use of in the same way that overload capabilities of such apparatus as transformers and rectifiers are utilized.

This paper describes the methods which the author and his co-workers have developed for the practical application of rigorous theory to the routine calculation of short-time overload ratings of solid-type and oil-filled cables installed in ducts and for the oil demands of Pirelli-type oil-filled cables installed in ducts. In a previous paper[1] a treatment of the problems of single-conductor cables was given. In the present paper a novel method of extending this treatment to the problems of 3-conductor cables will be given and the methods of making routine calculations will be described in detail. These methods have been applied to all the practical problems of this type which have occurred in the last 20 years in a large utility company operating one of the most extensive cable systems on the American continent. They have proved convenient and fully adequate. It is hoped that they will be of value to other engineers. The author has not had occasion to solve such problems for pipe-type cables or cables buried directly in the earth and the paper does not deal with them.

The particular methods to be described have certain advantages not found in other methods. A different solution for the problem of cable temperatures under variable loading has been published by E. Church.[2] This solution is rigorous but does not cover the problem of oil demands. An approximate solution for the problem of cable temperatures under variable loading has been published by W. B. Kirke.[3] It is not applicable to the problem of oil demands and has the further disadvantage of introducing certain approximations which are not present in rigorous solutions. A rigorous solution which covers both transient temperature problems and oil demand problems has been published by G. B. Shanklin and F. H. Buller[4] but convenient methods of making numerical computations have not been made available. The present method is rigorous, it is applicable to both transient temperature problems and oil demand problems and considerable simplification of computing procedure has been worked out. Although its use in transient temperature problems entails more computing labor than the approximate method noted in reference 3, the facility gained in handling oil-demand problems more than compensates for the extra effort.

Temperature Transient of 3-Conductor Cables

The first problem which will be dealt with is the temperature change of a 3-conductor cable produced by a change in loading. The ampere loading of a cable

---

Paper 49-268, recommended by the AIEE Insulated Conductors Committee and approved by the AIEE Technical Program Committee for presentation at the AIEE Fall General Meeting, Cincinnati, Ohio, October 17-21, 1949. Manuscript submitted May 25, 1949; made available for printing September 1, 1949.

F. O. Wollaston is with the British Columbia Electric Railway Company, Ltd., Vancouver, B. C., Canada.

The author wishes to express his appreciation to Mr. E. H. Grosser, Jr., for his assistance in calculating several of the temperature transients given in the paper and to Mr. L. R. Horne for his assistance in the preparation of the numerical example.

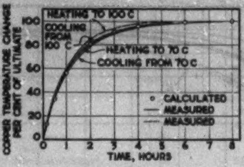

Figure 1. Attainment curve for 3-conductor type-H cable

Cable has 500,000-circular mil compack sector conductors, 125 mils insulation, 117 mils sheath

can change either abruptly or gradually. The abrupt change is easier to solve mathematically and is used here. Since it is heat loss, not loading, that controls the temperature, the problem is worked out in terms of losses. The losses are assumed to have been constant for sufficient time to allow the cable to reach a constant temperature. The loss then changes abruptly by one watt and produces a temperature transient.

This problem has been solved rigorously for single-conductor cables, as noted earlier. However, it has not been solved rigorously for 3-conductor cables, for the reason that no satisfactory mathematical formula for the thermal resistance of the insulation has been developed. It is therefore necessary to adopt the device of converting a 3-conductor cable into an equivalent single-conductor cable, after which the single-conductor solution can be applied. Formerly, the usual method of doing this was to treat each core of a 3-core cable as though it were a separate single-conductor cable. It was assumed that in shielded-type cables the heat in each core flowed uniformly in all directions from the conductor to the metallic shielding tape, which in turn conducted it with negligible thermal drop to the sheath. This permitted the calculation to be carried out as though only one phase of the cable were present, the thermal resistances of the sheath and duct being multiplied by three to adjust them to the single-phase basis. For want of a better method, the same procedure was proposed for belted cables, with the expectation that it would not be very accurate.

These assumptions were reviewed in 1942 when starting design calculations on the first 3-conductor oil-filled lines to be installed by the company with which the author was then associated. Common sense indicated that they were not true for belted cables with sector-shaped conductors. The insulation between conductors is relatively thin compared to the size of the conductors, since such cable is used only in the lower voltage classes. Thus it forms a thin sandwich between masses of metal which are at the same temperature. It seemed inconceivable that any appreciable amount of heat would flow into the insulation between the conductors. Accordingly it was concluded that the three conductors and the insulation between them could be considered as a sort of composite single conductor. This is the concept that is developed in this paper and is used as a means of converting 3-conductor cables into equivalent single-conductor cables.

That this concept was applicable to shielded-type solid cable with sector conductors was already known. Halperin[5] had originated it in connection with studies of the measured values of insulation thermal resistance of such cables. He found that the values measured in his tests were substantially higher than would be obtained by calculation using the usually accepted method, that is, the method of reference 6. He showed that the formula for single-conductor cables could be made to give acceptable results, provided an empirical correction was applied. The correction was less for cables with thin insulation and relatively large conductors of pronounced sector shape than for thicker insulation and more rounded conductors.

These results established the soundness of the basic idea of the composite single conductor. The idea could not be used for direct calculation of the insulation thermal resistance or of problems involving the insulation thermal resistance, since the proper correction factors to apply for various types and designs of cables had not been determined. However, it was seen that if the correct value of the insulation thermal resistance were already known, it could be used to calculate the diameter of an equivalent single conductor which would have the correct ultimate temperature rise. It seemed evident, too, that the calculated temperature transient of the equivalent cable would be very nearly correct. Even if the insulation thermal resistance were not accurately known, the best available value could be used. In that case the results would still be the best that the accuracy of the available data would permit. Trial calculations were made for several cables whose temperature transients were known from tests. An example for a shielded cable is given in Figure 1 and for a belted cable in Figure 2. The agreement between the calculated temperature transients and the measured transients is quite sufficient for all practical purposes. The results proved the value of the method and it was adopted as standard.

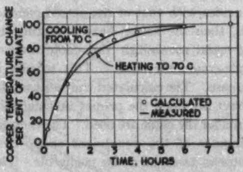

Figure 2. Attainment curve for 3-conductor belted cable

Cable has 500,000-circular mil standard stranded sector conductors, 141 mils conductor insulation, 78 mils belt insulation, 125 mils sheath

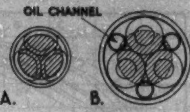

Figure 3. Equivalent single conductors for 3-conductor cables

Shaded areas delineate the equivalent single conductors

A. 500,000-circular mil type-H cable, compack sector conductors, 125 mils insulation, 117 mils sheath

B. 450,000-circular mil 69-kv oil-filled cable, compack round conductors, 315 mils insulation, 156 mils sheath

The author is indebted to the Commonwealth Edison Company for the test curves in Figures 1, 2, and 5. In Figure 5 the test data shown are averages. To bring out a point of interest, Figures 1 and 2 show details of certain individual test runs on cables 5 and 6 respectively of Figure 5. All tests were made with the cables installed in the open air of a testing laboratory. It is noticeable that the measured heating curves in Figures 1 and 2 do not coincide with the cooling curves, nor do the heating curves for the cable of Figure 1 coincide in the two test runs to different maximum temperatures. This is probably due to the variability in the thermal "constants" of each cable, particularly the thermal resistance of the sheaths. The sheath thermal resistance is known to decrease[5,6,7] as the dissipated losses increase. The losses being dissipated through the sheath are always less at the start of a heating transient than at the finish, even though the losses generated within the cable remain constant throughout. The reverse is true for a cooling transient. Consequently the sheath thermal resistance will vary during a test and the heating and cooling curves will usually not coincide. In theoretical

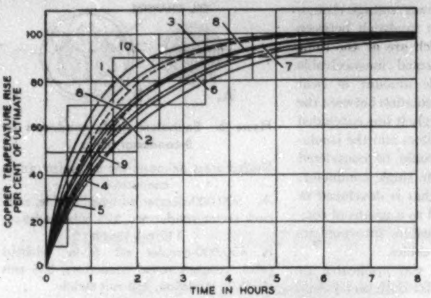

Figure 4. Calculated attainment factors for single-conductor cables

No.	Cond. Size, Cir. In.	Core Size, In.	Kv	Type	Nominal Thickness Mils Insul.	Nominal Thickness Mils Sheath	R_i
1	1.25	0.75	12	Ord, rope core	250	125	1.01
2	1.75	1.00	12	Ord, rope core	250	141	0.852
3	0.5	None	33	Ordinary	406	109	2.44
4	2.1	0.69	69	Oil-filled	315	141	0.855
5	2.1	None	69	Ord, segmental cond	688	169	1.86
6	1.0	None	69	Ordinary	750	141	2.60
7	0.75	None	69	Ordinary	750	141	2.88
7	0.6	0.69	132	Oil-filled	720	190*	2.48
7	0.6	0.50	132	Oil-filled	720	156	2.48
8	0.6	0.40	132	Oil-filled	720	250**	2.48
9	1.1	0.69	132	Oil-filled	720	156	2.0
10	0.25	0.69	132	Oil-filled	560	133	2.24

* Double. ** Fluted.

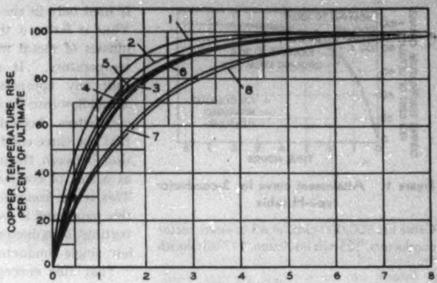

Figure 5. Attainment factors for 3-conductor cables

Curve No.	Cond. Size, Cir. In.	Stranding	Type of Cable	Nominal Thickness Mils Cond.	Nominal Thickness Mils Belt	Nominal Thickness Mils Sheath	R_i
1	#0 Awg	Compackround	"H" 12 kv	165		109	1.49
2	0.375	Standard sector	Belted, 5kv	78	47	109	0.56
3*	0.350	Compacksector	"H" experimental	110		109	0.535
4*	0.5	Compacksector	"H" experimental	90		109	0.569
5*	0.5	Compacksector	"H" experimental	125		117	0.587
6*	0.5	Compacksector	Belted 13 kv	141	78	125	1.11
7	0.4	Compackround	Oil-filled 69 kv	315		156	1.23
8	0.45	Compackround	Oil-filled 69 kv	315		156	1.195

*These attainment curves were determined by tests. Other attainment curves were calculated.

calculations the thermal constants of the cable are assumed to be truly constant and therefore the calculated heating and cooling curves are identical.

The desirability of having correct values of insulation thermal resistance deserves comment. As indicated by the tests reported in reference 5, part III, already referred to, the correctness of the values calculated by the usual method of reference 6 for shielded cables is open to question. The insulation thermal resistance is an essential factor in the determination of steady-state ratings as well as short-time ratings and oil-flow problems. It is suggested that the matter is important enough to justify obtaining demonstrably correct values by actual measurement. This might be done by adding a clause to the cable purchase specifications which would require the manufacturer to furnish the guaranteed value of the insulation thermal resistance. When sufficient background data had been established, it would be quite easy to estimate the values sufficiently closely for use in design studies where the cables have not been actually constructed.

It is not necessary that the periphery of the equivalent single conductor coincide with the periphery of the actual conductors. Two typical examples of equivalent single conductors are shown in Figure 3. In Figure 3(A) for a solid-type shielded cable the peripheries do coincide. In Figure 3(B) for a 66-kv oil-filled cable with round conductors they do not. This merely means that in the shielded cable example the actual heat flow is entirely from the backs of the conductors, whereas in the oil-filled cable example it is not. In both cases, however, the equivalent single-conductor method will give the correct result for the ultimate copper temperature rise above sheath, which is the most important consideration.

It also is necessary, of course, that the transient temperature rise be correct, or nearly so, throughout the transient. In the case of solid-type cable, either belted or shielded, it is obvious that if the periphery of the equivalent single conductor coincides with that of the actual conductors, then the actual heat flow must be the same as though the cable were a single-conductor cable. This usually is the case. The calculated transient will be correct provided the proper thermal constants for the cable are used. The thermal resistance of the equivalent single conductor is assumed to be negligible. The thermal capacity is calculated separately for the coppers and for the impregnated-paper insulation within the periphery of the equivalent single conductor. The sum of the two values is the total thermal capacity. The specific thermal capacity and the thermal resistivity p of the insulation also are required. The insulation is not uniform in composition due to the presence of the filler materials in the filler spaces. This nonuniformity is unimportant in solid-type cable since the thermal constants of the filler materials are the same as for the insulation. For modern solid-type cables p can usually be taken as 600 watts per degree centigrade per centimeter cube. The thermal resistance of the metal of the sheath is assumed to be negligible. The thermal capacity is calculated for the volume of lead in the sheath. If shielding tapes are present, the thermal capacity for the portions adjacent to the sheath can be added to that of the sheath if this refinement is thought desirable. The physical properties of cables are given in Table I.

APPLICATION OF METHOD TO OIL-FILLED CABLES

The determination of the physical constants of the equivalent single conductor for oil-filled cables requires a certain amount of judgment. This may be seen by considering the equivalent single-conductor in Figure 3(B). Some of the filler spaces are left open to provide extra channels for oil flow. The physical constants of the insulating oil must be used for the material in these spaces. The conductors project into the insulation space between the surface of the equivalent

Table I. Properties of Cable Materials

Material	Specific Gravity	Cubical Expansion Coefficient	Specific Thermal Capacity		Thermal Resistivity °C/watt per cm. cube
			Joules/cm. cube/C°	Joules/in. cube/C°	
Copper	8.95	5.01×10^{-5}	3.44	56.4	0.285
Lead	11.37	8.4×10^{-5}	1.43	23.4	2.990
Transformer oil	0.90	75×10^{-5}	1.90	31.1	611
Dry paper	1.41	10×10^{-5}	2.26	37.1	770
Oil-filled insulation*	1.15	45.75×10^{-5}	2.06	33.8	550

* Assumed 55 per cent oil, 45 per cent paper.

single conductor and the sheath. This is not permissible mathematically, as the treatment requires the insulation space to be occupied wholly by insulation. In addition, the mathematics requires the insulation to be uniform in its thermal properties. This latter requirement is not met in the actual cable, since parts of the insulation space are occupied by free oil and the remainder by impregnated paper. It is necessary to use compromise values. In addition to the thermal constants, coefficients of expansion also are required if the oil-flow transient is to be calculated. These too must be appropriate compromise values.

The recommended procedure is to assume that the copper conductors are located wholly within the equivalent single conductor. The remainder of the equivalent single conductor is considered to be occupied by insulation and oil. The thermal and physical constants are calculated for the appropriate volume of each material separately and then combined to get the total for the composite conductor. This is illustrated in detail in the sample calculation given later in the paper. The volume of the free oil in the tubes in the insulation space of the equivalent single conductor cable is next calculated and the remainder of the insulation space is assumed to be occupied by impregnated paper. The thermal and physical properties of the free oil and the impregnated paper are calculated separately and then combined in the same manner as for the conductor. It is very helpful to have a sample of the cable before one, to aid in deciding the relative volumes to use for oil and impregnated paper. The mathematics assumes that the unit thermal resistivity, the specific thermal capacity, and the coefficient of expansion of the insulation are uniform throughout the insulation. The unit values are required, not the total values. The unit thermal resistivity p can be taken as 550 degrees centigrade per watt per centimeter cube. The specific thermal capacity is obtained by dividing the total thermal capacity by the total volume of the equivalent insulation space. This procedure gives an average value which is assumed to be uniform throughout the insulation. The average coefficient of expansion is obtained in the manner shown in the numerical example.

The thermal capacity of the metal in the sheath is calculated in the same way as for solid-type cable. The spiral tubes of the oil channels are close to the sheath and relatively far from the conductors. The thermal capacity of the metal spirals and of the segments of metallic shielding close to the sheath can therefore be added to that of the sheath, if desired. This is considered an unnecessary refinement.

The temperature of the oil in these tubes is probably close to the temperature of the sheath. The viscosity of the oil will be controlled by sheath temperature. Consequently the calculation of the pressure drop of the oil during transients requires the transient sheath temperature to be calculated. This is done very readily along with the calculation of the copper temperature transient, as detailed in the section on Numerical Example. It is worth noting that the transient temperature of any location inside the insulation can be calculated just as readily as the transient sheath or copper temperature by the methods of this paper. If it is felt that it is too conservative to assume that the oil in the channels is at the same temperature as the sheath, the channels can be assumed to be further inside the insulation and the temperature transient calculated for that location.

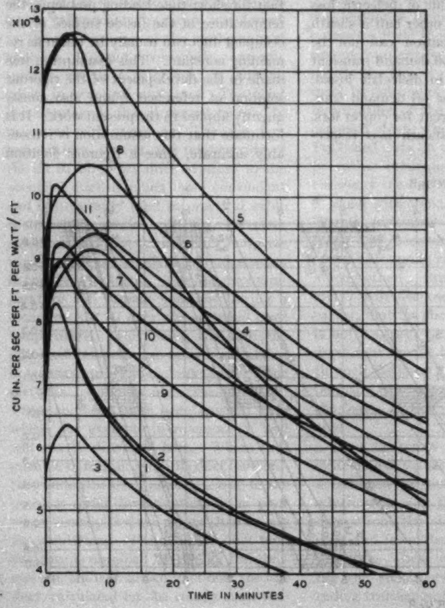

Figure 6 (left). Transient oil demand caused by unit change in copper loss

Curve No.	Conductor		Oil Tube Size (In.)	Kv	Nominal Thickness Mils	
	Size, Cir. In.	No.			Insul.	Sheath
1	2.8	1	0.69	69	330	156
2	2.1	1	0.69	69	315	141
3	2.0	1	None	69	315	235**
4	1.1	1	0.69	132	720	156
5	0.6	1	0.69	132	720	190*
6	0.6	1	0.50	132	720	156
7	0.6	1	0.40	132	720	250**
8	0.25	1	0.69	132	560	133
9	0.55	3	0.39	69	315	160
10	0.45	3	0.55	69	315	156
11	0.40	3	0.55	69	315	156

* Double. ** Fluted.

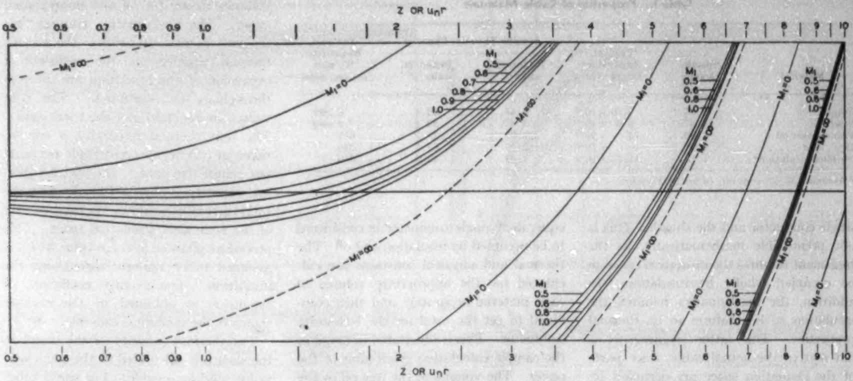

Figure 7

Treatment of Dielectric Losses in Transient Problems

The equivalent single-conductor conception is not capable of handling the problem of dielectric losses in an acceptable manner. This is because there is no equivalence between the actual dielectric field in a 3-conductor cable and the dielectric field in a single-conductor cable. In this respect the equivalent single-conductor method falls short of the capabilities of the rigorous solution for single-conductor cables, which includes the feature of dielectric losses properly distributed throughout the insulation. Fortunately, this is not of much importance. Dielectric losses are usually negligible in modern cables at the voltages at which 3-conductor cables are operated. In addition, most practical problems do not involve the switching on or off of the voltage, which is the only condition under which the dielectric losses can change. A rough approximation of the copper temperature transient caused by a change in dielectric loss can be made, if desired, by the well-known method of assuming that half the calculated value of dielectric loss is copper loss and the other half is sheath loss. This approximation can not be used to calculate the oil demand transient caused by a change in dielectric losses, since the nature of the oil demand transient is entirely different for copper loss, dielectric loss, and sheath loss respectively.

This is shown clearly in Figures 3 and 4 of reference 1.

Temperature of the Ducts

As a general rule, a cable responds much more quickly to loss changes than a duct structure. The cable temperature transient completes itself in less than eight hours, while the duct temperature transient will usually go on for two days or more. The difference is so pronounced that for short-time loading problems, the temperature of the inside surface of the occupied duct can usually be taken as remaining constant. This assumption was made in the development of the rigorous solution of reference 1 and also consequently applies to the present work. It is fortunate that this assumption is reasonably accurate, since a rigorous solution

Figure 8

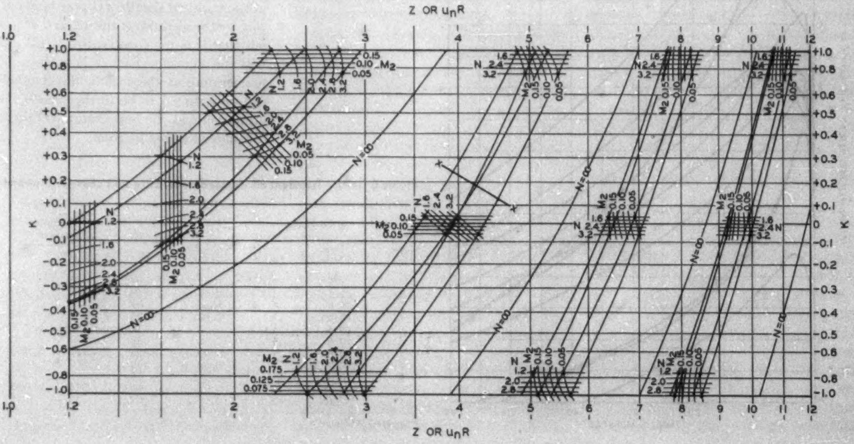

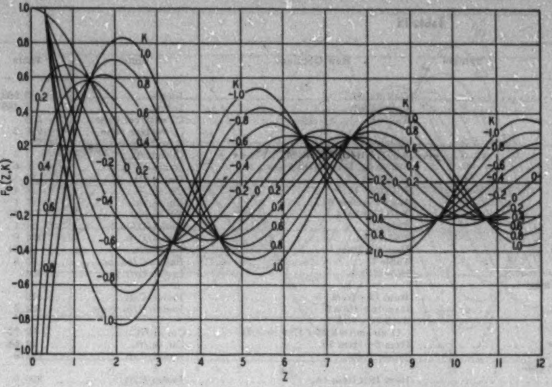

Figure 9. Function F_0

for the transient temperatures of duct structures in a form suitable for routine practical use has not yet become available.

The temperature of the inside surface of the occupied duct is the reference or ambient temperature to which the transient temperature rise must be added to get the total temperature of the cable. The choice of the occupied duct temperature as the reference temperature was forced by the requirements of the mathematical analysis. It is not a convenient temperature to use as a reference, or starting point, in practical problems. The chief disadvantage is that it cannot be readily measured with accuracy. The idle duct temperature, that is, the temperature of the air in an empty duct adjacent to the occupied duct, is much more convenient and is invariably used in practical cable temperature work. It is therefore recommended that the idle duct temperature be used as the reference temperature in transient problems. The idle duct temperature will remain constant during a transient just as does the occupied duct temperature. This being the case the idle duct temperature can be calculated in transient problems by exactly the same methods as for steady-state problems. These methods have been covered elsewhere, for example in reference 6, and will not be discussed here. Where it is possible to measure the idle duct temperature under the conditions applying to the problem under investigation, it is preferable usually to do so rather than to rely on calculations. The occupied duct temperature is obtained by adding the thermal rise of the occupied duct over the idle duct, calculated for the steady-state condition which is assumed to precede the initiation of the transient. The order of magnitude of this rise is indicated by the very general statement that the thermal resistance from the inside surface of an occupied duct to the air in an adjacent idle duct may be anywhere from 0.5 to 1.5 degrees centigrade per watt per foot of duct.

SHEATH THERMAL RESISTANCE

The choice of the value of sheath thermal resistance to use in a given problem requires a little thought. In the calculation of transient temperatures and oil demands, the temperature rise of the sheath must be calculated with reference to the temperature of the inside surface of the occupied duct, which remains constant. Published data on this subject are felt to be rather inadequate. A valuable discussion of the subject is given in reference 8, along with some test values of sheath thermal resistance determined for cables in air and in conduits. Additional data are to be found in references 3, 5, 6, and 7 among others. Study of references 3, 5, and 7 will disclose the fact mentioned earlier, that the sheath thermal resistance is not constant but is quite appreciably dependent on the losses being dissipated through the sheath. An endeavor should be made to select a value appropriate to the losses in the problem being considered.

Some operators of underground cable systems use values of thermal resistance determined by field measurements and which represent the combined thermal drops from the sheath to the occupied duct and from the occupied duct to the idle duct. These may be used in calculating the steady-state temperatures preceding transients, but it is not correct to use them in the calculation of the transients themselves.

Numerical Example

A numerical example is worked out to illustrate the equivalent single-conductor method. The cable is a 3-conductor 450,000-circular mil 69-kv oil-filled type with compact round conductors, as illustrated in Figure 3(B). It is assumed that the best available value for the insulation thermal resistance, R_t, has been obtained, either by actual test or by calculation. The thermal resistivity ρ of the insulation, other necessary physical properties of the cable, and cable data are listed in Tables I and II. All symbols are listed and explained as they occur in the calculation.

Table II. Cable Data

Conductor size	450,000 cir. mil (0.45 cir. inches)
Diameter of conductor	0.700 inches
Diameter over insulation	1.347 inches
Diameter over shielding	1.363 inches
Thickness of lead sheath	0.156 inches
Overall diameter	3.290 inches
Diameter under lead sheath, (D)	2.978 inches
Inside diameter of oil tubes	0.550 inches
Outside diameter of oil tubes	0.650 inches
Insulation thermal resistance, (R_t)	1.195 degrees °C/watt/ft.
Thermal resistivity of insulation, (ρ)	550 degrees °C/watt/cm. cube

DETERMINATION OF CONDUCTOR AND SHEATH TEMPERATURE TRANSIENTS

Solve equation 1 for d, the diameter of the equivalent single conductor which will have the correct steady-state temperature rise

$$R_t = 0.00522\rho \ln D/d \qquad (1)$$

$$\ln D/d = 1.195/550(0.00522) = 0.416;$$

$$D/d = 1.515$$

$$d = 2.978/1.515 = 1.966 \text{ inches}$$

Insulation thickness on equivalent conductor $= (2.978 - 1.966)/2 = 0.506$ inches.

The next step is to consider that the copper conductors are located wholly within the circle bounded by diameter d, irrespective of their actual location and that the rest of the volume contained within d consists of impregnated paper. This means that the equivalent conductor in this hypothetical cable is composed of copper and impregnated paper, see Figure 3(B). The annular space between d and D is the insulation space of the equivalent single-conductor cable and therefore is considered to be wholly occupied by insulation, consisting partly of impregnated paper and partly of the free oil in the oil feed tubes.

Table III

Item	Symbol	How Obtained	Units	Value
1. Equivalent conductor radius	r	Calculated	Inches	0.983
2. Radius over insulation	R	Calculated	Inches	1.489
3. Thermal resistivity of insulation	p	Table I	C/watt/cm. cube C/watt/in. cube	550 216.2
4. Thermal resistivity of sheath	B	Selected by calculator	C/watt/sq.cm.	1,200
5. Surface thermal resistance, sheath to duct	E	0.00411 B/O.D. of cable	C/watt/ft.	1.5
6. Thermal capacity of sheath	Q_2	883 (Avg. Diam.)(thickness)/12	Joules/C/in.	36.0
7. Volume inside sheath	V	$\pi(1.489)^2\ 12$	Cu. in./ft.	83.5
8. Volume of equivalent conductor	C	$\pi(0.983)^2\ 12$	Cu. in./ft.	36.4
9. Volume of equivalent insulation (including oil tubes)		Item 7 − Item 8	Cu. in./ft.	47.1
10. Volume of oil in the three tubes		$3\pi(0.55)^2\ 12/4$	Cu. in./ft.	8.56
11. Specific thermal capacity of oil		Table I	Joules/C/cu. in.	31.1
12. Thermal capacity of oil in feed tubes		8.56×31.1	Joules/C/ft.	266.0
13. Volume of impregnated paper in equivalent insulation		Item 9 − Item 10	Cu. in./ft.	38.54
14. Specific thermal capacity of impregnated paper		Table I	Joules/C/cu. in.	33.8
15. Thermal capacity of impregnated paper portion of insulation		38.54×33.8	Joules/C/ft.	1,304
16. Total thermal capacity of insulation (including oil in feed tubes)		Item 12 + Item 15	Joules/C/ft.	1,570
17. Avg. specific thermal capacity of equivalent insulation	q	Item 16 ÷ Item 9	Joules/C/in. cube	33.3
18. Actual volume of copper		3×0.45×9.43 (1 cir. mil = 9.43×10^{-6} in. ^{3}/ft.)	Cu. in./ft.	12.72
19. Volume of impregnated paper in equivalent conductor		Item 8 − Item 18	Cu. in./ft.	23.68
20. Thermal capacity of copper conductors, see Table I		551(3)(0.45)	Joules/C/ft.	744.0
21. Thermal capacity of impregnated paper in equivalent conductor		Item 19 × Item 14	Joules/C/ft.	800.0
22. Total thermal capacity of equivalent conductor	Q_1	$\frac{\text{Item 20} + \text{Item 21}}{12}$	Joules/C/in.	128.7
23. $M_1 = Q_1/2\pi qr^2$		$128.7/2\pi(33.3)(0.983)^2$	Numeric	0.635
24. $M_2 = Q_2/2\pi qR^2$		$36.0/2\pi(33.3)(1.489)^2$	Numeric	0.078
25. $N = p/2\pi E$		$216.2/2\pi(1.5)(12)$	Numeric	1.91
26. R/r		1.489/0.983	Numeric	1.514
27. $p\ q$		Item 3 × Item 17	Sec./sq. in.	7,240

The calculation is continued in Table III using only the dimensions of the equivalent single-conductor cable.

Next obtain values of K and Z from Figures 7 and 8. These Figures together with Figure 9 solve the transient temperature equation graphically, as described in reference 1. Figure 8 must be traced on transparent paper for practical use. If Figures 7 and 8 are to be used frequently in routine work, they should be replotted to a scale about five times larger. The symbol Z represents the quantity ux, where x is any radius measured from the center of the cable. Thus at the surface of the conductor, $x=r$ and $Z=ur$; at the surface of the insulation, $x=R$ and $Z=uR$. At the general radius x, Z would equal ux. u is a number which the calculations will evaluate. In Figure 7, Z always represents ur. In Figure 8, Z always represents uR. In Figures 9 and 10, referred to later, Z represents any value of ux from ur to uR.

1. Lay Figure 8 over Figure 7 with the Z axes coinciding and with $Z=R/r=1.514$ on Figure 8 coinciding with $Z=1$ on Figure 7.

2. Interpolate on Figure 7 the sequence of curves $M_1=0.635$ and interpolate on Figure 8 the sequence of curves for $M_2=0.078$ and $N=1.91$.

3. Note the points where the interpolated curves of Figure 7 intersect those of Figure 8. Only two intersections usually occur for cables with thin insulation. For cables with thick insulation three intersections usually occur. The third intersection can be ignored without much sacrifice in accuracy and this will save a great deal of computing labor later on.

4. Two intersections are obtained in the present problem. For the first point of intersection (starting at the left hand side of the figures) read off K_1 from the vertical scale on Figure 8; read off u_1r from the horizontal scale of Figure 7; and read off u_1R from the horizontal scale of Figure 8. For the second intersection read off in the same way the values of K_2, u_2r and u_2R.

These values now are tabulated. The making of a complete and orderly tabulation of every step of the calculation is of the utmost importance in obtaining a correct final result. The values of u_n also are required. They are calculated from $u_n=u_nR/R$ and entered in the tabulation. The values of $u_n{}^2$ and of $\lambda_n=u_n{}^2/pq$ are calculated and tabulated in Table IV.

The multiplier 60 is used in evaluating λ_n so that the time can be expressed in minutes instead of seconds in the final equation.

It now is necessary to obtain from Figure 9 the values of $F_o\ (Z,K)$. As already explained Z represents u_nr or u_nR. The values of $F_o\ (Z,K)$ corresponding to the tabulated values of K_n, u_nr and u_nR are set down in Table V.

It can be checked easily from Figure 9 that $F_o(u_1r,\ K_1)=+0.73$ is obtained by entering with $K_1=-0.045$ and $Z=u_1r=0.984$. $F_o(Z,K)$ is read from the left-hand scale. The remaining values of

Table IV

Quantity	How Obtained	Value	
		n = 1 (First Intersection)	n = 2 (Second Intersection)
K_n	Figures 7 and 8	$K_1=-0.045$	$K_2=-\ 0.78$
u_nr	Figures 7 and 8	$u_1r=\ 0.984$	$u_2r=\ 3.62$
u_nR	Figures 7 and 8	$u_1R=\ 1.491$	$u_2R=\ 5.47$
u_n	Calculated from u_nR/R	$u_1=\ 1.002$	$u_2=\ 3.68$
$u_n{}^2$	Calculated	$u_1{}^2=\ 1.004$	$u_2{}^2=\ 13.55$
$\lambda_n=60u_n{}^2/pq$	Calculated	$\lambda_1=\ 0.00832$	$\lambda_2{}^2=\ 0.1124$

Table V

Quantity	How Obtained	Value	
		n = 1 (First Intersection)	n = 2 (Second Intersection)
$F_o(u_nr,\ K_n)$	Figure 9	$F_o(u_1r,\ K_1)=+0.73$	$F_o(u_2r,\ K_2)=-0.225$
$F_o(u_nR,\ K_n)$	Figure 9	$F_o(u_1R,\ K_1)=+0.47$	$F_o(u_2R,\ K_2)=+0.42$

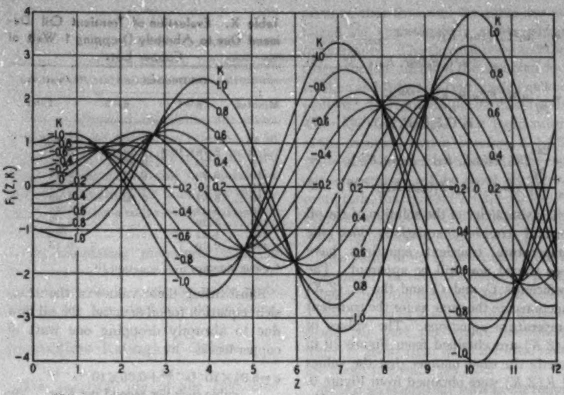

Figure 10. Function F_1

$F_0(Z,K)$ are obtained in similar fashion.

The last major step is to evaluate the quantities C_n in the following simultaneous equations, in which all other terms have already been evaluated

$$C_1F_0(u_1r,\ K_1)+C_2F_0(u_2r,\ K_2)=R_i+E \quad (2)$$

$$C_1F_0(u_1R,\ K_1)+C_2F_0(u_2R,\ K_2)=E \quad (3)$$

Substituting in these equations, there is

$$0.73C_1-0.225C_2=1.195+1.5=2.695$$
$$0.47C_1+0.42C_2=1.5$$

Solving

$$C_1=3.56$$
$$C_2=-0.414$$

These values now may be substituted in the equations for the temperature transients, which are given below.

Conductor temperature transient due to abruptly dropping one watt of copper loss

$$T_c=C_1F_0(u_1r,\ K_1)\epsilon^{-\lambda_1t}+C_2F_0(u_2r,\ K_2)\epsilon^{-\lambda_2t} \quad (4)$$

Sheath temperature transient due to abruptly dropping one watt of copper loss

$$T_s=C_1F_0(u_1R,\ K_1)\epsilon^{-\lambda_1t}+C_2F_0(u_2R,K_2)\epsilon^{-\lambda_2t} \quad (5)$$

Substituting numerical values, the final equations are

$$T_c=2.60\epsilon^{-0.00832t}+0.093\epsilon^{-0.1124t} \quad (4)$$

$$T_s=1.67\epsilon^{-0.00832t}-0.174\epsilon^{-0.1124t} \quad (5)$$

The evaluation of equation 4 is tabulated in the second column of Table VI. It is important to note that the whole calculation has been carried through for a change in loss of one watt per foot. The results can be used for any other change in loss by simply multiplying the tabulated results by the actual change in loss. This is illustrated by examples in the section on Short-Time Ratings of Cables. The right-hand column of Table VI contains an evaluation of the attainment factor. This is the per cent of ultimate temperature rise attained at any time during a transient caused by increasing the copper loss by one watt per foot. It is obtained by subtracting column three from 100. Column three is column two expressed in per cent of the initial temperature. The use of the attainment factor is explained in the section on Short-Time Ratings of Cables.

Table VI. Evaluation of Attainment Factor

Time (t), Minutes	T_c for Dropping One Watt of Copper Loss Per Foot of Cable	Decrement Factor Per Cent	Attainment Factor, Per Cent
0	2.693	100	0
2.5	2.615	97.1	2.9
5	2.548	94.7	5.3
10	2.422	90.0	10.0
15	2.312	85.8	14.2
30	2.028	75.7	24.3
60	1.580	58.7	41.3
120	0.957	35.5	64.5
240	0.354	13.1	86.9
480	0.047	1.7	98.3

Attainment factors for a wide variety of single-conductor cables are given in Figure 4. These can be useful for estimating the temperature transients of similar cables. In Figure 5 the attainment factors are given for a variety of three-conductor cables. The numerical value of the insulation thermal resistance R_i also is given in these figures for each of the cables concerned. The copper temperature rise above the occupied duct temperature in degrees centigrade at any point in the transient can be obtained by multiplying the ordinate of the attainment factor curve by (R_i+E) and by the watts loss.

For the sake of clarity only the conductor and sheath temperature transients due to a change in copper loss have been worked out in the example. In the Appendix the procedure is given for calculating the conductor and sheath temperature transients due to a change in sheath loss or a change in dielectric loss. The latter is only applicable to single-conductor cables, for the reason given in the section on Treatment of Dielectric Losses in Transient Problems. The Appendix also contains the procedure for obtaining the temperature transient at any point in the insulation due to a change in copper loss, or sheath loss, or dielectric loss.

DETERMINATION OF THE OIL DEMAND TRANSIENTS

The oil demands of the component parts of the cable, namely, the conductor, the insulation, and the sheath are obtained separately by calculating the volume of the respective components times their effective expansion coefficients times their individual rates of temperature change. The total oil demand is the algebraic sum of the above component demands.

When load is dropped, the cable cools and the conductor shrinks in volume. Oil must be supplied to the cable to fill the resulting space. The insulation also is shrinking in volume and consequently additional oil must be supplied to the cable.

As the sheath contracts, however, the volume within the sheath is reduced and oil is expelled from the cable. Thus the effect of the sheath component is negative and must be subtracted when the over-all demand of the cable is being determined.

Volumetric expansion coefficients are used for all the component parts of the cable.

The method of calculating the sheath expansion is of some interest. The volume enclosed within the sheath is multiplied by the volumetric expansion coefficient of metallic lead. To see that this is valid, imagine that the sheath fits tightly around a solid cylinder of lead, instead of around the normal cable insulation and copper. No matter what temperature change may occur, the lead cylinder will always exactly fit within the enclosing sheath. Consequently the volumetric expansion of the sheath is correctly calculated by multiplying the volume enclosed within the sheath by the volumetric coefficient of expansion of metallic lead. Suitable compromise values for the expansion coefficients of the equivalent conductor and insulation respectively are required. The expansions of the component parts of the equivalent conductor are individually determined and totalled for unit temperature change. The total is then divided by the total conductor volume to arrive at the effective expansion coefficient. A similar procedure is followed when dealing with the insulation. The actual values are given in Table VII.

Let

a_1 = conductor component of the oil demand
a_2 = sheath component of the oil demand
a_3 = insulation component of the oil demand
a = total oil demand = $a_1+a_3-a_2$

The equations for the component transient oil demands are as follows where only two terms are to be retained in the solution

$$a_1=\frac{Cc}{pq}[u_1^2C_1F_0(u_1r, K_1)\epsilon^{-\lambda_1 t}+ u_2^2C_2F_0(u_2r, K_2)\epsilon^{-\lambda_2 t}] \quad (6)$$

$$a_2=\frac{Vv}{pq}[u_1^2C_1F_0(u_1R, K_1)\epsilon^{-\lambda_1 t}+ u_2^2C_2F_0(u_2R, K_2)\epsilon^{-\lambda_2 t}] \quad (7)$$

$$a_3=\frac{2\pi e}{pq}\{C_1[F_1(u_1R, K_1)-F_1(u_1r,K_1)]\epsilon^{-\lambda_1 t}+ C_2[F_1(u_2R, K_2)-F_1(u_2r, K_2)]\epsilon^{-\lambda_2 t}\} \quad (8)$$

The simplicity of the solution of the oil demand transient equations once the temperature transient equations have been solved now will be apparent. The coefficients C_1 and C_2 and the $F_0\ (Z,K)$ functions are the same as for the transient temperature equations. The values of $F_1(Z,K)$ are obtained from Figure 10 in exactly the same manner that the values of $F_0(Z,K)$ were obtained from Figure 9.

These values must now be tabulated in order to obtain the numerical values for oil flow coefficients, as shown in Table IX.

Table X. Evaluation of Transient Oil Demand Due to Abruptly Dropping 1 Watt of Copper Loss

t Minutes	Oil Demand (in³/sec./ft./watt/ft.) n=1	n=2	Total
0			7.42×10^{-6}*
2.5	8.76×10^{-6}	0.49×10^{-6}	9.25
5	8.58	0.37	8.95
10	8.23	0.21	8.44
15	7.90	0.12	8.02
30	6.97	0.02	6.99
60	5.43		5.43
120	3.29		3.29
240	1.22		1.22
480	0.16		0.16

* Value obtained from equation 10.

Substituting these values in the transient equation for oil demand, the oil flow due to abruptly dropping one watt of copper loss is

$$a=8.94\times10^{-6}\epsilon^{-\lambda_1 t}+0.65\times10^{-6}\epsilon^{-\lambda_2 t}$$
cubic inch per second per foot (9)

The evaluation of equation 9 is given in Table X.

If the oil flow due to a change in sheath loss or a change in dielectric loss is required, it can be obtained simply by substituting the proper values of C_1 and C_2 in the component transient equations. The equations for evaluating these constants when sheath loss or dielectric loss is being considered are given in the Appendix. As in the transient temperature calculation, the oil demand has been worked out for a change in loss of one watt per foot.

At $t=0$, equations 6, 7, and 8 are not accurate since only the first two terms of an infinite series[1] are retained in the solution. After the first few moments the neglected terms rapidly become insignificant, but at $t=0$ they are important. For the initial instant ($t=0$) the following equations should be used

Oil flow due to abruptly dropping one watt of copper loss

$$a_1=Cc/Q_1; \quad a_2=0; \quad a_3=0 \quad (10)$$

Oil flow due to abruptly dropping one watt of dielectric loss

$$a_1=0; \quad a_2=0; \quad a_3=e/q \quad (11)$$

Oil flow due to abruptly dropping one watt of sheath loss

Table VII. Cubical Expansion Coefficients of Equivalent Conductor and Equivalent Insulation

	Volume (in³/ft.)	Expansion Coefficient	Product
Equivalent Conductor			
Copper	12.72	5.01×10^{-5}	63.7×10^{-5}
Paper—45 per cent of 23.68	10.66	10×10^{-5}	106.6×10^{-5}
Oil—55 per cent of 23.68	13.02	75×10^{-5}	976.5×10^{-5}
	36.40		1146.8×10^{-5}
Equivalent Insulation			
Paper—45 per cent of 38.54	17.34	10×10^{-5}	173.4×10^{-5}
Oil—55 per cent of 38.54	21.20	75×10^{-5}	1592×10^{-5}
Free oil in feed tubes	8.56	75×10^{-5}	642×10^{-5}
	47.10		$2,407.4\times10^{-5}$

Additional quantities now are shown in Table VIII.

Table VIII

Item	Symbol	How Obtained	Units	Value
28. Average cubical expansion coefficient of conductor	c	$1,146.8\times10^{-5}/36.40$	Vol/Vol/C	31.5×10^{-5}
29. Average cubical expansion coefficient of insulation	e	$2,407.4\times10^{-5}/47.10$	Vol/Vol/C	51.1×10^{-5}
30. Cubical expansion coefficient of sheath	v	Table I	Vol/Vol/C	8.4×10^{-5}
31. Cc/pq		$36.4(31.5\times10^{-5})/7,240$	in³/ft./Csec.	15.85×10^{-7}
32. Vv/pq		$83.5(8.4\times10^{-5})/7,240$	in³/ft./Csec.	9.68×10^{-7}
33. $2\pi e\times12/pq$		$24\pi(51.1\times10^{-5})/7,240$	in³/ft./Csec.	53.2×10^{-7}

Table IX

Quantity	Value n=1 (First Intersection)	n=2 (Second Intersection)
34. C_n	$C_1=3.56$	$C_2=-0.414$
35.	$C_1F_0(u_1r, K_1)=2.60$	$C_2F_0(u_2r, K_2)=0.093$
36.	$a_1=\frac{Cc}{pq}u_1^2C_1F_0(u_1r, K_1)=4.13\times10^{-6}$	$\frac{Cc}{pq}u_2^2C_2F_0(u_2r, K_2=2.0\times10^{-6}$
37.	$C_1F_0(u_1R, K_1)=1.672$	$C_2F_0(u_2R, K_2)=-0.174$
38.	$a_2=\frac{Vv}{pq}u_1^2C_1F_0(u_1R, K_1)=1.63\times10^{-6}$	$\frac{Vv}{pq}u_2^2C_2F_0(u_2R, K_2)=-2.28\times10^{-6}$
39.	$F_1(u_1r, K_1)=+0.48$	$F_1(u_2r, K_2)=-1.79$
40.	$F_1(u_1R, K_1)=+0.82$	$F_1(u_2R, K_2)=-0.14$
41.	$a_3=\frac{24\pi e}{pq}C_1[F_1(u_1R, K_1)-F_1(u_1r, K_1)]=6.44\times10^{-6}$	$\frac{24\pi e}{pq}C_2[F_1(u_2R, K_2)-F_1(u_2r, K_2)]=-3.63\times10^{-6}$
42. Total oil demand ($a_1+a_3-a_2$) =	8.94×10^{-6}	$=0.65\times10^{-6}$

$$a_1=0; \qquad a_2=Vv/Q_2; \qquad a_3=0 \qquad (12)$$

There is no error in the transient temperature equations at $t=0$ because the mathematical form of solution automatically avoids it.

The oil demand transients are given in Figure 6 for the cables referred to in Figures 4 and 5 which are of the oil-filled type. These curves can be useful for quickly estimating the maximum oil demands of cables similar to those shown in the figure.

The calculating procedures given in the foregoing example can be used just as well for single-conductor cable problems as for 3-conductor cable problems.

Short-Time Ratings of Cables

The practical use of the calculated thermal transients is chiefly in the field of short-time ratings. Another but more limited field of practical use is in the designing of oil-filled cable lines. The pressure drop of the oil along the hollow core or oil-feed tubes in such lines is the controlling design factor. The pressure drop is directly proportional to the rate of flow of the oil and to its viscosity. The rate of flow is obtained from the calculated transient oil demands. The viscosity is obtained from the calculated transient temperature of the conductor if the cable is of the hollow-core type, or from the transient temperature of the sheath if the cable is of the 3-conductor type or the fluted-sheath type. It is, of course, necessary to have the characteristic viscosity-temperature curve of the oil used in the cable. The designing of oil-filled lines is a rather extensive subject which this paper does not attempt to cover, other than the calculation of the fundamental oil demand and temperature transients.

Short-time ratings consist essentially of answering the following question: "If the cable under consideration has been operating at approximately such-and-such a stable temperature, how much more load can be suddenly thrown on it for X hours without exceeding the maximum permissible copper temperature?"

This formulation of the question makes the calculating procedure almost obvious, once the transient temperature characteristics of the cable have been determined. Suppose that the shielded 500,000-circular mil 3-conductor cable number 5 of Figure 5 is installed in a duct bank with other cables, the idle duct temperature of the bank being 40 degrees centigrade, at, say 5 p.m. The load on the 500,000-circular mil cable is 250 amperes at that time and the cable has attained an approximately stable copper temperature. The thermal resistance between the idle duct and the occupied duct is taken as 1.0 degrees centigrade per watt per foot. The total conductor losses in the cable are 4.67 watts. The temperature of the occupied duct is therefore $40+4.67\times1=44.67$ degrees centigrade. The copper temperature will be about 58 degrees centigrade, that is, $3\times I^2R\,(R_t+E)+44.67$ degrees centigrade $=(4.67)(2.855)+44.67=58$ degrees centigrade.

The value of R_t is given in Figure 5. The sheath thermal resistance E is calculated from the formula given in item 5, Table III, using $B=1{,}200$ degrees centigrade per watt per square centimeter, which is about right when the total losses are about five watts per foot.

Now if an emergency such as the failure of a parallel cable occurs, how much additional load can be carried through the peak period? The peak will probably be over at 7 p.m. Accordingly the extra load will be applied for two hours, that is, from 5 p.m. to 7 p.m. The normal maximum allowable copper temperature for the cable, which will be assumed to be rated in the 12-kv class, is 83 degrees centigrade. Thus the additional copper temperature rise is to be $83-58=25$ degrees centigrade. The ultimate steady-state rise above the occupied duct temperature for one watt loss is $1\times(R_t+E)=2.855$. From Figure 1, the rise in two hours will be 81.5 per cent of the ultimate or 2.32 degrees centigrade. Hence the additional losses that can be allowed are $25/2.32=10.8$ watts. The allowable current will be

$$\sqrt{\frac{4.67+10.8\text{ watts}}{3R}}=442\text{ amperes}$$

or an increase in load of 192 amperes or 4,000 kva at 12 kv.

To be conservative in the calculation of the allowable current, the copper resistance is taken at the final temperature of 83 degrees centigrade instead of the initial temperature of 58 degrees centigrade.

It is interesting to note that to hold the temperature constant at the new level, the load must be sharply reduced after the 2-hour overload. Holding the temperature constant at this point requires the application of a transient which will cancel that part of the transient in Figure 1 which extends beyond the 2-hour point. Thus a negative transient must be applied, or in other words a load reduction.

To illustrate further the value of short-time overloads, the case will be considered for the same cable where it is decided that a higher temperature than 83 degrees centigrade will be permitted in an emergency. Suppose, for example, that the permissible temperature is to be 98 degrees centigrade as permitted for emergency operation by the Association of Edison Illuminating Companies Cable Specifications.[9] Following the same procedure as before, the permissible loading for two hours will be found to be 514 amperes or an increase of 264 amperes over the initial loading of 250 amperes. For one hour the maximum loading would be 578 amperes and for one-half hour the permissible loading would be 710 amperes. These are substantial increases which can be of much value, as for instance in making possible the elimination or deferment of a proposed additional cable line.

In many practical cases a utility has no means of controlling an overload caused by the trip-out or failure of one of a group of parallel lines. In such cases the practical question becomes "Did the overload damage the overloaded cables?" This question is readily answered by calculating the increase in watts loss caused by the overload. From the attainment factor for the cable the transient temperature rise is determined. This is added to the initial temperature to get the total temperature at the end of the overload. It can be said that if such an occurrence happens only occasionally, an experienced cable engineer will usually not consider that any appreciable damage has been done if the copper temperature has not exceeded 110 or 120 degrees centigrade for an hour or two.

The operating procedure to be followed in emergencies deserves some comment. As a rule the direct control of the cable circuits will be in the hands of the load dispatcher or the operating division rather than the cable engineer. It is considered good practice to furnish the operating division with a list of normal permissible ratings for all cables on the system, accompanied by a standing instruction to notify the cable engineer immediately when the load on any cable exceeds its rating. The cable engineer will then learn from the operating division how long the overload is expected to continue. The engineer should have at hand the transient temperature characteristic, or attainment curve, of each type of cable on the system. From this, along with his intimate knowledge of duct temperatures throughout the system, he can estimate in a few minutes whether or not the cable will be damaged seriously. Usually there will be no means of reducing the overload by a controlled amount. It will be a question of either permitting it to continue or of taking the line out of service. The latter is nearly always a drastic, last-resort procedure. However, if the overload is going to result in "cooking" the cable, then taking the line out of service for a few hours will be preferable to damaging it so badly that complete replacement is necessitated. The latter may require months of time and the expenditure of many thousands of dollars. The cable engineer should have the authority to order the line taken out of service when in his opinion such action is justified, no matter how important the customer load may be that is interrupted.

It is not considered good practice to attempt to foresee all emergencies that might arise and to calculate in advance for the use of the operating division the overload capabilities of all system cable lines under such hypothetical conditions. With the aid of the transient temperature characteristics of the cables, any emergency can be promptly and more intelligently met as it arises by the cable engineer. The needs of many systems will be adequately met by the attainment curves given in Figures 4 and 5, without the necessity of calculating curves for the specific cables that may happen to be on the system. This is so because the attainment curves given are for a very wide variety of cable designs and the attainment curves are, in general, not very different even for considerable variations in cable make-up.

A type of operating problem which differs markedly from the problem of emergency short-time overloads is that of variable loading. It may be desired to take advantage of the fact that the carrying capacity of a cable operating under a load cycle of the type common to light and power feeders is somewhat greater than for a continuous steady load. The attainment curves can be used to calculate such problems, by a step-by-step procedure. The procedure has been fully covered elsewhere[3] and will not be repeated here. However, it seems desirable for the sake of completeness to draw attention to this important application of transient temperature calculations.

Appendix I

The transient temperature equations for changes in sheath loss or dielectric loss are evaluated in a similar manner to that illustrated for copper loss. The transient due to sheath loss will be explained first. The procedure is identical with the numerical example up to equations 2 and 3. The right-hand side of equation 2 is the copper temperature rise above ambient due to one watt of copper loss. This is replaced in the sheath loss transient by the copper temperature rise due to one watt of sheath loss, which is E. The right-hand side of equation 3 is the sheath temperature rise due to one watt of copper loss. This is replaced by the sheath temperature rise due to one watt of sheath loss, which again is E. The equations now become

$$C_1F_0(u_1r,\ K_1)+C_2F_0(u_2r,\ K_2)=E \qquad \text{(2A)}$$

$$C_1F_0(u_1R,\ K_1)+C_2F_0(u_2R,\ K_2)=E \qquad \text{(3A)}$$

These equations are to be solved for C_1 and C_2. The values of C_1 and C_2 so obtained when used in equation 4 transform it into the equation for the conductor temperature transient due to dropping one watt of sheath loss. When used in equation 5, they transform it into the equation for the sheath temperature transient due to dropping one watt of sheath loss.

The dielectric loss transients cannot be handled for 3-conductor cables for reasons explained in the section on Treatment of Dielectric Losses in Transient Problems. The following procedure, therefore, applies only to single-conductor cables for obtaining the dielectric loss transients. The right-hand side of equation 2 is replaced by the copper temperature rise due to one watt of dielectric loss, which is $(R_i/2+E)$. The right-hand side of equation 3 is replaced by the sheath temperature rise due to one watt of dielectric loss, which is E. The equations now become

$$C_1F_0(u_1r,\ K_1)+C_2F_0(u_2r,\ K_2)=Ri/2+E \qquad \text{(2B)}$$

$$C_1F_0(u_1R,\ K_1)+C_2F_0(u_2R,\ K_2)=E \qquad \text{(3B)}$$

These equations are to be solved for C_1 and C_2. The values so obtained when used in equation 4 transform it into the equation for the conductor temperature transient due to dropping one watt of dielectric loss. When used in equation 5 they transform it into the equation for the sheath temperature transient due to dropping one watt of dielectric loss.

If it is desired to calculate the temperature transient for some point in the insulation at radius x from the center of the cable, equation 4 is used but with the F_0 functions evaluated from Figure 9 for $(u_nx,\ K_n)$. The final equation for the transient thus becomes

$$T_x=C_1F_0(u_1x,\ K_1)\,\epsilon^{-\lambda_1t}+C_2F_0(u_2x,\ K_2)\,\epsilon^{-\lambda_2t} \qquad \text{(4A)}$$

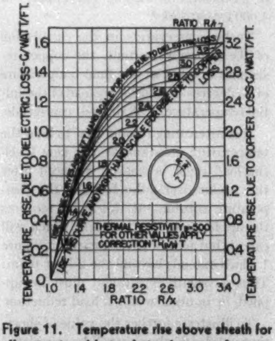

Figure 11. Temperature rise above sheath for all points in cable insulation from conductor to sheath

For the transient due to copper loss, the quantities C_1 and C_2 would be the same as determined from equations 2 and 3, that is, 3.56 and -0.414 respectively. For the transient due to sheath loss, they would have the values determined from equations 2A and 3A. For the transient due to dielectric loss they would have the values determined from equations 2B and 3B.

The procedure for handling problems in which three intersections occur on Figures 7 and 8 and the third intersection is not ignored will now be explained. Equations 2 and 3 are used as before for the transients due to change in copper loss, but they will have a third term, as follows

$$C_1F_0(u_1r,\ K_1)+C_2F_0(u_2r,\ K_2)+C_3F_0(u_3r,\ K_3)=R_i+E \qquad \text{(2C)}$$

$$C_1F_0(u_1R,\ K_1)+C_2F_0(u_2R,\ K_2)+C_3F_0(u_3R,\ K_3)=E \qquad \text{(3C)}$$

A third simultaneous equation is needed in order to be able to solve for C_1, C_2, and C_3. The third equation is written for any convenient point in the insulation, for example, at $x=(r+R)/2$. The right-hand side of the equation is the temperature rise at $x=(r+R)/2$ due to one watt of copper loss and is $p/2\pi \ln R/(r+R)/(2)$. The complete equation thus becomes

$$C_1F_0\left(u_1\frac{r+R}{2},K_1\right)+C_2F_0\left(u_2\frac{r+R}{2},\ K_2\right)+C_3F_0\left(u_3\frac{r+R}{2},\ K_3\right)=p/2\pi \ln R/\frac{(r+R)}{2} \qquad \text{(13)}$$

The F_0 functions in equation 13 are evaluated from Figure 9, after which the three simultaneous equations 2C, 3C, and 13 are solved for C_1, C_2, and C_3. These three coefficients are then carried into the final equations. The final equation for copper temperature transient due to dropping one watt of copper loss becomes, for example

$$T_c=C_1F_0(u_1r,\ K_1)\,\epsilon^{-\lambda_1t}+C_2F_0(u_2r,\ K_2)\,\epsilon^{-\lambda_2t}+C_3F_0(u_3r,\ K_3)\,\epsilon^{-\lambda_3t} \qquad \text{(4B)}$$

Similarly the equation for sheath temperature transient due to dropping one watt of copper loss becomes

$$T_s=C_1F_0(u_1R,\ K_1)\,\epsilon^{-\lambda_1t}+C_2F_0(u_2R,\ K_2)\,\epsilon^{-\lambda_2t}+C_3F_0(u_3R,\ K_3)\,\epsilon^{-\lambda_3t} \qquad \text{(5A)}$$

For the transients due to sheath loss or dielectric loss, equations 4B and 5A are again used but with new values of C_1, C_2, and C_3 determined in the same manner as described for the case of two coefficients. In this case it will be necessary to evaluate the temperature rise at the point x in the insulation due to one watt of dielectric loss. This is given by the following expression

$$T_x=\frac{p}{4\pi(\ln R/r)}(\ln R/x)(\ln Rx/r^2) \qquad \text{(14)}$$

Figure 11 evaluates this quantity graphically, and also evaluates the temperature rise at any point X in the insulation due to one watt of copper loss, which is expressed by $T_x = \rho/2\pi \ln R/x$. It is to be noted that "any point x in the insulation" includes the conductor surface, for which $x = r$. Thus Figure 11 also will give the copper temperature for both copper loss and dielectric loss. The use of Figure 11 will save considerable calculation and avoid errors which might occur if numerical computation were used.

From all of the foregoing, it will be obvious that carrying a problem through in two coefficients is comparatively simple, whereas it is much more laborious for three coefficients. Hence the recommendation that the third term be dropped unless great accuracy is sought.

References

1. Thermal Transients and Oil Demands in Cables, K. W. Miller, F. O. Wollaston. *AIEE Transactions*, volume 52, March 1933, pages 98–110.

2. Temperatures in Electric Power Cables under Variable Loading, Elwood A. Church. *AIEE Transactions*, volume 50, September 1931, pages 982–92.

3. The Calculation of Cable Temperatures in Subway Ducts, W. B. Kirke. *AIEE Journal*, volume 49, October 1930, pages 855–59.

4. Theory of Oil-Filled Cables, G. B. Shanklin, F. H. Buller. *General Electric Review* (Schenectady, N. Y.), July and September 1931.

5. Load Ratings of Cable—II, Herman Halperin. *AIEE Transactions*, volume 61, part III, December 1942, pages 940–42.

6. Calculation of Electrical Problems of Underground Cables, D. M. Simmons. *Electric Journal* (East Pittsburgh, Pa.), May–November, 1932.

7. Thermal Properties of Underground Cables, P. Barenscher, A. R. McCann. *NELA Publication Number 267–91*, Edison Electric Institute (New York, N. Y.), August 1927, pages 267–91.

8. Current Carrying Capacity of Rubber Insulated Conductors, S. J. Rosch. *Electrical Engineering* (*AIEE Transactions*), volume 57, March 1938, pages 155–67.

9. Specifications for Impregnated Paper-Insulated Lead-Covered Cable, Solid Type. Association of Edison Illuminating Companies (New York, N. Y.) seventh edition.

Discussion

E. H. Grosser (Commonwealth Edison Company, Chicago, Ill.): This paper furnishes very useful tools to engineers faced with the problem of determining transient temperatures and oil demands of power cables. While the earlier paper by Miller and Wollaston[1] gave the essential theoretical basis for calculations of this type, the present paper puts this theoretical information into a directly usable practical form. In addition, an ingenious solution of the 3-conductor cable is given, using the equivalent single-conductor concept.

This method of calculation has been applied in the design of 3-conductor low-pressure oil-filled 66-kv cable lines in Chicago, totalling approximately 78 miles, of which 51 miles have been completed or are now under construction.

It is unfortunate that no means is available for including the effect of dielectric loss on the oil demand transient of the 3-conductor cable. The usual limiting case that determines line design from the standpoint of transient pressures is the very practical one in which a load-carrying line trips or fails. Dielectric losses, which may amount to as much as 10 to 12 per cent of the total losses of a 69-kv 3-conductor cable, thus are of importance. Perhaps the best way of including their effect is to design so that minimum pressures, using oil demands based on copper loss only, include some small allowances for additional pressure drop due to the dielectric loss transient.

The author states that the temperature of the oil in the oil channels of 3-conductor cable is probably close to the sheath temperature. We believe that the oil tube temperature can be represented more accurately as the temperature at a point with 20 to 30 per cent of the temperature rise between conductor and sheath. If the copper and sheath temperature transients are calculated, we may thus determine the approximate intermediate temperatures of the oil in the tubes as

$$
\begin{aligned}
T_o &= T_s + 0.25(T_c - T_s) \\
&= 0.75T_s + 0.25T_c
\end{aligned}
$$

where the subscripts o, s, and c denote temperatures of the oil, sheath, and conductor, respectively.

It is sometimes desirable to have an idea of the approximate peak value of the oil demand transient without taking the time to make a complete determination. This situation may arise in making preliminary estimates, or even in final design calculations where the amount of cable involved is very small, as, for example, in the termination of a long 3-conductor cable line with short lengths of single-conductor cable. The estimating curve of Figure 1 of this discussion has proved useful for this purpose. The abscissa is the total copper cross-section in the cable. For 3-conductor cables, it is the total area of the three conductors. The ordinate gives the maximum value of oil demand attained, a few minutes after the initiation of the transient, on assuming or dropping unit copper loss. This curve is based on the oil demands of actual cables as determined by calculation. The peak value of oil demand is thus shown to be roughly a function of the cable size, approximately independent of the voltage rating and number of conductors.

Reference

1. See reference 1 of the paper.

E. R. Thomas (Consolidated Edison Company of New York, Inc., New York, N. Y.): Mr. Wollaston is to be congratulated on preparing an excellent treatise on temperature transients in cable due to short time loading. Short time overloading on high-voltage cable has been of general concern to the industry at large in the last decade or so. However, I might point out that transient temperature phenomena was one of the fundamental factors required to be evaluated some 25 years ago in the early design of the a-c network. It obviously became necessary to design a secondary network system of cables where a short circuit would be capable of heating up a cable sufficiently rapid to melt a conductor of the cable in one branch of the circuit permitting that branch to burn clear without having developed too great heating in the parallel branch feeds of the network system to have damaged the rest of the network cable system. While these were temperature time transients generally much shorter in period than are being considered in this paper, they represent another type of thermal relation in which the distribution engineer is vitally concerned.

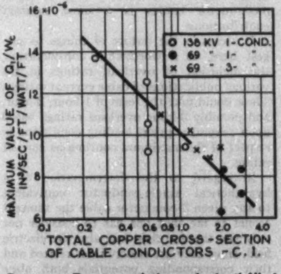

Figure 1. Transient oil demand of oil-filled cable due to dropping copper loss

M. H. McGrath (General Cable Company, Perth Amboy, N. J.): This paper provides a valuable and welcome addition to a 1933 AIEE paper by Miller and Wollaston. It not only contains important new material but, in addition, presents this material in a manner that will save much work in cases where temperature transients or oil demand calculations are involved, a matter of some consequence to those concerned with specific values rather than the general picture.

The new material, namely the new approach to the solution for the 3-conductor case, is of course quite important in itself, not only because of its practical value in duct lay installations but also because it suggests a possible basis of attack for the transient temperature and oil demand problem on pipe-type systems. The Wollaston method for three conductor is also quite timely in that it takes into account the fact that recent tests have failed to verify the generally accepted method of calculating the thermal resistance from copper to lead of a 3-conductor type-*H* cable.

Experience has shown one imperfection of the earlier Miller-Wollaston paper to be that the example given was, because of space considerations, condensed to the point where it is only with a very material expenditure of time and effort that an uninitiated computer can arrive at a suitable calculation format that will permit practical problems to be handled with speed and accuracy. The unabridged and unpublished report on which the earlier AIEE paper is based and which Miller and Wollaston made available to some of us, served at that time to offset to some extent this disadvantage. However, as time goes on, it has become increasingly evident that there was a very real need for something of a permanent nature in the AIEE record to amplify the brief example given previously. The example included by Wollaston in his present paper fills in this gap in admirable fashion. Although it applies specifically to the 3-conductor method which Wollaston has developed, the format used applies equally well to the single-conductor problem. Furthermore, Wollaston has materially reduced the computation work by showing that in many cases it is possible to obtain a completely satisfactory answer by using only two roots.

The earlier paper laid so much stress on the oil demand and other of the more complicated aspects of the oil-filled cable problem that it unintentionally concealed the fact, so clearly brought out in the new Wollaston paper, that the Miller-Wollaston methods provide a simple and at the same time the most accurate procedures yet developed for securing temperature attainment characteristics for use in determining emergency loadings for times up to the order of several hours on any type of duct installation.

In preliminary work on new projects one is frequently confronted with a number of alternate constructions. To carry through detail calculations for each alternate is often impractical. On the other hand, at least an approximate knowledge of the temperature or oil demand transient is often essential in making any significant comparative economic study of the alternates under consideration. The measured and calculated temperature attainment factor curves and the curves of unit oil demand transient given by Wollaston for the wide range of single and 3-conductor cable constructions employed by Commonwealth Edison Company will be invaluable in such cases because from this very extensive data one can obtain directly from one of the plots in the paper a reasonably accurate "guess" as to the general magnitude of either transient for most constructions of practical interest.

The engineer occasionally is confronted with a temperature transient or oil demand problem on a long submarine installation. It would appear that this problem can be readily approximated by the author's methods. Due to the excellent heat transfer by the water, there will be little if any thermal resistance between the sheath and the water. Thus the pertinent M_2, N curves of Figure 8 will be those shown for N=infinity. The intersection of these curves with the particular value of the M_1 group of Figure 7, will provide two roots. In setting up the simultaneous equations to determine the C coefficients, one would be similar to the author's equation 2 but with zero surface thermal resistance and the other equation would be written for, say, the midpoint of the insulation in much the same manner as suggested by the author for cases where three roots are employed on duct lay installations. The author's comments on this suggestion would be of interest.

Herman Halperin and C. A. Bauer (Commonwealth Edison Company, Chicago, Ill.): This paper is of considerable practical interest and value for various reasons, including the fact that it makes it feasible to determine accurately how much load can be carried within set temperature limits during a short-time emergency for 3-conductor cable. In addition to E. H. Grosser's discussion, the following remarks are made regarding the sections entitled Temperature of the Ducts and Sheath Thermal Resistance.

Many field measurements of duct temperatures cause agreement with the author that the duct temperature may be assumed as remaining constant during short-time heavy loading. In that period, the additional heat generated is so relatively small and the thermal time lag of ducts and associated earth is so extremely large that the change in duct temperature will be only a few per cent of the total ultimate possible change.

The author in his discussion in Item 4 of Table III may not seem explicitly clear as to the value to use for thermal resistivity of the sheath in determining the surface thermal resistance from sheath to the duct structure. He gives a value of 1,200 in the table which seems reasonable for determining the thermal resistance from the sheath to an unoccupied duct. In calculations using the thermal resistance of sheath to the surface of the duct in which the cable is located, the constant should be perhaps 550.

Regarding author's figures on thermal resistance from the inner surface of an occupied duct to the air in an adjacent idle duct, field measurements have indicated that at locations where the duct structure is fairly moist, the lower value applies, while at quite dry locations the higher value applies.

H. D. Short (Canada Wire and Cable Company Limited, Toronto, Ont., Canada): We have in the past found the Miller-Wollaston thermal transient formulas very useful tools in the practical design of high-voltage Pirelli-type single-conductor oil-filled cable lines in Canada. Mr. Wollaston's extension of these formulas to the case of 3-conductor cables is indeed most appropriate. In the 3-conductor case one is confronted more particularly with many practical applications where short-time current ratings are very valuable to the cable user in assessing fully the earning capacity of a given cable line. More especially is this true today when capital costs are high and the tendency prevails to maintain the present selling price of electric energy. From these points of view the author's method of computing the short-time current rating of 3-conductor cables is a most salutary contribution.

It seems in the nature of things to suggest here, as a worthwhile consideration, the inclusion of overload ratings in the various publications of cable current ratings. These could take the form of 1-hour, 2-hour, and possibly 3-hour overload ratings based upon several a priori loading conditions in respect of the maximum continuous current rating.

In regard to the determination of a hypothetical single-conductor equivalent to any given 3-conductor cable the thought occurs to me that one has to consider not only the thermal field but also the electric field, since they are closely inter-related and their corresponding potentials both obey the homogeneous Laplace equation for 2-dimensional flow. Thermal flux is analogous to electric flux and for any given configuration the same potential function is manifested, thereby establishing the well known equivalency of thermal resistance and electrical elastance. Hence I would like to propose the following method of determining the dimensions of the hypothetical single conductor which obviates the need of choosing a value for either D or d (the paper's nomenclature), and which brings to bear the effect of the electric field. It may be shown that

$$R_{TH1}C_s = \frac{pk}{4}$$

where

R_{TH1} = thermal resistance of the three conductors of the given 3-conductor cable in parallel to the lead sheath outer surface
= R_i of the paper

C_s = electric capacity between the three conductors of the given 3-conductor cable connected together as one electrode and the sheath as the other electrode, (electrostatic units per centimeter)

p = thermal resistivity of the insulation in question

k = dielectric constant of the insulation in question

Knowing R_{TH1}, p, and k, C_s may be readily found, and taking this value of capacity as that of the hypothetical single-conductor cable the following transpires

C = electric capacity of the hypothetical single-conductor cable

$$= \frac{k}{2 \log_e \frac{D_i}{d_h}} = C_s$$

and

$$\log_e \frac{D_i}{d_h} = \frac{k}{2C_s}$$

where D_i and d_h are respectively the diameter over the insulant and over the conductor of the hypothetical single-conductor cable

Now in order to assimilate in the hypothetical single-conductor cable the electric field obtaining in the 3-conductor cable between the outer surfaces of the three conductors and the lead sheath we may proceed as follows

Let g_c' = stress on the surface of the conductor in the 3-conductor cable towards the sheath

and g_c = stress on the surface of the conductor in the hypothetical single-conductor cable

$$= \frac{E}{r_h \log_e \frac{D_i}{d_h}}$$

where

E = voltage to neutral

and

$$r_h = \frac{d_h}{2}$$

putting

$$g_e = g_e'$$

we obtain another expression for $\log_e \frac{D_t}{d_h}$ thusly

$$\log_e \frac{D_t}{d_h} = \frac{E}{r_h g_e'}$$

hence

$$r_h = \frac{2EC_2}{g_e' k}$$

from which the corresponding value of D_t may be readily computed.

Maybe this approach is a bit too pendantic, but in any case I should like to have Mr. Wollaston's comments in respect to its practical significance to the temperature phenomena in hand.

I should like to know whether the values of R_t given in Figures 4 and 5 are measured or calculated values; and if calculated what value of thermal resistivity was used therein. In addition, what value of thermal resistivity was used in calculating the time-temperature rise data of Figures 1 and 2; were the specimen cables used to determine Figures 1 and 2 new or old cables?

F. O. Wollaston: Mr. Grosser has discussed the effect of dielectric losses. The oil demand due to dielectric loss change in a 3-conductor shielded cable can be computed by the device mentioned in the section on Temperature Transient of 3-Conductor Cables, that is, by treating each core of the cable as a separate single-conductor cable. This component of oil demand can then be added to the component due to copper loss computed by the equivalent single-conductor method. This procedure would double the computing labor and would contain some error but may be worthwhile in the circumstances stated by Mr. Grosser. Mr. Grosser's finding that peak oil demand has a consistent relationship to total copper cross-section in cables of various designs is surprising to me. It will be valuable for estimating purposes.

I am indebted to Mr. McGrath for pointing out the application of the method to submarine cables. It would not be necessary to write a new equation for the midpoint of the insulation. Equations 2 and 3 are correct and sufficient. It would only be necessary to set the sheath thermal resistance E equal to zero in these two equations and proceed in the manner described in the paper. It may be helpful in this connection to note that equations 2 and 3 are the general transient temperature equations 4 and 5, written for $t=0$, that is, for the steady-state condition preceding the transient. The steady-state condition is a convenient known boundary condition which the general equations must fit correctly. In equations 2 and 3 we are determining the proper values of the constants C_1 and C_2 so that this fit will take place. In the case of submarine cable, the steady-state copper temperature rise above ambient for 1 watt of copper loss is correctly stated by equation 2 with E set equal to zero. The steady-state sheath temperature rise above ambient for 1 watt of copper loss is correctly stated by equation 3 with E set equal to zero, that is, the sheath temperature rise is zero. Accordingly these equations will correctly determine the constants C_1 and C_2. Of course submarine cable would usually be armored, with jute bedding under the armor and perhaps over it. The jute bedding has some thermal resistance and thus E in a practical case would be larger than zero.

Mr. Short's use of the electrostatic field to calculate the diameter of the equivalent single conductor is ingenious, but I do not see how it can be applied to shielded cable. The electrostatic field is not analogous to the thermal field in shielded cable, a fact which I endeavored to point out in the section headed Treatment of Dielectric Losses in Transient Problems. The values of R_t given in Figures 4 and 5 are calculated in some cases and experimental in others. For the calculated values, p in watt-centimeter units was taken as 550 for all the oil-filled cables, and as 650 for all the solid cables except the 66-kv single-conductor cables numbers 5, 6, and 7 in Figure 1, for which p was taken as 600. The value of p in the calculations for the cables in Figures 1 and 2 was 650. The cables were new but had been subjected to a number of load cycles on test. The terminations of the test lengths of cable were pressure tight and high internal pressures and some sheath expansion occurred during the tests before the experimental attainment factors given in Figures 1 and 2 were logged.

Mr. Halperin and Mr. Bauer state that the sheath thermal resistivity should be taken as about 550 instead of 1,200 when calculating the resistance from the sheath to the occupied duct. I am aware that Commonwealth Edison Company have a wealth of Chicago field observations which support this contention and which were discussed in one of Mr. Halperin's papers.[1] However, I have been unable to convince myself that these findings for Chicago would be generally applicable to other systems. The references on this subject listed in my paper state explicitly that the thermal resistivity of sheath (B) should be taken as 1,200 in calculating the thermal resistance from the sheath to the occupied duct and also from the sheath to still air. Reference 8 gives a good deal of laboratory test data supporting this value. In a recent paper[2] which was not available when my paper was written, J. H. Neher states that for fiber duct in concrete and cable losses in the neighborhood of 10 watts per foot, it is correct to calculate the sheath thermal resistance to the occupied duct wall by the formula given in my paper and taking B as 1,200. In working up my numerical example I assumed these conditions, that is, fiber ducts and moderate cable losses, although it was not so stated. It seems significant that Neher found that B should be much lower for ducts of higher thermal conductivity, for example 800 for terra cotta ducts. In Chicago the ducts are precast concrete and are quite generally damp or even very wet. It may be that the low value of B found in Chicago is peculiar to that type of duct, which is not generally used elsewhere and has not generally been used in laboratory tests. This suggestion is not entirely satisfactory, however, since Rosch, ref. 8 of the paper, found that B for cables in metallic conduits was in the order of 1,000 to 1,100. For such conduits, B should have been abnormally low, due to the low thermal resistance of the duct material. Another point which may be significant is that the Chicago data are for field conditions and we may expect that the air in the occupied ducts was heavily saturated with moisture. In the laboratory tests where B has almost invariably been found to be around 1,200, the surrounding air was presumably much drier. To sum up, I believe I have used the generally accepted and conservative value for B, but I feel that much more work will have to be done on the subject before we can all be sure of our ground and get into general agreement with each other.

REFERENCES

1. LOAD RATINGS OF CABLE, Herman Halperin. *Electrical Engineering* (*AIEE Transactions*) volume 58, October 1939, pages 535–52.

2. THE TEMPERATURE RISE OF CABLES IN A DUCT BANK, J. H. Neher. *AIEE Transactions*, volume 68, part I, 1949, pages 540–48.

Diagnosis of Rectifier Ailments

I. K. DORTORT
MEMBER AIEE

THE mercury-pool rectifier is a reliable machine fully accepted by industry. Incorrect operating conditions and internal deterioration lead to internal faults which are cleared by the protective gear. Unlike most other machines, the rectifier can be returned to service immediately after the fault is cleared. Now, even though no change has taken place in the circumstances which produced the fault, the rectifier can operate a long time before another failure takes place.

The explanation appears to be that a very improbable set of coincident phenomena have to occur to produce a failure. If this sounds far-fetched, consider the tremendous number of anode cycles which transpire without incident between faults, even in a very sick rectifier. A 12-anode rectifier with a bad record of one arc-back per day is averaging one bad anode cycle in 62 million.

Nevertheless, improper environment and internal disorders must be diagnosed and corrected early, and it is very important to the user that it be done with the least loss of service and minimum expense.

This paper is an attempt to assemble and correlate the known facts and experiences to provide a guide to a logical diagnostic procedure.

Scope

The most common type of failure is the arc-back, colloquially called a backfire. An occasional arc-back is no cause for concern about a rectifier properly applied and protected. However, almost anything that can go wrong with a rectifier or its associated equipment will eventually induce a progressively increasing arc-back rate. While the harm done by any one arc-back is very slight, the damage is cumulative. In the interest of continuity of service and minimum maintenance costs, the cause must be discovered and corrected as soon as possible.

In inverter service some of these same causes generally lead to arc-throughs or "spillovers." They also may induce arc-backs which are of little consequence but may themselves produce arc-throughs and interruptions. The detection of the faulty anode and the determination of the cause follows very closely the procedure to be outlined for arc-backs. Because of this and because inverters are still relatively few in number, diagnosis of arc-throughs will be treated chiefly by annotation.

Misfires, peculiar to Ignitrons, and excitation failures in general, are not particularly difficult to diagnose as a rule, and are therefore not included in this paper. However, some of the material contained herein will be found applicable.

Most other troubles that may cause service interruption (other than power short circuits) will be found lurking in control devices or control circuits, and do not differ from those experienced with comparable controls of other machines. They are outside the scope of this paper.

It appears then that the only subject remaining to be discussed here is the isolation and analysis of the causes of arc-backs. It will become apparent that the scope has not been unduly restricted.

Causes and Some Effects

Before we go into the discussion of procedure, it will be helpful to review the direct and indirect causes of arc-backs. Everyone interested in rectifiers already knows that an arc-back is a failure of the check-valve action, permitting a reversal of current flow between cathode and anode; in other words, the anode emits electrons and becomes in fact a cathode. This phenomenon may be caused by many things, such as poor vacuum, overtemperature, overloads, including those due to unbalance, high initial inverse voltage, voltage surges, deterioration of insulation, traces of foreign material on the anode, etc. An arc-back constitutes an unbalanced short circuit across the secondary winding of the rectifier transformer with reverse current in the faulted phase reaching values as high as 100 times the normal forward current.

In an otherwise sound rectifier the probability of arc-backs increases as a function of the residual ion concentration under the anode immediately after the completion of commutation, and of the value of the inverse voltage which appears suddenly between anode and cathode at that instant. The residual ion concentration depends, among other things, on the rate of decrease of the anode current near the end of commutation, and this rate of decrease in turn depends on the load, the commutating reactance, and phase control. The residual ionization also depends upon mercury vapor pressure and the presence of other gases. Again, the initial inverse voltage depends on load, commutating reactance, and phase control. An increase of any of these factors will increase the probability of arc-back.

Symptoms

In the initial phases of operation of a new rectifier, some arc-backs are to be expected. If the unit backfires excessively (or arcs-back, if you prefer), the seat of the trouble may be in the rectifier or in the rectifier transformer; it may be circuit trouble and may even be located in the connected a-c or d-c systems. The boundary between reasonable and excessive backfiring cannot be defined by formula, depending as it does on design, type of service, and past history. Trouble

---

Paper 49-270, recommended by the AIEE Electronic Power Converters Committee and approved by the AIEE Technical Program Committee for presentation at the AIEE Fall General Meeting, Cincinnati, Ohio, October 17-21, 1949. Manuscript submitted March 2, 1949; made available for printing September 7, 1949.

I. K. DORTORT is with the Allis-Chalmers Manufacturing Company, Milwaukee, Wis.

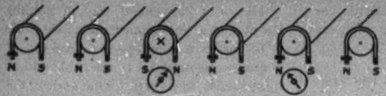

Figure 1 (left). U-bolt arc-back detector

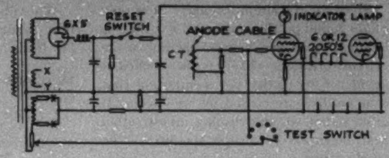

Figure 4 (right). Electronic arc-back detector

developing on rectifiers with past records of satisfactory service should be much easier to diagnose, since it can be assumed that the record is proof of the soundness of application and engineering.

Whatever base is used as a criterion, the arc-back rate is our most important symptom, signaling the existence of one or more unfavorable conditions. The arc-back itself is not visible so we depend on external manifestations, such as the tripping of circuit breakers, to announce their occurrence. With very few exceptions industrial rectifier installations include a cathode or an anode circuit breaker or both, and an a-c circuit breaker. If the d-c machine circuit breaker trips only on reverse current and the d-c system is capable of feed-back, an arc-back will be announced by the opening of the circuit breaker with a report that one is inclined to accept as sufficient proof. Nevertheless, it is advisable in all cases to analyze the control and protective systems of all circuit breakers involved to establish the validity of assumptions based on circuit breakers operations.

Poor vacuum, another important symptom, may be caused by a leak, loss of pumping capacity, or the presence of foreign volatile matter in the vacuum system. This symptom requires immediate investigations, as continued poor vacuum will result in rapid deterioration of the rectifier.

Abnormally high or low temperatures also may lead to arc-backs. Wide variations of temperature among anode or anode cables indicate severe current unbalance conducive to arc-backs.

High transformer temperature may be caused by overload or loss of interphase transformer function. Saturation of the interphase transformer due to anode unbalance or a short circuit in the interphase winding will generally produce arc-backs. It also may double the copper losses of the main transformer winding.

A marked change in the noise produced by the transformer, other than that caused by changes of load conditions, is a danger signal. This is particularly true if the noise becomes rough. Noisy anode-balancing reactors generally indicate poor anode current balance and sharp clicks or thumps indicate excitation failures, misfires, or arc-throughs. An arc-back also will cause a sharp noise in an anode-balancing reactor, but usually is drowned out by the noise of the circuit breakers unless the arc-back is cleared by arc suppression without operation of the circuit breakers.

The symptoms described previously are directly observable without special equipment.

The following also have deviations from the normal: anode current balance; anode current wave-shape; anode-to-cathode voltage wave-shape; grid current wave-shape; grid-to-cathode voltage wave-shape; interphase transformer voltage wave-shape; and internal insulation resistances.

The most important thing to look for in these quantities and wave-shapes, and the most easily spotted, is dissymmetry of any kind among anodes and grids.

Instruments and Aids

Below are listed a number of standard and a few special devices which can be used to observe and record various sustained and transitory symptoms. These are in addition to those with which the rectifier unit is organically equipped.

1. Clip-on ammeter or other means of determining anode current balance.
2. Megger—preferably 1,000 volts.
3. Oscillograph, magnetic or cathode ray.
4. U-bolts and compass to catch current reversal.
5. Surge crest ammeter.
6. Special electronic arc-back detector for logging the distribution of arc-backs or arc-throughs among the anodes.
7. Memory attachments for oscillographs.

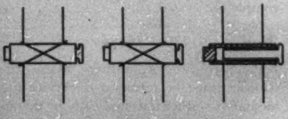

Figure 2. Magnetic links for surge-crest ammeter, installed on anode cables

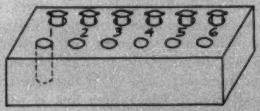

Figure 3. Magazine for magnetic links

The usual assortment of test voltmeters, ammeters, thermometers, and a McLeod vacuum gauge are assumed to be on hand.

It will be noted that all but the first three items on the list provide a "memory" of transitory phenomena. Sitting up with a sick rectifier to catch randomly occurring momentary symptoms can be a very tedious job.

Procedure

In order to illustrate most effectively the various phases of an investigation, we will assume a typical case of trouble and follow a step-by-step procedure to determine the cause. Instruments and aids will be described and their use explained as they are called for in the procedure.

We will assume for our purpose a rectifier that has been operating satisfactorily until recently, averaging less than two or three arc-backs per year. Over the last few months this rate has increased to three or four per month. The circuit breakers have reclosed properly each time so there is not as yet any interference with operation. However, the outages all seem to occur during the peak load hours, and should the rate continue to increase, serious service interruptions are to be expected.

To start at the beginning, if we assume the station unattended, the only fact known is that unscheduled circuit breaker operations occur, and targets are found down on the instantaneous overload relays after each interruption.

Analysis of Circuit Breaker Openings

The first step then is to determine whether or not the outages are caused by arc-backs. The d-c circuit breaker is equipped with a built-in reverse current trip and a shunt trip coil. There is no overload trip, overloads being cleared by the feeder circuit breakers. Opening of the a-c circuit breaker, water failure, and excitation failure will act on the shunt trip of the d-c circuit breaker. The only light found on the annunciator is the one indicating an unscheduled opening of the circuit breakers. There is then sufficient evidence to justify the assumption that the outages are caused by arc-backs. If this is not so, the ensuing investigation can be expected to show this during the early stages.

Vacuum, temperature, and all other observable conditions have been checked and found correct. However, no seepage test has been made on the rectifier because this would require a shut-down.

ANODE CURRENT BALANCE

The next test that can be made without shutting down the rectifier is a check of the anode current balance.

Although clip-on ammeters are particularly inaccurate on unidirectional pulse currents such as flow in the anode circuits, they are convenient and generally used to check anode current balance. Care must be exercised in positioning the clip-on ammeter, as neighboring cables have an influence on the reading and even the location of the cable within the window of the ammeter iron and the angle of the ammeter with respect to the cable may cause large errors in the readings.

If greater accuracy is desired and if suitable sections of the anode connections are accessible, a d-c millivoltmeter is much more satisfactory. It should preferably be shielded and used in conjunction with two probes rigidly mounted on a bar of insulating material.

A fluctuating load makes accurate reading of instruments difficult and may introduce considerable error. This error is minimized by taking readings as the total d-c load holds momentarily or passes slowly through a selected value. If the load fluctuates too wildly to follow this procedure, an attempt is made to catch simultaneous readings on the d-c ammeter and clip-on ammeter for each anode in turn, and proportional corrections are applied to the anode current readings.

Between half and full load, unbalances up to 5 per cent above or below average are acceptable. If anodes are paralleled through reactors, deviations up to $7^1/_2$ per cent can be expected, but should improve with increasing phase-control.

At light load the unbalance will be worse than at the higher loads. Should any anodes drop out and not carry current for appreciable intervals, arc-backs are to be expected.

Even when the percentage of unbalance is within permissible limits, any change for the worse in comparison to previous records should be investigated.

We will assume here that anode current balance is satisfactory at high and low loads.

DETERMINATION OF ARC-BACK DISTRIBUTION

If it is permissible to shut down the rectifier over week ends, the next logical steps would be the seepage and megger tests. Assuming it is desirable to postpone a shutdown as long as possible, preparations are made to determine next the distribution of arc-backs among the anodes.

U-Bolts and Compass

The U-bolt can hardly be classified as a scientific instrument, but together with an ordinary compass it provides a simple and certainly an inexpensive means for determining which anode has backfired.

One U-bolt is tied to each anode cable in as uniform and symmetrical an arrangement as possible. One end of each U-bolt should be marked so no mistakes will be made when they are removed for checking. They should be mounted on the cables with markings always in the same direction as shown in Figure 1.

Anode currents during normal operation will magnetize the U-bolts in one direction, whereas the heavy reverse current in the faulted phase will reverse the polarity of the U-bolt on that phase during arc-back.

The reversal of polarity can be checked easily with an ordinary compass. If there is sufficient distance between U-bolts, the polarity can be determined without removing the bolts from the cables. In most cases it is necessary to remove them to obtain reliable indications. The check must of course be made before the rectifier is returned to service, as otherwise the record may be erased.

Surge Crest Ammeter

The U-bolt is at best a makeshift affair for this purpose. The surge crest ammeter is more reliable, easier to use, and in addition to polarity provides a relative measure of the currents involved. With proper calibration a fair measure of the actual crest current can be obtained.

The complete surge crest ammeter consists of three component parts: (1) any desired number of magnetic links; (2) an indicating instrument with a holder in which the magnetic links are placed for measurement; and (3) a demagnetizing coil through which each link is passed after the measurement has been made and before the link is used again.

The most convenient way of holding the magnetic link against the anode cable is to fasten a small piece of tubing of nonmagnetic material to the cable and at right angles to its axis. One end of the tube should be closed, so the link has to be inserted from the same end each time and the diameter of the tube should be such that the nibs provided at one end of the link will not go into the tube. This arrangement makes it very easy to remove the magnetic links for measurement and return them with proper direction assured, see Figure 2.

To permit restoration of service with a minimum loss of time and provide definite association of each meter reading with the proper anode, it is common practice to use twice as many links as there are anodes so that a demagnetized replacement link can be substituted for each one as it is removed from the anode cable. A convenient magazine for the links is made by drilling two rows of holes in a block of wood, one hole for each link on the cables and one directly beneath it for the demagnetized replacement, as in Figure 3.

In the event of an arc-back and before the unit is restored to service, each link is removed in turn from the anode cable and inserted in the magazine in the correspondingly marked position. Its replacement link from the other row is removed from the block and inserted in the holder on the cable. Twelve links can be changed easily in one minute.

Using either the rough-and-ready U-bolts or the more refined surge crest ammeter, the distribution of arc-backs among the anodes is tabulated. With the surge crest ammeter it is also possible, with somewhat less reliability, to determine the distribution of arc-throughs in inverter service. The magnetic link on the anode which last carried arc-through current will probably give the highest reading in the forward direction. It will not tell if the arc-through was due to loss of control on that anode or if the next succeeding anode failed to pick up at the proper time.

The surge crest ammeter can be tried with immediate reclosure of the breaker if not too much time elapses before the links are checked. Otherwise there is a chance that the record will be obscured or completely erased.

Electronic Arc-Back Detector

For operating conditions where the rectifier must be returned to service immediately, either automatically or manually, or where other conditions make it impracticable for an operator to get at the

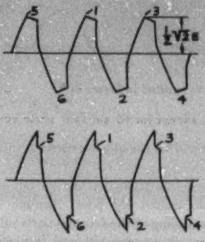

Figure 5(A) (top). Full interphase transformer voltage with no phase control

Figure 5(B) (bottom). Interphase transformer voltage with phase control

links installed on the anode cables, an electronic device has been built and used successfully, which lights a signal lamp corresponding to the phase on which the fault occurred. The diagram for the device is shown in Figure 4.

The circuit consists essentially of a number of thyratron tubes, six for a 6-phase rectifier, 12 for a 12-phase rectifier, and so forth, and a small d-c power supply. The grid of each tube is connected to a through-type current transformer in one of the anode leads. The tubes are normally blocked by negative bias on the grids. On the occurrence of an arc-back (or arc-through if an inverter is being investigated) the current transformer in the faulted phase produces a positive impulse on the grid of the corresponding tube and releases it. The resulting current flowing through the common cathode resistor increases the negative bias on all grids, so that all tubes except the one triggered are blocked. That tube will continue to fire until reset. The plate current is used to light a small signal lamp on the front of the cabinet.

In some cases two lamps may be lit simultaneously, but only the one corresponding to the leading phase should be recognized. Although arc-backs may occur on more than one anode for any given fault, it is improbable that they will be initiated at the same instant, and the one that leads off will most likely be the troublemaker.

A system using a large number of rectifiers would well justify building an electronic arc-back detector.

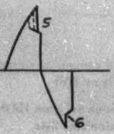

Figure 6. Interphase transformer voltage, showing erratic pick-up of anode 5

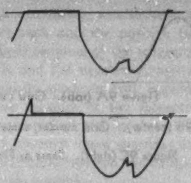

Figure 7(A) (top). Anode-to-cathode voltage with no phase control (double Y with interphase transformer)

Figure 7(B) (bottom). Anode-to-cathode voltage with phase control (same connections as 7A)

Failure to detect any arc-backs, even though circuit breaker openings continue to occur, calls for a review and thorough investigation of circuit breakers, protective relays and settings, interlocks, and control circuits. Power circuits all the way from the a-c circuit breaker to the d-c load should be checked carefully. The rectifier transformer should be scrutinized for intermittent faults. If oil-immersed, the oil should be checked for indications of under-oil arcing.

To avoid a premature ending, we will assume that arc-backs are taking place and most, but not all, are registered on anode 5. The cause is yet to be determined, with particular emphasis on its location in or external to the rectifier.

Oscillographic Analysis

As the cause of the arc-backs may lie outside the rectifier, it is still desired to avoid what might be an unnecessary shutdown. So we choose oscillographic analysis for our next step in the investigation.

The cathode-ray oscillograph, or oscilloscope, is one of the most useful and versatile implements in the investigation of rectifier disorders. The magnetic oscillograph is more cumbersome in every way and does not have the sensitivity of the oscilloscope. It does permit viewing as many as six separate quantities simultaneously and provides photographic film for careful study. However, the oscilloscope also can be equipped with a camera and is often used in that manner.

Either type of oscillograph is useful in investigating the important voltage and current wave-shapes listed in the chapter on symptoms.

The cathode-ray oscilloscope should be tried in several different positions to determine to what extent the image is being affected by stray fields. Twisted leads are important to avoid pick-up.

When using either instrument every precaution should be taken to insure personal safety. Whenever possible, the oscillograph is used in a grounded circuit and connected across the grounded end of a potentiometer if the voltage is high. These conditions, however, can seldom be fulfilled. It is wise to place the oscillograph on an insulated table and operate from an insulated stool or mat. When used on rectifiers of 600 volts, or even 250 volts, it is well to take the power supply of the cathode-ray oscilloscope through a small insulating transformer.

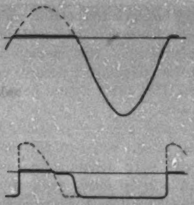

Figure 8(A) (top). Grid-to-cathode voltage, sinusoidal wave, with small amount of bias phase control

Figure 8(B) (bottom). Grid-to-cathode voltage, chopped sinusoidal voltage wave, negative loop suppressed

The first thing to look for is any dissymmetry or other irregularity in the firing of the anodes. The easiest way to do this is to check the wave-shape across the interphase transformer. Figures 5(A) and 5(B) show the normal wave-shape of the interphase transformer voltage, without and with phase control, for a 6-phase double-Y rectifier transformer. The sweep of the oscilloscope is adjusted for one cycle of the primary frequency so that each of the three positive and three negative loops of the curve will correspond to one of the six phases of the rectifier transformer secondary. The phases will, of course, appear in sequence, but the first loop will not necessarily coincide with phase one.

By various means it is possible to identify one loop of the resulting curve with its corresponding anode and from that all other loops can be properly identified. The sweep and synchronizing circuit of the oscilloscope must be stable, as any drift of the image across the screen will make identification almost impossible.

A quick way to identify a particular phase with a loop of the interphase transformer voltage wave is to disconnect momentarily the grid or grids of the anodes connected to that phase. The leading slope of one of the loops will continue forward, past the point where it normally breaks, to complete a sine wave. The point at which this particular curve normally breaks is the point at which the anode which was disabled would normally have picked up. This method applies only if the grids have a positive characteristic. This check should be made at light load.

Many other means of identification are possible. A sure way with less risk than the above is to determine the pick-up point of a given anode from either its voltage or current wave, without changing the sweep or synchronization.

The numbered points on curves, Figures 5(A) and 5(B), indicate the time at which the anodes connected to correspondingly numbered phases pick up.

Any deviation of the trace from the general character indicated or any difference between loops is cause for suspicion and further investigation.

Any difference in the height of the pips above the loops in Figure 5(B) denotes differences of phase control among the phases. Such differences will generally cause unbalance of anode current and may be caused by trouble in the phase control circuit, in the grid insulation, or even a break in the internal connections between the grid inlet bushing and the grid. A trace such as shown in Figure 6 is caused by erratic pick-up and may be caused by external or internal disorders.

Marked differences between the positive and negative loops indicate d-c saturation of the interphase transformer, and are generally caused by an unbalance between the two 3-phase systems. A marked reduction in the amplitude of either the positive or negative loops, or both, might be caused by one or more shorted turns in the interphase winding. The peak voltage across the total interphase winding, without phase control, should be exactly one-half of the peak voltage of the transformer secondary phase-to-neutral voltage. If this value is not attained, it means the interphase transformer is not fully effective. Should the interphase transformer be inoperative for any reason, the transformer will, if it has a delta primary or delta tertiary, act like a 6-phase star, producing anode currents of only 60 degrees' instead of 120 degrees' duration, and of twice the normal amplitude. This condition will be productive of arc-backs.

The foregoing illustrates why the interphase transformer voltage offers excellent advantages for a quick over-all check of the operation of the rectifier. It has limitations, particularly when two anodes are paralleled through anode reactors, and of course in many instances the interphase transformer terminals are not readily accessible.

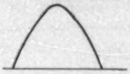

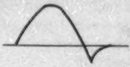

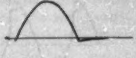

Figure 9A (top). Grid current for voltage as applied in Figure 8(A)

Figure 9B (center). Grid current, same as Figure 9(A), except for 15 per cent phase control

Figure 9C (right). Same as Figure 9(B), except grid has partially lost control

More specific investigations with the cathode-ray oscilloscope can be made directly on the anode and grid circuits of the rectifier. The anode-to-cathode voltage wave-shape, observed on all anodes, will disclose facts that cannot readily be deduced from the interphase transformer voltage. However, even using an electronic switch, it is not possible with standard equipment to observe all anodes simultaneously and comparison becomes more difficult unless the load is reasonably steady. The magnetic oscillograph is more useful for this work.

Figures 7(A) and 7(B), respectively, show the normal anode-to-cathode voltage without and with phase control. The particular points of interest are at the beginning and end of the conducting periods; the beginning showing any discrepancy in phase control, and the end showing the initial inverse voltage, which has a great effect on the arc-back rate.

The anode current wave-shape can be obtained by using current transformers or shunts, and the shunt may consist merely of a suitable length of the anode connection conductor. Differences of wave-shapes between anodes should be investigated.

Among the most revealing checks that can be made on the rectifier itself are the wave-shape of the grid-to-cathode voltage and grid current. A comparison of the grid-to-cathode voltage will reveal any discrepancy in the grid circuits, whether external or internal. Figure 8(A) shows a typical grid-to-cathode voltage where sinusoidal voltages are applied and Figure 8(B) shows a typical grid-to-cathode wave-shape for peaked voltages. Figures 9(A) and 9(B) show typical currents for sinusoidal voltages. In Figure 9(C) the grid has partially lost control.

Unlike anode currents, the amplitudes of the positive and negative grid currents are of the same order of magnitude permitting ready observation of the deionizing current at the grid. Figure 10(A) is a typical curve showing the rapid decay of deionizing current at the grid immediately after completion of the anode-conducting period. In Figure 10(B) the deionizing period is dragged out almost to the beginning of the next positive cycle. This condition may be inherent in the particular design but may also be caused by poor vacuum, improper cooling of the internal parts of the rectifier, or deteriorated grid insulation. It also may indicate a broken grid. If all grids of the machine show exactly the same characteristic and have not changed from the time when the machine was performing satisfactorily, no special significance should be attached to this image. For average rectifier service, stress should be placed on the uniformity and constancy of the deionizing current form rather than on the form itself. As a rule, the higher the rated voltage of the machine, the shorter the deionizing time should be. For inverter service, in particular, deionization must be complete before the step-limit is reached, that is, the point at which the anode becomes positive with respect to the cathode, and the total time available for deionization is generally quite small. A relatively small increase of deionizing time will cause arc-throughs.

Figure 6, showing erratic pick-up on phase 5, calls for a careful check of the grid circuits of that phase. If all external components are found in good order, the next step will be the megger test. A short shut-down is required.

MEGGER TEST

The 1,000-volt megger has been found to be most reliable, although the 500-volt megger is used more often because of its wider distribution. The 1,000-volt megger can be expected to discover weaknesses that do not show up on a 500-volt test.

The megger is used here primarily to

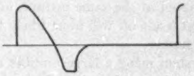

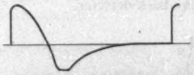

Figure 10(A) (top). Grid current for voltage as applied in Figure 8(B)

Figure 10(B) (bottom). Same as Figure 10(A) except for long deionizing time

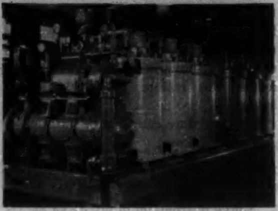

Figure 11. Rectifier with arc-back probability of less than 1 in 23 billion anode-cycles

test the internal insulating members of the rectifiers. Any external connections, electric and water, that might influence the readings should be removed.

Special care should be taken to see that the megger leads are supported so that they do not touch each other, ground, or anything that might influence the readings, as insulation resistances can be expected to run over 2,000 megohms.

As far as possible all insulating members should be tested and a record made of readings between anode and tank, grid to tank, tank to cathode if the cathode is insulated as on multiple-anode rectifiers, and tank to cooling coil where the rectifier has an internal cooling coil insulated from the tank. The value of insulation measured for the various component parts is a function of design and service. Significant differences between anodes of the same rectifier and between rectifiers of the same type should be investigated.

In certain designs of multianode tanks there are insulating members that have critical influence on the arc-back rate but cannot be checked from outside the rectifier by the usual means. One such insulating element is the support of the grid in the anode housing, and another, rarely used today, is a petticoat on the anode insulator serving as support for the anode housing.

With excitation established in the rectifier tank and the positive (usually grounded) terminal of the megger on the cathode and the negative (ungrounded) terminal on anode or grid, a good comparative measure of the respective insulating members can be obtained. The ionized mercury vapor provides an electric connection between the cathode and the anode housing.

SEEPAGE TEST

Again we assume that all results have been negative up to this point, and it is finally decided to shut down the rectifier to make a seepage test. For dependable results, the seepage rate should be averaged over at least six hours. The machine must be held at constant temperature, preferably room temperature, throughout the test. This means the rectifier will be out of service 10 to 12 hours or longer.

A McLeod vacuum gauge is generally provided for making seepage tests. With proper precautions a fair test can be made with the electric gauge but this is not recommended.

The general procedure for single-anode rectifiers is as follows:

1. Cool rectifier to room temperature, allowing sufficient time for internal parts to cool.
2. Pump rectifier down to best obtainable vacuum.
3. Close individual vacuum valves on rectifier tanks and the main vacuum valve.
4. After a period of not less than six hours, take a reading of the vacuum in the vacuum header. The rise of pressure in the header should not exceed 5 microns per hour.
5. Open main vacuum valve and restore good vacuum in the header.
6. Close main vacuum valve.
7. Open valve on one tank. After five minutes read vacuum. The increase in pressure divided by the number of hours the tank valve has been closed is approximately the average seepage rate. Close tank valve.
8. Repeat 5, 6, and 7 for each tank in turn.

1
2
3
4
5
6
7
8
9
10
11
12

Figure 13. Electronic arc-back detector

The permissible seepage rate is based on previous experience with the particular design of machine. The correct value can be obtained from the manufacturer. As a general rule it can be assumed that a seepage of 0.5 micron per hour is the maximum permissible. However, any increase in seepage on a given tank should be investigated.

This procedure must be modified when there is no valve between the vacuum pump and the vacuum gauge. In this case both the high vacuum and roughing pumps must be shut down after the tank valves (or valve in the case of a multianode rectifier) are closed.

About one hour before the end of the test the pumps are started again, in proper sequence, to pump down the vacuum pipe line. Then they are shut down again, and when the high vacuum

Figure 12 (below). Group of instruments used in checking rectifiers

Figure 14 (right). Cathode-ray oscillograph with automatic camera attached

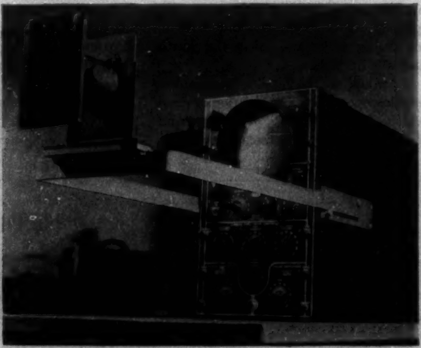

pump has cooled down sufficiently to be completely inoperative, the tank valves are opened, as above. Cooling water should flow continuously through the jacket of the high vacuum pump.

Naturally, no direct seepage test is possible in the case of sealed-off rectifiers. Where glass seals are employed and the light of the arc can be observed through them, a pinkish glow indicates a leaky tube. The excitation arc of a continuously excited rectifier will be unstable without the aid of the main arc when the vacuum is bad.

OSCILLOGRAMS UNDER FAULT CONDITIONS

Assuming that all checks and tests up to this point have produced negative results and a longer shutdown must still be avoided at this time, the rectifier will be returned to service for further observation. There is a possibility that progressive deterioration will produce more definite clues before serious damage is done.

During this period special attention should be given to the a-c and d-c systems for possible surges or other irregularities. Before going back in service, check the over-all circuit breaker speeds, including relay time, to make sure that slow tripping will not cause deterioration in parts of the equipment which are still sound.

Observation and analysis at this stage (or earlier) can be greatly enhanced by obtaining oscillograms under actual fault conditions. These oscillograms, to be of value, must show not only the fault itself, but what occurred immediately preceding it.

An excellent device for this purpose is a cathode-ray oscilloscope with a camera attachment for retaining the image that was on the screen at the time of the fault. Because of the retentivity of the oscilloscope screen, it is not difficult to have the fault trigger the shutter of the camera and photograph the image that was projected on the screen a cycle before the shutter actually opened.

It would not be feasible to have one oscilloscope-camera combination or memoscope for each anode. When the backfiring anode has been isolated and it is desired to obtain more specific information as to the phase relation of the fault, the magnitude, or other pertinent information, then this device can be applied directly. A single oscilloscope, however, can be connected across the interphase transformer to scan all anodes as previously described.

It might be difficult from the image so produced to decide with certainty which anode backfired, but since the timing of the shutter can be set to include in the image some of the phenomena preceding the fault, a clue to the cause might be found.

FINAL STEP

We have chosen for our example a difficult case which has stubbornly resisted diagnosis. Three more steps remain, the choice depending on circumstances:

1. Open for inspection and overhaul the tank or tanks with the poorest record.
2. If there is reasonable doubt that the trouble is internal, interchange the tank which has had the most arc-backs with one of the others.
3. If a spare tank and conditioning unit are available, interchange with each tank on the frame, one at a time, until the culprit is found by elimination.

The procedures, checks, and analyses outlined are directly applicable, or applicable with obvious modifications to rectifiers using the igniter principle.

Conclusion

Before embarking on any elaborate program of investigation, it is logical to carry out first the simpler tests requiring the least time and equipment. The actual order will be determined largely by service requirements and the severity of the trouble.

Load division, seepage, and megger tests are basic and should be carried out as soon as trouble is experienced, since any one of them might discover the source of trouble and indicate the remedy. The seepage and megger tests particularly are likely to determine at once whether trouble is in the rectifier itself or in associated equipment. A poor seepage test of course means that the leak has to be found and corrected. In many cases this requires opening the rectifier. Low megger tests invariably mean opening the rectifier to restore proper insulation levels.

The procedure can then be outlined in general as follows:

1. Ascertain that interruptions are being caused by arc-backs.
2. Check distribution of arc-backs among anodes.
3. Check anode current balance.
4. Megger test.
5. Seepage test.
6. Check operation of interphase transformer and wave-shape.
7. Check wave-shapes of: anode-to-cathode voltages; anode currents; grid-to-cathode voltages; and grid currents.
8. Detailed investigation of nature of arc-backs, including oscillograms obtained at the time of arc-back.
9. Investigation of a-c and d-c circuits.
10. Open tank or tanks for inspection and overhaul.
11. Check circuit breaker and relay speeds before restoring unit to service to make sure that slow tripping will not cause further deterioration.

This sequence is not fixed. Depending on local conditions, some steps may be eliminated and others added. Step 11, checking of relay and circuit breaker speeds, should always be included as a matter of routine.

The length of this paper should not be taken as a reflection on the reliability of rectifiers. If a rectifier installation is made with full understanding and due allowance for the fact that arc-backs do occur in normal operation with a frequency depending on the application and conditions of service, an occasional arc-back will have no serious consequences. If the arc-back rate increases beyond what could reasonably be expected, even though it causes no operational difficulty, the cause should be investigated. The seat of the trouble may be in the rectifier itself or in associated equipment, or it may even be in the supply or load circuits. An early diagnosis will reduce subsequent outage time and the cost of maintenance.

No Discussion

Rectifier Transformer Characteristics

AN AIEE COMMITTEE REPORT

AT EVERY installation of an electronic power converter, the voltage and phase characteristics of the power supply system are usually quite different from those required at the anode terminals of the rectifier. Because of this circumstance, a transformer having appropriate d-c windings is necessary to adapt the system to the rectifier requirements.

Many different converter circuits have been developed. In all of these the transformer connection influences the duty of the individual rectifying devices comprising the rectifier; therefore, the transformer connections used must be coordinated with the rectifying devices available.

Circuit Connections

Rectifier power circuits are of two general types. In one type, the transformer d-c windings are connected to the rectifying device so as to permit conduction in only one direction; while in the other type, current is carried in both directions during alternate half cycles. This classification is of considerable importance in the design of power transformers for rectifiers since the transformer utility, and winding arrangement to prevent core saturation, are different in the two types.

In power rectifier terminology, the terms single-way and double-way have been introduced to define the direction of current flow in the alternating voltage circuit elements which are conductively connected to the rectifying devices. A single-way rectifier is one in which the current between each terminal of the alternating voltage circuit and the rectifying device flows only in one direction. A double-way rectifier is one in which the current between each terminal of the alternating voltage circuit and the rectifying devices conductively connected to it flows in both directions.

In the single-way rectifier, which is the type most commonly used for power application, each rectifying device and its associated transformer d-c winding carry current in only one direction. There is, therefore, a direct component in each d-c winding current. In order to avoid saturation of the transformer core by this direct current, an even number of d-c windings must be associated with each a-c winding, and these d-c windings must be so connected that each conducts currents once per cycle, but at half cycle intervals, and in an opposite direction with respect to the a-c winding. This is shown clearly in Figure 1.

In this type of circuit, the a-c winding conducts current reflected from the pair of d-c windings and the current alternates in sign every half cycle. Since the a-c winding conducts current each half cycle while the d-c windings each conduct current only every other half cycle, the a-c winding kilovolt-amperes will be less than the sum of the kilovolt-amperes of the pair of d-c windings it supplies. Thus, for all single-way rectifier transformers, the a-c winding kilovolt-amperes will be less than the total d-c winding kva. The ratio between the a-c and d-c winding kilovolt-amperes depends upon the transformer connection.

In double-way rectifier circuits, the opposite directions of current conduction in the d-c windings are in alternate half cycles. The d-c winding current, therefore, contains no direct component and the a-c winding will conduct the reflected d-c winding current. Since the a-c and d-c windings are active simultaneously, their kilovolt-amperes will be equal and the winding arrangement is similar to the conventional transformer. It is, therefore, evident that the copper economy of the rectifier transformer for double-way circuits is greater than for single-way circuits.

Arrangement of Windings

The arrangement of rectifier transformer windings is similar to that of ordinary power transformers. The a-c winding may be either coaxial and concentric or coaxial and interleaved with respect to the d-c windings. Only the concentric arrangement will be discussed in this report. The d-c windings, usually the low voltage high-current windings, are on the inside next to the core, and the a-c winding, usually the high voltage, is on the outside. In some cases for low voltage

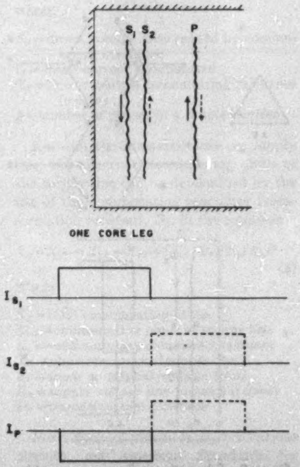

Figure 1. Winding arrangement and winding currents in a single-way rectifier transformer

---

Paper 49-271, recommended by the AIEE Electronic Power Converters Committee and approved by the AIEE Technical Program Committee for presentation at the AIEE Fall General Meeting, Cincinnati, Ohio, October 17–21, 1949. Manuscript submitted March 28, 1949; made available for printing September 7, 1949.

Personnel of the Rectifier Transformer Subcommittee of the AIEE Electronic Power Converters Committee: A. J. Maslin, *Chairman;* R. A. Nelson, F. D. Kaiser, and W. C. Sealey.

and very high direct current output, with a moderate voltage a-c winding, the reverse arrangement is found convenient.

In order to obtain balanced regulation, it is a necessary requirement that all d-c windings from anode to neutral have the same reactance to their associated a-c winding. This complicates the simple 2-winding arrangement when there is more than one d-c winding per phase, as in the single-way circuits.

It also is a necessary requirement that a-c and d-c windings which normally have balancing ampere turns be physically balanced with respect to the heights of the winding coil stacks. This balancing of winding lengths helps reduce the mechanical forces and minimizes stray losses.

With these general principles in mind, it may be helpful to discuss a few specific connections of the types most commonly used and see how these conditions are satisfied.

In all simple double-way rectifier transformers having one a-c and one d-c winding, such as the delta-Y 6-phase double-way connection, the current conductions are similar in manner to standard power transformers. The windings in these transformers can, therefore, be arranged in accordance with the established practices for power transformers, which satisfy the conditions mentioned.

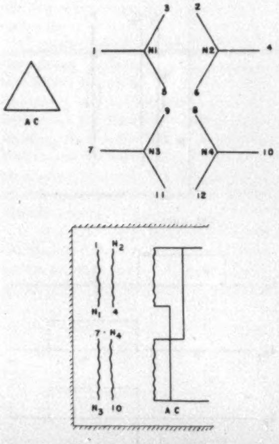

Figure 2. Schematic winding arrangement in a delta 6-phase parallel double-Y connected rectifier transformer

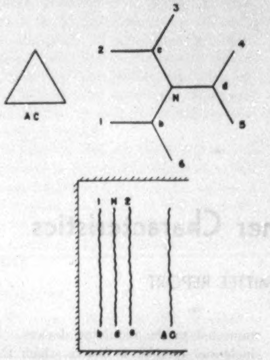

Figure 3. Schematic winding arrangement in a delta 6-phase fork connected rectifier transformer

The most common of all single-way circuits is the 6-phase double-Y having either a delta or Y a-c winding. For this connection, the two d-c windings, which are on the same core leg, can be made an interwound helical coil and located next to the core. An interwound helical coil consists of two or more windings, each having the same inside and outside diameters and the same number of turns, disposed to form a multiple pitched helix. Such a coil may be likened to nested helical springs having the same diameters and number of turns, or a multiple thread screw. The a-c winding is then concentric with the d-c windings and located on the outside. As stated before, the d-c windings may be the outside windings. In this case, these windings may consist of many multiple coils, with the coils of the two windings interleaved, so that each is spread over the full winding length.

A modification of the double-Y circuit is the 6-phase parallel double-Y connection. This connection is, in effect, two double-Y sets of windings on one core. The two d-c windings, which are on the same core leg, and part of the same 6-phase set of Y windings, may be an interwound helical coil located next to the core in the top half of the core window. The other two d-c windings, which are on this same core leg, and part of the other 6-phase set of windings, are then a similar interwound helical coil and located next to the core in the bottom half of the core window. The a-c winding on each core leg is divided into two multiple circuits, one associated with each set of d-c windings. The a-c windings are concentric with and located outside the d-c windings, one in the top half and one in the bottom half of the core window. This arrangement is shown schematically in Figure 2.

Another connection which has been used is the single-way 6-phase fork with either a delta- or Y-connected a-c winding. The three d-c windings, which are all on the same core leg, can be interwound as a helical coil. With the a-c winding on the outside, this arrangement gives approximately the same leakage reactance between any one of the three d-c windings and the a-c winding, and very low reactance between the d-c windings themselves, as shown schematically in Figure 3.

There are two general arrangements for the 12-phase quadruple zigzag single-way circuit. One has a single-circuit a-c winding with four long d-c windings which may be interwound as a helical coil and four short d-c windings which also may be interwound as a helical coil, on each core leg.

The long and short coils being of unequal turns cannot be interwound, but rather each is spread out over the entire stack height. The other arrangement for the 12-phase zigzag has two a-c circuits in multiple, one associated with one of the two 6-phase sets of d-c windings, and the other associated with the other 6-phase set.

This arrangement is then similar to the parallel double-Y connection described previously, with the paralleled a-c windings in the top and bottom halves of the core window opposite their respective sets of d-c windings. These two types of the 12-phase zigzag connection are shown schematically in Figures 4 (A) and 4(B) respectively.

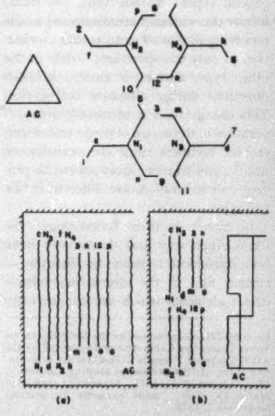

Figure 4. Schematic winding arrangements in delta 12-phase quadruple zigzag connected rectifier transformers

Structural Features

Rectifier transformers are essentially power transformers that have been modified in some important details to make them suitable for rectifier service. The modifications in winding arrangements have been described. A second and very important modification is an increase in the fault current limit of rectifier transformers over power transformers.

As will be shown later on, rectifier transformers are subjected to more severe stresses and at more frequent intervals than are power transformers. The mechanical strength must, therefore, be of the highest order, and all mechanical bracing must be ample for the forces involved and must be of such a nature as not to yield or fail under repeated stressing. The difficulty of successfully meeting these requirements increases with the size of the unit.

Adequate mechanical bracing, like cooling surface, is quite easily obtained in the smaller units; but with increasing rating the mechanical stresses, like losses, increase faster than in proportion to the capabilities of the structure. They therefore demand special consideration.

Rectifier transformer windings are usually wound with rectangular conductor of larger cross section than power transformer windings, so proportioned as to give high mechanical strength in the direction of greatest force. The outer coils in a concentric coil arrangement are designed so that the tensile stress under the most severe fault conditions is well below the elastic limit of the copper used. The inner coil is adequately supported on its inner surface to preclude buckling due to the compressive forces acting on its outer surface. Because of the axial component of forces, the coil supports between turns or coil sections must be adequate so that the beam strength of the conductors between supports will not allow deflections which could cause failure turn-to-turn or section-to-section.

Inasmuch as the axial net force between a-c and d-c windings is proportional to their net displacement of magnetic centers, it is desirable to have both windings as free as possible of taps so that the net magnetic displacement can be kept as small as possible. Also, the ampere turn distribution should be as nearly uniform as possible throughout the principal length of the leakage path so that internal coil forces or forces on individual sections are uniform and minimum. It is highly desirable to maintain a perfectly balanced winding both magnetically and mechanically and to avoid idle tap sections and extended windings for voltage control unless they can be achieved in a symmetrical manner in so far as winding layout is concerned. On the larger ratings it has become common to take care of direct voltage control, when required, by auxiliary means such as an autotransformer or voltage regulator, in order not to impair the rectifier transformer design as regards unbalanced magnetic forces.

The use of spirally-wound coils with a large pitch should be avoided because of the unbalanced magnetic distribution and resulting torque on the coil, which tends to unwind an outer coil or otherwise seriously deflect the copper conductors.

In addition to the forces on the windings themselves, the forces on leads and bus bars must be considered and adequate bracing provided for these structures. The optimum lead arrangement should minimize the stress without employing a configuration which produces stray losses or heating of tank wall and core clamps. The objectives of minimum stress and minimum stray losses and tank heating are mutually incompatible.

Some of the forces mentioned are ultimately transmitted to the top and bottom core clamps, which are made adequately strong and are tied together by means of steel members. Winding clamping surfaces are supported by the core clamps, thus making tight clamping of the winding structure possible.

Electrical Characteristics—Voltage

In a power rectifier, the transformer is of primary importance because many characteristics of the rectifier such as direct voltage, regulation, and power factor depend upon the transformer connection and characteristics.

For single-way rectifiers, the direct voltage is equal to the average voltage during the conducting period, between the transformer neutral and the conducting anode.

At no load, the reactance drop is zero and the direct voltage wave follows the envelope of d-c winding voltage, waves inherent to the circuit or, according to the general equation

$$E_{d0} = (p/\pi)\sqrt{2}E_s \sin(\pi/p) \qquad (1)$$

where

E_{d0} = average direct voltage at no load assuming no overlap, no phase control, and zero arc drop
E_s = anode-to-neutral voltage (rms)
p = number of phases in a simple rectifier

Electrical Characteristics—Reactance

The commutating reactance is the reactance which opposes the current transfer between rectifying elements which conduct consecutively. In an actual installation, the commutating reactance includes the reactance of the anode leads, the transformer reactance, and the a-c supply system reactance, which must be considered irrespective of whether or not the rms value of the supply voltage is maintained constant at the transformer a-c winding terminals. The commutating reactance is usually expressed as a lumped value, anode-to-neutral ohms, referred to d-c winding of the transformer.

In accordance with the principles of rectifier operation in which the load current is successively conducted by the various anodes and their associated transformer d-c windings, it can be shown that the effect of commutating reactance is to increase the length of time of current transfer between the successive anodes, without altering the average or maximum value of anode current. It also can be shown that the length of time to effect a current transfer varies with load, and that the voltage-time integral, during the period of current transfer, represents a wattless voltage drop in so far as the average direct voltage is concerned. This voltage or commutation drop may be represented by the equation

$$E_x = (I_c X_c p)/(2\pi) \qquad (2)$$

where

E_x = direct voltage drop caused by commutating reactance
I_c = direct current commutated
X_c = line-to-neutral commutating reactance in ohms
p = number of phases in a simple rectifier

Knowing the ohms reactance per supply line, the effective commutating ohms of the supply line can be determined by the use of the commutating reactance transformation constant, D_x, in the equation

$$X_c = X_{cT} + X_{cL} = X_{cT} + (X_L/D_x)(E_s/E_n)^2 \qquad (3)$$

where

X_c = total commutating ohms
X_{cL} = commutating ohms of supply line
X_{cT} = commutating ohms of transformer
X_L = ohms reactance of supply line
E_s = anode-to-neutral voltage (rms)
E_n = supply voltage line-to-neutral (rms)
D_x = transformation constant

For a table of values of D_x for various circuits, see American Standards for Transformers, Regulators, and Reactors.[1]

For the case of double-way rectifier

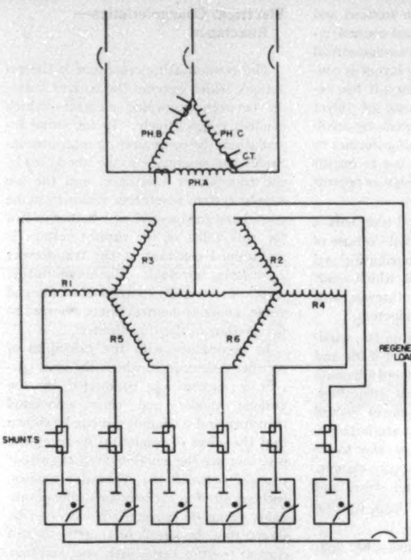

Figure 5. Schematic diagram for artificial arc-back tests

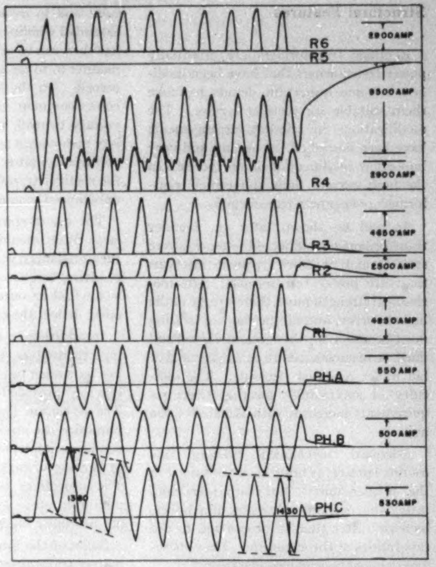

Figure 6. Oscillogram of an artificial arc-back test in the laboratory

transformers having a single d-c winding, or single-way rectifier transformers assumed to have perfect interlacing between the pairs of d-c windings, the commutating ohms due to the transformer can be readily calculated from the transformer reactance.

The total transformer commutating reactance line-to-line is the leakage reactance between the d-c windings undergoing commutations and their respective a-c windings. The anode-to-neutral reactance is one-half the line-to-line reactance. We may, therefore, write

$$X_c = \frac{3E^2}{VA} X_t \tag{4}$$

where

X_c = commutating reactance line-to-neutral (ohms)

E = rms volts, anode-to-junction point of successive conducting phases

X_t = per unit transformer reactance on a-c winding—volt ampere base

VA = volt amperes of the a-c winding associated with commutating d-c windings

For all of the connections discussed here, the value E is actually E_s, the line-to-neutral d-c winding volts with the single exception of the fork-connected transformer. For the fork connection $E = 0.577E_s$. This fact is obvious when commutation is between two directly connected outer fork windings as $R_2 - R_3$, Figure 3. It also is true for commutation between anodes such as $R_1 - R_2$. This is because the commutating current is equal and opposite in the two outer fork windings in the circuit and it has been assumed that there is perfect interlacing and hence no leakage reactance between these two windings.

The VA is the total a-c winding volt amperes with the exception of the quadruple zigzag connection having two a-c winding circuits, each associated with separate 6-phase d-c windings.

In calculating the commutating ohms for the single-way circuits, we have assumed perfect interlacing between pairs of d-c windings on the same core leg. Actually, of course, the condition of zero reactance betweens pairs is not realized. However, with the usual arrangement of interwound helical coils or interleaved paralleled coils, the reactance between pairs is small. Considering the various reactances in a 3-winding equivalent diagram, where the a-c winding to each d-c winding reactance is equal, and the interlacing reactance is small, it can be shown readily that the major portion of the transformer reactance is in the a-c winding. In general, the reactance between d-c windings on the same core leg will be in the range of 0.5 to 2 per cent on the a-c winding kilovolt-ampere base.

This imperfect interlacing of d-c windings will have the effect of increasing the commutating reactance 2 to 10 per cent

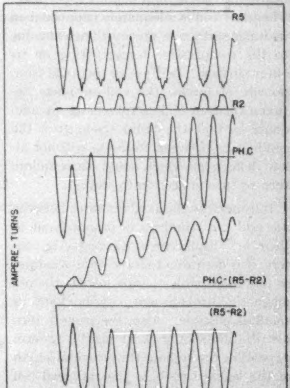

Figure 7. Magnetizing forces on one transformer core leg during arc back

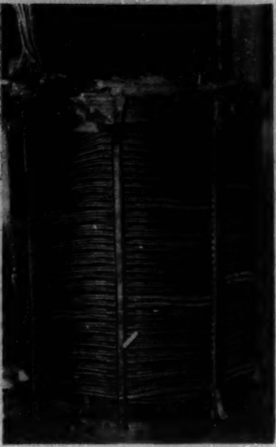

Figure 8. Interwound helical coil comprising two d-c windings damaged by repeated arc-backs

higher than the value calculated from the transformer reactance as given before.

Having calculated the X_c as above, the actual voltage drop caused by commutation can be determined from equation 2, or knowing the per cent reactance based on the a-c winding rating of the transformer considered as a normal power transformer (information which is usually given on the nameplate), the approximate per cent regulation due to commutating reactance may be determined from Table I.

Table I

Circuit	Per cent E_s*
Delta-6-phase Y double-way	0.5 per cent IX**
Delta-6-phase fork	0.5 per cent IX
Delta-6-phase double-Y	0.5 per cent IX
Delta-6-phase parallel double-Y	0.5 per cent IX
Delta-12-phase quadruple zigzag with single-circuit a-c winding	0.258 per cent IX
Delta-12-phase quadruple zigzag with multiple-circuit a-c winding	0.516 per cent IX

* Per cent E_s = regulation due to commutating reactance expressed as a per cent of the no load d-c voltage.

$$= 100 \times \frac{E_s}{E_{do}}$$

** Per cent IX = a-c to total d-c winding reactance in per cent.

The equations shown in Table I are approximate as they assume that the reactances of the a-c winding to each of the d-c winding groups, or commutating pairs, are equal, and that the commutating pairs are perfectly interlaced. They may yield results as much as 10 per cent low.

While transformer reactance is one of the largest factors in rectifier regulation, it also is one of the largest factors in limiting rectifier fault currents. It would, therefore, seem desirable to design rectifier transformers with higher values of reactance than are standard for power transformers of the same voltage and kilovolt-ampere rating. This is actually the case; however, since high reactance means high regulation, the application of the rectifier also must be considered.

Rectifiers are used in three general classifications of service. These are railway or mining service, industrial service, and electrochemical service.

Rectifiers in railway service usually have a regulation of approximately 5 to 6 per cent. This fixes the value of transformer reactance at 6 to 7 per cent for the usual 6-phase transformer connections. If the 12-phase quadruple zigzag connection having a single-circuit a-c winding is used, the transformer reactance may be increased to approximately 13 per cent and still not exceed a rectifier regulation of 6 per cent. This is an advantage of this connection in that it allows high reactance for limitation of fault currents and gives normal regulation. The 12-phase quadruple zigzag connection having a double-circuit a-c winding is similar to the 6-phase connections in regard to reactance and regulation.

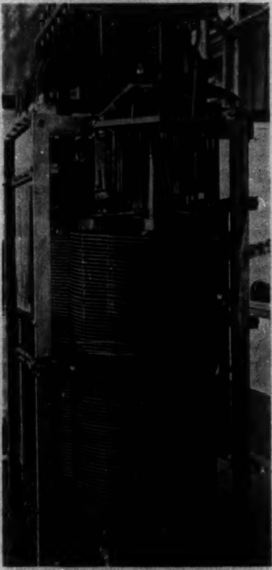

Figure 9. Delta 6-phase parallel double-Y connected rectifier transformer damaged by repeated arc backs

Figure 10. Bus bar leads deflected during arc-back tests

Rectifiers for industrial service are usually provided with phase control voltage regulation. The voltage is maintained at rated value to 100 per cent load. Phase control has the disadvantage of reducing the power factor and increasing the harmonic content of the supply line current. Because high reactance would increase the amount of phase control required, the inherent regulation of rectifiers for this type of service also is limited to approximately 6 per cent, and the transformer reactance is limited to approximately 7 per cent for the usual 6-phase connections.

Rectifier installations in electrochemical plants are usually considerably larger in kilowatt capacity than in railway or industrial service. These installations often comprise several rectifier transformers operating with phase shifting auto-transformers to give multiphase systems. Under the fault condition of arc back, d-c feed from the paralleling rectifier equipment is present until cleared by the d-c switchgear. This being a very severe condition, it is desirable to increase the transformer reactance above that provided for the smaller railway or industrial systems. Accordingly, the transformer reactance may be in the range 7 to 9 per cent.

Regulation in these installations is not so important because a current regulator, operating on phase control, is usually provided; also taps are generally included in the rectifier transformer or separate regulating transformers for direct voltage control. The transformer taps are used for coarse voltage adjustment and phase control for fine adjustment.

Electrical Characteristics—Resistance

In addition to the regulation due to reactance, there also is a voltage drop due to the losses of the circuit. The circuit losses include the copper or load losses of the main transformer and interphase transformer, and generally can be lumped into a single resistance or voltage drop, which is equal to P_r/I_d where P_r is total resistance loss in watts, and I_d is the d-c load current of the rectifier. The resistance loss should not include the core loss of the main transformer or interphase transformer, as these losses are supplied by the a-c source with negligible regulation through the transformer. In general, the resistance losses will range from 0.9 to 1.5 per cent of the rectifier rating, or for the larger ratings (above 3,000 kw) generally about 1 per cent.

In the consideration of short-circuit and arc-back calculations, the ratio X/R is used quite often. This ratio theoretically concerns the actual value of reactance and resistance in the equivalent or simplified circuit. If the arc drop is neglected, this ratio may be approximated by the ratio X_c/R_c, where X_c is the line-to-neutral commutating reactance, and R_c the line-to-neutral commutating resistance. The value of this ratio may range from 2.5 to 8.5, with the higher values in the larger 3,000-volt rectifiers, and the smaller values in 250-volt rectifiers.

Fault Currents

In many applications, rectifiers are arranged to operate in parallel with other converting equipment such as d-c generators, synchronous converters, or other rectifiers. Arc backs in rectifiers connected to such a system are equivalent to a short circuit on both the a-c and d-c systems. In cases such as this, the winding fault current may be much greater than the 25 times normal current, which according to American Standards Association, is the maximum current a power transformer must be capable of withstanding for two seconds.

In the case of a power transformer, the number of short circuits is few, if any, during any one year and relatively few during the life of the transformer. The occurrence of arc backs in rectifiers is basically random in nature. It is apparently not practical to absolutely eliminate the possibility of arc backs. Realizing this, the transformer designer must make allowances for the cumulative effects of repeated short circuits or arc backs which may occur at a rate of several per year.

On 600-volt class rectifier transformers under conditions of fault with d-c feed, it has been found advisable to consider the stresses in the coil sections and coil leads, based upon peak currents of the order of 50 times normal rms current in the respective windings and leads.

The magnitude of fault currents, especially during arc back, is importantly influenced by saturation of the rectifier transformer core for some sequences of switching. Some data on this phenomenon were obtained using a 6-tube Ignitron rectifier fed from a 252-kva transformer in conventional delta double-Y connection, as indicated in Figure 5.

Specially designed current transformers connected within the delta of the a-c windings were used to measure the three a-c winding currents, while six shunts, one in each of the anode leads, were used to record the d-c winding currents *R1* to *R6*. Alternating current was supplied through an oil circuit breaker, and the regenerative load was connected to the set through a high-speed cathode circuit breaker. Anode circuit breakers were not used. Artificial arc backs were applied by connecting transformer terminal *R5* to the tube cathode, using a short circuiting switch.

Figure 6, traced from the oscillogram, shows the currents recorded during one test. With the rectifier carrying approximately rated load at zero phase control, the artificial arc back was initiated substantially at the end of the normal conducting period, which time of initiation may be expected to yield the maximum first cycle of fault current. Reverse power from the regenerative load was interrupted in approximately one-half cycle by the high speed cathode circuit breaker, and the fault completely cleared by the opening of the a-c circuit breaker after about ten cycles. It will be noted that during the first half-cycle of fault, windings *R2*, *R4*, and *R6* do not contribute to the fault current, while the regenerative load does. During the second half-cycle, *R6* makes a substantial contribution, *R4* begins to contribute, *R2* does not contribute, and the reverse current from the load is out of the picture. As a result, the crest value of fault current (*R5*) changes but little during the entire fault period. A large amount of test data such as this supports the contention that, when high-speed anode switching is employed, the contribution from the unfaulted Y can be neglected without significant error.

Windings *R2*, *R5*, and phase *C* are on the same core leg of the transformer. Figure 7 was obtained from an enlargement of Figure 6 by multiplying measured deflections, calibration factors, and winding turns. All curves in Figure 7 are to the same scale. The net magnetomotive forces acting on this core leg are shown by the trace phase $C-(R5-R2)$, and contains both alternating and direct components. The alternating component reaches its approximate ultimate value within about three cycles, while the d-c component continues to increase for at least eight cycles. From a comparison of the traces phase *C* and $(R5-R2)$ in Figure 7, it is apparent that saturation of the transformer core is not an important factor during the first cycle or two, but is significant later. The effect of the increased alternating component of exciting magnetomotive forces on the alternating component of current in phase *C* winding is indicated in Figure 6. The crest-to-crest amplitude of this current changes from about 1,380 to 1,430 amperes—an increase of less than five per cent.

The mechanical force acting on the phase *C* winding during this fault is proportional to the ampere turn product

Phase C by $(R5-R2)$

as obtained from Figure 7. This is a maximum at the time of the second crest of current through winding *R5* and subsequently diminishes to roughly 65 per cent of that value for the ninth crest. If the transformer core were capable of carrying unlimited flux and required zero magnetizing force (an ideal core), the phase *C* current and magnetomotive forces would not be reduced with time, but would be as shown by $(R5-R2)$ in Figure 7, and the maximum force on the winding would be sustained for the duration of the fault. Thus, in spite of an increase in alternating component of fault current in the a-c winding, it is significant that core saturation is effective in reducing the severity of the mechanical forces acting on the windings of the transformer during long faults.

In connection with the oscillogram, Figure 6, it is interesting to note that anodes *R1-R2-R3-R5* are all conducting at the instant of interruption of the a-c supply. The d-c transients, on the traces of *R5-R3-R2-R1* and all three primary phases, after interruption, are due to the dissipation of the energy stored in the magnetic field of the saturated core. This energy is dissipated as I^2R loss in the circuit and transformer and is in the same direction in all three primary phases (phase *C* is inverted in the oscillogram).

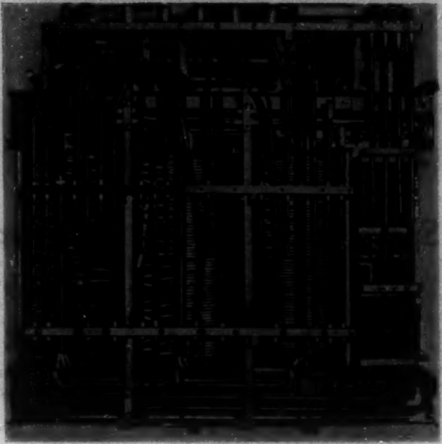

Figure 11. D-c winding leads deflected during service arc backs

Mechanical Forces

Rectifier transformers are subject to severe mechanical stresses due to abnormal currents that flow in the windings during short circuits or arc backs. Since the severest forces occur in the transformer during an arc back with d-c feed, the mechanical strength should be coordinated for this condition.

The accumulated data from laboratory tests and field experiences have contributed greatly to the art of rectifier transformer design and manufacture. These data have repeatedly substantiated the magnitude of fault currents to be expected and the destructive forces which result therefrom. In one early test a 3,000-kw 600-volt delta parallel double-Y rectifier transformer was tested to destruction by the repeated application of artificial arc backs in the laboratory. Figure 8 shows one inner coil, comprising a pair of interwound helical d-c windings, from this transformer. It will be noted that the deflections between radial spacers are greatest at the ends of the coil and are in opposite directions; that is, toward the center from each end. Electrical failure occurred at the bottom end, presumably because there the deflection between radial spacers was large enough to cause a winding-to-winding short circuit. Over-all mechanical failure of the coil also ensued as a result of the failure of the insulating member at the top end of the coil.

Figure 9 shows the transformer from which the coil, Figure 8, was taken. The repeated impacts of the large number of arc backs caused mechanical failure of the upper coil of the a-c winding. It will be noted that the coil support strips, which dovetail with the spacers between coil sections, have inched themselves upward between the upper core clamps, allowing the spacers to become detached and fall out. The resulting downward deflection of the portion of the coil thus released was unquestionably a factor in the failure of the insulating member at the top of the d-c coil in Figure 8. This a-c winding failure was due to lack of stability under repeated stressing, and not due to insufficient strength.

Figure 10 shows the deformation in bus bar leads on a rectifier transformer which was subjected to a large number of laboratory arc backs. While the deformation in the busses did not cause a failure, the need of adequate bracing is apparent.

In the design of braces for bus bar leads, it is essential that proper consideration be given to the allowable working stresses for the copper used; annealed copper has an allowable stress approximately one-third that of hard copper.

Figure 11 shows the deformation in bus rod leads on a rectifier transformer which had been subjected to a large number of arc backs with resulting d-c feed. This unit had not failed but was untanked for inspection after four years of continuous service.

Figures 8 to 11 are units of older designs and show the need of additional bracing. They are not representative of modern rectifier transformers.

Summary

This report briefly discusses the circuit, winding, structural, and electrical characteristics of rectifier transformers as they are required by the application, and as they in turn affect the over-all operation of the rectifier installation. Some data which permit approximate interpretation of rectifier transformer characteristics in terms of over-all rectifier performance are presented. The magnitude of fault currents, their frequency of occurrence, and their importance as factors in the design of rectifier transformers are emphasized. Examples of their destructive effect are cited.

Reference

1. TEST CODE FOR RECTIFIER-TRANSFORMER EQUIPMENT, American Standards Association (New York, N. Y.), *C57.28-1948*, page 11.

No Discussion

Space Code Selector Supervisory System

E. F. FORREST
ASSOCIATE AIEE

P. W. SCHIRMER
NONMEMBER AIEE

DURING the past 20 years there have been numerous supervisory systems using various designs and basic principles of transmitting signals such as tone, counting chain codes, or sequence chain codes.

The purpose of this paper is to summarize what requirements a system should meet to obtain the maximum benefits and economies from the viewpoint of the user, and to describe a commercially available equipment which meets these requirements.

Requirements

A supervisory system should fulfill the following essential operating requirements:

1. Transmit control circuit selection code and check this transmission before the control operation is performed.
2. Prevent control operation if the correct checking signal is not received.
3. Be suitable for operation over any commonly available type of channel.
4. Be suitable for operating a number of outlying stations from a single control station.
5. Components should harmonize with other switchboard devices and be suitable for building into standard switchboards.
6. Equipment should be easy to expand to take care of future growth.
7. Equipment should be easy to install, maintain, and test.
8. Be available for either 48-volt or 125-volt d-c operation.
9. Include provision for telemetering and telephone communication.
10. Should operate over the same standard range of battery voltage as the remainder of the switchgear devices.
11. Be simple and easy to operate.
12. Be rapid, uniform speed of operation for all points.

Space Code Selector Supervisory System

The system described in this paper known as the space code selector system meets these requirements. It uses a signal resembling the telegraph code which is transmitted and received by circuits composed of telephone-type relays. Where the telegraph uses short and long impulses, the space code system uses impulses of the same length. However, the time between impulses determines the code. Figure 1 shows a code consisting of two impulses. Impulse 1 is on for one unit of time and impulse 2 is on for one unit of time with one unit of time spacing between the two impulses. Thus a code with a definite number of impulses and a definite characteristic is established.

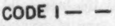

Figure 1

Again, if the same two impulses are used but the time spacing between impulses 1 and 2 is doubled, a new code results. The increased time element will be referred to as pause time. Figure 2 will show the relation between codes 1 and 2.

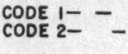

Figure 2

If three impulses are used, the codes can be increased, as shown in Figure 3, to four.

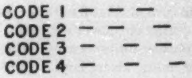

Figure 3

If four impulses are used, the codes are again increased, as shown in Figure 4, to eight.

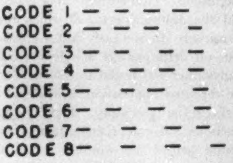

Figure 4

It is, therefore, shown that for each impulse added to the code the total number of codes is doubled. Five impulses will produce 16 codes, six impulses 32 codes, seven impulses 64 codes and eight impulses 128 codes.

A supervisory system requiring more than 128 codes would be rare. Therefore, the equipment described later is designed for a maximum of 128 code selections. The complete system of 128 codes is divided into 16 groups. Each group contains eight codes or selection points and the system may have from 1 to 16 groups depending on the number of points required. Figure 5 shows the codes used for the first eight points of 128-point system.

The codes in Figure 5 are divided into the first four impulses (point code) and the second four impulses (group code). The first four impulses with pauses denote the selection of the point within the group. The lack of pauses in the second four impulses place all the point codes in the first group.

Paper 49-272, recommended by the AIEE Substations Committee and approved by the AIEE Technical Program Committee for presentation at the AIEE Fall General Meeting, Cincinnati, Ohio, October 17–21, 1949. Manuscript submitted July 19, 1949; made available for printing September 13, 1949.

E. F. FORREST and P. W. SCHIRMER are both with the General Electric Company, Philadelphia, Pa.

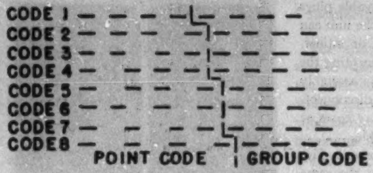

Figure 5 (left)

Figure 6 shows the relation between code 3 in the first group and code 11 in the second group. The first four impulses of code 11 are the same as the first four impulses for code three. The second four impulses have a pause inserted between impulses 4 and 5 denoting it as the third point in the second group or code 11.

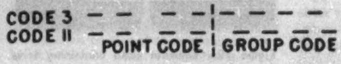

Figure 6 (left)

Figure 7 shows the relation between codes 3, 11, and 19 which are in the first, second, and third group respectively. Again the unit code is the same, but the pause between impulses 5 and 6 places code 19 in the third group. Other codes are established in the same manner.

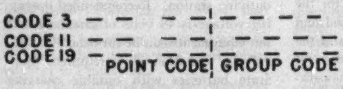

Figure 7 (left)

After the selection of a point is completed, a code of four impulses is used to perform a control operation or transmit an indication. Figure 8 shows the codes used for close and trip.

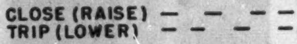

Figure 8 (left)

To complete a point selection on this system, the following steps take place:

1. The control station transmits the code for the point selection and registers its own transmission.
2. The outlying station will register this code and transmit the same code back to the control station. At the same time it registers its own transmission checking itself against the code originally received.
3. The control station registers the code received from the outlying station checking this code against the original transmission.
4. When the control station receives the same code it transmitted, a check feature is established and is so indicated by the lighting of the amber lamp, Figure 9.
5. When an automatic operation occurs, this exchange of codes is reversed.

After a point selection is completed, the check key, Figure 9, can be operated to check the indication of the point without operating the supervised unit.

This system also provides the following protection against misoperation:

1. It must always transmit and receive eight impulses for a selection.
2. It always transmits and receives four impulses for control and indication. If a selection code were to replace a control code, the receiving equipment would reset.
3. If more or less than the correct number of impulses are received due to channel interference, a selection or control will be incomplete and equipment must be reset.
4. If an impulse is received during pause time, the equipment will prevent a selection or operation.

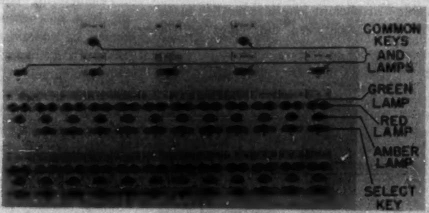

Figure 9 (right). Control and indication equipment

The system operates on a single polarity impulse and, therefore, can be used for any type of channel which will carry signal intelligence such as single polarity direct current, unmodulated carrier, single audio tone or microwave.

The equipment may be used for multistation operation where one control station will operate several remote stations. For example, a 24-point system can be divided into three remote stations with eight points in each station. Station 1 will only respond to the eight codes assigned to that station. Stations 2 and 3 will lock out until the selection established in station 1 is complete. Likewise any code assigned to station 2 will lock out stations 1 and 3. The division of points may be any multiple of eight.

Equipment

The space code selector supervisory system consists of control station equipment interconnected with one or more outlying station equipments. See Figures 9, 10, and 11. The interconnecting channel may be either a 2-conductor metallic line, a single-frequency carrier current, or microwave system.

The control station equipment, Figures 10 and 11, includes the cases containing telephone relays, a key and lamp group for control and indication of each apparatus unit, and a set of common operating keys and lamps.

Each key and lamp group, Figure 9, consists of:

1. A push button select key used to select the apparatus unit to be controlled.
2. An amber lamp to indicate that a selection has been made and checked and equipment is ready to transmit control codes.
3. Red and green lamps to provide continuous indication of the position or condition of the apparatus unit. An automatic change in position of apparatus unit will be indicated by flashing a red or green lamp.

A common key and lamp group consists of:

1. Two push button control keys "close" and "trip" controlling the selected unit.
2. A green start lamp which indicates that the equipment is in a normal at-rest position.
3. A red alarm lamp which lights whenever an operation originates at the outlying station. An alarm bell sounds simultaneously.
4. A push button bell key which extinguishes the alarm lamp and silences the bell, but does not stop the flashing of the indicating lamps.
5. A push button reset key which resets

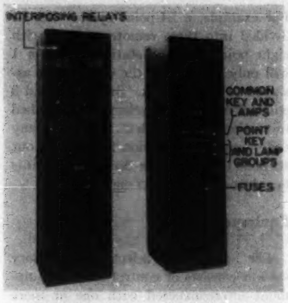

Figure 10. Front view supervisory equipment. Control station on right, outlying station on left

the equipment to its normal condition and stops the flashing of the indicating lamps.

6. A push button check key which causes the equipment to check the position of any selected apparatus unit or to perform station check operation of all points when the equipment is in a normal reset position.

The supervisory relay cases, Figure 11, consist of the following:

1. Two common cases (1 and 2) containing the supervisory relays required to transmit and receive codes for any system up to 128 points.
2. One point relay case for each eight apparatus units controlled. Point 1 is always used for station check.
3. One line case containing the equipment required to adapt the supervisory system to the particular channel involved.

The relay cases are semiflush mounted, standard switchboard type of drawout construction, see Figure 12. A flexible cable of sufficient length is used to make connections between the relays on the drawout cradle and the removable plugs at the rear of the case so that the unit can be withdrawn for inspection or adjustment of relays without disconnecting the leads, see Figure 13. The relay assembly may be entirely removed by disconnecting the plugs. The point relay cases at any terminal are interchangeable.

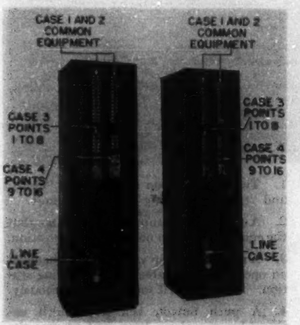

Figure 11. Rear view supervisory equipment. Control station on right, outlying station on left

The outlying station equipment, Figures 10 and 11, is essentially the same except for the substitution of interposing auxiliary relays instead of the key and lamp groups.

Future Growth

Since the common relay cases (1 and 2), Figure 11, always contain the necessary code transmitting and receiving relays for 128 points, additional points can be added in groups of eight by simply adding another point relay case. A standard switchboard unit 24 inches wide will accommodate 32 points (see Figures 10 and 11). A 28 inch unit will cover 56 points, a 32-inch unit 96 points. For systems larger than 96 points, two units are required. To facilitate easy expansion the switchboard units are originally drilled for the maximum number of point key and lamp groups and relay cases. For unequipped points the holes for the key and lamp groups are buttoned and cover plates are provided in place of the relay cases not required at that time.

Any system can be changed from operation over one type of channel to another by simply substituting the proper line relay case.

Telemetering Selection

Telemetering equipment, suitable to the type of channel used, can be connected by supervisory selection to give intermittent readings over the supervisory channel. Torque balance telemeters are used for direct metallic wire channels, and impulse or frequency-type telemeters are used for operation through insulating transformers or over a carrier current channel. A separate additional metering channel is recommended for readings directly associated with a control function, or if a continuous reading of a selected quantity is desired.

Telephone Communication

Telephone equipment can be provided to operate over the supervisory channel between the control and outlying stations. Carrier current equipments are usually provided with integral telephone equipments which do not require a supervisory selection point for ringing.

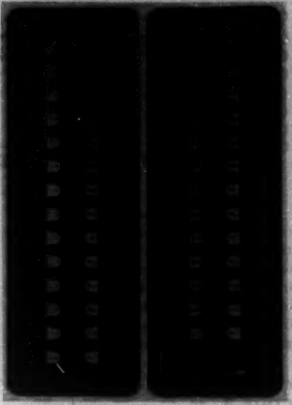

Figure 12. Drawout cases containing telephone relays. Right-hand view cover in place, left-hand cover removed

Control Power

A storage battery is required to furnish control power to the supervisory equipment at the control station and each outlying station. Recommended operating voltage is 48 volts of direct current but equipments can be furnished for 125-volt d-c operation where required. Separate batteries with suitable charging equipments are usually provided for the

Figure 13. Drawout carriage being removed from case for inspection

supervisory system, but station control batteries can be used as sources of control power provided they are ungrounded and will maintain a voltage within the operating limits of the equipment. These limits are 42 to 56 volts for 48-volt systems and 105 to 140 volts for 125-volt systems. The actual current requirements are quite low, and the continuous drain required for the average size system is approximately two amperes.

Conclusions

The space code selector supervisory system described in this paper meets all the essential operating requirements previously outlined. In the design of the equipment, special emphasis on providing maximum flexibility resulted in the following:

1. The system can be expanded to take care of future growth by the simple addition of point relay cases in the previously drilled switchboard units.

2. The system can be expanded to handle multiple outlying stations.

3. Any type of channel can be used by changing the line case.

4. The system can be furnished for either 48 or 125 volts of direct current.

5. The system can be built as an integral part of the switchboard with all devices harmonizing with standard switchboard equipment.

Discussion

W. A. Derr (Westinghouse Electric Corporation, East Pittsburgh, Pa.): Mr. Forrest and Mr. Schirmer have listed what they feel are the basic requirements of a supervisory control system without placing any particular emphasis on any of these requirements. There are two basic requirements of a supervisory control system which warrant special stress. These two basic requirements are accuracy and reliability. The degree of accuracy and reliability obtained with a supervisory control system is determined by the principle of operation and the caliber of the component parts. The list of requirements presented by the authors could be expanded to include other items which are just as important as some of those listed. Following are several such additional items:

1. The component parts should be chosen so that maintenance requirements are kept to a minimum.

2. The number of signal responsive elements at each station should be kept to a minimum.

3. Design should provide maximum flexibility as concerns the types of operations which can be performed.

4. For operation over telephone line wires the continuity of the circuit should be continuously supervised.

5. For circuit breaker operation the supervisory control itself should be inherently antipumping.

6. There should be no critical timing in the operation of the system.

An all-relay coded impulse supervisory control system known as Visicode[1,2] has been available for many years. This system meets all of the requirements listed in this discussion as well as all of those listed by the authors. In the Visicode system all impulses are of the same length and polarity. Also, the space time between impulses is not varied. Requirement number 12 in the paper is not clear. The uniform speed mentioned could refer to the operate time after selection or to the selection time itself. It is assumed that it refers to the operate time after selection. If it was meant to refer to the point selection time, the statement is not correct. Actually the system described in the paper does not have uniform selection time for all points.

The paper indicates the system described is designed for a maximum of 128 selections. While the necessity of more than 128 selections in one station is rare, the necessity of more than 128 selections for a single multistation system is not rare. There are many multistation systems in operation which already involve more than 128 selections or which are designed for expansion to more than 128 selections.

The paper states that the selection and check codes are based on differentiation between spaces of one and two units of time. However, no mention is made as to the actual length of these times. Due to the change in release time of relays over the operating voltage range, it appears that the units of space time would have to be relatively long for reliable operation if the 2-to-1 ratio is maintained.

The arrangement of the individual circuit control indicating lamps and keys as well as the arrangement of the common keys as described in the paper has been used with the all-relay coded impulse system mentioned previously[1,2] for a number of years.

The use of drawout relay cases appears to offer no advantage for the following reasons:

1. The expense of stocking completely assembled relay units probably could not be economically justified. Relatively few individual spare relays should be required for an all-relay supervisory control system.

2. Since properly applied telephone-type relays require such infrequent attention, connecting jack contacts could well result in more difficulty than the relays themselves.

3. Experience indicates that difficulty with a particular relay can best be located as it operates as part of a complete system rather than as it operates individually. Removing an assembly of relays from a switchboard panel after having located the relay in difficulty is of no more advantage than having the relays readily accessible on the switchboard.

4. The drawout case has not eliminated the necessity of unsoldering and soldering for individual relay replacement.

Figures 12 and 13 of the paper indicate that the relays employed are somewhat smaller than the type normally used. The reason for this is not obvious since there is a negligible saving in space at the possible sacrifice of durability and ease of relay maintenance.

The paper recommends the use of a separate channel for telemetered indications associated with a control function. This is an economic disadvantage since a large number of applications require telemetered indications in conjunction with control functions. It is essential to have simultaneous telemetering with the control of tap changers, speed and load control of generators, and the like. Providing a separate channel for such telemetered indications usually would be difficult to justify. The providing of telemetered indications directly associated with control functions without the use of a separate additional channel has been a standard arrangement with the Visicode system for the past 15 years. This is true for operation over telephone-type line wires and carrier or microwave channels.

The paper also indicates that a separate channel is required for any continuous telemetered reading. Providing a single continuous reading over the supervisory control channel which is only momentarily interrupted while some other operation is taking place has also been a standard arrangement with the Visicode system. The equipment can be arranged so that any one of several telemetered indications can be provided over the supervisory control channel, with the operator being provided with the necessary keys and lamps to select any one of the quantities for continuous indication. This is known as continuous selective telemetering.

A 3-wire supervisory control system with selection based on the location of long and short impulses was developed in 1923. An all-relay single channel system employing the same number of impulses for all selection codes with selection being determined by the location of long and short impulses was developed and applied by the Westinghouse Electric Corporation in 1936. The system described by Mr. Forrest and Mr. Schirmer is similar to these systems except for the use of long and short pauses between impulses instead of long and short impulses.

In conclusion, the system described in the paper does not employ operating principles which are new to the art or which have not been employed previously. However, the detailed circuit design of the system described by the authors has apparently imposed certain operating limitations which do not exist in other modern all-relay supervisory control systems.

REFERENCES

1. Development of a Two-Wire Supervisory Control System with Remote Metering, **R. J. Wensley, W. M. Donovan.** *AIEE Transactions*, volume 49, October 1930, pages 1339–43.

2. Visicode Supervisory Control, **L. J. Cissna**, *Electric Journal* (East Pittsburgh, Pa.), volume 28, July 1931, pages 424–30.

G. S. Lunge (General Electric Company, Schenectady, N. Y.): It is interesting to compare the characteristics and construction of the supervisory control system described by the authors with the type of code selector supervisory control equipment built for many years by the same manufacturer and of which there are numerous installations still in operation.

The older equipment utilized selection codes consisting of combinations of impulses of two different polarities. Where a direct metallic pilot wire channel without insulating transformers was not available, two audio-frequencies ordinarily were used to represent the two polarities required. Thus a simple telegraph-type channel, such as an unmodulated carrier pilot relay channel, to handle impulses of one polarity only would not have been enough. This was a particularly severe handicap for carrier supervisory control applications.

Instead of using only one length of impulse and two widely different lengths of spaces between impulses, the older equipment used three different lengths of impulses, thus requiring more careful relay timing adjustment to distinguish between them.

Only one (long) impulse was used for the final control (close or trip) operation, whereas now a 4-impulse code is used for this, for greater safety.

The older equipment was designed for 125-volt battery operation only and also required a mid-tap from the battery, whereas the equipment described in the paper can be designed for either 48 volts or 125 volts and needs no mid-tap from the battery. In common with most types of supervisory control equipment, it was not convenient to add to it beyond the number of points for which wiring and drilling had been provided in the initial equipment.

The older (polarized) code selector supervisory equipment contained, besides many telephone-type relays, numerous step-by-step selectors similar to line switches used in automatic telephone practice. These selectors required occasional lubrication and adjustment. In contrast to this, the supervisory equipment described in the paper is an all-relay system intended to operate without maintenance other than periodic inspection.

E. F. Forrest and **P. W. Schirmer:** The authors wish to thank the discussors of this paper for their remarks and for calling attention to some additional requirements which were not specifically mentioned. The supervisory system described in this paper meets all the requirements outlined by Mr. Derr in the opening paragraph of his discussion.

The time required to complete a point selection (select a point and check the selection) with the supervisory system described in this paper is approximately 2.5 seconds ± 0.3 seconds. This variation in selection time is so small that in ordinary operation it is very difficult to detect. The operate time after selection is always uniform.

In the design of a standard supervisory system such as this, it is very desirable to include initially in the common equipment all of the components required to transmit and receive the number of codes that ultimately might be required in the majority of cases. From the nature of the scheme it is evident that 128 is not an inherent limit on the number of points for which the base equipment could be designed. However, our experience shows that even multistation systems requiring more than 128 selections are very rare. An important feature of this standard design is that the first two relay cases always contain the necessary relays required to transmit and receive the codes for the maximum number of points, and expansion up to that point can be accomplished by the addition of "point" relay cases without modifying the basic common equipment.

The supervisory system described in this paper does not necessitate the use of a separate channel for telemetered indications. Selected or continuous readings, interrupted only momentarily while control or indication codes are being transmitted, can be transmitted readily over the supervisory channel. However, if uninterrupted readings are necessary, a separate telemetering channel is required. Even a separate channel does not necessarily mean a separate pair of wires, as several channels can be provided over one pair of wires by the use of audio-tone equipment or over carrier by the use of a number of different frequencies.

The drawout relay case construction used in this design was not adopted to make possible the stocking of completely assembled relay units nor to make it easier to locate troubles and replace relays. However, in some installations, these points do have some merit. The primary reasons for utilizing the drawout relay case construction are as follows:

1. The common or basic equipment required to transmit and receive codes for the maximum number of points can be included in two standard cases (numbers 1 and 2). Any size system can be built or expanded up to the maximum without modifying this basic equipment.

2. A system can be expanded to take care of future growth by the simple addition of point relay cases. It is much simpler to install and connect complete relay cases than individual telephone relays.

3. Special features or channel conditions can be accommodated by varying the components in the line case. This makes it possible to change the type of channel or operating features after an equipment has been installed by changing the line case without modifying the basic supervisory system.

4. The drawout relay case provides a dust-proof construction which harmonizes with standard switchboard devices.

The telephone-type relays used in this equipment were selected as a result of extensive tests on the many available types, some of which were the result of wartime developments for the aircraft industry where light weight and extreme reliability were major requirements. The selection was made primarily upon the basis of reliability and long life, size having been a secondary consideration. These comparative tests led to the conclusion that the type selected was the best available regardless of size. Some of the features described in the paper obviously were not new, but we believe it is fair to say that the salient ones, such as drawout relay cases containing standard assemblies that can be put together to build any size system, in general represent definite improvements over previous designs.

A Convenient Method for Determining Generator Reserve

HOWARD P. SEELYE
FELLOW AIEE

THE study of generator reserve requirements by methods using probability mathematics has received a considerable amount of attention in recent years and several papers have been published describing such methods. For the most part the calculations required are quite long and involved, and the underlying principles are somewhat complex. Although appreciable benefits are to be derived from studies of system reserve requirements by these means, it is doubtful if they have had very general or widespread use. There would seem to be a need for some short, direct method or guide whereby any system could arrive at the order of its reserve requirements directly, provided certain simple basic factors are known.

In a paper presented in 1947[1] certain rather simple algebraic formulas for the study of the reserves necessary to take care of forced or emergency outages of generators were developed, and their method of application was indicated. These formulas provided for the use of individual basic data as to average frequency and duration of outage for the system being studied. They also cover the use of any variety of different sizes of machines and different running times. It was indicated in that paper, however, that for most systems, consisting of a diverse assortment of generator sizes, the work could be greatly simplified and no great error introduced, if it were assumed as an approximation that all of the machines were of the same size, that is, the average for the system.

This simplified approximate method now has been extended to the development of a few charts whereby the percentage of reserve in terms of total system capability or total system load may be found directly. These charts are given in this paper with a brief explanation of how they were derived from the preceding paper and how similar charts for other variations could be determined if required.

Basic Formula

The formula given in the preceding paper,[1] which is used in developing the charts, is as follows:

The expectancy of outages of *j machines or more*, is

$$E_{j+} = \left(\frac{n}{T}\right)^j \frac{d^{j-1}}{(j-1)!} \epsilon^{-\frac{nd}{T}}$$

where

n = the number of generators running
d = the average duration of individual outages (in years)
T = the average interval between individual outages (in years)
j = the number of generators out at the same time
ϵ = the base of Naperian logarithms, 2.7183

An outage refers to the whole group of individual generator outages characterized by j, the largest number of generators out together at any time during the continuous duration for the whole group. E_{j+} is the expectancy, given in terms of a decimal. For example, if $E_{j+} = 0.05$ it means that the outage of the corresponding j machines (three perhaps) *or more* may be anticipated 5/100, or five times in 100 years, or once in 20 years on the average.

The quantities d, the average duration of individual outages, and T, the average interval between outages can best be obtained from records on the system being studied, if such records are available. If not, they may be assumed from the records of other systems, national averages, or other such sources, or they may be estimated from experience. For example, an average of one outage each two years ($T = 2$) of an average duration of one week ($d = 0.02$) might be assumed to apply.

Application of Average Size

As explained previously, the formula can be applied directly if all of the machines on the system are of the same size and have the same percentage of running time to total time, or a good approximation reached if all machines are assumed to be of the same size, that is the average size, and to have the same average running time. Figure 3 of the previous paper shows how a simple chart can be plotted with such average values. For this chart the basic outage data $d = 0.02$ and $T = 2$ were chosen. It also was assumed that an expectancy of once in 30 years would be satisfactory ($E_{j+} = 0.033$) that is an outage would not be expected to equal or exceed the reserve oftener than once in 30 years. This chart is repeated here as Figure 1 for reference. The curve shows the relation between the total number of generators and the indicated total reserve required—150 megawatts for 15 machines for example.

Development of New Charts

It is a rather obvious operation to convert the lower scale of this chart, which now shows megawatts of reserve, to *number* of generators (of average size) which should be in reserve by dividing by the average size. If the average size were 50 megawatts for example, the scale divisions would read 1, 2, 3, 4, and 5. It also is quite obvious that by a further conversion the curve could be replotted to show

---

Paper 49-278, recommended by the AIEE Joint Subcommittee on Application of Probability Methods to Power System Problems and approved by the AIEE Technical Program Committee for presentation at the AIEE Fall General Meeting, Cincinnati, Ohio, October 17-21, 1949. Manuscript submitted June 17, 1949; made available for printing September 1, 1949.

HOWARD P. SEELYE is Chief Engineer of the Engineering Department of The Detroit Edison Company, Detroit, Mich.

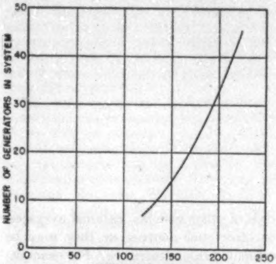

Figure 1. Variation of reserve requirement with number of generators

Average size of generators = 50 megawatts
Reserve will not be exceeded oftener than once in 30 years
Average interval between forced outages of each generator = 2.0 years running time
Duration of outages = 0.02 year

the percentage of the total number of generators which should be held in reserve.

The values for this replot would be obtained by dividing the number in reserve by the total number of generators for various points along the curve.

This is essentially the method used in obtaining the curve shown in Figure 2. The percentages are determined directly by calculation, without the intermediate steps just described.

The method can probably best be illustrated by a sample calculation:

$$E_{j+}=\left(\frac{n}{T}\right)^j \frac{d^{j-1}}{(j-1)!}\,\epsilon^{-\frac{nd}{T}}$$

If $E_{j+}=0.033$; $d=0.02$; $T=2$

Then

$$0.033=\left(\frac{n}{2}\right)^j \frac{0.02^{j-1}}{(j-1)!}\,\epsilon^{-0.01n}$$

For a system with 20 generators, with average running time 75 per cent

$$n=0.75\times 20=15$$

$$0.033=\left(\frac{15}{2}\right)^j \frac{.02^{j-1}}{(j-1)!}\,\epsilon^{-0.15}$$

This equation may be solved for j by calculating the value of the left-hand member for various simple values of j and then interpolating to obtain the value of j corresponding to $E_{j+} = 0.033$.

$$\text{If } j=2 \ldots \frac{15}{2}\Big)^2 \frac{0.02^{(2-1)}}{(2-1)!}\,\epsilon^{-0.15}=$$

$$7.5^2\times 0.02\times 0.86071=0.9683$$

$$j=3 \ldots\ldots \left(\frac{15}{2}\right)^3 \frac{0.02^{(3-1)}}{(3-1)!}\,\epsilon^{-0.15}=$$

$$7.5^3\times\frac{0.0004}{2}\times 0.86071=0.07262$$

$$i=4 \ldots\ldots \left(\frac{15}{2}\right)^4 \frac{0.02^{(4-1)}}{(4-1)!}\,\epsilon^{-0.15}=$$

$$7.5^4\times\frac{2^3\times 10^{-6}}{6}\times 0.86071=0.003631$$

It has been discovered that the plotted curve of j against n is approximately a straight line on semilog paper. The value of j corresponding to $E_{j+}=0.033$ may therefore be calculated by use of the formula

$$j=3+\frac{\log E_3-\log E_j}{\log E_3-\log E_4}=$$

$$3+\frac{\log 0.07262-\log 0.03333}{\log 0.07262-\log 0.003631}$$

$$=3+\frac{0.33822}{1.30103}=3.260$$

Converting to percentage of total generators, 3.260/20 = 16.3 per cent.

Similarly, for a system with 40 generators, 75 per cent running time, n = 30.

$$E_{j+}=0.033=\left(\frac{30}{2}\right)^j \frac{0.02^{j-1}}{(j-1)!}\,\epsilon^{-0.3}$$

For

$$j=2 \ldots\ldots 15^2\times 0.02\times 0.74082=3.3337$$
$$j=3 \ldots\ldots 15^3\times 0.0002\times 0.74082=0.5000$$
$$j=4 \ldots\ldots 15^4\times 1.33\times 10^{-6}\times 0.74082=0.05000$$
$$j=5 \ldots\ldots 15^5\times 0.667\times 10^{-8}\times 0.74082=0.00375$$

$$j=4+\frac{\log 0.04995-\log 0.0333}{\log 0.04995-\log 0.003746}=4.1566$$

In percentage of total number of generators 4.1566/40 = 10.39 per cent.

Criterion for Expectancy

It would seem that an outage which would be expected to occur somewhat less frequently than once in 30 years could be reasonably faced without providing full reserve for it. That is, such an outage might require unusual measures of dropping voltage or frequency or even of some load. This period has, therefore, been used as the criterion for expectancy throughout all of the calculations in this paper and the charts shown: $E_{j+} = 0.033$. The reserve provided by this criterion would take care of all outages which might be expected more frequently than once in 30 years, and also would take care of most of the amount of the outage in the more infrequent cases where the reserve would be exceeded. Similar charts could be calculated by the methods indicated for other expectancies such as once in 20 years or once in 50 years. It should be noted, however, that, as was indicated in the preceding paper, the curve between reserve and expectancy is relatively steep in this range and not much advantage is gained for the more frequent expectancy nor is the penalty very large for the less frequent one. The effect would be approximated from the charts given here, if desired, by slightly modifying the reserve percentages indicated.

Reserve in Terms of Load

In Figure 2, the per cent reserve is expressed in terms of the total capability of the system. It is probably more frequently desired to have reserve in terms of system load. When loads are estimated in advance, the total capability which should be provided to serve them will be at least equal to the load plus the necessary amount of reserve. In most cases it will be more convenient to know the capability needed for a given load than the load for which a given capability will provide. In the calculations here described it has been assumed that the capability remaining after the greatest outage within the expectancy used would be sufficient to carry the load. It is a simple matter, therefore, to convert the reserve percentage in terms of capability to reserve percentage in terms of load. For the 40-generator example used previously, the reserve indicated was 10.39 per cent of capability

$$\frac{10.39}{100-10.39}=11.6 \text{ per cent of load}$$

Figure 3 has been plotted on this basis.

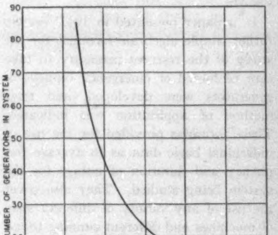

Figure 2. Generator emergency reserve in per cent of system capability

Reserve will not be exceeded oftener than once in 30 years
Average interval between forced outages of each generator = 2.0 years running time
Duration of outages = 0.02 year
Average running time = 75 per cent

Variations in Basic Data

In order that the charts may be useful for a wide variety of local conditions, the effect of several variations in the basic data is included in them, as follows:

Variation in Outage Frequency: The average frequency of individual outages may vary considerably with different systems, depending on type of equipment, maintenance policy, loading and operating practices, and other local conditions. Separate curves have therefore been plotted on Figure 3 for several values of average interval (*T*), namely 1.5, 2, and 2.5 years respectively. The curves are approximately parallel so values for other intervals such as $T = 1$ or $T = 3$ or for intermediate values can be approximated easily if needed.

Variation in Average Length of Outage: The average length of individual machine outages used in calculating the charts was $d = 0.02$, or approximately one week. On some systems the average outage period may be appreciably different. A variation in this factor makes a variation in the reserve values throughout the range of the chart, which may be approximated by applying a constant percentage of change to each of these values. Figure 4 gives these modifying percentages for any change in *d* from the assumed value of 0.02. For example, if the average duration of outage were 0.03 (about 11 days) the reserve would be about 13 per cent greater than the value obtained from Figure 3 for the system in question. For a system of 30 generators with $T = 2$, the figure shows 14.3 per cent reserve. For $d = 0.03$ this would become $14.3 \times 1.13 = 16.2$ per cent.

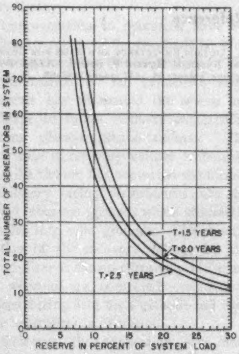

Figure 3. Generator emergency reserve in per cent of system load

Reserve will not be exceeded oftener than once in 30 years

T = average interval between forced outages of each generator in years of running time

Duration of outages = 0.02 year

Average running time = 75 per cent

Variation in Running Time: In the calculations for Figure 2 and 3, an average running time of 75 per cent of total time was used for all generators. If a different value is experienced, the reserves obtained from the charts will be varied accordingly. The effect may be approximated by a constant percentage applied to the whole range of values. These percentages for any variation for the assumed 75 per cent are shown in Figure 5. For example, if the average running time is only 60 per cent, the reserve values given by Figure 3 should be reduced by about 8 per cent. For the 30 generator system, therefore, the reserve required would be reduced from the 14.3 per cent given by the chart to $14.3 \times 0.92 = 13.2$ per cent.

New Charts: The effect of the several variations have been indicated by the supplementary curves and charts for convenience in using them for a specific problem without appreciable calculation. If frequent use of the charts is to be made with such variations, it will be more satisfactory to alter the chart scale accordingly or plot a new chart for the individual conditions.

Use of Charts

The practical use of the charts is fairly obvious and has been pretty well indicated in the preceding discussion. They are particularly applicable to systems having all steam-driven generators for which seasonal variations in availability are not a large factor, as might be the case with hydro. It also was assumed initially that the system would have seasonal variations in load which would provide margins of capability and these would be quite fully used for scheduled maintenance. On such a system, an outage at one time of the year is just as important as one at any other time, so the basic data have all been taken on a full yearly basis. For other conditions, the results could be modified, of course, as was indicated in the preceding paper.

For any system which reasonably well fits these conditions, if the values of the basic data (*T*, *d*, and running time) are known, or can be assumed, the charts will give a good idea of the order of the reserve required for emergency outages. Referring to Figure 3, a system with 15 generators should have about 25 per cent of its peak load as reserve ($T = 2$) to meet the criterion of not being exceeded by an outage oftener than once in 30 years. If, however, the system increases so as to have 25 generators, the reserve percentage need be only about 16.5 per cent. If the latter system is interconnected with another system having 20 generators, or 45 in all, the reserve for the pool need be only 10.7 per cent. The advantage of interconnection in reducing required reserve is evident. It is interesting to note, however, that this advantage becomes progressively smaller as the pool grows larger, the curves becoming relatively steep.

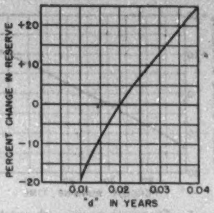

Figure 4. Change in reserve with variation of duration of outage

In per cent of reserve for $d = 0.02$

It is significant that these charts show the reserve required as dependent upon the number of machines rather than upon their ratings. A system would require less reserve for 30 machines than for 20 even with the same system load. This is reasonable since a large machine is just as likely to go out as a small one but the effect of an outage on the total system capability will be much greater with the larger one. The magnitude of this factor in the decision on the size of a new generator for a system might be approximated from the chart.

Smaller Systems

For systems with a comparatively small number of generators, say less than 15, the charts are not as applicable in the form given as they are to larger systems. This is due to the fact that individual generator units are a larger percentage of the total capability, and the assumption of a smooth curve rather than a stepped curve, for the relation between reserve and the expectancy of its use, upon which this development was based, may lead to appreciable discrepancies. This was shown in the previous paper in its Figure 1. The greater the diversity in the sizes of the machines used, the nearer the smooth

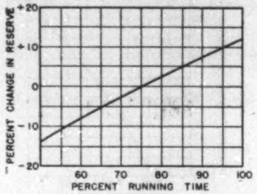

Figure 5. Change in reserve with variation of running time

In per cent of reserve for per cent of running time = 75

curve will fit, since there are more intermediate values of possible outage. For the extreme case of all machines of the same size, the problem may better be considered from the standpoint of the order of protection which is provided by one, two, or three units as reserve.

Figure 6 has been developed to show this, using the same basic data as for the previous charts, that is $T = 2$, $d = 0.02$, and 75 per cent running time. It is plotted on semilog paper for convenience. The left-hand curve shows the expectancy of a simultaneous outage of two units or more in terms of the average expected interval in years. The right-hand curve shows the expectancy of outage of three units or more.

For example, on a system having five units, a 2-unit outage (or more) might be expected about once in 15 years, hence one of the five generators (20 per cent of capacity or 25 per cent of load) in reserve would protect against the more frequent occurrence of less magnitude. On the other hand, a 3-generator reserve would probably never be called upon, the expectancy of such an outage being of the order of hundreds of years, and there are no intermediate possibilities, assuming all units to be the same size. Similarly, for a 10-generator system, a single generator reserve (10 per cent of capacity or 11.1 per cent of load) would be exceeded by an outage of two units or more once in four years.

If such operation is not to be tolerated, a 2-unit reserve (20 per cent of capacity or 25 per cent of load) would be required and this would be exceeded by an outage of three or more units once in 100 years, and should therefore be very good protection.

It should be kept in mind that comparisons of the figures taken from Figure 6 should be made with those from Figure 2 rather than Figure 3 since Figure 2 and Figure 6 are both in terms of generator capability, whereas Figure 3 is in terms of load. For 10 generators, Figure 2 would indicate a reserve of about 25 per cent for a 30-year criterion, or $2^1/_2$ generators. This is intermediate between the 4-year interval for two generators and the 100-year interval for three generators from Figure 6.

Other Reserves

It should be emphasized that the reserve covered by the calculations and charts in this paper are only the reserves for emergency outages of generators. On many systems, additional reserves will be found advisable or necessary to provide for scheduled maintenance or for unforeseen loads or other conditions. It is recognized that these matters are part of the total consideration of reserves, but they are subject to other controlling factors than those upon which this present study has been based. It is believed that for the purpose of getting a quick estimate of the reserves required for emergency outages, without prolonged calculations, these charts will be found very useful to many power systems. It must be recognized, however, that neither this method nor that of the longer more accurate calculations can be depended upon solely to give the final answer. They are at best merely guides and the results indicated must always be tempered and qualified by good judgment based upon experience and the peculiar conditions of the case being studied.

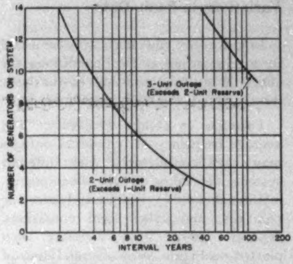

Figure 6. Protective value of 1-unit and 2-unit reserve of small systems

Average running time = 75 per cent

Reference

1. OUTAGE EXPECTANCY AS A BASIS FOR GENERATOR RESERVE, Howard P. Seelye. *AIEE Transactions*, volume 66, 1947, pages 1483–88.

No Discussion

Operation of a Ground-Fault Neutralizer on a Regulated Distribution System

H. R. TOMLINSON
MEMBER AIEE

F. B. HUNT
ASSOCIATE AIEE

ARCING grounds occurring on an underground delta-connected distribution system produce oscillatory overvoltage stresses which result in simultaneous failures of the cable insulation. These have been the predominant cause of primary circuit outages in the operation of a 2,400-volt ungrounded, distribution system serving a load of 12,000 kva in five square miles of urban territory. With a view toward improving service by the suppression of arcing grounds, a ground-fault neutralizer has been installed in accordance with the well-known neutralizer theory.

Improvements to operation have resulted by reason of the two basic benefits to be gained by the neutralizer. The neutralization of the capacitive fault currents has eliminated the severe arc damage to cables formerly experienced during phase-to-ground failures. The slow rate of recovery voltage tending to restrike the arc has converted the former oscillatory arcing disturbances into delayed recurrent grounds which ultimately resolve into solid grounds. This modification of the recovery voltage by the neutralizer is shown effectively in Figure 1, wherein are compared oscillograms taken during field tests without and with the neutralizer in operation.

However, the application of a neutralizer to a distribution system has given rise to some special problems, particularly by the effects of the zero sequence voltages produced by single-phase feeder voltage regulators. These effects have been analyzed for both ground-free and grounded conditions, after having been observed during field tests. Field tests also have been made to accumulate oscillograph records of the recovery voltages obtainable on an extensive cable system by variations of neutralizer tuning, in addition to wave form records of the fault currents.

Description of System

The distribution system on which the neutralizer has been applied is supplied by a substation having delta-connected step-down transformers of 17,000-kva total capacity, and consists of 15 primary circuits each of which is regulated by two single-phase induction regulators connected in open delta. Feeder primaries, which for the most part are underground, utilize 141 conductor miles of single-conductor lead-sheathed cable. The ground fault current of this primary system, previous to the neutralizer installation with 2,400 volts maintained on the bus and all feeder regulators in neutral positions, was 47 amperes.

The neutralizer equipment consists of three standard distribution transformers connected 2,400 volts Y-grounded to 240 volts open-cornered delta, with three air-core current-limiting reactors connected in series across the opened corner to control the quadrature lagging neutralizer current. This arrangement was selected for the reason that current-limiting reactors of the proper ohmic value were available for this use. The neutralizer performs the same as one with $(N/3)^2$ ohms reactance installed in the primary neutral, where N is the transformation ratio of the neutral deriving transformer.

The neutralizer equipment is connected to the station service feeder which is unregulated and at all times energized from the operating main bus.

When the system is in normal operation, the cable capacitance and the neutralizer inductance are in series resonance. This is changed to parallel resonance when a ground fault occurs. Hence, the application of a neutralizer to a regulated distribution system requires an analysis of the effects of feeder voltage regulators on the two resonant circuits.

This discussion will be confined to the effects of open delta-connected regulators. However, similar results will be obtained with other single-phase regulator connections.

Zero Sequence Voltage Due to Regulators

The open delta-connected regulators in any off-neutral position cause a zero sequence voltage to be impressed upon the series circuit containing the neutralizer inductance and cable capacitance. As shown in Figure 2, the vector representation of this voltage can range from the system neutral to any point within a rhombus, the center of which is at the neutral of the bus voltages, and the major and minor axes of which are $E_R/\sqrt{3}$ and $E_R/3$ respectively. The maximum zero sequence voltage, as resulting from all regulators being in the extreme positions, is in phase with or in phase opposition to the neutral voltage

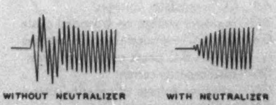

Figure 1. Oscillograms of recovery voltages

Paper 49-282, recommended by the AIEE Protective Devices Committee and approved by the AIEE Technical Program Committee for presentation at the AIEE Fall General Meeting, Cincinnati, Ohio, October 17–21, 1949. Manuscript submitted July 18, 1949; made available for printing September 8, 1949.

H. R. TOMLINSON and F. B. HUNT are both with the New England Power Service Company, Boston, Mass.

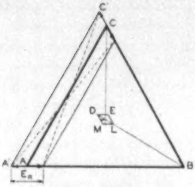

Figure 2. Range of zero sequence voltage due to voltage regulators

ACB—bus voltages

AA', *CC'*—regulator voltages

DELM—range of zero sequence voltage

E_R—voltage range of regulators

$DL = \frac{E_R}{\sqrt{3}}$; $EM = \frac{E_R}{3}$

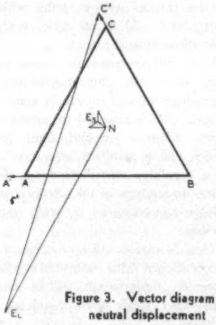

Figure 3. Vector diagram of neutral displacement

ACB—bus voltages

AA',*CC'*—regulator voltages

NE_s—zero sequence voltage

NE_L—quadrature voltage on neutralizer

E_LC'—maximum voltage to ground. Based on resonant tuning and coil constant = 40

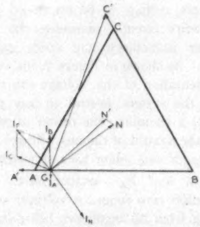

Figure 4. Vector diagram during fault

ACB—bus voltages

AA', *CC'*—regulator voltages

AG—regulator voltage on grounded cable

GA', *GB*, *GC'*—ground-to-phase voltages

I_A, I_B, I_C—A-B-C phase capacity currents

GI_F—total capacity current

GN'—effective voltage of capacity current

GN—voltage on neutralizer

GI_N—neutralizer current

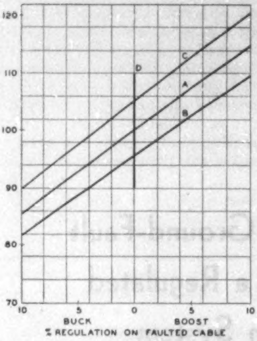

Figure 5. Range of capacity and neutralizer currents

A—neutralizer current

B—minimum capacity current (regulators full boost)

C—maximum capacity current (regulators full buck)

D—capacity current unregulated cable grounded

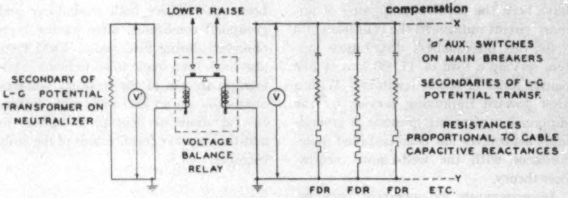
TO
NEUTRALIZER REGULATOR
LOWER RAISE
SECONDARY OF L-G POTENTIAL TRANSFORMER ON NEUTRALIZER
V'
V
VOLTAGE BALANCE RELAY
X
"a" AUX. SWITCHES ON MAIN BREAKERS
SECONDARIES OF L-G POTENTIAL TRANSF.
RESISTANCES PROPORTIONAL TO CABLE CAPACITIVE REACTANCES
Y
FDR
FDR
FDR
ETC.

Figure 6. Control scheme for zero sequence compensation

to the unregulated phase, depending on whether the regulators are bucking or boosting the bus voltages. This maximum voltage is considered in the following in order to determine the greatest effects upon the resonant circuits.

The Series Resonant Circuit

When the neutralizer is exactly tuned to the system capacitance, the zero sequence voltage causes a current to flow through the series resonant circuit limited only by the resistance component of the circuit. This current in the neutralizer causes a quadrature leading voltage drop across the inductance equal in magnitude to the resistance drop across it multiplied by its coil constant (coil constant equals ratio of reactance to effective resistance).[1] This quadrature voltage is impressed between ground and the system virtual neutral, and, as shown in Figure 3, causes a maximum voltage to ground several times the value of the normal phase-to-ground voltage. On a system with regulators having an over-all range of 20 per cent, this overvoltage to ground may be four to five times normal, which is counter to the purpose of the neutralizer and indicates that a method must be devised to imit the maximum ground voltage to a tolerable value.

The Parallel Resonant Circuit

In parallel resonance, as when a ground fault occurs on the system, any combination of regulators in the off-neutral position produces different effects in the two parallel branches, and hence complete neutralization of the capacity current under these conditions is not possible without compensating action. The effective voltage on the neutralizer is the ground-to-neutral voltage (zero sequence) of the unregulated system, whereas the voltage producing the flow of capacity current is the ground-to-neutral voltage (zero sequence) of the regulated system.

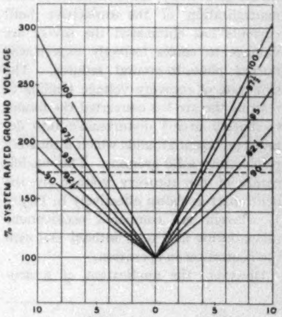

Figure 7. Maximum line-to-ground voltages. Based on neutralizer coil constant of 40

Dotted line is system rated phase-to-phase voltage. Figures on lines are neutralizer tuning in per cent of resonant value

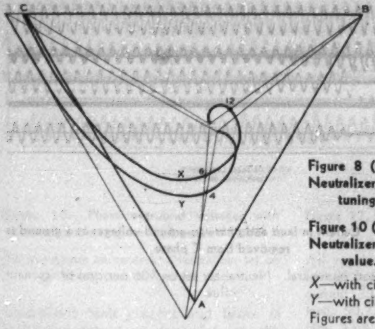

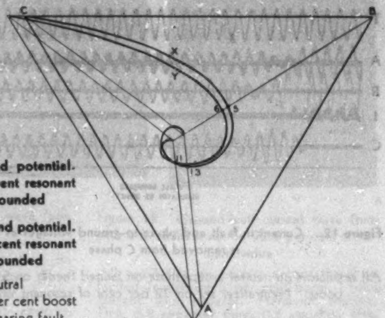

Figure 8 (left). Locus of ground potential. Neutralizer adjusted to 91 per cent resonant tuning. Regulated phase grounded

Figure 10 (right). Locus of ground potential. Neutralizer adjusted to 106 per cent resonant value. Regulated phase grounded

X—with circuit regulators on neutral
Y—with circuit regulators on 5 per cent boost
Figures are time in cycles after clearing fault

The first is affected only by the regulator on the faulted cable, the latter by all regulators on the system including that on the faulted cable. The vector difference of these two ground-to-neutral voltages is the zero sequence voltage of the feeder regulators. This voltage produces a residual current in the fault which has a maximum value, when referred to the capacitive fault current with no regulation, equal in percentage to the regulating range of the feeder regulators. The vector representation of a ground fault is shown in Figure 4, which is based on the case of all feeder regulators in the maximum boost position except the one on the faulted cable, which is in the maximum buck position. This is an improbable operating condition, but it clarifies the effects of regulators on the ground-to-neutral voltages. The residual fault current is the resultant of the neutralizer and capacity currents.

The position of the regulator on the faulted cable establishes the ground reference of the neutral voltages, and thereby affects both the magnitudes and angular positions of the effective voltages on the neutralizer and on the system capacitance. Hence an analysis of the currents resulting from these voltages must be referred to the position of the regulator on the faulted cable. This is done in Figure 5, wherein is shown the range in magnitude of the currents in the neutralizer and capacitance circuits.

As shown by line *A* in Figure 5, the maximum neutralizer current occurs when the regulator on the faulted phase is in the extreme boost position, and hence the current and kilovolt-ampere rating of the neutralizer equipment must be adequate for the conditions imposed on it by the extreme boost position of any regulator on the system.

The magnitude of the capacitive fault current is similarly affected by the operation of the regulator on the faulted phase, and, in addition, varies between lower and upper limits because of the operation of the system regulators. Lines *B* and *C* in Figure 5 are the lower and upper limits of capacitive currents obtainable within probable operating conditions. Both Figures 4 and 5 indicate that maximum capacitance currents result when the system regulators are in maximum buck positions.

Line *D* in Figure 5 indicates the range in magnitude of the resultant capacity current when a ground occurs on the unregulated phase.

Control of Ground Voltages

By reason of the regulator action, it is evident that a means must be devised to limit the ground voltages during normal operation when a neutralizer is applied to a regulated system. The following three methods are suggested to accomplish this:

1. Install voltage regulators on the neutralizer circuit.
2. Insert reactance in the series circuit by avoiding resonant tuning.
3. Install a saturable core reactor in the neutralizer.

A discussion of each method and their effects during ground fault and normal conditions follows:

1. By equipping the neutralizer circuit with voltage regulators, a compensating zero sequence voltage can be impressed on the neutralizer equal to the same effective voltage on the cable capacitance.

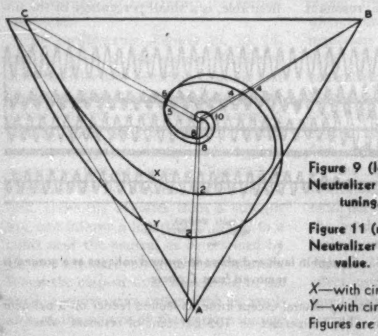

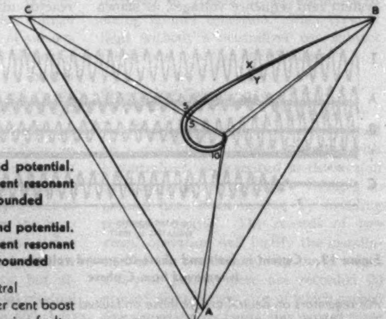

Figure 9 (left). Locus of ground potential. Neutralizer adjusted to 72 per cent resonant tuning. Regulated phase grounded

Figure 11 (right). Locus of ground potential. Neutralizer adjusted to 91 per cent resonant value. Unregulated phase grounded

X—with circuit regulators on neutral
Y—with circuit regulators on 5 per cent boost
Figures are time in cycles after clearing fault

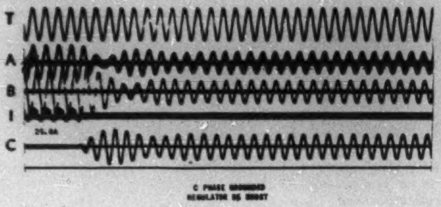

Figure 12. Current in fault and phase-to-ground voltages as a ground is removed from C phase

All regulators on neutral except those on faulted feeder on 5 per cent boost. Neutralizer set on 72 per cent of resonant value

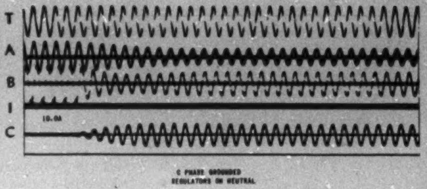

Figure 14. Current in fault and phase-to-ground voltages as a ground is removed from C phase

All regulators on neutral. Neutralizer set on 106 per cent of resonant value

During normal conditions the neutralizer and the system will assume the same neutral, no series resonant current will flow, and the performance will be the same as on an unregulated system. During a ground fault, the effective ground-to-neutral voltages on the neutralizer and the cable capacitances will be the same, hence neutralization of the fault current is obtainable. The performance during fault conditions will be the same as on an unregulated system except that the magnitudes of both quadrature currents will be influenced by the operation of the feeder regulators. The magnitude of the maximum current and voltage thus obtainable defines the rating of the neutralizer equipment.

The neutralizer regulators must have sufficient range to correct for other zero sequence contributions, such as unbalances in cable capacitances, in order to eliminate completely the undesirable effects of series resonance.

The main problem is to make the neutralizer regulators automatically responsive to the ever-changing zero sequence voltage of the system regulators. A suggested method is to use a voltage-balancing relay to match the neutralizer and the system zero sequence voltages, as shown in Figure 6. Line-to-ground potential transformers with loading resistors proportionate to cable capacitive reactances are employed on each feeder, and all are paralleled into the voltage matching relay which operates the neutralizer regulator until V' equals V. An identical control is required for each regulated phase.

By the elimination of neutral displacement, correct indications will be obtained on bus-connected ground-detecting equipment usually employed on ungrounded delta systems. This method also allows for the use of sensitive current or potential ground-indicating relays with the neutralizer equipment.

2. By avoiding resonant tuning with the neutralizer reactor, a net reactance will be inserted in the series circuit, which provides a ready means for controlling the extent of the neutral displacement. Inductive reactance of less than the resonant value will cause leading currents in the series circuit, and greater values will cause lagging currents to flow.

During normal conditions, any net reactance will result in a reduction of the maximum voltage to ground, the amount of which will be approximately the same for equal deviations of the neutralizer reactor above and below the resonant value. Figure 7 shows the resulting voltages to ground obtainable by a series capacitive circuit and with a neutralizer coil constant of 40.

As a precaution against the system resolving into tuned series resonance because of a switching operation, such as the clearing of sectionalizing fuses or the automatic operation of a feeder main circuit breaker, it is advisable to adjust the reactor to an ohmic value less than for resonant tuning, as shown in Figure 7. Planned switching operations that may result in additional capacitance to the system can be provided for by a preliminary adjustment of the reactor to the new conditions.

It is possible that the magnitude of the series current will exceed the required quadrature neutralizing current, in which case the series current will define the rating of the neutralizer equipment.

When a ground fault occurs on the system, the detuning of the neutralizer within the limits of 85 to 115 per cent of the resonant value has no serious detrimental effect on either the arc neutralization or the recovery voltage characteristics. It causes a fundamental frequency residual fault current which, although not desirable, is a small percentage of the un-

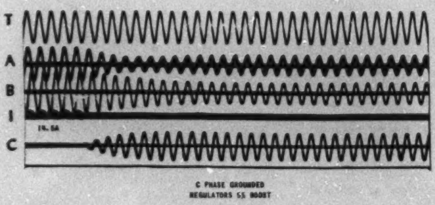

Figure 13. Current in fault and phase-to-ground voltages as a ground is removed from C phase

All regulators on neutral except those on faulted feeder on 5 per cent boost. Neutralizer set on 91 per cent of resonant value

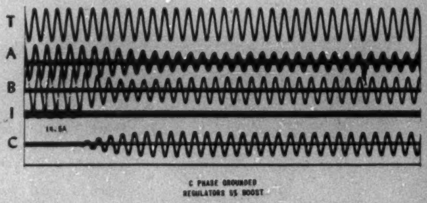

Figure 15. Current in fault and phase-to-ground voltages as a ground is removed from C phase

All regulators on neutral except those on faulted feeder on 5 per cent boost. Neutralizer set on 106 per cent of resonant value

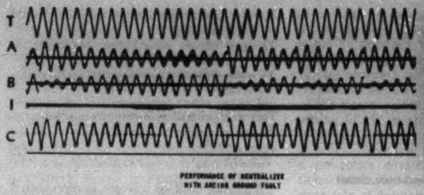

Figure 16. Phase-to-ground voltages with intermittent arcing on B phase of a feeder

All regulators on neutral. Neutralizer set on 97.5 per cent of resonant value

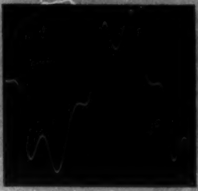

Figure 17. Ground-fault current wave form without a neutralizer

All regulators on neutral except those on faulted feeder on 5 per cent boost. Total current 53.7 amperes. Harmonic analysis: First, 50.7 amperes; third, 3.45 amperes; fifth, 13.5 amperes; seventh, 2.5 amperes

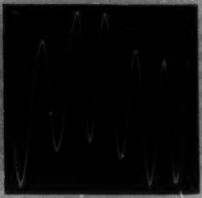

Figure 18. Ground-fault current wave form with a neutralizer set on 97.5 per cent of resonant value

All regulators on neutral except those on faulted feeder on 5 per cent boost. Total current 16.3 amperes. Harmonic analysis: First, 6.8 amperes; third, 0.5 amperes; fifth, 14.7 amperes; seventh, 1.6 amperes

neutralized fault current and hence is proportionately less damaging to the cable system. It alters the characteristics of the recovery voltage in the following manner.

When the system is tuned to resonance and a ground fault is extinguished, the line-to-ground voltage on the grounded phase returns to its normal value in accordance with the oscillogram in Figure 1. In an inverse manner the voltages to ground on the two unfaulted phases return gradually from line-to-line to their normal value. The time delay in restoring these voltages coincides with the decay of the neutralizer current to zero, the rate of which is determined by the time constant of the zero sequence circuit. Conditions are most favorable to arc extinction when this circuit is tuned to the system frequency.

When the neutralizer is not tuned for resonance, the natural frequency of the zero sequence circuit differs from the system, thus giving rise to oscillations in the phase-to-ground voltages as the two frequencies beat. This condition produces nodes in the recovery voltage exceeding the normal phase-to-neutral voltage.

Hence, any out-of-tune condition is less favorable to the return to normal operation.

Test oscillograms, Figures 12, 13, 14, and 15, taken on the system mentioned show the effects of neutralizer tuning and regulators upon the phase-to-ground recovery voltages. They can be illustrated best by polar plots of the locus of the neutral voltage amplitude on the 3-phase voltage vectors, as shown in Figures 8 to 11 inclusive. For any out-of-tune condition, the locus deviates from a straight line and follows a logarithmic spiral to a point near the neutral as determined by the zero sequence voltage of the regulators. When the elapsed time is included in the plots, a convenient comparison is available of the effects of the various tuning values on both the amplitude and rate-of-rise of the recovery voltage.

3. The use of a saturable iron core in the neutralizer reactor will allow for resonant tuning with a restricted displacement of the system neutral during ground free conditions. Saturation would occur at a marginal value over the maximum voltage to which the neutralizer may be subjected, thereby limiting the maximum voltage to ground to approximately twice the normal value. This method will provide the advantages of resonant tuning during ground faults. However, the resulting series resonant current will require equipment of higher current rating than needed for fault neutralization. Ground-indicating equipment will be accurate only at times when the net system regulation is at neutral.

Losses and Harmonics

Complete neutralization of the ground-fault current on a regulated distribution system is not possible because of the loss components of the neutralizer and cable system and because of currents of harmonic frequencies which are present where transformers and induction voltage regulators are overexcited and of various ages. The in-phase component of the unneutralized fault current on a system largely underground may exceed 5 per cent. Fault current wave forms on the system tested were analyzed, and the fifth and seventh harmonics were found to be the most pronounced; without a neutralizer the former being in the order of 25 per cent and the latter 5 per cent of the total fault current. After the neutralizer was installed, various ohmic values of the neutralizer coil had little effect upon harmonic currents, but altered their percentage of the total residual current. In one instance, the fifth harmonic was 90 per cent of the total when the fundamental was 42 per cent.

Typical wave forms of ground-fault current with and without a neutralizer are shown in Figures 17 and 18.

Wave forms of ground-fault currents were taken with various settings of the voltage regulators on the shortest feeder, all other regulators on the system remaining on neutral. The age of these two regulators exceeds 30 years. The effects on harmonics in the fault were not entirely consistent, but, in general, varied with regulator positions.

Other Test Results

At the start of a ground test, an interesting oscillogram, Figure 16, was obtained. An intentional ground was placed on *C* phase with an oil fuse cutout in series with the grounding lead. A simultaneous ground developed on *B* phase, causing the fuse to operate. The ensuing recurrent ground on *B* phase is pictured. The neutralizer, set on 97.5 per cent of resonant tuning, prevented any additional failures which otherwise would have occurred by reason of an uncontrolled arcing ground condition. This type of fault without a neutralizer can subject the system to severe overvoltages.[9]

Operating Experience

Operating experience has been obtained on a distribution system equipped with a neutralizer, as described in the section on Description of System. Voltages to ground have been limited by avoiding resonant tuning. The records of two years' operation well justify the installation of the neutralizer. In the previous 4$^{1}/_{2}$-year period there are recorded 20 ground disturbances, one of which caused five simultaneous faults, one caused three simultaneous faults, 11 caused two simultaneous faults, and seven remained as single grounds. Although no data are available to indicate the number of second grounds caused by raising the ground voltages on two unfaulted phases, it is reasonable to assume that a large percentage of the above multiple grounds were as a result of arcing conditions for the reason that periodic grounding tests were made to break down weak spots not capable of withstanding phase-to-phase voltage.

After the neutralizer was installed, a large number of faults were experienced, many caused by activities of postwar construction within the territory served. Of 23 disturbances recorded, two were double grounds and 21 remained single grounds.

Conclusions

The ground-fault neutralizer is a means for improving the reliability of an ungrounded distribution system. When applied to an underground delta-connected system, it provides for a high degree of reliability to service.

Distribution plant equipment influence both the operation and design of the neutralizer. The principal features are as follows:

1. Single-phase feeder voltage regulators give rise to the flow of zero sequence current, which, during normal operation, causes the neutralizer to displace the system neutral.

2. Losses in the cable system and harmonic currents of distribution transformers and regulators prevent complete neutralization of the ground-fault current.

3. In normal operation, a zero sequence current may influence the continuous current rating of the neutralizer.

4. When a ground fault occurs, the maximum boost position of the feeder regulator influences the kilovolt-ampere rating of the neutralizer.

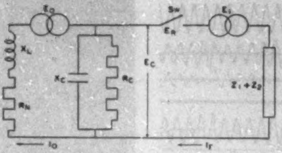

Figure 19. Zero sequence circuit

The displacement of the system neutral during normal operation may be controlled by:

1. Compensating the neutralizer with zero sequence voltage by means of automatically controlled voltage regulators.

2. Avoiding resonant tuning of the neutralizer.

Within limits, this has no serious effects on either the fault neutralization or the recovery voltage. The preferred setting is to an ohmic value less than for resonance to provide for loss of cable capacitance when a protective device operates.

Appendix I

The zero sequence circuit of an unfaulted delta system with one or more regulated feeders and a neutralizer is shown on the left-hand side of Figure 19. The zero sequence current in vector notation is given by the equation

$$\mathbf{I}_o=\frac{\mathbf{E}_o}{R_N+\dfrac{R_cX_c^2}{R_c^2+X_c^2}+j\left(X_L-\dfrac{R_c^2X_c}{R_c^2+X_c^2}\right)} \quad (1)$$

where

$\mathbf{I}_o$ = zero phase sequence current per phase
$\mathbf{E}_o$ = zero phase sequence voltage due to regulators
R_N = three times zero sequence resistance
R_c = per phase resistance of phase-to-ground insulation
X_c = per phase capacitative reactance to ground
X_L = three times neutralizer inductive reactance

This series circuit is in resonance when

$$X_L=\frac{R_c^2X_c}{R_c^2+X_c^2} \quad (2)$$

A ground fault on a feeder is represented by closing the switch in Figure 19, thereby forming a 2-loop network with two voltage sources. The steady-state fault current is

$$\mathbf{I}_F=\frac{\mathbf{Z}_o}{\mathbf{Z}_o\mathbf{Z}_A-\mathbf{Z}_{Ao}^2}(3\mathbf{E}_1)-\frac{\mathbf{Z}_{Ao}}{\mathbf{Z}_o\mathbf{Z}_A-\mathbf{Z}_{Ao}^2}(3\mathbf{E}_o) \quad (3)$$

where

$$\mathbf{Z}_o=R_N+\frac{R_cX_c^2}{R_c^2+X_c^2}+j\left(X_L-\frac{R_c^2X_c}{R_c^2+X_c^2}\right)$$

$$\mathbf{Z}_{Ao}=\frac{R_cX_c^2}{R_c^2+X_c^2}-j\frac{R_c^2X_c}{R_c^2+X_c^2}$$

$\mathbf{Z}_A=\mathbf{Z}_1+\mathbf{Z}_2+\mathbf{Z}_{Ao}$
$\mathbf{Z}_1+\mathbf{Z}_2$ = sum of positive and negative sequence impedances
$\mathbf{E}_1$ = positive sequence voltage to ground

At resonance $\mathbf{Z}_o$ is much less than $\mathbf{Z}_{Ao}$ so that the fault current is approximately proportional to $\mathbf{E}_o$.

References

1. **American Standard Definitions of Electrical Terms.** AIEE, Section 65.11.140, 1941, page 206.

2. **Effect of Restriking on Recovery Voltage, C. Concordia, W. F. Skeats.** *Electrical Engineering (AIEE Transactions)* volume 58, August 1939, pages 371–76.

3. **The Electrostatic Unbalance of Transmission Lines and Its Effect on the Application of Petersen Coils, John Alexander Melvin Lyon.** *Electrical Engineering (AIEE Transactions)* volume 58, March 1939, pages 107–12.

4. **Factors Affecting Arc Extinction on a Petersen-Coil System, J. R. Eaton.** *Electrical Engineering (AIEE Transactions)* volume 58, November 1939, pages 576–77.

5. **Electric Circuits (book), Electrical Engineering Staff, Massachusetts Institute of Technology. John Wiley and Sons, Inc., New York, N. Y., 1943.**

Discussion

C. B. Hinton (General Electric Company, Schenectady, N. Y.): There are only a few ground-fault neutralizers in use on distribution systems in the United States and consequently there have not been very many papers written on the subject. The installation described in this paper is the first on a regulated distribution system and so it opens up an entirely new field for the application of these protective devices. The authors are to be congratulated for the initiative shown in making the application and describing the problems which they had to overcome.

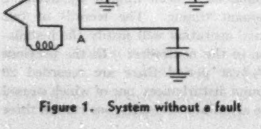

Figure 1. System without a fault

My discussion is concerned with the automatic voltage-limiting action which can be built into a ground-fault neutralizer application and which experience has shown to be a desirable feature. This particular subject was not mentioned in the paper.

The first neutralizer in this country was installed on the system of the Alabama Power Company. It was an air-core type coil in the neutral of the system and produced a good operating record. Some switching operations, however, caused a momentary single-phasing condition with the result that sizeable over-voltages occurred resulting in insulator flashover. Since that time General Electric neutralizers have been built with a steel core designed to

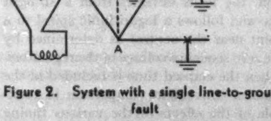

Figure 2. System with a single line-to-ground fault

saturate on the occurrence of voltages higher than normal, thereby detuning the system and effectively preventing excessive overvoltages.

The same automatic protection can be obtained in the Bauch-type neutralizer, which is the type described in the paper, by proper design of the grounding bank. The mechanism for throwing the system out of tune differs from that which acts in a conventional neutralizer but it is just as effective and is shown in Figure 1 of this discussion. Normally the voltage across each leg of the grounding bank is of line-to-neutral magnitude. When a single-line-to-ground fault occurs, the voltages on the two unfaulted legs approach line-to-line magnitude, Figure 2 of discussion. This increased voltage results in a slight change in the magnetizing current drawn by the grounding bank. The magnetizing component of current has the same phase relationship as the current supplied by the neutralizer, and therefore the two components add directly to produce the total reactive current in the fault, Figure 3 of discussion. If the voltage across the grounding bank tends to increase still more for any reason, the magnetizing current increases very rapidly, so that the total reactive component in the fault becomes relatively large, see Figure 4 of this discussion, and the system is detuned. Thus any increase in voltage at the terminals of the grounding bank causes an automatic voltage-limiting action to take place.

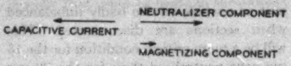

Figure 3. Components of current which flow in a single line-to-ground fault

If the grounding bank is designed judiciously, the increase in magnetizing current can be held to a low value for a normal voltage increase of 73 per cent during a single-line-to-ground fault and can be forced to a relatively high value when the voltage appreciably exceeds this amount. This can be accomplished by taking advantage of the familiar nonlinear saturation characteristic of core steel.

The grounding bank described in the paper consists of three standard distribution transformers rated 2,400-240 volts. The voltage on each leg of the bank is approximately 1,380 volts with no fault on the system. When a single line-to-ground fault occurs, the voltage on the two unfaulted legs increases to approximately 2,400 volts, resulting in a slightly higher magnetizing current. Any further increase in voltage would cause the valve action described previously to begin to operate. The maximum value the voltage would reach before it was effectively limited, however, is a function of the saturation characteristic of the grounding bank. The protection offered by this grounding bank made up of 2,400-volt transformers is not as good as that which would be provided by a bank designed to operate at approximately line-to-neutral voltage because a relatively higher voltage is required to initiate the limiting action.

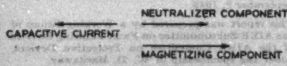

Figure 4. Components of current which flow when voltage at terminals of grounding transformer is excessive

The paper mentions that the preferred setting of the neutralizer is to an ohmic value less than that required for resonance to provide for loss of cable capacitance when a protective device operates. One additional reason for detuning on the low reactance side of resonance is that the sustained voltages on the unfaulted phases during a single line-to-ground fault are less than they are if detuning is on the high reactance side of resonance. Still another reason is that the arc at the point of fault is easier to extinguish if the net fault current is lagging rather than leading.

Eric T. B. Gross (Illinois Institute of Technology, Chicago, Ill.): This paper is of great value particular to the operating engineer, and for many reasons:

1. It indicates clearly that resonant grounding deserves much wider application in distribution systems[1] than this grounding method has had in the past.

2. It is emphasized that self-extinguishing of arcing grounds is accomplished by the prevention of restrikes, and that it is not necessary to keep the ground-fault neutralizer at resonant tuning. Previous discussions, published in the Transactions during the past 20 and more years, indicate that many engineers were under the impression it was of prime importance to keep the tuning always at exact resonance; they thought it was necessary to keep the fault current small, whereas only the out-of-tune ratio[2] is responsible for the rate of recovery voltage, and not the magnitude of the residual fault current as such.

3. It is pointed out that detuning in both directions, by ±15 per cent in this case from 85 to 115 per cent, has no detrimental effects on the self-extinguishing of arcing grounds; this statement is in agreement with experiences made in distribution and transmission system on numerous[3] coils at voltages up to 220 kv.

4. It is underlined that a complete analysis of tests[4] requires the resolution of the residual fault current into its harmonic components.

I am certain that the authors recognize the advantages of saturation of the ground-fault neutralizer at approximately phase voltage, and agree with me that such an iron-core coil is preferable to an air reactor. A properly designed ground-fault neutralizer will start to deviate from the linear characteristic on all its taps at or near phase voltage. However, if it does not, an air reactor will hardly do worse.

The equivalent diagram, Figure 19, is very helpful in studying ground-fault phenomena in resonant grounded systems; it may be worthwhile mentioning that a possible fault resistance would be added to Z_1+Z_2 and that E_0 (the neutral displacement of the system when $R_N+jx_L=\infty$) is really an equivalent electromotive force in the R_c and x_c branch and in series with it.[5] The particular type of ground-fault neutralizer described here is often referred to as Bauch Transformer[6] or indirect method of resonant neutral grounding, whereas the better known single-phase Petersen coil is the direct method of resonant neutral grounding.

It is hoped that this paper will lead many engineers to recognize resonant neutral grounding as a grounding method that provides one of the cheapest solutions of the problem by covering a high percentage of faults without voltage dips.

References

1. Resonant Grounding of Distribution Systems, E. Herzog. *Proceedings*, Midwest Power Conference (Chicago, Ill.), volume 11, 1949, pages 171–78.

2. The Arc Quenching Effect of Petersen Coils, W. Diesendorf. *Journal*, Institution of Engineers (Sydney, Australia), volume 18, 1946, pages 237–40.

3. The Why and How of Resonant Grounding, Eric T. B. Gross. *Electric Light and Power* (Chicago, Ill.), volume 25, July and August 1947.

4. *Discussion* by Eric T. B. Gross of Engineering Features of the 230-Kv Boulder-Chino Transmission Line of the Southern California Edison Co., Ltd., Alex A. Kroneberg, E. M. Hunter. *AIEE Transactions*, volume 59, 1940, page 1176.

5. Adjustment of Ground Fault Coils, E. Gross. *Bulletin*, Swiss Institute of Electrical Engineers, volume 28, 1937, pages 165–69.

6. Bauch Transformer Damps Cable Faults, L. M. Nelson, H. N. Muller. *Electrical World* (New York, N. Y.), volume 122, 1944, page 86.

H. R. Tomlinson and **F. B. Hunt:** Mr. Hinton has called attention to the preference for saturating the grounding transformers rather than the neutralizer reactor to control excessive voltages by the nonlinear method. The authors concur in view of the fact that the system can be thrown out-of-tune at a much lower voltage than with the saturable reactor method. However, in the application to the lower voltage regulated distribution systems, it is questionable if this especially designed equipment has any merit over the use of standard transformers with an air-core reactor set to 90 per cent of the resonant value. If the special grounding transformers can be made to saturate effectively at a voltage moderately higher than phase-to-phase voltage, the maximum ground voltage to a regulated phase during fault-free conditions is in the same order as obtained when a linear device is set to the 90 per cent value. On the system described in the paper, saturation at approximately 2,500 volts will result in a ground voltage to the furthest regulated phase of approximately 2,700 volts, or 195 per cent of the system rated ground voltage. This is slightly higher than that shown for the full boost condition in Figure 7, resulting by the use of a 90 per cent air-core reactor.

The authors believe that the resonantly tuned condition obtainable by the nonlinear design when the system becomes faulted has no practicable advantage, as experience and tests indicate that neutralizer objectives are attained when the reactance is 90 per cent, and even lower, than the resonant value.

Inspection of oscillograms and recovery voltage curves included in the paper indicate that a residual capacitive current at the fault is no more difficult to extinguish than an equal reactive current.

In answer to the discussion by Professor Gross, the authors do not believe that the use of a tuned saturable iron-core reactor will limit the ground voltages as effectively as an out-of-tune air-core reactor. For equal reactance values, some cost reduction may be realized with iron cores by savings in space and materials.

Additional units similar to the one described in the paper will be installed at other locations within the territory served by the company with which the authors are associated. These will afford an opportunity to gain further experience with this type of equipment. These units will be installed primarily to avoid the disturbances caused by arcing grounds on cable systems. However, it is recognized that additional benefits are realized on the overhead portions of the distribution systems. In particular, the neutralizer will extinguish ground-fault currents caused by lightning flashovers between primary and secondary bushings of a pole top transformer which otherwise are sustained by the flow of capacitive current if the magnitude of such is insufficient to cause operation of the transformer primary fuses. These sustained ground currents have caused damage to transformers and customers' equipment.

Report on Survey of Unbalanced Charging Currents on Transmission Lines as Affecting Ground-Fault Neutralizers

AN AIEE COMMITTEE REPORT

DURING the preparation of the standards material for ground-fault neutralizers, which forms a part of AIEE Standard Number 32 for Neutral Gounding Devices,[1] there was considerable discussion in reference to the requirement that all ground-fault neutralizers be capable of carrying continuously a circulating current equal to 30 per cent of the current rating. Some expressed the view that this value might be too low, and some thought it might be too high. The value chosen was assumed to represent a balance among such factors as: the investment cost of the neutralizer; the fact that tests are made on these devices when first installed and 30 per cent current may be possible; the possible cost of transposing or interchanging line conductors; and in some cases detuning is not an acceptable solution. The investment cost of the neutralizer can be estimated closely, but the possible cost of transposing is rather difficult to determine.

In view of the question as to whether the requirement of 30 per cent continuous circulating current capability for ground-fault neutralizers was correct, it was decided to conduct a survey to determine this point.

From data submitted by the manufacturers on neutralizers built to the 30 per cent requirement, it appears that in about 15 per cent of the applications, further transpositions of the circuits were necessary to reduce circulating current to a value below 30 per cent. However, after the transpositions were effected, only about half of the systems which were transposed to meet the 30 per cent requirement then had less than 15 per cent circulating current. This would have necessitated further transpositions for some systems if the neutralizers had had a 15 per cent requirement. Furthermore, the submitted data indicate that if the neutralizers had had a 15 per cent continuously circulating current rating, then in 43 per cent of the applications it would have been found necessary to transpose. This percentage compares to the 15 per cent that were required to transpose with the present 30 per cent requirement.

On the basis of these facts, an investigation of a 15 per cent ground-fault neutralizer was made. It was confirmed that to carry 30 per cent circulating current continuously requires a 10-minute time rated coil (standards had intended to include this correlation), and that the 15 per cent neutralizer resulted in a 1-minute rating. For a 13,800-volt application the 15 per cent rated neutralizer equipment would sell for 97 per cent of the price of the 30 per cent unit, a saving of $210. At 34.5, 46, and 69 kv, the 15 per cent rated neutralizer equipment would sell for approximately 94 per cent of the price of the 30 per cent unit, a saving of $500, $550, and $600 respectively.

There is some indication that the tendency to omit transpositions, except where telephone co-ordination requires them, is increasing. If this is the case, unbalanced charging current will be more prevalent in the future than in the past. There is a strong probability that the over-all cost to the industry would be greater with a 15 per cent neutralizer than with the present standard 30 per cent neutralizer.

It has been found that a system may have acceptably balanced charging current as a whole but be badly unbalanced when sections are disconnected. This will be a more critical condition for the 15 per cent neutralizer than for the 30 per cent unit and would tend to increase the percentage of installations for which additional transpositions would be required.

When the standards were being written, there was considerable discussion as to whether a 1-minute rating or a 10-minute rating for the neutralizer would be better. There was a decided tendency to prefer the 10-minute rating because it was thought that one minute was too short a time from operating considerations. The present 30 per cent neutralizer correlates with a 10-minute time rating, while the 15 per cent neutralizer correlates with a 1-minute time rating. This feature is a definite handicap for the 15 per cent neutralizer.

Summary

The committee finds that the requirement that neutralizers be capable of carrying a continuous circulating current not less than 30 per cent of its rating appears to be sound in view of the foregoing conclusions, and therefore recommends that no change be made.

Reference

1. STANDARD FOR NEUTRAL GROUNDING DEVICES. *AIEE Standard Number 32*, May 1947.

Paper 49-284, recommended by the AIEE Committee on Protective Devices and approved by the AIEE Technical Program Committee for presentation at the AIEE Fall General Meeting, Cincinnati, Ohio, October 17-21, 1949. Manuscript submitted August 31, 1949; made available for printing September 2, 1949.

This report was prepared by a Working Group of the AIEE Subcommittee on Fault Limiting Devices of the AIEE Committee on Protective Devices, under the sponsorship of W. D. Hardaway.

Personnel of the Working Group of the AIEE Subcommittee on Fault Limiting Devices: J. E. Clem, *Chairman;* H. H. Brown, S. S. Cook, N. B. Dillow, W. D. Hardaway, R. E. Neidig, P. B. Speer.

Discussion

Eric T. B. Gross (Illinois Institute of Technology, Chicago, Ill.): It seems worthwhile mentioning that "transposition," as used in this report, does not mean either a complete barrel of transpositions for each line section or "the interchange of the position of the several conductors of a circuit," as defined in ASA C42-1941[1] under 35.60.330. This report refers to electrostatic unbalances with respect to ground; it is desirable to equalize the capacitances-to-ground of all 3-phase conductors, irrespective of remaining unbalances of interphase capacitances. The transposition can be accomplished often by an interchange of two conductors only, and transposition towers are rarely necessary. In one of the severest cases that was considered in this country, altogether 28 transpositions were made; 26 of these were interchanges that could be made in substations and only two required transposition structures on overhead line towers: the system referred to comprised more than 200 miles of overhead line right of way. These figures indicate that it is not difficult nor expensive to balance an overhead line electrostatically with respect to earth.

I am in full agreement with the recommendation to design resonant neutral grounding devices, as defined in AIEE Standard No. 32[2] for not less than 30 per cent continuous circulating current. Some of the coils that have been in operation in this country for some time were designed rather conservatively and the operating companies have found out, through experiences with faults that were permitted to stay on for more than ten minutes, that the equipment may be used without overheating on permanent faults with full load, even if designed for "10-minute rating".

A recent survey concerning the application of resonant neutral grounding to systems at voltages up to 110 kv seems to indicate that there is a tendency towards preference of equipment that is designed for extended time rating. This tendency is in line with the established practices in foreign countries[3] to operate with permanent faults until the defective line has been located[4] with the help of sensitive ground relays, and may be switched off without voltage dips or service interruptions.

References

1. American Standard Definitions of Electrical Terms, ASA C42. AIEE, 1941.

2. Standard for Neutral Grounding Devices. *AIEE Standard Number 32*, May 1947.

3. The Why and How of Resonant Neutral Grounding, Eric T. B. Gross. *Electric Light and Power* (Chicago, Ill.), volume 25, July/August, 1947.

4. Sensitive Ground Protection for Transmission Lines and Distribution Feeders, Eric T. B. Gross. *Electrical Engineering (AIEE Transactions)*, volume 60, November 1941, pages 968–71.

Governors and the AIEE-ASME Governor Performance Specification

A. F. SCHWENDNER
NONMEMBER AIEE

WAYNE C. ASTLEY
NONMEMBER AIEE

THE Joint AIEE-ASME Committee on a Recommended Specification for Prime Mover Speed Governing recently issued a recommended specification[1] for steam turbines intended to drive electric generators rated 500 kw and up. A similar specification for hydraulic turbines intended to drive electric generators has been submitted to the AIEE Standards Committee for approval. These specifications include definitions and descriptions of terms relating to governor functions, and standards of performance.

The purpose of this paper is to show the application of the terms and definitions to modern speed-governing systems; and indicate how these systems meet the requirements of the specifications.

Steam-Turbine Speed-Governing Systems

Two types of speed-governing systems are illustrated in Figures 1 and 2 to indicate how the component parts are defined in the specification. The system shown in Figure 1 does not represent any particular make, but contains features common or comparable to most of the flyball governing systems. The system shown in Figure 2 is an oil governing system which is illustrated more in detail in Figure 3. In Tables I and II the components which are labeled in the figures are grouped under the proper terms as described in the specifications.

Table I. Flyball Type of Speed-Governing System

Term	Components	Description
Speed governor	1	Flyball element responsive to speed
Speed-control mechanism	2_1	Force amplifier
	2_2	Force amplifier
	2_3	Valve servomotor
Governor-controlled valves	3	Steam inlet valve
Speed changer	4	
Load-limiting device	5	

Table II. Hydraulic Type of Speed-Governing System

Term	Components	Description
Speed governor	1	Impeller responsive to speed
Speed control mechanism	2_1	Pressure amplifier
	2_2	Force amplifier
	2_3	Force amplifier
	2_4	Valve servomotor
Governor-controlled valves	3	Steam inlet valve
Speed changer	4	
Load-limiting device	5	

The component parts of an electronic-type governor can be similarly grouped, as may elements of other systems in use which perform within the limits of the specification.

Having established the definitions and the grouping of the components of governor systems, it is intended to show how the system functions to meet the specifications. Practically all of the performance specifications deal with governor characteristics which involve every component of the system. For that reason operation of the system as a whole will be described as necessary under each specification.

Performance Specifications

STEADY-STATE SPEED REGULATION

Steady-state speed regulation is defined as the change in sustained speed expressed in per cent of rated speed when the power output of the turbine is gradually reduced from rated power output to zero power output with identical settings of all adjustments of the speed-governing system.

From the definition it is obvious that we must start with the governor-controlled valve lift to check the performance of the governors shown in Figures 1 and 2. Under rated speed and steam conditions the valve motion from rated load to no load will be a definite value. In the hydraulic type of governor shown in Figure 2 this definite motion can be obtained only by a fixed proportional change in the control pressure acting on the power amplifying device, 2_2. This control pressure change is obtained by a change in the governor pressure in response to a speed change of the turbine. The governor pressure in turn acts on the bellows of the pressure amplifying device, 2_1, and the ratio of amplification is fixed by the bellows and cup areas.

When an increase in control pressure acts on the area of the power amplifying piston, 2_2, the extension spring attached to the return link is stretched. The piston moves down a fixed amount which is dependent on the pressure change, the piston area, and the scale of the extension spring. The lower end of the piston extends into the pressure chamber of the power amplifying device, 2_3. The extension of the piston is made in the shape of a cup valve which covers a drain hole extending through the length of the servomotor relay. This relay is held against the extension of the piston by a strong compression spring.

High-pressure oil is admitted into the pressure chamber through an orifice. As the oil pressure in the chamber increases, it acts on the exposed area of the relay and overcomes the upward force of

---

Paper 49-288, recommended by the AIEE Power Generation Committee and approved by the AIEE Technical Program Committee for presentation at the AIEE Fall General Meeting, Cincinnati, Ohio, October 17–21, 1949. Manuscript submitted October 29, 1948; made available for printing September 12, 1949.

A. F. SCHWENDNER is with the Westinghouse Electric Corporation, Philadelphia, Pa., and WAYNE C. ASTLEY is with the Philadelphia Electric Company, Philadelphia, Pa.

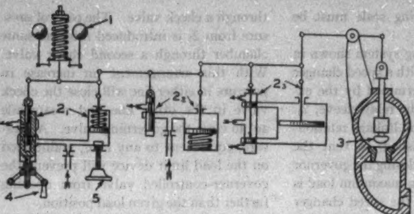

Figure 1. Flyball type of speed governing system

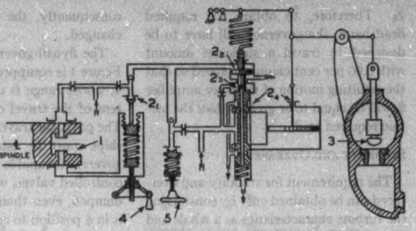

Figure 2. Hydraulic type of speed governing system

the compression spring. The relay is pushed down by oil pressure until the exposed drain area permits the pressure in the chamber to drop to a value where the spring force is balanced by the pressure acting on the area of the relay.

The motion of the relay has admitted high-pressure oil into the servomotor cylinder, 2_4, and moved the servomotor piston up. This motion of the servomotor piston continues until the return linkage, by means of the extended spring, moves the power amplifier piston and relay back to the neutral position. The travel of the servomotor piston depends on the change in control oil pressure. With a given ratio for the return linkage lever, it will require a given oil pressure change (and consequently a given speed change) to move the governor-controlled valve from the rated load-rated speed position to the no-load position.

A change in regulation is obtained by modifying the ratio of the return linkage lever, which controls the variation of spring extension for a given valve travel. The change in the extension of the spring changes the control pressure required to move the relay to the neutral position. The change in control pressure is obtained, of course, by a corresponding change in speed and impeller oil discharge pressure.

The procedure followed in tracing the operating of the hydraulic governor will be used in describing the flyball governing system, which has the same characteristics, Figure 1. The movement of the governor controlled valve from rated load to no load can be obtained only as a result of a proportional movement of the governor weight. This movement of the governor weights, due to a change in speed, moves the relay and operating mechanism of the force amplifier, 2_1. The operating piston of 2_1 moves the relay of the second force amplifier, 2_2, which in turn moves the relay valve of the governing valve servomotor. The ratio of the linkage between the governor-controlled valve and the governor establishes the governor speed regulation.

A change in speed regulation can be obtained by changing the lever ratio of any one of the force amplifying devices, as this changes the governor travel required to produce a given change in valve travel. Similarly, the spring scale of the governor could be changed, as this would produce the same effect without any change in the linkage. Both of these control systems require that the unit be stopped in order to change the regulation.

STEADY-STATE INCREMENTAL SPEED REGULATION

The steady-state incremental speed regulation at a given steady-state speed and power output is the rate of change of the steady-state speed with respect to the power output. Because of differences in steam flow at various governing valve openings, and the uneven characteristics of some governors' speed versus travel relationship, the incremental regulation can be different for each portion of the governing valve travel. In the two governing systems shown, the governors' response to a speed change will be identical at any load point when operating at rated speed. There is no change in the flyball position in Figure 1 regardless of valve position as long as rated speed is maintained. If, however, the speed is permitted to change, the uneven governor characteristics must be considered. The governing system shown in Figure 2 does not change its characteristics with changes in speed and/or load.

For the two governors described, the incremental regulation is dependent mostly on the governor-controlled valve flow versus travel characteristics and the valves have to be so designed that the resultant incremental regulation remains within the specified limits.

DEAD BAND

Dead band is the total magnitude of the sustained speed change within which there is no resulting measurable change in the position of the governor controlled valves. For turbines in excess of 5,000 kw, the specification states that the dead band shall not be greater than 0.06 per cent. This means that the motion of the governor-controlled valves must be reversed with a speed change not greater than 0.06 per cent of rated speed. The following analysis indicates the methods to be employed to bring the dead band of the governors illustrated within the required limits.

Considering the governor in Figure 2, it is evident that the governor-controlled valve is so attached to the operating piston of the servomotor, that all loads are taken in one direction and all dead travel between them is eliminated. That is not the case, however, in the relationship between the operating piston and the control pressure applied to the piston of the force amplifying device, 2_3. There is a slight dead travel in the relay, and the piston of the amplifying device is not completely frictionless. The control pressure change acting on the piston, 2_3, necessary to reverse the motion of the operating piston of the servomotor may be determined. Similarly, the oil pressure change, equivalent to a 0.06 per cent change in speed, which acts on the bellows of the pressure amplifier, 2_1, may be determined. To obtain the required dead band, it is then necessary to select a cup valve with an area such that the necessary control pressure change is obtained, as a result of the pressure change on the bellows. As an alternative, the area of the bellows could be changed.

Examination of the governor in Figure 1 indicates that again all dead travel is eliminated between the operating piston of the servomotor and the governor controlled valve. The lever moving the servomotor relay will have a small change in travel, however, before the operating piston will change its direction. The amount of travel is somewhat increased through the action of the force amplifier,

2_2. Therefore, to obtain the required dead band, the governor will have to be designed to travel a sufficient amount with 0.06 per cent change in speed so that the resulting motion of the force amplifier 2_1 will be equal to or greater than the motion required by 2_2.

STABILITY AND OVERSPEED

The requirement for stability and overspeed can be obtained only by considering the turbine characteristics as a whole and by building into the governor system the specified rate of response. In most cases, this means the selection of relay areas sufficient to pass the required quantities of oil with small displacement, oil pumps with sufficient capacity, and so forth. Each type and size of unit must be investigated as a governing system; that which is satisfactory for one design may not give identical performance on another design.

RANGE OF SPEED CHANGER ADJUSTMENT

In the hydraulic-type governor, Figure 2, the range of the speed changer is determined by the extent of travel of the speed changer 4 and the scale of the spring. The product of the two determines the force restraining the bellows against the governor pressure. The ratio of the bellows area to the cup valve area establishes the relationship between a change in governor pressure and the resultant change in control pressure. The force on the bellows, due to the tension of the speed changer spring, determines at what speed (governor pressure) the resultant control pressure will be equivalent to the no-load position or full-load position of the governor controlled valve. To change the range of the speed changer, consequently, the spring scale must be changed.

The flyball governing system shown in Figure 1 is equipped with a speed changer 4, whose range is determined by the extent of the travel of the relay sleeve, 2_1. The governor travel and linkage relationships must be established, so that the governor is capable of closing the governor controlled valves, when maximum load is dumped, even though the speed changer is in a position to carry maximum load at 102 per cent of rated speed. The speed changer also must have sufficient travel, so that at no load the speed can be carried 5 per cent below rated speed. To increase the range of the speed changer, it is necessary that the governor be designed for the increased travel necessary to cover this range.

ADJUSTMENT OF SPEED REGULATION WITH TURBINE IN OPERATION

A device to change the steady-state speed regulation with the turbine in operation is optional in the specification. This is accomplished by moving the fulcrum point of the follow-up linkage in either of the governing systems illustrated.

LOAD LIMITING DEVICE

The connection of a load limiting device to a hydraulic turbine governor is shown in Figure 2. It consists of a spring loaded cup valve supplied with high-pressure oil through an orifice. The compression of the spring and, consequently, the resultant oil pressure leaving the device is adjustable as indicated at 5. The oil pressure controlled by the load limit device is led into the top chamber of the force amplifying device, 2_2 in Figure 2, through a check valve. The control pressure from 2_1 is introduced into the same chamber through a second check valve. With this arrangement an increase in pressure in either line will close the check valve in the other line and meanwhile act to close the governing valve. A pressure, equivalent to any load, maintained on the load limit device will prevent the governor-controlled valve from opening further than the given load position.

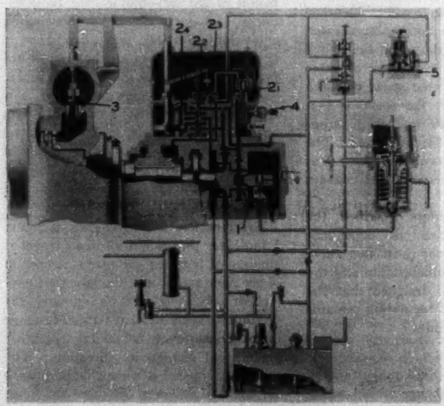

Figure 3. Steam turbine with a hydraulic type of speed governing system

During any period that the governor control pressure is higher, it will have full control over the governor-controlled valves, but as soon as the control pressure drops below the given load point, the pressure maintained by the load limit will open its check valve and close the check valve leading to the pressure amplifying device and hold the governor-controlled valve in one position. In the event that load is dropped from the system, the governor control pressure rises and assumes control of the governor-controlled valve.

A similar device can be used to limit the load on the flyball type of governor. This is accomplished by introducing an adjustable screw, 5, below the operating piston of the force amplifier 2_1 in Figure 1. The upper end of this screw prevents the piston from moving below the point for which it is set, and the governor will have full control over the governing valves above the setting of the load limit.

Care must be taken in the design of this system to allow sufficient over-travel between the relay of 2_1 and the sleeve adjusted by the speed changer. Otherwise, free travel of the governor for any position of the speed changer or load limit would not be permitted and excessive loads might be placed on the knife edges of the governor.

Summary

It is evident that either of the two conventional governing systems shown can satisfy the conditions laid down in the specification. Similar analysis will indicate how other systems of less conventional design also meet the specification. It has been the intention of the authors to indicate the steps in these analyses and show how modern systems can be adjusted to operate within the limits of the specification.

Reference

1. RECOMMENDED SPECIFICATION FOR SPEED-GOVERNING OF STEAM TURBINES INTENDED TO DRIVE ELECTRIC GENERATORS RATED 500 KW AND UP. *AIEE Standard Number 600*, May 1949.

No Discussion

Performance Characteristics of Lightning Protective Devices

AN AIEE COMMITTEE REPORT

THIS report presents data covering the performance characteristics of lightning protective devices of present-day manufacture. It combines in one report the data on lightning arresters of various types published previously by the AIEE Lightning Protective Devices Subcommittee in a number of separate reports,[1–4] with such modifications as required to bring this material up to date. In addition, data covering line expulsion-type lightning arresters, and data on rod gap spark-over voltages, for co-ordination with lightning arrester characteristics, are included.

The data presented are the results of tests made in accordance with methods of testing covered in the proposed combined AIEE Lightning Arrester Standards for Valve and Expulsion Lightning Arresters, under preparation by the Lightning Protective Devices Subcommittee. The data in this report were compiled from information supplied by the lightning arrester manufacturers. The values are for lightning arresters of present-day manufacture and do not necessarily apply for older types.

The data are presented in both tabular and graphical form. Data for valve-type lightning arresters in the distribution, line, and station classifications are shown in Table I and Figures 1 to 16, inclusive, and for expulsion-type lightning arresters in the distribution classification in Table II and Figures 17 and 18. The tables give the minimum, average, and maximum spark-over values for the lightning arrester, using the rate of voltage rise specified in the proposed AIEE Standards for Lightning Arresters; that is, 100 kv per microsecond per 12 kv of lightning arrester rating, with an impulse of the polarity that gives the higher spark-over values. This information is shown graphically in Figures 1, 5, 9, 13, and 17.

The complete impulse spark-over characteristics of valve and distribution expulsion-type lightning arresters are shown in Figures 2, 6, 10, 14, and 18. Average spark-over voltages for the front-of-wave test are indicated for each lightning arrester rating.

Table I, for valve-type lightning arresters, also includes values of discharge voltages that appear across the lightning

Table I. Performance Characteristics of Valve-Type Lightning Arresters

Lightning Arrester Type and Rated Voltage, Kv	Front of Wave Impulse: Rate of Rise,* Kv Per Microsecond	Front of Wave Impulse: Spark-over Kv**			Discharge Voltage-Kv on 10 by 20 Microsecond Current Wave**: 5,000 Amperes			10,000 Amperes			20,000 Amperes		
		Min	Avg	Max	Min	Avg	Max	Min	Avg	Max	Min	Avg	Max
Distribution													
3	25	12	18	23	9	14	17	10	16	20	12	18	23
6	50	22	34	45	16	26	34	19	30	38	22	34	44
9	75	32	48	62	24	39	51	28	44	57	33	51	66
12	100	42	61	77	32	49	62	37	55	69	43	62	78
15	125	52	73	91	39	61	77	44	69	87	52	79	99
Line													
20	167	56	75	94	66	83	100	73	92	110	81	101	121
25	208	70	93	116	81	101	121	89	111	133	97	121	145
30	250	82	110	138	97	121	145	108	135	162	119	149	179
37	308	102	136	170	119	149	179	131	164	197	145	181	217
40	333	110	147	181	129	161	193	140	177	213	157	196	235
50	417	137	183	229	161	202	242	177	222	265	194	243	292
60	500	165	220	274	193	242	290	217	271	325	238	298	358
73	608	200	267	333	237	297	355	261	328	392	288	360	432
Station													
3	25	10	13	16	9	10	11	9	11	13	10	12	14
6	50	18	23	28	17	20	23	19	22	25	20	24	28
9	75	28	35	42	26	30	34	28	33	38	30	35	40
12	100	34	43	52	34	40	46	37	44	51	40	47	54
15	125	42	53	64	43	50	57	46	54	62	50	59	68
20	167	58	72	86	57	67	77	61	72	83	66	78	90
25	208	71	89	107	71	83	95	77	90	103	85	100	115
30	250	85	106	127	85	100	115	92	108	124	100	118	136
37	308	105	131	157	105	124	143	112	132	152	123	145	167
40	333	109	136	163	114	134	154	122	144	166	130	153	176
50	417	143	178	213	142	167	192	152	179	206	163	191	219
60	500	171	214	257	170	200	230	185	217	249	199	234	269
73	608	209	261	313	208	245	282	223	262	301	241	283	325
97	808	276	345	414	275	323	371	297	349	401	321	377	433
109	908	310	388	465	309	363	417	335	394	453	361	424	487
121	1,008	344	430	516	343	403	463	372	438	504	400	470	540
145	1,208	412	515	618	414	487	560	445	523	601	480	564	648
169	1,408	482	602	722	481	566	651	519	610	701	559	658	757
196	1,633	553	691	829	550	647	744	593	698	803	642	755	868
242	2,017	688	860	1,032	685	806	927	741	872	1,003	799	940	1,081

* 100-kv per microsecond per 12-kv of lightning arrester rating.

** Impulse of polarity giving higher spark-over voltage.

Paper 49-286, recommended by the AIEE Protective Devices Committee and approved by the AIEE Technical Program Committee for presentation at the AIEE Fall General Meeting, Cincinnati, Ohio, October 17–21, 1949. Manuscript submitted August 2, 1949; made available for printing September 2, 1949.

Personnel of AIEE Lightning Protective Devices Subcommittee: H. R. Stewart, *Chairman*, H. A. Cornelius, F. M. Defandorf, R. H. Earle, M. Getting, I. W. Gross, E. H. Grosser, H. W. Hartzell, T. H. Mawson, T. I. Eldridge, W. A. McMorris, A. M. Opsahl, W. E. Rushlow, A. H. Schirmer, J. M. Towner, E. R. Whitehead, E. H. Yonkers.

Working group membership includes R. H. Earle, T. I. Eldridge, W. A. McMorris, A. M. Opsahl, under chairmanship of E. H. Grosser.

arrester following spark-over and during passage of discharge current. Test values are given for 10 by 20 microsecond current waves of 5,000, 10,000, and 20,000 amperes crest, of the polarity giving the higher voltage values. Figures 3, 7, 11, and 15 show graphically the minimum, average, and maximum discharge voltages at 5,000 amperes for distribution and line lightning arresters, and at 10,000 amperes for station lightning arresters. Average discharge voltages at 5,000, 10,000, and 20,000 amperes are given in Figures 4, 8, 12, and 16.

Data on the critical impulse spark-over voltages of line expulsion-type lightning arresters are shown in Table III and Figure 19. For shorter times to sparkover, the different laboratories have been unable to agree on comparable spark-over values.

Data are available, however, showing the co-ordination to be expected between these lightning arresters and line insulation. These data are included in Table III.

Table II. Performance Characteristics of Distribution Expulsion-Type Lightning Arresters

Rated Voltage of Lightning Arrester, Kv	Front of Wave Impulse Spark-over: Rate of Rise,* Kv Per Microsecond	Kv** Min	Kv** Avg	Kv** Max	Average Critical Impulse Spark-over 1.5 by 40 Microsecond Wave, Kv**
3	25	23	33	45	29
6	50	32	50	70	41
9	75	48	71	97	53
12	100	63	84	94	61
15	125	77	101	114	70

* 100-kv per microsecond per 12-kv of lightning arrester rating.

** Impulse of polarity giving higher spark-over voltage.

Table III. Performance Characteristics of Line Expulsion-Type Lightning Arresters

Rated Circuit Voltage,* Kv	Rated Voltage of Lightning Arrester, Kv	Average Critical Impulse Spark-over 1.5 by 40 Microsecond Wave Kv Positive	Average Critical Impulse Spark-over 1.5 by 40 Microsecond Wave Kv Negative	Number of 10-Inch Diameter-5¾-Inch Spacing Insulator Disks Protected
13.8	8.4	100	110	1
23	14	150	155	2
34.5	21	200	220	2
46	28	260	285	3
69	42	375	420	5
92	56	475	540	6
115	70	575	635	7
138	84	680	760	9

* Usual circuit voltage for grounded neutral systems.

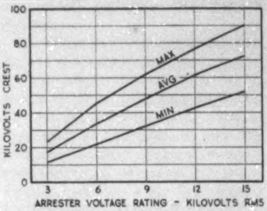

Figure 1. Front-of-wave impulse spark-over* of distribution valve-type lightning arresters

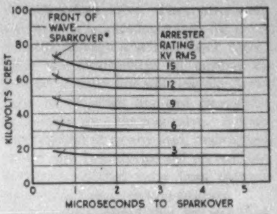

Figure 2. Average impulse spark-over volt-time characteristic of distribution valve-type lightning arresters

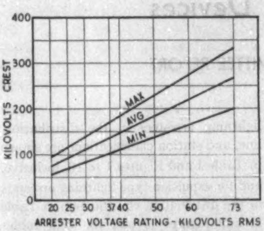

Figure 5. Front-of-wave impulse spark-over* of line valve-type lightning arresters

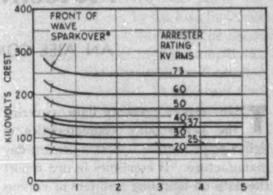

Figure 6. Average impulse spark-over volt-time characteristic of line valve-type lightning arresters

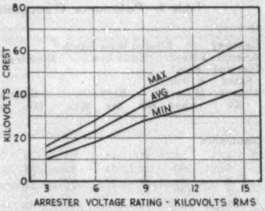

Figure 9. Front-of-wave impulse spark-over* of station valve-type lightning arresters rated 3–15 kv

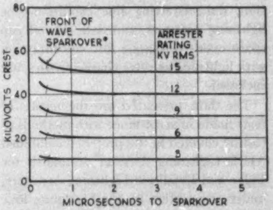

Figure 10. Average impulse spark-over volt-time characteristic of station valve-type lightning arresters rated 3–15 kv

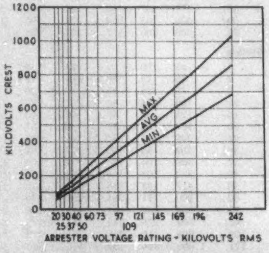

Figure 13. Front-of-wave impulse spark-over* of station valve-type lightning arresters rated 20–242 kv

* 100-kv per microsecond per 12-kv of lightning arrester rating

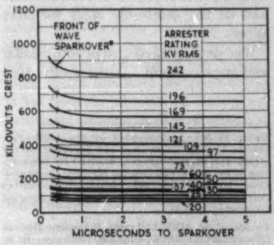

Figure 14. Average impulse spark-over volt-time characteristic of station valve-type lightning arresters rated 20–242 kv

* 100-kv per microsecond per 12-kv of lightning arrester rating

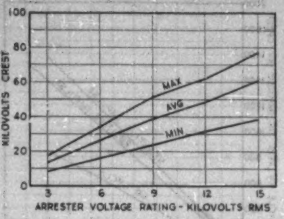

Figure 3. Discharge voltage at 5,000 amperes of distribution valve-type lightning arresters

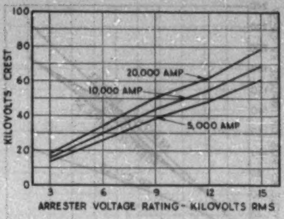

Figure 4. Average discharge voltage characteristic of distribution valve-type lightning arresters

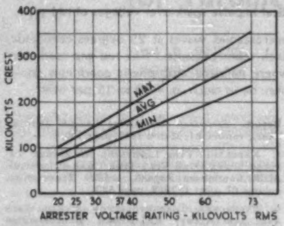

Figure 7. Discharge voltage at 5,000 amperes of line valve-type lightning arresters

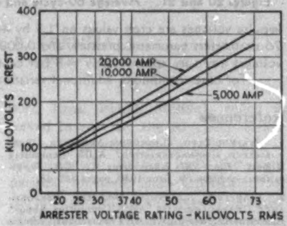

Figure 8. Average discharge voltage characteristic of line valve-type lightning arresters

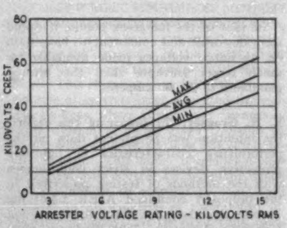

Figure 11. Discharge voltage at 10,000 amperes of station valve-type lightning arresters rated 3–15 kv

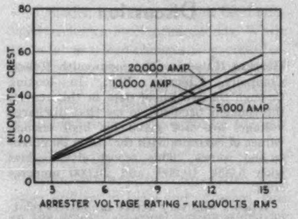

Figure 12. Average discharge voltage characteristic of station valve-type lightning arresters rated 3–15 kv

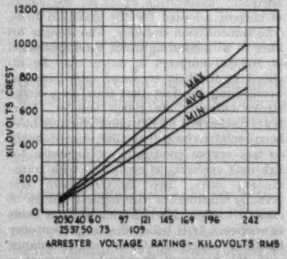

Figure 15. Discharge voltage at 10,000 amperes of station valve-type lightning arresters rated 20–242 kv

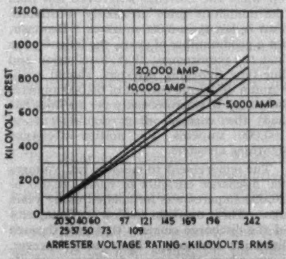

Figure 16. Average discharge voltage characteristic of station valve-type lightning arresters rated 20–242 kv

Rod-gap spark-over voltages are given in Table IV and Figures 20 and 21. These data have been taken from the latest available information, given in the report by the EEI-NEMA Subcommittee on Correlation of Laboratory Data.[5] Sixty-cycle and critical impulse spark-over voltages are included for the standard 1/2-inch square cut rod gap (AIEE Standards Number 4).[6] The rod-gap spark-over voltages may vary approximately ±8 per cent, where standard atmospheric conditions apply. For other conditions, additional variations may be as much as ± 10 to 15 per cent. As in the case of line expulsion-type lightning arresters, for times to spark-over shorter than those at which critical spark-over occurs, no agreement on spark-over voltages of rod gaps has been reached between various laboratories. Hence it is not possible to publish the complete volt-time spark-over characteristics of rod gaps at this time.

The data show variations in the characteristics of lightning arresters of all makes as high as ± 35 or 40 per cent. For lightning arresters of any one make, however, the tolerances permitted by the manufacturer do not exceed the following values: distribution and line valve- and expulsion-type lightning arresters, ± 25

Table IV. Rod-Gap Spark-over Voltages

Gap Spacing, Inches	60-Cycle Spark-over Voltage, Kv Rms	Critical Impulse Spark-over Voltage 1.5 by 40 Microsecond Wave, Kv Crest	
		Positive	Negative
0.5	11.5	22	23
0.75	17.5	30	
1.0	22.5	38	38
1.5	32	51	51
2	40	60	62
3	50	75	82
4	58	91–95	102
5	66	106–114	123
6	74	128–141	143
7		141–155	163
8	89	159–166	183
9		175–178	203
10	105	190	224
12			259–271
14			293–318
15	150	275	309–342
16			323–339
18			360–386
20	200	350	395–415
25			490
30	295	505	575
40	385	650	740
50	480	800	910
60	575	945	1,070
70	665	1,095	1,235
80	755	1,240	1,405
90	835	1,385	1,570
100		1,530	

Test conditions: temperature 25 degrees centigrade; barometric pressure 76 centimeters mercury; humidity 0.6085-inch vapor pressure.

Dual values are due to unstable conditions, the cause of which is not known.

The rod-gap spark-over voltages may vary approximately ±8 per cent, where standard atmospheric conditions apply. For other conditions, additional variations may be as much as ±10 to 15 per cent.

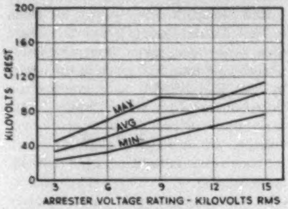

Figure 17. Front-of-wave impulse spark-over* of distribution expulsion-type lightning arresters

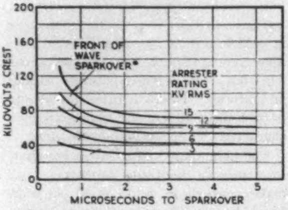

Figure 18. Average impulse spark-over volt-time characteristic of distribution expulsion-type lightning arresters

* 100-kv per microsecond per 12-kv of lightning arrester rating

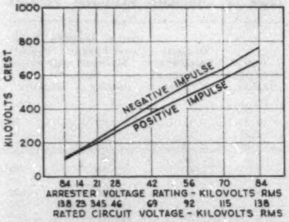

Figure 19. Average critical impulse spark-over voltage in 1.5 by 40 microsecond wave of line expulsion-type lightning arresters

per cent for spark-over voltages and (for valve-type lightning arresters only) ± 20 per cent for discharge voltages; station valve-type lightning arresters, ± 20 per cent for spark-over voltages and ± 15 per cent for discharge voltages.

Lightning arresters covered by this report have a 60-cycle spark-over voltage that is at least 1.5 times the voltage rating of the lightning arrester. The discharge current withstand test on a 5 by 10 microsecond wave is 65,000 amperes for distribution and line arresters of both valve- and expulsion-type, and 100,000 amperes for the station valve-type arresters.

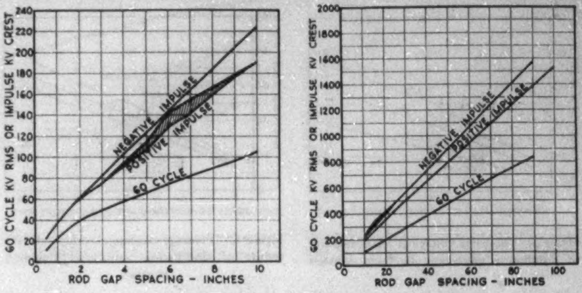

Figures 20 and 21. Average 60-cycle and critical impulse spark-over voltages of rod gaps

Impulse voltages are crest values on 1.5 by 40 microsecond waves at 25 degrees centigrade, 76 centimeters barometric pressure, and 0.6085-inch vapor pressure. The rod-gap spark-over voltages may vary approximately ±8 per cent where standard atmospheric conditions apply. For other conditions, additional variations may be as much as ±10 to 15 per cent

References

1. Station-Type Lightning-Arrester Performance Characteristics, **AIEE Committee Report.** *Electrical Engineering* (*AIEE Transactions*), volume 59, June 1940, pages 347–48.

2. Line-Type Lightning-Arrester Performance Characteristics, **AIEE Committee Report.** *Electrical Engineering* (*AIEE Transactions*), volume 60, November 1941, pages 982–83.

3. Distribution-Type Lightning-Arrester Performance Characteristics, **AIEE Committee Report.** *Electrical Engineering* (*AIEE Transactions*), volume 61, March 1942, page 132.

4. Expulsion-Type Lightning Arresters' Impulse Spark-Over Volt-Time Characteristics **AIEE Committee Report.** *AIEE Transactions*, volume 67, part 1, 1948, page 520.

5. Flashover Characteristics of Rod Gaps and Insulators, **EEI-NEMA Subcommittee Report.** *Electrical Engineering*, volume 56, June 1937, pages 712–14.

6. Measurement of Test Voltage in Dielectric Tests. **AIEE Standard Number 4, 1942.**

Discussion

Herman Halperin (Commonwealth Edison Company, Chicago, Ill.): In looking through the wealth of data in this report, the thought occurred to me that discharge voltages are not given for high enough values of currents with the 10 by 20 microsecond waves. This report gives values with 5,000, 10,000, and 20,000 amperes crest.

When I was very active in matters relating to lightning and lightning protection 15 to 25 years ago, test values for such currents would have seemed quite satisfactory. It had been found in the 1920's that many distribution lightning arresters would blow up when the currents were even less than the minimum value previously mentioned, that is, less than 5,000 amperes. However, for a good number of years, the industry has had the requirement that distribution and line-type lightning arresters should withstand a discharge current of 65,000 amperes on a 5 by 10 microsecond wave and also has had the corresponding requirement of 100,000 amperes for station-valve-type lightning arresters.

The requirement to measure test voltages for discharge currents of 5,000, 10,000 or 20,000 amperes was formulated many years ago. Those currents cover a good majority of the discharge currents that pass through lightning arresters. There are, however, cases where the actual discharge currents approach in magnitude the discharge-current capabilities of lightning arresters, and sometimes exceed them.

In view of the foregoing points, it would seem desirable and consistent to have data on discharge voltages made available for much larger currents than the present maximum of 20,000 amperes.

E. H. Grosser: In preparing this report, the intention was to present data on the performance characteristics of lightning protective devices in strict conformance with the methods of testing prescribed in the proposed combined AIEE Lightning Arrester Standards for Valve and Expulsion Lightning Arresters. The discharge voltages were therefore reported for the surge current values specified in the proposed Standards, namely 5,000, 10,000, and 20,000 amperes.

It might be pointed out, however, that adequate justification exists for the values of current adopted for the standard tests. The transmission engineer, who designs his lines to withstand lightning stroke currents of 100,000 amperes or more, may be inclined to think in terms of such currents, overlooking the fact that usual or average stroke currents are much smaller. Currents discharged by lightning arresters have been found to be still smaller, due probably to less severe conditions of exposure for lightning arresters as compared with transmission lines. The 20,000-ampere test actually approaches the highest values of current measured in lightning arrester leads in service. It is believed that present-day lightning arresters, tested in accordance with the proposed Standards, represent a reasonable design compromise in being able to maintain good protective characteristics for moderately large surge currents.

A New Automatic Load Control for Turbine Generators

H. B. RUUD
NONMEMBER AIEE

S. B. FARNHAM
MEMBER AIEE

Synopsis: In an interconnected power system, load changes of sufficient magnitude to affect system frequency are normally shared by all the generators on the system in proportion to their ratings and the characteristics of their governors. This inherent sharing of load changes is highly desirable in the majority of cases. It may, however, present a problem in a few instances if some of the generators are remote geographically and electrically from that part of the system which includes a large fluctuating load. In such cases it would sometimes be preferable if the load changes could be confined in whole or in part to the local generators, thereby relieving the remainder of the system from having to respond to distant load fluctuations. This situation may become acute in the case of systems interconnected through long tie lines, where abrupt load changes in either system result in large transfers of synchronizing power through the interconnecting ties. This paper describes a new automatic load control arrangement which has the ability to respond to local load changes in anticipation of their effect on system frequency. At the same time, however, it does not deprive the conventional speed governor of its ability to control the prime mover input to help maintain constant system frequency. In this latter respect lies its essential and unique difference from other somewhat similar arrangements described previously.[1,2,3]

Introductory Background

THE decision to install automatic load-regulating control on the turbines at the Riverside Power Station of the Iowa-Illinois Gas and Electric Company near Davenport, Iowa, was prompted by the Aluminum Company of America constructing a rolling mill adjacent to that power station with all power requirements of the mill to be supplied by the utility company. The construction of this large capacity mill made automatic load-regulating control desirable for two reasons. First, the Tri-City area, (Davenport, Rock Island, Moline), which is served in part by the Riverside Power Station, was experiencing peak loads of approximately 100,000 kw. For comparison, the peak loads anticipated for the proposed rolling mill were in the order of 40,000 kw. The nature of the forthcoming load meant that the utility was to be faced with relatively large, sudden, and rapidly reoccurring load changes. The power company's previous experience with sudden load changes had been confined to electric steel furnace loads. While these furnace load changes were considerably smaller than those anticipated for the rolling mill, operating experience gained through them indicated that automatic load-regulating control for the new mill load would be highly desirable.

Second, the Iowa-Illinois Gas and Electric Company, in co-operation with other utilities in Iowa and Missouri, was in the process of constructing a 161-kv interconnecting transmission line, Figure 1. In order to achieve the maximum benefits from the interconnection facilities, the participating power companies agreed that each participant was to carry the load variations occurring in its own area. In brief, the interconnection facilities were to be essentially base loaded. This comprised the second reason for the installation of automatic load regulator control to carry the Alcoa mill load swings.

The Aluminum Company of America furnished the utility with representative kilowatt load curves taken at a similar, but smaller, rolling mill in Tennessee. From these curves the severity and frequency of the load swings for the mill under construction were predicted. It was estimated that the load swings would vary in magnitude from 10,000 kw to 16,000 kw. That is, the mill load would vary between 5,000 and 8,000 kw above and below the mean load. The frequency of the load swings was expected to be about one per minute. The rate of load change was estimated to vary between 2,000 and 5,000 kw per second.

Load-Regulating Equipment

Turbine Parts

A schematic diagram of the turbine speed-governing and control mechanism as applied to two of the four major generating units at Riverside is shown in Figure 2. This will be recognized as essentially the conventional speed governor and oil-actuated valve arrangement, although for purposes of this application it has several distinguishing modifications.

First, the synchronizing motor is sufficiently oversized to provide a travel time between the "full-open" and "full-closed" positions of approximately four to five seconds, as contrasted with a time of approximately 20 to 30 seconds achieved with the conventional governor motor. This higher speed of operation is essential in order to accomplish the desired objective of forcing the controlled generator to assume the local load fluctuations in advance of their tendency to change system frequency.

Second, instead of the split series field type of motor usually employed, this application makes use of a separately excited d-c shunt motor. This selection is determined by considerations of the control circuit, as will become apparent.

Third, a follow-up arrangement is added, which provides a voltage output whose magnitude is proportional to the speed-changer lead screw position. At constant system frequency, this voltage therefore also is essentially proportional

Paper 49-289, recommended by the AIEE Power Generation Committee and approved by the AIEE Technical Program Committee for presentation at the AIEE Fall General Meeting, Cincinnati, Ohio, October 17-21, 1949. Manuscript submitted July 14, 1949; made available for printing September 12, 1949.

H. B. Ruud is Chief System Supervisor, Iowa-Illinois Gas and Electric Company, Rock Island, Ill., and S. B. Farnham is with the General Electric Company, Schenectady, N. Y.

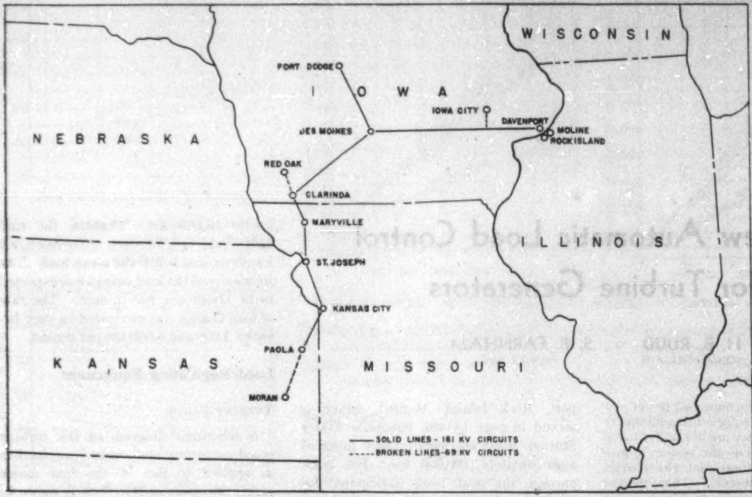

Figure 1. Map of interconnected system

to the kilowatt load on the turbine generator. If, however, for any reason there should be an appreciable nonlinearity between kilowatt load and mechanism position as might result for example from the inherent characteristics of the steam inlet valves and passages, this can be compensated for in the gearing or linkage through which the follow-up device is actuated. While the device itself may be anything capable of producing a voltage whose magnitude is proportional to position, such as a potentiometer, a selsyn, operating as an induction-voltage regulator, was chosen for convenience in this application.

Fourth, an initial steam-pressure regulator is included, whose function it is to prevent the possible "carry-over" of water from the boiler to the turbine inlet should excessive demands be placed upon the boiler by the load regulator. Normally the anticipated load increases will be within the ability of the boilers to handle without suffering an excessive pressure drop. If, however, for any reason circumstances were such that a sudden load demand might reduce the boiler pressure to a point where water carry-over could result, this initial pressure regulator is designed to assume control by pulling apart a telescoping connection, Figure 2, and thereby prevent any further increase in the loading of this machine until normal boiler pressure has been re-established. Rated steam pressure for this unit is 850 pounds per square inch. The initial steam pressure regulator is calibrated to assume control if the pressure falls below 750 pounds.

Electrical Controls

The controlling quantity which initiates operation of the automatic load-regulating control equipment is current in the feeder circuits to the Alcoa mill. This current is totalized in the secondaries of two current transformers, one each in the same phase of the two 13.8-kv mill feeder circuits, as indicated in Figures 3 and 4. The totalized current produces a voltage drop across resistor *R*, of a bridge circuit, as indicated in Figure 4. Two arms of the bridge are the opposing control fields of a continuously driven amplidyne generator, connected through rectifiers. The other two arms are formed by a potentiometer or variable autotransformer, across which are established the reference voltages E_1 and E_2. The proportionality between these voltages determines the base load at which the controlled machine operates. Hence, the position of the movable arm of the potentiometer or variable autotransformer may actually be calibrated in base-load kilowatts. At each value of steady base load on the generator, the follow-up device described previously on the turbine governor re-establishes the balance of the bridge.

Any current in the Alcoa feeders, by producing a voltage across resistor *R*, unbalances the bridge, and thus causes the amplidyne generator to produce a direct voltage of the correct polarity to cause rotation of the synchronizing motor in the direction to pick up load. The magnitude of the direct voltage, and, consequently the rate at which load is picked up, depends on the magnitude of the Alcoa load change. Once the turbine generator output satisfies the new load requirements, the voltage from the follow-up device re-establishes the balance of the bridge, the amplidyne generator output voltage returns to zero, and the synchronizing motor comes to rest. These sequences take place with such rapidity that the turbine generator output follows the fluctuating Alcoa load demands within approximately 1 to $1^1/_2$ seconds; and at this rate the load swings do not cause a measurable change in system frequency.

It will be apparent that by adjusting the ohmic value of resistor *R* across which the Alcoa load current produces the controlling voltage drop, the controlled generator can be made to assume all or any desired part of the Alcoa load changes. In this manner, with all four of the large turbine generators at Riverside similarly equipped, the total fluctuating load can be carried by any one machine, or divided among them in any ratio desired.

It is to be noted in Figure 4 that the reference voltages and the follow-up voltages are supplied from a common source. Not only must these voltages be in phase with one another, but also they must be derived from the same phase in which the current transformers for the Alcoa load

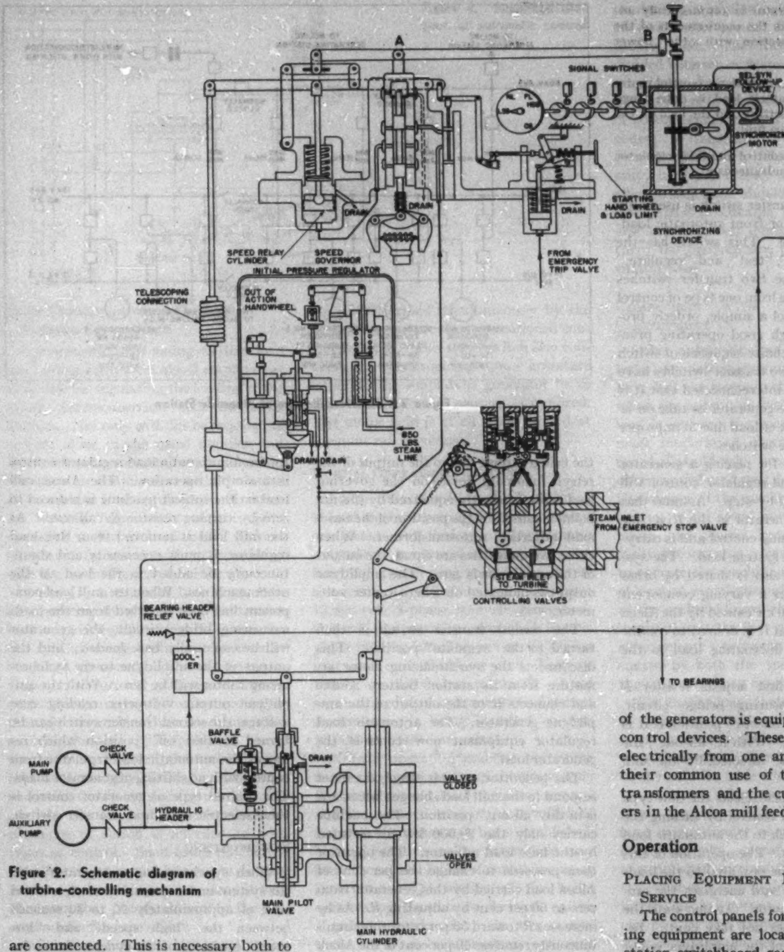
A
B
SIGNAL SWITCHES
SELSYN FOLLOW-UP DEVICE
SYNCHRONIZING MOTOR
STARTING HAND WHEEL & LOAD LIMIT
DRAIN
SYNCHRONIZING DEVICE
FROM EMERGENCY TRIP VALVE
DRAIN
DRAIN
SPEED RELAY CYLINDER
SPEED GOVERNOR
INITIAL PRESSURE REGULATOR
TELESCOPING CONNECTION
OUT OF ACTION HANDWHEEL
650 LBS. STEAM LINE
DRAIN DRAIN
STEAM INLET FROM EMERGENCY STOP VALVE
STEAM INLET TO TURBINE
CONTROLLING VALVES
BEARING HEADER RELIEF VALVE
COOLER
TO BEARINGS
BAFFLE VALVE
CHECK VALVE
MAIN PUMP
CHECK VALVE
HYDRAULIC HEADER
AUXILIARY PUMP
DRAIN
VALVES CLOSED
VALVES OPEN
MAIN PILOT VALVE
MAIN HYDRAULIC CYLINDER

Figure 2. Schematic diagram of turbine-controlling mechanism

are connected. This is necessary both to reflect in the bridge circuit a full measure of the quantities involved, rather than only a component dependent on vector relationships, and also to avoid operation of the controls in response to the reactive power or kilovar demands of the Alcoa load. With the connections as indicated, or with any comparable arrangement in which the reference voltages and kilowatt component of load current are in phase, the bridge is insensitive to kilovars, since the kilovar component of load current produces a voltage vector which is at right angles to the reference voltages, and thus affects both sides of the balanced bridge equally. Hence the kilovar component produces no net change in the amplidyne control fields. In this manner, the over-all system is responsive to kilowatts alone, in spite of the fact that the controlling quantity is load current.

Single-phase quantities are utilized, both in the interest of simplicity, and because, with the expected loads being essentially balanced, an entirely acceptable degree of accuracy can be realized. Each of the generators is equipped with its own control devices. These are independent electrically from one another, except for their common use of the bus potential transformers and the current transformers in the Alcoa mill feeders.

Operation

Placing Equipment In and Out of Service

The control panels for the load-regulating equipment are located in the power station switchboard room near the conventional generator control panels. The switchboard operator is responsible for the loading of the generator, whether the unit is on manual or either of three different automatic controls. On the generator load regulating control panel there are mounted along with the necessary indicating instruments, two transfer switches. The first transfer switch selects the desired type of control. The controls available are:

1. Manual control.
2. Tie-line bias control under which the

load on the generator is automatically adjusted to maintain the requirements of the 161-kv interconnection with other power companies.

3. Automatic load regulator control under which the generator's load is determined by the base load setting and the load on the feeders to the Alcoa mill.

4. Tie-line bias control and load regulator control acting simultaneously.

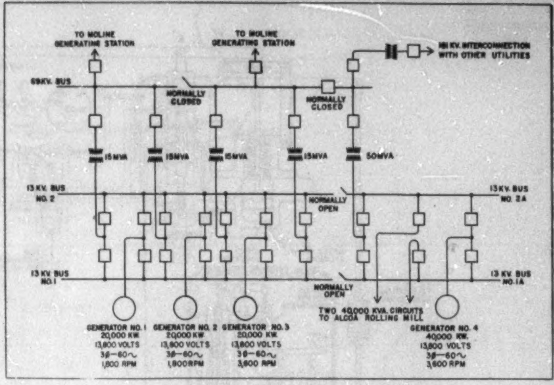
TO MOLINE GENERATINE STATION
TO MOLINE GENERATING STATION
161 KV. INTERCONNECTION WITH OTHER UTILITIES
69KV. BUS
NORMALLY CLOSED
NORMALLY CLOSED
15MVA
15MVA
15MVA
15MVA
50MVA
13 KV. BUS NO. 2
13 KV. BUS NO. 2A
NORMALLY OPEN
13 KV. BUS NO. 1
13 KV. BUS NO. 1A
NORMALLY OPEN
TWO 40,000 KVA. CIRCUITS TO ALCOA ROLLING MILL
GENERATOR NO. 1 20,000 KW. 13,800 VOLTS 3ϕ—60～ 1,800 RPM
GENERATOR NO. 2 20,000 KW. 13,800 VOLTS 3ϕ—60～ 1,800 RPM
GENERATOR NO. 3 20,000 KW. 13,800 VOLTS 3ϕ—60～ 3,600 RPM
GENERATOR NO. 4 40,000 KW. 13,800 VOLTS 3ϕ—60～ 3,600 RPM

Figure 3. Electrical diagram of Riverside Station

The second transfer switch is used only for changing to or from automatic load-regulator control. This switch has the positions of "off", "test", and "regulate." The use of these two transfer switches makes the change from one type of control to another control a simple, orderly procedure. Although good operating practice requires a definite sequence of switch operations, the two transfer switches have their contacts so interconnected that it is impossible for the generator to take on or drop a large block of load due to improper operation of these switches.

The procedure for placing a generator on automatic load-regulator control will be explained step-by-step. Assume that the 40,000-kw generator in the Riverside Station is on manual control and is carrying 20,000 kw of system load. The system load, which also is shared by other machines, includes a varying component of 30,000 to 40,000 kw caused by the Alcoa mill. Assume that it is desired to confine one-half of this fluctuating load to the subject machine.

The operator first adjusts resistor R in the load-measuring bridge circuit, Figure 4, to the "all-out" position if it is not already so set. With R "all-out", the bridge cannot be affected by the mill load.

The operator then selects the new type of automatic load control by turning the first transfer switch to the automatic load regulator position. The operation of this switch connects the potential to the load-measuring bridge and energizes the amplidyne driving motor. At this state the load regulator does not take control because the output of the amplidyne is not connected to the synchronizing motor.

The second transfer switch is then turned to the "test" position. This position permits the operation of the motor-operated base-load adjustor by the operator. It also makes operative a synchronizing motor control switch located at the load regulator control panel. The operator then adjusts the actual load on the generator with this control switch, if this is necessary. With the generator carrying 20,000 kw, the variable autotransformer, which serves as base-load adjustor, is set so that the unbalance in the bridge circuit due to the output of the selsyn follow-up device on the governor lead screw is exactly equalized by the unbalance caused by the position of the base-load adjusting autotransformer. When these two quantities are equal, the output of the amplidyne is zero. The amplidyne output is indicated on a zero-center voltmeter.

The second transfer switch is then turned to the "regulate" position. This disconnects the synchronizing motor armature from its station battery source and connects it to the output of the amplidyne generator. The automatic load regulator equipment now controls the generator load.

The generator, at this stage, does not respond to the mill load changes, because R is in the "all-out" position. The machine carries only the 20,000 kw as dictated by the base load adjustor. The operator then proceeds to change the per cent of Alcoa load carried by this generator from zero to 50 per cent by adjusting R. As he increases R toward 50 per cent, this simultaneously removes 50 per cent of the Alcoa load from the other machines on the system.

The generator now carries 20,000 kw plus one-half of the Alcoa load; that is, the generator load varies from 35,000 to 40,000 kw as the Alcoa load changes. If the system load or the Alcoa mill load changes sufficiently to demand a new base load on the generator, this is accomplished by simply resetting the base load adjusting autotransformer. As indicated previously, this adjustment is actually calibrated in base load kilowatts.

The procedure for removing a generator from automatic load regulator control is a simple operation. The Alcoa mill load on the subject machine is reduced to zero by turning resistor R "all-out." As the mill load is removed from this load regulator, it must necessarily and simultaneously be added to the load on the other machines. When the mill load component has been removed from the load-measuring bridge circuit, the generator will be essentially base loaded; and the output of the amplidyne to the synchronizing motor will be zero. With the amplidyne output voltmeter reading zero voltage, the second transfer switch can be turned to the "off" position which removes the automatic load regulator from control with no shifting of generator loads. The desired type of generator control is then selected with first transfer switch.

SYNCHRONIZING

When synchronizing a generator with the system under manual control, a travel time of approximately 20 to 30 seconds between the "high speed" and "low speed" positions of the synchronizing device is desirable in order to give the operator the requisite degree of control. The 4- to 5-second travel time as provided in this application to realize the objective of automatically confining local load swings to the controlled machine must therefore be extended to approximately 20 or 30 seconds when the machine is under manual control. This is accomplished by supplying the synchronizing motor armature at reduced voltage obtained from the station battery through an appropriate series resistor or potentiometer.

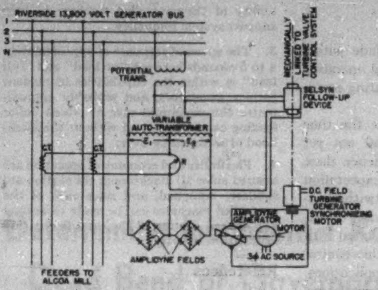
RIVERSIDE 13,800 VOLT GENERATOR BUS
1
2
3
N
POTENTIAL TRANS.
MECHANICALLY LINKED TO TURBINE VALVE CONTROL SYSTEM
SELSYN FOLLOW-UP DEVICE
VARIABLE AUTO-TRANSFORMER
E_1
E_2
CT
CT
R
D.C. FIELD
TURBINE GENERATOR SYNCHRONIZING MOTOR
AMPLIDYNE GENERATOR
MOTOR
3φ AC SOURCE
AMPLIDYNE FIELDS
FEEDERS TO ALCOA MILL

Figure 4. Simplified diagram of automatic control circuit

Joint Operation with Tie Line Loading Controller

Conventional slow-acting tie-line load bias control equipment also is employed at Riverside for regulating the loading of the 161-kv interconnection with the other utilities. Not only will this be required to operate alone in the usual manner, but also it must be suitable for simultaneous operation in conjunction with the automatic turbine load-regulating equipment. An obvious requirement of this joint operation is that each controller perform its alloted functions without interfering with the normal operation of the other.

During such times as both controllers are operating simultaneously, the turbine load control equipment will operate on the synchronizing motor in the manner described previously. The tie-line controller, however, will not operate directly on the synchronizing motor, but indirectly through the turbine base load adjusting autotransformer. Its operation, therefore, will be to reset the turbine base-load adjustment periodically, in accordance with the dictates of the tie-line loading. In this way, full freedom and independence of action is afforded to both types of control. Such could not be the case if both attempted to operate directly on the synchronizing motor, since it may be shown that one would nullify the corrective effects of the other.

When the Aluminum Mill is not operating, or if for any other reason the turbine load control equipment is removed from service, the tie-line controller is transferred directly to the synchronizing motor. The motor speed, however, is then reduced as described previously to a level consistent with that normally employed in such cases, that is, approximately 20 to 30 seconds for the range of travel between the "fully-open" and "fully-closed" valve positions.

The operations incident to transferring the control to conform to any of the several available methods of operation are all performed simultaneously by the first of the two previously mentioned control switches. This same switch also connects the synchronizing motor armature either to the amplidyne generator or to the reduced voltage source, as required. The motor field is at all times excited at constant rated voltage.

Normal Operating Practice

At the time of writing, the installation of load regulating equipment has not been completed, but this type of automatic control is in process of installation on the four major generating units at the Riverside Station. All four machines have 13,800-volt 3-phase 60-cycle generators. Control equipment as described in this paper is being installed on one 40,000-kw unit and one 20,000-kw unit, both of which are 3,600-rpm machines. Load regulating control equipment of a different manufacture is being installed on two 20,000-kw 1,800-rpm units.

Normal operating practice pertaining to the number of machines simultaneously under automatic load regulator control and the proportioning of Alcoa mill load between them has not been established. Normal practice can be determined only after the accumulation of actual operating experience. The ability of the boiler systems to respond to the demands will be a prime consideration. In the station there are three boiler systems operating at different pressures and temperatures. The reserve steaming capacity varies between systems. All boilers are equipped with full automatic control and normally burn either powdered coal or natural gas.

In view of the nature of the fuel, full automatic boiler control, and the fact that four generators will be equipped with automatic load regulator control, the proportioning of mill load between machines is not expected to pose a serious problem. The actual proportioning will vary from day to day and from hour to hour, dependent upon available steaming capacity on each boiler system and total system electric load. The Alcoa load will be divided between as many generators as is practical so as to cause the greatest number of boilers to share the sudden changes of steam demand. This practice will, of course, be modified by generating unit over-all efficiencies. For greatest economy, it appears that the newer, more efficient machines should be base loaded insofar as is practicable, leaving the older and generally less efficient machines to carry the predominant part of the fluctuating load.

Comparison With Other Similar Equipment

Other automatic load-control systems have been described previously.[1,2,3] They have had the common characteristic that when the automatic load control feature was in service, the speed governor was made inoperative, except that on overspeed it could take precedence over the other controls and shut down the machine. Conversely, if the machine was under the control of its speed governor, the automatic load control features were necessarily disconnected. Never was it possible to operate the machine under both types of control simultaneously. To the best of the authors' knowledge, the Riverside installation is the first embodiment of an arrangement permitting simultaneous control by both the speed governor and the automatic load regulating equipment.

The earlier load controls were applied to machines serving industrial power systems, wherein the generating capacity was relatively small compared with that of the utilities with which they were interconnected. The purpose of the automatic controls was to confine the local load swings insofar as practicable to the industries' own generators, and this was accomplished successfully. However, in the event of a drop in the frequency of the interconnected system, as might be occasioned by the tripping out of a transmission line or the loss of a major unit of the utilities' generation, there was no expectation that the industries' machine would pick up load in an endeavor to support frequency. This was entirely rational, since the industries' machines in general are relatively so small a part of the interconnected system generation as to be ineffectual in attempting to maintain sagging frequency.

Such a situation, however, could not be tolerated in load control equipment applied to the generators of a power company. In this service, every generating unit must, at all times it is in operation, be able to pick up load in response to its speed governor. Stated another way, even though the machine may be performing its intended functions under the control of the automatic load regulator as long as system frequency remains normal, any drop in frequency must be the signal for the machine to increase its output to help offset the drop. The new control equipment described herein fulfills this criterion.

Its operation may be visualized as simply that of a load regulator, so long as system frequency remains constant. Under this condition, the governor arm, top of Figure 2, pivots about point *A* as a fulcrum. If system frequency changes, point *B* becomes the fulcrum. Practically, of course, both motions can and do occur continually and simultaneously. Hence the load regulating function in no way impairs the ability of the machine to "step into the breach" whenever a system emergency calls for its full capabilities toward helping to maintain system frequency.

Conclusions

It had been hoped to include within this paper the results of actual operating experience with the new regulating equipment.

Unfortunately, however, at the time of writing the equipment had not yet been completely installed. Hence these remarks necessarily reflect expectation rather than realization. Notwithstanding this, the wide background of experience that has been accumulated with the essential components of this control as used for other governor applications, amplidyne generator voltage regulators, current controllers, and locomotive controls gives a basis for the following summary:

1. **The control arrangement described herein affords a means for confining load swings to near-by generators, thereby relieving tie lines and distant generators from handling large fluctuating loads.**

2. **For the first time, the load-regulating function is obtained without sacrificing the ability of the controlled machine to help support system frequency.**

3. **The speed of response of approximately 4 to 5 seconds between "no load" and "full load" is within the capabilities of modern turbine generators, and probably approximates the maximum rate at which boiler loading can be increased without the likelihood of water carry-over.**

4. **Flexibility and economy of operation are assured since all machines in the station are similarly equipped, and since each of the controlled machines can be made to assume any desired portion of the total fluctuating load within its rating.**

References

1. **Automatic Load Control for Turbine Generators, F. E. Crever, R. L. Jackson.** *Electrical Engineering (AIEE Transactions)* volume 64, September 1945, pages 656–60.

2. **Automatic Regulation of Turbine Generators to Relieve Power-Supply Systems of Steel-Mill Load Swings, W. W. Eberhardt, C. W. Harrison, E. J. Kohn, A. G. Darling.** *Electrical Engineering (AIEE Transactions)* volume 64, November 1945, pages 751–58.

3. **Suddenly Applied Loads Carried by a Variable-Ratio Synchronous Induction Frequency Changer, A. G. Darling, G. A. Kaufman.** *AIEE Transactions*, volume 67, part II, 1948, pages 91–94.

Discussion

G. S. Lunge (General Electric Company, Schenectady, N. Y.): This load regulator, if connected in accordance with Figure 4 of the paper, is obviously applicable if the line or lines feeding the fluctuating load leave the controlled generating station itself, so that instrument transformer secondary circuits can be connected directly to the regulator.

However, this load regulator is equally applicable if the generating station is many miles from where the active power flow to the fluctuating load can be measured, provided that this measurement is telemetered to the generating station and converted back to a suitable proportional value of single-phase alternating current. Both the telemetering and the reconversion to alternating current must take place continuously and with negligible time lag, as discontinuous action could not be tolerated.

Depending on the nature of the channel for transmitting the telemetered quantity, either a torque balance telewattmeter or a frequency-type telewattmeter would be suitable. If more than one fluctuating load circuit is involved, the telemetering equipment would be arranged in the usual manner to totalize the kilowatt load in the various circuits. A torque balance converter would be suitable for converting the d-c milliampere output of the telemetering equipment to a proportional single-phase alternating current. For this particular application, the restraining element of the torque balance converter would have its potential coils energized from a regulated (constant) voltage a-c source. This feature is essential in order that the converter current output (rather than its power output) may be linearly proportional to the power flow measurement telemetered to it.

A suitable amplifier would be needed to step up the 0.5-ampere 3-volt-ampere output of the torque balance converter to that required by the amplidyne field circuit.

In this case the regulated voltage a-c supply also should be used to supply the amplidyne field bridge circuit and the follow-up Selsyn supply circuit, to eliminate the effects of variation in generating station voltage.

The over-all time lag of the instrument combination suggested in this discussion is less than one second, regardless of whether a torque balance or a frequency-type telemeter is used, and there are no rotating parts involved in the instruments, other than the jewelled bearing shaft and disk assembly in the frequency-type telemeter transmitter.

Determining Incremental Regulation and Dead Band of Governors on Steam Turbine Generators Under System Load Conditions

E. L. TORNQUIST
MEMBER AIEE

I. L. WADE
NONMEMBER AIEE

Synopsis: The purpose of this paper is to present some of the reasons for testing steam turbine governors and to describe a method which makes it possible to determine the incremental regulation, dead band and stability of a governor connected to a large power system. The test equipment described has no mechanical inertia or lost motion and requires only connections to the potential and current metering circuits of the generator. The values obtained show the corresponding load change on the generator for any change in frequency. It is believed that these are the values which are most desired and are obtained directly under actual operating conditions of the unit without resort to assumptions as to the relationship between inlet valve movement and generator output. Some difficulties have been encountered and these are discussed with the hope that the work so far completed may be of interest to others and may stimulate thought towards a more simplified system for determining governor performance.

THE need for a method of testing that will determine the characteristics of a steam turbine governor is somewhat self-evident. However, a review of some of the factors that were considered important in the design of the test equipment described herein will be of interest since the objectives of the test dictated to a large extent the type of equipment desired.

The purpose of the test can be divided into the following:

1. To determine the performance of a governor with respect to purchase specifications.
2. To determine the necessity for and the results of maintenance work on the governor.
3. To determine the optimum settings of the governor through a knowledge of the governor characteristics and system requirements in order that each unit will perform most satisfactorily considering its size, heat rate, location on the system, and local plant steam generating conditions.

If the need is only for determining (1) above, somewhat elaborate equipment can be permitted, but to be effectively used for (2) and (3) the equipment should be simple to operate and provide the necessary data quickly.

The information necessary to evaluate the performance of a governor is the incremental regulation, dead band, and stability at all load points. The average steady-state speed regulation is only important in estimating the performance of the machine upon being disconnected from the system, since seldom is a turbine subject to frequency changes in the order of 4 or 5 per cent while connected to a large power system. However, each machine is being constantly influenced by small frequency changes in the order of 0.1 per cent and frequently 0.3 per cent. The response of the governor to these changes determines to a large extent the steadiness of the frequency, the division of a fluctuating load between the generators on the system, and the tendency for excessive changes in steam demand on the boiler room.

To maintain tie line loads at some predetermined value and to keep a constant integration of frequency for control of clocks most large power systems have installed remote automatic control on a number of turbines. A knowledge of the performance of a governor, therefore, is useful in determining which machines can best be used for load control. It can be seen, for instance, that if the remote load control calls for an increase of load at the moment the frequency is influencing the governor to reduce the load there will be a conflict between the sensitive governors on machines with load control and machines without load control. An understanding of these factors coupled with a knowledge of governor characteristics should assist in obtaining optimum performance of all machines on the system.

Method of Testing

A method of testing is desired that can be applied simply and does not require special attachments to the turbine. Around this principle a method was designed using a sensitive frequency bridge and a sensitive watt-converter connected into the current and potential metering circuits of the machine in such a manner that changes in both frequency and kilowatt output are converted into electrical quantities and these quantities appropriately indicated or recorded. These quantities are applied to an oscilloscope with a long persistence screen and the oscilloscope beam deflected horizontally with changes in frequency and deflected vertically with changes in kilowatts. The long persistence screen permits the pattern of the light beam to be observed for approximately 30 seconds. In this time a rotatable grid is adjusted to the slope of the figure and the degree of inclination read on a dial. If it is desired to obtain a record of the figure, a camera is placed in front of the oscilloscope. This gives a record of the type shown in Figure 1. The slope of line (*b*) is the incremental regulation. The line (*a*) is an index of the

---

Paper 49-290, recommended by the AIEE Power Generation Committee and approved by the AIEE Technical Program Committee for presentation at the AIEE Fall General Meeting, Cincinnati, Ohio, October 17–21, 1949. Manuscript submitted July 20, 1949; made available for printing September 12, 1949.

E. L. Tornquist and I. L. Wade are both with the Public Service Company of Northern Illinois, Chicago, Ill.

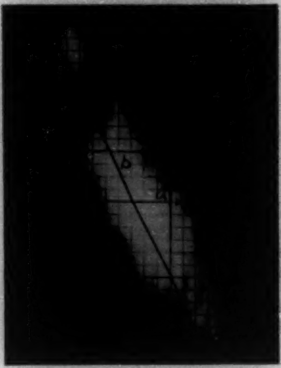

Figure 1. Kilowatts change versus frequency change with a 45-megawatt load on a 65-megawatt unit

Kilowatt change on vertical scale is 159 kw per small division and frequency change on horizontal scale is 0.005 cycle per small division

dead band. These readings are repeated at any desired intervals of load and the results plotted.

General Description of Equipment

The equipment used is shown in Figure 2. The standard cathode-ray oscilloscope with a long persistence screen comprises the heart of the system, and with the aid of the camera, gives a graphic record of the test data. The principle used to obtain these data by means of the oscilloscope is to apply an amplified direct voltage to the deflecting plates of the cathode-ray tube in such a manner that one set of deflecting plates will cause a horizontal deflection of the electron beam for changes in frequency and the other two deflecting plates will cause a vertical deflection of the electron beam for changes in kilowatt output. This principle is comparable to two mechanical forces displaced by 90 degrees. The resulting movement or deflection of the electron beam is, therefore, a combination of the two electrical forces acting upon the two sets of deflecting plates of the cathode-ray tube. The instrument thus becomes an X-Y recorder and the diagram thus obtained consists of a multiplicity of diagrams superimposed on a common axis and it usually resembles a parallelogram.

The amplifier, watt-converter, and bridge circuit are the means by which the various factors, such as frequency change and kilowatt output, are translated into proportional electrical quantities to be applied to the cathode-ray oscilloscope. The equipment and the method of operation is further described in Appendix I.

The AIEE Recommended Specifications for Speed-Governing of Steam Turbines Intended to Drive Electric Generators Rated 500 Kw and Up[1] defines incremental regulation in terms of kilowatt change with respect to speed change, or frequency change. These same specifications define dead band in terms of the speed change or frequency change over which there is no change in the position of the inlet steam valve, see Appendix II. Changes in the position of the steam valve are reflected in changes in the kilowatt output at some time interval later due to the inertia of the machine itself and the time it takes for the turbine to translate the changed steam flow into a changed power flow. Therefore, the method of determining dead band from the kilowatt output of the machine rather than from the valve movement does not conform to the AIEE specifications, but does give an index of the performance of the machine on the system under actual load conditions. Furthermore, it recognizes such factors as the inertia of the machine which may be useful in determining the response wanted or expected on a given machine. To illustrate, a machine that has a large dead band as determined by this method of testing may not be a good machine upon which to apply load control.

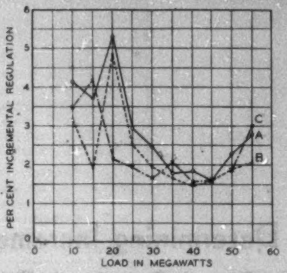

Figure 3. Comparison of three methods of obtaining Incremental Regulation on a 65 megawatt unit with one overload valve

Results of Incremental Regulation Tests

Curve A, Figure 3, shows the results of a test for incremental regulation on a 65,000-kw reheat turbine with one overload valve.

In order to compare this method of testing with other methods of testing, arrangements were made with one of the manufacturers to conduct a test on the above unit. This manufacturer's method, it is believed, determines incremental regulation in accordance with the AIEE specifications, but the equipment does not readily lend itself to quick determinations in the field. The incremental regulation obtained according to this manufacturer's procedure is shown as curve B, Figure 3. Another method of testing for incremental regulation was tried in which valve movement instead of kilowatt change was recorded on the vertical axis, and the kilowatts represented by this change in the valve movement were calculated, using the inlet valve characteristics curve, Figure 6. Curve C, Figure 3, represents incremental regulation as de-

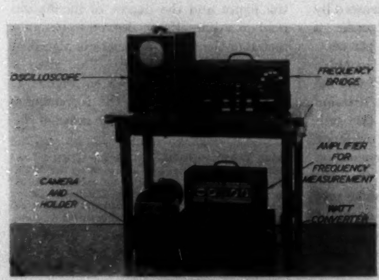

Figure 2 (left). Apparatus for determination of kilowatts change versus frequency change

Figure 4 (right). Apparatus for determination of valve movement versus frequency change

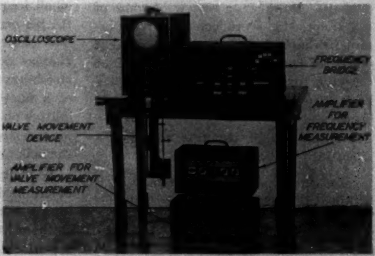
OSCILLOSCOPE
FREQUENCY BRIDGE
AMPLIFIER FOR FREQUENCY MEASUREMENT
VALVE MOVEMENT DEVICE
AMPLIFIER FOR VALVE MOVEMENT MEASUREMENT

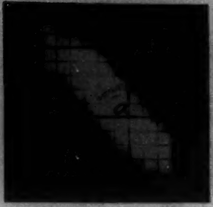

Figure 5. Valve movement versus frequency change with a 45-megawatt load on a 65-megawatt unit

Valve movement on vertical scale is 0.0075 inch per small division and frequency change on horizontal scale is 0.005 cycle per small division

Figure 7. Dead band tests on 10,000-kw unit by kilowatts change versus frequency change method and by valve movement versus frequency change method

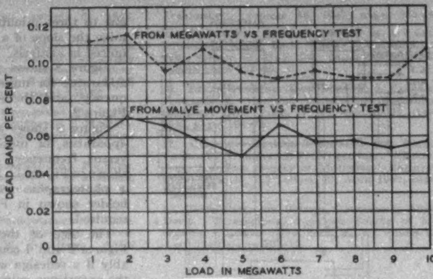

termined by this method on the same unit. It will be seen that the three methods of test give reasonably close agreement. The method of making these calculations is shown in Appendix II.

Results of Dead Band Determination

The dead band as determined by frequency change versus kilowatt change is not true dead band as defined in the aforementioned AIEE specifications. These specifications define dead band in terms of valve movement and frequency change. In order to study true dead band, a device as illustrated in Figure 4 was designed. The frequency bridge, amplifier and oscilloscope are the same as previously described. In place of the watt measuring equipment, a sensitive valve movement device was mounted on the inlet steam valve, and this movement electronically amplified so that changes in movement of the inlet valve are applied to the oscilloscope as an electrical quantity. A record obtained with this equipment is shown in Figure 5. Line (*a*) on Figure 5 therefore represents true dead band as interpreted from the AIEE specifications.

Figure 7 shows results of dead band obtained by these two methods. It is felt, however, that the index of dead band obtained by the kilowatt change versus frequency change method, although it cannot be used to determine conformance to purchase specifications, is a valuable index of the performance of the machine under load conditions, and when interpreted as such, and not as true dead band, has considerable value. While some of the tests show almost identical results by the two methods, many of the tests show the differences as indicated in Figure 7.

Difficulties Encountered

One of the difficulties encountered in applying this method of testing is the presence of oscillations in the kilowatt output of the generator having a frequency of about one cycle every 0.8 seconds. These are quite noticeable with the sensitive test apparatus used, and also may require recognition in other problems incident to the operation of a large power system. These oscillations are independent of system frequency changes and seem to be exaggerated by fluctuating loads. Under these conditions it is difficult to obtain a reliable index of performance. In one case, after a large fluctuating load was transferred to another generator, satisfactory results could be obtained. However, the cyclic variations under some load conditions have been sufficient to make determinations difficult and attention now is being directed towards eliminating these fluctuations from affecting the test apparatus. These cyclic changes in kilowatt output are natural phenomena in the operation of a generator on an interconnected system, and the frequency, but not the magnitude, of the fluctuations can be calculated quite readily from the constants of the system.

Future Work

The greatest need is for the development of test apparatus which will satisfactorily cancel out these oscillations. Recent tests show that this can be neutralized in the test circuit by using capacitors in the oscilloscope circuit. This gives excellent results for incremental regulation, but at the expense of the true picture of dead band.

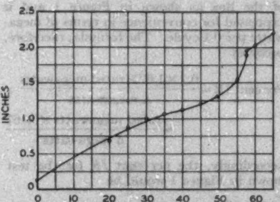

Figure 6. Inlet valve characteristics curve for 65-megawatt unit with one overload valve

Slope at 45 megawatts is 42.6 megawatts per inch of valve movement

Further work is needed to improve the technique of testing with the long persistence screen.

The equipment that is mounted on the inlet valve for determining true dead band also can be moved to other parts of the governor system for tracking down lost motion. It is planned to do some work along this line.

The frequency-sensitive bridge, watt-converter, and amplifiers were assembled or purchased separately and temporary connections used. A more compact and permanently wired instrument should be designed.

Summary

It is believed that there is need for a field method of determining incremental regulation and dead band of steam turbines under actual load conditions. The equipment described appears to be satisfactory for determining incremental regulation according to the AIEE specifications without making attachments to the turbine. Also an index of dead band can be determined by this method. True dead band as defined by the AIEE specifications can be obtained by the use of the auxiliary equipment described. However, this requires the attachment of a device on the inlet valve so that the small movements of the valve can be converted into electrical quantities suitable for the test apparatus.

Appendix I

Method of Test

To obtain the "power output (kilowatts) versus frequency" values, the watt-sensitive or watt-converter device is connected directly into the current and potential metering circuits of the generator under

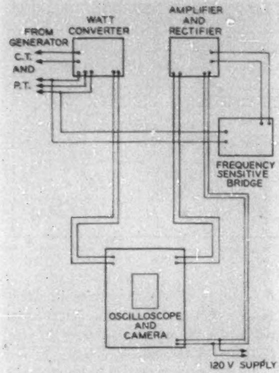

Figure 8. Block diagram of the apparatus used for the determination of kilowatts change versus frequency change

test and the frequency-sensitive bridge device or circuit is connected to the generator potential circuit. The watt-converter converts kilowatt output change directly to a proportional direct voltage change and the inherent characteristic of the converter circuit supplies sufficient amplification so that the direct output voltage can be applied directly to the cathode-ray oscilloscope. The frequency bridge is detuned to provide a polarizing effect so as to differentiate between increasing and decreasing frequency changes. The voltage output thus obtained from the bridge is a very small alternating voltage which is in turn amplified, rectified, and applied to the cathode-ray oscilloscope. Thus, the two corresponding forces proportional to kilowatt change and frequency change are applied to the cathode-ray deflecting plates and the resulting diagram is observed or photographed to obtain a measure of the machine performance.

The "valve movement versus frequency" test, which was mentioned in connection with "check tests" shown in Figure 3, is obtained in a similar manner, except that the watt-converter is replaced by a valve-movement detector. A variable inductance, comprising one leg of an inductive bridge circuit, is coupled mechanically to the main inlet valve or power piston of the turbine. This inductive bridge circuit is unbalanced in a manner somewhat similar to the detuning of the frequency bridge circuit, thereby polarizing the output voltage. Likewise, as with the frequency bridge, the output voltage is amplified and rectified and then applied to the cathode-ray tube. The resulting diagram thus obtained is another measure of the machine performance.

The feasibility of using a cathode-ray tube having a screen with extra long persistence, and thereby eliminating the need for photographing the screen, has proved satisfactory. This eliminates the need for the camera and holder shown in Figure 2, except in cases in which a photographic record is desired.

Experience has shown that a test run of one to three minutes is sufficient to determine the slope of a common major axis required in analysis.

Figure 8 shows a block diagram of the apparatus for measuring watts versus frequency, and the equipment is shown in Figure 2.

Figure 9 shows a block diagram of the apparatus for measuring valve movement versus frequency, and the equipment is shown in Figure 4. If it is necessary to make a photographic record, the camera and holder shown in Figure 2 also would be required.

The size of the equipment shown in Figures 2 and 4 could be reduced considerably if a redesign were made incorporating the experience gained and using parts that now are available but were not at the time of the original design. Such a redesign would probably incorporate the amplifier and frequency bridge of Figure 2 in one cabinet of about the same size and weight as the present frequency bridge. In Figure 4, the valve-movement amplifier should be much smaller, and as mentioned before, the frequency bridge and its amplifier would be combined.

Appendix II

Incremental Regulation

1. From an unpublished AIEE paper Recommended Specifications for Speed Governing of Steam Turbines Intended to Drive Electric Generators Rated 500 KW and Up, dated Nov. 1947, it is determined that, on a 60-cycle system

Steady-state incremental speed regulation in per cent

$$=\frac{\text{cycles change in speed}\times 100}{\text{system frequency}}\div\frac{\text{change in power output}}{\text{rated output}}$$

therefore

$$\text{Per cent IR}=\frac{\Delta\ \text{cycles}\times 100}{60}\times\frac{\text{Rated output}}{\Delta\ \text{power output}}$$

or

$$\frac{\Delta\ \text{cycles}\times 1.67\times\ \text{Rated output}}{\Delta\ \text{power output}}$$

Δ power output is obtained by the slope of the line as shown in Figure 1 and is expressed for convenience in terms of megawatts per 0.1 cycle. The formula, therefore, becomes

$$\text{Per cent IR}=\frac{0.1\times 1.67\times\text{rated megawatts}}{\Delta\ \text{megawatts}}=\frac{\text{rated megawatts}\times 0.167}{\Delta\ \text{megawatts}}$$

Accordingly, the per cent *IR* for the test shown in Figure 1 would be

$$\frac{0.167\times 65}{6.8}=1.6\ \text{per cent}$$

2. Also Δ megawatts = valve movement in inches per 0.1 cycle (from Figure 5) by megawatts per inch of valve movement (from inlet valve characteristics curve, Figure 6.) Valve movement per 0.1 cycle is proportional to the slope of the parallelogram as shown in Figure 5, therefore, per cent *IR* = rated megawatts by 0.167 ÷ Δ valve movement by megawatts per inch, from inlet valve curve as per Figure 6. Accordingly, the per cent *IR* for the test shown in Figure 5 would be

$$\frac{0.167\times 65}{0.16\times 42.6}=1.6\ \text{per cent}$$

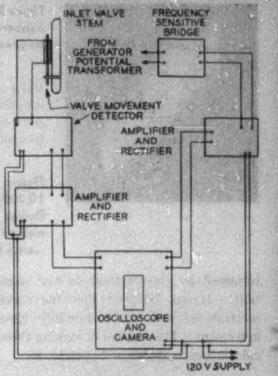

Figure 9. Block diagram of the apparatus used for the determination of valve movement versus frequency change

Dead Band

Dead band is the total magnitude of the sustained speed change within which there is no resulting measurable change in the position of the governor-controlled valves. Dead band is a measure of the insensitivity of the speed-governing system and is expressed in per cent of rated speed.

Therefore

Per cent dead band on a 60-cycle system

$$=\frac{\text{cycles of no movement}\times 100}{60}$$

The total magnitude of sustained speed change within which there is no change in valve position is considered to be the change in frequency represented by the line (*a*) in Figure 1 which is 6.0 divisions or 6 by 0.005 cycles or 0.030 cycles.

Accordingly

Per cent index of dead band would be

$$\frac{0.03\times 100}{60}=0.05\ \text{per cent}$$

Similarly, dead band can be determined from valve movement versus frequency change, as shown in Figure 5, the line (*a*) represents five divisions, or 5.0 by 0.005 cycles or 0.0250 cycles. Accordingly

$$\text{Per cent dead band would be }\frac{0.0250\times 100}{60}=0.0416\ \text{per cent}$$

References

1. Speed-Governing of Steam Turbines Intended to Drive Electric Generators Rated 500 Kw and Up. *AIEE Standard Number 600*, May 1949.

2. Oscillograph Analyzes Governor Performance, J. E. Allen. *Power* (New York, N. Y.) volume 78, November 1934, pages 610–12.

3. Prime-Mover Speed Governors for Interconnected Systems, R. J. Caughey, J. B. McClure. *AIEE Transactions*, volume 60, 1941, pages 147–51. Discussion by J. E. Allen, pages 729–30.

4. A Turbine-Governor Performance Analyzer, W. O. Osbon. *Electrical Engineering* (*AIEE Transactions*) volume 60, November 1941, pages 963–67. Discussion, R. Sheppard, C. Concordia. *AIEE Transactions*, volume 61, 1942, pages 393–94.

5. Effect of Prime-Mover Speed Governor Characteristics on Power-System Frequency Variations and Tie-Line Power Swings, C. Concordia, S. B. Crary, E. E. Parker. *AIEE Transactions*, volume 60, 1941, pages 559–67.

6. Prime-Mover Speed Governors for Interconnected Systems, R. J. Caughey, J. B. McClure. *AIEE Transactions*, volume 60, April 1941, pages 147–50.

7. Power System Governing—The Problem, J. J. Dougherty, A. P. Hayward, A. C. Monteith, S. B. Griscom. *AIEE Transactions*, volume 60, 1941, pages 547–58.

8. Testing Governor Performance on Electric Power Systems with Improved Instruments, J. E. Allen, W. B. Hess. *AIEE Transactions*, volume 66, 1947, pages 329–39.

9. Methods of System Control in a Large Interconnection, Earle Wild. *AIEE Transactions*, volume 60, May 1941, pages 232–36. Discussion pages 737–39.

10. Steam Turbine Governors, R. J. Caughey. *Transactions*, American Society of Mechanical Engineers (New York, N. Y.) volume 62, April 1940, pages 191–98.

11. Constant System Speed and the Steam-Turbine Governor, A. F. Schwendner. *Transactions*, American Society of Mechanical Engineers (New York, N. Y.) volume 62, April 1940, pages 199–206.

12. The Field of System Governing, Albion Davis. *Transactions*, American Society of Mechanical Engineers (New York, N. Y.) volume 62, April 1940, pages 207–19.

No Discussion

The Performance of a Topped Steam Power Plant on Sudden Load Reduction

JOHN G. NOEST
MEMBER AIEE

AT THE present stage of the development of the system of the Consolidated Edison Company of New York, one of the company's power generating stations, namely the Sherman Creek Station, with a generating capacity considerably in excess of its local bus load, depends upon a single high-capacity tie feeder for the purpose of interconnecting it with the remaining system. The utilization of the major portion of the plant's capacity, therefore, depends on this tie feeder carrying the difference between the plant capacity and the local bus load. At certain times, the local plant load may be as little as 10 per cent of generation.

This situation exposes the plant to unusual operating conditions in that the trip-out of the single tie feeder will result in a sudden, severe unloading of the plant.

To discover whether or not this condition involved particular hazards to the continuity of service to the local consumer load and to plant equipment, as well as to formulate operating instructions for the guidance of the plant operating personnel, a study was undertaken to disclose the performance of the component parts of the plant when the plant was subjected to a sudden reduction of its load. This study was aimed particularly towards the determination of the performance of the local electric system, the turbine plant, and the steam generation equipment. This study was later expanded to include actual tests, involving the dropping of various percentages of the plant generation, and it includes the experience gained during unstaged, accidental trip-out of the tie feeder.

Description of the Plant and Its Interconnections

Prior to the year 1943, when the first of the present two topping units was being installed, the Sherman Creek Station had been developed to a point where it had eight condensing turbogenerators, varying in size from 15 to 30 megawatts, with a total capacity of 171 megawatts. The steam generating equipment consisted of 50 boilers, which were initially provided with stokers and some of which were later converted to oil burning. The steam pressure was 185 pounds per square inch gauge and the steam temperature was 500 degrees Fahrenheit. The steam conditions after the installation of the topping units remained, of course, the same as far as the eight low-pressure units, all of which are still in service, are concerned.

At that time, the eight generators were connected to a 13-kv bus of four sections and there were six 13-kv ties to the Company's Hell Gate Station, with a total capacity of 60 megawatts; there were two 45-kv ties, with a total capacity of 42 megawatts to the system via Laconia Avenue Substation, which still exist, but which now are operated from an isolated bus section at Sherman Creek; and there was and still is another 13-kv 8-megawatt tie to the system via Columbus Avenue Substation. The total tie capacity was therefore 110 megawatts and the locally distributed peak load was 80 megawatts.

As mentioned before, the first topping turbogenerator unit, rated 50 megawatts, at 0.8 power factor, was installed in 1943. By that time the two end bus sections had been modernized by the installation of metal-clad phase-isolated busses with modern switchgear. The tie feeder situation remained virtually unchanged. By this installation the station capacity was increased from 171 to 221 megawatts.

The steam generating equipment for the first topping turbogenerator consists of a Combustion Engineering Company pulverized coal-fired wet-bottom boiler with a capacity of 1,000,000 pounds per hour at 950 degrees Fahrenheit. The furnace is equipped with gas ignition torches, operable from the control board. Automatic combustion control and boiler water level control are provided. The boiler feed pumps and fans are turbine-driven. In 1947 the second topping turbogenerator was installed and the 138-kv tie feeder, connected at the Dunwoodie Substation to an existing tie from Hell Gate to the Niagara-Hudson System, was established. This turbogenerator also is 50 megawatts, 0.8 power factor, and its installation added another 50 megawatts to the existing station capacity of 221 megawatts, giving a new total of 271 megawatts.

The steam generation equipment for the second topper is a duplicate of that provided for the first, except for the provision for pulverized coal and oil firing for load carrying, and for oil ignition using steam atomizing burners, and the bifurcation of the lower coal burner to provide better air-coal mixing to minimize sulphiding. The oil ignition torches must be lit manually at the burners.

To provide space for these installations, 18 of the old boilers were removed, leaving 32, with a total capacity of 190,000 pounds per hour.

With the installation of the new 138-kv tie, which has a capacity of 179 megavolt-amperes, the then existing six Hell Gate ties had to be discontinued since they could not be operated in parallel with the new 138-kv tie at high loads.

Paper 49-291, recommended by the AIEE Power Generation Committee and approved by the AIEE Technical Program Committee for presentation at the AIEE Fall General Meeting, Cincinnati, Ohio, October 17–21, 1949. Manuscript submitted July 20, 1949; made available for printing September 2, 1949.

JOHN G. NOEST is Division Engineer in the Electrical Engineering Department of the Consolidated Edison Company of New York, Inc., New York, N. Y.

The author wishes to acknowledge the valuable contributions made to this paper by W. J. Roberts and R. W. Clement, of the Consolidated Edison Company of New York.

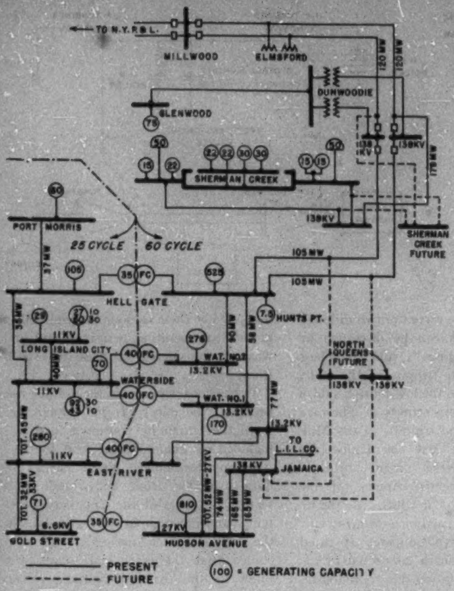
TO N.Y. R & L.
MILLWOOD
ELMSFORD
120 MW
120 MW
DUNWOODIE
GLENWOOD
75
50
15
22
22
22
30
30
SHERMAN CREEK
15
15
50
138 KV
138KV
179 MW
138KV
SHERMAN CREEK FUTURE
60
PORT MORRIS
25 CYCLE
60 CYCLE
37 MW
105 MW
105 MW
105
35 FC
525
HELL GATE
7.5
HUNTS PT.
35 MW
29
27
10
20
30
11KV
LONG ISLAND CITY
40MW
70
40 FC
275
WAT. NO.2
13.2KV
60MW
58 MW
NORTH QUEENS FUTURE
138KV
138KV
WATERSIDE
11KV
92
30
43
10
40 FC
WAT. NO.1
13.2KV
77MW
170
13.2KV
TO L.I.L.CO.
280
TOT. 40 MW
11KV
40 FC
EAST RIVER
138 KV
JAMAICA
TOT. 32 MW 33KV
71
810
TOT. 52 MW-27KV
74MW
165MW
165MW
6.6KV
35 FC
27KV
GOLD STREET
HUDSON AVENUE
PRESENT
FUTURE
(100) = GENERATING CAPACITY

Figure 1. Diagram of the Consolidated Edison Company's Metropolitan System

The presently existing interconnection of the Sherman Creek Station with the remainder of the Company's system is shown on Figure 1, which also shows the planned future development. Figure 2 shows the present bus arrangement at the Sherman Creek Station together with planned future expansion. Figure 3 shows schematically the connections of the steam equipment.

The generating capacity versus the station bus load and tie-feeder capacity situation at the Sherman Creek Station is summarized in Table I. This tabulation shows that the Sherman Creek Station may be exposed to a sudden load reduction of up to 179 megawatts on trip-out of the 138-kv tie feeder at times when the station local bus load may be at any value between 20 and 100 megawatts.

The Operating Problem

Under normal operating conditions the load, served from the Sherman Creek Station, is essentially of the metropolitan type in that load changes are small in amount and of slow nature. For this reason it has never been found necessary to use automatic voltage regulation on any of the generators. Automatic load-frequency regulation is available for the purpose of maintaining the tie-feeder load.

Since the Sherman Creek Station is located on the northern end of the metropolitan system of the company, where, because of the available charging kilovolt-amperes from the capacitances of the 138-kv ties, of which the Sherman Creek-Dunwoodie tie is one, (the Hell Gate-Dunwoodie and the Sherman Creek-Dunwoodie ties being cable circuits) and where, because of the small local load, the reactive kilovolt-ampere requirements are small, this station normally operates with power factors ranging between 0.90 to 0.95.

The operating problem, which presents itself on sudden load reduction because of the trip-out of the 138-kv tie feeder, may be resolved into three major phenomena, which are, of course, interrelated:

1. The effect of the voltage and frequency rise upon the remaining consumer load.
2. The effect upon the low-pressure steam header pressure, to which the major boiler auxiliaries, such as the induced and forced draft fan and the boiler feed pumps, all of which are turbine-driven, are connected.
3. The effect on the high-pressure boilers with respect to water level and the maintenance of ignition.

Within these three divisions there is a question not only in relation to the performance of equipment but in relation to the performance of the operating personnel as well.

The Theoretical Investigation

Beginning with the effect of voltage rise on the remaining consumer load, there is the question of magnitude and duration. Since automatic voltage regulation is not available in this station, the duration of overvoltage depends largely upon the time it will take the operators to

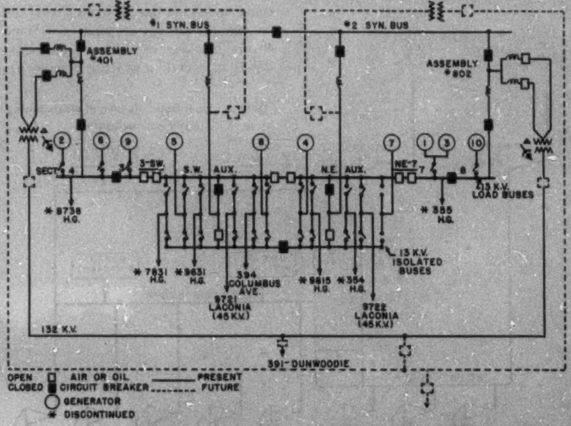
#1 SYN. BUS
#2 SYN. BUS
ASSEMBLY #401
ASSEMBLY #802
2
6
9
5
8
4
7
1
3
10
SECT. 4
3-SW.
S.W.
AUX.
N.E.
AUX.
NE-T
7
8
13 K.V. LOAD BUSES
* 8736 H.G.
* 355 H.G.
13 K.V. ISOLATED BUSES
* 7631 H.G.
* 9631 H.G.
394 COLUMBUS AVE.
9721 LACONIA (45 K.V.)
* 9615 H.G.
* 354 H.G.
9722 LACONIA (45 K.V.)
132 K.V.
391-DUNWOODIE
OPEN
CLOSED
AIR OR OIL CIRCUIT BREAKER
PRESENT
FUTURE
GENERATOR
* DISCONTINUED

Figure 2. Diagram of the electric connections of Sherman Creek Station

Table I

Generating capacity	271 megawatts
Local bus load, incl. the Laconia Ave & Columbus Ave ties	100 megawatts peak 20 megawatts off-peak
Dunwoodie 138-kv tie capacity	179 megawatts

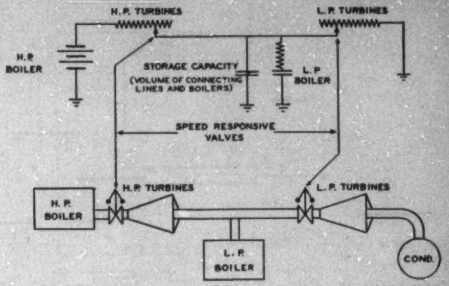

Figure 4. Electric analogue of steam flow

restore conditions to normal. In the theoretical investigation it therefore is assumed that the activities of the operators will have no effect upon the maximum voltage which is reached in a few seconds. In effect, therefore, it is assumed that the voltage will have reached steady-state conditions before the operator is able to intervene.

The factors, which affect the voltage rise, are:

1. Initial conditions, that is: tie-line load, bus load, power factor, and generator capacities.

2. The effect of the change of load and power factor on the generator voltage at constant speed.

3. The effect of the change of load on the frequency or the turbine speed, which in turn is a function of the behavior of the turbine governors, and which affects voltage cumulatively because of the action of pilot and main exciters with increasing speed.

Although the calculation of the first two factors is simple and straightforward, difficulty was experienced with the third, not so much because of the difficulties in the basic approach as because of the difficulty in obtaining the necessary governor constants. Appendix I shows the methods used in the calculation of the above three factors. The result of these calculations is given in Table II.

In the calculation of factor 2, the effect of load and power factor change on the generator voltage, there are two different conditions, which can be discerned by inspection of Figures 1 and 2. These two conditions are tripping of the 13-kv circuit breakers on the low-tension side of the tie-feeder transformers at Sherman Creek Station, and tripping of the Millwood Substation and the Dunwoodie Substation tie-feeder circuit breakers without simultaneous tripping of the Sherman Creek end, in which case the tie feeder with its capacitance charging current of 30 megavolt-amperes at rated voltage would remain connected to the Sherman Creek Station bus. Obviously, as far as voltage rise is concerned, the latter situation would represent the most severe case. However, since this case cannot arise under fault conditions without the simultaneous failure of the Sherman Creek Station, tie-feeder circuit breaker operating mechanisms or their control circuits, the probability of it happening is negligible. Under normal conditions, the tie-feeder capacitance could be left on the Sherman Creek bus only by the erroneous operation of three circuit breakers at different locations; this is an operation which is equally unlikely. For these reasons the probability of such an operation is insignificant and was not considered in these investigations.

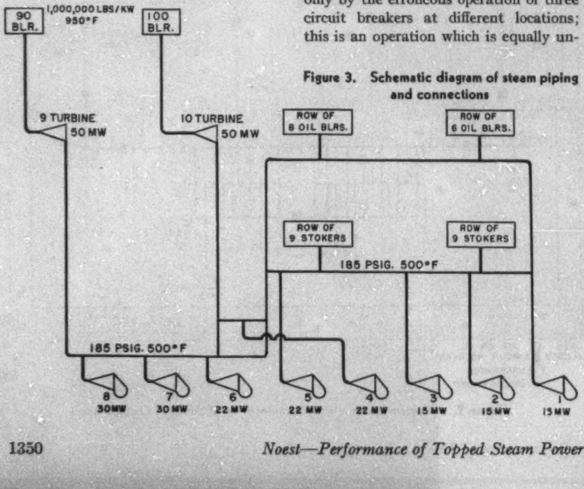

Figure 3. Schematic diagram of steam piping and connections

In the consideration of the voltage rise problem, the effect of the voltage rise upon the remaining consumer load was included by assuming the load to have constant impedance. From checks of data available from tests made previously on parts of the Company's system and from comparison with data in the technical literature[1,2,3] it was concluded that the error thus made was small in the expected voltage range. However, no consideration was given to the possible reduction of the consumer load because of lamp burnout, since it was known from previous experience that a voltage rise up to 25 per cent is acceptable from this standpoint, provided that the duration of such a rise does not exceed one minute.

In the study of the second part of the operating problem, namely the effect of sudden load reduction upon the behavior of the low-pressure steam header pressure, there also are a number of factors to be considered. These are:

1. The performance of the high-pressure and low-pressure turbine governors.

2. The amount of low-pressure boiler capacity and the amount of steam storage capacity, represented by banked boilers and by the volume of the steam piping.

3. The time limit imposed on the operators by the restrictions in motoring time on the topping turbines.

The data available for the study of the first of the above listed factors was meager indeed. Although the regulation at steady state was known for the different governors, there was no information available on the incremental regulation, nor on the time constants involved in the problem. Because of this lack of definite information, assumptions were made as follows:

1. That the steady-state regulation curves

Table II. Calculated Performance

		Nominal Load Drop in Megawatts 50	100	170
Assumed conditions, adjustments*		None	None	None
Total load	Megawatts	76	122	220
	Megavars	43	60	107
Tie-line load	Megawatts	51	100	170
	Megavars	24	43	70
Bus load	Megawatts	25	22	50
	Megavars	19	17	37
Generating capacity on bus, megavolt-amperes	Initial	133	220	254
	Final	133	220	254
Bus voltage, kilovolts	Initial	13.5	13.6	13.6
	Maximum	15.6	15.9	17.1
	Final**	15.4	15.9	17.1
Frequency, cycles per second	Initial	60	60	60
	Maximum	62.7	63.3	63.3
	Final**	61.2	61.5	61.9
Low-pressure header pressure, pounds per square inch gauge	Initial	200	202	200
	Final**	216	196	—

* No manual adjustments were assumed to be made for a 15-second period following the trip-out.

** At 15 seconds.

are combinations of straight lines within the range involved, and that these curves would give the ultimate speed.

2. That governors, having reasonably equal regulation and time constants, may be lumped together and represented by an equivalent governor.

3. That for the low-pressure turbine governors a maximum valve gear travel time could be assigned, and that the valve gear travel speed would be proportional to the instantaneous difference between the actual speed at the moment and the speed called for by the regulation curves for the respective units.

4. That a linear relation exists between the output of the generator and the position of the valve gear.

For the determination of the behavior of the low-pressure steam header pressure, the system can be represented by an electric circuit as shown in Figure 4. From this representation it can be seen that the two regulating devices, representing the turbine governors, are not independent so far as the regulation of the steam flow is concerned. They do, however, independently affect the low-pressure header pressure.

Using the method outlined in Appendix I, the set of curves shown in Figure 5, as well as the data given in Table II, were derived.

From this study the following conclusions can be reached:

1. With the usual power factor of the load on the tie feeder of 0.95 or higher, the voltage rise would not exceed 25 per cent.

2. For the maximum load reduction by tie-feeder trip-out, the frequency rise would not exceed 6 per cent.

3. The faster governors of the topping turbogenerators are primarily effective in limiting the frequency or speed rise.

4. The behavior of the low-pressure steam header pressure is determined by the incremental regulations of the two groups of governors, which also determine the load division, and by initial loading.

5. Low-pressure steam storage helps in reducing the rate at which the pressure in the low-pressure header changes.

6. The ratio of available low-pressure steam generation to the remaining bus load determines the extent to which the topping units will tend to motor.

7. Judicious removal of excess generating capacity is the quickest way for the restoration of normal conditions.

With the data obtained from these theoretical investigations on hand, the boiler operating problem was discussed. The outcome of these discussions is summarized below:

If on trip-out at high loads the operator promptly removes one of the high-pressure generators together with the proper number of low-pressure generators, the low-pressure header pressure can be kept within reasonable limits so that the boiler feed pumps will be available to prevent

Figure 5. Comparison of theoretical computations with test results—50-megawatt load drop

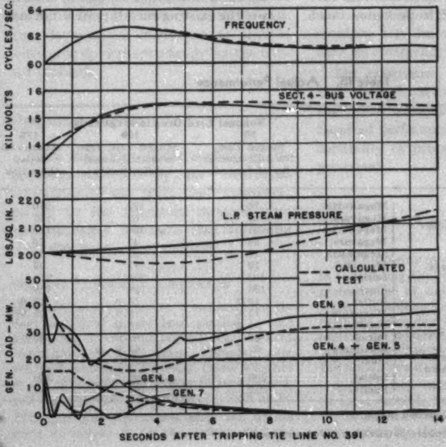

Figure 6. Comparison of theoretical computations with test results—100-megawatt load drop

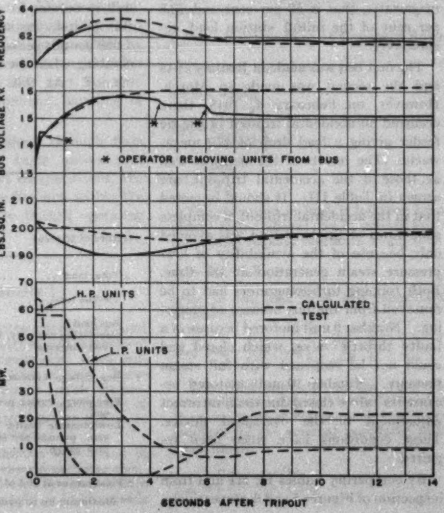

dangerously low-water levels in the high-pressure boilers, while these boilers are blowing off steam through their safety valves. Since number 90 boiler has gas ignition, it should be removed rather than the number 100 boiler (number 100 boiler is being changed to gas ignition).

The prompt removal of excess generating capacity also will reduce the tendency toward motoring of the remaining high-pressure unit, thereby avoiding the need to shut it down when the permissible motoring time of 30 seconds on one, 45 seconds on the other, has expired. By avoiding shutdown, because of motoring, the boiler operation problem was considered well within the capability of the operating personnel and no damage to station equipment was anticipated.

Tests and Actual Unstaged Trip-outs

Because the investigation discussed previously shows that the Sherman Creek Station would be able to ride through the most severe sudden load reduction without damage to company or consumer equipment, provided that the operators act quickly and correctly, it was decided to stage tests. Such tests would provide the means for checking the method of calculation and the correctness of the assumptions as well as give valuable training to the operators. In accordance with the foregoing, arrangements were made for two tests the first involving a load drop of 50 megawatts, and the second, 100 megawatts, that is 52 per cent and 60.5 per cent of the initial station load, respectively.

The first test was made in January 1948 and the second was made in March. However, on February 4, 1948, there occurred an accidental trip-out of the tie feeder giving a load drop of 170 megawatts. The results of the tests, as well as those of the accidental trip-out, are shown in Table III. It should be noted that in the accidental trip-out, a complete shut-down of the local load was avoided only because of the availability of low-pressure steam generation at the time. Both topping turbogenerators had to be removed from the bus because of motoring. Number 9 unit motored because of a faulty throttle valve, which closed and could not be reopened with full steam pressure. Number 10 unit motored because its valves closed due to an incorrect adjustment of the overspeed device. These conditions have since been repaired.

By comparing Tables II, III and from inspection of Figures 5 and 6, respectively, it can be seen that the theoretical method employed in these investigations can closely predict the actual performance.

In respect to boiler operation during both staged tests for which the operating personnel was fully prepared and armed with detailed instructions, all equipment functioned correctly and the operators easily controlled all essential boiler operating functions without difficulty. Prolonged motoring of the high-pressure turbines was avoided and there was no trouble with the maintenance of the boiler drum water levels.

However, the unstaged trip-out of February 4, 1948, because of the closing of the turbine valves on both topping units, created additional problems.

Because of the loss of both topping units, the electrical operator did not trip low-pressure units, but tried to maintain the remaining station load with them. In so doing, he caused the low-pressure header pressure to drop to 145 pounds per square inch gauge, which, in turn, resulted in water carry-over and, because of the sudden chilling, leakage in all flanged joints in the low-pressure piping system.

Delayed by having to manually light the oil ignition on the boiler, it was ten minutes before number 10 could be synchronized, whereas, if remote controlled gas ignition had been available, number 10 could have been back on load in one or two minutes.

Anticipating the momentary opening of number 9 throttle, the number 90 boiler operator cut in the gas ignition and held a mill in service for one minute. During this period, the steam pressure rose to 1,950 pounds per square inch and was still climbing when the ignition and mill were cut off. At this high pressure, much steam escaped through the safety valve expansion slip joints and clouded the entire area, rendering the boiler water columns invisible. However, the drop in drum water level was held to 13 inches by manual operation of the boilerfeed pumps. (The safety valve piping joints have since been modified to prevent a recurrence of the condition.) As number 9 throttle had closed due to unbalanced pressures, the boiler pressure had to be reduced materially before the valve could be reopened. As a result, it was 17 minutes before number 9 unit was returned to service.

The exact sequence of events and operations was made more difficult to reconstruct as some of the instruments did not record rapidly enough. These were principally the multipoint recording type. Some of the instruments were not set exactly on the correct time. Some of them stopped at the crucial moment due to blown fuses following overvoltage at the time of trip-out. The operators were busy and many of the indicating instruments went unread and unlogged.

Automatic Devices for Alleviating the Problem

During one stage of the investigation, consideration was being given to the installation of various automatic devices for assisting the operators in controlling the voltage rise and for controlling the low-pressure header pressure.

For the control of overvoltages, consideration was given to the installation of standard voltage-regulating equipment on all generators. This would have involved the installation of new exciter field rheostats on all but the two topping units because the existing rheostats were not suit-

Table III. Actual Performance

Nature of trip-out		Nominal Load Drop in Megawatts 50 Staged Test, No Adjustments for 15 Seconds	100 Staged Test, Immediate Manual Adjustments	170 Accidental Relay Operation
Total load	Megawatts	76	122	220
	Megavars	43	60	107
Tie-line load	Megawatts	51	100	170
	Megavars	24	43	70
Bus load	Megawatts	25	22	50
	Megavars	19	17	37
Generating capacity, megavolt-amperes	Initial	133	220	254
	Final	133	98	129
Bus voltage, kilovolts	Initial	13.5	13.6	13.6
	Maximum	15.5	15.6	16.9**
	Final*	15.2	15.0	
Frequency, cycles per second	Initial	60	60.0	60
	Maximum	62.7	62.8	
	Final*	61.2	61.6	
Low-pressure header pressure, pounds per square inch gauge	Initial	200	202	200
	Final*	212	198	

* Final means at end of 15-second period.

** Maximum up to point where potential transformer fuse blew.

able for use with automatic voltage-regulating equipment. The costs of such an installation would have had to be justified purely on the basis of alleviating a rather infrequently expected emergency condition.

As a cheaper means of reducing voltage rise, a scheme, using voltage relays, set above the normal operating voltage, to lower the exciter field rheostats to a preset position, was investigated. This would have obviated the need to purchase new field rheostats. This scheme was abandoned because of the possibility of creating instability by depriving a loaded generator of a sufficiently high field excitation to assure maintenance of synchronism.

For the purpose of maintaining low-pressure header pressure and to prevent prolonged motoring of the remaining high-pressure turbine, an automatic scheme for tripping excess generator capacity was considered. With this scheme, the operator would preselect the units he would want quickly removed from the bus in case of a trip-out of the tie feeder. A voltage relay, set to a certain overvoltage, would then trip these preselected units. Because of the operator's understandable aversion to a scheme which would automatically remove the generating capacity several units in case of failure of a single device, such as a relay, this scheme was abandoned.

No additional automatic devices were ever considered for application to the boilers; in fact, the operators invariably resort to manual control of the boiler in all emergencies.

In view of the tests, and on the basis of actual unstaged trip-out experience of which, to date, five cases have occurred, a final decision was made not to provide automatic devices specifically for the trip-out problem.

Operating Guides

From the wider understanding of the problem, provided by the theoretical investigation and from the experience, gained by the operators through tests and unstaged trip-outs, the following operating guides were derived:

FOR THE ELECTRICAL OPERATOR

He must be prepared for a sudden load reduction, equal to the load carried by the 138-kv tie feeder, under all station load conditions and at all times. Depending on the load conditions, he must know whether or not generating units have to be dropped, and if so, he must have decided which units. The electrical operator's plan for action must be agreed on by the turbine and the boiler operators, and all three must be kept informed of changing conditions and plans. Depending on load conditions, the electrical operator is to proceed as follows on sudden loss of load:

Trip off the preselected units promptly.

Reduce frequency further, if required, by reducing the load on the heaviest loaded remaining units.

Reduce voltage if required, by reducing the excitation, beginning with the lightest loaded units, and taking care to maintain lagging power factor.

In reducing load, be guided by the low-pressure header pressure and by motoring limitations on the higher pressure generators.

FOR THE TURBINE OPERATOR

Secure all turbines, tripped by the electrical operator and prepare them for resynchronizing when required.

FOR THE BOILER OPERATOR

Switch to manual combustion and feed water control.

If a high-pressure turbine has been tripped, secure associated boiler in a normal manner.

On the remaining high-pressure boiler, keep a heavy coal feed on the bottom burners to prevent loss of ignition. Cut in the ignition torches immediately. Should the drum water level drop below the danger point, cut off all coal feed.

Cut in low-pressure boilers and force these to steaming in accordance with the prearranged program.

Conclusion

Theoretical investigation, staged tests, and actual case experiences show that a topping turbine steam generating station can successfully operate through sudden load reductions up to 90 per cent of initial load without damage to plant or remaining consumer load equipment. The complete understanding of the problem by the operators, together with preparedness and co-operation on their part, is a prerequisite for the successful handling of such an emergency.

The experience, gained through tests and through actual cases, shows that even with unforeseen complications, the required performance lies well within the capability of properly trained operating personnel.

Appendix I

The following describes the methods used in calculating the electrical and mechanical performance of turbogenerators when subjected to sudden reduction of load. These methods were developed to enable the prediction by relatively simple calculations of voltage and frequency rises, as well as of the unbalance in steam flows.

Step-by-step calculations were found to be most suitable because of the large number of variables involved. The calculations were made for the periods up to 15 seconds following the load drop, by which time equilibrium conditions are generally reached (except for the low-pressure boilers).

All generators on the load busses were assumed to be combined in an equivalent generator, having the adjusted synchronous and transient reactance, and the adjusted transient short-circuit time constant, of the paralleled units. The inertia of this equivalent generator was taken as equal to the sum of the inertias of the rotating assemblies of the paralleled units.

When only a few units are involved, the output of each turbine may be considered separately and derived from its governor characteristic curve. When many units are involved, a simplification may be achieved by use of an equivalent high-pressure turbine and an equivalent low-pressure turbine to combine the characteristics of all the high- and low-pressure turbines, respectively. The turbine output, derived from the governor characteristic curve, is the steady-state condition, which must be modified for the travel time and dead time of the governors for the transient condition.

In calculating the generator behavior, the d-c and subtransient components were neglected as is done usually in cases involving load impedances.

Although the electrical and the mechanical factors of the problem are not mutually independent, the following division establishes the primary factors of each group:

1. VOLTAGE RISE
   - A. At constant speed.
   - B. Effect of the speed variations.
2. SPEED VARIATION
   - A. Governor characteristics.
   - B. Computations.
3. STEAM PRESSURE
   - A. Effect of the volume of the steam piping and effect of low-pressure steam generation.

1 (A). Voltage Rise at Constant Speed

The basic equations are

$$\mathbf{e} = \mathbf{E}_{Tb} + \mathbf{I}_b\mathbf{X}_{eq}$$

$$\mathbf{E}_{Ta} = \mathbf{e}\left[\frac{\mathbf{Z}_L}{\mathbf{Z}_L + \mathbf{X}_{eq}}\right]$$

$$\mathbf{I}_{La} = \frac{\mathbf{E}_{Ta}}{\mathbf{Z}_L}$$

The reduction in load is followed by an almost instantaneous rise in voltage due to the smaller leakage reactance drop; thus

$$\mathbf{e}_b' = \mathbf{E}_{Tb} + \mathbf{I}_b\mathbf{X}_e$$

prior to the load drop and immediately thereafter

$$\mathbf{E}_{Ta}' = \mathbf{e}_b' - \mathbf{I}_a\mathbf{X}_e = \mathbf{e}_b'\left[\frac{\mathbf{Z}_L}{\mathbf{Z}_L + \mathbf{X}_e}\right]$$

The time constant of the equivalent generator was computed from the weighted time constants of the paralleled units and modified for the external impedance in the usual manner.

$$T_{da}' = \left[\frac{X_d' + X_e}{X_d + X_e}\right] T_{do}'$$

Table IV. Sample Calculation, 50-Megawatt Load Drop Test

Time-Seconds	Bus Kv		Megawatts			Degrees Per Second Squared	Δt	Incremental Degrees Per Second $\Delta\omega$	Cumulative Degrees Per Second ω	N	Valve Position						Steam MW		
	From Curve	Corresponding for Speed	Input	Load	Accel.						Unit	Initial	Corresponding to Speed	Final	MW		High-Pressure Units	Low-Pressure Units	Unbalance
Before Trip = 0	13.5	13.5	76	76	0	0		0	0	1.000	9	0.88	0.88	0.88	44	=76	44	32+20*	0
											8	0.50	0.50	0.50	15				
											7	0.57	0.57	0.57	17				
0–0.1	14.0	14.0	76	27	49	720	0.1	72	72	1.003	9	0.88		0.88	44	=76	44	52	0
											8	0.50		0.50	15				
											7	0.57		0.57	17				
0.1–0.2	14.01	14.05	76	27	49	720	0.1	72	144	1.006	9	0.88	0.80	0.80	40	=72	40	52	−4
											8	0.50		0.50	15				
											7	0.57		0.57	17				
0.2–0.4																			

* Includes units 4 and 5 on isolated bus.

Unit Number	Rating		M	Governor		Rate
	Megavolt-Amperes	Megawatts		Dead Time	Travel Time	
9	62.5	50	3.7	0.1	1.0	Uniform
8	35.3	30	5.5	1.0	2.5	Proportional to
7	35.3	30	5.5	1.0	2.5	Proportional to

Total M 14.7 seconds per 100 megavolt-amperes

$$K=\frac{360f}{M(MVA)}=\frac{360\times 60}{14.7\times 100}=\frac{1}{0.068}$$

$\alpha=K.\Delta MW$

$\Delta\omega=\alpha.\Delta t$

$N=1+w/21{,}600$

$M=$ inertia constant

$$=\frac{0.462(WR^2)(RPM)^2}{100}10^{-8}$$

This time constant was of the order of six seconds for most calculations and was not critical in affecting the results. The range of correct application of this equation is questionable in view of the large resistance component of the load. However, the difference between T_{de}' and T_{do}' was found to be small.

Using the preceding time constant, the bus voltage at any time after the load drop is

$$E_T=E_{Ta}+(E_{Ta}'-E_{Ta})\left(\epsilon^{-\frac{t}{T_{de}'}}\right)$$

[constant speed]

It will be recognized that this treatment assumes all the paralleled units to have the same internal angles as well as the same terminal voltages. This is approximately true prior to the load drop, when the units operate at comparable per-unit loads, while having similar per-unit reactances. However, following the load drop, the regulation of the governors may result in some machines motoring (even in the steady state) and the internal voltages of the different units will be too far out of phase to yield sufficiently accurate results. Therefore a second, more accurate method is given. This method may be used with almost equal facility where the number of units is not too great.

The vector diagram of Figure 7 shows the internal voltages prior to the load drop while Figure 8 gives the vector diagram following the load drop. From these diagrams the following equations are derived

$h_1-E_{Ta}=I_{a1}X_1 \sin \theta_{a1}$

$h_2-E_{Ta}=I_{a2}X_2 \sin \theta_{a2}$

$h_n-E_{Ta}=I_{an}X_n \sin \theta_{an}$

$I_L \sin \theta_L=I_{a1} \sin \theta_{a1}+I_{a2} \sin \theta_{a2}+I_{an}\times \sin \theta_{an}$

Substituting and reducing

$$E_{Ta}=\frac{\frac{h_1}{X_1}+\frac{h_2}{X_2}+---+\frac{h_n}{X_n}-I_L \sin \theta_L}{\frac{1}{X_1}+\frac{1}{X_2}+---\frac{1}{X_n}}$$

Since

$$I_L \sin \theta_L=\frac{E_{Ta}}{Z_L}.\frac{X_L}{Z_L}=E_{Ta}b_L$$

$$E_{Ta}=\frac{\frac{h_1}{X_1}+\frac{h_2}{X_2}+---+\frac{h_n}{X_n}}{\frac{1}{X_1}+\frac{1}{X_2}+---\frac{1}{X_n}+b_L}$$

The values of K_n are proportional to $I_nX_n \cos \theta_{an}$ and hence to the load carried by these units in the steady state following the load drop, and they may be determined from the governor characteristic curves and the approximate loads.

The advantage of deriving E_{Ta} in this form lies in the resulting good accuracy because the measured quantities (h_n) are in phase with the voltage and therefore little affected by errors in approximating the loads.

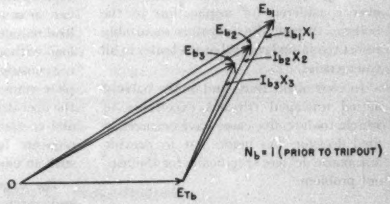

Figure 7. Voltage vector diagram prior to trip-out

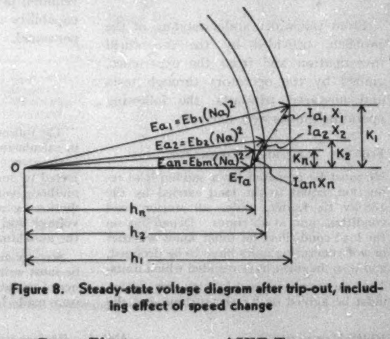

Figure 8. Steady-state voltage diagram after trip-out, including effect of speed change

1(B). Effect of Speed Variation on Voltage

The load saturation characteristic of the pilot exciter, the main exciter, and the generator may be approximated between two points lying sufficiently close together, by

$$I_f = K'E^n = K''\phi^n \text{ or } \phi = K'''E^{1/n}$$

where $n > 1$.

For the pilot exciter and the main exciter

$$E_p = K_p \phi_p N$$
$$\phi_p = K_p' E_p^{1/n_1}$$
$$E_p = K_p'' N^{\left(\frac{n_1}{n_1-1}\right)}$$
$$E_m = K_m \phi_m N$$
$$\phi_m = K_m' E_p^{1/n_2}$$
$$E_m = K_m'' N^{\left[\frac{n_1}{n_2(n_1-1)}+1\right]}$$

respectively. The time delays in both the main and pilot exciters are neglected, since they are small compared with that of the generator field.

For the generator, then

$$E_g = K_g \phi_g N$$
$$\phi_g = K_g' E_m^{1/n_3}$$
$$\frac{E_N}{E} = \left[1 + \left\{ N^{\left[\frac{n_1}{n_2(n_1-1)}+1\right]\frac{1}{n_3}} - 1 \right\} \times \{1 - \epsilon^{-t/T}\} \right] N$$

Since in most units $n \approx 2$ the equation reduces to

$$\frac{E_N}{E} = N[1 + (N-1)(1 - \epsilon^{-t/T})]$$

E_N = voltage at speed N
E = voltage at $N = 1.0$
$T \approx T_{do}'$

The foregoing equations are based on sudden speed change. When used in a step-by-step method the result will be approximately correct. For steady state the ratio $E_N/E = N^3$. This relationship was used for rough work.

2(A). Speed Variations—Governor Characteristics

With the steady-state governor characteristics available for different loads, the steady-state load division is easily determined. For the transient performance, however, the steady-state characteristics must be modified, which was done through the following assumptions:

	Dead Time, Seconds	Travel Time, Seconds
High-pressure governors	0.1	1.0
Low-pressure governors	1.0	2.5

The travel rate of the high-pressure governor valves is assumed constant, because of the relatively high speed of valve travel, while that of the low-pressure governors was assumed to be proportional to the difference between the actual turbine speed at the moment and the speed required by the steady-state regulation.

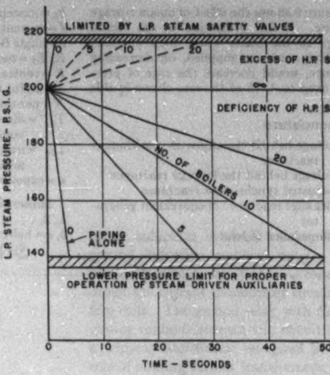

Figure 9. Effect of banked low-pressure boilers on steam pressure for 5-megawatt unbalance in steam flow, flash steam not included

2(B). Computations

The step-by-step calculation is performed as shown in Table IV. Starting with the initial conditions of no steam flow unbalance, and with no turbine accelerating torque, $t = 0$ marks the time at which the tie line load is assumed to be dropped. The difference between the prior load and the bus load is applied to accelerate the rotating masses.

Using methods similar to those used in stability studies, the speed is found. Intervals of 0.1 to 1.0 second are used; the smaller, when changes are rapid, and the larger, when steady state is approached. After the first 0.1 second, the high-pressure turbine governors are assumed to move to a position corresponding to the speed at the end of the next interval, providing that the assumed travel rate is not exceeded. From the turbine input (assumed to be proportional to the instantaneous position of the valve gear) a new accelerating torque is derived.

When the dead time of the low-pressure turbine governors has been passed, they are treated in a similar manner, except that an allowance is made for the rate of travel being a function of displacement.

The load is treated as a constant impedance; it varies, therefore, as the square of the bus voltage. The bus voltage, corrected for the actual speed, is plotted as previously developed.

Curves of governor position versus load for actual speed-changer settings are used to obtain governor valve position.

Starting from the initial condition of balanced steam flow, any decrease in high-pressure turbine generation, not matched by a corresponding decrease in low-pressure generation, is considered to result in a deficiency of high-pressure steam flow, thus decreasing the low-pressure header pressure, and vice versa.

The power contribution of each unit represents the turbine input, which, during acceleration, may be quite different from the generator output.

3(A). Low-Pressure Steam Pressure as Affected by Load Drop and by Low-Pressure Steam Generation

Due to the different valve gear travel speeds and governor regulations, the steam flow balance, which existed before the load drop, will generally be destroyed and the low-pressure steam header pressure will either rise or fall, depending on the direction of the unbalance. The larger the volume of stored steam, the slower will be the change in pressure.

Three conditions may exist:

No Low-Pressure Boilers On. In that case the available energy is only that stored in the volume of the connecting piping.

Low-Pressure Boilers Floating on the Line. With this condition, there is considerable stored energy available which is utilized when the low-pressure header pressure drops because of the inherent volume and the release of flash steam. If the low-pressure header pressure rises, the boiler stop-check valves may prevent the complete utilization of this energy. However, the rate of rise of pressure generally is so slow, and the pressure differential usually small enough, that the loss of energy from this cause may be inconsequential.

Low-Pressure Boilers on the Line and Steaming. This is similar to the second condition, except that more low-pressure steam will be available with dropping pressure. Even if the stop-check valves should close on rising pressure, the low-pressure steam flow will be reduced by the amount of initial low-pressure boiler contribution.

The energy available to the turbines may be corrected for the change in the low-pressure header pressure in the step-by-step calculations. For the cases at hand, the net change was relatively slow for the first 15 seconds. After a few check steps, this correction generally could be ignored.

It should be noted that, where very little storage volume exists, very severe low-pressure header pressure drops may occur because of the faster action of the high-pressure turbine governors shutting off the supply of steam while the slower low-pressure turbine governor valves are still nearly wide open.

Figure 9 shows the effect of steam storage volume. If full utilization of the stored energy in the boiler water were possible, the flash steam so supplied, on decreasing pressure, would decrease the rate of pressure drop to 1/15 of the rate shown in this graph.

Nomenclature

e = voltage behind the adjusted synchronous reactance
e' = voltage behind the leakage reactance
X = adjusted synchronous reactance
X_e = leakage reactance of equivalent generator
Z_L = inpedance of load
b_L = susceptance of load
I = current
θ = angle between current and bus voltage
E, E_T = bus voltage
K = constant
ϕ = useful magnetic flux
N = per unit speed
T_{do}' = direct axis transient open circuit time constant
T_{de}' = transient short circuit time constant, adjusted for the load reactance
n = exponent a = constant

Subscripts 1, 2, . . . n, refer to generators 1, 2, . . . n
b, a = before or after load drop, respectively
eg = equivalent generator
p = pilot exciter
m = main exciter
E_n = voltage at speed N

References

1. WESTINGHOUSE TRANSMISSION AND DISTRIBUTION REFERENCE BOOK. Westinghouse Electric Corporation (East Pittsburgh, Pa.) 1942.

2. SYSTEM LOAD SWINGS, H. A. Bauman, O. W. Manz, Jr., J. E. McCormack, H. B. Seeley. *AIEE Transactions*, volume 60, 1941, pages 541–47.

3. GENERATOR STABILITY AT LOW EXCITATION, E. L. Michelson, L. F. Lischer. *AIEE Transactions*, volume 67, part I, 1948, pages 1–9.

No Discussion

A-C Tripping and Reclosing of Line Sectionalizing Circuit Breakers

C. E. WINEGARTNER
MEMBER AIEE

H. E. BONHEIMER
ASSOCIATE AIEE

THE application of power supply for control at a remote unattended station is discussed. This problem requires a design for automatic sectionalizing and reclosing two 34.5-kv circuits without the use of a control battery.

The control and tripping scheme for the two 34.5-kv oil circuit breakers uses a-c tripping and reclosing power. Circuit breakers automatically sectionalize and re-energize the overhead portions of two overhead-underground cable circuits when faulted. The use of a-c tripping in a remote unattended small sheet-steel building, normally unheated, eliminates the hazards and difficulties of battery maintenance. This description covers the operation of the various control devices for manual and automatic switching during fault condition.

General

In this application of automatic switching, Figure 1, a large transmission station *W* feeds two 34.5-kv underground cable circuits of 18-megavolt-ampere capacity. The underground cable parts are tapped to feed one or more distribution stations *X* through step-down transformers paralleled on the low side only. To utilize all the capacity of the underground cables, they were connected through circuit breakers at sectionalizing station *Y*, to overhead lines which feed one or more distribution stations *Z*. These small stations *Z* are fed through step-down transformers which are paralleled on the low side only.

The control scheme provides for automatically isolating the overhead portion of a faulted circuit at sectionalizing station *Y* by tripping the circuit breaker; phase induction overload relays and ground induction overload relays actuate the tripping. Backfeed is removed at distribution stations *Z* by circuit breaker tripping from reverse power relays.

After clearing the fault, automatic reclosure is made at sectionalizing station *Y* by a conventional timer. The circuit breaker on the low side of transformer recloses by an induction-type potential relay after line is re-energized. The closing and tripping controls of the circuit breakers are alternating current at all stations except station *W*.

Control and Tripping of 34.5-Kv Circuit Breakers at Sectionalizing Station *Y*

Normal Operation

Normally all circuit breakers and air switches, Figure 1, are closed. Supply station *W* feeds distribution stations *X* through underground cable. Supply station *W* also feeds distribution stations *Z* through underground cable to sectionalizing station *Y* and by overhead line beyond.

Fault on Overhead Line

1. A fault on overhead line at *A*, Figure 1, is cleared by tripping circuit breakers at sectionalizing station *Y* and distribution stations *Z*.

At sectionalizing station *Y*, the 34.5-kv circuit breaker trips (Figure 2) by either: phase induction overload relays; or a ground induction overload relay. The phase relays with circuit opening contacts direct the current transformer circuits to trip coils. The ground relay with circuit closing contacts connect trip circuit from a tripping transformer energized by two sets of bushing current transformers.

At distribution station *Z*, Figure 1, reverse power relays with circuit opening contacts provide protection; control of circuit opening contacts is similar to overload relay trip circuit at station *Y*, Figure 2.

2. Automatic re-energizing of overhead line and power transformer is attempted immediately at sectionalizing station *Y*.

An a-c operated timer introduces three impulses to closing relay *X* of oil circuit breaker, Figure 3. The first impulse through contact *BC* is instantaneous with

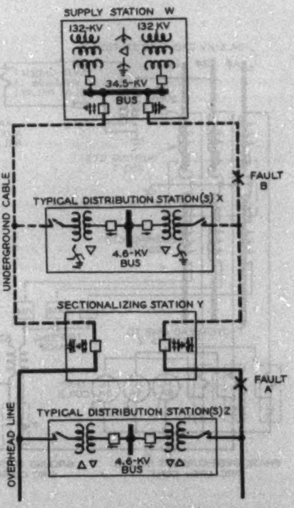

Figure 1. 1-line diagram of 34.5-kv underground-overhead circuits

---

Paper 49-293, recommended by the AIEE Switchgear Committee and approved by the AIEE Technical Program Committee for presentation at the AIEE Fall General Meeting, Cincinnati, Ohio, October 17–21, 1949. Manuscript submitted February 16, 1949; made available for printing September 7, 1949.

C. E. Winegartner and H. E. Bonheimer are both with The Cleveland Electric Illuminating Company, Cleveland, Ohio.

the second and third at 15 and 150 second intervals respectively.

3. Automatic reconnecting the main power transformer to 4.6-kv bus at distribution stations *Z*, Figure 1, follows successful energizing of transformers. A potential time delay relay actuates an a-c closing coil of 4.6-kv circuit breaker after three seconds of sustained voltage.

Fault in Cable

1. A fault at *B* in cable is cleared by trippings at supply station *W*, distribution stations *X* and *Z*; a single-phase-to-ground fault will clear at sectionalizing station *Y* instead of stations *Z*. No automatic reclosure is attempted for cable faults.

At stations *W* and *X*, grounded neutral of power transformers provide tripping current for phase-to-ground faults. At attended station *W*, phase and ground overload relays initiate d-c impulse to trip coils.

At distribution stations *X* and *Z*, reverse power relays with circuit opening contacts control current transformer output by a circuit similar to overload relays at station *Y*, Figure 2. Phase-to-ground faults in cable are cleared from load end at sectionalizing station *Y* instead of *Z*. With no neutral grounding beyond load side of station *Y*, an over-under voltage relay instead of ground overload relay was required to detect phase-to-ground faults. Both over- and under-voltage contacts are circuits closing, Figure 2. An *AA* auxiliary time delay relay discriminates to prevent false trippings from surges. Automatic reclosure is locked-out by a back contact on *AA* auxiliary relay, Figure 3, opening the timer closing circuit. In this manner the cable is protected from over-voltage to ground, which would result if an arcing ground were not removed, as well as an automatic reclosure into the grounded cable.

Solenoid Operating Mechanism

Tripping

The maximum number of trip coils available per oil circuit breaker is limited to four by standard design, Figure 2. Having used three trip coils for phase overload relays, it was necessary to have triple control on the fourth trip coil. This fourth trip coil is operated by a common circuit from (1) the manual remote control switch, (2) the ground overload relay for "overhead-line" phase-to-ground faults, and (3) the over-under voltage relay for underground cable phase-to-ground faults.

For overhead line phase-to-ground faults, this fourth 3-ampere trip coil is actuated by current transformers feeding through a tripping transformer. Remote manual control and underground cable phase-to-ground faults also actuate this same 3-ampere trip coil from a distribution feeder 230-volt a-c supply. The 230-volt a-c supply is connected to a 3-ampere trip coil through a suitable resistor.

Reclosing

The use of alternating current to actuate this size solenoid operated mechanism requires a large size rectifier. Automatic reclosure and remote manual closing become impossible during interruptions of the a-c distribution feeder supply.

Pneumatic-operated mechanism for this type of circuit breaker of present design was offered with: a-c operation of compressor motor; d-c operation of one trip coil standard, with one manufacturer adding three current transformer trip coils special; and an exhaust valve used for pneumatic trip-free operation requiring d-c operation (one large manufacturer has mechanical trip-free operation).

Change to complete a-c operation was not generally available. Hence, the advantage of reliable stored operating capacity of the pneumatic mechanism at sectionalizing station *Y* was not advisable without installing a battery.

Conclusions

The control and tripping schemes described demonstrate the feasibility of

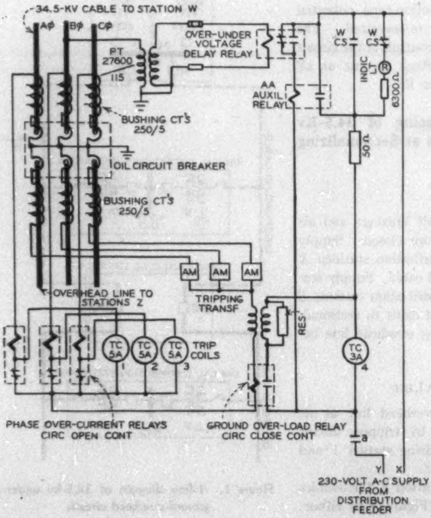
34.5-KV CABLE TO STATION W
Aϕ
Bϕ
Cϕ
PT
27600
115
OVER-UNDER VOLTAGE DELAY RELAY
W CS
W CS
INDIC LT
R
6300 Ω
AA AUXIL RELAY
BUSHING CT'S 250/5
OIL CIRCUIT BREAKER
BUSHING CT'S 250/5
50 Ω
AM
AM
AM
OVERHEAD LINE TO STATIONS Z
TRIPPING TRANSF
RES
TC 5A 1
TC 5A 2
TC 5A 3
TRIP COILS
TC 3A 4
PHASE OVER-CURRENT RELAYS CIRC OPEN CONT
GROUND OVER-LOAD RELAY CIRC CLOSE CONT
a
Y
X
230-VOLT A-C SUPPLY FROM DISTRIBUTION FEEDER

Figure 2 (left). Schematic wiring diagram of tripping control for solenoid-operated mechanism at station *Y*

Figure 3 (below). Schematic wiring diagram of closing control for solenoid-operated mechanism at station *Y*

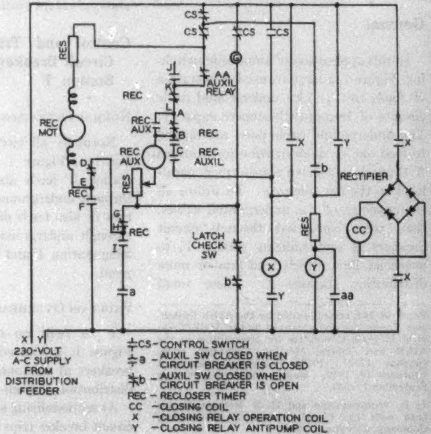
CS
CS
CS
CS
RES
G
J
K
AA AUXIL RELAY
REC
L
A
REC MOT
REC AUX
B
REC
C
REC AUX
REC AUXIL
X
Y
X
b
D
E
REC
F
RES
RECTIFIER
G
H
REC
I
LATCH CHECK SW
RES
CC
X
Y
b
X
a
Y
aa
X
Y
230-VOLT A-C SUPPLY FROM DISTRIBUTION FEEDER
CS – CONTROL SWITCH
a – AUXIL SW CLOSED WHEN CIRCUIT BREAKER IS CLOSED
b – AUXIL SW CLOSED WHEN CIRCUIT BREAKER IS OPEN
REC – RECLOSER TIMER
CC – CLOSING COIL
X – CLOSING RELAY OPERATION COIL
Y – CLOSING RELAY ANTIPUMP COIL

using alternating current to eliminate battery maintenance problems at remote unattended stations.

The applications of circuit opening relays and tripping transformer, while not generally used, have proved satisfactory in service. However, it would improve this a-c tripping if a 3-phase network transformer could be developed. Such a network transformer, into which 3-phase currents were fed, could connect its output to one trip coil through circuit closing contacts. Thus three trip coils, and the objection to relay contacts in the current transformer circuits would be eliminated.

The use of large rectifiers to close a-c solenoid operated circuit breakers from an a-c source is common. However, a complete a-c pneumatic operated circuit breaker would insure faster operation and several reclosures with stored air, if a-c control supply failed. Development of an a-c operated exhaust valve, operation from the main trip bar or a change to a mechanically trip-free mechanism, would give added stimulus to a-c tripping and automatic reclosing.

No Discussion

Transients in 2-Phase Synchronous Machines

N. E. WILSON
MEMBER AIEE

Synopsis: The analytical study of 3-phase synchronous machines has been well covered by many authors.[1,2,3,4] Not so much attention has been devoted to the 2-phase machine because much of the development of the methods of analysis occurred after the trend away from 2-phase systems was well established. Although the present use of 2-phase generators represents a small percentage of total generation, it is believed that there is some justification for analytical study of 2-phase machine performance. Such a study has value for the 2-phase systems now in use, and it has value in an analytical sense by showing how the relations developed for 3-phase generators may be adapted to generators with a different number of phases.

The discussion in this paper is confined to L-connected, or quarter-phase machines with salient poles and without damper windings. It is limited to short-circuit or transient conditions. The inductances are defined and the relations expressing the variations of the several inductances of the windings are developed. The general flux-linkage equations for all windings are determined in terms of stator and rotor currents. With this basis the operation of the machine under all possible short-circuit conditions is considered with the object of determining the transient and steady-state currents. The possible short-circuit conditions for the L-connected quarter-phase machine are the double line-to-neutral fault, the line-to-line fault, and the single line-to-neutral fault. The equations developed are compared with similar relations for 3-phase machines to show the similarities and the differences.

The method of solution for the currents uses the theorem of constant flux linkages. This theorem has been used[5] successfully to obtain an approximate solution for fault conditions on 3-phase machines. It has been shown[6,7] that the solution for a symmetrical short circuit on a 3-phase generator is but very little modified when it is based on rigorous analysis instead of the theorem of constant flux linkages. Since this theorem is the basis of most of the analytical study of the behavior under transient conditions of synchronous machines, and even of d-c machines,[8] it is used here.

Inductances of the Windings

THE SELF inductance of a winding on the stator of a machine with salient poles is not a constant, but varies with rotor position. This is shown in Figures 1 and 2. In Figure 1 the self inductance of phase A is greatest when the centerline of the poles (direct axis) is in line with the centerline of the phase. The self inductance of phase B is minimum at this time. When the poles have rotated through 90 electrical degrees so that an interpolar space (quadrature axis) is in line with the centerline of phase A the self inductance of this winding is minimum and of phase B it is maximum. If the variation in reluctance of the magnetic circuit is sinusoidal, then

$$L_{aa}=L_{sa}+L_{sv}\cos 2\sigma \tag{1}$$

$$L_{bb}=L_{sa}+L_{sv}\cos 2(\sigma-\pi/2)=L_{sa}-L_{sv}\cos 2\sigma \tag{2}$$

where L_{aa} and L_{bb} are the self inductances of phases A and B respectively, L_{sa} is the average value of these inductances, and L_{sv} is the amplitude of variation from the average value. The instantaneous angular displacement, σ, of the direct axis of the poles from the reference point, the centerline of phase A, is measured in electrical radians. The double frequency variation in reluctance of the magnetic circuit causes the double frequency variation in inductance.

Nomenclature

L_{aa}, L_{bb} = self inductance of phase A or B
L_{sa} = average value of L_{aa} or L_{bb}
L_{sv} = amplitude of variation of L_{aa} or L_{bb}
L_{ab} = mutual inductance between phases A and B
L_{mv} = amplitude of variation of L_{ab}
L_{af}, L_{bf} = mutual inductance between phase A or B and the field
L_{afM} = maximum value of L_{af} or L_{bf}
L_{ff} = self inductance of the field
L_d = direct-axis inductance
L_d' = direct-axis transient inductance
L_q = quadrature-axis inductance
X_d, X_d', X_q = reactance values of L_d, L_d', and L_q
$T_{d\phi}'$ = time constant used with transient terms arising from direct current in the field with the armature circuits open
T_d' = time constant used with transient terms arising from direct current in the field with one or more armature circuits closed
T_a = time constant used with transient terms arising from direct current in the armature circuit
σ = instantaneous displacement of the direct axis from the center-line of phase A
$\psi=\sigma+\pi/4$
Λ = instantaneous value of the flux linkages of a circuit
ϕ = angle of lead or lag of the armature current with respect to the internally generated voltage
i = instantaneous current in a winding
E_t = effective value of the voltage generated in one phase of the armature on open circuit by the flux linkages with the field circuit
E_{tM} = maximum value of E_t

The mutual inductance between phase A and phase B is the mutual inductance between windings which are $\pi/2$ electrical radians apart. Therefore, the average value of such an inductance will be zero. However, in a machine with a salient-pole rotor, the unsymmetrical distribution of flux produced by current in one phase produces at times during one cycle of variation of σ a net linkage of flux with the other phase. When σ is zero, the distribution of flux produced by cur-

---

Paper 49-294, recommended by the AIEE Rotating Machinery Committee and approved by the AIEE Technical Program Committee for presentation at the AIEE Fall General Meeting, Cincinnati, Ohio, October 17–21, 1949. Manuscript submitted March 21, 1949; made available for printing September 13, 1949.

N. E. WILSON is Associate Professor of Electrical Engineering at the University of Massachusetts.

This paper is based upon a thesis supervised by Dr. W. A. Lewis, Dean of Graduate School, Illinois Institute of Technology, and submitted by Mr. Wilson as Westinghouse Fellow in Power Systems Engineering to the faculty of the Illinois Institute of Technology in partial fulfillment of the requirements for the degree of Master of Science in Electrical Engineering.

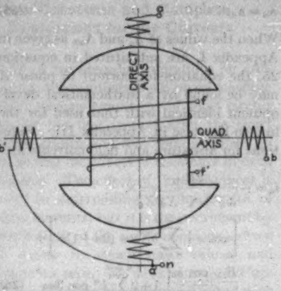

Figure 1. Position of the rotor for maximum self inductance of phase A

rent in phase A is symmetrical and the net flux linkages with phase B are zero. As the rotor turns toward phase B (assumed to be $\pi/2$ radians behind phase A), the flux is shifted toward the axis of this winding and a positive linkage of flux with phase B occurs. This effect reaches a maximum when $\sigma=\pi/4$ radians. When the rotor has turned $\pi/2$ radians, the flux is again symmetrically disposed and the flux linkages are again zero. When the rotor turns beyond $\pi/2$ radians, the flux again is distorted, being shifted backward so that there is a negative linkage of flux with phase B when phase A carries current. The effect reaches its maximum value when $\sigma=3\pi/4$. This variation in mutual effect may be stated in equation form as

$$L_{ab}=L_{mv}\cos 2(\sigma-\pi/4)=L_{mv}\sin 2\sigma \qquad (3)$$

in which L_{ab} is the mutual inductance between phase A and phase B, and L_{mv} is the amplitude of variation of the mutual inductance.

It has been shown[9] that for 3-phase machines the amplitudes of variation of the self and mutual inductances are very nearly equal. The assumption of equality is normally made in the analysis of 3-phase machine performance, and since the pole structure would be the same for a 2-phase machine, the same relationship will be assumed here. Thus, since $L_{sv}=L_{mv}$,

$$L_{ab}=L_{sv}\sin 2\sigma \qquad (4)$$

The self inductance of the field winding is constant since the reluctance of the magnetic path of the flux produced by current in this winding does not change with rotor position (slot effects not considered).

The mutual inductances between rotor and phase windings are variables, being maximum for a particular phase when the direct axis of the field is in line with the axis of the phase winding. These variations for a 2-phase machine may be expressed as

$$L_{af}=L_{afM}\cos\sigma \qquad (5)$$

$$L_{bf}=L_{afM}\cos(\sigma-\pi/2)=L_{afM}\sin\sigma \qquad (6)$$

in which L_{afM} is the maximum value of the mutual inductance, L_{af}, between phase A and the rotor winding, and of the mutual inductance, L_{bf}, between phase B and the rotor winding.

It is convenient in 3-phase work to resolve the inductance of each phase winding into components, one to be used with the component of armature current producing magnetization along the direct axis, and the other to be used with the component of armature current producing magnetization in the quadrature axis. These are called the direct-axis inductance and the quadrature-axis inductance respectively. It also is useful in 2-phase machine work to make this separation because of the simplification it brings to the form of the equations, and as a means of comparison with the 3-phase case. In Appendix I it is shown that these inductances are

$$L_d=L_{sa}+L_{sv} \qquad (7)$$

$$L_q=L_{sa}-L_{sv} \qquad (8)$$

from which L_{sa} and L_{sv} may be obtained as

$$L_{sa}=(L_d+L_q)/2 \qquad (9)$$

$$L_{sv}=(L_d-L_q)/2 \qquad (10)$$

Double Line-to-Neutral Short Circuit

In applying the theorem of constant flux linkages, it is necessary to determine the flux linkages before the fault when the phase currents are zero (for short circuits occurring on an unloaded machine), and to equate the expressions thus obtained to those for flux linkages at any time with armature currents present. The equations resulting then may be solved for the currents for the first instant after short circuit. In Appendix I the general flux-linkage equations are developed. The circuit for a double line-to-neutral short circuit is shown in Figure 3. For this condition $e_{an}=e_{bn}=0$. Since each of the phase windings has zero voltage and is closed on itself, the constant-linkage theorem applies to these windings directly and

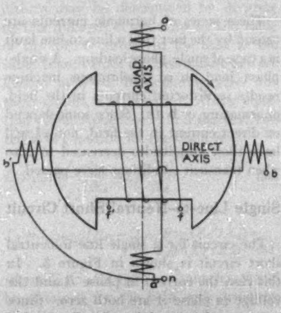

Figure 2. Position of the rotor for minimum self inductance of phase A

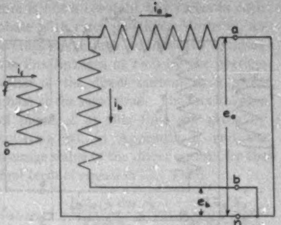

Figure 3. Circuit for a double line-to-neutral short circuit

$$\Lambda_a=\Lambda_{a0} \qquad (11)$$

$$\Lambda_b=\Lambda_{b0} \qquad (12)$$

The process indicated by these equations carried out in Appendix II and the solutions for i_a, i_b, and i_f are obtained. The result is

$$\begin{aligned} i_a=&\frac{\sqrt{2}E_i(X_d'+X_q)}{2X_d'X_q}\cos\sigma_0-\\ &\frac{\sqrt{2}E_i}{X_d'}\cos(\omega t+\sigma_0)-\\ &\frac{\sqrt{2}E_i(X_d'-X_q)}{2X_d'X_q}\cos(2\omega t+\sigma_0) \end{aligned} \qquad (13)$$

$$\begin{aligned} i_b=&\frac{\sqrt{2}E_i(X_d'+X_q)}{2X_d'X_q}\sin\sigma_0-\\ &\frac{\sqrt{2}E_i}{X_d'}\sin(\omega t+\sigma_0)-\\ &\frac{\sqrt{2}E_i(X_d'-X_q)}{2X_d'X_q}\sin(2\omega t+\sigma_0) \end{aligned} \qquad (14)$$

$$\begin{aligned} i_f=&i_{f0}+i_{f0}(X_d-X_d')/X_d'-\\ &i_{f0}[(X_d-X_d')/X_d']\cos\omega t \end{aligned} \qquad (15)$$

In these equations some new terms have been introduced. All are defined in Appendix IV. All have the same significance as they do when used for 3-phase machines, but the values of the reactances involve the actual winding reactances in a slightly different relationship as will be discussed later.

Present in these equations are five components of current. They are:

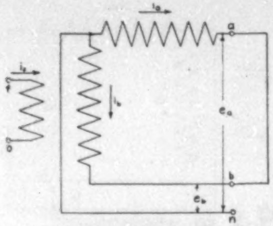

Figure 4. Circuit for a line-to-line short circuit

1. A d-c transient in the field resulting from the demagnetizing effect of the steady magnetomotive force which is a result of balanced currents in the armature.

2. An a-c fundamental-frequency component in the armature caused by the direct current in the field,

3. A d-c transient component in the armature. This is the usual d-c transient that occurs whenever an alternating voltage is suddenly applied to an inductive circuit. It depends on the value of the voltage at the time the switch is closed.

4. An a-c component of twice fundamental frequency in the armature. This is part of component 3 and would not be present if the inductances of the windings were constant. The variation of inductances is caused not only by saliency, but also by the presence of rotor circuits in one axis.

5. An a-c fundamental-frequency component in the field which results from the efforts of the field in preventing components 3 and 4 from making any changes in the field flux linkages.

Equations 13, 14, and 15 are for the currents at the first instant after short circuit occurs. If resistances were not present, these currents would continue unchanged in amplitude. The resistances will cause exponential changes in the amplitudes with time constants to be determined in a later section.

Line-to-Line Short Circuit

The circuit diagram for a line-to-line short circuit is shown in Figure 4. The phase voltages, e_{an} and e_{bn}, are not zero as in the previous case, but

$$i_a=-i_b \tag{16}$$

$$e_{an}-e_{bn}=e_{ab}=0 \tag{17}$$

With resistances neglected

$$e_{ab}=-d\Lambda_a/dt-(-d\Lambda_b/dt)=-d(\Lambda_a-\Lambda_b)/dt$$

and the flux linkages comprising those of phases A and B may be defined as

$$\Lambda_{ab}=\Lambda_a-\Lambda_b \tag{18}$$

Therefore

$$-\Lambda_{ab}=0 \tag{19}$$

This being the case, Λ_{ab} must be constant at the initial value once the short circuit has been established, and

$$\Lambda_{ab0}=\Lambda_{ab} \tag{20}$$

The substitutions for equation 20 are made in Appendix III and the resulting equation solved for i_a and i_b. With these currents known, i_f also may be found and the resulting equations are

$$i_a=-i_b=-\frac{\sqrt{2E_{tM}}}{X_d'+\sqrt{X_d'X_q}}\times \left[\cos\psi+\sum_{n=1}^{n=\infty}b^n\cos(2n+1)\psi\right]+ \frac{\sqrt{2}E_{tM}\cos\psi_0}{2\sqrt{X_d'X_q}}\left[1+2\sum_{n=}^{n=\infty}b^n\cos 2n\psi\right] \tag{21}$$

$$i_f=i_{f0}+\frac{(X_d-X_d')i_{f0}}{X_d'+\sqrt{X_d'X_q}}\times \left[1+\frac{1+b}{b}\sum_{n=1}^{n=\infty}b^n\cos 2n\psi-2\cos\psi_0\times \left(\cos\psi+\sum_{n=1}^{n=\infty}b^n\cos(2n+1)\psi\right)\right] \tag{22}$$

In these equations

$$\psi=\sigma+\pi/4=\omega t+\sigma_0+\pi/4 \tag{23}$$

$$b=(\sqrt{X_d'X_q}-X_d')/(X_d'+\sqrt{X_d'X_q}) \tag{24}$$

Equations 21 and 22 contain the five components of current listed for the double line-to-neutral short circuit. They also contain two additional sets of harmonic currents. These are:

1. A series of even harmonics in the field and of odd harmonics in the armature which are dependent on the direct current in the field.

2. A series of even harmonics in the armature and of odd harmonics in the field which are dependent on the direct current in the armature.

These series of harmonic currents are caused by the fact that a line-to-line fault is a case of single-phase loading. A single-phase load on a synchronous machine results in distorted currents in the field, or armature, or both. Since some depend on direct current in the field, not all will have their amplitudes decreased to zero when transient conditions have passed.

Single Line-to-Neutral Short Circuit

The circuit for a single line-to-neutral short circuit is shown in Figure 5. In this case the current in phase B and the voltage in phase A are both zero. Since e_{an} is zero, the theorem of constant flux linkages applies to phase A, and

$$\Lambda_a=\Lambda_{a0} \tag{25}$$

When the values of Λ_a and Λ_{a0}, as given in Appendix I, are substituted in equation 25, the equation for current in phase A may be found by a mathematical development identical with that used for the line-to-line case in Appendix III. Solutions for armature and field currents are

$$i_a=-\frac{2E_{tM}}{X_d'+\sqrt{X_d'X_q}}\times \left[\cos\sigma+\sum_{n=1}^{n=\infty}b^n\cos(2n+1)\sigma\right]+ \frac{E_{tM}\cos\sigma_0}{\sqrt{X_d'X_q}}\left[1+2\sum_{n=1}^{n=\infty}b^n\cos 2n\sigma\right. \tag{26}$$

$$i_f=i_{f0}+\frac{(X_d-x_d')i_{f0}}{X_d'+\sqrt{X_d'X_q}}\times \left[1+\frac{1+b}{b}\sum_{n=1}^{n=\infty}b^n\cos 2n\sigma-2\cos\sigma_0\times \left(\cos\sigma+\sum_{n=1}^{n=\infty}b^n\cos(2n+1)\sigma\right)\right] \tag{27}$$

In these equations, b has the value given in equation 24.

Inspection of equations 26 and 27 for the single line-to-neutral short circuit, and of equations 21 and 22 for the line-to-line short circuit shows that the two faults are very little different for the 2-phase machine. The differences are: the magnitude of each component in the armature is greater by the factor $\sqrt{2}$ for a single line-to-neutral short circuit; and the angular position of the currents in phase A is shifted by $\pi/4$ radians for the line-to-line fault. The reaction on the field circuit is the same for both faults if the rotor occupies the same position relative to the axis of the single winding short-circuited that it occupies relative to the two windings short circuited. If the positions are not the same, the amplitudes of the odd-harmonic components are affected by the difference in initial position. The maximum possible amplitudes are the same in each case.

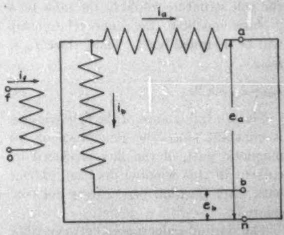

Figure 5. Circuit fo r a single line-to-neutral short circuit

Time Constants and Complete Expressions for the Currents

All of the preceding equations for currents in the windings of a 2-phase machine under various conditions of short circuit are for the first instant after the short circuit occurs, and they were obtained by neglecting the effects of resistance in each winding. The effect of the resistances is small in determining the amplitudes of these currents, but it is the instrument by which some of the components are caused to decay to steady-state values, and others to zero. In determining and applying the time constants to be used with these equations, all components of current in the field and armature which are related to direct current in the field are assumed to decay together at a rate governed by a time constant determined from field circuit parameters. The ratio of the final to initial amplitudes of these components will be the same as the ratio of final to initial values of direct current in the field.

Further, all of the components of current in the field and armature which are related to direct current in the armature are assumed to decay together at a rate governed by a time constant determined from armature circuit parameters. The ratio of final to initial amplitudes of these components will be the same as the ratio of final to initial values of direct current in the armature.

In general, the fundamental-frequency and odd-harmonic components of current in the armature are associated with the direct and even-harmonic components in the field. The fundamental-frequency and odd-harmonic components of current in the field are associated with the direct and even-harmonic components in the armature. The first of these two groups of components will not decay to zero. The direct current in the field is increased on short circuit to counteract the demagnetizing effect of the armature reaction. The increase in direct current diminishes until the total direct current in the field has returned to its original value (before short circuit) because there is no additional field voltage to support the increase.

Thus, the final value of field current for each of the cases of short circuit is i_{f0}.

The second of these two groups of components will decay to zero. All of this group are dependent on direct current in the armature, and, there being no source of sustained direct current in that circuit, their final values will become zero.

Double Line-to-Neutral Short Circuit

The initial value of direct current in the field is contained in the first two terms of equation 15. The ratio of final to initial values is, then

$$i_{f0}/i_{f(d\text{-}c)}=X_d'/X_d \tag{28}$$

When this ratio is applied to the amplitude of the fundamental-frequency components of current in armature-phase A, the result is

$$I_{aM(ss)}=\frac{E_{tM}}{X_d} \tag{29}$$

where $I_{aM(ss)}$ is the amplitude of the steady-state current in phase A. By separating the initial amplitude into its steady-state and transient parts, and remembering that the final amplitudes of all other components in the armature, and of the transient components in the field, are zero, the equations for current in phase A and in the field may be written

$$i_a=\left[\frac{E_{tM}}{X_d}+\left(\frac{E_{tM}}{X_d'}-\frac{E_{tM}}{X_d}\right)\epsilon^{-\frac{t}{T_d'}}\right]\times \cos\,(\omega t+\sigma_0)+\frac{E_{tM}}{2X_d'}\left(\frac{X_d'+X_q}{X_q}\cos\sigma_0-\frac{X_d'-X_q}{X_q}\cos\,(2\omega t+\sigma_0)\right)\epsilon^{-\frac{t}{T_a}} \tag{30}$$

$$i_f=i_{f0}\left[1+\frac{X_d-X_d'}{X_d'}\,\epsilon^{-\frac{t}{T_d'}}-\frac{X_d-X_d'}{X_d'}\,\epsilon^{-\frac{t}{T_a}}\cos\,\omega t\right] \tag{31}$$

In these equations T_d' and T_a are the short-circuit time constants of the field and armature respectively for a double line-to-neutral fault.

The time constant of an inductive circuit is the ratio of its inductance to its resistance. The effective inductance of the field circuit during short-circuit conditions may be determined by dividing its flux linkages at any time by the value of the direct current in the field at the same time. Both of these quantities are known at $t=0$, immediately after the short circuit is established. Using equation 65, in Appendix I, and the first two terms of equation 15, the result is

$$L_{ff(eff)}=\frac{L_{ff}I_{f0}}{i_{f0}\dfrac{X_d}{X_d'}}=L_{ff}\,\frac{X_d'}{X_d} \tag{32}$$

$$T_d'=L_{ff(eff)}/R_{ff}=(L_{ff}/R_{ff})(X_d'/X_d)=T_{d\phi}'(X_d'/X_d) \tag{33}$$

where $T_{d\phi}'$ is the time constant that would be obtained for the field with armature circuits open.

The effective inductance of the armature is not a constant but varies in each phase with rotor position. However, an average value may be found by dividing the flux linkages at $t=0$ by the average value of the direct current in a given phase at the same time. The flux linkages of phase A at this time are given by equation 63, in Appendix I, and the average value of the direct current by the first term of equation 13. Then

$$L_{a(eff)}=\frac{L_{afM}i_{f0}\cos\sigma_0}{E_{tM}\dfrac{X_d'+X_q}{2X_d'X_q}\cos\sigma_0}=\frac{2X_d'X_q}{\omega(X_d'+X_q)} \tag{34}$$

and

$$T_a=\frac{L_{a(eff)}}{R_a}=\frac{2X_d'X_q}{\omega R_a(X_d'+X_q)} \tag{35}$$

Line-to-Line Short Circuit

The initial value of direct current in the field is contained in the first two terms of equation 22. The final value is the same as before. Thus

$$\frac{i_{f0}}{i_f}=\frac{X_d'+\sqrt{X_d'X_q}}{X_d+\sqrt{X_d'X_q}} \tag{36}$$

The steady-state value of the amplitude of the fundamental-frequency and odd-harmonic components in the armature is obtained as before by multiplying the initial value by the ratio given in equation 36. The result is

$$I_{aM(ss)}=-\left(\frac{\sqrt{2}E_{tM}}{X_d'+\sqrt{X_d'X_q}}\right)\times\left(\frac{X_d'+\sqrt{X_d'X_q}}{X_d+\sqrt{X_d'X_q}}\right)=-\frac{\sqrt{2}E_{tM}}{X_d+\sqrt{X_d'X_q}} \tag{37}$$

Then the complete approximate equation for armature current becomes

$$i_a=-i_b=-\left[\frac{\sqrt{2}E_{tM}}{X_d+\sqrt{X_d'X_q}}+\left(\frac{\sqrt{2}E_{tM}}{X_d'+\sqrt{X_d'X_q}}-\frac{\sqrt{2}E_{tM}}{X_d+\sqrt{X_d'X_q}}\right)\epsilon^{-\frac{t}{T_d'(LL)}}\right]\times\left(\cos\psi+\sum_{n=1}^{n=\infty}b^n\cos\,(2n+1)\psi\right)+\frac{\sqrt{2}E_{tM}\cos\psi_0}{2\sqrt{X_d'X_q}}\times\left(1+2\sum_{n=1}^{n=\infty}b^n\cos 2n\psi\right)\epsilon^{-\frac{t}{T_{a(LL)}}} \tag{38}$$

The amplitude of the even-harmonic currents in the field change in the same ratio as the direct current there, and with a field time constant. The amplitude of the odd-harmonic components in the field follow the direct current in the armature to zero with an armature time constant.

Therefore

$$i_f=i_{f0}+i_{f0}\left[\frac{X_d-X_d'}{X_d+\sqrt{X_d'X_q}}+\left(\frac{X_d-X_d'}{X_d'+\sqrt{X_d'X_q}}-\frac{X_d-X_d'}{X_d-\sqrt{X_d'X_q}}\right)\epsilon^{-\frac{t}{T_{d'(LL)}}}\right]\times\left(\frac{1+b}{b}\sum_{n=1}^{n=\infty}b^n\cos 2n\psi\right)+i_{f0}\left[\frac{X_d-X_d'}{X_d'+\sqrt{X_d'X_q}}\epsilon^{-\frac{t}{T_{d'(LL)}}}-\frac{2(X_d-X_d')\cos\psi_0}{X_d'+\sqrt{X_d'X_q}}\times\left(\cos\psi+\sum_{n=1}^{n=\infty}b^n\cos(2n+1)\psi\right)\epsilon^{-\frac{t}{T_{a'(LL)}}}\right] \tag{39}$$

The effective inductances are determined as for the preceding case by dividing the flux linkages of each circuit at $t=0$ by the average value of direct current in the respective circuit required to maintain these flux linkages. The ratios of these inductances to the resistances of the circuits are the time constants. For the field circuit, equation 65 is divided by the first two terms of equation 22 to obtain the effective inductance.

$$L_{ff(eff)}=\frac{L_{ff}i_{f0}}{\dfrac{X_d+\sqrt{X_d'X_q}}{X_d'+\sqrt{X_d'X_q}}i_{f0}}=L_{ff}\frac{X_d'+\sqrt{X_d'X_q}}{X_d+\sqrt{X_d'X_q}} \tag{40}$$

$$T_{d'(LL)}=\frac{L_{ff(eff)}}{R_{ff}}=\frac{L_{ff}}{R_{ff}}\frac{X_d'+\sqrt{X_d'X_q}}{X_d+\sqrt{X_d'X_q}}=T_{d0}'\frac{X_d'+\sqrt{X_d'X_q}}{X_d+\sqrt{X_d'X_q}} \tag{41}$$

For the armature circuit the flux linkages are required from equation 81 (in Appendix III). They are

$$\Lambda_{ab0}=L_{afM}i_{f0}(\cos\sigma_0-\sin\sigma_0)=\sqrt{2}L_{afM}i_{f0}\cos(\sigma_0+\pi/4)=\sqrt{2}L_{afM}i_{f0}\cos\psi_0 \tag{42}$$

The direct current of the armature is contained in equation 21 so that

$$L_{ab(eff)}=\frac{\sqrt{2}L_{afM}i_{f0}\cos\psi_0}{\dfrac{\sqrt{2}E_{1M}\cos\psi_0}{2\sqrt{X_d'X_q}}}=\frac{2\sqrt{X_d'X_q}}{\omega} \tag{43}$$

$$T_{a(LL)}=\frac{L_{ab(eff)}}{2R_a}=\frac{\sqrt{X_d'X_q}}{\omega R_a} \tag{44}$$

Single Line-to-Neutral Short Circuit

The final and initial values of direct current in the field are the same for this case as for the line-to-line short circuit. Since the amplitude of the fundamental-frequency and odd-harmonic components of current in the armature are also the same except for a factor $\sqrt{2}$, the result for the steady-state current amplitude may be written as

$$I_{aM(ss)}=\frac{-2E_{1M}}{X_d+\sqrt{X_d'X_q}} \tag{45}$$

Then the approximate complete expression for armature current is

$$i_a=-\left[\frac{2E_{1M}}{X_d+\sqrt{X_d'X_q}}+\left(\frac{2E_{1M}}{X_d'+\sqrt{X_d'X_q}}-\frac{2E_{1M}}{X_d+\sqrt{X_d'X_q}}\right)\epsilon^{-\frac{t}{T_{d'(LN)}}}\right]\left(\cos\sigma+\sum_{n=1}^{n=\infty}b^n\cos(2n+1)\sigma\right)+\frac{E_{1M}\cos\sigma_0}{\sqrt{X_d'X_q}}\times\left(1+2\sum_{n=1}^{n=\infty}b^n\cos 2n\sigma\right)\epsilon^{-\frac{t}{T_{a(LN)}}} \tag{46}$$

For the field, the result is

$$i_f=i_{f0}+i_{f0}\left[\frac{X_d-X_d'}{X_d+\sqrt{X_d'X_q}}+\left(\frac{X_d-X_d'}{X_d'+\sqrt{X_d'X_q}}-\frac{X_d-X_d'}{X_d+\sqrt{X_d'X_q}}\right)\epsilon^{-\frac{t}{T_{d'(LN)}}}\left(\frac{1+b}{b}\sum_{n=1}^{n=\infty}b^n\cos 2n\sigma+\right)\right]+i_{f0}\left[\frac{X_d-X_d'}{X_d'+\sqrt{X_d'X_q}}\epsilon^{-\frac{t}{T_{d'a(LN)}}}-\frac{2(X_d-X_d')\cos\sigma_0}{X_d'+\sqrt{X_d'X_q}}\left(\cos\sigma+\sum_{n=1}^{n=\infty}b^n\cos(2n+1)\sigma\right)\epsilon^{-\frac{t}{T_{a(LN)}}}\right] \tag{47}$$

Since the amplitude of the direct current in the field is the same for both the line-to-line and the single line-to-neutral faults, both initially and immediately after short circuit, the effective inductance is the same for the two cases, as will be the time constant also. Thus

$$T_{d'(LN)}=T_{d'(LL)}=T_{d\phi}'\frac{X_d'+\sqrt{X_d'X_q}}{X_d+\sqrt{X_d'X_q}} \tag{48}$$

The effective inductance per phase of the armature circuit is determined as before. The flux linkages at $t=0$ are given by equation 63 (in Appendix I). The direct current in the armature is obtained from equation 26. Then

$$L_{a(eff)}=\frac{L_{afM}i_{f0}\cos\sigma_0}{\dfrac{E_{1M}\cos\sigma_0}{\sqrt{X_d'X_q}}}=\frac{\sqrt{X_d'X_q}}{\omega} \tag{49}$$

Thus the effective inductance of phase A of the armature circuits under the conditions of a line-to-neutral short circuit is one-half the effective inductances of phases A and B in series for a line-to-line short circuit. Since the resistance of the circuit involved is also one-half as large in the present case, the armature circuit time constant is the same as given by equation 44. Therefore

$$T_{a(LN)}=T_{a(LL)}=\frac{\sqrt{X_d'X_q}}{\omega R_a} \tag{50}$$

Comparison With 3-Phase Machines

Some of the essential differences between the 2-phase and 3-phase synchronous machines have been absorbed in the definitions of the inductances in the direct and quadrature axes. The result is that the equations for the short-circuit currents in the 2-phase machine, when expressed in terms of these inductances, are very similar to equivalent equations for 3-phase machines. The differences in the inductances are shown in Table I. In the expressions for 3-phase machine inductances is the term L_{ma} which is the average value of the mutual inductance between phases. For the 2-phase case this term is zero, as noted previously.

Equations 30 and 31 for the currents in phase A and in the field for a double line-to-neutral short circuit are identical with equivalent equations for a 3-phase machine with a 3-phase short circuit. Thus, the only differences here are included in the definitions of inductances.

Equation 38 for the current in phase A for a line-to-line short circuit is the same as the equivalent equation for a 3-phase machine with a similar fault excepting a common multiplier of $\sqrt{2}$ for the 2-phase, and $\sqrt{3}$ for the 3-phase cases. There is a necessary difference in phase angle because in this paper the equation is written for the reference phase, and for 3-phase work it is usually written for one of the two nonreference phases. The equation for field current is the same in both cases.

Equations 46 and 47 for a single line-to-neutral fault are considerably different from the equivalent equations for a 3-phase machine. The difference involves a term X_0 used to account for the zero-sequence reactance of 3-phase systems. The value of X_0 is given by

$$X_0=\omega L_0=\omega(L_{aa}-2L_{ma})$$

The term L_0 does not appear in this paper because of the absence of an average mutual inductance, L_{ma}. Thus the various inductances of the 2-phase machine may

Table I. Inductances and Time Constants for 2-Phase and 3-Phase Machines

Quantity	2-Phase	3-Phase
L_d	$L_{sa}+L_{sv}$	$L_{sa}+L_{ma}+3/2L_{sv}$
L_q	$L_{sa}-L_{sv}$	$L_{sa}+L_{ma}-3/2L_{sv}$
L_d'	$L_d-L_{afM}^2/L_{ff}$	$L_d-(3/2)(L_{afM}^2/L_{ff})$
$T_{d\phi}'$	L_{ff}/R_{ff}	L_{ff}/R_{ff}
T_d'*	$T_{d\phi}'\dfrac{X_d'}{X_d}$	$T_{d\phi}'\dfrac{X_d'}{X_d}$
$T_{d'(LL)}$	$T_{d\phi}'\dfrac{X_d'+\sqrt{X_d'X_q}}{X_d+\sqrt{X_d'X_q}}$	$T_{d\phi}'\dfrac{X_d'+\sqrt{X_d'X_q}}{X_d+\sqrt{X_d'X_q}}$
$T_{d'(LN)}$	$T_{d\phi}'\dfrac{X_d'+\sqrt{X_d'X_q}}{X_d+\sqrt{X_d'X_q}}$	$T_{d\phi}'\dfrac{X_d'+\dfrac{X_0}{2}+\sqrt{\left(X_d'+\dfrac{X_0}{2}\right)\left(X_q+\dfrac{X_0}{2}\right)}}{X_d+\dfrac{X_0}{2}+\sqrt{\left(X_d'+\dfrac{X_0}{2}\right)\left(X_q+\dfrac{X_0}{2}\right)}}$
T_a*	$\dfrac{2X_d'X_q}{\omega R_a(X_d'+X_q)}$	$\dfrac{2X_d'X_q}{\omega R_a(X_d'+X_q)}$
$T_{a(LL)}$	$\dfrac{\sqrt{X_d'X_q}}{\omega R_a}$	$\dfrac{\sqrt{X_d'X_q}}{\omega R_a}$
$T_{a(LN)}$	$\dfrac{\sqrt{X_d'X_q}}{\omega R_a}$	$\dfrac{2}{3\omega R_a}\sqrt{\left(X_d'+\dfrac{X_0}{2}\right)\left(X_q+\dfrac{X_0}{2}\right)}$

* T_d', T_a are for a double line-to-neutral fault on a 2-phase machine and for a 3-phase fault on a 3-phase machine.

be completely defined by L_d and L_q alone. This would not be the case for short circuits involving neutral impedance. However, it can be shown[10] that when neutral impedance is not involved, zero-sequence voltages do not enter the equations for 2-phase 3-wire generators. If equation 26, for current in phase A for a single line-to-neutral short circuit, is written in terms of machine inductances, L_{sa}, L_{sv}, L_{afM} and L_{ff} instead of with the fictitious inductances, L_d, L_d', and L_q, a result will be obtained as follows

$$i_a=-\frac{2E_{iM}}{L_{sa}-L_{afM}^2/L_{ff}+\sqrt{(L_{sa}+L_{sv}-L_{afM}^2/L_{ff})(L_{sa}-L_{sv})}}\times\left(\cos\sigma+\sum_{n=1}^{n=\infty}b^n\cos(2n+1)\sigma\right)+\frac{E_{iM}\cos\sigma_0}{\sqrt{(L_{sa}+L_{sv}-L_{afM}^2/L_{ff})(L_{sa}-L_{sv})}}\times\left(1+2\sum_{n=1}^{n=\infty}b^n\cos(2n\sigma)\right)$$

Equations 7, 8, and 72, in Appendix II, were used to effect this change. If the same procedure is followed in writing an equivalent equation for a 3-phase machine with a single line-to-neutral short circuit, an identical expression results when the various inductances are defined in the same manner, and the analysis is carried out by the method of constant flux linkages. The effect of L_{ma} cancels. This is, of course, as it should be since, with equal windings in each case and no other armature windings involved in the fault, it can make no difference how many other windings are on the armature.

Included in Table I are the expressions for the various time constants of both 2-phase and 3-phase machines. They are alike for all but the single line-to-neutral case. However, if the same procedure is followed in expressing these time constants in terms of winding inductances, they become identical. That they should do so is evident when it is considered that in each case but one winding is involved. It should be noted that for the other two faults the expressions appear alike when written in terms of direct- and quadrature-axis inductances (or their reactances) but would be dissimilar if expressed in terms of winding inductances because L_{ma} would not cancel.

Appendix I. Flux Linkages of the Windings

The flux linkages of the phase A and B windings are given by

$$\Lambda_a=L_{aa}i_a+L_{ab}i_b+L_{af}i_f \tag{51}$$

$$\Lambda_b=L_{bb}i_b+L_{ab}i_a+L_{bf}i_f \tag{52}$$

Substituting for the inductances from equations 1, 2, 4, 5, and 6, these become

$$\Lambda_a=L_{sa}i_a+L_{sv}i_a\cos 2\sigma+L_{sv}i_b\sin 2\sigma+L_{afM}i_f\cos\sigma \tag{53}$$

$$\Lambda_b=L_{sa}i_b-L_{sv}i_b\cos 2\sigma+L_{sv}i_a\sin 2\sigma+L_{afM}i_f\sin\sigma \tag{54}$$

The flux linkages of the field winding are

$$\Lambda_f=L_{ff}i_f+L_{af}i_a+L_{bf}i_b \tag{55}$$

where L_{ff} is the constant self inductance of the field winding. Substituting again equations 5 and 6 gives

$$\Lambda_f=L_{ff}i_f+L_{afM}i_a\cos\sigma+L_{afM}i_b\sin\sigma \tag{56}$$

Equations 53, 54, and 56 are general for the three windings on an L-connected salient-pole 2-phase machine and apply under all conditions if there are no additional windings carrying current. If the armature currents are known, the expressions for flux linkages may be used to determine the armature and field voltages.

It is useful to determine the flux linkages for the particular case where the armature windings are carrying symmetrical, sinusoidal currents. Thus, let

$$i_a=I_{aM}\sin(\sigma+\phi_i) \tag{57}$$

$$i_b=I_{aM}\sin(\sigma+\phi_i-\pi/2) \tag{58}$$

where I_{aM} is the amplitude of the armature current and ϕ_i is the angle between the armature current and the internally generated voltage. Using these equations to substitute in equation 53, and combining terms gives

$$\Lambda_a=I_{aM}[L_{sa}\sin(\sigma+\phi_i)+L_{sv}\sin(-\sigma+\phi_i)]+L_{afM}i_f\cos\sigma \tag{59}$$

When the sines of the double angles are expanded and terms combined, this equation becomes

$$\Lambda_a=I_{aM}[(L_{sa}+L_{sv})\sin\phi_i\cos\sigma+(L_{sa}-L_{sv})\cos\phi_i\sin\sigma]+L_{afM}i_f\cos\sigma \tag{60}$$

If ϕ_i is zero, representing unity power factor, the first term in brackets becomes zero and the flux linkages become those caused by field current plus a component at right angles to the flux linkages caused by field current; that is, a component in the quadrature axis, and the inductance used is $L_{sa}-L_{sv}$. If ϕ_i is $\pm\phi/2$, representing leading or lagging zero power factor, the second term inside the brackets becomes zero and the flux linkages become those produced by the field current plus or minus a component produced by armature current that is in the same (direct) axis, and the inductance to be used is $L_{sa}+L_{sv}$. Thus two values of inductance become apparent, one for the direct axis, and one for the quadrature axis. They are

$$L_d=L_{sa}+L_{sv} \tag{61}$$

$$L_q=L_{sa}-L_{sv} \tag{62}$$

L_d and L_q are called the direct-axis inductance and the quadrature-axis inductance respectively. These quantities have the same significance as their counterparts in 3-phase machines, but their values are different. This point is discussed in a later section.

The values of initial flux linkages, before short circuit occurs, are found by substituting for the values of current at that time. They are

$$i_a=i_b=0$$
$$i_f=i_{f0}$$

From these equations and equations 53, 54, and 56 the flux linkages are

$$\Lambda_{a0}=L_{afM}i_{f0}\cos\sigma_0 \tag{63}$$

$$\Lambda_{b0}=L_{afM}i_{f0}\sin\sigma_0 \tag{64}$$

$$\Lambda_{f0}=L_{ff}i_{f0} \tag{65}$$

If the flux linkages of the field before short circuit are equated to the flux linkages of this circuit after short circuit, an expression may be obtained for the instantaneous value of field current in terms of i_a and i_b. Performing this operation gives

$$L_{ff}i_{f0}=L_{ff}i_f+L_{afM}i_a\cos\sigma+L_{afM}i_b\sin\sigma$$

$$i_f=i_{f0}-(L_{afM}/L_{ff})(i_a\cos\sigma+i_b\sin\sigma) \qquad (66)$$

When this equation is substituted in equations 53 and 54, expressions for the phase flux linkages are obtained which contain only armature currents.

$$\Lambda_a=L_{sa}i_a+L_{sv}i_a\cos 2\sigma+L_{sv}i_b\sin 2\sigma+ L_{afM}i_{f0}\cos\sigma-(L_{afM}^2/L_{ff})\times (i_a\cos\sigma+i_b\sin\sigma)\cos\sigma \qquad (67)$$

$$\Lambda_b=L_{sa}i_b-L_{sv}i_b\cos 2\sigma+L_{sv}i_a\sin 2\sigma+ L_{afM}i_{f0}\sin\sigma-(L_{afM}^2/L_{ff})\times (i_a\cos\sigma+i_b\sin\sigma)\sin\sigma \qquad (68)$$

Appendix II. Currents for a Double Line-to-Neutral Short Circuit

Applying the method of the theorem of constant flux linkages, equations 63 and 64 for the flux linkages before short circuit are set equal to equations 67 and 68 for the flux linkages before short circuit are set equal to equations 67 and 68 for the flux linkages after short circuit. When this is done for phase A, the result is

$$L_{afM}i_{f0}\cos\sigma_0=L_{sa}i_a+L_{sv}i_a\cos 2\sigma+ L_{sv}i_b\sin 2\sigma+L_{afM}i_{f0}\cos\sigma- (L_{afM}^2/L_{ff})(i_a\cos\sigma+i_b\sin\sigma)\cos\sigma \qquad (69)$$

The values of L_{sa} and L_{sv}, as given in equations 9 and 10, may now be substituted. When this is done, and simplification accomplished, the result is

$$2L_{afM}i_{f0}(\cos\sigma_0-\cos\sigma) =i_a[L_d-L_{afM}^2/L_{ff}+L_q+ (L_d-L_{afM}^2/L_{ff}-L_q)\times\cos 2\sigma]+ i_b[(L_d-L_{afM}^2/L_{ff}-L_q)\sin 2\sigma] \qquad (70)$$

The expression $L_{afM}i_{f0}$ gives the maximum flux linkages of the phase windings caused by initial current in the field. When this is multiplied by ω, the angular velocity of the field, it is equal to the maximum value of the voltage generated in the phase windings for a field current i_{f0}. Thus

$$E_{tM}=\sqrt{2}E_t=\omega L_{afM}i_{f0} \qquad (71)$$

This equation may be used to simplify equation 70.

Before this is done, a further simplification can be made by defining the direct-axis transient inductance as

$$L_d'=L_d-L_{afM}^2/L_{ff} \qquad (72)$$

and

$$X_d'=\omega L_d'=X_d-\omega L_{afM}^2/L_{ff} \qquad (73)$$

Using equations 71, 72, and 73, equation 70 may finally be written

$$2E_{tM}(\cos\sigma_0-\cos\sigma)=i_a[X_d'+X_q+ (X_d'-X_q)\cos 2\sigma]+i_b(X_d'-X_q) \sin 2\sigma \qquad (74)$$

Similarly, a relation for phase B may be written

$$2E_{tM}(\cos\sigma_0-\cos\sigma)=i_a(X_d'-X_q)\sin 2\sigma+ i_b[X_d'+X_q-(X_d'-X_q)\cos 2\sigma] \qquad (75)$$

Equations 74 and 75 are two equations in i_a and i_b and may be solved simultaneously for these currents. These solutions are

$$i_a=\frac{E_{tM}(X_d'+X_q)}{2X_d'X_q}\cos\sigma_0-\frac{E_{tM}}{X_d'}\cos(\omega t+\sigma_0)- \frac{E_{tM}(X_d'-X_q)}{2X_d'X_q}\cos(2\omega t+\sigma_0) \qquad (76)$$

$$i_b=\frac{E_{tM}(X_d'+X_q)}{2X_d'X_q}\sin\sigma_0-\frac{E_{tM}}{X_d'}\sin(\omega t+\sigma_0)- \frac{E_{tM}(X_d'-X_q)}{2X_d'X_q}\sin(2\omega t+\sigma_0) \qquad (77)$$

The equation for current in the field may be obtained by substituting these values of i_a and i_b in equation 66. The equation for field current may first be put into better form as follows

$$i_f=i_{f0}-\frac{\omega L_{afM}^2}{L_{ff}}\;\frac{i_{f0}}{\omega L_{afM}i_{f0}}(i_a\cos\sigma+i_b\sin\sigma)$$

$$=i_{f0}-\frac{X_d-X_d'}{E_{tM}}i_{f0}(i_a\cos\sigma+i_f\sin\sigma) \qquad (78)$$

Then, on substituting the armature currents and making use of trigonometric identities, equation 78 becomes

$$i_f=i_{f0}+\frac{X_d-X_d'}{X_d'}\,i_{f0}-\frac{X_d-X_d'}{X_d'}\,i_{f0}\cos\omega t \qquad (79)$$

Appendix III. Currents for a Line-to-Line Short Circuit

The starting point is with equations 67 and 68, the expressions for the general flux linkages of each phase winding. These may be simplified by the fact that $i_a=-i_b$. When the two flux-linkage equations are substituted in equation 18, Λ_{ab} is obtained as

$$\Lambda_{ab}=2L_{sa}i_a-2L_{sv}i_a\sin 2\sigma+ L_{afM}i_{f0}(\cos\sigma-\sin\sigma)- (L_{afM}^2/L_{ff})(1-2\sin\sigma\cos\sigma)i_a \qquad (80)$$

The relation for flux linkages at $t=0$ may be obtained from equation 80 by the fact that $i_a=0$. Thus

$$\Lambda_{ab0}=L_{afM}i_{f0}(\cos\sigma_0-\sin\sigma_0) \qquad (81)$$

After the short circuit is established, $\Lambda_{ab}=\Lambda_{ab0}$. Then setting equation 80 equal to equation 81 and making use of equations 9 and 10, the result for i_a is obtained as

$$i_a=-i_b= \frac{\sqrt{2}E_{tM}[\cos(\sigma_0+\pi/4)-\cos(\sigma+\pi/4)]}{X_d'+X_q-(X_d'-X_q)\sin 2\sigma} \qquad (82)$$

Equation 82 will be easier to manipulate if the following changes in angles are made

$$\psi=\sigma+\pi/4=\omega t+\sigma_0+\pi/4$$
$$\psi_0=\sigma_0+\pi/4$$

The field current may be obtained from equation 66 by substituting the values of i_a and i_b and making the change in angle. It is

$$i_f=i_{f0}+(X_d-X_d')\times \frac{1+\cos 2\psi-2\cos\psi_0\cos\psi}{X_d'+X_q+(X_d'-X_q)\cos 2\psi}i_{f0} \qquad (83)$$

Equation 82 with the change in angle, and equation 83 may be expanded as series by means of the following equations

$$\frac{1}{A+B\cos 2\psi}=\frac{1}{\sqrt{A^2-B^2}}\times \left(1+2\sum_{n=1}^{n=\infty}b^n\cos 2n\psi\right)$$

$$\frac{\cos\psi}{A+B\cos 2\psi}=\frac{1+b}{\sqrt{A^2-B^2}}\times \left(\cos\psi+\sum_{n=1}^{n=\infty}b^n\cos(2n+1)\psi\right)$$

$$\frac{\cos 2\psi}{A+B\cos 2\psi}=\frac{1}{\sqrt{A^2+B^2}}\times \left(b+\frac{1+b^2}{b}\sum_{n=1}^{n=\infty}b^n\cos 2n\psi\right)$$

$$\frac{1+\cos 2\psi}{A+B\cos 2\psi}=\frac{1+b}{\sqrt{A^2+B^2}}\times \left(1+\frac{1+b}{b}\sum_{n=1}^{n=\infty}b^n\cos 2n\psi\right) \qquad (84)$$

where

$$b=\frac{\sqrt{A-B}-\sqrt{A+B}}{\sqrt{A+B}+\sqrt{A-B}}+\frac{\sqrt{X_q}-\sqrt{X_d'}}{\sqrt{X_d'}+\sqrt{X_q}} =\frac{\sqrt{X_d'X_q}-X_d'}{\sqrt{X_d'X_q}+X_d'} \qquad (85)$$

for the equations under consideration. When equations 82 and 83 are expanded in accordance with equation 84, the results for i_a and i_f are

$$i_a=-i_b=-\frac{\sqrt{2}E_{tM}}{X_d'+\sqrt{X_d'X_q}}\times \left(\cos\psi+\sum_{n=1}^{n=\infty}b^n\cos(2n+1)\psi\right)+ \frac{\sqrt{2}E_{tM}\cos\psi_0}{2\sqrt{X_d'X_q}}\left(1+2\sum_{n=1}^{n=\infty}b^n\cos 2n\psi\right) \qquad (86)$$

$$i_f=i_{f0}+i_{f0}\frac{X_d-X_d'}{X_d'+\sqrt{X_d'X_q}}\times \left[\frac{1+b}{b}\sum_{n=1}^{n=\infty}b^n\cos 2n\psi-2\cos\psi_0\times \left(\cos\psi+\sum_{n=1}^{n=\infty}b^n\cos(2n+1)\psi\right)\right] \qquad (87)$$

References

1. Synchronous Machines—I and II, R. E. Doherty, C. A. Nickle. *AIEE Transactions*. volume 45, June 1926, pages 912–47.

2. Synchronous Machines—IV, R. E. Doherty, C. A. Nickle. *AIEE Transactions*, volume 47, April 1928, pages 457–92.

3. Synchronous Machines—V, R. E. Doherty, C. A. Nickle. *AIEE Transactions*, volume 49, April 1930, pages 700–14.

4. Initial and Sustained Short-Circuits in Synchronous Machines, Vladimir Karapetoff. *AIEE Transactions*, volume 44, April 1925, page 403.

5. A SIMPLIFIED METHOD OF ANALYZING SHORT-CIRCUIT PROBLEMS, R. E. Doherty. *AIEE Transactions*, volume 42, June 1923, pages 841–49.

6. TWO-REACTION THEORY OF SYNCHRONOUS MACHINES—I, R. H. Park. *AIEE Transactions*, volume 48, July 1929, page 716.

7. TWO-REACTION THEORY OF SYNCHRONOUS MACHINES—II, R. H. Park. *AIEE Transactions*, volume 52, June 1933, page 352.

8. THE SHORT-CIRCUIT CHARACTERISTICS OF D-C GENERATORS, G. E. Frost. *Electrical Engineering* (*AIEE Transactions*) volume 65, June 1946, pages 394–402.

9. FUNDAMENTAL CONCEPTS OF SYNCHRONOUS MACHINE REACTANCES, B. R. Prentice. *AIEE Transactions*, volume 56 (supplement), 1937, pages 1–21.

10. SYMMETRICAL COMPONENTS (book), C. F. Wagner, R. D. Evans. McGraw-Hill Book Company, Inc., New York, N. Y., 1933, pages 332–36.

11. SYNCHRONOUS MACHINERY, W. A. Lewis. Illinois Institute of Technology, Chicago, Ill.

No Discussion

The Dynamoelectric Amplifier—Class A Operation

ROBERT M. SAUNDERS
MEMBER AIEE

Synopsis: Previous papers have described the basic operating principles of several dynamoelectric amplifiers and their behavior under d-c transient conditions. This paper compares the various dynamoelectric amplifiers to the electronic amplifier, and discusses the static and dynamic characteristics of both the single- and 2-stage dynamoelectric amplifiers from an a-c steady-state point of view. The dynamic characteristics are calculated from equivalent circuits and compared with test results in the form of frequency response and phase angle curves. Negative feed-back circuits and response curves also are presented and the effects of feedback pointed out. Methods of obtaining the equivalent circuit parameters from test are discussed briefly.

RECENTLY there have been several papers describing the various dynamoelectric amplifiers individually which discuss their characteristics when operating under transient conditions. It is the purpose of this paper to point out the similarity of the dynamoelectric amplifiers to each other as far as external effects are concerned, to show the similarity to electronic amplifiers (on which there is a wealth of literature), and to present equivalent circuits that can be used to predict satisfactorily the performance of these amplifiers under a-c steady-state conditions.

The American Standards Association[1] definition of an amplifier is "... a device for increasing the power associated with a phenomenon without appreciably altering its quality, through control by the amplifier input of a larger amount of power supplied by a local source to the amplifier output."

There are several rotating machines that can qualify as amplifiers under the above definition and those considered here are: the separately excited d-c generator, the Amplidyne, the Rototrol, and the Regulex. In each of these machines a large amount of output power can be controlled by a small control field current, the power being supplied in the form of mechanical power through the shaft.

Figure 1(A) shows the separately excited d-c generator with its circuit parameters indicated. The inductance and resistance of the control field are shown as L_c and R_c respectively. The total inductance of the armature circuit is shown as L_A and includes the armature, interpoles, and inductive effects of commutation. The resistance R_A represents all of the resistance in the armature circuit including the armature winding, interpoles, and brushes. If a direct voltage, E_c, is placed on the control field, a voltage E_G will be developed across the brushes. The relationship between E_c and E_G is indicated as the curve *BA* in Figure 2, this curve being the usual saturation curve for the machine. If the direct voltage now is replaced by the smaller sine wave, Figure 2, which requires swings of voltage over only the straight line portion of the curve, the variation of the generated voltage also will be sinusoidal in nature. However, if the amplitude of the sine wave of Figure 2 is increased so that operation ensues over a curved portion of the saturation curve, the output voltage will no longer be a true representation of the input and distortion now will be present. Hence, operation along the straight line portion of the curve results in distortionless amplification, usually referred to as class *A* amplification.

The operation of the d-c machine as a dynamoelectric amplifier is analogous in many respects to the electronic amplifier shown in Figure 1(B); yet there are several distinct differences:

1. The source of power is mechanical instead of electrical.
2. There is no direct current present in the output circuit.
3. Control is effected by a current instead of a voltage.
4. The control and output circuits contain inductance.

As a consequence of (1) and (2), there is no problem of blocking the direct current from the load in the dynamoelectric amplifier circuit, thus obviating the necessity for capacitor *C*, Figure 1(B), used in the electronic amplifier. It is this capacitor that limits the low frequency response of the latter; and its absence in the dynamoelectric amplifier permits the frequency response to extend to zero frequency or direct current. As a consequence of (3), the driving circuit must have sufficient power associated with it to excite the dynamoelectric amplifier even for class *A* operation, whereas the electronic amplifier normally requires essentially no power for similar operation. As a consequence of (4), the high-frequency response will be affected by the inductances present. The inductances, especially the control field inductance, are usually so high that the d-c machine is not suitable for use as an amplifier where the frequency response must be greater than approximately 0.5 cycle per second.

The Amplidyne, the Rototrol, and the Regulex are dynamoelectric machines in which the time constant of the control field has been materially reduced by various means so that a higher frequency response can be achieved. In this paper it is assumed that the basic principles of these machines are familiar to the reader.[2-6] For each of these machines, as well as for the d-c machine, a plot of E_c or I_c versus

---

Paper 49-295, recommended by the AIEE Rotating Machinery Committee and approved by the AIEE Technical Program Committee for presentation at the AIEE Fall General Meeting, Cincinnati, Ohio, October 17–21, 1949. Manuscript submitted May 2, 1949; made available for printing September 13, 1949.

ROBERT M. SAUNDERS is with the Division of Electrical Engineering, University of California, Berkeley, Calif.

The author wishes to express his appreciation to Dr. Troy D. Graybeal, Assistant Professor of Electrical Engineering, University of California, for his many valuable suggestions contributed during the preparation of this paper.

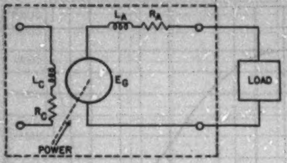

Figure 1A. Single-stage dynamoelectric amplifier with circuit parameters

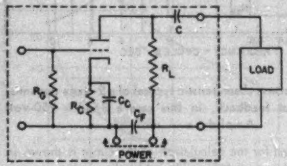

Figure 1B. Comparable single-stage resistance-coupled electronic amplifier with circuit parameters

E_G may be obtained for each stage, and for class A operation, the swings of control field current confined to the straight line portion of that curve. Likewise an equivalent circuit similar to that for the d-c machine may be employed for the purpose of obtaining the characteristics.

Static Characteristics

The static characteristics of an electronic amplifier are of interest since they determine the necessary supply voltage, circuit parameters, and the permissible operating range for linear operation. Similarly the static characteristics are needed for the dynamoelectric amplifier to determine the linear operating range and the induced voltage per ampere of field current for the various stages; this latter quantity is called the transresistance in this paper. It will be noted that the transresistance has a reciprocal analogy to the transconductance in the vacuum tube. There are several types of static characteristics. Those the author has found the most useful and the easiest to obtain are the control field current versus generated voltage for each stage, and the control field current versus over-all output voltage for constant resistance loads.

Figure 3 depicts a set of these over-all static characteristics for a 3/4-kw 250-volt Amplidyne. The open and short-circuit tests described by Graybeal[7] also have been found useful. These characteristics permit the calculation of the transresistances for the various stages and provide a check on the resistive components of the equivalent circuit. One also may calculate the power amplification, the voltage amplification, and the transconductance, but these quantities serve little use except to act as figures of merit when discussing amplifiers qualitatively.

Dynamic Characteristics

There are two methods of analyzing the dynamoelectric amplifier from a dynamic point of view: the transient method and the a-c steady-state method. This paper is concerned with the latter. If the transient analysis is preferred, the $j\omega$ terms used herein may be replaced with the operator, $p=d/dt$. In examining an amplifier from an a-c steady-state viewpoint, one usually is concerned with its amplification, frequency response characteristics, and zones of stability. To consider the dynamic characteristics an equivalent circuit is used in this paper, and the response of the equivalent circuit to various frequencies is explored. First, the single- and 2-stage amplifiers are discussed, and then the two types of negative feed-back amplifiers are considered. To illustrate the validity of the assumptions, the agreement with test values is indicated where such test data are available.

The following general assumptions apply to the dynamic analysis made in this paper:

1. Prime mover speed is constant.
2. Only straight line portion of saturation curve is used.
3. Residual effects are negligible.
4. Hysteresis effects are negligible.
5. Parameters are linear.

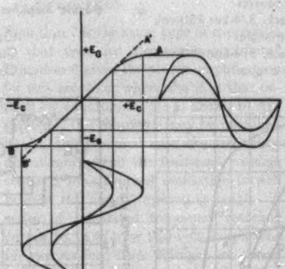

Figure 2. Relationship between control field voltage and generated voltage

Distortion is introduced as soon as the swings of control voltage extend over the straight line portion of the curve

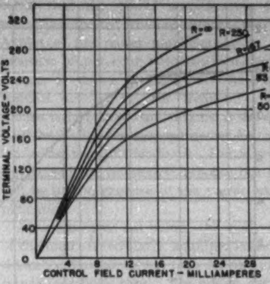

Figure 3. Over-all static characteristics of a 3/4-kw 250-volt Amplidyne

Resistance values are in ohms

First, a single-stage amplifier similar to that of Figure 1(A) will be considered. This circuit would be appropriate for the d-c generator or the single-stage Rototrol or Regulex units. For a constant alternating voltage applied to the control field, the voltage developed across the load is

$$E_L=\frac{E_G Z_L}{Z_L+Z_A}=\frac{NI_c Z_L}{Z_L+Z_A}=\frac{NE_c Z_L}{Z_c(Z_L+Z_A)} \qquad (1)$$

where

$$N=\left(\frac{\partial E_G}{\partial I_c}\right)_{I_A=0}=\text{slope of } E_G \text{ versus } I_c \text{ curve}$$

Z_L = load impedance
Z_A = armature circuit impedance
Z_c = control field self impedance
E_c = applied voltage to control field

The complex voltage amplification

$$A=\frac{E_L}{E_c}=\frac{NZ_L}{Z_c(Z_L+Z_A)} \qquad (2)$$

The power amplification

$$B=\frac{P_L}{P_c}=\frac{|I_L|^2R_L}{|I_c|^2R_c}=\frac{|E_L|^2|Z_c|^2R_L}{|Z_L|^2|E_c|^2R_c}$$
$$=|A|^2\frac{|Z_c|^2R_L}{|Z_L|^2R_c} \qquad (3)$$

Equation 3 is a very general one and applies to all dynamoelectric amplifiers irrespective of the numbers of stages. For any amplifier to serve as an oscillator the criterion is that one term in the denominator of equation 2 have a zero. Defining θ_L, θ_A, and θ_c as the phase angle of the load, armature, and control field impedances respectively, it is noted that in all cases $-\pi/2\leq\theta_L\leq\pi/2$; $0\leq\theta_A\leq\pi/2$; $0\leq\theta_c\leq\pi/2$. Hence $|Z_L|>0$ and $|Z_c|>0$ in all instances and therefore this amplifier is inherently stable, and cannot serve as an oscillator under the conditions imposed, namely, constant speed and linear constants.

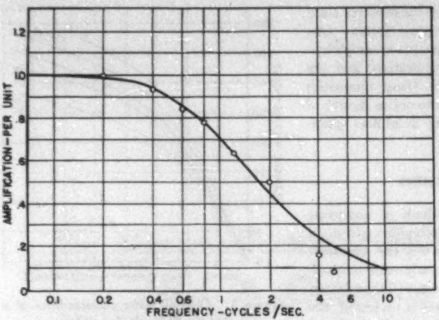

Figure 4. Frequency response characteristic typical of a single-stage dynamoelectric amplifier without feedback, in this case a 100-watt Rototrol

Test points are indicated by the circles

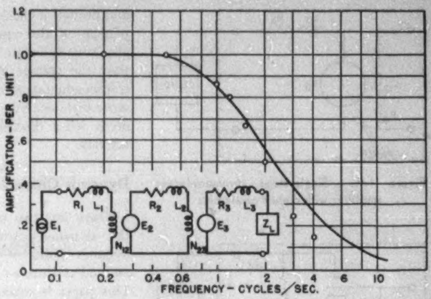

Figure 6. Frequency response characteristic typical of a 2-stage dynamoelectric amplifier without feedback, in this case a 3/4-kw 250-volt Amplidyne

The equivalent circuit used for the calculation of the curve is shown in the insert, and the test values indicated by the circles

The calculated frequency response characteristics of a 100-watt 125-volt single-stage Rototrol operating into a resistance load is shown in Figure 4 and the phase angle characteristic as curve A, Figure 5, with the test values indicated. For the single-stage amplifier it can be seen that there is very close agreement between the response determined by the equivalent circuit and the actual test values. The equivalent circuit for a 2-stage dynamoelectric amplifier is shown in the insert of Figure 6. This circuit would be suitable for two d-c generators in cascade, a critically compensated Amplidyne, or a critically compensated 2-stage Rototrol. For a constant alternating voltage applied to the control field, the voltage developed across the load is

$$E_L = E_1 \frac{N_{12} N_{23} Z_L}{Z_1 Z_2 (Z_3 + Z_L)} \tag{4}$$

and the complex voltage amplification

$$A = \frac{N_{12} N_{23} Z_L}{Z_1 Z_2 (Z_3 + Z_L)} \tag{5}$$

The power amplification expression is very similar to equation 3 except that the term Z_c is replaced by Z_1, and the A is, of course, that of equation 5.

$$B = |A|^2 \frac{|Z_1|^2 R_L}{|Z_L|^2 R_1} \tag{6}$$

A test for stability again is to examine the denominator for possible zeros. In this case: $0 \leqq \theta_1 \leqq \pi/2$; $0 \leqq \theta_2 \leqq \pi/2$; $0 \leqq \theta_3 \leqq \pi/2$; $-\pi/2 \leqq \theta_L \leqq \pi/2$; hence $|Z_1| > 0$, $Z_2| > 0$, $|(Z_3 + Z_L)| > 0$ and no zeros can exist. The 2-stage amplifier is therefore inherently stable.

The calculated and test frequency response characteristics of a 3/4-kw 250-volt Amplidyne operating at no load ($Z_L = \infty$) are shown in Figure 6, and the phase

Figure 5. Phase angle characteristics of single- and 2-stage dynamoelectric amplifiers

Curve A—single-stage no-feedback 100-watt Rototrol
Curve B—2-stage no-feedback 3/4-kw 250-volt Amplidyne, test values indicated by circles
Curve C—2-stage, 10 per cent negative feedback, 3/4-kw 250-volt Amplidyne, test values indicated by squares
Curve D—2-stage, 20 per cent negative feedback, 3/4-kw 250-volt Amplidyne, test values indicated by triangles
Curve E—2-stage, 100 per cent negative feedback, 3/4-kw 250-volt Amplidyne, test values indicated by circles

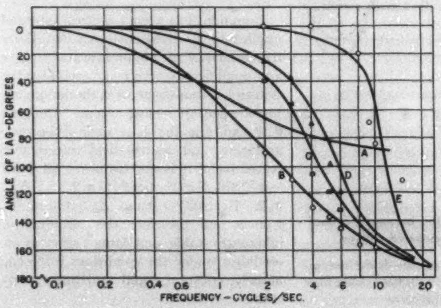

Figure 7. Frequency response characteristics of a 2-stage dynamoelectric amplifier for various degrees of negative feedback

Curve A—10 per cent feedback
Curve B—20 per cent feedback
Curve C—100 per cent feedback

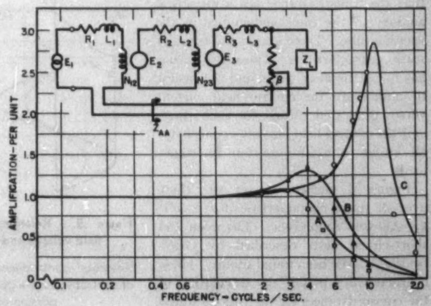

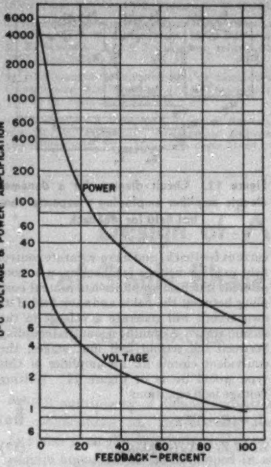

Figure 8. Variation of power and voltage amplification of a 3/4-kw 250-volt Amplidyne as a function of the amount of negative feedback

angle-frequency characteristic shown as curve *B*, Figure 5.

Feedback

The general advantages of the use of negative or inverse feedback in electronic amplifiers are well known and have been rather thoroughly explored by many observers. For a brief treatment of this subject and a bibliography the reader is referred to Terman[8] or for a more complete treatment to Bode.[9] The chief advantage of negative feedback in the dynamoelectric amplifier is that it improves the frequency response by reducing the over-all time constant by a factor of from six to ten times. The disadvantages are that the amplification is seriously reduced, and the possibility of unstable operation becomes greater.

For the purposes of this paper, negative feedback is defined as being present if at zero frequency (direct current), the over-all amplification of the amplifier is reduced from that without feedback.

The feedback may be introduced in the dynamoelectric amplifier by two methods. In the first method, called the external feed-back circuit, a fraction of the output voltage or current is placed in series with the input voltage or current as illustrated by the insert of Figure 7. The second method, called the internal feed-back circuit, involves the use of a separate control field for the purpose of injecting the feed-back signal. The second method has the advantage of keeping the input and output circuits electrically isolated, but has the disadvantage of being somewhat more awkward to handle from an analytical point of view. An example of this method is shown in Figure 11 where both current and voltage feedback are employed.

In the case of the Amplidyne and the 2-stage Rototrol, current feedback may be present as a result of the overcompensation or the undercompensation of the machine. A noncritically compensated unit will inject a magnetomotive force in the control circuit which will be proportional to the load current and will act in every way as if a separate field were used for this purpose. Of course, in many applications current feedback is intentionally employed, and the injection is made through the use of a separate control field winding. The overcompensated unit will display positive current feedback and the undercompensated unit will display negative current feed-back characteristics. Because the positive feedback may lead to oscillations, it is quite essential that the dynamoelectric amplifier be under or critically compensated for most applications.

The analysis of the external feed-back circuit is fairly straightforward and is developed in Appendix I for the case of voltage feedback. The voltage amplification for a 2-stage amplifier is

$$A=\frac{A_o}{1-\beta A_o} \tag{7}$$

where

$$A_o=\frac{N_{12}N_{22}Z_L}{Z_1Z_2(Z_2+Z_L)} \tag{8}$$

Equation 7 is the same type of expression as that used for electronic amplifiers.[8] Equation 6 gives the power amplification for this amplifier where the *A* is that defined by equation 7. As is shown in Appendix I, this amplifier may be unstable, but in the practical case the frequency and magnitude of the feed-back voltage required for sustained oscillation is well beyond the normal operating range. A series of calculated frequency response curves for a 3/4-kw 250-volt Amplidyne for various feed-back voltages are shown in Figure 7, and the phase characteristics are shown in Figure 5 with the test values being plotted as circles, triangles, and so forth. While these response curves are plotted in the customary fashion (that is, with 100 per cent for the zero-frequency point of all curves), it must be remembered that the power amplification is seriously impaired when feedback is used. A plot of the power amplification as a function of per cent negative feed-back voltage is shown in Figure 8. As was pointed out before, the frequency response is improved, and Figure 9 shows how the 70.7 per cent response can be extended by negative feedback. Hence one can extend the frequency response but it will be at the expense of the power amplification.

As was pointed out before, the analysis of the internal feed-back amplifier is considerably more involved than for the external feed-back case. The added complications are contributed by the mutual effects between the various field windings. The method of attack is very similar to the previous situations, that is, to write the voltage loop equations and to solve the resulting equations simultaneously. As an example, a 2-stage amplifier with internal feedback, Figure 11, is analyzed in Appendix II. It is theoretically possible to correlate equation 22 of Appendix II with the form of equation 7; however, β will no longer be a simple ratio, but will be a complex quantity. It is usually much easier to make a Nyquist plot to find when Δ_o vanishes to determine the point of instability.

Determination of Parameters

Thus far it has been assumed that all the necessary circuit parameters are known. The ensuing discussion suggests the means of finding the parameters. The parameters may be separated into four categories: the resistances (R_m); the self-inductances, (L_m); the mutual inductances (M_{mn}); and the speed transresistances (N_{mn}). The resistances of the field windings can be determined by the usual methods such as the bridge or the voltage drop methods. The armature resistance is a rather elusive quantity. At this stage the most reliable method

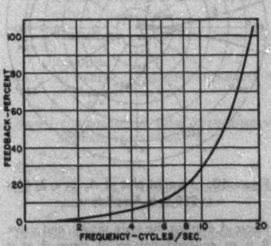

Figure 9. Variation of the 0.707 amplification point with frequency and feedback

seems to be to run the open and short-circuit tests described by Graybeal,[7] or to use data obtained from static tests. The self and mutual inductances can best be determined by means of 60-cycle impedance tests with the machine operating at normal speed somewhat as suggested by Bower.[10] Care must be exercised that the slot ripple voltage does not enter into the impedance calculations. If the slot ripple voltage is too large, it may be preferable to use static tests taking the average values for the various positions of the armature. The use of a rotating test procedure is considered superior since any short circuiting effects of the coils undergoing commutation then will be reflected in the inductances.

The determination of the transresistances has been described in the section on Static Characteristics.

Conclusions

1. The dynamoelectric amplifier has sufficient similarity to the electronic amplifier that the literature pertaining to the latter may be used to an advantage in predicting performance characteristics.

2. All the recent dynamoelectric amplifiers operating under class *A* conditions can be represented by an equivalent circuit containing resistances, self-inductances, mutual inductances, and transresistances.

3. The dynamic characteristics can be accurately predicted from a-c steady-state analysis using the equivalent circuits suggested before.

4. Negative feedback extends the frequency-response at the expense of amplification.

5. Either external or internal feedback may be employed.

6. The parameters can be determined from direct current and 60-cycle measurements with sufficient accuracy to use in the above equivalent circuits.

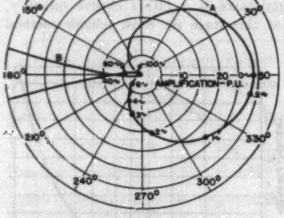

Figure 10. Nyquist plot of A_o for a 3/4-kw 250-volt Amplidyne

Curve *A* employs the scale shown, and curve *B* is an enlarged portion of curve *A* as it crosses the 180 degree line. For values of curve *B*, multiply radial scale by 0.01

Appendix I

The analysis of an external feed-back circuit is based upon the insert diagram of Figure 7. If the impedance of the control field $(R_1+j\omega L_1)$ is much greater than the impedance looking back at *AA*

$$E_L=\frac{N_{12}N_{23}Z_LE_1}{Z_1Z_2(Z_3+Z_L)\left(1-\beta\frac{N_{12}N_{23}Z_L}{Z_1Z_2(Z_3+Z_L)}\right)} \tag{9}$$

$$A=\frac{E_L}{E_1}=\frac{N_{12}N_{23}Z_L}{Z_1Z_2(Z_3+Z_L)\left(1-\beta\frac{N_{12}N_{23}Z_L}{Z_1Z_2(Z_3+Z_L)}\right)} \tag{10}$$

when

$$\beta=0$$

$$A_o=\frac{N_{12}N_{23}Z_L}{Z_1Z_2(Z_3+Z_L)} \tag{11}$$

so that

$$A=\frac{A_o}{1-\beta A_o} \tag{12}$$

The power amplification

$$B=\frac{|A|^2|Z_1|^2R_L}{R_1|Z_L|^2}=\frac{|A_o|^2|Z_1|^2R_L}{|(1-\beta A_o)|^2R_1|Z_L|^2} \tag{13}$$

The power amplification is reduced from that of the nonfeedback case since

$$\frac{|A_o|^2}{|(1-\beta A_o)|^2}<|A_o|^2 \text{ for } \beta<0 \tag{14}$$

The amplifier will be unstable and oscillate if

$$\beta A_o=1.0+j0 \tag{15}$$

The complex expression is used since A_o is complex so that both the real and imaginary quantities must satisfy the explicit condition given. Since, for a given dynamoelectric amplifier, all the quantities comprising A_o are known, a Nyquist plot of A_o in the complex plane affords a convenient means of finding if the function βA_o encloses the point 1, *j*0. The Nyquist plot for A_o of a 3/4-kw 250-volt Amplidyne is shown in Figure 10. This plot shows an instability point for approximately 50 cycles but requires that β be a large negative number. The quantity A_o is approximately 0.07 for instability so that β would have to be −142 to enclose 1, *j*0, a value well beyond the usually encountered. Hence, this particular amplifier will be very stable.

Appendix II

As an example of internal feedback, a dynamoelectric amplifier such as the Amplidyne or 2-stage Rototrol which is noncritically compensated (thus resulting in current feedback) and has a separate control field used for voltage feedback may be considered. Such an amplifier has mutual coupling between the fields and each field of its own accord will generate a voltage in the second stage. Assuming no mutual coupling between the second and first stages, the equivalent circuit for an amplifier of this type would be as in Figure 11. Writing voltage loop equations

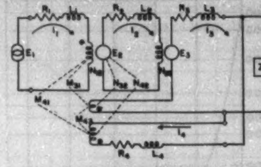

Figure 11. Circuit diagram for a dynamoelectric amplifier employing a separate control field for feedback

$$E_L=(I_3-I_4)Z_L \tag{16}$$

$$E_1=I_1Z_1+jX_{31}I_3+jX_{41}I_4 \tag{17}$$

$$\begin{aligned}E_3=N_{23}I_2&=\frac{N_{23}}{Z_2}(N_{12}I_1+N_{32}I_3+N_{42}I_4)\\&=I_3Z_3+E_L+jX_{13}I_1+jX_{43}I_4\end{aligned} \tag{18}$$

$$E_L=jX_{14}I_1+jX_{34}I_3+I_4Z_4 \tag{19}$$

The characteristic determinant is (after rearrangement)

$$\Delta_o=\begin{vmatrix}-1, & \frac{N_{23}N_{12}}{Z_2}-jX_{13}, & \frac{N_{23}N_{32}}{Z_2}-Z_3, & \frac{N_{23}N_{42}}{Z_2}-jX_{43}\\ 0 & Z_1 & jX_{31} & jX_{41}\\ -1 & jX_{14} & jX_{34} & Z_4\\ -1 & 0 & Z_L & -Z_L\end{vmatrix} \tag{20}$$

$$E_L=\frac{1}{\Delta_o}\times\begin{vmatrix}E_1 & Z_1 & jX_{31} & jX_{41}\\ 0 & \frac{N_{23}N_{12}}{Z_2}-jX_{13}, & \frac{N_{23}N_{32}}{Z_2}-Z_3, & \frac{N_{23}N_{42}}{Z_2}-jX_{43}\\ 0 & jX_{14} & jX_{34} & Z_4\\ 0 & 0 & Z_L & -Z_L\end{vmatrix} \tag{21}$$

$$A=\frac{E_L}{E_1}=\frac{1}{\Delta_o}\times\begin{vmatrix}\frac{N_{23}N_{12}}{Z_2}-jX_{13}, & \frac{N_{23}N_{32}}{Z_2}-Z_3, & \frac{N_{23}N_{42}}{Z_2}-jX_{43}\\ jX_{14} & jX_{34} & Z_4\\ 0 & Z_L & -Z_L\end{vmatrix} \tag{22}$$

The power amplification is again described by equation 6 where *A* is defined by equation 22. This amplifier will oscillate freely when $\Delta_o=0$.

References

1. AMERICAN STANDARD DEFINITIONS OF ELECTRICAL TERMS. American Standards Association

(New York, N. Y.), 1942, paragraph 05.45.155.

2. Dynamoelectric Amplifier for Power Control, E. F. W. Alexanderson, M. A. Edwards, K. K. Bowman. *AIEE Transactions*, volume 59, 1940, pages 937–39.

3. The Design Characteristics of Amplidyne Generators, Alec Fisher. *AIEE Transactions*, volume 59, 1940, pages 939–944.

4. Rototrol—A Versatile Electric Regulator, W. H. Formahls. *Westinghouse Engineer* (East Pittsburgh, Pa.), May 1942, pages 51–54.

5. The Multistage Rototrol, M. M. Liwschitz. *AIEE Transactions*, volume 66, 1947, pages 564–68.

6. Two-Stage Rototrol for Low Energy Regulating Systems, A. W. Kimball. *AIEE Transactions*, volume 66, 1947, pages 1507–11.

7. Steady-State Theory of the Amplidyne Generator, T. D. Graybeal. *Electrical Engineering* (*AIEE Transactions*) volume 61, 1942, pages 750–56.

8. Radio Engineers' Handbook (book), F. E. Terman. McGraw-Hill Book Company, Inc., New York, N. Y., 1943, pages 395–406.

9. Network Analysis and Feedback Amplifier Design (book), H. W. Bode. D. Van Nostrand Company, New York, N. Y., 1945.

10. Fundamentals of the Amplidyne Generator, J. L. Bower. *AIEE Transactions*, volume 64, 1945, pages 873–81.

No Discussion

Design of Auxiliary Circuits of Single-Phase Induction Motors

M. S. THACKER
FELLOW AIEE

H. V. GOPALAKRISHNA
NONMEMBER AIEE

THE multiplicity of difficult industrial specifications for the starting performance of single-phase induction motors require equations to be developed in an ideal manner. In their AIEE paper of January 1944,[1] Lloyd and Karr have dealt with the design of starting windings of split-phase motors and plotted useful curves. And Veinott's AIEE paper of June 1944[2] presents calculation methods for the determination of the best starting winding and the best capacitor required to meet any specified requirement on the basis of the equation developed by Boothby[3] but with a slight modification. The methods outlined have merits; but a lengthy process of trial-and-error may lead to the desired result. The importance of accurate design methods to meet the increasing diversity and severity of the starting conditions especially in single-phase induction motors cannot be overemphasized.

In this paper, mathematical procedures are evolved to arrive at the best proportions of the auxiliary circuit constants for a given set of conditions on the basis of the equations developed by the method of symmetrical components in the paper entitled Suggested Improvements in the Performance Calculations of Single-Phase Induction Motors by the authors.[4]† Appendices III and IV indicate results by authors' method as compared with other methods. Tables I and II give the summary of results.

Table I contrasts the values obtained for a split-phase motor by the authors' method with those of Lloyd and Karr. According to the present investigation it is significant that for a given starting torque a smaller size of wire could be used for the starting winding; the magnitude of current in the auxiliary circuit as well as in the line also is lower.

Table II presents the design values for a capacitor-start motor and contrasts with Veinott's figures. The analysis of this paper yields a greater starting torque for a prescribed starting current in the line; or if the starting torque is the criterion in design a smaller size of capacitor could be employed with reduced line current.

It is believed that the methods presented in this paper will contribute to the most economical design of the auxiliary circuits of single-phase induction motors which are being manufactured in very large numbers.

Symbols and Factors

V_m = applied rms volts across main and start phases
I_m = main phase rms amperes
I_s = start phase rms amperes
I_m^+ = positive sequence component of I_m
I_m^- = negative sequence component of I_m
I_s^+ = positive sequence component of I_s
I_s^- = negative sequence component of I_s
Z_m^+ = total positive sequence impedance of M phase
Z_m^- = total negative sequence impedance of M phase
Z_s^+ = total positive sequence impedance of S phase
Z_s^- = total negative sequence impedance of S phase
X_{1m} = reactance of M phase primary winding
R_{1m} = resistance of M phase primary winding

$$a=\frac{\text{effective conductors of } S \text{ phase}}{\text{effective conductors of } M \text{ phase}}=a'\sqrt{\frac{X_s}{X_m}}$$

a^2R_{1s} = primary resistance of S phase
a^2X_{1s} = primary leakage reactance of S phase
R_c = capacitor resistance
X_c = capacitor reactance
R_2 = equivalent M phase secondary resistance referred to primary winding
X_2 = equivalent M phase secondary reactance referred to primary winding
Z_2^{+1} = apparent secondary positive sequence impedance of M phase
Z_2^{-1} = apparent secondary negative sequence impedance of M phase
R_2^{+1} = apparent positive sequence M phase secondary resistance
R_2^{-1} = apparent negative sequence M phase secondary resistance
X_2^{+1} = apparent positive sequence M phase secondary reactance
X_2^{-1} = apparent negative sequence M phase secondary reactance
R_2'' = standstill apparent secondary resistance
X_2'' = standstill apparent secondary reactance
Z_2'' = standstill apparent secondary impedance

$$b=\frac{R_\varphi^2+X_\varphi^2}{(R_2+R_\varphi)^2+(X_2+X_\varphi)^2}$$

R_φ = resistance representing core loss when connected in series with X_φ $=\frac{\text{core loss}}{i_m^2}$
X_φ = equivalent M phase mutual or magnetizing reactance
$X_0=X_\varphi+X_{1m}$ = reactance of the primary winding with the secondary open circuited
$i_m=\frac{V_m}{X_0}$ = primary current with the secondary open
R_m = real component of total impedance of M phase at standstill $=R_{1m}+R_2''$
X_m = j component of total impedance of M phase at standstill $=X_{1m}+X_2''$
$Z_m=R_m+jX_m$
$Z_m=\sqrt{R_m^2+X_m^2}$ = total impedance of the main winding at standstill $=K$
R_s = real component of total impedance of S phase at standstill $=a^2R_{1s}+a^2R_2''$
X_s = j component of total impedance of S

---

† This paper is scheduled for presentation at the AIEE Winter General Meeting, New York, N. Y., January 30–February 3, 1950, and should be available for distribution shortly thereafter.

Paper 49-296, recommended by the AIEE Rotating Machinery Committee and approved by the AIEE Technical Program Committee for presentation at the AIEE Fall General Meeting, Cincinnati, Ohio, October 17–21, 1949. Manuscript submitted August 23, 1948; made available for printing September 9, 1949.

M. S. Thacker and H. V. Gopalakrishna are both with the Indian Institute of Science, Bangalore, India.

Table I

Items	Maximum Torque Winding Lloyd and Karr Trial and Error Solutions					Authors' Method
Conductors, starting winding	1,056	1,056	1,056	850	850	1,091
Ratio, 1/a	1.21	1.21	1.21	1.5	1.5	1.17
Resistance, starting winding	12.7	16.0	10.0	12.7	8.22	20.2
Starting winding current	6.53	5.55	7.55	7.4	10.13	4.6
Total starting amperes	14.4	13.3	15.45	13.96	17.9	12.35
Starting torque, ounce feet	16.80	16.10	16.15	19.2	20.6	15.0
Torque per ampere	1.165 (best solution)	1.208	1.042	1.286	1.15	12.15.

Table II

Items	Given: Line Current 24.8 Amperes		Given: Max. Start. Torque 82.5 ounce feet	
	Veinott's Maximum Torque/ampere Method	Authors' Maximum Torque Method	Veinott's Maximum Torque Method	Authors' Maximum Torque Method
Capacitance in microfarads	228	234	284	198
Total resistance of the auxiliary winding	8.5	4.63	8.5	6.6
Voltage across capacitor	118	115.9	104.2	138.1
Line current			27.1	23.03
Maximum starting torque ounce feet	78.5	111.7		
Maximum starting torque per ampere of line current	3.16	4.5	3.04	3.58

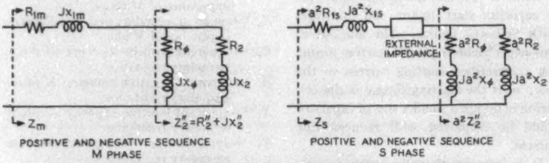

POSITIVE AND NEGATIVE SEQUENCE M PHASE

POSITIVE AND NEGATIVE SEQUENCE S PHASE

Figure 1. Equivalent circuits of a single-phase induction motor at standstill

External impedance: for capacitor motor $= R_c - jX_c$; for split-phase motor $= 0$

phase at standstill

$= a^2X_{1s} + a^2X_2''$

$Z_s = R_s + jX_s$

$Z_s = \sqrt{R_s^2 + X_s^2}$ = total impedance of the auxiliary winding at standstill

R_{sc} = real component of total impedance of the auxiliary winding with capacitor at standstill

$= R_c + R_s = R_c + a^2R_{1s} + a^2R_2''$

X_{sc} = j component of total impedance of the auxiliary winding with capacitor at standstill

$= -X_c + X_s = -X_c + a^2X_{1s} + a^2X_2''$

$Z_{sc} = R_{sc} + jX_{sc}$

$Z_{sc} = \sqrt{R_{sc}^2 + X_{sc}^2}$ = total impedance of the auxiliary winding with capacitor at standstill

θ = time angle, I_m and I_s of split-phase motors

φ = time angle, I_m and I_s of capacitor-start motors

The equivalent circuits of a single phase induction motor at standstill conditions are represented by Figure 1. These circuits and the following equations from 1 to 7 are derived by substituting $s=1$ in the corresponding equivalent circuits of Figure 3 and equations (numbered with*) of the paper entitled Suggested Improvements in the Performance Calculations of Single-Phase Induction Motors by the authors.[4]

Starting Performance

Under starting conditions the apparent secondary resistance of M phase at standstill is

$$R_2'' = R_2^{+1} = R_2^{-1} = \frac{(R_2R_\varphi - X_2X_\varphi)(R_2+R_\varphi) + (R_2X_\varphi + X_2R_\varphi)(X_2+X_\varphi)}{(R_2+R_\varphi)^2 + (X_2+X_\varphi)^2} \qquad (1)\ (10)^*(13)^*$$

and the apparent secondary reactance of M phase at standstill is

$$X_2'' = X_2^{+1} = X_2^{-1} = \frac{(R_2X_\varphi + X_2R_\varphi)(R_2+R_\varphi) - (R_2R_\varphi - X_2X_\varphi)(X_2+X_\varphi)}{(R_2+R_\varphi)^2 + (X^2+X_\varphi)^2} \qquad (2)\ (11)^*(14)^*$$

The total impedance of the M phase at standstill is

$$Z_m = Z_m^+ = Z_m^- = (R_{1m} + R_2'') + j(X_{1m} + X_2'') = R_m + jX_m \qquad (3)(15)^*(16)^*$$

The total impedance of the S phase at standstill is

$$Z_{sc} = Z_s^+ = Z_s^- = (R_c + a^2R_{1s} + a^2R_2'') + j(-X_c + a^2X_{1s} + a^2X_2'') \qquad (4)$$
$$= R_{sc} + jX_{sc} \qquad (17)^*(18)^*$$

The starting torque in synchronous watts is obtained from equation 35*, so that

$$T_{st} = 2bR_2[|I_m^+|^2 - |I_m^-|^2] \qquad (5)$$

where

$$b = \frac{R_\varphi^2 + X_\varphi^2}{(R_2+R_\varphi)^2 + (X_2+X_\varphi)^2}$$

The positive and negative sequence currents of the main winding are found from equations 23* and 24* in conjunction with equations 3 and 4. Thus

$$I_m^+ = \frac{V_m}{2}\,\frac{(R_{sc} + aX_m) + j(X_{sc} - aR_m)}{(R_mR_{sc} - X_mX_{sc}) + j(R_mX_{sc} + X_mR_{sc})} \qquad (6)$$

$$I_m^- = \frac{V_m}{2} \times \frac{(R_{sc} - aX_m) + j(X_{sc} + aR_m)}{(R_mR_{sc} - X_mS_{sc}) + j(R_mX_{sc} + X_mR_{sc})} \qquad (7)$$

giving

$$|I_m^+|^2 - |I_m^-|^2 = aV_m^2\,\frac{R_{sc}X_m - X_{sc}R_m}{Z_m^2Z_{sc}^2}$$

Equation 5 for the starting torque of capacitor start motors now may be written as

$$T_{st} = \frac{2abR_2V_m^2(R_{sc}X_m - X_{sc}R_m)}{Z_m^2Z_{sc}^2} \qquad (8)$$

In Appendix I the starting conditions for a capacitor motor are calculated and compared with the double revolving field and cross field methods.

If core loss is neglected

$$T_{st} = \frac{2aR_2''V_m^2(R_{sc}X_m - X_{sc}R_m)}{Z_m^2Z_{sc}^2} \qquad (9)$$

This equation is identical with the equation 103 of Veinott's paper[2] (see also Appendix II) which is a modification of the original equation given by Boothby[3] and also with equation 14 of Morrill's[12] paper.

For split-phase motors $R_c = 0$ and $X_c = 0$. Deleting the subscript c in equation 9, the starting torque for split-phase motors

$$T_{st} = \frac{2abR_2V_m^2(R_sX_m - X_sR_m)}{Z_m^2Z_s^2} \qquad (10)$$

Neglecting core loss

$$T_{st} = \frac{2aR_2''V_m^2(R_sX_m - X_sR_m)}{Z_m^2Z_s^2} \qquad (11)$$

The locked-rotor current in the line

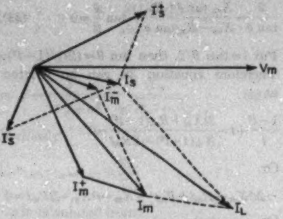

Figure 2. Vector relationships at instant of starting in a split-phase motor

being the vector sum of the main and start phase currents, Figures 2 and 3, is

$$I_L=I_m+I_s=I_m{}^++I_m{}^-+I_s{}^++I_s{}^-$$
$$=I_m{}^++I_m{}^-+\frac{j}{a}I_m{}^+-\frac{j}{a}I_m{}^-$$
$$=V_m\frac{(R_{sc}+R_m)+j(X_{sc}+X_m)}{(R_mR_{sc}-X_mX_{sc})+j(R_mX_{sc}+X_mR_{sc})}$$

from equations 6 and 7

Therefore for capacitor motors

$$|I_L|=V_m\frac{\sqrt{(R_{sc}+R_m)^2+(X_{sc}+X_m)^2}}{Z_mZ_{sc}} \quad (12)$$

and for split-phase motors

$$|I_L|=V_m\frac{\sqrt{(R_s+R_m)^2+(X_s+X_m)^2}}{Z_mZ_s} \quad (13)$$

Equations 12 and 13 are convenient expressions for calculating the line current.

The starting torque per ampere of line current is obtained by dividing equation 8 by equation 12 for capacitor motors so that

$$T_{st}/I_L=\frac{2abR_2V_m(R_{sc}X_m-X_{sc}R_m)}{Z_mZ_{sc}\sqrt{(R_{sc}+R_m)^2+(X_{sc}+X_m)^2}} \quad (14)$$

Neglecting core loss

$$T_{st}/I_L=\frac{2aR_2''V_m(R_{sc}X_m-X_{sc}R_m)}{Z_mZ_{sc}\sqrt{(R_{sc}+R_m)^2+(X_{sc}+X_m)^2}} \quad (15)$$

The starting torque per ampere of line current for split-phase motors is obtained by dividing equation 10 by equation 13 so that

$$T_{st}/I_L=\frac{2abR_2V_m(R_sX_m-X_sR_m)}{Z_mZ_s\sqrt{(R_s+R_m)^2+(X_s+X_m)^2}} \quad (16)$$

Neglecting core loss

$$T_{st}/I_L=\frac{2aR_2''V_m(R_sX_m-X_sR_m)}{Z_mZ_s\sqrt{(R_s+R_m)^2+(X_s+X_m)^2}} \quad (17)$$

The voltage across the capacitor E_c

$$=I_s\sqrt{R_c^2+X_c^2}=\frac{V_m}{Z_{sc}}\sqrt{R_c^2+X_c^2} \quad (18)$$

Optimum Auxiliary Circuit Constants

The main winding is designed by efficiency and breakdown torque considerations and the problem now is to find the best possible companion starting winding to produce the maximum starting torque, and the maximum starting torque per ampere of line current for single-phase induction motors.

Maximum Starting Torque Winding for Split-Phase Motors

The winding ratio a may be considered as equal to

$$a'\sqrt{\frac{X_s}{X_m}}$$

where a' is a constant.

Equation 10 may be written as

$$T_{st}=\frac{2bR_2V_m^2}{Z_m^2}a\frac{R_sX_m-X_sR_m}{R_s^2+X_s^2}$$
$$=\frac{2a'bR_2V_m^2\sqrt{X_s}}{Z_m^2\sqrt{X_m}}\left[\frac{R_sX_m-X_sR_m}{R_s^2+X_s^2}\right]$$
$$=\text{constant}\sqrt{X_s}\frac{R_sX_m-X_sR_m}{R_s^2+X_s^2} \quad (19)$$

The standstill resistance R_m and reactance X_m are known for a given main winding. The standstill resistance R_s and reactance X_s of the starting winding will have to be specified in terms of the constants of the main winding to produce maximum torque. The magnitude of the current in the starting winding may be arbitrarily fixed up thereby fixing the total impedance $Z_s=\rho$ of the starting winding and its position varied. The problem, therefore, reduces to investigating the maximum value of

$$T_{st}\propto\alpha\sqrt{X_s}\frac{R_sX_m-X_sR_m}{R_s^2+X_s^2} \quad (20)$$

T_{st} being positive, R_s and X_s being variables, with the condition

$$R_s^2+X_s^2=\rho^2$$

being constant.
Now from equation 19

$$T_{st}^2=\text{ constant }X_s\frac{(R_sX_m-X_sR_m)^2}{(R_s^2+X_s)^2=\rho^4}$$

Let

$$R_m^2+X_m^2=Z_m^2=K^2$$

Putting

$$R_sX_m-X_sR_m=K\rho\sin\theta \quad (21)$$

and

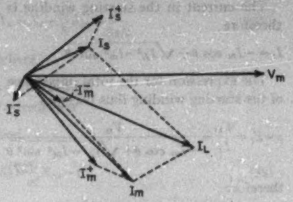

Figure 3. Vector relationships at instant of starting in a capacitor motor

$$X_sX_m+R_sR_m=K\rho\cos\theta \quad (22)$$

and solving for R_s and X_s from these, the following equations are obtained

$$R_s=\frac{\rho}{K}(X_m\sin\theta+R_m\cos\theta) \quad (23)$$

$$X_s=\frac{\rho}{K}(X_m\cos\theta-R_m\sin\theta) \quad (24)$$

The problem modifies to finding the maximum value of

$$(X_m\cos\theta-R_m\sin\theta)\sin^2\theta$$

Taking logarithms and differentiating and equating to zero gives

$$\frac{\varphi'(\theta)}{\varphi(\theta)}=\frac{2\cos\theta}{\sin\theta}-\frac{R_m\cos\theta+X_m\sin\theta}{X_m\cos\theta-R_m\sin\theta}=0$$

Or

$$2(X_m-R_m\tan\theta)-\tan\theta(R_m+X_m\tan\theta)=0$$

that is

$$\tan^2\theta+3\alpha\tan\theta-2=0$$

where

$$\alpha=\frac{R_m}{X_m}$$

that is

$$\tan\theta=\frac{-3\alpha+\sqrt{9\alpha^2+8}}{2} \quad (25)$$

It is, therefore, clear that for all maximum torque windings the phase displacement θ, Figure 4, between the main and auxiliary circuit currents is fixed; it is independent of the constants of the auxiliary winding. For the value of θ lying between zero and $\pi/2$ both X_s and $R_sX_m-X_sR_m$ will be positive and the values of R_s and X_c are determined from equations 23 and 24, which completely specify the auxiliary winding that gives the maximum starting torque for a given main winding. ρ could be determined easily to give the desired total locked-rotor current thus:

Referring to Figure 4, the total locked-rotor current in the line is

$$I_L=\sqrt{I_m^2+I_s^2+2I_mI_s\cos\theta} \quad (26)$$

The current in the starting winding is therefore

$$I_s=-I_m\cos\theta+\sqrt{I_L^2-I_m^2\sin^2\theta}$$

The expression for the total impedance of the starting winding thus becomes

$$\rho=Z_s=\frac{V_m}{I_s}=\frac{V_m}{-I_m\cos\theta+\sqrt{I_L^2-I_m^2\sin^2\theta}}\tag{27}$$

therefore

$$T_{st\ \max}=\frac{2a'bR_2V_m^2\sin\theta}{Z_m^{3/2}}\times\sqrt{\frac{X_m\cos\theta-R_m\sin\theta}{\rho X_m}}\tag{28}$$

It may be noticed that for a given starting torque θ is definite and hence R_s and X_s.

If core loss is neglected

$$T_{st\ \max}=\frac{2a'R_2''V_m^2\sin\theta}{Z_m^{3/2}}\times\sqrt{\frac{X_m\cos\theta-R_m\sin\theta}{\rho X_m}}\tag{29}$$

The procedure for determining the starting winding constants for a given main winding to meet a specified starting torque, and a specified starting current, is as follows:

For a Specified Starting Torque (*See Appendix III*):

1. $I_m=(V_m)/(Z_m=K)$
2. Calculate θ from equation 25.
3. Substitute the value of θ in equation 28 and get the value of ρ.
4. Determine R_s and X_s from equations 23 and 24.
5. $I_s=(V_m)/(Z_s=\rho)$
6. Calculate the value of I_L from equation 26 and check with the limit of total locked-rotor current prescribed by rules.

For a Specified Starting Current:

1. $I_m=(V_m)/(Z_m=K)$
2. Calculate θ from equation 25.
3. Substitute the value of θ in equation 27 and get the value of ρ.
4. Determine R_s and X_s from equations 23 and 24.
5. Substitute the above values in equation 28 and check with the minimum value of starting torque prescribed by rules.

CONDITIONS FOR MAXIMUM STARTING TORQUE PER AMPERE OF LINE CURRENT FOR SPLIT-PHASE MOTORS

The expression for the starting torque per ampere of line current may be written in the form

$$T_{st}/I_L=\text{constant}\times\sqrt{X_s}\sqrt{\frac{R_sX_m-X_sR_m}{(R_s^2+X_s^2)(\overline{R_s+R_m}^2+\overline{X_s+X_m}^2)}}\tag{30}$$

R_s and X_s being the variables. As in the previous problem the following relations hold good

$$R_s^2+X_s^2=\rho^2;\quad R_m^2+X_m^2=K^2$$
$$R_sX_m-X_sR_m=K\rho\sin\theta$$
$$X_sX_m+R_sR_m=K\rho\cos\theta$$

Solving for R_s and X_s yields

$$KR_s=\rho(X_m\sin\theta+R_m\cos\theta)\tag{31}$$

$$KX_s=\rho(X_m\cos\theta-R_m\sin\theta)\tag{32}$$

and

$$(R_m+R_s)^2+(X_m+X_s)^2=K^2+\rho^2+2K\rho\cos\theta\tag{33}$$

The problem reduces to that of finding the maximum, when ρ and θ vary, of

$$(\rho,\theta)=\frac{\sin\theta(X_m\cos\theta-R_m\sin\theta)^{1/2}\rho^{1/2}}{(K^2+\rho^2+2K\rho\cos\theta)^{1/2}}\tag{34}$$

On differentiating log $f(\rho,\theta)$ with respect to ρ and θ and equating the expressions to zero gives

$$\frac{1}{2\rho}-\frac{2(\rho+K\cos\theta)}{2(\rho^2+K^2+2K\rho\cos\theta)}=0\tag{35}$$

and

$$\frac{2\cos\theta}{\sin\theta}-\frac{X_m\sin\theta+R_m\cos\theta}{X_m\cos\theta-R_m\sin\theta}+\frac{2K\rho\sin\theta}{\rho^2+K^2+2K\rho\cos\theta}=0\tag{36}$$

Simplifying equation 35

$$\rho^2+K^2+2K\rho\cos\theta-2\rho^2-2K\rho\cos\theta=0$$

or

$$\rho=K$$

that is

$$R_m^2+X_m^2=R_s^2+X_s^2\tag{37}$$

Substituting $\rho=K$ in equation 36 and simplifying results in

$$2\cot\theta-\frac{X_m\tan\theta+R_m}{X_m-R_m\tan\theta}+\frac{\sin\theta}{1+\cos\theta}=0$$

that is,

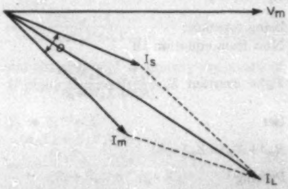

Figure 4. Maximum starting-torque diagram for a split-phase motor. θ is determined by the main winding constants—equation 25

$$\frac{2}{\tan\theta}-\frac{X_m\tan\theta+R_m}{X_m-R_m\tan\theta}+\tan\frac{\theta}{2}=0\tag{38}$$

Put $t=\tan\theta/2$, then $\tan\theta=(2t)/(1-t^2)$. Therefore equation 38 can be written as

$$\frac{1-t^2}{t}+t-\frac{2tX_m+R_m(1-t^2)}{X_m(1-t^2)-2R_mt}=0$$

Or

$$-2t^2X_m-R_mt+R_mt^3+X_m-t^2X_m-2R_mt=0$$

Or

$$R_mt^3-3X_mt^2-3R_mt+X_m=0$$

Let

$$\frac{R_m}{X_m}=\alpha$$

as before then $\tan\theta/2=t$ satisfies the equation

$$\varphi(t)=t^3-\frac{3}{\alpha}t^2-3t+\frac{1}{\alpha}=0\tag{39}$$

As it has two changes of sign it has at most two positive roots, and

$$\varphi(0)=\frac{1}{\alpha}>0$$

$$\varphi(1)=1-\frac{3}{\alpha}-3+\frac{1}{\alpha}=-2\left(1+\frac{1}{\alpha}\right)<0$$

Hence it has exactly one root in (0,1), another in $(1,\infty)$, and another negative root. For the value of $t=\tan\theta/2$ in (0,1), T_{st}/I_L will be maximum. From the form of $f(\rho,\theta)$ for $\rho=K$ it is clear that this gives the maximum value of T_{st}/I_L and for this value X_s is really positive. The solution of equation 39 is obtained by writing in the form

$$\left(t-\frac{1}{\alpha}\right)^3-\frac{3t}{\alpha^2}-3t+\frac{1+\alpha^2}{\alpha^3}=0$$

Or

$$\left(t-\frac{1}{\alpha}\right)^3-\frac{3(1+\alpha^2)}{\alpha^2}\left(t-\frac{1}{\alpha}\right)-\frac{2(1+\alpha^2)}{\alpha^3}=0\tag{40}$$

Put

$$\left(t-\frac{1}{\alpha}\right)=\beta\cos\frac{\psi}{3}$$

Then equation 40 assumes the form

$$\beta^3\cos^3\frac{\psi}{3}-\frac{3(1+\alpha^2)\beta}{\alpha^2}\cos\frac{\psi}{3}-\frac{2(1+\alpha^2)}{\alpha^3}=0\tag{41}$$

Multiplying by $4/\beta^3$

$$4\cos^3\frac{\psi}{3}-\frac{12(1+\alpha^2)}{\alpha^2\beta^2}\cos\frac{\psi}{3}-\frac{8(1+\alpha^2)}{\alpha^3\beta^3}=0\tag{42}$$

Let β be such that

$$\frac{4(1+\alpha^2)}{\alpha^2\beta^2}=1\text{ or }\beta=\frac{2\sqrt{1+\alpha^2}}{\alpha}$$

Then equation 42 becomes

$$4\cos^3\frac{\psi}{3}-3\cos\frac{\psi}{3}-\frac{8(1+\alpha^2)\alpha^2}{\alpha^2 8(1+\alpha^2)^{3/2}}=0$$

or

$$\cos\psi=\frac{1}{\sqrt{1+\alpha^2}}=\frac{X_m}{\sqrt{R_m^2+X_m^2}} \tag{43}$$

Obviously

$$\psi=\tan^{-1}\alpha=\tan^{-1}\frac{R_m}{X_m}$$

ρ is calculated from

$$\tan\frac{\theta}{2}=t=\frac{1}{\alpha}+\beta\cos\frac{\psi}{3}=\frac{1}{\alpha}+\frac{2\sqrt{1+\alpha^2}\cos\frac{\psi}{3}}{\alpha} \tag{44}$$

Substitute instead of $\psi/3$, $\psi/3+120$ degrees or $\psi/3+240$ degrees, so that $\tan\theta/2$ lies in (0,1). The values of R_s and X_s are obtained by substituting θ in equations 31 and 32 and since $\rho=K$

$$R_s=X_m\sin\theta+R_m\cos\theta \tag{45}$$

$$X_s=X_m\cos\theta-R_m\sin\theta \tag{46}$$

The expression for the maximum starting torque per ampere of line current becomes

$$(T_{st}/I_L)_{\max}=\frac{a'bR_2V_m\sin\theta}{Z_m}\times\sqrt{\frac{2(X_m\cos\theta-R_m\sin\theta)}{X_m(1+\cos\theta)}} \tag{47}$$

If core loss is neglected

$$(T_{st}/I_L)_{\max}=\frac{a'R_2''V_m\sin\theta}{Z_m}\times\sqrt{\frac{2(X_m\cos\theta-R_m\sin\theta)}{X_m(1+\cos\theta)}} \tag{48}$$

Substituting the values of R_s and X_s from equations 45 and 46 in equation 19 for the expression of the starting torque, the following relation is obtained

$$T_{st}=\frac{2a'bR_2V_m^2\sin\theta}{Z_m^2}\times\sqrt{\frac{X_m\cos\theta-R_m\sin\theta}{X_m}} \tag{49}$$

Neglecting core loss

$$T_{st}=\frac{2a'R_2''V_m^2\sin\theta}{Z_m^2}\times\sqrt{\frac{X_m\cos\theta-R_m\sin\theta}{X_m}} \tag{50}$$

CONDITIONS FOR MAXIMUM STARTING TORQUE OF CAPACITORS START MOTORS

Depending on the voltage the capacitor is able to withstand a certain number of turns and distribution of the starting winding is assumed fixing the reactance X_s. The current in the starting winding may be arbitrarily fixed up thereby fixing the locked-rotor impedance of the starting winding, $Z_{sc}=\rho_1$.

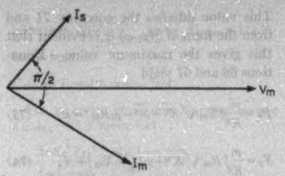

Figure 5. Maximum starting-torque diagram for a capacitor-start motor

The expression for the starting torque may be written as

$$T_{st}=\text{constant}\ \frac{R_{sc}X_m-X_{sc}R_m}{R_{sc}^2+X_{sc}^2}$$

$$=\text{constant}\times\frac{(R_c+R_s)X_m-(-X_c+X_s)R_m}{(R_c+R_s)^2+(-X_c+X_s)^2} \tag{51}$$

Taking

$$(R_c+R_s)X_m-R_m(-X_c+X_s)=K\rho_1\sin\varphi \tag{52}$$

$$(-X_c+X_s)X_m+R_m(R_c+R_s)=K\rho_1\cos\varphi \tag{53}$$

where

$$R_m^2+X_m^2=Z_m^2=K^2$$

The problem now reduces to that of finding the maximum value of

$$K\rho_1\sin\varphi \tag{54}$$

The maximum obviously occurs when $\varphi=\pi/2$, Figure 5. Substituting this in equations 52 and 53

$$(R_c+R_s)X_m-R_m(-X_c+X_s)=K\rho_1 \tag{55}$$

$$(-X_c+X_s)X_m+R_m(R_c+R_s)=0 \tag{56}$$

yielding

$$X_c=X_s+\frac{\rho_1}{K}R_m=\frac{10^6}{2\pi fc} \tag{57}$$

where

c = microfarads
f = frequency

and

$$R_s=\frac{\rho_1}{K}X_m-R_c \tag{58}$$

giving the total resistance of the starting winding; the capacitor resistance R_c is treated as a known quantity.

The expression for the maximum starting torque may be written as

$$T_{st\max}=\frac{2abR_2V_m^2}{Z_m\rho_1} \tag{59}$$

Neglecting core loss

$$T_{st\max}=\frac{2aR_2''V_m^2}{Z_m\rho_1} \tag{60}$$

Then the starting torque per ampere of line current is

$$T_{st\max}/I_L=\frac{2abR_2V_m}{\sqrt{Z_m^2+\rho_1^2}} \tag{61}$$

Neglecting core loss

$$T_{st\max}/I_L=\frac{2aR_2''V_m}{\sqrt{Z_m^2+\rho_1^2}} \tag{62}$$

For a given locked-rotor current in the line I_L, the current in the start phase is

$$I_s=\sqrt{I_L^2-I_m^2} \tag{63}$$

so that

$$\rho_1=Z_{sc}=\frac{V_m}{\sqrt{I_L^2-I_m^2}} \tag{64}$$

For a given maximum starting torque ρ_1 is definite. Equations 57 and 58 will give the required X_c and R_s.

The procedure for determining the starting winding constants of capacitor start motors (See Appendix IV), X_s being assumed on considerations already indicated, is as follows:

For a Given Line Current I_L:

1. Calculate

$$I_m=\frac{V_m}{Z_m},I_s=\sqrt{I_L^2-I_m^2}\text{ and }\rho_1=\frac{V_m}{I_s}$$

2. Find X_c and R_s from equations 57 and 58.

3. $C_{\text{mfd}}=\dfrac{10^6}{2\pi fX_c}$

4. $E_c=I_s\sqrt{R_c^2+X_c^2}$

5. Find the maximum starting torque from equations 59 or 60 and the starting

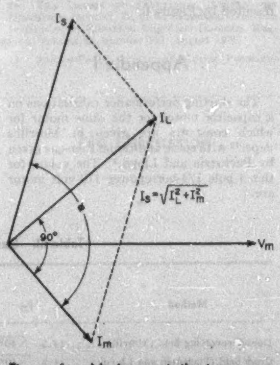

Figure 6. Maximum starting-torque per ampere diagram for a capacitor-start motor

torque per ampere of line current from equations 61 or 62.

For a Given Maximum Starting Torque $T_{st\,\max}$:

Calculate ρ_1 from equation 59 or 60. The other items are calculated as in the previous case.

Conditions for Maximum Starting Torque Per Ampere of Line Current for Capacitor Start Motors

The expression for the starting torque per ampere of line current is

$$T_{st}/I_L=\text{constant}\times\frac{R_{sc}X_m-X_{sc}R_m}{Z_{sc}\sqrt{(R_{sc}+R_m)^2+(X_{sc}+X_m)^2}}$$

$$=\text{constant}\times\frac{(R_c+R_s)X_m-(-X_c+X_s)R_m}{\sqrt{\dfrac{[(R_c+R_s)^2+(-X_c+X_s)^2]}{[(R_c+R_s+R_m)^2+(-X_c+X_s+X_m)^2]}}}\tag{65}$$

As in the previous problem the following relations may be written

$$R_m^2+X_m^2=Z_m^2=K^2$$

$$(R_c+R_s)^2+(-X_c+X_s)^2=\rho_1^2$$

also

$$(R_c+R_s)X_m-(-X_c+X_s)R_m=K\rho_1\sin\varphi$$

$$(-X_c+X_s)X_m+(R_c+R_s)R_m=K\rho_1\cos\varphi$$

Solving for (R_c+R_s) and $(-X_c+X_s)$ the following are obtained

$$(R_c+R_s)=\frac{\rho_1}{K}(X_m\sin\varphi+R_m\cos\varphi)\tag{66}$$

$$(-X_c+X_s)=\frac{\rho_1}{K}(X_m\cos\varphi-R_m\sin\varphi)\tag{67}$$

and

$$(R_c+R_s+R_m)^2+(-X_c+X_s+X_m)^2 = K^2+\rho_1^2+2K\rho_1\cos\varphi\tag{68}$$

The problem reduces to that of finding the maximum value when φ varies, of the following expression

$$\xi(\rho_1,\varphi)=\frac{\sin\varphi}{\sqrt{\rho_1^2+K^2+2K\rho_1\cos\varphi}}\tag{69}$$

where $0<\varphi<\pi$.

Differentiating $\log\xi(\rho_1,\varphi)$ with respect to ρ_1 and φ and equating the expressions to zero gives

$$-\frac{2(\rho_1+K\cos\varphi)}{2(\rho_1^2+K^2+2K\rho_1\cos\varphi)}=0\tag{70}$$

and

$$\frac{\cos\varphi}{\sin\varphi}+\frac{2K\rho_1\sin\varphi}{2(\rho_1^2+K^2+2K\rho_1\cos\varphi)}=0\tag{71}$$

Simplifying equation 70 results in

$$\cos\varphi=-\frac{\rho_1}{K}\tag{72}$$

This value satisfies the equation 71 and from the form of $\xi(\rho_1,\varphi)$ it is evident that this gives the maximum value. Equations 66 and 67 yield

$$R_s=\frac{\rho_1}{K^2}[X_m\sqrt{K^2-\rho_1^2}-\rho_1R_m]-R_c\tag{73}$$

$$X_c=\frac{\rho_1}{K^2}[R_m\sqrt{K^2-\rho_1^2}+\rho_1X_m]+X_s\tag{74}$$

These two equations completely define the auxiliary circuit.

From the foregoing, it follows that the expression for the maximum starting torque per ampere of line current may be put down as

$$(T_{st}/I_L)_{\max}=\frac{2abR_2V_m}{Z_m}\tag{75}$$

Neglecting core loss

$$(T_{st}/I_L)_{\max}=\frac{2aR_2''V_m}{Z_m}\tag{76}$$

The starting torque is given by

$$T_{st}=\frac{2abR_2V_m^2\sqrt{Z_m^2-\rho_1^2}}{Z_m^2\rho_1}\tag{77}$$

Neglecting core loss

$$T_{st}=\frac{2aR_2''V_m^2\sqrt{Z_m^2-\rho_1^2}}{Z_m^2\rho_1}\tag{78}$$

For a given locked-rotor current in the line I_L, the current in the start phase is expressed by the relation

$$I_s=\sqrt{I_L^2+I_m^2}\tag{79}$$

so that

$$\rho_1=Z_{sc}=\frac{V_m}{\sqrt{I_L^2+I_m^2}}\tag{80}$$

The time angle between the line current and the main phase current is 90 degrees, the starting conditions being represented by Figure 6.

Appendix I

The starting performance calculations on a capacitor motor for the same motor for which constants are given in Morrill's paper[12] with some additional items as given by Puchstein and Lloyd.[9] The values for this 4-pole 1/4-horsepower 110-volt motor are

$R_{1m}=2.02$; $a^2R_{1}s=1.39\times5.12=7.13$; $R_2=4.12$; $R_c(\text{at start})=3$; $X_c(\text{at start})=14.5$; $X_{1m}=2.79$; $a^2X_{1s}=1.39\times2.31=3.22$; $X_2=2.12$; $a=1.18$; $a^2=1.39$; $X_\varphi=66.8$; iron losses $=24$ watts

Calculations

$X_e=69.59$; $i_m=1.58$; $R_\varphi=9.6$

Equations 1 and 2 give
$R_2''=3.84$ and $X_2''=2.25$

From equations 3 and 4

$$Z_m=5.86+j5.04\quad I_m=\frac{V_m}{Z_m}=14.23\ \overline{\diagdown 40^\circ 42'}$$

$$Z_{sc}=15.47-j8.15\quad I_s=\frac{V_m}{Z_{sc}}=6.29\ \underline{/27^\circ 49'}$$

Substituting in equation 8 $T_{st}=749$ synchronous watts, see Table III.

Appendix II

Example of Starting Torque Calculations

Machine data are taken from the example given by Veinott[3] for a capacitor start motor, 115 volts, 4 poles 60 cycles. In the notations of this paper they become

$R_{1m}=1.47$; $a^2R_2''=3.67$; $X_c=11.62$; $X_m=3.72$; $a^2R_{1s}=4.83$; $a=1.172$; $Z_m=5.57$; $R_c=0.98$; $R_2''=2.67$; $a^2(X_{1s}+X_2'')=X_s=5.14$

Then

$R_{sc}=9.43$; $X_{sc}=-6.48$; $R_m=4.14$

Equation $9\times\dfrac{112.7}{\text{synchronous rpm } 1{,}800}$ gives

$T_{st}=78.7$ ounce feet (same as Veinott's result)

Equation $15\times\dfrac{112.7}{\text{synchronous rpm } 1{,}800}$ gives

$Tst/I_L=3.15$ ounce feet (same as Veinott's result)

Appendix III

Example of Maximum Starting Torque Calculations

Machine data are taken from the example given by Lloyd and Karr[1] for a split-phase induction motor.

A starting winding is to be designed for a motor rated 1/8th horsepower, 60 cycles, 1,150 rpm, 115 volts. The following con-

Table III. Starting Conditions

Method	I_m	I_s	T_{st} in Synchronous Watts
Double revolving field (Morrill)	14.2 $\overline{\diagdown 40^\circ 50'}$	6.30 $\underline{/27^\circ 55'}$	755
Cross field (Puchstein and Lloyd)	14.2 $\overline{\diagdown 40^\circ 0'}$	6.25 $\underline{/27^\circ 50'}$	759
Symmetrical components	14.23 $\overline{\diagdown 40^\circ 42'}$	6.29 $\underline{/27^\circ 49'}$	749

stants are known. In the symbols of this paper they become

$R_m=9.26$; $X_m=10.7$; $R_2''=4.85$

Series turns in main winding = 1,248; winding factor for main winding = 0.856; and winding factor for the auxiliary winding = 0.837. The starting torque is to be 15 ounce-feet and the starting current limited to 15 amperes.
Then

$$Z_m=14.15 \qquad I_m=8.13$$
$$\theta=30°58'$$

Assume that the ratio of transformation obtained from the effective turns is exactly the same as the ratio obtained from the leakage reactances, that is, $a'=1$. Multiplying the right-hand side of equation 29 by 112.7/1,200 to convert synchronous watts into ounce feet and inserting the foregoing values in the equation yields $\rho_1=25.0$.

Equations 23 and 24 give $R_s=23.74$ and $X_s=7.80$, also

$$\frac{1}{a}=\sqrt{\frac{X_m}{X_s}}=1.17.$$

The resistance of the starting winding $=R_s-a^2R_2''=20.2$; $I_s=4.6$. From equation 26 $I_L=12.35$.

Therefore,

$$\text{starting torque per ampere}=\frac{15}{12.35}=1.215$$

ounce feet

$$\text{Starting winding conductors}=\frac{0.856\times 1{,}248}{0.837\times 1.17}$$

$=1{,}091$.

Appendix IV

Determination of the Optimum Auxiliary Circuit Constants of a Capacitor Start Motor

Machine data are taken out from the example given in Appendix II.

Maximum Starting Torque Winding

For a given line current $I_L=24.8$; $I_m=20.6$; $I_s=13.8$; $\rho_1=8.33$; $X_c=11.33$; $R_s=4.63$; $C_{mfd}=234$; $E_c=115.9$.

Equation $60\times\frac{112.7}{1{,}800}$ gives $T_{st\,max}=111.7$ ounce feet

$T_{st\,max}/I_L=4.5$ ounce feet

For a given maximum starting torque $T_{st\,max}=82.5$ ounce feet.

$$\rho_1=\frac{2aR_2''V_m^2}{Z_mT_{st\,max}}\times\frac{112.7}{1{,}800}=11.28$$

and $X_c=13.52$; $R_s=6.60$; $C_{mfd}=198$; $I_s=10.19$; $E_c=138$; $I_m=20.6$.
Therefore

$$I_L=\sqrt{I_m^2+I_s^2}=23.03$$

$$T_{st\,max}/I_L=\frac{82.5}{23.03}=3.58 \text{ ounce feet}$$

References

1. Design of Starting Windings for Split-Phase Motors, **T. C. Lloyd, J. H. Karr.** *Electrical Engineering (AIEE Transactions)* volume 63, January 1944, pages 9–13.

2. Starting Windings for Single-Phase Induction Motors, **C. G. Veinott.** *Electrical Engineering (AIEE Transactions)* volume 63, June 1944, pages 288–94.

3. Discussions, **C. R. Boothby.** *AIEE Transactions*, volume 48, 1929, pages 629–30.

4. Suggested Improvements in the Performance Calculations of Single-Phase Induction Motors, **M. S. Thacker, H. V. Gopalakrishna.** *AIEE Transactions*, volume 69, 1950 (*Proceedings* 50-1).

5. Single-Phase Induction Motors, **W. J. Branson.** *AIEE Transactions*, volume 31, 1912, part II, pages 1749–87.

6. The Cross-Field Theory of A-C Machines, **H. R. West.** *AIEE Journal*, February 1926, pages 160–66.

7. Performance Calculations on Induction Motors, **C. G. Veinott.** *AIEE Transactions*, volume 51, September 1932, pages 743–54.

8. Single-Phase Induction-Motor Performance, **A. F. Puchstein, T. C. Lloyd.** *Electrical Engineering (AIEE Transactions)* volume 56, October 1937, pages 1277–84.

9. The Cross-Field Theory of the Capacitor Motor, **A. F. Puchstein, T. C. Lloyd.** *Electrical Engineering (AIEE Transactions)* volume 60, February 1941, pages 58–62.

10. The Design of Fractional Horsepower Induction Motors, **N. F. T. Saunders.** *Journal*, Institution of Electrical Engineers (London, England) volume 85, number 502, August 1939.

11. Single-Phase Induction-Motor Performance Calculations, **F. S. Himebrook.** *Electrical Engineering (AIEE Transactions)* volume 60, February 1941, pages 55–58.

12. The Revolving Field Theory of the Capacitor Motor, **W. J. Morrill.** *AIEE Transactions*, volume 48, April 1929, pages 614–29.

13. Symmetrical Components as Applied to the Single-Phase Induction Motor, **F. W. Suhr.** *Electrical Engineering (AIEE Transactions)* volume 64, September 1945, pages 651–66.

14. Segregation of Losses in Single-Phase Induction Motors, **C. G. Veinott.** *Electrical Engineering (AIEE Transactions)* volume 54, December 1935, pages 1302–06.

15. Performance Calculations on Capacitor Motors, **P. H. Trickey.** *Electrical Engineering (AIEE Transactions)* volume 60, February 1941, pages 73–76.

16. Design of Capacitor Motors for Balanced Operation, **P. H. Trickey.** *AIEE Transactions*, volume 51, September 1932, pages 780–84.

17. The Equal-Volt-Ampere Method of Designing Capacitor Motors, **P. H. Trickey.** *Electrical Engineering (AIEE Transactions)* volume 60, November 1941, pages 990–92.

18. Current Loci for the Capacitor Motor, **T. C. McFarland.** *Electrical Engineering (AIEE Transactions)* volume 61, March 1942, pages 152–56.

19. The Fundamental Theory of the Capacitor Motor, **H. C. Specht.** *AIEE Transactions*, volume 48, April 1929, pages 607–13.

20. The Condenser Motor, **B. F. Bailey.** *AIEE Transactions*, volume 48, April 1929, pages 596–606.

21. Method of Symmetrical Co-ordinates Applied to the Solution of Polyphase Networks, **C. L. Fortescue.** *AIEE Transactions*, volume 37, 1918, part II, pages 1027–1140.

22. Analysis of Unsymmetrical Machines, **W. V. Lyon, Charles Kingsley.** *Electrical Engineering (AIEE Transactions)* volume 55, May 1936, pages 471–76.

23. The Apparent-Impedance Method of Calculating Single-Phase Motor Performance, **W. J. Morrill.** *Electrical Engineering (AIEE Transactions)* volume 60, December 1941, pages 1037–41.

24. Principles of Alternating-Current Machinery (book), **Ralph R. Lawrence.** McGraw-Hill Book Company Inc., New York, N. Y., 1940.

25. Theory of Alternating-Current Machinery (book), **A. S. Langsdorf.** McGraw-Hill Book Company, Inc., New York, N. Y., 1937.

26. Fractional Horsepower Electric Motors (book), **C. G. Veinott.** McGraw-Hill Book Company Inc., New York, N. Y., 1948.

27. Electric Power Circuits—Theory and Applications (book), **O. G. C. Dahl.** McGraw-Hill Book Company, Inc., New York, N. Y., first edition, pages 80–89 and 138–44, 1938.

28. Symmetrical Components as Applied to the Analysis of the Unbalanced Electrical Circuits (book), **C. F. Wagner, R. D. Evans.** McGraw-Hill Book Company, Inc., New York, N. Y., 1933.

No Discussion

Measuring Commutation with an Indicating Instrument

R. T. LUNDY
ASSOCIATE AIEE

BLACK bands[1] have been used for years to compare the commutating ability of d-c machines and to set the brushes in the proper place. A black band, as used here, is defined as the number of amperes by which the current through the commutating winding can be changed without producing sparking at the brush faces. This band width is usually taken at 25, 50, 75, 100, 125, and 150 per cent of rated load. This is plotted as shown in Figure 1, the black band being the shaded portion.

When developing new brushes it is necessary to have a fairly fast and accurate way of comparing the commutating ability of the various brushes. The conventional black band was first used for this purpose. It was thought, however, that changing the load to obtain these bands disturbed the commutator film, making it difficult to duplicate results. Consequently, it was decided to make these comparative tests at full load only, which saves time as well as giving more consistent results. Of course this gives only the band width at full load, not a complete band as shown in Figure 1. The complete band can be taken if required. Even when holding the load constant, results varied considerably with different observers and with different light conditions. Other variables which affect commutation are atmospheric conditions (especially humidity), contaminated atmospheres, brush fit, end play of shaft, and commutator surface condition. In our work we attempted to eliminate as many of these variables as possible.

Studies were first made with a cathode-ray oscilloscope and then with an electronic voltmeter and a radio noise meter. Not all electronic voltmeters are suitable for this service. Two makes were tried that showed very little difference in reading between black commutation and bad sparking. The trouble with these voltmeters was, evidently, their lack of sensitivity at high frequencies. The meter giving the best results has a frequency error of less than 1 per cent between 20 cycles and 50 megacycles. This instrument which now has been used almost daily for two years, is a peak reading voltmeter calibrated in terms of the rms value of a pure sine wave. The voltage indicated is 0.707 of the positive peak of the applied voltage. There are five ranges making it easy to select a suitable scale for the voltage being read. Since the voltmeter is connected across the positive and negative studs it has to stand the full direct voltage of the generator. The instrument as received is limited to 700 direct volts if the negative lead is connected to the high terminal, and to 300 volts if the positive lead is connected to the high terminal. The voltage is limited by the rating of the 0.006-microfarad input capacitor which blocks out the direct current. This voltage rating can be increased by using an external capacitor of the same size with no effect other than raising the lower frequency limit from 20 cycles to about 40 cycles. Specific instructions should be obtained for the instrument when used on direct voltages above scale reading. Tests were made with the shielded probe of the electronic voltmeter connected directly on a brush stud. This was repeated with the shielded probe in the meter box and with unshielded connections between the voltmeter terminals and the machine. Since little or no differences were observed in the results the latter and simpler method of connection is now used.

Most of our evaluation of commutating ability of various brush grades has been done on a type *CD87* motor rated at 230 volts, 575 to 2,300 rpm, 10 to 15 horsepower , 39/58 amperes full load current. Our tests were all run at 1,800 rpm and approximately 30-volts output. This machine is directly connected and driven as a generator by a similar motor, both being mounted on a rigid steel frame. A thrust bearing was installed to eliminate end play. When first operated this equipment was located in a large room, but we soon found that the commutation was affected by changes in atmospheric conditions. The whole set was then moved inside of our altitude chamber[2] where we could hold the temperature at 85 degrees Fahrenheit and 35 per cent relative humidity. The steel shell of the altitude chamber also makes a good shield to eliminate interference when using the radio noise meter and the electronic voltmeter. The shield is not essential, however, as we have obtained good vacuum-tube voltmeter bands on a transportation traction motor outside the chamber.

Before starting a test with a new grade of brush the film was removed from the commutator with a commutator dresser stone and the new test started on a raw

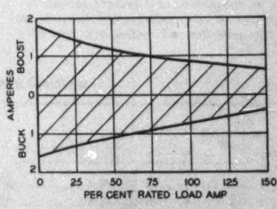

Figure 1. Representative black band

Paper 49-31, recommended by the AIEE Rotating Machinery Committee and approved by the AIEE Technical Program Committee for presentation at the AIEE Winter General Meeting, New York, N. Y., January 31–February 4, 1949, and represented at the Fall General Meeting, Cincinnati, Ohio, October 17–21, 1949. Manuscript submitted November 16, 1948; made available for printing December 16, 1948.

R. T. Lundy is with the General Electric Company, Schenectady, N. Y.

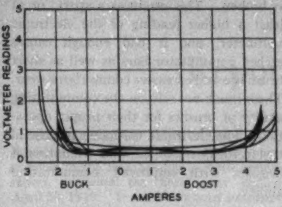

Figure 2. Representative voltmeter band for brush number 6, a very good commutating brush

commutator. Brushes were carefully sanded to fit the commutator and finally seated with soft white seater stone. Hourly readings were taken with the electronic voltmeter and then plotted against amperes buck and boost. Amperes buck or boost were changed in half-ampere steps, starting at the middle of the band and going in the buck direction until a voltmeter reading of over 1.0 volt was obtained, then returning to the middle of the band and increasing the boost current to the same limit. From this family of curves, see Figures 2 and 3, taken each day, an average band width at one volt was obtained. The comparison was made at one volt on this machine because the curve had definitely turned up and sparking was evident at this point. Carrying the buck and boost current much further caused excessive sparking which damaged the film and then required considerable time to return to normal. Table I is a summary of test results obtained on five different electrographitic brush grades. Brushes numbers *1* and *5* were useful commercial grades but did not have especially good commutating ability. Brushes numbers *2* and *3* were commercial grades recognized as better than average commutating brushes, while numbers *4* and *6* were experimental brushes. Brush number *6* shows exceptionally good commutating qualities. Visible sparking occurred near the bend in the curve of Figure 2 where the first increase in voltage was read, or at the half-ampere step of buck or boost current immediately preceding it. This has been checked many times while taking the voltmeter bands.

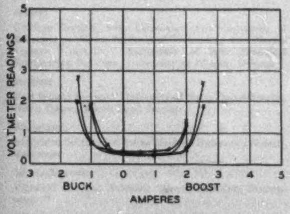

Figure 3. Representative voltmeter band for brush number 1, a poor commutating brush

A cathode-ray oscilloscope, connected between one brush and a pencil probe about one-half commutator bar from the trailing edge of the brush, produces the standing voltage wave shown in Figure 4. The high peaks occur at a frequency of approximately 1,260 per second, which is the calculated slot frequency. The minor peaks between are probably due to the three coils per slot in this machine. The sharp points at the tops and bottoms of the wave are caused by sparks when the brush leaves a commutator bar before the current is reduced to zero. The frequency of this spark is high. When the oscilloscope is connected across the brush studs, instead of from one brush to the pencil probe, the pattern is less sharply defined due to the influence of all eight brushes, but the slot frequency is still evident.

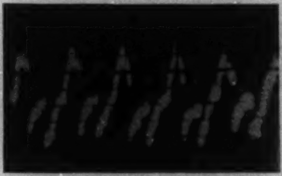

Figure 4. The wave obtained on an oscilloscope with leads connected between one brush and a pencil probe about one-half commutator bar from the trailing edge of the brush

Table I. Summary of Commutation Tests Using Electronic Voltmeter

Brush	Date of Test	Amperes, Buck	Amperes, Boost	Band Width
1	1-21-47	1.2	2.0	3.2
1	1-27-47	1.2	2.0	3.2
2	12-16-46	1.6	2.6	4.2
2	1-24-47	1.3	2.8	4.1
3	12-12-46	1.3	2.1	3.4
3	12-19-46	1.4	2.4	3.8
4	12-26-46	1.7	2.8	4.5
4	12-30-46	1.7	2.7	4.4
4	1-28-47	1.2	2.8	4.0
5	12-24-46	—0.3	1.8	1.5
5	12-23-46	—0.3	1.7	1.4
5	12-20-46	—0.3	1.9	1.6
6	2-11-47	1.9	4.2	6.1
6	2-18-47	1.8	4.5	6.3

Note:
Full load current of 58 amperes, room temperature 85 degrees Fahrenheit, 35 per cent relative humidity.

Average band width corresponding to a reading of one volt on the voltmeter.

These were 14-hour tests starting with a raw commutator each day.

Following this work an investigation of radio noise generation was made in cooperation with C. W. Frick. Readings were taken with a Ferris model *32* radio noise meter connected across the brushes at the following frequencies: 0.16, 0.2, 0.35, 0.6, 1, 1.5, 2, 3, 5, 8, 11, 15, and 20 megacycles. These readings show a maximum disturbance at 0.35 megacycle, which explains the necessity of using an electronic voltmeter sensitive to high frequencies. For comparison of results with those obtained with the electronic voltmeter the values plotted are the summation of the readings taken at the different frequencies, converted to an arbitrary scale. This comparison is shown in Figure 5. It is seen readily that these curves are similar in shape and, as indicated, sparking started near the bend in the curves. Some precautions must be taken when using the indicating instrument as a commutation meter. Erroneous results may be obtained if the generator supplying the buck and boost current sparks, as the disturbance will follow the wires to the voltmeter. Also, if the machine is loaded by "pump back" or on a line with other generators, sparking of the other machines may be read on the meter. We have used a resistance load bank for our tests to eliminate interference. At one time our generator was separately excited by an electronic current regulator to hold constant load. The current regulator rectified alternating current, supplying pulsating current to the generator field. These pulsations were transmitted to the armature and raised the electronic voltmeter readings over the full width of the band. If it is

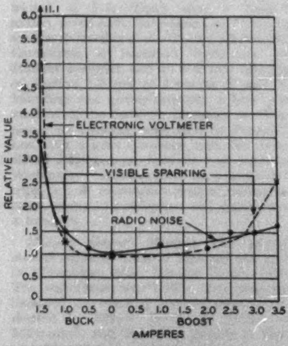

Figure 5. Comparison of radio noise meter readings and electronic voltmeter readings (relative values)

necessary to make a test on a generator running in parallel with other machines, it should be possible to block out the high frequency from the other machines by using a filter. Nevertheless, there are several reasons for our preferring the electronic voltmeter for measuring commutation instead of observing the visual sparking. One advantage is the elimination of the variations in readings due to different observers. This is important as there are considerable differences in the ability of the human eye to detect the first sparks. The local lighting conditions also effect the ability of the eye to see the small sparks. Another important point is that the electronic voltmeter shows sparking on all the brushes with one reading since it is connected directly across the brushes, while with visual observation it is necessary to look at all the brushes and on many machines this is physically impossible.

This more accurate method of comparing commutation makes it possible to study the effect of atmospheric conditions on brushes and machine performance. Besides being useful in evaluating brush performance the electronic voltmeter should be useful on production tests in setting the brushes in the neutral position, for checking pole shims, and to be sure each machine is within design limits. The requirement of preventing any sudden changes in current, especially at the trailing edge of the brush, has been fairly well taken care of in some machines by the machine designers. In many others current is still flowing between the commutator bar and the brush when contact is broken. This produces a spark, or at least a higher reading of the electronic voltmeter, and if bad enough causes etched commutator bars as well as short brush life and excessive commutator wear. These machines rely on the commutating ability of brushes for their proper operation. The electronic voltmeter is a useful tool in the development and evaluation of brushes with improved commutating ability.

References

1. **The "Black Band" Method of Commutation Observation, T. W. Schroeder, J. C. Aydelott.** ***AIEE Transactions*, volume 60, 1941, pages 446–51.**

2. **New Test Chambers for Aircraft Electric Apparatus with Particular Reference to Carbon Brushes, E. R. Summers, J. F. Settle.** ***AIEE Transactions*, volume 63, 1944, pages 1205–12.**

No Discussion

Report of the Board of Directors

THE BOARD OF DIRECTORS of the American Institute of Electrical Engineers presents to the membership its 65th annual report, covering the fiscal year ending April 30, 1949. It contains a brief summary of the principal activities of the Institute during the year, a general balance sheet showing the financial condition of the Institute at the close of the fiscal year, a statement of cash receipts and disbursements, and a schedule of securities owned. Additional information regarding the activities appeared in issues of *Electrical Engineering*.

BOARD OF DIRECTORS' MEETINGS

Five meetings of the Board of Directors were held during the year, two in New York, N. Y., one in Mexico, Federal District, Mexico, one in Milwaukee, Wis., and one in Dallas, Tex.

Information regarding many of the more important matters which were considered by the Board of Directors appeared in various issues of *Electrical Engineering*.

INSTITUTE VISITS BY PRESIDENT LEE

Alabama

Southern District Meeting, Birmingham

Arizona

Arizona Section and University of Arizona Branch, Phoenix

California

Stanford University Branch, Stanford; University of California Branch, Berkeley; University of Santa Clara Branch officers, Santa Clara; San Francisco Section; California Institute of Technology Branch, Pasadena; University of Southern California Branch, Los Angeles; Los Angeles Section; San Diego Section

Canada

Vancouver Section and University of British Columbia Branch officers; Toronto Section; Montreal Section; St. Maurice Valley Subsection, Shawinigan Falls; Ottawa Subsection; Niagara International Section, Niagara Falls, N. Y.

Colorado

Denver Section and University of Wyoming, Colorado Agricultural and Mechanical College, University of Denver, and University of Colorado Branches; University of Colorado Branch, Boulder

District of Columbia

Middle Eastern District Meeting, Washington; Joint AIEE-Institute of Radio Engineers-National Bureau of Standards Conference on High-Frequency Measurements, Washington

Florida

South Florida Subsection, Miami; North Florida Subsection, Gainesville; University of Florida AIEE-IRE Joint Student Branch, Gainesville

Illinois

Chicago Section, with Counselors and Chairmen of Branches at Illinois Institute of Technology and Northwestern University; dedication of new Electrical Engineering Building, University of Illinois, Urbana

Indiana

Fort Wayne Section; University of Notre Dame Branch, Notre Dame; South Bend Section

Maryland

Maryland Section and Johns Hopkins University Branch, Baltimore

Massachusetts

Pittsfield Section; Summer General Meeting, Swampscott

Michigan

Michigan Section, Detroit; joint meeting of University of Detroit and Wayne University Branches, Detroit; Michigan State College Branch, East Lansing; University of Michigan Branch, Ann Arbor; luncheon for Counselors of these Branches, Detroit

Missouri

St. Louis Section; luncheon meeting of St. Louis Section Executive Committee with Counselors and Chairmen of University of Missouri, Washington University, and Missouri School of Mines Branches, St. Louis; Washington University Branch, St. Louis; Kansas City Section and University of Kansas and Kansas State College Branches, Kansas City

Montana

Montana Section, Butte

New York

Joint meeting of Student Branches in New York City District, New York, with ten Branches represented; New York Section; Winter General Meeting, New York; Schenectady Section; Union College and Rensselaer Polytechnic Institute Branches, Schenectady; Syracuse Section; University of Syracuse Branch; Rochester Section; Ithaca Section with Binghamton Area Subsection; District 1 Executive Committee, Schenectady

North Carolina

North Carolina Section and University of North Carolina and Duke University Branches, Raleigh

Ohio

Toledo Section; Dayton Section; Columbus Section and Ohio State University Branch; Cleveland Section, Case Institute of Technology Branch, and Fenn College Branch, Cleveland; Mansfield Section; Akron and Canton Sections joint meeting, Akron; University of Akron Branch; Cincinnati Section and University of Cincinnati Branch

Oregon

Portland Section; Oregon State College professors of electrical engineering, Corvallis

Pennsylvania

University of Pennsylvania and Drexel Institute of Technology Branches, Philadelphia; Philadelphia Section; Lafayette College Branch, Easton; Lehigh University Branch, Bethlehem; Lehigh Valley Section, Reading; Pittsburgh Section and Carnegie Institute of Technology, University of Pittsburgh, West Virginia University, and Pennsylvania State College Branches, Pittsburgh; Erie Section; I.S.A. Convention joint with AIEE Committee on Instruments and Measurements, Philadelphia; Johnstown Subsection

Tennessee

Memphis Section

Texas

South West District Meeting, Dallas

Utah

Utah Section and University of Utah Branch, Salt Lake City

Vermont

North Eastern District Conference on Student Activities, Burlington

Virginia

Virginia Section with Western Virginia Subsection and Virginia Polytechnic Institute and Virginia Military Institute Branches and professors representing the University of Virginia Branch, Roanoke

Washington

Richland Section; Seattle Section; Pacific General Meeting, Spokane

West Virginia

West Virginia Section, Charleston

Wisconsin

Midwest General Meeting, Milwaukee

ANNUAL MEETING

The 65th annual business meeting of the Institute was held in Mexico, Federal District, Mexico, June 23, 1948. The annual report of the Board of Directors for the fiscal year which ended April 30, 1948, was presented in abstract by Secretary H. H. Henline, who also presented reports of the Committee of Tellers on the vote of the membership on constitutional amendments, and on the election of officers whose terms were to begin on August 1, 1948. In the absence of Treasurer W. I. Slichter, his report on Institute finances was presented by Secretary Henline. President-Elect Everett S. Lee was introduced, and responded with a brief address. Institute prizes for technical papers were presented.

The Lamme Medal for 1947 was presented to Past-President A. M. MacCutcheon, retired Vice-President of the Reliance Electric and Engineering Company, Cleveland, Ohio. The president's address was delivered by Blake D. Hull.

GENERAL MEETINGS

Four general meetings were held during the year, and a brief report on each follows.

Summer General Meeting. The 64th Summer General Meeting was held in Mexico, Federal District, Mexico, June 21–25, 1948, with a registration of 1,074. The program included the special opening inauguration ceremony presided over by President Miguel Aleman of the United States of Mexico, 19 technical sessions, 2 administrative conferences, and the official annual business meeting of the Institute. Social and entertainment features included a banquet Monday noon sponsored by the Secretary of National Economy and by the Federal Commission of Electricity, at which about 1,300 persons were present by invitation; a reception and luncheon in honor of the Board of Directors; a banquet and grand ball; a symphonic concert; exhibition of Mexican dances; ladies' events; and closing ceremonies and reception.

Pacific General Meeting. The Pacific General Meeting was held in Spokane, Wash., August 24–27, 1948, with a registration of 375. There were a general session, seven technical sessions, two Student sessions, a meeting of the District 9 Executive Committee, a luncheon conference on Student activities, and an informal meeting of Section officers of Districts 8 and 9. Members and guests attended a luncheon meeting of the Spokane Chamber of Commerce on Tuesday, addressed by President Lee, and a joint luncheon with the Associated Engineers of Spokane was held on Wednesday. Other events were inspection trips, a golf tournament, ladies' entertainment, president's reception and dance, and a banquet.

Midwest General Meeting. The second annual Midwest General Meeting was held in Milwaukee, Wis., October 18–22, 1948. The registration was 1,507. The program included an opening general session, addressed by Mayor Frank P. Zeidler of Milwaukee, and President Everett S. Lee, and 34 technical sessions and conferences, with 125 papers of wide variety in the fields of power, industry, communication, and basic sciences. There were about 30 committee meetings and luncheons. Many members and guests attended a luncheon in the Allis-Chalmers clubhouse Tuesday. Other events included inspection trips, a stag-smoker with entertainment, a banquet and dance, an extensive ladies' program, and a "Gemuetlichkeit."

Winter General Meeting. The Winter General Meeting was held in the Hotel Statler, New York, N. Y., January 31–February 4, 1949, with a registration of 2,896, and a record program of 55 technical sessions and conferences, and presentation of 233 papers. In a general session, the Edison Medal for 1948 was presented to Dr. Morris E. Leeds, Chairman of the Board, Leeds and Northrup Company, Philadelphia; an address on "The Professional Estate" was delivered by Charles E. Wilson, President of the General Electric Company; and President Everett S. Lee gave an address on "Our Institute." Approximately 80 meetings of technical and administrative committees were held. In addition, there were inspection trips, a smoker, a dinner-dance, and ladies' entertainment events.

DISTRICT MEETINGS

Middle Eastern District Meeting. The largest meeting ever held by the Middle Eastern District was held in Washington, D. C., October 5–7, 1948. The registration was 715. In 20 technical sessions, 70 technical program and District papers were presented. In a general session, addresses were given by President Lee, and Dr. F. B. Silsbee, Chief of the Division of Optics and Electricity of the National Bureau of Standards. Dr. Silsbee was introduced by Past-President William McClellan, honorary Chairman of the Meeting Committee. The program included inspection trips, a smoker, a dinner-dance, and events for the ladies.

Southern District Meeting. A Southern District Meeting was held in Birmingham, Ala., November 3–5, 1948, with a registration of 334. The program included an opening session with addresses by the Honorable Cooper Green, President o City Commission of Birmingham, F. B. Weiss, Chairman of the Meeting Committee, President Everett S. Lee, and Vice-President J. H. Berry, who were introduced by H. J. Scholz, Chairman of the Alabama Section. In five technical sessions, many papers of particular interest in the South were presented. There were inspection trips, two banquets, a District Executive Committee meeting, and ladies' events.

South West District Meeting. A highly successful meeting was held in Dallas, Tex., April 19–21, 1949, with a registration of 783, including slightly more than 300 students. The features included two general sessions, one with addresses by President Lee and Dr. Jack T. Wilson, and the other with five addresses on "The Electrical Engineers' Contribution to the Growth of the Southwest," a meeting of the Board of Directors, seven technical sessions with 27 papers, two student sessions, two luncheons, a smoker and buffet supper, a banquet and dance, inspection trips, and ladies' events.

SPECIAL TECHNICAL CONFERENCES

A special technical conference is a relatively new type of meeting, which is held independent of general and District meetings. It may be defined as a program of panel discussions, technical papers, or exhibits under the auspices of a national technical committee in co-operation with an AIEE local Section. The purpose of these meetings is to expand technical committee activities on individual specialized subjects and to serve the interest of members and nonmembers on that subject. The scope of the conference is meant to be national in interest, technical in character, and concentrated as to subject matter toward one particular industry or objective. It also is intended to further the program of expanded Institute activities by taking the Institute to members, and at the same time to stress its potential value in advancing the AIEE into new fields by demonstrating in a forceful manner to engineers inside and outside the membership that the Institute does have a place for all, and is definitely interested in providing ways and means for discussing and ironing out their technical problems.

Operating under the foregoing principles, the following conferences were held during the past fiscal year.

Conference on Electric Welding was held in the Rackham Memorial Building, Detroit, Mich., December 6–8, 1948, sponsored by the Committee on Electric Welding, in co-operation with the AIEE Michigan Section, the Detroit Section of American Welding Society, and the Industrial Electrical Engineers Society of Detroit. The conference provided an opportunity for the presentation of papers and discussions among an audience of persons primarily interested in arc and resistance welding. The program was planned to cover many timely and vital topics of interest to manufacturers, designers, users, and the utilities which supply the power. Six sessions provided for the presentation of 31 papers. The total attendance at the conference was 436; advance registration was 178. Orders for proceedings at the conference were 235. A special inspection trip was planned to the Ford Motor Company's River Rouge Plant, and was attended by 194 persons. During the 3-day conference, 336 persons attended the special luncheons.

Conference on Electronic Instrumentation in Medicine and Nucleonics was held in the Engineering Societies Building, New York, N. Y., November 29–December 1, 1948, sponsored jointly by committees of AIEE and the Institute of Radio Engineers. Committees included the Subcommittee on Nucleonic Instrumentation of the Committee on Nucleonics and the Subcommittee on Electronic Aids for Medicine of the Committee on Electronics; also the Committee on Nuclear Studies of the Institute of Radio Engineers. These three groups found an area of common interest, and combined their efforts to conduct an interesting and informative conference. The program was planned to interest the several groups of technical specialists: one day for papers of interest to medical people, one for engineers and physicists, and another combined the interests of both medical and technical people. Six sessions provided for the presentation of 26 papers. The total attendance at this conference was 547 persons; advance registration 250. An interesting exhibit of nuclear radiation instruments, which was provided by the Atomic Energy Commission, accompanied this conference.

Conference on High-Frequency Measurements was held in Washington, D. C., January 10–12, 1949, sponsored jointly by the AIEE, the Institute of Radio Engineers, and the National Bureau of Standards. It brought together those interested in high-frequency measurements and measuring apparatus. The program was planned to include surveys of various branches of the art and the presentation of the latest developments in measuring technique. Four sessions provided for the presentation of 25 technical conference papers. The total attendance at this conference was 584; advance registration more than 200.

In addition to the technical sessions, inspection trips were arranged to the Naval Research Laboratory, the Naval Ordnance Laboratory, and the National Bureau of Standards. At a special luncheon at the Roger Smith Hotel on January 11, the guests were addressed by President Everett S. Lee, Dr. Stuart L. Bailey, President of IRE, and Dr. E. U. Condon, Director of the Bureau of Standards, each expressing the belief that many benefits to all and encouragement for future progress would be derived from the exchange of technical knowledge at these conferences.

Conference on Industrial Application of Electron Tubes was held at the Statler Hotel, Buffalo, N. Y., April 11 and 12, 1949. This conference was sponsored by the Subcommittee on Electron Tubes of the Committee on Electronics, and the Subcommittee on Electronic Control of the Committee on Industrial Control, jointly with the Niagara Frontier Section. The conference provided an opportunity to discuss the application of electron tubes in the industrial field, with presentation and discussion encouraged among the audience of people primarily interested in the application and operation of tubes in this field. A program was planned to cover experiences of manufacturers, designers, and users. Four sessions provided for the presentation of 20 papers. The total attendance was 229; with an advance registration of 152. Orders for proceedings at the conference were 118.

A special inspection trip was planned to Westinghouse Electric Corporation's Motor and Control Plant in Buffalo. A portion of the control division of this plant is devoted to the manufacture of electronic control equipment. The Monday evening dinner featured an address on the control aspects of atomic power by Dr. Karl H. Kingdon of the General Electric Company.

Conference on Electrical Engineering Problems in the Rubber and Plastics Industries was held at the Hotel Portage, Akron, Ohio, April 26, 1949, sponsored by the Subcommittee on Rubber and Plastics of the Committee on General Industry Applications, in co-operation with the Akron Section. This conference provided an opportunity for the presentation of papers and discussions of electrical problems in the rubber and plastics industry. Two sessions provided for the presentation of ten papers, with full discussion at the end of each session. The total attendance at this conference was 191; with an advance registration of 168. Orders for proceedings at the conference were 99.

Because of the lack of time at the one-day conference, the committee was unable to schedule any special events except the noonday luncheon. For next year's conference, the committee is hoping to extend the time to two days in order to cover more fully the problems at hand. This was the second conference conducted by the committee on this subject.

General Committees

FINANCE COMMITTEE

The fiscal year ending on April 30, 1949, as was indicated by preliminary figures, shows an operating deficit of about $18,000. This shortage, together with temporary needs for cash during the latter part of the year, has been met by withdrawals from the reserve capital fund. These transfers will be repaid early in the new fiscal year. Certain remedial factors are now in operation, which, it is hoped, will minimize or obviate such transfers in the near future. They were reflected in the adoption in October 1948 of a balanced budget for the year October 1, 1948, to September 30, 1949; and performance under this budget so far has been approximately in line with its provisions. Principal among these remedial factors are

1. Substantially increased advertising rates in *Electrical Engineering*.
2. Establishment of registration fees for general and District meetings.
3. Price scales for Institute publications designed to make them approximately self-supporting.
4. Wholehearted co-operation by those committees responsible for sizable expenditures in the effort to confine their expenditures within limits set by the budget.

In spite of these encouraging signs, the financial future of the Institute is by no means a clear picture, and the Special Committee on Institute Dues appointed a year ago by President Hull is continuing to function. In response to one of its recommendations, the principal spending committees have submitted 5-year forecasts of their financial requirements, which now are being studied by the Finance Committee with the objective of preparing a 5-year budget. The special committee then will use this and other information to assist it in recommending a policy concerning the dues situation. In the meantime, the existence of the reserve capital fund is the "shock absorber" which enables our activities to continue unimpaired and to be enlarged where necessary to meet the demands of the ever-enlarging electrical industry.

COMMITTEE ON PLANNING AND CO-ORDINATION

The committee held four meetings during the fiscal year, in August and October, 1948, February and April, 1949. It is expected that a meeting will be held during the Summer General Meeting.

Meetings. Consideration and approval was given to a number of Institute general and District meetings scheduled to be held during 1950, 1951, and 1952, at various locations. It has been found desirable to schedule these at least two, and preferably three, years in advance in order to obtain suitable hotel accommodations.

Registration Fees. The matter of registration fees to be charged at general and District meetings has been reviewed at various times. A fixed schedule of fees was adopted in 1948, whereby, at general meetings members pay a registration fee of $3 and nonmembers $5, while at District meetings members pay $2 and nonmembers $3. Families of members and Student members are not charged any registration fee. The purpose of these fees is to assist in defraying the expenses of the technical activities of the meetings. Recently the Committee on Planning and Co-ordination reviewed this situation to determine what fees, if any, should be paid by guest speakers, nonmembers presenting papers, applicants, and so on. The committee recommended, and the Board of Directors approved, the following supplemental schedule:

Guest speaker—No fee.

Nonmember presenting paper—Nonmember fee.

Applicant for membership—Member fee.

Attendance at meetings jointly sponsored with other societies—Fees are to be agreed upon beforehand with the other society, either *a* each society charging its members according to its own rules, or *b* all in attendance being charged in accordance with AIEE rules; means of identification to be agreed upon.

Attendance at social functions only—No fee.

From all reports, the charging of registration fees during the past year has not aroused any substantial adverse criticism, and the money so collected has been decidedly beneficial in assisting to maintain a balanced budget.

Technical Activities. The Technical Activities Subcommittee has well served as the correlating agency of the several co-ordinating committees, and has handled a number of specific projects, including the preparation of "Administrative Scope for Technical Co-ordinating Committees" and a manual for technical conferences.

Several organization changes have been arranged for in the co-ordinating and technical committee setups. Several important subcommittees have been elevated to full committee status, and this has proved advantageous. The co-ordination group on Communication and Science has been enlarged and split into two co-ordinating groups, Communication, and Science and Electronics. The Communication Co-ordinating Group will have seven technical committees, and the Science and Electronics Co-ordinating Group will have eight technical committees.

The scopes of several new technical committees now are being prepared.

Professional Group. The Professional Activities Subcommittee has provided a scope for the Bylaws for the Committee on Education, which recently was transferred to the list of general committees and placed under the Professional Group Co-ordinating Committee.

Legislation and Tax Status. The committee has given a great deal of consideration to the tax status of the AIEE as it might be affected by activities in the field of legislation pertaining to engineers. The New York State Tax Department recently ruled the Institute to be exempt from New York State Unemployment Tax.

Uniform Grades of Membership. The committee has endorsed the statement of uniform grades of membership as adopted by the ECPD committee on Professional Recognition, and this has been approved by the Board of Directors.

Volta Memorial Fund. A specific procedure for handling this memorial fund was drafted, and it is expected this will be submitted to the Board of Directors for approval at the June meeting.

Prize Awards. Action has been initiated for a detailed review and analysis of the Institute's procedure for handling prize awards.

Technical Conferences. The policy to be followed in planning and conducting technical conferences has been discussed in detail, and the manual which is being prepared on this subject is expected to facilitate and encourage holding of such conferences, which have proved to be highly successful.

PUBLICATION COMMITTEE

The publication policy, which became effective January 1, 1947, has been continued in operation. This policy provides for three publications: *Electrical Engineering*, *Transactions*, and *Proceedings*, together with advance photographic copies of papers regularly approved for presentation at meetings. Each of these publications was described briefly in an article entitled: 'AIEE Publication Services Reviewed for Membership" (*EE, Apr '49, pp 348–9*), with a detailed statement telling how each publication might be procured. The number of pages of published material is reported in Table I for the calendar year 1948, so that it readily may be compared with the amount of material published during previous years.

Electrical Engineering. With the growth of the Institute in numbers of members and Student members, the circulation of *Electrical Engineering* has increased steadily from an average of 40,375 copies for the preceding

Table I, Numbers of Pages of Published Material

	Electrical Engineering			Transactions Only		
Year	Technical Articles	News	Transactions Sections	Technical Papers	Discussions	Totals
1941	337	281	600	542	268	2,028
1944	246	214	738	493	231	1,922
1945	255	225	736	121	143	1,480
1946	285	315	832	254	120	1,806
1947	806	474		1,463*	153*	2,896
1948	832	395		1,815†	172†	3,214*

* Preprinted in 227 sections of AIEE *Proceedings*, except for a 17-page technical paper in *Electrical Engineering*.

† Preprinted in 247 sections of AIEE *Proceedings* requiring a total of 2,090 pages.

Table II. Classification of Articles in Electrical Engineering in Seven Broad Fields

	May	June	July	Aug.	Sept.	Oct.	Nov.	Dec.	Jan.	Feb.	Mar.	Apr.	Total
General interest			2	2							3		7
Educational						2		2	2	1		1	8
Scientific	3.5*	4	6	2	4	3	2	3	2		0.5*	2	32
Communication	0.5*	2	1	1					1	3	3	1	12.5
Power	2.5*	2	1	1	4	3	5	3		3		1	25.5
Industry	3.5*	1		2		2	1		4	1	0.5*	1	16
General applications	1.0	1			1	1		1	2	3	3	1	14
	11	10	10	8	9	11	8	9	11	11	10	7	115.0

* Half values assigned to articles which fall in two fields.

year, as compared with 47,800 copies for the current year, with an all-time high of 52,100 copies for the April issue. The increase in circulation, combined with a ten per cent increase in the cost of printing and an advance in paper prices has been partly offset by reducing the yearly content by 135 pages, and using a paper of slightly less weight. In Table II, is presented a classification of articles in *Electrical Engineering* in seven broad fields. By judicious selection of technical papers of broader interest, and by giving preference to the papers which are shorter (six pages or less), the table shows that about the same number of articles have been published in the last half of the year, under the reduced page budget, as was published during the first half of the year. On inquiry in various sections of the country, it has been reported that the 135 pages have not been missed.

In the selection of articles for each issue, an attempt has been made to carry one or two articles in each of the six broad fields shown in Table II. The increase in the numbers of communication, educational, and general appliance engineering articles in recent months has met with favor. As time goes on, the totals for each of these six broad fields will be more nearly proportional to the number of members in these fields of endeavor.

Advertising. The amount of advertising received has held up very well, and it is expected that the gross revenue will total approximately the $180,000 estimated at the beginning of the appropriation year. The $33^{1}/_{3}$ per cent increase in rates, which became effective February 1, 1948, still has not been in effect for a sufficient time to derive the full gross revenue for the duration of the appropriation year. In view of the large circulation, and, after consideration of the circulation and rates of eight similar magazines, the committee thought the rates for *Electrical Engineering* were disproportionate. However, on recommendation of the advertising director, the committee agreed that now was not an appropriate time to raise the advertising rates further.

Transactions. Volume 67 of the 1948 *Transactions* has been made available in two parts—part I, which consists of 862 pages, contains the papers which were presented during the first half of the year, and it was made available last December. Part II, which consists of 952 pages, includes the papers which were presented during the last half of the year, the Board of Directors' report, and a complete index, was made available in May. In this way, half of the papers have been made available six months sooner, and the bulk of the volume has been reduced. On recommendation to the Board of Directors, the Student subscription rate to the *Transactions* has been raised to $5, the same as for members.

AIEE Proceedings. As an interim service to members who are specialists, and Student members only, single copies of the 1948 papers correlated with discussion, if any, have been made available in 247 sections to those filling out order forms published every few months in *Electrical Engineering*. Ten per cent of the papers are free to members and additional papers are available at ten cents each. In the case of Student members, there is no free allowance. A total of 6,295 orders for *Proceedings* were received during 1948. These orders average $8^{1}/_{3}$ papers per order form, and represent a distribution of 53,500 copies. Most of the copies ordered are free copies, and the total receipts were $644. By publishing a reference on the cover of the April issue to the location of the *Proceedings* order form in the advertising section, 54 per cent more orders have been received during the first ten days than were received during the same interval for the December order form. At this date, it is not known whether the procedure has merely advanced the time for ordering the papers, or there has been a substantial increase in the number of orders.

Review of Publication Policy. The present publication policy is being reviewed, a number of suggestions and constructive criticisms have been received from members and officers, and all of them are being given careful study. Among them, two important suggestions are listed:

(*a*). To abandon the *Proceedings* entirely and issue quarterly *Transactions* with the papers correlated in six subject divisions: communication, electronics and science, power systems, power equipment, general applications, and industry. This plan involves providing one or two such *Transactions* each quarter to each member without charge, and with a nominal price for any others. According to a preliminary estimate, one free division would cost approximately $3,700 less than the present cost of *Proceedings* and *Transactions*. Two divisions free would cost approximately $22,000 more.

(*b*). As an alternate to *a:* To publish more technical material in full in *Electrical Engineering* to the extent of the additional expense in *a*.

Special Publications. During the year, the following four special publications have been made available, and others are in prospect. These special publications fill a specialized need—they are published entirely on a self-supporting basis, and made available to members at cost, and in general at double the cost to nonmembers, through announcements published in *Electrical Engineering* from time to time.

1. Telemetering, Supervisory Control, and Associated Circuits (September 1948).

2. Electrical Engineering Problems in the Rubber and Plastics Industries.

3. Electron Tubes for Instrumentation and Industrial Use.

4. Elements of Nucleonics for Engineers.

Preprints. Technical papers approved for presentation at meetings have been made available in advance by a photolithographic process. A few of the papers not considered of permanent-record value have been made available as miscellaneous papers on an advance-copy-only basis. For the purposes of discussion, the free allowance to authors has been increased to ten copies, and the allowance to committees has been liberalized to 50 copies to the sponsoring committee. Other copies are sold to members at a price of 30 cents each, and to nonmembers at a price of 60 cents each. In general the system has been working satisfactorily, and it is believed to be more nearly on a self-supporting basis.

SECTIONS COMMITTEE

Section Activities. Section activities have continued to expand at accelerated postwar levels. A new Section has been formed at Miami, Fla., and several new Sections are in the process of formation. New Subsections have been formed in various Sections.

Booklet—"The Electrical Engineer." A subcommittee of the Sections Committee and of the Committee on Student Branches has revised the booklet, "The Electrical Engineer," and presented it to the headquarters staff for reprinting.

Prize Award Rules. A subcommittee of the Sections Committee has prepared a revision of the Institute Prize Paper Rules for final consideration at the June meeting of the Section Delegates. After approval, it will be presented to the Committee on Planning and Co-ordinating and the Committee on Award of Institute Prizes for final approval.

Meetings of the Sections Committee. A meeting of the Sections Committee was held during the Winter General Meeting. Three meetings are scheduled for Section delegates during the Summer General Meeting. These will include the Delegates' Get-together on Monday evening, June 20; a meeting to initiate an aggressive publicity program by the Sections on Tuesday morning, June 21; and a Section Delegates' Conference on Tuesday afternoon, June 21.

Co-operation With Other Institute Committees. The Sections Committee has actively cooperated with several Institute general committees, including Transfers, Membership, Student Branches, and the Technical Activities Subcommittee of the Committee on Planning and Co-ordination. At the request of the Technical Activities Subcommittee, a revised draft of the proposed policy on conduct of technical conferences was prepared and submitted.

Section Finances. A subcommittee of the Sections Committee under the chairmanship of G. W. Bower, Vice-President of District 2, is conducting a survey and study of the problem of Section finances for the next 5-year period. This study is being made in accordance with the action of the Board of Directors during the Winter General Meet-

Table III. Section and Branch Statistics

	For Fiscal Year Ending April 30					
	1944	1945	1946	1947	1948	1949
sections						
Number of Sections	73	73	75	75	81	84
Number of meetings held	738	884	1,210	1,333	1,340	1,561
Total attendance	83,120	96,346	113,531	155,649	109,637	128,025
Branches						
Number of Branches	125	125	125	126	127	129
Number of meetings held	755	547	716	1,018	1,172	1,350
Total attendance	24,768	17,132	22,844	40,669	77,040	103,828

ing, wherein a recommendation of the Special Committee on Institute Dues requested a survey of Institute finances for the coming 5-year period.

COMMITTEE ON RESEARCH

The activity of the committee consisted of the sponsorship of a symposium at the Winter General Meeting on the subject "New Tools for Research and What They Promise for Electrical Engineering." Several papers were presented, all of which were well received. Attendance was approximately 200. Plans for a similar session on a different subject are being formulated for the 1950 Winter General Meeting.

STANDARDS COMMITTEE

During the year, the administration of the Standards Committee was unfortunately interrupted by the untimely death of its Chairman, Dr. Reginald L. Jones, who had for many years past given tirelessly of his time and of his tremendously capable capacity.

The Secretary, H. E. Farrer, who served the committee exceptionally well for more than 25 years, was retired at the end of the calendar year 1948 under the Institute's retirement system, and has been succeeded in this assignment by J. J. Anderson, Jr.

In the field of Standards or Codes developed or revised, the past year saw the completion of the following: Industrial Control (revised); Marine Rules (further revision); Master Test Code for Temperature Measurement in Electric Apparatus; Graphical Welding Symbols; Mercury Arc Rectifiers (revision); Letter Symbols for Electrical Quantities; Transformers, Regulators and Reactors (revision); Steam Turbine Generators (revision); Speed Governing of Prime Movers (revision).

It has been determined finally between ASA and co-operating bodies that the size of published Standards will be changed to $8^1/_2$ by 11 inches, and for the AIEE this was put into effect during the year. New binders for the $8^1/_2$ by 11 size now have been provided, and the Institute's entire existing stock of Standards on hand have been repunched so they will fit both old and new binders.

A new Standards co-ordinating committee, designated as number 8, to be known as the Committee on Co-ordination of Insulation, has been formed under the chairmanship of J. H. Foote. This committee includes the entire AIEE delegation to the Joint Committee on Insulation between AIEE, Edison Electric Institute, and the National Electrical Manufacturers Association. The scope of this activity encompasses insulation levels, insulation strengths, apparatus design, and similar technical aspects.

The C40 Sectional Committee on Storage Batteries, one of the important ASA activities for which AIEE is sponsor, is being reactivated pursuant to getting at the revision of the storage battery Standards.

In the international field, a very successful conference session was conducted in Mexico City during the Summer General Meeting. Papers were presented outlining the standardization procedures employed in the United States, the use of Standards as tools by industry, emphasis on safety codes, and papers indicating the application of Standards to two specific types of apparatus. The entire top echelon of the Mexican Department de Normas participated in the conference, and were very cordial in conducting interested visitors through their facilities and in discussing together standards problems. Senőr Rafael Illescas Frisbie, Director General de Normas, visited this country soon after the meeting, and it is believed a real forward step in understanding and co-operation was accomplished.

Further in the international field, the AIEE Committee on Marine Transportation was asked to assume international standards work in the marine field. Representatives thereof met in London.

One knotty problem entered into during the year and carrying over is that of temperature limits for switchgear in enclosures as controlled by cable insulation. This problem was assigned to a special subcommittee under the chairmanship of J. E. Clem.

UNITED STATES NATIONAL COMMITTEE OF THE INTERNATIONAL ELECTROTECHNICAL COMMISSION

Meetings of the following advisory committees of the International Electrotechnical Commission were held: A.C. 6: Lamp Caps and Holders, March 1948, The Hague; A.C. 28: Co-ordination of Insulation, June 1948, Paris; A.C. 18: Electrical Installations on Shipboard, July 1948, London; A.C. 30: Extra-High Voltages, July 1948, Paris; A.C. 31: Flameproof Enclosures, July 1948, London; A.C. 32: Fuses, July 1948, London. In Stockholm, Sweden, October, 1948—Council; Committee of Action; A.C. 6: Lamp Caps and Holders; A.C. 9: Electric Traction; A.C. 12: Radio Communication; A.C. 23: Electrical Accessories; A.C. 33: Capacitors.

The advisory committees have under way considerable technical work and much progress has been made. None of this work has resulted as yet in the submission of proposals for international agreement. Due to the lapse in the work during World War II, it is to be expected that some time will elapse before standard proposals can be put into shape for international adoption.

The meetings of the council and the Committee of Action were devoted to the administrative and financial affairs of the commission. Due to the transfer of the central office of the IEC from London to Geneva, Switzerland, during the previous year, adjustments were necessary. The offices in Geneva are now completely equipped and in a position adequately to service the work of the IEC. At Stockholm, work was actively begun on a revision of the Statutes, Rules of Procedure, and Directives for the Advisory Committees. The statutes were last revised in September 1913, and in the intervening years had become partially out of date. It is hoped that the revision of these fundamental documents of the IEC will be completed in the near future.

To date, a meeting of A.C. 14: Transformers, has been held in London, March 1949. The following meetings have been scheduled for the coming year: A.C. 32: Fuses, May 1949, Paris; and at Stresa, Italy, June 1949: A.C. 1: International Electrotechnical Vocabulary; A.C. 8: Standard Voltages and Current Ratings, High-Voltage Insulators; A.C. 10: Insulating Oils; A.C. 17: Switchgear; A.C. 22: Electronic Devices; Council; Committee of Action.

TECHNICAL PROGRAM COMMITTEE

Technical Programs. The technical activities of the Institute are at the highest level in history as a result of the efforts of 31 technical committees, the largest number ever to serve the Institute. The Winter General Meeting program was enlarged to provide for the presentation of 233 papers, 145 of which were conference papers. Both of these figures are new meeting records.

In Table IV, the number of papers presented at each of the seven meetings which were held during the year are given, together with the attendance. This table would show a greater increase in the yearly number of papers presented but for the fact that only half as many papers as usual were presented at the Summer General Meeting. One of the reasons for the smaller number of papers at the Mexico City meeting was the great amount of time required to provide preprints in both English and Spanish. The Mexican members were responsible for translating and reproducing the preprints in Spanish. The local members were most appreciative of having the papers available in their native language and, of course, the results were made available to a much larger number of engineers. The large number of sessions, conferences, and papers would indicate that the Institute is on its way toward a greatly expanded program of technical activities. This increase may be attributed to growth in membership and the increase in the number of technical committees from 21 to 31. In addition the Institute is served also by six joint subcommittees.

Planning for Programs. The recent creation of seven new technical committees has increased the number of these committees serving the Institute to a total of 38, which in itself will continue to make available to the Institute an increased number of technical meetings and papers. The committee

Table IV. Number of Papers Presented During the Year Ending April 30, 1949*

Meeting	District	Advance Copy Only	Conference Papers	Transactions	Total	Attendance
Summer, Mexico City		26		31	57	1,074
Pacific Coast, Spokane		2	11	19	32	375
Middle Eastern, Washington	33	8		29	70	715
Midwest, Milwaukee		10	57	58	125	1,507
Southern, Birmingham	17			1	18	334
Winter, New York		14	145	74	233	2,896
South West, Dallas	20	4		3	27	783
	70	64	213	215	562	7,684

* Repeated presentations not included.

now is reviewing papers for the Summer General Meeting, the meeting having been designed to fit in with the meeting of the American Society for Engineering Education to be held concurrently in Troy, N. Y. This kind of co-ordinated activity with other technical organizations also has added to the general activity in the electrical engineering field; each technical committee is attempting to work jointly, in so far as possible, with other technical bodies whose work affects it. In the arrangements of programs, an attempt has been made to cover all new developments in the field of electrical engineering and the allied arts. The geographical location of meetings also has been taken into consideration, and papers have been presented which were of particular interest in certain regions.

Analysis of Subject Matter. With special reference to the 1948 Summer General Meeting, the technical program was planned to present the latest trends and developments in a number of specialized fields of electrical engineering that were of particular interest to Mexican engineers. Among these were papers on paper and textile mills, petroleum and steel production applications, hydroelectric power and irrigation and mining operations. At the Pacific General Meeting, the emphasis was on transmission and distribution, while at the Middle Eastern District Meeting the larger number of papers were on subjects in the fields of air and marine transportation. A field relatively new to electrical engineers was covered at the Midwest General Meeting in a conference on ore beneficiation. Also presented, in the industrial field, was a symposium on speed regulating systems for sectional paper machine drives and an all-day conference on automatic contouring for machine tools. At the Winter General Meeting, a widely diversified program was highlighted by a conference on energy sources and symposiums on gas turbines for power generation and new tools for research.

Future Meetings. The program for the Summer General Meeting has been completed, and those for the Pacific General Meeting and the Fall General Meeting are well under way.

BOARD OF EXAMINERS

Statistics relating to the number of cases handled by the Board of Examiners during the year 1948–49 are given in Table V. The current total represents an increase of 60 per cent over 1947–48. These figures are exclusive of those covering "enrolled Students," which rose from 5,894 to 9,265, or about 58 per cent. The increase in the current total is principally in the applications for admission to the grade of Associate, this increase being 85 per cent.

Due to the increase in the membership of the Board of Examiners to 30, it has been possible to handle this larger volume of work with only one meeting over those regularly scheduled.

The large increase in Associate admissions and Student enrollments is principally due to the greatly increased enrollment in schools under the G. I. Bill of Rights. The Associate increase has come from those whose schooling was interrupted by the war and who have now finished the two or three remaining years. The Student enrollment has come largely from those who have taken advantage of the G. I. Bill of Rights to start their electrical engineering education.

There is need to re-emphasize the statement in last year's report to the effect that it is still necessary to ask frequently for more detailed statements of record and additional supporting references. A mere statement of dates and titles of positions held is not sufficient to enable the Board of Examiners to arrive at a decision on eligibility.

The Board of Examiners regrets the loss, through retirement, of its former Secretary, H. E. Farrer. His services to the Board through the years have been invaluable.

COMMITTEE ON CONSTITUTION AND BYLAWS

Submitted by the committee on June 2, 1948, and adopted by the Board of Directors on June 24, 1948, were the following recommendations:

Bylaws. A new section defining the scope of the Committee on Institute Publicity was added and became Section 78 in the 1948 "Year Book." The name was changed in October to Committee on Public Relations. Section 83 was amended to give the Standards Committee increased authority in the adoption of Standards.

A new section regarding the establishment of Subsections (or Divisions) was added, and became Section 41 in the 1948 "Year Book."

A new section relating to the disfranchisement of a Section of the Institute was added, and became Section 44 in the 1948 "Year Book."

Submitted by the committee on September 24, 1948, and adopted by the Board of Directors on October 19, 1948, were the following recommendations:

Bylaws. Section 105 (Section 107 in 1948 "Year Book") was amended to omit any reference to a limiting price for *Transactions*.

Sections 67, 69, 71, 72, 75, 81, 84, and the new section on Committee on Transfers (became Sections 66, 77, 82, 69, 74, 81, 80, and 86 in 1948 "Year Book") were amended to add the sentence, "At least one member of the committee shall be a member of the Board of Directors."

Submitted by the committee on January 20, 1949, and adopted by the Board of Directors on February 3, 1949, were the following recommendations:

Bylaws. A new section defining the scope of the Members-for-Life-Fund Committee was added, and will be placed between Sections 73 and 74, as printed in the 1948 "Year Book."

Section 31 was amended to clarify the matter of voting privileges of alternates to District Executive Committee meetings.

Submitted by the committee on March 29, 1949, and adopted by the Board of Directors on April 20, 1949, were the following recommendations:

Bylaws. Section 55 was amended to allow Student members to purchase current *Transactions* at the same price extended to members. A new section defining the scope of the Committee on Education was added, and will be placed between Sections 70 and 71, as printed in the 1948 "Year Book."

HEADQUARTERS COMMITTEE

The principal activities of the committee were the supervision of the cleaning of all rugs in the Directors' room, Members Room, and the hallways; shampooing of all upholstered furniture in these rooms; reupholstering of three overstuffed chairs in the Directors' room, and repainting of all venetian blinds in both rooms; and the submission to United Engineering Trustees of a suggestion that AIEE participate in proposed changes in the first floor lobby of the Engineering Societies Building, and contribute proportionately to the cost of such changes on the basis that: AIEE retain its own Board room for meetings of Directors and other large groups, and AIEE make use of smaller rooms as necessary for meetings of small groups.

The committee has under consideration the matter of polishing the table in the Board of Directors room, and provision of a sectionalized glass top. Some further upholstering may be necessary during the coming year, and the possibility of new lighting fixtures in the Directors' room will be considered.

COMMITTEE ON PUBLIC RELATIONS

The Committee on Public Relations, formerly known as the Committee on In-

Table V. Applications for Admission and Transfer, 1948–1949

Applications for Admission		
Recommended for grade of Associate	4,061	
Re-elected to the grade of Associate	98	
Not recommended	3	
		4,162
Recommended for grade of Member	308	
Re-elected to the grade of Member	10	
Not recommended	73	
		391
Recommended for grade of Fellow	6	
Not recommended	2	
		8
Applications for Transfer		
Recommended for grade of Member	485	
Not recommended	38	
		523
Recommended for grade of Fellow	118	
Not recommended	4	
		122
Students		
Recommended for enrollment as Students		9,265
Total		14,471

stitute Publicity, has been guided in its activities during the past season by a statement of policy adopted by the Board of Directors during the summer of 1948. This statement reads in part as follows:

> It is the policy of the Institute that public knowledge and understanding of the Institute's activities and public confidence in its members and their work be as widespread as possible....
>
> To accomplish these purposes and to promote the prestige of membership in the Institute, an active publicity program is necessary. Such a program should be integrated and continuous. It should reflect the Institute's position of responsible leadership in the scientific and engineering world and as the authoritative source of information regarding broad advances in the art of electrical engineering

In former years the committee had as its principal duty the publicizing of the Winter General Meeting. To implement the Board's statement of policy, a program was undertaken which promises to widen greatly the public's appreciation of Institute activities. This program is based largely on active co-operation with Section officers throughout the United States.

Publicity for the Winter General Meeting again was handled by professional counsel, Raymond C. Mayer, who has served effectively in the past, provided press releases and services which resulted in broad news coverage. The Committee on Public Relations assisted as far as possible in the publicity activities of the local committee covering the South West District Meeting, and will assist in connection with the Summer General Meeting.

The program of "integrated and continuous" publicity has enlisted the lively support of the Sections Committee. As an experimental part of the program, a publicity kit of instructions, suggestions, and samples of written material has been distributed to the Sections for trial and comment. It is expected that experience with this material during the next year will lead to the exploration and improvement of means for co-operation between the Committee on Public Relations and the AIEE leaders throughout the country. A half-day session of the Sections Committee at Swampscott, Mass., will be devoted to the discussion of the kit and other phases of Institute public relations.

Plans to provide more active publicity for general and District meetings are also under way. A great deal remains to be done to carry out the Board's policy, but a good beginning has been made.

COMMITTEE ON SAFETY

The Committee on Safety has been active, both in holding a conference and meetings of importance to the Institute, and in launching projects for promoting a better appreciation of safety and for implementing safety into practice.

A project of outstanding importance which has been considered intensively throughout the year by the committee and by a special subcommittee is that relating to research on resuscitation from electric shock. Analysis of reports of electric shock accidents shows that about a third of the victims made unconscious, but given artificial respiration with the promptness that should promise success, fail to recover for causes generally unknown. The doubtful and unknown elements in this situation long have blocked any substantial improvement in the resuscitation ratio of shock victims. In this committee's considered opinion, this block will continue until removed by research.

A research program for this purpose, therefore, has been carefully drawn up by members of the committee, including engineering and medical authorities on electric shock. The three Schools of Engineering, Hygiene, and Medicine of the Johns Hopkins University have offered to carry out this research jointly if the necessary financial support can be secured. The program has the endorsement of the Accident Prevention Committee of the Edison Electric Institute. The carrying out of this research not only should provide information on reasons for present failures, but also explore promising improvements in methods of resuscitation. The Board of Directors of the Institute has endorsed this proposed research, and hopes the electrical industry can provide the necessary financial support.

During the year, the steering committee held numerous meetings for the purpose of preparing an authoritative pamphlet which would present the hazards of low-voltage electric shocks, how electrocution occurs, and the safety features of electrical codes in prescribing proper wiring and vigilant maintenance as means of mitigating the hazards of low-voltage shocks. The preparation of such a pamphlet which would be worthy of the dignity of the Institute was proposed at the 1948 Winter General Meeting as a means of aiding in the dissemination of information on electrical hazards and safety practices. Although its context is still in the formative period, the pamphlet is being pressed for early completion.

A comprehensive bibliography on safety is under preparation to supplement a prior edition which covered safety conferences up to 1942, and it is planned that it will be available during the next administrative year.

The committee has co-operated with the Sections and Student Branches Committees with the objective of promoting continuing interest in safety throughout the AIEE membership by the nationwide activities of these committees.

Various committee members gave addresses on pertinent phases of safety before AIEE Sections, chapters of the National Safety Council, meetings of the American Society of Safety Engineers, industrial accident prevention groups, electrical association meetings, and other technical groups. W. R. Smith, C. F. Dalziel, and W. B. Kouwenhoven have given addresses on different aspects of low-voltage shock hazards, and Robin Beach on electrostatic fire and explosion hazards in industry. Other members have been active in promoting safety within their respective organizations.

Several members of the committee were appointed to serve as liaison representatives with correlated committees of the Institute and with national organizations, such as, the American Society of Safety Engineers, Edison Electric Institute, National Fire Prevention Association, and others.

W. R. Smith, representing AIEE on the National Fire Waste Council, attended the annual meeting in Washington. The chairman, Robin Beach, represented the Institute on The President's Conference on Industrial Safety—being a member of the steering committee and of the Subcommittee on Machine Safeguarding. During the year, he attended three meetings of this conference in Washington. W. B. Kouwenhoven and W. T. Rogers, of the Committee on Safety, also attended the general conference meetings.

During the 1949 Winter General Meeting the Committee on Safety held a well-attended Conference on Control of Electrical Hazards in Rural Areas. The program included a treatise by Professor C. F. Dalziel on American and European practice in the manufacture and operation of electric fences and on the hazards of improvised or improperly designed systems. The papers on low-voltage shocks to cattle and to personnel on farm properties by W. B. Buchanan and J. H. Waghorne of the Hydro-Electric Power Commission of Ontario were reports of several years' investigations into this phase of the electrical hazards. A. H. Schirmer supplemented these papers on shock hazards arising from improper grounding by graphically presenting the code requirements for their elimination. These papers are being prepared for *Transactions*, as they summarize the findings from a long-range study, the collection of extensive field data, and recommendations for safe practices which possess outstanding value on this subject.

COMMITTEE ON TRANSFERS

The present Committee on Transfers has endeavored to continue the efforts of its predecessor committees in complying with the requirements of the bylaws calling for encouragement of the Sections in their local transfers work, co-operation with the Sections committees, acting as a medium of exchange of ideas, and working toward the preparation and maintenance of an operations guide for the local committees. Encouragement of and co-operation with the local Sections has been accomplished through answering all inquiries addressed to the committee and through issuance of a letter and questionnaire to all Section committees on transfers.

The committee met at the Winter General Meeting, at which time a clarification of the principles, policies, and objectives of grade transfer work was developed. These may be stated as follows:

1. Each member of the Institute should be in the highest grade for which he is qualified.
2. The impetus for transfer should come from without. No member should be overlooked. The initiative for advancing a man in grade preferably should come from his fellow engineers (although the prerogative to take the initiative himself should remain unimpaired).
3. The initiating and follow-through action for transfer best can be undertaken by each Section through the medium of a hard working standing Committee on Transfers.
4. Each Section committee on transfers should be, in effect, a "Junior Board of Examiners" undertaking the careful preliminary screening of each and all members of the Section.

Also on February 1, 1949, an informal report on transfers work was presented at a meeting of the Sections Committee.

The importance and status of Section committees on transfers cannot be overemphasized. There seems to be general agreement with the idea of Section committees on transfers having the status and importance of being in effect "Junior Boards of Examiners."

D. E. Moat, Chairman of the Committee on Transfers for the past two committee-years, perhaps has stated this conception best in his report presented at the Summer General Meeting in 1948:

> The primary determination of when a member is qualified for a higher grade should be in the hands of the local committee on transfers. The procedure of trial application to the Board of Examiners should be abandoned except in borderline cases when for some peculiar reasons the local committee cannot decide.
>
> The Board of Examiners, of course, should be the last word, charged with the maintenance of the standards and quality of membership, but the local committee should be, in effect, a "Junior Board of Examiners" which nine times out of ten could come up with the recognized correct answer.
>
> The whole problem is one of definition placed in the hands of recognized people in each Section and which people should so clearly understand the requirements that they can fairly judge, approve, or disapprove, the qualifications of an applicant.

As an example, the Committee on Transfers of a Section having a membership of approximately 800 submitted 132 cases for transfer to the Board of Examiners over a two year period, of which only one case was disapproved.

A guide or manual of recommended procedure for Section transfer work is regarded as one of the most important objectives of the committee. Such a manual can be prepared best as the result of polling the Sections as to how past transfer suggestions have been received and acted on, and how the various Sections conduct their transfers work. From this information, the best material can be selected and combined into a master plan or manual of procedure. Toward this end, a questionnaire was sent to the Sections under date of March 18, 1949. In addition to questions as to committee procedures and suggestions, questions were included for the purpose of revealing the present extent and nature of Sections transfer activities throughout the Institute.

Other projects in which the Committee on Transfers is active are as follows:

1. Assistance in publicizing advantages of the higher grades.
2. Assistance in working toward improvement of the AIEE system of grades.
3. Improvement of proposal and application transfer forms.

Replies to the questionnaire are being currently received, and it is hoped that returns will be adequate to permit analysis and preparation of a proposed manual of procedure for presentation at the scheduled meeting of the committee at the Summer General Meeting.

In the letter of transmittal accompanying the questionnaire sent to the Sections on March 18, 1949, the following statements were included by way of encouragement to the Section committees on transfers:

> The importance of Section work on transfers cannot be overestimated. We, on the national committee on transfers, have come to regard a Section committee on transfers as a "Junior Board of Examiners," a "Court of Honor," sitting in accurate appraisal of a man's professional record in an endeavor to determine whether or not he merits the honor of advancement to a higher grade as a badge of recognition conferred on him by his professional associates. It is to be emphasized, however, that such a committee performs a screening function only, and in no way:
>
> 1. Replaces or changes the present constitutional procedure whereby the final decision as to whether or not an applicant qualifies rests with the national Board of Examiners.
> 2. Replaces the present right of individual members to take the initiative for their own transfer.

The committee's reaction from contact with the Sections over the past year is that interest in transfers work is very much on the increase throughout the Institute. The committee will continue to endeavor to move ahead in this very important work.

MEMBERSHIP COMMITTEE

Membership in the Institute increased by 2,391 members in the year ending April 30, 1949. This was the largest growth on record, amounting to 373 more than the previous maximum of 2,018 in 1946. Total membership reached 30,791. Table VI of membership statistics shows the nature of the changes in membership during the year.

Applications from new members shows the basis for the new records being set in Institute growth. Applications from Student members for Associate grade reached a new high of 2,286, compared with 1,481 in 1948. This trend of increased applications from students reflects the large enrollment in colleges, growth in Student membership, which reached a total of 19,428 as of April 30, 1949, and the active solicitation of students for election to Associate grade. See Table VII.

This trend of growth from the student group is still on the increase due to the fact that the peak graduation of electrical engineering students in the war-swollen cycle will not be reached before 1950 or 1951.

The accelerated activity of the membership committees among the college graduates tends to reduce the number of eligible members in other categories. This is reflected in the decrease in applications from all others in this fiscal year, as shown in Table VII.

Members in arrears for dues for the fiscal year ended April 30, 1949, reached a total of 1,376, compared with 1,288 last year. This represented a delinquency of 0.448 per cent, compared with 0.453 per cent a year ago, showing slight improvement. It is also encouraging to note that only 685 were dropped during the year, compared with 693 in the previous period.

Activity of the District vice-chairmen was outstanding during the year. From two to four letters were sent by each vice-chairman

Table VII. Number of Applications Received From Student Members and From All Others

Year Ending April 30	Students	All Others	Total
1949	2,286	2,192	4,478
1948	1,481	2,272	3,753
1947	938	2,331	3,269
1946	308	2,453	2,761
1945	249	2,179	2,428
1944	466	1,908	2,374
1943	783	1,431	2,214

Table VIII. Number of Student Members as of April 30

Year	New Applications	Renewals	Total
1949	9,967	9,461	19,428
1948	7,876	6,041	13,917
1947	5,092	3,929	9,021
1946	2,574	2,513	5,087
1945	2,326	2,287	4,613
1944	2,242	2,656	4,898
1943	2,512	3,200	5,712

Table IX. Record of AIEE Membership

Year	Total May 1	Year	Total May 1	Year	Total May 1
1884	71	1906	3,870	1928	18,265
1885	209	1907	4,521	1929	18,133
1886	250	1908	5,674	1930	18,003
1887	314	1909	6,400	1931	18,334
1889	333	1910	6,681	1932	18,003
1890	427	1911	7,117	1933	17,010
1891	541	1912	7,459	1934	15,230
1892	615	1913	7,654	1935	14,269
1893	673	1914	7,876	1936	14,600
1894	800	1915	8,054	1937	15,308
1895	944	1916	8,202	1938	16,078
1896	1,035	1917	8,710	1939	16,605
1897	1,073	1918	9,282	1940	17,213
1898	1,098	1919	10,352	1941	17,886
1899	1,133	1920	11,345	1942	18,944
1900	1,183	1921	13,215	1943	20,161
1901	1,260	1922	14,263	1944	21,407
1902	1,549	1923	15,298	1945	23,072
1903	2,229	1924	16,455	1946	25,090
1904	3,027	1925	17,319	1947	26,470
1905	3,460	1926	18,158	1948	28,408
		1927	18,344	1949	30,791

Table VI. Membership Statistics for Fiscal Year Ending April 30, 1949

	Honorary Members	Fellows	Members	6-Year Associates	Associates	Subtotals	Totals
Membership							
April 30, 1948	8	1,088	8,117	8,106	11,081		28.400
Additions							
New members qualified		5	249		3,009	3,263	
Former members re-instated or re-elected		4	96	64	134	298	
Subtotals		9	345	64	3,143	3,561	
Transfers		115	514	1,296		1,925	
Totals		124	859	1,360	3,143	5,486	
Deductions							
Died		36	71	68	33	208	
Resigned		2	46	110	119	277	
Dropped		2	75	232	376	685	
Subtotals		40	192	410	528	1,170	
Transfers			115	419	1,391	1,925	
Totals		40	307	829	1,919	3,095	
Net Changes		84	552	531	1,224	2,391	
Membership							
April 30, 1949	8	1,172	8,669	8,637	12,305		30,791

Table X. Deaths of AIEE Members Reported in Electrical Engineering

Name	Date of Election	Date of Death	Grade at Death	Obituary Notice in Electrical Engineering
Adams, Lee F.	A '09	Oct. 14, '48	F	Dec. '48, p. 1217
Adamson, Ralph T.	A '44	Mar. 19, '48	A	June '48, p. 613
Archibold, William K.	A '94	Oct. 27, '48	M	Dec. '48, p. 1219
Atwater, De Nyse W.	A '34	Apr. 13, '48	A	June '48, p. 613
Bachman, Elwood	M '40	Dec. 14, '48	M	Mar. '49, p. 271
Baker, Carey W.	M '34	July 5, '48	M	Sept. '48, p. 920
Bancroft, Charles F.	A '95	Oct. 25, '48	F	Dec. '48, p. 1219
Barrett, Sampson K.	A '11	Dec. 23, '48	M	Mar. '49, p. 269
Bassett, Allen	A '23	Nov. 19, '47	A	May '48, p. 503
Becker, Alvin G.	A '47	Oct. 18, '48	A	Jan. '49, p. 79
Bergrun, Ted	A '44	Apr. 1, '48	A	June '48, p. 613
Bijl van der, Hendrik J.	M '17	Dec. 2, '48	M	Feb. '49, p. 177
Bonine, Charles E.	A '03	Oct. 25, '48	M	Dec. '48, p. 1218
Booth, William T.	A '03	Apr. 11, '48	M	Aug. '48, p. 791
Borden, Stephen W.	M '16	May 13, '48	M	Aug. '48, p. 791
Bowman, Sr., James C.	A '40	June 30, '48	M	Sept. '48, p. 920
Brainerd, Frank K.	A '08	Dec. 6, '48	F	Feb. '49, p. 177
Buell, Henry H.	A '11	Jan. 12, '48	M	May '48, p. 503
Burkholder, Charles I.	A '03	Mar. 13, '48	F	June '48, p. 612
Cadwallader, James A.	A '15	Dec. 20, '48	F	Mar. '49, p. 270
Carr, John O.	A '22	Aug. 24, '48	A	Dec. '48, p. 1219
Champlin, Franklin J.	A '20		A	Nov. '48, p. 1115
Chipperfield, John W.	A '22	Mar. 16, '48	M	June '48, p. 613
Colpitts, Edwin H.	A '11	Mar. 6, '49	F	May '49, p. 460
Colvin, Clare W.	A '12	Oct. 9, '48	M	Jan. '49, p. 79
Davis, Benjamin	A '39	Oct. 8, '48	A	Dec. '48, p. 1219
Day, George C.	A '45	Nov. 13, '48	A	Mar. '49, p. 271
Diamond, Harry	F '47	June 21, '48	F	Aug. '48, p. 790
Dubs, Ford H.	A '27		A	Jan. '49, p. 79
Durland, D. C.	A '08	Oct. 19, '48	A	Dec. '48, p. 1219
Elson-Dew, William	A '08	Dec. 16, '47	F	June '48, p. 613
Flood, Jr., Henry	A '10	June 17, '48	F	Aug. '48, p. 790
Forman, Alexander H.	A '16	June 30, '48	F	Sept. '48, p. 920
Frankenfield, Budd	A '97	Feb. 1, '48	M	June '48, p. 612
Garretson, Harry D.	A '07	Feb. 12, '49	ML	Apr. '49, p. 366
George, Frederick R.	A '13	June 1, '48	ML	Sept. '48, p. 919
Glasso, John G.	A '03		F	Aug. '48, p. 791
Gordon, Leslie B.	A '25	Apr. 8, '48	M	June '48, p. 613
Gorsuch, William S.	A '07	June 13, '48	M	Sept. '48, p. 919
Gowan, Arthur J.	A '23	Aug. 17, '48	A	Dec. '48, p. 1219
Graf, Robert J.	A '11	Jan. 2, '49	A	Mar. '49, p. 271
Haar, Selby	A '07	Sept. 5, '48	M	Jan. '49, p. 79
Haller, Cecil E.	A '43	July 6, '48	A	Dec. '48, p. 1218
Hamlin, Edwin W.	A '35	Apr. 27, '48	M	July '48, p. 714
Hancock, Edward A.	M '38	Feb. 26, '48	M	May '48, p. 503
Herring, Edgar J. C.	A '29	Oct. 28, '48	M	Mar. '49, p. 271
Herron, James H.	M '35	Mar. 29, '48	F	Aug. '48, p. 790
Hill, E. Rowland	A '99	Aug. 25, '48	F	Dec. '48, p. 1217
Hill, Frederick W. L.	M '24	Jan. 12, '49	F	Mar. '49, p. 271
Horley, R. E. G.	A '21		A	Dec. '48, p. 1219
Hoseason, Donald B.	A '22	July 16, '48	M	Oct. '48, p. 1021
Humphrey, Clifford W.	A '03	July 6, '48	F	Nov. '48, p. 1115
Jackson, John P.	A '92	Apr. 2, '48	F	June '48, p. 612
James, Tudor C.	A '18	July 3, '48	M	Oct. '48, p. 1021
Jones, Archer K.	A '16	Sept. 6, '48	A	Dec. '48, p. 1219
Jones, Reginald L.	A '11	Jan. 14, '49	F	Mar. '49, p. 270
Kelsall, George A.	A '10	Jan. 4, '49	A	Mar. '49, p. 270
Kenyon, Otis A.	A '06	Feb. 3, '49	M	Apr. '49, p. 365
Knight, George L.	A '11	Mar. 27, '48	F	June '48, p. 612
Knouse, Walter E.	A '27	Dec. 4, '48	A	Feb. '49, p. 177
Lately, Harry N.	A '04	July 11, '48	F	Sept. '48, p. 920
Law, Raymond K.	A '47	Feb. 23, '49	A	Apr. '49, p. 365
Lawson, John E.	A '22	July 23, '48	A	Oct. '48, p. 1022
Lear, John E.	A '03	Aug. 17, '48	M	Nov. '48, p. 1116
Lee, Lloyd L.	A '46	Aug. 14, '48	A	Nov. '48, p. 1115
Linebaugh, Jesse J.	A '06	Aug. 2, '48	A	Nov. '48, p. 1116
Littler, Raymond G.	M '44	May 1948	M	Oct. '48, p. 1022
Long, Thomas H.	M '44	Jan. 18, '49	M	Apr. '49, p. 366
Mackenzie, Norman	A '43	Dec. 13, '48	A	Mar. '49, p. 270
Mahoney, Francis W.	A '09	Aug. 21, '48	M	Dec. '48, p. 1219
Manion, William J.	A '33	Feb. 18, '48	A	May '48, p. 503
Mapes, Leland R.	M '29	May 1, '48	F	Sept. '48, p. 920
Marti, Othmar K.	A '21	Feb. 15, '49	F	Apr. '49, p. 365
Martin, Allan F.	A '36	Mar. 2, '48	A	May '48, p. 503
Mason, Frank H.	A '10	Dec. 17, '48	A	Mar. '49, p. 270
Maurer, Keith L.	M '30	Feb. 23, '49	M	Apr. '49, p. 365
Meyers, Robert S.	A '37	Dec. 12, '48	M	Mar. '49, p. 270
Miller, Eugene H.	M '25	Mar. 12, '48	M	June '48, p. 612
Mills, John	A '11	June 14, '48	F	Aug. '48, p. 790
Milnor, Joseph W.	A '13	Mar. 30, '49	F	May '49, p. 460
Moloney, Thomas O.	A '12	Jan. 30, '49	F	Apr. '49, p. 366
Moritz, Charles J. H.	A '02	June 27, '48	F	Oct. '48, p. 1022
Moser, Matthew X.	A '25	Feb. 3, '49	M	Apr. '49, p. 366
MacFadden, Samuel P.	A '19	May 23, '48	M	Sept. '48, p. 920
MacGregor, Willard H.	A '97	Dec. 19, '48	M	Feb. '49, p. 177
MacMuray, Charles F.	A '13	Aug. 24, '48	A	Nov. '48, p. 1116
McClure, Earl L.	A '37	Sept. 2, '48	M	Dec. '48, p. 1218
McKearin, James P.	A '11	Apr. 24, '48	F	Aug. '48, p. 791
McKinney, Henry H.	M '47	Apr. 13, '48	M	Aug. '48, p. 791
McLean, William	M '42	Dec. 17, '48	M	Mar. '49, p. 271
Needham, Robert J.	M '23	Oct. 25, '48	M	Mar. '49, p. 270
Nill, Edwin P.	A '41	May 20, '48	A	Aug. '48, p. 791
Orwell, Albert E.	A '44		A	Mar. '49, p. 271
Peterson, Arthur P.	A '32	July 16, '48	M	Nov. '48, p. 1115
Post, Charles R.	A '39	Feb. 18, '48	A	June '48, p. 613
Powell, David A.	M '45	Dec. 19, '48	M	Mar. '49, p. 270
Powell, James A.	M '31	June 9, '48	M	Aug. '48, p. 790
Pratt, William H.	A '02	May 29, '48	F	Sept. '48, p. 919
Price, Bernard	A '10	July 9, '48	A	Dec. '48, p. 217
Pufler, William L.	A '93	Mar. 8, '48	F	June '48, p. 614
Rawkins, Herbert L.	A '30	Feb. 17, '48	M	May '48, p. 503
Reid, William E.	M '36	Jan. 23, '48	M	June '48, p. 613
Rentschler, Harvey C.	M '40	Mar. 23, '49	M	May '49, p. 460
Riggs, Arthur F.	M '16	Oct. 30, '48	F	Feb. '49, p. 177
Rockwell, Robert L.	A '13	Feb. 11, '48	M	May '48, p. 503
Rockwood, Jr., George H.	A '26		M	July '48, p. 715
Rushmore, Samuel W.	A '00	Aug. 16, '48	A	Dec. '48, p. 1218
Sah, Adam Pen-Tung	A '35	Feb. 14, '49	F	Apr. '49, p. 366
Samuels, Maurice M.	F '24	Jan. 29, '49	F	Mar. '49, p. 271
Shire, Leo E.	A '27	July 31, '48	A	Nov. '48, p. 1116
Sloan, Kenneth H.	A '38	Dec. 31, '48	M	Apr. '49, p. 365
Smeaton, James H.	A '07	Oct. 30, '48	A	Jan. '49, p. 79
Smith, Howard E.	A '44	Apr. 25, '48	A	June '48, p. 612
Smith, Jr., Walter F.	A '23	Feb. 9, '49	M	Apr. '49, p. 366
Snow, Wilber C.	A '20	May 20, '48	M	Dec. '48, p. 1218
Spencer, Charles G.	M '22	Aug. 16, '48	M	Nov. '48, p. 1116
Stayner, Charles M.	A '20	Nov. 19, '48	M	Mar. '49, p. 270
Sterne, William C.	A '23	Nov. 28, '48	M	Feb. '49, p. 177
Thompson, Jesse L.	M '40	Jan. 13, '49	M	Apr. '49, p. 365
Twyford, George T.	A '21	Dec. 6, '48	A	Mar. '49, p. 271
Unger, Arthur M.	A '40	Sept. 1948	A	Dec. '48, p. 1218
Warren, Aldred K.	A '95	Nov. 20, '48	M	Jan. '49, p. 79
Watts, Frank W.	A '24		F	May '48, p. 503
Werwath, Oscar	A '19	Mar. 20, '48	M	June '48, p. 613
White, Peter	A '37	Dec. 12, '48	A	Feb. '49, p. 177
White, William M.	M '21	Feb. 9, '49	M	Apr. '49, p. 366
Wilson, Charles C.	M '43	Aug. 12, '48	M	Oct. '48, p. 1021
Wilson, Jr., Joseph C.	A '44	July 14, '48	A	Sept. '48, p. 920
Wilson, William	M '23	May 6, '48	M	July '48, p. 715
Wood, Albert C.	A '10	Mar. 13, '49	M	May '49, p. 460
Work, William R.	A '08	Oct. 3, '48	F	Dec. '48, p. 1218

to the Section membership chairmen suggesting ways of increasing membership and committee activities. In addition to this, the vice-chairmen made many personal visits to Sections encouraging membership work. All Districts showed a gain in membership applications except District 8. The greatest gain was 57 per cent by District 9, with District 7 close behind. District 7 showed the greatest activity per member, having applications totaling 21.1 per cent of the membership at the beginning of the period.

Individual membership committees are of course primarily responsible for these gains. The committees had more members on the average and were particularly active in handling personal contacts with prospects. The greatest difficulty is still in the delay in organizing committees. Few Section membership committees begin active solicitation before the first of the year, which leaves only four months of concentrated effort.

The new program for soliciting Associate applications from Student members before departure from college was inaugurated this year. It is expected that this will stimulate membership and aid the Membership Committees. This program was developed through the efforts of the Membership and Student Branches Committees.

Two active subcommittees are working on membership problems. J. C. Woods, Vice-Chairman of the Membership Committee, is acting as chairman of a joint subcommittee with the Committee on Student Branches to study Student membership in the Branches. It is expected that this group will recommend methods of increasing Student membership and standardizing practices among the various universities and colleges.

Walter C. Bloomquist, Vice-Chairman, District 1, is acting as chairman of a subcommittee to prepare a proposal for improving the function of interesting prospective members in the Institute. A revision of the "Membership Information" bulletin has been proposed.

The key to a successful membership promotion program still rests with the individual initiative of the Section membership chairmen. Earlier selection of committees, use of larger committees, and more activity in finding and soliciting prospects are the three objectives to which each must strive. These committee chairmen have done an outstanding job this year but much ground is still to be gained in the year ahead.

Professional Group Committees

COMMITTEE ON CODE OF PRINCIPLES OF PROFESSIONAL CONDUCT

The committee has dealt with only two matters of importance, beyond incidental correspondence upon minor matters not requiring further attention. These were a new Statement or Code of Principles of Professional Conduct, and action of the Southwestern Power Authority, United States Department of the Interior, in soliciting competitive bids for engineering service.

In regard to the first matter, work held over from last year has continued upon the formulation of a formal Statement of Principles of Professional Conduct which will combine the newer Engineers Council for Professional Development canons, or ethical principles, with certain additional rules of practice which have had a long and honorable history in the Institute code.

The second matter involved a case where a Federal bureau advertised for competitive proposals for professional electrical engineering services. That matter was closed with our detailed report to the Board of Directors. It appeared that the bureau officials needed outside engineering service, but were advised that under existing law and regulations they had no other way of securing it. This committee found no violation of the new canons or the old code, but believed that the Institute should not approve or encourage such practice, and that necessity for it should be removed by legislative or executive action.

COMMITTEE ON EDUCATION

Four sessions have been individually or jointly sponsored at general meetings as follows.

1. At the Summer General Meeting, papers by two Mexican and three American authors dealt with education in Mexico, and with philosophical side of engineering education.

2. At the Midwest General Meeting, a conference was sponsored jointly with the Committee on Student Branches to promote interest among engineering students and faculties in electric power engineering. This activity was undertaken because the committees thought that students have been preparing for careers in electronics and communication in numbers proportionately much greater than employment opportunities warrant. Four papers, on careers in power engineering, unsolved problems, and better ways of teaching in the field were given to a large audience whose interest was exhibited by a spirited discussion.

3. At the Winter General Meeting, one conference was held on the theme "Industry's Active Part in Education." Four papers were presented, two from industry, two from educational institutions. The papers dealt with co-operation between colleges and industry at the undergraduate and graduate levels and with the development of the young engineer after entering industry. Another conference was sponsored jointly with the Subcommittee on electronic Education of the Committee on Electronics on the theme "Education in Power Electronics." Five papers were presented showing how the subject of power electronics could be employed to great advantage as a medium of instruction.

A session is planned for the Summer General Meeting on the accreditation of electrical engineering curricula. It is thought that the value of Engineers Council for Professional Development accreditation will be enhanced by a wider understanding of its objectives and procedures. At later meetings, it is planned to present and discuss other activities of the ECPD within the field of electrical engineering education. With these subjects and others, the committee looks forward to being able to sponsor interesting sessions at three of the general meetings each year.

At the invitation of the Engineers Council for Professional Development, the committee has undertaken a revision of Section IV, Electrical Engineering, of the ECPD Selected Bibliography of Engineering Subjects. The efforts of many members of the committee who have given generously of their time have brought this work very near to its completion.

In addition to these activities, the committee has considered and is currently considering other questions: the report of the President's Commission on Higher Education, industrial experience for foreign students, co-operation with Sections of the Institute in educational programs, and the acquainting of students with the facts of professional registration and licensing, the last jointly with the Committee on Registration of Engineers.

The committee thinks it can be most effective if it deals with problems that require the co-ordinated efforts of the engineering teacher, the practicing engineer, and industrial and governmental organizations. Thus, it is recommended that in appointing new personnel, there be more nearly equal representation from industry and colleges than at present.

COMMITTEE ON REGISTRATION OF ENGINEERS

The committee has continued its activities in connection with efforts to advise AIEE membership regarding the advantages of registration as a professional engineer and also as to the procedures for registration in the several states. Particular emphasis has been placed upon acquainting the young engineer, both while a senior in college and during his early years of professional activity, with professional registration.

Meetings of the committee were at the Midwest General Meeting and at the Winter General Meeting. Another meeting of the committee is scheduled for the Summer General Meeting, at which time special consideration will be given to suggested changes in the Model Law.

The committee has asked Professor R. W. Sorensen and Professor A. H. Lovell to prepare a paper entitled "Registered Professional Engineers." This paper has been prepared and presented for publication in *Electrical Engineering*, with the expectation of distributing several thousand copies to the Student Branches and the Sections of the Institute, calling their attention to professional registration, its advantages, and its procedures.

The committee has addressed a letter to each of the Student Branches, suggesting that they arrange a meeting at which the Sorensen-Lovell paper could be discussed, and at which time the Student membership could be given full information regarding registration. A letter also has been addressed to the officers of each Section of the Institute, directing their attention to the Sorensen-Lovell paper, and suggesting that they give all possible assistance to the Student Branches; also that some time be devoted at a Section meeting to acquaint the general membership with registration facts.

The individual Sections also have been asked to give assistance wherever possible to the State Boards of Examination, particularly in helping them to prepare suitable questions for the examinations covering the field of electrical engineering. Encouragement wherever possible has been given to the Sections to establish refresher courses to prepare their membership for the written and oral examinations.

At the suggestion of the committee, a question regarding the status of registration was included on the "Year Book" card circulated by AIEE headquarters to the membership. It is hoped that the returns will provide additional information regarding the extent of registration among our membership.

COMMITTEE ON STUDENT BRANCHES

During the past year, the Committee on Student Branches held three meetings, each at a general meeting of the Institute. At these meetings, there were unusually important agenda items which are summarized in the following.

At the committee meeting in Mexico City, a means of revising and expediting the timetable and processes of admission of Student members to Associate grade was recommended to the Board of Directors. This was the result of a study made jointly with the Membership Committee.

The committee met at the Midwest General Meeting. Pursuant to remarks made by Past President Hull and endorsed by President Lee, the committee set up a subcommittee to work jointly with the Institute of Radio Engineers to work out recommended bylaws for the establishment of Joint Student Branches that would be acceptable to both Institutes. The committee endorsed the action of the previous committee relative to using ECPD accreditation as a necessary qualification in the establishment of Student Branches in schools within the United States.

The third meeting was at the Winter General Meeting. At this time, the Subcommittee on Joint Student Branches reported in full and presented a model set of bylaws that had been worked out with IRE representatives. The committee endorsed this report, and referred it to the Secretary of the Institute for Board of Directors' consideration. This is an important step allowing many schools now having Branches to operate in a clearcut fashion jointly with many IRE branches now in existence.

At the New York meeting, a new joint

subcommittee was established with the Membership Committee and the Sections Committee. This group will organize and undertake surveys of Student Branch membership as a function of maximum potential membership at each school. It is investigating methods used by Counselors in promoting a larger percentage of admissions of Student Members as Associates, and will inquire concerning active steps taken by Branches to insure closer co-ordination with AIEE Sections located in the same geographical area.

The committee approved the revision of "The Electrical Engineer," which was accomplished jointly with the Sections Committee, and this revision was referred to headquarters for publication.

The Committee on Student Branches jointly sponsored with the Committee on Education a session at the Midwest General Meeting covering career opportunities, teaching methods, and growth in the electrical engineering power field. This session was very well received, and all of the four papers, each by an outstanding author, have been since published in *Electrical Engineering*.

During the past year, the committee has had referred to it seven requests for permission to establish new Student Branches. After complete consideration in each case, the committee recommended four for favorable consideration of the Board of Directors, and to date three charters have been approved. These Branches are located at the following schools:

Louisiana Polytechnic Institute

Fenn College

Instituto Tecnologico y De Estudios Superiores De Monterrey

Technical Committees

Co-ordinating Committees

POWER, INDUSTRY, COMMUNICATION AND SCIENCE, GENERAL APPLICATIONS

Organizational Changes. The technical committees have continued to function under four co-ordinating groups as established by the Board of Directors on April 23, 1947. It has been found that the co-ordinating committee meetings have been very valuable to the work in each group, and they have, to a considerable extent, facilitated the efforts of the individual technical committees. Problems relating to organization of technical committees received careful study by the co-ordinators, culminating in the following:

1. The Committee on Electronic Power Converters was transferred from the Power Group to the Communication and Science Group. This action was taken to reduce the number of technical committees within the Power Group from 12 to 11, also placing the committee in the group where it could carry out its work more effectively. At the same time, this change tended to equalize the number of committees within the co-ordinating groups. The creation of additional co-ordinating groups with the numbers of committees similarly limited will insure more effective operation under the co-ordinating group plan of organization.

2. A fifth co-ordinating group was created by splitting the Communication and Science Group into two groups, one for Communication and the other for Science and Electronics. This gives more prominence to Communication and Electronics, and elevates these subjects to positions commensurate with their importance in the field of electrical engineering.

3. The Metallic Rectifier Subcommittee has been advanced to full technical committee status. Upon recommendation of the Chairman of the Committee on Chemical, Electrochemical, and Electrothermal Applications of the Industry Group, this committee has been transferred to the Science and Electronics Group. It is believed that this arrangement will provide desirable liaison between the several technical committees of relatively common interests, since metallic rectifiers appear to have much in common with electronics and basic sciences.

4. The growing importance of servomechanism applications would seem to indicate the need of a full technical committee on this subject, which currently is being handled by subcommittees of several technical committees. The matter has been under study, which will be continued during the ensuing year.

5. In accordance with a resolution by the Committee on Planning and Co-ordination to the effect

> "That it is the sense of the Committee on Planning and Co-ordination that the number of committees (11) in the Power Group may be too large for effective operation, and, therefore, the Power Group Co-ordinating Committee should give consideration to the desirability of dividing it into two groups,"

a letter ballot canvass was conducted among the members of the Power Co-ordinating Committee on the proposal to split the Power Group into two groups, one for Power Equipment, and the other for Power Systems. A majority favored the proposal, with a strong minority in opposition thereto. The matter remains unsettled, pending further study and consideration.

Committee Scopes. Experience during the year has demonstrated successful operation under the scope previously prepared for each technical committee. Accordingly, the policy of having scopes available for all committees at Institute headquarters was extended to include all subcommittees, working, and project committees.

Technical Conferences. The number of technical conferences on specialized subjects scheduled during this year has been greatly increased, and this development promises to become one of the more important Institute activities. A written statement on the policy with respect to technical conferences has been completed in the form of a manual for the guidance of technical committee chairmen who may plan to sponsor such conferences. The co-operation and contribution of J. C. Strasbourger, Chairman of the Sections Committee, toward completion of this project is gratefully acknowledged. Plans for joint sponsorship with IRE of annual technical conferences on semiconductors have been completed, with recommendation for approval of this undertaking pending.

Committee Publicity. With the April 1949 issue of *Electrical Engineering*, a new department was created titled "Committee Notes," the object being to provide publicity on technical committee activities, which it is hoped will be interesting and beneficial to the Institute members.

Power Group

COMMITTEE ON CARRIER CURRENT

The Committee on Carrier Current held three meetings. In addition to the committee meetings, a full technical session was sponsored at the Midwest General Meeting, and a combined technical and conference-type session at the Winter General Meeting. At these meetings, a total of four *Transactions*-type papers, three committee reports, and four conference-type papers were presented.

The following projects are being followed actively, or have been completed during the past year, as indicated by the individual listings in the following:

1. A project committee is preparing a general-interest paper covering the status of carrier current in power system operation.

2. A survey was made and a report presented in Milwaukee outlining the subject of methods of measurements at carrier frequency. Project completed.

3. A working group is collecting data on the carrier current characteristics of transmission lines and systems.

4. A working group is collecting information on the carrier current characteristics of power equipment.

5. A subcommittee has been appointed to prepare information that would permit writing an application guide for carrier-current equipment. A working group prepared and presented a report on coupling capacitors and traps for rural line carrier telephone applications. Work completed.

6. A working group prepared and presented a report on the use of microwave equipment for relaying, telemetering, and supervisory control. This study of the application of microwave equipment for power system uses will continue.

7. A working group has been appointed to obtain data as to the operating experience with carrier current channels with the intention of publishing a committee report indicating the expected reliability of such channels.

8. A subcommittee has been appointed to study the requirements for tubes for carrier current applications and to report from time to time on the status of this subject.

COMMITTEE ON INSULATED CONDUCTORS

This report covers the work of the committee, which until 1947 functioned on a limited basis as the Cable Subcommittee of the Committee on Transmission and Distribution.

Committee Meetings. Committee meetings have grown from 1- to 2-day sessions, the first portion being devoted to individual subcommittee meetings. The committee held two meetings during the past year with an average attendance of 47.5.

Subcommittee Organization. To effect functioning of this newly created committee it was organized into 12 standing subcommittees as follows: Administration, Standards and Publications, Cable Characteristics, Conductors, Insulations, Sheaths and Coverings, Cable Supply Systems, Utilization Wiring Systems, Special-Purpose Cable, Accessories, Structures, and Tests and Measurements. It is recommended that the standing subcommittee type of organization be continued. This plan is preferred to the project type because it is more productive of sponsored papers, which is one of the primary objectives of an AIEE committee. Also, it avoids the administrative detail and time lag involved in setting up new working groups as each project is suggested for study.

Technical Papers. The committee has reviewed a number of papers, and 11 were scheduled at meetings held during the past year. In addition, five papers will be on the program of the Summer General Meeting. The committee is making an effort to sponsor papers on topics neglected heretofore, or inadequately covered recently, and to include papers on engineering practices as well as on new developments in the art.

Standards. During the past 30 or so years the AIEE has not been a factor in the field of standards for either bare or insulated conductors. To some extent, this situation is attributable to the fact that, until 1947, the subject of conductors was not recognized with autonomous technical committee status. At present, the generally accepted major industry standards and specifications for conductors are sponsored by eight organizations. It is evident that the AIEE plays a very minor role in standards for conductors, and will continue to do so unless there is a major change in policy by the established sponsoring organizations. Standards under consideration by the committee are as follows: Wires and Cables (AIEE 30–1944); Low-Voltage Air Circuit Breakers (AIEE 20A–1946); Recommended Practice Electric Installations on Shipboard (AIEE 45–1948); Potheads (AIEE 48–1948); Cable Limiters; and Test Code for Paper-Insulated Power Cables.

Subcommittee Projects. A project numbering system for the numerous activities of the subcommittees has been adopted. The advantages of this system are

1. Helps the chairman co-ordinate and follow the various subcommittee activities.
2. Assists the secretary in preparing co-ordinated and continuous issues of minutes.
3. Assists in the preparation of annual reports.
4. Tends to keep letters confined to one subject.
5. Provides an automatic filing system.
6. Helps to provide continuity of effort and to avoid repetition of work from one administrative year to the next with changing chairmen and personnel.

Numerous projects are being considered by the subcommittees.

Co-ordination With EEI and AEIC. To avoid duplication of effort, an informal working agreement was effected with the Edison Electric Institute and the Association of Edison Illuminating Companies. In general, it is based on the principle that in case of possible duplication the AIEE will not actively engage in the project, provided the EEI and AEIC intend to publish the results of their work. In some cases the publication facilities of the AIEE will be utilized for this purpose.

General. At the request of the Power Group Co-ordinating Committee, consideration was given to the formation of a Pacific Coast Subcommittee. However, it was decided not to organize this subcommittee, as few if any meetings could be held because of the distances involved. Since the participation in subcommittee work would be by correspondence in either event, it was thought preferable for the Pacific Coast members to be in contact directly with the subcommittees rather than through a Pacific Coast Subcommittee. Studies are being conducted through the subcommittees on many interesting and valuable projects.

COMMITTEE ON POWER GENERATION

Five technical sessions were sponsored by the Committee on Power Generation during the year. A total of 13 technical and 5 conference papers were presented at these sessions. In addition, the committee held two meetings during the year, the first at the Midwest General Meeting, and the second at the Winter General Meeting. Subjects covered by the papers were

1. Hydroelectric station design and operation.
2. Speed governing of multivalved steam turbines.
3. Speed governing of automatic-extraction steam turbines.
4. System load division by accurate time control.
5. Hydraulic model of liquid-cooled turbine-alternator rotor.
6. Outage rates of steam turbines, boilers, and hydro units.
7. Gas turbine design, theory, and testing.

At the last meeting, plans were laid to hold a technical conference on the subject of "Problems of Meeting Load Demands With Limited Reserve in Light of Maintenance and Forced Outages." Time and place of the proposed conference are to be settled later.

Activities of the committee are delegated to the subcommittees which reported as follows during the year:

Prime Movers. Two sessions on gas turbines were presented at the Winter General Meeting. Three technical papers and four conference papers were presented on different aspects of these new prime movers in respect to stationary power generation. Plans are under way to organize a joint committee with the American Society of Mechanical Engineers to consider the problem of standardizing steam turbogenerators, 7,500-kw capacity and under.

Speed Governing. During the year, the speed governing specifications that had been in trial use were recommended to be accepted for standard practice. One session at the Midwest General Meeting was sponsored to present two papers on speed governing, one paper on load division, and one paper on liquid-cooled rotor. Four papers on speed governing are being organized for the Fall General Meeting.

Station Design. A session of two or three papers on station auxiliaries is being organized for the Summer General Meeting. A program of papers for the Winter General Meeting, 1950, is being planned on the subject of centralized control in generating stations.

Excitation Systems. Two papers had been initiated by this group during the year and presented at jointly-sponsored sessions held during the Winter General Meeting. The working group on definitions has produced about 12 definitions relating to excitation systems. These will be presented to ASA Committee *C-42* for consideration and inclusion in its project on electrical definitions.

Application of Probability Methods. Outage data on steam and hydro-units collected under the auspices of the Edison Electric Institute have been published by the AIEE as a project of this subcommittee. A bibliography on probability methods is being compiled as well as a collection of definition of terms. A survey is under way of the load scheduling methods and spinning reserve practices being used by various utility systems in the United States. Papers are being solicited for the 1950 Winter General Meeting on the development of short-cut methods in probability calculations and on the probability of forecasting errors.

Hydroelectric Systems. Seven papers were presented at the Summer General Meeting, and at the Pacific General Meeting. Three papers are in preparation or available for future meetings.

Pacific Coast. A paper describing the available test procedures for determining performance of large hydroelectric turbogenerator units will be solicited. Plans are being made to collect statistical data on electrical characteristics of recently installed hydro generators feeding extensive high-voltage long-distance transmission systems. It is intended to make qualitative and quantitative analyses of these data and to determine the reasons for selecting the various characteristics.

COMMITTEE ON PROTECTIVE DEVICES

The activities of the committee, carried on by three subcommittees, were as reported in the following.

Fault Limiting Devices Subcommittee. The "Application Guide for the Grounding of Synchronous Generator Systems," will deal with the different methods of grounding synchronous generator systems, such as unit, more than one generator on a bus without feeders, generators on a bus with feeders, and so forth. It will discuss the various methods of grounding, such as potential transformer, distribution transformer, resistance, reactance, and direct grounding. The basic considerations in grounding will be discussed, and the accepted and preferred methods will be summarized with the advantages and disadvantages of the various methods pointed out. It is expected that the guide will be presented at the Fall General Meeting.

The "Application Guide for the Grounding of Transmission Systems," will deal with the basic factors and the different methods of grounding transmission systems of 22 kv and above. It will present the acceptable methods of providing grounding connections on transmission systems. It discusses in general terms ground relaying, limitation of ground fault currents, arrester protection, and transient overvoltages. Grounding transformers, grounding reactors, grounding resistors, and ground fault neutralizers are reviewed with regard to their proper application. This guide is intended to summarize briefly those methods of grounding transmission systems which are considered to be best practice.

The "Guide for Application of Ground Fault Neutralizers," reviews the voltage, current, frequency, and time ratings of ground fault neutralizers, application criteria dealing with location and number of units, system insulation levels, electric-static balance to ground, system interconnections, and possible effect on loading of transformers. Operating information dealing with tuning and testing after installation is discussed. It is expected that the guide will be presented at the Fall General Meeting.

The "Bibliography of Literature on Grounding Devices," will be divided into two parts: Bibliography on Resonant Grounding (Neutralizer Grounding), which will be complete through 1947 for presentation at the Fall General Meeting, and Neutral Grounding Devices in general, which is still incomplete, with no definite indication as to its completion date.

The "Field Survey of Unbalanced Charging Currents," is intended to determine whether the unbalanced charging currents of transmission lines were sufficiently large to justify the requirements in the AIEE Standard for Neutral Grounding Devices, which requires the ability of ground fault neutralizers to be capable of carrying 30 per cent circulating current continuously. This survey has been completed and the results will be presented at the Fall General Meeting.

The "Power System Fault Limitation" report is being prepared on methods used to limit fault currents on a metropolitan underground system; a system composed of overhead transmission and use of series reactors. With the increases in generating, transmission, and distribution facilities that are being made, it is important to limit the short-circuit kilovolt-amperes to a reasonable value. This is true both from the standpoint of the installation of new equipment and also from the standpoint of overduty on existing circuit breaker installations.

Lightning Protective Devices Subcommittee. The "Application Guide for Lightning Protection of Substations," will deal with the selection and application of lightning protective devices for the protection of equipment in substations. Factors taken into consideration will include system operating conditions, distance of protective devices from apparatus protected, grounding conditions, and other related factors. Included in the guide will be problems peculiar to some unit-type stations where, because of cable connections, the location of lightning protection equipment may be a considerable distance from protected equipment. It is expected that this guide will be completed and presented at the Fall General Meeting.

The subcommittee is preparing a revision and combination of AIEE Standards 24, Protective Tubes; 28, Lightning Arresters for A-C Power Circuits; and 47, Expulsion-Type Distribution Lightning Arresters. Agreement has been reached on all of this proposed Standard, except for the dielectric tests on the insulation assemblies of the so-called grounded neutral arresters. It is expected that values for these tests will be agreed upon shortly so that the Standard may be reported to the main committee, with the possibility that a covering paper could be presented at the Fall General Meeting.

A report on "Performance Characteristics of Lightning Protective Devices," of present-day station-type 20- to 73-kv line-type 3- to 15-kv distribution arresters, line-type expulsion arresters (expulsion tubes), and rod gap characteristics, is in preparation. It will combine in one place the important characteristics of the various types of protective devices available. It is expected to be presented at the Fall General Meeting. This activity is followed closely by the AIEE delegation to the Triple Joint AIEE-EEI-NEMA Committee on Insulation Co-ordination.

A symposium on "Recovery Voltage Characteristics of Distribution Systems," was presented at the 1949 Winter General Meeting, covering both field and laboratory test data on the recovery voltage characteristics of distribution systems. These data now are being correlated with the probable range of pertinent parameters of existing systems, and the next step will be to make use of them in setting up duty cycle test specifications for incorporation in a future revision on that part of the combined arrester Standard dealing with expulsion arresters. These data also should prove useful to other groups concerned with Standards on distribution circuit fuses, circuit reclosures, and so on.

This activity has been carried on by a joint working group sponsored by both the Lightning Protective Devices Subcommittee and by the General Systems Subcommittee of the Committee on Transmission and Distribution.

Co-ordination of Insulation Subcommittee. This subcommittee was established to handle problems within the Committee on Protective Devices dealing with co-ordination of insulation. Its function has been to keep the members of the main committee informed concerning the activities of other committees that are doing work dealing with insulation co-ordination.

COMMITTEE ON RELAYS

The technical activities of the committee have required three meetings, and one to three meetings of each of its ten project committees. The 11 formal and six conference papers presented have included one final committee report and one preliminary report. A conference session was sponsored at the Winter General Meeting. Revised Standards for power relays have been prepared and are being submitted to the Standards Committee. The principal technical activities were carried on through project committees, which are appointed to fulfill specific assignments.

Generator Protection. Investigation of loss of excitation of generators and associated protection methods has provided further data for a committee report now being formulated to summarize the protection of a-c generators. Two conference papers on this phase of the problem will be presented at the Summer General Meeting. The influence of partial winding faults to ground on the capability of relaying systems to provide positive protection is receiving particular attention, especially in view of neutral grounding schemes which limit fault current to small values with faults at the generator terminals. Papers are being encouraged to provide better methods for calculating the currents associated with partial winding faults with various grounding methods.

Bibliography of Relay Literature. An interim report covering references to technical articles on relaying in the American and foreign press which have been published since the last formal report of this project committee has been distributed to the committee and other interested individuals. It is planned that another formal report covering three years will be available in 1950.

Co-ordination of Construction and Protection of Distribution Circuits (Joint Group). This joint working group of the AIEE Committee on Relays, the AIEE Distribution Subcommittee, and the EEI is continuing with the study of correlation of distribution circuit construction and protection practices. Three meetings of the group were held. As a result of these activities, some 30 electrical utilities are participating in a study which will provide performance data on representative distribution circuits. Special records are being kept on the number of transient and sustained faults, the extent and duration of interruptions to customers, and the correlation of this information with construction and protection details such as, relay settings, protection, conductor size, material, covering and spacing, span length, surge protection.

Standards for Power Relays. The project committee has completed a final draft of a proposed revision of ASA Standard C-42, "American Standard for Relays Associated with Electric Power Apparatus." This draft has been approved by the project committee and the Committee on Relays, and is being transmitted to the Standards Committee. The proposed new Standard would modernize previous definitions, amplify the bases of rating, including current, voltage, temperature, range of operating voltage, and dielectric tests. For the purpose of future revisions, information is being formulated on additional performance data such as fidelity of characteristics as influenced by variations in temperature, wave form, and the like.

Insulation Levels for Relays and Control Circuits. A value of 1,500 volts alternating current has been adopted as being an adequate test voltage for the current, potential, and trip circuits of relays and associated circuits. An investigation of the standard recommended contact spacings for various types of high-speed relays showed that all of these are adequate to withstand a test of at least 1,500 volts alternating current across contacts (provided any arc suppressive devices are disconnected).

An individual paper, "Voltage Surges in Relay Control Circuits," was presented at the Midwest General Meeting, outlining the origin of transient voltages in relay circuits and reviewing methods for reducing these voltages. The Committee on Switchgear has been asked to consider a provision in future revisions of circuit breaker Standards which would require limiting the transient voltage produced by inductive "kicks" of operating solenoids to 1,500 volts crest (or lower if feasible).

Sensitive Ground Protection. A preliminary report of this project committee was presented at the Winter General Meeting. Based on additional discussions, the project committee is preparing a final report which will summarize available methods for sensitive ground protection of 3-wire systems and outline the limitations of present available methods for the protection of systems with multigrounded neutrals.

Transmission Line Protection. Back-up protection and its influence on transmission-line relaying has been given special emphasis. Three conference papers on back-up protection were presented at a conference session during the Winter General Meeting. Discussion developed that recent trends toward heavier loading of transmission lines have minimized the available inherent "back-up protection" formerly obtained as a by-product of sensitive relay settings. Several schemes for providing local back-up protection have been developed, but all appear to have undesirable limitations. A survey is underway to determine present and preferred practices in back-up protection.

Electronic Relay Applications. This project committee is seeking to develop additional favorable applications of electronic devices to protective relaying. Two individual papers were presented, one at the Midwest General Meeting, describing an actual installation of all-electronic distance relays, and the other at the Winter General Meeting covering laboratory models of electronic distance and other relays with test information. The project committee also is studying the application of microwave channels to protective relaying.

Relaying of Interconnections Between Industrial and Utility Generating Systems. This project committee is continuing its investigation of the special relaying problems encountered in the parallel operation of industrial generating systems with those of interconnected transmission systems.

Protection of Stations Without High-Voltage Switching. In line with modern trends toward simplified switching schemes, this project committee has completed a survey of present and preferred practices in the protection of stations without high-voltage switching. Increasing costs of equipment and improved reliability of power transformers have emphasized the desirability of dispensing with high-voltage circuit breakers wherever justifiable. Protection schemes include single- and 3-pole automatic grounding switches actuated by local differential relays and also various schemes of remote tripping of line circuit breakers. The work of the group was completed with the presentation of a project committee report at the Winter General Meeting. However, it is expected that certain phases of the problem may justify additional investigation, and consideration is being given to this as one of the future projects of the Committee on Relays.

Joint and Associated Projects. Through representation, the committee has participated in the activities of the Instrument Transformer Subcommittee of the Committee on Transformers with special attention to the relaying performance of current transformers and the transient performance of capacitance potential devices. Close co-ordination has been maintained with activities of the Committee on Carrier Current and a special subcommittee to study circuit breaker duty on out-of-phase switching.

COMMITTEE ON ROTATING MACHINERY

A total of 48 papers, sponsored by this committee, were presented at the AIEE meetings during the past fiscal year. Of these, 29 were presented at the Winter General Meeting. The main committee meeting was held during the Winter General Meeting. Subcommittee activities reported at this meeting are briefed in the following:

Insulation Resistance Subcommittee. Report 43A "Recommended Practice for Insulation Testing of Rotating Machinery," was presented to the committee. Final agreement on this report is expected shortly, after which it will be published as an AIEE Standard.

D-C Machine Subcommittee. Results of the 3-year motor test program on motors from 1/2 to 50 horsepower and 1,750 rpm, conducted by five co-operating electrical manufacturers, were reported at the technical sessions of the Winter General Meeting. The results indicate that a revision of Standards is necessary relative to the measurement of temperature rise on d-c machines; results on large machines differ from those obtained on small machines and additional data must be obtained on large units. Further work of the committee includes obtaining further data on temperature rises on large d-c machinery, revision of Standards on temperature rise measurements on d-c machines, the investigation of a standard method for determining short-circuit currents on d-c machines.

Fractional-Horsepower Subcommittee. Current activities of the committee include the formulation of a test code for fractional-horsepower motors. Future plans of the committee include the formation of an application guide for fractional-horsepower motors. It was agreed in committee that fractional-horsepower d-c machines, as well as a-c machines, will be covered by this committee.

Induction Machine Subcommittee. A test code for induction machines is in preparation and it is hoped that this will be completed in time for consideration at the Summer General Meeting. A session on the application of induction motors is contemplated for a future meeting.

Synchronous Machine Subcommittee. Minor revisions in the test code are contemplated.

Test Code Subcommittee. A co-ordinating subcommittee of this committee has been formed to integrate and co-ordinate test code activities.

During the discussion of these reports and other business by the main committee the following recommendations were made:

1. The Committee on Instruments and Measurements be asked to establish Master Test Code for Power Measurements.
2. The publication policy of the Institute be reviewed to permit the publication of a greater number of papers resulting from the increasing activities of the technical committees.

A report on the compilation of a bibliography on rotating machinery indicated this project is nearly complete with a total of 394 volumes having been reviewed, from which 1,408 articles have been catalogued under 12 major and 47 minor classifications. It is expected that this bibliography will be published when completed.

COMMITTEE ON SUBSTATIONS

Work in Progress. This committee, formerly the Committee on Automatic Stations, recently completed organization of its subcommittees and working groups to cover the greatly expanded scope of the committee. The main committee has assigned the projects mentioned in the following for study and possible action by the subcommittees concerned. So far, little has been accomplished on any of these projects, because they were only recently assigned.

The Automatic and Supervisory Control Subcommittee has been assigned projects relating to investigating the reliability of supervisory and automatic control for substations, and also revision of American Standard C37.2–1945 covering such equipment.

The Transmission Substations Subcommittee and the Distribution and Conversion Substations Subcommittee have in hand projects dealing with the relative merits and standardization possibilities of the 1-line diagram connections and structural design of the substations falling within their jurisdiction, also the problem of safety considerations in substation design, station lighting practices, and the problem of station auxiliary power supply for substations.

The Distribution and Conversion Substations Subcommittee also has been assigned projects covering the relative merits of circuit breakers versus reclosing fuses for small distribution substations and the choice of bus regulation versus feeder regulation for distribution substations.

The Working Group on Device Function Numbers has prepared and recently circulated a questionnaire regarding the adequacy of the present standard device numbers as established in American Standard C37.2–1945. The work of that group will be very valuable in considering the next revision of that American Standard.

The Working Group on Rectifier Switchgear, which is responsible for treatment of all matters pertaining to the design, construction, and application of switching devices, instrumentation, and protective and functioning relays for electronic power converters, has prepared a conference paper on Electronic Power Rectifier Protection that was presented at the Winter General Meeting. This paper will be followed by a formal paper of similar scope intended for presentation at the Summer General Meeting.

The Working Group on Substation Grounding Practice is responsible for investigation and study of substation grounding system design and testing practices, including consideration of the relative merits of galvanized iron versus copper electrodes. This group includes representation from two of the subcommittees of the Committee on Protective Devices.

AIEE Papers. This committee sponsored papers at a joint technical session at the Midwest General Meeting, with the Committee on Transmission and Distribution. This committee expects to sponsor a technical session at the Summer General Meeting, and also one at the Fall General Meeting.

Committee Meetings. The main committee met in Milwaukee on October 20, and in New York on January 31. A meeting also is scheduled for June 20 at Swampscott.

COMMITTEE ON SWITCHGEAR

The Committee on Switchgear sponsored technical sessions at the Midwest and Winter General Meetings. It will sponsor a similar session in June.

The committee held one meeting during the Winter General Meeting.

Proposed Standards for Automatic Circuit Reclosers for A-C Distribution Systems have been submitted to the Standards Committee with the recommendation that they be approved for a 1-year trial.

A Guide for Application of Low-Voltage Circuit Breakers has been prepared and submitted to the committee for letter-ballot. The balloting is nearly completed and indicates the acceptance by a large majority of the committee. This guide will be discussed at the Summer General Meeting.

The Subcommittee on Circuit Breakers is working on a proposed revision of ASA Standards for Power Circuit Breakers.

Last year the committee approved for submission to the Standards Committee a proposed Standard on Air Interrupter Switches and a proposed revision of Standard 22 covering "Air Switches and Bus Supports." At the committee meeting in January, it was pointed out that these two Standards had much in common and were very closely related. It was agreed that they would be combined into one, to be submitted to the Standards Committee. This combination has been made, and the combined Standard is being submitted to the Standards Committee for action.

Proposed revision of the Standard on Switchgear Assemblies, 27, was approved by the committee for submission to the Standards Committee, and has been so submitted.

COMMITTEE ON SYSTEM ENGINEERING

This report covers the work of the second year of the committee. The general program of subcommittees was continued. However, there was considerable enlarging of the committee in that 14 new members were added at the end of the first year to give broader diversification, geographically, and to strengthen the important System Planning Subcommittee.

The committee sponsored three sessions during the year—two at the Midwest General Meeting, and one at the Winter General Meeting. A total of 13 formal papers and 8 conference papers have been presented by the committee. There were two committee meetings during the year. At these meetings, plans of the committee for future meetings were outlined. The report of the program of the Power Group Co-ordinating Committee has been presented, and the reaction of the committee to the publication policies of the Institute have been discussed. In general, it has been the policy of this committee to present a full and adequate review of one phase of system engineering at any session it sponsors.

It prepared two papers for the Summer General Meeting, one covering the broad subject of the principles in the design of a utility system from the generating station through to the ultimate distribution system, and the second covering a basic change in the system frequency of one system and the problems associated therewith. Both papers were well received. The committee also prepared a paper which was presented at the Pacific General Meeting, dealing with the economics of transmission design in overall system planning.

System Planning Subcommittee. This subcommittee sponsored two papers at the Midwest General Meeting, one on the development and growth of a large all-hydro system and the second on a similar development of a metropolitan steam system. These papers emphasized the fundamental factors influencing the development of these systems and demonstrated the influence of these factors in future planning. Similar papers are scheduled for the Summer General Meeting on another type of metropolitan system using extensive subtransmission voltages, and a smaller system where the generation is located away from the load centers. There was also a paper presented at the Winter General Meeting on the use of the calculating board in system planning.

System Controls Subcommittee. This subcommittee sponsored a group of conference papers at the Midwest General Meeting, dealing with the subject of turbine and boiler design to meet fluctuating loads. These conference papers provoked so much discussion, not only at the meeting, but also in the technical press afterwards, that they were made the basis for three formal papers and two conference papers at the Winter General Meeting. This subcommittee also sponsored two papers on load control apparatus at the Midwest General Meeting, and has prepared a committee report on the status of automatic load control equipment.

System Operations Subcommittee. This subcommittee sponsored a companion group of three papers at the Midwest General Meeting on the subject, "Emergency Control of System Loads." The subcommittee also has undertaken a study of the problem of load pickup on radial and network feeders following prolonged shutdowns, made at the request of the Committee on Substations. This study is planned for presentation at the 1949 Fall General Meeting.

Interconnection Contracts Subcommittee. This subcommittee has prepared a committee report on various aspects of interconnection operations as influenced by the types of contracts. This report is being circulated only within the committee for future study.

Joint Subcommittees. Representatives also have served on two joint subcommittees, one on probability study of equipment outage, and the other on out-of-phase high-voltage switching. The Probability Studies Subcommittee presented a very complete report at the Winter General Meeting on outage records of steam and hydro-generators and boilers. It is continuing its study of variations in load and load estimating on a probability analysis basis.

COMMITTEE ON TRANSFORMERS

The committee held three meetings, with an average attendance of 21 members. The activities of this committee have been quite varied, and, at the present time, 14 main subjects are under consideration.

Co-ordinated Study of Life of Transformer Insulation Working Group. A program was drawn up for a set of pilot tests on selected class *B* and class *H* materials to be carried out by the four participating laboratories: Allis-Chalmers, Dow-Corning, General Electric, and Westinghouse. The pilot tests are intended: to permit a choice between the test methods proposed by General Electric and by Westinghouse; to train laboratory personnel in the techniques of making the tests. Apparatus and materials now are being accumulated and the pilot tests will be under way shortly.

Temperature Gradients and Hot-Spot Temperatures for Dry-Type Transformers Working Group. The work of this committee was conducted principally by correspondence without formal meetings being held. A tentative value of 110 degrees centigrade was accepted by the Committee on Transformers as the tentative limiting hot-spot temperature rise, after which this working group was dismissed.

Joint Subcommittee on Instrument Transformers. Inasmuch as the interest in instrument transformers is rather broad, an effort has been made to obtain broad coverage by obtaining representatives from other interested technical committees as well as from the Committee on Transformers.

Meetings have been held, and considerable progress has been made. Inasmuch as the subcommittee is rather large, all the work has been carried on in working groups. The following working groups have been established: Relaying Performance of Current Transformers, Test Code, Rating Factors, Grounding Instrument Transformer Secondaries, Definitions, Revision of Test Code for Metering, Separate Publication of Instrument Transformer Standards, Transient Characteristics of Potential Devices.

Subcommittee on Papers. There are nine papers available for the Summer General Meeting. The Committee on Transformers has been assigned two sessions at this meeting.

Operating Guides for Regulators Working Group. The draft of the proposed guide for the loading of oil-immersed step-voltage and induction-voltage regulators was revised several times by correspondence. Each revision was acceptable in all respects except on several fundamental points. These points were agreed upon at a meeting of the working group held on January 31, 1949.

The guide "Proposed American Standard Guide for Loading of Oil-Immersed Step-Voltage and Induction-Voltage Regulators" has been completed by the working group. A letter-ballot is being sent to each member of the Committee on Transformers for approval.

Short-Circuit Thermal Ratings of Oil-Immersed Step-Voltage and Induction-Voltage Regulators Working Groups. The work of this group is to amplify section 15.050 in ASA C57.15 to cover regulators which supply feeders having automatic reclosing circuit breakers; also to check if the regulators will withstand 25 times normal current both thermally and mechanically for the times given in the standard. Since this question was primarily one of determining from the manufacturers the short-circuit thermal and mechanical rating of regulators, the manufacturers of this equipment were consulted. In view of all of the variables involved, the following statement was generally agreed upon:

> When used on circuits with breakers having reclosing cycles, the accumulated time a regulator is subjected to short-circuit current shall not exceed that given in the above table.

This statement was to be added to ASA C57.15 immediately after the table in section 15.050. The Standard now states that regulators must withstand 25 times rated current for four per cent impedance for two seconds. All manufacturers agree that their regulators will meet this requirement.

A letter-ballot was sent to each member of the Committee on Transformers asking for approval of the statement, as a result, the original statement was changed as follows, the words in italics being added:

> When used on circuits with breaker *or other devices, such as fuses*, having reclosing cycles, the accumulated time a regulator is subjected to short-circuit current, *during one reclosing cycle*, shall not exceed that given in the above table.

This question was discussed by the Committee on Transformers. After many comments and suggestions, the problem was referred back to the working group for further consideration.

The suggestion was made that the interpretation of section 15.050 may belong in the Guide for Loading of Regulators. This will be considered, and a recommendation will be made to the Committee on Transformers by the working group at a later date. It was suggested also that similar changes should be made in the guide for loading transformers on the same point.

Subcommittee on Magnetization Characteristics of Transformers. The work of this subcommittee has been divided into three natural divisions:

1. Magnetization characteristics of transformers.
2. Effect of magnetization current on operation o air break switches.
3. Effect of magnetization current on relay problems.

Meetings have been held, and reasonable progress is being made.

Short-Circuit Requirements of Transformers Working Group. At a meeting of the working group, a proposal was drafted for revising sections of ASA C 57–12. In September, the proposal was submitted by letter-ballot to the members of the main committee. After minor revisions, it was approved and adopted by the committee.

Guides for Operation and Maintenance of Dry-Type Transformers With Class B Insulation Working Group. One meeting was held to review data assembled by means of a questionnaire to the working group members and to determine what material should be included in the guides. As a result of this meeting, a draft of a proposed guide was prepared and submitted to the members of the committee for review. Comments have been received on this draft, and a second meeting is being arranged, at which time it is hoped that a revised guide can be prepared for submission to the main committee.

Co-ordination of Insulation Working Group. This is essentially a 1-man committee, whose assignment is liaison between the committee and the AIEE group of the Joint AIEE-EEI-NEMA Committee on Co-ordination of Insulation. Two meetings of the AIEE group have been held and considerable progress has been made.

Electronic Power Converters Working Group. One man was appointed to act as the liaison representative between the Committee on Transformers and the committee on Electronic Power Converters to take care of such subjects as required co-ordination between the two groups.

Subcommittee on Method of Making Transformer Heat Runs. The work of this subcommittee is essentially a continuation of that carried on previously, and has to do primarily with the change in the ASA C 57 Transformer Standard necessary to indicate that the short-circuit method is the standard method and will be used unless otherwise specified and agreed upon. Because of a misunderstanding, serious opposition to the proposed change has arisen in one of the

EEI committees. The immediate task of the working group is to rewrite the proposal so that a misunderstanding will be impossible, and to secure sufficient data to prove that the short-circuit method is reliable and gives correct results within the same degree of accuracy as the back-to-back method.

Revision of Dielectric Tests Working Group. The working group was set up to consider changes in the insulation tests, both as to the magnitude and the technique of testing. Several changes in test procedure have been proposed. One in particular was due to an editorial error, but still remains to be corrected. Another involved changes in testing technique, particularly the use of current neutral measurements during impulse tests. A meeting was held, and tentative plans for changes were made. In order that the group should have broad coverage in the industry, it included several manufacturers' representatives and operators' representatives. Proposals were made, but several differences of opinion were expressed which were of so serious a nature that further work will be required.

COMMITTEE ON TRANSMISSION AND DISTRIBUTION

The past year was marked by continued intensive activity within the subcommittees. The product of this work will come to fruition shortly in the form of five subcommittee reports. In addition to the subcommittee meetings, there were two meetings of the general committee—the first in Milwaukee on October 20, and the second in New York on January 31. A third meeting is planned for Chicago on May 4.

Technical Meetings. Two technical sessions were sponsored by the Committee on Transmission and Distribution at the Summer General Meeting, and two at the Pacific General Meeting. At the Midwest General Meeting, one separately-sponsored session, and one jointly-sponsored session with the Committee on Substations were held. Two solely-sponsored sessions and one jointly-sponsored session with the Committee on Protective Devices were held at the Winter General Meeting. For the Summer General Meeting, one separately-sponsored session and one jointly-sponsored session with the Committee on System Engineering are scheduled.

Capacitor Subcommittee. A revision of AIEE Standard 18 on capacitors is nearing completion by the Capacitor Subcommittee. This Standard has been circulated through the main committee, and requires only slight modifications before submission to the Standards Committee for final approval. A joint report with a corresponding working group of the EEI on the performance of shunt capacitors is likewise nearing completion, and should be available for presentation at the Fall General Meeting. The Capacitor Subcommittee also will have available for presentation at that meeting a report on the maintenance of shunt capacitors.

Distribution Subcommittee. A report of this subcommittee entitled "Preliminary Report on Electric Power Distribution System Practices and Trends in the United States," was presented at the Summer General Meeting. This since has been made a final report and published in *Electrical Engineering.* A Symposium on Primary Network Systems, at which four papers will be presented, is being sponsored by the Distribution Subcommittee for the Summer General Meeting. Consideration also is being given by the subcommittee to an economic study of different values of primary voltages. The subcommittee also is engaged jointly with other groups of the AIEE and EEI in a study of the construction and protection of distribution circuits.

General Systems Subcommittee. A report by this subcommittee on "Power System Overvoltages Produced by Faults and Switching Operations," was presented at the Summer General Meeting. A co-operative survey with a corresponding group of EEI is being made on the causes of outages and operating experience on transmission lines of 100 kv and over. A session at the Winter General Meeting was sponsored in co-operation with the Committee on Protective Devices on "Recovery Rates of Voltage on Distribution Systems."

Lightning and Insulator Subcommittee. One of the active projects of this subcommittee is the preparation of a bibliography of material relating to lightning. This is a compromise with the original plan, which contemplated the correlation and publication of papers relating to the subject similar to the previous Lightning Reference Book prepared by the same subcommittee. This plan was abandoned because of cost. The subcommittee is concerning itself also with a study of recommendations for lightning-proof transmission lines. A symposium of five papers on the subject of insulator contamination and corrective measures was sponsored by this subcommittee and presented at the Midwest General Meeting.

Towers, Poles, and Conductors Subcommittee. A report by this subcommittee on the types of conductors available for use on high-voltage transmission lines was presented at the Summer General Meeting. A report on transposition is under preparation, and should be available for presentation at the Fall General Meeting.

Other Activities. The Committee on Transmission and Distribution is jointly active with other committees in two projects, the first being the investigation of high-voltage switching when out-of-phase voltage exists at the time of arc interruption, and the second is the calculation of short-circuit currents on low-voltage systems.

Co-ordination With Edison Electric Institute. Close co-operation between the Committees on Transmission and Distribution of the EEI and the AIEE has continued during the past year. As mentioned previously, the Capacitor Subcommittee, the Distribution Subcommittee, and the General Systems Subcommittee have active projects that they are carrying on with groups of the Transmission and Distribution Committee of EEI.

Industry Group

COMMITTEE ON CHEMICAL, ELECTROCHEMICAL, AND ELECTROTHERMAL APPLICATIONS

The committee held one meeting, in New York during the Winter General Meeting. The accomplishments of the past year were reviewed and plans discussed for the coming year. The scope of each subcommittee was reviewed and specific projects outlined for 1949.

This technical committee is now composed of the following subcommittees: Arc Furnaces and Electrothermal Processes; Electrolytic Processes; Cathodic Protection; Metallic Rectifiers; Petroleum Refining and Production; Batteries, Battery Forming, and Charging; Chemical Industries. The subcommittees engaged in the following activities during the year.

Arc Furnaces and Electrothermal Processes. This subcommittee is studying to establish good engineering practices in these fields. Problems relating to design and installation are of particular interest and a number of papers covering selected phases of the subject will be sponsored in 1949.

Electrolytic Processes. This subcommittee held a meeting during the Winter General Meeting to discuss future plans. It is continuing its work on matters relative to theory, technique, plant efficiency, application of power conversion equipment, and operating hazards. It is engaged in the preparation of a subcommittee report on the influence of electrolytic cell line characteristics on the selection of electric power and conversion equipment.

Cathodic Protection. This subcommittee now is working on a report relative to design and operation of apparatus and systems to minimize corrosion. A number of papers on corrosion prevention will be sponsored this year.

Metallic Rectifiers. This subcommittee is continuing its standardization work on metallic rectifiers. Two technical sessions are planned for the Summer General Meeting on theory, design, and application of metallic rectifiers.

Petroleum, Refining and Production. This subcommittee sponsored two papers at the Summer General Meeting on the electrification of pipe lines and oil well pumping by electric power. It also sponsored a conference at the Winter General Meeting on wiring and distribution systems for petroleum refineries.

Batteries, Battery Forming, and Charging. This subcommittee is actively studying battery ratings and battery applications to clarify inconsistencies in present Standards, and it also is sponsoring a conference at the Summer General Meeting on batteries and battery charging.

Chemical Industries. This subcommittee sponsored a conference at the Winter General Meeting on wiring and distribution systems for chemical plants, and jointly sponsored, with the Committee on Transmission and Distribution, a conference on heat balance in chemical plants. The subcommittee is actively studying the application of electric equipment to the chemical industry, particularly switchgear and control devices, to establish good engineering practices to meet the exacting requirements of this industry.

COMMITTEE ON ELECTRIC HEATING

The principal activity of the committee during the past year has been the sponsorship of two conference sessions on electric heating at the Midwest General Meeting, which were well attended. The papers covered resistance heating, induction and dielectric heating, and radiant heating. The committee met in New York on February 3, 1949. At this meeting, each of the subcommittee chairmen reported on the activity of his subcommittee during the past year. Since the major work of the committee is carried on through the subcommittees, the remainder of this report consists of abstracted portions from the subcommittee reports.

The Subcommittee on Electronic Heating has proceeded with an agenda agreed upon by the Joint AIEE, IRE, NEMA Co-ordination Committee on Induction and Dielectric Heating. Various working groups within the subcommittee have been given specific assignments, some of which already have been completed. A Standard has been formulated on good engineering practice in the case of radio interference, which covers the proper methods of shielding, grounding, and installation of this equipment. The report has been accepted by the subcommittee and has been tentatively approved by the IRE. The report will be presented at the 1949 Summer General Meeting.

A data sheet for use by the FCC in reporting cases of radio interference has been formulated. This form has been accepted by the FCC, and is now in use by all their field engineers for cases of radio interference from industrial equipment. A set of standard definitions for induction and dielectric heating is being prepared. It is planned eventually to incorporate all such information in a formal Standard.

The Subcommittee on Radiation Measurements Above 200 Megacycles met five times during the year, the work following closely the pattern set during the preceding year. It is still thought that the best method for measuring radiation field strengths in the range of 200 megacycles and above is by the substitution method, using a standard signal generator, a suitable calibrated receiver, and a pickup device having known characteristics. Through a study of the literature and the building and testing of dipoles, dipoles with corner reflectors, and horns, the subcommittee has become convinced that it will be possible to give constructional details for various pickup devices which, when constructed according to specification, will permit the measurement of field strengths in the range from 200 megacycles to 7,350 megacycles with an accuracy of plus or minus approximately 20 per cent. This assumes the use of proper equipment, smooth lines, and proper technique, all of which must be described in a final specification of recommended procedure. Preparing such a Standard will be the major work of the coming year.

The Subcommittee on Resistance Heating and Electric Furnaces met twice during the year, and played a prominent part in the conference on electric heating held in Milwaukee in October 1948. Several project groups have been formed within the subcommittee to collect and prepare technical data with the hope it can be made available ultimately in some well edited form for the use of engineers. Close co-ordination is maintained with the Subcommittee on Radiant Heating because of the overlapping nature of resistance and radiant heating.

The Radiant Heating Subcommittee has 22 members, and is organized with 11 project groups working on specific problems. The subcommittee met four times in places widely separated geographically. Nine inspection trips were held in conjunction with these meetings, and several pages of publicity including photographs on these activities have been obtained in such publications as *Electrical Engineering, Electrical World, Industrial Heating, Industrial Finishing, American Paint Journal, Products Finishing.*

The subcommittee currently is assisting the National Fire Protection Association in connection with a code revision on industrial ovens and furnaces. It is further preparing numerous recommendations although to date only one official action has been taken, namely that the AIEE adopt and recommend through C-42 that infrared be spelled without a hyphen. The subcommittee activities now fully embrace industrial radiation heating with both lamp and glassless high-temperature resistance heaters.

COMMITTEE ON ELECTRIC WELDING

Conference on Electric Welding. The committee in co-operation with the Michigan Section sponsored a 3-day Conference on Electric Welding in Detroit. The purpose of this conference was to provide a forum on welding in Detroit, which is the center of this activity. One day was devoted to arc welding, and two days to resistance welding. The results of this conference were very gratifying because an attendance of over 400 was obtained. This is to be compared with a usual attendance, at similar sessions held during general meetings, of 35 to 100, depending on subject and location. The conference was so well received that plans are being made to repeat it in 1950.

Bibliography. The committee published a bibliography of resistance welding, prepared by Mr. Zucker.

Subcommittee on Power Supplies for Resistance Welding. Additional papers have been prepared and presented, also data gathered for a revision of the present report on "Power Supplies for Resistance Welding." Work of this subcommittee is about 40 per cent complete. This work will go on until possibly 1950 before being ready to publish.

COMMITTEE ON GENERAL INDUSTRY APPLICATIONS

Principles of Work. The committee has endeavored to follow the principles which were laid down when it was formed in the summer of 1947: (*a*) To study, discuss, and clarify electrical engineering problems in the several industries assigned to the committee, and (*b*) to attract to AIEE and to this work the electrical engineers interested in the foregoing industries.

In order to carry out this work effectively, it was necessary to subdivide it among several subcommittees, each to cover an industry or a group of related industries. The subcommittees are the Subcommittee on Machine Tools, Subcommittee on Rubber and Plastics Industries, Subcommittee on Textile Industry, Subcommittee on Pulp and Paper Industry, Subcommittee on Materials Handling. This list does not cover, by any means, all industries which come within the scope of the committee. One of the problems discussed at the February 3 meeting was: "Shall we organize additional subcommittees to cover additional industries?"

Subcommittee on Machine Tools. This subcommittee organized a very successful all-day session at the Midwest General Meeting. The topic selected was "Automatic Contour Follower Control for Machine Tools." Nine papers were presented. The meeting was very well attended. Discussions were interesting and lively. It is hoped these papers and their discussions can be published in one pamphlet, which will be an authoritative reference book on this subject.

This subcommittee did not plan on holding any additional machine tool sessions in 1948–49, but is working on the program for a session at the Fall General Meeting. The plans call for a 2-day session, with trips to several machine tool manufacturing plants in the area.

Subcommittee on Rubber and Plastics Industries. This group has arranged to hold annual meetings. Considering the geographical location of the rubber industry, Akron, Ohio, has been selected as the preferred place for the meetings, which will be arranged jointly with the Akron Section. The date for the 1948–49 meeting was set for April 26, 1949. This was an all-day affair. The program included discussion of: banbury drives, mill drives, calender drives, tuber drives, electrical standards for industrial equipments, and preventive maintenance. The papers and discussions will be published in pamphlet form, as has been done in connection with the April 20, 1948, meeting in Akron.

Subcommittee on Textile Industry. A session was held during the Winter General Meeting. This was devoted to the synthetic fibres industry, and consisted of four papers, one a presentation by title only. Two conferences are scheduled for the spring, one in Boston on May 3, and one in Atlanta on May 26 and 27.

Subcommittee on Pulp and Paper Industry. This group held a technical session at the Midwest General Meeting. The theme of the session was the "Speed Regulators for Sectional Paper Machines." Three papers were presented. The meeting was well attended (about 125) with many paper mill engineers present. This subcommittee is planning to hold the next session at the Summer General Meeting, the theme being "Electric Drives for Supercalenders and Winders." Two committee reports will be presented.

Subcommittee on Materials Handling. One technical session was held at the Midwest General Meeting. Two papers were presented. The topics were discussed at great length by many engineers attending the meeting. The subcommittee is planning the organization of a special one-day conference on May 13, 1949, in Cleveland, jointly with the Cleveland Section. The theme of this meeting will be heavy materials handling equipment such as needed for ore bridges and unloaders.

Reviewing the activities for the last year and a half, it appears that the committee met with some degree of success in its main task: "To bring AIEE closer to engineers working on industrial problems." The technical sessions organized by the subcommittees represent the sole ground on which these engineers can meet others in the same fields and discuss the problems which loom the largest in their professional lives. It is noted that there are no engineering organizations in existence (except these subcommittees), which discuss electrical engineering problems in such industries as machine tools, rubber, textile, paper, and materials handling. Hence, this work begins to fill a definite need. Efforts will be made to make it more effective, and to lay plans for the future.

Note: L. A. Umansky, Chairman of the Committee on General Industry Applications, his committee, and subcommittees merit special mention due to the number of successful technical committee conferences which they have conducted during the year and for the number planned for the future.

COMMITTEE ON INDUSTRIAL CONTROL

The committee has continued to take an active part in the work of the Industry Co-ordinating Committee, and every effort has been made to interest industrial engineers by preparation and presentation of papers relating to control problems in industry.

The Subcommittee on Standards has completed its work on the revision of Standard 15—Industrial Control Apparatus. The new Standard has been forwarded to the American Standards Association through the Standards Committee.

The Subcommittee on Electronic Control has been active in the formation of five working groups. These groups are concerned with: electronic control of d-c motors, photoelectric control systems, electronic relaying devices, electronic regulators and regulating systems, and electronic control of a-c power. Considerable work has been done by these groups on definitions in close co-operation with corresponding groups of the American Standards Association.

The Subcommittee on Electronic Control, in co-operation with the Committee on Electronics, sponsored a 2-day Conference on the Industrial Applications of Electron Tubes, in Buffalo, in April.

The Subcommittee on Test Codes is proceeding with a code on interrupting ability of contactors and endurance tests on a-c contactors. Numerous other subjects are under consideration by the subcommittee. The bibliography referred to in last year's report has been brought up to date, and final abstracting is now in progress.

The Subcommittee on Servomechanisms, jointly sponsored by this committee and those on Basic Sciences and Instruments and Measurements, conducted a well-attended session at the Winter General Meeting, and joined in a second session with the Committee on Industrial Control. It is hoped that in the near future a close liaison will be established between this joint subcommittee and the Subcommittee on Electronic Control.

During the year, the committee sponsored two sessions at the Midwest General Meeting and two at the Winter General Meeting. The sessions were well attended, and the papers presented were freely discussed by the members.

COMMITTEE ON INDUSTRIAL POWER SYSTEMS

This committee sponsored a session on industrial power distribution systems at the Midwest General Meeting. Three papers were presented at this meeting. Chemical and petroleum industry problems were covered at the Winter General Meeting. Papers on power generation and steam balance were given at this meeting.

The committee has three subcommittees: the Subcommittee on Wiring Design for Commercial Buildings is expected to complete its work and issue its final report at the Summer General Meeting; the Subcommittee on Revision of the Red Book is now actively engaged in revising and bringing up to date the so-called Red Book on Industrial Power Distribution Systems; the Subcommittee on Transformer Ratios was appointed mainly as a group to watch developments in the EEI-NEMA Transformer Voltage Standardization Program.

COMMITTEE ON MINING AND METAL INDUSTRY

The Committee on Mining and Metal Industry was newly formed in 1947, at which time it was called the Committee on Mining, Metal Forming and Rolling. At the present time it has 33 members, and is divided into two subcommittees, one covering the metal industry, and the other covering the mining industry. The members of this committee have been very active and have co-operated to the fullest extent in the committee program.

The first major activity of this committee was the presentation at the 1948 Winter General Meeting of 22 papers in six sessions. Much interest in these sessions was exhibited by men from the steel and mining industries. The committee sponsored a session on steel and a session on mining at the Summer General Meeting. The committee also sponsored two papers for the Pacific General Meeting. At the Midwest General Meeting, the committee presented 11 papers in three sessions, which covered mining, ore beneficiation, and steel mills. Because of the lack of space, the committee was asked not to sponsor sessions for the Winter General Meeting and the Summer General Meeting.

The committee has held several meetings, the last of which was at the Winter General Meeting. A good percentage of the committee attended. Glenn B. Southward, Mechanization Engineer of The American Mining Congress, also attended and gave many helpful suggestions on the work of the committee and on co-operation with The American Mining Congress.

The committee now is making preparations for three sessions at the Fall General Meeting.

Communication and Science Group

COMMITTEE ON BASIC SCIENCES

The Committee on Basic Sciences, as its name implies, deals with the investigation and presentation of subjects of fundamental nature likely to be of present or future interest to electrical engineers. It is the duty and purpose of the committee to sponsor, and present to the members of the Institute the results of activity in newly developing fields not easily assignable—at least in the initial stages of their development—to one of the established technical committees of the Institute. When, in the opinion of the members of the committee, fundamental activity in a field becomes great enough, a subcommittee for the particular field is formed, which concerns itself with this field exclusively. Often the fundamental activity in a new field leads to practical engineering applications not fitting well into an established technical committee, in which case the subcommittee becomes a full-fledged new technical committee of the Institute. For instance, the Committee on Basic Sciences had a Joint Subcommittee on Servomechanisms with the Committee on Industrial Control and the Committee on Instruments and Measurements; this subcommittee now is being considered for elevation to full technical committee status with the suggested name of "Committee on Feedback Control Systems."

The Committee on Basic Sciences sponsored technical sessions at the Midwest General Meeting, and at the Winter General Meeting. At these two meetings, a total of nine papers were presented.

The committee also held two meetings, one at the Midwest General Meeting, and one at the Winter General Meeting, at which it dealt with the question of standardization of voltage notation, the reports and plans of its subcommittees, and the possible formation of new subcommittees.

Activities of the five subcommittees operating through the year are reported in the following:

Energy Sources. The subcommittee sponsored its third conference on energy sources at the Winter General Meeting. Four papers were presented, dealing with the effect of electricity on the human body and on the subject of nerve electricity. The close correlation of this subject with the phenomena of electric fishes was discussed, and a demonstration with electric eels was presented. The attendance at this meeting proved the great interest in this subject. The committee is trying to arrange for publication, in pamphlet form, of most of the 14 papers presented since the formation of the subcommittee in 1946.

Electric Circuit Theory. The Subcommittee on Electric Circuit Theory presented a symposium on circuit analysis at the Midwest General Meeting, consisting of three papers dealing with the history and present state of operational calculus and of the application of matrix algebra, as well as with circuit analysis in servomechanisms. The subcommittee continues to participate in the defining of terms in network theory and electrical measurements, and the chairman of the subcommittee has undertaken to trace out the historical origin of the terms used in circuit theory.

Applied Mathematics. This subcommittee sponsored a Conference on Applied Mathematics jointly with the American Mathematical Society. The conference was held during the Winter General Meeting, four papers having been presented at this time. The subcommittee has further plans for participation in the International Mathematical Convention to be held in Boston, September 1949, and the ASEE meeting in Troy, June 1949. It also is scheduling another conference at the Winter General Meeting of 1950.

Magnetics. This subcommittee formed this year, sponsored a symposium on magnetics at the Winter General Meeting, consisting of morning and afternoon sessions, in the course of which six papers were presented. The attendance at these two sessions indicated that the formation of this subcommittee had filled a definite need. The subcommittee is planning another symposium on the subject for the Winter General Meeting of 1950.

Electrical Properties of Solids. This subcommittee was formed during the past year. The properties of semiconductors only recently have begun to be understood a little more clearly, and the development of the transistor has attracted a great deal of interest. Recognizing this, the subcommittee has prepared a symposium on the electrical properties of semiconductors and transistors to be given at the Summer General Meeting. Owing to the great interest in these devices by other technical societies, activities are under way to establish a joint AIEE-IRE committee on jointly sponsored annual symposia on this subject, so that duplication of effort will be avoided. Initial plans have been made by the subcommittee for a future symposium on "Electrical Properties of Dielectrics."

Electrical Properties of Gases. This subcommittee is still in the process of formation but can be expected to become active in 1950.

COMMITTEE ON COMMUNICATION

The Committee on Communication has continued its policy of allocating practically full responsibility to the subcommittees and the associated chairmen for the initiation of the technical programs in their particular fields of interest, solicitation and review of timely papers, and conduct of the sponsored sessions. The general steering of these communication activities has been under the guidance and direction of a co-ordinating committee including the three administrative officers and the chairmen of the nine technical subcommittees. Functioning essentially on a group basis for the past two years, the committee has requested Board of Directors' approval of the advancement of the subcommittees to full committee status in an autonomous Communication Group, effective August 1, 1949.

During the past fiscal year, the committee sponsored 11 complete technical sessions, at which 48 papers were presented that specifically covered the fields of telephone switching, wire and radio communication systems, aural and television broadcasting, railroad, and other special communication applications.

The Summer General Meeting was supported by the committee with four papers on telephone, telegraph, and radio subjects. Two papers on the status of radio telephone service in the United States were contributed to a joint electronic and communication session at the Pacific General Meeting.

Participation in the Midwest General Meeting was extended by sponsoring five complete sessions that covered a comprehensive list of subjects including home radio receivers, microgroove recording, television broadcasting and associated coaxial and radio relay facilities, development in semiconductors and the transistor, and telephone and telegraph switching systems. In view of the locale for the meeting a full session was devoted to "Radio on the Great Lakes."

For the Winter General Meeting, the committee sponsored a 5-paper home radio and broadcasting session; radio communication systems session with four papers; 5-paper session relative to wire communication systems; and a fifth session composed of five papers on special communication applications.

Two meetings of the main committee were held for the consideration of general policy matters. The co-ordinating committee met three times during the year in order to formulate the general program of activities and for the discussion and approval of the arrangements worked out by the subcommittees.

The communication program for the Summer General Meeting has been finalized to provide for three sessions, and a total of 12 technical papers, with the principal emphasis being focused on a telephone switching symposium that will deal with the fundamental and functional design of relay switching circuits. Tentative plans are under way for the 1949 Fall General Meeting with a possibility of underwriting five sessions highlighted by a symposium on coaxial systems.

COMMITTEE ON COMPUTING DEVICES

Activities of the Committee on Computing Devices so far have been to sponsor several sessions at AIEE meetings, including a session on analog computers at the last Winter General Meeting, as well as several articles on computing machine developments in *Electrical Engineering*. A session is planned for the Summer General Meeting.

Two major subcommittees have been formed, one on analog computers with Dr. E. L. Harder as Chairman, and one on digital computers with Dr. J. W. Mauchly as Chairman.

Professor G. D. McCann is compiling a bibliography on computing machines, and Dr. W. H. MacWilliams, Jr., is co-ordinating with the IRE and ACM (Association for Computing Machinery) on nomenclature and definitions. Professor S. H. Caldwell maintains contact with the Committee on Instruments and Measurements, while C. Concordia (Chairman) and Dr. J. G. Brainerd (Vice-Chairman) are also members of the Committee on Basic Sciences. Professor W. C. Johnson, Jr., is Secretary.

COMMITTEE ON ELECTRONIC POWER CONVERTERS

The committee activities were concentrated largely on projects initiated during the preceding year. The committee held two meetings—on October 11 in Pittsburgh, and on April 12 in Buffalo. Meetings were held also by several of the subcommittees. A committee report, "Mercury-Arc Power Converters in North America," was presented at the 1948 Summer General Meeting. This is a comprehensive report on the designs and applications of mercury-arc rectifiers.

Protection of Electronic Power Converters. Part 1 of the report on protection, which deals with the calculation of fault currents in rectifier circuits, was completed by the Electronic Converter Circuits Subcommittee, and was presented during the Winter General Meeting, at a technical session on protection sponsored by the committee. Part 2 of the report, which deals with protection systems and devices, is nearing completion and will be presented at the Fall General Meeting. It is being prepared by representatives of the Committees on Substations and Switchgear, in co-operation with the Circuits Subcommittee. The complete report will be published after part 2 has been completed.

Survey of Rectifier Operation. The Electronic Converter Application Subcommittee is making a survey of operating experience and system characteristics in mercury-arc rectifier installations, by means of questionnaires sent to rectifier users. The subcommittee expects to have a preliminary report on the survey ready for presentation at the Fall General Meeting. The complete report probably will be ready for the next Winter General Meeting.

Rectifier Transformer Characteristics. The Rectifier Transformer Subcommittee prepared a report on rectifier transformer characteristics, which was presented at the Winter General Meeting. The report has been submitted to the AIEE for publication.

Bibliography on Electronic Power Converters. The Papers and Speakers Subcommittee has completed a bibliography on electronic power converters, and it has been submitted to the AIEE for publication. The bibliography covers the years from 1903 to the end of 1947. It has 1,550 references to articles in English-language and foreign-language publications.

Inductive Co-ordination on D-C Side of Rectifier Installations. A report on inductive co-ordination aspects relating to the d-c side of rectifier installations is being prepared by a working group under the auspices of the committee. The first draft of the report has been completed. It is expected to have the report completed in time for presentation at the Winter General Meeting.

Conference on Education in Power Electronics. A conference on education in power electronics was held during the Winter General Meeting, under the joint sponsorship of the Committees on Electronic Power Converters, Electronics, and Education. The program included speakers from engineering schools and industry. A report on the conference was published in the April issue of *Electrical Engineering*.

West-Coast Subcommittee. The first organization meeting of this subcommittee was held in Spokane, Wash., on August 26, 1948. The membership of the subcommittee and the scope of its activities were discussed.

COMMITTEE ON ELECTRONICS

One of the very important activities of the committee is that of insuring that early and adequate attention be given by the AIEE to new techniques and engineering practices employing electronic devices. In pursuit of that objective, the committee has added, during the past year, a Subcommittee on Magnetic Amplifiers, and a Subcommittee on Electronic Applications of Semiconductors, and has changed the Subcommittee on Infrared Applications to a Subcommittee on Industrial Spectroscopy, thus enlarging its scope.

The practice of operating with two distinctive types of subcommittees has been continued. One type deals with general functions, such as the processing of Standards, papers solicitations and Section contacts, maintenance of national and informational contacts, education, and liaison with other professional groups. The other type is responsible for attention to specific technical fields. The committee ended the year with seven general-function subcommittees and with 14 subcommittees dealing with specific technical activities.

Plans of operation for the 1948–49 period were formulated at a meeting of subcommittee chairmen in New York, N. Y., in September 1948. A meeting of the entire committee was held in Chicago, in November 1948, in connection with the National Electronics Conference. A meeting was held at the Winter General Meeting.

At the Summer General Meeting, the committee sponsored a technical session dealing with general trends in: electron tube design, mercury-arc converters, and radio-type equipment. Also, the committee assisted in arranging for a discussion of "Electronics in Engineering Education," in a program sponsored by the Committee on Education.

At the Winter General Meeting, the committee sponsored:

1. A technical session dealing with recent developments in electron tubes and circuits.
2. The usual conference session on new electronic devices.
3. A technical session on high-frequency cables.
4. A conference session on education in power electronics.
5. A technical session on electrostatic precipitation.

One of the committee's policies is to encourage the presentation, in sessions sponsored by other committees of the Institute, of papers having an important electronics content. It is interesting to note in this connection that approximately one-half of all of the papers which were presented at the Winter General Meeting referred to some phase of electronics as an essential feature of the treatment.

For the 1949 Summer General Meeting, the committee will sponsor a technical session on infrared applications, and a technical session on magnetic amplifiers; it also will add support to the symposium on semiconductors, sponsored by the Committee on Basic Sciences.

Late in November 1948, a 3-day Conference on Electronic Instrumentation in Nucleonics and Medicine was held in New York, N. Y., sponsored jointly by the Committees on Electronics and Nucleonics of the AIEE, and the Nucleonics Studies Committee of the IRE. This conference was very well attended, and indications are that a similar conference will be held in the late fall of 1949.

In April 1949, a 2-day Conference on Industrial Electron Tubes was held in Buffalo, jointly sponsored by the Subcommittee on Electron Tubes of the Committee on Electronics and the Subcommittee on Electronic Control of the Committee on Industrial Control. This conference consisted of five technical sessions and a dinner meeting. In general, the objective was to permit exchange of information between industrial electronic circuit engineers and industrial electron tube engineers. The conference was very well attended, there was active discussion by those who attended, and it is believed the program was a valuable contribution.

Activities of the subcommittees of the general-function type were as follows:

Electronic Papers Solicitation and Section Contacts. This subcommittee accepts the responsibility for organizing technical sessions at general meetings, for following through to procurement suggestions for technical papers originating within its own members and from members of the technical subcommittees, for encouraging and stimulating papers involving electronics but sponsored by other committees, and for assisting Sections in stimulating electronic contacts.

Electronic Standards. This subcommittee is the channel for processing Standards through to the American Standards Association, and renders active assistance toward familiarizing the committee as a whole with Standards procedures.

Liaison With IRE. This subcommittee has the responsibility of maintaining satisfactory co-ordination with the Institute of Radio Engineers.

Liaison With JETEC. This subcommittee has maintained active co-ordination with JETEC, particularly in regard to matters of policy and areas of standardization activity.

Education in Electronics. This subcommittee has been very active in strengthening contacts as to electronics between industry and universities, and in providing exchange as to points of view among universities in relation to methods of education in electronics. The most significant contribution this year was the technical session on this subject at the Winter General Meeting.

West Coast Subcommittee. This subcommittee has been active in maintaining local contact in the West Coast area, particularly California, between the various electronics activities of importance to the AIEE. Plans are being formulated for a symposium on electronic instrumentation to provide an interchange of ideas between electronic industries in the West Coast area.

Canadian Liaison Subcommittee. This subcommittee is functioning actively in maintaining close contact with electronic developments in Canada, and in addition has maintained a link with electronic developments in Europe.

Activities of subcommittees in technical fields have been as follows:

Electron Tubes. This subcommittee has four working groups in the field of industrial electron tube standards in the following fields: vacuum tubes, cathode-ray tubes, gas-filled thermionic and cold cathode tubes, and mercury-pool cathode tubes. This subcommittee was responsible for the share of the Committee on Electronics in the sponsoring of the Industrial Electron Tube Conference in Buffalo.

X-Ray Tubes and Apparatus. This subcommittee provided two technical papers for a technical session at the Winter General Meeting, has completed its recommendations for changes in regard to X-ray graphical symbols, and has undertaken a revision of the American Standards Association X-ray terms. A study of specifications of characteristics and ratings of tubes used for X-ray equipment is under way.

Electronic Instruments. Activity in the electronic instrument field is handled through the Joint Subcommittee on Electronic Instruments, sponsored co-operatively with the Committee on Instruments and Measurements. This joint subcommittee sponsored two technical sessions at the Winter General Meeting, one on electronic instruments, and one on electronic digital computers. It has actively reviewed the results of the Conference on Instrumentation Tubes held in March 1948 in Philadelphia, and has used the results of that conference for furthering subsequent activities of smaller groups in the same field, and for initiating a Standards program.

Electronic Precipitation. This subcommittee sponsored a technical session at the Winter General Meeting.

High-Frequency Conductors, Cables, and Connectors. This subcommittee was responsible for a technical session at the Winter General Meeting.

Hot-Cathode Electronic Power Converters. This subcommittee has continued to be very active in bringing nearer to completion standard definitions properly correlated with similar standards in mercury-pool rectifiers. Close liaison is being maintained in all respects between this group and the AIEE committee dealing with mercury-pool converters.

Liaison With Nucleonics. This subcommittee has been responsible for maintaining close contact with the activities of the Committee on Nucleonics and other similar groups, and has been instrumental in clarifying judgment as to the proper relationship of the main committee to nuclear studies.

Electronic Aids to Medicine. This subcommittee was the avenue of the sponsorship by the Committee on Electronics of the 1948 Conference on Electronic Instrumentation in Nucleonics and Medicine in New York, N. Y., and is carrying forward plans for a similar conference late next fall. Also, the subcommittee is canvassing the proper setup for adequate liaison with the American Medical Association.

Electronic Aids to Navigation. The responsibility of this subcommittee has been for maintaining close contact with, and making contributions to, the activities of an IRE committee active in this field. Closely associated through overlapping membership is a committee of the Radio Technical Commission for Aeronautics. Liaison is also maintained with the Institute of Aeronautical Sciences, the Joint Technical Advisory Committee, the Air Materiel Command, and the Institute of Navigation. There recently has been achieved by the IRE group agreement on a tentative list of terms and definitions, and other standards procedures are under way.

Electronic Aids to Geophysics. This subcommittee sponsored last fall, jointly with an IRE group, a symposium on electronic circuitry in geophysical work, held in the Texas area where the greatest activity in this field exists. An important objective of this subcommittee's work is to enlarge the area of contact, by means of technical publication and otherwise, between geophysical electronic work and other areas of electrical engineering.

Infrared Applications. This subcommittee arranged a technical session for the Summer General Meeting. At present it is planned to extend the scope of this subcommittee to include industrial spectroscopy, thus broadening the base of its activities.

Electronic Preparation and Preservation of Food. This recently organized subcommittee is looking forward to activity in providing for presentation to the Institute of technical papers regarding progress in this field.

Magnetic Amplifiers. This new subcommittee was organized during the past year in recognition of the facts that magnetic amplifiers recently have become of substantial importance, that the circuit principles involved are basically the same as those in purely electronic circuits, and that nearly all magnetic amplifiers include important electron tube elements in their circuits. This subcommittee has arranged a technical session for the Summer General Meeting, and is maintaining a close liaison with the Committee on Basic Sciences. Standards activities are being planned.

Electronic Applications of Semiconductors. It is the responsibility of this newly organized subcommittee to give adequate attention, in the way of technical sessions and papers within the AIEE, to engineering applications to the newer solid-state devices, including transistors, crystal rectifiers, and related devices. Standards activities are under consideration.

COMMITTEE ON INSTRUMENTS AND MEASUREMENTS

Because measurement is fundamental to scientific progress, the activities of the committee are related to all branches of Institute work, and close liaison is paramount. The work of the committee has been aimed at the stimulation of interest in instruments and measurements and the co-ordination of effort in this field, including the preparation of appropriate Standards. To keep pace with the expansion of the measuring art, the membership was increased to 49. Meetings were held on November 9, 1948, and March 30, 1949. The latter was at the National Bureau of Standards, with Dr. F. B. Silsbee as host, and included an inspection trip of a number of the laboratories of the Bureau of Standards, as well as a visit to the Naval Ordnance Laboratory the following day.

About 50 technical and conference papers were presented during the year under the auspices of the main committee and its direct subcommittees, and about 50 additional papers were sponsored by the joint subcommittees. The range of subject matter testifies to the extreme diversity of measurement work.

In considerable measure, the instruments and measurements work is carried out through nine subcommittees whose activities have been as follows:

Subcommittee on Revision of Standard 4 (Measurement of Test Voltage in Dielectric Tests). The most important item on the program of this subcommittee is the standardization of methods for short-time impulse measurements. This problem is being studied by the NEMA Laboratory Co-ordination Subcommittee.

Subcommittee on Revision of C39 (Electrical Indicating Instruments). This subcommittee has co-operated with the ASA subcommittee on the revision of the C39 Standard. The first part of the Standard, covering switchboard and panel instruments, has been approved by ASA and printed for general distribution. Work on the second part, covering portable and laboratory standard-type instruments, is nearing completion.

Subcommittee on Master Test Code for Resistance Measurements. A revised draft of the trial code published in September 1947 is being circulated for approval of the Standards Committee and final printing.

Subcommittee on Master Test Code for Temperature Measurements. A proposed new code was published in October 1948 for one year's trial use.

Subcommittee on Marking of Varmeters and Related Instruments. A questionnaire has been circulated to obtain data on present practices regarding the connection and scale markings of the varmeter and related instruments. Further activities of the subcommittee will be based on the results of this survey.

Subcommittee on Watt-Hour Meters. This subcommittee sponsored nine technical and conference papers.

Subcommittee on Electrical Tests on Dielectrics in the Field. This subcommittee sponsored two sessions at the Winter General Meeting, at which eight conference papers were presented.

Subcommittee on High-Frequency Measurements. This subcommittee was responsible for planning the Conference on High-Frequency Measurements, held in Washington, D. C., January 10–12, 1949, under the joint sponsorship of AIEE, IRE, and the National Bureau of Standards. Attendance totaled 584. The community of interest in the subject gave rise to animated discussion.

Subcommittee on Definitions. The activities of this subcommittee have been limited to review of the definitions prepared by Subcommittee 6 of ASA C42.

Necessary co-ordination with the work of the other technical committees of the Institute is achieved through a number of joint subcommittees and in some instances, by cross representation. The increasing number of technical committees has augmented the problem of maintaining proper liaison. While present arrangements have proved highly satisfactory, a study is being made of intercommittee relationships to see whether any modifications in the existing scheme might be advantageous. The activities of the joint subcommittees are summarized in the following:

Joint Subcommittee on Electronic Instruments. This subcommittee sponsored two sessions at the Winter General Meeting. Work is underway on the development of specifications for the performance of vacuum tube voltmeters and cathode-ray oscilloscopes.

Joint Subcommittee on Servomechanisms. This subcommittee sponsored one session at the Winter General Meeting.

Joint Subcommittee on Nucleonic Instruments. This subcommittee, in co-operation with the Committee on Nucleonics and the Committee on Electronics Subcommittee on Electronic Aids to Medicine, sponsored a joint AIEE-IRE Conference on Electronic Instrumentation in Nucleonics and Medicine in New York, N. Y., November 29–December 1, 1948. The conference was quite successful with a total attendance of 540. Also, the subcommittee sponsored sessions at the Pacific General Meeting and the Midwest General Meeting.

Joint Subcommittee on Telemetering. A revision of the October 1941 report on "Telemetering, Supervisory Control, and Associated Circuits," has been issued. Three technical papers were sponsored by the subcommittee.

Joint Subcommittee on Instrument Transformers. Working groups are active on current transformers, test code, and rating factors.

COMMITTEE ON NUCLEONICS

This committee continued its activities in the field of nucleonics with a membership of approximately 25, and with four subcommittees as follows: Joint Subcommittee on Nucleonic Instruments (Joint with Committee on Instruments and Measurements); Subcommittee on Isotopic Tracers; Subcommittee on Safety and Health Protection Against Radiation; Subcommittee on Nuclear Physics.

Committee meetings were held in Spokane, Wash., Washington, D. C., and New York, N. Y., and a meeting of the committee officers and subcommittee chairmen was held in Cambridge, Mass., on August 10, 1948.

The committee activities were directed mainly toward bringing nucleonic information to the Institute membership, and thus stimulating interest in this field in which the electrical engineer must play an increasingly important part. To this end the following meetings were arranged.

Conference session at Pacific General Meeting, with four papers covering health physics, nucleonic instruments, accelerators, and atomic power reactors, sponsored by the Subcommittee on Nucleonic Instruments.

Conference session at Middle Eastern District Meeting, with four papers by different authors covering the same subjects for the different audience, sponsored by the Subcommittee on Nucleonic Instruments.

Conference session at the Winter General Meeting, with four papers covering health physics, and industrial and research applications and techniques for radioactive tracers, sponsored by the Subcommittees on Isotopic Tracers and on Safety and Health Protection.

Conference session at South West District Meeting, with three papers covering accelerators and radioactive tracer applications in medicine and biology, sponsored by the Subcommittee on Nuclear Physics.

Joint AIEE-IRE Conference on Electronic Instrumentation in Nucleonics and Medicine held in the Engineering Societies' Building, in New York, on November 29, 30, and December 1, with 26 papers.

The last-named meeting was sponsored jointly with the Committee on Electronics Subcommittee on Electronic Aids to Medicine, in co-operation with the Institute of Radio Engineers. Approximately 540 people attended. The program was well received. A questionnaire was sent to those who attended, and, on the basis of replies, it has been decided that a similar conference should be held in 1949.

In addition to meetings, the committee sponsored the publication of additional papers on nucleonic subjects, and the nucleonic series in *Electrical Engineering* was completed. A bibliography was prepared covering other literature on the subject, and the complete series has been published in pamphlet form under the title "Elements of Nucleonics for Engineers."

Finally, the committee participated in arrangements for the co-ordination of the various glossaries on nucleonics under the National Research Council, and is collaborating on the preparation of the section on instrumentation.

General Applications Group

COMMITTEE ON AIR TRANSPORTATION

The Committee on Air Transportation held one meeting of the entire committee during the year. This meeting was held in Washington on the occasion of the Middle Eastern District Meeting. The activities of the committee for the coming year in the field of Standards were discussed, and plans were made for technical sessions at the 1949 Pacific General Meeting. Because of the wide geographical spread of the electrical engineers interested in aircraft transportation, it is thought that technical sessions on this subject should be concentrated at one principal meeting during the year. For this reason it is planned to concentrate efforts on technical papers at the coming Pacific General Meeting. The Standards activities of the committee are carried on by its several subcommittees, and the status of the committee's work is described under the headings of the several subcommittees in the following paragraphs.

Aircraft Electric Rotating Machinery. The "Proposed Test Code for D-C Aircraft Electric Rotating Machines," AIEE Report 800, which was issued in March 1947 for one year's trial use, is being revised for reissue. It was thought that in the present form this report was not ready for standardization in the form of a test code, and it is expected that this will be available for reissue within the next few months.

Joint Subcommittee on Carbon Brushes. This subcommittee, which is joint with the Committee on Rotating Machinery and the Committee on Air Transportation, was formed for the purpose of writing a code for testing carbon brushes and brush materials. It made an interim report at the recent Winter General Meeting. At that time, a recommendation was made that the present subcommittee be disbanded and a new joint subcommittee formed with the fore-named AIEE committees and the Carbon Brush Committee of the NEMA Technical Committee. This action now is awaiting the approval of the Standards Committee. It is hoped that the new joint subcommittee may be completed at an early date.

Aircraft Electrical Control, Protective Devices, and Cable. This subcommittee has prepared a "Proposed Test Code for Aircraft Circuit Interrupting Devices (12-, 24-, and 120-Volt D-C Systems)," which has been submitted to the Committee on Air Transportation for approval, with the view of recommending it to the Standards Committee for issue for one year's trial use. This subcommittee also is preparing a test code for aircraft generator voltage regulators. It is expected that this code also will be issued for one year's trial use by the industry before being proposed as a Standard. This subcommittee is planning next to prepare a code for testing the interrupting capacity of aircraft d-c circuit breakers. It is expected also that this group will undertake the preparation of a report on the "Recommended Practice for the Installation and Protection of Electric Wiring in Aircraft."

Basic Principles of Altitude Rating. This subcommittee has been assigned the task of preparing an AIEE Standard on the basic principles of altitude rating of electric machinery. It is expected that this rating will extend the altitude considerations to 50,000 feet and take into consideration such factors as temperature, pressure, and humidity, and will furnish data for determining safe rating of aircraft electric machinery. It is planned that a survey will be conducted of the users of altitude chambers to determine the correlation of data obtained in flight with that obtained in altitude chambers, and it is hoped that this survey may result in a more unified practice in the use of altitude chambers.

Aircraft Electric Systems. This subcommittee was engaged in the preparation of new material for inclusion in the report "Report on Aircraft Electric System Guide," AIEE 750, which was published in July 1947. The guide was issued in an incomplete state, and it is expected that revision will be a continual process in order that it may be kept up to date in regard to aircraft electric system development. It is planned that other subcommittees will furnish information pertaining to their assigned fields of activity for inclusion in the "Systems Guide."

COMMITTEE ON DOMESTIC AND COMMERCIAL APPLICATIONS

The committee has been active in the preparation and presentation of papers, and in promoting a greater awareness among the engineers in the appliance field both of the value of the Institute and of the part which appliance engineers play in developments in the electrical industry.

The scope of the Committee on Domestic and Commercial Applications is such that the engineering requirements do not lend themselves readily to standardization such as is normally considered within the field of the Institute's activities. As a consequence, no work on Standards has been conducted or contemplated. Many excellent papers have been prepared, however, and presented at various Institute meetings. Papers were presented at the Summer General Meeting and at the Midwest General Meeting, and a symposium of six papers on the control and protection of household electric equipment was held at the Winter General Meeting.

All sessions where papers were presented under the auspices of this committee were well attended, and four of the papers were considered to be of sufficient general interest to be acceptable for publication in *Electrical Engineering*.

Interest in the program sponsored by the committee resulted in six engineers affiliating with the Institute and the renewal of activity on the part of members in several Districts who had believed that their particular field was not adequately covered.

COMMITTEE ON LAND TRANSPORTATION

The committee held one well-attended and very full business meeting on February 1, 1949. At this meeting, the committee heard a very interesting discussion by T.M.C. Martin on the question "Will Complete Dieselization Save Oil?" The following activities also were discussed and organized.

Technical Meetings. Two transportation papers were presented at the Summer General Meeting, and four were presented at the Midwest General Meeting. These related to short-time ratings of diesel-electric locomotives, energy sources for railroad motive power, head end power on railroad passenger trains, and handling of suburban traffic on steam railroads. Seven papers were presented at the Winter General Meeting. These covered application of diesel-electric locomotives, 25 years progress in the design of traction motors (report on the progress of the art), the renaissance of the electric motive power, the electric equipment for Chesapeake and Ohio steam turbine-electric locomotives, selenium rectifiers in motor vehicle power systems, trackless trolley operations in Rhode Island, and a review of cities where trolley coaches have replaced busses.

Subcommittee Activities. The review of AIEE Standard 16, "Standards for Electric Railway Control Apparatus," has been completed, and this Standard now includes coverage of the electric portions of the electropneumatic brake system. This Standard is being issued for trial use.

COMMITTEE ON PRODUCTION AND APPLICATION OF LIGHT

One meeting of the entire committee was held. This meeting was held at the Winter General Meeting. A conference on fluorescent lighting, which was sponsored by the committee, was held on the afternoon of the same day. One of the subjects which was discussed at the committee meeting was the scope of the committee's activities. As a result of this discussion, it was concluded that one of the primary objectives is to keep AIEE membership advised on lighting matters, by encouraging meetings on the subject at general meetings, and Section meetings. Earlier in the year, the chairman had proposed to the Sections Committee that a list of speakers available for various local activities be distributed to the Sections. The Sections Committee had responded by indicating that it would like to consider the inauguration of such a procedure for all technical committees.

Reports were presented on the activities of the following subcommittees:

Subcommittee on Ultraviolet Radiation. This subcommittee has been working on a paper giving general background material on ultraviolet radiations. The manuscript was distributed to the committee, and several suggestions made for bringing it to completion.

Subcommittee on Infrared Radiation. This subcommittee is working in co-operation with two other AIEE infrared subcommittees: Radiant Heating Subcommittee under the Committee on Electric Heating; Infrared Applications Subcommittee under the Committee on Electronics. This subcommittee will encourage the use of electric infrared radiation for those processes for which it is suitable, by the collection and dissemination of available data, as well as the encouragement of new research. Investigations are being carried on at the present time on infrared sources, techniques, and measuring instruments. A program is also under way for the collection of fundamental application data.

Subcommittee on Nomenclature of Electric Discharge Lamps. The report which had been prepared by this subcommittee had been circulated to members of the committee prior to the meeting. A number of written comment had been received, and these were discussed, together with other comments which were brought in by other committee members or evolved out of the discussion. The chairman of the subcommittee agreed to prepare an additional draft, incorporating the suggestions which the committee had agreed should be included. The final draft should be ready for circulation shortly.

COMMITTEE ON MARINE TRANSPORTATION

Two well-attended meetings of the committee were held at Institute headquarters, one in January, and one in April, 1949.

The latest revision of "Recommended Practice for Electrical Installation on Shipboard," was issued in December 1948. The committee has been working on the matter of international standardization of electrical installation on shipboard. This work was delegated to the Committee on Marine Transportation by action of the Board of Directors of the Institute.

Technical Meeting. Four marine transportation sessions were held at the Middle Eastern District Meeting. The sessions were very well attended, each having from 50 to 125 people present. The first session covered the subjects of insulating materials and magnetic amplifiers, and the second covered the subjects of circuit breakers and shipboard degaussing installations. Three papers were presented at each. The third session covered the subject of power on shipboard, with four papers presented and discussed. The fourth session covered the subject of shipboard lighting, with three papers presented and discussed. These sessions all created considerable interest in the work of the committee.

Subcommittee Activities. These subcommittees have been quite active, each reviewing the sections of Standards 45 under its cognizance, and making reports to the main committee.

Awards

COMMITTEE ON AWARD OF INSTITUTE PRIZES

On account of the adoption of the new rules, with a shift from the calendar year to the administrative year, no awards were made this spring. The committee held one meeting for consideration of the proposed changes in rules submitted by a subcommittee of the Sections Committee, and will consider the proposals again when they are in final form.

CHARLES LEGEYT FORTESCUE FELLOWSHIP

During the year, one meeting of the committee was held to select the recipient of the Fortescue Fellowship award for the scholastic year 1949–50. One full fellowship of $1,500 was awarded to E. F. Koncel, Jr. A continuing fellowship in the amount of $500 was awarded to last year's recipient to assist him in completing the second year of his graduate work.

Consideration is being given to several proposals to arouse more interest on the part of faculty members so that competition or this fellowship will be more widespread.

COMMITTEE ON MEMBERS-FOR-LIFE FUND

The committee took no further action during the past year. The Board of Directors approved its recommendations that a statement regarding the use of the fund be published in *Electrical Engineering* and mailed to each new Member-for-Life with the notification; that a specially designed card be mailed to all living Members-for-Life and in the future be mailed with the official notice; and that, when the growth of the fund warrants, prize winners from all Districts be included in the provision for traveling expense allowance to the Summer General Meeting.

EDISON MEDAL

The Edison Medal for 1948 was awarded to Dr. Morris E. Leeds, Chairman of the Board, Leeds and Northrup Company, Philadelphia, Pa., "for his contributions to the industry through development and production of electrical precision measuring devices and controls," and was presented to him on February 2, 1949, in a general session of the Winter General Meeting.

The medal may be awarded annually for meritorious achievement in electrical science, electrical engineering, or the electrical arts, Awards are made by a committee of 24 members of the Institute.

LAMME MEDAL

The Lamme Medal for 1948 was awarded to Dr. V. K. Zworykin, Vice-President and Technical Consultant of the RCA Laboratories Division, Radio Corporation of America, Princeton, N. J., "for his outstanding contribution to the concept and design of electronic apparatus basic to modern television." The medal will be presented to him on June 22, 1949, during the Summer General Meeting.

The medal may be awarded annually by a committee of nine members to a member of the AIEE for "meritorious achievement in the development of electrical apparatus or machinery."

HOOVER MEDAL

The Hoover Medal is awarded periodically to an engineer for distinguished public service by a board representing the American Society of Civil Engineers, American Institute of Mining and Metallurgical Engineers, American Society of Mechanical Engineers, and AIEE. The medal was awarded, in 1948, to Malcolm Pirnie, Consulting Engineer, New York, N. Y., with a citation as: "Engineer, leader of engineers and servant of his fellowman, whose ideals and accomplishments in public life beyond the call of his profession have benefited men in his own and other countries of the world." The medal was presented to him on January 19, 1949, at the annual meeting of the ASCE, of which he is a past president.

JOHN FRITZ MEDAL

The John Fritz Medal may be awarded annually for notable scientific or industrial achievements, by a board of award composed of representatives of the ASCE, AIME, ASME, and AIEE. The 1949 medal was awarded to Charles M. Allen, Professor Emeritus of Hydraulic Engineering, Worcester Polytechnic Institute, with the citation:

"Exceptional achievements in hydraulic engineering. Founder of notable hydraulic laboratory; prominent teacher, consultant, inventor and author." The medal was presented to him on January 19, 1949, at the annual meeting of the ASCE.

MARSTON MEDAL

The Marston Gold Medal is awarded to an alumnus of Iowa State College, of at least 30 years' standing, for achievement in engineering in a broad field. The board of award includes representatives of the college, and five engineering societies: ASCE, AIME, ASME, AIEE, and AIChE. The 1948 award was to Roy W. Crum, Director of the Highway Research Board of the National Research Council, Washington, D. C.

WASHINGTON AWARD

The Washington Award for 1949 was made to John L. Savage, Consulting Engineer, Tennessee Valley Authority, and Chief Designing Engineer, United States Bureau of Reclamation, Denver, Colo. The award is made annually to an outstanding engineer, a citizen or resident of the United States, who ably has served human needs, and is administered by a commission representing the Western Society of Engineers, ASCE, AIME, ASME, and AIEE.

ALFRED NOBLE PRIZE

This prize was established in 1929 to perpetuate the name and achievements of Alfred Noble, Past President of the ASCE and the Western Society of Engineers. It may be made to a member of any of the cooperating societies, ASCE, AIME, ASME, AIEE, or WSE, for a technical paper of particular merit accepted by the publication committee of any of these societies, provided the author is not more than 30 years of age at the time of such acceptance.

Joint Activities

UNITED ENGINEERING TRUSTEES, INC.

The funds and property held jointly by the four Founder Societies, including the Engineering Societies Building, the Engineering Societies Library, and the endowment funds of the Engineering Foundation, are administered by the United Engineering Trustees, Inc., which also serves as treasurer of the Engineers' Council for Professional Development.

The building has recently required some major repairs. It is fully occupied at present, and two of the Founder Societies have substantial amounts of space in other buildings.

ENGINEERING FOUNDATION

The Engineering Foundation is a department of the United Engineering Trustees, Inc., and its general objective is "the furtherance of research in science and engineering."

With the income from its endowment funds, it supports a broad range of research projects, now numbering about 16. Some of its most effective contributions are those supporting studies and analyses necessary in the early stages of organizing projects on such bases that financial support from other sources becomes available. A special study is being devoted to the future employment of Foundation funds towards advancing research.

ENGINEERING SOCIETIES LIBRARY

The library is a department of the United Engineering Trustees, Inc., and was formed by combining the separate libraries of the ASCE, AIME, ASME, and AIEE, and is conducted as a free public reference library.

In addition to affording the use of a large collection of engineering books and periodicals, the library renders special services such as bibliographies, translations, photostats, searches, and book loans by mail.

A broad survey is in progress for the purpose of reorienting the library with other technical libraries in the United States and for obtaining greater financial support. The bylaws governing the Library Board have been amended to reduce the number of board members from 22 to 12.

ENGINEERS' COUNCIL FOR PROFESSIONAL DEVELOPMENT

The principal activities of ECPD include programs for the guidance of young persons thinking of entering the engineering field, the accrediting of curricula of engineering schools, and encouragement and assistance to individuals in their engineering and cultural studies during several years following graduation. The council represents ASCE, AIME, ASME, AIEE, American Institute of Chemical Engineers, the Engineering Institute of Canada, the American Society for Engineering Education, and the National Council of State Boards of Engineering Examiners.

ENGINEERS JOINT COUNCIL

The membership of this council includes the two most recent available past presidents and the secretaries, also the presidents as ex-officio members without votes, of the five member societies; ASCE, AIME, ASCE, AIEE, and AIChE. Its purpose is to promote co-operation among the branches of engineering by seeking and studying matters of mutual interest to the member societies, to recommend joint action, and to administer activities authorized by a majority of the societies. A constitution was recently adopted and referred to the societies for approval.

REPRESENTATIVES

A complete list of about 40 joint bodies upon which the Institute is represented appears in the Year Book and in the October issue of *Electrical Engineering* each year.

Appreciation

The continuing rapid increase in the membership and the income of the Institute are tangible symbols of the highly effective work of the national committees, and the District, Section, and Branch officers and committees. For their enthusiasm and excellent co-operation, the Board of Directors expresses sincere thanks and appreciation. It also thanks the members in general for their keen interest in the activities and for their splendid support of established policies.

Respectfully submitted for the Board of Directors.

H. H. HENLINE
Secretary

HASKINS & SELLS
CERTIFIED PUBLIC ACCOUNTANTS

1 EAST 44TH STREET
NEW YORK 17

ACCOUNTANTS' CERTIFICATE

American Institute of Electrical Engineers:

We have examined the balance sheet of American Institute of Electrical Engineers, and schedule of securities owned, as of April 30, 1949, and the related statements of cash receipts and disbursements of operating and restricted funds for the year then ended. Our examination was made in accordance with generally accepted auditing standards, and accordingly included such tests of the accounting records and such other auditing procedures as we considered necessary in the circumstances.

In our opinion, the accompanying balance sheet, schedule of securities owned, and statements of cash receipts and disbursements, respectively, present fairly the financial position of, and securities owned by, the Institute at April 30, 1949, and its recorded cash receipts and cash disbursements for the year then ended, in conformity with generally accepted accounting principles applied on a basis consistent with that of the preceding year.

(Signed) HASKINS & SELLS

New York,
May 19, 1949

AMERICAN INSTITUTE OF ELECTRICAL ENGINEERS

Balance Sheet, April 30, 1949

Exhibit A

ASSETS		
Property Fund Assets:		
One-fourth interest in physical properties of United Engineering Trustees, Inc.:		
Land, buildings, and equipment (less depreciation and renewal reserve)	$332,383.85	
Funded depreciation and renewal reserve	166,064.63	
Total	$498,448.48	
Equipment:		
Library (volumes and fixtures)—estimated value	36,366.37	
Office furniture and fixtures (less reserve for depreciation, $31,567.26)	15,746.17	
Works of art, etc.	3,001.35	
Total property fund assets		$ 553,562.37
Restricted Fund Assets:		
Securities—at cost, less reserve, $1,788.15 (quoted market value, $533,172.52)—Schedule 1	$523,824.26	
Cash (Exhibit *C*)	56,399.79	
Accrued interest receivable	184.98	
Total restricted fund assets		580,409.03
Operating Fund Assets:		
Cash (not including $1,674.87 for Federal taxes withheld from employees)—(Exhibit *B*)	$14,795.59	
Accounts receivable:		
Members—for dues (less reserve, $5,750.00)	11,675.34	
Advertisers	2,572.37	
Miscellaneous	6,638.63	
Technical Conference loans outstanding	650.00	
Accrued interest receivable	2,042.33	
Inventories:		
Transactions, etc.	1,308.00	
"Electrical Definitions"	537.00	
Work in process *Transactions* (Part II 1948), etc.	5,726.96	
Text and cover paper	11,311.46	
Badges	7,601.64	
Deferred charges—Production charges for May issue of *Electrical Engineering*	16,127.61	
Total operating fund assets		80,986.93
Total		$1,214,958.33

LIABILITIES		
Property Fund Reserve		$ 553,562.37
Restricted Fund Reserves:		
Reserve capital fund	$531,660.79	
Life membership fund	8,312.51	
Member-for-Life fund	9,632.17	
International Electrical Congress of St. Louis library fund	6,442.30	
Lamme Medal fund	4,440.44	
Mailloux fund	1,012.15	
Volta Memorial fund	18,908.67	
Total restricted fund reserves		580,409.03
Operating Fund Reserves, Liabilities, etc.:		
Accounts payable	$ 30,007.57	
Deferred income:		
Dues received in advance	3,501.36	
Entrance fees and dues advanced by applicants for membership	2,309.08	
Subscriptions to publications received in advance	20,597.00	
Miscellaneous (including unallocated receipts)	1,753.57	
Operating fund reserves	22,818.35	
Total operating fund reserves, liabilities, etc.		80,986.93
Total		$1,214,958.33

Exhibit B Statement of Cash Receipts and Disbursements of Operating Fund for the Year Ended April 30, 1949

Cash on Deposit with The National City Bank of New York, May 1, 1948 (not including $2,031.98 for Federal taxes withheld from employees)			$ 22,394.58
Receipts:			
Dues (including $168,882.00 allocated to *Electrical Engineering* subscriptions)		$363,816.95	
Advertising in *Electrical Engineering*		169,325.25	
Transaction subscriptions		15,874.93	
Electrical Engineering subscriptions		30,662.92	
Miscellaneous publications (preprints, Standards, special reports, etc.)		49,246.60	
Students' fees		39,356.25	
Entrance fees		19,584.56	
Registration fees—Institute Meetings and Technical Conferences		13,585.71	
Membership badges		5,264.20	
Transfer fees		3,440.00	
Interest and dividends on investments of Reserve Capital Fund		29,958.02	
Miscellaneous		496.90	
Total		$740,612.29	
Refund from Radio Technical Planning Board		722.28	
Refund of expenses paid, 1947 Summer General Meeting		53.03	
Contribution from Committee on Instrumentation and Measurements		94.00	
Transfer from Property Fund		612.91	
Transfer from Reserve Capital Fund–net (see Exhibit *C*)		11,817.00	
Total receipts			753,911.51
Total			$776,306.09
Disbursements:			
Publications expense:			
Electrical Engineering text	$175,472.46		
Electrical Engineering advertising	93,594.98	$269,067.44	
Transactions		21,166.69	
Proceedings		37,636.58	
"Year Book"		12,168.99	
Special publications		2,528.15	
Miscellaneous publications (preprints, Standards, etc.)		32,498.14	
Institute meetings		32,396.51	
Institute Sections		91,039.35	
Institute Branches, including prizes, etc.		7,706.99	
Finance Committee		850.00	
Headquarters Committee		344.86	
Membership Committee		19,512.63	
Standards Committee		20,711.33	
Technical Committees		11,684.65	
Committee on Public Relations		1,183.88	
Edison Medal Committee		296.51	
Forward		$560,792.70	
Total (forward)			$776,306.09
Total (forward)			$776,306 09
Disbursements (forward)		$560,792.70	
Traveling expenses:			
Geographical Districts:			
Executive committees		6,278.69	
Vice-Presidents		1,770.67	
Conferences on Student activities		8,783.72	
Board of Directors		15,750.87	
Nominating Committee		1,568.85	
President's appropriation		4,294.33	
Administrative expenses		90,436.12	
Geographical Districts—Branch paper prizes		100.11	
Institute prizes—National		532.70	
Retirement system AIEE—normal contribution		8,395.31	
American Standards Association		1,875.00	
Canadian Radio Technical Planning Board		10.00	
Canadian Council of Professional Engineers and Scientists		278.71	
Engineers' Council for Professional Development		1,808.50	
Engineering Foundation Project—Welding research		250.00	
Engineers Joint Council—General expenses		759.50	
John Fritz Medal		75.00	
National Committee State Board Engineering Examiners		500.00	
U. S. National Committee—International Commission on Illumination		300.00	
Constitution and Bylaws Committee		1,152.48	
United Engineering Trustees, Inc.:			
Building assessments		19,547.48	
Library assessments		13,053.35	
Library Retirement Plan		3,615.43	
Lamme Medal expense (see Exhibit *C*)		124.30	
Membership badges		5,768.42	
Legal services		987.53	
Office furniture and fixtures and repairs		3,067.03	
Rent, etc., Editorial Department, 500 Fifth Avenue		6,963.30	
Total		$758,840.10	
Transfer to Member-for-Life fund		2,020.40	
Technical Conference—Loans outstanding		650.00	
Total disbursements			761,510.50
Cash on Deposit, April 30, 1949:			
The National City Bank of New York (not including $1,674.87 for Federal taxes withheld from employees)		$ 12,441.23	
The Canadian Bank of Commerce, Toronto		2,354.36	$ 14,795.59

Exhibit C Statement of Cash Receipts and Disbursements of Restricted Funds for the Year Ended April 30, 1949

	Restricted Funds							
	Total	Reserve Capital Fund	Member-for-Life Fund	Life Membership Fund	International Electrical Congress of St. Louis Library Fund	Lamme Medal Fund	Mailloux Fund	Volta Memorial Fund
Cash on Deposit With The National City Bank of New York and Various Savings Banks, May 1, 1948	$ 39,398.08	$ 25,489.06	$ 8,416.86	$3,435.68	$ 891.47	$150.00	$1,015.01	
Receipts:								
Proceeds from sales, etc. of securities	$ 82,902.20	$ 82,902.20						
Income from bonds	545.34		$ 62.50	$ 127.56	$ 135.28	$160.00		$ 60.00
Interest on bank balances	63.14			48.00			$ 15.14	
Transfer from operating fund	1,957.90		1,957.90					
Life membership fees	209.56			209.56				
Gift from Italy America Society, Incorporated	16,759.51							16,759.51
Total receipts	$102,437.65	$ 82,902.20	$ 2,020.40	$ 385.12	$ 135.28	$160.00	$ 15.14	$16,819.51
Total	$141,835.73	$108,391.26	$10,437.26	$3,820.80	$1,026.75	$310.00	$1,030.15	$16,819.51
Disbursements:								
Purchase of securities	$ 71,791.32	$ 66,791.32	$5,000.00					
Transfers to operating fund:								
To be repaid when adequate funds become available	11,817.00	11,817.00						
Other	709.36			$ 709.36				
Purchase of medal, cost of engraving, etc. (exclusive of $124.30 paid from operating fund)	150.00					$150.00		
Library purchases	111.09				$ 93.09		$ 18.00	
Traveling expenses	857.17		857.17					
Total disbursements	$ 85,435.94	$ 78,608.32	$5,857.17	$ 709.36	$ 93.09	$150.00	$ 18.00	
Cash on Deposit With The National City Bank of New York and Various Savings Banks, April 30, 1949	$ 56,399.79	$ 29,782.94	$4,580.09	$3,111.44	$ 933.66	$160.00	$1,012.15	$16,819.51

AMERICAN INSTITUTE OF ELECTRICAL ENGINEERS

Securities Owned, April 30, 1949

Schedule 1

	Principal Amount of Bonds or Number of Shares of Stock	Reserve Capital Fund	Restricted Funds					Total
			Life Membership Fund	Member for Life Fund	International Electrical Congress Library Fund	Lamme Medal Fund	Volta Memorial Fund	
Railroad Bonds:								
Atlantic Coast Line First Consolidated 4%, due 1952	$ 4,000.00					$4,253.78		$ 4,253.78
Baltimore & Ohio, Pittsburgh, Lake Erie & West Virginia System Refunding 4%, due 1980	10,000.00	$ 6,450.00						6,450.00
Chicago & Erie Railroad Company 5% first mortgage, due 1982, registered	1,000.00	1,105.00						1,105.00
New York Central Railroad Company 4% series *A* consolidated mortage, due 1993	15,000.00	9,812.50						9,812.50
Northern Pacific Railway Company 4 1/2% collateral trust, due 1975	15,000.00	15,307.50						15,307.50
St. Louis-San Francisco Railway Company 4% series *A*, first mortgage, due 1997	1,200.00	1,200.00						1,200.00
St. Louis-San Francisco Railway Company 4% series *A*, first mortgage, scrip	198.00	198.00						198.00
St. Louis-San Francisco Railway Company 4 1/2% series *A*, second mortgage income bonds, due 2022	1,300.00	1,300.00						1,300.00
St. Louis-San Francisco Railway Company 4 1/2% series *A*, second mortgage income bonds, scrip	61.10	61.10						61.10
Total railroad bonds		$ 35,434.10				$4,253.78		$ 39,687.88
Public Utility Bonds:								
American Telephone & Telegraph Company 2 3/4% convertible debentures, due 1961	$40,000.00	$ 33,154.75	$5,153.12		$5,457.85			$ 43,765.72
Consolidated Edison Company of New York, Incorporated 3% convertible debentures, due 1963	25,000.00	27,281.25						27,281.25
Total public utility bonds		$ 60,436.00	$5,153.12		$5,457.85			$ 71,046.97
United States Government Bonds:								
Treasury bonds 2%, due March 15, 1952/50	$ 3,000.00	$ 3,074.22						$ 3,074.22
Treasury bonds 3%, due September 15, 1955/51	2,000.00						$2,081.66	2,081.66
Defense bonds series *G*, 2 1/2%, due December 1, 1954	18,000.00	13,000.00		$5,000.00				18,000.00
Treasury Savings bonds series *G*, 2 1/2%, due September 1, 1955	40,000.00	40,000.00						40,000.00
Treasury Savings bonds series *G*, 2 1/2%, due November 1, 1956	17,000.00	17,000.00						17,000.00
Treasury Savings bonds series *G*, 2 1/2%, due May 1, 1957	20,000.00	20,000.00						20,000.00
Treasury Savings bonds series *G*, 2 1/2%, due October 1, 1957	30,000.00	30,000.00						30,000.00
Total United States Government bonds		$123,074.22		$5,000.00			$2,081.66	$130,155.88
Capital Stocks:								
American Can Company	60 shares	$ 4,988.40						$ 4,988.40
American Gas & Electric Company	400 shares	15,137.62						15,137.62
Atchison, Topeka & Santa Fe Railway Company preferred	200 shares	19,174.71						19,174.71
Atlantic City Electric Company	40 shares	612.00						612.00
Boston Edison Company	200 shares	4,927.50						4,927.50
Commonwealth Edison Company	200 shares	7,580.68						7,580.68
Consolidated Natural Gas Company	100 shares	4,428.80						4,428.80
Dow Chemical Company $4 cumulative preferred, series A	100 shares	11,547.50						11,547.50
Eastman Kodak Company	315 shares	10,694.11						10,694.11
E. I. du Pont de Nemours & Company	80 shares	13,096.68						13,096.68
General Electric Company	200 shares	7,748.66						7,748.66
General Motors Corporation $5 preferred	200 shares	25,820.00						25,820.00
General Motors Corporation	100 shares	4,235.53						4,235.53
Gulf Oil Corporation	200 shares	12,264.20						12,264.20
Insurance Company of North America	100 shares	10,847.50						10,847.50
International Harvester Company	300 shares	5,030.50						5,030.50
International Match Realization Co. capital stock	6 shares	1,788.15*						1,788.15*
Louisville & Nashville Railroad Company	100 shares	6,278.13						6,278.13
Ohio Edison Company 4.40% preferred	200 shares	21,279.25						21,279.25
Pacific Gas and Electric Company	200 shares	8,420.99						8,420.99
Public Service Electric and Gas Company $1.40 dividend preference common stock	370 shares	11,150.00						11,150.00
St. Louis-San Francisco Railway Company voting trust certificates for 5% series *A* preferred stock	21 1800/10000ths shares	582.75						582.75
St. Louis-San Francisco Railway Company voting trust certificates for common stock	42 6000/10000ths shares	357.00						357.00
Scoville Manufacturing Company 3.65% cumulative preferred	100 shares	10,111.25						10,111.25
Sears, Roebuck and Co.	400 shares	6,014.97						6,014.97
Socony Vacuum Oil Company	408 shares	8,381.20						8,381.20
Standard Oil Company of Indiana	200 shares	8,170.32						8,170.32
Standard Oil Company of New Jersey	$212^{36}/_{100}$ shares	9,761.26						9,761.26
Texas Gulf Sulphur Company	$3^{8}/_{64}$ shares	144.60						144.60
Union Carbide & Carbon Corporation	300 shares	7,277.42						7,277.42
United Fruit Company	300 shares	11,985.00						11,985.00
United States Steel Corporation 7% cumulative preferred	100 shares	14,885.00						14,885.00
Total capital stocks		$284,721.68						$284,721.68
Total		$503,666.00	$5,153.12	$5,000.00	$5,457.85	$4,253.78	$2,081.66	$525,612.41
* Less reserve in full for securities considered to be of doubtful value		1,788.15						1,788.15
Total Securities, Less Reserve		$501,877.85	$5,153.12	$5,000.00	$5,457.85	$4,253.78	$2,081.66	$523,824.26

Officers of A.I.E.E. for 1949–1950

PRESIDENT

JAMES F. FAIRMAN
New York, N. Y.
(Term expires July 31, 1950)

PAST PRESIDENTS

Blake D. Hull, Dallas, Tex.
(Term expires July 31, 1950)

Everett S. Lee, Schenectady, N. Y.
(Term expires July 31, 1951)

VICE-PRESIDENTS

District	
1	Victor Siegfried, Worcester, Mass.
3	J. L. Callahan, New York, N. Y.
5	E. W. Seeger, Milwaukee, Wis.
7	G. N. Pingree, Dallas, Tex.
9	Richard McKay, Spokane, Wash.

(Terms expire July 31, 1950)

District	
2	C. G. Veinott, Lima, Ohio
4	W. J. Seeley, Durham, N. C.
6	W. C. DuVall, Boulder, Colo.
8	Ralph A. Hopkins, Los Angeles, Calif.
10	A. H. Frampton, St. Catharines, Ont.

(Terms expire July 31, 1951)

DIRECTORS

W. J. Barrett, Newark, N. J.
R. T. Henry, Buffalo, N. Y.
E. P. Yerkes, Philadelphia, Pa.
(Terms expire July 31, 1950)

W. L. Everitt, Urbana, Ill.
A. C. Monteith, Pittsburgh, Pa.
Elgin B. Robertson, Dallas, Tex.
(Terms expire July 31, 1951)

C. W. Fick, Cleveland, Ohio
M. D. Hooven, Newark, N. J.
F. O. McMillan, Corvallis, Oreg.
(Terms expire July 31, 1952)

E. W. Davis, Cambridge, Mass.
N. B. Hinson, Los Angeles, Calif.
H. J. Scholz, Birmingham, Ala.
(Terms expire July 31, 1953)

TREASURER

W. I. Slichter, New York, N. Y.
(Term expires July 31, 1950)

SECRETARY

H. H. Henline, New York, N. Y.
(Term expires July 31, 1950)

LOCAL HONORARY SECRETARIES

Australia—V. J. F. Brain, Electricity Authority of N.S.W., Box 2600 G.P.O., Sydney, New South Wales

Brazil—Richard H. Bowles, Sao Paulo Tramway Light and Power Company, Caixa Postal 26-B, Sao Paulo

England—Sir A. P. M. Fleming, Metropolitan Vickers Electric Company, Trafford Park, Manchester 17

India, Northern—S. S. Kumar, P.W.D. Electricity Secretariat, Ellerslie, Simla-E, East Punjab

India, Southern—S. M. Zubair, Tata Hydro Electric Company, Bombay House, Bruce Street, Fort Bombay

New Zealand—P. H. Powell, 130 Glandovey Road, Fendalton, Christchurch, N. W. 1 (Acting)

Sweden—Edy Velander, Box 5073, Stockholm 5

Transvaal—Francis E. Ingham, Box 6067, Johannesburg, Transvaal, South Africa

PAST PRESIDENTS—*1884–1949*

*Norvin Green	1884–85–86
*Franklin L. Pope	1886–87
*T. Commerford Martin	1887–88
*Edward Weston	1888–89
*Elihu Thomson	1889–90
*William A. Anthony	1890–91
*Alexander Graham Bell	1891–92
*Frank Julian Sprague	1892–93
*Edwin J. Houston	1893–94–95
*Louis Duncan	1895–96–97
*Francis Bacon Crocker	1897–98
*A. E. Kennelly	1898–1900
*Carl Hering	1900–01
*Charles P. Steinmetz	1901–02
*Charles F. Scott	1902–03
*Bion J. Arnold	1903–04
*John W. Lieb	1904–05
*Schuyler Skaats Wheeler	1905–06
*Samuel Sheldon	1906–07
*Henry G. Stott	1907–08
*Louis A. Ferguson	1908–09
*Lewis B. Stillwell	1909–10
Dugald C. Jackson	1910–11
Gano Dunn	1911–12
Ralph D. Mershon	1912–13
*C. O. Mailloux	1913–14
*Paul M. Lincoln	1914–15
*John J. Carty	1915–16
H. W. Buck	1916–17
*E. W. Rice, Jr.	1917–18
Comfort A. Adams	1918–19
*Calvert Townley	1919–20
*A. W. Berresford	1920–21
William McClellan	1921–22
Frank B. Jewett	1922–23
*Harris J. Ryan	1923–24
*Farley Osgood	1924–25
*M. I. Pupin	1925–26
*C. C. Chesney	1926–27
*Bancroft Gherardi	1927–28
*R. F. Schuchardt	1928–29
*Harold B. Smith	1929–30
*William S. Lee	1930–31
C. E. Skinner	1931–32
H. P. Charlesworth	1932–33
J. B. Whitehead	1933–34
*J. Allen Johnson	1934–35
*E. B. Meyer	1935–36
A. M. MacCutcheon	1936–37
W. H. Harrison	1937–38
John Castlereagh Parker	1938–39
F. Malcolm Farmer	1939–40
R. W. Sorensen	1940–41
David C. Prince	1941–42
Harold S. Osborne	1942–43
Nevin E. Funk	1943–44
C. A. Powel	1944–45
*W. E. Wickenden	1945–46
J. Elmer Housley	1946–47
B. D. Hull	1947–48
Everett S. Lee	1948–49

*Deceased.

Past and Present Officers of the Institute

Abbott, Arthur V., *V-P.*, 1900–02.
Adams, Comfort A., *M.*, 1912–15; *V-P.*, 1915–17; *P.*, 1918–19.
*Adsit, C. G., *V-P.*, 1921–23.
Alger, P. L., *D.*, 1944–48.
*Anthony, Wm. A., *V-P.*, 1886–89; *P.*, 1890–91; *V-P.*, 1894–96.
*Armstrong, A. H., *M.*, 1903–06; *V-P.*, 1906–08.
*Arnold, Bion J., *M.*, 1895–98; *V-P.*, 1902–03; *P.*, 1903–04.
Auty, K. A., *V-P.*, 1932–34.

*Babcock, A. H., *V-P.*, 1918–19.
Barker, J. W., *V-P.*, 1940–42.
Barnes, H. H., Jr., *M.*, 1910–13; *V-P.*, 1913–15.
*Barstow, W. S., *M.*, 1900–03; *V-P.*, 1903–05.
Barton, T. F., *V-P.*, 1939–40; *D.*, 1940–44.
†Bates, D. H., *V-P.*, 1885–87.
*Baum, Frank G., *V-P.*, 1906–08.
Beardsley, C. R., *D.*, 1937–41.
Beaver, J. L., *V-P.*, 1927–29.
Bedell, Frederick, *M.*, 1914–17; *V-P.*, 1917–18.
*Behrend, B. A., *M.*, 1913–16; *V-P.*, 1916–18.
*Bell, Alexander G., *V-P.*, 1884–85; *P.*, 1891–92.
*Bell, Louis, *M.*, 1891–94.
Bennett, Edward, *V-P.*, 1924–26.
*Berresford, A. W., *M.*, 1909–12; *V-P.*, 1912–14; *P.*, 1920–21.
Berry, J. H., *V-P.*, 1947–49.
Bettis, A. E., *V-P.*, 1926–28; *D.*, 1928–32.
Bickelhaupt, C. O., *V-P.*, 1927–29.,
Bingham, L. A., *V-P.*, 1943–45.
†Black, R. G., *M.*, 1910–13.
Blackwell, O. B., *V-P.*, 1936–38.
Blaisdell, L. T., *V-P.*, 1936–38.
Bolton, F. C., *V-P.*, 1938–40.
Bonney, R. B., *V-P.*, 1933–35.
Bower, G. W., *V-P.*, 1947–49.
*Brackett, Cyrus F., *M.*, 1886–89.
*Bradley, Chas. S., *M.*, 1894–97; *V-P.*, 1897–99, *M.*, 1899–1902.
*Brooks, David M., *M.*, 1885–88.
*Brooks, Morgan, *M.*, 1907–10; *V-P.*, 1910–12.
*Brush, Chas. F., *M.*, 1884–87.
Bryant, J. M., *M.*, 1924–28.
Buck, Harold W., *M.*, 1907–10; *V-P.*, 1910–12; *P.*, 1916–17.
*Buckingham, Chas. L., *M.*, 1885–88.
Buckley, O. E., *V-P.*, 1946–48.
Bush, Vannevar, *D.*, 1937–41.
Bussey, H. E., *V-P.*, 1923–25.

Callahan, J. L., *V-P.*, 1948–50.
Carle, N. A., *M.*, 1916–19; *V-P.*, 1919–20.
*Carlton, W. G., *M.*, 1908–11; *V-P.*, 1911–13.
Carpenter, C. B., *V-P.*, 1944–46.
*Carpenter, H. V., *V-P.*, 1930–32.
*Carty, John J., *M.*, 1893–96, 1900–03, 1903–04, 1906–08; *V-P.*, 1904–06, 1908–11; *P.*, 1915–16.
*Chamberlain, J. C., *M.*, 1890–93.
Charlesworth, H. P., *M.*, 1923–27; *V-P.*, 1930–32; *P.*, 1932–33.
*Chesney, C. C., *M.*, 1905–08; *V-P.*, 1908–10; *P.*, 1926–27.
Chesterman, F. J., *D.*, 1926–30.
Christie, C. V., *V-P.*, 1935–37.
Chubb, L. W., *D.*, 1931–35.
Chubbuck, L. B., *V-P.*, 1931–33.
†Church, W. Lee, *M.*, 1887–88.
*Clarke, Chas. L., *M.*, 1904–05.
Clifford, H. E., *M.*, 1908–11.
Coldwell, O. B., *V-P.*, 1921–22.
*Compton, Alfred G., *M.*, 1891–94.
Cone, D. I., *V-P.*, 1947–49.
Cooper, A. B., *V-P.*, 1927–29; *D.*, 1930–34.
Coover, M. S., *D.*, 1940–44; *V-P.*, 1944–46.
Copley, A. W., *V-P.*, 1931–33.
*Craft, E. B., *M.*, 1920–24.
Craft, F. M., *V-P.*, 1933–35.
*Crocker, Francis B., *M.*, 1888–90; *V-P.*, 1890–92, 1894–96; *P.*, 1897–98.
†Crosby, Oscar T., *V-P.*, 1892–94.
*Cross, Chas. R., *V-P.*, 1884–85.
*Cuttriss, Chas., *M.*, 1888–91.

Danner, R. F., *V-P.*, 1946–48.
Davis, Ernest W., *V-P.*, 1946–48; *D.*, 1949–53.
Dawes, Chester L., *V-P.*, 1938–40.
*Delany, Patrick B., *M.*, 1890–93; *V-P.*, 1893–95.
Del Mar, Wm. A., *M.*, 1917–21; *V-P.*, 1921–22.
Dewars, A. G., *V-P.*, 1942–44.
Dobson, W. P., *V-P.*, 1925–27.
*Dolbear, A. E., *V-P.*, 1885–87.
*Don Carlos, H. C., *D.*, 1926–30.
*Downing, P. M., *V-P.*, 1925–27.
*Duncan, Louis, *P.*, 1895–97.
Dunn, Gano, *M.*, 1897–1900; *V-P.*, 1900–02; *M.*, 1902–05; *V-P.*, 1905–07; *P.*, 1911–12.
DuVall, W. C., *V-P.*, 1949–51.

†Eales, H. W., *V-P.*, 1921–26.
*Eckert, W. H., *M.*, 1884–85.
*Edgar, Chas. L., *M.*, 1905–08.
*Edison, Thos. A., *V-P.*, 1884–85.
*Eglin, W. C. L., *M.*, 1903–06; *V-P.*, 1907–09.
Eldredge, M., *V-P.*, 1935–37; *D*,. 1939–43.
Ellestad, I. M., *V-P.*, 1947–49.
*Emmet, W. L. R., *V-P.*, 1900–02.
Evans, Herbert S., *V-P.*, 1929–31.
Evenson, F. F., *V-P.*, 1945–47.
Everitt, W. L., *D.*, 1947–51.
Ewart, F. R., *V-P.*, 1921–23.

*Faccioli, G., *M.*, 1918–22; *V-P.*, 1922–24.
†Fair, R. H., *V-P.*, 1935–37.
Fairman, J. F., *V-P.*, 1944–46; *D.*, 1946–49; *P.*, 1949–50.
Farmer, F. M., *D.*, 1934–38; *V-P.*, 1938–39; *P.*, 1939–40.
*Ferguson, Louis A., *M.*, 1904–07; *V-P.*, 1907–08; *P.*, 1908–09.
Ferguson, O. J., *V-P.*, 1927–29.
Fick, C. W., *D.*, 1948–52.
*Field, Stephen D., *M.*, 1884–86.
Fields, E. S., *V-P.*, 1945–47.
*Finney, John H., *M.*, 1914–17; *V-P.*, 1917–18.
*Fisken, John B., *M.*, 1916–19; *V-P.*, 1919–20.
Flanigen, J. M., *D.*, 1945–49.
Fleager, C. E., *V-P.*, 1929–31.
*Foster, Horatio A., *M.*, 1890–93.
*Fowle, F. F., *M.*, 1919–23.
*Fowler, A. C., *M.*, 1887.
Fowler, M. M., *D.*, 1925–29.
Frampton, A. H., *V-P.*, 1949–51.
*Freeman, W. E., *V-P.*, 1931–33.
Funk, N. E., *D.*, 1934–38; *P.*, 1943–44.

Gamble, Lester R., *V-P.*, 1938–40; *D.*, 1941–45.
Gaylord, J. M., *V-P.*, 1943–45.
Gear, H. B., *D.*, 1934–38.
Geiger, D. G., *V-P.*, 1947–49.
*Geyer, Wm. E., *M.*, 1888–92.
*Gherardi, Bancroft, *M.*, 1905–08, 1914–17; *V-P.*, 1908–10; *P.*, 1927–28.
Gilson, Walter J., *V-P.*, 1943–45.
Goldsborough, W. E., *M.*, 1901–04; *V-P.*, 1904–06.
*Gray, Elisha, *M.*, 1884–86.
*Green, Norvin, *P.*, 1884–86; *V-P.*, 1886–88.
*Greene, S. Dana, *M.*, 1899.

Hall, Walter A., *M.*, 1917–21; *V-P.*, 1921–22.
*Hamblet, Jas., *M.*, 1891–94; *V-P.*, 1894–96.
*Hamilton, George A., *V-P.*, 1884–86; *Natl. Treas.*, 1895–1930.
Hamilton, J. L., *V-P.*, 1940–42.
*Hammer, William J., *V-P.*, 1891–93; *M.*, 1893–96.
Hanker, F. C., *D.*, 1927–31.
Hansen, K. L., *V-P.*, 1940–42; *D.*, 1942–46.
*Harding, C. F., *V-P.*, 1936–38.
*Harisberger, John, *V-P.*, 1924–26.
Harrison, W. H., *V-P.*, 1935–37; *P.*, 1937–38.
*Haskins, Chas. H., *V-P.*, 1884–86.
*Hasson, W. F. C., *V-P.*, 1895–97; *M.*, 1897–1900.
*Hazard, Rowland R., *Treas.*, 1884–86; *V-P.*, 1887–89.
*Hellings, M. L., *M.*, 1884–85.
*Hellmund, R. E., *D.*, 1939–42.
*Henderson, S. E. M., *V-P.*, 1923–25.
Henline, H. H., *Act. Secy.*, 1932; *Secy.*, 1933–.
Henry, R. T., *V-P.*, 1944–46; *D.*, 1946–50.
*Hering, Carl, *V-P.*, 1891–93, 1895–98; *P.*, 1900–01.
*Herzog, F. Benedict, *M.*, 1887–92.
†Hewitt, Chas., *M.*, 1893–96.
†Hibbard, Angus S., *M.*, 1892–95; *V-P.*, 1895–97.
Hibshman, N. S., *V-P.*, 1941–43.
*Higson, C. R., *V-P.*, 1932–34.
Hinson, N. B., *V-P.*, 1935–37; *D*, 1949–53.
Hitchcock, H. W., *V-P.*, 1939–41.
*Hobart, H. M., *M.*, 1922–26; *V-P.*, 1926–28.
Hooven, M. D., *D.*, 1948–52.
Hopkins, Ralph A., *V-P.*, 1949–51.
Housley, J. B., *V-P.*, 1941–43; *P.*, 1946–47.
*Houston, Edwin J., *M.*, 1884–87; *P.*, 1893–95.
*Howell, John W., *M.*, 1888–90.
Hull, A. H., *V-P.*, 1933–35.
Hull, B. D., *V-P.*, 1928–30; *D.*, 1931–35; *P.*, 1947–48.
*Humphrey, H. H., *V-P.*, 1906–08.
Hunting, F. S., *M.*, 1911–14; *V-P.*, 1914–16.
*Hutchinson, Cary T., *M.*, 1895–98; *V-P.*, 1898–1900.
*Hutchinson, F. L., *Natl. Secy.*, 1912–32.

*Imlay, L. E., *M.*, 1919–23.
Jackson, Dugald C., *V-P.*, 1897–99; *P.*, 1910–11.
*Jackson, W. B., *M.*, 1912–15; *V-P.*, 1918–19.
†James, Wm. F., *V-P.*, 1923–25.
Jamieson, B. G., *V-P.*, 1926–28.
Jewett, F. B., *M.*, 1915–18; *V-P.*, 1918–19; *P.*, 1922–23.
Johnson, F. Ellis, *D.*, 1936–39.
*Johnson, J. Allen, *D.*, 1928–32; *V-P.*, 1932–34; *P.*, 1934–35.
Jollyman, J. P., *V-P.*, 1937–39.
Jones, A. L., *V-P.*, 1941–43.
Jones, C. R., *D.*, 1935–39; *V-P.*, 1942–44.
*Jones, Francis W., *M.*, 1884–85; *V-P.*, 1885–87.
*Jorgensen, L. R., *V-P.*, 1919–20.
Juhnke, P. B., *D.*, 1933–37.
*Junkersfeld, P., *M.*, 1913–16; *V-P.*, 1916–18.

Kearns, J. E., *D.*, 1929–33.
*Keith, Nathaniel S., *Secy.*, 1884–85.
*Kelsch, Raymond S., *V-P.*, 1918–19.
*Kennelly, Arthur E., *V-P.*, 1892–94; *M.*, 1894–97; *V-P.*, 1897–98; *P.*, 1898–1900.
Kidder, H. A., *M.*, 1925–28; *V-P.*, 1928–30.
*Knight, G. L., *M.*, 1922–26; *V-P.*, 1926–28.
Knowlton, A. E., *D.*, 1930–34.
Kositzky, G. A., *D.*, 1932–36.
Kouwenhoven, W. B., *V-P.*, 1931–33; *D.*, 1935–39.

Lacy, T. N., *V-P.*, 1930–32.
Laffoon, C. M., *D.*, 1942–47.
*Lamme, Benj. G., *M.*, 1907–10.
Lane, F. H., *D.*, 1937–41.
Lardner, H. A., *M.*, 1913–16.
Lawton, F. L., *V-P.*, 1945–47.
LeClair, T. G., *D.*, 1941–45; *V-P.*, 1946–48.
Lee, Everett S., *D.*, 1933–37; *V-P.*, 1940–42; *P.*, 1948–49.
*Lee, William S., *M.*, 1911–14; *D.*, 1929–30; *P.*, 1930–31.
*Leonard, H. Ward, *M.*, 1890–93; *V-P.*, 1893–95.
*Lieb, John W., *M.*, 1896–99; *V-P.*, 1899–1901; *M.*, 1901–03; *V-P.*, 1903–04; *P.*, 1904–05.
*Lighthipe, J. A., *V-P.*, 1913–15.
Lincoln, J. F., *M.*, 1920–24.
*Lincoln, Paul M., *M.*, 1906–09; *V-P.*, 1909–11; *P.*, 1914–15.
Liversidge, H. P., *D.*, 1927–31.
*Lloyd, Herbert *M.*, 1898–1901.
*Lockwood, Thos. D., *V-P.*, 1886–87; *M.*, 1888–90; *V-P.*, 1891–93.
Lovell, A. H., *D.*, 1932–36; *V-P.* ,1938–40.
*Lozier, R. T., *M.*, 1902–04.
†Lunn, Ernest, *M.*, 1922–26.

MacCutcheon, A. M., *D.*, 1928–32; *P.*, 1936–37.
*Macdonald, J. E., *V-P.*, 1923–25.
*Macfarlane, Alexander, *M.*, 1897–1900.
Maclachlan, Wills, *V-P.*, 1919–20.
*Magnusson, C. E., *V-P.*, 1920–21.
Mahood, E. T., *V-P.*, 1942–44.
*Mailloux, C. O., *M.*, 1886–89; *V-P.*, 1898–99; *M.*, 1899–1902; *V-P.*, 1902–04; *M.*, 1905–07; *P.*, 1913–14.
*Mapes, L. R., *D.*, 1938–42.
*Martin, T. Commerford, *Act. Secy.*, 1884–85; *M.*, 1885–87; *P.*, 1887–88; *V-P.*, 1888–90.
Martindale, E. H., *M.*, 1917–20; *V-P.*, 1920–21.
*Maver, Wm., Jr., *M.*, 1888–91.
Maxwell, Fred R., Jr., *V-P.*, 1939–41; *D.*, 1941–45.
*Maynard, Geo. C., *V-P.*, 1886–88.
*McAllister, A. S., *M.*, 1914–17; *V-P.*, 1917–18.
McClellan, L. N., *V-P.*, 1937–39.
McClellan, William, *M.*, 1912–15, *V-P.*, 1915–17, *P.*, 1921–22.
†McConahey, W. M., *M.*, 1923–27.
McDowell, C. S., *V-P.*, 1920–21.
McEachron, K. B., *D.*, 1936–40; *V-P.*, 1942–44.
McHenry, M. J., *V-P.*, 1937–39; *D.*, 1944–48.
McKay, Richard, *V-P.*, 1948–50.
McMillan, F. O., *V-P.*, 1934–36; *D.*, 1948–52.
*Merriam, E. B., *M.*, 1924–28; *V-P.*, 1928–30.
Mershon, Ralph D., *M.*, 1900–03; *V-P.*, 1903–05; *P.*, 1912–13.
*Meyer, E. B., *D.*, 1927–31; *V-P.*, 1932–34; *P.*, 1935–36.
Meyer, F. J., *V-P.*, 1934–36; *D.*, 1939–43.
*Michaelis, O. E., *M.*, 1886–89; *V-P.*, 1889–90.
Mier, C. W., *D.*, 1943–47.
Mills, G. A., *V-P.*, Aug.–Oct. 1932.
Mitchell, W. E., *V-P.*, 1925–27.
Montieth, A. C., *D.*, 1947–51.
*Morehouse, L. F., *M.*, 1919–23; *V-P.*, 1924 26.
*Morrow, L. W. W., *D.*, 1933–37.
Mortensen, S. H., *D.*, 1943–47.
Morton, W. B., *D.*, 1941–46.
Moultrop, I. E., *D.*, 1926–30; *V-P.*, 1930–32.
*Mullin, E. H., *M.*, 1902–04.
*Murray, Wm. S., *M.*, 1908–09, 1909–12; *V-P.*, 1912–14.

Newbury, F. D., *M.*, 1918–22.
*Nichols, E. L., *V-P.*, 1889–91.
*Norris, H. H., *M.*, 1909–12.
North, J. R., *D.*, 1945–49.
Northmore, E. R., *V-P.*, 1927–29.

Osborne, H. S., *D.*, 1938–42; *P.*, 1942–43.
*Osgood, Farley, *M.*, 1911–14; *V-P.*, 1914–16; *P.*, 1924–25.
†Owens, R. B., *V-P.*, 1898–1900.

Parker, John Castlereagh, *V-P.*, 1921–22; *P.*, 1938–39.
†Patton, P. H., *V-P.*, 1931–33.
*Peek, F. W., Jr., *D.*, 1930–33.
Pender, Harold, *M.*, 1915–18; *V-P.*, 1918–19.
*Perrine, Frederick A. C., *M.*, 1898–1900.
*Phelps, Geo. M., Jr., *M.*, 1885–87; *Treas.*, 1886–95.
*Pickernell, F. A., *M.*, 1896–99.
Pierce, A. G., *M.*, 1921–25; *V-P.*, 1925–27.
Pingree, G. N., *V-P.*, 1948–50.
Plumb, H. T., *V-P.*, 1922–24.
*Pope, Franklin L., *V-P.*, 1884–86; *P.*, 1886–87; *V-P.*, 1887–89.
*Pope, Ralph W., *Secy.*, 1885–1911; *Hon. Secy.*, 1911–29.
Post, G. G., *V-P.*, 1934–36.
Powel, C. A., *D.*, 1936–40; *V-P.*, 1942–43; *P.*, 1944–45.
†Pratt, H. A., *M.*, 1921–25.
*Prescott, Geo. B., *M.*, 1884.
*Prescott, G. B., Jr., *M.*, 1888–91.
†Price, C. A., *V-P.*, 1941–43.
Prince, D. C., *D.*, 1938–41; *P.*, 1941–42.
*Puffer, Wm. L., *M.*, 1896–99.
*Pupin, Michael I., *M.*, 1892–95; *V-P.*, 1895–97, 1901–03; *P.*, 1925–26.

Quarles, D. A., *D.*, 1944–48.
Quinan, G. E., *V-P.*, 1928–30.

*Reber, Samuel, _M._, 1901-04; _V-P._, 1904-06.
*Rice, Calvin W., _M._, 1900-03; _V-P._, 1903-05.
*Rice, E. W., Jr., _P._, 1917-18.
Ricker, Claire W., _V-P._, 1943-45.
†Robbins, Chas., _M._, 1916-20; _V-P._, 1920-21.
Robertson, Elgin B., _D._, 1947-51.
Robertson, L. M., _V-P._, 1945-47.
*Robinson, L. T., _M._, 1913-16; _V-P._, 1916-18, 1920-21.
*Rodman, W. S., _V-P._, 1929-31.
Rogers, C. E., _V-P._, 1936-38.
*Ruffner, Chas. S., _M._, 1916-20; _V-P._, 1920-21.
*Rugg, W. S., _M._, 1910-13.
*Rushmore, D. B., _M._, 1908-11; _V-P._, 1911-13.
*Ryan, Harris J., _M._, 1893-96; _V-P._, 1896-98; _P._, 1923-24.
*Ryan, W. T., _V-P._, 1928-30.

*Sands, Herbert S., _V-P._, 1923-27.
*Sargent, W. D., _M._, 1885-86.
Schilling, E. W., _V-P._, 1942-44.
*Schoen, A. M., _M._, 1906-09; _V-P._, 1919-20.
Scholz, H. J., _D._, 1949-53.
Schoolfield, H. H., _V-P._, 1926-28.
*Schuchardt, R. F., _V-P._, 1922-24; _P._, 1928-29.
*Scott, Chas. F., _M._, 1895-98; _V-P._, 1899-1901; _P._, 1902-03.
*Scribner, Chas. E., _M._, 1910-13; _V-P._, 1913-15.
Seeley, W. J., _V-P._, 1949-51.
Sever, Geo. F., _M._, 1898-1901; _V-P._, 1901-03; _M._, 1903-06.
*Shaad, G. C., _V-P._, 1930-32; _D._, 1935-36.
*Shelbourne, Sidney, F., _M._, 1886-87.
*Sheldon, Samuel, _M._, 1898-1901; _V-P._, 1901-03; _M._, 1903-06; _P._, 1906-07.
Sibley, R., _V-P._, 1921-23.
Siegfried, Victor, _V-P._, 1948-50.
Sinclair, C. T., _V-P._, 1939-41.
Sisson, C. E., _V-P._, 1929-31.
Skinner, C. E., _M._, 1915-19; _V-P._, 1919-20; _P._, 1931-32.
Slichter, Walter I., _M._, 1918-22; _V-P._, 1922-24; _Treas._, 1930-.
*Smith, H. B., _M._, 1920-24; _V-P._, 1924-26; _P._, 1929-30.
Smith, Walter Charles, _V-P._, 1941-43; _D._, 1945-49.
Smith, W. R., _D._, 1942-46.
*Smith, W. W., _M._, 1884-85.
Sorensen, R. W., _V-P._, 1933-35; _D._, 1936-40; _P._, 1940-41.
*Spencer, Paul, _M._, 1906-09; _V-P._, 1909-11.
*Sprague, Frank J., _V-P._, 1890-92; _P._, 1892-93.
*Springer, F. W., _V-P._, 1921-23.
*Sprong, S. D., _M._, 1909-12; _V-P._, 1912-14.
*Stanley, Wm., _V-P._, 1898-1900.
Stein, I. Melville, _V-P._, 1937-39.
*Steinmetz, Chas. P., _M._, 1892-95; _V-P._, 1896-98; _M._, 1898-1901; _P._, 1901-02.
*Stephens, C. E., _D._, 1928-33.
Stevens, A. C., _D._, 1932-36; _V-P._, 1936-38.
*Stevens, J. Franklin, _M._, 1912-15; _V-P._, 1915-17.
*Stillwell, Lewis B., _M._, 1896-99; _V-P._, 1899-1901; _P._, 1909-10.
†Stine, Wilbur M., _V-P._, 1896-98.
Stokes, Stanley, _V-P._, 1932-34.
*Stone, Chas. W., _M._, 1908-11; _V-P._, 1911-13.
Stone, E. C., _D._, 1925-29; _V-P._, 1929-31.
*Storer, Norman W., _M._, 1911-14; _V-P._, 1914-16, 1921-23.
*Stott, Henry G., _M._, 1904-07; _P._, 1907-08.
Sykes, Wilfred, _M._, 1917-21.

Tapscott, R. H., _D._, 1930-34; _V-P._, 1934-36.
Taylor, A. LeRoy, _V-P._, 1940-42.
Taylor, John B., _M._, 1915-18; _V-P._, 1918-19.
Terrell, C. F., _V-P._, 1946-48.
*Terry, Chas A., _M._, 1902-05; _V-P._, 1905-07.
Terry, I. A., _V-P._, 1948-50.
*Tesla, Nikola, _V-P._, 1892-94.
*Thomas, B. F., _M._, 1885-87.
Thomas, Percy H., _M._, 1907-10; _V-P._, 1910-12.
†Thompson, Edward P., _M._, 1887-88.
*Thomson, Elihu, _V-P._, 1887-89; _P._, 1889-90.
Thomson, J. M., _V-P._, 1939-41.
Timbie, W. H., _V-P._, 1934-36.
*Townley, Calvert, _M._, 1905-08; _V-P._, 1908-10; _P._, 1919-20.
*Townsend, Henry C., _M._, 1899-1902.
*Trowbridge, Wm. P., _M._, 1884-86.
Turner, A. L., _V-P._, 1939-41.

*Upton, Francis R., _V-P._, 1889-90; _M._ 1890-92.

*Vail, Theo. N., _M._, 1884-86.
*Vanderpoel, W. K., _M._, 1923-27.
*Van Hoevenbergh, H., _M._, 1888-90.
Veinott, C. G., _V-P._, 1949-51.
*Vonsize, W. B., _M._, 1894-97.

*Wallace, Wm., _V-P._, 1893-95.
Warner, R. G., _D._, 1940-44.
Warner, R. W., _V-P._, 1944-46.
*Weaver, W. D., _M._, 1894-97; 1899-1902.
†Webb, Herbert L., _M._, 1891-94; 1897-1900.
*Weston, Edward, _M._, 1884-87; _P._, 1888-89; _V-P._, 1889-91.
*Wetzler, Jos., _M._, 1888-90; _V-P._, 1890-92.
*Wheeler, Schuyler S., _M._, 1887-90; _V-P._, 1890-91; 1902-04; _M._, 1904-05; _P._, 1905-06.
*White, Jas. G., _M._, 1904-07; _V-P._, 1907-09.
Whitehead, John B., _M._, 1924-28; _P._, 1933-34.
*Wickenden, W. E., _V-P._, 1943-45; _P._, 1945-46.
*Williamson, R. B., _M._, 1921-25.
*Wilson, A. M., _V-P._, 1933-35.
*Wirt, Chas., _M._, 1892-95.
*Wolcott, Townsend, _M._, 1902-05; _V-P._, 1905-07.
Wolf, H. B., _V-P._, 1945-47.
*Wood, Edwin D., _V-P._, 1937-39.
*Woodrow, H. R., _D._, 1931-35.

Yerkes, E. P., _D._, 1946-50.

Abbreviations: _P._, President; _V-P._, Vice-President; _M._, Manager; _D._, Director; _Natl. Secy._, National Secretary; _Secy._, Secretary; _Hon. Secy._, Honorary Secretary; _Natl. Treas._, National Treasurer; _Treas._, Treasurer.

*Deceased. †Non-members at present.

Honorary Members, 1884-1949

*Sir William Preece	1884
*Norvin Green	1889
*Moses G. Farmer	1890
*Lord Kelvin	1892
*Cyrus Field	1892
*E. W. von Siemens	1892
*Andre E. Blondel	1912
*C. E. L. Brown	1912
*Emil A. Budde	1912
*S. Z. de Ferranti	1912
*Antonio Pacinotti	1912
*S. P. Thompson	1914
*Guglielmo Marconi	1917
*Oliver Heaviside	1918
*Ferdinand Foch	1921
*Thomas A. Edison	1928
*John J. Carty	1928
*M. I. Pupin	1928
*Ambrose Swasey	1928
*Elihu Thomson	1928
Herbert Hoover	1929
* CharlesF. Scott	1929
*Charles F. Brush	1929
Motoji Shibusawa	1929
*Frank J. Sprague	1932
*W. L. R. Emmet	1933
*G. A. Hamilton	1933
*Arthur E. Kennelly	1933
R. A. Millikan	1933
*E. W. Rice, Jr.	1933
*Edward Weston	1933
*Bion J. Arnold	1937
*Alex Dow	1937
*Cummings C. Chesney	1938
Andrew G. L. McNaughton	1942
Dugald C. Jackson	1944
Charles E. Skinner	1945
Gano Dunn	1945
Frank B. Jewett	1945
Vannevar Bush	1949

* Deceased

Headquarters Staff

33 West 39th Street, New York 18

Secretary	H. H. Henline
Office Manager and Business Manager of Publications	F. A. Norris
Editor	C. S. Rich
Associate Editor	E. B. Grazda
Secretary, Technical Program Committee	Edward C. Day
Secretary, Board of Examiners and Standards Committee	J. J. Anderson, Jr.
Technical Committee Activities	R. S. Gardner
Advertising Manager	J. S. Lopes

General Counsel

Simon Presant........55 Liberty St., New York 5

Sections

Name	District	When Organized	Membership Aug. 1, 1949	Chairman	Secretary	Secretary's Address
Akron	2	Aug. 12, '20	118	H. P. Davis	R. F. Miller	2284 14th St., Cuyahoga Falls, Ohio
Alabama	4	May 22, '29	199	J. W. Davis	Gayle Riley	Alabama Power Co., 600 No. 18th St., Birmingham 2, Ala.
Arizona	8	Mar. 22, '41	131	W. B. Bustard	I. G. Jenkins, Jr.	Central Arizona Light & Power Co., 2215 No. 25th St., Phoenix Ariz.
Arkansas	7	Apr. 23, '47	79	W. A. Lewis, Jr.	R. B. Newman	Reynolds Metals Co., Jones Mills Plant, Jones Mills, Ark.
Arrowhead	5	Apr. 23, '47	43	P. A. Beckjord	Roy B. Wiprud	137 Greenwood Lane, Duluth 3, Minn.
Beaumont	7	June 27, '45	81	R. W. Parker	T. G. Smith	490 Bowie St., Beaumont, Tex.
Boston	1	Feb. 13, '03	833	J. J. Loustaunau	Leslie J. Weed	Boston Edison Co., 182 Tremont St., Boston 11, Mass.
Canton	2	Nov. 5, '47	79	C. L. Lucal	R. V. Kelch	4520 13th St., N. W., Canton 7, Ohio
Central Indiana	5	Jan. 12, '12	232	G. M. Grabbe	J. W. Sears	Indiana Bell Tel. Co., 240 No. Meridian St., Indianapolis 9, Ind.
Chicago	5	1893	1587	H. E. Nason	E. L. Michelson	Commonwealth Edison Co., 72 West Adams St., Chicago, Ill.
Cincinnati	2	June 30, '20	236	F. E. Wiatt	D. T. Michael	Cincinnati Gas & Elec. Co., 4th & Main Sts., Cincinnati 2, Ohio
Cleveland	2	Sept. 27, '07	708	R. L. Oetting	J. A. Cortelli	Clark Controller Co., 1146 East 152nd St., Cleveland 10, Ohio
Columbus	2	Mar. 17, '22	137	N. L. Greene	C. E. Warren	Ohio State Univ., Columbus 10, Ohio
Connecticut	1	Apr. 16, '21	490	J. B. Powell	F. W. Buck	United Illuminating Co., 80 Temple St., New Haven 6, Conn.
Dayton	2	June 9, '43	341	E. Herzog	J. G. Tolentino	2 Palermo Place, Dayton 4, Ohio
Denver	6	May 18, '15	367	F. A. Eastom	E. R. Jones	Mountain States Tel. & Tel. Co., Box 960, Denver 1, Colo.
East Tennessee	4	Sept. 2, '36	415	T. D. Talmage	J. D. Sharp, Jr.	3004 Pope Drive, Chattanooga, Tenn.
Erie	2	Jan. 11, '18	130	M. J. Kolhoff	J. F. Davis	General Elec. Co., 2901 East Lake Road, Erie, Pa.
Florida	4	Jan. 28, '31	137	Jess D. Thomas	J. D. Griffin	P. O. Box 26, Station G, Jacksonville, Fla.
Fort Wayne	5	Aug. 14, '08	125	J. F. Eitman	J. H. Capps	General Elec. Co., 1635 Bway, Fort Wayne 2, Ind.
Georgia	4	Jan. 14, '04	220	E. S. Lammers	H. P. Peters	Georgia Inst. of Tech., Engg. Experiment Sta. Atlanta, 3 Ga.
Houston	7	Aug. 7, '28	271	W. O. Ray	W. E. Silvus	P. O. Box 2537, Houston, Tex.
Illinois Valley	5	June 30, '45	151	E. W. Stone	E. Krefting	317 Persimmon St., Peoria 6, Ill.
Iowa	5	June 29, '29	187	T. W. Schroeder	F. E. Keith	Keith Elec. Construction Co., 1213 Walnut St., Des Moines 9, Iowa
Ithaca	1	Oct. 15, '02	180	H. L. Livingood	S. W. Zimmerman	102 Valley Road, Ithaca, N. Y.
Kansas City	7	Apr. 14, '16	272	R. M. Kerchner	A. J. Nicholson	Kansas City Power & Light Co., P.O. Box 679, Kansas City 10, Mo.
Lehigh Valley	2	Apr. 16, '21	324	C. H. Sprague	A. L. Price	Pennsylvania Power & Light Co., Hazleton, Pa.
Los Angeles	8	May 19, '08	1289	E. L. Bettannier	E. K. Sadler	Kelman Elec. & Mfg. Co., 1650 Naud St., Los Angeles 12, Calif.
Louisville	4	Oct. 15, '26	115	R. D. Spalding	H. T. Smith	2816 Virginia Ave., Louisville 11, Ky.
Lynn	1	Aug. 22, '11	266	R. S. Schlotterbeck	A. M. Bjontegard	General Elec. Co., 920 Western Ave., West Lynn, Mass.
Madison	5	Jan. 8, '09	75	Leonard Hesse	Rubin A. Imm	102 Electrical Lab., Univ. of Wis., Madison, Wis.
Mansfield	2	Mar. 6, '39	74	E. C. Ryan	F. L. Hanson	The Ideal Elec. & Mfg. Co., Mansfield, Ohio
Maryland	2	Dec. 16, '04	626	F. H. Rogers	J. W. Magee	Westinghouse Elec. Corp., Std. Oil Bldg., Baltimore 3, Md.
Memphis	4	May 22, '30	124	W. B. Thompson	J. R. Owens	3563 Mimosa St., Memphis, Tenn.
Mexico	7	June 29, '22	216	E. D. Luque	F. Aubert	Apartado Postal 1399, Mexico,Federal District, Mexico
Miami	4	Feb. 3, '49	97	C. H. Summers	W. T. Edwards, Jr.	Southern Bell Tel. & Tel. Co., 1410—20th St., Miami Beach, Fla.
Michigan	5	Jan. 13, '11	805	E. F. Dissmeyer	O. E. Bowlus	18628 Lauder, Detroit 19, Mich.
Milwaukee	5	Feb. 11, '10	688	F. J. Van Zeeland	C. P. Feldhausen	Cutler-Hammer, Inc., 315 No. 12th St., Milwaukee 2, Wis.
Minnesota	5	Apr. 7, '02	279	Lincoln Rietow	R. E. Willey	Northwestern Bell Tel. Co., 224 So. 5th St., Minneapolis 2, Minn.
Montana	9	June 24, '31	90	J. R. Walker	Marion O. Hansen	112—14th St., Great Falls, Mont.
Montreal	10	Apr. 16, '43	296	N. L. Morgan	A. Malkin	Canadian Car & Foundry Co. Ltd., 621 Craig St. W., Montreal, Quebec 3, Canada
Nebraska	6	Jan. 21, '25	108	F. C. Howard	C. N. Allen	Allis-Chalmers Mfg. Co., 9th & Farnam Sts., Omaha 8, Nebr.
New Mexico-West Texas	7	Mar. 7, '40	148	Oscar Gutsch	G. R. Yelderman	General Elec. Co., 109 North Oregon, El Paso, Tex.
New Orleans	4	Dec. 8, '33	246	E. I. Blanchard	H. E. Pritchard, Jr.	5836 General Haig St., New Orleans 19, La.
New York	3	Dec. 10, '19	4894	D. W. Taylor	J. P. Neubauer	402 Fairway Road, Ridgewood, N. J.
Niagara Frontier	1	Feb. 10, '25	266	F. C. Rushing	C. J. Brumbaugh	129 Hunt Ave., Hamburg, N. Y.
Niagara International	10	Aug 5, '48	101	W. G. A. Barr	E. A. Dillon	11 York St., St. Catharines, Ontario, Canada
North Carolina	4	Mar. 21, '29	229	G. G. Mattison	B. V. Martin	Westinghouse Elec. Corp., 210 East Sixth St., Charlotte 1, N. C.
North Texas	7	May 18, '28	385	P. G. Wallace	A. L. Jones, Jr.	General Elec. Co., 1801 North Lamar St., Dallas, Tex.
Oklahoma City	7	Feb. 16, '22	180	E. W. Allen	J. C. Turner	Southwestern Bell Tel. Co., 1004 Telephone Bldg., Oklahoma City 2, Okla.
Ottawa	10	June 23, '49	56	Fred Fleming	Gordon Cathcart	137 Clarendon Ave., Ottawa, Ontario, Canada
Panhandle Plains	7	June 12, '47	131	George Dupree	G. R. Bunton	Box 631, Lubbock, Tex.
Philadelphia	2	Feb. 18, '03	1344	W. F. Henn	H. H. Sheppard	Rumsey Elec. Co., 1007 Arch St., Philadelphia 7, Pa.
Pittsburgh	2	Oct. 13, '02	1050	F. H. Schlough	L. N. Grier	Aluminum Co. of America, 801 Gulf Bldg., Pittsburgh, Pa.
Pittsfield	1	Mar. 25, '04	283	T. E. Rodhouse	G. L. Vallin	General Elec. Co., Pittsfield, Mass.
Portland	9	May 18, '09	438	R. B. Temple	Waldo Porter	Aluminum Co. of America, Vancouver, Wash.
Providence	1	Mar. 12, '20	132	O. E. Sawyer	C. B. Leathers	General Elec. Co., 111 Westminster St., Providence, R. I.
Richland	9	Apr. 23, '48	94	W. J. Dowis	R. B. Crow	206 Barth Ave., Richland, Wash.
Rochester	1	Oct. 9, '14	214	J. H. Rogers	E. M. Morecock	817 Chili Ave., Rochester, N. Y.
Rock River Valley	5	Apr. 23, '47	84	S. A. Coxhead	W. C. Busch	1421 North Church St., Rockford, Ill.
St. Louis	7	Jan. 14, '03	521	R. C. Horn	J. C. Lebens, Jr.	7322 Melrose Ave., University City, Mo.
San Diego	8	Jan. 18, '39	157	J. F. Sinnott	O. L. Doolittle	4738 Works Place, San Diego 4, Calif.
San Francisco	8	Dec. 23, '04	1259	T. C. McFarland	Remi Bollaert	Westinghouse Elec. Corp., 410 Bush St., San Francisco 8, Calif.
Schenectady	1	Jan. 26, '03	928	J. C. Page	L. T. Rader	General Elec. Co., Bldg. 69, Schenectady 5, N. Y.
Seattle	9	Jan. 19, '04	422	Ray Rader	H. R. Loew	General Elec. Co., 710 Second Ave., Seattle 11, Wash.
Sharon	2	Dec. 11, '25	178	G. R. Monroe	A. J. Maslin	Westinghouse Electric Corp., Sharon, Pa.
Shreveport	4	June 12, '47	74	L. T. Williams	C. M. L. Pons	3536 Del Rio, Shreveport 65, La.
South Bend	5	Feb. 26, '41	102	R. A. Cliff	Rayhue Neighbours	526 So. Twyckenham Drive., South Bend 15, Ind.
South Carolina	4	Mar. 2, '40	122	E. P. Miller	W. E. Dent, Jr.	The Springs Cotton Mills, Lancaster, S. C.
South Texas	7	May 23, '30	163	L. L. Antes	R. R. Kreadorn	153 Engg. Bldg., University of Texas, Austin, Tex.
Spokane	9	Feb. 14, '13	128	T. W. MacLean	R. M. Gilbert	Westinghouse Elec. Corp., 1023 West Riverside Ave., Spokane 8, Wash.
Springfield	1	June 29, '22	88	W. E. Maxwell	W. L. Vest, Jr.	54 Churchill Road, West Springfield, Mass.
Syracuse	1	Aug. 12, '20	237	J. D. Hershey	H. H. Graley	Central New York Power Corp., 300 Erie Blvd., W. Syracuse, N. Y.
Toledo	2	June 3, '07	117	F. A. Furfari	W. M. Campbell	2145 Central Grove Ave., Toledo, Ohio
Toronto	10	Sept. 30, '03	557	J. M. Somerville	W. R. Harmer	Hydro-Elec. Power Co. of Ont., 49 Bathurst St., Toronto, Ontario, Canada
Tulsa	7	Oct. 1, '37	139	Dick Ray	W. H. Plumer	Southwestern Bell Tel. Co., 424 So. Detroit, Tulsa, Okla.
Urbana	5	Nov. 25, '02	99	H. N. Hayward	P. R. Egbert	University of Illinois, Urbana, Ill.
Utah	9	Mar. 9, 17	115	F. O. Wald	J. A. McDonald	General Elec. Co., P. O. Box 779, Salt Lake City 1, Utah
Vancouver	10	Aug. 22, "11	182	W. J. Lind	F. O. Wollaston	B. C. Elec. Ry. Co., Ltd., 425 Carrall St., Vancouver, British Columbia, Canada
Virginia	4	May 19, '22	168	L. Saunders	P. R. Spracher	P. O. Box 1194, Richmond 19, Va.
Washington	2	Apr. 9, '03	832	Dixon Lewis	L. V. Berkner	7213 Bradley Blvd., Bethesda 14, Md.
West Virginia	2	Apr. 9, '40	120	E. B. Ellerbe	J. J. Fitzgibbon	306 McCorkle Ave., Charleston 28, W. Va.
Western Virginia	4	June 23. '49	86	Ira H. McMann	E. L. Munday, Jr.	P. O. Box 2021, Appalachian Elec. Power Co., Roanoke, Va.
Wichita	7	Sept. 16, '37	82	R. F. Dice	J. E. McNicol	Kansas Gas & Elec. Co., 201 No. Market, Wichita 2, Kans.
Worcester	1	Feb. 18, '20	88	D. R. Percival	W. G. Coleman	General Elec. Co., 507 Main St.. Worcester 8, Mass.
Total Sections	85		30,460			

Subsections

Name	Chairman	Secretary	Secretary's Address
Albuquerque (New Mexico-West Texas Section)	W. O. McCord, Jr.	A. D. Taylor	1722 East Gold Ave., Albuquerque, N. Mex.
Baton Rouge (New Orleans Section)	F. R. Adams	E. F. Tims	3155 Lakeshore Drive, Baton Rouge 15, La.
Billings (Montana Section)	Frank M. Holly	Curtis B. Brown	751 Lewis Ave., Billings, Mont.
Binghamton Area (Ithaca Section)	K. S. Koon	J. P. Peterson	Westinghouse Elec. Corp., 86 Court St., Binghamton 62, N. Y.
Boulder City (Los Angeles Section)	W. H. Taylor	F. A. Latham	Los Angeles Water & Power Dept., 600 Nevada Highway, Boulder City, Nev.
Casper, Wyo. (Denver Section)			
Central Texas (North Texas)			
Centre County (Pittsburgh Section)	R. J. E. Hemman	R. M. Smith	Ord. Res. Lab., Penna. State Col., State College, Pa.
Charleston (South Carolina Section)			
Charlotte (North Carolina Section)	M. F. Leftwich	I. G. Wallace, Jr.	205 Wales Ave., Charlotte, N. C.
Columbia (South Carolina Section)	H. K. Walker	J. F. Rader, Jr.	1307½ Gladden St., Columbia, S. C.
Corpus Christi (South Texas Section)	A. B. Weaver	J. H. Watts, Jr.	Westinghouse Elec. Corp., 508 Medical Professional Bldg., Corpus Christi, Tex.
Fort Worth (North Texas Section)	J. L. Candry	Karl J. Ratliff	1101 Electric Bldg., Fort Worth 2, Tex.
Fox River Valley (Milwaukee Section)	Herbert F. Weckwerth	Donald Christison	209 Frederick St., Menasha, Wis.
Freeport (Houston Section)	H. K. Brown	R. B. Adams	P. O. Box 413, Lake Jackson, Tex.
Fresno (San Francisco Section)	C. L. Smith	William Green	U. S. Bureau of Reclamation, T. W. Patterson Bldg., Fresno 1, Calif.
Great Falls (Montana Section)			
Hamilton (Toronto Section)			
Hampton Roads (Virginia Section)	C. E. Hastings	S. H. Fletcher	Va. Electric & Power Co., Newport News, Va.
Hudson Valley (New York Section)	W. E. Smalley	J. E. Rusher	49 Carroll St., Poughkeepsie, N. Y.
Jackson (Miss.) (New Orleans Section)	J. B. Fountain	A. N. Saxon	Graybar Electric Co., 758 Ricks St., Jackson, Miss.
Jacksonville (Florida Section)			
Johnstown (Pittsburgh Section)	W. R. Wood	R. S. Baum	Univ. of Pittsburgh, 325 Cypress Ave., Johnstown, Pa.
Lake Charles (New Orleans Section)	G. B. S. Ricketts	J. J. Alleman	29 Hibiscus Road, Maplewood, La.
Lancaster-York (Maryland Section)	W. H. Freund	H. H. Wittenberg	RCA Victor Div., Radio Corp. of America, Lancaster, Pa.
Lima (Dayton Section)	B. O. Austin	O. M. Swain	Westinghouse Elec. Corp., Engg. Dept., Lima, Ohio
Mid-State (North Carolina Section)	F. R. Jackson, Jr.	L. H. Allcorn, Jr.	2425 Elizabeth Ave., Winston-Salem 7, N. C.
Muscle Shoals (East Tennessee Section)	Lyle W. Jenkins	Arthur R. Rifkin	Apt. 4, Spring Creek Apts., Village 1, Sheffield, Ala.
Nashville (Memphis Section)	Walter Criley	E. R. Boruch	1229 Stahlman Bldg., 234—3rd Ave., North, Nashville 3, Tenn.
New Hampshire (Boston Section)			
New Jersey (New York Section)	J. S. Bell	Max Enderlin	Federal Telephone & Radio Corp., 900 Passaic Ave., East Newark, N. J.
Northern New York (Syracuse Section)	J. B. Pitman	L. F. Pries	New York State Agric. & Tech. Inst., 8 College St., Canton, N. Y.
Northwest Arkansas (Arkansas Section)	W. B. Stelzner	R. E. Anderson	Southwestern Gas & Elec. Co., De Queen, Ark.
Oak Ridge (East Tennessee Section)	M. C Becker	M. P. Falls	105 Vermont Ave., Oak Ridge, Tenn.
Quad-Cities (Iowa Section)	E. H. Breckenfelder	M. P. Roller	Iowa-Illinois Gas & Elec. Co., United Light Bldg., Davenport, Iowa
Red River Valley (Minnesota Section)	M. R. Hughes	H. K. Ugelstad	Northern States Power Co., 612 N. P. Ave., Fargo, N. Dak.
Richmond (Virginia Section)	C. L. Gilkeson	L. D. Johnson, 3rd	R. F. D. 7, Box 201, Richmond, Va.
Sacramento (San Francisco Section)	C. R. Day	G. A. Fleming	3711 17th St., Sacramento 18, Calif.
Saginaw Valley (Michigan Section)	E. L. Holmgren	F. H. Justin	401 W. Sugnet Road, Midland, Mich.
St. Maurice Valley (Montreal Section)	E. A. McKeagan	H. T. Ball	11 Wayagamack Island, Three Rivers, Que., Canada
San Jose (San Francisco Section)	L. O. Templeton	Warren Raab	1188 Thornton Way., Campbell, Calif.
Sangamon (Illinois Valley Section)	G. E. Sangster	J. T. Youngblood	Sangamo Elec. Co., Springfield, Ill.
Shasta (San Francisco Section)	W. G. Whitney	G. A. Thompson	U. S. Bureau of Reclamation, Redding, Calif.
Tacoma (Seattle, Section)	Glen H. Walker	Harry M. Manning	Tacoma City Light, 402 City Hall, Tacoma 2, Wash.
Tri-State (West Virginia Section)			
West Central Texas (North Texas Section)	R. D. Henley	C. B. Herbert	Route 2, Hamlin, Tex.
West Coast (Florida)	J. G. Ennis		
West Michigan (Michigan Section)	R. M. Chermak	L. A. Zahorsky	127 Colfax, N.E., Grand Rapids, Mich.
Wilmington (Philadelphia Section)	E. W. Randall, Jr.	E. R. Streed	R. F. D. 3, Box 156, Wilmington, Del.
Zanesville (Columbus Section)	R. W. Hartsook	C. G. Winters	1115 Seborn Ave., Zanesville, Ohio

Geographical District Executive Committees

District	Chairman (Vice-President, AIEE)	Secretary (District Secretary)	Chairman, District Committee on Student Activities
1 North Eastern	Victor Siegfried, American Steel & Wire Co., Worcester 7, Mass.	Frederick G. Webber, 9 Federal Court, Springfield 5, Mass.	A. G. Conrad, Yale University, New Haven, Conn.
2 Middle Eastern	C. G. Veinott, Westinghouse Electric Corp., Lima, Ohio	W. A. Dynes, 312 Lonsdale Ave., Dayton 9, Ohio	K. F. Sibila, University of Akron, Akron 4, Ohio
3 New York City	J. L. Callahan, R. C. A. Laboratories, Radio Corporation of America, 66 Broad St., New York 4, N. Y.	R. T. Oldfield. Public Service Commission, 233 Broadway, New York 7, N. Y.	F. A. Wahlers, Polytechnic Inst. of Brooklyn, 99 Livingston St., Brooklyn 2, N. Y.
4 Southern	W. J. Seeley, Duke University, Durham, N. C.	T. H. Mawson, Commonwealth & Southern Corp., 600 North 18th St., Birmingham 2, Ala.	H. B. Duling, Georgia Institute of Technology, Atlanta, Ga.
5 Great Lakes	E. W. Seeger, Cutler-Hammer, Inc., 315 N. 12th St., Milwaukee 1, Wis.	N. C. Pearcy, Pioneer Service & Engineering Co., 231 S. LaSalle St., Chicago 4, Ill.	E. W. Kane, Marquette Univ., 1515 W. Wisconsin Ave., Milwaukee 3, Wis.
6 North Central	W. C. DuVall, University of Colorado, Boulder, Colo.	G. E. Gless, Jr., University of Colorado, Boulder, Colo.	C. H. Chinburg, Colorado A. & M. College, Fort Collins, Colo.
7 South West	G. N. Pingree, General Electric Co., 1801 N. Lamar St., Dallas 2, Tex.	Gibbs A. Dyer, Southwestern Bell Telephone Co., Dallas 1, Tex.	Ralph W. Tapy, University of New Mexico, Albuquerque, N. Mex.
8 Pacific	R. A. Hopkins, Westinghouse Electric Corp., 600 St. Paul Ave., Los Angeles 14, Calif.	T. M. Blakeslee, Dept. of Water & Power, City of Los Angeles, Box 3669 Terminal Annex, Los Angeles 54, Calif.	R. C. Lewis, University of Southern Calif., Los Angeles 7, Calif.
9 North West	Richard McKay, Washington Water Power Co., West 825 Trent Ave., Spokane 6, Wash.	H. C. Glaze, Jr., General Electric Co., S. 162 Post St., Spokane 8, Wash.	G. D. Sheckels, Montana State College, Bozeman, Mont.
10 Canada	A. H. Frampton, English Elec. Co. of Canada Ltd., St. Catharines, Ontario, Canada	J. I. Gram, Hydro-Electric Power Comm. of Ont., Box 237, Niagara Falls, Ontario, Canada	

NOTE: Each District executive committee includes also the chairmen and secretaries of all Sections within the District, the District vice-chairman of the AIEE membership committee, and a member of the Sections Committee who is resident in the District.

Student Branches

Name and Location	District	Counselor (Member of Faculty)
Akron, University of, Akron, Ohio	2	K. F. Sibila
Alabama Polytechnic Inst., Auburn	4	R. D. Spann
Alabama, University of, University	4	W. F. Gray
Alberta, University of, Edmonton, Canada	10	R. E. Phillips
Arizona, University of, Tucson	8	J. C. Clark
Arkansas, Univ. of, Fayetteville	7	N. H. Barnette
British Columbia, Univ. of, Vancouver, Canada	10	W. B. Coulthard
Brooklyn, Polytechnic Inst. of, Brooklyn, N. Y., (Day)	3	F. A. Wahlers
Brooklyn, Polytechnic Inst. of, Brooklyn, N. Y., (Evening)	3	Anthony B. Giordano
Brown University, Providence, R. I.	1	F. N. Tompkins
Bucknell University, Lewisburg, Pa.	2	Ralph C. Walker
California Inst. of Technology, Pasadena	8	William H. Pickering
California, University of, Berkeley	8	R. M. Saunders
Carnegie Inst. of Technology, Pittsburgh, Pa.	2	George M. Anderson
Case Inst. of Technology, Cleveland, Ohio	2	Carl F. Schuneman
Catholic University of America, Washington, D. C.	2	J. C. Michalowicz
Cincinnati, Univ. of, Cincinnati, Ohio	2	A. C. Herweh
Clarkson College of Technology, Potsdam, N. Y.	1	George W. Reed
Clemson A. & M. College, Clemson, S. C.	4	F. T. Tingley
Colorado A. & M. College, Fort Collins	6	C. H. Chinburg
Colorado, University of, Boulder	6	W. G. Worcester
Columbia University, New York, N. Y.	3	W. A. LaPierre
Connecticut, Univ. of, Storrs	1	Clarence W. Schultz
Cooper Union, New York, N. Y.	3	E. W. Starr
Cornell University, Ithaca, N. Y.	1	M. S. McIllroy
Delaware, University of, Newark	2	H. S. Bueche
Denver, University of, Denver, Colo.	6	A. M. Stiles
Detroit, University of, Detroit, Mich.	5	H. O. Warner
Drexel Inst. of Technology, Philadelphia, Pa.	2	F. C. Powell
Duke University, Durham, N. C.	4	Otto Meier, Jr.
Fenn College, Cleveland, Ohio	2	R. W. Schindler
Florida, University of, Gainesville	4	Paul H. Nelson
George Washington Univ., Washington, D. C.	2	Jerome S. Antel, Jr.
Georgia Inst. of Technology, Atlanta, Ga.	4	H. B. Duling
Harvard University, Cambridge, Mass.	1	John C. Fisher
Idaho, University of, Moscow	9	J. Hugo Johnson
Illinois Inst. of Technology, Chicago	5	E. T. B. Gross
Illinois, University of, Urbana	5	E. A. Reid
Iowa State College, Ames	5	G. Richardson
Iowa, University of, Iowa City	5	E. B. Kurtz
Johns Hopkins University, Baltimore, Md.	2	T. Larsen
Kansas State College, Manhattan	7	Earl L. Sitz
Kansas, University of, Lawrence	7	E. B. Phillips
Kentucky, University of, Lexington	4	H. Alex Romanowitz
Lafayette College, Easton, Pa.	2	J. G. Reifsnyder
Lehigh University, Bethlehem, Pa.	2	W. Lyle Donaldson
Louisiana Polytechnic Inst., Ruston, La.	4	Milton R. Johnson, Jr.
Louisiana State University, Baton Rouge	4	A. K. Ramsey
Louisville, University of, Louisville, Ky.	4	Harry T. Smith
Maine, University of, Orono	1	P. M. Seal
Manhattan College, New York, N. Y.	3	Robert T. Weil
Marquette University, Milwaukee, Wis.	5	E. W. Kane
Maryland, University of, College Park	2	L. J. Hodgins
Massachusetts Inst. of Technology, Cambridge	1	E. W. Boehne
Michigan College of Mining & Technology, Houghton	5	G. W. Swenson
Michigan State College, East Lansing	5	C. E. Goodell
Michigan, University of, Ann Arbor	5	John J. Carey
Milwaukee School of Engineering, Milwaukee, Wis.	5	R. J. Ungrodt
Minnesota, University of, Minneapolis	5	J. H. Kuhlmann
Mississippi State College, State College	4	Paul B. Jacobs, Jr.
Missouri School of Mines & Metallurgy, Rolla	7	I. H. Lovett
Missouri, University of, Columbia	7	G. V. Lago
Montana State College, Bozeman	9	G. D. Sheckels
Nebraska, University of, Lincoln	6	F. J. Ballard, Jr.
Nevada, University of, Reno	8	I. J. Sandorf
Newark College of Engineering, Newark, N. J.	3	C. R. Moore
New Hampshire, University of, Durham, N. H.	1	A. J. Merlini
New Mexico College of A. & M. Arts, State College	7	Russell Riese
New Mexico, University of, Albuquerque	7	J. Lawton Ellis
New York, College of the City of, New York, N. Y.	3	Harry Baum
New York, University of, New York	3	James Ley
North Carolina State College, Raleigh	4	W. D. Stevenson, Jr.
North Dakota Agri. College, Fargo	5	Harry S. Dixon
North Dakota, University of, Grand Forks	5	K. B. MacKichan
Northeastern University, Boston, Mass.	1	Roland G. Porter
Northwestern University, Evanston, Ill.	5	A. H. Wing
Norwich University, Northfield, Vt.	1	
Notre Dame, University of, Notre Dame, Ind.	5	L. F. Stauder
Ohio Northern University, Ada	2	W. R. Ankrom
Ohio State University, Columbus	2	Edmund D. Ayres
Ohio University, Athens	2	D. B. Green
Oklahoma A. & M. College, Stillwater	7	David L. Johnson
Oklahoma, University of, Norman	7	Gerald Tuma
Oregon State College, Corvallis	9	Melvin J. Kofoid
Pennsylvania State College, State College	2	A. P. Powell
Pennsylvania University of, Philadelphia	2	Kenneth C. Fegley
Pittsburgh, University of, Pittsburgh, Pa.	2	R. C. Gorham
Pratt Institute, Brooklyn, N. Y.	3	Robert B. Morgan
Princeton University, Princeton, N. J.	2	Norman W. Mather
Puerto Rico, University of, Mayagues, P. R.	3	Miguel Wiewall, Jr.
Purdue University, Lafayette, Ind.	5	C. R. Nichols
Rensselaer Polytechnic Institute, Troy, N. Y.	1	Emerson D. Broadwell
Rhode Island State College, Kingston	1	John L. Hummer
Rice Institute, Houston, Tex.	7	J. S. Waters
Rose Polytechnic Institute, Terre Haute, Ind.	5	C. C. Knipmeyer
Rutgers University, New Brunswick, N. J.	3	P. H. Daggett
Santa Clara, Univ. of, Santa Clara, Calif.	8	Henry P. Nettesheim
South Carolina, Univ. of, Columbia	4	S. A. Ferguson
South Dakota School of Mines & Tech., Rapid City	6	J. O. Kammerman
South Dakota State College, Brookings	5	Wm. H. Gamble
Southern California, Univ. of, Los Angeles	8	Rodney C. Lewis
Southern Methodist Univ., Dallas, Tex.	7	F. W. Tatum
Stanford University, Stanford, University, Calif.	8	W. G. Hoover
Stevens Inst. of Technology, Hoboken, N. J.	3	W. L. Sullivan
Swarthmore College, Swarthmore, Pa.	2	C. J. Garrahan
Syracuse University, Syracuse, N. Y.	1	Henry F. Cooke
Tennessee, University of, Knoxville	4	W. O. Leffell
Texas, A. & M. College of, College Station	7	N. F. Rode
Texas Technological College, Lubbock	7	
Texas, University of, Austin	7	A. J. McCrocklin, Jr.
Texas Western College Sub-Branch, El Paso		
Toronto, University of, Toronto, Ontario, Canada	10	L. S. Lauchland
Tufts College, Medford, Mass.	1	A. H. Howell
Tulane University, New Orleans, La.	4	Marion E. Forsman
Union College, Schenectady, N. Y.	1	Owen G. Owens
Utah, University of, Salt Lake City	9	O. C. Haycock
Vanderbilt University, Nashville, Tenn.	4	Walter Criley
Vermont, University of, Burlington	1	Howard M. Smith, J
Villanova College, Villanova, Pa.	2	John B. Clothier
Virginia Military Institute, Lexington	4	J. S. Jamison
Virginia Polytechnic Institute, Blacksburg	4	Claudius Lee
Virginia, University of, Charlottesville	4	Gordon K. Carter
Washington, State College of, Pullman	9	O. E. Osburn
Washington, University of, Seattle	9	H. M. Rustebakke
Washington University, St. Louis, Mo.	7	Pierre M. Honnell
Wayne University, Detroit, Mich.	5	Edward L. Fairchild
West Virginia University, Morgantown	2	Everette C. Dubbe
Wisconsin, University of, Madison	5	Vincent C. Rideout
Worcester Poly. Institute, Worcester, Mass.	1	Donald C. Alexander
Wyoming, University of, Laramie	6	R. O. Trueblood
Yale University, New Haven, Conn.	1	A. G. Conrad

Total Branches........129

Committees and Representatives for 1949-1950

General Committees

Executive

J. F. Fairman, *chairman*, Consolidated Edison Company of New York, Inc, 4 Irving Place, New York 3, N. Y.

J. L. Callahan	New York, N. Y.
W. L. Everitt	Urbana, Ill.
R. T. Henry	Buffalo, N. Y.
Everett S. Lee	Schenectady, N. Y.
W. I. Slichter	New York, N. Y.
E. P. Yerkes	Philadelphia, Pa.

Board of Examiners

E. D. Doyle, *chairman*, Leeds & Northrup Company, 4901 Stenton Ave., Philadelphia 44, Pa.

P. H. Adams, *vice-chairman*	Newark, N. J.
John J. Anderson, Jr., *secretary*	AIEE Headquarters
A. E. Anderson	Phildelphia, Pa.
R. W. Atkinson	Bayonne, N. J.
R. H. Barclay	New York, N. Y.
Robin Beach	Brooklyn, N. Y.
H. A. Dambly	Philadelphia, Pa.
E. W. Davis	Cambridge, Mass.
C. W. Franklin	New York, N. Y.
W. N. Goodwin, Jr.	Newark, N. J.
I. W. Gross	New York, N. Y.
N. S. Hibshman	Brooklyn, N. Y.
L. F. Hickernell	Hastings-on-Hudson, N. Y.
C. R. Jones	New York, N. Y.
I. F. Kinnard	West Lynn, Mass.
A. E. Knowlton	Short Beach, Conn.
C. M. Laffoon	East Pittsburgh, Pa.
Henry Logan	New York, N. Y.
L. G. Pacent	New York, N. Y.
R. F. Penman	New York, N. Y.
J. J. Pilliod	New York, N. Y.
R. C. Roe	New York, N. Y.
F. J. Scudder	Manhasset, N. Y.
George Sutherland	New York, N. Y.
Gordon Thompson	New York, N. Y.
H. M. Trueblood	Dobbs Ferry, N. Y.
S. S. Watkins	New York, N. Y.
H. H. Weber	New York, N. Y.
John Westbye	New York, N. Y.
Sidney Withington	New Haven, Conn.

Constitution and By-Laws

N. B. Hinson, *chairman*, Southern California Edison Company, Edison Building, Los Angeles 53, Calif.

F. M. Farmer	New York, N. Y.
W. Scott Hill	Baltimore, Md.
W. W. Lewis	Schenectady, N. Y.
W. S. Peterson	Los Angeles, Calif.
Walter C. Smith	Palo Alto, Calif.

Finance

E. P. Yerkes, *chairman*, Bell Telephone Company of Pennsylvania, 1401 Arch Street, Philadelphia 2, Pa.

W. J. Barrett	Newark, N. J.
R. T. Henry	Buffalo, N. Y.
H. J. Scholz	Birmingham, Ala.
Victor Siegfried	Worcester, Mass.

Headquarters

C. S. Purnell, *chairman*, Westinghouse Electric Corporation, 40 Wall Street, New York 5, N. Y.

H. H. Henline	New York, N. Y.
H. H. Race	Schenectady, N. Y.
E. P. Yerkes	Philadelphia, Pa.

Members-for-Life Fund

C. R. Beardsley, *chairman*, Consolidated Edison Company of New York, Inc., 4 Irving Place, New York 3, N. Y.

T. F. Barton	New York, N. Y.
N. E. Funk	Philadelphia, Pa.
A. H. Hull	Toronto, Ontario, Canada
E. H. Martindale	Cleveland, Ohio
F. D. Newbury	Pittsburgh, Pa.
W. I. Slichter	New York, N. Y.
R. W. Sorensen	Pasadena, Calif.
J. F. Tritle	Erie, Pa.

Membership

F. S. Black, *chairman*, *Electrical World*, 330 West 42 Street, New York 18, N. Y.

J. C. Woods, *vice-chairman*	Chicago, Ill.
F. A. Norris, *secretary*	AIEE Headquarters
C. H. Cutter	Seattle, Wash.
J. A. Duncan, Jr.	New York, N. Y.
C. W. Fick	Cleveland, Ohio
H. R. Heckendorn	Chicago, Ill.
R. C. Horn	St. Louis, Mo.
Thomas Ingledow	Vancouver, British Columbia, Canada
F. H. Knapp	Cleveland, Ohio
M. J. Lantz	Portland, Oreg.
W. Stone Leake	New Orleans, La.
W. W. Morris	Los Angeles, Calif.
H. N. Muller, Jr.	East Pittsburgh, Pa.
C. G. Rumohr	Denver, Colo.
A. M. Spaulding	Denver, Colo.

District Vice-Chairmen

W. C. Bloomquist (1)	Schenectady, N. Y.
M. L. Lehman (2)	Philadelphia, Pa.
Charles Clos (3)	New York, N. Y.
J. D. Harper (4)	Alcoa, Tenn.
H. M. Craig (5)	Detroit, Mich.
A. S. Anderson (6)	Denver, Colo.
E. W. Allen (7)	Oklahoma City, Okla.
P. L. Savage (8)	Los Angeles, Calif.
C. R. Kingsbury (9)	Seattle, Wash.
C. L. Roach (10)	Montreal, Quebec, Canada

Ex-officio

Chairman of membership committees of Sections

Planning and Co-ordination

M. D. Hooven, *chairman*, Public Service Electric and Gas Company, 80 Park Place, Newark 1, N. J.

D. I. Anzini	San Francisco, Calif.
W. R. G. Baker	Syracuse, N. Y.
G. W. Bower	Haddonfield, N. J.
H. C. Coleman	East Pittsburgh, Pa.
F. E. Harrell	Cleveland, Ohio
L. F. Hickernell	Hastings-on-Hudson, N. Y.
N. B. Hinson	Los Angeles, Calif.
T. G. LeClair	Chicago, Ill.
Everett S. Lee	Schenectady, N. Y.
K. B. McEachron	Pittsfield, Mass.
J. R. North	Jackson, Mich.
J. J. Orr	New York, N. Y.
Elgin B. Robertson	Dallas, Tex.
H. I. Romnes	New York, N. Y.
M. J. Steinberg	New York, N. Y.
J. D. Tebo	New York, N. Y.
C. H. Willis	Princeton, N. J.
E. P. Yerkes	Philadelphia, Pa.

Publication

K. B. McEachron, *chairman*, General Electric Company, 100 Woodlawn Ave., Pittsfield, Mass.

F. R. Benedict	Pittsburgh, Pa.
J. M. Flanigen	Atlanta, Ga.
P. B. Garrett	Chicago, Ill.
H. H. Henline	New York, N. Y.
R. K. Honaman	New York, N. Y.
B. M. Jones	Pittsburgh, Pa.
F. O. McMillan	Corvallis, Oreg.
G. C. Quinn	Milwaukee, Wis.
B. R. Teare, Jr.	Pittsburgh, Pa.
G. C. Tenney	San Francisco, Calif.
C. H. Willis	Princeton, N. J.

Public Relations

R. K. Honaman, *chairman*, Bell Telephone Laboratories, Inc., 463 West Street, New York 14, N. Y.

G. T. Minasian, *vice-chairman*	New York, N. Y.
Guy Bartlett	Schenectady, N. Y.
G. W. Bower	Haddonfield, N. J.
M. Getting	Pittsburgh, Pa.
H. H. Henline	New York, N. Y.
A. E. Knowlton	Short Beach, Conn.
H. W. Marquardt	New York, N. Y.
K. B. McEachron	Pittsfield, Mass.
H. J. Scholz	Birmingham, Ala.
D. W. Taylor	Newark, N. J.
A. R. Thompson	New York, N. Y.
C. H. Willis	Princeton, N. J.

(Continued in next column)

Research

M. J. Kelly, *chairman*, Bell Telephone Laboratories, Inc., 463 West Street, New York 14, N. Y.

J. A. Hutcheson, *vice-chairman*	East Pittsburgh, Pa.
M. B. Long, *secretary*	New York, N. Y.
B. G. Ballard	Ottawa, Ontario, Canada
J. W. Barker	New York, N. Y.
R. D. Bennett	Silver Spring, Md.
L. V. Berkner	Washington, D. C.
E. W. Boehne	Cambridge, Mass.
Cledo Brunetti	Stanford, Calif.
C. R. Burrows	Ithaca, N. Y.
A. G. Conrad	New Haven, Conn.
H. P. Corwith	New York, N. Y.
H. E. Edgerton	Cambridge, Mass.
W. L. Everitt	Urbana, Ill.
R. S. Glasgow	Annapolis, Md.
T. A. Hopkins	Spokane, Wash.
T. J. Kilan	Washington, D. C.
J. T. Littleton	Corning, N. Y.
A. D. Moore	Ann Arbor, Mich.
B. K. Northrop	Ithaca, N. Y.
W. H. Pickering	Pasadena, Calif.
C. S. Schifreen	Philadelphia, Pa.
E. F. Seaman	Washington, D. C.
C. G. Suits	Schenectady, N. Y.
J. B. Thomas	Fort Worth, Tex.
Eric Walker	State College, Pa.
V. K. Zworykin	Princeton, N. J.

Safety

W. B. Kouwenhoven, *chairman*, The Johns Hopkins University, Baltimore 18, Md.

M. M. Brandon, *vice-chairman* and *secretary*	New York, N. Y.
Robin Beach	Brooklyn, N. Y.
J. H. Berry	Norfolk, Va.
Hendley Blackmon	New York, N. Y.
W. B. Buchanan	Toronto, Ontario, Canada
C. F. Dalziel	Berkeley, Calif.
G. S. Diehl	Lancaster, Pa.
W. P. Dobson	Toronto, Ontario, Canada
J. P. Ferguson	Los Angeles, Calif.
L. P. Ferris	New York, N. Y.
J. M. Flanigen	Atlanta, Ga.
J. A. Glenger	Rochester, N. Y.
M. C. Goodspeed	Harborcreek, Pa.
Floyd Goss	Los Angeles, Calif.
N. B. Hinson	Los Angeles, Calif.
O. S. Hockaday	Fort Worth, Tex.
J. O. Leslie	Reading, Pa.
R. L. Lloyd	Washington, D. C.
Albrecht Naeter	Stillwater, Okla.
G. R. Radley	Milwaukee, Wis.
C. N. Rakestraw	Cleveland, Ohio
P. X. Rice	State College, Pa.
W. T. Rogers	New York, N. Y.
A. H. Schirmer	New York, N. Y.
A. B. Smith	New York, N. Y.
W. R. Smith	Newark, N. J.
E. E. Turkington	Boston, Mass.
H. H. Watson	Bridgeport, Conn.
H. B. Williams	New York, N. Y.
William R. Wood	Windber, Pa.

Medical Consultants

Dr. Anna Baetjer, The Johns Hopkins University, Baltimore, Md.

Dr. Cecil K. Drinker, Harvard University, Cambridge, Mass.

Dr. T. L. Hazlett, Westinghouse Electric Corporation, Pittsburgh, Pa.

Dr. B. L. Vosburgh, General Electric Company, Schenectady, N. Y.

Sections

D. I. Anzini, *chairman*, General Electric Company, 806 Russ Building, San Francisco 4, Calif.

C. S. Purnell, *vice-chairman* (East)	New York, N. Y.
Walter C. Smith, *vice-chairman* (West)	Palo Alto, Calif.
F. S. Benson, *secretary*	San Francisco, Calif.
W. J. Barrett	Newark, N. J.
F. S. Black	New York, N. Y.
G. W. Bower	Haddonfield, N. J.
T. C. D. Churchill	Toronto, Ontario, Canada
Bradley Cozzens	Los Angeles, Calif.
H. A. Dambly	Philadelphia, Pa.
O. R. Enriquez	Mexico, D. F., Mexico
C. W. Fick	Cleveland, Ohio
R. C. Horn	St. Louis, Mo.
R. E. Kistler	Seattle, Wash.
C. P. Knost	New Orleans, La.
C. W. Lethert	Minneapolis, Minn.
A. L. O'Banion	Boston, Mass.
L. R. Patterson	Denver, Colo.
F. H. Pumphrey	Gainesville, Fla.
R. V. Shepherd	Schnectady, N. Y.
E. W. Stone	Peoria, Ill.
J. C. Strasbourger	Cleveland, Ohio
H. H. Wagner	Canonsburg, Pa.

(Continued in next column)

Ex-officio

Chairman of Sections

Standards

F. E. Harrell, *chairman*, Reliance Electric and Engineering Company, 1088 Ivanhoe Road, Cleveland 10, Ohio

E. B. Paxton, *vice-chairman*	Schenectady, N. Y.
John J. Anderson, Jr., *secretary*	AIEE Headquarters
Joseph Wm. Allen	Teterboro, N. J.
R. W. Atkinson	Bayonne, N. J.
E. L. Bailey	Highland Park, Mich.
Sterling Beckwith	Milwaukee, Wis.
F. R. Benedict	Pittsburgh, Pa.
R. C. Bergvall	East Pittsburgh, Pa.
M. M. Brandon	New York, N. Y.
J. E. Clem	Schenectady, N. Y.
C. L. Dawes	Cambridge, Mass.
R. D. de Kay	New York, N. Y.
W. P. Dobson	Toronto, Ontario, Canada
C. M. Gilt	New York, N. Y.
I. W. Gross	New York, N. Y.
John Grotzinger	Akron, Ohio
R. T. Henry	Buffalo, N. Y.
H. R. Huntley	New York, N. Y.
H. E. Kent	New York, N. Y.
A. C. Muir	Philadelphia, Pa.
J. R. North	Jackson, Mich.
J. E. O'Brien	Washington, D. C.
G. H. O'Sullivan	New York, N. Y.
F. B. Silsbee	Washington, D. C.

Ex-officio

Chairman of Standards subcommittees and co-ordinating committees

Chairman of AIEE technical committees

Chairman of AIEE delegations on other standardizing bodies or sole representative thereon

President, U. S. National Committee of the International Electrotechnical Commission

President, Canadian National Committee of the International Electrotechnical Commission

Standards Coordinating Committees

No. 1—REFERENCE VALUES FOR STANDARDS

P. L. Bellaschi, *chairman*	Sharon, Pa.
J. J. Clark	East Pittsburgh, Pa.
R. F. Field	Cambridge, Mass.
E. J. Rutan	New York, N. Y.
F. B. Silsbee	Washington, D. C.
J. J. Smith	Schenectady, N. Y.
I. M. Stein	Philadelphia, Pa.
Gordon Thompson	New York, N. Y.

No. 2—STANDARD VOLTAGES AND CURRENTS

C. A. Powel, *chairman*	East Pittsburgh, Pa.
W. P. Dobson (*ex-officio*)	Toronto, Canada
R. A. Hentz	Philadelphia, Pa.
D. M. Jones	Schenectady, N. Y.

No. 3—Surge Testing and Insulation

V. M. Montsinger, *chairman*	Schenectady, N. Y.
F. R. Benedict	East Pittsburgh, Pa.
F. E. Harrell	Cleveland, Ohio
Philip Sporn	New York, N. Y.

No. 4—Basic Principles for Rating of Electric Machinery and Apparatus

W. R. Hough, *chairman*	Cleveland, Ohio
P. L. Alger	Schenectady, N. Y.
R. T. Henry	Buffalo, N. Y.
H. E. Kent	New York, N. Y.
C. M. Laffoon	East Pittsburgh, Pa.
T. H. Morgan	Worcester, Mass.
J. J. Orr	Schenectady, N. Y.
E. B. Paxton	Schenectady, N. Y.
R. Rudenberg	Cambridge, Mass.

No. 5—Basic Theories and Units

E. E. Bennett, *chairman*	Madison, Wis.
E. C. Crittenden	Washington, D. C.
H. L. Curtis	Washington, D. C.
H. L. Hazen	Cambridge, Mass.
E. S. Lee	Schenectady, N. Y.
F. B. Silsbee	Washington, D. C.
J. Slepian	East Pittsburgh, Pa.
E. Weber	Brooklyn, N. Y.

No. 6—Interference, Sound, and Vibration Problems

R. S. Tucker, *chairman*	New York, N. Y.
P. L. Alger	Schenectady, N. Y.
W. F. Davidson	New York, N. Y.
H. E. Kent	New York, N. Y.
L. J. Plucknett	Washington, D. C.
Gordon Thompson	New York, N. Y.

No. 7—Conduction in Vacuum, Gases, Liquids, and Solids

Disbanded in 1944

No. 8—Insulation Coordination

J. H. Foote, *chairman*	Jackson, Mich.
J. E. Clem	Schenectady, N. Y.
I. W. Gross	New York, N. Y.
R. T. Henry	Buffalo, N. Y.
S. E. Schultz	Portland, Oreg.
T. G. A. Sillers	Milwaukee, Wis.
J. J. Taylor	Barberton, Ohio
C. F. Wagner	East Pittsburgh, Pa.

Technical Program

C. H. Willis, *chairman*, Princeton University, Princeton, N. J.

M. M. Brandon, *vice-chairman* New York, N. Y.

Edward C. Day, *secretary*	AIEE Headquarters
J. L. Callahan	New York, N. Y.
P. H. Light	Schenectady, N. Y.
F. O. McMillan	Corvallis, Oreg.
Robert D. Miller	San Francisco, Calif.
S. H. Mortensen	Milwaukee, Wis.
M. J. Steinberg	New York, N. Y.
Frank Thornton, Jr.	East Pittsburgh, Pa.
H. M. Turner	New Haven, Conn.

Ex-office

Chairman of
- Technical co-ordinating committees
- Technical committees
- Committee on Education
- Committee on Planning and Co-ordination
- Committee on Research
- Committee on Safety
- Standards Committee

Transfers

F. W. Willcutt, *chairman*, Potomac Electric Power Company, 10th & E Streets, N. W., Washington 4, D. C.

C. W. Fick, *vice-chairman*, Cleveland, Ohio

L. F. Hunt, *secretary*	Los Angeles, Calif.
F. A. Cooper	St. Louis, Mo.
O. A. Demuth	Portland, Oreg.
John Gammell	Philadelphia, Pa.
J. D. Harper	Alcoa, Tenn.
W. R. Hough	Cleveland, Ohio
M. M. Moore	Washington, D. C.
L. R. Patterson	Denver, Colo.
F. H. Pumphrey	Gainesville, Fla.
John Wm. Robinson	San Francisco, Calif.
H. K. Smith	Chicago, Ill.
H. B. Wood	Boston, Mass.

(*Continued in next column*)

Ex-officio

Chairman of transfers committees of Sections

Professional Group Committees

Professional Group Co-ordinating

T. G. LeClair, *chairman*, Commonwealth Edison Company, 72 West Adams Street, Chicago 90, Ill.

W. Scott Hill

Chairman of professional group committees

Charles LeGeyt Fortescue Fellowship

H. N. Muller, Jr., *chairman*	East Pittsburgh, Pa.
H. P. Sedwick	Chicago, Ill.
	(*Terms expire July 31, 1950*)
J. W. Barker	New York, N. Y.
R. I. Wilkinson	New York, N. Y.
	(*Terms expire July 31, 1951*)
F. W. Bush	Milwaukee, Wis.
A. G. Conrad	New Haven, Conn.
	(*Terms expire July 31, 1952*)

Code of Principles of Professional Conduct

Harry Barker, *chairman*, Barker and Wheeler, 11 Park Place, New York 7, N. Y.

P. L. Alger	Schenectady, N. Y.
D. D. Ewing	Lafayette, Ind.
E. S. Fields	Cincinnati, Ohio
E. H. Flath	Dallas, Tex.
Harold Goodwin, Jr.	Wyncote, Pa.
Dugald C. Jackson	Cambridge, Mass.
R. D. Maxson	Chicago, Ill.
R. W. Sorensen	Pasadena, Calif.

Edison Medal

Appointed by the President for term of five years

C. V. Christie,	Montreal, Quebec, Canada
Zay Jeffries	Pittsfield, Mass.
Harold Pender	Philadelphia, Pa.
	(*Terms expire July 31, 1950*)
C. A. Corney	Boston, Mass.
J. R. North	Jackson, Mich.
I. M. Stein	Philadelphia, Pa.
	(*Terms expire July 31, 1951*)
Marvin W. Smith	Philadelphia, Pa.
H. S. Osborne	New York, N. Y.
H. A. Winne	Schenectady, N. Y.
	(*Terms expire July 31, 1952*)
D. I. Cone	San Francisco, Calif.
J. B. MacNeill, *chairman*	East Pittsburgh, Pa.
Philip Sporn	New York, N. Y.
	(*Terms expire July 31, 1953*)
J. L. Callahan	New York, N. Y.
J. M. Flanigen	Atlanta, Ga.
R. I. Wilkinson	New York, N. Y.
	(*Terms expire July 31, 1954*)

Elected by the Board of Directors from its own membership for term of two years

R. T. Henry	Buffalo, N. Y.
M. D. Hooven	Newark, N. J.
Victor Siegfried	Worcester, Mass.
	(*Terms expire July 31, 1950*)
W. L. Everitt	Urbana, Ill.
A. H. Frampton	St. Catharines, Ontario, Canada
A. C. Monteith	Pittsburgh, Pa.
	(*Terms expire July 31, 1951*)

Ex-officio

James F. Fairman, president	New York, N. Y.
W. I. Slichter, treasurer	New York, N. Y.
H. H. Henline, secretary	New York, N. Y.

Education

B. R. Teare, Jr., *chairman*, Carnegie Institute of Technology, Pittsburgh, Pa.

(*Continued in next column*)

R. D. Bennett	Silver Spring, Md.
R. L. Biesele	Dallas, Tex.
D. S. Bridgman	New York, N. Y.
E. E. Dreese	Columbus, Ohio
W. L. Everitt	Urbana, Ill.
A. W. Friend	Princeton, N. J.
H. E. Hartig	Minneapolis, Minn.
A. R. Hellwarth	Detroit, Mich.
T. G. LeClair	Chicago, Ill.
T. C. Lloyd	Springfield, Ohio
A. H. Lovell	Ann Arbor, Mich.
K. B. McEachron, Jr.	Schenectady, N. Y.
H. N. Muller, Jr.	East Pittsburgh, Pa.
J. A. Northcott, Jr.	Notre Dame, Ind.
R. C. Putnam	Cleveland, Ohio
Walther Richter	West Allis, Wis.
J. D. Ryder	Urbana, Ill.
E. M. Strong	Ithaca, N. Y.
G. F. Tracy	Toronto, Ontario, Canada
C. E. Tucker	Cambridge, Mass.
E. A. Walker	State College, Pa.
M. L. Waring	New York, N. Y.
S. Reid Warren, Jr.	Philadelphia, Pa.

Lamme Medal

F. E. Harrell	Cleveland, Ohio
D. A. Quarles	New York, N. Y.
J. B. Thomas, *chairman*	Fort Worth, Tex.
	(*Terms expire July 31, 1950*)
J. H. Berry	Norfolk, Va.
T. H. Morgan	Worcester, Mass.
L. A. Umansky	Schenectady, N. Y.
	(*Terms expire July 31, 1951*)
C. B. Jolliffe	Princeton, N. J.
A. H. Kehoe	New York, N. Y.
J. B. MacNeill	East Pittsburgh, Pa.
	(*Terms expire July 31, 1952*)

Management

A. C. Monteith, *chairman*, Westinghouse Electric Corporation, 306 Fourth Avenue, Pittsburgh 30, Pa.

P. L. Alger	Schenectady, N. Y.
K. P. Applegate	Hartford, Conn.
C. J. Beller	Cleveland, Ohio
R. D. Bennett	Silver Spring, Md.
H. K. Breckenridge	Pittsburgh, Pa.
F. W. Bush	Milwaukee, Wis.
W. L. Cisler	Detroit, Mich.
E. E. Hill	New York, N. Y.
E. L. Moreland	Boston, Mass.
H. A. Peterson	New York, N. Y.
D. A. Quarles	New York, N. Y.
F. M. Roberts	Schenectady, N. Y.
D. D. Smalley	San Francisco, Calif.
O. Van Rye	Boston, Mass.

Prizes, Award of Institute

C. H. Willis, *chairman*, Princeton University, Princeton, N. J.

D. I. Anzini	San Francisco, Calif.
H. C. Coleman	East Pittsburgh, Pa.
H. L. Davis, Jr.	Philadelphia, Pa.
L. F. Hickernell	Hastings-on-Hudson, N. Y.
W. C. Kalb	Cleveland, Ohio
M. J. Kelley	New York, N. Y.
T. G. LeClair	Chicago, Ill.
K. B. McEachron	Pittsfield, Mass.
F. O. McMillan	Corvallis, Oreg.
J. J. Orr	New York, N. Y.
H. I. Romnes	New York, N. Y.
F. M. Sebast	Troy, N. Y.
J. D. Tebo	New York, N. Y.
H. M. Turner	New Haven, Conn.

Registration of Engineers

Elgin B. Robertson, *chairman*, P. O. Box 745, Dallas 1, Tex.

E. H. Bancker	Schenectady, N. Y.
L. H. Cleary	Washington, D. C.
J. M. Flanigen	Atlanta, Ga.
J. H. Foote	Jackson, Mich.
N. L. Freeman	Schenectady, N. Y.
J. E. Hobson	Stanford, Calif.
J. T. Hood	Tacoma, Wash.
K. B. McEachron	Pittsfield, Mass.
E. W. Oesterreich	Pittsburgh, Pa.
William W. Perry	Binghamton, N. Y.
L. M. Robertson	Denver, Colo.
E. W. Seeger	Milwaukee, Wis.
R. W. Sorensen	Pasadena, Calif.
P. G. Wallace	Dallas, Tex.
R. G. Warner	New Haven, Conn.
E. R. Whitehead	Brookfield, Ill.

Student Branches

F. O. McMillan, *chairman*, Oregon State College, Corvallis, Oreg.

F. W. Tatum, *vice-chairman*	Dallas, Tex.
R. G. Porter, *secretary*	Boston, Mass.
Sterling Bechwith	Milwaukee, Wis.
R. A. Galbraithe	Syracuse, N. Y.
J. H. Kuhlmann	Minneapolis, Minn.
H. N. Muller, Jr.	East Pittsburgh, Pa.
L. T. Rader	Schenectady, N. Y.
E. A. Reid	Urbana, Ill.
E. W. Spring	Detroit, Mich.
W. G. Warren	Santa Clara, Calif.
B. S. Wills	Ames, Iowa

Chairman, District Committee on Student Activities

A. G. Conrad (1)	New Haven, Conn.
K. F. Sibila (2)	Akron, Ohio
F. A. Wahlers (3)	Brooklyn, N. Y.
H. B. Duling (4)	Atlanta, Ga.
E. W. Kane (5)	Milwaukee, Wis.
C. H. Chinburg (6)	Fort Collins, Colo.
R. W. Tapy (7)	Albuquerque, N. M.
R. C. Lewis (8)	Los Angeles, Calif.
G. D. Sheckels (9)	Bozeman, Mont.

Ex-officio

Counselors of Student Branches

Volta Scholarship Trustees

W. L. Everitt	Urbana, Ill.
	(*Term expries July 31, 1951*)
C. A. Powel	Cambridge, Mass.
	(*Term expires July 31, 1953*)
H. S. Osborne, *chairman*,	New York, N. Y.
	(*Term expires July 31, 1955*)

(The functions of the foregoing committees are stated in Secs. 65–86 of the By-laws.)

Technical Committees

Communications Group

Communication Co-ordinating Committee

H. I. Romnes, *chairman*; American Telephone and Telegraph Company, 195 Broadway, New York 7, N. Y.

F. B. Bramhall, *vice-chairman*	New York, N. Y.
A. J. Busch, *secretary*	New York, N. Y.

Members-at-Large

J. L. Callahan, representing Board of Directors	New York, N. Y.
Rothwell E. Smith	New York, N. Y.

Ex-officio members

Chairman of the technical committees in the Communication Group

Aural Broadcasting Systems

E. G. Ports, *chairman*; Federal Telephone and Radio Corporation, 100 Kingsland Road, Clifton, N. J.

J. L. Middlebrooks, *vice-chairman*	New York, N. Y.
M. L. Levy, *secretary*	New York, N. Y.
T. M. Bloomer	Baltimore, Md.
T. J. Boerner	Camden, N. J.
L. E. Closson	Philadelphia, Pa.
E. W. Davis	New York, N. Y.
C. E. Dean	Little Neck, N. Y.
P. G. Edwards	New York, N. Y.
L. K. Findley	Cedar Rapids, Iowa
J. C. Gaudio	Chicago, Ill.
R. W. Masters	Columbus, Ohio
Gerard Mountjoy	Rochester, N. Y.
R. M. Sprague	Waltham, Mass.
J. K. Tyler	Sunbury, Pa.
R. H. Williamson	Syracuse, N. Y.

Transmission Systems Subcommittee

J. L. Middlebrooks, *chairman*; American Broadcasting Company, Inc., 30 Rockefeller Plaza, New York 21, N. Y.

G. M. K. Baker	Princeton, N. J.

(*Continued on page 1417*)

T. M. Bloomer	Baltimore, Md.
E. W. Davis	New York, N. Y.
P. G. Edwards	New York, N. Y.
L. K. Findley	Cedar Rapids, Iowa
R. W. Masters	Columbus, Ohio
R. M. Sprague	Waltham, Mass.
R. H. Williamson	Syracuse, N. Y.

Receivers Subcommittee

C. E. Dean, *chairman;* Hazeltine Electronics Corporation, 58-25 Little Neck Parkway, Little Neck, L. I., N. Y.

L. E. Closson	Philadelphia, Pa.
J. C. Gaudio	Chicago, Ill.
M. L. Levy	New York, N. Y.
Gerard Mountjoy	Rochester, N. Y.
J. K. Tyler	Sunbury, Pa.

Communication Switching Systems

R. C. Davis, *chairman;* Bell Telephone Laboratories, Inc., 463 West Street, New York 14, N. Y.

J. Meszar, *vice-chairman*	New York, N. Y.
A. E. Frost, *secretary*	New York, N. Y.
L. L. Burns	Dallas, Tex.
D. G. Geiger	Toronto, Ontario, Canada
G. H. Gray	New York, N. Y.
L. B. Haigh	New York, N. Y.
C. F. Lynch	Poughkeepsie, N. Y.
A. B. Smith	Chicago, Ill.
D. L. Solomon	Rochester, N. Y.
W. G. Storey	Chicago, Ill.
C. M. Tomlinson	Philadelphia, Pa.

No subcommittees

Radio Communication Systems

G. T. Royden, *chairman;* MacKay Radio and Telegraph Company, 67 Broad Street, New York 4, N. Y.

E. D. Becken, *vice-chairman*	New York, N. Y.
A. C. Dickieson, *secretary*	New York, N. Y.
C. M. Backer	Clifton, N. J.
E. H. B. Bartelink	New York, N. Y.
I. F. Byrnes	New York, N. Y.
F. H. Cusack	New York, N. Y.
D. D. Grieg	Nutley, N. J.
G. R. Messmer	Washington, D. C.

Mobile Radio Subcommittee

A. C. Dickieson, *chairman;* Bell Telephone Laboratories, Inc., 463 West Street, New York 14, N. Y.

C. M. Backer	Clifton, N. J.
I. F. Byrnes	New York, N. Y.

Point-to-Point Radio Subcommittee

E. D. Becken, *chairman;* RCA Communications, Inc., 66 Broad Street, New York 4, N. Y.

E. H. B. Bartelink	New York, N. Y.
F. H. Cusack	New York, N. Y.
D. D. Greig	Nutley, N. J.
G. R. Messmer	Washington, D. C.

Special Communications Applications

E. W. Kenefake, *chairman;* Electronics Department, General Electric Company, Syracuse, N. Y.

L. A. Smith, *vice-chairman*	New York, N.Y.
L. C. Holmes, *secretary*	Rochester, N. Y.
S. C. Bartlett	New York, N. Y.
G. W. Baughman	Swissvale, Pa.
I. F. Byrnes	New York, N. Y.
Melville Eastham	Cambridge, Mass.
W. D. Hailes	Rochester, N. Y.
L. E. Kearney	New York, N. Y.
R. H. Kline	Baltimore, Md.
Newton Monk	New York, N. Y.
W. A. Ready	Malden, Mass.
H. H. Spencer	Camden, N. J.
R. B. Vaile, Jr.	Stanford, Calif.
A. J. Warner	Nutley, N. J.

Electro-Acoustics Subcommittee

R. B. Vaile, Jr., *chairman;* Stanford University, Stanford Research Institute, Stanford, Calif.

I. F. Byrnes	New York, N. Y.
L. C. Holmes	Rochester, N. Y.
H. H. Spencer	Camden, N. J.

Railroad Communications Subcommittee

W. D. Hailes, *chairman;* General Railway Signal Company, 801 West Avenue, Rochester 11, N. Y.

G. W. Baughman	Swissvale, Pa.
L. E. Kearney	New York, N. Y.
Newton Monk	New York, N. Y.

Special Activities Subcommittee

A. J. Warner, *chairman;* Federal Telecommunication Laboratories, 500 Washington Avenue, Nutley 10, N. J.

Melville Eastham	Cambridge, Mass.
R. H. Kline	Baltimore, Md.
Newton Monk	New York, N. Y.
H. H. Spencer	Camden N. J.

Telegraph Systems

I. S. Coggeshall, *chairman;* Western Union Telegraph Company, 60 Hudson Street, New York 13, N. Y.

J. A. Duncan, Jr., *vice-chairman*	New York, N. Y.
E. C. Chamberlain, *secretary*	New York, N. Y.
M. Alden	Brockton, Mass.
E. P. Bancroft	New York, N. Y.
A. S. Benjamin	Chicago, Ill.
A. G. Cooley	New York, N. Y.
W. G. H. Finch	New York, N. Y.
H. H. Haglund	New York, N. Y.
J. V. L. Hogan	New York, N. Y.
Grosvenor Hotchkiss	New York, N. Y.
Alfred Kahn	New York, N. Y.
J. A. Krechek	Washington, D. C.
R. E. Mathes	Hartford, Conn.
R. B. Steele	Toronto, Ontario, Canada
L. A. Thompson	Cleveland, Ohio
E. F. Watson	New York, N. Y.
R. J. Wise	New York, N. Y.
G. B. Worthen	New York, N. Y.
C. J. Young	Princeton, N. J.

Facsimile Subcommittee

W. G. H. Finch, *chairman;* Finch Telecommunications, Inc., 10 East 40th Street, New York, N. Y.

M. Alden	Brockton, Mass.
A. S. Benjamin	Chicago, Ill.
A. G. Cooley	New York, N. Y.
J. V. L. Hogan	New York, N. Y.
J. A. Krchek	Washington, D. C.
R. E. Mathes	Hartford, Conn.
L. A. Thompson	Cleveland, Ohio
R. J. Wise	New York, N. Y.
G. B. Worthen	New York, N. Y.
C. J. Young	Princeton, N. J.

Television Broadcasting Systems

J. B. Coleman, *chairman;* Radio Corporation of America, RCA Victor Division, Camden, N. J.

L. G. Cumming, *vice-chairman*	New York, N. Y.
L. M. Rodgers, *secretary*	Philadelphia, Pa.
G. H. Brown	Princeton, N. J.
D. G. Fink	New York, N. Y.
J. C. Gaudio	Chicago, Ill.
P. C. Goldmark	New York, N. Y.
T. T. Goldsmith, Jr.	Passaic, N. J.
W. R. Hewlett	Palo Alto, Calif.
E. M. Johnston	New York, N. Y.
I. J. Kaar	Syracuse, N. Y.
W. L. Lawrence	Camden, N. J.
G. M. Nixon	New York, N. Y.
D. W. Pugley	Syracuse, N. Y.
F. M. Rives	Syracuse, N. Y.
R. E. Shelby	New York, N. Y.
S. C. Spielman	Philadelphia, Pa.
V. E. Trouant	Camden, N. J.
N. H. Young	Nutley, N. J.

Transmission Systems Subcommittee

W. L. Lawrence, *chairman;* Radio Corporation of America, RCA Victor Division, Camden, N. J.

G. H. Brown	Princeton, N. J.
P. C. Goldmark	New York, N. Y.
E. M. Johnson	New York, N. Y.
G. M. Nixon	New York, N. Y.
F. M. Rives	Syracuse, N. Y.
V. E. Trouant	Camden, N. J.
N. H. Young	Nutley, N. J.

Receivers Subcommittee

S. C. Spielman, *chairman;* Philco Corporation, C and Tioga Streets, Philadelphia 34, Pa.

D. G. Fink	New York, N. Y.
J. C. Gaudio	Chicago, Ill.
T. T. Goldsmith, Jr.	Passaic, N. J.
W. R. Hewlett	Palo Alto, Calif.
I. J. Kaar	Syracuse, N. Y.
D. W. Pugsley	Syracuse, N. Y.
R. E. Shelby	New York, N. Y.

Wire Communications Systems

H. A. Affel, *chairman;* Bell Telephone Laboratories, Inc., 463 West Street, New York 14, N. Y.

G. B. Ransom, *vice-chairman*	New York, N. Y.
L. G. Abraham, *secretary*	New York, N. Y.
A. L. Albert	Corvallis, Oreg.
W. M. Allen	Portland, Oreg.
E. H. B. Bartelink	New York, N. Y.
J. D. Booth	Baltimore, Md.
Hezzie Clark	Houston, Tex.
A. B. Credle	Mineola, N. Y.
G. E. Dodrill	Washington, D. C.
H. E. Ellithorn	Notre Dame, Ind.
L. G. Erickson	San Carlos, Calif.
G. H. Gray	New York, N. Y.
W. D. Hailes	Rochester, N. Y.
E. B. Harmon	Denver, Colo.
H. R. Hunkins	Clifton, N. J.
R. R. O'Connor	Chicago, Ill.
F. M. Rives	Syracuse, N. Y.
A. L. Rumsey	Albany, N. Y.
J. O'D. Shepherd	Atlanta, Ga.
Arthur Bessey Smith	Chicago, Ill.
W. T. Smith	New York, N. Y.

Power Line Carrier Subcommittee

F. M. Rives, *chairman;* General Electric company, Electronics Park, Syracuse, N. Y.

J. D. Booth	Baltimore, Md.
G. E. Dodrill	Washington, D. C.
W. D. Hailes	Rochester, N. Y.
E. B. Harmon	Denver, Colo.
W. T. Smith	New York, N. Y.

General Applications Group

General Applications Co-ordinating Committee

H. C. Coleman, *chairman;* Marine and Aviation Section of Industry Engineering Department Westinghouse Electric Corporation, East Pittsburgh, Pa.

C. C. Whipple, *vice-chairman*	Brooklyn, N. Y.
O. A. Wilde, *secretary*	Chester, Pa.

Member-at-Large

Elgin B. Robertson, representing Board of Directors	Dallas, Tex.

Ex-officio members

Chairman of the technical committees in the General Applications Group

Air Transportation

W. V. Boughton, *chairman;* Phaostron Company, 151 Pasadena Avenue, South Pasadena, Calif.

D. E. Fritz, *vice-chairman*	Cleveland, Ohio
W. L. Berry, *secretary*	Culver City, Calif.
J. W. Allen	Teterboro, N. J.
G. W. Almassy	Los Angeles, Calif.
J. H. Blankenbuehler	Troy, Ohio
W. C. Bryant	Burbank, Calif.
J. P. Dallas	Culver City, Calif.
Peter Duyan, Jr.	Santa Monica, Calif.
D. W. Exner	Seattle, Wash.
Alec Fisher	Lynn, Mass.
Elio Fueyo	Miami, Fla.
C. E. Gagnier	Los Angeles, Calif.
S. H. Hanville, Jr.	Washington, D. C.
W. T. Harding	Dayton, Ohio
J. G. Hutton	Schenectady, N. Y.
R. R. Jenner	Wichita, Kans.
R. D. Jones	Fort Wayne, Ind.

(*Continued in next column*)

W. B. Keller	Cleveland, Ohio
R. J. Lusk	East Pittsburgh, Pa.
Karl Martinez	Seattle, Wash.
C. F. McCabe	San Diego, Calif.
R. E. McDonald	St. Paul, Minn.
R. S. Mead	Kansas City, Mo.
R. A. Millermaster	Milwaukee, Wis.
J.D. Miner	Lima, Ohio
C. R. Moore	Los Angeles, Calif.
W. F. Moore	Schenectady, N. Y.
Joseph Nader	Chicago, Ill.
W. E. Pakala	East Pittsburgh, Pa.
H. F. Rempt	Burbank, Calif.
R. A. Rugge	Columbus, Ohio
K. R. Smythe	Baltimore, Md.
S. D. Summers	Washington, D. C.
Harold Tanke	Washington, D. C.
S. H. Webster	Burbank, Calif.

Aircraft Electrical Rotating Machinery Subcommittee

L. R. Larson, *chairman;* Naval Research Laboratory, Washington, D. C.

J. W. Allen	Teterboro, N. J.
J. B. Crockford	Lima, Ohio
William Fell	Cleveland, Ohio
Alec Fisher	Lynn, Mass.
S. H. Hanville, Jr.	Washington, D. C.
R. D. Jones	Fort Wayne, Ind.
G. W. Sherman	Dayton Ohio
R. R. Smith	Baltimore, Md.

Aircraft Electrical Systems Subcommittee

G. A. Phillips, *chairman;* Aviation Division, General Electric Company, Schenectady, N. Y.

J. W. Allen	Teterboro, N. J.
G. W. Almassy	Los Angeles, Calif.
Phil. Binderman	Washington, D. C.
H. B. Bunce	East Pittsburgh, Pa.
L. M. Cobb	Baltimore, Md.
D. W. Exner	Seattle, Wash.
H. L. Hildebrandt	Dayton, Ohio
C. S. Milliken	Burbank, Calif.
W. F. Moore	Schenectady, N. Y.
D. H. Scott	Washington, D. C.
A. J. Snyder	Tulsa, Okla.
A. F. Trumbull	Santa Monica, Calif.

Principles of Altitude Rating of Electrical Apparatus Subcommittee

Karl Martinez, *chairman;* Boeing Airplane Company, Plant 1, Seattle, Wash.

J. W. Allen	Teterboro, N. J.
S. H. Hanville, Jr.	Washington, D. C.
V. C. Holloway	Washington, D. C.
J. G. Hutton	Schenectady, N. Y.
C. A. Maple	Dayton, Ohio
R. A. Rugge	Columbus, Ohio

Aircraft Electrical Control Protective Devices and Cable Subcommittee

B. O. Austin, *chairman;* Westinghouse Electrical Corporation, Small Motors Division, Lima, Ohio

Earl Barlow	Baltimore, Md.
E. E. Magee	Dayton, Ohio
R. A. Millermaster	Milwaukee, Wis.
H. S. Moore	New Haven, Conn.
W. F. Moore	Schenectady, N. Y.
J. Ottmar	Attleboro, Mass.
Milton Schach	Washington, D. C.
Omar Wally	Cleveland, Ohio
W. W. West	New York, N. Y.

Domestic and Commercial Applications

Carl F. Scott, *chairman;* General Electric Company, 1285 Boston Avenue, Bridgeport, Conn.

O. K. Coleman, *vice-chairman*	Lafayette, Ind.
V. G. Vaughan, Sr., *secretary*	Attleboro, Mass.
J. C. Beckett	San Francisco, Calif.
M. M. Brandon	New York, N. Y.
A. C. Bredahl	Pittsburgh, Pa.
W. B. Buchanan	Toronto, Ontario, Canada
O. K. Buck	Los Angeles, Calif.
T. H. Cline	Newark, Ohio
T. H. David, Jr.	Chicago, Ill.
M. D. Duffy	Portland, Oreg.
R. W. Fleming	South Bend, Ind.
R. R. Herrmann	Minneapolis, Minn.
T. C. Johnson	Bloomfield, N. J.
F. W. Linder	La Crosse, Wis.
B. H. Martin	Chattanooga, Tenn.

(*Continued on page 1418*)

L. W. McCullough	New York, N. Y.
W. G. Meese	Detroit, Mich.
R. F. Parr	Mansfield, Ohio
A. L. Riche	Freeport, Ill.
L. N. Roberson	Seattle, Wash.
H. P. Seelye	Detroit, Mich.
G. S. Smith	Seattle, Wash.
G. C. Tenney	San Francisco, Calif.
Wesley Weinerth	Philadelphia, Pa.

No subcommittees

Land Transportation

H. F. Brown, *chairman;* New York, New Haven and Hartford Railroad, Railroad Station, New Haven 6, Conn.

L. W. Birch, *vice-chairman*	Mansfield, Ohio
R. L. Kimball, *secretary*	New York, N. Y.
J. C. Aydelott	Erie, Pa.
I. S. Billau	Baltimore, Md.
H. R. Blomquist	Providence, R. I.
W. A. Brecht	East Pittsburgh, Pa.
D. M. Burckett	Boston, Mass.
C. N. Chase	Coney Island, N. Y.
Andrew Costic	Hoboken, N. J.
Llewellyn Evans	Chattanooga, Tenn.
J. C. Fox	Princeton, W. Va.
A. P. Frey	Baltimore, Md.
K. H. Gordon	Philadelphia, Pa.
W. S. H. Hamilton	New York, N. Y.
P. H. Hatch	New Haven, Conn.
G. L. Hoard	Seattle, Wash.
J. G. Inglis	Toronto, Ontario, Canada
Charles Kerr, Jr.	East Pittsburgh, Pa.
Paul Lebenbaum	San Francisco, Calif.
S. B. Lent	Boston, Mass.
T. M. C. Martin	Portland, Oreg.
P. A. McGee	New York, N. Y.
E. B. Meissner	St. Louis, Mo.
S. R. Negley	Philadelphia, Pa.
I. S. Nippes	Ridgway, Pa.
A. G. Oehler	New York, N. Y.
W. R. Simmons	Montreal, Quebec, Canada
D. L. Smith	Highwood, Ill.
Jacob Stair, Jr.	Philadelphia, Pa.
M. C. Swanson	Schenectady, N. Y.
R. G. Thring	Washington, D. C.
J. P. Tretton	Indianapolis, Ind.
R. S. Warren	Elkhart, Ind.
R. A. Williamson	Erie, Pa.
G. M. Woods	East Pittsburgh, Pa.
H. P. Wright	Baltimore, Md.
Lawrence Wylie	Seattle, Wash.

Heavy Traction Electrification Data Subcommittee

L. W. Birch, *chairman;* Ohio Brass Company, Mansfield, Ohio

H. F. Brown	New Haven, Conn.
A. G. Oehler	New York, N. Y.
R. A. Williamson	Erie, Pa.
G. M. Woods	East Pittsburgh, Pa.

Projects:

(*1*). Catenary overhead systems
(*2*). Third rail systems
(*3*). Electric locomotives
(4). Substations
(*5*). Power supply

The personnel of the projects is as follows:

(*1*) and (*2*). L. W. Birch, *chairman,* Ohio Brass Company, Mansfield, Ohio; H. F. Brown, New Haven, Conn.

(*3*), (*4*), and (*5*). A. G. Oehler, New York, N. Y.; R. A. Williamson, Erie, Pa.; G. M. Woods, East Pittsburgh, Pa.

Heavy Traction Papers and Plans Subcommittee

H. F. Brown, *chairman;* New York, New Haven, and Hartford Railroad, Railroad Station, New Haven, Conn.

A. L. Brecht	East Pittsburgh, Pa.
R. L. Kimball	New York, N. Y.

Light Traction Papers and Plans Subcommittee

G. M. Woods, *chairman;* Industry Engineering Department, Westinghouse Electric Corporation, East Pittsburgh, Pa.

H. R. Blomquist	Providence, R. I.
D. L. Smith	Highwood, Ill.

Subcommittee on Revision of AIEE Standard Number 16 (Electric Railway Control Apparatus) ASA C48

(*Continued in next column*)

R. A. Williamson, *chairman;* Railroad Rolling Stock Division of Locomotive and Car Equipments Divisions, General Electric Company, Erie, Pa.

W. S. H. Hamilton	New York, N. Y.
P. H. Hatch	New Haven, Conn.
J. G. Inglis	Toronto, Ontario, Canada
G. M. Woods	East Pittsburgh, Pa.

Marine Transportation

Oscar A. Wilde, *chairman;* Sun Shipbuilding and Dry Dock Company, Chester, Pa.

E. C. Alger, *vice-chairman*	Quincy, Mass.
W. N. Zippler, *secretary*	New York, N. Y.
W. B. Armstrong	Washington, D. C.
R. A. Beekman	Schenectady, N. Y.
H. C. Coleman	East Pittsburgh, Pa.
P. J. DuMont	New York, N. Y.
J. B. Feder	Washington, D. C.
A. R. Gatewood	New York, N. Y.
L. M. Goldsmith	Philadelphia, Pa.
P. A. Guise	New York, N. Y.
H. F. Harvey, Jr.	Newport News, Va.
W. E. Jacobsen	Schenectady, N. Y.
J. E. Jones	Milwaukee, Wis.
Cornelius Krommenhock	Brooklyn, N. Y.
Clarence Lynn	East Pittsburgh, Pa.
V. W. Mayer	Washington, D. C.
S. N. Mead	Amesbury, Mass.
W. H. Reed	New York, N. Y.
E. M. Rothen	New York, N. Y.
L. B. Sinclair	Sparrows Point, Md.
C. W. Souder	Great Neck, N. Y.
E. H. Stivender	Milwaukee, Wis.
G. O. Watson	London, England

Power Generator Subcommittee

Clarence Lynn, *chairman;* Westinghouse Electric Corporation, East Pittsburgh, Pa.

W. B. Armstrong	Washington, D. C.
R. A. Beekman	Schenectady, N. Y.
H. C. Coleman	East Pittsburgh, Pa.
L. M. Goldsmith	Philadelphia, Pa.
W. E. Jacobsen	Schenectady, N. Y.
E. H. Stivender	Milwaukee, Wis.
O. A. Wilde	Chester, Pa.

Power Application Subcommittee

L. M. Goldsmith, *chairman;* Atlantic Refining Company, 260 South Broad Street, Philadelphia, Pa.

W. B. Armstrong	Washington, D. C.
H. C. Coleman	East Pittsburgh, Pa.
W. E. Jacobsen	Schenectady, N. Y.
J. E. Jones	Milwaukee, Wis.
Clarence Lynn	East Pittsburgh, Pa.
E. H. Stivender	Milwaukee, Wis.

Wires and Cables Subcommittee

W. N. Zippler, *chairman;* Gibbs and Cox, Inc., 1 Broadway, New York 4, N. Y.

P. J. DuMont	New York, N. Y.
J. B. Feder	Washington, D. C.
A. R. Gatewood	New York, N. Y.
W. E. Jacobsen	Schenectady, N. Y.
V. W. Mayer	Washington, D. C.
W. H. Reed	New York, N. Y.

Switches and Control Subcommittee

H. C. Coleman, *chairman;* Westinghouse Electric Corporation, East Pittsburgh, Pa.

R. A. Beekman	Schenectady, N. Y.
P. J. DuMont	New York, N. Y.
H. F. Harvey, Jr.	Newport News, Va.
J. E. Jones	Milwaukee, Wis.
C. Krommenhock	Brooklyn, N. Y.
L. B. Sinclair	Sparrows Point, Md.
E. H. Stivender	Milwaukee, Wis.

Distribution Subcommittee

H. F. Harvey, Jr., *chairman;* Newport News Shipbuilding and Dry Dock Company, Newport News, Va.

W. B. Armstrong	Washington, D. C.
A. R. Gatewood	New York, N. Y.
L. M. Goldsmith	Philadelphia, Pa.
P. A. Guise	North Bergen, N. J.
V. W. Mayer	Washington, D. C.
W. N. Zippler	New York, N. Y.

Fittings and Appliances Subcommittee

J. B. Feder, *chairman;* United States Coast Guard, Merchant Marine Technical Division, 1300 E. Street, N. W., Washington 25, D. C.

E. C. Alger	Quincy, Mass.

(*Continued in next column*)

P. J. DuMont	New York, N. Y.
P. A. Guise	North Bergen, N. J.
H. F. Harvey, Jr.	Newport News, Va.
V. W. Mayer	Washington, D. C.
E. M. Rothen	New York, N. Y.
L. B. Sinclair	Sparrows Point, Md.
O. A. Wilde	Chester, Pa.

Communications and Alarm Subcommittee

W. H. Reed, *chairman;* Bruce Electric Company, 196 West Houston Street, New York 14, N. Y.

E. C. Alger	Quincy, Mass.
J. B. Feder	Washington, D. C.
A. R. Gatewood	New York, N. Y.
C. Krommenhock	Brooklyn, N. Y.
S. N. Mead	Amesbury, Mass.
E. M. Rothen	New York, N. Y.
L. B. Sinclair	Sparrows Point, Md.
C. W. Souder	Great Neck, N. Y.

Navigation Equipment Subcommittee

S. N. Mead, *chairman;* Henschel Corporation, 14 Cedar Street, Amesbury, Mass.

E. C. Alger	Quincy, Mass.
P. A. Guise	New York, N. Y.
C. Krommenhock	Brooklyn, N. Y.
E. M. Rothen	New York, N. Y.
C. W. Souder	Great Neck, N. Y.

Publicity, Personnel, and History Subcommittee

R. A. Beekman, *chairman;* General Electric Company, Federal and Marine Department, Schenectady, N. Y.

H. F. Harvey, Jr.	Newport News, Va.
W. H. Reed	New York, N. Y.

Editing Subcommittee

W. N. Zippler, *chairman;* Gibbs and Cox, Inc., 1 Broadway, New York, N. Y.

J. B. Feder	Washington, D. C.
H. F. Harvey, Jr.	Newport News, Va.
W. H. Reed	New York, N. Y.

Production and Application of Light

E. H. Salter, *chairman;* Electrical Testing Laboratories, Inc., 2 East End Avenue, New York 21, N. Y.

R. C. Putnam, *vice-chairman*	Cleveland, Ohio
R. L. Oetting, *secretary*	Cleveland, Ohio
J. F. Angier	Washington, D. C.
L. H. Brown	Stanford, Calif.
S. W. Bruun	New York, N. Y.
H. S. Bull	Ann Arbor, Mich.
M. J. Dring	South Bend, Ind.
Frank Hansen	Los Angeles, Calif.
C. P. Hayes	Fort Wayne, Ind.
S. G. Hibben	Bloomfield, N. J.
O. W. Holden	Los Angeles, Calif.
R. W. Loehr	Cleveland, Ohio
H. E. Mahan	West Lynn, Mass.
J. A. McDermott	Corona, N. Y.
F. H. Murphy	Portland, Oreg.
Harris Reinhardt	Flushing, N. Y.
D. W. Rowten	Cleveland, Ohio
R. G. Slauer	Salem, Mass.
E. M. Strong	Ithaca, N. Y.
H. F. Wall	Detroit, Mich.
C. C. Whipple	Brooklyn, N. Y.

Ultraviolet Radiations Subcommittee

Allen J. Dusalt, *chairman;* Westinghouse Lamp Division, Bloomfield, N. J.

W. T. Anderson, Jr.	Newark, N. J.
H. W. Scott	Cleveland, Ohio

Nomenclature of Electronic Lamps Subcommittee

R. C. Putnam, *chairman;* Case Institute of Technology, Cleveland, Ohio

G. S. Evans	Bloomfield, N. J.
L. R. Keiffer	Cleveland, Ohio
T. C. Sargent	Salem, Mass.

Infrared Radiation Subcommittee

E. A. Linsday, *chairman;* General Electric Company, Nela Park, Cleveland 12, Ohio

George Parmallee	Cleveland, Ohio

Industry Group

Industry Co-ordinating Committee

J. J. Orr, *chairman;* United States Rubber Company, 1230 Avenue of the Americas, New York 20, N. Y.

T. R. Rhea, *vice-chairman*	Schenectady, N. Y.
R. S. Gardner, *secretary*	New York, N. Y.

Member-at-Large

Victor Siegfried, representing Board of Directors	Worcester, Mass.

Ex-officio members

Chairmen of the technical committees in the Industry Co-ordinating Group

Chemical, Electrochemical, and Electrothermal Applications

F. R. Benedict, *chairman;* Industry Engineering Department, Westinghouse Electric Corporation, East Pittsburgh, Pa.

L. W. Roush, *vice-chairman*	South Charleston, W. Va.
F. V. Andreae	Chattanooga, Tenn.
F. T. Bowditch	Cleveland, Ohio
J. D. Brance	Houston, Tex.
A. B. Campbell	Houston, Tex.
W. H. Dickinson	Elizabeth, N. J.
W. C. Dreyer	Houston, Tex.
Felix S. Glaza	Freeport, Tex.
L. M. Goldsmith	Philadelphia, Pa.
W. E. Gutzwiller	Milwaukee, Wis.
E. A. Hanff	Pittsburgh, Pa.
J. D. Harper	Alcoa, Tenn.
T. G. Hieronymus	Kansas City, Mo.
J. E. Hobson	Stanford, Calif.
H. E. Houck	Wilmington, Del.
J. D. Huntsberger	Trenton, N. J.
M. A. Hyde, Jr.	East Pittsburgh, Pa.
Rollin Kennard	Great Falls, Mont.
R. J. Kuhn	New Orleans, La.
E. H. Lamberger	East Pittsburgh, Pa.
D. H. Levy	Dallas, Tex.
J. J. Loustaunau	Boston, Mass.
J. A. McLellan	Linden, N. J.
G. H. Orcutt	Wyandotte, Mich.
Waldo Porter	Vancouver, Wash.
R. L. Rayner	Detroit, Mich.
T. R. Rhea	Schenectady, N. Y.
H. C. Riggs	Philadelphia, Pa.
G. B. Scheer	Oakland, Calif.
E. H. Scheick	New York, N. Y.
H. P. Sherer	Cleveland, Ohio
E. O. Scott	Welland, Ontario, Canada
Joel Tompkins	Massena, N. Y.
J. J. Unger	Cleveland, Ohio
G. W. Vinal	Washington, D. C.
H. W. Wahlquist	New York, N. Y.
H. H. Zielinski	Schenectady, N. Y.

Arc Furnace and Electrothermal Processes Subcommittee

E. H. Browning, Jr., *chairman;* Westinghouse Electric Corporation, East Pittsburgh, Pa.

F. V. Andreae	Chattanooga, Tenn.
W. L. Bundy	Wilson Dam, Ala.
R. A. Geiselman	East Pittsburgh, Pa.
E. A. Hanff	Pittsburgh, Pa.
A. R. Oltrogge	Schenectady, N. Y.
E. Scheick	New York, N. Y.
H. H. Zielinski	Schenectady, N. Y.

Cathodic Protection Subcommittee

A. E. Archambault	New York, N. Y.
J. D. Brance	Houston, Tex.
A. S. Brooks	Newark, N. J.
Guy Corfield	Los Angeles, Calif.
G. C. Cox	Charleston, W. Va.
I. A. Dennison	Washington, D. C.
L. J. Gorman	New York, N. Y.
T. G. Hieronymus	Kansas City, Mo.
R. J. Kuhn	New Orleans, La.
D. H. Levy	Dallas, Tex.
R. L. Rayner	Detroit, Mich.
H. W. Wahlquist	New York, N. Y.

Electrolytic Processes Subcommittee

W. E. Gutzwiller, *chairman;* Allis-Chalmers Manufacturing Company, Milwaukee, Wis.

(*Continued on page 1419*)

Felix Glaza Freeport, Tex.
J. D. Harper Alcoa, Tenn.
H. E. Houck Wilmington, Del.
F. L. Kaestle Schenectady, N. Y.
Rollin Kennard Great Falls, Mont.
F. L. Lawton Montreal, Quebec, Canada
G. H. Orcutt Wyandotte, Mich.
Waldo Porter Vancouver, Wash.
G. B. Scheer Oakland, Calif.
Joel Tompkins Massena, N. Y.

PETROLEUM REFINING AND PRODUCTION SUBCOMMITTEE

Lester Goldsmith, *chairman;* Atlantic Refining Company, 260 South Broad Street, Philadelphia 1, Pa.
H. J. Appel New York, N. Y.
W. H. Dickinson Elizabeth, N. J.
J. B. Glasby Philadelphia, Pa.
E. L. Hoyle East Chicago, Ind.
D. H. Levy Dallas, Tex.
E. L. Nopper Philadelphia, Pa.

STORAGE BATTERIES SUBCOMMITTEE

H. C. Riggs, *chairman;* Electric Storage Battery Company, 19th and Allegheny Avenue, Philadelphia 32, Pa.
J. D. Huntsberger Trenton, N. J.
L. A. Murray Providence, R. I.
E. T. Rummel Cleveland, Ohio
J. J. Unger Cleveland, Ohio
K. A. Vaughn Depew, N. Y.
H. H. Zielinski Schenectady, N. Y.

CHEMICAL INDUSTRIES SUBCOMMITTEE

L. W. Roush, *chairman;* Carbide and Carbon Chemicals Corporation, South Charleston, W. Va.
Felix Glaza Freeport, Tex.
E. M. Hansford Montgomery, W. Va.
J. A. Horacek Fairport Harbor, Ohio
H. E. Houck Wilmington, Del.
M. A. Hyde East Pittsburgh, Pa.
S. J. Rosch Hastings-on-Hudson, N. Y.

Electric Heating

J. C. Handy, *chairman;* Consolidated Gas, Electric Light and Power Company, Lexington Building, Baltimore, Md.
P. H. Goodell, *vice-chairman* Detroit, Mich.
L. M. Duryee, *secretary* Waterbury, Conn.
E. L. Bailey Highland Park, Mich.
R. M. Baker Baltimore, Md.
E. H. Browning East Pittsburgh, Pa.
Harold Bunte Chicago, Ill.
F. T. Chestnut Trenton, N. J.
R. H. Ellis Pittsburgh, Pa.
E. M. Guyer Corning, N. Y.
L. P. Hynes Haddonfield, N. J.
T. P. Kinn Baltimore, Md.
G. F. Leland Schenectady, N. Y.
W. H. Meyer Toronto, Ontario, Canada
A. E. Opdenweyer Portland, Oreg.
C. E. Peck Meadville, Pa.
Kennard Pinder Wilmington, Del.
W. C. Rudd Brooklyn, N. Y.
E. H. Scheick New York, N. Y.
E. A. Schmotzer Cleveland, Ohio
W. R. Schofield Philadelphia, Pa.
G. W. Scott, Jr. Lancaster, Pa.
G. S. Smith Seattle, Wash.
T. H. Story Camden, N. J.
J. T. Thwaites Hamilton, Ontario, Canada
G. E. Walters Peoria, Ill.
H. R. Winemiller Chicago, Ill.

INDUCTION AND DIELECTRIC HEATING SUBCOMMITTEE

W. C. Rudd, *chairman;* Induction Heating Corporation, 181 Wythe Avenue, Brooklyn 11, N. Y.
W. R. G. Baker Syracuse, N. Y.
G. P. Bosomworth Akron, Ohio
E. W. Chapin Laurel, Md.
F. T. Chesnut Trenton, N. J.
H. E. Dinger Washington, D. C.
L. M. Duryee Waterbury, Conn.
J. E. Eiselein Camden, N. J.
C. W. Frick Schenectady, N. Y.
H. C. Gillespie Camden, N. J.
W. H. Hickok Louisville, Ky.
R. J. Hunn Wilmington, Del.
T. R. Kennedy Trenton, N. J.
T. P. Kinn Baltimore, Md.
W. H. Meyer Toronto, Ontario, Canada

(Continued in next column)

L. R. Milburn Detroit, Mich.
Eugene Mittleman Chicago, Ill.
G. W. Scott, Jr. Lancaster, Pa.
J. T. Thwaites Hamilton, Ontario, Canada
R. L. Uphoff Bound Brook, N. J.
G. E. Walters Peoria, Ill.
D. E. Watts Syracuse, N. Y.
Otto Weitmann New York, N. Y.
H. R. Winemiller Chicago, Ill.
A. C. Wooldridge Newark, N. J.

RADIANT HEATING SUBCOMMITTEE

Paul H. Goodell, *chairman;* Jensen Specialties, Inc., 9331 Freeland Avenue, Detroit 28, Mich.
C. E. Russell, *secretary* Philadelphia, Pa.
I. J. Barber Fostoria, Ohio
E. J. Bates Dayton, Ohio
Earl Benson Salem, Mass.
P. O. Blackmore Newark, N. J.
A. H. Canada Schenectady, N. Y.
C. A. Casey Charlottesville, Va.
H. J. Garber Knoxville, Tenn.
M. M. Greer Pittsburgh, Pa.
S. G. Hibben Bloomfield, N. J.
W. F. Hickes Foxboro, Mass.
J. E. Johanson St. Louis, Mo.
E. A. Linsday Cleveland, Ohio
R. C. Machler Philadelphia, Pa.
A. D. Moore Ann Arbor, Mich.
C. T. Prendergast Chicago, Ill.
C. L. Raynor Detroit, Mich.
D. Y. Robinson Chicago, Ill.
Lawrence Stout St. Louis, Mo.
J. E. Sump Detroit, Mich.
W. H. Wannamaker Philadelphia, Pa.

SUBCOMMITTEE ON RADIATION MEASUREMENTS ABOVE 200 MEGACYCLES

R. M. Baker, *chairman;* Westinghouse Electric Corporation, 3601 Washington Boulevard, Baltimore, Md.
C. W. Frick, *secretary* Schenectady, N. Y.
H. H. Beizer Bradley Beach, N. J.
Marvin Bock Waltham, Mass.
R. E. Burgess Washington, D. C.
E. W. Chapin Laurel, Md.
H. E. Dinger Washington, D. C.
J. E. Eiselein Camden, N. J.
R. M. Showers Philadelphia, Pa.
H. E. Sorrows Washington, D. C.
A. J. Vadasz Syracuse, N. Y.

RESISTANCE HEATING AND ELECTRIC FURNACE SUBCOMMITTEE

J. C. Handy, *chairman;* Consolidated Gas, Electric Light and Power Company, Lexington Building, Baltimore 3, Md.
M. M. Greer, *secretary* Pittsburgh, Pa.
F. E. Bash Harrison, N. J.
Harold Bunte Chicago, Ill.
A. G. Hotchkiss Schenectady, N. Y.
F. J. Jolly Detroit, Mich.
C. E. Peck Meadville, Pa.
Kennard Pinder Wilmington, Del.
D. Y. Robinson Chicago, Ill.
E. H. Scheick Perth Amboy, N. J.

Electric Welding

Myron Zucker, *chairman;* Myron Zucker Engineering Company, 1708 Crooks Road, Royal Oak, Mich.
R. C. McMaster, *vice-chairman* Columbus, Ohio
R. S. Gardner, *secretary* New York, N. Y.
J. H. Blankenbuehler Troy, Ohio
W. G. Bostwick Cincinnati, Ohio
G. M. Chute Detroit, Mich.
C. N. Clark Pittsburgh, Pa.
J. F. Deffenbaugh Warren, Ohio
D. D. Douglass Oakland, Calif.
R. C. Freeman Fitchburg, Mass.
J. W. Gore Baltimore, Md.
E. M. Guyer Corning, N. Y.
W. B. Kouwenhoven Baltimore, Md.
E. J. Limpel Milwaukee, Wis.
S. W. Luther Detroit, Mich.
R. S. Phair Philadelphia, Pa.
C. M. Rhoades, Jr. Schenectady, N. Y.
M. S. Shane Cleveland, Ohio
C. E. Smith Warren, Ohio
H. W. Snyder Bozeman, Mont.
C. B. Stadum Buffalo, N. Y.
H. I. Stanback Milwaukee, Wis.
E. F. Steinert Buffalo, N. Y.
G. I. F. Theriault Dayton, Ohio
H. W. Tietze Newark, N. J.

(Continued in next column)

L. P. Winsor Troy, N. Y.
B. L. Wise Bay City, Mich.

POWER SUPPLY FOR RESISTANCE WELDING MACHINES SUBCOMMITTEE

C. N. Clark, *chairman;* Duquesne Light Company, 435 Sixth Avenue, Pittsburgh, Pa.
N. A. Kieb, *vice-chairman;* Detroit, Mich.
W. K. Boice Schenectady, N. Y.
W. G. Bostwick Cincinnati, Ohio
W. W. Brumby St. Catharines, Ontario, Canada
J. F. Deffenbaugh Warren, Ohio
E. F. Dissmeyer Jackson, Mich.
S. W. Luther Detroit, Mich.
R. S. Phair Philadelphia, Pa.
C. E. Smith Warren, Ohio
J. L. Solomon Chicago, Ill.
C. B. Stadum Buffalo, N. Y.
H. W. Tietze Newark, N. J.
Myron Zucker Royal Oak, Mich.

General Industry Applications

Kennard Pinder, *chairman;* E. I. du Pont de Nemours and Company, 10th and Market Streets, Wilmington, Del.
J. C. Fink, *vice-chairman* East Pittsburgh, Pa.
V. O. Johnson, *secretary* New York, N. Y.
B. T. Anderson Rockford, Ill.
A. T. Bacheler East Pittsburgh, Pa.
V. B. Baker East Pittsburgh, Pa.
E. L. Blankenbeker Pittsburgh, Pa.
S. A. Bobe Atlanta, Ga.
M. A. de Ferranti Schenectady, N. Y.
J. M. Delfs Schenectady, N. Y.
R. J. Demartini Schenectady, N. Y.
A. W. Frankenfield Wilmington, Del.
John Gammell Philadelphia, Pa.
E. M. Hays Pittsburgh, Pa.
L. W. Herchenroeder East Pittsburgh, Pa.
K. W. John Detroit, Mich.
G. W. Knapp Schenectady, N. Y.
A. F. Lukens Lynn, Mass.
H. B. Mathieu Pampa, Tex.
E. F. Mekelburg Milwaukee, Wis.
J. F. Moore Toronto, Ontario, Canada
E. K. Murphy New York, N. Y.
D. R. Percival Worcester, Mass.
G. E. Plaisted San Francisco, Calif.
N. L. Platt Binghamton, N. Y.
H. A. Rose Seattle, Wash.
R. G. Rudrow Wilmington, Del.
H. L. Smith New York, N. Y.
R. H. Smith Cleveland, Ohio
F. D. Snyder Boston, Mass.
R. F. Snyder Akron, Ohio
Ray Stroppel Cincinnati, Ohio
J. A. Tudor Portland, Oreg.
H. C. Uhl Sylacauga, Ala.
L. A. Umansky Schenectady, N. Y.

MACHINE TOOLS SUBCOMMITTEE

D. R. Percival, *chairman;* Machinery Electrification, Inc., 98 Union St., Worcester 8, Mass.
B. T. Anderson Rockford, Ill.
R. W. Brown Windsor, Vt.
J. M. Delfs Schenectady, N. Y.
R. T. Fenn Springfield, Vt.
L. W. Herchenroeder East Pittsburgh, Pa.
J. J. Jaeger West Hartford, Conn.
E. F. Mekelburg Milwaukee, Wis.
W. J. Piper Springfield, Vt.
S. Rice Worcester, Mass.
E. J. Rivoira Cincinnati, Ohio
R. E. Stroppel Cincinnati, Ohio
W. B. Wigton Cincinnati, Ohio

MATERIALS HANDLING SUBCOMMITTEE

M. A. de Ferranti, *chairman;* Industrial Engineering Division, General Electric Company, Schenectady 5, N. Y.
E. L. Blankenbeker, *secretary* Pittsburgh, Pa.
F. W. Atz Philadelphia, Pa.
S. P. Blakeman Philadelphia, Pa.
E. O. Dunham Battle Creek, Mich.
D. C. Gray St. Paul, Minn.
E. M. Hays Pittsburgh, Pa.
J. R. Kilander Schenectady, N. Y.
C. B. Rissler East Pittsburgh, Pa.
George Thompson Memphis, Tenn.
H. W. Williams Jersey City, N. J.
G. W. Yanney Alliance, Ohio

PULP AND PAPER INDUSTRY SUBCOMMITTEE

V. B. Baker, *chairman;* Industry Engineering Department, Westinghouse Electric Corporation, East Pittsburgh, Pa.
D. C. Christison, *secretary* Neenah, Wis.
H. B. Barrow Atlanta, Ga.
G. C. Ehemann Rittman, Ohio
O. O. Fisk Cumberland Mills, Maine
G. W. Knapp Schenectady, N. Y.
E. K. Murphy New York, N. Y.
H. A. Rose Seattle, Wash.
J. L. Van Nort Cleveland, Ohio

RUBBER AND PLASTICS INDUSTRY SUBCOMMITTEE

R. F. Snyder, *chairman;* Goodyear Tire and Rubber Company, 1144 East Market Street, Akron, Ohio
A. T. Bacheler, *secretary* East Pittsburgh, Pa.
E. J. Dalton Schenectady, N. Y.
John Gammell Philadelphia, Pa.
F. A. Green Akron, Ohio
K. W. John Detroit, Mich.
V. O. Johnson New York, N. Y.
G. V. Kullgren Akron, Ohio
J. F. Moore Toronto, Ontario, Canada
B. D. Morgan New Brunswick, N. J.
W. L. Ringland Milwaukee, Wis.
C. E. Robinson Cleveland, Ohio
R. G. Rudrow Wilmington, Del.
H. J. Secrest Akron, Ohio
R. E. Seddon Wilmington, Del.
H. L. Smith New York, N. Y.

TEXTILE INDUSTRY SUBCOMMITTEE

H. C. Uhl, *chairman;* Avondale Mills, Sylacauga, Ala.
R. J. Demartini, *secretary* Schenectady, N. Y.
A. T. Bacheler East Pittsburgh, Pa.
S. A. Bobe Atlanta, Ga.
I. S. Bull Greenville, S. C.
S. O. Cowan Charlotte, N. C.
W. E. Dent, Jr. Lancaster, S. C.
R. B. Flowers Atlanta, Ga.
A. W. Frankenfield Wilmington, Del.
H. Haley Philadelphia, Pa.
C. F. Hedlung Boston, Mass.
L. T. Jester Boston, Mass.
A. P. Lewis New Bedford, Mass.
A. F. Lukens Lynn, Mass.
Dan McConnell Greensboro, N. C.
Victor Sepavich Worcester, Mass.
F. D. Snyder Boston, Mass.

Industrial Control

G. W. Heumann, *chairman;* Control Engineering Division, General Electric Company, Schenectady 5, N. Y.
J. A. Cortelli, *vice-chairman* Cleveland, Ohio
H. L. Palmer, *secretary* Schenectady, N. Y.
E. H. Alexander Schenectady, N. Y.
H. H. Angel Bethlehem, Pa.
John Baird Madison, Wis.
T. H. Bloodworth Milwaukee, Wis.
G. S. Brown Cambridge, Mass.
L. J. Conover Easton, Pa.
W. H. Elliot Milwaukee, Wis.
C. T. Evans Milwaukee, Wis.
J. E. Gahagan Binghamton, N. Y.
J. A. Gienger Rochester, N. Y.
F. Y. Grepe Toronto, Ontario, Canada
K. W. John Detroit, Mich.
R. W. Jones Evanston, Ill.
J. D. Leitch Cleveland, Ohio
E. F. Mekelburg Milwaukee, Wis.
E. E. Moyer Troy, N. Y.
J. J. O'Connor New York, N. Y.
J. W. Picking Cleveland, Ohio
J. E. Ryan Schenectady, N. Y.
F. E. Strauss Oakland, Calif.
E. H. Vedder Buffalo, N. Y.

BIBLIOGRAPHY SUBCOMMITTEE

R. W. Jones, *chairman;* Department of Electrical Engineering, Northwestern University, Evanston, Ill.
H. H. Angel Bethlehem, Pa.
L. J. Conover Easton, Pa.
J. A. Cortelli Cleveland, Ohio
C. T. Evans Milwaukee, Wis.
D. K. Frost Rockford, Ill.
J. E. Gahagan Binghamton, N. Y.
J. A. Gienger Rochester, N. Y.
J. D. Leitch Cleveland, Ohio

(Continued on page 1420)

L. H. Matthias Milwaukee, Wis.
E. F. Mckelburg Milwaukee, Wis.
E. E. Moyer Troy, N. Y.
E. H. Vedder Buffalo, N. Y.

ELECTRONIC CONTROL SUBCOMMITTEE

H. L. Palmer, *chairman;* General Electric Company, 1 River Road, Schenectady 5, N. Y.
F. T. Bailey East Pittsburgh, Pa.
H. B. Black Ampere, N. J.
S. L. Burgwin East Pittsburgh, Pa.
C. J. Collom Detroit, Mich.
E. T. Davis Philadelphia, Pa.
L. H. Dee Schenectady, N. Y.
W. H. Elliot Milwaukee, Wis.
William Few Cleveland, Ohio
E. W. Hutton Schenectady, N. Y.
L. U. C. Kelling Schenectady, N. Y.
O. W. Livingston Schenectady, N. Y.
E. B. McDowell Schenectady, N. Y.
F. O. Nottingham Lafayette, Ind.
J. W. Picking Cleveland, Ohio
V. J. Porter Philadelphia, Pa.
K. P. Puchlowski Pittsburgh, Pa.
W. G. Roman East Pittsburgh, Pa.
C. A. Schurr Cleveland, Ohio
W. W. Snyder Kew Gardens, N. Y.
H. I. Stanback Milwaukee, Wis.
B. B. Stuart Chicago, Ill.
C. M. Summers Fort Wayne, Ind.
B. F. Tellkamp Milwaukee, Wis.

Working Groups:

(*1*). Electronic Control of D-C Motors
J. W. Picking, *chairman;* Reliance Electric and Engineering Company, 1068–1088 Ivanhoe Road, Cleveland 10, Ohio
H. B. Black Ampere, N. J.
C. J. Collom Detroit, Mich.
L. H. Dee Schenectady, N. Y.
W. H. Elliot Milwaukee, Wis.
William Few Cleveland, Ohio
W. G. Roman East Pittsburgh, Pa.
H. I. Stanback Milwaukee, Wis.
B. B. Stuart Chicago, Ill.
B. F. Tellkamp Milwaukee, Wis.

(*2*). Photoelectric Pickup Systems
L. U. C. Kelling, *chairman;* General Electric Company, 1 River Road, Schenectady 5, N. Y.
F. T. Bailey East Pittsburgh, Pa.
H. A. Lindsay Charleston, W. Va.
E. M. Pritchard Boston, Mass.
L. L. Worner Rankin, Ill.

(*3*). Electronic Relaying Devices
E. B. McDowell, *chairman;* General Electric Company, 1 River Road, Schenectady 5, N. Y.
C. A. Schurr Cleveland, Ohio
B. F. Tellkamp Milwaukee, Wis.

(*4*). Electronic Regulators and Regulating Systems
O. W. Livingston, *chairman;* General Electric Company, 1 River Road, Schenectady 5, N. Y.
H. B. Black Ampere, N. J.
S. L. Burgwin East Pittsburgh, Pa.
E. T. Davis Philadelphia, Pa.
W. H. Elliot Milwaukee, Wis.
William Few Cleveland, Ohio
J. W. Picking Cleveland, Ohio
W. W. Snyder Kew Gardens, N. Y.

(*5*). Electronic Control of A-C Power
E. W. Hutton, *chairman;* General Electric Company, 1 River Road, Schenectady 5, N. Y.
H. B. Black Ampere, N. J.
W. H. Elliot Milwaukee, Wis.
W. G. Roman East Pittsburgh, Pa.
B. F. Tellkamp Milwaukee, Wis.

STANDARDS SUBCOMMITTEE

G. W. Heumann, *chairman;* General Electric Company, Control Engineering Division, Schenectady 5, N. Y.

TEST CODES SUBCOMMITTEE

C. T. Evans, *chairman;* Cutler-Hammer, Inc., 315 North 12th Street, Milwaukee, Wis.
D. K. Frost Rockford, Ill.
B. W. Jones Schenectady, N. Y.
H. E. Nason Chicago, Ill.
W. E. Pakala East Pittsburgh, Pa.
J. E. Ryan Schenectady, N. Y.
C. A. Schaefer Milwaukee, Wis.

Industrial Power Systems

J. S. Gault, *chairman;* Electrical Engineering Department, University of Michigan, Ann Arbor, Mich.
H. G. Barnett, *vice-chairman* East Pittsburgh, Pa.
S. A. Warner, *secretary* New York, N. Y.
D. L. Beeman Schenectady; N. Y.
E. S. Dibble Los Angeles, Calif.
Leo Dolkart Chicago, Ill.
D. D. Douglass Oakland, Calif.
Felix Glaza Freeport, Tex.
W. S. Gordon, Jr. Tacoma, Wash.
C. R. Johnson New York, N. Y.
R. E. Johnson Rockford, Ill.
C. M. Lathrop Elizabeth, N. J.
M. C. Mapes New Haven, Conn.
A. E. Marshall St. Louis, Mo.
J. L. McKeever Peterboro, Ontario, Canada
J. S. Morgan Milwaukee, Wis.
W. A. Mosteller Detroit, Mich.
J. S. Parsons East Pittsburgh, Pa.
Dick Ray Tulsa, Okla.
W. H. Rollman Dallas, Tex.
C. C. Saunders Wilmington, Del.
C. W. Schemm St. Louis, Mo.
J. M. Smith Cleveland, Ohio
J. F. Spease Portland, Oreg.
W. D. Stevenson, Jr. Raleigh, N. C.
T. O. Sweatt New York, N. Y.
H. T. Theis Bristol, Pa.
B. F. Thomas New York, N. Y.
William Zelley Roebling, N. J.
T. O. Zittel Lackawanna, N. Y.

SUBCOMMITTEE ON REVISION OF ELECTRIC POWER DISTRIBUTION FOR INDUSTRIAL PLANTS

John Grotzinger, *chairman;* Goodyear Tire and Rubber Company, 1144 East Market Street, Akron, Ohio
J. A. Arberry Pittsburgh, Pa.
H. G. Barnett East Pittsburgh, Pa.
Y. T. Chaney Plainville, Conn.
William Deans Philadelphia, Pa.
L. E. Fisher Detroit, Mich.
N. B. Lainge Detroit, Mich.
S. W. Luther Detroit, Mich.
R. B. McKinley Schenectady, N. Y.
J. S. Parsons East Pittsburgh, Pa.
E. E. Turkington Boston, Mass.
R. C. Waldron Passaic, N. J.
R. M. Wilson, Jr. Schenectady, N. Y.
J. A. Yetter Schenectady, N. Y.

Mining and Metal Industry

T. B. Montgomery, *chairman;* Control Section, Allis-Chalmers Manufacturing Company, West Allis, Wis.
A. C. Muir, *vice-chairman* Philadelphia, Pa.
J. E. Breth Bessemer, Ala.
Graham Bright Pittsburgh, Pa.
A. B. Chafetz Carlsbad, N. Mex.
R. J. Corfield Garfield, Utah
J. A. Cortelli Cleveland, Ohio
F. W. Cramer Pittsburgh, Pa.
E. W. Davis Cambridge, Mass.
J. M. Downie Erie, Pa.
J. H. Edwards Huntington, W. Va.
Sam Ein Chicago, Ill.
R. H. Ellis Pittsburgh, Pa.
Cecil Farrow Cleveland, Ohio
J. J. Fitzgibbon Charleston, W. Va.
Lanier Greer Cleveland, Ohio
L. N. Grier Pittsburgh, Pa.
C. L. Gust Lead, S. Dak.
W. R. Harris East Pittsburgh, Pa.
L. H. Harrison Birmingham, Ala.
G. A. Hornbecker Waterbury, Conn.
J. G. Ivy Chicago, Ill.
L. H. James Scranton, Pa.
J. Z. Linsenmeyer East Pittsburgh, Pa.
R. C. McMaster Columbus, Ohio
W. E. Miller Schenectady, N. Y.
H. P. Musser Charleston, W. Va.
F. C. Nicholson Wilkes-Barre, Pa.
B. E. Price New York, N. Y.
D. E. Renshaw East Pittsburgh, Pa.
V. E. Schlossberg East Chicago, Ind.
E. G. Schlup Middletown, Ohio
F. O. Schnure Sparrows Point, Md.
Victor Siegfried Worcester, Mass.
H. I. Stanback Milwaukee, Wis.
O. J. Swanson Gary, W. Va.
C. L. Tyler Irwin, Pa.
T. R. Weichel Wilkes-Barre, Pa.

(*Continued in next column*)

C. O. Wood Chicago, Ill.
C. D. Woodward Butte, Mont.

METAL INDUSTRIES SUBCOMMITTEE

(Chairman not yet selected)

J. A. Cortelli Cleveland, Ohio
F. W. Cramer Pittsburgh, Pa.
Sam Ein Chicago, Ill.
R. H. Ellis Pittsburgh, Pa.
Cecil Farrow Cleveland, Ohio
Lanier Greer Cleveland, Ohio
L. N. Grier Pittsburgh, Pa.
W. R. Harris East Pittsburgh, Pa.
G. A. Hornbecker Waterbury, Conn.
W. E. Miller Schenectady, N. Y.
B. E. Price New York, N. Y.
V. E. Schlossberg East Chicago, Ind.
E. G. Schlup Middletown, Ohio
F. O. Schnure Sparrows Point, Md.
Victor Siegfried Worcester, Mass.
H. I. Stanback Milwaukee, Wis.

MINING SUBCOMMITTEE

(Chairman not yet selected)

J. E. Breth Bessemer, Ala.
Graham Bright Pittsburgh, Pa.
A. B. Chafetz Carlsbad, N. Mex.
R. J. Corfield Garfield, Utah
E. W. Davis Cambridge, Mass.
J. M. Downie Erie, Pa.
J. H. Edwards Huntington, W. Va.
J. J. Fitzgibbon Charleston, W. Va.
C. L. Gust Lead, S. Dak.
L. H. Harrison Birmingham, Ala.
J. G. Ivy Chicago, Ill.
L. H. James Scranton, Pa.
G. F. Johnson Valparaiso, Ind.
J. Z. Linsenmeyer East Pittsburgh, Pa.
R. C. McMaster Columbus, Ohio
A. C. Muir Philadelphia, Pa.
H. P. Musser Charleston, W. Va.
F. C. Nicholson Wilkes-Barre, Pa.
D. E. Renshaw East Pittsburgh, Pa.
O. J. Swanson Gary, W. Va.
C. L. Tyler Irwin, Pa.
T. R. Weichel Wilkes-Barre, Pa.
C. O. Wood Chicago, Ill.
C. D. Woodward Butte, Mont.

Feedback Control Systems (Servomechanisms)

G. S. Brown, *chairman;* Massachusetts Institute of Technology, Building 32, Cambridge 39, Mass.
(Exact title, scope, and personnel to be announced later)

Power Group

Power Co-ordinating Committee

L. F. Hickernell, *chairman;* Anaconda Wire and Cable Company, Hastings-on-Hudson 6, N. Y.
W. R. Brownlee, *vice-chairman* Jackson, Mich.
R. S. Gardner, *secretary* New York, N. Y.

Members-at-Large

R. T. Henry, representing Board of Directors Buffalo, N. Y.
L. F. Kennedy Schenectady, N. Y.
A. E. Knowlton New York, N. Y.
C. F. Wagner East Pittsburgh, Pa.

Ex-officio members

Chairmen of the technical committees in the Power Group

Carrier Current

S. C. Bartlett, *chairman;* American Gas and Electric Service Corporation, 30 Church Street, New York 8, N. Y.
C. W. Boadway, *vice-chairman* Toronto, Ontario, Canada
E. W. Kenefake, *secretary* Syracuse, N. Y.
W. H. Blankmeyer Butte, Mont.
J. M. Dunham New York, N. Y.
L. G. Eaton Boston, Mass.
J. R. Ellison Oklahoma City, Okla.
R. C. Ericson Hammond, Ind.
L. F. Ferri Elyria, Ohio
L. F. Kennedy Schenectady, N. Y.

(*Continued in next column*)

S. C. Leyland Newark, N. J.
Samuel Lubin Washington, D. C.
L. E. Ludekens Los Angeles, Calif.
D. M. MacGregor New York, N. Y.
T. W. MacLean Spokane, Wash.
R. H. Miller San Francisco, Calif.
F. M. Rives Syracuse, N. Y.
T. T. Smith Vancouver, Wash.
O. A. Starcke Kansas City, Mo.
B. W. Storer Chicago, Ill.
H. J. Sutton Beaumont, Tex.
T. D. Talmage Chattanooga, Tenn.
Mead Warren, Jr. Alcoa, Tenn.
M. H. Wood Baltimore, Md.

SUBCOMMITTEE FOR PREPARATION OF A GENERAL INTEREST PAPER ON CARRIER CURRENT

M. H. Wood, *chairman;* Westinghouse Electric Corporation, Electronics and X-Ray Division, 2519 Wilkens Avenue, Baltimore 3, Md.
S. C. Bartlett New York, N. Y.
J. D. Booth Baltimore, Md.
L. F. Kennedy Schenectady, N. Y.

SUBCOMMITTEE TO REPORT ON APPLICATION GUIDANCE FOR CARRIER CURRENT

D. M. MacGregor, *chairman;* Ebasco Services, Inc., 2 Rector Street, New York 6, N. Y.
C.W.Boadway Toronto, Ontario, Canada
T. D. Talmage Chattanooga, Tenn.

METHODS OF MEASUREMENT SUBCOMMITTEE

E. W. Kenefake, *chairman;* General Electric Company, Electronics Department, Syracuse, N. Y.
S. C. Bartlett New York, N. Y.
C.W.Boadway Toronto, Ontario, Canada
M. H. Wood Baltimore, Md.

HIGH-FREQUENCY CHARACTERISTICS OF POWER EQUIPMENT SUBCOMMITTEE

S. C. Leyland, *chairman;* Westinghouse Electric Corporation, 95 Orange Street, Newark 2, N. J.
T. A. Cramer Schenectady, N. Y.

CARRIER CURRENT CHARACTERISTICS OF TRANSMISSION LINES AND SYSTEMS SUBCOMMITTEE

R. C. Ericson, *chairman;* Northern Indiana Public Service Company, 5265 Hohman Avenue, Hammond, Ind.
W. H. Blankmeyer Butte, Mont.
W. J. Googe Shreveport, La.
L. E. Ludekens Los Angeles, Calif.
T. D. Talmage Chattanooga, Tenn.

STANDARD TERMINOLOGY FOR CARRIER CURRENT SUBCOMMITTEE

S. C. Leyland, *chairman;* Westinghouse Electric Corporation, 95 Orange Street, Newark 2, N. J.

LONG-LIFE TUBES SUBCOMMITTEE

L. G. Eaton, *chairman;* New England Power Service Company, 441 Stuart Street, Boston 16, Mass.
R. W. Beckwith Syracuse, N. Y.
L. F. Ferri Elyria, Ohio
Samuel Lubin Washington, D. C.
M. H. Wood Baltimore, Md.

USE OF MICROWAVE EQUIPMENT FOR RELAYING, TELEMETERING, AND SUPERVISORY CONTROL SUBCOMMITTEE

S. C. Leyland, *chairman;* Westinghouse Electric Corporation, 95 Orange Street, Newark 2, N. J.

OPERATING EXPERIENCE WITH CARRIER CURRENT RELAYING CHANNELS SUBCOMMITTEE

O. A. Starcke, *chairman;* Kansas City Power and Light Company, Box 679, Kansas City, Mo.
T. A. Cramer Schenectady, N. Y.
J. R. Curtin Portland, Oreg.
W. J. Googe Shreveport, La.
V. J. Hayes Waterbury, Conn.
H. W. Lensner Newark, N. J.
L. E. Ludekens Los Angeles, Calif.
B. W. Storer Chicago, Ill.
Mead Warren, Jr. Alcoa, Tenn.

Insulated Conductors

Herman Halperin, *chairman;* Commonwealth Edison Company, 72 West Adams Street, Chicago 90, Ill.
V. A. Sheals, *vice-chairman* Schenectady, N. Y.
C. T. Hatcher, *secretary* New York, N. Y.
G. W. Acock Trenton, N. J.
C. F. Avila Boston, Mass.
H. G. Barnett East Pittsburgh, Pa.
C. E. Baugh San Francisco, Calif.
E. D. Bent Montreal, Quebec, Canada
Andrew Bodicky St. Louis, Mo.
A. S. Brookes Newark, N. J.
T. J. Brosnan Buffalo, N. Y.
W. R. Bullard New York, N. Y.
H. W. Clark Washington, D. C.
E. W. Davis Cambridge, Mass.
W. A. Del Mar Yonkers, N. Y.
C. D. Eash Jackson, Mich.
D. M. Farnham Montreal, Quebec, Canada
G. H. Fiedler Rochester, N. Y.
L. E. Fogg Phillipsdale, R. I.
J. D. Frantz Portland, Oreg.
M. W. Ghen N. S. Pittsburgh, Pa.
L. F. Hickernell Hastings-on-Hudson, N. Y.
R. A. Hopkins Knoxville, Tenn.
A. H. Kidder Philadelphia, Pa.
R. H. Kolks Cincinnati, Ohio
L. I. Komives Detroit, Mich.
M. J. Lowenberg Boston, Mass.
C. G. Mansfield Los Angeles, Calif.
R. E. Morse New York, N. Y.
Lawrence Palmer Seattle, Wash.
W. T. Peirce Worcester, Mass.
M. L. Perry Kansas City, Mo.
R. S. Peterson Chicago, Ill.
A. D. Pettee Bayonne, N. J.
R. A. Schatzel Rome, N. Y.
V. E. Schlossberg East Chicago, Ind.
G. B. Shanklin Schenectady, N. Y.
H. D. Short Toronto, Ontario, Canada
F. V. Smith Chicago, Ill.
L. G. Smith Baltimore, Md.
G. M. L. Sommerman Evanston, Ill.
E. G. Sturdevant Bristol, R. I.
Gordon Thompson New York, N. Y.
H. H. Watson Bridgeport, Conn.
R. J. Wiseman Passaic, N. J.
R. K. Woodson Kansas City, Mo.
K. S. Wyatt New York, N. Y.
C. W. Zimmerer New York, N. Y.
W. N. Zippler New York, N. Y.

ADMINISTRATION SUBCOMMITTEE

Herman Halperin, *chairman;* Commonwealth Edison Company, 72 West Adams Street, Chicago 90, Ill.
V. A. Sheals, *vice-chairman* Schenectady, N. Y.
C. T. Hatcher, *secretary* New York, N. Y.
L. F. Hickernell, *ex-chairman* Hastings-on-Hudson, N. Y.

Subcommittee Chairmen:
G. W. Acock Trenton, N. J.
W. A. Del Mar Yonkers, N. Y.
G. H. Fiedler Rochester, N. Y.
L. E. Fogg Phillipsdale, R. I.
M. W. Ghen Pittsburgh, Pa.
L. I. Komives Detroit, Mich.
W. T. Peirce Worcester, Mass.
R. S. Peterson Chicago, Ill.
G. M. L. Sommerman Evanston, Ill.
Gordon Thompson New York, N. Y.
H. H. Watson Bridgeport, Conn.

STANDARDS AND PUBLICATIONS SUBCOMMITTEE

L. E. Fogg, *chairman;* Kennecott Wire and Cable Company, Phillipsdale, R. I.
A. S. Brookes Newark, N. J.
M. H. McGrath Bayonne, N. J.
V. A. Sheals Schenectady, N. Y.
H. D. Short Toronto, Ontario, Canada
C. W. Zimmerer New York, N. Y.

CABLE CHARACTERISTICS SUBCOMMITTEE

W. A. Del Mar, *chairman;* Phelps Dodge Copper Products Company, Habirshaw Cable and Wire Division, Yonkers, N. Y.
E. D. Bent Montreal, Quebec, Canada
C. T. Hatcher New York, N. Y.
A. H. Kidder Philadelphia, Pa.
C. G. Mansfield Los Angeles, Calif.
M. H. McGrath Bayonne, N. J.
J. H. Neher Philadelphia, Pa.
G. B. Shanklin Schenectady, N. Y.
F. V. Smith Chicago, Ill.
E. R. Thomas New York, N. Y.
R. J. Wiseman Passaic, N. J.
R. K. Woodson Kansas City, Mo.

(*Continued in next column*)

CONDUCTORS SUBCOMMITTEE

G. W. Acock, *chairman;* J. A. Roebling's Sons, South Broad Street, Trenton 2, N. J.
R. C. Waldron Passaic, N. J.
G. W. Zink Yonkers, N. Y.

INSULATIONS SUBCOMMITTEE

G. M. L. Sommerman, *chairman;* Department of Electrical Engineering, Northwestern Technological Institute, Evanston, Ill.
J. C. Balsbaugh Cambridge, Mass.
C. E. Betzer Chicago, Ill.
F. M. Clark Schenectady, N. Y.
A. S. Dana Seymour, Conn.
E. W. Greenfield Hastings-on-Hudson, N. Y.
Thorstein Larson Baltimore, Md.
E. L. Lotz Irvington, N. J.
R. B. McKinley Bridgeport, Conn.
J. D. Piper Detroit, Mich.
R. A. Schatzel Rome, N. Y.
E. G. Sturdevant Bristol, R. I.
A. J. Warner New York, N. Y.
K. S. Wyatt Yonkers, N. Y.

SHEATHS AND COVERINGS SUBCOMMITTEE

G. H. Fiedler, *chairman;* Rochester Gas and Electric Company, Rochester, N. Y.
C. F. Avila Boston, Mass.
C. E. Betzer Chicago, Ill.
Andrew Bodicky St. Louis, Mo.
A. S. Brockes Newark, N. J.
A. H. Kidder Philadelphia, Pa.
F. E. Kulman New York, N. Y.
A. D. Pettee Bayonne, N. J.
V. A. Sheals Schenectady, N. Y.
R. C. Waldron Passaic, N. J.
G. W. Zink Yonkers, N. Y.

CABLE SUPPLY SYSTEMS SUBCOMMITTEE

L. I. Komives, *chairman;* Detroit Edison Company, 2000—2d Avenue, Detroit 26, Mich.
C. F. Avila Boston, Mass.
T. J. Brosnan Buffalo, N. Y.
W. R. Bullard New York, N. Y.
H. W. Clark Washington, D. C.
D. M. Farnham Montreal, Quebec, Canada
J. D. Frantz Portland, Oreg.
C. T. Hatcher New York, N. Y.
M. J. Lowenberg Boston, Mass.
A. D. Pettee Bayonne, N. J.
C. S. Schifreen Philadelphia, Pa.
G. B. Shanklin Schenectady, N. Y.
H. D. Short Toronto, Ontario, Canada
C. F. Titus Jacksonville, Fla.
R. J. Wiseman Passaic, N. J.
K. S. Wyatt Yonkers, N. Y.

UTILIZATION WIRING SYSTEMS SUBCOMMITTEE

H. H. Watson, *chairman;* General Electric Company, 1285 Boston Avenue, Bridgeport 2, Conn.
E. L. Bailey Detroit, Mich.
H. G. Barnett East Pittsburgh, Pa.
A. L. Barrett Franklin, Pa.
T. P. Branch Washington, D. C.
G. B. Dodds Pittsburgh, Pa.
C. A. Finkel Passaic, N. J.
R. W. Foster Canton, N. C.
F. S. Glaza Freeport, Tex.
Lester Goldsmith Philadelphia, Pa.
J. E. Huguelet Detroit, Mich.
M. J. Lowenberg Boston, Mass.
J. B. MacLean New York, N. Y.
S. J. Rosch Hastings-on-Hudson, N. Y.
R. A. Schatzel Rome, N. Y.
V. E. Schlossberg East Chicago, Ind.
J. S. Waddington Brockville, Ontario, Canada
C. W. Zimmerer New York, N. Y.
G. W. Zink Yonkers, N. Y.

SPECIAL-PURPOSE CABLE SUBCOMMITTEE

W. T. Peirce, *chairman;* American Steel and Wire Company, Worcester, Mass.
G. W. Acock Trenton, N. J.
J. F. Atkinson Washington, D. C.
A. L. Barrett Franklin, Pa.

(*Continued in next column*)

E. D. Bent Montreal, Quebec, Canada
E. W. Davis Cambridge, Mass.
R. I. Fort Chicago, Ill.
R. A. Hopkins Knoxville, Tenn.
J. E. Huguelet Detroit, Mich.
R. H. Kolks Cincinnati, Ohio
R. B. McKinley Bridgeport, Conn.
S. B. Pennell New York, N. Y.
M. L. Perry Kansas City, Mo.
V. E. Schlossberg East Chicago, Ind.
F. V. Smith Chicago, Ill.
E. G. Sturdevant Bristol, R. I.
C. F. Titus Jacksonville, Fla.
A. D. Whamond Philadelphia, Pa.
R. K. Woodson Kansas City, Mo.
W. N. Zippler New York, N. Y.
Myron Zucker Royal Oak, Mich.

ACCESSORIES SUBCOMMITTEE

M. W. Ghen, *chairman;* Duquesne Light Company, 1241 Reedsdale St., N. S., Pittsburgh 12, Pa.
C. Christianson Melrose Park, Ill.
C. D. Eash Jackson, Mich.
J. D. Frantz Portland, Oreg.
G. G. Grissinger East Pittsburgh, Pa.
Fred Heller New York, N. Y.
J. E. Johnson Philadelphia, Pa.
R. H. Kolks Cincinnati, Ohio
E. L. Lotz Irvington, N. J.
H. E. Martin Brooklyn, N. Y.
R. E. Morse New York, N. Y.
J. H. Nicholas Chicago, Ill.
Lawrence Palmer Wenatchee, Wash.
M. L. Perry Kansas City, Mo.
F. P. West New York, N. Y.
L. Wetherill Pittsfield, Mass.
D. S. Young Toronto, Ontario, Canada

STRUCTURES SUBCOMMITTEE

R. S. Peterson, *chairman;* Commonwealth Edison Company, 72 West Adams Street, Chicago 90, Ill.
C. E. Baugh San Francisco, Calif.
Andrew Bodicky St. Louis, Mo.
T. J. Brosnan Buffalo, N. Y.
H. W. Clark Washington, D. C.
C. D. Eash Jackson, Mich.
G. H. Fiedler Rochester, N. Y.
Lawrence Palmer Wenatchee, Wash.
C. G. Mansfield Los Angeles, Calif.
L. G. Smith Baltimore, Md.
F. P. West New York, N. Y.
R. K. Woodson Kansas City, Mo.

TESTS AND MEASUREMENTS SUBCOMMITTEE

Gordon Thompson, *chairman;* Electrical Testing Laboratories, Inc., 2 West End Avenue, New York 21, N. Y.
J. C. Balsbaugh Cambridge, Mass.
A. L. Brownlee Chicago, Ill.
A. S. Dana Seymour, Conn.
E. W. Davis Cambridge, Mass.
W. A. Del Mar Yonkers, N. Y.
E. W. Greenfield Hastings-on-Hudson, N. Y.
Thorstein Larson Baltimore, Md
J. C. Parker Memphis, Tenn.
G. M. L. Sommerman Evanston, Ill.
R. F. Tener Washington, D. C.
E. R. Thomas New York, N. Y.
R. C. Waldron Passaic, N. J.
C. W. Zimmerer New York, N. Y.

Power Generation

B. G. A. Skrotzki, *chairman; Power*, McGraw-Hill Publishing Company, Inc., 330 West 42d Street, New York 18, N. Y.
J. A. Brooks, *vice-chairman* New York, N. Y.
Giuseppe Calabrese, *secretary* New York, N. Y.
R. E. Appleyard Milwaukee, Wis.
J. E. Barkle, Jr. East Pittsburgh, Pa.
C. S. Bowden Cleveland, Ohio
E. P. Bryant Los Angeles, Calif.
R. M. Bush Washington, D. C.
Hubbell Carpenter Duluth, Minn.
A. D. Caskey Chicago, Ill.
H. E. Deardorff Dayton, Ohio
S. M. Denton Denver, Colo.
E. F. Dissmeyer Jackson, Mich.
Alex Dovjikov Portland, Oreg.
John Finlaw Philadelphia, Pa.
C. B. Fontaine Lynn, Mass.
C. A. Harrington Cleveland, Ohio
H. R. Harris Detroit, Mich.

(*Continued in next column*)

A. F. Hartung Kansas City, Mo.
A. P. Hayward Pittsburgh, Pa.
B. V. Hoard Portland, Oreg.
W. R. Johnson San Francisco, Calif.
L. A. Kilgore East Pittsburgh, Pa.
A. J. Krupy Chicago, Ill.
F. L. Lawton Montreal, Quebec, Canada
J. T. Madill Arvida, Quebec, Canada
E. F. Maryatt San Francisco, Calif.
J. B. McClure Schenectady, N. Y.
G. H. McDaniel New York, N. Y.
D. R. Pattison Johnstown, Pa.
M. L. Perry Kansas City, Mo.
W. W. Perry Binghamton, N. Y.
A. L. Pollard Seattle, Wash.
C. S. Randall Washington, D. C.
H. B. Robinson Raleigh, N. C.
G. M. Tatum Richmond, Va.
C. W. Watchorn Baltimore, Md.
C. C. Whelchel San Francisco, Calif.
R. R. Wisner Boston, Mass.
G. R. Woodman Los Angeles, Calif.

PRIME MOVERS SUBCOMMITTEE

B. G. A. Skrotzki, *chairman;* Associate Editor, *Power*, 330 West 42d Street, New York 18, N. Y.
J. A. Brooks New York, N. Y.
E. P. Bryant Los Angeles, Calif.
A. D. Caskey Chicago, Ill.
John Finlaw Philadelphia, Pa.
A. F. Hartung Kansas City, Mo.
C. S. Randall Washington, D. C.
H. B. Robinson Raleigh, N. C.
C. C. Whelchel San Francisco, Calif.

SPEED GOVERNING SUBCOMMITTEE

J. B. McClure, *chairman;* General Electric Company, Central Station Engineering Divisions, Schenectady 5, N. Y.
R. E. Appleyard Milwaukee, Wis.
C. P. Almon, Jr. Chattanooga, Tenn.
R. M. Beville Chicago, Ill.
A. P. Hayward Pittsburgh, Pa.
T. H. Mawson Birmingham, Ala.
G. H. McDaniel New York, N. Y.
F. L. Reinmann Michigan City, Ind.

EXCITATION SYSTEMS SUBCOMMITTEE

A. J. Krupy, *chairman;* Commonwealth Edison Company, 72 West Adams Street, Chicago 90, Ill.
J. B. McClure, *vice-chairman* Schenectady, N. Y.
J. E. Barkle, Jr. East Pittsburgh, Pa.
E. F. Dissmeyer Jackson, Mich.
Alex. Dovjikov Portland, Oreg.
C. B. Fontaine, Jr. Lynn, Mass.
L. A. Kilgore East Pittsburgh, Pa.
J. H. Kinghorn New York, N. Y.
H. A. P. Langstaff Pittsburgh, Pa.
T. B. Montgomery Milwaukee, Wis.
G. M. Tatum Richmond, Va.
F. D. Troxel Chicago, Ill.
R. L. Witzke East Pittsburgh, Pa.

STATION DESIGN SUBCOMMITTEE

H. R. Harris, *chairman;* The Detroit Edison Company, 2000—2d Avenue, Detroit 26, Mich.
C. S. Bowden Cleveland, Ohio
R. M. Bush Washington, D. C.
Hubbell Carpenter Duluth, Minn.
H. E. Deardorff Dayton, Ohio
C. A. Harrington Cleveland, Ohio
W. R. Johnson San Francisco, Calif.
D. R. Pattison Johnstown, Pa.
M. L. Perry Kansas City, Mo.
W. W. Perry Binghamton, N. Y.
R. R. Wisner Boston, Mass.

HYDROELECTRIC SYSTEMS SUBCOMMITTEE

F. L. Lawton, *chairman;* Aluminum Laboratories, Ltd., 1800 Sun Life Building, Montreal, Quebec, Canada
S. M. Denton Denver, Colo.
J. T. Madill Arvida, Quebec, Canada
A. L. Pollard Seattle, Wash.
G. R. Woodman Los Angeles, Calif.

PACIFIC COAST SUBCOMMITTEE

Alex. Dovjikov, *chairman;* Bonneville Power Administration, Engineering Department, Portland, Oreg.
E. P. Bryant Los Angeles, Calif.
S. M. Denton Denver, Colo.
B. V. Hoard Portland, Oreg.

(*Continued on page 1422*)

W. R. Johnson San Francisco, Calif.
E. F. Maryatt San Francisco, Calif.
A. L. Pollard Seattle, Wash.
C. C. Whelchel San Francisco, Calif.
G. R. Woodman Los Angeles, Calif.

Protective Devices

W. J. Rudge, *chairman;* General Electric Company, 100 Woodlawn Avenue, Pittsfield, Mass.
H. R. Stewart, *vice-chairman* Boston, Mass.
A. A. Johnson, *secretary* East Pittsburgh, Pa.
L. J. Blaire Dallas, Tex.
V. J. Cissna Chattanooga, Tenn.
J. E. Clem Schenectady, N. Y.
J. O. Coleman Boston, Mass.
L. M. Connors Toronto, Ontario, Canada
H. A. Cornelius Chicago, Ill.
F. M. Defandorf Washington, D. C.
G. K. Ditlow Washington, D. C.
G. B. Dodds Pittsburgh, Pa.
R. H. Earle Milwaukee, Wis.
T. I. Eldridge Philadelphia, Pa.
W. D. Hardaway Denver, Colo.
E. B. Harmon Denver, Colo.
E. M. Hunter Schenectady, N. Y.
P. A. Jeanne New York, N. Y.
W. A. Lewis, Jr. Chicago, Ill.
F. R. Longley Springfield, Mass.
Cort Lowerison Los Angeles, Calif.
T. H. Mawson Birmingham, Ala.
Corbett McLean Portland, Oreg.
E. G. Norell Chicago, Ill.
A. M. Opsahl East Pittsburgh, Pa.
H. L. Rorden Portland, Oreg.
H. D. Ruger Sparrows' Point, Md.
W. E. Rushlow Washington, D. C.
O. L. Sidenfaden Los Angeles, Calif.
W. T. Smith New York, N. Y.
J. M. Towner Baltimore, Md.
S. S. Watkins New York, N. Y.
E. H. Yonkers Chicago, Ill.

Fault Limiting Devices Subcommittee

E. G. Norell, *chairman;* Sargent and Lundy, 140 South Dearborn Street, Chicago 3, Ill.
(Personnel to be selected)

Lightning Protective Devices Subcommittee

E. H. Yonkers, *chairman;* Joslyn Manufacturing and Supply Company, 3700 S. Morgan Street, Chicago 9, Ill.
(Personnel to be selected)

Insulation Co-ordination Subcommittee

J. E. Clem, *chairman;* Central Station Engineering Division General Electric Company, Schenectady 5, N. Y.
(Personnel to be selected)

Relays

E. L. Michelson, *chairman;* Commonwealth Edison Company, 72 West Adams Street, Chicago 90, Ill.
A. J. McConnell, *vice-chairman* Schenectady, N. Y.
J. R. Linders, *secretary* Cleveland, Ohio
C. E. Asbury Jackson, Mich.
M. A. Bostwick Portland, Oreg.
G. E. Brooks Oklahoma City, Okla.
R. J. Cooper Atlanta, Ga.
R. E. Cordray Philadelphia, Pa.
G. E. Dana Binghamton, N. Y.
G. B. Dodds Pittsburgh, Pa.
M. A. Faucett Urbana, Ill.
F. S. Fehr Reading, Pa.
L. F. Ferri Elyria, Ohio
L. L. Fountain East Pittsburgh, Pa.
Sidney Goldsmith Cincinnati, Ohio
E. T. B. Gross Chicago, Ill.
T. R. Halman Detroit, Mich.
E. L. Harder East Pittsburgh, Pa.
V. J. Hayes Waterbury, Conn.
B. C. Hicks Montreal, Quebec, Canada
J. H. Kinghorn New York, N. Y.
R. A. Larner Fort Worth, Texas
W. A. Lewis, Jr. Chicago, Ill.
S. C. Leyland Newark, N. J.
H. F. Lindemuth New York, N. Y.
Cort Lowerison Los Angeles, Calif.

(*Continued in next column*)

W. E. Marter Pittsburgh, Pa.
W. A. Morgan Denver, Colo.
C. E. Parks Indianapolis, Ind.
H. R. Paxson Philadelphia, Pa.
F. C. Poage New York, N. Y.
E. G. Ratz Hamilton, Ontario, Canada
K. N. Reardon Pittsburgh, Pa.
H. P. Sleeper Newark, N. J.
W. K. Sonnemann Newark, N. J.
George Steeb Buffalo, N. Y.

Project Committee on Bibliography of Relay Literature

E. T. B. Gross, *chairman* and *sponsor;* Illinois Institute of Technology, 3300 Federal Street, Chicago 16, Ill.
S. Goldsmith Cincinnati, Ohio
C. E. Parks Indianapolis, Ind.
C. L. Smith Rochester, N. Y.

Project Committee on Generator Protection

H. R. Paxson, *chairman* and *sponsor;* Philadelphia Electric Company, 900 Sansom Street, Philadelphia 5, Pa.
L. L. Draper Los Angeles, Calif.
B. C. Hicks Montreal, Quebec, Canada
S. C. Leyland Newark, N. J.
H. F. Lindemuth New York, N. Y.
W. E. Marter Pittsburgh, Pa.
J. B. McClure Schenectady, N. Y.
A. J. McConnell Schenectady, N. Y.
C. E. Parks Indianapolis, Ind.
F. C. Poage New York, N. Y.
C. L. Smith Rochester, N. Y.

Project Committee on Co-ordination of Construction and Protection of Distribution Circuits (Joint with Distribution Subcommittee and Edison Electric Institute)

G. B. Dodds, AIEE *chairman* and *sponsor;* Duquesne Light Company, 435 Sixth Avenue, Pittsburgh 19, Pa.
R. O. Askey Chicago, Ill.
T. J. Brosnan Buffalo, N. Y.
W. B. Fisk, Jr. New York, N. Y.
H. W. Haberl Montreal, Quebec, Canada
C. L. Headley Baltimore, Md.
C. Lowerison Los Angeles, Calif.
A. L. Malmstrom Detroit, Mich.
H. F. Ostman St. Louis, Mo.
C. E. Parks Indianapolis, Ind.
J. S. Parsons East Pittsburgh, Pa.
R. F. Quinn Schenectady, N. Y.
H. P. Sleeper Newark, N. J.
C. L. Smith Rochester, N. Y.
C. J. Belier, EEI *chairman* and *sponsor;* Cleveland Electric Illuminating Company, 75 Public Square, Cleveland 1, Ohio
G. H. Fiedler Rochester, N. Y.
E. W. Knapp Montreal, Quebec, Canada
William McLean Baltimore, Md.

Project Committee on Revision of Standards for Power Relays

S. C. Leyland, *chairman* and *sponsor;* Westinghouse Electric Corporation, 95 Orange Street, Newark 2, N. J.
R. E. Cordray Philadelphia, Pa.
V. L. Cox Philadelphia, Pa.
L. L. Fountain East Pittsburgh, Pa.
W. A. Lewis, Jr. Chicago, Ill.
J. R. Linders Cleveland, Ohio
E. L. Michelson Chicago, Ill.
W. A. Morgan Denver, Colo.
H. P. Sleeper Newark, N. J.
George Steeb Buffalo, N. Y.

Project Committee on Sensitive Ground Protection

E. T. B. Gross, *chairman* and *sponsor;* Illinois Institute of Technology, 3300 Federal Street, Chicago 16, Ill.
C. J. Berghs Glencoe, Ill.
R. J. Cooper Atlanta, Ga.
T. R. Halman Detroit, Mich.
P. A. Jeanne New York, N. Y.
C. Lowerison Los Angeles, Calif.
W. K. Sonnemann Newark, N. J.
A. R. van C. Warrington Philadelphia, Pa.

Project Committee on Transmission Line Protection

E. L. Harder, *chairman* and *sponsor;* Westinghouse Electric Corporation, East Pittsburgh, Pa.

(*Continued in next column*)

L. J. Audlin Syracuse, N. Y.
W. R. Brownlee Jackson, Mich.
B. C. Hicks Montreal, Quebec, Canada
J. H. Kinghorn New York, N. Y.
W. A. Lewis, Jr. Chicago, Ill.
W. E. Marter Pittsburgh, Pa.
A. J. McConnell Schenectady, N. Y.
M. S. Merritt Chattanooga, Tenn.
E. L. Michelson Chicago, Ill.
C. E. Parks Indianapolis, Ind.
K. N. Reardon Pittsburgh, Pa.

Project Committee on Electronic Relay Applications

A. J. McConnell, *chairman* and *sponsor;* General Electric Company, Schenectady 5, N. Y.
J. E. Barkle, Jr. East Pittsburgh, Pa.
R. J. Cooper Atlanta, Ga.
F. S. Fehr Reading, Pa.
L. F. Ferri Elyria, Ohio
E. L. Harder East Pittsburgh, Pa.
J. H. Kinghorn New York, N. Y.
D. M. MacGregor New York, N. Y.
E. L. Michelson Chicago, Ill.
E. G. Ratz Hamilton, Ontario, Canada

Project Committee on Insulation Levels of Relays and Control Circuits

E. L. Michelson, *chairman* and *sponsor;* Commonwealth Edison Company, 72 West Adams Street, Chicago 90, Ill.
R. E. Cordray Philadelphia, Pa.
S. Goldsmith Cincinnati, Ohio
T. R. Halman Detroit, Mich.
V. J. Hayes Waterbury, Conn.
W. K. Sonnemann Newark, N. J.

Project Committee on Relaying of Interconnections Between Industrial and Utility Generating Systems

K. N. Reardon, *chairman* and *sponsor;* West Penn Power Company, 14 Wood Street, Pittsburgh, Pa.
J. E. Barkle, Jr. East Pittsburgh, Pa.
G. E. Dana Binghamton, N. Y.
F. S. Fehr Reading, Pa.
T. R. Halman Detroit, Mich.
J. R. Linders Lakewood, Ohio

Project Committee on Relaying Performance of Current Transformer (Emphasis on High Impedance Secondary Types)

W. E. Marter, *chairman* and *sponsor;* Duquesne Light Company, 435—6th Avenue, Pittsburgh 19, Pa.
J. E. Barkle, Jr. East Pittsburgh, Pa.
J. E. Clem Schenectady, N. Y.
R. E. Cordray Philadelphia, Pa.
W. K. Dickinson Lynn, Mass.
T. R. Halman Detroit, Mich.
W. A. Lewis, Jr. Chicago, Ill.
W. K. Sonnemann Newark, N. J.
E. C. Wentz Sharon, Pa.

Rotating Machinery

W. R. Hough, *chairman;* Reliance Electric and Engineering Company, 1088 Ivanhoe Road, Cleveland 10, Ohio
C. G. Veinott, *vice-chairman* Lima, Ohio
J. L. Fuller, *secretary* Cleveland, Ohio
J. E. Allen Lancaster, Pa.
W. R. Appleman Dayton, Ohio
E. L. Bailey Detroit, Mich.
Sterling Beckwith Milwaukee, Wis.
B. H. Caldwell Schenectady, N. Y.
A. G. Conrad New Haven, Conn.
James DeKiep Minneapolis, Minn.
E. F. Dissmeyer Jackson, Mich.
L. O. Dorfman New York, N. Y.
W. H. Fifer Washington, D. C.
D. E. Fritz Cleveland, Ohio
J. S. Gault Ann Arbor, Mich.
C. B. Hathaway Buffalo, N. Y.
V. P. Hessler Urbana, Ill.
L. E. Hildebrand Lynn, Mass.
J. W. Jones Philadelphia, Pa.
C. E. Kilbourne Schenectady, N. Y.
A. A. Kronberg Los Angeles, Calif.
I. M. Levy Dayton, Ohio
T. M. Linville Schenectady, N. Y.
M. R. Lory East Pittsburg, Pa.
Clarence Lynn East Pittsburgh, Pa.
W. E. Meserve Ithaca, N. Y.

(*Continued in next column*)

R. C. Moore Milwaukee, Wis.
J. G. Noest New York, N. Y.
E. I. Pollard Ridgway, Pa.
C. P. Potter St. Louis, Mo.
F. C. Rushing Buffalo, N. Y.
V. E. Schlossberg East Chicago, Ind.
M. L. Schmidt Fort Wayne, Ind.
J. F. Sellers Milwaukee, Wis.
P. H. Trickey St. Louis, Mo.
R. W. Wieseman Schenectady, N. Y.
W. W. Wishard Chicago, Ill.
S. S. Wolff St. Louis, Mo.

Administrative Subcommittee

W. R. Hough, *chairman,* Reliance Electric and Engineering Company, 1068–1088 Ivanhoe Road, Cleveland 10, Ohio
C. G. Veinott, *vice-chairman* Lima, Ohio
J. L. Fuller, *secretary* Cleveland, Ohio
B. H. Caldwell Schenectady, N. Y.
James DeKiep Minneapolis, Minn.
J. L. Fuller Cleveland, Ohio
J. W. Jones Philadelphia, Pa.
I. M. Levy Dayton, Ohio
S. S. Wolff St. Louis, Mo.

Synchronous Machinery Subcommittee

James DeKiep, *chairman;* Electric Machinery Manufacturing Company, 1331 Tyler Street, Minneapolis 13, Minn.
Sterling Beckwith Milwaukee, Wis.
J. F. Calvert Evanston, Ill.
S. B. Crary Schenectady, N. Y.
L. O. Dorfman New York, N. Y.
E. L. Harder East Pittsburgh, Pa.
R. A. Hopkins Knoxville, Tenn.
L. F. Hunt Los Angeles, Calif.
J. W. Jones Philadelphia, Pa.
C. E. Kilbourne Schenectady, N. Y.
M. R. Lory East Pittsburgh, Pa.
G. W. McIver Toledo, Ohio
W. P. Monroe Chicago, Ill.
J. G. Noest New York, N. Y.
E. I. Pollard Ridgway, Pa.
S. S. Wolff St. Louis, Mo.

Induction Machinery Subcommittee

S. S. Wolff, *chairman;* Century Electric Company, 1806 Pine Street, St. Louis 3, Mo.
R. E. Arnold West Lynn, Mass.
E. C. Barnes Cleveland, Ohio
S. F. Henderson Buffalo, N. Y.
C. J. Koch Schenectady, N. Y.
I. M. Levy Dayton, Ohio
T. C. Lloyd Springfield, Ohio
R. C. Moore Milwaukee, Wis.
J. E. Noest New York, N. Y.
C. P. Potter St. Louis, Mo.
F. C. Rushing Buffalo, N. Y.
P. H. Trickey Finderne, N. J.
F. M. Winterhalter Norwood, Ohio

D-C Machinery Subcommittee

B. H. Caldwell, *chairman;* General Electric Company, 1 River Road, Schenectady 5, N. Y.
Florence F. Buckland Schenectady, N. Y.
A. G. Conrad New Haven, Conn.
A. G. Darling Schenectady, N. Y.
W. H. Fifer Washington, D. C.
D. E. Fritz Cleveland, Ohio
Lanier Greer Cleveland, Ohio
C. B. Hathaway Buffalo, N. Y.
V. P. Hessler Urbana, Ill.
V. B. Honsinger Cincinnati, Ohio
Paul Lebenbaum, Jr. Lynn, Mass.
T. M. Linville Schenectady, N. Y.
Clarence Lynn East Pittsburgh, Pa.
A. T. McClinton Washington, D. C.
J. G. Noest New York, N. Y.
L. G. Opel Buffalo, N. Y.
J. H. Schneider Ridgway, Pa.
J. F. Sellers Milwaukee, Wis.
P. H. Trickey Finderne, N. J.
S. S. Wolff St. Louis, Mo.

Single-Phase and Fractional-Horsepower Subcommittee

I. M. Levy, *chairman;* Delco Products Division, General Motors Corporation, Dayton, Ohio
W. R. Appleman Dayton, Ohio
J. S. Gault Ann Arbor, Mich.
E. E. Kimberly Columbus, Ohio
T. C. Lloyd Springfield, Ohio

(*Continued on page 1423*)

R. F. Munier	St. Louis, Mo.
C. P. Potter	St. Louis, Mo.
M. L. Schmidt	Fort Wayne, Ind.
P. H. Trickey	Finderne, N. J.
C. G. Veinott	Lima, Ohio
S. S. Wolff	St. Louis, Mo.

Test Code Subcommittee

J. L. Fuller, *chairman;* Reliance Electric and Engineering Company, 1088 Ivanhoe Road, Cleveland 10, Ohio

J. E. Allen	Lancaster, Pa.
Sterling Beckwith	Milwaukee, Wis.
J. S. Gault	Ann Arbor, Mich.
L. E. Hildebrand	Lynn, Mass.
Clarence Lynn	East Pittsburgh, Pa.
R. F. Munier	St. Louis, Mo.

Insulation Resistance Subcommittee

J. W. Jones, *chairman;* Philadelphia Electric Company, Edison Building, Philadelphia 5, Pa.

J. E. Allen	Lancaster, Pa.
L. J. Berberich	East Pittsburgh, Pa.
E. B. Curdts	Philadelphia, Pa.
E. F. Dissmeyer	Jackson, Mich.
Orville Fawcett	Pittsburgh, Pa.
D. D. Higgins	Chicago, Ill.
J. L. Kuehlthau	Milwaukee, Wis.
V. E. Schlossberg	East Chicago, Ind.
H. R. Stewart	Boston, Mass.
J. B. Swering	Hartford, Conn.
A. L. Van Emden	Washington, D. C.
R. W. Wieseman	Schenectady, N. Y.

Substations

G. S. Lunge, *chairman;* Central Station Engineering Divisions, General Electric Company, Schenectady 5, N. Y.

R. C. Ericson, *vice-chairman*	Hammond, Ind.
Marino Fraresso, *secretary*	Toronto, Ontario, Canada
T. J. Allen	Atlanta, Ga.
Herman Bany	Philadelphia, Pa.
Harris Barber	Boston, Mass.
R. O. Bell	Milwaukee, Wis.
F. J. Berger	Philadelphia, Pa.
M. K. Brown	Buffalo, N. Y.
C. C. Crane	Madison, Wis.
B. D. Dexter	San Francisco, Calif.
M. V. Eardley	Los Angeles, Calif.
G. P. Fallon	Baltimore, Md.
H. F. Gidlund	Denver, Colo.
K. B. Hoffman	New York, N. Y.
E. M. Hunter	Schenectady, N. Y.
S. C. Killian	Chicago, Ill.
W. J. Lank	Washington, D. C.
N. G. Larson	Chicago, Ill.
J. T. Lienert	Portland, Oreg.
W. M. McCauley	Greensburg, Pa.
J. L. McKee	New York, N. Y.
I. S. Mendenhall	Detroit, Mich.
D. C. Millard	Denver, Colo.
M. E. Reagan	East Pittsburgh, Pa.
J. H. Rixse, Jr.	Washington, D. C.
W. S. Scheering	Springfield, Mass.
C. H. Smoke	Portsmouth, Va.
R. F. Stevens	Portland, Oreg.
K. L. Wheeler	Cleveland, Ohio

Executive Subcommittee

G. S. Lunge, *chairman;* Central Station Engineering Divisions, General Electric Company, Schenectady 5, N. Y.

M. V. Eardley	Los Angeles, Calif.
R. C. Ericson	Hammond, Ind.
Marino Fraresso	Toronto, Ontario, Canada
H. B. Hoffman	New York, N. Y.
M. E. Reagan	East Pittsburgh, Pa.

Automatic and Supervisory Control Subcommittee

M. E. Reagan, *chairman;* Switchboard Engineering Department, Westinghouse Electric Corporation, East Pittsburgh, Pa.

T. J. Allen	Atlanta, Ga.
Herman Bany	Philadelphia, Pa
R. O. Bell	Milwaukee, Wis.
B. D. Dexter	San Francisco, Calif.
R. C. Ericson	Hammond, Ind.
J. L. McKee	New York, N. Y.

Distribution and Conversion Substation Subcommittee

M. V. Eardley, *chairman;* Department of Water and Power, City of Los Angeles, Los Angeles 54, Calif.

(Continued in next column)

T. J. Allen	Atlanta, Ga.
Herman Bany	Philadelphia, Pa.
R. O. Bell	Milwaukee, Wis.
M. K. Brown	Buffalo, N. Y.
C. C. Crane	Madison, Wis.
G. P. Fallon	Baltimore, Md.
E. M. Hunter	Schenectady, N. Y.
J. T. Lienert	Portland, Oreg.
I. S. Mendenhall	Detroit, Mich.

Transmission Substation Subcommittee

K. B. Hoffman, *chairman;* Burns and Roe, Inc., 233 Broadway, New York 7, N. Y.

T. J. Allen	Atlanta, Ga.
Harris Barber	Boston, Mass.
F. J. Berger	Philadelphia, Pa.
H. P. Cadario	Toronto, Ontario, Canada
C. C. Crane	Madison, Wis.
Marino Fraresso	Toronto, Ontario, Canada
H. F. Gidlund	Denver, Colo.
E. M. Hunter	Schenectady, N. Y.
S. C. Killian	Chicago, Ill.
N. G. Larson	Chicago, Ill.
W. M. McCauley	Greensburg, Pa.
D. C. Millard	Denver, Colo.
J. H. Rixse, Jr.	Washington, D. C.
W. S. Schering	Springfield, Ill.
R. F. Stevens	Portland, Oreg.

Working Group on Device Function Numbers

R. C. Ericson, *chairman;* Northern Indiana Public Service Company, 5265 Hohman Avenue, Hammond, Ind.

Herman Bany	Philadelphia, Pa.
L. B. LeVesconte	Chicago, Ill.
M. E. Reagan	East Pittsburgh, Pa.
M. S. Schneider	Cincinnati, Ohio

Working Group on Substation Grounding Practice

H. F. Gidlund, *chairman;* Public Service Company of Colorado, 810—15th Street, Denver 2, Colo.

F. J. Berger	Philadelphia, Pa.
M. K. Brown	Buffalo, N. Y.
F. R. Longley	Springfield, Mass.
J. M. Towner	Baltimore, Md.

Working Group on Rectifier Switchgear

M. E. Reagan, *chairman;* Switchgear Engineering Department, Westinghouse Electric Corporation, East Pittsburgh, Pa.

D. C. Hoffman	Philadelphia, Pa.
H. V. Nye	West Allis, Wis.

Working Group on Basic One-Line Diagrams

E. M. Hunter, *chairman;* General Electric Co., Central Station Engg. Div., Schenectady 5, N. Y.

(Personnel to be selected)

Switchgear

F. A. Lane, *chairman;* American Gas and Electric Service Corporation, 30 Church Street, New York 8, N. Y.

H. V. Nye, *vice-chairman*	West Allis, Wis.
Otto Naef, *secretary*	New York, N. Y.
F. S. Benson	San Francisco, Calif.
C. K. Beyette	Fort Worth, Tex
Harry Brown	New Haven, Conn.
J. S. Brown	Pittsburgh, Pa.
E. A. Childerhose	Boston, Mass.
H. W. Codding	Newark, N. J.
V. L. Cox	Philadelphia, Pa.
G. K. Ditlow	Washington, D. C.
G. H. Doan	Detroit, Mich.
J. A. Elzi	Jackson, Mich.
W. E. Enns	Portland, Oreg.
K. J. C. Falck	Philadelphia, Pa.
R. M. Ferrill	Chattanooga, Tenn.
J. M. Geiger	Buffalo, N. Y.
W. J. Gilson	Toronto, Ontario, Canada
J. W. Graff	Birmingham, Ala.
C. W. Gragg	Amarillo, Tex.
W. D. Hardaway	Denver, Colo.
V. J. Hayes	Waterbury, Conn.
M. H. Hobbs	East Pittsburgh, Pa.
L. M. Hovey	Winnipeg, Manitoba, Canada
C. L. Killgore	Denver, Colo.
I. T. Knight	Kansas City, Mo.
H. A. P. Langstaff	Pittsburgh, Pa.

(Continued in next column)

H. J. Lingal	East Pittsburgh, Pa.
F. W. McCloska	Chicago, Ill.
W. J. McLachlan	Schenectady, N. Y.
R. G. Meyerand	St. Louis, Mo.
E. F. Miller	Rock Island, Ill.
V. G. Mussenay	Schenectady, N. Y.
M. L. Perry	Kansas City, Mo.
H. H. Rudd	Greensburg, Pa.
E. K. Sadler	Los Angeles, Calif.
A. W. Shelhorse	Atlanta, Ga.
O. L. Sidenfaden	Los Angeles, Calif.
J. F. Sinnott	San Diego, Calif.
Garland Stamper	Dayton, Ohio
A. Van Ryan	South Milwaukee, Wis.
J. H. Vivian	Los Angeles, Calif.
R. L. Webb	New York, N. Y.
C. E. Winegartner	Cleveland, Ohio
J. D. Wood	Philadelphia, Pa.
J. C. Woods	Chicago, Ill.
S. W. Zimmerman	Ithaca, N. Y.

Circuit Breaker Subcommittee

R. L. Webb, *chairman;* Consolidated Edison Company of New York Inc., 4 Irving Place, New York 3, N. Y.

F. W. Cramer	Pittsburgh, Pa.
R. M. Ferrill	Chattanooga, Tenn.
M. D. Hardaway	Denver, Colo.
A. W. Hill	East Pittsburgh, Pa.
M. H. Hobbs	East Pittsburgh, Pa.
C. L. Killgore	Denver, Colo.
W. J. McLachlan	Schenectady, N. Y.
J. R. North	Jackson, Mich.
H. V. Nye	West Allis, Wis.
F. V. Smith	Chicago, Ill.
A. Van Ryan	South Milwaukee, Wis.
J. H. Vivian	Los Angeles, Calif.
C. E. Winegartner	Cleveland, Ohio
J. D. Wood	Philadelphia, Pa.
J. C. Woods	Chicago, Ill.
B. W. Wyman	Philadelphia, Pa.

Working Groups:

A—Power Circuit Breakers
B—Low-Voltage Air Circuit Breakers
C—Automatic Reclosers
D—Calculations of Short-Circuit Currents in Low-Voltage Systems

Switchgear Assemblies Subcommittee

H. V. Nye, *chairman;* Allis-Chalmers Manufacturing Company, West Allis, Wis.

F. W. Cramer	Pittsburgh, Pa.
J. M. Geiger	Buffalo, N. Y.
C. H. Kreger	Chicago, Ill.
E. F. Miller	Rock Island, Ill.
G. M. Reed	Philadelphia, Pa.
H. H. Rudd	Greensburg, Pa.
B. K. Sturgis	Philadelphia, Pa.
O. B. Vikoren	Philadelphia, Pa.
C. P. West	East Pittsburgh, Pa.
W. F. Wetmore	Detroit, Mich.

Switches, Fuses, and Insulators Subcommittee

H. H. Rudd, *chairman;* Railway and Industrial Engineering Company, Greensburg, Pa.

K. J. C. Falck	Philadelphia, Pa.
A. H. Powell	Philadelphia, Pa.
J. M. Wallace	East Pittsburgh, Pa.
R. L. Webb	New York, N. Y.
J. C. Woods	Chicago, Ill.

Working Groups:

A—Air Switches and Insulators
B—Interrupter Switches
C—Fuses

Subcommittee on High-Voltage Switching (Where Out-of-Phase Voltages Exist at Time of Arc Interruption)

K. J. C. Falck, *chairman;* Philadelphia Electric Company, 1000 Chestnut Street, Philadelphia 5, Pa.

C. H. Black	Philadelphia, Pa.
W. E. Enns	Portland, Oreg.
R. M. Ferrill	Chattanooga, Tenn.
G. D. Floyd	Toronto, Ontario, Canada
I. W. Gross	New York, N. Y.
E. L. Harder	East Pittsburgh, Pa.
M. H. Hobbs	East Pittsburgh, Pa.
C. B. Kelley	Davenport, Iowa
H. V. Nye	West Allis, Wis.

System Engineering

Earle Wild, *chairman;* Commonwealth Edison Company, 72 West Adams Street, Chicago 90, Ill.

(Continued in next column)

Robert Brandt, *vice-chairman*	Boston, Mass.
O. W. Manz, Jr., *secretary*	Brooklyn, N. Y.
C. G. Adams	Schenectady, N. Y.
C. P. Almon, Jr.	Chattanooga, Tenn.
John Bankus	Portland, Oreg.
M. L. Blair	Spokane, Wash.
W. R. Brownlee	Jackson, Mich.
O. E. Charlton	Birmingham, Ala.
O. A. Demuth	Portland, Oreg.
A. G. Dewars	Minneapolis, Minn.
W. B. Fisk	New York, N. Y.
G. D. Floyd	Toronto, Ontario, Canada
A. P. Fugill	Detroit, Mich.
E. E. George	New York, N. Y.
E. T. B. Gross	Chicago, Ill.
W. D. Hardaway	Denver, Colo.
H. L. Harrington	Buffalo, N. Y.
A. P. Hayward	Pittsburgh, Pa.
R. G. Hooke	Newark, N. J.
L. R. Janes	Chicago, Ill.
A. A. Johnson	East Pittsburgh, Pa.
W. R. Johnson	San Francisco, Calif.
C. B. Kelley	Des Moines, Iowa
C. L. Killgore	Denver, Colo.
M. H. Lovelady	Corpus Christi, Tex.
N. M. Lovell	Tucson, Ariz.
C. W. Mayott	Hartford, Conn.
G. H. McDaniel	New York, N. Y.
W. E. Montgomery	Los Angeles, Calif.
S. B. Morehouse	Philadelphia, Pa.
W. H. Osterle	Pittsburgh, Pa.
H. P. Peters	Atlanta, Ga.
H. W. Phillips	Philadelphia, Pa.
C. B. Signor	Binghamton, N. Y.
W. O. Smith	Mineola, N. Y.
G. M. Tatum	Richmond, Va.
J. J. Tesar	Cleveland, Ohio
R. M. Walker	El Paso, Tex.
C. W. Watchorn	Baltimore, Md.
G. S. Whitlow	St. Louis, Mo.
A. L. Williams	Los Angeles, Calif.

Administrative Subcommittee

Earle Wild, *chairman;* Commonwealth Edison Company, 72 West Adams Street, Room 506, Chicago 90, Ill.

C. P. Almon, Jr.	Chattanooga, Tenn.
R. Brandt	Boston, Mass.
E. E. George	New York, N. Y.
H. L. Harrington	Buffalo, N. Y.
A. P. Hayward	Pittsburgh, Pa.
O. W. Manz, Jr.	Brooklyn, N. Y.
C. W. Mayott	Hartford, Conn.
C. N. Metcalf	New York, N. Y.

System Planning Subcommittee

H. L. Harrington, *chairman;* Buffalo, Niagara and Eastern Power Company, Electric Building, Buffalo 3, N. Y.

C. G. Adams	Schenectady, N. Y.
O. E. Charlton	Birmingham, Ala.
A. G. Dewars	Minneapolis, Minn.
W. B. Fisk	New York, N. Y.
A. P. Fugill	Detroit, Mich.
E. T. B. Gross	Chicago, Ill.
W. D. Hardaway	Denver, Colo.
R. G. Hooke	Newark, N. J.
L. R. James	Chicago, Ill.
A. A. Johnson	East Pittsburgh, Pa.
C. L. Kilgore	Denver, Colo.
A. A. Kroneberg	Los Angeles, Calif.
W. H. Osterle	Pittsburgh, Pa.
H. P. St. Clair	New York, N. Y.
C. B. Signor	Binghamton, N. Y.
N. N. Smeloff	Allentown, Pa.
J. J. Tesar	Cleveland, Ohio
R. M. Walker	El Paso, Tex.
Matthew Ward	Toronto, Ontario, Canada

System Operations Subcommittee

O. W. Manz, Jr., *chairman;* Consolidated Edison Company of New York, Inc., 1 Hudson Avenue, Brooklyn 1, N. Y.

J. Bankus	Portland, Oreg.
M. L. Blair	Spokane, Wash.
O. A. Demuth	Portland, Oreg.
G. D. Floyd	Toronto, Ontario, Canada
W. R. Johnson	San Francisco, Calif.
C. B. Kelley	Des Moines, Iowa
W. E. Montgomery	Los Angeles, Calif.
H. W. Phillips	Philadelphia, Pa.
W. O. Smith	Glenwood Landing, N. Y.
G. M. Tatum	Richmond, Va.

System Economics Subcommittee

A. P. Hayward, *chairman;* Duquesne Light Company, 435—6th Avenue, Pittsburgh 19, Pa.

E. C. Brown	Hartford, Conn.
E. E. George	New York, N. Y.
N. M. Lovell	Tucson, Ariz.
H. P. Peters	Atlanta, Ga.
R. T. Purdy	Chicago, Ill.
J. A. Rose	Newark, N. J.
C. W. Watchorn	Baltimore, Md.
A. L. Williams	Los Angeles, Calif.

System Controls Subcommittee

G. P. Almon, Jr., *chairman;* Tennessee Valley Authority, Chattanooga 4, Tenn.

W. R. Brownlee	Jackson, Mich.
D. H. Cameron	Kansas City, Mo.
T. E. Curtis	San Francisco, Calif.
A. A. Johnson	East Pittsburgh, Pa.
G. H. McDaniel	New York, N. Y.
C. N. Metcalf	New York, N. Y.
S. B. Morehouse	Philadelphia, Pa.
G. S. Whitlow	St. Louis, Mo.

Interconnection Contracts Subcommittee

C. W. Mayott, *chairman;* Hartford Electric Light Company, 266 Pearl Street, Hartford, Conn.

Bradley Cozzens	Los Angeles, Calif.
E. D. Early	Birmingham, Ala.
E. E. George	New York, N. Y.
G. A. Grimm	St. Petersburg, Fla.
C. B. Kelly	Davenport, Iowa
M. H. Lovelady	Corpus Christi, Tex.
Roy Martindale	Los Angeles, Calif.
G. H. McDaniel	New York, N. Y.

Transformers

J. B. Hodtum, *chairman;* Allis-Chalmers Manufacturing Company, N. S. Station, Pittsburgh 12, Pa.

F. J. Vogel, *vice-chairman*	Chicago, Ill
M. K. Brown, *secretary*	Buffalo, N. Y.
J. A. Adams	Philadelphia, Pa.
F. S. Brown	Pittsburgh, Pa.
R. J. Brown	Toronto, Ontario, Canada
J. L. Cantwell	Pittsfield, Mass.
J. H. Chiles	Sharon, Pa.
J. E. Clem	Schenectady, N. Y.
G. W. Clothier	Milwaukee, Wis.
Merrill De Merit	Chattanooga, Tenn.
J. A. Elzi	Jackson, Mich.
M. M. Ewell	Portland, Oreg.
I. W. Gross	New York, N. Y.
W. G. James	Sharon, Pa.
A. A. Johnson	East Pittsburgh, Pa.
H. B. Keath	St. Louis, Mo.
D. L. Levine	Chicago, Ill.
C. M. Lovell	St. Louis, Mo.
M. L. Manning	Canonsburg, Pa.
J. R. Meador	Pittsfield, Mass.
V. M. Montsinger	Pittsfield, Mass.
M. H. Pratt	Syracuse, N. Y.
T. D. Reimers	New York, N. Y.
S. E. Schultz	Portland, Oreg.
W. C. Sealey	Milwaukee, Wis.
F. L. Snyder	Sharon, Pa.
K. M. Stevens	Alhambra, Calif.
J. M. Towner	Baltimore, Md.
P. A. Vance	Fort Wayne, Ind.
H. H. Wagner	Canonsburg, Pa.
C. E. Winegartner	Cleveland, Ohio

Co-ordinated Study of Life of Transformer Insulation Subcommittee

J. L. Cantwell, *chairman;* General Electric Company, 100 Woodlawn Avenue, Pittsfield, Mass.

C. E. Arntzen	East Pittsburgh, Pa.
F. M. Clark	Pittsfield, Mass.
J. F. Dexter	Midland, Mich.
C. F. Hill	East Pittsburgh, Pa.
Myron Kin	Midland, Mich.
V. M. Montsinger	Pittsfield, Mass.
T. D. Reimers	New York, N. Y.
F. L. Snyder	Sharon, Pa.
W. M. Terry, Jr.	Pittsburgh, Pa.
F. J. Vogel	Chicago, Ill.
H. G. Zambell	Pittsburgh, Pa.

Instrument Transformers Subcommittee

J. E. Clem, *chairman;* Central Station Engineering Division, General Electric Company, Schenectady 5, N. Y.

Herman Bany	Philadelphia, Pa.
J. H. Chiles	Sharon, Pa.
R. E. Cordray	Philadelphia, Pa.
A. B. Craig	Boston, Mass.
F. E. Davis, Jr.	Jackson, Mich.
K. J. C. Falck	Philadelphia, Pa.
R. E. Franck	Lynn, Mass.
J. M. Geiger	Buffalo, N. Y.
T. R. Halman	Detroit, Mich.
E. K. Huntington	Rochester, N. Y.
L. F. Kennedy	Schenectady, N. Y.
W. E. Marter	Pittsburgh, Pa.
E. V. Sayles	Jackson, Mich.
J. P. Scott	St. Louis, Mo.
F. B. Silsbee	Washington, D. C.
W. K. Sonnemann	Newark, N. J.
W. M. Terry, Jr.	Pittsburgh, Pa.
E. C. Wentz	Sharon, Pa.
C. A. Woods	East Pittsburgh, Pa.

(*Continued in next column*)

AIEE Papers Subcommittee

J. El Clem, *chairman;* Central Station Engineering Division, General Electric Company, Schenectady 5, N. Y.

Short-Circuit Thermal Ratings of Induction and Step Type Regulators Subcommittee

A. A. Johnson, *chairman;* Westinghouse Electric Corporation, East Pittsburgh, Pa.

J. E. Clem	Schenectady, N. Y.
W. C. Sealey	Milwaukee, Wis.

Magnetization Characteristics of Transformers Subcommittee

J. E. Clem, *chairman;* Central Station Engineering Divisions, General Electric Company, Schenectady 5, N. Y.

J. A. Elzi	Jackson, Mich.
T. D. Gordy	Pittsfield, Mass.
J. H. Kinghorn	New York, N. Y.
W. E. Marter	Pittsburgh, Pa.
A. J. Maslin	Sharon, Pa.
A. H. Powell	Philadelphia, Pa.
W. C. Sealey	Milwaukee, Wis.
J. M. Wallace	East Pittsburgh, Pa.

Revision of Dielectric Tests Subcommittee

F. J. Vogel, *chairman;* Illinois Institute of Technology, Chicago, Ill.

V. F. Christen	St. Louis, Mo.
I. W. Gross	New York, N. Y.
J. H. Hagenguth	Pittsfield, Mass.
D. M. MacGregor	New York, N. Y.
W. R. McCarty	St. Louis, Mo.
J. R. Meador	Pittsfield, Mass.
C. W. Miller	Sharon, Pa.
V. M. Montsinger	Pittsfield, Mass.
W. C. Sealey	Milwaukee, Wis.
W. L. Teague	Sharon, Pa.

Guides for Operation and Maintenance of Dry-Type Transformers With Class B Insulation

J. A. Adams, *chairman;* Philadelphia Electric Company, 900 Sansom Street, Philadelphia 5, Pa.

G. J. Johnston	Pittsburgh, Pa.
T. D. Reimers	New York, N. Y.
T. E. Rodhouse	Pittsfield, Mass.
W. W. Satterlee	Sharon, Pa.
H. H. Wagner	Canonsburg, Pa.
C. E. Winegartner	Cleveland, Ohio

Co-ordination of Insulation Subcommittee

J. E. Clem, *chairman;* Central Station Engineering Division, General Electric Company, Schenectady 5, N. Y.

Electronic Power Converters Subcommittee

W. C. Sealey, *chairman;* Allis-Chalmers Manufacturing Company, Post Office Box 512, Milwaukee 1, Wis.

Methods of Making Heat Runs Subcommittee

E. Clem, *chairman;* General Electric Company, Central Station Engineering Division, Schenectady 5, N. Y.

J. A. Adams	Philadelphia, Pa.
M. F. Beavers	Pittsfield, Mass.
M. K. Brown	Buffalo, N. Y.
H. B. Keath	St. Louis, Mo.
A. J. Maslin	Sharon, Pa.
W .H. Mutschler	Pittsburgh, Pa.

Power Factor Measurements Subcommittee

J. B. Hodtum *chairman;* Allis-Chalmers Manufacturing Company, N. S. Station, Pittsburgh 12, Pa.

Audible Noise in Transformers Subcommittee

J. H. Chiles, *chairman;* Westinghouse Electric Corporation, Transformer Engineering Department, Sharon, Pa.

J. E. Clem	Schenectady, N. Y.
D. L. Levine	Chicago, Ill.
A. J. Maslin	Sharon, Pa.
J. R. Meador	Pittsfield, Mass.
T. D. Reimers	New York, N. Y.
J. M. Towner	Baltimore, Md.

Transmission and Distribution

I. W. Gross, *chairman;* American Gas and Electric Service Corporation, 30 Church Street, New York 8, N. Y.

S. B. Crary, *vice-chairman*	Schenectady, N. Y.
R. E. Pierce, *secretary*	New York, N. Y.
C. E. Baugh	San Francisco, Calif.
A. E. Beattie	Beaumont, Tex.
P. L. Bellaschi	Sharon, Pa.
H. C. Bingham	Cleveland, Ohio
D. K. Blake	Schenectady, N. Y.
P. W. Blye	New York, N. Y.
C. A. Booker	Boston, Mass.
Bryce Brady	Oklahoma City, Okla.
T. J. Brosnan	Buffalo, N. Y.
Harold Cole	Detroit, Mich.
E. R. Coulbourn	Birmingham, Ala.
A. E. Curtis	Montreal, Quebec, Canada
H. A. Dambly	Philadelphia, Pa.
A. E. Davison	Toronto, Ontario, Canada
T. C. Duncan	New York, N. Y.
H. A. Frey	Baltimore, Md.
J. H. Hagenguth	Pittsfield, Mass.
K. E. Hapgood	Chattanooga, Tenn.
E. R. Hendrickson	Maywood, Ill.
J. B. Hodtum	Pittsburgh, Pa.
E. K. Huntington	Rochester, N. Y.
E. L. Kanouse	Los Angeles, Calif.
C. H. Kraft	St. Louis, Mo.
A. A. Kroneberg	Los Angeles, Calif.
J. T. Lusignan	Mansfield, Ohio
D. W. Nethercut	Elyria, Ohio
J. E. O'Brien	Washington, D. C.
E. W. Oesterreich	Pittsburgh, Pa.
J. S. Parsons	East Pittsburgh, Pa.
C. K. Poarch	New York, N. Y.
L. M. Robertson	Denver, Colo.
R. R. Robinson	Niles, Mich.
W. E. Rushlow	Washington, D. C.
E. V. Sayles	Jackson, Mich.
A. N. Shealy	Baltimore, Md.
F. V. Smith	Chicago, Ill.
K. M. Smith	Chicago, Ill.
E. C. Starr	Corvallis, Oreg.
C. F. Wagner	East Pittsburgh, Pa.
R. L. Witzke	East Pittsburgh, Pa.

Capacitor Subcommittee

F. V. Smith, *chairman;* Sargent and Lundy, 140 South Dearborn Street, Chicago 3, Ill.

M. I. Alimansky	Pittsfield, Mass.
G. Appleman	Allentown, Pa.
C. E. Baugh	San Francisco, Calif.
P. L. Bellaschi	Sharon, Pa.
E. W. Dillard	Boston, Mass.
K. E. Hapgood	Chattanooga, Tenn.
E. R. Hendrickson	Maywood, Ill.
S. Lubin	Washington, D. C.
R. E. Marbury	East Pittsburgh, Pa.
N. A. Miller	Chicago, Ill.
R. B. Miller	Rock Island, Ill.
C. E. Parks	Indianapolis, Ind.
E. V. Sayles	Jackson, Mich.
E. C. Starr	Corvallis, Oreg.
R. A. Wood	South Milwaukee, Wis.

Distribution Subcommittee

T. J. Brosnan, *chairman;* Buffalo Niagara Electric Corporation, 300 Electric Building, Buffalo, N. Y.

C. E. Baugh	San Francisco, Calif.
H. C. Bingham	Cleveland, Ohio
D. K. Blake	Schenectady, N. Y.
Bryce Brady	Oklahoma City, Okla.
Harold Cole	Detroit, Mich.
H. A. Dambly	Philadelphia, Pa.
E. R. Hendrickson	Maywood, Ill.
J. B. Hodtum	Pittsburgh, Pa.
E. K. Huntington	Rochester, N. Y.
C. H. Kraft	St. Louis, Mo.
J. E. O'Brien	Washington, D. C.
E. W. Oesterreich	Pittsburgh, Pa.
J. S. Parsons	East Pittsburgh, Pa.
E. V. Sayles	Jackson, Mich.

(*Continued in next column*)

General Systems Subcommittee

R. L. Witzke, *chairman;* Industry Engineering Department, Westinghouse Electric Corporation, East Pittsburgh, Pa.

P. W. Blye	New York, N. Y.
R. W. Caswell	Chicago, Ill.
O. A. Demuth	Portland, Oreg.
G. D. Floyd	Toronto, Ontario, Canada
R. G. Hooke	Newark, N. J.
E. K. Huntington	Rochester, N. Y.
I. B. Johnson	Schenectady, N. Y.
A. A. Kroneberg	Los Angeles, Calif.
L. B. LeVesconte	Chicago, Ill.
L. M. Robertson	Denver, Colo.
H. M. Trueblood	New York, N. Y.

Lightning and Insulator Subcommittee

J. T. Lusignan, *chairman;* Ohio Brass Company, Engineering Department, Mansfield, Ohio

L. V. Bewley	Bethlehem, Pa.
H. N. Ekvall	Philadelphia, Pa.
H. A. Frey	Baltimore, Md.
I. W. Gross	New York, N. Y.
J. H. Hagenguth	Pittsfield, Mass.
E. L. Harder	East Pittsburgh, Pa.
W. W. Lewis	Schenectady, N. Y.
G. D. McCann, Jr.	Pasadena, Calif.
S. K. Waldorf	Baltimore, Md.
E. R. Whitehead	Chicago, Ill.

Towers, Poles, and Conductors Subcommittee

A. E. Davison, *chairman;* Hydro-Electric Power Commission of Ontario, 620 University Ave., Toronto, Ontario, Canada

H. W. Biskeborn	Newark, Ohio
A. A. Booker	Boston, Mass.
K. E. Hapgood	Chattanooga, Tenn.
E. L. Kanouse	Los Angeles, Calif.
W. H. Knutz	Hammond, Ind.
A. A. Osipovich	Portland, Oreg.
J. A. Rawls	Richmond, Va.
A. S. Runciman	Montreal, Quebec, Canada
F. E. Sanford	Chicago, Ill.
A. N. Shealy	Baltimore, Md.
E. J. Staubitz	Pittsburgh, Pa.
J. Tompkins	Massena, N. Y.

Science and Electronics Group

Science and Electronics Co-ordinating Committee

J. D. Tebo, *chairman,* Bell Telephone Laboratories, Inc., 463 West Street, New York 14, N. Y.

Charles Concordia, *vice-chairman*	Schenectady, N. Y.
W. F. Davidson, *secretary*	New York, N. Y.

Members-at-Large

Walter J. Seeley, representing Board of Directors	Durham, N. C.
I. Melville Stein	Philadelphia, Pa.

Ex-officio members

Chairmen of the technical committees in the Science and Electronics Group

Basic Sciences

Walther Richter, *chairman;* Allis-Chalmers Manufacturing Company, P. O. Box 512, West Allis, Wis.

M. G. Malti, *vice-chairman*	Ithaca, N. Y.
N. S. Hibshman, *secretary*	Brooklyn, N. Y.
J. A. Becker	Murray Hill, N. J.
L. V. Bewley	Bethlehem, Pa.
C. R. Burrows	Ithaca, N. Y.
F. M. Clark	Schenectady, N. Y.
Charles Concordia	Schenectady, N. Y.
P. C. Cromwell	Knoxville, Tenn.

(*Continued on page 1425*)

L. A. Finzi	Pittsburgh, Pa.
E. A. Gaugler	Silver Spring, Md.
W. C. Hall	Washington, D. C.
C. W. Hansell	Rocky Point, N. Y.
F. K. Harris	Washington, D. C.
V. P. Hessler	Urbana, Ill.
T. J. Higgins	Madison, Wis.
G. B. Hoadley	Raleigh, N. C.
W. C. Johnson	Princeton, N. J.
W. A. Lewis, Jr.	Chicago, Ill.
W. H. MacWilliams, Jr.	Whippany, N. J.
P. C. Magnusson	Corvallis, Oreg.
R. C. Mason	East Pittsburgh, Pa.
L. W. Matsch	Chicago, Ill.
G. D. McCann	Pasadena, Cal
K. W. Miller	Chicago, Ill.
W. E. Phillips	Philadelphia, Pa.
H. J. Plumley	Silver Spring, Md.
Dimiter Ramadanoff	Cleveland, Ohio
W. J. Seeley	Durham, N. C.
H. H. Skilling	Stanford, Calif.
Joseph Slepian	East Pittsburgh, Pa.
J. J. Smith	Schenectady, N. Y.
V. G. Smith	Toronto, Ontario, Canada
F. G. Tappan	Norman, Okla.
J. D. Tebo	New York, N. Y.
G. S. Timoshenko	Storrs, Conn.
J. S. Waters	Houston, Tex.
A. H. Waynick	State College, Pa.
T. D. Yensen	East Pittsburgh, Pa.

Applied Mathematics Subcommittee

M. G. Malti, *chairman;* Cornell University, School of Electrical Engineering, Ithaca, N. Y.

P. L. Alger	Schenectady, N. Y.
H. B. Hansteen	Ithaca, N. Y.
E. W. Kimbark	Evanston, Ill.
Joseph Slepian	East Pittsburgh, Pa.
J. J. Smith	Schenectady, N. Y.
Harry Sohon	Philadelphia, Pa.

Electric Circuit Theory Subcommittee

T. J. Higgins, *chairman;* University of Wisconsin, Department of Electrical Engineering, Madison 6, Wis.

J. G. Brainerd	Philadelphia, Pa.
H. J. Carlin	Brooklyn, N. Y.
R. L. Dietzold	Murray Hill, N. J.
E. A. Guillemin	Cambridge, Mass.
F. J. Maginnis	Schenectady, N. Y.
W. O. Osborn	East Pittsburgh, Pa.
E. B. Payne	New York, N. Y.
W. E. Phillips	Philadelphia, Pa.
M. C. Reed	Urbana, Ill.
H. I. Tarpley	State College, Pa.
Ernst Weber	Brooklyn, N. Y.

Energy Sources Subcommittee

L. W. Matsch, *chairman;* Armour Research Foundation, Electrical Engineering Department, 35 West 33rd Street, Chicago 16, Ill.

W. C. Brown	Bradley Beach, N. J.
M. A. Gartens	Washington, D. C.
W. A. Lewis, Jr.	Chicago, Ill.
Walther Richter	Milwaukee, Wis.
J. J. Smith	Schenectady, N. Y.
B. R. Teare	Pittsburgh, Pa.
J. D. Tebo	New York, N. Y.

Electrical Properties of Solids and Liquids Subcommittee

Joseph A. Becker, *chairman;* Bell Telephone Laboratories, Inc., Murray Hill, N. J.

Stephen Angello	East Pittsburgh, Pa.
C. B. Brown	Washington, D. C.
F. M. Clark	Schenectady, N. Y.
W. C. Dunlap	Schenectady, N. Y.
R. W. Engstrom	Lancaster, Pa.
K. Lark-Horovitz	Lafayette, Ind.
P. H. Miller, Jr.	Philadelphia, Pa.
Fred Seitz	Pittsburgh, Pa.
Lloyd Smith	Ithaca, N. Y.
A. von Hippel	Cambridge, Mass.
D. W. Wooldridge	Culver City, Calif.

Magnetics Subcommittee

T. D. Yensen, *chairman;* Westinghouse Research Laboratories, Ardmore Boulevard, East Pittsburgh, Pa.

H. G. Zambell, *secretary*	Pittsburgh, Pa.
J. P. Barton	Pittsburgh, Pa.
R. M. Bozorth	Murray Hill, N. J.
F. J. Brockman	Irvington-on-Hudson, N. Y.
G. H. Cole	Middletown, Ohio
E. A. Gaugler	Silver Spring, Md.
S. L. Quimby	New York, N. Y.
W. E. Ruder	Schenectady, N. Y.

(*Continued in next column*)

The Electrical Properties of Gases Subcommittee

Joseph Slepian, *chairman;* Westinghouse Electric Corporation, Research Laboratories, East Pittsburgh, Pa.

T. B. Jones, *vice-chairman*	Baltimore, Md.
J. D. Cobine	Schenectady, N. Y.
L. H. Fisher	New York, N. Y.
L. H. Germer	New York, N. Y.

Computing Devices

J. G. Brainerd, *chairman;* Moore School of Electrical Engineering, University of Pennsylvania, Philadelphia 4, Pa.

W. H. MacWilliams, Jr., *vice-chairman*	Whippany, N. J.
W. C. Johnson, *secretary*	Princeton, N. J.
S. N. Alexander	Washington, D. C.
S. H. Caldwell	Cambridge, Mass.
Charles Concordia	Schenectady, N. Y.
G. V. Eltgroth	Philadelphia, Pa.
E. L. Harder	East Pittsburgh, Pa.
J. W. Mauchly	Philadelphia, Pa
G. D. McCann	Pasadena, Calif.
M. S. McIlroy	Ithaca, N. Y.
J. C. McPherson	New York, N. Y.
P. L. Morton	Berkeley, Calif.
G. R. Stibitz	Burlington, Vt.

Continuous-Variable Computers Subcommittee

E. L. Harder, *chairman;* Westinghouse Electric Corporation, East Pittsburgh, Pa.

(Personnel to be selected)

Digital Computers Subcommittee

John W. Mauchly, *chairman;* Eckert-Mauchly Computer Corporation Broad and Spring Garden Streets, Philadelphia 23, Pa.

Electronic Power Converters

C. C. Herskind, *chairman;* Power Electronics Division, General Electric Company, 1 River Road, Schenectady 5, N. Y.

W. N. Farquhar, *vice-chairman*	Pittsburgh, Pa.
C. R. Marcum, *secretary*	East Pittsburgh, Pa.
H. R. Blomquist	Providence, R. I.
W. F. Bonner	East Newark, N. J.
J. L. Boyer	East Pittsburgh, Pa.
J. H. Cox	Sunnyvale, Calif.
F. W. Cramer	Pittsburgh, Pa.
A. G. Dickinson	Trail, British Columbia, Canada
J. B. Donnelly	Philadelphia, Pa.
I. K. Dortort	Milwaukee, Wis.
William Fraser	Arvida, Quebec, Can.
W. E. Gutzwiller	Milwaukee, Wis.
G. N. Hughes	Alcoa, Tenn.
Otto Jensen	Philadelphia, Pa.
W. K. MacAdam	New York, N. Y.
D. E. Marshall	Bloomfield, N. J.
A. J. Maslin	Sharon, Pa.
L. W. Morton	Schenectady, N. Y.
R. A. Nelson	Pittsfield, Mass.
Waldo Porter	Vancouver, Wash.
M. E. Reagan	East Pittsburgh, Pa.
W. J. L. Rupprecht	Midland, Mich.
August Schmidt, Jr.	Schenectady, N. Y.
W. C. Sealey	Milwaukee, Wis.
F. W. Smith	Easton, Pa.
S. L. Smith	Philadelphia, Pa.
H. C. Steiner	Schenectady, N. Y.
O. J. Swanson	Gary, W. Va.
J. T. Thwaites	Hamilton, Ontario, Canada
D. E. Truckses	New York, N. Y.
C. H. Willis	Princeton, N. J.
Harold Winograd	Milwaukee, Wis.

Administrative Subcommittee

Main Committee Officers:

C. C. Herskind, *chairman;* General Electric Company, Power Electronics Division, Schenectady 5, N. Y.

W. N. Farquhar, *vice-chairman*	Pittsburgh, Pa.
C. R. Marcum, *secretary*	East Pittsburgh, Pa.
Harold Winograd, *preceding chairman*	Milwaukee, Wis.

(*Continued in next column*)

Subcommittee Chairmen:

J. H. Cox	Sunnyvale, Calif.
I. K. Dortort	Milwaukee, Wis.
R. A. Nelson	Pittsfield, Mass.
August Schmidt, Jr.	Schenectady, N. Y.
D. E. Truckses	New York, N. Y.

Electronic Converter Application Subcommittee

W. N. Farquhar, *chairman;* Aluminum Company of America, 801 Gulf Building, Pittsburgh 19, Pa.

F. W. Cramer	Pittsburgh, Pa.
J. B. Donnelly	Philadelphia, Pa.
William Fraser	Arvida, Quebec, Canada
C. E. Buterbaugh	
N. W. Geist	
W. E. Gutzwiller	Milwaukee, Wis.
R. N. Hunter	New York, N. Y.
W. K. MacAdam	New York, N. Y.
W. J. L. Rupprecht	Midland, Mich.
S. L. Smith	Philadelphia, Pa.
O. J. Swanson	Gary, W. Va.
J. T. Thwaites	Hamilton, Ontario, Canada

Electronic Converter Circuits Subcommittee

I. K. Dortort, *chairman;* Allis-Chalmers Manufacturing Company, Electrical Department, Milwaukee 1, Wis.

W. F. Bonner	East Newark, N. J.
J. L. Boyer	East Pittsburgh, Pa.
G. N. Hughes	Alcoa, Tenn.
Otto Jensen	Philadelphia, Pa.
W. K. MacAdam	New York, N. Y.
A. H. Mittag	Schenectady, N. Y.
R. A. Nelson	Pittsfield, Mass.
R. J. Pogorzelski	Detroit, Mich.
M. E. Reagan	East Pittsburgh, Pa.
August Schmidt, Jr.	Schenectady, N. Y.

Papers and Speakers Subcommittee

August Schmidt, Jr., *chairman;* General Electric Company, 1 River Road, Schenectady 5, N. Y.

J. B. Rice	West Allis, Wis.
J. T. Thwaites	Hamilton, Ontario, Canada
H. E. Zuvers	Schenectady, N. Y.

Rectifier Transformers Subcommittee

R. A. Nelson, *chairman;* General Electric Company, 100 Woodlawn Avenue, Pittsfield, Mass.

F. D. Kaiser	Sharon, Pa.
A. J. Maslin	Sharon, Pa.
W. C. Sealey	Milwaukee, Wis.

Rectifying Devices Subcommittee

Harold Winograd, *chairman;* Allis-Chalmers Manufacturing Company, Electrical Department, Milwaukee 1, Wis.

D. V. Edwards	Newark, N. J.
D. E. Marshall	Bloomfield, N. J.
H. C. Steiner	Schenectady, N. Y.

West Coast Subcommittee

J. H. Cox, *chairman;* Westinghouse Electric Corporation, Sunnyvale, Calif.

W. M. Allen	Portland, Oreg.
E. D. Barcus	Los Angeles, Calif.
E. S. Benson	San Francisco, Calif.
H. L. Burris	Pittsburg, Calif.
R. J. Corfield	Garfield, Utah
R. H. Denyer	Portland, Oreg.
A. G. Dickinson	Trail, British Columbia, Canada
E. F. Donatic	Ontario, Calif.
Alex. Dovjikov	Portland, Oreg.
R. H. Duguid	Los Angeles, Calif.
S. R. Durand	Milwaukee, Wis.
L. E. Dye	Los Angeles, Calif.
T. F. Hadwin	Vancouver, British Columbia, Canada
D. R. Hoopes	Salt Lake City, Utah
J. V. Kresser	San Francisco, Calif.
C. A. Langlois	Portland, Oreg.
H. F. Lickey	Pullman, Wash.
M. McCoy	Portland, Oreg.
A. L. Munn	San Leandro, Calif.
S. J. Pope	Spokane, Wash.
Waldo Porter	Vancouver, Wash.
H. H. Skilling	Stamford, Calif.
E. C. Starr	Corvallis, Oreg.
H. V. Strandberg	Seattle, Wash.
J. R. Tenney	Geneva, Utah

Hot-Cathode Power Converter Subcommittee

D. E. Truckses, *chairman;* Bell Telephone Laboratories, Inc., 463 West Street, New York 14, N. Y.

H. R. Butler	Newark, N. J.
F. W. Cramer	Pittsburgh, Pa.
E. V. DeBlieux	Pittsfield, Mass.
D. V. Edwards	Newark, N. J.
C. E. Hamann	Lynn, Mass.
J. F. Harris	Newark, N. J.
E. W. Hutton	Schenectady, N. Y.
W. E. Large	East Pittsburgh, Pa.
F. G. Logan	St. Louis, Mo.
Roman Pogorzelski	Detroit, Mich.
E. J. Rathsack	Milwaukee, Wis.
F. M. Rives	Schenectady, N. Y.
W. C. Rudd	Brooklyn, N. Y.
J. W. Sanborn	Camden, N. J.
H. C. Steiner	Schenectady, N. Y.
H. L. Thorson	Schenectady, N. Y.
J. C. Walter	Washington, D. C.

Electronics

W. G. Dow, *chairman;* Department of Electrical Engineering, University of Michigan, Ann Arbor, Mich.

J. T. Thwaites, *vice-chairman* (East)	Hamilton, Ontario, Canada
A. M. Zarem, *vice-chairman* (West)	Los Angeles, Calif.
E. M. Boone, *secretary*	Columbus, Ohio
W. R. G. Baker	Syracuse, N. Y.
Rawson Bennett	San Diego, Calif.
C. J. Breitwieser	San Diego, Calif.
C. B. Brown	Washington, D. C.
R. S. Burnap	Harrison, N. J.
A. H. Canada	Schenectady, N. Y.
W. R. Clark	Philadelphia, Pa.
L. G. Cowles	Houston, Tex.
C. F. Crandell	Dallas, Tex.
G. J. Crowdes	Cambridge, Mass.
A. V. Eastman	Seattle, Wash.
G. V. Eltgroth	Philadelphia, Pa.
Rudolf Feldt	Clifton, N. J.
G. H. Fett	Urbana, Ill.
D. G. Fink	New York, N. Y.
H. L. Flowers	Washington, D. C.
W. A. Geohegan	New York, N. Y.
E. R. Haberland	Silver Spring, Md.
E. L. Harder	East Pittsburgh, Pa.
G. W. Hewitt	East Pittsburgh, Pa.
J. E. Hobson	Stanford, Calif.
J. R. Hyneman	New York, N. Y.
T. P. Kinn	Baltimore, Md.
K. S. Koon	Endicott, N. Y.
W. A. Leidigh, Jr.	Portland, Oreg.
O. W. Livingston	Schenectady, N. Y.
D. E. Marshall	Bloomfield, N. J.
R. C. Mason	East Pittsburgh, Pa.
S. T. Maunder	Pittsfield, Mass.
H. R. Meahl	Schenectady, N. Y.
H. R. Mimno	Cambridge, Mass.
G. A. Morton	Princeton, N. J.
R. E. Mumma	Dayton, Ohio
B. K. Northrop	Ithaca, N. Y.
J. K. Nunan	Hollywood, Calif.
David Packard	Palo Alto, Calif.
H. L. Palmer	Schenectady, N. Y.
G. W. Penney	Pittsburgh, Pa.
W. H. Pickering	Pasadena, Calif.
O. W. Pike	Schenectady, N. Y.
A. J. Quigley	Notre Dame, Ind.
Simon Ramo	Culver City, Calif.
J. G. Reid, Jr.	Washington, D. C.
L. E. Reukema	Berkeley, Calif.
R. W. Reynolds	Wilmington, Del.
J. D. Ryder	Urbana, Ill.
Hubert Sharp	Denver, Colo.
M. R. Shaw	Corning, N. Y.
E. T. Sherwood	Milwaukee, Wis.
S. W. Smith	Washington, D. C.
E. P. Spandau	Dayton, Ohio
H. C. Steiner	Schenectady, N. Y.
C. M. Summers	Fort Wayne, Ind.
E. R. Thomas	New York, N. Y.
F. N. Tompkins	Providence, R. I.
D. E. Truckses	New York, N. Y.
D. C. Ulrey	Lancaster, Pa.
R. F. Wall	College Station, Tex.
A. S. Waxman	Sparrows Point, Md.
W. C. White	Schenectady, N. Y.
C. H. Willis	Princeton, N. J.
D. G. Wilson	Lawrence, Kans.
Harold Winograd	Milwaukee, Wis.

Electronic Papers, Meetings, and Section Contacts Subcommittee

W. C. White, *chairman;* General Electric

(*Continued on page 1426*)

Research Laboratory, The Knolls, Schenectady, N. Y.
(Personnel to be selected)

Electronic Standards and Definitions Subcommittee

O. W. Pike, *chairman;* Vacuum Tube Engineering Department, General Electric Company, Schenectady 5, N. Y.
(Personnel to be selected)

Electronic Education Subcommittee

J. D. Ryder, *chairman;* Department of Electrical Engineering, Iowa State College, Ames, Iowa
(Personnel to be selected)

Liaison With IRE Subcommittee

R. S. Burnap, *chairman;* RCA Victor Division, Radio Corporation of America, Harrison, N. J.

Liaison With JETEC Subcommittee

O. W. Pike, *chairman;* Vacuum Tube Engineering Department, General Electric Company, Schenectady 5, N. Y.

Electron Tubes Subcommittee

H. C. Steiner, *chairman;* Electrical Department, General Electric Company Schenectady 5, N. Y.
(Personnel to be selected)

X-Ray Tubes, Apparatus, and Applications Subcommittee

Scott W. Smith, *chairman;* National Bureau of Standards, Washington, D. C.
(Personnel to be selected)

Electronic Precipitation Subcommittee

G. W. Hewitt, *chairman;* Westinghouse Electric Corporation, East Pittsburgh, Pa.
(Personnel to be selected)

High-Frequency Conductors, Cables, and Connectors Subcommittee

G. J. Crowdes, *chairman;* Simplex Wire and Cable Company, 79 Sidney Street, Cambridge 39, Mass.
(Personnel to be selected)

Liaison With Nucleonics Subcommittee

G. A. Morton, *chairman;* RCA Laboratories, Princeton, N. J.

Electronic Aids to Navigation Subcommittee

H. R. Mimno, *chairman;* Gordon McKay Professor, Engineering Sciences and Applied Physics Department, Harvard University, Cambridge, Mass.

Electronic Aids to Geophysics Subcommittee

L. G. Cowles, *chairman;* Superior Oil Company, Houston, Tex.

Infrared Applications Subcommittee

A. H. Canada, *chairman;* General Engineering Laboratory, General Electric Company, Schenectady 5, N. Y.
(Personnel to be selected)

Electronic Processing and Preservation of Foods and Biological Products Subcommittee

(Personnel to be selected)

Magnetic Amplifiers Subcommittee

E. L. Harder, *chairman;* Industry Engineering Department—11-L, Westinghouse Electric Corporation, East Pittsburgh, Pa.
(Personnel to be selected)

Applications of Semiconductor Devices Subcommittee

C. B. Brown, *chairman;* Naval Ordnance Laboratory, Washington, D. C.
(Personnel to be selected)

Electronic Heating Liaison Subcommittee

T. P. Kinn, *chairman;* Westinghouse Electric Corporation, 2519 Wilkens Avenue, Baltimore 3, Md.

Instruments and Measurements

W. R. Clark, *chairman;* Leeds and Northrup Company, 4901 Stenton Avenue, Philadelphia 44, Pa.

J. H. Miller, *vice-chairman* (East)	Newark, N. J.
J. E. Hobson, *vice-chairman* (West)	Stanford, Calif.
J. G. Reid, Jr., *secretary*	Washington, D. C.
P. L. Bellaschi	Sharon, Pa.
H. W. Berry	Camden, N. J.
P. A. Borden	Waterbury, Conn.
D. L. Brown	Portland, Oreg.
G. S. Brown	Cambridge, Mass.
A. L. Brownlee	Chicago, Ill.
L. A. Burckmyer, Jr.	Ithaca, N. Y.
R. T. Capodanno	Philadelphia, Pa.
J. H. Chiles, Jr.	Sharon, Pa.
J. E. Clem	Schenectady, N. Y.
A. B. Craig	Boston, Mass.
C. L. Dawes	Cambridge, Mass.
F. C. Doble	Belmont, Mass.
E. D. Doyle	Philadelphia, Pa.
C. K. Duff	Toronto, Ontario, Canada
C. A. Duke	Chattanooga, Tenn.
G. W. Dunlap	Schenectady, N. Y.
W. N. Eddy	Cambridge, Mass.
G. V. Eltgroth	Philadelphia, Pa.
Rudolf Feldt	Clifton, N. J.
F. J. Gaffney	Brooklyn, N. Y.
W. A. Geohegan	New York, N. Y.
T. S. Gray	Cambridge, Mass.
E. I. Green	New York, N. Y.
G. B. Hoadley	Raleigh, N. C.
A. J. Hornfeck	Cleveland, Ohio
W. G. Knickerbocker	Detroit, Mich.
A. E. Knowlton	New York, N. Y.
H. C. Koenig	New York, N. Y.
E. S. Lee	Schenectady, N. Y.
B. E. Lenehan	Newark, N. J.
W. N. Lindblad	Emeryville, Calif.
J. T. Lusignan, Jr.	Mansfield, Ohio
Harold Lyons	Washington, D. C.
L. W. Matsch	Chicago, Ill.
Whitney Matthews	Washington, D. C.
W. J. Mayo-Wells	Silver Spring, Md.
David Packard	Palo Alto, Calif.
H. J. Plumley	Silver Spring, Md.
C. F. Savage	Lynn, Mass.
J. P. Scott	St. Louis, Mo.
F. B. Silsbee	Washington, D. C.
D. B. Sinclair	Cambridge, Mass.
Harry Sohon	Philadelphia, Pa.
M. B. Stout	Ann Arbor, Mich.
J. M. Vanderleck	Toronto, Ontario, Canada
A. H. Wing, Jr.	Evanston, Ill.
C. J. Zeller	New York, N. Y.

Organization Subcommittee

T. S. Gray, *chairman;* Massachusetts Institute of Technology, Cambridge 39, Mass.

C. F. Savage, *secretary*	Marblehead, Mass.
E. I. Green	New York, N. Y.
H. C. Koenig	New York, N. Y.
J. G. Reid, Jr.	Washington, D. C.

Revision of Standard Number 4 Subcommittee (Measurement of Test Voltage in Dielectric Tests)

J. T. Lusignan, *chairman;* Ohio Brass Company, Mansfield, Ohio

P. L. Bellaschi	Sharon, Pa.
A. L. Brownlee	Chicago, Ill.
J. S. Carroll	Stanford University, Calif.
J. J. Clark	East Pittsburgh, Pa.
J. E. Clem	Schenectady, N. Y.
E. W. Davis	Cambridge, Mass.
C. M. Foust	Schenectady, N. Y.
H. A. Frey	Baltimore, Md.
I. W. Gross	New York, N. Y.
J. H. Hagenguth	Pittsfield, Mass.
W. B. Kouwenhoven	Baltimore, Md.
R. S. Lapp	LeRoy, N. Y.
W. W. Lewis	Schenectady, N. Y.
M. Newman	Minneapolis, Minn.
J. H. Park	Washington, D. C.
W. C. Sealey	Milwaukee, Wis.
W. T. Smith	Washington, D. C.
R. W. Sorensen	Pasadena, Calif.
W. L. Teague	Sharon, Pa.
S. W. Zimmerman	Ithaca, N. Y.

(*Continued in next column*)

Watthour Meters Subcommittee

C. F. Savage, *chairman;* General Electric Company, Lynn, Mass.

H. A. Brown	Rochester, N. Y.
D. T. Canfield	Lafayette, Ind.
A. B. Craig	Boston, Mass.
C. K. Duff	Toronto, Ontario, Canada
F. C. Holtz	Springfield, Ill.
W. G. Knickerbocker	Detroit, Mich.
H. C. Koenig	New York, N. Y.
B. E. Lenehan	Newark, N. J.
F. H. Rogers	Baltimore, Md.
M. B. Stout	Ann Arbor, Mich.

Definitions Subcommittee

C. L. Dawes, *chairman;* Harvard University, Cambridge 39, Mass.

J. E. Clem	Schenectady, N. Y.
A. B. Craig	Boston, Mass.
H. C. Dickinson	Lynn, Mass.
W. N. Goodwin, Jr.	Newark, N. J.
E. S. Lee	Schenectady, N. Y.
B. E. Lenehan	Newark, N. J.
P. MacGahan	Haines Falls, N. Y.
F. B. Silsbee	Washington, D. C.

Dielectric Measurements in the Field Subcommittee

F. C. Doble, *chairman;* Doble Engineering Company, Belmont 78, Mass.

D. L. Brown	Portland, Oreg.
A. L. Brownlee	Chicago, Ill.
E. B. Curdts	Philadelphia, Pa.
C. L. Dawes	Cambridge, Mass.
E. D. Doyle	Philadelphia, Pa.
W. F. Dunkle	Hazleton, Pa.
I. G. Easton	New York, N. Y.
W. N. Eddy	Cambridge, Mass.
I. W. Gross	New York, N. Y.
E. S. Lee	Schenectady, N. Y.
W. N. Lindblad	Emeryville, Calif.
G. M. L. Sommerman	Evanston, Ill.
Lynn Wetherill	Pittsfield, Mass.

Master Test Code for Temperature Measurements Subcommittee

L. A. Burckmyer, Jr., *chairman;* Cornell University, Ithaca, N. Y.

P. A. Borden	Waterbury, Conn.
E. D. Doyle	Philadelphia, Pa.
J. [illegible]	Cleveland, Ohio
W. [illegible]	Cleveland, Ohio
A. R. [illegible]	New York, N. Y.
M. D. Ross	East Pittsburgh, Pa.
S. S. Stack	Schenectady, N. Y.

High-Frequency Measurements Subcommittee

H. Lyons, *chairman;* Microwave Measurement Laboratory, National Bureau of Standards, Washington, D. C.

R. T. Capodanno	Philadelphia, Pa.
F. L. Creager	Princeton, N. J.
I. G. Easton	New York, N. Y.
E. P. Felch	New York, N. Y.
F. J. Gaffney	Brooklyn, N. Y.
E. I. Green	New York, N. Y.
F. Hamburger, Jr.	Baltimore, Md.
G. B. Hoadley	Brooklyn, N. Y.
H. R. Meahl	Schenectady, N. Y.
H. J. Plumley	Silver Spring, Md.
H. E. Webber	Great Neck, N. Y.
Ernst Weber	Brooklyn, N. Y.
H. A. Wheeler	Great Neck, N. Y.
A. J. Wing, Jr.	Evanston, Ill.

Marking of Varmeters and Related Instruments

A. B. Craig, *chairman;* Boston Edison Company, 39 Boylston Street, Boston 12, Mass.

A. L. Brownlee	Chicago, Ill.
A. L. Carvill	New York, N. Y.
W. G. Knickerbocker	Detroit, Mich.
A. E. Knowlton	New York, N. Y.
F. A. Redding	Los Angeles, Calif.
F. B. Silsbee	Washington, D. C.
H. B. Smith	Buffalo, N. Y.
J. S. Wantland	Oklahoma City, Okla.

Co-operation With Instrument Society of America Subcommittee

J. P. Scott, *chairman;* Union Electric Company of Missouri, 414 North Tenth Street, St. Louis, Mo.

(*Continued in next column*)

W. R. Clark	Philadelphia, Pa.
J. G. Reid, Jr.	Washington, D. C.

Metallic Rectifiers

L. O. Grondahl, *chairman;* Union Switch and Signal Company and Westinghouse Air Brake Company, Pittsburgh 18, Pa.

I. R. Smith, *vice-chairman*	Buffalo, N. Y.
E. A. Harty, *secretary*	West Lynn, Mass.
W. F. Bonner	East Newark, N. J.
L. W. Burton	Lynn, Mass.
P. G. Cobb	Newark, N. J.
M. E. Gamble	Indianapolis, Ind.
K. S. Geiges	New York, N. Y.
E. A. Groeteke	St. Louis, Mo.
C. E. Hamann	Lynn, Mass.
C. W. Hansell	Rocky Point, N. Y.
C. C. Herskind	Schenectady, N. Y.
W. E. Phillips	Philadelphia, Pa.
N. Y. Priessman	Murray Hill, N. J.
Glen Ramsey	North Chicago, Ill.
D. E. Trucksess	New York, N. Y.
J. L. Wagner	Endicott, N. Y.
E. D. Wilson	East Pittsburgh, Pa.
Stanley Zwerling	Laurelton, N. Y.

Standard Definitions Subcommittee

I. R. Smith, *chairman;* Westinghouse Electric Corporation, Box 2025, Buffalo 5, N. Y.
(Personnel to be selected)

New Definitions Subcommittee

D. E. Trucksess, *chairman;* Bell Telephone Laboratories, Inc., 463 West Street, New York 14, N. Y.
(Personnel to be selected)

Bibliography Subcommittee

E. A. Harty, *chairman;* Lightning Engineering Division, General Electric Company, River Works, West Lynn 3, Mass.
(Personnel to be selected)

Test Standards Subcommittee

W. F. Bonner, *chairman;* Federal Telephone and Radio Corporation, 900 Passaic Avenue, East Newark, N. J.
(Personnel to be selected)

Patent Bibliography Subcommittee

Glen Ramsey, *chairman;* Fansteel Metallurgical Corporation, Rectifier Division, North Chicago, Ill.
(Personnel to be selected)

Papers and Speakers Subcommittee

N. Y. Priessman, *chairman;* Bell Telephone Laboratories, Inc., Murray Hill, N. J.
(Personnel to be selected)

Miniature Rectifiers Subcommittee

P. G. Cobb, *chairman;* Weston Electrical Instrument Corporation, 614 Frelinghuysen Avenue, Newark 5, N. J.
(Personnel to be selected)

Nucleonics

J. J. Smith, *chairman;* General Engineering and Consulting Laboratory, General Electric Company, Schenectady 5, N. Y.

W. F. Davidson, *vice-chariman*	New York, N. Y.
P. N. Ross, *secretary*	Pittsburgh, Pa.
W. E. Barbour, Jr.	Boston, Mass.
H. W. Bibber	Schenectady, N. Y.
H. W. Brackney	Upton, N. Y.
L. J. Bulliet	Rockford, Ill.
J. M. Cork	Ann Arbor, Mich.
G. W. Dunlap	Schenectady, N. Y.
J. R. Dunning	New York, N. Y.
I. A. Getting	Cambridge, Mass.
T. S. Gray	Cambridge, Mass.
M. M. Hubbard	Cambridge, Mass.
H. L. Hull	Chicago, Ill.
T. R. Kohler	Irvington-on-Hudson, N. Y.
E. H. Krieg	Boston, Mass.
R. G. Lorraine	Schenectady, N. Y.

(*Continued on page 1427*)

H. B. Marvin	Syracuse, N. Y.
J. K. Pickard	Washington, D. C.
Walther Richter	Milwaukee, Wis.
Frederick Seitz	Urbana, Ill.
W. E. Shoupp	Homestead, Pa.
Abe Tilles	San Francisco, Calif.
J. G. Trump	Cambridge, Mass.
R. E. Watson	Philadelphia, Pa.
J. T. Wilson	Milwaukee, Wis.

Isotopic Tracers Subcommittee

W. E. Barbour, Jr., *chairman;* Tracerlab, Inc., 55 Oliver Street, Boston 10, Mass.

A. J. Allen	Pittsburgh, Pa.
J. T. Burwell, Jr.	Cambridge, Mass.
C. Herzog	Bellaire, Tex.
M. D. Kamen	St. Louis, Mo.
W. W. Miller	Upton, N. Y.
Morris Muskat	Pittsburgh, Pa.
A. F. Reid	Dallas, Tex.
R. E. Watson	Philadelphia, Pa.
Nathan Woodruff	Oak Ridge, Tenn.

Studies of Nuclear Theory Subcommittee

J. T. Wilson, *chairman;* Allis-Chalmers Manufacturing Company, Milwaukee 1, Wis.

(Personnel to be selected)

Therapeutics

H. D. Moreland, *chairman;* Westinghouse Electric Corporation, 2519 Wilkens Avenue, Baltimore 3, Md.

S. Reid Warren, Jr., *vice-chairman*	Philadelphia, Pa.
Scott W. Smith, *secretary*	Washington, D. C.
F. B. Claussen	Portland, Oreg.
M. J. Gross	Milwaukee, Wis.
W. B. Kouwenhoven	Baltimore, Md.
R. H. Morgan	Baltimore, Md.
T. H. Rogers	Springdale, Conn.
C. M. Slack	Bloomfield, N. J.
W. R. Smith	Newark, N. J.
R. E. Watson	Philadelphia, Pa.

No subcommittees

Joint Subcommittees

Joint Subcommittee on Application of Probability Methods to Power-System Problems (Joint With Power Generation and System Engineering Committees)

G. Calabrese, *chairman;* Electrical Engineering Department, New York University, University Heights, New York, N. Y.

V. A. Thiemann, *secretary*	New York, N. Y.
W. R. Blakeley	Toronto, Ontario, Canada
Howard Duryea	Birmingham, Ala.
R. G. Hooke	Newark, N. J.
H. A. Lott	Los Angeles, Calif.
W. J. Lyman	Pittsburgh, Pa.
H. W. Phillips	Philadelphia, Pa.
C. A. Roberts	Chattanooga, Tenn.
H. B. Smith	Buffalo, N. Y.
H. P. St. Clair	New York, N. Y.
G. M. Tatum	Richmond, Va.
C. W. Watehorn	Baltimore, Md.

Joint Subcommittee on Carbon Brushes (Joint AIEE Technical Committees on Air Transportation and Rotating Machinery, and in Co-operation With NEMA on Codes)

T. M. Linville, *chairman;* General Electric Company, 1 River Road, Schenectady 5, N. Y.

W. H. Austry	St. Marys, Pa.
H. R. Brown	Seattle, Wash.
W. E. Clancy (NEMA)	St. Marys, Pa.
J. V. Dobson	St. Marys, Pa.
H. M. Elsey	East Pittsburgh, Pa.
C. J. Herman	Fort Wayne, Ind.
V. P. Hessler	Urbana, Ill.
L. H. Hildebrandt	Dayton, Ohio
H. E. Keneipp	Lima, Ohio
E. A. Lapham	Long Island City, N. Y.
D. Ramadanoff	Cleveland, Ohio
O. C. Rutledge (NEMA)	Schenectady, N. Y.
S. D. Summers	Washington, D. C.
A. L. Van Emden	Washington, D. C.

Joint Subcommittee on Nucleonic Instruments (Joint with Nucleonics and Instruments and Measurements Committees)

(*Continued in next column*)

G. W. Dunlap, *chairman;* General Engineering and Consulting Laboratory, General Electric Company, Schenectady 5, N. Y.

E. E. Goodale, *secretary*	Schenectady, N. Y.
W. E. Barbour, Jr.	Boston, Mass.
L. F. Curtiss	Washington, D. C.
F. J. Gaffney	Brooklyn, N. Y.
W. H. Hall	Syracuse, N. Y.
M. M. Hubbard	Cambridge, Mass.
P. S. Johnson	Washington, D. C.
J. B. H. Kuper	Upton, N. Y.
F. D. Lewis	Cambridge, Mass.
G. A. Morton	Princeton, N. J.
M. A. Princi	West Lynn, Mass.
M. A. Schultz	Pittsburgh, Pa.
R. E. Watson	Philadelphia, Pa.
H. G. Weiss	Los Alamos, N. Mex.

Joint Subcommittee on Electronic Instruments (Joint with Electronics and Instruments and Measurements Committees)

J. G. Reid, Jr., *chairman;* National Bureau of Standards, Division 13.1, Washington 25, D. C.

Rudolf Feldt, *vice-chairman*	Clifton, N. J.
W. H. Tidd, *secretary*	New York, N. Y.
G. E. Beggs, Jr.	Philadelphia, Pa.
H. W. Berry	Camden, N. J.
C. C. Chambers	Philadelphia, Pa.
H. F. Dart	Bloomfield, N. J.
G. V. Eltgroth	Philadelphia, Pa.
D. B. Fisk	West Lynn, Mass.
W. A. Geohegan	New York, N. Y.
Truman S. Gray	Cambridge, Mass.
E. R. Haberland	Silver Spring, Md.
C. E. Hastings	Hampton, Va.
G. B. Hoadley	Raleigh, N. C.
E. J. Isbister	Garden City, N. Y.
C. A. Mabey	West Orange, N. J.
G. N. Mahaffey	Washington, D. C.
C. W. Martel	Newton, Mass.
N. W. Matthews	Washington, D. C.
P. K. McElroy	Cambridge, Mass.
H. R. Meahl	Schenectady, N. Y
David Packard	Palo Alto, Calif.
T. B. Perkins	Harrison, N. J.
J. J. Slattery	Belmar, N. J.
E. R. Thomas	New York, N. Y.
J. T. Thwaites	Hamilton, Ontario, Canada
A. H. Waynick	State College, Pa.
W. P. Wills	Philadelphia, Pa.

(*Continued in next column*)

Joint Subcommittee on Telemetering (Joint with Instruments and Measurements, Carrier Current, and Substations Committees)

C. K. Duff, *chairman;* Hydro-Electric Power Commission, 620 University Avenue, Toronto, Ontario, Canada

J. L. McKee, *secretary*	New York, N. Y.
J. L. Blackburn	Newark, N. J.
P. A. Borden	Waterbury, Conn.
M. A. Bostwick	Newark, N. J.
E. C. Brown	Hartford, Conn.
W. A. Derr	East Pittsburgh, Pa.
A. J. Hornfeck	Cleveland, Ohio
G. S. Lunge	Schenectady, N. Y.
E. E. Lynch	West Lynn, Mass.
W. J. Mayo-Wells	Silver Spring, Md.
W. E. Phillips	Philadelphia, Pa.
Merle Robison	Toledo, Ohio
G. M. Thynell	Waterbury, Conn.
J. H. Vivian	Los Angeles, Calif.
B. G. Walker	Minneapolis, Minn.
C. E. Winegartner	Cleveland, Ohio

Joint Subcommittee on Electrical Aids to Medicine (Joint with Electronics, Instruments and Measurements, and Therapeutics Committees)

Dr. W. A. Geohegan, *chairman;* Department of Anatomy, Cornell University Medical College, 1300 York Avenue, New York 21, N. Y.

G. W. Dunlap	Schenectady, N. Y.
Dr. Harry Grundfest	New York, N. Y.
Dr. J. P. Hervey	Baltimore, Md.
L. W. Matsch	Chicago, Ill.
G. A. Morton	Princeton, N. J.
J. G. Reid, Jr.	Washington, D.C.
S. W. Smith	Washington, D. C.
Dr. C. A. Tobias	Berkeley, Calif.
S. R. Warren, Jr.	Philadelphia, Pa.
A. M. Zarem	Los Angeles, Calif.

Institute Representatives

Aeronautical Electrical Equipment Standardization

W. V. Boughton, liaison representative with NASC and SAE	South Pasadena, Calif.

Alfred Noble Prize Committee, ASCE

T. M. Linville	Schenectady, N. Y.

American Association for the Advancement of Science, Council

J. W. Barker	New York, N. Y.
I. Melville Stein	Philadelphia, Pa.

American Research Committee on Grounding

C. T. Sinclair	Pittsburgh, Pa.

American Standards Association, Standards Council

F. E. Harrell	Cleveland, Ohio
Charles Rufus Harte	New Haven, Conn.
R. T. Henry	Buffalo, N. Y.

Alternates

R. C. Bergvall	East Pittsburgh, Pa.
J. R. North	Jackson, Mich.
E. B. Paxton	Schenectady, N. Y.

American Year Book, Advisory Board

H. H. Henline	New York, N. Y.

Construction Industry Advisory Council

Henry A. Lardner	New York, N. Y.

Electrical Standards Committee, ASA

John Grotzinger	Akron, Ohio
F. E. Harrell	Cleveland, Ohio
J. J. Pilliod	New York, N. Y.

Alternates

H. E. Farrer	New York, N. Y.
I. W. Gross	New York, N. Y.
E. B. Paxton	Schenectady, N. Y.

Division Assignment

Division on Communication and Electronics

H. E. Farrer	New York, N. Y.
F. E. Harrell	Cleveland, Ohio
J. J. Pilliod	New York, N. Y.

Division on Power

I. W. Gross	New York, N. Y.
John Grotzinger	Akron, Ohio
E. B. Paxton	Schenectady, N. Y.

Engineering Foundation Board

J. W. Barker	New York, N. Y.
C. G. Suits	Schenectady, N. Y.

Engineering Societies Monographs Committee

W. I. Slichter	New York, N. Y.

Engineers' Council for Professional Development

M. S. Coover	Ames, Iowa
E. W. Davis	Cambridge, Mass.
M. D. Hooven	Newark, N. J.

Engineers Joint Council

J. F. Fairman	New York, N. Y.
H. H. Henline	New York, N. Y.
B. D. Hull	Dallas, Tex.
Everett S. Lee	Schenectady, N. Y.

General Electric Educational Fund Fellowship Committee

J. F. Fairman	New York, N. Y.

Hertz Award Committee

M. S. Coover	Ames, Iowa

Hoover Medal Board of Award

H. S. Osborne	New York, N. Y.
David C. Prince	Schenectady, N. Y.
J. G. Tarboux	Ithaca, N. Y.

Industry Committee on Interior Wiring Design

M. M. Brandon	New York, N. Y.
L. C. Peterman	New York, N. Y.

John Fritz Medal Board of Award

J. F. Fairman	New York, N. Y.
J. Elmer Housley	Alcoa, Tenn.
B. D. Hull	Dallas, Tex.
Everett S. Lee	Schenectady, N. Y.

Joint Committee for Development of Statistical Applications in Engineering and Manufacturing

W. P. Dobson	Toronto, Ontario, Canada

Library Board, United Engineering Trustees, Inc.

N. S. Hibshman	Brooklyn, N. Y.
George Sutherland	New York, N. Y.

Marston Medal Board of Award

Harry B. Gear	Chicago, Ill.

National Association of Corrosion Engineers, Inter-Society Committee on Corrosion

L. J. Gorman	New York, N. Y.
H. M. Trueblood	Dobbs Ferry, N. Y.

National Bureau of Engineering Registration, Advisory Board

Elgin B. Robertson	Dallas, Tex.

National Electronics Conference, Board of Directors

W. G. Dow	Ann Arbor, Mich.

National Fire Protection Association, Electrical Committee

W. B. Kouwenhoven	Baltimore, Md.
Robin Beach, alternate	Brooklyn, N. Y.

National Fire Waste Council

Robin Beach	Brooklyn, N. Y.
W. B. Kouwenhoven	Baltimore, Md.

National Research Council, Division of Engineering and Industrial Research

W. B. Kouwenhoven	Baltimore, Md.

National Technological Advisory Committee Quarterly of Applied Mathematics

M. G. Malti	Ithaca, N. Y.

United Engineering Trustees, Inc.

J. F. Fairman	New York, N. Y.
W. H. Harrison	New York, N. Y.
D. A. Quarles	New York, N. Y.

United States National Committee of the International Commission on Illumination

Ward Harrison	Cleveland, Ohio
Harris Reinhardt	Flushing, N. Y.
E. H. Salter	New York, N. Y.

United States National Committee of the International Electrotechnical Commission

W. P. Dobson	Toronto, Ontario, Canada
H. E. Farrer	New York, N. Y.
F. E. Harrell	Cleveland, Ohio
E. B. Paxton	Schenectady, N. Y.
J. J. Pilliod	New York, N. Y.

Washington Award Commission

W. A. Lewis, Jr.	Chicago, Ill.
Frank V. Smith	Chicago, Ill.

World Power Conference, Executive Committee of United States National Committee

J. F. Fairman	New York, N. Y.